Japan Geoscience Union Meeting 2014
(28 April - 02 May 2014 at Pacifico YOKOHAMA, Kanagawa, Japan)

U01-01 Room:419 Time:May 1 09:00-09:15

International Activities of Science Council of Japan (TBD)

KASUGA, Fumiko[1*]

[1]Science Council of Japan

International activities of Science Council of Japan will be reviewed and discussed, including Future Earth, ICSU-WDS, and CODATA etc. (TBD)

Keywords: Future Earth, ICSU-WDS, GEOSS

Japan Geoscience Union Meeting 2014
(28 April - 02 May 2014 at Pacifico YOKOHAMA, Kanagawa, Japan)

U01-02 Room:419 Time:May 1 09:15-09:30

Global Data Framework and Japanese Contribution

MURAYAMA, Yasuhiro[1*]

[1]National Institute of Information and Communicatoins Technology

Open data is not only the subject discussed in the last G8 meeting 2013, but also can be a wide-spread argument and can become substantially important factor in conducting science. Of course we cannot make all the research data publicly open immediately after its creation. But also data and paper are important in the modern science scheme, for validating results of a scientific research, e.g., its reproduction or statistical significance particularly in fields such as physics, earth science, or so. Recently there are found scientific results in certain percentage of original papers which are not necessarily reproducible in life science fields. Today's society has increasingly big concern with climate change and huge earthquake etc., where scientific research may directly affect real worlds like political and people's decision making. Validation of scientific papers is important since it may affect mutual trust between science and society. Here electronic data which can be linked to scientific papers in data citation scheme, are part of evidence of our scientific truth. In comparison to the history for a couple of hundred year of the printing culture in scholarly communications, the modern technology like Internet, hard disk drives, etc., have only the tens-of-years history. Human beings are now challenging this new system of electronic way to conduct science with society, seeking the right strategy for management of scholarly information. International data management activity like ICSU-WDS from the academic side, and RDA related to governmental arrangement are part of such big challenges of the international community. Furthermore Future Earth, the international 10-year transdisciplinary research programme are promoted by ICSU, UN bodies, Belmont Forum, etc. for future of the planetary earth and human beings, where ICSU-WDS and CODATA are required to support Future Earth's international scientific data management. We need careful discussions to promote those activities, but with a bright hope for the human society who has the indispensable intellectual infrastructure called "science".

Keywords: Scientific data, World Data System, open data, data management, data science, geophysics

Japan Geoscience Union Meeting 2014
(28 April - 02 May 2014 at Pacifico YOKOHAMA, Kanagawa, Japan)

U01-03 Room:419 Time:May 1 09:30-09:45

The ICSU World Data System: Trusted Data Services for Global Science

EDMUNDS, Rorie[1*] ; MOKRANE, Mustapha[1]

[1]ICSU-World Data System International Programme Office

This presentation will give a brief overview of the current activities of the International Council for Science – World Data System (ICSU-WDS). In particular, it will focus on ICSU-WDS' close involvement in the new Future Earth initiative and the Belmont Forum e-Infrastructure Steering Committee. It will also highlight joint projects between ICSU-WDS and the Research Data Alliance.

Keywords: ICSU-WDS, trusted data, long-term preservation, interoperability

Japan Geoscience Union Meeting 2014
(28 April - 02 May 2014 at Pacifico YOKOHAMA, Kanagawa, Japan)

U01-04 Room:419 Time:May 1 09:45-10:05

Issues and Agenda toward Data Era

IWATA, Shuichi[1*]

[1]MPD

Issues and agenda toward ”Data Era” will be dicsussed.

Keywords: Science Council of Japan, data, CODATA

Japan Geoscience Union Meeting 2014
(28 April - 02 May 2014 at Pacifico YOKOHAMA, Kanagawa, Japan)

U01-05 Room:419 Time:May 1 10:05-10:25

Importance of Future Earth in Asia

YASUNARI, Tetsuzo[1*]

[1]Research Institute for Humanity and Nature

Future Earth (FE) has been launched as an international initiative to promote research for global sustainability by the international science and technology alliance with partnership of the International Council for Science (ICSU), the International Social Science Council (ISSC), the Belmont Forum of funding agencies, the United Nations Educational, Scientific, and Cultural Organization (UNESCO), the United Nations Environment Programme (UNEP), the United Nations University (UNU), and the World Meteorological Organization (WMO) as an observer (Future Earth, 2013). Future Earth will provide a single overarching structure for researchers, funders, service providers, and users, and integrates the existing Global Environmental Change (GEC) programmes. The GEC programmes have provided foci for several extensive international and multi-disciplinary networks of researchers investigating key human-environmental dynamics. Future Earth would develop a new generation network building on these. Future Earth proposes national and regional level committees, in addition to the regional nodes. The most essential issue for the overall FE activity towards global sustainability will be how to integrate efforts and activity of solving environmental problems and achieving sustainability for local to regional scales.

This paper introduces a strategic science plan for FE in Asia, which should be a guideline for implementing the overall FE activity in the whole of Asia, including a comprehensive archive of data in natural science as well humanity and social science fields.

Keywords: Global Environmental Change, Asia, Future Earth

Japan Geoscience Union Meeting 2014
(28 April - 02 May 2014 at Pacifico YOKOHAMA, Kanagawa, Japan)

U01-06 Room:419 Time:May 1 10:25-10:45

Integrated Data System on Climate, Water and Disaster Risk Reduction

KOIKE, Toshio[1*]

[1]School of Engineering, The University of Tokyo

Increased water cycle variability impacts primarily through water, biological processes and human dimensions with implications for land use and societal development. It is critically important to recognize the fundamental linkages among water; land use, including deforestation; carbon cycle and ecosystem services; and food-, energy- and health- securities. By sharing coordinated, comprehensive and sustained water cycle and related Earth observations and information for sound decision making, we are now in developing effective interdisciplinary collaborations for working together based on coordinated and integrated efforts and subsequently to both mitigation and adaptation benefits at a river basin scale. Reducing disaster risk and building resilience to the climate change and variability is essential for establishment toward the final goal, the sustainable development of Earth societies and ecosystems.

Keywords: Earth Observation, Water Cycle, Climate Change, Disaster Risk Reduction, Data Integration

Japan Geoscience Union Meeting 2014
(28 April - 02 May 2014 at Pacifico YOKOHAMA, Kanagawa, Japan)

U01-07 Room:419 Time:May 1 11:00-11:15

Synergetic approach of bottom-up/top-down studies on CO2 and CH4 emissions from biomass burning and rice paddy in East A

IMASU, Ryoichi[1] ; TAKEUCHI, Wataru[2] ; SEKIYAMA, Ayako[2] ; SAITOH, Naoko[3] ; MATSUMI, Yutaka[4*] ; KAWASAKI, Masahiro[4] ; HAYASHIDA, Sachiko[5] ; ONO, Akiko[5]

[1]Atmosphere and Ocean Research Institute, The University of Tokyo, [2]Institute of Industrial Science, The University of Tokyo, [3]Center for Environmental Remote Sensing, Chiba University, [4]Solar-Terrestrial Environment Laboratory, Nagoya University, [5]Nara Women's University

There has been still a large discrepancy in estimations between bottom-up and top-down approaches for both CO_2 emissions from biomass burning and CH4 from rice paddy in East Asia. The purpose of this study is to update the emission inventory databases as to be more consistent between these two approaches through a synergetic usage of satellite data, ground-based remote sensing measurements, and in situ data. The most important parameter to estimate total CO_2 emissions from biomass burning is the biomass amount of the forests. In this study the amount is estimated based on the normalized vegetation index (NDVI) observed by satellites and, CO_2 emissions from burning area are estimated by multiplying the fire strength evaluated from hot spot data with some auxiliary data such as soil moisture and groundwater level. As for the top-down approach, CO_2 concentration data observed from space are useful for constraining the inverse analysis of CO_2 emission strength. The greenhouse gas observing satellite (GOSAT) dedicated to observe atmospheric CO_2 and CH_4 concentrations was launched in 2009 and has been operated for more than five years. The main band of its sensor can measure the columnar CO_2 concentration, however, it cannot be directly converted into the concentration near the surface. One of our attempts is to develop a retrieval method to estimate CO_2 concentration in the lower troposphere, particularly in the boundary layer, from a synergy of spectrum data in a wide spectral range covering from short wavelength infrared to the thermal infrared. In order to validate this method we have carried out CO_2 sonde observations around Tokyo city where GOSAT has been operated in a specific observation mode (targeting mode) to obtain sufficient number of data over this area. Based on the validated results, this method will be applied to analyze the data observed in biomass burning areas. One of our important targets is Kalimantan (Indonesia) where peat fire is the main CO_2 emission source. We started the ground-based measurement of columnar CO_2 concentration using an optical spectrum analyzer (OSA), and expect that these temporally continuous data would be effective for achieving the consistency between bottom-up and top-down approaches. Also started are observations of columnar CH_4 concentration using the same type of spectrometer in Sichuan basin (China) and Karnal (India) where are identified as the extremely high CH_4 concentration area based on the almost decadal record of observations by SCIAMACHY and GOSAT. It is expected that the synergetic analysis of data from satellite and ground-based measurements could contribute to make clear the cause of high concentration of CH_4 in these areas.

Keywords: carbon dioxide, methane, GOSAT, top down approach, bottom up approach, ground-based remote sensing

Japan Geoscience Union Meeting 2014
(28 April - 02 May 2014 at Pacifico YOKOHAMA, Kanagawa, Japan)

U01-08 Room:419 Time:May 1 11:15-11:30

Estimation of Ecological Function based on Biodiversity and Ecosystem Information

ITO, Motomi[1*]

[1]Graduate School of Arts and Sciences, University of Tokyo

In the Green Network of Excellence (GRENE) - environmental information project, we are working on collecting biodiversity and ecosystem information, and developing methods to use them for evaluation. In the past three years, more than 500,000 plant distribution information and information of more than 10,000 localities of vegetation had been databaed, and now they become available for users. Based on those information, together with several kinds of environmental information and land use data, it is possible to estimate distribution probability of each plant species, and to estimate some ecosystem functions of the forests with higher accuracy by considering composition of tree species. Here, I will present some examples of estimation of ecological function in Japanese forests, such as forest biomass, CO2 FLUX, and amount of pollination services for crops by insects. I also discuss a way from those ecosystem function to estimating Ecosystem Services, which is a total benefits for us provided by biodiversity and ecosystems function.

Keywords: Biodiversity Informatics, Eco Informatics, Ecosystem Function, Ecosytem Services, IPBES

Japan Geoscience Union Meeting 2014
(28 April - 02 May 2014 at Pacifico YOKOHAMA, Kanagawa, Japan)

U01-09 Room:419 Time:May 1 11:30-11:45

Environmental Monitoring of Soil contaminated by Radiocaesium in Iitate Village using FMS developed in GRENE project

MIZOGUCHI, Masaru[1*]

[1]Graduate School of Agricultural and Life Sciences, The University of Tokyo

Most of radiocaesium released from Fukushima Daiichi nuclear power plant has been accumulated in the topsoil within 5 cm. For decontamination of the top soil, Japanese government (Ministry of Agriculture, Forestry and Fisheries) has authorized three methods: topsoil stripping method, puddling method, and plowing method to replace surface soil with subsoil. Among three methods, the topsoil stripping method is being carried out and a lot of flexible container bags containing contaminated topsoil are piled up in the paddy field. We have not yet found the final disposal site of the contaminated soil. For agricultural regeneration and early return village, it is urgent and important to find a feasible decontamination method that farmers can conduct by themselves. Therefore, we are challenging a field test that buried the contaminated soil in the ground by a combination of the topsoil stripping method and the plowing method in Iitate Village in Fukushima Prefecture. We named this method ”Madei-method” that means we treat contaminated soil carefully. Currently, we are monitoring the radiation level from the buried contaminated soil by using a soil radiation sensor combined to the Field Monitoring System (FMS) that we developed for agricultural use in GRENE project. At the moment, leakage of radiocaesium has not been confirmed from the buried contaminated soil despite rapid changes in ground water due to rainfall and irrigation to the paddy. In the presentation, I explain outline of the FMS we developed in GRENE project and would like to propose to build a useful soil radiation database in Fukushima as one of important global data.

Keywords: decontamination, radiation, soil, monitoring, database, GRENE project

Japan Geoscience Union Meeting 2014
(28 April - 02 May 2014 at Pacifico YOKOHAMA, Kanagawa, Japan)

U01-10 Room:419 Time:May 1 11:45-12:00

Framework of Applications of Environmental Information for Realizing Resilient and Sustainable National Land Design

HAYASHI, Yoshitsugu[1*] ; KATO, Takaaki[2] ; SUZUKI, Yasuhiro[1] ; TANIKAWA, Hiroki[1] ; SATO, Shinji[3] ; SHIBASAKI, Ryosuke[4] ; TSUKAHARA, Kenichi[5] ; KATO, Hirokazu[1] ; KAWAZOE, Yoshiyuki[2] ; SHIBAHARA, Naoki[1] ; AKIYAMA, Yuki[6] ; KACHI, Noriyasu[5]

[1]Graduate School of Environmental Studies, Nagoya University, [2]Institute of Industrial Science, The University of Toyko, [3]Graduate School of Engineering, The University of Tokyo, [4]Center for Spatial Information Science, The University of Tokyo, [5]Faculty of Engineering, Kyushu University, [6]Earth Observation Data Integration and Fusion Research Initiative, The University of Tokyo

1. Introduction

This research project, GRENE-City, aims to construct a methodology to design and realize ”resilient and sustainable national land” with mitigation and adaptation measures against vulnerabilities of national land and society. This ”resilient” concept is derived from an understanding of ”natural providence”. The proposed system takes advantage of a broad range of information includes disaster risk caused by meteorological phenomena and others from DIAS (Data Integration and Analysis System) by the Earth Observation Data Integration and Fusion Research Initiative (EDITORIA), the University of Tokyo. As such the system will be developed as a ”Progressive Integrated Database” based on various environmental information infrastructures provided by DIAS. In addition, this project aims to cultivate experts who can construct and utilize this database in actual policy making fields.

To achieve this goal, a re-design of national land and society for a reduplicative system in both normal and emergency situations is necessary. Both a ”safety and security” concept, which takes account of damage reduction, and a ”sustainability” concept which tackles low carbon, energy saving, and prevention of climate change, are needed in order to keep pace with the threats of predicted huge earthquakes and climate change.

2. Contents

Natural hazards caused by climate change, earthquakes and other disasters may be increasing, and could strike in the near future our vulnerable society which is characterized by with declining birth rate and a growing proportion of elderly people, population decline, urban sprawl and etc. Based on the common recognition on these problems, this research project sets out to construct a methodology to lead to safer peaceful mind and sustainable national land and society by using DIAS.

The system needs to use data on natural and social situations. The data on natural situations includes earthquakes, climate change and disasters. The data on social situations include population structure, economic conditions, infrastructure, and land use. Additionally, not only the present data, but also historical data, such as land use and infrastructure change, record of disasters, population structures, and other information, are collected. Therefore ”four-dimensional GIS” will be constructed to allow quantitative prediction and to evaluate policies considering historical faces, past place names, and other qualitative information.

In consequence, the system will analyze the vulnerability of national land and society caused by social, geographical, and other conditions, and natural variations and disaster risks. This system supports the examination of various policies, especially, the effectiveness of ”Smart shrink” which could stop urban sprawl.

3. Results and future works

1) Information archives

This project collected historical data on earthquakes, tsunamis, and other natural disasters from old documents and other resources. In particular, records of tsunami damages of the Great East Japan Earthquake are stored. A prototype Web-GIS is developed to show these photos and tsunami height with map information.

2) Analysis and design

This project offers the evaluation of national land and cities with a view to safety, security, and sustainability. The system introduces QOL (Quality of Life) indicators. Data about accessibility, amenity, and disaster vulnerability to calculate QOL indicators are collected and added to the system. This will be utilized to illustrate conditions of residential amenity and disaster vulnerability in each area of the national land.

3) Utilization and deployment

This evaluation system will be applied to case study cities and regions. The problems and demands of the system will also

be clarified. As a result, the system and database will be developed to accommodate requests from policy planning of city and national land.

Keywords: resilient national land, sustainability, natural disaster, triple bottom line

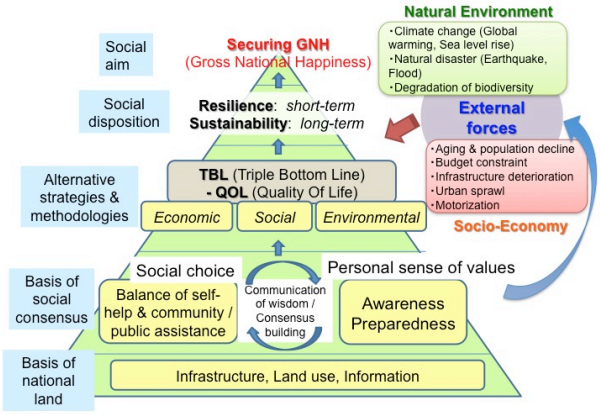

Japan Geoscience Union Meeting 2014
(28 April - 02 May 2014 at Pacifico YOKOHAMA, Kanagawa, Japan)

U01-11 Room:419 Time:May 1 12:00-12:15

Population health and global data sciences in Grene Ecohealth project

KANEKO, Satoshi[1*] ; WATANABE, Chiho[2] ; MOJI, Kazuhiko[3] ; NISHIMOTO, Futoshi[4] ; TIENGKHAM, Pongvongsa[5]

[1]Institute of Tropical Medicine, Nagasaki University, [2]School of International Health, Graduate School of Medicine, The University of Tokyo, [3]Graduate school of international health development, Nagasaki University, [4]Research institute for humanity and nature, [5]Savannakhet Provincial Health Department, the Lao People's Democratic Republic

Age of global and big data has come. The amount of data explosively increase and the expectations of exploring such data and effective utilization of data analysis results go wide of the mark. We enjoyed somehow the benefits from the big data analysis in daily life and some of the field in sciences; however, how can it be delivered to the health field, especially in areas or regions where the data collection is difficult due to the luck of data collection system? In developed countries, we can have data related to health and it has been already used for improvement public health service system. Furthermore, it has been linked to environmental data to know the results from climate and environmental changes. But this is only limited to developing countries and data or information from developing countries or regions, where the most vulnerable people from climate changes live and no information exists even on population, is still lack in identifying and monitoring the real situation. To sort out such information lack situation, the GRENEcoH project, a GRENE-Ecohealth project that is running under the GRENE-environmental information program, has started data collection of population health in areas in the Lao People's Democratic Republic using up-to-date technology to collect and link individual data. The system called in general as Health and Demographic Surveillance System (HDSS), which collect information about residents in the certain given areas for research. The HDSS programs are run in different areas and by different organization in African and Asian countries, however, in Japan; the HDSS is not paid enough attention. In this presentation, the introduction and the scientific and social values of HDSS and our technology will be presented.

Keywords: developing countries, marginal areas, population health, infectious disease

Japan Geoscience Union Meeting 2014
(28 April - 02 May 2014 at Pacifico YOKOHAMA, Kanagawa, Japan)

U01-12 Room:419 Time:May 1 12:15-12:30

Development of DIAS Metadata System

YOSHIKAWA, Masatoshi[1*] ; SHIMIZU, Toshiyuki[1] ; LI, Jiyi[1] ; NAKAHARA, Yoko[1] ; KINUTANI, Hiroko[2]

[1]Graduate School of Informatics, Kyoto University, [2]Institute of Industrial Science, The University of Tokyo

We are developing a metadata system in the Data Integration and Analysis System (DIAS) project sponsored by Japan Ministry of Education, Culture, Sports, Science and Technology. A major goal of the DIAS metadata system is to collect all metadata of earth observation data produced under the projects sponsored by Japanese government. The DIAS metadata system is comprised of metadata registration system, metadata retrieval system, and download system.

Cooperation with other data centers is also an important goal of the DIAS metadata system. We have imported metadata from JAMSTEC (Japan Agency for Marine-Earth Science and Technology) data catalog and JaLTER (Japan Long Term Ecological Research Network) database, and supported integrated metadata search through the DIAS retrieval system. On the other hand, by exporting DIAS metadata, DIAS is now listed in the Earth Observation Catalogs of GEOSS Portal. We are developing a metadata coordination system to make it possible more comprehensive exchange of metadata among data centers.

Keywords: earth observation data, metadata

Japan Geoscience Union Meeting 2014
(28 April - 02 May 2014 at Pacifico YOKOHAMA, Kanagawa, Japan)

U01-13 Room:419 Time:May 1 12:30-12:45

Design and proposal of operational DIAS

NISHIMURA, Hajime[1] ; KAKUTA, Shinya[1*] ; KOIKE, Toshio[2] ; FUKUDA, Toru[3] ; NOJIRI, Yukihiro[4]

[1]Japan Agency for Marine-Earth Science and Technology, [2]Department of Civil Engineering, School of Engineering, The University of Tokyo, [3]Earth Observation Research Center, Japan Aerospace Exploration Agency, [4]National Institute for Environmental Studies

Data Integration and Analysis System (DIAS) is intended to create new scientific knowledge and public benefits through integration of various data under collaboration with stakeholders, in order to become a social infrastructure to make new innovations and social growth. DIAS will provide information toward resilient society and mitigation on social problems related to global environment, including resource management, bio-diversity, and natural hazards, by utilizing data on earth observation, climate-variability prediction, socio-economy, and so on.

Data Integration and Analysis System Program (DIAS-P) started in 2011 as the second phase, aiming at (a) designing and proposing an operational scheme (operational DIAS) to realize public benefits through its operational application for global-scale solutions with sustainable scientific cutting-edge advancement, as well as (b) prototyping the operational regime with intelligent infrastructure to create new value, and (c) enabling stakeholders in various fields to together leverage the fusion of super-large-scale various data sets and information.

Japan Agency for Marine-Earth Science and Technology (JAMSTEC) is collaborating with the University of Tokyo EDITORIA, Japan Aerospace Exploration Agency (JAXA), and National Institute for Environmental Studies (NIES) to design the operational DIAS and present a tentative reference model including its roles. The infrastructure and schemes shown in the reference model will be the first practice if realized. This reference model has been designed in consideration with relevant progresses in relating research programs, and will be annually amended.

To achieve the above-mentioned objectives, DIAS comprehensively manages and publishes metadata as an integrated portal to provide and distribute the following data; (1) observation data listed in ”Japan Earth Observation Implementation Plan,” (2) observation data collected in each state to contribute toward nine social benefit areas of ”Global Earth Observation System of Systems” (GEOSS), (3) observation data available in partner states under bilateral or multilateral collaboration, (4) data obtained through Application Workbenches, which are intelligent infrastructure to support projects toward application to each field, and (5) data provided by Function-Improvement Partners, which are inter-organization partnership to sustainably improve functions of DIAS. Their targeted fields include socio-economy, agriculture and fishery, land use and land cover, transportation network on roads and ports, landscape, and hazards. It is to be discussed how to create an environment where archives are acknowledged as research results.

The core infrastructure of DIAS will consist of large-scale storages to archive the data, and of analysis space and tools to analyze large-scale data.

The operational DIAS expects decision-makers (in domestic and developing countries) on resource management, disaster-protection, etc. to be the major users. The major users of integrated data and analysis function of DIAS will be not only researchers (science communities) who provide decision-makers with evidence but also stakeholders who collaborate on Application Workbenches. Moreover, end-users, social movements, and civilian services are also expected to use DIAS through access to the DIAS portal site.

For the above-mentioned purposes, we developed a remote collaboration system (ubiDIAS) utilizing open sources, and studied various policies and United Nations’ Sustainable Development Goals.

Keywords: DIAS, operation, design

Japan Geoscience Union Meeting 2014
(28 April - 02 May 2014 at Pacifico YOKOHAMA, Kanagawa, Japan)

U01-14 Room:419 Time:May 1 14:15-14:40

Activities of the Union Commission for Data and Information of the International Union of Geodesy and Geophysics

FOX, Peter[1*] ; BARTON, Charles[2]

[1]Rensselaer Polytechnic Institute, [2]Australian National University

The data and information activities of IUGG, International Union of Geodesy and Geophysics, will be introduced, from a viewpoint of IUGG's Union Commission for Data and Information.

Keywords: IUGG, Data and Information, eGY

Japan Geoscience Union Meeting 2014
(28 April - 02 May 2014 at Pacifico YOKOHAMA, Kanagawa, Japan)

U01-15 Room:419 Time:May 1 14:40-14:55

The Laud Use Information System (LUIS) Database which has been developed under the GRENE-ei biodiversity area

NAKAJIMA, Hideaki[1*] ; HIMIYAMA, Yukio[2] ; SAIGUSA, Nobuko[1] ; NOJIRI, Yukihiro[1]

[1]National Institute for Environmental Studies, [2]Hokkaido University of Education, Asahikawa Branch

We, the Office for Global Environmental Database, at the Center for Global Environmental Research (CGER), in National Institute for Environmental Studies (NIES), has been developing a new database called the Land User Information System (LUIS). LUIS is a database which was provided from NIES as one of the databases of GRID-Tsukuba before. LUIS is a database to visualize the land use in Japan which was extracted from the topographical maps of the Geospatial Information Authority of Japan in three different eras, i.e., Meiji-to-Taisyo era (around 1900s), early Syowa era (around 1950s), and late Syowa era (around 1985). The land use information was extracted in each 2x2 km mesh of 1:50,000 topographical map for the upper left corner, the maximum land use, and existing land use. We have developed a program to plot the land use, on a simple Japanese map and on Google Earth view screen. The figure shows the distribution of broadleaf trees in 1900s and 1985. Red area represents the existence in both era, blue represents the extinction, and yellow represents the appearance. We are thinking of distributing the map from the CGER's Database Web server in future. Current status and future plan of the LUIS database will be presented.

Keywords: database, land use, LUIS, topographical map, GRID-Tsukuba

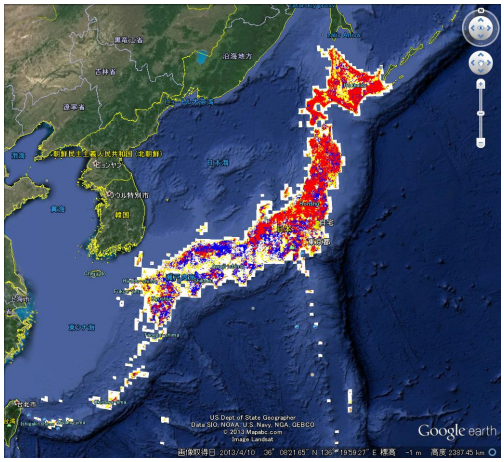

Japan Geoscience Union Meeting 2014
(28 April - 02 May 2014 at Pacifico YOKOHAMA, Kanagawa, Japan)

U01-16 Room:419 Time:May 1 14:55-15:10

Arctic Data archive System(ADS)

YABUKI, Hironori[1*] ; SUGIMURA, Takeshi[2]

[1]Japan Agency for Marine-Earth Science and Technology, [2]National Institute of Polar Research

Of all the regions on the planet, the Arctic currently shows the biggest rise in average temperature due to global warming, and is one of the regions expected to become most affected by climate change on the Earth in the future. The change in the Arctic area brings a profound impact to the global climate system through changes in interactions between the atmosphere, ocean circulation, and the cryosphere. These climate changes not only impact upon human activities, but also the Arctic flora and fauna ecosystem.

Large parts of the observations and mechanisms of the environmental change, including the climate of the Arctic region, are still not well understood. In order to further our understanding of these complex systems, an integrated study carried out with continuous observations in the Arctic is proposed. In the Arctic Environmental Observation Center in the National Institute of Polar Research, operations began on the Arctic Data archive System (ADS) in March 2012, in order to promote the mutual use of scientific data.

The purpose of the Arctic Data archive System is to archive and distribute multiple observational (atmosphere, ocean, terrestrial, and ecology) and model simulation datasets, and promote utilization of these datasets. ADS is the central repository of archived data on Arctic research in Japan.

Keywords: Arctic, Environment, Global Warming, ADS

Japan Geoscience Union Meeting 2014
(28 April - 02 May 2014 at Pacifico YOKOHAMA, Kanagawa, Japan)

U01-17 Room:419 Time:May 1 15:10-15:25

JAXA's contributions for Earth and Planetary research using earth observation data

FUKUDA, Toru[1*]

[1]Earth Observation Research Center, JAXA

JAXA's earth observation satellites play an important role in providing essential information for Earth science and applications regarding global warming, climate change, water cycle change, agriculture, public health and disaster management.

JAXA have been operating Greenhouse gas Observing SATellite (GOSAT), and Global Change Observation Mission-Water 1 (GCOM-W1) successfully. These satellites are collecting geophysical data of the earth's surfaces and atmosphere those are important for the earth and planetary researches.

In addition to those ongoing earth observation satellite missions, new satellites will be added to the line.

One is GPM (Global Precipitation Measurement), the successor of TRMM focusing to measure precipitation. Another one is ALOS-2 (Advanced Land Observing Satellite) carrying an L-band synthetic aperture radar. Those new generation satellites will contribute to observe disaster, earth resources, climate change, water cycle, etc.

JAXA will make continuous efforts to create and provide satellite-based information for not only scientists but also decision makers and stakeholders in order to contribute to solving global and regional issues. In order to make such information useful, close collaboration with various players in various sectors is essential.

Keywords: GCOM, ALOS, GPM, TRMM, GOSAT

Japan Geoscience Union Meeting 2014
(28 April - 02 May 2014 at Pacifico YOKOHAMA, Kanagawa, Japan)

U01-18 Room:419 Time:May 1 15:30-15:45

IUGONET project and its products for multidisciplinary study on upper atmospheric physics

ABE, Shuji[1*] ; YATAGAI, Akiyo[2] ; KOYAMA, Yukinobu[3] ; TANAKA, Yoshimasa[4] ; SHINBORI, Atsuki[5] ; UENO, Satoru[6] ; UMEMURA, Norio[2] ; SATO, Yuka[4] ; YAGI, Manabu[7] ; HORI, Tomoaki[2]

[1]International Center for Space Weather Science and Education, Kyushu Univ., [2]Solar Terrestrial Environment Laboratory, Nagoya Univ., [3]Data Analysis Center for Geomagnetism and Space Magnetism Graduate School of Science, Kyoto Univ., [4]National Institute of Polar Research, [5]Research Institute for Sustainable Humanosphere, Kyoto Univ., [6]Kwasan & Hida Observatories, School of Science, Kyoto Univ., [7]Planetary Plasma and Atmospheric Research Center, Graduate School of Science, Tohoku Univ.

In order to investigate the mechanism of long-term variations in the upper atmosphere, it is crucially important to make cross-cutting studies with various kinds of data observed between Sun and Earth region. Thus, it is needed to combine databases which maintained by each institute and to accelerate to make data-sharing network in the STP community. The IUGONET (Inter-university Upper atmosphere Global Observation NETwork) project was established in 2009 as a six-year research project supported from the Ministry of Education, Culture, Sports, Science and Technology (MEXT), Japan. It consists of the five Japanese universities and institutes (NIPR, Tohoku University, Nagoya University, Kyoto University, and Kyushu University, that have been leading ground-based observations of the upper atmosphere for decades), and collaborates with many domestic (for example, the National Institute of Information and Communications Technology (NICT), the National Astronomical Observatory of Japan (NAOJ), and the Kakioka magnetometer observatory, Japan Meteorological Agency) and overseas institutes/projects (for example, ESPAS in EU). One of our products in the IUGONET data management framework is developing systems for searching metadata of these observational data, and the metadata database (MDB). In the STP community, there are various kinds of archived data observed by many instruments, for example radars, magnetometers, photometers, radio telescopes, helioscopes, and so on. The IUGONET MDB is based on DSpace as a metadata registering system, which is mainly used in literature management. It also adopts an extension of the SPASE data model as a metadata format, which is widely used in the upper atmospheric community in USA. As a result, this system can deal with all kind of data belonging to IUGONET institutes, including cosmic ray, meteorological information observed by automatic weather station, etc. The system can also get flexibility to other type of data including the satellites and the numerical simulation which are used in the STP community. It is one of our challenges to apply the IUGONET system to many kinds of data in other communities. This MDB system is in operation since 2011 with over 10 million metadata. Other challenge of the IUGONET is developing software which can use for scientific research and publication. The iUgonet Data Analysis Software (UDAS) is a plug-in software of Themis Data Analysis Software (TDAS), which is upgraded to Space Physics Environment Data Analysis System (SPEDAS). The UDAS provides many routines for loading the ground-based observational data from various types of instruments, and performing scientific data analysis. This platform made it easier for STP community to analyze a various kind of data in a unified way. The IUGONET project will be closed at the end of fiscal year 2014. In this presentation, we will introduce the achievements and problems of our six-year project and discuss futures for global data sharing and research.

Keywords: Solar-Terrestrial Physics, metadata database, data analysis software, IUGONET

Japan Geoscience Union Meeting 2014
(28 April - 02 May 2014 at Pacifico YOKOHAMA, Kanagawa, Japan)

U01-19 Room:419 Time:May 1 15:45-16:00

Introduction of NICT ionospheric data archive system

ISHII, Mamoru[1*] ; MARUYAMA, Takashi[1] ; TSUGAWA, Takuya[1]

[1]NICT

NICT has a long history of operational ionospheric observation with ionosondes since IGY 1957. On the beginning, we had four domestic observatories, Wakkanai, Akita, Kokubunji and Yamagawa. After that Akita was closed and Okinawa joined and we operate these four observatories continuously. In addition, Syowa station in Antarctica has been observing ionosphere by NICT since IGY, too. In addition as the World Data Center for ionosphere, we have a lot of number of ionospheric data obtained by foreign institutes.

The present ionosonde system named 10C provides digital image of ionogram. However, all other previous systems provide analog image and recorded on films. Now it becomes a serious problem to lose data by corrupted of films. The only solution of this issue is to digitize the film image but usually the cost is very high. We search the way to keep low cost and comfortable quality for future analysis and find a method named ribbon scanning. In this method we keep whole of one film data in one file, which makes cost low and avoid losing data by frame skipping. We had trial of resolution of digital image and confirm the quality is same level of original image.

We already had some fruitful results using these data archive. Maruyama et al. [2012] shows the statistic results of ionospheric variation after large earthquakes. Other than these kinds of study we expect the archive is useful for discussion of long-term variation of ionosphere with climate change. For improving the use of these dataset we need to solve another issue. Film-digitized images are suitable to manual scaling with naked-eye but we cannot use these data automatically because the axes vary in each image. To solve the issue we need to try image analysis to detect the axes automatically.

Reference

Maruyama, T., T. Tsugawa, H. Kato, M. Ishii, and M. Nishioka, Rayleigh wave signature in ionograms induced by strong earthquakes, J. Geophys. Res., DOI: 10.1029/2012JA017952.

Keywords: WDS, WDC, ionosphere, space weather

Japan Geoscience Union Meeting 2014
(28 April - 02 May 2014 at Pacifico YOKOHAMA, Kanagawa, Japan)

U01-20 Room:419 Time:May 1 16:15-16:35

The Current and the Future of AIST GEO Grid Technologies- A Case Study of Fukushima Radiation Monitoring Application

KOJIMA, Isao[1*] ; NAKAMURA, Ryosuke[1] ; OGAWA, Hirotaka[1] ; TANAKA, Yoshio[1] ; MATONO, Akiyoshi[1]

[1]National Institute of Advanced Industrial Science and Technology

The Current status and future perspetive will be discussed of ”GEO Grid” Technologies which have been studied and developed at AIST (National Institute of Advanced Industrial Science and Technology). Also a case study of Fukushima Radiation Monitoring Application will be reviewed.

Keywords: GRID computing, geoscience data, database technology, information technology, RDA, ICSU-WDS

Japan Geoscience Union Meeting 2014
(28 April - 02 May 2014 at Pacifico YOKOHAMA, Kanagawa, Japan)

U01-21 Room:419 Time:May 1 16:35-17:05

Making Dynamic Data Citable: Approaches to Data Citation within the Context of the RDA Working Group

RAUBER, Andreas[1*]

[1]Vienna University of Technology

Being able to reliably and efficiently identify entire or subsets of data in large and dynamically growing or changing datasets constitutes a significant challenge for a range of research domains. In order to repeat an earlier study, to apply data from an earlier study to a new model, we need to be able to precisely identify the very subset of data used. While verbal descriptions of how the subset was created (e.g. by providing selected attribute ranges and time intervals) are hardly precise enough and do not support automated handling, keeping redundant copies of the data in question does not scale up to the big data settings encountered in many disciplines today. Furthermore, we need to be able to handle situations where new data gets added or existing data gets corrected or otherwise modified over time. Conventional approaches, such as assigning persistent identifiers to entire data sets or individual subsets or data items, are thus not sufficient.

In this talk we will review the challenges identified above and discuss solutions that are currently elaborated within the context of the working group of the Research Data Alliance (RDA) on Data Citation: Making Dynamic Data Citable. These approaches are based on versioned and time-stamped data sources, with persistent identifiers being assigned to the time-stamped queries/expressions that are used for creating the subset of data. We will further review examples of how these can be implemented for different types of data and see how this fits into the larger context of activities on Data Citation.

Keywords: Research Data Alliance, data citation, dynamic data, information technology, interoperability

Japan Geoscience Union Meeting 2014
(28 April - 02 May 2014 at Pacifico YOKOHAMA, Kanagawa, Japan)

U01-22 Room:419 Time:May 1 17:05-17:20

Recent activity of DOI-minting to database by WDCs in Japan

NOSE, Masahito[1*] ; KOYAMA, Yukinobu[1] ; IYEMORI, Toshihiko[1] ; ISHII, Mamoru[2] ; MURAYAMA, Yasuhiro[3] ; KADOKURA, Akira[4] ; SHINOHARA, Iku[5]

[1]WDC for Geomagnetism, Kyoto University, [2]WDC for Ionosphere and Space Weather, NICT, [3]WDS Scientific Committee, NICT, [4]WDC for Aurora, National Institute of Polar Research, [5]WDC for Space Science Satellites, JAXA

Recent electronic journals are published with DOI (digital object identifier) such as doi:10.1029/2012SW000785. DOI is a persistent name that is resolved into URL, where readers can obtain digital objects of the journal articles; for example, abstract, figures, and pdf files. The DOI system was launched around 2000 and becomes popular these days so that DOI is ordinarily indicated in references and citations.

The next development of the DOI system is to extend it to database. It makes possible for researchers to cite the data used in a scientific publication, which is called ”data citation”. Data citation provides the following benefits:

• Readers can more easily locate the data used in the paper, obtain necessary information of the data (i.e., metadata), and validate the findings of the paper.

• Readers can also easily discover datasets which are relevant to their interests but has not been noticed.

• Data contributors can gain professional recognition and rewards for their published data in the same way as for traditional publications.

• Data centers can measure the impact of individual datasets and receive proper credit of their work.

Recognizing the importance of data citation, World Data Centers (WDCs) in Japan including WDC for Aurora (National Institute of Polar Research), WDC for Geomagnetism (Kyoto University), WDC for Ionosphere and Space Weather (National Institute of Information and Communications Technology), and WDC for Space Science Satellites (Japan Aerospace Exploration Agency) started discussion to mint DOI to their own database in August 2013. The discussion finds that Japan Link Center (JaLC) is a proper agency to register DOI-URL mapping, because JaLC aims at public information services to promote science and technology in Japan and it handles scientific and academic metadata and content from holders nationwide, including national institutes, universities. Two representatives of the above 4 WDCs are working closely with JaLC to define a registration scheme to implement the DOI-URL mapping. We are also developing a web-based system to register metadata with JaLC and create landing pages for database. We expect to start a pilot program to mint DOI to the database from the middle of 2014.

Keywords: DOI, Database, Data Citation, Data Publication

Japan Geoscience Union Meeting 2014
(28 April - 02 May 2014 at Pacifico YOKOHAMA, Kanagawa, Japan)

U01-23 Room:419 Time:May 1 17:20-17:45

Interlinking Articles And Data? The Past, Present, And Future

KOERS, Hylke[1*]

[1]Elsevier

Activities of linking scholarly articles and scientific data will be introduced.

Keywords: data publication, scholarly article, data citation

Japan Geoscience Union Meeting 2014
(28 April - 02 May 2014 at Pacifico YOKOHAMA, Kanagawa, Japan)

U01-24 Room:419 Time:May 1 17:45-18:00

Open Science Data Discovery Platform

ZETTSU, Koji[1*]

[1]National Institute of Information and Communicatoins Technology

Technology and use case studies of ”Open Science Data Discovery Platform” will be introduced. So far we have harvested approximately 0.6 million metadata of data citation (DOIs and related metadata given to datasets) from publicly open databases of ICSU-WDS, PANGEA, ICPSR, etc., and have been developing new technology to leverage those data-citation link information and scholarly article archives. This technology, including linguistic, time-space, and ontological analysis techniques, is expected to have potential to enable new knowledge finding from various relations between datasets and articles, as well as analysis of higher-class clustering and grouping structures of relationships and links between science-technology information sources and even various communities which are related to science and technology data and articles. Through this process, perhaps to be like easy user-interface in future (like Web of Science), even international perspectives will be easily captured of more general science and technology research information pieces, links, and inter-relations to each other. For example, regarding climate change prediction and related decision making we may be able to find easily by an online search system how different earth observation datasets are used in political papers and meteorological papers.

Keywords: Scientific data, ICSU-WDS, database technology, data search, data citation

Japan Geoscience Union Meeting 2014
(28 April - 02 May 2014 at Pacifico YOKOHAMA, Kanagawa, Japan)

U01-P01 Room:Poster Time:May 1 18:15-19:30

Construction of spatio-temporal data mining system for time-series satellite imagery using Hadoop

NISHIMAE, Kou[1] ; MIYOSHI, Tomoya[1] ; HONDA, Rie[1*]

[1]Kochi University

A large number of spatio-temporal data have been stored in various fields of science, such as remote sensing, numerical simulation, and astronomical observation, in which data often appears as time-series images. To extract spatio-temporal knowledge from spatio-temporal data including time-series images, spatio-temporal cross section relevant to a target task has to be extracted from a mass of data. Since these data are stored as a large number of files, utilization of distributed processing framework such as Hadoop or Gfarm is promising.

We constructed distributed data mining system for time-series satellite images using 53 nodes (3 masters and 50 slaves at maximum) of iMac and Hadoop which enables distributed file system and distributed processing using MapReduce. We evaluated the scalability and performance of the system for the task extracting time-series data from a large number of images carefully and found that partitioning the images into optimum numbers and reducing the data between map phase and reduce phase is essential.

The system was then applied to two different tasks focusing on time-series data analysis extracted from satellite imagery: statistical modeling of seasonal changes in vegetation index and spatio-temporal correlation analysis of weather satellite images. The tasks were successfully implemented on the system and the computational time was decreased in inverse proportion to the number of slave nodes, thus usefulness of the distributed system to spatio-temporal data mining for time-series images.

Keywords: distrubuted processing, Hadoop, MapReduce, data mining, spatio-temporal, satellite imagery

Japan Geoscience Union Meeting 2014
(28 April - 02 May 2014 at Pacifico YOKOHAMA, Kanagawa, Japan)

U01-P02 Room:Poster Time:May 1 18:15-19:30

Basic Technologies, Integrated Systems and Applications of the NICT Science Cloud

MURATA, Ken T.[1*] ; WATANABE, Hidenobu[1] ; UKAWA, Kentaro[2] ; MURANAGA, Kazuya[2] ; YUTAKA, Suzuki[2] ; KASAI, Yasuko[1] ; SATOH, Shinsuke[1] ; ISHII, Shoken[1] ; YAMAMOTO, Kazunori[1] ; NAGATSUMA, Tsutomu[1] ; TSUGAWA, Takuya[1] ; NISHIOKA, Michi[1] ; GUO, Zhihong[3] ; KUROSAWA, Takashi[4] ; MIZUHARA, Takamichi[5]

[1]National Institute of Information and Communications Technology, [2]Systems Engineering Consultants Co., LTD., [3]SURIGIKEN Co.,Ltd., [4]Hitachi Solutions East Japan, Ltd., [5]CLEALINKTECHNOLOGY Co.,Ltd.

This paper is to propose a cloud system for science, which has been developed at NICT (National Institute of Information and Communications Technology), Japan. The NICT science cloud is an open cloud system for scientists who are going to carry out their informatics studies for their own science. The NICT science cloud is not for simple uses. Many functions are expected to the science cloud; such as data standardization, data collection and crawling, large and distributed data storage system, security and reliability, database and meta-database, data stewardship, long-term data preservation, data rescue and preservation, data mining, parallel processing, data publication and provision, semantic web, 3D and 4D visualization, out-reach and in-reach, and capacity buildings.

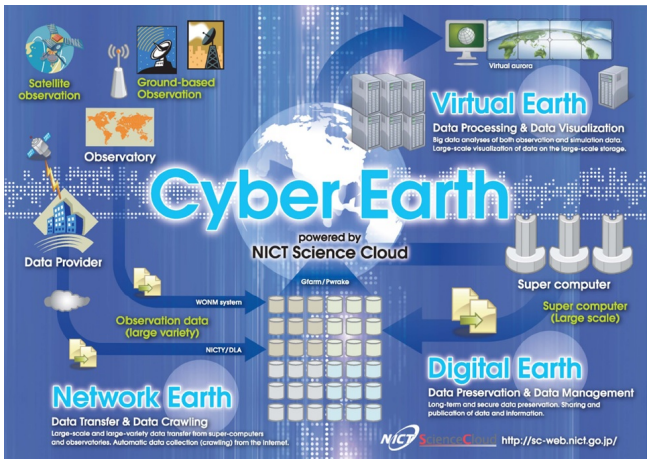

Japan Geoscience Union Meeting 2014
(28 April - 02 May 2014 at Pacifico YOKOHAMA, Kanagawa, Japan)

U01-P03 Room:Poster Time:May 1 18:15-19:30

Global spectral crustal model

TENZER, Robert[1*] ; CHEN, Wenjin[1]

[1]School of Geodesy and Geomatics, Wuhan University

We compile the harmonic coefficients, which describe the Earth crustal density structure with a spectral resolution complete to degree/order 180. These coefficients can be used in gravimetric studies of the Earth lithosphere structure, isostasy, crustal loading, sedimentary basins and related topics. The global spectral crustal model is separated into 9 specific layers of the topography, bathymetry, polar ice sheets, sediments (3-layers) and consolidated crust (3-layers). The harmonic coefficients describe uniformly the geometry and density (or density contrast) distribution within each crustal component. The topographic and bathymetric coefficients are generated from the topographic/bathymetric model ETOPO1 and the global geoid model GOCO03s. A uniform density model is adopted for the topography. The ocean density distribution is approximated by the depth-dependent seawater density model. The ETOPO1 topographic and the DTM2006.0 ice thickness data are used to generate the ice coefficients, while assuming a uniform density of the glacial ice. The geometry and density distribution within sediments is described by the 3 stratigraphic layers of a laterally varying density model, and the same structure is used to describe the density distribution within the consolidated crust down to the Moho interface. The sediment and consolidated crust coefficients are generated from the global crustal model CRUST1.0. The density contrasts of the ocean, ice, sediments and remaining crustal structures are taken relative to the reference crustal density.

Keywords: crust, density, gravimetric forward modeling, harmonic analysis

Japan Geoscience Union Meeting 2014
(28 April - 02 May 2014 at Pacifico YOKOHAMA, Kanagawa, Japan)

U02-01 Room:419 Time:April 28 10:00-10:15

Muographic observations in Satsuma Iwojima, Japan

TANAKA, Hiroyuki[1*]

[1]Earthquake Research Institute, The University of Tokyo

Satsuma-Iwojima volcano continuously discharges large amounts of volcanic gasses without significant magma discharge. One of the proposed mechanisms of this continuous gas discharge is conduit magma convection. In this hypothesis, a magma conduit is connected to a deep magma chamber and a ”degassing” phenomenon drives convection. Once the volatile component is released (by degassing) at the top of the magma conduit, the degassed magma sinks through the non-degassed magma occupying the pathway. A continuous supply of non-degassed magma from the magma chamber ensures that there is compensation for the degassed magma and the cycle continues. In 2008, a muography detector was placed at the foot of Satsuma-Iwojima volcano, and it captured an image of a large, shallow depth, low-density region existing beneath the crater floor. Degassing magma, with its high proportion of bubbles, has been interpreted as being the low-density region, and its dimension (location and size) was compared to the results from other field measurements, laboratory and theoretical studies. In 2013, an improved muography detector was developed and placed at the same location as the 2008 observation to exploit advanced muographic images in Satsuma-Iwojima. The recent progress in muographic observations will be reported.

Keywords: Muography, Muon, Volcanic Conduit, Imaging

Japan Geoscience Union Meeting 2014
(28 April - 02 May 2014 at Pacifico YOKOHAMA, Kanagawa, Japan)

U02-02 Room:419 Time:April 28 10:15-10:30

Conduit magma convection: Constraints from Muography

SHINOHARA, Hiroshi[1*] ; TANAKA, Hiroyuki[2]

[1]GSJ, AIST, [2]ERI, Univ. Tokyo

Muographic imaging is a powerful tool to radiographically reveal density structure of a shallow volcanic edifice with high energy muons and was applied to the rhyolitic dome of Iwodake, Satsuma-Iwojima in order to understand the conduit magma convection in this volcano. In this paper, we will discuss the constraints obtained by the muographic measurements performed in 2008 and their implication to the conduit magma convection model.

Conduit magma convection is a model to explain persistent degassing, that is continuous emission of large amount of volcanic gases without eruption and is driven by the density contrast between the ascending non-degassed magma and the descending degassed magma that is created by outgassing at the top of a magma column (Kazahaya et al., 1994). This model is commonly applied to less viscous basaltic magma systems but the application to andesitic or rhyolitic magma system is a matter of debate, because the large viscosity of these magmas can slow down the magma flows in the conduit. Although theoretical evaluation indicated that a larger diameter of a conduit can compensate the larger magma viscosity and can cause the rapid magma flows in the conduit, it is difficult to prove its occurrence under the ground, as the conduit magma convection is a steady state process with few seismic signals nor deformation. In contrast, the conduit magma convection suggests that intensive degassing occurs at top of a magma column, which is likely detectable as a low density zone in a shallow magma conduit system. Therefore the density structure survey the muon-radiography is an ideal method to reveal the size, shape and magnitude of density anomaly at the shallow volcanic edifice.

Quantitative re-evaluation of the muon radiography data at the Iwodake rhyolitic cone obtained by Tanaka et al. (2009) confirms the existence of a low-density body of 300 m in diameter and with 0.9-1.0 g cm^{-3} at depths of 135-190 m from the summit crater floor. The low-density material is interpreted as rhyolitic magma with 60% vesicularity on average, and existence of this unstable highly vesiculated magma at shallow depth without any recent eruptive or intrusive activity is considered evidence of conduit magma convection. The structure of the convecting magma column top was modeled based on density calculations of vesiculated ascending and outgassed descending magmas, compared with the observed density anomaly. The existence of the low-density anomaly was confirmed by comparison with published gravity measurements, and the predicted degassing at the shallow magma conduit top agrees with observed heat discharge anomaly distribution localized at the summit area. This study confirms that high viscosity of silicic magmas can be compensated by a large size conduit to cause the conduit magma convection phenomena. The rare occurrence of conduit magma convection in a rhyolitic magma system at Iwodake is suggested to be due to its specific magma features of low H_2O content and high temperature.

Keywords: Conduit magma convection, muon-radiography, shallow volcanic edifice, density structure

Japan Geoscience Union Meeting 2014
(28 April - 02 May 2014 at Pacifico YOKOHAMA, Kanagawa, Japan)

U02-03 Room:419 Time:April 28 10:30-10:45

Development of coupled Stokes–DEM simulation scheme for geodynamical magmatic studies

FURUICHI, Mikito[1*] ; NISHIURA, Daisuke[1]

[1]Japan Agency for Marine-Earth Science and Technology

For geodynamical magmatic studies such as crystal settling at the melting roof of a magma chamber, we develop a robust and efficient simulation scheme for solving high-viscosity fluid and particle dynamics in a coupled computational fluid dynamics and discrete element method (CFD–DEM) framework. The high-viscosity fluid is treated by the Stokes-flow approximation, where the fluid interacts with particles via the drag force in a cell-averaged manner. The particles are tracked with contact forces by DEM. To efficiently solve such Stokes–DEM coupled equations, we propose two key techniques. One is formulation of particle motion without the inertial term, allowing a larger time step at higher viscosities. The other is a semi-implicit treatment of the cell-averaged particle velocity in the fluid equation to stabilize the calculation. We will explain some details of our model developments in the presentation. A series of numerical experiments shows that our proposed scheme can handle sinking particles in a high-viscosity fluid; such problems are difficult for the conventional CFD–DEM method. Then we will discuss our targeting geodynamical problems tackled with this simulation method.

Keywords: Magma, Particle-Laden flow, Stokes flow, Discrete element method, Melt roof, Numerical simulation

Japan Geoscience Union Meeting 2014
(28 April - 02 May 2014 at Pacifico YOKOHAMA, Kanagawa, Japan)

U02-04 Room:419 Time:April 28 11:00-11:15

Recent updates on the DIAPHANE project of muon tomography

MARTEAU, Jacques[1*] ; GIBERT, Dominique[2] ; DE BREMOND D'ARS, Jean[2] ; JOURDE, Kevin[3]

[1]Institut de Physique Nucleaire de Lyon, Univ Claude Bernard, UMR 5822 CNRS, Lyon, France, [2]Geosciences Rennes, Univ Rennes 1, UMR 6118 CNRS, Rennes, France., [3]Institut de Physique du Globe de Paris, Sorbonne Paris Cite, Univ Paris Diderot, UMR 7154 CNRS, F.

Density radiography with atmospheric muons aims at determining the density variations or the absolute densities of geological or large volume bodies. The density is measured through the screening effect on the incident muons flux induced by the presence of matter, like for the X rays in a standard medical radiography. We will present recent updates on the DIAPHANE project which studies volcanoes with this technique since many years and is now deployed in the Lesser Antilles (Guadeloupe, Montserrat), Italy (Etna), the Philippines (Mayon) and in underground sites (France and Switzerland). Time-of-flight techniques have been developed to improve the data analysis and provide significant results.

Keywords: Volcanology, Muon tomography, Particles detector, Inverse problem

Japan Geoscience Union Meeting 2014
(28 April - 02 May 2014 at Pacifico YOKOHAMA, Kanagawa, Japan)

U02-05 Room:419 Time:April 28 11:15-11:30

Muon radiography by nuclear emulsions - Report on activity in Italy

BOZZA, Cristiano[1*]

[1]University of Salerno and INFN

The nuclear emulsions technology has entered the field of muon radiography of volcanic edifices and faults in the last decade, and progressively attracted the interest of nuclear emulsion laboratories and experts from various countries. The historical first muographic image of a volcano was indeed generated by using this nuclear emulsion technology. In earlier times, large-scale application was limited by the readout time and manpower needs as the emulsion films had to be scanned by eye; modern fast automatic microscopes solved both issues with limited cost, and the readout and analysis speed increased by several orders of magnitude, opening the door to access muography that requires large statistics. The Italian nuclear emulsion groups of the Universities of Salerno, Napoli and Padova and the Laboratori Nazionali del Gran Sasso (INFN) have built an Italian network of scientists working on muography, establishing tight collaboration links with the Tokyo University Earthquake Research Institute; more Italian groups could join in the near future. The network performs many activities, from the preparation of emulsion film exposure, on-site data taking campaigns, to readout and data analysis.

Nuclear emulsions are usually cast in the shape of thin films (thickness in the range of 20-100 micrometers) coating transparent plastic bases. Even a single film can provide 3D tracks marking the passage path of ionizing particles, when observed by a dedicated microscope. Normally emulsions films are exposed in stacks, piling several sheets, so that a single particle, after development, leaves several aligned tracks, one in each film.

Automatic emulsion readout systems allow track detection and measuring on several m^2 of surface in few weeks, collecting large statistics, which is needed to investigate regions of high cosmic muon absorption. Angular resolution of the order of a few milliradians is commonly achieved, which gives the ability to discriminate relatively small details, depending on the distance between the detector and the observed volume. Currently, one line of research aims at developing faster and cheap film readout systems, based on commercial hardware, to increase the current data-taking speed by a factor 10 or better.

Emulsions are continuously sensitive, since the time of their production: while this is an advantage because they need no power supply, the lack of time discrimination makes data analysis for such detectors a delicate task. The high combinatorial background of 3D tracks, due to many months' pile-up, can be greatly reduced by exploiting the micrometric alignment precision of emulsion tracks. Application of nuclear emulsion data to muon radiography requires also particle identification. Multi-film stacks with interleaved slabs of dense scatterers (such as iron or lead), allow distinguishing soft particles, typically electrons/positrons from electromagnetic showers, from hard muons with 1 GeV/c momentum or higher. Dedicated simulation of the passage of hard muons through rock and in the emulsion-instrumented volume allows optimizing selection criteria and estimating purity and efficiency of the selection. Systematic errors on the predicted integrated flux, which is compared to the measured integrated flux, should be kept as small as possible; in turn, this requires proper modelling of the expected cosmic-ray muon flux, which demands specific efforts in some regions of the angular and energy spectrum, where the statistics is intrinsically lower. Simulation and modelling activities require specific software and sizeable computing resources and are shared amoung the collaborating groups.

Accounts are given of the status of muon radiography campaigns in which the Italian groups are mostly involved. The cases covered are Stromboli, Teide and the La Palma fault. For each case, the present situation, possible developments and future plans are also envisaged.

Keywords: nuclear, emulsion, muography, Italy, volcano, fault

Japan Geoscience Union Meeting 2014
(28 April - 02 May 2014 at Pacifico YOKOHAMA, Kanagawa, Japan)

U02-06 Room:419 Time:April 28 11:30-11:45

Development of Nuclear Emulsion Detector for Cosmic-ray Muon Radiography and Its Applications

MORISHIMA, Kunihiro[1*] ; NISHIO, Akira[1] ; KATO, Yoshito[1] ; NAKANO, Toshiyuki[1] ; NAKAMURA, Mitsuhiro[1]

[1]Nagoya University

We are developing nuclear emulsion and its automatic analysis system for cosmic-ray muon radiography (muography). Nuclear emulsion is very high-sensitive photographic film for detecting 3-demensional trajectories of charged particles like muon in its volume with the very high position resolution (sub-micron), which gives us the very high angular resolution (a few mrad). In addition, nuclear emulsion does not require electronic power, the size is very compact and the weight is very light. And also, it is easy to perform the tomographic analysis using multiple detectors placed around the target. These features have advantages in the field observation for the measurement of geoscience object, archeological object, or in the disaster area like Fukushima Dai-ichi nuclear power plant.

In the case of Fukushima Dai-ichi nuclear power plant, high radioactivity shielding and lack of electronic power supplies should be taken into account. Nuclear emulsion is the powerful candidate used in such area. We have conducted the basic study of muon radiography of reactor core at fast reactor Joyo, which belongs to Japan Atomic Energy Agency (JAEA), in order to demonstrate the imaging of the reactor core. The result validates the observation of the reactor core with high resolution.

We will present technical developments of nuclear emulsion, latest scientific results including other observed objects and future prospects.

Keywords: cosmic-ray muon radiography, nuclear emulsion, non-destructive observation, Fukushima Dai-ichi nuclear power plant

Japan Geoscience Union Meeting 2014
(28 April - 02 May 2014 at Pacifico YOKOHAMA, Kanagawa, Japan)

U02-07 Room:419 Time:April 28 11:54-12:09

Muon radiography Monitoring for Structural Survey of the Prambanan World Heritage Temple

HANAZATO, Toshikazu[1*] ; TANAKA, Hiroyuki[2] ; KUSAGAYA, Taro[1] ; OKAMOTO, Yumiko[1]

[1]Mie University, [2]University of Tokyo

Muon cosmic-ray can penetrate rocks and soils and give us projection of the path' density, therefore, muography technology has been successfully developed in the geological field for disaster prevention of volcano explosion 1). Furthermore, it was utilized to survey the inner condition of a blast furnace in a steel mill during its operation time. On the other hand, non-destructive tests are required, in general, to conduct structural survey of heritage structures with cultural and historical values. In particular, when World Heritage Monuments are surveyed, we have to follow this principle strictly. There are a number of World Cultural Heritages of masonry in seismic regions in the World. When their seismic safety is assessed, seismic structural survey is conducted by employing non-destructive tests. Considering that muography technology can be useful for structural survey of massive masonry structures as a non-destructive test, we installed the muon detecting system at the Prambanan Temples, World Cultural Heritage in Indonesia and monitored the muon cosmic-ray for 5 months. Here, the Prambanan Temples of stone masonry structures were severely damaged by Central Java Earthquake of 2006. We have been successfully involved in architectural and structural survey project conducted by an international and interdisciplinary team. The damaged masonry monuments have been restored after the earthquake, however, restoration work of Candi Siva, the oldest and highest monument of the Prambanan Temples, was not started yet, as its inner structural condition was unknown. If the inner structural conditions are revealed, 3-D finite element model is available for seismic structural diagnosis of such massive masonry structures. The scope of the present paper is to describe this challenge of non-destructive test utilizing muography technology for the Prambanan restoration project and to demonstrate applicability of this advanced technology to structural survey of World Cultural Heritages of masonry. The muon data obtained at the site indicated that the monument must have inner chambers that had been unknown. The date also indicated their sizes and locations. This information will be useful to provide analysis model for seismic evaluation.

References

1)Tanaka,H.K.M.,Taira,H.,Uchida,T.,Tanaka,M.,Takeo,M.,Ohiminato,T.,Aoki,R.,Nishiyama,et al. :
Three-dimensional computational axial tomography scan of a volcano with cosmic ray muon radiograph,
J. Geophys., Res.,115, B12332, 2010

Keywords: muon, structural survey, masonry, World Heritage, seismic safety

Japan Geoscience Union Meeting 2014
(28 April - 02 May 2014 at Pacifico YOKOHAMA, Kanagawa, Japan)

U02-08 Room:419 Time:April 28 12:09-12:24

An Application of Muography to Exploring Gigantic Masonry Architectures: Evolution in Pyramid ConstructionTechnique

OHSHIRO, Michinori[1*]

[1]Komazawa University

Since the technique of Muography was used for the pyramid of Khafre (second pyramid of Giza) by L. W. Alvarez in 1970, academic researches using non-destructive testing methods have been applied to some huge stone structures (ex. the Pyramid of the Sun in Teotihuacan, Mexico, by A. Menchaca-Rocha). Although Alvarez and his team attempted to find a new chamber in the pyramid, they couldn't find any hidden chambers. However, now it is thought that the result was unreliable because their muon detector was an old type. After Alvarez the muon detector was developed and contributed to the elucidation of mechanism of a volcanic eruption in recent years (e.g. Asama volcano and Satsuma-Iwojima Volcano by H. Tanaka et al). Applying this technique, the internal structures of the Shiva temple in the Prambanan temple compounds (Indonesia) and the Parthenon (Greece) is explorable. On the basis of those results, we are going to go back to the roots of Muography by Alvarez by revisiting the pyramid.

It is assumed that if it is possible to use Muography for the pyramids in Egypt (the oldest huge stone building in the world), in terms of the usage and volume of differing density of the stone (limestone and granite), it would make clear the developmental sequence and construction way of pyramids which has been impossible to know until now. Therefore, we can confirm the human ingenuity of earthquake-proof structures by ancient Egyptians. Most of the pyramids were made of limestone. Harder granite was sometimes used to encase the pyramids. If it can be made clear where two different kinds of stones were used and how much stone were used for the pyramids, we can take possession of previously-unattainable new information in the study of earthquake-proof structures of pyramids.

The developmental sequence of burial of ancient Egyptian kings and the transition of the outer shape are as follows:1.Simple graves, 2.Mastabas, 3.Step Pyramids, 4.Bent Pyramid, 5.Red Pyramid (true pyramid), 6.Pyramid of Khufu (true pyramid), 7.Pyramid of Khafre (true pyramid), 8.Pyramid of Menkaure (true pyramid).

Judging from the above-mentioned process, it is assumed that there were further stages in the development of pyramids. However, it is still not clear. If we have the opportunity to use muongraphy to the above pyramids (from the step pyramid of Netjerykhet to three true pyramids in Giza), we can put an end to speculation as to the evolution theory of the pyramid from the viewpoint of earthquake-proof structures and advancement of civilization.

References

(1) L. W. Alvarez et al, Search for Hidden Chambers in the Pyramids: The Structure of the Second Pyramid of Giza is Determined by Cosmic-ray Absorption, Science 167 (1970), pp.832-839.

(2) A. Dodson, The Pyramids of Ancient Egypt (London, 2003).

(3) M. C. Gonzalez-Garcia, Francis Halzen, Michele Maltoni, and Hiroyuki K. M. Tanaka, Radiography of Earth's Core and Mantle with Atmospheric Neutrinos, Physical Review Letters, 100, 061802, 2008.

(4) Hiroyuki K.M. Tanaka, Tomohisa Uchida, Manobu Tanaka, Minoru Takeo, Jun Oikawa, Takao Ohminato, Yosuke Aoki, Etsuro Koyama and Hiroshi Tsuji, Detecting a mass change inside a volcano by cosmic-ray muon radiography (muography): First results from measurements at Asama volcano, Japan, Geophysical Research Letters, 36, L17302, 2009.

(5) Hiroyuki K.M. Tanaka, Tomohisa Uchida, Manobu Tanaka, Hiroshi Shinohara, Cosmic-ray muon imaging of magma in a conduit: Degassing process of Satsuma-Iwojima Volcano, Japan, Geophysical Research Letters, 36, L01304, 2009.

Keywords: muongraphy, pyramid, civilization, earthquake-proof structures

Japan Geoscience Union Meeting 2014
(28 April - 02 May 2014 at Pacifico YOKOHAMA, Kanagawa, Japan)

U02-09 Room:419 Time:April 28 12:27-12:42

Overview of Neutrino Geoscience

DYE, Steve[1*]

[1]Hawaii Pacific University

Radiogenic heating is a key component of the energy balance and thermal evolution of the Earth. Geo-neutrino observations from Japan and Italy are now measuring the radiogenic power of our planet. Although the error on the present measurement is too large to significantly constrain geological models, the potential of geo-neutrino observations is clearly demonstrated. This contribution traces the development of neutrino geosciences and discusses the prospects for geo-neutrino observations to inform geology.

Keywords: neutrino geoscience, radiogenic heat

Japan Geoscience Union Meeting 2014
(28 April - 02 May 2014 at Pacifico YOKOHAMA, Kanagawa, Japan)

U02-10 Room:419 Time:April 28 14:15-14:30

KamLAND: geo-neutrino result

SHIMIZU, Itaru[1*]

[1]RCNS, Tohoku University

Geo-neutrinos are anti-neutrinos (elementary particles) produced in radioactive decays within the Earth. Those anti-neutrinos can be detected in a terrestrial experiment using interaction via weak force, however, due to extremely low reaction probabilities, there were no feasible experiments for a long time. Owing to the development of large-size anti-neutrino detectors, the observation of geo-neutrinos has been finally made, and then composition models of the Earth are constrained from the radiogenic heat estimate. In this talk, a precise measurement of geo-neutrino flux from the Kamioka Liquid-scintillator Anti-Neutrino Detector (KamLAND) in Japan will be presented. In addition, the recent situation of KamLAND anti-neutrino data will be reviewed. Following the Fukushima nuclear accident in 2011, the most of Japanese nuclear reactors has been subjected to a protracted shutdown, resulting in the low reactor anti-neutrino background. It provides a unique opportunity to measure the geo-neutrinos with an improved sensitivity. Based on this low background data, prospects of geo-neutrino sensitivity with KamLAND data in the near future will be shown, and discuss the ability of discriminating between Earth models.

Keywords: geo-neutrino

Japan Geoscience Union Meeting 2014
(28 April - 02 May 2014 at Pacifico YOKOHAMA, Kanagawa, Japan)

U02-11 Room:419 Time:April 28 14:30-14:45

Borexino: geo-neutrino results

SUVOROV, Yury[1*]

[1]Yury Suvorov

Geo-neutrinos are the electron anti-neutrinos produced by long-lived radioactive isotopes (such as U, Th and K) in the earth crust and mantle. Geo-neutrinos can be detected in kiloton scale organic liquid scintillator detectors located in underground laboratories. The detection reaction is the inverse-beta decay, which has a particular signature given by two correlated in space and time prompt and delayed signals.

In spite of the strong signature geo-neutrino can only be detected in massive low background set-ups designed for low energy (1 MeV) neutrinos.

Borexino at the GranSasso underground laboratory in Italy has been in operation since 2007 to search for sub-MeV solar neutrinos.

At present experimental studies of geo-neutrinos are carried out with Kamland at the Kamioka mine in Japan and with Borexino at GranSasso. The first attempt of a geo-neutrino measurement was done in Kamland in 2005. Only in 2010 and 2011 both Borexino and Kamland observed at more the 4sigma C.L. a signal from geo-neutrinos. The search of geo-neutrinos likewise the one of solar neutrinos for the sun provides a unique tool to probe the interior of the earth. Uranium and thorium from the crust and the mantle make the geo-neutrino flux on surface. The energy spectrum of the detected geo-neutrinos depends on the abundance of uranium and thorium and on the different beta decays in the two radioactive chains. A spectroscopy determination of the geo-neutrino signal can be done. This has been recently shown by Borexino. By means of this analysis the ultimate goal of the geo-neutrino search will be the determination of the uranium and thorium content in the mantle. For this purpose a combined analysis of more than one experiment results will be necessary. In this talk we will review the present status of geo-neutrino research. We elaborate on the recent results from Borexino and Kamland. The experimental difficulties and background sources will be discussed.

Keywords: neutrinos, geo neutrinos, Earth, crust, mantle

Japan Geoscience Union Meeting 2014
(28 April - 02 May 2014 at Pacifico YOKOHAMA, Kanagawa, Japan)

U02-12 Room:419 Time:April 28 14:45-15:00

A reference Earth model for geoneutrinos

HUANG, Yu[2] ; MANTOVANI, Fabio[1*] ; RUDNICK, Roberta L.[2] ; MCDONOUGH, William F.[2]

[1]University of Ferrara - INFN of Ferrara - Italy, [2]University of Maryland, College Park, MD, USA

Geoneutrino data from the KamLAND and Borexino experiments provide insights into Earth's energetics and global radiogenic heat production. In 2014, SNO+ will begin to collect data; the era of the exploration of our planet through geoneutrinos is definitely open.

Detection of geoneutrinos provides quantitative information about the total amounts of U and Th in the Earth and their distribution within the different reservoirs (crust, mantle and possibly core). One of the greatest potentials of geoneutrino is to discriminate among the different models for the bulk composition of the Earth, which are based on cosmochemical arguments and geochemical and geophysical observations. In order to determine the U and Th concentration of the deep Earth from the geoneutrino signal, the regional and crustal contribution to the geoneutrino flux needs to be determined from detailed geological studies.

We developed a geophysically based, three-dimensional global reference model for the abundances and distributions of U and Th in a Bulk Silicate Earth (BSE) model. The structure and composition of the outermost portion of the Earth, the crust and underlying lithospheric mantle, are detailed in the reference model; this portion of the Earth has the greatest influence on the geoneutrino fluxes. The structure of the crust is based on 1^{o} x1^{o} surface map of the Earth discriminating layers of sediments, upper, middle and lower crust. For the first time three geophysical global crustal models based on reflection and refraction seismic body wave (CRUST 2.0), surface wave dispersion (CUB 2.0), and gravimetric anomalies (GEMMA) are studied with the aim to estimate the contribution of geophysical uncertainties to the reference crustal model.

On the base of new compilations of geochemical data for sediments, oceanic and continental crust, we estimate the expected geoneutrino signal and its uncertainties for the crust of the Earth. Evaluating the U and Th abundances and their uncertainties in middle and lower crust are a focus of this model, along with using seismic velocity data to determine the lithological nature of these layers. The fraction of felsic and mafic rocks in the deep portions of the continental crust has been estimated by comparing the velocities of longitudinal and transverse seismic waves reported in the crustal model with the laboratory values obtained for ultrasonic velocities of different rock types.

An updated xenolithic peridotite database is used to represent the average composition of continental lithospheric mantle. The geoneutrino signal from this reservoir is calculated for the first time and it exceeds that from the oceanic crust at all three existing detectors.

Geoneutrino signal at Earth's surface is calculated in TNU (Terrestrial Neutrino Unit) (see figure) and Monte Carlo simulation is used to track the asymmetrical uncertainties of different crustal inputs. The combination of the global crust model, detailed local crust models, and the measured signal for each detector provides the critical inputs needed to assess the global mantle signal and its uncertainty. Thus, the mantle signal at each detector and its uncertainty can be independently combined to place limits on acceptable models for the mantle's radiogenic power.

Keywords: geoneutrino flux, heat producing element, radiogenic heat power, reference crustal model, deep crust composition, bulk silicate Earth composition

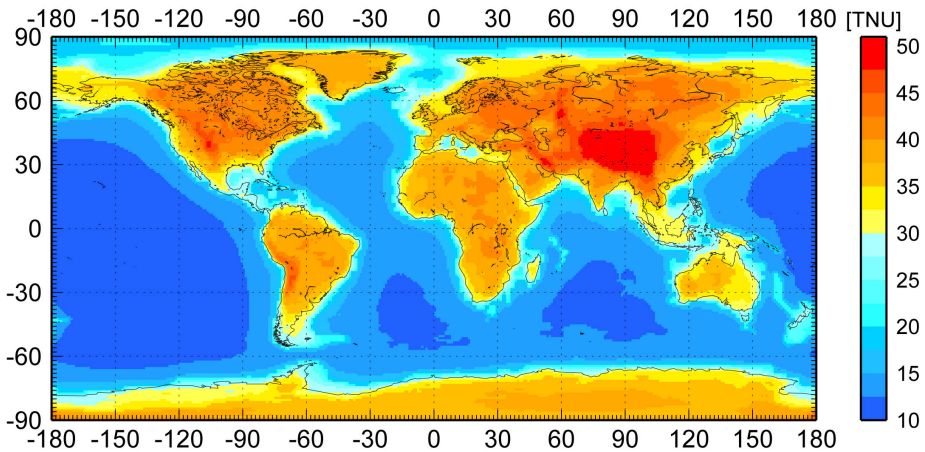

Japan Geoscience Union Meeting 2014
(28 April - 02 May 2014 at Pacifico YOKOHAMA, Kanagawa, Japan)

U02-13 Room:419 Time:April 28 15:00-15:15

Can noble gas reservoirs in Earth's mantle be identified from the geoneutrino distribution?

SUMINO, Hirochika[1*] ; BALLENTINE, Chris[2]

[1]Geochemical Research Center, Graduate School of Science, University of Tokyo, [2]Department of Earth Sciences, University of Oxford

Noble gas isotopes in mantle-derived samples are key tracers of chemical heterogeneity in the Earth's mantle and of the origin of the atmosphere. Samples of mid-ocean ridge basalt (MORB) and ocean island basalt (OIB) provide a comprehensive understanding of mantle noble gases. MORBs show relatively uniform $^{3}He/^{4}He$ ratios and in a $^{21}Ne/^{22}Ne$-$^{20}Ne/^{22}Ne$ diagram form a mixing line between the atmospheric composition and the MORB-source endmember. The latter is formed by the addition of nucleogenic ^{21}Ne to the primordial Ne ("solar" or "Ne-B" composition, Ballentine et al., 2005; Honda et al., 1991; Trieloff et al., 2000; Mukhopadhyay, 2012). In contrast, OIB samples, which are derived from a deeper region of the mantle, can exhibit higher $^{3}He/^{4}He$ ratios and less nucleogenic Ne isotope compositions. The OIB characteristics provide evidence for a mantle source in which primordial He and Ne has been less diluted by addition of radiogenic ^{4}He and nucleogenic ^{21}Ne produced by the decay of U- and Th-series elements. Therefore, noble gas isotopic evolution in the mantle is directly related to the U and Th contents in their reservoirs. However, the reasons for the less-radiogenic/nucleogenic character of the plume source are under debate; it may be less degassed (e.g., Allegre et al. 1983; Kaneoka, 1983; Kurz et al. 1982; Porcelli and Ballentine, 2002; Porcelli and Elliott, 2008), re-gassed through volatile recycling (Holland and Ballentine 2006; Ballentine and Holland 2008), or depleted in U and Th by ancient melt extraction events (Parman, 2007; Albarede, 2008). Recent finding of different $^{129}Xe/^{130}Xe$ ratios (^{129}Xe is a product of extinct isotope ^{129}I, while ^{130}Xe is primordial) in the MORB and Icelandic plume source requires that a portion of the latter has been isolated from the MORB-source mantle over geological timescales (Mukhopadhyay, 2012). This finding is consistent with that the less degassed nature is essential for the high $^{3}He/^{4}He$ ratio of the plume source because high noble gas concentrations in the plume source is required to preserve Xe isotope heterogeneity against dilution by depleted or surface-recycled material with atmospheric or MORB-like $^{129}Xe/^{130}Xe$. If the plume source corresponds to the large low-shear-wave-velocity provinces (LLSVPs) or D" layer at the base of the mantle, it may indeed have existed since the formation of the Earth and cannot exclusively be composed of subducted slabs (Mukhopadhyay, 2012). This is consistent with high $^{3}He/^{4}He$ (primordial) and low $^{3}He/^{4}He$ (recycled) components in Polynesian OIBs (Parai et al., 2009). The geoneutrino distribution will shed light on this issue; the less degassed (i.e., primordial) plume source is expected to contain 30-40% of the total mantle U and Th and if the LLSVPs is dominated by undiluted primordial material this feature will generate a significantly higher geoneutrino flux than a LLSVPs dominated by ancient subducted slabs with U and Th contents most likely lower than the convecting mantle.

Subcontinental lithospheric mantle (SCLM) exhibits slightly lower $^{3}He/^{4}He$ ratio and more nucleogenic Ne feature (Gautheron and Moreira, 2002; Buikin et al., 2005), indicating it is enriched in U and Th relative to noble gases. Although U and Th concentrations in SCLM is estimated as 10-30 times those in the convecting mantle, its small volume fraction (ca. 1.5%) results in insignificant contribution to global geoneutrino flux. However, it may be significant for existing detectors located in or close to continental region such as KamLAND (Japan) and Borexino (Italy). An ocean-based or transportable detector like Hanohano (Sramek et al., 2013) is therefore expected to have a great advantage to reveal geoneutrino flux from the deep mantle.

Keywords: Noble gas, Mantle, Uranium and Thorium, Geoneutrino, LLSVP, D" layer

Japan Geoscience Union Meeting 2014
(28 April - 02 May 2014 at Pacifico YOKOHAMA, Kanagawa, Japan)

U02-14 Room:419 Time:April 28 15:15-15:30

On the origin of large-scale heterogeneity in the deep mantle: Thermo-chemical mantle convection in a spherical geometry

NAKAGAWA, Takashi[1*]

[1]IFREE, JAMSTEC

The origin of large-scale heterogeneous structure in the deep mantle, that is, large low shear velocity provinces (LLSVP) is still debated, which is between thermo-chemical [e.g. Nakagawa et al., 2012] and purely thermal [e.g. Davies et al., 2012]. If the large-scale heterogeneous anomalies in the deep mantle are generated by basaltic piles, the large-scale anomalies such as LLSVP may be enhanced for huge amount of heat source compared to the ambient mantle. Current efforts of geoneutrino observations attempt to detect the large-scale anomalous region of radioactive elements in the deep mantle [personal communication with H. Tanaka], which may have large-scale enhanced region of radioactive element in the deep mantle beneath the southern Pacific from test simulations of geoneutrino detectors. In addition, this approach could give an answer for the origin of large-scale heterogeneous structure in the deep mantle. Here we introduce our current numerical modeling of thermo-chemical mantle convection in a spherical geometry with self-consistently calculated mineralogy. The advantage of this approach is to include all phase transitions in the mantle without any linearization of physics of phase transition in mantle minerals and calculate seismic anomalies from thermo-chemical structure obtained from numerical modeling directly. In this presentation, we will show several important information on resolving this issue.

Keywords: thermo-chemical mantle convection, large-scale heterogeneity, mineral physics, radioactive heat source

Japan Geoscience Union Meeting 2014
(28 April - 02 May 2014 at Pacifico YOKOHAMA, Kanagawa, Japan)

U02-15 Room:419 Time:April 28 15:30-15:45

Anti-Neutrino Directionality with KamLAND

XU, Benda[1*]

[1]RCNS, Tohoku University

KamLAND holds its novelty in the observation of reactor anti-neutrino disappearance. After the great Tohoku earthquake in 2011, almost all nuclear power plants of Japan are closed for safety inspection. This Reactor-Off period offers a unique opportunity to study the directionality of anti-neutrinos from the earth and the remaining nuclear reactors with the liquid scintillator detector.

Keywords: neutrino

Japan Geoscience Union Meeting 2014
(28 April - 02 May 2014 at Pacifico YOKOHAMA, Kanagawa, Japan)

U02-16 Room:419 Time:April 28 15:45-16:00

Tracking geo-neutrinos towards the future geo-neutrinography

WATANABE, Hiroko[1*]

[1]RCNS, Tohoku University

Directional sensitive neutrino detectors contributed to astronomy and particle physics. The solar neutrino problem was firmly believed by the directional measurement of solar neutrinos, and the atmospheric neutrino oscillation was confirmed by the zenith angle distribution for two types of neutrinos. Liquid scintillator detectors are marked by the ability to detect low energy neutrino signals, such as reactor, geo, and extraterrestrial neutrinos. On the other hand, liquid scintillator detectors do not have sensitivity of neutrino direction.

KamLAND (Kamioka, Japan) and Borexino (Gran Sasso, Italy) have showed the geo anti-neutrino detection realized by the event rate and energy spectra. We have begun to use neutrinos as " probe " to observe the Earth's interior. Geo-neutrino measurement does not have the sensitivity of its direction, so we can not distinguish the crust and mantle contribution.

It is hoped the development of new measurement technology to measure neutrino direction. Lithium-loaded liquid scintillator has the potential to have the high sensitivity of coming anti-neutrino direction. Directional sensitive detectors will contribute to the better understanding of the earth interior using geo anti-neutrino flux information. Other motivations are the earlier determination of supernova direction and improvement of oscillation sensitivity for reactor anti-neutrinos.

Keywords: geo-neutrino

Japan Geoscience Union Meeting 2014
(28 April - 02 May 2014 at Pacifico YOKOHAMA, Kanagawa, Japan)

U02-17 Room:419 Time:April 28 16:15-16:30

Geophysical Inversion of Geo-Neutrino Flux Data: Formulation for Reveling Chemical Structure in the Earth

TAKEUCHI, Nozomu[1*]

[1]Earthquake Research Institute, University of Tokyo

Observation of geo-neutrino flux enables us to constrain distribution of radiogenic heat sources in the Earth (e.g., Enomoto et al. 2007, EPSL). Although the data provides unique information, resolution was limited because the observed data has been just one scalar quantity (geo-neutrino flux at the observational site). However, recent challenge to directional measurements by the RCNS group will greatly improve the resolution, because the observed data becomes a vector quantity with large dimension (geo-neutrino flux as a function of incident angle and azimuth).

In this study, I will formulate geophysical inverse problem to effectively constrain where and how much we have radiogenic heat sources in the Earth. Following procedures by Enomoto et al. (2007), we first categorize reservoirs of radiogenic elements (e.g., crust, bulk mantle, slab and LLSVP) and develop a reference distribution model of radiogenic elements in the Earth. We then compute a synthetic geo-neutrino flux pattern (as a function of incident direction) for each reservoir category. We assume that the observed flux can be expressed by linear combination of synthetic patterns and define their coefficients as model parameters.

The optimal coefficients can be obtained by solving an inverse problem. If the reference model is perfect, every coefficients should be equal to one. If the optimal coefficient deviates from one, it suggests that the assumed concentration was not appropriate for that reservoir category. This formulation should be useful for geophysical interpretation. For example, if the coefficient for LLSVP is large, we can suggest that a large amount of crustal material is accumulated in the LLSVP.

At the time of presentation, besides the details of the above formulation, I plan to show expected resolution when we use data obtained by the ongoing KamLAND experiment.

Keywords: geo-neutrino, KamLAND, geophysical inversion

Japan Geoscience Union Meeting 2014
(28 April - 02 May 2014 at Pacifico YOKOHAMA, Kanagawa, Japan)

U02-18 Room:419 Time:April 28 16:30-16:45

Hanohano: Future deep ocean geo-neutrino measurement

LEARNED, John[1*]

[1]University of Hawaii

Neutrinos from the decay chains of Uranium and Thorium from within the Earth's mantle constitute a vital signature of the origin of most of the heat thought to be driving all of geodynamics. The only means conceived as yet to study the magnitude and geographical distribution of the flux of mantle geo-neutrinos is from a large and mobile deep ocean detector. This study cannot be done from crustal locations due to the ovewhelming flux of neutrinos from local rocks. We present a description of the Hanohano Project, aimed at opening this new discipline.

Keywords: neutrino, uranium, thorium, geoneutrino, tomography

Japan Geoscience Union Meeting 2014
(28 April - 02 May 2014 at Pacifico YOKOHAMA, Kanagawa, Japan)

U02-19 Room:419 Time:April 28 17:03-17:18

Prospects of Earth Composition Measurements via Neutrino Tomography at Next-generation Neutrino Detectors

ROTT, Carsten[1*]

[1]Sungkyunkwan University

The Earth matter density is well determined through seismological measurements, however the chemical composition of the Earth has not yet been measured and only been inferred from meteorite samples. The Earth interior composition could be determined using neutrino tomography. Neutrinos are naturally produced in the Earth atmosphere and can be detected at neutrino telescopes. Neutrinos are elementary particles that are extremely light and only rarely interact, so that they can traverse the entire Earth without being absorbed. For the measurement, one can utilize a unique property of neutrinos, which is known as matter induced neutrino oscillations. This effect changes the neutrino properties based on the electron density of the medium through which the neutrino travels.

The dependence on electron density is what allows us to get a handle on the composition of the Earth. While seismological measurements determine the matter density, so to speak the average mass of nuclei, the oscillation effects depend on the electron density. In combination we can determine the average Z/A, where Z is the proton number (number of protons per nucleus) and A is the atomic mass (number of protons and neutrons per nucleus). The talk will introduce the measurement and discuss prospects at next-generation neutrino detectors like PINGU and Hyper-K, that could perform it.

Keywords: Neutrino, Tomography, IceCube, PINGU, Hyper-K, Earth Composition

Japan Geoscience Union Meeting 2014
(28 April - 02 May 2014 at Pacifico YOKOHAMA, Kanagawa, Japan)

U02-20 Room:419 Time:April 28 17:18-17:33

The Hyper-Kamiokande Project

YOKOYAMA, Masashi[1*]

[1]The University of Tokyo

In this paper, we present the baseline design and expected performance of the Hyper-Kamiokande detector (Hyper-K)[1,2], a next generation underground water Cherenkov detector proposed in Japan. Hyper-Kamiokande is a successor of Super-Kamiokande (Super-K), which has been producing epoch-making results in particle physics and astrophysics, most notably the discovery of neutrino oscillation, since 1996. A water Cherenkov detector measures properties of elementary particles by detecting Cherenkov light, which is emitted when a charged particle travels faster than the velocity of light in water. Although neutrino itself does not emit Cherenkov light, it can be detected via particles produced in interaction with matter. Because the interaction probability is very small, a gigantic detector is necessary for the study of neutrinos. Water Cherenkov technique is the only solution to realize a Megaton scale detector with currently available technology. The design of Hyper-K is based on the highly successful Super-K, taking full advantage of a well-proven technology. The science goals of Hyper-K include not only the study of neutrino properties, but also broad topics in particle physics, astrophysics and geophysics.

Hyper-K consists of two cylindrical tanks lying side-by-side, the outer dimensions of each tank being 48 (W) 54 (H) 250 (L) m^3. The total (fiducial) mass of the detector is 0.99 (0.56) million metric tons, which is about 20 (25) times larger than that of Super-K. The inner detector region is viewed by 99,000 20-inch PMTs, corresponding to the PMT density of 20% photo-cathode coverage (one half of that of Super-K). In order to enhance the performance of the detector and to reduce the construction cost, new types of photosensors are under development. The design of critical components such as excavation of large caverns, mechanical structure of the tank, and water purification system is established. Further R&D towards detailed technical design, together with study of science cases, is ongoing by an international working group consisting of more than hundred scientists from eleven countries over the world.

Hyper-K presents unprecedented potential for precision measurements of neutrino oscillation parameters and discovery reach for CP violation in the lepton sector. Hyper-K can extend the sensitivity to nucleon decays beyond what was achieved by Super-K by an order of magnitude or more. The scope of studies at Hyper-K also covers high precision measurements of solar neutrinos, observation of both supernova burst neutrinos and supernova relic neutrinos, and dark matter searches.

Although the main motivation of the Hyper-K project arises from particle physics and astrophysics, thanks to its large volume and excellent performance, Hyper-K will be also able to contribute to geophysics by detection of neutrinos coming through the inside of the earth as discussed in [1]. The prospects for geophysics using Hyper-K will be discussed.

References

[1] K. Abe, T. Abe, H. Aihara, Y. Fukuda, Y. Hayato, K. Huang, A. K. Ichikawa and M. Ikeda et al., Letter of Intent: The Hyper-Kamiokande Experiment — Detector Design and Physics Potential —, arXiv:1109.3262 [hep-ex].

[2] Hyper-Kamiokande Working Group, Hyper-Kamiokande Physics Opportunities, arXiv:1309.0184 [hep-ex].

Keywords: neutrino, radiography

Japan Geoscience Union Meeting 2014
(28 April - 02 May 2014 at Pacifico YOKOHAMA, Kanagawa, Japan)

U02-21 Room:419 Time:April 28 17:33-17:48

Testing Geological Hypotheses Using Particle Physics

HERNLUND, John[1*] ; TANAKA, Hiroyuki[2]

[1]Earth-Life Science Institute, Tokyo Institute of Technology, [2]Earthquake Research Institute, Tokyo University

Installations of muon and neutrino observatories are yielding an increasing spirit of collaboration between particle physicists and Earth scientists interested in leveraging their resources and techniques and to apply them to major outstanding scientific problems in both fields. This comes at a very good time, as experimental methods and seismological analysis has increasingly illuminated the frontier of Earth's deep geological structure, leading to new ideas and hypotheses regarding the evolution of Earth since its formation. Particle geophysics offers unique new tools to test hypotheses regarding the geological evolution of the entire Earth, some of which should help to break through non-uniqueness hurdles that arise using more traditional approaches. Here we discuss some of the frontier problems in Earth science, and describe some potentially novel approaches that may lead to breakthroughs in our understanding of our planet. One already well-known application involves detection of anti-neutrinos generated by naturally occurring radioactive decay processes in Earth's interior, the strength and distribution of which is sensitive to different hypotheses regarding Earth's origin and evolution. Other approaches, which will be made possible using the high energy detectors in Antarctica, is the determination of the electron density inside the Earth. This is especially useful, since the electron density is sensitive to the molar fraction of elements in solution inside bodies like the core, while seismology is only sensitive to the weight percent of those solutes. Here we show how combining this independent information will help to solve major questions such as the composition of the core.

Keywords: Thermal Evolution, Chemical Evolution, Composition of Earth, Earth Formation, Hadean Geology, Deep Earth

Japan Geoscience Union Meeting 2014
(28 April - 02 May 2014 at Pacifico YOKOHAMA, Kanagawa, Japan)

U02-P01 Room:Poster Time:April 28 18:15-19:30

Review of the recent muon radiography observations by using nuclear emulsion detector

MIYAMOTO, Seigo[1*]

[1]The University of Tokyo

Nuclear emulsion is one of three dimensional particle tracker which have micron position resolution and the feature that no electricity so we can put this detector everywhere easily and also this is suitable for non-fixed point observation.

Several observations for volcanoes were done and will be done from 2011 to 2014. The imaging the of Unzen lava dome, which was formed from 1991 to 1995, was done by Miyamoto et al and they found the detector got many back ground particles and the amount is more than several times than expected muon signal. this implies that we are on the stage of background particle study.

The emulsion cloud chamber (ECC) is a modular structure made of a sandwich of passive material plates such as lead interleaved with emulsion film layers. Nishiyama et al studied the source of background noise in cosmic-ray muon radiography using ECC. They found that the origin of background is expected to be electromagnetic components of air-showers or cosmic-ray muons scattered in topographic material whith momentums is less than 2GeV/c.

The shallow conduit shape of Stromboli will provide the important information for eruption dynamics modeling by Tioukov et al. Hernandez et al put the emulsion detector near the top of summit of Teide volcano to investigate the past eruption histroy of Teide. Teide volcano is located in Teferife, Canary Islands, Spain. They are also under observation of the fault appeared in La Palma, Canary Island, in 1949, which is the sign of huge land collapse or not. The width of the fault is expected to be 1 meter or less, so high position resolution of emulsion detector is suitable for this observation. They will measure the width, delth and the porosity of this fault.

Japan Geoscience Union Meeting 2014
(28 April - 02 May 2014 at Pacifico YOKOHAMA, Kanagawa, Japan)

U02-P02 Room:Poster Time:April 28 18:15-19:30

Simultaneous inversion of muon radiography and gravity anomaly data for 3-D density structural analysis of lava domes

NISHIYAMA, Ryuichi[1*] ; MIYAMOTO, Seigo[1] ; OSHIMA, Hiromitsu[2] ; OKUBO, Shuhei[1] ; TANAKA, Hiroyuki[1]

[1]Earthquake Research Institute, University of Tokyo, [2]Usu Volcano Observatory, Hokkaido University

Cosmic-ray muon radiography (muography) has been utilized for obtaining the density profiles of volcanoes (eg. Tanaka et al., 2007; Lesparre et al., 2010; Cârloganu et al., 2013). Since gravity measurement is also sensitive to the internal density of the Earth, a combination of muography and gravimetry is expected to provide density profiles with fine resolutions (Okubo and Tanaka, 2012). Nishiyama et al. (2014) has developed a simultaneous inversion method of both two data for determining the 3-D density structures of volcanoes and has presented the feasibility of the hybrid measurement through a case study of a small (500 m in diameter) lava dome, Showa-Shinzan, Hokkaido, Japan. This study revealed that a vent extends downward beneath the dome.

We are now planning another hybrid measurement at Tarumai Lava Dome on the Shikotsu caldera, Hokkaido, Japan, in order to perform a comparative study on the internal structures of lava domes. The Tarumai lava dome has formed at the top of Mt. Tarumai during the 1909 eruption. We conducted gravity measurements at 23 stations spanning 1.5 km (NS) x 1.5 km (EW). We are preparing the muography detector for the coming measurement. We report the possible detector sites and the result of the resolution test of this new hybrid measurement.

References:
Tanaka et al., Earth Planet. Sci. Lett., 263, 104-113 (2007).
Lesparre et al., Geophys. J. Int., 183, 1348-61 (2010).
Cârloganu et al., Geosci. Instrum. Method. Data Syst., 2, 55?60 (2013).
Nishiyama et al., J. Geophys. Res. Solid Earth, 119, doi:10.1002/2013JB010234 (2014, in press).

Keywords: cosmic-ray muon radiography, gravity anomaly, density, lava dome

Japan Geoscience Union Meeting 2014
(28 April - 02 May 2014 at Pacifico YOKOHAMA, Kanagawa, Japan)

U02-P03 Room:Poster Time:April 28 18:15-19:30

Introduction about test measurement of the muon detection system for monitoring a groundwater (With some observations)

SANNOMIYA, Akira[1*] ; TANAKA, Hiroyuki[2] ; SUENAGA, Hiroshi[3] ; SUZUKI, Kouichi[3]

[1]Electric Power Development Co., Ltd, [2]Earthquake Research Institute,U of Tokyo, [3]Central Research Institute of EPI

The technique to radiographically image the internal structure of gigantic objects by utilizing muon's significant penetration power (muography) enabled us to investigate the internal structure of volcanoes and the city foundation with higher spatial resolution than possible with the conventional techniques.

This observation technique is applicable to exploring a large-scale civil engineering structure, the internal state of a base rock, etc. However, feasibility of muographic application to monitoring inside the large-scale civil engineering structure has not confirmed yet. Therefore, we decided to carry out test measurements in order to explore the possibility of muography for monitoring groundwater levels.

We are currently investigating the response of the groundwater levels to major rainfall events in the landslide area. We selected this area as an observation area. The measurement was carried out from the inside of a scupper tunnel in the base rock. Our muon detection system consists of plastic scintillator, photomultipliers (PMTs), and a high voltage (HV) power supply.

The muography detector was installed to the observation site in August, 2012 and measurement was started on the same date.

The result will be compared with the independent measurement results of groundwater levels and soil resistivity in order to quantitatively assess the technological limit of muography.

So far, we obtained the preliminary result that showed variations in the penetrating muon intensity; hence the density as a response of major rain fall events by plotting a moving average of the 48-hour observation time at different time intervals of one hour, two hours, three hours, and six hours. It showed a clear rainfall effect when the time interval is 6 hours. The future prospect includes further case studies for different rainfall-underground water coupling scenarios.

Keywords: muography, muon detection system, groundwater, test measurement, landslide

Japan Geoscience Union Meeting 2014
(28 April - 02 May 2014 at Pacifico YOKOHAMA, Kanagawa, Japan)

U02-P04 Room:Poster Time:April 28 18:15-19:30

A Historical View on the Degradation on Seismic Performance of The Parthenon, Greece and Muography as the Potential Eval

AOKI, Shimpei[1*] ; TANAKA, Hiroyuki[2] ; OHSHIRO, Michinori[3] ; YAMASHITA, Maria[4]

[1]Faculty of Letters, Kansai University, [2]Earthquake Research Institute, the University of Tokyo, [3]Faculty of Letters, Komazawa University, [4]Graduate Division of Arts and Sciences, Komazawa University

To reinforce the Parthenon against earthquakes, the process of disassembling and reassembling Doric columns is obligatory. For this, the column strength and durability is required to withstand the reconstruction process. Wooden rods in the dowels of each drum provide the mechanical strength of each column, however some of these rods may have been damaged during the Venetian bombardment of the Acropolis on September 26, 1687. Due to the size of the Parthenon's Doric columns, muography is more appropriate to image the internal structure than conventional radiographic techniques. Muography may be utilized as a non-destructive technique targeting the inside composition of the Parthenon's Doric columns, potentially providing the following information: (1) the durability of the columns against future earthquakes, and (2) the magnitude of the internal damage sustained during the Venetian bombardment. The results of this muographic survey would aid conservator's efforts to protect the Parthenon along with the possibly of applying to other cultural properties. Secondly, the state of the wooden rod inside the column will provide evidence for the time and temperature around the column (based on the geometrical structure and thermal conductivity of the column) which would contribute further evidence to historical discussions particular to the Parthenon, such as estimates of the amount of gun powder stored in the Parthenon by the Ottoman Empire and information on the aforementioned siege. Muography may supplement efforts to preserve and protect the Parthenon as well as contributing to our understanding of the historical events that have occurred in this ancient structure.

Keywords: a Historical View, the Degradation on Seismic Performance, the Parthenon, Muography

Japan Geoscience Union Meeting 2014
(28 April - 02 May 2014 at Pacifico YOKOHAMA, Kanagawa, Japan)

U02-P05 Room:Poster Time:April 28 18:15-19:30

Geo-neutrinos and reactor anti-neutrinos expected in Daya Bay II and in LENA

BALDONCINI, Marica[1*] ; ESPOSITO, Juan[2] ; LUDHOVA, Livia[3] ; MANTOVANI, Fabio[1] ; RICCI, Barbara[1] ; XHIXHA, Gerti[1] ; ZAVATARELLI, Sandra[4]

[1]University of Ferrara, [2]INFN, Legnaro National Laboratories, [3]University of Milan, [4]University of Genova

Geo-neutrinos produced by beta decays occurring in ^{238}U and ^{232}Th decay chains are presently detected via inverse beta reaction in liquid scintillation detectors (KamLAND and Borexino). Geo-neutrinos are a unique direct probe of our planet's interior since they instantaneously bring to the Earth's surface information concerning the total amount and distribution of U and Th in the crust and in the mantle, which are thought to be the main reservoirs of these elements. The geo-neutrino spectrum allows to discriminate the different Th and U components. Measuring geo-neutrino fluxes and spectra can shed light on the radiogenic contribution to the terrestrial heat power and on the Earth's nowadays composition, providing a direct test of the Bulk Silicate Earth models and giving additional constraints on the Earth's evolution models.

A better discrimination among different Earth's global models can be reached combining the results from several sites: new measurements of geo-neutrino fluxes are highly awaited from experiments entering operation, such as SNO+, or proposed to the scientific community, as LENA or Daya Bay II. In particular, LENA and Daya Bay II would provide a substantial increase of the detection sensitivity and of the event rate thanks to their large target masses (50 kton and 20 kton, respectively) compared to the 1 kton mass of KamLAND and SNO+ and to the 0.3 kton of Borexino.

The main background in geo-neutrino measurements is due to the electron anti-neutrinos produced by nuclear power plants, which are the strongest man-made anti-neutrino sources. Many fission products decay through beta processes with the consequent emission of electron anti-neutrinos, the so called reactor anti-neutrinos. The reactor anti-neutrino spectrum covers an energy range extending up to about 8 MeV, which results in a significant overlap between geo-neutrino and reactor anti-neutrino signals in the geo-neutrino energy window (1.8 $-$ 3.3 MeV). The events of reactor anti-neutrinos are strongly dependent on the distance of the closeby commercial nuclear power plants. Therefore, a careful analysis of the expected reactor anti-neutrino event rate at a given experimental site is mandatory.

In this framework, we estimate the expected reactor anti-neutrino signals at ongoing geo-neutrino experiments sites, in particular at Pyhasalmi and JUNO (Jiangmen Underground Neutrino Observatory), which are the candidate sites for hosting the LENA and Daya Bay II experiments, respectively. The inputs required to evaluate the reactor anti-neutrino flux come from neutrino properties, nuclear physics in the reactors and features of nuclear power plants. In our calculation we take into account the three neutrino oscillation mechanisms in vacuum, the most updated reactor anti-neutrino spectra and standard fuel compositions. According to the International Atomic Energy Agency (IAEA) database, we use detailed information on the locations and on the monthly time profiles of the thermal power for each nuclear core.

In Table 1 we report the expected geo-neutrino and reactor anti-neutrino signals for different locations, expressed in TNU (Terrestrial Neutrino Units). Nuclear power plants data refer to IAEA database reporting information of year 2012, when all of the Japanese nuclear power plants were still switched off. The ratio between the expected reactor anti-neutrino signal in the geo-neutrino energy window (R_G) and the expected geo-neutrino signal (G) is calculated all over the world in order to produce a R_G/G map. The values of R_G/G for future sites (Phyasalmi and JUNO) are almost comparable to the operating ones (LNGS and Kamioka), with a slight preference for the Finnish location. The total uncertainty on the reactor signal predictions is on the order of 5%: among all the accounted sources of uncertainties, the ones giving the main contributions originate from the θ_{12} mixing angle, the anti-neutrino spectrum, the fuel composition and the thermal power.

Keywords: geo-neutrino, anti-neutrino from reactor, neutrino detector

Sites	R [TNU]	R_G [TNU]	G [TNU]	R_G/G
LNGS	85.8 ± 4.6	22.8 ± 1.1	$40.3^{+7.3}_{-5.8}$	0.6
KAMIOKA	70.1 ± 3.7	18.7 ± 1.1	$31.5^{+4.9}_{-4.1}$	0.6
SUDBURY	174.6 ± 9.0	43.1 ± 2.1	$45.4^{+7.5}_{-6.3}$	0.9
PHYASALMI	69.2 ± 3.7	17.5 ± 0.8	$45.3^{+7.0}_{-5.9}$	0.4
FREJUS	587.9 ± 31.0	134.0 ± 7.1	$42.4^{+7.6}_{-6.2}$	3.2
HOMESTAKE	27.7 ± 1.5	7.3 ± 0.3	$48.7^{+8.4}_{-6.9}$	0.1
HAWAII	3.4 ± 0.2	0.9 ± 0.04	$12.0^{+0.7}_{-0.6}$	0.1
CURACAO	9.5 ± 0.5	2.5 ± 0.1	$29.3^{+4.2}_{-3.3}$	0.1
JUNO	99.0 ± 5.1	27.4 ± 1.4	$39.7^{+6.5}_{-5.1}$	0.7

Table 1: Comparison between expected reactor (R) and geo (G) antineutrino signal. R_G indicates the reactor signal expected in the geo neutrino energy window ($E_{\bar{\nu}} < 3.26$ MeV). 1 TNU = 1event/year/10^{32} protons.

Japan Geoscience Union Meeting 2014
(28 April - 02 May 2014 at Pacifico YOKOHAMA, Kanagawa, Japan)

U02-P06 Room:Poster Time:April 28 18:15-19:30

Towards a refined regional geological model for predicting geoneutrinos flux at Sudbury Neutrino Observatory (SNO+)

STRATI, Virginia[1*] ; HUANG, Yu[2] ; MANTOVANI, Fabio[1] ; SHIREY, Steven B.[3] ; RUDNICK, Roberta L.[2] ; MCDONOUGH, William F.[2]

[1]University of Ferrara, [2]University of Maryland, [3]Carnegie Institution of Washington

The SNO+ detector is the redeployment of the illustrious Sudbury Neutrino Observatory (SNO) at SNOLAB in Ontario (Canada). After the substitution of heavy water (D_2O) with liquid scintillator (CH_2) inside the inner vessel, in 2014 the 1 kton detector will come on-line and together with KamLAND in Japan and Borexino in Italy will accumulate geoneutrino events. Geoneutrinos are electron antineutrinos originating from beta decays of natural radioactive nuclides in the Earth interior. A fraction of them, generated from ^{214}Bi and ^{234}Pa of ^{238}U decay chain and from ^{228}Ac and ^{212}Bi of ^{232}Th decay chain, are above the threshold for inverse beta reaction on free protons and can be detected by SNO+. Geoneutrinos are a real time probe of Earth interior, because the flux at the terrestrial surface depends on the amount and distributions of U and Th in the Earth's reservoirs. To extract global information such as terrestrial radiogenic heat power or to test compositional models of the Bulk Silicate Earth (BSE), the regional contribution to the geoneutrino signal has to be controlled by study of regional geology.

We present the 3-D refined geological model of the main reservoirs of U and Th in the regional crust extended for approximately 2×10^5 km^2 around SNOLAB, including estimates of the volumes and masses of Upper, Middle and Lower crust, together with their uncertainties. According to the existing global reference model (Huang et al., 2013), this portion of the crust contributes for 43% of the total expected signal at SNO+. The remaining contributions come from the far field crust (34%), from continental lithospheric mantle (5%) and from the mantle (18%). Since SNO+ will accumulate statistically significant amounts of geoneutrino data in the coming years, the calculated signal that is predicted to be derived from the lithosphere can be subtracted from the experimentally determined total geoneutrino signal to estimate the mantle contribution.

The main crustal reservoirs are modeled by identifying three main surfaces: the Moho discontinuity, the top of the Lower Crust and the top of the Middle Crust. About 400 depth-controlling data points obtained from deep crustal refraction surveys and from teleseismic receivers are the inputs for the spatial interpolation performed with the Ordinary Kriging estimator. This method takes into account the spatial continuity of the depths and it provides the uncertainties of the crustal volumes. The Upper Crust is further modeled in detail combining information from vertical crustal cross sections and Geological Map of North America at 1:5,000,000 scale. Seven sub-reservoirs with distinctive characteristics lithologies, metamorphism, tectonic events and chemical composition are identified. The density and the abundances of U and Th in the seven sub-reservoirs are evaluated from the published litho-geochemical databases, including analyses of representative outcrop samples. The Middle and Lower Crust densities and radioactivity contents are evaluated from seismic constraints.

The numerical 3D model consists of about 9×10^8 cells of 1 km $\times$ 1 km $\times$ 0.1 km dimensions. For each of them geophysical information, such as latitude, longitude, depth and reservoir type, are combined with estimates of the U and Th abundances to predict the geoneutrino signal at SNO+ originated from the regional crust. The total geoneutrino signal at SNO+ is about 12% less than that calculated using the global reference model (Huang et al., 2013).

Keywords: geoneutrinos, SNO+, uranium, thorium, geological modeling

Japan Geoscience Union Meeting 2014
(28 April - 02 May 2014 at Pacifico YOKOHAMA, Kanagawa, Japan)

U02-P07 Room:Poster Time:April 28 18:15-19:30

Upgrade plan of the KamLAND detector for improvement of sensitivity to geo-neutrino

OBARA, Shuhei[1*]

[1]RCNS, Tohoku University

Neutrino, which is a kind of elementary particles, interacts with other particles only via weak interaction. RCNS, Tohoku University, researches the neutrino science with the large neutrino detector, KamLAND. Measuring the geo-neutrinos that are produced in beta decays within the Earth ′ s interior, is only way to estimate the Earth ′ s radiogenic heats production and constrain composition models of the Earth.

The KamLAND detector is marked by the ability to detect low energy electron-type anti-neutrinos. Radioactive isotopes, such as ^{238}U and ^{232}Th decay as follows, and produce the electron-type (anti-) neutrinos (geo-neutrino).

^{238}U$\rightarrow$ ^{206}Pb+8 ^{4}He+6e^{-}+6$\nu^{bar}{}_{e}$+51.7[MeV]

^{232}Th$\rightarrow$ ^{208}Pb+6^{4}He+4e^{-}+4$\nu^{bar}{}_{e}$+42.7[MeV]

Geo-neutrino flux directly informs us the radiogenic heat generation. In fact, previously, the KamLAND experiment has given the result; the radiogenic heat production in the Earth ′ s interior by ^{238}U and ^{232}Th is estimated to be $20.1_{-9.1}{}^{+9.1}$ TW through measuring the geo-neutrinos, and it is obviously smaller than the Earth ′ s total heat flow (44 ± 1TW).

In order to improve the sensitivity of the KamLAND detector, the upgrade plans (KamLAND2 experiment) are in progress. Large light intensity liquid scintillator, light collection mirror, high quantum efficiency photomultiplier, imaging device, scintillation film, etc...

In the KamLAND2 experiment, improving energy and vertex resolution are expected. Therefore it will be possible to observe geo-neutrinos with higher accuracy and statistics. This experimental improvement will have higher ability to discriminate between models and separate contributions from ^{238}U and ^{232}Th. The KamLAND2 will play a contribution to the geo physics in that way.

In this presentation, future prospects and R&D are discussed.

Keywords: geo-neutrino

Japan Geoscience Union Meeting 2014
(28 April - 02 May 2014 at Pacifico YOKOHAMA, Kanagawa, Japan)

U02-P08 Room:Poster Time:April 28 18:15-19:30

The next-generation KamLAND electronics

HAYASHIDA, Shingo[1*]

[1]Research Center for Neutrino Science, Tohoku University

KamLAND was constructed to detect the low energy anti-neutrinos. And then, KamLAND detected reactor neutrinos and solved solar neutrino problem on 2003. And furthermore, KamLAND detected geo-neutrinos for the first time in the world on 2005. Currently, KamLAND has already been beginning to search several new physics. However, searching new physics in the detector of 10 years ago is difficult. So, it is necessary to update the detector. We are planning to update the KamLAND. As this updating, KamLAND electronics will be renewed using the latest technologies. The next-generation KamLAND electronics will certainly contribute to geoscience.

Keywords: Neutrino detector, Data taking, electronics

Japan Geoscience Union Meeting 2014
(28 April - 02 May 2014 at Pacifico YOKOHAMA, Kanagawa, Japan)

U02-P09 Room:Poster Time:April 28 18:15-19:30

Imaging detector

MITSUI, Tadao[1*]

[1]RCNS, Tohoku University

Geo-neutrinos are emitted from radioactive elements, such as Uranium and Thorium, in the Earth's interior. Those elements contribute about one half of Earth's heat source. With high transmissivity of neutrinos, geo-neutrino may enable us to measure heat sources in the deep mantle. Since 1-kton liquid scintillator detector "KamLAND" detected geo-neutrinos in 2005, it has been expected as a new probe of Earth's interior. At present, an Italian detector "Borexino" is also observing geo-neutrinos, realizing a "stereo observation". However, observation points are still not enough. In addition, lack of the directional information of geo-neutrinos are serious disadvantage in making the data more precise. We are now developing a new detector for directional measurement of geo-neutrinos, aiming at installing it in KamLAND in the near future. Geo-neutrinos are electron antineutrinos being detected with an inverse beta decay channel with a free proton. Directional information of the neutron, emitted in the inverse beta decay channel, should be measured, in order to measure the direction of the incoming electron antineutrino. To this purpose, we are developing liquid scintillators doped with Lithium-6, which has large neutron capture cross section, and imaging detectors, which detect the vertex position of neutron capture precisely. In this poster, imaging detectors, that we are developing, are reviewed. To detect feeble light emission of the scintillator (actually one photon level), and determine the emission position precisely, optics with large acceptance and small aberration, together with a light detector with high quantum efficiency and positional sensitivity should be employed. In our current R&D, a hopeful design is that with a mirror of diameter 50 cm, and a 256-channel multi-anode photomultiplier tube. Highlighting that design, we will review the latest progress, plan of installing it, expected geophysical results.

Keywords: neutrino, geo-neutrino, radiogenic heat source

Japan Geoscience Union Meeting 2014
(28 April - 02 May 2014 at Pacifico YOKOHAMA, Kanagawa, Japan)

U02-P10 Room:Poster Time:April 28 18:15-19:30

Li loaded liquid scintillator for directional measurement

SHIRAHATA, Yutaka[1*]

[1]RCNS, Tohoku University

By the detection of the electron antineutrino using the current liquid scintillator, we can suppress the large background by the delayed coincidence of positron and neutron released by the inverse β-decay that proton and electron antineutrino cause. And we can observe electron antineutrino in the low energy scale.

On the other hand, we cannot know the coming direction of the electron antineutrino like the water Cerenkov method with the existing detector.But we can know the coming direction of the electron antineutrino by observing both reaction point of positron and capture point of neutron.If we could observe the coming direction of the electron antineutrino in the low energy scale, we would distinguish a neutrino every observation object and be able to expect observation with high precision.

There are three necessary conditions to detect the coming direction of the electron antineutrino by a liquid scintillator; (i)capture a neutron before losing directional information, (ii)cause luminous phenomenon at a neutron capture point, (iii)develop a new detection technology with the high position identification performance to detect the reaction points.

In current liquid scintillator, it takes about 200μs until a positron captures a thermal neutron released by inverse β-decay and this reaction emits 2.2MeV gamma ray. The released thermal neutron scatters about 10 cm, and so the neutron loses antineutrino $'$ s directional information. The neutron produces 2.2MeV capture gamma ray and it obscures the neutron capture point. To solve this problem, we developed ^{6}Li loaded liquid scintillator. ^{6}Li has large neutron capture cross section (940barn) and when ^{6}Li captures neutron, it releases alpha ray that it cannot move a long distance in the liquid scintillator. We can expect to solve two problems by using this new liquid scintillator and also to detect the coming direction of the electron antineutrino using imaging detector that has high position resolution.

In presentation, I will talk about the lithium loaded liquid scintillator developed by an original method.

Keywords: geo-neutrino

Japan Geoscience Union Meeting 2014
(28 April - 02 May 2014 at Pacifico YOKOHAMA, Kanagawa, Japan)

U02-P11 Room:Poster Time:April 28 18:15-19:30

Tomography of the earth with large-scale neutrino experiments

HOSHINA, Kotoyo[1*]

[1]Earthquake Research Institute, the University of Tokyo, [2]Wisconsin IceCube Particle Astrophysics Center

Experimental techniques to study inside of the Earth have been developing remarkably in the past decades. For example, in-situ x-ray diffraction measurements under high-pressure and high-temperature opened new era for studying about possible chemical components and structures of deep Earth. In the next ten years, we will obtain yet another technique for direct measurements of the Earth's interior.

Probing inner structures of the Earth with neutrinos has been discussed for more than 30 years. Neutrinos are chargeless particles and have very small cross-sections. They normally penetrate the Earth without any interaction, and from the rare interactions that do occur we obtain information on the density profile of the Earth's interior. However, the elusive characteristic of neutrinos poses a challenge for detecting them at experimental sites. To compensate for the small interaction cross-section, one needs a large volume neutrino detector.
The IceCube[1] neutrino observatory, completed in 2011 and has 1 cubic kilo-meter volume of detector size, is a possible candidate for this study. Current status of a study for measuring the core density of the Earth with atmospheric neutrino will be presented.

Another characteristic of neutrino is that they change their flavor periodically (neutrino oscillation). These oscillation patterns are affected by the density profile of electrons along the path of the neutrino. Comparisons between the Earth's mass-density profile and the electron-density profile give us ratio profiles of atomic number vs mass number (A/Z), which contains information of chemical composition of the Earth.

It is crucial to use a specific energy range for source neutrinos in order to perform the neutrino oscillation tomography. For Earth's core, the energy range is ˜1GeV to 30GeV. To detect the GeV-range neutrinos with sufficient statistics, next-generation experiments Hyper Kamiokande[2] and PINGU[3] have been proposed. Possible discrimination powers of some chemical models of the Earths core will be discussed.

Fig.1
Left: Exclusion of a pyrolite core model with respect to a pure iron core a time range of ten years. Right: The accuracy, measured in units of sigma, of the Z/A measurement for the assumption of an iron core. Calculated for PINGU[3].

References

1.IceCube Collaboration, Astroparticle Physics 26, 155(2006)
2.LoI: The Hyper-Kamiokande experiment, arXiv:1109.3262(2011)
3.LoI: The Precision IceCube Next Generation Upgrade, arXiv:1401.2046 (2014)

Keywords: neutrino tomography, neutrino radiography, IceCube

U02-P11 Room:Poster Time:April 28 18:15-19:30

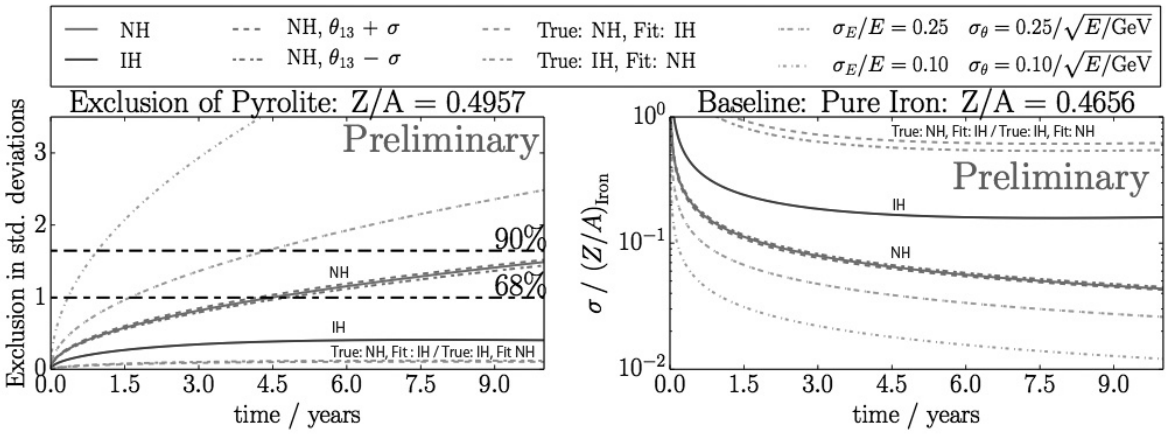

Japan Geoscience Union Meeting 2014
(28 April - 02 May 2014 at Pacifico YOKOHAMA, Kanagawa, Japan)

U02-P12 Room:Poster Time:April 28 18:15-19:30

Muographic imaging of Usu volcano with a multilayer detector

KUSAGAYA, Taro[1*] ; TANAKA, Hiroyuki[1] ; OSHIMA, Hiromitsu[2] ; MAEKAWA, Tokumitsu[2] ; YOKOYAMA, Izumi[3]

[1]Earthquake Research Institute, University of Tokyo, [2]Graduate School of Sciences, Hokkaido University, [3]The Japan Academy

Usu volcano is one of the most active volcanoes in Japan and has erupted for four times in the recent 100 years (1910, 1943, 1977-1978 and 2000). In the 1977-1978 eruption, 18 craterlets and a U-shaped fault were formed in the summit crater. The eruption also caused the deformation in the summit crater area with a diameter of 1.8 km and formed an upheaval called Usu-Shinzan.

Preceding studies suggested that the cooling magma intrusion with a height of 600 m and a width of 300 m was located below the Usu-Shinzan by magnetotelluric soundings (e.g. Ogawa et al., 1998, Matsushima et al., 2001). And Yokoyama and Seino (2000) built a tilt model to interpret the formation of Usu-Shinzan. In this model, a block with a width of 800 m tilted approximately 11^o on a pivot at a depth of 800 m. So, in the present work, we conducted the muographic imaging (radiography with cosmic-ray muon) of Usu volcano to confirm the existence of magma intrusion beneath Usu-Shinzan.

But there is the issue of background (BG) noise of muographic imaging for a large volcano (>1 km thick). Since the integrated intensity of traversing cosmic-ray muons steeply decays as a function of the thickness of the target, the signal-to-noise (S/N) ratio also decreases seriously as the size of target becomes larger, and thus the density distribution cannot be accurately measured at a large volcano. The background (BG) noise that reduces the S/N ratio mainly consists of the fake tracks that are generated by the accidental coincidence of the electromagnetic (EM) shower particles. The values of BG noise were 10^{-6} cm^{-2} sr^{-1} s^{-1} (Lesparre et al., 2012) and 10^{-7} cm^{-2} sr^{-1} s^{-1} (Carloganu et al., 2013). BG noise of 10^{-7} cm^{-2} sr^{-1} s^{-1} corresponds to integrated cosmic-ray muon intensity after traversing 1 km of 2.65-g cm^{-3} rock.

In order to solve this problem, we developed a novel muon detection system that consists of multiple layers of position sensitive detectors (PSDs) in conjunction with a trajectory analysis method to effectively reduce the BG noise. In this method, the EM shower-originated fake tracks are rejected by requesting a linear trajectory for a muon event (linear cut method) since EM shower particles randomly hit each PSD layer and make a non-linear trajectory in the detection system. This detection system was applied to Usu volcano, Hokkaido, Japan to image its internal density structure (the spatial distribution of the density). In this measurement, we utilized a muon detection system that consisted of 7 layers of PSDs. One PSD consisted of x- and y- arrays of plastic scintillator strips with an active area of 1.21 m^2 and a segmented area of 10x10 cm^2. The angular resolution was +/- 3^o. The measurement duration was 1977 hours (82 days).

In this measurement, we compared the integrated cosmic-ray muon intensity traversing 2500 m of 1.5-g cm^{-3} rock with observed data at an elevation angle of 55.6 mrad. Assuming that the residual between the calculated intensity and data is BG noise, we obtained the BG noises of 5.4x10^{-5} cm^{-2} sr^{-1} s^{-1} with two PSDs and 1.9x10^{-6} cm^{-2} sr^{-1} s^{-1} with seven PSDs. The multilayered muon detector was effective to reduce the BG noise. However, BG noise remains and they may be attributed to another source of BG noise such as upward-going particles(Jourde et al., 2013). This measurement yielded the following results: (A) by analyzing the region that has a thickness of more than 1000 m, we confirmed that our detection system is sensitive to a density variation of 10% in 1300-m rock; and (B) there are high- and low-density anomalies beneath between Oo-Usu and Usu-Shinzan peaks, which is consistent with the magma intrusion and the resultant fault generation suggested by Yokoyama and Seino (2000), Ogawa et al. (1998) and Matsushima et al. (2001).

For the future prospect, we will try to use the shield in order to distinguish the upward-going particles from muons arriving from a volcano side.

Keywords: muography, muon, radiography

Japan Geoscience Union Meeting 2014
(28 April - 02 May 2014 at Pacifico YOKOHAMA, Kanagawa, Japan)

U03-01 Room:Main Hall Time:May 1 14:15-14:20

Expecting great development of PEPS

TSUDA, Toshitaka[1*]

[1]Research Institute for Sustainable Humanosphere (RISH), Kyoto University

JpGU is going launch ”Progress in Eaerth and Planetary Science; PEPS” as a new open acceess E-journal, covering all scientific fields of JpGU.

Keywords: open access, e-journal, PEPS

Japan Geoscience Union Meeting 2014
(28 April - 02 May 2014 at Pacifico YOKOHAMA, Kanagawa, Japan)

U03-02 Room:Main Hall Time:May 1 14:20-14:45

Open Access Issues in Physics Journals

UEDA, Ken-ichi[1*]

[1]Institute for Laser Science, University of Electro-Communications

I introduce some of Open Access activities in Physics journals.

1. arXiv, INSPIRE, SCOAP3

Open Access activities in Physics area have a long history and culture. The standard of judgement of physics papers is based on whether they give new knowledges or informations on human or not. We developed open access databases like arXiv and INSPIRE in 1991 at the beginning of WWW technology. High energy physics (HEP) has been a front runner of open data and open articles. SCOAP3 is a challenging program to serve OA services for top existing HEP journals not only to readers but also to the authors; most of the authors are poor theoretical physicists. Redirection of budget flow from subscription to SCOAP3 scheme is proposed. SCOAP3 started and challenge to stablish a long term sustainable model.

2. Public Access activities

Physics communities have delivered charge-free access to the journal database of societies via public libraries and high school libraries since early 90's. All physics papers are open to the people in US when they visit these libraries. Researchers and teachers of developing countries have a charge-free-acceess to the physics papers through International Center of Theoretical Physics (ICTP). Most of physical societies and publishing companies join the ICTP OA library. ICTP developed a lot of research support and educational programs under a support of UNESCO.

3. Charge-free Reading vs Charge-free Publishing

There are intense discussions on Gold-OA, which means charge-free reading journal. In 1997, the first Gold-OA journals such as Optics Express (OSA) and New Journal of Physics (IOP) were published. In 2003, Optics Expres reached breakeven point. Today OSA published more than 50% articles in Gold-OA journals with top IF in Optics. These Gold-OA journals demonstrated a sustainable model which satisfies high quality, article volume, and financial condition, altogether. Such a success was achieved by extraordinal efforts of editors group toward the new generation academic journals by online pubishing techniques. APS developed Gold-OA Physical Review X for the real top journal under a diffrect scope and vision. We understand Gold-OA is not a single issue, there are many variations in their scope and functions.

APS journals (Physical Review A-E, Physical Review Letters, etc) published more than 60% articles in Physics with high quality. The publicatin cost in APS journals is relatively low because authors send their manuscripts in REVTEX fromat. APS returned the benefit of electronic publication to the authors. The author-fee for Physical Review is zero when they send the manuscript in a manner of electronically acceptable format. The increase of subcriptions from Chinese institutions by WTO scheme contributed to their financial balance significantly.

How to share the scientific information with a reasonable cost, this is a main topics of OA movement today. However, we have to remind that the final target of information sharing is stimulation and activation of scientific activities. Physics communites have payed significant attention to the benefit of authors and readers in equal weight.

4. Try and Error, this is our principle.

Physics communities have made big efforts to improve the publication and access to the scientific informations last 20 years. Fortunately, Gold-OA journals in physics keep high quality by the effort of top societies like APS, IOP and OSA. The financial gain of Gold-OA is directly connected to the acception volume. This is an internal mechanism of Gold-OA. We need additional feedback mechanis to keep the scientific quality independently to the rejection rate. We have no rigid model for OA publishing and economical sustainability even now. It depends on the real situation of research and educational condition. Every academic community and every contry have to develop their own model accorting to their requirement, scope and decision.

Keywords: Open Access Journals, IUPAP WG, Gold OA, Public Access, Subscription Model, Author fee

Japan Geoscience Union Meeting 2014
(28 April - 02 May 2014 at Pacifico YOKOHAMA, Kanagawa, Japan)

U03-03 Room:Main Hall Time:May 1 14:45-15:10

Open Access to Academic and Scholarly Information and Scientific Data

MURAYAMA, Yasuhiro[1*]

[1]National Institute of Information and Communicatoins Technology

Scholarly and scientific information is the infrastructure of science and humanity in a broad sense. The first successful academic journal, Philosophical Transactions, in 17 century have resulted in open and sharing of academic literature or information. In modern Science and Technology research, information which cannot be expressed in a written journal paper, including numerical data, 3-dimensional geospatial information, voice and sounds, and movies. are increasingly being recognized important in international community. Considering that Open Access (OA) of academic journals is to support further advancement of science and technology in coordination with transition from printing culture to electronic media, scientific research data which can be open should be subject to the scientific information infrastructure. International data management activity like ICSU-WDS from the academic side, and RDA related to governmental arrangement are part of such big challenges of the international community. Data citation, using DOI as a persistent identifier attached to a data set, is promoted by international organizations such as WDS, RDA, DataCite, ICSTI, Force11, etc., jointly with science publishers such as Thomson Reuter, Elsevier, Wiley, and so on.

Keywords: Open Data, Scientific Data, ICSU-WDS, RDA, G8

Japan Geoscience Union Meeting 2014
(28 April - 02 May 2014 at Pacifico YOKOHAMA, Kanagawa, Japan)

U03-04 Room:Main Hall Time:May 1 15:10-15:30

Toward the Founding of a Scholarly Publishing Consortium: UniBio Press Activities

NAGAI, Yuko[1*]

[1]The Zoological Society of Japan

This is a report on UniBio Press activities toward the founding of a scholarly publishing consortium as suggested by the Science Council of Japan Special Committee on Scholarly Publishing in August of 2012.

UniBio Press has, in collaboration with 8 other academic societies, adopted Strengthening International Dissemination of Information (A), and has spent this last year actively pursuing the creation of arenas for information sharing among, not only the participant academic societies, but for the whole of academic societies across Japan.

Keywords: the Science Council of Japan, Scholarly Publishing, Consortium, UniBio Press

Japan Geoscience Union Meeting 2014
(28 April - 02 May 2014 at Pacifico YOKOHAMA, Kanagawa, Japan)

U03-05 Room:Main Hall Time:May 1 15:30-15:40

Renovation and future perspective of journal ”Earth, Planets and Space”

ODA, Hirokuni[1*] ; OGAWA, Yasuo[2]

[1]National Institute of Advanced Industrial Science and Technology, [2]Tokyo Institute of Technology

Earth, Planets and Space (EPS) is an academic journal published by the following five societies; The Society of Geomagnetism and Earth, Planetary and Space Sciences, The Seismological Society of Japan, The Volcanological Society of Japan, The Geodetic Society of Japan, and The Japanese Society for Planetary Sciences. The publication of EPS started in 1998 as continuations of the *Journal of Geomagnetism and Geoelectricity* and the *Journal of Physics of the Earth*. EPS is accepting scientific articles in the earth and planetary sciences covered by the five societies, in particular, geomagnetism, aeronomy, space science, seismology, volcanology, geodesy, and planetology. The 5-year publication project proposal on EPS to Grant-in-Aid for Publication of Scientific Research Results was accepted and open access publication has started from Jan. 2014. EPS is going to strengthen its international scholarly communication prioritizing letters, and will start publishing in cooperation with Japan Geosciences Union from Jan. 2016. Renovations of EPS including change of publishers and business model transition into open access carried out in FY2013 and the future perspectives will be presented.

Keywords: Earth, Planets and Space, open access, Grant-in-Aid for Publication of Scientific Research Results, business model transition, academic publisher, scholarly communication

Japan Geoscience Union Meeting 2014
(28 April - 02 May 2014 at Pacifico YOKOHAMA, Kanagawa, Japan)

U03-06 Room:Main Hall Time:May 1 15:40-15:50

Editorial policy and goal of Progress in Earth and Planetary Science

IRYU, Yasufumi[1*]

[1]General Chief Editor, Progress in Earth and Planetary Science

We at the Japan Geoscience Union (JpGU) launched a new open access e-journal called Progress in Earth and Planetary Science (PEPS) in October 2013. As its name suggests, the purpose of this journal is to publish papers that present new discoveries, ideas and unifying concepts in the various fields of earth and planetary sciences (space and planetary sciences, atmospheric and hydrospheric sciences, human geosciences, solid earth sciences, and biogeosciences). In addition to normal research papers and review articles we would also like to publish material based on the best presentations given at the JpGU Annual meetings, and we have asked and will ask session conveners from the meetings to recommend those presentations that they consider to be the most scientifically interesting.

Because PEPS is an open access journal, the following benefits can be provided to authors:
- All articles published by PEPS are made freely and permanently accessible online immediately upon publication, without subscription charges or registration barriers.
- Authors of articles published in PEPS are the copyright holders of their articles and have granted to any third party, in advance and in perpetuity, the right to use, reproduce or disseminate the article.

The authors will benefit from the e-journal as follows:
- No restrictions or limitations for pages, figures, tables, or additional files to enrich the content, including videos, animations, and large original data files.
- No cost for color figures/pictures.
- Fast publication?generally papers/articles can be published 3?4 months earlier in e-journals than in standard print publications.

By taking these advantages, we intend to make PEPS a top-level international journal, and therefore all submitted papers (including invited papers) will go through a full peer review process. In order to publish high level research papers and review articles, we have organized a strong editorial board composed exclusively of active scientists and asked them to ensure that the refereeing process is strict as well as fair.

The PEPS editorial team works and will work hard for PEPS. However success of this journal relies primarily on whether JpGU members submit many high quality manuscripts or not. We earnestly wait for your submission to PEPS.

Keywords: Progress in Earth and Planetary Science, Editorial policy, Open access, E-journal

Japan Geoscience Union Meeting 2014
(28 April - 02 May 2014 at Pacifico YOKOHAMA, Kanagawa, Japan)

U03-07 Room:Main Hall Time:May 1 15:50-16:00

Publication of Progress in Earth and Planetary Science by JpGU

KAWAHATA, Hodaka[1*]

[1]Atmosphere and Ocean Research Institute, The University of Tokyo

JpGU started Open Access e-journal of Progress in Earth and Planetary Science (PEPS). The purpose of this new journal is to strengthen international communication in the field of geo- and planetary-science, and in particular: 1) To establish a geoscience open access leading e-journal; 2) To publish the best presentations from the JpGU Annual Meeting and the high quality of articles from authors based anywhere in the world, both those concerning specific areas of research and general unifying concepts and 3) To work on this together with the JpGU member societies. Efforts for the Promotion of PEPS are 1) to receive the list of the best presentation recommended by the session conveners at the JpGU annual meeting for PEPS submission and 2) to provide travel support and submission fee to submit a review (overview)/high quality articles. We will have the JpGU Journal special international session as part of the JpGU Meeting 2014, the JpGU Journal special symposium (relevant to JpGU research activity), invitation of big scientists recommended by each Science Section in JpGU, and enhancement of communication of the latest information on current research activity (e.g., published) among JpGU members and others. We are developing new application software that will be used at JpGU annual meeting place and at home. Also special effort is required to make PEPS recognized as a leading international journal by many scientists abroad. We will put an advertisement in AGU, EGU, AOGS and others. Our policy for JpGU journal is to publish high quality of articles in order to contribute to geoscience community globally. We present the latest information about JpGU journal and discuss its future development in this session.

Keywords: JpGU, open access e-journal, PEPS, earth planetary science, Participating society, JSPS

Japan Geoscience Union Meeting 2014
(28 April - 02 May 2014 at Pacifico YOKOHAMA, Kanagawa, Japan)

U04-01 Room:211 Time:April 29 09:00-09:15

Promotion of Scientific Research on Atmosphere and Climate System Using Aircrafts: Proposal of MSJ to SCJ

NIINO, Hiroshi[1*] ; KONDO, Yutaka[2] ; SATOH, Masaki[1] ; KOIKE, Makoto[2]

[1]Atmosphere and Ocean Research Institute, The University of Tokyo, [2]Graduate School of Science, The University of Tokyo

Aircraft observation systems along with artificial satellite and ground-based measurement systems are one of the most important tools for earth observations. Rapidly on-going climate change is already influencing our social and economic activities and water and food resources, which are bases for the civilization. Therefore it is important to understand the current status of the earth system and make reliable predictions of its future to avoid serious risks caused by the climate change.

The Working Group for Earth Observation Promotion, Subdivision on Research Planning and Evaluation, the Council for Science and Technology of the MEXT has summarized critical scientific issues for understanding of the global change in its annual guidelines in 2013. These include circulation and budget of the greenhouse gases, cloud and precipitation processes, changes in tropospheric species, climate change in polar regions, and changes in water circulation. The necessity of establishing aircraft observation system for conducting well organized long-term research of the global change is also mentioned. In-situ measurements by the state-of-the-art instruments on board aircraft provide accurate data of key parameters with high spatial resolutions, which lead to improved understanding of the critical processes.

The needs for research aircrafts have long been discussed among the Japanese research communities of atmospheric science and earth science. The Meteorological Society of Japan recently proposed a research project entitled ”Promotion of Scientific Research on Atmosphere and Climate System Using Aircraft” as a candidate for Master Plan of Large Research Project announced by the Japan Council of Science. This presentation gives a brief overview of the proposal. We plan to further polish up the research plans in the proposal and enrich the proposal by including possible subjects from other fields of earth science.

Keywords: Atmospheric Science, Climate System, Research Aifrcrafts, Meteorological Society of Japan, Science Council of Japan, Master Plan of Large Reserach Projects

Japan Geoscience Union Meeting 2014
(28 April - 02 May 2014 at Pacifico YOKOHAMA, Kanagawa, Japan)

U04-02 Room:211 Time:April 29 09:15-09:30

Long-term Observation of Atmospheric Greenhouse Gases using Aircraft

MACHIDA, Toshinobu[1*] ; MATSUEDA, Hidekazu[2] ; SAWA, Yousuke[2] ; MORIMOTO, Shinji[3] ; AOKI, Shuji[3]

[1]National Institute for Environmental Studies, [2]Meteorological Research Institute, [3]Graduate School of Science, Tohoku University

The more reliable prediction for future level of atmospheric greenhouse gases such as carbon dioxide (CO2) requires the quantitative understanding of global cycles in these gases. Comprehensive observation in atmospheric mixing ratios of trace gases can reduce the uncertainties of emission and absorption of these gases at earth's surface. The atmospheric observations, however, are not enough in several areas in the world, especially observations in upper atmosphere are quite limited compared to surface measurements.

Aircraft is one of the most reliable tools to observe the atmospheric compositions in troposphere and lower stratosphere. Several activities have been conducted to understand the 3-dimensional distribution and temporal variation of atmospheric greenhouse gases.

Mixing ratios of atmospheric CO2 have been measured from 200 to 10,000 m over Japan using chartered and commercial airliner since 1979 by Tohoku University (TU). Obtained data set is the longest record for CO2 mixing ratio in upper air. Latitudinal distributions of CO2 in upper troposphere are observed by commercial airliner operated by Japan Airlines (JAL) between Sydney, Australia and Narita, Japan, and Narita and Anchorage, USA from 1984 to 1985 by TU. The JAL observation in Australia-Japan route started again in 1993 using an Automatic Air Sampling Equipment (ASE) by Meteorological Research Institute (MRI). The new JAL observation named "Comprehensive Observation Network for Trace gases by AIrLiner (CONTRAIL)" have been done using improved ASE and Continuous CO2 Measuring Equipment (CME) since 2005 by National Institute for Environmental Studies (NIES) and MRI. Time series of CO2 mixing ratio in upper troposphere observed by old ASE and improved ASE are shown in the Figure. CONTRAIL-CME provides a large amount of CO2 data in upper air which contribute to solve global carbon cycle, atmospheric transport, model validation and satellite validation.

When dedicated aircraft is introduced in Japan, we propose to make a long-term observation for atmospheric greenhouse gases using above techniques and instruments.

Keywords: Greenhouse gases, Aircraft, CO2, Long-term observation, Troposphere

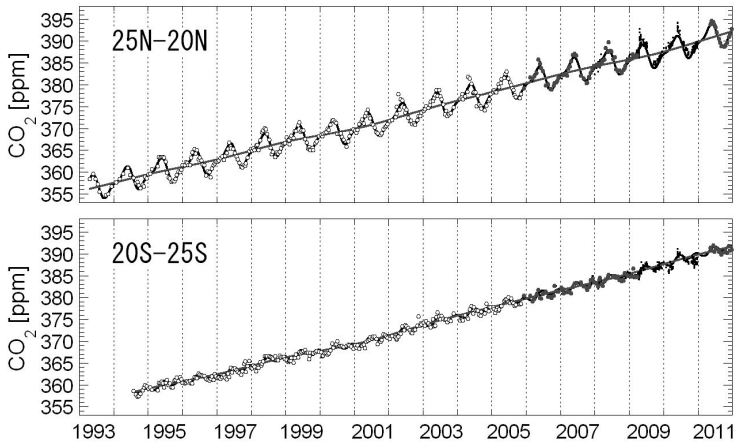

Japan Geoscience Union Meeting 2014
(28 April - 02 May 2014 at Pacifico YOKOHAMA, Kanagawa, Japan)

U04-03 Room:211 Time:April 29 09:30-09:45

Elucidation of atmospheric chemistry of reactive gases from airborne observations

KANAYA, Yugo[1*]

[1]JAMSTEC

Knowledge on spatio-temporal variations in the concentrations of tropospheric NOx, CO, and VOC is critical for closing the budget of OH radical, controlling oxidative capacity, and of O3, as a pollutant and a warming substance. Although recent satellite observations of tropospheric NO2, for example, have revealed regional/global distribution and seasonal features, they are based on column concentrations and thus limitation is present regarding information on vertical profiles and also on the spatial resolution.

In-situ airborne observations could provide complementary information with improved resolution in space, critical for validation of chemical transport model simulations. Validation of future satellite observations based on multi-spectral approach (e.g., O3 and CO), which could provide a piece of vertical profile information, is also important. Successful retrieval of near-surface concentrations, having impact on health and ecosystems, should be targeted.

Remote sensing from aircraft could enhance spatial (horizontal and vertical) coverage and resolution. For example, an airborne multi-channel imaging spectrometer in a nadir view could detect detailed inhomogeneity of NO2 and other gases present within cities at a 100-m resolution, contributing to studies on meso-scale atmospheric chemistry and physics. Limb observations in multiple angles could provide detailed vertical profile information.

In the presentation, observations of halogen and other unprecedented species, and observations to reveal air-sea or air-land interactions are also highlighted.

Keywords: vertical profile, nitrogen oxides, carbon monoxide, ozone, remote sensing from aircraft, spatial resolution

Japan Geoscience Union Meeting 2014
(28 April - 02 May 2014 at Pacifico YOKOHAMA, Kanagawa, Japan)

U04-04 Room:211 Time:April 29 09:45-10:00

Aerosol measurements by aircraft and modeling studies

OSHIMA, Naga[1*] ; KONDO, Yutaka[2] ; KOIKE, Makoto[2] ; MOTEKI, Nobuhiro[2] ; TAKEGAWA, Nobuyuki[3] ; KITA, Kazuyuki[4] ; NAKAMURA, Hisashi[3]

[1]Meteorological Research Institute, [2]Department of Earth and Planetary Science, Graduate School of Science, The University of Tokyo, [3]Research Center for Advanced Science and Technology, The University of Tokyo, [4]Faculty of Science, Ibaraki University

Most aerosol components scatter solar radiation; however, black carbon (BC) aerosols efficiently absorb it and lead to heating of the atmosphere. Because of these effects, the role of BC particles in the climate system has been recognized to be particularly important. However, there remain large uncertainties in the calculations of the spatial distributions of BC and its light absorption in current global models. One of the main causes is considered to be large uncertainties in the vertical transport and wet removal processes of BC adopted in aerosol models. Understandings of the vertical transport and wet removal processes of BC are critically important because they directly controls spatial distribution of BC and its radiative effects. To improve our understanding of these processes, aircraft measurements covering the entire altitude range of the troposphere are needed; however, there have been no aircraft observations of BC measurements covering the entire altitude range of the troposphere over East Asia since the ACE Asia and TRACE-P campaigns in spring 2001.

The Aerosol Radiative Forcing in East Asia (A-FORCE) aircraft campaign was conducted over the Yellow Sea, the East China Sea, and the western Pacific Ocean in March-April 2009 (Oshima et al., 2012; Moteki et al., 2012; Koike et al., 2012; Takegawa et al., 2013). During the campaign, 120 vertical profiles of BC particles, carbon monoxide (CO) concentrations, aerosol number concentrations, and cloud microphysical properties were measured at 0-9 km in altitude. The A-FORCE measurements showed that concentrations of BC were greatly enhanced in the free troposphere (FT) over the Yellow Sea. In this study (Oshima et al., 2012), the transport efficiency of BC (namely the fraction of BC particles not removed during transport) for sampled air parcels was estimated from changes in observed BC-to-CO ratios, because CO can be used as an inert combustion tracer within a timescale of a few weeks. The transport efficiency of BC decreased primarily with the increase in the precipitation amount that air parcels experienced during transport, and its value was about 70-90% and 30-50% at 2-4 km and 4-9 km levels, respectively.

Vertical transport and removal processes of BC over East Asia in spring were examined through numerical simulations for the A-FORCE campaign using a modified version of the regional-scale three-dimensional chemical transport model WRF-CMAQ (Oshima et al., 2013). The simulations reproduced the vertical distributions of the transport efficiency of BC observed by the A-FORCE campaign reasonably well, indicating the validity of the treatment of the wet removal processes of aerosols in the model. We identified three major transport pathways for BC export from East Asia to the western Pacific in spring. One pathway was the planetary boundary layer (PBL) outflow through which BC was advected by the low-level westerlies without uplifting out of the PBL (weak BC removal). The second pathway was through uplifting from the PBL to the FT by migratory cyclones over northeastern China and the subsequent eastward transport in the lower FT (moderate BC removal). The third pathway was orographic uplifting and/or convective upward transport from the PBL to the FT over inland-southern China followed by westerly transport in the mid-FT (strong BC removal).

We will introduce our studies with a particular focus on the importance of the aerosol measurements by aircraft and its importance for modeling studies in this presentation.

References

Koike, M., et al. (2012), J. Geophys. Res., 117, D17205, doi:10.1029/2011JD017324.
Moteki, N., et al. (2012), Geophys. Res. Lett., 39, L13802, doi:10.1029/2012GL052034.
Oshima, N., et al. (2012), J. Geophys. Res., 117, D03204, doi:10.1029/2011JD016552.
Oshima, N., et al. (2013), J. Geophys. Res. Atmos., 118, 13175-13198, doi:10.1002/2013JD020262.
Takegawa, N., et al. (2013), Aerosol Sci. Technol., 47(10), 1059-1065.

Keywords: Aircraft measurements, Aerosols, Black carbon, Aerosol model, Transport, Removal

Japan Geoscience Union Meeting 2014
(28 April - 02 May 2014 at Pacifico YOKOHAMA, Kanagawa, Japan)

U04-05 Room:211 Time:April 29 10:00-10:15

Aircraft measurements of aerosol-cloud interactions

KOIKE, Makoto[1*] ; MOTEKI, Nobuhiro[1] ; KONDO, Yutaka[1] ; TAKEGAWA, Nobuyuki[2]

[1]Graduate School of Science, University of Tokyo, [2]Research Center for Advanced Science and Technology, University of Tokyo,

1. Importance of aerosol ? cloud interactions

By serving as cloud condensation nuclei and ice nuclei, aerosols affect cloud droplet number concentrations and phase of cloud particles. These cloud microphysical changes cause cloud albedo changes and cloud adjustments (fast cloud response), such as changes in cloud liquid water path and/or cloud fraction. However, there are large uncertainties in estimations of these aerosol ? cloud interactions

2. Aircraft measurements

Satellite measurements can provide global view of the aerosol ? cloud interactions, however, quantities retrieved from satellite measurements are limited. Several artifacts are also known. Although aircraft measurements are limited in space and time, they can provide critical information to study aerosol ? cloud interactions, namely, aerosol and cloud droplet number size distributions. In fact, aircraft measurements have been intensively made over off the coast of California, Peru, and West Africa, tropical Pacific, Indian ocean, and Arctic ocean. Aircraft measurements act as a driving force to study aerosol ? cloud interactions.

3. Aircraft measurements in Asia

Aerosol concentrations in Asia are highest level in the world and they can potentially affect clouds forming over the Western Pacific. However, a number of aircraft measurements is limited. In this paper, results from aircraft measurements made over the Western Pacific during the A-FORCE-2009 and 2013S campaigns are shown. Future science of aerosol ? cloud interactions using aircraft is also discussed.

Keywords: aerosol, cloud, aircraft measurement, Asia

Japan Geoscience Union Meeting 2014
(28 April - 02 May 2014 at Pacifico YOKOHAMA, Kanagawa, Japan)

U04-06 Room:211 Time:April 29 10:15-10:30

Evaluation of a result of a coupled atmosphere-ocean model around a tropical cyclone center using aircraft observations

SHINODA, Taro[1*] ; KUBO, Keishi[1] ; AIKI, Hidenori[2] ; YOSHIOKA, Mayumi[3] ; KATO, Masaya[1] ; TSUBOKI, Kazuhisa[1] ; UYEDA, Hiroshi[1]

[1]HyARC, Nagoya Univ., [2]JAMSTEC, [3]CAOS, Tohoku Univ.

Aircraft observations are enable us to understand the dynamical, thermodynamical, and microphysical structure of an inner region of TCs, such as their eye and eyewall. Numerical simulation is also a useful tool to clarify the structure of TCs, however, the reproducibility around the inner region of TCs could not be confirmed. This study shows an application of aircraft observations to evaluate the structure of a simulated TC using a coupled atmosphere-ocean non-hydrostatic model, Cloud Resolving Storm Simulator (CReSS) and Non-Hydrostatic Ocean model for Earth Simulator (NHOES), CReSS-NHOES.

The target typhoon is T1013 (Megi) developed over the tropical western Pacific Ocean in October 2010. During the Impact of Typhoons on the Ocean in the Pacific (ITOP), 200 dropsondes are dropped into and around T1013, including its eye and eyewall regions, from a height of about 2.5 km. Dropsondes can observe a vertical profile of pressure (height), temperature, humidity, wind direction, and wind speed. The profiles of these parameters are used to evaluate the simulation result using CReSS-NHOES. A simulation with horizontal grid resolution of 0.02 degree (approximately 2 km) is conducted for 7 days from 00 UTC on October 14, 2010, after one day of the formation of the T1013.

The simulation well reproduces its track and the tendency of the minimum central pressure. The reproduced minimum central pressure is 889 hPa and corresponds the observed one (885 hPa). To conduct the direct comparison between dropsonde observations and the simulation result, the target time of the simulation to compare with the observed one is determined to consider the value of minimum central pressure and its tendency. At the observed target time when conducted the dropsonde observations, the observed TC center is determined by the linear interpolation of the best track data provided by Japan Meteorological Agency. The simulated TC center at the target time is defined by the application to the Braun's method to the CReSS-NHOES output data. The location of the simulated profiles are determined by that of the dropsonde observations relative to the center of the TC at the simulated target time.

The eyewall region in this study is defined as the region that relative humidity of all layers is greater than 95% and maximum wind speed exceeds 25 m s^{-1} below a height of 2 km. The eye and outer region are defined by the inner and outer ones of the eyewall. The simulated potential temperature, mixing ratio of water vapor, and wind speed in the outer region are in the range of 1-sigma (standard deviation), thus, the simulated thermodynamic parameters are well reproduced statistically. After the rapid intensification of T1013, weak and maximum wind speed regions are reproduced in the eye and lower level of the eyewall, respectively. High potential temperature in the low-level of the eye is also reproduced. Thus, qualitative properties of the TC are well reproduced in the simulation. However, the simulated potential temperature is 3 K greater than that in the observation. And the simulated wind speed is 25 m s^{-1} lesser than that in the observation. The quantitative differences are expected to be caused by the difference of the structure of the eye. The problem on the structure of the eye appears in comparison with the application of the aircraft observations for the first time.

Keywords: aircraft observation, tropical cyclone, cloud-resolving model, coupled atmosphere-ocean model, model evaluation

Japan Geoscience Union Meeting 2014
(28 April - 02 May 2014 at Pacifico YOKOHAMA, Kanagawa, Japan)

U04-07 Room:211 Time:April 29 10:30-10:45

Aircraft observations over the Sea of Japan and the Sea of Okhotsk in winter

FUJIYOSHI, Yasushi[1*]

[1]Inst. Low Temp. Sci., Hokkaido Univ.

It is well known that the Sea of Okhotsk is one of the southernmost seasonal sea ice zones in the Northern Hemisphere. The importance of the relationship between the Sea of Okhotsk ice cover and regional/global climate has long been recognized. Indeed, recent research work has tied the extreme maximum and minimum wintertime extents of sea ice cover to large scale changes in atmospheric circulation patterns. Recent studies suggest that a possible origin of the North Pacific Intermediate Water (NPIW) is produced in the Sea of Okhotsk. Thus, there are important climate issues that are associated with the Sea of Okhotsk. It is also known that Japan, especially along the coast of the Sea of Japan, is one of the heaviest snowfall regions in the world. Snowfall is brought by banded snow clouds formed when winter monsoon air from Siberia is supplied latent and sensible heat from the Sea of Japan. These banded snow clouds are also frequently formed in the lee side of the sea ice over the Sea of Okhotsk, and play an important role in the growth of the sea ice.

Despite of the scientific importance of these areas in regional/global climate system, in-situ observations there are extremely few, especially in winter. This is due to the fact that the wintertime environment is generally harsh and is not conductive to making high quality measurements. However, in recent years instrumentation and technology have improved to the point where it is now possible to make the requisite wintertime measurements. In this regard, we conducted aircraft observations over the Sea of Okhotsk and the Sea of Japan.

We had deployed an X-band Doppler radar at Monbetsu on November of 2005, and started observation on 16 January of 2006. The height of sea-ice is different from place to place. Air-born laser altimeter is only the tool that can make horizontal distribution of the height of sea-ice. However, this method is very expensive and severely affected by weather condition. We tried to make a three dimensional display of sea-ice and suggested that our radar system could be used to study the irregularity of the height of sea-ice. Therefore, we measured horizontal distribution of height of sea-ice by using aerial cameras and compared it with 3Dimages of our X-band radar.

Keywords: snow clouds, sea ice, marine boundary layer

Japan Geoscience Union Meeting 2014
(28 April - 02 May 2014 at Pacifico YOKOHAMA, Kanagawa, Japan)

U04-08 Room:211 Time:April 29 11:00-11:15

Use of Aircraft for Coastal and Oceanographic Research and Observations

ISHIZAKA, Joji[1*]

[1]Hydrospheric Atmospheric Research Center, Nagoya University

Aircraft should be useful to observe coastal and ocean environments, including physical, chemical and biological properties, especially under the raid, unexpected and dangerous conditions, such as typhoon or volcanic eruption, where ship operation is difficult. It is expected that there are two methods of observations from aircraft, other than seaplane, for oceanographic research; one is remote sensing and another is use of air-deployable sensors or platforms. Various remote sensing sensors are available using visible, infrared, microwave and sound waves. They have advantage to satellite-based remote sensors with high resolution and more flexible overflight, and they should be useful for coastal applications. Most of the remote sensing sensors can only obtain surface information; however LIDAR can detect vertical profiles of some parameters such as plankton distribution. Air-deployable sensors have been used for measurements of vertical profiles of temperature (AXBT; Airborne eXpendable BathyThermograph), salinity (AXCTD; Airborne eXpendable Conductivity Temperature and Depth probes), and current (AXCP; Airborne eXpendable Current Profilers). More recently, vertical profiling floats are developed and deployed for Argo project. There were attempts to deploy one of the vertical profiling floats, Electromagnetic Autonomous Profiling Explorer (EX-APEC), from airplane for typhoon observation and obtained profiles of temperature, density and currents. Autonomous profiling floats are now developing equipped with chemical, optical and biological parameters, and should be deployable from aircraft. Other various types of small autonomous underwater vehicles (AUV) are also underdevelopment and may be deployable from airplane in future. Combination studies of those physical, chemical, and biological parameters in coastal and ocean environments with atmospheric information, such as weather condition and chemical properties, are necessary to understand coupled atmospheric-ocean system.

Keywords: aircraft, coast, ocean, remote sensing, float, typhoon

Japan Geoscience Union Meeting 2014
(28 April - 02 May 2014 at Pacifico YOKOHAMA, Kanagawa, Japan)

U04-09 Room:211 Time:April 29 11:15-11:30

Earth Observation by using airborne SAR

URATSUKA, Seiho[1*] ; UEMOTO, Jyunpei[1] ; KOJIMA, Shoichiro[1] ; UMEHARA, Toshihiko[1] ; SATAKE, Makoto[1] ; KOBAYASHI, Tatsuharu[1] ; MATSUOKA, Takeshi[1] ; NADAI, Akitsugu[1]

[1]National Institute of Information and Communications Technology

Pi-SAR2 and Pi-SAR are high resolution airborne SAR. We will present possibilities of these sensors for application to the erath science.

Keywords: Synthetic Aperture Radar, Polarimetry, Interferometry, Pi-SAR2

Japan Geoscience Union Meeting 2014
(28 April - 02 May 2014 at Pacifico YOKOHAMA, Kanagawa, Japan)

U04-10 Room:211 Time:April 29 11:30-11:45

Applicability of airborne remote sensing to terrestrial ecosystem sciences

SUZUKI, Rikie[1*]

[1]Japan Agency for Marine-Earth Science and Technology

Although the airborne remote sensing generally cannot be conducted repeatedly for a region during a multi-year long time period like satellite (space borne) remote sensing, the airborne remote sensing has many advantages in the observation of terrestrial ecosystem. One of them is, of course, the spatial resolution of the airborne remote sensing can be much higher than that of the satellite because the airborne platform flies at much lower altitude than satellite. Although WorldView-2 and GeoEye-1 provide high resolution images of land surfaces, it is practically hard to identify the individual tree in a forest, while the image of airborne remote sensing allows us to observe the tree crown structure and the forest floor condition. In 2000, an airborne remote sensing was conducted from spring to summer over forests around Yakutsk, eastern Siberia, and forest images were recorded by the onboard video camera from heights of 100 to 150m above the land surface. We examined the presences of green leaves in the crown of forest and the snow cover on the floor, and the spectral reflectance of the forest was investigated in relation to those conditions. The result suggested the reflectance from the forest floor significantly influenced the satellite-derived vegetation index (e.g. NDVI) in case of sparse boreal forests. The airborne remote sensing at a further lower height, several tens meters, enables us to indentify the individual leaf and insect, and subsequently, to study the biodiversity on individual basis. Recently, the remote sensing technique by airborne hyperspectral camera and LiDAR has explored a feasibility to identify species and retrieve the chemical trait and structure of vegetation. This methodology made a breakthrough for investigating the ecosystem function and biodiversity. Another advantage of airborne remote sensing is the capacity to select the observation geometry such as the incident angle of solar illumination and the view angle of the sensor. This capacity leads a robust development of radiative transfer model of vegetation based on the bidirectional reflectance distribution function (BRDF).

Keywords: forest ecosystem, LiDAR, ecosystem function, biodiversity

Japan Geoscience Union Meeting 2014
(28 April - 02 May 2014 at Pacifico YOKOHAMA, Kanagawa, Japan)

U04-11 Room:211 Time:April 29 11:45-12:00

Ground Truth of Earth Observation Satellites using UAV

HONDA, Yoshiaki[1*] ; KAJIWARA, Koji[1] ; TANIGAWA, Satoshi[1] ; ONO, Yusaku[2]

[1]Center for Environmental Remote Sensing, Chiba University, [2]Earth Observation Research Center, Japan Aerospace Exploration Agency

Japan Aerospace Exploration Agency (JAXA) is going to launch new Earth observation satellite GCOM-C1 in near future. The core sensor of GCOM-C1, Second Generation Global Imager (SGLI) has a set of along track slant viewing Visible and Near Infrared Radiometer (VNR). These multi-angular views aim to detect the structural information from vegetation canopy, especially forest canopy, for estimating productivity of the vegetation. SGLI Land science team has been developing the algorithm for 10 standard products (above ground biomass, canopy roughness index, shadow index, etc).

In this paper, we introduce the ground observation method developed by using Unmanned Aerial Vehicle (UAV) in order to contribute the algorithm development and its validation. Mainly, multi-angular spectral observation method and simple BRF model have been developed for estimating slant view response of forest canopy. The BRF model developed by using multi-angular measurement has been able to obtain structural information from canopy. In addition, we have conducted some observation campaigns on typical forest in Japan in collaboration with other science team experienced with vegetation phenology and carbon flux measurement. Primary results of these observations are also be demonstrated.

Keywords: UAV, Second Generation Global Imager (SGLI), Multi-angular observation, Forest canopy, Vegetation productivity

Japan Geoscience Union Meeting 2014
(28 April - 02 May 2014 at Pacifico YOKOHAMA, Kanagawa, Japan)

U04-12 Room:211 Time:April 29 12:00-12:15

New phase remote sensing stimulated by the use of airborne observation

KUZE, Hiroaki[1*]

[1]Center for Environmental Remote Sensing, Chiba University

Center for Environmental Remote Sensing (CEReS), Chiba University, is processing, archiving, and disseminating satellite data and related ground observation data to wide communities in remote sensing and environment-related areas. In the field of atmospheric remote sensing, we have established a radiometer network (SKYNET), which contributes to satellite data validation through characterization of atmospheric aerosols and clouds in East Asia. Also, the radiometer data are valuable for studying air pollutants due to anthropogenic activities when coupled with data from lidar and high spectral resolution spectroradiometer observations. Quantitative analysis of global biomass can be implemented by means of vegetation remote sensing. Methodology for obtaining highly accurate vegetation reflectance has been sought using satellite- and ground-based observations, as well as directional observation using unmanned helicopters. This approach has been exploited for developing an algorithm to be used for GCOM-C1, JAXA's next-generation satellite. In the field of microwave remote sensing, sensors based on circularly polarized synthetic aperture radar (CP-SAR) technique have been developed for both small satellites and unmanned aircraft applications.

Currently a new cooperative study plan is being discussed among university research institutes/centers based on chartering a manned airplane for scientific observation purposes. Through this initiative, it is expected that atmospheric science and climate system studies (University of Tokyo), cloud and precipitation system studies (Nagoya University), as well as high-level scientific application of remote sensing data (Chiba University) will be promoted. The primary goal of CEReS activity will be to achieve highly accurate remote sensing of vegetation, snow and ice fields, and coastal areas through the realization of high-precision atmospheric correction of satellite data, which would have been impossible without resorting to aircraft observation.

As more and more high resolution satellite data are becoming available, needs are growing for high-precision retrieval of physical quantities such as land or ocean surface reflectance. The largest obstacle for this improvement is the spectral changes due to atmospheric scattering and absorption. The influence of air molecules (Rayleigh scattering) can be corrected relatively easily. In contrast, correcting the effects of clouds and aerosols (Mie scattering) tends to be much more difficult, due to their temporal and spatial variability. Conventionally, network observation using a number of sunphotometers and skyradiometers has been implemented for measuring the optical properties of atmospheric aerosols and clouds. Also helicopter and unmanned air vehicle (UAV) measurements have been undertaken covering altitude ranges lower than 150 m above ground. Still, it is difficult to carry out the validation of satellite remote sensing imagery over an extended region.

The aircraft project currently under discussion will enable the measurements of radiation quantities and surface reflectance from high altitudes. The radiometer and hyperspectral camera measurements from both unmanned (low altitude) and manned (high altitude) platforms will allow us to improve radiative transfer algorithms indispensable for high-precision atmospheric correction. This, in turn, will contribute to dramatically improving the accuracy of algorithm for estimating biomass amount based on reflectance measurements. In addition, all-weather and both day- and nighttime surface observation can be demonstrated by equipping the CP-SAR instrumentation.

Keywords: remote sensing, airborne observation, vegetation, atmosphere, microwave sensor

Japan Geoscience Union Meeting 2014
(28 April - 02 May 2014 at Pacifico YOKOHAMA, Kanagawa, Japan)

U04-P01 Room:Poster Time:April 29 14:00-15:15

Aerosol particles collected using aircrafts from anthropogenic sources and biomass burning and electron microscopy

ADACHI, Kouji[1*]

[1]Meteorological Research Institute

Aerosol particles collected during four sampling campaigns using aircrafts were analyzed using transmission electron microscopes (TEM). The samples were collected from two A-Force campaigns in 2013 (winter and summer) conducted in Japan and Korea, BBOP campaign in 2013 in the USA, and MILAGRO campaign in 2006 in Mexico. These campaigns aim to characterize aerosol particles from regional transportation, biomass burning, and both. The samples collected using aircrafts are useful for characterization of particle agings, especially changes of their mixing states, from emissions as the aircrafts can chase plumes of different aging periods. An example of such aerosol-particle aging is tar ball formation in biomass burning smoke. Tar ball is spherical, organic aerosol particles commonly from combustion smoke of a wide range of biomass burning. At the early stage of the emission, tar balls are liquid but as they age in the smoke, they become solid and spherical. Sets of biomass burning aerosol samples with different aging stages collected using an aircraft revealed such processes in atmosphere. I will also discuss the samples collected over Japan during the A-Force campaigns.

Keywords: Electron microscope, East Asia, Northwest US, A-Force, BBOP, MILAGRO

Japan Geoscience Union Meeting 2014
(28 April - 02 May 2014 at Pacifico YOKOHAMA, Kanagawa, Japan)

U04-P02 Room:Poster Time:April 29 14:00-15:15

Aerial observations for nitrogen compounds over the East China Sea

SADANAGA, Yasuhiro[1*] ; BANDOW, Hiroshi[1] ; ARAKAKI, Takemitsu[2] ; KATO, Shungo[3] ; KAJII, Yoshizumi[4] ; ZHANG, Daizhou[5] ; WATANABE, Izumi[6] ; FUJIMOTO, Toshiyuki[7] ; OKUYAMA, Kikuo[8] ; OGI, Takashi[8] ; SETO, Takafumi[9] ; TAKAMI, Akinori[10] ; SHIMIZU, Atsushi[10] ; HATAKEYAMA, Shiro[6]

[1]Osaka Prefecture University, [2]University of the Ryukyus, [3]Tokyo Metropolitan University, [4]Kyoto University, [5]Prefectural University of Kumamoto, [6]Tokyo University of Agriculture and Technology, [7]Muroran Institute of Technology, [8]Hiroshima University, [9]Kanazawa University, [10]National Institute for Environmental Studies

In order to clarify long-range transport of air pollutants from the Asian continent, we have conducted aerial observation over the East China Sea and measured air pollutants centering on aerosols, as part of Grant-in-Aid for Scientific Research on Innovative Areas " Impacts of Aerosols in East Asia on Plants and Human Health (ASEPH) " . In this presentation, the results of nitrogen compounds such as nitrate are mainly described.

The aerial observations were conducted in October, 2009 (autumn), December, 2010 (winter) and March, 2012 (spring) over the East China Sea. The flights were performed between Fukue Island and the southern offing of Jeju Island and the flight altitudes were 500, 1000, 2000 and 3000 m. Onboard measurements of gaseous total odd nitrogen species, gaseous nitric acid (HNO_3(g)), O_3, SO_2, CO and black carbon were made and particles were collected on filters for ionic and metal component analyses.

The concentration ratios of particulate nitrate (NO_3^-(p)) to inorganic total nitrate (T.NO_3 = HNO_3(g) + NO_3^-(p)) were less than 0.5 in most of the flights except under high concentrations of dust particles (Kosa) or transboundary air pollutants. Most of NO_3^-(p) would be $NaNO_3$ formed by the reaction of gaseous nitric acid (HNO_3(g)) with sea salt aerosols during the observations in autumn and winter except on October 17 and December 11, when high concentrations of Kosa were transported. In the spring observation, the fraction of $NaNO_3$ in NO_3^-(p) was low and a large part of NO_3^-(p) would be originated from reactions of HNO_3(g) with gas phase ammonia and soil dust particles.

O_3 concentrations decreased with altitude in autumn and increased in winter. Positive and negative correlations between NO_y-T.NO_3 and O_3 concentrations were observed throughout the flights in autumn and winter, respectively. This indicates that the major components of NO_y-T.NO_3 were secondary photochemical nitrogen oxides such as PANs and NO_x, in autumn and winter, respectively. The differences of vertical distribution and NO_y components between autumn and winter may be caused by the variation of solar radiation intensity.

Keywords: aerial observation, nitrate, total odd nitrogen species, East Asia

Japan Geoscience Union Meeting 2014
(28 April - 02 May 2014 at Pacifico YOKOHAMA, Kanagawa, Japan)

U04-P03 Room:Poster Time:April 29 14:00-15:15

Airborne lidar measurements of water-vapor profiles

ABO, Makoto[1*] ; NAGASAWA, Chikao[1] ; SHIBATA, Yasukuni[1] ; UCHINO, Osamu[2] ; NAGAI, Tomohiro[2] ; SAKAI, Tetsu[2] ; SHIBATA, Takashi[3]

[1]Tokyo Metropolitan University, [2]MRI, [3]Nagoya University

Measurements of water vapor profiles are very important in studies of the atmospheric dynamics, aerosol growth effect and the eartlfs radiation effects. Water vapor is the predominant greenhouse gas and its vertical distributions are important parameters in model simulation of the global climate system. Passive remote sensing techniques from space provide global coverage of water vapor distribution but do not provide good vertical resolution, while lidar remote sensing techniques can provide high resolution measurements of water vapor distributions.

For future spaceborne water vapor DIAL systems, we developed a high power diode-pumped Nd:YLF laser and Ti:sapphire laser for water vapor DIAL. A Ti:sapphire laser is pumped by the SHG of the Nd:YLF laser. Tuning of the Ti:sapphire laser to a strong absorption line (ON1), a weak absorption line (ON2) of water vapor and an off line (OFF) is made by an injection seeder which consists of two single longitudinal mode laser diode modules. Two on-line laser diodes are locked to water vapor absorption lines using an absorption cell or a photo-acoustic cell. These three laser lines (ON1, OFF and ON2) are transmitted into the atmosphere with a triple pulse technique for measurements of water vapor profiles from the ground up to 10 km. The laser spectral width of the on line was 0.045 pm with a stability of 0.06 pm. The output energy of each laser line is more than 45 mJ. We have demonstrated airborne measurements of water vapor profile using this laser system.

Keywords: water vapor, airborne, lidar

Japan Geoscience Union Meeting 2014
(28 April - 02 May 2014 at Pacifico YOKOHAMA, Kanagawa, Japan)

U05-01 Room:419 Time:April 30 09:00-09:30

Bioavailable energy distributions in the hydrothermal systems on Enceladus and early Earth

SHIBUYA, Takazo[1*] ; SEKINE, Yasuhito[2] ; RUSSELL, Michael[3] ; TAKAI, Ken[1]

[1]JAMSTEC, [2]University of Tokyo, [3]Jet Propulsion Laboratory

A recent research by Cassini spacecraft suggests that there are silica nanoparticles in Saturn ′ s E-ring derived from the Enceladus plume (Hsu et al., submitted). The findings of silica nanoparticles imply active water-rock reactions. Furthermore, an experimental study simulating the reactions between chondritic material and alkaline seawater revealed that the formation of silica nanoparticles requires hydrothermal reactions at temperatures higher than 100 deg. C (Sekine et al., submitted). Considering a short residence time of nanoparticles in the ocean, these studies imply geologically-recent or on-going hydrothermal activity in the Enceladus ′ subsurface ocean. Therefore, we modeled possible hydrothermal fluid/rock reactions and bioavailable energy in the mixing zone between hydrothermal fluid and seawater on Enceladus. The thermodynamic calculations of reactions between CI chondrite and alkaline NaCl-NaHCO3 seawater at 100 deg.C indicate that the pH of fluid increases up to about 10 and hydrogen concentration in the fluid is elevated up to 20 mmolal through the water/rock reaction. Based on the estimated fluid compositions, we calculated chemical property of the mixing zone between seawater and hydrogen-rich alkaline hydrothermal fluid, which revealed that the a certain level of bioavailable energy is derived from redox reactions based on CO2 and H2 in the mixing zone whereas there are unlikely other electron accepters such as sulfate and nitrate that are abundant in the terrestrial seawater. Thus, the CO2-H2 pair can be used for possible metabolic reaction, namely hydrogenotrophic methanogenesis and acetogenesis. In the low-temperature zone, the available energy of the Enceladus methanogenesis is higher than that of methanogenesis in the Rainbow field (Mid-Atlantic Ridge) where methanogens are certainly separated. It is therefore highly possible that H2-based energy metabolisms have been generated in the Enceladus hydrothermal vent system. Considering that the most ancient metabolisms in the Hadean terrestrial hydrothermal vent system could be also H2-based redox reactions, there is an energetic similarity between hydrothermal vent systems on Enceladus and Hadean Earth. The future exploration of Enceladus ′ plume would potentially provide clues to the origin of life on Earth.

Japan Geoscience Union Meeting 2014
(28 April - 02 May 2014 at Pacifico YOKOHAMA, Kanagawa, Japan)

U05-02 Room:419 Time:April 30 09:30-09:45

Impact-induced D/L chiral changes of valine in early Earth's oceans

SEKINE, Toshimori[1*] ; TAKASE, Atsushi[1] ; FURUKAWA, Yoshihiro[2] ; KAKEGAWA, Takeshi[2] ; KOBAYASHI, Takamichi[3]

[1]Hiroshima University, [2]Tohoku University, [3]National Institute for Materials Science

It has widely known that proteins are composed of L-amino acid mononers and that nucleic acids contains exclusively D-sugars. Homochirality selection may be contributed to the consequence of life materials and their generation conditions. Regarding the enantiomeric excess in biomolecules, there are several proposals at present. Because the enantiomeric excess occurs in photoreactions by circularly polarized light, it has been believed that interstellar environments play an important role to the formation of chiral amino acids identified in chondrites and interstellar ices. However, it is also important to know whether the enantiomeric excess of amino acids occurs during oceanic impacts or not, because the enantiomeric enrichments are known under critical states of fluids due to density fluctuations.

We have investigated the shock-induced chiral changes of valine in aqueous solution coexisting with given solids. Powders of olivine, hematite, and calcite were selected to represent solids. Hypervelocity plane impact experiments were carried out using a propellant gun. Sample solution of each of L- and D-valine in sealed steel containers was subjected to impact at velocities of about 1 km/s. The calculated shock pressures are 5-6 GPa by the impedance match solution. The recovered solutions were analyzed with LC/MS (2695 separation module; Waters Corp. and Quattro micro API; Waters Corp) after the FDLA derivatization that makes a difference in hydrophobicity between D- and L-valine. The enantiomeric excess (ee(%)=100(L-D)/(L+D)), the yield of the initial valine, and shock pressure are plotted to see their relationship. The results indicate a difference among the solid. Although there was no significant change from the racemic valine solution, the reaction from L-valine to D-valine was significantly faster than that from D-valine to L-valine in calcite. The adsorption of calcite powders was checked to display no difference between D- and L-valine. These results may suggest that oceanic impacts may change the chirality of amino acids in oceans. However the enrichment of L-amino acids on the Earth need another mechanism.

Keywords: Impact-induced D/L chiral changes, D/L valine, Calcite

Japan Geoscience Union Meeting 2014
(28 April - 02 May 2014 at Pacifico YOKOHAMA, Kanagawa, Japan)

U05-03 Room:419 Time:April 30 09:45-10:15

The oldest remnant of life in 3.8 Ga old early Archaean rocks

OHTOMO, Yoko[1*] ; KAKEGAWA, Takeshi[2]

[1]Kochi Institute for Core Sample Research, JAMSTEC, [2]Graduate School of Science, Tohoku University

The suggestion that graphite in early Archaean rocks represents materials of biogenic origin has met with a degree of scepticism. Isotopic compositions of graphite in >3.7-billion-year-old rocks from the Isua Supracrustal Belt (ISB), western Greenland, which are believed to be of sedimentary origin, suggest that vast microbial ecosystems were present in early Archaean oceans. However, results of more recent studies suggest that most of graphite-bearing rocks were formed through interactions between crustal fluids and surrounding igneous rocks during later metasomatic events, thereby casting doubt on the existence of an extensive sedimentary sequence in the ISB and on the biogenic origin of constituents. In contrast, ^{13}C-depleted graphite globules, which are considered to form from biogenic precursors, have been reported from the metamorphosed clastic sedimentary rocks in the ISB. However, these were found at a single locality. It therefore remains unclear whether traces of life at other localities in the ISB were lost during metamorphism or were originally absent. The presence of additional clastic sedimentary rocks containing graphite may provide evidence for the preservation of organic constituents in early Archaean rocks, thus supporting the notion that microbes were active in early Archaean oceans.

We conducted a geological survey along the northwestern area of the ISB. Banded iron formations contain interbedded black to grey schist layers, typically 40-80 cm thick. Rare earth element patterns in samples lie close to that in Post Archaean Australian Shale, suggesting that the protoliths of the schist was clastic marine sediments. The black-grey schist samples contain abundant reduced carbon (0.1-8.8 wt%), identified as graphite by X-ray diffraction analysis. The range of δ^{13}C values was -23.8 to -12.5 per mil (average, -17.9 per mil), which is within the range of values reported in previous studies. Scanning transmission electron microscope and high-resolution electron microscope observations present different nanoscale morphologies between the graphite of metasediment and secondary vein samples. Examined metasediment included graphitic polygonal grains and nanotubes. Sheeted flakes were a dominant morphology of secondary graphite, whereas polygonal grains and nanotubes were absent from them, suggesting a different origin from the secondarily derived graphite.

We modelled the theoretical δ^{13}C values of fluid-precipitated graphites. The lowest δ^{13}C values exceed -16.4 per mil when Rayleigh-type isotope fractionation operates in the fluids. Therefore, ^{13}C-depleted biogenic organic matter in Isua clastic sediments is postulated as an initial carbon source to explain the lightest carbon isotope compositions (e.g., -23.8 per mil) in the present study. Distorted structures are common in pyrolysed and pressurized organic compounds. Such precursors commonly contain non-planar carbon ring compounds associated with abundant pores. Biogenic organic matter, which contains various molecules and functional groups, is suggested as the precursors of the graphite observed in metasediment.

In summary, the graphite in metasediment from the northwest ISB is distinct from the graphite in secondary vein samples. The combined information on geological occurrences, graphite morphologies, nanoscale structures, and isotopic compositions of the graphite in the metasediment suggests a biogenic origin of the graphite. High concentrations of ^{13}C-depleted graphite in these rocks would require widespread biological activity to support the high rate of production and sedimentary delivery of organic matter to the >3.7-billion-year-old ocean floor.

Keywords: origin of life, Greenland, Isua Supracrustal Belt, graphite, remnants of life

Japan Geoscience Union Meeting 2014
(28 April - 02 May 2014 at Pacifico YOKOHAMA, Kanagawa, Japan)

U05-04 Room:419 Time:April 30 10:15-10:30

Mineralogical and geochemical study of clastic sedimentary rocks in Barberton greenstone belt, South Africa

KAWAI, Shohji[1*] ; KAKEGAWA, Takeshi[1]

[1]Graduate School of Science, Tohoku University

Cyanobacteria became active and oxidize surface ocean water in Archean. However, chronological constraint is still uncertain as to when ocean water became oxic. Some redox sensitive minerals in clastic sediments are often used to indicate the absence or presence of oxidative weathering, oxic sea water and diagenesis. Clastic sedimentary rocks in Barberton Greenstone Belt are studied by many previous investigators. However, detailed examination of redox sensitive minerals and elements are rare. Therefore, we set objectives of the present study (1) to investigate mineralogical and geochemical characteristics of clastic sedimentary rocks deposited in shallow water environments in ca.3.2Ga Moodies Group, (2) to discuss the origin of redox sensitive minerals in clastic sediments and (3) to decipher the redox conditions of the surface environments at the time of Moodies sedimentation.

We examined clastic sedimentary rocks (mainly sandstone) of the Joes Luck Formation in the Moodies Group. Samples were collected from drilled core collections of Sheba mine. All samples are belonging to Eureka Syncline blocks. Those samples are not affected by modern weathering.

The examined sandstones contained rounded quartz, K-feldspar, albite, minor zircon, and rutile. These minerals were detrital origins mainly from felsic crustal materials. Rounded chromite also occurs and we interpret that such chromite is a weathering product from mafic to ultramafic rocks. Rounded chromite is always surrounded by forming aggregates Cr-rich micas, and chromite never occurs without micas. We interpret that chromite was protected by micas, and survived from dissolution during weathering, transportation and diagenesis. Detrital pyrite and uraninite were not seen in these samples. Those mineral features indirectly indicate that presence of oxidative weathering, transportation and/or diagenesis at the sedimentation of Moodies Group. Geochemical analyses of the bulk samples indicate that most elements (e.g., Ti, Zr and V) are correlated to Al. Therefore, chemistry of examined samples are controlled by detrital components. On the other hand, Cu, Pb, Mn, and Mo are not correlated to Al, and apparently enriched in clastic sediments. Cu and Pb were mobilized in sediments during early to late diagenesis associated with late sulfide formations. Enrichment of Mn and Mo in the examined samples more reflected precipitation process from ocean water and diagenesis. In particular, enrichment of Mo is found in some samples with moderate amount of organic carbon. This suggests that Mo was dissolved in Moodies ocean water as oxidized species, and then reduced by microbial activities followed by sedimentation with organic matter. Overall results of this study suggested that oxygenic phototrophs already flourished in the photic zone of the 3.2 Ga ocean, making surface ocean water oxic.

Keywords: Cyanobacteria, Chromite, Barberton, RSE

Japan Geoscience Union Meeting 2014
(28 April - 02 May 2014 at Pacifico YOKOHAMA, Kanagawa, Japan)

U05-05 Room:419 Time:April 30 10:30-10:45

Cerium stable isotopic fractionation as a potential paleo-redox proxy

NAKADA, Ryoichi[1*] ; TANAKA, Masato[1] ; TANIMIZU, Masaharu[2] ; TAKAHASHI, Yoshio[1]

[1]Department of Earth and Planetary Systems Science, Graduate School of Science, Hiroshima University, [2]Kochi Institute for Core Sample Research, JAMSTEC

Cerium (Ce) anomaly that appears in rare earth element (REE) pattern is a tool to estimate paleoredox condition and has been used for many studies. Discussion in previous studies, however, has been limited to qualitative one based on the REE pattern. This study, therefore, aims to provide more quantitative information on the redox condition in paleoenvironment by Ce stable isotope ratio related to the redox-sensitive property of Ce. If fractionations of Ce stable isotope responds differently to various geochemical processes such as (i) oxidative scavenging on Mn oxide, (ii) precipitation as $Ce(OH)_4$, and (iii) adsorption of Ce^{3+} without oxidation, it is possible that Ce stable isotope ratio can give more information on redox condition in paleoenvironment.

Cerium(III) chloride solution was added to manganese oxide and iron hydroxide, respectively, with the concentration of Ce systematically changed. In both systems, pH was adjusted to 5.00, 6.80, 8.20, and 11.0 ($\pm$0.05) and shaken for 6 hours before the filtration using 0.2 μm membrane filter. In addition, precipitation of Ce was obtained by bubbling of O_2 gas in the same $CeCl_3$ solution. Stable isotope ratios of Ce in both liquid and solid phases were determined using MC-ICP-MS at Kochi Institute for Core Sample Research. The $CeCl_3$ solution used in the adsorption experiment was employed as standard solutions and the isotope ratio of each element was expressed in delta notation relative to the average standards, which is shown in the equation as follows: δ^{142}Ce = [(142Ce/140Ce)$_{sample}$ / (142Ce/140Ce)$_{CeCl3}$ — 1] $\times$ 10^3.

Assuming equilibrium isotopic fractionation, the mean isotopic fractionation factor between the liquid and solid phases $\alpha_{Lq?So}$ of Ce adsorbed on ferrihydrite was within the analytical uncertainty for all the pH conditions. Meanwhile, the $\alpha_{Lq?So}$ of Ce adsorbed on δ-MnO_2 was gradually decreased with increasing pH. Most surprisingly, the $\alpha_{Lq?So}$ of spontaneous precipitation of Ce showed that, with increasing pH, the direction of the isotopic fractionation was in contrast to those in the adsorbed systems. These results suggests that the degree of mass-dependent fractionation of Ce can be used to clearly distinguish spontaneous precipitation from oxidative adsorption on δ-MnO_2, that occurs under more oxic conditions than the Ce(III)/Ce(IV) boundary. Our results suggest that the combination of the degrees of mass-dependent fractionation and chemical state of Ce can be used to classify the redox condition into the three stages based on Ce geochemistry, thereby offering a powerful tool for exploring redox conditions in paleo-ocean environments.

Keywords: cerium, stable isotope, redox

Japan Geoscience Union Meeting 2014
(28 April - 02 May 2014 at Pacifico YOKOHAMA, Kanagawa, Japan)

U05-06 Room:419 Time:April 30 11:00-11:30

Decoding the Evolution of Early Atmosphere: Experimental Reconstraction of the D36S/D33S Chemostratigraphy

UENO, Yuichiro[1*] ; ENDO, Yoshiaki[1] ; MISHIMA, Kaoru[1] ; DANIELACHE, Sebastian[4]

[1]Department of Earth and Planetary Sciences, Tokyo Institute of Technology, [2]Earth-Life Science Institute (ELSI), Tokyo Institute of Technology, [3]Precambrian Ecosystems Laboratory, JAMSTEC, [4]Faculty of Science & Technology, Sophia University

Sulfur Mass-Independent Fractionation (S-MIF) has potential to monitor chemistry of the Earth's early atmosphere (Farquhar et al., 2000). Nonetheless, detailed mechanism of the S-MIF occurred in the Archean atmosphere is still poorly understood. Previous laboratory experiments indicate the anomalous isotopic fractionation depends largely on (1) wavelength or spectrum of the incident light source and (2) partial pressure of SO2, though none of these experiments have not yet succeeded to fully reproduce the S-MIF recorded in the Archean sedimentary rocks (e.g., Danielache et al., 2008; Masterson et al., 2011; Whitehill & Ono, 2012). We have developed a new photochemical chamber for determining isotopic effect of the SO2 photolysis under optically thin condition. Also, a new direct fluorination technique of carbonyl sulfide allowed us precise isotopic analysis down to 50 nmolS of photolysis product. The results indicate that the basic character of the S-MIF observed in the Archean record can be reproduced when SO2 column density is reasonably low (i.e. 10 to 50 times higher than preindustrial atmosphere). The results with a numerical modeling of the atmospheric reaction network suggest that the observed change in D36S/D33S ratio can be adequately explained by the two factors: (1) SO2 partial pressure and (2) amount of reducing gas (H2, CH4 and CO). In light of the new perspective, we have re-evaluated the geological record of the D36S/D33S ratio with additional analyses of Archean sedimentary sulfides from South Africa and India. Based on the magnitude of the S-MIF and the D36S/D33S ratio, the Archean period can be subdivided into four stages (i.e. › 3.0 Ga, 3.0-2.7 Ga, 2.7-2.5 Ga and 2.5-2.4 Ga). These changes probably reflect both intensity of volcanic SO2 emission and concentration of reducing gasses under the O2-free atmosphere. Particularly, the maximum scatter of D33S values observed in the stage 3 (2.7-2.5 Ga) requires high volcanic emission as well as very reducing atmospheric condition in the atmosphere at that time.

Keywords: Archean, atmospheric chemistry, mass independent fractionation

Japan Geoscience Union Meeting 2014
(28 April - 02 May 2014 at Pacifico YOKOHAMA, Kanagawa, Japan)

U05-07 Room:419 Time:April 30 11:30-11:45

Archean Atmospheres Modeled with the KROME Chemistry Package

DANIELACHE, Sebastian[1*] ; UENO, Yuichiro[3] ; SIMONCINI, Eugenio[2]

[1]Sophia University, Faculty of Science & Technology, Department of Materials and Life Sciences, [2]INAF, Astrophysical Observatory of Arcetri, Italy., [3]Earth & Planetary Sciences, Tokyo Institute of Technology, [4]Earth-Life Science Institute (ELSI), Tokyo Institute of Technology

Sulfur isotopic fractionation has been used as a tool to understand the composition of reducing atmospheres. Our previous work (Danielache et al., 2008 and 2012) have shown that UV-light triggers a large Sulfur Mass-Independent Fractionation (S-MIF) on the SO_2 photodissociation products. However photodissociation of unshielded UV-light alone cannot reproduce the S-MIF signals reported for the Archean and Early Proterozoic (>2300 Ma) nor its large variability mainly at 2600 Ma (D33S = +11 ‰) (Johnston, 2011). In order to study a planetary-like chemical network capable of accounting for a sulfur cycle in reducing conditions we have introduced a high-order solver (DLSODES) administrated by the KROME (Grassi et al.,) chemistry package. The package automatically generates a set of FORTRAN subroutines with build-in rate equations and solves them with accuracy and e?ciency for sparse networks. This technique allows us to couple a detailed 4 sulfur isotopes chemistry to a 1D transport model capable of calculating the opacities influencing photochemistry and the temperature structure of an Archean atmosphere. We present preliminary results showing the ability of the code to deal with small isotopic fractionations and compare with already existing model studies of the Archean atmosphere.

Danielache, S. O., et al., (2008), High-precision spectroscopy of 32S, 33S, and 34S sulfur dioxide: Ultraviolet absorption cross sections and isotope effects, J. Geophys. Res., 113(D17), D17314,

Danielache, S. O., et al., (2012), Photoabsorption cross-section measurements of 32S, 33S, 34S, and 36S sulfur dioxide for the B1B1-X1A1 absorption band, J. Geophys. Res. Atmos., 117(D24),

Johnston, D. T. (2011), Multiple sulfur isotopes and the evolution of Earth's surface sulfur cycle, Earth Science Review., 106(1-2), 161-183.

Grassi T., et al., (2014), KROME - a package to embed chemistry in astrophysical simulations, Monthly Notices of the Royal Astronomical Society., DOI: 10.1093/mnras/stu114 (arXiv:1311.1070 [astro-ph.GA]).

Keywords: Archean Atmosphere, Sulphur, Stable Isotopes

Japan Geoscience Union Meeting 2014
(28 April - 02 May 2014 at Pacifico YOKOHAMA, Kanagawa, Japan)

U05-08 Room:419 Time:April 30 11:45-12:00

Effects of atmospheric composition on apparent activation energy of silicate weathering

KANZAKI, Yoshiki[1*] ; MURAKAMI, Takashi[1]

[1]Department of Earth and Planetary Science, Graduate School of Science, University of Tokyo

Silicate weathering is a major sink of atmospheric CO_2. Because CO_2 is an important greenhouse gas, silicate weathering regulates not only the partial pressure of atmospheric CO_2 ($P\mathrm{co}_2$) but also the surface temperature (T). The apparent activation energy of silicate weathering represents the temperature dependence of silicate weathering and thus interrelates the intensity of silicate weathering, $P\mathrm{co}_2$ and surface temperature. It has been reported that solution composition can affect the apparent activation energy of dissolution/precipitation of silicates (e.g., Casey and Sposito, 1992; Lasaga, 1995; Cama et al., 1999). However, the relationship between the solution composition and the apparent activation energy of silicate reaction is not yet fully understood.

To investigate the apparent activation energy of silicate weathering in a natural weathering system, we formulated the apparent activation energy of silicate weathering in three different scales, namely, (i) dissolution/precipitation of each mineral, (ii) elemental loss as the net reactions of the minerals and (iii) weathering flux from a weathering profile, based on the rate expressions in the three scales. It was found that, due to the effects of solution composition on the apparent activation energy, the temperature dependence of atmospheric CO_2 ($\Delta H^*\mathrm{co}_2$) affects the apparent activation energy of silicate weathering. Based on the formulated apparent activation energy, we estimated the apparent activation energy of silicate-weathering flux as a function of $\Delta H^*\mathrm{co}_2$. Then, the compensation law between the pre-exponential factor and the apparent activation energy of silicate-weathering flux was introduced from the literature, leading to the establishment of the relationship between silicate-weathering flux ($F\mathrm{co}_2$), T and $\Delta H^*\mathrm{co}_2$.

Based on the $F\mathrm{co}_2$-T-$\Delta H^*\mathrm{co}_2$ relationship and the greenhouse effects of atmospheric CO_2 in the literature, we calculated the ratio of change in $F\mathrm{co}_2$ to that in $P\mathrm{co}_2$ as an indicator of silicate-weathering feedback in the Precambrian. The calculation revealed that when $P\mathrm{co}_2 > \sim 10^{-0.5}$ atm, the feedback is negative and independent of $P\mathrm{co}_2$ and surface temperature. On the other hand, when $P\mathrm{co}_2 < \sim 10^{-0.5}$ atm, the feedback is independent of $P\mathrm{co}_2$ but dependent on surface temperature; at low ($< \sim 30$ ℃) and high ($> \sim 30$ ℃) temperatures, the feedback is negative and positive, respectively. Due to the positive feedback, the conditions of $P\mathrm{co}_2 < \sim 10^{-0.5}$ atm and $T > \sim 30$ ℃ are unstable, and immediately change, with a slight change in $P\mathrm{co}_2$, to either the conditions of $P\mathrm{co}_2 > \sim 10^{-0.5}$ atm or those of $P\mathrm{co}_2 < \sim 10^{-0.5}$ atm and $T < \sim 30$ ℃. When $P\mathrm{co}_2 < \sim 10^{-0.5}$ atm and $< \sim 30$ ℃, the feedback is not only negative, but also becomes more negative as temperature decreases, suggesting that global glaciations are harder to bring about than previously thought.

Keywords: silicate weathering, carbon dioxide, feedback, Precambrian

Japan Geoscience Union Meeting 2014
(28 April - 02 May 2014 at Pacifico YOKOHAMA, Kanagawa, Japan)

U05-09 Room:419 Time:April 30 12:00-12:15

Kinetics and Mechanisms of Zeolite Crystallization at Hyperalkaline Conditions

FRANCISCO, Paul clarence[1*] ; SATO, Tsutomu[1] ; OTAKE, Tsubasa[1]

[1]Graduate School of Engineering, Hokkaido University

The predicted precipitation of zeolites in geologic barrier systems for radioactive wastes due to the alkaline alteration of bentonite may result in the modification or loss of favorable physicochemical properties of the bentonite as a suitable barrier material. Zeolites formation is typically preceded by an amorphous precursor, the transformation of which is seen as the rate-controlling step. However, the structure of the precursor phase and the rates and mechanisms by which it transforms into crystalline zeolites are poorly understood. In this study, we investigated the rates and mechanisms of zeolite crystallization from solutions.

Batch synthesis experiments were carried out over a range of solution compositions (Si/Al = 0.1 to 8.0), pH (9.5 to 13.5) and temperature (25C to 90C) conditions in order to clarify the effects of these parameters on zeolite crystallization. Solid products were characterized using XRD, SEM-EDX, FTIR spectroscopy, Raman spectroscopy and MAS NMR spectroscopy.

Zeolite crystallization proceeds by the rapid formation of an amorphous precursor phase, followed by the slower transformation of this precursor into crystalline zeolite. Depending on the Si/Al ratio of the parent solution, the species of zeolite may vary. At Si/Al >1, Faujasite forms slowly, whereas for Si/Al <1, Zeolite A forms more rapidly. Higher pH and temperatures favor transformation.

Morphological information from SEM shows intimate physical relationship between crystalline zeolites and the amorphous precursor phase. Spectroscopic results from FTIR, Raman and MAS NMR indicate that ring structures are present in both amorphous and crystalline phases, indicating structural similarity between the two phases. These data may suggest that amorphous phases transform directly into crystalline zeolites. The activation energy of crystallization suggests that solid-state processes occur alongside dissolution of the amorphous phase in order for the transformation of the amorphous phase into crystalline zeolite to proceed.

Keywords: zeolite, mechanisms, transformation, spectroscopy

Japan Geoscience Union Meeting 2014
(28 April - 02 May 2014 at Pacifico YOKOHAMA, Kanagawa, Japan)

U05-10 Room:419 Time:April 30 12:15-12:30

Effects on Phosphate Ion for the Phase Changes of Amorphous Calcium Carbonate

SUGIURA, Yuki[1*] ; ONUMA, Kazuo[2] ; YAMAZAKI, Astushi[1]

[1]Department of Creative Science and Technology, Waseda University, [2]National Institute of Advanced Industrial Science and Technology, Central 6

Under the biometric simulated environment, amorphous calcium carbonate (ACC) appears as initiation phase by reaction of calcium and carbonate ions. There is a strong relationship between the ACC phase and the forming crystalline polymorphs. We have shown a significant inhibit effect on the vaterite formation and calcite crystallized instead, and also stabilize ACC under higher PO4 concentration conditions. We hypothesized that PO4 ions incorporated in the ACC in that suspect that the adjusting the transfer mechanism of the amorphous phase. The structure and stability of ACC under various PO4 concentrations were examined using in situ ultra violet/visible spectroscopy (UV/Vis). Further, in order to observe in detail the coupling state, the ex situ measurement of ACC by Raman spectroscopy and by using a Ca ion electrode were performed to evaluation of the presence time of the ACC phase. The bicarbonate buffer was mixed with supersaturated solution of calcium chloride and sodium bicarbonate solution to precipitate the ACC, under conditions of pH ˜8.6. By mixing the potassium hydrogen phosphate at a concentration of any carbonate solution side during mixing, PO4 ions was adjusted between 0-50μM concentrations. The ACC contains no PO4 ions shows a spectrum similar to calcite. However the concentration of PO4 ions increase, UV / Vis absorption spectrum was carried out changed to spectrum like vaterite gradually. The similar behavior showed in the spectrum observed by Raman spectroscopy. By results of measurements of the molecular weight and particle size of the ACC by scattered light spectroscopy, the increasing both density and particle size of ACC was obsereved. Ion electrode measurements showed that the residence time of the ACC increased exponentially as increasing PO4 concentration.

In the presence of PO4 ion, ACC showed a structure similar to vaterite and its stability was increased. Moreover, the type of forming polymorphs greatly changes in variation of PO4 ions in μM scale, and stability amorphous structure is also highly variable. The results suggest a need to consider the effects of coexisting PO4 ions on ACC, when calcium carbonate tissue is formed in the organism.

Keywords: Amorphous, Calcium carbonate, Phosphate, Phase transformation, Biomineralization

Japan Geoscience Union Meeting 2014
(28 April - 02 May 2014 at Pacifico YOKOHAMA, Kanagawa, Japan)

U05-11 Room:419 Time:April 30 12:30-12:45

Re-evaluation of mineral particles in geothermal fluid: Focus on polysilicic acid and adsorbed particles

YONEZU, Kotaro[1*] ; MASUDA, Chisato[1] ; MASUNAGA, Sachi[2] ; ETOU, Mayumi[2] ; WATANABE, Koichiro[1] ; YOKOYAMA, Takushi[2]

[1]Dept. of Earth Resources Engineering, Kyushu Univ., [2]Dept. of Chemistry, Faculty of Sciences, Kyushu Univ.

In geothermal system, the solubility of monosilicic acid concentration in geothermal fluid is controlled by physicochemical conditions. Once the supersaturated condition with respect to amorphous silica attained, the polymerization of silicic acid begins followed by the formation of the particles of polysilicic acid. In addition, the particles adsorbed on the solid surface can be a trigger for the further siliceous deposit. Therefore, in order to investigate the formation mechanism of siliceous deposit, the polysilicic acid particles formed by polymerization of silicic acid and the particles adsorbed on the solid surface in geothermal fluid are focused in terms of those size and chemical composition.

In this study, the polymerization mechanism of silicic acid is discussed based on the size variation of polysilicic acid in geothermal fluid as a function of time measured by dynamic light scattering (DLS) in addition to TEM observation of fractionated polysilicic acid. The filtered particles with different pore size and the adsorbed particles on the copper pipe are analyzed by SEM-EDX to characterize the particle size and chemical composition of the particles.

We expect that these results can be basic information for the prevention technology of siliceous deposit formation on the surface of heat exchanger during geothermal binary power generation.

Keywords: polysilicic acid, geothermal fluid, binary power generation, polymerization of silicic acid, mineral particles

Japan Geoscience Union Meeting 2014
(28 April - 02 May 2014 at Pacifico YOKOHAMA, Kanagawa, Japan)

U05-12 Room:419 Time:April 30 14:15-14:45

Geomicroiology of Uranium - Challenges for the Deep Geological Environment

SUZUKI, Yohey[1*]

[1]Department of Earth & Planetary Science, The University of Tokyo

Our understanding of uranium mobility in the environment has been rapidly expanding in the past decades, especially due to problems associated with environmental remediation of uranium-contaminated sites and geological disposal of spent fuels composed mostly of UO_2. Although neither of these environmental problems was relevant in Japan, Fukushima Daiichi nuclear disaster has dramatically changed our situation. Despite the significant advancement, it is still difficult to predict the form, distribution and fate of uranium in the deep subsurface, as exemplified by studies of a Swedish geological disposal site where high concentrations of uranium was unexpectedly found in the granitic aquifer. In this presentation, the state of the art investigations of microbially mediated redox reactions and uranium mobility in the deep granitic aquifer at Mizunami Underground Research Laboratory (URL) will be presented to discuss factors controlling long-term uranium migration, as well as the relevance to the formation processes of Tono uranium deposit nearby the URL.

Keywords: uranium, microorganisms, redox transformation, underground research laboratory

Japan Geoscience Union Meeting 2014
(28 April - 02 May 2014 at Pacifico YOKOHAMA, Kanagawa, Japan)

U05-13 Room:419 Time:April 30 14:45-15:00

Haloarcula strains regulate transcription of two types of 16S rRNA genes by growth temperatures

SATO, Yu[1*] ; KIMURA, Hiroyuki[1]

[1]Graduate school of Science, Shiuzoka university

Translation is the process in which ribosome creates protein. The ribosome consists of two major components, the small and large subunits. In prokaryotes, small subunit of ribosome is composed of 16S rRNA and some ribosomal proteins. Many microbiologist use the 16S rRNA gene sequence for phylogenetic analysis and identification of prokaryotes. Previous studies have reported that the 16S rRNA gene sequence is naturally inscribed with the temperature adaptations of the prokaryotic host. This observation was based on the high correlation between the growth temperatures of prokaryotes and the guanine-plus-cytosine (G+C) contents of the 16S rRNA sequences. Thermophilic and hyperthermophilic prokaryotes generally have high G+C contents of 16S rRNA genes (56-69%). In contrast, mesophilic and psychrophilic prokaryotes have relatively low G+C contents of 16S rRNA genes (51-59%).

Haloarcula strains, belonging to a diverse group of salt-loving organisms in the archaeal phylum Euryarchaeota, have two types of 16S rRNA genes on the genome. These 16S rRNA genes indicate different sequences and G+C contents. Here, we proposed a hypothesis that *Haloarcula* strains preferentially expresses the high G+C contents of 16S rRNA gene (58%), having the stability to heat, during growth in high temperature, whereas they express low G+C contents of 16S rRNA gene (56%) during growth in low temperature. In order to verify this hypothesis, we surveyed transcriptional responses of *Haloarcula* strains in a wide range of temperature conditions by using RT-qPCR method. As the result, high G+C contents of 16S rRNA gene showed significant upregulation in high temperature conditions (40 to 55^{o}C). In contrast, low G+C contents of the 16S rRNA gene expressed at significantly higher levels in low temperature conditions (25 to 35^{o}C). The results suggest that *Haloarcula* strains regulate the transcription of two types of 16S rRNA genes by growth temperatures.

Keywords: halophilic archaea, 16S rRNA, G+C contents, translation, environmental temperature

Japan Geoscience Union Meeting 2014
(28 April - 02 May 2014 at Pacifico YOKOHAMA, Kanagawa, Japan)

U05-14 Room:419 Time:April 30 15:00-15:15

The effect of methane concentration on methanotrophic bathymodiolid mussels in the Okinawa Trough hydrothermal fields

MIYAZAKI, Yukari[1*] ; SUNAMURA, Michinari[1] ; ISHIBASHI, Junichiro[2] ; WATANABE, Hiromi[3] ; KONNO, Uta[3] ; SUZUKI, Yohey[1]

[1]Graduate School of Science, the University of Tokyo, [2]Graduate School of Science, the University of Kyusyu, [3]JAMSTEC

As methane (CH_4) is a greenhouse effect gas, the emergence and activity of CH_4-oxidizing organisms is suggested to have triggered global glaciation. Although the threshold concentrations of CH_4 for the growth of CH_4-oxidizing microorganisms under laboratory conditions are well known, CH_4-oxidizing organisms in the field is poorly constrained for the threshold concentration of CH_4 for growth. This information is critical to reconstruct atmospheric and oceanic CH_4 levels when the activities of methanotrophic organisms are indicated from geologic records with ^{12}C-enriched organic matter. We investigated sediment-hosted deep-sea hydrothermal fields in the Okinawa Trough where abundantly emitted $CH_4$is known to support methanotrophic ecosystem represented by Bathymodiolid mussels. The distribution of Bathymodiolid mussels and the CH_4 concentrations of their habitats were determined in five hydrothermal fields throughout the Okinawa Trough, and it is suggested that approximately 10μM is a threshold CH_4 concentration for the methanotrophic organism in the deep-sea ecosystem.

Keywords: hydrothermal vent, Bathymodiolus sp., Neoverruca sp., methanotroph, Okinawa Trough

Japan Geoscience Union Meeting 2014
(28 April - 02 May 2014 at Pacifico YOKOHAMA, Kanagawa, Japan)

U05-15 Room:419 Time:April 30 15:15-15:30

Biogeochemical cycles of iron and carbon in biogenic iron-rich sediment

KIKUCHI, Sakiko[1*] ; MAKITA, Hiroko[2] ; KONNO, Uta[2] ; SHIRAISHI, Fumito[1] ; TAKAI, Ken[2] ; TAKAHASHI, Yoshio[1]

[1]Department of Earth and Planetary Systems Science, Graduate School of Science, Hiroshima University, [2]Japan Agency for Marine-Earth Science and Technology

Biogenic iron oxides are the mixture of iron oxyhydroxides and organic materials which are produced by the metabolic activities of bacteria. These biogenic iron oxides work not only as adsorbent for various trace elements, but also as a source of iron and carbon for microorganisms. However, there is only little information about the degradation process of biogenic iron oxides and the effect to microbial activities after their sedimentation. Thus, the purpose of our study is to identify the spatial changes of iron species and microbial communities in biogenic iron-rich sediment (10 cm long).

We observed the existence sharp shifts for iron mineral species and microbial communities in the sediment. The dominance of ferrihydrite at the surface sediment (0-2 cm) subsequently turned into goethite and siderite at sediment depth 2-5 cm, corresponding to the iron reduction. However, iron reduction was depleted at depth deeper than 5 cm, as opposed to the remarkable increase of methane concentration. The microbial clone libraries were dominated by iron-oxidizing chemolithoautotrophic bacteria in the sediment 0-2 cm. In contrast, phylotypes represented by iron reducing and fermenting bacteria at 4 cm, and uncultured delta-proteobacteria and methnogenic archaea were recovered at 10 cm depth. These changes of iron mineral species, carbon metabolisms, and microbial communities only within a few centimeter intervals will also couple to the drastic change in cycles of trace element around the biogenic iron-rich sediment.

Keywords: iron oxides, iron-oxidizing bacteria, Ferrihydrite, Siderite, iron-reducing bacteria, methane

Japan Geoscience Union Meeting 2014
(28 April - 02 May 2014 at Pacifico YOKOHAMA, Kanagawa, Japan)

U05-16 Room:419 Time:April 30 15:30-16:00

Interaction of nanoparticles with microorganisms

UTSUNOMIYA, Satoshi[1*] ; SHIOTSU, Hiroyuki[1] ; MASAKI, Shota[1] ; JIANG, Mingyu[1] ; OHNUKI, Toshihiko[2]

[1]Kyushu University, [2]JAEA

Nano-mineralization by microorganisms is a key process that can constrain the migration of actinides and REEs. This study demonstrates the REEs accumulation experiments to understand the effect of pH, coexistent REEs and the functional group of cells surfaces on the crystal chemistry of biogenic nanoparticle formation. During the experiment at 25 oC, all REEs were removed from the solution by 24 h at pH 4 and 5, while 50 % of the initial amount remained in the solution at pH 3 after 24 h. The nano-particles at pH 3 had monazite structure, while the particles forming at pH 4 and 5 were amorphous. The REE pattern at 24 h indicated the preferential uptake of LREEs. In case transuranic elements coexist, those elements should be preferentially incorporated into the particles compared to REEs. No cytotoxicity of CeNPs was detected; however, CeNPs induced an excess expression of two proteins: Eno2p and Rps24bp. The released organic substances enhanced anion adsorption and changed surface property of CeNPs. This leads to high colloid stability in solutions. This process is of great importance in the migration of radionuclides in the subsurface environment.

Keywords: Nanoparticles, Microorganisms, Rare earth elements

Japan Geoscience Union Meeting 2014
(28 April - 02 May 2014 at Pacifico YOKOHAMA, Kanagawa, Japan)

U05-17 Room:419 Time:April 30 16:15-16:45

Microbial methanogenesis in coal seams and diatomaceous formations: Topics and application prospects

SHIMIZU, Satoru[1*]

[1]Horonobe Research Institute for the Subsurface Environment

1. Introduction

Microbial methanogenesis occurs in diverse subsurface environments. For example, biogenic methane has been detected from all representative ecosystems of the world and has been reviewed[1)]. However, the process of methanogenesis in those subsurface environments has yet to be revealed. Understanding the methanogenesis process is necessary for discerning the global-scale carbon-cycle and for a more effective utilization of biological methane as an energy resource from subsurface environments.

2. Methanogenic archaea from coal-beds and diatomaceous rock

Research topics on biogenic methanogenesis in the Ishikari (bituminous coal)[2)] and Tenpoku (brown coal) basin and the diatomaceous formations[3,4,5)] of northernmost Japan will be introduced in this presentation. We were successful in isolating and culturing methanogens from these habitats. In particular, the dominant methanogens isolated from diatomaceous shale formation[4,5)] will help in understanding some of the processes of methanogenesis in subsurface environments.

3. Biological methanogenic potential of coal-beds and diatomaceous rock formations as geobioreactors

The bottleneck of methanogenesis in subsurface environments is the production of suitable substrates for methanogens from persistent geomacromolecules. One of our approaches for eliminating the bottleneck is a geobioreactor for methanogenesis using hydrogen peroxide. Oxidation of low-rank coal using hydrogen peroxide produces a high yield of small-molecule substrates for methanogenic microorganisms (e.g., methanol, acetate, formate)[6)]. Substrate production from diatomaceous rock is considerably less than that from low-rank coal. However, the stratum thickness of diatomaceous rock (1 km or more) is much more than that of coal seams (several meters). Therefore, although the methanogenic potential of diatomaceous rock is low, by quantity, it constitutes an abundant resource. Furthermore, we have had success in microbial methanogenesis from small molecules produced from brown coal using hydrogen peroxide.

References)

1) Strapoc et al. (2011) Annu. Rev. Earth Planet Sci. 39, 617-656.
2) Shimizu et al. (2007) Geobiology 5, 423-433.
3) Shimizu et al. (2006) Geobiology 4, 203-213.
4) Shimizu et al. (2011) Int. J. Syst. Evol. Microbiol. 61, 2503-2507.
5) Shimizu et al. (2013) Int. J. Syst. Evol. Microbiol. 63, 4320-4323.
6) Miura et al. (1996) Energy & Fuels 10, 1196-1201.

Keywords: Methane, Coal, diatomaceous rock, subsurface microorganisms, methanogenesis, Geo-bioreactor

Japan Geoscience Union Meeting 2014
(28 April - 02 May 2014 at Pacifico YOKOHAMA, Kanagawa, Japan)

U05-18 Room:419 Time:April 30 16:45-17:00

Transportation process of As in surface and shallow ground waters

MASUDA, Harue[1*]

[1]Osaka City University

Natural As contaminated groundwater has been a serious problem in the world. Instead of numerous studies, sources and pollution mechanism are still in debate. Most accepted source of As is Fe-oxyhydroxides that adsorb the As, and reduction-dissolution of the Fe-oxyhydroxides is believed to release the As into groundwater. Biotite and pyrite would be candidate sources of As, however, few studies assured the presence of As in those minerals. Here, transportation process of the As in surface water and As release mechanism in shallow sediments.

Arsenic is transported as dissolved components and suspended matters. Total As concentration of Red River water is ˜10 ppb, and dissolved As and As with suspended particles are 6:4. Although the Red River water contained gibbsite and goethite as suspended matters, those do not but clay minerals host the As as adsorbent. Concentrations of As of the riverbed sediments of Ganges-Bramaptra and Red Rivers are a few to 15 ppm, most of which are in insoluble detrital phases such as silicates and sulfides. Chlorite was the host phase of As in As contaminated groundwater aquifer in our study areas of Bangladesh and Pakistan, although different detrital minerals can host As in each rivers, of which tributaries As contaminated groundwater occurs. These results suggest that the transportation of As with detrital minerals is more important than that as dissolved components and adsorbed phases onto clay minerals and goethite.

In the shallow sediments, As concentration changes with redox potential and pH. Geochemical condition would be controlled by microbial activity in the aquifer. Dissolution of As occurs at the depths where detrital As host minerals are decomposed via oxidation. Newly formed Fe-oxyhydroxides would adsorb parts of the As but not all. Thus, the dissolution of As host minerals are the main reaction to cause As contaminated groundwater.

Keywords: arsenic contaminated groundwater, microbial geochemical reactio, chlorite, goethite, gibsite

Japan Geoscience Union Meeting 2014
(28 April - 02 May 2014 at Pacifico YOKOHAMA, Kanagawa, Japan)

U05-19 Room:419 Time:April 30 17:00-17:15

Adsorption behavior of organoarsenic compounds in soils

TANAKA, Masato[1*] ; TAKAHASHI, Yoshio[1]

[1]Graduate School of Science, Hiroshima University

The arsenic pollution is a world problem. Natural originated inorganic arsenic compounds are predominant cause of the water-related disease. In addition, anthropogenic originated organoarsenic compounds such as phenylarsonic acid (PAA) and diphenylarsinic acid (DPAA) are also pollution source. For example, DPAA polluted well water caused serious health problems in Kamisu, Japan [1]. These phenyl arsenic compounds are considered as a decomposition product of chemical warfare agents produced during World Wars I and II, and even now such compounds still remain in the ground [2]. Recently, adsorption and mobility of these aromatic arsenic compounds in agricultural soils have been investigated [3]. However, their adsorption mechanisms on soil are still unknown. In general, the adsorption property of chemical compounds influences its migration process in natural environments such as soil-water system. Thus, it is important to understand the adsorption mechanism of the arsenic compounds to predict future fate of them in environment. Recently, we reported adsorption structures of PAA and DPAA on ferrihydrite obtained by X-ray absorption fine structure (XAFS) analysis and quantum chemical calculations [4]. In this study, we conducted As K-edge XAFS measurements for organoarsenic compounds adsorbed on soil, as well as a sequential extraction, to understand their adsorption behavior in the soil. EXAFS analysis suggests that all arsenic compounds in this study adsorbed on Fe or Al (oxyhydr)oxide in the soil mainly regardless of the organic functional groups. This fact indicates that the Fe/Al (oxyhydr)oxide can control the mobility of organorasenic compounds in the ground.

References:
[1] Hanaoka S, Nagasawa E, Nomura K, Yamazawa M and Ishizaki M 2005 Appl. Organometal. Chem. 19 265.
[2] Wang A, Li S, Teng Y, Liu W, Wu L, Zhang H, Huang Y, Luo Y and Christie P 2013 J. Environ. Sci. 25 1172.
[3] Maejima Y, Murano H, Iwafune T, Arao T and Baba K 2011 Soil Sci. Plant Nutr. 57 429.
[4] Tanaka M, Togo Y S, Yamaguchi N and Takahashi Y 2014 J Colloid Interface Sci., 415, 13.

Keywords: soil, adsorption, XAFS, organoarsenic

Japan Geoscience Union Meeting 2014
(28 April - 02 May 2014 at Pacifico YOKOHAMA, Kanagawa, Japan)

U05-P01 Room:Poster Time:April 30 18:15-19:30

Impact-induced produtcs from glycine polymers in early Earth's oceans

SEKINE, Toshimori[1*] ; KATSUKI, Yuto[1] ; SUGUMURA, Kousuke[1] ; KOBAYASHI, Takamichi[2]

[1]Hiroshima University, [2]National Institute for Materials Science

Early oceans may have contained appreciable amounts of prebiotic organic molecules, since previous studies have indicated that simple organic molecules are capable to be formed through oceanic impact processes by meteorites. Geologic evidence suggests that the root for the origin of life materials occurred just after or during the heavy bombardment period. At that time the impact energy is considered to have been important for molecules present in oceans to react. Shock reactions of organic molecules in aqueous solutions have been subject to few studies.

Here we investigate the reactions for glycine polymers (dimer G2, trimer G3, and tetramer G4) and alanilglyine (AG) in aqueous solutions in order to know their stability and reaction products during impacts. The starting G2 (>99.o% Tokyo Chemical Industry Co. Ltd), G3 (>98.0%, Tokyo Chemical Industry Co. Ltd), G4 (>95%, Tokyo Chemical Industry Co. Ltd), and AG (>98.0%, Tokyo Chemical Industry Co. Ltd) were used in the present study. Hypervelocity plane impact experiments were carried out using a propellant gun. Sample solutions of glycine polymers in sealed steel containers were subjected to impact at velocities of about 1 km/s. The calculated shock pressures are 5-6 GPa by the impedance match solution. The recovered solutions were analyzed with a hybrid Fourier transform mass spectrometer (Thermo Fisher Scientific LTQ Orbitrap XL) at Hiroshima University.

The analytical results for the recovered samples were compared with those for the initial sample. Limited numbers of amino acids of Glycine, alanine, and their polymers, amines from propylamine to octylamine, and carboxylic acids from acetic acid to decanoic acid were selected due to a measured range of their m/z values. The identification of a molecule was done by the presence of a peak with the calculated m/z value ($\pm$0.002). The results are discussed.

Keywords: Glycine polymers in early Earth's oceans, Impact-induced products

Japan Geoscience Union Meeting 2014
(28 April - 02 May 2014 at Pacifico YOKOHAMA, Kanagawa, Japan)

U05-P02 Room:Poster Time:April 30 18:15-19:30

Effect of mineral species on the glycine polymerization

ONISHI, Hiroyuki[1*] ; KITADAI, Norio[2] ; FUKUSHI, Keisuke[3]

[1]Department of Nature System, Kanazawa Univ., [2]Earth Life Science Institute, Tokyokogyo Univ., [3]Inst Nature and Environmental Technology, Sci., Kanazawa Univ.

Protein is a major constituent of life on the earth, and is produced by polymerization due to dehydration condensation of amino acids. Polymerization of amino acids is an important process for the origin of life. The understanding of amino acid polymerization process in the earth surface environment is important for the origin of life. It is well known that polymerization of amino acids under the ambient condition is thermodynamically difficult. Therefore, how the amino acids polymerization in the early earth environment proceeded is still under debates.

Many model experiments for amino acid polymerization had been designed so far. Among them, one of the promising method is mixing the mineral powder with glycine solution with heating (e.g., Bujdak and Rode, 1997a). Bujdak and Rode, (1997b) was confirmed that alumina could promote alanine polymerization than Quartz. They suggested that the effect of mineral type is important on the polymerization of amino acids. However, it is not known which functions of the mineral affect the amino acid polymerization. After Bujdak and Rode, (1997b), amino acid polymerization experiments by using various type of mineral species has been widely examined. However, the experiment condition has not been unified among the studies. We cannot compare the effect of amino acid polymerization on each mineral. In present study, we conducted the experiments of amino acid polymerization using t various types of minerals (Rutile, Anatase, Amorphous silica, Quartz, gamma-Al2O3, Corundum, Hematite, Magnetite, Forsterite) under the unified experimental conditions. The purpose of the study is to clarify the factors for promoting the amino acid polymerization in mineral species.

Keywords: amino acid, polymerization, mineral

Japan Geoscience Union Meeting 2014
(28 April - 02 May 2014 at Pacifico YOKOHAMA, Kanagawa, Japan)

U05-P03 Room:Poster Time:April 30 18:15-19:30

Role of minerals for hydrogen generation in the interaction between ultramafic rocks and water

FUKUHARA, Naoki[1*] ; SATO, Tsutomu[1] ; OTAKE, Tsubasa[1]

[1]Laboratory of Environmental Geology, Hokkaido university, Graduate School of Engineering, Hokkaido U

Hydrogen generation by high temperature serpentinization is understood as hydration of mafic and ultramafic rocks, owing to the oxidation of reduced iron present in the olivine or pyroxene. On the other hand, in the Oman Ophiolite and Lost City Hydrotherrmal Field (LCHF) in the Mid-Atlantic Ridge, hydrogen is generated via low temperature serpentinization. Moreover, previous experimental study shown generating hydrogen at low temperatures (<100 degrees C). However, since even the rate of hydrogen generation by high temperature serpentinization is slow, the mechanism of hydrogen generation by low temperature in short period is yet to be explained. Therefore, the objective of this study is to clarify the mechanism of hydrogen generation via low temperature serpentinization for a short period. Batch experiments were conducted at 30 degrees C, 60 degrees C and 90 degrees C using minerals which constitute ultramafic rocks (olivine, Magnetite, Fe-Ni alloy), and serpentinite. Samples were taken after various reaction times (3h, 6h, 12h, 24h, and 1week). Liquid samples were analyzed by ICP-AES, ion chromatography, UV-Vis, pH, and ORP. Mineral phase changes in the solid samples were characterized by TG-DTA, SEM-EDX and XRD. The concentration of hydrogen gas was determined by GC-RGD.

Hydrogen generation was observed in all samples. Highest concentration of hydrogen gas was observed in the experiment using Fe-Ni alloy. In the experiment using Fe-Ni alloy, apparent surface change was not observed at the surface of Fe-Ni alloy. Therefore, hydrogen gas was generated by catalysis of Fe-Ni. The generation of hydrogen gas by this catalysis would be higher than that of generated hydrogen accomplished by the dissolution of olivine, which is the dominant mineral in the ultramafic rocks.

In this study, the hydrogen generation was confirmed at a temperature of less than 90 degrees C. The hydrogen generation process is catalyzed by Fe-Ni alloys or magnetite present in secondary minerals by serpentinization.

Japan Geoscience Union Meeting 2014
(28 April - 02 May 2014 at Pacifico YOKOHAMA, Kanagawa, Japan)

U05-P04 Room:Poster Time:April 30 18:15-19:30

Spatial distribution of chromium enrichment in 3.2 Ga Moodies BIF, Barberton Greenstone Belt, South Africa

ISHIKAWA, Ko[1*] ; OTAKE, Tsubasa[1] ; KAWAI, Shohji[2] ; SATO, Tsutomu[1] ; KAKEGAWA, Takeshi[2]

[1]Division of Sustainable Resource Engineering, Graduate School of Engineering, Hokkaido University, K, [2]Department of Earth Science, Graduate School of Science, Tohoku University, Aoba 6-3, Aoba-ku, Senda

Geochemical data for ferruginous chemical sedimentary rocks (e.g., Banded Iron Formation: BIF) have been used to understand surface environments on early Earth. For example, enrichment of Cr relative to Ti in BIFs that occurred ˜2.48 billion years ago has been considered as a result of the chemical mobilization of Cr in acidic aqueous environments due to sulfide oxidation after the oxygenation of atmosphere. While the Archean sedimentary environments studied in most previous works are limited to deeper settings, the 3.2 Ga Moodies BIF in the Barberton Greenstone Belt, South Africa also indicated that Cr was enriched in the BIF and was therefore chemically mobile in a shallow marine environments. This finding could be significant because it may indicate the oxidation of, at least, some parts of the ocean and therefore, imply the emergence of oxygenic photosynthesis. However, spatial distribution of Cr enrichment in the BIF has not been well understood because the data were obtained from an outcrop and an underground mine. Therefore, the objective of this study is to investigate sedimentary environments and Cr enrichment of the Moodies BIF at another locality.

We conducted a geological survey of another outcrop of the Moodies BIF in the Eureka syncline located ˜10 km northeast of Barberton. The section of the BIF exposed in the outcrop was underlain by a conglomeratic quartzite, which is stratigraphically correlated with the BIF at Moodies Hills block in the previous study. Whereas the BIF at Moodies Hills block are 22m in the thickness and overlain by 122m thick silty sandstone and sandstone, the BIF in this study has a thickness of 36m and is overlain by a 103m thick layer of greywacke and silty sandstone. Petrographic observation of the BIF samples shows that the reddish layers are composed of microcrystalline quartz and fine grains of hematite (˜15μm), and that the black layers are composed of large grains of magnetite (˜50μm). These observations indicate that they are typical oxide-type BIF and therefore were originally formed as precipitates from seawater. Although chromite, which is a host mineral for Cr, was found in both BIF and clastic sedimentary rock (e.g., silty sandstone) samples, chromite in the BIF was always overgrown by magnetite. This observation is also consistent with results from previous studies. The chemical compositions of the chromite determined by FE-EPMA were low Mg# (0.001˜0.01) and high Cr# (0.76˜0.89). No significant difference in chemistry was observed in chromite between BIF and clastic sedimentary rock samples. Bulk chemical compositions of the samples were also analyzed by XRF. The results show that the Cr/Ti ratio was not significantly different between BIF and clastic sedimentary rock samples. Therefore, Cr enrichment was not observed in the BIF in this study. The apparent contradiction to the previous study at Moodies Hills block can be explained by the difference in (1) analytical method used or (2) the sedimentary environment. The Ti contents of BIF at Moodies Hills block were determined by ICP-MS after acid decomposition, by which the detection limit is one order of magnitude lower than XRF used in this study. Therefore, the high detection limit in this study may lose the sensitivity for Cr enrichment in samples in which Ti content was low. Alternatively, the BIF in this study could have been deposited in a deeper setting than that at the Moodies Hills block. Therefore, the results may suggest that oxygenated seawater was only localized in very shallow parts.

Keywords: Banded Iron Formation, chromium, chromite, Barberton Greenstone Belt, surface environments on early Earth

Japan Geoscience Union Meeting 2014
(28 April - 02 May 2014 at Pacifico YOKOHAMA, Kanagawa, Japan)

U05-P05 Room:Poster Time:April 30 18:15-19:30

Change by a diagenesis of first minerals in 1.9 Ga sedimentary rocks of the Gunflint Formation

NIKAIDO, Emi[1*] ; KAKEGAWA, Takeshi[1]

[1]Graduate School of Science, Tohoku University

Some microfossils in the 1.9 Ga Gunflint Formation show clear morphology of aerobic microorganisms. However, carbon isotope compositions of microfossils and other geochemical characteristics suggest the activity of anaerobic microorganisms in the same rock sample. This leads to the skepticism if the 1.9 Ga surface ocean environments were essentially anoxic and oxic environments were very limited.

In order to examine if oxic world were more common or anoxic world were more common, shallow water sedimentary rocks were collected from Kakabeka (the bottom of the Gunflint) and Telly Fox (the top of the Gunflint) areas. The following features were found in the present study. (1) Chemistry of carbonate change into either Fe-rich or Mg-rich from calcite during diagenesis. Fe-rich feature is only found at the bottom of the Gunflint Formation, suggesting wide injection of reduced fluids in sediments. (2) Carbon isotope compositions were similar to cyanobacteria value, and feature of anaerobic bacteria were not detected. This suggests that previous report of carbon isotope compositions of anaerobic bacteria was limited in a few places and not widespread in the Gunflint Formation. Therefore, aerobic microorganism was the major life forms. (3) Sulfur isotope compositions of pyrite range from -2 to +15 per mil, suggesting closed system sulfate reduction. The closed system was most likely isolated oxic seawater from anoxic sediments, probably high sedimentation of SiO2 and CaCO3. In addition, isolated sediments were anaerobic bacterial world, where organic matter from the oxic world was largely consumed.

Keywords: diagenesis, oxic, anoxic, closed system

Japan Geoscience Union Meeting 2014
(28 April - 02 May 2014 at Pacifico YOKOHAMA, Kanagawa, Japan)

U05-P06 Room:Poster Time:April 30 18:15-19:30

Origin of phosphate stromatolite formed after the snowball Earth

SHIRAISHI, Fumito[1*] ; OKUMURA, Tomoyo[2] ; TAKASHIMA, Chizuru[3] ; KANO, Akihiro[4]

[1]Hiroshima University, [2]JAMSTEC, [3]Saga University, [4]Kyushu University

The sedimentary rocks formed after Neoproterozoic snowball Earth distribute near Irece, Bahia, Brazil. Salitre Formation is one of them, and contains unique phosphate (apatite) stromatolites. They show dense columnar shape, and are surrounded by laminated dolomite. The relationship between stromatolite and dolomite is mostly sharply bounded, although some parts appear transitional. Stromatolite contains various shape of microfossils. Filamentous microfossil (5-10 μm diameter, about 300 μm long) is most abundant and resembles to filamentous cyanobacteria, and thus, photosynthetic microorganisms such as cyanobacteria are considered to be involved in the formation of stromatolite.

In order to understand the influence of microbial photosynthesis on apatite precipitation, saturation state of apatite after removing 200 μM of CO_2 from seawater was calculated by Phreeqc. The result indicated that photosynthesis can significantly increase saturation state of apatite, when the concentration of dissolved phosphate is at least1 μM. Although the saturation state of $CaCO_3$ is also increased by photosynthesis, its degree is much smaller than that of apatite. As a result, apatite is more likely to precipitate than carbonate, and phosphate stromatolite is formed.

The concentration of dissolved phosphate is extremely low at the surface ocean due to the uptake by phytoplankton, and its concentration is as high as several μM even at the deep ocean. At the time of post-snowball Earth, similar situation is expected for the surface ocean, while the concentration of phosphate in the deep ocean is considered to be much higher than today. If occasional upwelling transported such water mass to the shallow sedimentary basin where cyanobacterial mat is developed, phosphate stromatolite will be formed even if dissolved phosphate concentration is several μM.

Japan Geoscience Union Meeting 2014
(28 April - 02 May 2014 at Pacifico YOKOHAMA, Kanagawa, Japan)

U05-P07 Room:Poster Time:April 30 18:15-19:30

Large Fe isotope fractionations in ferruginous sedimentary rocks above Kuroko deposits in the Hokuroku district

SUZUKI, Ryohei[1*] ; TSUBASA, Otake[1] ; YAMADA, Ryoichi[2] ; SHIN, Ki-cheoul[3] ; KON, Yoshiaki[4] ; YONEDA, Tetsuro[1] ; SATO, Tsutomu[1]

[1]Laboratory of Environmental Geology, Graduate School of Engineering, Hokkaido University, [2]Tohoku Univ., [3]Research Institute for Humanity and Nature, [4]National Institute of Advanced Industrial Science and Technology

The Hokuroku district in Akita Prefecture, Japan, hosts many large volcanogenic massive sulfide (VMS) deposits called Kuroko deposits formed around 15.3 million years ago by ancient submarine hydrothermal activity. VMS deposits were formed by the precipitation of metals from hydrothermal fluids and could have contacted with seawater in geological timescales. Because they are composed of sulfide minerals that are stable in a reducing environment, such as pyrite and chalcopyrite, an anoxic environment in the Hokuroku basin may play an important role in the preservation of the sulfide ores containing valuable metals in Kuroko deposits. However, geochemical evidence of such an environment occurring in Hokuroku district is currently lacking. Therefore, objective of this study is to investigate the distribution of REEs and the variation of Fe isotope compositions in the Fe-Mn-rich sedimentary rocks associated with VMS deposits in the Hokuroku district to understand the depositional environments and ancient sea-floor hydrothermal systems in the Hokuroku basin. Sedimentary rock samples obtained from both outcrops and mines in the Hokuroku district include ferruginous cherts occurring directly on or above a Kuroko deposit, manganese-rich siliceous mudstone, and amber in mudstone or tuff. Samples were analyzed by XRD, petrography, and SEM-EDS for mineralogy, by XRF and LA-ICPMS for chemical composition and MC-ICPMS for iron isotope composition (δ^{56}Fe (‰) = $1000*[(^{56}Fe/^{54}Fe)_{sample}/(^{56}Fe/^{54}Fe)_{IRMM-14}$ -1]).

The results of these analyses show the δ^{56}Fe values of mine samples occurring directly on and above Kuroko deposits were -1.5 to 0.5 ‰. These values are largely fractionated from δ^{56}Fe value that is similar with igneous rock ' s δ^{56}Fe. Iron isotopic fractionation occurs when ferrioxide precipitate part of the bivalent iron present in the reservoir. These values are largely fractionated from the δ^{56}Fe value of the standard (i.e., 0 ‰), which is a similar to that of igneous rocks. The samples that have a large negative value also bears negative Ce anomaly. These signatures indicate that partial oxidation of dissolved ferrous iron occurred by mixing ferrous iron-bearing anoxic water with oxygen-bearing seawater, and therefore that the sea-floor of the Hokuroku Basin was anoxic. On the other hand, δ^{56}Fe values of chemical sedimentary rocks formed during 2 -3 Ma after Kuroko deposits formed ranges from -0.8 to -0.3 ‰. These values are similar to that of dissolved ferrous ion in a modern sea-floor hydrothermal fluid. Therefore, the δ^{56}Fe values of the samples indicate near complete oxidation of dissolved ferrous iron in an oxic environment. Therefore, the results of this Fe isotope study suggest that the depositional environment in the Hokuroku basin shifted from anoxic to oxic after the formation of Kuroko deposit.

Keywords: iron isotope, rare earth pattern, anoxic environment, Volcanogenic massive sulfide, hydrothermal system

Japan Geoscience Union Meeting 2014
(28 April - 02 May 2014 at Pacifico YOKOHAMA, Kanagawa, Japan)

U05-P08 Room:Poster Time:April 30 18:15-19:30

SEM and TEM observations of carbonate, Fe-oxide and silica minerals in Okuoku-hachikuro hot spring, Akita Prefecture

TERAJIMA, Shogo[1*] ; KAKEGAWA, Takeshi[1]

[1]Graduate School of Science, Tohoku University

Recent studies of biomineralization mainly treated biominerals produced by evolved life. It is uncertain if primordial microbes are capable to precipitate biominerals. If biomineralization by early life is well documented, it will help to understand the Precambrian environments more in details.

Abundant carbonates are precipitating at Okuoku-hachikuro hot spring, located in Kosaka, Akita Prefecture, Japan. We collected sinters, soft to solidified sediments and microbial mats. Then, those constituents were observed using field emission-scanning electron microscopy (FE-SEM). Minerals around microbial sheath were also observed by transmitted electron microscopy (TEM). Analyses of X-ray diffraction, pH, DO, dissolved amino acids, carbon isotope compositions and chlorophyll compositions were also performed.

Hot spring water does not contain appreciable amounts of dissolved oxygen, but Fe-oxides immediately precipitated after discharge. Chlorophyll analyses indicate no presence of anoxic photosynthesizing bacteria. These results suggest that Fe were precipitated by Fe-oxidizing bacteria dominantly, supported by SEM observation of characteristic morphology of the sheath. Cyanobacteria become more dominant in the distance.

Most samples contain radial aggregates of needle-shape aragonite. Such morphology was found in bubble in the ”first” discharging fluid. Each needle in radial aggregates seems to be bigger depending on a distance from the discharging point. Aggregates of coarser and random orientated needles of aragonite are found in lower stream zone, where evaporation and cooling of hot spring water are more visible. Because of no systematic correlation to biological activities (microbial mat, amino acid, organic carbon, etc.) to those morphological changes, all aragonites are formed inorganically. On the other hand, Fe-oxide covering sheath are found locally. Using dilute hydrochloric acid etching, Fe-oxide is observed clearly, especially in zone 1. It has 3 morphological types: sheath-like, agglomerated and needle in radial aggregates. It is noteworthy that Fe-oxides never grow in large crystals. This can possibly because microbial activities or organic molecules may prohibit the growth of Fe-oxides. Furthermore Si was detected in Fe-oxide. This result suggests that Fe-oxide probably adsorbs amorphous silica selectively. Such unique morphology may help to interpret the origin of hematite in Precambrian banded iron formations.

Keywords: aragonite, Fe-oxide, Fe-oxidizing bacteria, SEM, TEM

Japan Geoscience Union Meeting 2014
(28 April - 02 May 2014 at Pacifico YOKOHAMA, Kanagawa, Japan)

U05-P09 Room:Poster Time:April 30 18:15-19:30

Microbial processes forming lamination in hot spring stromatolites by sulfur oxidizing bacteria and cyanobacteria.

OKUMURA, Tomoyo[1*] ; TAKASHIMA, Chizuru[2] ; HIRANO, Misa[2] ; KANO, Akihiro[3]

[1]JAMSTEC, [2]Faculty of Culture and Education, Saga Univ., [3]SCS, Kyushu Univ.

Travertines are carbonate precipitates from hot-spring water containing a sufficient amount of calcium and carbon dioxide. Most of travertines show sub-mm order laminations that were resemble to ancient stromatolites. Recently, daily microbial processes were identified in some travertines precipitated from some sulfide-poor and moderate temperature (<55 degree C) springs. In the process, daily growth of biofilms consisting cyanobacteria or heterotrophic bacteria, which inhibited inorganic mineral precipitation (1,2). While, lamination is less common in the travertines at higher temperature (>60 degree C) and sulfide-rich springs (3) likely because such daily microbe-mineral interaction might not be occurred. In order to understand the geomicrobiological system in high temperature and sulfide-rich spring, this study investigates a travertine in Sipoholon, Northern Sumatra, Indonesia.

Sipoholon hot spring forms the hugest travertine mound among the hot springs in Tarutung area located about 30 km south from the Lake Toba. The travertine mound spread in total area of 50,000 km^2. The actively precipitated region was separated 3 areas; A is natural mound without artificial effect, B is the mounds in a quarry, C is exposes the rim pools behind spa facilitates. In all area, sulfur-rich yellow sediments were formed near the vents, while white laminated sediment was formed from midstream to downstream. The surface color of the laminated travertine was changed with water temperature; pale pink around 55 degree C and green below 50 degree C. Lamination in the green travertine consisted of light colored crystalline layer and dark colored biofilm-rich porous layer in the interval of 0.5-1.0 mm. While, some lamination in the pink travertine was not clear.

12 sequences of water and travertine samples were collected at a green travertine and a pink travertine in Area C every 4 hours during 48 hours. Samples of both types of the travertine showed that the dark layer was formed during daytime and light colored layer was formed during nighttime without variation in pH, water temperature, Ca ion concentration, alkalinity, and flow. Only dissolved oxygen concentration showed the daily variation in the water chemistry, which was higher during the daytime and lower during the nighttime. Phylogenetic analysis on 16S rRNA gene showed that the pink and green travertines have a microbial composition dominated by obligatory chemolithoautotophic sulfur-oxidizing bacteria. Phototrophs, cyanobacteria and chloroflexus were more diverse in the green travertine than in the pink one. Epifluorescence microscopy showed that phototrophs were concentrated in the diurnal dark layer in the green travertine, while sparsely distributed near the surface in the pink travertine.

These results suggest that formation of phototroph biofilm in daily cycle was responsible for lamina formation in the green travertine same as previous study. On the other hand, formation of sulfur-oxidizer biofilm stimulated daytime increment of oxygen concentration was likely responsible for lamina formation in the pink travertine. The obscure lamination in the pink travertine possibly due to growth of chemolithoautotophs stimulated by extrinsic factor that is daily supplement of oxygen, in contrast to intrinsic daily growth of phototrophs. This novel microbial process could be occurred in ancient stromatolites formed under the anoxic sulfide-rich ancient ocean.

[Ref]
(1) Takashima, C. & Kano, A. (2008) Sediment. Geol. 208, 114-119.
(2) Okumura, T., Takashima, C., Shiraishi, F., Nishida, S., Kano, A. (2013) Geomicrobiol. J. 30, 910-927.
(3) Fouke, B.W., Farmer, J.D., Des Marais, D.J., Pratt, L., Sturchio, N.C., Burns, P.C., Discipulo, M.K. (2000) J. Sediment. Res. 70, 565-585.

Keywords: travertine, lamination, stromatolite, cyanobacteria, sulfur-oxidizing bacteria

Japan Geoscience Union Meeting 2014
(28 April - 02 May 2014 at Pacifico YOKOHAMA, Kanagawa, Japan)

U05-P10 Room:Poster Time:April 30 18:15-19:30

Influences of silica and embedding on thermal alteration of aliphatic hydrocarbons in cyanobacteria as evaluated by FTIR

IGISU, Motoko[1*] ; YOKOYAMA, Tadashi[2] ; UENO, Yuichiro[3] ; NAKASHIMA, Satoru[2] ; MARUYAMA, Shigenori[3]

[1]JAMSTEC, [2]Osaka University, [3]Tokyo Institute of Technology

To study influences of the presence of silica and embedding on thermal changes of aliphatic hydrocarbons in prokaryotic cells, cyanobacteria Synechocystis sp. PCC6803 were isothermally heated at 250-400 ℃ and the changes in IR signals were monitored by micro-Fourier transform infrared (FTIR) spectroscopy. The absorbance of aliphatic C-H decreased with heating time, indicating the degradation of aliphatic hydrocarbons. Both the presence of silica and embedding delayed the degradation of the aliphatic C-H. The absorbance ratios of 2960 cm-1 band (aliphatic CH3) to 2925 cm-1 band (aliphatic CH2) (R3/2 values) increased or changed little by the heating. Raman spectral features showed that some experimental products had a structural ordering similar to the Proterozoic microfossils, indicating that they were carbonized to a degree similar to the microfossils. These results reveal that the presence of silica and embedding affect the thermal degradation rate of aliphatic C-H in cyanobacteria but do not lead to the decrease in R3/2 values. The low R3/2 values of Proterozoic prokaryotic fossils from Bitter Springs and Gunflint Formations are not considered to be due to thermal degradation upon fossilization during diagenesis. Although other possibility cannot be ruled out, the results suggest that precursor lipids, having low R3/2 values, were selectively preserved in microfossils.

Keywords: micro-FTIR, cyanobacteria, silica, thermal alteration, aliphatic hydrocarbon

Japan Geoscience Union Meeting 2014
(28 April - 02 May 2014 at Pacifico YOKOHAMA, Kanagawa, Japan)

U05-P11 Room:Poster Time:April 30 18:15-19:30

Role(s) of extracellular polymeric substance in microbial mineralization

NAKAMURA, Yuki[1*] ; SHIRAISHI, Fumito[1]

[1]Hiroshima University

Microbialites are defined as organosedimentary deposits that have accreted as a result of benthic microbial community binding detrital sediment or forming the locus of mineral precipitation. Most of microbialites are consisted of carbonate minerals, and considered to be formed by microorganism, such as cyanobacteria and sulfate reducing bacteria. Microbialite records the history of interaction between life and Earth environment, and therefore, it is important to understand their formation. Microbialites are formed mainly by three processes, including grain-trapping, mineral precipitation by metabolism and mineral nucleation by extracellular polymeric substances (EPS). Grain-trapping is locally important, but key processes are precipitation and nucleation. The knowledge of precipitation process by bacterial metabolism has increased, while that of EPS is still limited. Therefore, this study aims to investigate the influences of EPS on microbialite formation. We examined carbonate deposit developed at Kibedani hot spring, Shimane Prefecture. Calcite was despite of undersaturation in bulk water. Microerectrode measurement revealed that this deposit is formed as a result of photosynthesis-induced $CaCO_3$ precipitation. The result of EPS staing observation by Confocal Laser Scanning Microscope revealed that this deposit contains abundant acidic EPS, which is generally considered to have important roles in mineral nucleation. This deposit composed of two layers: the upper layer is consisted of empty EPS sheaths and the lower layer is of cyanobacteria with EPS sheaths. Both layers contain acidic EPS, while only lower layer was mineralized. This observation implies that acidic EPS cannot solely cause nucleation, and requires high mineral saturation state induced e.g.by photosynthesis.

Japan Geoscience Union Meeting 2014
(28 April - 02 May 2014 at Pacifico YOKOHAMA, Kanagawa, Japan)

U05-P12 Room:Poster Time:April 30 18:15-19:30

Controlling factors of microbialite textures inferred by a tufa deposit

HANZAWA, Yuhsaku[1*] ; OKUMURA, Tomoyo[2] ; SHIRAISHI, Fumito[1]

[1]Hiroshima university, [2]Japan Agency for Marine-Earth Science and Technology

Microbialite is organosedimentary deposits that are formed by the interaction between life, water and mineral. It has accreted as a result of a benthic microbial community trapping and binding detrital sediment and/or forming the locus of mineral precipitation. Typical examples of microbialite are laminated stromatolite, and clotted thrombolite. In the Earth history, stromatolite appeared from about 3500 Ma, followed by its peak at 1300 Ma. At about 500 Ma, stromatolite rapidly declined, and thrombolite appeared. Although this transition is considered to reflect evolution of life and Earth environment, its detail is still not well understood. To understand the basic mechanisms forming microbialites, the geomicrobiological studies of recent samples are essential. While microbialite in modern marine environment is scarce, it is relatively common at freshwater environment as a tufa. The present study focuses on tufa for investigating the relationship between depositional structure and microbial composition. Tufa deposit usually has laminated structure resembling stromatolite. However, tufa deposit developed in Takahashi city (Okayama prefecture) exhibits both stromatolitic and thrombolitic structures by reflecting the difference of hydrodynamic condition. The chemical compositions of creek water at the sites where stromatolitic and thrombolitic tufa are depositing are almost the same, and similar to that of common tufa-depositing creek. Extracellular polymeric substances (EPS) staining observation applied for deposits surface by Conforcal Laser Scanning Microscope (CLSM) showed that the distribution patterns of phototrophs and EPS were different between stromatolitic and thrombolitic tufa. At the surface of thrombolitic tufa, coccoid cyanobacteria densely colonized to form small mounds (500 μm in diameter) and EPS located inner and marginal part of the mounds. On the other hand, at the surface of stromatolitic tufa, filamentous cyanobacteria distributed sparsely with EPS, and calcite was widely exposed. Vertical thin section observation revealed that there were large calcite crystals (500 μm in diameter) at the surface of thrombolitic tufa, and filamentous one colonized around them. Stromatolitic tufa, on the other hand, was consisted of fine grained calcite (10 μm in diameter) with filamentous cyanobacteria colonized perpendicular to the lamination. Microbial composition of both deposits was examined by 16S rRNA gene analysis. The result indicated that cyanobacteria were abundant and some strains were common between thrombolitic and stromatolitic tufa. However, the diversity of microbial population microbial population was higher in thrombolitic tufa than stromatolitic ones.

From the results above, it is inferred that the transition from stromatolite to thrombolite in $\sim$500 Ma was caused by microbial diversification and resultant EPS composition change.

Keywords: microbialite, stromatolite, thrombolite, tufa, carbonate rock

Japan Geoscience Union Meeting 2014
(28 April - 02 May 2014 at Pacifico YOKOHAMA, Kanagawa, Japan)

U05-P13 Room:Poster Time:April 30 18:15-19:30

Soil micromorphology and the effect of biotic activity

SUZUKI, Shigeyuki[1*] ; HATTORI, Tsutomu[2] ; HATTORI, Reiko[2] ; MIMURA, Kaori[3] ; ISHIGURO, Munehide[4]

[1]Okayama University, [2]Atic Laboratory, [3]Kanematsu-NNK Corporation, [4]Hokkaido University

Soil is formed on a boundary between geosphere and biosphere in relation with hydrosphere and atmosphere. The major component is quite very fine-grained particles which are not still unknown in detail. A great variety of microbes are associated in soil (e.g., Hattori, 1987). Hattori (2006) suggests that there is a possibility some bacteria produce very fine-grained mineral particles, silica-nano particle as a part of soil material. Micromophology is observed under petrological microscope. The technique for preparation to make thin section from unconsolidated soil is followed by method in FitzPatrick (1993). Soil fragments are examined by scanning electron microscope. Samples are collected from recent cultivated soil (Okayama University Farm), fluvial soil (Sendai City), rice field soil (150 to 2000 years old fluvial soil from Okayama University), paleosol (about 3000 years old organic rich fluvial soil from Dhaka City, Bangladesh).

The formation of microaggregates: The structure of soil macroaggregate (1∼2mm) which is composed of microaggregates (0.05∼0.3mm) and sand grains of mineral and rock fragments is observed in the recent cultivated soil from Okayama University Farm. Similar microaggregates (0.1∼0.5mm), structure with heterogeneous granular domains is observed in rice field soil from Okayama University. A paleosol from Dhaka, which is not considered to have artificial effects, also consists of microaggregate. The aggregates do not have distinctive boundary but are distinguished by different compositions (content of organic materials, deposited ferri-hydrite and .manganese dioxide, particles of mineral and rock fragment). Root pipes and cracks are associated in the soil. The compound structure is interpreted to be formed under effects of microorganisms, root and physical process as demonstrated by previous soil research (e.g., FitzPatrick, 1993).

The formation of silica-nano particle: Under scanning electron microscope, surface of mineral grain has structures caused by weathering, for example embayment, fracture and etch pit. Crystallized nano-sized minerals are formed on weathered surface of a mineral. A bacterial cell surrounded by radiate fibrous mineral is found. The feature indicates a possibility that some bacteria promote to form minerals. And also there is a possibility that a part of inorganic soil materials might be formed relation with organism.

FitzPatrick, E.A. (1993) Soil Microscopy and Micromorphology, Wiley
Hattori, T. (1987) Microbial life in the soil, Iwanami
Hattori, T. (2006) Soil Microorganisms, 60(2), 105-107

Keywords: soil, microaggregate, silica-nano particle, bacteria

Japan Geoscience Union Meeting 2014
(28 April - 02 May 2014 at Pacifico YOKOHAMA, Kanagawa, Japan)

U05-P14 Room:Poster Time:April 30 18:15-19:30

A novel remediation method for nickel-bearing wastewater at neutral conditions

OKAHASHI, Haruko[1*] ; NISHIUCHI, Toru[1] ; SATO, Tsutomu[2] ; OTAKE, Tsubasa[2] ; YONEDA, Tetsuro[2]

[1]Graduate School of Engineering, Hokkaido University, [2]Faculty of Engineering, Hokkaido University

Advances in technology such as the electronics and metal plating industries have increased the demand of Ni year by year. On the other hand, the resources are unevenly distributed in a few countries and the supply is highly dependent on strategic policies. Moreover, since Ni is not produced in Japan and it is dependent on imports from foreign countries, the supply structures of Ni are vulnerable. Because of this, the necessity of recovering Ni from wastewaters and other waste forms has been increasing. Some industrial wastewaters contain large amounts of Ni. Generally, the removal of Ni from contaminated wastewater by adding antalkaline and flocculants to increase the pH to 10 or above would result in the generation of Ni-hydroxides after treatment. After that, it is necessary to adjust the pH below the effluent standard (pH 5.8∼8.6). However, this method suffers from some disadvantages, such as the high cost for chemical reagents, problems in the disposal of alkali sludge and inefficient treatment system. Therefore, a more sustainable remediation method must be developed to achieve sustainable wastewater treatment operations. This study focused on natural attenuation processes which are safer, cost-effective and more environmentally friendly than traditional methods. For example, at Dougamaru abandoned mine in Japan, high concentrations of Cu and Zn in wastewater are naturally incorporated in the structure of layered double hydroxides (LDH), which forms in the presence of Al ions, hence, natural attenuation of Cu and Zn occurs (Okamoto et al., 2010). Because LDH has the hydroxide structure, six-coordinated heavy metals such as Cu, Ni and Co can be incorporated into the structure during the formation process. Therefore the objective of this study is to develop a remediation method for Ni-bearing wastewaters at neutral conditions, and to clarify the behavior of Ni in the neutralization and precipitation process.

In this context, to check the applicability of LDH in the treatment of Ni-bearing wastewaters, synthesis experiments were carried out by co-precipitation of Ni-bearing LDHs containing SO_4^{2-} as the interlayer anion with different concentrations of dissolved Al ions. Analysis of water chemistry before and after the co-precipitation show that the removal efficiencies of Ni from the synthetic wastewaters increased with increasing dissolved Al concentration. The results further show that the presence of Al in the formation of LDH removed Ni at pH values lower than previous methods which precipitated Ni-hydroxides. It is expected that treatment costs will be reduced in actual wastewater treatment systems because Al addition leads to the reduction of antalkaline use and the neutralization process.

Ni adsorption experiments and extraction experiments were conducted to investigate the sorption behavior of Ni. Only a small amount of Ni was adsorbed to LDH and basaluminite (major minerals in coprecipitation experiments) as inner- and outer-sphere complexes. From the result of XAFS analysis, Ni was incorporated into the structure by being able to precipitate LDH selectively. This shows Ni is fixed securely in the structure of LDH and that the mobility of Ni will be governed by the solubility of LDH. Thermodynamic modeling suggests that the precipitation of LDHs with the optimum Al/Ni molar ratio (0.25∼0.50) is determined by the initial conditions (e.g. pH, Al, Ni concentrations). Furthermore, modeling results reproduce the experimental results such as removal efficiency and mineral species well, opening the possibility of its application in actual wastewater treatment operations.

Keywords: Remediation, Layered double hydroxide, Nickel

Japan Geoscience Union Meeting 2014
(28 April - 02 May 2014 at Pacifico YOKOHAMA, Kanagawa, Japan)

U05-P15 Room:Poster Time:April 30 18:15-19:30

Changes in water properties and microbial facies along a flow path of a travertine developed in northern Sumatra Island,

TAKASHIMA, Chizuru[1*] ; HIRANO, Misa[1] ; OKUMURA, Tomoyo[2] ; KANO, Akihiro[3]

[1]Saga Univ., [2]JAMSTEC, [3]Kyushu Univ.

Sumatra Island has many hot springs related with volcanoes belonged to the Ring of fire. Geothermal studies for these hot springs have been performed actively, but hot spring sediments including travertines have rarely been reported. Travertine is a useful modern analog for the Precambrian stromatolites (Takashima and Kano, 2008; Okumura et al., 2013).

We studied travertines at Sipoholon hot spring located about 30 km south from the Lake Toba which is the largest caldera lake in the world. The travertines spread in total area of 50,000 km^2, in which active deposition occurs mainly in three separated sites; Area A, B and C from north to south, respectively. This study focused on Area A that lacks artificial effect.

In this study, we measured chemical components and stable isotopes of water and observed textures and bacteria of the travertine. Based on these results, we cleared that relationship between water properties, travertine textures and distribution of bacteria.

The travertine deposit occurs along ~35-m-long flow path. The water from the vent first flows 15 m on a narrow (50 cm) and gentle passage and then widely on a steep slope on the travertine dome. Below the dome, the water passes on terrace-like rim pools and finally flows into a pool about 5 m in diameter.

The water with sulfurous smell emits from a vent at a rate of 286 L/min. This water is high temperature (61.4 degree Celsius), neutral pH (6.48) and microaerobic (DO of 0.6 mg/L). The water is rich in Ca^{2+} and $SO_4{}^{2-}$, and poor in Mg^{2+} and Cl^-. To the downstream, the water temperature decreases, pH increase, and conversely alkalinity and Ca^{2+} concentration decrease. These and increased carbon isotope of dissolved inorganic carbon indicate that CO_2 degassing increased supersaturation and induced deposition of calcium.

The travertine in Sipoholon hot spring is mainly composed of aragonite, but in one place, calcite coexists. It tends to become softer from the upstream to the downstream. This may reflect difference in crystal shape and texture. The harder travertines consist of tightly packed spherical aggregates of aragonite needles, while softer travertines have loose textures containing dumbbell-shape crystals.

Microbial facies on the travertine surface changes obviously from the upstream to the downstream. A white sulfur-turf in upper stream is composed of sulfur oxidizing bacteria with sulfur particles (Maki et al., 2004). It is known that the sulfur-turf prefers in high temperature, neutral pH and rich in hydrogen sulfide, which corresponds the conditions of the upstream. On high flow parts of the travertine dome, the travertine colored in pale pink likely due to the occurrence of purple sulfur bacteria. Green microbial mat covers the travertine deposited in in lower part with low flow rate. The mat is composed of filamentous bacteria with photosynthesis pigment identified in fluorescence observation. These are cyanobacteria. Water temperatures on the mat are all below 45 degree Celsisu. Thus, color change of travertine surface reflect that of microbial composition responded to water properties, such as water temperature, flow rate, flow volume, nutrient.

[References]

Takashima, C. and Kano, A. (2008) Microbial processes forming daily lamination in a stromatolitic travertine. Sedimentary Geology, 208, 114-119.

Okumura, T., Takashima, C., Shiraishi, F., Nishida, S., Kano, A. (2013) Processes forming daily lamination in a microbe-rich travertine under low flow condition at the Nagano-yu Hot Spring, Southwestern Japan. Geomicrobiology Journal, 30, 910-927.

Maki, Y., Ogawa, K. and Shimizu, A. (2004) A model for syntrophic cooperations in microbial mats on pristine Earth: Structure-function relationship of sulfur-oxidation in sulfur-turf microbial mat vegetating in hot spring effluents. Viva Origino, 32, 96-108.

Keywords: travertine, aragonite, sulfur oxidizing bacteria, cyanobacteria

Japan Geoscience Union Meeting 2014
(28 April - 02 May 2014 at Pacifico YOKOHAMA, Kanagawa, Japan)

U05-P16 Room:Poster Time:April 30 18:15-19:30

A study of irregular shaped tests formation of planktonic foraminifera

HORI, Masako[1*] ; SHIRAI, Kotaro[1] ; TAKAHATA, Naoto[1] ; SANO, Yuji[1] ; KURASAWA, Atsushi[2] ; KIMOTO, Katsunori[2]

[1]Atmosphere and Ocean Research Institute, The University of Tokyo, [2]Japan Agency for Marine-Earth Science and Technology

Planktonic foraminifera are protist forming carbonate tests. They are used as useful index fossils, and moreover, the oxygen isotopic and trace element compositions in their calcite tests are recognized as a promised archive representing paleo-ocean environments. Foraminifera generally consist of multipul chambers, and each chamber forms spirally for the center of the first chamber. Culturing observations have contributed for understanding relationships between trace elements and isotopic indices, and environmental factors. However, the transfer of elements and trigger of test formation are poorly understood. Cultured specimens sometimes show irregular-shaped tests, which are unlikely formed under natural condition in the ocean.

In this study, we focused the test formation of planktonic foraminifera, and cultured two species (*Globigerina bulloides*, *Globigerinoides ruber*) collected at Sagami bay. Culturing temperature was controlled at 19, 21, 23 and 25 ℃. Calcium isotopic reagents were added to the culturing seawater to mark the timing of test formation. Moreover, we also investigated the other specimens cultured with seawater, whose calcium concentration was raised for 10% respective to the original concentration. In those cases, the pH of calcium reagents were adjusted to appropriate pH, and therefore, the seawater pH was kept at constant during the observation.

As a result, three of ten specimens of *G. ruber* have newly formed a regular test at 19, 21 and 23 ℃. On the other hand, 5 of 7 specimens of *G. bulloides* have formed new tests, three of which have formed irregular shaped tests. These three specimens are ones survived more than a couple of weeks after sampling. The water temperature of irregular test formation was 21 or 25 ℃, suggesting that the temperature was not a direct controlling factor of irregular test formation. Potential factors are concentrations of dissolved oxygen or dissolved organic matters. Foraminifera first forms organic layer called POM at the beginning of test formation. Anomalously high organic concentration in crystallization liquid may impede the regular formation of POM, consequently resulting in the formation of irregular-shaped tests.

For the specimens with increasing calcium concentration of seawater, the spines fell out within 12 hours. Because calcium is an essential element not only for test formation but also various biological reactions, rapid increase of calcium concentration might disturb the biofunction of planktonic foraminifera.

Keywords: planktonic foraminifera, laboratory culture

Japan Geoscience Union Meeting 2014
(28 April - 02 May 2014 at Pacifico YOKOHAMA, Kanagawa, Japan)

U05-P17 Room:Poster Time:April 30 18:15-19:30

Anion adsorption and post-adsorption behavior of metastable iron hydroxides

KODAMA, Ritsu[1*] ; OKAHASHI, Haruko[1] ; YAMAMOTO, Takato[1] ; SATO, Tsutomu[1] ; OTAKE, Tsubasa[1] ; YONEDA, Tetsuro[1]

[1]Laboratory of Environmental Geology, Hokkaido university, Graduate School of Engineering, Hokkaido U

Pollution by dissolved anions has been a pertinent environmental concern in many areas around the world. For example, acid mine drainage from abandoned mines and contaminated waters resulting from the Fukushima nuclear power plant accident emphasize the importance of predicting the behavior of the dissolved trace elements on Earth ' s surface environments. Iron minerals may play a potentially important role in the control of dissolved trace elements in the environment. In particular, poorly crystalline iron minerals exhibit excellent adsorption capacities for toxic anions due to their high specific surface areas and reactivity. In order to evaluate the potential of poorly crystalline iron minerals as stable sinks of dissolved hazardous ions, it is necessary to investigate the adsorption mechanism on these minerals and their post-adsorption behaviors.

Adsorption experiments using arsenate, phosphate, chromate, sulfate, selenate, fluoride, and chloride were performed to investigate the selectivity of Schwertmannite and Ferrihydrite for various anions. Adsorption selectivity decreases in the following order: $H_2AsO_4^-$ › $H_2PO_4^-$ › $HCrO_4^-$ › $SeO_4^{2-} \fallingdotseq SO_4^{2-} \gg F^- \fallingdotseq Cl^-$. Schwertmannite and Ferrihydrite didn ' t have an ability to adsorb F^- and Cl^-.The adsorption mechanism of these anions was investigated using zeta potential measurements. The results indicated that $H_2AsO_4^-$, $H_2PO_4^-$ and $HCrO^{4-}$ formed inner-sphere complexes while SeO_4^{2-} and SO_4^{2-} formed outer-sphere complexes. The adsorption mechanism of these anions to both Scwertmannite and Ferrihydrite is generally similar, except in the case of $HCrO_4^-$.

Accelerated alteration experiments were performed to observe post-adsorption behaviors of Schwertmannite and Ferrihydrite. Oriented specimens loaded with varying amounts of adsorbed anions were aged under saturated water vapor pressure conditions at 50 ℃ for 30 days and analyzed by XRD. Results show that larger amounts of adsorbed anions delay the transformation of Schwertmannite and Ferrihydrite into more stable phases, indicating that adsorption of anions, particularly as inner-sphere complexes, stabilizes poorly crystalline iron minerals.

These results show that poorly crystalline iron minerals are capable of taking up a range of toxic anions from contaminated waters and that the stability of these minerals will be affected by the amount of anions sorbed on the surface. These suggest that poorly crystalline iron minerals may serve as stable, long-term sinks for toxic anions.

Japan Geoscience Union Meeting 2014
(28 April - 02 May 2014 at Pacifico YOKOHAMA, Kanagawa, Japan)

U05-P18 Room:Poster Time:April 30 18:15-19:30

Anion adsorption and post-adsorption behavior of metastable calcium carbonate polymorph

YAMAMOTO, Takato[1*] ; KODAMA, Ritsu[1] ; SATO, Tsutomu[1] ; OTAKE, Tsubasa[1]

[1]Laboratory of Environmental Geology, Hokkaido University

In Japanese transuranic (TRU) waste disposal facilities, I-129 is the most important radionuclide that must be considered in long-term safety assessments of the repository. However, the degradation of cement materials used in the repositories can produce high pH pore fluids that can affect to anion transport behavior. Therefore, it is necessary to understand the behavior of anions such as I- in hyperalkaline conditions. Examples of I- behavior in natural hyperalkaline environments, such as in Oman, show that I^- is taken up by aragonite, opening up the possibility of calcium carbonates as inhibitors of I^- migration. This concept is currently being applied in the development of the Advanced Liquid Processing System (ALPS), which employs carbonate coprecipitation to treat contaminated waters resulting from the Fukushima Daiichi nuclear power plant accident. However, the stability of the carbonate phases precipitated in this system as well as the anion uptake capacities of these phases are poorly understood. In a previous study, (Kasahara, 2012), it was found that monohydrocalcite (MHC), a precursor of aragonite, affects the iodine capacity of aragonite, making it a possibly important material that can control the behavior of anions..The objective of this study therefore, is to investigate the sorption capacity of MHC for anions and its stability. MHC (Mg^{2+}/Ca^{2+}=6; $Ca^{2+}/{CO_3}^{2-}$=1) was synthesized and used for sorption experiments involving F^-, Br^-, I^-, ${IO_3}^-$, ${SO_4}^{2+}$, ${CrO_4}^{2-}$, ${HAsO_4}^{2-}$, and phase transformation experiments. Results show that Kd values of ${HAsO_4}^{2-}$ and F^- on MHC are high, while ${IO_3}^-$, ${SO_4}^{2-}$ are relatively low. On the other hand, Br^-, I^-, ${NO_3}^-$, ${CrO_4}^{2-}$ were not taken up. It is because MHC has high chemical reactivity and high specific surface (4 times large of aragonite, 15 times large of calcite), in addition MHC is most low density of calcium carbonate, so MHC can takes up relatively large amount of anions than other calcium carbonate. And other thing, MHC involves Mg^{2+} abundantly. This study indicates that Mg^{2+} form fluoride adsorption site. Results of the transformation experiments show that MHC with no adsorbed anions easily transforms into a stable phase, whereas MHC loaded with increasing amounts of anions transform after longer durations. It is because the driving force for the transformation decreases with the anions content in the solution. In conclusion, MHC can take up fluoride and oxyanions that ionic radii is similar to carbonate but larger than that. In addition, MHC is stabilized as a function of uptake amount of anions.

Japan Geoscience Union Meeting 2014
(28 April - 02 May 2014 at Pacifico YOKOHAMA, Kanagawa, Japan)

U06-01 Room:503 Time:April 28 09:00-09:15

On activities in the interdisciplinary science of Hayabusa-2

KOBAYASHI, Naoki[1*] ; WATANABE, Sei-ichiro[2] ; THE INTERDISCIPLINARY SCIENCE TEAM, Hayabusa-2[1]

[1]ISAS/JAXA, [2]Division of Earth and Planetary Sciences, Graduate School of Science, Nagoya University

Hayabusa-2 is an asteroid sample return mission of which target asteroid is 1999JU3, a near Earth asteroid of type C, and it is scheduled to be launched late in this year. As on-board scientific instruments, Hayabusa-2 has a near infrared spectrometer (NIRS3), thermal IR imager (TIR), optical navigation camera (ONC-T) used as a multi-band imager with seven band-pass filters, laser altimeter (LIDAR), sampler (SMP), small carry-on impactor (SCI), separation digital camera (DCAM-D), and small lander (MASCOT). Using these instruments, we try to characterize the surface properties and materials of 1999JU3 and select three sampling points from which material samples will be obtained to reveal physical and chemical processes on the asteroid and its history from the formation to the present. Thus scientific success of Hayabusa-2 strongly depends on a strategy for characterizing the surface and selecting sampling sites, which can be achieved making the best use of data from the above all sensors. We, for this purpose, organize a working team called as the Interdisciplinary Science Team (IDST) of Hayabusa-2. In this presentation, we introduce the activity of the IDST.

The IDST was established in the first meeting held on Dec. 2012. Its purposes are to obtain the general picture of a scientific scenario of Hayabusa-2, define interdisciplinary science themes and contribution of individual instruments to the themes, define scientific constraints and validations on the mission scenario, and promote planetary sciences and think out planetary sciences from a standpoint of the asteroid mission. The discussion in the IDST is open to the project members. So far, we have discussed deeply a strategy in return sample analyses, heterogeneity detection by the remote sensing sensors, surface temperature detection, crater chronology, morphology produced by meteoroid impacts, reflectance spectra of C-type asteroids, space weathering, and so on. As a result of these discussion, we produce a logical flow chart to characterize the surface material and property. In the chart, mutual relations between basic observation quantities, quantities inferred by multiple sensors, their indexes, identified characters and general inferences on primitiveness are described. Contributions from each sensor are clarified in the chart. In addition, we also depicted an operational picture of SCI which is a grand experiment for an impact process in the low gravity space and exposes material in a depth that can be less suffered by space weathering, but SCI is wasteful of the satellite resources. It is necessary to polish up the operation plan of SCI from the view point of the system resources.

The logical flow chart is a guiding principle in the science of the Hayabusa-2 mission. We continue to refine the chart and complete the logic. For this purpose, we make several working groups to reinforce the logic flows. As closing the development phase of on-board instruments, we now rush up to make the IDST of Hayabusa-2 more active. We think that the activity in the IDST is a key point to succeed in the science mission and promote planetary sciences and explorations in Japan.

Keywords: Hayabusa-2, asteroid, exploration, surface material, interdisciplinary science, sample return

Japan Geoscience Union Meeting 2014
(28 April - 02 May 2014 at Pacifico YOKOHAMA, Kanagawa, Japan)

U06-02 Room:503 Time:April 28 09:15-09:30

Detectability of 0.7 um absorption band of hydrous minerals using the Hayabusa2 ONC-T Flight Model

KAMEDA, Shingo[1*] ; AKITO, Takei,[1] ; SATO, Masaki[1] ; OKUMURA, Yu[1] ; CHO, Yuichiro[2] ; ONC, Science team[3]

[1]Rikkyo University, [2]The University of Tokyo, [3]JAXA

Hayabusa2 has three cameras for optical navigation to the asteroid 1999JU3. ONC-T is one of them and it can be used also for reflectance spectroscopy. The results of the ground-based observation suggested that hydrous materials might remain on the 1999JU3 but on the small part of the surface. To bring them to the Earth, we should perform reflectance spectroscopic observation near the asteroid using ONC-T to locate the point where hydrous mineral is rich.

In this presentation, we will report the result of final calibration test of ONC-T and discuss the detectability of hydrous minerals on 1999JU3.

Japan Geoscience Union Meeting 2014
(28 April - 02 May 2014 at Pacifico YOKOHAMA, Kanagawa, Japan)

U06-03 Room:503 Time:April 28 09:30-09:45

Development and tests of Hayabusa-2 LIDAR

NAMIKI, Noriyuki[1*] ; MIZUNO, Takahide[2] ; SENSHU, Hiroki[1] ; YAMADA, Ryuhei[3] ; NODA, Hirotomo[3] ; SHIZUGAMI, Makoto[3] ; HIRATA, Naru[4] ; IKEDA, Hitoshi[5] ; ABE, Shinsuke[6] ; MATSUMOTO, Koji[3] ; OSHIGAMI, Shoko[3] ; YOSHIDA, Fumi[3] ; HIRATA, Naoyuki[7] ; MIYAMOTO, Hideaki[7] ; SASAKI, Sho[8] ; ARAKI, Hiroshi[3] ; TAZAWA, Seiichi[3] ; ISHIHARA, Yoshiaki[2] ; KOBAYASHI, Masanori[1] ; WADA, Koji[1] ; DEMURA, Hirohide[4] ; KIMURA, Jun[9] ; HAYAKAWA, Masahiko[2] ; KOBAYASHI, Naoki[2] ; MITA, Makoto[2] ; KAWAHARA, Kousuke[2] ; KUNIMORI, Hiroo[10]

[1]PERC/Chitech, [2]ISAS/JAXA, [3]NAOJ, [4]The University of Aizu, [5]ARD/JAXA, [6]Nihon University, [7]The University of Tokyo, [8]Osaka University, [9]Tokyo Institute of Technology, [10]NICT

The Japanese first asteroid mission, Hayabusa, visited at the small asteroid 25143 Itokawa in September, 2005. Images taken by Hayabusa are combined with other remote sensing observations and revealed that the asteroid as small as 500 m in the longest axis is the first rubble-pile body identified in our solar system. Despite of several serious failures of the spacecraft occurred during and after rendezvous, Hayabusa successfully retrieved samples from the surface of 25143 Itokawa to the Earth in 2010 to disclose unpredicted nature of a very small asteroid.

JAXA and collaborating scientists are now developing the second asteroid mission named ”Hayabusa-2”. Hayabusa-2 is based on a heritage of the first Hayabusa. At the same time, Hayabusa-2 is intended to improve engineering and scientific achievements of the first Hayabusa, and also to challenge new technologies. Furthermore, target asteroid is different from that of the first Hayabusa. The asteroid 25143 Itokawa is a silicate-rich S-type. On the other hand, Hayabusa-2 is visiting a C-type asteroid, (162173) 1999 JU3. Needless to say, C-type is more primitive than S-type, therefore is expected to be a key to understand chemical evolution of the early solar system.

LIDAR measures altitudes of the spacecraft from the surface of the asteroid by taking a time of flight of laser pulse. As a part of Attitude and Orbit Control System (AOCS), the LIDAR data are used for navigation of the spacecraft. The data are particularly important during touchdown operation. Besides, the LIDAR data are served for scientific analysis of the shape, mass, and surface properties of the asteroid in order to elucidate physical evolution of minor bodies such as impact fragmentation and coagulation. We also wish to expand outcomes of Itokawa exploration by examining uniformity and variation of porosity within rubble-pile body and detecting dusts levitating above the surface of asteroid. The remote sensing observations of Hayabusa-2 will be carried out from Home Position (HP), middle altitude, and low altitude whose distances from the asteroid surface are nominally 20 km, 5 km, and 1 km, respectively. We report recent progress of LIDAR development anticipating the launch in December 2014.

Keywords: Hayabusa, asteroid, exploration, LIDAR

Japan Geoscience Union Meeting 2014
(28 April - 02 May 2014 at Pacifico YOKOHAMA, Kanagawa, Japan)

U06-04 Room:503 Time:April 28 09:45-10:00

A strategy to estimate thermal properties using Thermal Infrared Imager on board Hayabusa-2.

SENSHU, Hiroki[1*] ; TAKITA, Jun[2] ; TANAKA, Satoshi[3] ; OKADA, Tatsuaki[3]

[1]PERC/Chitech, [2]Graduate School of Science, Tokyo University, [3]ISAS/JAXA

Thermal InfraRed imager (TIR) on board Hayabusa-2, an upcoming japanese mission to C-type asteroid 1999JU3, is non-cooled bolometer which image mid-infrared thermal emission from the asteroidal surface. The field-of-view (FOV) of TIR is 16x12 degrees and ts effective pixels are 320x240. So the spacial resolution, which depends on distance from the suface, is about 18m from an altitude of 20km (Home position) and less than 1m from an altitude of 1km.

By comparing the temperature distribution obtained by TIR and thermal evolution model, we can get thermophysical properties such as thermal inertia and emissivity. These parameters are diagnostic for the characteristic size of surafce grain.

In this presentation we will present our strategy to estimate the thermophysical properties from TIR observation.

Keywords: hayabusa-2, thermal infrared imager, surface temperature, thermal properties, thernal inertia, emissivity

Japan Geoscience Union Meeting 2014
(28 April - 02 May 2014 at Pacifico YOKOHAMA, Kanagawa, Japan)

U06-05 Room:503 Time:April 28 10:00-10:15

Relationship on Surface Morphology of Small Asteroids and Geopotential

HIRATA, Naru[1*] ; MATSUMOTO, Koji[2] ; KIMURA, Jun[3]

[1]ARC-Space/CAIST, The University of Aizu, [2]RISE Project, The National Astronomical Observatory of Japan, [3]The Earth-Life Science Institute (ELSI) of Tokyo Institute of Technology

We compared the distribution of smooth terrains with the geopotential map of the asteroid Itokawa, and demonstrate that the distribution of smooth terrains on Itokawa is strongly controlled by the geopotential distribution. Because the geopotential distribution of an asteroid can be estimated from its shape, rotation state and density, we can predict the distribution of smooth terrains on the asteroid from these observations.

Keywords: Asteroid, geopotential, smooth terrain, Itokawa, 1999JU3

Japan Geoscience Union Meeting 2014
(28 April - 02 May 2014 at Pacifico YOKOHAMA, Kanagawa, Japan)

U06-06 Room:503 Time:April 28 10:15-10:30

Spectral evolution of s-type asteroids suggested by principal component analysis of multi-band images of Itokawa

KOGA, Sumire[1*] ; SUGITA, Seiji[1] ; KAMATA, Shunichi[2] ; ISHIGURO, Masateru[3] ; HIROI, Takahiro[4] ; SASAKI, Sho[5]

[1]Graduate School of Frontier Sciences, The University of Tokyo, [2]Dept. of Earth and Planetary Sci., UC Santa Cruz, [3]Depertment of Physics and Astronomy, Seoul National University, [4]Depertment of Geological Science, Brown University, [5]Department of Earth and Space Science, Graduate School of Science, Osaka University

Objective

Itokawa is covered with materials from the same initial material with different degree of space weathering[1,2]. However, it has not been verified sufficiently if there is other factors that change the spectra. Our analyses of principal component analysis (PCA) using multi-band images taken by Hayabsa's AMICA (Asteroid Multi-band Imaging CAmera) so far have provided the results that a component of spectral reddening, a typical trend of space weathering effect, is the first principal component (PC1) with comparison to laser-irradiated meteorites spectra. The comparison with main-belt asteroids suggests how the spectra of the asteroids develop in their PC space with weathering (by micrometeorites bombardment[3])[4]. However, further analysis had been impeded by electromagnetic noise. In this study, we remove the noise and examine spectral change trends caused by processes other than space weathering.

Methods

We used 2 sets of images of six visible bands (Central wavelengths of 381, 429, 553, 700, 861, 960 nm) taken by AMICA. Periodic electromagnetic noise is imposed on most of the images. We removed it by subtracting superposition of sine waves. The images were calibrated following [4] and coresistrated. Normalized ratio images were obtained by dividing the images by those of 553 nm.

We performed PCA on the normalized reflectance spectra. We used a set of images of a Itokawa semisphere and another set including a dark rock (Black Boulder). Shock darkening is indicated as a possible origin of it [5].

We also performed PCA on spectra of main-belt asteroids obtained in ECAS [6] and each Itokawa spectrum superimposed. Because AMICA and ECAS filter wavelengths are approximately same, we can compare the Itokawa surface in the PC space defined by ECAS data set.

Results

The PC1 of spectra of only Itokawa had a shape rising to the right with a steep rise in 430-700nm. The PC1 score spatial distribution was consistent with the distribution of space weathering degree obtained by [7]. PC2 had positive coefficients at the wavelengths except 553nm, and the spectrum shape was upward to both sides. The PC2 is different from sillicate spectra, therefore interpretation in a context of material science is difficult. We found a feature that PC1 score is low and PC2 score high in boulder-rich regions, but the muximum area of PC2 score lay around a boulder where PC1 score were minimum. Proportion of variance of PC1 and PC2 was 60-75% and 20-30%.

In the ECAS-defined PC space, the spectra of Black Boulder were distributed apart from the cluster of the other parts.

Discussion

The proportions of variance of PC1 and PC2 would suggest that the heterogeneity in Itokawa surface spectrum is dominated by two processes. The PC1 and PC2 score distribution might suggest that the process which changes PC2 score occurs where space weathering has moderately developed. We have observed only a part of the surface, and features observed in a global analysis will be reported in our presentation.

The fact Black Boulder spectral trend is different from that of the other parts suggests that another process than space weathering (shock darkening is a candidate) is the origin of its peculiar spectrum.

In this analysis, another trend than the general space weathering was captured. Consideration of an evolution caused by larger impacts together as well as the space weathering caused by micrometeorites bombardment may enable us to constrain the spectral evolution processes of asteroids and derive relationships among asteroids of different spectral classes.

References

[1] Abe, M et al. (2006) Sci. 312, 1334. [2] Hiroi, T. et al. (2006) Nature 443, 56. [3] Sasaki, S. et el. (2001) Nature 410, 555-557. [4] Koga, S. et al. (2014) 45th LPSC, Abstract #1721 [5] Ishiguro, M. et al., (2010) Icarus,207, 714. [6] Hirata, N. and Ishiguro, M., (2011) 42nd LPSC, Abstract #1821. [7] Tedesco, E.F. et al. (1982) Astron.J. 87, 1585. [8] Ishiguro, M. et al. (2007) MAPS 42, 1791.

Japan Geoscience Union Meeting 2014
(28 April - 02 May 2014 at Pacifico YOKOHAMA, Kanagawa, Japan)

U06-07 Room:503 Time:April 28 11:00-11:15

Small carry-on impactor of Hayabusa2

SAIKI, Takanao[1*] ; IMAMURA, Hiroshi[1] ; SAWADA, Hirotaka[1] ; ARAKAWA, Masahiko[2] ; TAKAGI, Yasuhiko[3] ; KADONO, Toshihiko[4] ; WADA, Koji[5] ; HAYAKAWA, Masahiko[1] ; SHIRAI, Kei[1] ; OKAMOTO, Chisato[1] ; OGAWA, Kazunori[6] ; IIJIMA, Yuichi[1]

[1]Japan Aerospace Exploration Agency, [2]Kobe University, [3]Aichi Toho University, [4]University of Occupational and Environmental Health, [5]Chiba Institute of Technology, [6]University of Tokyo

Small Carry-on Impactor of Hayabusa2

A Japanese spacecraft, Hayabusa2, the successor of Hayabusa, which came back from the Asteroid Itokawa with sample materials after its 7-year-interplanetary journeys, is a current mission of Japan Aerospace Exploration Agency (JAXA) and scheduled to be launched in 2014. Hayabusa2 is a similar sample return mission to Hayabusa, however the type of the target asteroid is different from that of Hayabusa. Asteroid Itokawa, explored by Hayabusa is a rock-rich S-type one. Hayabusa2 will go to a C-type asteroid. Both C-type and S-type asteroids consist of rocks, but C-type asteroids are considered to have organic and water materials. Hayabusa2 has two objectives to discover: organic matters and water in the solar system and relationship between life and ocean water. C-type asteroids are the most common variety and many of them are in the outer part of the asteroid belt beyond 2.7 AU. An asteroid, called 1999 JU3, is chosen as the target of Hayabusa2 mission because it is considerably easy to reach. It has a similar orbit as that of Itokawa and it is in the orbit that occasionally comes close to the earth orbit.

The design of Hayabusa2 basically follows Hayabusa. Its configuration, size and weight are almost same as Hayabusa and the touch-down operation will be performed in much the same way. However, it is planned to be equipped with some new components. Small Carry-on Impactor (SCI) is one of the new challenges. The observations by Hayabusa discovered that Itokawa was rubble-pile body with the macro-porosity. No direct observational data as for their internal structures and sub-surface materials were available, however. One of the most important scientific objectives of Hayabusa2 is to investigate chemical and physical properties of the internal materials and structures in order to understand the history of formation of small bodies such as small, un-differentiated asteroids. In order to achieve this objective, the SCI is required to remove the surface regolith and create an artificial crater on the surface of the asteroid. Different from other impact missions, Hayabusa2 can make a detailed observation of the resultant crater after the impact. Observing the size of the crater is very important to investigate the physical properties of the asteroid. Additionally, Hayabusa2 will try to touchdown near the crater to get the fresh material of the asteroid.

It is very difficult to create a meaningful crater on the asteroid. High kinetic energy (i.e. about 2km/s impact speed and 2kg impact mass) is required to make a crater, but the high speed is difficult to realize. The famous impact mission, Deep Impact was the direct impact mission, which used the interplanetary velocity for the impact speed. Consequently, the impact energy became very high. On the other hand, SCI of Hayabusa2 is a carry-on type impactor and it should accelerate itself after the separation from the mother spacecraft. Therefore, how to accelerate the impact body is a big challenge of SCI. The traditional acceleration devices such as rocket motors and thrusters are difficult to hit the asteroid without a guidance system because the acceleration distance is large. To overcome this difficulty, the powerful explosive is use in SCI. The special type of shaped charge makes it possible to accelerate the impact head in a very short amount of time (less than 1 millisecond) and it becomes possible to crash into the asteroid.

The development of SCI is now almost finished. A lot of tests were conducted during the development period. The overview of the small carry-on impactor system and the results of the development tests will be presented in the conference.

Keywords: Hayabusa2, Impactor, Artificial Crater

Japan Geoscience Union Meeting 2014
(28 April - 02 May 2014 at Pacifico YOKOHAMA, Kanagawa, Japan)

U06-08 Room:503 Time:April 28 11:15-11:30

Small Carry-on Impactor Elucidates the Nature of Craters and the Evolution of our solar system

WADA, Koji[1*] ; SCI, Team[2] ; DCAM3, Team[2]

[1]PERC/Chitech, [2]Hayabusa-2 Project

Hayabusa-2, the Japanese next asteroid exploration mission, equips Small Carry-on Impactor (SCI) to launch a decimeter scale projectile on an asteroid surface. This is a novel apparatus to excavate the asteroid surface, and hopefully it will enable us to observe a fresh surface without space weathering and thermal alteration. Furthermore, we will be able to recover the asteroid sample excavated from several 10 cm depth at the deposit of the impact ejecta. The SCI impact on the asteroid is very good chance to examine the projectile scale on the crater scaling law in addition to the study on the gravity effect on the crater formation process. In this presentation, I will introduce the scientific goals of Hayabusa-2 mission using SCI and the scientific problems to be solved in the near future to maximize the scientific outputs of the SCI impact.

Keywords: Hayabusa-2, SCI, impact, asteroid

Japan Geoscience Union Meeting 2014
(28 April - 02 May 2014 at Pacifico YOKOHAMA, Kanagawa, Japan)

U06-09 Room:503 Time:April 28 11:30-11:45

The final impact tests of Small Carry-on Impactor(SCI) equipped on HAYABUSA-2

HAYAKAWA, Masahiko[1*] ; SAIKI, Takanao[1] ; IMAMURA, Hiroshi[2] ; SHIRAI, Kei[2] ; WADA, Koji[3] ; ARAKAWA, Masahiko[4] ; OKAMOTO, Chisato[2] ; TSUDA, Yuichi[1] ; TAKAGI, Yasuhiko[5] ; KADONO, Toshihiko[6] ; NAKAZAWA, Satoru[2] ; IIJIMA, Yuichi[1] ; YANO, Hajime[2] ; KAMITOMAI, Hideo[7] ; MATSUZAKI, Shinichi[7]

[1]ISAS/JAXA, [2]JSPEC/JAXA, [3]Planetary Exploration Research Center/Chiba Institute of Technology, [4]Graduate School of Science, Kobe University, [5]Aichi Toho University, [6]University of Occupational and Environmental Health, [7]NIPPONN KOHKI Co. ltd

HAYABUSA-2(the next Japanese Aseroid Sumple Return Explorer) is now at the final integrated test. Before this test, all sub-systems experienced final test individually. The Small Carry-on Impactor:SCI has been adopted the new sub-system of HAYABUSA-2, it is one of the self forging fragment which will be able to eject the 2kg projectile by 2km/sec velocity by detonation.

In this paper we show the outline and results of the final performance test of the SCI explosive part on Oct. 2013. The test bodies have be made by the same rot of flight model, and experienced environmental stress tests. The projectiles formed explosion impacted on the sand target and made craters.

A point of view of understunding of impact phenomina, these tests are larger scale impact experiments than thats made in labolatory, between space scale and labolatory scale. Therefore we observed and measured the crater formation prosesses by two high-speed video cameras, a infrared video camera, accelerometers, geophons, and digital handy video cameras. We succeeded to obtaine five cratering prosesses.

Keywords: HAYABUSA-2, Small Carry-on Impactor, impact experiment, crater, explosion

Japan Geoscience Union Meeting 2014
(28 April - 02 May 2014 at Pacifico YOKOHAMA, Kanagawa, Japan)

U06-10 Room:503 Time:April 28 11:45-12:00

Optical performance verification of DCAM3-D/Hayabusa 2

ISHIBASHI, Ko[1*] ; ARAKAWA, Masahiko[2] ; IIJIMA, Yuichi[3] ; OGAWA, Kazunori[4] ; SHIRAI, Kei[3] ; WADA, Koji[1] ; HONDA, Rie[5] ; SAWADA, Hirotaka[3] ; SAKATANI, Naoya[6] ; KADONO, Toshihiko[7] ; KOBAYASHI, Masanori[1] ; NAKAZAWA, Satoru[3] ; HAYAKAWA, Hajime[3] ; IKEDA, Yuji[8]

[1]Chiba Institute of Technology, [2]Kobe University, [3]Japan Aerospace Exploration Agency, [4]University of Tokyo, [5]Kochi University, [6]The Graduate University for Advanced Studies, [7]University of Occupational and Environmental Health, [8]Photocoding

Small Carry-on Impactor (SCI) is one of the instruments carried on Hayabusa-2 space craft. It will be used for an active exploration on the surface of asteroid 1999JU3. The SCI consists of a disk impactor made of copper. This disk will be accelerated to a velocity of ˜2km/s for the collision onto the asteroid surface, creating an artificial crater on 1999JU3. Then, samples in the crater and/or around the crater will be recovered by the Hayabusa-2 mother ship. Observation of the crater is expected to reveal the surface structure of 1999JU3. This SCI impact also has an aspect of an ”impact experiment” on an asteroid that elucidates the impact phenomena on small bodies.

A miniaturized optical camera unit (DCAM3) is being developed for observations of the SCI impact. DCAM3 will be detached from Hayabusa-2 mother ship and obtain a close-up image of the SCI impact. The detached part of DCAM3 has two cameras; one is an analog camera (DCAM3-A) and the other is a digital camera (DCAM-3D). The purposes of DCAM3-D are (1) the detection of SCI explosion and impact on the asteroid and (2) the observation of ejecta created by the SCI impact.

DCAM3-D optical system has to satisfy strict required specifications to fulfill these purposes: it requires a large view angle (74 deg) to detect both the SCI and the asteroid, high imaging capability for whole sensor area, a bright optical system (F $>$1.7) to detect dark SCI and ejecta, resistance to radiation, and limited size and weight . Moreover, these conditions have to be accomplished without active temperature control.

In this presentation we report the results of the optical performance verification of a flight model of DCAM3-D. The optical performance verification tests consist of electrical test, collimator test, and integration sphere test. The electrical test evaluated the performance of the CMOS sensor. In the collimator test, lens-sensor distance and lens-sensor angle were adjusted. Then, imaging capability (i.e., ensquared energy), spatial resolution, and distortion were evaluated under vacuum condition ($<$1 torr) with various temperatures, wavelength regions, and angles of view. In the integration sphere test, sensitivity, limb darkening, and stray light were evaluated. We confirmed that the results of these evaluations were favorable and that the strict required specifications of the optical system are almost satisfied.

Keywords: asteroid, planetary exploration, Hayabusa-2, scientific payload

Japan Geoscience Union Meeting 2014
(28 April - 02 May 2014 at Pacifico YOKOHAMA, Kanagawa, Japan)

U06-11 Room:503 Time:April 28 12:00-12:15

The effect of substrate structure of rubble-pile bodies on cratering process

TATSUMI, Eri[1*] ; SUGITA, Seiji[1]

[1]Graduate School of Frontier Science, The University of Tokyo

Introduction: Hayabusa obtained many high-resolution images and revealed that this asteroid has many unique morphological features which are not seen on other small planetary bodies. One of the most symbolic configurations are quasi-circular depressions (QCD) on boulder-rich surfaces, which are inferred as impact craters (Hirata et al,. 2009). If the QCDs are impact craters, then the surface crater retention age of Itokawa can be estimated based on crater chronology approach. However, age estimates has great uncertainty: 75Myr-1Gyr (Michel et al., 2009). The uncertainty in age results mostly from the uncertainty in crater scaling formed on the boulder-rich surface observed on rubble-pile bodies. The impact energy required for forming a crater on a small body is much smaller than that on a large body because of the limitation of catastrophic disruption energy (Benz and Asphaug, 1999). Impact cratering with such small energy on rubble-pile bodies are expected to follow a scaling low between the strength-regime rates and the gravity-regime cratering. The impactor destroys a surface boulder and dissipates its energy, then leading to a smaller crater: an armoring effect.

Moreover, impact induced mass loss is a critical value for estimating the life time of small bodies. The escape velocity of small bodies is very small. For example, Itokawa has an escape velocity of 10-20cm/sec. Thus, small bodies can easily lose their mass upon impact cratering.

As mentioned above, crater size and ejecta mass are important parameters for calculating the life-time of small bodies. However, these values for the rubble-pile bodies are not constrained well. Cratering process may be influenced greatly by the substrate structure of small bodies. In this study, the effect of the substrate structure of the rubble-pile bodies on the impact process is examined experimentally.

Experiment: Sintered glass beads blocks crashed into 8-15 mm chips and 200 micro meter glass beads are used as boulder simulants and regolith simulant in our experiments, respectively. We employ two types of targets: one consists of all boulders simulants (target 1) and the other consists of a surface layer of boulders simulants and regolith substrate (target 2). Polycarbonate projectiles 10mm diameter were launched at 160-180 m/sec of velocities. The impact cratering process was observed by a high-speed camera. We also measured the size of final crater and the ejecta mass.

Result: Crater size of target 1 is smaller by $\sim$20% than target 2, and ejecta mass of target 1 is smaller than by a factor of five than target 2. High-speed camera observations revealed that the surface boulders are destroyed by the impactor more heavily in the target 1. This difference occurs because the shock impedance of boulder simulants are larger than that of regolith simulant by a factor of ten and much stronger reflected stress waves comes back to the surface boulders for target 1, but the stress wave transmits efficiently from surface boulders to legolith layer in target 2.

These results suggest that the substrate structure of small bodies changes the impact process greatly. Crater size varies by $\sim$20% depending on substrate layers: boulders or regolith. Crater forming on bodies consisting of only boulder is smaller than bodies with regolith substrate but still much larger than crater on monolith (i.e., the scaling in strength-regime scaling). Consequently, the surface age of Itokawa could be on the younger side of the previous estimates as 75Myr-1Gyr with the strength-regime crater scaling. Furthermore, the substrate structures of the rubble pile bodies change the ejecta mass by 5 times. Rubble-pile bodies consisted of boulders possibly live longer.

Keywords: rubble-pile bodies, impact cratering, mass loss, fragmentation

Japan Geoscience Union Meeting 2014
(28 April - 02 May 2014 at Pacifico YOKOHAMA, Kanagawa, Japan)

U06-12 Room:503 Time:April 28 14:15-14:35

Computer Vision in Space: Optical Navigation Technology Development for Hayabusa-2

OHTA, Naoya[1*]

[1]Gunma University

Computer vision (CV) is a research field aiming to establish technologies by which information of objects is extracted from their images. Using CV technologies, our research group are developing methods to construct shape model of an asteroid for Hayabusa-2 navigation. We report this activity in this article. In addition, applying CV technologies to space environment has a potential to drive CV itself to a new research direction. We also touch on this observation.

For Hayabusa-2 navigation, we need to know shape of the destination asteroid, but the long distance between the asteroid and the earth prevent us from measuring it from the earth. Therefore we have to measure it after the arrival to the asteroid. Because active measurement methods need too much power, we are developing methods using images taken from the spacecraft.

Our project is mainly run by Dr. Seiji Sugita at Univ. of Tokyo and Dr. Naru Hirata at Aizu Univ., who are researchers in planetary science. However, because shape reconstruction techniques using images have intensively been studied in CV and CG (computer graphics) areas, the project is contributed by Dr. Hiroshi Ishikawa at Waseda Univ. and the author from CV area, and Dr. Shigeo Takahashi at Univ. of Tokyo from CG area.

We have applied a structure from motion technique developed in CV without modifications to the shape reconstruction of asteroids. We have had a minimum result required for Hayabusa-2 navigation, but more precise model is needed to make the navigation more certain and flexible. Therefore, we are combining photometric stereo to it.

Photometric stereo is a shape reconstruction method utilizing reflectance information of objects. However, we cannot directly apply such techniques developed in CV to the asteroid, because the conditions assumed in CV are fairly different from our case. The CV techniques assume that a number of images are taken from the same position, but the spacecraft cannot be controlled in such a way because it requires too much fuel. In addition, the reflectance models are different; Lambertian and Phong, for example, are used in CV, but we need algorithms based upon models such as Hapke and Minnaert, which describe reflectance of planet materials. Therefore, we are developing new algorithms that match the space environment for Hayabusa-2 navigation.

Looking at the origin of CV, it was regraded as a part of artificial intelligence research and has been motivated by artificially realizing functions of visual systems of human beings, or creatures in general. It seems that, from this reason, methods developed in CV tend to be general-purpose, and also that environments on the earth are implicitly assumed. Therefore, algorithms in CV are sometimes not applicable to problems in space science. However, viewing the situation from a different point, it may inspire CV itself to a new research direction by giving clear purposes.

When assuming usage in space, the following peculiarities are observed. The light source is usually only the sun, so it often suffice to consider only parallel light as the illumination. We can develop algorithms fully taking advantage of this simplicity. As mentioned above, reflectance models special to planet are used. If the process is executed in spacecrafts, the amount of computation is very limited, so the view point to develop a minimum algorithm to fulfill the objective becomes important. On the other hand, if images are transferred to the earth, the number of images is limited, but usually no limitation exists in amount of the computation. In such a case, CG-CV loop where a CG model is iteratively modified so that the generated images match to the observed images becomes to have reality. In addition to stated above, computing other information needed for space science than shape, estimating error information (variance), and so on, are important tasks for space science. We believe developing these techniques is an important direction of CV research.

Keywords: image measurement, shape reconstruction, optical navigation, Hayabusa-2

Japan Geoscience Union Meeting 2014
(28 April - 02 May 2014 at Pacifico YOKOHAMA, Kanagawa, Japan)

U06-13 Room:503 Time:April 28 14:35-14:55

Analytical chemistry of organic compounds in the Solar System: An attempt to link with planetary science

YABUTA, Hikaru[1*]

[1]Osaka University, Department of Earth and Space Science

Analytical chemistry of organic compounds in the Solar System small bodies is a microscopic approach for understanding of the origin and evolution of building blocks of the Solar System and life, which has a complementary relationship with macroscopic approaches such as observational and theoretical astronomy. This approach would provide a significance of considering organic compounds in the planetary formation theory, which has been constructed only by silicate and ice dusts. Indeed, significant roles of organic compounds in the early Solar System are explained by (1) high abundances of C, H, O, N in the Solar System, (2) major components of dusts in interstellar clouds, (3) high reactivity to heat, light, shock, water, and minerals (chemical indicator recording the processes in the Solar System), (4) possible contribution to accretion of dusts, due to their stickiness (Kouchi et al. 2002), and (5) possible contribution to redox imbalance in solar nebula (that determined the chemical compositions of chondrules) (Yurimoto and Kuramoto, 1998). Despite these significant roles, however, organic cosmochemistry was not a very popular field in planetary science until several years ago. One of the reasons may be because of difficulty in visualization of organic compounds, i.e., drawing of a big picture. In this point, I attempt to show a simple example. When starch-syrup is heated, how is it changed. One would tell that the color is changed from colorless to brown, the originally sticky syrup becomes less sticky candy, and water-soluble syrup becomes an insoluble solid. These descriptions are based on visuality and are easy to understand. On the other hand, if these phenomena are translated to organic analytical chemistry, the description becomes quite different from the former; hydroxyl groups of glucose changes to carbonyl groups via dehydration as well as aromaticity increases with heating. However, it should be noted that two ways of descriptions explain exactly the same phenomenon. That demonstrates that physical properties (color, stickiness, and solubility) are determined by molecular chemical structures. Likewise, analytical chemistry of organic compounds in the Solar System has a potential to reveal the molecular science that determines physics of macroscopic planetary formation, such as the color of asteroids (albedo). This will become possible by improvements of the in-situ organic analyses such as spectromicroscopy (e.g., STXM), electron microscopy (TEM), and ion probe mass spectrometry (e.g., nanoSIMS), through visualization of the distributions of organics and minerals in the Solar System materials which record the chemical evolution from dusts to planetesimals.

Keywords: Organic compounds, Solar System, Analytical chemistry, small bodies, planetary formation, visualization

Japan Geoscience Union Meeting 2014
(28 April - 02 May 2014 at Pacifico YOKOHAMA, Kanagawa, Japan)

U06-14 Room:503 Time:April 28 14:55-15:15

Formation Process of Complex Organic Molecules in Protoplanetary Disks

NOMURA, Hideko[1*]

[1]Tokyo Institute of Technology

It is believed that chemical reactions in protoplanetary disks will lead the origin of materials in our Solar System. Recently, many complex organic molecules (COMs) have been found in molecular clouds by radio observations of molecular transition lines. Meanwhile, amino-acids are found in a comet and meteorites in our Solar System. In this work we investigate the synthesis of complex organic molecules in protoplanetary disks using a large gas-grain chemical network together with a 2D steady-state physical model of a disk irradiated by UV and X-rays from the central star. We find COMs are efficiently formed on cold and warm grains in the disk midplane via grain-surface reactions through efficient migration of icy species on grain surface. Radiation processing on ice forms reactive radicals and helps build further complexity. We find the grain-surface abundances predicted by our calculations are consistent with those derived from cometary comae observations. We also predict line spectra of COMs, which are partly photodesorbed into gas from grain surface, will be observable in nearby protoplanetary disks with ALMA. In this talk I would like to discuss further on formation process of COMs on grains in the asteroid belt region, too.

Keywords: protoplanetary disks, formation of organic molecules

Japan Geoscience Union Meeting 2014
(28 April - 02 May 2014 at Pacifico YOKOHAMA, Kanagawa, Japan)

U06-15 Room:503 Time:April 28 15:15-15:30

Status report of curation of Hayabusa-returned samples

YADA, Toru[1*] ; ABE, Masanao[1] ; UESUGI, Masayuki[1] ; KAROUJI, Yuzuru[1] ; ISHIBASHI, Yukihiro[1] ; OKADA, Tatsuaki[1] ; SATAKE, Wataru[1] ; FUJIMOTO, Masaki[1]

[1]Japan Aerospace Exploration Agency

Hayabusa spacecraft returned samples from S-type Near-Earth Asteroid (NEA) Itokawa in June 2010. After the return, Extraterrestrial Sample Curation Team (ESCuTe) of JAXA have recovered particles from a sample catcher of Hayabusa, and more than 400 particles initially described have been presented in public (Yada et al., 2014a). In this presentation, we review the recovery and initial description of Hayabusa-returned samples and mention their future schedule.

A sample container had been extracted from the reentry capsule of Hayabusa and cleaned in cleanrooms of the Extraterrestrial Sample Curation Center (ESCuC) of JAXA. It was introduced into a clean chamber No.1 and opened in vacuo, and then a sample catcher, which enclosed samples captured on the surface of asteroid Itokawa, was extracted to be transferred to a clean chamber No.2 which is designed to handle Hayabusa-returned samples in highly purified nitrogen condition. The sample catcher is mainly composed of a rotational cylinder through which captured samples had been transferred, a room A in which samples obtained by the second touchdown on Itokawa and a room B in which captured those of the first one. At first, we had prepared quartz glass disks of the same size with covers of the room A and B, on which particles inside each room were fallen by tapping. The particles on the quartz disks have been picked up one by one with a specially designed electrostatically-controlled micromanipulator to be placed onto a SEM holder which can seal the samples in nitrogen condition and initially described by SEM-EDS. Then they sent back to the clean chamber No.2 to be placed onto gridded quartz glass slides to be given their ID and preserved. In fiscal year of 2013, we started to describe particles on a cover of the room B with SEM-EDS directly, utilizing a SEM holder specially designed for the cover of the catcher (Yada T. et al., 2014b).

The initial description method using the quartz glass disks has disadvantages in inefficiency and risk of particles transportation one by one with the micromanipulator. In order to resolve these disadvantages, we have developed metal disks which particles can be fallen on by tapping and can be set to the SEM holder designed for the covered of the catcher in fiscal year of 2013. We are planning to start sample recovery by the metal disks in fiscal year of 2014, and going to confirm vast majority of particles inside the catcher for more than two years (Yada T. et al., 2014a).

The ESCuTe of JAXA started the international AO for Hayabusa-returned samples in the beginning of 2012. In the international AO, worldwide researchers can apply their proposals and the committee composed manly of top scientists outside JAXA reviews the proposals to determine which proposal the precious samples should be distributed. The AO have been published approximately annually, and the third AO will be published in the beginning of fiscal year 2014. The research results of the AOs are presented in the international symposium held by JAXA, named as ”Hayabusa 2013: Symposium of Solar System Materials”, and its proceedings will be published in the international journal.

Particles having rare features have not been provided to the international AOs, but to consortium studies led by ESCuTe of JAXA until 2013. So far, four consortia, including the maximum-sized particle, a NaCl-bearing one, an iron sulfide one, and ones containing phosphates Uesugi et al., 2013; Yada et al., 2013; Karouji et al., 2013). Particles having other rare features will be provided to consortium studies in future.

References:

Abe M. et al. (2011) LPS XLII, Abstract #1638.
Karouji Y. et al. (2013) 76th Ann. Meteorit. Soc. Meeting, Abstract #5148.
Uesugi M. et al. (2013) 76th Ann. Meteorit. Soc. Meeting, Abstract #5186.
Yada T. et al. (2013) 76th Ann. Meteorit. Soc. Meeting, Abstract #5150.
Yada T. et al. (2014a) LPS XLV, Abstract #1759.
Yada T. et al. (2014b) MAPS, in press.

Keywords: Hayabusa, asteroid, curation, sample return

Japan Geoscience Union Meeting 2014
(28 April - 02 May 2014 at Pacifico YOKOHAMA, Kanagawa, Japan)

U06-16 Room:503 Time:April 28 15:30-15:45

Examination of the origin of carbonaceous particles in Hayabusa-returned samples

UESUGI, Masayuki[1*] ; NARAOKA, Hiroshi[2] ; ITO, Motoo[3] ; YABUTA, Hikaru[4] ; KITAJIMA, Fumio[2] ; TAKANO, Yoshinori[3] ; MITA, Hajime[5] ; KEBUKAWA, Yoko[6] ; YADA, Toru[1] ; KAROUJI, Yuzuru[1] ; ISHIBASHI, Yukihiro[1] ; SATAKE, Wataru[7] ; OKADA, Tatsuaki[1] ; ABE, Masanao[1]

[1]Japan aerospace exploration agency, [2]Department of Earth and Planetary Sciences, Kyushu University, [3]Kochi Institute for Core Sample Research JAMSTEC, [4]Osaka University, Department of Earth and Space Science, [5]Fukuoka Institute of Technoology, Faculity of Engineering, Department of Life, Environment and Mater, [6]Department of Natural History Sciences Hokkaido University, [7]Department of Earth and Planetary Science, University of Tokyo

Extraterrestrial Sample Curation Team (ESCuTe) recovered more than 50 carbonaceous particles from the sample catcher of the Hayabusa spacecraft. Those carbonaceous materials, named as category 3, were found in the form of particles with similar size range of the silicate particles those confirmed as Itokawa regolith particles. Initial description by the SEM-EDS analysis shows variable textures and chemical compositions of them, suggesting the multiple origins of the carbonaceous materials.

Preliminary examinations of category 3 particles were carefully processed in parallel with those of silicate materials. However, we could not obtain the information for the origin of category 3 particles before the opening of international announcement of opportunity (A/O). The ESCuTe and preliminary examination team of category 3 particles have continued the investigations. In this paper, we report the several recent results obtained from the sequential analyses.

Samples allocated for the preliminary examinations of category 3 are RA-QD02-0008, RA-QD02-0120, RA-QD02-0180, RB-QD04-0001, RB-QD04-0037-01 and RB-QD04-0047-02. RA-QD02-0008 was lost during the manipulation at first preliminary examination. Three samples, RA-QD02-0120, RB-QD04-0001, and RB-QD04-0047-02, were pressed on the Au plate and fixed without any adhesive materials. We analyzed H, C and N isotopic composition by nano-SIMS in the beginning of the sequential study, in order to investigate the isotopic anomaly which is a direct evidence of extraterrestrial origin of organic materials [8]. FT-IR and micro-Raman spectroscopy were also applied for the pressed samples [9]. After ToF-SIMS analysis of those particles, the samples were sliced by FIB in order to investigate the fine structure of the samples by XANES and TEM/STEM [10].

We performed those analyses with determining the effect on the subsequent analyses, such as sample damages and contaminations. The rest two particles, RA-QD02-0180 and RB-QD04-0037-01 were pressed on indium plates, because significant disturbance by Au on the ToF-SIMS analyses was found. We will also report the construction of the sequential analysis flow of tiny carbonaceous particles.

In parallel with the Hayabusa-returned particles, we processed observation and analysis of insoluble organic matter (IOM) of A881458 (CM2) and several possible materials of the origin of the category 3 particles, such as viton, silicon rubber, vectran and particles collected from the Hayabusa2 clean room.

We did not obtain any signature of extraterrestrial origin from category 3 particles so far. We are planning to continue the preliminary examination of category 3 by the end of March 2014. We are also planning to open the category 3 particles to the future International A/O, with the data of preliminary examinations before the end of 2014.

References: [1] Yada et al. 2011. Meteoritics & Planetary Science 32:A74. [2] Nakamura et al. 2011. Science 333:1113-1116. [3] Yurimoto et al. 2011. Science 333:1116-1119. [4] Ebihara et al. 2011. Science 333:1119-1121. [5] Noguchi et al. (2011) Science 333:1121-1125. [6] Tsuchiyama et al. 2011. Science 333:1125-1128. [7] Nagao et al. 2011. Science 333:1128-1131. [8] Ito et al. 2013. Abstract of Hayabusa Symposium, [9] Kitajima et al., 2013 Abstract of Hayabusa Symposium, [10] Uesugi et al. 2013. Abstract of Hayabusa Symposium

Japan Geoscience Union Meeting 2014
(28 April - 02 May 2014 at Pacifico YOKOHAMA, Kanagawa, Japan)

U06-17 Room:503 Time:April 28 15:45-16:00

H, C and N isotopic compositions of HAYABUSA Category 3 organic samples

ITO, Motoo[1*] ; UESUGI, Masayuki[2] ; NARAOKA, Hiroshi[3] ; YABUTA, Hikaru[4] ; KITAJIMA, Fumio[3] ; MITA, Hajime[5] ; TAKANO, Yoshinori[6] ; KAROUJI, Yuzuru[2] ; YADA, Toru[2] ; ISHIBASHI, Yukihiro[2] ; OKADA, Tatsuaki[2] ; ABE, Masanao[2]

[1]Kochi Institute for Core Sample Research, JAMSTEC, [2]Japan Aerospace Exploration Agency, [3]Department of Earth and Planetary Sciences, Kyushu University, [4]Osaka University, Department of Earth and Space Science, [5]Fukuoka Institute of Technology, Department of Life, Environment and Materials Science, [6]Institute of Biogeosciences, JAMSTEC

Hayabusa spacecraft had brought back asteroid Itokawa particles to the Earth on June 2010. More than 1,500 mineral particles were identified on the Qz glass after the compulsive free fall, and most of them were very small ranging from 10 to 300 μm but are mostly smaller than 50 μm (Nakamura et al., 2011). In addition several amount of carbonaceous materials were found that is called Category 3. Based on FE-SEM and EDS observations at JAXA Extraterrestrial Sample Curation Team, those samples mainly composed of C, N, O and some of them contain NaCl and KCl (JAXA Hayabusa sample catalogue).

H, C and N isotopic compositions of extraterrestrial organic materials in Stardust cometary samples (McKeegan et al., 2006), IDPs (Messenger, 2000), IOM (Busemann et al. 2006) and nanoglobules in primitive chondrite (Nakamura-Messenger et al., 2006) provide a clue for understanding of origin and nature of the Solar System. Large D and 15N isotopic enrichments were observed, and C isotope is slightly enriched in 13C in extraterrestrial organic materials (Pizzarello, 2005). Those data suggest that extraterrestrial organics are probably interstellar material that was survived through formation processes (planetesimals) of the Solar System (Sanford et al., 2001), and may also have material that formed in the cold molecular cloud region of the protoplanetary disk (Aikawa et al., 2002).

Here we report H, C and N isotopic measurement of organic materials from Hayabusa Category 3 samples, RB-QD04-0047-02, RA-QD02-0120 and RB-QD04-0001, by an ion imaging with the JAMSTEC NanoSIMS ion microprobe. The purposes of this study are to evaluate terrestrial contaminations in the Hayabusa spacecraft and in the JAXA curation facility, and to find extraterrestrial organic materials on the basis of H, C and N isotope measurements.

Each Hayabusa organic sample was pressed on Au plate together with terrestrial organic standards of 1-hydroxybenzotriazole hydrate and BBOT with known H, C and N isotopic compositions. Following the SEM study to check the sample condition, texture and morphology, the samples were analyzed for H, C and N isotopic compositions by an isotopic imaging with the JAMSTEC NanoSIMS 50L at Kochi Institute for Core Sample Research.

We studied three Hayabusa organic samples, RB-QD04-0047-02, RA-QD02-0120 and RB-QD04-0001. All of the samples have been initially investigated by a FE-SEM and EDX observation at JAXA Hayabusa curation facility, and the EDX spectra of the samples contain C, N and O; the dominant elements are C, and N (Hayabusa sample catalogue).

Based on NanoSIMS isotopic images of H, C and N in RB-QD04-0047-02, RA-QD02-0120 and RB-QD04-0001, all three samples show homogeneous and terrestrial H, C and N isotopic compositions within an error (δD = 60 $\pm$ 13 permil, δ13C = 3 $\pm$ 3 permil and δ15N = -4 $\pm$ 2 permil for RB-QD04-0047-02; δD = 81 $\pm$ 54 permil, δ13C = -20 $\pm$ 8 permil and δ15N = 2 $\pm$ 2 permil for RA-QD02-0120; δD = 135 $\pm$ 32 permil, δ13C = -20 $\pm$ 9 permil and δ15N = 16 $\pm$ 12 permil for RB-QD04-0001).

The IOMs in CI and CM chondrites show heterogeneous distributions of delta-D at the molecular (Remusat et al. 2009) and micron scale level (Busemann et al., 2006). The IOMs of CR, CM and CI have D and 15N isotopic enrichments in micron-sized regions (hot spots). The IOMs in ordinary chondrites are heterogeneous, however, they do not show many micron-scale anomalies as IOMs in carbonaceous chondrite (Remusat et al., 2013). It is obvious that H, C and N isotope signatures of Hayabusa organic samples are different from those of IOMs in carbonaceous and ordinary chondrites: i.e., No hot spots, terrestrial values for H, C and N isotopes.

We have not found strong evidence of extraterrestrial origin because isotope compositions of H, C and N in Hayabusa organic samples show terrestrial values, and homogeneous distributions of H, C and N in the samples, which are unlike to IOM in various types of chondrites.

Japan Geoscience Union Meeting 2014
(28 April - 02 May 2014 at Pacifico YOKOHAMA, Kanagawa, Japan)

U06-18 Room:503 Time:April 28 16:15-16:35

Albedo properties of main belt asteroids based on the infrared all-sky surveyors

USUI, Fumihiko[1*]

[1]University of Tokyo

Presently, the number of asteroids is known to be more than 620,000, and more than 90% of asteroids are classified as the main-belt asteroids (MBAs). The spatial distribution of compositions among MBAs is of particular interest, because the main belt is the largest reservoir of asteroids in the solar system. Asteroids are thought to be the remnants of planetesimals formed in the early solar system, and have a clue to study the formation and evolution of asteroids, origin of meteoroids and the near-Earth asteroids, as well as the formation of the solar system. Size and albedo are one of the most basic physical quantities of asteroid. Knowledge of size and albedo is essential in many fields of asteroid research, such as chemical composition and mineralogy, the size-frequency distribution of dynamical families and populations of asteroids, and the relationship between asteroids in the outer solar system and comets.

Several techniques have been developed to determine the size of asteroids. One of the most effective methods for measuring asteroidal size and albedo indirectly is through the use of radiometry, where a combination of the thermal infrared flux and the absolute magnitude as the reflected sunlight. Using radiometric measurements, a large number of objects can be observed in a short period of time, providing coherent data for large populations of asteroids within the asteroid belt. Infrared observations can be made still better under ideal circumstances, from space. The first space-borne infrared telescope is the Infrared Astronomical Satellite (IRAS; Neugebauer et al. 1984), launched in 1983 and performed a survey of the entire sky. To date, there are two other infrared astronomical satellites dedicated to all-sky survey: the Japanese infrared satellite AKARI (Murakami et al. 2007), and the Wide-field Infrared Survey Explorer (WISE; Wright et al. 2010). Based on the all-sky survey data obtained by IRAS, AKARI, and WISE, the largest asteroid catalogs containing size and albedo data were constructed (e.g., Tedesco et al. 2002; Usui et al. 2011; Mainzer et al. 2011). The total number of asteroids detected with size and albedo information with these three surveyors is 138,285, which is 22% of currently known asteroids with orbits.

In addition, several outstanding works have provided the taxonomic classification of asteroids (e.g., Tholen 1989; Bus & Binzel 2002; Lazzaro et al. 2004; Carvano et al. 2010), based on ground-based spectroscopic observations within optical and near-infrared wavelengths. Along with these taxonomic classifications, size and albedo data also contribute to our understanding of asteroid compositions. In general, the albedo of C-types is considered as low and that of S-types is high (e.g., Zellner & Gradie 1976). The relationship between taxonomic types and albedo is, however, complex and type determinations cannot be made on the basis of albedo values alone. Recently albedos of C- and S-type asteroids are found to vary widely, especially for sizes smaller than several tens km (Usui et al. 2013). Furthermore, in spite of the albedo transition process like space weathering, the heliocentric distribution of the mean albedo of asteroids in each taxonomic type is found to be nearly flat. In the total distribution, on the other hand, the mean albedo value gradually decreases with increasing the semimajor axis, presumably due to the compositional mixing ratios of taxonomic types.

In this talk, we present the details of data compiling of size, albedo, and taxonomy of MBAs, and discuss the compositional distribution in the main belt regions.

Keywords: asteroids, main belt, infrared surveys, size and albedo, taxonomic classifications

Japan Geoscience Union Meeting 2014
(28 April - 02 May 2014 at Pacifico YOKOHAMA, Kanagawa, Japan)

U06-19 Room:503 Time:April 28 16:35-16:50

Lightcurve Survey of Vestoids in the Inner Asteroid Belt

HASEGAWA, Sunao[1*] ; MIYASAKA, Seidai[2] ; MITO, Hiroyuki[3] ; SARUGAKU, Yuki[1] ; OZAWA, Tomohiko[4] ; KURODA, Daisuke[5] ; YOSHIDA, Michitoshi[6] ; YANAGISAWA, Kenshi[5] ; SHIMIZU, Yasuhiro[5] ; NAGAYAMA, Shogo[5] ; TODA, Hiroyuki[5] ; OKITA, Kouji[5] ; KAWAI, Nobuyuki[7] ; SEKIGUCHI, Tomohiko[8] ; ISHIGURO, Masateru[9] ; ABE, Masanao[1]

[1]Institute of Space and Astronautical Science, Japan Aerospace Exploration Agency, [2]Tokyo Metropolitan Government, [3]Kiso Observatory, Institute of Astronomy, The University of Tokyo, [4]Misato Observatory, [5]Okayama Astrophysical Observatory, National Astronomical Observatory, [6]Hiroshima Astrophysical Science Center, Hiroshima University, [7]Graduate School of engineering, , Tokyo Institute of Technology, [8]Asahikawa Campus, Hokkaido University of Education, [9]Department of Physical and Astronomy, Seoul National University

We have made the lightcurve observation of 13 vestoids ((1933) Tinchen, (2011) Veteraniya, (2508) Alupka, (3657) Ermolova, (3900) Knezevic, (4005) Dyagilev, (4383) Suruga, (4434) Nikulin, (4796) Lewis, (6331) 1992 FZ_1, (8645) 1998 TN, (10285) Renemichelsen, and (10320) Reiland).

Lightcurves in the R-band of rotation periods were found for (1933) Tinchen, (2011) Veteraniya, (2508) Alupka, (3657) Ermolova, (3900) Knezevic, (4005) Dyagilev, (4383) Suruga, (4796) Lewis, (6331) 1992 FZ_1, (8645) 1998 TN, and (10320) Reiland.

The distribution of rotational rates of 59 vestoids in the inner main belt, including 29 members of the Vesta family that are regarded as ejecta from the asteroid (4) Vesta, is inconsistent with the best-fit Maxwellian distribution.

This inconsistency may be due to the effect of thermal radiation Yarkovsky- O'Keefe-Radzievskii-Paddack (YORP) torques, and implies that the collision event that formed vestoids is sub-billion to several billion years in age.

Keywords: asteroid, vesta

Japan Geoscience Union Meeting 2014
(28 April - 02 May 2014 at Pacifico YOKOHAMA, Kanagawa, Japan)

U06-20 Room:503 Time:April 28 16:50-17:05

Near-infrared spectral measurements of zodiacal light by CIBER rocket experiments

MATSUURA, Shuji[1*] ; ARAI, Toshiaki[1] ; ONISHI, Yosuke[1] ; SHIRAHATA, Mai[1] ; TSUMURA, Kohji[1] ; MATSUMOTO, Toshio[2] ; BOCK, James[3] ; CIBER, Team[3]

[1]JAXA, [2]ASIAA, [3]Caltech

We have observed the cosmic near-infrared background light as the integrated light along the line of sight, which is the near-infrared diffuse radiation in wide range of the cosmic structure from the solar system to extragalactic universe, with the CIBER (Cosmic Infrared Background ExpeRiment) rocket experiments. One of scientific objectives of CIBER is to measure the zodiacal light in the near-infrared, which is the scattered sun light by interplanetary dusts. From the results of CIBER, we first observed the zodiacal light spectrum and its polarization in the near-infrared range from 0.8 to 2 mincrons. In this paper, we present the observation results.

CIBER is an international collaboration study among Japan, US and Korea, and a sounding rocket program by NASA. In a term from 2009 to 2013, we have carried out four times of launch and obtained high quality data at the altitudes above 200 km with no contamination by the earth atmosphere. In order to measure the extragalactic background light, we selected the observation field to have solar elongation over 90 degrees with relatively low brightness. We extracted the zodiacal light component from the total sky brightness by using the ecliptic latitude dependence. As the result, we could obtain information of spectrum, polarization and seasonal variation of the zodiacal light.

The observed infrared spectrum shows neither ecliptic latitude dependence nor time variation, and reddened color compared with the solar spectrum at wavelengths below 1.5 microns. From this result, size of interplanetary dust is larger than the order of micron, and there may be absorption of dust minerals at shorter wavelengths. We found the polarization of 20-25% at the maximum at the north ecliptic pole, which is higher than that previously observed in the visible wavelength range. The polarization result also suggest that the majority of the dust size is much larger than the observation wavelength.

In this paper, we report the observation result, and we discuss the optical properties of interplanetary dust by comparing our result with the spectral reflectance of meteorites and cometary dust.

Keywords: zodiacal light, interplanetary dust, infrared, observation

Japan Geoscience Union Meeting 2014
(28 April - 02 May 2014 at Pacifico YOKOHAMA, Kanagawa, Japan)

U06-21 Room:503 Time:April 28 17:05-17:20

Reflectance Spectra of Jovian Small Satellites and Implication of their Origin

TAKATO, Naruhisa[1*] ; TERADA, Hiroshi[1] ; YOSHIDA, Fumi[1] ; OHTSUKI, Keiji[2]

[1]National Astronomical Observatory of Japan, [2]Kobe Univ.

Abstract

Jupiter has many small satellites other than the four giant Galilean satellites. Four of them revolve inside Io's orbit and others revolve outside Calisto's orbit. Based on the similarities of their photometric and orbital properties, these small satellites are thought to be captured asteroids. However, it is still unknown where and when these satellites were captured by Jupiter. We can reveal the dynamic history of our solar system evolution by investigating these questions.

Here, we have made optical spectroscopies of 11 small satellites which were not yet taxonomically classified by spectroscopy so far. We compared the number ratio of C- and X-type to D-type of the 11 satellites, and the Hilda and Trojan groups observed recently by Grav et al. (2012) as a function of diameter. We found that the diameter-(C,X)/D relation of the Jovian irregular satellites is similar to that of Hilda's, not Trojan's. This result suggests that the Jovian irregulars and the Hilda members originate from the same source of asteroids.

We also observed the 3.05 μm narrow-band photometry of the inner small satellite Thebe and found that there is absorption. This can be attributed to hydrated minerals.

Keywords: satellites, Jupiter, spectrum, Hilda group, Trojan

Japan Geoscience Union Meeting 2014
(28 April - 02 May 2014 at Pacifico YOKOHAMA, Kanagawa, Japan)

U06-22 Room:503 Time:April 28 17:20-17:35

Weathering effect of solar wind proton on hydrated silicate minerals

NAKAUCHI, Yusuke[1*] ; ABE, Masanao[2] ; KITAZATO, Kohei[3] ; TSUCHIYAMA, Akira[4] ; YASUDA, Keisuke[5]

[1]The Graduate University for Advanced Studies, [2]Japan Aerospace Exploration Agency, [3]University of Aizu, [4]Kyoto University, [5]The Wakasa Wan Energy Reserch Center

NIRS3 is an on-board near infrared spectrometer of Hayabusa-2 project which is aimed at returning samples from C-type asteroid 1999 JU3. In this project, it is important to characterize mineralogical and heterogeneities on the asteroid surface for the sampling site selection. Observing wavelength of NIRS3 is including the 3 μm band which is charactering C-type asteroid (*Rivkin et al. LPSC 2002, Milliken et al. 2007*). The NIRS3 will measure reflectance spectra of asteroid surface in the wavelength range of 1.8 - 3.2 μm. This wavelength region includes features mainly related to OH and H_2O.

The spectral properties of the surface, however, would have different trend to the subsurface, because the surface of asteroids would be exposed to solar wind and micrometeorite. As for the reflectance spectrum of the moon, the absorption feature from 2.8 μm to 3.0 μm was reported in M^3 data (*Pieters et al. 2009*). It is thought that the implantation of solar wind proton is one of the causes (*McCord et al. 2011*). The solar wind protons will affect the spectral shape of 3μm region of air less bodies. Thus we study effect of irradiation of solar wind protons on near-infrared reflectance spectra by laboratory experiment.

We executed the simulation of irradiation of solar wind protons using ion implantation device at the Wakasa Wan Energy Research Center (WERC), Fukui. This device can irradiate $H_2{}^+$ beam with 10 keV in a vacuum (under 1×10^{-5} Pa). The total amount of $H_2{}^+$ was about 10^{18} ion/cm^2. Three samples were prepared; olivine (San Carlos, Arizona), antigorite (Sangenchaya, Kyoto), saponite (synthetic: Kunimine Industries Co., Ltd.). Antigorite and saponite were sieved between 50 μm and 75 μm and olivine served between 75 μm and 105 μm, and then they were heated for 24 hours at 423 K. They were packed into Cu cups and formed pellets. After irradiated the spectra were measured using FTIR, which resolution was 2.0 cm^{-1} in wavenumber. We adopted the analysis method of *Ichimura et al. (2012)*, which is to compare the reflectance spectra of altered sample, R, with unaltered sample, R_0, to determine the alteration ratio of spectra, R/R_0, without absorption water.

The alteration ratios of irradiated samples were different between minerals. The alteration ratio of olivine showed increasing of broad absorption feature from 2.8 μm to 3.8 μm due to OH/H_2O production. In antigorite and saponite, the alteration ratio, additionally, showed characteristic change related to coupling state of -OH. In the alteration ratio of antigorite, stretching of -OH bonded water molecule (-OH $\cdots$ ^{H}OH) at 2.77 μm and stretching of -OH $\cdots$ ^{H}OSi at 2.85 μm was increased conspicuously. On the other hands, the alteration ratio of saponite was changed conspicuously at 2.77 μm.

We think that the difference of the bands which showed conspicuously change is related with structure of minerals. Antigorite have -OH into the crystal. Therefore the irradiated protons broke bonds of Si-O and produced newer hydrogen bonds which are -OH $\cdots$ ^{H}OH or -OH $\cdots$ ^{H}OSi. Saponite has H_2O as interlayer water. It would be similarly broken bands of Si-O and produced newer hydrogen bonds which are -OH $\cdots$ ^{H}OH. These spectral changes can explain same process. These features support that the irradiated protons react with bonds of Si-O in the crystal.

In this study, we showed that the alteration of feature related with OH/H_2O is different from each mineral. Next step, we will examine the other minerals against determination minerals and the amount of water from reflectance spectra.

Keywords: Hayabusa-2, space weathering, solar wind, OH/H_2O, C-type Asteroid, proton implantation

Japan Geoscience Union Meeting 2014
(28 April - 02 May 2014 at Pacifico YOKOHAMA, Kanagawa, Japan)

U06-23 Room:503 Time:April 28 17:35-17:50

The effect of coexisting iron sulfide on space weathering by nanosecond pulse laser irradiation

OKAZAKI, Mizuki[1*] ; SASAKI, Sho[1] ; HIROI, Takahiro[2]

[1]School of Science, Osaka University, [2]Brown University

High-velocity impacts of micrometeorites and solar-wind particles change the surface optical properties of airless silicate bodies such as asteroids and the Moon. This process is called ”space weathering”. Experiments using nanosecond pulse laser confirmed the prediction that the formation of nanometer-size metallic iron particles should cause darkening, reddening and attenuation of absorption bands in visible and near infrared reflectance. The space weathering may explain the spectral mismatch between S-type asteroids and ordinary chondrites.

Previously sulfur depletion from asteroid surface was advocated on the basis of low sulfur abundance on Eros.

Recently on the surface of dust particles from Itokawa’s surface returned by Hayabusa, a thin layer containing nano particles of FeS over amorphous zone containing nano iron particles. A 10 micron size FeS crystal is also found in one Itokawa-derived grain.

To examine the effect of FeS on the space weathering, we conducted simulation experiments of the space weathering of silicate-FeS mixture using nanosecond pulse laser irradiation.

Then S is rich in volatility, so we guessed if sulfur has a certain influence on space weathering at the astronomical surface, and the experiments on chondrites with S by using nanosecond pulse laser.

We prepared pellet samples of powdered olivine and pyroxene (45-75 micrometer) mixed with iron sulfide particles (of 10, 20wt%) with same (and smaller) size range. We also prepared olivine pellet samples containing metallic iron particles of 10 to 20 wt%.

We found that the addition of Fe should enhance reddening and also darken near infrared reflectance (about 20% in the case of 10-20wt % FeS)., as compared with the case of the addition of Fe.

Although it was space weathering which has so far attracted attention from reddening, such as reddening by weathering in case Fe is contained, in the case where FeS is added, darkening was also seen and it has checked that space weathering became strong. Although existence of nano iron particulates can be considered about reddening, about overall darkening, it is under examination.

The samples were irradiated by nano-second pulse laser.

Keywords: space weathering, iron sulfide, experiments using pulse laser, asteroids, Itokawa

Japan Geoscience Union Meeting 2014
(28 April - 02 May 2014 at Pacifico YOKOHAMA, Kanagawa, Japan)

U06-P01 Room:Poster Time:April 28 18:15-19:30

Photometric Properties of (162173) 1999 JU3 in Preparation for JAXA Hayabusa 2 Sample Return Mission

ISHIGURO, Masateru[1*] ; KURODA, Daisuke[2] ; HASEGAWA, Sunao[3] ; HAYABUSA 2, Observation sub-group[4]

[1]Department of Physical and Astronomy, Seoul National University, [2]Okayama Astrophysical Observatory, National Astronomical Observatory of Japan, [3]Institute of Space and Astronautical Science, Japan Aerospace Exploration Agency, [4]Japan Aerospace Exploration Agency

A near-Earth asteroid, (162173) 1999 JU3 (hereafter 1999 JU3), is a primary target asteroid for Hayabusa 2 sample return mission. We conducted a worldwide campaign to make photometric observations of the asteroid to determine the physical properties. 1999 JU3 is classified into C-type asteroid having a nearly spherical shape and the synodic rotational period of 7.6312±0.0010 hr.

In this presentation, we will report further information about 1999 JU3 determined since last JpGU meeting in 2013. We investigated the magnitude-phase angle relation. We obtained the parameters for IAU H-G formalism, H =19.20±0.12 and G=0.077±0.011 (V-band, 550nm), respectively. In combination of our result with infrared photometry, the geometric albedo is updated to be 0.05 (Mueller et al. in preparation), which is typical to but slightly smaller than the average of C-type asteroids in main-belt. We found that the magnitude-phase angle relation has a linear behavior in a wide range of the phase angles (5-80 degree) and show a possible non-linear opposition brightening within the phase angle of ‹ 5 degree. The phase slope is consistent to those of tens-km C-type asteroids, that is, 0.04 mag degree^{-1}. The opposition effect amplitude, ≈10% or less, is slightly weaker than that of a precursor C-type mission target body, (253) Mathilde, but the difference seems to reflect the diversity of C-type asteroids. Recently, Shevchenko & Belskaya (2010) reported that ˜20% of all studied low albedo asteroids did not show detectable opposition effect. We explore the significance of 1999 JU3 data with remote-sensing devices in terms of the opposition effect.

Keywords: Hayabusa 2, 1999 JU3, Ground-based observations

Japan Geoscience Union Meeting 2014
(28 April - 02 May 2014 at Pacifico YOKOHAMA, Kanagawa, Japan)

U06-P02 Room:Poster Time:April 28 18:15-19:30

Observation of geometric albedo of the C-type asteroid by the laser altimeter on Hayabusa-2 spacecraft

YAMADA, Ryuhei[1*] ; SENSHU, Hiroki[2] ; ABE, Shinsuke[3] ; YOSHIDA, Fumi[1] ; HIRATA, Naoyuki[4] ; ISHIHARA, Yoshiaki[5] ; HIRATA, Naru[6] ; NODA, Hirotomo[1] ; NAMIKI, Noriyuki[2]

[1]National Astronomical Observatory of Japan, [2]Chiba Institute of Technology, [3]Nihon University, [4]University of Tokyo, [5]Japan Aerospace Exploration Agency, [6]The University of Aizu

The Japanese asteroid explorer 'Hayabusa2' will be launched at end of 2014, and it will probe the near-Earth C-type asteroid '1999JU3'. In this mission, we have a plan to utilize the laser altimeter (LIDAR) to investigate the distribution of geometric albedo of 1999JU3 at laser wavelength (1064 nm). The LIDAR on-board Hayabusa2 has functions to measure the intensities of sending laser pulse and receiving laser pulse reflected from the asteroid surface in addition to measurement of distance between the spacecraft and the asteroid. We can evaluate the geometric albedo of the 1999JU3 using the measured intensities of sending and receiving pulses.

In this presentation, we will indicate results of the performance tests of the LIDAR and expected accuracy of the albedo evaluated from the results of the tests. We will also describe not only effect of characteristic of the LIDAR but also effects of inclination and roughness of the asteroid surface on estimation of the albedo.

In our study, three types of scientific topics using information of the albedo on asteroid surface estimated from the LIDAR data with other equipment data are considered; they are (1) rock and mineral category of 1999JU3, (2) degree of water content on asteroid surface and (3) variation of asteroid surface caused from space weathering and/or exterior material. We will report prospects to obtain information about these science topics applying the LIDAR which has our evaluated performance.

Keywords: Albedo of Asteroid, C-type asteroid, 1999JU3, Hayabusa-2, Laser Altimeter

Japan Geoscience Union Meeting 2014
(28 April - 02 May 2014 at Pacifico YOKOHAMA, Kanagawa, Japan)

U06-P03 Room:Poster Time:April 28 18:15-19:30

Performances of Flight Model of NIRS3: the Near Infrared Spectrometer on Hayabusa-2

IWATA, Takahiro[1*] ; KITAZATO, Kohei[2] ; ABE, Masanao[1] ; ARAI, Takehiko[1] ; NAKAUCHI, Yusuke[3] ; NAKAMURA, Tomoki[4] ; HIROI, Takahiro[5] ; MATSUOKA, Moe[4] ; MATSUURA, Shuji[1] ; OZAKI, Masanobu[1] ; WATANABE, Sei-ichiro[6]

[1]Institute of Space and Astronautical Science, JAXA, [2]University of Aizu, [3]Graduate University for Advanced Studies, [4]Tohoku University, [5]Brown University, [6]Nagoya University

NIRS3: the Near Infrared Spectrometer is one of the candidate scientific instruments which will be equipped on Hayabusa-2 mission. It aims to observe near infrared spectroscopy at the wave length band of 1.8-3.2 micrometer to detect specific molecular absorption lines, including the absorption by hydrated minerals at 3 micrometer, on the target C-type asteroid. The major purpose of NIRS3 is to observe the absorption bands of hydrated minerals in the 3 micrometer band on the candidate target C-type asteroid 1999JU3. C-type asteroids are thought to be mother celestial bodies of carbonaceous chondrites (C-chondrites). C-chondrites have been classified into sub-groups by their composition, organization, and isotope ratio of oxygen. The spectra of C-type asteroids have also been classified into sub-types by their inclination and the existence of absorption bands detected in ground observations. However, the relationship between the sub-groups of C-chondrites and the sub-types of C-type asteroids has not been clarified due to the effects of solar radiation and space weathering. Therefore, we will directly observe the surface of a C-type asteroid without the terrestrial atmospheric absorption in the 3 micrometer band using NIRS3. Detecting younger terrain by global mapping of the asteroid and the ejecta of new crater by the Small Carry-on Impactor (SCI) will also provide the spectra of surface less affected by space weathering. To estimate the quantities of the hydrated minerals with accuracies of 1 to 2 wt%, we designed the NIRS3 system to have a signal-to-noise ratio (SNR) exceeding 50 at 2.6 micrometer for global mapping.

The ground tests for NIRS3 flight model started in 2013. Results of the flight model tests implied that the dark current at the InAs sensor is much lower than that of the engineering model which improves SNR. The projected on-board SNR was confirmed to be sufficient during the one-year observation period of 1999JU3 assuming the asteroid surface temperature estimated from the heliocentric range and solar phase angle. The SNR exceeds 300 after 2.5 ms integration and 1024-stacking at the home position observations. The data obtained after the vibration tests and thermal-vacuum tests indicate that NIRS3 is sufficiently durable for the launching and on-orbit environments. The observed spectra for samples of serpentine, olivine, and C-chondrites (Murchison, Murray, and Jbilet Winselwan) demonstrated that the derived reflectances are almost the same as those obtained by Fourier-transform infra-red (FTIR) spectroscopy. These design results show that NIRS3 has sufficient performance for scientific objectives.

Keywords: Hayabusa-2, asteroid, 1999JU3, NIRS3, near infrared, spectrometer

Japan Geoscience Union Meeting 2014
(28 April - 02 May 2014 at Pacifico YOKOHAMA, Kanagawa, Japan)

U06-P04 Room:Poster Time:April 28 18:15-19:30

Thermal Infrared Imager TIR on Hayabusa2: Instrumentation and Ground Calibration

OKADA, Tatsuaki[1*] ; FUKUHARA, Tetsuya[3] ; TANAKA, Satoshi[1] ; TAGUCHI, Makoto[4] ; ARAI, Takehiko[2] ; IMAMURA, Takeshi[1] ; SENSHU, Hiroki[5] ; DEMURA, Hirohide[6] ; OGAWA, Yoshiko[6] ; KITAZATO, Kohei[6] ; HASEGAWA, Sunao[1] ; SEKIGUCHI, Tomohiko[7] ; NAKAMURA, Ryosuke[8] ; KOUYAMA, Toru[8] ; MATSUNAGA, Tsuneo[9] ; WADA, Takehiko[1] ; TAKITA, Jun[10] ; SAKATANI, Naoya[10] ; HORIKAWA, Yamato[11] ; HELBERT, Jorn[12] ; MUELLER, Thomas[13] ; HAGERMANN, Axel[14] ; HAYABUSA2, Tir team[2]

[1]ISAS/JAXA, [2]JSPEC/JAXA, [3]Hokkaido University, [4]Rikkyo University, [5]Chiba Institute of Technology, [6]University of Aizu, [7]Hokkaido University of Education, [8]AIST, [9]NIES, [10]University of Tokyo, [11]Sokendai, [12]German Aerospace Center (DLR), [13]Max Planck Institute for Extraterrestrial Physics (MPE), [14]Open University

Thermal Infrared Imager TIR onboard Hayabusa2 is to map thermo-physical properties of Near-Earth C-class asteroid (162173) 1999JU3 through thermal imaging. Scientific significance must be placed on physical properties of asteroids as well that imply the planetesimal formation in solar nebula and its mechanical evolution to current small bodies, although planetary material science is often more focused in small body missions.

In the typical solar system evolution scenario, very fluffy porous bodies are formed in solar nebula and then become denser due to high-speed collision and thermal metamorphism. Some C-class asteroids are less dense, implying a highly porous assembly of densely compacted rocks or a loosely bound rubble-pile of porous rocks and soils. Those features will be identified by thermo-physical properties derived with TIR. Some C-class asteroids must have experienced dehydrated process whose clues might be found as veins or grooves on the asteroid. Those features are expected to be investigated by TIR. Granular flows which were found on asteroid Itokawa and ejecta sediments around impact craters will be measured by TIR as different thermal inertia zones because they have smaller particle size or higher porosity. Floating boulders (or moons), surrounding dust or vapor clouds ejected from asteroid surface could be detected by TIR if they exist sufficiently. Furthermore, on-site TIR observation will contribute to more confident and accurate determination of asteroid thermo-physical properties by ground observation.

TIR is a thermal infrared imager using two-dimensional micro-bolometer array, which has 328 x 248 effective pixels, 16 x 12 degrees field of view, and 0.05 degree per pixel, so that pixel resolution is 20m when observed from 20km altitude Home Position (HP), and less than 1m from 1km altitude covering 280m x 210m. The imaging feature is suitable for obtaining asteroid global feature from HP and investigating local geological context before and after sample collection. Hayabusa2 will observe asteroid 1999JU3 at the heliocentric distance from 0.96 to 1.42 AU and the dayside surface temperature is estimated -40 to 150 ℃ assuming the albedo is 0.05 and emissivity is 0.90 to 0.95. Detection range of TIR is 8 to 12 μm, which is best for observing thermal radiation from asteroid.

We have calibrated TIR performance for the target temperature ranging from -40 to 150 ℃. Goal is to construct the calibration curves for each pixel by 3 ℃ absolute temperature as well as 0.3 ℃ NETD. The apparatus for TIR calibration are the vacuum chamber for cold target and the clean-booth for hot target, with adjusting the optics and mounted panel temperatures. It is ideal that a single OFPN (Onboard Flat Pattern Noise) data is applicable for all the temperature range. Now efforts have been taken to improve its performance by interrelation between cold and hot calibration cases, adjusting bias levels due to different thermal energy input to detector, as well as geometric calibration. Instrumentation and results of calibration for TIR will be reported in detail.

Keywords: asteroid, Hayabusa2, thermo-physical property, Thermal Infrared, bolometer, planetary exploration

Japan Geoscience Union Meeting 2014
(28 April - 02 May 2014 at Pacifico YOKOHAMA, Kanagawa, Japan)

U06-P05 Room:Poster Time:April 28 18:15-19:30

Relationship between Regolith Particle Size and Porosity on Small Bodies

KIUCHI, Masato[1*] ; NAKAMURA, Akiko[1]

[1]Department of Earth and Planetary Sciences, Kobe University

Planetary small bodies are covered by a particulate layer called regolith. The particle size and porosity of the regolith surface of small bodies are important physical properties. The responses of the surface to solar irradiation are dependent on the particle size and porosity. The particle size and porosity have influences on the dynamic responses of the surface, such as cratering efficiency. By Apollo missions, the particle size was directly measured and estimated the mean porosity of the regolith 51% (Mitchell et al., 1974). The near-surface bulk porosity of asteroid was estimated using ground-based radar data to have a mean of 51∓14% (Magri et al., 2001). The angular width of opposition surge in optical reflectance was interpreted in terms of porosity and particle size distribution : surface porosities of S-class asteroidswere ranging from 40 to 80 % (Hapke, 1986; Domingue et al., 2002).

An empirical relationship between porosity and the ratio of the magnitudes of the interparticle force that was estimated as the capillary force and gravity which act on a particle was presented by Yu et al. (2003). The porosity was measured for the particles in the loose packing state and different porosities were interpreted as due to the difference of particle size. In this study we assume that the van der Waals force is predominant in the interparticle forces. A model formula of the van der Waals force in which the effect of adsorbate molecules is taken into account by a parameter is defined as

$Fv=AS^2r/48\Omega^2$ (1)

where A is Hamaker constant, r is particle radius, Ω is diameter of an O^{-2} ion, S is cleanliness ratio which shows the smallness of a number of the adsorbate molecules (Perko et al., 2001). It was shown that cleanliness ratio, S, is approximately 0.1 on the Earth, and is almost unity in the interplanetary space. In addition to the data of the several past studies, our own measurement result of micron-size fly ash particles in atmospheric condition.

We calculate Fv of all data using Eq.2, and obtain a revised relationship between porosity and the ratio RF of the magnitudes of the van der Waals force and gravity Fg , $R_F = F_V/F_g$. An empirical formula used in the previous study (Yu et al., 2003) ,

$p=p_0+(1-p_0)\exp(-mR_F^{-2})$ (2)

is applied to fit the data, where p_0, m and n are constants. Substituting Eq.1 to Eq.2 yields,

$p=p_0+(1-p_0)\exp\{-m(AS^2/64\pi\Omega^2\rho gr^2)^{-n}\}$ (3)

where $\rho$is particle density and g is gravitational acceleration.

We apply Eq. 3 to the conditions of small bodies ' surfaces to derive the relationship between particle radius and porosity. For example, we obtained the relationship for asteroid 25143 Itokawa surface. The particle size of Itokawa is ranging from millimeter to centimeter in the area of fine particles, smooth terrain of the Muses Sea (Yano et al., 2006). The result shows the range of porosity would be 0.55-0.8. Similarly, we can calculate the above relationships for other small bodies.

Gundlach and Blum (2013) estimated the particle size of small bodies by using the thermal inertia data and a heat conductivity model for regolith. By combining the relationship described for Eq.3 with those of Gundlach and Blum (2013), we can estimate the particle size and the porosity of regolith for the small bodies simultaneously.

Keywords: asteroid, regolith, porosity

Japan Geoscience Union Meeting 2014
(28 April - 02 May 2014 at Pacifico YOKOHAMA, Kanagawa, Japan)

U06-P06 Room:Poster Time:April 28 18:15-19:30

How to detect a small crater produced by Small Carry-on Impactor (SCI) using Thermal InfraRed Camera (TIR)

WADA, Koji[1*] ; NAKAMURA, Akiko[2] ; KUROSAWA, Kosuke[1] ; SCI, Team[3] ; TIR, Team[3]

[1]PERC/Chitech, [2]Department of Earth and Planetary Sciences, Kobe University, [3]Hayabusa-2 Project

In Hayabusa-2 mission, a crater will be formed on the surface of a C-type asteroid 1999JU3 using Small Carry-on Impactor (SCI) and the crater should be quickly detected from the mother ship. The detection, however, will become difficult when the crater is very small with a diameter of only 30 cm, near to the resolution limit of on-board cameras. On the other hand, Thermal InfraRed Camera (TIR) mounted on Hayabusa-2 has a possibility to detect such a small crater even if the crater size is sub-pixel of TIR resolution, because the temperature on the surface of a small crater is expected to be different from that around the crater. We, therefore, have started examination about the possibility and method to detect a SCI-formed small crater using TIR. In this presentation, we introduce the basic idea and the preliminary results of our modeling.

Keywords: Hayabusa-2, Impact, SCI, TIR, cater thermal model, asteroid

Japan Geoscience Union Meeting 2014
(28 April - 02 May 2014 at Pacifico YOKOHAMA, Kanagawa, Japan)

U06-P07 Room:Poster Time:April 28 18:15-19:30

Hayabusa 2/SCI: calibration impact experiments

KADONO, Toshihiko[1*] ; ARAKAWA, Masahiko[2] ; TSUJIDO, Sayaka[2] ; YASUI, Minami[3] ; HASEGAWA, Sunao[4] ; KUROSAWA, Kosuke[5] ; SHIRAI, Kei[4] ; HAYAKAWA, Masahiko[4] ; OKAMOTO, Chisato[4] ; SAIKI, Takanao[4] ; IMAMURA, Hiroshi[4] ; YANO, Hajime[4] ; NAKAZAWA, Satoru[4] ; OGAWA, Kazunori[4] ; IIJIMA, Yuichi[4] ; HIRATA, Naru[6] ; TAKAGI, Yasuhiko[7] ; WADA, Koji[5]

[1]University of Occupational and Environmental Health, [2]Graduate School of Science, Kobe University, [3]Organization of Advanced Science and Technology, Kobe University, [4]Japan Aerospace Exploration Agency, [5]Planetary Exploration Research Center, Chiba Institute of Technology, [6]Dep. of Computer Science and Engineering, Univ. of Aizu, [7]Aichi Toho University

SCI (Small Carryon Impactor" boarded on "Hayabusa 2" is a hollow Cu sphere with a mass of 15 kg, a diameter of 15 cm, which will impact a surface of asteroid 1999JU3. To estimate the conditions of the surface of the asteroid, such as composition and structure, we should investigate the results of the impact experiments with similar projectiles and various targets. We carried out impact experiments with gypsum and basalt targets and small hollow projectiles accelerated by a two-state light-gas gun at ISAS/JAXA, and sand targets and real scale projectiles at Kamioka. We report a summary of the results of these experiments.

Keywords: Hayabusa 2, Small Carryon Impactor, Impact experiments

Japan Geoscience Union Meeting 2014
(28 April - 02 May 2014 at Pacifico YOKOHAMA, Kanagawa, Japan)

U06-P08 Room:Poster Time:April 28 18:15-19:30

Impact crater formation on quartz sand: the effect of projectile density on ejecta velocity distributions

TSUJIDO, Sayaka[1*] ; ARAKAWA, Masahiko[1] ; WADA, Koji[2] ; SUZUKI, Ayako[3]

[1]Graduate School of Science, Kobe University, [2]Planetary Exploration Research Center, Chiba Institute of Technology, [3]Institute of Space and Astronautical Science, Japan Aerospace Exploration Agency

Introduction : Regolith formation and surface evolution on asteroid are caused by high velocity impacts of small bodies. The ejecta velocity distribution is one of the most important physical properties related to the crater formation and it is necessary to reconstruct the planetary accretion process among planetesimals. The surface of small bodies in the solar system has a various property on the porosity, strength and density. Therefore, the impact experiment on the target with the various properties is necessary to clarify the crater formation process applicable to the small bodies in the solar system. However, there have not enough studies on the effect of projectile density on the ejecta velocity distribution. Therefore, we would try to determine the effect of projectile density on the ejecta velocity distribution using 8 projectiles with different density by means of the observation of the each ejecta grain.

Experimental method: The cratering experiment was made by using a vertical type one-stage light gas gun (V-LGG) set at Kobe Univ. We used 3 types of targets: that is, they are the 100micron-glass beads target (porosity 37.6%), the 500 micron-glass beads target (porosity 37.6%), and 500-micron quartz sand (porosity 44.7%). These granular materials were put into the stainless steel container with the diameter of 30cm and the depth of 11cm. The target container was set in a large chamber with the air pressure less than 10^3 Pa or 10^5Pa. The material of the projectile that we used was a lead, a copper, an iron, a titanium, a zirconia, an alumina, a glass, and a nylon (1.1-11.3g/cm^3), and it had a diameter of 3mm and was launched at the impact velocity (v_i) of 24 to 217m/s.

We made an impact experiment using 8 types of projectiles on the 500-micron quartz sand target and observed each ejecta grain by using a high speed digital video camera taken at 2000-10000 FPS. Then, we measured the ejection velocity and the initial position of each grain. We successfully obtained the relationship between the initial position and the initial ejection velocity or ejection angle for the quartz sand grains.

Result: In (Eq.1), mu is proportional to density of projectile in the range less than 6g/cmˆ3. (Eq.2)

$v_e/v_i=a(x/R)^{(-1/mu)}$?(1)

, where ve is an ejection velocity of grain, x is the initial position of ejecting quartz sand grains and R is the crater radius.

mu=0.05ρ+038 -(2)

Moreover, we obtain the relation between crater size and projectile density.(Eq.3)

[R$*$(ρt/m)ˆ(1/3)]=11$*$[ρt/ρp]ˆ0.096 ?Eq(3)

The ejection angle of quartz sand grains is also obtained. For all projectiles, the grain that ejects from near impact point have high ejection angle and the more distant that grain ejects from, the lower the eject angle is. There are no effect of projectile density.

The obtained empirical equation between the ejection velocity and the initial position is as follows Eq(4),

$ve/vi=1.5*10^{-3}(x/R)^{-1.8}$ (0.3<x/R <0.9) -(4)

Japan Geoscience Union Meeting 2014
(28 April - 02 May 2014 at Pacifico YOKOHAMA, Kanagawa, Japan)

U06-P09 Room:Poster Time:April 28 18:15-19:30

Impact cratering experiments on granular slopes

HAYASHI, Kosuke[1*] ; SUMITA, Ikuro[1]

[1]Graduate School of Natural Science and Technology

Impact cratering is an important process for the evolution of planetary surfaces. Many experiments of impact cratering into granular media have been conducted to understand its basic physics (e.g., Walsh et al., 2003, de Vet and Bruyn, 2007). These studies have shown that as impact energy becomes larger, simple craters transform into complex craters. In addition when gravity is more important than the target strength, the crater diameter increases in proportion to the 1/4 power of the impact energy. Peculiar craters on asteroids have been discovered in recent planetary missions. Some craters on asteroids are likely to be in the transitional regime between the gravity and strength dominated regimes. In order to better understand how such craters may have formed, we have recently conducted experiments around the transitional regime (Takita and Sumita, 2013). In addition, because asteroids have large topography relative to its size, some craters seem to have formed by impact on slopes (Jaumann et al., 2012). However, since most previous experiments were performed on horizontal targets, impact cratering on slopes is still poorly understood. In this study, we report the results of experiments to understand the effects of slope angle on crater formation.

The experiments in this study were performed by dropping spherical projectiles into an inclined granular target. Projectiles are made of stainless steel (density: 7.70g/cm^3) and their diameters are 11.0mm and 22.2mm. We use sand (mean diameter of 0.204mm, density of 2.66g/cm^3, angle of repose of 37.2○, volumetric packing fraction of 0.56) for the granular target. The slope angle ϑ was 0○,11○,16○,22○,34○. Impact energy E was 0.055 , 0.073 and 0.58 J. Crater formation process was recorded by a high speed camera. The 3-D topographies of the granular target before and after the impact were measured by a laser displacement meter which we move by a stepping motor. Resolution of the laser displacement meter is about 0.024mm for vertical direction, and about 0.1mm for horizontal direction. The stepping motor moves at 0.2mm intervals. We obtained the vertical displacement of the granular target caused by the impact by subtracting the topography of the target before and after the impact. We defined the maximum vertical displacement as the crater depth, the length of the crater in the dip direction projected to the horizontal plane as the crater length, and the width in the strike direction as crater width.

We find that the part of the crater rim disappears when ϑ is larger than about 20○. From studying the images recorded by high speed camera, we find that when ϑ becomes large, the slope above the impact point collapses and this causes the partial disappearance of the rim.

Comparing with the Vestan craters (Jaumann et al., 2012), we find that both laboratory and Vestan craters have common asymmetric shape with ejecta spreading down slope and the location of the maximum depth also shifted towards downslope. We find that the crater depth decreases with ϑ . On the other hand, crater length and crater width remains unchanged from 0○to 22○and increased when ϑ was larger than 22○. As a result, the depth / length ratio decreased from 0.25 to 0.05 with the increase of ϑ.

We also analyzed the impact energy dependence of the crater scales and fit them by a power law relation AE $\wedge$ α. We find that with the increase of ϑ, both the prefactor A, and the exponent α changes. This shows that the scaling law obtained for the horizontal granular target cannot be directly applied to impacts on slopes.

References:

de Vet and Bruyn., 2007. Phys.Rev E 76, 041306
Jaumann et al., 2012. Science 336, 687
Takita and Sumita, 2013. Phys.Rev E 88, 022203
Walsh et al., 2003, PRL 91.104301

Keywords: impact cratering, granular matter

Japan Geoscience Union Meeting 2014
(28 April - 02 May 2014 at Pacifico YOKOHAMA, Kanagawa, Japan)

U06-P10 Room:Poster Time:April 28 18:15-19:30

Size Dependence of Impact Disruption Threshold of Iron Meteorites

KATSURA, Takekuni[1] ; NAKAMURA, Akiko[1*] ; TAKABE, Ayana[1] ; OKAMOTO, Takaya[1] ; SANGEN, Kazuyoshi[1] ; HASEGAWA, Sunao[2] ; LIU, Xun[3] ; MASHIMO, Tsutomu[3]

[1]Graduate School of Science, Kobe University, [2]Institute of Space and Astronautical Science, [3]Institute of Pulsed Power Science, Kumamoto University

Iron meteorites and some M-class asteroids are generally understood to be fragments that were originally part of cores of differentiated planetesimals or part of local melt pools of primitive bodies. On these primitive bodies and planetesimals, a wide range of collisional events at different mass scales, temperatures, and impact velocities would have occurred between the time when the iron was segregated and the impact that eventually exposed the iron meteorites to interplanetary space.

In this study, we performed impact disruption experiments of iron meteorite specimens as projectiles or targets at room temperature to increase our understanding of the disruption process of iron bodies. Our iron specimens (as projectiles or targets) were almost all smaller in size than their counterparts (as targets or projectiles, respectively), with one exceptional shot. Experiments of impacts of steel specimens were also conducted for comparison.

The fragment size distribution of iron material is different from that of rocks because in iron fragmentation, a higher percentage of the mass is concentrated in larger fragments, probably due to its ductility. The largest fragment mass fraction is dependent not only on the energy density but also on the size of the specimen. We show the largest fragment mass fraction has a power-law dependence to initial peak pressure normalized by a dynamic strength, which is defined to be dependent on the size of the iron material.

This work was supported by the Space Plasma Laboratory, ISAS, JAXA, Japan and by the Global Center of Excellence Program of Pulsed Power Science, Kumamoto University.

Keywords: Small Bodies, Iron Meteorite, Impact Process

Japan Geoscience Union Meeting 2014
(28 April - 02 May 2014 at Pacifico YOKOHAMA, Kanagawa, Japan)

U06-P11 Room:Poster Time:April 28 18:15-19:30

Cratering chronology models for the near-Earth asteroid 1999 JU3

ANDO, Kosuke[1*] ; MOROTA, Tomokatsu[1] ; SUGITA, Seiji[2] ; HONDA, Rie[3] ; KAMEDA, Shingo[4] ; YAMADA, Manabu[5] ; HONDA, Chikatoshi[6] ; SUZUKI, Hidehiko[4] ; WATANABE, Sei-ichiro[7]

[1]Graduate School of Environmental Studies, Nagoya University, [2]Department of Complexity Science and Engineering, Graduate School of Frontier Sciece, The University, [3]Departmant of information Sciemce, Kochi University, [4]School of Science, Rikkyo University, [5]Planetary Exploration Research Center, Chiba Institute of Technology, [6]The University of Aizu, [7]Division of Earth and Planetary Sciences, Graduate School of Science, Nagoya University

The Japanese asteroid explorer Hayabusa-2, that is scheduled for launch in 2014, will be observe a near Earth C-type asteroid 1999 JU3 and will return to Earth with its samples. In this study, we model cratering and crater erasure processes on 1999 JU3 to provide an age estimate for 1999 JU3 based on high-resolution images that will be obtained by Hayabusa-2. The impact rate on 1999 JU3 is calculated from population models of main-belt asteroids (MBAs) and near-Earth asteroids (NEAs) and the average collision probabilities for the main belt and for NEAs. By converting the impactor size to the size of consequent crater based on crater scaling law and the average collision velosities for the main belt and for NEAs, the cratering rate on 1999 JU3 is calculated. For comparison, we use two population models of asteroids, two crater scaling laws and five conditions of surface of 1999JU3. In addition, two crater erasure processes, seismic shaking and saturation of craters, are considered in our model. As a result, our models indicate that age estimate of 1999 JU3 primary depends on crater scaling laws used and assumptions of surface conditions of 1999 JU3 rather than population models of asteroids.

Japan Geoscience Union Meeting 2014
(28 April - 02 May 2014 at Pacifico YOKOHAMA, Kanagawa, Japan)

U06-P12 Room:Poster Time:April 28 18:15-19:30

Scaling analysis of cavity morphology and disruption threshold for highly porous targets

OKAMOTO, Takaya[1*] ; NAKAMURA, Akiko[1] ; HASEGAWA, Sunao[2]

[1]Graduate School of Science, Kobe University, [2]Institute of Space and Astronautical Science

The morphology of the cavity formed by an impact can be dependent on parameters such as porosity, bulk density and strength of target bodies and size, bulk density, strength and impact velocity of impactors. Laboratory impact experiments have been conducted and cavity diameter and depth have been studied in previous studies in which highly porous targets up to 60% in porosity were used (e.g. gypsum, sintered glass and snow). Based on recent spacecraft missions and ground-based observation, it is shown that small bodies have even higher bulk porosities up to 86% (Consolmagno et al., 2008). Experiments using further highly porous targets are necessary for understanding collisional evolution of such bodies in the formation period. We study cavity morphology of highly porous targets and compile the result with previous studies. We also study disruption threshold of targets and compile the results.

We prepared porous targets with three different porosities, which have porosity of 94%, 87% and 80% (Okamoto et al.,2013). Various projectiles with different density and strength were used; titanium, aluminum, stainless steel and nylon spheres of 1 and 3.2 mm in diameter, and basalt cylinder of 3.2 mm in diameter and 2.0 mm in height. The impact velocity was ranged from 1.7 to 7.2 km/s.

The track was long and thin, in carrot-shape, when the projectile was intact, while it was short and thick, in bulb-shape, when the projectile was fragmented. We report the results of bulb-shape cavity in this presentation.

We apply crater scaling law in strength regime for maximum diameter and entrance hole diameter of the cavity. We compile data of previous studies and ours to obtain empirical relationships. A correlation is shown between the distance from entrance hole to maximum diameter and characteristic depth where initial kinetic energy of projectile becomes 1/e. Characteristic length is a function of drag coefficient. Since the drag coefficient depends on the fragmentation degree of projectile, it is shown that disruption of projectile affects the distance from the entrance hole to the maximum diameter.

Volume, maximum diameter and depth of cavity during its growth were measured on flash X-ray images. Normalized cavity volume and time (Schmidt and Housen., 1987) are applied for the analyses of the results. They have a power law relationship. The power law index for shots with larger density ratio (target density / projectile density) is slightly larger than those with smaller density ratio. Similarly power law relationships between normalized depth of cavity, maximum diameter and normalized time were obtained, respectively. The power indices are consistent of the power index determined for the normalized volume and time. Thus the growth of cavity volume can be explained by growth of maximum diameter and depth.

The threshold energy density for disruption $Q^*$is defined by energy density leading to a largest remnant having half the mass of the target. Q^*increases slightly with porosity of the targets. $Q^*$for the targets with equal diameter-height ratio is slightly larger than those with longer shape (diameter /height=0.5). In this presentation, we will discuss scaling of $Q^*$with various previous study.

Keywords: impact experiment, small body, crater, catastrophic disruption

Japan Geoscience Union Meeting 2014
(28 April - 02 May 2014 at Pacifico YOKOHAMA, Kanagawa, Japan)

U06-P13 Room:Poster Time:April 28 18:15-19:30

A consortium study of the largest particle of Hayabusa-returned samples

UESUGI, Masayuki[1*] ; KAROUJI, Yuzuru[1] ; YADA, Toru[1] ; ISHIBASHI, Yukihiro[1] ; SATAKE, Wataru[2] ; OKADA, Tatsuaki[1] ; ABE, Masanao[1]

[1]Japan Aerospace Exploration Agency, [2]Department of Earth and Planetary Science, University of Tokyo

Hayabusa-returned samples retrieved by the Hayabusa spacecraft were already distributed and investigated in the preliminary examinations and international A/Os. Through the investigations, several insights have been obtained on the formation process of 25143 Itokawa and surface processes occurred on the asteroid, as well as the confirmation that the particles were certainly regolith particles from there [1-6].

There are several particles, however, which have not been distributed for those examinations because of their rare features appeared in the initial description done by extraterrestrial sample curation team (ESCuTe) of JAXA. Though those particles will provide us further information for Itokawa and evolution of the asteroid, the samples should be investigated as carefully as possible to reduce consumption and damage of the samples. RA-QD02-0136-01 is currently the largest sample of Hayabusa-returned samples recovered from the sample catcher. The major axis of the particle ra is around 310 μm, and weight of the particles is estimated around 20 μg, assuming the volume V= $4/3\pi r_a r_b r_c \sim 4/3\pi/(2\sqrt{2})r_a{}^3$ and density of the particle as 3.4 g/cm^3, where r_a, r_b and r_c are major axis, semi-major axis and minor axis, respectively. The RA-QD02-0136-01 is mainly composed of Ca-rich pyroxene, and also contains minor amount of low-Ca pyroxene, olivine, plagioclase and troilite. In order to maximize scientific gain from the Hayabusa-returned samples, we decided to investigate this particle by constructing a specific consortium for the analysis.

6 teams were joined the consortium, and following analyses were proposed.
M. Uesugi and A. Tsuchiyama : CT observation of 3D texture and surface observation
J. Park and Rutger team : Ar age analysis to determine the shock ages
K. Nishiizumi and K. Nagao : Analysis of cosmogenic nuclides to estimate the erosion rate of Itokawa
N. Kita and D. Nakashima : O-isotope analysis of high-Ca pyroxenes and plagioclases by SIMS
F. Langenhorst : TEM observation of the dislocations for estimating shock effect by small impacts
L. Keller : TEM observation of the space weathering rims

Currently, we prepare the sample cutting method, and evaluate effect of the cutting and sample transfer on the subsequent analysis. We will report the sequential flow of the analyses and results of the rehearsals.

References: [1] Nakamura et al. 2011. Science 333:1113-1116. [2] Yurimoto et al. 2011. Science 333:1116-1119. [3] Ebihara et al. 2011. Science 333:1119-1121. [4] Noguchi et al. (2011) Science 333:1121-1125. [5] Tsuchiyama et al. 2011. Science 333:1125-1128. [6] Nagao et al. 2011. Science 333:1128-1131.

Japan Geoscience Union Meeting 2014
(28 April - 02 May 2014 at Pacifico YOKOHAMA, Kanagawa, Japan)

U06-P14 Room:Poster Time:April 28 18:15-19:30

Present status of a consortium study of a NaCl bearing Itokawa particle

YADA, Toru[1*] ; UESUGI, Masayuki[1] ; KAROUJI, Yuzuru[1] ; NOGUCHI, Takaaki[2] ; ITO, Motoo[3] ; ISHIBASHI, Yukihiro[1] ; OKADA, Tatsuaki[1] ; ABE, Masanao[1]

[1]Japan Aerospace Exploration Agency, [2]Faculty of Science, Ibaraki University, [3]Japan Agency for Marine-Earth Science and Technology

Hayabusa spacecraft returned samples from S-type Near-Earth Asteroid (NEA) Itokawa in June 2010. After the return, Extraterrestrial Sample Curation Team (ESCuTe) of JAXA have recovered particles from a sample catcher of Hayabusa, and more than 400 particles initially described have been presented in public (Yada et al., 2014). Among them, some types of particles having rare features are assigned to consortium studies, because they are supposed to be applied by multiple proposals so that they could not be distributed. Members of the ESCuTe would lead consortium studies to ask for research plans from worldwide researchers, discuss a research flow for the particles with the researchers to maximize their scientific gain, and push the plan forward.

One of the consortium studies is for a silicate particle bearing NaCl. The sample ID RA-QD02-0129 is 40 micron in size, mainly composed of silicate similar to plagioclase in chemical composition, and have euhedral NaCl particles of 3-5 micron in size on its surface. This is the only silicate particle bearing NaCl among those initially described so far.

In planetary material samples, NaCl is very rare and unique component. It has been discovered only in Monahan and Zag H chondrites among all ordinary chondrites so far. Trace of extinct 129I was discovered in the NaCl in the meteorites, which means that it should have formed in their parent body(ies), H chondrite or other, in the early solar system and involved in the meteorites in some processes afterward (Zolensky et al., 1999; Whitby et al., 2000). The formation of NaCl should be linked with water in their parent bodies, so it could provide important information about the origin of its parent body. Additionally, water and salt should be closely linked with organic material revolution and might provide interesting suggestion for the origin of life.

One of the most important purposes of this consortium is to prove extraterrestrial origin of the particle (silicate) and NaCl. And next step is to clarify whether its parent body would be Itokawa and/or LL chondrite parent body or other ones. What can prove the extraterrestrial origin of the NaCl is (1) discovery of solar flare tracks in the NaCl, (2) detection of solar wind He on its surface, (3) presence of space weathering layer on its surface. Transmitted electron microscope (TEM) observation for ultrathin section of the NaCl made by focused ion beam (FIB) system will be necessary for (1) and (3), and a laser ionization mass spectrometer is necessary for (2). In the research plan so far, terrestrial NaCl with instrumentally implanted He and NaCl in Monahan meteorite will be prepared for the rehearsal analyses to establish analytical techniques and then we will try the real particle.

References:
Abe M. et al. (2011) LPS XLII, Abstract #1638.
Whitby J. et al.(2000) Science 288, 1819.
Yada T. et al. (2014) LPS XLV, Abstract #1759.
Zolensky M. E. et al. (1999) Science 285, 1377.

Keywords: Itokawa, asteroid, NaCl, consortium

Japan Geoscience Union Meeting 2014
(28 April - 02 May 2014 at Pacifico YOKOHAMA, Kanagawa, Japan)

U06-P15 Room:Poster Time:April 28 18:15-19:30

Three-dimensional structures of aggregate-type Itokawa particles

YADA, Toru[1*] ; UESUGI, Masayuki[1] ; KAROUJI, Yuzuru[1] ; UESUGI, Kentaro[3] ; TSUCHIYAMA, Akira[2] ; ISHIBASHI, Yukihiro[1] ; OKADA, Tatsuaki[1] ; ABE, Masanao[1]

[1]Japan Aerospace Exploration Agency, [2]Graduate school of science, Kyoto University, [3]Japan Synchrotron Radiation Research Institute

Regolith particles, which should have been formed by fragmentation and abrasion due to impact and impact-induced vibration, exist on surfaces of minor bodies. Their formation processes and causes will tell us physical and chemical condition of the surfaces of the minor bodies and their parent bodies.

Hayabusa spacecraft returned samples from S-type Near-Earth Asteroid (NEA) Itokawa in June 2010 (Abe et al., 2011). Among the returned regolith particles, we focus on aggregate-type particles composed of tiny component grains to analyze their three-dimensional (3D) structure in order to clarify their formation processes and environments.

In this study, we chose five aggregate-type Itokawa particles, which are 55-128 micron in size, assigned for JAXA's research among more than 400 particles initially described. They were firstly analyzed by synchrotron X-ray computed tomography (CT). Because they might be fragile, they were placed inside tiny, upside-down pyramid-shaped sample holder made of SiN. They were irradiated in beam line (BL) 47XU of SPring-8 by photon light source of both 7keV and 8keV in energy and obtained their transmitted X-ray images. The obtained images were calibrated by computers, and their 3D structure could be reconstructed. Mineral species in the particles could be estimated by the different X-ray adsorption factors of different energy X-ray in each of the minerals.

The obtained data are under calibration so far. We will clarify their 3D structure and discuss about their formation processes. Additionally, we are planning to make their ultrathin sections by focused ion beam fabrication system (FIB) and confirm detailed structures between the tiny component grains with transmitted electron microscope (TEM).

References:

Abe M. et al. (2011) LPS XLII, Abstract #1638.
Tsuchiyama et al. (2013) GCA 116, 5.

Keywords: Itokawa, asteroid, aggregate, three-dimensional structure, synchrotron CT

Japan Geoscience Union Meeting 2014
(28 April - 02 May 2014 at Pacifico YOKOHAMA, Kanagawa, Japan)

U06-P16 Room:Poster Time:April 28 18:15-19:30

Consortium Study of Troilite and Phosphate-bearing HAYABUSA Returned Samples

KAROUJI, Yuzuru[1*] ; UESUGI, Masayuki[1] ; YADA, Toru[1] ; ISHIBASHI, Yukihiro[1] ; SATAKE, Wataru[2] ; OKADA, Tatsuaki[1] ; ABE, Masanao[1]

[1]Japan Aerospace Exploration Agency, [2]Department of Earth and Planetary Science, University of Tokyo

HAYABUSA returned samples have been shown as Itokawa origin by the preliminary examinations (e.g. Nakamura et al., 2011). Furthermore, international AO study has begun last year, and a formation process of asteroid Itokawa is becoming revealed.

HAYABUSA returned samples are described initially by JAXA Extraterrestrial Sample Curation Team (ESCuTe), and a sample catalogue is prepared based on the data of initial description (e.g. Yada et al., 2014). More than 400 returned samples were described so far. These described samples are classified into four categories. A number of samples of each category to be distributed for international AO are decided based on the sample catalogue. But it is difficult to distribute such samples with rare characteristics in composition, mineralogy, structure, or size, although those samples should maintain scientifically important information.

Therefore, in JAXA, ESCuTe started to organize the consortium studies in order to obtain the scientific information as many as possible from these samples (e.g. Yada et al., 2014; Uesugi et al., 2014). In this paper, we report the research plan for the particles mainly composed of FeS and which contain phosphate minerals.

RA-QD02-0245 composed mainly of FeS (40 micron) with smaller attached olivine and pyroxene grains. This particle was analyzed by X-ray CT at SPring-8 for 3D texture without atmosphere. Two ultra-thin section will be made from the edge of this particle by FIB. The ultra-thin sections will be examined by TEM in detail for space-weathering effect on FeS surface. The main mass of this particle will be analyzed for chemical composition. Especially, the siderophile element composition gives us information on the formation process of Itokawa parent body.

Some particles including phosphate mineral were found by the initial description. Because Ca-phosphate tends to be enriched in incompatible elements such as REEs, Th and U, we propose the investigation of U-Pb systematics using Nano-SIMS in order to study the history recorded in the phosphates. We will perform the U-Pb dating of the phosphates as many as possible and aim to understand the thermal history of Itokawa parent body such as crystallization age and the catastrophic collition if recorded.

Keywords: HAYABUSA, Itokawa, troilite, phosphate, siderophile element, U-Pb dating

Japan Geoscience Union Meeting 2014
(28 April - 02 May 2014 at Pacifico YOKOHAMA, Kanagawa, Japan)

U06-P17 Room:Poster Time:April 28 18:15-19:30

Asteroid Shape Reconstruction by Structure-from-Motion Method with Bundler and PMVS2

HIRATA, Naru[1*] ; MORI, Yohei[1] ; HAYABUSA-2 SHAPE RECONSTRUCTION, Study group[2]

[1]ARC-Space/CAIST, The University of Aizu, [2]Hayabusa-2 project

Here we report results on application of open source shape reconstruction tools to an asteroid image data set. We test two tools that cooperatively work to reconstruct an object shape from images. Bundler is an open source implementation of a stereo shape reconstruction method called Structure from Motion (SfM). PMVS2 gives a more dense shape model, since Bundler only estimates 3D locations of a limited number of feature points. A global image data set of the asteroid Itokawa taken by AMICA on board the Hayabusa spacecraft is employed to our test data set. An obtained model satisfies that most requirements from the Hayabusa-2 mission on the shape model that used during the mission phase. An important advantage of these new tools compared to previous ones is its short processing time. This advantage will be effective in quick evaluation of observation data and decision making during the mission operations. More precise and high definition models will be reconstructed by other method such as shape-from-shading or photometric stereo.

Keywords: Asteroid, shape reconstruction, bundler, PMVS2, Structure-from-Motion, Hayabusa-2

Japan Geoscience Union Meeting 2014
(28 April - 02 May 2014 at Pacifico YOKOHAMA, Kanagawa, Japan)

U06-P18 Room:Poster Time:April 28 18:15-19:30

Feature matching in planetary images with multiple spatial resolutions by using SIFT algorithm

KODAMA, Hiroyuki[1] ; HONDA, Chikatoshi[1*]

[1]The University of Aizu

This study uses feature matching in planetary images with multiple spatial resolution. To know where lower altitude images are taken in high altitude images is performed based on images without the position and attitude of spacecraft in this study. The lower altitude images of AMICA on-board the Hayabusa spacecraft, asteroid probe are found as a correspondence of image features (keypoint) in higher altitude images. We adopted the Scale Invariant Features Transform (SIFT) to represent a kind of key-point of image for image feature matching. In generally, the SIFT keypoint is robust to scale transition, change of lighting condition, parallel displacement, and rotation of image, so this keypoint is suitable to feature matching of planetary image which contains of scale and rotation between different images. As a result, for the improvement of accuracy of feature matching, it is important to have a preprocessing of image (e.g., equalizing).

Keywords: planetary image, SIFT, feature matching, AMICA

Japan Geoscience Union Meeting 2014
(28 April - 02 May 2014 at Pacifico YOKOHAMA, Kanagawa, Japan)

U06-P19 Room:Poster Time:April 28 18:15-19:30

Grooves on Phobos: Spatial distributions and their implications to the formational mechanism

KIKUCHI, Hiroshi[1*] ; MIYAMOTO, Hideaki[1]

[1]The University Museum, The University of Tokyo

Grooves are roughly-defined as trough-like depressions commonly found on asteroids and small satellites. Among the various features categorized as grooves, the most typical are considered as those found on the surface of Phobos. Grooves on Phobos are the most extensively-existing geological features on the satellite, and thus are documented and discussed for years. However, their formational processes remain controversial. Previously-proposed hypotheses are (1) grooves are some kind of intentional fractures and (2) they are results of impacts caused likely by linearly-aligned impactors ejected from Mars.

Former hypothesis has difficulty in explaining the geographical distribution of grooves (Murray 2011). In fact, because of this difficulty, Murray (2011) concluded that the latter (i.e., secondary impactors derived from Mars) could only be the reasonable explanation for the observed characteristics of grooves on Phobos, including their morphological features, distributions, and hemispheric coverage. Nevertheless, Ramsley and Head (2013) recently showed that, in order to form grooves well organized as those found on Phobos, each of fragments ejected from Mars should have no relative velocity, which is difficult to be achieved for ejecta from Mars. They also showed that most grooves on the northern hemisphere cannot be formed as secondary impacts from Mars because the impactors ejected from Mars do not impact in the directions normal to the equatorial plane of Phobos. Therefore, neither hypothesis remains satisfactory to explain the observational facts.

We carefully reevaluate previous hypothesis based on recently-acquired data, which are partly not available at the time of previous studies. We scrutinize all of the high-resolution images obtained so far to map them out on a numerical shape model. As a result, we identify 488 grooves, whose spatial distributions are precisely mapped three dimensionally. We newly find that each of grooves is always aligned on a certain plain even though it sometimes appears to be an undulating curved depression. We consider this strongly indicates that a groove is a result of a series of impacts of aligned fragments.

We statistically study the angle between the equatorial plane of Phobos and the plane, which contain each groove and find that the distributions of the angles have three peaks at 25, 90 and 155 degrees (hereafter we call A, B, and C type, respectively). Most of the B type grooves exist on the northern hemisphere.

To explain our mapping results, we propose a new hypothesis for the formation of Phobos as follows: (1) An asteroid of a collection of smaller fragments held together by self-gravity in the form of a rubble-pile is pulled apart and stretched straightly by tides during a close approach to Mars; (2) The asteroid (now separates into a train of fragments) is caught by the Mars gravity and revolves around Mars; (3) Every time it revolves around Mars, a part of the fragments hit Phobos and form a lineated depression, which is observed as a type A or C groove; (4) When the eccentricity of the impartor becomes low until the overlapping the trajectory of Phobos, type B grooves are formed.

Our hypothesis is along the idea that grooves are formed by aligned impactors as proposed by Murray (2011) but essentially different in the origin of the fragments, which can resolve the difficulty pointed out by Ramsley and Head (2013). Not only that, our hypothesis has advantage of completely satisfying both the morphological and geographical characteristics of grooves on Phobos. Furthermore, our hypothesis can also explain the deficiency of grooves on Deimos.

Reference

[1]Murray, J.B., Iliffe, J.C., 2011. Geomorphology. Geol, Soc, Spec, Publ., London, pp.21-41
[2]Ramslay, K.R., James, W. H., 2013. Planetary and Space Science, 69-95

Keywords: Phobos, groove, Mars, tidal-disruption, impact

Japan Geoscience Union Meeting 2014
(28 April - 02 May 2014 at Pacifico YOKOHAMA, Kanagawa, Japan)

U06-P20 Room:Poster Time:April 28 18:15-19:30

Visible wavelength spectroscopy of sub-km-sized Near-Earth Asteroids with low delta-v

KURODA, Daisuke[1*] ; ISHIGURO, Masateru[2] ; TAKATO, Naruhisa[3] ; HASEGAWA, Sunao[4] ; ABE, Masanao[4] ; TSUDA, Yuichi[4] ; SUGITA, Seiji[5] ; USUI, Fumihiko[6] ; HATTORI, Takashi[3] ; IWATA, Ikuru[3] ; IMANISHI, Masatoshi[3] ; TERADA, Hiroshi[3] ; CHOI, Young-jun[7] ; WATANABE, Sei-ichiro[8] ; YOSHIKAWA, Makoto[4]

[1]Okayama Astrophysical Observatory, National Astronomical Observatory of Japan, [2]Department of Physics and Astronomy, Seoul National University, [3]Subaru Telescope, National Astronomical Observatory of Japan, [4]Institute of Space and Astronautical Science, Japan Aerospace Exploration Agency, [5]Graduate School of Frontier Science, The University of Tokyo, [6]Graduate School of Science, The University of Tokyo, [7]Korea Astronomy and Space Science Institute, [8]Graduate School of Science, Nagoya University

We present a unique data set of the taxonomic type of near-Earth asteroids (NEAs) accessible with available spacecraft.

The research on NEAs has entered a new phase thanks to sample-return space explorations together with state-of-the-art large ground-based telescopes. We made observations of twelve asteroids with Subaru, GEMINI-North, GEMINI-South and Okayama 188cm telescopes. They have low delta-v orbits with potential to be investigated by manned/unmanned spacecraft. Also, ten sub-km-sized bodies are included in them, and are one of remarkable characteristics in terms of an evolutionary scenario.

We find that eleven asteroids are classified as S-complex and one asteroid as V-type. Most S-complex asteroids (eight out of eleven, $\sim$70%) have spectra similar to subgroups of Q or Sq-type, suggesting that these objects are less matured against space weathering.

In this presentation, we show their spectra and discuss dominance of S-complex asteroids based on the previous research.

Keywords: asteroid, visible spectroscopy, taxonomic classification

Japan Geoscience Union Meeting 2014
(28 April - 02 May 2014 at Pacifico YOKOHAMA, Kanagawa, Japan)

U06-P21 Room:Poster Time:April 28 18:15-19:30

Development of a wide-band optical filter optimized for deep imaging of small solar-system bodies

OKUMURA, Shin-ichiro[1*] ; NISHIYAMA, Kota[1] ; URAKAWA, Seitaro[1] ; SAKAMOTO, Tsuyoshi[1] ; TAKAHASHI, Noritsugu[1] ; YOSHIKAWA, Makoto[2]

[1]Japan Spaceguard Association, [2]JAXA

We developed a newly designed wide-band optical filter and evaluated its performance. It is optimized for deep imaging of small solar-system bodies. The new filter, which we denote as *Wi*, is designed to reduce contamination by light pollution from street lamps, especially strong mercury and sodium emission lines. For the reasons that (1) much of artificial light pollution concentrates in the *V* band, (2) the photon numbers peak at a wavelength of 6350 $\AA$ in the spectrum of sunlight, and (3) many asteroids have their peak/plateau reflectance at around 7000 $\AA$ in the optical range, the new filter's cut-on wavelength is set to 5880 $\AA$ by using an OG590 Schott color glass filter. On the other hand, the cut-off wavelength, which is achieved by a short-pass interference coating, is set to 9380 $\AA$ in consideration of worst of the OH night sky emission and the atmospheric water vapor absorption band at 9400 $\AA$.

Compared with the use of a commercially available long-wave cut wide-band filter (*W* filter, 4900-9100 $\AA$), the sky brightness is 10-20 % reduced by the *Wi* filter under bright-sky conditions by not only artificial light pollution but scattered moonlight. In the detection of asteroids, the detected total flux of an asteroid through the *Wi* filter has been 3% larger than that through the *W* filter, though the width of the *Wi* filter response function is 16% narrower than that of the *W* filter. By using the *Wi* filter, the S/N ratios in the detection of asteroids were improved by about 6%, on average, compared with the use of the *W* filter, and the improvements were slightly larger in a brighter sky. The use of the CCD with high sensitivity at longer wavelength, such as the back-illuminated, fully-depleted CCD, will show a larger improvement in the S/N ratio by using the *Wi* filter.

Reference:
Wide-Band Optical Filter Optimized for Deep Imaging of Small Solar-System Bodies,
Okumura *et al*. Publications of the Astronomical Society of Japan, **64**, 47 (2012)

Keywords: optical, small solar system body, light pollution, wide-band filter

Japan Geoscience Union Meeting 2014
(28 April - 02 May 2014 at Pacifico YOKOHAMA, Kanagawa, Japan)

U06-P22 Room:Poster Time:April 28 18:15-19:30

Prediction of Phoeincid in 2014

SHUTO, Hironobu[1] ; SATO, Isao[2*]

[1]Nihon Univ., [2]Astronomical Society of Japan

Phoenicid appeared in 1956 is a meteors yielded by the comet 289P/Blanpain founded in 1819. We calcurated a prediction of Phoenicid in 2014.

Comet Blanpain has a mean motion resonance of 9:4 with Jupiter. Therefore Phoenicid has 95 year cycle. The next big apparition will be in 2051.

Keywords: Meteors

Japan Geoscience Union Meeting 2014
(28 April - 02 May 2014 at Pacifico YOKOHAMA, Kanagawa, Japan)

U06-P23 Room:Poster Time:April 28 18:15-19:30

Solidified and mixed materials on Asteroid body

MIURA, Yasunori[1*]

[1]In & Out University

The results of the present study are summarized as follows:

1) Study of the Asteroids provides characteristic formation processes of primordial terrestrial and extraterrestrial celestial bodies.

2) Identification of crystalline solids are almost similar between the Asteroids and Earth, though the Asteroid rocks might be formed by similar formation processes of terrestrial rocks based on the crystalline parts. However, extraterrestrial Asteroids show irregular mixtures of multiple states solidified amorphous solids.

3) Formation of non-spherical Asteroid body formed mainly by impact-related melting process is observed as heterogeneous and irregular distribution of impacted grains.

4) Local fluid-bearing depositions irregularly distributed on the surface and interior of the Asteroids might be based on storages on the interior formed by solidified mixtures of multiple states triggered by impact process on the Asteroids.

5) Different processes of solids between the Asteroids and Earth can be observed silica Si-O frameworks which can be obtained by the ion bombardment experiments. Crystalline rocks with hard silicate structures on Earth show higher ion-peaks of alkali ions (Na, K and Ca etc.), whereas solid-aggregates of the Asteroids show higher ion-peaks of Si and Al ions which are relatively destroyed by ion bombardments.

6) Ion-peaks by the sputtering of terrestrial impact-breccias are clearly higher than those of the Asteroid meteorites, which the main differences are not rock textures of breccias but atomic bonding of slow or rapid cooling process.

7) The air- and water-less Asteroids with solidified materials with multi-states are formed from nano-grains to macroscopic rocks by impact-related evolution process,

8) The primordial planet Earth with remained heterogeneous surface by impact-related process is considered to be cyclic system of three material states (air, liquid and solid) with macro-life activity which is formed by huge production from the interior triggered by huge collision process of the giant impact. On the other hand, the Asteroids without global cyclic changes of three materials states, microscopic quasi life-like materials might be locally found (mainly by high-resolution electron microscopy on in-situ or returned samples finally).

9) It should be avoided to collect artificial impacted samples, because irregular mixtures of solidified amorphous solids from vapor and liquid states are easily destroyed to be escaped to be exaggerated solids with less volatiles.

Keywords: Asteroids, solid aggregates, amorphous materials, fluid, ion bombardment run, micro quasi life-like materials

Japan Geoscience Union Meeting 2014
(28 April - 02 May 2014 at Pacifico YOKOHAMA, Kanagawa, Japan)

U06-P24 Room:Poster Time:April 28 18:15-19:30

The Origin of The Moon and The Earth in Multi-Impact Hypothesis

TANEKO, Akira[1*]

[1]SEED SCIENCE Lab.

Origin of the moon and the earth in the multi-impact hypothesis

This new hypothesis to the origin of the Moon and Earth,This is the proposal of solutions that satisfy unified manner new hypothesis
to the origin of the Earth and the Moon, all of the following questions.

(1).Why, large biological extinction of five times or more were happened on the earth?
(2).The meteorite falling on Earth, why stony-meteorites, stony-iron meteorite, iron-meteorite, such as differentiated and undifferentiated chondrites, what mixed in there?
(3).The old theory, why cosmic dust or did not become a planet in the asteroid belt?I think Itokawa's aggregate piece of crust differentiated?
(4).We have proposed a theory of the origin of the original description to solve the problems of the giant planet collision theory, all of the earth and the moon and deep sea bottom.
(5).Why, protoplanetary Serra did they destruction? = The tragedy caused by tidal forces and deformation due to Jupiter orbit perturbation.
(6).Increase in the aspect ratio of Serra orbital perturbation by Jupiter, destruction by tidal force of the approaching Jupiter.
(7).Plate boundary formation of plate tectonics,I suggest the formation origin of the deep sea bottom crust by peeling.
(8).The origin of deep-sea bottom update and continental drift and Mystery of the driving force was solved.
(9).Why diamond pipe did formed in South Africa?
(10).Why core eccentric (about ten percent) of what is happening? Radiation anomaly of Brazil over the Van Allen belt.
(11).New hypothesis at the origin of Jupiter's Great Red Spot, I think about How and Why to that Mystery !
(12).Why is whether the silicate star (asteroid now) Pluto of the outer planets?

Until now, Giant impact hypothesis is a theory only for making the moon.Protoplanet is the result of accidental collision with the Earth there Mars core size to the Earth,
It only has to calculate the conditions formed by the mantle further moon.

It is the original collision hypothesis.

Protoplanetary Serra was born in Ceres position of Bode's law.The planet Serra that differentiated, elliptical orbit was flattened by the Jupiter perturbations.
Major axis is constant because of energy conservation law.Eccentricity of Serra increases, the orbit that focus of the solar get closer so as to extend to the point of near-side Jupiter.
Just before the collision with Jupiter, Serra was rupture in tidal forces of Jupiter.By the mantle debris collides with the Earth, the moon was formed.
Position Serra collides to the Earth becomes the Pacific Ocean, it becomes the origin of the plate boundary crack.In addition, deep-sea of multiple formed with Impact of Multi-attack which is the time difference.
Eccentricity of the moment of inertia is estimated to be the driving force of the seabed update theory and theory of continental drift.
Mantle debris energy is large becomes Pluto, heavy and high density Koaritchi debris became Mercury with scattered to the inner planet side.
I estimated that the debris of Serra collide to Jupiter, it became the origin of the Jupiter's Great Red Spot.
The fact that iron meteorites, stony-iron meteorites, stony meteorites are differentiated, and chondrite undifferentiated are mixed, Ceres is present in the asteroid belt, the origin of the meteorite is convinced straightforwardly with this hypothesis.
Multi-impact theory be the basis of large organism extermination repeated, it is also the reason sea accounts for 70%, it was possible to understand the origin of the plate boundary crack.
Multi-impact hypothesis can be explained in a unified manner present condition of the earth as well as make the moon in this manner.

It is believed that asteroid Itokawa could check a set? Like Serra crust, then it becomes even proof of this hypothesis.

Keywords: Serra tidal disruption, Perturbation of Jupiter, Orbit transition of Serra, Match of the planets revolving surface, Feedengue zone (integrated range), Origin of Deep Sea Bottom

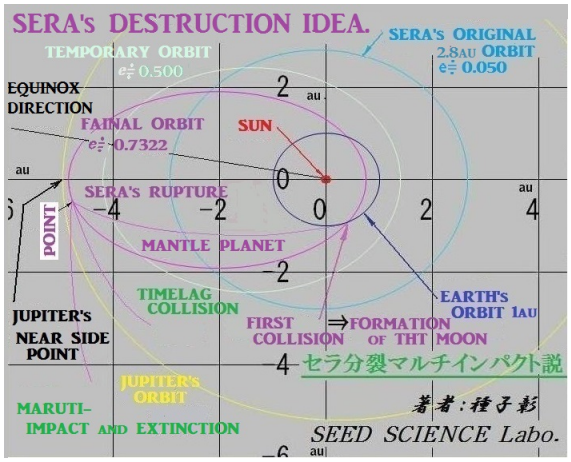

Japan Geoscience Union Meeting 2014
(28 April - 02 May 2014 at Pacifico YOKOHAMA, Kanagawa, Japan)

U07-01 Room:501 Time:May 1 09:00-09:30

Importance of Future Earth in Asia

YASUNARI, Tetsuzo[1*]

[1]Research Institute for Humanity and Nature

Future Earth (FE) has been launched as an international initiative to promote research for global sustainability by the international science and technology alliance with partnership of the International Council for Science (ICSU), the International Social Science Council (ISSC), the Belmont Forum of funding agencies, the United Nations Educational, Scientific, and Cultural Organization (UNESCO), the United Nations Environment Programme (UNEP), the United Nations University (UNU), and the World Meteorological Organization (WMO) as an observer (Future Earth, 2013). Future Earth will provide a single overarching structure for researchers, funders, service providers, and users, and integrates the existing Global Environmental Change (GEC) programmes. The GEC programmes have provided foci for several extensive international and multi-disciplinary networks of researchers investigating key human-environmental dynamics. Future Earth would develop a new generation network building on these. Future Earth proposes national and regional level committees, in addition to the regional nodes. The most essential issue for the overall FE activity towards global sustainability will be how to integrate efforts and activity of solving environmental problems and achieving sustainability for local to regional scales.

This paper introduces a strategic science plan for FE in Asia, which should be a guideline for implementing the overall FE activity in the whole of Asia, including part of the Pacific/Australasia and the Indian Ocean basin region.

Keywords: Future Earth, Asia

Japan Geoscience Union Meeting 2014
(28 April - 02 May 2014 at Pacifico YOKOHAMA, Kanagawa, Japan)

U07-02 Room:501 Time:May 1 09:30-09:55

Trade-offs in climate risks and societal risk decision

EMORI, Seita[1*]

[1]National Institute for Environmental Studies

The need to take mitigation measures in order to hold the increase in global average temperature below 2 degree C above pre-industrial levels are recognized in international negotiations of the United Nations Framework Convention on Climate Change (UNFCCC). According to the fifth assessment report by the Working Group I of Intergovernmental Panel on Climate Change (IPCC) which was published last September, attaining the temperature goal with a probability of 50% will require cumulative CO2 emissions from all anthropogenic sources to stay approximately 300 GtC from the present. If the current level of anthropogenic CO2 emission, 10 GtC yr-1, continues, the cumulative emissions will reach this upper limit in only 30 years. If we will seriously pursue the goal of temperature increase below 2 degree C, global CO2 emission should be turned to decline as soon as possible, and to be reduced at nearly zero by around the end of this century.

A great deal of research on climate change impacts and mitigation measures exist; however, large uncertainties remain in their overall pictures. So far, nobody can grasp clearly risks for human society and ecosystem associated with global warming exceeding ”2 degree C”, and risks for socioeconomics due to severe emission reductions of greenhouse gases. Furthermore, the risks will be realized in different ways by country, region, generation, and social attribution, and therefore, either if no specific response measures are conducted or if strong measures are conducted, a part of people in the world will have benefits and another part of people will make a loss. Climate change impact is not just an issue on benefits and losses of each person; but it relates to issues how we feel distress on risks for ecosystem, developing countries, and future generations. It relates to different value judgment among people. Deliberate work will be necessary in order to lead a decision-making which have both scientifically high rationality and socially high consensus, by connecting expert knowledge with social value judgment.

Japan Geoscience Union Meeting 2014
(28 April - 02 May 2014 at Pacifico YOKOHAMA, Kanagawa, Japan)

U07-03 Room:501 Time:May 1 09:55-10:20

Integrated MRV system using Monitoring-Sensing-Modeling in Tropical Peatland and Wet/lowland

OSAKI, Mitsuru[1*] ; HIROSE, Kazuyo[2]

[1]Research Faculty of Agriculture, Hokkaido University, [2]Earth Remote Sensing Division, Japan Space Systems

The Earth ' s remaining tropical forests are found mainly in the peatlands of the Amazon, Central Africa, and Southeast Asia, especially in regions of Kalimantan, Sumatra, and Papua New Guinea, where rich biodiversity can still be found and large amounts of carbon are stored in peat soils. Also, Wet/low-land where locate especially in South-East Asia is globally one of most important Bioproduction Ecosystem on food production, livelihood, mitigation and adaptation on climate change. This kind of Bioproduction Ecosystem have been supporting to feed large population, because of sustainability of soil fertility and nature friendly production system, calling as human-nature coexistence such as Satoyama in Japan. This human-nature coexistence Ecosystem (Satoyama Ecosystem) in wet/low-land is widely distributed in South-East Asia and South Asia, such as Cambodia, Thailand, Myanmar, Malaysia, Indonesia, Philippines and Bangladesh. Thus, peatland and wet/low-land Ecosystem has a role to stock large amount of Carbon, especially in peat and organic soils, and Mangrove soil. However, this human-nature coexistence Ecosystem (Satoyama Ecosystem) has been gradually or quality degrading and breaking down because of human-impact and climate change. Thus Sustainability of this human-nature coexistence Ecosystem (Satoyama Ecosystem) is one of key issue in not only regional, but also global. As SBSTA38 and Workshop of UNFCCC in 2013 have been focusing on ”Ecosystem of High Carbon Resorvoirs” such as peatland, costal ecosystem including Mangrove and Coral, and Permafrost, South-East Asia is key in this aspect.

Focusing on carbon emission estimation related with the REDD (Reducing Emissions from Deforestation and Forest Degradation in Developing Countries) Mechanism, at COP15 in Copenhagen, MRV (Measurement, Reporting and Verification) focused on establishing reference emission levels, national monitoring systems. At COP15 of Copenhagen, it was declared that an MRV system that should be coupled with two components ? satellite sensing and grand truth- is urgently required. Presently, our JST-JICA Project (SATREPS) on ”Wild Fire and Carbon Management in Peat-Forest in Indonesia” is the only project in the world to propose all aspects of MRV in tropical peatlands, enabling it to contribute significantly to also in tropical wet/low-land. Actually, carbon stock mapping and carbon flux mapping in peatland were obtained. Therefore, this paper describes our MRV system as a sensing standard for REDD+, biodiversity, and LLULUCF in tropical peatland and Wet/low lands.

Keywords: Satoyama Ecosystem, MRV, REDD+, Tropical peatland, Wet/low lands, High Carbon Resorvoir Ecosystem

Japan Geoscience Union Meeting 2014
(28 April - 02 May 2014 at Pacifico YOKOHAMA, Kanagawa, Japan)

U07-04 Room:501 Time:May 1 10:20-10:45

Current state of international governance on conservation and sustainable use of marine ecosystem services

YAGI, Nobuyuki[1*]

[1]Graduate School of Agricultural and Life Sciences, The University of Tokyo

Conservation and sustainable use of marine ecosystem services has been discussed internationally. For instance, discussions on EBSA (Ecologically or Biologically Significant Areas) are ongoing at meeting under the CBD (Convention on Biological Diversity). Likewise, the issues of VME (vulnerable marine ecosystem) are also discussed at FAO (Food and Agriculture Organization of the United Nations). In addition, General Assembly Ad Hoc Open-ended Informal Working Group to study issues relating to the conservation and sustainable use of marine biological diversity beyond areas of national jurisdiction has been held by the United Nations in order to discuss the need for creating an international instrument under UNCLOS to address the issue of the conservation and sustainable use of marine biological diversity of areas beyond national jurisdiction before the end of the 69th Session of the United Nations General Assembly (which is winter time in 2014).

The author has closely monitored the development of the discussions on the above meetings and found that their discussions were narrowly focused upon the control of fishing activities and they lacked considerations on the ecosystem services as a whole. This is most likely because stakeholder identifications, such as polluters and users of ecosystem services, are difficult and creating a legal framework is extremely hard. Under this situation, it can be argued that agreeing economical tools such as payment for ecosystem services would be more practical.

Keywords: Ecosystem services, UNCLOS, CBD, FAO, EBSA

Japan Geoscience Union Meeting 2014
(28 April - 02 May 2014 at Pacifico YOKOHAMA, Kanagawa, Japan)

U07-05 Room:501 Time:May 1 11:00-11:25

Global and regional platforms for integrated environmental and sustainability studies

TANIGUCHI, Makoto[1*]

[1]Research Institute for Humanity and Nature

Future Earth is a new 10 years initiative of international research program for global sustainability. The objectives of the Future Earth are to provide the knowledge required for societies in the world to face risks posed by global environmental change and to seize opportunities in a transition to global sustainability. Future earth was launched at 2013 by international academic, funding, organizations as alliances including ICSU, ISSC, IGFA, Belmont Forum, UNEP, UNESCO, and UNU. Future Earth focuses on co-design, co-production, and co-delivery, transdisplinarity, vertical (global-regional-local) and horizontal (multi issue with different sectors and stakeholders) integrations, and the involvement of young scientists. There are three themes, 1) Dynamic Planet, 2) Global Development, and 3) Transformation towards Sustainability. Researches on global environment and sustainability are urgent in Asia, because more than 50 percent of the world population lives in Asia, and drastic changes (both increase and decrease) of population, urbanization, material consumptions, environmental deteriorations, natural and social disasters, occurs in Asia, i.e. Asia is a hot spot area in terms of human and nature drives. Therefore core research hubs of the global environment and sustainability study such as Future Earth are needed in Asia, where is the hot spot area for global sustainability. Structures of the global and regional hubs for the Future Earth, core projects, and others are now under discussion during the interim period. Japan is expected to be Asian regional hub and a part of global hubs because many experiences and good practices on global environmental researches with stakeholders. Methodology, data, and knowledge for interdisciplinary and transdisciplinary researches, should be established in a platform and networking as regional hub of the Future Earth in Asia Pacific and others. Capacity building and education for global sustainability are also very important in Future Earth. Beyond the existing one-way capacity building and environmental education, knowledge transfers between different stakeholders may be a key for the next step of capacity building and education for global sustainability.

Keywords: global environmental change studies, global sustainability, future earth, platform, capacity building

Japan Geoscience Union Meeting 2014
(28 April - 02 May 2014 at Pacifico YOKOHAMA, Kanagawa, Japan)

U07-06 Room:501 Time:May 1 11:25-11:50

On Sustainability Initiative for Marginal Seas in East Asia

YAMAGATA, Toshio[1*] ; CRUZ, Lourdes J.[2] ; HASAN, Nordin M.[3]

[1]Application Lab, JAMSTEC, [2]National Research Council, the Philippines, [3]ICSU, Regional Office for Asia and the Pacific

The marginal seas of East Asia (MSEA hereafter) along the western Pacific, geologically as the interface between the Pacific Ocean and the Asian land mass, have islands spread from the Bering Sea down to the Indonesian seas consisting mainly of the Japanese, Philippine, and Indonesian Archipelagos. The MSEA is very important to international commerce and global security as linkage of heavily populated megacities with active societal, economical and industrial activities.

The MSEA is also the region of the highest marine biodiversity in the world, and its coral reefs and waters around atolls and small islands serve as the spawning ground and nursery of many marine species including tuna and other pelagic species that serve as very important food commodities in the Pacific islands, the Asia mainland and North America. To conserve the health of the MSEA under the pressure from the global change is of our urgent need. The region also lies along the path of destructive typhoons that originate in the western North Pacific and affect the Philippines, Vietnam, Hong Kong, China, Korea, and Japan. It is known that the western North Pacific is one of the most active basins where about 26 typhoons are generated annually, majority of which enter the Philippine area. The latest typhoon, Haiyan, the strongest storm recorded at landfall and the deadliest Philippine typhoon causing storm surges ever recorded, impinged heavily on human life, food security, energy supply, health, wellbeing, and transportation and communication systems in addition to extreme destruction of property, the economy and the ecosystem of Central Philippines. The outpouring of support from the international community to help the Philippines rise out of the disaster is well appreciated particularly by the victims of typhoon Haiyan and its storm surges. Many lessons now learned can be shared to minimize the impact, improve the resiliency of communities and to ensure protection of people against the anticipated increase in the number of future disasters due to global climate change. The cold phase of the Interdecadal Pacific Oscillation which brought the apparent hiatus of the global warming will eventually change and we expect a dramatic climate regime shift as observed in 1976.

In the spirit of the Future Earth initiative of ICSU, we are proposing a collaboration mechanism to share knowledge and expertise for better well-being among ICSU members around the MSEA to work for solutions of relevant problems in the region. While focusing on the maritime region, the researchers will aim to contribute to the attainment of the goals of Future Earth, namely: 1) to develop the knowledge for responding effectively to the risks and opportunities of global environmental change, and 2) to support transformation towards global sustainability in the coming decades. The main region of the proposed study will be the Exclusive Economic Zone beyond the territorial limit (generally 12 nautical miles from shore) in MSEA as well as international waters relevant to the sustainable use of common areas. The collaboration will involve joint researches and capacity building particularly of young scientist in developing countries. We had the brainstorming pre-scoping workshop for SIMSEA in February in Yokohama, of which purposes are:

1) To exchange information and knowledge on the existing discipline-oriented research programs on the marginal seas in Asia and the western Pacific for integrative sustainability research program involving natural, social, economic, engineering and technological sciences.

2) To discuss and co-design a collaborative interdisciplinary research program on the marginal seas of Asia and the western Pacific that meets the criteria of research toward global sustainability under the framework of Future Earth.

We will summarize the outcome of the pre-scoping meeting and envisage the future of SIMSEA in accord with Future Earth.

Keywords: Future Earth, Marginal Seas, East Asia, Interdecadal Pacific Oscillation, Global Change, Climate Variations

Japan Geoscience Union Meeting 2014
(28 April - 02 May 2014 at Pacifico YOKOHAMA, Kanagawa, Japan)

U07-07 Room:501 Time:May 1 11:50-12:15

Digital Earth as a communication platform for Future Earth

FUKUI, Hiromichi[1]*

[1]International Digital Earth Applied Science Research Center, Chubu Univ.

As we can see in problematique, such as environmental issues and disasters, the various risks we face at both local and global scale are all interrelated to each other, and also tend to suddenly emerge at very local level. Conventional science has only been able to deal with parts of these problems. The first step to build a sustainable and disaster resilient society is to monitor, identify, store the data of phenomena on the earth, then process and interpret the raw data, turn them into understandable information to display, publish and distribute. We must share a common recognition of the issues. Therefore we need the Digital Earth (DE) that is a virtual representation of our planet on the internet, and enables a person to explore and interact with the vast amounts of natural, socio-economic and cultural information gathered about the earth. These infrastructures are using for the ESD (Education for Sustainable Development) that focus on systems thinking, critical thinking and holistic views. The Digital Earth can also facilitate collaborative, data-intensive studies for problematiques of Future Earth Project in the 21st century

It was reviewed Digital Earth concept, applications, and some of projects for promoting disaster resilient and sustainable society with information and communication technology in this paper.

We propose Digital Earth platform as the public information base which has cloud-based geospatial information system and services in cooperation with multi stakeholder as shown in Fig. These information systems should be autonomous, distributed and coordinated, interoperable as well. They work for ESD especially for the multi-risks, both mitigation and preparedness in ordinary time and emergency to reduce the vulnerability of our society. It would be a comprehensive facility and social system dedicated to disaster and environment management for sustainable future, with the capacity to supply the necessary staff and equipment such as sensor web supporting by a wide range of associated organizations.

Keywords: Digital Earth, Geographic Information System, Citizen Sciences, Data Journalism, Education for Sustainable Development, Future Earth

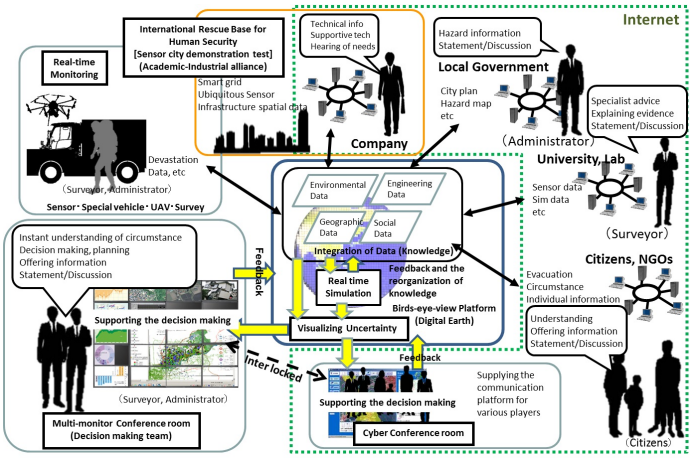

Japan Geoscience Union Meeting 2014
(28 April - 02 May 2014 at Pacifico YOKOHAMA, Kanagawa, Japan)

U07-08 Room:501 Time:May 1 12:15-12:40

Future Earth and Sustainable Development Goals

KANIE, Norichika[1*]

[1]Tokyo Institute of Technology

One of the next major challenges for research and policy in the field of sustainable development is the agreement of the post-2015 development agenda. This challenge is a direct result from the 2012 United Nations Conference on Sustainable Development (Rio+20), as well as from the formal ending of the Millennium Development Goals (MDG) in 2015. Governments, supported by civil society, now need to agree on a series of new global sustainable development goals and on the related governance mechanisms. At the Rio+20 Conference, governments decided on a process to develop such novel Sustainable Development Goals (SDG), to be integrated into the post-2015 global development agenda. Differently from the MDGs that target developing countries, the new Sustainable Development Goals are meant to apply to both developing and developed countries.

The research community that works in this field is faced with essentially two research tasks:
? First, we need to analyze the goal setting and implementation processes (governance questions);
? Second, we need to analyze and identify the goals and indicators themselves.

The first task entails an inquiry into who will be involved in setting these goals (Agency, Accountability), by which decision making mechanisms (Architecture, Adaptiveness), what these goals will be (Allocation and Access), and how to arrive at the framework for formulating the goals as well as an inquiry into how these goals will be translated into outcomes. The second task includes the question on how to elaborate the global development goals to facilitate achieving human well-being for all within resource constraints and environmental boundaries set by the earth system. A related question is the conceptual framework for the goals, and what goals, targets and indicators need to be developed. This in turn poses questions on enabling institutions and governance processes. We have witnessed in the past years that the development model that underpinned the post-1945 decades appears to be unable to handle the crises that many societies and institutions are struggling with (financial, demographic, environmental, etc.).

Therefore, questions related to the Post-2015 development agenda are not solely about SDGs, but are rather fundamental questions on how to achieve sustainability in the 21st century. To do so requires knowledge innovation, and it is possible through transdisciplinary research, one of the purposes of Future Earth, including co-design, co-production and co-design. This is a theme that should be explored in the year to come.

Keywords: Future Earth, Sustainable Development, Sustainable Development Goals, Post 2015 Development Agenda, Governance

Japan Geoscience Union Meeting 2014
(28 April - 02 May 2014 at Pacifico YOKOHAMA, Kanagawa, Japan)

U07-09 Room:501 Time:May 1 14:15-14:45

How will Humanity Survive and Flourish on Future Planet Earth?

DE MULDER, Eduardo[1*]

[1]Earth Science Matters Foundation

In the past half century the world has changed in an unprecedented way. For the first time ever humans observed their planet from outer space. Our species also has become a geologic factor while beginning to interfere with natural forces in the Earth to a scale which can no longer be ignored. These caused geographic modifications at the Earth' surface and geographic maps begin to show more and more distinct human imprints. Simultaneously, our knowledge about the Earth has increased to a level that the Earth crust's anatomy and composition is increasingly known and that we begin to understand how our planet works. Knowing the basic principles of the Earth processes paves the way to forward modelling and more and more accurately predicting the impacts of human interaction with planet Earth. That, in turn, provides tools to anticipate on both assets and threats for an increasingly large and complex human population. As long as we remain dependent on our home planet societies should benefit more from such rapidly increasing knowledge to balance development with the Earth' bearing capacity. Here, we describe recent progress in our knowledge of the Earth and some trends in human development. In combination, these may point to knowledge-based options on how human societies may cope with potentials and limitations posed by planet Earth in view with the ambitions expressed by the Future Earth science initiative.

Planet Earth by itself is not in danger and humans will never threaten its existence for another 5 billion years. But human activities will continue and possibly aggravate impacting the biosphere, the hydrosphere, and to a lesser degree, also the geosphere. Dimensions of such changes will be determined by physical factors in the first place but ability of human societies to cope with such changes also depends on cultural diversity.

Five global trends in human development are discussed: population, urbanisation, living standard, environmental awareness and science & technology. Together these trends point to a growing need for physical space to accommodate future human ambitions. Science and technology trends demonstrate accelerating potential abilities of human society to address such needs. As we proceed in the Anthropocene the need to integrate humanity issues and the geosciences will further increase while reconfirming the growing relevance of the discipline of the Human Geosciences.

So far, the Earth sciences play a modest role in the Future Earth initiative. That is in sharp contrast with global ambitions to arrive at a Green Economy, as expressed in Rio+20, to be developed in balance with the Earth' bearing capacities. Recent progress in geoscientific and technological research demonstrate the potential of such development. This has been widely exposed during the International Year of Planet Earth (IYPE, 2007-2009). This global initiative was proclaimed by the UN and was particularly successful in its outreach programme. In turn, the IYPE served as a model for developing the International Year of Global Understanding, spearheaded by the IGU, and for the UN Year of the Soil (2015).

Human ingenuity spurred discovery of larger natural resources than ever before to drive our economies to unprecedented heights. Future Earth might mobilize the brain powers accumulated in the heads of 400,000 Earth scientists around the world towards a sustainable economy.

Japan Geoscience Union Meeting 2014
(28 April - 02 May 2014 at Pacifico YOKOHAMA, Kanagawa, Japan)

U07-10 Room:501 Time:May 1 14:45-15:10

Scientific Knowledge Creation Supported by Data Integration and Information Fusion

KOIKE, Toshio[1*]

[1]School of Engineering, The University of Tokyo

What is scientific knowledge? We create some hypothesis based on theories, develop models, and implement experimental observation for validation of the hypothesis. This approach is called deductive inference. Based on the accumulation of factual knowledge, we can form the hypothesis. This approach is called inductive inference. Scientific knowledge is called formal knowledge which can be transferred and shared among wide scientific communities. By publishing paper and promoting communication, we exchange the factual knowledge. Such widely shared factual knowledge is defined as scientific knowledge. We are doing science in this way. During past one hundred years, this scientific knowledge has been increasing explosively. Differentiation and systematization have proceeded, and then a large number of disciplines have been established.

However, it is very difficult to reflect accumulated sub-system knowledge to holistic knowledge. Knowledge on a whole system can be rarely introduced to a targeted subsystem. In many cases, knowledge in one discipline is inapplicable to others. We are far from solution of issues across disciplines. It is critically important to establish inter-disciplinarity and create scientific knowledge crossing disciplines. To realize the benefits of scientific knowledge in society, we need to combine scientific knowledge in the natural world, the socio-economic world and the recognition world and to develop trans-disciplinarity as well as inter-disciplinarity.

How can we develop inter-disciplinarity and trans-disciplinarity? We need to share the data and information and develop inter-linkage of our knowledge by developing models and exchanging tools. Based on this kind of scientific activities, we can corporate between science community and society by making effective use of opportunities.

Data Integration and Analysis System (DIAS) coordinates the cutting-edge information science and technology and the various research fields addressing the earth environment, constructs data infrastructure that can integrate earth observation data, numerical model outputs, and socio-economic data effectively, creates knowledge enabling us to solve the earth environment problems, and generates socio-economic benefits, aiming to create knowledge to be shared among different disciplines, to create knowledge to be shared throughout the world, and to disseminate data and information that brings awareness.

Keywords: Data Integration, inter-disciplinarity, trans-disciplinarity

Japan Geoscience Union Meeting 2014
(28 April - 02 May 2014 at Pacifico YOKOHAMA, Kanagawa, Japan)

U07-11 Room:501 Time:May 1 15:10-15:35

Geospatial data and Future Earth: a case of digital elevation models

OGUCHI, Takashi[1*]

[1]CSIS, Univ. Tokyo

Future Earth is related to the concept of Digital Earth, proposed by US Vice-President Al Gore in 1998. Digital Earth aimed to compile global geospatial data with various resolutions and make them open to public worldwide for efficient solution of environmental problems. Although some related projects were launched, such activities in the 21st century have been relatively limited, partly because Gore lost in the 2000 presidential election. However, some of the elements of Digital Earth have been realized in the form of Internet virtual globes such as Google Earth and Bing Maps. These services allow us to browse maps, satellite images and airphotos with various resolutions. Although Digital Earth planned to provide more varied geospatial data related to science and culture, compilation and broad distribution of such data have been more delayed. It is important to understand the current state of available geospatial data and utilize them for activities associated with Future Earth. This presentation deals with digital elevation models (DEMs), one of the most basic geospatial data. It introduces currently available DEMs and application examples related to Future Earth.

Keywords: Future Earth, geospatial data, digital elevation model, Digital Earth

Japan Geoscience Union Meeting 2014
(28 April - 02 May 2014 at Pacifico YOKOHAMA, Kanagawa, Japan)

U07-12 Room:501 Time:May 1 15:35-16:00

Promoting Studies under Future Earth supported by Super-High Resolution Simulations on the Global Environment

OKI, Taikan[1*]

[1]Institute of Industrial Science, The University of Tokyo

The new terminology ”Anthropocene”, the geological era when anthropogenic activities substantially altering global environmental systems in which human beings are also a part of it, has been a popular word, but how the Anthropocene evolved? Population growth, economic development, and urbanization are inducing the climate change, the depletion of non-renewable resources, and the degradation of ecosystem services through the enhancement of the waste of resources, the emission of greenhouse gases, and the land use-land cover changes. Consequently, economic equity and the stable accesses to food, water, and energy are threatened, the potential risks to natural disaster are increased, and the minimum standards of wholesome and cultured living are in danger. How socio-ecological systems are changing and interacting with global and local environment?

In order to answer to these questions, it is necessary to understand the inter-linkages among factors of the socio-ecological systems through earth observations, field studies, data archive of social statistics and historical information on local and global changes, and the synthesis of them with integrated analysis and mapping. The study should have a scope with multi-spatial scale including Japan, Asia, and the globe, and with the target period of drastic changes for human beings in 300 years from the 150 years from the industrial revolution till now, and the 150 years from now on.

A research project of ”Super-High Resolution Simulations on the Global Environment” is proposed in order to promote various studies under Future Earth. Cycles and budgets of energy, water, and materials such as carbon, will be eventually simulated by 1km (30 arc second) over global continent for past 150 and future 150 years considering social and climatic changes. Past and projected changes will prevail the historic transition and future anticipations in sustainable energy, renewable resources such as food and water, impacts and transition of health and ecosystem services with super-high resolution.

Research components to enable the study are mostly ready to start feasibility studies. Motivated researchers are welcome to join.

Keywords: future earth, offline simulation, super-high resolution, anthropocene

Japan Geoscience Union Meeting 2014
(28 April - 02 May 2014 at Pacifico YOKOHAMA, Kanagawa, Japan)

U07-13 Room:501 Time:May 1 16:15-16:35

Asian Economic Development and Global Environmental Sustainability

SUGIHARA, Kaoru[1*]

[1]National Graduate Institute for Policy Studies

During the last twenty years or so, growth economies of Asia collectively became the largest importer of resources (particularly of energy resources) in the world, as not only resource-poor countries like Japan but counties like Indonesia and China, which used to be resource exporters, turned to net importers. Meanwhile, East Asia historically pursued a path of economic development, different from that of capital- and resource-intensive industrialization developed in the West, by fostering relatively labour-intensive and resource-saving technology. The energy intensity (energy consumption per GDP) has been kept low in many Asian countries, and Japan's energy-saving technology still leads the world in a number of respects. Thus, growth economies of Asia (now including most of South and Southeast Asia) are major players in the global market of resources, influencing both demand and supply.

Needless to say, monsoon Asia creates the world's largest circulation of water and heat energy around the Himalayas (and the Tibetan Plateau), and about a half of world population live in this environment. It has formed a uniquely coherent civilization and economy, such as densely populated society based on rice farming, transcending the geospheric and biospheric boundaries between the tropics and temperate zones. Today, this region is going through comprehensive industrialization and urbanization, and the resource and energy use there is beginning to affect the health of the entire world economy.

In what ways has Asian economic development been affecting global environmental sustainability? If Asia has long fostered a path of economic development under the unique environmental outfit of monsoon Asia, how would it influence the region's ability to address global environmental issues? This presentation offers a review of recent history literature on these questions, with comments on its utility for the understanding of the future of global sustainability.

I am currently serving for the Future Earth Committee at the Science Council of Japan, to promote humanities and social science research for this global initiative. I hope to have an opportunity to exchange ideas with members of this Union, and to explore possibilities of interdisciplinary research, specifically designed for the activities of Future Earth.

Keywords: Asia, economic development, global environmental sustainability, path dependency

Japan Geoscience Union Meeting 2014
(28 April - 02 May 2014 at Pacifico YOKOHAMA, Kanagawa, Japan)

U07-14 Room:501 Time:May 1 16:35-16:55

International Earth Science Olympiad from the viewpoint of Future Earth

TAKIGAMI, Yutaka[1*] ; HISADA, Ken-ichiro[2]

[1]Kanto Gakuen University, [2]Graduate School of Life and Environmental Sciences, University of Tsukuba

When considering the Future Earth-sustainable Earth, it is important to know the whole Earth and the international cooperation. As the study of the whole Earth is Earth Science, we consider International Earth Science Olympiad (IESO) which is the international competition for high school students from the viewpoint of Future Earth.

IESO was hold on 2007 (Korea), 2008(Philippine), 2009(Taiwan), 2010(Indonesia), 2011(Italia), 2012(Argentina) and 2013(India). In 2016, we will have IESO at Mie.

1) International Team Field Investigation (ITFI)

ITFI is the typical event which is not existed on other science Olympiads. This event is the presentation event after high school students from other countries investigated some subjects with international cooperation. At this event, communication language is English and sometimes subjects of this investigation include the regional social life. This experience will guide the consideration of Future earth to students in future.

2) Increase of participating countries

Participating countries were increased from about 6 (2007,2008) to over 20 (2011-). One of the reason might be due to the understanding the importance of Earth Science for Future Earth.

3) Examination questions at IESO

At present, questions are consisting from three disciplines; Geology and Solid Earth, Metrology and Oceanology, Astronomy. However, members of IESO want to include multidisciplinary questions which are important for considering Future Earth. At 2016 IESO at Mie, we want include these examination questions aggressively.

4) Japan Earth Science Olympiad (JESO)

The half of students for participating the JESO will enter the universities of art divisions and 30% of students are girls. This fact is good for consideration of Future Earth because many peoples, not scientist, have basic earth science knowledge. However, it is regret that more high school students study another science curriculum than earth science.

I think that it is very important for Future earth to learn Earth Science and to join the Earth Science Olympiad.

Keywords: Earth Science Olympiad

Japan Geoscience Union Meeting 2014
(28 April - 02 May 2014 at Pacifico YOKOHAMA, Kanagawa, Japan)

U07-15 Room:501 Time:May 1 16:55-17:15

The education for sustainable earth - The International Geography Olympiad

IDA, Yoshiyasu[1*]

[1]University of Tsukuba

The International Geography Olympiad (iGeo) is a competition for the best 16 to 19 year old geography students from all over the world. Four students represent each country in a series of Geography tests in (generally) a four-five day program. An adult Team leader and International Board Member accompany each national team. The official language of the iGeo is English.(from iGeo home page)

There are three aims of iGeo. First is to stimulate active interest in geographical and environmental studies among young people, second to contribute positively to debate about the importance of geography as a senior secondary school subject by drawing attention to the quality of geographical knowledge, skills and interests among young people, third to facilitate social contacts between young people from different countries and in doing so, contribute to the understanding between nations.

The test questions in iGeo are presented from each country and are made. The international standard test is aimed by these questions. These questions are divided into three types that are multimedia, description, and fieldwork. The aim of each type test is to make students develop the ability to look the future society and earth on underlying knowledge, skills and view points of the geography. Particularly, in the fieldwork test, students can learn not only the present understanding but also the future by observing local natural phenomenon and the life of people, directly. Regarding geography education of our country, though present understandings more importance, a point of view to inquire the relation between nature and human in the future is not enough. In factually, the Japanese team in iGeo really tends that the point of the fieldwork test is low. As for this, the main factor would be that thinking the future is not educated in geography education in Japan. In addition, students have few chances to experience the fieldwork in geography class of our country.

In the geography education of Japan, it is necessary for the learning content including the consideration for the future based on geographical knowledge, skill and inquires.

Keywords: sustainable earth, future earth, geography education, international geography olympiad, fieldwork

Japan Geoscience Union Meeting 2014
(28 April - 02 May 2014 at Pacifico YOKOHAMA, Kanagawa, Japan)

U07-16 Room:501 Time:May 1 17:15-17:35

Sustainable Future of Coastal and Marine Ecosystems in the Indo-Pacific Ocean

UEMATSU, Mitsuo[1*]

[1]Atmosphere and Ocean Research Institute, The University of Tokyo

The Indo-Pacific Ocean Region encompasses diverse coastal ecosystems, as represented by coral reefs, mangrove forests, seagrass beds, and even deep basin over 4000 m deep. These diverse environments harbor the unique and extremely high biodiversity of the region, known as the major biodiversity hotspot in the world. However, the region is also under serious threat of environmental decline from various human impacts due, for example, to loads of pollutants from land and habitat destruction associated with resort development and fisheries. There are also concerns about negative impacts of global climate change associated with ocean acidification.

As one of Future Earth initiatives, we should establish future perspectives and needs for strengthening sustainable ocean environment and development. A project aims at further expanding the network of the scientific and socio-economic studies and education on the Indo-Pacific Ocean Region, through (1) research collaboration applying new approaches and methodologies such as satellite remote sensing, molecular genetic analyses, and high-precision analyses of biogeochemical parameters, (2) integrative, inter-disciplinary ecosystem researches, and (3) establishment of core of coastal marine science and socio-economy in each country and multilateral network. Through these activities the project aims at enhancing education of researchers who will play major roles not only in domestic but also in international activities on global issues.

As a practical matter that impeded harmonized implementation of the program, there will be a large gap among the member countries in their funding capabilities, resulting in the shortage of funding in some countries. This may be partly due to the differences in political priorities for basic environmental and/or socio-economic research among countries. There are also problems that the importance and practical application of basic research to urgent environmental issues have not effectively been reflected in the response of funding organizations, policy makers, and/or popular audience, despite our efforts to demonstrate and disseminate these issues in various occasions.

Keywords: Indo-Pacific Ocean region, marine ecosystem, coastal region, biodiversity, inter-disciplinary research, impacts of global climate change

Japan Geoscience Union Meeting 2014
(28 April - 02 May 2014 at Pacifico YOKOHAMA, Kanagawa, Japan)

U07-17 Room:501 Time:May 1 17:35-18:00

Geoscientific Perspective for Sustainable Future Earth

HIMIYAMA, Yukio[1*]

[1]Hokkaido University of Education

The world global environmental studies are being re-organized under the flag of Future Earth led by ICSU, ISSC etc. Geoscience, which specializes in the dynamic nature and phenomena of the earth's surface, including lithosphere, hydrosphere, atmosphere, biosphere and human-geosphere, assumes unique responsibility in contributing to Future Earth. It was highly relevant for JpGU to establish Human Geoscience Section as one of its five academic sections when it was born in 2005 in response to the restructuring of the Science Council of Japan. The paper discusses the roles and the roadmaps of the geoscience community in general and those of the human geoscience in particular in implementing Future Earth.

Keywords: geoscience, Future Earth, global environmental problem, human geoscience, sustainability

Japan Geoscience Union Meeting 2014
(28 April - 02 May 2014 at Pacifico YOKOHAMA, Kanagawa, Japan)

U08-01 Room:Main Hall Time:May 2 09:00-09:15

Actions to the Eastern Japan earthquake disaster by SSJ and to disaster and environmental issues in academic communities

TADOKORO, Keiichi[1*]

[1]Graduate School of Environmental Studies, Nagoya University

The Seismological Society of Japan (SSJ) has organized the Investigation Committee for disaster. The committee corrected preliminary research outputs and opened them as a link correction on the SSJ ' s web site at the 2011 eastern Japan great earthquake disaster.

One of the important tasks of the committee is the contact point for other related academic societies dealing with earthquake and tsunami. The SSJ participated in the Liaison Committee on the off the Pacific coast of Tohoku Earthquake established with the related societies, as well as in the Environmental Hazard Countermeasure Committee of the Japan Geoscience Union (JpGU). The Outreach Committee of SSJ performed enlightening actions for general public and mass media. The SSJ cooperated the action also by the Science Council of Japan.

What we learn from the 2011 eastern Japan great earthquake and tsunami disaster is global environmental issues and natural disaster are inseparable. Earth and planetary sciences should integrate such problems that we have considered completely different problems in the past. For this purpose, cooperative action among our community is a matter of course. In addition, cooperation with the community outside of us is indispensable to earth and planetary sciences, studies about basis of the prosperity of the human, contribute for building sustainable human society. The JpGU is expected to be a core for such cooperative actions. It is important to make careful preparations to be successful in the actions and cooperation between the societies during the emergence period. I propose a workshop such as " global environmental issues among natural disaster " for brainstorming.

Japan Geoscience Union Meeting 2014
(28 April - 02 May 2014 at Pacifico YOKOHAMA, Kanagawa, Japan)

U08-02 Room:Main Hall Time:May 2 09:15-09:30

Activities of the Geological Society of Japan in support of reconstruction after the 2011 Tohoku earthquake disaster

TAKAGI, Hideo[1*]

[1]Waseda University (JGS Director of Outreach and Geopark Affairs)

I introduce the activities of the Geological Society of Japan (JGS) in support of the reconstruction after the 2011 Tohoku earthquake disaster on behalf of the Social Contribution Committee of the JGS. The JGS asked its members to submit proposals in support of the disaster recovery, and six of nine research programs in 2011 and one of two in 2012 were adopted and supported by funds of the Society. The seven projects can be categorized into three research categories: 1. recovery of specimens from museums destroyed by the tsunami, 2. development of methods of decontamination to help deal with the radioactive material spread by the Fukushima Daiichi nuclear power plant accident, and 3. surveys to recognize and quantify liquefaction caused by the Tohoku earthquake. The results of these studies were reported in poster presentations given at the JGS annual meetings and in newsletter articles published in 2012 and 2013. This report also introduces briefly the geopark activity that has been promoted by the JGS and its importance for local education in earth science including disaster prevention and mitigation in the eastern Tohoku coastal area (Sanriku area).

Keywords: Geological Society of Japan, 2011 Tohoku earthquake disaster, tsunami, liquefaction, decontamination of radioactive materials, recovery of museum specimens

Japan Geoscience Union Meeting 2014
(28 April - 02 May 2014 at Pacifico YOKOHAMA, Kanagawa, Japan)

U08-03 Room:Main Hall Time:May 2 09:30-09:45

Reframing the academic responsibility of JSAF on the basis of its activities after the 2011 Tohoku earthquake

SHISHIKURA, Masanobu[1*]

[1]Active Fault and Earthquake Research Center, AIST

The Japanese Society for Active Fault Studies (JSAF) is devoted to the study of not only inland active faults but also offshore active faults including subduction zone mega-thrusts. The members of JSAF have been conducted emergently survey for every earthquake disasters related to active fault since the establishment of 2007. One of the important purposes of the survey is to identify and to describe any geological and geomorphological phenomena associated with earthquake and tsunami such as trace, geometry and displacement of surface rupture, coastal change and tsunami deposit. These modern analogues are key to reveal the past phenomena. And clarifying the past is key to estimate the future. This philosophy of paleoseismology and active fault study has been socially recognized in its importance for measuring low frequent great disaster after the 2011 great Tohoku earthquake (M9.0). However, as the lessons from the 2011 event and its triggered 2011 Fukushima Prefecture Hamadori earthquake (M7.0), we also recognized a limit of the current investigation technique of geological and geomorphological methods. The JSAF has an important role as a community for discussing new technique.

Keywords: Japanese Society for Active Fault Studies, 2011 great Tohoku Earthquake, 2011 Fukushima Prefecture Hamadori Earthquake, Active Fault Study, Paleoseismological Study

Japan Geoscience Union Meeting 2014
(28 April - 02 May 2014 at Pacifico YOKOHAMA, Kanagawa, Japan)

U08-04 Room:Main Hall Time:May 2 09:45-10:00

Activity of the AJG to the Great East Japan Earthquake Disaster: Role of academic societies at a big disaster

KUMAKI, Yohta[1*]

[1]Association of Japanese Geographers / Senshu Univ.

The activity of the Association of Japanese Geographers (AJG) responding to the Great East Japan Earthquake Disaster was as follows:

1) "The Headquarters for Disaster Response," the general manager of which was the chairperson of the executive committee of AJG, was set up just after the disaster occurrence. It performed correspondence to a various inquiries, liaison and information exchange with other associations, communication to geographers in the fields, uploading quick reports and proposals to the web site, etc.

2) Based on a geographical property to make much of air-photo interpretation and mapping, AJG organized a working group for clarifying the entire surface of the tsunami inundation and published the first report on March 28 (revised eight times until December).

3) AJG gave the geography teaching materials to damaged schools by the members' contribution.

4) Until March, 2014, ten symposia relating to the Great East Japan Earthquake Disaster were held. The theme were of physical geography (tsunami, liquefaction, slope disaster, disaster of land developed for housing, radioactive contamination, etc.) and of human geography (life of damaged inhabitants, the revival way, etc).

On the occasion of a big disaster, societies of geosciences should do not only the academic activity but also take a social role as follows:

1) dispatching the research results in a easily understandable way quickly and broadly

2) Supporting people and governments based on specialized intellect.

3) Supporting to school education.

It is important for JpGU to have an open window for the society for disaster outbreak as well as to support the researchers who act in the field.

Japan Geoscience Union Meeting 2014
(28 April - 02 May 2014 at Pacifico YOKOHAMA, Kanagawa, Japan)

U08-05 Room:Main Hall Time:May 2 10:00-10:15

Cartographic society's contributions to crisis resolution of environmental issues and disasters

ARIKAWA, Masatoshi[1*] ; MORITA, Takashi[1] ; KAMADA, Kouzou[1] ; KUMAKI, Yohta[1] ; SATO, Jun[1]

[1]Japan Cartographers Association

Maps are important for crisis management in environmantal issues and disasters, however it is not clear if the current situations of providing and using maps for crisis management are appropriate or not. We try to clarify contributions and problems on map provisions and uses for crisis management from the viewpoint of cartographic society in our talk. Particularly, we focus on the following points.

(1) prompt action and quality
(2) appropriateness of map provisoins to suffered communities
depending on their situation
(3) designing action plans of map provisions for levels of situations
(4) paper maps and digital maps
(5) appropriateness of current hazard maps
(6) weak map literacy in decision making, communication, and media
(7) international contributions
(8) volunteered geographic information, location-based SNS, and ubiquitous mappings
(9) use of spatio-temporal big data

Keywords: maps, disaster maps, aerial photographs, geospatial information, hazard maps, Volunteered Geographic Information

Japan Geoscience Union Meeting 2014
(28 April - 02 May 2014 at Pacifico YOKOHAMA, Kanagawa, Japan)

U08-06 Room:Main Hall Time:May 2 10:15-10:30

Disaster Response Support Activity based on Geospatial Information

HATAYAMA, Michinori[1*]

[1]Disaster Prevention Research Institute, Kyoto University

In this presentation, the history of major disasters and progress of information communication technology related to geospatial information after 1994.

In 1995 Great Hanshin-Awaji Earthquake, GIS and Remote Senescing got a lot of attention to manage disaster information.

In 2004 Chuetsu Earthquake, GSI and voluntary base research group tried to share damage and recovery process information through Web GIS.

After launch of Google Earth, ordinary person can share his/her geospatial information though internet. And in 2011 Great East Japan Earthquake, most layers of geospatial information were shared.

Keywords: Geospatial Information, GIS, Disaster Response Support Activity

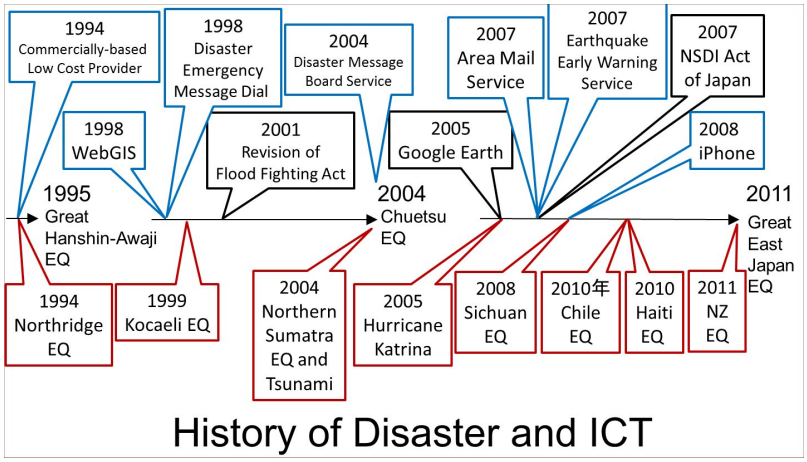

Japan Geoscience Union Meeting 2014
(28 April - 02 May 2014 at Pacifico YOKOHAMA, Kanagawa, Japan)

U08-07 Room:Main Hall Time:May 2 10:30-10:45

Environmental pollution by the Fukushima Daiichi nuclear power plant accident and role of the atmospheric science

NAKAJIMA, Teruyuki[1*]

[1]Atmosphere and Ocean Research Institute

There are several past and future issues to be discussed regarding the role of the atmospheric science in the accident of the Fukushima Daiichi nuclear power plant. SPEEDI model results were not effectively used in the evacuation plan by the government. It was found, on the other hand, that the performance of atmospheric chemistry transport models are comparable to or better than that of SPEEDI, for simulation of distribution of radioactive material over the wide area contaminated by the accident. In that situation, a bottom-up process were useful to gather results of simulation and in situ measurements by volunteer scientists to be utilized in the decision process of the government. The Science Council of Japan is now under discussion of establishing an emergency action manual for gathering data and knowledge by scientists to be shared by professionals to make useful outputs to government and public. As also indicated by the IPCC assessment process for climate change, it is important to present uncertainties included in the scientific knowledge to be released. In this regard, it is important for the atmospheric science to contribute to reducing the uncertainties through a further progress of the atmospheric dynamics, physics, and chemistry modeling system and through establishing more robust monitoring system of weather and other quantities. I like to discuss these issues for improving our ability to reduce damage caused by future disasters that may happen.

Japan Geoscience Union Meeting 2014
(28 April - 02 May 2014 at Pacifico YOKOHAMA, Kanagawa, Japan)

U08-08 Room:Main Hall Time:May 2 11:00-11:15

How JAHS will manage the Great East Japan Earthquake?

KONDOH, Akihiko[1*] ; YASUHARA, Masaya[2] ; TSUKAMOTO, Hitoshi[2]

[1]CEReS, Chiba University, [2]The National Institute of Advanced Industrial Science and Technology

JAHS (Japanese Association of Hydrological Sciences) is an academic society that treat hydrological cycle on the Earth. Water is one of the most important component that makes feature of earth's surface. Water also is indispensable resources for human's life and activity, so hydrological sciences involves the relationship between hydrological cycle and human activities. JAHS have deep concern to human dimensions of environmental changes. To realize "Hydrological Sciences in the society" becomes important subject to be accomplished after the great earth quick in March 11, 2011.

After the great disaster, we carried out the studies both on Tsunami and on nuclear disaster. At a lecture, we will focus on the nuclear disaster in Fukushima District, because we think our knowledge and experiences on hydrology will be useful to understand the actual situation and future perspectives of radioactive contamination, and also useful to propose measures to restore the region contaminated by radioactive fallout.

The research works on the behavior of radioactive nuclides in the environment are divided into mechanism study and distribution study. In the latter, the distribution map should be discussed with the scales, because often what looks important at one scale is less important at another.

The small scale dose rate maps published by the government was useful to determine the evacuation area at the initial stage of the nuclear disaster, however, large scale map is necessary at the restoration stage. In the mountain village, the life and livelihood are strongly dependent to water and material cycles in SATOYAMA watershed. We have to know the distribution of radioactive materials, water and material cycles in the watershed. The knowledge and experiences in hydrology have great effect to make measures to cope with radioactive materials based on the SATOYAMA watershed scale. We are now conducting hydrological research in the small watershed in one of evacuation area. The outcomes are shared with local people and make them the materials to discuss the future of the region.

At the Fukushima Dai-ichi nuclear power plant, control of polluted water flowing from nuclear reactor buildings becomes an urgent issue to be solved. The buildings are located on the independent plateau. At this situation, local groundwater flow system, recharged on the surface and discharge to surrounding lowland, is the main system of hydrologic cycle. Groundwater from Abukuma Mountains belongs regional groundwater system, and its flux should be very low and residence time should be extremely long. This is hydrological knowledge, however, why accumulated knowledge does not apply to the field in problem?

Science is in the society, and supported by the society. We, scientists, have to consider how to use scientific knowledge in the framework that have common purpose.

Keywords: Japanese Association of Hydrological Sciences, nuclear disaster, FUKUSHIMA, the roll of hydrological sciences, distribution map and its scale, groundwater flow system

Japan Geoscience Union Meeting 2014
(28 April - 02 May 2014 at Pacifico YOKOHAMA, Kanagawa, Japan)

U08-09 Room:Main Hall Time:May 2 11:15-11:30

Transfer of radionuclides to river by Fukushima Daiichi NPP

ONDA, Yuichi[1*]

[1]Center for Research in Isotopes and Environmental Dynamics, University of Tsukuba

A number of studies have been conducted to monitor and model the time series change of radiocesium transfer through aquatic systems after significant fallout, especially from the Chernobyl disaster. Our research team has been monitoring the environmental consequences of radioactive contamination just after the Fukushima Daiichi NPP accident in Yamakiya-district, Kawamata town, Fukushima prefecture. Research items are listed below.

1. Radiocesium wash-off from the runoff-erosion plot under different land use.
2. Measurement of radiocesium transfer in forest environment, in association with hydrological pathways such as throughfall and overlandflow on hillslope.
3. Monitoring on radiocesium concentration in soil water, ground water, and spring water.
4. Monitoring of dissolved and particulate radiocesium concentration in river water, and stream water from the forested catchment.
5.Measurement of radiocesium content in drain water and suspended sediment from paddy field.

Our monitoring result demonstrated that the Cs-137 concentration in eroded sediment from the runoff-erosion plot has been almost constant for the past 3 years, however the Cs-137 concentration of suspended sediment from the forested catchment showed slight decrease through time. On the other hand, the suspended sediment from paddy field and those in river water from large catchments exhibited rapid decrease in Cs-137 concentration with time. The decreasing trend of Cs-137 concentration were fitted by the two-component exponential model, differences in decreasing rate of the model were compared and discussed among various land uses and catchment scales. Such analysis can provide important insights into the future prediction of the radiocesium wash-off from catchments with different land uses.

Keywords: Cs-137, Fukushima Daiichi NPP, soil erosion, suspended sediment, river, flux

Japan Geoscience Union Meeting 2014
(28 April - 02 May 2014 at Pacifico YOKOHAMA, Kanagawa, Japan)

U08-10 Room:Main Hall Time:May 2 11:30-11:45

Stock and Flow of Environmental radionuclides in Lake ecosystem

NOHARA, Seiichi[1*]

[1]National Institute for Environmental Studies

Stock and Flow of Environmental radionuclides in Lake ecosystem

Keywords: Fukushima daiichi nuclear plant accident, environmental radioactivity, Lake ecosystem

Japan Geoscience Union Meeting 2014
(28 April - 02 May 2014 at Pacifico YOKOHAMA, Kanagawa, Japan)

U08-11 Room:Main Hall Time:May 2 11:45-12:00

Activities of JAGH relating to the earthquake disaster and disaster relief

NAKAGAWA, Kei[1*] ; TOKUNAGA, Tomochika[2] ; SUGITA, Fumi[3] ; KAIHOTSU, Ichirow[4] ; SHIMADA, Jun[5]

[1]Graduate School of Fisheries Science and Environmental Studies, Nagasaki University, [2]Graduate School of Frontier Sciences, The University of Tokyo, [3]Faculty of Commerce and Economics, Chiba University of Commerce, [4]Graduate School of Integrated Arts and Sciences, Hiroshima University, [5]Graduate School of Science and Technology, Kumamoto University

Followings are the activities of Japanese Association of Groundwater Hydrology (JAGH) relating to the 2011 off the Pacific coast of Tohoku Earthquake.

Program Committee (Chair: Makoto Nakashima) organized the symposium " The way of groundwater use as the emergency water source at the time of the earthquake " on May 26, 2012, at the Kashiwa Campus of the University of Tokyo. In the symposium, following presentations were given; " Ensuring safety and security of the water supply system " by Kenichi Yamamoto (Ministry of Land, Infrastructure, Transport and Tourism), " The securing water in areas affected by the Great East Japan Earthquake Tsunami " by Yoshiharu Ueno (Iwate prefecture), " About the use of groundwater as a domestic water at the time of the disaster in Nagoya " by Kazuhiro Takemoto (Nagoya City), " Investigation of the effect of tsunami induced by the Great East Japan Earthquake on groundwater " by Kei Nakagawa (Nagasaki University). Then, the panel discussion was coordinated by Makoto Taniguchi (Research Institute for Humanity and Nature). In this symposium, difference of water usage between emergency and non-emergency times, management method and registration system were discussed based on the presentations.

Editorial Committee (Chair: Tomochika Tokunaga) organized and published two special issues. In the special issue of " The 2011 off the Pacific Coast of Tohoku Earthquake and groundwater " (Vol.54, No.1, Feb, 2012), Technical Report of " Change in groundwater environment caused by the 2011 off the Pacific Coast of Tohoku Earthquake in the southern part of Sendai Plain " by Kazushi Mori et al. and Research-in-Progress of " Impact of Tsunami caused by the 2011 off the Pacific coast of Tohoku Earthquake on groundwater usage and quality in Asahi-city, Chiba Prefecture Japan " by Fumi Sugita are published. In the special issue of " Earthquake Hazard and Groundwater " (Vol.55, No.1, Feb, 2013), Review of " Importance of groundwater as security " by Makoto Taniguchi, Research-in-progress of " Field study on the damages of a well due to the Great East Japan Earthquake " by Kunio Ohtoshi et al., Data of " Effect of Tsunami induced by the 2011 off the Pacific coast of Tohoku Earthquake on groundwater " by Kei Nakagawa et al., Data of " Treatment and effective utilization of debris and tsunami deposits generated by the Great East Japan Earthquake " by Takeshi Katsumi et al., and Data of " Symposium, The way of groundwater use as the emergency water source at the time of the earthquake " by Makoto Taniguchi and Makoto Nakashima were published. All these papers have been published in the J-stage (https://www.jstage.jst.go.jp/browse/jagh/-char/ja/).

Prof. Ichirow Kaihotsu organized the joint investigation team of JAGH and JSHWR (Japan Society of Hydrology and Water Resources). They visited public water works offices and collected water samples at the wells of the city in Kamaishi city, Rikuzen Takata city, and Minami Sanriku town during June 16-19 and August 1-3, 2011. They also sampled water at the well for disaster in Wakaba-ku, Sendai City at that time. As a follow up of these investigations, the team of University of Tokyo and Nagasaki University sampled groundwater, river water and soil in Minami Sanriku town. In these investigations, we mainly focused on recovery from the salinization of groundwater due to tsunami induced by the earthquake.

Keywords: JAGH, The 2011 off the Pacific coast of Tohoku Earthquake, Symposium, Special issue, Joint investigation team, Salinization of groundwater

Japan Geoscience Union Meeting 2014
(28 April - 02 May 2014 at Pacifico YOKOHAMA, Kanagawa, Japan)

U08-12 Room:Main Hall Time:May 2 12:00-12:15

Oceanic dispersion model intercomparison for the Fukushima accident

MASUMOTO, Yukio[1*]

[1]The University of Tokyo

There are several attempts to simulate oceanic dispersion of radionuclides discharged into the ocean after the accident of Fukushima Daiichi Nuclear Power Plant on March 11, 2011. In order to understand a present status of model capability to simulate the dispersion of radionuclide and uncertainty in the model simulations, detailed comparisons of model results with observations and also among the model results are necessary. A model intercomparison project, launched by a working group established under the Oceanographic Society of Japan, and then under Japan Science Council, compared results from several downscaling dispersion models focusing on Cesium 137 dispersion for the Fukushima case. Eleven model results from ten groups are participating in the project. Although there are general similarities in basic flow fields and dispersion patterns, significant differences among the simulated results also exist, due to differences in model settings and uncertainty in the forcing fields. This presentation introduces the model intercomparison activity and discuss some preliminary results of the comparisons.

Keywords: Oceanic Dispersion Model, Radionuclides, Model Intercomparison

Japan Geoscience Union Meeting 2014
(28 April - 02 May 2014 at Pacifico YOKOHAMA, Kanagawa, Japan)

U08-13 Room:Main Hall Time:May 2 12:15-12:30

Development of Composite Materials with Zeolite and Magnetite for Radioactive Cs Decontamination in Soil

AONO, Hiromichi[1*]

[1]Ehime University

1. Intorduction

The decontamination of radioactive Cs from the accident at the Fukushima No.1 nuclear power plant is an urgent problem. Zeolites are the most promising material for the Cs decontamination in water such as ponds and rice fields. The movement of the Cs^+ ions in the soil to the zeolite should be possible when the powdered zeolite mixes with the soil during the wet process using a K^+ or $NH_4{}^+$ ion-containing solution for ion exchange with the Cs^+ ions in the soil. However, the collection of the zeolite after the decontamination of the radio Cs^+ ions is impossible when the powder material mixes with the soil. Magnetic collection is one of the methods using a composite material composed of the zeolite and a magnetic material after the Cs^+ ion adsorption.

An Na-P1 type artificial zeolite ($Na_6Al_6Si_{10}O_{32}?12H_2O$) having a high cation exchange capacity (CEC) is able to be synthesized at a low cost using alkali from the waste coal fly ash of thermal power stations. On the other hand, the synthesis method using alkali for the nano-sized magnetite (Fe_3O_4) is very similar to that for the Na-P1 type artificial zeolite. We considered that a new composite material using alkali from a suspension of both starting materials would be a promising material for the Cs decontamination.

In this study, we synthesized the composite material (magnetic zeolite) of the Na-P1 type zeolite and nano-sized magnetite by alkali processing from a mixed solution of the fly-ash and iron chlorides for the magnetic collection of the zeolite after Cs^+ ion adsorption.

2. Experimentals

Fly ash (JIS II type) from thermal power stations (Shikoku Electric Power Co.) was used for the preparation of the Na-P1 type zeolite. For the preparation of the Na-P1 type zeolite, the fly ash and 2M NaOH were mixed and refluxed at 100 ^{o}C for 24 h. The powder was collected and washed several times by centrifugal separation, and then dried at 80 ^{o}C. For the preparation of the nano-sized magnetite, $FeCl_2?4H_2O$ and $FeCl_3?6H_2O$ (mole ratio=1:2) were dissolved in pure water. The mixed solution was placed in a water bath at 100 ^{o}C, and then a 2M NaOH solution was added with stirring and held at the same temperature for 30 min. For the preparation of the composite material (magnetic zeolite) of the Na-P1 type zeolite and magnetite, the synthesized magnetite in water and then fly ash was added to the mixed solution. A 2M NaOH solution was added to the mixed solution and refluxed at 100 ^{o}C for 24 h.

3. Results and discussion

For the material without magnetite , the main peaks for the XRD were the Na-P1 type zeolite with mullite ($Al_6Si_2O_{13}$) as the second phase. The peak intensity of the magnetite increased with an increase in the magnetite content. The peaks of the magnetite were very broad due to its small crystalline size. The particle size for the magnetic zeolite was 5˜30 μm for a SEM observation. These particles of the magnetic zeolite were easily attracted by the neodymium magnet. For the TEM observation, the Na-P1 zeolite, the magnetite, and amorphous phases were confirmed using the electronic diffraction of the center of the particle. The nano-sized and aggregated magnetite particles were observed in the bright-field image. Due to the slow formation of the zeolite crystals after formation of the nano-sized magnetite, the magnetite particles existed at the grain boundary between the polycrystalline zeolites.

We tested that the magnetic zeolite (200 g) and the soil (2 kg) obtained from the rice fields in Fukushima were mixed using a shaking apparatus with $NH_4{}^+$ ion containing solution. The magnetic zeolite with radioactive Cs collected using neodymium magnet (8000 gauss). We succeeded to decontaminate ca. 80 % radio active Cs from the soil using the magnetic zeolite.

Keywords: Racioactive Cs Decontamination, Na-P1 type zeolite, Magnetite, Composite Material

Japan Geoscience Union Meeting 2014
(28 April - 02 May 2014 at Pacifico YOKOHAMA, Kanagawa, Japan)

U08-14 Room:Main Hall Time:May 2 12:30-12:45

The Mission of Human Geoscience in the Study of Disasters and Global Environmental Problems

HIMIYAMA, Yukio[1*]

[1]Hokkaido University of Education

The Human Geoscience Section of JpGU has been emphasizing the importance of studying increasing disasters and global environmental problems together in an integrative way, and has worked together with the Human Geoscience Committee of the Science Council of Japan to organize various meetings and issued proposals related with global environmental problems and hazards/disasters. The lecture reviews these activities and their achievements, the harsh reality of the still continuing Great East Japan Disaster, and the worsening global environmental problems and the efforts to combat them, and discusses the missions of human geoscience now and towards future.

Keywords: human geoscience, Great East Japan Disaster, global environmental problem, sustainability, disaster

Japan Geoscience Union Meeting 2014
(28 April - 02 May 2014 at Pacifico YOKOHAMA, Kanagawa, Japan)

U08-15 Room:Main Hall Time:May 2 14:15-14:30

A new research field after the 2011 Tohoku earthquake and tsunami

IMAMURA, Fumihiko[1*]

[1]International Research Institute of Disaster Science, Tohoku University

The Tohoku region in Japan was hit by a gigantic earthquake of M=9.0 subsequently followed by a huge tsunami which occurred off the Pacific ocean. Both of them have caused huge damage on the eastern coast of Japan, having a huge inundation area more than 500km2 with the attack of destructive wave forces. There are several issues why this tragedy occurred, and what unrecognized factors contributed to the high vulnerability of the area, and how the risk at each region in the future earthquake and tsunami.

The damage actual situation of the East Japan great earthquake disaster and the study base formation of practical disaster prevention studies based on the lesson are big problems and develop the situation of the damage, a future evaluation, prediction from elucidation of a giant earthquake and the outbreak mechanism of the tsunami and must record a then lesson to earthquake disaster archives. Furthermore, study such as the ways of the disaster prevention that stood on improvement of the trust of the risk evaluation, the construction of support studies, cooperation with the disaster medicine, the history culture will be necessary to prepare for domestic and foreign disasters.

In natural disaster scientific research, I arrest prior measures, the outbreak of the disaster, influence of the damage, urgent correspondence, restoration, revival, forehandedness with a series of disaster cycles and elucidate the phenomenon in each process, and it is necessary to make the lesson generalization, unification. Social incorporate result of the natural disaster scientific research that assumed knowledge and the world provided from the research in the East Japan great earthquake disaster, the action to reconstruction contracts a field and a human being, society is smart and copes for a disaster cycle to become complicated and systematizes study to build society system keeping a lesson alive through hardship as ”practical disaster prevention studies”, and a wound wants to form the scientific value.

Keywords: Disaster Science, 2011 Tohoku earthquake and tsunami

Japan Geoscience Union Meeting 2014
(28 April - 02 May 2014 at Pacifico YOKOHAMA, Kanagawa, Japan)

U08-16 Room:Main Hall Time:May 2 14:30-14:45

How volcanology will manage environment and hazard?

FUJII, Toshitsugu[1*]

[1]Crisis & Environment Management Policy Institute (CeMI)

In order to mitigate volcanic disaster, it is necessary to understand the timing and magnitude of eruption before eruption, and to evaluate the transit of eruption properly, indicating the development of volcanology is essential. Therefore, the roles of volcanology and volcanologist are important to mitigate the volcanic disaster.

Japanese volcanologists have contributed to mitigate the volcanic disaster in case of volcanic unrest or eruption. A few examples will be reviewed during the session.

However, these contributions have not been made by the volcanological society, but by volcanologists personally. It is not clear how the academic society such as volcanological society should contribute to mitigate the natural disaster. Academic society could be an organ to contribute in risk evaluation through the scientific discussion within the society, but may not be an organ to engage in risk management.

Keywords: Volcanology, volcanic hazard, volcanic disaster mitigation

Japan Geoscience Union Meeting 2014
(28 April - 02 May 2014 at Pacifico YOKOHAMA, Kanagawa, Japan)

U08-17 Room:Main Hall Time:May 2 14:45-15:00

Recent transformation of the snow and ice disaster and emerging issues

KAWASHIMA, Katsuhisa[1*] ; KAMIISHI, Isao[2]

[1]Research Institute for Natural Hazards and Disaster Recovery, Niigata University, [2]Snow and Ice Research Center, National Research Institute for Earth Science and Disaster Prevention

Recently, the natural environment and social environment surrounding Japan, such as the increased global warming and the acceleration of demographic aging, have changed greatly. A few decades ago, there was a view that snowfall will decrease sharply with the progress of global warming and the resultant snow disaster will be drastically alleviated. However, since heavy snowfall appears frequently after the 21st century, it is being accepted widely that the impact of global warming on variations in snow cover is not a simple problem. The heavy snowfall events which appeared in three consecutive years from 2010/11 winter to 2012/13 winter are good examples, and consequently more than 100 people were killed each year. Moreover, it is noteworthy that the aspect of snow disaster has greatly differed from the time of Showa. In relation to earthquakes and heavy rainfalls which occurred frequently in the heavy-snow region of Japan, new issues of the compound disaster events, hardly taken note until now, began to gain prominent attention recently. In this study, I am going to discuss about the research perspective towards mitigation of the snow disaster.

Keywords: snow and ice disaster

Japan Geoscience Union Meeting 2014
(28 April - 02 May 2014 at Pacifico YOKOHAMA, Kanagawa, Japan)

U08-18 Room:Main Hall Time:May 2 15:00-15:15

Space disasters and space weather studies

KIKUCHI, Takashi[1*]

[1]Solar-Terrestrial Environment Laboratory

When the solar flare occurs, the high energy particles hit the satellite and cause serious troubles in the communication and broadcasting systems. The geomagnetic storm causes induced currents giving damages to the power transmission system. To avoid the damages due to the solar flare and geomagnetic storms, we are doing research to achieve the prediction model of the solar flare and magnetospheric and ionospheric storms. This talk will present examples of the satellite failures and power outage and also the simulation studies which will enable us to predict the space weather.

Keywords: Space weather, magnetic storm, geomagnetically induced current, radiation particles, satellite anomaly, power outage

Japan Geoscience Union Meeting 2014
(28 April - 02 May 2014 at Pacifico YOKOHAMA, Kanagawa, Japan)

U09-01 Room:502 Time:May 1 14:20-14:45

Estimation of the paleotsunami size using tsunami deposits along the eastern Nankai Trough

FUJIWARA, Osamu[1*]

[1]Active Fault and Earthquake Research Center, AIST

Repeated great earthquakes (M8 class) and accompanying tsunamis occurred along the Nankai Trough have severely damaged the coastal areas along the trough. In response to the 2011 Tohoku-oki earthquake and tsunami, Cabinet office, Government of Japan came up with a new policy to the damage assumptions for the great earthquake and tsunami generated from this plate boundariy. That is, a doctrine that gives serious consideration to the greatest class of earthquake and tsunami, which take every possibility into account, was announced.

The announced ”greatest class of earthquake and tsunami” along the Nankai Trough by the Central Disaster Management Council of the Cabinet Office (2011, 2012) has a rupture zone covering the almost entirely of the Nankai Trough (Mw 9.1) and is much larger than formerly estimated one. As this great earthquake and tsunami would hit the area with clustered population and industries, disaster prevention measure for these catastrophes increasingly attracts public attention.

Japanese historical documents cover the past 1300 year records of the great tsunami-inducing earthquakes generated from the Nankai Trough, so called Nankai and Tokai/Tonankai earthquakes. However, M9-class mega earthquake as mentioned above has never reported in this area. In considering whether out-sized earthquake and tsunami announced for the Nankai Trough will do occur or not, it is necessary to verify whether unknown out-sized earthquake has occurred in the geological time scale. Paleo-seismological studies including the tsunami deposit researches are also needed to expand the time range of the earthquake and tsunami records beyond the historical documents and to make the reliable and realistic size estimation for the palate boundary earthquakes and tsunamis based on their recurrence history.

In reconstructing the paleotsunami size, it is needed to consider the influence of coastal geomorphic developments in centennial to millennium time-scale. Seaward expansion of alluvial lowland (migration of coast line) and coastal uplift are primary factors for these topographic changes, which can function as ”natural barrier” for the tsunami inundation. For this reason, the older tsunami deposits tend to distribute the deeper inland and higher altitude. If the effect of these natural barrier is not considered, there is a risk that will come into the over estimation for the size of palerotsunamis. In considering the effect of natural barrier, tsunami deposits suggesting the out-sized earthquake have not found from the sedimentary sequence formed along the Enshu-nada and Suruga Bay coast in the last 4000-5000 years.

Keywords: Nankai Trough, Tokai earthquake, Tsunami, Tsunami deposit

Japan Geoscience Union Meeting 2014
(28 April - 02 May 2014 at Pacifico YOKOHAMA, Kanagawa, Japan)

U09-02 Room:502 Time:May 1 14:45-15:10

Tsunami Sediment along the Nankai Trough and Nuclear Power Plants

OKAMURA, Makoto[1*]

[1]Science Research Center

We know well interplate megathrust earthquakes have been occurred repeatedly through several decades to centuries. Based on this common knowledge, huge earthquakes and tsunamis must be occured within a period of several thousand years. We research on tsunami sediment from lacustrine deposits along the Nankai Trough for prehistoric Nankai Trough Earthquake. As a result, large tsunami has been occurred 300 years interval through past 6,000 years. The Hoei Earthquake, AD1707 was the biggest tsunami through last millennium as mentioned after ancient manuscripts. Nevertheless, over the Hoei Earthquake tsunami sediments were found in several cores collected from lacustrine deposits.

However, we only have poor knowledge about these interplate earthquakes through millennium. Actually, the Fukushima Accident after the Kashiwazaki, we cannot evaluate even small-sized earthquake (Mw6.8), and 3.11 tsunami. We, seismologists and engineers, said ”out of image” just after 3.11 off Tohoku District Earthquake. Never say ”safe or safety” again about future earthquake and tsunami related nuclear power plants.

Keywords: mega-quake, Nankai Trough, tsunami sediment, nuclear power plant

Japan Geoscience Union Meeting 2014
(28 April - 02 May 2014 at Pacifico YOKOHAMA, Kanagawa, Japan)

U09-03 Room:502 Time:May 1 15:10-15:35

Change of giant tsunami study and the risk evaluation of the NPP before and after the 2011 Tohoku earthquake

OKAMURA, Yukinobu[1*]

[1]The National Institute of Advanced Industrial Science and Technology

When the 2011 Tohoku earthquake occurred, the study of the 869 Jogan earthquake by AIST has finished the first stage and the evaluation of the Jogan earthquake was almost concluded in the Headquarters for Earthquake Research Promotion, and also the back check of nuclear power plants seem to have been slowing down.

The study of Jogan earthquake by AIST started 2004 and was included in the project supported by MEXT from 2005 to 2009. The final report of the project submitted to MEXT in 2010, which concluded that a giant tsunami was generated during the AD869 Jogan earthquake which was larger than M 8.4 based on tsunami deposits survey in the Sendai and Ishinomaki plains, and that the recurrence interval of the giant tsunamis was 450 to 800 years. The AIST study team understands that the source area could extend to the north and south because the survey area of tsunami deposits was insufficient, and tsunami inundation was wider than the distribution of tsunami deposits. The survey of tsunami deposits of wider area had been started from 2010, but it was difficult to find coastal plains which preserve tsunami deposits.

The re-evaluation of all of the nuclear power plans started in 2007 based on new criteria of the safety assessment. The plants were evaluated by three sub-committees and the result was reported to the joint committee. Evaluation against strong motion by earthquake was preceded putting tsunami evaluation off later. In 2009, the middle reports of the Fukushima No.1 NPP was submitted to the joint committee which did not mentioned to the Jogan earthquake, and then only the minimum model of the Jogan earthquake was evaluated. The further discussion of its magnitude and tsunami has not been conducted before March 11, 2011.

The study of Jogan earthquake have been presented in meetings of earth science societies by AIST and medias reported several times since 2005, but the possibility of giant earthquake along the Japan trench was not discussed in the community of earthquake science. In addition, it is not easy to change the society that was not ready to giant earthquake. In these circumstances, nuclear power plants were working during the re-evaluatio, while many problems have been pointed out.

The situation has changed dramatically after the 2011 Tohoku earthquake. Society shares sense of crises against giant tsunami. The tsunami assessment has been made not based on known maximum earthquakes but unknown possible maximum. The safety of nuclear power plant were in doubt and the operation can be started after the safety of the plant was confirmed. Government dose not hesitated to assume maximum earthquake and tsunami, then possibility to point put unknown giant tsunami has been declined. But there is still unknown in earthquake, so it is necessary to continue study and to tell the society truce what we know and do not.

Keywords: tsunami deposits, giant tsunami, Jogan earthquake, Tsunami evaluation

Japan Geoscience Union Meeting 2014
(28 April - 02 May 2014 at Pacifico YOKOHAMA, Kanagawa, Japan)

U09-04 Room:502 Time:May 1 16:15-16:40

Strong motion characteristics of Mega-Thrust earthquake and the seismic response of NPP as a massive, stiff structure

KAWASE, Hiroshi[1*]

[1]DPRI, Kyoto University

The 2011 Tohoku earthquake generated a large number of strong motion records with high acceleration at many observation points, mainly in Miyagi and Ibaraki Prefectures. The distribution of seismic intensities observed or collected by JMA shows that intensity 7 was recorded only at K-NET Tsukidate (MYG004) in Kurihara City, but that intensity 6 upper were recorded at 40 points in four prefectures. When we compare the distribution of the peak ground acceleration (PGA) and velocity (PGV) of the strong motion records observed by K-NET and KiK-net of NIED with the empirical attenuation relation of Si and Midorikawa we can see that PGAs exceeded 500 Gals extensively along the coast from the Central Sanriku to Ibaraki Prefecture, but that PGVs in the area were lower than 80 cm/s. Because of the stochastic nature of the strong motion generation from the large-sized ruptured area there is no site with the coherent intermediate-period (around 1 s) velocity pulse with PGA larger than 800 Gals and PGV higher than 100 cm/s, which is the primary reason for not having severe seismic damage onto the ordinary low-rise buildings.

Prof. Sakai of Tukuba Universiy investigated the structural damage around the site with JMA intensity 6 upper to find that there are no site with heavy damage. We also found that, by using the nonlinear response models which can reproduce the damage ratios caused by the 1995 Hyogo-ken Nanbu (Kobe) earthquake, the structural damage potentials of the observed strong motions were relatively minor for most of the sites. These facts suggest that the current ordinary buildings in Japan, which is basically designed by using the rigid-structure concept, are capable to survive to the strong shakings from the mega-thrust earthquakes.

On the other hand the structural damage prediction by the Cabinet Office of the Japanese Government is made from the empirical relations with respect to seismic intensities of the predicted strong motions. Since such empirical relationship are all based on the damage observed during the 1995 Kobe earthquake, the relationship is good for the inland earthquake but not appropriate to the strong motions pervasively observed during the mega-thrust earthquakes with high PGAs but not so high PGVs. To prove this we independently predict strong motions and using the nonlinear response models we estimated structural damages and found heavily damaged sites only close to the shore line with soft ground conditions.

The same kind of smaller responses were predicted for the nuclear power plant (NPP) structures by using the strong motions predicted by the Cabinet Office in 2003 (Seckin et al., 2008, WCEE). The response of the NPP for predicted strong motions were about twice larger than the elastic limit of the structure, in terms of the relative shear deformation ratios. This is because on one hand the rigid body design concept makes structures sufficiently strong to the high PGA input and on the other hand the elastic limit used for the design is quite low compared to the ordinary buildings. Thus from the structural point of view strong motions during future mega-thrust earthquakes would not be a primary risk for NPPs despite of the spectral amplitude higher than the design input.

Keywords: strong motion, Mega-thrust earthquake, Stiff structure, shear deformation

Japan Geoscience Union Meeting 2014
(28 April - 02 May 2014 at Pacifico YOKOHAMA, Kanagawa, Japan)

U09-05 Room:502 Time:May 1 16:40-17:05

Safety regulations of nuclear power plant for tsunami after the 2011 great Tohoku-oki earthquake

TANIOKA, Yuichiro[1*]

[1]Institute of Seismology and Volcanology

Due to large tsunamis caused by the 2011 great Tohoku-oki earthquake, at First Fukushima Nuclear Power plant, cores were melted and explosions were occurred. Many inhabitants are still evacuated now because of radioactive contamination on land. About four months after this accident, the Nuclear Safety Commission of Japan made the committee for earthquake and tsunami related regulation guidance. In the committee, the revision of the earthquake-resistant design examination guidance was discussed. Before the accident, tsunami was treated as ”consideration for the earthquake accompanying phenomenon”. In the new guidance, ”the safe design policy for tsunami” became an item different from ”the earthquake-resistant safe design policy”. In March, 2012, a new examination guidance including the safe design policy for tsunami was made.

Then, in September, 2012, the Nuclear Regulation Authority was newly established in Japan. Under the Authority, ”the study team on the regulatory requirement for light water nuclear power plants - earthquake and tsunami ?” was established. The study team discussed about ”new safety design standard for earthquake and tsunami”. That was finalized in June, 2013.

In this new safety design standard, concept of the multiplex defense is adopted. 1) Tsunami should not get into a site. 2) When a tsunami get into a site with any reasons, the tsunami should be protected from a house or constructions. 3) When a tsunami get into a house, the power should be supplied from higher place near a site to prevent a severe accident. For tsunami should assume the largest tsunami source from the largest expected event. It is important to understand the concept of the multiplex defense. Some people may think that it is OK to have small inundation from small holes because the houses are protected from water. If such a thought comes out for the multiplex defense, a risk may increase ironically. I wish that the concept of the multiplex defense should be applied closely.

Japan Geoscience Union Meeting 2014
(28 April - 02 May 2014 at Pacifico YOKOHAMA, Kanagawa, Japan)

U09-06 Room:502 Time:May 1 17:05-17:30

Seismic Safety Regulations and Earthquake Science

KOKETSU, Kazuki[1*]

[1]Earthq. Res. Inst., Univ. Tokyo

The first parts of seismic safety regulations for nuclear power plants consist of seismic and tsunami hazard evaluations as in the regulations for other structures. Although there are probabilistic and scenario assessments for the seismic hazard evaluation, the scenario assessment is mainly used and the probabilistic assessment is only in auxiliary use to evaluate remaining risk. Therefore, knowledge of earthquake science mostly contributes to making choices of scenario earthquakes in the scenario assessment.

This presentation mostly discusses the seismic hazard evaluation for nuclear power plants as the conveners requested, but also discusses the tsunami hazard evaluation as related to large subduction zone earthquakes. In addition, various phenomena occurring at nuclear power plants due to the 2011 Tohoku earthquake and their relation to these hazard evalutions and choices of scenario earthquakes are discussed.

We finally show from the above that the earthquake science cannot contribute to the real safety of a nuclear power plant unless unknown phenomena can be foreseen. We also discuss the danger of the idea that real safety can be reached if ”decision is made without prejudice only from the scientific and technical point of view.”

Japan Geoscience Union Meeting 2014
(28 April - 02 May 2014 at Pacifico YOKOHAMA, Kanagawa, Japan)

U10-01 Room:Main Hall Time:May 1 09:15-09:45

Collaboration beyond the difference between science and government

YAMAOKA, Koshun[1*]

[1]Graduate School of Environmental Studies, Nagoya University

Government and public take actions with decisions and judgments based on scientific knowledge. Science community widens and deepens human knowledge with continual research efforts. Therefore, any scientific conclusion, which is once regarded as true, can be denied by later researches. This is the origin of disagreement between science, which has essential uncertainties, and government and society, which require definite decisions. They need to acknowledge such differences that exist between science and government to improve the society.

In the volcano eruption prediction in Japan, the relationship between science community and government-public functions well. The reason is ”reasonable distance” between them. Japan Meteorological Agency (JMA) is responsible for issuing volcano information for evacuations. The information is justified in the discussion of the Coordinating Committee for the Prediction of Volcanic Eruption (CCPVE), where both scientists, geologists to geophysicists, and government personnel participate. Scientists often devoted themselves to the disaster reduction plan in local society near volcanoes, also contributing establishment of reasonable-distance between scientists and local government-public.

The Headquarters of Earthquake Research Promotion (HERP) is responsible for making use of the scientific knowledge of earthquakes in disaster reduction. In contrast to the volcano eruption prediction, it is rather difficult to keep reasonable distance between scientists and government-public for the following reason. The community of earthquake science is much bigger than that of volcano eruption prediction. Government personnel are changed in two years. Most of earthquake scientists live in Mega cities, and many prefectures have no earthquake scientists to ask for advices.

Volcanic Alert Levels were established following the requirement by the public. The level is designed so that each level corresponds to a definite evaluation action of the residents. Although, this is more than that volcano science can provide, the level functions so far with a conservative operations. For example, in the 2011 eruption of Kirishima nobody was insured or killed in spite of no precursors are observed. The alert level was kept level 2 after the small eruption of the previous year.

HERP issues long-term probability of earthquake occurrence in Japan, which was a strong requirement of the public after the 1995 Kobe earthquake. Characteristic earthquake model is used for the evaluation, because this the only usable model for the calculation of long-term probability of earthquake. To meet the responsibility for the public the government have to evaluate earthquake probability for all of major active faults and plate boundaries in Japan territory, in spite of large uncertainty. In the evaluation the off-Tohoku area are divided into several regions, each of which was assigned its own characteristic earthquake. Interaction of asperities, which represents the region division, was not taken into account. The off the coast of Tohoku earthquake is really a result of such interaction. After the earthquake the ”Off-the-coast-of-Tohoku-type” earthquake are introduced in the evaluation process, but still based on the characteristic earthquake hypothesis. The disaster reduction plan based on the long-term evaluation depends on the polity of the Cabinet Office or local governments.

The above examples are the results of interaction among social demands, governmental policy and state-of-the art of scientific knowledge. Though we have to admit that they are more than the present achievement of volcano and earthquake science, it is inevitable to issue some information for practical disaster reduction. We need to make continual efforts to improve the disaster reduction measure through effective communication between governmental personnel, public and scientists.

Japan Geoscience Union Meeting 2014
(28 April - 02 May 2014 at Pacifico YOKOHAMA, Kanagawa, Japan)

U10-02 Room:Main Hall Time:May 1 09:45-10:15

Space Policy in Japan after new decision system

MATSUI, Takafumi[1*]

[1]Planetary Exploration Research Center, Chiba Institute of Technology

In 2012, decision system on space policy in Japan changed. Since then, new space policy has been decided under the supervision of national committee on space policy. In this talk I will introduce the structure of this new system and vision of space exploration of our country in the next decade.

Japan Geoscience Union Meeting 2014
(28 April - 02 May 2014 at Pacifico YOKOHAMA, Kanagawa, Japan)

U10-03 Room:Main Hall Time:May 1 10:15-10:45

The relationship between Earth and Planetary Science and polyiics from the stand point of oceanography

KOIKE, Isao[1*]

[1]University of Ryukyus

Ocean political issue is one of the most critical issues in recent Japan including continental shelf, recources, fishing, conservation of living resources, and ottal environment of the Earth. Science has been required to give contribution to policy making, which means that to keep balance is important for us. I will discuss the situation of science in recent Japanese ocean politics and how we should go.

Japan Geoscience Union Meeting 2014
(28 April - 02 May 2014 at Pacifico YOKOHAMA, Kanagawa, Japan)

U10-04 Room:Main Hall Time:May 1 11:00-11:30

Transdisciplinary approach for global environment and Future Earth

YASUNARI, Tetsuzo[1*]

[1]Research Institute for Humanity and Nature

The global environmental studies are now required to make progress toward global sustainability and futurability of the earth system. RIHN is now stepping forward to transdisciplinary approach for tackling these issues. This approach involves strong collaboration with the international Future Earth initiative. We also emphasize the importance of Asia-Pacific region as a complex tectonic-environmental hot spot region on these issues.

Japan Geoscience Union Meeting 2014
(28 April - 02 May 2014 at Pacifico YOKOHAMA, Kanagawa, Japan)

U10-05 Room:Main Hall Time:May 1 11:30-12:00

Relationship between scientists and government - public

YOKOYAMA, Hiromi[1*]

[1]Department of Earth and Planetary Science

How scientists should be saying to the government and society? Based on the norms of scientists, I will discuss the social role of scientists.

Keywords: scientists, goverment, public

Japan Geoscience Union Meeting 2014
(28 April - 02 May 2014 at Pacifico YOKOHAMA, Kanagawa, Japan)

U10-06 Room:Main Hall Time:May 1 12:00-12:30

Earth science, community, and government

NAGAHARA, Hiroko[1*]

[1]Dept. Earth Planet. Sci., The Univ. Tokyo

Earth and planetary science stands on a special position between natural science and the community and government, which in turn means an importance of our community from both sides. We have encountered various difficulties in March 2011, when our words gave a great influence on community and we had flustration how we presented scientific results that might have caused social confusion. We will discuss how Earth and planetary sicence keep good distances from social community and government and how we should play our role.

Keywords: earth and planetary science, community, government

Japan Geoscience Union Meeting 2014
(28 April - 02 May 2014 at Pacifico YOKOHAMA, Kanagawa, Japan)

O01-01 Room:503 Time:April 29 09:00-09:30

Action of the disaster prevention education in Kochi˜development and practice of the Kochi safety education program˜

KAMIOKA, Norimasa[1*]

[1]Kochi prefectual board of education secretariat,School safety management division

In 2013, the Kochi prefectural Board of Education created teacher's instructional documents for disaster prevention education called "the Kochi Safety Education Program (for earthquakes)" and handed it out to all the teachers in Kochi. It explains the outline of the program and introduces some specific efforts to promote disaster prevention education in Kochi.

Keywords: Disaster prevention education, the Kochi Safety Education Program (for earthquakes), Nankai trough quake, Instruction ten items

Japan Geoscience Union Meeting 2014
(28 April - 02 May 2014 at Pacifico YOKOHAMA, Kanagawa, Japan)

O01-02 Room:503 Time:April 29 09:30-10:00

Advancing disaster preparedness in Okinawa Prefecture

MATSUMOTO, Takeshi[1*] ; FUJIWARA, Ayako[1]

[1]University of the Ryukyus

Okinawa Prefecture located in the south-westernmost part of Japanese Islands and in the subtropical area is often attacked by characteristic natural disasters which are different from the other areas in Japan, such as, destructive typhoons after passing the Western Pacific Warm Pool, high tide due to typhoons and warm water eddies, many earthquakes of both plate convergent type and due to active across-arc fault slip, most of them may induce tsunamis because their hypocentres are mostly sub-seafloor. Disaster preparedness, especially in Okinawa Prefecture is to be taught at the school education. Currently, 'Home Economics' is the only subject in which disaster preparedness is taught in junior and senior high schools in Japan. Therefore the articles on disaster preparedness in the current official textbooks on 'Home Economics' for junior and senior high school education were investigated in order to search if they contain descriptions enough to fulfil the disaster preparedness education in these schools. The results, however, show that the description in all the official textbooks was poor and that the volume of the description was half page in the minimum case and two pages even in the maximum case. The authors therefore started the following practice to fulfil the disaster preparedness education at schools.

A brochure to explain the nature of these natural disasters characteristic of Okinawa Prefecture and to teach how to prepare for the natural disasters was printed for auxiliary materials for school education. It includes the aspects of both natural science (earth science) and home economics, such as preparedness in the viewpoint of food clothing and shelter.

Japanese government established the system for renewing educational personnel certificates in 2007 and mandated the adoption of it in April 2009. The new system shows that only persons who have attended the certificate renewal courses over 30 hours and passed the examination before the expiration of the valid period can renew their certificate which is valid for next ten years. The purpose of this system is for teachers to acquire the latest knowledge and skills. Since 2012, the author has offered a 6-hour certificate renewal course titled by 'Disaster preparedness in Okinawa ? practicing development of teaching materials for school pupils'. This course was targeted mainly for science and home economics teachers of junior and senior high schools to tell the school pupils how to save their lives in case of devastated natural disasters.

Japan Geoscience Union Meeting 2014
(28 April - 02 May 2014 at Pacifico YOKOHAMA, Kanagawa, Japan)

O01-03 Room:503 Time:April 29 10:00-10:30

Lesson from the great east earthquake and future education for safety

SATO, Hiroki[1*]

[1]Ministry of Education Culture Sports Science and Technology - Japan

Lesson from the great east earthquake and future education for safety

Keywords: Safety education

Japan Geoscience Union Meeting 2014
(28 April - 02 May 2014 at Pacifico YOKOHAMA, Kanagawa, Japan)

O01-04 Room:503 Time:April 29 11:00-11:30

Urban Disaster

KAWATA, Yoshiaki[1*]

[1]Faculty of safety Science

Disasters in urban area have evolved with urbanization such as urbanizing disaster, urbanized disaster, urban disaster and Super-urban disaster. These changes of the disasters are discontinuous due to phase tradition. The condition will be proposed by the worst damage scenario. The disaster vulnerability depends on several conditions such as rapid urbanization and inadequate land use management, over-population and its density, imbalance of natural environment, over-dependence on social infrastructure and public service. Disaster resilience was proposed in Hyogo Framework of Action (HFA), the 3rd United Nation Conference on Disaster Reduction in 2005. Japanese government will promote the disaster resilient policy, but it does not include community based projects which is also supported by people in any community. In the case of retrofit of houses, community based promotion is necessary because the cause of a fire is an earthquake vulnerable old house in the community.

Keywords: Urban disaster, Disaster evolution, Phase tradition

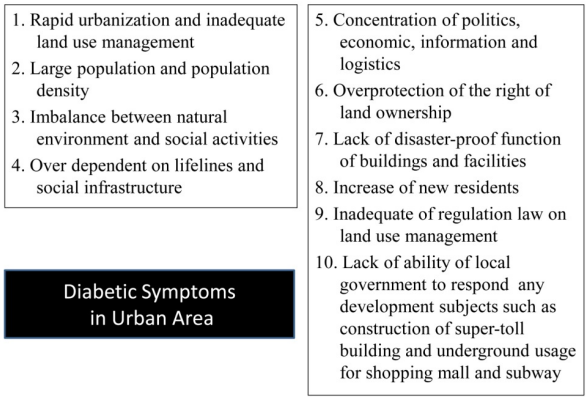

Fig. 1 Factors of acceleration of vulnerability in urban area

Japan Geoscience Union Meeting 2014
(28 April - 02 May 2014 at Pacifico YOKOHAMA, Kanagawa, Japan)

O01-05 Room:503 Time:April 29 11:30-12:00

Natural Disaster in The World

KAWATA, Yoshiaki[1]*

[1]Faculty of Safety Science

Natural disasters have two characteristics. The former is that disaster history repeats itself and the latter is locality. In Istanbul, Turkey, plate boundary earthquakes have occurred 27 times since 438. Mayon Volcano, Philippines had erupted 50 times in 400 years since 17th century, therefore average time interval is 8 years. In Asia, natural disasters hold a certain percent of the world such as number of occurrences : 36%, property damage : 47%, death toll : 62% and number of injured : 89%. The last two has increased due to rapid growth of population in urban area. The combination with gigantic earthquake and tsunami and volcano eruption had occurred in Japan as 1) 864 to 887 with Mt. Fuji eruption, Jougan earthquake and tsunami and Nankai-trough earthquake and 2) 1703 to 1707 with Genroku earthquake in Tokyo, Nankai-trough earthquake and Mt. Fuji eruption. We are now under clear effect of global warming. For example, in South Asia, the number of flooding has increased nearly twice in next ten years. Since 1995 in China, river flood disasters occurred five time with the victims of more than one hundred million. In 2005, hurricane Katrina with category 5 hit New Orleans and just three weeks after hurricane Rita also hit the damaged area. She was also category 5 and they made compound disaster. Finally, we proposed vicious cycle among population increase, disaster occurrence and poverty in rural area and urban area. The pair of two vortexes is very stable, therefore it is necessary to become economic growth to break the voltexes.

Keywords: Natural disaster, Global warming, Vicious cycle

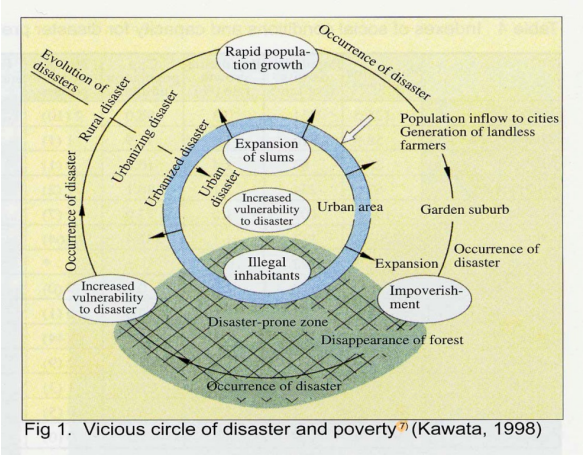

Fig 1. Vicious circle of disaster and poverty[7] (Kawata, 1998)

Japan Geoscience Union Meeting 2014
(28 April - 02 May 2014 at Pacifico YOKOHAMA, Kanagawa, Japan)

O01-06 Room:503 Time:April 29 12:00-12:30

Support by the health care providers in the reconstruction phase of disaster

TAKADA, Satosho[1*]

[1]Graduate School of Health Sciences, Kobe University

In the reconstruction phase, health care providers should pay particular attention to vulnerable groups which include the poor, women, children, elderly, handicapped and people with preexisting mental disorders.

Japanese people have experienced two severe natural disasters for the last two decades. The Hanshin-Awaji Earthquake occurred in the early morning of the January 17, 1995. Approximately 6,433 people perished and more than 43,792 people were injured. Homes of more than 300,000 people were totally or partially destroyed. Citizens not directly affected by the earthquake had to endure extreme disruption and confusion in their daily lives due to the long time disruption of daily activities resulting from the severely damaged infrastructure.

The Great East Japan Earthquake measuring a magnitude of 9.0 created a devastating tsunami that resulted in the destruction of a nuclear power station with the release of radioactive materials into the environment. The disaster occurred on March 11, 2011, and created one of the most severe humanitarian disasters in modern day Japan. According to the most recent estimates, 15,870 people perished during the disaster, with an additional 2,814 missing, and more than 329,777 being internally displaced. Some statistical models estimated that 727 of those who perished were children.

Three aspects were focused in this paper. The first is the data of psychological reactions in the small children and their mothers following the Hanshin-Awaji Disaster, and the second is the data obtained of children with intellectual or physical disabilities. Thirdly, I would like to introduce our activities in Indonesia and Tohoku based on our experiences gained after the Hanshin-Awaji Earthquake.

Keywords: reconstruction phase, support, PTSD, disability, family

Japan Geoscience Union Meeting 2014
(28 April - 02 May 2014 at Pacifico YOKOHAMA, Kanagawa, Japan)

O02-01 Room:503 Time:April 29 14:15-14:40

Some recent efforts and future activities of JpGU for the next high school national curriculum revision

MIYAJIMA, Satoshi[1*] ; ABE, Kunihiro[2] ; IIDA, Kazuaki[3] ; UEMURA, Takeshi[4] ; OBI, Yasushi[5] ; KAWAGATA, Shungo[6] ; KAWAMURA, Norihito[7] ; KOBAYASHI, Norihiko[8] ; TAKIGAMI, Yutaka[9] ; NEMOTO, Hiroo[10] ; NOUMI, Fuminaga[11] ; HATAKEYAMA, Masatsune[12] ; MANNEN, Kazutaka[13] ; MINAMISHIMA, Masashige[14] ; YAJIMA, Michiko[15] ; YAMASHITA, Satoshi[16] ; WATANABE, Masato[17]

[1]Saitama prefectual Fukaya dai-ichi High School, [2]NPO corporation nature reproduction center toward ”the rich sea mingled with fresh water area clean, [3]Urawahigashi high school,Saitama, [4]Kaijo Junior and Senior High school, [5]Kanagawa Prefectual Sagamihara Seiryo High School, [6]Faculty of Education and Human Sciences, Yokohama National University, [7]Faculty of Education and Human Studies, Akita University, [8]Seibu Gakuen Bunri High School, [9]Kanto Gakuen University, [10]J.F.Oberlin University, [11]Saitama Municipal Sashiougi Jumior High school, [12]Seiko Gakuin High School, [13]Hot Springs Research Institute of Kanagawa Prefecture, [14]Tokyo Metropolitan Ryogoku Senior Hight School, [15]Tokyo Medical and Dentel University, [16]Saitama Prefecural Kumagaya Girls’ Upper Secondary School, [17]Miyamaedaira elementary school

From 2012, the new national curricula standards has been in effect according to Ministry of Education, Culture, Sports, Science and Technology guidelines.

Among most high school students three or more subjects are chosen from the following four subjects; Basic Physics, Basic Chemistry, Basic Biology and Basic Geoscience.

As a result, The number of students who choose Basic Geoscience in 2014 has increased by about 3.5 times compared with that of the number under the former national curriculum guidelines, and some improvement came to be seen in people’s geoscience literacy.

During this time, the Educational Affairs Committee of JpGU, in preparation for the next national curriculum revision, consider the way of desirable high school geoscience education through preliminary discussion in the study meeting (December 2012) and symposium (May 2013).

In order to raise geoscience literacy, it is necessary for the number of students studying geoscience to increase even more.

It is necessary to discern what is asked of high school geoscience education by society, and include the appropriate contents.

In order to allow students to learn the content effectively, we need to discuss what kind of subject setup is desirable.

In this session, based on the discussions so far, we present three drafts about the subject setting of a high school geoscience with different points of view. In addition, we plan to deepen discussion about the future direction of geoscience education taking into consideration the presentation about expectations for geoscience education from people who do not specialize in science.

Keywords: next national curriculum revision, high school geoscience education, subject setting

Japan Geoscience Union Meeting 2014
(28 April - 02 May 2014 at Pacifico YOKOHAMA, Kanagawa, Japan)

O02-02 Room:503 Time:April 29 14:40-15:05

Suggestion of the modified selective subject based on the current Basic Earth Science

OBI, Yasushi[1*] ; KAWAGATA, Shungo[2] ; KOBAYASHI, Norihiko[3] ; TAKIGAMI, Yutaka[4] ; NOUMI, Fuminaga[5] ; MINAMISHIMA, Masashige[6] ; MIYAJIMA, Satoshi[7] ; YAJIMA, Michiko[8] ; WATANABE, Masato[9]

[1]Kanagawa Prefectual Sagamihara Seiryo High School, [2]Yokohama National University, [3]Seibu Gakuen Bunri High School, [4]Kanto Gakuen University, [5]Saitama Municipal Sashiougi Jumior High school, [6]Tokyo Metropolitan Ryogoku Hight School, [7]Saitama Prefectural Fukaya dai-ichi High School, [8]Tokyo Medical and Dentel University, [9]Kawasaki Municipal Miyamaedaira elementary school

Current basics subjects (2 credits) are subjects set based on mind of science for all, and the contents are veneer knowledge. However, it is thought that these basic subjects contribute to the improvement of good scientific literacy upbringing of the balance of the high school student's knowledge because a study rate of all subjects of four subjects of science rose because three subjects of science choice are required. In addition, it is realistic subject setting when based on the situation to teach the subject that does not match a specialty of a high school science teacher.

However, as contents of basics subjects are broad and veneer and have not the learning a principle and structure, the memorized tendency of the item is deeply concerned. Based on this reflection, we want to propose a new Basic Earth Science including contents learning a principle and structure by the selection of contents of the current basics subject carefully.

Keywords: Basic Earth Science, careful selection of contents, selective subject

Japan Geoscience Union Meeting 2014
(28 April - 02 May 2014 at Pacifico YOKOHAMA, Kanagawa, Japan)

O02-03 Room:503 Time:April 29 15:05-15:30

Suggestion of the new high school general science with the contents necessary as earthian

YAMASHITA, Satoshi[1*] ; ABE, Kunihiro[2] ; IIDA, Kazuaki[3] ; UEMURA, Takeshi[4] ; KAWAMURA, Norihito[5] ; HATAKEYAMA, Masatsune[6]

[1]Saitama Prefectural Kumagaya Girls' Upper Secandary School, [2]NPO corporation nature reproduction center, [3]Urawahigashi high school,saitama, [4]Kaijo Junior and Senior High school, [5]Faculty of Education and Human Studies,Akita University, [6]Seiko Gakuin High Scool

Existing national curricula standards(N.C.S) in high school require 3 basic sciences of the 4 basic sciences, an improvement on the former N.C.S. But it is not enough for students to only study 3 basic subjects for coming to a deeper understanding of their place in earth's ecological system.

Therefore we would like to propose two new types of 'General Science' which need 4 credits or 6 credits in school classes.

One type integrates four science subjects into one compulsory subject with the aim of developing better understanding of the global environment and sustainable society,and is based on learning of the problem solution type with high regard for key competency. The other type is to divide 4 basic sciences into 2 subjects in order to understand science literacy, and consists of 'physics and chemistry' and 'biology and earth science' at this time, we want to suggest the former, which integrates four basic science subjects.

Keywords: general science, compulsory subject, problem solution type, understanding global environment scientifically

Japan Geoscience Union Meeting 2014
(28 April - 02 May 2014 at Pacifico YOKOHAMA, Kanagawa, Japan)

O02-04 Room:503 Time:April 29 15:45-16:10

Proposal of novel compulsory subject which is mixed Geoscience, Geography, environment, and natural disaster prevention

NEMOTO, Hiroo[1*] ; MIYAJIMA, Satoshi[2] ; HATAKEYAMA, Masatsune[3]

[1]Division of Natural Sci., J. F. Oberlin Univ., ERI(Guest), [2]Saitama Prefectural Fukayadai-ichi Upper Secondary Sch., [3]Seikou Gakuin Secondary Sch.

The subcommittee of school curriculumme at the committee of school education at Japan Geoscience Union (JpGU) has investigated into the contents of Earth and Planetary Sciences and its related Sciences of next and future subjects of upper secondary schools based on the next and future national standard curricula in Japan. We would like to make 3 types of subjects and their contents. In this presentation, we will report novel compulsory subject of them.

This novel compulsory subject will be invented based on new concepts which break down long-established the framework of current subjects. The contents of this subject consist of geoscience, geography, environment, natural disaster prevention, and so forth. The educational purpose of this subject is to acquire the scientific literacy and the attainment ability of type of PISA, Programme for International Student Assessment, through the ability of natural and social sciences. As a result, students will be able to get ability to take action and thinking faculty for environmental problem and natural disaster prevention by themselves scientifically.

Keywords: Novel Compulsory Subject, Upper Secondary School, Geoscience, Geography, Natural Disaster Prevention, Environment

Japan Geoscience Union Meeting 2014
(28 April - 02 May 2014 at Pacifico YOKOHAMA, Kanagawa, Japan)

O02-05 Room:503 Time:April 29 16:10-16:35

My Expectations to High School Subject ”Earth Science” under the New National Curriculum Standard in Japan

ABIKO, Tadahiko[1*]

[1]Kanagawa University

The new national courses of study in science education of high schools implemented formally in 2013 have asked high school students to choose 3 science subjects from 4 subjects such as physics, chemistry, biology and earth science. This revision has led to following changes; First, the number of students to choose earth science has drastically increased and most of them tend not to study earth science deeply, but to regard it as sort of general education. Second, and what counts most is, their interests in the most important problems of the global environmental issues are increasing. If these tendencies are continued to be seen, new earth science as a high school subject shall have a very serious and critical mission to enhance student’s general science literacy and their motivations for engagement or action in solving those real life problems, while they must be active to make effective conditions of the sustainable development in our human life as well as in all kinds of life on the earth.

Keywords: science education, earth science education, global environmental issues, education for sustainable development (ESD)

Japan Geoscience Union Meeting 2014
(28 April - 02 May 2014 at Pacifico YOKOHAMA, Kanagawa, Japan)

O03-01 Room:Main Hall Time:April 29 09:45-10:20

Hunting mega-quakes -What we can and cannot find out from tsunami deposit-

SHISHIKURA, Masanobu[1*]

[1]Active Fault and Earthquake Research Center, AIST

The giant tsunami of 2011 Tohoku was inundated into further inland and transported sand and mud from the coast. Such sand and mud are called tsunami deposit. Researchers have surveyed past tsunami deposits before the 2011 tsunami, and have revealed that the 869 Jogan tsunami had very large inundation in the Tohoku area. Because the inundation area was eventually almost similar between the 2011 and 869, studying past earthquakes and tsunamis (paleoseismology) came to be recognized in its importance for forecasting magnitude of tsunami. However finding out past phenomena beyond several thousand years is not easy. In this talk, I would like to introduce how to reconstruct the past earthquake and tsunami from historical records, tsunami deposits and coastal topography, including episode of field survey and relationship with society.

Keywords: great earthquake, tsunami, tsunami deposit, paleoseismology

Japan Geoscience Union Meeting 2014
(28 April - 02 May 2014 at Pacifico YOKOHAMA, Kanagawa, Japan)

O03-02 Room:Main Hall Time:April 29 10:20-10:55

Recent eruptions in Japan (review): past and future

NAKADA, Setsuya[1*]

[1]ERI, Univ. of Tokyo

In late November of 2013, eruption started in Nishinoshima approximately 1,000km south of Tokyo, and the activity continued. Including this eruption characterized by gentle lava outflow, various types of eruptions occurred in Japan during recent decades. For instance, Shinmoe-dake (Kirishima) woke up with explosive pumice eruption in 2011 after a quiescent period of 300 years. Sakurajima repeats explosions every day. Miyakejima erupted with subsidence of the volcano peak area in 2000. Eruption at Unzen issued pyroclastic flows for several years in early 1990s. Except some people damaged directly by it, volcanic eruption itself fascinates people, and the resultant landforms, hot springs, and fertile plateaus bring blessings to people. Therefore, eruption activity is different from other natural hazards. In the volcanic belts surrounding the Pacific, such as Indonesia, Chile and so on, eruption activity in the Japanese Islands was very low in magnitude during these centuries. After the large earthquake on March 11, 2011 which caused a extensive crustal movement in the whole East Japan, seismic activity increased in several volcanoes in the East Japan including Mount Fuji. Volcanologists were worried about eruptions triggered. However, no volcanic eruptions were triggered during, at least, three years. Does an earthquake trigger volcanic eruption really?

In this lecture, I review recent major volcanic eruptions in and outside the Japanese Islands with their research results. In addition, I will mention on the possibility of large-scale eruptions near future, especially at Mount Fuji stopping eruption for these 300 years and at volcanoes that experienced caldera-forming eruptions in the past.

Keywords: volcanic eruption, Nishinoshima, natural hazards, triggering eruption, Mount Fuji, Caldera eruption

Japan Geoscience Union Meeting 2014
(28 April - 02 May 2014 at Pacifico YOKOHAMA, Kanagawa, Japan)

O05-01 Room:313 Time:April 29 09:05-09:35

Career path of young scientists

NAKAMURA, Masato[1*]

[1]Institute of Space and Astronautical Science of Japan Aerospace Exploration Agency

For sustainable development of geosciences, it is necessary to consider supporting and training system of geoscientists, especially for young geoscientists who hardly get permanent academic positions under recent condition surrounding Japanese young scientists. They are worrying about their carrier paths, with considering their work-life balances in parallel. Due to anxious of invisible future, some of them quit trying to become scientists when they face to life events such as childbirth and care of their children or parents, If this situation will continue still more, our academic field, geosciences, will reduce gradually. Therefore, I will introduce to them mental attitude required for geoscientists and successful role models, i.e., active senior geoscientists by doing continuous efforts.

Japan Geoscience Union Meeting 2014
(28 April - 02 May 2014 at Pacifico YOKOHAMA, Kanagawa, Japan)

O05-02 Room:313 Time:April 29 09:35-10:05

Effort for Diversity Promotion, University of Tsukuba

HABAZAKI, Makiko[1*]

[1]Office of Diversity, University of Tsukuba

The University of Tsukuba promotes the gender equality based on the 3rd Basic Act for Gender-Equal Society and the 4th Science and Technology Basic Plan in Japan, recognizing our social role and responsibility to form a gender equal society. In 2007, the Committee on Gender Equality and the Office of Gender Equality were established, and 'Basic Principles and Policies on Gender Equality' has been enacted in 2008. For the three years from 2009 to 2012, a project of 'University of Tsukuba Style: Sustainable Support for Women Researchers' program was adopted as a strategic fund of a model of support for women researchers for Promoting Science and Technology. Therefore we endeavor to develop its environment of the gender equality. In April 2012, 'the Office of Gender Equality' was reorganized to 'the Office of Diversity', and 'Basic Principals and Policies on Diversity' was designed to become a university where human potential and diversity are respected and all stakeholders can experience pride and joy in their work. In March 2013, 'Action Plan of Diversity, University of Tsukuba' was designed, and in August, new project was adopted as 'Fund for supporting activities for female researchers'. In response, we are going on amplification of environment for gender equality and diversity.

We are promoting various projects based on following five purposes in 'Action Plan of Diversity (from 2013 to 2018)'.

1. Promotion for diversification in university management
2. Offering of assistance in the balancing of education, research, and work with family life
3. Expansion of diversity in next generation
4. Pursuit of awareness-raising activities targeting faculties, staffs, and students
5. Pursuit of gender equality through partnerships with the local community and international society

Workers during a Childbirth, Child Care, and Family Care can employ for tenured faculty members and secure of substitute teachers. The University also opened Au Work-Life Balance Counselling Room for such workers. For educational activity, we have held some seminar of awareness of diversity for managerial staff, and class of 'Work-Life I and II' for university student. Then, we have been focused 'Expansion of lower' that educate young generation (especially women) wanted to be scientist. As a result of these efforts, the ratio of women researcher has increased year by year at University of Tsukuba.

Japan Geoscience Union Meeting 2014
(28 April - 02 May 2014 at Pacifico YOKOHAMA, Kanagawa, Japan)

O05-03 Room:313 Time:April 29 10:05-10:35

Balance with caring for parents, caring for children, and studying-My experience in caring for my parents-

OHYA, Hiroyo[1*]

[1]Graduate School of Engineering, Chiba University

Suddenly one day, if your parents are given half a year to live and you become care for your parents-. The caring for parents suddenly comes to you and may continue for a long time. When I was caring for my little children, my father was given half a year to live due to cancer. I will talk about my experience for caring for my father, caring for children, and studying in this session. Shall we think about caring for parents from each point of view regardless that you experienced or not?

Now my children are university and high school students. I will also talk about the difference of life-work balance between the childhood and adolescence.

Japan Geoscience Union Meeting 2014
(28 April - 02 May 2014 at Pacifico YOKOHAMA, Kanagawa, Japan)

O05-04 Room:313 Time:April 29 11:00-11:30

An Encouragement of doing *Ikumen* and taking *paternity leave*

YOSHIDA, Hiroki[1*]

[1]Fathering Japan, Nonprofit Organization

The author has a confident to contribute to all male scientists, who have an idea of taking a *paternity leave*. We can learn many things and grow up ourselves by taking care of children. However, the time as to be a current parent especially for a small child is too short. Thus, male scientists should do *Ikumen* right now and take *paternity leave* if necessary.

The term parental leave includes maternity, *paternity*, and adoption leave. The minimum benefits are stipulated by Japanese law. Although such valuable supports are provided by the government, there are few people experienced *paternity leave*. One of the reasons is too worry about eyes of surrounding people such as colleagues and neighbors. Even they take *paternity leave*, they may have a hard time to take care of children. Parenting is different from repeating same things as just for feeding, substituting diapers, etc. It is an important work to bring up and to educate children, precious talented people in the near future. Praising, encouraging and smiling are the most important for education not only for children but also for all people. *Ikumen* experience will be sure to help your private life as well as academic and scientific works.

Japan Geoscience Union Meeting 2014
(28 April - 02 May 2014 at Pacifico YOKOHAMA, Kanagawa, Japan)

O05-05 Room:313 Time:April 29 11:30-11:50

Now and Future Thailand’s Family

TANGWATTANANUKUL, Ladda[1*]

[1]Graduate School of Engineering and Resource Science, Akita University

In Thailand, families reside with their family size either in cities or countryside. The family size in countryside is larger than one in cities. The marriage practice allows women to move into husband’s family.

Family member are delegated household each other. Women do household: cooking, cleaning and washing. Instead, men do heavy work in their house. When children reach about 8 years old, they need to assist their mother and father like cooking and taking care of younger siblings. Most men of Thailand can cook and taken care of kids. Recently, the family likes to pay money to housekeeper to clean house and wash clothes. Some family’s grandmother and grandfather are in house. They take care of kids when the parent goes to work out. Women worked in company or government ask maidservant to stay with her family. Maidservant will take care of baby and cooking for the host family. They get foods and salary about 20000 yen per month. Most of the maidservants are teenager and the maidservants are from Myanmar or Laos. However, recently women who graduate from colleges or universities become choosing to work for long period before marriage.

Japan Geoscience Union Meeting 2014
(28 April - 02 May 2014 at Pacifico YOKOHAMA, Kanagawa, Japan)

O06-01 Room:Main Hall Time:April 30 09:00-09:26

Geopark

OIKE, Kazuo[1*]

[1]Chairman, Japan Geopark Committee, Kyoto University of Art and Design

Looking at the landscape constructed by the activity of the earth, tasting vegetables and fruits produced by the blessing of nature, we learn the natural phenomena, regional history and culture of the geoparks.

The basic characteristics of nature of Japan islands are earthquake occurrence, volcanic eruption and tsunami. Japan’s geoparks are located along the deformation belt and are also the parks of the earth where the culture of the Japanese people who have lived in natural disasters is intoruduced.

On December 2013, thirty three geoparks has been certified by the Japan Geopark Committee. Six of them have been certified to join the Global Geopark Network. We will continue to learn from the beauty of nature of Japanese archipelago, and introduce it to people of the world.

Keywords: Geopark, Japan Geopark Committee, Japanese Geoparks Network

Japan Geoscience Union Meeting 2014
(28 April - 02 May 2014 at Pacifico YOKOHAMA, Kanagawa, Japan)

O06-02 Room:Main Hall Time:April 30 09:26-09:51

Nature parks as a tool for local sustainable community

MATSUDA, Hiroyuki[1*]

[1]Yokohama National University

Abstract

Biosphere reserve (BR) of UNESCO's Man and the Biosphere (MAB) Programme seeks balance between sustainable use of natural capitals and biodiversity conservation, rather than protection of primeval nature. In the early stage of the MAB programme, BR encouraged academic research in the site and usually consisted of core area and buffer zone. Forest Ecosystem Reserve of Japan follows the concept of BR zoning.

Since 1995, BR consists of core, buffer and transition areas. Transition area supports sustainable use of natural capitals (Figure 1). Therefore, BR becomes a good arena of development of local economy. Also global trend of environmental movement shifts from protection of primeval nature to conservation of natural resources.

BR recommends involvement of all actors in management and decision-making processes. New forms of institutional cooperation and links between different levels of economic and political decision making. Aya BR, designated in 2013 as the 5th Japanese BR, is recognized as one of the best models of participatory approach for BRs in the world. Bokova (Director-General of UNESCO) said, "From the Luberon-Lure BR in France and the Aya BR in Japan to the Dana BR in Jordan, local communities are developing bio-products that meet both local and global needs, and in ways that contribute to a healthy environment and reduce waste."

Fig. 1 Role of core, buffer and transition areas in biosphere reserves

Keywords: UNESCO, MAB, biosphere reserve

Japan Geoscience Union Meeting 2014
(28 April - 02 May 2014 at Pacifico YOKOHAMA, Kanagawa, Japan)

O06-03 Room:Main Hall Time:April 30 09:51-10:16

Geopark from the viewpoint of residencial research

KIKUCHI, Naoki[1*]

[1]Research Institute for Humanity and Nature

Residential research is a new method being proposed for use in problem-solving research that corresponds to the actual local circumstances and from the stance of the scientist/researcher not only being a resident but also a member of the local society concerned. I participated in a project involving storks, an endangered species, being returned to the wild, which took place in the area around Toyooka City in Hyogo Prefecture, and in researching the environmental sociology of Hyogo Park of Oriental White Stork, and thus also gaining experience as a residential researcher. The Sanin Kaigan Global Geopark is also in the area, and hence the storks being returned to the wild and the activities of the geopark are correlated, with also having been involved in the geopark's activities to a certain extent. Based on this personal experience I discuss the potential of geoparks being a tool to use in solving local problems , from the point of view of residential research.

Keywords: residential research, integrated local environmental knowlede, re-introduce project of the oriental white stork, adaptive governance

Japan Geoscience Union Meeting 2014
(28 April - 02 May 2014 at Pacifico YOKOHAMA, Kanagawa, Japan)

O06-04 Room:Main Hall Time:April 30 10:16-10:41

Think about the Geopark - After landslides disaster from the eyes of the guide

NISHITANI, Kana[1*]

[1]Izu Oshima Geopark

Three and a half years have passed since I met the Geopark. I have continued to guide because I have been fascinated by the story of plants, animals and human beings and the earth involved each other. So everyone‘s sensitivity and eyes for wonder, knowledge and experience was always different that I felt every tour would be the only one story in the world.

October 16 of this year, 36 people died, three people were still missing in Izu-Oshima. Because of the landslide disaster caused by heavy rain of typhoon No. 26. We thought ” Water drainage is good in this islands because it is young volcano here.” We were scary the eruption and tsunami, but not worry about floods. We couldn’t imagine the landslide disaster.

”Why we could not notice the danger? Why we could not tell it to the person who become a victim? ”. I felt unbearable thought. If I could worn it, a life would not to be lose. Then, I realized that there is lots of sadness in the back of words ”We are living on the land that volcanoes made ”.

Now, We are starting the reconstruction in Izu-Oshima. There are various problems, which are always changing. I feel that facing the reconstruction and disaster is just a Geopark itself.

We had the seminar by volcanic expert, and inviting lecturers from Miyakejima, Unzen Geopark, and Sanriku Geopark, for residents.

Are there any changes to the residents by sharing the information with different Geoparks?

We consider the role of a network of Geoparks through various activities after the disaster.

Keywords: geopark, guide, Izu Oshima, net work, disaster, rule

Japan Geoscience Union Meeting 2014
(28 April - 02 May 2014 at Pacifico YOKOHAMA, Kanagawa, Japan)

O06-05 Room:Main Hall Time:April 30 11:00-11:19

Summary of the evaluation process of Japan Geopark Committee

WATANABE, Mahito[1*]

[1]Geological Museum, Geological Survey of Japan, AIST

Japan Geopark Committee (JGC) has started its evaluation of prospective geoparks in 2008. Geopark specialists from the geoparks of Japanese Geoparks Network (JGN) joined as on-site evaluators in 2012.

Dossiers are evaluated by the JGC member and they decide which candidate should be further evaluated on-site. JGC decides a on-site evaluator and a assistant evaluator for each candidate area from those who are well experienced person in one of Geopark. One JGC member and two evaluator conduct a on-site evaluation for 2-3 days. Detailed evaluation report based on the dossier and the on-site survey is written by them and submitted to the JGC. JGC that is composed of eleven member make a final decision on each application.

Check list for the evaluation are revised every year by JGC and on-site evaluation from the geoparks.

Keywords: Geopark, UNESCO, Global Geoparks Network, Japanese Geoparks Network, Japan Geopark Committee

Japan Geoscience Union Meeting 2014
(28 April - 02 May 2014 at Pacifico YOKOHAMA, Kanagawa, Japan)

O06-06 Room:Main Hall Time:April 30 11:19-11:49

volcano gifts from the south Izu Peninsula Geopark

YOSHIKAWA, Kaoru[1*] ; HORINO, Yoshiaki[1] ; ISHII, Chiharu[1] ; TUKUDA, Hiromi[1] ; KOYAMA, Masato[2]

[1]Izu Peninsula Geopark Promotion Council, [2]Shizuoka University

The Izu Peninsula was situated to the south of the Japanese archipelago long time back. Due to the movement of the Philippine sea plate, it moved gradually to the North and collided with Honshu. In the Izu Peninsula, which was formed out of this mutual collision a great range of natural diversity can be seen, which makes it unique as a peninsula on the global scale. It is possible to observe the geological mechanisms that formed the peninsula in different locations. The peninsula is ideal to observe the geological processes ranging from submarine volcanism, land volcanism due to the collision of landmasses and ongoing volcanic activities. As a geopark, Izu Peninsula is attempting to collaborate with other geoparks and raise awareness on natural disasters as results of tectonic level processes, while preserving local nature, culture and history.

In March 2011, 13 cities and towns came together to form the core of the geopark. In September 2012 the geopark was accredited by the Japanese Geoparks Network. In December 2013 two more towns joined the geopark area. The geopark employed a new researcher on human geography in 2013 and published its newsletter.

Apart from these the geopark is working to assess the volcanic gas conditions in Teishi Kaikyu area with the Natural Disaster prevention unit of the Shizuoka University, giving guide programs, popularizing earth science for children, and participating in childrens summer school camps. In the Asia Pacific Geoparks Networks Conference (APGN 2013) the geopark put up its poster and introduced its activities.

Keywords: geopark, Izu Peninsula

Japan Geoscience Union Meeting 2014
(28 April - 02 May 2014 at Pacifico YOKOHAMA, Kanagawa, Japan)

O06-07 Room:Main Hall Time:April 30 11:49-12:19

Action of Mt. Apoi Geopark for the accession of GGN

HARADA, Takumi[1*] ; SAKASHITA, Kazuyuki[1] ; KATO, Satomi[1] ; NIIDA, Kiyoaki[1]

[1]Mt. Apoi Geopark Promotion Council

2013, Mt. Apoi Geopark sought a recommendation to the GGN to JGC. However, wish was dismissed. I will introduce the approach to solving the problems of the Mt.Apoi Geopark.

Keywords: guide, Information tool, Traditional Culture of Ainu, cultural exchange, Nature conservation activities

Japan Geoscience Union Meeting 2014
(28 April - 02 May 2014 at Pacifico YOKOHAMA, Kanagawa, Japan)

O06-08 Room:Main Hall Time:April 30 12:19-12:45

Mt. Naeba foot geopark concept -The person from 30,000 years before to the present, and relation of the ground -

SATOU, Nobuyuki[1*] ; NAKAZAWA, Hidemasa[1]

[1]Tsunan town Board of Education

Here we present the outlines of the Mt. Naeba foothills geopark concept.The geopark is located in the northwest of Mt. Naeba, which area includes both Tsunan town of Niigata prefecture and Sakae village of Nagano prefecture. It is characterized by the facts that while the area has 3 to 4 meter of annual snowfall the population of over 10,000 is maintained, and that 30,000 years of history and cultures of people interacting with the earth can be learned.Numerous environmental changes have occurred on the earth, in the air, in the oceans and on the lands. Studies on the rocks, clays, volcanic ashes, plant and pollen remains in the peat layers, information from archaeological remains and various meteoric factors, enable us to know the influences of the environmental changes to the lives of the people.The Mt. Naeba foothills emerged about 3 million years ago and the base of the land was formed by the lava flow of the Mt. Naeba. Through the development of river terraces, snowfalls and waters from springs, a rich natural environment was formed. The present environment as the snowy country began about 8,000 years ago. Tendency towards the sedentary way of life increased in the prehistoric times with the development in the exploitations of resources. The land formation and the peoples lives are closely related.For example, during the Jomon period, 5000 years ago, people formed very unique flame-style pottery using indigenous clays, made stone tools using volcanic flows or sedimentary rocks and lived in the settlements constructed on the river terraces. There are plenty of archaeological data showing the relations of the land and the people.We began to think about our land seriously placing the Mt. Naeba foothills geopark as a keyword. This idea is to reflect our land which is a precious treasure with geo-eco-culture, to love, to learn, to protect and to pass on the region to the next generations. A group of local people called Geo-egg emerged recently, and many inhabitants began to have consciousness to learn more about the land they were born and bred visiting the local heritages.For us, the Mt. Naeba foothills geopark is one of the hopes for overcoming the disaster of the Northern Nagano earthquake.

Keywords: Mt.Naeba, geopark, river terrace, tephra, archeological remains

Japan Geoscience Union Meeting 2014
(28 April - 02 May 2014 at Pacifico YOKOHAMA, Kanagawa, Japan)

O06-09 Room:Main Hall Time:April 30 14:15-14:41

Amakusa Geopark plan

KUNITAKE, Yuko[1*] ; KANAZAWA, Hiroyoshi[1] ; UGAI, Hiroaki[1] ; HASE, Yoshitaka[1]

[1]Amakusa Geopark planning promotion committee

The Amakusa Islands, consisting of about 120 islands are located in the southwest area of Kumamoto Prefecture: a beautiful archipelago with geologic and geographic characteristic landscapes and a 100 million year history, not to mention a treasure of ancient fossils offering its visitors a fantastic glimpse into times gone by. A unique culture has been carved out of life on these islands by its inhabitants adding to the many breath-taking sightseeing opportunities. The plan of the Amakusa Geopark is to show off the diversity of geology, geography, history, culture, industry and ecology in Amakusa with a mind of ecologic conservation and economic growth.

Residents and officials alike collaborate to preserve the geologic inheritance of Amakusa with an educational perspective. Exposing the unique beauty of this inheritance as a tourist attraction in conjunction with the history and culture of the area, an attractive geo-tourism will be founded aimed at the promotion of the Amakusa area.

Keywords: Island, sea, geopark, guide

Japan Geoscience Union Meeting 2014
(28 April - 02 May 2014 at Pacifico YOKOHAMA, Kanagawa, Japan)

O06-10 Room:Main Hall Time:April 30 14:41-15:07

Shimokita Peninsula Geopark Design;The glory of 4 oceans,one land 4 geological elements

ARAYA, Tomofumi[1*] ; MIYASHITA, Junichiro[1] ; UEDA, Hayato[1] ; ITO, Michio[1] ; MITSUNO, Yoshiatsu[1]

[1]shimokita peninsula geopark design promotion meeting

About Shimokita Peninsula

Shimokita Peninsula is located on the northeastern side of Aomori Prefecture, and the northernmost point of Honshu Island. It stretches across 1 city, 1 town and 3 villages surrounded by 4 bodies of water; the Pacific Ocean in the east, the Sea of Japan in the west, Mutsu Bay in the south, and the Tsugaru Straight in the north.

Shimokita Peninsula Geopark contains the 4 major geological elements that make up the island of Japan, including Osorezan ' s gold ore deposit and caldera, Hotokegaura ' s green-tuff series, the vast coastal exposure of quaternary strata in the Tanabu area, and Cape Shiriya ' s accretionary body. Shimokita also has a rich history and culture influenced by the Kitamaebune shipping trade, the Abeshiro kuroko mine, the northernmost distribution of monkeys in the world, the Tsugaru Straight ' s Blakiston ' s line, etc. Shimokita is blessed with amazing resources in a wide variety of fields.

Reason for applying to the JGN

The Shimokita Peninsula lacks universities and public museums so many people don ' t have a chance to study at a higher level, and realize how lucky we are to have many valuable natural treasures and learning resources.

Turning this area into a geopark will give people a chance at higher education and help create pride and love for Shimokita.

Through this geopark we hope to educate and explore Shimokita together with the next generation so that we can all learn of its value and importance.

Shimokita Peninsula Geaopark Desgin: Theme and Story

Japan is made up almost entirely of four basic geological elements; the non-volcanic Pacific coastal range consisting of the accretionary body, the axial volcanic chain, the sedimentary basin between the coastal and axial ranges, and the green-tuff mountains and hills which record the genesis of the Sea of Japan.

This geopark is the only one that touches both the Pacific Ocean and the Sea of Japan making it the only place where we can see all four basic elements in one place.

Also the peninsula is surrounded by four bodies of water and each body of water supports its own unique type of fishing. Fishing is the main industry that supports Shimokita.

Thus the theme of this project is [Shimokita Peninsula Geopark: The glory of 4 oceans, one land 4 elements.] The sub-themes are [East Coast Zone: Gift from the Pacific Ocean,] [Tanabu Plains Zone: Competition between land and sea,] [Osorezan and Mutsu Hiuchidake Volcanic Zone: Volcano and hot spring blessings,] [West Coast Zone: Split land.]

Contribution to JGN

As a place without universities or museums we hope to exchange ideas with other members of the JGN so that we may develop higher education and lifelong learning opportunities here in Shimokita. We hope to contribute to the JGN by demonstrating a system of higher education without the support of a university.

In Japan we believe that spirits live in mountains, trees and rocks. Osorezan and Hotokegaura are famous places for praying to the spirits. People come from all over Japan to talk to Itako, blind mediums who speak with the deceased at Osorezan.

With Osorezan at the center of the Shimokita Peninsula Geopark another contribution to the JGN is a geopark not only with amazing geology, but with the intangible resource of faith.

In Conclusion

The Shimokita Peninsula Geopark may not have anything that no other geoparks have or anything more amazing, but it is unique in that it is the only geopark in Japan which touches both the Pacific Ocean and the Sea of Japan.

The people of Shimokita want to protect, preserve and share the amazing natural resources of Shimokita with others. We hope that by taking pride in our home, our love for Shimokita will be carried on for generations and visitors will see it as a special place too.

Applying to join the JGN will allow the people of Shimokita to realize the value of our natural resources. It will also give us a new reason to love the peninsula and create a new type of tourism.

Keywords: Japanese national geopark, 4 oceans, 4 geological elements, Love for Shimokita(Love for one's home), Faith;Mt.Osorezan

Japan Geoscience Union Meeting 2014
(28 April - 02 May 2014 at Pacifico YOKOHAMA, Kanagawa, Japan)

O06-11 Room:Main Hall Time:April 30 15:07-15:33

The Promotion of Nanki Kumano Geopark Plan

HIGASHIKAWA, Tomoaki[1*] ; HASHIZUME, Masaki[1] ; TAWARA, Takaharu[1] ; TANIWAKI, Tomokazu[1]

[1]Nanki Kumano Geopark Promotion Council

The area of Nanki Kumano Geopark Plan is located in the southern part of the KiiPeninsula, the southernmost point of Honshu. It consists of a city, 7 towns and a village: Shingu City, Shirahama Town, Kamitonda Town, Susami Town, Nachikatsuura Town, Taiji Town, Kozagawa Town, Kushimoto Town and Kitayama Village.

The total area of Nanki Kumano Geopark Plan is approximately 1,356 km^2; the area stretches 60 km from east to west and 60 km from north to south. It includes various landforms ranging from steep mountains over 1,000 m to deeply-indented coastlines formed by the submerged coast.

The area of Nanki Kumano is blessed with mild and moist climate, but does not have many plain fields because it consists largely of steep mountains. Besides, roads were not built in earlier times. Therefore, the livelihoods of people have relied on forestry, fishery, and shipping industry since a long time ago. In addition, the geography, nature and culture of this area inspired a feeling of awe in city people away from the area. Historically, many people have visited this area and it has prospered as sacred sites of Kumano worship. In modern times, it has become a key area of forestry, fishery, and shipping and has also thrived on diggings of mineral resources, papermaking industry, hot springs and tourism.

However, in recent years, regional disparity between urban and rural areas has widened. We can see depopulation, aging and industry decline in rural areas, although pavements, railroads, ports and an airport have been developed and traffic has become more convenient than before.

In this situation, the progress of earth science gradually revealed the formation process of geological and geographical features peculiar to this area. Moreover, it has turned out that those features are quite unique. This area consists of three kinds of geological conditions formed by a series of plate movements. The central part is made up of accretionary prism formed by subduction of oceanic plate near the ocean trench. The eastern and western parts are respectively composed of forearc-basin sediments formed on accretionary prism. Additionally, igneous rocks are distributed in the eastern part. These three landforms exist in this area due to the encounter of plates. Thus, we can learn typical three geological formations showing the formation process of the land in addition to dynamic planet activity, namely, subduction of plate.

Culture, history, industry and people's life have been developed in this area by using geological and geographical features. People feel a sense of pride in each of them and gradually recognize that they are valuable assets that should be left to future generations.

The area of Nanki Kumano is the core of Sacred Sites and Pilgrimage Routes in the Kii Mountain Range registered as a World Heritage Site in 2004. Sacred Sites, Pilgrimage Routes, Cultural Landscapes are already regarded highly as worthwhile. However, we think not only they but also charm and value of this area can be enhanced by exploring dynamism of a land formation, the formation process of nature and contacts between people and nature in this area. We are working on the geopark project with the idea that charm and value of this area will give local people confidence and pride and will create new jobs and opportunities for human interaction. We believe it important for sustainable local development to advance this project in the area of Nanki Kumano. Therefore, we apply for membership in Japanese Geoparks Network.

We would like to contribute to Japan Geoparks Network by demonstrating a new model of geopark activities; we can enhance each value of the sites by connecting the geological heritage with the existing property: the UNESCO World Heritage Site, Kushimoto Coral Communities (a registered wetland under the Ramsar Convention) and Yoshino-Kumano National Park.

Keywords: Nanki Kumano, Geopark

Japan Geoscience Union Meeting 2014
(28 April - 02 May 2014 at Pacifico YOKOHAMA, Kanagawa, Japan)

O06-12 Room:Main Hall Time:April 30 15:33-15:59

Geographic History of the Purple Mountain and Suigo and the Life Carried on to the Future

SHIBAHARA, Toshitsugu[1*]

[1]Mt.tsukuba Area Geopark promotion Council

Mount Tsukuba is located in the northeast of Kanto Plain. From the distance, the mountain looks like a single peaked mountain which is a rare view in Kanto area. The mountain is called ”Shiho”, meaning a purple mountain, since the color of the mountain surface looks purple in the evening reflected by the setting sunlight.

The crest has steep double peaks constructed of solid gabbros which were intruded and risen approximately 75 million years ago.

The mountainside (declive) and the base of the mountain (piedmont) are covered with debris of gabbro and weathered debris of granite.

The gentle curves of the mountain skirts make its mountain shape beautiful. Additionally, as the northeast tip of Kanto Plain, the surrounding regions centering the Kasumigaura Lake make the scenic beauties of ”Suigo” with broad platforms and lowlands formed by the 4th period of the sea level change.

Therefore, blessed with the ”geological inheritance”, the Mount Tsukuba is renowned as we have an expression, ”Mt.Fuji in the west, Mt.Tsukuba in the east.” So, the mountain has been regarded as the landmark of Kanto. Also, even competing with Mt.Fuji, which has just been approved as one of the World Heritages, the mountain worship and many Japanese traditional culture and art have originated in this area.

The activities typified by the water transport in Kasumigaura Lake, stone manufacturing and pottery, have had developed its own style independently even though the region was located near Edo(Tokyo). It is particularly worth noting that they supported the modernization of Japan. Inada granite was used for architectures such as the Diet Building, Bank of Japan and Nihon-bashi Bridge in the Meiji Era.

In the modern age, Tsukuba Science City is established on the platform at the base of Mount Tsukuba. The area is vitalized from both inside and outside Japan and has started to create the future.

Evaluating the features of this area-the nature, the history and people’s activities-from the geological and geographical points of view, each element may not seem to relate to each other. However, once you change your perspectives, you can find fascinating, charming and attractive aspects in them.

So, in Tsukuba Area Geopark, we view every geographical and geological feature of this area as a series of the eternal history and rediscover the value of the geological features of this area, share it with people inside and outside of the region and carry on to the future.

Japan Geoscience Union Meeting 2014
(28 April - 02 May 2014 at Pacifico YOKOHAMA, Kanagawa, Japan)

O06-13 Room:Main Hall Time:April 30 16:15-16:41

Concept for the Tateyama Kurobe geopark:Feel the tales of dynamic time-space, 3800Ma history and 4000m topography !

MASUBUCHI, Yoshiko[1*] ; OONO, Hiromi[1] ; TANBO, Toshiya[1] ; FUJITA, Masato[1] ; ISHIZU, Hidetomo[1] ; TAKEUCHI, Akira[1] ; NAKAO, Tetsuo[1] ; HORIUCHI, Yasuo[2]

[1]Tateyama Kurobe geopark Promotion Conference, [2]Tateyama Kurobe geopark Support Municipalities Conference

”4000 meters times 3.8 billion years”; this is how we could express the geological history and geography of the eastern part of Toyama Prefecture. Nature guides activities in each of 9 municipalities have made it a duty to transmit the scale of those numbers, protect the land and make good use of it. And this, in turn, has been the founding principle behind the Tateyama Kurobe geopark.

The region of the Tateyama Kurobe geopark is now located in the geologically very active region. The volcanic and tectonic activities that have been ongoing since the Mesozoic Era create the Toyama bay that is over 1000 meters deep, and the Tateyama Mountain Range that is over 3000 meters tall. Since they place in a very compact location, the eastern part of Toyama Prefecture has a dynamic and unique landscape and geology. Besides, the region has the youngest granite on Earth which is said to be around 800 thousand years old and it shows rapid tectonic activity. While the oldest mineral on Japan, Eoarchean?Paleoproterozoic zircon (over 3.8 billion years old), was also identified. This turns the region into a life-size ”encyclopedia of geology”. It encompasses various minerals and sings of the multiple events occurred during the long history of Earth, including rests of the collision that created the Asian continent during the Paleozoic. In the present time, large quantities of precipitation which comes from the Sea of Japan to the Tateyama Mountain Range return to the Sea of Japan through the mountain glaciers located in the southernmost in the Far East, rivers and numerous springs in the alluvial fans. This water circulation maintains unique natural environment in this region.

Since the earliest times, the people had come to understand the importance to protect the resources of the land and sea and the voluntary nature guides system was established in 1970s by Toyama prefecture. This is pioneer in nature guides system in our country. The nature guides activities become widespread throughout the northern Japanese Alps and the coastal plain by Toyama Bay. We cannot still say that many citizens and travelers in the region understand the whole story above. However, recently we have found that more people are aware of the importance of the land and began to grow a strong wish to know more about what makes their land special.

All of this above makes us think that ”that is on what our region and landscape is based”. We want to use the geopark activities as catalyzer to bring together all those actors in order to bring out the interest of the people about the region. However, we believe that we need an organization at the center of it all that is ”built by the people, for the people”. Therefore, instead of limiting ourselves to the various organizational forms in existence, we decided to pioneer an organization that would make this possible, having the local actors themselves create it, receiving support from both private and public sectors. This is because we believe that, in our region, the people and the governments should work as partners together for the management of the geopark.

Keywords: Tateyama Kurobe geopark conception

Japan Geoscience Union Meeting 2014
(28 April - 02 May 2014 at Pacifico YOKOHAMA, Kanagawa, Japan)

O06-P01 Room:Poster Time:April 30 18:15-19:30

JGN National Training meeting Summary - The current state and issue of Geoguide development -

SAKANOUE, Hiroyuki[1*] ; ISHIKAWA, Toru[1]

[1]The Council for the Promotion of the Kirishima Geopark

In the various geoparks around the country special features, required knowledge, and original curriculum has been established and geoguide training is progressing. However, in Kirishima, there are more than a few areas that have concerns over the content, length and so forth of the curriculum. Also, due to the differences in shape and environment of the features such as mountains, beaches, and islands the crisis management skills required of guides is substantial and various forms of support will be needed.

At the November 2013 JGN National Training Meeting held in Kirishima Geopark, geoguide development was the chosen theme. Local guides gave presentations and shared information on current conditions and issues and then participated in a lively group debate on the topic of risk management. With the information gleaned from this training meeting compiled with general information a report detailing the objectives of Kirishima Geopark guide development will follow.

Keywords: Geopark, Kirishima, Geoguide development, JGN National Training Meeting, risk management.

Japan Geoscience Union Meeting 2014
(28 April - 02 May 2014 at Pacifico YOKOHAMA, Kanagawa, Japan)

O06-P02 Room:Poster Time:April 30 18:15-19:30

Authorization System of San'in Kaigan Geopark Guide

FUKUHARA, Youichiro[1*] ; SAN'IN KAIGAN GEOPARKE, Promotion council[1]

[1]San'in Kaigan Geopark Promotion Council

San'in Kaigan Geopark Promotion Council established an authorization system which authorizes local guides who fulfill a certain criteria as "San'in Kaigan Geopark Guide", to improve the guide information for visitors and develop the skills of local guides.

San'in Kaigan Geopark includes three cities and three towns in three prefectures, and tour guides has been existed since before this area became one of geoparks. Various tour guide services were provided, showing visitors around the town and coastal area, for free or with charge. To add the geological elements to these guide services and fascinate visitors even more, the council and local guides in the San'in Kaigan Geopark spent a lot of time discussing about the training and requirements to set a uniform criteria in 2012-2013, aiming to promote geotourism.

There are two levels in the authorization system of San'in Kaigan Geopark Guide. Local guides must guide a specific geosite in the area and explain about the geopark system and overview to receive a level 1 certificate. To receive a level 2 certificate, in addition to the skill of level 1, local guides must help the council's events as representative guides of the San'in Kaigan Geopark.

The requirements of level 1 guide are 1) Taking training courses about basic knowledge of geopark, geosite, guide and risk management admitted by the council, 2) Being covered by general liability insurance, and 3) a person who belongs to tourism facilities registered in the council. This certificate is valid for three years.

In addition to active experiences as a level 1 guide, the requirement of level 2 guide is passing qualification test conducted by the council.

In the near future, by operating this authorization system, we aim to boost the skills of San'in Kaigan Geopark Guide and promote active geopark activities.

Keywords: San'in Kaigan Geopark, Geopark guide, Authorization system

Japan Geoscience Union Meeting 2014
(28 April - 02 May 2014 at Pacifico YOKOHAMA, Kanagawa, Japan)

O06-P03 Room:Poster Time:April 30 18:15-19:30

The Tour Guide Training program for Sanriku Geopark

SEKI, Hiromitsu[1*] ; UENO, Ayumi[1]

[1]Sanriku Geopark Promotion Conference

The Sanriku Geopark promotion conference conducted the tour guide training program based on PDCA cycle as many visitors can enjoy the Sanriku Geopark.

We will report the program this year.

We will continue to systematically train human resources held on a regular basis to promote the Sanriku Geopark.

Keywords: Tour Guide Training Program, Sanriku Geopark, PDCA cycle

Japan Geoscience Union Meeting 2014
(28 April - 02 May 2014 at Pacifico YOKOHAMA, Kanagawa, Japan)

O06-P04 Room:Poster Time:April 30 18:15-19:30

About the ideal Geopark guide in the Geopark

KONOMATSU, Masahiko[1*] ; ONISHI, Nao[1]

[1]Wakayama University

As of January, 2014, there is the Geopark of 33 areas in Japan. It is predicted that the numbers increase from local sightseeing promotion more. When a tourist observed the geo-site in the Geopark, they are impressed by mentioning a creature, the history, the culture of scenery and the topography, geological feature, and knowing the local splendor, and it become a repeater. However, the tourist cannot often understand the knowledge of the earth science including the origin of a geological feature, the topography only by watching merely scenery and the topography by oneself, and reading a guidance signboard. Therefore the guide can tell charm and an impression to a tourist to a tourist as a story concerning the geo-site because a Geopark guide exists. In addition, I can go to the attractive geo-site in usual times because a guide goes together at the place that I cannot go. Furthermore, as for the guide, a climate, a creature, culture are concluded based on a geological feature, the topography; remind you of it.

I am shown that even the guidelines on member standard to the Global Geopark Network (GGN) train a guide and perform the tour with the guide. Therefore, in the Geopark, a Geopark guide and the training become the important matter. The training lecture of the Japanese Geopark guide sets a curriculum while devising information sharing in what I do by Geopark meeting and JGN whole country workshop in Japan in each Geopark and is carried out.

Therefore, through an expert Geopark guide, there was what kind of skill and, in this study, examined a tourist what kind of response you gave. Furthermore, about the training system of the Geopark guide, I investigated nationwide tendencies and extracted the points that I weighed it, and were common. I compared it with the training system of a common ecotourism.

In addition, in Wakayama where the writer is, there is Nanki-Kumano Geopark design, and the training of the Geopark guide is carried out from 2013. What kind of person took lectures, and questionary survey did what kind of skill the body had there.

In consideration of the tendencies that were a common point and the whole country, I suggested it about a curriculum of the necessary geo-guide training based on real attendance true satisfaction to a minimum.

Keywords: Geopark, Geopark guide, The training of the Geopark guide, Nanki-Kumano Geopark design

Japan Geoscience Union Meeting 2014
(28 April - 02 May 2014 at Pacifico YOKOHAMA, Kanagawa, Japan)

O06-P05 Room:Poster Time:April 30 18:15-19:30

Trainning of Geoguides by Nankikumano Geopark

YAMAMOTO, Toshio[1*] ; TANIWAKI, Tomokazu[2]

[1]Pacific Consultant, [2]Wakayama Prefecture

The Nanki Kumano geopark concept is an area of the southern part of Kii Peninsula used as the southernmost tip of the main island of Japan, and is an area which consists of1 city 7 town 1 village in Shingu-ctiy, Shirahama-cho, Kamitonda-cho, Susami-cho, Nachikatsuura-cho, Taiji-cho, Kozagawa-cho, Kitayama-village, and Kushimoto-cho.

East and west and the north and south of this area are about 60 km, and a gross area is as wide range as about 1400 km2, and it is an area which has complicated coastline by a drowned coast, and various geographical features from the steep mountain land over 1000m. About geology, it consists of three geology objects produced by the motion of a series of a plate. The central part consists of an accretionary prism made by subduction of an oceanic plate near the trench, and the eastern part and the western part consist of front arc basin deposition objects formed on the accretionary prism. Furthermore, the huge eruptive rock object is distributed over the eastern part.

On these grounds, a respectively characteristic geographical feature scene and ecosystem, and culture are cherished, and they are connected deeply mutually. With such a background in Nanki Kumano, various attractive ”encounter” between the ground, a living thing, and a person has always been produced.

From these things the Nanki Kumano geopark concept was born by the theme which meets with the nature and culture of Kumano cherished on the three grounds which the plate met and were produced.

In the Nanki Kumano geopark promotion conference, 100 or more persons’ geopark guide is scheduled to be trained between the fiscal 2013 and the fiscal 2015 . There is an application of attendance exceeding 70 persons and the geopark guide of the 1st term (about 60 persons) was born in the fiscal 2013 . It is carrying out the curriculum which thought local training, practice of geo-tour, etc. as important on the basis of acquisition of a guide technique or a safety control on the occasion of geopark guide cultivation, and trained the geopark guide with high quality which can guide for counter value.

Trial geo-tour to which a participant takes the lead and performs it in order to develop having learned by a lecture or local inspection training in geopark guide cultivation as practical skill is included in the curriculum. By this measure, in which it is difficult to attach to the body in the guide cultivation lecture of a lecture,the practice power about the importance of a safety control or time management was able to be trained, and the bottom raising effect of the whole geopark guide ,an improving point when performing the geopark guide in the evaluation meeting after enforcement can be clarified,was able to be acquired.

Moreover, it became an important opportunity to consider the composition of the tour for having a visitor enjoy oneself by planning and carrying out trial geo-tour and actually looking back upon it. In this trial geo-tour, the opportunity that it will perform making the tool of the area for greeting a visitor, and it will heap geopark activity that the guide cultivation lecture attendance student itself works on a local contractor for development of the Geo-bowl,is also growing.

About the geopark guide after cultivation, opportunities, such as a school and skull session, are prepared and continuous skill improvement is aimed at. Moreover, cultivation of an upper geopark guide is also scheduled to be tackled

Keywords: Geopark, Geoguide, NankiKumano, trial geo-tour

Japan Geoscience Union Meeting 2014
(28 April - 02 May 2014 at Pacifico YOKOHAMA, Kanagawa, Japan)

O06-P06 Room:Poster Time:April 30 18:15-19:30

Hakone Geopark -The activities by cooperation with various organizations

AOYAMA, Tomofumi[1*]

[1]Hakone Geopark Promotion Council

The Hakone Geopark Promotion Council, established in 2011, is consisting of 72 affiliates including educational institutions, volunteer groups, a wide variety of companies and NPOs in the area. They are not only working for Geopark's activities independently, but acting by cooperating with each organization.

We introduce some examples of the investigative commission by council members about development of goods and maintenance of signboards.

Japan Geoscience Union Meeting 2014
(28 April - 02 May 2014 at Pacifico YOKOHAMA, Kanagawa, Japan)

O06-P07 Room:Poster Time:April 30 18:15-19:30

Concept behind the Tateyama Kurobe geopark: towards the cooperation of private and administrative organizations

MASUBUCHI, Yoshiko[1*] ; TANBO, Toshiya[1] ; FUJITA, Masato[1] ; TAKEUCHI, Akira[1] ; ISHIZU, Hidetomo[1] ; NAKAO, Tetsuo[1] ; KOSHIMIZU, Kazunori[2] ; HORIUCHI, Yasuo[2]

[1]Tateyama Kurobe Geopark Promotion Conference, [2]Tateyama Kurobe Geopark Support Municipalities Conference

The Toyama plain is divided roughly into two equal parts by the centrally located Kureha hills: the east side, called Gotou (East of Kureha), and the west side, called Gosai (West of Kureha). Each side has its own landscape and traditions. On the west side, in Gosai, you have a region where the influence of the Kaga clan is still felt strongly; on the east side, in Gotou, you have a region influenced by the unique shape of the land, with a steep mountain range over 3000 meters tall overlooking many coastal alluvial fans, where the many people live. The Tateyama Kurobe geopark is based in Gouto, this east side, with its landscape and traditions, and with its people's industriousness and thoughts that shaped the region.

A peculiarity in this region is that, in order to protect the land and understand its value, governments have supported many residents and organizations, which would then pursue various activities on their own.

With this in mind, various local regional study groups, field researchers, university and high school teachers, and other professionals gathered together and, on January 20th 2013, created the Kurobe Tateyama geopark Research Group. The Group has proposed to turn the whole region into a geopark, conducting various researches about the current amount of human activity and natural resources in the region, as well as about the future tasks and responsibilities that would come with the organization of a geopark. At the same time, they contacted the various local governments situated in the region to promote the idea of geopark, as well as to receive their support regarding its current and future activities. Also, and this is the peculiarity of this region's geopark, the group also made contact with the region's business community, where they not only promoted the geopark but also promoted their direct participation in its activities, making the local businesses, which are at the base the local industries and economy, have a strong role in all the geopark activities.

This is how, on December 9th 2013, the Kurobe Tateyama geopark Association was founded, upon what would become its predecessor, the aforementioned Kurobe Tateyama geopark Research Group. This Association, receiving support from both local businesses and local governments, was given the responsibility of all activities pertaining to the realization of the geopark in terms of human resources. The Association itself is privately run, their members linked to regional development and local business leaders. The organization currently consists of the following groups: activity planning group, research and education group, Geo-guide formation group, Geo-tourism group. While, at this moment, the geopark is supported by a volunteer staff, in the future, the organization seeks to have the geopark fully supported economically by local firms and touristic businesses.

Also, the Association seeks support from the local governments, mostly in three forms: support in the protection and usage of the designated geosites through bylaws and regulations, usage of the geopark in local and environmental education and disaster prevention by inclusion into the school curriculum, and making of the various public museum employees' currently volunteer work in the geopark organization into a part of their duties. At this moment, the Association is preparing the "Tateyama Kurobe geopark Support Municipalities Conference", in order to get a hold on their support to fully start the geopark's activities during 2014.

The association aims to have the geopark activities supported by the partnership of both private and public sectors, by having them be responsible for the maintenance of both activities and installations. This is how we are aiming for regional development through the Tateyama Kurobe geopark.

Keywords: The concept of Tateyama Kurobe Geopark

Japan Geoscience Union Meeting 2014
(28 April - 02 May 2014 at Pacifico YOKOHAMA, Kanagawa, Japan)

O06-P08 Room:Poster Time:April 30 18:15-19:30

Activities and work for the future in the Hakusan Tedorigawa Geopark.

HIBINO, Tsuyoshi[1*]

[1]Hakusan Tedorigawa Geopark Promotion Council

We have advanced various activities since 2010 in the Hakusan Tedorigawa geopark. Hakusan Tedorigawa Geopark was certified as a Japanese geopark in 2011. We carried out various activities, such as the activities to promote the geopark, educational activities, training for guides, environmental maintenance for geopark and so on, after the cetrification.

In 2013, we had the domestic examination for application to the Global Geopark Network, but the result was not reached. Although we received some good evaluation about the activities of the geopark by this examination, and we were able to share it among various people who pushed forward the activities for the geopark. Furthermore, the work that should be solved became more clear and also became the index in pushing forward the future activities. We will promote various activities for solving these works in the Hakusan Tedorigawa Geopark.

Keywords: geopark, Mt. Hakusan, Tedorigawa river, educational activity, training for guides, geotour

Japan Geoscience Union Meeting 2014
(28 April - 02 May 2014 at Pacifico YOKOHAMA, Kanagawa, Japan)

O06-P09 Room:Poster Time:April 30 18:15-19:30

Joint Management of Geopark and Biosphere Reserve - The Case Study in the Hakusan Tedorigawa National Geopark in Japan

AOKI, Tatsuto[1*]

[1]School of Regional Development Studies, Kanazawa University

Area of the Hakusan Tedorigawa National Geopark (GP) in Japan is partly overlapped with that of Hakusan Biosphere Reserve (BR). The organizing committee of the Hakusan Tedorigawa GP has started to manage Hakusan BR for making to coexist these two programs within the same region (see our poster presentation for in details).

As well known, both program is controlled by UNESCO, and the purposes of these programs are became almost the same after the Sevilla strategy of BR in 2002 as follows.
>Conservation the regional nature and natural heritage
>Encourage the scientific research and education for regional nature
>Encourage the local community and economy though the scientific based sustainable using the regional natural resource

The local ecological diversity can’t exist without local geodiversity. Furthermore, the local geo-diversity provides much of effect for the local people through the local ecosystem. Fundamentally, the general ideas of these two programs are inseparable. On the other hand, these two programs must be separate on the park system. The authors think that it is necessary to take care following points to for making to coexist these two programs.

For inside of the park
>promoting the scientific relationships between two programs
>making relationships between organizing committees of each program
>organizing the TPO for using each brand and trademark
>organizing budget and human resources

For outside of the park
>promoting the scientific relationships between two programs
>organizing the methods for advertises these two programs

Keywords: Hakusan Tedorigawa National Geopark, Hakusan Biosphere Reserve, UNESCO, Co-exsistence

Japan Geoscience Union Meeting 2014
(28 April - 02 May 2014 at Pacifico YOKOHAMA, Kanagawa, Japan)

O06-P10 Room:Poster Time:April 30 18:15-19:30

Networking of geology, history and culture in the Izumo region

RITSUO, Nomura[1*] ; TAKASU, Akira[1] ; IRIZUKI, Toshiaki[1] ; HAYASHI, Masahisa[1] ; TASAKA, Ikuo[1] ; TSUJIMOTO, Akira[1]

[1]Kunibiki Geopark Project Center, Shimane University

The ground of Izumo, Shimane Prefecture, was formed in association with the creation of the Chugoku Mountains, the Sea of Japan and the largest brackish lakes, Shinjiko and Nakaumi, in Japan, all of which were episodic in the Earth history. A lot of geologists have investigated such characteristic features of Izumo area and have found its unique geological figures such as magnetite-rich granite of the late Mesozoic and early Cenozoic Era, severely deformed Neogene sediments, huge alluvial plane, and the Quaternary volcanoes. A varied nature of such geologic basements leads the birth of local industry, using diversified biological and mineral resources, and as a consequence led to the formation of so called " Izumo culture. " There was much folklore in a long human history, such as well known " Kunibiki legend. " Izumo is thus very famous as the place of mythical world. We enhance interdisciplinary research on the geological, geographical and biological nature linking to the history and culture of the Izumo region. Main goal of our project is to make a plan of national and international geo-park for the Izumo region

Our research project is based on the fruits resulted from the active investigation that mainly carried out by the geologists in the Department of Geoscience, Shimane University, as a plan to make a geopark for the San ' in and Shimane districts. The 38 geological places in the Izumo region were introduced in the publication, " 100 geosites selected in the San ' in and Shimane districts, " that was published in 2013. On our schedule, we will set up a social organization to promote our geopark project in coming April, 2014.

Keywords: Izumo region, Culture and Geography of Izumo, Kunibiki legend, Shimane Peninsula, Tatara iron industry

Japan Geoscience Union Meeting 2014
(28 April - 02 May 2014 at Pacifico YOKOHAMA, Kanagawa, Japan)

O06-P11 Room:Poster Time:April 30 18:15-19:30

Device and the present conditions of ***Mine-Akiyoshidai Geopark Plan***

OBARA, Hokuto[1*] ; FUJIKAWA, Masayuki[1] ; YAMAGATA, Tomoko[1]

[1]Mine-city Geopark Promotion Council

The geopark activities in Mine area located in the middle western part of Yamaguchi Prefecture have been promoted from 2011. The geopark name and the theme are decided as follows; "***Mine-Akiyoshidai Geopark Plan***" and "**The history of the earth and the life to breathe on the karst plateau**". The contents of Geopark Plan and its present status will be presented.

The name and theme spotlight Akiyoshidai Karst Plateau in Mine area. The limestone which forms the karst plateau originated from coral reef of oceanic island. It has various information of natural history, so that contains academic value very much. Scientific and cultural values concerning the geology, geography, biology, ecology and human culture in Akiyoshidai are very high. Therefore, Akiyoshidai Karst Plateau is very precious worldwide.

In Mine area, as well as Akiyoshidai Karst Plateau, there are Omine Coalfield which is mined high quality anthracite (hard coal) and Naganobori Copper mine which is the oldest public copper mine in Japan. We aim to keep those geo-resources, use them for an instructional activity positively, and apply them in local promotion.

Keywords: ***Mine-Akiyoshidai Geopark Plan***, Akiyoshidai, karst plateau, Mine area, Yamaguchi Prefecture

Japan Geoscience Union Meeting 2014
(28 April - 02 May 2014 at Pacifico YOKOHAMA, Kanagawa, Japan)

O06-P12 Room:Poster Time:April 30 18:15-19:30

Creating new geo business and the role of key persons in the San'in Kaigan Geopark

IMAI, Hiroko[1] ; NIINA, Atsuko[2] ; MATSUBARA, Noritaka[3*]

[1]NPO Tajima Marine School, [2]Regional Innovation Research Center, Tottori University of Environmental Studies, [3]Division of Geo Environmental Sciences,University of Hyogo

The economical success is essential for the sustainable development of geoparks. Local business is the main actor to offer high quality products and service in a geopark. If they can satisfy of the demand of consumers and visitors, the geopark itself will become a higher quality one. This presentation reports on the case studies of geo business from the beginning to the present in the San'in Kaigan Geopark.

Keywords: geobusiness,, geo product and service, regional promotion, San'in Kaigan Global Geopark

Japan Geoscience Union Meeting 2014
(28 April - 02 May 2014 at Pacifico YOKOHAMA, Kanagawa, Japan)

O06-P13 Room:Poster Time:April 30 18:15-19:30

Effects and Issues of Resident Involvement in Walking Model Route Map

MATSUBARA, Noritaka[1*] ; SAKIYAMA, Tohru[1]

[1]Division of Geo Environmental Sciences,University of Hyogo

One of the important roles of geopark activities is resident understanding of the geopark concept, territory and its features. For this purpose, it is important that local residents participate in geopark activities positively. However, in Japan, where local development has been undertaken by governmental organizations, it is difficult for local residents to take part in geopark activities.

This time, we planned ”Geopark Walking Model Route Map” across the San’ in Kaigan Geopark in cooperation with local people, to promote better understanding and communication with local people, government and academia involved in geopark activities.

<San’ in Kaigan ”Geopark Walking Model Route Map”>

In a geopark, creating a tour route and map which allow visitors to explore the geosites easily is required. We have therefore prepared a ”Geopark Walking Model Route Map” for walking tours in half-day or one day, and for enjoying the feature of each area. Each map includes outlines of about twelve must-see geological spots, allowing visitors to enjoy sightseeing and learn about the San’ in Kaigan Geopark. 20 model courses extending to three prefectures (Kyoto, Hyogo and Tottori) were created until fiscal year 2012.

<The process for planning a ”Geopark Walking Model Route Map” >

1) San’in Kaigan Geopark Promotion Council Academic Group selects the candidate sites from the area where geopark activities are prosperous, and if requested to create a map by local residents.

2) Local guides, tourism facilities, local residents, geopark-related officials and academic members form a working group on creating a draft of map.

3) The working group surveys the field and checks the highlights, safety, estimated walking time, etc.

4) Academic Group creates a map.

5) The working group checks the content of the map.

Since Academic Group directly got involved in creating a map, the contents were thought to become difficult. To make it understandable to the general public, we posted images and descriptions on the map to Facebook and modified them to more simply by collecting public opinions through SNS during the process 5).

<Effects and issues of resident involvement in ”Geopark Walking Model Route Map”>

We were able to make ”Geopark Walking Model Route Map” useful for local residents, by involving experienced local guides and people in the area. It is important that geopark guides take part in map creation especially in the process 2) and 3). Firstly, geopark guide’s participation made the map more practical. Secondly, by working together by local residents and researchers, scientific information could be shared among local people.

As mentioned above, we think that resident involvement in planning ”Geopark Walking Model Route Map” was effective, however, some problems were found in its operation. The map is not used effectively in the area which has fewer visitors and no local guides. From now on, it is also necessary to accept visitor’s opinions and correct continuously so that the map may come to be more effective and useful for both visitors and local residents.

Keywords: geopark, San’ in Kaigan Geopark, Geopark Walking Model Route Map, resident participation

Japan Geoscience Union Meeting 2014
(28 April - 02 May 2014 at Pacifico YOKOHAMA, Kanagawa, Japan)

O06-P14 Room:Poster Time:April 30 18:15-19:30

Shimonita geopark and regional construction

KANBE, Satoru[1*] ; OKAWARA, Junjiro[1] ; SEKIYA, Tomohiko[1]

[1]Shimonita geopark promoting office

Shimonita Geopark is a Geopark comprised of the farming and mountain village Shimonita town that assumed Shimonita-negi and konjac located in Southwest Gunma a special product.It is the farming and mountain village that is full of nature among the Mt. Myogi and Kanto mountains and is a town historical as a stage of the branch road of Nakasendo Road.

I am said to be the sacred place of the geological feature study from old days, and the geological feature phenomena that they hid a secret of the Japanese Islands birth. Those geological features bring about the unique life and culture of people of the land.

I introduce sightseeing, citizen-based town planning of Shimonita town utilized these area resources.

In a sightseeing side, we open a course in a guide training lecture so that a local guide guides you and begin the sightseeing taxi which I matched with a world heritage as tourlists who came by a train.

In an eduction side, because the teaching materials becoming the help of the science education of the elementary and junior high school are abundant, we perform an invitation from Tokyo and wrestle for activity to have local children know the charm of the hometown more, and to bring up regionalism

In addition, the symposium of the theme ”how protected local treasure” held a symposium last year and, as the place that thought about the sustainability of local resources, utilized the network of the Geopark and had you report the example of sustainable resources utilization from many aspects.

In Shimonita town, I wrestle as consistency of the local promotion that is sustainable by Geopark activity.

Keywords: geopark, shimonita, regional construction, education of earth

Japan Geoscience Union Meeting 2014
(28 April - 02 May 2014 at Pacifico YOKOHAMA, Kanagawa, Japan)

O06-P15 Room:Poster Time:April 30 18:15-19:30

a

ITAYA, Daiki[1*]

[1]Happo Tourism Association

a

Japan Geoscience Union Meeting 2014
(28 April - 02 May 2014 at Pacifico YOKOHAMA, Kanagawa, Japan)

O06-P16 Room:Poster Time:April 30 18:15-19:30

Total Design Strategy of Sakurajima-Kinkowan Geopark

ISHIMIYA, Satoshi[1*]

[1]Sakurajima-Kinkowan Geopark Promotion Council

The Geopark is thought of as a place where, across a long period of time, the local peoples' thoughts on community planning and improvement can be expressed as a single goal.

With that idea in mind, the Sakurajima-Kinkowan Geopark's information sharing and role as a geopark are based on a Total Design strategy.

The Total Design strategy, logo, character design, etc. are products of a team of local designers and illustrators who work both in and outside of Kagoshima.

The results of these design specialists' work are a friendly character and design, which draw interest from a wide age group, and allow them to enjoy the Geopark and its activities at their own pace.

The current poster uses this Total Design to introduce Sakurajima-Kinkowan Geopark.

Keywords: Total Design

Japan Geoscience Union Meeting 2014
(28 April - 02 May 2014 at Pacifico YOKOHAMA, Kanagawa, Japan)

O06-P17 Room:Poster Time:April 30 18:15-19:30

Aso Geopark Infrastructure Development; International Students Monitoring Tour

KATAYAMA, Akira[1*] ; ISHIMATSU, Akinobu[1] ; YAMAUCHI, Mariko[1]

[1]Aso Geopark Promotion Council

Aso Geopark has been applied for joining the Global Geopark Network (GGN) in December 2013.The Promotion Council has been maintaining both the hard and soft elements of the park infrastructure for not only Japanese tourists but also visitors from abroad as we expect more visitors after becoming the GGN member. In November 2013, international university students in the Tokyo area, who are from Canada, UK, Czech Republic, Korea, China and Taiwan, are interested in Aso region, carried out 3days monitoring tours to evaluate Aso Geopark's foundations to meet visitor satisfaction. The group researched geological sites, public transport systems, the Geopark's base facilities, guiding leaflets and foreign language service at tourists' information and accommodations. During the tour, related people from municipalities, accommodation unions and the council staff gathered together with students and discuss about findings which students discover as native tourists.From the monitoring tour, overall performance includes guide's skill, numbers of signboards and omotenashi at accommodations are relatively highly satisfied. However, explanations in multilingual signboards at public transport stations and base facilities and also automatically translation service on the geopark official website were pointed out and need of immediate development.Even though there are many experiment activities in Aso Geoaprk, most of students suggested having more kindly information service from an entrance to a goal for main tourist's route to look around Aso region with stress free. Explanations for Japanese culture such as use of Ryokan and Onsen, hot spas are essential.This monitoring tour has been programed to have sustainable relationship between the council staff and students as an adviser for future infrastructure developments. Only long-term stay students were selected and asked to check the geopark's official website both before and after the monitoring tour.The promotion council will boost our infrastructures from this research and continue to have more monitoring activities.

Keywords: Aso, geopark, monitor

Japan Geoscience Union Meeting 2014
(28 April - 02 May 2014 at Pacifico YOKOHAMA, Kanagawa, Japan)

O06-P18 Room:Poster Time:April 30 18:15-19:30

Minami-alps geopark

KASUGA, Hiromi[1*] ; KOIKE, Yutaka[1] ; FUJII, Rieko[1]

[1]Minami-Alps geopark conference

The measure of the Minami-Alps geopark

Keywords: geopark, Mountains, Person, Meeting

Japan Geoscience Union Meeting 2014
(28 April - 02 May 2014 at Pacifico YOKOHAMA, Kanagawa, Japan)

O06-P19 Room:Poster Time:April 30 18:15-19:30

The earth science learning tourism Let’s enjoy learning The Chichibu Geopark!

MIYAGI, Satoshi[1*] ; YOSHIDA, Ken-ichi[1]

[1]The Chichibu Geopark Promotion Council Japan

People avoid taking part in the Geo-tourism on focus the geology or topography due to its image as difficult and not-interesting.
However, once you go to Geo-tourism, you can enjoy learning the history, culture and the local life by talking with local guide.
The Chichibu Geopark held monitor tours The earth science learning tourism which set on the several themes, by bus and train this year.
People who participated in the monitor tour commented as follows:
-Hope many people to understand the importance of nature.
-Nice to hear the details by local people.
-Hope to conserve and restore the industrial heritage.
-Hope to continue the Geopark monitor tour.
Geo-tourism is the journey to make us enjoy by local guide as interpreter of the earth.
We continue to discover, to familiarize and also to conserve and utilize the goodness of Chichibu as the local treasure.

Keywords: The Chichibu Geopark, monitor tours, The earth science learning tourism, Geo-tourism

Japan Geoscience Union Meeting 2014
(28 April - 02 May 2014 at Pacifico YOKOHAMA, Kanagawa, Japan)

O06-P20 Room:Poster Time:April 30 18:15-19:30

Private organization for lifelong learning in the Geopark -San-in Kaigan Geopark Saloon (tentative name)

SAKIYAMA, Tohru[1*] ; NIINA, Atsuko[2] ; MATSUBARA, Noritaka[1] ; IMAI, Hiroko[3] ; IMAI, Manabu[3]

[1]Graduate School of Regional Resource Management, University of Hyogo, [2]Regional Innovation Institute, Tottori University of Environmental Studies, [3]NPO Tajima Umino Gakko

Local branding is required in a geopark, and therefore the lifelong education is one of the important activities of the geopark. The staffs of many education and research organizations such as universities and museums are working in the San-in Kaigan Geopark. They do research activities and take part in the operation of the geopark as the member of the committee. Furthermore, they educate for geopark guides and general citizens. These educations are carried out by each organization in cooperation with municipalities individually. There are many small educational facilities and community center in the geopark and some of them provide some educational programs related to geopark. Furthermore, individual guide groups and nonprofit organizations related geopark activity also provide opportunity of learning of training for guides and improving their skill. Summarizing and provision of information by promotion council of San-in Kaigan Geopark are expected, but all programs cannot be grasped by following reasons.

(1)Most of events are not for full area but close to a municipality.

(2)Most of promoting offices of the geopark belong to industry and tourism division, but most of educational facilities belong to education board in the city or town.

(3)Some information on the private offices, NPO and university are not easily spread, because of operating system of the organization led by local government.

(4)Secretariat has very much work because of the wide geopark.

Then we started up a private group (San-in Kaigan Geopark Research Group) for the lifelong education. Members of San-in Kaigan Geopark Research Group belong to universities , NPO, corporations, guide groups and administrative officers.

The San-in Kaigan Geopark Research Group supports the San-in Kaigan Geopark through following educating programs.

(1)Holding regular meetings

(2)Coordination of seminars provided by many educational facilities

(3)Providing original seminars

(4)Planning and execution of out-reach program (geo-caravan)

(5)Providing lecturer

(6)Execution of continuous professional development for geopark guide (Geo-CPD)

The group is composed mainly of staffs of NPO, personal organization and university, and can provide the educational activities across the administrative division. Participation of staffs from various fields makes the geopark expect spreading cooperation in the San-in Kaigan Geopark.

Keywords: geopark, San-in Kaigan, lifelong learning, earth science education

Japan Geoscience Union Meeting 2014
(28 April - 02 May 2014 at Pacifico YOKOHAMA, Kanagawa, Japan)

O06-P21 Room:Poster Time:April 30 18:15-19:30

Past action in the instructional activity of the Shikoku Seiyo Geopark

MAKITA, Takanori[1]*

[1]Shikoku Seiyo Geopark promotion meeting

I performed an instructional activity over many divergences until now in the Shikoku Seiyo Geopark, but, please let the instructional activity in the Seiyo municipal institution Kaida elementary school introduce in that here.

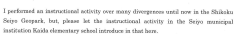

Japan Geoscience Union Meeting 2014
(28 April - 02 May 2014 at Pacifico YOKOHAMA, Kanagawa, Japan)

O06-P22 Room:Poster Time:April 30 18:15-19:30

A Five Senses Sensation in Oga City Geopark Study Center -Geological Geo-Cite and Human History&Culture Meeting Point-

IGARASHI, Yusuke[1*] ; KIKUCHI, Mitukazu[2] ; OYAMADA, Tomoko[2]

[1]Oga City Board of Education, [2]Oga City Geopark Study Center

The Oga City Geopark Study Center was officially opened on August in 2012. This opening followed on from the establishment of the Oga Peninsula-Ogata region as one of the Japanese Geopark sites on September in 2011. The creation of this center focused on the idea that by coming to visit, you would be able to learn everything that there is to know about the Oga Peninsula-Ogata Geopark and surrounding area.

Since the opening of this facility, more than half of the guests at the Geopark center have consisted of arranged educational institution visits - among these visits, Elementary School guests have been the most in number so far. Recently, we are seeing an increase in visits to the center when the weather is poor outside, as this is the biggest issue for people who are traveling to visit the area as part of a 'Geo-Tour'.

Depending upon the guest, we have aimed to provide a wide range of learning materials considering the age and the purpose of the visit. We have also given a high priority to hands-on, participatory ways of learning that will require the use of all five senses of the visitor.

For the lower grade Elementary School learners, we have also provided a range of picture-story style shows which are related to both the Geopark, as well as the legends and stories of Oga City. During the summer and winter vacation times, a workshop is held for Elementary School guests where rock specimen and stones from the Oga area are used to make replicas and models of various common fossils. We are very keen to promote these hands-on activities to the enjoyment of our guests.

Aside from the geological elements of our center, it is also felt that we should promote and educate visitors to the human history of the region in order to preserve our cultural and traditional assets. We aim to cover both of these points comprehensively and widely.

Going forward, it is our aim to promote the human and geological connection and to explore this intertwined relationship. We wish to further our success in this by cooperation with the Ogata Village Polder Museum of Reclaimed Agricultural Land, located only a few kilometers away from our Geopark's location.

It is with this announcement that we would like to introduce you to our facility and activities and express the wish for prospects which lead us to a bright and successful future.

Keywords: The Oga City Geopark Study Center, education, history, culture

Japan Geoscience Union Meeting 2014
(28 April - 02 May 2014 at Pacifico YOKOHAMA, Kanagawa, Japan)

O06-P23 Room:Poster Time:April 30 18:15-19:30

How the precise geological model is utilized in education at schools

YOSHIKAWA, Hirosuke[1*] ; HATANAKA, Takenori[1] ; OTSUKA, Masahiro[2]

[1]Dinosaur Valley Fukui Katsuyama Geopark Promotion Council, [2]Arado elementary school

In 2013, a precise geological model of this region was created with the help of a scientist. This model has mainly been utilized in schools to develop various lessons about Geo-visualization.

The point of this project is not simply to reveal this regions geological features; rather, it aims to awaken the children spirit of inquiry and provide them with the educational opportunity to experience surprise and discovery. We will now present an example of how this geological model was utilized and explain how it may be applied in the future.

Keywords: precise geological model, education at schools, lessons about Geo-visualization, spirit of inquiry, educational opportunity

Japan Geoscience Union Meeting 2014
(28 April - 02 May 2014 at Pacifico YOKOHAMA, Kanagawa, Japan)

O06-P24 Room:Poster Time:April 30 18:15-19:30

The summary of Mt. Apoi geopark project and introduction of earth science education program.

KATO, Satomi[1*]

[1]Mt. Apoi Geopark promotion council

I will introduce earth science education program of Mt. Apoi Geopark.

Keywords: town of Samani, Mt. Apoi, geopark, earth science education, lifelong learning, rock

Japan Geoscience Union Meeting 2014
(28 April - 02 May 2014 at Pacifico YOKOHAMA, Kanagawa, Japan)

O06-P25 Room:Poster Time:April 30 18:15-19:30

To decipher a volcano story from the south.

NAKAGAWA, Kazuyuki[1*] ; MATSUMOTO, Shota[2] ; COMMITTEE OF 14TH EARTHQUAKE & VOLCANO, Summer school for children.[3]

[1]JijIPress, [2]Kobe University, [3]SSJ,VSJ,GSJ,Izu Peninsula Geopark Promotion Council

The Seismological Society of Japan,The Volcanological Society of Japan,The Geological Society of Japan has held the ” earthquake volcano Children Summer School ” every summer . The 2013 marks the 14 th , August 3 , 4 days , it was held in the Izu Peninsula Geopark in Shizuoka Prefecture .The theme is ” the volcano story from the south .” We report an overview of the program, such as the announcement of children.

Keywords: Education for disaster-prevention, Geopark, Izu Peninsula

Japan Geoscience Union Meeting 2014
(28 April - 02 May 2014 at Pacifico YOKOHAMA, Kanagawa, Japan)

O06-P26 Room:Poster Time:April 30 18:15-19:30

Geo-tour program for children during summer vacation in Choshi Geopark

YAMADA, Masahito[1*] ; IWAMOTO, Naoya[1] ; NAKAMURA, Kizuna[1]

[1]Geopark Promotion Office, Choshi City Hall

1.Purpose

Choshi Geopark Promotion Council organized geo-tour for children during summer vacation last year, which is in collaboration with the Association of Chiba Institute of Science (hereafter CIS), Choshi Ryokan union Choshi Inn union, Choshi GeoParty. The purpose of this geo-tour is to provide unique experiences for the children that can also be used as part of their summer homework, and to create a model of overnight package tour.

2.Schedule of geo-tour

The geo-tour was held four times. The first (Jul 24 to 25), the second (Jul 31 to Aug 1) and the fourth round (Aug 27 to 28) have activities such as ”biological observation at rocky shore, touch the nature fun”. The third round (Aug 8) was one day trip with ”observation of the stratum, that can also be submitted to the children’s school as their summer homework.

For the overnight program, we first gathered at Choshi Station at 9:30am, according to the arrival time of the JR limited express. After giving an orientation in CIS, the next event was biological observation at the rocky shore in Nagasaki coast. Then there was plant observation in Kimigahama followed by lunch break in the Culture Center for Youth and Children. In the afternoon, we made star plates and watched a planetarium show. Next, we explored at Inubosaki in the late afternoon. On the next day, there were observation of the landscape at the top of the Mt. Atago-yama, moved to climax forest and had summary of the experiences learned during the programs. The last event was a closing ceremony that all the children were given a participation certificate.

For the one day trip, after giving an orientation in CIS, there were interpretation of layers and sampling of tephra at Byobugaura, and lunch time at CIS. In the afternoon, we observed the sampling using stereoscopic microscope.

3.Advance preparation

Preparation of this geo-tour was started around late April. The events were organized primarily by exchanging information using e-mails. A Working Group meeting was carried out about once a month.

Application of this geo-tour was started from Jun 10 through the ”Jaran” internet version, that reservation was received at each accommodation.

We posted advertisement on the web site of the Choshi Tourism Association and the Choshi Geopark Promotion Council. In addition, we made flyers and sent to each museum and Secretariat of Geopark Promotion Council in Kanto region on July 9. Also, an article was published to the local newspaper on July 20.

The number of participants did not increase as expected. Thus, we changed the program to accept participants from the local people who do not need accommodation.

4.On geo-tour days

The numbers of children for round one to four were 6, 2, 2 and 21, respectively. Many of them were delighted to join the tour.

According to the questionnaire results, many children enjoyed playing at rocky shore. A mother of participants who is born and raised in Choshi commented that she can feel the enjoyable part of Choshi again and another mother would like to learn more about Geopark.

5.Evaluation meeting

Evaluation meeting was held on Sep 19 with a total of 16 participants. The discussion was held by dividing the participants into groups in a workshop format with sticky notes.

The positive comments raised in the meeting were ”The children have fun”, ”Various organizations have cooperate”, ”Various projects could be introduced”, ”Overall framework was constructed ”, ”Accident-free” and so on.

On the other hand, the problems are ”Difficult to understand how to apply”, ”Necessary to devise PR activities”, ”The program was too packed ”, ”Setting of dates”, ”Few participants”, ”Consideration for participants”, ”Difficult to understand the interpretation”.

In addition, the solutions suggested are ”Take action as soon as possible”, ”Separate geo-tour from accommodation”, ”Learn from other Geoparks”, ”Consider the situation of the day” and ”Have a better contact system and role-sharing”.

Japan Geoscience Union Meeting 2014
(28 April - 02 May 2014 at Pacifico YOKOHAMA, Kanagawa, Japan)

O06-P27 Room:Poster Time:April 30 18:15-19:30

Towards the practice of Disaster prevention education and measures using an application of Japanese Geoparks

KUMAGAI, Makoto[1*] ; IMAI, Masayuki[1] ; TAMAOKI, Masashi[1] ; SUGIYAMA, Toshiaki[2] ; KONDO, Masato[3]

[1]Engaru Town Hall, [2]Engaru High school, [3]Hokkaido-Chizu Co.,Ltd.

The core concept of Shirataki Geopark is Where Nature and Culture Meet. Its biggest attractions are the sites of the unique volcanic activity that formed the obsidian, and relics showing how people in the Paleolithic period used the obsidian as an essential resource.

Keywords: disaster prevention education, geographic information systems, school education, tourists correspondence

Japan Geoscience Union Meeting 2014
(28 April - 02 May 2014 at Pacifico YOKOHAMA, Kanagawa, Japan)

O06-P28 Room:Poster Time:April 30 18:15-19:30

The resident seminar after the landslide disaster, and support of research.

NISHITANI, Kana[1*] ; KAJIYA, Akimi[1] ; NAKADA, Setsuya[2] ; NAKAGAWA, Kazuyuki[3]

[1]Izu Oshima Geopark, [2]ERI, [3]Jiji Press Ltd.

The resident seminar was hold about a disaster by Earthquake Research Institute of the University of Tokyo and the Izu-Oshima Geopark. Four specialists explained to residents what has happened and how far it understands in perfection now. 160 persons participated.

We thought our Geopark cauld help a research goes into Oshima, and we opened a window for support of study.

We represented our progress and a subject about the questionnaire result of a resident seminar.

Keywords: geopark, disaster, Izu-Oshima, volcano, information, measure

Japan Geoscience Union Meeting 2014
(28 April - 02 May 2014 at Pacifico YOKOHAMA, Kanagawa, Japan)

O06-P29 Room:Poster Time:April 30 18:15-19:30

What's the meaning of sharing the thought and the experience? The report what we learned through symposium in Izu-Oshim

NISHITANI, Kana[1*] ; SHIRAI, Iwahito[1]

[1]IZU Oshima Geopark

What is sharing of a thought or experience?
The report what we learned through the symposium in Izu-Oshima

After the landslide disaster of the typhoon 26, we will take a symposium in order to learn how to faced the trouble after a disaster and how to live on this island. We will invite people from Miyake-island and the Sanriku Geopark where have experience of eruptions or tsunami, and we will exchange opinions.

Moreover, in order to send some information all of residents equally, we planed to make a booklet for shearing the experience of disaster.

We will consider about the role as a network of the Geopark from our measures.

Keywords: geopark, network, protection against disasters, disaster, jointly , a role

Japan Geoscience Union Meeting 2014
(28 April - 02 May 2014 at Pacifico YOKOHAMA, Kanagawa, Japan)

O06-P30 Room:Poster Time:April 30 18:15-19:30

Exhibition of ”Geohistory of Hachirogata” Established in Polder Museum of Ogata Village

SHINDO, Tomoya[1*] ; WATANABE, Akira[1] ; USUI, Noriyuki[1]

[1]Polder Museum of Ogata Village

Polder museum of Ogata village was opened in 2000. Main theme of the exhibition was Hachirogata reclamation project and history of Ogata village, such as the reclamation works, start of Ogata Village, settlement project as colonists and the lives of the settled people. In the preparation of the museum, Natural History in Ogata also was nominated for the exhibition theme, exhibition on ”Geography of Hachirogata” were also included in it. However, it was decided that the exhibition plan is excluded completely in the process of planning reduced for various reasons.

In 2011, Oga Peninsula-Ogata Geopark was certified by the Japan Geopark Committee for the first

Japan Geoscience Union Meeting 2014
(28 April - 02 May 2014 at Pacifico YOKOHAMA, Kanagawa, Japan)

O06-P31 Room:Poster Time:April 30 18:15-19:30

The picture book about geo-stories of Toay-Usu global geopark

KAGAYA, Nire[1*] ; HATA, Yoshiaki[1] ; NAKAYA, Asami[1] ; ENDO, Kazuya[1] ; TAKEKAWA, Masato[1] ; HIROSE, Wataru[1] ; SASAKI, Hikaru[2] ; SASAKI, Mayuko[2]

[1]Toya-Usu Global Geopark Council, [2]SESENSITKA

Toya-Usu global geopark is a volcanic geopark located in Hokkaido in northern Japan. There are major farms producing vegetables and fruits in this area, and the lands the crops are grown on contain a moderate amount of alkaline ash and pumice from the Toya volcano and the Usu volcano. Therefore, the soil is well suited for cultivation, with a balanced pH and good runoff of water. Also, there are forests in various transition stages around Mt. Usu. This produces bio-diversity with each environmentally-accepted creature. This is due to frequent disturbance and restoration by the eruptions of Usu volcano in recent years. Because of this, we can find a lot of hidden tales ”Geo-Stories”, associated with the activity of the living Earth when we focus on the different aspects of local industry, people’s livelihood, and the natural habitats of living things.

In 2014, Toya-Usu global geopark produced the picture book Toya-Usu Global Geopark Storybook in order to comprehend the relationship between the worlds above and under the ground world. It is edited to include easy-to-understand text and illustrations to reach local people of all ages.

Keywords: Geopark, geo-story, Toya, Usu

Japan Geoscience Union Meeting 2014
(28 April - 02 May 2014 at Pacifico YOKOHAMA, Kanagawa, Japan)

O06-P32 Room:Poster Time:April 30 18:15-19:30

Winter is the Time for Geo-tour!! : The Recommended Winter Trekking Course in Toya-Usu

KAGAYA, Nire[1*] ; HATA, Yoshiaki[1] ; NAKAYA, Asami[1] ; ENDO, Kazuya[1] ; TAKEKAWA, Masato[1]

[1]Toya-Usu Global Geopark Council

In Hokkaido, Japan the number of tourists in the period from April to September 2012 (34 million) was double that of the period from October 2012 to March 2013 (17 million). This gap between the number of tourists in summer and in winter is large when compared with any other region of Japan. This is because the low temperatures and snow in the winter months is standing in the way of winter tourism in Hokkaido, which is a high latitude location.

The downturn in the tourism industry during the winter is an old challenge. In our Geopark, it continues to disturb local employment and industrial growth, and marks it hard to have a stable income throughout the year. Creating new attractions in the region is a solution of vital importance for the promotion of our Geopark and the sustainable development of the local economy.

The winter is actually the best season for enjoying the outdoors of our Geopark, when you can easily see the steaming active lava domes and craters due to the low temperature, as well the beautiful landscape covered with snow. Snow-shoe trekking is becoming popular these days in Japan. There is a lot of potential for a successful tour in the winter months. Here I will present our recommended winter trekking course.

Keywords: geopark, foot path, snow-shoe, geo tour

Japan Geoscience Union Meeting 2014
(28 April - 02 May 2014 at Pacifico YOKOHAMA, Kanagawa, Japan)

O06-P33 Room:Poster Time:April 30 18:15-19:30

Selecting potential geosites in the eastern Kii Peninsula, SW Japan

KAPUSCIK, Dorota[1*]

[1]Waseda University

The geologic structure formed by plate subduction along trenches is well preserved in Southwest Japan. Formed from Jurassic to Paleogene eastward trending belts of accretionary complexes with metamorphic rocks characterize the geology of the Kii Peninsula.

The eastern Kii Peninsula presents varied geological features, such as rocks exposures and fossils, which displays the history of formation of the Japanese Islands. The aim of this work is to identify significant geological sites in the region and set the basis for establishing geosites in future. A geo-site, in the field of geo-tourism, is a geological attraction with the highest value rank, which identification would play the essential role in development of geo-tourism in this region.

Scientifically important geosites has been picked up together with the sites of unique history and culture within the study area including Ise, Toba and Shima City in eastern Kii Peninsula. The valorization of selected objects, from the aspect of geo-tourism development in the region, is based on field studies and detailed petrographic analyzes by using samples from rock exposures on the surface. The thin sections analyze provides information about more precise surface trace of the Median Tectonic Line (MTL) in the eastern Kii peninsula, which can be use as the most attractive point of geological trips in the region.

This work also focus on the lack of geo-touristic infrastructure that would make available all their advantages for educational and tourism purposes. Though several MTL outcrops are visible among local roads in relatively close distance to popular touristic spots, most visitors do not notice this fact. Sufficient information about geosites, as well as the access facility, is the most important for visitors. Establishing a tentative geo-touristic course in the study area would increase public awareness of geoscience education, protection and conservation important landscapes for future generation and help tourists with better understanding the geology of visited area.

Keywords: MTL, geo-site, geo-tourism, Kii Peninsula

Japan Geoscience Union Meeting 2014
(28 April - 02 May 2014 at Pacifico YOKOHAMA, Kanagawa, Japan)

O06-P34 Room:Poster Time:April 30 18:15-19:30

Virtual Poster Geotour of Unzen Volcanic Area Global Geopark Part 2 : Unzen Hell

OHNO, Marekazu[1*]

[1]Unzen Volcanic Area Geopark Promotion Office

Main theme of Unzen Volcanic Area Global Geopark is ”coexisting between active volcanoes and human beings”. However this geopark also has another highlights; e.g. hot springs, human histories and local foods which are closely related to natural environments. In this poster presentation, we introduce highlights of ”Unzen Hell”(geothermal area) on the basis of a view of a geopark.

Keywords: Unzen Volcanic Area Global Geopark, Virtual geotour, Sulfate hot springs, Unzen Hell, Geothermal Area, Solfatalic cray

Japan Geoscience Union Meeting 2014
(28 April - 02 May 2014 at Pacifico YOKOHAMA, Kanagawa, Japan)

O06-P35 Room:Poster Time:April 30 18:15-19:30

Strata Observation Party Evolved into the Geo-Tour -The Oga Peninsula-Ogata Geopark's Trial-

WATANABE, Kosei[1*] ; TAKEUCHI, Hirokazu[1] ; SUGAWARA, Sinichi[1]

[1]Oga Peninsula-Ogata Geopark Promotion Council

The Oga Peninsula-Ogata Geopark is a suitable place for geological learning and research. We could examine the strata for 70 million year-long doramatic history. Every year, many students and researchers in the field of geology come to visit. At the beginning of Geopark's authorization period, due to desired efforts in education and research, this area was considered to be particularly "difficult" Geopark compared to other locations. However, more recently due to the interaction and exchange of ideas from various geological conventions and from within the community of Geopark inspectors, we are happy to announce this area is now more "fun" Geopark.

With this announcement, we would like to introduce our progress and the results, the bright future prospects.

Keywords: Oga Peninsula-Ogata Geopark, Geo-Tour, Oga no Namahage

Japan Geoscience Union Meeting 2014
(28 April - 02 May 2014 at Pacifico YOKOHAMA, Kanagawa, Japan)

O06-P36 Room:Poster Time:April 30 18:15-19:30

The geopark which feels the sound which turns over the page of the history of the earth

SATO, Misao[1] ; SATO, Hidekazu[1*] ; MIURA, Go[1]

[1]miyagi kuriharacity

The causes for Kurihara to aim at a geopark were Heisei 20 Iwate and the Miyagi inland earthquake.

In this earthquake, very various types and destructive movement of the slope of a scale which exceed 3000 from the summit of the mountain of the volcano which constitutes the Ou mountain range to foot arose.

Inland epicentral earthquake.

This is business of the earth in the Ou mountain range repeated since ancient ancient times, the natural wonder itself can be felt here and it is thought that Nature is moving.

”The sound which turns over the page of the history of the earth is felt.”

In the Ou mountain range, this meaning has only the history for the 1 million ? 2 million years the history for earth 4,600 million years, and in it, and Iwate and the Miyagi inland earthquake in the meantime are new occurrences of five years ago.

We should make it the hit of a between, should feel it and must merely have felt the dreadfulness of the earth.

We have helped the moment which turns over rightly 1 page that the Ou mountain range will change greatly, in the history of It continues for a long time endlessly.

Since it seethes with the senses rather than explaining, it is expressing it in the word of ”feeling sound” by the Mt. Kurikoma foot geopark concept.

Japan Geoscience Union Meeting 2014
(28 April - 02 May 2014 at Pacifico YOKOHAMA, Kanagawa, Japan)

O06-P37 Room:Poster Time:April 30 18:15-19:30

Locality exploration of archaeological relics and a theme of geopark - an example of the Yakumo geopark plan

OYA, Shigeyuki[1*] ; KATOH, Takayuki[2] ; THE ASSOCIATION OF GEOPARK PLAN, In yakumo[3]

[1]Yakumo education comittee, [2]Earth Science Co.Ltd, [3]Yakumo town

Yakumo-cho is a town that has the chief industries of the dairy farming and the fishery which owns the two seas of the Pacific Ocean and Sea of Japan, being in the narrowest part in Oshima Peninsula.

Since 2012, it is doing an activity while the geopark conception preparatory meeting of the private base gets the support from Yakumo town, too.

Oshima Peninsula is the peculiar place which was the corridor connect with Honshu , like a geological feature like landform and also for the people to come and go since the Old Stone Age.

Therefore, the one of archaeological relic which was carried from Honshu in the converse to the one from the inland in Hokkaido is jumbled up around Yakumo town. These relics are also beautiful for modern human beings.

Accordingly, the tour by which an use and an origin are explained about the stone and it observes relics and observes the geological feature of the source of supply and the candidate site can be organized. It thinks of that the case cooperates with some geoparks in each place, too.

The examples are as follows {The archaeology relic (the stone quality)-Locality-The way of visiting}.

1. Jadeite→Itoigawa City→ Visit to the Itoigawa geopark
2. Obsidian-→Akaigawa village and Shirataki area of Engaru town→Visit to the Shirataki geopark
3. Blue schist→Kamuikotan belt→Visit to the Asahikawa geopark (plan)
4. So-called ”Aotora” (Greenshist to blueshist facies metamorphosed bannded pyrocrastic rock brocks in a serpentinite mass) →Nukabira serpentinite mass, Kamuikotan belt→Visit to the Hidaka mountains museum (Hidaka town)
5. Rodingite metazomatized from serpentinite itself with Cr-spinel→Nukabira serpentinite mass, Kamuikotan belt→Visit to the Hidaka mountains museum (Hidaka town)
6. Welded tuff bearing hornblend (house-formed production) →Nigorikawa pyroclastic flow→Visit to around the Nigorikawa caldera
7. Silicified shale→The Yakumo formation with the contact zone of intrusive rocks→Visit to several localities around Yamumo town
8. Marlite→The nodule in Yakumo formation→Visit to Kami-Yakumo area, Yakumo town
9. Agate→The area of volcanic rocks of submarine such as Kunnui-, Yakumo-, Kuromatunai- formations→The Kuroiwa in Yakumo town, R. Kunnui-gawa in Oshamanbe town, and R.Shiribeshi-toshibetu-gawa in Imakane town
10. Talc→Era area in Matsumae town→Visit to Matsumae town
11 .Asphalt→Yamakoshi area in Yakumo town, Kuji city in Iwate prefecture→Visit to the oil showing of Yamakoshi, and the Sannriku geopark

Keywords: Yakumo geopark plan, archaeological relics

Japan Geoscience Union Meeting 2014
(28 April - 02 May 2014 at Pacifico YOKOHAMA, Kanagawa, Japan)

O06-P38 Room:Poster Time:April 30 18:15-19:30

East and West found in the Jomon Pottery - Example from the Archeological Geo-diversity

YAMAGISHI, Yoichi[1*]

[1]Itoigawa Geopark Council (Itoigawa CIty Geopark Promotion Office)

The Itoigawa Global Geopark is interesting place where you can see the difference between the east and west culture. Geo - divercity is deeply refrected to archeological feachers too.

Japan Geoscience Union Meeting 2014
(28 April - 02 May 2014 at Pacifico YOKOHAMA, Kanagawa, Japan)

O06-P39 Room:Poster Time:April 30 18:15-19:30

Mini Geotourism Centered on Itoigawa's Old Town

II, Toru[1*] ; WATANABE, Seigou[1] ; TAKENOUCHI, Ko[1]

[1]Itoigawa Geopark Council(Itoigawa City Geopark Promotion Office)

One of the main points of entry for the Itoigawa Geopark is Itoigawa Station,located in the middle of Itoigawa's Old Town.The north side of the station has since long ago been a shopping area.Once lively with activity, it now sees little foot traffic. This problem is shared with many rural cities,the causes include:loss of customers to large suburban box stores, the recent trend away from public transport,and declined enthusiasm among shop owners due to decreased sales and difficulty in finding successors.In 2009 came Global Geopark certification and plans were undertaken to further utilize and revitalize the Old Town in time for the new Hokuriku Shinkansen Line in March 2015.In this session,we will introduce how we are using Geotourism in order to increase foot traffic in the Old Town.The center of the old town district is an area called 'Ro-no-Ji' for its square shape resembling the Japanese character 'ro'. It is largely commercial and is often used for events such as festivals.Itoigawa Station lies at one corner of Ro-no-Ji alongside a tourism information center which includes geopark information.In the Old Town are a statue of Princess Nunakawa,a local deityp;and historical landmarks including the beginning of the old Salt Trail,Kaga-no-I Brewery,and a gangi-lined street.Gangi are traditional roofs built over streets Japan's snowy regions.This street preserves the image of Japan before modern shopping malls.A number of Geopark-related sights show ways in which the land has changed.These are all valuable tools in the development of the Old Town District.The Itoigawa Machinaka Collection is an event that has been held every year since 2006.Participation is increasing yearly and in 2013 a Town Walking Tour attracted many participants looking to enjoy the Old Town.The 'Increase Shop Charms Women's Club' was formed in 2010 by 50 women working in the Old Town to help revitalize the area in preparation for the new Shinkansen.They now help with the Machinaka Collection, sell limited edition sweets, and participate in events in the area,helping to reenergize the district.The Itoigawa Geopark Council promotes downtown walking through pedestrian maps. These maps include interesting sights around the station as well as specialty products available at downtown shops.The leaflet targeted toward women has been particularly well-received.Itoigawa Station is a hub which connects the Hokuriku Main Line with the Oito Line,and so travelers occasionally must wait for their connection. Wanting to capitalize on this,a Geopark Guide Walking Tour program was tested. Over 10 days in late October,8 people participated in these impromptu tours.All 8 were women who,having time to spend before their next train,enquired at the tourism desk about things to do. The guides primarily focused on the gangi street,Kaga-no-I Brewery,the seaside viewing platform, and downtown shops, from which some visitors bought gifts.Others declined the tour,but took leaflets to walk the town alone.To improve secondary transport from Itoigawa Station,a Town Loop Bus began operation in 2011.Running weekends and holidays, the bus starts at the station and makes a 40 min.loop through central Itoigawa's main tourist sites.Among these are the Fossa Magna Museum,Chojagahara Archaeological Museum,and the Itoigawa Folk History Museum.These are all indispensable facilities within the Geopark and the new bus line is important for visiting Geotourists.Since starting an all-day pass program in 2013, ridership has increased.The Old Town has many sites of interest,but they are being overlooked.Few people visit the Old Town outside of events.In order to help people understand the charms of this area, we must improve information transmission and hospitality.We mustn't miss the opportunity afforded to us by the opening of the new Hokuriku Shinkansen to increase visitors to this forgotten gem.

Keywords: town strolling, shopping streets, partnerships, Hokuriku Shinkansen

Japan Geoscience Union Meeting 2014
(28 April - 02 May 2014 at Pacifico YOKOHAMA, Kanagawa, Japan)

O06-P40 Room:Poster Time:April 30 18:15-19:30

Investigation and preservation of old Coalmine in the Mikasa Geopark

NII, Tadahiro[1*] ; KURIHARA, Ken'ichi[2]

[1]Promotion Policy Division, Mikasa City Office, [2]Mikasa City Museum

Mikasa city is the area of Mikasa Geopark had many coalmines.
Therefore, Mikasa created prosperity by coalmine, which has many remains of them.

To consider using those remains, we investigated worth of them from point of architecture.
Then, based on the results, We tried to safety state of around the Nishiki headframe in 2013.The Nishiki headframe is believed to have completed in December 1920, and it is the oldest remaining headframe in Hokkaido.The headframe is approximately 10 meters high, and the shaft is approximately 197 meters deep.

So, we introduce you the action of preservation and reuse those remains in the Miasa Geopark.

Keywords: coalmine, remains, preservation and reuse, geopark activity, Mikasa Geopark

Japan Geoscience Union Meeting 2014
(28 April - 02 May 2014 at Pacifico YOKOHAMA, Kanagawa, Japan)

O06-P41 Room:Poster Time:April 30 18:15-19:30

Rice farming and culture in Yuzawa Geopark

KAWABE, Kenichiro[1*]

[1]Yuzawa Geopark Promotion Group

Yuzawa Geopark is a member of the Japan Geopark Network from 2012. In 2013, Yuzawa Geopark have created a catch copy and story. We are using the word ”Life and History”, in this copy.In this presentation, I will introduce the rice farming and culture in Yuzawa Geopark.

People have been praying for a good harvest. Also, a lot of the daily necessities and equipment used in religious ceremonies were made from rice straw. It was born from rice farming that praying for a good harvest and making daily necessities. And then, we are inheriting the culture from old generations. The inheriting is supported in rice farming that has been actively.

Japan Geoscience Union Meeting 2014
(28 April - 02 May 2014 at Pacifico YOKOHAMA, Kanagawa, Japan)

O06-P42 Room:Poster Time:April 30 18:15-19:30

Diversity of ”freezing” and its application to activities in the Tokachi-Shikaoi Geopark

ONISHI, Jun[1*] ; SAWADA, Yuki[2]

[1]Tokachi shikaoi geopark Promotion conference, [2]Fukuyama city university

“ Freezing ” is one of the main themes of Tokachi-Shikaoi Geopark. It appears in many different features: periglacial phenomena and landform, ecology, and life-style of residents in this region. We show some examples of geomorphic features related to cold climate, and activities of residents adapting to the “ freezing ” winter and even using ice to build hot spa, ice bar and other activities on “ freezing ” Lake Shikaribetsu.Our poster will show introduction to the world of freezing.

Keywords: tokachi shikaoi, geopark, freezing

Japan Geoscience Union Meeting 2014
(28 April - 02 May 2014 at Pacifico YOKOHAMA, Kanagawa, Japan)

O07-01 Room:Main Hall Time:April 29 10:55-11:30

Viewing the Earth's Climate from Space

FREILICH, Michael[1*]

[1]Director, Earth Science Div. NASA Headquarters

Earth is a complex, dynamic system we do not yet fully understand.
The Earth system, like the human body, comprises diverse components that interact in complex ways.
We need to understand the Earth's atmosphere, lithosphere, hydrosphere, cryosphere, and biosphere as a single connected system.
Our planet is changing on all spatial and temporal scales.
This presentation will highlight how satellite observations are revolutionizing our understanding of and its response to natural or human-induced changes, and to improve prediction of climate, weather, and natural hazards.

Japan Geoscience Union Meeting 2014
(28 April - 02 May 2014 at Pacifico YOKOHAMA, Kanagawa, Japan)

PPS01-01 Room:418 Time:April 30 14:15-14:35

The Solar Power Sail for Round Trip Exploration to Jupiter Trojans and Deep Space Cruising Observation

YANO, Hajime[1*] ; NAKAMURA, Ryosuke[2] ; MATSUURA, Shuji[1] ; SEKINE, Yasuhito[3] ; TOYODA, Michisato[4] ; AOKI, Jun[4] ; YOSHIDA, Fumi[5] ; TAKATO, Naruhisa[5] ; KINOSHITA, Daisuke[6] ; YONETOKU, Daisuke[7] ; YOSHIKAWA, Makoto[1] ; MORI, Osamu[1] ; SOLAR SYSTEM SMALL BODY EXPLORATION WGT, .[1] ; SOLAR POWER SAIL WG, .[1]

[1]JAXA/ISAS, [2]AIST, [3]The University of Tokyo, [4]Osaka University, [5]NAOJ, [6]Taiwan Central University, [7]Kanazawa University

Since 2002, the Solar Power Sail WG has been studying a mission design of Japan's first outer planet region exploration, by demonstrating the solar power sail technology, and it is bound to Jupiter Trojan asteroids, which may hold fundamental clues of the Solar System formation and revolution discussed by two competing hypotheses between the classic model and the planetary migration model. The former suggests that Trojan asteroids are mainly survivors of building blocks of the Jupiter system, while the latter claims that they must be intruders from outer regions after the planetary migration of gas planets settled.

After Jupiter flyby, the spacecraft will reach to a candidate Trojan asteroid, hopefully being larger than a few 10's of km in size. Both global remote observation and deployment of an autonomous lander will be conducted. On the surface of the Trojan asteroid, sampling will be attempted for in-situ TOF mass spectrometry and passing the sample container to the mothership for a possible sample return option.

Also during the cruising operation, "dust free" astronomical platform beyond the cocoon of the zodiacal light formed by the main asteroid belt for the benefit of infrared astronomy searching for the first generation light of the Universe, let alone continuous observation of the zodiacal light structure of the Solar System. Extremely long baseline with the observation from the Earth, gamma-ray burst observation can identify their sources.

This presentation discusses major scientific objectives of an exploration mission to Jupiter Trojans for the first time in the history, its mission design and spacecraft system using solar power sail, a hybrid propulsion system of electric propulsion and photon sail, which inherited from the IKAROS deep space solar sail spacecraft, together with major engineering challenges, in-situ observation instruments and operational options including landing and sample return from the surface of a Trojan asteroid.

Keywords: Solar Power Sail, Jupiter Trojans, Deep Space Exploration, Deep Space Astronomy, Zodiacal Light, Sample Return

Japan Geoscience Union Meeting 2014
(28 April - 02 May 2014 at Pacifico YOKOHAMA, Kanagawa, Japan)

PPS01-02 Room:418 Time:April 30 14:35-14:55

EUROPA CLIPPER MISSION CONCEPT OVERVIEW

PAPPALARDO, Robert[1] ; GOLDSTEIN, Barry[1] ; MAGNER, Thomas[2] ; PROCKTER, Louise[2] ; SENSKE, David[1] ; PACZKOWSKI, Brian[1] ; COOKE, Brian[1] ; VANCE, Steven[1*] ; PATTERSON, G. wesley[2]

[1]Jet Propulsion Laboratory, California Institute of Technology, Pasadena, CA 91109, [2]The Johns Hopkins University, Applied Physics Laboratory, Laurel, MD, 20723

A NASA-appointed Science Definition Team (SDT) recently considered options for a future strategic mission to Europa, with the stated science goal: Explore Europa to investigate its habitability. The team worked closely with a technical team from the Jet Propulsion Laboratory (JPL) and the Applied Physics Laboratory (APL). Together, the group considered several mission options, which were fully technically developed, then costed and reviewed by technical review boards and planetary science community groups. Study results strongly favored an architecture consisting of a spacecraft in Jupiter orbit, making many close flybys of Europa, and concentrating on remote sensing to explore the moon. The resulting nominal mission design is innovative for its use of gravitational perturbations of the spacecraft trajectory to permit flybys at a wide variety of latitudes and longitudes. The design enables globally distributed regional coverage of the moon's surface, nominally with 45 close flybys at altitudes from 25 to 100 km. We will present the science and reconnaissance goals and objectives, a mission design overview, and the notional spacecraft for this concept, which has become known as the Europa Clipper. The Europa Clipper concept provides a cost-efficient means to explore Europa and investigate its habitability, through understanding the satellite's ice and ocean, composition, and geology. The set of investigations derived from these science objectives traces to a notional payload for science, consisting of: Ice Penetrating Radar (for sounding of ice-water interfaces within and beneath the ice shell), Topographical Imager (for stereo imaging of the surface), ShortWave Infrared Spectrometer (for surface composition), Neutral Mass Spectrometer (for atmospheric composition), Magnetometer and Langmuir Probes (for inferring the satellite's induction field to characterize an ocean), and Gravity Science (to confirm an ocean). Among the many science investigations addressed, Europa Clipper could potentially characterize plumes linked to Europa's internal lakes or ocean. The mission would also include the capability to perform reconnaissance for a future lander, with the Reconnaissance goal: *Characterize safe and scientifically compelling sites for a future lander mission to Europa*. To accomplish these reconnaissance objectives and the investigations that flow from them, principally to address issues of landing site safety, two additional instruments would be included in the notional payload: a Reconnaissance Camera (for high-resolution imaging) and a Thermal Imager (to characterize the surface through its thermal properties). These instruments, in tandem with the notional payload for science, could assess the science value of potential landing sites. This notional payload serves as a proof-of-concept for the Europa Clipper during its formulation stage. The actual payload would be chosen through a NASA Announcement of Opportunity. If NASA were to proceed with the mission, it could be possible to launch early in the coming decade, on an Atlas V or the Space Launch System (SLS).

Keywords: Europa, Icy Worlds, Astrobiology, Europa Clipper, Missions, Planetary Science

Japan Geoscience Union Meeting 2014
(28 April - 02 May 2014 at Pacifico YOKOHAMA, Kanagawa, Japan)

PPS01-03 Room:418 Time:April 30 14:55-15:10

Investigation of the Galilean Moons with the Ganymede Laser Altimeter (GALA)

HUSSMANN, Hauke[1*] ; LINGENAUBER, Kay[1] ; MICHAELIS, Harald[1] ; KOBAYASHI, Masanori[2] ; THOMAS, Nicolas[3] ; LARA, Luisa M.[4] ; ARAKI, Hiroshi[5] ; BEHNKE, Thomas[1] ; GWINNER, Klaus[1] ; KIMURA, Jun[6] ; NAMIKI, Nori[2] ; NODA, Hirotomo[5] ; OBERST, Juergen[1] ; ROATSCH, Thomas[1] ; RODRIGO, Rafael[4] ; SASAKI, Sho[7] ; SEIFERLIN, Karsten[3] ; SPOHN, Tilman[1] ; BARNOUIN, Olivier[8] ; BREUER, Doris[1] ; CASOTTO, Stefano[9] ; CASTRO, Jose[4] ; CHOBLET, Gael[10] ; CHRISTENSEN, Ulrich[11] ; FERRAZ-MELLO, Sylvio[12] ; GIESE, Bernd[1] ; KALLENBACH, Reinald[11] ; KURITA, Kei[13] ; LAINEY, Valery[14] ; LICHOPOJ, Alexander[1] ; LOETZKE, Horst-georg[1] ; LUPOVKA, Valery[15] ; MOORE, William B.[16] ; RODRIGUEZ, Adrian[6] ; SANTOVITO, Maria rosaria[17] ; SCHREIBER, Ulrich[18] ; SCHROEDTER, Rolf[1] ; SOHL, Frank[1] ; DEL TOGNO, Simone[1] ; VERMEERSEN, Bert[19] ; WIECZOREK, Mark[20] ; YSEBOODT, Marie[21]

[1]DLR Institute of Planetary Research, Berlin, Germany, [2]Chiba Institute of Technology, Planetary Exploration Research Center, Chiba, Japan, [3]Physics Institute, University of Bern, Switzerland, [4]CSIC, Instituto de Astrofisica de Andalucia, Granada, Spain, [5]National Astronomical Observatory of Japan, Mizusawa, Japan, [6]Earth-Life Science Institute, Tokyo Institute of Technology, Japan, [7]Osaka University, Toyonaka Japan, [8]Space Dept., The Johns Hopkins University Applied Physics Laboratory, Laurel, MD, USA, [9]University of Padua, Dept. of Physics and Astronomy and Center for Space Studies, Padova, Italy, [10]Laboratoire de Planetologie et Geodynamique de Nantes, France, [11]Max Planck Institute for Solar System Research, Katlenburg-Lindau, Germany, [12]Institute of Astronomy, Geophysics and Atmospheric Science, Sao Paulo, Brasil, [13]University of Tokyo, Earthquake Research Institute, Tokyo, [14]IMCCE-Observatoire de Paris, France, [15]Moscow State University of Geodesy and Cartography, (MIIGAiK), Russia, [16]Hampton University, National Institute of Aerospace, USA, [17]CO.RI.S.T.A. Consortium of Research on Advanced Remote Sensing Systems, Napoli, Italy, [18]Technische Universitat Munchen, Fundamentalstation Wettzell, Germany, [19]Astrodynamics & Space Missions, Faculty of Aerospace Engineering, TU Delft, Netherlands, [20]Institut de Physique du Globe de Paris, France, [21]Royal Observatory of Belgium , Brussels, Belgium

The icy moons of Jupiter ? Europa, Ganymede, and Callisto ? are believed to contain global subsurface water oceans underneath their icy crusts. The possibility is intriguing that these large liquid water oceans represent ”habitable” environments. Investigation of the latter is a major objective of ESA’s Jupiter Icy Moons Explorer (JUICE) mission. The Ganymede Laser Altimeter (GALA) is one of the instruments focusing on aspects related to the presence and characterization of subsurface water oceans by measuring Ganymede’s tidal deformation. GALA will further contribute (a) to the exploration of the surface morphology and physical properties of Ganymede, Europa and Callisto, (b) to determination of their interior structures from a combination of shape, topography and gravitational field data, and (c) to understanding the satellites formation and evolution especially with respect to subsurface water oceans. GALA will investigate the surface and topography of Ganymede in particular. Topography data is needed to account for the effects of topographic heights on the gravity field and to account for near surface mass distribution anomalies above the reference figure; to support geological studies, e.g. to identify and characterize tectonic and cryo-volcanic regions on the icy moons and to identify periodic variations of Ganymede’s shape due to tides.

Investigations by GALA will furthermore contribute to determine the orientation and rotational state of Ganymede and to study surface characteristics (roughness, slopes, and albedo) on Ganymede, Europa, and Callisto.

The instrument can be operated from ranges smaller than about 1000 to 1300 km (depending on the different albedo values and surface slopes of Europa, Ganymede and Callisto) during flybys and orbital pericenter passages. The main phases for acquiring data at Ganymede are the final circular orbit phases, where continuous operations are possible from altitudes around 500 km and 200 km, respectively.

Here, we will give an overview on the GALA experiment focusing on its scientific goals and performance.

Keywords: Laser altimetry, Satellites of Jupiter, Ganymede, Tides

Japan Geoscience Union Meeting 2014
(28 April - 02 May 2014 at Pacifico YOKOHAMA, Kanagawa, Japan)

PPS01-04 Room:418 Time:April 30 15:10-15:25

Longevity of an internal ocean in Ganymede

KIMURA, Jun[1*] ; VANCE, Steven[2] ; HUSSMANN, Hauke[3] ; KURITA, Kei[4]

[1]Earth-Life Science Institute, Tokyo Institute of Technology, [2]Jet Propulsion Laboratory, [3]DLR Institute of Planetary Research, [4]Earthquakle Research Institute, The University of Tokyo

The outer solar system may provide a potential habitat of extra-terrestrial life. Most moons orbiting planets in the outer Solar System, at orbits beyond the snow line, such as Jupiter or Saturn, are covered with water ice and are referred to as ”icy moons”. Galileo’s detection of induced magnetic fields combined with imaged surface characteristics and thermal equilibrium modeling of the moons, support that the Jovian icy moons Europa and Ganymede, and possibly Callisto, may harbor liquid water oceans underneath the icy crusts. The presence of internal oceans in the icy moons means that a deep habitat different from Earth’s biosphere may exist, located beyond the ”habitable zone” of the Sun. Evidence for oceans is not definitive, however, and awaits confirmation measurements. Also, the depth and composition of the oceans remain unclear, as do their variability through time.

Here we focus on Ganymede, the largest moon in the Solar System and the primary target of a new mission to the Jupiter system, the Jupiter Icy Moons Explorer (JUICE), which is planned by the European Space Agency (ESA). The bulk density of Ganymede, 1.936 g/cc, indicates a composition of approximately equal amounts of rocky material and water. Previous measurements of Ganymede’s gravitational field and intrinsic magnetic field by the Galileo orbiter suggest that its interior is completely differentiated into three layers, a convecting metallic core at the center, a rocky mantle surrounding the core, and an outermost water-ice shell. The water-ice layer in total has a thickness of 800-1000 km. A layer of melted, salty water that lies beneath the icy crust would be the best way to explain the signal of magnetic induction.

To investigate the lifetime of an ocean (thickness change through time) assumed to be initially in an entirely liquid state, we performed numerical simulations for the internal thermal evolution using a spherically symmetric model for the convective and conductive heat transfer with radial dependence of viscosity, heat source distribution, and other material properties. Here we take into account the energy due to decay of long-lived radioactive elements and also evaluate the effect of tidal heating. If the ocean were composed of pure water, a primordial ocean would have disappeared (completely solidified) within 1 Gyr even if tidal heating for the current orbital state were included. Consistent with previous predictions , this result indicates that significant tidal heating in the past, or strong antifreeze components (e.g., salts or ammonia),

are needed if the presence of the internal ocean in Ganymede would be confirmed from future JUICE observations. We numerically investigate their effect on the lifetime of the ocean.

Keywords: satellite, evolution, ocean, habitability, ice, Ganymede

Japan Geoscience Union Meeting 2014
(28 April - 02 May 2014 at Pacifico YOKOHAMA, Kanagawa, Japan)

PPS01-05 Room:418 Time:April 30 15:25-15:40

Impact basin relaxation on Pluto: Implications for the presence of a subsurface ocean

KAMATA, Shunichi[1*] ; NIMMO, Francis[2]

[1]Hokkaido University, [2]UC Santa Cruz

Large-scale topographies, such as impact basins, on solid planetary bodies deform in geologically long timescales. The degree of deformation depends mainly on the viscosity, and the viscosity is strongly controlled by temperature. Consequently, viscous relaxation of large impact basins has been studied to investigate the thermal evolution of terrestrial planets as well as that of icy satellites of giant planets [e.g., 1-4].

Pluto, an icy dwarf planet, is likely to possess large impact basins. In this study, we investigate long-term viscoelastic deformation of impact basins on Pluto which can be compared with forthcoming observational data from New Horizons, the first Pluto explorer.

Although little is known for Pluto, its interior is likely differentiated into a rocky core and an outer H_2O layer [e.g., 5]. The presence of a subsurface ocean, however, is highly uncertain. If the outer (solid) H_2O layer is convective, the radiogenic heat from the rocky core is efficiently transferred to the surface, and temperature of the H_2O layer can be lower than its melting temperature. On the other hand, if the outer H_2O layer is conductive, the heat from the core can melt the H_2O layer. The main controlling factor whether the H_2O layer is convective or conductive is the reference viscosity: the ice viscosity at its melting temperature [6]. In this study, we calculate viscoelastic deformation of impact basins assuming different viscosity profiles and examine the effect of the presence of a subsurface ocean on basin relaxation.

For the initial study, we use two time-independent viscosity profiles; one profile assumes a stiff top shell overlying a thick subsurface ocean, and the other assumes a completely solidified interior. The same viscosity profile in the shell is assumed.

Our results indicate that the instantaneous elastic response largely differ between the viscosity models. However, long-term relaxation does not differ much because it is controlled by the viscosity profile in the shell, which is identical in our calculations. Nevertheless, long-term relaxation strongly depends on the reference viscosity, the main controlling factor whether the shell is convective. Consequently, relaxation state of impact basins can be used to infer the reference viscosity as well as the presence of a subsurface ocean. This result would be applicable to icy satellites of Jupiter and Saturn.

Our next step is to use time-dependent viscosity profiles. To do so, we have modified our relaxation code to take into account the temporal change in the shell thickness. The results will be discussed.

[1] Kamata et al. JGR 118, 398-415, 2013. [2] Mohit and Phillips, GRL, 34, L21204, 2007. [3] Robuchon et al. Icarus 207, 959-971, 2010. [4] Solomon et al. JGR 87, 7763-7771, 1982. [5] McKinnon et al. in Pluto and Charon, pp. 295-343, 1997. [6] Robuchon and Nimmo, Icarus 214, 426-439, 2011.

Keywords: Impact basin, Relaxation, Pluto, Viscoelasticity

Japan Geoscience Union Meeting 2014
(28 April - 02 May 2014 at Pacifico YOKOHAMA, Kanagawa, Japan)

PPS01-06 Room:418 Time:April 30 15:40-15:55

Sub-millimeter observations of icy bodies toward understanding of planetary formation and cosmochemistry

SEKINE, Yasuhito[1*] ; KASAI, Yasuko[2] ; SAGAWA, Hideo[2] ; KURODA, Takeshi[3] ; KODAMA, Kenya[1] ; HORI, Yasunori[4] ; IKOMA, Masahiro[1] ; KURAMOTO, Kiyoshi[5] ; YURIMOTO, Hisayoshi[5]

[1]University of Tokyo, [2]NICT, [3]Tohoku University, [4]NAOJ, [5]Hokkaido University

The present-day composition of regular icy satellites consists of combinations of initial conditions and subsequent evolution. These icy satellites are considered to have been formed in a circumplanetary disk associated with giant planet formation. Thus, icy satellites that are not geologically active, such as Callisto, would serve as solar system fossils, which may preserve the information of the protoplanetary disk and planetary formation. On the other hand, geologically active satellites, such as Europa and Enceladus, would provide particular geological processes and consequent products of geochemical reaction. Sub-millimeter observations are capable of providing unique isotopic and chemical compositions of gas molecules in atmospheres and plumes of the icy satellites. In this paper, we discuss key observational targets and their importance for planetary formation theory and geo/cosmochemistry, especially focusing on sub-millimeter observations of Galilean satellites by the Jupiter Icy moons Explorer mission, JUICE.

Keywords: sub-millimeter observation, icy satellite, planetary formation, cosmochemistry

Japan Geoscience Union Meeting 2014
(28 April - 02 May 2014 at Pacifico YOKOHAMA, Kanagawa, Japan)

PPS01-07 Room:418 Time:April 30 16:15-16:30

Proto-atmospheres on giant icy satellites forming within gaseous circum-planetary disks

MIKAMI, Takashi[1*] ; KURAMOTO, Kiyoshi[1]

[1]Department of Cosmosciences, Graduate School of Science, Hokkaido University

In spite of the great similarity in size and mean density, the giant icy satellites Ganymede, Callisto, and Titan have very different surface environments. In particular, only Titan holds a thick atmosphere dominated by N_2. Recent data of the Cassini spacecraft indicated that atmospheric N_2 is probably originated from other nitrogen-bearing species like NH_3. However, it still remains an open question when and how N_2 was generated. This is partly because the physical states of giant icy satellites have been poorly understood.

According to a widely-accepted theory of regular satellites formation, the giant icy satellites were formed in subnebulae with low temperature and low pressure taking a long accretion time. Some models assert that their surfaces were kept too cold to induce significant differentiation during accretion. However, these satellites may capture a significant amount of subnebula gas, which possibly forms proto-atmospheres along with gases volatilized from icy components. Such a hybrid-type proto-atmosphere may have significant blanketing effect.

Here, we numerically analyze the structure and effect of a hybrid-type proto-atmosphere. Our model atmosphere is hydrostatically connected with subnebula at the satellite Hill radius. It contains H_2 and He as nebula gas components, H_2O and NH3 as volatilized ice components. The radiative-convective equilibrium structure is solved as a function of surface temperature. The subnebula conditions are given by Canup and Ward (2002), the temperatures are 150 K at Ganymede, 120 K at Callisto, and 50 K at Titan, and the corresponding subnebula pressures are varied over 0.1-10 Pa.

For all the boundary conditions, the proto-atmosphere is opaque due to water vapor, so that the outgoing thermal radiation (OTR) flux at top of the atmosphere is smaller than that of black body radiation without atmosphere when the surface temperature is higher than 273 K. When the surface temperature is lower, the OTR fluxes from the proto-atmospheres of Ganymede and Callisto are close to black-body radiation because these atmospheres have low surface pressure and are optically thin due to large scale height under high background temperature. On the other hand, the proto-atmosphere of Titan has another type of solution with the OTR fluxes significant lower than blackbody radiation under low surface temperature. This is due to the formation of optically thick atmosphere tightly bounded by gravity because of low background temperature.

These results imply that a warm proto-atmosphere near 200 K could be kept on Titan for a long time after the end of accretion. Our stability analysis suggests that the proto-atmospheres of Ganymede and Callisto were lost associated with the dissipation of the Jovian subnebula, but that of Titan survived after the dissipation of the Saturnian subnebula.

In the case, NH_3 vapor pressure would be kept high under the irradiation of the solar UV for a long time. The present atmospheric N_2 of Titan may be generated by photochemical reaction of NH_3 vapor in such a warm proto-atmosphere.

Keywords: Giant icy satellites, Atmosphere, Circum-planetary disks

Japan Geoscience Union Meeting 2014
(28 April - 02 May 2014 at Pacifico YOKOHAMA, Kanagawa, Japan)

PPS01-08 Room:418 Time:April 30 16:30-16:45

The difference of cloud formation process between Jupiter and Saturn.

TAKAHASHI, Yasuto[1*] ; HASHIMOTO, George[2] ; ISHIWATARI, Masaki[1] ; TAKAHASHI, Yoshiyuki[3] ; ONISHI, Masanori[3] ; KURAMOTO, Kiyoshi[1]

[1]Hokkaido Univ, [2]Okayama Univ, [3]Kobe Univ

Gas giant planets have hydrogen-rich, thick atmospheres, and their styles of cloud activities are thought to be closely related to the profile of radiative cooling rate in troposphere. For example, Recent studies indicate that it basically controls the intermittency of cumulonimbus clouds. In spite of its significance, however, no systematic estimate has been made for the radiative cooling profiles of gas giant planets.

Recently, we have developed a 1D radiative-convective equilibrium model for such hydrogen-rich atmospheres. The model atmosphere continues to a lower boundary where the optical depth from the top of atmosphere is sufficiently large and the thermal structure follows convective equilibrium. The atmospheric composition and potential temperature of each planet are given from observational constraints. The mixing ratios of H2O, CH4, NH3, H2S, PH3 and NH4SH follow their saturation vapor pressure in the altitudes where their condensation occurs. Collision induced absorption of H2-H2 and H2-He, and line absorption of H2O, CH4, NH3, H2S, PH3 are included while the extinction by condensates is neglected. Under these settings, our model can calculate a reasonable atmospheric vertical structure by the iteration of radiative transfer calculation and convective adjustment.

For the case of Jupiter, the peak of radiative cooling rate is 1.6e-7 K/sec at 0.7 bar level. Also, our model predicts the radiative-convective boundary i.e., tropopause to be located around 0.3-0.4 bar level, where is slightly higher than the uppermost NH3 condensation layer ˜0.5 bar. For the case of Saturn, the peak of radiative cooling rate is 3.5e-8 K/sec at 0.53 bar, and the separation of tropopause and NH3 cloud layer is larger than that of Jupiter. This implies that the Saturnian NH3 cloud formation is essentially confined in the troposphere, whereas the Jovian one is also affected by the stratospheric processes.

Figure description : Radiative heating rate profile (solid lines, bottom x axis, K/sec) and Volume mixing ratio of NH3 profile (dashed lines, top x axis, mole fraction). Y axis is pressure (bar). Shaded area represents between NH3 condensation level and tropopause level. Red means Jovian model, and blue means Saturnian model. Note that these results are calculated with the polytropic temperature profiles for preliminary calculation, not thermal equilibrium profiles.

Keywords: Jupiter, Saturn, Cloud, Radiative transfer, Convection

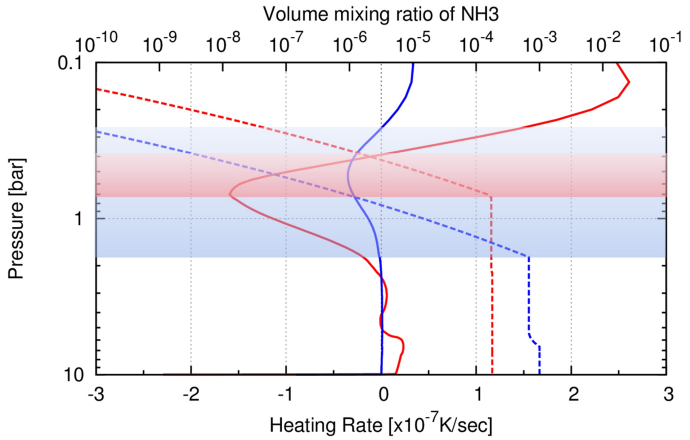

Japan Geoscience Union Meeting 2014
(28 April - 02 May 2014 at Pacifico YOKOHAMA, Kanagawa, Japan)

PPS01-09 Room:418 Time:April 30 16:45-17:00

Near-infrared detections of surprisingly bright Ganymede and Callisto in the Jovian shadow

TSUMURA, Kohji[1*] ; ARIMATSU, Ko[2] ; EGAMI, Eiichi[3] ; HAYANO, Yutakla[4] ; HONDA, Chikatoshi[5] ; KIMURA, Jun[6] ; KURAMOTO, Kiyoshi[7] ; MATSUURA, Shuji[1] ; MINOWA, Yosuke[4] ; NAKAJIMA, Kensuke[8] ; NAKAMOTO, Taishi[9] ; SHIRAHATA, Mai[1] ; SURACE, Jason[10] ; TAKAHASHI, Yasuto[7] ; WADA, Takehiko[1]

[1]Institute of Space and Astronautical Science, Japan Aerospace Exploration Agency, [2]University of Tokyo, [3]Arizona University, [4]Subaru Observatory, Natinal Astronomical Observatory of Japan, [5]The University of Aizu, [6]Earth-Life Science Institute, Tokyo Institute of Technology, [7]Hokkaido University, [8]Kyushu University, [9]Tokyo Institute of Technology, [10]California Institute of Technology

The Galilean satellites (Io, Europa, Ganymede, and Callisto) are expected to be dark when eclipsed by the Jovian shadow. However, we have discovered that Ganymede and Callisto are still surprisingly bright at 1.5 μm even when not directly lit by sunlight, based on observations from the Hubble Space Telescope and the Subaru Telescope. Their eclipsed luminosity was one-millionth of their uneclipsed brightness (i.e. $\sim$50 μJy for Ganymede and $\sim$30 μJy for Callisto in eclipse), which is low enough that this phenomenon has been undiscovered until now. In contrast, Europa in eclipse was not detected ($<$5.5 μJy), a potential clue to the origin of the source of luminosity. Likewise, Ganymede was observed at 3.6 μm by the Spitzer Space Telescope but it was not detected either ($<$3.6 μJy), suggesting a significant wavelength dependence. Why are they luminous even when in the Jovian shadow? These facts may be consistent with sunlight scattered by dust in the Jovian upper atmosphere, and if this is the case, observations of Ganymede and Callisto while eclipsed by the Jovian shadow provide us with a new method to investigate Jupiter's atmospheric composition.

Keywords: Galilean satellite eclipse, Ganymede, Callisto, Europa, Jovian upper atmosphere

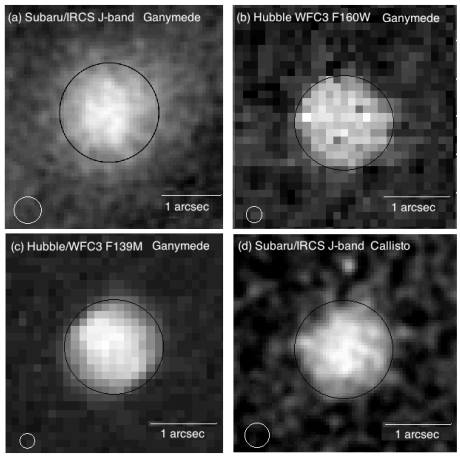

Japan Geoscience Union Meeting 2014
(28 April - 02 May 2014 at Pacifico YOKOHAMA, Kanagawa, Japan)

PPS01-10 Room:418 Time:April 30 17:00-17:15

Simulated radiative forcing by molecules in Jupiter's stratosphere

KURODA, Takeshi[1*] ; MEDVEDEV, Alexander[2] ; HARTOGH, Paul[2]

[1]Tohoku Univ., [2]MPS

We present the radiative heating and cooling rates by molecules for Jupiter's upper troposphere and stratosphere (10^3 to 10^{-3} hPa) with a newly developed parameterization which is suitable for general circulation models. The scheme is a band model based on the correlated *k*-distribution approach, which accounts for the heating due to absorption of solar radiation by CH_4, and cooling in the infrared by C_2H_6, C_2H_2, CH_4 and collision-induced transitions of H_2-H_2 and H_2-He.

The band model achieved the accuracy of within 10% in comparison with the line-by-line calculations. We show the sensitivity of the heating/cooling rates due to variations of the mixing ratios of hydrocarbon molecules calculated with this scheme, in addition to the calculated radiative-convective equilibrium temperature which is in agreement with observations in the equatorial region. Our results suggest that the radiative forcing in the upper stratosphere is much stronger than it was thought before [Conrath et al., 1990]. In particular, the characteristic radiative relaxation time decreases exponentially with height from 10^8 s near the tropopause to 10^5 s in the upper stratosphere.

Keywords: Jupiter, atmospheric radiation, gas giants, JUICE

Japan Geoscience Union Meeting 2014
(28 April - 02 May 2014 at Pacifico YOKOHAMA, Kanagawa, Japan)

PPS01-11 Room:418 Time:April 30 17:15-17:35

EXCEED EUV spectral images of Jupiter and Venus

YOSHIKAWA, Ichiro[1*] ; YOSHIOKA, Kazuo[2] ; MURAKAMI, Go[2] ; TSUCHIYA, Fuminori[3]

[1]University of Tokyo, [2]ISAS, [3]Tohoku University

An earth-orbiting Extreme Ultraviolet (EUV) spectroscopy is the first mission of the Small scientific satellite Platform for Rapid Investigation and Test -A (Sprint-A) conducted by ISAS/JAXA. A single science instrument (EXCEED) is boarded on Sprint-A. We have started to observe the solar planets in the EUV spectral range, and will extend to the identification of extrasolar planet atmosphere.

I will show the first light of the EXCEED and the next.

Keywords: Planetary Airglows, Sprint-A, EUV, plasma, visualization

Japan Geoscience Union Meeting 2014
(28 April - 02 May 2014 at Pacifico YOKOHAMA, Kanagawa, Japan)

PPS01-12 Room:418 Time:April 30 17:35-17:50

Occurrence characteristics of Saturn's short-term radio burst

MARUNO, Daichi[1] ; KASABA, Yasumasa[1*] ; KIMURA, Tomoki[2] ; MORIOKA, Akira[1] ; CECCONI, Baptiste[3]

[1]Tohoku Univ., [2]ISAS/JAXA, [3]Obs. Paris

Saturn kilometric radiation (SKR) is emitted from auroral electrons and suggested to be correlated with Saturn's auroral processes. We extracted northern SKR (N-SKR) and southern SKR (S-SKR) burst events, by newly defined selection criteria, with radio data observed by the Cassini Radio and Plasma Wave Science (RPWS) instrument in the period from day 250 of 2005 to day 200 of 2006. The data was separated into northern and southern components according to its circular polarization degree. As a result, 16 N-SKR burst events and 36 S-SKR burst events were identified in this period. Based on statistical studies of these events, we obtained the following results: (1) We derived typical frequency profiles of N- and S-SKR during SKR bursts to compare the intensity of N- and S-SKR bursts. The profiles show that the S-SKR burst was more intense than the N-SKR by 7 dB in the main frequency range. From the recent studies, the north-south asymmetry could be explained by the difference in solar illumination due to the tilted the magnetic and rotational axis. (2) By comparing onset timings of N- and S-SKR bursts, we found that 67 % of S-SKR burst events were accompanied by N-SKR bursts or burst-like enhancements. (3) To elucidate what determines the timing of SKR burst onsets, we compared the onset timing of N- and S-SKR bursts with each SKR phase of the periodic modulations. The result showed that the timing of SKR burst onsets generally depends on both the N- and S-SKR modulation phases. This suggests the existence of the internal control of SKR burst onsets. It is, however, noted that some SKR bursts occurred out of phases with SKR modulation phases. That indicates the timing of SKR bursts can also be determined by the external process, i.e., solar wind compressions. (4) We investigated the time evolutions of SKR intensities in the main frequency range and the low frequency range before and after SKR bursts. By comparing them with AKR intensity evolutions at AKR breakup, we found that they had two similarities: the enhancement of lower-altitude source regions prior to onsets and the formation of the distinct higher source regions. On the other hand, their timescales are quite different. In addition, this study pointed out that the two-step evolution scenario could not be directly applied to Saturn's case.

In conclusion, our study demonstrated the north-south asymmetry, the conjugacy and the dependence on the SKR periodic modulations of SKR bursts. These results would be helpful for understanding the auroral process at Saturn's magnetotail reconnections by elucidating the relationship between SKR bursts and reconnections. We consider the third result is particularly important because this suggests that both northern and southern periodicities would affect magnetotail reconnections.

Keywords: Saturn, SKR, aurora, Cassini

Japan Geoscience Union Meeting 2014
(28 April - 02 May 2014 at Pacifico YOKOHAMA, Kanagawa, Japan)

PPS01-P01 Room:Poster Time:April 30 18:15-19:30

Submillimeter-Wave Instrument (SWI) for JUICE: Current Status of the Instrumental Development

SAGAWA, Hideo[1*] ; KASAI, Yasuko[1] ; KIKUCHI, Kenichi[1] ; NISHIBORI, Toshiyuki[2] ; MANABE, Takeshi[3] ; OCHIAI, Satoshi[1] ; KURODA, Takeshi[4] ; SEKINE, Yasuhito[5] ; HARTOGH, Paul[6]

[1]National Institute of Information and Communications Technology (NICT), [2]Japan Aerospace Exploration Agency, [3]Osaka Prefecture University, [4]Tohoku University, [5]University of Tokyo, [6]Max Planck Institute for Solar System Research

The Submillimetre-Wave Instrument (SWI) is a passive submillimeter-wave heterodyne instrument proposed as one of the scientific payload instruments for the Jupiter Icy Moons Explorer (JUICE) mission. It measures the thermal emission from atmosphere of Jupiter and its moons at the frequency region of 500 - 600 GHz (with keeping 1200 GHz range as an optional concept). Thermal emission from the surface of moons will also be measured. JUICE/SWI provides unique observational data for characterization of the Jovian stratosphere such as thermal structure, dynamics, and distribution of minor species; and for exploration of tenuous-atmosphere and surface environment of the Jovian moons. By detecting hydrogen and oxygen isotopes in the water vapor of Jovian moons' atmosphere, SWI can also contribute to understanding the origin and distribution of water in our solar system.

This paper presents the current status of the development of SWI instrument, including the updates on the science targets and their feasibility studies. The SWI instrument is being developed through international cooperation. The Japanese team contributes to the development of the submillimeter reflector (mirror). The submillimeter reflector is one of the key components of SWI, and it determines the spatial resolution of observations. Currently a 30-cm aperture diameter reflector is considered, providing a spatial resolution of 2 mrad (FWHM) at 600 GHz. In order to fulfill the stringent requirement of weight reduction, we evaluated the material of the reflector and optimized its rib structure. The side lobe suppression is also an important factor to improve the quality of observations.

Keywords: Jupiter, Icy moon, JUICE, Submillimeter wave, Heterodyne

Japan Geoscience Union Meeting 2014
(28 April - 02 May 2014 at Pacifico YOKOHAMA, Kanagawa, Japan)

PPS01-P02 Room:Poster Time:April 30 18:15-19:30

Development of JUICE/Ganymede Laser Altimeter (GALA)

NAMIKI, Noriyuki[1] ; KIMURA, Jun[2*] ; KOBAYASHI, Masanori[1] ; HUSSMANN, Hauke[3] ; LINGENAUBER, Kay[3] ; TEAM, Gala-japan[4]

[1]PERC/Chitech, [2]Earth-Life Science Institute, Tokyo institute of Technology, [3]DLR Institute of Planetary Research, [4]JUICE Japan Group

The overarching theme for JUICE is: The emergence of habitable worlds around gas giants, and the focus is to characterise the conditions that may have led to the emergence of habitable environments among the Jovian icy satellites, with special emphasis on the three oceanbearing worlds, Ganymede, Europa, and Callisto. JUICE will be launched in 2022, and will arrive at Jupiter in 2030. After several fly-bys to Europa and Callisto, JUICE will be inserted into an orbit around Ganymede in 2032 and will continue scientific observations for eight months until the end of nominal mission in 2033. Ganymede Laser Altimeter, GALA, measures distance between the spacecraft and the surface of the satellite from time of flight of a laser pulse. Together with positions of the spacecraft and mass center of the satellite, surface topography of the satellite is calculated from measured distances. The GALA data are particularly important for finding of internal ocean.

1) if the ocean exists beneath icy crust, tidal deformation of the satellite is so large that temporal variation of the topography as great as a few tens meter shall be detected.

2) small eccentricity of orbit of Ganymede causes libration that will be observed as lateral shifts of footprint of laser beam at the surface.

3) improved determination of spacecraft orbits by cross over analysis results in precise estimate of low degree harmonics of gravity field. Thus accurate Love number will be calculated to infer internal density structure of the satellite.

Global topographic data derived by GALA are also important for the study of tectonic history at the surface, elastic and viscous structure of ice crust, and thermal evolution of interior of the icy satellite. For example, linear structures such as ridges and grabens reveal extension stresses due to past variation of thermal states. As well, flat surface and thin crust may indicate partial melting of the crust and consequent internal lake. These observations on various geologic activities lead to understanding of transport of heat and materials from interior to the surface. Further, a comparison of styles of tectonics of ice crust and that of silicate lithosphere will likely shed a new light on the theory of plate tectonics of the Earth.

GALA is developed by international collaboration of scientists and engineers in Germany, Switzerland, and Japan. Its conceptual design is based on the laser altimeter on board of Mercury orbiter, BepiColombo, and consists of transceiver unit (TRU) with laser optics and appropriate electronics, electronic unit (ELU) with digital range finder module, digital processing module and power converter module, and laser electronic unit (LEU) with laser control electronics. Japanese team provides receiver telescope, backend optics, detector, and analogue electronics of TRU. The transmission optics of TRU and entire LEU are developed at DLR in Germany, and ELU is developed at Bern University in Switzerland. Assembly and integration are conducted at DLR under a supervision of the principal investigator of GALA. We therefore need to pay special caution on interfaces between analogue electronics and range finder, low-temperature environment, and radiation environment that Japanese space scientists have never experienced before.

Keywords: Jupiter, Ganymede, Laser Altimeter, Exploration, Spacecraft, Habitability

Japan Geoscience Union Meeting 2014
(28 April - 02 May 2014 at Pacifico YOKOHAMA, Kanagawa, Japan)

PPS01-P03 Room:Poster Time:April 30 18:15-19:30

Accretion of Solid Materials onto Circumplanetary Disks from Protoplanetary Disks

TANIGAWA, Takayuki[1*] ; MARUTA, Akito[2] ; MACHIDA, Masahiro[2]

[1]ILTS, Hokkaido University, [2]Kyushu University

We investigate accretion of solid materials onto circumplanetary disks from heliocentric orbits rotating in protoplanetary disks, which is a key process for the formation of regular satellite systems. In the late stage of gas-capturing phase of giant planet formation, the accreting gas from protoplanetary disks forms circumplanetary disks. Since the accretion flow toward the circumplanetary disks affects the particle motion through gas drag force, we use hydrodynamic simulation data for the gas drag term to calculate the motion of solid materials. We consider wide range of size for the solid particles (10^{-2}-10^{6}m), and find that the accretion efficiency of the solid particles peaks around 10m-sized particles because energy dissipation of drag with circumplanetary disk gas in this size regime is most effective. The efficiency for particles larger than 10m size becomes lower because gas drag becomes less effective. For particles smaller than 10m, the efficiency is lower because the particles are strongly coupled with the back-ground gas flow, which prevent particles from accretion. We also find that the distance from the planet where the particles are captured by the circumplanetary disks is in a narrow range and well described as a function of the particle size.

Keywords: satellite formation, circumplanetary disks

Japan Geoscience Union Meeting 2014
(28 April - 02 May 2014 at Pacifico YOKOHAMA, Kanagawa, Japan)

PPS02-01 Room:418 Time:April 28 09:00-09:25

Hydrogen Isotope Ratio and Thickness of Martian Ground Ice: Implication from Multi-Water-Reservoir Model

KUROKAWA, Hiroyuki[1*] ; USUI, Tomohiro[2] ; DEMURA, Hirohide[3] ; SATO, Masahiko[4]

[1]Nagoya University, [2]Tokyo Institute of Technology, [3]University of Aizu, [4]Kyushu University

Martian surface ice is currently observed only as polar layered deposits (PLDs), whereas Mars Odyssey Gamma Ray Spectrometer (Boynton et al., 2002; Boynton et al., 2007) and Mars Express radar sounder observations (Mouginot et al., 2012) propose the presence of much larger amount of ground ice in the mid- to high-latitudes. The total volume of PLDs is 20-30 m in Global Equivalent Depth (Zuber et al., 1998; Plaut et al., 2007). Ground-ice region is expected to spread over a few tenths of percent of the total Martian surface, yet the thickness (i.e. volume) is poorly constrained (Mouginot et al., 2012).

The thickness of the ground ice is related to the evolution history of the Martian water reservoirs. After ancient oceans became extinct (˜4Ga), the oceanic water would become ”surface ice”, which currently occur as PLDs, and ”ground ice” which would extend from high latitude to mid- or low-latitude. Atmospheric escape of hydrogen and oxygen through the Martian history causes decrease of the amount of the ice. The signature of the evolution history is recorded by hydrogen isotope ratio (D/H). Martin atmosphere and soil have D/H ratio of ˜6 (relative to SMOW) (Owen et al., 1988; Webster et al., 2013), which is higher than the Martian primitive D/H ratio of ˜1.3 (Usui et al., 2012).

We constrain the hydrogen isotope ratio of surface ice and ground ice, and estimate the thickness of ground ice, using a multi-water-reservoir box model (see figure shown below). The model solves the evolution of water inventories and D/H ratio of atmosphere, surface ice, and ground ice during the ice age. Atmospheric escape and sublimation are considered as D/H fractionation processes. We adapt our model to the Matian ice age (4Ga to present). The initial D/H ratio is that of ancient ocean, which is informed by D/H data of the Martian meteorite ALH84001 formed at ˜4.1Ga (Lapen et al., 2010): D/H = 2.2-4.0 (relative to SMOW) (Boctor et al., 2003,Greenwood et al., 2008).

First, we show the results from two water-reservoir box model (ice and atmosphere). The ratio of atmospheric D/H and ice D/H is in a quasi-equilibrium state of the fractionation caused by atmospheric escape and sublimation. The ratio of the present Mars is mainly determined by the fractionation caused by sublimation.

Second, we show the results from four water-reservoir box model (surface ice, ground ice, high-latitude atmosphere, and mid- to high-latitude atmosphere). Assuming the atmospheric condition of the present Mars, the mixing of two atmospheric reservoir is inefficient in D/H exchange between surface ice and ground ice, which results in the independent growth of D/H ratio of the surface ice and the ground ice. To fractionate the D/H ratio of the surface ice and the ground ice into ˜6, the thickness of active ground ice which can exchange water with atmosphere is constrained. Thin active ice causes high deuterium concentration. The required thickness is a few hundred meters, which is distinctly large value compared to the thickness that HDO diffusion works (˜10 m in 1 Gyrs). Nature of this active ground ice might be partially melted ice suggested by recent observations of recurring slope lineae (McEwen et al., 2014), hydrated clathrates in underground cryosphere, or breathing porous permafrosts.

Keywords: ground ice, hydrogen isotope ratio, atmospheric escape

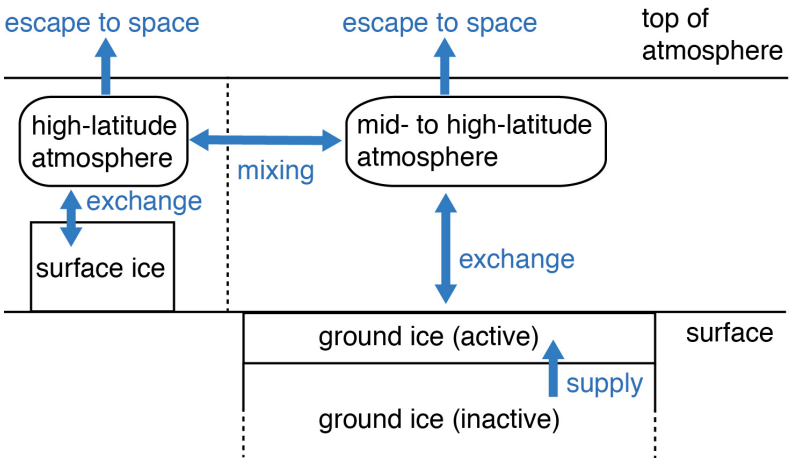

Japan Geoscience Union Meeting 2014
(28 April - 02 May 2014 at Pacifico YOKOHAMA, Kanagawa, Japan)

PPS02-02 Room:418 Time:April 28 09:25-09:50

New evidence for plate tectonism on Mars: Accreted Terrains

DOHM, James[1*] ; MARUYAMA, Shigenori[1]

[1]Earth-Life Science Institute, Tokyo Institute of Technology

Reported evidence for plate tectonism has included spatial association among magnetic anomalies, large (thousands of kilometers long) structures, and highly degraded promontories interpreted to be andesitic domes, thrust faults, folds, structurally-controlled basins, large mountain ranges, and topographic and crustal-thickness-model signatures of structural control (including plate movement) within and along the margin of the northern plains. Significant evidence for an ancient phase of plate tectonism on Mars, newly identified, is accretionary complexes, informed through Earth analogs exquisitely detailed here in Japan. This finding represents a new frontier in the geologic investigation of Mars, bringing greater attention to pre-Tharsis (˜>4.0 Ga) terrains, which record Earth-like conditions. Pre-Tharsis, Earth-like conditions include an active dynamo and plate tectonism, as well as Habitable-Trinity conditions?an ocean, relatively thick atmosphere, and primordial crustal materials enriched in phosphorous, iron, among other elements important to life, all of which interact due to hydrological cycling driven by the Sun. Accreted terrains, which mark major crustal shortening through subduction of oceanic crustal materials and associated accumulation of andesites and granites, could comprise rock records on Mars dating back more than 4.2 Ga. Considering planetary evolution of Mars, largely informed through our understanding of the evolution of Earth, the accretionary complexes are likely to record environmental conditions during a time range of several hundred million years, which includes possible fossil life if initiated and evolved during the extremely ancient (>4.0 Ga) Habitable-Trinity conditions. A prime example of an extremely ancient accretionary complex is located to the west of Claritas rise, southwest margin of the Tharsis superplume. At the meeting we will present evidence of a Martian accretionary complex and discuss the implications of such a significant finding, including highlighting the next phase of geologic investigation of the evolution of Mars and its bearing on Astrobiology.

Keywords: Plate tectonics, accretional complex, OPS

Japan Geoscience Union Meeting 2014
(28 April - 02 May 2014 at Pacifico YOKOHAMA, Kanagawa, Japan)

PPS02-03 Room:418 Time:April 28 09:50-10:15

Environmental monitoring camera system for the Martian aerosols and water vapor for the Japanese Mars rover, MELOS

MANAGO, Naohiro[1*] ; NOGUCHI, Katsuyuki[2] ; OGOHARA, Kazunori[3] ; SUZUKI, Makoto[4] ; HASHIMOTO, George[5]

[1]Chiba University, [2]Nara Women's University, [3]University of Shiga Prefecture, [4]Japan Aerospace Exploration Agency, [5]Okayama University

We propose the environmental monitoring camera system of aerosols and water vapor in the Martian atmosphere for the Japanese Mars rover, MELOS. The meteorology and the climate of Mars are strongly controlled by the aerosols, which consists of dust and clouds in the Martian atmosphere, and the better understanding of the basic parameters such as optical depth, radius distribution and composition of the aerosols enables us to describe the effect on the Martian meteorology and climate quantitatively. The water vapor also affects the Martian meteorology and climate through the infrared radiation and the generation of clouds. The MELOS aims at the search for life, and it needs the basic knowledge of the meteorology and climate at the landing site for detailed discussion. Therefore we should conduct the measurements of aerosols and water vapor at the MELOS landing site simultaneously.

To satisfy the requirement of monitoring the aerosols and water vapor in the MELOS rover mission, we propose a three-CMOS-camera system, which consists of a direct sunlight camera, a scattering light camera and a high-resolution color camera. The direct sunlight camera has four wavelength band (340 or 450nm and 550nm for aerosols and 870 and 940nm for water vapor). The scattering light camera also has the same wavelength band, but it is directed at the neighborhood of the sun and at several points along the great circle including the sun and is utilized for aerosol measurements. The arrangement proposed here basically follows the previous Mars missions, e.g., Viking lander, Mars Pathfinder and Mars Exploration Rover. The high-resolution color camera obtains pseudo color pictures around the rover and is intended to support the navigation for the life search experiment.

Keywords: MELOS rover mission, Martian atmosphere

Japan Geoscience Union Meeting 2014
(28 April - 02 May 2014 at Pacifico YOKOHAMA, Kanagawa, Japan)

PPS02-04 Room:418 Time:April 28 10:15-10:30

Examination of Mission Scenario and Spacecraft System to Study Martian Atmospheric Escape

MATSUOKA, Ayako[1*] ; SEKI, Kanako[2] ; TERADA, Naoki[3] ; YOKOTA, Shoichiro[1] ; YAMAZAKI, Atsushi[1] ; KAWAKATSU, Yasuhiro[1] ; ABE, Takumi[1] ; FUTAANA, Yoshifumi[4] ; HIRAHARA, Masafumi[2] ; IMAMURA, Takeshi[1] ; ISHISAKA, Keigo[5] ; KUMAMOTO, Atsushi[3] ; KURIHARA, Junichi[6] ; NAKAGAWA, Hiromu[3] ; OGURA, Satoshi[1] ; SAKANOI, Takeshi[7] ; TAGUCHI, Makoto[8] ; YAGITANI, Satoshi[9]

[1]ISAS/JAXA, [2]STEL, Nagoya Univ., [3]Dept. Geophys., Grad. Sch. Sci., Tohoku Univ., [4]IRF, Sweden, [5]Toyama Pref. Univ., [6]Planet. Plasma Atmos. Res. Cent., Tohoku Univ., [7]Cosmosciences, Hokkaido Univ., [8]Rikkyo Univ., [9]Kanazawa Univ.

The atmospheric escape from Mars is considered to be closely associated with the evolution of the Martian atmosphere as well as the existence of the water on Mars. We are now investigating a project to study the global feature and the physical process of the atmospheric escape from Mars. It is expected to consist of at least two orbiters; one of the orbiters is aimed to make in-situ observation of plasma and thin atmosphere at about 100 km altitude, and the other is for the atmospheric imaging and solar-wind monitor. We are planning to make simultaneous observation of the atmospheric escape by the interaction with the solar wind by both of in-situ measurement orbiter and remote-sensing one. Now we are examining the quantitative measurement targets to fully understand the Martian atmospheric escape. At the same time, the sorts and performance of scientific instruments on these orbiters are examined. And furthermore, the preliminary spacecraft design, orbit design and mission plan to achieve the scientific goal are investigated.

Japan Geoscience Union Meeting 2014
(28 April - 02 May 2014 at Pacifico YOKOHAMA, Kanagawa, Japan)

PPS02-05 Room:418 Time:April 28 10:30-10:45

Development of a dust imager for Mars landing mission

SATOH, Takehiko[1*] ; OGOHARA, Kazunori[2] ; HASHIMOTO, George[3] ; MIURA, Kazuhiko[4] ; MANO, Takaaki[5]

[1]Japan Aerospace Exploration Agency, [2]University of Shiga Prefecture, [3]Okayama University, [4]Tokyo University of Science, [5]National Institute for Materials Science

We report progress in developing a dust imager for future Mars landing missions. As Martian dust is a key element of its environment and a potential hazard for human exploration, it is essential to know what is Martian dust and how it works. However, little is known about the Martian dust due primarily to lack of measurements. Direct imaging would greatly increase our knowledge about the Martian dust (previously, an Atomic-Force Microscope onboard Phoenix acquired just one image).

The dust imager under development is not a microscope but a ”bare” imaging sensor of which pixels are fine pitched. After exposing the sensor to the air with dust for a while, we illuminate the sensor with a parallel beam so that shadows of particles on the sensor are directly imaged. In this way, the imager does not need a focusing mechanism and is expected to be very light-weighted and robust. Although the status is still the laboratory-experiment level, this small tool would greatly contribute to the Mars science and exploration.

Keywords: Mars, dust, imager, landing, mission

Japan Geoscience Union Meeting 2014
(28 April - 02 May 2014 at Pacifico YOKOHAMA, Kanagawa, Japan)

PPS02-06 Room:418 Time:April 28 11:00-11:25

Life Detection Microscope: Search for Microbes on the Mars Surface with a Fluorescent Microscope

YAMAGISHI, Akihiko[1*] ; SATOH, Takehiko[2] ; ENYA, Keigo[2] ; MIYAKAWA, Atsuo[1] ; SASAKI, Satoshi[3] ; YOSHIMURA, Yoshitaka[4] ; HONDA, Hajime[5] ; DEMURA, Hirohide[6] ; IMAI, Eiichi[5] ; USUI, Tomohiro[7] ; FUJITA, Kazuhisa[8] ; ISHIGAMI, Genya[9] ; OZAWA, Takashi[8] ; OHNO, Sohsuke[10] ; SASAKI, Sho[11] ; MIYAMOTO, Hideaki[12]

[1]Tokyo University of Pharmacy and Life Sciences, [2]ISAS/JAXA, [3]Tokyo University of Technology, [4]Tamagawa University, [5]Nagaoka Univ. Tech., [6]The University of Aizu, [7]Tokyo Institute of Technology, [8]JAXA, [9]Keio University, [10]Chiba Institute of Technology, [11]Osaka University, [12]The University of Tokyo

Past trial of direct detection of life on Mars by 1970's Viking mission reported a negative conclu-sion, whereas numbers of circumstances provided by recent Mars exploration missions in the last dec-ade indicate that there are good reasons to perform another life detection program.

Here we propose Life Detection Microscope that has much higher sensitivity than the instrument onboard Viking. Indeed Life Detection Microscope (LDM) that we propose here could detect less than 104 cells in 1 gram clay. Our life detecting instru-ment has the sensitivity that is three orders of mag-nitude higher than the one onboard Viking that issued the negative conclusion. LDM is capable of identifying what we think to be the most fundamen-tal features that a cell should possess to constitute life.

Our Investigation Goals are:

1: High-resolution characterization of regolith and dust particles.

2: Search for any type of organic compounds in Mars surface samples. The compounds include cells, other biological materials, and abiotic polycyclic aromatic hydrocarbon (PAH).

3: Identify cell-like structure in which organic compounds are enveloped by membrane, which may represent Martian life.

Keywords: Mars, Life search, Fluorescence microscope, Microbe, Organic compounds

Japan Geoscience Union Meeting 2014
(28 April - 02 May 2014 at Pacifico YOKOHAMA, Kanagawa, Japan)

PPS02-07 Room:418 Time:April 28 11:25-11:40

Landing-site candidates for the Life Detection Microscope instrument

MIYAMOTO, Hideaki[1*] ; USUI, Tomohiro[2] ; KOMATSU, Goro[3] ; DOHM, James[2] ; NIIHARA, Takafumi[4] ; OGUMA, Midori[1] ; SATOH, Takehiko[5] ; YAMAGISHI, Akihiko[6]

[1]University of Tokyo, [2]TiTech, [3]IRSPS, [4]National Institute of Polar Research, [5]ISAS, [6]Tokyo University of Pharmacy and Life Science

Mars explorations of past decades indicate that ancient Mars had environment somehow similar to that of Earth. Existence of large bodies of water, chemical building blocks of life, a wide range of oxidation states, and a magnetic field indicate that Mars would have been habitable. Recent studies of microbes in extreme environments show that some terrestrial microbes have possibilities for surviving and proliferating under the current martian environment, if these are placed in some specific conditions such as with sufficient shield from UV light (attained only at more than several centimeters below the surface) and with the existence of gradients of free energy. Such environmental conditions likely exist at some specific locations even the present Mars. For this reason, we are developing a new instrument called LDM (Life Detection Microscope), which is designed to detect less than 10^4 cells in 1 gram clay, orders of magnitude higher than previous attempts performed by Viking landers. To maximize the chances of the detection of organisms, the landing sites should be carefully selected in terms of the possibility of the existence of near-surface water, as well as recent geological activities and release of volatiles. Traces of possible liquid water flow have been reported at a number of locations including those recognized as the recurring slope lineae, seasonal flows on slopes of several craters, and anastomosing slope streaks. These are proposed to be the result of small and continuous seeps of subsurface brine water, which could persist for a longer period providing a habitable environment. In this talk, we examine the morphologic characteristics of these features and discuss their origins in the line of geological contexts for selecting appropriate landing sites for the LDM instrument.

Keywords: Mars, extraterrestrial life, life detection microscope, landing site, water

Japan Geoscience Union Meeting 2014
(28 April - 02 May 2014 at Pacifico YOKOHAMA, Kanagawa, Japan)

PPS02-P01 Room:Poster Time:April 28 18:15-19:30

Interannual analyses of the meridional distributions of Martian dust and clouds obtained by MRO-MCS

NOGUCHI, Katsuyuki[1*] ; IMAE, Kaori[1] ; KAWANISHI, Mai[1]

[1]Nara Women's University

We investigated the interannual variability of the meridional distributions of dust and clouds in the Martian atmosphere by using Mars Reconnaissance Orbiter Mars Climate Sounder (MRO-MCS) measurements. As the previous analyses did not consider measurement errors to depict the zonal averages, we took a criterion of 10% for the measurement error. Results show that Mars Year (MY) 29, which is regarded as a standard year in the previous analyses, had an enhancement of dust in the high altitudes (above 10 Pa) in the tropical region, and such an enhancement was not found in other MYs (28, 30 and 31). On the other hand, the distribution of ice clouds in MY 29 roughly agreed with other MYs' distribution.

Japan Geoscience Union Meeting 2014
(28 April - 02 May 2014 at Pacifico YOKOHAMA, Kanagawa, Japan)

PPS02-P02 Room:Poster Time:April 28 18:15-19:30

Implementing Martian dust lifting scheme into DCPAM, and a diagnosis experiment of surface dust flux

OGIHARA, Hirotaka[1*] ; TAKAHASHI, Yoshiyuki O.[2] ; ISHIWATARI, Masaki[1] ; ODAKA, Masatsugu[1] ; HAYASHI, Yoshiyuki[3]

[1]Department of Cosmosciences, Graduate school of Science, Hokkaido University, [2]Graduate School of Science, Kobe University, [3]Department of Earth and Planetary Sciences, Graduate School of Science, Kobe University

The Martian dust cycle influences thermal states of its atmosphere, hence it plays an important role for determining states of the Martian atmosphere(Gierasch and Goody, 1968). Dust processes to be considered are dust lifting, turbulent mixing, advection, and gravitational sedimentation. Parameterizations of lifting by model resolved wind stress and by model unresolved vortices such as dust devils are considered. The Martian dust cycle has been simulated with general circulation models implemented above dust process schemes by some research groups. For example, Kahre et al.(2006) roughly simulated a seasonal variation of dust loading. The seasonal variation of dust loading has a peak in during northern autumn and winter. In contrast, DCPAM (Takahashi et al., 2012), which is a general circulation model developed by our group, has not been implemented above dust process schemes. Aims of this study are to implement dust process schemes into DCPAM, and to perform numerical experiments on the dust cycle with it. In the future, we will consider about interannual variability of the Martian dust distribution, which still has not been reproduced. In this work, we implement dust lifting scheme by model resolved wind stress into DCPAM. Addtionally, we perform an experiment with dust lifting to investigate behavior of this dust lifting scheme. And, we compare our model's results with thoses of Kahre et al.(2006).

The model utilized is DCPAM which is developed by GFD Dennou Club. DCPAM adopted three dimensions primitive equations. A radiative scheme by Takahashi et al.(2003, 2006) is used. This include the radiative effects of gaseous CO_2 and suspended dust. And, used suspended dust distribution is spatially and temporally fixed. A turbulent process is estimated by used vertical diffusivity based on Mellor and Yamada(1974). A surface process is estimated based on Louis et al.(1982). Each parameter are selected as Martian values. We use a surface distribution of thermal inertia, albedo and topography observed by Mars Grobal Surveyor. A horizontal discretization is the spectral method, and the trauncation wavenumber is 21. A vertical discretization is the finite difference method, and the number of layor is 32. We integrate 3 Mars year, and use the last 1 Mars year for analysis.

First, we implement a dust lifting scheme called by KMH scheme(Kahre et al., 2006) into DCPAM. Then, we perform a diagnosis experiment of surface dust flux with this. This result is similar to result by Kahre et al.(2006) as follows. In regions around latitude 50N degree and 30S degree, strongly dust lifting occurs during northern autumn and winter. At latitude 50N degree, it appears that eastward waves, which have zonal wavenumber 1 and period 6 Mars days, contribute to dust lifting. it is to be considered the baroclinic wave(Briggs et al., 1979). At latitude 30S degree, it appears that westward waves, which have zonal wavenumber 1 and period 1 Mars days, contribute to dust lifting. It is to be considered the diurnal thermal tidal wave(Joshi et al., 1979), and dust lifting tends to occur at 16 o'clock local time. These results qualitatively are consistent with these of Kahre et al. (2006), but are not quantitatively consistent with these of Kahre et al.(2006). For example, our model's surface dust flux is greater by a degree of magnitude then these of Kahre et al.(2006) in the northen polar cap. The reason is probably that the number of vertical levels and the method for estimating turbulent mixing are diffrent from those of Kahre et al.(2006). In this work, we implemented dust lifting scheme by model resolved wind into DCPAM. We are now implementing dust lifting scheme by dust devils into DCPAM. Then, we are going to implement advective scheme and gravitational sedimentation scheme into DCPAM in turn, and perform numerical experiments for their implementation test.

Keywords: Dust, Mars, General Circulation Model

Japan Geoscience Union Meeting 2014
(28 April - 02 May 2014 at Pacifico YOKOHAMA, Kanagawa, Japan)

PPS02-P03 Room:Poster Time:April 28 18:15-19:30

Assessment of Mars surface environment for MELOS1 lander using Planetary General circulation model DCPAM

ODAKA, Masatsugu[1*] ; SUGIYAMA, Ko-ichiro[2] ; TAKAHASHI, Yoshiyuki O.[3] ; NISHIZAWA, Seiya[4] ; HAYASHI, Yoshiyuki[5] ; HASHIMOTO, George[6]

[1]Department of Cosmosciences, Hokkaido University, [2]Institute of Space and Astronautical Science, Japan Aerospace Exploration Agency, [3]Center for Planetary Science, [4]RIKEN Advanced Institute for Computational Science, [5]Department of Earth and Planetary Sciences, Graduate School of Science, Kobe University, [6]Department of Earth Sciences, Okayama University

1. Introduction

The Mars exploration program MELOS1, which is to mainly challenge life and surface environment exploration, is now planning by space engineering and planetary science community in Japan. To support designing the landing module and observation instruments and ensure safety experiments during entry, decent and landing phase, plausible range of meteorological conditions at MELOS1 landing site is required.

We try to assess the Mars surface environment from planetary to atmospheric boundary layer scale by using simulation results obtained by General Circulation Model (GCM), Regional Meteorological model, and Large Eddy Simulation (LES) model (LES). For mesoscale assessment, CReSS which is developed by HyArc Nagoya University will be used. For boundary layer scale, SCALE-LES which is developed by RIKEN AICS will be used as LES model. Both numerical model are now tuned to Mars and preliminary experiments are performed (Sugiyama et al. 2013; Nishizawa et al. 2013). For planetary scale assessment, we use a planetary atmospheric general circulation model DCPAM which is developed by GFD Dennou Club (Takahashi et al. 2012). In this study, we compare simulation results of DCPAM to observation results of Viking and Mars Path Finder (MPF) and investigate proper method for assessment of Mars surface environment by using DCPAM data. By using this method, we show some assessment results at proposed landing sites of MELOS1.

2. Data

DCPAM is a spectral GCM including physical processes appropriate for Martian atmosphere. The topography, surface albedo and thermal inertia in the model is based on observation results obtained by Mars Global Surveyor (MGS). The horizontal truncation wave number is 31, which corresponding horizontal resolution is about 200 km. The number of vertical layer is 16 and the height of lowest level is about 3 m. The seasonal variation of atmospheric dust distribution is given which is based on typical case of MGS observation. Numerical integration is performed for 7 Mars years with isothermal no motion initial condition. The data of last two years are used for analysis. The proposed landing sites are Newton Crater, Nili Fossae, and Isidis Planitia. The period of analysis is 90 sols from Ls = 331, 324, 14, and 135 which are corresponding to four mission window. In each period, diurnal variations every 15 sols are investigated.

3. Methods of analysis and results

In comparing the DCPAM results to observation results of Viking and MPF, the atmospheric temperature and wind velocity at observed altitude are estimated assuming the boundary layer similarity theory in neutral case is valid near the model surface. The surface pressure at actual altitude is estimated assuming hydrostatic balance with constant scale height which is calculated by the using model temperature. The comparison between estimated values from DCPAM results and observations show that the observed diurnal variation of atmospheric temperature is well reproduced by using 2nd level (about 12.5 m height) temperature of DCPAM, and seasonal variation of surface pressure is almost represented by using the scale hight corresponding to 10th level (about 1.35 km height) model temperature and subtracting offset value (60 Pa).

Based on above results, analysis of the DCPAM data at the three proposed landing site during four mission periods are performed. At Newton Crater, which is the first proposed site, during 90 sols from Ls = 331, the diurnal mean atmospheric temperature ranges from 190 to 220 K. The amplitude of diurnal change of atmospheric temperature is about 50 - 70 K. The air temperature is almost constant during this period and its value is about 140 K. The maximum values of direct and diffuse solar radiative flux are 480 Wm^{-2} and 40 Wm^{-2}, respectively. We will also estimate the extent of variation of meteorological variables, such as temperature and pressure, at the proposed landing sites by analyzing DCPAM data with different dust distribution.

PPS02-P03 Room:Poster Time:April 28 18:15-19:30

Keywords: Exploration of Mars, General Circulation Model, Surface environment of Mars

Japan Geoscience Union Meeting 2014
(28 April - 02 May 2014 at Pacifico YOKOHAMA, Kanagawa, Japan)

PPS02-P04 Room:Poster Time:April 28 18:15-19:30

Estimation of Martian atmospheric composition change caused by CO2 condensation and its application to radio occultation

IKEDA, Sayaka[1*] ; NOGUCHI, Katsuyuki[1] ; KURODA, Takeshi[2] ; PAETZOLD, Martin[3]

[1]Nara Women's University, [2]Tohoku University, [3]University of Cologne

We estimated the Martian atmospheric composition change caused by CO_2 condensation using the Ar measurements obtained by Gamma Ray Spectrometer (GRS) onboard the 2001 Mars Odyssey. We applied this estimation of the composition change to the rederivation of the radio occultation (RO) measurements of Mars Global Surveyor (MGS) obtained at polar latitudes of the winter hemisphere, because the MGS RO standard product which is available to the public did not consider the atmospheric composition change by CO_2 condensation. Using the rederived MGS RO measurements, we investigated the occurrence of CO_2 supersaturation in the Martian polar winter atmosphere and found that there were more supersaturation in the rederived data than in the original data.

Keywords: Mars, CO2, supersaturation, condensation, radio occultation

Japan Geoscience Union Meeting 2014
(28 April - 02 May 2014 at Pacifico YOKOHAMA, Kanagawa, Japan)

PPS02-P05 Room:Poster Time:April 28 18:15-19:30

Equation of state of $(Fe,Ni)_3S$ phase - Implications for Mars internal structure

AKAGI, Shunsuke[1] ; SAKAI, Takeshi[1*] ; HIRAO, Naohisa[2]

[1]Geodynamics Research Center, Ehime University, [2]Japan Synchrotron Radiation Research Institute

The existence of lower mantle ($MgSiO_3$-perovskite layer) has an important role on Mars thermal evolution. The layer thickness of Mars lower mantle depends on the depth of the core-mantle boundary (CMB). The depth of CMB is related to the Mars core density. Although the structure model of Mars core was discussed based on the equation of state of pure iron and FeS (e.g., Urakawa et al., 2004), Fe_3S phase and also the effect of nickel on the density should be considered.

We newly established the equation of state (EoS) of $(Fe_{0.89},Ni_{0.11})_3S$ up to about 40 GPa by high pressure experiment using diamond anvil cell. Considering EoSs of γ-Fe (Tsujino et al., 2013), γ-FeNi (Tsujino, 2012), Fe_3S (Seagle et al., 2006), and $(Fe_{0.89},Ni_{0.11})_3S$, the effects of nickel and sulfur on the density was determined. Then, we determined the Mars core density corresponding to the composition model based on SNC meteorites. Our new model shows relatively thin lower mantle compare to previous one. Moreover, if Mars core contains 16 wt.%S and 7 wt.%Ni (Sanloup et al., 1999) and if Mars has an entirely liquid core (Fei and Bertka, 2005), there is a possibility of disappearance of Mars lower mantle.

Keywords: Mars core, equation of state, Mars lower mantle

Japan Geoscience Union Meeting 2014
(28 April - 02 May 2014 at Pacifico YOKOHAMA, Kanagawa, Japan)

PPS03-01 Room:424 Time:April 29 09:00-09:15

About drift, oscillations and steps of the center of mass of the Moon

BARKIN, Yury[1*] ; HANADA, Hideo[2]

[1]Sternberg Astronomical Institute, Moscow, Russia, [2]National Astronomical Observatory of Japan, Mizusawa, Japan

We have previously predicted and studied a step (abrupt) shift of the center of mass of the Earth in 1997 - 1998 years relatively to the mantle (Zotov, Barkin, Lubushin, 2009). In accordance with the basic provisions of the geodynamic model of excitation of planets and satellites shells (Barkin, 2002) we expected and we expect similar displacements of the centers of mass for other bodies in the solar system (for Mercury, Moon, Sun, Titan, Mars, etc.). Moreover, according to our hypothesis these abrupt geodynamic phenomena for solar system bodies are synchronous (Barkin, 2000) and, in particular, it should appear in 1997-1998. On the Earth, the similar jumps in 1997-1998 were observed in almost all planetary processes (Barkin, 2009). In the case of the Moon similar jump of center of mass obtains a confirmation in the data of laser observations and accounts for a specified period of time 1997-1998.

The jump (step) in the center of mass of the Moon in 1997 on data of laser ranging of reflectors on the lunar surface. On the basis of current laser measurements of distances to reflectors mounted on the Moon the preliminary estimates of the parameters of drift, oscillations and jump of the center of mass of the Moon were obtained. Their dynamic interpretation on the base of a geodynamic model of forced relative oscillations of the shells of planets and satellites has been done (Barkin, 2002). In the paper of G.A. Krasinskii (2003) from the analysis of lunar laser range measurements (or rather their residual differences compared with the theoretical celestial-mechanical design values of ranges) an abrupt (step) changes (in 1997 - 1998) in the coordinates of reflectors on the very substantial distances of about 15 -25 cm in selenographic coordinate system of the epoch have been discovered. Since jumps of coordinates for all four observed reflectors were quite close, it is natural to assume that the jump occurred in the position of the center of mass of the Moon by about 25-35 cm relatively to the lunar crust (in direction toward the Earth). Extremely important here is the fact that the jumps occurred in 1997-1998, as it was predicted by the theory of the unified geodynamic synchronous rhythms in variations of the activity of natural processes on the bodies of the solar system (Barkin, 2000). For the mean values of displacements of reflectors the following values were obtained (in meters): -0.15 +/- 0.04 m (offset along x coordnate - from the Earth), 0.23 +/- 0.07 m (offset on y - east), - 0.23 +/- 0.07 m (offset along z - to the north). Thus in 1997, the center of mass of the Moon abruptly shifted to a geographical point on the lunar surface with coordinates 40.0o N, 32.1o W approximately on distance in 0.36 +/- 0.11 m. According to the Krasinskii work (2003) we have identified trends in the changes of distances to reflectors and their abrupt changes before 1997 and after 1998, with rates of about 0.036 ns / year (before the jump) and at a rate of 0.128 ns / year (after the jump). If we consider only the drift relatively to the axis x, then estimates the drift velocities decrease: 0.98 cm / year - until 1997 and 1.47 cm / year - since 1998. It is expected to perform a spectral analysis of the residual differences of distances in order to identify their cyclic variations (with lunar months periods and with multiple periods).

Keywords: center of mass of the Moon, jumps and trends of center of mass of the Moon, LLR data

Japan Geoscience Union Meeting 2014
(28 April - 02 May 2014 at Pacifico YOKOHAMA, Kanagawa, Japan)

PPS03-02 Room:424 Time:April 29 09:15-09:30

Interpretation of unexplained secular changes of the lunar orbit

BARKIN, Yury[1*]

[1]Sternberg Astronomical Institute, Moscow, Russia

Unexplained secular effects in the orbital motion of the Moon are consequences of the observed phenomenon of remove of the center of mass of the Moon relatively to its mantle and crust toward the back-side. An explanation of anomalous part of secular variation in the longitude of the Moon and in the eccentricity of the lunar orbit has been obtained.

Unexplained secular variation of the eccentricity of the lunar orbit. In the works of James Williams and his colleagues showed that the observed rate of secular change of the eccentricity of the orbit of the Moon in 2.3x10 (-11) 1/year can not be explained within the framework of the classical model of the tides. Earth tides give only a fraction of the value specified in 1.3x10 (-11) 1/year and lunar tides result even effect with the opposite sign and give part of the acceleration in -0.6x10 (-11) 1/year. Remains unexplained an anomalous part of the secular change in the eccentricity (1.6 +/- 0.4) x10 (-11) 1/year. This value corresponds to abnormal changes in the distances to the perigee and apogee at 6 mm / year. ”Abnormal speed distances to the perigee and apogee of the lunar orbit is up to 6 mm / year and its cause is unknown” (Williams J.,2006).

Tidal acceleration and evolution of the Moon’s orbit. Laser ranging method proved to be very sensitive to the tidal acceleration of the Moon. Tides on the Earth dominate in the transfer of angular momentum, and energy in the orbital motion, in particular in the removal of the Moon from the Earth. Tidal effects on the Moon are separable from the effects of Earth tides in laser range measurements to the Moon (Chapront et al., 2002; Williams et al., 2009). Full tidal acceleration in the mean orbital longitude (due to the tides of the Earth and the Moon) is estimated at -25.85” 1/cy2, corresponding to the removal of the Moon from the Earth at a speed of 3.81 cm / year (Williams et al., 2009). The rate of secular variation of the eccentricity of the lunar orbit e = (9 +/- 3) x10 (-12) 1/year also detected on the basis of long laser observations over a period of 38.7 years (March 16, 1970 - November 22, 2008) (Williams, Boggs, 2009). The basis of dynamical studies makes a precision lunar ephemeris DE421, taking into account all of Newtonian and Einsteinian effects. The authors believe that the study of the evolution of the lunar orbit is an important and surprisingly difficult task. Lunar laser ranging provides the numerical values for the two sources of dissipation on the Earth and the Moon.

Possible secular drift of the center of mass of the Moon relative to its crust and mantle toward the back side and an explanation of the anomalies of the orbital motion. In this report we give some first estimations of the possible rate of the secular drift of the Moon center of mass with respect to its crust and mantle in the 10 - 15 mm / year toward the back-side of the satellite. This secular drift of the center of mass of the Moon should be considered by the studying of the orbital motion of the Moon on laser-based observations. Namely, to add to the value obtained by laser observations. The result will be an estimate of the secular increasing of semi-major axis is the center of mass of the Moon. It should be expected that this will obtain the interpretation and explanation of the unexplained part of the secular acceleration of the Moon orbit and the anomalous part of the secular variation of the eccentricity of the lunar orbit, identified according to the perennial laser observations of the Moon. An anomalous part of the orbital acceleration (unexplained) of the Moon is 0.7” / cy2, and the anomalous part of the secular variation of the eccentricity is characterized by rate in 1.23x10 (-11) 1/year (Williams et al., 2011). Found offset - drift of the center of mass of the Moon (12 - 15 mm / year) is explained by the mechanism of excitation and the relative displacements of the shells of the Moon (solid core, liquid core, mantle) (Barkin, 2002).

Keywords: anomalous secular variation of the eccentricity of the lunar, tidal and non-tidal acceleration of the Moon, the center of mass of the Moon drift

Japan Geoscience Union Meeting 2014
(28 April - 02 May 2014 at Pacifico YOKOHAMA, Kanagawa, Japan)

PPS03-03 Room:424 Time:April 29 09:30-09:45

Deep interior structure of the Moon inferred from Apollo seismic data and the latest selenodetic data

MATSUMOTO, Koji[1*] ; YAMADA, Ryuhei[1] ; KIKUCHI, Fuyuhiko[1] ; KAMATA, Shunichi[2] ; IWATA, Takahiro[3] ; ISHIHARA, Yoshiaki[3] ; HANADA, Hideo[1] ; SASAKI, Sho[4]

[1]RISE Project Office, NAOJ, [2]University of California Santa Cruz, [3]JAXA, [4]Osaka University

Internal structure and composition of the Moon provide important clue and constraints on theories for how the Moon formed and evolved. The Apollo seismic network has contributed to the internal structure modeling. Efforts have been made to detect the lunar core from the noisy Apollo data (e.g., [1], [2]), but there is scant information about the structure below the deepest moonquakes at about 1000 km depth. On the other hand, there have been geodetic studies to infer the deep structure of the Moon. For example, LLR (Lunar Laser Ranging) data analyses detected a displacement of the lunar pole of rotation, indicating that dissipation is acting on the rotation arising from a fluid core [3]. Bayesian inversion using geodetic data weakly suggests a fluid core and partial melt in the lower mantle region [4]. Further improvements in determining the second-degree gravity coefficients and the Love numbers will help us to better constrain the lunar internal structure.

Recent analyses of GRAIL data have achieved the improved k_2 accuracy; JPL solution is 0.02405 ± 0.00018 [5], and GSFC solution is 0.02427 ± 0.00026 [6]. The two solutions are consistent with each other within their error bounds, and the accuracy of k_2 is now about 1 %. By introducing the improved gravity coefficients and k_2 from GRAIL mission, the updated LLR data analysis has also resulted in a better h_2 determination. Such accurately-determined Love numbers will contribute to constrain the structure of the lunar deep interior, such as the radius of the possible liquid core. It is difficult, however, to tightly constrain the internal structure from the geodetic data only because there are trade-offs among the structures of crust, mantle, and core. The combination of the Apollo seismic data and the geodetic data therefore afford the key to better determination of the lunar interior structure. We included geodetic data of the mass, the mean moment of inertia, the Love numbers h_2 and k_2, and 262 P and S travel time data in the analysis.

Markov Chain Monte Carlo (MCMC) method is used to infer the model parameters. When we used a five-layer model consisting of crust, upper-mantle, mid-mantle, lower-mantle, and core, the core radius is estimated to be 483 ± 22 km, and the core density values tend to be sampled around the assumed lower limit of 3600 kg/m^3. However, the inferred core radius is significantly larger than the magnetic constraint from SELENE data [7] which predicts the upper bound of the core radius to be 400 km. This discrepancy might be attributed to a possible low velocity layer above the core-mantle boundary which was not included in the five-layer model. We will discuss the results when such a low velocity layer is taken into account.

[1] Weber et al. (2011), Science, 331, 309-312, doi:10.1126/science.1199375
[2] Garcia et al. (2011), PEPI, doi:10.1016/j.pepi.2011.06.015
[3] Williams et al. (2001), JGR, 106, E11, 27,933-27,968
[4] Khan and Mosegaard (2005), GRL, 32, L22203, doi:10.1029/2005GL023985
[5] Konopliv et al (2013), JGR, 118, doi:10.1002/jgre.20097
[6] Taken from the PDS label of GRAIL Derived Data Products
[7] Simizu et al. (2013), Icarus, 222, doi:10.1016/j.icarus.2012.10.029

Keywords: Moon, internal structure, gravity field, tidal Love number, GRAIL

Japan Geoscience Union Meeting 2014
(28 April - 02 May 2014 at Pacifico YOKOHAMA, Kanagawa, Japan)

PPS03-04 Room:424 Time:April 29 09:45-10:00

Observations of lunar rotation on the Moon: possibility and problems.

HANADA, Hideo[1*] ; TSURUTA, Seiitsu[1] ; ASARI, Kazuyoshi[1] ; CHIBA, Kouta[2] ; INABA, Kenta[2] ; FUNAZAKI, Ken-ichi[2] ; SATOH, Atsushi[2] ; TANIGUCHI, Hideo[2] ; KATO, Hiromasa[2] ; KIKUCHI, Mamoru[2] ; ARAKI, Hiroshi[1] ; NODA, Hirotomo[1] ; KASHIMA, Shingo[1]

[1]RISE Project, National Astronomical Observatory, [2]Faculty of Engineering, Iwate University

The lunar rotation is one of the essential and basic target of selenodetic observations for investigation of the interior of the Moon as well as those of gravity fields, and high accuracy of the observations have a potential to detect signals related to the structure of lunar deep interior including the core. We have developed a small telescope like a PZT (Photographic Zenith Tube) for observations of Lunar rotation with the target accuracy of 1 milli-seconds of arc (1 mas)[1]. Theoretical investigation shows that observations by the telescope in the polar area of the Moon will open great possibilities for determining the libration in inclination ρ and node Iσ with the accuracy much better than before, although the determination of the libration in longitude will not be very well. It also showed that the determination error in the libration angles will not exceed $\sqrt{2}\varepsilon$, where ε is the positioning error of stars and is regarded as 1 milli-seconds of arc [2].

There are several technical problems to be solved in the development of the telescope. Effect of large temperature change is one of the most serious problem for such a precise observation, and we can loosen thermal condition by about ten times by introducing a diffraction lens compared with the case not introducing it. It is possible, on the other hand, that the vibrations of the mercury surface caused by the ground vibrations lead to fluctuations of star positions on CCD as large as 1 second of arc judging from laboratory experiments. The amplitude of the fluctuations depend on the amplitude of the ground vibrations and the depth of mercury pool. We can reduce the effect of the vibrations by making the mercury pool shallow down to the minimum depth. In the case of the mercury pool of 64mm diameter, the depth of 0.5mm is the best according to our experience [3]. It is important to keep the proper period of the mercury pool away from the period of ground vibrations in order to avoid the resonance. It is also effective to lengthen the integration time, and it can improve the reliability of the mean value of the center of a star image by statistical procedure.

We have already made a bread board model (BBM) and we will observe the deflection of the vertical on the ground by using the BBM for the time being in order to evaluate the characteristics of the total system of the telescope.

References

[1] Hanada, H. et al., Development of a digital zenith telescope for advanced astrometry, Science China, 55, 723?732, 2012.
[2] Petrova, N. and H. Hanada, Computer simulation of observations of stars from the Moon using the polar Zenith Telescope of the Japanese Project ILOM, Solar Sys. Res., 47, 504-517, 2013.
[3] Tsuruta, S. et al., Stellar imaging experiment using a mercury pool as a ground test of the telescope for In-situ Lunar Orientation Measurements(ILOM), Proc. 14th Space Science Symposium, 2014.

Keywords: rotation, moon, telescope, PZT, librations

Japan Geoscience Union Meeting 2014
(28 April - 02 May 2014 at Pacifico YOKOHAMA, Kanagawa, Japan)

PPS03-05 Room:424 Time:April 29 10:00-10:15

THE EARTH ORIENTATION PARAMETERS AND THE VARIATION OF THE SECOND ZONAL HARMONIC OF THE GEOPOTENTIAL

BARKIN, Mikhail[1*] ; FILIPPOVA, Alexandra[1] ; NOVIKOVA, Daria[1] ; PEREPELKIN, Vadim[1]

[1]Moscow Aviation Institute, Moscow, Russia

The study of the time variations of the geopotential as a result of the rotary-oscillatory processes of the Earth motion is of a significant natural-sciences and practical interest. Oscillations of the Earth ′ s inertia tensor components depend on many factors, among them the mechanical and physical parameters of the planet, the motions of tide-forming bodies, and the observed large-scale phenomena in nature. Time-dependent variations of these and other factors (regular and irregular oscillations, stochastic fluctuations, secular variations) affect the Earth rotary-oscillatory processes and the rotational parameters of the planet. The dynamic processes of the Earth orientation parameters (EOP) in turn have an effect on its figure and lead to the fluctuations of the gravitation field. Observed variations of the EOP, the variations of the Earth ′ s gravitational field and oscillations in the large-scale geophysical events appear to be in a considerable correlation.

An amplitude-frequency analysis of the rotary-oscillatory Earth motion under the action of gravitational-tidal perturbing torques from the Sun and the Moon is carried out using the classical mechanics' methods. The simulation results of the oscillatory process in the motion of the Earth pole and the variations of the second zonal harmonic of the geopotential are studied. Based on the dynamic Euler-Liouville equations expressions for amplitude and phase of the Earth pole oscillations are obtained. A comparison of the spectral power densities of the time series between the Earth pole coordinates and the variations of the gepotential is carried out. A functional dependence of the aforementioned component of the geopotential from the amplitude and phase of the Earth ′ s pole oscillatory process is shown.

Keywords: the rotary-oscillatory processes, secular variations, stochastic fluctuations, geopotential

Japan Geoscience Union Meeting 2014
(28 April - 02 May 2014 at Pacifico YOKOHAMA, Kanagawa, Japan)

PPS03-P01 Room:Poster Time:April 29 18:15-19:30

The free and forced librations of the Moon with liquid shell and solid core

BARKIN, Yury[1*] ; HANADA, Hideo[2] ; MATSUMOTO, Koji[2] ; BARKIN, Mikhail[3]

[1]Sternberg Astronomical Institute, Moscow, Russia, [2]National Astronomical Observatory of Japan, Mizusawa, Japan, [3]Moscow Aviation Institute, Moscow, Russia

In report we present our results of the study of lunar physical libration of the Moon on the base of its two and three layers models. On the base of analytical solution for two layers model (the Moon with liquid core) and empirical theory of the Moon ′ s rotation (Rambaux, Williams, 2011), we have identified period, amplitude, and the initial phase of the forth mode of free libration of the Moon, caused by liquid ellipsoidal core. Preliminary results of studies of three-layers model of physical librations of the Moon have been obtained on the base of some simplified approach for the problem of rotation of the Moon with liquid and rigid cores. The plans for future studies of the Moon rotation are discussed.

The modern view of internal structure of the Moon planet takes into account a complex two- or three-layer model. In our work the analytical theory of lunar physical libration based on its two-layer model consisting of a non- spherical solid mantle and of the ellipsoidal liquid core has been developed. The Moon moves on high-accurate perturbed orbit in the gravitational field of the Earth and other celestial bodies. On the base of two layers model of the Moon we have fulfilled systematic studies of the Moon physical librations. And in first we have presented a solution of the problem in components of vector of angular velocity of the Moon. An analytical presentation of LOD of the Moon with high accuracy in form of trigonometric series has here the progressive value. In first we have determined the fourth mode of free libration of the Moon caused by the influence of the liquid core oscillations of pole axis of rotation of the Moon (its mantle), with a long period in 205.7 yr, with an amplitude of 0 ″ 0395 and the initial phase of -134 ^{0} (for the initial epoch 2000.0). This oscillation reflects the so-called phenomenon of free oscillation of the liquid core. The estimates for the dynamic (meridional) oblatenesses of the ellipsoidal liquid core of the Moon: 0.000442 and 0.000283 have been obtained. These fundamental parameters of geodynamics of the Moon could be determined only on the base of data of observations. Earlier the attempts to determine the period of free core nutation undertaken. Our results were obtained by comparing of the developed analytical theory of lunar physical libration with empirical theory libration of the Moon, constructed on the basis of laser observations in last about 40 years (Rambaux, Williams, 2011).

Preliminary results of studies of three-layers model of physical librations of the Moon have been obtained on the base of some simplified approach for the problem of rotation of the Moon with liquid and rigid cores. We have analyzed the Cassini ′ s motion of the decoupled solid core and its librations in longitude to compare with the Moon motions. On the base of Getino, Ferrandiz et al. approach we give estimations of the periods of free librations of this system. We have constructed differential equations of rotational motion of three layers Moon from positions of the Hamiltonian formalism with application of Andoyer ′ s and Poincare ′ s variables. Now we construct analytical theory of rotation of the Moon system consisting from the non-spherical mantle, ellipsoidal liquid core and solid core.

Keywords: Moon rotation, free libration, liquid core, solid core

Japan Geoscience Union Meeting 2014
(28 April - 02 May 2014 at Pacifico YOKOHAMA, Kanagawa, Japan)

PPS03-P02 Room:Poster Time:April 29 18:15-19:30

Viscosity structure dependence of large-scale polar wander rate of the Earth: A potential impact of a low-viscosity zone

HARADA, Yuji[1*] ; XIAO, Long[1]

[1]China University of Geosciences

In this study, we make an attempt to quantitatively evaluate an effect of presence of a low-viscosity layer inside the mantle of the Earth on the timescale of its polar wander. In particular, we perform model calculation of the viscoelastic Love number which characterizes the mechanical response of the interior of the Earth, and then investigate how the timescales and strengths of some relaxation modes in the Love number depend on the viscosity structure. I compare the structure dependence of these relaxation modes with that of the polar wander speed. For the sake of convenience of this numerical calculation, we simplify the multilayered structure of the Earth and assume its incompressibility to compute the relaxation modes.

In this calculation, we apply the quasi-fluid approximation which makes it possible to integrate the polar motion equation as a non-linear one. Its reason is because the linear approximation is not allowed for the large-scale polar wander as dealt with in here. Following the applicable condition of the quasi-fluid approximation, we consider load history which timescale is slower than the characteristic one of the viscoelastic deformation of the asthenosphere.

As a result of the calculation mentioned above, we find that the timescale of the polar wander depends almost only on the longest relaxation mode. It is a remarkable point here that, in fact, the ratio of the strength of this relaxation mode governing the polar wander to the total viscoelastic Love number is not so large. In other words, this fact means that the other modes which amplitudes of tidal deformation are more dominant have almost no effect with respect to the timescale of the polar wander. Apparently, this might seem to be a peculiar result.

The reason for this dependence is because the timescale only of the above-mentioned longest mode is much longer by a few orders of magnitude compared to those of the other modes. A mode with a longer time constant of viscous relaxation has an effect which stabilizes rotation axis in a longer term even if its strength is smaller. Oppositely, a mode with a shorter time constant contributes less to the long-term rotational stability because of its faster relaxation even if its strength is larger.

In the light of this result, we can tell that the structure dependence of the true polar wander rate also basically reflects just that of the relaxation time of this longest mode. Actually, even assuming the internal structure without the low-viscosity layer inside the mantle, we still find the influence of this mode to be prominent. Once we take the existence of the low-viscosity layer into account, lower its viscosity is, shorter the timescale of the longest mode is. It can be less than forty percent at shortest. However, if this viscosity becomes lower than a certain value, the timescale of this mode is asymptotic to a constant value. Such a trend results from that this layer behaves as a fluid rather than a viscoelastic body in a sufficiently long timescale due to its too low viscosity.

Here we conclude from the calculation result shown above that the presence of the low-viscosity layer inside the Earth generally shortens the timescale of the large-scale polar wander, and also that this impact mainly stems from the variation in the timescale of the longest relaxation mode. Indeed, the preexisting works have already discussed the dependence of the timescale of the large-scale polar wander on the internal structure of the Earth as well. However, they have not examined the impact of the low-viscosity layer therein, considering a more simplified viscosity structure. Also, they have not clearly stated that the major controlling factor on the true polar wander speed. On the contrary, this work estimates the timescale of the polar wander with explicitly including the impact of this layer, and shows the non-negligible effect of the heterogeneous viscosity structure on the large-scale polar wander.

Keywords: true polar wander, the Earth, mantle, low-viscosity layer, relaxation mode, time constant

Japan Geoscience Union Meeting 2014
(28 April - 02 May 2014 at Pacifico YOKOHAMA, Kanagawa, Japan)

PPS03-P03 Room:Poster Time:April 29 18:15-19:30

Effects of global geodynamics in a series of astrometry observations of latitude at Poltava

KHALYAVINA, Lydmila[1] ; BARKIN, Yury[2*]

[1]Gravimetry Observatory, Poltava, Ukraine, [2]Sternberg Astronomical Institute, Moscow, Russia

Diverse geodynamic phenomena observed in the modern era, received a convincing explanation in the framework of the northern drift of Earth's core. Model proposed and developed by Yuri Barkin relative to the set of ancient geodynamic processes: the secular drift of the Earth's pole, non-tidal acceleration of the Earth's rotation, secular change of gravity, the evolution of the earth's figure, plate tectonics, the formation of specific geological structures, etc.

The North drift of the core generates mass redistribution of the Earth and leads to changes in the gravitational field. Since astrometry instruments have as a reference axis direction of the local plumb line, then this process should be displayed in the slow position changes no polar zenith Observatory. It is shown that for locations in the northern hemisphere, the north drift of the core causes the displacement of local plumb in a southerly direction. Is the picture of long-term changes in the direction of gravity (NST) in the meridian of Poltava for the period 1962 - 2013 based on long-term observations of latitude prismatic astrolabe taking into account: 1) high-precision catalogs (HIPPARCOS, ARIHIP, Tycho-2), 2) improved model of the pole C01 IERS; 3) the theory of the precession-nutation IAU2000; 4) plate tectonics (NUVEL1A-NNR). The resulting long-period changes in NST can be represented as the sum of three components: a linear trend with velocity ~-0.0003 ″ /yr, the nonlinear part of the trend, consisting of two branches (descending - in 1962 to 1996. And rising - in 1998 and 2010.), which can be regarded as a fragment of a wave with period T~50 years and amplitude A~0.02 ″ ; quasi cyclic part with 11 - year period, close to the main period of index of solar activity period and amplitude <0.01 ″ .

The linear part of the translational displacement means the plumb line to the south of Poltava, which is consistent with the above Barkin ′ s model. The observed velocity of motion of zenith corresponds to moving the center of mass of the Earth in a northerly direction at the velocity in 1.4 cm/yr. Found that the nonlinear part of the trend and the 11-year cyclicity in the shifts of plummet quite clearly reproduce the form of low-frequency polar latitude variations at Poltava derived from model C01 (EOP IERS). Actually observed amplitude of long-period oscillations of latitude caused by pole motion, in 2 times higher than the calculated amplitude. The non-linear part of the trend is the projection on the Poltava meridian of the Markowitz wave.

It is shown that both low-frequency cycles are negatively correlated with the corresponding components of the index of solar activity. The most probable mechanism of solar activity influence on the motion of the pole is the North Atlantic Oscillation. An increase in the amplitude of low-frequency polar displacements of Poltava zenith in astrometric observations requires a special study. One from possible explanations - the influence of the features of the geological structure in the vicinity of Poltava, which is located in the center of the so-called rift Poltava site.

Keywords: plate tectonics, secular change of gravity, Markowitz wave

Japan Geoscience Union Meeting 2014
(28 April - 02 May 2014 at Pacifico YOKOHAMA, Kanagawa, Japan)

PPS03-P04 Room:Poster Time:April 29 18:15-19:30

Minerals detection on Mars from Mars Reconnaissance Orbiter (MRO) CRISM data

JIN, Shuanggen[1] ; BARKIN, Yury[2*]

[1]Shanghai Astronomical Observatory, Chinese Academy of Science, [2]Sternberg Astronomical Institute, Moscow State Uniersity

Martian mineral detection and mapping can provide important information and constraints on Martian aqueous history, which can be used to assess the potential habitability of Mars. Degrees of addressing the key question for Martian aqueous alteration are dictated by the depth and extent of grasping the Martian hydrous mineral. Therefore, it is important to know detailed minerals and chemical induction of the existence of water on the Martian surface at past or present. In-situ observations of the Martian rovers, such as Spirit, Opportunity and Curiosity have provided the mineralogical analysis of Martian surface, but restricting in a limited areas. Compact Reconnaissance Imaging Spectrometer for Mars (CRISM) aboard the Mars Reconnaissance Orbiter (MRO) with enhanced spectral resolution can provide more information at spatial and time scale. In this paper, CRISM near-infrared spectral data are used to identify mineral classes and distribution at Martian Gale region, including kaolinite, chlorites, smectite, jarosite, northupite and salts. The detection of northupite that is indicative of evaporation in Gale region suggests that the Gale region has experienced the climate change from moist condition with mineral dissolution to dryer climate with water evaporation.

Keywords: Martian minerals, Mars Reconnaissance Orbiter, CRISM

Japan Geoscience Union Meeting 2014
(28 April - 02 May 2014 at Pacifico YOKOHAMA, Kanagawa, Japan)

PPS21-01 Room:416 Time:April 29 09:00-09:15

The solidification of a magma ocean of Vesta

KAWABATA, Yusuke[1*] ; NAGAHARA, Hiroko[1]

[1]Earth and Planetary Science, The University of Tokyo

Asteroid 4 Vesta is the only preserved intact example of a large, differentiated protoplanet. Observations of surface spectra of Vesta provide convincing evidence for a differentiated interior. Vesta is considered as the parent body of HED meteorites.

Whether growing mineral grains remain suspended in the magma ocean or settled out is crucial for the primary interior structure of a planet.

The purpose of this study is to understand the role of grain size of crystals on solidification of a magma ocean under a turbulent flow. We select asteroid 4 Vesta as a subject of this study due to the presence of HED chondrites as a reference. In this study, we consider the solidification before the rheological transition occurs.

We assume that the interior structure of Vesta had already differentiated to form a core. We use the bulk silicate Vesta composition proposed by Righter and Drake (1998), which is a mixture of L and CV chondrites with the ratio of 7 to 3 adjusted for core separation. We calculate liquidus, solidus and solid fractions using the MELTs program (Ghiorso and Sack 1995; Asimow and Ghiorso 1998).In vigorously convective systems such as magma oceans, the temperature distribution is nearly adiabatic and isentropic (Solomatov, 2000).

The heat flux can be calculated with the help of the blackbody radiation. This heat flux must match the heat flux transported to the surface by convection. Convection changes to a regime sometimes called hard turbulence at very high Rayleigh number such as those in the magma ocean, of which heat flux is shown by Siggia (1994).

To describe the rate at which particles settle out of a turbulently convective fluid, we use the model by Martin & Nokes (1989).The particle number is calculated by

$dN/dt=N(-g\triangle\rho a^2)/(18\rho\nu h)$

where N is the particle number, g is the acceleration due to gravity, a is the diameter of the particle, $\triangle\rho$ is the density difference between the crystal and the magma, ν is the kinematic viscosity, and h is the depth of the fluid layer (Martin & Nokes, 1989).

The adiabat, liquidus and solidus of the magma ocean of Vesta are very steep, that is, they have negligibly small dependence on pressure.

Thermodynamic calculations with the MELTs program showed that olivine is the first liquidus phase at ˜1900K, followed by orthopyroxene and spinel. At the very late stage, clinopyroxene appears consuming orthopyroxene if chemical equilibrium is maintained.

The fluid dynamic evaluation shows that a very small fraction of crystals are separated from the magma ocean until the rheological transition which varied from 100um to 1cm in the current work. The thickness increases with time, which is shown in Figure.

Evaluation of fluid dynamic regime shows that the magma ocean on Vesta was at the hard turbulence regime, suggesting near equilibrium crystallization until the rheological transition takes place at the crystal fraction of 60% at 1649K.

The role of grain size on fluid dynamics is very small, but the amount of crystals settled down to the bottom of the magma ocean has small dependence on the grain size. If the crystal size is 1cm, 1km thickness bottom layer is formed.

The fluid dynamic regime changes into soft turbulence in 100 years in the order in the magma ocean of Vesta.

The summary of our conclusion is as follows.

(1)The pressure effect in the interior of Vesta is negligibly small.
(2)The solidification of a magma ocean of Vesta before the rheological transition follows batch solidification.
(3)The size of crystallizing grains has a minor effect on the evolution of magma ocean until the rheological transition.
(4)The mantle would be harzburgite if the interstitial melt was effectively extracted at the later soft turbulence stage.

Fig. The thickness of the bottom layer consisting of settled crystals from the main body of a magma ocean.

PPS21-01 Room:416 Time:April 29 09:00-09:15

Keywords: Vesta, magma ocean

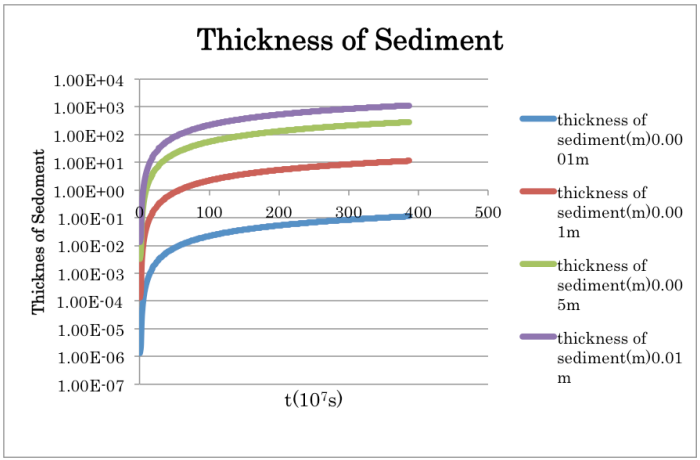

Japan Geoscience Union Meeting 2014
(28 April - 02 May 2014 at Pacifico YOKOHAMA, Kanagawa, Japan)

PPS21-02 Room:416 Time:April 29 09:15-09:30

Thermal evolution simulation of Vesta including convection and melt migration

NOGAMI, Tatsuhiko[1*] ; SIRONO, Sin-iti[2]

[1]Division of Earth and Planetary Sciences, Graduate School of Science, Nagoya University, [2]Division of Earth and Planetary Sciences, Graduate School of Science, Nagoya University

Vesta has been regarded as the parent body of the HED meteorites. From the observation of DAWN spacecraft, the uppermost layer of Vesta is composed of howardite and its thickness ranges from 50km to 80km (Jutzi et al. 2013). It is known that the ratio of the number of eucrites to diogenites is around two. Based on these facts, rapidly cooled magma layer on Vesta should be more than 10km in thickness.

In this work, I studied the evolution of internal thermal evolution of Vesta due to heating of decay of 26Al. I calculated the temperature distribution by solving numerically heat conduction equation. According to Formisano et al.(2013), if Vesta completed its formation within 1.4Ma from the injections of 26Al into the solar nebula, the degree of silicate melting inside Vesta exceeds 50 vol%. But in that work, convection and melt migration were not taken into account. These two mechanisms contribute to cool down Vesta. It is expected that the formation of Vesta should be completed earlier if these effects are taken into account. On the other hand, it is known that it takes about a few million years for Vesta-size planet to complete its formation according to the standard model of planetary formation.

As a convection model, I adopted the model of Kaula (1979). It was assumed that generated melt migrates to the surface instantaneously, and the migrating melt to the surface was accounted as the rapidly cooled magma. There are two parameters in this study, including a (the percentage of melt migration) and t0 (formation time of Vesta), and perform simulation taking into account the convection and melt migration.

As a result, convection and melt migration substantially change the evolution of internal thermal structure, and total volume of magma considerably depends on a and t0. The magma volume increases as a increases. On the other hand, the magma volume decreases as t0 increases.

When t0=0, corresponding to no decay of 26Al at the beginning, and if $a>0.3$, the erupting magma layer of 10km in thickness is formed. When a=1, corresponding to total melt migration, the magma layer of 10km is formed if $t0<0.9$Ma. According to these results, Vesta should be completed its formation within 0.9Ma after CAI formation, and more than 30% of generated melt should migrate the surface. But total generated melt migration is not reasonable . If $a<1$, Vesta has to be formed earlier than a=1.

Therefore, it is suggested that the formation time of Vesta should be earlier than the estimate by Formisano et al.(2013), and rapid formation mechanism of 100km sized objects is needed.

Japan Geoscience Union Meeting 2014
(28 April - 02 May 2014 at Pacifico YOKOHAMA, Kanagawa, Japan)

PPS21-03 Room:416 Time:April 29 09:30-09:45

Thermal conductivity measurements of sintered glass beads and application to planetesimal thermal evolution

TSUDA, Shoko[1] ; SAKATANI, Naoya[2*] ; OGAWA, Kazunori[3] ; TANAKA, Satoshi[3] ; ARAKAWA, Masahiko[4] ; HONDA, Rie[5]

[1]University of Tokyo, [2]The Graduate University for Advanced Studies, [3]Institute of Space and Astronautical Science, [4]Kobe University, [5]Kochi University

In the planetary formation process, dusts in the early solar nebula would have formed into planetesimals. Planets and asteroids have been formed by collisions of planetesimals. To constrain planetesimal ' s formation process and internal structure is an important issue. Especially, thermal evolution of planetesimal is key phenomenon for this purpose, and thermal conductivity of the planetesimal constituents is an essential parameter for understanding the thermal evolution.

As planetesimals are treated as dust aggregates, they would experience sintering when their temperature increases as a result of thermal evolution. The sintering makes neighbor particles bonded. The thermal conductivity of powered materials before sintering has been researched recently. However, thermal conductivity of sintered dust has not been measured under vacuum. Once dusts undergo the sintering, contact faces, so-called neck, are formed between dusts. The sintering causes growth of the neck and decrease of the porosity. It is thought that these changes make thermal conductivity higher than not-sintered dusts.

Based on our previous measurements of the thermal conductivity of glass beads, a positive correlation between thermal conductivity and compressional stress (thus, the inter-particle contact area) was observed with sample porosity remaining constant. Therefore, the thermal conductivity should be expressed as a function of not only porosity but also contact area between the particles.

This study aims at investigating thermal conductivity of the sintered materials under vacuum condition, in order to estimate effect of the sintering on thermal evolution of planetesimals. Especially, we focus on the dependence of neck size on the thermal conductivity.

We used three sizes of glass beads (250, 500, and 1000 μm) as analogous samples of dusts. For respective glass beads, we made three sintered samples with different degrees of sintering, or different neck size, in order to investigate the neck size dependence of the thermal conductivity. To measure the neck size, the sintered particles were separated and the neck crack size was observed using optical microscope. The thermal conductivity was measured by line heat source method under vacuum.

As a result of these experiments, we confirmed that the neck sizes of the nine samples had different ratio of neck size to beads radius, whose average values were ranged from 0.075 to 0.30. The thermal conductivity was ranged from 0.036 to 0.25 W/mK. These values were more than 10 times higher than that of not-sintered glass beads. Combining the results of neck size and thermal conductivity measurements, it was found that the thermal conductivity is proportionally related to the neck size ratio independent of the particle size. In these experiments, the porosity was constant about 40%. Therefore, when we calculate thermal evolution of planetesimals under sintering, the thermal conductivity should be estimated from the neck size at least until the neck size ratio grows up to 0.3 (initial stage of sintering).

Finally, we calculated the thermal evolution of the planetesimal using the relation of the thermal conductivity and the neck ratio we found in this experiment. Hypothesized planetesimals have radius between 100 m and 1000 m, formation age between 1 Myr and 3 Myr after CAI formation, and dust diameter of 1 and 1000 μm. As a result of the calculation, it was found that the sintering and resulting increase of the thermal conductivity make internal peak temperature more than 1000 K lower than the case when the sintering effect is not included in the calculation. In addition, internal temperature structure and neck size (or material strength) distribution in the planetesimals vary widely depending on the size and formation age of the planetesimals and particle size of dust.

Japan Geoscience Union Meeting 2014
(28 April - 02 May 2014 at Pacifico YOKOHAMA, Kanagawa, Japan)

PPS21-04 Room:416 Time:April 29 09:45-10:00

The effect of melt on frictional behavior and the implication for deep moonquake

AZUMA, Shintaro[1*] ; KATAYAMA, Ikuo[1]

[1]Department of Earth and Planetary Systems Science, Hiroshima University

Apollo program (Passive Seismic Experiment) investigated a number of seismic events in moon (e.g., Nakamura 2003). These seismic events (moonquakes) are classified to four categories; thermal moonquake, shallow moonquake, impact moonquake and deep moonquake (Latham et al., 1969). In kinds of moonquake, deep moonquake is especially interesting because the occurrence depth of deep moonquake (700?1200 km) is obviously in plastic deformation region where frictional behavior and fracture does not occur. Analysis of PSE (Passive Seismic Experiment) data and modelling in previous studies suggest that the partial melt layer underlies near the occurrence depth of deep moonquake (Weber et al., 2011). Therefore partial melt possibly is one of important factor on the deep moonquake. Here we show the results of frictional experiments using a borneol?diphenylamine which can be adjusted in melt fraction and dihedral angle (Takei 2000). When dihedral angle is 30o, frictional coefficient becomes small with decrease of melt fraction. Although frictional coefficient is significantly decreased when dihedral angle is 0o, frictional coefficient does not depend on melt fraction. When dihedral angle of partial melt is 0o, frictional behavior is fully dominated by partial melt. Partial melt is considered to have the three effects on the shear strength. First, our frictional experiments found that partial melt decrease frictional coefficient. Second, partial melt behave as the pore pressure. Third, partial melt extracts the water from the surrounded rocks, and induces the shear localization (the stress concentration). Considering these effects of partial melt on frictional behavior, partial melt might be one of important factors on deep moonquake.

Keywords: melt, deep moonquake, moon, frictional behevior

Japan Geoscience Union Meeting 2014
(28 April - 02 May 2014 at Pacifico YOKOHAMA, Kanagawa, Japan)

PPS21-05 Room:416 Time:April 29 10:00-10:15

Velocity scaling of granular convection and its application to timescale of regolith migration

YAMADA, Tomoya[1*] ; KATSURAGI, Hiroaki[1]

[1]Graduate School of Environmental Studies, Nagoya University

On the basis of accurate surface observation of asteroid Itokawa, it has been thought that regolith migration and sorting could occur [1]. Besides, Nagao et al. revealed that cosmic-ray exposure age of Itokawa's surface grains is less than 8 Myr [2]. As a possible explanation for such active and young surface of Itokawa, regolith convection caused by impact-induced seismic shaking has been considered [1]. Indeed, granular convection can be readily observed in the laboratory experiment of vertically vibrated granular matter (e.g. [3]). However, the quantitative feasibility of granular convection under the microgravity environment has not been studied well so far. Although the direct control of gravity is quite difficult, we instead employ the scaling approach to figure out the gravity dependence of granular convective velocity. Specifically, we measure the granular convective velocity under various experimental conditions. Then, using the systematically obtained data, we find a scaling relation among the convective velocity, gravitational acceleration, and other control parameters such as vibration frequency, grain size, and so on. We also estimate the timescale of regolith migration due to the granular convection by using the obtained scaling.

The grains used in this experiment are glass beads of diameter d = 0.4, 0.8, or 2 mm (AS-ONE corp. BZ04, BZ08, BZ2). The experimental setup consists of a cylinder made by plexiglass of its height 150 mm and inner radius R = 16.5, 37.5, or 75 mm. The cylindrical cell is filled by glass beads to make a granular bed of the height H = 20, 50, 80, or 110 mm. The system is mounted on an electromechanical vibrator (EMIC 513-B/A) and shaken vertically. The vibration frequency f is varied from 100 to 300 Hz and the maximum dimensionless acceleration is varied from 2 to 6. Motions of glass beads on the sidewall of the container are captured by a high-speed camera (Photoron SA-5) with a macro lens. PIV (Particle imaging velocimetry) method is used to compute the vertical component of the convective velocity, v_z. The maximum value of the velocity is nondimensionalized as $v_{zmax}/(gd)^{1/2}$, where g is the gravitational acceleration. Using the obtained experimental data, we scale $v_{zmax}/(gd)^{1/2}$ by the shaking parameter S [4] and the dimensionless system size L. S represents the energy balance between vibration and gravity, $S=(2\pi Af)^2/gd$, where A is shaking amplitude. L is the scaled system size defined by $L=(RH)^{1/2}/d$.

As a result of systematic dimensional analysis, we obtain a scaling form, $v_{zmax}/(gd)^{1/2} \sim S^{0.47}L^{0.82}$. From this scaling form, we find that the granular convective velocity v_{zmax} depends on the gravitational acceleration g as $v_{zmax} \propto g^{0.97}$ when the maximum dimensionless acceleration is fixed. This means that the granular convective velocity is almost proportional to the gravitational acceleration. We also find that the timescale of regolith migration due to the granular convection is almost independent of its roll size, by assuming that L is the dimensionless convective roll size. In the presentation, we are going to discuss the consistency between the regolith migration timescale and cosmic-ray exposure age of Itokawa's surface grains.

[1]H. Miyamoto *et al.*, Science **316**, 1011 (2007)
[2]K. Nagao *et al.*, Science **333**, 1128-1131 (2011)
[3]A. Garcimartín *et al.*, Physical Review E **65**, 031303 (2002).
[4]P. Eshuis *et al.*, Physics of Fluids **19**, 123301-1 (2007)

Keywords: granular convection, scaling analysis, gravitational acceleration, regolith migration, Itokawa

Japan Geoscience Union Meeting 2014
(28 April - 02 May 2014 at Pacifico YOKOHAMA, Kanagawa, Japan)

PPS21-06 Room:416 Time:April 29 10:15-10:30

Experimental study on impact-induced seismic wave propagating in granular materials

MATSUMOTO, Eri[1] ; YASUI, Minami[2*] ; ARAKAWA, Masahiko[1]

[1]Graduate school of Science, Kobe University, [2]Organization of Advanced Science and Technology, Kobe University

Introduction:

A seismic wave survey is a direct method to investigate the sub-surface structures of solid bodies, so we measured and analyzed these seismic waves propagated through these interiors. Earthquake and Moonquake are the only two phenomena that have been observed to explore these interiors until now, while the future surveys on the other bodies, (solid planets and/or asteroids) are now planned. To complete the seismic wave survey during the mission period, the artificial method that activates the seismic wave is necessary and the one candidate for the artificial one is a projectile collision on the target body. However, to utilize the artificial seismic wave generated on the target body, the relationship between the impact energy and the amplitude and the decay process of the seismic wave should be examined. If these relationships are clarified, we can estimate the required sensitivity of seismometers installed on the target body and the distance from the seismic origin measurable for the seismometer. Furthermore, if we can estimate the impact energy from the observed seismic wave, it is expected to estimate the impact flux of impactors collided on the target body. In this study, we carried out impact experiments in the laboratory, observed the seismic waves by accelerometers, and examined the effects of projectile properties on the amplitude and the decay process of the seismic wave.

Experimental methods:

We did impact experiments by using the one-stage gas gun at Kobe University. The projectile was a polycarbonate cylinder with the diameter of 10 mm and the height of 10 mm, and a stainless and an alumina ball with the diameter of 3 mm. The stainless and the alumina balls was accelerated with the sabot made by polyethylene. The impact velocity was $\sim$100 m/s. The target was prepared by putting 200 μm glass beads into the container with the diameter of 300 mm and the height of 100 mm, up to 80 mm depth. Three accelerometers (response frequency $<$10 kHz) were set on the target surface at different distances from the impact point. The observed seismic waves were recorded as voltage on the data logger (A/D conversion efficiency 100 kHz).

Experimental results:

We calculated the propagation velocity of seismic wave by using the traveling time from the impact point to the site of accelerometer and the impact velocity, and obtained 105 $\pm$ 15 m/s. Additionally, the relationship between the maximum acceleration, g_{max}, and the normalized distance, x/R (x: distance from impact point, R: crater radius), was determined as g_{max} =268$(x/R)^{-2.8}$. From these results, it is found that the seismic wave attenuates with similar waveform on the same target, irrespective of projectile type. The duration keeping the maximum acceleration was estimated to be $\sim$0.3 ms, and this value was almost consistent with the penetration time of projectile estimated by using the model proposed by Niimi *et al.* (2011). McGarr *et al.* (1969) studied the energy conversion efficiency from impact energy to seismic momentum and obtained the ratio of the impulse of projectile during the penetration, I, to the kinetic energy of projectile, E_k. As a result of this study, the I/E_k was obtained to be $1.6 \times 10^{-2} \pm 1.0 \times 10^{-2}$. On the other hand, McGarr *et al.* (1969), which the lexan projectile collided on the sand target with the impact velocity of 2-8 km/s, was obtained to be $6 \times 10^{-6} \pm 4 \times 10^{-6}$. This difference might be caused by the dependence of impact velocity on the energy conversion efficiency.

Keywords: impact-induced seismic wave, granular materials, decay process, planetary exploration, crater formation, accelerator

Japan Geoscience Union Meeting 2014
(28 April - 02 May 2014 at Pacifico YOKOHAMA, Kanagawa, Japan)

PPS21-07 Room:416 Time:April 29 10:30-10:45

Velocity measurements of impact jetting during oblique impacts

KUROSAWA, Kosuke[1*] ; NAGAOKA, Yoichi[1] ; HASEGAWA, Sunao[2] ; SUGITA, Seiji[3] ; MATSUI, Takafumi[1]

[1]PERC, Chitech, [2]ISAS, JAXA, [3]Dept. of Complexity Sci. & Eng., The Univ. of Tokyo

Impact jetting is a widely-known phenomenon in both hypervelocity impact experiments and hydrocode calculations. There are two important features in impact jetting, which are (1) extremely high velocity greater than the impact velocity and (2) the high degree of shock heating. Jetting has been considered as a mechanism for the origin of chondrules, tektites and impact glasses, Pluto, and the Moon. Jetting during a symmetric collision between two thin plates has been well studied. However, the understanding of jetting for spherical impactors is essential for planetary applications and it has not been obtained. One of the reasons for this is the lack of the experimental data of hypervelocity jetting of obliquely-impacted spherical projectiles. Although the temperature of jetted vapor has been investigated under a wide range of experimental conditions, only 3 data points, including unpublished data, have been reported as the jet velocity, which is one of the important anchors for developing a jetting model.

In this study, we conducted a series of oblique impact experiments using spherical projectiles and 3 different targets and investigated the jet velocity as a function of impact velocity and target materials. The frame rate of a high-speed imaging was 100 ns/frame to resolve the jetting initiation during projectile penetration. We found that the velocity ratio of the jet velocity to the impact velocity increases as the shock impedance of target increases at a given impact velocity and decreases with as impact velocity increases.

We obtained the first systematic data set for the jet velocity of spherical projectiles during oblique impacts. Using the data set, we constructed a physical model to explain the observed jet velocities. We found that (1) a classical phenomenological model constructed by Ang (1990) predicts well observed jet velocities if we use the vertical component of impact velocity instead of impact velocity in his model and that (2) observed jet velocities can be obtained by the sum of the horizontal component, the deformation velocity of the shocked projectile, and the particle velocity after isentropic release. The latter model may provide a physical basis of the jet formation

Both the standard and our physical model predict the jet velocity during oblique impacts reaches 2.5 times than the impact velocity. Although the mass of jetted materials must be small for energy conservation, the aerodynamic interaction between such hypervelocity jet and an ambient atmosphere may be significant because the heating rate of aerodynamic ablation is proportional to the cube of the velocity. In the case for an oblique impact on Titan, the jet velocity may reach 30 km/s in the case of typical cometary impacts and may generate strong EUV radiation from produced high-temperature plasma in the N2CH4 atmosphere via aerodynamic interaction near the surface of Titan. Active chemical reactions of C-bearing species may be driven by the produced EUV. The available energy source near the current Titan surface is only cosmic rays. Thus, hypervelocity jetting may be a new energy source for atmospheric chemistry on Titan.

Keywords: Hypervelocity impacts, Oblique impacts, High-speed video camera, Ultrafast imaging observation, Impact jetting, Titan

Japan Geoscience Union Meeting 2014
(28 April - 02 May 2014 at Pacifico YOKOHAMA, Kanagawa, Japan)

PPS21-08 Room:416 Time:April 29 11:00-11:15

The stability of amino acids in early ocean by meteorite impacts: Implication for chemical evolution of biomolecules

UMEDA, Yuhei[1*] ; SEKINE, Toshimori[1] ; FURUKAWA, Yoshihiro[2] ; KAKEGAWA, Takeshi[2] ; KOBAYASHI, Takamichi[3]

[1]Graduate School of Science, Hiroshima University, [2]Graduate School of Science, Tohoku University, [3]National Institute for Materials Science

Prebiotic oceans may have contained abundant amino acids, and were subject to meteorite impacts, especially during the late heavy bombardment. It has been unknown how meteorite impacts affected such dissolved amino acids in the early oceans. Experiments in the present study were performed using aqueous solutions containing olivine or hematite powders and ^{13}C-labeled glycine and alanine. In particular, the reaction products from ^{13}C-labeled amino acids are expected to compose ^{13}C, distinguishing if they are contaminants or not. Two powders of olivine and hematite help to keep the oxygen fugacity low and high during experiments, respectively in order to investigate the effect of oxygen fugacity on chemical reaction of amino acids. The run product of selected amino acids and amines in samples were analyzed with liquid chromatography-mass spectrometry (LC/MS). Some experiments were carried out in the presence of ammonia and/or benzene. The results revealed that amino acids survived partially or reacted out in early ocean through meteorite impacts. It was found that glycine changes into alanine and large amounts of methylamine and ethylamine are formed. Amine formation from alanine was increased considerably in the presence of Fe_2O_3 rather than olivine under similar impact conditions. XRD for the recovered hematite powders indicated the presence of a small amount of magnetite, suggesting that the oxygen fugacity was kept high enough to be close to the Fe_2O_3-Fe_3O_4 buffer. The formation of n-butylamine, detected as the largest number of carbon species in the recovered samples from the solutions with ammonia and benzene, suggests that chemical reactions to form new biomolecules can proceed through marine impacts. These results suggest that amino acids in early oceans can proceed further by impact-induced reactions, implying that impact energy plays a role in the prebiotic formation of various biomolecules, although the reactions depend upon the chemical environments as well.

Japan Geoscience Union Meeting 2014
(28 April - 02 May 2014 at Pacifico YOKOHAMA, Kanagawa, Japan)

PPS21-09 Room:416 Time:April 29 11:15-11:30

Organic aerosol experiments for CH_4/CO_2 atmospheres using a hydrogen/helium UV lamp

HONG, Peng[1*] ; SEKINE, Yasuhito[1] ; SUGITA, Seiji[1]

[1]Complexity Sci. & Eng., Univ. of Tokyo

Organic aerosols are photochemically produced in CH_4-rich reducing atmospheres, but their production mechanisms are not well constrained. Organic aerosol layers are believed to influence the surface temperature of early Earth, through its anti-greenhouse (Pavlov et al., 2001) and/or indirect greenhouse effects (Wolf and Toon, 2010), however, because of the uncertainty of the aerosol production mechanism, there are large uncertainties inherent in previous estimates of the aerosol production rate and optical depth of aerosol layers (Trainer et al., 2006). In order to put a constraint to the production mechanism and obtain aerosol production rate applicable to CH_4/CO_2 atmospheres, we conducted laboratory experiments to form organic aerosol analogues using a hydrogen/helium lamp that simulates solar far UV (FUV) with wavelengths longer than 110 nm. We measured the aerosol production rate as functions of UV flux and of CH_4/CO_2 ratio in the reactant gas. The aerosol production rates were determined by ellipsometrically measuring the growth rates of thin organic films deposited on a substrate. The UV fluxes from the hydrogen/helium lamp were measured by N_2O/CO_2 actinometry. Our experimental results show that the aerosol production rate is not a second-order function but a linear function of UV flux. This leads to a lower estimate for aerosol production rate due to FUV irradiation, when extrapolating the production rate in Titan's atmosphere to early Earth and exoplanets. We also found that the aerosol production exhibits a steep decrease when the CH_4/CO_2 ratio becomes less than unity. In order to interpret the dependence of aerosol production rate on the CH_4/CO_2 ratio, we also performed one-box photochemical calculations, including 791 reactions and 134 species up to C_8 hydrocarbons. The one-box photochemical model was validated against some basic carbon species (CH_4, C_2H_2, C_2H_4, C_2H_6, CO, CO_2), in which the abundances of those species calculated with the model and observed with a quadruple mass spectrometer (QMS) show a good agreement. We found that the observed production rate is in a good agreement with polymerization reaction rates involving aromatic hydrocarbons (i.e., benzene), suggesting benzene is the key parent molecule controlling the aerosol production. On the other hand, polymerization reactions involving polyynes do not account for the experimental data, suggesting that they are not the limiting molecules. This implies that aerosol production rate in an early Earth atmosphere due to solar FUV would become significantly lower than a previous estimate which includes polymerizations of polyynes as formation reactions of aerosols (Pavlov et al., 2001), resulting in an optically thinner aerosol layer by a factor of 100. Thus the optical depth of organic aerosol layers produced by solar FUV in an early Earth atmosphere would not have had efficient anti-greenhouse effect or indirect greenhouse effect, which makes other greenhouse effect important for the Archean climate, such as greenhouse effect of ethane. We will also discuss the possibility of aerosol formation through nitrile reactions driven by high-energy particle irradiation, which could be more efficient than the aerosol production due to solar FUV.

Keywords: organic aerosol, photochemistry, laboratory experiment, reducing atmosphere

Japan Geoscience Union Meeting 2014
(28 April - 02 May 2014 at Pacifico YOKOHAMA, Kanagawa, Japan)

PPS21-10 Room:416 Time:April 29 11:30-11:45

Proto-atmosphere on giant icy satellites forming within gaseous circum-planetary disks

MIKAMI, Takashi[1*] ; KURAMOTO, Kiyoshi[1]

[1]Department of Cosmosciences, Graduate School of Science, Hokkaido University

In spite of the great similarity in size and mean density, the giant icy satellites Ganymede, Callisto, and Titan have very different surface environments. In particular, only Titan holds a thick atmosphere dominated by N_2. Recent data of the Cassini spacecraft indicated that atmospheric N_2 is probably originated from other nitrogen-bearing species like NH_3. However, it still remains an open question when and how N_2 was generated. This is partly because the physical states of giant icy satellites have been poorly understood.

According to a widely-accepted theory of regular satellites formation, the giant icy satellites were formed in subnebulae with low temperature and low pressure taking a long accretion time. Some models assert that their surfaces were kept too cold to induce significant differentiation during accretion. However, these satellites may capture a significant amount of subnebula gas, which possibly forms proto-atmospheres along with gases volatilized from icy components. Such a hybrid-type proto-atmosphere may have significant blanketing effect.

Here, we numerically analyze the structure and effect of a hybrid-type proto-atmosphere. Our model atmosphere is hydrostatically connected with subnebula at the satellite Hill radius. It contains H_2 and He as nebula gas components, H_2O and NH_3 as volatilized ice components. The radiative-convective equilibrium structure is solved as a function of surface temperature. The subnebula conditions are given by Canup and Ward (2002), the temperatures are 150 K at Ganymede, 120 K at Callisto, and 50 K at Titan, and the corresponding subnebula pressures are varied over 0.1-10 Pa.

For all the boundary conditions, the proto-atmosphere is opaque due to water vapor, so that the outgoing thermal radiation (OTR) flux at top of the atmosphere is smaller than that of black body radiation without atmosphere when the surface temperature is higher than 273 K. When the surface temperature is lower, the OTR fluxes from the proto-atmospheres of Ganymede and Callisto are close to black-body radiation because these atmospheres have low surface pressure and are optically thin due to large scale height under high background temperature. On the other hand, the proto-atmosphere of Titan has another type of solution with the OTR fluxes significant lower than blackbody radiation under low surface temperature. This is due to the formation of optically thick atmosphere tightly bounded by gravity because of low background temperature.

These results imply that a warm proto-atmosphere near 200 K could be kept on Titan for a long time after the end of accretion. Our stability analysis suggests that the proto-atmospheres of Ganymede and Callisto were lost associated with the dissipation of the Jovian subnebula, but that of Titan survived after the dissipation of the Saturnian subnebula.

In the case, NH_3 vapor pressure would be kept high under the irradiation of the solar UV for a long time. The present atmospheric N_2 of Titan may be generated by photochemical reaction of NH_3 vapor in such a warm proto-atmosphere.

Keywords: Giant icy satellite, Atmosphere, Circum-planetary disk

Japan Geoscience Union Meeting 2014
(28 April - 02 May 2014 at Pacifico YOKOHAMA, Kanagawa, Japan)

PPS21-11 Room:416 Time:April 29 11:45-12:00

Atmospheric formation and thermal evolution of a proto-Mars growing in the solar nebula

SAITO, Hiroaki[1*] ; KURAMOTO, Kiyoshi[1]

[1]Cosmo Sci., Hokkaido Univ

It is widely accepted that Mars is a survivor of proto-planets formed by oligarchic growth i.e., the runaway accretion of planetesimals. Numerous planetesimals impacts onto the growing proto-Mars likely cause shock-melting, resulting into the early core formation as constrained by the chronology of Martian meteorites. Such impacts should also induce the degassing of H_2O and other molecular species from accreting materials, which contributes to atmosphere formation. Since the oligarchic growth proceeds within the solar nebula, a growing Mars probably acquired a proto-atmosphere consisting of the mixture of nebula gas component and degassed component. Such a hybrid-type proto-atmosphere may play important role in thermal balance and volatile partitioning between the planetary surface and interior. However, the structure and behavior of such atmosphere has been poorly investigated so far.

In this study, we build a one-dimensional radiative-convective (RT) equilibrium model for a hybrid-type proto-atmosphere assuming a compositional double layer structure. Here the upper layer is dominated by H_2-He continuing from the solar nebula and the lower one is dominated by degassed components enriched in H_2O. Radiative transfer is modeled, taking into account the absorptions by H_2, He and H_2O. RT equilibrium structures are obtained as a function of thermal luminosity that would be balanced with accretional heating rate and the amount of degassed component. The degassed component consists of H_2O and H_2 with molar ratio 1:5 in equilibrium with metal and silicate. The accretion time is taken 10^6-10^7 years.

For the pure H_2-He atmosphere, the surface temperature is kept lower than 700 K. Supply of degassed component increases the surface temperature that can exceed 1500 K given the mass of degassed component more than 1% of the Mars mass. If planetesimals contain enough proportions of H_2O and other heavy volatiles, growing Mars would have global magma ocean sustained by the blanketing effect of proto-atmosphere. This would promote core formation and transport of dissolved volatiles.

Japan Geoscience Union Meeting 2014
(28 April - 02 May 2014 at Pacifico YOKOHAMA, Kanagawa, Japan)

PPS21-12 Room:416 Time:April 29 12:00-12:15

Line-by-line calculations of radiation properties for exoplanets with steam atmosphere

ONISHI, Masanori[1*] ; HASHIMOTO, George[2] ; KURAMOTO, Kiyoshi[3] ; TAKAHASHI, Yoshiyuki O.[1] ; TAKAHASHI, Yasuto[3] ; ISHIWATARI, Masaki[3] ; HAYASHI, Yoshi-yuki[1]

[1]Department of Earth and Planetary Sciences, Kobe University, [2]Department of Earth Sciecnes, Okayama University, [3]Department of Cosmosciences, Graduate School of Science, Hokkaido University

For a hot water rich atmosphere, there is an upper limit on the thermal emission that is unrelated to surface temperature (Simpson, 1927, Nakajima et al., 1992). The radiation limit is deeply related to evolution of planetary atmosphere. Hamano et al., 2013 showed that terrestrial planets can be divided into two distinct types on the basis of their evolutionary history during solidification from the initially hot molten state depending on whether incoming flux from a host star is larger or less than the radiation limit. On the other hand, the first direct image of an exoplanet has finally occurred in 2004 (Chauvin et al., 2004), it is expected to observe radiation spectrum from terrestrial planets near future. If we can observe the spectrum, we have potential to clarify the atmospheric and surface environment and history of the planets. In order to estimate the planetary environment from the observation, numerical simulation of radiative transfer is needed. The most reliable calculation method of the radiation is line-by-line treatment. Goldblatt et al., 2013 calculates the radiative transfer of a pure water atmosphere by line-by-line treatment. Goldblatt et al., 2013 investigates only one case of surface water amount, one current ocean mass case. In this study, we calculate the radiative transfer in steam atmosphere by line-by-line treatment in several surface water amount cases.

Absorption cross section of water vapor was calculated from HITEMP2010 (Rothman et al., 2010) and MT_CKD continuum model (Mlawer et al., 2012). We used a 1D convective model in pure water atmosphere. The surface temperature was varied from 250 to 2000 K. The total water amount of water was varied from 0.01 to 5 current Earth ocean mass (270 bar). For rapid calculation, we prepared absorption cross section table and calculated required absorption cross section by cubic spline interpolation. A two-stream approximation (Toon et al., 1989) was used to calculate radiative transfer by line-by-line treatment with resolution of 0.01 cm^{-1} wavelength.

A radiation limit of our study is 282 W m^{-2}. The value is good agreement with that of Goldblatt et al., 2013. When the total water amount is lesser, increasing of outgoing thermal flux over radiation limit occurs in lower surface temperature conditions. In 0.01 current ocean mass condition, increasing of flux occurs in lower than 1000 K. In this case, most of flux radiate from 10 micron and 4 micron window region. Results of optical depth calculation indicate that we can't detect NIR and IR radiation from the surface of planets with surface temperature higher than 1500 K, even if the planet has 0.01 water amount.

Keywords: steam atmosphere, radiative property, radiation limit

Japan Geoscience Union Meeting 2014
(28 April - 02 May 2014 at Pacifico YOKOHAMA, Kanagawa, Japan)

PPS21-13 Room:416 Time:April 29 12:15-12:30

Dependence of the runaway threshold on water distributions on the surface of Earth-like planets

NITTA, Akira[1*] ; ABE, Yutaka[1] ; O'ISHI, Ryouta[2] ; ABE-OUCHI, Ayako[2]

[1]Department of Earth and Planetary Science, Graduate School of Science, University of Tokyo, [2]Atmosphere and Ocean Research Institute, University of Tokyo

Liquid water is one of the most important material not only for its large effect on planetary climate but also as a controlling factor of the habitability [e.g. Kasting et al., 1993]. Water planets, which are planets with liquid water on their surface, can be divided in 3 types: 'ocean planets', 'partial-ocean planets', and 'land planets'. Ocean planets have enough water to cover their surface entirely. Partial-ocean planets, which are like the Earth, have an interconnected ocean and lands. Land planets have little water in scattered lakes around both Poles [Abe et al., 2013, Hawaii, Kona]. The type of the water planet is determined by the balance between the surface water transport, which depends on the amount of water and topography, and the atmospheric water transport, which depends on the global circulation.

Surface water on each water planet is unstable and entirely vaporized when the planet receives insolation above a certain critical value. It is because of the positive feedback of the greenhouse effect of water vapor. This phenomenon is called the runaway greenhouse. In the following, the critical insolation is called 'runaway threshold' [e.g. Abe and Kasting 1988; Nakajima et al, 1992; Kopparapu et al., 2011].

Abe et al. [2011] discussed the difference of the runaway threshold between Earth-sized ocean planets and land planets using a 3-D model for the first time. They found that the surface water of land planet is significantly stable than that of ocean planet against the large insolation. While an ocean planet gets unstable and the runaway greenhouse occurs when the insolation reaches about 130% of that on the present Earth, a land planet remains stable until the insolation reaches 170%. However, a land planet that they represented is only one of the various situations of land planets, and they didn't mention the effect of variety of surface water distributions on the planetary climate.

Takao [2013] showed the dependence of the runaway threshold on latitudinal surface water distribution using the combination of meridional energy balance model (EBM) and the vertical radiative-convective equilibrium model. He suggested that runaway threshold of the Earth-sized water planet varies with the degree of latitudinal localization of surface water. Nevertheless, his 1-D EBM was so simple that he could neither discuss about the effects of longitudinal distribution of surface water, nor include dynamical global circulation.

In this study, we perform numerical experiments to clarify the effects of the surface water distribution on runaway threshold of Earth-sized planets with a 3-D model, GCM.

We use CCSR/NIES AGCM 5.4g [Numaguchi, 1999], which includes dynamical atmospheric circulation, radiative transfer, formation of clouds, and so on. While this model is adapted to the present Earth, it cannot calculate the change of surface water distribution determined by the water amount and topography. Therefore, we assumed the surface water distribution, which is determined as a result of the balance between the surface and atmospheric water transport in reality, and used it as the boundary condition. Then, we raised the insolation gradually until the surface water got unstable for each surface distribution, and evaluated the runaway threshold.

We found that the degree of localization of surface water significantly affects the runaway threshold, and it varies from 180% (extremely localized land planet) to 130% (ocean planet) continuously. Even if no surface water is given low latitudes area initially, because the Hadley circulation transports water to such area, when the initial surface water area reaches adequately low latitudes, the runaway threshold is almost the same as that of ocean planets, that is, 130%. We also investigated the dependence on the longitudinal water distribution. As a result, even if the total area of surface water is the same, there are about 10% of differences in the runaway threshold depending on its distribution.

Keywords: runaway greenhouse, GCM, Earth-like planet

Japan Geoscience Union Meeting 2014
(28 April - 02 May 2014 at Pacifico YOKOHAMA, Kanagawa, Japan)

PPS21-14 Room:416 Time:April 29 14:15-14:30

Dead zones by electric heating in protoplanetary disks

MORI, Shoji[1*] ; OKUZUMI, Satoshi[1]

[1]Tokyo Institute of Technology

Turbulence driven by magnetorotational instability (MRI) is a viable mechanism of angular momentum transport in accretion disks. In protoplanetary disks, however, there is a region where the ionization degree is too low for MRI to be active (e.g., Gammie 1996; Sano et al. 2000). Whether turbulence is present or not strongly affects the growth of dust particles to planetesimals. Therefore, a good knowledge of the size of dead zones is essential to understanding planet formation.

In this study, we focus on the heating of electrons by turbulent electric fields and its effect on the ionization state of protoplanetary disks. Previous studies have assumed that electrons in the disks have the same temperature as the neutral gas. However, this is not necessarily the case in MRI-driven turbulence, in which turbulent electric fields can significantly heat up electrons (Inutsuka & Sano 2005). Heated electrons efficiently adsorb onto dust grains, and therefore electron heating leads to a reduction of the ionization degree (Okuzumi & Inutsuka, in prep.). This could effectively increase the dead zone size by reducing the saturation level of MRI turbulence outside the conventional dead zone.

The aim of this study is to show where in protoplanetary disks the effect mentioned above becomes important. We calculate the ionization degree of disks assuming that MRI operates outside the dead zone. For a minimum-mass solar nebula with the dust grain radius of 0.1um and dust-to-gas mass ratio of 0.01, we find that the effect becomes significant in a region extending from the outer edge of the dead zone (at ˜20 AU from the central star) out to 70 AU. Furthermore, our analytic estimate suggests that the saturation level of turbulence in this region is significantly low.

Keywords: protoplanetary disk, ionization degree, dust grains, MHD turbulence, electric heating

Japan Geoscience Union Meeting 2014
(28 April - 02 May 2014 at Pacifico YOKOHAMA, Kanagawa, Japan)

PPS21-15 Room:416 Time:April 29 14:30-14:45

Collisional disruption of sintered dust aggregates

SIRONO, Sin-iti[1*] ; UENO, Haruta[1]

[1]Graduate School of Environmental Sciences, Nagoya University

Planets are formed in a protoplanetary nebula consisting of gas and dust grains. The first step of planetary formation is coagulation of dust grains, leading to the formation of dust aggregates. Further growth of the dust aggregates is promoted by mutual collisions between them. The motion of dust aggregates gradually decouples from that of the gas as aggregates grow. Dust aggregates drift inward due to gas drag. If the inward drift is faster than aggregate growth, solid components in a protoplanetary nebula disappears and planets cannot be formed. To prevent infalling, many mechanisms have been proposed (Kretke & Lin 2007, Lyla et al.2009, Sandor et al.2011). Fast collisional growth during the infalling of icy dust aggregates (Okuzumi et al. 2012) is another possibility. These studies are based on the assumption that the motion of aggregates decouples from gas. The infalling velocity is on the order of 1m/s when substantial decoupling is attained. Aggregates should grow to the sizes corresponding to the infalling velocity. Is it possible?

Experimentally, collisional breakup velocity of micron-sized SiO2 dust aggregates is on the order of 1m/s(Blum 2010). Breakup velocity for H_2O ice aggregates is also on the same order(Shimaki & Arakawa 2012). However, it is difficult to produce highly porous dust aggregates experimentally due to the Earth's gravity. I conducted two-dimensional numerical simulation of sintered dust aggregates in this study. It has been pointed out that sintering of H_2O ice proceeds in wide region of a protoplanetary nebula (Sirono 2013). As sintering proceeds, a neck between adjacent grains grows and mechanical interactions between grains greatly change. The effects of sintering are taken into account by changing breaking forces of a contact. The interactions between non-sintered contacts (Dominik & Tielens 1997) are adopted for newly formed contacts.

If sinterng proceeds sufficiently such that a neck is disappeared, catastrophic disruption was observed at low collision velocities (˜10cm/s). This is because a contact is broken by rolling of a grain. On the other hand, catastrophic disruption at low collision velocities was not realized for less-sintered aggregates. This is due to immediate reconnection between grains with a non-sintered mode. These results depends on the tensile strength of H_2O ice. The breakup velocity increases as the strength increases. From the results obtained in this study, the evolution of icy dust aggregates is various, depending on the location in a protoplanetary nebula.

Keywords: dust aggregate, protoplanetary nebula, collisional disruption, sintering

Japan Geoscience Union Meeting 2014
(28 April - 02 May 2014 at Pacifico YOKOHAMA, Kanagawa, Japan)

PPS21-16 Room:416 Time:April 29 14:45-15:00

Planetesimal size and protoplanetary disk turbulence

KOBAYASHI, Hiroshi[1*] ; TANAKA, Hidekazu[2] ; OKUZUMI, Satoshi[3]

[1]Nagoya University, [2]Institute of Low Temperature Science, Hokkaido University, [3]Tokyo Institute of Technology

When the random velocities of bodies are greater than their surface escape velocities, the runaway growth of bodies occurs, which produces a single large bodies surrounded by leftover bodies in each annual of a protoplanetary disk. The slope of the size distribution of bodies becomes steeper through runaway growth. The slope of runaway growth is seen in the size distribution of 100km sized or larger bodies in the main belt. Since the random velocities rises by turbulent stirring in the disk, the planetesimal size above which runaway growth occurs is determined by the strength of turbulence. We discuss turbulence strength in the solar nebula.

Keywords: Planetesimal, Protoplanetary disk, Asteroids, The size distribution of bodies, Planet formation

Japan Geoscience Union Meeting 2014
(28 April - 02 May 2014 at Pacifico YOKOHAMA, Kanagawa, Japan)

PPS21-17 Room:416 Time:April 29 15:00-15:15

The formation of gas planets from cores in type I migration

MAESHIMA, Naohiko[1*] ; WATANABE, Sei-ichiro[1]

[1]Division of Earth and Planetary Sciences, Graduate School of Science, Nagoya University

Many gas planets have been discovered. The formation of the gas planets requires that solid planets, which correspond to cores of gas planets, must achieve the critical core mass M_{crit} before the disk gas have entirely diffused. The cores moves radialy by torques caused by interaction with disk gas (type I migration). It was long thought that the cores fall into the star with very short timescale before achieveing M_{crit} by strong negative torque (Ward 1997, Tanaka et al. 2002). Recent study have showed that the region where positive torque operates is formed on the disk by corotation torque if we consider the non-isothermal process of the gas (Baruteau & Masset 2008,Paardekooper & Papaloizou 2008). As a result, equilibrium radii, where torque is zero, are created. The cores may accrete gas without falling into the star if they are trapped by equilibrium radius because the timescale of radial migration slows down to that of disk evolution. However, positive torque only operates for cores in limited mass range ($M_{p,min}<M_p<M_{p,max}$). If it takes long time for achieving $M_{p,min}$, the cores moves inward largely by negative torque. In this study, we examine how the orbit and mass of cores evolve depending on the disk model, and find the condition the disk must have for the gas planet formation.

The distribution of the gas surface density evolves by viscous diffusion and photoevaporation. The temperature distribution is determined by viscous heating and stellar irradiation. In the disk, an equilibrium radius is formed on the region where the main heating source shifts from the viscous heating to stellar irradiation. In this study, we investigate the possibility of the formation of gas planets at the equilibrium raidus. Cores grow by accreting planetesimals in their gravitational radius, and capture the disk gas if they achieve M_{crit}.

We find that the condition of gas planet formation is determined as follows. In diks evolving fast (α parameter of viscosity = 0.005), cores born in the middle region ($\sim$ 10AU) is captured by the equilibrium radius and capture the disk gas by achieving M_{crit} if core growth stars at the time when disk mass is still large (initial mass accretion rate $\sim 10^{-7} M\odot yr^{-1}$) and the ingredient of the cores is abundant (ratio of the solid material to gas is large $>$0.03). On the other hand, in the disks evolving slowly (α = 0.001), gas planets can be formed even if core growth stars at the stage when disk mass has been decreased (initial mass accretion rate $\sim 10^{-8} M\odot yr^{-1}$). In this case, the dependence on the ratio of the solid to gas is very weak.

Keywords: type I migration

Japan Geoscience Union Meeting 2014
(28 April - 02 May 2014 at Pacifico YOKOHAMA, Kanagawa, Japan)

PPS21-18 Room:416 Time:April 29 15:15-15:30

Protoplanet Spin by Planetesimal Accretion

SHIBATA, Takashi[1*] ; KOKUBO, Eiichiro[2]

[1]University of Tokyo, [2]National Astronomical Observatory of Japan

In the standard scenario of planet formation, protoplanets or planetary embryos are formed through runaway and oligarchic growth of planetesimals. We investigate the spin parameters of protoplanets using N-body simulations. By N-body simulations we can calculate consistently the orbital, accretionary, and spin evolution of planetesimals. The spin of protoplanets are important for terrestrial planet formation since it affects the accretion condition of protoplanets and determines the spin of terrestrial planets. For the standard model of a planetesimal disk, a Mars-sized protoplanet forms in 0.5 million years around 1 AU. We find that the spin angular velocity of planetesimals decreases as their mass increases. Planetesimals obtain their spin angular momentum on the early stage of accretion where their mass ratio is not so large. Once a runaway-growing planetesimal (protoplanet) becomes large enough, it mainly accretes smaller planetesimals whose collisional angular momentum tends to cancel out since they collide from random directions. Thus the protoplanet increases its mass but not the spin angular momentum, which leads to smaller angler velocity for larger protoplanets. When a protoplanet reaches the isolation mass, its typical spin angular velocity is as high as 10% of the critical angular velocity for rotational instability under the assumption of perfect accretion in collisions. We find that the obliquity of planetesimals is well expressed by an isotropic distribution. During the protoplanet growth, the scale height of the planetesimal system is much larger than the size of planetesimals. Thus, collisions are three-dimensional and isotropic, which leads to the isotropic obliquity distribution. We show the dependence of the spin parameters on the initial planetesimal system parameters. The spin angular velocity increases with the bulk density of planetesimals. The dependence of the spin angular velocity on the planetesimal mass becomes weaker as the initial mass of planetesimals increases. However, these system parameters do not affect the obliquity distribution.

Japan Geoscience Union Meeting 2014
(28 April - 02 May 2014 at Pacifico YOKOHAMA, Kanagawa, Japan)

PPS21-19 Room:416 Time:April 29 15:30-15:45

Gravitational accretion of particles onto moonlets embedded in Saturn's rings

YASUI, Yuki[1*] ; OHTSUKI, Keiji[1] ; DAISAKA, Hiroshi[2]

[1]Department of Earth and Planetary Sciences, Kobe University, [2]Graduate School of Commerce and Management, Hitotsubashi University

Collision and gravitational accretion of particles is an important issue related to the origin of ring-satellite systems of giant planets in the solar system. The Hill radii of Pan, Daphnis, Atlas, and Prometheus are found to be within 15 % of the observed long axes of these satellites given by the best-fit model ellipsoids. Also, the densities of these satellites (0.4 - 0.6 g cmˆ-3) are very low compared to the density of water ice and all approximately equal to the critical density at that distance, which is defined as the density of a body that entirely fills its Hill sphere. From these results, the small satellites within the orbit of Pandora are thought to be formed by accretion of small porous ring particles onto large dense cores, and further accretion seems to have been suppressed when the density of the satellite reaches the critical density at that distance. Local N-body simulations also demonstrated that a Hill sphere-filling body is produced by accretion of small porous particles onto a large dense core. However, it has not been studied how the degree of particle accretion onto moonlets in the inner parts of Saturn's rings depends on the distance from Saturn.

The shapes of these small ringmoons would also provide clues to the dynamical evolution of Saturn's rings. The fact that the shapes of these ringmoons approximately match those of their associated Hill sphere suggests that the moonlet cores were surrounded by a number of particles when they were formed. On the other hand, Pan and Atlas have the characteristic shapes with equatorial ridges, and are thought to be formed by two stages. First, their precursors whose shapes are similar to their Hill sphere without equatorial ridges were formed when the rings were thick. Then, equatorial ridges were formed through particle accretion onto the equatorial planes of the above formed objects after the rings became sufficiently thin and also before ring particles diffused. However, effects of dynamical properties of the rings on the shaping of moonlets formed by particle accretion have not been examined in detail.

Propeller-shaped structures have also been found in Cassini images of Saturn's rings. These propeller-shaped features are explained by gravitational interaction between ring particles and unseen embedded moonlets. From these observations, the sizes and orbital distributions of these unseen embedded moonlets are obtained, and such information provide us with clues to the evolution of the ring-satellite system. The propeller-shaped structures are mainly observed in the A ring. Recently, observations of similar structures have also been reported for the Cassini Division, and the B and C rings. Although some of these moonlets either may be collisional shards resulting from the breakup of a bigger icy progenitor ring body or may have formed by accretion of small low-density ring particles onto larger dense fragments, the origin of these moonlets is not clear.

Using local N-body simulation, we examine gravitational accretion of ring particles onto moonlets in Saturn's rings. We find that gravitational accretion of ring particles onto moonlets is unlikely to occur at radial locations interior to the outer edge of the C ring, unless the density of the moonlets is much larger than that of water ice or non-gravitational cohesive forces play a major role. Detailed analysis of accretion process of individual particles onto moonlets shows that particle accretion onto high-latitude regions of the moonlet surface occurs even if the rings' vertical thickness is much smaller than the moonlet's radius. The degree of particle accretion in outer rings is found to depend significantly on rings' vertical thickness and optical depth. Our results suggest that large boulders recently inferred from observations of transparent holes in the C ring are likely to be collisional shards, while propeller moonlets in the A ring would be gravitational aggregates formed by particle accretion.

Keywords: gravitational accretion, moonlet, Saturn's rings

Japan Geoscience Union Meeting 2014
(28 April - 02 May 2014 at Pacifico YOKOHAMA, Kanagawa, Japan)

PPS21-20 Room:416 Time:April 29 16:15-16:30

Mass-Loss Evolution of Super-Earths: Constraints on Their Compositions and Origins

KUROKAWA, Hiroyuki[1*] ; KALTENEGGER, Lisa[2] ; NAKAMOTO, Taishi[3]

[1]Nagoya University, [2]Max Planck Institute for Astronomy, [3]Tokyo Institute of Technology

Recent progress of he search for exoplanets, for example the transit observations with Kepler space telescope, has pushed toward small planets. Especially, ”Super-Earths”, that are planets having sizes from Earth to Neptune, are revealed as quite common: ˜30% of solar-type stars have super-Earths (Howard et al., 2012). Therefore, an understanding of their compositions, which is related to their origins, is important for planet formation and evolution.

We can speculate the compositions of super-Earths both whose masses and radii are known by using theoretical mass-radius relations for different compositions. Some fraction of super-Earths have low density, which suggests the presence of H/He envelopes formed by protoplanetary-disk gas capture. There exist. on the other hand. high-density super-Earths possibly having rocky- or water-rich compositions. The origin of this dichotomy is one problem that we address in this study, which possibly arises from the difference of the amount of captured disk gas due to different masses and disk temperature in their formation stages, or from XUV (X-ray and EUV)-driven atmospheric escape in later evolution stages (e.g., Lopez et al., 2012). Another problem that we address in this study is ”the degeneracy of composition”: The compositions of super-Earths can be fitted by various ratios of H/He envelope, rock, and water. Their atmospheric compositions have been speculated by measuring their transmission spectra, but recent observations using Hubble Space Telescope suggested that cloudy atmospheres of super-Earths (Kreidberg et al., 2014; Knutson et al., 2014). If clouds are common in atmospheres of Super-Earths, direct measurements of their compositions are difficult because clouds obscure any features of atmospheric species.

In this study, we show constraints on these problems of compositions and origins of super-Earths by calculating their mass-loss evolution due to XUV-driven atmospheric escape considering the differences of host-stellar types. The ratio of XUV luminosity and bolometric luminosity differs among stellar types, which enables us to distinguish formation origin and mass-loss origin of the dichotomy of super-Earths with or without H/He envelopes. Also, the degeneracy of compositions can be solved by considering stability criteria to lose H/He envelopes.

We calculated the critical orbital radii to lose H/He envelopes for different stellar types, that corresponds to different equilibrium temperature depending on stellar types. The obtained critical separations are consistent with the distribution of the observed super-Earths with or without H/He envelopes, suggesting that the observed dichotomy has a mass-loss origin.In this case, we expect that super-Earths having moderate density and orbiting inside the critical separation are water-rich super-Earths without H/He envelope.

We also evaluated uncertainty caused by mass-loss model and XUV luminosity and discuss the validity of our results.

Keywords: exoplanet, atmospheric escape, composition, super-Earth

Japan Geoscience Union Meeting 2014
(28 April - 02 May 2014 at Pacifico YOKOHAMA, Kanagawa, Japan)

PPS21-21 Room:416 Time:April 29 16:30-16:45

Exoplanet exploration for brown dwarfs with infrared astrometry

YAMAGUCHI, Masaki[1*] ; YANO, Taihei[1] ; GOUDA, Naoteru[1]

[1]National Astronomical Observatory of Japan

The astrometry is one of the oldest method for the exoplanet exploration. However, only one exoplanet has been found with the method. This is because the planet mass is sufficiently smaller than the mass of the central star, so that it is hard to observe the fluctuation of the central star by the planet. Therefore, we investigate the orbital period and mass of planets which we can discover by the future astrometric satellites for brown dwarfs with the mass less than a tenth of the solar mass.

So far five planetary systems have been found, whose mass ratios are larger than a tenth. For example, for the system whose distance, orbital period and mass ratio are 10 pc, 1 year and a tenth, respectively, the apparent semi-major axis reaches 3 milli-arcsecond, which can be well detected with the future astrometric satellites such as Small-JASMINE and Gaia. With these satellite, we can discover even super-Earth for the above system.

We further investigate where in the period-mass plane we can explore the planet for individual brown dwarf with Small-JASMINE and Gaia. As a result, we find that we can explore a wide region where period and mass are within 5 years and larger than 3 earth mass. In addition, we can explore the region around 0.1 day and 10 jovian mass, where planets have never found for any central star, and where we can explore only with Small-JASMINE for most target brown dwarfs.

Keywords: astrometry, brown dwarf, exoplanet exploration, infrared, Small-JASMINE, Gaia

Japan Geoscience Union Meeting 2014
(28 April - 02 May 2014 at Pacifico YOKOHAMA, Kanagawa, Japan)

PPS21-22 Room:416 Time:April 29 16:45-17:00

Experimental study on organic aerosol formation in super-Earths' atmosphere: Implications for transit observations

KOBAYASHI, Jumpei[1*] ; SEKINE, Yasuhito[2] ; HONG, Peng[2]

[1]Dept. Earth & Planet. Sci., Univ. Tokyo, [2]Dept. Complexity Sci. & Engr., Univ. Tokyo

A super-Earth is an extrasolar planet with a mass greater than Earth and below Neptune. Although there is no super-Earth in our solar system, astronomical observations demonstrate that it is one of the major categories of planets beyond the solar system. Recent transit observations of super-Earths, including GJ 1214b, indicate that their atmospheres contain opaque clouds or haze at high altitudes. One candidate for the opaque materials is metallic or salt dusts, such as KCl and ZnS, which would condense in the upper atmospheres of super-Earths. Another candidate is organic haze, such as those observed in the atmosphere of Saturn's moon Titan, which would be composed of high-molecular-weight hydrocarbon aerosols produced through photochemical reactions involving CH_4. Given the proposed formation mechanisms of nearby super-Earths, e.g., planetary migration, they would have a wide variety in chemical composition of atmosphere. However, previous laboratory experiments have mainly focused on organic aerosol formation in Titan's and early Earth's atmospheres. Thus, both the formation rate and optical property of organic haze for various atmospheric compositions have been poorly constrained by laboratory experiments.

In this study, we investigate the formation rate and optical property of organic aerosols formed by laboratory experiments simulating super-Earths' atmospheres with a wide variety in chemical composition. We used initial gas mixtures of H_2 and CH_4 or CO_2 and CH_4, and varied the H_2/CH_4 or CO_2/CH_4 ratios. The experiments were conducted at a total pressure of 1 Torr in a flow system. Cold plasma irradiation was used to initiate aerosol formation. We measured the aerosol formation rate, chemical compositions of intermediate gas molecules, and optical property of aerosol using a spectroscopic ellipsometer, a quadrupole mass spectrometer, and a UV/VIS spectrometer, respectively.

Our experimental results show that the aerosol formation rate decreases with increasing the H_2/CH_4 ratio, suggesting that recycling of high-molecular-weight hydrocarbons to CH_4 occurs through reactions with H and H_2 under H_2-rich conditions. We also show that organic aerosols are produced less efficiently at higher CO_2/CH_4 ratios. The results of gas analyses also show that formation of high-molecular-weight hydrocarbons are inhibited at higher CO_2/CH_4 ratios. These results indicate that oxygen-bearing molecules and radicals formed by CO_2 dissociation oxidizes hydrocarbons produced from CH_4, which results in a lower aerosol formation rate at higher CO_2/CH_4 ratios. Optical constant of the aerosols formed under the conditions simulating super-Earths' atmospheres is significantly lower than those of Titan aerosol analogs.

Based on the experimental results, we discuss the chemical composition and formation process of transiting super-Earths, such as GJ 1214b, by comparing the observed transmittance spectra with the model spectrum. We suggest that organic aerosol production in a H_2-rich or CO_2-rich atmosphere is inefficient so that organic haze would not be capable of explaining the observed transit spectra of super-Earths, even if they contains gaseous CH_4 in the atmospheres.

Keywords: exoplanet, super-Earth, organic aerosol, haze, atmospheric composition

Japan Geoscience Union Meeting 2014
(28 April - 02 May 2014 at Pacifico YOKOHAMA, Kanagawa, Japan)

PPS21-23 Room:416 Time:April 29 17:00-17:15

Transmission spectrum models of low-mass exoplanet atmospheres with haze: Application to GJ 3470b

KAWASHIMA, Yui[1*] ; IKOMA, Masahiro[1] ; FUKUI, Akihiko[2] ; NARITA, Norio[2]

[1]The University of Tokyo, [2]National Astronomical Observatory of Japan

Since the first exoplanet was discovered in 1995, detection of more than 1000 exoplanets has been reported. Recently, transit observations of an exoplanet have been done at multiple wavelengths. From a decline in apparent stellar brightness due to a planetary transit, we can measure the plantary radius. In addition, observed dependence of the planetary radius on wavelength (which is often called the transimission spectrum) provides the information of absorption and scattering by molecules and small particles such as haze and clouds in the planetary atmosphere. Thus, the composition of the planetary atmosphere can be constrained by comparison between the observational and theoretical transmission spectra. The constraint on atmospheric composition gives an important clue to the origin of the planet.

Our observational group has recently observed transits of two low-mass exoplanets, GJ 3470b and GJ 1214b, at multiple wavelengths. For both planets, the observed transit radii in the optical wavelength region are greater than those in the near-infrared region, inferring the existence of haze in the atmosphere. While the observed transmission spectrum was already analysed theoretically in detail as for GJ 1214b, there are few researches discussing the theoretical spectrum models incorporating the effect of haze systematically for GJ 3470b. In this study, we have modeled theoretical transmission spectra of low-mass exoplanets orbiting close to their host stars. Then, applying the calculated spectrum models to GJ 3470b and GJ 1214b, we discuss the property of the atmospheres of both planets.

In calculating theoretical spectrum models, we have taken into account the vertical distribution of molecular abundances from the chemical equilibrium calculations, in addition to absorption and scattering of the incident radiation from the host star by molecules and haze particles in the planetary atmosphere. We explore the dependences of the atmosphere's metallicity, C/O ratio and water vapor abundances on the transmission spectrum. We also probe the dependences of haze's height, particle sizes and number density. In comparing the observed and theoretical transmission spectra, we have performed the chi-squared analysis to quantify the validity of each atmospheric model.

Keywords: exoplanets, transits, transmission spectrum models, atmospheric composition, haze

Japan Geoscience Union Meeting 2014
(28 April - 02 May 2014 at Pacifico YOKOHAMA, Kanagawa, Japan)

PPS21-24 Room:416 Time:April 29 17:15-17:30

The SEEDS Exoplanet and Circumstellar Diks Survey

KUZUHARA, Masayuki[1*] ; TAMURA, Motohide[2] ; KUDO, Tomoyuki[3] ; HASHIMOTO, Jun[4] ; KUSAKABE, Nobuhiko[5] ; MATSUO, Taro[6] ; MCELWAIN, Michael[7] ; JANSON, Markus[8] ; TAKAHASI, Yasuhiro[2]

[1]Department of Earth and Planetary Sciences, Tokyo Institute of Technology, [2]Department of Astronomy, The University of Tokyo, [3]Subaru Telescope, [4]H. L. Dodge Department of Physics and Astronomy, University of Oklahoma, [5]National Astronomical Observatory of Japan, [6]Department of Astronomy, Kyoto University, [7]NASA Goddard Space Flight Center, [8]Astrophysics Research Centre, Queen's University Belfas

About 1,000 extrasolar planets (or exoplanets) have been discovered by now. Furthermore, Kepler survey has reported the presences of more than 3,000 exoplanet candidates (Huber et al. 2013). Thus, the planetary systems are common in our Galaxy, but it has known that those exoplanets have a variety of properties. Meanwhile, studies for circumstellar disks, which are the birth-places of planets, have also progressed. In particular, the radio telescope ALMA, whose operations have recently started, have provided intriguing data for the structure properties of protoplanetary disks (e.g., van der Marel et al. 2013; Casassus 2013). ALMA should provide a deep insight to the studies of circumstellar disks.

Direct imaging observations enable the discovery and study of exoplanets orbiting their host stars at wide orbital separations comparable to a few tens of AU, but the detections of those are impractical with indirect techniques such as radial velocity or transit method. Direct imaging is also useful to characterize circumstellar disks. The high-resolution observations of scattered light from protoplanetary disks or debris-disks have provided many important clues to reveal the physical disk-planet connections. We have progressed the SEEDS project, which aims at detecting and characterizing giant exoplanets and circumstellar disks with the Subaru 8-m ground-based telescope, state-or-the-art adaptive optics AO188, and a high-sensitivity infrared camera HiCIAO that we have newly developed. The total SEEDS sample will reach 500 targets, and this target sample adequately covers stellar ages ranging from 1 to 1000 Myr for solar-type stars. Also, intermediate-mass or low-mass stars are included in our SEEDS sample. The survey is currently in its fifth year, and to date, it has identified intriguing structures, such as gaps or spirals, in more than 10 transitional or debris disks (e.g., Hashimoto et al. 2012; Grady et al. 2013). Furthermore, SEEDS has discovered a massive giant planet candidate orbiting the B-type star Kappa Andromedae (Carson et al. 2013) and a Jovian planet in orbit with a size of about 44 AU (GJ 504b) around the G0-type Sun-like star GJ 504. GJ 504b has an estimated mass of about 4 Jupiter masses and effective temperature of 500 K. Among such the wide-orbit exoplanets directly imaged so far, GJ 504b represents the lowest-mass Jovian planet, and the inferred effective temperature is the coldest. The follow-up observations for GJ 504b have revealed the presences of methane in its atmosphere (Janson et al. 2013), allowing us to report the first methane detection in an atmospheres of directly imaged exoplanet. Thus, SEEDS has successfully identified and studied the exoplanets with the previously unknown properties. After the end of SEEDS survey, the comprehensive and statistical analysis of entire survey sample will be carried out. This analysis leads to improve our understanding about exoplanets and circumstellar disks. In addition, it should become a promising clue that connects to future exoplanet/disk studies, such as a survey of extrasolar Earths.

Here, we report the latest achievements of SEEDS project, such as the detection of GJ 504b. Moreover, its whole survey status and progress are also reported, as well as the future plan of SEEDS project.

Keywords: extrasolar planet, debris disk, protoplanetary disk, giant planet, direct imaging observation

Japan Geoscience Union Meeting 2014
(28 April - 02 May 2014 at Pacifico YOKOHAMA, Kanagawa, Japan)

PPS21-P01 Room:Poster Time:April 29 18:15-19:30

Sonic Boom Analysis of Meteorite at Hypersonic Speeds in Earth Atmosphere

YAMASHITA, Rei[1*] ; SUZUKI, Kojiro[1]

[1]Graduate School of Frontier Sciences, The University of Tokyo

The sonic boom followed by the passage of shock waves may cause serious damage on the ground, when a meteorite falls at hypersonic speeds as experienced at the Chelyabinsk meteorite event in February 2013. Therefore, it is important to evaluate the sonic boom generated by the meteorite. In this study, the prediction method of the sonic boom developed in the aeronautical engineering is applied to the case of the meteorite. The nature of the sonic boom propagation in the earth atmosphere is evaluated by the whole-domain simulation technique, which is based on the computational fluid dynamics in the domain bounded by the flying object and the ground (R. Yamashita and K. Suzuki, APISAT2013, No. 02-05-3). The flowfield around the sphere with 20 m diameter is numerically obtained by solving the three dimensional Navier-Stokes equations with the gravity term. The earth ' s atmospheric model is based on the international standard atmosphere (ISO 2533:1975). The flight Mach number is 10 (about 3 km/s), the flight altitude is 10 km and the flight condition is the steady level flight. The computational grid is constructed by rotating the two dimensional grid about the body axis and the number of the grid points is about 5.5 million. After the numerical calculation is conducted by using the initial grid, the calculation is performed again with the adaptive grid reconstructed to align the bow shock wave to avoid the artificial smearing of the shock wave. For computational efficiency, the domain is divided into several sectors from the body to the ground. The shape of the meteorite is approximated as a sphere and the axi-symmetric flowfield is assumed in the sector near the body. The numerical fluxes are evaluated by SHUS scheme (E. Shima and T. Jounouchi, NAL SP, pp.7-12, 1997) with the third order accuracy by MUSCL interpolation technique. The time integration is conducted by MFGS (E. Shima, proceedings of 29th Fluid Dynamic Conference, pp.325-328, 1997) method. The gravity term is added to the governing equations as a source term.

The flowfield around the sphere is composed of the bow shock wave in front of the body and the trailing shock wave in the wake. Both the waves propagating downward are merged into a single wave at 8 km altitude. In such case, the sonic boom sounds only once, while the sonic boom generated by a supersonic airplane creates explosive sounds twice without merging of the shock waves. It is reported that Chelyabinsk meteorite has been broken into three big pieces and the sonic boom sounds three times at the ground (NHK COSMIC FRONT, June 2013). Hence, the number of the pieces is equal to that of the sound of explosion. This fact seems consistent with the present simulation result. The pressure rise across the shock wave decreases with the distance from the body because of the geometric spreading. In the actual earth's atmosphere, however, the rate of decrease becomes smaller near the ground, because the atmospheric pressure and temperature increase toward the ground. Assuming the pressure augmentation factor of 1.9 at the reflection of the shock wave at the ground, the peak pressure rise is estimated at about 1.5 kPa, which is 63 times as large as the maximum allowable pressure rise (24 Pa) determined in the environmental regulation for the supersonic airplane. In the case of the Chelyabinsk meteorite, the pressure rise is estimated at 3.2±0.6 kPa (Nature 12741) from the observation of the damage of the glass windows there. Although the numerical condition is not the same as the actual flight condition of the meteorite, the pressure rise due to the passage of a meteorite at hypersonic speeds is expected to be in the order of 1 kPa or higher.

As mentioned above, the prediction method developed in the aeronautical engineering has a great potential to predict the flight condition, say, the size, altitude and Mach number, from the magnitude of the sonic boom measured on the ground by conducting the parametrical study.

Keywords: Sonic Boom, Meteorite, Hypersonic Flow, CFD, Shock Wave

Japan Geoscience Union Meeting 2014
(28 April - 02 May 2014 at Pacifico YOKOHAMA, Kanagawa, Japan)

PPS21-P02 Room:Poster Time:April 29 18:15-19:30

The brightness and the color temperature of the Chelyabinsk bolide

YANAGISAWA, Masahisa[1*]

[1]Univ. Electro-Communications

The bolide explosion on Feb. 15, 2013 over Chelyabinsk, Russia was the next most violent to the probable bolide explosion in Tunguska, Siberia in 1908. It was recorded by many dashboard movie cameras in a wide area around the city, and the movies are released on the Internet. We analyzed one of them and obtained the lightcurves of the bolide for three colors (see the figure for the temporal variations of the brightness). More than 95% of the radiant energy in the visible wavelengths was released in its flare-up for about 2 seconds. The luminosity ratios among the R (red), G (green), and B (blue) color bands are consistent with the 3500 K black-body radiation during the flare, while the pre-flare bolide was greenish-blue in color and the ratios do not agree to the black-body spectra. The maximum luminosity was 1.0 x 10^{15} W. The impact energy is estimated to be 1.9 x 10^{15} J or 450 kton in TNT equivalent (1 kton = 4.185 x 10^{12} J), based on an empirical formula for the radiant efficiency of bolides. The lightcurves and the impact energy almost agree to the results reported thus far.

Figure caption: Temporal variations of the source luminosities of the bolide in logarithmic scales. The thick (red), dotted (green), and thin (blue) lines correspond to the RGB color bands. The calculated intensities are negative in the periods without plot. The vertical scale on the right side shows the luminosity integrated over the wavelengths assuming 3500 K black body radiation. Seconds of 3:20 on Feb. 15, 2013 (UT) are shown in abscissa.

Keywords: bolide, meteoroid impact, small solar system objects, Chelyabinsk, Space guard, meteorites

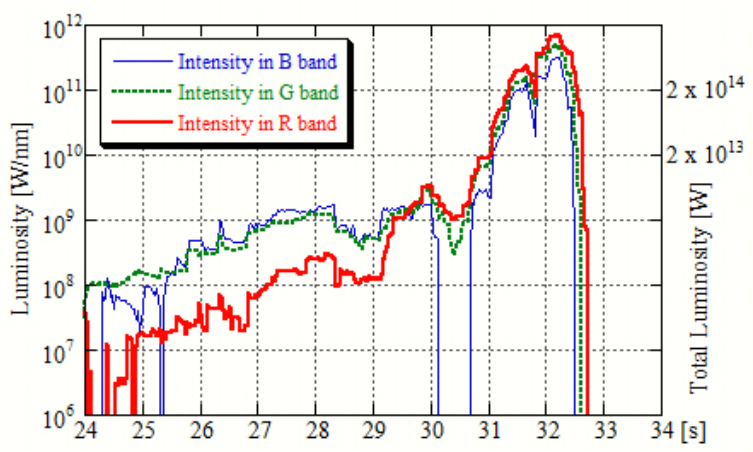

Japan Geoscience Union Meeting 2014
(28 April - 02 May 2014 at Pacifico YOKOHAMA, Kanagawa, Japan)

PPS21-P03 Room:Poster Time:April 29 18:15-19:30

Statistical distribution of the solar system dusts by meteor head echo observations with the large-aperture radar

ABE, Shinsuke[1*] ; KERO, Johan[2] ; NAKAMURA, Takuji[3] ; FUJIWARA, Yasunori[4] ; WATANABE, Jun-ichi[5]

[1]Department of Aerospace Engineering, College of Science and Technology, Nihon University, [2]Swedish Institute of Space Physics (IRF), [3]National Institute of Polar Research (NIPR), [4]Nippon Meteor Society, [5]National Astronomical Observatory of Japan

A meteor head echoes is caused by radio waves scattered from the intense region of the plasma surrounding and co-moving with a meteoroid during atmospheric entry at about 70-130 km altitude. Meteor head echo observations were carried out using the high-power large-aperture (HPLA) Kyoto university Shigaraki middle and upper atmosphere (MU) radar in Japan (34.85deg N, 136.10deg E). Since 2009 the atmospheric trajectories and interplanetary orbital elements have been derived by the MU radar meteor head echoes (e.g.; Kero et al. (2012); Kero et al. (2011)). Approximately 120,000 orbital elements of meteors with excellent accuracy were obtained until January 2014. Typical error for velocity and semi-major axis are 0.3 km/s and 0.1 AU, respectively. Such a huge number of meteoroid orbits with the precise orbital accuracy has not been observed before. Here we report some results obtained by the statistical analysis of the database, such as orbital distributions and associations of comets and asteroids.

Keywords: meteors, dusts, meteoroids, comets, asteroids, MU radar

Japan Geoscience Union Meeting 2014
(28 April - 02 May 2014 at Pacifico YOKOHAMA, Kanagawa, Japan)

PPS21-P04 Room:Poster Time:April 29 18:15-19:30

Laboratory experiment simulating Martian surface observation with submillimeter-wave polarimetric radiometry

ARIMURA, Taketo[1*] ; OCHIAI, Satoshi[2] ; KIKUCHI, Kenichi[2] ; KITA, Kazuyuki[3] ; KASAI, Yasuko[2]

[1]Graduate School of Science and Engineering, Ibaraki University, [2]National Institute of Information and Communications Technology, [3]Faculty of Science, Ibaraki University

Energies and materials exchange between the ground and atmosphere on Mars play important roles in the Martian general circulation. It is necessary to observe the spatial and temporal variability of the Martian surface from orbiter. However, it has been quite difficult to continually monitor the Mars surface in optical observation due to opaqueness of the Martian dust. Millimeter/submillimeter radiometers enable to observe the Martian surface through dust, though such measurement has never been conducted in planetary exploration. We assess the effectiveness of this observation method by laboratory experiment.

By observing millimeter/submillimeter emission from the Martian surface in several emission angles and two polarizations, we can derive physical temperatures, permittivity and roughness of the surface from brightness temperatures. In order to estimate each property from polarized brightness temperatures, we need to know relationship between emissivity or/and reflectivity in millimeter/submillimeter wave region and the parameters of surface.

We developed an experiment system to examine millimeter/submillimeter scattering and emission characteristics of the simulated Martian surface in a chamber. Measurement samples in the chamber are coolable at Martian surface temperature. The chamber is designed to measure emission of samples using a receiver and reflection of samples using a transmitter and a receiver. We can also obtain arbitrary-polarized emission with arbitrary incident angle by controlling mirrors in our system.

To discuss relationship between emission and surface parameters on the Martian surface, it is necessary to know influences of permittivity and surface roughness on the reflectivity. Therefore, we measured reflectance of Acrylic plate and Alumina grain at millimeter/submillimeter waves region. We discuss effects of permittivity and roughness on measured reflectivity of measurement samples in known polarization and incident angle. Moreover, we retrieve the permittivity and the roughness of sample from measured reflectivity. Using this measurement results, we expect a step closer to explanation of relationship between emission and surface parameters in the Martian surface at millimeter/submillimeter waves region.

Keywords: Mars, surface observation, submillimeter-wave

Japan Geoscience Union Meeting 2014
(28 April - 02 May 2014 at Pacifico YOKOHAMA, Kanagawa, Japan)

PPS21-P05 Room:Poster Time:April 29 18:15-19:30

Scientific importance and possibility of HCN detection in Enceladus plumes by ALMA

KODAMA, Kenya[1*] ; SEKINE, Yasuhito[1] ; IINO, Takahiro[2] ; SAIGO, Kazuya[6] ; KASAI, Yasuko[3] ; SAGAWA, Hideo[4] ; MAEZAWA, Hiroyuki[5]

[1]Dept. Complexity Sci. and Engr. Univ. of Tokyo, [2]Solar-Terrestrial Environment Laboratory,Graduate school of science,Nagoya University, [3]Senior Researcher Global Environment Division National Institute of Information and Communications, [4]National Institute of Information and Communications Technology, [5]Department of Physical Science Osaka Prefecture University, [6]National Astronomical Observatory of Japan

Saturn's icy moon, Enceladus, exhibits ongoing geological activities, including eruption of water-rich plumes from warm fractures near the south-pole region. These geological activities together with the findings of Na-rich salts in the plumes suggest the presence of an interior liquid ocean beneath the icy crust. This demonstrates that Enceladus' plumes provide a unique opportunity to investigate the chemical composition of oceanic water, possible geochemical reactions, and habitability of the icy moon. However, due to limitations of in-situ measurements of the plumes by the Cassini spacecraft, it is not able to identify or quantify some key molecules, which could probe physical and chemical conditions of the ocean.

Here we discuss scientific importance and possibility of detection of HCN in the plumes by large ground-based, sub-millimeter telescope, ALMA. Because HCN is one of the fundamental materials contained in icy planetasimals in the outer solar system, and because it readily hydrolyzes in warm water($>$50 ℃), a lack of HCN suggests that Enceladus' interior would have experienced relatively high temperatures, i.e., a presence of hydrothermal activity. On the other hand, if HCN were presence in the plumes, this in turn means that Enceladus would have been cold throughout its history. Given the results of thermal evolution model, the latter case suggests late formation of the Saturnian system($>$5Myr) after CAI formation, which would result in a depletion of short-lived radiogenic heat source in Enceladus.

To evaluate the possibility to detect HCN in the plumes by ALMA, we first estimate a special distribution of H_2O gas density based on results from Cassini's observations and plume eruption modeling. Then, we calculate radiactive temperatures of HCN in the field of view of ALMA as a function of HCN concentration. Finally, the upper limit of HCN as a function of observation time will be obtained. For instance, if HCN were not detected within 4-6 hours of observation time, an upper limit of the HCN concentration in the plumes becomes 0.2% relative to water, which is comparable to a typical concentration of HCN in comets. Thus, the ALMA telescope is capable of detecting HCN in Enceladus' plumes within a reasonable observation time, if it were present in an amount comparable to that of comets. In either case whether HCN were presence or not, we would be able to constrain geochemical reactions and thermal history of Enceladus as well as the timing of formation of Saturnian system.

Japan Geoscience Union Meeting 2014
(28 April - 02 May 2014 at Pacifico YOKOHAMA, Kanagawa, Japan)

PPS21-P06 Room:Poster Time:April 29 18:15-19:30

Development of SPH: Toward Understanding of Disk-planet Interaction Near the Disk Inner Edge

FUJII, Yuri[1*] ; IWASAKI, Kazunari[1] ; TSUKAMOTO, Yusuke[1] ; INUTSUKA, Shu-ichiro[1]

[1]Nagoya University

Recent observations of exoplanets reveal the existence of close-in planets. These planets are thought to form in outer disks and migrate inward because of the disk-planet interaction. If there are disk inner cavities, planets can stop migrating and stay in close-in orbit. Disk evolution is highly affected by these planets. Thus, the understanding of the interaction between disks and close-in planets is crucial. In this study, we develop a numerical scheme to investigate the interaction between disks and planets. Although the grid-based schemes are widely used in this context, there are difficulties in calculating with a disk inner cavity or eccentric planets. These difficulties can be removed by smoothed particle hydrodynamics (SPH) with high accuracy. In this presentation, we will talk about the development of code and the performance evaluation.

Keywords: exoplanet, protoplanetary disk, smoothed particle hydrodynamics

Japan Geoscience Union Meeting 2014
(28 April - 02 May 2014 at Pacifico YOKOHAMA, Kanagawa, Japan)

PPS21-P07 Room:Poster Time:April 29 18:15-19:30

Evolution of a protoplanetary disk and chemical composition of planetesimals

NAGAHARA, Hiroko[1*] ; OZAWA, Kazuhito[1]

[1]Dept. Earth Planet. Sci., The Univ. Tokyo

We investigate physico-chemical evolution of the proto-solar disk at the early stage by developing a new model that combines physics and chemistry with special interest to temporal and spatial evolution of the disk. Then, we discuss how the composition of planetesimals varies depending on the time and space for their formation including refractory or volatile rich ones.

The basic of the model is a radial advection-diffusion equation, which includes drift and dispersion by turbulence with stochastic diffusion term calculated by the Monte Carlo method and which shows the diffusivity by the viscosity of the disk. The difference from conventional disk models is that the present method stands on the Lagrangean differentiation, and it is able to trace the movement of individ- ual particles.

A considerable amount of materials in the inner regions are transported outward at the early stage (t <10^5 yrs), which is because the surface density is much larger in the inner region at the early stage of the disk evolution. Although the outward flux is large at the early stage, there comes a larger amount of materials from the outer region even within ~10^5 yrs. The mixing ratio of materials from the inner regions to outer regions is almost unity within several AU all through the disk evolution, suggesting that thermally processed materials and unprocessed materials were mixed in the inner region of the disk. It is important that the relative abundance of materials from outer regions becomes larger with time, which implies that planetesimals formed within several AU at the early stage of the disk evolution consists partly of materials initially located at the inner regions and partly from outer regions, but those formed at the later stage contain more abundant law materials transported from the outer regions.

The mixing ratio of materials from the inner and outer regions is almost unity at the early stage but the fraction of materials from the outer regions increases with time. Combining the information about the maximum temperature that the particles experienced, we can constrain that early differentiated planetesimals such as the parent body of angrites and planetesimals with refractory-rich compositions such as CV chondrites were formed at the inner region of the disk in ~10^5 yrs. On the other hand, planetesimals for other carbonaceous chondrites or ordinary chondrites that are depleted in sulfur were formed later, possibly at ~10^6 yrs.

Keywords: protoplanetary dsik, chemical evolution, dust movement

Japan Geoscience Union Meeting 2014
(28 April - 02 May 2014 at Pacifico YOKOHAMA, Kanagawa, Japan)

PPS21-P08 Room:Poster Time:April 29 18:15-19:30

Simulating global dust coagulation with grain charging

OKUZUMI, Satoshi[1*] ; TANAKA, Hidekazu[2]

[1]Graduate School of Science and Engineering, Tokyo Institute of Technology, [2]Institute of Low Temperature Science, Hokkaido University

Growth of dust particles by collisions is the initial step of planet formation. Conventionally, the theory of dust coagulation in protoplanetary disks assumed electrically neutral dust particles, but in reality dust in the disks is likely to be charged given that the disks are ionized by cosmic rays and stellar X-rays. In our previous work (Okuzumi 2009; Okuzumi et al. 2011a,b), we extensively studied the role of grain charging in protoplanetary dust growth, and concluded that dust growth stalls at its early stage because of the excessively large (negative) charges carried by small dust aggregates. We also predicted that this ”charge barrier” could be overcome (albeit on a very long timescale) if dust in the disks is globally transported by radial drift and turbulent diffusion.

The purpose of the present work is to demonstrate the breakthrough of the charge barrier in a global setup. In order to do this, we have developed a new simulation code for global dust coagulation including the effect of grain charging. The new code is based on a previous code for planetesimal formation (Brauer et al. 2008; Okuzumi et al. 2012) but now calculates charging and Coulomb repulsion of dust particles at each location in a disk consistently with the particle size distribution at the same location. To verify the code, we perform some test simulations and compare them with the prediction from our previous theory.

Keywords: dust, charging, planet formation, protoplanetary disk

Japan Geoscience Union Meeting 2014
(28 April - 02 May 2014 at Pacifico YOKOHAMA, Kanagawa, Japan)

PPS21-P09 Room:Poster Time:April 29 18:15-19:30

N-body simulations of Rubble pile Collisions in Tidal fields

HYODO, Ryuki[1*] ; OHTSUKI, Keiji[1]

[1]Kobe University, Graduate School of Science

We examine collisional disruption of gravitational aggregates in the tidal environment by using local N-body simulations. We find that outcomes of such collision largely depend on impact velocity, direction of impact, and radial distance from the planet. In the case of a strong tidal field corresponding to Saturn's F ring, collisions in the azimuthal direction is much more destructive than those in the radial direction. Numerical results of collisions sensitively depend on impact velocity, and complete disruption of aggregates can occur even in impacts with velocity much lower than their escape velocity. In such low-velocity collisions, deformation of colliding aggregates plays an essential role in determining collision outcomes, because the physical size of the aggregate is comparable to its Hill radius. On the other hand, the dependence of collision outcomes on impact velocity becomes similar to the case in free space when the distance from the planet is sufficiently large. We submitted the results to the Astrophysical Journal.

Keywords: rings, satellites, aggregates

Japan Geoscience Union Meeting 2014
(28 April - 02 May 2014 at Pacifico YOKOHAMA, Kanagawa, Japan)

PPS21-P10 Room:Poster Time:April 29 18:15-19:30

An improved fragmentation model on outcome of planetesimal collisions

FUJITA, Tomoaki[1] ; GENDA, Hidenori[2*] ; KOBAYASHI, Hiroshi[3] ; TANAKA, Hidekazu[4] ; ABE, Yutaka[1]

[1]Department of Earth and Planetary Science, University of Tokyo, [2]Earth-Life Sicence Institute, Tokyo Institute of Technology, [3]Department of Physics, Nagoya University, [4]Institute of Low Temperature Science, Hokkaido University

Collisions between planetesimals or a planetesimal and a protoplanet are thought to occur frequently in the stage of planet formation, and these planetary bodies grow up through these collisions. However, if destructive collisions between them occur frequently, these bodies break up into fragments rather than promote the growth of them. Therefore, in order to understand the process of the growth for planetesimals and protoplanets, it is important to know the impact conditions under which a collision is destructive. The critical specific impact energy for catastrophic disruption $Q_D{}^*$, where the largest remnant has half the target mass, has been well investigated under various conditions so far (Holsapple et al., 2002; Benz & Asphaug, 1999; Leinhardt & Stewart, 2009). Such catastrophic impacts have been regarded as important process for planet formation. The values of $Q_D{}^*$ which has been referred and used most frequently were calculated by Benz and Asphaug (1999). Although they performed many impact simulations to determine $Q_D{}^*$, the resolution of their numerical simulation were quite low and they did not check the resolution convergence of $Q_D{}^*$. In addition, recent studies (Kobayashi & Tanaka, 2010; Kobayashi et al., 2010) have suggested that non-disruptive small-scaled impacts were also important to the growth of protoplanets, because these small-scaled impacts are much more frequent than disruptive impacts.

In order to discuss more correctly the growth of planets, a correct value of $Q_D{}^*$ and the relation between ejecta mass and impact energy for small-scaled impacts should be required. In this thesis, I investigate the resolution dependence of $Q_D{}^*$ and obtain a correct value of $Q_D{}^*$ for planetesimal collisions by numerical impact simulations with sufficient resolution. I also investigate small-scaled impacts, and formulate the relation between the ejecta mass and impact energy.

Using the smoothed particle hydrodynamics method (SPH) with self-gravity and without strength, I systematically perform the hydrodynamic simulations of collisions between rocky planetesimals. I consider collisions of 10 km and 100 km rocky targets and various sized impactors under various conditions such as impact velocity, impact angle and resolution.

I found that the value of $Q_D{}^*$ depended on resolution. This is because distribution ratio of initial impact energy to kinetic and internal energy of a target differs depending on resolution due to shear flows which appears during propagation of shock wave and rarefaction wave and ejection process. This energy distribution ratio, probably also $Q_D{}^*$, converges in using 7.5×10^7 particles. The resolution in Benz & Asphaug (1999), where they performed impact simulations with 5×10^4 particles, was insufficient. The $Q_D{}^*$ obtained by higher-resolution simulations is about a half order of magnitude smaller than that of Benz and Asphaug (1999). This means collisions between planetesimals or a planetesimal and a protoplanet are more destructive than previously thought. I applied improved $Q_D{}^*$ to the growth of protoplanets using analytical method proposed by Kobayashi et al. (2010). As a result, the mass of the finally formed protoplanet is a half smaller than the case for previous $Q_D{}^*$. In addition, I derived the formulation of scaling law representing the relation between ejecta mass and impact energy from small-scaled impacts to destructive impacts. I found that this relation can be scaled by target size, impact energy normalized by $Q_D{}^*$, and impact velocity, but it depend on impact angle. With $Q_D{}^*$ and the scaling law obtained in this study, the final grown mass of a protoplanet is 0.058 M_{earth} at 1AU and 0.17M_{earth} at 5 AU, where M_{earth} represents the Earth mass.

Japan Geoscience Union Meeting 2014
(28 April - 02 May 2014 at Pacifico YOKOHAMA, Kanagawa, Japan)

PPS21-P11 Room:Poster Time:April 29 18:15-19:30

Numerical modeling of impact phenomena using iSALE shock physics code

KUROSAWA, Kosuke[1*] ; SENSHU, Hiroki[1] ; WADA, Koji[1] ; MIKAMI, Takashi[2] ; HIRATA, Naru[3] ; KAMATA, Shunichi[2] ; ISHIHARA, Yoshiaki[4] ; GENDA, Hidenori[5] ; NAKAMURA, Akiko[6] ; TAKATA, Toshiko[7]

[1]PERC, Chitech, [2]Dept. of CosmoSciences, Hokkaido Univ., [3]Dept. of Computer Sci. & Eng., The University of Aizu, [4]ISAS, JAXA, [5]ELSI, Titech, [6]Dept. of Earth and Planetary Sciences, Kobe University, [7]Division of Science Education, Miyagi University of Education

iSALE (impact-SALE) is a shock physics code based on the SALE hydrocode (Simplified Arbitrary Lagrangian Eulerian), which is an open code for planetary scientist. iSALE contains a number of option to model impact phenomena of geological materials. The calculation results can be easily visualized and analyzed using included software. A number of ANEOS tables and strength models of geological materials, including water ice, silicate rocks, and iron are also included. We have formed a user community called " iSALE users group in Japan " to introduce iSALE to the Japanese society for planetary science and to share information on the usage of iSALE. The URL of our wiki page and the mailing list are as follows.

The URL of the wiki page of iSALE users group in Japan
https://www.wakusei.jp/~impact/wiki/iSALE/

Mailing list
isale-users-jp@perc.it-chiba.ac.jp

In the presentation, we show the results of a number of test calculations using iSALE.

We gratefully acknowledge the developers of iSALE, including Gareth Collins, Kai W$\bar{u}$
nnemann, Boris Ivanov, Jay Melosh and Dirk Elbeshausen.

Keywords: Hypervelocity impacts, Shock physics code, Hydrocode calculation, Equations of state, strength model, iSALE

Japan Geoscience Union Meeting 2014
(28 April - 02 May 2014 at Pacifico YOKOHAMA, Kanagawa, Japan)

PPS21-P12 Room:Poster Time:April 29 18:15-19:30

Study on fundamental characteristics of penetration dynamics into icy target

NAMBA, Kazuya[1*] ; SUZUKI, Kojiro[2]

[1]Grad. Sch. Eng., The University of Tokyo, [2]GSFS, The University of Tokyo

A penetrator, which penetrates the surface of a planet, a satellite and so on to investigate the interior by high-speed hard landing, is expected to play an important role in the solar system exploration of the future. Comparing to soft lander, penetrator has advantages of consuming less fuels, enabling us to launch multiple probes at a time because of its low mass, and so on. However, probe must survive hard impact in collision, thus no penetrator missions have been successfully achieved so far. The icy object, such as 24 Themis and Europa, is expected to contain organics which serve as the precursor of life in their subsurface. Therefore, the cryo-penetrator, which penetrates the icy object and investigate specimens of subsurface which have not been contaminated by cosmic rays, should have a high importance. For a penetrator into regolith, a fully-developed flyable penetrator has been successfully developed for the Lunar-A mission, though the mission itself has been cancelled. For icy target, however, the number of studies from the engineering viewpoint is quite limited, for example, the conceptual study on CRAF mission to a comet nucleus (Adams et al., NASA CR-177393, 1986). In this study, we investigated the fundamental properties of the penetration dynamics of the cryo-penetrator, by conducting penetration experiments into the target made from H_2O ice.

Penetration experiments were conducted by using a ballistic range in our laboratory. The projectile is accelerated by the compressed air, launched horizontally and crashed into a target body. Impact speed is set from 100 m/s to 300 m/s. Two types of projectile, a needle-like one (iron, size: ϕ2.45x15mm, mass: 1.71g) and a blunt cone-like one (brass, ϕ8.4x15mm, 2.33g) are used. Three types of target, pure H_2O ice (size: 270x175x130mm, mass: 5.5kg, density: 0.90g/cm^3, porosity: 3%), low purity H_2O ice (150x120x100mm, 1.5kg, 0.75g/cm^3, 19%) and an oil clay (155x120x70mm, 2.2kg, 1.7g/cm^3) are used. A high-speed camera (frame rate: 2200-8800fps, exposure time: 15μs) is used to observe a sequence of events: the free-flight of the projectile, impact, crater formation, penetration, and so on.

We found that the penetration into H_2O ice produces ejecta of icy fragments, which erupt conically immediately after collision, and then produces the jet-like ejecta in the almost perpendicular direction to the surface that continues more than 100 msec. On the other hand, the penetration into clay target produces ejecta outward-conically for duration of a few msec. Moreover, we found that the penetrator tends to be pushed back from the target by the ejecta, since the ice around the projectile has been almost broken into pieces erupting as the ejecta and the penetrator cannot be fixed inside the target without receiving the gripping force from the ice. We also found that eruption was continued even after the projectile has completely bounced from the target. This phenomena is frequently observed when the projectile with a less slender body. In the case of a slender penetrator, however, it is hardly subject to bounce-back. Consequently, a slender shape seems more suitable to the penetrator for icy target. The shape of crater consists of the pit region on the center, the spall region which is a shallow depression on the periphery of the pit, and cracks spread a wide range of target. It is qualitatively consistent with previous researches using bullet shape (e.g. Kato et al., Icarus 113(2) 423-441, 1995., Arakawa, Low Temperature Science 66 113-121, 2008). The pressure at a point of impact is estimated by using the one-dimensional planar impact approximation (Wada, JSIAM 16(4) 19-31, 2006): the result shows that it is beyond the Hugoniot elastic limit (HEL), thus the H_2O ice is expected to behave like fluid in the vicinity of the impact point.

This work is supported by Grant-in-Aid for Scientific Research (B) No. 25289301 of Japan Society for the Promotion of Science.

Keywords: icy object, penetrator, crater, ballistic range

Japan Geoscience Union Meeting 2014
(28 April - 02 May 2014 at Pacifico YOKOHAMA, Kanagawa, Japan)

PPS21-P13 Room:Poster Time:April 29 18:15-19:30

Experimental study of compaction process of powder bed by centrifuge experiment

OMURA, Tomomi[1*] ; KIUCHI, Masato[1] ; GUETTLER, Carsten[2] ; NAKAMURA, Akiko[1]

[1]Graduate School of Science, Kobe University, [2]Max-Planck-Institute for Solar System Research

Dust aggregates in protoplanetary disk are compacted by dust-dust collisions, ram pressure of the disk gas and self-gravity (Kataoka et al., 2013). At reaccumulation phase of asteroids, porosity of rubble pile and regolith would be determined by collisional pressure and self-gravity.

Relationship of porosity of powder layer and particle's radius is given by (Yu et al., 2003; Kiuchi and Nakamura, 2014)

$p=p_0+(1-p_0)\exp\{-mR_F^{-n}\}$ (1)

where R_F is the ratio between the magnitudes of the van der Waals force between two particles and gravity force on particles, therefore a function of particle radius. p_0, m, and n are constants. p_0 should be understood as the porosity without any interparticle force.

It is not clear if Eq.1 can be applied for powder layer under different gravity from 1 G. Eq.1 was originally derived for particles at surface, and we don't know to what extent this equation is able to be applied for the interior of planetary bodies, i.e., it has not examined for the porosity evolution of bodies due to the accumulation of new grains and blocks onto the surface. If Eq.1 is applicable to such case, porosity given by Eq.1 should be consistent with the result of the case in which R_F is reduced by increasing the gravity. In this study we perform experiments, under different gravitational accelerations, and we compare the results with Eq.1.

We use silica sand, 60 wt% of grains have sizes ranging from 7.5 μm and 80 μm and fly ash, 60 wt% of grains have sizes ranging from 1 μm and 8 μm. They were sieved into a cylindrical container of diameter 5.8 cm and depth 3 cm. After that, the top part of the bed over the height of the container was leveled off. Porosity of each granular bed is approximately 60 % and 70 %. The experiments were performed at elevated acceleration on a centrifuge to provide 1-18 G and observed with a video camera. In contrast with unidirectional compressive compaction using a piston, centrifugal compaction is capable of applying uniform compressive force at any place of the container without causing any local disturbance (Mizuno et al., 1991). After the materials were compressed, bed height was measured with a laser displacement meter and the difference between the initial bed height and the average bed height after acceleration was calculated.

As a result, it is shown that Eq.1 is consistent with experimental result within 6 % (silica sand) and 5% (fly ash) in porosity when assuming the grain diameter=24 μm and 4.5 μm, respectively. This diameter corresponds to the median of cumulative weight distribution of the grains. Also, the diameter of the small silica sand grains sticked with large grains is close to 24 μm.

Keywords: planetesimal, asteroid, porosity, high gravity, powder and granular material

Japan Geoscience Union Meeting 2014
(28 April - 02 May 2014 at Pacifico YOKOHAMA, Kanagawa, Japan)

PPS21-P14 Room:Poster Time:April 29 18:15-19:30

High velocity impact cratering experiments on ice-sand mixture simulating the surface of icy satellites

TAKANO, Shota[1*] ; ARAKAWA, Masahiko[1] ; YASUI, Minami[2]

[1]Graduate School of Science, Kobe University, [2]Organization of Advanced Science and Technology, Kobe University

It is well known that ice-rock mixtures could be a main component of icy satellites, the surface crust of asteroid Ceres. Ceres' icy crust could be impacted by various asteroids with different components and physical properties will affect the crater morphology. Therefore, we would obtain various information from the investigation of the observed craters such as material properties of impacted asteroids and the internal structures of the icy crust and so on. To conduct these investigation, the laboratory experiments would be necessary to derive such information from the observed crater. Then, we should carry out the cratering experiments on ice, ice-rock mixtures and the layered target.

Impact experiments on ice has been conducted systematically under various conditions. However, the cratering experiments on ice-rock mixture were limited in the impact velocity range and the rock contents. It is necessary to experiment at the velocity higher than 4km/s to apply to craters on Ceres, but it is not done now. Therefore, we made cratering experiments on ice?rock mixtures at the impact velocity higher than 1km/s using the several types of the projectile, and compared them with the pure ice to clarify the effects of rock inclusion on the crater morphology and crater scaling law.

We installed and used a new two-stage light gas gun at Kobe University in 2013. We prepared ice-rock mixture targets simulating Ceres crust which consisted of water ice and quartz sand having a particle size of about 500μm, and the quartz content was regulated to be 81$\pm$2wt%. The ice-sand mixture was made in a cylindrical metal container with the height of 5$\sim$10cm and the diameter of 15cm. The water-sand mixture was frozen in a freezer with the temperature from -23 ℃ to -15 ℃. Used spherical projectiles were made of aluminum (2.7g/cm3), titanium (5g/cm3), and zirconium (5.7g/cm3), respectively. We lunched projectiles at 1.6$\sim$5.1km/s with nylon sabots to use various types of projectiles. To prevent targets from melting, the vacuum chamber was evacuated for insulation. The chamber pressure during the experiments was from 200 to 230Pa. A crater formation process was taken by an image-converter camera every 5μs, and 18 successive images were obtained for each shot. From these images, we examined the characteristics of impact eject such as the growth rate, and the shape, and it was compared with that of pure ice. We measured the crater shapes by a caliper.

We found that the spallation was difficult to occur on the ice-rock mixture targets compared to pure ice targets. So, the depth-diameter ratio of the crater for ice-rock mixtures, these dependencies on the velocities, and the projectile densities was different from that of pure ice targets. We found that the crater diameter on the ice-rock mixture is about a half of that on pure ice at the same impact energy. Hiraoka et al. (2004) made the cratering experiments on ice-rock mixture with the rock contents from 0 to 50 wt% at the constant impact energy. We compared their results with our results obtained for 80 wt% and found that our result is almost consistent with their results of 50 wt% content. This means that the crater size stop decreasing at 50 wt%, then it becomes almost constant until 80 wt%. We speculate that the crater size might drastically change to be small between 80 to 100 wt% corresponding to rock itself. It might be possible that the crater size could be controlled by the ice strength from 0 to 80wt% and by the rock strength at the range of content near 100 wt%. The crater scaling law proposed by Housen and Holsapple (2012) was applied, and the scaled crater radius π_R and the scaled strengthπ_Y were investigated in our results. Our results were compared with that of pure ice and the ice-rock mixture's dynamic tensile strength was supposed to be 100MPa if the ice-rock mixture was scaled by the same parameter as that of pure ice.

Keywords: icy satellites, ice-sand mixture, impact crater, high velocity impact experiments

Japan Geoscience Union Meeting 2014
(28 April - 02 May 2014 at Pacifico YOKOHAMA, Kanagawa, Japan)

PPS21-P15 Room:Poster Time:April 29 18:15-19:30

Experimental study on the decay process of impact-induced stress propagating through granular materials

MATSUE, Kazuma[1*] ; ARAKAWA, Masahiko[1] ; YASUI, Minami[2]

[1]Graduate School of Science, Kobe University, [2]Organization of Advanced Science and Technology, Kobe University

Introduction: Impact process is one of the most important physical processes in the solar nebula. In order to understand the impact histories related to planetary formation process, it is important to study the impact cratering process and the scaling law. Impact cratering experiments have been performed on granular material, and the crater size is found to be different depending on the target material. So, it is necessary to study how physical properties affect the cratering process, especially for excavation stage. Excavation flow is a main process that controls the crater size, so we should examine the effects of material properties. However, it is difficult to observe the flow inside the target, so we used the in-material sensor to measure the pressure. The pressure distribution in the granular target would show the flow and we can compare the crater size and the pressure distribution to clarify the effect of target materials on the crater formation process.

Experimental method: We prepared a target container with a pressure sensor to measure the stress generated by impact. It is made of aluminum with the size of 10cm×10cm×10cm, and we changed the depth of the granular target from 1 to 10cm. The pressure sensor (20kPa, ≤2kHz)was attached on the bottom of the container just below the impact point, and impact experiments were conducted by a free-fall or by a one-stage vertical He-gas gun in Kobe University. We studied the effects of projectile size and impact velocity on the crater size and the stress wave. We used glass beads and quartz sand with the diameter of 100 and 500μm as granular target, and glass balls (ϕ=7.75, 10, 15mm) in free-fall, nylon and alumina (ϕ= 3mm) in vertical gun experiments as projectile. Impact velocity is 2-5.5m/s in free-fall and 60-70m/s in vertical gun experiments. We observed crater size and pressure wave in each experiment.

Results: We found that the size of the impact crater strongly depends on the granular materials, that is, the crater formed on the quartz sand was systematically smaller than that formed on the glass beads. Then, we found that the pressure wave increased suddenly and decreased with a relaxation time depending on target materials. The relaxation time is small for quartz sand and long for glass beads, and the relaxation time of 100μm quartz sand was not measured because of normal mode oscillation of the pressure sensor: it means that the time is less than 0.5ms.

Although the normal mode oscillation of the sensor was observed in the high velocity impact and the shallow depth impact in the case of gas gun experiments, we analyzed the peak of measure pressure waves (P_{max}) and obtained the relaxation time (τ) by fitting them with the following function: $P(t)$-$P(\infty)$=$A\exp(-t/\tau)$, where t is time after the impact. As a result, τ is obtained to be 1ms for glass beads target irrespective of the bead size, and 0.1ms for 500μm quartz sand. The relationship between the pressure and the propagation distance was described by $P(r)=P_0(r/L)^{-b}$, where L is a projectile radius, r is distance, P_0 is an initial impact pressure, and b is a decay constant. The decay constant was found to change with the impact velocity and the target materials: it was derived to be 0.79,0.94 in a low velocity range, 1.61,1.71 in a high velocity range for glass beads, quartz sand.

We found that the relationship between the crater size and P_{max} at 4cm depth was different in each granular material. The crater size of the glass beads target was larger than that of the quartz sand at the same P_{max} . Then, we introduce a new parameter expressed by τ times P_{max}, so called impulse, I. We renewed the relationship using I instead of P_{max} and found that all data set were merged on one line. This means that I could be a suitable parameter to describe the material dependence of the cratering efficiency. We would like to clarify what material properties determine the τ and how it changed with the physical condition in the future.

Keywords: Excavation flow, Granular material, Cratering process

Japan Geoscience Union Meeting 2014
(28 April - 02 May 2014 at Pacifico YOKOHAMA, Kanagawa, Japan)

PPS21-P16 Room:Poster Time:April 29 18:15-19:30

Effects of impact angles on the impact strength of icy and rocky planetesimals for the collision among equal size bodies

KOMOTO, Yasunari[1] ; ARAKAWA, Masahiko[1] ; YASUI, Minami[2*]

[1]Graduate School of Science, Kobe University, [2]Organization of Advanced Science and Technology, Kobe University

Introduction: There are a lot of impact experiments to simulate planetesimals collisions, and most of them had a large mass difference between a projectile and a target. The impact strength is well known that they are described by the energy density: the ratio of the projectile kinetic energy to the mass of the target and the projectile. So, when the projectile is rather smaller than the target (this is an usual situation in the lab. experiments), the very high speed more than 1 km/s is necessary to disrupt the target. This is an analogy of the present asteroid collisions, but it might be far from the simulation expected in planetesimals collisions. Because we speculate the collisions among the similar size small bodies in the solar nebula, and the relative collisional velocity among them could be several 10 m/s. Therefore, it should be important that the planetesimals were disrupted or not at the impact speed around several 10m/s for the collisions among similar size small bodies, then we must conduct the collisional experiments to derive the impact strength of planetesimals in the similar size collisions. In this study, we carried out the impact experiments using the equal size ball made of ice, gypsum, and gypsum-glass beads mixture. These samples simulate icy planetesimals, planetesimlas for chondrite parent bodies. We also conducted not only head-on collision but also oblique collision and studied the effects of impact angles on the impact disruption.

Experimental methods: We prepared three types of ball sample with the size of 25 mm and 30 mm made of ice, gypsum-glass beads mixture, and gypsum. They were made by putting each solution in a round mold to form spherical sample. The impact experiments were made by using three types of accelerators: they are a spring gun for low velocity collision, a vertical gas gun for ice and a horizontal gas gun for gypsum, and the achieved velocity is from 4 to 160m/s. The oblique impact was also conducted by shifting the impact point from the geometrical center of the target. The impact angle was changed from 0 deg. (normal impact) to 80 deg. (nearly passing away impact). Impact experiments were observed by a high-speed camera and all of the impact fragments were collected to measure the weight and establish the size distribution. We looked for the recovered fragments to identify the same fragment found in the video image, and tried to construct the velocity-mass distribution of the impact fragments.

Results: We used the reduce mass to calculate the impact energy in the center-of-mass system, so the energy density Q_g was defined by the ratio of the kinetic energy of two bodies in the center-of-mass system to the mass of the two equal balls. The impact strength was obtained for the similar size collisions by using this Q_g. As a result, the impact strength ${Q_g}^*$ of ice and gypsum was derived to be almost similar to that obtained for the impact experiments with the mass difference more than 10. However, the ${Q_g}^*$ of glass beads-gypsum mixture was derived to be rather smaller than that obtained in the previous experiments. In the oblique impacts, the mass of the maximum impact fragment was found to decrease with the increase of the impact angle. So, we modify the energy density by using the velocity component normal to the impact surface which effectively work for the disruption, then this modified energy density enabled us to fit all of the data on one line for each target. Finally, we estimated the re-accumulation condition of planetesimals according to the velocity distribution of the impact fragments that obtained in this study. As a result, it is speculated that icy planetesimals could re-accumulate for the bodies larger than 20 km in the diameter, and this threshold size for the planetesimals of ordinary chondrite parent bodies is 5.2km and that for the planetesimals of carbonaceous chondtite parent bodies is 6.7km.

Keywords: Planetesimals, Oblique impact, Impact strength, Energy partition, Re-accretion

Japan Geoscience Union Meeting 2014
(28 April - 02 May 2014 at Pacifico YOKOHAMA, Kanagawa, Japan)

PPS21-P17 Room:Poster Time:April 29 18:15-19:30

Dynamic compaction experiments of porous materials: Implications for impact compaction of pre-planetesimals

YASUI, Minami[1*] ; YOKOTA, Mizuki[2] ; SAKAMOTO, Kana[2] ; ARAKAWA, Masahiko[3]

[1]Organization of Advanced Science and Technology, Kobe University, [2]Faculty of Science, Kobe University, [3]Graduate School of Science, Kobe University

Introduction: Two theories are proposed for the growth mechanism of bodies with the diameter from cm to several hundreds meters (pre-planetesimals). One is that planetesimals could form by a gravitational instability in the dust layer of a protoplanetary disk. The other is that planetesimals could form by a repeating impact coagulation of dust aggregates. In this study, we focus on the latter theory. There are some problems that planetesimals could not grow because of rebound and catastrophic disruption among pre-planetesimals caused by the increase of average density. Sakamoto (2013) did free-fall impact experiments of porous snow simulating icy pre-planetesimals by using the stainless cylinder to examine the compaction conditions, and clarified the relationship between the impact stress and the final density profile and the size of compaction area. However, the impact velocities in her study were 0.7 to 3.5 m/s, relatively lower compared to the average impact speed of pre-planetesimals. In this study, we conducted impact experiments of porous materials at $>$5 m/s to examine the compaction mechanism, impact stress, and density profile.

Experimental methods: The target was high porous snow with the initial porosities of 70 and 80% and perlite particles with the density of 85 kg/m^3 simulating the icy and rocky pre-planetesimals. We did impact experiments of snow in the cold room (-10 ℃) at ILTS, Hokkaido University, and perlite at Kobe University, by using the one-stage vertical and horizontal light gas guns. The vertical gun was used for only snow targets. The target was prepared by packing ice grains or perlite particles into the acrylic tube, up to 120 mm depth, and the blue ice grains or the red perlite particles were put into the target every 20 mm from the bottom due to measure the density changing with depth. The piston was set on the target surface in the acrylic tube, and accelerated by the projectile to compress the target. The projectiles were an elastic ball with the diameter of 25 mm for horizontal gun and same ball installed on the cylindrical sabot with the diameter of 30 mm for vertical gun. The pistons were a polycarbonate, an aluminum, and a polyacetal cylinders with the diameter of 30 mm and the height of 10-30 mm to examine the effects of piston type. The impact velocities were 2-118 m/s. The impact compaction of the target was observed by a high-speed digital camera. The shutter speed was set to be 20 to 100 μs, and the frame rate was set to be 6000 to 10000 fps.

Results: First, we measured the impact stress from the motion of piston, σ_p, and compared σ_p with the strength calculated by Kinoshita method, Y. As a result, the σ_p was almost same with the Y for both perlite and snow targets.

Next, we measured the final density of target, ρ_f, and obtained the relationship between the ρ_f and the kinetic energy or the momentum of projectile. As a result, we found that the ρ_f for perlite was determined by the kinetic energy while that for snow was determined by the momentum. Furthermore, we proposed the model of ρ_f for perlite and snow by assuming these compaction mechanisms: the perlite compressed due to the fracture of perlite particles while the snow compressed due to the decrease of area among ice grains. We compared these models with our experimental results and found that they were almost consistent with each other.

Finally, we examined the relationship between the σ_p and the final density of top layer in the target, ρ_{f1}. As a result, we obtained as ρ_{f1}=3.0${\sigma_p}^{0.8}$ for perlite and ρ_{f1}=127${\sigma_p}^{0.3}$ for snow in kPa. The data for snow at σ_p $>$100 kPa was scattered because the compaction mechanism was changed at σ_p $>$100 kPa.

Keywords: pre-planetesimal, dynamic compaction, impact experiment, final density, Kinoshita strength, compression viscosity

Japan Geoscience Union Meeting 2014
(28 April - 02 May 2014 at Pacifico YOKOHAMA, Kanagawa, Japan)

PPS21-P18 Room:Poster Time:April 29 18:15-19:30

Effect of particle size distribution on thermal conductivity of powdered materials

SAKATANI, Naoya[1*] ; OGAWA, Kazunori[2] ; HONDA, Rie[3] ; ARAKAWA, Masahiko[4] ; TANAKA, Satoshi[2]

[1]The Graduate University for Advanced Studies, [2]Institute of Space and Astronautical Science, [3]Kochi University, [4]Kobe University

Understanding about heat transport mechanism of powdered materials, such as lunar surface regolith, is important issue in order to estimate planetary thermal evolution and present thermal state. Thermal conductivity of powdered materials depends on various parameters (particle size and its distribution, temperature, compressional stress, etc.). Depending on these parameters, thermal conductivity can vary by one order of magnitude. Due to insufficiency of the experimental studies, heat transfer mechanism is not understood enough, and it is difficult to constrain in-situ thermal conductivity on planetary surface.

Our purpose is to understand the heat transfer mechanism of powdered materials under vacuum conditions by means of systematic survey of parameter dependences of the thermal conductivity. This will enable us to model the thermal conductivity, which can apply the estimation of thermal conductivity structure on planetary surface. Most of previous studies focus on the powdered samples with uniform particle size. However, actual planetary regolith has wide range of particle size from sub-μm to mm. Moreover, parent bodies of chondritic meteorites would be composed of mixture of meteoritic matrix and chondrule. In this presentation, we will report the effect of particle size distribution on the thermal conductivity under vacuum.

Glass beads mixtures of 100 μm and 200 μm in diameters were used. Prepared samples had volume mixing ratio of 1:0, 2:1, 1:1, 1:2, and 0:1. Porosity of each sample was 0.38, 0.35, 0.32, 0.35, and 0.38, respectively. The thermal conductivity of these samples was measured by line heat source method.

As a result, 100 and 200 μm glass beads of uniform sizes had 0.0023 and 0.0035 W/mK, respectively. This difference in the conductivity would be caused by the difference of radiative heat transfer. On the other hand, mixing samples had thermal conductivity of 0.0039, 0.0029, and 0.0039 W/mK for mixing ratio of 2:1, 1:1, and 1:2, respectively. These conductivities related well to porosity. There were no linear relation between thermal conductivity and mixing ratio. We found M-shaped correlation between them.

The measured thermal conductivity can be represented by the sum of solid conductivity, which is conductive contribution through contact area between the particles, and radiative conductivity, which is radiative contribution through the pore between the particle surfaces. Our results will be explained by the variation of these conductivities with particle size distribution. Therefore, it is necessary to separate the measured values into solid and radiative conductivities for explanation of our experimental results. This can be accomplished by investigation of temperature dependence of the conductivity. In this presentation, we will report dependence of solid and radiative conductivities on the particle size distribution.

Japan Geoscience Union Meeting 2014
(28 April - 02 May 2014 at Pacifico YOKOHAMA, Kanagawa, Japan)

PPS21-P19 Room:Poster Time:April 29 18:15-19:30

Measurement experiments of thermal conductivity and sound velocity in sintered glass beads

TSUDA, Shoko[1] ; OGAWA, Kazunori[1*] ; SAKATANI, Naoya[2] ; ARAKAWA, Masahiko[3] ; YASUI, Minami[3]

[1]The University of Tokyo, [2]The Graduate University for Advanced Studies, [3]Kobe University

The thermal conductivity and sound velocity of sintered particle materials (glass beads) were experimentally measured, and a correlation between them was investigated. Particles have often played important roles in the solar system history. Especially dust particles condensed in the early solar nebula formed planetesimals, and they remained as the main structure material of the bodies. The particles were then gradually sintered as temperature increased by disintegrations of radioactive isotopes. Finally, a part of planetesimals might be completely sintered and began to melt. Currently the sintered materials may also exist on the lunar and asteroid subsurface for example. Mechanical and thermal properties of such sintered materials are essential information for investigating the history of these bodies.

In the thermal issues, particles are known as a strong thermal insulator in vacuum. Although the thermal conductivity of sintered materials has never been measured, it is considered to be a value between the unsintered and a continuous rock, depending on degree of the sintering process. Concerning the sound velocity, characteristic feature depending on the sintering degree is expected to be similar to the thermal conductivity, because basically the phonon conduction is a common mechanism for both the thermal and sound phenomena in electrical insulation materials.

In this presentation, we report results of the first experiments of the thermal conductivity and sound velocity measurements in sintered particle materials. For measurement samples, 9 different blocks of sintered soda-lime glass beads were prepared: three bead diameters of 180-255, 355-500, and 710-1000 μm, and three degrees of sintering that have nearly the same porosity 40%. The cross section of sintering contact sites (neck) was evaluated for each sample. The thermal conductivity was measured by the line heat source method by a line heater and temperature sensors given in the sample in advance. The sound velocity was directly measured by a transmitter and receiver put at both ends of the block samples.

As results of the experiments, both the thermal conductivity and the sound velocity had an apparent correlation with each other, and with degree of sintering. They appeared almost in proportion to the neck diameter, which feature obviously indicates that the neck or contact size controls the bulk thermal and sound conductions, in weakly-sintered particle systems at least. These results can be directly applied to estimation of thermal and mechanical property of the ancient planetesimals. These results also suggest that the thermal conductivity of sintered materials, and also of unsintered particles probably, can be evaluated by measurements of the sound velocity.

Keywords: Particle material, Regolith, Thermal Conductivity, Sound velocity, Glass beads

Japan Geoscience Union Meeting 2014
(28 April - 02 May 2014 at Pacifico YOKOHAMA, Kanagawa, Japan)

PPS21-P20 Room:Poster Time:April 29 18:15-19:30

Experiment to know the power to pull mutually between things that are axisymmetric for the Saturn's-like magnetic axis

MASE, Hirofumi[1*]

[1]none

The magnetic axis of magnetic field in the Saturn is corresponding to the rotation axis(1). And, Saturn's rings revolve on the equatorial plane of the Saturn(2). I want to think that the reason why beautiful rings exist miraculously is related to these miraculous features. The power to pull against each other between things that are axisymmetric for the magnetic axis is generated on the plane that passes center of the axial dipole field and intersects vertically for the magnetic axis. Because the material that composes the ring is tied to the material on the 180-degree other side by the surcharge-gravitation, Saturn's rings are generated and maintained. I am making the experiment that proves the truth of this hypothesis. I introduce the result of it.

∗∗∗∗Composition of experiment (Please refer to the drawing)∗∗

"A","C":the one(34L∗25W∗25H) that natural whetstone(sandstone) was cut

"B":the one(40L∗40W∗40-80H) that 4-8 pieces of permanent magnet(anisotropic ferrite,40L∗40W∗10H,B=79mT,F=2.746kgf)s were piled up

Device box:I used "two step box" on the market and remodeled it. The front side of the left cell of this box is glazed. The front side of the right cell of this box is opening. Plywood in which "B" is set is put on the medium plate of this box to close the hole in the plate. The left cell is airtight exclusive of the top of the vinyl chloride pipe. "A" is hung from the ceiling by two strings(1,700L) and can swing freely in the left cell. The space of "B" and "A" in geostationary point is about 20mm. "C" is hung from the top board in the right cell by the string. The edge of another string is bonded on the right side of "C". (State:"C1")"C" can be separated from "B" by pulling this string from the right side of this box. (State:"C2")"C" can approach "B" by loosening this string.

∗∗∗∗Condition of experiment∗∗I experimented on the following three kinds of by changing the composition and direction of "B". Condition 1:pile 8 pieces vertically(magnetic axis is perpendicular) Condition 2:pile 4 pieces vertically(axis, perpendicular) Condition 3:pile 4 pieces horizontally(axis, horizontal right and left)

∗∗∗∗Procedure of one experiment∗∗1.I wait as much as possible until the swing of "A" stops(now"C1"). 2.I begin taking a picture of the animation of "A" with the video camera(now"C1"). 3.After 2 minutes pass, I change State from "C1" into "C2"(now"C2"). 4.After 4 minutes pass, from "C2" into "C1"(now"C1"). 5.After 6 minutes pass, from "C1" into "C2"(now"C2"). 6.After 8 minutes pass, I end taking a picture.

∗∗∗∗Result of experiment∗∗"A" swung faintly when taking a picture was begun. 1.In case of Condition 1 and 2, the swing was controlled at time zone in State "C2" of the first times, and was amplified at time zone in State "C2" of the second times. 2.In case of Condition 3, I could not confirm special change of "A" during all time.

∗∗∗∗Consideration∗∗I seem I can conclude that static electricity and magnetism don't influence the result by the comparison between Condition 2 and 3. There is a possibility that the power that I had expected was detected.

Reference literature

(1)Hori/"The School of the Universe (13th)"/NAOJ
http://th.nao.ac.jp/MEMBER/hori/pdf/HORI_2013Mar26_part1.pdf P23
(2)Hiratsuka City Museum http://www.hirahaku.jp/hakubutsukan_archive/tenmon/00000050/59.html

PPS21-P20 Room:Poster Time:April 29 18:15-19:30

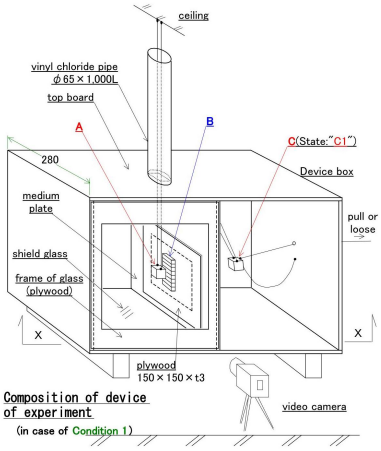

Composition of device of experiment
(in case of Condition 1)

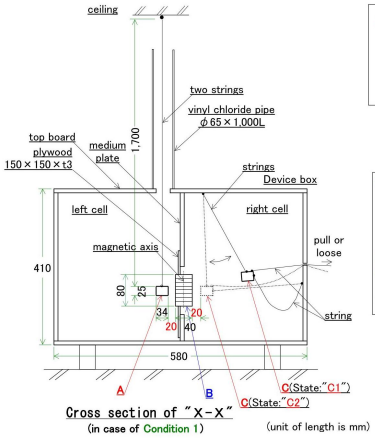

Cross section of "X-X"
(in case of Condition 1)
(unit of length is mm)

A, C : natural whetstone(sandstone)
34L × 25W × 25H

B : permanent magnet(anisotropic ferrite,40L × 40W × 10H, B=79mT,F=2.746kgf) piled up 4～8 pieces
40L × 40W × 40～80H

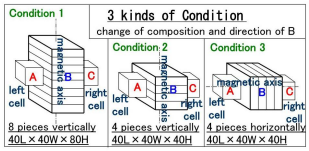

Japan Geoscience Union Meeting 2014
(28 April - 02 May 2014 at Pacifico YOKOHAMA, Kanagawa, Japan)

PPS22-01 Room:415 Time:May 1 09:00-09:15

Compositional and textural inhomogeneity of Chelyabinsk meteorites

ARAI, Tomoko[1*] ; ABE, Shinsuke[2] ; OHTSUKA, Katsuhito[3] ; HIROI, Takahiro[4] ; KOMATSU, Mutsumi[5] ; FAGAN, Tim[5]

[1]Chiba Inst. of Technology, Planetary Exploration Research Center, [2]Nihon University, [3]Tokyo Meteor Network, [4]Brown University, [5]Waseda University

Meteorites are important sources of information on composition and age of the solar system materials. However, collected meteorites are likely biased and unrepresentative of the near-Earth meteoroid population. Mineralogy and reflectance spectra of meteorites are used to link specific classes of meteorites and asteroids, but are not definitive enough. Meteorites of which fall were witnessed are rare and substantial case when meteorites and their parent bodies are directly linked, and both orbital and material data of the near-Earth bodies are known. The fireball was eye-witnessed near Chelyabinsk city of Russia in 15 February 2013, and associated meteorites of total mass of 4-6 ton, were subsequently recovered. Survey of physical and chemical nature of small bodies with an Earth-crossing orbit is crucial in understanding the origin and evolution of the near-Earth materials and in planetary defense. While near-Earth objects (NEO) >1 km dia. have been largely identified by NEO survey programs, most NEOs <?100 m dia. remain unknown. Thus, it is important to study the Chelyabinsk-sized objects. We present mineralogy and reflectance spectra of several chips of Chelyabinsk meteorites, which indicate chemical and spectral inhomogeneity, suggesting the complex history of the parent body.

Keywords: Chelyabinsk meteorites, Meteoroid impacts, Inhomogeneity

Japan Geoscience Union Meeting 2014
(28 April - 02 May 2014 at Pacifico YOKOHAMA, Kanagawa, Japan)

PPS22-02 Room:415 Time:May 1 09:15-09:30

Classification and petrologic features of chondrites of petrologic type 7

KIMURA, Makoto[1*] ; YAMAGUCHI, Akira[2] ; FRIEDRICH, Jon[3]

[1]Ibaraki University / National Institute of Polar Research, [2]National Institute of Polar Research, [3]Fordham University / American Museum of Natural History

Chondrites are classified into petrologic types 1-6, which distinguish the degrees of aqueous alteration (types 1-2), and thermal metamorphism (types 4-6). In addition, a petrographic type 7 has also been proposed to indicate an even higher degree of thermal metamorphism [1]. Such chondrites contain only relict chondrules, and plagioclase is commonly coarse-grained. Low-Ca pyroxene contains >1% CaO. However, most of these chondrites may actually be melt rocks or melt breccias [2], and the occurrence of a type 7 is controversial problem. However, LEW 88663 seems to be a genuine type 7 chondrite [3], not a melt rock.

Here we report the preliminary results of our petrographic study on ordinary chondrites classified as type 7, to explore their thermal history, classification, and genetic relationships to melt breccia and others.

Many chondrites are classified as type 7 in NIPR and other collections (77 chondrites at present). However, the detailed petrography has been rarely reported for these chondrites. Here we studied 4 H7, 4 L7, and 4 LL7 in NIPR collections. We also examined Uden (LL7).

All of the chondrites studied here show a well recrystallized texture. Triple junctions among olivine and pyroxene is commonly observed. However, Y-790124 and -790446 include many chondrules, indicative of type 6. A-880844 and -880993 contain clasts of various petrologic types, and are genomict breccias (H5-6 and LL4-6, respectively). Although Y-790144 does not seemto contain any chondrules, it is shock-darkened chondrite, and has lost its original texture.

Y-74160 has been extensively studied [e.g., 4]. This chondrite, Y-791067, and Uden consist of clasts among fine-grained matrix. The clasts comprise coarse-grained olivine, low-Ca pyroxene, and plagioclase. Olivine is typically included as chadacryst in pyroxene. The matrix is also highly recrystallized. Friedrich et al. [5] suggested that Y-74160 and Uden were subjected to Fe-FeS mobilization. These chondrites experienced partial melting, recrystallization, and brecciation, and may be classified as recrystallized breccias.

On the other hand, five chondrites, Y-75008, -790120, and -790960 (H7s), Y-82088 (L7), and Y-82067 (LL7), contain no or only a few relic chondrule in each section. They show highly recrystallized texture, and are not subjected to brecciation and melting. Y-82067 has composition identical to equilibrated LL chondrites [5]. These five chondrites are temporarily classified as type 7, if type 7 chondrite is defined to have experienced only a high degree of thermal metamorphism.

We are now examining modal mineral abundances and conducting mineral analyses, which will shed light on the classification criteria for type 7 chondrites.

References: [1] Dodd et al. (1975) GCA, 39, 1585-1594. [2] Huss et al. (2006) in Meteorites and the Early Solar System II. [3] Mittlefehldt and Lindstrom (2001) MAPS, 36, 439-457. [4] Takeda et al. (1984) EPSL, 71, 329-339. [5] Friedrich et al. (2014) submitted to GCA.

Keywords: ordinary chondrite, type 7, thermal metamorphism

Japan Geoscience Union Meeting 2014
(28 April - 02 May 2014 at Pacifico YOKOHAMA, Kanagawa, Japan)

PPS22-03 Room:415 Time:May 1 09:30-09:45

Origin of eclogitic clasts in a CR2 chondrite: Evidence of frequent collisions and disruptions of large planetesimals?

HIYAGON, Hajime[1*] ; SUGIURA, Naoji[1] ; KITA, Noriko T.[2] ; KIMURA, Makoto[3] ; MORISHITA, Yuichi[4] ; TAKEHANA, Yoshie[1]

[1]Graduate School of Science, The University of Tokyo, [2]Department of Geoscience, University of Wisconsin -Madison, USA, [3]Faculty of Science, Ibaraki University, [4]Department of Geosciences, Shizuoka University

Achondritic clasts found in the Northwest Africa 801 (NWA801) CR2 chondrite have significant importance in planetary science (Sugiura et al., 2008; Kimura et al., 2010, 2013): (i) it provides strong evidence that achondrites formed earlier than chondrites, (ii) the clasts contain eclogitic high mineral assemblages (garnet and omphacite), suggesting formation at a high pressure (˜3 GPa and ˜1000 C; Kimura et al., 2013), and (iii) the clasts contain two lithologies, graphite-bearing (GBL) and graphite-free (GFL), and the presence of graphite in GBL implies some relations to ureilite.

We performed ion microprobe studies of oxygen isotopes and rare earth element (REE) abundances for selected minerals in the clasts (Hiyagon et al., 2014). Based on the newly obtained data and diffusion calculations, we discuss possible origin of the clasts, esp., whether they formed under a static high pressure in a large planetesimal or formed under a shock high pressure.

Key observations are as follows. (1) Olivine (ol) grains in the clasts (˜20 micrometers in size) are chemically homogeneous with Mg# 66-68. (2) Most of orthopyroxene (opx) grains (˜20 micrometers in size) are homogeneous with Mg# 70-75, but a few large opx grains (50-80 micrometers in size) have Mg-rich cores with Mg# 78-87. (3) Various geothermobarometers (7 equations for mineral pairs of opx-cpx, garnet-cpx, garnet-opx and garnet-olivine) consistently give a high P-T condition of 940-1080 C and 2.8-4.2 GPa. (4) All the oxygen isotopic data of ol and opx fall on a correlation line with a slope of ˜0.6. Data for GFL (ol) are homogeneous with delta18O ˜+5 permil, located close to the CCAM line and the ureilite field, but data for GBL (ol +opx) are variable with delta18O from +2.4 to +4.3 permil. (5) Major host minerals of REEs are chlorapatite (both LREEs and HREEs) and garnet (for HREEs). The estimated bulk REE patterns for GBL and GFL are almost flat (unfractionated) with ˜1.2 x CI and ˜1.8 x CI, respectively.

We consider that the presence/absence of graphite in the two lithologies may be due to absence/presence of smelting reactions, FeO (in silicates) + C (graphite) = Fe (metal) + CO (gas). This means that GBL might form at a deeper portion and GFL might form at a shallower portion, respectively, of a planetesimal.

We consider two different models: a shock high-P model and a static high-P model. Based on careful diffusion calculations, we argue that (1) almost homogeneous Fe/Mg ratios in ol and opx (with some Mg-rich cores) can be explained by heating at 1000 C for 120-800 years, (2) oxygen isotopic variations in GBL must have established before homogenization of Fe/Mg ratios in olivine, (3) consistency of different geothermobarometers requires equilibration of different elements among different mineral pairs, strongly suggesting a static high-P model, (4) in a static high-P model, ˜3 GPa corresponds to the pressure at the center of a large planetesimal with a radius of ˜1500 km, almost the size of the Moon, (5) consistency of different geothermobarometers also suggests a rapid cooling after heating several hundreds of years at ˜1000 C at ˜3 GPa, suggesting possibe disruption of the parent body.

In conclusion, the present results suggest frequent collisions and disruptions of a large planetesimals at a certain stage of the solar system evolution.

References: Kimura M. et al. (2010) (abstract) Meteoritics and Planetary Science 45, A105; Kimura M. et al. (2013) American Mineralogist, 98, 387-393; Sugiura N. et al. (2008) (abstract) Meteoritics and Planetary Science 43, A149. Hiyagon H. et al. (2014) in preparation.

Keywords: eclogite, CR chondrite, oxygen isotopes, rare earth elements, collisions of planetesimals, diffusion

Japan Geoscience Union Meeting 2014
(28 April - 02 May 2014 at Pacifico YOKOHAMA, Kanagawa, Japan)

PPS22-04 Room:415 Time:May 1 09:45-10:00

Estimation of the size of the angrite parent body

SUZUKI, Hiroko[1*] ; OZAWA, Kazuhito[1] ; NAGAHARA, Hiroko[1] ; MIKOUCHI, Takashi[1]

[1]Department of Earth and Planetary Science, University of Tokyo

Angrites has very old crystallization age yielding 4557 - 4564Ma (Brennecka and Wadhwa, 2012; Kleine et al., 2012) and are igneous rocks come from differentiated planetesimal or protoplanet (e.g. Prinz and Weisberg 1995; Baker et al., 2005; Weiss et al., 2008). Angrites preserve information on such differentiated planets, and are one of the best targets for studying processed operated in the early stages of planetary evolution of the solar system. However, the angrite parent body has not been found, and we have scarce knowledge on its planet size, which is one of the most important information in planetary science. The radius of angrite parent body is believed to be larger than 100 ? 200km because of the operation of dynamo, which requires prolonged high temperature of the planet interior due to heat production of ^{26}Al decay to achieve its core formation (Weiss et al., 2008; Elkins-Tanton et al., 2011). The upper limit of radius is not constrained at all, although 2440km is proposed based on ambiguous evidence for Mercury as the angrite parent body (Papike et al., 2003; Kuehner et al., 2006). The radius of the angrite parent body, particularly its upper limit, needs to be further constrained. In this study, we try to constrain the upper limit of the planet size from the presence of spherical voids as large as 25mm in D'Orbigny angrite.

D'Orbigny has many spherical voids suggesting that they formed in 100% molten magma before crystallization. The vesicles are deformed while ascending in the melt depending on several physical parameters such as, melt viscosity and the size of vesicles. There are two dimensionless numbers that determine the shape, Reynolds number and Eotvos (or Bond) number. Reynolds number is a ratio of inertia force and viscous force and Eotvos number is a ratio of buoyancy force and surface tension. These two numbers depends on gravity of the parental body, and the gravity depends on the radius of the parental body. Therefore, spherical shape of the largest void enables us to estimate the upper limit of the radius of the angrite parent body. The boundary conditions for spherical and nonspherical regimes have been determined by Bhaga and Weber (1981) based on fluid dynamic experiments and by Hua and Lou (2007) based on numerical simulations.

Spherical voids in D'Orbigny are armored by fine-grained olivine and plagioclase crystals, where are the first liquidus phases, suggesting that the spherical shape was frozen by heterogeneous nucleation and growth of these phases on the bubble wall. In order to know relationship between Reynolds and Eotvos numbers for D'Orbigny, accurate estimation of density and viscosity is very important, which are strongly dependent on temperature of shape freezing. The temperature was estimated by MELTS (Ghiorso and Sack, 1995) as metastable olivine liquidus for the D'Obigny bulk composition to be ˜1100 ℃, from which the density and viscosity of D'Obigny magma are estimated to be ˜3000 kg/m^3 and ˜1.0 Pa s, respectively. Surface tension of the melt is 0.35N/m according to Walker and Mullins (1981), which is corrected by 50% occupation of olivine and plagioclase on the bubble-melt interface. We assume the average density of the parent body as 4000kg/m^3 for the planet having core, such as asteroid 4 Vesta (Zuber et al., 2011). By using these parameters, we estimated the upper limit of radius to be 700±100 km, which is clearly much smaller than that of Mercury.

Keywords: angite, planetesimal, parent body radius, parent body internal structure, D'Orbigny, protoplanet

Japan Geoscience Union Meeting 2014
(28 April - 02 May 2014 at Pacifico YOKOHAMA, Kanagawa, Japan)

PPS22-05 Room:415 Time:May 1 10:00-10:15

Crystallization experiment of alpha-Fe, gamma-Fe and iron compounds found in the Almahata Sitta and Antarctic ureilites

AOYAGI, Yuya[1*] ; MIKOUCHI, Takashi[1] ; SUGIYAMA, Kazumasa[2] ; YOKOYAMA, Yoshihiko[2] ; GOODRICH, Cyrena A.[3] ; ZOLENSKY, Michael E.[4]

[1]Dept. of Earth & Planet. Sci., Univ. of Tokyo, [2]Inst. for Materials Research, Tohoku Univ., [3]Planet. Sci. Inst., [4]NASA-JSC

Ureilites are ultramafic achondrites whose origin and petrogenesis are still controversial. The cooling rate of ureilites estimated from silicates is approximately a few degrees per hour, and it was considered to reflect catastrophic disruption of the ureilite parent body. Ureilites were broken into meter-sized fragments and then formed daughter body(ies) by re-accumulation.

Fe-Ni metal is one of the major components of all types of ureilites. Almahata Sitta, having fallen on the earth in October 2008, was classified as a polymict ureilite and ureilitic fragments from the Almahata Sitta contain abundant Fe-Ni metal. In previous studies, some grain boundary metals in Almahata Sitta ureilites show unique textures, not found in main group ureilites. These textures show characteristic assemblages with various combinations of α-iron (bcc), γ-iron (fcc), cohenite ($[Fe,Ni]_3C$) and schreibersite ($[Fe,Ni]_3P$).

Those metal textures resemble the product by steelmaking process in the earth, for example martensite (α-iron and γ-iron). Generally, these textures require rapid cooling equivalent to quenching by water ($>$100 ℃/s). However, the cooling rate estimated from silicates (ca. several ℃/h) is much slower than that in producing the martensite. Thus, these metal textures may record the event separated from the event that recorded in the silicates, that is, disruption of parent body. Therefore, studying these complicated metal textures will contribute to a better understanding of the formation and origin of metal in ureilites with the information about their thermal histories.

Those metal textures were only found in Almahata Sitta fragment #44, in previous studies, but we found similar assemblages composed of iron metal and its compounds in other fragments of Almahata Sitta and Antarctic ureilites. Forms and abundances are variable depending on samples, but it is suggested that those mineral assemblages in Fe-Ni metal are commonly found in ureilites.

To estimate the cooling rate which can form these iron and iron compounds textures, we performed cooling experiments by the electric furnace to heat and quench metal whose compositions correspond to metals showing complex metal phase assemblages in Almahata Sitta ureilite. The results suggest that those metal textures can be achieved in the cooling rate faster than the lowest limit between 10 ℃/s and 0.83 ℃/s, whose chemical composition is $Fe_{79.2}Ni_{3.4}P_{2.5}Si_{2.7}C_{12.2}$. At lower cooling rate (0.83 or 0.04 ℃/s) and 10 ℃/s of other starting material ($Fe_{86.4}Ni_{2.8}P_{0.7}Si_{4.1}C_{6.0}$), interstitial schreibersite among rounded iron was detected and neither cohenite nor γ-iron has been formed. In the carbon-free composition ($Fe_{91.2}Ni_{3.9}P_{0.5}Si_{4.4}$), similar textures were not generated at all cooling rates. This cooling rate, forming metal textures, is much faster than that estimated from silicates, and thus it is concluded that the event recorded by the silicates and the event formed the metal textures were truly separated.

Before disruption of ureilite parent body, primary metals probably melted and mixed with surrounding materials (graphite, phosphide and other iron compounds) to various extents at high temperature. The iron phase was considered to be uniformly γ-iron. Then, the ureilite parent body was destroyed and silicate minerals obtained cooling rate by quenching. Later, daughter body(ies) formed by accumulation of meter-size fragments. If daughter body(ies) was either shocked while still hot or heated by shock and then disrupted into smaller fragments (cm-size), the formation of iron textures may be achieved by super rapid cooling exceeding 1 ℃/s. The metal grains without γ-iron would experience relatively slow cooling due to larger fragment size. Consequently, it is considered that the complex coexistences of iron and iron compounds found in ureilites have recorded temperature change and fragmentation process due to the impacts on the parent body and daughter body(ies).

Japan Geoscience Union Meeting 2014
(28 April - 02 May 2014 at Pacifico YOKOHAMA, Kanagawa, Japan)

PPS22-06 Room:415 Time:May 1 10:15-10:45

Early impact events on differentiated protoplanets: Evidence from basaltic achondrites

YAMAGUCHI, Akira[1*]

[1]National Institute of Polar Research

Impact events are a ubiquitous geological process on planetesimals and protoplanets, evidenced by the presence of shock and brecciated textures in asteroidal meteorites. However, evidence for early impact events were obliterated by overprints of later thermal events such as volcanism and thermal metamorphism. We investigated early impact events in these meteorites on the basis of mineralogical and geochemical data.

At present, there are ˜5 eucrites which were derived from distinct protoplanets. An anomalous eucrite, Ibitira, is a strongly recrystallized rock. Low-Ca pyroxene shows homogeneous compositions, indicating that these rocks experienced prolonged thermal metamorphism (˜900-1000 C), as did most basaltic eucrites. The presence of unequilibrated pyroxenes related to oxide grains can be explained by short reheating event (and partial melting) and rapid cooling. Normal eucrites, EET 90020 and Y 86763, and a cumulate eucrite Moore County seem to have experienced a similar history. Most likely explanation for this thermal history is that they were excavated by impact from hot interior.

Anomalous cumulate eucrites Dho 700 and EET 92023 are medium-grained granular rocks similar to cumulate eucrites. Anomalous basaltic eucrite, NWA 011 shows a recrystallized texture. These rocks are crystalline (unbrecciated) but contain significant amounts of impactor materials. Dho 700 and EET 92023 contain taenite which is not common in pristine eucrites. The high abundances of siderophile elements are explained by addition of ˜1% iron meteorites. Thus, these rocks experienced impact event before or during crystallization and thermal metamorphism.

All anomalous eucrites studied here show crystalline textures, but have evidence for impact melting or brecciation before thermal events. These meteorites record early collisional history possibly during the stage of runaway growth.

Japan Geoscience Union Meeting 2014
(28 April - 02 May 2014 at Pacifico YOKOHAMA, Kanagawa, Japan)

PPS22-07 Room:415 Time:May 1 11:00-11:15

Shock features in a Martian meteorite, Tissint

MIYAHARA, Masaaki[1*] ; OHTANI, Eiji[2] ; EL GORESY, Ahmed[3] ; GILLET, Philippe[4]

[1]DEPSS, Graduate School of Science, Hiroshima Univ., [2]Institute of Mineralogy, Petrology and Economic Geology, Graduate School of Science, Tohoku Uni., [3]BGI, [4]EPFL

Tissint is the fifth fall Martian meteorite collected in Morocco on 2011 [1]. The nomination of a fall Martian meteorite is since 1962. Tissint will bring new clues for Martian evolution because it is less contaminated with terrestrial materials. Tissint is a member of shergottite. Many shergottites experienced a heavy shock event on Mars [e.g., Ref. 2]. We expected that Tissint should be also heavily shocked. A high-pressure polymorph is one of clear evidences for such a dynamic event. Accordingly, we described shock features, especially a high-pressure polymorph by FEG-SEM, EMPA, Raman spectroscopy and FIB-TEM techniques to clarify shock history recorded in Tissint.

We prepared several petrographic thin sections of Tissint for this study. EMPA analysis show that Tissint studied here consists mainly of olivine (Fa_{18-66}), pigeonite or augite ($En_{43-62}Fs_{23-37}Wo_{10-34}$) and labradoritic feldspar ($An_{62-66}Ab_{34-37}Or_{0-1}$). There are many melt-pockets, which is suggestive of a heavy shock event. FEG-SEM and FIB-TEM observations show that olivine grains entrained in the melt-pockets dissociated into silicate-perovskite (now almost amorphous or poorly-crystallized) and magnesiowustite, which is found in a Martian meteorite DaG 735 for the first time [3]. Silicate-perovskite and magnesiowustite show equigranular texture and less than ˜100 nm in dimension. We also identified ringwoodite lamella in some olivine grains adjacent to the melt-pockets. TEM images show that ringwoodite has a dimension of less than ˜500 nm. Raman spectroscopy analysis indicates that most feldspar now transforms into maskelynite. Jadeite-like crystals appear in some feldspar grain adjacent to the melt-pockets.

Considering the dissociation reaction of olivine into silicate-perovskite and magnesiowustite, shock pressure condition recorded in Tissint is beyond ˜23 GPa based on phase diagram deduced from static synthetic experiments [4]. Phase transformation from olivine to ringwoodite also occurs besides the olivine dissociation reaction. Phase transformation from olivine to ringwoodite occurs instead of olivine dissociation reaction with decreasing temperature but under same pressure condition [5], which is due to thermal gradient in the olivine grains adjacent to the melt-pockets although pressure condition should be almost homogeneous. The nucleation and grain growth of a high-pressure polymorph is kinetically controlled. Baziotis et al. (2013)[6] propose that Tissint experienced the largest impact event among known Martian meteorites because ringwoodite appear to be a huge single crystal based on their SEM observations. However, our TEM images clearly depict that ringwoodite is a fine-grained grain assemblage, suggesting that it is unlikely that Tissint experienced the largest impact event.

References

[1] Chennaoui Aoudjehane H. et al. Tissint Martian Meteorite: A fresh look at the interior, surface, and atmosphere of Mars. Science 338, 785-788 (2012).

[2] El Goresy A. et al. Shock-induced deformation of Shergottites: Shock-pressures and perturbations of magmatic ages on Mars. Geochim.Cosmochim.Acta 101, 233-262 (2013).

[3] Miyahara M. et al. Natural dissociation of olivine to (Mg,Fe)SiO_3 perovskite and magnesiowustite in a shocked Martian meteorite. Proc.Nat.Acad.Sci.U.S.A. 108, 5999-6003 (2011).

[4] Presnall D.C. Phase diagrams of Earth-Forming Minerals. 248-268, in Mineral Physics & Crystallography, A Handbook of Physical Costants, T. J. Ahrens ed., AGU, Washington D. C (1995).

[5] Akaogi M. et al. Low-temperature heat capacities, entropies and enthalpies of Mg_2SiO_4 polymorphs, and a?b?c and post-spinel phase relations at high pressure. Phys.Chem.Minerals 34, 169-183 (2007).

[6] Baziotis I.P. et al. The Tissint Martian meteorite as evidence for the largest impact excavation. Nat.Commun., doi: 10.1038/ncomms2414 (2013).

Keywords: Tissint, Martian meteorite, Shock, High-pressure polymorph

Japan Geoscience Union Meeting 2014
(28 April - 02 May 2014 at Pacifico YOKOHAMA, Kanagawa, Japan)

PPS22-08 Room:415 Time:May 1 11:15-11:30

Estimation of bulk major element composition for Centimeter-Sized Impact Melt Clasts in Lunar Rocks using EPMA

NIIHARA, Takafumi[1*] ; KRING, David A.[2]

[1]NIPR / LPI / SSERVI, [2]LPI / SSERVI

Most of lunar surface rocks are brecciated and mixed with various types of rock fragments and impact melt clasts during multiple impact events. We are testing the Late Stage Heavy Bombardment on the Moon surface [1-3] using Apollo 16 centimeter-sized impact melt clasts in ancient regolith breccias. Bulk composition is a key to understand original (pre-impact) lithologies where the clasts come from [4, 5]. Large-sized impact melt rocks (>5 cm) have been classified into 4 major group (Group 1 to 4) according to Sm and Sc compositions [6]. We compiled major element compositions of the previously classified impact melt rocks [6] and found that we can classify major impact melt groups even when we use major element compositions. However, our samples, centimeter-sized impact melt clasts, are highly restricted on their masses and makes us difficult to obtain bulk composition using conventional techniques (e.g. INAA and XRF). Defocused beam analyses (DBA) with EPMA is used to estimate the bulk compositions for limited mass samples using petrological sections, however, nobody tested accuracy of DBA techniques using certified geochemical standard.

We use a thin section of BCR-2 (fine-grained basalt supplied from USGS) and tested accuracy of DBA method using an EPMA (CAMECA SX-100) at NASA Johnson Space Center. We measured 12 elements (Na, Mg, Si, Al, P, K, Ca, Ti, Fe, Mn, Cr, and Ni) at >250 points with 20 micrometer beam diameter. We corrected density effect following the Warren (1997) method [7]. Averaged SiO_2 and FeO have larger difference from USGS values (+4.4 wt.% for SiO_2, -4.68 Wt.% for FeO) relative to other elements (up to +/- 2.4 wt.%). Although there are major changes in SiO_2 and FeO values after correct the density effect (difference from USGS values are up to -4.1 Wt.% for SiO_2 and up to +4.6 Wt.% for FeO), we suggest the DBA compositions can useable for the fine-grained materials to estimate the bulk major element composition for Apollo 16 impact melt clasts.

We estimated the bulk composition by averaged DBA method for two impact melt clasts in an Apollo 16 ancient regolith breccia 61135 which have optically different 5 regions (Clast1 R1, R2, and R3; and Clast 2 R1 and R2) to reveal the original lithology of the impact melt clasts. Five regions from the two impact melt clasts can be divided into three chemical groups of high-K, low-K and intermediate compositions. Clast 1 R3 has high K (K_2O=0.72 wt.%) and P (P_2O_5=0.35 wt.%), and low Al (Al_2O_3=20.7 wt.%) and Ca (CaO=12.0 wt.%). On the other hand, Clast 1 R1 and R2 have low K (K_2O=0.31-0.27 wt.%) and P (P_2O_5=0.08-0.07 wt.%) with high Al (Al_2O_3=26.1-25.2 wt.%) and Ca (CaO=14.5-14.0 wt.%). Clast 2, in both dark and bright regions, has an intermediate composition between high-K and low-K melts (e.g. K_2O=˜0.46, P_2O_5=˜0.16 wt.%, Al_2O_3=˜22.9 wt.%, CaO=˜12.8 wt.%). The bulk Mg# of the 5 regions are similar (Mg#=80-78).

If the melts in the two clasts are related, there are two possible origins: (1) A single impact event hit a complex lithological target and incompletely mixed the melts, to produce high-K, intermediate-K, and low-K melt fractions. (2) An impact produced either a high- or low-K melt. A second impact produced a melt at the other end of the K spectrum. The melts in Clast 1 represent those two end member melts. If the second impact melt digested older fragments of the first impact melt, then that may have produced the intermediate compositions of Clast 2. Alternatively, the melts are not related and require three or more impact events.

Reference: [1] Papanastassiou D.A. and Wasserburg G.J. 1971. EPSL 11. 37-62. [2] Turner G. et al., 1973. Proc. LPSC 4, 1889-1914. [3] Tera F. et al., 1974. EPSL 22, 1-21. [4] Niihara, T. and Kring, D. A., 2012. LPSC. #1229. [5] Niihara, T. et al., 2013. LPSC. #2083. [6] Korotev, R.L. 1994. GCA 58, 3931-3969. [7] Warren, P.H., 1997. LPSC28, #1406.

Keywords: EPMA, Bulk composition, Apollo 16, Impact melt clast

Japan Geoscience Union Meeting 2014
(28 April - 02 May 2014 at Pacifico YOKOHAMA, Kanagawa, Japan)

PPS22-09 Room:415 Time:May 1 11:30-11:45

Formation processes of silica polymorphs in lunar meteorites

KAYAMA, Masahiro[1*] ; TOMIOKA, Naotaka[2] ; SEKINE, Toshimori[1] ; GöTZE, Jens[3] ; NISHIDO, Hirotsugu[5] ; OHTANI, Eiji[4] ; MIYAHARA, Masaaki[1] ; OZAWA, Shin[4]

[1]Department of Earth and Planetary Systems Science, Graduate School of Science, Hiroshima University, [2]Institute for Study of the Earth's Interior, Okayama University, [3]Department of Mineralogy, TU Bergakademie Freiberg, [4]Department of Earth and Planetary Materials Science, Graduate School of Science, Tohoku University, [5]Depertment of Biosphere-Geosphere Science, Okayama University of Science

Asteroid and meteorite collisions lead to formation of impact craters and thick regoliths on the Moon and also contribute to revolution of the Earth, e.g. Giant impact, the late heavy bombardments and the origin of life. Although lunar meteorites and Apollo samples have experienced such impact events during the ejection from the lunar surface or formation of immense basin, they were believed to contain few high-pressure mineral because of the volatilization during collision in the high vacuum (Papike 1998; Lucey et al., 2006). Recently, Ohtani et al. (2011) and Miyahara et al. (2013) discovered high-pressure silica polymorphs (coesite, stishovite and seifertite) in lunar meteorites, Asuka-881757 and NWA4734. Their existences provide constraints on the shock condition and give us valuable information on impact history on the Moon and the Earth.

The shock condition of meteorites has been estimated based on the pressure-temperature phase diagram obtained from high-pressure experiments using shock gun, multi-anvil press and diamond anvil cell (DAC) for various types of minerals including in silica polymorphs. There have been many investigations of the high-pressure experiments for quartz and amorphous silica glass, but not for the other polymorphs, regardless of dominant occurrence of cristobalite and tridymite in lunar meteorites. Since the transition pressure to high-pressure phase depends on a type of starting material (Kubo et al. 2012; Bläβ, 2013), it is necessary for understanding the detailed impact history of the Moon to conduct the high-pressure experiments for various types of silica polymorphs.

In this study, silica polymorphs in various types of lunar meteorites (anorthositic breccia, basalt, and gabbro and basalt clast-dominated breccia) were described using Raman spectroscopy, Scanning and Transmission Electron Microscope and X-ray diffraction analysis and the obtained results were compared with the data of high-pressure experiments for various types of silica polymorphs to clarify the phase transition process, interpret the formation process on the Moon and constrain shock pressure and temperature that the lunar meteorites have experienced.

Keywords: Lunar meteorite, Silica polymorph, High-pressure mineral, Collision, Shock experiment, Static compression experiment

Japan Geoscience Union Meeting 2014
(28 April - 02 May 2014 at Pacifico YOKOHAMA, Kanagawa, Japan)

PPS22-10 Room:415 Time:May 1 11:45-12:00

Discovery of stishovite in an Apollo 15 sample and impact record on the Moon

KANEKO, Shohei[1] ; OHTANI, Eiji[1*] ; MIYAHARA, Masaaki[2] ; OZAWA, Shin[1] ; ARAI, Tomoko[3]

[1]Tohoku University, [2]Hiroshima University, [3]Chiba Institute of Technology

Thick regolith layers and many craters on the Moon indicate that the Moon has been heavily bombarded after the lunar formation. Short time intervals of high-pressure and high-temperature occurred on the lunar surface during the collision of asteroids on the Moon, and the constituent minerals of the Moon and asteroids transformed into high-pressure polymorphs during the high-pressure and high-temperature conditions. Although many brecciated lunar rocks have been recovered by the Apollo missions, any high-pressure polymorph has not been observed in Apollo samples so far. Silica is one of constituent minerals of terrestrial planets and asteroid. We investigated a lunar regolith collected by the Apollo 15 mission with a special interest on silica, because high-pressure polymorphs of silica are recently reported from shocked lunar meteorites (Ohtani et al., 2011; Miyahara et al., 2013). Here, we show stark evidence for stishovite from a sample collected by the Apollo 15 mission. X-ray diffraction analysis and transmission electron microscopic observations clearly confirmed the existence of a high-pressure polymorph of silica, stishovite, in the Apollo sample, which suggests that the lunar legolith preserves records of early shock events. Considering radio-isotope ages, lithologies, and shock features, stishovite was formed by an impact event in the near side Moon ca. 3.8-4.1 Ga ago.

Keywords: Stishvite, Apollo mission, Impact, High pressure and temperature, Lunar sample

Japan Geoscience Union Meeting 2014
(28 April - 02 May 2014 at Pacifico YOKOHAMA, Kanagawa, Japan)

PPS22-11 Room:415 Time:May 1 12:00-12:30

Experimental constrains on shock conditions of meteorites based on non-equilibrium behaviors of silica and plagioclase

KUBO, Tomoaki[1*] ; KONO, Mari[1] ; KATO, Takumi[1]

[1]Dept. Earth Plant. Sci., Kyushu Univ.

Recent studies on shocked meteorites have revealed non-equilibrium behaviors of silica and plagioclase at high pressures. We focus on the following three points observed in meteorites to deduce the P-T-t shock conditions from high-pressure kinetic experiments. 1) The formation of seifertite as a high-pressure polymorph of silica, 2) The occurrence of jadeite from plagioclase that does not contain stishovite, 3) The formation of lingunite as a high-pressure polymorph of albite-rich plagioclase.

Seifertite is a polymorph of silica with alpha-PbO2 type structure that was found in shocked Martian and lunar meteorites (e.g., Sharp et al., Science1999; Miyahara et al., PNAS2013). Although this phase is thermodynamically stable at more than 90 GPa corresponding to the base of the lower mantle (Murakami et al., GRL2003), it has also been known that it metastably appears from cristobalite at around more than 40 GPa and room temperature (Dubrovinsky et al., CPL2001). We have carried out high-pressure and high-temperature in-situ XRD experiments of cristobalite using a Kawai-type multi-anvil (KMA) apparatus, and determined the formation kinetics of metastable seifertite and the following stable phase of stishovite. Because the activation energy for the seifertite formation is very low (˜10 kJ/mol), which is consistent with the recently proposed formation mechanism (Blab, PCM2013), it can metastably appear at low T conditions beyond the negative PT boundary from ˜10 GPa and 400C to ˜30 GPa and room T. We found the clear difference in the formation kinetics between seifertite and stishovite, which enables to estimate the P-T-t shock conditions from the coexistence of these phases in various ratios in meteorites.

The occurrence of jadeite from plagioclase that does not contain stishovite has been often reported in shocked meteorites (e.g., Kimura et al., MAPS2000). In-situ XRD study using KMA apparatus have revealed that jadeite forms first from (amorphous) plagioclase, whereas the nucleation of other minerals such as stishovite or garnet is significantly delayed (Kubo et al., NGEO2010). The missing stishovite problem can be explained owing to the differences in crystallization kinetics of high-pressure phases from plagioclase. The hybrid shock indicator combining these non-equilibrium behaviors of silica and plagioclase mentioned above consistently and strongly constrains the P-T-t shock conditions of Martian meteorites.

The formation of lingunite (albite-rich hollandite) in shocked meteorites (e.g., Gillet et al., Science2000; Tomioka et al., GRL2000) has remained unsolved. This phase appears in lase-heated diamond anvil cell (LHDAC) experiments as a minor phase at around ˜20-24 GPa and ˜1000C (Liu, PEPI1978) and ˜2000C (Tutti, PEPI07). However, KMA experiments indicate that the maximum solubility of NaAlSi3O8 component in hollandite structure is limited to ?50 mol% (Yagi et al., 1994, Liu, 2006). This clear contradiction may be due to the non-equilibrium origin. It has been suggested that the rapid T quenching in LHDAC experiments is important for the survival of lingunite metastably to the ambient condition. Our previous in-situ XRD study using KMA apparatus have indicated that lingunite is not formed at least ˜1200C at these pressure conditions (Kubo et al., NGEO2010). We are also preliminarily conducting some LHDAC experiments, however we have not observed lingunite at least ˜1400C. Further studies on the formation process of lingunite are needed to solve this problem, which may lead to construct another P-T-t shock indicator.

Japan Geoscience Union Meeting 2014
(28 April - 02 May 2014 at Pacifico YOKOHAMA, Kanagawa, Japan)

PPS22-P01 Room:Poster Time:May 1 18:15-19:30

Laboratory impact experiments of rock projectiles onto simulated asteroid regolith: Impactor fragmentation and capture

NAGAOKA, Hiroki[1] ; NAKAMURA, Akiko[1*] ; SUZUKI, Ayako[2] ; HASEGAWA, Sunao[2]

[1]Graduate School of Science, Kobe University, [2]Institute of Space and Astronautical Science

We conducted laboratory impact experiments of rock projectiles onto target consist of silica sand used as simulated regolith surface. We investigate the relationship between degree of projectile fragmentation and impact velocity and particle size of silica sand.

Laboratory impact experiments have been performed to study the degree of target fragmentation, however, much less attention has been paid to the fate of the impactors. Experiments with impact velocity lower than 1 km/s were conducted using a powder gun and a gas gun at Kobe University, while experiments with higher impact velocity up to 5 km/s were conducted using a two-stage light-gas gun at Institute of Space and Astronautical Science. We collected the projectile fragments in the sand and weighed the mass of the largest fragments.

Destruction of rock projectiles is found to occur when the peak pressure is about equal to the dynamic tensile strength of the rock in the low velocity impact experiments (Nagaoka et al., 2014, MAPS). The largest fragment mass fractions in the high velocity impact experiments are higher than the expected from the result of low velocity impact experiments. The discrepancy is larger for the target with smaller silica sand particles. The larger fragments consist of multiple fragments and silica sand particles which were consolidated into larger particles by compression and the heating due to compaction of silica sand.

Keywords: meteorites, impact process, asteroids

Japan Geoscience Union Meeting 2014
(28 April - 02 May 2014 at Pacifico YOKOHAMA, Kanagawa, Japan)

PPS22-P02 Room:Poster Time:May 1 18:15-19:30

Secondary Ion Mass Spectrometry (SHRIMP) U-Pb dating of Chelyabinsk meteorite

KAMIOKA, Moe[1*] ; TERADA, Kentaro[1] ; HIDAKA, Hiroshi[2] ; KIMURA, Kosuke[2] ; SKUBLOV, Sergey[3]

[1]Osaka University, Department of Earth and Space Science, [2]Guraduate school of Science, Hiroshima University, [3]Institute of Precambrian Geology and Geochronology,

On Feburuary 15,2013, a meteorite fell into the area of Chelyabinsk in Russia .The petrographic and chemical analysis of the Chelyabinsk meteorite unambiguously classifies it as an LL5 ordinary chondrite (Galimov et al.2013). The reported Sm-Nd age of 3.7 Ga and Rb-Sr age of 0.29 Ga suggest that the Chelyabinsk meteorites could have suffered from the secondary event possibly due to shock metamorphism.For further understanding of the thermal history of Chelyabinsk meteorite, we carried out an in-situ U-Pb dating of phosphates of which closure temperatures is high (~600 ℃), using Hiroshima-SHRIMP.(Sensitive High-Resolution Ion MicroProbe).

Keywords: Chelyabinsk meteorite, SHRIMP, phosphate, U-Pb dating

Japan Geoscience Union Meeting 2014
(28 April - 02 May 2014 at Pacifico YOKOHAMA, Kanagawa, Japan)

PPS22-P03 Room:Poster Time:May 1 18:15-19:30

Crystallization and subsolidus processes of the NWA 6704 ungrouped achondrite

TAKAGI, Yasunari[1] ; NOGUCHI, Takaaki[1*] ; KIMURA, Makoto[1] ; YAMAGUCHI, Akira[2]

[1]Ibaraki University, [2]National Institute of Polar Research

Introduction: NWA 6704 is an unique ungrouped achondrite. It consists of low-Ca pyroxene, less abundant olivine and plagioclase, minor chromite and merrilite, and trace awaruite, heazlewoodite, and pentlandite (1, 2). Although its bulk oxygen isotopic ratio is within the ranges of the acapulucoite-lodranite and CR chondrites, its petrography and mineralogy are evidently different from both of them (1). The U-Pb dating of this meteorite gives a $^{207}Pb/^{206}Pb$ date of 4563.75 +/- 0.41 Ma (3). To deduce its formation processes is important to understand formation of its parent body that may have predated the formation of chondrite parent bodies.

Methods: Polished thin sections were investigated by optical microscopes, electron microprobe analyzer (EPMA), field-emission scanning electron microscope (FE-SEM), Raman spectroscopy, and electron backscattered diffraction (EBSD).

Results: The most abundant mineral in NWA 6704 is orthopyroxene containing blobs of augite. Both Raman spectroscopy and EBSD data indicate that this pyroxene is orthopyroxene. The texture of the blob-bearing orthopyroxene is very similar to Kintokisan-type orthopyroxene (inverted pigeonite) (4). We call it early formed (ef-) pigeonite. There are another less abundant low-Ca pyroxenes: augite blob-free orthopyroxene, and pigeonite containing sub-micrometer-size augite exsolution lamellae. Here we call them primary orthopyroxene and later formed (lf-) pigeonite. Lf-pigeonite occurs as coherent overgrowth of the primary orthopyroxene and discrete grains in the interstices of large ef-pigeonite. Lf-pigeonite also occur as inclusions in olivine. Based on the EBSD data, modal abundances of ef-pigeonite, olivine, lf-pigeonite, primary orthopyroxene, feldspar, chromite, awaruite are 67.2, 16.8, 3.4, 0.6, 10.9, 0.4, and 0.4 vol.%, respectively. Crystallization sequence estimated based on the petrography is following: primary orthopyroxene =>awaruite =>ef-pigeonite =>chromite =>lf-pigeonite =>olivine =>augite (quite rare crystallized from melt) =>heazlewoodite =>pentlandite =>merrilite =>feldspar. Early formed pigeonite (blob-bearing orthopyroxene) shows a LPO of the [010] axis. Lf-pigeonite contains complex exsolution lamellae of augite. The thickest lamellae have ˜0.2 micrometer in width and 1-2 micrometer wavelength. Finest lamellae have <0.1 micrometer thick and ˜0.2 micrometer wavelength.

Discussion: Because [010] lattice preferred orientation of pyroxene in terrestrial rocks has been interpreted as settling of tabular pyroxene crystals in a stagnant magma chamber (5), ef-pigeonite could have settled in a stagnant magma chamber. Presence of Fe^{3+} in chromite and high NiO concentration in olivine (0.89 wt.% on average) suggest that this meteorite crystallized under an oxidized condition. About 1100 ^{o}C equilibrium temperature was estimated by using two pyroxene geothermometry and ˜950 ^{o}C by using olivine-spinel geothermometry. These high temperatures suggest that the meteorite cooled rapidly in this range of temperature. Multiple exsolution lamellae with thickness and wavelength similar to this meteorite were observed in Zagami martian meteorite. Its cooling rate between 1100 ^{o}C to 950 ^{o}C was estimated to be ˜0.02 ^{o}C/hr (6). This meteorite could be cooled as slow as Zagami did. Further studies are needed to clarify if a monotonous cooling can accomplish both high equilibrium temperatures estimated by geothermometers and sub-micrometer-size exsolution lamellae in lf-pigeonite. NWA 6704 has petrography similar to that of NWA 6693. However, there is a stark difference between these two meteorites. Blob-bearing orthopyroxene is the most abundant pyroxene in the former. On the other hand, low-Ca pigeonite is the most abundant in the latter. Therefore, it is possible that NWA 6704 is not mere a pair of NWA 6693.

References: (1) Irvine et al. (2011), (2) Warren et al. (2012), (3) Iizuka et al. (2013), (4) Ishii and Takeda (1974), (5) Jackson (1961), (6) Brearley (1991).

Keywords: NWA 6704, achondrite

Japan Geoscience Union Meeting 2014
(28 April - 02 May 2014 at Pacifico YOKOHAMA, Kanagawa, Japan)

PPS22-P04 Room:Poster Time:May 1 18:15-19:30

Petrologic type from plagioclase size distribution

KAWASAKI, Takehiro[1] ; KIMURA, Makoto[1*] ; NOGUCHI, Takaaki[1]

[1]Faculty of Science, Ibaraki University

Ordinary chondrites are classified into petrologic types 3-6, reflecting thermal metamorphism. One of the criteria to classify types 5 and 6 is the size distribution of plagioclase. The size, 50 microns, has been commonly used to classify types 5 and 6. However, no any statistic study for plagioclase size has been conducted. Here we measured the size distribution, and discuss the classification of types 5 and 6. We studied 26 thin sections of types 5 and 6 from the H, L, and LL chondrite groups. Our study indicates that plagioclase of 50 microns are commonly encountered both in types 5 and 6. However, plagioclase of 80-100 microns is more abundant in type 6 than type 5. We also noticed that the size distribution of plagioclase in H6 is similar to that in type H5. The different criteria to classify H from L and LL are necessary.

Keywords: ordinary chondrite, petrologic type, plagioclase, thermal metamorphism

Japan Geoscience Union Meeting 2014
(28 April - 02 May 2014 at Pacifico YOKOHAMA, Kanagawa, Japan)

PPS22-P05 Room:Poster Time:May 1 18:15-19:30

Systematic isotopic studies of REE, Sr and Ba in eucrites

SERA, Kohei[1*] ; HIDAKA, Hiroshi[1] ; YONEDA, Shigekazu[2]

[1]Department of Earth and Planetary Systems Science, Hiroshima University, [2]National Museum of Nature and Sci.

The eucrites is meteorites that probably originate from the crust of asteroid 4-Vesta. Cosmochemical and chronological information of eucrites puts important constraints of on the evolutional history of the eucrite parent body (EPB). In this study, systematic istopic isotopic studies of Sr, Ba, Ce, Nd, Sm and Gd were performed on eight eucrites for better understanding of differentiation on the EPB. ^{138}Ce, ^{142}Nd, and ^{143}Nd include radiogenic components, and their isotopic variations correlate with La/Ce and Sm/Nd elemental ratios, respectively. The results were consistent with the isochron from previous studies (Makishima and Masuda, 1991; Boyet and Carlson, 2005; Andreasen and Sharma, 2007). The Rb-Sr chronometer consisting of ^{87}Sr/^{86}Sr and Rb/Sr for these eucrites is now in progress. Sm and Gd isotopic compositions of the eucrites showed the isotopic shifts caused by neutron caputure reactions due to cosmic rays irradiation. These isotopic shifts correspond to the neutron fluences ranging from 0.28 to 4.05 $\times$ 10^{15} n cm^{-2}, but these are almost consistent with their cosmic-ray exposure ages, suggesting no strong evidence of initial cosmic-ray irradiation on the surface of EPB. Most previous Ba isotopic studies of meteorites focused on the variation of r- and s-process nucleosynthetic components due to additional inputs in the early solar system. ^{135}Ba and ^{137}Ba isotopes are sensitive to s- and r-process variations, and often have deficits and/or excesses in chemical separates in carbonaceous chondrites due to the existence of presolar grains. In case of eucrites, there are no isotopic variations of all Ba isotopes, but some samples showed the slight excess of radiogenic ^{135}Ba probably from ^{135}Cs decay. Systematic isotopic data obtained in this study provide a hint to understand the evolution processes of differentiated meteorites. We are now applying this technique for the analyses of cumulate eucrites and diogenites.

Keywords: eucrite, REE, chronology, isotope

Japan Geoscience Union Meeting 2014
(28 April - 02 May 2014 at Pacifico YOKOHAMA, Kanagawa, Japan)

PPS22-P06 Room:Poster Time:May 1 18:15-19:30

Preliminary experiments on the formation process of lingunite in shocked meteorites

KONO, Mari[1*] ; KUBO, Tomoaki[1] ; KATO, Takumi[1] ; KONDO, Tadashi[2]

[1]Kyushu Univ., [2]Osaka Univ.

Albite-rich hollandite (lingunite) has been frequently found in shocked meteorites with other high-pressure minerals (Gillet et al., 2000; Tomioka et al., 2000). According to the laser-heated diamond anvil cell (LHDAC) experiments by Liu (1978), following the decomposition of albite ($NaAlSi_3O_8$) into jadeite ($NaAlSi_2O_6$) plus quartz (SiO_2) at 2-3 GPa, these phases recombine to form lingunite in the range of pressure between 21 and 24 GPa at about 1000 ℃, and then it decomposes again into calcium ferrite-type NaAlSiO4 plus stishovite at pressures above 24 GPa. Similarly, Tutti (2007) observed $NaAlSi_3O_8$ lingunite at 21-23 GPa and 2000 ℃ using LHDAC. In contrast to these LHDAC studies, high-pressure experiments using multi-anvil type (MA) apparatus revealed that the maximum solubility of $NaAlSi_3O_8$ component in hollandite structure is limited to ˜50 mol% at 14-25 GPa and 800-2400 ℃ (Yagi et al., 1994, Liu, 2006). This contradiction has not been solved yet, which makes it difficult to understand the shock conditions for the presence of lingunite in shocked meteorites. Tutti (2007) suggested that the stability of lingunite might be sensitive to temperature and could transform back when quenching rate is slow like MA experiments. However, the formation conditions of lingunite has not been well constrained even by LHDAC experiments.

To investigate the formation process of lingunite, we preliminarily carried out LHDAC experiments using a powder of natural albite as a starting material. The samples were compressed at room temperature, and then heated by the double-sided laser heating method using a Nd:YAG laser. The emission spectra were measured on both side of the heated sample, and used to estimate temperature. Heating duration at the maximum temperature was several minutes. Recovered samples were analyzed by X-ray diffraction method at BL-ARNE7 and BL-ARNE1 of photon factory, KEK. The results obtained suggest that jadeite and stishovite are present at 22 GPa and 1230 ℃. The assemblage changed into calcium ferrite-type structure and stishovite at 25 GPa and 1400 ℃. Hydrous aluminum silicate (phase egg) was also present in both samples probably due to the effect of absorbed water in the powdered stating material. We measured X-ray diffraction patterns at several points in the sample, which showed changes of the ratio of the constituent minerals due to the presence of pressure and temperature gradients, however we did not observe lingunite in any measured points. Although experimental conditions are still rather limited, our preliminary results suggest that the formation condition of lingunite is more than 1400 ℃ at these pressure ranges.

Keywords: lingunite, high pressure, LHDAC, shocked meteorite

Japan Geoscience Union Meeting 2014
(28 April - 02 May 2014 at Pacifico YOKOHAMA, Kanagawa, Japan)

PPS23-01 Room:413 Time:May 2 09:00-09:15

Surface roughness effect on KAGUYA LRS surface echo observation and its calibration

KOBAYASHI, Takao[1*] ; LEE, Seung ryeol[1]

[1]Korea Institute of Geoscience and Mineral Resources

KAGUYA Lunar Radar Sounder (LRS) was an HF (5MHz) radar whose primary mission was to explore subsurface of the Moon. Its footprint covered whole surface of the Moon in its operation period. All the data was processed by applying Synthetic Aperture Radar (SAR) algorithm so that the signal-to-noise ratio of target echoes as well as the spatial resolution was improved.

The data was further processed to extract nadir surface echoes so that the surface property of the Moon was studied in a spectral range of the HF band. The physical property that can be known directly from the data was the apparent reflectivity of the lunar surface in the frequency range of the HF band: The data contains scattering effect of surface roughness due to the surface terrain. We need to separate this scattering effect from the data so that we can make quantitative evaluation of the surface reflectivity. In order to meet this requirement, we carried out simulation of KAGUYA LRS observation to evaluate the surface scattering effect due to the lunar surface terrain.

The simulation was based on Kirchhoff approximation method. The Lunar Imager/SpectroMeter (LISM) Digital Elevation Model (DEM) data was utilized to simulate actual lunar surface terrain. Flat surface observation was simulated as the reference case before the simulation of actual LRS observation was carried out. We assumed that the dielectric constant of the lunar surface material was 4.0.

Our simulation revealed that even a mare surface where the surface is often regarded to be flat certainly behaved as a rough surface which gave a rise to decrease of the nadir echo intensities for a few decibels in comparison to the flat surface reflection. This effect gives a significant influence on estimation of regolith thickness in maria. Newly estimated regolith thickness was approximately a meter smaller than previously estimated value: it turned out to be 6 - 7 m in Mare Imbrium.

Keywords: KAGUYA, LRS, HF radar, surface echo, scattering

Japan Geoscience Union Meeting 2014
(28 April - 02 May 2014 at Pacifico YOKOHAMA, Kanagawa, Japan)

PPS23-02 Room:413 Time:May 2 09:15-09:30

Determination of the dielectric constant of the lunar surface based on the radar echo intensity observed by the Kaguya

KUMAMOTO, Atsushi[1*] ; ISHIYAMA, Ken[1] ; KOBAYASHI, Takao[2] ; OSHIGAMI, Shoko[3] ; HARUYAMA, Junichi[4]

[1]Tohoku Univ., [2]KIGAM, [3]NAOJ, [4]JAXA

In the planetary radar observation, echo power and delay time depend on the effective dielectric constant, or equivalent dielectric constant including the voids in the planetary uppermost media. As for the Moon, because there is almost no material whose dielectric constant is far from the basalt rocks, the effective dielectric constant of the lunar uppermost media is considered to depend mainly on their porosity. So if we can determine the effective dielectric constant of the lunar uppermost media, we can derive their bulk density, or density including the voids based on the empirical relation between the dielectric constant and bulk density of the Apollo samples [Carrier et al., 1991].

If we are going to use echo power for determination of the permittivity, we should note that the radar echo intensity depends not only on the dielectric constant but also on the roughness of the surface. Therefore, we have determined the permittivity of the lunar surface with considering the surface roughness. In the analysis, the dielectric constant is determined by using the radar echo intensity obtained by Kaguya Lunar Radar Sounder (LRS) [Ono et al, 2000; 2008; 2010], and the surface roughness parameters derived from Digital Terrain Model (DTM) based on Kaguya Terrain Camera (TC) observation [Haruyama et al., 2008]. The global distributions of the echo powers in a frequency range of 4-6 MHz were derived from the Kaguya/LRS dataset. We have used the intensity of off-nadir echoes in an incident angle from 5 to 15 degree. The reason why nadir echoes are not used in the analysis is because the echo intensity changes drastically in small incident angle range due to the poor range resolution from the spacecraft to the off-nadir reflection point. The echoes arrived after the arrival of the nadir surface echo were identified as off-nadir echoes in this study. In addition, we have also derived the global distribution of the surface roughness parameters. The RMS height of the surface can be obtained by <(z(x+L)-z(x))ˆ2>, where z(x) is height of the surface derived from the Kaguya TC/DTM, L is baseline length, and <>denotes the average. If we assume the self-affine surface model, the roughness parameters H and s can be obtained by the least square fitting of the RMS heights to s LˆH. The off-nadir surface echo power can be calculated based on the radar equation. Assuming Kirchhoff Approximation (KA), the backscattering coefficient in the radar equation can be obtained from the roughness parameters H and s, and assumed dielectric constant [cf. Bruzzone et al., 2011]. Using the backscattering coefficient, we can calculate the expected off-nadir surface echo powers. By performing the comparison between calculated and observed echo powers, we can determine most plausible dielectric constant. In the calculation of the echo powers, the transmitting loss of LRS have to be determined, which are however difficult to measure in the ground tests. So we estimated the transmitting loss to be 5.8 dB by assuming that the average dielectric constant is to be 5.3, which are derived from bulk density of 2.55 g/cm3 in the highlands reported based on GRAIL observations[Wieczorek et al., 2013].

The obtained Hurst exponent H is less than 0.5 in the maria, and about 0.9 in the highland. The parameter s is about 1 in the maria, and about 0.3 in the highland. By applying the analysis method mentioned above, we could obtain the observed and calculated surface echo powers in the regions where H˜0.5, and H˜0.9. Based on them, we could estimate the average dielectric constant in the maria (H?0.5) to be 7, and that in the highland (H?0.9) to be 4. The bulk densities are therefore estimated to be 3.0g/cm3 in the maria (H˜5), and 2.1g/cm3 in the highland. It suggests that there are more voids in the highland than in the maria due to longer exposure to the meteorite impacts.

Keywords: Kaguya (SELENE), Lunar Radar Sounder (LRS), Terrain Camera (TC), Surface roughness, Bulk density, Dielectric constant

Japan Geoscience Union Meeting 2014
(28 April - 02 May 2014 at Pacifico YOKOHAMA, Kanagawa, Japan)

PPS23-03 Room:413 Time:May 2 09:30-09:45

Tectonic evolution of Sinus Iridum and northwestern Imbrium regions

DAKE, Yuko[1*] ; YAMAJI, Atsushi[1] ; SATO, Katsushi[1] ; HARUYAMA, Junichi[2] ; MOROTA, Tomokatsu[3] ; OHTAKE, Makiko[2] ; MATSUNAGA, Tsuneo[4]

[1]Graduate School of Science, Kyoto University, [2]Japan Aerospace Exploration Agency / Institute of Space and Astronautical Science, [3]Graduate School of Environmental Studies, Nagoya University, [4]National Institute for Environmental Studies

Tectonic features, including mare ridges and lobate scarps, visualize the permanent strains of the lunar crust, and show ancient stress field in the shallow part of the crust, which can further places constraint on global thermal history [1], orbital evolution [2] or basin-scale mascon loading [3, 4]. Their formation ages are clues to understand the origin of tectonic movements. The subsidence of mare basalts began to affect the lithosphere as soon as they were deposited, but global tectonics can affect it long after their deposition. Some of the lobate scarps were recently estimated to be younger than 0.1 Ga [5]. It was pointed out there are some mare ridges even on the youngest mare basalts. These young tectonic structures suggest their origins other than the mascon loading. However, the amount of contraction induced by mascon loading have not yet been elucidated. The formation age of each mare ridge is not well understood. In this study, we estimated the ages of mare ridges in northwestern Imbrium and Sinus Iridum regions.

By means of optical data taken by the cameras onboard SELENE, we estimated the depositional ages of mare units and constrained the formation ages of ridges. Mare basalt lavas were so inviscid that the lava field initially made level surfaces. Therefore, the ages of deformed and dammed mare units by tectonic structures help us to determine the upper and lower bound of formation ages of the structures. We defined geological units by spectral features. The absolute ages of the units were estimated by crater-size frequency distribution measurements, applicable to craters with diameters ranging from 0.25 to 1 km, where the production and chronology functions of Neukum and Ivanov [6, 7].

The prominent mare ridges in the study area are ENE-WSW trending ridge system, hereafter Ridge System A, and NE-SW trending ridge system, Ridge System B. They are located at just to the south of Promontorium Laplace. They are parts of the concentric ridge system of Mare Imbrium, suggesting that the ridges are results of mascon loading. The eastern part of Ridge System A branches into three relatively small ridges. There is a unit boundary runs along the southern foot of Ridge System A. Relatively Ti-poor basalt [8] makes up the ridge, and relatively Ti-rich one [8] lies on the plain at the foot of the ridge. This indicates that the unit was dammed by the ridge. Therefore, the upper and lower limits of ridge formation are determined by the ages of the deformed and dammed basalt units. As a result, we estimated the ages of nine units and constrained the ages of tectonic structures as follows. Western part of Ridge System A and northern part of Ridge System B were formed between 3.0 to 2.1 Ga and 3.3 to 2.1 Ga, respectively. However, Ridge System A partially reactivated and become higher after 2.1 Ga. The middle part of Ridge System B also partially reactivated after 2.1 Ga. The southern part of Ridge System B deforms the youngest basalt indicating it was formed after 2.1 Ga.

Most of mare ridges in the study area can not be explained by mascon loading, because the major subsidence by mare basalt was occurred before 3.0 Ga in Mare Imbrium. Accordingly, this area was tectonically active after the deposition of mare basalts.

We also report other young tectonic features, such as lobate scarps and arcuate rilles in the study area.

References: [1] Prichard M.E. and Stevenson D.J., in Origin of the Earth and Moon, Canup R.M. and Righter K., Eds. (Arizona Univ. Press, 2000), 179-196. [2] Melosh H. (1980) Icarus, 43, 334-337. [3] Solomon S.C. and Head J.W. (1979) JGR, 84,148-227. [4] Freed A.M. et al. (2001) JGR, 106, 20603-30620. [5] Watters T.R. et al. (2010) Science, 329, 936-940. [6] Neukum G. (1983) Meteoritenbombardment und Datierung planetarer oberflachen, Habil. Thesis, Univ. Munich. [7] Neukum G. et al. (2001) Space Sci. Rev. 96, 55-86. [8] Lucey P.G. et al. (1998) JGR, 103, E2, 3679.

Keywords: Mare ridges, Deformation ages, Crater ages, Mascon tectonics

Japan Geoscience Union Meeting 2014
(28 April - 02 May 2014 at Pacifico YOKOHAMA, Kanagawa, Japan)

PPS23-04 Room:413 Time:May 2 09:45-10:00

Evaluation of the horizontal shortening in the shallow part of the lunar crust

YAMAJI, Atsushi[1*] ; DAKE, Yuko[1] ; SATO, Katsushi[1] ; HARUYAMA, Junichi[3] ; MOROTA, Tomokatsu[2] ; OHTAKE, Makiko[3] ; MATSUNAGA, Tsuneo[4]

[1]Divisin of Earth and Planetary Scieces, Kyoto University, [2]Graduate School of Environmental Studies, [3]Institute of Space and Astronautical Science, JAXA, [4]Center for Environmental Measurement and Analysis, National Institute for Environmental Studies

The topography of tectonic features in northwestern Imbrium and Sinus Iridum were studied in detail using SELENE-LISM data to estimate the horizontal shortening achieved by the formation of the features. As a result, it was found that the shortening by the formation of mare ridges was smaller than previous estimations by two orders of magnitudes except for a ridge, along which shortening was as large as ~500 m at maximum.

Keywords: tectonics, wrinkle ridge, graben, restoration

Japan Geoscience Union Meeting 2014
(28 April - 02 May 2014 at Pacifico YOKOHAMA, Kanagawa, Japan)

PPS23-05 Room:413 Time:May 2 10:00-10:15

Volcanic activity of lunar maria: Verification of super hot plume event at 2.0 Ga ago

KATO, Shinsuke[1*] ; MOROTA, Tomokatsu[1] ; WATANABE, Sei-ichiro[1] ; YAMAGUCHI, Yasushi[1] ; OTAKE, Hisashi[2] ; OHTAKE, Makiko[2]

[1]Nagoya University Graduate School of Environmental Studies, [2]Japan Aerospace Exploration Agency

Because the Moon is an endmember of terrestrial planetary bodies, to understand the thermal evolution of the Moon is necessary for understanding that of terrestrial planetary bodies. However, the process of magma ocean solidification and the thermal and structural evolution of the lunar mantle are still unknown.

Lunar mare basalts provide insights into compositions and thermal history of lunar mantle. Using image data from orbital satellites, a considerable number of maria have been dated by various techniques such as crater degradation measurement, crater size?frequency measurement, and stratigraphic relationship. Mare basalt ages indicate that eruptive activity has a second peak at the end of lunar volcanism (∼2 Ga), and the latest eruptions were limited in the Oceanus Procellarum and Mare Imbrium regions.

Using multiband images data obtained by SELENE/Kaguya, we have reinvestigated the relationship between titanium contents and eruption ages of mare basalts. Although the systematic relationship is not observed globally, an obvious increase in mean titanium content occurred at 2.3 Ga in the Oceanus Procellarum and Mare Imbrium regions, suggesting that the magma source changed at that time (hereafter, we call the volcanism before 2.3 Ga as Phase 1 volcanism, the volcanism after 2.3 Ga as Phase 2 volcanism.) The high-titanium basaltic eruption, which occurred at the late stage of mare volcanism, can be correlated with the second peak of volcanic activity at ∼2 Ga. The latest volcanic activity can be explained by the occurrence of a super hot plume originated from the core-mantle boundary.

To verify the super hot plume hypothesis, we calculate the difference between topography and selenoid in the mare region. We found a plateau structure around the center of the PKT region, whose the diameter is 1,000 km from southwest to northeast and 1,200 km from northwest to southeast and the altitude is 700 m. This plateau structure may be formed with ascending of super hot plume. Then, Phase 2 basaltic lava flows formed. If the ascending of super hot plume occurred ∼2.0 Ga ago, most mare formation had finished at that time and some transitional structures may have been left. In this presentation, we will discuss the relationship between Phase 2 high-titanium volcanisms and the super hot plume.

Keywords: Moon, lunar mare, titanium content, the Procellarum KREEP Terrane, super hot plume, selenoid

Japan Geoscience Union Meeting 2014
(28 April - 02 May 2014 at Pacifico YOKOHAMA, Kanagawa, Japan)

PPS23-06 Room:413 Time:May 2 10:15-10:30

Numerical models of mantle evolution in the moon

OGAWA, Masaki[1*]

[1]Graduate School of Arts and Sciences, Univ. of Tokyo

Numerical models of magmatism in convecting mantle are presented to understand the lunar magmatism that was active for the first 1 Gyr but rapidly declined after that. In the model, the characteristic time of magmatism is on the order of several hundred million years, much longer than that of the model of magmatism on larger planets like Mars, because a positive feedback between magmatism and mantle convection does not work: Upwelling flow of mantle convection induces magma by decompression melting. The buoyancy of the magma enhances the upwelling flow itself, and hence makes magmatism vigorous in a large planet. This positive feedback, however, does not work in the moon because of its low Rayleigh number. The long characteristic time of magmatism in the model is consistent with observations. The suggested mild magmatism implies that the heat extraction by magmatism is inefficient in the moon. Since the convective heat extraction is also inefficient in the moon because of its low Rayleigh number, this inefficient heat extraction by magmatism suggests that the most important mechanism of mantle cooling in the moon is thermal diffusion. Indeed, the thickening of the lithosphere with time by thermal diffusion makes the activity of magmatism decline within the first 1 Gyr of its history regardless of the initial content of heat producing elements in the mantle and other parameters that controls magmatism and mantle convection in the models. It may be necessary to carry out further numerical studies that include the early chemical differentiation of the mantle by magma-ocean to understand the magmatism that remained active till 2 Ga locally in some areas of the moon.

Keywords: mantle evolution, mantle convection, magmatism, the moon

Japan Geoscience Union Meeting 2014
(28 April - 02 May 2014 at Pacifico YOKOHAMA, Kanagawa, Japan)

PPS23-07 Room:413 Time:May 2 10:30-10:45

Identification of secondary craters based on the Voronoi diagram of the lunar craters

KINOSHITA, Tatsuo[1] ; HONDA, Chikatoshi[1*] ; HIRATA, Naru[1] ; MOROTA, Tomokatsu[2]

[1]The University of Aizu, [2]Graduate School of Environmental Studies, Nagoya University

We developed an automatic method for detecting crater clusters with crater spatial distribution based on the Area Voronoi tessellation technique. In the method based on the hierarchical cluster analysis, the evaluation of crater strongly depends on the closest one crater (or one cluster). In the method based on Voronoi tessellation on the other hand, it depends on the adjacent all craters. Since, this approach does not misjudge the pair craters evaluated cluster by the method based on the hierarchical cluster analysis. When a small crater is close adjacent a large crater, a boundary line of Voronoi tessellation is in the rim of the crater. This is different from the line a person pulls by intuition. So, we select Area Voronoi tessellation. For estimate an area of Voronoi, we adopted the wave front method (Watanabe and Murashima, 2006). We applied the Area Voronoi tessellation to observed crater spatial distribution. If the area of Voronoi cell is small, the crater becomes the candidate of the crater cluster. As a result, for the evaluation of crater spatial distribution, we propose that the Area Voronoi diagram is suitable to identify candidates of secondary crater.

Keywords: secondary crater, Voronoi diagram

Japan Geoscience Union Meeting 2014
(28 April - 02 May 2014 at Pacifico YOKOHAMA, Kanagawa, Japan)

PPS23-08 Room:413 Time:May 2 11:00-11:15

Development of a web application for dynamic analysis of the Kaguya Spectral Profiler data

SUGIMOTO, Kohei[1] ; HAYASHI, Yohei[2] ; OGAWA, Yoshiko[1*] ; HIRATA, Naru[1] ; TERAZONO, Junya[1] ; DEMURA, Hirohide[1] ; MATSUNAGA, Tsuneo[3] ; YAMAMOTO, Satoru[3] ; YOKOTA, Yasuhiro[3] ; OHTAKE, Makiko[4] ; OTAKE, Hisashi[4]

[1]University of Aizu, [2]AIST, [3]NIES, [4]ISAS/JAXA

Kaguya is a Japanese lunar orbiter launched on September 14, 2007 and observed the moon for about 2 years. The Spectral Profiler (SP) on board Kaguya was a spectrometer which provided global data set of visible-near infrared continuous reflectance spectra of the Moon. GEKKO is a web-application used to visualize the data observed by SP. GEKKO displays the graph of SP spectra and tables of ancillary data with thumbnail images simultaneously taken by Kaguya imager/camera. The current version of GEKKO is very useful for viewing SP spectra, but does not include analysis functions.

The goal of this study is to develop a framework for implementing analysis functions of the SP data. For transferring the data from the client, the original GEKKO connects to the server using MapServer. However, in case of MapServer, the client-researchers can only analyze in a predetermined manner. Therefore, we prepared CGI scripts and incorporated them into GEKKO.

By using the new GEKKO system, the clients-researchers will be able to dynamically analyze the SP data. The clients can select, coordinate and add the functions according to their objectives. We prepared the basic functions commonly used for the spectral analysis, such as running average, normalization and also similarity measurement.

Japan Geoscience Union Meeting 2014
(28 April - 02 May 2014 at Pacifico YOKOHAMA, Kanagawa, Japan)

PPS23-09 Room:413 Time:May 2 11:15-11:30

Rock and mineral distribution of the lunar South Pole-Aitken basin

UEMOTO, Kisara[1*] ; OHTAKE, Makiko[2] ; HARUYAMA, Junichi[2] ; YAMAMOTO, Satoru[3] ; NAKAMURA, Ryosuke[4] ; MATSUNAGA, Tsuneo[3] ; IWATA, Takahiro[2]

[1]The University of Tokyo, [2]Japan Aerospace Exploration Agency, [3]National Institute for Environmental Studies, [4]National Institute of Advanced Industrial Science and Technology

South Pole-Aitken (SPA) basin is one of the largest basin (2500 km in diameter [1]) on the lunar farside. In pre-vious studies, it has been suggested that most of the crustal material was excavated and that the mantle materials have been exposed [e.g., 1]. Particularly, because this excavation was the biggest at the central area of the basin, mantle materials exposed. Mantle material of this area is melted by the basin impact and produced impact melt [e.g., 2], therefore we suggest that investigation within this impact melt area lead up to understand mantle material conpo-sition. However, because SPA is very old and large, we cannot identify the impact melt area. In our study, we pro-duce a new mineralogical map of SPA basin interior, based on data derived from SELENE Multiband Imager (MI). In particular, we investigated mineralogy within the central depression of SPA by iron and titanium concentration and altitude data derived from SELENE. Using these method, we identified the impact melt area of SPA.

We prodused a mineralogical map within the central depression of SPA. As a result, we classified into three mineral type layers on this map ; low-Ca pyroxene layer, high-Ca pyroxene layer and very high-Ca pyroxene layer. From correlations of these layers and occurrences, we created the column diagrams of respective areas. Then, we suggested origins of these mineral type layers : The high-Ca pyroxene layer is impact melt area of the basin. The low-Ca pyroxene layer and the very high-Ca pyroxene layer is the ejecta of SPA basin and mare erupted after SPA basin formation, respectively. In fact, the area of the high-Ca pyroxene layer is impact melt area of SPA. In the fu-ture work, we will analyze mineral and chemical compositions within this area.

References: [1] Spudis et al., 1994. [2] Pieters et al., 2000

Keywords: South Pole-Aitken, lunar, rock, mineral

Japan Geoscience Union Meeting 2014
(28 April - 02 May 2014 at Pacifico YOKOHAMA, Kanagawa, Japan)

PPS23-10 Room:413 Time:May 2 11:30-11:45

Global Distribution Trend of High-Ca Pyroxene on the Lunar Highland by Satellite Hyperspectral Remote Sensing

YAMAMOTO, Satoru[1*] ; NAKAMURA, Ryosuke[2] ; MATSUNAGA, Tsuneo[1] ; OGAWA, Yoshiko[3] ; ISHIHARA, Yoshiaki[4] ; MOROTA, Tomokatsu[5] ; HIRATA, Naru[3] ; OHTAKE, Makiko[4] ; HIROI, Takahiro[6] ; YOKOTA, Yasuhiro[1] ; HARUYAMA, Junichi[4]

[1]NIES, [2]AIST, [3]Univ. of Aizu, [4]JAXA, [5]Nagoya Univ., [6]Brown Univ.

The studies using the spectral data obtained by Spectral Profiler (SP) and Multiband Imager (MI) onboard the Japanese lunar explorer SELENE/Kaguya revealed the global distributions of the purest anorthosite (PAN), olivine-rich materials, orthopyroxene-rich, and spinel-rich materials over the entire Moon. However, the global distribution of high-Ca pyroxene (HCP)-rich sites has been unclear so far. In addition to mare region, which is dominated by HCP, it has been reported that several ray craters on highland regions show HCP-dominant spectra. Thus, the global distribution of HCP-rich sites, especially for the lunar highland regions, would provide important information for the structure and evolution of the lunar crust and mantle. Thus, using the global data set of the SP, we conducted the global survey to find HCP-rich sites on the Moon, especially for the lunar highland regions. Here, we report the global distribution trend of the HCP-rich sites based on this survey.

Keywords: Remote-sensing, Hyperspectral, Kaguya

Japan Geoscience Union Meeting 2014
(28 April - 02 May 2014 at Pacifico YOKOHAMA, Kanagawa, Japan)

PPS23-11 Room:413 Time:May 2 11:45-12:00

Solidification of the lunar magma ocean suggested by composition of the highland crust

OHTAKE, Makiko[1*] ; KOBAYASHI, Shingo[2] ; TAKEDA, Hiroshi[3] ; MOROTA, Tomokatsu[4] ; ISHIHARA, Yoshiaki[1] ; MATSUNAGA, Tsuneo[5] ; YOKOTA, Yasuhiro[5] ; HARUYAMA, Junichi[1] ; YAMAMOTO, Satoru[5] ; OGAWA, Yoshiko[6] ; KAROUJI, Yuzuru[1] ; SAIKI, Kazuto[7]

[1]Japan Aerospace Exploration Agency, [2]National Institute of Radiological Sciences, [3]Chiba Inst. of Technology, [4]Nagoya University, [5]National Institute for Environmental Studies, [6]The University of Aizu, [7]Osaka University

Introduction: Previously we reported that highland materials with higher Mg# (Mg/[Mg+Fe] in mole percent in mafic minerals) (up to 80) than those on the lunar nearside were found on the lunar farside [1]. The observed higher Mg# on the lunar farside indicates that the farside crust consists of rocks that crystallized from less-evolved magma than the nearside crust. One of the other key parameters for evaluating solidification of the lunar magma ocean is Th abundance. Th is an incompatible element and concentrates in the liquidus phase when magma cools, therefore highland material that solidified earlier must have lower Th abundance than the highland material that solidified later. Th abundance distribution and its dichotomic nature were found to be lower on the farside than on the nearside [2].

If the dichotomic distribution of lunar highland Mg# and the Th abundance were formed by lunar magma ocean solidification, as the solidification proceeds, Mg# will decrease while Th abundance will increase, giving the two parameters a negative correlation. This study investigated the correlation of the two observed parameters of the lunar highland to validate the magma ocean origin of Mg# and Th abundance distribution on the lunar surface. We also tried to estimate the chemical composition of the lunar magma ocean by combining two remote-sensing data sets.

Method: Using Kaguya gamma-ray data, we derived the relative Th abundance (count of the observed gamma-ray data) map of the Moon as gridded data. We then derived the Mg# map of the lunar highland so that it had the same grid as the Th abundance map. For comparison with the derived Mg# and Th abundance correlation trend, we calculated the Mg# of the lunar magma ocean starting with different bulk chemical compositions by using the MELTS program [3]. The calculated starting magmatic compositions were bulk silicate Earth and bulk lunar magma ocean.

Results: The derived Mg# and Th concentration ratio of the same location indicates a negative correlation of the two parameters. In addition to the negative correlation, another interesting feature is that there seems to be two separate trends with lower and higher Th concentration ratios. Comparison of the observed Mg# and Th concentration ratio trend with that of the model calculation suggests that the observed data of the lower Th concentration ratio group matches the bulk silicate Earth composition better than the lunar magma ocean.

Discussion: The negative correlation of observed Mg# and Th concentration ratio suggests that current values of these parameters on the lunar surface are likely due to cooling of the lunar magma ocean as each location crystallized at a different solidification stage though the origin of the two apparent sets of the observed trends is not clear. The fact that the observed data of the lower Th concentration ratio group matches the bulk silicate Earth model better may imply that the chemical composition of the lunar magma ocean needs to re-evaluated and that the Mg# of the actual bulk lunar magma ocean may be higher than previously estimated although we need to further evaluate the effect of calculation conditions. The possibly higher Mg# of the bulk lunar magma ocean agrees with the reported higher Mg# (up to 80) in the farside highland than previously estimated based on the nearside sampled FAN compositions.

[1] Ohtake, M. et al. (2012) Nature GeoSci. 5, 384-388. [2] Kobayashi, S. et al. (2012) Earth Planet. Sci. Lett. 337, 10?16. [3] Ghiorso and Sack (1995) Contrib. Mineral. Petrol. 119, 197?212.

Keywords: Moon, Kaguya, SELENE, Crust, Magma Ocean

Japan Geoscience Union Meeting 2014
(28 April - 02 May 2014 at Pacifico YOKOHAMA, Kanagawa, Japan)

PPS23-12 Room:413 Time:May 2 12:00-12:15

Plagioclase with High Ca Contents from the Central Farside Highland.

TAKEDA, Hiroshi[1*] ; NAGAOKA, Hiroshi[2] ; KAROUJI, Yuzuru[3] ; OHTAKE, Makiko[4] ; YAZAWA, Yuuki[5] ; YAMAGUCHI, Akira[6]

[1]Graduate School of Sciences, The University of Tokyo, [2]Waseda Univ., [3]JAXA/ISAS, [4]JAXA/ISAS, [5]Faculty of Engineering, Chiba Institute of Technology, [6]National Inst. of Polar Research

Some lunar meteorites contain clasts of nearly pure calcic plagioclase with high An values and low FeO (1). We proposed that these meteorites are derived from the lunar farside on the basis of estimated low concentrations of Th and FeO by the remote sensing data on the farside of the Moon (2). The Lunar Magma Ocean (LMO) model deduced from the Apollo samples is not able to explain such dichotmy of the Moon. Nyquist et al. (3) performed Sm-Nd and Ar-Ar studies of pristine ferroan anorthosites (FANs) of the returned Apollo samples and showed that a whole rock Sm-Nd isochron for selected FANs yields an isochron age of 4.47 Ga . Mineralogical studies of lunar meteorites of the Dhofar 489 group (2) and Yamato 86032 , all possibly from the farside highlands, showed some aspects of the farside crust. Nagaoka et al. (1) reported that many fragments in such meteorites contain clasts of nearly pure calcic plagioclase with high An values.

Mineralogy of magnesian anorthosite clasts in Dhofar 489, 309 and 307 (2) was used to deduce the ejection site of the Dhofar 489 group. Presence of fine-grained magnesian granulitic clast, and many crystalline clasts with rapid growth features were interpreted in terms of a large impact basin associated with small cratering. Among a few large basins of the farside, the Dirichlet-Jackson (DJ) basin has a few large craters on the floor, and the formation age by Morota et al. (4) is 4.25 Ga, which agrees with the Ar-Ar age (4.23 Ga) of Dhofar 489 (2). Based on the Th map made by KGRS, Kobayashi et al. (5) showed that the lowest Th regions in the lunar farside occurs near the equatorial region and noted that the regions well correspond to the high Mg number region (DJ) measured by SP, of the farside crust (6). These rocks with low Th may be crystallized from less-evolved magma than the nearside crust. Anorthosites composed of nearly pure anorthite (PAN) with low Th at many locations in the farside highlands and a map of the Mg numbers (6) also showed that the region around the DJ basin is consistent with the Mg numbers (70 to 76) of the magnesian anorthositic clast in Dhofar 489 (2). A large impact, which excavated a basin of the farside might have produced granulites in deep ejecta of a smaller impact.

We investigated a process of decomposition of Ca-rich plagioclase with fulvic acid, which is a complex natural organic acid produced in humified soils (7). The Ca ion released from plagioclase can be used to fix carbon dioxide as calcite as in oolites, and is useful for reducing carbon dioxide from the atmosphere on the Earth.

References: (1) Nagaoka H., Takeda H. et al. (2012) 75th Ann. Meet. Meteorit Soc. Abstr no. 5197. (2) Takeda et al. (2006) Earth Planet Sci Lett 247, 171-184. (3) Nyquist L. E. et al (2013) LPSC 45th no. 1125. (4) Morota T. et al. (2011) JGU Meeting, PPS024-10. (5) Kobayashi S. et al. (2012) EPSL, 337-338, 10-16. (6) Ohtake M. et al. (2012) Nature Geosci., 5, 384-388. (7) Yazawa Y. et al. (2012) Chapter. 5, in Moon, B. Viorel Ed., XXXVIII, 750 p, 105-138, Springer.

Keywords: plagioclase, lunar crust, farside highland, resource utilization

Japan Geoscience Union Meeting 2014
(28 April - 02 May 2014 at Pacifico YOKOHAMA, Kanagawa, Japan)

PPS23-13 Room:413 Time:May 2 12:15-12:30

Volatile accretion on the Moon - A clue for the emergence of a habitable Earth.

HASHIZUME, Ko[1*] ; HARUYAMA, Junichi[2]

[1]Osaka University, Graduate School of Science, [2]Japan Aerospace Exploration Agency / Institute of Space and Astronautical Science

I would like to introduce the recent advancement in deciphering the information on accretion of planetary volatile compounds to the moon using lunar regolith samples. I will also make a brief comment on the future lunar explorations, toward a better understanding of volatile accretion to the early Earth-Moon system that possibly lead to the emergence of the habitable Earth.

Keywords: Lunar Regolith, Volatile Compound, Isotope Composition, Accretion Rate

Japan Geoscience Union Meeting 2014
(28 April - 02 May 2014 at Pacifico YOKOHAMA, Kanagawa, Japan)

PPS23-14 Room:413 Time:May 2 12:30-12:45

Extraterrestrial solidified materials with multi-mixture on the Moon

MIURA, Yasunori[1*]

[1]In & Out Universities

The results of the present study are summarized as follows:

1) Study of the Moon provides largely valuable information on formation processes of primordial Earth and extraterrestrial celestial-bodies.

2) Identification of crystalline solids are almost similar between the Moon and Earth, though the Moon rocks might be formed by similar formation processes of terrestrial (Earth) rocks based on the crystalline parts. However, extraterrestrial solids are mixtures of multiple states shown as amorphous solids.

3) Formation of quasi-spherical Moon body formed mainly by impact-related melting process is found as heterogeneous and irregular distribution of lunar rocks with impact craters.

4) Fluid-bearing depositions irregularly distributed on the surface and interior of the Moon are largely based on storages on the interior formed by solidified mixtures of multiple states triggered by impact process on the Moon.

5) Different processes of solids between the Moon and Earth can be observed silica Si-O frameworks which can be obtained by the ion bombardment experiments. Crystalline rocks with hard silicate structures show higher ion-peaks of alkali ions (Na, K and Ca etc.), whereas solid-aggregates of the Moon rocks show higher ion-peaks of Si and Al ions which are easily destroyed by ion bombardment relatively.

6) Ion-peaks by the sputtering of Earth impact-breccias are clearly higher than those of the Moon breccias, which main differences are not rock textures but atomic bonding.

7) The air- and water-less Moon with solidified materials with multi-states is formed from nano-grains to macroscopic rocks by impact-related evolution process.

8) The primordial planet Earth with remained heterogeneous surface by impact-related process is considered to be different cyclic system of three states (air, liquid and solid) with macro-life activity which is formed by huge production from the interior triggered by huge collision process of the giant impact.

Keywords: the Moon, mixture, solidified material, material state, ilicate framework, ion bombarment run

Japan Geoscience Union Meeting 2014
(28 April - 02 May 2014 at Pacifico YOKOHAMA, Kanagawa, Japan)

PPS23-15 Room:413 Time:May 2 14:15-14:30

Re-examination of Excavation Cavity of the Impact Basins of the Moon based on GRAIL based Crustal Thickness Model

ISHIHARA, Yoshiaki[1*] ; NAKAMURA, Ryosuke[2]

[1]JAXA, [2]AIST

Large impact features, whose diameters are more than hundreds of kilometers, are called impact basins. Large impact basins can provide comparatively clear information of the cratering process and/or constrain the lunar thermal history. The internal or subsurface structures of basins can be assessed through an analysis of their associated gravitational and topographic signatures. The recently Kaguya/SELENE mission has improved the crustal thickness model not only for the nearside but also for the farside based on the first direct farside gravity and global topography mapping. Moreover most recent GRAIL mission vastry improved spatial resolution and overall accuracy of the lunar gravity models and lunar crustal thickness models. The GRAIL crustal thickness model gives us the opportunity to re-analyse excavation depth and diameter of basin forming impact processes anywhere on the Moon with improved accuracy. This study uses the GRAIL crustal thickness model, to reconstruct the excavation cavity geometry of large impact basins on the Moon.

Our method of reconstructing the excavation cavity of large impact basins is fairly simple. We assume that the thinned crust and uplifted Moho beneath features is a direct consequence of (1) the amount of crustal material excavated during the cratering process and (2) the subsequent rebound of the crater (basin) floor. We first construct azimuthally averaged profiles for the surface topography, mare thickness and subsurface structure of the Moho for each basin. Next, we restored the uplifted Moho and overlying crust to its pre-impact position. Estimating procedures of pre-impact position is almost the same as previous analysis. After removing mare fill, this process resulted in a roughly parabolic surface depression, that we interpret as being the first-order representation of the basin's excavation cavity.

One of the most important values of understanding the large impact basin is the depth-to-diameter ratio of the excavation cavity. We examine the depth versus the diameter of our reconstructed excavation cavities (excluding the Imbrium Basin and the South Pole-Aitken Basin). It seems that up to 400 km cavity diameter, the depth (hex) and diameter (Dex) are linearly related. Further more, the linear relationship (hex/Dex=0.079+/-0.006) is almost consistent with, though slightly smaller than, the value for craters orders of magnitude smaller in size (hex/Dex=0.1), suggesting that proportional scaling is valid for basin scale impact structures except the largest impact structures on the Moon. One of the reasons of smaller depth-to-diameter ratio are probably effects due to the post impact modifications. Impact basins which has excavation cavity diameter larger than 400 km show the different state. The average crustal thickness of GRAIL lunar crustal thickness model is 34 to 43 km. So excavation cavity diameter of 400 km is located the ragime boundary between the excavation/melting cavity within crust ragime and the excavation/melting cavity exeed the Moho interface ragime.

Keywords: Impact Basin, Excavation Cavity, Melting Cavity, Moon

Japan Geoscience Union Meeting 2014
(28 April - 02 May 2014 at Pacifico YOKOHAMA, Kanagawa, Japan)

PPS23-16 Room:413 Time:May 2 14:30-14:45

Lunar gravity anomaly recovery with the GRAIL level-1b and level-2 data

HASHIMOTO, Mina[1*] ; HEKI, Kosuke[1]

[1]Department of Natural History Sciences, Faculty of Science, Hokkaido University

First, we will talk about the lunar gravity anomaly recovery with the GRAIL level-1b data. Among several global lunar gravity field models available now, GRAIL offers the highest resolution. The Doppler tracking between Earth-based stations and lunar satellites can directly observe gravity field of the lunar nearside. SELENE could measure the farside, for the first time, by inter-satellite tracking using the high-altitude relay satellite. GRAIL employs the low-low inter-satellite tracking method, often called as ″ Tom and Jerry ″ . This is similar to GRACE, the twin satellites for the gravimetry of the earth. It observes the gravity field by ranging between the satellites using microwave. In this way, GRAIL got the global lunar gravity anomaly map. In our study, we use the GRAIL level-1b and level-2 data. Both data have become open to public at the PDS Geoscience Node at the Washington University, Saint Lewis. The level-1b data include satellite position data compiled as the GNV1b files, and inter-satellite ranging data (ranges, range rates, and range accelerations every five seconds) are compiled in the KBR1b files. In this study, we used these two data sets and estimated the mass distribution on the moon. We remodeled the moon ' s gravity anomaly program of the Lunar Prospector developed by Sugano and Heki (EPS 2004; GRL 2005). Using this program, we estimated the gravity anomaly of the specific parts of the lunar surface. We found the Level-1b data are able to recover them clearly. Then, we will introduce the next-stage study by using the GRAIL level-2 data set, and explain the scientific targets of our study. Recent study (Miljkovi?, K. et al., 2013) suggested that the size and depth of the crater depends on the mantle temperature as well as the size and speed of the projectile. We here study the gravity signatures of small to medium sized craters, and will find systematic difference between the lunar near and far sides.

Japan Geoscience Union Meeting 2014
(28 April - 02 May 2014 at Pacifico YOKOHAMA, Kanagawa, Japan)

PPS23-17 Room:413 Time:May 2 14:45-15:00

Consideration of the seismic moment distribution of deep moonquake and the lunar deep structure

YAMADA, Ryuhei[1*] ; NODA, Hirotomo[1] ; ARAKI, Hiroshi[1]

[1]National Astronomical Observatory of Japan / RISE Project

The Apollo seismic network consists of 4 seismic stations (Apollo12, 14, 15 and 16) have observed deep moonquakes which occur repeatedly from specific source regions at depth of 700-1200 km in the lunar deep region. The deep moonquake occurs periodically related with positions of the Earth, the Moon and the Sun; that is tidal forces (e.g., Lammlein, 1977, Bulow et al., 2007). The 106 deep moonquake sources are currently located (Nakamura, 2005), the activity and largeness of the deep event and maybe occurrence mechanism are different among the sources (Araki, 2001).

Yamada et al., (2013) have investigated seismic moment of each deep event occurred from active and well-located 15 deep sources from analysis of data obtained in Apollo 12 station. To derive the seismic moment, we have to correct for characteristics of the Apollo seismometers, elastic and attenuation parameters of the lunar interior where the seismic phase passes, geometrical spreading and radiation pattern of the fault at source region from amplitude of the seismic event (Goins et al., 1981). In Yamada et al., (2013), recent lunar interior model VPREMOON (Garcia et al., 2013) are used, and the results have shown that the values of seismic moments are different among active 15 sources and far deep sources occur the events which have larger seismic moment than near sources.

In this study, we have derived the seismic moments of identical deep events observed in Apollo 15 and 16 stations to verify the previous results derived from analysis of Apollo 12 data. This analysis indicates that the values of seismic moments derived from each station data are respectively different from even if the events are identical. We found a tendency which deep moonquakes occur from far sources indicates larger differences in seismic moments derived from each station data than near source events. This may mean that the recent lunar interior model applied in this study has some problems. Especially, seismic quality factor in the mantle mainly affects on amplitudes of the seismic events. Previous studies (e.g., Nakamura and Koyama, 1982) have described that values of seismic quality factor had large uncertainty in lunar deep region. We, therefore, derived appropriate seismic quality factor so as to minimize differences of the seismic moments derived from each station data. In this analysis, we considered effects of possible radiation patterns because these values also have large uncertainty and effect on derivation of the seismic moments. We will report and discuss our new seismic moment distribution of deep moonquakes and new values of seismic quality factor in this presentation.

Keywords: Deep Moonquake, Seismic Moment, Lunar Seismic Activity, Lunar Mantle, Lunar Seismic Quality Factor, Lunar Deep Structure

Japan Geoscience Union Meeting 2014
(28 April - 02 May 2014 at Pacifico YOKOHAMA, Kanagawa, Japan)

PPS23-18 Room:413 Time:May 2 15:00-15:15

Variation of the ionized lunar sodium and potassium exosphere

YOKOTA, Shoichiro[1*] ; SAITO, Yoshifumi[1] ; ASAMURA, Kazushi[1] ; NISHINO, Masaki n[2] ; TSUNAKAWA, Hideo[3]

[1]ISAS/JAXA, [2]STE Lab., [3]Tokyo Institute of Tech.

Lunar exosphere has been observed and studied on many occasions by ground-based telescopes since the discovery of surface-bounded alkali exosphere. The observed exospheric components were alkali atoms such as Na and K because the emission lines are much brighter than for other conceivable components. The structure, source, and the transport mechanisms of the lunar exosphere have been discussed based on these ground-based observations of the alkali atoms. As for the source mechanism of the thin lunar alkali exosphere, five processes were proposed as follows: thermal desorption, electron-stimulated desorption (ESD), photon-stimulated desorption (PSD), ion-induced desorption (sputtering), and vaporization by micrometeoroid impacts. Structure of the lunar exosphere gives us the key parameters to investigate the source mechanism. The observed Na exosphere distribution suggested that PSD and/or sputtering do not simply release the exospheric particles. Since PSD is capable of releasing alkali atoms only out of very shallow region in the lunar soils, PSD has relatively limited store of the exospheric particles in the lunar surface. If there was no replenishing process, PSD would deplete surface alkalis. We present latitude and longitude distributions of Na+ and K+ fluxes from the Moon derived from the Kaguya low-energy ion data. Although the latitude distribution agrees with the previous ground-based telescope observations, dawn-dusk asymmetry has been found in the longitude distribution. Our model of the lunar surface abundance and yield of Na and K demonstrates that the abundance decreases to around 50%, at dusk compared to that at dawn due to the emission of the exospheric particles. It is also implicated that the surface abundance of Na and K need to be supplied during the night in order to explain the observed lunar exosphere with the dawn-dusk asymmetry.

Keywords: Moon, Exosphere, Alkali atmosphere, Mass analyses

Japan Geoscience Union Meeting 2014
(28 April - 02 May 2014 at Pacifico YOKOHAMA, Kanagawa, Japan)

PPS23-19 Room:413 Time:May 2 15:15-15:30

Various appearances of whistler-mode waves observed near the Moon in the solar wind

TSUGAWA, Yasunori[1*] ; KATOH, Yuto[1] ; TERADA, Naoki[1] ; TSUNAKAWA, Hideo[2] ; TAKAHASHI, Futoshi[2] ; SHIBUYA, Hidetoshi[3] ; SHIMIZU, Hisayoshi[4] ; MATSUSHIMA, Masaki[2]

[1]Department of Geophysics, Tohoku University, [2]Department of Earth and Planetary Sciences, Tokyo Institute of Technology, [3]Department of Earth and Environmental Sciences, Kumamoto University, [4]Earthquake Research Institute, University of Tokyo

Narrowband whistler-mode waves whose frequencies close to 1 Hz have been observed near the Moon [Farrell et al., 1996; Nakagawa et al., 2003; Halekas et al., 2006; Tsugawa et al., 2011]. Broadband whistler-mode waves in the frequencies up to about 10 Hz with no preferred polarity have also been observed near the Moon [Halekas et al., 2008; Nakagawa et al., 2011, Tsugawa et al., 2012]. In addition, the lunar magnetometer (LMAG) aboard Kaguya detected right-hand polarized broadband waves, which is relatively weak and appears in the frequency range of several Hz. Since the angle between the wave vector and the sunward direction is large, the waves are not significantly Doppler shifted, indicating that they are whistler-mode waves. We also reveal the existence of harmonic waves whose fundamental waves appear in the frequencies near 1-2 Hz. The fundamental waves resemble the narrowband whistler-mode waves.

We construct criteria to select these waves and perform statistical analyses. Based on the statistical properties, we suggest possible scenarios of the generation and propagation of the four types of waves around the Moon. Whistler-mode waves in the frequency near the lower hybrid frequency generated through the reflection of ions by the Moon would be observed as (1) the narrowband waves in the spacecraft frame when the group velocity vector points to the sunward and is cancelled by the solar wind velocity, as (2) the broadband waves in the interaction region with various wave components, as (3) the right-hand polarized broadband waves when the wave vector points perpendicular to the sunward, and as (4) the harmonic waves in the same condition with NR with a large compressional component enough to be steepened.

Japan Geoscience Union Meeting 2014
(28 April - 02 May 2014 at Pacifico YOKOHAMA, Kanagawa, Japan)

PPS23-20 Room:413 Time:May 2 15:30-15:45

Detection experiment of Ar emission lines for K-Ar dating using Laser-Induced Breakdown Spectroscopy

OKUMURA, Yu[1*] ; SHIBASAKI, Kazuo[1] ; OISHI, Takahiro[1] ; CHO, Yuichiro[2] ; KAMEDA, Shingo[1] ; MIBE, Kenji[2] ; MIURA, Yayoi N.[2] ; SUGITA, Seiji[2]

[1]Rikkyo University, [2]The University of Tokyo

JAXA is currently planning the lunar lander SELENE-2 project, a follow-up mission of SELENE. This project involves the dispatch of a lunar rover to investigate the lunar surface and rocks. We propose Laser-Induced Breakdown Spectroscopy (LIBS) as an instrument for mounting rovers. The LIBS conducts in-situ analysis of elemental composition.

The LIBS instrument uses a high intensity laser pulse and induced plasma. The plasma emits energy in the form of photons. The spectroscopic analysis of the plasma enables the determination of the elemental composition.

K-Ar dating is a radiometric method used in geochronology. It is based on the measurement of the product of the radioactive decay of ^{40}K into ^{40}Ar with a half-life of 1.25 Gyr. K is found in many rocks. Therefore, we can determine the solidification age of rocks by measuring the ratio of ^{40}K to ^{40}Ar in the rock. In the existing K-Ar dating method, K is measured using LIBS and Ar is measured using quadrupole mass spectrometry (QMS); thus, the method needs two measuring instruments. Our method can be applied to measure both K and Ar using only LIBS. Therefore, the instrument weight will be reduced if our method is applied successfully. The Curiosity rover, a part of NASA's Mars Science Laboratory mission, used LIBS to obtain the spectra of rocks present on the surface of Mars. The Curiosity rover's LIBS instrument detected K in the rocks. However, Ar has not been detected using LIBS. We conducted experiments to detect the Ar emission lines using LIBS.

Commonly, the temperature of plasma induced using LIBS is approximately 1eV (11600K) in the atmosphere. When temperature of plasma was 1eV, we expected that it is possible to detect the Ar emission lines at the wavelengths of 104.8nm and 106.7nm in the vacuum ultraviolet spectral range because no emission lines of neutrals and singly-charged ions of major elements exist in the range. However, as a result, we found that the plasma temperature might be several tens of eV in vacuum. We found that relative intensity of multiply-charged ions (e.g. Si(Ⅳ), Fe(Ⅱ)) emission lines is much stronger than the Ar emission lines. Therefore, we decreased the temperature of plasma in vacuum by decreasing the pulse laser intensity and conducted experiments. In addition, we conducted experiments to investigate the Ar emission lines, which we might be able to detect when the plasma temperature is higher than 1eV, in the vacuum ultraviolet (VUV)-near infrared (NIR) range in vacuum.

Keywords: LIBS, elemental compositions, K-Ar dating, Planetary Explora, Moon

Japan Geoscience Union Meeting 2014
(28 April - 02 May 2014 at Pacifico YOKOHAMA, Kanagawa, Japan)

PPS23-21 Room:413 Time:May 2 15:45-16:00

Unprecedented Zipangu Underworld of the Moon Exploration (UZUME)

HARUYAMA, Junichi[1*] ; KAWANO, Isao[1] ; KUBOTA, Takashi[1] ; OTSUKI, Masatsugu[1] ; NISHIBORI, Toshiyuki[1] ; IWATA, Takahiro[1] ; ISHIHARA, Yoshiaki[1] ; YAMAMOTO, Yukio[1] ; NAGAMATSU, Aiko[1] ; HASENAKA, Toshiaki[3] ; SHIMIZU, Hisayoshi[4] ; MOROTA, Tomokatsu[5] ; MICHIKAMI, Tatsuhiro[6] ; SHIRAO, Motomaro[7] ; MIYAMOTO, Hideaki[4] ; KOBAYASHI, Kensei[2] ; YAMAMOTO, Satoru[8] ; YOKOTA, Yasuhiro[8] ; HASHIZUME, Ko[9] ; SAIKI, Kazuto[9] ; KOMATSU, Goro[10]

[1]Japan Aerospace Exploration Agency, [2]Yokohama National University, [3]Kumamoto University, [4]University of Tokyo, [5]Nagoya University, [6]Kinki University, [7]Planetary Geology Institute, [8]National Institute for Environmental Studies, [9]Osaka University, [10]Universita d'Annunzio

Japanese lunar explorer SELENE (Kaguya) discovered gigantic vertical holes of 100 m in diameters and depths in the Marius Hills, Mare Tranquillitatis, and Mare Ingenii of the Moon. These holes are possibly skylights of underground large caverns such as lava tubes, magma chambers, or faults. There are lots of scientific interests on the holes and associating caverns. In addition, these holes and underground structures are the best candidate locations for future lunar base. Similar holes have been also found on the Mars. The caverns connecting to the Martian holes may be the best place for Martian lives to emerge, evolve and survive because of their safer conditions than the Martian surface. We are now planning to establish a project working group to explore the lunar holes and caverns associating to the holes. We call the project as UZUME (Unprecedented Zipangu Underworld of the Moon Exploration).

Keywords: Moon, SELENE, hole, cavern

Japan Geoscience Union Meeting 2014
(28 April - 02 May 2014 at Pacifico YOKOHAMA, Kanagawa, Japan)

PPS23-P01 Room:Poster Time:May 2 16:30-17:30

Development of ILOM using DOE and situation of trial manufacturing of DOE

KASHIMA, Shingo[1*] ; ARAKI, Hiroshi[1] ; HANADA, Hideo[1] ; TSURUTA, Seiitsu[1] ; SUZUKI, Hirofumi[2] ; YASUDA, Susumu[3] ; UTSUNOMIYA, Shin[3]

[1]RISE Project Office, National Astronomical Observatory of Japan, [2]Mechanical Engg.,Chubu University, [3]Japan Aerospace Exploration Agency

We have a plan to install the photo-zenith telescope on the moon as part of a next SELENE project. The purpose is to explain the internal structure and the origin of the moon by measuring the small vibration and movement with very high accuracy. In this presentation, we show the development of ILOM using DOE that actualize the very high performance, i.e.,1 mas, in the severe thermal condition of the moon and show the situation of the trial manufacturing of DOE that is the key technology of this telescope.

Keywords: ILOM, DOE, SELENE

Japan Geoscience Union Meeting 2014
(28 April - 02 May 2014 at Pacifico YOKOHAMA, Kanagawa, Japan)

PPS23-P02 Room:Poster Time:May 2 16:30-17:30

Angle, deformation and DAO (Dihedral Angle Off-set) Analysys of the corner cube mirror for LL

KASHIMA, Shingo[1*] ; NODA, Hirotomo[1] ; ARAKI, Hiroshi[1] ; HANADA, Hideo[1] ; KUNIMORI, Hiroo[2] ; OTSUBO, Toshimichi[3]

[1]RISE Project Office, National Astronomical Observatory of Japan, [2]National Institute of Information and Communications Technology, [3]Social Sciences, Hitotsubashi University

We have a plan to install the corner cube mirror which has about 20cm aperture on the moon as part of a next SELENE project. The purpose is to explain the internal structure and the origin of the moon by measuring and analysing the distance between the moon and the earth with cm order accuracy. In order to actualize such a precise measurement, we have to manufacture the CCM with 0.1 sec angular precision and less the lambda/10 flatness for the mirror surface. In this presentation, we show the optical response analysis for deriving these degree of precision.

Keywords: LLR, CCM, SELENE

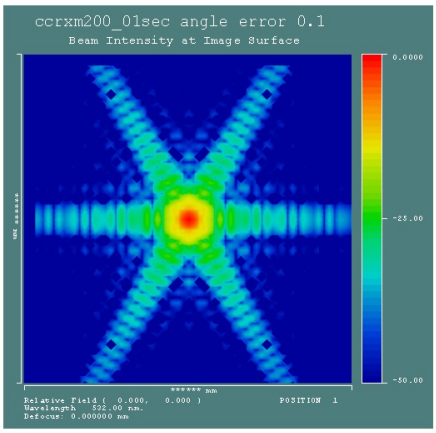

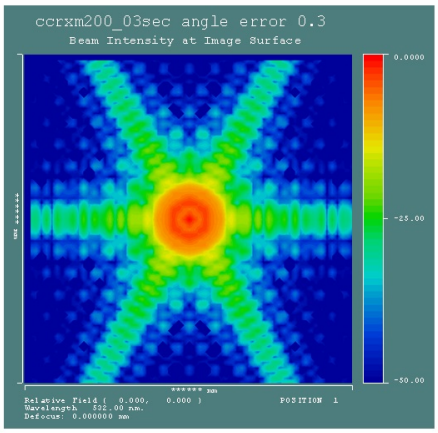

Japan Geoscience Union Meeting 2014
(28 April - 02 May 2014 at Pacifico YOKOHAMA, Kanagawa, Japan)

PPS23-P03 Room:Poster Time:May 2 16:30-17:30

Development of the Retroreflector on the Moon for the Future Lunar Laser Ranging

ARAKI, Hiroshi[1*] ; KASHIMA, Shingo[1] ; NODA, Hirotomo[1] ; KUNIMORI, Hiroo[2] ; CHIBA, Kouta[3] ; OTSUBO, Toshimichi[4] ; UTSUNOMIYA, Makoto[5] ; MATSUMOTO, Yoshiaki[6]

[1]National Astronomical Observatory of Japan, [2]National Institute of Communication and Technology, [3]Iwate University, [4]Hitotsubashi University, [5]Japan Aerospace Exploration Agency, [6]PLANET Co. Ltd.

Lunar Laser Ranging (LLR) data are important for the investigations of the lunar rotation, tide, and lunar deep interior structure. The range accuracy of LLR has been less than 2 cm for the last 20 years due to the progress of laser transmit/receive system on the ground stations and the atmospheric signal delay model, however, one order or more accurate ranging than 2cm is needed for better understanding of the lunar deep interior. We are developing 'single aperture and hollow' retroreflector (Corner Cube Mirror; CCM) to be aboard future lunar landing missions. The aperture of CCM is 20cm because the reflection efficiency of that size is found to be higher than that of Apollo 11 array CCP (Corner Cube Prism). For the CCM ultra low expansion glass-ceramic (ClearCeramRZ-EX, OHARA Inc.; hereafter CCZ-EX)' or 'single crystal Si' is selected for candidate material of CCM taking into account small |CTE|/K (Thermal expansion coefficient over thermal diffusivity) and large specific Young modulus. The optical performance of CCM deformed by lunar gravity or solar illumination in the holder model is presented for some cases.

Keywords: LLR, corner cube mirror, hollow, single crystal Si, deformation, optical performance

Japan Geoscience Union Meeting 2014
(28 April - 02 May 2014 at Pacifico YOKOHAMA, Kanagawa, Japan)

PPS23-P04 Room:Poster Time:May 2 16:30-17:30

Lunar Laser Ranging Trial at Koganei SLR station

NODA, Hirotomo[1*] ; KUNIMORI, Hiroo[2] ; ARAKI, Hiroshi[1]

[1]National Astronomical Observatory of Japan, [2]National Institute of Information and Communications Technology

Introduction: The Lunar Laser Ranging (LLR) is a technique to measure the distance between laser stations on the Earth and retroreflectors on the Moon, by detecting the time of flight of high-powered laser emitted from the ground station. Since the Earth-Moon distance contains information of lunar orbit, lunar solid tides, and lunar orientation and rotation, observation data of LLR have contributed to the lunar science, especially for the estimation of the inner structure of the Moon through orientation, rotation and tide. There are five refroreflectors on the Moon, Apollo 11, 14, 15 (U. S. A.), Lunokhod 1 and 2 (french-made, carried by former U. S. S. R.). The Apollo 15 has largest aperture among them, and almost 75 % of the total LLR data are from Apollo 15 site.

System Description: Since there is no Japanese station which can range the Moon so far, a precursor ranging experiment by using the Satellite Laser Ranging (SLR) facility in the NICT Koganei campus in Tokyo is ongoing. The SLR station has a 1.5 m Cassegrain telescope with Coude focus. Normally it is equipped with a laser with 20mJ, 20Hz repetition rate, and 35 picoseconds pulse width for satellite ranging. In addition to it, a wide-pulse width laser (3 nanoseconds, which corresponds to 45 cm in 2-way range) with energy of about 350 mJ per shot, repetition rate of 10Hz, wavelength of 532 nm is introduced to detect photons from the lunar retroreflectors for demonstration. As the pulse width is broad, the high accuracy ranging is not expected, therefore it is solely used for the confirmation of the optical link budget between the ground station and retroreflectors on the Moon. As the photon detector, we use a SPAD (Single Photon Avalanche Diode) and also an MCP (Micro Channel Plate) photo multiplier whose quantum efficiency is twice as much as that of the SPAD in use. For the pointing, a CCD imager is also available in the same detector box. They can be switched by reflecting mirrors. To suppress the background noise, a bandpass filter (0.3 nm FWHM, 50 % transparency) and spatial filter (pinhole) with diameter of 400 microns are installed and checked. For better link budget, the contamination of optical elements of the telescope and on the optical bench was checked. The alignment of the laser emission path with respect to the laser receiving path and laser beam divergence has been adjusted to maximize the efficiency of the laser emission.

Pointing: Because the retroreflectors are small and they are not visible from ground telescopes, we point the telescope to known small-sized craters (˜10 km in diameter) whose positions are known in selenographic coordinate and thus in topocentric coordinate at the observation site. Then the offset angles in azimuth and elevation direction from the predicted pointing direction are determined so that the center of the crater comes to the center of the CCD images which are coalligned with the SPAD and the MCP. This procedure confirms the pointing of the telescope.

Observations: Trials for the lunar return have been conducted since autumn 2013. As of the date of submission, the ranging to the Moon is not successful. Therefore we need to detect the return from the Apollo 15 site by using the nanosecond laser pulse for the first step. As the next step, we need to know the condition on which lunar ranging is successful in Koganei, for example, lunar phase, distance to the retroreflectors, libration angles, and atmospheric conditions.

Keywords: Lunar Laser Ranging, Satellite Laser Ranging, Moon, internal structure

Japan Geoscience Union Meeting 2014
(28 April - 02 May 2014 at Pacifico YOKOHAMA, Kanagawa, Japan)

PPS23-P05 Room:Poster Time:May 2 16:30-17:30

SELENE-2/Lunar ElectroMagnetic Sounder (LEMS): a test of inversion

MATSUSHIMA, Masaki[1*] ; SHIMIZU, Hisayoshi[2] ; TOH, Hiroaki[3] ; YOSHIMURA, Ryokei[4] ; TAKAHASHI, Futoshi[1] ; TSUNAKAWA, Hideo[1] ; SHIBUYA, Hidetoshi[5] ; MATSUOKA, Ayako[6] ; ODA, Hirokuni[7] ; OGAWA, Kazunori[6] ; TANAKA, Satoshi[6]

[1]Tokyo Institute of Technology, [2]ERI, University of Tokyo, [3]Kyoto University, [4]DPRI, Kyoto University, [5]Kumamoto University, [6]ISAS/JAXA, [7]AIST

Understanding of lunar origin and evolution can be advanced through investigation of the lunar interior structure. The present thermal state of the Moon can be clues to the Moon's thermal history. In the SELENE-2 mission, we propose a lunar electromagnetic sounder (LEMS) to estimate the electrical conductivity structure of the Moon, which can be used to deduce the thermal structure of the Moon.

Temporal variations in the magnetic field of lunar external origin induce eddy currents in the lunar interior depending on the electrical conductivity structure and frequencies of the temporal variations. The eddy currents, in turn, generate temporal variations in the magnetic field of lunar internal origin. Therefore electromagnetic response of the Moon is obtained from magnetic field measurements by magnetometers onboard a lunar orbiter and a lunar lander. The response function is then used to estimate the electrical conductivity structure by solving an inverse problem. Here we assume a one-dimensional structure for electrical conductivity distribution. We show some results for a test of inversion.

Japan Geoscience Union Meeting 2014
(28 April - 02 May 2014 at Pacifico YOKOHAMA, Kanagawa, Japan)

PPS23-P06 Room:Poster Time:May 2 16:30-17:30

Moonquake observation and lunar interior exploration by one penetrator station

YAMADA, Ryuhei[1*] ; ISHIHARA, Yoshiaki[2] ; KOBAYASHI, Naoki[2] ; MURAKAMI, Hideki[3] ; SHIRAISHI, Hiroaki[2] ; HAYAKAWA, Masahiko[2] ; TANAKA, Satoshi[2]

[1]National Astronomical Observatory of Japan / RISE Project, [2]Japan Aerospace Exploration Agency, [3]Kochi University

The penetrator developed through Japanese lunar explorer 'LUNAR-A' mission is system to deploy on-board sensors on the planetary surface by free-fall from an orbiter. The penetrator is smaller and lighter than typical soft-landers because it does not require complicated landing system and thermal control system, and it has an advantage to construct geophysical network on the planetary surface. However, on-board sensors require high shock durability to survive a penetrating impact. Through previous studies, we have already shown that seismometers for the penetrator can maintain the performance to detect moonquakes even after a shock over the impact to the lunar surface (Yamada et al., 2009) and the communication instrument on the penetrator properly operate for data transmission (Tanaka et al., 2010).

Although high shock durability of the penetrator was established, deployment of the penetrator has not been executed due to cancel of the LUNAR-A mission. We, therefore, have a plan to load the penetrator on a small satellite launched by the Epsilon Launch Vehicle. In the plan, we can carry only one penetrator due to strict weight limitation of the vehicle. For the reason, we currently study the expected scientific results obtained from the observation by one penetrator station.

The seismometers deployed through the NASA Apollo missions have detected some types of moonquakes; deep moonquake, shallow moonquake and meteoroid impacts. The seismometer for the penetrator has performance capable of observing these moonquakes, and verification of activities of these lunar seismic events through comparison with results from the Apollo mission will be one of important topics. Then, we can expect to obtain information about the lunar crustal thickness and structure if we can locate meteoroid impacts by their impact flashes from ground observation. In this presentation, we report that expected detection numbers of the lunar seismic events can be observed by the penetrator and the scientific results, and appropriate installation locations of the one penetrator to obtain good scientific results be described. Then, we also discuss the prospects for future network observation using the penetrator after the small satellite exploration.

Keywords: Penetrator, Moonquake Observation, Lunar Interior Exploration, Small Satellite Exploration, Meteoroid Impact Flash

Japan Geoscience Union Meeting 2014
(28 April - 02 May 2014 at Pacifico YOKOHAMA, Kanagawa, Japan)

PPS23-P07 Room:Poster Time:May 2 16:30-17:30

On the attenuation of reflected echoes of Lunar Radar Sounder onboard Kaguya

TOH, Hiroaki[1*] ; KUMAMOTO, Atsushi[2]

[1]Graduate School of Science, Kyoto University, [2]Graduate School of Science, Tohoku University

The successful Japanese Moon probe, KAGUYA, was equipped with a variety of state-of-the-art scientific instruments including the Lunar Radar Sounder (LRS; Ono et al., 2010). LRS is a frequency modulated continuous wave (FMCW) radar with carrier frequencies from 4 to 6 MHz, and succeeded in observing distribution of reflectors beneath almost all the Moon's surface (Ono et al., 2009). Pommerol et al. (2010) further pointed out that the presence of the reflectors in lunar maria is negatively correlated with abundance of TiO2 because of its high electrical conductivity.

Loss tangent is defined as a ratio of the conduction to displacement current within an electric medium and hence an indicator of high electrical conductivity. If loss tangent is small enough, the permittivity and the electrical conductivity of the Moon's surface can be determined at the same time by comparing the reflected echo of LRS with its source pulse. Namely, by estimating the complex ratio of the received signal to the transmitted pulse, the dielectric constant can be known from the phase difference while the electrical conductivity can be derived by the observed amplitude attenuation and the permittivity obtained from the phase difference.

However, determination of the complex ratios is not straightforward because the reflected echoes are the product of a pulse compression technique and thus needs deconvolution to restore the true amplitude and phase of the echoes. Preliminary analysis of the LRS waveform data collected at the end of the fast down-link (21.3 Gbpd) mode [Jun. - Sep. 2008] showed that quality of the data is sufficient enough to perform necessary deconvolution. This implies that LRS can also be used as a ground penetrating radar.

In this presentation, the principle and the method for estimating the permittivity and electrical conductivity are first described in addition to the data used. Interpretation of the derived complex ratios and its spatial distribution on the Moon's surface is finally discussed and summarized.

REFERENCES

Ono, T. et al., Lunar Radar Sounder Observations of Subsurface Layers Under the Nearside Maria of the Moon, Science, 323, 909-912 doi:10.1126/science.1165988, 2009.

Ono, T. et al., The Lunar Radar Sounder (LRS) onboard the KAGUYA (SELENE) spacecraft, Space Sci. Rev., 154, 145-192, doi:10.1007/s11214-010-9673-8, 2010.

Pommerol, A. et al., Detectability of subsurface interfaces in lunar maria by the LRS/SELENE sounding radar: Influence of mineralogical composition, Geophys. Res. Lett., 37, L03201, doi:10.1029/2009GL041681, 2010.

Keywords: Ground penetrating radar, Electrical conductivity, Permittivity, Source pulse, Reflected echo, Loss tangent

Japan Geoscience Union Meeting 2014
(28 April - 02 May 2014 at Pacifico YOKOHAMA, Kanagawa, Japan)

PPS23-P08 Room:Poster Time:May 2 16:30-17:30

The accmulation ages of subsurface layer in Mare Imbrium based on the SELENE observation data

ISHIYAMA, Ken[1*] ; KUMAMOTO, Atsushi[1] ; NAKAMURA, Norihiro[1]

[1]Graduate School of Science, Tohoku University

Lunar Radar Sounder (LRS) onboard SELENE succeeded in detecting the electromagnetic wave reflected at subsurface layer in low-titanium regions [Ono et al., 2009; Pommerol et al., 2010]. Multiband Imager (MI) and Terrain Camera (TC) onboard SELENE respectively investigated the lunar surface composition [e.g., Otake et al., 2012] and the eruption ages of lunar lava flows [e.g., Morota et al., 2011]. Besides, the studies combined the LRS, MI, and TC data revealed the subsurface structure around the impact crater [Oshigami et al., 2012], and suggests the brittle subsurface layer with a high-porosity [Ishiyama et al., 2013]. This study investigates the accumulated age of subsurface layer in lava flow units (Unit 12 and 8 [Bugiolacchi and Guest, 2008]) in the north Mare Imbrium. This investigation is significant for discussing lunar volcanic activity because we can estimate a eruption rate of lunar lava flow.

We identified three subsurface echoes under Unit 8 from the LRS data, and revealed that the margin of the deepest subsurface echo was consistent with the surface boundary between Unit 12 and Unit 8; Unit 8 is accumulated on Unit 12. These ages of the units were estimated to be 3.31±0.19 Ga [Bugiolacchi and Guest, 2008]. However, the previous study estimated these ages by using a lunar map data with a low spatial resolution (60 – 150 m/pixel). This low spatial resolution data causes a large error for estimating the age. Thus, this study used the lunar high-resolution ortho map data obtained from TC, which has 10 m/pixel. The age of Unit 12 was estimated to be ∼3.6 Ga, which was older than the age of Unit 8. This result is consistent with the order of the stratification identified from the LRS data.

In addition, we identified that Unit 8 can be divided into several units by using the plagioclase, FeO, and TiO2 Map data, produced from the MI data. We investigate the correspondence relationship between the subsurface echoes and the identified units, and then the history of lunar volcanic activity will be discussed in the presentation.

Japan Geoscience Union Meeting 2014
(28 April - 02 May 2014 at Pacifico YOKOHAMA, Kanagawa, Japan)

PPS23-P09 Room:Poster Time:May 2 16:30-17:30

Experimental evidence for the deep high-Ti basalt magma in the lunar mantle

IGARASHI, Mako[1*] ; SUZUKI, Akio[1] ; OHTANI, Eiji[1] ; ASAHARA, Yuki[1] ; SAKAMAKI, Tatsuya[1]

[1]Division of Earth and Planetary Materials Science, School of Science, Tohoku University

The existence of high seismic attenuation zone at the depths greater than about 800 km implies that the lower mantle of the Moon could be partially molten (Nakamura et al., 1973; 1974). There is a longstanding hypothesis that the last fraction of the lunar magma ocean crystallized into a layer of dense Ti-rich cumulates at the shallow depths (˜100 km) early in the lunar history. It has been suggested that the cumulates subsequently sank into the deep interior of the moon because of its gravitational instability (e.g., Ringwood and Kesson, 1976). It is necessary to investigate the melting relations of the high-Ti basalt that may be erupted from the depths at high pressure (>4 GPa).In this study, melting relations of Apollo 14 black glass (Delano, 1986), the most Ti-rich lunar ultramafic glasses, were experimentally determined at the pressure of 4 GPa and the temperature range from 1300 C to 1450 C.

The high-pressure and high-temperature experiments were performed by using 3000 ton Kawai-type multi-anvil apparatus of Tohoku University. The samples were packed into graphite capsules and the experimental temperatures were measured by using W-Re thermocouples. The compositions of run products were analyzed by using FE-SEM (Field Emission Scanning Electron Microscopy). Our experiments depicted that the liquidus and solidus temperatures were determined to be 1450 C and 1325 C respectively at 4 GPa.

The liquidus phase is garnet, and the first consuming phase is ilmenite. Estimated temperature profile of the Moon at depths of 700 km -1200 km are between 1100 C and 1400 C (e.g., Gagnepain-Beyneix et al., 2006). The densities of partial melts and total melt were calculated by using the partial molar volume of the oxide components at one atmosphere (Lange and Carmichael, 1987) and the Birch-Murnaghan equation of state (Sakamaki et al., 2010). The densities of the melts formed by partial and total melting of the Apollo 14 black glass were heavier than those of the lunar deep mantle. Crystal-liquid density crossover is inevitable at the depth around 800 km, the pressure corresponding to 4 GPa. Therefore, the high-Ti basalt magma can exist stably if the lunar temperature profile is close to the upper bound of the estimated lunar temperature profile, suggesting existence of the low-velocity and low attenuation anomalies caused by chemical heterogeneities in the lunar deep mantle.

Keywords: high pressure, lunar mantle, high-Ti basalt, mantle over turn

Japan Geoscience Union Meeting 2014
(28 April - 02 May 2014 at Pacifico YOKOHAMA, Kanagawa, Japan)

PPS23-P10 Room:Poster Time:May 2 16:30-17:30

History of heavenly bodies collision of the solar system inside of the past one billion years studing from a lunar crate

KATO, Mami[1*] ; MOROTA, Tomokatsu[1]

[1]Nagoya University Graduate School of Environmental Studies

The moon preserve the record of the bodies impact history of the past 4.0 Ga as a crater, it is important the information to solution impact and orbit evolution of the bodies of the solar system.

Standard lunar cratering chronologies have been based on combining Luna and Apollo sample radiometric ages and impact crater densities. However, the bombardment history cannot be resolved in the past 3.0Ga because of the absence of samples with radiometric age ranging from 3.0 to 1.0 Ga. On the other hand, from crater density of lunar rayed craters, radiometric ages of lunar glass spherules, and statistics of terrestrial craters it has been suggested the hypothesis that the production function has increased in recent.

In this study, we determine formation ages of rayed craters using SELENE image data. Based on the finding, we will discuss a temporal variation of the cratering rate in the past 1.0 Ga.

Keywords: Moon, crater, cratering chronology

Japan Geoscience Union Meeting 2014
(28 April - 02 May 2014 at Pacifico YOKOHAMA, Kanagawa, Japan)

PPS23-P11 Room:Poster Time:May 2 16:30-17:30

Formation process of linear gravity anomalies and thermal evolution of the Moon

SAWADA, Natsuki[1*] ; MOROTA, Tomokatsu[1] ; ISHIHARA, Yoshiaki[2] ; HIRAMATSU, Yoshihiro[3]

[1]Graduate School of the Enviromental studies, Nagoya University, [2]JAXA, [3]Graduate School of Natural Science and Technology, Kanazawa University

The investigation of the subsurface structure in the Moon through a gravity distribution is one of means to understand the early evolution history of the Moon. Andrew-Hanna et al. (2013) analyzed gravity data, obtained by GRAIL (The Gravity Recovery and Interior Laboratory) and identified linear gravity anomalies (LGAs). They suggested that the LGAs resulted from ancient intrusions formed by magmatism with globally expansion. We can expect that such intrusions leave other evidences on the surface. In this study, we analyze topography data and FeO concentration distribution to find some characters corresponding to the LGAs and magma intrusion, and, together with the thermal history of the Moon, discuss the formation process of the LGAs on the Moon.

In this study, we focus 20 of LGAs reported by Andrew-Hanna et al. (2013) that show clear gravity anomaly. We use the 1/1024-degree gridded lunar topographic data from LOLA and the 10pixel/degree lunar FeO concentration distribution map from Clementina.

For topography data analysis, we set a study area that ranges 300km in orthogonal direction from a LGA. We apply a filter to remove topographical perturbation due to small craters. On a vertical profile to a LGA, the average, the standard deviation, and the average gradient of relative altitude are calculated with a reference altitude on a LGA. We define a vicinity area as an area within 50km from a LGA and a surrounding area as an area farther than 100km from a LGA on a vertical profile. Based on topographical features of both a vicinity area and a surrounding area, we categorize the topographic feature of LGAs into three types: mountain type, valley type, and unclassified type.

For FeO concentration data analysis, we calculate the average and the standard deviation of FeO concentration in vicinity areas of a LGA from the FeO concentration map.

The topographical data analysis reveals that most of the LGAs regions are categorized as the valley type. This result suggests that the LGAs regions are distributed over trough regions formed by tensile stress in the early history of the Moon. The FeO concentration distribution analysis reveals that the average FeO concentration of the vicinity areas in highland is 6.72 ± 1.62 wt%. This value is higher than that in the highland (<6 wt%) of the Moon, suggesting that an ancient intrusion is possibly exposed by later crater gardening.

We propose a following hypothesis on the formation process of the linear structures as a cause of LGAs from these results and the thermal history of Head and Wilson (1992). The stress state in the early period of the Moon is tensile stress for thermal expansion process. After crack formation due to the tensile stress before 4.0 Ga, the linear structures are formed by magma intrusion. The linear structures are covered by magmatism that forms mare during 4.0-3.0Ga. Ridges are formed in mare during 3.8-3.0Ga because of the compressive stress with the cooling of the Moon or in the impact basin. The formation of the ridges occurs in association with cracks near the linear structures.

Keywords: magmatism intrusions event, expansion, ridge, FeO concentration, Lunar topography data

Japan Geoscience Union Meeting 2014
(28 April - 02 May 2014 at Pacifico YOKOHAMA, Kanagawa, Japan)

PPS23-P12 Room:Poster Time:May 2 16:30-17:30

Source of the lunar magnetic anomalies estimated with the prism model

YOKOYAMA, Takashi[1*] ; TAKAHASHI, Futoshi[1] ; TSUNAKAWA, Hideo[1]

[1]Department of Earth and Planetary Sciences, Tokyo Institute of Technology

Many magnetic anomalies have been observed on the Moon since the Apollo project, although the Moon has no global intrinsic magnetic field at present. The lunar magnetic anomalies are considered to be caused by remanent magnetization of the lunar crust. Several models of the lunar magnetic anomalies have been proposed (e.g. Hood et al., 2001, 2013; Richmond et al., 2008; Purucker et al., 2012; Nicholas et al., 2007; Hemingway and Garrick-Bethell, 2012; Wieczorek et al., 2012). However, the magnetized material and its magnetizing process have been still controversial. In the present study, we have analyzed several magnetic anomalies with the prism model, in which three dimensional position, size, horizontal direction and magnetization are parameterized. The observation data by Lunar Prospector and Kaguya at the low altitude were used in the analysis. We adapt a forward modeling approach, in which the source parameters are changed iteratively till the minimum RMS (Root-Mean-Squares) misfit between the model and data is achieved. The optimal number of the prisms for modeling is objectively determined using Akaike's Information Criterion.We will discuss possible source materials on the basis of the modeling results.

Keywords: moon, magnetic anomaly, prism source model, swirl

Japan Geoscience Union Meeting 2014
(28 April - 02 May 2014 at Pacifico YOKOHAMA, Kanagawa, Japan)

PPS23-P13 Room:Poster Time:May 2 16:30-17:30

Lunar Electromagnetic responses to the stepwise changes in the IMF

HIGA, Tetsuya[1*] ; YOSHIMURA, Ryokei[2] ; OSHIMAN, Naoto[2] ; SHIMIZU, Hisayoshi[3] ; MATSUSHIMA, Masaki[4] ; TAKAHASHI, Futoshi[4] ; SHIBUYA, Hidetoshi[5] ; TSUNAKAWA, Hideo[4]

[1]Graduate School of Science, Kyoto University, [2]Disaster Prevention Reseach Institute, [3]Earthquake Research Institute, University of Tokyo, [4]Department of Earth and Planetary Sciences, Tokyo Institute of Technology, [5]Department of Earth and Environmental Sciences, Kumamoto University

The electrical conductivity structure of the lunar interior provides us very important information for investigation of the lunar origin and evolution. We attempted to estimate on the lunar electrical conductivity from magnetic field measurements by LMAG on board KAGUYA (SELENE) during the period from 21 December 2007 to 31 October 2008, when KAGUYA was in the orbit of 100-km altitude.

Magnetic fields are induced in the moon by changes in the interplanetary magnetic field (IMF). In order to confirm whether the lunar electromagnetic induction signals are observed in KAGUYA data, we compared KAGUYA data and data of ACE and WIND satellites, which locate around the Lagrange point (Sun-Earth L1), when the stepwise changes are shown in each data. LMAG measured the sum of the inducing and the induced fields, while ACE and WIND measured only the inducing field. It was found that LMAG recorded the lunar electromagnetic responses to the stepwise changes in the IMF.

Dyal and Parkin (1971) gave the homogeneous moon model and estimated lunar conductivity. Their estimation was carried out using the data measured by Apollo 12 magnetometer fixed on the lunar surface. In this study, we applied their method to the data of the orbiting satellite, KAGUYA. The homogeneous moon model was able to explain the electromagnetic response against the stepwise changes in the IMF well, and the estimated homogeneous lunar conductivity was 1×10^{-4} - 4×10^{-4} S/m. On the other hand, we found that LMAG data also recorded the anomalous signals in the minor components, not predicted from the above model. In order to confirm whether such signals are unique to KAGUYA data, we scrutinized the data obtained by Apollo and Lunar Prospector. As a result, we concluded that such signals are common when the stepwise changes penetrate the moon.

In this presentation, we will report the new analysis results of KAGUYA, Apollo, and Lunar Prospector data, and discuss the anomalous signals in the minor component of the responses to the stepwise changes in the IMF.

Keywords: Moon, KAGUYA, SELENE, LMAG, induction, conductivity

Japan Geoscience Union Meeting 2014
(28 April - 02 May 2014 at Pacifico YOKOHAMA, Kanagawa, Japan)

PPS23-P14 Room:Poster Time:May 2 16:30-17:30

Plasma observations above strong lunar crustal fields in the solar-wind wake

NISHINO, Masaki n[1*] ; SAITO, Yoshifumi[2] ; TSUNAKAWA, Hideo[3] ; TAKAHASHI, Futoshi[3] ; YOKOTA, Shoichiro[2] ; MATSUSHIMA, Masaki[3] ; SHIBUYA, Hidetoshi[4] ; SHIMIZU, Hisayoshi[5] ; FUJIMOTO, Masaki[2]

[1]Nagoya University, [2]ISAS/JAXA, [3]Tokyo TECH, [4]Kumamoto University, [5]Earthquake Research Institute, The University of Tokyo

Plasma signature around crustal magnetic fields is one of the most important topics of the lunar plasma sciences. Although recent spacecraft measurements are revealing solar-wind interaction with the lunar crustal fields on the dayside, plasma signatures around crustal fields on the night side have not been fully studied yet. Here we show evidence of plasma trapping on the closed field lines of the lunar crustal fields in the solar-wind wake, using SELENE (KAGUYA) plasma and magnetic field data at 15 km altitude. In contrast to expectation on plasma cavity formation at the strong crustal fields, electron flux is enhanced above one of the strongest crustal fields, Crisium Antipode (CA), where the magnetic field along the spacecraft orbit is as strong as 80 nT. The enhanced electron fluxes above CA are characterized by bidirectional beams in the lower energy range (typically lower than 100 eV), which shows that these electrons are trapped on the closed field lines of the crustal magnetic fields, although a possibility of opened field configuration with cusps is not totally excluded. The observed electrons on the closed field lines may come from the lunar night side surface, while the mechanism of electron supply onto the closed field line remains to be solved.

Keywords: Lunar crustal field, Lunar plasma environment, Lunar wake, SELENE (KAGUYA)

Japan Geoscience Union Meeting 2014
(28 April - 02 May 2014 at Pacifico YOKOHAMA, Kanagawa, Japan)

PPS23-P15 Room:Poster Time:May 2 16:30-17:30

A long-term all-sky imager observation of lunar sodium tail

NISHINO, Masaki n[1*] ; SHIOKAWA, Kazuo[1] ; OTSUKA, Yuichi[1]

[1]Solar-Terrestrial Environment Laboratory, Nagoya University

The Moon possesses long tail of neutral sodium atoms that are emitted from the lunar surface and transported anti-sunward by the solar radiation pressure. Since the earth crosses the lunar sodium tail for a few days around the new moon, the resonant light emission from sodium atoms can be detected from the ground. Although it has been reported that bright emissions from sodium atoms of the tail is observed during the Leonids meteor shower, only few events without meteor shower have been investigated so far. Here we show a long-term (over 15 years) observation of the lunar sodium tail using all-sky imager at Shigaraki Observatory (35N, 136E), Japan. We have surveyed our database of all-sky sodium images at a wavelength of 589.3 nm to find that a bright spot emerges around the anti-lunar point for a few days around the new moon. Although the sodium spot is the brightest during the Leonids meteor shower, a weaker sodium spot is detected in the period without meteor shower as well. The sodium spot gradually moves eastward (roughly, 0.2 hours a day), which shows that the sodium tail is strongly affected by the earth's gravity. We will present the latest results of our data analysis to discuss signatures of the lunar sodium tail as well as the origin of the lunar sodium exosphere.

Keywords: Lunar sodium tail, Lunar exosphere, All-sky imager observation

Japan Geoscience Union Meeting 2014
(28 April - 02 May 2014 at Pacifico YOKOHAMA, Kanagawa, Japan)

PPS24-01 Room:415 Time:May 1 14:15-14:30

Crystal structure, morphology, and isotopic compositions of presolar alumina grains in unequibrated ordinary chondrites

TAKIGAWA, Aki[1*] ; STROUD, Rhonda M.[2] ; NITTLER, Larry, R.[3] ; VICENZI, Edward, P.[4]

[1]Department of Geology and Mineralogy, Kyoto University, [2]The U.S. Naval Research Laboratory, [3]Carnegie Institution of Washington, [4]Smithsonian Institution, [5]National Institute of Standards and Technology

Corundum, the thermodynamically stable phase of Al_2O_3, is predicted to be the most abundant refractory dust species condensed in envelopes around oxygen-rich asymptotic giant branch (AGB) stars. Many presolar Al_2O_3 grains, which are the survival circumstellar dust grains, have been identified from acid-residues of chondrites. The grain morphology and crystal structure of presolar grains may reflect condensation conditions in circumstellar envelopes of AGB stars and processing in the interstellar medium (ISM) and protosolar disk.

Using scanning electron microscopy (SEM) we obtained detailed secondary electron images, energy dispersive X-ray spectroscopy (EDS), electron backscattered diffraction (EBSD) patterns, and cathodoluminescence (CL) spectra of each Al_2O_3 grain prior to isotopic measurements. Focused ion beam (FIB) lift-out sections were made from the identified presolar grains and the interior structures were observed with a transmission electron microscope (TEM).

The Al_2O_3 grains were identified from acid residues of QUE97008 (LL3.05) by EDS and observed in detail by field emission (FE) SEM at the Carnegie Institution of Washington (CIW). Previously identified alumina grains from Semarkona (LL3.0), Roosevelt County 075 (H3.1), and Bishunpur (LL3.15) were also used in this study. CL spectra were obtained with a FE-SEM equipped with a Gatan Mono CL4 system at NIST. EBSD analysis was performed with an FEI Nova 600 FIB-SEM equipped with an HKL EBSD system at the Naval Research Laboratory (NRL). Isotope measurements were performed with the Cameca NanoSIMS 50L ion-microprobe at CIW. Oxygen isotopes of 163 grains were measured using ~100 nm Cs^+ beam rastered over each of the grains. An O^- beam was used to measure the Mg-Al isotopic compositions of the presolar and some solar Al_2O_3 grains. Ultra-thin sections of presolar grains QUE053, 060, and 067 were prepared with the NRL FIB-SEM. TEM studies were carried out at NRL with a JEOL 2200FS field-emission scanning transmission electron microscope (STEM).

Eight presolar grains from QUE97008 and one from RC 075 were newly found. Grain QUE060 is classified into Group 2 and has a subhedral shape with clear flat facets. The surface is smooth except for a face with a cavity. TEM diffraction patterns of the FIB section indicated that the grain consists of multiple corundum crystallites. Dark-field TEM image showed large (>100 nm) and small (<30 nm) scale orientation variation. The large-scale misorientation observed on the right side of the grain seems to relate to the cavity. Small-scale distortions occur uniformly within the grain. EDS spectra showed that the Mg/Al ratio of QUE060 is ~0.01, and the NanoSIMS measurement revealed this high Mg content to be essentially pure radiogenic ^{26}Mg, with inferred initial $^{26}Al/^{27}Al$~0.01, similar to other Group 2 grains.

QUE067 is a thin Group 4 grain with very irregular morphology. Its $^{27}Al/^{24}Mg$ ratio was three times lower than in QUE060, but its inferred $^{26}Al/^{27}Al$ ratio was similar. No EBSD patterns of crystals were obtained from the grain surface but TEM observation on the FIB section showed that the interior of QUE067 was corundum, not amorphous.

The subhedral shape and smooth surface of QUE060 suggest that this grain was likely single crystalline corundum when it condensed in a circumstellar envelope of a low-mass AGB star, and that the polycrystalline nature, voids and distorted crystal structure inside the grain are secondary features.

A possible process to form large-scale misorientation and the cavity is grain-grain collisions in a SN shock in the ISM. A high velocity collision creates a shockwave propagating inside the grain, finally forming a crater. Small-scaled distortions may have also formed by collisions with small particles in the ISM. Such collisions are less destructive than with larger grains, but their probability is high. Ion bombardment in the ISM may also contribute to the small-scale distortions.

Keywords: dust, early solar system, chondrite, presolar grain, transmission electron microscopy, evolved star

Japan Geoscience Union Meeting 2014
(28 April - 02 May 2014 at Pacifico YOKOHAMA, Kanagawa, Japan)

PPS24-02 Room:415 Time:May 1 14:30-14:45

3-D observation of GEMS by electron tomography

MATSUNO, Junya[1*] ; MIYAKE, Akira[1] ; TSUCHIYAMA, Akira[1] ; NAKAMURA-MESSENGER, Keiko[2] ; MESSENGER, Scott[2]

[1]Dep. of Geology and Mineralogy, Kyoto Univ., [2]NASA Johnson Space Center

Amorphous silicates in chondritic porous interplanetary dust particles (CP-IDPs) coming from comets are dominated by glass with embedded metal and sulfides (GEMS). GEMS grains are submicron-sized rounded objects (typically 100-500 nm in diameter) with nanometer-sized (10-50 nm) Fe-Ni metal and sulfide grains embedded in an amorphous silicate matrix. Several formation processes for GEMS grains have been proposed so far, but these models are still being debated [2-5].

Bradley et al. proposed that GEMS grains are interstellar silicate dust that survived various metamorphism or alteration processes in the protoplanetary disk and that they are amorphization products of crystalline silicates in the interstellar medium by sputter?deposition of cosmic ray irradiation, similar to space weathering [2,4]. This consideration is based on the observation of nano-sized crystals (~10 nm) called relict grains in GEMS grains and their shapes are pseudomorphs to the host GEMS grains.

On the other hand, Keller and Messenger proposed that most GEMS grains formed in the protoplanetary disk as condensates from high temperature gas [3,5]. This model is based on the fact that most GEMS grains have solar isotopic compositions and have extremely heterogeneous and non-solar elemental compositions. Keller & Messenger (2011) also reported that amorphous silicates in GEMS grains are surrounded by sulfide grains, which formed as sulfidization of metallic iron grains located on the GEMS surface.

The previous studies were performed with 2D observation by using transmission electron microscopy (TEM) or scanning TEM (STEM). In order to understand the structure of GEMS grains described above more clearly, we observed 3D structure of GEMS grains by electron tomography using a TEM/STEM (JEM-2100F, JEOL) at Kyoto University. Electron tomography gives not only 3D structures but also gives higher spatial resolution (~a few nm) than that in conventional 2D image, which is restricted by the sample thickness (~>50 nm). Three cluster IDPs (L2036AA5 cluster4, L2009O8 cluster13 and W7262A2) were used for the observations. IDP W7262A2 was collected without silicon oil, which is ordinary used to collect IDPs, so this sample has no possibility of contaminations caused by silicon oil or solvent to rinse it [6].

The samples were embedded in epoxy resin and sliced into ultrathin sections (50-300 nm) using an ultramicrotome. The sections were observed by BF-TEM (bright field-TEM) and HAADF-STEM (high angle annular dark field-scanning TEM) modes. Images were obtained by rotating the sample tilt angle over a range of $\pm$65 degree in 1 degree steps. The obtained images were reconstructed to slice images. Mineral phases in the slice images were estimated by comparing with a 2D elemental map obtained by an EDS (energy dispersive X-ray spectroscopy) system equipped in the TEM/STEM.

Careful examination of the slice images confirmed that iron grains are embedded in the amorphous silicate matrix of the GEMS grains, but sulfide grains were mainly present on the surface of the amorphous silicate. These results are consistent with the model that GEMS grains formed as condensates [3,5], although more data are needed to conclude the origin of GEMS grains. The present study is the first successful example adapting the electron tomography to the IDPs. This type of analysis will be important for planetary material sciences in the future.

[1] Bradley et al. (1999) Science, 285, 1716
[2] Bradley and Dai (2004) ApJ, 617, 650
[3] Keller and Messenger (2011) GCA, 75, 5336
[4] Bradley (2013) GCA, 107, 336
[5] Keller and Messenger (2013) GCA, 107, 341
[6] Messenger et al. (2012) 43rd LPSC, 2696 (abstr.)

Keywords: IDP, GEMS, TEM, tomography

Japan Geoscience Union Meeting 2014
(28 April - 02 May 2014 at Pacifico YOKOHAMA, Kanagawa, Japan)

PPS24-03 Room:415 Time:May 1 14:45-15:00

Condensation experiments of Si-rich gas into the chondrule melt for rapid low-Ca pyroxene formation using a new furnace

IMAE, Naoya[1*] ; ISOBE, Hiroshi[2]

[1]National Institute of Polar Research, [2]Kumamoto University

Introduction

Low-Ca pyroxenes (mainly enstatites) and the high-pressure polymorphs are the most major phases constituting rocks in the solar system. The formation mechanism of low-Ca pyroxenes in the solar nebula is problematic. It has been thermodynamically predicted that enstatite forms from forsterite by the reaction with Si-rich gas since enstatite and the preceding condensate Mg-silicate, forsterite, are in reaction relation (Grossman, 1972). However, the rate of the reaction is sluggish because of the solid diffusion-controlled in the enstatite layer, and the reaction is nearly treated as maximum fractional condensation (Imae et al., 1993). Also, the amount of enstatite condensed directly from the residual gas is very small. Tissandier et al. (2002) experimentally showed that pigeonite (CaO˜5-7 wt%) crystallized from chondrule melt by the interaction with Si-rich gas. In the present study, a new technique to simulate the solar nebula was developed and massive low-Ca pyroxenes (CaO˜1 wt%) were produced using the furnace.

Experiments

The total pressure was mainly controlled to be 100Pa under the hydrogen gas flow, using a butterfly valve indicated from the diaphragm-seal type pressure gauge. The maximum temperature for each run was 1200-1450^{o}C, in which pyroxene is in stable region and the cooling rate was mainly 100^{o}C/h. A tiny fragment of the Allende meteorite (˜30-50 mg for each run) was used as a starting material of the experiments. The staring material and silica powder were put avoiding the direct contact into the alumina cruicible with the 1 mm orifice. The experiments without silica powder were also carried out as reference experiments.

Result

Minor amount of low-Ca pyroxenes were found mainly with dominant olivines under the experiments without Si-rich gas source. While, a drastic change was observed from the experiments with Si-rich gas source: completely changed to low-Ca pyroxenes poikilitically enclosing rounded olivines were observed for the charges at 1450^{o}C, and low-Ca pyroxenes were observed mainly on the rim for the charges at 1350^{o}C and 1250^{o}C. The iron content increased on the decreasing temperatures.

Discussion

The collision frequency of the Si-rich gas on the melt of the Allende chondrite as a starting material is not so large to derive the crystallization of the massive low-Ca pyroxenes from the melt. Rather, the Si-rich gas helped the nucleation of low-Ca pyroxenes in the stability filed of low-Ca pyroxene. Massive crystallization of pyroxenes did not occur for the experiments without Si-rich gas source and here the forsterite continued to grow under metastable condition.

References

Grossman L. (1972) GCA 36, 597.
Imae N., et al. (1993) EPSL 118, 21.
Tissandier L., et al. (2002) MAPS 37, 1377.

Keywords: primordial solar nebula, condensation, low-Ca pyroxene, Si-rich gas, low-pressure experiments, chondrule

Japan Geoscience Union Meeting 2014
(28 April - 02 May 2014 at Pacifico YOKOHAMA, Kanagawa, Japan)

PPS24-04 Room:415 Time:May 1 15:00-15:15

Hydration of amorphous forsterite grains in protoplanetary disks

YAMAMOTO, Daiki[1*] ; KURODA, Minami[1] ; TACHIBANA, Shogo[2]

[1]Department of Natural History Sciences, Hokkaido University, [2]Department of Natural History Sciences, Hokkaido University

Hydrous silicate dust can be thermodynamically stable at low temperatures (~200K) in protoplanetary disks with the solar-system abundance of elements. Theoretical and experimental investigation (Fegley and Prinn, 1989; Imae et al., 1999) have shown that the hydration reaction between crystalline Mg-silicates and water vapor is too sluggish to occur during a lifetime of protoplanetary disks. However, infrared spectroscopic observation and investigation of extraterrestrial materials have shown that both crystalline and amorphous Mg-silicates may be present in protoplanetary disks and in the protosolar disk. Amorphous silicates are thermodynamically unstable, and thus could be hydrated more rapidly at higher temperatures than crystalline silicates (Nagahara and Ozawa, 2011). If hydration of amorphous silicates occurs within a disk lifetime, hydrated dust could be a source of water to terrestrial planets.

In this study, in order to investigate hydration of amorphous Mg-silicates, we conducted closed-system reaction experiments of amorphous forsterite and water vapor in sealed glass tubes at temperatures of 1023-423K and P_{H2O} of 0.05 -50 bar for 2-1344 hours. Run products were analyzed with FT-IR and XRD. We found that samples reacted at temperatures below 723K and P_{H2O} of 5-50 bar showed sharp 3μm absorption features, clearly suggesting the formation of hydrous phase(s). XRD analyses of some run products showed that the hydrous phase was serpentine. Because the stable temperature of hydrous phase(s) at P_{H2O} of 5-50 bar is~523K, the present results indicate that hydrous Mg-silicates can be formed metastably from amorphous forsterite at higher temperatures than the thermodynamic prediction. Moreover, hydration of amorphous forsterite occurred after 2-hour heating at 623K and P_{H2O} of 5 and 50 bar, implying that the activation energy for hydration of amorphous forsterite is much smaller than that for crystalline forsterite.

Hydration reaction seems to have little P_{H2O} dependence at P_{H2O} of 5-50 bar, indicating that hydration is controlled by a reaction between amorphous forsterite with saturated adsorbing water molecules. No hydration occurred, however, at 523K and P_{H2O} <1 bar, which could be due to less effective adsorption of water molecules at low-pressure conditions.

Keywords: protoplanetary disk, Mg-silicate, crystalline, amorphous, forsterite, hydrous mineral

Japan Geoscience Union Meeting 2014
(28 April - 02 May 2014 at Pacifico YOKOHAMA, Kanagawa, Japan)

PPS24-05 Room:415 Time:May 1 15:15-15:30

Sticking probability for homogeneous nucleation of iron dust

KIMURA, Yuki[1*] ; TANAKA, Kyoko[2] ; INATOMI, Yuko[3] ; TAKEUCHI, Shinsuke[3] ; TSUKAMOTO, Katsuo[1]

[1]Tohoku University, [2]Hokkaido University, [3]ISAS/JAXA

Nucleation theories have been used to understand the condensation sequence, number density and size of cosmic dust in a gas outflow of dying stars or a gas plume after shock wave heating in the primitive solar nebula. However, it has been well known that nucleation rates obtained by nucleation theories and by experiments have a large difference. We believe that the reason is uncertainties of the physical parameters of nanometer sized particles. Therefore, it is still not successful to explain the characters of cosmic dust by a nucleation theory. To determine the physical parameters of nanoparticles and evaluate nucleation theories, we constructed an in-situ observation system of temperature and concentration during homogeneous nucleation in vapor phase using interferometry for both of ground based and microgravity experiments.

Nanoparticles are formed from a supercooled vapor after evaporation by electrical heating in a controlled gas atmosphere. Using the new system in lab, we succeeded to determine surface free energy and sticking probability of manganese nanoparticle from timescale for gas cooling and condensation temperature based on nucleation theories [1]. In this laboratory experiment, convection of gas atmosphere caused by thermal heating generates heterogeneity of nucleation environment, such as temperature and concentration profiles around evaporation source. If same kinds of experiments are performed in microgravity, evaporated vapor defuses uniformly and the temperature profile becomes concentric around the evaporation source. As the result, nucleation will occur at concentric position. Then, we can obtain physical properties with relatively smaller error bars and then we may be able to evaluate nucleation theories more precisely. Therefore, we also performed a microgravity experiments using an aircraft and the sounding rocket S-520-28 launched on December 17^{th}, 2012.

We prepared specially designed Mach-Zehnder-type interferometers with an evaporation chamber and camera recording systems to fit the space and weight limitations of the rocket. Three systems, named DUST 1 to 3, with same configuration except evaporation source and gas pressure in the chamber were installed into the nosecone of the rocket. The evaporation source and gas atmosphere were tungsten and gas mixture of oxygen (4000 Pa) and argon (36000 Pa) for DUST 1, iron and argon (20000 Pa) for DUST 2, and iron and argon (40000 Pa) for DUST 3. The experiments were run sequentially and automatically started from 100 s after launch of the rocket. The evaporation source of iron was electrically heated under microgravity. Evaporated iron vapor was diffused, cooled and condensed in the gas atmosphere. The temperature and concentration at the nucleation site are determined from the movement of the fringe in the interferogram. Here, we will show the results of the homogeneous nucleation and determine the sticking probability of iron atoms into a nanoparticle based on nucleation theories. The results will be compared with that by ground based experiment.

[1] Y. Kimura, K. K. Tanaka, H. Miura, K. Tsukamoto, Direct observation of the homogeneous nucleation of manganese in the vapor phase and determination of surface free energy and sticking coefficient, *Crystal Growth & Design*, **12** (2012) 3278?3284.

Keywords: Nucleation, Sounding Rocket, Interferometer, In-situ Observation, Cosmic Dust

Japan Geoscience Union Meeting 2014
(28 April - 02 May 2014 at Pacifico YOKOHAMA, Kanagawa, Japan)

PPS24-06 Room:415 Time:May 1 15:30-15:45

Ion-induce nucleation experiment I: development of a new apparatus

WATANABE, Naoki[1*] ; HIDAKA, Hiroshi[1] ; NAKAI, Yoichi[2] ; KOJIMA, Takao[3]

[1]Institute of Low temperature Science, Hokkaido University, [2]Nishina Center, RIKEN, [3]Atomic Physics Laboratory, RIKEN

Mechanisms of grain nucleation have attracted researchers in various fields of science in connection with e.g. atmospheric aerosols and cosmic dust grains. Although there have been many theoretical and experimental works approaching this issue, the details of nucleation mechanism is still in debate. Most of works are performed assuming homogeneous nucleation in gas phase or heterogeneous nucleation on the bulk surfaces. The homogeneous nucleation often suffers from a ”critical size” of particle and requires high supersaturation condition to gain the efficient formation rate, while the nucleation on the bulk surface may not be relevant to the first stage of grain formation in realistic environments. It is know that ion-induce heterogeneous nucleation would play an important role in the particle formation because in this mechanism ion-neutral interaction overcome difficulties expected in neutral-gas-phase homogeneous nucleation. We recently developed a new experimental apparatus to investigate the elementary process of the ion-induced nucleation. We present the importance of ion-induced nucleation and advantages of the newly developed apparatus. Using this apparatus, we have been successful in obtaining an important physical parameter, free energy, of water cluster ions.

Keywords: cluster ion, ion-induced nucleation

Japan Geoscience Union Meeting 2014
(28 April - 02 May 2014 at Pacifico YOKOHAMA, Kanagawa, Japan)

PPS24-07 Room:415 Time:May 1 15:45-16:00

Mid-infrared Observation of sungrazing comet C/2012 S1 (ISON) with Subaru+COMCIS

OOTSUBO, Takafumi[1*] ; USUI, Fumihiko[2] ; TAKITA, Satoshi[3] ; WATANABE, Jun-ichi[4] ; KAWAKITA, Hideyo[5] ; FURUSHO, Reiko[6] ; HONDA, Mitsuhiko[7]

[1]Tohoku University, [2]University of Tokyo, [3]ISAS/JAXA, [4]NAOJ, [5]Kyoto Sangyo University, [6]Tsuru University, [7]Kanagawa University

Comets are the frozen reservoirs of the early solar nebula and are made of ice and dust. Dust grains in comets have been used to investigate the formation conditions of the solar system. A silicate feature is often observed in comet spectra in mid-infrared region, for example 11.3-micron, and may be used for probing early history of the solar system. In most cases the feature shows the existence of crystalline silicate together with amorphous silicate. Since the crystalline silicate grains are generally made through high-temperature annealing above 800K from amorphous ones, it is believed that the crystalline silicate grains produced at the inner part of the disk were transported to the outer cold regions where comet nuclei formed.

Comet C/2012 S1 (ISON) is a long-period Oort cloud comet, discovered in September 2012. In particular, comet ISON is a sungrazing comet, which is predicted to pass close by the Sun and Earth and becoming a bright object. Mid-infrared observations of this new comet and investigation of the 10-micron silicate feature help us to understand the formation of crystalline silicate grains in the early solar nebula.

We observed comet ISON in mid-infrared wavelength region using Cooled Mid-Infrared Camera and Spectrometer (COMICS) mounted on the Subaru Telescope on Mauna Kea, Hawaii. The observation of comet ISON was carried out on 2013 October 19th and 21st UT. Since the weather condition was not so good when we observed, we carried out N-band imaging observations (8.8 and 12.4 micron) and N-band low-resolution spectroscopy. The spectrum of C/ISON can be fit with 260–265 K blackbody spectrum when we use the 7.8–8.2 and 12.4–13.0 micron region as the continuum. The spectrum has only a weak silicate excess feature, which may be able to attribute to small amorphous olivine grains. We could not detect a clear crystalline silicate feature in the spectrum. We will compare the spectrum with other Oort cloud comets, such as comets C/2011 L4 (PanSTARRS) and C/2013 R1 (Lovejoy), and discuss the dust properties and the birthplace of the comet C/ISON.

Keywords: comet, dust, silicate, infrared

Japan Geoscience Union Meeting 2014
(28 April - 02 May 2014 at Pacifico YOKOHAMA, Kanagawa, Japan)

PPS24-08 Room:415 Time:May 1 16:15-16:30

Observation of surface structure of amorphous solid water by atomic force microscope at low temperatures

HIDAKA, Hiroshi[1*] ; SUGIMOTO, Yoshiaki[2] ; NAKATUBO, Syunichi[1] ; WATANABE, Naoki[1] ; KOUCHI, Akira[1]

[1]Inst. of Low Temp. Sci., Hokkaido Univ., [2]Grad. Sch. of Eng., Osaka Univ.

Amorphous solid water (ASW) is one of the important materials in space because it exists an abundant and effects to evolution of interstellar molecules. In molecular clouds, it is well known that chemical reactions on icy interstellar dust grains which consist of ASW mantle and mineral particle core are key processes in the formations of important organic molecules (ie. H_2CO, CH_3OH) and deuterium-enriched molecules. Although ASW surface play an important role as a field of chemical reactions, the surface structure of ASW has yet to be revealed.

Recently, we developed a low temperature atomic force microscope (AFM) for study of the surface structure of ASW. AFM is a powerful tool to study the surface structure of ASW because it can work even if the surface do not have a conductive property. In this presentation, we show AFM images of ASW surfaces which were formed at several conditions. ASW were formed on Si(111) 7×7 at 103-135 K with various deposition rate (0.08-0.8 nm/min) and various thickness(2.5-22 nm). From the observations of surface structure, we discuss the relation between the surface structure and the condition of ASW formation.

Keywords: amorphous ice, interstellar dust, molecular clouds, atomic force microscopy

Japan Geoscience Union Meeting 2014
(28 April - 02 May 2014 at Pacifico YOKOHAMA, Kanagawa, Japan)

PPS24-09 Room:415 Time:May 1 16:30-16:45

Experimental approach to the formation of organic molecules following vacuum-ultraviolet irradiation of interstellar ice

HAMA, Tetsuya[1*] ; TACHIBANA, Shogo[2] ; LAURETTE, Piani[2] ; ENDO, Yukiko[2] ; FUJITA, Kazuyuki[1] ; NAKATSUBO, Shunichi[1] ; FUKUSHI, Hiroki[1] ; MORI, Shoichi[1] ; CHIGAI, Takeshi[1] ; KOUCHI, Akira[1]

[1]Institute of Low Temperature Science, Hokkaido University, [2]Department of Natural History Scieces, Hokkaido University

Cosmic gases and dust grains ejected from dying stars gradually assemble under the influence of gravity to form interstellar clouds. Among these gases, heavy elements such as magnesium (Mg) and silicon (Si) are incorporated in dust. Lighter and chemically active elements (e.g., hydrogen, carbon, oxygen, and nitrogen; H, C, O, N, respectively) play important roles in the chemistry of interstellar clouds. After the temperature and photon field decrease when the density of dust particles increases in interstellar clouds, atoms (e.g., H, O, C, N) and molecules (e.g., CO) deposit onto the dust surfaces. Cold-surface reactions proceed on the grain surface, and an ice mantle, which is predominantly composed of H_2O combined with other molecules such as CO, CO_2, NH_3, CH_4, H_2CO, and CH_3OH, is formed.

The ice mantles are also subjected to substantial energetic processing by the prevailing ultraviolet radiation during the lifetime of a interstellar cloud. Followed by repeated processing when cycling between diffused clouds and dense clouds, new refractory organic molecules are formed in the ice mantles. The ice mantles undergo further photon radiations upon the formation of protoplanetary disks, and finally evolve to non-volatile complex organic residues by irradiation and thermal processing. However, the detail of the chemical evolution of the organic molecules has still been ambiguous. Although the previous laboratory studies using infrared spectroscopy can provide the presence of polar compounds such as amines, carboxylic acid or amides functions, it often suffers from the low sensitivity and the difficulty to obtain precise identifications of molecular species due to the overlapping of broad solid-state bands. Since dust grains and ice mantles are the precursors of planetary material, studying the photoprocesses is essential to understanding the origin of our solar system, and more powerful analytical techniques are required to unveil rich chemistry of the ices in interstellar clouds and protoplanetary disks.

Here, we are going to present a talk about a new apparatus which is now under construction to shed light on the chemical evolution of organic molecules in interstellar clouds and protoplanetary disks. The apparatus consists of three basic parts, i.e., a vacuum system, a copper-substrate equipped with a closed cycle helium refrigerator, and a vacuum ultraviolet source. Multi-component interstellar ice analogues are created on the cold (10 K) substrate by vapor deposition, and subjected to irradiation by the ultraviolet. The irradiated ice is subsequently heated up to 800 K. The gas composition desorbed from the ice during heating is analyzed by a high-resolution quadrupole mass spectrometer in the vacuum chamber. The survived organic residue from heating are studied using gas chromatography coupled to mass spectrometry (GC-MS) and high performance liquid chromatography coupled to mass spectrometry (HPLC-MS).

Keywords: interstellar cloud, protoplanetary disk, ice mantles, complex organic molecules

Japan Geoscience Union Meeting 2014
(28 April - 02 May 2014 at Pacifico YOKOHAMA, Kanagawa, Japan)

PPS24-10 Room:415 Time:May 1 16:45-17:00

Hydrogen addition reactions of C_2H_2 on cold grains; clue to the formation mechanism of cometary C_2H_6

KOBAYASHI, Hitomi[1*] ; WATANABE, Naoki[2] ; HIDAKA, Hiroshi[2] ; HAMA, Tetsuya[2] ; WATANABE, Yoji[1] ; KAWAKITA, Hideyo[1]

[1]Koyama Astronomical Observatory, Kyoto Sangyo Univeristy, [2]Institute of Low temperature Science, Hokkaido University

Volatiles incorporated into comets were formed in the pre-solar molecular cloud and probably chemically altered in the proto-planetary disk of the Sun. Although physico-chemical evolution from a molecular cloud to the disk is basically understood, detailed evolutional processes are still in debate; e.g., the fraction of the materials originated in the molecular cloud incorporated into the disk without physico-chemical alterations (some fraction of materials might sublimate via accretion shock) and physical conditions (temperature, densities of materials, etc.). To reveal those links, we focused on the molecules formed through grain surface reactions, which occurred under quite low temperature conditions like 10K. We discuss the origin of such molecules in comets (icy small body of the Solar system), which might preserve the information about chemical and physical conditions of proto-planetary disk. Cometary ethane (C_2H_6) and acetylene (C_2H_2) have been observed in multiple comets since 1996 and their abundances relative to H2O (the major component of cometary ices) is ~10^{-3} but with variations. This variation might be caused by the difference in the mixing ratios between the materials originated in the molecular cloud and the disk-processed materials. C_2H_6 has never been detected in the molecular cloud and the formation mechanism of C_2H_6 detected in comets is still in debate. One of the candidates of formation reactions of C_2H_6 is the hydrogen addition reaction of C_2H_2 on the cold grain surface (C_2H_2 ->C_2H_3 ->C_2H_4 ->C_2H_5 ->C_2H_6). In the previous experimental studies, those reactions were evaluated qualitatively and it was concluded that the reaction from C_2H_4 to C_2H_6 occurred more rapidly than the reactions from C_2H_2 to C_2H_4 and it would be a reason for the nondetection of C_2H_4. To investigate these reactions more quantitatively in realistic conditions for molecular clouds, we performed the laboratory measurements of hydrogen addition reactions of C_2H_2 and C_2H_4 on the amorphous solid water (ASW), respectively.

The experiments were conducted by using laboratory setup for surface reaction in interstellar environment (LASSIE) at the institute of low temperature science, Hokkaido University3. A cryogenic aluminum substrate is located in the center of the main chamber and surrounded by a large copper shroud connected to a liquid-nitrogen reservoir. Atomic hydrogen used for the reactions were produced by the dissociation of H2 molecules in microwave-induced plasma. The kinetic temperature of hydrogen atoms were ~120 K and the H-atom flux was ~10^{13} cm^{-2} s^{-1}. The samples of pure solid C_2H_2, C_2H_4, and those on ASW were produced on the substrate at 10, 15 and 20K. Infrared absorption spectra of the ices were measured by FTIR before and during the exposure of H-atom.

Our measurements show basically the same trend as shown in the previous studies. We will discuss the temperature and thickness dependence of the time constant for the sample ices in the poster.

Keywords: molecular formation, grain surface chemistry, Inter Stellar Medium

Japan Geoscience Union Meeting 2014
(28 April - 02 May 2014 at Pacifico YOKOHAMA, Kanagawa, Japan)

PPS24-11 Room:415 Time:May 1 17:00-17:15

High Resolution Spectroscopy of Laboratory-Produced Interstellar Molecule having Response to Visible Light

ARAKI, Mitsunori[1*] ; WAKO, Hiromichi[1] ; NIWAYAMA, Kei[1] ; TSUKIYAMA, Koichi[1]

[1]Tokyo University of Science

Diffuse interstellar bands (DIBs) still remain the longest standing unsolved problem in spectroscopy and astrochemistry, although several hundreds of DIBs have been already detected. It is expected that identifications of DIBs can give us crucial information for extraterrestrial organic molecule. One of the best approaches to identify carrier molecules of DIBs is a measurement of DIB candidate molecule produced in the laboratory to compare their absorption spectra with astronomically observed DIB spectra.

Radical in a gas phase is a potential DIB candidate molecule. The electronic transitions of polyaromatic hydrocarbon radicals result in optical absorption. However, because radicals are unstable, their electronic transitions are difficult to observe using a laboratory spectrometer system. To solve this difficulty, we have developed a glow-discharge cell using a hollow cathode in which radicals can be effectively produced as a high-density plasma. The radicals produced were measured by using the cavity ringdown (CRD) spectrometer and the discharge emission spectrometer.

The CRD spectrometer, which consists of a tunable pulse laser system, an optical cavity and a discharge device, is an apparatus to observe an high-resolution optical absorption spectrum. The electronic transition of thiophenoxy radical C_6H_5S was observed in the discharge emission of thiophenol C_6H_5SH. The frequency of the electronic transition of thiophenoxy radical was measured.

A optical discharge emission was examined by a HORIBA Jobin Yvon iHR320 monochromator. We detected the phenoxy radical C_6H_5O in the discharge of phenol C_6H_5OH. The band observed at 6107 A in the discharge was assigned to the electronic transition of phenoxy radical on the basis of the sample gas dependences and the reported low resolution spectra. The frequency of the electronic transition of phenoxy radical was measured.

Comparison studies of thiophenoxy and phenoxy radicals were made with known DIB spectra.

Keywords: Diffuse Interstellar Band, interstellar molecule, spectroscopy, cavity ringdown, molecular cloud, discharge

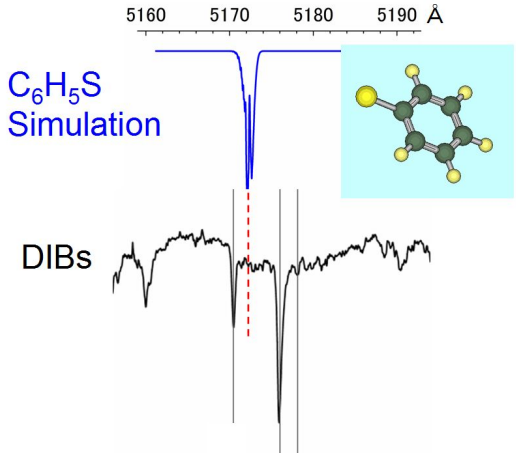

Japan Geoscience Union Meeting 2014
(28 April - 02 May 2014 at Pacifico YOKOHAMA, Kanagawa, Japan)

PPS24-12 Room:415 Time:May 1 17:15-17:30

Variation of organic compounds in the polar extract of Murchison meteorite

NARAOKA, Hiroshi[1*] ; YAMASHITA, Yohei[1] ; MITA, Hajime[2]

[1]Dept. Earth & Planet. Sci., Kyushu Univ., [2]Fukuoka Inst. Tech.

Various organic compounds have been found in carbonaceous chondrites, in which water-soluble bio-related organic compounds such as amino acids and carboxylic acids are fully studied mainly because of their great interests to origins of life in the universe and standards available for the analyses. The concentrations of these acids increase significantly after acid hydrolysis of the water extract. Even though a few studies attempted to identify the chemical structures of their precursors (Cooper and Cronin, 1995), the original structures remain largely unclear. The aqueous activity on the meteorite parent body also could proceed in a chemical oxidation (i.e. incorporation of oxygen by hydrous reaction), resulting in the alteration of original organic matter (Oba and Naraoka, 2009). The large abundance of carboxylic acids in the water extract may be attributable to such oxidation processes.

In contrast to the water extract, less polar methanol extract of chondrites has not been characterized well in spite of relatively high content of organic matter with the D- and 15N enrichment. Recently, ultrahigh-resolution mass spectral analysis on various solvent extracts of the Murchison meteorite (CM2) was performed by electrosplay ionization (ESI) using Fourier transform-ion cyclotron resonance/mass spectrometry (FT-ICR/MS) to reveal significant chemical diversity to tens of thousands of different mass peaks having CHO, CHOS, CHNO and CHNOS elemental compositions (Schmitt-Kopplin et al., 2010). With the assumption for molecular formulae calculation and no chromatographic separation, however, the detailed chemical structures of the compounds cannot be determined. In particular, the organic compounds with their elemental compositions of CH and CHN were not discussed. In this study, we performed high-performance liquid chromatography/high resolution mass spectrometry (HPLC/HRMS) analysis of organic compounds in polar solvent extracts of the Murchison meteorite.

Homologous series of alkylpyridines have been identified in the polar solvent extracts of the Murchison meteorite by liquid chromatography/high- resolution mass spectrometry. The wide range of saturated- and unsaturated-alkylated (C1 to C21) pyridines is more diverse relative to that previously found, which could be produced by aldehydes and NH3 through aldol condesation and Chichibabin-type synthesis on the meteorite parent body. This finding implies a high aldehyde activity under an alkaline condition with ammonia for the chemical evolution of organic matters in carbonaceous meteorites. In addition to the compound distribution of alkylpyridines, the occurrence of other compounds in the water extract will be also discussed with respect to their formation mechanisms in carbonaceous meteorites.

Keywords: polar organic compounds, carbonaceous meteorite, Murchison, high-resolution mass spectrometry

Japan Geoscience Union Meeting 2014
(28 April - 02 May 2014 at Pacifico YOKOHAMA, Kanagawa, Japan)

PPS24-13 Room:415 Time:May 1 17:30-17:45

Heating and evaporation of icy dust in transient heating events induced by nebular shocks

MIURA, Hitoshi[1*] ; YAMAMOTO, Tetsuo[2] ; NAKAMOTO, Taishi[3]

[1]Nagoya City University, [2]Kobe University, [3]Tokyo Institute of Technology

Icy dust plays an important role in chemical evolution from molecular clouds to protoplanetary disks. Simple organic molecules such as formaldehyde (H_2CO) and methanol (CH_3OH) can form in H_2O-CO ice by consecutive addition of hydrogen atoms to CO molecule (Watanabe & Kouchi 2002). Deuterium enrichment in these organic molecules was confirmed to occur by H-D substitution on icy dust surfaces (Nagaoka et al. 2005). More complex organic molecules such as amino acids were detected in the room-temperature residue of an interstellar ice analogue that was ultraviolet-irradiated in a high vacuum at 12 K (Munoz Caro et al. 2002). Sublimation of such icy dust will change the chemical composition of a gas phase in molecular clouds or protoplanetary disks. It is important to elucidate the thermal history of icy dust because it affects the chemical evolution of these organic molecules significantly.

In this paper, we investigated the transient heating event of icy dust induced by nebular shocks. In protostellar or protoplanetary disks, gas accretion from its parent molecular cloud or formation of planetary systems induces shock waves in various conditions. When icy dust passes through the shock front together with the ambient gas, the gas changes its velocity suddenly but the icy dust retains its velocity because of its large inertia. This results in a large relative velocity between them. The high-velocity collision of gas molecules to the icy dust surface raises the dust temperature and leads to its evaporation. Since the relative velocity is reduced by collisions with gas molecules, the heating event should cease within a short period of time. We calculated thermal history and evaporation experienced by icy dust during shock passage for various shock conditions systematically.

The physical model is as follows. We assume that the temperature and density of the post-shock gas are uniform. For simplicity, we consider a spherical icy dust composed of pure H_2O or CO. The icy dust temperature changes much faster than its velocity because of its small thermal inertia. It is shown that the evaporation fraction of individual icy dust defined by the ratio of the decrease in radius to the initial one depends only on the post-shock gas density (ρ_g) and the relative velocity between icy dust and gas just behind the shock front (v_0). We calculated the equations of motion and evaporative shrinkage of the icy dust to obtain the peak temperature and evaporation fraction experienced by the icy dust.

In general, icy dust experiences high temperature and significant evaporation for large v_0 and ρ_g. In addition, we obtained the results as follows: (i) Icy dust does not evaporate completely before it stops relative to the ambient gas even for quite large v_0 and ρ_g. This is due to a negative feedback between the evaporative shrinkage and the duration of heating. (ii) Icy dust hardly evaporates if v_0 is smaller than a certain value. For example, when $v_0 <\sim 3$ km/s for pure H_2O ice or $v_0 <\sim 1$ km/s for pure CO ice, the icy dust shrinks less than by 1% in radius for any gas density. (iii) Icy dust can experience an extremely high temperature at which it would evaporate completely if it were in equilibrium. This is a remarkable feature of the transient heating event that the short heating duration allows the icy dust to survive against superheating.

We elucidated the conditions of icy dust evaporation induced by nebular shocks for various shock conditions systematically. Our results would be useful to discuss the relation between the changes in chemical composition of molecular clouds or protostellar/protoplanetary disks and the evaporation of icy dust by shocks.

Keywords: icy dust, shock heating, evaporation, chemical evolution, protostellar disk, protoplanetary disk

Japan Geoscience Union Meeting 2014
(28 April - 02 May 2014 at Pacifico YOKOHAMA, Kanagawa, Japan)

PPS24-P01 Room:Poster Time:May 1 18:15-19:30

Importance of deuterium fractionation of ethanol by grain surface reactions: experiment of H-D tunneling substitution

OSAKA, Kazuya[1*] ; OBA, Yasuhiro[1] ; KOUCHI, Akira[1] ; WATANABE, Naoki[1]

[1]Inst Low Temp Sci, Hokkaido University

Since we have demonstrated the importance of tunneling grain surface reactions in deuterium fractionation of molecules, many works have targeted this process. To date, we have shown that the grain surface reactions play a crucial role in deuterium enrichments of water, formaldehyde, methanol, and methylamine. In this talk, we present the results of experiment on H-D substitution tunneling reactions of ethanol on cryogenic surfaces. Although C_2H_5OH was observed toward interstellar clouds, its deuterated species have not been detected. However, it was found that its homologous, CH_3OH can be highly deuterated by H-D substitution reactions on grain surfaces and thus it should be reasonable to focus on the potential importance of this process for ethanol. We demonstrated that deuterated methanol is efficiently produced by tunneling reaction of H atoms at very low temperatures relevant to grain surfaces in clouds. H-D reactions predominantly occur in CH_3-CH_2- groups but were hardly observed in an ?OH group which is consistent with the methanol case.

Keywords: deuterium enrichment, ethanol, grain surface reaction

Japan Geoscience Union Meeting 2014
(28 April - 02 May 2014 at Pacifico YOKOHAMA, Kanagawa, Japan)

PPS24-P02 Room:Poster Time:May 1 18:15-19:30

Ion-induce nucleation experiment II: free energy of the water-cluster ion

HIDAKA, Hiroshi[1*] ; NAKAI, Yoichi[2] ; KOJIMA M., Takao[3] ; WATANABE, Naoki[1]

[1]Inst. Low Temp. Sci., Hokkaido Univ., [2]RIKEN Nishina Center, [3]RIKEN Atomic Physics Laboratory

Ion-induce nucleation in gas phase is an important mechanism for grain formation in various circumstances. However, the number of works regarding this formation mechanism is very limited. To investigate the elementally processes of ion-nucleation mechanism, we recently developed a new apparatus (See, the presentation by N. Watanabe in this session). Using this apparatus, the cluster ion formation with an ion core mass-selected, which is the first stage of nucleation, can be observed quantitatively. In this presentation, we show the results of experiment on water-cluster ion formation in which free energies with the size of cluster have been determined. The experiment was performed at temperatures in range of 230-400 K with the supersaturation ratio of about 10^{-3}-10^{-2}.

Keywords: interstellar grain, cluster ion, nucleation

Japan Geoscience Union Meeting 2014
(28 April - 02 May 2014 at Pacifico YOKOHAMA, Kanagawa, Japan)

PPS24-P03 Room:Poster Time:May 1 18:15-19:30

Detection of levitation dust around the asteroid by Hayabusa-2 LIDAR

OSHIGAMI, Shoko[1*] ; SENSHU, Hiroki[2] ; WADA, Koji[2] ; KOBAYASHI, Masanori[2] ; NAMIKI, Noriyuki[2] ; MIZUNO, Takahide[3]

[1]National Astronomical Observatory of Japan, [2]Planetary Exploration Research Center, Chiba Institute of Technology, [3]Institute of Space and Astronautical Science, Japan Aerospace Exploration Agency

The micron-size particles are continuously produced at the surface of airless bodies like the Moon and asteroids by innumerable micro impacts and thermal stress related to large temperature difference between daytime and nighttime. Previous asteroid missions have revealed smooth appearance of topography on 951 Gaspra, 243 Ida, and 433 Eros suggesting that these asteroids are covered with particles smaller than resolution of camera images. Particularly, the exploration of Eros by NEAR Shoemaker has revealed as smooth surface as a liquid water at the base of craters whose diameter is between 20 and 300 m. This ”pond” is consistent with stagnant dusts of diameter smaller than 50 microns. Based on this observation, dust levitation hypothesis was proposed. According to this hypothesis, a photoelectric effect of solar UV positively charges both dust and the surface. Then a balance between electric repulsion and gravity causes 0.5-microns dusts to oscillate vertically over the surface of Eros long period of time. When a dust has a horizontal velocity, it transfers laterally until it reaches to a shadow of topography where electrostatic field is weaker than surroundings. Thus topographic depression such as a crater becomes a sink of levitating dusts.

LIDAR is one of four remote-sensing instruments onboard Hayabusa-2, and is used to measure altitudes of the spacecraft from a surface of the asteroid, 1999 JU3, for not only secure navigation but also scientific investigation of a C-type asteroid. Hayabusa-2 LIDAR has been improved from that onboard Hayabusa which explored and returned samples from asteroid 25143 Itokawa. A new function called dust count mode is implemented to Hayabusa-2 LIDAR to observe spatial distribution of dust number density in 8 levels with resolution of 20 m in bore sight direction. LIDAR can hardly observe lateral distribution of dusts, but distinguish a weak reflection of thin dust cloud from that of the surface. To plan an operation of the dust count mode observation is difficult because the number density of asteroid dust is not known at all. Instead, we evaluate the lower bound of number density that is geologically important for morphology of asteroid surface. For a given number density of dusts and under an assumption that a characteristic time of levitation is the rotation period of 1999 JU3, the rate of embayment of craters is calculated. If this rate of embayment is greater than that of crater production, we need to take into account a modification process for the study of crater morphology and crater counts of 1999 JU3. This lower bound is calculated to be 10^6 m^{-3} for a cloud of dusts whose radius is larger than a few microns. Then we set this value as a target of the dust count mode observation.

A detectability of dust count mode is dependent on sensitivity of Hayabusa-2 LIDAR and an altitude of the spacecraft. We calculate a reflection from dusts using Mie scattering model assuming that a diameter of dust particle is constant and is larger than the wavelength of laser, that is, 1064 nm. A characteristic distance between dusts is also assumed to be sufficiently larger than the wavelength so that interaction between dust particles is negligible. Using a lidar equation, we calculate a peak power of backscattering light from a dust cloud for various sets of the distance, the number density, and the dust radius. The peak power of reflection is generally stronger than noise level of the detector. The reflection from dust cloud is so weak that the targeted number density of 10^6 m^{-3} is hardly higher than the detection limit. Even at the lowest altitude, the reflection from a dust cloud of 10-microns radius for 10^6-m^{-3} number density is equivalent to the detection limit. If the dust radius is 5 microns, number density more than 10^7 m^{-3} is necessary to be detected. Therefore we plan to start the dust count operation from the HP and attempt to conduct as much operations as possible at low altitude.

Japan Geoscience Union Meeting 2014
(28 April - 02 May 2014 at Pacifico YOKOHAMA, Kanagawa, Japan)

PPS24-P04 Room:Poster Time:May 1 18:15-19:30

Condensation of forsterite under protoplanetary disk conditions

TACHIBANA, Shogo[1*] ; TAKIGAWA, Aki[2] ; MIYAKE, Akira[2] ; NAGAHARA, Hiroko[3] ; OZAWA, Kazuhito[3]

[1]Dept. Natural History Sci., Hokkaido Univ., [2]Dept. Geol. Mineral., Kyoto Univ., [3]Dept. Earth Planet. Sci., Univ. Tokyo

Meteoritic evidence indicates that dust condensation occurred in the early stage of solar system evolution. In this study, we succeeded in performing condensation experiments of forsterite under controlled protoplanetary-disk conditions, which will make significant contribution to understanding silicate formation and chemical fractionation in protoplanetary disks.

Condensation experiments were carried out in the system of Mg_2SiO_4-H_2-H_2O. A mixed gas of H_2 and H_2O was flowed into a continuously evacuated infrared vacuum furnace at a controlled rate to keep a pressure constant. Synthetic forsterite powder in an It crucible was heated as a gas source. A part of evaporated gases were condensed on a Pt mesh located at a cooler region in the chamber. The pressure and temperature conditions were close to those of protoplanetary disks. The total pressure of the system was 5.5 Pa, and the substrate temperature ranged from 1320 to 1160 K. The H_2O/H_2 ratio was set at 0.015, which was about 15 times larger than the solar ratio. The SiO/H_2 ratio was evaluated to be about 0.7-2 % of the solar ratio from the weight loss rate of the gas-source forsterite. Experimental duration ranged from 6 to 237 hours.

Sub-micron to micron-sized condensates covered with Pt substrates at 1160 and 1275 K, but no condensates were found at 1320 K. The typical size of condensates at 1160 K was less than 1 micron irrespective of experimental duration and no effective growth of each condensed grain was observed. Condensates at 1275 K for $>$40 hours partly had several micron-sized flat regions. EDS analyses showed that chemical compositions of condensates were consistent with the stoichiometry of forsterite, and their EBSD patterns were well fitted with the patterns from crystalline forsterite. Coincident EBSD patterns were obtained from the flat region of condensates at 1275 K, suggesting that the area was covered with a single crystal. TEM observation of condensates at 1160 K also found that the condensates were polycrystalline forsterite with a thickness of 30-150 nm, and infrared absorption spectra of condensates show clear 10-micron absorption features resembling those of crystalline forsterite. These evidence indicates that polycrystalline forsterite condensed at 1275 and 1160 K.

The mean free path of gas molecules under the present experimental conditions is less than 1 mm, and the evaporated forsteritic gas and the ambient H_2-H_2O gas are expected to be well mixed. Supersaturation ratios (S) for experiments at 1320, 1275, and 1160 K are thus estimated to be $<$1.2, $<$10, and $<$1000-2000. These supersaturation ratios correspond to the supercooling of $<$5, $<$60 and $<$170 K, respectively.

No condensates were found at 1320 K because the degree of supersaturation was too small for nucleation of forsterite or even the vapor was not saturated with forsterite ($S<1$). The condensates at the supercooling of $<$170 K (1160 K) imply that heterogeneous nucleation of new grains occurred successively on preexisting grains. On the other hand, with the supercooling of $<$60 K (1275 K), some grains seem to have grown up to several microns, and some seem to have newly nucleated on preexisting grains, suggesting that both nucleation and growth of each condensate occurred.

These differences would result in a structural difference in forsterite dust condensed in protoplanetary disks. Fluffy aggregates of sub-micron sized fine particle would form with a supersaturation of $>$1000, while aggregates of micron-sized grains would form with S of 10 that could be an analogue of amoeboid olivine aggregates in chondrites.

Keywords: forsterite, condensation, protoplanetay disk

Japan Geoscience Union Meeting 2014
(28 April - 02 May 2014 at Pacifico YOKOHAMA, Kanagawa, Japan)

PPS24-P05 Room:Poster Time:May 1 18:15-19:30

A New Experiment for Organic Molecule Formation by Catalytic Reactions on the Surface at Low Temperature and Pressure

KIMURA, Yuki[1*] ; TSUCHIYAMA, Akira[2] ; NAGAHARA, Hiroko[3]

[1]Tohoku University, [2]Division of Earth and Planetary Sciences, Graduate School of Sciece, Kyoto University, [3]Department of Earth and Planetary Science, Graduate School of Science, The University of Tokyo

Abundant H_2, CO and N_2 gases react to be more complex molecules mainly on the cooled surface of cosmic dust particles in the molecular cloud and/or primitive solar nebula [1]. The production of organic molecules and subsequent evolution to organic materials in the solar nebula may contribute to the primordial organic system of the Earth. Catalytic chemical reactions are possible production pathway of organic materials in the solar nebula after the formation of simple molecules on nanometer sized cosmic dust particles in the molecular clouds. Experimentally, organic molecules ranging from methane (CH_4), ethane (C_2H_6), benzene (C_6H_6) and toluene (C_7H_8), to more complex species such as acetone (C_3H_6O), methyl amine (CH_3NH_2), acetonitrile (CH_3CN) and N-methyl methylene imine (H_3CNCH_2) have been produced using such as the Fischer-Tropsch type (FTT) and Haber-Bosch type (HBT) reactions on analogs of naturally occurring grain surfaces [2]. Previous studies were performed at higher-temperature ($>$573 K) and pressure ($\sim$1 atm) than the expected conditions in the solar nebula [3-6]. However, since the actual environment is at lower temperature and pressure, it is not clear whether the previous experimental results can be extrapolated to the solar nebula. Our group seeks to elucidate the reaction rates of chemical reactions including isotopic fractionation at lower temperature (100-500 K) and pressure (10^{-3}-10^{0}) and their contribution to the primordial organic system of the Earth.

We are constructing a vacuum chamber based on a new concept to conduct the experiments mentioned above. The chamber with a differential pumping system has a temperature-controlled substrate, a Fourier transform infrared spectrometer (FT-IR), and two quadrupole mass spectrometers (Q-MSs). The substrate has an iron or silicate thin film for FTT and HBT reactions and the FT-IR measures the vibration modes of adsorbed and produced molecules on the surface and the Q-MSs detect volatile and nonvolatile molecules, respectively. As a result, reaction rates of molecules such as H_2, CO, N_2 and NH_3 on iron or silicate substrate will be obtained as a function of temperature and pressure.

[1] J. Llorca and I. Casanova, *Meteorit. Planet. Sci.* **35**, 841 (2000).
[2] H. G. G. M. Hill, and J. A. Nuth, *Astrobiology* **3**, 291 (2003).
[3] J. A. Nuth, N. M. Johnson, and S. Manning, *The Astrophysical Journal* **673**, L225 (2008).
[4] J. A. Nuth, N. M. Johnson, and S. Manning, *Organic matter in space, Proc.* **IAU Symp. 251**, edited by S. Kwok and S. Sandford, Cambridge Univ. Press, NY (2008), pp. 403-408.
[5] J. A. Nuth, Y. Kimura, C. Lucas, F. Ferguson, and N. M. Johnson, The *Astrophysical Journal Letters* **710**, 98 (2010).
[6] Y. Kimura, J. A. Nuth, N. M. Johnson, K. D. Farmer, K. P. Roberts, and S. R. Hussaini, *Nanoscience and Nanotechnology Letters* **3**, 4 (2011).

Keywords: Organic molecules, Catalytic reactions, Protoplanetary system

Japan Geoscience Union Meeting 2014
(28 April - 02 May 2014 at Pacifico YOKOHAMA, Kanagawa, Japan)

PPS24-P06 Room:Poster Time:May 1 18:15-19:30

Dust movement and chemical evolution of proto-solar disk

NAGAHARA, Hiroko[1*] ; NAKATA, Mamoru[1] ; OZAWA, Kazuhito[1]

[1]Hiroko Nagahara

Origin and evolution of the protoplanetary system have been developed mostly from the dynamic point of view, which includes two competing theories, and whichhas been improved by astrophysical observation of exoplanets and extrasolar planetary systems. On the other hand, examination of meteorites and samples by planetary explorations such as lunar samples, cometary particles, and regolith particles of the asteroid Itokawa enable us to gain insight into the evolution of the Solar System. Although those primitive materials give various information, they are not linked to the physical processes in the primary Solar System.

The purpose of this study is to demonstrate how chemical composition distribution evolves over time in the early stage of the proto-solar disk. In order to combine physical processes and chemistry, we have developed a new model consisting of chemical equilibrium calculation and particle tracking equations. At first, we calculate the chemical composition of starting particles at each position in the protoplanetary disk, to track their each motion in the evolving disk, and to analyze the bulk composition of particles that came from various positions in particular time and space. Then, the dynamic evolution of individual particles is calculated in one-dimensional steady-state disk model. In an early stage, particle located in the inner region of the disk have a composition rich in refractory components and those outside have unfractionated CI-like composition. Particles in average move inward by the angular momentum conservation, but a little fraction of them move outward by the turbulent diffusion. Therefore, mixing of refractory particles from inside and CI-like materials from outside takes place, and the mixing ratio vary with time and space.

Because of inward movement of many particles, the relative fraction of particles from outside increases with time for one particular region in the disk, that is, the bulk chemical composition of particles is getting more CI-like. Similarly, the bulk chemical composition of particles at particular place is getting more CI-like with time. Calculations with model parameters of higher temperature of the disk suggest that longer time is needed to replace refractory-rich compositions by a CI-like composition. It is because the radial distance between fractionated particles with refractory-rich composition and unfractionated CI-like materials is longer in a high temperature disk.

Comparing these results and the composition of CM, CO, CV chondrites, it is concluded that CV composition can be reproduced at the most inner region, CO in the next, and CM most outer region in the disk. The present work shows that the composition of carbonaceous chondrites were formed at the asteroid belt region at the early stage of disk evolution with the wide spread of high temperature region.

Keywords: protoplanetary disk, chemical evolution, dust movement, chemical equilibrium

Japan Geoscience Union Meeting 2014
(28 April - 02 May 2014 at Pacifico YOKOHAMA, Kanagawa, Japan)

PPS25-01 Room:213 Time:May 2 09:00-09:15

Age-cytometry : new approach for meteorite anatomy

HIRATA, Takafumi[1*] ; ITOH, Shoichi[1]

[1]School of Science, Kyoto University

The chronology for meteorite samples has played an important role to decode the early sequence of the solar system. Among the chronometers based on the radio-active decay of long-lived nuclides, because of the high time resolution of the resulting age data, the U-Pb chronometry has been widely used to define the timing of formation of refractory inclusions or to understand the formation sequence of the chondrite parental body. The high time resolution on the U-Pb chronometers was achieved by the small contribution of the analytical uncertainties in the isotope ratio measurements onto the resulting age data, and also because of the well-defined decay constants for ^{238}U, ^{235}U and ^{232}Th nuclides. Moreover, the U-Pb isotope systematics has further advantages of evaluating of system closure since the sample formation or crystallization of minerals, and therefore, reliability of the resulting age data can be rigorously tested. Using the U-Pb chronometer, the resulting time-resolution can become as small as 0.2 ? 1 Ma range for chondritic materials, but this could not be high enough to understand the planetary formation during the runaway growth or to understand the timing of the core formation. To overcome this, we are trying to measure in-situ 238U/235U ratio from individual minerals by means of combination of two ion collectors. Details of the instrumentation and operational conditions would be demonstrated in this talk.

Cytometry is the quantitative analysis of cells and cell systems. Cytometry measures optical properties of cells, and most often uses fluorescence to measure specific antigen molecules, intracellular ions and DNA/RNA using antibodies, indicator dyes, or nucleic acid-specific probes. Cells may be live or fixed, depending on the application, and individual cells can often be physically sorted. ? Advantage of the cytometry are the analysis speed, detection sensitivity, the ability to measure many parameters simultaneously, and the ability to sort individual cells, and therefore, mechanism or process of elemental metabolism could be precisely evaluated based on the extensive number of cells (e.g., Benfall et al., Science, 2011; Bodenmiller et al., Nature Biotechnology, 2012). This approach can also be applied to understand the solar system evolution based on the numerous number of age data. In recent ten years, we have demonstrated the unique study approach using the distribution pattern of sample ages based on the series of precise age data collected from large number of samples (i.e., age-cytometry) [e.g., Rino et al., PEPI, 2008; Iizuka et al., Geology, 2008; Iizuka et al., Iizuka et al., Chem. Geol., 2009; Iizuka et al., GCA, 2010]. With the high-time resolution age data obtained by present analytical technique using the LA-ICPMS, further precise and quantitative discussion could be made on the solar system evolution through the age-cytometry. The newly developed high-resolution and high-throughput age determination system using a laser ablation-ICP mass spectrometry has a potential to become a significant tool to promote an age-cytometry.

Keywords: meteorite anatomy, cytometry, solar system evolution, multiple collector mass spectrometry, laser ablation-ICPMS, ICP-mass spectrometry

Japan Geoscience Union Meeting 2014
(28 April - 02 May 2014 at Pacifico YOKOHAMA, Kanagawa, Japan)

PPS25-02 Room:213 Time:May 2 09:15-09:30

147Sm-143Nd and 146Sm-142Nd chronology of a basaltic eucrite, Juvinas

KAGAMI, Saya[1*] ; YOKOYAMA, Tetsuya[1]

[1]Dept. Earth and Planetary Sciences, Tokyo Tech

Eucrites are interpreted to have originated from the asteroid 4-Vesta which differentiated into crust and mantle. The chronology of eucrites is important to understand the formation and differentiation of planets/ planetesimals in the early Solar System. The combination of two chronometers, short-lived ^{146}Sm-^{142}Nd system ($T_{1/2}$=6.8×10^{7}yr) and long-lived ^{147}Sm-^{143}Nd ($T_{1/2}$=1.06×10^{11}yr), is useful to decode the thermal history of the eucrite parent body, because they have the same closure temperature [1]. To obtain precise Sm-Nd ages for eucrites and other achondrites, it is indispensable to develop highly precise Nd isotope analysis.

We investigated the ^{147}Sm-^{143}Nd and ^{146}Sm-^{142}Nd chronometers for a brecciated basaltic eucrite, Juvinas. We examined samples of whole rock powder (W.R.), 400 mesh grains, plagioclase (Pl), and pyroxene (Px). Plagioclase and pyroxene grains were obtained by handpicking. Samples were dissolved using a mixture of concentrated pure acid ($HClO_4$, HF, and HNO_3) and heating at 195 ℃. About ten percent of the solution was removed and spiked with ^{149}Sm-^{145}Nd in order to precisely measure Sm and Nd concentrations by ID-ICP-MS (Thermo X-series II at Tokyo Tech). We separated Nd from the rest of the solution via a four-step column chemistry. Nd isotope ratios in W.R., 400mesh, Pl, and Px were analyzed by TIMS (Thermo TRITON-plus at Tokyo Tech) with the dynamic multicollection method.

The ^{147}Sm-^{143}Nd mineral isochron diagram of Juvinas, yielded an age of 4610±410 Ma. In contrast, the ^{146}Sm-^{142}Nd systematic for Juvinas yielded an initial ^{146}Sm/^{144}Sm ratio of 0.0157±0.0074. This gives ?4618?_(-63)^(+38) Ma for the age of Juvinas when an initial solar system ratio of ^{146}Sm/^{144}Sm=0.0094 at 4568 Ma is assumed [1]. The self-consistency of the ^{147}Sm-^{144}Nd and ^{146}Sm-^{142}Nd ages for Juvinas supports early crust-mantle differentiation on the eucrite parent body as was proposed by previous chronological studies on basaltic eucrites (e.g., Pb-Pb, Al-Mg, Mn-Cr, and Hf-W; [2-5]).

It has been suggested that cumulate eucrites provide internal isochron ages younger than basaltic eucrites due to a longer history in the deep crust or late thermal disturbance during later meteorite bombardment event(s) [6]. Because of the limited Sm/Nd variation in the meteorite components analyzed, the Sm-Nd ages obtained in this study have uncertainties several times larger than those in previous studies [6]. The ^{147}Sm-^{143}Nd age and the initial ^{143}Nd/^{144}Nd ratio for Juvinas are consistent with those obtained by the mineral isochrons of three cumulate eucrites within analytical error (4546±8 Ma; [6]). However, our ^{146}Sm-^{142}Nd age is older than the proposed ^{147}Sm-^{143}Nd age for cumulate eucrites, indicating that the crystallization of basaltic eucrites predates the timing when the Sm-Nd systematics for cumulate eucrites reached a closure temperature. It should be noted that Juvinas is a brecciated basaltic eucrite which may not record a correct Sm-Nd age. Further investigation is required to obtain more precise Sm-Nd ages utilizing unbrecciated basaltic eucrite to reveal the thermal history on the eucrite parent body.

References: [1] N. Kinoshita et al., (2012) Science, 335, 1614 [2] S.J.G. Galer and G.W. Lugmair, (1996) MAPS, 31, A47. [3] M. Wadhwa et al., (2003) LPSC XXXIV, 2055. [4] G.W. Lugmair and A. Shukolyukov, (1998) GCA 62, 2863. [5] T. Kleine et al., (2004) GCA 68, 2935.
[6] M. Boyet et al., (2010) EPSL 291, 172.

Japan Geoscience Union Meeting 2014
(28 April - 02 May 2014 at Pacifico YOKOHAMA, Kanagawa, Japan)

PPS25-03 Room:213 Time:May 2 09:30-09:45

Al-Mg mineral isochron of a Type C CAI from Allende

KAWASAKI, Noriyuki[1*] ; KATO, Chizu[2] ; ITOH, Shoichi[3] ; ITO, Motoo[4] ; WAKAKI, Shigeyuki[4] ; YURIMOTO, Hisayoshi[1]

[1]Hokkaido University, [2]Washington University in St. Louis, [3]Kyoto University, [4]JAMSTEC

Ca-Al-rich inclusions (CAIs) show the record of ^{26}Al, which is a short-lived radionuclide with a half-life of 0.73 Myr (e.g., MacPherson et al., 1995), thus a relative chronometer with Al-Mg systematics is applicable for determining a precise time interval of individual CAI formation process. In this work, we report full petrologic and mineralogical studies of a Type C CAI from Allende, EK1-04-2, with more detailed analyses of O isotopic distributions and Al-Mg systematics than presented by Ito et al. (2000).

FE-SEM equipped with EDS and EBSD system (JEOL JSM-7000F; Oxford X-Max 150; Oxford HKL) was used for petrologic and mineralogical studies. O and Al-Mg isotopic compositions were measured by SIMS (Cameca ims-1270).

The EK1-04-2 is a CAI fragment with a size of ~2 mm across. The CAI mainly consists of spinel, anorthite, olivine and diopside. The CAI has mantle and core structure. In the core part, euhedral spinel crystals are enclosed by other mineral grains. Anorthite and olivine grains show euhedral or subhedral shape. Diopside grains show anhedral shape and include spinel and olivine grains. Thus, crystallization sequences of core minerals are spinel, anorthite, olivine and diopside. The mantle part has a same mineral assemblage as the core part, however, amount of spinel is lower than the core part, and anhedral spinel and anorthite grains are present, and the diopside is more Mg-rich and Ti-poor comparing with core diopside.

O isotopic compositions of the minerals are distributed along CCAM line (delta-^{18}O = -44 to +9 permil). Spinel is ^{16}O-rich (delta-^{18}O ~-43 permil), while anorthite is ^{16}O-poor (delta-^{18}O ~9 permil). Any differences of O isotopic compositions are not observed for these minerals among core and mantle parts while olivine and diopside show different O isotopic compositions between core and mantle parts. Olivine and diopside in the core have an intermediate O isotopic composition between spinel and anorthite (delta-^{18}O ~-15 permil). In contrast, the oxygen isotopic compositions of olivine and diopside in the mantle are not homogeneous and distributed to ^{16}O-poor direction compared with those in the core (delta-^{18}O = -13 to -4 permil). Olivine and diopside grains in the mantle are not in chemically equilibrium with those in the core. The O isotopic distributions among mineral grains indicate that the CAI experienced multiple and individual crystallization events: a crystallization of spinel, a crystallization of core olivine and diopside, and a crystallization of mantle olivine and diopside.

On the Al-Mg isochron diagram, spinel grains are plotted on a line of $^{26}Al/^{27}Al_0 = (3.52\pm0.15) \times 10^{-5}$, while olivine, diopside and anorthite grains of core are plotted on a line of $^{26}Al/^{27}Al_0 = (5\pm5) \times 10^{-7}$. The difference of the initial values corresponds to a relative age of ~4.6 Myr. In contrast, olivine and diopside grains in mantle are plotted below the line of olivine and diopside in core. The ^{16}O-poor and low delta-$^{26}Mg_0$ compositions of mantle olivine and diopside suggest mixing of Al-rich chondrule-like materials. The composition of the mantle diopside is consistent with this scenario.

The petrographic, oxygen isotopic and chronological studies indicate that the CAI experienced multiple heating events after a precursor CAI formation. After ~4.6 Myr later than the precursor CAI formation, the CAI partially melted at ~1600K. The melt exchanged oxygen isotopes with the surrounding ^{16}O-poor solar nebular gas. ^{16}O-poor olivine, diopside and anorthite grains recrystallized from the partial melt. Subsequently, Al-rich chondrule-like materials accreted on the CAI and experienced partial melting and recrystallization, again. Distinctive ^{16}O-poor composition of anorthite is a result of a thermal metamorphism at the Allende parent body.

Our study revealed that the CAI has retained in the protosolar nebula at least for 4.6 Myr and experienced multiple melting events.

Keywords: Al-Mg, CAI, SIMS, oxygen isotopes, solar nebula

Japan Geoscience Union Meeting 2014
(28 April - 02 May 2014 at Pacifico YOKOHAMA, Kanagawa, Japan)

PPS25-04 Room:213 Time:May 2 09:45-10:00

Water contents and hydrogen isotopic compositions of phosphate minerals from LL4-6 ordinary chondrites.

YANAI, Kaori[1] ; ITOH, Shoichi[2*] ; GREENWOOD, James[3] ; RUSSELL, Sara[4] ; YURIMOTO, Hisayoshi[1]

[1]Department of Natural History Sciences, Hokkaido University, [2]Department of Earth and Planetary Sciences, Kyoto University, [3]Department of Earth and environment Sciences, Wesleyan University, [4]Department of Earth Sciences, Natural History Museum, London

The origin of water on the earth is discussed by many researcher. The hydrogen isotopic compositions of earth ' s water were also studied to discuss the origin of water for Earth, Lunar and comet through the planetary scale in the solar system [Greenwood et al., 2011]. One of siginificant possible precursor of H20 in Earth ' s orbitary could be cometary ice but it is unclear. In preliminary results, we reported the hydrogen isotopic compositions of phosphate minerals (Merrilite and apatite) from Ensisheim LL6 ordinary chondrite (OC) on 2012 at JPGU and NIPR meeting in Japan. These D/H ratio are extremely duetrium-rich value (δD ˜15000permil). In addition, Deloule and Robert (1995) also reports that the hydrogen isotopic compositions of phyllosilicate from LL3.0 Semarkona OC is D-rich (˜4000permil) and suggest the origin of this D-rich isotopic compositions come from the interstellar space or in the outer regions of the solar nebula, like cometary ice. These results suggest that, as the Itokawa S-type asteroids with Earth ' s orbitary, the heavily hydrogen isotopic compositions of LL OCs resulted from cometary ice close to the earth. However, there is no sytematic study of hydrogen isotopic compositions of LL4-6 OCs because it is difficult to estimate the planetsimal hydrogen isotopic compositions of water due to very low water contents and contamination from adsorbed water. In this study, we applied the in-situ measurement technique of water content and hydrogen isotopic compositions of phosphate minerals from LL4-6 OCs by SIMS. All D/H ratio in the phosphate minerals are D-rich (δD ˜+2000 to +25000). The D/H ratio in the phosphate minerals from LL4 Soko-Banja and LL5 Tuxtuac could be resulting from degassing of H2 during Fe-water oxidation reaction but it is difficult to apply it for those of LL6 Ensisheim and Bandong LL6. These results suggest that the origin of D-rich hydrogen isotopic compositions of LL6 phosphate mineral is resulting from extra-planetary with cometary ice beause of extremely heavily hydrogen isotopic compositions.

Keywords: Hydrogen isotope, SIMS, phosphate, apatite

Japan Geoscience Union Meeting 2014
(28 April - 02 May 2014 at Pacifico YOKOHAMA, Kanagawa, Japan)

PPS25-05 Room:213 Time:May 2 10:00-10:15

Oxygen diffusion in perovskite with different Ca/Ti ratio

HASHIGUCHI, Minako[1*] ; SAKAGUCHI, Isao[1] ; HIROSE, Sakyo[2] ; OHASHI, Naoki[1]

[1]National Institute for Materials Science (NIMS), [2]Murata Manufacturing Co., Ltd.

<**Introduction**> Calcium-aluminum-rich inclusions (CAIs) in chondrites are believed to be the first solid formed in solar nebula and are composed of refractory minerals, such as spinel, mellilite, anorthite, and perovskite ($CaTiO_3$). Previous studies have been reported heterogeneous oxygen (O)-isotopic compositions among the CAI minerals [Clayton et al. (1973)]. The isotopic compositions are considered to be a marker of O-isotopic composition in the solar nebula [Yurimoto et al. (1998); Itoh and Yurimoto (2003); Park et al. (2012)]. Diffusion processes are important processes to affect the O-isotopic compositions of CAI minerals. To understand the effect, oxygen diffusivity of minerals should be investigated.

Perovskite crystals showed several order of larger oxygen diffusion coefficients than other CAI minerals [Gautason and Muehlenbachs (1993); Ryerson and McKeegan (1994); Sakaguchi and Haneda (1996)]. Thus, its O-isotopic compositions can provide us an important key to understand whether O-isotopic compositions of the CAI minerals have been modified or not. However, there still were a few reports on the oxygen diffusivity of perovskite, and the previously reported values are different by about one order of magnitude [Gautason and Muehlenbachs (1993); Sakaguchi and Haneda (1996)]. In this study, we focus on Ca/Ti ratio of perovskite and determined oxygen diffusion coefficients in perovskite with different Ca/Ti ratio experimentally.

<**Experimental**> Polycrystalline perovskite samples were prepared by a conventional sintering technique. High-purity reagent-grade powders of $CaCO_3$ and TiO_2 were used as the starting materials. These powders were mixed as Ca/Ti=0.098-1.002 by ball milling with PSZ balls. The powders were pressed as a sheet and were sintered at 1350 degC for 2 h in the atmosphere.. Then, perovskite samples with different Ca/Ti ratio were obtained. Because of a contamination of ZrO_2 from PSZ balls, Ca/Ti ratio of the samples may differ by 0.001-0.0015 from initial value.

The samples were polished and finished by a mechanical polishing using the several grade of diamond pastes. To remove damages by the polishing, the samples were annealed at 1200 degC for 1h in the atmosphere. The samples were annealed under $^{18}O_2$ gas at 750-1050 degC for several hours. Oxygen diffusion coefficients in the samples were determined using depth profiles of ^{18}O concentration of the samples obtained by secondary ion mass spectrometry (Cameca ims-4f).

<**Results and discussion**> Two contributions to the oxygen bulk diffusion mechanism are observed in depth profiles of ^{18}O concentration obtained from Ti-rich perovskite samples. One starts near surface (diffusion A) and the other starts from about a few 100 nm depth (diffusion B) of the sample. In Ca-rich perovskite samples, only a diffusion mechanism is observed.

We found that the oxygen bulk diffusion coefficients (D_b) in Ca-rich perovskite samples were larger than that of Ti-rich samples, in both diffusion A and B. The D_b value of 950 degC in a perovskite sample prepared by a powder with Ca/Ti=0.098 was $7x10^{-13}$ cm^2/s (diffusion A), $1x10^{-11}$ cm^2/s (diffusion B), whereas the value of a sample prepared by a powder with Ca/Ti=1.002 was $7x10^{-10}$ cm^2/s.

Previous reports showed ^{16}O-poor [Ito et al. (2004)] or ^{16}O-rich [Park et al. (2012)] perovskite in carbonaceous chondrites. It has been suggested that the former was changed from its original isotopic composition during thermal processes, the later was escaped the secondary processes. Larger oxygen diffusion coefficients of perovskite than that of other CAI minerals suggested that perovskite record the final thermal process, which the CAI experienced. Moreover, this study may suggest shorter timescale required for change of O-isotopic composition of perovskite than previously estimated and also indicates the importance of investigation on Ca/Ti ratio of perovskite to understand its oxygen diffusivity.

Keywords: Perovskite, Oxygen diffusion

Japan Geoscience Union Meeting 2014
(28 April - 02 May 2014 at Pacifico YOKOHAMA, Kanagawa, Japan)

PPS25-06 Room:213 Time:May 2 10:15-10:30

Newly identified hibonite-bearing FUN inclusions with low Al/Mg ratios

FUKUDA, Kohei[1*] ; HIYAGON, Hajime[1] ; SASAKI, Shogo[1] ; MIKOUCHI, Takashi[1] ; FUJIYA, Wataru[2] ; TAKAHATA, Naoto[3] ; SANO, Yuji[3] ; MORISHITA, Yuichi[4]

[1]Graduate School of Science, The Univ. of Tokyo, [2]Max Planck Institute for Chemistry, [3]AORI, The Univ. of Tokyo, [4]Graduate School of Science, Shizuoka Univ.

It has been recognized that a minor group of CAIs named FUN (*F*ractionation and *U*nknown *N*uclear effects) and some types of hibonite ($CaAl_{12}O_{19}$) inclusions show isotopic anomalies in ^{48}Ca, ^{50}Ti, and no or small excesses in ^{26}Mg from the decay of ^{26}Al. The existence of isotopic anomalies in Ca and Ti suggests that these inclusions formed at the earliest stage of the solar system evolution, when isotopic heterogeneity still existed. The lack of ^{26}Al may also be interpreted as their formation before the homogenization of ^{26}Al distribution in the early solar system. Hence, FUN inclusions and hibonite-bearing inclusions may have significant importance in studying the earliest stage of the solar system evolution.

In order to better understand the isotopic homogenization process(es) in the early solar system, I have conducted multiple isotopic analyses of three hibonite-bearing inclusions from the Murchison (CM2) meteorite using two ion microprobes (Cameca ims-1270 & NanoSIMS 50). I identified three new hibonite-bearing FUN inclusions (MC037, MC040, and MC003), which exhibit extremely large mass-dependent fractionation in Mg (up to ∼55 ‰/amu) but almost no excess in ^{26}Mg, and have resolvable isotopic anomalies in ^{48}Ca and ^{50}Ti. The results suggest that these inclusions formed during the isotopic homogenization process(es). The results of Mg isotopic compositions (extremely large isotopic fractionation) and elemental abundances (rather low Al/Mg ratios of 20-150) indicate that the precursors of these inclusions might have more Mg-rich (less refractory) compositions than the previously reported hibonite-bearing F(UN) inclusions (Al/Mg ratios from ∼500 up to ∼60000). In addition, their oxygen isotopic compositions are plotted on a mass-dependent fractionation line with Δ^{17}O values of ∼-23 ‰, similar to the value for the majority of typical CAIs. This suggests that oxygen isotopic compositions of their precursors are also ^{16}O-rich ($\delta^{17,18}$O ∼-50 ‰), identical to those of typical CAIs. Furthermore, the textual signatures suggests that a molten precursor of MC040 may have been quenched. Although the origin of FUN inclusions is still not known, the present results and previous works show that there are further variations in their precursor compositions, isotopic anomalies, and thermal processes.

Keywords: FUN inclusion, hibonite, ion microprobe, Mg isotopes, Ca and Ti isotopes, oxygen isotopes

Japan Geoscience Union Meeting 2014
(28 April - 02 May 2014 at Pacifico YOKOHAMA, Kanagawa, Japan)

PPS25-07 Room:213 Time:May 2 10:30-10:45

O-16-rich olivine in igneous rim from NWA 3118 (CV)

MATSUDA, Nozomi[1*] ; SAKAMOTO, Naoya[2] ; YURIMOTO, Hisayoshi[3]

[1]Natural History Sciences, Hokkaido University, [2]CRIS, Hokkaido University, [3]Natural History Sciences, Hokkaido University

Ca-Al-rich inclusions (CAIs) and chondrules in chondrites show mass independent oxygen isotopic fractionation. Normally, CAIs are enriched in O-16 whereas chondrules are depleted in O-16. However, olivine grains having O-16-rich composition were reported in chondrule rims from CR2 chondrites (Takeda et al., 2002; Nagashima et al., 2013). Existence of O-16-rich grains in the rims indicates that the chondrule rims preserve information about chondrule precursor components with oxygen isotope in the chondrule formation region. In addition, abundance and distribution of O-16-rich olivine in chondrule rims have not been studied for other chondrite groups. Therefore, we study petrology and oxygen isotopic mapping of an igneous chondrule rim from a CV3 chondrite in order to reveal the distribution of O-16-rich materials.

The sample used in this study is a polished thin section from NWA 3118 CV3 chondrite. The petrographic observation and chemical analysis were performed by FE-SEM-EDS (JEOL JSM-7000F + Oxford X-Max 150). Crystal orientation analysis was studied by EBSD (Oxford HKL). Isotope mapping technique for oxygen was applied by an isotope microscope (Cameca ims-1270 + SCAPS).

The chondrule studied here has 1.4 millimeters in diameter and Mg-rich (type I) porphyritic texture mainly composed of forsterite, low-Ca pyroxene and feldspathic mesostasis. The chondrule is surrounded by rim that shows an evidence of igneous process with the thickness of up to 400 micrometers. The rim is mostly composed of ferromagnesian olivine and also contains low-Ca pyroxene, high-Ca pyroxene, Fe-Ni metal and sulfide. The Fe-rich olivine grains often show Fe-Mg zoning, suggesting that diffusional Fe-Mg exchange has occurred during metamorphism on the parent body.

In this study, seven O-16-rich olivine grains with 10-30 micrometers in diameter were found in the igneous rim. O-16-enrichments are observed in core of the olivine crystals. The oxygen isotope heterogeneity and the chemical composition are not correlated. This result suggests that these O-16-rich parts are relict and overgrown by O-16-poor olivine crystallized from melt during rim formation.

The existence of O-16-rich olivine in the rim from CV chondrite indicates that both O-16-rich and O-16-poor materials exist in the chondrule formation region.

Keywords: chondrule rim, chondrule, oxygen isotopes, carbonaceous chondrite, SIMS

Japan Geoscience Union Meeting 2014
(28 April - 02 May 2014 at Pacifico YOKOHAMA, Kanagawa, Japan)

PPS25-08 Room:213 Time:May 2 11:00-11:15

Internal structure of chondrules and their possible origin

TAKAHASHI, Eiichi[1*] ; NAKAMOTO, Taishi[1]

[1]Earth & Planetary Sciences, Tokyo Institute of Technology

In order to clarify 3D shapes and internal structure of chondrules in Allende chondrite, we have separated 180 chondrules grains and investigated them with X-ray CT apparatus (Scan Xmate-D180RSS270) recently installed at the Museum of Natural History, Tohoku University (Tsuda et al., JPGU 2013). We also developed an optical device to measure 3D shape of chondrules or other spherical objects (Nishida et al. JPGU 2013). Our results revealed that chondrules shapes show wide distribution consisting of true spheres, prolate-spheres and oblate-spheres. Chondrules with porphyritic textures distribute in all shape categories. Chondrules with barred olivine texture (quenched from super-heated melt) show a distribution between true sphere and oblate-shape. Implication of the 3D shapes and internal texture of chondrules are consistent with the shock-wave heating model (e.g., Miura & Nakamoto, 2002, 2008).

Due to the density contrast, textures of Fe-FeS phase are most easily observed by X-ray tomography. By melting, coagulation and growth of Fe-FeS phase occur in chondrules. In some chondrules, coagulation resulted in mini-core formation (driven by surface energy minimization, see Fig.1). It is suggested that duration of heating episodes could be estimated by coagulation textures of Fe-FeS. If chondrules were formed by shock heating mechanism (e.g., Miura & Nakamoto, 2002, 2008), separation of molten silicate and coagulated Fe-FeS droplets would have taken place during acceleration and slow down of chondrules. Accordingly, significant chemical fractionation took place by dynamic processes during chondrules formation.

In X-ray CT images, many chondrules are surrounded by 50-200 micron thick rims. Coagulation and growth of Fe-FeS grains are observed in chondrules-rims as well as inside of chondrules indicating that temperature may have exceeded ˜1000C (eutectic point in the Fe-FeS) in the chondrule-rims. The common appearance of growth texture of Fe-FeS grains supports high-temperature origin of chondrule-rims rather than metasomatic origin. Clear textural distinction between chondrules and their ambient rims may correspond with presence or absence of melting in silicates. Most abundant element that volatilized below 1000C is sulfur. It is suggested that sulfur would have acted as a glue to coagulate dust particles onto molten droplets (chondrules) during shock heating episodes.

Keywords: meteorite, chondrule, texture, origin, X-ray CT

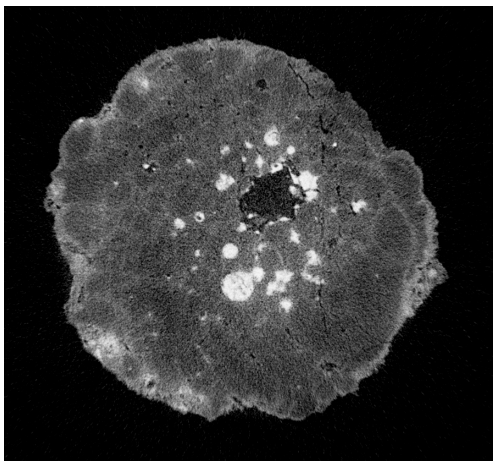

Japan Geoscience Union Meeting 2014
(28 April - 02 May 2014 at Pacifico YOKOHAMA, Kanagawa, Japan)

PPS25-09 Room:213 Time:May 2 11:15-11:30

Artificial cosmic spherules produced by heating and quenching experiments

GONDO, Takaaki[1*] ; ISOBE, Hiroshi[1]

[1]Grad. Sch. Sci. Tech., Kumamoto Univ.

Micrometeorites (MMs) are extraterrestrial fine particles derived from asteroids and comets and continuously falling to the Earth. Depending on their velocity, mass and entry angle, micrometeorites have undergone various degrees of heating during the atmospheric entry within a few seconds. This heating lead to significant textural, mineralogical and chemical modifications to MMs. The MMs larger them 70 micron meters in diameter show variously melted textures. In particular, completely melted micrometeorites are known as cosmic spherules. Cosmic spherules have experienced large degrees of melting of primary phases during atmospheric entry, and form molten droplets. In this study, we carried out rapid heating and quenching experiments on fine particles of three kinds of meteorites (CV, CM and H chondrite) to reproduce cosmic spherules by atmospheric entry.

The run products of meteorites as starting materials show quite analogous textures to cosmic spherules including porphyritic olivine and barred olivine. The most of molten particles show spherical shape due to surface tension of the silicate melt. The outside shape of the particles is various depending on melt fraction of the particle. We successfully reproduced artificial cosmic spherules with remarkably analogous textures to natural ones. We can compare textural variations of cosmic spherules to run products and possible precursors of cosmic spherules. Analogy of the run products to cosmic spherules can be applied from textural, mineralogical and chemical modifications during atmospheric entry to estimate abundance of the interplanetary fine particles in the vicinity of the Earth’s orbit.

Keywords: micrometeorite, carbonaceous chondrite, H chondrite, atmospheric heating, cosmic spherule

Japan Geoscience Union Meeting 2014
(28 April - 02 May 2014 at Pacifico YOKOHAMA, Kanagawa, Japan)

PPS25-10 Room:213 Time:May 2 11:30-11:45

Experimental reproduction of microtexutures of chondrules and CAIs by reducing-gas levitation technique

SETO, Yusuke[1*] ; ICHIMURA, Shun[1] ; MATSUNO, Junya[2] ; TAKAHASHI, Ryohei[2] ; TSUCHIYAMA, Akira[2] ; KOHARA, Shinji[3]

[1]Kobe Univ. Sci., [2]Kyoto Univ. Sci., [3]JASRI

Chondrules are the most abundant component in chondrites. They are mm-sized round (or irregularly) shaped particles mainly composed of silicates, which formed by the rapid cooling of droplets of molten or partially molten rock in space before they accreted. They show unique and diverse internal micro-textures (e.g., porphyritic olivine, barred olivine, radial pyroxene, etc.), even if they have same bulk compositions. These internal textures, therefore, should reflect not only stating material compositions, but also nebular conditions, such as gas species and their partial pressures, heating and cooling rate. CAIs are another major component in chondrites, which are also known to show the evidence of molten and quenching textures. The conditions of chondrule formation, however, remain poorly constrained, because the reproduction of the chondrule formation processes in a laboratory is experimentally difficult, especially in terms of container-less arrangement and reducing (low-fO_2) ambient. In the present study, we conducted gas-levitation and laser heating experiments in order to reproduce micro-textures of chondrules and CAIs, and constrain their formation conditions.

As stating materials, we used (i) natural olivine (Fo_{90}) from San Carlos, USA, (ii) matrices of Murchison CM meteorite, and (iii) mixed compounds of melilite ($Ca_2Al_2SiO_7$) + spinel ($MgAl_2O_4$) which are analogue to CAIs. The molten-quenched droplets of these samples were obtained using the gas-levitation and laser-heating experiments, which avoided both contamination of the molten samples and heterogeneous nucleation by crucible surfaces, at SPring-8 BL04B2. 1-2 mm-sized droplets were heated by a continuous-wave CO_2 laser, and were levitated in 96% Ar + 4% H_2 gas to achieve reducing ambient. The temperature during heating was monitored by a pyrometer. Surfaces and internal textures of the recovered samples were analyzed using SEM-EDX and -EBSD (JEOL, JSM-6480LAII and JSM-7100F).

(i) As a result of experiments using San Carlos olivine, olivine was re-crystallized under any condition. They show micro-porphyritic texture consisting of fine grained (1 to 5 μm) olivine, which are equal in composition to the starting material. Magnetite (Fe_3O_4) or hematite (Fe_2O_3) was completely absence, which suggests the low fO_2 (at least MFQ buffer) was maintained during the present experiments. (iii) The recovered sample of Murchison CM chondrite shows barred-olivine like texture. The platy (10 μm thickness) olivine crystals (Fa_{20-40}) are embedded in a FeO-SiO_2-rich glass. Idiomorphic fine (1 μm) magnetite are also observed in the glass. EBSD analyses revealed that most of the olivine plates are normal to b-axis, and the crystallographic orientations in a parallel platelet domain are identical. (iii) As a result of experiments using melilite and spinel compounds, dendritic spinel was always crystallized from surfaces to core irrespective of sample size and cooling rates, and they are embedded in Al-rich glass phase. The demonstrations of the present study show that reducing-gas levitation experiments is a powerful technique to simulate the molten-quenched texture of early solar materials.

Keywords: Chondrule formation, Molten-quenched texture, Crystal growth, Containerless heating, Barred olivine

Japan Geoscience Union Meeting 2014
(28 April - 02 May 2014 at Pacifico YOKOHAMA, Kanagawa, Japan)

PPS25-11 Room:213 Time:May 2 11:45-12:00

A unique lithology in the NWA 1232 CO3 chondrite containing clasts of different metamorphic grades

MATSUMOTO, Megumi[1*] ; TOMEOKA, Kazushige[2] ; SETO, Yusuke[2] ; YAMAMOTO, Yukiko[2] ; UMEHARA, Mariko[2] ; MIYAKE, Akira[3] ; HAMANE, Daisuke[4]

[1]CSREA, Kobe Univ., [2]Graduate School of Science, Kobe Univ., [3]Graduate School of Science, Kyoto Univ., [4]ISSP, Tokyo Univ.

Northwest Africa 1232 (NWA 1232) is a CO3 carbonaceous chondrite consisting of three lithologies (A, B, and C) that went through different thermal histories [1,2]. Kiriishi et al. [3] found that lithology A contains many small clasts (100-400 micron in diameter) scattering throughout the lithology. These small clasts typically consist of one chondrule surrounded by matrix and show little evidence of thermal metamorphism. Such unique lithology has not been known in other CO3 chondrites and potentially provides new insights into the formation of CO3 chondrites. Here we report the results of detailed mineralogical and petrological study of NWA 1232. The study was performed using SEM-EDS, TEM (STEM)-EDS, EPMA, and SR-XRD.

The thin section of NWA 1232 studied consists of lithologies A (738 mm^2), B (624 mm^2), and C (196 mm^2) that are separated by sharp boundaries. In lithology C, olivine phenocrysts in type I chondrules have relatively homogeneous compositions (Fa_{3-13}) and exhibit weak Fe-Mg zoning; these correspond to metamorphic grade 3.4. The matrix consists mainly of fine grained (100-500 nm in diameter) olivine that is relatively homogeneous in composition ($\sim Fa_{60}$). In lithology B, olivine phenocrysts are more Fe-rich (Fa_{19-42}) and exhibit distinct Fe-Mg zoning; these correspond to metamorphic grade 3.7. The matrix is mainly composed of relatively coarse-grained ($>$500 nm in diameter) olivine that is very homogeneous ($\sim Fa_{40}$).

In contrast, chondrules and matrix in lithology A exhibit considerable chemical and textural diversities. Olivine phenocrysts in chondrules vary widely in composition from Fa_1 to Fa_{43}. Most of Mg-rich olivine phenocrysts in Mg-rich chondrules show almost no Fe-Mg zoning; these are similar to those in CO 3.0 chondrites. Their surrounding matrix consists mainly of very fine-grained Mg-Si-Fe-rich amorphous material. On the other hand, most of Fe-rich phenocrysts in Fe-rich chondrules show distinct Fe-Mg zoning and their surrounding matrix consists mainly of coarse-grained ($>$500 nm in diameter) Fe-rich ($\sim Fa_{40}$) olivine; these are similar to those in highly metamorphosed CO 3.7 chondrite. There are also many other chondrules whose olivine phenocrysts have compositions intermediate between the Mg-rich and Fe-rich olivines described above. The matrix surrounding these chondrules mainly consist of fine-grained (100-500 nm in diameter) Fe-rich olivine similar to those mildly metamorphosed CO chondrites.

The chemical and textural heterogeneities observed in lithology A cannot be explained by thermal metamorphism of a single lithology. The results suggest that lithology A is composed of many clasts that underwent various degrees of thermal metamorphism in different locations of the parent body. The results further imply that CO chondrites had once experienced various degrees of thermal metamorphism in different locations in the parent body and subsequently went through extensive brecciation and mixing.

References: [1] Kiriishi and Tomeoka (2008), JMPS, 103, 161?165. [2] Umehara et al. (2009), JAMS Annual Meeting (abstract). [3] Kiriishi et al. (2009), JAMS Annual Meeting (abstract).

Keywords: CO chondrite, thermal metamorphism, brecciation, clast, TEM, SR-XRD

Japan Geoscience Union Meeting 2014
(28 April - 02 May 2014 at Pacifico YOKOHAMA, Kanagawa, Japan)

PPS25-12 Room:213 Time:May 2 12:00-12:15

Hydrothermal alteration experiments of the Allende meteorite

IIKUNI, Tsuneyuki[1*] ; TOMEOKA, Kazushige[1] ; SETO, Yusuke[1]

[1]Graduate school of Science, Kobe University

Among the processes that have affected early cosmic materials including carbonaceous chondrites, water perhaps played the most significant role in the chemical and mineralogical evolution of a range of small asteroidal bodies, by modifying the primary mineralogical characteristics of precursor materials. The obvious effect of aqueous alteration is the formation of secondary phases, such as serpentine and smectite. The diversity in alteration assemblages among various chondrites likely reflect the aqueous environment (e.g., temperature, dissolved ion, duration, water/rock ratio, fO_2, etc.) of the parent bodies. Although several hydrothermal experiments were made on olivine or pyroxene as starting materials[#1−#2], little is known about the actual behavior of chondrite toward aqueous fluid[#3]. Here we report hydrothermal alteration experiments of Allende meteorites.

We use Allende meteorites as starting materials. In order to observe micro-textures before and after alterations, we cut out block-shaped samples (2.5 mm×2.5 mm×6 mm) and never crushed. Hydrothermal alteration experiments were performed with PTFE double-vessels (1 ml and 25 ml) loaded into a steel autoclave. In order to maintain a reducing ambient, H_2 gas was generated in the outer vessel by reaction with HCl and magnesium,. All experiments were carried out at temperature of 200 deg.C, where the saturated vapor pressure reaches about 15 bar. As to reaction fluids, we use different pH solution (7, 8.5, 10, 14)[#4] with different water/rock (W/R) ratios (0.5, 2, 8 vol./vol.)[#5]. All run durations are 168 hours. Recovered products were analyzed by synchrotron X-ray diffraction (SR-XRD), scanning electron microscope (SEM) equipped with an energy-dispersive X-ray spectrometer (EDS).

As the results, except for condition of pH 7 and W/R 0.5, serpentine is observed in matrix, which formed at interstitial space of olivine grains of the matrix. As pH value increases, more abundance of matrix olivine are replaced by serpentine. Smectite is observed only under the condition of pH 14 and W/R 0.5. Calcite ($CaCO_3$) is formed on the sample surface under almost all conditions. Under pH 7 condition, anhydrite ($CaSO_4$) is also formed on the sample surface. The results of this study indicate that hydrated mineral formation easily proceeds compared with the previous studies where olivine or pyroxene were used as starting materials.

#1 Ohnishi and Tomeoka (2007) MPS, 42, 49-61. #2 Iishi and Han (2000) Neues Jahrbuch Fur Mineralogie-Monatshefte 2:49-59. #3 Jones and Brearley (2006) GCA, 70, 1040-1058. #4 Zolensky et al. (1989) Icarus, 78, 411-425. #5 Clayton and Mayede (1998) GCA, 63, 2089-2104.

Keywords: carbonaceous chondrite, hydrothermal experiments, hydrated minerals, Allende

Japan Geoscience Union Meeting 2014
(28 April - 02 May 2014 at Pacifico YOKOHAMA, Kanagawa, Japan)

PPS25-13 Room:213 Time:May 2 12:15-12:30

Electron Holography Reveals Nanometer Scale Magnetic Structure of Framboidal Magnetite and its Formation Process

KIMURA, Yuki[1*] ; SATO, Takeshi[2] ; NAKAMURA, Tomoki[1] ; NAKAMURA, Norihiro[1] ; NOZAWA, Jyun[3] ; TSUKAMOTO, Katsuo[1] ; YAMAMOTO, Kazuo[4]

[1]Tohoku University, [2]Hitachi High-Technologies Corporation, [3]Tohoku University, [4]Japan Fine Ceramics Center

Small solar system bodies were formed as agglomerates of dust and ices 4.6 billion years ago. Several million years after asteroid formation [1], the ice melted due to radioactive heating inside the larger asteroids [2] and/or highly energetic impacts [3]. Then, water plays several major roles in the chemistry of asteroids, both in mineralization and in the formation of organic compounds. Currently, bulk liquid water no longer exists in meteorites. We see only the signature of water in ancient asteroids as veins of hydrothermally deposited minerals [4] or water trapped in salt crystals [5] in meteorites. The Tagish Lake meteorite, which is a unique Type 2 carbonaceous chondrite, has a signature of aqueous process in the matrix that is abundant micrometer-sized polyhedral particles of magnetite [6]. The framboids are three-dimensionally ordered colloidal crystals of magnetite nanoparticles. The uniformity of the size distribution and the similar morphology of the magnetite nanoparticles in each of the colloidal crystals suggest that they were formed through homogeneous nucleation from a highly supersaturated isolated solution in a single nucleation event.

Here we show evidence of how magnetite nanoparticles assembled into periodic structures based on a nanometer scale paleomagnetic method using electron holography in an examination of the framboidal magnetite in the Tagish Lake carbonaceous chondrite [7]. An attractive force such as magnetism never contributes to the formation of colloidal crystals [8], but the repulsive force caused by the surface charge of the magnetite is able to work. To overcome the repulsive force, the density of magnetite nanoparticles in a solution must be sufficiently high in an isolated solution as a water droplet parches in microgravity. We used electron holography to visualize the magnetization of the meteoritic minerals for the first time and found that magnetite grains in the framboid have no external magnetic force, i.e., they have a flux-closure vortex structure, which allowed the formation and preservation of the colloidal crystals. We conclude that these framboids formed in tiny water droplets with pH of 7-12 containing ions such as Ca^{2+} and Mg^{2+} at levels of 10^{-14}-10^{-15} mol m^{-2}, just before exhaustion of water during thermal alteration in a hydrous asteroid.

[1] Fujiya, W., Sugiura, N., Hotta, H., Ichimura, K. & Sano, Y. Evidence for the late formation of haydrous asteroids from young meteoritic carbonates. *Nature Communications* **3**, 627 (2012).

[2] Endress, M., Zinner, E. & Bischoff, A. Early aqueous activity on primitive meteorite parent bodies. *Nature* **379**, 701-703 (1996).

[3] Rubin, A. F. Collisional facilitation of aqueous alteration of CM and CV carbonaceous chondrites. *Geochim. Cosmochim. Acta* **90**, 181-194 (2012).

[4] Tomeoka, K. Phyllosilicate veins in a CI meteorite: evidence for aqueous alteration on the parent body. *Nature* **345**, 138-140 (1990).

[5] Zolensky, M. E. *et al*. Asteroidal water within fluid inclusion-bearing halite in an H5 chondrite, Monahans (1998). *Science* **285**, 1377-1379 (1999).

[6] Nozawa, J. et al. Magnetite 3-D Colloidal Crystals Formed in the Early Solar System 4.6 Billion Years Ago, *Journal of the American C* **133**, 8782-8785(2011).

[7] Kimura, Y. et al. Vortex magnetic structure in framboidal magnetite reveals existence of water droplets in an ancient asteroid, *Nature Communications*, **4** (2013) 2649 doi: 10.1038/ncomms3649.

[8] Philipse, A. P. & Maas, D. Magnetic colloids from magnetotactic bacteria: chain formation and colloidal stability. *Langmuir* **18**, 9977-9984 (2002).

Keywords: Magnetite, Electron holography, Tagish Lake meteorite

Japan Geoscience Union Meeting 2014
(28 April - 02 May 2014 at Pacifico YOKOHAMA, Kanagawa, Japan)

PPS25-14 Room:213 Time:May 2 12:30-12:45

C-XANES analyses of carbonaceous solid inclusions from Monahans halite

KEBUKAWA, Yoko[1*] ; ZOLENSKY, Michael[2] ; KILCOYNE, David[3] ; RAHMAN, Zia[4] ; FRIES, Marc[2] ; CODY, George[5]

[1]Department of Natural History Sciences, Hokkaido University, [2]NASA Johnson Space Center, [3]Lawrence Berkeley National Laboratory, [4]Jacobs-Sverdrup, [5]Geophysical Laboratory, Carnegie Institution of Washington

Monahans meteorite (H5) contains fluid inclusion-bearing halite (NaCl) crystals [1]. Microthermometry and Raman spectroscopy showed that the fluid in the inclusions is an aqueous brine and they were trapped near 25^{o}C [1]. Their continued presence in the halite grains requires that their incorporation into the H chondrite asteroid was post metamorphism [2]. Abundant solid inclusions are also present in the halites. The solid inclusions include abundant and widely variable organics [2]. Analyses by Raman microprobe, SEM/EDX, synchrotron X-ray diffraction and TEM reveal that these grains include macromolecular carbon similar in structure to CV3 chondrite matrix carbon, aliphatic carbon compounds, olivine (Fo_{99-59}), high- and low-Ca pyroxene, feldspars, magnetite, sulfides, lepidocrocite, carbonates, diamond, apatite and possibly the zeolite phillipsite [3]. Here we report organic analyses of these carbonaceous residues in Monahans halite using C-, N-, and O- X-ray absorption near edge structure (XANES).

Approximately 100 nm-thick sections were extracted with a focused ion beam (FIB) at JSC from solid inclusions from Monahans halite. The sections were analyzed using the scanning transmission X-ray microscope (STXM) on beamline 5.3.2.2 at the Advanced Light Source, Lawrence Berkeley National Laboratory for XANES spectroscopy. C-XANES spectra of the solid inclusions show micrometer-scale heterogeneity, indicating that the macromolecular carbon in the inclusions have complex chemical variations. C-XANES features include 284.7 eV assigned to aromatic C=C, 288.4-288.8 eV assigned to carboxyl, and 290.6 eV assigned to carbonate. The carbonyl features obtained by C-XANES might have been caused by the FIB used in sample preparation. No specific N-XANES features are observed. Various degrees of 1s-$\sigma*$exciton shown in the C-XANES spectra indicate that the solid inclusions contain macromolecular carbon which experienced various degree of thermal processing. The natures of the macromolecular carbon in the solid inclusions observed by C-XANES are consistent with the previous studies showing that the solid inclusions have not originated from Monahans parent body [1-3].

References: [1] Zolensky et al. 1999. Science 285: 1377-1379. [2] Fries et al. 2011. 74th MetSoc #5390. [3] Zolensky et al. 2013. 76th MetSoc #5200.

Keywords: C-XANES, Halite, Carbon, Chondrite, Organic matter

Japan Geoscience Union Meeting 2014
(28 April - 02 May 2014 at Pacifico YOKOHAMA, Kanagawa, Japan)

PPS25-15 Room:213 Time:May 2 14:15-14:30

3D shapes of Itokawa regolith particles: comparison with lunar regolith particles

TSUCHIYAMA, Akira[1*] ; MATSUSHIMA, Takashi[2] ; MATSUMOTO, Toru[3] ; NAKANO, Tsukasa[4] ; MATSUNO, Junya[1] ; SHIMADA, Akira[3] ; UESUGI, Kentaro[5] ; TAKEUCHI, Akihisa[5] ; SUZUKI, Yoshio[5] ; OHTAKE, Makiko[6] ; NAKAMURA, Tomoki[7] ; UESUGI, Masayuki[6] ; YADA, Toru[6] ; NISHIIZUMI, Kunihiko[8]

[1]Graduate School of Science, Kyoto University, [2]Graduate School of Systems and Information Engineering, [3]Graduate School of Science, Osaka University, [4]AIST/GSJ, [5]JASRI/SPring-8, [6]JAXA/ISAS, [7]Graduate School of Science, Tohoku University, [8]Space Sciences Laboratory, University of California

Regolith particles were returned from the surface of asteroid Itokawa by the Hayabusa spacecraft. The sample analysis elucidated a variety of surface processes on the asteroid (e.g., [1]): (1) Formation of regolith by impacts of small objects, with selective escape of the finest-scale particles. (2) Implantation of solar wind into the uppermost particle surfaces and formation of space-weathering rims. (3) Grain abrasion, probably due to seismic-induced particle motion. Processes (5) and (6) might have been repeated. (7) Final escape of particles from the asteroid by impact within the past 8 million years (1-3 million years [3]).

During the course of the analysis, 3D size and shape features of the Itokawa particles were obtained by SR-based x-ray microtomography to understand the origin and evolution of the regolith particles on Itokawa ' s surface [2,3]. In particular, the particle shape distribution with respect to their three-axial ratios was obtained and compared with that of fragments formed by high-speed impact in laboratory experiments [4,5] and of lunar regolith samples [6]. The 3D shapes of the lunar samples have been examined by tomography [6] but not grain-by-grain as performed for the Itokawa samples. In addition, the procedure for measuring the three axial lengths was different between the regolith particles and the impact fragments: the former was obtained from 3D external particle shapes by ovoid approximation [2,3,6], while the latter by bounding box method using a calliper [4,5]. In order to make strict comparison between them, lunar regolith particles were examined by the same method as the Itokawa particles, and the three axial lengths were measured from the tomography data by bounding box method that was newly developed in the present study.

The 3D shapes of 70 particles from 105-250 μm sieved fraction of Descartes highland (60501) and 74 particles from $<$1 mm sieved fraction of Mare Tranquillitatis (10084) were obtained by microtomography at BL47XU of SPring-8. Furthermore, the 3D shapes of new 24 Itokawa particles (3 of them are from Dr. M. Meier, personal communication) were also examined in addition to the previous 48 particles [3]. The three axial lengths were measured in the orders of short to long and long to short axes to compared with the data of [3] and [4], respectively. The shape distribution in a Zingg diagram was compared using the Kolmogorov-Smirnoff test.

The shape distribution of the Itokawa particles cannot be distinguished from that of the impact fragments of [4] but can be distinguished from that of [3]. This may suggest that the Itokawa particles resulted from mechanical disaggregation, as a response to impacts with a specific condition. In contrast, the shape distribution of the lunar regolith particles can be distinguished from that of the Itokawa particles and the impact fragments although lunar regolith is the product of impact on the lunar surface. The lunar particle shapes are more equant than the others. The both lunar samples examined are matured (Is/FeO = 80 and 78 for 60501 and 10084, respectively [7]). These regolith particles should become equant from the shapes similar to the impact fragments by mechanical disaggregation or abrasion due to repeated impacts during a long residence time in the regolith layer although a specific process for the shape change is not known.

[1] Tsuchiyama (2013) Elements, 10: in print. [2] Tsuchiyama et al. (2011) Science, 333: 1125. [3] Tsuchiyama et al. (2013) Meteor. & Planet. Sci., 1-16. doi: 10.1111/maps.12177. [4] Fujiwara et al. (1978) Nature 272: 602. [5] Capaccioni et al. (1984) Nature 308: 832. [6] Katagiri (2010) Proc. 12th Internat. Conf. Engin., Sci., Constr., Operat. in Challeng. Environ., 254?259. [7] Morris et al. (1978) Proc. Lunar Planet. Sci. Conf., 9th, 2287.

Keywords: Hayabusa mission, particle shape, SPring-8, x-ray tomography, Apollo mission, impact

Japan Geoscience Union Meeting 2014
(28 April - 02 May 2014 at Pacifico YOKOHAMA, Kanagawa, Japan)

PPS25-16 Room:213 Time:May 2 14:30-14:45

Surface micromorphology of regolith particles from Asteroid Itokawa: Implication for space weathering of regolith

MATSUMOTO, Toru[1*] ; TSUCHIYAMA, Akira[2] ; MIYAKE, Akira[2] ; NOGUCHI, Takaaki[3] ; NAKAMURA, Tomoki[4] ; NAKAMURA, Michihiko[4] ; MATSUNO, Junya[2] ; SHIMADA, Akira[1] ; UESUGI, Kentaro[5] ; NAKANO, Tsukasa[6]

[1]Osaka University, [2]Kyoto University, [3]Ibaraki University, [4]Tohoku University, [5]JASRI/SPring-8, [6]GSJ/AIST

Spectral features of airless bodies are known to be modified by processes called space weathering. From Analysis of lunar samples, the space weathering is considered to be caused by mainly nano phase iron (npFe^0) formed by mainly vapor deposition produced by micrometeorite bombardments and solar wind irradiation [1].Space weathering of asteroid is also considered to progress by mainly solar wind irradiation and micrometeorite bombardments [1]. Detailed Space weathering processes on asteroids are expected to be revealed by analysis of asteroidal regolith samples. Hayabusa spacecraft recovered regolith particles from S-type asteroid 25143 Itokawa. In previous study, implantation of solar wind to Itokawa regolith particles was detected by noble gas isotope analysis [2]. The space weathering rims including npFe^0 were observed on regolith particles using transmission electron microscopes [3][4]. Surface micromorphology of regolith particles are expected to have information to reveal space weathering processes related to surface activity on Itokawa and applied to. So far, general surface features of regolith particles have not yet been clearly understood. Therefore, this study investigates Itokawa regolith particles focusing on their surface micromorphology.

Three-dimensional (3D) external shapes of the regolith particles were analyzed by microtomography. Surface morphologies of the regolith particles were observed by field-emission scanning electron microscopy (FE-SEM). It is revealed that the regolith surfaces can be classified into fractured surfaces formed by impact and surfaces formed by condensation from vapor in microdruses of original chondritic materials. Regardless of these surface types, there are matured surfaces, which have rounded edges. The matured surfaces are considered to be formed by abrasion processes on Itokawa [5]. Internal structures of space weathering rim of regolith particles was observed by transmission electron microscopy (TEM/STEM) and this was compared with the surface morphologies of the same surface observed by FE-SEM. Observed space weathering rim have vesicles and form blister structures. The blisters can be identified by FE-SEM, indicating that space weathering rims with blisters can be observed by FE-SEM without any destructive methods. Space weathering processes related to the surface activities on Itokawa is considered from observation of blister distribution on the regolith particles. It is revealed that there is no correlation between blister distribution and the roundness of the surface morphologies, indicating that dominant mechanism of the abrasion process is not solar wind sputtering but mechanical abrasion. The abrasion processes can peel off the space weathering rims. In addition, there are heterogeneous distribution of blisters suggesting migration and fragmentation of regolith particles. Two distinct time-scales for the spectral reddening of S-type asteroids due to space weathering were proposed [7]: solar wind irradiation for about 10^6 years and micrometeorite bombardment for about 10^9 years. This study proposes that spectral change of Asteroid Itokawa by space weathering would have gradually occurred for 10^6 years at the latest by regolith activities on Asteroid Itokawa such as mechanical abrasion, migration and fragmentation of regolith particles, while space weathering rims are developed on local surface of individual regolith particles for 10^3-10^4 years[4].

[1]Clark B. E. (2002) Asteroid, 585-599. [2] Nagao K. et al. (2011) Science, 333, 1128-1131. [3] Noguchi T. et al. (2011) Science, 333, 1121-1125. [4] Noguchi T. et al. (2013) Met. Planet. Sci.27, 1-27 [5] Tsuchiyama A. et al. (2011) Science, 333, 1125-1128. [6] Matsumoto T. et al. (2013) LPSC XLIV, 1441. [7] Vernazza et al. (2009) Nature, 458, 993-995.

Keywords: Itokawa, regolith, space weathering

Japan Geoscience Union Meeting 2014
(28 April - 02 May 2014 at Pacifico YOKOHAMA, Kanagawa, Japan)

PPS25-17 Room:213 Time:May 2 14:45-15:00

Extraction and Identification of Primitive Grains Driven by Magnetic Volume Force.

HISAYOSHI, Keiji[1*] ; UYEDA, Chiaki[1]

[1]Institute of Earth and Space Science, Graduate School of Science, Osaka University

Magnetic volume force caused by a field gradient has been commonly used to extract ferro-(or ferri-) magnetic materials from weak magnetic materials. The separation was realized because the field-gradient forces that operated on the spontaneous magnetizations of the above category of materials were considerably large with respect to terrestrial gravity. It was considered that dynamic motion of a weak magnetic material generally require a strong field above B = 10T .

Primitive materials are generally obtained as an ensemble of grains with different elemental composition with heterogeneous origins. At an initial stage of investigating this type of material, it is important to extract and identify the material of individual particles included in the ensemble. Such method should be non-destructive and easily performed. Moreover, it should be based on a well-established physical or chemical concept. In the case of analyzing a fluid sample of organic molecules, the stage separation and identification has been established by introducing the technique of chromatography; such method has not been established as yet on mixture of solid samples. Here we propose a new principle of grain separation that is driven by magnetic volume force. By comparing the measured χ_{DIA} of a particle by their published values, material of the particle is identified. This is because an intrinsic χ_{DIA} value is assigned to a material.

Microgravity was generated using a compact drop shaft system, which can be introduced in an ordinary laboratory. The length of the shaft was 1.8m, and the duration of microgravity time was about 0.5 second. The sample is released in the field-gradient produced by a by a magnetic circuit composed by a NdFeB permanent magnet. Maximum field intensity of the circuit was 0.8 T. The experimental apparatus was set inside a rectangle box which had a size of 30x30x20cm. The vacuum chamber equipped with an electric actuator, sample releasing signal reception device, the sample holder controller, the magnet, the battery, and the high-vision video camera are installed in the above box. [1-3]

The present results achieved on sub-millimetre-sized diamagnetic grain have a large significance as a step to realize the extraction and identification of micron-sized grains that compose the primitive materials. The technique described is useful in the search for new types of pre-solar grains that are not identified as yet.

Reference

[1] K. Hisayoshi, S. Kanou and C. Uyeda : Phys.:Conf. Ser., 156 (2009) 012021.
[2] K. Hisayoshi, C. Uyeda, K. Kuwada, M. Mamiya and H. Nagai, : Phys.:Conf. Ser., 327 (2011) 012058.
[3] C. Uyeda, K. Hisayoshi, and S. Kanou : Jpn. Phys. Soc. Jpn. 79 (2010) 064709.

Keywords: magnetic ejection,, nondestructive identification, magnetic extraction, microgravity, translational motion, magnetic volume force

Japan Geoscience Union Meeting 2014
(28 April - 02 May 2014 at Pacifico YOKOHAMA, Kanagawa, Japan)

PPS26-01 Room:418 Time:April 30 09:00-09:15

Summay of the third stage of Next Decade Initiatives for Lunar Planetary Explorations

WATANABE, Sei-ichiro[1*]

[1]Dept. of Environmental Studies, Nagoya University

The Next Decade Initiatives for Lunar Planetary Explorations is now in the final phase of the third stage selection. The concept and progress of the third stage selection will be presented.

We have been discussed the mid-range (the next decade or two) future vision of planetary explorations providing the best mix of medium- to large-size flagship missions, small-size missions, and missions of opportunity for science payloads on foreign missions; the compelling concepts of the flagship missions that are central to the mid-range future vision, and strategy for unifying the planetary science community to the flagship missions. The final candidates for the flagship missions are (1) the lunar (or planetary) chronological mission based on the in-situ geochronology instruments, (2) the Mars lander and rover exploration with science payloads including the life-detection experiment system, and (3) the solar power sail mission for Trojan asteroids with cruising phase observation of the cosmic infrared background radiation. The selection committee are now reviewing the three mission concepts to polish up. I will report on the activity of the committee and discuss the relation to the ISAS's roadmap for space science approved by the Japanese Strategic Headquarter for Space Policy in September 2013.

Keywords: planetary science, Solar System exploration, Future missons

Japan Geoscience Union Meeting 2014
(28 April - 02 May 2014 at Pacifico YOKOHAMA, Kanagawa, Japan)

PPS26-02 Room:418 Time:April 30 09:15-09:30

A status report of future geospace satellite projects

MIYOSHI, Yoshizumi[1*] ; TERADA, Naoki[2] ; FUJIMOTO, Masaki[3]

[1]STEL, Nagoya University, [2]Graduate School of Science, Tohoku University, [3]ISAS/JAXA

In this presentation, we report several plans for future geospace exploration projects including magnetosphere and ionosphere, and discuss a possible roadmap for the future mission.

Keywords: future mission, solar-terrestrial physics, geospace exploration

Japan Geoscience Union Meeting 2014
(28 April - 02 May 2014 at Pacifico YOKOHAMA, Kanagawa, Japan)

PPS26-03 Room:418 Time:April 30 09:30-09:45

MELOS1 Mars Exploration for Life-Organism Search

SATOH, Takehiko[1*] ; KUBOTA, Takashi[1] ; FUJITA, Kazuhisa[1] ; YAMAGISHI, Akihiko[2] ; MIYAMOTO, Hideaki[3] ; HASHIMOTO, George[4] ; SENSHU, Hiroki[5] ; USUI, Tomohiro[6] ; KOMATSU, Goro[7] ; DEMURA, Hirohide[8] ; ISHIGAMI, Genya[9] ; OGAWA, Naoko[1] ; OKADA, Tatsuaki[1]

[1]Japan Aerospace Exploration Agency, [2]Tokyo University of Pharmacy and Life Sciences, [3]University of Tokyo, [4]Okayama University, [5]Chiba Institute of Technology, [6]Tokyo Institute of Technology, [7]Universita' d'Annunzio, [8]Aizu University, [9]Keio University

Mars exploration is uniquely significant as it includes all of "scientific", "engineering", and "exploration" importances almos equally. Visiting Mars is, therefore, an essential milestone to expand the frontier of human being. In this paper, as part of JSPS "next decade" activity, we discuss MELOS1 with view points of science and engineering.

The target of MELOS1 is direct detection of lives on Mars. It will be a simplified mission with just a rover plus a cruise stage, no orbiter at all. It may not be unreasonable to expect relay orbiters in Mars orbit when MELOS1 will arrive at the red planet as there are a number of mission plans from the U.S.A., Europe, and Russia.

The MELOS1 rover will weigh about 60 kg, equipped with a life-detection microscope (LDM) and meteorology sensors to monitor its environment. Details of LDM will be presented elsewhere. In brief, the LDM uses the highest possible sensitivity technique, dyeing cells with pigment and observe them by fluorescent light. This technique will give us 3 orders of magnitudes higher sensitivity of life detection than was done on Viking Landers.

If discovered, it should undoubtedly be the biggest discovery in science. The surface area of Mars is so wide and so different from one place to another. Yet, we had only 7 landers, basically at places similar to each other. The best places for life-detection experimetn, fluvial feasures or mud volcanoes (may be methane hot spots) are still intact. In MELOS1, we will perform high-precision landing to such a place and will search for lives for the first time. The current status of planning will be presented. In addition, the position in Japan's future missions will be discussed with

audience of greater variety.

Keywords: Mars, exploration, landing, life, rover

Japan Geoscience Union Meeting 2014
(28 April - 02 May 2014 at Pacifico YOKOHAMA, Kanagawa, Japan)

PPS26-04 Room:418 Time:April 30 09:45-10:00

Lunar chronological mission based on the in-situ geochronology instruments

MOROTA, Tomokatsu[1*] ; SUGITA, Seiji[2] ; CHO, Yuichiro[2] ; MIURA, Yayoi N.[2] ; WATANABE, Sei-ichiro[1] ; OHTAKE, Makiko[3] ; KOBAYASHI, Naoki[3] ; KAROUJI, Yuzuru[3] ; FURUMOTO, Muneyoshi[1] ; HONDA, Chikatoshi[4] ; SUGIHARA, Takamitsu[5] ; ISHIHARA, Yoshiaki[3] ; ISHIBASHI, Ko[6] ; ARAI, Tomoko[6] ; TAKEDA, Hiroshi[2] ; TERADA, Kentaro[7] ; KAMATA, Shunichi[8] ; SAIKI, Kazuto[7] ; KOBAYASHI, Shingo[9] ; KAMEDA, Shingo[10] ; YOSHIOKA, Kazuo[3] ; OKAZAKI, Ryuji[11] ; NAMIKI, Noriyuki[6] ; KOBAYASHI, Masanori[6] ; OHNO, Sohsuke[6] ; SENSHU, Hiroki[6] ; WADA, Koji[6] ; TACHIBANA, Shogo[8] ; TANAKA, Satoshi[3] ; MUKAI, Toshifumi[3]

[1]Nagoya Univ., [2]Univ. Tokyo, [3]JAXA, [4]University of Aizu, [5]JAMSTEC, [6]Chiba Institute of Technology, [7]Osaka Univ., [8]Hokkaido Univ., [9]NIRS, [10]Rikyo Univ., [11]Kyushu Univ.

In-situ geochronology measurements have long been a key goal for planetary science.We propose a mission, which is designed to determine formation age of young Aristillus crater of the Moon. The correlation of crater frequency measured with remote-sensing data with the obtained age provides information about the cratering history in the inner solar system.

Keywords: Lunar and Planetary explorations, Moon, chronology, crater, K-Ar dating

Japan Geoscience Union Meeting 2014
(28 April - 02 May 2014 at Pacifico YOKOHAMA, Kanagawa, Japan)

PPS26-05 Room:418 Time:April 30 10:00-10:15

Applicability of a laser-ablation in-situ K-Ar dating method on the Moon: insights from lunar samples

CHO, Yuichiro[1*] ; MIURA, Yayoi N.[2] ; MOROTA, Tomokatsu[3] ; SUGITA, Seiji[4]

[1]Department of Earth and Planetary Science, University of Tokyo, [2]Earthquake Research Institute, University of Tokyo, [3]Nagoya University, [4]Department of Complexity Science and Engineering, University of Tokyo

We have been developing an in-situ K-Ar isochron dating method for future landing missions. Potassium-argon ages are measured with the combination of laser-induced breakdown spectroscopy (LIBS) and mass spectrometry using a quadrupole mass spectrometer (QMS). In our previous studies, we reported that isochron ages for gneiss samples with 30% accuracy and 10-20% precision.

However, such experimental results using test samples do not guarantee the applicability of our LIBS-QMS isochron method for actual rock samples on planetary surfaces. Depending on geologic units, the types of rocks and K concentration vary greatly on planetary surfaces.

Thus, we assess the capability of our in-situ K-Ar dating method taking the petrologic properties including K abundance and possible age range of the lunar surfaces into account. First, we examined the global maps of K obtained with the Gamma Ray Spectrometers onboard remote sensing satellites. We found that the concentrations of K and Ar of KREEPy materials are well above the detection limits of our LIBS-QMS approach. Then, the elemental compositions and textures of KREEP basalt were investigated. We found that Si-rich glasses contained in mesostasis are measurable with K-Ar dating on the Moon because of the high K concentration (˜7 wt%), while other minerals (i.e., pyroxene, olivine, and plagioclase) contain virtually no K. Since the textures of these samples were heterogeneous at the scale of laser spot (˜500 microns), the ”isochron” ages would be obtained by measuring the different portions containing K-bearing phases in various ratios.

The major problem concerning in-situ K-Ar dating is partial 40Ar loss due to thermal events after crystallization. This suggests that K-Ar dating only yields the lower limit for the real crystallization age. Furthermore, brecciation by impacts and contamination by solar wind will inhibit accurate in-situ dating. In order to avoid such problems and obtain meaningful age data by in-situ dating, we aim to measure fresh impact melt rocks exposed by a very recent (tens of Ma) impact on the Aristillus crater floor.

Finally, we evaluated how our method can constrain the absolute chronology models of the Moon and Mars based on the precisions of age measurements achieved by this study. For example, the absolute age of impact melt rocks in Aristillus crater, whose ages correspond to the ”missing ages” of the current lunar crater chronology model (i.e., between 3.0 Ga and 0.1 Ga), would be measured with ˜20% precision when the K concentration of the glass in KREEP basalt is assumed. Then, our method would be able to discriminate the constant flux model [Neukum, 1983] and the decreasing flux model [Hartmann et al., 2007]. The implications of in-situ dating in Aristillus crater include refining the crater chronology model, determining the age of the youngest mare basalts, and understanding the dynamical evolution of the asteroids in the last three billion years.

Japan Geoscience Union Meeting 2014
(28 April - 02 May 2014 at Pacifico YOKOHAMA, Kanagawa, Japan)

PPS26-06 Room:418 Time:April 30 10:15-10:30

Exploration of Jovian Trojan asteroids by Solar Power Sail

NAKAMURA, Ryosuke[1] ; SEKINE, Yasuhito[2*] ; MATSUURA, Shuji[3] ; YANO, Hajime[3] ; MORI, Osamu[3] ; SOLAR SAIL, Working group[3]

[1]AIST, [2]Universit of Tokyo, [3]JAXA

Solar Power Sail is a novel concept with hybrid propulsion of large-area solar sail and ion engine driven by thin-film solar panel. It enables us to bring relatively large mission payloads to the outer solar system without nuclear technology. The Solar Power Sail spacecraft is currently planned in Japan to explore Jovian Trojan astereoids. There exist two competing hypotheses on their origin. The classic model suggests that Trojan asteroids are mainly survivors of building blocks of the Jupiter system, while NICE model claims that they must be intruders from outer regions after the planetary migration of gas planets settled. This mission will provide invaluable clues to the genesis of the planets, asteroids ana comets through remote sensing, in-situ sample analysis and comparison of the results with other small body missions, such as Dawn, Rosetta, Osiris-ReX and Hayabusa-2. Another target of this mission is novel astronomy; measurement of the infrared extragalactic background light without foreground contamination of the zodiacal light thanks to low-density environment at deep space, polarization measurement of the gamma-ray burst and accurate determination of its direction based on the interplanetary network technique. The Solar Power Sail mission will thus develop a new direction of space astronomy and planetary science providing us an interplanetary telescope site and will play an important roll to form a new interdisciplinary science field.

Keywords: Jupiter, Trojan, asteroids, exploration, Solar Sail

Japan Geoscience Union Meeting 2014
(28 April - 02 May 2014 at Pacifico YOKOHAMA, Kanagawa, Japan)

PPS26-07 Room:418 Time:April 30 11:00-11:15

Current status of mission study for small scale planetary exploration in JSPS

ARAKAWA, Masahiko[1*]

[1]Graduate School of Science, Kobe University

Recent success of launching a new Japanese rocket named as Epsilon gives us a new chance for planetary exploration. So, we just begin to discuss a new planetary exploration mission suitable for this Epsilon rocket in Japanese Society of Planetary Science (JSPS) . Future planning section in JSPS has examined the small size mission for planetary exploration since last summer, and the special working group for this purpose in this section was organized to submit our report showing the scientific feasibility in a small size mission to a vice-president of JSPS. The final report is shown on the web-site of https://www.wakusei.jp/~shourai/wiki/epsilon/. A new load map for space science in Japan by JAXA was released last september, and it showed that the exploration of solar system would be planned in a small scale mission in order to overcome technical problems and develop new devices for the future planetary exploration planned after 10 years. According to this new load map related to planetary science, we have decided to discuss a future mission of small scale planetary exploration by using Epsilon rocket in JSPS fall meeting. We are going to hold a symposium to discuss a future plan regularly in 2014, and our symposium is open not only for JSPS member but also for every scientist and engineer who are interested in a small scale planetary exploration.

Keywords: Epsilon rocket, small scale planetary exploration

Japan Geoscience Union Meeting 2014
(28 April - 02 May 2014 at Pacifico YOKOHAMA, Kanagawa, Japan)

PPS26-08 Room:418 Time:April 30 11:15-11:30

This is what I learned from the development of EXCEED

YOSHIKAWA, Ichiro[1*]

[1]University of Tokyo

I will present my plan for the next 10-year instrumental development based on my heritage on the Sprint-A/EXCEED.

An earth-orbiting Extreme Ultraviolet (EUV) spectroscopy (EXCEED) is the first mission of the Small scientific satellite Platform for Rapid Investigation and Test -A (Sprint-A) conducted by ISAS/JAXA. A single science instrument (EXCEED) is boarded on Sprint-A. EXCEED has started to observe the solar planets in the EUV spectral range, and will extend to the identification of extrasolar planet atmosphere.

Keywords: Sprint-A, EUV, Planetary airglow

Japan Geoscience Union Meeting 2014
(28 April - 02 May 2014 at Pacifico YOKOHAMA, Kanagawa, Japan)

PPS26-09 Room:418 Time:April 30 11:30-11:45

Deep Space Explorer DESTINY

KAWAKATSU, Yasuhiro[1*]

[1]ISAS/JAXA

DESTINY which stands for "**D**emonstration and **E**xperiment of **S**pace **T**echnology for **IN**terplanetary vo**Y**age" is a mission candidate for the next space science small program. The next mission is planned to be decided in 2014, and the select one is scheduled to be launched in 2018.

As illustrated in the Figure, DESTINY will be launched by an Epsilon launch vehicle and firstly placed into a low elliptical orbit, where then its altitude raised by the use of ion engine. When the orbit raising reaches the Moon, DESTINY subsequently is injected into transfer orbit for L_2 Halo orbit of the Sun-Earth system by using lunar gravity assist. Upon arrived at L_2 Halo orbit, DESTINY will conduct its engineering experiment as well as scientific observations for at least a half year. If conditions permit, DESTINY will leave L_2 Halo orbit, and transfer to the next destination.

On the way to L_2 Halo orbit, DESTINY will conduct demonstration and experiment on key advanced technologies for future deep space missions. Major items of the technology demonstration are listed as follows.

1) High energy mission by Epsilon rocket.

We investigate appropriate rocket configurations and flight path designs, and evaluate the performance of Epsilon rocket to insert spacecrafts into high energy orbits. It provides basic data of Epsilon rocket application to deep space missions.

2) Ultra-Lightweight solar panel.

In order to generate large electric power to run μ20 ion engine, "Ultra-Lightweight Solar Panel", which is under development at JAXA, is applied and its performance is evaluated. This solar panel is estimated to achieve power to mass ratio at least double to conventional ones. Future application is expected in outer planet probes (JMO, MELOS) or probes with large ion engines.

3) Large scale ion engine μ20.

DESTINY is inserted into an elliptical orbit and reaches to a Halo orbit by its own orbital maneuver. For this maneuver, a large ion engine (μ20) which is under R&D at JAXA will be adopted and its performance is evaluated. This ion engine has thrust five times as much as μ10 used by Hayabusa and will be expected to be applied to large probes such as SOLAR-D or Hayabusa Mk2.

4) Advanced thermal control.

In order to manage large amount of heat generated by the large ion engine, advanced thermal control techniques by way of Loop Heat Pipe will be adopted.

5) Orbit determination under low thrust operation.

DESTINY will reach to Halo orbit by running ion engine over long duration. In order to reduce burdens to shut down the ion engine each time of orbit determinations, orbit determination under ion engine operation is conducted and its performance is evaluated.

6) Automatic/autonomous onboard operation.

In order to increase the efficiency of operation, autonomous and highly functioned spacecraft management system is developed demonstrated on board. This technique is expected to be adopted especially in the deep space missions usually operated under severe communication condition.

7) Halo orbit transfer and maintenance.

DESTINY will reach to Halo orbit and maintains the orbit more than one period. In order to reduce the risks of Halo orbit insertion and suppress the amount of orbital maneuvers, the orbit control technique using dynamical system theory is used and its operability is evaluated. This technique will be adopted in SPICA, which will be operated in Halo orbit.

DESTINY itself is an engineering experiment probe which destines L_2. However, its mission profile is naturally applied to lunar missions and escape missions by forking the profile at the lunar encounter. Moreover, the spacecraft's high astronautic performance makes its application to other launch method attractive, such as dual launch with GEO satellite or another deep space probe. The significance of DESTINY from the point of its opening new opportunities for low-cost deep space mission is discussed in the presentation as well.

PPS26-09 Room:418 Time:April 30 11:30-11:45

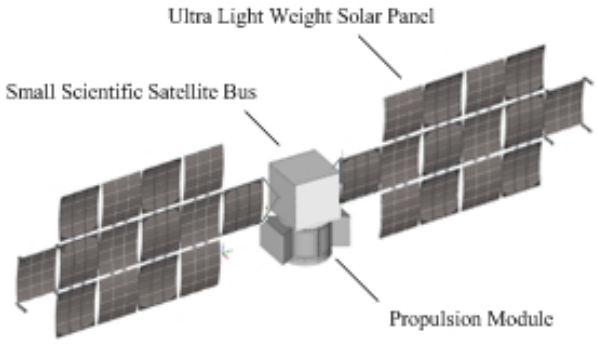

DESTINY Overview

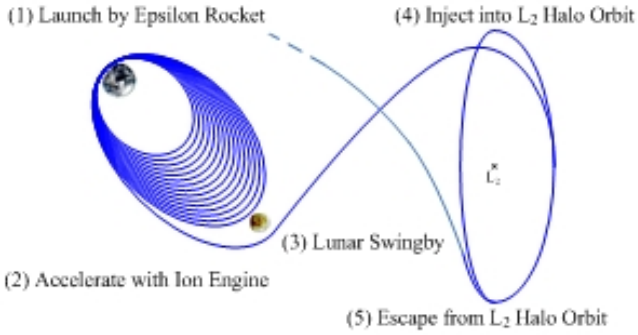

Mission Profile

Japan Geoscience Union Meeting 2014
(28 April - 02 May 2014 at Pacifico YOKOHAMA, Kanagawa, Japan)

PPS26-10 Room:418 Time:April 30 11:45-12:00

Introduction of SLIM, a small and pinpoint lunar lander

SAKAI, Shin-ichiro[1*] ; SAWAI, Shujiro[1] ; SLIM, Working group[1]

[1]ISAS/JAXA

Small experimental spacecraft ”SLIM” is proposed to demonstrate accurate ”pinpoint” landing technology on a celestial body with gravity. Conventional landing missions, such as Apollo or Chang’e achieved lunar landing with km-order accuracy. Since modern spacecraft provided extensive high-resolution data on the Moon, such as the fruits of SELENE spacecraft, now the place of interest comes to be ”exactly that point”, not ”somewhere on the Moon”. Marius Hill’s Hall (MHH), which is one of the candidates of SLIM landing target, is an interesting vertical hall, for example, and to carry out some exploration on MHH, pinpoint-landing with 100 meter-order accuracy is desired. To enable such 100 meter-order landing accuracy on a celestial body with gravity, several novel technologies has been researched and developed with the effort of SLIM working group members. Practical crater detection and recognition algorithms were proposed for image based guidance system, which can be implemented on an existing space qualified FGPA device. Novel landing radar system was newly developed, and was already evaluated with a bread board model in the field flight test. Detection and avoidance of harmful obstacles around the landing point based on camera image were also researched.

SLIM spacecraft is designed as a small 500 kg-class spacecraft, to pursue lower project cost and shorter development time. To realize lunar lander in this restricted size and weight, unique ideas have been also investigated. Improved ceramic thruster will be applied based on the heritage from AKATSUKI mission, and inherited one is now discussed to be a candidate main thruster for future ESA mission. Propellant tank is designed as a part of spacecraft main structure, to minimize the total weight of SLIM spacecraft. Unique aluminum foam based landing gear is also studied and experimentally demonstrated, and electrical power system is designed with novel ultra-lightweight space solar sheet. Numbers of these engineering researches have been carried out in many universities, and with these efforts, the SLIM is just proposed to the third mission of Epsilon launch vehicle.

SLIM mission is important for its original purpose, to demonstrate the accurate landing technology, and at the same time, key technologies to realize lunar lander in small size and light weight will contribute a lot to the future exploration missions based on Epsilon launcher. In the presentation, the detail of each technology researched and developed by the member of SLIM working group will be introduced, with the result of the system design of SLIM spacecraft. The future perspective on the Epsilon exploration missions based on the SLIM design will be also discussed.

Keywords: Moon and Planetary survey, Lunar landing, Guidance and Navigation for landing, Precise landing, Epsilon Rocket

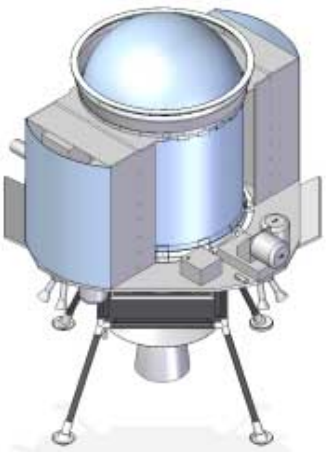

Japan Geoscience Union Meeting 2014
(28 April - 02 May 2014 at Pacifico YOKOHAMA, Kanagawa, Japan)

PPS26-11 Room:418 Time:April 30 12:00-12:15

Proposal for Demonstration of Penetrator Technology by Small Satellite and Epsilon Launch Vehicle

SHIRAISHI, Hiroaki[1*] ; YAMADA, Ryuhei[2] ; ISHIHARA, Yoshiaki[1] ; OGAWA, Kazunori[1] ; OKAMOTO, Taro[3] ; TAKEUCHI, Nozomu[4] ; ISHIHARA, Yasushi[5] ; MURAKAMI, Hideki[6] ; TANAKA, Satoshi[1] ; KOBAYASHI, Naoki[1] ; HAYAKAWA, Masahiko[1] ; HAYAKAWA, Hajime[1] ; ARAYA, Akito[4] ; GOTO, Ken[1] ; MIZUNO, Takahide[1] ; ISHII, Nobuaki[1] ; TSUDA, Yuichi[1] ; HABU, Hiroto[1] ; KAKEHASHI, Yuya[1] ; ISHIMURA, Kosei[1] ; TOKUDOME, Shinichiro[1]

[1]Department of Solar System Sciences, Institute of Space and Astronautical Science, JAXA, Japan, [2]National Astronomical Observatory of Japan, RISE project, [3]Department of Earth and Planetary Sciences, Tokyo Institute of Technology, [4]Earthquake Research Institute, University of Tokyo, [5]IFREE, JAMSTEC, [6]Department of Applied Science,Faculty of Science,Kochi University

A new mission to validate the penetrator technology and to investigate the shallow structure of the Moon, using a small satellite and a penetrator module developed for the former LUNAR-A project is proposed. The lunar penetrator module consists of a penetrator main body, a de-orbit motor and an attitude control system. The de-orbit motor attached at the rear end of the penetrator module is used to cancel the orbital velocity, and the attitude control system which consists of a small gas jet and a sun-sensor is also attached to the central part of the module. The penetrator probe is a missile-shaped instrument carrier and is about 75 cm in length, 14 cm in maximum diameter and about 14 kg in weight. The penetrator contains a two-component seismometer and a heat flow probe, together with electronics, primary batteries, a tiltmeter, an accelerometer, and radio communication system. The primary objective of this mission is to demonstrate the technical issues in penetrator system; (1) holding and separation mechanism, (2) sequence of de-orbit, attitude control and subsurface deployment, (3) data-relay and remote operation by way of an orbital spacecraft, and (4) long-term geophysical observation on the Moon. The flight-proven penetrator system could be applied to the future lunar mission for a full-scale network.

The Epsilon launch vehicle lifts off a spacecraft (or lunar orbiter) with a solid propellant motor newly developed as the upper stage. The spacecraft, which should be play roles of the carrier of penetrator module and of data-relay orbiter, is assumed to revolve in a near-circular orbit of 100-200 km by 25-45 km altitude around the Moon and to release the penetrator module to deploy on the low latitude zone of the lunar nearside or terminator. The penetrator will hit on the lunar surface with a velocity of 270 to 300 m/sec and penetrate into the regolith up to a depth of 2 or 3 meters, and then it will measure the acceleration record and the stop angle at the rest position. These data would be also useful for data reduction of seismic and heat-flow data. After that, it will observe the near-surface and internal structures on the geological unit different from the past Apollo and Luna landers. Ground-based optical telescopes will continuously monitor meteoroid impact flashes on the night side of the Moon, which should frequently occur during the observation period of penetrator seismometer. These landmarks detected in the vicinity of the penetrator will be available for seismological study as known moonquake foci.

This paper describes the spacecraft design, the mission profile from launch to deployment and an operational scenario of geophysical instruments.

Keywords: small satellite, Epsilon rocket, penetrator, seismometer, heat flow probe

Japan Geoscience Union Meeting 2014
(28 April - 02 May 2014 at Pacifico YOKOHAMA, Kanagawa, Japan)

PPS26-12 Room:418 Time:April 30 12:15-12:30

Lunar and planetary explorations in a coming decade: Summary of 4 years and problems remained

NAMIKI, Noriyuki[1*] ; KOBAYASHI, Naoki[2] ; DEMURA, Hirohide[3] ; OHTSUKI, Keiji[4]

[1]PERC/Chitech, [2]Department of Planetary Science, ISAS, [3]The University of Aizu, [4]Kobe University

Future Planetary Exploration Working Group of Japanese Planetary Science Society is discussing next generation of planetary explorations that need to be strongly supported by planetary science community. We started ”Planetary Exploration in a Coming Decade” activity in 2010 aiming to organize a new mission to be launched between 2017 and 2027. The first stage of the activity is ending in March, 2011. A summary of the first stage was reported by 5 panels; (1) terrestrial solid planets, (2) terrestrial atmosphere and magnetosphere, (3) minor body, (4) Jovian planets, icy satellites, and exoplanets, and (5) astrobiology. Each panel received proposals regarding ”top sciences” of each category from the community in the summer of 2010. On September 10 in 2010, an open meeting was held at Kobe University to discuss top sciences among the community of planetary scientists. From the summer of 2011, the second stage began. Proposals for new mission and instruments were submitted by 13 groups and were adivsed by the second-stage committee not only to improve the proposal, but also to raise and develop exploration groups. In 2012 May, the thrid stage started. The main purpose of the third stage is to polish up the proposls in the view of feasibility. In September 14 and 15, 2012, we held a workshop to integrate individual proposals into a few comprehensive mission plans, such as in-situ chronology and interior exploration of the moons and planets, primitive small body exploration, and sercha of life on Mars. The mission concepts of these comprehensive mission plans are now being discussed for later evaluation by the third stage committee. Thsi activity will be closing in the summer of 2014, and the final report will be published in October.

Keywords: moon, planets, exploration, road map

Japan Geoscience Union Meeting 2014
(28 April - 02 May 2014 at Pacifico YOKOHAMA, Kanagawa, Japan)

PPS26-13 Room:418 Time:April 30 12:30-12:45

Approach of the next decade panel

DEMURA, Hirohide[1*]

[1]University of Aizu

Report of the next decade panel.

Keywords: Planetary Science, Space Science, Future Planning, Exploration, Epsilon Launch Vehicle, JAXA

Japan Geoscience Union Meeting 2014
(28 April - 02 May 2014 at Pacifico YOKOHAMA, Kanagawa, Japan)

PPS26-P01 Room:Poster Time:April 30 18:15-19:30

Development and evaluation of heat flow probe for the precise measurement of lunar and planetary heat flow

HORIKAWA, Yamato[1*] ; TANAKA, Satoshi[2] ; SAKATANI, Naoya[1] ; TAKITA, Jun[3]

[1]The Graduate University for Advanced Studies, [2]Japan Aerospace Exploration Agency, [3]The University of Tokyo

The precise measurement of lunar and planetary heat flow contributes to a better understanding of bulk composition and thermal history of the solid bodies. In order to conduct the in situ measurement, a high speed penetration probe, penetrator, which can be buried into a depth of 1 to several meters, has been developed. Since the shock durability at the penetration and the weight saving are required prior to scientific measurements, the heat flow sensors are installed on the surface of the penetrator. However, the sensors must have an uncertainty by disturbances of temperature distribution around the penetrator due to a large difference of thermal conductivities between the penetrator and the surrounding regolith.

In this study, we propose to develop an extension mechanism of needle probes from the buried penetrator which can avoid the thermal disturbance and measure heat flux with an uncertainty better than 10%. The temperature sensing part is required to be placed at a distance as far as possible from the penetrator body. Although the theoretical solution has been obtained to estimate thermal conductivity of the particulate material at the tip part of the probe, no research has yet been carried out to measure thermal conductivity of regolith by the needle probes whose temperature sensing parts are at the tip part. We developed a prototype model of the probe and evaluated the measurement uncertainty of thermal conductivity of glass beads as the regolith simulant material under vacuum condition.

The prototype of the needle probe consists of a wire heater, a K-type thermocouple, a stainless pipe as the needle probe's sheath, and epoxy resin fixing the heater and the thermocouple in the pipe. The length of the probe is 10cm which is the equivalent size of inner diameter of the penetrator body. Thermal conductivity of the glass beads under 200Pa can be controlled to be about 0.02W/m/K, which is almost the same thermal conductivity of the lunar environment at a depth of 1 to several meters. The needle probe was placed at the center of the sample container and surrounded by three sets of line heat source conductivity sensors for reference calibration.

Under 200Pa, we obtained 0.0165W/m/K by the theoretical solution of the probe, and 0.0207W/m/K by the average values of three line heat source sensors. The measurement uncertainty of thermal conductivity by the probe was calculated to be about 31%. However, the thermal conductivity by the probe can't be estimated directly from the theoretical solution because the conditions of the solution differ from the properties of the actual probe, such as the diameter of the probe, the thermal contact between the probe and the glass beads, and the axial heat flow of the probe. Therefore, we conducted the heat-transfer simulation whose numerical model included the properties of the actual probe, and estimated the thermal conductivity by the probe from increases in temperature after heating of the simulation. In addition, we confirmed an agreement with the temperature profiles of the theory and the simulation whose model condition was the same as the condition of the theory.

As a result, the thermal conductivity by the probe was estimated to be 0.0212W/m/K, and the measurement uncertainty of thermal conductivity was calculated to be about 3%, which was well satisfied with the requirement uncertainty of better than about 5%. In future, in order to estimate thermal conductivity of the regolith in lunar and planetary surface layer by using our probe, the measurement uncertainties are required to determine for the probable thermal conductivities by using the heat-transfer simulation.

Keywords: heat flow, thermal conductivity, moon, planet, penetrator, needle probe

Japan Geoscience Union Meeting 2014
(28 April - 02 May 2014 at Pacifico YOKOHAMA, Kanagawa, Japan)

PEM04-01 Room:311 Time:April 28 11:00-11:15

ERG project

MIYOSHI, Yoshizumi[1*] ; TAKASHIMA, Takeshi[2] ; ASAMURA, Kazushi[2] ; SHIOKAWA, Kazuo[1] ; SEKI, Kanako[1] ; SHOJI, Masafumi[1] ; SHINOHARA, Iku[2] ; HIRAHARA, Masafumi[1] ; HIGASHIO, Nana[2] ; MATSUMOTO, Haruhisa[2] ; KASAHARA, Satoshi[2] ; MITANI, Takefumi[2] ; KASABA, Yasumasa[3] ; MATSUOKA, Ayako[2] ; KOJIMA, Hirotsugu[4] ; FUJIMOTO, Masaki[2] ; ONO, Takayuki[3]

[1]STEL, Nagoya University, [2]JAXA, [3]Graduate School of Science, Tohoku University, [4]RISH, Kyoto University

The ERG (Exploration of energization and Radiation in Geospace) is Japanese geospace exploration project. The project focuses on relativistic electron acceleration mechanism of the outer belt in the context of the cross-energy coupling via wave-particle interactions. The project consists of the satellite observation team, the ground-based network observation team, and integrated-data analysis/simulation team. The ERG satellite will be launched in FY2015. Comprehensive instruments for plasma/particles, and field/waves are installed in the ERG satellite to understand the cross-energy coupling system. In the ERG project, several ground-network teams join; magnetometer networks, radar networks, optical imager networks, etc. Cooperative observations between the in-situ satellite and ground-based observations are important. Some simulation codes including both macro-scale phenomena and micro-physics are developed in Japan, which are very helpful quantitatively to understand the observational results and to incorporate the observations. In this presentation, the overview of the projects will be presented and possible collaborations with other geospace satellite missions as well as the ground-based observations will be discussed.

Keywords: ERG project, inner magnetosphere, future mission

Japan Geoscience Union Meeting 2014
(28 April - 02 May 2014 at Pacifico YOKOHAMA, Kanagawa, Japan)

PEM04-02 Room:311 Time:April 28 11:15-11:35

Upper Atmosphere phenomena in Geomagnetic Anomaly Region in association with Magnetosphere Disturbances

MAKITA, Kazuo[1*]

[1]Takushoku University

Since 1999, we continuously study/observe upper atmosphere phenomena in Geomagnetic Anomaly Region (South Atlantic Anomaly: SAA) by using several equipments and obtained several interesting results. We show several remarkable phenomena in SAA on the basis of imaging riometer data and CCD imager data obtained at Southern Space Observatory (SSO; 29.4S, 307E) in Brazil and other stations.

(1) Particle precipitation in SAA seems to be related with polar disturbances. From imaging riometer data, enhancement of Cosmic Noise Absorption (CNA) occurs simultaneously with magnetic disturbances in polar region. On the other hand, CNA at Kakioka imaging riometer can be also seen during polar disturbance (not so frequently observed). It may suggest that particle precipitations are occurred in association with substorm at Kakioka as well as SAA.

(2) In sometimes, strong CNA is observed in association with sharply decreasing of electron flux (GOES satellite data) after moderate polar disturbance period. It may indicate that injection and drifting of electrons after polar disturbances precipitate in SAA during this period.

(3) It is well known that VLF waves trigger precipitation of radiation belt particles.

Although the longitudinal difference is 94 degrees (6 hours local times) between Syowa Station, Antarctica and SSO, CNA at SSO is nearly simultaneously observed with VLF emissions at Syowa Station. It may suggest that particles are more easily precipitating and observed in SAA through the wave particle interactions in radiation belt.

(4) Static multiple bands are singularly observed at SSO. The characteristics of static multiple bands are different from atmospheric gravity waves. They are fixed at the ground and rotate with earth rotation. This phenomena is very seldom and looks like occurs in winter season. The luminosity of these phenomena are not clear but less than 150R like airglow level..

We almost finished to construct South America Riometer Network (SARINET; 7 stations) and hope to collect data continuously during one solar cycle.

Keywords: South Atlantic Geomagnetic Anomaly, Cosmic noise absorption, Imaging riometer, Radiation belt, Airglow

South America Riometer Net work (SARINET)

Japan Geoscience Union Meeting 2014
(28 April - 02 May 2014 at Pacifico YOKOHAMA, Kanagawa, Japan)

PEM04-03 Room:311 Time:April 28 11:35-11:55

Loss of geosynchronous relativistic electrons by EMIC waves during quiet geomagnetic conditions

KIM, Khan-hyuk[1*] ; HYUN, Kiho[1] ; LEE, Ensang[1] ; LEE, Dong-hun[1]

[1]School of Space Research, Kyung Hee University, Gyeonggi, Korea.

We have examined relativistic electron flux losses at geosynchronous orbit under quiet geomagnetic conditions. Two 3-day periods, from 11 to 13 October and from 29 November to 1 December, in 2007 were chosen for analysis because geomagnetic conditions were very quiet (3-day average of Kp $<$1) and significant losses of geosynchronous relativistic electrons were observed. During both intervals, there were no geomagnetic storm activities. Thus, the loss processes associated with geomagnetic field modulations caused by ring current buildup can be excluded. The flux of geosynchronous relativistic electrons with energy $>$2 Mev shows typical diurnal variations with a maximum near noon and a minimum near midnight for each day. The flux level of the daily variation gradually decreased from first day to third day for each 3-day period. The total magnetic field strength (Bt), however, is relatively constant for each day. Unlike electron flux decreases, the flux of protons with energy between 0.8 and 4 MeV adiabatically responses to the daily variation of Bt. That is, there is no significant decrease of the proton flux when the electron flux decreases. During both 3-day periods, well-defined electromagnetic ion cyclotron (EMIC) waves were detected at geosynchronous spacecraft. Low-altitude polar orbiting spacecraft observed the precipitation of energetic electrons and protons in the interval of EMIC waves enhancement. From these observations, we suggest that the EMIC waves are a major factor to control the electron flux decrease under quiet geomagnetic conditions.

Keywords: Relativistic electron flux, geosynchronous orbit, EMIC waves

Japan Geoscience Union Meeting 2014
(28 April - 02 May 2014 at Pacifico YOKOHAMA, Kanagawa, Japan)

PEM04-04 Room:311 Time:April 28 11:55-12:10

Characteristics of dayside SAPS structures observed by the SuperDARN Hokkaido radar

NISHITANI, Nozomu[1*] ; HORI, Tomoaki[1] ; NAGANO, Hiroki[1]

[1]Solar-Terrestrial Environment Laboratory, Nagoya University

Sub-Auroral Polarization Streams (SAPS) are intense westward ionospheric flows in the subauroral ionosphere, and considered to be generated as a result of magnetosphere-ionosphere coupling during relatively disturbed periods. SAPSs are usually located in the evening to midnight sector, but occasionally it extends to earlier magnetic local times close to local noon. Owing to limitation of the observation techniques, no detailed studies of its local time extent have been made so far. In this study we use the data from the SuperDARN Hokkaido radar, one of the midlatitude SuperDARN radars located at the lowest geomagnetic latitude, to discuss the detailed characteristics of dayside SAPS, with focus on their relation to solar wind and geomagnetic parameters.

Keywords: dayside, SAPS, SuperDARN, Hokkaido radar, magnetosphere, ionosphere

Japan Geoscience Union Meeting 2014
(28 April - 02 May 2014 at Pacifico YOKOHAMA, Kanagawa, Japan)

PEM04-05 Room:311 Time:April 28 12:10-12:25

Amplification of EMIC waves by Pc3-4 waves

NOMURA, Reiko[1*] ; KEIKA, Kunihiro[2] ; TERAMOTO, Mariko[4] ; KLETZING, Craig[3]

[1]IGEP, TU Braunschweig, [2]Solar-Terrestrial Environment Laboratory, Nagoya University, [3]Japan Aerospace Exploration Agency, [4]Department of Physics and Astronomy, The University of Iowa

Electromagnetic ion cyclotron (EMIC) wave is one of the key phenomena for the dynamics of high energy electrons in the radiation belt, since EMIC waves can scatter particles and make them precipitate into the ionosphere from the inner magnetosphere. The EMFSIS of Van Allen Probes observed the proton-band EMIC wave with the frequencies 2-6Hz at ∼3RE in the GSM coordinates at 1110-1140UT on 29 June 2013. It was during the recovery phase of the magnetic storm started on 27 June. This event has significant enhancements of wave amplitudes up to ∼10nT at 1123 and 1130UT. At these times, the magnetic field variations in the Pc3-4 range are also observed. We present the relation between amplitudes of EMIC waves and Pc3-4 wave occurrences, and discuss the amplification mechanism of EMIC waves by ULF waves with longer periods.

Keywords: EMIC waves, Pc3-4

Japan Geoscience Union Meeting 2014
(28 April - 02 May 2014 at Pacifico YOKOHAMA, Kanagawa, Japan)

PEM04-06 Room:311 Time:April 28 12:25-12:40

Study of Pc1 pearl structures observed at multi-point ground stations at Russia, Japan and Canada

JUN, Chae-woo[1*] ; SHIOKAWA, Kazuo[1] ; SCHOFIELD, I.[2] ; CONNORS, M.[2] ; PODDELSKY, I.[3] ; SHEVTSOV, B.[3]

[1]Solar-Terrestrial Environment Laboratory, Nagoya University, Nagoya, Japan, [2]Center for Science, Athabasca University, Athabasca, Canada, [3]Institute of Cosmophysical Research and Radiowave Propagation, Far Eastern Branch of the Russian Aca

We have investigated possible generation mechanisms of pearl structures of Pc1 geomagnetic pulsations using ground-based multi-point induction magnetometers at Athabasca in Canada, at Magadan in Russia and at Moshiri in Japan. During 3-years of observation (January 1, 2009 to December 31, 2011), we found two Pc1 pulsations with similar dynamic spectrum shapes at three stations simultaneously. For the case 1, which occurred on April 8, 2010, Pc1 pulsations were clearly identified at the three stations in the frequency range of 0.4 to 1.2 Hz. Coherence between the two stations was high ($r > 0.8$). The cross-correlation of the upper envelope of Pc1 waves between the ATH and the MGD, which indicates amplitude modulation of Pc1 due to pearl structures, was also high ($r > 0.8$). In some time interval during the case 1, however, correlation decreased down to 0.5. The case 2 occurred on April 11, 2010 in the frequency range of 0.2 to 0.8 Hz showed that the coherence and cross-correlation between ATH and MGD were both high ($r > 0.8$) throughout the event. The high coherence indicates that the Pc1 pulsations observed at these different stations were propagated from the same source region. However, in case 1, the Pc1 pearl structures were slightly different for different stations. The case 1 showed polarization angle variation depending on frequencies, while the case 2 does not show such dependence, suggesting that the case 1 has a spatially-distributed ionospheric source at high latitudes. In order to understand these different features of Pc1 pearl structures, we made two model calculations of Pc1 peal structures under the different conditions. One model is that the Pc1 waves come from a north-south extended ionospheric source region with slightly different frequencies at different latitudes. This source distribution, causes the Pc1 pearl structure by beating during the duct propagation in the ionosphere. The other model is that the Pc1 waves with different frequencies are mixed at the point source in the ionosphere, assuming that the pearl structures were already made in the magnetosphere. The Pc1 from the point source shows an identical waveform among the different stations. On the other hand, the Pc1 from distributed source region shows slightly different waveforms at different stations. This result suggests that the distributed source region is able to create the different Pc1 pearl structures at different stations through the beating, as observed for the case 1. We conclude that the Pc1 pearl structures are created by both magnetospheric processes and ionospheric beating processes before they reach the ground-based magnetometer at low latitudes.

Keywords: Pc1 pulsation, Pearl structures, multi-point ground observations

Japan Geoscience Union Meeting 2014
(28 April - 02 May 2014 at Pacifico YOKOHAMA, Kanagawa, Japan)

PEM04-07 Room:311 Time:April 28 14:15-14:35

Gradual Diffusion and Punctuated Enhancements of Highly Relativistic Electrons: Van Allen Probes Observations

BAKER, Daniel N.[1*]

[1]University of Colorado Boulder

The dual-spacecraft Van Allen Probes mission has provided a new window into megaelectron Volt (MeV) particle dynamics in the Earth′ s radiation belts. Observations (up to E ˜10 MeV) show clearly the behavior of the outer electron radiation belt at different time scales: months-long periods of gradual inward radial diffusive transport and weak loss being punctuated by dramatic flux changes driven by strong solar wind transient events. Analysis of multi-MeV electron flux and phase space density (PSD) changes during March 2013 are presented in the context of the first year of Van Allen Probes operation. This March period demonstrates the classic signatures both of inward radial diffusive energization as well as abrupt localized acceleration deep within the outer Van Allen zone (L ˜4.0±0.5). This reveals graphically that both ″ competing ″ mechanisms of multi-MeV electron energization are at play in the radiation belts, often acting almost concurrently or at least in very rapid succession. It also shows in remarkable ways how the coldest plasmas in the magnetosphere intimately control the most highly energetic particles.

Keywords: Van Allen Probes, Radiation belts, Solar wind, Electron energization

Japan Geoscience Union Meeting 2014
(28 April - 02 May 2014 at Pacifico YOKOHAMA, Kanagawa, Japan)

PEM04-08 Room:311 Time:April 28 14:35-14:55

Particle Acceleration in Kinetic Eigenmodes from the Van Allen Probes

CHASTON, Christopher[1*] ; BONNELL, John[2] ; WYGANT, John[3] ; KLETZING, Craig[4] ; MOZER, Forrest[2] ; BALE, Stuart[2] ; KURTH, William[4] ; HOSPARDARSKY, George[4] ; KERSTEN, Kris[3] ; BRENEMAN, Aaron[3] ; SMITH, Charles[5] ; MACDONALD, Elizabeth[6]

[1]School of Physics, University of Sydney, Sydney, NSW, Australia, [2]Space Sciences Laboratory, University of California, Berkeley, CA, USA, [3]School of Physics and Astronomy, University of Minnesota, Minneapolis, MN, USA, [4]Department of Physics and Astronomy, University of Iowa, Iowa City, IA, USA, [5]Department of Physics and IEOS, University of New Hampshire, Durham, NH, USA, [6]Los Alamos National Laboratory, Los Alamos, NM, USA

The Van Allen Probes have revealed the presence of a broad spectrum of narrow scale Alfvén eigenmodes in the inner magnetosphere during geomagnetic storms. Here we use observations from the Van Allen Probes to build a reduced MHD model for these waves in a dipolar geomagnetic field. This model is then used to explore the manner through which particles may be accelerated in these wavefields. Test particle simulations show that the narrow perpendicular scale and parallel electric fields carried by these waves lead to the violation of the 1st and 2nd adiabatic invariants for ions. This can drive the heating of the thermal ion population to multi-keV temperatures and the acceleration of a small fraction of these particles to energies exceeding 100 keV. This process has obvious implications for the storm time ring current, but also for the acceleration/loss of radiation belt electrons.

Keywords: Particle acceleration, Alfven waves, van allen probes, field lines resonances, ring current, radiation belts

Japan Geoscience Union Meeting 2014
(28 April - 02 May 2014 at Pacifico YOKOHAMA, Kanagawa, Japan)

PEM04-09 Room:311 Time:April 28 14:55-15:10

Van Allen Probes observations of oxygen torus in the inner magnetosphere

NOSE, Masahito[1*] ; KEIKA, Kunihiro[2] ; KLETZING, C. A.[3] ; SMITH, C. W.[4] ; MACDOWALL, R. J.[5] ; KURTH, W. S.[3] ; DE PASCUALE, S.[3]

[1]Graduate School of Science, Kyoto University, [2]Solar-Terrestrial Environment Laboratory, Nagoya University, [3]Department of Physics and Astronomy, University of Iowa, [4]Institute for the Study of Earth, Oceans and Space, University of New Hampshire, [5]NASA Goddard Space Flight Center

The oxygen torus is found in the deep inner magnetosphere as enhancements of O^+ ion density in a limited L range. It was first reported by Chappell [1982] who used the DE-1/RIMS instrument. Horwitz et al. [1984, 1986] showed that the O^+ density sometimes becomes comparable to or exceeds the H^+ density at L=3-4. Following studies revealed that the oxygen torus is observed just inside the plasmasphere at all local time with higher occurrence frequency in the late evening and morning sectors. A recent study by Nosé et al. [2010] cast a new light on the oxygen torus as a one of essential factors of O^+-rich ring current generation. They proposed that thermal O^+ ions preexisting in the oxygen torus are locally and nonadiabatically accelerated by fluctuations associated with dipolarization in the deep inner magnetosphere and contribute to ring current O^+ ions. Therefore investigation of the oxygen torus is important to understand the dynamics of ions of ionospheric origin in the inner magnetosphere.

We study the oxygen torus, using the magnetic field and plasma wave data obtained by the Electric and Magnetic Field Instrument Suite and Integrated Science (EMFISIS) instrument onboard the Van Allen Probes. We examine a few events on the dawnside in which toroidal standing Alfven waves appear clearly. From the frequency of the toroidal waves, the magnetospheric local mass density (ρ) is estimated by solving the MHD wave equation for realistic models of the magnetic field and the field line mass distribution. We also estimate the local electron number density (n_e) from the plasma wave spectrograms by identifying narrow-band emission at the upper-hybrid resonance frequency. Assuming the quasi-neutral condition of plasma, we infer the local average ion mass (M) by ρ/n_e. It is found that M is generally less than 4 amu in the plasma trough, while it shows an enhancement of $>$6 amu near the plasmapause. This indicates an existence of the oxygen torus in the vicinity of the plasmapause. We will present the result and discuss possible formation mechanisms of the oxygen torus. Possible contribution of the oxygen torus to the formation of the O^+-rich ring current will be also discussed.

Japan Geoscience Union Meeting 2014
(28 April - 02 May 2014 at Pacifico YOKOHAMA, Kanagawa, Japan)

PEM04-10 Room:311 Time:April 28 15:10-15:25

Akebono observations of EMIC waves in the slot region of the radiation belts

SAKAGUCHI, Kaori[1*] ; KASAHARA, Yoshiya[2] ; SHOJI, Masafumi[3] ; OMURA, Yoshiharu[4] ; MIYOSHI, Yoshizumi[3] ; NAGATSUMA, Tsutomu[1] ; KUMAMOTO, Atsushi[5] ; MATSUOKA, Ayako[6]

[1]National Institute of Information and Communications Technology, [2]Information Media Center, Kanazawa University, [3]Solar-Terrestrial Environment Laboratory, Nagoya University, [4]Reserach Institute for Sustainable Humanosphere, Kyoto University, [5]Department of Geophysics, Graduate School of Science, Tohoku University, [6]Institute of Space and Astronautical Science, Japan Aerospace Exploration Agency

We present a unique observation of electromagnetic ion cyclotron (EMIC) waves in the deep inner magnetosphere at L = 2.5-5 made by the Akebono satellite at altitudes of 3,300-8,700 km. The mode conversion, i.e., L mode (He+ band)→R mode (He+ band)→L mode (O+ band) was clearly identified from the equator to high latitudes. In addition, we found rising tone structures, recently identified as EMIC triggered emissions, which could lead to bursty precipitation of relativistic electrons. First, we estimated the ion composition ratio (H+, He+, O+) = (83%, 16%, 1%) from polarization analysis. Second, we estimated minimum resonant electron energies with the observed EMIC waves and triggered emissions to be 1?10 MeV. The satellite trajectory during the wave observation was primarily through the slot region of electron radiation belts. The collocation implies possible contribution of EMIC waves to formation of the slot region of radiation belts after a magnetic storm.

Keywords: EMIC wave, slot region of the radiation belt, mode conversion, triggered emission, ion compotision ratio, Akebono satellite

Japan Geoscience Union Meeting 2014
(28 April - 02 May 2014 at Pacifico YOKOHAMA, Kanagawa, Japan)

PEM04-11 Room:311 Time:April 28 15:25-15:40

Oxygen ion acceleration and transport in the near-Earth plasma sheet during an isolated substorm

NAKAYAMA, Yohei[1*] ; EBIHARA, Yusuke[1] ; TANAKA, Takashi[2]

[1]Research Institute for Sustainable Humanosphere (RISH), Kyoto university, [2]SERC, Kyushu University

Rapid enhancements of energetic ions during a substorm are one of the unsolved issues in the inner magnetospheric research (<7 Re). Previously, two distinct processes have been suggested to explain the enhancements. The first one is transport from the near-earth plasma sheet, and the other one is local acceleration. To test the both process, we performed test particle simulation under the electric and magnetic fields that are self-consistently obtained by the global MHD simulation developed by Tanaka et al. (2010, JGR). Oxygen ions are released in the lobe region with an interval of 1 minutes. The distribution function in the lobe is assumed to be drifting Maxwellian. The temperature is assumed to be 20 eV, the density is 105 cm-3, and the parallel velocity is given by the MHD simulation. In total, a few hundreds of millions of particles are traced. Each test particle carries the real number of particles in accordance with the Liouville theorem. After tracing particles, we reconstruct 6-dimensional phase space density of the oxygen ions, as well as the directional differential number flux so as to be able to make a direct comparison with in-situ satellite observations. Just after a substorm onset, the differential flux of the ions is rapidly enhanced in the energy range from 50 to 150 keV at radial distance R greater than 7 on the nightside in the equatorial plane. The region of the enhanced flux propagates duskward, then to dayside because of grad-B and curvature drift of the ions. We also plotted energy versus time spectrograms of the differential flux at a fixed position to make a direct comparison with the CRRES satellite observation. At 7.2 Re and at 22.4 MLT, the ion flux is suddenly enhanced about 10 minutes after the onset. The enhancement appears first at 120 keV, followed by lower energy as time proceeds. The energy-time dispersion is similar to that observed by CRRES [Fu et al., 2002]. The steepness of the energy-time dispersion depends on the source location of the ions. After a while, a high energy ion flux appears first, followed by that at lower energies. This is a called a drift echo, arising from the ions that encircled the Earth by the grad-B and curvature drift. We will discuss the acceleration processes in more detail, the role of pre-existing ions, and the total kinetic energy of the oxygen ions and its dependence on the source distribution function in terms of the ring current development.

Reference:

Fu, S. Y., Q. G. Zong, T. A. Fritz, Z. Y. Pu, and B. Wilken, Composition signatures in ion injections and its dependence on geomagnetic conditions, J. Geophys. Res, 107(A10), 1299, doi:10.1029/2001JA002006, 2002.

Tanaka, T., A. Nakamizo, A. Yoshikawa, S Fujita, H. Shinagawa, H. Shimizu, T. Kikuchi, and K. K. Hashimoto, Substorm convection and current system deduced from the global simulation, J. Geophys. Res. 115, A05220, doi:10.1029/JA014676, 2010.

Japan Geoscience Union Meeting 2014
(28 April - 02 May 2014 at Pacifico YOKOHAMA, Kanagawa, Japan)

PEM04-12 Room:311 Time:April 28 15:40-15:55

On the formation of overshielding triggered by a substorm onset: Global MHD simulation study

EBIHARA, Yusuke[1*] ; TANAKA, Takashi[2] ; KIKUCHI, Takashi[3]

[1]RISH, Kyoto Univerisity, [2]Emeritus Professor, Kyushu University, [3]Emeritus Professor, Nagoya University

The dawn-dusk convection electric field is a significant driver of transport of charged particles in the inner magnetosphere. When the dawn-disk convection electric field is enhanced, the ring current is developed, and the plasmasphere is shrunk. Ground-based observations have shown that, sometimes, the polarity of the convection electric field is reversed after a substorm onset. The presence of the dusk-dawn electric field is called an overshielding condition. Here, we demonstrate that the overshielding condition can appear after a substorm onset on the basis of a global MHD simulation. Immediately after the substorm onset manifested by a sudden decrease in the AL index and auroral brightening, the plasma pressure is enhanced in the inner magnetosphere. The simulated magnetic field on the ground shows a negative excursion in the polar cap, a positive excursion at auroral latitudes, and a negative excursion at sub-auroral latitudes at dusk. At noon and at equator (0 MLAT), the eastward electrojet starts to decrease just after the onset, and the westward electrojet appears about 10 min after the onset. All these variations are consistent with the observations. We discuss generation mechanisms, evolution of the overshielding condition in the ionosphere and the magnetosphere, and the redistribution of the charged particles trapped in the inner magnetosphere during the overshielding condition on the basis of the simulation solving drift transport equations.

Japan Geoscience Union Meeting 2014
(28 April - 02 May 2014 at Pacifico YOKOHAMA, Kanagawa, Japan)

PEM04-13 Room:311 Time:April 28 16:15-16:30

Nonlinear wave particle interactions in oblique whistler-mode chorus emissions

NUNN, David[2] ; OMURA, Yoshiharu[1*]

[1]RISH, Kyoto University, [2]ECS School, Southampton University

The highly nonlinear phenomena of VLF chorus and triggered VLF emissions are of great interest due to their role in electron heating and precipitation, and are widely believed to be due to nonlinear cyclotron resonance between the narrow band wavefield and the anisotropic energetic electron population (∼keV), the dominant mechanism being identified as nonlinear phase trapping. Considerable advances have been made in the theory and numerical simulation by assuming parallel (ducted) propagation [Nunn et al., 1997, 2009;Omura et al., 2008, 2009; Omura and Nunn, 2011]. Here we address the important issue of nonlinear wave particle interaction in oblique VLF wavefields. The treatment is of necessity non self-consistent. The narrow band wavefield is arbitrarily, but here chosen to be a CW field or a sophisticated model of a VLF chorus element based upon the theory of Omura et al.[2008, 2009]. We develop the electron equations of motion and then by backward trajectory integration compute resonant particle distribution function , resonant currents and thus local nonlinear growth rates. This may be done for any resonance order n and any field. As shown in Omura et al. [2008] nonlinear trapping for n=1 cyclotron resonance gives rise to a phase space hole in distribution function at the trap. Such a hole is also noted at higher order resonances (e.g. n=2) for sufficient wave amplitude and obliquity. For n=1 we find a marked saturation effect due to adiabatic effects, growth maximising at about 25pT and 2000km from the equator. For moderate obliquity ϑ<20 degrees the n=1 resonance is relatively unaffected but growth rolls off sharply at high obliquity. For the n=0 resonance for obliquity ϑ >20 degrees nonlinear trapping may occur giving a peak in phase space density. As trapped electrons are moving away from the equator adiabatic effects do not occur and maximum damping rates are at ∼6000kms and at obliquities ∼55 degrees. For the lower band rising chorus element model maximum n=1 growth is close to the equator, but maximum n=0 damping is found at the top of the frequency band at ∼10000km downstream. Due to the coincidence of group and resonance velocities particles may be trapped near the equator and dragged a long way before detrapping.

References

Nunn, D., Y. Omura, H. Matsumoto, I. Nagano, and S. Yagitani (1997), The numerical simulation of VLF chorus and discrete emissions observed on the Geotail satellite using a Vlasov code, J. Geophys. Res., 102, 27,083?27,097.

Nunn, D., O. Santolik, M. Rycroft, and V. Trakhtengerts (2009), On the numerical modelling of VLF chorus dynamical spectra, Ann. Geophys., 27, 2341?2359.

Y. Omura,Y. Katoh, and D. Summers (2008), Theory and simulation of the generation of whistler-mode chorus, J. Geophys. Res., 113, A04223.

Y. Omura, , M. Hikishima, Y. Katoh, D. Summers, and S. Yagitani (2009), Nonlinear mechanisms of lower band and upper band VLF chorus emissions in the magnetosphere, Journal Geophysical Research, 114, A07217.

Omura, Y., and D. Nunn (2011), Triggering process of whistler mode chorus emissions in the magnetosphere, J. Geophys. Res., 116, A05205.

Keywords: whistler wave, wave-particle interaction, simulation, nonlinear, inner magnetosphere, chorus emissions

Japan Geoscience Union Meeting 2014
(28 April - 02 May 2014 at Pacifico YOKOHAMA, Kanagawa, Japan)

PEM04-14 Room:311 Time:April 28 16:30-16:45

Relativistic electron microbursts induced by EMIC triggered emissions in the dipole magnetic field

KUBOTA, Yuko[1*] ; OMURA, Yoshiharu[1]

[1]Research Institute for Sustainable Humanosphere, Kyoto University

We perform test particle simulations of relativistic electrons interacting with electromagnetic ion cyclotron (EMIC) triggered emissions with rising-tone frequencies. We assume that the geomagnetic field is dipole because EMIC triggered emissions and radiation belt electrons are observed in the inner magnetosphere [1]. EMIC triggered emissions are generated by energetic protons injected into the inner magnetosphere and drifting westwards in the longitudinal direction. We study trajectories of relativistic electrons drifting eastwards interacting with EMIC triggered emissions over different longitudinal ranges. When relativistic electrons in the radiation belt interact with EMIC triggered emissions, some of them are trapped by a wave potential and efficiently guided down to lower pitch angles. Repeated interactions result in scattering of relativistic electrons into the loss cone [2]. Counting relativistic electrons which fall into the polar region, we find that half of the relativistic electrons interacting with EMIC triggered emissions are precipitated. We derive conditions of kinetic energies and pitch angles for efficient precipitation of relativistic electrons.

References

[1] Pickett, J. S., et al. (2010), Cluster observations of EMIC triggered emissions in association with Pc1 waves near Earth's plasmapause, Geophys. Res., 37, L09104.

[2] Omura, Y., and Zhao, Q., (2013), Relativistic electron microbursts due to nonlinear pitch-angle scattering by EMIC triggered emissions, J.Geophys.Res., 118, 5008-5020.

Japan Geoscience Union Meeting 2014
(28 April - 02 May 2014 at Pacifico YOKOHAMA, Kanagawa, Japan)

PEM04-15 Room:311 Time:April 28 16:45-17:00

Investigating the upper and lower energy cutoffs of EMIC-wave driven precipitation events

HENDRY, Aaron[1*] ; RODGER, Craig[1] ; CARSON, Bonar[1] ; CLILVERD, Mark[2] ; RAITA, Tero[3]

[1]University of Otago, New Zealand, [2]British Antarctic Survey, UK, [3]SGO, Sodankyla, Finland

For some time theoretical modelling has shown that electromagnetic ion cyclotron (EMIC) waves should play an important role in the loss of relativistic electrons from the radiation belts, through precipitation of the electrons into the polar ionosphere. However, there are limited direct experimental observations of relativistic electron precipitation occurring, despite the indirect evidence for its importance.

Relativistic electron resonance takes place through ”anomalous resonance” where the electron overtakes the wave. Until recently, it was through that EMIC wave scattering interactions were limited to electrons with energies greater than 1-2 MeV. Recent theoretical modelling [Omura et al., JGR, 2012] has suggested that this lower limit may be as small as 100 keV when considering EMIC waves more like those experimentally observed (i.e. non-constant frequency which ramps with time on one second timescales). Using data from the POES satellites we confirm the presence of lower energy ($<$1 MeV) electron precipitation most likely driven by EMIC waves.

We report on a continuing study that determines the typical flux impacting the ionospheric D-region during EMIC-driven precipitation events, and the effect this has on ionospheric conditions. We examine a very large set of EMIC-driven electron precipitation events detected using data from the POES satellite constellation [Carson et al., JGR, 2013] and determine the typical precipitating electron and proton fluxes.

As part of this study, we investigate the response of the MEPED instruments on-board the POES satellites to better characterise the EMIC-driven precipitation. Using the results of a previously reported Monte-Carlo simulation of the MEPED electron and proton telescopes [Yando et al., JGR, 2011], we characterise the typical energy range and flux for both the precipitating electrons and protons observed in these events. We go on to show that such events will produce very significant D-region changes detectable using the ground-based Antarctic-Arctic Radiation-belt (Dynamic) Deposition - VLF Atmospheric Research Konsortium (AARDDVARK) worldwide VLF receiver network.

Keywords: EMIC waves, electron precipitation, POES spacecraft, AARDDVARK, radiation belts, particle precipitation

Japan Geoscience Union Meeting 2014
(28 April - 02 May 2014 at Pacifico YOKOHAMA, Kanagawa, Japan)

PEM04-16 Room:311 Time:April 28 17:00-17:15

Plasmaspheric Content as Revealed by Spaceborne GPS Observations

TSAI, Ho-fang[1*] ; CHOU, Min-yang[1] ; CHEN, Chao-yen[2] ; LIN, Charles[1] ; LIU, Jann-yenq[2]

[1]Dept. of Earth Sciences, National Cheng Kung University, Taiwan, [2]Institute of Space Science, National Central University, Taiwan, [3]National Space Organization, Taiwan

The FORMOSAT-3/COSMIC (F3/C) mission has been operating for more than seven years. The F3/C low earth orbit (LEO) satellites receive the signals from the global positioning system (GPS) for sounding of the atmosphere and the ionosphere of the earth, including the plasmasphere. The plasmasphere above ionosphere acts like a reservoir; it takes plasma from the ionosphere by day, stores it in a loss-free environment, and returns it to the ionosphere at night. For the non-radio occultation observation of the F3/C, we study the morphology of the plasmaspheric electron content (PEC) derived from F3/C raw observation data, which includes the diurnal variations of the time-series PEC, two-dimensional distribution and the interaction with the ionosphere.

Keywords: plasmasphere, FORMOSAT-3/COSMIC, GPS

Japan Geoscience Union Meeting 2014
(28 April - 02 May 2014 at Pacifico YOKOHAMA, Kanagawa, Japan)

PEM04-17 Room:311 Time:April 28 17:15-17:30

Polarization and occurrence statistics of VLF/ELF chorus waves at sub-auroral latitudes at Athabasca, Canada.

MARTINEZ CALDERON, Claudia[1*] ; SHIOKAWA, Kazuo[1] ; MIYOSHI, Yoshizumi[1] ; OZAKI, Mitsunori[2] ; SCHOFIELD, Ian[3] ; CONNORS, Martin[3]

[1]Solar-Terrestrial Environment Laboratory, Nagoya University, Nagoya, Japan, [2]Kanazawa University, Kanazawa, Japan, [3]Athabasca University, Athabasca, Canada

Chorus waves are whistler-mode emissions in the very low frequency (VLF) range that are one of the most intense and common natural emissions. They are generated in the inner magnetosphere at the geomagnetic equator and follow the geomagnetic field lines into the ionosphere and the ground. They are believed to be *one of the major contributions to the acceleration and scattering of radiation belt particles* (e.g., Inan et al., 1982; Omura et al., 2007). Consequently we are interested in the *spatial and temporal motion of the acceleration region of radiation belt electrons*, which might be directly linked to the motion of the Ionospheric footprints of VLF/ELF waves.

For a period of 9 days, from February 17 to 25, 2012, the VLF-CHAIN campaign observed VLF/ELF emissions at sub-auroral latitudes using two loop antennas at Athabasca (MLAT=61.31, L=4.3) and Fort Vermillion (MLAT=64.51, L=5.4), Canada.

Several interesting features of chorus emissions have been observed such as quasi-periodic emissions, falling-tone and rising-tone chorus, as well as *Bursty-Patch* emissions. We have applied polarization and spectral analysis to make **the first comprehensive study of the physical properties of VLF/ELF chorus waves at sub-auroral latitudes**. Combining these analyses with a triangulation method we have also identified the location and motion of the Ionospheric exit points of these various types of chorus waves.

Furthermore, after September 24, 2012, continuous measurements of VLF/ELF waves with a sampling rate of 100 kHz have been made at Athabasca. Based on this data we show in this presentation the preliminary results of a one-year statistical analysis of frequency and occurrence rate of VLF/ELF chorus waves at sub-auroral latitudes.

Keywords: VLF, Chorus Waves, Polarization analysis, Ionospheric exit point, Sub-auroral latitudes

Japan Geoscience Union Meeting 2014
(28 April - 02 May 2014 at Pacifico YOKOHAMA, Kanagawa, Japan)

PEM04-18 Room:311 Time:April 28 17:30-17:45

Nonlinear analysis of magnetospheric wave-particle interactions

SUMMERS, Danny[1*] ; TANG, Rongxin[2] ; OMURA, Yoshiharu[3]

[1]Memorial University of Newfoundland,St John's,Canada, [2]Nanchang University,China, [3]Kyoto University,Japan

The dynamics of the Earth's radiation belts are largely controlled by wave-particle interactions. Gyro-resonant whistler-mode chorus - electron interactions can generate relativistic (MeV) electrons in the outer zone during magnetic storms. Whistler-mode waves can pitch-angle scatter electrons and induce precipitation loss from the inner magnetosphere. Here we analyze the growth of magnetospheric whistler mode waves with particular emphasis on the nonlinear growth phase. We show that nonlinear wave growth can only take place over a restricted parameter space. We examine the conditions under which chorus wave growth can take place,and discuss how the results can be compared with computer simulations and experimental observations.

Keywords: wave-particle interactions, whistler-mode waves, radiation belts, nonlinear cyclotron resonance, chorus wave growth

Japan Geoscience Union Meeting 2014
(28 April - 02 May 2014 at Pacifico YOKOHAMA, Kanagawa, Japan)

PEM04-P01 Room:Poster Time:April 28 18:15-19:30

Retrieval of plasmaspheric He+ density field-aligned distributions from EUV imaging data

KEIKA, Kunihiro[1*] ; BRANDT, Pontus C.[2] ; TOIGO, Anthony[2] ; ROBERT, Demajistre[2]

[1]Solar-Terrestrial Environment Laboratory, Nagoya University, [2]The Johns Hopkins University Applied Physics Laboratory

We retrieve the spatial distributions of He+ density (n_{He+}) in the Earth ' s plasmasphere from EUV imaging data, by using a forward modeling technique. We use a parametric model for the density distribution to simulate line-of-sight integrated He+ densities (i.e., EUV images), and then find parameters that give the best fit to real EUV images. The parametric model used in this study is described as a function of L and magnetic latitude (λ): $n_{He+} = n_0 (L_0/L)^{alpha\_L} \times (r_0/L_0 \cos\lambda^2)^{alpha\_f}$, where n_0 and L_0 are He^+ density and L value at the inner boundary of this model (i.e., the topside ionosphere), and α_L and α_f are parameters that represent L and field-aligned dependence of He^+ density, respectively.

In this paper, we evaluated how well our forward model can retrieve the He^+ density spatial distribution, by performing the following analysis. (1) EUV emission intensities were simulated through the EUV camera response function, given a vantage point of the IMAGE satellite. (2) EUV images were simulated for a large number of (α_L, α_f) pairs: α_L was chosen from 4.0 to 6.0 with 0.1 increment, and α_f was from 0.0 to 2.0 with 0.1 increment. (3) The EUV image corresponding to the (α_L, α_f)=(5.0, 1.0) pair was chosen as our synthetic EUV image. After noise was added to the synthetic image, the forward modeling was applied to all simulated images made in (2). The reduced χ^2 ($\chi_r{}^2$) was used to determine how well simulated image data fit to the synthetic image. The results of this analysis confirm that the He^+ density distributions can be retrieved with good certainty within |40 deg.|MLAT. However, beyond this magnetic latitude it is difficult to determine the L dependence or field-aligned dependence of plasmaspheric He^+ density.

Next, in order to decouple the synthetic data from the parametric formula, we will use density distributions provided by physics-based ionosphere/plasmasphere models as our synthetic data. We will also apply our forward simulation model to real EUV image data from the EUV imager onboard the IMAGE spacecraft.

Keywords: Plasmasphere, Helium ion density, Inner magnetosphere, Plasma refilling, Forward modeling

Japan Geoscience Union Meeting 2014
(28 April - 02 May 2014 at Pacifico YOKOHAMA, Kanagawa, Japan)

PEM04-P02 Room:Poster Time:April 28 18:15-19:30

Solar-cycle variation of the plasmasphere observed from the Akebono PWS data

HASEGAWA, Shuhei[1*] ; MIYOSHI, Yoshizumi[1] ; KITAMURA, Naritoshi[1] ; KEIKA, Kunihiro[1] ; SHOJI, Masafumi[1] ; KUMAMOTO, Atsushi[2] ; MACHIDA, Shinobu[1]

[1]Solar-Terrestrial Environmment Laboratory, Nagoya University, [2]Department of Geophysics, Graduate School of Science, Tohoku University

Plasmaspheric density structures have been studied for a long time. Although it has been clarified that the density is roughly constant along field lines in the outer plasmasphere, field-aligned density distributions of the inner plasmasphere has not been studied intensively. Moreover, continuous observations longer than one-solar cycle have not been reported. Consequently, long-term variations of the plasmaspheric density over a solar cycle remain unknown. In this study, using electron density data based on plasma wave observations from the PWS experiments on board the Akebono satellite from 1989 to 2008, we conduct statistical analyses on variations of structures of the plasmasphere and plasmatrough. In order to investigate the latitudinal distribution of the electron density, we assumed that electron density distribution along field lines are described by a power law form N_e = $N_{e0}(LR_E/R)\alpha, where N_{e0}$ is the equatorial electron density. Using the dataset during geomagnetically quiet periods and altitude higher than 4000 km, we derived solar cycle variations of the equatorial density N_{e0} and field-aligned density distributions α. N_{e0} and α are almost constant for the solar cycle ($N_{e0} \approx$ 2000 cm^{-3} and α = 0 – 1) in the inner plasmasphere at L = 2.1 – 2.3, which distribution is close to diffusive equilibrium. In contrast, $N_{e0}\sim$200 cm^{-3} and α=0 – 1 at solar minimum which distribution is close to diffusive equilibrium and N_{e0} $\sim$30 cm^{-3} and α= 2 – 3 at the solar maximum which distribution is close to collisionless in the outer plasmasphere at L = 4.2 – 4.7.

Keywords: plasmasphere, electron density, akebono satellite, solar-cycle

Japan Geoscience Union Meeting 2014
(28 April - 02 May 2014 at Pacifico YOKOHAMA, Kanagawa, Japan)

PEM04-P03 Room:Poster Time:April 28 18:15-19:30

Statistical analysis of EMIC waves in the inner magnetosphere from the Akebono observations

KATO, Yuichi[1*] ; MIYOSHI, Yoshizumi[1] ; SAKAGUCHI, Kaori[2] ; KASAHARA, Yoshiya[3] ; KEIKA, Kunihiro[1] ; KITAMURA, Naritoshi[1] ; SHOJI, Masafumi[1] ; HASEGAWA, Shuhei[1] ; KUMAMOTO, Atsushi[4] ; SHIOKAWA, Kazuo[1]

[1]Solar-Terrestrial Environment Laboratory, Nagoya University, Japan, [2]National Institute of Information and Communications Technology, [3]Information Media Center, Kanazawa University, [4]Department of Geophysics, Graduate School of Science, Tohoku University

Electromagnetic ion cyclotron (EMIC) waves in the inner magnetosphere are important since EMIC waves cause the pitch angle scattering of ring current ions as well as relativistic electrons of the radiation belts. Although the spatial distributions of EMIC waves have been investigated by several spacecraft such as CRRES, THEMIS and AMPTE, there have been little studies on their latitudinal distributions. Up to this point, we developed the automatic detection algorithm to use the magnetic field data observed by the ELF instrument on board the Akebono satellite, and demonstrated that EMIC waves exist inside the plasmasphere. Since the Akebono satellite measures the thermal plasma density, we investigate the fp(plasma frequency)/fc(cyclotron frequency) dependence and derive the resonance energies of the observed EMIC waves. In this presentation, we report the spatial distributions of EMIC waves, and discuss the dependence of fp/fc and the resonant energy.

Keywords: Electromagnetic Ion Cyclotron, EMIC wave, Statistical analysis, inner magnetosphere

Japan Geoscience Union Meeting 2014
(28 April - 02 May 2014 at Pacifico YOKOHAMA, Kanagawa, Japan)

PEM04-P04 Room:Poster Time:April 28 18:15-19:30

Dispersion relation of Pc1 geomagnetic pulsations using ground-magnetometer observations

NOMURA, Reiko[1*] ; PLASCHKE, Ferdinand[2] ; NARITA, Yasuhito[2] ; GLASSMEIER, Karl-heinz[1] ; FUJITA, Shigeru[3] ; MANN, Ian[4]

[1]IGEP, TU Braunschweig, [2]Space Research Institute Austrian Academy of Sciences, [3]Meteorological College, Japan Meteorological Agency, [4]University of Alberta

Pc1 geomagnetic pulsation (Pc1) observed on the ground at subauroral latitudes (L∼4) is the signature of ion cyclotron waves with frequencies 0.2-5.0Hz near the plasmapause. When the waves reach onto the ionosphere, they induce the Pedersen and Hall currents which generate both Alfven and fast mode waves in the ionospheric duct. On the ground we observe the variations of the magnetic field caused by both of the Alfven and the fast mode wave in the ionospheric duct. Previous studies based on the theoretical models showed the frequency dependence of attenuations, and the spatial distribution of wave polarisations, and furthermore, predicted the dispersion relation in the ionospheric duct. Especially for the characteristics of attenuations and polarisations, previous studies have been established using ground magnetometer observations. Yet, no study has demonstrated the Pc1 dispersion relation experimentally. In our presentation, we show the Pc1 dispersion relation obtained by the wave telescope analysis using CARISMA ground magnetometers.

Keywords: Pc1, EMIC waves, dispersion relation, ionospheric duct

Japan Geoscience Union Meeting 2014
(28 April - 02 May 2014 at Pacifico YOKOHAMA, Kanagawa, Japan)

PEM05-01 Room:424 Time:May 2 09:00-09:15

A Brief History of Collaborative Study on Equatorial MLT Dynamics using Meteor and MF Radars in Indonesia

TSUDA, Toshitaka[1*] ; DJAMALUDDIN, Thomas[2] ; YATINI, Clara[2] ; BUDIYONO, Afif[2] ; VINCENT, Robert[3] ; REID, Iain[3]

[1]Research Institute for Sustainable Humanosphere (RISH), Kyoto University, [2]Indonesian National Institute of Aeronautics and Space (LAPAN), [3]Department of Physics, University of Adelaide

In the tropics active cumulus convection generates various atmospheric waves, such as Kelvin waves, planetary waves, tides, and gravity waves. The wave energy and momentum are transported upward though propagating of these waves. Wave-mean flow interactions are crucially important for understanding of dynamical processes in the equatorial atmosphere, including the formation of peculiar long-term variations such as quasi-biennial oscillation (QBO) and semi-annual oscillation (SAO) in both the stratosphere and the MLT (mesosphere and lower thermosphere) region (70-120 km).

We constructed a total of five meteor and medium frequency (MF) radars in Indonesia since 1992 under close collaboration between RISH, LAPAN and the University of Adelaide. The MLT radar network has been expanded in India, Central and Eastern Pacific, and China. These radars have clarified the behavior of atmosphere dynamics in the MLT region. This paper gives an overview of our collaborative studies as well as highlights of scientific achievements using the MLT radar network

Keywords: mesosphere and lower thermosphere, equaotrial atmosphere, atmospheric waves, meteor radar, medium frequency radar, Indonesia

Japan Geoscience Union Meeting 2014
(28 April - 02 May 2014 at Pacifico YOKOHAMA, Kanagawa, Japan)

PEM05-02 Room:424 Time:May 2 09:15-09:45

Atmospheric Waves in the MLT: A Review

VINCENT, Robert[1*]

[1]University of Adelaide

Through their efficient transfer of energy and momentum, atmospheric waves propagating up from the lower atmosphere play an important role in determining the structure of the Mesosphere/Lower Thermosphere (60-100 km). A wide range of wave types are involved, with periods ranging from minutes to days. Here we review developments in our understanding of wave coupling and impacts on the MLT, with an emphasis on developments in the past decade.

Keywords: MLT Dynamics, Gravity Waves, Atmospheric Tides, Planetary Waves

Japan Geoscience Union Meeting 2014
(28 April - 02 May 2014 at Pacifico YOKOHAMA, Kanagawa, Japan)

PEM05-03 Room:424 Time:May 2 09:45-10:00

Behavior of non-migrating tides in the MLT region

MIYOSHI, Yasunobu[1*] ; FUJIWARA, Hitoshi[2]

[1]Kyushu University, [2]Seikei University

It is well established that non-migrating tides have significant amplitudes in the mesosphere and lower thermosphere (MLT). Using a general circulation model that contain the region from the ground surface to the upper thermosphere, behavior and excitation sources of non-migrating tides are examined. In this study, behaviors of the westward moving semidiurnal tide with zonal wavenumber 1 (SW1), the semidiurnal tide with zonal wavenumber 0 (S0) and the diurnal tide wit zonal wavenumber 0 (D0) are examined in detail. There are two main sources for non-migrating tides. One is latent heat release due to the cumulus convection in the troposphere. The other is the nonlinear interaction between the migrating tide and the stationary planetary wave in the middle atmosphere. Our results indicate that the amplitudes of SW1, S0 and D0 are enhanced when the stationary planetary wave in the stratosphere and mesosphere is active. This means that SW1, S0 and D0 are mainly excited by the nonlinear interaction between the migrating tide and the stationary planetary wave. Furthermore, we discuss excitation sources of other non-migrating tides, such as the eastward moving diurnal tide with zonal wavenumber 3 (DE3) and the eastward moving semidiurnal tide with zonal wave number 2 (SE2).

Keywords: Tides, General Circulation Model

Japan Geoscience Union Meeting 2014
(28 April - 02 May 2014 at Pacifico YOKOHAMA, Kanagawa, Japan)

PEM05-04 Room:424 Time:May 2 10:00-10:15

Long-term observations of MLT zonal wind variations in relation to stratospheric zonal winds over low-latitudes

GRANDHI, Kishore kumar[1*] ; KARANAM, Kishore kumar[2] ; SINGER, Werner[1] ; ZULICKE, Christoph[1] ; S, Gurubaran[3] ; GERD, Baumgarten[1] ; RAMKUMAR, Geetha[2] ; S, Sathishkumar[4] ; RAPP, Markus[5]

[1]Leibniz Institute of Atmospheric Physics, University of Rostock, Kuhlungsborn, Germany, [2]Space Physics Laboratory, Vikram Sarabhai Space Center, Trivandrum, India, [3]Indian Institute of Geomagnetism, Navi Mumbai, India, [4]Equatorial Geophysical Research Laboratory, Indian Institute of Geomagnetism, Tirunelveli, India, [5]German Aerospace Center Institute of Atmospheric Physics (IPA), Oberpfaffenhofen, Wessling, Germany

Long-term observations from medium-frequency and meteor radars (1993-2012) and rocket soundings (1979-1990 and 2002-2007) are used to study mesosphere lower thermosphere (MLT) zonal wind variations in relation to the stratospheric winds over Northern low-latitudes. The combined dataset provide a complete height profile of amplitude of semiannual oscillation (SAO) up to 100 km, with an exception around 75-80 km. The SAO signal has maxima around 50 km and 82 km and a minimum around 65 km. The MLT zonal winds show remarkable inter-annual variability during spring equinox and much less during fall equinox. Zonal wind mesospheric spring equinox enhancements (MSEE) appear with a periodicity of 2-3 years suggesting a modulation by the quasi-biennial oscillation, which we identified with the strength of stratospheric westward winds. Out of 20 years of observations, the stratospheric westward winds are strong during 11 years (non-MSEE) and weak during 9 years. Six of these years show large MLT winds (MSEE) and 3 years (1999, 2004 and 2006) show small MLT winds (missing-MSEEs). These unexpected small winds occur in years with global circulation anomalies as identified with strong sudden stratospheric warmings and an early spring transition of zonal winds, along with a minor enhancement in the tidal amplitudes.

Keywords: MLT winds, MSAO, Meteor radar, MF radar, QBO

Japan Geoscience Union Meeting 2014
(28 April - 02 May 2014 at Pacifico YOKOHAMA, Kanagawa, Japan)

PEM05-05 Room:424 Time:May 2 10:15-10:30

The saturation of gravity waves traveling from the lower to the upper atmosphere observed by the MU radar and understood

KATO, Susumu[1*] ; TSUDA, Toshitaka[1] ; YAMAMOTO, Mamoru[1] ; NAKAMURA, Takuji[2]

[1]Research Institute for Sustainable Humanosphere, Kyoto University, [2]National Polar Research Institute)

The MU radar of Kyoto University was constructed in 1984. One of the main purpose of the radar construction is to observe atmospheric gravity waves particularly to find how gravity waves saturate in traveling from the lower atmosphere to the upper atmosphere. In the 1980s Matsuno, Geller and others put forwards an idea suggesting that the gravity wave saturation may release momentum for driving the mesosphere general circulation. Their idea is based on rocket and satellite global- observation of winds and temperature varying peculiarly with seasons in the mesosphere.

Our MU radar observation has been successful in proving the gravity wave momentum release to be in a good agreement with the required quantity for the mesosphere general circulation. Also our success of precise measurements of the saturated gravity wave power spectrum strongly supports to explain the gravity wave saturation idea in terms of a simple theory based on the linear or monochromatic gravity wave theory by Hines in 1960.

Our theory on the basis of our MU radar observation shows that the gravity wave saturation is attained for each gravity wave in amplitude reaching the phase speed due to a balance between the increasing amplification expected by the linear theory and non-linear braking effects. We can consider that the original gravity wave dispersion relation is maintained upon the saturation.

Gravity waves should experience a number of such saturations before
reaching the thermosphere on the way.

Japan Geoscience Union Meeting 2014
(28 April - 02 May 2014 at Pacifico YOKOHAMA, Kanagawa, Japan)

PEM05-06 Room:424 Time:May 2 10:30-10:45

Ducted Concentric Gravity Wave Observed by IMAP/VISI Associated with Super Typhoon Haiyan

PERWITASARI, Septi[1*] ; SAKANOI, Takeshi[1] ; YAMAZAKI, Atsushi[2] ; OTSUKA, Yuichi[3] ; HOZUMI, Yuta[4] ; AKIYA, Yusuke[4] ; SAITO, Akinori[4] ; SUZUKI, Shin[3]

[1]PPARC, Tohoku University, [2]JAXA/ISAS, [3]STEL, Nagoya University, [4]Geophysics Dept., Kyoto University

Although the convection activity in the troposphere is generally accepted as one of important source of gravity waves in the mesosphere and lower thermosphere, however it is still uncertain how these waves can reach these regions and what types of waves are generated. For decades, the study of gravity waves has been classified into two categories; first is that the waves travel directly from the source and the second is that the waves are ducted or trapped. Many studies tried to explain both categories yet all studies focused on gravity waves produced by transient events. There were almost no observation reports of airglow emissions during a large storm and what type of gravity waves and typical wavelength can be produced from such event. To address this issue, a space-based observation is more preferable since it covers wider area. Until recently, IMAP/VISI is the only space-based instrument that capable of imaging gravity waves above the troposphere in the nadir direction. The Visible and near-Infrared Spectral Imager (VISI) of the IMAP mission was launched successfully on July 21, 2012 with H-IIB/HTV-3 and installed onto the International Space Station (ISS). IMAP/VISI is now operated in the night side hemisphere with a range of +/- 51 deg. GLAT. IMAP/VISI is measuring three different airglow emissions of OI at 630 nm, the OH Meinel band at 730 nm and the O_2 (762 nm) atmospheric band at 762 nm at an altitude of ˜400 km with the typical spatial resolution of 16-50 km.

We found concentric gravity waves events in the southeastern part of Australia that was observed around 13-15 UT for 3 days from 6-8 November 2013 in O_2 (0-0) airglow emission by IMAP/VISI. The waves have horizontal wavelength vary from 80 – 210 km. By using the least squares method, the curvature of the waves was fitted to a perfect circle. The center of the wave was found to be around 155^0E; -42^0S with the radius varies from 400-1200 km. From the meteorological satellite, we cannot locate any convective source around the center of the wave. The nearby local convective source was located a few hundreds km to the south of the wave center and the rainfall rate was less than 10 mm/hr. Therefore, we rule out the possibility of local convective activity as the source of these waves. From the past studies, there were evidences that the gravity waves may be ducted and traveled a great distance away from a specific convective source (e.g. Nakamura et al., 1999; Walterscheid et al., 1999; Hecht et al., 2001). Their studies suggested that the gravity waves observed in Australia were originated from convective activity several thousands km north of Australia. During the observed events, the Typhoon Haiyan was underway. On November 6, the typhoon was categorized as 5 – equivalent of super typhoon and reached its peak on November 7 and then made a landfall in Philippine on November 8. In this study, we argue that the concentric gravity waves seen by IMAP/VISI could be generated by the intense convective activity associated with the Haiyan Typhoon event. Background wind data from TIDI (TIMED Doppler Interferometer) and MF Radar will be used to examine the plausibility for the formation of a ducted/trapped region that can explain the long distance propagation of these waves. The temperature profile from MSISE-90 model will also be used to examine the mesospheric inversion layer and if it ′ s possible to get the data, we will also use the ground-based airglow imager data from Adelaide and Alice Spring.

Keywords: IMAP/VISI, O2 (0-0), concentric gravity wave, ducted, typhoon Haiyan

Japan Geoscience Union Meeting 2014
(28 April - 02 May 2014 at Pacifico YOKOHAMA, Kanagawa, Japan)

PEM05-07 Room:424 Time:May 2 11:00-11:30

The MF Radar Technique: a Review

REID, Iain[1*]

[1]Department of Physics, University of Adelaide, [2]ATRAD Pty Ltd

The Medium Frequency (MF) radar technique has been applied for more than five decades to measure winds and turbulence in the upper atmosphere in the region between 60 and 100 km during the day, and between 80 and 100 km at night. It is one of the few techniques able to provide winds reliably in the 60 to 80 km height region during the day. Although some care is needed in interpretation of the results, it remains a powerful and very useful technique. In this paper, we review the technique and highlight some recent recent results.

Keywords: Radar, Medium Frequency, Spaced Antenna, Mesosphere Lower Thermosphere, Winds, Turbulence

Japan Geoscience Union Meeting 2014
(28 April - 02 May 2014 at Pacifico YOKOHAMA, Kanagawa, Japan)

PEM05-08 Room:424 Time:May 2 11:30-11:45

Tidal periodicity of mesospheric gravity waves observed with MF radar at Poker Flat, Alaska and at Tromso, Norway

MURAYAMA, Yasuhiro[1*] ; KINOSHITA, Takenari[1] ; KAWAMURA, Seiji[1] ; NOZAWA, Satonori[2] ; HALL, Chris[3]

[1]National Institute of Information and Communicatoins Technology, [2]Solar-Terrestiral Physics Laboratory, [3]Toromso University

The interaction between gravity waves and tidal waves has been studied by using observations, although the phase relation between them was not fully understood (e.g., Saskatoon, Canada (Manson et al. 1998), Rothera, Antarctica (Beldon and Mitchell, 2010)). The neutral wind velocity data from mesosphere to lower thermosphere observed by MF radars at Poker Flat in Alaska and Tromso in Norway has been observed since the late 1990s. The long-term wind velocity data at Poker Flat and Tromso was analyzed for 10 years of 1999 ? 2008 to show daily and seasonal behaviors and climatology of mesospheric gravity waves and horizontal wind of the 12 and 24 hour components. First, we extracted these waves from the MF radar observation data. In this study, harmonic analysis was carried out for periods of 48, 24, 12, and 8 hours, which are extracted from the 5 day time series of wind velocity using. Gravity waves are defined as the 1 ˜12 hour period component of difference between observed wind velocity and these harmonic components. The method is applied to 30-minute-average data to calculate the 5 day running mean amplitude and phase of zonal wind of the 12 and 24 hour components. We made 1- day composite plots of kinetic energy of gravity waves for periods of 1 ˜4 hours and harmonic components. The results show that the kinetic energy of gravity waves in Tromso has a peak in 6UT from November to February which tends to coincide with the time when zonal wind of 24 hour component is easterly maximum and easterly wind of 12 hour components is switched westerly. This feature is different from results in Poker Flat and Saskatoon. On the other hand, the phase relation between 12 hour components of zonal wind and kinetic energy of gravity waves shows that their phase agrees for more than 10 days in several years in both observation points. We confirmed the phase agreement in Tromso continued about 10 days at the same time when that in Poker Flat is continued more than 20 days from November to December in 2000. However, the phase of gravity wave kinetic energy is shifted 90 degrees between Tromso and Poker Flat. We plan to discuss more detail of underlying physical processes, focusing on migrating and non-migrating tidal waves and background state of horizontal wind velocities.

Japan Geoscience Union Meeting 2014
(28 April - 02 May 2014 at Pacifico YOKOHAMA, Kanagawa, Japan)

PEM05-09 Room:424 Time:May 2 11:45-12:00

Characteristics of Short Period Tidal Components in Antarctic MLT above Syowa and Davis

TSUTSUMI, Masaki[1*] ; MURPHY, Damian[2]

[1]National Institute of Polar Research, Japan, [2]Australian Antarctic Division

The behaviour of short period atmospheric tidal components in the Antarctic mesosphere and lower thermosphere is studied based on long term observations over Syowa (69.0S, 39.6E) and Davis (68.6S, 78.0E) stations. Semidiurnal tides in the Antarctic mesosphere and lower thermosphere have been extensively studied through the recently established Antarctic radar network [e.g., Murphy et al., 2006; 2008]. However, details of shorter period components such as terdiurnal and six-hour tides are less investigated and poorly known because of their smaller amplitudes compared to the semidiurnal and diurnal tides in the height region of conventional MF radar observations of around 70-90 km. These short period tides also fall in the frequency range of inertial gravity waves and are often hard to distinguish from these waves.

The characteristics of the terdiurnal tide above Davis and Syowa have been measured on a short-term to seasonal basis in the mesosphere and lower thermosphere using long-term simultaneous MF radar data at the two sites (1999-). The terdiurnal tide achieves moderate amplitudes in the winter at these heights but there are subtle differences between the two stations. These differences are explored further by differencing tide phasors in local time and checking the amplitude of the result on a seasonal basis. If the terdiurnal tide was made up entirely of migrating components, this difference would yield a zero-average amplitude. However, the observed non-zero values suggest that the terdiurnal tide at these latitudes contains strong non-migrating tidal components.

The Syowa MF radar has a great advantage over other MF radars in that it has been conducting simultaneous meteor wind measurements together with the conventional correlation based measurements, which enables wind observations in a very wide height range of 65-120km [Tsutsumi and Aso, 2005]. A clear enhancement in terdiurnal amplitudes is seen in early winter months of March-June. The amplitudes can reach 20 m/s around 110 km even in the composite plot made with more than 10 years of data. These amplitudes can be comparable or sometimes even larger than those of diurnal and semidiurnal tides, and indicate a possible significant role of short period tidal components in the polar lower thermosphere.

Keywords: Antarctic, mesosphere and lower thermosphere, short period atmospheric tidal waves

Japan Geoscience Union Meeting 2014
(28 April - 02 May 2014 at Pacifico YOKOHAMA, Kanagawa, Japan)

PEM05-10 Room:424 Time:May 2 12:00-12:15

The SMILES observations of mesospheric ozone during the solar eclipse

IMAI, Koji[1*] ; AKIYOSHI, Hideharu[2] ; TAKAHASHI, Kenshi[3] ; YAMASHITA, Yousuke[2] ; IMAMURA, Takashi[2] ; SUZUKI, Makoto[1] ; EBISAWA, Ken[1] ; SHIOTANI, Masato[3]

[1]Institute of Space and Astronautical Science, Japan Aerospace Exploration Agency, Sagamihara, [2]National Institute for Environmental Studies, [3]Research Institute for Sustainable Humanosphere, Kyoto University

Solar eclipse temporally reduces the amount of solar radiation, providing an opportunity to verify the ozone photochemistry under changing solar radiation. During the longest annular solar eclipse in this millennium occurred on 15 January 2010, Superconducting Submillimeter-Wave Limb-Emission Sounder (SMILES) successfully captured increased ozone mostly in the mesosphere with a decrease in solar illuminations. The ozone increment shows altitude dependence in the mesosphere. Using an atmospheric chemistry box model, it is found that the dependence results from the difference in chemical reaction rates to the solar radiation change. The model also predicts the difference in the ozone concentration evolution between the sunlight decreasing and increasing phases, although SMILES observation does not resolve the difference.

Keywords: SMILES, ozone, mesosphere

Japan Geoscience Union Meeting 2014
(28 April - 02 May 2014 at Pacifico YOKOHAMA, Kanagawa, Japan)

PEM05-11 Room:424 Time:May 2 12:15-12:30

Contribution of the IUGONET data analysis system to upper atmospheric researches

SHINBORI, Atsuki[1*] ; YAGI, Manabu[2] ; TANAKA, Yoshimasa[3] ; SATO, Yuka[3] ; YATAGAI, Akiyo[4] ; UMEMURA, Norio[4] ; UENO, Satoru[5] ; KOYAMA, Yukinobu[6] ; ABE, Shuji[7]

[1]Research Institute for Sustainable Humanosphere (RISH), Kyoto University, [2]Planetary Plasma and Atmospheric Research Center, Graduate School of Science, Tohoku University, [3]National Institute of Polar Research, [4]Nagoya University Solar Terrestrial Environment Laboratory Geospace Research Center, [5]Kwasan & Hida Observatories, School of Science, Kyoto University, [6]Data Analysis Center for Geomagnetism and Space Magnetism Graduate School of Science, Kyoto Universi, [7]International Center for Space Weather Science and Education, Japan

Various kinds of atmospheric disturbances and long-term variation as seen in several parameters (temperature, mean wind etc.) in the upper atmosphere (mesosphere, thermosphere and ionosphere) is caused by energy input from solar radiation, momenta and energies from the lower atmosphere (stratosphere and troposphere) via atmospheric waves, and chemical reaction. Such atmospheric phenomena observed by ground-based and satellite instruments are the result of such complicated processes. In order to investigate the mechanisms of the atmospheric disturbances and long-term variations in the upper atmosphere, which may be affected by solar activities and global warming, researchers need to conduct comprehensive analyses with various kinds of long-term observation data that have been continued by means of a global network of MST (Mesosphere-Stratosphere-Troposphere) radars, optical sensors, radiosondes, etc. The IUGONET (Inter-university Upper atmosphere Global Observation NETwork) project initiated in 2009 aims at the establishment of a cross-reference system for various kinds of ground-based observation data. The IUGONET participants consist of five universities/institutes: the National Institute of Polar Research (NIPR), Tohoku University, Nagoya University, Kyoto University, and Kyushu University. We have developed a metadata database (MDB) of ground-based observations and IUGONET data analysis software (UDAS) in order to provide researchers in a wide range of disciplines with a seamless data environment to link databases spread across the IUGONET institutions. In particular, the MDB and UDAS will be of great help in data acquisition and integrated analyses to understand the dynamics on the mesosphere-lower thermosphere (MLT) throughout the Sun-Earth system. Therefore, the IUGONET MDB and UDAS will greatly contribute to upper atmospheric researches on the basis of integrated analysis of various kinds of long-term observation data covering a wide region from both the poles to the equator. In this talk, we introduce a brief overview of the IUGONET project and an application of the IUGONET products for upper atmospheric researches.

Keywords: Upper atmosphere, Grand-based observation data, IUGONET, metadata search system, IUGONET data analysis tool

Japan Geoscience Union Meeting 2014
(28 April - 02 May 2014 at Pacifico YOKOHAMA, Kanagawa, Japan)

PEM05-12 Room:424 Time:May 2 12:30-12:45

Vertical and lateral wave coupling observed with network of MLT/MST Radars over Indian region

M, Venkat ratnam[1*] ; S., Eswariah[2] ; N., Venkateswara rao[1] ; S., Vijayabhaskar rao[2] ; K., Kishore kumar[3] ; S., Sathish kumar[4] ; S., Gurubaran[4]

[1]National Atmospheric Research Laboratory, [2]Sri Venkateswara University, [3]Space Physical Laboratory, [4]Indian Institute of Geomagnetism

It is well known that gravity waves and tides play an important role in delineating the middle atmospheric structure and dynamics. There have been several studies in recent years, using different measurement techniques, to understand significant roles played by gravity waves and tides in the lower, middle and upper atmospheres. However, only a few studies addressed this problem with simultaneous observations of all the three regions. Moreover, no efforts have been made so far to understand the lateral forcing of these waves and tides since such a study needs a network of radars located nearby which was missing. With the establishment of an advanced meteor radar at Sri Venkateswara University, Tirupati (13.63oN, 79.4oE), India, and up gradation of MF radar at Kolhapur (16.8oN, 74.2oE) together with MST radar at Gadanki (13.5oN, 79.2oE), Meteor radar at Thumba (8.5oN, 77oE) and MF radar at Tirunalveli (8.7oN, 77.8oE) forms a unique network of radars in the tropical region. Importantly, all these radars are located within 1000 km distance. Accordingly, this network is suitable to study the lower atmospheric forcing and its impacts on middle and upper atmospheric structure and dynamics. For the present study, all these radars were simultaneously operated for a few days in September 2013. These observations show the presence of short period gravity waves and tides (diurnal, semi-diurnal and ter-diurnal) at all locations. Large day-to-day day variability in gravity waves and tides is observed within a station and among different stations providing insight on lateral coupling. Phase propagations of the three tidal components at different stations is used to further understand the lateral coupling. Using simultaneous MST radar, Rayleigh lidar and SVU meteor radar (which are nearly co-located), lower atmospheric forcing and its impacts on the mesosphere and lower thermosphere are investigated. This study showed need for long-term measurements, with simultaneous operation of all the above mentioned network of radars, to effectively address the problem of vertical and latitudinal wave forcing.

Keywords: Coupling, Meteor/MF radars, Tropical MLT region

Japan Geoscience Union Meeting 2014
(28 April - 02 May 2014 at Pacifico YOKOHAMA, Kanagawa, Japan)

PEM05-P01 Room:Poster Time:May 2 16:15-17:30

Diurnal tide and QTD wave in the tropical stratosphere and MLT region: Long-term trends and solar cycle influence

NARUKULL, Venkateswara rao[1*] ; M., Venkat ratnam[1] ; C., Vedavathi[2] ; S., Gurubaran[3] ; B.V., Krishna murthy[4] ; S., Vijaya bhaskara rao[2]

[1]National Atmospheric Research Laboratory, [2]Sri Venkateswara University, [3]Indian Institute of Geomagnetism, [4]B1, CEEBROS, 47/20, IIIrd Main Road, Chennai

In the present study, long-term trends and solar cycle influence on the diurnal tide (DT) and quasi two day wave (QTDW) in the stratosphere, mesosphere and lower thermosphere (MLT) region over a tropical station Tirununveli (8.7oN, 77.7oE) are investigated using ERA-Interim datasets and MF radar observations available since 1993. As no ground truth is available over Tirununveli, suitability of the ERA-Interim data for the present study is ascertained using simultaneous radiosonde and MST radar observations over Gadanki (13.5oN, 79.2oE) and good consistency is found between the two. Amplitudes of the DT and QTDW over Tirununveli show a long-term linear increasing trend, which becomes prominent in the MLT region. Role of solar cycle on the DT and the QTDW is investigated by separating them with respect to the solar activity (minimum and maximum of solar cycles). Both the DT and QTDW show higher amplitudes during solar minimum and vice versa. Significant higher amplitudes in the recent extended solar minimum are noticed in the MLT region. However, no consistent relation is found between solar activity and DT in the stratosphere although increasing trend is clearly observed. Though increasing trend in the tropical convection is noticed at nearby locations, similar to the DT, it varies from location to location which may be due to large scale circulation effects. This demands data from network of radars located across the globe to see the combined effects of lower atmospheric forcing, circulation and their effects on MLT region.

Keywords: Diurnal Tide, Quasi-two day wave, Long-term trends, Solar cycle, Extended minimum

Japan Geoscience Union Meeting 2014
(28 April - 02 May 2014 at Pacifico YOKOHAMA, Kanagawa, Japan)

PEM05-P02 Room:Poster Time:May 2 16:15-17:30

MQBE and Amplitude Modulation of SAO in the MLT

MATSUMOTO, Naoki[1*] ; SHINBORI, Atsuki[2] ; TSUDA, Toshitaka[2]

[1]Division of Earth and Planetary Sciences, Graduate School of Science, Kyoto University, [2]Research Institute for Sustainable Humanosphere (RISH), Kyoto University

Characteristics of various atmospheric waves in the mesosphere and lower thermosphere (MLT) have been investigated by long-term ground-based and satellite-based observation. In the equatorial region, the westward monthly mean wind is enhanced in March in 2 or 3 years in MLT, which is called Mesosphere Quasi-Biennual Enhancement (MQBE) [Rao et al., 2012]. Recently, They showed that MQBE appears once in 2 or 3 years until 2002, based on data analysis of meteor/MF radars in the Asia-Oceania region. However, the occurrence features remained unknown due to no sufficient wind data with high-time resolution from 50 to 80 km.

We analyzed the long-term wind data from 1990 to 2013 obtained from meteor/MF radars in the Asia-Oceania region, such as Kauai, Christmas island, Tirunelveli, Koto Tabang in order to identify the occurrence features and mechanism of MQBE. And also we investigated relationship of the monthly-mean wind between MLT stratosphere using MERRA retrospective-analyses data provided by NASA. We used integrated analysis tool " UDAS " provided by " IUGONET " (Inter-university Upper atmosphere Global Observation NETwork). And We use Stockwell-transform to detect the temporal variation of frequency and amplitude in time series data.

As a result, we found that MQBE occurred in spring of 2005, 2008 and 2011 with amplitude over 32 m/s in an altitude from 80 to 100 km . From an S-transform spectral analysis of zonal wind in MLT, MQBE coincides with the enhancement of the amplitude of 6-months component of zonal wind. Furthermore, comparing the 6-month component in the lower thermosphere at 90 km and stratosphere using retrospective-analyses data of MERRA, 6-months component of lower thermosphere(90 km) and stratopause (1 hPa) are well negative correlated. And also 6-months component of lower thermosphere and lower stratosphere (70 hPa) are well positive correlated. Their correlation coefficients are about 0.6, and lags are under 3 month. the former result is consistent with the fact that the phase of SAO are reversal in the lower thermosphere and in the stratosphere.

Although Rao et al.,[2012] reported that MQBE did not appear after 2002, the present results showed that MQBE takes place after 2002. Next, the SAO amplitude in MLT obtained from the S-transform analysis tends to be enhanced significantly, corresponding to the occurrence of MQBE. This relationship can be a clue of occurrence features of MQBE. Furthermore, the relationship of mean wind between in MLT and stratosphere indicates that MQBE is driven by coupling process of the mesosphere-stratosphere system. We can infer that MQBE is caused by atmospheric gravity waves, which is similar to the generation mechanism of QBO.

In addition, we need to detect and analyze the gravity wave in equatorial region to identify the mechanism of MQBE.

Keywords: meteor radar, MF radar, stratosphere, SAO, MQBE

Japan Geoscience Union Meeting 2014
(28 April - 02 May 2014 at Pacifico YOKOHAMA, Kanagawa, Japan)

PEM05-P03 Room:Poster Time:May 2 16:15-17:30

Meteor Wind Radar Application for the study the dynamics of the neutral winds above at Kototabang and Biak station

ACHMAD, Effendy[1] ; TSUDA, Toshitaka[2] ; SHINBORI, Atsuki[2*]

[1]National Institute of Aeronautics and Space Indonesia (LAPAN), [2]Research Institute for Sustainable Humanosphere

Currently for meteor observations is not only done with the naked eye and optical equipment such as a telescope, the latest development to detect natural phenomena meteor shower rained almost every day the Earth can be detected using radar technology. Meteor Wind Radar (MWR) is a radar system used to detect, analyse and display meteor entrance events to the Earth's atmosphere. By using of radar meteors (SKiYMET Meteor Radar) was used to observe the meteor trail (ionized air columns) that moves with the wind neutral layer of mesosphere. When a meteor enters the atmosphere it rapidly vaporises leaving behind a trail of ionised gas along its path of travel, this trail can form a target for a radar transmission. Generally the frequencies used for the detection of radar, located on the VHF band wave spectrum. The results of the analysis of radar data output consists of 7th meteor parameter can be used to study the behavior of neutral winds in the Mesosphere. In this paper the utilization of SKiYMet shown to detect Wind speed Meridional and Zonal Wind speed, Temperature in the Mesosphere and the number and received Flux meteor in the Earth, as a sources of data to better understand the dynamics of the neutral winds at an altitude of 70-110 km region of observation locations. Simultaneously measurement data will be shown at Kototabang observations that have been operating since year 2006 and in Biak Station since year 2011. All of the radar installation is a collaboration between LAPAN and RISH - Kyoto, NICT Japan.

Keywords: Meteor radar, Indonesia, Equatorial regiona, Koto Tabang, Biak

Japan Geoscience Union Meeting 2014
(28 April - 02 May 2014 at Pacifico YOKOHAMA, Kanagawa, Japan)

PEM05-P04 Room:Poster Time:May 2 16:15-17:30

Concentric structures in molecular oxygen emission observed by ISS-IMAP/VISI

AKIYA, Yusuke[1*] ; SAITO, Akinori[1] ; SAKANOI, Takeshi[2] ; HOZUMI, Yuta[1] ; YAMAZAKI, Atsushi[3] ; OTSUKA, Yuichi[4] ; NISHIOKA, Michi[5] ; TSUGAWA, Takuya[5]

[1]Department of Geophys., Kyoto Univ., [2]PPARC, Tohoku University, [3]ISAS/JAXA, [4]STE Lab., Nagoya Univ., [5]NICT

Concentric structures in airglow emissions were often observed from ground based imagers. Some of them were thought to be caused by the active clouds in the troposphere. It was not able to observe the overall structures from the imagers on the ground under the cloudy condition. Field of views of the imagers were not enough to observe whole structure. Space borne imagers are able to observe the structures caused by the disturbances in the lower atmosphere with wider field of view. Concentric structures of the O_2 airglow emission in 762-nm wavelength were found by the Visible and near-infrared imager on the International Space Station on June 1, 2013 over the U. S. This is the first case which took the image from edge to the center of the concentric structure. Spatial scale of this concentric structures were estimated to be 1,200 km. Fine structures with 80 km wavelength and no dumping in the intensity were observed in this VISI observation. Amplitude in these fine structures were about 10 % to the background intensity. Circular structures were also observed in the GPS-TEC observations before the VISI observation. These concentric structures were estimated to be caused from the active clouds after tornado and atmospheric gravity waves had propagated in horizontal direction in the emission layer.

Keywords: Near infrared, Airglow, Concentric structure, the Mesosphere, Atmospheric gravity waves

Japan Geoscience Union Meeting 2014
(28 April - 02 May 2014 at Pacifico YOKOHAMA, Kanagawa, Japan)

PEM05-P05 Room:Poster Time:May 2 16:15-17:30

Background Lamb waves coupled with thermospheric gravity waves

NISHIDA, Kiwamu[1*] ; KOBAYASHI, Naoki[3] ; FUKAO, Yoshio[2]

[1]ERI, Univ. of Tokyo, [2]IFREE, Jamstec, [3]ISAS, JAXA

Lamb waves of the Earth's atmosphere in the millihertz band have been considered as transient phenomena excited only by large events. Nishida et al. (2014) showed the first evidence of background Lamb waves in the Earth's atmosphere from 0.2 to 10 mHz, based on the array analysis of microbarometer data from the USArray in 2012. The observations suggest that the probable excitation source is atmospheric turbulence in the troposphere. Theoretically, their energy in the troposphere tunnels into the thermosphere at a resonant frequency via thermospheric gravity wave because the Lamb-wave branch intersects that of thermospheric gravity waves at 3.5 mHz and that of acoustic waves trapped near the mesopause at 6.5 mHz [Garrett 1969]. The observed FK spectrum shows a local minimum of Lamb-wave amplitudes at around 3.5 mHz, where the Lamb-wave branch is crossed by the thermospheric gravity-wave branch. Coupled Lamb waves leak a certain amount of energy from the troposphere to the thermosphere, reducing the Lamb-wave amplitudes at the crossover frequency relative to those at neighboring frequencies, when their excitation sources exist in the troposphere. The energy tunnels from the troposphere to the thermosphere at the resonant frequency, although Lamb waves themselves cannot induce an upward flux [Lindzen 1972]. The RMS amplitudes of the coupled modes are estimated to be 0.3 m/s at 150 km and 0.1 m/s at 120 km, respectively. These modes might contribute to the thermosphere energy balance by heating via viscous dissipation [Hickey et al. 2001]. The amplitude suggests that the Lamb waves partly contribute to the excitation of thermospheric wave activity associated with severe convection activity [Hunsucker1982].

Keywords: Atmospheric Lamb wave, Thermospheric gravity wave

Japan Geoscience Union Meeting 2014
(28 April - 02 May 2014 at Pacifico YOKOHAMA, Kanagawa, Japan)

PEM05-P06 Room:Poster Time:May 2 16:15-17:30

A proposal of simple resonance scattering lidar using an alkali metal vapor laser for monitoring the MLT region

ABO, Makoto[1*] ; MIURA, Natsumi[1] ; NAGASAWA, Chikao[1] ; SHIBATA, Yasukuni[1]

[1]Tokyo Metropolitan University

Many observations of metal atomic layers such as Na, Fe, K, Ca and Ca ion in the mesopause region have been conducted in many parts of the world. We have observed several mesospheric metallic layers at Tokyo and Indonesia using resonance scattering lidars consisting of a dye laser and a Ti:Sapphire laser [1]. Especially, in order to solve the formation mechanism of metallic sporadic layers occurred in the mesopause region, the simultaneous observation of Ca ion and the neutral metal atom is necessary. However since the output power of the Ti:Sapphire laser has a low damage threshold of a crystal, it is difficult to improve the output average power. We propose the resonance scattering lidar consisting of the alkali vapor laser for monitoring the MLT region. Optically pumped alkali vapor lasers have attracted increasing attention because of their potential of achieve high power in a high quality beam. The alkali vapor laser can easily realize narrow-linewidth and precise tuning.

Metal atomic layers in the mesosphere are an excellent tracer of the atmospheric wave motion in the region between 80 and 100km. sudden formation of thin metallic layers, superposed in the background mesospheric metallic layers was discovered and these enhanced layers are called the sporadic metallic layers. We have observed frequently the sporadic sodium layers (Nas) at Hachioji, Japan (35.6N, 139.4E) and the sporadic sodium and iron layers (Fes) at Kototabang, Indonesia (0.2S, 100.3E). The ion recombination mechanism invoking wind shear and sporadic E layers appears to be consistent with many observed characteristics, but their cause is still an open question.

Zhdanov et al. presented optically pumped continuous wave potassium vapor laser operating in a single longitudinal and a single transverse mode at 770 nm [2]. Zweiback et al. demonstrated a high efficiency potassium vapor laser using a 0.15nm bandwidth alexandrite laser as the pump source [3]. The alkali vapor laser operates in a three level scheme. The optical pump source excites the D2 line of alkali atom and lasing occurs on the D1 line. To provide a population inversion, fast quenching must be provided by using a buffer gas. We are developing a high peak power pulsed potassium vapor laser using alexandrite laser as the optical pump source. Sealed potassium vapor cell had AR coated windows, and filled with metallic potassium and helium. The cell was assembled inside an oven which had temperature controlled heaters. A pump beam polarized in the horizontal plane was focused through the polarizing beam splitting cube into the potassium vapor cell with a lens. A laser cavity was created for the vertical polarization by two mirrors and the beam splitting cube.

The development of these kinds of lasers is identified as one of the key topics for advancing the application of resonance scattering lidar systems.

References

[1] Y. Shibata et al., J. Meteor. Soc. Jap., 84A, 317-325, 2006.
[2] B. Zhdanov et al., Opt. Commun., 270, 353-355, 2007.
[3] J. Zweiback et al., Opt. Commun., 282, 1871-1873, 2009.

Keywords: mesopause, metal atomic layer, resonance scattering lidar, metal vapor laser

Japan Geoscience Union Meeting 2014
(28 April - 02 May 2014 at Pacifico YOKOHAMA, Kanagawa, Japan)

PEM06-01 Room:312 Time:April 30 11:00-11:30

Study of Coupling Processes in the Solar-Terrestrial System: Project Overview

TSUDA, Toshitaka[1*]

[1]Research Institute for Sustainable Humanosphere (RISH), Kyoto University

We promote a project named ”Coupling Process in the Solar-Terrestrial System” under close collaboration among universities and research institutess. We aim to study the solar energy inputs to the Earth, and responses of the Geospace (magnetosphere, ionosphere and atmosphere) to them. The solar energy can manly be divided into two parts; the solar radiation, involving infra-red, visible, ultra-violet and X-ray, and the solar wind, which is a high-speed flow of plasma particles.

The solar radiation becomes the maximum on the equator, then, atmospheric disturbances are actively generated near the Earth’s surface. They further excite various atmospheric waves, which propagate upward carrying energy and momentum. On the other hand, electro-magnetic energy associated with the solar wind converges into the polar regions. Disturbances are also generated there, and a part of the energy is transported toward lower latitudes and lower atmospheric regions. We propose to establish large atmospheric radars with active phased array antenna on the equator and the Arctic region. Among the equatorial regions, we focus on Indonesia where the atmospheric disturbances are most intense in the world, and we will establish a comprehensive observatory in Indonesia with the Equatorial MU radar as its main facility. While, we will also construct the state-of-the-art radar, called EISCAT-3D, in Scandinavia under international collaboration. An observation network of portable equipment for will be expanded in Asia and Africa to clarify the global flow of energy and materials.

Keywords: Equatorial fountain, Equatorial MU Radar, EISCAT_3D, Global observation network

Japan Geoscience Union Meeting 2014
(28 April - 02 May 2014 at Pacifico YOKOHAMA, Kanagawa, Japan)

PEM06-02 Room:312 Time:April 30 11:30-11:45

A Review on Equatorial Atmosphere Radar (EAR) Observations of Lower Atmosphere

HASHIGUCHI, Hiroyuki[1*] ; TSUDA, Toshitaka[1] ; YAMAMOTO, Mamoru[1] ; YAMAMOTO, Masayuki[1] ; SHIBAGAKI, Yoshiaki[2] ; SHIMOMAI, Toyoshi[3] ; EDDY, Hermawan[4]

[1]Research Institute for Sustainable Humanosphere (RISH), Kyoto University, [2]Osaka Electro-Communication University, [3]Shimane University, [4]National Institute of Aeronautics and Space (LAPAN), Indonesia

The Equatorial Atmosphere Radar (EAR) is an atmospheric radar located in Kototabang, West Sumatra in Indonesia (0.20S, 100.32E). The EAR has a circular antenna array of approximately 110 m in diameter, consisting of 560 three-element Yagis. It is an active phased array system with each Yagi driven by a solid-state transceiver module. It is operated by collaboration between the Research Institute for Sustainable Humanosphere (RISH), Kyoto University and National Institute of Aeronautics and Space of Indonesia (LAPAN), Indonesia since 2001. RISH has conducted a collaborative research program (EAR collaboration) by using the EAR and its related facilities since 2005. The EAR can observe winds and turbulence in the lower atmosphere and echoes from ionospheric irregularities. In the presentation, observation results of the lower atmosphere with the EAR are reviewed.

Keywords: Equatorial Atmosphere Radar, Equatorial MU Radar, Equatorial Atmosphere

Japan Geoscience Union Meeting 2014
(28 April - 02 May 2014 at Pacifico YOKOHAMA, Kanagawa, Japan)

PEM06-03 Room:312 Time:April 30 11:45-12:00

Ionospheric observations by SEALION and the Equatorial Atmosphere Radar

YOKOYAMA, Tatsuhiro[1*] ; TSUGAWA, Takuya[1] ; ISHII, Mamoru[1]

[1]National Institute of Information and Communications Technology

Equatorial spread F (ESF) is a well-known phenomenon in the equatorial ionoshperic F region. As it causes severe scintillation in the amplitude and phase of radio signals, it is important to understand and forecast the occurrence of ESF from a space weather point of view. Ionospheric observation with the 47-MHz Equatorial Atmosphere Radar (EAR) in West Sumatra, Indonesia (0.20S, 100.32E, 10.36S dip latitude) has been conducted since 2001, and its unique observational data has been obtained for more than one solar cycle. The EAR is sensitive to 3-m scale ionospheric irregularities, which can be regarded as a tracer of ESF. Along with the EAR observations, Southeast Asia Low-latitude Ionospheric Network (SEALION) project by NICT started in 2003 for the purpose of monitoring and forecasting ESF. The SEALION consists of multiple ionosondes, GPS receivers and several other instruments in the Southeast Asian region. Since the developed ESF usually drifts eastward, monitoring ESF in this region can provide important space weather information for the Japanese longitude sector. We will summarize observational results with the SEALION and EAR, and discuss future potential of the ionospheric observation in the Southeast Asian region.

Keywords: SEALION, EAR, equatorial spread F, equatorial ionosphere

Japan Geoscience Union Meeting 2014
(28 April - 02 May 2014 at Pacifico YOKOHAMA, Kanagawa, Japan)

PEM06-04 Room:312 Time:April 30 12:00-12:15

Development of Indonesian Monsoon Index (IMI) Based on EAR and other Facilities at Kototabang

EDDY, Hermawan[1] ; HASHIGUCHI, Hiroyuki[2*]

[1]National Institute of Aeronautics and Space (LAPAN), Indonesia, [2]Research Institute for Sustainable Humanosphere (RISH), Kyoto University

This study is mainly concerned on developing of the Indonesian Monsoon Index (IMI) based on the Equatorial Atmosphere Radar (EAR) at Kototabang, West Sumatera (0.2S; 100.32E, 865 m from MSL). We have analyzed the zonal and meridional wind data of EAR for period of July 2001 to July 2008. By applying the bandpass filtering method that we call as the Fast Fourier Transform (FFT) and Wavelet (WL) technique, we have identified the characteristics of meridional wind velocity in frequency domain. The predominant peak oscillation that appear is Annual Oscillation (AO) for the meridional wind velocity between 8 to 18 km above mean sea level (MSL). While, the strongest is located around 14.1 km from MSL (It's equal to 200 hPa). At the same time period observation of EAR, we analyzed also the Global Monsoon Index as represented by the Indian Summer Monsoon Index (ISMI), Western North Pacific Monsoon Index (WNPMI), and Australian Monsoon Index (AUSMI), respectively. We found a 12 months oscillation for Global Monsoon Index that we call as the AO. By comparing them with meridional wind velocity of EAR, we found a good agreement between AUSMI and the meridional wind velocity of EAR, especially. By this preliminary result, we suspect that we can use the AUSMI parameter to detect the Monsoon Signal over Indonesia, especially for the Western part of Indonesia region, especially at about the 200 hPa. We wish to develop these results by investigating the Monsoonal Onset, especially, including their anomalies, since we know that Monsoon is still a pre dominant peak oscillation at the Indonesian Maritime Continent (IMC) which have big effect to control the complexity of atmospheric dynamic over Indonesia. If it looks possible, we wish also to develop the IMI model that suitable for Indonesia region. Detailed information due to that preliminary results including the basic idea of this proposal research will be discussed at our presentation.

Keywords: IMI, EAR, AUSMI, Model

Japan Geoscience Union Meeting 2014
(28 April - 02 May 2014 at Pacifico YOKOHAMA, Kanagawa, Japan)

PEM06-05 Room:312 Time:April 30 12:15-12:30

Vertical and horizontal coupling processes in the equatorial atmosphere

YAMANAKA, Manabu D.[1*]

[1]JAMSTEC/Kobe U

Future targets of the equatorial atmosphere dynamics are discussed from viewpoints of recent progress of the lower-atmospheric parts including increase of climatological interests and rapid developments of tropical countries. From recognition of the importance of land-sea heat contrast on Earth we must consider again two types of diurnal cycles: sea-land breeze circulations and atmospheric tides, which have local and global phase structures, respectively. We must consider also two types of Earth rotation effects: solar radiation heating and Coriolis force, which are stronger and weaker, respectively, in the equatorial region. Furthermore, in the lower atmosphere, clouds govern winds in the equatorial region, in contrast to opposite relationship in middle and high latitudes. Because the equatorial convective clouds are dependent not only on dynamical and thermal instabilities but also by water and electrical budgets, we need to study again dynamical-chemical and atmosphere-ionosphere couplings.

Keywords: atmosphere vertical coupling, atmosphere observation network

Japan Geoscience Union Meeting 2014
(28 April - 02 May 2014 at Pacifico YOKOHAMA, Kanagawa, Japan)

PEM06-06 Room:312 Time:April 30 12:30-12:45

Vertical wind measurement in the equatorial troposphere by the Equatorial Atmosphere Radar: A review

YAMAMOTO, Masayuki[1*] ; HASHIGUCHI, Hiroyuki[1] ; YAMAMOTO, Mamoru[1]

[1]Research Institute for Sustainable Humanosphere, Kyoto University

Measurements of vertical wind are important not only for clarifying transportation processes of energy and momentums but also for quantifying dynamical processes of precipitation and clouds. Because 50-MHz atmospheric radars measure vertical and horizontal wind velocity by using scatterings caused by irregularities of radio refractive index, they can measure vertical wind both in clear and precipitation regions. Using the capability, EAR has resolved the fine-scale vertical wind motions in the equatorial troposphere. In the presentation, the measurement results of vertical wind obtained by the EAR are reviewed. Future plans of vertical wind measurement using the Equatorial MU radar are also proposed.

Keywords: Equatorial Atmosphere Radar, Equatorial MU Radar, equatorial atmosphere, vertical wind measurement

Japan Geoscience Union Meeting 2014
(28 April - 02 May 2014 at Pacifico YOKOHAMA, Kanagawa, Japan)

PEM06-07 Room:312 Time:April 30 14:15-14:45

Science and design overview of the EISCAT_3D radar

MCCREA, Ian[1*]

[1]STFC Rutherford Appleton Laboratory

For thirty years, the EISCAT Scientific Association (www.eiscat.se) has operated a network of leading facilities for ground-based research in solar-terrestrial physics. The UHF and VHF radars at Tromso in northern Norway, together with the receiver sites at Kiruna, Sweden and Sodankyla, Finland and the EISCAT Svalbard Radar near Longyearbyen, represent a uniquely capable group of instruments serving a worldwide user community. The EISCAT mainland radars in particular, however, are based on ageing transmitters and antennas which are slow-moving and increasingly hard to maintain. For several years now, EISCAT (with support from international partners including the European Union) has been planning to replace the current set of mainland radars with a new state-of-the-art radar system, better suited to the current needs of the research community. EISCAT_3D (www.eiscat3d.se) will be the next-generation radar for the high-latitude atmosphere and geospace, with capabilities going beyond anything currently available. The facility will consist of large phased arrays in three countries. EISCAT_3D will comprise tens of thousands, up to more than 100 000, antenna elements. The new facility combines volumetric imaging and tracking, aperture synthesis imaging, multistatic configuration, improved sensitivity and transmitter flexibility. EISCAT_3D will be the first multistatic phased array ISR. A network of five sites is planned, with receivers located around 120 km and 250 km from the active site, providing optimal geometries for vectors in the middle and upper atmosphere. At the passive sites, the design allows the transmitted beam to be imaged using multi-beam techniques. EISCAT_3D will be a modular system, allowing an array to be split into sections for imaging. The result will be a new data product, range-dependent images of small structures, with sizes down to a few tens of metres. The antenna gain and array size will deliver large increases in the figure-of-merit relative to the existing EISCAT radars. An active site comprising 16,000 elements will exceed the sensitivity of the present VHF radar by an order of magnitude. In this talk the technical specifications and science case for EISCAT_3D will be discussed and the current progress reviewed. Studies of the atmospheric energy budget, exploration of small-scale and large-scale processes, as well as geospace environment monitoring and potential space weather service applications will be presented.

Keywords: EISCAT, Incoherent Scatter, Radar, Ionosphere, Solar-Terrestrial Physics, Space Weather

Japan Geoscience Union Meeting 2014
(28 April - 02 May 2014 at Pacifico YOKOHAMA, Kanagawa, Japan)

PEM06-08 Room:312 Time:April 30 14:45-15:00

The EISCAT_3D System and Status

HEINSELMAN, Craig[1*]

[1]EISCAT Scientific Association

The EISCAT Scientific Association has been operating incoherent scatter radars in the arctic since the early 1980s. Those systems have been extremely productive over the decades, supporting a wide range of scientific topics within geospace research and resulting in more than 2000 publications in peer-reviewed journals. For the past several years the EISCAT community, with significant support from the European Commission, has been working toward a new set of radar systems to replace the now aging infrastructure. This distributed radar, called EISCAT_3D, will provide the scientific community with new measurement capabilities that far exceed, both quantitatively and qualitatively, those presently available.

EISCAT_3D, when it is fully implemented, will consist of five phased array antennas strategically positioned in northern Norway, Sweden, and Finland. One of the antennas will include a distributed 10 MW peak power transmitter with full polarization capabilities, rapid steering, and antenna aperture coding options. The receive antenna arrays will be capable of instantaneously covering the entire transmit beam, thus providing a large number of intersecting volumes for vector drift measurements. The overall system will, furthermore, have sufficient sensitivity to provide order of magnitude improvements in both spatial and temporal resolution over the present radars.

We will present an overview of the system in this talk along with an update on the present status of the overall project.

Keywords: Incoherent Scatter Radar, ionosphere

Japan Geoscience Union Meeting 2014
(28 April - 02 May 2014 at Pacifico YOKOHAMA, Kanagawa, Japan)

PEM06-09 Room:312 Time:April 30 15:00-15:15

Thermospheric neutral density observations using the EISCAT incoherent scatter radars

KOSCH, Michael[1*] ; VICKERS, Hannah[2] ; OGAWA, Yasunobu[3]

[1]Physics Dept., Lancaster University, Lancaster, UK, [2]Institute for Physics and Technology, University of Tromso, Norway, [3]National Institute of Polar Research, Tachikawa, Japan

We exploit a recently-developed technique, based on ion-neutral coupling, to estimate the thermospheric neutral density at ˜350 km using measurements of ionospheric plasma parameters made by the EISCAT radars. The passive version of the technique is applied to a 13-year long data set from the EISCAT Svalbard Radar (ESR). Here we show that the thermospheric density in the polar cap is decreasing, consistent with satellite drag estimates at lower latitudes. The active version of the technique requires the EISCAT Heater to artificially induce ion up-flow by heating the electrons, with observations from the EISCAT UHF radar. Here we show that ion up-flow is consistent with the plasma pressure gradient, and we extract the thermospheric neutral density. At an altitude of ˜500 km, where neutral composition is not always pure atomic oxygen, problems with the technique are discussed.

Keywords: Thermospheric density, Incoherent scatter radar

Japan Geoscience Union Meeting 2014
(28 April - 02 May 2014 at Pacifico YOKOHAMA, Kanagawa, Japan)

PEM06-10 Room:312 Time:April 30 15:15-15:30

3D ionospheric electron density determination in Scandinavia with TomoScand and EISCAT 3D

AMM, Olaf[1*] ; NORBERG, Johannes[1] ; VIERINEN, Juha[3] ; ROININEN, Lassi[4] ; LEHTINEN, Markku[4] ; NAKAMIZO, Aoi[1]

[1]Finnish Meteorological Institute, Arctic Research Unit, Helsinki, Finland, [2]STEL, Nagoya University, Japan, [3]Haystack Observatory, Massachusetts Institute of Technology, Westford, Massachusetts, USA, [4]Sodankyla Geophysical Observatory, University of Oulu, Finland

The TomoScand network for ionospheric tomography in Scandinavia consists of a network of newly designed Beacon receivers and an extensive, dense array of GPS receivers. A novel tomographic inversion technique allows for a multi-frequency analysis for reconstruction of ionospheric electron densities, and is also able to include information of a multitude of ground-based measurements into the inversion, such as data from ionosondes, from the EISCAT radar, and from the magnetometers of the MIRACLE network in Scandinavia. We present the current status of the TomoScand network, and show latest inversion results on 2D profiles in meridional direction, together with test results that allow to evaluate the performance of the inversion technique. Further, we discuss the future development into a full 3D inversion scheme, and how the TomoScand network can be used as a ”partner instrument” for the upcoming EISCAT 3D radar.

Keywords: ionospheric tomography, ionospheric electron density, ground-based observations, EISCAT 3D

Japan Geoscience Union Meeting 2014
(28 April - 02 May 2014 at Pacifico YOKOHAMA, Kanagawa, Japan)

PEM06-11 Room:312 Time:April 30 15:30-15:45

Advancement of geospace and atmospheric sciences with EISCAT_3D

MIYAOKA, Hiroshi[1*] ; NOZAWA, Satonori[2] ; OGAWA, Yasunobu[1] ; OYAMA, Shin-ichiro[2] ; NAKAMURA, Takuji[1] ; FUJII, Ryoichi[2] ; HEINSELMAN, Craig[3]

[1]National Institute of Polar Research, [2]STEL, Nagoya University, [3]EISCAT Scientific Association

The EISCAT(European Incoherent SCATter) Scientific Association is an international research organization, which operates incoherent scatter radars at 931MHz, 224MHz and 500MHz in northern Scandinavia and Svalbard for studies of physical and environmental processes in the middle/upper atmosphere and near-Earth space. Affiliated in the EISCAT scientific association in 1996, Japanese science community has jointly contributed to achieve further understanding of the magnetosphere-ionosphere-thermosphere coupling processes using the integrated ground-based instruments and rocket/satellite simultaneous observations with EISCAT radars.

EISCAT_3D is the major upgrade of the existing EISCAT radars in the northern Scandinavia.With a multi-static phased array system composed of one central active (transmit-receive) site and several receive-only sites, the EISCAT_3D system is expected to provide us 10 times higher temporal and spatial resolution and capabilities than the present radars.

In this presentation, we will overview our scientific activity and achievements with the EISCAT facility and our strategic plan of national funding for EISCAT_3D as well as the science targets which we expect to be unraveled by EISCAT_3D.

Keywords: Incoherent scatter radar, EISCAT, Ionosphere, Thermosphere, Mesosphere, 3D imaging observation

Japan Geoscience Union Meeting 2014
(28 April - 02 May 2014 at Pacifico YOKOHAMA, Kanagawa, Japan)

PEM06-12 Room:312 Time:April 30 15:45-16:00

Study on ion upflow and outflow based on EISCAT_3D and its related observations

OGAWA, Yasunobu[1*]

[1]National Institute of Polar Research, JAPAN

An important phenomenon of magnetosphere-ionosphere coupling is the formation of upwelling ions in the topside polar ionosphere. These upflows can be a significant loss of atmospheric gasses into interplanetary space and a significant source of magnetospheric plasma, which may also affect the dynamics of the magnetosphere. Key processes for upward ion flows in the topside ionosphere are suggested to be frictional heating, ambipolar diffusion driven by a heated electron gas, and transverse ion acceleration produced by plasma waves. It is critical to determine the relative importance of the different mechanisms in operation and to understand the 3D distribution and composition of the upflowing ions and neutrals. Moreover, there are several transitions of upflowing ions, for examples, from chemical to diffusion dominance at 500-800 km altitude, from subsonic to supersonic flow at 1000-2000 km altitude, and from collisional to collisionless region at 1500-2500 km altitude.

EISCAT_3D is one of the most suitable measurements to investigate such transitions because of its wider height coverage (up to about 2000 km) along the field line. EISCAT_3D will have more transmitter power density and higher sensitivity than those of the current Tromso UHF radar, and will give information of accurate thermal ion velocity, upward flux, and ion composition (O^+, H^+, and hopefully NO^+). A combination of the EISCAT_3D, ground-based optical instruments, and in-situ measurements is definitely essential to solve several key questions of ion upflow and outflow study. In this paper, we show potential investigations of ion upflow and outflow using the EISCAT_3D, and also discuss a desirable combination of the EISCAT_3D and its related observations for the ion upflow and outflow study.

Keywords: EISCAT, ionosphere, M-I coupling

Japan Geoscience Union Meeting 2014
(28 April - 02 May 2014 at Pacifico YOKOHAMA, Kanagawa, Japan)

PEM06-13 Room:312 Time:April 30 16:15-16:30

Meteor head echo observation with a high power large aparture (HPLA) radar and an open database of precise meteor orbit

NAKAMURA, Takuji[1*] ; KERO, Johan[2]

[1]National Institute of Polar Research, [2]Swedish Institute of Space Physics (IRF)

Mass influx from the space into the terrestrial atmosphere is mainly caused by meteors. Meteors delivers various elements into the atmosphere, but the meteoric dust particles are also of great importance in the terrestrial atmosphere, as they act as nucleus for condensation and clouds and affect the various atmospheric phenomena both in physical and chemical aspects. Thus, to investigate the meteor flux, orbits and their interactions in the upper atmosphere is very important but at the same time the method of investigation is limited, especially for the precise measurements.

A high power large aperture (HPLA) radar technique is one of the recent technique to provide useful information on meteor influx and orbital information, as well as interactions with atmosphere. The recent development of the technique carried out using the middle and upper atmosphere radar (MU radar) of Kyoto University at Shigaraki (34.9N, 136.1S), which is a large atmospheric VHF radar with 46.5 MHz frequency, 1 MW output transmission power and 8330 m^2 aperture array antenna, has established very precise orbit observations with meteor head echoes. Since 2009, orbital data of about 120,000 meteors have been collected. A database is now being created as an open database for research and education. In this

study, we present the physical quantities and precisions obtained by our radar meteor head echo observations and the detail of the database.

Keywords: meteor, upper atmosphere, high power large aperture radar

Japan Geoscience Union Meeting 2014
(28 April - 02 May 2014 at Pacifico YOKOHAMA, Kanagawa, Japan)

PEM06-14 Room:312 Time:April 30 16:30-16:45

Comparison of Cloud Propagation over Sumatera during CPEA-I and II

MARZUKI, Marzuki[1*] ; RAHAYU, Aulya[1] ; VONNISA, Mutya[1] ; HASHIGUCHI, Hiroyuki[2] ; K. YAMAMOTO, Masayuki[2] ; D. YAMANAKA, Manabu[3] ; MORI, Shuichi[3] ; KOZU, Toshiaki[4] ; SHIMOMAI, Toyoshi[4]

[1]Department of Physics, Andalas University, Padang, Indonesia, [2]Research Institute for Sustainable Humanosphere (RISH) Kyoto University, Gokasho, Uji, Kyoto 611-001, [3]Japan Agency for Marine-Earth Science and Technology (JAMSTEC), Yokosuka, Japan, [4]Interdisciplinary Faculty of Science and Engineering, Shimane University, Japan

Maritime Continent of the Indonesian (MCI) archipelago is one of the world's most convectively active areas and thereby affects the global climate system. It consists of thousands of islands with different size. The island coastlines' complex shape and geography, as well as their orientation, contribute to the uniqueness of this region. Not surprisingly, maritime continent receives a large amount of rainfall throughout the year, and the precipitation varies considerably across the region. Global climate models exhibit systematic errors in their mean precipitation over the MCI due to such variability. In this study, the behavior of convective activity over Sumatera during the Coupling Processes in the Equatorial Atmosphere (CPEA) campaign I and II is examined using 1-hourly satellite infrared data. Sumatra Island is elongated and oriented from northwest to southeast and its elevated orography temporarily blocked the eastward propagation of precipitation system. The dynamics of Sumatra weather systems remains poorly understood and part of the problem lies in the lack of atmospheric data and high-resolution gridded data analyses and realistic model simulations. Therefore, the data of two intensive observation periods as the international observation campaign of the CPEA will also be used. Cloud propagation statistics (speed, span, life time, size, etc.) of the individual cloud episodes and the physical basis behind the results will be discussed.

Keywords: Cloud propagation, Sumatra, CPEA

Japan Geoscience Union Meeting 2014
(28 April - 02 May 2014 at Pacifico YOKOHAMA, Kanagawa, Japan)

PEM06-15 Room:312 Time:April 30 16:45-17:00

SuperDARN global observation of energy input and coupling processes and recent technical development

YUKIMATU, Akira sessai[1*] ; NISHITANI, Nozomu[2] ; NAGATSUMA, Tsutomu[3]

[1]NIPR/SOKENDAI, [2]STEL, Nagoya Univ., [3]NICT

SuperDARN (Super Dual Auroral Radar Network) [Greenwald, et al., 1995] is an international collaborative HF-radar network [Greenwald, et al., 1985] operated by more than 15 institutions in over 10 countries, and the number of the radars is currently more than 30 and it is still growing and the fields-of-view (FOVs) have been expanding to both higher and mid-latitudes covering considerable portions of global upper atmosphere in both hemispheres.

SuperDARN was originally designed to measure line-of-sight plasma Doppler spectra and ionospheric electric field to obtain global large scale two-dimensional polar ionospheric plasma convection patterns and polar cap potential drop in both hemispheres with a temporal resolution of 1 to 2 minutes in real time since 1995, which have never been possible by any other observational techniques, and this capability provides us very important and essential information on solar energy input to our geospace, magnetosphere and polar ionosphere, which has greatly contributed to basic understanding of coupling processes in Sun-Earth system as well as space weather researches.

SuperDARN is a powerful tool to be applied to many scientific issues [Chisham, et al., 2007 and references therein]. It can be used not only to deduce dynamics of global large-scale convection patterns, but also to study dynamics of transient meso-scale phenomena like FTEs and TCVs, and polar cap boundary or open-closed field line boundary (OCB), to detect reconnection sites and to deduce reconnection rates, to study substorms, storms and phenomena related to subauroral regions like sub-auroral polarisation stream (SAPS), to deduce field aligned currents (FACs), to study MHD waves in a variety of frequency ranges, and also to study ionospheric irregularities in D-, E-, and F-regions. Moreover, it can be utilised not only to ionospheric researches but also to neutral atmospheric studies, e.g., on atmospheric waves like TIDs, tides and gravity waves, neutral winds around mesopause region, and also polar mesospheric summer echoes (PMSEs), etc.

These days, the fields-of-view (FOVs) of SuperDARN have been expanded to higher latitude (PolarDARN) and mid-latitude (StormDARN) which covers considerable portions of mid- and polar latitudes of earth's ionosphere in both hemispheres and enables us to address much wider ranges of scientific questions including inner magnetospheric physics. There are also ongoing discussions to expand the SuperDARN radars field of view to even lower latitudes, up to low latitude and equatorial regions.

SuperDARN has extensively evolved successfully and has been extremely productive by strong cooperation and competitions within the community and also by collaborative studies with other ground-based and satellite/rocket observations and theoretical researches, which has greatly contributed to a variety of studies especially on magnetosphere-ionosphere coupling processes and ionosphere and neutral atmosphere coupling.

As SuperDARN could have provided basic and important physical parameters in global upper atmosphere, collaborative studies with other projects like IS-radars like EISCAT and PANSY providing many detailed physical parameters at fix points as well as satellite missions like THEMIS, VAP, and ERG and rocket campaigns providing in-situ measurements will be particularly important to contribute to our deeper understanding of the Sun-Earth coupling processes.

Also some SuperDARN radars has developed new technical upgrade including imaging radar capabilities providing higher spatial resolution. New science targets with SuperDARN with new capabilities will also be discussed.

Keywords: SuperDARN, HF radar, coupling processes, imaging radar, MI coupling, neutral wind

Japan Geoscience Union Meeting 2014
(28 April - 02 May 2014 at Pacifico YOKOHAMA, Kanagawa, Japan)

PEM06-16 Room:312 Time:April 30 17:00-17:15

Low Latitude Ionospheric Scintillation Research Using GISTM Network over Indonesia

HUSIN, Asnawi[1*] ; ABADI, Prayitno[1] ; JIYO, Harjoswito[1] ; YAMAMOTO, Mamoru[2] ; OTSUKA, Yuichi[3]

[1]Space Science Center, LAPAN, [2]RISH, Kyoto University, [3]STEL, Natoya University

The ionosphere plays an active role in the space weather relationships, so the permanent monitoring of the ionosphere state on global and regional is required. The advancement of Global Navigation Satellite Systems (GNSS) such as GPS (Global Positioning System) receiver technology provides a low cost solution for monitoring and research the ionosphere on global and regional basis. National Institute of Aeronautics and Space (LAPAN) Indonesia has been installed GPS Ionospheric Scintillation and TEC Monitor (GSV4004b) to monitor and study ionospheric irregularities.

This paper reports a statistical study of the occurrences characteristic of GPS ionospheric scintillation and irregularity in low latitude Indonesia sector. These measurements were made by GPS Ionospheric Scintillation and TEC Monitor System (GISTM) at Pontianak (0.03S 109.33E), Bandung (6.93S 107.6E), Manado (1.34N 124.83E), Kupang (10.16S 123.66E), and Kototabang (0.12S 100.12E). For the GPS station at Kototabang, we use ISM (ionospheric scintillation monitor) under collaboration with STELAB Nagoya Univeristy. We distinguish scintillation occurrences rate between post sunset and after midnight by using S4 index during maximum solar activity period in 2013. We analyze the occurrence rate using azimuth-elevation coordinate (sky plot). The following figure is to show observation geometry which is used in this study.

Keywords: Ionospheric Scintillation, Indonesia, GPS receiver

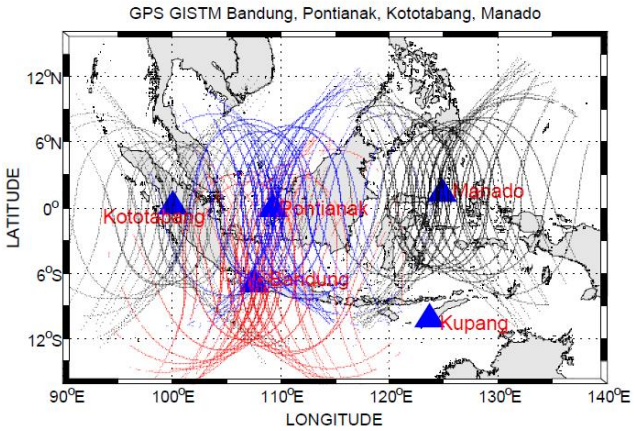

Japan Geoscience Union Meeting 2014
(28 April - 02 May 2014 at Pacifico YOKOHAMA, Kanagawa, Japan)

PEM06-17 Room:312 Time:May 1 09:00-09:30

Future direction of the ground-based network observations of the magnetosphere and the upper atmosphere

SHIOKAWA, Kazuo[1*] ; OTSUKA, Yuichi[1]

[1]Solar-Terrestrial Environment Laboratory, Nagoya University

Multi-point ground-based instruments are powerful tools to investigate global dynamics of the magnetosphere, ionosphere, and the upper atmosphere. Airglow imagers and multi-point GPS receivers provide two- and three-dimensional view of these regions. The ring-current and radiation-belt particles in the inner magnetosphere round the earth with a time scale from a few tens of minutes to a few hours. Interactions of these particles with Pc5 (times scale of ˜minutes), Pc1 (˜Hz) and VLF/ELF chorus (˜kHz) causes acceleration and loss of these particles. Thus, longitudinal chain of ground-based stations to observe these various waves and auroras is essentially needed to understand the acceleration and loss of the plasma in the inner magnetosphere. The auroral energy input from the solar wind and magnetosphere to the high-latitude ionosphere is a major energy source of the dynamic variation of the upper atmosphere. Intense convective activity in the equatorial troposphere gives another energy source of the dynamic variation of the upper atmosphere. Thus, meridional chain stations are essentially needed to understand these dynamic variations and their global coupling. In this presentation we discuss possible future directions of these ground-based network observations to understand the global dynamics of the magnetosphere, ionosphere, and the upper atmosphere.

Keywords: ground-based network observation, ionosphere, magnetosphere, upper atmosphere, future direction

Japan Geoscience Union Meeting 2014
(28 April - 02 May 2014 at Pacifico YOKOHAMA, Kanagawa, Japan)

PEM06-18 Room:312 Time:May 1 09:30-09:45

ICSWSE/ MAGDAS Project: Research for global electromagnetic coupling from polar to equatorial ionosphere

YOSHIKAWA, Akimasa[1*] ; NAKAMIZO, Aoi[2] ; OHTANI, Shinichi[3] ; TANAKA, Yoshimasa[4] ; IMAJO, Shun[5] ; MATSUSHITA, Hiroki[5] ; CARDINAL, Maria gracita[1] ; ABE, Shuji[1] ; UOZUMI, Teiji[1] ; YUMOTO, Kiyohumi[1]

[1]International Center for Space Science and Education, Kyushu University, [2]Finish Meteorological Institute, [3]The Johns Hopkins University Applied Physics Laboratory, [4]National Institute of Polar Research, [5]Earth and Planetary Science , Kyushu University

International Center for Space Weather Science and Education (ICSWSE) has developed a real time magnetic data acquisition system (the MAGDAS project) for space environment monitoring around the world. The number of observational sites is increasing every year with the collaboration of MAGDAS host countries. Now at this time, the MAGDAS Project has installed 73 real time magnetometers ? so it is the largest magnetometer array in the world.

Applying equivalent current method to this network data, we analyze a global ionospheric current system from polar to equatorial ionosphere. Our results suggest that Dp2 type disturbances excited by solar wind variation, Pi2 type pulsations accompanied by aouroral substorm onset process and Pc3 type pulsations accompanied by dayside cavity type oscillation show the same type of global current system, which are produced by primary bipolar electric field accompanied by field-aligned current system and Hall polarization electric field excited at the dawn-dusk conductivity terminator and at the magnetic dip equator.We will discuss how the electromagnetic coupling between polar and equatorial ionosphere is regulated by the formation of global Cowling channel in the ionosphere.

Keywords: Space Weather, Magnetosphere-Ionosphere-Atmosphere Coupling, Global Coupling

Japan Geoscience Union Meeting 2014
(28 April - 02 May 2014 at Pacifico YOKOHAMA, Kanagawa, Japan)

PEM06-19 Room:312 Time:May 1 09:45-10:00

Contribution of the IUGONET data analysis system to a study on coupling processes in the solar-terrestrial system

SHINBORI, Atsuki[1*] ; YAGI, Manabu[2] ; TANAKA, Yoshimasa[3] ; SATO, Yuka[3] ; YATAGAI, Akiyo[4] ; UMEMURA, Norio[4] ; HORI, Tomoaki[4] ; UENO, Satoru[5] ; KOYAMA, Yukinobu[6] ; ABE, Shuji[7]

[1]Research Institute for Sustainable Humanosphere (RISH), Kyoto University, [2]Planetary Plasma and Atmospheric Research Center, Graduate School of Science, Tohoku University, [3]National Institute of Polar Research, [4]Solar-Terrestrial Environment Laboratory, Nagoya University, [5]Kwasan & Hida Observatories, School of Science, Kyoto University, [6]Data Analysis Center for Geomagnetism and Space Magnetism Graduate School of Science, Kyoto Universi, [7]International Center for Space Weather Science and Education, Japan

Various kinds of disturbance phenomenon and long-term variation as seen in several observation parameters (electric and magnetic fields, temperature, mean wind etc.) in a wide area from space surrounding the Earth to the atmospheric layers are caused by energy input from solar radiation, solar wind, momenta and energies from the lower atmosphere via atmospheric waves, and chemical reaction. Such a disturbance phenomenon and long-term variation observed by various kinds of ground-based and satellite instruments are the result of such complicated processes. Then, in order to investigate the mechanisms of these phenomena in this region, researchers need to conduct comprehensive analyses with various kinds of long-term observation data that have been continued by means of a global network of radars, magnetometers, optical sensors, helioscopes, etc. The IUGONET (Inter-university Upper atmosphere Global Observation NETwork) project initiated in 2009 aims at the establishment of a cross-reference system for various kinds of ground-based observation data obtained from different techniques. The IUGONET participants consist of five universities/institutes: the National Institute of Polar Research (NIPR), Tohoku University, Nagoya University, Kyoto University, and Kyushu University. We have developed metadata database (MDB) and IUGONET data analysis software (UDAS) of ground-based observation data managed by these IUGONET universities/institutes with an international collaboration in order to promote a study on coupling process in the Sun-Earth system. The MDB provides researchers in a wide range of disciplines with a seamless data environment to link databases spread across the IUGONET universities/institutes. In particular, UDAS will be of great help in conducting integrated analyses and visualization of various kinds of solar-terrestrial observation data to investigate the long-term variation in the upper atmosphere throughout the Sun-Earth system. Then, the IUGONET products will greatly contribute to a study on coupling process in the Sun-Earth system on the basis of integrated analysis of various kinds of long-term observation data covering a wide region from both the pole to the equator. In this talk, we introduce a brief overview of the IUGONET project, and an application of the IUGONET products to typical examples of upper atmospheric researches.

Keywords: Upper atmosphere, Long-term variation, Solar activity, Metadata search system, Data analysis tool, Coupling process in the Sun-Earth system

Japan Geoscience Union Meeting 2014
(28 April - 02 May 2014 at Pacifico YOKOHAMA, Kanagawa, Japan)

PEM06-20 Room:312 Time:May 1 10:00-10:15

Statistical characteristics of nighttime MSTIDs observed by an airglow imager over sub-tropical site Yonaguni (19.3N dip)

VISWANATHAN, Lakshmi narayanan[1*] ; SHIOKAWA, Kazuo[1] ; OTSUKA, Yuichi[1] ; SAITO, Susumu[2]

[1]Solar Terrestrial Environment Laboratory, Nagoya University, Nagoya, Japan, [2]Electronic Navigation Research Institute, Tokyo, Japan

The nighttime medium-scale travelling ionospheric disturbances (MSTIDs) are frequently observed in the mid-latitude ionosphere. They very often moves toward the southwest direction in the northern hemisphere with phase fronts aligned along the northwest to the southeast. However they do not extend to the equatorial latitudes and are rarely sighted at dip latitudes below 15^o. In this study we investigate the characteristics of MSTID features observed over Yonaguni (24.5^oN, 123.0^oE; 19.3^oN dip latitude), Japan with all-sky imaging of OI 630.0 nm airglow emission. We selected two year period for analysis in which one year corresponds to the solar minimum conditions and another year corresponds to solar maximum conditions. It is found that the MSTIDs occur more frequently during solar minimum conditions. The observed range of wavelengths, phase speeds and directions of MSTIDs are similar to those observed at typical mid-latitude sites. On many occasions the phase fronts of the observed MSTIDs do not extend over the whole field of view of imager indicating that some process hinders their extension to further lower latitudes. Herein, we also investigate the possible reason for the disappearance of phase fronts when they reach lower latitudes.

Keywords: medium-scale travelling ionospheric disturbances, OI 630.0 nm airglow

Japan Geoscience Union Meeting 2014
(28 April - 02 May 2014 at Pacifico YOKOHAMA, Kanagawa, Japan)

PEM06-21 Room:312 Time:May 1 10:15-10:30

Thermospheric wind variations in the pulsating aurora measured with FPI and IS radars

OYAMA, Shin-ichiro[1*] ; KURIHARA, Junichi[2] ; TSUDA, Takuo[3] ; SHIOKAWA, Kazuo[1] ; MIYOSHI, Yoshizumi[1] ; WATKINS, Brenton J.[4]

[1]Solar-Terrestrial Environment Laboratory, Nagoya University, [2]Graduate School of Science, Hokkaido University, [3]National Institute of Polar Research, [4]Geophysical Institute, University of Alaska Fairbanks

Pulsating aurora is a typical phenomenon of the recovery phase of magnetic substorm and is frequently observed in the morning sector. While our understanding of pulsating aurora has not yet reached maturity, the widely accepted generation mechanism causing pulsations in precipitating electrons is related to wave-particle interactions around the equatorial plane in the magnetospheric tail. The closure current system in pulsating aurora may not be as strongly evolved as compared to that in the discrete arc because of smaller precipitation flux (or upward field-aligned current) and weaker perpendicular electric field (or the Pedersen current). Thus one may assume that Joule energy dissipation and/or Lorentz force does not play an important role for modifications of the thermospheric wind dynamics in pulsating aurora. However, we found thermospheric-wind variations in the pulsating aurora during simultaneous observations with a Fabry-Perot Interferometer (FPI; 557.7 nm), an all-sky camera (557.7 nm), and the European Incoherent Scatter (EISCAT) UHF radar. Of particular interest is that the location of the fluctuations was found in a darker area that appeared within the pulsating aurora. During the same time period, the EISCAT radar observed sporadic enhancements in the F-region backscatter echo power, which suggests the presence of low-energy electron (1 keV or lower) precipitation. Using other data sets archived by the EISCAT radar, a statistical analysis shows that the F-region enhancement tends to coexist with hard-particle precipitation or the pulsating aurora. This presentation will summarize our experimental evidences showing several events of the pulsating aurora, and discuss application of the phased-array IS radar to this study.

Keywords: pulsating aurora, thermosphere, FPI, IS radar

Japan Geoscience Union Meeting 2014
(28 April - 02 May 2014 at Pacifico YOKOHAMA, Kanagawa, Japan)

PEM06-22 Room:312 Time:May 1 10:30-10:45

Coordinated observation of space-borne imaging by ISS-IMAP and ground-based measurement by radars and GPS

SAITO, Akinori[1*] ; YAMAZAKI, Atsushi[2] ; SAKANOI, Takeshi[3] ; YOSHIKAWA, Ichiro[4] ; OTSUKA, Yuichi[5] ; YAMAMOTO, Mamoru[1] ; NAKAMURA, Takuji[6] ; AKIYA, Yusuke[1] ; HOZUMI, Yuta[1]

[1]Kyoto University, [2]JAXA/ISAS, [3]Tohoku University, [4]University of Tokyo, [5]Nagoya University, [6]National Institute of Polar Research

ISS-IMAP mission is a space-borne mission to investigate the mesoscale structures in the ionosphere, the mesosphere, and the plasmasphere by imaging observations of instruments on International Space Station. It consists of two imaging instruments. Visible-light and infrared spectrum imager (VISI) observes the airglow in the MTI region. Extra ultraviolet imager (EUVI) observes the resonant scattering from ions in the ionosphere and the plasmasphere. The objective of this mission is to clarify the upper atmospheric structures whose horizontal scale is 50-500km, and the effect of the structures on the space-borne systems in the low- and mid-latitude regions. VISI observes the airglow of 730nm (OH, Alt. 85km), 762nm (O2, Alt 95km), 630nm(O, Alt.250km) in the Nadir direction to investigate the mesoscale structures in the mesosphere and the ionosphere. The coordinated observations of ISS-IMAP with ground-based measurements have been carried out. The MU radar and Equatorial Atmosphere Radar (EAR) observe the ionosphric density structures and field-aligned irregularities while ISS-IMAP observe the large and mesoscale ionospheric structures with the 630nm airglow, and the atmospheric gravity waves in the mesosphere with the 762nm airglow. The two-dimensional distribution of total electron contents derived with the ground-base GPS receiver array is also compared with the ionospheric and mesospheric structures observed by ISS-IMAP. The results of the ISS-IMAP mission by VISI and EUVI, and its coordinated observations with the ground-based instruments will be introduced in the presentation.

Keywords: Ionosphere, Airglow, Atmospheric Gravity Wave, Plasma Bubble, Radar, GPS

Japan Geoscience Union Meeting 2014
(28 April - 02 May 2014 at Pacifico YOKOHAMA, Kanagawa, Japan)

PEM06-23 Room:312 Time:May 1 11:00-11:30

Current status of Program of the Antarctic Syowa MST/IS radar (PANSY)

SATO, Kaoru[1*] ; TSUTSUMI, Masaki[2] ; SATO, Toru[3] ; NAKAMURA, Takuji[2] ; SAITO, Akinori[3] ; TOMIKAWA, Yoshihiro[2] ; NISHIMURA, Koji[2] ; KOHMA, Masashi[1] ; YAMAGISHI, Hisao[2] ; YAMANOUCHI, Takashi[2]

[1]Dept Earth & Planetary Sci., The University of Tokyo, [2]National Institute of Polar Research, [3]Kyoto University

The PANSY radar is the first Mesosphere-Stratosphere-Troposphere/Incoherent Scatter (MST/IS) radar in the Antarctic. It is a VHF monostatic pulse Doppler radar operating at 47 MHz, consisting of an active phased array of 1,045 Yagi antennas and an equivalent number of transmit-receiver modules with a total peak output power of 500 kW. The first stage of the radar was installed at Syowa Station (69^{o}00'S, 39^{o}35'E) in early 2011, and is continuously operating with 228 antennas and modules since April 2012. The full radar system operation will start in 2015. This paper reports the project's scientific objectives, technical descriptions, and the preliminary results of observations made to date. The radar is designed to clarify the role of atmospheric gravity waves at high latitudes in the momentum budget of the global circulation in the troposphere, stratosphere and mesosphere, and to explore the dynamical aspects of unique polar phenomena such as polar mesospheric/stratospheric clouds. The katabatic winds as a branch of Antarctic tropospheric circulation and as an important source of gravity waves are also of special interest. Moreover, strong and sporadic energy inputs from the magnetosphere by energetic particles and field-aligned currents can be quantitatively assessed by the broad height coverage of the radar which extends from the lower troposphere to the upper ionosphere. From engineering points of view, the radar had to overcome restrictions related to the severe environments of Antarctic research, such as very strong winds, limited power availability, short construction periods, and limited manpower availability. We resolved these problems through the adoption of specially designed class-E amplifiers, lightweight and tough antenna elements, and versatile antenna arrangements. We will show highlights of several interesting results from the radar observations regarding severe snow storms, gravity waves, multiple tropopauses, and polar mesosphere summer/winter echoes.

Reference

Sato, K., et al., *J. Atmos. Solar-Terr. Phys.*, doi:10.1016/j.jastp.2013.08.022, 2013.

Keywords: MST/IS radar, polar atmosphere, middle atmosphere, gravity waves, general circulation

Japan Geoscience Union Meeting 2014
(28 April - 02 May 2014 at Pacifico YOKOHAMA, Kanagawa, Japan)

PEM06-24 Room:312 Time:May 1 11:30-11:45

Importance of coordinated ground-based, satellite observations

MIYOSHI, Yoshizumi[1*] ; OYAMA, Shin-ichiro[1] ; SAITO, Shinji[1]

[1]STEL, Nagoya University

The ERG (Exploration of energization and Radiation in Geospace) is Japanese geospace exploration project. The project focuses on the geospace dynamics in the context of the cross-energy coupling via wave-particle interactions. The project consists of the satellite observation team, the ground-based network observation team, and integrated-data analysis/simulation team. The ERG satellite will be launched in FY2015. Comprehensive instruments for plasma/particles, and field/waves are installed in the ERG satellite to understand the cross-energy coupling system. In the ERG project, several ground-network teams join; magnetometer networks, radar networks, optical imager networks, etc. Moreover, the modeling/simulations play an important role for the quantitative understanding. In this presentation, we will discuss the importance of coordinated observations toward the ERG era. As an example, we show the cooperative observations between the geospace satellite Van Allen Probes an EISCAT to observe the pulsating aurora. The EISCAT measured the height profile of the electron density that can provide the energy of the precipitating electrons. The Van Allen Probes measured the plasma waves in the magnetosphere, which can be used to investigate the origin of the pulsating aurora. In fact, the GEMSIS-RBW simulation that used the observed plasma waves as an input reproduces characteristics of the observed precipitation. Such coordinated observations including the modeling provide a comprehensive view on cause and result.

Keywords: satellite-ground observations, ERG project

Japan Geoscience Union Meeting 2014
(28 April - 02 May 2014 at Pacifico YOKOHAMA, Kanagawa, Japan)

PEM06-25 Room:312 Time:May 1 11:45-12:00

Synthetic Study on Solar-Terrestrial Phenomena with Widespread Observation Network in Antarctica

KADOKURA, Akira[1*] ; YAMAGISHI, Hisao[1] ; YUKIMATU, Akira sessai[1] ; MIYAOKA, Hiroshi[1] ; OKADA, Masaki[1] ; OGAWA, Yasunobu[1] ; TANAKA, Yoshimasa[1] ; KATAOKA, Ryuho[1] ; EBIHARA, Yusuke[2] ; MOTOBA, Tetsuo[3]

[1]National Institute of Polar Research, [2]Research Institute for Sustainable Humanosphere, Kyoto University, [3]Applied Physics Laboratory, Johns Hopkins University

A large observation network with the SuperDARN radars and other ground-based instruments at manned and unmanned stations is currently developed in the Antarctic area from sub-auroral latitudes to polar cap region and from nightside to dayside hours under international collaboration. Such a widespread circumpolar observation network is very unique and powerful for studies on the phenomena which occur due to the Sun-Earth interaction, e.g., direct entry of solar wind energy and momentum into the cusp and polar cap regions, explosive energy dissipation during substorm-time, highly energetic particle precipitation into the atmosphere during storm-time. Coordinated observations with several low-altitude satellites (e.g., NOAA, DMSP, etc.) and magnetospheric satellites (e.g., THEMIS/ARTEMIS, Geotail, MMS, ERG, etc.) can be also expected In our presentation, current status and future plan of NIPR-related project will be introduced, and importantce of such a widespread ground-based observation network in Antarctica will be explained and discussed.

Keywords: Antarctica, large area, observation network, Solar-Terrestrial Physics

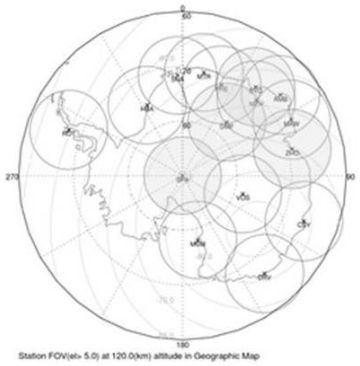

Figure 1. Field of views (FOVs) of Antarctic stations projected at 120 km altitude for elevation above 5 deg. The shaded FOV indicates the station where auroral optical observation is currently carried out. Geomagnetic latitudes are also shown in gray lines.

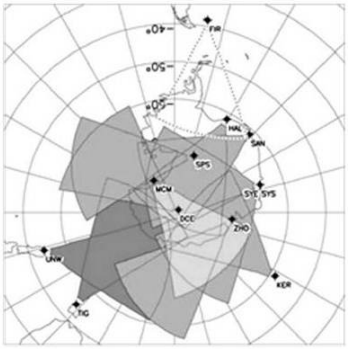

Figure 2. Field of views of the SuperDARN radars in the southern hemisphere in the magnetic coordinates, including two radars at Syowa Station (SYE and SYS).

Japan Geoscience Union Meeting 2014
(28 April - 02 May 2014 at Pacifico YOKOHAMA, Kanagawa, Japan)

PEM06-26 Room:312 Time:May 1 12:00-12:15

A review of selected data-analysis techniques for determining ionospheric electrodynamic parameters on mesoscales

VANHAMAKI, Heikki[1*] ; AMM, Olaf[1]

[1]Finnish Meteorological Institute, Helsinki, Finland

We present a review of selected data-analysis methods that are applied in studies of ionospheric electrodynamics and magnetosphere-ionosphere coupling using ground-based and space-based data sets. At present, there is no single measurement device that can measure all ionospheric electrodynamic parameters directly and simultaneously, with good spatial and temporal resolution and coverage. Therefore data-analysis techniques are needed to combine different types of measured data and to obtain unobserved ionospheric parameters from the observed ones, possibly using some additional assumptions in the process. We concentrate on methods that are data driven and applicable to single events (not simulations or statistical models), and which can be used in mesoscale studies, where the analysis area is typically some hundreds or thousands of km across.

The primary focus of this review is in ionospheric electrodynamics, so we do not include variables like chemical composition, temperature, etc. in our discussion. Furthermore we concentrate on analysis techniques that have been developed to be used with data from the MIRACLE network (Magnetometers - Ionospheric Radars - All-sky Cameras Large Experiment) situated in Northern Europe, possibly in combination with satellite observations, such as Cluster or CHAMP. However, the techniques can be applied to data from any other mesoscale network with similar observations.

The full set of ionospheric electrodynamic parameters that we are interested in consist of the ionospheric horizontal electric field, height integrated Hall and Pedersen conductances, horizontal sheet current and field aligned current (FAC). Additionally, the ground magnetic perturbation is an important input parameter in many analysis methods.

Most of the reviewed methods are used in 2-dimensional (latitude - longitude) regions of the ionosphere, but some methods have also 1-dimensional variants. In 1D analysis it is assumed that ionospheric parameters vary only in one horizontal direction (e.g. as a function of geomagnetic latitude), so input data is required along a single chain or a satellite track only. The 1D methods are especially useful when analyzing data from an overpassing satellite or from a meridional magnetometer chain.

Keywords: Ionosphere, Ionospheric electrodynamics, Ionospheric currents, Data-analysis methods

Japan Geoscience Union Meeting 2014
(28 April - 02 May 2014 at Pacifico YOKOHAMA, Kanagawa, Japan)

PEM06-27 Room:312 Time:May 1 12:15-12:30

Fine-scale electrodynamic structure behind auroral vortex street

HOSOKAWA, Keisuke[1*]

[1]University of Electro-Communications

One of the primary scientific objectives of the planned EISCAT_3D system would be “3D imaging of aurora”, especially 3D imaging of dynamically moving auroral arcs at the time of substorm expansion phase onset. In order to discuss the specification of the EISCAT_3D system in detail, we have to know how such an effort of multi-dimensional imaging of aurora has been made by using currently-working radar systems in the high-latitude region. For this purpose, I present a fine-scale electrodynamic structure behind an auroral vortex street observed immediately before substorm expansion phase onset, as inferred from high spatial and temporal resolution measurements of auroral breakup with an all-sky TV camera (ATV) and a coherent HF radar of Super Dual Auroral Radar Network (SuperDARN) in Iceland. During the interval of interest, the ATV observed eastward propagating auroral vortices in the initial brightening arc of a substorm just prior to the poleward expansion. During the sequential passage of the vortices across the radar beams, the radar detected large velocity flow shears whose magnitude was in excess of 1.5 km/s. The observations suggest that flow shears were located very close to the center of the vortices; thus, they corresponded to electric fields converging toward the vortices, which is consistent with the existence of upward field-aligned currents (FACs) flowing out of the vortices. The temporal and spatial resolutions of the current radar measurement were still insufficient for fully resolving the detailed electrodynamic structure behind the fast moving auroral vortices. At least, however, the observations suggest the existence of highly localized filamentary FAC structures behind the auroral vortex street. Such a fine-scale structuring process of an auroral arc would be one of the possible targets of the 3D imaging observations of the planned EISCAT_3D system.

Keywords: Aurora, Radar, Electric Field

Japan Geoscience Union Meeting 2014
(28 April - 02 May 2014 at Pacifico YOKOHAMA, Kanagawa, Japan)

PEM06-28 Room:312 Time:May 1 12:30-12:45

Study of the physical meanings of ionospheric tidal signatures using theoretical models

LIN, Charles[1*] ; CHEN, Yu-tsung[1] ; CHEN, Po-cheng[1] ; CHANG, Loren[2] ; LIN, Jia-ting[1] ; HUBA, Joseph[3] ; CHEN, Chia-hung[1]

[1]Department of Earth Science, National Cheng-Kung University, Tainan, Taiwan, [2]Institute of Space Science, National Central University, Chung-Li, Taiwan, [3]Plasma Physics Division, Naval Research Laboratory, Washington, D.C., USA

Variations the ionospheric electron density structures related to the tidal forcing propagating upward from the lower atmosphere have been studied intensively recently. The longitudinal variations of ionospheric electron density are related to the themospheric nonmigrating tidal signatures produced in-situ or propagating upward from below. During a stratospheric sudden warming, thermospheric migrating tidal signatures are modified and lead to the phase shift of ionospheric electron density structures at low latitudes. With the increasing number of global ionospheric observations, it is desirable to relate the thermospheric tidal signatures to corresponding tidal signatures of ionospheric electron density, since the neutral thermospheric temperature and wind observations are rather limited. In this paper we perform theoretical simulations to study the interconnections between tidal modes in thermospheric neutral parameters and ionospheric plasma. The migrating and nonmigrating tides of thermospehric winds output from NCAR GSWM/TIEGCM runs are incorporated to NRL SAMI-3 to investigate the responses of corresponding tidal modes in ionospheric electron density and their physical meanings.

Keywords: atmospheric tides, tidal signature of ionospheric electron density

Japan Geoscience Union Meeting 2014
(28 April - 02 May 2014 at Pacifico YOKOHAMA, Kanagawa, Japan)

PEM06-29 Room:312 Time:May 1 14:15-14:45

Wavelike Structures in the Low-Latitude F region Using Beacon Satellites

TSUNODA, Roland[1*]

[1]SRI International

The low-latitude F-region plasma is produced by solar radiation, and its gross structural features arise from plasma transport and re-distribution (1) along geomagnetic field (B) lines by a meridional neutral wind, and (2) in planes transverse to B by an electric field (E). The fundamental process is often referred to as the equatorial fountain, in which an eastward electric field, applied over the magnetic dip equator, drives the plasma upward; this transverse transport is accompanied by downward and outward transport along B, which is driven by gravity and diffusion. The enhancements in plasma density that form, one in each hemisphere, are known as the equatorial ionization anomalies. Embedded within these largest-scale structures is a hierarchy of smaller-scale wavelike perturbations that extend downward from perhaps 1000 km to nearly 10 cm. These structures include large-scale wave structure, traveling ionospheric disturbances, equatorial plasma bubbles, as well as the small-scale irregularities that are responsible for radio wave scintillations and radar backscatter. Because of the complex hierarchy of structures that can be present, comprehensive investigations require a network of sensors that can provide both spatial and temporal information with adequate spatial resolution, while providing the necessary geographical coverage. A brief review of some of the recent results regarding wavelike structures, obtained from studies using a broad network of instruments distributed throughout the Southeast Asian sector, is presented.

Keywords: Wavelike structures, Low Latitude F Region, Plasma Structures, Beacon Satellites

Japan Geoscience Union Meeting 2014
(28 April - 02 May 2014 at Pacifico YOKOHAMA, Kanagawa, Japan)

PEM06-30 Room:312 Time:May 1 14:45-15:00

Preliminary study of equatorial ionization anomaly characteristic from GRBR chain in southeast Asia

WATTHANASANGMECHAI, Kornyanat[1*] ; YAMAMOTO, Mamoru[1] ; SAITO, Akinori[2] ; MARUYAMA, Takashi[3]

[1]Research Institute for Sustainable Humanosphere, Kyoto University, [2]Department of Geophysics, Graduate School of Science, Kyoto University, [3]National Institute of Information and Communications Technology

To study the equatorial ionization anomaly (EIA) characteristic, comparison of total electron content (TEC) obtained from the GNU Radio Beacon Receiver (GRBR) network in southeast Asia with the data from SEALION ionosonde network, Equatorial Atmosphere Radar (EAR), and the SAMI2 model are employed. Five GNU Radio Beacon Receivers (GRBRs) were aligned along 100 degree geographic longitude. Their observations started in March 2012 to enable monitoring the ionosphere during the high solar activity. The GRBR network in southeast Asia is a unique observation network of which the field of view covers $\pm$ 20 degree magnetic latitude including the magnetic equator to capture the ionospheric irregularities including the EIA. As a preliminary result, the day-to-day variability of the EIA was captured by GRBR chain. The asymmetry of the EIA was investigated. As generally known, the neutral wind is a primary source of the EIA asymmetry, while the zonal electric field is the secondary one. Using the GRBR network, the EIA asymmetry is compared with the data from SEALION ionosonde network and from SAMI2 model to clarify the source mechanism of the EIA asymmetry.

Keywords: GRBR, EIA symmetry, Equatorial, Ionosphere, Ionosonde, SAMI2 model

Japan Geoscience Union Meeting 2014
(28 April - 02 May 2014 at Pacifico YOKOHAMA, Kanagawa, Japan)

PEM06-31 Room:312 Time:May 1 15:00-15:15

Performance evaluation of plasma bubble monitoring by VHF radars for GNSS augmentation systems

SAITO, Susumu[1*] ; YAMAMOTO, Mamoru[2] ; OTSUKA, Yuichi[3] ; YOSHIHARA, Takayuki[1]

[1]Electronic Navigation Research Institute, [2]RISH, Kyoto University, [3]STEL, Nagoya University

For global navigation satellite systems (GNSS), ionospheric plasma is one of the most serious error sources. Especially in air navigation where safety is extremely important, augmentation systems corresponding to flight phases are used. Even with augmentation systems of current design, such as ground-based augmentation system (GBAS) or satellite-based augmentation system (SBAS), probability of miss-detection of ionospheric anomalies prevent them from more advance operations. In the low latitude region, ionospheric anomaly detection is a challenge because of frequent occurrence of plasma bubbles.

In this study, plasma bubble detection by a VHF backscatter radar is proposed as an external ionospheric monitor. Multi-beam observation of plasma bubbles can detect two dimensional shapes of plasma bubbles in a plane perpendicular to the magnetic field. When satellite-receiver path of GNSS signals pass crosses the magnetic field line, the signals shall be discarded because it may be affected by plasma bubble.

To evaluate the performance of this system, a VHF radar-GNSS receivers combined experiment has been conducted. The Equatorial Atmosphere Radar (EAR) is used to detect plasma bubbles. Sets of GNSS receivers around the EAR and in Bangkok are used as the pseudo-user and reference station. The observation started from
October 2012, and continues with some technical interruptions.

At the meeting, first results of the experiment will be presented.

Keywords: Equatorial Atmosphere Radar, GNSS augmentation system, plasma bubble, ionospheric monitoring

Japan Geoscience Union Meeting 2014
(28 April - 02 May 2014 at Pacifico YOKOHAMA, Kanagawa, Japan)

PEM06-32 Room:312 Time:May 1 15:15-15:30

Future direction of operational ionospheric research

ISHII, Mamoru[1*]

[1]NICT

We are now facing new aspect of oprational ionospheric research. International Civil Aviation Organization (ICAO) is planning to revise their protocol and in near future all civil aviation must use space weather information for their operation.

Space weather information is important for aviation mainly in the following three factors; HF communication, aviation and radiation. Space weather phenomena in polar region are tend to be focused on in many cases, however, it is important also in equatorial region, e.g., equatorial plasma bubbles.

There are still some unknown process in space weather and they make the forecast difficult and low precision. We are required two different approach; understand the unknows process, and make empirical forecast methods which works even though we have still unknown process. Especially we need domestic/international cooperation in the former approach e.g., EISCAT-3D and Equatorial MU radar, because it is impossible to cover these ovservation in only one institute. ICAO issue is one of the important outcome for space weather and we should unify our activity to contribute the operation.

Keywords: space weather, ionosphere, ICAO

Japan Geoscience Union Meeting 2014
(28 April - 02 May 2014 at Pacifico YOKOHAMA, Kanagawa, Japan)

PEM06-33 Room:312 Time:May 1 15:30-15:45

Importance of EISCAT 3D as space weather reseach

NAGATSUMA, Tsutomu[1*]

[1]National Institute of Information and Communications Technology

These days, importance of space weather is significantly realized by international community, such as ICAO, WMO etc. NICT has been responsible for national space weather forecast in Japan for a long time. Since NICT's space weather forecast center belongs to the International Space Environment Service (ISES) as the Regional Warning Center (RWC) Japan, our operational activities are supported by international cooperation. To understand the current conditions of "space weather", monitoring networks of space weather observations are operated and used. For future objective and advanced space weather monitoring, we have been developing a space weather numerical simulation codes, too. These activities are strongly related to the space weather research for improving space weather forecasting.

EISCAT 3D is a quite unique facility to measure many kinds of physical parameters which cannot be obtained from other instruments. Therefore, it is expected that the EISCAT 3D can contirbute to the evaluation and improvement of space weather models. The future perspective of space weather research and our expectation to EISCAT 3D are introduced in our presentation.

Keywords: Space Weather, EISCAT 3D, Ground-Based Observation

Japan Geoscience Union Meeting 2014
(28 April - 02 May 2014 at Pacifico YOKOHAMA, Kanagawa, Japan)

PEM06-34 Room:312 Time:May 1 15:45-16:00

Thunderstorm Activity in Asia Maritime Continent and Global Cloud Variation

TAKAHASHI, Yukihiro[1*] ; SATO, Mitsuteru[1] ; YAMASHITA, Kozo[2]

[1]Department of Cosmosciences, Hokkaido University, [2]Salesian Polytechnic

Global relationship among the thunderstorm activities especially in Asia Maritime Continent, cloud variations in tropical regions and solar parameters was examined based on lightning data measured by Global ELF observation Network (GEON) operated by Hokkaido University and Outgoing Longwave Radiation (OLR) intensity. A correlated analysis between the number of the lightning strokes, cloud variation in the tropical regions, and solar parameters was examined, looking into the variation with ˜one month periodicity. It was found that the number of lightning stokes in Asia Maritime Continent (AMC) varies with about month periodicity in the period from February to June 2004 and shows positive correlation (R= ˜0.8) with OLR in the Western Pacific Warm Pool (WPWP). On the other hand, OLR in the central Africa shows negative correlation with the number of lightning stokes in the AMC in that period. It is also found that the galactic cosmic rays or UV intensity associated with solar activity shows good correlation with tropical OLR or lightning activity in AMC. One explanation to connect such global variations in thunderstorm / cloud amount with solar parameters would be the electrical circuit between lower and upper atmospheres. The radars distributed globally would provide some essential information for this hypothesis, such as conductivity in the lower ionosphere, which may determine the strength of electrical connection in the vertical and horizontal directions.

Keywords: Maritime Continent, thunderstorm, tropical region, cloud amount, OLR, solar activity

Japan Geoscience Union Meeting 2014
(28 April - 02 May 2014 at Pacifico YOKOHAMA, Kanagawa, Japan)

PEM06-P01 Room:Poster Time:April 30 18:15-19:30

Equatorial MU Radar project

YAMAMOTO, Mamoru[1*] ; HASHIGUCHI, Hiroyuki[1] ; TSUDA, Toshitaka[1]

[1]RISH, Kyoto University

Research Institute for Sustainable Humanosphere, Kyoto University (RISH) has been studying the atmosphere by using radars. The first big facility was the MU (Middle and Upper atmosphere) radar installed in Shiga, Japan in 1984. This is one of the most powerful and multi-functional radar, and is successful of revealing importance of atmospheric waves for the dynamical vertical coupling processes. The next big radar was the Equatorial Atmosphere Radar (EAR) installed at Kototabang, West Sumatra, Indonesia in 2001. The EAR was operated under close collaboration with LAPAN (Indonesia National Institute for Aeronautics and Space), and conducted the long-term continuous observations of the equatorial atmosphere/ionosphere for more than 10 years. The MU radar and the EAR are both utilized for inter-university and international collaborative research program for long time. National Institute for Polar Research (NIPR) joined EISCAT Scientific Association together with Nagoya University, and developed the PANSY radar at Syowa base in Antarctica as a joint project with University of Tokyo. These are the efforts of radar study of the atmosphere/ionosphere in the polar region. Now we can find that Japan holds a global network of big atmospheric/ionospheric radars. The EAR has the limitation of lower sensitivity compared with the other big radars shown above. RISH now proposes a plan of Equatorial MU Radar (EMU) that is to establish the MU-radar class radar next to the EAR. The EMU will have an active phased array antenna with the 163m diameter and 1055 cross-element Yagis. Total output power of the EMU will be more than 500kW. The EMU can detect turbulent echoes from the mesosphere (60-80km). In the ionosphere incoherent-scatter observations of plasma density, drift, and temperature would be possible. Multi-channel receivers will realizes radar-imaging observations. The EMU is one of the key element in the project ”Study of coupling processes in the solar-terrestrial system” for Master Plan 2014 of the Science Council of Japan (SCJ). We show the EMU project and its science in the presentation.

Keywords: Atmospheric radar, ionosphere observation, Indonesia, MST radar

Japan Geoscience Union Meeting 2014
(28 April - 02 May 2014 at Pacifico YOKOHAMA, Kanagawa, Japan)

PEM06-P02 Room:Poster Time:April 30 18:15-19:30

Development of a configurable digital receiver for atmospheric radars

YAMAMOTO, Masayuki[1*] ; GAN, Tong[1] ; FUJITA, Toshiyuki[1] ; NOOR HAFIZAH BINTI, Abdul aziz[1] ; OKATANI, Yoshikazu[1] ; HASHIGUCHI, Hiroyuki[1] ; YAMAMOTO, Mamoru[1]

[1]Research Institute for Sustainable Humanosphere, Kyoto University

Recent progress in radar imaging techniques enables high-resolution measurements of wind and turbulence by atmospheric radars. In order to implement radar imaging techniques to existing atmospheric radars, a cheap multi-channel receiver needs to be developed. Further, for improving and verifying radar imaging techniques, a digital receiver which can change its real-time signal processing is highly useful. We are now developing a low-cost configurable digital receiver. Because the digital receiver comprises a general-purpose software-defined radio receiver and a personal computer, its purchase cost is low and its real-time signal processing is easy to be implemented. In the presentation, we report the current development status of the digital receiver.

Keywords: atmospheric radar, wind profiler radar, digital receiver, software-defined radio technique, Universal Software Radio Peripheral (USRP)

Japan Geoscience Union Meeting 2014
(28 April - 02 May 2014 at Pacifico YOKOHAMA, Kanagawa, Japan)

PEM06-P03 Room:Poster Time:April 30 18:15-19:30

Statistical study of F-region field-aligned irregularities based on Equatorial Atmosphere Radar in Indonesia

DAO, Tam[1*] ; OTSUKA, Yuichi[1] ; SHIOKAWA, Kazuo[1] ; YAMAMOTO, Mamoru[2]

[1]STEL, Graduate School of Science, Nagoya University, [2]Research Institute for Sustainable Humanosphere, Kyoto University

I examined the statistical characteristics of Field-Aligned Irregularities (FAIs) echoes from the F-region of Ionosphere using Equatorial Atmosphere Radar (EAR) in Indonesia during three years from 2010 to 2012. We investigated the differences between post-sunset and post-midnight FAIs. Some results are analyzed in the daily and monthly average of echo power, spectral width, and Doppler velocity. We found that post-midnight FAIs occurred mostly in summer solstices from May to August in 2010 and 2011, and only in June and July in 2012. We realized some different characteristics between post-sunset and post-midnight FAIs observed from EAR as follow. (1) Echo intensity of the post-midnight FAIs is weaker than that of post-sunset FAIs. (2) The post-sunset FAIs often exceed an altitude of 450 km, whereas the post-midnight FAIs mostly occur in a range from 200 to 450 km in F-region. (3) Spectral width of the post-midnight FAIs is smaller than that of the post-sunset FAIs. These results suggest that plasma instability operates more actively at post-sunset than at post-midnight.

Keywords: F-region Ionosphere, Field-Aligned Irregularities (FAIs), VHF radar

Japan Geoscience Union Meeting 2014
(28 April - 02 May 2014 at Pacifico YOKOHAMA, Kanagawa, Japan)

PEM06-P04 Room:Poster Time:April 30 18:15-19:30

Statistical study of ionospheric irregularities by using Equatorial Atmosphere Radar

MARTININGRUM, Dyah rahayu[1*] ; YAMAMOTO, Mamoru[1]

[1]RISH, Kyoto University

The equatorial region is the source of many unique atmospheric processes that couple the entire atmosphere vertically from bottom to top and horizontally from equator to pole. The dynamical, electrodynamical, and electrical process of lower and upper atmosphere of equatorial region contribute to ionospheric irregularities through propagation of atmospheric waves, and magnetosphere-ionosphere interaction. Those process are responsible for the large degree of variabilities observed in the low latitude ionosphere.

Study of ionospheric irregularities was made during 2008-2013 by using 47 MHz Equatorial Atmosphere Radar (EAR) in Kototabang, Indonesia (0.20S, 100.32E; 10.36S dip latitude). Characteristic of echoes from ionospheric Field Aligned Irregularities (FAI) classified based on structure of E and F backscattered echoes power of EAR radar both of spatially and temporally. The results base on intermittent observations (2008-2010) and continuous observations (2011-2013). During the observations were obtained percentage of Equatorial Spread F (ESF) occurrences, diurnal and seasonal characteristics of ionospheric irregularities from the E region and also from F region. Furthermore, occurrence correlation between E and F region irregularities are also observed.

Keywords: Ionospheric Irregularity, Equatorial Atmosphere Radar, Statistical Study

Japan Geoscience Union Meeting 2014
(28 April - 02 May 2014 at Pacifico YOKOHAMA, Kanagawa, Japan)

PEM06-P05 Room:Poster Time:April 30 18:15-19:30

Lidar observations for study of coupling processes over the equatorial region

ABO, Makoto[1*] ; NAGASAWA, Chikao[1] ; SHIBATA, Yasukuni[1]

[1]Tokyo Metropolitan University

Stratosphere-troposphere exchange is important for the budget of ozone in the lower stratosphere as well as in the troposphere. Upward transport occurs in the tropical region (Brewer-Dobson circulation), but the exact mechanism controlling the transport is not clear. We have constructed the lidar facility for survey of atmospheric structure over troposphere, stratosphere, mesosphere and low thermosphere over Kototabang (100.3E, 0.2S), Indonesia in the equatorial region [1]. The lidar system consists of the Mie and Raman lidars for tropospheric aerosol, water vapor and cirrus cloud measurements, the Rayleigh lidar for stratospheric and mesospheric temperature measurements and the Resonance lidar for metallic species such as Na, Fe, Ca ion measurements and temperature measurements in the mesopause region. The laser system included in this lidar facility consists of three pulsed Nd:YAG lasers, a pulsed Ti:Sapphire laser seeded by a ring Ti:Sapphire laser and a dye laser. The most parts of this lidar system are remotely controlled via the Internet from Japan. The full lidar observations started from 2004. The routine observations of clouds and aerosol in the troposphere and stratosphere are continued now.

We found the top height of the stratospheric aerosol layer descend with time, synchronized with the QBO in the zonal wind. The QBO signals of the aerosol layer are noticed in the altitude range from 30 to 40 km. In addition, the tropospheric aerosol amount observed around the tropopause over Kototabang is much more than at mid-latitudes. They suspect that this is an evidence of active material exchange between the troposphere and the stratosphere over the equatorial region.

We have installed DIAL (differential absorption lidar) system for high-resolution measurements of vertical ozone profiles in the equatorial tropopause region over Kototabang, Indonesia. We will contribute to the elucidation of the climate change by getting observational information about high-resolution ozone density profiles, and the wave-propagation and material transportation using ozone as a tracer from the troposphere to the lower stratosphere over the equator.

There were many ozone DIAL systems in the world, but almost systems are optimized for stratospheric ozone layer measurement [2] or tropospheric ozone measurement [3]. Because of deep ozone absorption in the UV region, the wavelength selection is important. Simulation results show that we can measure above 20km with height resolution of 500m within 5% random error.

Acknowledgments

This work was financially supported by Grants-in-Aid for Scientific Research (No. 233401043).

References

1. Nagasawa C., M. Abo, Y. Shibata 23rd International Laser Radar Conference, No.2O-8, 43-46, 2006.
2. Megie G. J., G. Ancellet,, J. Pelon, Lidar measurements of ozone vertical profiles, Applied Optics 24, 3454-3463, 1985.
3. Nakazato M., T. Nagai, T. Sakai, Y. Hirose, Applied Optics, 46, 2269-2279, 2007.

Keywords: coupling process, equatorial region, lidar

Japan Geoscience Union Meeting 2014
(28 April - 02 May 2014 at Pacifico YOKOHAMA, Kanagawa, Japan)

PEM06-P06 Room:Poster Time:April 30 18:15-19:30

Microstructure of Precipitation over Indonesia from a Network of Parsivel disdrometers

MARZUKI, Marzuki[1*] ; HASHIGUCHI, Hiroyuki[2] ; YAMAMOTO, Masayuki[2] ; MORI, Shuichi[3] ; TAKAHASHI, Yukihiro[4]

[1]Department of Physics, Andalas University, Padang, Indonesia, [2]Research Institute for Sustainable Humanosphere (RISH) Kyoto University, Gokasho, Uji, Kyoto 611-001, [3]Japan Agency for Marine-Earth Science and Technology (JAMSTEC), Yokosuka, Japan, [4]Hokkaido University, Sapporo, Japan

Insight into the regional variability of raindrop size distribution (DSD), is of primary importance for estimation of rainfall using remote sensing techniques, cloud/precipitation microphysical processes and numerical weather modeling. In order to quantify the regional variability of the DSD over Indonesia, a network of 4 Parsivel disdrometers along equatorial Indonesia has been designed. The disdrometers were installed at Kototabang (KT; 100.32E, 0.20S), Pontianak (PT; 109.37E, 0.00S), Manado (MN; 124.92E, 1.55N) and Biak (BK; 136.10E, 1.18S). It was found that the DSD at PT has more large drops than at the other three sites. The DSDs at the four sites are influenced by both oceanic and continental systems, and majority of the data matched the maritime-like DSD that was reported in a previous study. Continental-like DSDs were somewhat dominant at PT and KT. The combination of World Wide Lightning Location Network, wind profiler and the Tropical Rainfall Measuring Mission (TRMM) Precipitation Radar (PR) allows a discussion on physical basis behind the regional variability of DSD over Indonesia.

Keywords: Indonesia, Parsivel, Raindrop

Japan Geoscience Union Meeting 2014
(28 April - 02 May 2014 at Pacifico YOKOHAMA, Kanagawa, Japan)

PEM06-P07 Room:Poster Time:April 30 18:15-19:30

Feature studies of the polar lower thermosphere by EISCAT_3D

NOZAWA, Satonori[1*]

[1]STEL, Nagoya University

The new EISCAT_3D radar will give us with great opportunities. Its 3D volumetric observations of ion velocity will provide high quality neutral wind data in the lower thermosphere. Furthermore, its continuous observations will make it possible to study planetary waves in the lower thermosphere in more detail as well as day-to-day variabilities of tides. In this talk, we will describe our future study targets.

The lower thermospheric wind dynamics has been paid great attention for several decades to understand the Magnetosphere-Ionosphere-Thermosphere coupling, since the neutral atmosphere plays a key role. In particular, it has been an issue how the lower thermosphere will response to the solar wind energy input. IS radar measurements of the polar lower thermosphere begun about 40 years ago by a pioneer work of Brekke et al. [JGR, 78, 8235, 1973], and significant number of studies have been conducted since then. However, our understanding of the lower thermosphere is still limited. One of reasons is that the lower thermosphere is significantly influenced by atmospheric waves propagating from below. Thus, the day-to-day variability is very prominent. Owing to high running cost, long term datasets are hard to be obtained by IS radar a decade ago. In 2007-2008, EISCAT Svalbard radar was operated almost continuously for 1 year. However, only about 20% of the data sets can be used for deriving the ion velocity vector. If we have wind velocity datasets on daily basis like meteor and MF radars usually made for the mesospheric wind measurements (70-100 km), our understanding of the lower thermosphere wind dynamics will be much more progressed. EISCAT_3D will make it possible.

Furthermore, the EISCAT_3D radar will give us higher temporal resolution data sets of neutral winds in the lower thermosphere with multi volumes. The observations will allow us to distinguish the temporal and spatial variations of winds. One of scientific targets is to investigate wind variations nearby the auroral arc in the E-region. By combining sodium and Rayleigh LIDARs as well as meteor and MF radars, which provide neutral temperature and wind velocity, respectively, we expect we can investigate dissipation process of gravity waves in more details as well as effects of auroral precipitation on the middle atmosphere.

Keywords: EISCAT_3D, polar ionosphere, lower thermosphere, planetary wave, tidal wave, gravity wave

Japan Geoscience Union Meeting 2014
(28 April - 02 May 2014 at Pacifico YOKOHAMA, Kanagawa, Japan)

PEM06-P08 Room:Poster Time:April 30 18:15-19:30

Observation of non-thermal planetary radio emissions with EISCAT 3D

TSUCHIYA, Fuminori[1*] ; MISAWA, Hiroaki[1]

[1]Tohoku University

EISCAT 3D is developing as incoherent scatter radar to study the terrestrial ionosphere and atmosphere. Due to large aperture area and low noise temperature of the receiving system of EISCAT 3D and the uniqueness of the receiving frequency of 233 MHz, it can also be a useful tool to study non-thermal radio emissions from the solar system planets. In this paper, feasibility and advantage of EISCAT 3D for observing non-thermal planetary radio emissions are presented. Following topics will be discussed. (1) Time variability of Jovian synchrotron radiation, (2) Radio emissions from lightning discharges occurred in the atmospheres of Mars and Saturn, and (3) Recent trials to detect incoherent radio emissions from extra-solar planets.

Japan Geoscience Union Meeting 2014
(28 April - 02 May 2014 at Pacifico YOKOHAMA, Kanagawa, Japan)

PEM06-P09 Room:Poster Time:April 30 18:15-19:30

Numerical simulation of Generalized Auroral Computed Tomography toward its application to the EISCAT_3D project

TANAKA, Yoshimasa[1*] ; OGAWA, Yasunobu[1] ; KADOKURA, Akira[1] ; GUSTAVSSON, Bjorn[2] ; ASO, Takehiko[3] ; BRANDSTROM, Urban[4] ; MIYAOKA, Hiroshi[1] ; UENO, Genta[5] ; SAITA, Satoko[6]

[1]National Institute of Polar Research, [2]University of Tromso, [3]The Graduate University for Advanced Studies (Sokendai), [4]Swedish Institute of Space Physics, [5]The Institute of Statistical Mathematics, [6]Research Organization of Information and Systems

The EISCAT_3D is a next-generation phased-array incoherent scatter radar, which is capable of measuring three-dimensional (3D) ionospheric plasma parameters at ten-times higher temporal and spatial resolution. Thus, it is expected that the EISCAT_3D will provide new insights into auroral physics. On the other hand, optical imaging observation will be still useful for studying the auroral dynamics, because high-sensitivity camera can generally measure horizontal 2D distribution of the aurora at higher temporal resolution than the radars. We demonstrate by numerical simulation how useful monochromatic auroral images taken at multi-point camera network are for the study of aurora dynamics in the EISCAT_3D project. We apply the generalized - aurora computed tomography (G-ACT) to simulated observational data from real instruments, that is, the Auroral Large Imaging System (ALIS) and the EISCAT_3D radar. The G-ACT is a method to reconstruct three dimensional (3D) distribution of auroral emission and ionospheric electron density (corresponding to horizontal 2D distribution of energy spectra of precipitating electrons) from multi-instrument data. It is assumed that a core site of the EISCAT_3D radar is located at Skibotn (69.35N, 20.37E), Norway, and scans an area of 0.8 degrees in geographic latitude and 3 degrees in longitude at 130km altitude with 21x21 beams. Two neighboring discrete arcs are assumed to appear in the observation region of the EISCAT_3D radar. The reconstruction results from the G-ACT are compared with those from the normal ACT as well as those from only the electron density observed by the EISCAT_3D radar. It is found that the G-ACT can interpolate the ionospheric electron density at much higher spatial resolution than the original one observed by the EISCAT_3D radar. Furthermore, the multiple arcs reconstructed by the G-ACT are more precise than those by the normal ACT. Even for the case that the reconstruction by the ACT is difficult due to unsuitable location of the camera sites relative to the discrete arcs and/or a small number of available images, the G-ACT allows us to achieve the reconstruction.

Keywords: aurora computed tomography, EISCAT_3D, simulation, multi-point camera observation

Japan Geoscience Union Meeting 2014
(28 April - 02 May 2014 at Pacifico YOKOHAMA, Kanagawa, Japan)

PEM06-P10 Room:Poster Time:April 30 18:15-19:30

Aurora-induced sodium layer variation detected by coordinated observation with sodium lidar and EISCAT radar

TSUDA, Takuo[1*] ; NOZAWA, Satonori[2] ; KAWAHARA, Takuya[3] ; KAWABATA, Tetsuya[2] ; SAITO, Norihito[4] ; WADA, Satoshi[4] ; OGAWA, Yasunobu[1] ; OYAMA, Shin-ichiro[2] ; HALL, Chris[5] ; TSUTSUMI, Masaki[1] ; EJIRI, Mitsumu K.[1] ; SUZUKI, Shin[2] ; TAKAHASHI, Toru[2] ; NAKAMURA, Takuji[1]

[1]National Institute of Polar Research, [2]Solar-Terrestrial Environment Laboratory, Nagoya University, [3]Faculty of Engineering, Shinshu University, [4]RIKEN, [5]University of Tromsoe

Sodium atom layer is generally distributed at 80-100 km. One of mysterious subjects on high-latitude sodium layers is relationship between auroral particle precipitation and sodium atom layer variation. A previous study suggested a sodium column density decrease during a geomagnetic active period due to that the particle precipitation accompanied by electron density enhancement could induce ionization of sodium atom through their ion-molecule chemistry. Another study pointed a possibility of sodium density increase. For this reason, it is suggested that auroral precipitating particle bombardment on meteoric smoke particles can sputter sodium atoms from the smoke particles. On the other hand, ionospheric electric field, which may become more significant near auroral precipitating regions, could induce ion motions (i.e. can generate sodium ion convergence and/or divergence), and then also could affect generation and/or loss processes of sodium atoms through their ion-molecule chemistry. Thus, for the examination of the causality, it is vitally important to distinguish the effects of auroral particle precipitation and ionospheric electric field. Using a sodium lidar (which was installed in early 2010) and European incoherent scatter (EISCAT) radar at Tromsoe, Norway (69.6N, 19.2E), we have investigated, for the first time, that the actual effect of the particle precipitation to the sodium density variations without electric filed injection. In the nighttime observation on 24-25 January 2012, we detected a significant decrease of sodium atom density coincied with electron density enhancements (implying strong particle precipitations) and low ion temperatures (implying no electric field injections). These results strongly suggested that auroral particle precipitations induced sodium atom density decrease. Furthermore we discuss observed time response in the sodium density decrease.

Keywords: Na lidar, EISCAT radar, Na layer, Auroral particle precipitation, Ionospheric electric field

Japan Geoscience Union Meeting 2014
(28 April - 02 May 2014 at Pacifico YOKOHAMA, Kanagawa, Japan)

PEM06-P11 Room:Poster Time:April 30 18:15-19:30

The spatial and temporal evolution of equatorial plasma bubble observed using ground based GPS TEC measurement.

M BUHARI, Suhaila[1*] ; ABDULLAH, Mardina[2] ; HASBI, Alina marie[3] ; OTSUKA, Yuichi[4] ; NISHIOKA, Michi[5] ; TSUGAWA, Takuya[5]

[1]Physics Department, Universiti Teknologi Malaysia, [2]Space Science Centre, Universiti Kebangsaan Malaysia, [3]Department of Electrical, Electronics & Systems Engineering, Universiti Kebangsaan Malaysia, [4]Solar-Terrestrial Environment Laboratory, Nagoya University, [5]National Institute of Information and Communications Technology

The equatorial plasma bubble (EPB) commonly occurs near the equatorial region after post sunset period. The generation process of EPB has been well understood where it is commonly developed near the magnetic equator and elongated along magnetic field lines through Rayleigh-Taylor instability mechanism. However, the source of seeding perturbation leads to the generation of Rayleigh-Taylor instability is still unknown. The temporal and spatial properties of EPB have been well studied using airglow imager. However, the observation using airglow imager is impossible during sunset time where the EPB starts to develop due to light from the sun while the observation during night time is always interfered by moon and clouds.

In this study, we obtain the GPS data from Malaysia Real-Time Kinematics GNSS Network (MyRTKnet), International Ground Station (IGS) network and Sumatera GPS Array (SUGAR) network. The networks contains 127 receivers in South East Asia (SEA) region covers 8^{o}N to -8^{o}S latitude and 92^{o}E to 120^{o}E longitude geographic coordinates. In this study, we detected the structure of EPB using two-dimensional map of rate of TEC index (ROTI) calculated from ground based GPS TEC measurement in. The average ROTI value for all visible satellites at 300 km altitude is binned into 0.45^o x 0.45^o grid in geographic latitude and longitude. The advantage of this technique is the GPS data is always available and we are able to observe the spatial and temporal properties of EPBs continuously without distracted by light.

On the 17th March 2011, we observed the appearance of EPB structure pass through the SEA territory for 5 hours from 1300 UT (2100 LT) - 1900 UT (0200 LT). The initial ROTI-enhancement region is at 1300 UT is propagating to eastward direction and the information of the structure is lost due to the limited coverage of GPS receiver. At 1340 UT, a new ROTI-enhancement region appeared as a point source at geographic coordinate 2^{o}N and 98^{o}E as shown in Figure (a). After 20 minutes, the point source of ROTI-enhancement region expand to ˜600 km in the North and ˜200 km South direction as shown in Figure (b) while the zonal size ˜50 km remains the same. The perturbation region is expanding faster towards dip magnetic equator might associated with field-aligned irregularities. The structure travelled in eastward direction with velocity ˜133 ms^{-1} until the development process stopped. After 60 minutes, we assumed the structure is fully developed as illustrated in Figure (c) when no development in zonal size and ROTI value is observed anymore. The developed structure has 200 km zonal size continuously moves to eastward directions with slower velocity ˜111 ms^{-1}. The slower velocity incidentally with no development in zonal size and ROTI value might indicates the ”fossil” bubble where the plasma density is equal with background density and the structure velocity following the background plasma density. At 1440 UT the second structure is coming ˜600 km away from the first structure with velocity ˜111 ms^{-1} and zonal size 200 km same as the previous structure as shown in Figure (d). The first and second structure has the same zonal sizes and velocities might due to the same temporal and spatial evolution during the generation process.

The two-dimensional structure of EPB has been presented using GPS networks in SEA region is an alternative tool to observe the temporal and spatial properties of EPB structure from the initial perturbation until the decaying process without being distracted by light. The temporal and spatial properties of EPB can contribute towards understanding the generation mechanism of the Rayleigh-Taylor instability process.

Keywords: equatorial plasma bubble, rate of TEC index, GPS TEC measurement

PEM06-P11 Room:Poster Time:April 30 18:15-19:30

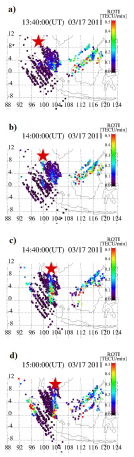

Japan Geoscience Union Meeting 2014
(28 April - 02 May 2014 at Pacifico YOKOHAMA, Kanagawa, Japan)

PEM06-P12 Room:Poster Time:April 30 18:15-19:30

Relationship between Latitudinal Extension of Scintillation and Pre-reversal Enhancement in the Southeast Asian Region

ABADI, Prayitno[1*] ; OTSUKA, Yuichi[2] ; HUSIN, Asnawi[1] ; JIYO, Jiyo[1] ; YAMAMOTO, Mamoru[3] ; TSUDA, Toshitaka[3]

[1]National Institute of Aeronautics and Space (LAPAN), [2]STEL, Ngoya University, [3]RISH, Kyoto University

We have investigated the relationship between the maximum latitude extension of observed scintillations (Lmax) and the maximum altitude of the equatorial F-region bottomside (h'Fmax), peak of eastward electric field (Emax), and time duration of eastward electric field (TE) during PRE period in the equatorial region. We used three GPS receivers installed in Kototabang (0.2S, 100.3E; 10.0N magnetic latitude), Pontianak (0.02S, 109.3E; 8.9S magnetic latitude), and Bandung (6.9S, 107.6E; 17.5S magnetic latitude), Indonesia for observing scintillation activity in period 18.00-22.00 LT (LT=UT+7h) and two frequency modulated-continues wave (FM-CW) ionosondes installed near equator magnetic, Chumphon (10.7N, 99.4E; 3.3N magnetic latitude), Thailand and Bac Lieu (9.3N, 105.7E; 1.7N magnetic latitude), Vietnam for measuring PRE parameters, such as h'F, vertical drift (dh'F/dt) which indicates eastward electric field, and TE. Our observation period is during equinox months (March, April, September, and October) in 2010, 2011, and 2012. We divide the relationships into two groups; 1) the relationships between PRE parameters obtained from Chumphon ionosonde and Lmax observed by Kototabang and Bandung GPS receivers and 2) PRE parameters obtained from Bac Lieu ionosonde and Lmax observed by Pontianak and Bandung GPS receivers. The following table is to show the coefficient correlation (R) of the relationships for each group. The results indicate that duration of eastward electric field does not play an important role for extension of the plasma bubble or latitudinal extension of scintillation, and that the peak of h'F and magnitude of E at the initial phase of plasma bubble generation (PRE period) is a primary factor for the plasma bubble extension. Therefore, the maximum latitude of scintillation is determined at the initial phase of plasma bubble generation (PRE period) in the equatorial region.

Relationship	R (group 1)	R (group 2)
h'Fmax vs Lmax	0.596	0.471
Emax vs Lmax	0.489	0.270
TE vs Lmax	0.054	0.090

Keywords: Ionosphere, Scintillation, Pre-reversal enhancement

Japan Geoscience Union Meeting 2014
(28 April - 02 May 2014 at Pacifico YOKOHAMA, Kanagawa, Japan)

PEM06-P13 Room:Poster Time:April 30 18:15-19:30

Geolocation of lightning discharge in the Maritime Continent based on radio observation in 0.1-40 kHz band

YAMASHITA, Kozo[1*] ; OHYA, Hiroyo[2] ; TAKAHASHI, Yukihiro[3] ; TSUCHIYA, Fuminori[4] ; MATSUMOTO, Jun[5]

[1]Salesian Polytechnic, [2]Chiba University, [3]Hokkaido University, [4]Tohoku University, [5]Tokyo Metropolitan University

Recent researches based on observation and data assimilation of lightning discharge indicate a possibility of now-cast and forecast of severe weather such as torrential rain. In these works, lightning data is focused on as a proxy for the presence or absence of deep convection which generates thunderstorm.

In previous works, occurrence of cloud-to-ground (CG) lightning discharges has been mainly used due to the ease of data availability. However, lighting observation based on electromagnetic measurement shows that there is extremely huge scale lightning whose scale is more than hundreds times bigger than that of averaged event. Lightning data including ″ occurrence ″ and ″ scale ″ enable us to evaluate not only existence but also intensity of atmospheric convection. Quantitative evaluation of atmospheric convection would make it possible to make a now-cast and forecast for intensity distribution of precipitation.

The Maritime Continent (MC) is one of the most important regions for lightning observation in the world. Thunderstorm activity causes enormous human and economic damage to countries in MC. However, until now, only few statistical studies on the lightning activity with scale information of lightning discharge have been done.

In this works, lightning observation network in the MC based on electromagnetic measurement in 0.1-40 kHz band is summarized. This network is developed to estimate not only spatial distribution but also scale one of lightning discharges. We have already constructed observation stations at Tainan in Taiwan (23.1N, 121.1E), Saraburi in Thailand (14.5N, 101.0E), Pontianak in Indonesia (0.0N, 109.4E), Los Banos in Philippines (14.2N, 121.25E) and Son Tay in Viet Nam (21.1N, 105.5E). Data obtained by multipoint observation is synchronized by GPS receiver installed at each station.

At the presentation, we show evaluation of accuracy for geolocation and detection efficiency of signal radiated from lightning discharge based on comparisons with World Wide Lightning Location Network (WWLLN) data.

Keywords: lightning discharge, thunderstorm, severe weather, VLF, the Maritime Continent

Japan Geoscience Union Meeting 2014
(28 April - 02 May 2014 at Pacifico YOKOHAMA, Kanagawa, Japan)

PEM06-P14 Room:Poster Time:April 30 18:15-19:30

A study on a low Earth orbit (LEO) satellite mission using radio propagation characteristics

TAKEDA, Yuji[1*] ; TSUDA, Toshitaka[1]

[1]Research Institute for Sustainable Humanosphere, Kyoto University

We study in this paper an Earth observation mission with a low Earth orbit (LEO) satellite using radio propagation characteristics on L (1.2-1.6 GHz for GPS) and Ka (17.3-20.2 GHz for O3b satellite) bands . In particular, applying GPS radio occultation (GPS RO) technique, we aim to obtain profiles of atmospheric parameters (humidity, temperature and electron density) with a good height resolution, covering a wide area. We also measure cloud water content and vapor distribution by using radiometer technique on Ka-band.

Radio occultation employs propagation delay and bending of radio waves in the atmosphere. Though GPS satellites hitherto has been used for observing radio occultation, we use not only GPS but also other GNSS satellites (GLONASS, Galileo, Beidou, and QZSS), moreover we further use O3b(Other 3 billion people), which is a communications satellite, then, we can increase number of observation points of RO.

Because the observation point of RO is determined by the relative location between the LEO satellite and transmitting satellites, we used a numerical model to investigate the data distribution of RO and proposed an optimal satellite orbit for a new LEO satellites mission. The model analysis shows that using GNSS and O3b satellites for RO the total number of RO data becomes approximately three times larger than those by using only GPS satellites. The analysis also shows that the longitudinal distribution of RO data does not depend on orbit of the LEO satellite, but, the latitudinal distribution is largely affected by an inclination angle of LEO satellite. Data distribution as function of local time varies by inclination and longitude of ascending node of LEO satellite.

We also investigate application of O3b operated on Ka-band, which is approximately ten times higher than L-band. So Ka-band is less sensitive to the ionosphere, but it is greatly attenuated by cloud water and vapor. In GPS RO on L band, atmospheric profiles at high-altitude (50km-) are not determined accurately because of influence of ionosphere. But using Ka-band of O3b we will be able to increase the maximum height of the profiles. Moreover, we expect to measure cloud water content and vapor distribution by using attenuation of Ka-band.

Keywords: GPS radio occultation, Low Earth orbit satellite, Global Navigation Satellite System, Ka-band

Japan Geoscience Union Meeting 2014
(28 April - 02 May 2014 at Pacifico YOKOHAMA, Kanagawa, Japan)

PEM07-01 Room:213 Time:April 30 14:15-14:30

Introdution to GLIMS mission

USHIO, Tomoo[1*] ; SATO, Mitsuteru[2] ; MORIMOTO, Takeshi[3] ; SUZUKI, Makoto[4] ; YAMAZAKI, Atsushi[4] ; HOBARA, Yasuhide[5] ; KIKKUCHI, Masayuki[6]

[1]Osaka University, [2]Hokkaido University, [3]Kinki University, [4]JAXA, [5]University of Electro Communications, [6]NIPR

The Global Lightning and sprIte MeasurementS (GLIMS) on the International Space Station (ISS) is a mission to detect and locate optical transient luminous events (TLEs) and its associated lightning simultaneously from the non-sun synchronous orbit, and was launched successfully in July, 2013 as part of the multi-mission consolidated equipment on Japanese Exposure Module (JEM). Our mission goals are to identify temporal and spatial evolutions of lightning and TLEs and to clarify the occurrence conditions of TLEs and global occurrence locations and rates of TLEs from the nadir observation. To achieve these goals, two CMOS cameras, six Photometers, VLF receiver, and VHF interferometer with two antennas, are installed at the bottom of the module to observe the TLEs as well as causative lighting discharges at nadir direction during day and night time. Though the luminous events so-called sprite, elves and jets have been investigated by numerous researchers all over the world based mainly on the ground observations, some important problems have not been fully understood yet such as generation mechanisms of columniform fine structure and horizontal offset of some sprites from the parent lightning discharges. In the JEM-GLIMS mission, observations from our synchronized sensors are going to shed light on above-mentioned unsolved problems regarding TLEs as well as causative lighting discharges.

The optical instruments are two CMOS cameras (LSI-1, LSI-2) and six-channel spectrophotometers (PH1 - PH6). The FOV of LSI is 28.3 deg. x 28.3 deg., and LSI-1 (LSI-2) equips a 766-832 nm wide band filter (a 762+/-7 nm narrow band filter). Each PH channel equips the optical band-pass filter, and these photometers measure the N2 1P, N2 2P, N2 LBH, and N2+ 1N emissions of lightning and TLEs. The radio receivers consist of one VLF receiver (VLFR) and two sets of VHF receivers (VITF). In order to detect TLE-associated whistler waves, VLFR employs a nadir-directing monopole antenna and an electronics unit recording waveform data with a sampling frequency of 100 kHz with 14-bit resolution. VITF consists of two patch-type antennas separated by 1.5 m and an electronics unit, and VITF mainly observes VHF pulses in the frequency range of 70-100 MHz excited by lightning discharges with a sampling frequency of 200 MHz with 8-bit resolution.

JEM-GIMS was successfully launched and transported to the ISS by the H-II Transfer Vehicle (HTV) No.3 cargo transporter at the end of July 2012, and started its operation from December 2013. So far, more than one thousand events were recorded. In this presentation, mission history and overview will be given as an introdution.

Keywords: Lightning, Sprite, ISS

Japan Geoscience Union Meeting 2014
(28 April - 02 May 2014 at Pacifico YOKOHAMA, Kanagawa, Japan)

PEM07-02 Room:213 Time:April 30 14:30-14:45

Estimating lightning characteristics by spaceborne spectrophotometric observation

ADACHI, Toru[1*] ; SATO, Mitsuteru[2] ; USHIO, Tomoo[3] ; YAMAZAKI, Atsushi[4] ; SUZUKI, Makoto[4] ; KIKUCHI, Masayuki[5] ; TAKAHASHI, Yukihiro[2] ; INAN, Umran[6] ; LINSCOTT, Ivan[6] ; HOBARA, Yasuhide[8] ; COHEN, Morris[6] ; LU, Gaopeng[9] ; CUMMER, Steven[9] ; HSU, Rue-ron[10] ; CHEN, Alfred[10] ; FREY, Harald[7]

[1]Waseda Institute for Advanced Study, Waseda University, [2]Department of Cosmosciences, Hokkaido University, [3]Division of Electrical, Electric and Information Engineering, Osaka University, [4]ISAS, JAXA, [5]NIPR, [6]Electrical Engineering Department, Stanford University, [7]Department of Electronic Engineering, The University of Electro-Communications, [8]Electrical and Computer Engineering Department, Duke University, [9]Physics Department, National Cheng Kung University, [10]SSL, University of California at Berkeley

The present study analyzes satellite optical data to evaluate the effectiveness of spaceborne spectrophotometric measurement in characterizing properties of lightning flash. The main data analyzed here are those obtained by FORMOSAT-2/ISUAL limb observation and ISS/GLIMS nadir observation. While ISUAL spectrophotometer observes optical emissions of 150-280, 316, 337, 392, 762, 600-900 nm at a sampling rate of 10 kHz, GLIMS observes emissions of 150-280, 337, 762, 600-900, 316, 392 nm at a rate of 20 kHz. These data for the first time derive fine spectral and temporal properties of lightning emission observed from space. By analyzing the ISUAL optical data and ground-based radio data, we found that spectral intensity ratio is a new parameter to discriminate intra-cloud (IC) and cloud-to-ground (CG) lightning discharges: the blue/red intensity ratio of CG strokes tends to be lower than that of IC pulses. We also found similar tendency in GLIMS lightning events. A case study showed that the color of lightning turned to red when a very bright impulsive emission, which is consistent with a ground return stroke, occurred. These results consistently suggest that the color of CG component is redder than that of IC component, and we explain this as a result of the Rayleigh scattering which effectively attenuates blue light emissions in the case of light sources located at lower-altitudes such as CGs. Using this technique, we will further examine the lightning characteristics on a global level, focusing on latitudinal dependences and land/ocean contrast for example.

Keywords: lightning, CG, IC, satellite, remote sensing

Japan Geoscience Union Meeting 2014
(28 April - 02 May 2014 at Pacifico YOKOHAMA, Kanagawa, Japan)

PEM07-P01 Room:Poster Time:April 30 18:15-19:30

VLF subionospheric disturbances and electrical properties of lightning discharges observed by JEM-GLIMS mission

KAKINUMA, Kanata[1*] ; HOBARA, Yasuhide[1] ; USHIO, Tomoo[2] ; SATO, Mitsuteru[3] ; MORIMOTO, Takeshi[4] ; TAKAHASHI, Yukihiro[5] ; SUZUKI, Makoto[6]

[1]Graduate School of Informatics and Communication Eng., The University of Electro-Communications, [2]Information and communication engineering department, Osaka University, [3]Department of Cosmoscience, Hokkaido University, [4]Faculty of Science and Engineering, Kinki University, [5]Department of Cosmosciences, Graduate School of Science, Hokkaido University, [6]Institute for Space and Astronautical Sciences, Japan Aerospace Exploration Agency

In this paper we report the preliminary results of ionospheric perturbation and causative lightning discharges observed by JEM-GLIMIS mission to study the electromagnetic coupling mechanism between the tropospheric lightning and overlaying ionosphere. Continuous nadir optical observations of lightning discharges are performed by ISS JEM-GLIMS mission and many lightning images have been observed globally. Ionospheric perturbations and electrical properties of causative lightning discharges such as polarity and vertical charge moment changes are derived by the data from UEC's ground-based observation networks of VLF/LF transmitter signal reception and of ELF waveforms respectively. We discuss the electrical coupling efficiencies from the tropospheric lightning to the ionosphere by comparing the area of the lightning flash and corresponding subionospheroic VLF disturbances and lightning properties.

Keywords: Transient Luminous Events, lightning discharges, GLIMS, ionospheric perturbation, charge moment

Japan Geoscience Union Meeting 2014
(28 April - 02 May 2014 at Pacifico YOKOHAMA, Kanagawa, Japan)

PEM07-P02 Room:Poster Time:April 30 18:15-19:30

The building of multipoint measurement network for observing electrostatic field changes caused by lightning discharge

SAKAI, Rikuma[1*] ; TAKAHASHI, Yukihiro[1] ; SATO, Mitsuteru[1] ; KUDO, Takeshi[1]

[1]Cosmosciences, Hokkaido Univ.

It’s not easy to understand the developing process of thunderstorm only with existing meteorological measurements because of its small spatial scale (less than an order of 1 km) and rapid change of the complicated structure. Electrostatic field under the thundercloud or its predecessor reflects the distribution of electrical charges, which is the result of frictions between ice crystal and hail due to strong vertical wind inside the thundercloud. If we measure the vertical electric field at multipoints on the ground, we could estimate the 3 dimensional distribution or the changes of the distribution of electrical charges, from which we may know the detailed development of thunderstorm. The traditional equipment for atmospheric electrostatic filed measurement is filed-mill sensor, which costs an order of 1 M JPY. In order to increase the number of observing stations, we should reduce the price of the instrument. Here we introduce a thunderstorm observation campaign, carried out in mountain area of Yamanashi prefecture, August 2013.We developed new plate-type electric filed sensor, which costs about 0.2 M JPY or less including recording device and battery for one site.This sensor was placed at seven locations in every 4 km with recording system and GPS clock.As a result, we succeeded to record the electrostatic field changes at the same time in multi points, which occured due to lightning strikes for three days.

Keywords: lightning discharge, electrostatic field, multipoint measurement

Japan Geoscience Union Meeting 2014
(28 April - 02 May 2014 at Pacifico YOKOHAMA, Kanagawa, Japan)

PEM07-P03 Room:Poster Time:April 30 18:15-19:30

Preliminary results of global lightning study by the DEMETER satellite

SUTO, Yushi[1*] ; NAKAMURA, Maho[1] ; KAMOGAWA, Masashi[1]

[1]Dpt. of Phys., Tokyo Gakugei Univ.

We investigate statistical property of global lightning activity by means of the DEMETER satellite. The DEMETER satellite which was launch by CNES, France, was operated from 2004 to 2010. In the study, we use electric field data to measure Whistler waves generated by lightning. In this presentation, we show preliminary results of this study.

Keywords: Ionosphere, Lightning, Whistler waves

Japan Geoscience Union Meeting 2014
(28 April - 02 May 2014 at Pacifico YOKOHAMA, Kanagawa, Japan)

PEM07-P04 Room:Poster Time:April 30 18:15-19:30

VHF lightning observations by digital interferometry on JEM-GLIMS

MORIMOTO, Takeshi[1*] ; KIKUCHI, Hiroshi[2] ; SATO, Mitsuteru[3] ; USHIO, Tomoo[2] ; YAMAZAKI, Atsushi[4] ; SUZUKI, Makoto[4]

[1]Kinki University, [2]Osaka University, [3]Hokkaido University, [4]ISAS/JAXA

Global Lightning and sprIte Measurements (GLIMS) mission is now ongoing on Exposed Facility of Japanese Experiment Module (JEM-EF) of the International Space Station (ISS). This paper focuses on an electromagnetic (EM) payload of JEM-GLIMS mission, very high frequency (VHF) broadband digital InTerFerometer (VITF). JEM-GLIMS mission is designed to conduct comprehensive observations with both the EM and the optical payloads for lightning activities and related transient luminous events (TLEs) expecting to give us many scientific impacts to the field.

VITF consists of two sets of antennas, band-pass filters, amplifiers, and 2-channel-AD-converter. Impulsive EM radiations received by the antennas are digitized by the AD converter synchronizing with another channel through the filters and the amplifiers. A patch type antenna is developed within the size of 200∗200 mm. It is mounted on the antenna base made of aluminum alloy and Teflon block with the total height of 100 mm to gain its bandwidth and to reduce the interference from other structural objects. The same two units of antennas are installed with the separation of 1.6 m. Their bandwidths with the higher return loss than -3 dB are from 70 to 100 MHz. The signals received by the antenna are transmitted along cables with the same lengths to the electronics. The AD converter records 130 waveforms as maximum of one dataset with the duration of 2.5 μs with 200 MS/s. The developments of VITF are based on the heritage of VHF sensor on Maido-1 satellite.

JEM-GIMS mission payload was successfully launched at the end of July 2012, and transported and installed to the ISS. After the initial checkout and maintenance, its nominal operation is continued from December 2012. Through the operation period, VITF corrects numerous VHF EM data synchronized with optical signals. About 650 VITF datasets were obtained in January and February 2013, for instance. The estimations of the EM direction-of-arrival (DOA) are attempted using the broadband digital interferometry. Some results agree with the optical observations, even though DOA estimation has difficulties caused by its very short baseline of the antennas and multiple pulses in short time, namely burst-type EM waveforms. VITF is designed expecting to estimate the DOA with about 10 km resolution that is equivalent to the scale of a thundercloud. The results on narrow bipolar pulses (NBPs) and/or transionospheric pulse pairs (TIPPs) are also expected as well as TLEs. The recorded VHF EM signals and the results of their DOA estimations, and the comparisons with optical observations will be introduced in the presentation.

Keywords: lightning, VHF radio observations, GLIMS, International Space Station

Japan Geoscience Union Meeting 2014
(28 April - 02 May 2014 at Pacifico YOKOHAMA, Kanagawa, Japan)

PEM08-01 Room:411 Time:May 1 16:15-16:30

Numerical Modeling of the Three-Dimensional Magnetic Fields and Eruption in the Solar Active Region 11158

INOUE, Satoshi[1*]

[1]School of Space Research, Kyung Hee University

Solar flares and coronal mass ejections (CMEs) are considered as sudden liberation of magnetic energy in the solar corona, which affect geospace in the form of electromagnetic disturbance called geomagnetic storms. Unfortunately, measurement based on vector field observations only provide the two-dimensional information of magnetic field on the photosphere, therefore, we could not reach on a common understanding yet regarding to the three-dimensional (3D) magnetic structure causing the eruptive phenomena and associated dynamics. In order to clarify them, in this study we first extrapolate a 3D coronal magnetic field under the Nonlinear Force-Free Field (NLFFF) approximation based on the vector field, using the Magnetohydrodynamic (MHD) relaxation method developed by Inoue et al. 2014, and then compare the 3D structures before and after the flare. Next we perform an MHD simulation to clarify the dynamics during the flare where the NLFFF prior to the flare is set as an initial condition. Photospheric vector field was observed at 00:00 UT and 03:00 UT on February 15 corresponding to before and after the X2.2-class flare taking place around at 01:50 UT, taken by the Helioseismic And Magnetic Imager (HMI) on board the Solar Dynamics Observatory (SDO) satellite.

As a result, we found that the NLFFF has strongly twisted field lines; most of them are in the range from half-turn to one turn twist, being resided above the polarity inversion line. Furthermore, we found that a distribution of these footpoints well captures the flare ribbons observed by Hinode where Ca II emission is strongly enhanced. On the other hand, because the most of these strongly twisted lines disappear after the flare, consequently the twisted field lines having more than half-turn twist play an important role on causing the large flare. The MHD simulation successfully shows an eruption of the more strongly twisted lines whose values are over one-turn twist, which are produced through the magnetic reconnection in strongly twisted lines of the NLFFF. Eventually, we found that they exceed a critical height at which the flux tube becomes unstable to the torus instability determining the condition that whether a flux tube might escape from the overlying field lines or not. In addition to these, during the eruption, we found that the distribution of the observed two-ribbon flares is similar to the spatial variance of the footpoints caused by the reconnection of strongly twisted lines with more than half-turn twist. Furthermore, because the post flare loops obtained from MHD simulation well capture that in EUV image taken by SDO, these results support the reliability of our simulation.

Keywords: Active Region, Coronal Magnetic Field, Solar Flare, Coronal Mass Ejections, Numerical Modeling

Japan Geoscience Union Meeting 2014
(28 April - 02 May 2014 at Pacifico YOKOHAMA, Kanagawa, Japan)

PEM08-02 Room:411 Time:May 1 16:30-16:45

Study on Triggering Process of Solar Flare on the basis of Satellite Observation

BAMBA, Yumi[1*] ; KUSANO, Kanya[1] ; IMADA, Shinsuke[1]

[1]STEL, Nagoya Univ.

Solar Flares are explosive phenomena driven by magnetic energy stored in the solar corona. Because interplanetary disturbances associated with solar flares sometimes impact terrestrial environments and infrastructure, understanding the flare-triggering process is important not only from a solar physics perspective but also for space weather forecasting. There are numerous observational studies and simulations which attempted to reveal the onset mechanism of solar flares. Because different observations support different models, the underlying mechanism of flare onset remains elusive. Thus the predictability of flare occurrence remains limited.

We have analyzed several flare events obtained by the Solar Optical Telescope (SOT) onboard the Hinode Satellite in order to elucidate flare trigger mechanism [*Bamba et al.* 2013]. We investigated the spatio-temporal correlation between the detailed magnetic field structure and the chromospheric pre-flare emission at the central part of flaring regions for several hours prior to the onset of flares. We observed that the magnetic shear angle in the flaring regions exceeded 70 degrees, as well as that characteristic magnetic disturbances developed at the centers of flaring regions in the pre-flare phase. The observed signatures strongly support the idea of flare trigger mechanism presented by *Kusano et al.* (2012), which proposed that solar flares can be triggered by the interaction between the sheared arcade and one of the two types of small magnetic disturbances. Hence, we could classify the events into two groups depending on the structure of their magnetic polarity inversion lines; to the so-called " Opposite-Polarity (OP) " and " Reversed-Shear (RS) " magnetic field. Furthermore, we studied how small magnetic field can work for triggering flares based on the Hinode observations. The results indicate that the critical amount of magnetic flux for the small magnetic field to trigger flares, depends on the magnetic connectivity in the flaring site, and it varies even within an active region.

However, only four Hinode data sets habe been utilizable for the analyze of this study because of the SOT ' s limited field of view (FOV) (328 " × 164 " for Narrow-band Filter Imager, 218 " × 109 " for Broad-band Filter Imager). Therefore, we applied the analysis method of *Bamba et al.* (2013) to the data obtained by the Helioseismic and Magnetic Imager (HMI) and the Atmospheric Imaging Assembly (AIA) onboard the Solar Dynamics Observatory (SDO), which has a full-disk FOV (2000 " × 2000 ") in order to increase the number of event analysis. We chose the flare events observed by SDO until 31 Jan. 2014, larger than M5.0 GOES class. Eleven X-class and twenty M-class events meet this condition, and we classified these events into independent 6 types by using following three conditions: (1) whether the initial flare kernels has obvious and sheared two-ribbon structure, (2) whether the chromospheric brightening was observed at the center of sheared ribbon, (3) the results of measurement of the magnetic shear angle θ and the azimuth of flare trigger field ϕ.

In this presentation, we would like to report the result of comparative study of Hinode and SDO. We would like to also introduce our preliminary result of statistical flare trigger study using SDO/HMI and AIA.

References:
[1] *Study on Triggering Process of Solar Flares Based on Hinode/SOT Observations,*
Y. Bamba, K. Kusano, T. T. Yamamoto, and T. J. Okamoto,
2013 ApJ 778 48 doi:10.1088/0004-637X/778/1/48
[2] *Magnetic Field Structures Triggering Solar Flares and Coronal Mass Ejections,*
K. Kusano, Y. Bamba, T. T. Yamamoto, Y. Iida, S. Toriumi, and A. Asai,
2012 ApJ 760 31 doi:10.1088/0004-637X/760/1/31

Keywords: Sun, solar flare, magnetic field, SDO, Hinode, space weather

Japan Geoscience Union Meeting 2014
(28 April - 02 May 2014 at Pacifico YOKOHAMA, Kanagawa, Japan)

PEM08-03 Room:411 Time:May 1 16:45-17:00

X5.4 flare on 7 March 2012: magnetic and velocity properties at the solar surface

SHIMIZU, Toshifumi[1*] ; LITES, Bruce[2] ; BAMBA, Yumi[3]

[1]ISAS/JAXA, [2]HAO/NCAR, [3]Nagoya University

Solar flares abruptly release the free energy stored as a non-potential magnetic field in the corona and may be accompanied by eruptions of the coronal plasma. Formation of non-potential magnetic field and the mechanisms on triggering the onset of flares are still unclear; Especially, dynamical behaviors observed around polarity inversion lines producing major flares observationally. This presentation will discuss X5.4 flare on 7 March 2012 with emphasis on magnetic and velocity field properties at the solar surface. The coronal mass ejection launched at the same time as the X5.4 flare propagated through interplanetary space and caused a large geomagnetic storm on 9 March. One of remarkable properties to be discussed is a high-speed material flow existing along the polarity inversion line located between flare ribbons at the main energy release side. The high-speed material flow was observed in the horizontally oriented magnetic field formed nearly in parallel to the polarity inversion line and it existed at least from 6 hours before the onset of the flare and continued at least for several hours after the onset of the flare. Observations suggest that the observed material flow represents neither the emergence nor convergence of the magnetic flux. It may be rather considered as material flows working for increasing the magnetic shear along the polarity inversion line and for developing the magnetic structures favorable for the onset of the eruptive flare.

Keywords: solar flare, Hinode, X-ray, Optical, magnetic field, Doppler shift

Japan Geoscience Union Meeting 2014
(28 April - 02 May 2014 at Pacifico YOKOHAMA, Kanagawa, Japan)

PEM08-04 Room:411 Time:May 1 17:00-17:15

Estimation of Astronaut Dose inside the Kibo Module during Large Solar Flare Events

SATO, Tatsuhiko[1*] ; KATAOKA, Ryuho[2] ; NAGAMATSU, Aiko[3]

[1]Japan Atomic Energy Agency, [2]National Institute of Polar Research, [3]Japan Aerospace Exploration Agency

Forecast of radiation doses for astronauts as well as aircrews due to the exposure to solar energetic particles (SEP) is one of the greatest challenges in space weather research. In last 3 years, we have developed a warning system of aviation exposure to solar energetic particles: WASAVIES, which can predict the SEP doses at any flight conditions within 2.5 hours after the onset of ground level enhancements (GLE). In this system, the SEP fluxes incident to the atmosphere are calculated by physics-based models [1,2], and they are converted to radiation doses using a database developed on the basis of air-shower simulation [3]. In this study, we applied the same physics-based models to the estimate of the SEP fluxes on the orbit of International Space Station, and converted the fluxes to radiation doses for astronauts staying inside the Kibo module. For this conversion, we performed Monte Carlo cosmic-ray transport simulation, using the Particle and Heavy Ion Transport code System PHITS [4] in combination with the realistic 3D model of the Kibo module. A brief outline of WASAVIES together with the results of the astronaut dose estimation will be presented at the meeting.

[1] Y. Kubo, submitted to Space Weather
[2] R. Kataoka et al. submitted to Space Weather
[3] T. Sato et al. (2013) Radiat. Prot. Dosim. doi:10.1093/rpd/nct332
[4] T. Sato et al. (2013) J. Nucl. Sci. Technol. 50, 913-923. http://phits.jaea.go.jp/

Keywords: solar flare, radiation dose, solar energetic particle, astronaut, space weather, PHITS

Japan Geoscience Union Meeting 2014
(28 April - 02 May 2014 at Pacifico YOKOHAMA, Kanagawa, Japan)

PEM08-05 Room:411 Time:May 1 17:15-17:30

WASAVIES: Warning System for Aviation Exposure to Solar Energetic Particles

KATAOKA, Ryuho[1*] ; SATO, Tatsuhiko[2] ; KUBO, Yuki[3] ; SHIOTA, Daikou[4] ; KUWABARA, Takao[5] ; YASHIRO, Seiji[6] ; YASUDA, Hiroshi[7]

[1]NIPR, [2]JAEA, [3]NICT, [4]Nagoya University, [5]Delaware University, [6]CUA, [7]NIRS

Solar energetic particles (SEP) sometimes induce air shower that significantly increase the radiation dose at flight altitudes. In order to inform the situation of such a space radiation hazard to aircrews, a physics-based forward model is developed as WASAVIES (Warning System for Aviation Exposure to SEP) based on focused transport equation and Monte Carlo particle transport simulation code PHITS. WASAVIES gives the fastest and simplest way to predict the time profile of dose rate during ground-level enhancements (GLEs).

Keywords: solar proton, radiation dose, flares, air shower

Japan Geoscience Union Meeting 2014
(28 April - 02 May 2014 at Pacifico YOKOHAMA, Kanagawa, Japan)

PEM08-06 Room:411 Time:May 1 17:30-17:45

Plan of large SPE search by the 14C content measurement in Japanese trees for the past 5000 years

MIYAKE, Fusa[1*] ; MASUDA, Kimiaki[1] ; HAKOZAKI, Masataka[2] ; NAKAMURA, Toshio[2] ; KIMURA, Katsuhiko[3]

[1]Solar-Terrestrial Environment Laboratory, Nagoya University, [2]Center for Chronological Research, Nagoya University, [3]Faculty of Symbiotic Systems Science, Fukushima University

Radiocarbon (^{14}C) is produced by incoming cosmic rays to the Earth. Produced ^{14}C becomes $^{14}CO_2$ and is absorbed by trees by photosynthesis. Then,tree-rings record the past cosmic ray intensity. Rapid yearly increases in the ^{14}C content have been detected for the period from AD 774 to AD 775 and from AD 993 to AD 994. Althogh some candidates for the cause of these cosmic-ray invents have been considered, it has been considered that the solar activity (large SPE) is the most plausible cause.

There is the possibility that a lot of ^{14}C increase events like the AD 775 one are hidden in the periods when the ^{14}C content has not been measured with a 1-year resolution. If we detect such events, we are able to discuss a detailed occurrence rate of large SPE which is very important factor to prepare for future large SPEs.

We are planning to search for ^{14}C increase events by the measurements of ^{14}C content in Japanese trees for this 5000 years. In this thesis, we are going to explain the plan and problems.

Keywords: radiocarbon, tree-rings, cosmic-ray, SPE

Japan Geoscience Union Meeting 2014
(28 April - 02 May 2014 at Pacifico YOKOHAMA, Kanagawa, Japan)

PEM08-07 Room:411 Time:May 1 17:45-18:00

End-Cretaceous mass extinction driven by the encounter with a dark cloud

NIMURA, Tokuhiro[1*] ; EBISUZAKI, Toshikazu[2] ; MARUYAMA, Shigenori[3]

[1]Okayama Astronomical Museum, [2]RIKEN, [3]Earth-Life Science Intitute, Tokyo Institute of Technology

We found that a significant positive broad component of iridium in a pelagic deep sea sediment core (886C) around an iridium peak by asteroid impact corresponds at the K-Pg boundary. The 886C is core sample was taken by the Ocean Drilling Program (ODP) in the central portion of the North Pacific. This site has been in Pelagic from the End-Cretaceous periods. The accumulation rate is 0.5 m Myr^{-1}. Kyte et al., (1995) measured iridium density in the 886C core of 0.75-72.2 m which corresponds of $\sim$80 Ma from the present. In this data, there is one sharp peak around 65.5 m correspond at K-Pg boundary. In addition, we found that there are broad components across $\sim$20 m above the back ground which have some sharp peak component. The Ir value of the broad component which is about dozen times of back ground. This broad component is difficult to be explained by the materials on the surface of the Earth, and requires the contribution from the iridium-rich extraterrestrial materials, such as CI chondrite. And it is difficult to explain the broad component by diffusion and bioturbation of an iridium peak by asteroid impact. Platinum-group-element such as Pt, Re and Ir are redistributed by changes in sedimentary redox condition. However such change can probably account for many of small $<$10 cm (Colodner et al., 1992) and the mean global depth of marine bioturbation was calculated to be 9.8$\pm$4.5 cm (Boudreau, 1994). And also an evidence of bioturbation was not found from lithofacies (Proc. ODP, Init. Repts., 145).

We consider that the broad component can be caused by an encounter of the solar system with a dark cloud with a size of $\sim$100 pc and the central density of over 2000 protons/cc in the galactic disk and estimated that the flux of exosolar material began $\sim$73 Ma and has run through $\sim$8 Myr. By the Kataoka's "Nebula Winter model" (Kataoka 2013), dark cloud can lead to an environmental catastrophe to the Earth from a few kiloannum to megaannum. The dark cloud encounter enhances a flux of cosmic dust particles and cosmic rays which lead to global cooling and destruction of the ozone layer.

The solid particles from the dark cloud accrete on the Earth and in the stratosphere, stay for a several months; their sunshield effect is as large as -9.3 W m^{-2}. The climate cooling in the End-Cretaceous period is also suggested by the variations of stable isotope rations in oxygen and strontium (Brian and Huber, 1990; Barrera and Savin, 1999; Li and Keller, 1998). Any photosynthetic plants had heavy damaged, and loss of biodiversity began to the top of food chain.

The mass extinction at K-Pg boundary, which is widely thought to be caused by an impact of an asteroid (e. g., Schulte et al., 2010). However, a complete extinction of level of family by asteroid impact seems rather difficult. First, a severe environment turn-over would finish few years after impact, the solid particles and sulphate launched by the asteroid impact was settled down for only few month (troposphere) to few years (stratosphere) and negative radiative forcing became negligible after a few years from the impact (Pierazzo, 2001).The number of individuals would recover completely after the environmental catastrophe was over, if a few percent of individuals of one species survived.

Second, in spite of there were similar impacts without catastrophic on the Earth, for example, Alamo, Woodleigh, and Popigai crater, there are no evidences of association for extinction. However, because the encounter with the dark cloud perturbs the orbit of asteroid or comet by its gravitational potential and may lead an asteroid or comet shower, the asteroid impact at K-Pg may be one of the consequences of the dark cloud. For a certainly, only an asteroid impact cannot involve mass extinction, however may be role cruncher. The multiple impact and volcanism in a short period of time (Keller, 2005) may have been caused by encounter the dark nebula and attendant cosmic ray, respectively.

Keywords: Nebula Winter, dark cloud, mass extinction, End-Cretaceous, K-Pg boundary, Ocean Drilling Program

Japan Geoscience Union Meeting 2014
(28 April - 02 May 2014 at Pacifico YOKOHAMA, Kanagawa, Japan)

PEM08-08 Room:411 Time:May 2 09:00-09:15

Update on the US GIC activities and generation of benchmark geomagnetic disturbance (GMD) scenarios

PULKKINEN, Antti[1*]

[1]NASA GSFC

The awareness about potential major impacts of geomagnetically induced currents (GIC) has drawn a high level action in the US and in Canada. More specifically, regulatory process has been launched to generate standards for GIC hazard assessments and mitigation procedures. All US high-voltage power transmission-related entities need to follow the standards in the near future. One of the central GIC activities in the US has been the North the American Electric Reliability Corporation's (NERC) GMD Task Force that has allowed in-depth communication and collaboration between US federal organizations, power transmission operators and scientific research community. I will discuss these activities in this paper and outline the road ahead for some of the key US GIC activities.

As a part of the GMD standards drafting process and the US GIC hazards assessments, substantial effort has been made for generating benchmark GMD scenarios. These scenarios that quantify extreme geoelectric field magnitudes and temporal waveforms of the field fluctuations are the foundation for subsequent engineering analyses. The engineering analyses will include the transmission system voltage stability and transformer heating assessments. The work on the GMD scenarios has been a major collaboration between a number of US and Canadian entities involved in GMD research and transmission system operations. I will discuss in this paper also the key elements of the benchmark GMD generation process and show the latest results from our NASA GSFC work on the topic.

Keywords: Space weather, geomagnetically induced currents, Extreme events

Japan Geoscience Union Meeting 2014
(28 April - 02 May 2014 at Pacifico YOKOHAMA, Kanagawa, Japan)

PEM08-09 Room:411 Time:May 2 09:15-09:30

Spatial distribution of nonthermal electrons in an X-class flare on 13 May 2013

MASUDA, Satoshi[1*]

[1]STEL, Nagoya Univeristy

Four X-class flares took place in May 2013. Fortunately three of four were observed with Nobeyama Radioheliograph (NoRH). One of them occurred behind the east limb on 13 May 2013. It is a good chance to investigate the height distribution of nonthermal electrons in the solar corona. In the framework of the standard flare model based on magnetic reconnection, Minoshima et al. (2011) showed that the height distribution of accelerated/heated electrons depends on the energy of the electrons. NoRH has a capability to observe a solar flare in 17 and 34 GHz with a high time resolution (100 ms). The energy of electrons emitting microwaves is very high (˜MeV), and the mean-energy emitting 34 GHz is higher than that for 17 GHz. Hard X-rays are emitted by relatively lower-energy (˜100 keV) electrons. So this dataset can cover a wide energy range of accelerated electrons. In order to understand the electron acceleration/transport/loss processes, multi-wavelength observation is crucially important. The 13 May 2013 flare was simultaneously observed with NoRH and RHESSI (The Reuven Ramaty High Energy Solar Spectroscopic Imager). Investigating the distribution of these emission sources in the solar corona, we discuss the electron acceleration/transport/loss processes.

Keywords: solar flare, particle acceleration, microwave, hard X-ray, solar corona, magnetic recconection

Japan Geoscience Union Meeting 2014
(28 April - 02 May 2014 at Pacifico YOKOHAMA, Kanagawa, Japan)

PEM08-10 Room:411 Time:May 2 09:30-09:45

An energetics study of X-ray jets using Hinode/XRT observation

SAKO, Nobuharu[1*] ; SHIMOJO, Masumi[2] ; WATANABE, Tetsuya[2] ; SEKII, Takashi[2]

[1]The Graduate University for Advanced Studies, [2]National Astronomical Observatory of Japan

For plasma acceleration in X-ray jets in the solar corona, three mechanisms have been considered, based on the model of X-ray jets by magnetic reconnection (Shibata et al. 1992); The reconnection jet produced by magnetic tension, the evaporation flow produced by pressure gradient, and the twisted jet produced by magnetic pressure. There are some evidences of X-ray jets in active regions (ARs) produced by pressure gradient. On the other hands, there is no observational evidence of X-ray jets by the other forces except the result of a high-speed jet. In order to distinguish the evaporation flow from the other types of jets, I have studied the energetics of the X-ray jets.

Using over 100 X-ray jets greater than 3×104 km in length in ARs, quiet regions (QRs), and coronal holes (CHs), I have found no large differences in the life time, the width of the jets, and the area of the footpoint flares in such regions. On the other hands, the plasma number density of the X-ray jets and flares in ARs is ten times larger than those in QRs and CHs. Assuming the energy balance between conductive flux and heat flux by the footpoint flare, we estimate the temperature of the jets. The AR jets has a wide range of the temperature (1 MK-9 MK), while the temperature of most X-ray jets in CH and QR is $1\sim2$ MK. In my presentation, I will discuss a relationship of the speed with the temperature of the jets.

Keywords: Sun, Solar Corona, X-ray jet, Energy release, Hinode

Japan Geoscience Union Meeting 2014
(28 April - 02 May 2014 at Pacifico YOKOHAMA, Kanagawa, Japan)

PEM08-11 Room:411 Time:May 2 09:45-10:00

Lower temperature response of an EUV wave observed by Hinode/EIS and SDO/AIA

LEE, Kyoung sun[1*] ; KWON, Ryun young[2] ; BROOKS, David[2] ; SHIMIZU, Toshifumi[1]

[1]ISAS/JAXA, [2]George Mason University

We investigate an EUV wave observed by Hinode/EIS and SDO/AIA on 2011 August 04. The EUV wave propagates across the solar disk and the wave front passing through a remote active region (AR 11263) is observed by EIS. This EUV wave has already been analyzed using coronal lines, but the lower temperature response to the EUV wave has not been investigated. Using multi-wavelength observations from EIS and AIA, we determined the intensity and Doppler velocity variation of different temperature lines and compared them. From the comparison, we found an enhancement of the intensity at lower temperatures before the intensity increase seen in the coronal filters of AIA. And a significant enhancement of the red shift (10 km/s) in the lower temperature line (Si VII, log T ˜5.8) compared to the increase of the red shift (˜3 km/s) in coronal lines (Fe XII, FeXIII, and Si X, log T ˜6.1-6.2) when the EUV wave interacts with the active region. We will discuss the impact of the EUV wave on the lower temperature emission.

Keywords: Spectroscopy, Corona, EUV wave

Japan Geoscience Union Meeting 2014
(28 April - 02 May 2014 at Pacifico YOKOHAMA, Kanagawa, Japan)

PEM08-12 Room:411 Time:May 2 10:00-10:15

Imaging, spectroscopic and stereoscopic observations of the bi-directional inflow in the solar flare

MATSUI, Yuki[1*] ; YOKOYAMA, Takaaki[1]

[1]University of Tokyo

The standard model of solar flares based on the magnetic reconnection includes bi-directional inflow toward the reconnection point. Corresponding to the bi-directional inflow, high temperature loops like a cusp shape are formed due to the magnetic reconnection. By combination of imaging, spectroscopic and stereoscopic observations, we succeeded in capture the three-dimensional structure of a bi-directional reconnection inflow of a solar flare.

We analyzed a C-class flare that occurred on 2012 September 11 beyond the solar limb. The bi-directional inflow was found in the images of coronal temperature filter taken by AIA onboard SDO. Hinode EUV Imaging Spectrometer (EIS) also observed this flare and provide the Doppler velocity of the bi-directional inflows. At the same time, cusp loops were observed with the raster scans of FeXXIV emission line (over 10 MK) at the region surrounded by the bi-directional inflow. This is clear evidence that 1MK loops are heated over 10MK by the magnetic reconnection. STEREO A/SECCHI was observing this flow from a different line of site. Inflowing angle in STEREO A/SECCHI images is consistent with the angle speculated by apparent velocity of SDO/AIA and line of sight velocity of Hinode/EIS. By combining these data sets, we constructed a self-consistent three-dimensional picture of the flows.

Keywords: solar flare, reconnection

Japan Geoscience Union Meeting 2014
(28 April - 02 May 2014 at Pacifico YOKOHAMA, Kanagawa, Japan)

PEM08-13 Room:411 Time:May 2 10:15-10:30

Diagnosis of coronal shock strength using the activation of large amplitude prominence oscillation

TAKAHASHI, Takuya[1*] ; ASAI, Ayumi[2] ; SHIBATA, Kazunari[3]

[1]Graduate School of Science, Kyoto University, [2]Unit of Synergetic Studies for Space, Kyoto University, [3]Kwasan and Hida Observatories, Kyoto University

X5.4 class solar flare occurred on March 7,2012 which was the second largest flare in this solar cycle. The flare was associated with very fast coronal mass ejection(CME) with the velocity of over 2500km/s. Associated with this flare, a wave-like coronal disturbance(known as EUV wave) was observed to propagate along the solar surface. The observed EUV wave propagated with the average speed of about 670km/s towards the north and 'hit' a polar prominence leading to its large amplitude oscillation. The activated prominence strongly brightened when EUV wave 'pushed' it.

Because of the difficulty in direct observation of physical quantities in the corona, the physical nature of the EUV waves is still under discussion. Two main interpretations of EUV waves are the 'fast mode MHD wave/shock' interpretation, and 'non-wave' interpretations.

In the images taken with Inner coronagraph(COR1) of the Sun Earth Connection Corona and Heliospheric Investigation(SECCHI) on board *Solar Terrestrial Relations Observatory(STEREO)-Behind*, we could see a coronal disturbance detached from expanding CME plasma. The time evolution of the disturbance seen in COR1 images was consistent with that of observed EUV wave. Also, Type II radio burst which is thought to be evidence of coronal shock wave was observed simultaneously. Because of that observational evidence, we regard the observed EUV wave as MHD fast mode shock front. Assuming the shock nature of the observed EUV wave, we could also explain prominence acceleration and brightening consistently.

Using the initial velocity of activated prominence, we could estimate the coronal shock strength of the EUV wave with the help of linear wave theory. We also check the applicability of linear theory to the shock problem with one dimensional numerical model and ascertained that it is applicable when the shock strength is not strong. Estimated fast mode mach number of the EUV wave was between 1.20 and 1.42, and we could say that the EUV wave was a weak shock front in the corona.

Keywords: solar flare, coronal mass ejection(CME), shock waves, solar prominence, magnetohydrodynamics(MHD)

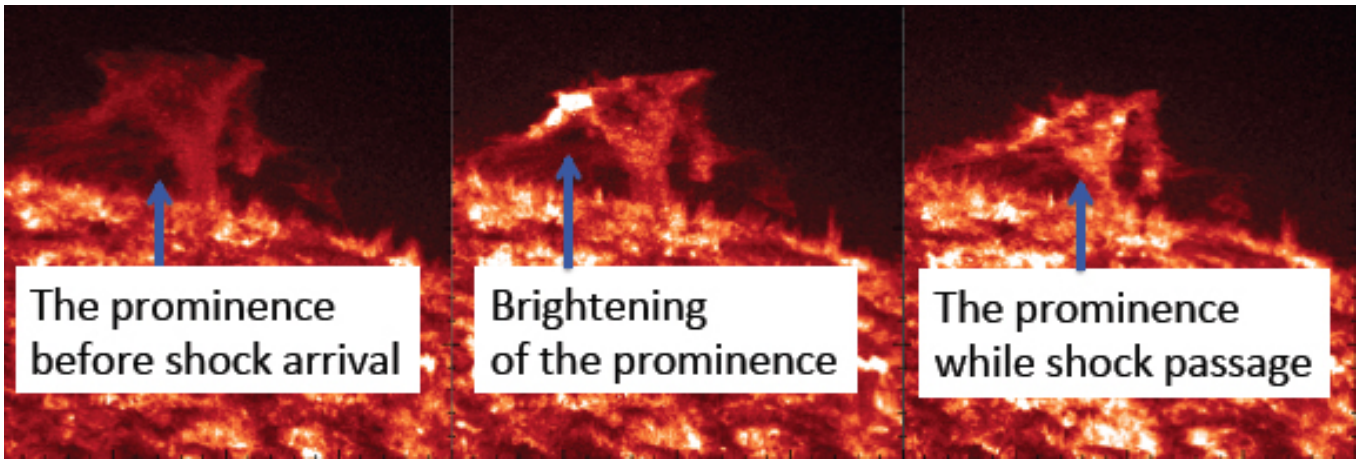

Japan Geoscience Union Meeting 2014
(28 April - 02 May 2014 at Pacifico YOKOHAMA, Kanagawa, Japan)

PEM08-14 Room:411 Time:May 2 10:30-10:45

Influence of interplanetary solar wind sector polarity on the ionosphere

LIU, Jing[1*]

[1]Beijing National Observatory of Space Environment, Institute of Geology and Geophysics, CAS

Knowledge of solar sector polarity effects on the ionosphere may provide some clues in understanding of the ionospheric day-to-day variability and 'hysteresis' effect on foF2. In this study, a solar-terrestrial connection ranging from solar sector boundary crossings, geomagnetic disturbances and ionospheric perturbations has been demonstrated. The increases in interplanetary solar wind speed within three days are seen after SB crossings, while the decreases in solar wind dynamic pressure and magnetic field intensity immediately after SB crossings are confirmed by the superposed epoch analysis results. Furthermore, the interplanetary magnetic field (IMF) Bz component turns from northward to southward in March equinox and June solstice as the Earth passes from a solar sector of outward to inward directed magnetic fields, whereas the reverse situation occurs for the transition from toward to away sectors. The IMF Bz component for the same solar sector polarity has opposite signs between March equinox and September equinox, and also between June solstice and December solstice. In order to know how the ionosphere reacts to the interplanetary solar wind variations linkage of SB crossings, the F2 region critical frequency (foF2) covering about four solar cycles and total electron content (TEC) during 1998?2011 are utilized to extract the related information, revealing that they are not modified significantly and vary within the range of 15% on average. The responses of the ionospheric TEC to SB crossings exhibit complex temporal and spatial variations and have strong dependencies on season, latitude, and solar cycle. This effect is more appreciable in equinoctial months than in solstitial months, which is mainly caused by larger southward Bz components in equinox. In September equinox, latitudinal profile of relative variations of foF2 at noon is featured by depressions at high latitudes and enhancements in low-equatorial latitudes during IMF away sectors. The negative phase of foF2 is delayed at solar minimum relative to it during other parts of solar cycle, which might be associated with the difference in longevity of major interplanetary solar wind drivers perturbing the near-Earth environment in different phases of solar cycle.

Japan Geoscience Union Meeting 2014
(28 April - 02 May 2014 at Pacifico YOKOHAMA, Kanagawa, Japan)

PEM08-15 Room:411 Time:May 2 10:55-11:15

Ensemble Data Assimilation for Thermospheric Mass Density Specification and Forecasting

MATSUO, Tomoko[1*] ; LEE, Ite[3] ; ANDERSON, Jeffrey[4]

[1]University of Colorado at Boulder, CO, USA, [2]National Oceanic and Atmospheric Administration, CO, USA, [3]National Central University, Taiwan, [4]National Center for Atmospheric Research, CO, USA

Even though the Earth's upper atmosphere density is tenuous, it is substantial enough to exert significant drag on orbiting spacecraft and debris. The largest uncertainty in low-Earth orbit prediction is aerodynamic drag estimation. Thermospheric mass density variation is the major source of drag estimation errors at altitudes below about 700 km. This paper demonstrates how the limit of predictability of thermospheric mass density variability can be extended by means of ensemble data assimilation.

To assimilate observations of the thermosphere and ionosphere, we use an ensemble data assimilation procedure constructed with the Data Assimilation Research Testbed and the Thermoshere-Ionosphere Electrodynamics General Circulation Model, two sets of community software offered by NCAR. An important attribute of our approach is that the ionosphere-thermosphere coupling is self-consistently treated in both the forecast model and the assimilation scheme. This enables the inference of unobserved thermospheric states from the relatively plentiful observations of the ionosphere. Given the ever-expanding global navigation satellite infrastructure, this is indeed a promising prospect for upper atmosphere data assimilation. Another relevant strategy is using data assimilation to estimate the model forcing parameters that control states of the thermosphere and ionosphere. In comparison to the lower atmosphere, the upper atmosphere is a dissipative, strongly forced dynamical system, so estimation of model forcing parameters can have a dramatic impact on the quality of ensemble forecasting and assimilation of the upper atmosphere.

In this paper, we present results from our ensemble assimilation experiments with thermospheric mass densities obtained from the accelerometer on board the CHAMP satellite, and electron density profiles obtained from the COSMIC/FORMOSAT-3 mission.

Keywords: thermosphere-ionosphere coupling, data assimilation, parameter and state estimation, thermospheric mass density, aerodynamic drag estimation, LEO orbit prediction

Japan Geoscience Union Meeting 2014
(28 April - 02 May 2014 at Pacifico YOKOHAMA, Kanagawa, Japan)

PEM08-16 Room:411 Time:May 2 11:15-11:30

Forecast of ionospheric disturbances using a high-resolution atmosphere-ionosphere coupled model

SHINAGAWA, Hiroyuki[1*] ; JIN, Hidekatsu[1] ; MIYOSHI, Yasunobu[2] ; FUJIWARA, Hitoshi[3] ; YOKOYAMA, Tatsuhiro[1]

[1]NICT, [2]Kyushu University, [3]Seikei University

Space weather forecasts are about to enter a stage incorporating numerical forecasts based on realistic numerical simulation, in addition to conventional methods used by forecasters to make predictions based on observational data and experience. At the National Institute of Information and Communications Technology (NICT) of Japan, we have developed an atmosphere-ionosphere coupled model, which includes the whole neutral atmosphere and the ionosphere. The model is called GAIA (Ground-to-topside model of Atmosphere and Ionosphere for Aeronomy). The present version has spatial resolution of about 1 degree in horizontal direction. In addition, we are also developing a high-resolution regional ionospheric model, which has a horizontal resolution of about 10 km. We plan to combine GAIA and the regional model to reproduce mesoscale ionospheric phenomena, such as plasma bubbles and SED (storm enhanced density). The model will be a useful tool for space weather forecast. We will report previous results, and a plan for the new model.

Keywords: space weather, ionosphere, atmosphere, simulation, model, disturbance

Japan Geoscience Union Meeting 2014
(28 April - 02 May 2014 at Pacifico YOKOHAMA, Kanagawa, Japan)

PEM08-17 Room:411 Time:May 2 11:30-11:45

Projection of substom processes from the plasma sheet to the polar ionosphere

TANAKA, Takashi[1*]

[1]Emeritus Professor, Kyushu University

It has been believed that auroras observed in the ionosphere have their corresponding counterpart in the plasma sheet (Haerendel, 2011). Localized auroral breakup should reveal the location of explosive dissipation in the plasma sheet. Similar correspondence is supposed even during the growth phase. While it is well known that the prebreakup arc breakups first during the substorm, the equatorial location and relating formation mechanism of equatormost arc are long-standing questions in the understanding of the growth phase (Sergeev et al., 2012). Another aurora during the growth phase is the poleward bright arc that is believed to be an ionospheric projection of the reconnection separatrix. Also the equatorward extension of the N-S auroral arc has been suggested to be associated with eathward fast bursty flows (Nishimura et al., 2010). The region of aurora indicates that the width of oval is 7^o (64^o to 71^o), near midnight just prior to the breakup. Pich angle isotropy boundary at 65.5^o is critical for the prebreakup arc, since the isotropy boundary coincides with the prebreakup arc. Seen from the structure of isotropy boundary, the breakup arc is somewhere in the transition region between the dipole-like region and the current sheet region. A phenomenon closely related to the projection of the aurora is the distribution of FAC and its tracing. A traditional understanding for the driver of disturbances is the fast flow, both for the growth phase and the onset. The BBF was expected for a wide range of activity including localized auroral brightenings, N-S auroras and streamers (Nakamura et al., 2001). At the same time, the BBF can be a source of the FAC. The cross-tail current is diverted via downward FAC into the ionosphere on the eastward side of the bubble and is connected to upward FACs west of the bubble. The overall region 1-sense FACs is expected to emerge from 64^o to 70^o (Yang et al., 2012). The plasma ahead of the bubble is compressed, resulting in a high plasma pressure and the region 2-sense FACs that are as thin as 1^o, centered at 63^o.

Recent M-I coupling simulation reproduces almost all signatures of the substorm, including the preonset arc, and the onset that start from the low-latitude side of the oval (Tanaka et al., 2010). From the numerical solution just prior tp the onset, the BBF region from x=-10 Re to x=-20 Re in the plasma sheet is projected down along the magnetic filed to a quite narrow region in the ionosphere from 65.7^o to 66.8^o latitudes. Even the outmost field line of the plasma sheet is traced down to 68^o latitude in the ionosphere. So that the observed high-latitude part of the oval (68^o~71^o) is outside the plasma sheet. The N-S arc that usually starts from higher latitude than 70^o cannot be the reflection of the BBF. Near the midnight, in the numerical solution, the region 1 FAC distributes from 65^o to 69^o (with strong part 67^o~68^o) and the region 2 FAC distributes from 62^o to 64^o latitude. From this result, the growth phase region 1 FAC cannot be from the plasma sheet. The result of current line tracing shows that the growth phase region 1 FAC extends into the magnetosphere as far as x=-20Re through the east-west flow shear between the tail plasma sheet and the lobe. If we look at only the latitude it is barely possible that the onset FAC strating from the lowest-latitude area of the region 1 FAC around 65^o could be from the CW that should to be inside x=-10 Re (65.7^o). However, it is implausible from the current line tracing. The onset region 1 FAC is mapped to the cusp-mantle region through the near earth flow shear between the plasma sheet and the lobe. Correspondence beween the plasma sheet and the ionosphere so far believed is quite confusing. It is doubtful to consider that all auroras observed in the ionosphere have their corresponding counterpart in the plasma sheet.

Keywords: substorm

Japan Geoscience Union Meeting 2014
(28 April - 02 May 2014 at Pacifico YOKOHAMA, Kanagawa, Japan)

PEM08-18 Room:411 Time:May 2 11:45-12:00

One-month periodicity in thunderstorm, OLR and solar parameters

TAKAHASHI, Yukihiro[1*] ; SATO, Mitsuteru[1]

[1]Department of Cosmosciences, Hokkaido University

Recently the relationship between the global circuit and solar-climate connection was pointed out. Here we introduce an example, which indicates the roles of thunderstorm or its resultant electric circuit in solar-climate connection. Global relationship between thunderstorm/cloud activities and solar parameters are examined based on lightning measurement by Global ELF observation Network (GEON) operated by Hokkaido University and Outgoing Longwave Radiation (OLR) intensity. It was found that the number of lightning stokes in Asia Maritime Continent (AMC) varies with about month periodicity in the period from February to June 2004 and shows positive correlation (R= ˜0.8) with OLR in the Western Pacific Warm Pool (WPWP). On the other hand, OLRs in the central Africa and some other tropical areas show negative correlation with the number of lightning stokes in the AMC in that period. It is also found that the galactic cosmic rays or UV intensity associated with solar activity indicates good correlation with tropical OLR or lightning activity in AMC. One explanation to connect such global variations in thunderstorm / cloud amount with solar parameters would be the electrical circuit involving lower and upper atmospheres. Global electric circuit model was proposed log time ago, in 1930s, in which thunderstorm plays a role of generator, and the ground and the ionosphere work as a spherical capacitor. However, now we need to reconstruct this simple model, taking into account 3 aspects: 1) global-scale nonuniformities both of ionospheric conductivity and of the distribution of the generators, 2) connections between the troposphere and D-region, considering the effects of TLEs, such sprites and blue jets, 3) establishing the observational methodology for global electric field, excluding the effect of cloud existing just above the observation sites. If the ionospheric electric field modulates the potential gradient in the lower atmosphere, it could cause the re-distribution of ionized atmospheric particles, which may, in turn, change the generation / reduction speed of cloud particles.

Keywords: thunderstorm, OLR, solar activity, one-month periodicity

Japan Geoscience Union Meeting 2014
(28 April - 02 May 2014 at Pacifico YOKOHAMA, Kanagawa, Japan)

PEM08-19 Room:411 Time:May 2 12:00-12:15

Influence of solar wind on climate: On the factors such as Quasi Biennial Oscillation

ITOH, Kiminori[1*] ; MATSUO, Shinya[1] ; YAMASHITA, Kazuyoshi[1]

[1]Yokohama National University, Graduate School of Env. & Inf. Sciences

In spite of long history of research, the influence of solar changes on the climate is not convincing enough yet. We have employed solar wind parameter (e.g., Pα (energy flowing into magnetosphere) and aa index) to successfully show their correlation with the temperatures of the stratosphere, troposphere and surface. For further analyses, OLR (outgoing longwave radiation) and the participation of QBO etc. are studied. For instance, January OLR during 1975-2011 showed high correlation with Pα at particular regions. At the QBO westerly phase, high correlation coefficient (r = 0.76) was found near Indonesia. The correlation map at the easterly phase resembled that for the Arctic Oscillation, and r = 0.81 at the Siberia region.

Keywords: Solar wind, climate, QBO, OLR, temperature

Japan Geoscience Union Meeting 2014
(28 April - 02 May 2014 at Pacifico YOKOHAMA, Kanagawa, Japan)

PEM08-20 Room:411 Time:May 2 12:15-12:30

Laboratory experiment with various radiation sources for verification of cloud condensation nucleation by cosmic rays

SUZUKI, Asami[1*] ; MASUDA, Kimiaki[1] ; TAKEUCHI, Yuya[1] ; ITOW, Yoshitaka[1] ; SAKO, Takashi[1] ; MATSUMI, Yutaka[1] ; NAKAYAMA, Tomoki[1] ; UEDA, Sayako[1] ; MIURA, Kazuhiko[2] ; KUSANO, Kanya[1]

[1]Solar-Terrestrial Environment Laboratory,Nagoya University, [2]Tokyo university of science

It is considered that the solar activity may affect the global climate,but the correlation mechanism is still not understood.

One of the possible mechanisms for the correlation is the cloud formation by the galactic cosmic rays, which are modulated by the variation of solar activity. This relation was clearly indicated by the good correlation observed for the galactic cosmic-ray intensity and the global low-cloud amount.

This hypothesis includes the ion-induced nucleation model, in which new particles in the atmosphere are created efficiently through atmospheric ions produced by cosmic rays, and finally these particles grow up to the size of

cloud condensation nuclei.

In this study, a laboratory experiment for verification of the hypothesis has been conducted with a reaction chamber. A flow of clean air, water vapor, ozone and sulfuric dioxide was introduced to a metallic chamber, where we irradiated UV light for solar irradiance and beta-rays or accelerator beam for cosmic rays. The beam of the heavy ion accelerator HIMAC at National Institute of Radiological Sciences was used in the present experiment.

As a result, ions produced by the ionizing radiation and increased particle density were observed for beta rays.

Some results with the accelerator beam are the following.

Ion density in the chamber increased as the beam intensity and particle density increased with ion density.

Particle size distribution was measured and the peak particle size and the particle density became to larger with time after start irradiation, but the density stopped to increase or decreased after irradiation stopped although the peak size continued to increase.

It is shown that our system is ready for more detailed measurements.

Keywords: cosmic rays, cloud, cosmoclimatology, cloud condensation nuclei

Japan Geoscience Union Meeting 2014
(28 April - 02 May 2014 at Pacifico YOKOHAMA, Kanagawa, Japan)

PEM08-21 Room:411 Time:May 2 14:15-14:30

Study on symmetry-breaking between the northern and southern hemispheres of the solar dynamo

SHUKUYA, Daishi[1*] ; KUSANO, Kanya[1]

[1]Solar-Terrestrial Environment Laboratory, Nagoya University

Solar dynamo is a mechanism whereby the kinetic energy of the plasma in the sun is converted to the magnetic energy. This mechanism works to generate and maintain all solar magnetic activities. Because the Earth's climate can be influenced by solar activities, variability of the solar dynamo is an important issue to understand long-term evolution of the Earth's climate.

Comparisons of the solar activities in each solar hemisphere show hemispheric asymmetry. Sunspots were found preferentially in one hemisphere and not the other in often long periods of time (Spoerer, 1889; Maunder, 1890, 1904). This asymmetry was extended to other measures of activity including faculae, prominences and flares (Waldmeier, 1971; Roy, 1977). The asymmetry happens in the solar polar magnetic field reversals. The polarity of the solar magnetic fields on the north and south poles periodically reverses at every sunspot maxima. However, the reversals at both poles actually don't occur at the same time. In other words, the reversal at one pole is followed by that on the other pole. This time difference of magnetic field reversals between the poles was first noted by Babcock (1959) from the very first observation of polar field. Recently, it was confirmed by detailed observations with the HINODE satellite (Shiota et al. 2012). As above, we have ever obtained many observation facts. However, the mechanisms of hemispheric asymmetry of the solar dynamo haven't been revealed theoretically yet.

In this paper, we study the asymmetric feature of the solar dynamo based on the flux transport dynamo model (Chatterjee et al. 2004) to explain the time difference of magnetic polarity reversal between the north and south poles. In order to calculate long-term variations of solar activities, we use the mean field kinematic dynamo model, which is derived from magnetohydrodynamics (MHD) equation through the mean field and other approximations. We carried out the mean field dynamo simulations using the updated SURYA code which was developed originally by Choudhuri and his collaborators (2004). We decomposed the symmetric and asymmetric components of magnetic field, which correspond respectively to the quadrupole and dipole-like components (Nishikawa and Kusano 2008), and analyzed the phase relation between them. As a result, we found that the two components are mixed even if the dipole-like component is predominant and that the two components spontaneously form 90 or -90 degree out of phase oscillation. The solutions with 90 and -90 degree out of phase oscillation form the different attracters of dynamo solutions. We found that the time difference of the polar field reversals between the different hemispheres can be explained by the out of phase relation between the different components of magnetic field.

Keywords: polar field reversal, solar dynamo, numerical simulation, hemispheric asymmetry

Japan Geoscience Union Meeting 2014
(28 April - 02 May 2014 at Pacifico YOKOHAMA, Kanagawa, Japan)

PEM08-22 Room:411 Time:May 2 14:30-14:45

Climate responses in central Japan and Taiwan to the cosmic ray intensifications during the Maunder Minimum

SAKASHITA, Wataru[1*] ; YOKOYAMA, Yusuke[1] ; MIYAHARA, Hiroko[2] ; AZE, Takahiro[3] ; YONENOBU, Hitoshi[4] ; OHYAMA, Motonari[5] ; HOSHINO, Yasuharu[6] ; NAKATSUKA, Takeshi[7]

[1]Atmosphere and Ocean Research Institute, The University of Tokyo, [2]College of Art and Design, Musashino Art University, [3]Interactive Research Center of Science, Tokyo Institute of Technology, [4]Graduate School of Education, Naruto University of Education, [5]The Center for Academic Resources and Archives, Botanical Gardens, Tohoku University, [6]National Research Institute for Cultural Properties, Nara, [7]Research Institute for Humanity and Nature

Relationship between solar variations and climate has been long discussed for various time scales. It is difficult to distinguish the impacts of the multiple solar parameters (total solar irradiance (TSI), solar ultraviolet (UV) radiation, and galactic cosmic rays (GCRs)) on climate, because these variations are nearly synchronized. However, GCR fluctuations related to solar magnetic activity have slightly different features compared to the other external forcing factors (TSI, UV). According to previous studies, the cosmic ray fluctuation was particularly unique during the Maunder Minimum (A. D. 1645-1715), when almost no sunspots were observed. Annually measured tree-ring Δ^{14}C and ice-core ^{10}Be data have shown that decadal variations of GCRs had been remarkably amplified during the Maunder Minimum. This characteristic amplification may be utilized to shed light on the GCR influence on climate.

In this study, we employ tree rings that can reconstruct both annual climate (δ^{18}O) and cosmic ray fluctuations (Δ^{14}C) during the Maunder Minimum. By using these proxies, we can directly compare these reconstructions without any dating error. Annually measured tree-ring δ^{18}O records from central Japan have shown significant wet climate at every remarkable GCRs enhancement. On the other hand, there is no significant climate response in tree-ring δ^{18}O record from Taiwan. We suggest that these climate responses may be related to a stationary position of the Baiu front. Recent satellite observations have shown that GCRs may cause the increase of low cloud amount at tropical western Pacific region. It can be suggested that cooling of tropical western Pacific region caused by GCR enhancement might have caused the weakening of Pacific high and indirectly brought wet rainy seasons in central Japan.

Keywords: Solar Magnetic Activity, Galactic Cosmic Ray, The Maunder Minimum, Tree-ring isotope

Japan Geoscience Union Meeting 2014
(28 April - 02 May 2014 at Pacifico YOKOHAMA, Kanagawa, Japan)

PEM08-23 Room:411 Time:May 2 14:45-15:00

Dynamical estimation of external/internal acceleration processes of the outer radiation belt using data assimilation

MIYOSHI, Yoshizumi[1*] ; TOYAMA, Haruto[1] ; UENO, Genta[2] ; KOSHIISHI, Hideki[3] ; MATSUMOTO, Haruhisa[3] ; SHIOKAWA, Kazuo[1]

[1]STEL, Nagoya University, [2]The Institute of Statistical Mathematics, [3]JAXA

Dynamical evolution of the outer belts should be a delicate balance among several processes. It has been believed that there exist two different acceleration mechanisms: the radial diffusion as the external source process, and the non-adiabatic wave particle interactions as the internal source process. In order to discriminate when and where these processes are dominant for the large flux enhancement of the outer belt electrons, we have developed a data assimilation code on the outer belt electrons. In our data assimilation, the particle filter and the particle smoother are used which are effective for non-linear/non-Gaussian distribution problems. We include the radial diffusion coefficient and the internal source model in the state vector and estimate the dynamical variations of these parameters. The Tsubasa satellite electron data are used as the observation vector. The results indicate that only the radial diffusion process is always too small to explain the observed flux enhancement and the internal source process should be necessary. The assimilation result suggests that the internal source process tend to take place around the storm recovery phase, which is consistent with the observations.

Keywords: radiation belts, data assimilation

Japan Geoscience Union Meeting 2014
(28 April - 02 May 2014 at Pacifico YOKOHAMA, Kanagawa, Japan)

PEM08-24 Room:411 Time:May 2 15:00-15:15

Evaluation of Relativistic Electron Flux Forecast at GEO Satellite

NAGATSUMA, Tsutomu[1*] ; SAKAGUCHI, Kaori[1] ; SAITO, Shinji[2] ; MIYOSHI, Yoshizumi[2] ; SEKI, Kanako[2]

[1]National Institute of Information and Communications Technology, [2]Solar Terrestrial Environment Laboratory, Nagoya University

We have developed near real time prediction model for relativistic electron flux at GEO satellite. This model is based on a multivariate autoregressive model with using solar wind speed, north-south component of the magnetic field and dynanmic pressure as inputs. Detailed description of this model can be found in Sakaguchi et al. [2013]. We have started relativistic electron flux forecast service as a test product since Apr. 2013. Forecast information can be found in the following web pages (URL: http://seg-web.nict.go.jp/radi/).

There are several difficulties in operating a near-real time forecast model. One is the quality of the real-time solar wind data. Because quality of real-time solar wind density data is quite poor, we avoid using solar wind density data for our operational model. The other one is the lead-time of the solar wind data. Currently, we can use only ACE data for solar wind input. The lead-time of this data is only about one hour. Threfore, we also 'predict' solar wind condition for two or three days in advance from current solar wind information. Anyway, prediction efficiencies of our forecast for 1day, 2day, and 3day ahead in 2013 are 81%, 63%, 48%, respectively. Evaluation and future parspective of our forecasting model will be introduced in our presentation.

Reference:

Sakaguchi, K., Y. Miyoshi, S. Saito, T. Nagatsuma, K. Seki and K. T. Murata (2013), Relativistic electron flux forecast at geostationary orbit using Kalman filter based on multivariate autoregressive model, Space Weather, 11, 79?89, doi:10.1002/swe.20020.

Keywords: Space Weather Forecast, Solar Wind - Magnetosphere Interaction, Magnetosphere, Radiation Belt, Inner Magnetosphere, Modeling

Japan Geoscience Union Meeting 2014
(28 April - 02 May 2014 at Pacifico YOKOHAMA, Kanagawa, Japan)

PEM08-25 Room:411 Time:May 2 15:15-15:30

Maps of ionospheric conductances, currents, and convection from the Swarm multi-satellite mission

AMM, Olaf[1*] ; VANHAMAKI, Heikki[1] ; KAURISTIE, Kirsti[1] ; STOLLE, Claudia[4] ; CHRISTIANSEN, Freddy[3] ; HAAGMANS, Roger[5] ; MASSON, Arnaud[6] ; TAYLOR, Matt[5] ; FLOBERGHAGEN, Rune[7] ; ESCOUBET, Philippe[5]

[1]Finnish Meteorological Institute, Arctic Research Unit, Helsinki, Finland., [2]STEL, Nagoya University, Japan, [3]Technical University of Denmark, DTU Space, Lyngby, Denmark, [4]Helmholtz-Centre Potsdam, GFZ German Research Center for Geosciences, Germany, [5]ESTEC, Noordwijk, The Netherlands, [6]ESAC, Madrid, Spain, [7]Directorate of Earth Observation Programmes, ESRIN, Frascati, Italy

The recently launched ESA Swarm spacecraft mission is the first dedicated multi-satellite ionospheric mission with two low-orbiting spacecraft that are flying in parallel in a distance of ˜100 km, thus allowing to derive spatial gradients of ionospheric parameters not only along the orbits, but also in the direction perpendicular to them. In addition, a third satellite with a slightly higher orbit regularly crosses the paths of the lower spacecraft pair. Using the Swarm magnetic and electric field instruments, we present a novel technique that allows to derive 2-dimensional (2D) maps of ionospheric conductances, currents, and convection in the area between the trajectories of the two parallel flying spacecraft, and even to some extent outside of it. This technique is based on Spherical Elementary Current Systems (SECS). We present several test cases of modelled ionospheric situations from which we calculate virtual Swarm data, and show that the technique is able to reconstruct the model electric field (or convection), horizontal currents, and conductances with very good to excellent accuracy. Larger errors arise for the reconstruction of the 2D field-aligned currents (FAC) map, especially in the area outside of the spacecraft orbits. However, even in this case the general pattern of the model FAC is recovered, and the magnitudes are valid in an integrated sense. Finally, using an MHD model run, we show how our technique allows to estimate the ionosphere-magnetosphere coupling parameter K, if conjugate multi-point observations of the magnetospheric magnetic and electric field are available, as they can be obtained, e.g., from the ESA Cluster mission.

Keywords: ionosphere, ionospheric electrodynamics, ionospheric currents, ionospheric convection, magnetosphere-ionosphere coupling, Swarm mission

Japan Geoscience Union Meeting 2014
(28 April - 02 May 2014 at Pacifico YOKOHAMA, Kanagawa, Japan)

PEM08-26 Room:411 Time:May 2 15:30-15:45

MLT and seasonal dependence of auroral electrojets: IMAGE magnetometer network observations

GUO, Jianpeng[1*] ; LIU, Huixin[2]

[1]SIGMA Weather Group, State Key Laboratory of Space Weather, CSSAR, Chinese Academy of Sciences, [2]Department of Earth and Planetary Sciences, Faculty of Sciences, Kyushu University

Total eastward and westward electrojet currents (EEJ and WEJ) and their central latitudes derived from the IMAGE network magnetic measurements are analyzed for the combined MLT and seasonal dependence during the period 1995-2009. EEJ shows a strong MLT variation with significant dependence on season. During summer months the maxima occur around 1600-1800 MLT, whereas during winter months the maxima occur at a later local time sector around 1800-2000 MLT. Moreover, the summer maxima are much larger than the winter maxima, and appear at higher latitudes. The summer maxima are mainly associated with the solar EUV conductivity effect, while the winter maxima are mainly due to the contribution of northward convective electric field. EEJ exhibits a dominant annual variation with maximum in summer and minimum in winter. WEJ also exhibits a strong MLT variation with significant dependence on season. The maxima occur around 0200-0400 MLT during summer months, around 0000-0200 MLT during winter months, and around 0000-0400 MLT during equinoctial months. Moreover, the equinoctial maxima are much larger than the summer and winter maxima, and appear at relatively lower latitudes. The seasonal variations in WEJ are the combinations of annual variations and semiannual variations. Both annual and semiannual variations show significant dependence on MLT. These results increase our knowledge on what factors contribute to the auroral electrojets as well as their magnetic signatures, and hence help us better understand the limitations of global auroral electrojet indices, such as the AE and SME indices.

Japan Geoscience Union Meeting 2014
(28 April - 02 May 2014 at Pacifico YOKOHAMA, Kanagawa, Japan)

PEM08-27 Room:411 Time:May 2 15:45-16:00

Temporal variations of nitric oxide in the mesosphere and lower thermosphere over Syowa station, Antarctica

ISONO, Yasuko[1] ; MIZUNO, Akira[1*] ; NAGAHAMA, Tomoo[1] ; MIYOSHI, Yoshizumi[1] ; NAKAMURA, Takuji[2] ; KATAOKA, Ryuho[2] ; TSUTSUMI, Masaki[2] ; EJIRI, Mitsumu[2] ; FUJIWARA, Hitoshi[3] ; MAEZAWA, Hiroyuki[4] ; UEMURA, Miku[1]

[1]Solar-Terrestrial Environment Laboratory, Nagoya University, [2]National Institute of Polar Research, [3]Seikei University, [4]Osaka Prefecture University

Energetic particle precipitation (EPP) related to solar proton events or geomagnetic storms induce ion-neutral reactions and change abundance of some minor molecules such as NO_x and HO_x in the mesosphere and lower thermosphere. To investigate the temporal variations of NO by EPP, we installed a millimeter-wave spectroscopic radiometer at Syowa Station (69.00S, 39.85E), and we have carried out ground-based observations of spectral line of nitric oxide (NO) at 250.796 GHz since January 2012.

We obtained 197 and 172 daily averaged NO spectra in 2012 and 2013 (until 30 September; DOY 273), respectively. The daily NO spectra are characterized by narrow line width with a Full-Width-at-Half-Maximum (FWHM) of about 0.5 MHz. These NO spectra are well fitted by a single Gauss function or by a single Lorenz function. From the spectral line shape, we conclude that the NO emitting region is between 75 and 100 km.

We found two temporal variation patterns of NO column density. One is a seasonal variation with a maximum in the winter and a minimum in the summer. The column density of NO during the winter was about 4 times larger than that during the summer. This seasonal variation is considered to be related to the atmospheric transport and the NO dissociation by solar radiation. The other is the short-term variation in a timeframe of 5-10 days associated with EPP events such as solar proton events and geomagnetic storms. At Syowa Station, short-term variations were caused mainly by the precipitation of electrons rather than that of protons. In the electron precipitation events, the column density of NO gradually increases just after the main phase of the geomagnetic storm and gradually decreases soon after its peak.

One of the short-term events related to a large geomagnetic storm in April 2012 was the most prominent single event among those observed at Syowa Station since January 2012. From the high time resolution (~ 3-hour) data, we revealed a diurnal tendency that NO column density increased about twice at UT 0, which is interpreted to be caused by the dawn-dusk asymmetry of the precipitated electrons with energies 30-300 keV.

Keywords: Nitric oxide, mesosphere and lower thermosphere, energetic particle precipitation, geomagnetic storm, solar proton event, Antarctica

Japan Geoscience Union Meeting 2014
(28 April - 02 May 2014 at Pacifico YOKOHAMA, Kanagawa, Japan)

PEM08-28 Room:411 Time:May 2 16:10-16:30

The Impacts of Space Weather on Society and the Economy

BAKER, Daniel N.[1*]

[1]University of Colorado Boulder

This presentation describes possible extreme space weather impacts and their economic and societal costs. Modern society depends heavily on a variety of technologies that are vulnerable to the effects of intense geomagnetic storms and solar energetic particle (SEP) events. Strong currents flowing in the ionosphere can disrupt and damage Earth-based electric power grids and contribute to the accelerated corrosion of oil and gas pipelines. Magnetic storm-driven ionospheric disturbances interfere with high-frequency radio communications and navigation signals from Global Positioning System (GPS) satellites. Exposure of spacecraft to solar particles and radiation belt enhancements can cause temporary operational anomalies, damage critical electronics, degrade solar arrays, and blind optical systems such as imagers and star trackers. Moreover, intense SEP events present a significant radiation hazard for astronauts during the high-latitude segment of the International Space Station (ISS) orbit as well as for future human explorers of the Moon and Mars. In addition to such direct effects as spacecraft anomalies or power grid outages, a thorough assessment of the impact of severe space weather events on present-day society must include the collateral effects of space-weather-driven technology failures. For example, polar cap absorption events due to solar particles can degrade — and, during severe events, completely black out — radio communications along transpolar aviation routes, requiring aircraft flying these routes to be diverted to lower latitudes. This can add considerable cost to the airlines and can greatly inconvenience passengers. Modern technological society is characterized by a complex set of interdependencies among its critical infrastructures. A complete picture of the socioeconomic impact of severe space weather must include both direct as well as collateral effects of space-weather-driven technology failures on dependent infrastructures and services.

Keywords: Space weather, Electric power grids, Radiation hazards, Infrastructure interdependencies, Socioeconomic impact of severe space weather

Japan Geoscience Union Meeting 2014
(28 April - 02 May 2014 at Pacifico YOKOHAMA, Kanagawa, Japan)

PEM08-29 Room:411 Time:May 2 16:30-16:45

GEMSIS-Sun Numerical Model of Sun-Earth System (SUSANOO): Application for Extremely Strong IMF CMEs

SHIOTA, Daikou[1*] ; KATAOKA, Ryuho[2] ; MIYOSHI, Yoshizumi[1] ; KUSANO, Kanya[1]

[1]STEL, Nagoya University, [2]National Institute of Polar Research

Solar wind including coronal mass ejections (CMEs) is a main driver of various space weather disturbances. MHD modeling of the solar wind is a powerful tool to understand the solar-terrestrial environment and to forecast space weather accurately. Recently, we developed an MHD model of the inner heliosphere on the basis of minimal input, namely, time series of daily synoptic observation of the photospheric magnetic field. The time series of MHD parameters at the Earth position is passed to a radiation belt model [Miyoshi et al. 2004] for forecasting of the radiation belt energetic electron flux. These programs are executed everyday on a server in STEL, Nagoya University and the results are uploaded on the web site (http://st4a.stelab.nagoya-u.ac.jp/susanoo/). This system is named as Space-weather-forecast-Usable System Anchored by Numerical Operations and Observations (SUSANOO).

Carrington event that occurred in September 1859 is the most violent solar storm in the human records. Since the magnetic storm associated with the event influenced globally, aurora was observed in wide area in the world. The magnetic response recorded in Bombay shows a rapid decrease of -1600 nT / h (Tsurutani et al. 2003). The induced electric field to explain the rapid decrease in the ground level is estimated to be 355 mV/m associated with a magnetic cloud influence. The time lag between onsets of solar flare and sudden commencement is 17.5 hours, and therefore shock propagation speed is estimated as 2380 km/s. The magnetic field strength in the associated magnetic cloud is needed to be 150nT. However, it is not clear how such a strong magnetic field can be kept while the strength of ordinary interplanetary magnetic field (IMF) is the order of 10 nT at 1 au.

In order to examine which condition of coronal mass ejections (CMEs) associated with an extreme event such as the Carrington event should be satisfied, we modeled a series of CMEs with the inner heliosphere MHD simulation (used in SUSANOO). In the model, multiple CMEs are injected as a twisted magnetic flux rope accompanying with a velocity pulse through the inner boundary of the simulation and propagate into the solar winds. Because there is almost no information associated with the Carrington event and the solar wind, instead, we used observational data of CMEs associated recent large-scale active regions: NOAA 10486 in October to November 2003 (Halloween event) and NOAA 11520 in July 2012 (far side STEREO event, Russell et al. 2013). Only fast (V $>\tilde{}$1000 km/s) and wide (angular width $>$60 degree) CME data are extracted from LASCO CME catalog (http://cdaw.gsfc.nasa.gov/CME_list/). As a result, the strength of compressed magnetic field becomes as high as about four times of background IMF when a CME interacts with the background solar wind. However, successive CMEs interact with each other to form much stronger magnetic filed due to compression of the magnetic cloud of the preceding CME by shock associated the following CME.

Keywords: MHD, coronal mass ejection, solar wind, IMF, geomagnetic storm, radiation belt

Japan Geoscience Union Meeting 2014
(28 April - 02 May 2014 at Pacifico YOKOHAMA, Kanagawa, Japan)

PEM08-30 Room:411 Time:May 2 16:45-17:00

Discovery of Two Sun-like Superflare Stars Rotating as Slow as the Sun

NOGAMI, Daisaku[1*] ; NOTSU, Yuta[1] ; HONDA, Satoshi[2] ; MAEHARA, Hiroyuki[3] ; NOTSU, Shota[1] ; SHIBAYAMA, Takuya[1] ; SHIBATA, Kazunari[1]

[1]Kyoto University, [2]University of Hyogo, [3]The University of Tokyo

We report on the results of high dispersion spectroscopy of two ‘superflare stars’, KIC 9766237, and KIC 9944137 with Subaru/HDS. Superflare stars are G-type main sequence stars, but show gigantic flares compared to the Sun, which have been recently discovered in the data obtained with the Kepler spacecraft. Though most of these stars are thought to have a rotation period shorter than 10 days on the basis of photometric variabilities, the two targets of the present paper are estimated to have a rotation period of 21.8 d, and 25.3 d. Our spectroscopic results clarified that these stars have stellar parameters similar to those of the Sun in terms of the effective temperature, surface gravity, and metallicity. The projected rotational velocities derived by us are consistent with the photometric rotation period, indicating a fairy high inclination angle. The average strength of the magnetic field on the surface of these stars are estimated to be 1-20 G, by using the absorption line of Ca II 8542. We could not detect any hint of binary in our spectra, although more data are needed to firmly rule out the presence of an unseen low-mass companion. These results claim that the spectroscopic properties of these superflare stars are very close to those of the Sun, and support the hypothesis that the Sun might cause a superflare.

Keywords: Sun-like stars, superflares, high dispersion spectroscopy

Japan Geoscience Union Meeting 2014
(28 April - 02 May 2014 at Pacifico YOKOHAMA, Kanagawa, Japan)

PEM08-P01 Room:Poster Time:May 2 16:15-17:30

Cosmic-ray exposure Space weather information during aircraft operation

AKUTSU, Retsu[1*] ; ASADA, Kazuaki[1]

[1]Airline Pilots' Association of Japan

Effects of exposure to cosmic-ray during aircraft operation are divided into exposure of aircrew and operational impact.

International Commision on Radiological Protection (ICRP) issued a recommendation to include occupational exposure of aircrew with a jet operated exposure from natural radiation source in 1990. Radiation Council consists of the Ministry of Education, Culture, Sports, Science and Technology, the Ministry of Health, Labour and Welfare, the Ministry of Land, Infrastructure, Transport and Tourism establised Guidelines for management of aircrew exposure to cosmic radiation in 2006. In response to this, airlines keep record of assessed doses on each aircrew using Japanese Internet System for Calculation of Aviation Route Doses (JISCARD-EX) developed by National Institute of Radiological Sciences (NIRS).

Impacts of space weather on aircraft operations can be classified into communications and navigations.

For communicaton, it includes difficulties on HF radio due to Dellinger Phenomenon while flying out of range of VHF coverages as international flight. And also includes difficulties on SATCOM voice communication and Controller Pilot Data Link Communication (CPDLC) in oceanic region.

Modern navigation by Global Navigation Satellite System (GNSS) is becoming mainstream. GNSS are used all phase of aircraft operation during on the ground, depareture, en-route, and approach. Future of operations aim high category precision approach using automatic approach and landing by GNSS even extremely low visibility until stop on runway. Cosmic-ray re-write the data in memory known as soft error on electronic equipment onboard aircrafts.

Use of SpaceWeather forecast, how to provide the information to aircrew and how to make decisions are urgent consideration.

For these problems International Airways VolcanoWatch Operations Group (IAWOPSG) which one of operations group of International Civil Aviation Organization (ICAO) is making draft Concept of Operations (ConOps) for international space weather information in support of international air navigation. Adoption of ConOps is targeted for ICAO/WMO divisional meeting in 2014.

Japan Geoscience Union Meeting 2014
(28 April - 02 May 2014 at Pacifico YOKOHAMA, Kanagawa, Japan)

PEM08-P02 Room:Poster Time:May 2 16:15-17:30

Rdiation exposure management for astronauts

MATSUMURA, Chiemi[1*] ; SATO, Masaru[1] ; KANEKO, Yuki[1] ; OGATA, Katsuhiko[1]

[1]JAXA

On the International Space Station (ISS), a habitable artificial satellite that orbits the Earth at an altitude of about 400 km, astronauts receive space radiation exposure 0.5-1.0mSv in one day which is equivalent to what humans on the Earth receive in six months.

The Japan Aerospace Exploration Agency (JAXA) employs radiation exposure management for JAXA astronauts to minimize the health damage caused by space radiation exposure.

Because of we must take action at space environment anomaly, the space environment monitoring and space weather is important information.

In this report, we introduce space radiation exposure management by JAXA.

Keywords: Astronaut, Space radiation exposure

Japan Geoscience Union Meeting 2014
(28 April - 02 May 2014 at Pacifico YOKOHAMA, Kanagawa, Japan)

PEM08-P03 Room:Poster Time:May 2 16:15-17:30

On a new antenna system for reception of real-time solar wind data

WATARI, Shinichi[1*] ; KUBO, Yuki[1] ; ISHII, Mamoru[1]

[1]National Institute of Information and Communications Technology

In-situ solar wind data are important for space weather to estimate effects of solar wind disturbances on magnetosphere and ionosphere of the Earth and investigate their solar sources. Since 1997, National Institute of Information and Communications Technology (NICT) contributes reception of real-time solar wind data from Advanced Composition Explorer (ACE), which observes solar wind at L1 point, for 24-hour data coverage. Deep Space Climate Observatory (DSCOVR) following on mission of ACE is plan to be launched in the end of 2014. NICT renews the antenna system, which enables to receive real-time data from DSCOVR. We will report on details of the new antenna system completed in March, 2014 and our application of real-time solar wind data in the presentation.

Keywords: solar wind, space weather, L1, ACE, DSCOVR

Japan Geoscience Union Meeting 2014
(28 April - 02 May 2014 at Pacifico YOKOHAMA, Kanagawa, Japan)

PEM08-P04 Room:Poster Time:May 2 16:15-17:30

Solar cell degradation of Akebono satellite due to space radiation and effect of temperature variation

MIYAKE, Wataru[1*] ; MIYOSHI, Yoshizumi[2] ; MATSUOKA, Ayako[3]

[1]Tokai University, [2]Solar Terrestrial Environment Laboratory, Nagoya University, [3]Institute of Space and Astronautical Science

Solar cells on any satellite degrade gradually due to severe space radiation environment. We have analyzed the degradation of the solar cells of the Akebono satellite, and found a fair correlation between the decrease rate of the solar cell output current and the trapped proton flux between 1989 and 1996. The previous studies demonstrated that we can deduce information of proton radiation belt from degradation of solar cells of the Akebono satellite. The relationship cannot be discernible after 1996. The previous studies suggested more prominent temperature effect in the later years because of progress of the degradation. In order to expand studies by using solar cells as a radiation monitor, we must separate exactly the contribution of temperature and of proton radiation. Since the sensor for solar cell temperature failed in 1991 and no temperature is available after 1991, we try to model the temperature variation at solar cells from the temperature of other surface parts. Once we establish the method, we correlate the temperature with solar cell output current and deduce the contribution of proton radiation.

Keywords: Akebono satellite, proton radiation belt

Japan Geoscience Union Meeting 2014
(28 April - 02 May 2014 at Pacifico YOKOHAMA, Kanagawa, Japan)

PEM08-P05 Room:Poster Time:May 2 16:15-17:30

Development of space weather prediction algorithm using big data analysis

HADA MURANUSHI, Yuko[1*] ; MURANUSHI, Takayuki[1] ; SHIBAYAMA, Takuya[1] ; ISOBE, Hiroaki[1] ; NEMOTO, Shigeru[2] ; SHIBATA, Kazunari[1]

[1]Kyoto University, [2]BroadBand Tower, Inc.

To predict and forecast the occurrence of solar flares and coronal mass ejections automatically without human power is one of the major goals in the space weather forecast research. Many studies have been performed in space weather prediction until today; For example, there are heuristics studies from the correlation of flares and the physical quantity being observed from the shape of the each sunspot. We always have required human power in such studies.

In recent years, the accuracy of the satellite and observation equipment has been increasing with the development of technology. Given that observation data is fast increasing, it is difficult for us to directly survey all data. On the other hand, big data analysis has developed rapidly in the field of information processing technology; Methods of machine learning and processing of unstructured large amounts of data by the parallel/distributed processing have been widely adopted in various fields of science. Therefore, we began to research fully automated flare prediction methods, in aim to utilize entire exhaustively large amount of data available for space weather forecast research. We set our goal to predict the X-ray flux with GOES satellites (Geostationary Operational Environmental Satellite.) More specifically, our goal is to predict the maximum of the X-ray flux from the present to 24 hours in the future.

First, we tried to predict GOES X-ray flux from past data of GOES X-ray flux and magnetic field data (Helioseismic and Magnetic Imager HMI) with SDO (Solar Dynamics Observatory), then evaluated the flare prediction accuracy using HSS (Heidke Skill Score) and TSS (True Skill Statistic) (see figure). Next, we added the extreme ultraviolet data observed with SDO/AIA (Atmospheric Imaging Assembly, wavelength: 193$\mathring{A}$) to the original dataset that consists of HMI and GOES data, and evaluated the flare prediction accuracy in the same way.

The reason for adding the AIA data is twofold. First, flare prediction studies using extreme ultraviolet full-disk image data with SOHO (Solar and Heliospheric Observatory) have revealed that we can construct a good indicator of flare activity of active regions by integrating over only pixels brighter than certain threshold in extreme ultraviolet images (threshold integral). Second, we expected to improve prediction accuracy by adding the AIA data, because magnetic field data cannot capture precursory phenomena of flare occurring in the rim of the sun, while AIA data can.

By our comparison study we found that adding full-disk integral of the AIA images to the data set improve the prediction accuracy, particularly that of X- class flares. In this presentation, we will try flare prediction based on the data set with additional features obtained by preprocessing AIA images, such as the threshold integral values, and report the results. This study is a joint research program with BroadBand Tower, Inc.

Keywords: Space weather, Solar flare, Active region, SDO/AIA, SDO/HMI, GOES

		GOES+MHI	AIA+GOES+MHI
X class Flare	HSS*1	0.209	0.215
	TSS*2	0.551	0.581
M class flare	HSS	0.439	0.402
	TSS	0.500	0.470
C class flare	HSS	0.521	0.542
	TSS	0.627	0.605

*1HSS=Heidke Skill Score

*2TSS=True Skill Statistic

Japan Geoscience Union Meeting 2014
(28 April - 02 May 2014 at Pacifico YOKOHAMA, Kanagawa, Japan)

PEM08-P06 Room:Poster Time:May 2 16:15-17:30

Statistical study on generating factors of white light solar flares

KITAGAWA, Jun[1*] ; MASUDA, Satoshi[1] ; WATANABE, Kyoko[2]

[1]STEL. Nagoya University, [2]JAXA/ISAS

'White Light Flare' is a flare with enhancement of visible continuum and is mainly associated with energetic flares like GOES X-class flares. But it could not be always observed in energetic flares and recently it is observed in relatively weak flares like GOES C-class flares (Matthews et al. 2003; Hudson et al. 2006). Its occurring mechanism has not been well understood yet and hence a key question remains; "What is needed to enhance white light emission in solar flares?"

In this study, we chose 37 events observed with Hinode/SOT and RHESSI among M- and X-class flares from January 2011 to August 2013. Out of the 37 events, Using running difference images of SOT three continuum bands (red, green, blue), we identified 13 White Light (WL) events. Remaining 24 events are classified into No White Light (NWL) events. We compare these two groups in several parameters (e.g., duration, distance between flare ribbons, and so forth) to find a generating factor of White Light event.

We found the following characteristics of WL events. (1) Most of WL events show a short duration within 20 minutes in GOES soft X-rays. (2) WL events show high (>15MK) temperature and relatively low emission measure at the peak of GOES soft X-rays. (3) The distance between two ribbons in WL events is short as 10arcsec. (4) Assuming the thick-target model, the mean dissipation rate of non-thermal energy in WL events is larger than that of NWL events. (5) WL events do not tend to coincide with CME comparing to NWL. These results indicate that precipitation of large amount of accelerated electrons into a compact area within a short time plays a key role to generate a WL event.

Keywords: solar flare, white light, hinode

Japan Geoscience Union Meeting 2014
(28 April - 02 May 2014 at Pacifico YOKOHAMA, Kanagawa, Japan)

PEM08-P07 Room:Poster Time:May 2 16:15-17:30

Influence of solar wind and ozone on the temperatures of the troposphere and stratosphere

YAMASHITA, Kazuyoshi[1*]

[1]YOKOHAMA National University

The correlation between global atmosphere and solar magnetic activity is evident though the cause is not clear. In this presentation, we analyze the influence that solar wind and ozone give to the global atmosphere to examine the cause on the basis of the previous observations [1].

The AE and Dst index data were used to detect the influence of the solar wind on the total ozone and the air temperature change of the troposphere and stratosphere.

In the analysis, the following factors were taken into account: 1)EPP-NOx effects on ozone at low latitudes may be comparable to the effects of solar UV radiation [Callis et al., 2000, 2001; Langematz et al., 2005; Rozanov et al., 2005]. 2) Since the ozone generated at low latitude is conveyed to the pole aria of the winter hemisphere, EPP-NOx has affected the ozone reduction of the pole area.

Thus, changes in the stratospheric ozone due to the influence of the solar wind appears to affect the climate of the troposphere.

References
[1]K.Itoh,JpGU 2008-2013

Keywords: troposphere, stratosphere, temperature, ozone, solar wind, geomagnetic activity

Japan Geoscience Union Meeting 2014
(28 April - 02 May 2014 at Pacifico YOKOHAMA, Kanagawa, Japan)

PEM08-P08 Room:Poster Time:May 2 16:15-17:30

On the influence of the luni-solar oscillation on the climate

ITOH, Kiminori[1*] ; AI, Yang[1] ; KAWANO, Shoh[1]

[1]Yokohama National University, Graduate School of Env. & Inf. Sciences

We have demonstrated a close relation between solar wind and regional temperatures, and suggested the participation of the Arctic oscillation. On the other hand, a link between the luni-solar oscillation and the Arctic oscillation has also been suggested [1]. Thus, both the sun and the moon appear to be important climatic factors to consider.

An interesting mechanism was proposed recently for the luni-solar oscillation cycle associated with the population change of the snowshoe hare in Canada [2]; that is, the position of the moon changes the intensity of the ionizing cosmic ray to induce changes in the activity of plants, which results in the changes in the forage quality.

This mechanism suggests a combination between the influences of the sun and the moon on the climate while their mutual independence is also possible. Thus, we try to examine the possible contribution of the luni-solar oscillation for establishing the effect of the solar wind on the climate.

1) Renato Ramos da Silva and Roni Avissar, The impacts of the Luni-Solar oscillation on the Arctic oscillation, Geophys. Res. Lett., VOL. 32, L22703 (2005)

2) Vidar Selås, Linking ’10-year’ herbivore cycles to the lunisolar oscillation: the cosmic ray hypothesis, Oikos, Volume 123, 194?202 (2014)

Keywords: Luni-solar oscillation, Arctic oscillation, Solar wind, Climate

Japan Geoscience Union Meeting 2014
(28 April - 02 May 2014 at Pacifico YOKOHAMA, Kanagawa, Japan)

PEM09-01 Room:211 Time:April 28 09:00-09:15

VarSITI - Variability of the Sun and Its Terrestrial Impact

SHIOKAWA, Kazuo[1*] ; GEORGIEVA, Katya[2]

[1]Solar-Terrestrial Environment Laboratory, Nagoya University, [2]Space Research and Technologies Institute, Bulgarian Academy of Sciences

The Scientific Committee on Solar Terrestrial Physics (SCOSTEP) is an interdisciplinary body of the International Council for Science (ICSU) to run international interdisciplinary scientific programs and promotes solar-terrestrial physics research. The last solar minimum in 2008-2009 and the current solar maximum of sunspot cycle 24 show much lower activities compared with the previous two solar cycles 22 and 23. The scientists in the solar-terrestrial physics are watching very low solar activities and their consequences on Earth, which have never been observed since modern scientific measurements become available. The SCOSTEP program "Variability of the Sun and Its Terrestrial Impact (VarSITI)" (2014-2018) will focus on this particular low solar activity and their consequences on Earth, for various times scales from the order of thousands years to milliseconds, and for various locations and their connections from the solar interior to the Earth's atmosphere. In order to elucidate various sun-earth connections, we encourage communication between solar scientists (solar interior, sun, and the heliosphere) and geospace scientists (magnetosphere, ionosphere, and atmosphere). Campaign observations will be promoted for particular interval in collaboration with relevant satellite and ground-based missions as well as modeling efforts. Four scientific projects will be carried out in VarSITI as (1) Solar Evolution and Extrema (SEE), (2) International Study of Earth-Affecting Solar Transients (ISEST/Minimax24), (3) Specification and Prediction of the Coupled Inner-Magnetospheric Environment (SPeCIMEN), and (4) Role Of the Sun and the Middle atmosphere/thermosphere/ionosphere In Climate (ROSMIC).

Keywords: VarSITI, solar activity, climate change, magnetosphere, ionosphere, atmosphere

Japan Geoscience Union Meeting 2014
(28 April - 02 May 2014 at Pacifico YOKOHAMA, Kanagawa, Japan)

PEM09-02 Room:211 Time:April 28 09:15-09:30

Specification and Prediction of the Coupled Inner-Magnetospheric Environment (SPeCIMEN)

MIYOSHI, Yoshizumi[1*] ; OMURA, Yoshiharu[2] ; KATOH, Yuto[3] ; JACOB, Bortnik[4] ; CRAIG, Rodger[5]

[1]Solar-Terrestrial Environment Laboratory, Nagoya University, [2]RISH, Kyoto University, [3]Graduate School of Science, Tohoku University, [4]UCLA, US, [5]University of Otago, NZ

Specification and Prediction of the Coupled Inner-Magnetospheric Environment (SPeCIMEN) is a focus group of next SCOSTEP project: VarSITI. The goals and objectives are the quantitative prediction and specification of the Earth inner magnetospheric environment based on Sun/solar wind driving inputs. Our question is how the inner magnetosphere responds as a coupled system to Sun/solar-wind driving, which will be solved by a combination of physical and statistical modeling, theory and observations from various platforms under this project. The satellite missions such as NASA/Van Allen Probes (US), JAXA/ERG (Japan) and ground-based network observations provide a comprehensive picture on the dynamical evolutions of geospace and reveal processes and consequences of the inner magnetosphere. Anticipated outcome should be a series of coupled, related models that quantitatively predict the dynamical evolution of the inner magnetospheric state including radiation belts, ring current, plasmasphere, plasma sheet. In this presentation, we give an overview of the SpeCIMEN project and the strategy of the project to gain the science output.

Keywords: future mission, inner magnetosphere

Japan Geoscience Union Meeting 2014
(28 April - 02 May 2014 at Pacifico YOKOHAMA, Kanagawa, Japan)

PEM09-03 Room:211 Time:April 28 09:30-09:45

Geotail observation of magnetic reconnection

NAGAI, Tsugunobu[1*] ; SHINOHARA, Iku[2]

[1]Tokyo Institute of Technology, [2]Institute of Space and Astronautical Science/JAXA

The spacecraft Geotail was launched on July 24, 1992. The main objective of the Geotail mission is to explore magnetic reconnection with in situ observations, and the Geotail mission has revealed various physical processes of magnetic reconnection. The ion-electron decoupling region where electron outflow speed differs from ion outflow speed is formed in the magnetic reconnection site. Ion and electron dynamics in the ion-electron decoupling region is derived with magnetic field and plasma observations by the spacecraft Geotail in near-Earth magnetotail magnetic reconnection. The ion-electron decoupling region has a spatial extent of approximately 11 ion inertial length along the GSM x direction, and the dawn-dusk current sheet with main current carriers of electrons exists over this region. An intense electron current layer with a spatial extent of 0.5?1 ion inertial length occupies in its center around the X line. High-speed electron outflow jets are formed just outside the central intense electron current layer. They are decelerated and become non-jet outflows with speed slightly higher than ion outflow speed. Electrons have flattop distribution functions indicating heating and acceleration in both the outflow jets and the non-jet outflows; however, heating and acceleration are weak in the central intense current layer. Inflowing ions enter the central intense electron current layer, and these ions are accelerated up to 10 keV inside the electron outflow jet regions. Ion acceleration beyond 10 keV and thermalization operate mostly in the non-jet electron outflow regions. Electrons show thermal distributions without any heating/acceleration signatures immediately beyond the edge of the ion-electron decoupling region, while higher-energy ions pervade even beyond the edge and hot MHD plasma flows are produced.

Keywords: magnetic reconnection, space plasma, substorm, magnetotail

Japan Geoscience Union Meeting 2014
(28 April - 02 May 2014 at Pacifico YOKOHAMA, Kanagawa, Japan)

PEM09-04 Room:211 Time:April 28 09:45-10:00

Global dynamics of the inner magnetosphere derived from long term observation by Akebono

KASAHARA, Yoshiya[1*] ; MATSUOKA, Ayako[2] ; NAGAI, Tsugunobu[3] ; KUMAMOTO, Atsushi[4] ; ABE, Takumi[2]

[1]Kanazawa University, [2]JAXA/ISAS, [3]Tokyo Inst. Tech., [4]Tohoku Univ.

Akebono is a Japanese scientific spacecraft which was launched in February, 1989 for observations of the Earth's magnetosphere, and has been operated successfully for 25 years. The regular data acquisition of MGF, PWS, VLF, TED, and RDM is still continued at stations in Japan and Sweden. The operation of the Akebono will be extended until March, 2015 (FY2014) in order to realize collaborative measurements with the Van Allen Probes, and further extension to the end of FY2016 is expected as an optional mission. Because of its unique orbit, the stored data is quite valuable for studying plasma physics in the auroral region as well as the radiation belt. In the present paper, we introduce important achievements of Akebono observation and discuss future science to be obtained from the long term observation data.

Keywords: Akebono, Inner Magnetosphere, Radiation belt, Aurora, Plasma wave

Japan Geoscience Union Meeting 2014
(28 April - 02 May 2014 at Pacifico YOKOHAMA, Kanagawa, Japan)

PEM09-05 Room:211 Time:April 28 10:00-10:15

ERG Science Center

KEIKA, Kunihiro[1*] ; MIYOSHI, Yoshizumi[1] ; SEKI, Kanako[1] ; HORI, Tomoaki[1] ; MIYASHITA, Yukinaga[1] ; SHOJI, Masafumi[1] ; SEGAWA, Tomonori[1] ; SHINOHARA, Iku[2] ; TAKASHIMA, Takeshi[2] ; TANAKA, Yoshimasa[3] ; ERG, Science center team[4]

[1]Solar-Terrestrial Environment Laboratory, Nagoya University, [2]Institute of Space and Astronautical Science, Japan Aerospace Exploration Agency, [3]National Institute of Polar Research, [4]ERG Science Center Team

ERG (Exploration of energization and Radiation in Geospace) is a Japanese geospace exploration project, and the ERG satellite will be launched in Japanese FY 2015. The project consists of the satellite observation team, the ground-based network observation team, and the integrated data analysis/simulation team. Besides these research teams, the ERG Science Center has been organized to promote close collaborations of these teams and thereby maximize scientific output. For studies of geospace, where different plasma populations are dynamically coupled with one another via cross-energy and cross-regional couplings, the environment for integrated data analysis is critical for comprehensive understanding using various kinds of data sets including data from physics-based models developed by the GEMSIS (Geospace Environment Modeling System for Integrated Studies) project of the Solar-Terrestrial Environment Laboratory, Nagoya University.

A standard data format and integrated data analysis tools are essential to realize the seamless data analysis environment. The ERG project data after Level-2 will be open to the public in the NASA CDF format. The integrated data analysis tool is developed as a plug-in tool of SPEDAS (Space Physics Environment Data Analysis System) in collaboration with the THEMIS (Time History of Events and Macroscale Interactions during Substorms) and IUGONET (Inter-university Upper atmosphere Global Observation NETwork) teams. It should be noted that other project data, such as THEMIS and Van Allen Probes, can be easily analyzed with SPEDAS if the data are converted to the CDF format. Thus the integrated data analysis using many kinds of data is truly realized through SPEDAS. Other useful tools in the web browser have been developed by the science center: ERGWAT (ERG Web Analysis Tool) is an interactive visualization tool, and CEF (Conjunction Event Finder) is a web-based tool enabling users to easily find conjunctions between satellites and ground-based observations. These tools will contribute to a part of the capacity building activity of the SPeCIMEN (Specification and Prediction of the Coupled Inner-Magnetospheric Environment) project carried out under the VarSITI (Variability of the Sun and Its Terrestrial Impact) program for 2014-2018.

Keywords: ERG, GEMSIS, IUGONET, Integrated analysis tool, SPEDAS, SPeCIMEN

Japan Geoscience Union Meeting 2014
(28 April - 02 May 2014 at Pacifico YOKOHAMA, Kanagawa, Japan)

PEM09-06 Room:211 Time:April 28 10:15-10:30

ICSWSE/MAGDAS Research Projects During the VarSITI Program Interval

KAWANO, Hideaki[1*] ; YOSHIKAWA, Akimasa[1] ; ABE, Shuji[1] ; UOZUMI, Teiji[1] ; CARDINAL, Maria gracita[1] ; MAEDA, George[1] ; YUMOTO, Kiyohumi[1] ; MAGDAS/CPMN, Group[1]

[1]International Center for Space Weather Science and Education

International Center for Space Weather Science and Education (ICSWSE) has developed a real time magnetic data acquisition system (the MAGDAS project) to monitor the space environment around the world. The number of observational sites is increasing every year in collaboration with MAGDAS host countries. Up to now, the MAGDAS Project has installed 73 real time magnetometers: It is the largest magnetometer array in the world. Using data from this global network, we are developing many research projects. In this talk, we introduce our research projects planned during the VarSITI program interval, as follows:

(1) Global electromagnetic coupling from polar to equatorial ionosphere
(2) Vertical coupling among the atmosphere, the ionosphere and the magnetosphere
(3) Plasmaspheric diagnosis using the Field line resonance
(4) Magnetospheric diagnosis using geomagnetic disturbances
(5) Monitoring of Space weather phenomena using solar and magnetospheric indices
(6) Modeling of Space weather parameters
(7) Sun-atmosphere coupling

Keywords: VarSITI, MAGDAS, CPMN

Japan Geoscience Union Meeting 2014
(28 April - 02 May 2014 at Pacifico YOKOHAMA, Kanagawa, Japan)

PEM09-07 Room:211 Time:April 28 10:30-10:45

Energetic electron precipitation during magnetic storm and substorm: Subionospheric VLF/LF observation

TSUCHIYA, Fuminori[1*] ; OBARA, Takahiro[1] ; MORIOKA, Akira[1] ; MISAWA, Hiroaki[1] ; YAGI, Manabu[1] ; MIYOSHI, Yoshizumi[2] ; SHIOKAWA, Kazuo[2] ; OGAWA, Yasunobu[3] ; CONNORS, Martin[4]

[1]Tohoku University, [2]Solar-Terrestrial Environment Laboratory, Nagoya University, [3]National Institute of Polar Research, [4]Athabasca University

Subionospheric VLF/LF radio observation is useful probe to investigate precipitation of high-energy (>100keV) electrons into the atmosphere and the observation at Ny-Alsound, Norway (NAL) and Athabasca, Canada (ATH) are used to detect energetic electron precipitation in auroral and sub-auroral regions during storm and substorm. At the NAL station, radio signals which are transmitted in mid-latitude and propagate across the auroral and sub-auroral regions are recorded. During magnetic storms, the strong phase variation associated with the substorm induced electron precipitation has been detected and the phase change quantitatively corresponds to the precipitating energetic electron flux observed by the NOAA/POES satellites over the radio propagation path. Onsets of the phase change were delayed by ten to several tens of minutes from the substorm onset in the morning and noon sectors, which is consistent with the drift time of energetic electrons with energy of ˜100 keV. On the other hand, the phase change in the dusk sector occurred shortly after the substorm onset and is often accompanied by Pc1 or Pi1B observed on the ground station near the radio path. These results show that the energetic electron precipitation is strongly connected with the dynamics of energetic ions and electrons and wave generations in the inner magnetosphere. The ATH station is located in the subautoral region and subionospheric signals from lower latitude are measured. The phase fluctuations with time scales of Pc5 or longer period were sometimes found during main and early recovery phases of magnetic storms. The phase fluctuations found on 5 June 2011 show good correlation with the GOES magnetic field data, suggesting Pc5 modulation of either electron injection or precipitation rates. Subionospheric radio observation provides opportunities to investigate various kinds of energetic electron precipitation processes. Part of observed data is provided through the IUGONET metadata database.

Japan Geoscience Union Meeting 2014
(28 April - 02 May 2014 at Pacifico YOKOHAMA, Kanagawa, Japan)

PEM09-08 Room:211 Time:April 28 11:00-11:15

A longitudinal network of VLF/ELF antennas and induction magnetometers at subauroral latitudes - Contribution to VarSITI

SHIOKAWA, Kazuo[1*] ; MIYOSHI, Yoshizumi[1] ; OZAKI, Mitsunori[2] ; NAGATSUMA, Tsutomu[3] ; ISHII, Mamoru[3] ; CONNORS, Martin[4] ; PODDELSKY, Igor[5] ; SHEVTSOV, Boris[5]

[1]Solar-Terrestrial Environment Laboratory, Nagoya University, [2]Kanazawa University, [3]National Institute of Information and Communications Technology, [4]Athabasca University, [5]Institute of Cosmophysical Research and Radiowave Propagation (IKIR), FEB RAS

We report observations of VLF/ELF chorus waves (~kHz) using loop antennas and Pc1 waves (~Hz) using induction magnetometers at longitudinally-distributed stations at subauroral latitudes. Continuous measurements of VLF waves with a sampling rate of 100 kHz have been made since September 2012 to monitor daily variations of chorus waves and their detailed structures at Athabasca (54.72N, 246.69E, MLAT=61.3). We observe various chorus emissions, such as quasi-periodic (Q-P) emissions, patchy burst emissions, rising and falling tone emissions at Athabasca. New loop antennas will be installed at Fredericton in the east-coast of Canada and at Zhigansk in the east-Siberia in Russia in 2014-2015. The induction magnetometer chain observes Pc1 geomagnetic pulsation which corresponds to electromagnetic ion cyclotron (EMIC) waves in the inner magnetosphere. The magnetometers have deployed in Athabasca, Magadan and Paratunka in far-eastern Russia, Moshiri and Sata in Japan, and will be deployed at Fredericton in the east-coast of Canada in 2014. These chorus waves and EMIC waves are known to contribute to the acceleration and loss of radiation belt particles. The longitudinal network of these measurements will provide continuous monitor of global distribution of the occurrence of these waves. These observations will contribute the next SCOSTEP program VarSITI, particularly to the SPeCIMEN Project.

Keywords: chorus wave, EMIC wave, Pc1 geomagnetic pulsations, ground-based multi-point observation, subauroral latitudes

Japan Geoscience Union Meeting 2014
(28 April - 02 May 2014 at Pacifico YOKOHAMA, Kanagawa, Japan)

PEM09-09 Room:211 Time:April 28 11:15-11:30

Solar Evolution and Extrema (SEE) under VarSITI Scientific Program

SAKAO, Taro[1*] ; SUZUKI, Takeru[2] ; KUSANO, Kanya[2] ; MARTENS, Petrus C.[3] ; NANDI, Dibyendu[4] ; OBRIDKO, Vladimir N.[5] ; SHIOKAWA, Kazuo[2] ; GEORIEVA, Katya[6]

[1]ISAS/JAXA, [2]Nagoya University, [3]CfA-Harvard, USA, [4]Indian Institute of Science Education and Research, India, [5]IZMIRAN, Russia, [6]SRTI, Bulgaria

Following the recent unsual solar activities, the next SCOSTEP international scientific program 'Variability of the Sun and Its Terrestrial Impact (VarSITI)' was launched as a 5 years program covering 2014-2018. It will focus on the the unusual solar activities and their consequences on Earth, for various times scales from the order of thousands years to milliseconds, and for various locations and their connections from the solar interior to the Earth's atmosphere.

The program consists of four elements:

(1) Solar Evolution and Extrema (SEE), (2) International Study of Earth-Affecting Solar Transients (ISEST/Minimax24), (3) Specification and Prediction of the Coupled Inner-Magnetospheric Environment (SPeCIMEN), and (4) Role Of the Sun and the Middle atmosphere/thermosphere/ionosphere In Climate (ROSMIC).

Among these elements, SEE will address, by promoting coordination of various projects between the Sun and the Earth, the following scientific questions:

(a) Are we at the verge of a new grand minimum? If not, what is the expectation for cycle 25? (b) Does our current best understanding of the evolution of solar irradiance and mass loss resolve the "Faint Young Sun" problem? What are the alternative solutions? (c) What is the largest solar eruption/flare possible? What is the expectation for periods with absence of activity?

An overview of SEE element will be presented.

Keywords: VarSITI Program, SEE Element, SCOSTEP, solar evolution, extreme solar events

Japan Geoscience Union Meeting 2014
(28 April - 02 May 2014 at Pacifico YOKOHAMA, Kanagawa, Japan)

PEM09-10 Room:211 Time:April 28 11:30-11:45

Solar Magnetic Activity and Their Influence on the Earth's Environment

SAKURAI, Takashi[1*]

[1]National Astronomical Observatory of Japan

The Sun affects the environment of the Earth in diverse ways. In a time scale of a few days, XUV emission and energetic particles from solar flares and disturbances in the solar wind (coronal mass ejections) cause various phenomena in the ionosphere and the magnetosphere. In a time scale of 2-4 weeks, the rotation of the Sun modulates its irradiance and solar wind properties. In a time scale of 11-year solar cycle, total and spectral irradiance changes in phase with the sunspot number. In this presentation I will pick up new results obtained with the Hinode mission and other ground-based instruments.

Hinode, launched on 23 September 2006, is a Japan-US-UK joint mission with contributions for downlink connections from ESA. The three primary instruments on Hinode are

(1) solar optical telescope/magnetograph (SOT),

(2) soft X-ray telescope (XRT), and

(3) extreme ultraviolet imaging spectrometer (EIS).

Ulysses spacecraft showed in 1998 that fast and steady solar wind comes from polar regions, and slow and variable solar wind comes from low-latitude regions. Since low-latitude regions are basically characterized by closed magnetic field lines by the presence of active regions with bipolar magnetic field configuration, it was not clear how the solar wind could flow out of the regions. However, Hinode/XRT discovered continuous outflow from the edges of active regions. Later, EIS observations confirmed the outflow by its Doppler shift. Now this outflow is believed to be the long-sought source of the slow solar wind.

The fast solar wind originates from polar regions which are basically unipolar. Since quiet-sun magnetic field of 10 gauss or less was known to consist of intense flux tubes with a kilo-gauss field strength occupying 1% of the area, the same might be expected for polar fields. Hinode/SOT showed clearly with its high spatial resolution observations of vector magnetic fields that it is the case. Hinode/SOT observations also track the polar field reversal with an unprecedented accuracy. The time delay of the south pole reversal compared with the north pole is seen in Hinode/SOT polar field observations as well as other indices, and is speculated to be related to an unusually low activity of the present solar cycle.

Coronal mass ejections (CMEs) are the major source of geomagnetic disturbances. How such an ejection of plasma cloud takes place is explained by several models. In one scenario, a solar magnetic configuration evolves by supplies of magnetic flux and magnetic helicity from below the surface. The accumulation of magnetic helicity leads to abrupt instability of magnetic configuration, leading to a CME. Magnetic helicity is distributed basically anti-symmetrically with respect to the equator, but anomaly is often observed. Long-term observations of magnetic helicity by ground-based instruments and high accuracy measurements of helicity by Hinode/SOT are providing interesting information on the nature of magnetic field generation in the solar convection zone.

Keywords: Sun, solar activity cycle, solar wind, solar magnetic field, helicity

Japan Geoscience Union Meeting 2014
(28 April - 02 May 2014 at Pacifico YOKOHAMA, Kanagawa, Japan)

PEM09-11 Room:211 Time:April 28 11:45-12:00

Modeling of the geomagnetically induced electric field in Japan

FUJITA, Shigeru[1*] ; ENDO, Arata[2] ; FUJII, Ikuko[3]

[1]Meteorological College, [2]Meteorological College, [3]Magnetic Observatory

The geomagnetically induced current (GIC) happens to damage transformers of electrical power line systems in high-latitude countries like Canada and Sweden where the geomagnetic disturbances are enhanced. Thus, since it is important to evaluate the GICs associated with geomagnetic disturbances in these countries, there have been many works about GIC [Pulkkinen et al., 2005]. On the other hand, the low-latitude countries like Japan seem to be regarded to be free from dangers of the GIC disasters [Pulkkinen et al., 2008]. Indeed, Watari et al. [2009] revealed that the GICs measured along the power line in Hokkaido (the northernmost part of Japan) are as small as several Ampere. These values are negligibly small compared with the permissible current of a transformer. It is noted that the measurements by Watari et al. [2009] were carried out in the period of extremely quiet solar activity.

The result by Watari et al. [2009] seems to indicate that Japan is safe from the GIC disasters. However, it should be noted that the ground conductivity structure is quite different between Hokkaido and other Japanese areas like the most industrialized and highly-populated Kanto plain. This difference invokes the following geoelectric characters in Japan; the geomagnetically induced electric field at Kakioka in Kanto plain is sometimes about 10-times larger than that at Memambetus in Hokkaido. This difference probably comes from difference in the ground conductivity structure. As a result, we have to employ a realistic 3D ground conductivity model to present a reliable conclusion on the GIC.

In the talk, we will present the first numerical result of the geomagnetically induced electric field in Japan based on the 3D electric conductivity in the Earth. The conductivity is compiled after the resistivity suitable to the characteristic layers based on the crustal layer structure after the database on the bathymetry and that on the thickness of the sediment layer together. Our initial results reveal several localized enhancements of the induced electric field in the coastline regions when the induced electric current tends to converge into a bay-shaped area. The enhanced electric field appears in the different areas depending on the direction of the external source current in the magnetosphere. Combination of the induced electric field calculated and quantities of the severe space weather event yields the info for evaluation of the extreme severe GIC in Japan.

References

Pulkkinen, A. et al. (2005), Space Weather, 3, S08C03, doi:10.1029/2004SW000123.
Pulkkinen, A. et al. (2008), Space Weather, 6, S07001, doi:10.1029/2008SW000388.
Watari, S., et al. (2009), Space Weather, 7, S03002, doi:10.1029/2008SW000417.

Keywords: geomagnetically induced current, space weather, electric conductivity, numerical modeling, nonuniformity

Japan Geoscience Union Meeting 2014
(28 April - 02 May 2014 at Pacifico YOKOHAMA, Kanagawa, Japan)

PEM09-12 Room:211 Time:April 28 12:00-12:15

Role of magneto-convection from the point of view of large-scale magnetic structure formation on the solar surface

IIDA, Yusuke[1*]

[1]ISAS/JAXA

The roles of magneto-convection on the solar surface in the formation of large scale magnetic field, which are revealed by the recent observation, are reported in this presentation.

Many energetic activities on the solar surface, e.g. filament formation, solar jet, and slow solar wind etc., root in the large-scale magnetic configurations. The circumstances around the photosphere, e.g. actual visible surface, is at high plasma beta condition. So the magnetic field is transported mainly by the surface convection there. Simultaneously its configuration is significantly affected and changed from its birth to solar surface. Hence, understanding of magneto-convection on the solar surface is thought to be a basic but an important issue in the solar physics for long time.

Despite of its importance, it is very difficult to give the conclusion to roles of solar surface convection to global structure, namely to answer how does it transport magnetic field and how does it change states of magnetic field. The difficulties come from the smallness and short time scale of the element structures of magneto-convection on the solar surface (<1,000km and order of minutes). The first difficulty is its smallness and short time scale in absolute value. We need stable high spatial and temporal resolution to catch up their element structure. We can say this difficulty is nearly solved thanks to the recent satellite observation. However, there is the second difficulty, smallness and short time scale compared to large scale structure (˜700,000km and order of years). We need a new method of analysis to overcome the problem, huge scale difference.

To solve this problem, we develop auto-recognition and tracking method of patches and apply it to the actual data. In the presentation, we report the results about reformation of patch structures by surface convection, especially the frequency distribution of flux content in each patch structure. We find that it is re-formed in 30 minutes, which is much shorter than flux supply time scale. This result indicates that most magnetic structures on the solar surface is decided by the local convection nature.

Keywords: the Sun, magnetic field, convection

Japan Geoscience Union Meeting 2014
(28 April - 02 May 2014 at Pacifico YOKOHAMA, Kanagawa, Japan)

PEM09-13 Room:211 Time:April 28 12:15-12:30

Solar Magnetism: Exploration with Local Convective Dynamo Modeling

MASADA, Youhei[1*]

[1]Department of Computational Science, Kobe University

A grand challenge in astrophysics is the origin of self-organizing properties of the magnetic field in highly turbulent flows. The solar magnetism is the front line in this area. The solar magnetic field shows a remarkable spatiotemporal coherence though it is generated by turbulent convective dynamo operating within its interior. Our understanding on the solar magnetism has been accelerated over the past decade in response to broadening, deepening and refining of numerical dynamo modelings. However, it is still unclear what dynamo mode is excited in the solar interior and how it regulates magnetic cycle with equatorward sunspot migration and periodicity of 22 years. To gain a deeper understanding of the solar dynamo mechanism, we are currently working on the convective dynamo simulation in a local stratified system.

Here we report a successful direct numerical simulation (DNS) of oscillatory large-scale dynamo spontaneously excited in a rotating stratified convection. The figure shown below is the simulation result; the time-radius diagram of the mean horizontal magnetic fields. Our simulation model consists of three layers like as the solar interior: bottom and top stably stratified layers and mid-convection zone (the area between white-dashed lines). It is found that the large-scale magnetic field is organized in the bulk of the convection zone and shows a well-regulated oscillatory behavior. The mean-field component is the strongest at around the mid-convection zone and propagates from there to top and base of the convection zone. The polarity is then gradually reversed over the period of about 200 convective turn-over time. It is noteworthy that there is a phase difference of about $\pi/2$ between B_x and B_y . The simulated spatiotemporal evolution of the large-scale magnetic field is quite reminiscent of the solar butterfly diagram although there is a difference in the propagation direction between the simulated field and the sunspot field.

To explore the underlying dynamo mechanism, we construct a mean-field electrodynamics model with dynamo coefficients directly computed from the DNS. The nonlinear back-reaction of the mean-field on the dynamo coefficients (both α- and η-quenching) is self-consistently taken into account. We demonstrate that the simulated large-scale dynamo is quantitatively reproduced by our DNS-driven mean-field dynamo model, and is interpreted as a manifestation of oscillatory α^2-dynamo mode. We will describe the basic physics which characterizes the cycle period and amplitude of the large-scale magnetic field sustained by the α^2-dynamo, and then discuss its playing role in the solar magnetism. This is the first to quantitatively demonstrate the presence of the oscillatory α^2-dynamo mode as a natural outcome of the rotating stratified convection, and raises an unignorable question about the conventional solar dynamo model relying strongly on the profiles of the mean flows, such as the differential rotation and meridional circulation.

Keywords: Sun, MHD, Convection, Dynamo

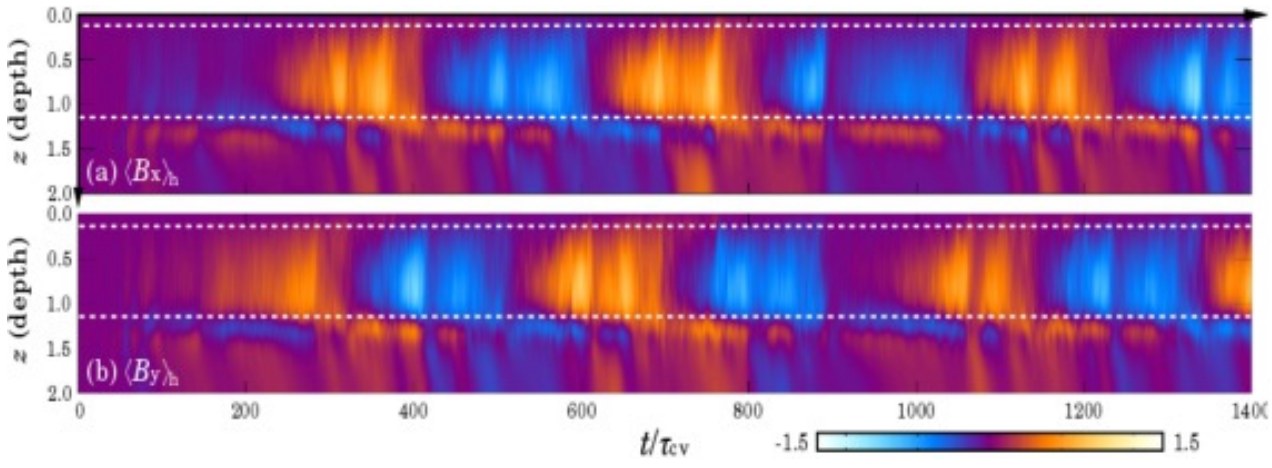

Japan Geoscience Union Meeting 2014
(28 April - 02 May 2014 at Pacifico YOKOHAMA, Kanagawa, Japan)

PEM09-14 Room:211 Time:April 28 12:30-12:45

From Deep Space Explorer DESTINY towards Solar Polar Region Observer SOLAR-D

KAWAKATSU, Yasuhiro[1*]

[1]ISAS/JAXA

DESTINY which stands for "**D**emonstration and **E**xperiment of **S**pace **T**echnology for **IN**terplanetary vo**Y**age" is a mission candidate for the next space science small program. The next mission is planned to be decided in 2014, and the select one is scheduled to be launched in 2018.

As illustrated in the Figure, DESTINY will be launched by an Epsilon launch vehicle and firstly placed into a low elliptical orbit, where then its altitude raised by the use of ion engine. When the orbit raising reaches the Moon, DESTINY subsequently is injected into transfer orbit for L_2 Halo orbit of the Sun-Earth system by using lunar gravity assist. Upon arrived at L_2 Halo orbit, DESTINY will conduct its engineering experiment as well as scientific observations for at least a half year. If conditions permit, DESTINY will leave L_2 Halo orbit, and transfer to the next destination.

On the way to L_2 Halo orbit, DESTINY will conduct demonstration and experiment on key advanced technologies for future deep space missions. Major items of the technology demonstration are listed as follows.

1) Ultra-Lightweight solar panel.

In order to generate large electric power to run μ20 ion engine, "Ultra-Lightweight Solar Panel", which is under development at JAXA, is applied and its performance is evaluated. This solar panel is estimated to achieve power to mass ratio at least double to conventional ones. Future application is expected in outer planet probes (JMO, MELOS) or probes with large ion engines.

2) Large scale ion engine μ20.

DESTINY is inserted into an elliptical orbit and reaches to a Halo orbit by its own orbital maneuver. For this maneuver, a large ion engine (μ20) which is under R&D at JAXA will be adopted and its performance is evaluated. This ion engine has thrust five times as much as μ10 used by Hayabusa and will be expected to be applied to large probes such as SOLAR-D or Hayabusa Mk2.

3) Advanced thermal control.

In order to manage large amount of heat generated by the large ion engine, advanced thermal control techniques by way of Loop Heat Pipe will be adopted.

4) Orbit determination under low thrust operation.

DESTINY will reach to Halo orbit by running ion engine over long duration. In order to reduce burdens to shut down the ion engine each time of orbit determinations, orbit determination under ion engine operation is conducted and its performance is evaluated.

5) Automatic/autonomous onboard operation.

In order to increase the efficiency of operation, autonomous and highly functioned spacecraft management system is developed demonstrated on board. This technique is expected to be adopted especially in the deep space missions usually operated under severe communication condition.

The technologies demonstrated by DESTINY will be applied to various future solar system exploration programs. One of them is a solar polar region observer, SOLAR-D, which is planned to be launched in 2020s.

SOLAR-D aims at the observation of the polar region of the Sun from out-of-ecliptic view point. It requires the observation from the high latitude point of the Sun, namely 45deg. To observe the Sun from the high latitude point, the space observatory (spacecraft) must be on the orbit largely inclined with the ecliptic plane. It is not an easy task to inject the spacecraft into the orbit largely inclined with the ecliptic plane. The mission plan under consideration supposes the use of solar electric propulsion, whose major technology challenges are going to be demonstrated in DESTINY.

The over view of DESTINY mission, and its effect on the future SOLAR-D mission will be introduced in the presentation.

PEM09-14 Room:211 Time:April 28 12:30-12:45

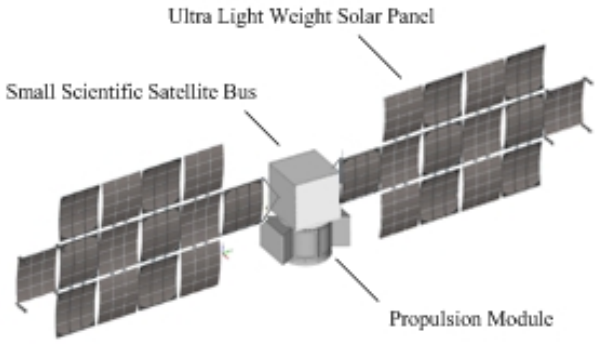

DESTINY Overview

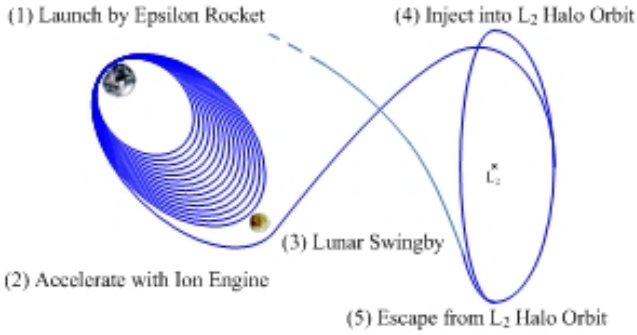

Mission Profile

Japan Geoscience Union Meeting 2014
(28 April - 02 May 2014 at Pacifico YOKOHAMA, Kanagawa, Japan)

PEM09-15 Room:211 Time:April 28 14:15-14:30

Overview of CAWSES II: Advancing the understanding of the Sun-Earth interaction

TSUDA, Toshitaka[1*]

[1]Research Institute for Sustainable Humanospherer (RISH), Kyoto University

CAWSES (Climate and Weather of the Sun-Earth System) was established as an international program by SCOSTEP (Scientific Committee on Solar-Terrestrial Physics) in order to enhance our understanding of the Solar Terrestrial relations, which impacts on life and society. In particular, we put special emphasis on the short and long-term variability of solar activity and its effects on the geospace and Earth's environment.

We carried out the first five-year project of CAWSES in 2003-2007. On the basis of its successful achievements, we conducted the second phase of CAESES during 2009-20013. CAWSES-Phase II especially promoted science and application of the following four themes, which are related to the fundamental questions of the Sun-Earth system.

TG1: What are the solar influences on the Earth's climate?
TG2: How will geospace respond to an altered climate?
TG3: How does short-term solar variability affect the geospace environment?
TG4: What is the geospace response to variable waves from the lower atmosphere?

We have enhanced international collaboration of ground-based observations, numerical modeling and satellite missions. Database is also very important for CAWSES-II. We also help capacity building activities to involve researchers in developing countries as well, and provide educational opportunities for students of all levels. We review in this talk recent achievements of CAWSES-II.

Keywords: CAWSES, SCOSTEP

Japan Geoscience Union Meeting 2014
(28 April - 02 May 2014 at Pacifico YOKOHAMA, Kanagawa, Japan)

PEM09-16 Room:211 Time:April 28 14:30-14:45

The Role of ICSU World Data System in VarSITI

WATANABE, Takashi[1*]

[1]Solar-Terrestrial Environment Laboratory, Nagoya University, [2]ICSU-WDS International Programme Office (NICT)

Solar-terrestrial physics is a typical example of interdisciplinary science, covering a wide variety of research fields. Interdisciplinary usage of observational data and information are essential in the research works to be conducted under VarSITI. ICSU has a long history to promote international collaborations in long-term provision of interdisciplinary data and information. In the IGY era (1957-58), the initial World Data Center (WDC) System was created under the policy of Full and Open Access to data and information. By the early 2000s, about 50 data centers were registered as WDCs, mainly for geophysical researches. ICSU also had another international data-oriented service under the name of Federation of Astronomical and Geophysical data-analysis Services (FAGS), which was created also in the IGY era, including ten services, e.g. International Space Environment Service (ISES). The World Data System (WDS) has been created by the 29th General Assembly of ICSU in 2008 as an Interdisciplinary Body to expand the range of data and information activities conducted by WDC and FAGS to much wider research fields, including social sciences. WDS strives to become a world-wide community of excellence providing trusted data services for global science with searchable common data directories and catalogues, which ensures the long-term stewardship and provision of quality-assessed data and data services. The VarSTEP will be one of the important partners of WDS because WDS includes many data centers came from former WDC and FAGS communities.

Keywords: VarSITI, Database, International collaboration, Interdisciplinary collaboration

Japan Geoscience Union Meeting 2014
(28 April - 02 May 2014 at Pacifico YOKOHAMA, Kanagawa, Japan)

PEM09-17 Room:211 Time:April 28 14:45-15:00

International Study of Earth-affecting Solar Transients (ISEST)/MiniMax24

KATAOKA, Ryuho[1*] ; SHIMIZU, Toshifumi[2] ; ASAI, Ayumi[3] ; ZHANG, Jie[4] ; MANUELA, Temmer[5] ; GOPALSWAMY, Nat[6]

[1]NIPR, [2]JAXA, [3]Kyoto University, [4]George Mason University, [5]University of Graz, [6]NASA/GSFC

We introduce the project ISEST (International Study of Earth-affecting Solar Transients)/Minimax24 of VarSITI, internationally led by Jie Zhang (USA), Manuela Temmer (Austria), and Nat Gopalswamy (USA). Goals and objectives are to understand the propagation of solar transients through the space between the Sun and the Earth, and develop space weather prediction capability. How do coronal mass ejections (CMEs) and corotating interaction regions (CIRs) propagate and evolve, drive shocks and accelerate energetic particles in the heliosphere? To answer this question, we need data/theory/modeling as follows: Establish a database of Earth-affecting solar transient events including CMEs, CIRs, flares, and energetic particle events based on remote sensing and in-situ observations from an array of spacecraft, run observation campaigns such as MiniMax24, develop empirical, theoretical, and numerical models of CME propagation and prediction, validate models using observations. As anticipated outcome, a comprehensive database of Earth-affecting solar transients will be created, and space weather prediction capability will be significantly improved.

Keywords: coronal mass ejection, corotating interaction region, flares, solar energetic particles

Japan Geoscience Union Meeting 2014
(28 April - 02 May 2014 at Pacifico YOKOHAMA, Kanagawa, Japan)

PEM09-18 Room:211 Time:April 28 15:00-15:15

The next-generation space solar observatory SOLAR-C

HARA, Hirohisa[1*]

[1]National Astronomical Observatory of Japan

The SOLAR-C is a planned satellite mission that is led by the JAXA SOLAR-C working group as the 4th Japanese space solar observatory that follows the 3rd satellite mission, Hinode. Hinode equips three major science payloads to cover from the photosphere to the corona simultaneously and has revealed the ubiquitous emergence/submergence of small-scale bipolar fields and the formation of kilo Gauss magnetic flux tubes from vector magnetic field measurements on the photosphere, unexpected dynamical phenomena in the chromosphere, spectral signatures of small-scale coronal heating events near the chromosphere below its spatial resolution, and so forth. These are the universal magnetized plasma activity in the nearest star, and the essential energy source of the phenomena is of magnetic-field origin coupled with photospheric convective motion. To elucidate the newly-found solar active phenomena and the problems that have been tackled for a long time in solar physics, we try to understand the causal linkage between solar magnetic fields and active phenomena on the Sun in the true sense by high-resolution (0.1-0.3 arcsecs) instruments in space. SOLAR-C will observe photospheric and chromospheric activity by imaging and measure chromospheric magnetic fields by spectro-polarimetry, in addition to photospheric magnetic fields. It visualizes the site of dynamical events for chromospheric and coronal heating by imaging and spectroscopy with comparable resolution and by high-resolution chromospheric magnetometry. In addition, SOLAR-C essentially contributes to space weather by estimating the stored magnetic energy in the corona via measurements of chromospheric magnetic fields.

Japan Geoscience Union Meeting 2014
(28 April - 02 May 2014 at Pacifico YOKOHAMA, Kanagawa, Japan)

PEM09-19 Room:211 Time:April 28 15:15-15:30

Statistical analysis of the gyroresonance sources using Nobeyama Radioheliograph and sunspot sketches

OTSUJI, Kenichi[1*] ; SHIBASAKI, Kiyoto[1] ; TANAKA, Yuuki[2] ; MIYAGOSHI, Takehiro[3]

[1]NAOJ, [2]Kyoto University, [3]JAMSTEC

Nobeyama Solar Radio Observatory of National Astronomical Observatory of Japan has continued the solar fulldisk observation using Radioheliograph (NoRH) since 1992. NoRH can measure the intensity and circular-polarization intensity of solar radio waves and identify the regions where the gyroresonance occurs. Gyroresonance is the mechanism in which the strongly circular-polarized radio waves are emitted from the resonance of the electrons gyrating around the magnetic field lines of sunspots. The radio flux coming from the gyroresonance mechanism depends on the magnetic field strength of its source and the observing wavelength. NoRH adopts 17 GHz radio waves and detects the gyroresonance emission from the strong magnetic field region with more than 2000 gauss. The statistical analysis combining gyroresonance sources and their magnetic field, or identifying them as the NOAA (National Oceanic and Atmospheric Administration) active region, however, has not been done sufficiently. So, the database including these informations is urgently needed.

In this study, we developed the database which combines the gyroresonance sources with NOAA active region number and the photospheric field strength. We listed up the location, radio flux and the circular-polarization ratio of each gyroresonance source with its area, using NoRH observation data. We also examined the area, McIntosh sunspot group classification, sunspot number and the magnetic classification of sunspots of each active region corresponding to the gyroresonance source. We used the sunspot sketches from Mt.Wilson and Crimea observatories because of the merits of covering solar fulldisk and being free from the saturation effect at the strong field. The temporal coverage of our database is from 1992 to 2013, which corresponds to almost two solar cycles.

The statistical analysis using our database clarified that the ratio of the active regions accompanied by the gyroresonance emissions increases in the latter half of cycle 23 (2002-2007). This phenomenon is not confirmed in cycle 22. There is a quadratic correlation between the number of occurrences of gyroresonance and the total number of active regions. This means that the ratio of the active regions accompanied by the gyroresonance emissions is proportional to the total number of active regions. Furthermore, we classified the active regions with the gyroresonance by their magnetic classification of sunspots and found that the complex magnetic configurations (beta-gamma-delta etc.) were predominant. Our statistical analysis provides new diagnostics to the past solar cycles and the prediction for the future solar activities.

Keywords: Sun, Radio, Sunspot

Japan Geoscience Union Meeting 2014
(28 April - 02 May 2014 at Pacifico YOKOHAMA, Kanagawa, Japan)

PEM09-20 Room:211 Time:April 28 15:30-15:45

Particle acceleration in a 3D current sheet of a Solar flare and comparison with solar radio observations

NISHIZUKA, Naoto[1*] ; NISHIDA, Keisuke[2]

[1]National Astronomical Observatory of Japan, [2]Kwasan and Hida observatories, Kyoto Uni.

Solar flares show intermittent time variability in nonthermal emissions, because particles are impulsively accelerated in small acceleration regions, i.e. multiple X-points, reconnection outflows, colliding plasmoids and internal shocks in a fragmented current sheet. We performed 3D MHD simulation of a solar flare, in which a horizontal flux rope in an unstable but equilibrium state are triggered by small amplitude of perturbation to be flown upward. The eruption of a flux rope forms a current sheet just below the flux rope, and when the width of a current sheet becomes enough thin, it becomes unstable for the tearing instability and generate small scale plasmoid inside. The formation and interaction of the plasmoids make the current sheet complex and turbulent structure. When a small scale plasmoid is ejected out or when two plasmoids collide with each other, the electric field in a current sheet is locally and intermittently enhanced.

In this 3D MHD simulation result, we inserted test particles, which are forced by electromagnetic field varying in time. Particles are trapped in the turbulent current sheet, or more exactly between multiple plasmoids, and accelerated by locally enhanced electric field along the current sheet. At that time, particles are intermittently accelerated at several heights and repeat multistep acceleration moving to other X-points. Sometimes, particles escape upward into the erupting flux rope and propagate along the field line of the flux rope. Particles are slightly accelerated by the curvature drift acceleration in the erupting flux rope and finally precipitate to another X-point connected to the different pair of loop-foot points. We also compared this simulation result with radio spectrograph data observed in Ondrejov observatory in Czech Republic. The radio spectrograph data shows similar intermittent time variability of type III bursts, i.e. electron beams, and sometimes slowly drifting pulsating structures, i.e. trapped electron beams in a plasmoid.

In this talk, we mainly talk about the test particle acceleration in 3D MHD simulation of an erupting solar flare and the comparison with the radio observation data. We are also aiming at simulating the propagation of a flux rope eruption into the interplanetary space, i.e. coronal mass ejection, forming a shock at the propagation front and reconnecting with open field in the interplanetary space. We welcome discussion and collaboration in VarSITI.

Keywords: Solar Flare, Coronal Mass Ejection, Particle Acceleration, Space Weather, Numerical Simulation, Radio Observation

Japan Geoscience Union Meeting 2014
(28 April - 02 May 2014 at Pacifico YOKOHAMA, Kanagawa, Japan)

PEM09-21 Room:211 Time:April 28 15:45-16:00

Role of the Japanese SuperDARN network in the VarSITI Program

NISHITANI, Nozomu[1*] ; YUKIMATU, Akira sessai[2] ; NAGATSUMA, Tsutomu[3]

[1]Solar-Terrestrial Environment Laboratory, Nagoya University, [2]National Institute of Polar Research, [3]National Institute of Information and Communications Technology

The Super Dual Auroral Radar Network (SuperDARN) is a network of HF radars operated under the international collaboration of 12 countries. At present, total of 33 radars have been operating in both hemispheres, monitoring important ionospheric parameters such as the global convection pattern and plasma density perturbations with high time (1 to 2 min) resolution. In addition to normal operaration modes, SuperDARN frequently operates special observation modes for conjunction studies with spacecraft programs, such as THEMIS, VAP and ERG missions. Japan has been operating total of 4 radars in Antarctica, Alaska and Hokkaido, contributing to the operation of the network. Judging from the characteristics of the network, it is expected to play important roles in several projects of the VartSITI programs, such as: ISEST (International Study of Earth-affecting Solar Transients/MiniMax24), SPeCIMEN (Specification and Prediction of the Coupled Inner-Magnetospheric Environment), and ROSMIC (Role Of the Sun and the Middle atmosphere/ thermosphere/ionosphere In Climate). Details of the SuperDARN network's role in the VarSITI program will be presented.

Keywords: SuperDARN, midlatitude, ionosphere, thermosphere, dynamics, VarSiti

Japan Geoscience Union Meeting 2014
(28 April - 02 May 2014 at Pacifico YOKOHAMA, Kanagawa, Japan)

PEM09-22 Room:211 Time:April 28 16:15-16:30

What determines the severity of space weather?

NANAN, Balan[5*] ; SKONG, R.[2] ; TULASI RAM, S.[3] ; RAJESH, P. K.[5] ; SHIOKAWA, Kazuo[1] ; HSU, R.[5] ; SU, T. H.[5] ; LIU, J. Y.[4]

[1]Solar-Terrestrial Environment Laboratory, Nagoya University, [2]Los Alamos National Laboratory, [3]Indian Institute of Geomagnetism, [4]National Central University, [5]National Cheng Kung University

Thanks to the works of a number of scientists it is known that severe space weather can cause extensive social and economic disruptions in the modern high-tech society. It is therefore important to understand what determines the severity of space weather, and whether it can be predicted. We present the results obtained from the analysis of solar-geophysical data during 30 space weather events that occurred since 1957 and produced geomagnetic storms of intensity less than -275 nT, and the Carrington event of 1859. The results seem to indicate that (1) space weather can become severe occasionally (7 since 1957) as experienced by satellite systems, Earth-based systems and Earth's environment. (2) It is the impulsive energy (or power) at the leading edge of the CMEs (coronal mass ejections) mainly due to impulsive leading edge velocity and partly due to density that determines the severity of space weather in the heliosphere; the higher the impulsive velocity (sudden increase by over 275 km s-1 over the background), the more severe the space weather. (3) Such CMEs with IMF Bz also southward from the leading edge cause severe space weather on Earth though the magnitude of southward Bz does not seem important, and the minimum impulsive velocity for severe space weather on Earth seems higher than that for severe space weather in heliosphere. (4) CMEs having northward IMF Bz at the leading edge do not seem to cause severe space weather on Earth though they can lead to geomagnetic storms of long duration main phase with intensity less than even -420 nT. Measurements of the rate of energy release during CME eruption (or measurements of the velocity and density of CMEs as close to the Sun as possible) and orientation of IMF Bz in CMEs may be used for predicting severe space weather.

Keywords: Severe space weather, solar flare, CME, geomagnetic storm

Japan Geoscience Union Meeting 2014
(28 April - 02 May 2014 at Pacifico YOKOHAMA, Kanagawa, Japan)

PEM09-23 Room:211 Time:April 28 16:30-16:45

Research and operatoinal activity of NICT space weather

ISHII, Mamoru[1*]

[1]NICT

ICT has been managing operational space weather forecast
since 1988 as a member of Inernational Space Environment Services (ISES). We provide the space weather forecast information every day including holidays with email and web site, and the number of subscribers is over 9,000.

In addition to these operational activity, we have research activities for improving the performance of space weather forecast.
We have three research projects, (1)sun and solar wind (2)magnetosphere, and (3)ionosphere with three approaches as follows: observation, simulation and informatics. These activities are progressing under the cooperation with domestic/international organizations which is suitable to the concept of VarSITI. Especially the connection to the operational users of space weather is important but very few institute only works for that including NICT. In this meaning we NICT can contribute to the activity of VarSITI.

Keywords: space weather

Japan Geoscience Union Meeting 2014
(28 April - 02 May 2014 at Pacifico YOKOHAMA, Kanagawa, Japan)

PEM09-24 Room:211 Time:April 28 16:45-17:00

Researches on solar eruptive phenomena and solar activities using chromospheric imaging data with the CHAIN

UENO, Satoru[1*] ; SHIBATA, Kazunari[1] ; ASAI, Ayumi[1] ; KITAI, Reizaburo[1] ; MORITA, Satoshi[2] ; OTSUJI, Kenichi[2] ; CABEZAS, Denis P.[3] ; G. ESCATE, Maria V.[3] ; ISHITSUKA I., Jose K.[4] ; YAMAGUCHI, Masashi[1] ; WATANABE, Hiroko[1] ; KIMURA, Goichi[1] ; ICHIMOTO, Kiyoshi[1] ; NAGATA, Shin'ichi[1] ; NAKATANI, Yoshikazu[1]

[1]Kyoto University, Japan, [2]NAOJ, [3]Presbiteriana Mackenzie University, Brazil, [4]Institute of Geophysics in Peru

In 2010, Kyoto University moved the Flare Monitoring Telescope (FMT) from Japan to Peru, and currently we are technically supporting two projects of building new solar telescopes in Saudi Arabia and Algeria under the Continuous H-Alpha Imaging Network (CHAIN) project. We also held international data analysis workshops three times during this four years to train foreign and domestic young researchers to analyze the data obtained by the FMT and Solar Magnetic Research Telescope (SMART) at Hida Observatory in Japan.

Current main scientific themes of the CHAIN project are

(1) 3D velocity field measurement of eruptive phenomena on the solar surface:
By applying "cloud model fitting" to multi-wavelength H-alpha chromospheric images, we can calculate physical parameters of moving features on the chromosphere. We especially focus on the 3D velocity field of erupting filaments to understand the process of growth and propagation of CMEs. Morimoto & Kurokawa (2003) statistically investigated time evolution of 3D velocity field of disappearing phenomena of chromospheric H-alpha filaments, and they observationally showed that if H-alpha filaments actually erupted, then CMEs necessary appears. On the other hand, however, when filaments are disappeared without eruption, sometimes CMEs occur. We have to know how to CMEs are generated in such a case, comparing with other observational data or MHD simulations. Moreover, we will statistically investigate relationship between characteristics of filament eruptions and geo-effectiveness of the CMEs .

(2) Detection of shock waves (Moreton wave) generated by solar explosive phenomena:
The FMT is quite effective to detect Moreton wave that was explained as the intersection of coronal shock wave on the solar chromosphere. Narukage et al. (2002) and Asai et al. (2012) observationally showed that Moreton waves detected in H-alpha chromospheric images actually correspond to foot-point of coronal shock waves observed with X-ray telescope or EUV telescope on satellites. On the other hand, even if flares that has almost the same intensity, sometimes they are accompanied by Moreton waves and sometimes they are not accompanied by them. We are investigating what are differences between flares "with" and "without" Moreton waves. According to our preliminary statistical study, the angle of filament eruption from the solar surface seems to be the most important parameter. We promote more investigation for more cases more accurately by combining with other satellite data or MHD simulations. Moreover, after that, we want to compare with characteristics of radio bursts and to investigate time evolution of various shock waves from solar surface to interstellar space.

(3) Estimation of solar UV radiation and comparison with ionospheric variation:
Solar radiation is also one of very important element for understanding the change of space weather. Especially solar UV around from 50 to 140 nm has strong influence for the ionosphere of the earth. One of good index of the change of ionosphere is the "geomagnetic solar daily quiet variation (Sq)". It basically changes well obeying the variation of solar UV radiation. When we investigate long-term variation of solar component and terrestrial component of Sq, currently we usually use F10.7 flux, sunspot number etc. as indexes of solar activity, because actual UV observations started just after around 1995. However, the indexes such as F10.7 do not accurately express variation of UV radiation and we cannot know accurate variation of terrestrial component of Sq. Therefore, we are currently trying to reproduce UV intensity from chromospheric images that have been obtained during longer-term than UV data. After this, by using estimated variation of solar UV radiation, we want to investigate relationship between solar activities and other physical parameters of ionosphere, too.

In this talk, we introduce our recent results and plans in VarSITI period on these themes.

Keywords: CHAIN, solar flare, filament eruption, Moreton wave, chromosphere, solar UV radiation

Japan Geoscience Union Meeting 2014
(28 April - 02 May 2014 at Pacifico YOKOHAMA, Kanagawa, Japan)

PEM09-25 Room:211 Time:April 28 17:00-17:15

The EISCAT_3D project

NOZAWA, Satonori[1*] ; MIYAOKA, Hiroshi[2] ; OGAWA, Yasunobu[2] ; OYAMA, Shin-ichiro[1] ; NAKAMURA, Takuji[2] ; FUJII, Ryoichi[1]

[1]STEL, Nagoya University, [2]NIPR

The EISCAT (European Incoherent SCATter) Scientific Association is an international research organization, which operates incoherent scatter (IS) radars in northern Scandinavia and Svalbard for studies of physical and environmental processes in the middle/upper atmosphere and near-Earth space. Since 1996, National Institute of Polar Research, in collaboration with STEL, Nagoya University, has promoted EISCAT collaborations for the user community in Japan to utilize the EISCAT facility as well as EISCAT data for their scientific subjects. Japanese scientists have been studying several scientific topics such as 3-D ionospheric current system, aurora dynamics, ion upflow, neutral wind dynamics, using EISCAT data, and published 110 papers from1995 to 2013.

EISCAT_3D is the major upgrade of the existing EISCAT radars in northern Scandinavia. The EISCAT_3D radar is a new phased array IS radar using the center frequency 233 MHz. The idea was firstly presented as 'E-prime' in 2003. The EISCAT community has been doing large efforts to make it happen since then. The design study was conducted from 2005 to 2009, and the preparatory phase program has been conducting since 2009 (until September 2014). With a multi static phased array system composed of one central active (transmiter-receiver) site and four receiver sites, the EISCAT 3D system is expected to provide us 10 times higher temporal and spatial resolution and capabilities than the present EISCAT radars. Furthermore, continuous observations can be made, and will provide us with long-term data sets of the polar ionosphere, which can be used to investigate variations of the ionosphere as well as the neutral wind dynamics (in particular, studies of planetary waves and tidal waves). In this presentation, we will overview the EISCAT_3D project, and present our strategic plan of national funding for the EISCAT_3D as well as science targets.

Keywords: EISCAT_3D, Incoherent Scatter radar, polar ionosphere, Magnetosphere-Ionosphere-Thermosphere coupling, 3D imaging observation, Mesosphere

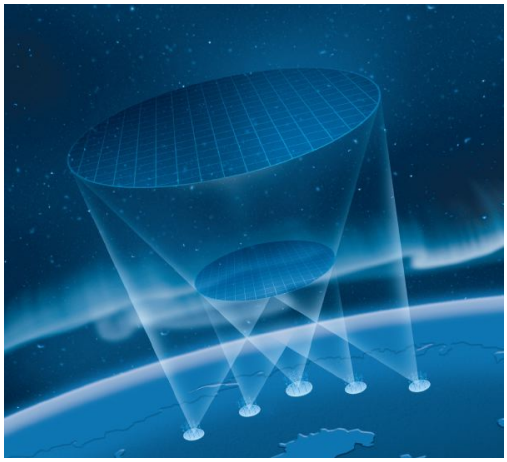

Japan Geoscience Union Meeting 2014
(28 April - 02 May 2014 at Pacifico YOKOHAMA, Kanagawa, Japan)

PEM09-26 Room:211 Time:April 28 17:15-17:30

Introduction of ROSMIC project in SCOSTEP/VarSITI program

OTSUKA, Yuichi[1*] ; NAKAMURA, Takuji[2] ; TAKAHASHI, Yukihiro[3] ; LUEBKEN, Franz-josef[4] ; WARD, William[5] ; SEPPALA, Annika[6]

[1]Nagoya University, [2]National Institute of Polar Research, [3]Hokkaido University, [4]Leibniz Institute of Atmospheric Physics, Germany, [5]University of New Brunswick, Canada, [6]Finnish Meteorological Institute, Finland

ROSMIC (Role Of the Sun and the Middle atmosphere/thermosphere/ionosphere In Climate, co-leaders: F.-J. Luebken, A. Seppala, W. Ward) is one of the four projects in VarSITI started in 2014 as a five year project. The goal of the project is to understand the impact of the Sun on the terrestrial middle atmosphere/lower thermosphere /ionosphere (MALTI) and Earth's climate and its importance relative to anthropenic forcing over various time scales from minutes to centuries. ROSMIC project consists of four sub-projects: 1) Coupling through solar variability (radiative, electrodynamics, ionospheric and photochemical effects), 2) Coupling by dynamics, 3) Trends in Mesosphere and Lower Thermosphere, 4) Trends and solar cycle effects in the thermosphere (incl. technological aspects). The project will be conducted under close collaborations between observations and modelings. Observations include both usage of existing data records and new measurements from a wide range of ground based (lidars, radars, mappers), in-situ (rockets, balloons, aircraft), and satellite (e.g., AIM, TIMED) instruments. Dedicated models are used and developed for a better understanding of specific processes (e.g. gravity wave breaking, ice formation). Global scale models will be modified and applied from the ocean to the thermosphere. Through the five year projects, we expect better understanding of the impact of solar activity on the entire atmosphere, relative to anthrogenic forcing and natural long term variability. In the paper, we will introduce outline of ROSMIC project and discuss how Japanese activities contribute to the ROSMIC project.

Keywords: Sun, middle atmosphere, thermosphere, ionosphere, climate

Japan Geoscience Union Meeting 2014
(28 April - 02 May 2014 at Pacifico YOKOHAMA, Kanagawa, Japan)

PEM09-27 Room:211 Time:April 28 17:30-17:45

Contribution of IUGONET to the VarSITI program

TANAKA, Yoshimasa[1*] ; YATAGAI, Akiyo[2] ; SHINBORI, Atsuki[3] ; KOYAMA, Yukinobu[4] ; ABE, Shuji[5] ; UMEMURA, Norio[2] ; SATO, Yuka[1] ; YAGI, Manabu[6] ; UENO, Satoru[7] ; HORI, Tomoaki[2]

[1]National Institute of Polar Research, [2]Solar-Terrestrial Environment Laboratory, Nagoya University, [3]Research Institute for Sustainable Humanosphere, Kyoto University, [4]World Data Center for Geomagnetism, Kyoto University, [5]International Center for Space Weather Science and Education, Kyushu University, [6]Planetary Plasma and Atmospheric Research Center, Tohoku University, [7]Kwasan and Hida Observatories, School of Science, Kyoto University

The Variability of the Sun and Its Terrestrial Impact (VarSITI) program aims at understanding the current extremely low solar activity and its influence on the Earth for various time scales and locations. In order to achieve these goals, it is necessary to conduct an interdisciplinary study that uses various types of data from multiple regions, such as solar interior, solar surface, heliosphere, magnetosphere, ionosphere, and atmosphere. The Inter-university Upper atmosphere Global Observation NETwork (IUGONET) project has developed the research infrastructure to promote such an interdisciplinary study. The IUGONET is an inter-university project by five Japanese institutes and universities (Tohoku University, Nagoya University, Kyoto University, Kyushu University, and the National Institute of Polar Research) that have been developing a worldwide ground-based observation network of the upper atmosphere, Sun and planets. The main tools developed by the IUGONET are metadata database and data analysis software.

The IUGONET metadata database (IUGONET-MDB) enables cross-searching of data distributed across the member institutes/universities of IUGONET. The metadata of various ground-based observational data have already been registered not only by the members of IUGONET but also by the other Japanese institutes, for example, the National Institute of Information and Communications Technology (NICT), the Solar Observatory of National Astronomical Observatory of Japan (NAOJ), and the Kakioka magnetometer observatory, Japan Meteorological Agency. We also consider including data from the satellites and the numerical simulation in the future. The iUgonet Data Analysis Software (UDAS) is a plug-in software of Space Physics Environment Data Analysis System (SPEDAS), which is an integrated analysis platform for visualizing and analyzing the ground-based and satellite observation data. The UDAS has provided many routines to load the ground-based observational data from various types of instruments, including solar telescope, solar radio telescope, ionosphere and atmosphere radars, imagers, magnetometers, and so on. The SPEDAS also includes a plug-in tool from a Japanese satellite mission, Energization and Radiation in Geospace (ERG), which will explore the dynamics of the radiation belts in the Earth's inner magnetosphere. Thus, they will be powerful tools for four projects of the VarSITI, in particular, Specification and Prediction of the Coupled Inner-Magnetospheric Environments (SPeCIMEN) and Role Of the Sun and Middle atmosphere thermosphere/ionosphere in Climate (ROSMIC). In the presentation we will show some examples of scientific researches that the IUGONET has done using the upper atmospheric data and discuss our possible contribution to the VarSITI program.

Keywords: IUGONET, upper atmosphere, ground-based observation, metadata database, data analysis software, interdisciplinary study

Japan Geoscience Union Meeting 2014
(28 April - 02 May 2014 at Pacifico YOKOHAMA, Kanagawa, Japan)

PEM09-28 Room:211 Time:April 28 17:45-18:00

Characteristics of airglow and auroral emissions in the lower- and upper-thermosphere obtained with IMAP/VISI on ISS

SAKANOI, Takeshi[1*] ; PERWITASARI, Septi[1] ; SAKAMOTO, Daiki[1] ; SAITO, Akinori[2] ; OTSUKA, Yuichi[3] ; AKIYA, Yusuke[2] ; HOZUMI, Yuta[2] ; YAMAZAKI, Atsushi[4] ; SUZUKI, Shin[3]

[1]Grad. School of Science, Tohoku University, [2]Grad. School of Science, Kyoto University, [3]STEL, Nagoya University, [4]ISAS / JAXA

We report the recent highlights of results on airglow and auroral distribution in the lower- and upper-thermosphere based on IMAP/VISI measurement data, and also report the current status of the operation VISI. IMAP/VISI is a visible imaging spectrometer which aims to measures nightglow emissions from ISS (˜400 km altitude) covering the wide range from +51 deg. to ? 50 deg. in geographical latitude. VISI adopts two field-of-views (+/-45 deg. to nadir) to make a stereoscopic measurement of the airglow and aurora emission to subtract background contaminations from clouds and ground structures. Each field-of-view has 90 deg width faced perpendicular to the orbital plane, which is mapped to ˜600 km width at 100 km altitude and ˜300 km width at 250 km altitude. A continuous line-scanning for all emissions lines in the nightside hemisphere in the latitudinal range from +51 deg. to -51 deg. is carried out by VISI with the successive exposure cycle with a time interval of 1 - several sec, which corresponds to a spatial resolution of 10 km ? a few tens km. From VISI data, we obtain the global distribution of airglow emissions (O 630 nm at 250 km alt., OH Meinel band 730 nm at 87km alt., and O2 (0-0) atmospheric band 762 nm at 95 km alt.) and auroral emissions (O 630 nm at 250 km alt., N2 1P 730 nm at ˜110 km alt. and O2 762 nm at ˜120 km alt.).

Since the successful launch of IMAP on August 2012, we found that meso-scale (˜10 - 50 km) wave pattern is always seen in the airglow emission at O2 762 nm mainly at mid-latitudes. The typical O2 airglow intensity is several hundreds R to several kR. Most of O2 airglow shows straight-shaped pattern, which indicates plane atmospheric gravity waves. In addition, we found more than 30 events on the concentric gravity wave (CGW) pattern in O2 airglow emission, which suggests that the local generation source in the lower-atmosphere. 26 CGW events out of total 30 events happened in March and April in 2013, which suggests its seasonal effect.

VISI sometimes measured auroral emissions at high-latitudes during geomagnetically disturbed period. One of major purposes of auroral measurement with VISI is to understand the generation process of gravity wave by auroral activity. However, we could not obtain the gravity wave event caused by aurora so far. Another target of VISI high-latitude measurement is SAR arc in the sub-auroral region. Even though the solar activity is expected to be maximum in 2012 ? 2013, we could not obtain the SAR arc data so far. However, we still expect to measure the SAR arc event caused with a major storm during a solar declining phase.

In addition, in the low-latitude region around the magnetic equator, we frequently obtained the enhanced O630 nm emission associated with equatorial ionization anomaly (EIA) overlapped with small-scale dark filament pattern, i.e., plasma bubble. We found the seasonal dependence of O630 nm intensity in the EIA which is consistent with the vertical motion of ionospheirc plasma due to the dragged by thermospheric day-to night tidal winds. The O630 nm intensity associated with EIA significantly decreased during the main phase of magnetic storm when the Dst index is larger than 90 nT. This fact suggests that the westward electric field associated with Region-2 current system penetrates to the ionosphere in the lower latitude that reduce the upwelling of EIA. We also obtained the MSTID pattern in O 630 nm emission in the eastside of North America on August 1 2013 by comparing the O 630 nm emission and TEC map. We carried the special operation for the measurement of MSTID last winter, and will summarize the result.

Acknowledgements

We thank the IMAP science team and the MCE team for their kind support.

Keywords: ISS, airglow, thermosphere, ionosphere, JEM, gravity wave

Japan Geoscience Union Meeting 2014
(28 April - 02 May 2014 at Pacifico YOKOHAMA, Kanagawa, Japan)

PEM09-29 Room:501 Time:April 29 11:00-11:15

The effect of Solar radiation on the Climate of Yakushima

MURAKI, Yasushi[1*] ; SHIBATA, Shoichi[2] ; SHIBATA, Takashi[3]

[1]Solar-Terrestrial Environment Laboratory, Nagoya University, [2]Department of Engeneering, Chubu University, [3]Graduate School of Environment Studies, Nagoya University

Yakushima (Yaku-island) is located to the south of Kyushu in Japan and is known as one of the world natural heritages of UNESCO. There are mountains on the island with heights of about 2,000m where cedar trees have lived for more than 2000 years. We analyzed meteorological data for the island from 1938 to 2013 and found several interesting results:

(1) Eleven and 20-30-year-periodicities are present in the data on daylight hours. Similar periodicities are, however, not seen in the data on temperature or water vapor pressure.
(2) The 11-year-periodicty appears strongly in June, the rainy season of the island, while the 20-30-year-periodicty is seen throughout the year except in April.
(3) An 11-year-periodicty can be also seen in the data for June and July at the other remote island Hachijyojima situated 300km to the south of Tokyo. Both islands are located on the Kuroshio warm current.
(4) The daylight hour data for January increased systematically around 1976. This may be related to the change of the North Hemisphere Temperature (NHT) in 1976.

In order to explain the observations, we examined the following hypothesis. Ocean waves produce large numbers of tiny salty droplets which contain plankton on the sea surface. These droplets (aerosols) are winded up and reach at the top of the mountain. They may act as cloud condensation nuclei (CCN).
It is known that the intensity of the UV light from the Sun is modulated by solar activity. It is also possible that the growth rate of CCN is affected by the solar UV radiation in the early stage of the aerosol formation process.
We speculate that this may be why solar activity is recognized in the daylight hour data. We have not accounted for the 20-30-year-periodicity in the data, but we speculate that this could be related to the Pacific Decadal Oscillation (PDO).
Details will be presented at the conference.

Keywords: solar activity, solar Ultra-Violet light, cloud, daylight hours, aerosols, Passific Decadal Oscillation

PEM09-29 Room:501 Time:April 29 11:00-11:15

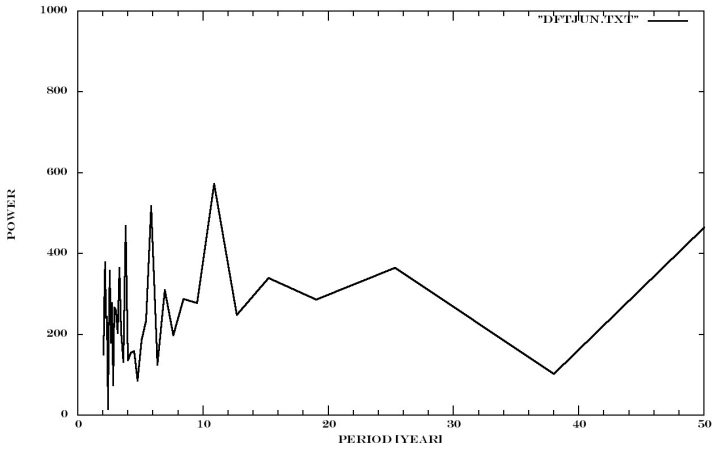

Japan Geoscience Union Meeting 2014
(28 April - 02 May 2014 at Pacifico YOKOHAMA, Kanagawa, Japan)

PEM09-30 Room:501 Time:April 29 11:15-11:30

Sounding rocket observation of the thermosphere-ionosphere-magnetosphere coupling

ABE, Takumi[1*] ; SAITO, Yoshifumi[1]

[1]Japan Aerospace Exploration Agency

The polar ionosphere is an open window of the Earth atmosphere to the outside space such as the magnetosphere and the solar wind, because energy and/or mass tends to be injected along the magnetic fields via various physical processes. In this connection, there exist numerous unique and unrevealed phenomena in the polar ionosphere.

Sounding rocket is a powerful platform which provides opportunity to make a vertical sounding through the lower thermosphere, ionosphere and magnetosphere while satellite generally flies in a horizontal direction, and it has an advantage so that it can enable us to make a brief survey of the upper atmosphere in the vertical direction. The Institute of Space and Astronautical Science (ISAS) of Japan Aerospace Exploration Agency (JAXA) has conducted sounding rocket experiments in Norway to investigate the upper atmospheric dynamics and chemistry induced by the auroral energy input. The primary objectives of these experiments include various topics; pulsating aurora, ozone chemistry affected by the auroral activity, fine structure of the auroral arc, and the cusp ion outflow. These subjects arise from phenomena that is caused by interaction between the solar wind or magnetospheric plasma and the upper atmosphere. It is necessary to make a comprehensive observation of the energy input, the response and consequences for better understanding of the causal relationship.

There are several candidates of the sounding rocket experiment which should be conducted in the auroral region for a direct measurement of the energy input from higher altitudes and the ionospheric response. To obtain the high-time resolution data of the ionospheric ion outflow which is one of the most significant phenomena of the magnetosphere-ionosphere coupling, it is necessary for the sounding rocket equipped with plasma and field instruments to reach up to 1000 km altitude. For such an experiment, it will be a key to get information on the wave-particle interaction which may play an important role in accelerating ionospheric ions. It is well known that the polar lower thermosphere has a significant response to auroral energy input from higher altitudes. This indicates an existence of energy inputs from the magnetosphere probably in the form of electric fields or energetic particles. It is important to understand quantitatively the momentum transfer between the neutrals and plasma by observing the neutral wind and ion drift simultaneously. The sounding rocket experiment to elucidate such a neutral-plasma coupling is also under consideration.

Thus, we are considering several candidates of the sounding rocket experiments which should be conducted in the auroral region to investigate the upper atmospheric response against the energy input from higher altitudes. In this presentation, we will briefly introduce some of the promising experiments.

Keywords: sounding rocket, thermosphere, M-I coupling, in-situ observation, aurora

Japan Geoscience Union Meeting 2014
(28 April - 02 May 2014 at Pacifico YOKOHAMA, Kanagawa, Japan)

PEM09-31 Room:501 Time:April 29 11:30-11:45

Trend of SST anomalies and Solar Activity

YAMASHIKI, Yosuke[1*]

[1]GSAIS, Kyoto University, [2]APL, JAMSTEC

The tendency of anomalies of SST during the fluctuation of Sunspot numbers are studied using composite SST and fluctuation of SSN.

In general, El Nino tendency is observed during Sunspot numbers (SSN) minimum, while La Nina tendency is observed in SSN maximum. It is generally accepted that the frequency of Solar Activity varies in 11 years, during those years there are SSN maximum and minimum. On the other hand, SST anomalies do not correspond well to the frequency of the solar activity. In addition, the thermal structure of sea surface temperature (SST) varies during El Nino and La Nina. Moreover, the impact of large-scale solar flare on the SST has not been clearly evident for the 4 days backward and forward comparison for the flare event on 2 April 2001 and 28 October 2003 on SST, wind velocity and OLR. Since the ocean has higher heat capacity, this might prevent the appearance of immediate SSN effect through the surge of any frequency in any band of electromagnetic waves from the SUN. The subtle impact might be confirmed either through cloud or wind. The long-term impact should also be considered by precise integration of the total energy on each wavelength. Numerical simulation is also expected to validate this issue.

Keywords: Solar activity, SST, Anomalies

Japan Geoscience Union Meeting 2014
(28 April - 02 May 2014 at Pacifico YOKOHAMA, Kanagawa, Japan)

PEM09-32 Room:501 Time:April 29 11:45-12:00

Recent observations by Rayleigh/Raman lidar and developments of tunable resonance scattering lidar system in JARE

EJIRI, Mitsumu K.[1*] ; TSUDA, Takuo[1] ; NISHIYAMA, Takanori[1] ; ABO, Makoto[2] ; TOMIKAWA, Yoshihiro[1] ; SUZUKI, Hidehiko[3] ; KAWAHARA, Takuya[4] ; TSUTSUMI, Masaki[1] ; NAKAMURA, Takuji[1]

[1]National Institute of Polar Research, [2]Graduate School of System Design, Tokyo Metropolitan University, [3]College of Science, Rikkyo university, [4]Faculty of Engineering, Shinshu University

The National Institute of Polar Research (NIPR) is leading a six year prioritized project of the Antarctic research observations since 2010. One of the sub-project is entitled ”the global environmental change revealed through the Antarctic middle and upper atmosphere”. Profiling dynamical parameters such as temperature and wind, as well as minor constituents is the key component of observations in this project, together with a long term observations using existent various instruments in Syowa, Antarctica (69S, 39E). As a part of the sub-project, Rayleigh/Raman lidar was installed at Syowa Station in January, 2011 and has been operated at more than 350 nights ($>$3000 hours clear sky) by February, 2014. The Rayleigh/Raman lidar observes temperature and clouds in the mesosphere, the stratosphere and part of the troposphere, and providing seasonal and yearly variations of temperature profiles and data of gravity wave characteristics in the middle atmosphere, as well as high altitude clouds of PMC (polar mesospheric clouds) and PSC (polar stratospheric clouds). In order to extend the height coverage to include mesosphere and lower thermosphere region, and also to extend the parameters observed, a new resonance scattering lidar system with tunable wavelengths is developed at NIPR in Tachikawa (36N, 139E). The lidar transmitter is based on injection-seeded, pulsed alexandrite laser for 768-788 nm (fundamental wavelengths) and a second-harmonic generation (SHG) unit for 384-394 nm (second harmonic wavelengths). The laser wavelengths are tuned in to the resonance wavelengths by a wavemeter that is well calibrated using a wavelength-stabilized He-Ne laser. The new lidar has capabilities to measure density variations of minor constituents such as atomic iron (Fe, 386 nm), atomic potassium (K, 770 nm), calcium ion (Ca^+, 393 nm), and aurorally excited nitrogen ion ($N_2{}^+$, 390-391 nm) and temperature profiles in the mesosphere and lower thermosphere (MLT) region using resonance scatter of K. Currently, the fundamental laser pulses are transmitted with 120-160 mJ/pulse at approximately 25 Hz (i.e., $\sim$3-4 W) and the backscattered signal is received with a 35 cm diameter telescope. The new lidar system will be installed two years later at Syowa Station and provide information on the mesosphere and lower thermosphere as well as the ionosphere. This unique observation is expected to make important contribution to studies on the atmospheric vertical coupling process and the neutral and charged particle interaction. In this talk, current status of the research, observations, and system developments will be presented.

Keywords: Lidar, Resonance scatter, Rayleigh/Raman, Antarctic observation, Syowa Station

Japan Geoscience Union Meeting 2014
(28 April - 02 May 2014 at Pacifico YOKOHAMA, Kanagawa, Japan)

PEM09-33 Room:501 Time:April 29 12:00-12:15

400 years interval of amplification in quasi bi-decadal climate variability: a case of summer precipitation in Japan

NAKATSUKA, Takeshi[1*]

[1]Research Institute for Humanity and Nature

Introduction

Quasi bi-decadal climate variability, often found in palaeoclimatological time series, should be not only attributed to internal climate variation such as ocean-atmosphere interaction, but also owing to astronomical climate forcing like 22 year cycle of solar activity. In long human history, the multi-decadal climate variations are sometimes enhanced to cause long abnormal meteorological conditions and result in numerous famines, wars and political regime shifts. Why does the amplitude of natural climate variation change? If we can understand mechanism of the amplitude modulation in climate variability and predict its future, it must be very helpful for improvement of our adaptability to climate change. In this presentation, I will discuss climatic mode of 400 year intervals of amplification in quasi bi-decadal climate variability found in last two millennial records of summer precipitation which were reconstructed annually by tree-ring cellulose isotope ratios.

Reconstruction of summer precipitation by tree-ring oxygen isotope ratio

Until recently, paleoclimatologists in Japan could not reconstruct precipitation before Edo era when weather descriptions in numerous diaries enable us to discuss climate change precisely. However, it is now possible to elucidate historical changes in summer precipitation with annual time resolution using tree-ring cellulose oxygen isotope ratios all over Asia monsoon area including Japan. Last two millennial summer precipitation variations have been reconstructed in central Japan using many wood samples of Japanese cypress from living trees, old architectures, archaeological remains and buried logs.

Amplification of quasi bi-decadal variability occurring at 400 years intervals.

By wavelet analysis of the two millennia length of summer precipitation record in central Japan, I have found that there are distinct periods of amplitude modulation for the multi-decadal variability, especially at quasi bi-decadal periodicity, in 2nd, 6th, 10th, 14th and 18th centuries when long lasting flood and drought occurred. In fact, 2nd, 6th and 14th centuries correspond to the end of Yayoi, Kofun eras and the medieval upheaval period (Namboku-cho, twin dynasty, era) in Japan, respectively. 10th and 18th centuries are also known as periods of the collapse of centralized political system and the occurrence of giant famines all over Japan, respectively. The amplitude modulation in quasi bi-decadal periodicity occurring at 400 years intervals always started with sudden decrease in tree ring d18O, accompanied with sudden increase and decrease in its d13C and 14C content, respectively. At present, I can propose the sudden enhancement of summer monsoon activity bringing tropical air mass to explain all signals of sudden changes in tree-ring isotope records. Especially, sudden increases in temperature during 14th century, which is corresponding to the precipitation increase in Japan, are found at low and middle latitudinal areas in both hemispheres, illustrating that they are actually owing to the summer monsoon enhancement originating from tropical areas. If the amplification in quasi bi-decadal variability at 400 year intervals is related to the periodical change in solar activity such as 800 year cycle, it must be very important to elucidate astronomical and climatic mechanisms combining cause (solar cycle) and effect (amplitude modulation) precisely.

Keywords: tree ring, oxygen isotope, bi-decadal change, precipitation

Japan Geoscience Union Meeting 2014
(28 April - 02 May 2014 at Pacifico YOKOHAMA, Kanagawa, Japan)

PEM09-34 Room:501 Time:April 29 12:15-12:30

Ionospheric studies using high-resolution GPS total electron content observations

TSUGAWA, Takuya[1*] ; NISHIOKA, Michi[1] ; SAITO, Akinori[2] ; OTSUKA, Yuichi[3] ; ISHII, Mamoru[1]

[1]National Institute of Information and Communications Technology, [2]Graduate School of Science, Kyoto University, [3]Solar-Terrestrial Environment Laboratory, Nagoya University

Two-dimensional total electron content (TEC) observations using dense GPS receiver networks have been applied to studies of various ionospheric disturbances since mid-1990s. For the purpose of monitoring and researching the ionospheric disturbances, we have developed high-resolution TEC maps using dense GPS receiver networks. We have been collecting all the available GNSS receiver data in the world to expand the TEC observation area. These GNSS data are provided by IGS, UNAVCO, SOPAC, and other regional data centers. Currently, we are providing global and regional maps of absolute TEC, detrended TEC, and rate of TEC change index (ROTI). These data and quick-look maps are archived and available in DRAWING-TEC website (http://seg-web.nict.go.jp/GPS/DRAWING-TEC/).

These high-resolution GPS-TEC maps have been applied to studies of various ionospheric disturbances. Sudden increase in TEC caused by solar flares were studied using global TEC observations. Regional TEC observations have revealed new characteristics of large- and medium-scale traveling ionospheric disturbances (LSTIDs and MSTIDs). Recently, clear concentric waves and short-period oscillations were observed after huge earthquakes/tsunamis and massive tornadoes, indicating that acoustic and/or gravity waves propagate upward from the lower atmosphere and reach the ionosphere.

These GPS-TEC observations will contribute the next SCOSTEP program VarSITI, particularly to the ROSMIC (Role Of the Sun and the Middle atmosphere/thermosphere/ionosphere In Climate) project.

Keywords: ionosphere, GPS, TEC, thermosphere

Japan Geoscience Union Meeting 2014
(28 April - 02 May 2014 at Pacifico YOKOHAMA, Kanagawa, Japan)

PEM09-35 Room:501 Time:April 29 12:30-12:45

Modulation of Greenland temperature through changes in solar activity

KOBASHI, Takuro[1*] ; KAWAMURA, Kenji[1] ; GOTO-AZUMA, Kumiko[1]

[1]National Institute of Polar Reseaerch

During the past decades, Greenland climate has undergone rapid warming and ice sheet ablation in coastal region with a nearly 1 mm/y sea level contribution. For sea level projection, it is critical to understand the mechanisms of Greenland temperature variability. Greenland temperature is known to be affected by the North Atlantic Oscillation (NAO), and it is also highly correlated with North Atlantic average temperature. Using the Greenland temperature reconstructed from argon and nitrogen isotopes in occluded air in GISP2 ice core (Kobashi et al., 2011), we found Greenland temperature deviated negatively (positively) from North Hemispheric (NH) temperature trend during stronger (weaker) solar activity over the past 800 years (Kobashi et al., 2013b). We also confirmed this effects continued over the past 4000 years (Kobashi et al., 2013a). Climate modeling suggests that the deviation was caused by solar induced atmospheric circulation changes (like NAO). The model also suggests that Atlantic meridional circulation weakens during the stronger sun by similar processes as enhanced greenhouse effect (Kobashi et al., 2013b). From the past relation between Greenland temperature anomaly and solar variability, it can be speculated that future gland solar minimum may induce additional 2 ^{0} C warming in Greenland with increased melting of the ice-sheet.

Kobashi, T., Kawamura, K., Severinghaus, J. P., Barnola, J.-M., Nakaegawa, T., Vinther, B. M., Johnsen, S. J., and Box, J. E.: High variability of Greenland surface temperature over the past 4000 years estimated from trapped air in an ice core, Geophysical Research Letters, 38, 10.1029/2011GL049444, 2011.

Kobashi, T., Goto-Azuma, K., Box, J. E., Gao, C.-C., and Nakaegawa, T.: Causes of Greenland temperature variability over the past 4000 years: Implications for Northern Hemispheric temperature change Climate of the Past, 9, 2299-2317, 2013a.

Kobashi, T., Shindell, D. T., Kodera, K., Box, J. E., Nakaegawa, T., and Kawamura, K.: On the origin of Greenland temperature anomalies over the past 800 years, Climate of the Past, 9, 583-596, 2013b.

Keywords: solar activity, Greenland, temperature, ice core, climate change

Japan Geoscience Union Meeting 2014
(28 April - 02 May 2014 at Pacifico YOKOHAMA, Kanagawa, Japan)

PEM09-36 Room:501 Time:April 29 14:15-14:30

Study of equatorial atmosphere/ionosphere under RISH/LAPAN collaboration

YAMAMOTO, Mamoru[1*] ; YATINI, Clara[2] ; BUDIYONO, Afif[2] ; HERMAWAN, Eddy[2] ; HASHIGUCHI, Hiroyuki[1]

[1]RISH, Kyoto University, [2]National Institute of Aeronautics and Space (LAPAN)

The Earth's atmosphere is vertically coupled with atmospheric waves. Momentum/energy transfer from lower to upper atmosphere through wave propagation plays an big role of determining the dynamics of the atmosphere. The energy input from the sun is the maximum at the equator that leads to the intense convection, and then variety of atmospheric waves are generated in the region. The equatorial atmosphere could be regarded as an engine for dynamics of the whole atmosphere. RISH-LAPAN started collaboration for the study of equatorial atmosphere/ionosphere since mid 1980s, and conducted radiosonde observation campaigns, meteor and MF radars, etc. The Equatorial Atmosphere Radar (EAR) was installed over the geographic equator on Sumatra Island in 2001. We continued long-term experiment for more than 10 years, and have found that troposphere-stratosphere airmass exchange is controlled by the modulation of the tropopause by Kelvin waves. Turbulent structures of the tropopause region is also revealed by the EAR. In the ionosphere, spatial and temporal variability of the equatorial Spread-F are clearly observed by the multibeam experiment. With research collaboration with other Japanese university/institutes, the EAR site now became a complete observatory that consists of many instruments, i.e., a meteor radar, a boundary-layer radar, a meteorological radar, lidars, an ionosonode, GPS receivers, etc. The next big project of our own is to improve the EAR ability by building the Equatorial MU radar (EMU) aside of the EAR, which is now included in the Japanese Master Plan. RISH-LAPAN recently obtained a fund of "JSPS Bilateral Joint Research Projects" for FY2014-2016. We will have more chances to discuss collaborative research program for the equatorial atmosphere/ionosphere. In the presentation we summarize our collaboration, and discuss future direction of research including the new EMU.

Keywords: Atmosphere, Ionospphere, Indonesia, Equatorial Atmosphere Radar

Japan Geoscience Union Meeting 2014
(28 April - 02 May 2014 at Pacifico YOKOHAMA, Kanagawa, Japan)

PEM09-37 Room:501 Time:April 29 14:30-14:45

Monitoring of molecular compositions in mesosphere with a network of ground-based millimeter-wave radiometers

NAGAHAMA, Tomoo[1*] ; MIZUNO, Akira[1] ; NAKAJIMA, Tac[1] ; OHYAMA, Hirofumi[1] ; ISONO, Yasuko[1] ; KOJIMA, Yasusuke[1] ; TSUTSUMI, Masaki[2] ; NAKAMURA, Takuji[2] ; MAEZAWA, Hiroyuki[3] ; OGAWA, Hideo[3]

[1]Solar-Terrestrial Environment Laboratory, Nagoya University, [2]National Institute of Polar Research, [3]Osaka Prefecture University

Chemical composition in mesosphere and lower thermosphere (MLT) region is strongly affected by changes of solar-terrestrial environment; for example, energetic particle precipitation into the earth atmosphere induces composition change in the mesosphere and lower thermosphere. Changes of gravity-wave activities also make the composition changes caused by temperature variations in various timescales.

To investigate these changes related to environment changes in the altitude region, we have started a project of network measurements of the distribution of mesospheric minor constituents, such as ozone, by using ground-based millimeter-wave spectral radiometers with a high-sensitivity superconducting (SIS) mixer receiver. We have been operating three millimeter-wave radiometers in the southern hemisphere; Atacama highland in Chile (23S, 68W), Rio Gallegos in Argentina (52S, 69W), and Syowa station in Antarctica (69S, 39E), and one radiometer in Rikubetsu, Japan(44N, 144E). Especially, at Syowa station, we have been monitoring ozone and nitric oxide (NO) spectra in 250 GHz band, and we have clearly detected temporal variations of NO column density in the MLT region including sudden enhancements of NO suggested to be associated with the energetic electron precipitation events.

In the presentation, we report features of observed variations of mesospheric ozone and NO as well as details of instruments, data validation and future extensions.

Keywords: mesosphere, composition change, millimeter-wave measurement

Japan Geoscience Union Meeting 2014
(28 April - 02 May 2014 at Pacifico YOKOHAMA, Kanagawa, Japan)

PEM09-38 Room:501 Time:April 29 14:45-15:00

Observations and modeling studies for understanding atmospheric responses to unusual solar activities

FUJIWARA, Hitoshi[1*] ; MIYOSHI, Yasunobu[2] ; JIN, Hidekatsu[3] ; SHINAGAWA, Hiroyuki[3] ; NOZAWA, Satonori[4] ; OGAWA, Yasunobu[5] ; KATAOKA, Ryuho[5]

[1]Faculty of Science and Technology, Seikei University, [2]Department of Earth and Planetary Sciences, Faculty of Sciences, Kyushu University, [3]National Institute of Information and Communications Technology, [4]Solar Terrestrial Environment Laboratory, Nagoya University, [5]National Institute of Polar Research

As pointed out by many researchers, the recent solar activities are very unusual; the solar activity during the last minimum in 2008-2009 was extremely low and that during the next maximum of sunspot cycle 24 shows much lower activities compared with the previous two solar maximums in cycle 22 and 23. In order to understand the complex system of the Earth's middle and upper atmosphere, these solar activities will give us important information and/or good opportunities for searching the basic states of the system both from the observations and GCM simulations. Comprehensive studies by observations from space, ground-based ones, and numerical simulations will enable us to understand the polar mesosphere, thermosphere, and ionosphere quantitatively. In order to understand variations of the polar ionosphere from the solar minimum to maximum periods, we have made EISCAT experiments in January 2011, March, 2012, and March 2013. For example, ionospheric variations were observed during solar flare and CME events on March 12, 2012. These EISCAT data clearly show an example of the solar wind, magnetosphere, and ionosphere coupling. In addition to the EISCAT observations, we have also investigated variations of the polar thermosphere during periods of significant solar activities from GCM simulations. In this presentation, we will introduce our research activities mainly related to the "Role Of the Sun and the Middle atmosphere/thermosphere/ionosphere In Climate (ROSMIC)" project in VarSITI.

Keywords: thermosphere, ionosphere, middle atmosphere, GCM, radar, aeronomy

Japan Geoscience Union Meeting 2014
(28 April - 02 May 2014 at Pacifico YOKOHAMA, Kanagawa, Japan)

PEM09-39 Room:501 Time:April 29 15:00-15:15

Enhancing our understanding of the atmosphere-ionosphere coupling with Low Earth Orbiting satellite missions

LIU, Huixin[1*] ; LUEHR, Hermann[2]

[1]Kyushu University, Japan, [2]GFZ, Germany

Low Earth Orbiting (LEO) satellites provide unique opportunities to observe the near-Earth space environment. Recent LEO satellite mission have been making rapid contribution to our understanding of the coupled atmosphere-ionosphere system by providing unprecedented observational evidences for the connection between ionospheric/thermosphric phenomena and their meteorological causes. This talk will briefly summarize the achievements of the decade-long CHAMP mission from the vertical coupling point of view, which is followed by a scientific perspective on the newly launched 3-satellite constellation SWARM mission.

Japan Geoscience Union Meeting 2014
(28 April - 02 May 2014 at Pacifico YOKOHAMA, Kanagawa, Japan)

PEM09-40 Room:501 Time:April 29 15:15-15:30

Multipoint airglow imaging measurements of mesospheric gravity waves over Japan

SUZUKI, Shin[1*] ; SHIOKAWA, Kazuo[1] ; OTSUKA, Yuichi[1]

[1]Solar-Terrestrial Environment Laboratory, Nagoya University

Atmospheric gravity waves significantly contribute to the wind/thermal balances in the mesosphere and lower thermosphere (MLT) through their vertical transport of horizontal momentum. It has been reported that the gravity wave momentum flux preferentially associated with the scale of the waves; the momentum fluxes of the waves with a horizontal scale of 10-100 km are particularly significant. Airglow imaging is a useful technique to observe two-dimensional structure of small-scale (<100 km) gravity waves in the MLT region and has been used to investigate global behavior of the waves. The Solar-Terrestrial Environment Laboratory, Nagoya University, has made long-term airglow imaging observations with ground-based all-sky airglow imagers using the Optical Mesosphere and Thermosphere Imager (OMTI) system. Each airglow imager of OMTI has interference filters on rotating wheels to observe airglow emissions in the vicinity of the mesopause (OI 557.7-nm, emission height ∼96 km; OH Meinel-bands, ∼86 km) and the ionosphere (OI 630.0-nm, ∼250 km). Four airglow imagers, which each has the field-of-view with a size of 5 deg x 5 deg in longitude and latitude at the mesopause height, has been in operation in Japan and, as a whole system, they nearly cover all part of Japan. This multipoint network enables us to detect propagation signatures and the spatial extent of MLT waves over a much wide range than ever.

In the presentation, we will report recent results of the MLT gravity waves having a very large spatial extent based on the OMTI multipoint measurements, such as a coherent gravity wave ducting and large concentric gravity wave rings possibly induced by a typhoon; these results offer new insight into dynamical coupling process between the lower and upper atmosphere.

Japan Geoscience Union Meeting 2014
(28 April - 02 May 2014 at Pacifico YOKOHAMA, Kanagawa, Japan)

PEM09-41 Room:501 Time:April 29 15:30-15:45

Exploration into evolution of solar-planetary environments: Solar variation and a variation and atmospheric escape

SEKI, Kanako[1*] ; TERADA, Naoki[2] ; YOKOYAMA, Takaaki[3] ; SUZUKI, Takeru[4] ; IMAMURA, Takeshi[5] ; NAKAMURA, Takuji[6] ; NAKAGAWA, Hiromu[2] ; KURODA, Takeshi[2] ; FUJIMOTO, Masaki[5] ; ESPE, Project team[1]

[1]Solar-Terrestrial Environment Laboratory, Nagoya University, [2]Graduate School of Science, Tohoku University, [3]School of Science, University of Tokyo, [4]School of Science, Nagoya University, [5]Institute of Space and Astronautical Science, JAXA, [6]National Institute of Polar Research

How has the atmosphere of terrestrial planets responded to the evolution of the sun, a center star of our solar system? In order to answer the question of the coevolution of our sun and the planetary environment " planetosphere ", planetary exploration missions have been promoted and related interdisciplinary researches are rapidly developing worldwide. It is scheduled that NASA ' s Mars mission MAVEN arrives at Mars in September 2014 and Venus weather explorer AKATSUKI arrives at Venus at the end of 2015. These missions will provide us new observations and insights in this field. Moreover, the solar evolution is included in one of the next emphasized problems in VarSITI program that starts in 2014, and the time of international collaborations is expected to come. On the other hand, the past researches in the solar-terrestrial sciences have had large emphasis on understanding of dynamic variations of the present sun and planetary environment. The interdisciplinary researches of understanding the coevolution of the sun and planetosphere over past four billion years or so are in the incunabula but start to develop rapidly. In this presentation, we will introduce an attempt to investigate the coevolution of the sun and planetosphere by combining large-scale numerical simulations and the latest observations based on international collaborations and cooperation of solar physics, solar-terrestrial physics, aeronomy, and meteorology.

Keywords: solar evolution, planetosphere, atmospheric escape, coupling of lower and upper atmosphere, climate change, evolution of planetary atmosphere

Japan Geoscience Union Meeting 2014
(28 April - 02 May 2014 at Pacifico YOKOHAMA, Kanagawa, Japan)

PEM09-42 Room:501 Time:April 29 15:45-16:00

Role of global electric circuit in solar-climate connection

TAKAHASHI, Yukihiro[1*] ; SATO, Mitsuteru[1]

[1]Department of Cosmosciences, Hokkaido University

Global electric circuit model was proposed log time ago, in 1930s, in which thunderstorm plays a role of generator, and the ground and the ionosphere work as a spherical capacitor. We need to reconstruct this simple model, taking into account 3 aspects: 1) global-scale nonuniformities both of ionospheric conductivity and of the distribution of the generators, 2) connections between the troposphere and D-region, considering the effects of TLEs, such sprites and blue jets, 3) establishing the observational methodology for global electric field, excluding the effect of cloud existing just above the observation sites. Recently, the relationship between the global circuit and solar-climate connection was pointed out. Here we introduce an example, which indicates the roles of thunderstorm or its resultant electric circuit in solar-climate connection. Global relationship between thunderstorm/cloud activities and solar parameters are examined based on lightning measurement by Global ELF observation Network (GEON) operated by Hokkaido University and Outgoing Longwave Radiation (OLR) intensity. It was found that the number of lightning stokes in Asia Maritime Continent (AMC) varies with about month periodicity in the period from February to June 2004 and shows positive correlation (R= ˜0.8) with OLR in the Western Pacific Warm Pool (WPWP). On the other hand, OLRs in the central Africa and some other tropical areas show negative correlation with the number of lightning stokes in the AMC in that period. It is also found that the galactic cosmic rays or UV intensity associated with solar activity indicates good correlation with tropical OLR or lightning activity in AMC. One explanation to connect such global variations in thunderstorm / cloud amount with solar parameters would be the electrical circuit involving lower and upper atmospheres. If the ionospheric electric field modulates the potential gradient in the lower atmosphere, it could cause the re-distribution of ionized atmospheric particles, which may, in turn, change the generation / reduction speed of cloud particles.

Keywords: global electric circuite, solar-climate connection, TLEs, thunderstorm activity, Asia Maritime Continent

Japan Geoscience Union Meeting 2014
(28 April - 02 May 2014 at Pacifico YOKOHAMA, Kanagawa, Japan)

PEM09-43 Room:501 Time:April 29 16:15-16:30

A Realistic Whole Atmosphere-Ionosphere Modeling and Collaboration with Observations

JIN, Hidekatsu[1*] ; MIYOSHI, Yasunobu[2] ; FUJIWARA, Hitoshi[3] ; SHINAGAWA, Hiroyuki[1] ; MATSUO, Tomoko[4]

[1]National Institute of Information and Communications Technology, [2]Kyushu University, [3]Seikei University, [4]National Oceanic and Atmospheric Administration

There has been an increasing number of collaboration between modeling and observation for the study of upper atmospheric variability and its relation to the lower atmosphere. Observations are used as the forcing inputs to models as well as for their validation. Outputs from models can be useful for the interpretation of observed phenomena owing to their sufficient spatial and temporal coverage, especially for the analysis of phenomena whose effects extend beyond the several atmospheric layers. Recently, we have examined the effects of a prominent stratospheric sudden warming (SSW) in January 2009 on the upper atmospheric variability, by using a whole atmosphere-ionosphere coupled model called GAIA. The model used the meteorological reanalysis data as realistic lower atmospheric forcing, and we compared the model outputs with the satellite observations of upper atmosphere [Jin et al., 2012; Liu et al., 2012]. The comparison suggests that the model can reproduce the overall major features of the observed perturbed variations in the upper atmosphere during the SSW period, which ensures the usage of model output for the detail analysis of vertical coupling mechanism during the event.

In this study, we applied the same method for the inclusion of realistic lower atmospheric forcing and carried out a whole atmosphere-ionosphere simulation for longer period. We will show the relation of ionospheric variability to the climatological and irregular variations in the lower atmosphere including several SSW events. Initial results from data assimilation experiment will also be shown as an example of model-observation collaboration.

Keywords: ionosphere, thermosphere, atmospheric vertical coupling, simulation, data assimilation, space weather

Japan Geoscience Union Meeting 2014
(28 April - 02 May 2014 at Pacifico YOKOHAMA, Kanagawa, Japan)

PEM09-44 Room:501 Time:April 29 16:30-16:45

Contribution of the Optical Mesosphere Thermosphere Imagers (OMTIs) to VarSITI

OTSUKA, Yuichi[1*] ; SHIOKAWA, Kazuo[1]

[1]Solar-Terrestrial Environment Laboratory, Nagoya University

The Optical Mesosphere Thermosphere Imagers (OMTIs) consist of thirteen all-sky cooled-CCD imagers, five Fabry-Perot interferometers (FPIs), three meridian scanning photometers, and four airglow temperature photometers. They measure two-dimensional pattern, Doppler wind, and temperature through airglow emissions from oxygen (wavelength: 557.7 nm) and OH (near infrared band) in the mesopause region (80-100 km) and from oxygen (630.0 nm) in the thermosphere/ionosphere (200-300 km). They are in automatic operation at Australia, Indonesia, Thailand, far-east Russia, Japan, Canada, Hawaii, and Norway. Station information and quick look plots are available at http://stdb2.stelab.nagoya-u.ac.jp/omti/. We show recent results obtained by OMTIs particularly focusing on the penetration of short-period gravity wave from the lower atmosphere to the thermosphere and the ionosphere, which are often recognized as meridum-scale traveling ionospheric disturbances (MSTIDs) in the ionosphere. We also show some results obtained by the multi-point Fabry-Perot interferometers. These observations will contribute the next SCOSTEP program VarSITI, particularly to the ROSMIC Project.

Keywords: airglow, ionosphere, thermosphere, mesosphere, gravity wave, traveling ionospheric disturbance

Japan Geoscience Union Meeting 2014
(28 April - 02 May 2014 at Pacifico YOKOHAMA, Kanagawa, Japan)

PEM10-01 Room:414 Time:April 29 14:15-14:35

Modeling Turbulence in Space Plasmas

CHO, Jungyeon[1*]

[1]Chungnam National University

Space plasmas are magnetized and in turbulent states. I will briefly introduce properties of turbulence in a strongly magnetized medium. Turbulence in space plasmas is involved with various length scales. In general, different descriptions should be used for different scales. On large scales, plasma turbulence can be described in the framework of magnetohydrodynamics (MHD). In the first par of the talk, I will focus on MHD turbulence in the presence of a strong mean field. I will discuss energy cascade and structure of turbulence in this regime. On the other hand, on small scales near the proton gyro-scale, we cannot use MHD. In the second part of the talk, I will discuss how we can treat magnetized turbulence on small scales. I will also discuss properties and scaling relations of waves and turbulence in this regime.

Keywords: turbulence, MHD, waves, magnetic field

Japan Geoscience Union Meeting 2014
(28 April - 02 May 2014 at Pacifico YOKOHAMA, Kanagawa, Japan)

PEM10-02 Room:414 Time:April 29 14:35-14:50

Nonlinear evolution of envelope-modulated Alfvenic turbulence in expanding accelerating solar wind plasmas

NARIYUKI, Yasuhiro[1*] ; HADA, Tohru[2] ; TSUBOUCHI, Ken[3]

[1]Faculty of Human Development, University of Toyama, [2]E.S.S.T., Kyushu University, [3]Tokyo Institute of Technology

It is well known that low-frequency Alfvenic turbulence is ubiquitously observed in solar wind plasmas. There is great interest in nonlinear evolution of the Alfvenic turbulence, since the observational studies clarified that the Alfvenic turbulence disappear with the increasing heliocentric distance and the fully-developed turbulence becomes dominant. Although most past studies on Alfvenic turbulence assumes uniform background plasmas and magnetic fields, the effects of the inhomogeneity may not be negligible in the inner-heliosphere, in which several future spacecraft missions are planned. It is important that even if the wave reflection due to the inhomogeneity is negligible, the inhomogeneity of background plasmas and magnetic field may affect the nonlinear interaction among waves through contraction and reflection of the waves and the radial dependence of the back ground parameters such as the Alfven velocity and the ion cyclotron frequency. In the present study, the nonlinear evolution of low-frequency, quasi-parallel propagating Alfvenic turbulence is studied by using the two-dimensional hybrid accelerating expanding box model. The dependence of the nonlinear evolution of Alfvenic turbulence on the effects of the inhomogeneity is discussed.

Keywords: solar wind, Alfvenic turbulence, ion kinetics

Japan Geoscience Union Meeting 2014
(28 April - 02 May 2014 at Pacifico YOKOHAMA, Kanagawa, Japan)

PEM10-03 Room:414 Time:April 29 14:50-15:10

Development and Properties of Compressible MHD Turbulence in High-Beta Plasmas

JONES, Thomas[1*] ; RYU, Dongsu[2] ; PORTER, David[1] ; EMMERICK, Andrew[1] ; CHO, Jungyeon[3]

[1]University of Minnesota, [2]Ulsan National Institute of Science and Technology, [3]Chungnam National University

Many cosmic plasmas, including those in the solar wind and extra-galactic environments, are high beta = P_g/P_B>1, so that as turbulence develops, magnetic stresses are, at least initially, weak. As the turbulence evolves, magnetic stresses become increasingly important on scales below the driving scales. Depending on the initial field strength and topology this evolution can take many large-scale eddy times to reach saturation. Even in subsonic turbulence, shocks can form and influence turbulence evolution and properties. We have carried out an extensive set of high resolution compressible MHD simulations of the evolution of such turbulence for a range of initial magnetic field strengths and topologies. Here we report on their properties and the astrophysical implications of those properties. This work is supported at the University of Minnesota by the US National Science Foundation and the Minnesota Supercomputing Institute.

Keywords: MHD Turbulence, High Beta Plasma

Japan Geoscience Union Meeting 2014
(28 April - 02 May 2014 at Pacifico YOKOHAMA, Kanagawa, Japan)

PEM10-04 Room:414 Time:April 29 15:10-15:30

Instabilities and turbulence near the heliopause

POGORELOV, Nikolai[1*] ; BOROVIKOV, Sergey[2] ; ZANK, Gary[1] ; ZHANG, Ming[3]

[1]Department of Space Science, University of Alabama in Huntsville, [2]CSPAR, University of Alabama in Huntsville, [3]Department of Physics and Space Sciences, Florida Institute of Technology

Recent observations from the Voyager 1 spacecraft show that it is sampling the local interstellar medium (LISM). This is quite surprising because no realistic, steady-state model of the solar wind (SW) interaction with the LISM gives the inner heliosheath width as narrow as 30. This includes such models that assume a strong redistribution of the ion energy to the tails in the pickup ion distribution function. We show that the heliopause (HP), which separates the SW from the LISM, is not a smooth tangential discontinuity, but rather a surface subject to Rayleigh-Taylor-type instabilities which can result in the LISM material penetration deep inside the SW. We also show that the HP flanks are always subject to a Kelvin-Helmholtz instability. The instabilities are considerably suppressed near the HP nose by the heliospheric magnetic field in steady-state models, but reveal themselves in the presence of solar cycle effects. We argue that Voyager 1 may be in one of such instability regions and therefore observing plasma densities much higher than those in the pristine SW. These results may be an explanation of the Voyager 1 early penetration into the LISM. We also show that there is a possibility that the spacecraft may enter the SW again before it finally leaves the heliosphere.

We demonstrate a spontaneous transition to chaotic behavior in the heliosheath region covered by the heliospheric current sheet. Additionally, we analyze the behavior of the heliopause in the heliotail and show that it becomes violently unstable beyond 1000 AU, which results in the interpenetration of the solar and interstellar plasma.

Keywords: ISM: kinematics and dynamics, ISM: magnetic fields, solar wind, Sun: heliosphere, turbulence

Japan Geoscience Union Meeting 2014
(28 April - 02 May 2014 at Pacifico YOKOHAMA, Kanagawa, Japan)

PEM10-05 Room:414 Time:April 29 15:30-15:45

Wave reflection-driven accretion in active solar-type star winds

SUZUKI, Takeru[1*] ; TERANISHI, Yasumasa[1]

[1]Nagoya University

In MHD simulations for winds from active solar-type stars by Suzuki et al.(2013), intermittent but long-time accretion phenomena were observed even though the Poynting flux associated with Alfven waves is directed outward. In this talk, we present the detailed mechanism how this counter-streaming accretion takes place. Alfven waves generated from a stellar surface are stochastically trapped in a transient density hole, and the magnetic pressure with the waves further dig the density hole. Eventually, this hole works as an efficient mirror against out-going Alfven waves. As a result, out-going waves are reflected and the reflected component excites counter streaming flow.

Keywords: Wave, MHD, stellar wind, accretion

Japan Geoscience Union Meeting 2014
(28 April - 02 May 2014 at Pacifico YOKOHAMA, Kanagawa, Japan)

PEM10-06 Room:414 Time:April 29 15:45-16:00

Physical Picture of 2-1/2D Driven Collisionless Magnetic Reconnection

CHENG, Chio[1*] ; INOUE, S.[2] ; ONO, Y.[3] ; HORIUCHI, R.[4]

[1]Plasma and Space Science Center, National Cheng Kung University, Taiwan, [2]Graduate School of Engineering, Universty of Tokyo, Japan, [3]Department of Advanced Energy, University of Tokyo, Japan, [4]National Institute of Fusion Science, Japan

The physical picture of how electrons and ions flow, how the electric and magnetic fields change, and how particles gain energy will be presented for the 2-1/2D collisionless driven magnetic reconnection. The 2-1/2 dimensional collisionless reconnection studies are performed using the particle simulation PASMO code [1] and theoretical analysis. In particular, we will provide the physical mechanism of how the poloidal current (including the Hall current in the downstream region) is generated and how the electrostatic potential is produced in the poloidal plane. The physical picture of how the quadrupole magnetic field and electrostatic potential are generated in the 2-dimensional (poloidal) plane is different from the one presented by Uzdensky and Kulsrud.[2]

[1] H. Ohtani and R. Horiuchi, Plasma Fusion Res., 4, 024 (2009)
[2] D. A. Uzdensky and R. M. Kulsrud, Phys. Plasma, 13, 062305 (2006)

Keywords: magnetic reconnection, numerical simulation, space plasma, laboratory experiment

Japan Geoscience Union Meeting 2014
(28 April - 02 May 2014 at Pacifico YOKOHAMA, Kanagawa, Japan)

PEM10-07 Room:414 Time:April 29 16:15-16:35

Turbulence and shocks in high-beta plasmas

RYU, Dongsu[1*]

[1]Department of Physics, UNIST

High-beta plasmas are common in astrophysical environments, such as the intracluster medium (ICM) of galaxy clusters and the interplanetary medium (IPM) of the solar system. Observations and theoretical arguments suggest that the plasmas in such environments are in the state of turbulence, where highly nonlinear and complex physics is involved. Here we report high-resolution simulations to study the turbulence in high-beta plasmas. Along with the properties of the turbulence, we discuss the role of shocks and the energy dissipation.

Keywords: turbulence, shock wave, high-beta plasma

Japan Geoscience Union Meeting 2014
(28 April - 02 May 2014 at Pacifico YOKOHAMA, Kanagawa, Japan)

PEM10-08 Room:414 Time:April 29 16:35-16:50

Acceleration and Diffusion of Cosmic Rays in Supernova Remnants in a Multi-Phase interstellar Medium

ROH, Soonyoung[1*] ; INUTSUKA, Shu-ichiro[2] ; INOUE, Tsuyoshi[3]

[1]Graduate School of Science, Nagoya University, [2]Graduate School of Science, Nagoya University, [3]Department of Physics and Mathematics, Aoyama Gakuin University

Supernova remnants (SNRs) are one of the most powerful cosmic phenomena and are thought to be the dominant source of Galactic cosmic rays (CRs). A recent report by Funk et al. (2013) has shown an unequivocal signature of pion-decay in the gamma-ray spectra of SNRs. This provides strong evidence that high-energy protons are accelerated in SNRs. On the other hand, Fukui et al. (2012) showed that pion-decay from protons dominates in emission from SNR RX J1713 based on the spatial correlation of gamma-rays and molecular line emission. The actual gamma-ray emission from pion-decay should depend on the diffusion of CRs in a multi-phase interstellar medium with molecular clouds (Inoue et al. 2012). In order to quantitatively describe the diffusion of high energy CRs from acceleration sites, we have performed test particle numerical simulations using a three-dimensional magnetohydrodynamics (MHD) simulation data cube provided by Inoue et al. (2012). In this presentation, we analyze a realistic diffusion coefficient of cosmic rays in simulated SNRs, and discuss the possible implications for X-ray and gamma-ray observations.

Keywords: Supernova Remnants, Diffusion of Cosmic Rays, Acceleration of Cosmic Rays, Pion-decay

Japan Geoscience Union Meeting 2014
(28 April - 02 May 2014 at Pacifico YOKOHAMA, Kanagawa, Japan)

PEM10-09 Room:414 Time:April 29 16:50-17:05

Superdiffusion in turbulence and shock acceleration

YAN, Huirong[1*]

[1]Kavli Institute of Astronomy & Astrophysics, Peking U

Cosmic ray (CR) transport and acceleration are determined by the properties of turbulent magnetic field. We use the models of magnetohydrodynamic turbulence that were tested in numerical simulation, in which turbulence is injected at large scale and cascades to to small scales. I shall address, in particular, the cross field transport of CRs. I shall demonstrate both analytically and numerically that particles are superdiffusive on small scales. We consider both super- and sub-Alfvenic cases. In the sub-Alfvenic case, the transport in the perpendicular direction is proportional with M_Aˆ4, consistent with our earlier analytical prediction. Implication for shock acceleration is discussed and we show that the difference between acceleration at perpendicular shock and parallel shock is marginalized in the presence of superdiffusion.

Keywords: turbulence, superdiffusion, particle, shock, acceleration, transport

Japan Geoscience Union Meeting 2014
(28 April - 02 May 2014 at Pacifico YOKOHAMA, Kanagawa, Japan)

PEM27-01 Room:421 Time:May 1 16:15-16:30

Micro-TypeIII radio bursts and outer corona

MORIOKA, Akira[1*] ; MIYOSHI, Yoshizumi[2] ; KASABA, Yasumasa[3] ; MASUDA, Satoshi[2] ; IWAI, Kazumasa[4] ; MISAWA, Hiroaki[1]

[1]PPARC, Tohoku University, [2]STEL, Nagoya University, [3]Dep. of Gephys. Tohoku University, [4]NSRO, NAOJ

We presents detailed features of micro-typeIII radio bursts and its relation to the outer corona, by using long-term observations made by the Geotail satellites. Micro-typeIII radio bursts are elements of the so-called type III storm, and are characterized by short-lived, continuous, and weak emissions. Their average power is estimated to be well below that of the largest type III burst by 6 orders of magnitude. The activity of micro-typeIII bursts with respect to the solar activity, lower frequency limit of the bursts and its relation to the solar activity, and the configuration of magnetic field line of which source electrons are trapped are investigated. The relationship between streamers and micro-typeIII bursts are discussed by using STEREO observations.

Keywords: micro-type-III burst, outer corona, solar radio burst, interplanetary space, inner-heliosphere

Japan Geoscience Union Meeting 2014
(28 April - 02 May 2014 at Pacifico YOKOHAMA, Kanagawa, Japan)

PEM27-02 Room:421 Time:May 1 16:30-16:45

Coronal vector magnetic field and the plasma beta determined from the NoRH and multiple satellites observations

IWAI, Kazumasa[1*] ; SHIBASAKI, Kiyoto[1] ; NOZAWA, Satoshi[2] ; TAKAHASHI, Takuya[3] ; SAWADA, Shinpei[2] ; KITAGAWA, Jun[4] ; MIYAWAKI, Shun[2] ; KASHIWAGI, Hirotaka[5]

[1]Nobeyama Solar Radio Observatory, National Astronomical Observatory of Japan, [2]Department of Science, Ibaraki University, [3]Graduate School of Science, Kyoto University, [4]Solar-Terrestrial Environment Laboratory, Nagoya University, [5]Planetary Plasma and Atmospheric Research Center, Tohoku University

In the solar corona, there are various kinds of eruptive phenomena, such as flares and coronal mass ejections, which are caused by interactions between the coronal magnetic field and plasma. Hence, it is important to precisely measure the coronal plasma parameters, including the magnetic field, plasma density, and temperature, in order to understand the mechanisms that generate these eruptive coronal phenomena.

The solar coronal vector magnetic field, plasma density, and temperature is derived from coordinated observations of the radio thermal free-free emission using the Nobeyama Radioheliograph (NoRH) and multiple line-of-sight extreme ultraviolet observations using the Solar Dynamic Observatory (SDO) and the Solar Terrestrial Relations Observatory (STEREO). We observed a post-flare loop on the west limb on 2013 April 11. The line-of-sight magnetic field was derived from the circularly polarized free-free emission observed by NoRH, which was combined with the tilt angle toward the Earth observed with STEREO and converted to a vector magnetic field. The emission measure and temperature were derived from the Atmospheric Imaging Assembly (AIA) onboard SDO. The derived temperature was used to estimate the emission measure from the NoRH radio free-free emission observations. The derived density from NoRH was 40% larger than that determined using AIA, which is due to the fact that the low temperature plasma is not within the temperature coverage range of the AIA filters used in this study. The derived plasma parameters (vector magnetic field, plasma density, and temperature) were used to derive the plasma beta, which is a ratio between the magnetic pressure and the plasma pressure. The derived plasma beta is about 6.2×10^{-3} at the pool top region. The plasma parameters derived in this study were all based on observational results, and the calculated vector magnetic field presented herein is one of the least affected by assumptions or modeling ever derived.

Keywords: Sun, corona, magnetic fields, polarization observation, Nobeyama Radioheliograph

Japan Geoscience Union Meeting 2014
(28 April - 02 May 2014 at Pacifico YOKOHAMA, Kanagawa, Japan)

PEM27-03 Room:421 Time:May 1 16:45-17:00

Relationships among cosmic ray intensity, the photospheric magnetic field, and solar wind speed

HAKAMADA, Kazuyuki[1*] ; TOKUMARU, Munetoshi[2] ; FUJIKI, Ken'ichi[2] ; KOJIMA, Masayoshi[2]

[1]Chubu University, [2]Solar-Terrestrial Environment Laboratory

We visualize three-dimensional structure of the coronal magneic field by using the Radial-Field model for the coronal magnetic field devised by Hakamada with synoptic maps of photospheric magnetic field observed by the NSO/Kitt Peak, USA. As the rsults, we obtained the radial component of the photospheric magnetic field (Br_pho) and the one of the coronal magnetic field (Br_sou) on the source surface on the same field line in the coronal magnetic field. We estimate the solar wind speed (SWS) by using IPS technique divised by STE Lab, Nagoya Univiersity. According to our previous analysis on the Carrignton rotation bases, Log10|Br_pho|, Log10|Br_sou|show good correlations with the SWS for the data of [-1.0 <= Log10|Br_pho|<= 1.5, (0.1 G <= |Br_pho|<= 31.6 G), -1.5 <= Log10|Br_sou|<= 0.0, (0.0316 G <= |Br_sou|<= 1.0 G)]. In this study, we add the intensity of Oulu neutorn monitor (NM), and study relations among rotation averages of these NM, SWS, and Log10|Br_pho|. We found good simple correrations coefficients between Log10|Br_pho|-NM (r=-0.773), and SWS-NM (r=0.703), as well as, a good multiple correlaion (r = 0.785) among them by using the regression equation in the form of NM = a + b ∗SWS + c ∗log10|Br_pho|with a = 6363, b = 1.186, and c = -1400.0. However, Log10|Br_pho|-SWS also shows good simple correlation (r=-0.802). We calculated partial correlation coefficients between (a) Log10|Br_pho|-NM, (b) SWS-NM, (c) Log10|Br_pho|-SWS and obtained (a) r=-0.294, (b) r=0.130, (c) r=-0.364. These results suggest that, althogh the cosmic ray intensities shown by NM is determined by the intensity of photospheric magnetic fields on the open field lines and the solar wind speed occupied by these field lines, the dpendence of magnetic field is stronger than the one of wind speed.

Keywords: cosmic ray intensity, photoshpheric magnetic field, solar wind speed

Japan Geoscience Union Meeting 2014
(28 April - 02 May 2014 at Pacifico YOKOHAMA, Kanagawa, Japan)

PEM27-04 Room:421 Time:May 1 17:00-17:15

Does a Plasma Tail of Comet ISON (C/2012 S1) Cause the Interplanetary Scintillation?

IJU, Tomoya[1*] ; ABE, Shinsuke[2] ; TOKUMARU, Munetoshi[3]

[1]Particle and Astrophysical Science, Nagoya-University, [2]Aerospace Engineering, CST, Nihon-University, [3]Solar-Terrestrial Environment Laboratory, Nagoya-University

C/2012 S1 (ISON) (referred to as Comet ISON) showed a well-developed plasma tail (longer than 0.1 AU) before its perihelion passage on November 28, 2013. A plasma tail consists of ionized gases emitted from a cometary nucleus and orients itself in the anti-solar direction by an interaction with the solar wind. In this study, we investigated the plasma tail of Comet ISON with interplanetary scintillation (IPS) data. The IPS is a scattering phenomenon of radio waves by density fluctuations of the solar wind, and it is well known that interplanetary disturbances such as coronal mass ejections (CMEs) cause an abrupt increase in IPS. A cometary plasma tail may also be a potential cause for the IPS enhancement, while observational studies for C/1972 E1 (Kohoutek), 1P/Halley and other are still controversial (*e.g.* Ananthakrishnan *et al.*, 1975, 1987; Slee *et al.*, 1987; Abe *et al.*, 1997; Roy *et al.*, 2007). We identified radio sources whose lines-of-sight approached to Comet ISON's plasma tail between November 1 and 28, and obtained their IPS data using the Solar Wind Imaging Facility (Tokumaru *et al.*, 2011) of the Solar-Terrestrial Environment Laboratory, Nagoya University. From examinations for them, we confirmed four IPS enhancement events, which is likely to be related to the plasma tail passage. In this session, we report this preliminary result for them and discuss an IPS of a cometary plasma tail origin.

Keywords: Comet ISON (C/2012 S1), Cometary plasma tail, Radio scintillation

Japan Geoscience Union Meeting 2014
(28 April - 02 May 2014 at Pacifico YOKOHAMA, Kanagawa, Japan)

PEM27-05 Room:421 Time:May 1 17:15-17:30

Effects of phase and group velocities on wave spectra observed in the solar wind

TSUGAWA, Yasunori[1*] ; KATOH, Yuto[1] ; TERADA, Naoki[1]

[1]Department of Geophysics, Tohoku University

Waves propagating in a plasma medium which has a relative velocity to the observer are differently observed in the spectra from those in the plasma rest frame. As known in general, the observed frequency is Doppler shifted by the relative velocity between the medium and the observer, V_{rel}. The frequency shift is the result of the difference of the phase velocities of the waves in the medium rest frame and in the observer frame. When the wave vector has a finite angle with respect to V_{rel} and the component of V_{rel} parallel to the wave vector is considerable to the phase velocity, the difference of the phase velocities between the frames and the frequency shift become significant.

We note that the observed spectral density is also modified by V_{rel}. The modification of the spectral density is the result of the difference of the group velocities of the waves in the medium rest frame and in the observer frame. When the component of V_{rel} parallel to the group velocity vector is considerable to the group velocity, the difference of the group velocities between the frames and the modification of the spectral density become significant. In order to estimate the amount of the modification, we derive the analytical expression of the modified spectral density in the observer frame.

It is important to consider not only the frequency shift but also the modification of the spectral density of waves observed by spacecraft in a moving plasma, such as the solar wind. Indeed, the phase and group velocities of whistler-mode waves cause significant frequency shift and modification of the spectral density in the solar wind. By the modification of the spectral density, we can explain the characteristic properties of '1 Hz waves', which have been generally observed in the upstream regions of various bodies, and suggest that the broadband upstream whistlers are the same source waves. The understanding of the effects is necessary to reveal the true nature of waves propagating in a moving plasma and to discuss their generation processes.

Japan Geoscience Union Meeting 2014
(28 April - 02 May 2014 at Pacifico YOKOHAMA, Kanagawa, Japan)

PEM27-06 Room:421 Time:May 1 17:30-17:45

Monochromatic whistler waves at 8 Hz observed by Kaguya above the terminator of the Moon

HASHIMOTO, Akira[1] ; NAKAGAWA, Tomoko[1*] ; TSUNAKAWA, Hideo[2] ; TAKAHASHI, Futoshi[2] ; SHIBUYA, Hidetoshi[3] ; SHIMIZU, Hisayoshi[4] ; MATSUSHIMA, Masaki[2]

[1]Information and Communication Engineering,Tohoku Institute of Technology, [2]Deparment of Earth and Planetary Sciences, Tokyo Institute of Technology, [3]Department of Earth and Environmental Sciences, Graduate School of Science and Technology, Kumamoto, [4]Earthquake Research Institute, University of Tokyo

Magnetic fluctuations around the moon are characterized with 2 major categories: (1) large amplitude monochromatic waves of 0.01 Hz and (2) monochromatic or non-monochromatic whistler waves, both observed on the dayside surface of the moon or above the terminator. Their generation is associated with (1) the solar wind ions or (2) electrons, respectively, reflected at the surface of the moon or the local crustal magnetic field. The monochromatic whistler waves are found at 1-2 Hz with left-handed polarization due to the Doppler shift caused by the solar wind flow. The frequency range is determined by the group velocity of the whistler waves that can overcome the solar wind speed.

Differently from the previously known characteristics, a new type of monochromatic waves was found at 8 Hz in the magnetic field data obtained by MAP/LMAG onboard Kaguya. They concentrated above the terminator. They propagated in the direction of the background magnetic field and showed right-hand polarization. They are thought to be whistler waves propagating down-stream, and the frequency was up-shifted due to the Doppler shift.

Keywords: moon, SELENE, KAGUYA, MAP/LMAG, whistler wave, solar wind

Japan Geoscience Union Meeting 2014
(28 April - 02 May 2014 at Pacifico YOKOHAMA, Kanagawa, Japan)

PEM27-P01 Room:Poster Time:May 1 18:15-19:30

Measurement result of the neutron monitor onboard the Space Environment Data Acquisition Equipment(SEDA-AP)

KOGA, Kiyokazu[1*] ; MURAKI, Yasushi[2] ; SHIBATA, Shoichi[3] ; YAMAMOTO, Tokonatsu[4] ; MATSUMOTO, Haruhisa[1] ; OKUDAIRA, Osamu[1] ; KAWANO, Hideaki[5] ; YUMOTO, Kiyohumi[5]

[1]JAXA, [2]Nagoya University, [3]Chubu University, [4]Konan University, [5]Kyushu University

To support future space activities, it is crucial to acquire space environmental data related to the space-radiation degradation of space parts and materials, and spacecraft anomalies. Such data are useful for spacecraft design and manned space activity.
SEDA-AP was mounted on ”Kibo” of the ISS (International Space Station) to measure the space environment at a 400-kilometer altitude.

Neutrons are very harmful radiation, with electrical neutrality that makes them strongly permeable. SEDA-AP measures the energy of neutrons from thermal to 100 MeV in real time using a Bonner Ball Detector (BBND) and a Scintillation Fiber Detector (FIB). BBND detects neutrons using He-3 counters, which have high sensitivity to thermal neutrons. Neutron energy is derived using the relative response function of polyethylene moderators of 6 different thicknesses. FIB measures the tracks of recoil protons caused by neutrons within a cubic arrayed sensor of 512 scintillation fibers. The charged particles are excluded using an anti-scintillator which surrounds the cube sensor, and the neutron energy is obtained from the track length of a recoil proton.

There are three sources of neutrons in space;
1. Albedo Neutrons
Produced by reactions of galactic cosmic rays or radiation belt particles with the atmosphere
2. Local Neutrons
Produced by the reactions of galactic cosmic rays or radiation belt particles with spacecraft
3. Solar Neutrons
Produced by accelerated particles in solar flares
An accurate energy spectrum of the solar neutrons includes important information on high-energy particle generation mechanism in a solar flare, because neutrons are unaffected by interplanetary magnetic fields. These data will become useful to forecast solar energetic particles in future. Some candidate events involving solar neutrons were found as a result of analyzing data of the solar flare of M>2 since September 2009.

Moreover, it is important to measure albedo neutrons, since protons generated by neutron decays are thought to originate from the radiation belt. This theory is called CRAND (Cosmic Ray Albedo Neutron Decay). Our observation result is consistent with the CRAND theory prediction in the case of low-energy parts. Moreover, the flux and angular distribution of local neutrons were estimated using the nuclear simulation code ”PHITS” to evaluate the influence of local neutrons on the structure of SEDA-AP and ”Kibo”.

The results of our analyses on solar and albedo neutrons are reported in this paper.

Japan Geoscience Union Meeting 2014
(28 April - 02 May 2014 at Pacifico YOKOHAMA, Kanagawa, Japan)

PEM27-P02 Room:Poster Time:May 1 18:15-19:30

Interplanetary emission observed by HISAKI (SPRINT-A) satellite

YAMAZAKI, Atsushi[1*] ; YOSHIOKA, Kazuo[1] ; MURAKAMI, Go[1] ; KIMURA, Tomoki[1] ; TSUCHIYA, Fuminori[2] ; KAGITANI, Masato[2] ; SAKANOI, Takeshi[2] ; TERADA, Naoki[3] ; KASABA, Yasumasa[3] ; YOSHIKAWA, Ichiro[4]

[1]Institute of Space and Astronautical Science / Japan Aerospace Exploration Agency, [2]Planetary Plasma and Atmospheric Research Center, Graduate School of Science, Tohoku University, [3]Dep. Geophysics Graduate School of Science Tohoku University, [4]The University of Tokyo

The HISAKI (SPRINT-A) satellite, which was launched last summer, has been observing the extreme ultraviolet emission around planets, such as Venus and Jupiter. In addition to the main observational target of Venus and Jupiter, HISAKI has detected the emission from interplanetary space. In this presentation the HISAKI observation of interplanetary emission is shown and its potential on the interplanetary issue is argued.

Keywords: HISAKI (SPRINT-A) satellite, extreme ultra violet emission, interplanetary, resonance scattering

Japan Geoscience Union Meeting 2014
(28 April - 02 May 2014 at Pacifico YOKOHAMA, Kanagawa, Japan)

PEM27-P03 Room:Poster Time:May 1 18:15-19:30

The Behavior of Distributions for Magnetic Polarities on the Surface of the Sun and Solar Minimum

SEINO, Mitsuhiro[1*] ; SHIMABUKURO, Tomomi[1]

[1]Department of Physics and Earth Sciences, Faculty of Science, University of the Ryukyus

Time series of satellite image data for SOHO/MDI Continuum and Magnetogram from 1997 to 2010, and for SDO/HMI Continuum and Magnetogram from 2011 to 2013 are analyzed. The new time series data derived from fractal analysis of the time series images illustrated in 1200x1200 pixels from 1997 to 2013 are generated and fractal measures and packing exponents are analyzed by box-counting method. Then the occupancies of sunspot pixels in Continuum and of pixels for the positive and negative magnetic polarities in Magnetogram are calculated and packing exponents for sunspot pixels in Continuum and packing exponents for positive polarity pixels and negative polarity pixels in Magnetogram are evaluated. For packing exponents of Continuum and Magnetogram from 1997 to 2013, power spectra with peaks are calculated by using Fourier transform, respectively. A first peak which appears the power spectra is determined, and time intervals between nearest neighbor peaks are valued. The correlations between sunspot numbers and occupancies of the positive and negative magnetic polarities for 17 years are anatomized. As the correlation coefficients are calculated by using the least squares method, the correlation between sunspot number and occupancy of positive magnetic polarities has a very high correlational relationship because the correlation coefficient is 0.86 and it for negative magnetic polarities is low.

Furthermore, the behavior of occupancies of sunspot pixels in Continuum and of pixels for the positive and negative magnetic polarities in Magnetogram and the packing exponents represented with time series are described in detail and discussed. Fluctuations for occupancies of positive magnetic polarities are similar to it for Zurich number from 1997 to 2013. As observing the occupancies and packing exponents of positive and negative magnetic polarities, the two and three different fluctuations appear in (1) 1997-2005 and 2009 and (2) 2006-2008 including the time period that solar cycle 24 began on January 4, 2008, respectively. In addition, the occupancies and packing exponents of them have a single fluctuation in (3) 2010-2013. Therefore, the periods for characterizing solar activity from 1997 to 2013 are divided into three periods in (1), (2), and (3). Specially, for 2 years before solar minimum on 2008, the packing exponents start fluctuating suddenly and sharply in 2006 and the fluctuation disappear in the end of 2009.

Keywords: Time Series Analysis, Fourier Analysis, SOHO/MDI Continuum, Magnetogram, Solar Minimum

Japan Geoscience Union Meeting 2014
(28 April - 02 May 2014 at Pacifico YOKOHAMA, Kanagawa, Japan)

PEM27-P04 Room:Poster Time:May 1 18:15-19:30

Fine spectral structures of a solar radio type-II burst observed with AMATERAS

SATO, Shintaro[1] ; MISAWA, Hiroaki[1*] ; TSUCHIYA, Fuminori[1] ; OBARA, Takahiro[1] ; IWAI, Kazumasa[2] ; MASUDA, Satoshi[3] ; MIYOSHI, Yoshizumi[3]

[1]PPARC, Tohoku Univ., [2]Nobeyama Solar Radio Observatory, NAOJ, [3]STE Lab., Nagoya Univ.

Solar radio type-II bursts are metric to hectometric radio bursts that show frequency drifting spectral structures caused by the plasma emission from shock-accelerated electrons. The bursts are known to sometimes show rapidly drifting fine structures; for example, about 20% of type-II bursts are composed of both negative and positive rapidly drifting elements, which are called as ”herringbone” structure (hereafter HB) [Roberts, 1959]. Such the drifting fine structures are interpreted as the motion of non-thermal energetic electron beams accelerated by the shock. However, their particle acceleration mechanisms and regions have not been understood well. The purpose of this study is to extract characteristics of the fine spectral structures of type-II bursts from high-resolution observations and investigate their acceleration processes.

AMATERAS is a ground-based solar radio receiving system developed in 2010 by Tohoku University [Iwai et al., 2012]. This system enables us to observe radio phenomena in 150 - 500 MHz with the 10 ms accumulation time and 61 kHz bandwidth. So far some type-II bursts with fine spectral structures have been observed. Among them, a type-II burst observed on November 12, 2010 around 200MHz showed distinctive fine structures whose spectral characteristics were different from those of HB. The fine structures showed no core structure which were normally confirmed in HB, but showed various rapidly drifting nature and composed whole body of a slowly negative-drifting type-II burst. The statistical drift rate analysis showed that negative drift cases were dominant and some of them indicated more than 100MHz/s. The particle speed for the drift rate by assuming a general coronal plasma density model, for example the Newkirk model [Newkirk, 1961], is estimated to be unrealistically fast. This implies that the rapidly drifting fine structures were generated by energetic electron beams in an outward moving steep density gradient region such as a shock front.

In this presentation, we will show revealed statistical characteristics of the fine structures and discuss inferred generation processes of the type-II burst. We will also introduce characteristics of fine spectral structures of the other events of type-II burst.

Keywords: Sun, radio wave, type-II burst, fine structure, generation process

Japan Geoscience Union Meeting 2014
(28 April - 02 May 2014 at Pacifico YOKOHAMA, Kanagawa, Japan)

PEM27-P05 Room:Poster Time:May 1 18:15-19:30

Spectral fine structure of solar radio bursts observed with IPRT/AMATERAS: Characteristics of Zebra Pattern

KANEDA, Kazutaka[1*] ; MISAWA, Hiroaki[1] ; TSUCHIYA, Fuminori[1] ; OBARA, Takahiro[1] ; IWAI, Kazumasa[2]

[1]PPARC, Tohoku University, [2]NSRO/NAOJ

It is known that there are a variety of complex fine structures in solar radio bursts in the meter to decimeter wave bands such as broadband pulsations, narrowband spikes, fiber bursts and zebra patterns (hereafter ZP). Since they are thought to be caused by some inhomogeneities or modulations of wave generation and/or radio propagation processes, they have significant information about plasma parameters and dynamical plasma processes in the solar corona. Among the various fine structures, ZP has a particularly characteristic spectral pattern with parallel drifting narrow stripes of enhanced emission. Although several models for generating ZP have been proposed so far, the generation mechanisms have not been revealed well yet.

AMATERAS (the Assembly of Metric-band Aperture Telescope and Real-time Analysis System) is a radio spectro-polarimeter installed in a large radio telescope named IPRT in Fukushima, which was developed for solar radio observations in 2010 by Tohoku University (Iwai et al., 2012). The specifications of this system are time resolution of 10 ms, frequency resolution of 61 kHz and the minimum detectable flux of 0.7 s.f.u. in the frequency range of 150 MHz to 500 MHz, which are enough to observe fine structures of solar radio bursts and analyze their spectral characteristics. In this study we focus on an event on June 21, 2011 associated with C7.7 class flare. In this event enhanced ZP appeared around 200MHz with about 30 stripes in fast drifting envelopes like type III bursts or broadband pulsations. The emission was strongly polarized in right-handed and shows a distinctive time delay of the left-handed component relative to the right-handed component by several tens msec increasing with emission frequency. In the presentation, we will show the characteristics of ZP precisely and also discuss the expected generation processes.

Keywords: solar radio, AMATERAS, zebra pattern

Japan Geoscience Union Meeting 2014
(28 April - 02 May 2014 at Pacifico YOKOHAMA, Kanagawa, Japan)

PEM27-P06 Room:Poster Time:May 1 18:15-19:30

Upgrade of the multi-station IPS system and solar wind observations at the cycle 24 maximum

TOKUMARU, Munetoshi[1*] ; FUJIKI, Ken'ichi[1] ; MARUYAMA, Kazuo[1] ; MARUYAMA, Yasushi[1] ; YAMASAKI, Takayuki[1] ; IJU, Tomoya[1]

[1]Solar-Terrestrial Environment Laboratory, Nagoya University

Since interplanetary scintillation (IPS) serves as a useful method to determine global distribution of the solar wind, IPS observations have been regularly conducted over more than 30 years using the multi-station system of the Solar-Terrestrial Environment Laboratory (STEL) of Nagoya University. Such long-term data collection is made possible by continuous maintenance and improvement of the system. The STEL has four antennas dedicated for IPS observations at Toyokawa, Fuji, Kiso, and Sugadaira. The system at Toyokawa was upgraded to a new antenna (called the Solar Wind Imaging Facility Telescope, SWIFT, Tokumaru et al., 2011) in 2008. After that, the observation control and data acquisition systems at Fuji and Kiso were upgraded in 2010 to enable 3-station IPS observations using Toyokawa, Fuji and Kiso antennas. However, the low-noise phased-array receivers of Fuji and Kiso antennas, which are a vital part to archive high sensitivity, remained unchanged, and some other parts such as reflectors, gears, motors, became superannuated. In order to improve these problems, we have performed extensive work for upgrading Fuji, Kiso and Sugadaira antennas since 2013.

The items for this upgrade are as follows; (1) installation of low-noise amplifiers using HEMTs (FE327-V5) and the phased-array control system, (2) development of the phase/gain calibration system using the loop method and the receiver temperature measurement system using a noise source for Fuji and Kiso antennas, (3) fabrication of reflector and replacement of gears and motors (for Kiso). The work at Fuji almost completed by the end of 2013, and that at Kiso will be made in this spring.

Owing to the upgrade project, IPS observations for 2013 was made for the period between April and August. Obtained IPS data clearly show that the fast wind reappears over the northern pole. This is not the case for the southern pole, and the slow wind is found to be dominant in the southern hemisphere. The disappearance and reappearance of the fast wind over the northern pole preceding that over the southern pole have been observed in solar maxima of two previous cycles, so that this is regarded as a common feature of the solar dynamo activity. While our IPS data for this cycle show good correlation between fast wind areas and polar fields, they reveal that the slope for this cycle differs from the ones for past cycle. This fact suggests that higher-order magnetic moments for this cycle may have more contribution for formation of fast winds than past cycles. The solar wind structure is expected to significantly change with declining solar activity toward the next minimum, and we intend to finish work for the upgrade project as soon as possible in order to miss observing this change.

Keywords: solar wind, interplanetary scintillation, heliosphere, solar cycle, space weather

Japan Geoscience Union Meeting 2014
(28 April - 02 May 2014 at Pacifico YOKOHAMA, Kanagawa, Japan)

PEM28-01 Room:413 Time:April 29 11:00-11:15

MLT dependence in the response of ionospheric electric fields at mid-low latitude during geomagnetic sudden commencement

TAKAHASHI, Naoko[1*] ; KASABA, Yasumasa[1] ; SHINBORI, Atsuki[2] ; NISHIMURA, Yukitoshi[3] ; KIKUCHI, Takashi[4] ; NAGATSUMA, Tsutomu[5]

[1]Graduate School of Science, Tohoku University, [2]Research Institute for Sustainable Humanosphere (RISH), Kyoto University, [3]University of California, Los Angeles, [4]Solar-Terrestrial Environment Laboratory, Nagoya University, [5]National Institute of Information and Communications Technology

The geomagnetic sudden commencement (SC) is one of the geomagnetic disturbance phenomena triggered by an enhancement of the magnetopause current associated with the compression of the magnetosphere due to solar wind disturbances [e.g., Araki, 1994]. Detailed evolution and propagating processes of the electromagnetic field associated with SCs are observed three-dimensionally in the entire geospace. Unlike magnetic storms and substorms which involve complex plasma physical processes, SCs can be identified as distinct magnetic variations that sharply change on a global scale. However, the characteristics of SCs have been extensively investigated mainly by means of the magnetic field variations obtained by ground-based observations, which could be affected by conductivities when deducing electric fields. Thus, investigating the electric field variations is needed to understand the transport of electromagnetic energy (Poynting fluxes, E$\times$B/μ) associated with SCs. In this study, we examined two critical subjects about the ionospheric electric field associated with SCs using the in-situ electric field data.

The in-situ ionospheric electric field was derived from the drift velocity observed by the Ionospheric Plasma and Electrodynamics Instrument (IPEI) onboard ROCSAT-1, which orbited at an ionospheric altitude (about 600 km), with magnetic field from the IGRF-10 model. We also used the geomagnetic field data from ground stations at the subauroral region, mid and low latitudes, and dip equator with a high time resolution of 1 second.

The first subject is the transmission time of the ionospheric electric field from the subauroral region to the dip equator. We found the simultaneous SC onset between the ionospheric electric field by the ROCSAT-1 observations and geomagnetic fields by ground-based observations, and the time delay in the peak amplitudes of the preliminary impulse (PI) and main impulse (MI) occur irrespective of the magnetic local time (MLT). In statistical analyses, we showed that peak signatures of the ionospheric electric field at the low latitude appeared simultaneously with that of the geomagnetic field at the subauroral region. We also found that the peak signature at the equatorial region was observed with the time delay, and its value is about 20-40 seconds in the PI peak and 80-140 seconds in the MI peak. The instantaneous onset can be explained by means of the TM_0 mode waves propagating at the speed of light in the Earth-ionosphere waveguide, while the time delay in the peaks is interpreted as the difference of the time constant L/R of an equivalent circuit. From these results, we demonstrated the transmission of the electric field from the subauroral region and the common energy transport process for both the PI and MI.

The second subject is the global structure of the ionospheric field. Ground-based observations are limited to mid and low latitudes, and provide only the horizontal component (E_{phi}) of the electric field. Thus, it is difficult to estimate the global electric field variation, especially at the terminator sector where SC signatures tend to appear in the radial component (E_r) of the electric field. We found the MLT dependence of the SC amplitude both the PI and MI signatures in the E_r and E_{phi} electric fields. In addition, the dayside characteristics of the PI signature extended to the evening terminator sector (18-21 h MLT) with an enhancement around 20 h MLT. This tendency is consistent with previous results obtained by the ground-based observations and model calculations. We consider that enhancements associated with SCs are influenced by the non-uniform ionospheric conductivity.

In the present study, we revealed the global instant response of the ionospheric electric field during SCs based on the in-situ ionospheric electric field observations. Our results can serve as a basis for understanding energy transmission paths during rapid reconfigurations of ionospheric convection.

Japan Geoscience Union Meeting 2014
(28 April - 02 May 2014 at Pacifico YOKOHAMA, Kanagawa, Japan)

PEM28-02 Room:413 Time:April 29 11:15-11:30

Evolution of convection vortices associated with sudden impulses observed by SuperDARN

HORI, Tomoaki[1*] ; SHINBORI, Atsuki[2] ; NISHITANI, Nozomu[1] ; FUJITA, Shigeru[3]

[1]STE lab, Nagoya Univ, [2]RISH, Kyoto Univ, [3]Meteorological College

Spatial evolution of transient ionospheric convection induced by sudden impulses (SIs) recorded by ground magnetometers is studied statistically by using SuperDARN (SD) data. An advantage of using SD data instead of ground magnetic fields is that ionospheric flows measured by the radars are not virtually biased by the spatially-varying ionospheric conductance or the magnetospheric currents. First we surveyed the Sym-H index for Jan., 2007 to Dec., 2012 to identify SI events with a peak amplitude |dSym-H|greater than 10 nT. Next we searched all SD data over the northern hemisphere during the SI events for ionospheric backscatters which give us the light-of-sight velocity of horizontal ionospheric flows. For each SI event, the collected ionospheric flow data were sorted into the four periods: the pre-SI period, the pre-Main Impulse (MI), middle-MI, and post-MI periods. In the present study, we examine the differences in flow velocity between the pre-SI period and the three MI periods to clarify how ionospheric flows change in association with SIs. As a result, the ionospheric flow shifts eastward on the dusk side and westward on the dawn side at the higher latitudes during positive SIs (SI+), while it shows a roughly westward/eastward shift on the dusk/dawn side, respectively, during negative SIs (SI-). These polarities of flow shifts are basically consistent with the higher latitude portions of the DP current for the MI phase as shown by Araki [1994] and Araki and Nagano [1988]. The high latitude flow shifts are basically larger for SI events with larger Sym-H variations, in the same fashion as ground magnetic field variations at high latitudes. In addition to the major dependence on SI amplitude, the flow shift magnitude shows a minor dawn-dusk asymmetry particularly under strong IMF-By conditions. We speculate that the interaction with pre-existing convection cells might cause the selective enhancement of either side of flow shifts.

Keywords: sudden impulse, SuperDARN, ionospheric convection

Japan Geoscience Union Meeting 2014
(28 April - 02 May 2014 at Pacifico YOKOHAMA, Kanagawa, Japan)

PEM28-03 Room:413 Time:April 29 11:30-11:45

Global distributions of storm-time ionospheric currents as seen in geomagnetic field variations

SHINBORI, Atsuki[1*] ; HORI, Tomoaki[2] ; TANAKA, Yoshimasa[3] ; KOYAMA, Yukinobu[4] ; KIKUCHI, Takashi[2] ; NAGATSUMA, Tsutomu[5]

[1]Research Institute for Sustainable Humanosphere (RISH), Kyoto University, [2]Nagoya University Solar Terrestrial Environment Laboratory Geospace Research Center, [3]National Institute of Polar Research, [4]Data Analysis Center for Geomagnetism and Space Magnetism Graduate School of Science, Kyoto Universi, [5]National Institute of Information and Communications Technology

To investigate temporal and spatial evolution of global geomagnetic field variations from high-latitude to the equator during geomagnetic storms, we analyzed ground geomagnetic field disturbances from high latitudes to the magnetic equator. The daytime ionospheric equivalent current during the storm main phase showed that twin-vortex ionospheric currents driven by the Region 1 field-aligned currents (R1 FACs) are intensified significantly and expand to the low-latitude region of ˜30 degrees magnetic latitude. Centers of the currents were located around 70 and 65 degrees in the morning and afternoon, respectively. Corresponding to intensification of the R1 FACs, an enhancement of the eastward/westward equatorial electrojet occurred at the daytime/nighttime dip equator. This signature suggests that the enhanced convection electric field penetrates to both the daytime and nighttime equator. During the recovery phase, the daytime equivalent current showed that two new pairs of twin vortices, which are different from two-cell ionospheric currents driven by the R1 FACs, appear in the polar cap and mid latitude. The former led to enhanced northward Bz (NBZ) FACs driven by lobe reconnection tailward of the cusps, owing to the northward interplanetary magnetic field (IMF). The latter was generated by enhanced Region 2 field-aligned currents (R2 FACs). Associated with these magnetic field variations in the mid-latitudes and polar cap, the equatorial magnetic field variation showed a strongly negative signature, produced by the westward equatorial electrojet current caused by the dusk-to-dawn electric field.

Keywords: geomagnetic storm, convection electric field, shielding electric field, ionospheric disturbance dynamo, interplanetary magnetic field, solar wind

Japan Geoscience Union Meeting 2014
(28 April - 02 May 2014 at Pacifico YOKOHAMA, Kanagawa, Japan)

PEM28-04 Room:413 Time:April 29 11:45-12:00

The forenoon-afternoon asymmetry of DP2 electric field penetrated to the dip equator

MATSUSHITA, Hiroki[1*] ; YOSHIKAWA, Akimasa[2] ; UOZUMI, Teiji[3] ; IKEDA, Akihiro[4] ; OHTANI, Shinichi[5]

[1]Department of Earth and Planetary Sciences, Graduate School of Science, Kyushu university, [2]Department of Earth and Planetary Sciences, Graduate School of Science, Kyushu university, [3]International Center for Space Weather Science and Education, Kyushu University, [4]Kagoshima National College of Technology, [5]The Johns Hopkins University Applied Physics Laboratory

DP2 oscillation is quasi-periodic disturbance whose period is from 30 min to a few hours, and it is well known that DP2 synchronize with IMF Bz oscillation [Nishida, 1968] and can be observed globally from polar to equator [Nishida, 1968], [Kikuchi et al., 1996]. These two characteristics indicate that the disturbance associated with solar wind comes into ionosphere at polar region and M-I coupled current system like penetrating to dip equator is produced, however, this mechanism of the inversion of electric field from polar to equator is not well understood.

The purposes of this study are to clarify how the electric field at polar region is penetrated to dip equator region and to identify the global distribution of DP2 current system. To attain these goals, we analyzed longitudinal and latitudinal distribution of DP2 oscillation observed at dip equator region that is the final destination of M-I coupling system. The electric field is calculated from magnetic field and electric conductivity based on Ohm ' s law, and magnetic field data used in this study are MAGDAS data [K. Yumoto et al., 2006 and 2007] and electric conductivity data are calculated using data of WDC for geomagnetism. We analyzed the real local time distribution of the electric field during DP2 event in 2007 and 2008 using these data. It is used the data Equatorial Magnetometer Network [T.-I. Kitamura, 1985] to derive latitudinal distribution of DP2 oscillation.

The result of this analysis shows that there is an asymmetry of electric field between forenoon and afternoon. It is difficult to explain this asymmetry from the view point of only the electric field at polar region on northern and southern hemisphere which makes global DP2 current system, so this result indicates that there is some mechanism to produce this asymmetry of electric field when the polar electric field is penetrated to equator. As this mechanism, we suggest that the polarization electric field along dip equator and the terminator line of day and night can change global potential structure by Cowling channel model [Yoshikawa et al., 2012, AGU], and the electrostatic potential distribution assumed from our observational result is consistent with the distribution derived from the calculation result based on this model.

Keywords: DP2 oscillation, dip equator, ionospheric current

Japan Geoscience Union Meeting 2014
(28 April - 02 May 2014 at Pacifico YOKOHAMA, Kanagawa, Japan)

PEM28-05 Room:413 Time:April 29 12:00-12:15

Substorm electric fields at nightside low latitude

HASHIMOTO, Kumiko[1*] ; KIKUCHI, Takashi[2] ; TOMIZAWA, Ichiro[3] ; NAGATSUMA, Tsutomu[4]

[1]Kibi International University, [2]Nagoya University, [3]University of Electro-Communications, [4]National Institute of Information and Communications Technology

The convection electric field penetrates from the polar ionosphere to low latitude and drives the DP2 currents in the global ionosphere with an intensified equatorial electrojet (EEJ). The electric field often reverses its direction, that is, the overshielding occurs and causes the equatorial counterelectrojet (CEJ) during storm and substorms. In this paper we report that the overshielding electric field is detected by the HF Doppler sounders at low latitude on the nightside. We analyzed the Doppler frequency of the HF radio signals propagated over 120 km in Japan at frequencies of 5 and 8 MHz and compared with the equatorial EEJ/CEJ during the substorm expansion phase. We found that the overshielding electric field reaches around 2 mV/m during major substorms (AL <-1800 nT). Taking the geometrical attenuation into account, we estimate the equatorial electric field to be about 1.5 mV/m. We also found that the electric field drives the eastward electrojets in the equatorial ionosphere on the night side. It is to be noted that the overshielding electric field is observed on the nightside at low latitude during the major substorms, while the convection electric field is dominant during smaller size substorms, as the CEJ flows on the dayside. These results suggest that the overshielding electric field associated with the Region-2 field-aligned currents becomes dominant during substorms at low latitude on the nightside as well as on the dayside. On the other hand, we found strong seasonal dependence of the overshielding in the sub-auroral latitudes. Although the substorm CEJs at Huancayo do not depend on season, the overshielding frequently occurs at subauroral latitudes during the winter period from November to February. In contrast, the convection electric field is dominant at the subauroral and low-latitudes during the summer period from April to August. The strong seasonal dependence may suggest that the Region-1 field aligned currents (FACs) have a constant voltage source, while the Region-2 FACs have a constant current source, which results in the convection and overshielding electric fields being dominant in summer and winter, respectively.

Keywords: subsotm, midlatitude ionosphere, convection electric field, overshielding, equatorial counter electrojet

Japan Geoscience Union Meeting 2014
(28 April - 02 May 2014 at Pacifico YOKOHAMA, Kanagawa, Japan)

PEM28-06 Room:413 Time:April 29 12:15-12:30

Comparing the ionospheric plasma drift obtained from the global MHD simulation and that measured by SuperDARN radars

SAITA, Satoko[1*] ; FUJITA, Shigeru[2] ; KADOKURA, Akira[3] ; TANAKA, Takashi[4] ; YUKIMATU, Akira sessai[3] ; TANAKA, Yoshimasa[3] ; OHTANI, Shinichi[5] ; MURATA, Ken T.[6] ; HIGUCHI, Tomoyuki[7]

[1]Research Organization of Information and Systems, [2]Meteorological College, [3]National Institute of Polar Research, [4]International Center for Space Weather Science and Education, Kyushu University, [5]Johns Hopkins University Applied Physics Laboratory, [6]National Institute of Information and Communications Technology, [7]The Institute of Statistical Mathematics

We present a parameter study of simulated processes of the magnetosphere-ionosphere (M-I) coupling using the global MHD simulation code developed by *Tanaka* (2010).

The boundary conditions for the M-I coupling include some scaling factors. These factors are adjustable and are determined through trial and error. The main goal of this study is optimization of these scaling factors in the boundary condition by use of a data assimilation technique.

In this paper, we combine the MHD simulation and solar wind parameters derived from the ACE satellite, and compare the ionospheric E x B plasma drift obtained from the global MHD simulation and that obtained from the SuperDARN HF Radar Network.

References:

Tanaka, T., A. Nakamizo, A. Yoshikawa, S. Fujita, H. Shinagawa, H. Shimazu, T. Kikuchi, and K. K. Hashimoto (2010), Substorm convection and current system deduced from the global simulation, J. Geophys. Res., 115, A05220, doi:10.1029/2009JA014676.

Keywords: the ionospheric convection, SuperDARN, simulation

Japan Geoscience Union Meeting 2014
(28 April - 02 May 2014 at Pacifico YOKOHAMA, Kanagawa, Japan)

PEM28-07 Room:413 Time:April 29 12:30-12:45

Toward construction of comprehensive proton and electron auroral substorm model: Ground-based observation at Syowa

KADOKURA, Akira[1*] ; FUKUDA, Yoko[2] ; I, Tomofumi[3] ; MIYAJI, Kohei[4] ; MIYAOKA, Hiroshi[1] ; SATO, Natsuo[1]

[1]NIPR, [2]Department of Earth and Planetary Science, Graduate School of Science, The University of Tokyo, [3]Kakioka Magnetic Observatory,Japan Meteorological Agency, [4]Graduate School of Science, Nagoya University

National Institute of Polar Research (NIPR) has been constructing an auroral optical observation system at Syowa Station during the 8th project term of 6 years of the Japanese Antarctic Research Expedition (JARE) program. Instruments categorized in the ”Monitoring observation” are (1) 4 sets of All-sky monochromatic digital CCD imagers (427.8, 557.7, 485.0, 481.0 nm) and (2) All-sky color digital camera, and those categorized in the ”Specific purpose observation” are (1) All-sky TV camera and (2) 8-color Scanning Photometer (SPM). Simultaneous observations with 2 electron and 2 proton CCD monochromatic imagers will be carried out in 2014. Interval of the 4 imagers are the same as each other, 15 sec, although the spatial resolution of the 2 proton imagers are reduced into 64x64, comparing with the full resolution of 512x512 of the electron imager.

Center (FWHM) wavelengths of the SPM are 482.5(0.6), 483.5(0.6), 484.5(0.6), 485.5(0.6), 486.5(0.6), 487.5(0.6),670.5(5.0), 844.6(0.6) nm.

Scanning speed and sampling rate are 180 deg/10 sec and 20 Hz, respectively.

Using these electron and proton auroral data observed with all-sky imager and scanning photometer, we would like to construct a comprehensive model of substorm including the information on energy characteristics of precipitating auroral electrons and protons.

Keywords: aurora, substorm, ground-based observation, Syowa Station

Japan Geoscience Union Meeting 2014
(28 April - 02 May 2014 at Pacifico YOKOHAMA, Kanagawa, Japan)

PEM28-08 Room:413 Time:April 29 14:30-14:45

Characteristics of Pi 2 pulsations around the dawn and dusk terminator

IMAJO, Shun[1*] ; YOSHIKAWA, Akimasa[2] ; UOZUMI, Teiji[2] ; OHTANI, Shinichi[3] ; NAKAMIZO, Aoi[4] ; MARSHALL, Richard[5] ; SHEVTSOV, Boris M.[6] ; AKULICHEV, Victor A.[7] ; SUKHBAATAR, Usnikh[8] ; YUMOTO, Kiyohumi[2]

[1]Dept. Earth Planet. Sci., Kyushu Univ., [2]ICSWSE, Kyushu Univ., [3]APL, Johns Hopkins Univ., [4]FMI, Arctic Research Unit, [5]IPS Radio and Space Services, Bureau of Meteorology, Australia, [6]Institute of Cosmophysical Researches and Radio Wave Propagation, [7]Pacific Oceanological Insititude, FEB RAS, [8]The Research Center of Astronomy and Geophysics of Mongolian Academy of Sciences

We statistically investigate low-latitude Pi 2 pulsations observed around the dawn and dusk terminator. The main observational results of this study are: (1) Pi 2 pulsations tended to have east-west polarity in the sunlit side of the dawn terminator, while these in the sunlit side of the dusk terminator tended to have north-south polarity. (2) Phase reversals of D-component oscillations occurred near the dawn terminator and 2-3 hours before the dusk terminator. (3) Peaks of D/H (maximum amplitude ratio between D and H component) appear 3 hours after the dawn terminator and near the dusk terminator.

We suggest that there is the dawn-dusk asymmetry of meridional ionospheric currents connecting between equatorial Cowling current and oscillating nightside FACs; meridional currents around dawn is more intense than around dusk. This asymmetry current system can be qualitatively explained by the deformation of potential pattern caused by polarization charges at the terminator.

Keywords: Pi 2 pulsations, The dawn and dusk terminator, Ionospheric currents, FACs

Japan Geoscience Union Meeting 2014
(28 April - 02 May 2014 at Pacifico YOKOHAMA, Kanagawa, Japan)

PEM28-09 Room:413 Time:April 29 14:45-15:00

Automatic identification of Pc5 waves using RBSP mode data from the SuperDARN Hokkaido HF radar

MATSUSHITA, Toshinori[1*] ; SEKI, Kanako[1] ; NISHITANI, Nozomu[1] ; HORI, Tomoaki[1]

[1]STEL, Nagoya University

Ultra-low-frequency Pc5 waves have been observed by many methods such as ground-based magnetometers, HF radars and satellites. It has been demonstrated by numerical experiments that magnetospheric Pc5 waves are globally and directly generated on the dayside by solar wind dynamic pressure variations and/or on the dawn/dusk flank by Kelvin-Helmholtz surface waves. In addition, there are storm-time Pc5 waves on the dusk side magnetosphere that are associated with instabilities in the storm time ring current caused by the particle injection. The Pc5 waves can play an important role in mass and energy transport within the inner magnetosphere such as the radial diffusion of outer radiation belt electrons, as suggested by previous studies. Outstanding problems in Pc5 studies include clarification of their global characteristics and distribution, generation mechanisms, and especially their dependence on the solar wind parameters.

In this study, we try to develop a new automatic identification method of Pc5 waves using ˜20-sec time resolution data obtained by the SuperDARN Hokkaido HF radar operated in the RBSP mode. In this method, we use the Doppler velocity data and the power spectrum density calculated by the wavelet transformation. We set criteria which can detect Pc5 waves even when harmonic oscillations coexist. We show an example for the identification method using the Doppler velocity data obtained by the SuperDARN Hokkaido HF radar in details. Then, the candidates of Pc5 event are verified by inspection. From the rate of error identification, we evaluate the accuracy of the automatic identification method statistically. In the presentation we will also report on the preliminary results of mid-latitude Pc5 characteristics such as frequency distribution and MLT dependence.

Keywords: SuperDARN, Pc5 waves

Japan Geoscience Union Meeting 2014
(28 April - 02 May 2014 at Pacifico YOKOHAMA, Kanagawa, Japan)

PEM28-10 Room:413 Time:April 29 15:00-15:15

A Simultaneous Observation of Pc 4 pulsation by Hokkaido HF Radar and Ground-Based Magnetometers

OBANA, Yuki[1*] ; NISHITANI, Nozomu[2] ; HORI, Tomoaki[2] ; TERAMOTO, Mariko[3] ; NOSE, Masahito[4] ; YOSHIKAWA, Akimasa[5]

[1]Department of Engineering Science, Osaka Electro-Communication University, [2]Solar-Terrestrial Environment Laboratory, Nagoya University, [3]Japan Aerospace Exploration Agency, [4]Graduate School of Science, Kyoto University, [5]Department of Earth and Planetary Sciences, Kyushu University

We studied a Pc 4 (6.7-22.2 mHz) oscillation of ionospheric Doppler plasma velocity observed around the dawn terminator on 16 Jul 2013 on an east-northeast pointing beam 14 of SuperDARN Hokkaido HF radar in Japan. We compared this ionospheric Pc 4 oscillation with magnetic field variation at St. Paratunka (PTK) in Russia, Kakioka (KAK) in Japan, Guam (GUA), Middlemarch (MDM) and Te Wharau (TEW) in New Zealand. PTK and conjugate points of MDM and TEW are located almost under the radar beam. The waveforms showed high similarity among the HF Doppler, the D (east-west) component of magnetic field at stations in the middle latitude of northern hemisphere (PTK and KAK). While, at the other stations (MDM, TEW, and GUA) the H (north-south) component of magnetic field showed high similarity to the HF Doppler. Using the value of the peak-to-peak amplitude of the HF Doppler velocity, we estimated amplitude of magnetic field variation with assuming a horizontal current sheet infinitely extended in the ionosphere. The estimated amplitude was comparable to the observed amplitude at PTK. We also studied longitudinal variation in amplitude using magnetic field data at Amsterdam Isl. (AMS) in South Indian Ocean and Fredericksburg (FRD) in the United States. The maximum amplitude was found at AMS which located around the midnight.

These results can be interpreted as follows. This event had its source from night side and the Doppler velocity oscillation was caused by an oscillating electric field in the east-west direction. In the northern hemisphere (PTK and KAK), the ionosphere above the observatory was sunlit, thus the ionospheric Hall current induced by the electric field makes D component of magnetic filed oscillation on the ground. On the other hand, in the southern hemisphere (MDM and TEW) and GUA, the ionosphere above the stations was still in the darkness, thus effective ionospheric current could not be induced due to low conductivity. The H component of magnetic field oscillation may reflect direct incidence of magnetic field oscillation from the magnetosphere to the ground.

Keywords: ULF, HF radar, M-I coupling, magnetic pulsation

Japan Geoscience Union Meeting 2014
(28 April - 02 May 2014 at Pacifico YOKOHAMA, Kanagawa, Japan)

PEM28-11 Room:413 Time:April 29 15:15-15:30

Solar zenith angle dependence of relationships between energy inputs to the ionosphere and O+ and H+ ion outflows

KITAMURA, Naritoshi[1*] ; SEKI, Kanako[1] ; KEIKA, Kunihiro[1] ; NISHIMURA, Yukitoshi[2] ; HORI, Tomoaki[1] ; STRANGEWAY, Robert J.[3] ; MCFADDEN, James P.[4] ; LUND, Eric J.[5]

[1]STEL, Nagoya University, [2]Dept. of Atmos. and Oceanic Science, UCLA, [3]Inst. of Geophys. and Planetary Phys.,UCLA, [4]Space Science Laboratory, UCBerkeley, [5]SSC, Univ. of New Hampshire

Recent satellite observations and simulations have clarified that plasma outflows play an important role in abrupt changes in the ion composition in the plasmasheet and ring current during geomagnetic storms. Statistical studies by Strangeway et al. [2005] and Brambles et al. [2011] indicated that the flux of ion outflows is correlated well with soft electron precipitation (precipitating electron density and electron density in the loss cone), and DC and Alfvenic Poynting fluxes using the data obtained by the FAST satellite near the cusp region in the dayside during the 24-25 September 1998 geomagnetic storm. To distinguish between O^+ and H^+ ion outflows, we performed statistical studies using the ion composition data in addition to the ion and electron data obtained by the FAST satellite at 3000-4150 km altitude during January 1998 and January 1999. The long-term dataset enables us to identify empirical formulas between the outflowing O^+ and H^+ ion fluxes and the precipitating electron density, the electron density in the loss cone, the net electron number flux, and the DC and Alfvenic Poynting fluxes in a wide solar zenith angle (SZA) range (for dayside, 50-110 degree; and for nightside, 90-150 degree). In the SZA range of 90-110 degrees, the above formulas in the dayside are almost similar to those in the nightside. While SZA dependence of the relationshps between the outflowing O^+ and H^+ ion fluxes and the DC and Alfvenic Poynting fluxes are weak, the empirical formulas between the outflowing O^+ and H^+ ion fluxes and soft electron precipitation, especially the precipitating electron density and the electron density in the loss cone, depend on SZA. Although the precipitating electron density and the electron density in the loss cone that correspond to the outflowing O^+ ion flux of about 10^7 /cm^2/s increase with decreasing SZA, the outflowing O^+ and H^+ ion fluxes become more sensitive to an increase in soft electron precipitation with decreasing SZA.

Keywords: ion outflow, polar ionosphere

Japan Geoscience Union Meeting 2014
(28 April - 02 May 2014 at Pacifico YOKOHAMA, Kanagawa, Japan)

PEM28-12 Room:413 Time:April 29 15:30-15:45

Inversion method for estimating the helium ion density distribution in the plasmasphere based on IMAGE/EUV data

NAKANO, Shin'ya[1*] ; FOK, Mei-ching[2] ; BRANDT, Pontus C.[3] ; HIGUCHI, Tomoyuki[1]

[1]The Institute of Statistical Mathematics, [2]NASA Goddard Space Flight Center, [3]The Johns Hopkins University Applied Physics Laboratory

The plasmasphere exhibits a variety of shapes as a result of the variation in the electric field in the inner magnetosphere due to the coupling processes between the solar wind, the magnetosphere, and the ionosphere. Global imaging observations from outside the plasmasphere provide striking evidence of the variability of the plasmasphere. In particular, the EUV imager on board the IMAGE satellite obtained global EUV images of the plasmasphere, which have provided important insights into the variation of the plasmasphere. Our aim is to obtain the information on the ion density distribution for individual events rather than simply the averaged distribution from IMAGE/EUV data. For this purpose, we propose a linear inversion technique by which to estimate the helium ion density distribution. We applied this technique to a synthetic EUV image generated from a numerical model. This technique was confirmed to successfully reproduce the helium ion density that generated the synthetic EUV data. We also demonstrate how the proposed technique works for real data using real EUV images.

Keywords: plasmasphere, inverse problem, magnetosphere

Japan Geoscience Union Meeting 2014
(28 April - 02 May 2014 at Pacifico YOKOHAMA, Kanagawa, Japan)

PEM28-13 Room:413 Time:April 29 15:45-16:00

Current availability and utilization prospect of data obtained by AKEBONO for the research on lightning whistler

OIKE, Yuta[1*] ; KASAHARA, Yoshiya[1] ; GOTO, Yoshitaka[1]

[1]Kanazawa University

The AKEBONO spacecraft (EXOS-D) was launched in 1989 to observe particles and plasma waves in the auroral region and the plasmasphere of the Earth. It covers the altitude region from 300 km to about 10,000 km with an orbital inclination of 75 degree, and has been operated for more than 25 years which exceed 2 cycles of solar activity or 1 cycle of solar magnetic polarity reversal. Therefore analyses of the data obtained by AKEBONO enable us to study how the magnetosphere varies comprehensively.

The WBA (Wide Band Analyzer) is one of subsystems of the VLF instruments onboard AKEBONO. It measures 1 component of electric or magnetic analogue waveform in the frequency band of 50 Hz - 15 kHz. Typical waves such as chorus, hiss and whistler were frequently observed by the WBA. Huge amounts of data obtained by the WBA for more than 25 years are originally recorded as analogue waveform format in the magnetic audio tapes. Data conversion from analogue to digital is now carried out and the converted data are stored in our computer storage as digital WAVE format. Total number of the data files of digital WAVE format is more than 6,000, the total file size exceeds 10 terabytes and the processable data amount corresponds to more than 5,000 hours observation.

An automatic detection system to detect lightning whistlers from spectrograms of the WBA was developed. The spectrum intensity is automatically calibrated inside the system referring to the status of automatic gain controller of the receiver before detecting lightning whistlers. The system can output observed time, frequency band and dispersion of each detected lightning whistler. Some statistics of the lightning whistlers such as spatial and local time dependence of the occurrence frequency were already performed and the comparison with lightning activities are now under study. Because the dispersion of lightning whistler strongly depends on the electron density profile along the propagation path of the wave so that global electron density profile can be estimated using trend of dispersions of lightning whistlers. It is also pointed out that the propagation behavior of lightning whistlers is important clue to understand the wave-particle interaction. Thus these data and statistics have potential to achieve more valuable knowledge of the plasma physics in the magnetosphere.

In this presentation, we introduce the current status of data availability of the WBA and the derived results so far. We also discuss prospect of the data utilization.

Keywords: AKEBONO (EXOS-D), VLF, wide band receiver, lightning whistler

Japan Geoscience Union Meeting 2014
(28 April - 02 May 2014 at Pacifico YOKOHAMA, Kanagawa, Japan)

PEM28-14 Room:413 Time:April 29 16:15-16:30

Simultaneous ground-based and satellite observations of MF/HF auroral radio emissions

SATO, Yuka[1*] ; KUMAMOTO, Atsushi[2] ; KATOH, Yuto[2] ; SHINBORI, Atsuki[3] ; KADOKURA, Akira[1] ; OGAWA, Yasunobu[1]

[1]National Institute of Polar Research, [2]Department of Geophysics, Graduate School of Science, Tohoku University, [3]Research Institute for Sustainable Humanosphere, Kyoto University

Ground-based and satellite observations have revealed that the Earth is a distinct radio source. The terrestrial auroral ionosphere emits electromagnetic waves in the MF/HF ranges (about 1-6 MHz) as well as well-known intense auroral kilometric radiation (AKR) and auroral hiss in the VLF/LF ranges. Terrestrial Hectometric Radiation (THR) is observed by satellite observations in a frequency range of 1-4.5 MHz at high latitudes during geomagnetic disturbances and is regarded as a counterpart of auroral roar which is one type of MF/HF auroral radio emissions observable from the ground. Both THR and auroral roar are attributed to mode conversions of upper hybrid waves favorably generated under the matching condition, $f_{UH} \sim nf_{ce}$, where previous studies confirmed n = 2,3,4 and 5 for auroral roar, and n = 2 for THR. However, no previous studies have tested the simultaneous appearance. In this study, we survey long-term observation data obtained by the ground-based passive receivers installed at the Husafell station, Iceland (after September 2005, latitude 64.67^{o}N, longitude -21.03^{o}E, 65.3^o magnetic latitude) and the Kjell Henriksen Observatory (KHO), Svalbard (after August 2008, latitude 78.15^{o}N, longitude 16.04^{o}E, 75.2^o magnetic latitude) and by the Plasma Waves and Sounder experiment (PWS) mounted on the Akebono satellite. This data set includes several simultaneous appearance events, while the frequency of aurora roar is different from that of THR observed by the Akebono satellite passing over the ground-based stations. This frequency difference supports the previously proposed idea that auroral roar and THR are generated at different altitudes near 250 km and 1000 km, respectively. There is hardly any possibility that simultaneous observations indicate the identical generation region of auroral roar and THR. We also find that auroral roar appearing during the time when the Akebono satellite passes over the ground-based stations tends to be accompanied by THR. However, when the Akebono satellite passing over the stations detects THR, auroral roar does not always appear. This tendency is explained in terms of the fact that the Akebono satellite can detect THR emissions coming from a wider region, and a considerable portion of auroral roar emissions generated in the F region is absorbed in the D/E regions.

Japan Geoscience Union Meeting 2014
(28 April - 02 May 2014 at Pacifico YOKOHAMA, Kanagawa, Japan)

PEM28-15 Room:413 Time:April 29 16:30-16:45

Spatiotemporal distribution of auroral brightening in the cusp

TAGUCHI, Satoshi[1*] ; HOSOKAWA, Keisuke[1] ; OGAWA, Yasunobu[2]

[1]University of Electro-Communications, [2]National Institute of Polar Research

Previous studies have shown that mesoscale auroral forms occur near the equatorward edge of the background, stable cusp aurora, and that they move in a direction that is consistent with the motion of the magnetic field line after reconnection on the dayside magnetopause. In this study we pay attention to its initial brightening using data from a high-sensitivity all-sky imager at Longyearbyen, Svalbard. The imager has a field-of-view that spans more than 4 hours in MLT, and can observe auroral brightenings that are widely separated in MLT. We determined the position of dayside auroral brightening using the 630-nm auroral images, and examined how these positions are distributed in the cusp, focusing on intervals when IMF was extremely stable. Results of analyses show that brightening occurs over a wide dayside MLT range. We show detailed spatiotemporal patterns for successive brightening events, and discuss the patterns in terms of the formation of intermittent reconnection on the dayside magnetopause.

Keywords: aurora, cusp, particle precipitation, magnetic reconnection, all-sky imager

Japan Geoscience Union Meeting 2014
(28 April - 02 May 2014 at Pacifico YOKOHAMA, Kanagawa, Japan)

PEM28-16 Room:413 Time:April 29 16:45-17:00

Height measurement from stereo imaging of aurora

KATAOKA, Ryuho[1*] ; SHIGEMATSU, Kai[2] ; MIYOSHI, Yoshizumi[2] ; MIYAHARA, Hiroko[3] ; ITOYA, Satoru[4]

[1]NIPR, [2]Nagoya University, [3]MAU, [4]JSF

A new stereoscopic measurement technique is developed (Kataoka+2013) to obtain an all-sky altitude map of aurora using two ground-based digital single-lens reflex (DSLR) cameras. Two identical full-color all-sky cameras were set with an 8 km separation across the Chatanika area in Alaska (Poker Flat Research Range and Aurora Borealis Lodge) to find localized emission height with the maximum correlation of the apparent patterns in the localized pixels applying a method of the geographical coordinate transform. It is successfully estimated that a typical ray structure of discrete aurora shows the broad altitude distribution above 100 km, while a typical patchy structure of pulsating aurora shows the narrow altitude distribution of less than 100 km. Recent new findings about the time variation of the emission height and further new challenges of February/March 2014 will also be reported.

Reference: Kataoka, R., Y. Miyoshi, K. Shigematsu, D. Hampton, Y. Mori, T. Kubo, A. Yamashita, M. Tanaka, T. Takahei, T. Nakai, H. Miyahara, and K. Shiokawa (2013), Stereoscopic determination of all-sky altitude map of aurora using two ground-based Nikon DSLR cameras, Ann. Geophys, 31, 1543-1548.

Keywords: aurora, ground-based imaging, digital single-lens reflex camera

Japan Geoscience Union Meeting 2014
(28 April - 02 May 2014 at Pacifico YOKOHAMA, Kanagawa, Japan)

PEM28-17 Room:413 Time:April 29 17:00-17:15

Statistical analysis of auroral structures related to the plasma instability based on ground optical observations

HASHIMOTO, Ayumi[1*] ; SHIOKAWA, Kazuo[1] ; OTSUKA, Yuichi[1] ; OYAMA, Shin-ichiro[1] ; NOZAWA, Satonori[1]

[1]Solar-Terrestrial Environment Laboratory, Nagoya University, Nagoya, Japan

Auroral complex shapes are formed due to the connection of the ionosphere and magnetosphere by geomagnetic field lines which project disturbance of the magnetosphere onto the ionosphere through auroral particles. Thus, study of the auroral dynamics is important in considering the disturbance of the magnetosphere. Shiokawa et al. [JGR, 2010] reported observations of small-scale finger-like auroral structures which appeared on the west side of auroral patches, using a high-resolution narrow field-of-view CCD camera at Gillam (geomagnetic latitude: 65.5 N), Canada. At the recovery phase of substorm in the night side, these structures appeared when the speed of the patches moving to the east was slowed down, due to the macroscopic Rayleigh-Taylor type instability in the magnetosphere. However, statistical characteristics of this phenomenon have not been investigated yet. In this study, based on observations by an all-sky imager at Tromso (magnetic latitude: 67.1 N), Norway from January 2009 to November 2012, we made statistical analysis of the occurrence conditions of 19 events of auroral structures that seem to be driven by pressure-driven plasma instability. We found fourteen large-scale finger-like structures which developed from auroral arcs and six small-scale finger-like structures which appeared in auroral patches. We investigated MLT dependence of the start time of these finger-like structures, their relationship with auroral substorms, scale sizes, eastward drift speeds, development speeds, and so on. The large- scale structures were seen from midnight to dawn and small-scale structures were seen at dawn mainly. Large-scale structures tend to appear at the beginning of substorms' recovery phase and small-scale structures tend to occur at the late recovery phase of substorms. The scale sizes of these large and small structures are larger than the gyro radius of the ions in the magnetospheric equatorial plane, indicating that the finger-like structures are caused by MHD instabilities. The eastward propagation speeds are slower than the typical midnight auroral drift speed. This fact indicates that the low-energy plasma may be source of the structures. However, this consideration may contradict with the idea that the high-energy particles lead to the pressure-driven instability.

Keywords: aurora, pressure-driven plasma instability, ground optical observation

Japan Geoscience Union Meeting 2014
(28 April - 02 May 2014 at Pacifico YOKOHAMA, Kanagawa, Japan)

PEM28-18 Room:413 Time:April 29 17:15-17:30

Auroral vortex street formation and cavity trapping of Alfven waves

HIRAKI, Yasutaka[1*]

[1]National Institute of Polar Research

The structuring of auroral arc has been studied to be understood in the context of magnetohydrodynamic (MHD) instabilities and their nonlinear evolution in the magnetosphere-ionosphere (MI) coupling system. It was demonstrated that feedback instability of field-line resonant and ionospheric Alfven resonant modes occurs, by means of linear analysis with non-uniformity of the Alfven velocity (v_A) in the dipole magnetic field and the convection electric field [Hiraki and Watanabe, 2011; 2012, Hiraki, 2013]. We performed 3D reduced-MHD simulations in the MI coupling system to examine nonlinear behavior of the initially assumed arc structure, where v_A is constant along the field line. Results show that i) the initial arc splits, intensifies, and just after that deforming into a vortex street, and ii) the transition of the growth pattern exists at the convection electric field of 20-40 mV/m. We also performed 3D simulations with non-uniformity of v_A, though without the initial arc, to examine changes in auroral structure and properties of Alfven waves due to the magnetospheric and ionospheric cavities. It was found that, if the ionospheric cavity becomes deep, the secondary instability in the magnetic equator side [Watanabe, 2010] is suppressed, alternatively, large-amplitude waves are trapped in the ionospheric cavity. In this talk, we report the initial results of the above two simulations. Furthermore, we would discuss on auroral electron acceleration in the cavity region, by means of extended analyses with two-fluid effects and parallel electric field.

Keywords: Auroral vortex street, Alfven wave, Ionospheric Alfven resonator, Electron acceleration, MHD simulation

Japan Geoscience Union Meeting 2014
(28 April - 02 May 2014 at Pacifico YOKOHAMA, Kanagawa, Japan)

PEM28-19 Room:413 Time:April 29 17:30-17:45

Relative timing of substorm-associated magnetic reconnection in the magnetotail and formation of auroral onset arc

MIYASHITA, Yukinaga[1*] ; IEDA, Akimasa[1] ; MACHIDA, Shinobu[1] ; HIRAKI, Yasutaka[2] ; ANGELOPOULOS, Vassilis[3] ; MCFADDEN, James P.[4] ; AUSTER, H. uli[5] ; MENDE, Stephen B.[4] ; DONOVAN, Eric[6] ; LARSON, Davin[4]

[1]STEL, Nagoya Univ., [2]NIPR, [3]Univ. of California, Los Angeles, [4]SSL, Univ. of California, Berkeley, [5]Technischen Universitat Braunschweig, [6]Univ. of Calgary

We have studied the relative timing of magnetic reconnection in the near-Earth magnetotail and formation of auroral onset arc, based on substorm events observed by the THEMIS spacecraft and ground-based all-sky imagers. The THEMIS all-sky imagers can observe auroras over a wide area with temporal and spacial resolutions higher than spacecraft-borne cameras. This enables us to investigate the timing of auroral development in more detail than before. A few min after the appearance and intensification of an auroral onset arc, it begins to form wave-like structure. Then auroral poleward expansion begins another few min later. Based on observations of plasmoids in the near-Earth magnetotail, we clearly show that magnetic reconnection is initiated at X∼-20 Re at least 1-3 min before the appearance of the auroral onset arc. This result suggests that magnetic reconnection plays some role in the formation of auroral onset arc.

Keywords: substorm, auroral onset arc, magnetotail, magnetic reconnection, plasmoid, GEMSIS

Japan Geoscience Union Meeting 2014
(28 April - 02 May 2014 at Pacifico YOKOHAMA, Kanagawa, Japan)

PEM28-20 Room:413 Time:April 29 17:45-18:00

Characteristics of eastward propagating aurora vortices obtained by aurora tomography

TANAKA, Yoshimasa[1*] ; OGAWA, Yasunobu[1] ; KADOKURA, Akira[1] ; MIYAOKA, Hiroshi[1] ; GUSTAVSSON, Bjorn[3] ; PARTAMIES, Noora[2] ; BRANDSTROM, Urban[4] ; WHITER, Daniel[2] ; ENELL, Carl-fredrik[5]

[1]National Institute of Polar Research, [2]Finnish Meteorological Institute, [3]University of Tromso, [4]Swedish Institute of Space Physics, [5]EISCAT Scientific Association

We investigate characteristics of three mesoscale aurora vortices observed in the Northern Scandinavia by aurora campaign observation in March, 2013, which was conducted in collaboration with the Swedish Institute of Space Physics (IRF) and the Finnish Meteorological Institute (FMI). The aurora vortices propagated eastward intermittently at about 15-minute intervals in the post-midnight sector (0:00-0:40 UT; 2:30-3:10 magnetic local time) after the substorm onset. They were simultaneously observed by three monochromatic (427.8nm wave length) all-sky EMCCD imagers at Tromso (69.6N, 19.2E), Norway, Kilpisjarvi (69.0N, 20.9E), Finland, and Abisko (68.4N, 18.8E), Sweden, with an exposure time of about 2 seconds and a sampling rate of about 10 seconds. In addition to these optical data, geomagnetic field data from the IMAGE magnetometer chain were also available.

The propagation speed of these vortices was approximately 3 to 10 km/s at 100 km altitude. The ionospheric equivalent current system accompanied by the aurora vortices indicated a two-vortex structure. By applying tomographic inversion analysis to the events, we also obtained 3D distributions of volume emission rate and ionospheric electron density, as well as horizontal distribution of auroral precipitating electrons. It is also possible to estimate horizontal distribution of the ionospheric conductivity from the electron density distribution at every 10-second interval. In the presentation we will discuss the magnetosphere - ionosphere coupling process of the aurora vortices and the relationship with the omega bands that are generally observed in the post-midnight sector.

Keywords: aurora, tomography, substorm, vortex structure, imager, ionospheric current

Japan Geoscience Union Meeting 2014
(28 April - 02 May 2014 at Pacifico YOKOHAMA, Kanagawa, Japan)

PEM28-P01 Room:Poster Time:April 29 18:15-19:30

Observation of 630 nm auroral polarization with a newly-developed imaging spectrograph

TAKASAKI, Shimpei[1*] ; SAKANOI, Takeshi[1] ; KAGITANI, Masato[1]

[1]PPARC, Tohoku University

From the recent result of observation of OI 630nm auroral emission related to polar rain at high-latitudes using a polarization photometer, linear polarization parallel to geomagnetic field with 2-7% was reported [Lilensten et al., 2013]. From a theoretical approach, OI 630nm emission can be polarized up to 17% [Bommier et al., 2011]. However, these past measurements were limited in the polar cap region and its polarimetry characteristics is not clear. Therefore, we developed an imaging spectrograph which can measure auroral polarization in the wide field-of-view of 130 deg. from 420 nm to 680 nm with a accuracy of 1% polarization degree, which enable us to obtain polarization degrees at 557.7 nm aurora and 630 nm auroral emission simultaneously at various geomagnetic angle configuration. Here we consider that 557.7nm aurora is useful as a standard light source because a theory predicts 557.7nm emission does not produce polarization. We installed it in the middle of auroral region at Poker Flat Research range in November 2013and carried out precise calibration to extract artificial polarization which may be produce inside the optical system using an LED light source with a linear polarizer. From the calibration, we found the acrylic dome does not produce serious artificial polarization. Since then, automatic operation is continuously going on till the beginning of April 2014.

From the result on January 1st 2014, we obtain the polarization of 630 nm aurora with degree of 10%. Then, there was elevation angle dependence in both degree and direction. But, we also observed the polarization of no polarized 557.7nm emission. It has same elevation angle dependence as former. So, it is indicated that they are polarized by same processes like atmospheric scattering on the path from emission region to instrument. In this presentation, we report these results.

Keywords: aurora, polarimetry

Japan Geoscience Union Meeting 2014
(28 April - 02 May 2014 at Pacifico YOKOHAMA, Kanagawa, Japan)

PEM28-P02 Room:Poster Time:April 29 18:15-19:30

Development of polarization photometer and observation of OI 630 nm auroral polarization

MONJI, Hiroyuki[1*] ; KAGITANI, Masato[1] ; SAKANOI, Takeshi[1]

[1]PPARC, TOHOKU Univ.

Auroral O630 nm emission is theoretically expected to be polarized due to the velocity anisotropy of precipitating electrons. On the other hand, auroral O557.7 nm emission should not be polarized because it is quadrupole transition [Lilensten et al., 2006].

Recent ground-based measurement data showed that auroral emission at OI 630 nm probably polarized with a degree of 1-4%, and the polarization is maximized in the magnetic perpendicular direction [Lilensten et al., 2008, Barthelemy et al., 2011]. This fact suggest that it would be possible to investigate auroral physical processes, like electron anisotropy, by remote-sensing the auroral polarization.

In this study, we aim to establish the procedures of polarimetry observation of aurora, and obtain its polarization degree by developing a new polarization photometer.

We developed the polarization photometer which measures the polarization parameters (Stokes vector) using a quartz waveplate mounted on rotation stage and a polarization beam splitter. We adopt a narrow band 630 nm for wavelength selection. The field-of-view of this photometer is 3 deg. Observation of OI 630 nm auroral polarimetry was performed at Poker Flat Research Range in Alaska for three weeks in January 2013. We rotated the waveplate and took data at nine positions in one rotation. The time resolution for one rotation is 30 s. In addition, we carried out the calibration at Polar Flat with a linear polarizer and LED lamp. Using the auroral polarization data set and calibration data, we estimated the linear polarization degree and circular polarization simultaneously for the world first time.

On January 17, aurora appeared in the whole sky around 14:00 UT. During this period, we estimated the auroral polarization degree at various points along geomagnetic meridian. The estimated polarization degree maximized at the point parallel to the local geomagnetic field, which is inconsistent with the past result. On January 18, the auroral linear polarization degree increased correlated with auroral enhancement at 11:30 UT. This fact suggest that auroral polarization may increase due to the change in anisotropy in precipitating electrons.

Keywords: aurora ground observation, polarization

Japan Geoscience Union Meeting 2014
(28 April - 02 May 2014 at Pacifico YOKOHAMA, Kanagawa, Japan)

PEM28-P03 Room:Poster Time:April 29 18:15-19:30

Approximate formula of daytime ionospheric conductance ratio

IEDA, Akimasa[1*] ; OYAMA, Shin-ichiro[1] ; FUJII, Ryoichi[1] ; NAKAMIZO, Aoi[2] ; HORI, Tomoaki[1] ; YOSHIKAWA, Akimasa[3] ; NISHITANI, Nozomu[1]

[1]STEL, Nagoya University, [2]Finish meteological institute, [3]Kyushu University

Solar zenith angle (SZA) dependences of daytime ionospheric conductances are studied. In particular, we developed a simple theoretical form for the Hall to Pedersen conductance ratio against SZA. The European incoherent scatter (EISCAT) radar observations located at Tromso (67 MLAT) on 30 March 2012 were used to calculate conductances.

Daytime electric conductances in the ionosphere are associated with plasmas created by Solar extreme ultraviolet radiation into the neutral atmosphere of Earth. Previous conductance models have been either consistent or not with the ideal Chapman theory of such plasma productions.

Our results indicate that the SZA dependence of the Pedersen conductance can be consistent with the Chapman theory after modifications. Such modifications include an approximation of vertically-uniform plasma densities in the topside E region, and taking atmospheric temperature upward gradient into account. The Hall conductance decreases with increasing SZA more rapidly than the Pedersen conductance does. This is because that the Hall conductivity layer thins from noon toward night.

Keywords: ionospheric conductivity, ionosphere, conductance, EISCAT, incoherent scatter radar

Japan Geoscience Union Meeting 2014
(28 April - 02 May 2014 at Pacifico YOKOHAMA, Kanagawa, Japan)

PEM28-P04 Room:Poster Time:April 29 18:15-19:30

Temporal variation of electron density in the vicinity of the ionospheric trough

ISHIDA, Tetsuro[1*] ; OGAWA, Yasunobu[2] ; KADOKURA, Akira[2] ; HOSOKAWA, Keisuke[3] ; OTSUKA, Yuichi[4]

[1]The Graduate University for Advanced Studies, [2]National Institute of Polar Research, [3]The University of Electro-Communications, [4]Nagoya University

The purpose of this study is to examine temporal variation of electron density in the vicinity of the ionospheric trough, and to understand its physical mechanisms on different geomagnetic activities.

Basu et al. [2008] showed that Subauroal Polarization Stream (SAPS) enhances in the south of the trough during storm main phase. At the same time, GPS-TEC map showed that the trough also extends longitudinally throughout the Northern American continent. In addition, they pointed out that the plasma density irregularities in the trough/SAPS region impact the GPS-based navigation systems.

So far, it remains unclear how the trough and such irregularities develop in a shorter time scale and what determines their spatial structure because adequate observation with sufficient temporal resolution has not been operated. Therefore, we had conducted EISCAT SP experiment (high speed meridional scans which take only 60-80 seconds to scan elevation angles from 25 to 89 degrees) in duskside-nightside (1630-2030 MLT) on Oct. 2013 - Dec. 2013, and obtained totally 9 events including 7 quiet-moderate events and 2 disturbed events.

We have been investigating on the following topics: (1) the difference of temporal variation of electron density between inside and outside the trough, (2) the characteristic of temporal variation of electron density in the vicinity of the trough. We have obtained the following results so far.

1. The quasi-periodic variations in electron density, on the time scale of 5-40 minutes, have been found outside the trough, which varies with time and altitude. Oh the other hand, such structures less occurs within the trough. This tendency is independent on geomagnetic activity.

2. The quasi-periodic variations in electron density, on the time scale of 5-10 minutes, have been found within the trough boundary, which is nearly consistent toward altitude in magnetically quiet-moderate condition. However, this cyclic pattern is inconsistent toward altitude in magnetically disturbed condition.

Keywords: ionosphere, trough

Japan Geoscience Union Meeting 2014
(28 April - 02 May 2014 at Pacifico YOKOHAMA, Kanagawa, Japan)

PEM28-P05 Room:Poster Time:April 29 18:15-19:30

Classification and occurrence characteristics of subauroral rapid plasma flows observed by SuperDARN Hokkaido HF radar

NAGANO, Hiroki[1*] ; NISHITANI, Nozomu[1] ; HORI, Tomoaki[1]

[1]STEL, Nagoya Univ.

The rapid ionospheric plasma flows equatorward of the auroral zone are called Sub-Auroral Polarization Stream (SAPS). As a result of the past studies of SAPS, Kataoka et al. [2009] reported that positions of SAPS shift toward lower latitude with developing Dst index using the SuperDARN Hokkaido HF radar.

In this study we investigate the occurrence characteristics of SAPS, with focus on the relationship between SAPS occurrence and solar wind / geomagnetic parameters, using the SuperDARN Hokkaido HF radar with the field of view covering the Far East region, which began its operation in 2006. In order to discuss characteristics of SAPS extensively, we take a wider range of velocity (>10 m/s) and MLAT (>40 deg) than the previous studies. As a result of the statistical analysis we identified two kinds of flows with a threshold of 150 - 200 m/s. MLAT of faster flows has correlation with SYM-H and AL index, whereas the slower ones have no such correlation. We will report on the details of correlation between flow characteristics of solar wind and geomagnetic parameters, including substorm and storm phases.

Japan Geoscience Union Meeting 2014
(28 April - 02 May 2014 at Pacifico YOKOHAMA, Kanagawa, Japan)

PEM28-P06 Room:Poster Time:April 29 18:15-19:30

Magnetic latitude and MLT dependence of the bandwidth of MF/HF auroral radio emissions in the topside ionosphere

SAKAI, Masataka[1*] ; KUMAMOTO, Atsushi[1] ; KATOH, Yuto[1] ; SATO, Yuka[2]

[1]Department of Geophysics, Tohoku University, [2]National Institute of Polar Research

In the ionosphere, auroral radio emissions are generated by precipitating auroral particles. Previous studies reported that the MF/HF auroral radio emissions emitted from the bottomside ionosphere were observed on the ground. The narrowband emissions are called auroral roar, and the broadband emissions are called MF burst. On the other hand, Sato et al. [2010] showed the spectrum and polarization of two events of MF/HF radio emissions observed in the topside ionosphere by the Akebono satellite. Based on the event studies, they suggested that the observed narrowband emissions are generated by the mode conversion of UHR waves enhanced in the auroral ionosphere where the upper hybrid frequency matches the harmonics of the electron cyclotron frequency as suggested for generation mechanism of the auroral roar observed on the ground [Weatherwax et al., 1995; Yoon et al., 1998; Weatherwax et al., 2002].

In this study, we have focused on broadband emissions observed in the topside ionosphere which are similar with broadband MF burst observed on the ground. We analyzed MF/HF broadband emissions (with wider bandwidth of $>$0.5 kHz) observed by the Akebono satellite. Because it is difficult to observe broadband emissions on the ground and in the topside ionosphere at the same time, we have performed statistical analysis. We found that the bandwidth of the MF/HF emissions was larger in the high latitude and in the dusk side. The bandwidth of the MF/HF emissions was greater than 1 MHz in higher geomagnetic latitude than 70 degree in the sector from 12 to 24 MLT. Previous studies suggested that the MF bursts observed on the ground were generated by the mode conversion of upper hybrid waves stimulated by the energetic auroral electrons [e.g. Sato et al., 2008]. Therefore, we can expect that the bandwidth of MF bursts depend on the generation processes of upper hybrid waves, mode conversion processes of upper hybrid waves, and propagation processes of converted electromagnetic waves in the auroral ionosphere.

Japan Geoscience Union Meeting 2014
(28 April - 02 May 2014 at Pacifico YOKOHAMA, Kanagawa, Japan)

PEM28-P07 Room:Poster Time:April 29 18:15-19:30

Time Variability of Characteristics of Pc5 during Passage of CIRs

KITAMURA, Kentarou[1*] ; SAITA, Satoko[2] ; TANAKA, Yoshimasa[3] ; KADOKURA, Akira[3] ; YAMAGISHI, Hisao[3]

[1]Tokuyma college of Technology, [2]The Institute of Statistical Mathematics, [3]National Institute of Polar Research

In this study, we analyzed the magnetic data observed at the high-latitude magnetic stations in Antarctica, H057 (-66.42, L=6.25), and Skallen (-66.42) to compare with the >2Mev electron flux observed by GOES 10 satellite. The pair of stations is located at the same latitude and within 1.7 degrees in longitude, which are quite suitable to estimate the azimuthal wave number.

We statistically analyzed the wave characteristics of the Pc5 pulsations by the superposed epoch (SPE) analysis for 14 magnetic storm events caused by the passage of CIRs (Corotating Interaction Region). The epoch time is defined as days from the passage of the stream interface (SI) of the CIR. The Pc5 power suddenly increases at 3-6 MLT sector from 0 day which is much stronger than that at dusk sectors. During 1-2 days, which is correspond to the recovery phase of the storms, the Pc5 power at the afternoon sectors (12-21 MLT) increases with the peak frequency of 2.5-3 mHz, whereas the Pc5 power at the morning sector does not become stronger.

On the other hand, the phase delay between the Pc5s at H057 and SKAL also shows the local time dependence especially during the epoch time of 1-2 day. At the noon and afternoon sectors, the Pc5 shows the eastward propagation and the phase lags between H057 and SKAL are less than 5 seconds. In contrast, at the morning sector, the Pc5 shows westward propagation with small azimuthal wave numbers.

These features indicate that the sources and generation mechanisms of Pc5 in the two periods (0-1 day and 1-2 day) are quite different. The premiere intensification of the Pc5 corresponds to the main phase of the moderate magnetic storm and can thought to be the forced oscillation caused by the strong disturbance of the solarwind dynamic pressure. In this case, the local time dependence of the phase structure does not show the obvious regularities. In the latter intensification of the Pc5 corresponds to the recovery phase of the storm (1-2 days). The westward (eastward) propagation at the morning (afternoon) sector and local time distribution of the Pc5 power could well correspond with the previous perception which could explain the Pc5 pulsations caused by the KH instability on the magnetopause.

The present result implies that the difference of the wave characteristics of Pc5s closely related the drift bounce resonance with the relativistic electrons. The drift bounce resonance might occur at the afternoon sector during the recovery phase of the moderate magnetic storm by the KH instability due to the passage of the high speed solar wind.

Keywords: Raadiation Belt, ULF wave

Japan Geoscience Union Meeting 2014
(28 April - 02 May 2014 at Pacifico YOKOHAMA, Kanagawa, Japan)

PEM29-01 Room:503 Time:April 30 09:00-09:25

Spontaneous excitation of Alfven waves and their interactions with high-energy ions in a magnetic mirror configuration

ICHIMURA, Makoto[1*] ; IKEZOE, Ryuya[1]

[1]Plasma Research Center, Univ. of Tsukuba

In laboratory fusion plasmas, high-energy ions are produced with DD and DT fusion reactions and are also created with high-energy neutral beam injection and electromagnetic waves for plasma heating. Special emphasis is given to plasma waves excited by such high-energy ions and their interactions with particles. For example, energetic alpha particles produced with DT fusion process can interact resonantly with shear Alfven waves during slowing-down process, and excite plasma instabilities, that is, so-called Alfven eigenmodes (AEs). Recently, enhancement of energetic ion transport caused by these instabilities has been remarked on its deleterious effects. When a small fraction of alpha particles is transported to the first wall in burning plasma devices, plasma facing materials can be damaged seriously. Many kinds of the experimental observations related to such wave-particle interactions are reported. In this report, spontaneously excited waves in Ion Cyclotron Range of Frequency (ICRF) and their interactions with high-energy ions in a mirror magnetic field configuration are presented.

The ICRF waves are frequently used for the plasma heating in laboratory fusion devices with the mirror magnetic field configuration. When the ICRF power and consequent wave energy levels are increased, it will become important to understand the detailed physics of wave-wave and wave-particle interactions. It is required to consider both linear and nonlinear processes for deposition of ICRF powers. In the ICRF heating experiments on the GAMMA 10 tandem mirror, the maximum ion temperature in the perpendicular direction has reached 10 keV and the temperature anisotropy (which is defined as the temperature ratio of perpendicular to parallel to the magnetic field line) becomes more than 10 in the central cell. Alfven-ion- cyclotron (AIC) waves are spontaneously excited owing to such the strong temperature anisotropy. The excitation of the AIC wave is one of the common physical phenomena in space plasmas with an anisotropic velocity distribution. High energy ions, of which energy is more than 50 keV, have been observed along the magnetic field line at the open end of the mirror magnetic field configuration. The transport of high-energy ions along the magnetic field line owing to the loss processes other than the classical Coulomb scattering has been suggested. The existence of considerable energy transport along the magnetic field line owing to the AIC waves is discussed theoretically. The AIC waves in GAMMA 10, which has several discrete peaks in the frequency spectrum, are excited as eigenmodes. Their spatial structures are measured with a microwave reflectometer inside the plasma and magnetic probes in the peripheral region. Low-frequency fluctuations around 0.1 MHz, which is a differential frequency between discrete peaks of the AIC waves, are observed in the central cell. These fluctuations are also observed in the high-energy ion signal detected by a semiconductor detector installed at the end for measuring ions along the magnetic field line. Pitch angle scattering in the velocity space owing to the spontaneously excited Alfven waves are indicated. The radial transport of high-energy ions owing to the low-frequency MHD instability has been observed, however, the transport across the magnetic field line owing to the AIC waves has not yet been detected.

Observations of spontaneously excited waves in ICRF in the large tokamak experiments are also reported as Ion Cyclotron Emissions (ICE). The fluctuations in ICRF are driven by the presence of non-thermal ion distribution in magnetically confined plasmas and plasmas with the strong anisotropy. Waves owing to fusion products of ^{3}He and T ions are clearly detected in D-plasma and alpha particles in DT-plasma experiments.

Keywords: magnetic mirror configuration, Alfven wave, wave-particle interaction, Alfven Ion Cyclotron wave

Japan Geoscience Union Meeting 2014
(28 April - 02 May 2014 at Pacifico YOKOHAMA, Kanagawa, Japan)

PEM29-02 Room:503 Time:April 30 09:25-09:45

Nonlinear wave particle interaction of electromagnetic ion cyclotron wave

SHOJI, Masafumi[1*] ; OMURA, Yoshiharu[2]

[1]Solar-Terrestrial Environment Laboratory, Nagoya University, [2]Research Institute for Sustainable Humanosphere, Kyoto University

Spacecraft observations and simulations show generation of coherent electromagnetic ion cyclotron (EMIC) triggered emissions with rising-tone frequencies. In the inner magnetosphere, the spontaneously triggered EMIC waves are generated by the energetic protons with large temperature anisotropy. We reproduced EMIC triggered emissions in the Earth's magnetosphere by real scale hybrid simulations with cylindrical magnetic geometry. We perform parametric analyses of electromagnetic ion cyclotron (EMIC) triggered emissions on the gradient of the non-uniform ambient magnetic field using a hybrid simulation. According to nonlinear wave growth theory, as the gradient of the ambient magnetic field becomes larger, the theoretical threshold of the wave amplitude becomes larger although the optimum wave amplitude for nonlinear wave growth does not change. With a larger magnetic field gradient, we obtain coherent rising tone spectra because the triggering process of the EMIC triggered emission takes place only under the limited condition of the wave amplitude. On the other hand, with a smaller magnetic field gradient, triggering of the emissions can be caused with various wave amplitudes, and then the sub-packets are generated at various locations at the same time. The concurrent triggerings of emissions result in incoherent waves, observed as "broadband" EMIC bursts. Broadband emissions induce rapid precipitation of the energetic protons into the loss cone since the scattering by the concurrent triggering takes place faster than that of the coherent emissions. The coherent triggered emission causes efficient proton acceleration around the equator because of the stable particle trapping by the coherent rising tone emission.

Keywords: triggered emission, electromagnetic ion cyclotron wave, wave particle interaction, acceleration, scattering

Japan Geoscience Union Meeting 2014
(28 April - 02 May 2014 at Pacifico YOKOHAMA, Kanagawa, Japan)

PEM29-03 Room:503 Time:April 30 09:45-10:00

Solar energetic particle spectrum at the Sun and the Earth

KUBO, Yuki[1*]

[1]National Institute of Information and Communications Technology

It is well accepted that high-energy solar energetic particles are accelerated at reconnection regions in a solar flare and coronal shock waves driven by a coronal mass ejection. The coronal shock waves accelerate particles through the first-order Fermi process. The original Fermi acceleration theory predicts a power law particle distribution in momentum with index depending on shock compression ratio. Solar energetic particle spectra have been well investigated and it is found that the observed spectra are represented by almost power law (with high energy rollover). This looks like natural results at first glance. However, the observed spectrum is the spectrum at the observation location not at the acceleration site, and it is not trivial if the observed spectrum is as same as the source spectrum. There are some evidences that typical observed power law index will be about 6 in ground level enhancement (GLE). If the source spectrum of accelerated particle at a coronal shock is assumed to be as same as observed one, a compression ratio of the coronal shock accelerating particles should be about 1.6 according to the Fermi acceleration theory. This shock strength may not be enough to accelerate particles to GeV energy range in a short time. This implies that the spectrum at the source may not be as same as one at the observation location. While a power law spectrum predicted by Fermi process is a steady state solution, a lot of study show that a shock accelerated particle spectrum is time dependent manner. This fact may also imply a different spectrum between at the Sun and at the Earth. In this study, we investigate an energetic particle spectrum difference between at the source region and at the observation location by the interplanetary particle transport simulations.

Keywords: Solar energetic particles, Spectra

Japan Geoscience Union Meeting 2014
(28 April - 02 May 2014 at Pacifico YOKOHAMA, Kanagawa, Japan)

PEM29-04 Room:503 Time:April 30 10:00-10:15

Coupling between ULF waves and high-energy particles in the inner geomagnetosphere based on a drift-kinetic simulation

SEKI, Kanako[1*] ; AMANO, Takanobu[2] ; SAITO, Shinji[3] ; MIYOSHI, Yoshizumi[1] ; KEIKA, Kunihiro[1] ; MIYASHITA, Yukinaga[1] ; MATSUMOTO, Yosuke[4] ; UMEDA, Takayuki[1] ; EBIHARA, Yusuke[5]

[1]Solar-Terrestrial Environment Laboratory, Nagoya University, [2]Graduate School of Science, University of Tokyo, [3]Graduate School of Science, Nagoya University, [4]Graduate School of Science, Chiba University, [5]Research Institute for Sustainable Humanosphere, Kyoto University

Understanding of acceleration mechanisms of electrons to cause drastic variation of the Earth's outer radiation belt is one of outstanding issues of the geospace researches. While the radial diffusion of the electrons driven by ULF waves has been considered as one of the candidate mechanisms, efficiency of the mechanism under realistic ULF characteristics and distribution is far from understood. GEMSIS (Geospace Environment Modeling System for Integrated Studies) of STEL, Nagoya University, is the observation-based modeling project for understanding energy and mass transportation from the Sun to the Earth in the geospace environment. The GEMSIS-Magnetosphere working team has developed a new physics-based model for the global dynamics of the ring current (GEMSIS-RC model). The GEMSIS-RC model is a self-consistent and kinetic numerical simulation code solving the five-dimensional collisionless drift-kinetic equation for the ring-current ions in the inner-magnetosphere coupled with Maxwell equations. In contrast to previous ring current models assuming a force-balanced equilibrium, the new model allows the force-imbalance to exist, which generates induced electric field through the polarization current. The most prominent advantage of the new model is the capability of describing fast time scale phenomena such as injections during substorms and MHD-time scale (ULF) waves.

We applied the GEMSIS-RC model for simulation of global distribution of ULF waves. Comparison between runs with/without ring current ions show that the existence of hot ring current ions can deform and amplify the original sinusoidal waveforms. The deformation causes the energy cascade to higher frequency range (Pc4 and Pc3 ranges). The cascade is more pronounced in the high beta case. It is also shown that the existence of plasmapause strengthens ULFs outside the plasmapause and widens the MLT region where the E_r (toroidal) component is excited from initially-given E_phi (poloidal) component. We also report the basic characteristics of the ring current driven ULF waves and its effects on the electron transport in the inner magnetosphere.

Keywords: drift-kinetic approximation, ring current, radiation belt, MHD wave, inner magnetosphere, drift resonance

Japan Geoscience Union Meeting 2014
(28 April - 02 May 2014 at Pacifico YOKOHAMA, Kanagawa, Japan)

PEM29-05 Room:503 Time:April 30 10:15-10:30

Radiation spectra from relativistic electrons moving in a Langmuir turbulence

TERAKI, Yuto[1*]

[1]Osaka University / RIKEN

We examine the radiation spectra from relativistic electrons moving in a Langmuir turbulence expected to exist in high energy astrophysical objects by using numerical method. The spectral shape is characterized by the spatial scale λ, field strength σ, and frequency of the Langmuir waves, and in term of frequency they are represented by {s:0188$_0$ $2\pi c/\lambda$, ω_{st} = eσ/mc, and ω_p, respectively. We normalize ω_{st} and ω_p by ω_0 as a $\equiv \omega_{st}/\omega_0$ and b $\equiv \omega_p/\omega_0$, and examine the spectral shape in the a ? b plane. An earlier study based on Diffusive Radiation in Lang- muir turbulence (DRL) theory by Fleishman & Toptygin showed that the typical frequency is $\gamma^2\omega_p$ and that the low frequency spectrum behaves as F$\omega\overline{\Gamma}\omega^1$ for b $>$1 irrespective of a. Here, we adopt the first principle numerical approach to obtain the radiation spectra in more detail. We generate Langmuir turbulence by superposing Fourier modes, inject monoenergetic electrons, solve the equation of motion, and calculate the radiation spectra using Lienard-Wiechert potential. We find different features from the DRL theory for a $>$b $>$1. The peak fre- quency turns out to be $\gamma^2\omega_{st}$ which is higher than $\gamma^2\omega_p$ predicted in the DRL theory, and the spectral index of low frequency region is not 1 but 1/3. It is because the typical deflection angle of electrons is larger than the angle of the beaming cone $\approx$ 1/γ. We call the radiation for this case " Wiggler Radiation in Langmuir turbulence " (WRL).

Keywords: Radiation mechanism, Relativistic particle, Turbulent electromagnetic field

Japan Geoscience Union Meeting 2014
(28 April - 02 May 2014 at Pacifico YOKOHAMA, Kanagawa, Japan)

PEM29-06 Room:503 Time:April 30 10:30-10:45

Fine Spectral Structures and Their Generation Mechanisms for Solar Radio Bursts Observed by AMATERAS

IWAI, Kazumasa[1*] ; MIYOSHI, Yoshizumi[2] ; MASUDA, Satoshi[2] ; TSUCHIYA, Fuminori[3] ; MORIOKA, Akira[3] ; MISAWA, Hiroaki[3]

[1]Nobeyama Solar Radio Observatory, NAOJ, [2]STEL, Nagoya University, [3]PPARC, Tohoku University

The solar corona contains many particle acceleration phenomena that are caused by the interactions between the coronal magnetic field and plasma. Non-thermal electrons accelerated in the corona emit radio waves in the metric range. As a result, many types of solar radio bursts are observed. There are many types of complex fine spectral structures in the solar radio bursts. They are thought to be caused by some inhomogeneity of particle acceleration, wave generation, radio emission, and radio propagation processes. Hence, metric solar radio bursts are very important to understand coronal plasma processes such as the particle acceleration and wave-particle interaction.

The fine spectral structures of solar radio type-I bursts were observed by the solar radio telescope AMATERAS. The spectral characteristics, such as the peak flux, duration, and bandwidth, of the individual burst elements were satisfactorily detected by the highly resolved spectral data of AMATEAS with the burst detection algorithm that is improved in this study. The peak flux of the type-I bursts followed a power-law distribution with a spectral index of 2.9?3.3, whereas their duration and bandwidth were distributed more exponentially. There were almost no correlations between the peak flux, duration, and bandwidth. That means there were no similarity shapes in the burst spectral structures. We defined the growth rate of a burst as the ratio between its peak flux and duration. There was a strong correlation between the growth rate and peak flux. These results suggest that the free energy of type-I bursts that is originally generated by non-thermal electrons is modulated in the subsequent stages of the generation of non-thermal electrons, such as plasma wave generation, radio wave emissions, and propagation. The variation of the time scale of the growth rate is significantly larger than that of the coronal environments. These results can be explained by the situation that the source region may have the inhomogeneity of an ambient plasma environment, such as the boundary of open and closed field lines, and the superposition of entire emitted bursts was observed by the spectrometer.

Keywords: Sun, Solar radio burst, corona, wave-particle interaction, radio emission processes

Japan Geoscience Union Meeting 2014
(28 April - 02 May 2014 at Pacifico YOKOHAMA, Kanagawa, Japan)

PEM29-07 Room:503 Time:April 30 11:00-11:15

Co-evolution of upstream waves and accelerated particles around parallel shocks

SUGIYAMA, Tooru[1*] ; FUJIMOTO, Masaki[2]

[1]JAMSTEC, [2]JAXA

We have investigated the co-evolution of upstream waves and the accelerated particles around the parallel shock. Hybrid particle simulations are performed in the exactly parallel shock configuration with Mach number of ˜10. The upstream waves convecting into the shock surface contribute the particles acceleration as reported in Sugiyama et al. (2001). The appropriate wave-length exists for the particle energization, that is, the longer wave-length wave leads the higher energy particles. Simultaneously, the higher energized particles excite the longer wave-length waves in the upstream region. Here we report that the higher energy particles and longer wave-length waves are observed as the time elapses later in the simulation runs. Therefore, the present process is ”co-evolution” of the upstream waves and accelerated particles.

Keywords: collisionless shock, particle acceleration, wave-particle interaction

Japan Geoscience Union Meeting 2014
(28 April - 02 May 2014 at Pacifico YOKOHAMA, Kanagawa, Japan)

PEM29-08 Room:503 Time:April 30 11:15-11:30

Colliding Two Oblique Shocks: Shock Structures and Particle Acceleration

NAKANOTANI, Masaru[1*] ; MATSUKIYO, Shuichi[1] ; HADA, Tohru[1]

[1]ESST, Kyushu univ.

Mechanisms of the particle acceleration at a collisionless shock have been intensively studied analytically, numerically, and observationally. Most of the previous studies assume that energetic particles interact with a single shock. However, shock waves are ubiquitous in space, and two shocks frequently come close to or even collide with each other. For instance, it is observed that a CME (coronal mass ejection) driven shock collides with the earth's bow shock [H. Hietala et al., 2011], or interplanetary shocks pass through the heliospheric termination shock [J. Y. Lu et al., 1999]. The detailed structures of such colliding shocks and the accompanied particle heating/acceleration processes have not been understood.

Cargill et al. [1986] performed one dimensional hybrid simulations to discuss the dynamic structure of colliding shocks and the accompanied ion acceleration. They showed that some ions are efficiently accelerated at the time of the collision of two supercritical shocks. However, since electron dynamics are neglected in a hybrid simulation, the microstructures of the colliding shocks, which may affect the early stage processes of particle acceleration, cannot be resolved.

Here, we perform full Particle-in-Cell (PIC) simulations to examine colliding two shocks. In particular, the following three points interacting with two colliding oblique shocks is discussed in detail.

1. Energetic electrons are observed upstream of the two shocks before their collision. These energetic electrons are efficiently accelerated through multiple reflections at the two shocks (Fermi acceleration). Moreover, a part of the accelerated electrons are farther energized by interacting with increasing magnetic field during the collision and/or one of the shocks after the collision.

2. Before two shocks collide, there is a large amplitude wave excited by electrons flowing out to the upstream. We discuss the excitation mechanism and the influence on particle propagation or shock structures.

3. After two shocks collide, we find that a plasma density and pressure in the downstream is lower than the value calculated by MHD. The reason is that energetic electrons run away to the upstream. In addition to this, we discuss kinetic influences by comparing PIC simulation's results with the value after two shocks collide (magnetic fields, the shock velocity and etc.) calculated by MHD.

Keywords: collisionless shock, multi-shock waves, particle acceleration, numerical simulation

Japan Geoscience Union Meeting 2014
(28 April - 02 May 2014 at Pacifico YOKOHAMA, Kanagawa, Japan)

PEM29-09 Room:503 Time:April 30 11:30-11:45

Particle acceleration in high Mach number quasi-parallel shocks

KATO, Tsunehiko[1*]

[1]Hiroshima University

We study particle acceleration process of electrons and protons in high Mach number (M_A~30) quasi-parallel collisionless shocks by particle-in-cell (PIC) simulation. We found that a fraction of protons which consist of the plasma are injected into acceleration mechanisms and efficiently accelerated around the shock. The energy spectrum of the accelerated protons becomes power-law like distribution. A part of electrons are also accelerated around the shock although they are roughly two orders of magnitude fewer than the accelerated protons. For both protons and electrons, the acceleration processes are often not diffusive and their time-scales are even shorter than the respective gyration times. We also found that protons reflected at the shock generate circularly polarized Alfven waves with very large amplitude in the upstream region of the shock and that, because of the strong perpendicular magnetic field of these waves, the structure of the collisionless shock itself is in fact similar to that of quasi-perpendicular shocks.

Keywords: particle acceleration, plasma, collisionless shocks

Japan Geoscience Union Meeting 2014
(28 April - 02 May 2014 at Pacifico YOKOHAMA, Kanagawa, Japan)

PEM29-10 Room:503 Time:April 30 11:45-12:00

Particle simulations on electron acceleration at Quasi-Perpendicular Shocks

SHINOHARA, Iku[1*] ; FUJIMOTO, Masaki[1] ; NAKAMURA, Takuma[2]

[1]Institute of Space and Astronautical Science / Japan Aerospace Exploration Agency, [2]Los Alamos National Laboratory

We found efficient production of non-thermal electrons up to $\gamma\sim20$ in results of three-dimensional full kinetic simulations of quasi-perpendicular shocks. The seed acceleration occurs in large-amplitude electromagnetic wave excited in the most front region of the shock foot. A small portion of electrons keeps staying in the foot region due to the scattering by the large-amplitude electromagnetic wave, and these electrons can get energy from the motional electric field in the shock rest frame. Since the large-amplitude electromagnetic wave is only possible in 3-D simulations, no electron acceleration is observed in previous 1-D and 2-D simulations. After the seed acceleration, these electrons can be further accelerated at the shock lamp region by the shock drift acceleration. The acceleration process occurs during the steepen phase of the self-reformation, and the acceleration efficiency depends on the phase of the shock self-reformation. In contrast to the standard Fermi acceleration at quasi-parallel shocks, the electron acceleration process at quasi-perpendicular shocks is much quicker (order of the ion cyclotron period); however, electrons cannot experience effective acceleration again and again so that there would be an energy limitation of the acceleration. In this presentation, we will discuss the energy limit of electron acceleration at quasi-perpendicular shocks by using simulation results obtained from the K computer.

Keywords: shock acceleration, particle simulation

Japan Geoscience Union Meeting 2014
(28 April - 02 May 2014 at Pacifico YOKOHAMA, Kanagawa, Japan)

PEM29-11 Room:503 Time:April 30 12:00-12:15

The fast acceleration of particles scattered by MHD wave in parallel shock

MURAKI, Koudai[1*] ; AMANO, Takanobu[2] ; HOSHINO, Masahiro[2]

[1]EPS. Univ. of Tokyo, [2]University of Tokyo

The origin of the galactic cosmic ray is believed to be generated around the supernova remnant shocks (SNR), and the first-order Fermi acceleration is widely recognized as the standard theory of cosmic ray acceleration. Yet this acceleration mechanism is not always efficient enough to explain high energy cosmic ray particles extending to the knee. The maximum attainable energy expected by the first-order Fermi acceleration is less than the observations. To overcome this problem, additional acceleration and/or other efficient acceleration processes are needed.

Scattering process is important to investigate diffusive shock acceleration(DSA). In the previous numerical simulations, scattering is often treated as just numerical way like Monte-Carlo methods or electromagnetic perturbation. Among these researches, a special attention is paid to the particle acceleration for the particles scattered by magnetohydrodynamic (MHD) waves around the shock wave front. In the uniform system, when the wave phases are strongly correlated spatially localized traveling wave packets can efficiently large angle scatter charged particles (*Kuramitsu & Hada, 2000*). The scattering process through monochromatic large amplitude MHD waves around the parallel shock (*Sugiyama et al. 2001*) is regarded as a possible pre-acceleration process injecting the thermal particles into the Fermi acceleration process and the subsequent fast Fermi acceleration process.By extending the previous researches, we study a fast particle acceleration process for MHD turbulence around the parallel shock. By using the test particle simulation, we argue about the particle acceleration in the quasi-linear regime and also about the case of strongly coherent waves and large amplitude waves.

Keywords: acceleration of particles, cosmic ray, shock, Alfven wave, coherence, large amplitude

Japan Geoscience Union Meeting 2014
(28 April - 02 May 2014 at Pacifico YOKOHAMA, Kanagawa, Japan)

PEM29-12 Room:503 Time:April 30 12:15-12:30

On statistics of a plasma in a nonuniform flow

HADA, Tohru[1*]

[1]IGSES, Kyushu University

It is well known that energetic particles such as cosmic rays can efficiently be accelerated by scatterers convected by a compressional flow (Fermi acceleration). Scatterers convected by an expanding flow decelerate the particles, but this is not the reverse process of the acceleration. Plasma in space is never uniform, but is rather composed of different plasmas with different propagation speeds. We analyze statistics of energetic particles in such nonuniform plasma flow analytically and numerically. Results will be compared with non-equilibrium plasma distributions in the solar wind.

Keywords: Fermi acceleration, Nonequilibrium distribution

Japan Geoscience Union Meeting 2014
(28 April - 02 May 2014 at Pacifico YOKOHAMA, Kanagawa, Japan)

PEM29-13 Room:503 Time:April 30 14:15-14:30

Helicon wave propagation, mode conversion, and plasma heating

ISAYAMA, Shogo[1*] ; HADA, Tohru[1] ; TANIKAWA, Takao[2] ; SHINOHARA, Shunjiro[3]

[1]Graduate School of Engineering Sciences, Kyushu University, [2]Research Institute of Science and Technology Tokai University, [3]Tokyo University of Agriculture and Technology, Institute of Engineering

Helicon plasma is a high-density (number density ˜10^{19} /m^3) and low-temperature (electron temperature ˜a few eV) plasma generated by the helicon wave, i.e., electromagnetic whistler wave in a bounded plasma. Helicon plasma is thought to be useful for various applications including plasma processing and electric thrusters. On the other hand, there remain a number of unsolved fundamental issues regarding how the plasma is generated. Some of the key processes involved are the wave propagation (dispersion relation), mode conversion, collisional and non-collisional damping and resultant plasma heating, ionization and re-combination of neutral particles due to electrons accelerated by the wave, and modification of the dispersion relation due to addition of newly produced plasma.

In this presentation, as a first step to understand the helicon plasma production mechanism, we study the helicon wave propagation, mode conversion, and the plasma heating. According to Shamrai (1996), the helicon wave is linearly mode converted to an electrostatic Trivelpiece-Gould (TG) wave, which can accelerate electrons efficiently. However, the mode conversion and the production of the TG wave strongly depend on the dissipation included in the plasma. Using fluid and particle-in-cell (PIC) simulations, we discuss the mode conversion efficiency, wave damping, and plasma heating due to wave-particle interactions. We show that direct damping of the helicon waves can play major roles in the plasma heating under circumstances relevant to actual laboratory experiments.

Keywords: Helicon plasma, Helicon wave, TG(Trivelpiece-Gould) wave, Mode conversion, PIC simulation

Japan Geoscience Union Meeting 2014
(28 April - 02 May 2014 at Pacifico YOKOHAMA, Kanagawa, Japan)

PEM29-14 Room:503 Time:April 30 14:30-14:45

Hamilton-Jacobi equation based on exterior derivative

NAKAMURA, Tadas[1*]

[1]Fukui Prefectural University

Analytical Mechanics of fields usually singles out the temporal coordinate as an independent parameter and calculates the time evolution regarding fields as dynamical parameters with infinite degree of freedom. Spatial coordinates are treated as infinit number of indexes of dynamical parameters. This approach has a disadvantage when applied to electromagnetism: the resulting equations are not manifestly covariant. Moreover, when applied to gauge fields, the canonical theory with this approach has extra degree of freedom, which need to be eliminated with some constraints. One must fix the gauge at the price of loosing manifest covariance, or introduce some
complicated technique such as Dirac brackets.

The author reported the way to treat four (time 1 + space 3) parameters equally to construct analytical mechanics at the fall SGEPPS meeting. The expression obtained is manifestly covariant, and there is no need for gauge fixing when applied to gauge fields. The present study is to extend it to Hamilton-Jacobi theory. Also, possible application to the fluid dynamics will be discussed at the presentation.

The name of Hamilton-Jacobi equation is well known by name, however, not many researchers try to understand its detail because it is not quite useful to solve actual problems. However, it is conceptually important for the deep understanding of analytical mechanics. Also, it is essential to introduce quantum mechanics based on the knowledge of classical mechanics.

Several attempts have been made to establish classical mechanics of relativistic fluid dynamics, but fully covariant expressions are yet to come. Kambe (2010) has reported the Euler equation can be cast into the form of Maxwell equation with appropriate definitions of variables. The present study has been successfully applied to the analytical mechanics of electromagnetism, therefore, it may be applicable to fluid dynamics based on Hasimoto's representation.

References:
T.K. Nakamura 2003 (http://hdl.handle.net/2433/97295)[In Japanese]
T. Kambe 2010, Fluid Dyn. Res.
Y. Kaminaga, Electronic Journal of Theoretical Physics, 2012 (http://www.ejtp.com/ejtpv9i26)

Keywords: exterior derivative, analytical mechanics, Hamilton-Jacobi Equation, fluid dynamics

Japan Geoscience Union Meeting 2014
(28 April - 02 May 2014 at Pacifico YOKOHAMA, Kanagawa, Japan)

PEM29-P01 Room:Poster Time:April 30 18:15-19:30

Study of the slowly drifting narrowband structure in type-IV solar radio bursts observed by AMATERAS

KATOH, Yuto[1*] ; IWAI, Kazumasa[2] ; NISHIMURA, Yukio[1] ; KUMAMOTO, Atsushi[1] ; MISAWA, Hiroaki[3] ; TSUCHIYA, Fuminori[3] ; ONO, Takayuki[1]

[1]Department of Geophysics, Graduate School of Science, Tohoku University, [2]Nobeyama Solar Radio Observatory, National Astronomical Observatory of Japan, [3]Planetary Plasma and Atmospheric Research Center, Graduate School of Science, Tohoku University

We show the type-IV burst event observed by AMATERAS on June 7, 2011, and reveal that the main component of the burst was emitted from the plasmoid eruption identified by the EUV images of SDO. The slowly drifting narrowband structure (SDNS) appear in the spectra of the burst. By a statistical analysis, we reveal that SDNS appeared with the duration of tens to hundreds of millisecond and with the typical bandwidth of 3 MHz. For the generation mechanism of SDNS, we propose the wave-wave coupling between Langmuir waves and whistler-mode chorus emissions generated in a post-flare loop, inferred from the similarities of the plasma environments between a post-flare loop and the equatorial region of the Earth's inner magnetosphere. We assume that a chorus element with a rising tone is generated at the loop-top of a post-flare loop. By referring to the propagation properties of chorus in the magnetosphere, we assume that the chorus element propagates downward along the magnetic field line and then propagates away from the central region of the flare-loop toward the outer edge of the loop where the plasma density is relatively small. By the magnetic field and plasma density models, we quantitatively estimate the expected duration of radio emissions generated through the coupling between Langmuir waves and chorus during its propagation in the post-flare loop and find that the observation properties of duration and bandwidth of SDNS are consistently explained by the proposed generation mechanism. The characteristics of SDNS are its intermittency in time and the negative frequency drift in the limited frequency band. While observation in the terrestrial magnetosphere shows that chorus is a group of large amplitude wave elements naturally generated intermittently, the mechanism proposed in the present study can explain both intermittency and slowly drifting narrowband structure in the observed spectra.

Keywords: solar radio burst, solar corona, wave-particle interaction

Japan Geoscience Union Meeting 2014
(28 April - 02 May 2014 at Pacifico YOKOHAMA, Kanagawa, Japan)

PEM29-P02 Room:Poster Time:April 30 18:15-19:30

Numerical simulation of magnetic field generation by relativistic effect in high intensity laser experiments

KAWAZURA, Yohei[1*] ; YOSHIDA, Zensho[1]

[1]Graduate School of Frontier Sciences, The University of Tokyo

It has been a big mystery how the seed (primordial) magnetic field is generated in the universe. In fluid description of plasma, a magnetic filed is coupled with a mechanical vorticity then represented as curl of canonical vorticity. Recently, Mahajan and Yoshida proposed a novel mechanism of vorticity generation by relativistic effect [1, 2]. The relativistic plasma have two vorticity generating terms, one is so-called baroclinic term(S_T). The baroclinic term is known to be weak except for strongly thermal nonequilibrium state (e.g. shock front). Mahajan and Yoshdia proposed that, even if the system is barotropic, there appears another term available to generate vorticity due to the relativistic effect (S_R).

Recent progress in high intensity laser experiment enables us to obtain relativistic electron plasma, and some of the workers established high accuracy measurement of the generated magnetic field [3]. The relativistic vorticity generation (RG) is expected to be verified in such high intensity laser experiments.

In this study, we conducted numerical simulation for the proposal of the experimental verification. We have following objectives; is RG sufficiently working in actual experiment? If not, in what parameters will RG effectively work? What is the characteristics of the magnetic field given by RG? We calculated for parameters relevant to the experiment in Ref. 3. Observing the ratio of relativistic baroclinicity to thermodynamic baroclinicity, we can state that thermal baroclinic effect is governing and RG is not sufficiently working. By raising the hot electron temperature or decreasing the ratio of skin depth to scale length, the ratio is improving (Fig).

[1] S. M. Mahajan and Z. Yoshida, Phys. Rev. Lett. 105, 095005 (2010).
[2] S. M. Mahajan and Z. Yoshida, Phys. Plasmas 18, 055701 (2011).
[3] S. Mondal et al., PNAS 109, 8011 (2012).

Keywords: relativistic plasma, high intensity laser experiment, magnetic field generation

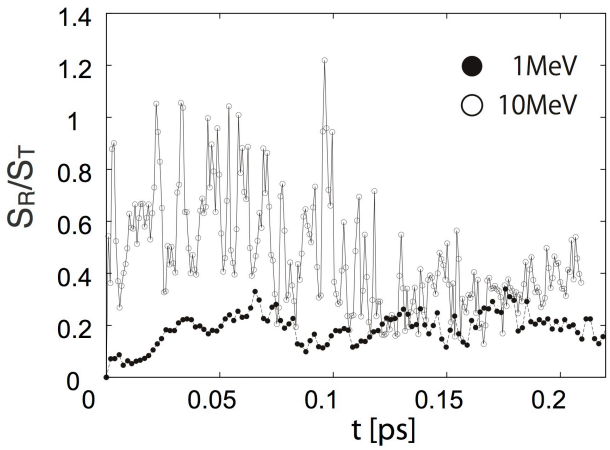

Japan Geoscience Union Meeting 2014
(28 April - 02 May 2014 at Pacifico YOKOHAMA, Kanagawa, Japan)

PEM29-P03 Room:Poster Time:April 30 18:15-19:30

The acceleration rate of cosmic rays in the cosmic ray modified shocks

SAITO, Tatsuhiko[1*] ; HOSHINO, Masahiro[1] ; AMANO, Takanobu[1]

[1]EPS, The University of Tokyo

It is a still controversial matter whether the production efficiency of cosmic rays (CRs) is relatively efficient or inefficient (e.g. Helder et al. 2009; Hughes et al. 2000; Fukui 2013). In upstream region of SNR shocks (the interstellar medium), the energy density of CRs is comparable to a substantial fraction of that of the thermal plasma (e.g. Ferriere 2001). In such a situation, CRs can possibly exert a back-reaction to the shocks and modify the global shock structure. These shocks are called cosmic ray modified shocks (CRMSs). In CRMSs, as a result of the nonlinear feedback, there are almost always up to three steady-state solutions for given upstream parameters, which are characterized by CR production efficiencies (efficient, intermediate and inefficient branch).

We evaluate qualitatively the efficiency of the CR production in SNR shocks by considering the stability of CRMS, under the effects of i)magnetic fields and ii)injection, which play significant roles in efficiency of acceleration.

By adopting two-fluid model (Drury & Völk, 1981), we investigate the stability of CRMSs by means of time-dependent numerical simulations. As a result, we show explicitly the bi-stable feature of these multiple solutions, i.e., the efficient and inefficient branches are stable and the intermediate branch is unstable, and the intermediate branch transit to the inefficient one. This feature is independent of the effects of i) shock angles and ii) injection.

Furthermore, we investigate the evolution from a hydrodynamic shock to CRMS in a self-consistent manner. From the results, we suggest qualitatively that the CR production efficiency at SNR shocks may be the least efficient.

Keywords: shocks, particle acceleration, feedback from cosmic rays

Japan Geoscience Union Meeting 2014
(28 April - 02 May 2014 at Pacifico YOKOHAMA, Kanagawa, Japan)

PEM29-P04 Room:Poster Time:April 30 18:15-19:30

2D Full Particle-In-Cell Simulation on a High Beta Collisionless Shock and Particle Acceleration

MATSUKIYO, Shuichi[1*] ; MATSUMOTO, Yosuke[2]

[1]Kyushu University, [2]Chiba University

High beta and relatively low Mach number shocks are commonly present in a vriety of space and astrophysical environments, like the earth's bow shock, the heliospheric termination shock (effective beta is rather high due to the presense of pickup ions), galaxy cluster merger shocks, etc. Even such high beta shocks show some evidences that high energy particles are possibly accelerated there. Voyager 2 spacecraft revealed that the fluxes of non-thermal electrons and ions (the latter are called as termination shock particles) are enhanced at the crossings of the termination shock. Radio synchrotron emissions from relics of galaxy cluster mergers imply the presence of relativistic electrons accelerated in the merger shocks. In this study we perform two-dimensional full particle-in-cell simulation to discuss structure of the shock as well as the acceleration process of electrons. The one-dimensional simulations performed in the past showed that under the high beta and relatively low Mach number conditions the shock is more or less laminar and time stationary and electron acceleration occurs through the so-called shock drift mechanism. Here, we reveal that two-dimensional structure of the shock is highly complex even for such a high beta and a low Mach number and further that some electrons are accelerated to high energy but their acceleration mechanism appears not to be so simple as that reproduced in one-dimensional simulations.

Keywords: collisionless shock, numerical simulation, particle acceleration

Japan Geoscience Union Meeting 2014
(28 April - 02 May 2014 at Pacifico YOKOHAMA, Kanagawa, Japan)

PEM30-01 Room:503 Time:April 30 14:45-15:10

Kelvin-Helmholtz turbulence in space and astrophysical plasmas

MATSUMOTO, Yosuke[1*]

[1]Graduate School of Science, Chiba University

Solar wind interactions with magnetized or un-magnetized planets destabilize planetary boundaries such as the magnetopause of the Earth magnetosphere and the ionopause of Mars and Venus. The Kelvin-Helmholtz (K-H) instability arising at a velocity shear layer has been considered to be important for momentum transport of the solar wind across the boundary layers, and been a universal nature of the planetary interactions. Linear and nonlinear growths of the instability depend on background plasma and magnetic field configurations. At the Martian ionopause, where the ionospheric ion escape is expected by the K-H instability, a fast (˜400 km/s), delute (˜1 /cc) plasma flow directly interacts with a high density (10^4-10^5 /cc), low temperature (a few thousand K) plasma. The situation can be found similarly at the terrestrial magnetopause, where in-situ observations have often indicated growth of the instability and resultant transport of the solar wind plasma into the magnetosphere, in the sense that the K-H instability grows in a strongly inhomogeneous plasma.

In this presentation, we review nonlinear evolutions of the K-H instability in strongly inhomogeneous plasmas. The evolutions are characterized by the secondary instabilities such as the Rayleigh-Taylor instability and the magnetic reconnection, by which a coherent eddy structure are destroyed and the energy is transported to smaller scales. Recent kinetic plasma simulations have shown that electron-scale structures are spontaneously generated as a consequence of the secondary instabilitties (Karimabadi et al., 2013). The micro-scale structure accompanied with the MHD-scale evolution enhanced mixing of collisionless plasmas. It was also found that the spatial size of the turbulent area was quickly broaden when coupled with a coalescence of large scale K-H modes, that is, the inverse energy cascade (Matsumoto & Seki, 2010). When nonlinear mode coupling was considered the time scale of the inverse energy cascade can be even faster than the fastest growing mode of the K-H instability. These nonlinear features in micro and macro scales have large impact on plasma transport process in the solar wind - planetary interactions as well as in astrophysical plasmas.

Keywords: Kelvin-Helmholtz instability, turbulence, Earth’s magnetosphere, Planetary atmosphere

Japan Geoscience Union Meeting 2014
(28 April - 02 May 2014 at Pacifico YOKOHAMA, Kanagawa, Japan)

PEM30-02 Room:503 Time:April 30 15:10-15:30

Experimental Study on Turbulent Transport using ElectroHydroDynamics Convection Turbulence

NAGAOKA, Kenichi[1*] ; YOSHIMURA, Shinji[1] ; HIDAKA, Yoshiki[2] ; TERASAKA, Kenichiro[2] ; YOKOI, Nobumitsu[3] ; MASADA, Yohei[4] ; MIURA, Hideaki[1] ; TSUNETA, Saku[5] ; KUBO, Masahito[6] ; ISHIKAWA, Ryoko[6]

[1]National Institute for Fusion Science, [2]Kyushu Univ., [3]Tokyo Univ., [4]Kobe Univ., [5]ISAS, [6]NAOJ

Turbulent transport is a very general subject in a wide area of physics research. The phenomena that we are interested in are very complex ones associated with structure formations in turbulence. It is well known that the Kolmogorov scaling appears in three-dimensional isotropic turbulence. However, it is less interested because nothing happens. In many cases of our interest, some structures appear in turbulence due to symmetry breaking such as temperature gradient, density gradient, intensity gradient of turbulence, rotation, velocity shear, magnetic field, etc. We have proposed a new experimental approach to turbulent transport using ElectroHydrodynamic Convection (EHC).

The EHC is a convection motion driven by the electric field in a liquid crystal, where the gravity and the temperature gradient in a Rayleigh Bernard convection (RBC) system can be replaced by the electric field alone. When the electric field is increased, the EHC becomes turbulent, which is the same feature as RBC with stronger buoyant force. Non-dimensional parameters characterizing EHC turbulence can be easily controlled with the biased voltage. The Rayleigh number is proportional to voltage squared and the Prandtl number is inversely proportional to the frequency of biased ac voltage, respectively. When the EHC turbulence experiment on a rotating table becomes possible in future, the Rossby number can be also controllable.

In the first step of the EHC turbulence experiment, particle transport in homogeneous EHC turbulence without rotation (symmetric case) was evaluated with a particle tracing technique. The small particles put in the liquid crystal can visualize local flow velocity in the EHC turbulence and the particle transport can be evaluated by the orbit tracing of particles. The diffusive nature (random walk process, the Hurst number ˜0.5) of particle transport was observed in the EHC turbulence. The effective diffusivity increases with the Rayleigh number with the power index of ˜0.85. These results are very similar to turbulent transport properties in viscos fluids (Navier-Stokes system).

The details of EHC turbulence experiment in laboratory frame without symmetry breaking and three experimental plans will be discussed. One is an investigation of non-uniformity effects on turbulent transport with inhomogeneity of turbulence intensity (spatial gradient of the Rayleigh number). Second one is an investigation of rotation effect on turbulent transport. These experiments on turbulent transport may reveal some general effects of symmetry breaking of scalar field and vector field, respectively. The last one is a laboratory simulation of the convection zone in stars and/or planet atmosphere with three-dimensional geometry identical to the real geometry (rotating spherical shell with radially driven convection). The radially-driven turbulence in rotating spherical shell have never realized in laboratory. Using ECH turbulence, turbulence can be driven in the radial direction with radial electric field. The convective zone in the Sun is the first target because of relatively large Rossby number˜0.1-1.

Keywords: turbulent transport experiment, symmetry breaking, EHC, liquid crystal

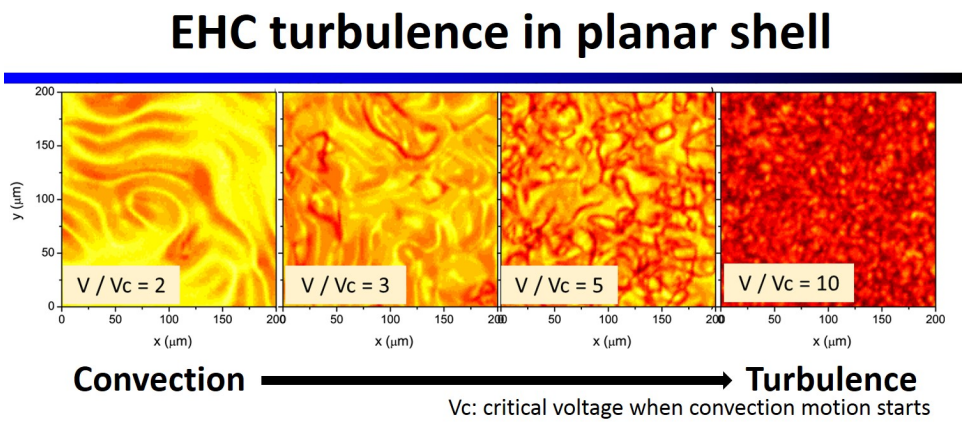

Japan Geoscience Union Meeting 2014
(28 April - 02 May 2014 at Pacifico YOKOHAMA, Kanagawa, Japan)

PEM30-03 Room:503 Time:April 30 15:30-15:45

Investigation of magnetic flux transport on the solar surface based on satellite data and auto-tracking technique

IIDA, Yusuke[1*]

[1]ISAS/JAXA

Spatial displacement of patch structure on the solar surface is investigated based on satellite data and auto-tracking technique.

Magento-convection system on the solar surface is thought to be important not only as a cause of various solar activities but also as an actual observable magneto-convection on the stellar surface. One important issue is how magnetic flux is transported there. In global scale, the transport of magnetic field is treated as a diffusion now. However it is not clear that diffusion treatment is appropriate in magneto-convection system. The aim of this study is to understand if the diffusion treatment of magnetic field transport in global scale is good or not.

I investigate the dependence of mean-square displacement on elapsed time by using auto-tracking technique, which is thought to be one of the critical characteristics for global-scale description of transport.

The longest magnetogram data obtained by Hinode/FG is used. In that data, number of tracked patches is enough for statistical study, more than 40000. The obtained dependence show a different character above and below the point of L˜10^4 km. Below that scale, it has a power-law dependence with an index of ˜-1.4, namely super-diffusion scheme. However, in the larger scale, the power-law dependence becomes ˜-0.6, namely sub-diffusion scheme. These characters can be explained by the network flow pattern qualitatively. Below the network scale, patch is transported by constant flow (˜0.3km s^{-1}) from center of network cell to edge of the cell addition to the large (˜1km s^{-1}) perturbing flow of granulation. On the other hand, above the network scale, patches experience the trapping around stagnation point of network flow, which makes displacement of patch shorter than that only by diffusion motion.

Keywords: the Sun, magnetic field, convection, diffusion, feature recognition

Japan Geoscience Union Meeting 2014
(28 April - 02 May 2014 at Pacifico YOKOHAMA, Kanagawa, Japan)

PEM30-04 Room:503 Time:April 30 15:45-16:00

Dynamic structure of convective motion depending on the height with line profile originating at solar photosphere

OBA, Takayoshi[1*] ; IIDA, Yusuke[2] ; SHIMIZU, Toshifumi[2]

[1]The Graduate University for Advanced Studies, [2]ISAS/JAXA

On the solar surface, there are bright cellular patterns which are called granules, separated by narrow dark regions named intergranular lanes. These spatial patterns result from surface convection. The surface convection induces the magnetic field dynamics and it is considered as an energy source of corona heating problem. Therefore, it is important to understand a convective motion in revealing the mechanism of corona heating problem. However, the smallness of its spatial structure prohibits us from resolving granular patterns in the observation. Furthermore, though the vertical structure is important in convection mechanism, it is difficult to observe it because there are few methods for a direct observation of solar interior. In this study, we investigate the height dependence of the vertical velocity and its spatial correlation with granular pattern based on the analysis of spectrum obtained by Solar Optical Telescope (SOT) on board the Hinode satellite. SOT/Spectropolarimeter (SP) obtains the spectrum including the Fe I 630.13/630.25nm lines, which corresponds the solar photosphere. The high spatial resolution of SP enables us to obtain spectra in granule and intergranular lanes separately. In addition, the seeing free condition in space observation enables the long time observation with high resolution, in this study, which is difficult for ground base observation. Consequently, we can remove the 5-min oscillation, which affects the radiative intensity and Doppler velocity, and then reduce errors of the analysis.

In this study, we focus on line profile of Stokes I originating in quiet region. Vertical velocity of convection is obtained from the Doppler shift of the line profile. We also analyze the wavelength structure of the line profile. Because of the dependence of absorption coefficient on wavelength, the intensity at different wavelength position reflects the structure at different height. The intensity at the line center reflects the structure in the higher layer, while the intensity at the line wings reflects the structure in the lower layer. We found that the difference of convective velocity between upper and lower level are typically 300 m s-1. At some locations, it exceeds 1km s-1. Taking into account that the speed of sound is approximately 7km s-1, it means that there are remarkable acceleration or deceleration around the solar surface. Further, there is a tendency between convective motion and acceleration, that granular region has upward motion with deceleration and intergranular region has downward motion with acceleration. In the presentation, we will discuss about the description of typical convective structure on the solar surface and what happens where has the different structure.

Keywords: sun, convection, spectrum, phtosphere

Japan Geoscience Union Meeting 2014
(28 April - 02 May 2014 at Pacifico YOKOHAMA, Kanagawa, Japan)

PEM30-05 Room:503 Time:April 30 16:15-16:30

Particle acceleration and magnetic field generation in the relativistic jet-plasma interactions

ARDANEH, Kazem[1*] ; CAI, Dongsheng[1]

[1]Department of Computer Science, University of Tsukuba, Ibaraki 305-8573, Japan

The aim of the current work is to analyze particle acceleration and magnetic field generation related to propagation of a relativistic electron-ion jet front into an unmagnetized ambient electron-ion plasma. We have focused on the earliest evolution in shock formation. The analysis is on the basis of a three-dimensional relativistic electromagnetic particle-in-cell (PIC) code. The results demonstrate that the Weibel instability is responsible for generation of strong small-scale magnetic fields and subsequent particles acceleration. In agreement with previous studies the majority of the particles acceleration occurs behind the jet front. Initially, the incoming electrons respond to field fluctuations growing as a result of the Weibel instability. Therefore, the electron channels are generated and the total magnetic energy grows linearly due to the mutual attraction between the channels, and downstream advection of the magnetic field fluctuations. When the magnetic fields become strong enough to deflect the much heavier ions, the linear growth rate of instability decreases as a result of oppositely directed electron-ion currents and topological change in the structure of magnetic fields. The Ion channels are then merged and magnetic energy increases more slowly at the expense of the energy stored in ion stream. It has been clearly illustrated that the ion channels develop through a larger scale in the longitudinal direction, while extension of the electron filaments is limited. Hence, the ions channels are the sources of deeply penetrating magnetic fields. Our results are in valid agreement with those reported in the literature.

Keywords: Relativistic jets, Particle acceleration, Magnetic field generation, Weibel instability

Japan Geoscience Union Meeting 2014
(28 April - 02 May 2014 at Pacifico YOKOHAMA, Kanagawa, Japan)

PEM30-06 Room:503 Time:April 30 16:30-16:45

Magnetohydrodynamic evolutions of the Richtmyer-Meshkov instability in astrophysical and laboratory plasmas

SANO, Takayoshi[1*]

[1]Institute of Laser Engineering, Osaka University

The Richtmyer-Meshkov instability (RMI) in magnetohydrodynamics is of great interest in many fields such as astrophysical phenomena, laboratory experiments, and inertial confinement fusion. The RMI occurs when an incident shock strikes a corrugated contact discontinuity. A strong shock wave traveling through the density inhomogeneity of magnetized interstellar medium is a promising site of the RMI. This astrophysically common event plays a key role in determining the dynamics of supernova remnants and gamma ray bursts. Recent laboratory experiments are designed to test the magnetic field amplification due to the RMI by the use of laser-induced shock waves. In inertial confinement fusion, the RMI excited at several capsule interfaces amplifies the perturbations that seed the Rayleigh-Taylor instability. For the fast ignition approach, the utilization of an external magnetic field to guide the fast electrons is discussed proactively and sheds light on the impact of magnetohydrodynamic (MHD) instabilities during the implosion.

The inclusion of a magnetic field brings two important consequences into the RMI, which are the amplification of an ambient field and the suppression of the unstable motions. The magnetic field can be amplified by the stretching motions at the interface associated with the RMI. A strong magnetic field inhibits the nonlinear turbulent motions of the RMI. The vorticity generated by the interaction between a shock front and a corrugated contact discontinuity is the driving mechanism for the RMI. For the cases of MHD parallel shocks, the role of the magnetic field is to prevent the deposition of the vorticity on the interface, and stabilize the RMI.

We have investigated that the critical strength of a magnetic field required for the suppression of the RMI numerically by using a two-dimensional single-mode analysis. For the cases of magnetohydrodynamic parallel shocks, the RMI can be stabilized as a result of the extraction of vorticity from the interface. A useful formula describing a critical condition for magnetohydrodynamic RMI is introduced and is successfully confirmed by direct numerical simulations. The critical field strength is found to be largely dependent on the Mach number of the incident shock. If the shock is strong enough, even low-beta plasmas can be subject to the growth of the RMI.

Keywords: MHD instability, astrophysical plasmas, laboratory plasmas

Japan Geoscience Union Meeting 2014
(28 April - 02 May 2014 at Pacifico YOKOHAMA, Kanagawa, Japan)

PEM30-07 Room:503 Time:April 30 16:45-17:00

Gyrokinetic simulation of multi-scale plasma turbulence

WATANABE, Tomo-hiko[1*]

[1]Graduate School of Science, Nagoya University

As is well known, spatio-temporal scales of plasma phenomena are characterized by multiple scale-lengths. As the scale-separation may not necessarily hold, multi-scale phenomena have been regarded as a common subject in the space and laboratory plasma studies. Magnetic reconnection is discussed as one of the examples. On the other hand, turbulence involves macro- and micro-scale structures simultaneously, and shows the fluctuation spectrum in a wide wavenumber range. Here, we discuss plasma turbulence with multiple scale-lengths, focussing on turbulent transport in magnetic fusion plasma.

By means of the gyrokinetic simulation, we have investigated transport phenomena in case with the electron temperature gradient (ETG) turbulence and the trapped electron mode (TEM) driven by a density gradient, where two scale-lengths characterizing the turbulence are involved. If both the two modes are unstable, after development of the ETG turbulence with a short spatio-temporal scale, the TEM instability grows with a long spatio-temporal scale. We have found an interesting case where the TEM drives a shear (zonal) flow with a longer spatio-temporal scale by which ETG and TEM fluctuations are regulated. The obtained result implies a possibility of turbulent transport reduction with a different driving source with a help of cross-scale interaction through zonal flows.

Furthermore, we have carried out a large-scale gyrokinetic simulation of multi-scale turbulence including the ion temperature gradient mode, where a turbulence spectrum from ion to electron scales as well as its dynamical evolution is studies. In the presentation, we will discuss characteristics of the multi-scale plasma turbulence and related transport.

∗This work is based on collaboration studies with Y. Aasahi (TiTech), S. Maeyama, M. Nakata, Y. Idomura (JAEA), A. Ishizawa, M. Nunami, and H. Sugama (NIFS). Under supports for the research collaborations, the numerical simulations are carried out by utilizing Plasma Simulator (NIFS), Helios (IFERC-CSC), and K (AICS, Riken). This work is also partly supported by by the MEXT grant for HPCI Strategic Program Field No.4, and by grants-in-aid of MEXT.

Keywords: turbulence, transport, kinetics, simulation

Japan Geoscience Union Meeting 2014
(28 April - 02 May 2014 at Pacifico YOKOHAMA, Kanagawa, Japan)

PEM30-08 Room:503 Time:April 30 17:00-17:15

Plasma heating by nonlinear development of a finite amplitude whistler wave

SAITO, Shinji[1*] ; NARIYUKI, Yasuhiro[2] ; UMEDA, Takayuki[3]

[1]Graduate School of Science, Nagoya University, [2]Faculty of Human Development, University of Toyama, [3]Solar-Terrestrial Environment Laboratory, Nagoya University

A two-dimensional, three-velocity (2D3V) particle-in-cell simulation has been done in order to study nonlinear development of a finite amplitude and long wavelength R-mode wave propagating parallel to the mean magnetic field, where the fluctuation energy is 10% of the mean magnetic field and the wavelength is about the ion inertial length. The simulation has shown that the bulk motion associated with the finite amplitude wave triggers the modified-two-stream instability that generates electrostatic field in the quasi-perpendicular direction. The electrostatic field scatters ions in the perpendicular direction and electrons in the parallel direction. About 70% of fluctuation energy of the initially imposed R-mode decreases in one gyro-period of ion. The dissipation through the modified-two-stream instability in the two-dimensional system is more effective than the parametric instability in the one-dimensional system. Further the simulation found that quasi-perpendicular-propagating electromagnetic fluctuations are enhanced through the nonlinear development of the R-mode. Discussion will focus on both the plasma heating and the nonlinearly enhanced fluctuations propagating quasi-perpendicular directions.

Keywords: Whistler wave, Solar wind, Nonlinear development, Plasma heating, Particle-in-cell simulation

Japan Geoscience Union Meeting 2014
(28 April - 02 May 2014 at Pacifico YOKOHAMA, Kanagawa, Japan)

PEM30-09 Room:503 Time:April 30 17:15-17:30

A theoretical model of nonlinear Alfven waves in expanding accelerating solar wind plasmas

NARIYUKI, Yasuhiro[1*]

[1]Faculty of Human Development, University of Toyama

During about forty years, a lot of studies have discussed the linear and nonlinear dynamics of Alfven waves in solar wind plasmas. Although the uniform plasmas are assumed in most past studies, the effects of the inhomogeneity of background plasmas cannot be negligible in the inner heliosphere, in which several future spacecraft missions are planned. In the present study, a nonlinear evolution equation of envelope-modulated Alfven waves is derived from the magnetohydrodynamic accelerating expanding box model by using the reductive perturbation method. The effects of the acceleration of solar wind to nonlinear evolution are discussed in detail.

Keywords: solar wind, Alfvenic turbulence

Japan Geoscience Union Meeting 2014
(28 April - 02 May 2014 at Pacifico YOKOHAMA, Kanagawa, Japan)

PEM30-P01 Room:Poster Time:April 30 18:15-19:30

Alfven wave resonance in density profile structure and the effect for nonlinear phenomenon

TSUTSUMI, Akihiro[1*] ; SUZUKI, Takeru[1]

[1]Nagoya University

Wave transport in plasma (e.g. Alfven wave) is a universal phenomenon for astrophysical fluid which is effected by electromagnetic force. Presence of

density structure in plasma causes these wave reflection, and prevents smooth transport for one direction. However, it is known that if the density structure is like square well form, Alfven wave is trapped in the structure and wave reflection does not occur. It seems that this wave trapping is a ordinary case and concerns with physical phenomenon, because density valley usual exist in plasma. For example, it is pointed out that Alfven wave energy is dissipated at low-density area which is located in surface of the sun, and this mechanism is relate to coronal heating.

At linear phase, we can understand analytically the property of Alfven wave transport on square well density profile. Therefore, we can also understand the condition that wave trapping and no reflection occurs. At this phase, the flow is well-regulated and steady state, and compressibility effect (e.g. pressure or density vary) doesn't appear because Alfven wave is essentially transverse wave. However, as the wave injection continues, the amplitude increases and nonlinear effect turns important. At this phase, the flow is complicated due to trapped wave's collision, and square well density profile can not keep the form. As a result, the resonance condition will change voluntarily. This density profile is universal in the plasma gas, so above physical mechanism is important for understanding plasma phenomenon.

In our numerical simulation, we pay attention voluntarily structural change due to linear phase shift to nonlinear phase. Consequently, the linear phase resonance condition directly affects the time evolution in nonlinear phase. We will introduce the result.

Japan Geoscience Union Meeting 2014
(28 April - 02 May 2014 at Pacifico YOKOHAMA, Kanagawa, Japan)

PEM30-P02 Room:Poster Time:April 30 18:15-19:30

The effect of the ion gyro motion to nonlinear processes of the Kelvin-Helmholtz instability

UENO, Satoshi[1*] ; UMEDA, Takayuki[1] ; NAKAMURA, Takuma[2] ; MACHIDA, Shinobu[1]

[1]Solar-Terrestrial Environment Laboratory, [2]Los Alamos National Laboratory

Nonlinear evolution of the Kelvin-Helmholtz instability (KHI) at a transverse velocity shear layer in an inhomogeneous space plasma is investigated by means of a four-dimensional (two spatial and two velocity dimensions) electromagnetic Vlasov simulation. When the rotation direction of the primary KH vortex and the direction of ion gyro motion are same, there exists a strong ion cyclotron damping. In this case, spatial inhomogeneity inside the primary KH vortex is smoothed and the secondary Rayleigh-Taylor instability is suppressed. The ion gyro motion also suppresses the formation of secondary vortices in the spatial scale smaller than the ion gyro radius, when the rotation direction of the vortex and the direction of ion gyro motion are same. As a result, the secondary instabilities take place at different locations in the primary KH vortex, where the rotation direction of the secondary vortex and the direction of ion gyro motion are opposite. These results indicate that secondary instabilities occurring in the nonlinear stage of the primary KHI at the Earth's magnetospheric boundaries might show dawn-dusk asymmetries.

Keywords: the Kelvin-Helmholtz instability, Vlasov simulation, space plasma, nonlinear processes, secondary instabilities

Japan Geoscience Union Meeting 2014
(28 April - 02 May 2014 at Pacifico YOKOHAMA, Kanagawa, Japan)

PEM30-P03 Room:Poster Time:April 30 18:15-19:30

Magnetohydrodynamic and Radiation Hydrodynamic Simulations of Tidal Disruption Events by a Supermassive Black Hole

KAWASHIMA, Tomohisa[1] ; OHSUGA, Ken[2] ; MATSUMOTO, Ryoji[3*]

[1]Shanghai Astronomical Observatory, [2]NAOJ, [3]Chiba University

Gas clouds or a star approaching a supermassive black hole can be disrupted by its tidal force. Such tidal disruption events enable us to observe the luminosity variations and state transitions triggered by the increase of the accretion rate, and give us hints to understand the transitions between different types of active galactic nuclei. Furthermore, the interval between the state transitions restricts the angular momentum transport rate, which determines the time scale of viscous evolution of an accretion disk. In 2014, tidal disruption flares are expected in two objects. One is the Galactic center supermassive black hole Sgr A$*$. A gas cloud named G2, whose mass is three times of the Earth mass is now approaching Sgr A$*$, and its pericenter passage will be in March, 2014. Since the distance from the black hole is well inside the radius of the accretion disk around Sgr A$*$, the tidally disrupted gas cloud will interact with the accretion disk. We carried out three-dimensional magnetohydrodynamic simulations of this interaction by applying a MHD code CANS+ based on the HLLD scheme. We found that the accretion rate increases more than 10 times during this outburst, and that magnetically driven jets are ejected. Increase of the X-ray and radio luminosity takes place within 1 month after the passage. The second object we expect an outburst is Swift J1644+57, which showed extremely high energy outburst in March 2011. This object locates at the center of a galaxy at redshift z=0.35. The energy released in this outburst indicates that the outburst was triggered by a disruption of a star. The luminosity of this source exceeded the Eddington luminosity for a 1-million solar mass black hole for period longer than a year but the X-ray luminosity decreased 100 times in August 2012. This darkening can be interpreted as the transition from a supercritically accreting slim disk state to a sub-critically accreting standard disk state. We carried out radiation hydrodynamic simulations of this event and showed that mass of the stellar debris is accumulating in the outer disk. When the surface density of the outer disk exceeds the threshold for the transition from a standard disk to a slim disk, the disk mass will accrete supercritically onto the black hole. Numerical results indicate that the luminosity of Swift J1644+57 may exceed the Eddington luminosity again in 1-2 years from the darkening.

Keywords: accretion disk, MHD, radiation hydrodynamics, black hole, tidal disruption, state transition

Japan Geoscience Union Meeting 2014
(28 April - 02 May 2014 at Pacifico YOKOHAMA, Kanagawa, Japan)

PEM31-01 Room:503 Time:May 1 15:15-15:40

Physics of weakly ionized dusty plasmas in planet formation

OKUZUMI, Satoshi[1*]

[1]Graduate School of Science and Engineering, Tokyo Institute of Technology

Planets form in gas disks around young stars. These protoplanetary disks are a typical example of weakly ionized plasmas in space: they are cool (∼10-1000 K) but are nonthermally ionized by galactic cosmic rays and stellar X-rays. The disks can also viewed as dusty plasmas as they contain micron-size dust particles from which planets form.

In this talk, we highlight interesting aspects of protoplanetary disks as weakly ionized dusty plasmas, and discuss their importance in planet formation as well as the MHD of the disks themselves. In particular, we focus on the interplay between charged dust particles and disk's MHD turbulence. Ionized accretion disks are prone to become turbulent because of the magnetorotational instability (MRI; Balbus & Hawley 1991). In protoplanetary disks, the activity of MRI strongly depends on how much dust has grown to larger solid bodies, as small dust particles determine the ionization degree of the disk gas. Meanwhile, turbulence, if present, drives the relative velocity of solid particles, which in turn affects how far the particles can grow by collisions. We briefly review recent developments in the numerical study of MRI-driven turbulence, and then discuss possible coevolution of MRI turbulence and dust particles as predicted by our latest self-consistent simulation (Okuzumi & Hirose 2012).

We will also highlight the importance of plasma heating by turbulent electric fields. A simple order-of-magnitude estimate shows that electric fields in MRI turbulence can significantly heat up electrons in the gas. This implies that Ohm's law can become *nonlinear* in the field strength. To study the nonlinearity of Ohm's law, we construct a gas-dust charge reaction model that takes into account the heating of ionized gas particles as well as impact ionization by hot electrons (Okuzumi & Inutsuka, in prep.). We find that the heating gives rise to negative differential resistivity at a high electric field strength. This occurs because heated electrons more frequently adsorb onto dust particles. The reduced conductivity will lead to suppressed MHD turbulence. Our ionization balance calculations predict that this effect become important in realistic protoplanetary disks (Mori & Okuzumi, in prep.).

Keywords: weakly ionized plasma, dust, planet formation, MHD, turbulence

Japan Geoscience Union Meeting 2014
(28 April - 02 May 2014 at Pacifico YOKOHAMA, Kanagawa, Japan)

PEM31-02 Room:503 Time:May 1 15:40-16:00

Ionospheric disturbances studied by high-resolution GPS total electron content observations

TSUGAWA, Takuya[1*] ; NISHIOKA, Michi[1] ; SAITO, Akinori[2] ; OTSUKA, Yuichi[3] ; ISHII, Mamoru[1]

[1]National Institute of Information and Communications Technology, [2]Graduate School of Science, Kyoto University, [3]Solar-Terrestrial Environment Laboratory, Nagoya University

The Global Positioning System (GPS) is a worldwide precise radio-navigation system formed from a constellation of at least 24 satellites at 20,200 km altitude, 4.2 R_E from the center of the Earth. GPS orbit configuration ensures that 5-10 satellites are visible from any single point on the Earth. The dual-frequency signals from the GPS satellites pass through the ionosphere to reach ground-based GPS stations. The phase and group velocities of radio waves vary in the ionosphere depending on the integrated electron density, that is total electron content (TEC), along the ray path and on the frequency of the radio waves. Using these characteristics, the TEC integrated along the ray path between a GPS satellite and a receiver can be accurately measured using two GPS signals in different frequencies. The TEC strongly reflects variations in the ionosphere at an altitude of about 300 km, where is the peak height of ionospheric electron density.

We have developed high-resolution TEC maps using dense GPS receiver networks. We have been collecting all the available GNSS receiver data in the world to expand the TEC observation area. These GNSS data are provided by IGS, UNAVCO, SOPAC, and other regional data centers. Currently, we are providing global and regional maps of absolute TEC, detrended TEC, and rate of TEC change index (ROTI). These data and quick-look maps are archived and available in DRAWING-TEC website (http://seg-web.nict.go.jp/GPS/DRAWING-TEC/).

These high-resolution GPS-TEC maps have been applied to studies of various ionospheric disturbances. Sudden increase in TEC caused by solar flares were studied using global TEC observations. Regional TEC observations have revealed new characteristics of large- and medium-scale traveling ionospheric disturbances (LSTIDs and MSTIDs). Recently, clear concentric waves and short-period oscillations were observed after huge earthquakes/tsunamis and massive tornadoes, indicating that acoustic and/or gravity waves propagate upward from the lower atmosphere and reach the ionosphere.

In this presentation, we will introduce recent studies of ionospheric disturbances using high-resolution GPS-TEC observations.

Keywords: ionosphere, GPS, TEC, thermosphere

Japan Geoscience Union Meeting 2014
(28 April - 02 May 2014 at Pacifico YOKOHAMA, Kanagawa, Japan)

PEM31-03 Room:503 Time:May 1 16:15-16:30

Observation of Lightning in Protoplanetary Disks by Ion Lines

MURANUSHI, Takayuki[1*] ; AKIYAMA, Eiji[2] ; INUTSUKA, Shu-ichiro[3] ; NOMURA, Hideko[4] ; OKUZUMI, Satoshi[4]

[1]Kyoto University, [2]The National Astronomical Observatory of Japan, [3]Nagoya university, [4]Tokyo Institute of Technology

Lightning in protoplanetary disks is an important elementary process in protoplanetary disk science. It has been studied as a candidate mechanism for chondrule formation, and it provides unique window to probe the electromagnetic state of the protoplanetary disks. As a consequence, multiple lightning models has proposed for protoplanetary disks, and it is important for protoplanetary disk astrophysics to observationally distinguish which model is correct. Here we study the possibility of observationally distinguishing lightning models in protoplanetary disks.

Lightning on Earth is discharge phenomenon in the air, and the gas discharge physics in air has been studied for centuries and is well understood process. But it has been observed that lightning takes place under electric field amplitude well below the dielectric strength of the air, the fact that has been a long standing mystery. Here, dielectric strength of an insulating material is the maximum amplitude of the electric field the subject material does not cause the electric breakdown. It is physical property of central importance for discharge physics.

In attempt to solve the mystery, traditional Townsend breakdown model has been challenged by new discharge models such as Druyversteyn-Penning breakdown model and runaway breakdown model. The values of the dielectric strength according to the latter two model are much smaller than it by Townsend breakdown model.

We can distinguish the breakdown models by their dielectric strength. Dielectric strength is the point where the electrons accelerated by the electric field reaches certain ionization energy. The electric field also accelerates the positively-charged ion species to the energy comparable to the electrons. Because the ionization energy is a universal constant, the accelerated ion energies are also constant. Observationally, this means that we will observe ion velocities much faster than the thermal velocity, and the observed velocities will be independent of the local density nor temperature among the lightning regions. This will be unique observational feature to detect and distinguish breakdown models in protoplanetary disks. For example, under disk gas that consists of 92% H_2 and 8% He, the characteristic ion speed of HCO^+ is 7.1km/s, 2.9km/s and 0.49km/s, respectively, for Townsend breakdown model, Druyversteyn-Penning breakdown model, and runaway breakdown model.

We have calculated the velocity distribution of the three ion species HCO^+, DCO^+ and N_2H^+, taking the lightning models into consideration. We have simulated the line profile and two-dimensional position-velocity images. We found lightning features of 10-100mJy appear in line profile. Recent ALMA observations e.g. by Mathews et al. (2013) and Qi et al. (2013) achives ˜10mJy sensitivity. Therefore we can reject some of the lightning models based on ALMA archive data, and distinguish lightning models by future ALMA observations.

Keywords: Protoplanetary disks, Discharge phenomena, Lightning, Weakly-ionized plasma, astrophysical plasma

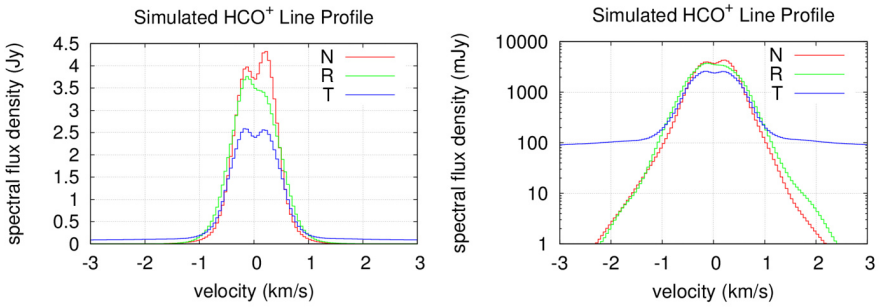

Simulated HCO^+ line profile of an MMSN disk located at distance d=56pc, inclination i = 7(deg). The three curves indicate disk without lightning (N), disk with runaway breakdown model (R), and with Townsend breakdown model (T), respectively.

Japan Geoscience Union Meeting 2014
(28 April - 02 May 2014 at Pacifico YOKOHAMA, Kanagawa, Japan)

PEM31-04 Room:503 Time:May 1 16:30-16:45

Investigation of attractive forces associated with overlapping Debye spheres using N-body simulations

ITOU, Hotaka[1*] ; AMANO, Takanobu[1] ; HOSHINO, Masahiro[1]

[1]Department of Earth and Planetary Science, Graduate School of Science, The University of Tokyo

Dust grains are quite common in space. They are thought to exist in, e.g., molecular clouds, protoplanetary disks, Earth's magnetosphere, and planetary rings. In addition, also in laboratories, the lattice formation of dust grains is the well-known phenomena and called Coulomb crystallization. Dust grains immersed in plasmas usually acquire large amount of charges due to several charging processes such as collisions with plasma partilcles and photoemission. Then the charged grains and the ambient plasma are strongly coupled with each other, and such plasmas are called dusty plasmas or complex plasmas. Since in situ observations in the solar system or Ikezi's prediction of Coulomb crystallization, dusty plasmas have been studied for not only astrophysical applications but also industrial applications.

When collisions between dust grains and plasma particles dominate charging processes, the dust grains are nagatively charged because generally the flux of electrons is larger than that of ions. Thus we expect that they repel each other. However, in realty, the force on dust grains is quite complex due to the interaction with the ambient plasma and several types of forces have been proposed (e.g., Shukla and Eliasson [2009]). Interestingly, some attractive forces may also exist and play important roles in aggregation or crystallization of dusty plsamas.

One of proposed attractive forces is that of due to the overlapping of Debye spheres (ODS). Resendes et al. [1998] showed that the potential between two dust grains is similar to Lennard-Jones potentials, which is repulsive at short distance and weakly attractive at longer distance. Moreover, Hou et al. [2009] showed that this type of attractive interaction has, if indeed it exists, the drastic aggregation and crystallization effect in dusty plasmas. On the other hand, it was suggested that the ODS attractive force does not exist when particles electrically trapped by grains are negligible ,i.e., the orbital motion limited (OML) theory is valid (Lampe et al. [2000]), and it has not been confirmed experimentally.

The aim of our study is to investigate the possibility of the ODS potential, by using direct N-body simulations, which allow us to investigate the electrostatic potential structure around the dust grains with minimun assumptions. By using a newly developed N-body simulation code implementing Ewald's sum algorithm, in which the short-range part of the potential is calculated in real space and the long-range part is calculated in wavenumber space, we have shown that in plasmas with a low plasma parameter there does not exist the ODS attractive force. In this study, we introduce the mesh and extend the code to implement the PM (particle-mesh) or PPPM (particle-particle particle-mesh) method allowing us to perform simulations with a much more particles to attempt the investigation of plasmas with the large plasma palameter.

Japan Geoscience Union Meeting 2014
(28 April - 02 May 2014 at Pacifico YOKOHAMA, Kanagawa, Japan)

PEM31-05 Room:503 Time:May 1 16:45-17:00

Test-particle simulation of electron-H2O elastic collision along the magnetic field line around Enceladus

TADOKORO, Hiroyasu[1*] ; KATOH, Yuto[2]

[1]Tokyo University of Technology, [2]Department of Geophysics, Graduate School of Science, Tohoku University

Saturn's inner magnetosphere is dominated by water group neutrals originated from Enceladus' water plume [e.g., Shemansky et al., 1993; Richardson et al., 1998; Esposito et al., 2005]. The neutrals in the inner magnetosphere contribute to one of the important loss processes of plasma through plasma-neutral collisions. However, little has been reported on a quantitative study of the electron loss process due to electron-neutral collisions. In this paper, we will focus on the collisional loss process with neutrals.

We examine the variation of equatorial electron pitch angle distribution and loss rate of precipitated electrons into Saturn's atmosphere through pitch angle scattering due to elastic collisions with neutral H_2O along Saturn's magnetic field line around Enceladus. We focus on 1 keV electrons as a typical energy in the present study. To examine the variation of those, we perform one-dimensional test-particle simulation when the co-rotating electron flux tube passes the dense H_2O region in the vicinity of Enceladus (˜6.4 minutes). Results show that the equatorial electron pitch angle distribution near the loss cone ($<$20 degrees and $>$160 degrees) decreases with time through pitch angle scattering due to elastic collisions. It is found that the electrons of ˜19 % to the total number of equatorial electrons at the initial condition are lost in ˜380 seconds. The calculated loss time is twice faster than the loss time under the strong diffusion.

Keywords: plasma-neutral collision, Saturn, Enceladus, elastic collision, pitch angle scattering

Japan Geoscience Union Meeting 2014
(28 April - 02 May 2014 at Pacifico YOKOHAMA, Kanagawa, Japan)

PEM31-06 Room:503 Time:May 1 17:00-17:15

MHD wave-driven mass loss from gas giants and effects on atmospheric structure

TANAKA, Yuki[1*] ; SUZUKI, Takeru[1] ; INUTSUKA, Shu-ichiro[1]

[1]Department of Physics, Nagoya University

Recently a number of exoplanets have been found, and some of them are close-in gaseous planets. Such planets are called hot Jupiters, and their surface temperatures are ˜1000K due to strong irradiation from central stars.

Information of radius and orbital period of exoplanet can be observed by transit method which is the one of method to detect exoplanets. Additionally, atmospheric composition can be estimated by variation of spectrum between transiting and non-transiting, and atmospheric structure can be estimated by multi-wavelength transit observation. From these observations, inflated hydrogen atmosphere of hot Jupiters and atmospheric escape are suggested. It is observed that escaping atmospheric flow is very fast, and mass loss rate is also estimated. However, detailed mechanism of mass loss from hot Jupiters are still unknown.

We propose a new mechanism of mass loss, which is mass loss driven by magneto-hydrodynamic wave, same as solar wind. Atmosphere is weakly ionized because surface temperatures of hot Jupiters are about 1000K, but it is good to treat as ideal MHD at upper atmosphere. If gas giant have magnetic field and turbulence exist on the surface of planet, magneto-hydrodynamic wave will be generated. The wave propagates upward and dissipates in upper atmosphere, then gas flow is accelerated. In this work, we apply numerical calculation of solar wind to mass loss from hot Jupiters. In consequence, mass loss by this magnetically driven wind is comparable to observed mass loss rate, therefore magnetically driven wind can be important role in mass loss from hot Jupiters.

We also derive an analytical solution for radius and mass dependence of mass loss rate, and it shows a good agreement with numerical results. Dissipation of MHD wave in the atmosphere also affects on atmospheric structure. The gas flow is accelerated to supersonic at upper atmosphere, and temperature become several tens of thousand kelvin. In this talk, we will discuss the possibility of mass loss from general gaseous planet and effects on atmospheric structure.

Keywords: exoplanet, atmospheric escape

Japan Geoscience Union Meeting 2014
(28 April - 02 May 2014 at Pacifico YOKOHAMA, Kanagawa, Japan)

PEM31-07 Room:503 Time:May 1 17:15-17:30

Group motion of heteromorphic fine particles in HF discharge plasma

MIENO, Tetsu[1*] ; MASUDA, Risa[2] ; MORIBAYASHI, Takashi[2] ; HAYASHI, Yasuaki[3]

[1]Grad. School Sci. Technol, Shizuoka Univ., [2]Dept. Phys., Shizuoka Univ., [3]Grad. School Eng., Kyoto Inst. Technol.

Related with complex systems, fine-particle plasmas have much attention to scientists and engineers [1, 2]. Hence, we are trying to make fine-particle plasmas with heteromorphic particle distributions by using a high-frequency (HF) Ar plasma. And the motions of charged particles are observed. In a stainless steel chamber (150 mm in diam, 150 mmh), 100 mm in diam disk electrodes and a 80 mm in diam metal ring are set. In this experiment, HF argon discharge is produced at 10˜13 Pa by applying HF voltage of about 270˜290 V_{rms} to the lower disk-electrode with respect to the upper grounded disk-electrode. And a ring is added on the lower electrode to confine fine-particles. The particles used are silicon carbide, which has diameter of about 8 um, or silicon-nitride (about 8 um), or short hemp (about 25 um diam. 10 ? 1500 um long). They are injected from a dust dropper. A digital microscope camera (SELMIC LWD100) and a CCD video camera are used to investigate the particle behaviors. Under a condition of discharge voltage V_d= 280 V_{rms}, discharge current I_d= 0.2 A_{rms} and pressure p(Ar)= 13 Pa, a disk-shaped cloud is generated as shown in Fig. 1. Each particle motion and the particle-group motion are recorded by the cameras. We could observe planet-like motions like Fig. 2 (track of a SiC particle). In case of the short hemp, there are spin motions and planet-like motions. We conjecture that these motions are activated by the dust-acoustic perturbation.

[1] Y. Hayashi, K. Tachibana, J. Vac. Sci. Technol. A 14 (2) (1996) 506.
[2] H. Thomas, G.E. Morfill, V. Demmel, Phys. Rev. Lett. 73 (1994) 652.

Keywords: fine particle plasma, heteromorphic particles, self organization, planetary motion, spin, dust plasma

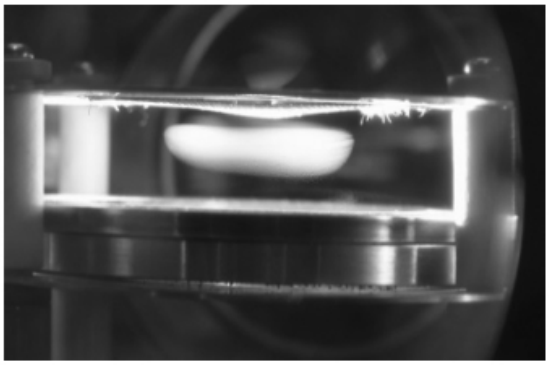

Fig. 1 Fine particles in the HF plasma.

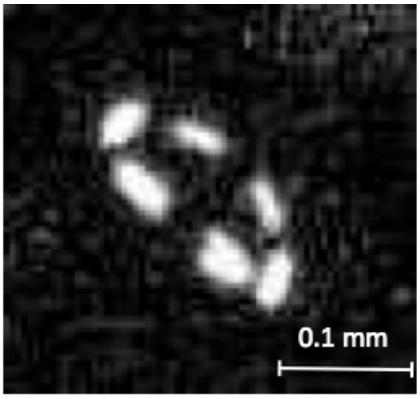

Fig. 2 Planet-like motion of a particle.

Japan Geoscience Union Meeting 2014
(28 April - 02 May 2014 at Pacifico YOKOHAMA, Kanagawa, Japan)

PEM32-01 Room:503 Time:May 2 09:00-09:15

A new instability along toroidal magnetic field in differentially rotating plasmas

HIRABAYASHI, Kota[1*] ; HOSHINO, Masahiro[1]

[1]Department of Earth and Planetary Science, The University of Tokyo

We discuss a new type of instability expected to take place in an accretion disk, which has a differentially rotating plasma threaded by a weak magnetic field, by performing linear eigenvalue analysis. We study the linear stability of a disk with a localized, toroidal magnetic field in the radial direction, which can be expected in an accretion disk during the nonlinear evolution of the magneto-rotational-instabilities (MRI).

The MRI is believed to be a strong source of magneto-hydro-dynamic (MHD) turbulence and the resultant angular momentum transport in the accretion disk, which is required for the gas to accrete onto the central object. Once the MRI grows, the system is chiefly governed by the toroidal and radial magnetic field newly generated by the dynamo action of MRI. Such a configuration allows the Alfven waves to propagate along toroidal direction.

In this talk, we study the linear stability of the Alfven wave in the local Cartesian coordinate, the so-called shearing periodic box, and show that the toroidally propagating Alfven wave can become unstable if its wavelength is larger than the length scale of the localized magnetic field gradient. We investigate our results of the linear eigenvalue analysis by changing the structure of the localized magnetic field, and discuss some properties of the instability with examining the eigenvectors and eigenvalues. It is revealed that this type of instability may also appear in non-rotating plasma, but it is highly suppressed in a rigid body rotating plasma. In addition to the linear analysis, the corresponding nonlinear behavior will also be discussed by using MHD numerical simulations. This instability plays an important role in the plasma transport because it probably couples with the magnetic reconnection occurring in the equatorial plane and then to contributes to the saturation mechanism of the MRI.

Japan Geoscience Union Meeting 2014
(28 April - 02 May 2014 at Pacifico YOKOHAMA, Kanagawa, Japan)

PEM32-02 Room:503 Time:May 2 09:15-09:30

Particle acceleration and angular momentum transport during magnetorotational instability in kinetic accretion disks

HOSHINO, Masahiro[1*]

[1]The University of Tokyo

Magneto-rotational instability (MRI) in a gravitational rotating system is known to play an important role on the formation of the astrophysical accretion disk and the angular momentum transport, and the nonlinear time evolution of magneto-rotational instability has been extensively investigated by using MHD simulations so far. The mean free path of plasma, however, is not necessarily smaller than the characteristic scale length for some classes of astrophysical accretion disks, and the collisionless behavior of MRI beyond the MHD approximation needs to be understood. In this talk, we study momentum transport and particle acceleration of the kinetic (collisionless) MRI by focusing on magnetic reconnection. We discuss that a strong pressure anisotropy is associated with the formation of the channel flow, and the anisotropic channel flow can lead to a rapid magnetic reconnection, that can occurs sporadically in three-dimensional system. As a result of the reconnection, non-thermal power law distribution with a hard spectral index p=1-1.5 is quickly formed. We also discuss that the so-called alpha parameter in the standard accretion disk model, which is numerically measured from the Reynolds and Maxwell stresses, can be dramatically enhanced during the nonlinear time evolution of MRI. The kinetic MRI is one of plausible mechanisms to explain much more efficient angular momentum transport and high-energy particle emissions observed from massive black holes such as Sgr A$*$.

Keywords: Space and astrophyiscal plasmas, accretion disk, particlle acceleration, magnetic reconnection, angular momentum transport

Japan Geoscience Union Meeting 2014
(28 April - 02 May 2014 at Pacifico YOKOHAMA, Kanagawa, Japan)

PEM32-03 Room:503 Time:May 2 09:30-09:45

Numerical Simulation of Kinetic Magnetorotational Instability using a new Hybrid Technique

SHIRAKAWA, Keisuke[1*] ; AMANO, Takanobu[1] ; HOSHINO, Masahiro[1]

[1]Faculty of Science, University of Tokyo

The evolution of Magnetorotational instability (MRI) is considered to be important in the context of efficient angular momentum transport in the accretion disks in our universe. Conventionally, the nonlinear evolution of MRI is studied under the MHD approximation which assumes the mean free path of the plasma is sufficiently small compared to the actual size of the disk. However some classes of the accretion disks, for example the disk around SgrA∗, are found to be constituted with a collision less plasma and therefore the kinetic effect of the plasma, such as generation and relaxation of the pressure anisotropy, should be taken into account.

For the inclusion of the kinetic plasma effects, hybrid code, which treats ions as particles and electrons as massless charge neutralizing fluid, may provide a robust approach resolving the ion scale physics and integrating over the Keplerian time scale. However in the 2 dimensional simulation of the MRI, it is well known that the system eventually grows to a set of channel flows. In this state, the density of the plasma is found to be extremely low in the region where the magnetic field is enhanced as a result of a strong dynamo effect of the differential rotation of the disk. In this low density, strong magnetic field region, the CFL condition determined by the R-mode wave is found to be severe. Moreover, since the extremely low density region is generated in the channel flow, the division-by-density operation in the conventional hybrid code leads to an unexpected termination of the calculation.

In this study we adopted a new approach of hybrid simulation to a differentially rotating system. In this approach, the finite electron inertia is taken into account which gives a upper bound in the phase velocity of the R-mode wave, providing a reduced CFL condition. In addition, the new approach is almost free from the division-by-density operation and the extremely low density region generated in the channel flow can then be calculated appropriately. With this new code we would like to discuss the nonlinear evolution of the 2 dimensional kinetic MRI.

Keywords: Magnetorotational Instability, Kinetic Plasmas, Accretion disks, Collisionless Plasmas, Hybrid code

Japan Geoscience Union Meeting 2014
(28 April - 02 May 2014 at Pacifico YOKOHAMA, Kanagawa, Japan)

PEM32-04 Room:503 Time:May 2 09:45-10:10

Self-organization and flow in high-beta magnetized plasmas

NAGATA, Masayoshi[1*]

[1]University of Hyogo, Graduate School of Engineering

The self-organized plasmas with high-beta such as spheromaks have the common features as magnetic reconnection, kinking behavior, particle acceleration and shock wave which are observed in space phenomena. Dynamical process of explosive plasmoid ejection, magnetic field's twisting and reconnection could account for the various phenomena called astrophysical jets, solar coronal loops and Jupiter's zonal flow driven by thermal convection. As for fusion plasmas, to control externally plasma flow or rotation plays an important role on maintaining high-beta confinements with an optimized pressure gradient. It is well known that for example, the H-mode transition in tokamak plasmas is created by inward radial electric field and poloidal shear flow. The diamagnetic configuration like Field Reversed Confinement (FRC) with super high beta, in which ion flows generate currents, is normally analyzed based on two-fluid MHD relaxation model. In helicity-driven system, non-axisymmetric dynamic processes create current due to the dynamo action in the plasmas and relax them toward certain minimum energy equilibria. The non-axisymmetric behavior, which arises from a helical kink instability on the open flux, could be responsible for the formation and sustainment of the configurations by helicity injection [1]. In this conference, we will present recent topics about dynamics and relaxed states relevant to MHD relaxations, plasmoid ejection, dynamo and kinking behavior which are recognized as analogical phenomena in astrophysical and fusion plasmas.

It is possible to replicate astrophysical plasma phenomena in the laboratory because MHD has no intrinsic scale. The governing MHD equations can be expressed in a dimensionless form that is equally applicable to systems having scale lengths with many orders of range. Now, a point is how to produce flexibly plasmoid eruptions like solar flares by taking critical issues of geometry and topology into consideration. We will introduce the magnetized coaxial plasma gun (MCPG) to make it possible to investigate such a bubble burst-like behavior. The MCPG is often used to produce spheromaks with poloidal and toroidal magnetic fields generated by internal current. Historically the spheromak was for the first time produced by Alfven et al. by using the MCPG.

The driven-relaxed configurations with open field lines, as well as closed systems, are described by the force-free equilibrium (Jensen-Chu) equation, $\nabla \times B = \lambda B$, where λ is the force-free parameter. The nature of the relaxed states in helicity-driven systems is characterized by the strength of the external toroidal field and the value of λ determined by coupling to the MCPG. Note that in the doubly connected helicity-driven system, the flipped spherical torus (ST) state appears in the regime of $\lambda < \lambda e$, where λe is the lowest eigenvalue, so that it could be observed in laboratory experiments. The structural formation of the flipped field configuration incorporates the self-reversal process of the toroidal and poloidal fields. This self-organizing phenomenon may have some analogy to reversal of the dipole field of Earth generated by a dynamo action. It is fundamentally important to elucidate a current-reversal phenomenon occurring in space and laboratory plasmas. We have observed this novel current-reversal phenomenon in our HIST experiment [2, 3]. The most important discovery of this experiment is that spherical torus plasmas tend to self-organize to the flipped states while reversing the direction of the external toroidal field [2, 3]. This experimental finding provides, for the first time, evidence for the existence of the relaxed states which were theoretically predicted.

References

[1] M. Nagata et al., Phys. Rev. Lett. 71, 4342 (1993)
[2] M. Nagata et al., Phys. Rev. Lett. 90, 225001 (2003)
[3] M. Nagata et al., Phys. Plasmas 10, 2932 (2003)

Keywords: plasmoid, spheromak, flow, self-organization, MHD relaxation, dynamo

Japan Geoscience Union Meeting 2014
(28 April - 02 May 2014 at Pacifico YOKOHAMA, Kanagawa, Japan)

PEM32-05 Room:503 Time:May 2 10:10-10:30

Observations of Alfvenic waves in the solar atmosphere

OKAMOTO, Joten[1*]

[1]ISAS/JAXA

Coronal heating and the acceleration of the solar wind are unsolved problems in solar physics. The propagation of Alfven waves along magnetic field lines is one of the candidate mechanisms to carry energy to large distances from the surface and heat the coronal plasma. However, such waves had not been observed for years.

The solar physics satellite, Hinode, was launched in 2006, and it opened the door to the world of coronal waves. Hinode observations have directly resolved small-scale transverse oscillations of field lines as a result of Alfven/Alfvenic waves in prominences (Okamoto et al. 2007) and spicules (De Pontieu et al. 2007) which are typical chromospheric features embedded in the corona. These waves had a period of 2-5 minutes (low frequency) and the velocity amplitudes are up to 20 km/s. If we assume these are propagating waves, the waves have enough power to heat the corona. However, since the wavelength of these waves is as long as or longer than the observed structures, it is difficult to resolve the phase difference along the field lines. This means we cannot know whether they are propagating or standing waves.

More recently, we had a challenge to detect ”propagating” waves (Okamoto and De Pontieu 2011). In this study, we developed an algorithm to detect spicules and phase difference of waves along them automatically. As a result, upward- and downward-propagating waves as well as standing waves were successfully detected. With statistical analyses, it is found that the behaviour of waves depends on the evolution of spicules, and numerous waves are reflected at the top of spicules. These waves detected in this study are high-frequency ones, and the energy is not larger than that of low-frequency ones. Hence, it is suggested that low-frequency waves are more important for coronal heating.

Finally, oscillations/waves shown here are ubiquitous in the solar atmosphere and ”wave hunting” is getting more active after the Hinode launch. In addition, investigation of coronal waves is important for the derivation of physical parameters such as coronal magnetic field strength, which it is difficult to measure in observations. In this talk, I will show these studies with Hinode and introduce a new result with a new satellite ”IRIS”.

Keywords: Sun, corona, wave, Hinode

Japan Geoscience Union Meeting 2014
(28 April - 02 May 2014 at Pacifico YOKOHAMA, Kanagawa, Japan)

PEM32-06 Room:503 Time:May 2 10:30-10:45

2.5D MHD Simulations of Solar Filament Formation by Condensation

KANEKO, Takafumi[1*] ; YOKOYAMA, Takaaki[1]

[1]Department of Earth and Planetary Science, The University of Tokyo

We investigate the formation mechanism of solar filaments by two-dimensional magnetohydrodynamic (MHD) simulations. Solar filaments are cool dense plasma clouds in the hot tenuous corona. Filaments abruptly erupt with flares, hence, they are the important objects to comprehend the explosive events in the solar atmosphere. On the other hand, their formation mechanism is still unclear as well as the mechanism for eruptions.

Filaments always appear inside the coronal arcade fields, and the cool dense plasma is sustained by the magnetic forces. Observations show that filaments are categorized as normal polarity filaments or inverse polarity filaments. The normal polarity filaments have the same polarity with the surrounding coronal magnetic fields, while the inverse polarity filaments have opposite polarity. One candidate to explain the origin of the cool dense plasma is condensation by the radiative cooling in the corona. The current condensation model can reproduce the normal polarity filaments, but not the inverse polarity filaments. We propose a new condensation model to reproduce the inverse polarity filaments, and demonstrate it by two-dimensional MHD simulations including radiative cooling, thermal conduction along the magnetic field and gravity. Our model starts from the formation of the magnetic flux rope. The relatively dense plasma at the lower corona is trapped inside the flux rope and lifted up to the upper corona. The dense plasma causes imbalance between the radiative cooling and the background heating, while the thermal conduction along the closed field line of the flux rope does not suppress the thermal imbalance. Consequently, the condensation process is triggered and the cool dense plasma is formed. We test two types of heating term (one depends on magnetic pressure and the other depends on density) and two types of formation mechanisms of the flux rope (one is the conversing motion at the footpoints of the coronal arcade field and the other is the interaction between the emerging flux and the coronal arcade field). As a result, the cool dense plasma is formed inside the flux rope in every case. We also show that our model has a possibility to reproduce the density of solar filaments, which is 10 -100 times larger than that of the surrounding corona, qualitatively.

Keywords: solar filament, prominence

Japan Geoscience Union Meeting 2014
(28 April - 02 May 2014 at Pacifico YOKOHAMA, Kanagawa, Japan)

PEM32-07 Room:503 Time:May 2 11:00-11:15

Comparative study of Observation and Calculation of Hot Fast Flow above a Solar Flare Arcade

IMADA, Shinsuke[1*]

[1]Nagoya Univ. STEL

Solar flares are one of the main forces behind space weather events. However, the mechanism that drives such energetic phenomena is not fully understood. The standard eruptive flare model predicts that magnetic reconnection occurs high in the corona where hot fast flows are created. However, there is not enough observational knowledge of the physical parameters in the reconnection region. The inflow into the reconnection region, the temperature of the plasma in the reconnection region, and the temperatures and densities of the plasma jets predicted by reconnection, have not been quantitatively measured in sufficient. First, we will show a flare that occurred on the west solar limb on 2012 January 27 observed by the Hinode EUV Imaging Spectrometer (EIS) and found that the hot (?30MK) fast (>500 km s?1) component was located above the flare loop and discuss how extent we understand the key-region of solar flare. Second, it is important to answer why the most observation cannot detect the predicted flow or temperature in the reconnection region. One of the reasons why we cannot observe inside the magnetic reconnection region is due to its darkness. Generally we can see the bright cusp-like structure during solar flare, although the reconnection region is faint/blind. One may think that the temperature in the reconnection region is enough higher than that of cusp-like flare loops. Thus the wavelength of emission from reconnection region is different from flare loops. However, this is not entirely true. Magnetic reconnection causes rapid heating. Thus ionization cannot reach to the equilibrium stage. We have calculated the ionization process in the down stream of Petschek type magnetic reconnection. From our result, we can clearly see that plasma cannot reach the ionization equilibrium in the down stream of slow-mode shock. The typical emissions from magnetic reconnection region are FeIXX or FeXX, although the plasma temperature is equal to 40MK. The typical temperature and density of post flare loops are 10 MK and 10ˆ11 /cc, and the dominant emissions from post flare loops are from FeIXX to FeXXIII. Thus the wavelength of emission from reconnection region is not so much different from post flare loops. We will discuss how the emissions from reconnection region looks like by using several ionization calculations of magnetic reconnection.

Keywords: flare, corona, non-equilibrium ionization, sun

Japan Geoscience Union Meeting 2014
(28 April - 02 May 2014 at Pacifico YOKOHAMA, Kanagawa, Japan)

PEM32-08 Room:503 Time:May 2 11:15-11:30

Magnetic Evolutions at Extremely High Latitude Region during Polarity Reversal Observed with Hinode

SHIOTA, Daikou[1*] ; SHIMOJO, Masumi[2] ; SAKO, Nobuharu[3] ; KAITHAKKAL, Anjali john[3] ; TSUNETA, Saku[4]

[1]STEL, Nagoya University, [2]National Astronomical Observatory of Japan, [3]The Graduate University for Advanced Studies, [4]ISAS, JAXA

The magnetic field in the Sun's polar region is a key ingredient of the solar dynamo mechanism because the polar field strength at a solar minimum has a correlation with solar activity of the following cycle. The evolution processes of the polar field (its polarity reversal and its build-up after the reversal) are thought to be caused by magnetic flux transport due to meridional flow and diffusion by turbulent convection. Nevertheless, our understanding of the meridional flow and diffusion in the polar region is still poor because of many difficulties in magnetic observation near the limb.

We recorded time evolution of magnetic polarity distribution within the whole of both polar regions derived from the high-accuracy spectropolarimetric observation with Solar Optical Telescope aboard Hinode. In the north polar region, the latitudinal polarity inversion line (PIL) between the preexisting negative polarity region and transported positive polarity region migrates from 60 degrees latitude at January 2012 to 68 degrees latitude at September 2012. Then the whole of the north polar region becomes positive at September 2013. The migration speed of the PIL is 5 m s^{-1} (January - September 2012) and then becomes 8.5 m s^{-1} (September 2012 - September 2013). According to a flux transport model, the speed-up is understood as a result of a diffusion process. In contrast, the whole of the south polar region observed in March 2013 has still ample positive field. The PIL locates out of the observed region (over 67 degrees latitude).

We examined a few parameter sets of the meridional flow pattern and the diffusion coefficient with an advection-diffusion model. The observed PIL migration in the north polar region can be explained well if there is slightly strong diffusion without the meridional flow.

Keywords: photosphere, magnetic fields, spectropolarimetry, polarity reversal, dynamo

Japan Geoscience Union Meeting 2014
(28 April - 02 May 2014 at Pacifico YOKOHAMA, Kanagawa, Japan)

PEM32-09 Room:503 Time:May 2 11:30-11:45

Properties of small-scale jets in a sunspot chromosphere revealed through spectroscopic observations

KATSUKAWA, Yukio[1*] ; OI, Akihito[2] ; REARDON, Kevin[3] ; TRITSCHLER, Alexandra[3]

[1]National Astronomical Observatory of Japan, [2]Kyoto University, [3]National Solar Observatory

High-resolution observations with HINODE Solar Optical Telescope (SOT) revealed that small-scale jets frequently occur in a sunspot chromosphere though their driving mechanism is not well understood yet because of lack of spectroscopic information, such as temperatures and Doppler velocities, in the chromospheric observations with Hinode SOT. Spectroscopic observations of the small-scale jets were attempted using an Interferometric BIdimensional Spectrometer (IBIS) at the National Soar Observatory (NSO), and suggested that temperature enhancements associated with the jets happened in the lower chromosphere though their upward flows were not clearly detected (Reardon, Tritschler, Katsukawa 2013). We've tried obtaining another spectroscopic data set of a sunspot chromosphere with better spectral resolution with IBIS, and carried out careful analysis of spectral profiles and their temporal evolution. The study shows majority of the heated plasma in the lower chromosphere has a bulk flow slower than the sound speed in the chromosphere. The spectral profiles indicate enhancements in the blue wing, which suggests a part of the heated plasma has a supersonic upflow. In addition, small temperature enhancements are also found in the upper chromosphere near the end of the duration of the jets. The supersonic upflows are possibly responsible for heating in the upper chromosphere. This study provides an important observational support for slow-mode waves as acceleration and heating mechanism in the chromospheric jets. We are going to present a new spectroscopic observation of chromospheric jets made by the Interface Regiong Imaging Spectrograph (IRIS) spacecraft that has just started observations since 2013.

Keywords: the Sun, chromosphere, jet, spectroscopy, HINODE, IRIS

Japan Geoscience Union Meeting 2014
(28 April - 02 May 2014 at Pacifico YOKOHAMA, Kanagawa, Japan)

PEM32-10 Room:503 Time:May 2 11:45-12:00

Fast magnetic reconnection with a moving X-point in resistive MHD

MIYOSHI, Takahiro[1*] ; KUSANO, Kanya[2]

[1]Graduate School of Science, Hiroshima University, [2]STEL, Nagoya University

Fast magnetic reconnection in high magnetic Reynolds number plasmas is one of the most important physical process of explosive phenomena in space and astrophysical plasmas. In recent years, using high-resolution MHD simulations with high magnetic Reynolds numbers, it has been indicated that fast magnetic reconnection may be triggered by the plasmoid instability in a thin current sheet [1]. Moreover, a state-of-the-art high-resolution MHD simulation revealed that some of multiple secondary reconnection are developed as Petschek-like reconnection [2]. However, the detailed structure and dynamics of individual secondary reconnection is not clarified yet.

The objective of this study is to reveal the structure and dynamics of resistive magnetic reconnection with a moving X-point paying attention to the motion of the secondary reconnection. Particularly, we propose an asymmetric reconnection model where a local anomalous resistivity including a shifting motion is added to the two-dimensional Harris equilibrium. A high-resolution MHD simulation for the asymmetric resistive reconnection was performed using the HLLD approximate Riemann solver and analyzed with respect to the structure in detail. Besides, we discussed the possibility of a self-sustaining mechanism of the asymmetric reconnection due to the flow driven by the reconnection itself.

[1] e.g, N. F. Loureiro, et al., Phys. Plasmas, 19, 042303 (2012)
[2] K. Kusano, K. Nakabou, et al., in preparation

Keywords: magnetic reconnection, MHD, anomalous resistivity model

Japan Geoscience Union Meeting 2014
(28 April - 02 May 2014 at Pacifico YOKOHAMA, Kanagawa, Japan)

PEM32-11 Room:503 Time:May 2 12:00-12:15

Dynamical Petscheck Reconnection

KUSANO, Kanya[1*] ; NAKABOU, Takashi[1] ; MIYOSHI, Takahiro[2] ; VEKSTEIN, Grigory[3]

[1]STEL, Nagoya University, [2]Graduate School of Science, Hiroshima University, [3]Manchester University

Magnetic reconnection is the major mechanism for explosive energy liberation in various plasmas. However, the mechanism of fast reconnection in high magnetic Reynolds number (S) plasmas like the solar corona, in which $S>10^{10}$, is still unclear. The observations suggested that the reconnection rate in solar flares is as large as 10^{-2}, although the classical theory by Sweet (1958) and Parker (1963) predicted that the reconnection rate is limited by $S^{-1/2}$. While Petscheck (1964) proposed the fast reconnection model driven by slow mode shock, the previous simulation study suggested that the Petscheck-type reconnection is not stable in uniform resistivity and some anomalous resistivity or non-MHD effects are needed for fast reconnection.

In this paper, we developed the high-resolution magnetohydrodynamics (MHD) simulation of magnetic reconnection for the high-S (S~10^4-10^6) regime aiming at revealing the acceleration mechanism of magnetic reconnection in the MHD regime of uniform resistivity. We applied the HLLD Riemann solver developed by Miyoshi and Kusano (2005) to the high resolution two-dimensional MHD simulation of current sheet dynamics. The initial state is given by the Harris sheet equilibrium plus perturbation, and the uniform and constant resistivity model is adopted.

As a result, we found a new type of fast reconnection. When S is larger than 10^4, multiple X-line reconnection appears as a result of the secondary tearing instability and magnetic reconnection is accelerated through the formation of multiple plasmoids. Furthermore, we found that the electric current sheets between some particular magnetic island bifurcate to V-shape current layers and that the reconnection at the apex of bifurcated current layers is preferentially accelerated. The bifurcated current layers create slow mode shocks which more increase the reconnection rate up to about 0.05. The slow mode shocks are repeatedly created and dissolved corresponding to the formation and transportation of plasmoids. These results indicate that, even though resistivity is uniform, when the magnetic Reynolds number is high enough, the multiple X-line reconnection of Sweet-Parker current sheets (plasmoid reconnection) is switched to a new regime called ”dynamical Petschek reconnection”. The mechanism of transition from the conventional plasmoid reconnection to the dynamical Petscheck reconnection will be discussed.

Keywords: reconnection, Petscheck reconnection, MHD, simulation, slow mode shock

Japan Geoscience Union Meeting 2014
(28 April - 02 May 2014 at Pacifico YOKOHAMA, Kanagawa, Japan)

PEM32-12 Room:503 Time:May 2 12:15-12:30

Thermal conduction effect on the Petschek magnetic reconnection

KONO, Shunya[1*] ; YOKOYAMA, Takaaki[1]

[1]University of Tokyo

We simulated the magnetic reconnection including the nonlinear thermal conduction effect with two-dimensional MHD equations. Magnetic reconnection is considered to be the basic process of the solar explosive phenomena. In the atmosphere with high temperature and low density like solar corona, time-scale of the nonlinear heat conduction becomes shorter and can become comparable to the Alfven time-scale. Thermal conduction effect should be considered. Previous studies have showed that, in the model of magnetic reconnection produced by Petschek, adiabatic slow mode shock wave generated from the localized diffusion region is dissociated into isothermal shock wave and conduction front due to the thermal conduction. However, the effect of the thermal conduction on the energy release rate in the magnetic reconnection is not explained enough in the past.

Here we investigated how the thermal conduction influences the energy conversion rate. We calculated the energy release rate in different magnitude of the magnetic diffusivity to see the dependence on the Lundquist number. As a result, due to the thermal conduction effect, adiabatic shock wave is dissociated into isothermal shock wave and conduction front and this makes temperature in the reconnection outflow jet smaller. In the outflow region with small temperature, density becomes larger. Considering mass conservation between the mass flux in the reconnection inflow and that in the outflow, inflow velocity is accelerated because of larger density in the outflow region. This causes increase of the energy release rate in the magnetic reconnection. That increase rate tends to become larger as the magnitude of magnetic diffusivity becomes smaller. Smaller magnetic diffusivity correponds to the larger Lundquist number. In the real solar atmosphere, plasma gas has larger Lundquist number than that in this numerical simulation. This means that thermal conduction effect on the energy release rate in magnetic reconnection might become more effective in the real solar atmosphere.

Keywords: solar flare, magnetic reconnection, thermal conduction, corona

Japan Geoscience Union Meeting 2014
(28 April - 02 May 2014 at Pacifico YOKOHAMA, Kanagawa, Japan)

PEM32-13 Room:503 Time:May 2 12:30-12:45

Analysis on turbulent reconnection of three-dimensional resistive MHD simulation

WANG, Shuoyang[1*] ; YOKOYAMA, Takaaki[1] ; ISOBE, Hiroaki[2]

[1]The University of Tokyo, [2]Kyoto University

This study starts from a three-dimensional current sheet with random perturbation on velocity, in order to understand more on the 3D reconnection in a more general way.

Due to the periodic boundary condition, the core of current sheet quickly develops a resonance netlike pattern under tearing instability. Small reconnection site mainly form two chains on either side of the current sheet center and constitute a zigzag arrangement. The outflow from one reconnection site is fed into the counterpart on the other side thus composes a positive feedback system resembles even double tearing mode. As the inflow being enhanced, slow-mode shocks are identified along the current sheet. The conversion of the magnetic energy is further raised. Total kinetic energy of the current sheet presents 4 steps of development while first 3 exhibit linear growing tendency. At the same time, reconnection rate increases by 5 times compared with the early phase. Thus we have achieved faster reconnection without localized resistivity in a more universal idea.

Japan Geoscience Union Meeting 2014
(28 April - 02 May 2014 at Pacifico YOKOHAMA, Kanagawa, Japan)

PEM32-14 Room:503 Time:May 2 14:15-14:30

Ion Acceleration Mechanisms in the Exhaust Region of Magnetic Reconnection

TAKAMOTO, Makoto[1*] ; FUJIMOTO, Keizo[2]

[1]Max-Planck-Institute for Nuclear Physics, [2]National Astronomical Observatory of Japan

Magnetic reconnection is considered to be a key mechanism to convert magnetic field energy into plasma kinetic and thermal energy in various plasma phenomena, in particular, in many astrophysical systems. In collisional plasma, many works assuming magnetohydrodynamic approximation have revealed that plasma jets can be accelerated up to the upstream Alfven velocity. However, in the case of the collisionless plasma, which is common in many astrophysical phenomena, there is still no conclusive theory of the ion acceleration mechanism and the maximum plasma jet velocity because of the complexities of plasma phenomena and the associated high numerical cost.

In this study, we performed a large-scale 2D particle-in-cell simulations with adaptive mesh refinement under an open boundary condition. The simulation was performed until the MHD condition is well-satisfied in the exhausts,
which allows us to study a long-time dynamical evolution of the structure of the diffusion region and exhausts.
To analyze the detailed mechanisms of the ion acceleration in the exhausts, we also performed test particle simulations on the dynamical background plasma. We found that the ions are accelerated mainly by the electric field perpendicular to the reconnection plane. However, effects from other electric field components are not negligible;
in particular, the contribution from the electric field along the exhausts becomes significant as the ions are accelerated. We also compared the results with the velocity distribution functions inside of the exhausts.

In this talk, we present our numerical results of the particle-in-cell simulation, and discussed its physical interpretations of the structure. We also discuss the ion kinetic mechanisms leading to the formation of reconnection jets.

Keywords: magnetic reconnection, ion acceleration

Japan Geoscience Union Meeting 2014
(28 April - 02 May 2014 at Pacifico YOKOHAMA, Kanagawa, Japan)

PEM32-15 Room:503 Time:May 2 14:30-14:45

Waves and particle acceleration around the separatrices of magnetic reconnection

FUJIMOTO, Keizo[1*]

[1]National Astronomical Observatory of Japan

Understanding the properties of waves in magnetic reconnection is very important in collisionless plasmas. The waves can transport the momentum and energy between the different species in plasmas, which results in the anomalous magnetic dissipation, particle heating, and formation of non-thermal particles. Therefore, the wave activities relevant to the kinetic interactions can have a significant impact on the dynamical behaviour of magnetic reconnection. Theoretical modeling of waves in the reconnection region is also beneficial to reveal the reconnection dynamics using in-situ satellite observations where wave properties are obtained in much higher time resolution than plasma distribution functions.

Recent satellite observations in the Earth's magnetotail have shown that the wave activities are significantly enhanced in a broad range of frequency around the separatrices of anti-parallel magnetic reconnection. The waves were recognized as lower hybrid waves, Langmuir waves, electrostatic solitary waves (ESWs), and whistler waves. In most cases, they were associated with cold electron beams and density cavity. However, because of the limited space-time resolutions of the observations, it has been difficult to identify the generation mechanisms of the waves and their roles in magnetic reconnection.

In this study, large-scale 2D particle-in-cell simulations with adaptive mesh refinement have been performed under an open boundary condition. The simulations use a set of more realistic parameters than those in most other simulations, achieving lower plasma beta in the upstream region that leads to stronger electron beams in the reconnection region. The wave activities are dominant in the inflow side of the separatrices. The waves are generated mainly due to the electron beams that constitute the Hall current. The relatively weak beams before strong acceleration trigger the Buneman instability which results in the waves with a frequency of the lower hybrid range. The strong acceleration occurs along the field line due to a localized potential hump and causes the density cavity. The intense electron beams excite the electron two-stream instability and the beam driven whistler instability. The former mode gives the Langmuir waves and the flat-top electron distributions in the parallel direction, both of which have been observed frequently in the Earth's magnetotail. The latter mode, on the other hand, scatters the electrons in the perpendicular direction, forming isotropic distribution with non-thermal high-energy tail. Both the Buneman and electron two-stream instabilities evolve the ESWs in the nonlinear phases.

In this talk, we present the generation mechanisms of the waves around the separatrices and their roles in magnetic reconnection. The mechanism of the intense electron acceleration along the field line will be discussed.

Keywords: magnetic reconnection, plasma waves, particle acceleration, particle-in-cell simulations

Japan Geoscience Union Meeting 2014
(28 April - 02 May 2014 at Pacifico YOKOHAMA, Kanagawa, Japan)

PEM32-16 Room:503 Time:May 2 14:45-15:00

Minimum spatial scale for maintaining vigorous magnetic reconnection

SHIMIZU, Kenya[1*] ; FUJIMOTO, Masaki[2] ; SHINOHARA, Iku[2]

[1]University of Tokyo, [2]Institite of Space and Astronautical Science, Japan Aerospace Exploration Agency

Magnetic reconnection drives the fast release of magnetic energy in explosive events such as magnetic substorms in the Earth's magnetosphere and flares in the solar corona. On the large scale, reconnection is an MHD-scale process but its rate is controlled by the compact electron diffusion region (EDR), where electrons are not magnetized. Recent kinetic simulations have revealed the structure of EDR in a quasi-steady reconnection rate. In some works, it is suggested that an elongated electron jet in the outflow region does not affect the reconnection rate. However, it is not clear the spatial scale for determining the rate. We find that the minimum spatial scale for maintaining magnetic reconnection by using kinetic simulations on periodic and reflective wall boundary conditions. On the periodic condition, an outflow jet extends a large distance downstream from the X-line with the fast rate of reconnection. However, the influence of periodicity shortens the jet to a narrow structure though the rate of reconnection is still fast. This structure is the minimum spatial scale for maintaining magnetic reconnection. On the other hand, asymmetric reconnection is performed on the reflective wall condition to lead a slow motion of the diffusion region away from the wall, the so called 'X-line retreat.' During the retreat motion an outflow jet is blocked by the wall though the rate of reconnection is maintained. The structure of the blocked jet is very similar to the minimum spatial scale on the periodic condition. We quantitatively show the minimum structure for maintaining magnetic reconnection by comparing the result on these periodic and reflective conditions. We also find the minimum structure is independent of domain sizes but gets smaller with decreasing electron mass.

Keywords: magnetic reconnection, electron diffusion region

Japan Geoscience Union Meeting 2014
(28 April - 02 May 2014 at Pacifico YOKOHAMA, Kanagawa, Japan)

PEM32-P01 Room:503 Time:May 2 16:15-17:30

Magnetothermal instability in the solar outer corona

YOKOYAMA, Takaaki[1*]

[1]The University of Tokyo

We discussed an application of the magnetothermal instability (MTI) to the solar atmosphere. This instability proposed by Balbus (2000) occurs in weakly collisionless plasmas where non-isotropic thermal conduction plays a role in a magnetized atmosphere. The time scale of the maximum growth is given as approximately sqrt(H/g) where H is the scale height, and g is the gravity. The magnetic field must be weak enough since its tension force contributes as a restoring force.

The solar corona is a dilute hot atmosphere where the thermal conduction is non-isotropic. The MTI is possible to work in the upper corona around a few solar radii above the photosphere where the temperature is decreasing outward and the scale height is about one solar radius. The condition for weak horizontal magnetic field might be satisfied above a closed loop in the lower corona. If the MTI is effective in such regions, it might contribute to generate the waves or perturbations in the solar wind.

We found that the MTI is unlikely to work in the upper corona because of its strong magnetic field that suppress the growth of the geometrically possible wavelength modes. It is found that when the field strength is 0.1 times the real corona, the wavelength for the maximum growth is comparable with the geometrical radius. The growth time for this setup can be consistent with the low frequency fluctuations in the solar wind.

Keywords: Sun, corona, plasma, magnetohydrodynamics

Japan Geoscience Union Meeting 2014
(28 April - 02 May 2014 at Pacifico YOKOHAMA, Kanagawa, Japan)

PEM32-P02 Room:503 Time:May 2 16:15-17:30

Cosmic-ray Parker Instability and Galactic Plane Symmetry

KUDOH, Takahiro[1*] ; YOKOYAMA, Takaaki[2] ; KUDOH, Yuki[3] ; MATSUMOTO, Ryoji[3]

[1]National Astronomical Observatory of Japan, [2]University of Tokyo, [3]Chiba University

We study two-dimensional MHD numerical simulations of the Parker instability with the cosmic-ray pressure under the circumstance of the galactic disk. Instead of the symmetric boundary conditions on the galactic plane as often used, we solve the entire region of the disk. Numerical simulations show that the symmetric mode on the disk also grows when the cosmic-ray pressure is relatively large, while the glide reflection symmetric mode dominates on the disk when the cosmic-ray pressure is small. We confirm that the results are consistent with those of the liner analyses: the growth rate of the symmetric mode approaches that of the glide reflection symmetric mode as the cosmic-ray pressure becomes relatively large.

In the nonlinear stage, some loop structures of the magnetic field lines expand rapidly and grow into large structure when the cosmic-ray pressure is relatively large. Other loops, which start to grow a little later, are suppressed by faster growing loops located nearby and do not reach the nonlinear expansions. Eventually, the loop structure at the nonlinear stage is larger than that is expected form the linear analysis when the cosmic-ray pressure is relatively large.

When the nonlinear fast growing loops collide with another loops, the high density thin gas layers are formed by the compression between the loops. The figure shows the logarithmic density at that stage. Some of the high density gas shows filament structures and some of them look like high density loops. Similarities of these structures with some observational features and the relation of star formation activities can be studied further.

Keywords: MHD, Interstellar gas, Cosmic rays

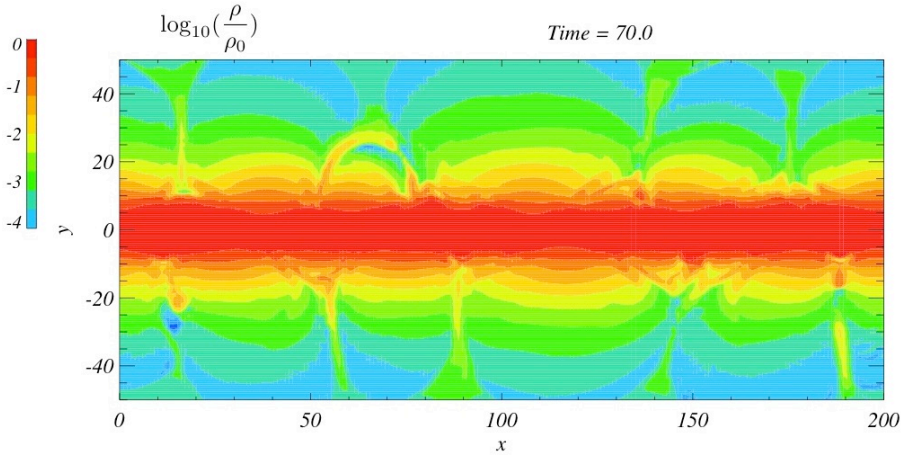

Japan Geoscience Union Meeting 2014
(28 April - 02 May 2014 at Pacifico YOKOHAMA, Kanagawa, Japan)

PEM32-P03 Room:503 Time:May 2 16:15-17:30

Formation of Dense, Cold Loops by Parker Instability in Galactic Gas Disks

PENG, Chih-han[1*] ; KUDOH, Yuki[1] ; ASAHINA, Yuta[1] ; MATSUMOTO, Ryoji[1]

[1]Faculty of Science, Chiba University

We performaced two dimensional numerical simulations of Parker instability taking into account the cooling and heating functions of the interstellar medium (Inoue et al. 2006). Our numerical experiment is based on the simulation code ”CANS+” in which the HLLD Riemann solver (Miyoshi & Kusano 2005) is used to solve the MHD equations. We found that the cold, dense filaments formed at the valley of magnetic field lines by Parker instability coupled with the cooling instability are deformed into loops of dense, cold gas when the Ram pressure at the left- and right-hand side of the filament is different. The maximum number density and the lowest temperature of cold, dense filament at 100Myrs is about 200 per cubic cm and 50K, respectively. These results support the model in which thermal instability triggered in the dense region formed by Parker instability is responsible for the formation of molecular loops found in the Galactic center region (e.g., Fukui et al. 2006).

Japan Geoscience Union Meeting 2014
(28 April - 02 May 2014 at Pacifico YOKOHAMA, Kanagawa, Japan)

PEM33-01 Room:503 Time:May 1 09:00-09:25

Effects of cosmological infall of galaxies: its discovery, plasma physical implications, and verification with ASTRO-H

MAKISHIMA, Kazuo[1*]

[1]Department of Physics, University of Tokyo

Clusters of galaxies are a system consisting of hundreds of galaxies that are gravitationally bound together. About 10% of the mass of each cluster is in the form of X-ray emitting hot plasmas, called Intra-Cluster Medium (ICM), that constitute the most dominant form of known baryonic components in the universe. The ICM is tenuous, hot, and magnetized, and is hence considered as the most ideal classical plasma ever known.

At central regions of many clusters, the ICM was considered to cool over the Hubble time by emitting X-rays, and lose its pressure. Then, the ICM would flow from outer to inner regions, and enhance the radiative cooling by raising the density. This catastrophy, called cooling flows, were long thought to be actually taking place, as X-ray observations kept discovering its evidence.(3) the energy is then transported to the cool ICM phase via Alfven waves and reconnection, (4) the two ICM phases are kept thermally stable by a mechanism known in Solar corona; and (5) the moving galaxies will gradually fall to the potential center as they transfer their dynamical energies to the ICM (Makishima et al., Publ. Astro. Soc. J. 53, 401, 2001). We have been striving to observationally enhance this novel scenario.

At central regions of many clusters, the ICM was considered to cool over the Hubble time by emitting X-rays, and lose its pressure. Then, the ICM would flow from outer to inner regions, and enhance the radiative cooling by raising the density. This catastrophy, called cooling flows, were long thought to be actually taking place, as X-ray observations kept discovering its evidence.

Through observations of clusters of galaxies with the 4th Japanese X-ray satellite ASCA launched in 1993, we found that the cooling flows are not taking place anywhere, even though the ICM ubiquitously shows mild temperature decrease towards the cluster center: there must be some unknown plasma heating source. We have hence proposed a novel plasma physical scenario; (1) the central galaxy has a magnetosphere, where the cooler plasma is confined and insulated from the surrounding hot ICM; (2) other galaxies, all moving in the cluster space, will receive resistance from the ICM and excite MHD turbulence therein; (3) the energy is then transported to the cool ICM phase via Alfven waves and reconnection, (4) the two ICM phases are kept thermally stable by a mechanism known in Solar corona; and (5) the moving galaxies will gradually fall to the potential center as they transfer their dynamical energies to the ICM (Makishima et al., Publ. Astro. Soc. J. 53, 401, 2001). We have been striving to observationally enhance this novel scenario.

Recently, we have obtained crucial evidence supporting (5). That is, we studied 34 clusters with various redshifts (0.1-0.9) with X-ray and optical wavelength. Then, galaxies in nearby clusters were confirmed to be much concentrated than the ICM, while these two components are nearly co-spatial at distant clusters (Gu et al., Astrophys. J. 767, id 157, 2013). That is, galaxies in each luster have been falling, on the Hubble time scale, to the center. This result not only provides the long-sought heating mechanism of the ICM and strengthen our hypothetical view, but means the discovery of a very large energy flow that has not been known. Furthermore, it can explain many other puzzles with clusters of galaxies.

We are now developing, under an extensive international collaboration, the innovative X-ray satellite ASTRO-H, to be launched in 2015. With ASTRO-H, we will be able to detect X-ray Doppler effects which is caused when moving galaxies drag the ICM around them, and study possible particle acceleration phenomena as a consequence of energy loss by galaxies.

Keywords: galaxies and their clusters, intra-cluster medium, X-ray emission, magnetoplasma effects, ASTRO-H satellite

Japan Geoscience Union Meeting 2014
(28 April - 02 May 2014 at Pacifico YOKOHAMA, Kanagawa, Japan)

PEM33-02 Room:503 Time:May 1 09:25-09:45

Direct measurement of the plasma momentum in a magnetic nozzle helicon plasma for electric propulsion

TAKAHASHI, Kazunori[1*] ; CHARLES, Christine[2] ; BOSWELL, Rod[2] ; CHIBA, Aiki[1] ; ANDO, Akira[1]

[1]Department of Electrical Engineering, Tohoku University, [2]Space Plasma, Power and Propulsion Laboratory, The Australian National University

The ion and electron energy distribution functions of a low-pressure, current-free helicon plasma in a magnetic nozzle configuration are experimentally investigated by electrostatic Langmuir probes including a radiofrequency compensated probe and a retarding field energy analyzer; the ions are electrostatically accelerated by a spontaneous potential drop of a double layer and/or ambipolar electric field, and only the energetic electrons can overcome the potential structure. The results indicate that the accelerated ions are spontaneously neutralized by the energetic electrons. These findings propose that the source system is applicable to an electrodeless and neutralizer-free plasma thruster.

Momentum of the plasma flow is one of essential physical parameters dominating the particle acceleration in both laboratory and space. Especially their interaction with magnetic fields have been significant subject associated with natural plasmas (astrophysical jets, magnetospheric physics, solar dynamics, aurora dynamics, etc.) and artificial plasmas (thermonuclear fusion devices, electric propulsion systems, plasma devices for material processing, etc.). The plasma momentum is equal in magnitude and opposite in direction to a thrust imparted from a plasma thruster for the electric propulsion device. The direct measurement of the thrust imparted from a magnetic nozzle helicon plasma thruster is successfully measured by using a pendulum thrust balance immersed in vacuum, where the thrust components arising from the presence of the physical boundaries and magnetic nozzle are also independently measured by attaching each component to the thrust balance. Further a laboratory experiment of a helicon plasma thruster is established to control only a plasma cross-field diffusion in a rapidly-divergent magnetic nozzle while maintaining a constant plasma injection into a magnetic nozzle. The thrust component due to a plasma pressure force inside the source cavity is constant and that due to the magnetic nozzle increases when inhibiting the cross-field diffusion in the nozzle. The latter force is well explained by an electron-diamagnetic-induced plasma momentum derived from two-dimensional momentum equations and approaches the theoretical limit derived from a one-dimensional model assuming an ideal magnetic nozzle with no plasma loss. Further a new source system approaching the ideal magnetic nozzle and the recent progress of the thruster performance will also be shown. It is noted that the above-described phenomena are occuring in current-free source system. These insights into the plasma thruster dynamics might include a common physics relating to the plasma acceleration in a non-uniform magnetic field in both the laboratory and space.

Keywords: plasma momentum, magnetic nozzle, helicon plasma, electric propulsion

Japan Geoscience Union Meeting 2014
(28 April - 02 May 2014 at Pacifico YOKOHAMA, Kanagawa, Japan)

PEM33-03 Room:503 Time:May 1 09:45-10:00

Laboratory in-situ experiments for plasma wave-particle interaction in linear magnetized plasma machine

KOGISO, Shun[1*] ; KATOH, Yuto[2] ; SHIMOYAMA, Manabu[1] ; KANEKO, Toshiro[3] ; MOON, Chanho[3] ; HIRAHARA, Masafumi[1]

[1]Solar-Terrestrial Environment Laboratory, Nagoya University, [2]Graduate School of Science, Tohoku University, [3]Graduate School of Engineering, Tohoku University

Wave-particle interactions are thought to play important roles to generate MeV electrons in the radiation belt. “ Wave-Particle Interaction Analyzer (WPIA) ” , which derives energy flaxes between wave and particle from simultaneous measurements of an electric field and particle velocity vector, has been developed to observe the interaction between wave and particle in space plasma. We have been conducting laboratory in-situ experiments of plasma wave-particle interaction.

We have carried out the laboratory simulation using the Q_T-Upgrade Machine in Tohoku University, which is linear magnetized plasma machine. The Q_T-Upgrade Machine consists of a vacuum chamber of 0.2 m in diameter and 4.5 m in length, and plasma sources, which generates high-temperature electrons using electron cyclotron resonance (ECR) and low-temperature thermal electrons. Thus, an electron temperature gradient (ETG) is formed in the apparatus by superimposing low temperature thermal electrons on the high temperature electrons of the ECR plasma. Moon et al. [Rev. Sci. Instrum., 2010] reported that low-frequency fluctuations of drift-wave mode with a frequency of 7 kHz were excited with ETG mode of 0.5 MHz. We focus on the low-frequency fluctuations and simultaneously measures an electric field vector (**E**) and current vector (**J**). Energy flaxes between wave and particle can be calculated from inner products of **E** and **J** vectors. For the simultaneous measurements, we have developed a combination probe, which is a combination of Mach probe for ion flow measurements and Twin probe for electric field measurements. Three-dimensional vector are measured by turning and moving the probe in the chamber.

In this presentation, we will report the performance of the combination probe, the phase relationship between the electric field fluctuation and the current fluctuation, and transient response of fluctuation growth in detail.

Japan Geoscience Union Meeting 2014
(28 April - 02 May 2014 at Pacifico YOKOHAMA, Kanagawa, Japan)

PEM33-04 Room:503 Time:May 1 10:00-10:15

Weibel instability mediated collisionless shock generation using large-scale laser systems

SAKAWA, Youichi[1*] ; MORITA, Taichi[1] ; KURAMITSU, Yasuhiro[2] ; KATO, Tsunehiko[3] ; MORITAKA, Toseo[1] ; SANO, Takayoshi[1] ; TOMITA, Kentaro[4] ; MATSUKIYO, Shuichi[4] ; OHNISHI, Naofumi[5] ; MIZUTA, Akira[6] ; WOOLSEY, N[7] ; GREGORI, G[8] ; KOENIG, M[9] ; SPITKOVSKY, A[10] ; HUNTINGTON, C[11] ; KUGLAND, N l[11] ; ROSS, J s[11] ; PARK, H-s[11] ; REMINGTON, B[11] ; TAKABE, Hideaki[1]

[1]ILE Osaka Univ, [2]National Central University Taiwa, [3]Hiroshjima Univ, [4]Kyushu Univ, [5]Tohoku Univ, [6]RIKEN, [7]York Univ UK, [8]Oxford Univ UK, [9]LULI France, [10]Princeton Univ USA, [11]LLNL USA

Collisionless shocks are considered to be sources of high-energy particles or cosmic rays, and occur when a coulomb mean-free-path is longer than the shock-front thickness. In such plasmas wave-particle interactions and collective effects play an essential role in the shock formation. In addition to local observations of spaces plasmas by spacecraft and global emission measurements of astrophysical plasmas, a laboratory experiment can be an alternative approach to study the formation of collisionless shocks.

In this paper, we investigate the formation of Weibel-instability mediated collisionless shocks in counter-streaming plasmas produced by large-scale laser systems. Kato and Takabe investigated the collisionless Weibel shock in two-dimensional PIC simulation using the injection method [1]. A scaling-law derived in simulation revealed that high-density (electron density $\sim 10^{20}$ cm^{-3}), high-flow velocity ($\sim$1000 km/s) plasmas are required to produce the collisionless Weibel shock. In order to achieve these plasma parameters, a MJ-class high-power laser system or the word largest laser, the NIF laser (LLNL, USA), is required. Before starting the NIF experiment, we conducted OMEGA laser (LLE, USA) experiment and measured plasma parameters such as electron and ion temperatures, electron density, and flow velocity of counter-streaming plasmas using collective Thomson scattering, and current filaments produced by the Weibel instability using proton-radiography.

[1] T. N. Kato and H. Takabe, The Astophys. J. Lett. 681, L93 (2008).

Keywords: collisionless shock, weibel instability, large-scale laser experiment

Japan Geoscience Union Meeting 2014
(28 April - 02 May 2014 at Pacifico YOKOHAMA, Kanagawa, Japan)

PEM33-05 Room:503 Time:May 1 10:15-10:30

Experimental study on collisionless shocks with high-power laser system ”Gekko-XII”

MORITA, Taichi[1*] ; SAKAWA, Youichi[1] ; ISHIKAWA, Taishi[1] ; YAMAURA, Yuta[1] ; SANO, Takayoshi[1] ; MORITAKA, Toseo[1] ; TOMITA, Kentaro[2] ; SHIMODA, Ryo[2] ; SATO, Yuta[2] ; MATSUKIYO, Shuichi[2] ; ISAYAMA, Shogo[2] ; HARADA, Daisuke[2] ; OYAMA, Tatsuya[2] ; FUJINO, Ryosuke[2] ; KURAMITSU, Yasuhiro[3] ; YONEDA, Hiroki[10] ; NAGAMINE, Kazuyoshi[10] ; KOENIG, Michel[4] ; YURCHAK, Roman[4] ; MICHAUT, Claire[5] ; WOOLSEY, Nigel[6] ; CROWSTON, Robert[6] ; PELKA, Alexander[7] ; LI, Yutong[8] ; YUAN, Dawei[8] ; YIN, Chuanlei[8] ; ZHONG, Jiayong[9] ; ZHANG, Kai[9] ; TAKABE, Hideaki[1]

[1]Institute of Laser Engineering, Osaka University, [2]Kyushu University, [3]National Central University, [4]LULI, Ecole Polytechnique, [5]LUTH, Observatoire de Paris, [6]University of York, [7]Helmholtz-Zentrum Dresden-Rossendorf, [8]Institute of Physics, Chinese Academy of Science, [9]National Astronomical Observatory, Chinese Academy of Science, [10]Institute for Laser Science, University of Electro-communications

Collisionless shocks play significant roles in particle acceleration, for example, in Earth’s bow shock and Supernova remnant shocks. In collisionless shocks, collisions between particles can not account for the formation mechanism and particle?field interactions are essential. Therefore, the shock thickness is much smaller than ion-ion mean free path and a large electromagnetic field exists at the vicinity of the shock. Laboratory experiments with high-power laser systems can be alternative to observations or in-situ measurements by satellites. Collisionless shocks have been produced and investigated in counter-streaming laser-produced plasmas. To investigate collisionless shocks, the measurements of an electric or magnetic field and of fundamental plasma parameters are required. Shocks have been measured by optical diagnostics such as interferometry, shadowgraphy, optical pyrometry, and Thomson scattering to obtain the fundamental plasma parameters: density, temperature, charge state, and flow velocity. We will present recent results from series of our experiments on collisionless shocks with Gekko-XII laser system.

Keywords: collisionless shock, laser, plasma, diagnostics

Japan Geoscience Union Meeting 2014
(28 April - 02 May 2014 at Pacifico YOKOHAMA, Kanagawa, Japan)

PEM33-06 Room:503 Time:May 1 10:30-10:45

Current status and issues of a study on collisionless shocks by using laser experiment

MATSUKIYO, Shuichi[1*] ; SAKAWA, Youichi[2] ; KURAMITSU, Yasuhiro[3] ; TOMITA, Kentaro[1] ; MORITA, Taichi[2] ; YAMAZAKI, Ryo[4] ; TAKABE, Hideaki[2]

[1]Kyushu University, [2]Osaka University, [3]National Central University, [4]Aoyama Gakuin University

Collisionless shocks are ubiquitous in various space and astrophysical environments like a termination shock of a stellar wind, planetary bow shocks, supernova remnant shocks, etc. Recently, collisionless shocks have been able to be experimentally generated by using high power laser facilities. One of the advantages in an experimental study is that both the global and the local structures of the phenomenon are simultaneously accessible in principle, which is inherently difficult in-situ or remote sensing observations in space. However, the shocks produced in the laser experiments and the method for measuring them are quite different from those in space. A majority of the shocks produced in laser experiments are unmagnetized shocks. The methodology for measuring their local quantities in the transition region has not been established.

On the other hand, basic structures and dissipation mechanisms in an unmagnetized shock have not been well understood theoretically. So far high Mach number electrostatic shocks are thought to be generated by the counter streams of two non-identical plasmas. In this study microstructures of such electrostatic shocks are studied by using a full particle-in-cell simulation. In addition, characteristics and issues of currently adopted method of measuring local quantities in shock transition region, known as Thomson scattering measurement, are also discussed.

Keywords: collisionless shock, laser experiment, numerical simulation

Japan Geoscience Union Meeting 2014
(28 April - 02 May 2014 at Pacifico YOKOHAMA, Kanagawa, Japan)

PEM33-07 Room:503 Time:May 1 11:00-11:15

Electromagnetic Field Excitation in Magnetized Plasmas by External Electrodes: 1D PIC Simulation Studies

OTSUKA, Fumiko[1*] ; HADA, Tohru[1] ; SHINOHARA, Shunjirou[2] ; TANIKAWA, Takao[3]

[1]Interdis. Grad. Sch. Eng. Sci., Kyushu Univ., [2]Inst. Eng.,TUAT, [3]RIST, Tokai Univ.

We perform one-dimensional particle-in-cell (PIC) simulation of external electromagnetic field excitation into magnetized plasmas. We consider two models for the electromagnetic field excitation: electrostatic excitation by electrodes and electromagnetic excitation by current antenna. Here, the external electrodes are placed outside plasma region, background magnetic field is perpendicular to the one-dimensional direction, and the externally applied field frequency is chosen in a range below the lower-hybrid frequency. For both models, we will discuss the electromagnetic field excitation processes by varying the externally applied field frequency and the plasma radius.

Keywords: external electromagnetic field, external electrodes, magnetized plasmas, electric thruster, electrodeless electric thruster

Japan Geoscience Union Meeting 2014
(28 April - 02 May 2014 at Pacifico YOKOHAMA, Kanagawa, Japan)

PEM33-08 Room:503 Time:May 1 11:15-11:30

Numerical simulation of satellite potential control using charged particle beam emission

HOSHI, Kento[1*] ; MURANAKA, Takanobu[2] ; KOJIMA, Hirotsugu[3] ; USUI, Hideyuki[4] ; SHINOHARA, Iku[5] ; YAMAKAWA, Hiroshi[3]

[1]Graduate School of Engineering Kyoto University, [2]School of Engineering Chukyo University, [3]Research Institute for Sustainable Humanosphere, Kyoto University, [4]Graduate school of system informatics Kobe University, [5]Japan Aerospace Exploration Agency/Institute of Space and Astronautical Science

It is known that a satellite is charged by plasma in space.

Satellite charging on surface is a cause of discharge and malfunction electric equipment, and affect plasma diagnostics by the satellite potential accelerate ambient plasma, therefore a satellite is designed to mitigate surface charging. However, a perfect mitigation of satellite charging is difficult.

Thereby, a charging mitigation technique using electron emitter and ion emitter is often adopted. Satellite charging will be caused due to collisions with charged particles in plasma. In general, surface potential is determined by the balance of inflow current and outflow current. It becomes a positive value in the sunshine, and a negative value in the shade. The potential balance point can be controlled using charged particle beam emission.

We investigate a feasibility of satellite potential control under various environments using numerical simulation.

Keywords: satellite charging, spacecraft charging, charged particle beam

Japan Geoscience Union Meeting 2014
(28 April - 02 May 2014 at Pacifico YOKOHAMA, Kanagawa, Japan)

PEM33-P01 Room:503 Time:May 1 18:15-19:30

New solar radio telescope in NICT - II

KUBO, Yuki[1*] ; WATARI, Shinichi[1] ; ISHII, Mamoru[1] ; ISHIBASHI, Hiromitsu[1] ; IWAI, Kazumasa[2]

[1]National Institute of Information and Communications Technology, [2]Nobeyama Solar Radio Observatory, National Astronomical Observatory of Japan

Solar radio burst is one of the most important events for not only space weather forecasting but also investigating high-energy phenomena in solar corona. The GHz solar radio waves are synchrotron radiation emitted by high energy electrons at lower corona. On the other hand, the MHz solar radio bursts, especially type II and III bursts, are radiated via mode conversion of Langmuir waves excited by high energy electrons. These high energy electrons are accelerated at reconnection regions in solar flare and shock waves in solar corona. Therefore, MHz and GHz solar radio waves are closely related each other through the accelerated high energy electrons. So, wide frequency range (MHz to GHz) radio wave observations with high time resolution are required to comprehensively understand high energy phenomena in solar corona. We have been operating solar radio spectrograph called HiRAS for over twenty years in Hiraiso Solar Observatory, National Institute of Information and Communications Technology (NICT), but the system has been decrepit and radio wave environment in Hiraiso is getting worse. So, we have developed a new solar radio telescope in Yamagawa radio observation facility, NICT. The frequency range and time resolution in the system is 70MHz to 9.0GHz and 8 msec. In this presentation, we introduce situation in progress for our new solar radio telescope.

Keywords: Solar radio waves, Solar corona, Radio spectrograph, Space weather

Japan Geoscience Union Meeting 2014
(28 April - 02 May 2014 at Pacifico YOKOHAMA, Kanagawa, Japan)

PEM34-01 Room:503 Time:May 1 11:30-11:55

Frontier of space plasma observations expanding from interplanetary space to interstellar medium

TOKUMARU, Munetoshi[1*]

[1]Solar-Terrestrial Environment Laboratory, Nagoya University

The Sun emits the super-sonic plasma flow, called the solar wind, to form the heliosphere in the ambient interstellar medium. The spatial scale of the heliosphere is about 100 AU. Since interesting physical phenomena such as the solar wind formation, excitation and propagation of shocks, acceleration of energetic particles arises through interaction between plasma and fields in the heliosphere, it is used as an experiment site to make various observational studies of the space plasma. Remote sensing measurements of the solar wind with the interplanetary scintillation (IPS) method are one of those studies. The obtained IPS data revealed the global distribution of the solar wind drastically changes its global distribution over short- and long-timescales being closely associated with the solar activities (Tokumaru, 2013).

At present, marked progress occurs in the heliospheric sciences, being driven by new observational facts. One of progress has been brought about by exploration of heliospheric boundary region by Voyager-1, 2 (V1,V2) and IBEX spacecraft (Gurnett et al., 2013, McComas et al., 2009). The V1 encountered the termination shock (TS) at 94 AU in 2004, and reached the heliopause at 120 AU in 2012, then entered the interstellar medium. The V2 encountered the TS at 87 AU in 2007, being expected to reach the heliopause in a few years. The IBEX revealed the large-scale ribbon structure surrounding the heliosphere from imaging observations of energetic neutral atoms (ENAs). In order to interpret those observations, information on 3-diminensional (3D) structure of the heliospheric boundary region is needed. Since IPS observations mentioned above give global distribution of the solar wind in the inner heliosphere, 3D structure of the heliospheric boundary region can be determined precisely by MHD simulation based on the IPS data. The IPS-based MHD simulation data are provided to both Voyager and IBEX teams to make collaborative studies of the heliospheric boundary region.

Another driver for progress in the heliospheric science is arrival of the peculiar solar activity. The level of the current solar cycle is 100 years low, and IPS observations revealed that significant changes including marked drop of the solar wind density and different distribution of fast and slow solar winds occurs in this cycle (Tokumaru et al., 2009, 2010, 2012). These facts are important not only for studies of the heliospheric boundary region and influence on the planetary magnetospheres (i.e. the space weather), but also for elucidating enigma of the solar wind acceleration mechanism. Besides, observations during the current peculiar activity provide a clue to understand a hidden process for cooling of the Earth's climate during the Maunder minimum in the 17th century.

The V2 encounter for the interstellar medium which is expected to occur within a few years will enable detailed investigation of plasma environment in the local interstellar cloud surrounding the heliosphere. Furthermore, the heliopshere is immersed in the low-density (but high-beta) region called the local bubble, whose plasma properties have been investigated from radio observations using pulsars (Spangler, 2009). In the future, space plasma study for the integrated region ranging from the heliosphere to the local bubble will significantly advance by using in situ and remote sensing observations.

Keywords: solar wind plasma, interplanetary scintillation, heliosphere, interstellar medium, solar cycle

Japan Geoscience Union Meeting 2014
(28 April - 02 May 2014 at Pacifico YOKOHAMA, Kanagawa, Japan)

PEM34-02 Room:503 Time:May 1 11:55-12:15

Scale hierarchy and self-organization in magnetospheric plasma

YOSHIDA, Zensho[1*]

[1]Graduate School of Frontier Sciences, University of Tokyo

Inhomogeneous magnetic field gives rise to interesting properties of plasmas which are degenerate in homogeneous (or zero) magnetic fields. Magnetospheric plasmas, as observed commonly in the Universe, are the most simple, natural realization of strongly inhomogeneous structures created spontaneously in the vicinity of magnetic dipoles. In this talk, we describe the experimental results form a ”laboratory magnetosphere” RT-1, and theoretical modeling of its spontaneous confinement.

The RT-1 device produces a magnetospheric plasma by a levitated superconducting magnet. Stable confinement (particle and energy confinement time = 0.5 s) of high-beta (local electron beta $>$0.7); electron temperature $>$10 keV) plasma has been demonstrated (which are promising characteristics for an innovative concept of advanced fusion; it is also applicable as a particle trap for experimental particle physics or atomic physics). The radial profile of the electron density n(r) is highly peaked. Fitting the data by a function $n(r) = n_0\ r^{-p}$,we estimate p=2.8$\pm$0.4 for a wide range of operating parameters. Multiplying n(r) by the magnetic flux tube volume, we can estimate the particle number N(r) in a unit magnetic-flux tube. While n(r) is a steep increasing function towards the center of the dipole magnetic field, N(r) is a decreasing function, hence interchange modes are stable. Whereas the simple kinetic model predicts a flat distribution of N(r) [1], the model of grand-canonical equilibrium explains the observed equilibrium state [2].

Theoretically, we can describe the self-organized confinement of the magnetospheric plasma as a grand-canonical equilibrium in a ”foliated phase space” of magnetized particles [3]. What makes the distribution function fundamentally different from the conventional Boltzmann distribution is the topological constraints on the phase space which limits the actual domain where the particles can occupy; the adiabatic invariants pose such constraints. Taking into account the constancy of the magnetic moment and the parallel action, we obtain a foliated phase space of coarse-grained variables, on with the invariant measure is distorted by the inhomogeneous magnetic field. The grand-canonical equilibrium has an inhomogeneous density when it is immersed in the laboratory flat space. Hence, the creation of a steep-density clump is a natural consequence of equipartition in the magnetic-coordinate phase space.

[1] A. Hasegawa, Phys. Scr. T116 (2005) 72.

[2] Z. Yoshida et al., Plasma Phys. Control. Fusion 55 (2013), 014018.

[3] Z. Yoshida and P.J. Morrison, in ”Nonlinear physical systems: spectral analysis, stability and bifurcation”, (ISTE and John Wiley and Sons, 2014) Chap. 18; http://arxiv.org/abs/1303.0887

Keywords: inward diffusion, adiabatic invariant, foliation, high-beta plasma, dipole magnetic field, non-neutral plasma

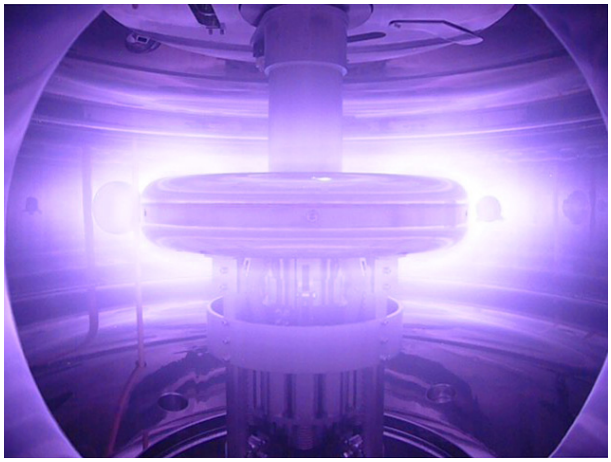

Japan Geoscience Union Meeting 2014
(28 April - 02 May 2014 at Pacifico YOKOHAMA, Kanagawa, Japan)

PEM34-03 Room:503 Time:May 1 12:15-12:30

Solar wind plasma entry into the wake behind an unmagnetized obstacle

NAKAGAWA, Tomoko[1*]

[1]Information and Communication Engineering, Tohoku Institute of Technology

Plasma entry into a wake downstream of a non-magnetized obstacle in the supersonic flow of the solar wind is studied by using a two-dimensional, electromagnetic particle-in-cell simulation. Importance of negative charging of the downstream-side surface of the obstacle is examined by comparing the simulation results of 3 different ratios 8, 16, 32 of the obstacle size to the Debye length.

Keywords: wake, solar wind, surface charging, electron thermal speed, Debye length, particle-in-cell simulation

Japan Geoscience Union Meeting 2014
(28 April - 02 May 2014 at Pacifico YOKOHAMA, Kanagawa, Japan)

PEM34-04 Room:503 Time:May 1 12:30-12:45

Global Vlasov simulation of a small body with a magnetic anomaly with the K-computer

UMEDA, Takayuki[1*]

[1]Solar-Terrestrial Environment Laboratory, Nagoya University

The interaction between a plasma flow and a small dielectric body with a weak intrinsic global magnetic field is studied by means of a five-dimensional (5D) full electromagnetic Vlasov simulation with two configuration spaces and three velocity spaces. In the present study, entry processes of ions into the nightside wake tail are examined. The simulation result shows that the bow shock and the magnetopause are formed on the dayside. However, most of solar-wind ions are reflected at the dayside magnetopause and are picked up by the interplanetary magnetic field. Then, a small part of the reflected ions are taken into the deep wake tail near the body by the E cross B cycloid motion. The present result, in which the spatial resolution is low and the Debye-scale charge separation on the dayside surface is not solved, is obtained by using a recent cluster computer system. Currently we are performing a 5D high-resolution global Vlasov simulation by using the K-computer. The direct comparison between the low- and high-resolution runs would show importance of fully kinetic global simulations.

Keywords: simulation, plasma, small geophysical body, magnetosphere, Vlasov code, K computer

Japan Geoscience Union Meeting 2014
(28 April - 02 May 2014 at Pacifico YOKOHAMA, Kanagawa, Japan)

PEM34-05 Room:503 Time:May 1 14:15-14:30

Dependence of Jovian Magnetopause Location on Solar Wind Dynamic Pressure

KITAGAWA, Hirotaka[1*] ; KASAHARA, Satoshi[2] ; TAO, Chihiro[3] ; KIMURA, Tomoki[2] ; FUJIMOTO, Masaki[2]

[1]Earth and Planetary Science, School of Science, University of Tokyo, [2]Institute of Space and Astronautical Science, Japan Aerospace Exploration Agency, [3]Research Institute in Astrophysics and Planetology

Past observations revealed that the probability density distribution of Jovian magnetopause stand-off distance has double-peak. The probability between two peaks is very low. Thus the stand-off distance of Jovian magnetopause changes from the peak distance to the other peak by solar wind dynamic pressure. However, the scatter plot of stand-off distance versus solar wind dynamic pressure was nearly on one line. But the solar wind dynamic pressure was considered by magnetic pressure in the Jovian magnetosphere, due to the absence of the solar wind monitor at the Jovian orbit. We approached the double-peaked distribution by using the calculated solar wind parameters via MHD equations whose input parameters are based on the observation at Earth's orbit. Referring the propagated solar wind parameters, we investigated the location of Jovian magnetopause observed by the Galileo spacecraft. We found that the peaks of the distribution seem to be a result of probability density distribution of solar wind dynamic pressure. The very low probability stand-off distance between the peaks seemed to be caused by unusual distribution of solar wind dynamic pressure.

Keywords: Jovian Magnetopause, Solar Wind Dynamic Pressure

Japan Geoscience Union Meeting 2014
(28 April - 02 May 2014 at Pacifico YOKOHAMA, Kanagawa, Japan)

PEM34-06 Room:503 Time:May 1 14:30-14:45

Pickup ion acceleration via multiple reflection between two successive CIRs

TSUBOUCHI, Ken[1*]

[1]Tokyo Institute of Technology

Interstellar neutral particles, during their propagation inside the heliosphere, become ionized by the charge exchange with the solar wind (SW) plasma. The interplanetary magnetic field picks up these newborn ions, called ”pickup ions” (PUIs), and carries them away into the outer heliosphere with SW. The gyrating velocity of PUIs around the magnetic field is equivalent to the SW flow speed, hundreds of km/s, which is much faster than the SW thermal velocity. This property enables PUIs to be accelerated more efficiently at the shock than the thermal SW particles. Thus PUIs are considered to be the dominant source of anomalous cosmic rays (ACRs) generated at the heliospheric termination shock.

However, the well-known diffusive shock acceleration (DSA) process alone is insufficient to raise the PUI energy up to the ACR range, typically in the order of MeV. This is because the primary PUI energy (10 keV at most) is still too low to be injected into DSA, where at least hundreds of keV is necessary. Therefore, some preacceleration should take place inside the heliosphere before SW and PUI reach the termination shock. Interplanetary shocks are the most possible source for it. In the present study, we focus on the shocks driven by the interaction of the fast SW with the ahead-flowing slow SW. The regions bounded by these shocks are called corotating interaction regions (CIRs); forward shock in the slow SW side and reverse shock in the fast SW side.

We demonstrate how particles are accelerated at this CIR system by performing hybrid simulations. The simulation results show that more efficient acceleration is identified in the PUI reflected at the shock than in those transmitted through the shock. The acceleration takes place while the PUI stays close to the shock surface. This situation is similar to the shock-drift or surfing acceleration mechanism. However, our results indicate that the acceleration is not dominant in the component transverse to the magnetic field, i.e., the direction of motional electric field. Rather, the net acceleration is confirmed in the field-aligned component. The mechanism will be discussed in terms of the characteristic of the Lorentz force balance acting on PUIs.

The periodic boundary condition applied in the present simulation virtually allows the successive appearance of two CIRs. After the reflected PUI travels the ”inter-CIR” space, it encounters the shock of another CIR, where the reflection again takes place. While one reflection increases the PUI energy only a few times, this multiple reflection process yields the most energetic PUI with its maximum energy up to 100 keV, probably enough for the injection into DSA. Recent CIR observations have confirmed the presence of the energetic PUI in the solar wind between two CIRs, which may prove the present results.

Japan Geoscience Union Meeting 2014
(28 April - 02 May 2014 at Pacifico YOKOHAMA, Kanagawa, Japan)

PEM34-07 Room:503 Time:May 1 14:45-15:00

Study on The Difference Between Proper-Motion of Balmer hydrogen line emission and Non-Thermal X-Ray emission in SNRs

SHIMODA, Jiro[1*] ; INOUE, Tsuyoshi[2] ; OHIRA, Yutaka[1] ; YAMAZAKI, Ryo[1] ; SOEDA, Masanobu[1]

[1]Aoyama Gakuin University, [2]National Astronomical Observatory of Japan

Balmer line emission (Hα) by neutral hydrogen and X-ray synchrotron emission by accelerated electrons are observed from some supernova remnants (SNRs), which are thought as accelerators of galactic cosmic rays (CRs). From these observations, the cosmic ray acceleration eciency is estimated. According to the theory of diusive shock acceleration (DSA), electrons are accelerated around the shock front, and emit the synchrotron radiation. Measurement of proper motion of the synchrotron X-rays gives the shock velocity. At the same time, we can estimate the post shock temperature from the line width of Hα emission, because neutral hydrogen collide with downstream hot protons and exchange their charge, so that the hot neutral component arises.

In the specific case of a SNR RCW86, measured expansion speed of Hα filament is about 1200km/s(Helder et al. 2013), while 6000km/s in X-rays (Helder et al. 2009). It is expected that the emission regions of the Hα and the synchrotron X-rays are dierent. However, they are overlaid in the same line of sight.

In this study, using three dimensional magnetohydrodynamics (MHD) simulations, we consider propagation of super

nova blast wave shock in realistic inhomogeneous interstellar medium. Interaction between the upstream density inhomogeneity and the shock wave causes rippled shock structure and uctuation of local shock velocity. We show that our synthetic observations of the MHD simulation data are consistent with actual observation results for RCW86.

Keywords: supernova remnants, shock wave, cosmic ray

Japan Geoscience Union Meeting 2014
(28 April - 02 May 2014 at Pacifico YOKOHAMA, Kanagawa, Japan)

PEM34-08 Room:503 Time:May 1 15:00-15:15

Magnetohydrodynamic Simulations of the Interaction of a Jet with Interstellar Neutral Hydrogen Clumps

ASAHINA, Yuta[1*] ; OGAWA, Takayuki[1] ; MATSUMOTO, Ryoji[1]

[1]Graduate School of Science, Chiba University

An astrophysical jet transfers the energy released near the gravitating object and interact with the interstellar medium. When the jet propagates in the interstellar medium interacting with its environment. We carried out magnetohydrodynamic simulations of the jet propagation in neutral hydrogen (HI) clumps taking into account the interstellar cooling. At the initial state, HI clumps are assumed to be in thermal equilibrium. As the clumps are compressed by the bow shock ahead of the jet, the shocked cloud is heated up but since the density enhancement increases cooling rate, the cloud is subsequently cooled down. As a result, cold, dense sheath is formed around the jet. The enhanced density triggers the cooling instability and prompts the formation of the cold, dense gas.

We studied the dependence of numerical results on the volume filling factor of the HI clumps. We found that when the volume filling factor is large, the propagation speed of the jet is slow and arc-shaped cold dense region is formed. When the volume filling factor is small, propagation speed does not decrease so much and dense cloud distribution is more elongated. The distribution of the cold, dense gas and the length of the jet propagation speed depend on the filling factor.

We report the application of this model to molecular clouds toward the stellar cluster Westlund 2 and TeV γ-ray source HESS J1023-575 observed by NANTEN2 and Mopra telescope. HESS J1023-575 is located between these molecular clouds. The shape of molecular cloud on the right of HESS J1023-575 is like an arc and molecular clouds on the other hand distribute linearly. The difference of the filling factor can explain the difference of the shape of these molecular clouds.

Keywords: jet, interstellar medium, magnetohydrodynamics

Japan Geoscience Union Meeting 2014
(28 April - 02 May 2014 at Pacifico YOKOHAMA, Kanagawa, Japan)

PEM34-P01 Room:503 Time:May 1 18:15-19:30

High beta plasma production and their diagnostics in magnetosphere RT-1 device

NISHIURA, Masaki[1*] ; YOSHIDA, Zensho[1] ; SAITOH, Haruhiko[1] ; YANO, Yoshihisa[1] ; KAWAZURA, Yohei[1] ; NOGAMI, Tomoaki[1] ; YAMASAKI, Miyuri[1]

[1]Graduate school of frontier sciences, The Univeristy of Tokyo

The magnetosphere plasma device is one of new concepts for nuclear fusion devices. A ring trap 1(RT-1) realizes the concept as a laboratory magnetosphere using a superconducting magnet levitated in a vacuum vessel, which produces a dipole magnetic field. We study the characteristics of confined plasmas in RT-1. In recent experiments, the RT-1 experiment has demonstrated the self-organization of a plasma clump with a steep density gradient; a peaked density distribution is spontaneously created through ”up-hill diffusion”.

The operation regime of RT-1 is extended into the electron density from 10^{17} to 10^{18} m^{-3} by optimizing the electron cyclotron heating (ECH) system. The line integrated density measured by an interferometer achieved 6.2x$10^{17}m^{-3}$ and diamagnetic flux 5.6 mWb. It is considered that the beta value (the ratio of plasma pressure to magnetic pressure) exceeds 100%. In such situation, a millimeter wave reflectometer is implemented to measure the density peaking and spatial structure. We observed the initial results and started the analysis of acquired signals.

When we use the electron heating by ECH system, the ion remains cold due to a collisionless situation. Therefore we installed three turn antenna into RT-1 to heat ions by a slow wave (ion cyclotron heating: ICH) in a MHz range. In the case of ˜$10^{18}m^{-3}$ as a target plasma of ICH by only use of ECH, the heating efficiency of ICH increases, and then leads to the increase of ion temperature. The effect has been observed by an electrostatic energy analyzer, which located at the plasma edge of RT-1.

We designed an ion probe to diagnose energies and pitch angles of ions in ICH experiments of RT-1. The principle of the ion probe is the same as that of fast ion loss measurement in a fusion machine, and is applied to the ion diagnostic in RT-1 plasmas. A scintillator is mounted inside the probe head with a pin hole. Ions with gyro motion enter into the probe head, and then hit the scintillator. We can know the energies and pitch angle simultaneously from the scintillation image.

We report the extension of plasma parameters by ECH optimization, progress on the installation of ion probe, and future perspective.

References

[1] Z. Yoshida et al., Phys. Rev. Lett. 104 (2010) 235004.
[2] H. Saitoh et al., Nucl. Fusion 51 (2011) 063034.

Keywords: plasma, magnetosphere, plasma diagnostics, plasma heating

Japan Geoscience Union Meeting 2014
(28 April - 02 May 2014 at Pacifico YOKOHAMA, Kanagawa, Japan)

PEM34-P02 Room:503 Time:May 1 18:15-19:30

Hybrid simulations of the interaction between the solar wind and the ion scale magnetosphere

NAKAMURA, Masao[1*]

[1]Osaka Prefecture University

The interaction between the solar wind and the ion scale magnetosphere with a dipole magnetic field is investigated by a three-dimensional hybrid simulation. In the present study, the ion scale magnetosphere has a dayside stand-off distance which is several to a hundred times larger than the ion Larmor radius of the solar wind proton in the magnetic field strength at the dayside magnetopause boundary. The hybrid simulation treats the ions as kinetic super particles via particle-in-cell method and the electrons as a massless fluid. In the interaction between the solar wind and the magnetosphere, the interplanetary magnetic field (IMF) condition controls not only the reconnection regions but also the subsolar sheath flow due to the ion kinetic effects. Those influence the structures of the bow shock and the magnetopause boundary layer. We will also discuss the momentum transfer process from the solar wind into the magnetosphere and to the magnetized object.

Keywords: Ion scale magnetosphere, Interaction between solar wind and mini-magnetosphere, 3D hybrid simulation

Japan Geoscience Union Meeting 2014
(28 April - 02 May 2014 at Pacifico YOKOHAMA, Kanagawa, Japan)

PEM35-01 Room:503 Time:May 2 15:00-15:25

Full PIC simulations on plasma electromagnetic disturbance in the vicinity of spacecraft

USUI, Hideyuki[1*] ; MIYAKE, Yohei[1]

[1]Graduate School of System Informatics, Kobe University

Space exploration has been rapidly increasing, and a strong demand arises regarding comprehensive understanding of spacecraft-plasma (SP) interactions [1]. This is clearly required to ensure survivability and proper operations of space-based systems, and also for correct interpretation of measurements and other information collected in situ by scientific spacecraft.

In space environments, spacecraft are electrically charged due to plasma contact to spacecraft surface and its floating potential is basically determined by the current balance at spacecraft surface. The current consists of incident background plasma, emission of photoelectrons/secondary electrons from spacecraft surface as well as active emission of plasma beam in electric propulsion system such as ion engine. Due to the spacecraft charging, plasma environment near spacecraft is influenced. Non-uniform plasma distributions such as sheath and wake structures are formed near spacecraft surface and in the downstream region with respect to the solar wind, respectively. Field components near spacecraft can be also disturbed by the plasma response to spacecraft. Understanding of the SP interactions is important from a view point of spacecraft observation of plasma environment as well as its data analysis. To discriminate plasma phenomena artificially disturbed by spacecraft from observational data, quantitative understanding of SP interactions is necessary. In designing science instruments such as electric field sensor, plasma disturbance near spacecraft has to be minimized as much as possible to obtain reliable and valuable data. To obtain self-consistent solution of these plasma disturbances near spacecraft, we perform plasma simulations including spacecraft body in a simulation domain.

For solving SP problems, we have developed the EMSES plasma particle simulation code [2]. EMSES is based on the standard electromagnetic PIC method, and also has the capability to include the conducting bodies of a spacecraft, based on the capacitance matrix method. In addition, a number of crucial physics such as the photoelectron emission and the secondary emission are modeled numerically in the latest version of EMSES. The code has been applied so far to some specific spacecraft, e.g., Geotail, Cluster, BepiColombo/MMO, and Solar Probe Plus.

In this talk, first we will briefly explain the numerical treatment of spacecraft in EMSES. Then we will show a few examples of EMSES applications to scientific spacecraft. One of such applications is an enhanced wake formed behind the Cluster satellite in tenuous streaming plasma [3]. In the simulation we have included the conducting surfaces of very thin (in an order of mm) wire booms by using the fictitious surface technique. We found that even the extremely thin wire booms can contribute substantially to the formation of an electrostatic wake because of highly positive spacecraft charging in the tenuous plasma environment. We will also show a recent research topic on the SP interactions in the near-Sun environment. Large photoelectron emission current caused by an intense solar flux forms a negative potential barrier on the spacecraft surface, leading to negative charging of the spacecraft. Electromagnetic environments around these specific spacecraft will be presented in the talk.

[1] D. Hastings and H. Garrett, Spacecraft-Environment Interactions, Cambridge University Press, 2004.

[2] Y. Miyake and H. Usui, A new electromagnetic particle code for the analysis of conductive spacecraft-plasma interactions, Physics of Plasmas 16, 062904, 2009.

[3] Y. Miyake, C. M. Cully, H. Usui and H. Nakashima, Plasma particle simulations of wake formation behind a spacecraft with thin wire booms, Journal of Geophysical Research: Space Physics, Volume 118, Issue 9, pages 5681-5694, September 2013.

Keywords: Spacecraft plasma environment, Spacecraft-plasma interactions, Electromagnetic Particle simulation, Spacecraft charging, electromagnetic disturbance

Japan Geoscience Union Meeting 2014
(28 April - 02 May 2014 at Pacifico YOKOHAMA, Kanagawa, Japan)

PEM35-02 Room:503 Time:May 2 15:25-15:45

General relativistic simulations of magnetized binary neutron star merger on K

KIUCHI, Kenta[1*] ; KYUTOKU, Koutarou[2] ; SEKIGUCHI, Yuichiro[1] ; SHIBATA, Masaru[1]

[1]Yukawa Institute for Theoretical Physics, [2]University of Wisconsin-Milwaukee

Binary neutron stars are a binary which is composed of two neutron stars and nine binaries have been observed so far. They gradually lose the orbital energy and angular momentum due to gravitation wave emission and merge in the end. Within the observed binaries, six of them will merger within the Hubble time. Gravitational waves emitted during the merger would be detectable with the ground-based gravitational wave detectors such as KAGRA, advanced LIGO, and advanced VIRGO at a frequency of about ten times per year. If we could observe the gravitational waves, they would tell us the validity of General Relativity in a strong gravitational field and the equation of state of neutron star matter which is poorly known to date as well.

This situation facilitates a theoretical study of binary neutron star mergers. During the merger, the density is as high as 10^{15} g/cc and the temperature rises as high as 10^{10} degrees. Therefore, any analytical approaches break down and we need a numerical modeling. Our group is approaching this problem in the framework of Numerical Relativity. It is a research field whose aim is figuring out phenomena in a strong gravitational field by solving the Einstein equation as well as the hydrodynamical equation and neutron radiation transfer.

The observations of the pulsars have revealed that the neutron stars are magnetized with about 10^{12} Gauss in general. Moreover, some of them could have 10^{14} Gauss. However, it is still unknown what the role of magnetic field during binary neutron star mergers is. There are several hydrodynamical instabilities which amplify the magnetic field and a short wavelength mode is essential in all cases. Therefore, it is mandatory to perform a high-resolution simulation. In the previous studies of this subject, it is hard to say that enough resolution is assigned to resolve these instabilities. Our group is performing a numerical simulation with the highest resolution on the supercomputer K and figuring out the role of the magnetic field during the merger of binary neutron stars. We summarize the result as follows.

When the two stars come into contact, the shear layer between the stellar surface becomes unstable against the Kelvin-Helmholts instability. The vortices are produce by this instability and the shorter the wavelength is, the larger the growth rate of the instability is. If there exists magnetic field lines, they are curled by these vortices and are expected to be amplified exponentially. By performing the convergence study against the numerical resolution, we have found the maximum magnetic field is amplified by the factor of about thirty at least at the merger.

After the merger, a hypermassive (HMNS) neutron star is transiently formed, which is supported by a rapid and strong differential rotation in addition to the thermal pressure. Although this star is unstable against the magnetorotational instability (MRI), it is difficult to resolve the MRI because the wavelength of the unstable mode is quite short due to the high density and high angular velocity of the HMNS neutron star. In our simulation, we have resolved this unstable mode and we have shown that the HMNS neutron star has the magnetic field as large as 10^{16}-10^{17} Gauss as a result.

In the HMNS neutron star, the angular momentum transport due to the non-axisymmetric structure as well as due to the MRI works. In addition, the star loses a significant amount of the angular momentum due to the gravitational wave emission. Then, the star collapses to a black hole which is surrounded by the accretion disk. Inside the accretion disk, the magnetohydrodynamical turbulence transports the angular momentum and its surface is unstable against the Kelvin-Helmoholts instability. Vortices produced by these two mechanisms transport the energy outwardly and the disk wind activates as a result. In this talk we will introduce the simulation result in details.

Japan Geoscience Union Meeting 2014
(28 April - 02 May 2014 at Pacifico YOKOHAMA, Kanagawa, Japan)

PEM35-03 Room:503 Time:May 2 15:45-16:00

Electromagnetic Vlasov simulations of magnetized plasma with a finite-volume multi-moment advection scheme

MINOSHIMA, Takashi[1*] ; MATSUMOTO, Yosuke[2] ; AMANO, Takanobu[3]

[1]Institute for Research on Earth Evolution, Japan Agency for Marine-Earth Science and Technology, [2]Graduate School of Science, Chiba University, [3]Department of Earth and Planetary Science, University of Tokyo

The Vlasov simulation, which directly discretizes the Vlasov equation on grid points in phase space, has been proposed as an alternative method to the common Particle-In-Cell simulation, to improve the accuracy of kinetic plasma simulations. Although the electrostatic Vlasov simulations have been successfully carried out thus far, the electromagnetic Vlasov simulation of magnetized plasma is still limited, owing to numerical difficulty in solving the distribution function in velocity space.

To overcome the difficulty, we develop a new numerical scheme, specifically designed to solve the Vlasov equation in magnetized plasma. The scheme advances multiple piecewise moments of a physical profile based on their governing equations, to preserve the profile with high accuracy. The scheme allows us to perform a long-time calculation of the distribution function of magnetized plasma with small numerical diffusion.

In this talk, we first present the scheme and its performance. Then, we report the application of the scheme to two-dimensional (2D3V) electromagnetic Vlasov simulations. Long-time simulations of the linear wave propagation in magnetized plasma are conducted with quite small numerical errors. We also conduct the simulation of collisionless magnetic reconnection. The simulation resolves macroscopic structure without numerical noise, and is in good agreement with previous studies. Furthermore, the simulation resolves microscopic structure of the non-Maxwellian plasma velocity distribution around the reconnection site, e.g., acceleration by the reconnection electric field at the X-point, high energy beams around the boundary layer, and heating by the magnetic compression at the downstream. Since the simulations have been successfully carried out with the grid size much larger than the Debye length, the Vlasov simulation is a powerful technique to treat global-scale kinetic plasma phenomena.

Keywords: Advection equation, Vlasov simulations, Magnetic reconnection

Japan Geoscience Union Meeting 2014
(28 April - 02 May 2014 at Pacifico YOKOHAMA, Kanagawa, Japan)

PEM35-04 Room:503 Time:May 2 16:15-16:30

Generalization of Plasma Hybrid Simulation Model

AMANO, Takanobu[1*] ; HIGASHIMORI, Katsuaki[1] ; SHIRAKAWA, Keisuke[1]

[1]Department of Earth and Planetary Science, University of Tokyo

The hybrid simulation model has been widely used as one of the self-consistent simulation methods in investigating nonlinear space plasma phenomena, which treats ions as kinetic macro-particles whereas electrons are assumed to be an inertialess fluid. It can correctly simulate from magnetohydrodynamic to the ion inertia length scale. However, the assumption of the inertialess electron makes it sometimes numerically difficult to handle high-frequency whistler waves. We have recently shown that the problem may be resolved by appropriately including finite electron inertia effect, which also makes it possible to handle vacuum regions in a hybrid code. In this report, we discuss extension of the model which may be able to incorporate electron kinetic effect. Ignoring the displacement current and assuming charge neutrality, we adopt the Vlasov-Ampere system of equations. An equation to determine the electric field is derived from the basic equation without any approximations. We demonstrate that by using the equation, the electron cyclotron resonance can be properly included.

Keywords: plasma, numerical simulation

Japan Geoscience Union Meeting 2014
(28 April - 02 May 2014 at Pacifico YOKOHAMA, Kanagawa, Japan)

PEM35-05 Room:503 Time:May 2 16:30-16:45

Optimization of Magnetohydrodynamic Simulation Code for Planetary Magnetosphere to Xeon Phi

FUKAZAWA, Keiichiro[1*]

[1]Research Institute for Information Technology, Kyushu University

For investigating the global structures of plasma, such as the planetary magnetospheres, the Magnetohydrodynamic (MHD) equations are often used, in which full kinetics of plasma are neglected by taking the moments of the Vlasov equations. The MHD equations are highly nonlinear and are very complex to solve by hand calculations. Thus computer simulations play essential roles in studies of global magnetosphere.

The numerical MHD code for the magnetosphere has been optimized for vector-type supercomputers for a long time because the MHD code is a kind of fluid code and most of supercomputers with vector processors have high performance to solve the fluid codes in 1990's. These codes often have achieved a very high computational efficiency (the ratio of the effective performance to the theoretical performance). However, almost 100% of the "Top 500" supercomputer systems in the world adopt the massively parallel scalar type processors and more than 85% of systems consist of the x86 processor architecture in these days. The other scalar type computers are POWER and SPARC architectures. Recently the new coprocessor Xeon Phi which has many cores (˜60 cores) of X86 architecture is introduced to the supercomputer system and achieved good performance of the Linpack benchmark.

In this study I evaluate the performance of MHD code for the planetary magnetosphere on the single Xeon Phi coprocessor. For the performance evaluation, I use the three-dimensional domain decomposition method and a cache-hit type of three-dimensional domain decomposition method with the flat MPI and hybrid MPI. As the results, I found that normal three-dimensional decomposition of the MHD model with the hybrid MPI is suitable for Xeon Phi coprocessor and achieved computing performance efficiency of ˜7%. Furthermore, I add the optimization to the MHD code based on the Xeon Phi architecture and obtained the computing performance efficiency of almost 10% which is the double performance of FX10 single node.

Japan Geoscience Union Meeting 2014
(28 April - 02 May 2014 at Pacifico YOKOHAMA, Kanagawa, Japan)

PEM35-06 Room:503 Time:May 2 16:45-17:00

A Study of Fluid Element Tracing in Global MHD Simulations via Parallel Data Processing on the NICT Science Cloud

MURATA, Ken T.[1*] ; FUKAZAWA, Keiichiro[2] ; GUO, Zhihong[3] ; EBIHARA, Yusuke[4] ; SAITA, Satoko[5] ; FUJITA, Shigeru[6] ; TANAKA, Takashi[7] ; KUBOTA, Yasubumi[1] ; WATANABE, Hidenobu[1] ; TATEBE, Osamu[8] ; TANAKA, Masahiro[8] ; KIMURA, Eizen[9]

[1]National Institute of Information and Communications Technology, [2]Kyushu University, [3]SURIGIKEN Co.,Ltd., [4]Kyoto University, [5]Research Organization of Information and Systems, [6]Meteorological College, Japan Meteorological Agency, [7]SERC, Kyushu University, [8]University of Tsukuba, [9]Ehime University

The NICT Science Cloud is a cloud system designed for scientific researches, and expected as a new infrastructure for big data sciences. Not only parallelization of CPU as in super-computers, but I/O and network throughput parallelization are crucial for the big data science. A high-performance visualization system is constructed on the NICT Science Cloud using Gfarm/Pwrake middleware. We examined performance of this parallel visualization environment for a set of computer simulation with 1000 files (2.3TB in all). After setting higher priority to access to local file on local disk, we finally achieved 124 times higher visualization using 192 core cpu.

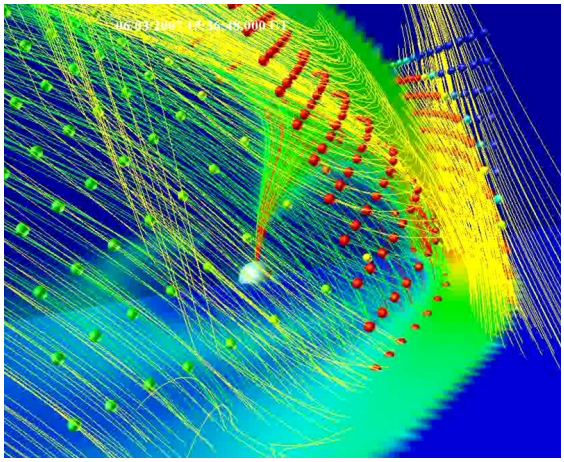

Japan Geoscience Union Meeting 2014
(28 April - 02 May 2014 at Pacifico YOKOHAMA, Kanagawa, Japan)

PEM35-P01 Room:503 Time:May 2 16:15-17:30

Development of magnetic field tracking module for analyzing a decaying sunspot

KATO, Shota[1*] ; IMADA, Shinsuke[1] ; MACHIDA, Shinobu[1]

[1]Solar-Terrestrial Environment Laboratory, Nagoya University

In order to analyze the structures of magnetic fields using the data from Solar Optical Telescope (SOT) on board the Hinode satellite, we have developed the automatic tracking module, which detects the magnetic region and tracks the time variation of each region.

The module, based on three thresholds, intensity, size, and distance, has main three functions: (1) detect the magnetic fields based on the intensity threshold, (2) remove the micro region by the size threshold, (3) based on move distance by time variation, detect the same regions and track them.

We made simple sample data for test and checked on the accuracy of our tracking module.

We applied the module to sunspot and analyzed the time variation of decaying sunspot which is one of the sources of magnetic element in the solar surface.

We have use the magnetograph data which was observed by Hinode/SOT from 29 Dec 2009 to 2 Jan 2010. We also discuss the north-south/east-west asymmetry of the decaying process in the active region.

Keywords: sunspot, development of module, auto detection, auto tracking

Japan Geoscience Union Meeting 2014
(28 April - 02 May 2014 at Pacifico YOKOHAMA, Kanagawa, Japan)

PEM35-P02 Room:503 Time:May 2 16:15-17:30

Application of feature recognition technique in the investigation of magneto-convection on the solar surface

IIDA, Yusuke[1*] ; HOTTA, Hideyuki[2]

[1]ISAS/JAXA, [2]High Altitude Observatory/JSPS

We show the recent feature recognition technique and its benefits in the investigation of magneto-convection on the solar surface using observational and numerical approaches.

The magneto-convection on the solar surface is important not only as a trigger of many surface energetic events, e.g. solar flare, jet, and X-ray bright point, but also as an actual example of the most detailedly observed and numerically simulated magneto-convection on the stellar surface owing to its closeness to the earth. However, the elements of magneto-convection (<1,000km), the basic convective cells and magnetic patches formed by convective motion, are much smaller than solar global scale(~70,0000km). It means that we need large field of view to catch up enough number of structures simultaneously with high spatial resolution to capture such small scale structures. Thanks to the improvement of engineering technique for satellite observation and computers for numerical calculation, we are now able to catch such a large scale structure at the same time. However, the new difficulty, how to investigate statistical characters of convective cells and magnetic structures in such huge data sets, has just shown up in the analysis.

Because of this situation, feature recognition and tracking technique is now focussed on. In this presentation, we want to introduce the auto-recognition and tracking code of magnetic patches and convective cells on the solar surface. Further it is shown that the statistical characters obtained through the analysis of observational data and numerical calculation data based on the auto-recognition and tracking code. We want to note that the feature tracking technique drastically improve statistics of the analysis drastically. We also want to discuss about the applicants of feature tracking technique with the scientists in the other fields though this collaborative session.

Keywords: the Sun, magneto-convection, feature recognition

Japan Geoscience Union Meeting 2014
(28 April - 02 May 2014 at Pacifico YOKOHAMA, Kanagawa, Japan)

PEM35-P03 Room:503 Time:May 2 16:15-17:30

On stability properties of the numerical Cherenkov instability in relativistic plasma flows

IKEYA, Naoki[1*] ; MATSUMOTO, Yosuke[1]

[1]Graduate School of Science, Chiba University

We examined stability properties of the numerical Cherenkov instability in relativistic plasma flows. Particle-in-cell simulation code package, pCANS, was used for the numerical analysis. With the implicit FDTD method for Maxwell equations, we found that the instability was greatly inhibited with the CFL number of 1.0. Numerical tests with various CFL numbers ranging from 0.5 to 1.0 showed that the growth rate remarkably decreased at CFL = 1.0 following a gradual decrease from the value at CFL=0.5. The implicitness factor (alpha=0.5 for Clank-Nicolson method) was also found to control the width of the dip. The present result contrasts with the recently reported results (Vay et al., 2011, Godfrey & Vay, 2013) in which the magical CFL number were 0.5 and 0.7 respectively for their different explicit field solvers. We present the result with the detailed dispersion relation of the implicit field solver and its application to relativistic collisionless shock simulations.

Keywords: particle-in-cell simulation, relativistic plasma, numerical Cherenkov radiation, shocks

Japan Geoscience Union Meeting 2014
(28 April - 02 May 2014 at Pacifico YOKOHAMA, Kanagawa, Japan)

PEM35-P04 Room:503 Time:May 2 16:15-17:30

Electron hybrid code simulations with OhHelp load balancer

KATOH, Yuto[1*] ; MIYAKE, Yohei[2] ; NAKASHIMA, Hiroshi[3] ; USUI, Hideyuki[2] ; OMURA, Yoshiharu[4]

[1]Department of Geophysics, Graduate School of Science, Tohoku University, [2]Graduate School of System Informatics, Kobe University, [3]Academic Center for Computing and Media Studies, Kyoto University, [4]Research Institute for Sustainable Humanosphere, Kyoto University

A spatially one-dimensional electron hybrid code has been developed for the study of the generation process of whistler-mode chorus emissions and relativistic electron acceleration in the Earth's inner magnetosphere [1-3]. In the electron hybrid code, we treat cold electrons as a fluid and energetic electrons as particles by the Particle-in-Cell (PIC) method. Since we assume an inhomogeneous background magnetic field in the simulation system so as to treat the bounce motion of energetic electrons along a magnetic field line, the distribution of energetic electrons in the system is non-uniform and energetic electrons move around the magnetic equator assumed at the center of the simulation system. While the electron hybrid code has been parallelized through the particle decomposition method, we need to improve the scalability of the electron hybrid code so as to use a large simulation system and billions of particles for simulations under initial conditions corresponding to the real magnetosphere.

In the present study, we have developed a spatially one-dimensional electron hybrid code domain-decomposed by OhHelp [4]. The OhHelp is a library which enables us to conduct PIC simulations by achieving both dynamic load balancing and scalability. The efficiency and scalability of OhHelp have been confirmed by a 3D full PIC simulations [5]. We show the efficiency and scalability of the developed code tested on the system A (Cray XE6) of Academic Center for Computing and Media Studies, Kyoto University. We compare the performance of the developed code and those of the code with the particle decomposition.

[1] Katoh Y., Y. Omura, Computer simulation of chorus wave generation in the Earth's inner magnetosphere, Geophys. Res. Lett., 34, L03102, doi:10.1029/2006GL028594, 2007.

[2] Katoh, Y., Y. Omura, and D. Summers, Rapid energization of radiation belt electrons by nonlinear wave trapping, Ann. Geophys., 26, 3451–3456, 2008.

[3] Katoh, Y. and Y. Omura, Effect of the background magnetic field inhomogeneity on generation processes of whistler-mode chorus and hiss-like broadband emissions, J. Geophys. Res. Space Physics, 118, 4189-4198, doi:10.1002/jgra.50395, 2013.

[4] Nakashima, H., Y. Miyake, H. Usui, and Y. Omura, OhHelp: A Scalable Domain-Decomposing Dynamic Load Balancing for Particle-in-Cell Simulations, Proc. 23rd Intl. Conf. Supercomputing, 90-99, 2009.

[5] Miyake, Y., H. Usui, and H. Nakashima, Development of a Scalable PIC Simulator and Its Application to Spacecraft-Plasma Interaction Problems, Proc. JSST 2012, OS6-8, pp. 262?267, 2012.

Keywords: dynamic load balancer, PIC simulation

Japan Geoscience Union Meeting 2014
(28 April - 02 May 2014 at Pacifico YOKOHAMA, Kanagawa, Japan)

PEM36-01 Room:312 Time:April 28 09:00-09:15

Effect of Surface BRDF on the Geostationary and Low Orbit Observations of Tropospheric NO_2

NOGUCHI, Katsuyuki[1*] ; RICHTER, Andreas[2] ; ROZANOV, Vladimir[2] ; ROZANOV, Alexei[2] ; BURROWS, John[2] ; IRIE, Hitoshi[3] ; KITA, Kazuyuki[4]

[1]Nara Women's University, [2]University of Bremen, [3]Chiba University, [4]Ibaragi University

We investigated the effect of surface reflectance anisotropy, Bidirectional Reflectance Distribution Function (BRDF), on geostationary and low orbit satellites' retrievals of tropospheric NO_2. We first develop an empirical model of the three BRDF coefficients for each land cover type over Tokyo, and then apply the model to the calculation of land cover type dependent AMFs and BAMFs. Results show that the variability of AMF among the land types is up to several tens percent, and if we neglect the reflectance anisotropy, the difference from BRDF's AMF reaches 10% or more. The evaluation of the BAMFs calculated shows that not to consider variations in BRDF will cause large errors if the concentration of NO_2 is high close to the surface, although the importance of BRDF for AMFs decreases for large AOD.

Japan Geoscience Union Meeting 2014
(28 April - 02 May 2014 at Pacifico YOKOHAMA, Kanagawa, Japan)

PEM36-02 Room:312 Time:April 28 09:15-09:30

R&D of passive radar -Water vapor estimation with digital terrestrial broadcasting wave-

KAWAMURA, Seiji[1*] ; OHTA, Hiroki[1] ; HANADO, Hiroshi[1]

[1]National Institute of Information and Communications Technology

In general, radars retrieve some information by transmitting radio waves and by receiving their scatted echoes. On the other hand, passive radars never transmit radio waves. They retrieve some information by receiving radio waves which are transmitted by others for other purposes. Passive radars do not need new radio wave frequencies, and just consist of rather simple and low cost receivers because they do not transmit radio waves. We, National Institute of Information and Communications Technology (NICT), are developing passive radar measurement systems whose targets are environmental monitoring.

In this study, we are developing a water vapor measurement system using digital terrestrial broadcasting wave as one of passive radars. Localized heavy rain in the urban area is a social issue in these days. Water vapor is an essential parameter for weather forecast because it is a state before rain drop. And it is one of the most difficult physical quantity to measure with remote sensing technique. If we can monitor water vapor around the ground surface with precise time and spacial resolutions, the weather forecast might be able to predict the localized heavy rain.

Radio waves are delayed due to water vapor through propagation. If we can measure this time delay, water vapor can be retrieved from it. Since delay doe to water vapor is quite small, very precise (sub-nano second order) measurements are needed. Radio waves used for digital terrestrial broadcasting are modulated with OFDM, and known signals are embedded. Complex delay profiles are calculated using these known signals. Using the phase of delay profile, we can measure propagation delay with precise accuracy (pico-second order).

When we consider the accuracy with order of sub-nano seconds, phase fluctuations of local oscillators at radio tower and receivers are essential error factors. We have developed a real-time delay (phase of delay profiles) measurement system with software-defined radio technique. Using this system, we can also measure phase fluctuations of local oscillator at each TV station by just receiving radio waves. With these systems at two receiving points on the same line including the radio tower, and with synchronization between their local oscillators, we can measure water vapor between two receiving points. After proving test of estimation of water vapor, we will distribute many small receivers and develop water vapor monitoring system in collaboration with many observations and data assimilations.

Keywords: passive radar, digital terrestrial broadcasting wave, water vapor, propagation delay

Japan Geoscience Union Meeting 2014
(28 April - 02 May 2014 at Pacifico YOKOHAMA, Kanagawa, Japan)

PEM36-03 Room:312 Time:April 28 09:30-09:45

Observation of local circulation in north area of Fukui prefecture by using two adjoining 1.3-GHz wind profiler radars

NAKAJO, Tomoyuki[1*] ; YAMAMOTO, Masayuki[2] ; AOYAMA, Takashi[1] ; HASHIGUCHI, Hiroyuki[2] ; UJIHASHI, Yasuyuki[3]

[1]Department of Electrical, Electronic and Computer Engineering, Fukui University of Technology, [2]Research Institute for Sustainable Humanosphere, Kyoto University, [3]Department of Architecture and Environmental Engineering, Fukui University of Technology

Global impact of our lifestyle to our own has been pointed out previously. In the field of atmospheric environment, it has been considered that heavy rainfall, of which occurrence and damages are increasing in recent years, to be related with global warming. In addition to influence of yellow dust and PM 2.5 on our health, it has been known that photochemical oxidant tends to increase again since 1980's. Furthermore, the severe accident of Fukushima Daiichi Nuclear Power Station has caused us the interest about diffusion of radioactivity.

Above atmospheric problems are not only global but also local because they are strongly affected by local circulation. Local circulation occurs in atmospheric boundary layer (ABL) which has different characteristics in each local area, therefore, it is essential to reveal the detailed characteristics of ABL for resolution of the atmospheric problems.

Under such a situation, Fukui University of Technology started a project named as "Formation of research base for measurement and conservation of environment in Hokuriku area" (H23 - H27) supported by MEXT. In the project, a 1.3-GHz wind profiler radar (FUT-WPR), which is same type atmospheric radar as that of JMA WINDAS network, was installed in the coastal area of northern part of Fukui prefecture in 2012. In Fukui prefecture, a WPR of WINDAS has worked at Fukui local meteorological observatory (WINDAS-FUKUI), and the distance between FUT-WPR and WINDAS-FUKUI is only 24 km. There is no area in Japan where two WPRs are located within such a short distance, which enables more detailed study of the local circulation in Fukui plain than previous studies.

The observation results of FUT-WPR have revealed the detailed characteristics of see and land breeze (SLB) which is well known local circulation in coastal areas; its temporal variation, structure in altitude, relation with ABL, occurrence probability, and effect on generating area of clouds. Especially, the comparison with WINDAS-FUKUI not only confirms the observation results by FUT-WPR but also shows the SLB reaches from the seashore to a few 10 km inland. Although the observation results are fundamental in meteorology, this is the first time that the real picture of SLB in Fukui plain was revealed in detail so far. The comparison with WINDAS-FUKUI also shows the horizontal winds under about 1 km in altitude often differs between FUT-WPR and WINDAS-FUKUI, which indicates the importance of measurement of ABL.

We also carried out the data analyses in the case of heavy rain. On September 3 in 2013, passage of the stationary front accompanying the typhoon No. 17 brought about the heavy rain reaching to 10 mm/10min in Fukui prefecture from 14:00 to 16:00 (JST). FUT-WPR observed not only a typical structure and temporal variation of horizontal wind followed by the passage of stationary front but also intermittent upward flow, of which velocity reaches 1 m/s in the altitude from 200 m to about 4 km, from 7 hours before the passage of front. Especially, a strong upward flow with the velocity of 4 m/s was observed around 12:00 in the altitude from 3.5 to 5 km although the duration was relatively short. The observations of MTSAT from 10:00 to 14:00 have shown that optically thick clouds, of which top altitude was estimated to reach about 10 km, had arrived over Fukui prefecture. Therefore, the upward flows observed by FUT-WPR should be a part of cumulonimbi system which brought about the heavy rain. On the other hand, upward flows observed by WINDAS-FUKUI was weaker than that of FUT-WPR, which indicates the horizontal scale of upward flow accompanying the cumulonimbi system was under 24 km at least.

The results of observations and data analyses obtained so far indicates the observation of ABL by adjoining WPRs will be useful in early detection of arriving cumulonimbi system or local weather prediction.

Keywords: atmospheric boundary layer, local circulation, see and land breeze, heavy rain, wind profiler radar

Japan Geoscience Union Meeting 2014
(28 April - 02 May 2014 at Pacifico YOKOHAMA, Kanagawa, Japan)

PEM36-04 Room:312 Time:April 28 09:45-10:00

Relationship between solar activity and disturbance in the middle atmosphere during Arctic winter

SAKANOI, Kazuyo[1*] ; KINOSHITA, Takenari[2] ; MURAYAMA, Yasuhiro[2]

[1]Komazawa Univ., [2]National Institude of Information and Communications Technology

Purpose of this research is to clarify relationship between solar activity and disturbance in the middle atmosphere during Arctic winter. In this research we consider stratospheric sudden warming (SSW), which is typical phenomenon in Arctic winter, as disturbance in the middle atmosphere including the mesosphere. Previous research reported effect of 11-year solar cycle on thermal structure only in the Stratosphere.

To get thing started, we selected daily bottom altitude of easterly wind area, which corresponds to SSW, in the zonal mean horizontal wind. Averaged value of those during one SSW event is used for quantitative comparison with solar activity and QBO index. No clear relationship was found between the selected new value (ZEW index) and two indexes. However we confirm that the ZEW index represents well the degree of disturbance. Next, we calculate AO index in the altitude range from 1000 hPa to 0.1 hPa (65km alt). AO index also represents the degree of disturbance.

In this presentation, we will examine and discuss in more detail about ZEW and AO index as those which indicate the degree of disturbance in the middle atmosphere for quantitative comparison with solar activity.

Keywords: Middle atmosphere disturbance, Solar activity, Arctic Oscillation, QBO, Arctic region, Stratospheric sudden warming

Japan Geoscience Union Meeting 2014
(28 April - 02 May 2014 at Pacifico YOKOHAMA, Kanagawa, Japan)

PEM36-05 Room:312 Time:April 28 10:00-10:15

Temporal variations of O3 and NO in the middle atmosphere above Syowa Station observed by a millimeter-wave radiometer

OHYAMA, Hirofumi[1*] ; ISONO, Yasuko[1] ; UEMURA, Miku[1] ; NAGAHAMA, Tomoo[1] ; MIZUNO, Akira[1] ; TSUTSUMI, Masaki[2] ; EJIRI, Mitsumu[2] ; NAKAMURA, Takuji[2]

[1]Solar-Terrestrial Environmental Laboratory, Nagoya University, [2]National Institute of Polar Research

Precipitation of energetic particle into the atmosphere impacts abundances of atmospheric constituents in the middle atmosphere. Highly energetic solar protons, which directly enter the middle atmosphere, cause increase of HOx and NOx species. Energetic electrons also increase NOx in the thermosphere, and the downward transport in the polar vortex moves the produced NOx to lower altitudes. These NOx species cause a decrease of O_3 in the middle atmosphere through catalytic reactions [Seppälä et al. 2006; Daae et al., 2012]. To investigate the effect of NOx on O_3 variation in the polar region, a ground-based millimeter-wave spectroscopic radiometer was installed at Syowa Station, Antarctica in March 2011. The instrument has recorded brightness temperature spectra of rotational emission from the atmospheric O_3 and NO molecules. From the NO spectra, both multiple short-term enhancements and seasonal variation of NO column are observed [Isono et al., 2014]. The short-term enhancements are correlated with the energetic particle precipitation. In the present study, O_3 profiles are retrieved from the brightness temperature spectra between 238.94-239.24 GHz, whose spectral range has sensitivity to the O_3 abundance between 20 and 70 km. The optimal estimation scheme is used for the O_3 profile retrieval, along with radiative transfer calculation through the use of the NCEP reanalysis data and spectroscopic parameters. Since the O_3 spectra are integrated over 1 hour every 6 hours, we usually derive four O_3 profiles in a day. We present the result of O_3 retrieval and discuss how the O_3 mixing ratios at given altitudes response to the short-term NO column enhancement.

Keywords: ozone, nitric oxide, remote sensing

Japan Geoscience Union Meeting 2014
(28 April - 02 May 2014 at Pacifico YOKOHAMA, Kanagawa, Japan)

PEM36-06 Room:312 Time:April 28 10:15-10:30

Current status of Syowa lidar project in the prioritized observation project for VIII-th term JARE

EJIRI, Mitsumu K.[1*] ; TSUDA, Takuo[1] ; NISHIYAMA, Takanori[1] ; ABO, Makoto[2] ; TOMIKAWA, Yoshihiro[1] ; SUZUKI, Hidehiko[3] ; KAWAHARA, Takuya[4] ; TSUTSUMI, Masaki[1] ; NAKAMURA, Takuji[1]

[1]National Institute of Polar Research, [2]Graduate School of System Design, Tokyo Metropolitan University, [3]College of Science, Rikkyo university, [4]Faculty of Engineering, Shinshu University

The National Institute of Polar Research (NIPR) is leading a six year prioritized project of the Antarctic research observations since 2010. One of the sub-project is entitled ”the global environmental change revealed through the Antarctic middle and upper atmosphere”. Profiling dynamical parameters such as temperature and wind, as well as minor constituents is the key component of observations in this project, together with a long term observations using existent various instruments in Syowa, Antarctica (69S, 39E). As a part of the sub-project, Rayleigh/Raman lidar was installed at Syowa Station in January, 2011 and has been operated at more than 350 nights (>3000 hours clear sky) by February, 2014. The Rayleigh/Raman lidar observes temperature and clouds in the mesosphere, the stratosphere and part of the troposphere, and providing seasonal and yearly variations of temperature profiles and data of gravity wave characteristics in the middle atmosphere, as well as high altitude clouds of PMC (polar mesospheric clouds) and PSC (polar stratospheric clouds). In order to extend the height coverage to include mesosphere and lower thermosphere region, and also to extend the parameters observed, a new resonance scattering lidar system with tunable wavelengths is developed at NIPR in Tachikawa (36N, 139E). The lidar transmitter is based on injection-seeded, pulsed alexandrite laser for 768-788 nm (fundamental wavelengths) and a second-harmonic generation (SHG) unit for 384-394 nm (second harmonic wavelengths). The laser wavelengths are tuned in to the resonance wavelengths by a wavemeter that is well calibrated using a wavelength-stabilized He-Ne laser. The new lidar has capabilities to measure density variations of minor constituents such as atomic iron (Fe, 386 nm), atomic potassium (K, 770 nm), calcium ion (Ca^+, 393 nm), and aurorally excited nitrogen ion ($N_2{}^+$, 390-391 nm) and temperature profiles in the mesosphere and lower thermosphere (MLT) region using resonance scatter of K. Currently, the fundamental laser pulses are transmitted with 120-160 mJ/pulse at approximately 25 Hz (i.e., $\sim$3-4 W) and the backscattered signal is received with a 35 cm diameter telescope. The new lidar system will be installed two years later at Syowa Station and provide information on the mesosphere and lower thermosphere as well as the ionosphere. This unique observation is expected to make important contribution to studies on the atmospheric vertical coupling process and the neutral and charged particle interaction. In this talk, current status of the research, observations, and system developments, as well as future plans will be presented.

Keywords: Lidar, Antarctic observation, middle and upper atmosphere, Resonance scattering, Rayleigh scattering, Raman scattering

Japan Geoscience Union Meeting 2014
(28 April - 02 May 2014 at Pacifico YOKOHAMA, Kanagawa, Japan)

PEM36-07 Room:312 Time:April 28 10:30-10:45

A daytime observation of polar mesospheric clouds with Syowa Rayleigh Raman lidar system equipped with a new etalon unit

SUZUKI, Hidehiko[1*] ; NAKAMURA, Takuji[2] ; EJIRI, Mitsumu[2] ; ABO, Makoto[3] ; YAMAMOTO, Akihiro[4] ; KAWAHARA, Taku d[4] ; TOMIKAWA, Yoshihiro[2] ; TSUTSUMI, Masaki[2] ; TSUDA, Takuo[2] ; NISHIYAMA, Takanori[2]

[1]Rikkyo University, [2]National Institute of Polar Research, [3]Tokyo Metropolitan University, [4]Shinshu University

A Rayleigh/Raman lidar system has been operated by the Japanese Antarctic Research Expedition (JARE) since February, 2011 (JARE 52nd) in Syowa Station Antarctica (69.0S, 39.5E). Polar Mesospheric Cloud (PMC) was detected by the lidar at 22:30UT (+3hr for LT) on Feb 4th, 2011, the first day of a routine operation. This event is the first time to detect PMC over Syowa Station by a lidar [Suzuki et al., 2013]. However, signal to noise ratio (SNR) of the PMC event was not so good due to a large shot noise from a daytime background signal. Moreover, a receiver system was mainly designed for nighttime observations. Therefore, observation of PMC during the midnight Sun, which also corresponds to PMC most active period, was difficult. Thus, to improve SNR of the PMC observation with Syowa Rayleigh/Raman lidar during daytime, a narrow bandpass Fabry-Perot etalon system has been developed and installed in the receiver system on Dec 2013 by JARE 55th. In this paper, Prompt report of a PMC observation with Syowa Rayleigh Raman lidar system equipped with the new etalon unit is presented.

Keywords: polar mesospheric cloud, noctilucent cloud, lidar, Antarctic

Japan Geoscience Union Meeting 2014
(28 April - 02 May 2014 at Pacifico YOKOHAMA, Kanagawa, Japan)

PEM36-08 Room:312 Time:April 28 11:00-11:15

Study on generation and sustaining mechanism for an SSL during a night of high auroral activity above Tromsoe

TAKAHASHI, Toru[1*] ; NOZAWA, Satonori[1] ; TSUDA, Takuo[2] ; OYAMA, Shin-ichiro[1] ; FUJIWARA, Hitoshi[3] ; TSUTSUMI, Masaki[2] ; KAWAHARA, Takuya[4] ; SAITO, Norihito[5] ; WADA, Satoshi[5] ; KAWABATA, Tetsuya[1] ; MATUURA, Nobuo[1] ; HALL, Chris[6]

[1]STEL, Nagoya Univ., [2]NIPR, [3]Faculty of Science and Technology, Seikei Univ., [4]Faculty of Engineering, Shinshu Univ., [5]RIKEN, [6]Univ. of Tromso

We will report observational results about an SSL (Sporadic Sodium Layer) that appeared on 22 January 2012 above Tromso, Norway (69.6deg N, 19.2deg E). An SSL is sudden formation (more precisely, from observer's viewpoint) of a dense thin sodium layer superposed on a normal sodium layer. Characteristic of an SSL is suitable for investigating, in particular, fine structures in the atmosphere such as small scale waves and turbulences. For example, Tsuda et al., GRL, 2011GL048685 [2011] found out a short-period wavelike structure on an SSL with sodium lidar operated Tromso, Norway.

Some generation mechanisms for SSLs have been proposed and discussed. A high correlation between an SSL and a sporadic E (Es) layer occurrences has been reported, and several authors proposed mechanisms how SSLs are generated by association of the Es layers [e.g., von Zahn and Hansen, JATP, 50, 93-104, 1988]. Kirkwood and von Zahn, JAP, 53, 389-407 [1991] have suggested that a strong electric field that generates an Es layer plays an important role for generation of an SSL as well in the auroral region. Recently, Matuura et al. JGR, 118, 1-12, jgra.50414 [2013] have proposed another mechanism that an electric current loop plays an important role for the convergence of positive ions including metallic ions.

Altitudinal temperature gradients have been also discussed as a candidate for an SSL generation. Clemesha et al., JASTP, j.jastp.2010.03.017 [2010] showed that an SSL tended to be located in the region where the temperature gradient is negative. A sodium lidar measurement exhibited a 40 K temperature increase on the topside of the SSL [Gardner et al., JGR, 98, 16,865-16,873, 1993].

We like to point out two concerns to be improved for the previous studies. First, although an SSL is complex phenomenon resulting from the confluence of various mechanisms, most studies focused on one mechanism alone. Second is a temporal resolution to calculate the neural temperature and sodium density. Since the sodium density inside an SSL varies largely and quickly in an order of seconds, data with insufficient resolution mislead our understanding. The temporal resolutions of five minutes used in previous studies are insufficient. In this study, we have derived neutral temperature and sodium density with a 15 second. Furthermore, we have used data obtained with the EISCAT UHF radar, meteor radar and photometer together with the sodium LIDAR at Tromso.

On 22 January 2012, an SSL was observed by the sodium lidar at about 94 km about 19 minutes after hard auroral precipitations. From 2118 UT to 2142 UT, the sodium density inside the SSL was from 2 and 6 times greater than the background sodium density. After 2142 UT the peak of the SSL went up to 96 km and the SSL became thinner than it was. The peak sodium density decreased, but it was still a few times higher than the background sodium density from 2142 UT to 2400 UT. We have calculated the temperature with a 15 second resolution, and have found that there are no remarkable enhancements in temperature profiles inside the SSL from 2118 to 2142 UT. It would be worth to point out that from 2200 to 2400 UT the SSL stayed in the local temperature minimum of the background atmosphere. Gardner et al. JGR. 2004JD005670 [2005] argued that the sodium density has a negative correlation with temperature at topside of the sodium layer. Therefore, our result is likely to indicate that the temperature profile contributes sustention of the SSL in this event. To investigate other candidate mechanisms for the SSL generation, we have analyzed the EISCAT radar data. The EISCAT radar detected an Es layer simultaneously with the SSL. The Es layer was located on about 94 km altitude where the SSL was located from 2118 UT to 2200 UT. However, after 2200 UT the Es layer was located on 2 km below the SSL. This result is likely to indicate that the Es layer contributes the SSL generation.

Keywords: Sporadic sodium layer, sodium lidar, aurora, EISCAT radar, meteor radar

Japan Geoscience Union Meeting 2014
(28 April - 02 May 2014 at Pacifico YOKOHAMA, Kanagawa, Japan)

PEM36-09 Room:312 Time:April 28 11:15-11:30

Seasonal variation of Polar Mesosphere Winter Echo (PMWE) observed by PANSY radar

NISHIYAMA, Takanori[1*] ; SATO, Kaoru[2] ; TSUTSUMI, Masaki[1] ; SATO, Toru[3] ; NAKAMURA, Takuji[1] ; NISHIMURA, Koji[1] ; KOHMA, Masashi[2] ; TOMIKAWA, Yoshihiro[1] ; EJIRI, Mitsumu[1] ; TSUDA, Takuo[1]

[1]National Institute of Polar Research, [2]Department of Earth and Planet Science, Graduate School of Science, The University of Tokyo, [3]Graduate School of Informatics, Kyoto University

In the lower thermosphere at the altitude of around 100 km, both neutral turbulence and ionization of atmosphere due to solar radiations cause irregularities of reflective index, and as a result back scatter echoes from that altitude are frequently observed by radars on the ground. In the mesosphere, Polar Mesosphere Summer Echo (PMSE) is reported to be a strong echo associated with ice particles, which are produced around the coldest mesopause region in the polar summer, by a number of past radar observations [*Cho and Rottger*, 1997; *Rapp and Lūbken*, 2004]. It should be also noted that occurrence rate of PMSE is very high (80-90%) [*Bremer et al*., 2003]. On the other hand, Polar Mesosphere Winter Echo (PMWE) is also known as back scatter echo from 55 to 85 km in the mesosphere, and it has been observed by MST and IS radar in polar region during winter [e.g., *Ecklund and Balsley*, 1981; *Czechowsky et al*., 1989; *Lūbken et al*., 2006; *Strelnikova and Rapp*, 2013]. Due to the lack of of free electrons and ice particles in the dark and warm mesosphere during winter, it is suggested that PMWE requires strong ionization of neutral atmosphere associated with precipitations of Solar Energetic Particles (SEPs) during geomagnetically disturbed periods [*Kirkwood et al*., 2002; *Zeller et al*., 2006]. However, the detailed generation process of PMWE has not been identified yet, partly because the reported PMWE occurrence rate was quite low (2.9%) [*Zeller et al*., 2006].

In the Ⅷ-th six-year project of the Japanese Antarctic Research Expedition (JARE) from 2010, the middle and upper atmosphere research is one of the sub-projects of the prioritized research project entitled 'Global warming revealed from the Antarctic', and comprehensive ground based observations with various remote sensing instruments for the middle and upper atmosphere have been operating continuously in Syowa station. We analyzed data obtained by PANSY (Program of the Antarctic Syowa MST/IS) radar, which is the core instrument of the project, focusing on PMWE in the context of neutral-plasma atmospheric coupling process between the middle and upper atmosphere. PANSY radar is a 47 MHz VHF radar with 125 kW (full system 500 kW) output power, and it is the largest MST radar composed 5,000 m^2 (full system 20,000 m^2) antenna array in Antarctica at the moment. PANSY has already identified a number of PMWE near local noon since operation of mesosphere observation mode was started in June 2012.

We would like to show seasonal variations of occurrence characteristics of PMWE between June 2012 and July 2013. Taking full advantage of PANSY radar's detectability, we calculated monthly-averaged height-time section of backscatter echo power in austral winter between 2012 and 2013. The result demonstrated that durations of PMWE strongly depended on hours of sunlight, although occurrence heights of PMWE, which range from 60 to 80 km, were fixed on every month and year. These statistical characteristics of PMWE were consistent with previous studies suggesting ionization at the PMWE height due to solar radiation play a dominant role in generation of PMWE [*Zeller et al*., 2006; *Lūbken et al*., 2006]. However, the mean occurrence rate of PMWE estimated by our study was 20-30%, which was considerably higher than that of previous studies. It implies that atmospheric turbulence in the mesosphere would be driven by breakings of atmospheric gravity waves more frequently than past observations, especially in Antarctica, and the role of atmospheric gravity waves cannot be ignored when considering the long-termed climate changes.

Keywords: Polar Mesosphere Winter Echo, PANSY radar, Atmospheric gravity wave, Neutral-plasma interaction

Japan Geoscience Union Meeting 2014
(28 April - 02 May 2014 at Pacifico YOKOHAMA, Kanagawa, Japan)

PEM36-10 Room:312 Time:April 28 11:30-11:45

Analysis of atmospheric gravity waves observed by airglow imaging at Syowa Station (69S,39E), Antarctica

MATSUDA, Takashi S.[1*] ; NAKAMURA, Takuji[2] ; EJIRI, Mitsumu K.[2] ; TSUTSUMI, Masaki[2] ; SHIOKAWA, Kazuo[3] ; TAGUCHI, Makoto[4] ; SUZUKI, Hidehiko[4]

[1]Graduate University for Advanced Studies, [2]National Institute of Polar Research, [3]Solar-Terrestrial Environment Laboratory, Nagoya University, [4]Rikkyo University

Atmospheric gravity waves (AGWs), which are generated in the lower atmosphere, transport significant amount of energy and momentum into the mesosphere and lower thermosphere and cause the mean wind accelerations in the mesosphere. This momentum deposit drives the general circulation and affects the temperature structure. Among many parameters to characterize AGWs, horizontal phase velocity is very important to discuss the vertical propagation. Airglow imaging is a useful technique for investigating the horizontal structures of AGWs at around 90 km altitude. Recently, there are many reports about statistical characteristics of AGWs observed by airglow imaging. However, it is difficult to compare these results obtained at various locations because each research group uses its own method for extracting and analyzing AGW events. In order to deal with huge amounts of imaging data obtained on different years and at various observation sites, without bias caused by different event extraction criteria for the observer, we have developed a new statistical analysis method for obtaining the power spectrum in the horizontal phase velocity domain from airglow image data. This method was applied to the data obtained at Syowa Station, Antarctica, in 2011 and compared with a conventional event analysis in which the phase fronts were traced manually in order to estimate horizontal characteristics. This comparison shows that our new method is suitable for deriving the horizontal phase velocity characteristics of AGWs observed by airglow imaging technique.

We plan to apply this method to airglow imaging data observed at Syowa Station in 2002 and between 2008 and 2013, and also to the data observed at other stations in Antarctica (e.g. Rothera Station (67S, 68W) and Halley Station (75S, 26W)), in order to investigate the behavior of AGWs propagation direction and source distribution in the MLT region over Antarctica. In this presentation, we will report interim analysis result of the data at Syowa Station.

Keywords: atmospheric gravity wave, airglow imaging

Japan Geoscience Union Meeting 2014
(28 April - 02 May 2014 at Pacifico YOKOHAMA, Kanagawa, Japan)

PEM36-11 Room:312 Time:April 28 11:45-12:00

First detection of daytime tweek atmospherics observed at Moshiri and Kagoshima, Japan

OHYA, Hiroyo[1*] ; SHIOKAWA, Kazuo[2] ; MIYOSHI, Yoshizumi[2]

[1]Graduate School of Engineering, Chiba University, [2]Solar-Terrestrial Environment Laboratory, Nagoya University

It is well known that tweek atmospherics can be observed only at night except for solar eclipse days, because daytime attenuation rate of the tweeks is much larger (˜70 dB/1000 km) than that in nighttime (˜3 dB/1000 km). In this presentation, we firstly report detection of daytime tweeks at Moshiri (Geographic coordinate: 44.37^{o}N, 142.27^{o}E) and Kagoshima (31.48^{o}N, 130.72^{o}E), Japan, on non-solar eclipse days in December, 1980. The daytime tweeks were observed both before and during a large magnetic storm during 16-20 December, 1980. The minimum Dst value was -240 nT at 04:00 UT on 20 December. The average occurrence numbers of the daytime tweeks at Moshiri and Kagoshima were 2.7 and 0.3 tweeks per minute, respectively. The local times (LT) when the daytime tweeks occurred were through 07:00 - 17:00 LT at Moshiri, while they were 07:00 - 09:00 LT and 15:00 - 17:00 LT at Kagoshima. All the daytime tweeks show clear frequency dispersion. The average duration was 18.94 ms, while that of nighttime tweeks is ˜50 ms. The average reflection heights of daytime tweeks at Moshiri and Kagoshima were 86.2 km and 94.7 km, respectively. The average reflection heights of nighttime tweeks at Moshiri and Kagoshima in same period were 87.1 km and 92.1 km, respectively. The variation of the daytime tweek reflection height was higher than that of nighttime tweeks. The horizontal propagation distance in daytime cannot be estimated from the dispersion, because the duration was too short to estimate the distance.

We found through a theoretical consideration that the VLF/ELF attenuation on the D-region ionosphere depends not only on the ionospheric height, but also the sharpness of electron density profiles, β. The β is a conventional parameter proposed by Wait and Spies [1964]. When the β increases, the attenuation decreases. Even daytime, when the β is occasionally large, the attenuation would become less down to be able to observe the tweeks. In this talk, we will show the results of the daytime tweeks and discuss their occurrence mechanism.

Japan Geoscience Union Meeting 2014
(28 April - 02 May 2014 at Pacifico YOKOHAMA, Kanagawa, Japan)

PEM36-12 Room:312 Time:April 28 12:00-12:15

Long term variation of geomagnetic Sq field over 100 years

TAKEDA, Masahiko[1*]

[1]Data Analysis Center for Geomag. and Space Magnetism, Kyoto Univ

The long-term variation of the geomagnetic Sq field over 100 years at several observatories was studied in the Y-component as well as the ionospheric conductivity estimated by the IRI model. The amplitude of the geomagnetic Y-component (Sq(Y)) depended strongly on solar activity, and showed features similar to those in the solar activity even when 11-years running averages were employed. The solar activity dependence of Sq(Y) can be fully explained by that of the ionospheric electrical conductivity, and wind velocity tends to be large for low solar activity; and slower in the middle of the 1900s in response to higher long-term solar activity. On the other hand, other long-term variations were not clear in the wind velocity. Although the dynamo theory predicts that the Sq current is enhanced when geomagnetic main field intensity decreases, the result of the present analysis does not necessarily support this prediction.

Keywords: geomagnetic daily variation, long-term variation, solar activity, main field strength, elecric conductivity, wind velocity

Japan Geoscience Union Meeting 2014
(28 April - 02 May 2014 at Pacifico YOKOHAMA, Kanagawa, Japan)

PEM36-13 Room:312 Time:April 28 12:15-12:30

Long-term variation in the upper atmosphere as seen in the geomagnetic solar quiet (Sq) daily variation

SHINBORI, Atsuki[1*] ; KOYAMA, Yukinobu[2] ; NOSE, Masahito[2] ; HORI, Tomoaki[3] ; OTSUKA, Yuichi[4] ; YATAGAI, Akiyo[4]

[1]Research Institute for Sustainable Humanosphere (RISH), Kyoto University, [2]Data Analysis Center for Geomagnetism and Space Magnetism Graduate School of Science, Kyoto Universi, [3]Nagoya University Solar Terrestrial Environment Laboratory Geospace Research Center, [4]Solar-Terrestrial Environment Laboratory, Nagoya University

It has been well-known that the geomagnetic field on the ground shows a regular variation with a fundamental period of 24 hours during a solar quiet day. This daily variation depends on local time, latitude, season and solar cycle and has been called solar quiet (Sq) geomagnetic field daily variation. The Sq variation is mainly produced by magnetic effects due to ionospheric currents flowing in the E region of the ionosphere around 105 km. The global pattern of the Sq variation of the H-component shows positive and negative changes in the equatorial and middle-latitude regions around noon, respectively. The Sq current system expected from the geomagnetic field perturbations consists of two large current vortices: one is an anticlockwise current in the northern hemisphere and the other is a clockwise current in the southern hemisphere. The Sq current is dominant in the daytime ionosphere where ionospheric conductivity is relatively large, and is driven by electric fields originating from the ionospheric dynamo via the interaction between ionized and neutral particles. According to the Ohm's law, the main variables in the Sq amplitude are the ionospheric conductivity, the polarization electric field, the solar diurnal tide, and the intensity of the ambient magnetic field at the E-region height. Then, to investigate the long-term variation in the Sq amplitude is important for understanding the physical mechanism of long-term variation in the upper atmosphere related to solar activity and lower atmospheric change such as global warming. In this study, we investigated long-term variation in the Sq amplitude using 1-hour geomagnetic field data obtained from 184 geomagnetic observation stations within a period of 1947-2012 in order to clarify the physical mechanism of long-term variation in the upper atmosphere. For the analysis of long-term observation data obtained from a lot of geomagnetic stations, we took advantage of the IUGONET data analysis system (metadata database search system and data analysis software). The Sq amplitude is defined as a difference of the H-component of geomagnetic field between the maximum and minimum values each solar quiet day. We identified the solar quiet day as the day when the maximum Kp value is less than 4 for each day. As a result, the Sq amplitude observed at all the geomagnetic stations showed a clear dependence on the 11-year solar activity and it tended to be enhanced significantly during solar maximum. The Sq amplitude became the smallest around the minimum of 23/24 solar cycle in 2008-2009. The relationship between the Sq amplitude and F10.7 solar activity index was not linear but nonlinear. This nonlinearity could be interpreted as the decrease of production rate of electrons and ions in the ionosphere for the strong extreme ultraviolet (EUV) and ultraviolet (UV) fluxes. In order to minimize an effect of solar activity including the long-term variation in the Sq amplitude, we calculated second orders of fitting curve between the F10.7 solar index and Sq amplitude during 1947-2012, and examined the residual Sq amplitude defined as the deviation from the fitting curve. As a result, majority of the residual Sq trends passed through the trend test showed a negative value without dependence on geographical latitude and longitude. The tendency was strong in India, the southern part of Africa, and the northern part of America and Europe. In a region of northern part of America and Europe, the secular variation of magnetic inclination becomes relatively large, compared with other regions. Therefore, the long-term trend in the residual Sq amplitude could be linked to a change in the ionospheric conductivities associated with the secular variation of the ambient magnetic field and the upper atmosphere and electro motive force (UxB) via the interaction between ionized and neutral particles.

Keywords: Geomagnetic solar quiet daily variation, Solar activity, Long-term variation, Geomagnetic secular variation, Ionospheric conductivity, Global warming

Japan Geoscience Union Meeting 2014
(28 April - 02 May 2014 at Pacifico YOKOHAMA, Kanagawa, Japan)

PEM36-14 Room:312 Time:April 28 12:30-12:45

Temporal increases of horizontal speed of frontal Es observed by HFD

TOMIZAWA, Ichiro[1*] ; MIYAWAKI, Masami[1]

[1]Center for Space Science and Radio Engineering, The University of Electro-Commnunications

In the yearly analysis of the horizontal speed of frontal Es by using the HFD observation data of the year 2012, we found some events which showed temporal increase and then decrease within the time scale from 40 to 270 minutes. The rate of the temporal speed enhancements were only 2.4 % in all frontal Es events in 2012, and the enhances were mainly observed aroun 21h JST in summer. The rate of the speed enhancement were less than 30 %, but some peak speeds increased up to more than 200 m/s. The duration times varied from 40 to 300 min, but most of the events terminated within 150 min. The average leading and trailing times were 35 and 50 min, respectively, so the trailing part took long time. The cause of temporal speed variation can be related to time variation of horizontal electric field or of horizontal wind speed of neutral atmosphere in the E layer. The former should show coincidence over the wide area but the latter would show some time difference. Analyzing pair data over 100 km separation, we obtained time delay less than 20 min. It is therefore interpreted that the temporal speed increase is caused by the change of the horizontal wind speed. Because the distance between successive Es front shows the minimum of less than 50 km around the speed peak, and increases upto 200 km both to the start and to the end, it can be attributed to the inequally spaced Es front. Combining all separation distances for each event, we get the outer size of the temporal variation as 400 km for 65 %, and as the maximum of 1400 km. On the otherhand, it can be related to a non-isotropic structure because the peak speed did show different values for the separate stations. Based on those observational results, it is concluded that the temporal speed increase may be introdued by a spiral-like, instead of linear, structure.

Keywords: frontal Es, horizontal speed, temporal increase, HF Doppler observation

Japan Geoscience Union Meeting 2014
(28 April - 02 May 2014 at Pacifico YOKOHAMA, Kanagawa, Japan)

PEM36-15 Room:312 Time:April 28 14:15-14:30

Study of medium-scale traveling ionospheric disturbances (MSTID) with sounding rockets and ground observations

YAMAMOTO, Mamoru[1*] ; KATO, Tomohiro[1] ; ISHISAKA, Keigo[2] ; YOKOYAMA, Tatsuhiro[3] ; IWAGAMI, Naomoto[3] ; TAKAHASHI, Takao[5] ; TANAKA, Makoto[5] ; ENDO, Ken[6] ; KUMAMOTO, Atsushi[6] ; WATANABE, Shigeto[7] ; YAMAMOTO, Masa-yuki[8] ; ABE, Takumi[9] ; SAITO, Susumu[10] ; TSUGAWA, Takuya[3] ; NISHIOKA, Michi[3] ; BERNHARDT, Paul[11] ; LARSEN, Miguel[12]

[1]RISH, Kyoto University, [2]Toyama Prefectural University, [3]NICT, [4]School of Science, University of Tokyo, [5]ICT Education Center, Tokai University, [6]School of Science, Tohoku University, [7]School of Science, Hokkaido University, [8]Kochi University of Technology, [9]JAXA/ISAS, [10]ENRI, [11]NRL, [12]Clemson University

Medium-scale traveling ionospheric disturbance (MSTID) is an interesting phenomenon in the F-region. The MSTID is frequent in summer nighttime over Japan, showing wave structures with wavelengths of 100-200 km, periodicity of about 1 hour, and propagation toward the southwest. The phenomena are observed by the total electron content (TEC) from GEONET, Japanese dense network of GPS receivers, and 630 nm airglow imagers as horizontal pattern. It was also measured as Spread-F events of ionograms or as field-aligned echoes of the MU radar. MSTID was, in the past, explained by Perkins instability (Perkins, 1973) while its low growth rate was a problem. Recently 3D simulation study by Yokoyama et al (2009) hypothesized a generation mechanism of the MSTID, which stands on electromagnetic E/F-region coupling of the ionosphere. The hypothesis is that the MSTID first grows with polarization electric fields from sporadic-E, then show spatial structures resembling to the Perkins instability. We recently conducted a observation campaign to check this hypothesis. We launched JASA ISAS sounding rockets S-310-42 and S-520-27 at 23:00 JST and 23:57JST on July 20, 2013 while an MSTID event was monitored in real-time by the GPS-TEC from GEONET. We found 1-5mV/m northeastward/eastward electric fields during the flight. Variation of electric fileds were associated with horizontal distribution of plasma density. Wind velocity was measured by the TME and Lithium releases from S-310-42 and S-520-27 rockets, respectively, showing southward wind near the sporadic-E layer heights. These results are consistent to the expected generation mechanism shown above. In the presentation we will discuss electric-field results and its relationship with plasma density variability together with preliminary results from the neutral-wind observations.

Keywords: MSTID, Sounding rocket, Electric field, GPS-TEC, Observation campaign

Japan Geoscience Union Meeting 2014
(28 April - 02 May 2014 at Pacifico YOKOHAMA, Kanagawa, Japan)

PEM36-16 Room:312 Time:April 28 14:30-14:45

Characteristics of O630nm emission associated with equatorial ionization anomaly obtained with IMAP/VISI

SAKAMOTO, Daiki[1] ; SAKANOI, Takeshi[1*] ; PERWITASARI, Septi[1] ; OTSUKA, Yuichi[2] ; SAITO, Akinori[3] ; AKIYA, Yusuke[3] ; HOZUMI, Yuta[3] ; YAMAZAKI, Atsushi[4]

[1]Grad. School of Science, Tohoku University, [2]STEL, Nagoya University, [3]Grad. School of Science, Kyoto University, [4]ISAS / JAXA

The Equatorial Ionization Anomaly (EIA) is occurred by plasma upwelling due to eastward electric field in the dayside magnetic equator, and descends to both northern and southern hemispheres along the field line. Density maximum appears around geomagnetic latitudes of +/-15 degree at both hemispheres. Since most of the past studies carried out with ground experiments, it is difficult to observe a wide area and study the variability of the northern and southern O630nm emission associated with EIA.

IMAP/VISI on the International Space Station(ISS) measures O630 nm airglow emission in the nightside hemisphere at an altitude of 400km. It covers the latitudinal range between +/-52 degrees with a typical spatial resolution of 1x14 km. Because of the wide observation coverage, it is possible to observe the variability of O630nm airglow associated with the EIA.

In this study, we carried out a statistical analysis using IMAP/VISI data from September 2012 to December 2013 to understand the variability of O630nm airglow associated with the EIA, particularly on its local time dependence, seasonal variation and geomagnetic activity. We derived the integrated intensity of O630nm emission along latitude with the four criteria as follows: (1) The O630nm emission in the EIA is greater than the background airglow that was determined by emission intensity in the middle latitude. (2) Latitudinal distribution of O630nm emission in the EIA is fully measured. (3) The northern and southern O630nm emission in the EIA is clearly separated. (4) The moon phase is smaller than 0.5. In case that the moon phase is bigger than 0.5 then we used the data when the moon did not appear.

We find that the time dependence of O630nm emission which is decreased from the evening toward the post mid-night. But there is a large variance in the intensity at the same local time. This fact suggests that other process, such as the longitude and/or seasonal variation, may affect the O630nm emission associated with the EIA in addition to the local time dependence.

On the seasonal dependence, we find that O630nm emission in the EIA in the winter hemisphere is greater than that in the summer hemisphere. This is consistent with the model that the thermospheric tidal wind affects the 630 nm intensity, namely, the tidal wind decreases the altitude of O630 nm emission layer and finally gain the O630 nm intensity.

To examine the longitudinal dependence, we used the data in equinox (September and October, 2013) and find that O630nm emission in the EIA in the northern hemisphere is greater than that in the southern hemisphere where the dip equator is the south of geographic equator (longitude is between 200 degree ? 310 degree). This is also consistent with the model that the thermospheric tidal wind controls the O630 nm intensity by making a vertical motion of emission layer.

Finally, we investigate the magnetic storm dependence on O630 nm intensity and find that significant decrease of O630nm intensity in the EIA happens during the period when the Dst index is larger than 90. From this fact, it is plausible that westward electric field in Region 2 current system penetrates to the low latitude region during the main phase of magnetic storm and reduce the formation of EIA.

Keywords: ISS, airglow, thermosphere, ionosphere, equatorial ionization anomarly, IMAP

Japan Geoscience Union Meeting 2014
(28 April - 02 May 2014 at Pacifico YOKOHAMA, Kanagawa, Japan)

PEM36-17 Room:312 Time:April 28 14:45-15:00

Analysis of the airglow structures using the simultaneous observations by ISS-IMAP and all-sky imagers

YUKINO, Hideko[1*] ; SAITO, Akinori[1] ; OTSUKA, Yuichi[2] ; SAKANOI, Takeshi[3]

[1]Dept. of Geophysics, Kyoto Univ., [2]STEL, Nagoya Univ., [3]Grad. School of Science, Tohoku Univ.

The spatial structure of the atmospheric gravity waves in the mesosphere was analyzed using the simultaneous observational data of ISS-IMAP and the all-sky imager at Hawaii. There are a plenty of ground-based observations of the atmospheric gravity waves in the mesosphere and the thermosphere. The problem of the ground-based observation is that it cannot distinguish spatial variations from temporal variations for the structures whose scale size is larger than its field-of-view. ISS-IMAP was launched on July 21, 2012 to observe the atmospheric gravity waves whose scale size is larger than 100 km. The altitude of the International Space Station (ISS) flies around 400 km altitude, and its orbital inclination angle is 51.6 degrees. ISS-IMAP/VISI (Visible-light and infrared Spectrum Imager) observes the airglow in the mesosphere and the ionosphere. The spatial resolution of the VISI imaging observation is from 10 km to 25 km. The airglow wavelengths observed by VISI are 630 nm, 730 nm, and 762 nm and by the ground-based all-sky image of Hawaii (20.48 N, 156.2 W) are 630 nm and 557.7-nm with 5.5 minutes interval. The observational data of ISS-IMAP/VISI and an all-sky imager in Hawaii were investigated for the nights when VISI made the observation over Hawaii, and the sky over the imager was clear. The night when the plasma bubble was detected by the ground-based all-sky imager, the plasma bubble was detected by the 630nm airglow observation of ISS-IMAP/VISI. The spatial and vertical structures of the airglow that were observed by the ground-based imager and the ISS-IMAP/VISI were analyzed. The sensitivity of the observation of ISS-IMAP/VISI will also be discussed in the comparison of the ground-based observation.

Keywords: airglow, plasma bubble, ISS-IMAP

Japan Geoscience Union Meeting 2014
(28 April - 02 May 2014 at Pacifico YOKOHAMA, Kanagawa, Japan)

PEM36-18 Room:312 Time:April 28 15:00-15:15

Horizontal structures of ionized Helium in the topside ionosphere of dusk side observed by ISS-IMAP/EUVI

HOZUMI, Yuta[1*] ; SAITO, Akinori[1] ; YAMAZAKI, Atsushi[2] ; MURAKAMI, Go[2] ; YOSHIKAWA, Ichiro[3]

[1]Department of Geophysics, Graduate School of Science, Kyoto University, [2]Institute of Space and Astronautical Science / Japan Aerospace Exploration Agency, [3]The University of Tokyo

Horizontal structures of ionized Helium in the topside ionosphere of dusk side were obtained with the Extreme Ultra Violet Imager (EUVI) of the ISS-IMAP (Ionosphere, Mesosphere, upper Atmosphere and Plasmasphere mapping) mission. EUVI has taken image of He He II radiation (30.4 nm) from the International Space Station (ISS) since October 2012. In this work, images taken in 2013 were analyzed. North-south asymmetry and longitudinal structure of ionized Helium were found. Seasonal dependence of these horizontal structures will be discussed.

Keywords: Topside ionosphere, ISS-IMAP, Ionoized Helium

Japan Geoscience Union Meeting 2014
(28 April - 02 May 2014 at Pacifico YOKOHAMA, Kanagawa, Japan)

PEM36-19 Room:312 Time:April 28 15:15-15:30

Study of ionospheric disturbance characteristics during solar flare events using the SuperDARN Hokkaido radar

WATANABE, Daiki[1] ; NISHITANI, Nozomu[1*]

[1]Solar-Terrestrial Environment Laboratory, Nagoya University

Ionospheric disturbances during solar flare events have been studied by various kinds of observation instrument in the last few decades. Kikuchi et al. (1985) reported on the positive Doppler shift in the HF Doppler system data during solar flare events, and indicated that there are two possible factors of Doppler shift, i.e., (1) apparent ray path decrease by changing refraction index due to increasing electron densities in the D-region ionosphere, and (2) ray path decrease due to descending reflection point associated with increasing electron density in the F-region ionosphere.

In this study, we use the SuperDARN Hokkaido Radar to investigate the detailed characteristics of solar flare effects on ionospheric disturbances. We focus on the positive Doppler shift of ground / sea scatter echoes just before sudden fade-out of echoes. Davies et al. (1962) showed that if the factor (1) is dominant, the Doppler shift should have positive correlation with slant range and negative correlation with elevation angle and frequency. On the other hand, if the factor (2) is dominant, the Doppler shift should have negative correlation with slant range and positive correlation with elevation angle and frequency. While Kikuchi et al. (1985) studied solar flare events and mainly discussed frequency dependence of Doppler shift, we study mainly slant range and elevation angle dependence, for the first time to the best of our knowledge. We found that the factor (1), in other words, increase of electron densities at D-region ionosphere, is dominant during solar flare events. This result is consistent with that of Kikuchi et al. (1985). In order to study characteristics of ionospheric disturbance in more detail, we are studying relationship between timing / amplitude of ionospheric disturbance and that of the solar irradiation changes, by comparing the HF radar data with high wavelength resolution irradiation data for X-ray and EUV from RHESSI and SDO satellites. Generally, X-ray radiation becomes more important for the changes in the D-region during solar flare events. Therefore we investigate relationship between X-ray flux changes and electron density variation in the D-region ionosphere intensively. Furthermore, we estimated electron density changes in the ionsosphere by analyzing elevation angle dependence of Doppler shift in radar echoes quantitatively. We are estimating electron density by considering chemical reaction and photoreaction caused by solar radiation. We will compare the two electron density changes deduced from different two ways and evaluate the amplitude of ionospheric disturbance observed by the HF radar. More detailed analysis result will be reported.

Keywords: SuperDARN, Hokkaido radar, solar flares, ionospheric disturbances, photochemical reaction, range dependence

Japan Geoscience Union Meeting 2014
(28 April - 02 May 2014 at Pacifico YOKOHAMA, Kanagawa, Japan)

PEM36-20 Room:312 Time:April 28 15:30-15:45

Thermospheric tidal effects on the ionospheric midlatitude summer nighttime anomaly

CHEN, Chia-hung[1*] ; LIN, Charles[1] ; CHANG, Loren[2] ; HUBA, J. D.[3] ; SAITO, Akinori[4] ; LIU, Jann-yenq[2]

[1]Department of Earth Science, National Cheng Kung University, Tainan, Taiwan, [2]Institute of Space Science, National Central University, Chung-Li, Taiwan, [3]Plasma Physics Division, Naval Research Laboratory, Washington, D. C., USA, [4]Department of Geophysics, Kyoto University, Kyoto, Japan

This study use a 3D physics-based ionospheric model, SAMI3, coupled with the National Center for Atmospheric Research Thermosphere Ionosphere Electrodynamics General Circulation Model (TIEGCM) and Global Scale Wave Model (GSWM) to simulate the mesospheric and lower thermosphreic tidal effects on the development of midlatitude summer nighttime anomaly (MSNA). Using this coupled model, the diurnal variation of MSNA electron densities at 300 km altitude is simulated on both June solstice (day of year (DOY) 167) and December solstice (DOY 350) in 2007. Simulation results show successful reproduction of the southern hemisphere MSNA structure including the eastward drift feature of the southern MSNA, which is not reproduced by the default SAMI3 runs using the neutral winds provided by the empirical Horizontal Wind Model 93 (HWM93) neutral wind model. A linear least squares algorithm for extracting tidal components is utilized to examine the major tidal component affecting the variation of southern MSNA. Results show that the standing diurnal oscillation component dominates the vertical neutral wind manifesting as a diurnal eastward wave-1 drift of the southern MSNA in the local time frame. We also find that the stationary planetary wave-1 component of vertical neutral wind can cause diurnal variation of the summer nighttime electron density enhancement around the midlatitude ionosphere.

Keywords: Midlatitude Summer Nighttime Anomaly, thermospheric tidal effect

Japan Geoscience Union Meeting 2014
(28 April - 02 May 2014 at Pacifico YOKOHAMA, Kanagawa, Japan)

PEM36-21 Room:312 Time:April 28 15:45-16:00

Horizontal ion drag effect on the thermospheric mass density anomaly in the cusp

MATSUMURA, Mitsuru[1*] ; TAGUCHI, Satoshi[2]

[1]Center for Space Science and Radio Engineering, University of Electro-Communications, [2]Graduate School of Informatics and Engineering, University of Electro-Communications

CHAMP satellite observations have revealed that the thermospheric mass density in the cusp region is statistically larger by a factor of about 1.3 than that in its adjacent region. Many studies have pointed out that the upward mass transport due to heating is important for the generation of the mass density anomaly, but what confines the heating rate to the cusp is controversial. We have paid attention to the effect of the horizontal mass transport. Our reasoning on this point is as follows. Ionospheric convection gives momentum to the neutral air through ion drag, and the ion drag can modify the distribution of the neutral mass density. Our recent results from numerical simulations have indicated that the ion drag enhances the neutral mass density in the cusp that the terminator overlaps. In this paper, we report on the result about more general situations including cases when the terminator is located away from the cusp. Our results show that the mass density anomaly is confined to the cusp by ion drag, irrespective of the location of the terminator. We show detailed relations between the ion drag distribution and the mass density enhancement or depletion.

Keywords: thermosphere, mass density, cusp, CHAMP satellite

Japan Geoscience Union Meeting 2014
(28 April - 02 May 2014 at Pacifico YOKOHAMA, Kanagawa, Japan)

PEM36-22 Room:312 Time:April 28 16:15-16:30

Edge of polar cap patches

HOSOKAWA, Keisuke[1*] ; TAGUCHI, Satoshi[1] ; OGAWA, Yasunobu[2]

[1]University of Electro-Communications, [2]National Institute of Polar Research

A highly sensitive all-sky EMCCD airglow imager (ASI) has been operative in Longyearbyen, Norway (78.1N, 15.5E) since October 2011. One of the primary targets of this optical observation is a polar cap patch which is defined as an island of enhanced plasma density in the F region drifting anti-sunward across the central polar cap. Since the electron density within patches is often increased by a factor of 2?10 above that in the surrounding region, all-sky airglow measurements at 630.0 nm wavelength are capable of visualizing their spatial distribution in 2D fashion.

During a 4-h interval on the night of December 4, 2013, a series of polar cap patches was observed by the ASI in Longyearbyen. By using the high-quality ASI images, we estimated the gradients in the leading/trailing edges of the patches and found that the gradient in the leading edge is 2-3 times steeper than that in the trailing edge. We also identified finger-like undulating structures growing along the trailing edge of the patches. Generation of these fingers is probably governed by a structuring through the gradient-drift instability which is known to occur only along one side of patches.

From these observations, we suggest that such a structuring process can transport and mix the patch plasma across their trailing edges so that the scale size of the edges get extended. This means that the structuring through the plasma instability can strongly influence the large-scale shape of patches. Such a knowledge is of particular importance for better understanding the space weather effects of patches on the trans-ionospheric satellite communications in the polar cap region.

Keywords: Polar cap ionosphere, Airglow, Polar patches, Plasma instability

Japan Geoscience Union Meeting 2014
(28 April - 02 May 2014 at Pacifico YOKOHAMA, Kanagawa, Japan)

PEM36-23 Room:312 Time:April 28 16:30-16:45

Correlation analysis between equatorial electrojet,pre-reversal enhancement and equatorial spread F in Southeast Asia

KUNITAKE, Manabu[1*] ; TSUGAWA, Takuya[1] ; YOKOYAMA, Tatsuhiro[1] ; NISHIOKA, Michi[1] ; YAMAMOTO, Kazunori[1] ; ISHIBASHI, Hiromitsu[1] ; NAGATSUMA, Tsutomu[1] ; MARUYAMA, Takashi[1] ; ISHII, Mamoru[1] ; SHIOKAWA, Kazuo[2]

[1]NICT, [2]STE Lab., Nagoya Univ.

At the equatorial latitudes, the reversal of dayside eastward electric field to westward around sunset is often accompanied by a strengthened eastward electric field. The strengthened eastward electric field is called as the pre-reversal enhancement (PRE). PRE is considered to be the primary process acting on the equatorial spread F (ESF) onsets. Relationships between PRE strength, ESF onsets, and equatorial electrojet (EEJ) strength have been investigated by using ionosonde observation and magnetometer observation. Uemoto et al. (2010) found that PRE strength and ESF onsets are suppressed when pre-sunset integrated EEJ from 2 hours to 1 hour prior to sunset is negative owing to the evening counter electrojet, by statistical analysis of observations in the Southeast Asia low-latitude ionospheric network (SEALION). Their analyzing period is from November 2007 to October 2008. The period is in solar minimum phase.

We use SEALION data from 2007 to 2013. Therefore, our analyzing period covers not only solar minimum phase but also solar maximum phase. Statistical analyses for each year are conducted. Further, detailed case study is conducted. Significant day-to-day variations of EEJ strength, PRE strength, and ESF onsets are picked up from these seven years data. Then, we investigate how and to what extent day-to-day variations of EEJ strength relate to the day-to-day variations of PRE strength and ESF onsets. The magnetometer data in our study were obtained at Phuket (geographic lat. 8.09N, geographic long. 98.32E, dip lat. -0.2) and Kototabang (0.20S, 100.32E, dip lat. -10.1). The ionosonde data in our study were obtained at Chumphon (10.72N, 99.37E, dip lat. 3.0), Chiang Mai (18.76N, 98.93E, dip lat. 12.7), and Kototabang (0.20S, 100.32E, dip lat. -10.1).

Reference

Uemoto J., T. Maruyama, S. Saito, M. Ishii, and R. Yoshimura, Relationships between pre-sunset electrojet strength, pre-reversal enhancement and equatorial spread-F onset, Ann. Geophys., vol. 28, pp. 449-454, 2010.

Acknowledgements

The ionosonde at Chiang Mai is operated under agreements between NICT, Japan and Chiang Mai University (CMU), Thailand. The ionosonde at Chumphon and the magnetometer at Phuket are operated under agreements between NICT and King Mongkut ′ s Institute of Technology Ladkrabang (KMITL), Thailand. The magnetometer at Kototabang has been operated in collaboration among the Solar-Terrestrial Environment Laboratory (STEL), Nagoya University, Japan, the Research Institute for Sustainable Humanosphere (RISH), Kyoto University, Japan, and the National Institute of Aeronautics and Space (LAPAN), Indonesia. The ionosonde at Kototabang has been operated in collaboration among NICT, RISH and LAPAN. We thank Mr. Yamazaki for manual scaling of ionosonde data.

Keywords: electrojet, equatorial spread F, day-to-day variation, SEALION

Japan Geoscience Union Meeting 2014
(28 April - 02 May 2014 at Pacifico YOKOHAMA, Kanagawa, Japan)

PEM36-24 Room:312 Time:April 28 16:45-17:00

Low-latitude ionosphere dynamics as deduced from meridional ionosonde chain: Ionospheric ceiling

MARUYAMA, Takashi[1*] ; UEMOTO, Jyunpei[1] ; ISHII, Mamoru[1] ; TSUGAWA, Takuya[1] ; SUPNITHI, Pornchai[2] ; KOMOLMIS, Tharadol[3]

[1]National Institute of Information and Communications Technology, [2]King Mongkut's Institute of Technology Ladkrabang, [3]Chiang Mai University

Peculiar ionospheric features at low latitudes originate in the earth's magnetic field configuration that has a shape of arch. Near the magnetic equator, the daytime eastward electric field raises the ionosphere to high altitudes where the ion-neutral collision frequency reduces. The ionospheric plasma slips down over off-equatorial latitudes along the arch-shaped magnetic field line by the earth's gravity acceleration and the reduced ion-neutral drag, which is called the fountain effect. As a consequence, the latitudinal distribution of ionospheric critical frequency (foF2) forms two crests at low latitudes and a trough above the magnetic equator, which is well-known equatorial anomaly in foF2 distribution. As for the diurnal variation of the ionosphere above the magnetic equator, foF2 once increases in the morning and decreases before noon along with the development of the equatorial anomaly, which is called noon bite-out. Another feature at the magnetic equator, associated with the fountain effect, is the relatively steady ionospheric peak height (hmF2) around noon, even though the EXB drift is upward throughout the daytime. However, not much attention has been paid to hmF2 except for the time rate of change of it in connection with the vertical plasma drift velocity.

Interest in the equatorial anomaly has been focused mostly on foF2 (or NmF2), and there have been a few studies on hmF2 variations associated with equatorial anomaly development. In this paper, we revisit the equatorial anomaly in terms of height variations. For this purpose, we analyzed scaled ionogram parameters from three stations located along the magnetic meridian that is a primary component of Southeast Asia low-latitude ionospheric network (SEALION); one at the magnetic equator and the others at conjugate off-equatorial latitudes near 10 degrees magnetic latitude.

The daytime hmF2 was investigated for each season during the solar minimum period, 2006-2007 and 2009. The peak height increased for approximately 3 hr after sunrise at all locations, as expected from the daytime upward EXB drift. The apparent upward drift ceased before noon at the magnetic equator, while the layer continued to increase at the off-equatorial latitudes, reaching altitudes higher than the equatorial height around noon. The noon time restricted layer height at the magnetic equator did not depend on the season, while the maximum peak height at the off-equatorial latitudes largely varied with season. The daytime specific limiting height of the equatorial ionosphere was termed ionospheric ceiling. Numerical modeling using the SAMI2 code reproduced the features of the ionospheric ceiling quite well. Dynamic parameters provided by the SAMI2 modeling were investigated and it was shown that the ionospheric ceiling is another aspect of the fountain effect, in which increased diffusion of plasma at higher altitudes has a leading role.

Keywords: equatorial anomaly, fountain effect, ionospheric ceiling, EXB drift, SEALION

Japan Geoscience Union Meeting 2014
(28 April - 02 May 2014 at Pacifico YOKOHAMA, Kanagawa, Japan)

PEM36-25 Room:312 Time:April 28 17:00-17:15

Three-dimensional high-resolution plasma bubble modeling

YOKOYAMA, Tatsuhiro[1*] ; SHINAGAWA, Hiroyuki[1] ; JIN, Hidekatsu[1]

[1]National Institute of Information and Communications Technology

Equatorial plasma bubble (EPB) is a well-known phenomenon in the equatorial ionospheric F region. As it causes severe scintillation in the amplitude and phase of radio signals, it is important to understand and forecast the occurrence of EPB from a space weather point of view. The development of EPB is known as a evolution of the generalized Rayleigh-Taylor instability. Numerical modelings of the instability on the equatorial two-dimensional plane have been conducted since the late 1970's, and the nonlinear evolution of the instability has been clearly presented. Recently, three-dimensional (3D) modelings became popular tools for further understanding of the development of EPB such as 3D structure of EPB, meridional wind effects and gravity wave seeding. One of the biggest advantages of the 3D model is that the off-equatorial E region which is coupled with the equatorial F region can be included in the model. It is known from observations that the conductance of the off-equatorial E region controls the growth rate of the Rayleigh-Taylor instability, that is, sudden decrease of the E-region conductance around the sunset accelerates the evolution of the instability. We have developed a new 3D high-resolution model for EPB, and studied internal structure of EPB and the contribution of the off-equatorial E region. As it is necessary to use high-order numerical schemes to capture sharp plasma density gradient of EPB, we adopted the CIP scheme which can keep the third-order accuracy in time and space. The simulated EPB has asymmetrical density gradients at east and west walls, and the growth rate changes significantly depending on the condition of the off-equatorial E region. In the future, we will integrate the high-resolution model into whole atmosphere-ionosphere coupled model (GAIA) to study the growth of EPB under the realistic background conditions.

Keywords: plasma bubble, equatorial spread F, equatorial ionosphere, numerical simulation

Japan Geoscience Union Meeting 2014
(28 April - 02 May 2014 at Pacifico YOKOHAMA, Kanagawa, Japan)

PEM36-P01 Room:Poster Time:April 28 18:15-19:30

Basic development of a small balloon-mounted telemetry with its operation system

KONO, Hiroki[1*] ; KAKINAMI, Yoshihiro[1] ; YAMAMOTO, Masa-yuki[1]

[1]Kochi Univ. of Tech

1. Introduction

In Japan, the high altitude balloon for scientific observation has been continuously launched by JAXA. The balloon has a possibility to reach 50 km altitude without severe environmental condition for onboard equipments, being operated with lower cost than sounding rockets, however, development of such large-scale scientific observating balloons by university laboratories is still difficult. Being coupled with rapid improvement of tiny semiconductor sensors recently, laboratory-basis balloon experiments using small weather balloons have been becoming easily in these years (e.g. Near Space Ventures, Inc., 2013).

Although the balloon is very small as its diameter of 6 feets, excluding its extra buoyancy and the weight of the balloon itself, it is expected that loading mass capacity of about 2 kg is remained for payloads to send it up to about 35 km. However, operation of such small balloons in Japan is not in general because precise prediction of a landing area of the payload is difficult, thus high-risk situation for balloon releases is still remained. In this study, we aim to achieve practical engineering experiments of weather balloons in Japan in order to operate laboratory level scientific observation within a university. Here we report an approach of developing many devices currently in progress.

2. Equipments development

We have been developing devices onboard a small tethered balloon for the future weather balloon release experiments. That is, one is a small-size and light-weight telemeter system of about 250 g that can be mounted on a commercially available balloon, while another is a ground station device that receives data from the telemeter. A combination of a wireless module, a GPS receiver, a barometer, a temperature and humidity meter, a camera, an accelerometer, an electronic compass, a power monitor sensor is mounted on the telemeter, and the measured values by each sensors can be transmitted in real time to the ground station device. Newly developed software for balloon operation can be run on a PC connected with the ground station device, it is possible to provide the operator the sensor information visualized in real time based on the position coordinates set on the ground station device using the software before the launch.

Real-time mapping of the balloon coordinates can be realized to rewrite a KML file to be input into the Google Earth continuously. In addition, azimuth and elevation of the balloon can be calculated by spherical trigonometry from obtained the GPS position. Providing these angles to a newly developed rotater to be mounted on a camera tripod, it is possible to track a small antenna automatically to the balloon direction continuously.

3. Result of the experiment

A tethered balloon experiment was performed for evaluating the developed telemeter system, however, there occurred unexpected issue in the communication distance. As a result, in the telemeter line, operating limit of the distance between the ground station and the telemeter is significantly shortened to approximately 110 m. It was almost different from our pre-experiment confirmation of a packet loss rate of 0% at 270 m distance in a preliminary experiment on ground.

Therefore, evaluation of the antenna rotator was carried out only at close range, i.e., in severe condition. It is because maximum elevation of the rotator was limited physically at 50 degrees or less, and there exists about 5 to 10 m error in the GPS positioning operated in the single receiver mode.

Nevertheless, it was possible to track the balloon continuously in a stable situation even in the shortened communication distance. In addition, the software and telemeter system worked as expected, the problem was not found in particular.

In this presentation, the data obtained by the tethered balloon experiment and detail of the developed equipments will be shown.

Keywords: Weather balloon, Tethered balloon, Stratosphere, Upper atmosphere, Telemeter, Embedded system

Japan Geoscience Union Meeting 2014
(28 April - 02 May 2014 at Pacifico YOKOHAMA, Kanagawa, Japan)

PEM36-P02 Room:Poster Time:April 28 18:15-19:30

Impacts of stratospheric sudden warming events in the mesosphere and lower thermosphere

WATANABE, Kumiko[1*] ; TANAKA, Takashi[1] ; MIYOSHI, Yasunobu[2]

[1]Department of Earth and Planetary Sciences, Graduate School of Sciences, Kyushu University, [2]Department of Earth and Planetary Sciences, Faculty of Sciences, Kyushu University

Impacts of stratospheric sudden warming (SSW) events on the middle and upper atmosphere have been widely recognized. However, due to an insufficient number of global observations, SSW's effects on the general circulation in the mesosphere and lower thermosphere (MLT) are not well known. In this study, we investigate the short term variation of the temperature, zonal wind and meridional wind in the MLT region during SSW events using a general circulation model that contains the region from the troposphere to the thermosphere. We conducted GCM simulation with meteorological reanalysis data during the period from November 1, 2008 to March 31, 2010. Our results show that the temperature drop occurs in the Southern hemisphere, during SSW events. This means that SSW influences the general circulation in the summer hemisphere. Furthermore, it is found that the temperature in winter polar region in the lower thermosphere increases during SSW events. This is related to upward propagation of the planetary wave excited in the mesosphere.

Keywords: stratospheric sudden warming, mesosphere, lower thermosphere

Japan Geoscience Union Meeting 2014
(28 April - 02 May 2014 at Pacifico YOKOHAMA, Kanagawa, Japan)

PEM36-P03 Room:Poster Time:April 28 18:15-19:30

Vertical profiles of atmospheric temperature between upper troposphere and mesosphere obtained from Rayleigh/Raman lidar

NISHIYAMA, Takanori[1*] ; NAKAMURA, Takuji[1] ; EJIRI, Mitsumu[1] ; ABO, Makoto[2] ; KAWAHARA, Taku d[3] ; TSUDA, Takuo[1] ; SUZUKI, Hidehiko[4] ; TSUTSUMI, Masaki[1] ; TOMIKAWA, Yoshihiro[1]

[1]National Institute of Polar Research, [2]Graduate School of System Design, Tokyo Metropolitan University, [3]Faculty of Engineering, Shinshu University, [4]Faculty of Science, Rikkyo University

Atmospheric gravity waves (AGWs) propagating upward from lower atmospheric sources play a dominant role in transportating and depositing energy and momentum from upper troposphere (UT) to lower mesosphere (LM). Particularly, in polar region, these effects of AGWs are well-known to strongly decelerate the polar night jet and drive large scale meridional circulation from the summer pole towards the winter pole. In addtion, it is suggested that considerations of the realistic propagation property of AGWs may largely improve a significant bias of climate model. Therefore, investigation of the activity of AGWs between UT and LM based on continuous observational studies can be regarded as one of important isuues.

The National Institute of Polar Research (NIPR) is leading a six year prioritized project of the Antarctic research observations since 2010. One of the sub-projects is entitled 'the global environmental change revealed through the Antarctic middle and upper atmosphere'. As a part of the sub-project, a Rayleigh/Raman lidar (RR lidar) was installed at Syowa, Antarctica (69S, 39E) in January, 2011. The operation has been conducted since February 2011 and the RR lidar has kept measuring temperature profiles continuously between approximately 10 and 80 km for almost 3 years.

The RR lidar system in Syowa can obtain photon count data for 4 channels simultaneously, and each data is recorded separately in binnary format. The data from 3 channeles, i.e., Raman (10-30km), Rayleigh-Low (20-65km), Rayleigh-High (30-80km), corresponding to differenet height ranges are used for estimations of temperature profiles from UT to LM. In oreder to estimate height continuous profiles of atmospheric temperature based on the 3 different channeles, we are examing the following analysis methods. (1) The temperature for Rayleigh-High and Rayleigh-Low channels estimated by solving the lidar equation can be assigned to temperature at an initial height for the lidar equation in Rayleigh-Low and Raman channels, respectively. (2) The initial heights for the lidar equation can be determined automatically taking into account time and height dependent shot noises due to background luminosity. (3) The error propagations from the initial height to lower heights are evaluated by assigning artificial temperature offset ranging from -50 to 50 K.

The height continuous temperature profiles between UT and LM obtained from improved analysis methods would allows us to investigate important scientific issues such as temporal and height variabilities of potential energy per unit mass of AGWs and the relationship between occurrence of Polar Stratospheric Clouds and background atmospheric temperature. In this presentation, we will report the detail of the analysis methods and future perspectives including open data base of temperature profiles.

Keywords: Rayleigh/Raman lidar, Atmospheric temperature, Mesosphere, Stratosphere, Atmospheric Gravity Waves, Polar Stratospheric Clouds

Japan Geoscience Union Meeting 2014
(28 April - 02 May 2014 at Pacifico YOKOHAMA, Kanagawa, Japan)

PEM36-P04 Room:Poster Time:April 28 18:15-19:30

Tunable resonance scattering lidar system for Antarctic observation: Current status

TSUDA, Takuo[1*] ; EJIRI, Mitsumu[1] ; NISHIYAMA, Takanori[1] ; ABO, Makoto[2] ; MATSUDA, Takashi[1] ; KAWAHARA, Takuya[3] ; NAKAMURA, Takuji[1]

[1]National Institute of Polar Research, [2]Graduate School of System Design, Tokyo Metropolitan University, [3]Faculty of Engineering, Shinshu University

We are developing a new resonance scattering lidar system to be installed at Syowa Station (69S, 39E) in Antarctica. For the new lidar system, we have employed a tunable alexandrite laser covering the resonance scattering wavelengths of two neutral species, which are atomic potassium (K, 770.11 nm) and atomic iron (Fe, 386.10 nm), and two ion species, which are calcium ion (Ca^+, 393.48 nm) and aurorally excited nitrogen ion ($N_2{}^+$, 390.30 nm, 391.08 nm). Thus the tunable resonance scattering lidar system will provide information on the mesosphere and lower thermosphere as well as the ionosphere. Using the tunable lidar and co-located other instruments, we will conduct a comprehensive ground-based observation of the low, middle, and upper atmosphere above Syowa Station. This unique observation is expected to make important contribution to studies on the atmospheric vertical coupling process and the neutral and charged particle interaction. In this presentation, we report current status of the tunable lidar system in development and test observations at National Institute of Polar Research in Tachikawa, Japan.

Keywords: Resonance scattering lidar, Antarctica, Syowa Station, K layer, Fe layer

Japan Geoscience Union Meeting 2014
(28 April - 02 May 2014 at Pacifico YOKOHAMA, Kanagawa, Japan)

PEM36-P05 Room:Poster Time:April 28 18:15-19:30

Doppler-free spectroscopy experiments for the Antarctic Potassium resonant lidar

KAWAHARA, Takuya[1] ; TSUDA, Takuo[2*] ; NISHIYAMA, Takanori[2] ; EJIRI, Mitsumu[2] ; ABO, Makoto[3] ; NAKAMURA, Takuji[2]

[1]Faculty of Engineering, Shinshu University, [2]National Institute Polar Research, [3]System Design, Tokyo Metropolitan University

The National Institute of Polar Research (NIPR) is leading a six year prioritized project of the Antarctic research observations since 2010. One of the sub-projects is entitled ”the global environmental change revealed through the Antarctic middle and upper atmosphere”. Profiling dynamical parameters such as temperature and wind, as well as minor constituents is the key component of observations in this project, together with long-term observations using existent various instruments in Syowa, the Antarctic (39E, 69S). As one of the instruments in this project, a new resonance scattering lidar system with tunable wavelengths is developed to be installed and operated at the Syowa Station. The lidar transmitter is based on injection-seeded, pulsed alexandrite laser for 768-788 nm (fundamental wavelengths) and a second-harmonic generation (SHG) unit for 384-394 nm (second harmonic wavelengths). In order to tune the seeder laser to absolute Potassium resonance line, Doppler-free spectroscopy with a Potassium cell is crucial. The measurement was done at NIPR and the Doppler-free spectrum was recorded with 0.005 pm wavelength resolution. Three absorptions spaced with 0.05pm at the cross-over wavelength were clearly measured. In this talk, details of the experiment will be shown.

Keywords: Antarctica, lidar, Potassium, resonant scattering, Doppler Free

Japan Geoscience Union Meeting 2014
(28 April - 02 May 2014 at Pacifico YOKOHAMA, Kanagawa, Japan)

PEM36-P06 Room:Poster Time:April 28 18:15-19:30

Development of a 3D sodium lidar: synchronous experimentation and validation

MURANAKA, Wataru[1*] ; KAWAHARA, Taku d[2] ; NOZAWA, Satonori[3]

[1]GSI, Shinshu University, [2]Faculty of Engineering, Shinshu University, [3]STE Lab., Nagoya University

Shinshu University, Nagoya University and RIKEN developed an all solid-state, high-power Na lidar for the temperature/wind measurements in the MLT region over EISCAT radar site in Tromso (69 N), Norway. Current observation is five-direction mode applied to the fixed direction such as vertical and 30 degree tilted to the north, south, east and west from the vertical.

We are now updating the lidar to multi-direction system which has never been done with resonant lidars. The transmission system uses two mirrors with electric rotary stages to emit laser light to any direction of the sky. Receiver system uses a telescope controlled by a PC. The coordination of the telescope is done with direction of so me blight stars. This repeatability pointing to the same direction is 5.3 mrad.

In this talk, we will discuss the experimental results of the synchronized experiments with the laser direction and telescope field-of-view.

Keywords: sodium, lidar, three diminutional

Japan Geoscience Union Meeting 2014
(28 April - 02 May 2014 at Pacifico YOKOHAMA, Kanagawa, Japan)

PEM36-P07 Room:Poster Time:April 28 18:15-19:30

Analysis of the factors of seasonal variation of the thermosphere-mesosphere NO observed at Syowa Station

UEMURA, Miku[1] ; ISONO, Yasuko[1] ; MIZUNO, Akira[1] ; NAGAHAMA, Tomoo[1] ; EJIRI, Mitsumu K.[2] ; TSUTSUMI, Masaki[2] ; NAKAMURA, Takuji[2*]

[1]Solar-Terrestrial Environment Laboratory, Nagoya University, [2]National Institute of Polar Research

When high-energy particles such as solar protons and energetic electrons fall down to the earth's atmosphere, the nitrogen oxides (NO, NO2) are increased in the mesosphere and the upper stratosphere in the polar regions (e.g. Lopez-Puertas et al. 2005). In collaboration with the National Institute of Polar Research, Nagoya University Solar-Terrestrial Environment Laboratory installed a millimeter-wave spectroscopic radiometer at Syowa Station in Antarctica. We have conducted continuous observation of the NO spectrum since January 2012. The NO column density derived from this observation shows a seasonal variation that the NO column density increases up to about 1.7×10^{15} cm^{-2} in winter and decreases down to about 0.5×10^{15} cm^{-2} in summer. In order to understand the mechanism of the seasonal variation, we compared it with seasonal variation of CO vertical distribution in thermosphere-mesosphere and the length of sunshine hours at Syowa Station. Since CO photochemical lifetime is longer than or equal to the horizontal and vertical transport in the thermosphere and the stratosphere, CO can be considered as a good tracer of atmospheric transport. We used CO data obtained by AULA / MLS (Version3.3).

The CO volume mixing ratio in a latitude range of 65 S-75 S and an altitude range of 0.1-0.01 hPa shows a tendency that the mixing ratio increased in winter and decreased in summer. The peak altitude of the mixing ratio changed from upper altitude to lower altitude during winter, suggesting downward transport of the atmosphere. The commencements of the increment of the NO column density and the CO mixing ratio were almost coincident, but the temporal variation patterns of NO and CO did not agree well with each other especially in the decrement phase. On the other hand, the temporal variation pattern of the NO column density and the length of night time showed good correlation throughout the period during which the NO enhancement was significant. Thus the variation of the NO column density in the lower thermosphere-mesosphere is considered to be caused by both the descending of the air mass and the photochemical process.

In this poster, we will present more detailed discussion on the relationship among the NO column density, CO mixing ratio, and length of the night time based on the dataset including the new data acquired this year.

Keywords: microwave spectroscopy, Nitric Oxide

Japan Geoscience Union Meeting 2014
(28 April - 02 May 2014 at Pacifico YOKOHAMA, Kanagawa, Japan)

PEM36-P08 Room:Poster Time:April 28 18:15-19:30

Small spatial scale field aligned currents in middle and low latitudes as observed by the CHAMP satellite

NAKANISHI, Kunihito[1*] ; IYEMORI, Toshihiko[1] ; AOYAMA, Tadashi[1] ; LUHR, Hermann[2]

[1]Department of Geophysics, Graduate School of Science, Kyoto University, [2]GeoForschungsZentrum, GFZ, Potsdam, Germany

The magnetic field observation by the CHAMP satellite shows the ubiquitous existence of small scale (1-5 nT) magnetic fluctuations with period around a few tens seconds along the satellites. From characteristics of the amplitude and period, they can be interpreted as the spatial structure of small scale field-aligned currents generated by the ionospheric dynamo driven by atmospheric gravity waves propagating from the lower atmosphere. The mechanism is the following; first, the gravity waves generated by the lower atmospheric disturbance propagate to the ionosphere; the neutral winds oscillate, cause ionospheric dynamo and Pedersen and Hall currents flow; because the dynamo region is finite, the currents cause polarized electric fields; and the polarized electric fields propagate along the geomagnetic filed as Alfven waves accompanied by field-aligned currents, at the same time, the ionospheric currents divert to the filed aligned currents; finally the CHAMP satellite observes the spatial structure of the filed aligned currents generated in this way as a temporal change along the path, because the temporal variation of the gravity waves are slow enough, i.e., more than a few minutes, that is, that of field aligned current can be ignored and nearly constant for the satellite crossing the currents.

This time we analyze correlation relation of the two components perpendicular to the geomagnetic field to find the following tendencies. About the magnetic data at the observed point, 1) if inclination and declination are plus and plus respectively, a correlation coefficient tends to be minus; 2) if inclination and declination are plus and minus respectively, it tends to be plus; 3) if inclination and declination are minus and plus respectively, it tends to be plus; 4) if inclination and declination are minus and minus respectively, it tends to be minus.

We report the model of the current system consistent to the characteristics of the magnetic fluctuations including the tendency of the correlation relation.

Keywords: spatial structure of field aligned currents, middle and low latitudes, the CHAMP satellite, atmospheric gravity wave, the lower atmospheric origin, correlation relation

Japan Geoscience Union Meeting 2014
(28 April - 02 May 2014 at Pacifico YOKOHAMA, Kanagawa, Japan)

PEM36-P09 Room:Poster Time:April 28 18:15-19:30

Atmospheric origin of small-scale magnetic fluctuations as observed by CHAMP above the ionosphere

AOYAMA, Tadashi[1*] ; IYEMORI, Toshihiko[2] ; NAKANISHI, Kunihito[1]

[1]Graduate School of Science, Kyoto University, [2]Graduate School of Science, Kyoto University

We analyzed magnetic field data obtained by a LEO(Low Earth Orbit) satellite, CHAMP(altitude 300˜450 km), and found out the global distribution of the short-period(10˜40 s) and small-amplitude(0.1˜5 nT) magnetic fluctuations in middle and low latitudes. We have reported that these fluctuations are small-scale structure(˜100 km) of the field-aligned currents generated by dynamo action in the ionospheric E-layer and the dynamos are caused by the atmospheric gravity waves (horizontal scale is ˜100 km) because of the characteristics of geographical and seasonal dependence of their amplitude.

In this paper, we focus on the mesoscale meteorological events to clarify the atmospheric origin such as typhoon which is possible to generate atmospheric gravity waves, and compare with magnetic fluctuations as observed by the CHAMP satellite above the ionosphere. We trace from the location of CHAMP to each footpoint in the E-layer along geomagnetic field line, and then compared with meteorological phenomena beneath the footpoint.

As a result, we detected large amplitudes of geomagnetic fluctuation above typhoons.

Keywords: field-aligned current, ionospheric dynamo, atmospheric gravity wave, acoustic resonance, CHAMP satellite, typhoon

Japan Geoscience Union Meeting 2014
(28 April - 02 May 2014 at Pacifico YOKOHAMA, Kanagawa, Japan)

PEM36-P10 Room:Poster Time:April 28 18:15-19:30

Optimization of notification system for bright meteor signals by using wide angle images at multiple sites

IYONO, Atsushi[1*] ; WADA, Naoki[2]

[1]Dept. of Fundamental Science, Okayama university of Science, [2]Graduate School of Science, Okayama university of Science

1. Purpose and Background

The sky monitoring system by using wide angle images have been maintained until Nov. 2011 at Okayama University of Science. The CCD camera system provides the slow shutter images every 3 second, and they have been transferred simultaneously to data storage server via the Internet connection. This system enables to monitor the real time condition of the sky. In the obtained images, bright meteors and sometimes fire balls were registered. We have been developing our new system which can provide quick analysis results for meteor and fire ball at the moment of observations. In this report, we describe the new sensor systems of thermography and low frequency sounds to increase the detection efficiency of brighter meteors and fire balls.

2. System

In the sky monitor system, CCD camera with wide angle lens and image server system have been operated in 24 hours/day. The exposure of CCD cameras has been set to be 4 second. The acquired image data have been stored in PC system via the internet ftp command. 28,800 images(500MB data

size) are stored in each day. In offline mode, images are processed with contrast enhancement module, image differentiating and object detection module. To detect meteors and fire balls effectively, we activated the IR image seosors and low frequency sound sensors as well as imaging devices.

3. Development

Our purposes are that new analysis system for online processing of images, IR sensors and low frequency seonsors have been developed in order to provied the information of the arrival of meteor and fireballs, arrival directions and brightness profiles. We are going to present new system and analysis result in this reports

Keywords: meteor, fireball, simultaneous? observation, meteor shower

Japan Geoscience Union Meeting 2014
(28 April - 02 May 2014 at Pacifico YOKOHAMA, Kanagawa, Japan)

PEM36-P11 Room:Poster Time:April 28 18:15-19:30

Measurement of propagation characteristics of MF band radio waves in lower ionosphere by S-310-40 sounding rocket

ISHISAKA, Keigo[1*] ; ITAYA, Keita[1] ; ASHIHARA, Yuki[2] ; ABE, Takumi[3] ; ENDO, Ken[4] ; KUMAMOTO, Atsushi[4]

[1]Toyama Prefectural University, [2]NARA National College of Technology, [3]ISAS/JAXA, [4]Tohoku University

The ionospheric D region is important in radio wave propagation because it absorbs energy from waves at MF, HF and VHF, and it reflects LF and VLF signals. Then D region is present only during daylight hours. Therefore, in the night-time, the MF band radio waves are propagated as far as an area where its radio waves cannot be propagated in the daytime. This reason why the radio waves cannot receive is that the D region is disappeared at night. However, the MF band radio waves that transmit from distant place have not been often received at the mid latitude in the night-time. In this time the sporadic E region cannot be observed by the ionogram. We guess that the D region appear in the lowest ionosphere like a daytime. To farther study the structure of the lowest ionosphere, we propose a method to measure the very low electron densities that occur at altitudes from 50 km to 90 km using the partial and perfect reflection characteristics of electromagnetic waves.

S-310-40 sounding rocket experiment was carried out at Uchinoura Space Center (USC) at 23:48 JST on 19 December, 2011. The purpose of this experiment is the investigation of characteristics of radio wave propagation in the ionosphere and the estimation of electron density structure in the lower ionosphere, when the intensity of radio wave measured on the ground will be attenuate at night-time. In order to measure the radio waves, a LF/MF band radio receiver (LMR) is installed on the sounding rocket. The LMR has measured the propagation characteristics of four radio waves at frequencies of 60 kHz (JJY signal from Haganeyama radio station), 405 kHz (NDB station from Minami-Daito), 666 kHz (NHK Osaka broadcasting station) and 873 kHz (NHK Kumamoto broadcasting station) in the region from the ground to the lower ionosphere. The LMR consists of a loop antenna, a pre-amplifier and a detector circuit. The loop antenna is set up in the nose cone, which is transparent to the LF/MF band radio waves, and is not deployed during the flight. Therefore, the LMR can measure the relative attenuation of radio waves from the ground up to the ionosphere. Furthermore the loop antenna consists of three loop antennas in order to measure three components of four radio waves. Then we can obtain the propagation directions of radio waves in the ionosphere directly.

A propagation vector can be obtained from the propagation characteristic of radio wave. It is possible to estimate electron density profile from a propagation vector, because the propagation vector is dependent on the electron density profile in the radio wave propagation region. We have estimated the electron density profile by the propagation vector. When the electron density profile estimated by the propagation vector was compared with the electron density profile measured with the Langmuir probe and the impedance probe onboard the S-310-40 sounding rocket, it was found that electron density becomes the maximum at an altitude of 104 km.

We show the results of propagation characteristics of radio waves in the ionosphere and explain the propagation vector of radio wave in the ionosphere. And the electron density profile in the ionosphere can be estimated by the propagation vector. We will show the result that it is investigated the influence the lowest ionosphere region has on a MF band radio wave in this study.

Keywords: ionosphere, propagation characteristic of radio wave, rocket experiment

Japan Geoscience Union Meeting 2014
(28 April - 02 May 2014 at Pacifico YOKOHAMA, Kanagawa, Japan)

PEM36-P12 Room:Poster Time:April 28 18:15-19:30

Measurement of LF Standard-Frequency Waves JJY along the track of Shirase during JARE55: Preliminary Report

KITAUCHI, Hideaki[1*] ; NOZAKI, Kenro[1] ; ITO, Hiroyuki[1] ; KONDO, Takumi[1] ; TSUCHIYA, Shigeru[1] ; IMAMURA, Kuniyasu[1] ; NAGATSUMA, Tsutomu[1]

[1]NICT

We developed a highly sensitive, reliable receiving system for the purpose of reception of low frequency (LF) radio waves. The system consists of digital lock-in amplifiers and crossed-loop antennas. Digital lock-in amplifier (DLA) employs phase-sensitive detection (PSD) of periodic signal multiplied by the input reference source of the known signal frequency. This makes it possible to realize very narrow bandpass filter around the reference frequency, detecting/measuring that of very weak signal even in noisy environment. The antenna, on the other hand, consists of orthogonally crossed, larger double loops (receivers R_X, R_Y) and smaller doubles (transmitters T_X, T_Y): the former receivers R_X, R_Y receive LF radio signals of x-, y-components, the latter transmitters T_X, T_Y transmit an instant, weak signal from each x-, y-component for self calibration purpose. The self calibration test is performed by transmitting a weak LF signal for an instant every an hour from the transmitter T_X, T_Y respectively, and receiving this signal from the receivers R_X, R_Y to obtain preassigned field strength. This test indicates if the receivers of the system are working properly and allows us to obtain reliable measurements.

We apply the receiving system to measure the field intensity and phase of the standard frequency and time signals (SFTS) JJY of LF 40 kHz and 60 kHz during the summer expedition of the 55th Japanese Antarctic Research Expedition (JARE), from November 2013 to April 2014. Figure 1 shows temporal evolution of the field intensities JJY 40 kHz (light blue dots) and 60 kHz (brown dots) as well as the self-calibrating radio signals. Our receiving system detects both the LF JJY radio signals even offshore Syowa Station, Antarctic, about 14,000 km away from those transmitting stations. Also the field intensities of the self calibration test show about a consistent preassigned value, assuring the measurements.

Keywords: low frequency (LF) radio waves, call sign JJY of 40 kHz and 60 kHz, standard frequency and time signals (SFTS), self calibration, Japanese Antarctic Research Expedition (JARE), Japanese Antarctic Research Icebreaker Shirase

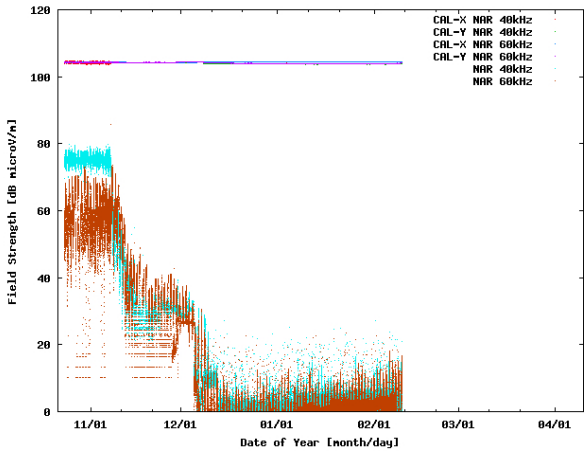

Japan Geoscience Union Meeting 2014
(28 April - 02 May 2014 at Pacifico YOKOHAMA, Kanagawa, Japan)

PEM36-P13 Room:Poster Time:April 28 18:15-19:30

Velocity distribution of electrons generating plasma waves around the wake of an ionospheric sounding rocket

ENDO, Ken[1*] ; KUMAMOTO, Atsushi[1] ; KATOH, Yuto[1]

[1]Department of Geophysics, Graduate School of Science, Tohoku University

When a body moves in plasma at supersonic velocity, a rarefied plasma region called 'plasma wake' is formed behind the body. Wakes can develop behind a solar system body immersed in solar-wind plasma as well as behind spacecraft such as satellites and ionospheric sounding rockets. There are several studies which report plasma waves around the wakes of a satellite and of the moon. Although there are not so many studies which report plasma waves generated in association with the rocket wake, observational results from two rocket experiments performed in 1998 and 2012 have shown generation of plasma waves around the wake of a rocket. It is very important to reveal the generation process of plasma waves near the rocket wake for understanding the universal physics related to the interaction between streaming plasma and a non-magnetized body as well as for interpreting wave data obtained in rocket experiments more accurately.

Our analysis has revealed three kinds of plasma waves observed in the S-520-26 rocket experiment in 2012. They are likely to be electrostatic electron cyclotron harmonic (ESCH) waves, upper hybrid resonance (UHR) mode waves, and whistler mode waves. They have spin-phase dependence in characteristic manners. These results indicate that the plasma waves should be generated inhomogeneously around the rocket. We have performed numerical calculations of plasma dispersion relations by assuming anisotropic velocity distribution functions such as electron beam and temperature anisotropy. As a result, positive linear growth rates have been obtained in the wave number and frequency ranges of UHR mode waves and ESCH waves in addition to electrostatic whistler mode waves. Accordingly, there have to be electrons with some anisotropic velocity distribution functions which are equivalent to those we assumed in the calculations. However, we have to clarify what kind of velocity distribution can be generated around the actual wake through the interaction between a sounding rocket and ionopsheric plasma.

Singh et al. (1987) has performed a one-dimensional simulation of plasma entering a void region from the two sides using a Vlasov-Poisson code. They have found counterstreaming electron beams in the very near wake. However, their study concentrates on electrons on the wake axis and does not indicate distribution functions in other areas. Besides, temperature anisotropy could not be treated in their simulation because it is performed in one dimension in velocity space.

In order to investigate inhomogeneity of electron distribution functions around the rocket wake, we are developing a Vlasov-Poisson code with one-dimensional space and two-dimensional velocity space, which is redesigned from the simulation code used in Singh et al. (1987). In this simulation, we deal with cases that electrons and ions are filling in a void space. The time evolution can be understood as spatial distribution along the wake axis. The direction of one-dimensional space is along the geomagnetic fields, along which electrons and ions can move easily. The size of space is 10 m, which is divided into 1024 grids in the calculation.

In this presentation, we clarify the frequency range and spatial distribution of the plasma waves around the wake based on the analyses of S-520-26 rocket experiment data. We also discuss the velocity distribution of the electrons which can generate the plasma waves as observed. In addition, we report initial results of our simulation for investigating the velocity distribution of electrons around the wake.

Keywords: ionosphere, sounding rocket, wake, plasma wave, Vlasov simulation

Japan Geoscience Union Meeting 2014
(28 April - 02 May 2014 at Pacifico YOKOHAMA, Kanagawa, Japan)

PEM36-P14 Room:Poster Time:April 28 18:15-19:30

Atmospheric Neutral Analyzer for mass-resolved velocity distribution measurements: Verification of mass analyzer

SHIMOYAMA, Manabu[1*] ; HAYASHI, Ayuko[1] ; ITO, Fumihiro[1] ; HIRAHARA, Masafumi[1]

[1]STEL, Nagoya University

In order to understand the temporal and spatial variability of the ionosphere-thermosphere system, simultaneous measurements of the composition and density of the neutral atmosphere and the velocity distribution of individual species are essential. However, most conventional types of instruments for neutral atmosphere lack the simultaneous capability of measuring neutral atmospheric velocity and resolving neutral mass.

We have designed the Atmospheric Neutral Analyzer (ANA) instrument to measure the detailed, mass-resolved 2-dimensional velocity distribution of neutral species, from which the corresponding density, mass composition, bulk velocity and temperature were derived. In this presentation, we will report the results from laboratory experiments for the performance verification on the prototype of mass analyzer along with the detailed and overall design determined by numerical simulation.

Keywords: neutral upper atomosphere, velocity distribution function, mass analysis

Japan Geoscience Union Meeting 2014
(28 April - 02 May 2014 at Pacifico YOKOHAMA, Kanagawa, Japan)

PEM36-P15 Room:Poster Time:April 28 18:15-19:30

Observation of resonance scattering light of Lithium vapor under daytime and moonlight condition and neutral wind analys

KIHARA, Daiki[1*] ; KAKINAMI, Yoshihiro[1] ; YAMAMOTO, Masa-yuki[1] ; WATANABE, Shigeto[2] ; HARD, Lucas[3] ; LARSEN, Miguel[3] ; YAMAMOTO, Mamoru[4] ; HABU, Hiroto[5] ; ABE, Takumi[5]

[1]Kochi Univ. of Tech., [2]Hokkaido Univ., [3]Clemson Univ., [4]Kyoto Univ., [5]ISAS/JAXA

1.Introduction

For the purpose of measurement of neutral atmospheric wind in lower thermosphere, we observed resonance scattering light of sunlit Lithium vapor released from a sounding rocket in the evening thermosphere in 2007 (e.g. Yamamoto et al., 2008). At that time, we successfully measured thermospheric neutral wind profile between 110 km and 400 km. In 2012, we observed resonance scattering light of sunlit Lithium at dawn, and estimated lower thermospheric neutral wind between 76 km and 127 km.

On July 4, 2013, a U.S.-Japan collaborative rocket experiment to observe neutral wind profile in daytime lower thermosphere with Lithium release was carried out at WFF (Wallops Flight Facility), NASA. A rocket to operate chemical release of Lithium was launched at 10:31:40 EDT (14:31:40 UTC). The rocket launched to southeastern direction released Lithium vapor three times between at about 90 km and 130 km altitude during the upleg, at about 40 km horizontally away from a ground-based observation site in WFF. Here we tried to observe of Lithium clouds from the ground-based and airborne observations with collaboration of Kochi University of Technology (KUT) and Clemson University.

On July 20, 2013, a rocket experiment to observe neutral wind profile in moonlit lower thermosphere with Lithium release was carried out at USC (Uchinoura Space Center), Japan. The S-520-27 rocket to operate chemical release of Lithium was launched at 23:57:00 JST and released Lithium vapor three times between at about 80 km and 120 km altitude during the downleg under the almost full moon condition (Moon age was 12). Here we tried to observe of Lithium clouds from 3 ground-based sites and an airplane.

2.Observations

Airborne observation of Lithium cloud was carried out under a condition with the sun at the backward direction while it flew to north-northeast at about 10 km (33,000 feet) altitude and at about 300 km away from the ground site at the southeastern direction. An observation site was set in WFF on ground. In order to detect the Lithium clouds in daytime skies with good S/N ratio, digital cameras (Canon EOS Kiss X4, Nikon D90) with 2 nm band pass filters (BPF) at 671 nm wavelength were used for all digital cameras. We installed three digital cameras in the aircraft NASA-8 and set two digital cameras on the ground site. A video camera (Watec, WAT-120N) with a 12 nm BPF was also used in the aircraft and on ground, respectively.

The Lithium clouds under moonlight condition was observed by using digital cameras, Watec, and cooled EM-CCD (BITRAN BQ-87EM) with 2 nm and 12 nm BPF from the JAXA airplane Hisyo as well as three ground-based observation sites (USC, Tanegashima and Muroto).

3.Results

A Lithium cloud under daytime sky condition was observed for about 25 minutes from the aircraft. The released Lithium vapor formed red clouds along the rocket trajectory just after the release. Afterwards, the Lithium trails were spread into complex shapes by strong wind shear in the altitude. We successfully observed Lithium clouds by the airborne observation.

A Lithium cloud under moonlight sky condition was observed for about 90 seconds from the aircraft and two ground sites.

4.Summary

We successfully observed 2 chemical releases of Lithium from the aircrafts and ground sites on July, 2013, in daytime and midnight. We succeeded the detection of resonance scattering light of Lithium vapor under daytime and moonlight sky condition in lower thermosphere. Owing to this experiment, we confirmed that we can measure altitude profile of the neutral atmospheric wind in lower thermosphere at almost all local time by using the chemical release of Lithium.

In this paper, we will discuss that the observed emission intensity of the resonance scattering light of Lithium vapor under daytime and moonlight sky condition in lower thermosphere, obtained results of the S/N ratio, preliminary results and problems of the neutral atmospheric wind measurement in daytime lower thermosphere.

Keywords: sounding rocket, thermosphere, neutral wind, Lithium Ejection Systems, airborne observation

Japan Geoscience Union Meeting 2014
(28 April - 02 May 2014 at Pacifico YOKOHAMA, Kanagawa, Japan)

PEM36-P16 Room:Poster Time:April 28 18:15-19:30

Improvement of the method for estimating thermospheric temperature using small FPIs and evaluation of their temperatures

NAKAMURA, Yoshihiro[1*] ; SHIOKAWA, Kazuo[1] ; OTSUKA, Yuichi[1] ; OYAMA, Shin-ichiro[1] ; NOZAWA, Satonori[1]

[1]Solar-Terrestrial Environment Laboratory, Nagoya University

Fabry-Perot interferometer (FPI) is an instrument that can measure the temperature and wind velocity of the thermosphere from the ground through observation of airglow emission at a wavelength of 630.0nm. The Solar-Terrestrial Environment Laboratory (STEL), Nagoya University, has five FPIs as parts of the Optical Mesosphere Thermosphere Imagers. Two of those FPIs, possessing a large aperture etalon (diameter: 116mm), were installed at Shigaraki, Japan in 2000 and in Tromso, Norway, in 2009. The other three small FPIs, using 70-mm diameter etalons, were installed in Thailand, Indonesia, and Australia in 2010-2011. They use highly-sensitive cooled-CCD cameras with 1024-1024 pixels to obtain interference fringes. However, appropriate temperature has not been obtained from the interference fringes using these new small-aperture FPIs. In the present study we aimed to improve the procedure of temperature derivation using these small etalon FPIs, to evaluate the accuracy for obtained temperatures and to perform statistical analysis of the temperature data obtained for 2-3 years.

The FPIs scan the sky in north, south, east, and west directions repeatedly by rotating a light receiving mirror. We determined each center of the laser fringe and sky fringes for north, south, east, and west directions. Then we found that they are slightly a few pixels different depending on the mirror directions. This difference of fringe centers seems to be due to distortion of the optics body, which is caused by the motion of the heavy scanning mirror on top of the optics. Thus, we decided to determine the fringe center for each direction. After this revision, we could make a reliable temperature determination. In this presentation, we show these procedures of temperature derivation and relation between airglow intensity and standard deviations of obtained temperatures as accuracy of temperature derivation. We also discuss effects of the etalon gap drift due to changes in etalon temperature for accuracy of measured thermospheric temperatures and winds.

Keywords: Fabry Perot Interferometers, thermospheric temperature

Japan Geoscience Union Meeting 2014
(28 April - 02 May 2014 at Pacifico YOKOHAMA, Kanagawa, Japan)

PEM36-P17 Room:Poster Time:April 28 18:15-19:30

Statistical characteristics of MSTIDs observed by 630-nm airglow imager and HF-radar echoes at Paratunka, Russia

MINOURA, Takeshi[1*] ; SUZUKI, Shin[1] ; SHIOKAWA, Kazuo[1] ; OTSUKA, Yuichi[1] ; NISHITANI, Nozomu[1] ; HOSOKAWA, Keisuke[2]

[1]Solar-Terrestrial Environment Laboratory, Nagoya University, [2]Department of Communication Engineering and Informatics, University of Electro-Communications

Medium-scale traveling ionospheric disturbances (MSTIDs), which typically have a horizontal scale of 100-500 km and a period of ˜1 h, are frequently observed in the F region ionosphere at middle latitudes. To date, quite a few observations of MSTIDs have been carried out especially in the middle latitudes; they predominantly had a northwest-southeast, (northeast-southwest) frontal structure and propagated southwestward (northeastward) in the northern (southern) hemisphere, however their generation and propagation mechanisms are not clear yet. Suzuki et al. [2009] investigated two dimensional characteristics of a nighttime MSTID using the SuperDARN Hokkaido HF radar at Rikubetsu, (43.5 N, 143.6 E), Japan, and an OI 630-nm airglow imager located at Paratunka (53.0 N, 158.2 E), Russia, within the radar field of view (FOV). The Doppler velocities of MSTID echoes observed by the SuperDARN radar showed systematic polarity changes which were consistent with airglow intensity variations. The electric field estimated from the airglow and SuperDARN observations, however, seems to be improbable and the E-F coupling processes would be important to explain the inconsistency. We investigated statistical characteristics of nighttime MSTIDs. Based on the coordinated airglow and SuperDARN measurements from 2011 to 2013, we investigated the relation between the MSTID amplitudes in the 630-nm airglow intensity and the Doppler velocities of the FAI echoes associated with the MSTID pattern. This study may give an observational insight into the E-F coupling quantitatively.

In this presentation, we will report the statistics of the relation of the FAI echoes and airglow signatures of the observed MSTIDs (5 events), which showed spatially conjugation in the radar FOV.

Keywords: airglow imager, Hokkaido SuperDARN radar, MSTID

Japan Geoscience Union Meeting 2014
(28 April - 02 May 2014 at Pacifico YOKOHAMA, Kanagawa, Japan)

PEM36-P18 Room:Poster Time:April 28 18:15-19:30

Detection of ionospheric disturbances caused by the earthquake using HFD

TAKABOSHI, Kazuto[1*] ; NAKATA, Hiroyuki[1] ; TAKANO, Toshiaki[1] ; TOMIZAWA, Ichiro[2]

[1]Graduate shool of Engineering, Chiba University, [2]Center for Space Science and Radio Engineering,Univ. Electro-Comm

Many studies have reported that ionospheric disturbances occur after giant earthquakes. This is because the acoustic wave and/or atmospheric gravity wave are excited by the ground perturbations or tsunami. The HF Doppler observation is suitable for detection of ionospheric disturbances since this can observe ionospheric vertical drift from Doppler shift of radiowaves (5006 and 8006 kHz) transmitted from the Chofu campus of UEC. In this study, usng Doppler shift data of 5006 kHz, ionospheric disturbances associated with earthquakes are ditected. When Doppler shift is fluctuated intensely after propagation time of Rayleigh wave from the seismic center to the observation points, the fluctuation is determined as a disturbance associated with the earthquakes.

In 55 events of earthquakes (M≥6.0) occurred around Japan since 2003, fluctuations by earthquakes are detected in 14 events and the smallest magnitude is 6.4. No fluctuation is detected in some larger earthquakes than M6.4. Since the ionosphere is unstable at night, received frequency is disturbed and it is hard to determine the fluctuations caused by earthquake. In addition, the observation points are not always located near the seismic centers. When earthquakes occur near observation points at the daytime, it is expected that the fluctuations caused by earthquakes are observed even if the magnitudes of the earthquakes is smaller than M6.4.

We also examined the relationship between direction of fault and fluctuations of HFD data. Most of the earthquakes in Japan are reverse fault type. Because a hanging wall slides up in this type of an earthquake, it is expected that initial perturbation of a sound wave excided by the hanging wall is upward. Actually, in most of the events Doppler shifts are negative, which means that the ionosphere moves upward. Next we examined a normal-fault-type earthquake (Fukushima hama-dori earthquake, 2011/4/11), in which a hanging wall slips down. In this event, the epicenter is located at the east of Fukushima prefecture. Doppler data of three observation points (Iitate, Sugadaira, Kiso) are examined. In Iitate observatory, which is the closest to the epicenter, Doppler data shows that ionosphere moved only upward. On the contrary, in the other two points, Doppler data shows that ionosphere moved downward first and then upward, or upward first and then downward. Therefore, fluctuations of ionosphere can not be determined only by a type of fault. More detailed analysis using the seismometer is necessary.

Keywords: ionosphere, HFD, earthquake, acoustic wave, atmospheric gravity wave, fault

Japan Geoscience Union Meeting 2014
(28 April - 02 May 2014 at Pacifico YOKOHAMA, Kanagawa, Japan)

PEM36-P19 Room:Poster Time:April 28 18:15-19:30

Observations of seismo-traveling ionospheric disturbance during the 2011 Tohoku earthquake using HF Doppler

CHOU, Min-yang[1*] ; TSAI, Ho-fang[1] ; LIU, Jann-yenq[2]

[1]Department of Earth Science,National Cheng-Kung University,Taiwan, [2]Institute of Space Science, National Central University, Taiwan

This paper reports seismo-traveling ionospheric disturbances (STIDs) induced by the 11 March 2011 M9.0 Tohoku-oki earthquake and following pan-Pacific tsunami by two networks of HF (high-frequency) Doppler sounding systems in Japan and Taiwan. The Hilbert-Huang Transform (HHT) is applied to analyze Doppler frequency shifts (DFSs) detecting STIDs, while the time delay, circle, ray-tracing, and beam-forming methods are used to compute the propagation of the detected STIDs. Both STIDs induced by the Rayleigh waves and tsunami of the Tohoku-oki earthquake are detected and discussed.

Keywords: STIDs, Ionosphere, earthquake, tsunami

Japan Geoscience Union Meeting 2014
(28 April - 02 May 2014 at Pacifico YOKOHAMA, Kanagawa, Japan)

PEM36-P20 Room:Poster Time:April 28 18:15-19:30

Spectrum of the neutral atmospheric waces derived from a numerical simulation of an earthquake

SHIMIZU, Yuki[1*] ; NAKATA, Hiroyuki[1] ; TAKANO, Toshiaki[1] ; MATSUMURA, Mitsuru[2]

[1]Grad. School of Eng. , Chiba Univ., [2]Center for Space Science and Radio Engineering, University of Electro-Communications

It is important to examine the ionospheric disturbances excited by earthquakes, since this contributes to monitoring tsunamis from satellites. There are many reports of ionospheric disturbances occurred by giant earthquakes, such as the 2011 off the Pacific coast of Tohoku Earthquake. But characteristics of atmospheric disturbances, connecting the ionospheric disturbances with the ground and the sea surface, is not clarified because broad observation of the atmosphere in high resolution is difficult. In this study, calculating the spectra from the temporal variations of neutral atmospheric waves determined by a numerical simulation, we derived the features of the propagation of the atmospheric waves.

In this simulation, two dimensional model is used. The atmospheric perturbation is created by a vertical velocity assuming an upward motion of the sea surface or ground surface. Calculating the temporal variations of neutral density, we derived their spectra.

As a result, it is shown that behavior of atmospheric waves is different for the frequency. For a notable example, variations around 1 mHz propagate to high altitudes 450 km ˜500 km and long distance 800 km. On the other hand, variations around 10 mHz propagate almost the same distance in lower altitude of 300 km or less. In addition, variation at 4 mHz are located above the epicenter at 350 km. This causes the variation of GPS-TEC at 4 mHz associated with earthquakes that have ever been reported.

Keywords: ionosphere, earthquake, acoustic wave, gravity wave

Japan Geoscience Union Meeting 2014
(28 April - 02 May 2014 at Pacifico YOKOHAMA, Kanagawa, Japan)

PEM36-P21 Room:Poster Time:April 28 18:15-19:30

Ionospheric effects on the F region during the Sunrise for the annular solar eclipse over Taiwan on 21 May 2012

CHUO, Yu-jung[1*]

[1]Department of Information Technology, Ling Tung University

On 21 May (20:56, Universal Time; UT, on 20 May), 2012, an annular solar eclipse occurred, beginning at sunrise over southeast China and moving through Japan, sweeping across the northern Pacific Ocean, and completing its passage over the western United States at sunset on 20 May (02:49 UT, 21 May), 2012. We investigated the eclipse area in Taiwan, using an ionosonde and global positioning system (GPS) satellites measurements. The measurements of foF2, hmF2, bottomside scale height around the peak height (Hm), and slab thickness (B0) were collected at the ionosonde station at Chung-Li Observatory. In addition, we calculated the total electron content (TEC) to study the differences inside and outside the eclipse area, using 3 receivers located at Marzhu (denoted as MATZ), Hsinchu (TNML), and Henchun (HENC). The results showed that the foF2 values gradually decreased when the annularity began and reached a minimum level of approximately 2.0 MHz at 06:30 LT. The hmF2 immediately decreased and then increased during the annular eclipse period. The TEC variations also appeared to deplete in the path of the eclipse and opposite to the outside passing area. Further, the rate of change of the TEC values (dTEC/dt measured for 15 min) was examined to study the wave-like fluctuations. The scale height near the F2 layer peak height (Hm) also decreased and then increased during the eclipse period. To address the effects of the annular eclipse in the topside and bottomside ionosphere, this study provides a discussion of the variations between the topside and bottomside ionospheric parameters during the eclipse period.

Keywords: ionospheric physics, ionospheric disturbances, solar radiation effects

Japan Geoscience Union Meeting 2014
(28 April - 02 May 2014 at Pacifico YOKOHAMA, Kanagawa, Japan)

PEM36-P22 Room:Poster Time:April 28 18:15-19:30

Horizontal shapes of mid-latitude sporadic-E observed with GPS-TEC

MAEDA, Jun[1*] ; HEKI, Kosuke[1]

[1]Graduate school of Science, Hokkaido University.

The horizontal shapes of sporadic-E (Es) have remained uncovered due to the lack of effective observation methods. We use a dense array of Global Positioning System (GPS) receivers in Japan to map horizontal shapes of mid-latitude sporadic-E layers and explore their diversity. The spatial and temporal resolutions of the GPS array are ˜25 km (in horizontal) and 30 s, respectively, which is ideal for studying the horizontal shape and movement of sporadic-E. Sporadic-E can be identified as positive anomalies of total electron content (TEC) along the line of sight between a satellite and a ground-based GPS station.

The results of GPS-TEC observation, i.e., mapping of positive TEC anomaly caused by mid-latitude sporadic E are presented in this presentation with a special emphasis on latitudinal and temporal variations of horizontal shapes of Es-layers. We analyzed ˜100 Es events in 2010-2013 to examine the latitudinal dependence of Es frontal structures with three study areas at different latitudes near ionosondes, namely Sarobetsu (geographical latitude: 45.16 N), Kokubunji (35.71 N) and Yamagwa (31.20 N).

As a result, strong Es shares the large-scale frontal structure as a common shape regardless of the occurrence latitude and time (e.g., morning, afternoon, and the evening). The horizontal structures of large-scale fronts are typically elongated in east-west (E-W) with the length and width of ˜300 km and ˜30 km, respectively. However, lengths vary from 30 to 300 km by occasion. The alignment of frontal structures prefers E-W, ENE-WSW and NE-SW alignment with some exception of NW-SE and NNW-SSE aligned structures.

We will also discuss the possible mechanisms for formation, development, and movement of mid-latitude sporadic-E based on the results of our observations and proposed theories.

Keywords: Sporadic-E, GPS, TEC

Japan Geoscience Union Meeting 2014
(28 April - 02 May 2014 at Pacifico YOKOHAMA, Kanagawa, Japan)

PEM36-P23 Room:Poster Time:April 28 18:15-19:30

GPS-TEC observation using two-frequency software receiver

ASHIHARA, Yuki[1*] ; KOMATSU, Kazuki[1]

[1]Dept. of Electrical Engineering, Nara National College of Technology

Global Positioning System (GPS) is a high accuracy positioning system that uses radio waves transmitted from several GPS satellites. The carrier signals of GPS satellites, there are two frequencies of L1 (1575.42MHz) and L2 (1227.60MHz). In the ionospheric plasma, the refractive index depends on the electron density. In addition, since the plasma is dispersive medium, each of L1 and L2 waves has different refractive indexes. Therefore, it is occurred propagation delay time (phase difference) in between these signals.

GPS-TEC (GPS Total Electron Contents) is a method to obtain the total electron contents along the line of satellite (LOS) from the phase difference between these signals. GPS-TEC is very useful technique to observe ionospheric electron density, but two-frequency GPS receiver is very expensive. Therefore, GPS-TEC has calculated by using GEONET data in most cases in Japan.

In the informatics and communication field, software receiver is being widely for demodulating the baseband signal, as a background of higher performance of computers. In this study, we build a software GPS receiver system, and receive the two-frequency signals. And we will evaluate the GPS-TEC data obtained by this observation.

Keywords: ionosphere, GPS-TEC, software receiver

Japan Geoscience Union Meeting 2014
(28 April - 02 May 2014 at Pacifico YOKOHAMA, Kanagawa, Japan)

PEM36-P24 Room:Poster Time:April 28 18:15-19:30

Total electron content observation by using GPS, QZSS and BeiDou

KINUGASA, Natsuki[1*] ; TAKAHASHI, Fujinobu[1]

[1]Yokohama National University

There are several methods for observation of total electron content (TEC). TEC can be obtained from the measurement of global navigation satellite system (GNSS) such as GPS. Recently, RNSS (regional navigation satellite system) has been developed in China and Japan. We are trying to use RNSS for TEC observation.

RNSS makes TEC observation stable since a satellite is tracked continuously for long time. It is of benefit to study of plasmasphere because the altitude is higher than GNSS. There is also drawback. Since the direction of vector from grand receiver to satellite is not so variable, it is hard to observe the horizontal electron density distribution of ionosphere. This problem can be solved by combining with measurements of RNSS and GNSS. That is called multi-GNSS.

TEC can be caluculated from the difference of delay between dual-frequency. The inter-frequency bias which remain in TEC measurement are required to estimated and removed. We will present model of ionospheric electron density distributionfor the bias estimation procedure. We have constructed the observation system for GPS, Japanese QZSS, and Chinese BeiDou in Yokohama National University. Various observational results will be shown and discussed.

Keywords: TEC, QZSS, BeiDou, GPS, ionosphere, plasmasphere

Japan Geoscience Union Meeting 2014
(28 April - 02 May 2014 at Pacifico YOKOHAMA, Kanagawa, Japan)

PEM36-P25 Room:Poster Time:April 28 18:15-19:30

Total Electron Content prediction model over Japan using an artificial neural network

NISHIOKA, Michi[1*] ; TSUGAWA, Takuya[1] ; MARUYAMA, Takashi[1] ; ISHII, Mamoru[1]

[1]National Institute of Information and Communications Technology

Forecasting Total Electron Content (TEC) is important for Space Weather; for predicting propagation delay of the radio waves in the ionosphere. Although several empirical and theoretical models have been developed, no model is available for forecasting TEC over Japan. Our purpose is to accomplish an operational TEC model over Japan using an artificial neutral network (ANN) technique which is developed by Maruyama [2007]. In our model, absolute TEC values for each day from 27^{o}N to 45^{o}N in latitude and 127^{o}E to 145^{o}E in longitude were projected on a two-dimension TEC map, that is, a local-time and latitudinal map. Then the time-latitudinal variation was fitted by using the surface harmonic function. The coefficients of the expansions were modeled by using a neural network technique. For the learning process, we used absolute TEC value from 1997 to 2013. The input parameters are proxies of the season, the solar activity, and the geomagnetic activity. Thus, daily two-dimensional TEC maps can be obtained for any day when the input parameters are provided. We used input parameters which are available in real-time by some institutes and achieved one-day TEC prediction over Japan.

Keywords: Ionosphere, Total Electron Content, Operational model, artificial neural network

Japan Geoscience Union Meeting 2014
(28 April - 02 May 2014 at Pacifico YOKOHAMA, Kanagawa, Japan)

PEM36-P26 Room:Poster Time:April 28 18:15-19:30

Statistical Analyses of Ionospheric Storms Over 50 Years In Japan

NAKAMURA, Maho[1*] ; KAMOGAWA, Masashi[1]

[1]Dpt. of Phys., Tokyo Gakugei Univ.

Statistical analyses of the ionospheric storms over Japan are carried out based on the long-term observations over 50 years in Japan. While there are many types of ionospheric variations such as ionospheric storms, plasma bubbles, TIDs and so on, ionospheric storms are most large fluctuations of electron density in the ionosphere. In general, the increase of the electron density is termed positive storm and the decrease of it is termed negative storm [1]. The positive storms cause satellite-positioning errors due to the delay of radio propagation and negative storms cause HF radio communication outages due to lowering the maximum usable frequency. Because these two types of ionospheric storms shows different characteristics on the duration, scale, and the seasonal dependences, we analyzed ionospheric storm occurrences using critical frequency of the F2 layer; foF2 obtained from ionograms over 4 observation sites (Wakkanai, Kokubunji, Yamagawa, and Okinawa) operated by National Institute of Information and Communications Technology, Japan (NICT) [2]. We extracted ionospheric storms based on the differences between the daily observation values and the one-month median in Japan for more than 50 years. Extracted storms of each station will be analyzed by the occurrences, duration, seasonal dependence and geomagnetic variations.

References
[1] G. W. Prolss, Ionospheric F-region storms, Vol. 2 of Hand book of Atmospheric Electro- dynamics, CRC Press, 1995.
[2] World Data Center for Ionosphere, http://wdc.nict.go.jp/.

Keywords: ionospheric storms, eritical frequency F2 layer, satelite navigation

Japan Geoscience Union Meeting 2014
(28 April - 02 May 2014 at Pacifico YOKOHAMA, Kanagawa, Japan)

PEM36-P27 Room:Poster Time:April 28 18:15-19:30

Statistical analysis of the Speckle applying the ”Hinode” / XRT

YAMADA, Masanori[1*] ; NOZAWA, Satoshi[1] ; SHIMIZU, Toshifumi[2]

[1]Graduate School of Science and Engineering, Ibaraki University, [2]Institute of Space and Astronautical Science, Japan Aerospace Exploration Agency (ISAS/JAXA)

“ When a charge-coupled device (CCD) image is taken, white noise will appear identically main CCD image. For examlpe, the trajectory of noise is watched like scar, small spot and snowstorm, which is call as spike, unwanted signal, and so on. In this study, noise is called “ Speckle ” . The speclke is due to the particle nature of photon when CCD is hitted by Solar Energitc Particle(SEP) or cosmic ray.
SEPs have high energy of 10 keV - 10 GeV, which are generated by solar flare, coronal mass ejection(CME). This reason is that SEP plays an important role in space weather. When SEPs with hige energy of GeV order will come to earth magnetosphere, low earth orbit (LEO) stellite would be damaged the potential of single events like SEPs effect.

For this reason, this study analyzed Hinode / X-Ray Telescope (XRT) images and detected speckles. Analysis period is from January 2011 to July 2013. As a result speckles were periodic fluctuations and significant increased, when on 00:04 UT March 7 2012, X5.4 Flare occurred.
Number of detected speckles had a time zone is 3 or 4 times as high as before the occurrence of the Flare. In addition periodic fluctuations are synchronized with orbital period. Moreover information of the satellite orbit indicates speckles increases over the High Latitude Zone (HLZ). Although this is suggested SEPs flow in HLZ, there is a region with high geomagnetic latitude, so speckles are caused by charged particles of non-SEPs.

This study reports on detailed consequence. Besides it looks at the correlations between decrease or increase in speckles and information of the satellite orbit or solar activity.

Keywords: Space Weather, SEP, Flare, CME, Hinode/X-Ray Telescope(XRT)

Japan Geoscience Union Meeting 2014
(28 April - 02 May 2014 at Pacifico YOKOHAMA, Kanagawa, Japan)

PEM36-P28 Room:Poster Time:April 28 18:15-19:30

Seasonal-longitudinal dependence of the occurrence of equatorial plasma bubbles obserbed by ISS-IMAP

TAKAHASHI, Akira[1*] ; NAKATA, Hiroyuki[1] ; TAKANO, Toshiaki[1] ; SAITO, Akinori[2]

[1]Chiba University, [2]Kyoto University

Equatorial plasma bubbles (EPBs) are local depletions of the electron density in the ionosphere. Ionospheric irregularities are included in EPBs and cause radio signal scintillation. Recently, reseach on applying GNSS to Air Navigation System has progressed, therefore, it becomes more necessary to investigate the generation mechanism and the morphology of EPBs.

In this study, we analyzed seasonal-longitudinal dependence of the occurrence of EPBs using airglow-images obtained by ISS-IMAP (Ionosphere, Mesosphere, upper Atmosphere, and Plasmasphere mapping).In 630-nm airglow images, EPBs are visualized as black lines. 181 events are selected during 2012/09 - 2013/08. To calculate the longitudinal denpendence of occurence rate, we divide the ionosphere into 36 longitude bins, each 10 degrees wide. Since EPBs are observed at low and middle latitude, the total obserbation time is accumlated when |latitude| $<$30. We calculate the occurrence rate as the number of EPBs detected over the total observation time.

The occurrence rate is high at the African-Atlantic-American regeions in the equinoctial seasons. On the other hand, the occurance rate is also high at American-Pacific resions in summmer, which is not obtained in the previous study, Burke et al. [2004], in which EPBs are detected using plasma density data on DMSP satellite. The altitude of DMSP is 840 km, which is higher than the observation altitude of ISS-IMAP, that is about 250 km. Therefore, it is conceivable that the difference of occurrence rate of EPB is due to the altitude of the observations. This imply that ISS-IMAP observation could detect EPBs not developed to higher altitude.

Based on above, we will present seasonal-longitudinal variability of the Rayleigh-Taylor instability growth rate, contributing the development of EPBs using ionosphere model and other observational data.

Keywords: Equatorial ionosphere, Plasma bubble, airglow, ISS-IMAP

Japan Geoscience Union Meeting 2014
(28 April - 02 May 2014 at Pacifico YOKOHAMA, Kanagawa, Japan)

PEM37-01 Room:414 Time:April 30 11:00-11:15

A coherent modulation of pulsating aurora at Pc5 frequency

SAKA, Osuke[1*] ; HAYASHI, Kanji[2] ; KLIMUSHKIN, Dmitri[3] ; MAGER, Pavel[3]

[1]Office Geophysik, [2]U. Tokyo, [3]Russian Academy of Sciences

Ground and satellite magnetometer observations and all-sky video images revealed that the Pc5 pulsations that occurred in 17 January 1994 showed a wide distribution in longitude from Alaska, USA (0 MLT) to the Hudson bay, Canada (11 MLT) and in latitudes from 62N (L=4.5) to 70N (L=8.5).

Auroras in all-sky image were composed of field line resonance (FLR) in higher latitudes in 67-70N and pulsating aurora (PsA) in lower latitudes in 62-67N.
It is found that the PsA, FLR, and field magnitude at the geosynchronous altitudes were all oscillated coherently at Pc5 periodicities.

We conclude that the coherent modulation of FLR and PsA are attributable to toroidally and poloidally polarized Pc5 pulsations, respectively, generated by the polarization splitting of the Alfven spectrum by the finite plasma pressures.(1), (2).

References
1. Klimushkin, D.Yu., Mager, P.N., Glassmeier, K.-H., 2004. Ann.Geophys.
2. Saka, O., Hayashi, K., Klimushkin, D.Yu, Mager, P.N., 2014. JASTP.

Keywords: Pc5 pulsations, pulsating aurora, poloidal mode

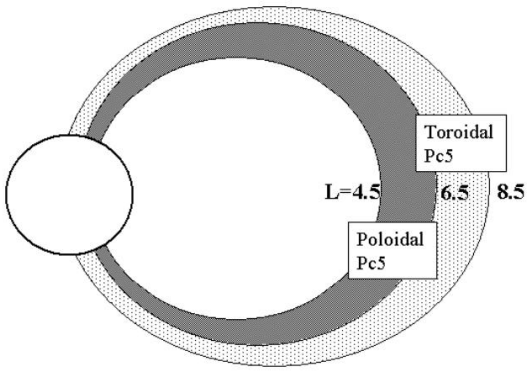

Japan Geoscience Union Meeting 2014
(28 April - 02 May 2014 at Pacifico YOKOHAMA, Kanagawa, Japan)

PEM37-02 Room:414 Time:April 30 11:15-11:30

Generation of pulsating aurora: Role of cold electron and electric field

SATO, Natsuo[1*] ; KADOKURA, Akira[1] ; TANAKA, Yoshimasa[1] ; NISHIYAMA, Takanori[1]

[1]National Institute of Polar Research

Pulsating auroras are common phenomena, which are observed universally during the recovery phase of substorm in the auroral and subauroral zones. But, even today, generation mechanism of fundamental characteristics of pulsating aurora, such as, their periodicity, their shapes, and their motion are not understood. Simultaneous observations onboard satellites and on the ground are important method to examine such fundamental characteristics of pulsating aurora. We examined some selected pulsating auroral events, which obtained onboard THEMIS spacecraft and the THEMIS ground-based all-sky camera network. THEMIS satellites were located in the post midnight sector near the equatorial plane in the magnetosphere. We found following signatures of particle, field and wave in the magnetosphere at the onset and during pulsating aurora; 1) All pulsating aurora associate with high-energy (>5 keV) electron flux enhancement, 2) Cold electron flux (<20 eV) and electric field intensity show QP (quasi-periodic) modulation in association with pulsating aurora, 3) and their QP modulation sometimes show one-to-one correspondence to QP modulation of ELF wave intensity, for both type of electromagnetic lower-band chorus wave and electrostatic ECH (electron cyclotron harmonic) wave, 4) But, not all pulsating aurora associate with ELF wave enhancement.

In this talk we focus on the event which THEMIS-A, D, E spacecraft crossed a clear boundary between strong pulsating auroral region and non-pulsating auroral region. In this strong pulsating auroral region, electric field, ULF-ELF (<300Hz) electric field waves, and cold electron flux are modulated in association with pulsating aurora, but the activity of lower-band chorus wave is very low or nothing. When the spacecraft entered into non-pulsating auroral region all of QP activity became quiet/stop. It is interesting to note that high-energy electron (>10 keV) flux was almost the same for both of the regions, but cold electron flux suddenly decreased and temperature suddenly increased when the spacecraft entered into non-pulsating auroral region. We will discuss the role of cold electron, electric field and ELF waves for the generation of pulsating aurora.

Keywords: aurora, pulsating aurora, chorus wave, magnetosphere, ionosphere, polar region

Japan Geoscience Union Meeting 2014
(28 April - 02 May 2014 at Pacifico YOKOHAMA, Kanagawa, Japan)

PEM37-03 Room:414 Time:April 30 11:30-11:45

High-resolution correlation analysis between VLF/ELF chorus waves and pulsating aurora observed at Athabasca, Canada

SUNAGAWA, Naoki[1*] ; SHIOKAWA, Kazuo[1] ; MIYOSHI, Yoshizumi[1] ; KATAOKA, Ryuho[2] ; OZAKI, Mitsunori[3] ; SAWAI, Kaoru[3] ; IAN, Schofield[4] ; MARTIN, Connors[4]

[1]Solar-Terrestrial Environment, [2]National Institute of Polar Research, [3]Kanazawa University, [4]Athabasca University

We investigate dynamic switching of arrival time difference between pulsating aurora intensity and chorus waves which were observed on 7 February 2013 at Athabasca in Canada (L=4.4), using a crossed-loop antenna and a narrow field-of-view EMCCD camera. Power spectra of pulsating auroral intensity and chorus wave intensity at 1.5-2.5 kHz show a same pulsation period at 0.1-0.15 Hz. Arrival time difference between pulsating aurora intensity and chorus waves are evaluated by using cross-correlation analysis. We found that two patterns of arrival time difference switches with a time scale of a few tens seconds. One pattern shows that electrons reached ionosphere later than the associated chorus waves with a delay time of 2 s, consistent with the theoretical value for south-going electrons reflected at the ionosphere in the southern hemisphere. The other pattern shows that electrons reached ionosphere earlier by 4.5 s than the associated chorus waves, consistent with the theoretical value for south-going chorus waves reflected at the ionosphere in the southern hemisphere. These results firstly show that interaction process of high-energy electrons and chorus waves are changing with a time scale of a few tens seconds.

Keywords: pulsating aurora, chorus waves, Wave-particle interactions, ground-based observation

Japan Geoscience Union Meeting 2014
(28 April - 02 May 2014 at Pacifico YOKOHAMA, Kanagawa, Japan)

PEM37-04 Room:414 Time:April 30 11:45-12:00

Relativistic electron precipitations in association with diffuse aurora

KURITA, Satoshi[1*] ; KADOKURA, Akira[2] ; MIYOSHI, Yoshizumi[3] ; SATO, Yuka[2] ; MISAWA, Hiroaki[1] ; MORIOKA, Akira[3]

[1]Tohoku Univ., [2]National Institute for Polar Research, [3]STEL, Nagoya Univ.

It has been widely thought that diffuse auroras are generated by electron precipitations in the energy range from a few keV to tens keV. Recent simulation results based on the quasi-linear theory showed that the scattering by whistler-mode waves plays an important role in the production of precipitating electrons responsible for diffuse auroras. A test particle simulation on electron-whistler interactions shows that relativistic electrons can be scattered into the loss cone simultaneously with the electrons in the energy range from a few keV to tens keV. Thus, it is expected that relativistic electrons precipitate into the atmosphere in association with diffuse auroras if whistler-mode waves contribute to generation of diffuse auroras. To examine this hypothesis, we investigated conjugate observations of SAMPEX and the all sky camera at Syowa Station on the dawn side, where diffuse auroras are frequently observed. In this study, we show a case study that relativistic electron ($>$1 MeV) precipitations observed by SAMPEX are associated with the diffuse aurora observed at Syowa Station. The SAMPEX observation shows that the enhancement of precipitating relativistic electrons are well correlated with that of precipitating $>$150 keV electrons, indicating that electrons in the energy range from a few keV to 1 MeV precipitate into the atmosphere simultaneously. It is observational evidence that whistler mode waves contribute to generation of diffuse auroras.

Keywords: diffuse aurora, whistler mode wave, relativistic electron, radiation belts, wave-particle interaction

Japan Geoscience Union Meeting 2014
(28 April - 02 May 2014 at Pacifico YOKOHAMA, Kanagawa, Japan)

PEM37-05 Room:414 Time:April 30 12:00-12:15

Refilling of Plasmasphere

WATANABE, Shigeto[1*]

[1]Hokkaido University

Satellite observations have revealed that ions are heated in the ionospheric polar region and are flowing to the magnetosphere. The fluxes of H+, He+, and O+ are ˜1011 ions m-2 s-1, ˜1011 ions m-2 s-1, ˜1010 ions m-2 s-1, ˜1010 ions m-2 s-1 during the solar maximum and ˜1010 ions m-2 s-1, ˜109 ions m-2 s-1, ˜109 ions m-2 s-1 near the solar minimum condition, respectively. The large amount of ions, including heavy ions such as O+, contributes the refilling of plasmasphere and inner magnetosphere. The ions are formed often as conics / transversely accelerated ion in the topside polar ionosphere. To understand the refilling process, the refilling time scale and the effects to the structure and dynamics of plasmasphere and inner magnetosphere, we have developed a three dimensional model of Atmosphere ? Plasmasphere including Electrodynamics (APE model). The model calculates densities, velocities and temperatures for electron, O2+, N2+, NO+, O+, He+ and H+ at altitudes from 90 km to 10 Re and for N2, O2, O, He and H in the thermosphere, and electric fields in the ionosphere, plasmasphere and inner magnetosphere. We calculate also parallel and perpendicular components of ion and electron temperatures to include the effect of perpendicular heating of ion in the polar ionosphere. The results show clearly the importance of ion heating in the polar region for the structure of plasmasphere, the refilling and the response to the magnetic disturbance.

Japan Geoscience Union Meeting 2014
(28 April - 02 May 2014 at Pacifico YOKOHAMA, Kanagawa, Japan)

PEM37-06 Room:414 Time:April 30 12:15-12:30

M/Q=2 Ion Cyclotron Whistlers Observed by Akebono

MATSUDA, Shoya[1*] ; KASAHARA, Yoshiya[1] ; GOTO, Yoshitaka[1]

[1]Kanazawa University

It is well known that lightning whistler wave is caused by lightning discharge, and propagates along geomagnetic field lines as R-mode plasma wave below several tens kHz. Ion cyclotron whistler wave, which is one of Electromagnetic Ion Cyclotron (EMIC) mode waves, has close relation to lightning whistler [1]. One of most important features is the lowest frequency of ion cyclotron whistler which denotes the local crossover frequency of the EMIC mode wave. R-mode lightning electron whistler is converted into L-mode ion cyclotron wave at local crossover frequency between electron whistler and ion cyclotron branches along the propagation path. Propagation characteristics of ion cyclotron whistler strongly depend on ion concentrations in plasma as well as nature of general EMIC waves. These facts suggest that we can estimate ion species and concentrations at observation point and/or along the propagation paths of the ion cyclotron whistlers.

Watanabe at al. [2] reported first observation of M/Q=2 ion cyclotron whistler measured by the ISIS-2 satellite. According to their analysis, M/Q=2 ion cyclotron whistlers were observed at an altitude region around 1,360 km. They suggested that these M/Q=2 ion cyclotron whistlers are caused by deuterons (D^+) from ionosphere of the Earth, and they named them ”deuteron whistlers”.

In the current study, we report M/Q=2 ion cyclotron whistlers observed by the Akebono satellite at an altitude region around 4,500 km, which is the highest altitude where M/Q=2 ion cyclotron whistlers were observed so far. We found that these events had obvious frequency gap near the cyclotron frequency at half of cyclotron frequency of H^+. Hence, these events are precious evidence that some amount of M/Q=2 ion exists in the inner magnetosphere.

In this paper, we study ion concentration in the inner magnetosphere estimated from crossover frequencies of ion cyclotron whistlers observed by Akebono. Recently, it is pointed out that wave-particle interaction is important process to control innermagnetospheric physics. Our results become prior information of future satellite mission such as ERG [3] in the inner magnetosphere and/or simulations such as ray tracing method.

[1]Gurnett, D. A., S. D. Shawhan, N. M. Brice, and R. L. Smith (1965), Ion cyclotron whistlers, *J. Geophys. Res.*, 70(7), 1665-1688, doi:10.1029/JZ070i007p01665.

[2]Watanabe, S., T. Ondoh (1975), Deuteron whistler and trans-equatorial propagation of the ion cyclotron whistler, *Planet. Space Sci.*, vol. 24, 359-364.

[3]Miyoshi, Y., Ono, T., Takashima, T., Asamura, K., Hirahara, M., Kasaba, Y., Matsuoka, A., Kojima, H., Shiokawa, K., Seki, K., Fujimoto, M., Nagatsuma, T., Cheng, C.Z., Kazama, Y., Kasahara, S., Mitani, T., Matsumoto, H., Higashio, N., Kumamoto, A., Yagitani, S., Kasahara, Y., Ishisaka, K., Blomberg, L., Fujimoto, A., Katoh, Y., Ebihara, Y., Omura, Y., Nose, M., Hori, T., Miyashita, Y., Tanaka, Y.-M. and Segawa, T. (2013) The Energization and Radiation in Geospace (ERG) Project, in *Dynamics of the Earth's Radiation Belts and Inner Magnetosphere* (eds D. Summers, I. R. Mann, D. N. Baker and M. Schulz), American Geophysical Union, Washington, D. C.. doi: 10.1029/2012GM001304

Keywords: ion cyclotron whistler, M/Q=2 ion, EMIC wave, Akebono satellite

Japan Geoscience Union Meeting 2014
(28 April - 02 May 2014 at Pacifico YOKOHAMA, Kanagawa, Japan)

PEM37-07 Room:414 Time:April 30 12:30-12:45

Sub-packet structures in the EMIC triggered emission observed by the THEMIS probes

NAKAMURA, Satoko[1*] ; OMURA, Yoshiharu[2] ; SHOJI, Masafumi[3] ; NOSE, Masahito[4]

[1]Department of Geophysics, Graduate School of Science, Kyoto University, [2]Reserach Institute for Sustainable Humanosphere, Kyoto University, [3]Solar-Terrestrial Environment Laboratory, Nagoya University, [4]Graduate School of Science, Kyoto University

We analyse Electromagnetic Ion Cyclotron (EMIC) triggered emission by the data from the THEMIS probes. These phenomena have recently received much attention because of the possibility of their strong interaction with energetic particles in the inner magnetosphere in spite of their scarceness in observations[1,2,3]. For 1400-1445 UT on 9 September 2010, THEMIS A, D and E observed strong EMIC waves with rising tone emissions. The probes were located near the dayside magnetopause at 8 R_E of the radial distance from the Earth, 13 MLT, and a few degrees of the geomagnetic latitude. During this time interval, the geomagnetic field was very distorted by the variation in the solar wind. We assume these emissions were excited around minimum-B pockets in accordance with the magnetospheric compression. It is found the rising tone emissions comprise of some smaller rising tones, which are called ”sub-packet structures”[4]. We compare these observed sub-packet structures with the nonlinear wave growth theory developed by Omura et al. [5]. The observed relationship between the amplitudes and frequencies of the emissions are well explained by the theory, and it is also found that the threshold and optimum amplitudes for the nonlinear growth agree well with the observed dynamic spectra.

[1]Pickett, J. S., et al. (2010), Cluster observations of EMIC triggered emissions in association with Pc1 waves near Earth’s plasmapause, Geophys. Res. Lett., 37 (9), doi: 10.1029/2010GL042648.

[2]Shoji, M., and Y. Omura (2012), Precipitation of highly energetic protons by helium branch electromagnetic ion cyclotron triggered emissions, J. Geophys. Res., 117 (A12), doi:10.1029/2012JA017933

[3]Omura, Y., and Q. Zhao (2012), Nonlinear pitch angle scattering of relativistic electrons by EMIC waves in the inner magnetosphere, J. Geophys. Res., 117 (A8), doi:10.1029/2012JA017943.

[4]Shoji, M., and Y. Omura (2013), Triggering process of electromagnetic ion cyclotron rising tone emissions in the inner magnetosphere, J. Geophys. Res. Space Physics, 118, 5553?5561, doi:10.1002/jgra.50523.

[5]Omura, Y., J. Pickett, B. Grison, O. Santolik, I. Dandouras, M. Engebretson, P. M. E. Decreau, and A. Masson (2010), Theory and observation of electromagnetic ion cyclotron triggered emissions in the magnetosphere, J. Geophys. Res., 115 (A7), doi:10.1029/2010JA015300.

Japan Geoscience Union Meeting 2014
(28 April - 02 May 2014 at Pacifico YOKOHAMA, Kanagawa, Japan)

PEM37-08 Room:414 Time:April 30 14:15-14:30

Statistical analysis of ionospheric Pi2 pulsations observed at mid and low latitude by the SuperDARN Hokkaido radar

TERAMOTO, Mariko[1*] ; NISHITANI, Nozomu[2]

[1]JAXA, ISAS, [2]Solar-Terrestrial Environment Laboratory, Nagoya University

Ultra-low-frequency waves with the periods of 40-150 s are categorized as Pi2 pulsations, which occur over a wide rage of latitude in the night side at substorm onsets. To identify the generation mechanism of Pi2 pulsations, a number of studies using different devices such as ground-based magnetometers and satellites have been carried out. These study provide spatial properties of Pi2 pulsations on the ground and in the inner magnetosphere and suggested that high- and mid-latitude Pi2 pulsations are associated with Alfven waves in the auroral region, while the cavity mode resonance established in the plasmasphere by the fast mode waves has been proposed as a possible Pi2 source at mid and low latitudes.

The interaction of Pi2 pulsations with the ionosphere creates current systems that modify the amplitude and spatial scale size of the waves. In order to construct a coherent view of Pi2 signals measured by ground-based magnetometers, radars and satellites, the effect of the ionosphere needs to be understood.

In present study, statistical studies of Pi2 pulsations in the ionosphere were performed with the SuperDARN Hokkaido radar at Rikubetsu (AACGM magnetic coordinates: 36.5○, 214.7○). The radar can observe the Doppler velocity of ionospheric plasma due to the electric field of Pi2 pulsations in the mid- and low-latitude ionosphere. We investigated the spatial characteristics of the similarity, amplitude ratio, and cross phase between Pi2 pulsations observed by the radar and a ground magnetometer Memanbetsu (MMB) which is located close to the radar site. We will present the results and discuss the interaction of Pi2 pulsations with the ionosphere.

Japan Geoscience Union Meeting 2014
(28 April - 02 May 2014 at Pacifico YOKOHAMA, Kanagawa, Japan)

PEM37-09 Room:414 Time:April 30 14:30-14:45

Pi pulsations in the near-earth magnetotail at substorm onset

SAKURAI, Tohru[1*] ; KADOKURA, Akira[2] ; TANAKA, Yoshimasa[2] ; SATO, Natsuo[2]

[1]Tokai University, [2]National Institute of Polar Research

The THEMIS satellite observations showed that Pi 1 and Pi 2 period range oscillations of the magnetic and electric fields play an important role at a substorm onset in the near-Earth magnetotail. They associated energetic particle accelerations toward the inner magnetosphere. The energetic particle accelerations were observed with very similar oscillation signatures to the Pi 1 and Pi 2 period range oscillations observed in the magnetic and electric fields.. This observation suggests that the Pi 1 and Pi 2 period range oscillations might play an important role for contribution to the auroral particle accelerations at substorm onset in the near-Earth magnetotail . The examination has been done on a substorm event observed on 28 February, 2009 at a THEMIS GBO station, Kuujjuaq (KUUJ) (Mag. Lat.=66.89 N, Mag. Lon.=13.23 E, Mag. Midnight =4.15 UT, L-value = 6.4) in the west coast at the high latitude of the North America Continent. This substorm event was simultaneously observed in the near-Earth magnetotail by the three THEMIS satellites, THEMIS-A, -E, and ?D located in the midnight region at ˜8 Re, ˜8 Re and ˜11 Re, respectively. The data examined in this study are the magnetic field, all-sky images (ASI) and keograms (ASK) obtained at KUUJ and the satellite observations of the magnetic field, electric field, and the electron and ion energy spectra in the ESA peir, and peer data. The results show very interesting facts of the Pi 1 and Pi 2 period range oscillations in the magnetic field and auroral activities observed on the ground and their conjunctions of the magnetic, electric fields, and the associated accelerated particles in the near-Earth magnetotail. The implication of this work provides the importance of the Pi 1 and Pi 2 period range oscillations for controlling the substorm onset plasma processes in the near-Earth magnetotail.

Keywords: Magnetospheric Physics, Substorm, Pi pulsations

Japan Geoscience Union Meeting 2014
(28 April - 02 May 2014 at Pacifico YOKOHAMA, Kanagawa, Japan)

PEM37-10 Room:414 Time:April 30 14:45-15:00

Substorm onset process: Ignition of auroral acceleration and related substorm phases

MORIOKA, Akira[1*] ; MIYOSHI, Yoshizumi[2] ; KASABA, Yasumasa[3] ; SATO, Natsuo[4] ; KADOKURA, Akira[4] ; MISAWA, Hiroaki[1] ; MIYASHITA, Yukinaga[2]

[1]PPARC, Tohoku University, [2]STEL, Nagoya University, [3]Dep. of Gephys. Tohoku University, [4]NIPR

The substorm onset process was studied on the basis of the vertical evolution of auroral acceleration regions derived from auroral kilometric radiation (AKR) spectra and Pi pulsations on the ground. The field-aligned auroral acceleration at substorm onset demonstrated two distinct phases. Low-altitude acceleration (h˜3000-5000 km), which accompanied auroral initial brightening, pre-breakup Pi2, and direct current of ultra-low frequency (DC-ULF) pulsation, was first activated and played an important role (pre-condition) in the subsequent substorm expansion-phase onset. Pre-breakup Pi 2 is suggestive of the ballooning-mode wave generation, and negative decrease in DC-ULF suggests increasing field-aligned current (FAC). We called this stage the substorm initial phase. A few minutes after this initial phase onset, high-altitude acceleration, which accompanied auroral breakup and poleward expansion with breakup Pi 1 and Pi 2 pulsations, suddenly broke out in an altitude range from 8000-16000 km. Thus, substorm expansion onset originated in the magnetosphere-ionosphere (M-I) coupling region, i.e., substorm ignition in the M-I coupling region. It is suggested that current disruption and subsequent violent energy release from the tail region take place after this ignition. Statistical investigations revealed that about 65% of earthward flow bursts observed in the plasma sheet were accompanied by enhanced low-altitude AKR, suggesting that flow braking of bursts causes FAC and resulting low-altitude field-aligned acceleration in the M-I coupling region. On the basis of these observations, we propose a substorm onset scenario in which FAC that originated from the braking of plasma flow bursts first enhances low-altitude acceleration (substorm initial phase onset), and then the increasing FAC induces current-driven instability in the M-I coupling region, which leads to high-altitude acceleration and resulting substorm expansion-phase onset.

Keywords: substorm, aurora, acceleration region, substorm onset

Japan Geoscience Union Meeting 2014
(28 April - 02 May 2014 at Pacifico YOKOHAMA, Kanagawa, Japan)

PEM37-11 Room:414 Time:April 30 15:00-15:15

drivers of the magnetospheric convection

FUJITA, Shigeru[1*] ; TANAKA, Takashi[2]

[1]Meteorological College, [2]Kyushu University

We present here the role of the plasma bulk flow in generation of the magnetosphere-ionosphere convection. Traditionally, the magnetospheric convection is studied with the perpendicular flow because this flow is equivalent with the speed of migration of the magnetic field. For example, the perpendicular force balance equations are utilized in discussion of the dynamo generation ($E*J<0$) in the cusp-mantle region [Tanaka, 1995]. However, since the plasma kinetic energy flux and the internal energy flux are transported along the plasma bulk flow, it is evident that the plasma bulk flow should be considered in generation of the magnetospheric convection. In
addition, the global MHD simulation reveals that the plasmas are accelerated into the cusp from the magnetosheath along the magnetic field. Thus, the plasma bulk flow transports energy into the magnetosphere.

At first, we discuss the dynamo in the cusp-mantle region based on the full set of physical principles (mass conservation, momentum conservation, and energy conservation). As a result, the load in the lower-latitude side of the cusp is invoked by plasma compression due to sudden deceleration of the field-aligned flow from the magnetosheath. The adiabatic assumption invokes pressure enhancement associated with plasma compression. Thus, energy should be supplied to compensate increase in the plasma pressure. As the kinetic energy is much smaller than the electromagnetic energy in the magnetosphere, the electromagnetic energy is converted to the thermal energy. Therefore, the load appears in the lower-latitude side of the cusp. On the other hand, in the cusp-mantle region, plasmas are squeezed with the field-aligned flow toward the lobe region. This yields plasma rarefaction, which eventually invokes energy conversion from the thermal energy to the electromagnetic energy. Thus, the dynamo appears. This process is also explained in terms of the slow mode expansion fan in the cusp-mantle region.

Next, we define an unique magnetospheric energy convection in the dayside magnetosphere. It is noted that the Poynting flux activated in the cusp-mantle region is transported across the dayside magnetosphere to the dayside magnetopause. The electromagnetic energy is totally deposited here. The deposited electromagnetic energy is converted into the thermal energy in the magnetopause. Then we need a mechanism of transporting this thermal energy elsewhere. The MHD simulation shows the thermal energy and the high-speed solar-wind kinetic energy are transported into the cusp from the magnetosheath. This flow goes to the mantle region. Then, the thermal energy transported from the magnetosheath via the cusp is partially converted into the electromagnetic energy in the cusp-mantle region. Finally, the loop of energy convection is completed.

The magnetospheric energy convection is unique because the energy convection and the mass convection show quite different behavior. On the other hand, in the normal fluid like the atmosphere, the energy convection is related to the mass convection in the atmospheric global circulation (convection).

Keywords: magnetospheric convection, MHD simulation, bulk flow, energy conversion, magnetospheric energy convection, cusp dynamo

Japan Geoscience Union Meeting 2014
(28 April - 02 May 2014 at Pacifico YOKOHAMA, Kanagawa, Japan)

PEM37-12 Room:414 Time:April 30 15:15-15:30

Sudden pressure enhancement and tailward retreat in the near-Earth plasma sheet: THEMIS observation and MHD simulation

YAO, Yao[1*] ; EBIHARA, Yusuke[1] ; TANAKA, Takashi[2]

[1]Research Institute for Sustainable Humanosphere, Kyoto University, [2]SERC, Kyushu University

Plasma pressure enhancement is one of the drastic substorm-associated phenomena in the inner magnetosphere. In a substorm occurred on 1 March 2008, four of THEMIS (Time History of Events and Macroscale Interactions during Substorms) probes were almost aligned along the sun-Earth line, which was suitable for investigating spatial-temporal evolution of the near-Earth plasma sheet in a substorm. They observed a sudden increase in the plasma pressure at the inner probe (at ∼7.2 Re), followed by the outer probes (at ∼7.5, ∼8.3, and ∼10.4 Re), that is the high pressure region propagates tailward. Hereinafter, we call this sudden pressure enhancement (SPE). We compared the observations with simulation results of a global magnetohydrodynamics (MHD) simulation, and found a fairly good agreement between them in terms of the followings. (1) Tailward propagation of the SPE can be seen only at off-equator after the substorm onset. In the equatorial plane, an earthward propagation of the SPE precedes the tailward propagation. (2) Observations from the three inner probes show that the SPE consists of two enhancements. The first one is attributed to the convergence of bulk flow energy flux, namely flow braking. The latter one is due to the convergence of the thermal energy flux and subsequent inflation of the plasma sheet. (3) Plasma flow turned from the tailward-and-toward-the-equatorial-plane to earthward-and-away-from-the-equatorial plane near the onset from the simulation results. We discuss the spatial-temporal evolution of the plasma flow and the magnetic field during the substorm.

Keywords: substorm, THEMIS observation, Global MHD simulation, Sudden pressure enhancement

Japan Geoscience Union Meeting 2014
(28 April - 02 May 2014 at Pacifico YOKOHAMA, Kanagawa, Japan)

PEM37-13 Room:414 Time:April 30 15:30-15:45

Evolution of theta aurora during strong positive IMF Bz and varying IMF By condition

OBARA, Takahiro[1*]

[1]PPARC, Tohoku University

Formation of the theta aurora, which appears under the condition of northward IMF and greater IMF magnitude, is investigated from the analysis of the numerical MHD simulation. The theta aurora is caused by the transient convection after a sign change of IMF By. This transient convection must include a replacement of lobe field lines from old IMF orienting fields, a rotation of plasma sheet to opposite inclination, and a reformation of ionospheric convection cells. In the midst of these reconfigurations, old and new convection system must coexist in the magnetosphere-ionosphere system. In this stage, the polar cap and tail lobes are continuously encroached by the new open field lines connected to the new IMF. Whereas magnetic field lines accumulated in new lobes tend to rotate the outer plasma sheet in the opposite direction, the old merging cell convection still continues to generate closed field lines that must return to dayside against the new lobe formation. As time progresses, the growth of new lobes results in the blocking of the return path toward dayside of closed field lines generated in the old merging cell to form the kink structure in the plasma sheet. Losing their return path, these closed field lines generated from old lobes accumulated on the night side. The theta aurora appears at the foot point of these accumulated closed field lines. In the presentation, we will demonstrate some observational results brought by satellites and ground based instruments, which support above mentioned hypothesis for theta aurora foramation.

Keywords: IMF, Strong northward IMF, Varying IMF By, Theta aurora, Simulation, Observation

Japan Geoscience Union Meeting 2014
(28 April - 02 May 2014 at Pacifico YOKOHAMA, Kanagawa, Japan)

PEM37-14 Room:414 Time:April 30 15:45-16:00

Substorm Onset: Correlation between Ground and Space Observations

CHENG, Chio[1*] ; CHANG, T. F.[2]

[1]Plasma and Space Science Center, National Cheng Kung University, [2]Institute of Space and Plasma Sciences, National Cheng Kung University

The observations of substorm onset phenomena in the magnetosphere and ionosphere are examined to study their correlation and to understand the substorm onset mechanism. In particular, we examine the Pi2 wave structure, propagation, frequency and growth rate in the magnetosphere observed by the THEMIS satellites in the near-Earth plasma sheet and the structure and propagation of the substorm auroral onset arcs. We show the correlation between the substorm onset wave-like arcs and the Pi2 pulsations in terms of wave structure, propagation, and the exponential growth of arc intensity and Pi2 wave amplitude. In particular, the azimuthal mode numbers of the Pi2 waves and the wave-like arc structure are estimated to be ˜100-200. The correlation between the ground and space phenomena strongly supports the kinetic ballooning instability (KBI) as the cause of substorms. KBI is the most natural mechanism for explaining the unstable Pi2 waves in the strong cross-tail current region and the KBI parallel electric field can accelerate electrons along the magnetic field lines into the ionosphere to produce the substorm onset wave-like arcs.

Keywords: substorm, magnetospheric dynamics, THEMIS observation

Japan Geoscience Union Meeting 2014
(28 April - 02 May 2014 at Pacifico YOKOHAMA, Kanagawa, Japan)

PEM37-15 Room:414 Time:April 30 16:15-16:30

Investigation of substorm triggering mechanism based on THEMIS data

MACHIDA, Shinobu[1*] ; MIYASHITA, Yukinaga[1] ; IEDA, Akimasa[1] ; ANGELOPOULOS, Vassilis[2] ; MCFADDEN, James P.[3]

[1]Solar-Terrestrial Environment Laboratory, Nagoya University, [2]IGPP/EPSS, UCLA, [3]SSL, UC Berkeley

In this study, we show the result of superposed epoch analysis on the THEMIS probe data during the period from November, 2007 to April, 2009 by setting the origin of time axis to the substorm onset determined by Dr. Toshi Nishimura based on the THEMIS all sky imager (THEMS/ASI) data. We have restricted the time interval from t = -100 sec to t = 100 sec and the region to -7.5 >X(Re) >-23, and investigated various variations associated with substorm onset.

It was confirmed that earthward flows start at t = -60 sec in the region around X = -14 Re, and then they move toward the Earth. At t = 0, the dipolarization of the magnetic field starts at X ˜-10 Re, and simultaneously the magnetic reconnection starts at X ˜-20 Re. These variations support the validity of our Catapult Current Sheet Relaxation model for substorm onset.

Interestingly, the absolute value of dawnward plasma flow velocity |Vy|decreases in the plasma sheet and the plasma sheet boundary layer during the interval -20 <t(sec) <20. By analyzing individual event of |Vy|decrease, it was confirmed that the plasma flows turn from the duskward convective flows (Vy >0) to the dawnward flows (Vy <0) on average, associated with substorm onset, so that the value of Vy once becomes to zero around t = 0. This variation was found to be related to the deflection of the flows when they encounter with the Earth's dipole magnetic field as they approach to the Earth, which is the same reason already known to cause the tailward flows around X = -10 Re when the earthward flows reach that region.

Keywords: substorm, magnetotail, magnetic reconnection, dipolarization, THEMIS probes

Japan Geoscience Union Meeting 2014
(28 April - 02 May 2014 at Pacifico YOKOHAMA, Kanagawa, Japan)

PEM37-16 Room:414 Time:April 30 16:30-16:45

Global MHD simulations of magnetosphere and 3-dimensional visualization

OGINO, Tatsuki[1*]

[1]Solar-Terrestrial Environment Laboratory, Nagoya University

A study on perpendicular and parallel current generation mechanism in the magnetosphere is important problems in interaction between the solar wind and earth's magnetosphere-ionosphere. Moreover, classification to fundamental MHD quantities and MHD modes is also essential for understandings of the mechanism. Thus we have executed a high resolution global 3D MHD simulation and a 3D graphic diagnostics.

As the solar wind and IMF becomes abnormal conditions, plasma turbulence are strongly excited near boundary layers in the magnetosphere. In the plasma sheet magnetic reconnection occurs in patchy and intermittent manner to produce streamer-like structure. At the magnetopause, more regular vortex train in association with current generation is formed for northward IMF.

Dayside reconnection occurs in patchy and intermittent manner to give seeds of plasma turbulence. As the results, complicated and strong vortex turbulence appears in flank magnetopause. We will demonstrate those phenomena from 3-dimensional visualization method of simulation results to discuss relationship between the currents and vortices in boundary layers. In particularly we will stress relationship among parallel and perpendicular components of vorticity and current, and also compressibility in order to understand the fundamental picture of magnetospheric dynamics. Moreover we will separate the fundamental MHD quantities to various MHD modes in the whole volume, which can make clear their roles on the vorticity and current generation mechanisms.

Keywords: global MHD simulation, current generation mechanism, vorticity and compressibility, roles of MHD modes, magnetic reconnection, magnetospheric dynamics

Japan Geoscience Union Meeting 2014
(28 April - 02 May 2014 at Pacifico YOKOHAMA, Kanagawa, Japan)

PEM37-17 Room:414 Time:April 30 16:45-17:00

Two-spacecraft reconstruction of a three-dimensional magnetic flux rope at the Earth's magnetopause

HASEGAWA, Hiroshi[1*] ; SONNERUP, Bengt[2] ; ERIKSSON, Stefan[3] ; NAKAMURA, Takuma[4]

[1]Institute of Space and Astronautical Science, JAXA, [2]Dartmouth College, [3]University of Colorado, [4]Los Alamos National Laboratory

We present first results of a data analysis method, developed by Sonnerup and Hasegawa [2011], for reconstructing three-dimensional (3-D), magnetohydrostatic structures from data taken as two closely spaced satellites traverse the structures. The method is applied to a flux transfer event (FTE), which was encountered on 27 June 2007 by at least three (TH-C, TH-D, and TH-E) of the five THEMIS probes and was situated between two oppositely directed reconnection jets near the subsolar magnetopause under a southward interplanetary magnetic field condition. The recovered 3-D field indicates that a magnetic flux rope with a diameter of about 3000 km was embedded in the magnetopause. The FTE flux rope obviously had a significantly 3-D structure, because the 3-D field reconstructed from the data from TH-C and TH-D (separated by 390 km) better predicts magnetic field variations actually measured along the TH-E path than does the 2-D Grad-Shafranov reconstruction [Hau and Sonnerup, 1999] using the data from TH-C (which was closer to TH-E than TH-D and was at about 1000 km from TH-E). Such a 3-D nature suggests that reconnected field lines from the two reconnection sites may have been entangled in a complicated way through their interaction with each other. The generation process of the observed 3-D flux rope is discussed on the basis of the reconstruction results and anisotropy of observed electron pitch-angle distributions.

Reference:
Hau, L.-N., and B. U. O. Sonnerup (1999), Two-dimensional coherent structures in the magnetopause: Recovery of static equilibria from single-spacecraft data, J. Geophys. Res. Space Physics, 104, 6899-6917.
Sonnerup, B. U. O., and H. Hasegawa (2011), Reconstruction of steady, three-dimensional, magnetohydrostatic field and plasma structures in space: Theory and benchmarking, J. Geophys. Res. Space Physics, 116, A09230, doi:10.1029/2011JA016675.

Keywords: magnetopause, magnetic flux rope, magnetic reconnection, magnetohydrostatic equilibrium, formation-flying observations

Japan Geoscience Union Meeting 2014
(28 April - 02 May 2014 at Pacifico YOKOHAMA, Kanagawa, Japan)

PEM37-P01 Room:Poster Time:April 30 18:15-19:30

Auroral vortex, auroral surge, and vortical current in the ionosphere associated with the Pi2 pulsations

SAKA, Osuke[1*] ; HAYASHI, Kanji[2]

[1]Office Geophysik, [2]U. Tokyo

The auroral breakup event occurred at 0500UT 27 January 1986 in central Canada is studied using all-sky video image from two optical stations (GWR and SHM) and magnetometer data from three ground stations including the optical stations.

The spatiotemporal motion of the ionospheric vortical current explained the ground magnetometer data in the auroral zone. During the activation of the current vortex, auroras composed of the shear layers rotating clockwise and the auroral surge propagating westward were observed.

It is found that the auroral surge first appeared at the onset latitudes propagated poleward passing through the auroral vortex and became the poleward boundary aurora-surge (PBAS)(1).

References
1. Saka, O., K. Hayashi, D. Koga (2012), JASTP.

Keywords: Aurora dynamics, Pi2 pulsation, Ionospheric current vortex

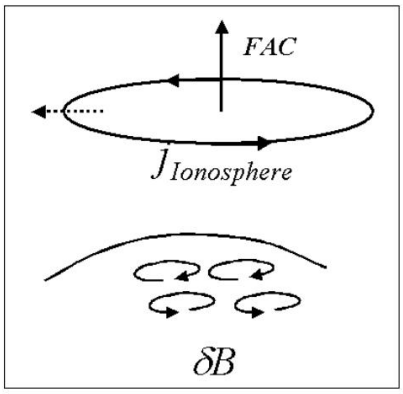

Japan Geoscience Union Meeting 2014
(28 April - 02 May 2014 at Pacifico YOKOHAMA, Kanagawa, Japan)

PEM37-P02 Room:Poster Time:April 30 18:15-19:30

Generation mechanism of steady-state field-aligned currents: A general theory in terms of plasma convection

WATANABE, Masakazu[1*]

[1]International Center for Space Weather Science and Education, Kyushu University, [2]Department of Earth and Planetary Sciences, Faculty of Sciences, Kyushu University

It is well known that field-aligned currents (FACs) play an important role in that they transfer electromagnetic energy and momentum from the magnetosphere to the ionosphere. Recent global magnetohydrodynamic (MHD) simulations indicate that in almost all cases the pressure gradient force is the major driver of FACs [Tanaka, 2003, 2007]. The inertia force becomes appreciable only in very special cases such as the preliminary impulse (PI) in sudden commencements (SCs) [Fujita et al., 2003]. Thus the pressure gradient mechanism is working universally and represents the essence of the dynamical nature of the magnetosphere. What is less or not at all understood, however, is the role of plasma convection in FAC generation. One misconception is that plasma convection is irrelevant to pressure gradient-driven FACs. In fact, convection plays a vital role in energy conversion. This paper describes a general theory of steady-state FACs, with an emphasis on the importance of plasma convection. FACs are created and maintained through the following two processes that occur spatially contiguously with each other. (1) A ”dynamo” process in which plasma thermal energy is converted to electromagnetic energy. A magnetospheric dynamo is necessary in order to sustain a steady-state FAC system. This dynamo is generated by expanding plasma flow (div($\mathbf{v}$) $>$0) that is characterized by the slow mode in MHD waves. The wave normal is directed to the $-$ grad(B) direction, and the flow speed in the wave normal direction (the ”normal” component) becomes the phase speed of the slow mode wave. Slow mode disturbances do not associate FACs. (2) A process in which field-perpendicular currents transform into field-aligned currents. This process occurs by a mode conversion of the waves from slow to Alfvenic. If the pressure gradient has a component perpendicular to both the wave normal and the magnetic field (the ”tangential” component), it produces a magnetic tension and consequently excites Alfven mode disturbances. The flow speed in the wave normal direction becomes the phase speed of the Alfven mode wave. The Alfven mode is associated with tangential plasma flow, and consequently the plasma motion becomes rotational.

References

Fujita et al. (2003), J. Geophys. Res., 108(A12), 1416, doi:10.1029/2002JA009407.
Tanaka (2003), J. Geophys. Res., 108(A8), 1315, doi:10.1029/2002JA009668.
Tanaka (2007), Space Sci. Rev., 133, 1, doi:10.1007/s11214-007-9168-4.

Keywords: field-aligned current, dynamo, convection

Japan Geoscience Union Meeting 2014
(28 April - 02 May 2014 at Pacifico YOKOHAMA, Kanagawa, Japan)

PEM37-P03 Room:Poster Time:April 30 18:15-19:30

Multi-spacecraft analysis of tailward plasma flows in the near-Earth plasma sheet : THEMIS observations

OKAMOTO, Shunichi[1*] ; TAKADA, Taku[2]

[1]Kochi National of College of Technology Department of Electrical Engineering and Information Science, [2]Kochi National of College of Technology

In the near-Earth's plasma sheet, the magnetic field is abruptly dipolarized, associated with an aurora activity. In this region, most of plasma flows are earthward, while some are tailward. Although the candidate mechanism for such tailward flow is considered as rebound flows and/or a part of vortex flows, the quantitative occurrence rate is not fully understood. In this work, we selected events that THEMIS spacecraft observed tailward flows near the magnetic dipolarization region, and then categorized in flow patterns before the tailward flows. Based on the results, we statistically analyzed the categolized events, and estimated the space structure of tailward flows by multi-spacecraft analysis. Consequently, we show the occurrence rate of such rebound flows and the vortex flows.

Keywords: Dipolarization, Tailward flow

Japan Geoscience Union Meeting 2014
(28 April - 02 May 2014 at Pacifico YOKOHAMA, Kanagawa, Japan)

PEM37-P04 Room:Poster Time:April 30 18:15-19:30

Simultaneous observation of a field-aligned current by the JAXA QZS satellite and a MAGDAS ground observatory

TAKEUCHI, Yuuto[1] ; KAWANO, Hideaki[2*] ; HIGASHIO, Nana[3] ; MATSUMOTO, Haruhisa[3] ; BAISHEV, Dmitry G.[4] ; UOZUMI, Teiji[2] ; ABE, Shuji[2] ; YUMOTO, Kiyohumi[2] ; YOSHIKAWA, Akimasa[2] ; MAGDAS/CPMN, Group[2]

[1]Department of Earth and Planetary Sciences, Kyushu University, [2]International Center for Space Weather Science and Education, Kyushu University, [3]Japan Aerospace Exploration Agency, [4]Yu.G.Shafer Inst. of Cosmophysical Research and Aeronomy, Siberian Branch, Russian Academy of Sci.

In this paper we conduct a QZS-MAGDAS conjunction study of a field-aligned current (FAC). QZS (Quasi-Zenith Satellite) is operated by JAXA, and MAGDAS is the ground magnetometer network mainly operated by ICSWSE (International Center for Space Weather Science and Education), Kyushu Univ.

There have been only limited number of papers on satellite-ground conjunction studies of FACs, because satellites usually passes overhead at a ground observatory in a short time.
On the other hand, the footpoint of QZS stays near one ground point in Siberia, Russia, because the orbit of QZS is close to that of geosynchronous satellites on the Japanese meridian. Moreover, a few Siberian MAGDAS observatories exist near the QZS footpoint.

Another advantage of QZS is that, unlike geosynchronous satellites, QZS has 41deg inclination and 0.1deg eccentricity which enable QZS to stay for a long time at northern high latitudes in the magnetosphere; this high-latitude feature increases the detectability of FACs, because the FAC magnitude is in general smaller near the equator, i.e., the FAC source region in the magnetosphere. Thus, the pair of QZS and Siberian MAGDAS is expected to have more chances of simultaneously observing the same FAC than past satellite-ground pairs.

We have been searching for events in which, when QZS and a Siberian MAGDAS observatory were located near the same field line (calculated by the Tsyganenko 96 model), QZS and MAGDAS simultaneously observed transient magnetic field perturbations.

In this paper we present such an event observed by QZS and a Siberian MAGDAS observatory CHD (Chokurdakh). We have found that the transient magnetic perturbations of this event can be interpreted to have been generated by the motion of a local current circuit consisting of line FACs and an ionospheric current. More details will be presented at the meeting.

Japan Geoscience Union Meeting 2014
(28 April - 02 May 2014 at Pacifico YOKOHAMA, Kanagawa, Japan)

PEM37-P05 Room:Poster Time:April 30 18:15-19:30

Comparison between particle environment around GEO from global MHD simulation and that from LANL satellite

NAGATSUMA, Tsutomu[1*] ; YAMAMOTO, Kazunori[1] ; KUBOTA, Yasubumi[1] ; TANAKA, Takashi[1]

[1]National Institute of Information and Communications Technology

Substorm injection is one of the important element of magnetospheric substorm, like auroral break up. Studying substorm injection is important to understand the physics of substorms. Also, substorm injection temporaly changes the particle environment around satellites at GEO. And dynamical variations of particle environment around GEO is one of the causes of satellite anomaly due to surface charging. We try to evaluate our magnetospheric global MHD simulation code by comparing output from global MHD code and LANL satellite particle data. Previous work has be done by Nakamura [2009]. We will examine the possibility of substorm injection prediction using global MHD simulation. Detailed comparison between simulation and observation will be shown in our presentation.

Keywords: Space Weather Forecast, Magnetosphere, Substorm, Modeling, Global MHD simulation, Geosynchronous orbit

Japan Geoscience Union Meeting 2014
(28 April - 02 May 2014 at Pacifico YOKOHAMA, Kanagawa, Japan)

PEM37-P06 Room:Poster Time:April 30 18:15-19:30

Energy dispersion and trajectory of particles injected from the magnetotail in magnetospheric quiet conditions

YAMAUCHI, Satoko[1*] ; NAGAI, Tsugunobu[2]

[1]Tokyo Institute of Technology, [2]Tokyo Insutitute of Technology

Particle injection is sudden enhancement in flux of energetic charged particles, commonly observed at geosynchronous orbit ($6.6R_E$), and associated with magnetospheric substorms. Since 2007, dispersive particle injections have been observed in the further dawnside of the magnetosphere ($>10R_E$) than geosynchronous orbit in quiet conditions with the spacecraft Geotail and THEMIS. Although only electron injections are observed in most cases, both electron and ion injections are observed in some cases. The injected population displays energy dispersion in which more energetic particles arrive at a given location earlier than less energetic particles. This dispersion occurs because of energy dependence of particle drift in the magnetospheric magnetic field. In order to investigate the time delay, we have calculated electron trajectories in the inner magnetosphere. We assume that the magnetospheric magnetic field is a simple dipole and the magnetospheric electric field is sum of a convection electric field and a corotation electric field, and obtain the particle trajectories in the equatorial plane using particle drift velocity. We find that the time delay is related to the intensity of the convection electric field. The simulations and observations show that electrons drift from the nightside through the dawnside to the dayside while ions drift from the nightside through the duskside to dayside. However, in the range given by the dipole field, it is not possible to explain the energy dispersion as observed. The shape of the magnetic field is different from the magnetic dipole in the magnetic tail region because the magnetosphere is stretched by the solar wind. In order to provide a more realistic magnetic field model in the magnetosphere, we use the Tsyganenko model that is an empirical magnetic field model of the magnetosphere. In this study, multi-satellite observations and test particle simulations are carried out to explore mechanisms in energization and transport of electrons in the quiet magnetosphere.

Keywords: magnetosphere, perticle injection, energy dispersive, Tsyganenko, quiet condition, trajectory

Japan Geoscience Union Meeting 2014
(28 April - 02 May 2014 at Pacifico YOKOHAMA, Kanagawa, Japan)

PEM37-P07 Room:Poster Time:April 30 18:15-19:30

Time development of the Dipolarization Front and its interactions with the dipole-field region obtained by 2-1/2 dimensi

UCHINO, Hirotoshi[1*] ; MACHIDA, Shinobu[2]

[1]Earth and Planetary Sciences Graduate School of Schience, Kyoto University, [2]Solar-Terrestrial Environment Laboratory, Nagoya University

Bursty bulk flows with increasing B_z (northward component of the magnetic field), which are caused by magnetic reconnections in the magnetotail, are called Dipolarization Front (DF). Under the picture of the Near Earth Neutral Line model, which is one of the models explaining the triggering of substorms, the compression of the dipole region by DF and the pileup of DF itself around the near-Earth plasma sheet boundary cause a wide increase of B_z in the night magnetosphere. Although there are many observational studies of DFs by spacecraft, there are no full-particle simulations that examine the case in which the DF approaches to the dipole region.

In this context, we have performed two-dimensional full-particle simulations for the initial magnetic configuration which is akin to Earth's dipole magnetic field together with a stretched magnetic field by the thin current sheet. We have generated the magnetic reconnection and earthward plasma flows accompanied by B_z, and examined the time development of the flows and the interactions with Earth's dipole-field.

In our simulations, a minimal region of the northward magnetic field where B_z does not increase have been formed between the dipole region and flux pileup region, different from the common picture of Dipolarization. The reason of this can be considered as follows; (1) the earthward flows transport and accumulate the plasmas of the current sheet around the near-Earth plasma sheet boundary, (2) the pressure of the accumulated plasmas decelerate the flow, (3) B_z piles up in the tailward of the boundary. This result is different from the common effect of the DF that it broadly increases B_z in the night side of the magnetosphere. Because of the two-dimensionality in our simulations, the accumulated plasmas cannot leave in the Y-direction (eastward), producing such characteristic region. We also discuss on the structure of the particle flow velocity and particle density distributions near the DF by comparing with observational results.

Keywords: Substorm, Dipolarization Front, Dipolarization

Japan Geoscience Union Meeting 2014
(28 April - 02 May 2014 at Pacifico YOKOHAMA, Kanagawa, Japan)

PEM37-P08 Room:Poster Time:April 30 18:15-19:30

3D Full kinetic simulations of plasma flow interaction with meso- and micro-scale magnetic dipoles

USUI, Hideyuki[1*] ; ASHIDA, Yasumasa[2] ; SHINOHARA, Iku[3] ; NAKAMURA, Masao[4] ; YAMAKAWA, Hiroshi[2] ; MIYAKE, Yohei[1]

[1]Graduate school of system engineering, Kobe University, [2]Research Institute for Sustainable Humanosphere, [3]Japan Aerospace Exploration Agency/Institute of Space and Astronautical Science, [4]Osaka Prefecture University

Plasma flow response to a magnetic dipole and the resulting formation of a magnetosphere depends on the intensity of the magnetic moment of the dipole. In this study, we examined plasma flow interactions with a magnetic dipole which is much smaller than the Earth's intrinsic magnetic dipole by performing three-dimensional full Particle-In-Cell simulations. The size of a magnetic dipole immersed in a plasma flow is characterized by distance L from its center at which the equilibrium is satisfied between the pressure of the magnetic field of the dipole and that of the plasma flow. In the Earth's magnetosphere, L implies the magnetopause location. We particularly focused on meso- and micro-scale magnetic dipoles in which L is comparable to and smaller than the gyroradius of ions in the flow. In the meso-scale case, ions kinetics should be dominantly considered while electrons whose gyroradius is sufficiently small can be treated as fluid. In the micro-scale, however, electrons as well as ions should be treated particles because L becomes small and the electron kinetics cannot be ignored either. Our interest is in the formation of current layer at the magnetosphere boundary in the both scales. Corresponding to the formation of a magnetosphere, the boundary current also depends on the size of the magnetosphere.

In the meso-scale case, the boundary current is dominated by the electron diamagnetic current at the large density gradient found at the distance of L. This signature is similar to the case of the Earth's magnetosphere. In the micro-scale case, however, the trajectories of ions and electrons gyration play an important role to determine the boundary current. Since the ion's gyroradius is larger than L, charge separation between ions and electrons occurs in the upstream region. As particles approach to the inner dipole, the electron gyroradius becomes small and electron drift motion becomes dominant. It is also confirmed that static electric field caused by the charge separation affect the plasma dynamics and the resulting current flow.

Keywords: Magnetic dipole, Meso-scale, Plasma response, Boundary current layer, Plasma particle simulation

Japan Geoscience Union Meeting 2014
(28 April - 02 May 2014 at Pacifico YOKOHAMA, Kanagawa, Japan)

PEM37-P09 Room:Poster Time:April 30 18:15-19:30

Estimation of the plasma sheet thickness in the Mercury's magnetosphere from the MESSENGER observations: IMF dependence

MORIMOTO, Yuya[1*] ; TAKADA, Taku[2]

[1]Kochi National College of Technology Department of Electrical Engineering and Information Science, [2]Kochi National College of Technology

Only two of spacecraft arrived at the Mercury until now: NASA's MESSENGER which went into orbit around Mercury in 2011 and Mariner 10 which investigated Mercury for two years from 1974. Although the Mercury's magnetosphere was first found by the Mariner 10, the magnetosphere has not been quantitatively understood. With the observations of magnetic field, we deduced the thickness of the plasma sheet and examined its dependence on the IMF (Interplanetary Magnetic Field) As a result, the plasma sheet thickness is estimated as 0.12-0.19 R_M during the northward IMF, and 0.02-0.08 R_M during the southward IMF. Bi-polar magnetic field signatures, which can be associated with the plasma flow in the plasma sheet, are observed both during northward and southward IMF. We then discuss the substorm-related phenomena in the Mercury's plasma sheet.

Keywords: MESSENGER, Mercury's Magnetsphere, plasma sheet, plasma flow, substorm

Japan Geoscience Union Meeting 2014
(28 April - 02 May 2014 at Pacifico YOKOHAMA, Kanagawa, Japan)

PCG11-01 Room:421 Time:April 28 10:00-10:15

Problems of DC Probe Measurement onBoard Mini/Microsatellite

OYAMA, Koichiro[1*]

[1]Plasma and Space Science Center, National Cheng Kung Universoty,Taiwan, [2]International Center for Space Weather Study and Education

DC Langmuir probe is one of the key instruments to study ionosphere by satellite. It needs a counter electrode whose conductive surface are is at least 1000 times larger than that of surface area of the electrode. This requirement is usually fulfilled for large satellites which have been launched so far for ionosphere study. Now we are jumping into an era to use tiny satellites. Then we will encounter serious problems for DC Langmuir probe measurements. Conductive surface area of the satellite becomes much less than 1000 times, or even equal to the surface area of electrode. As a result, measurement of electron density becomes unreliable, because potential of the electrode with respect to the satellite (counter electrode) cannot reach ambient plasma potential where electron density is calculated. For the worst case, DC Langmuir probe is in double probe region, where the maximum current is controlled by ion current. An electronics needs to measure low current. although to measure the low current is not impossible with low frequency response. Another more serious problem is contamination of electrode as well satellite surface. To avoid the effect of contamination, probe bias of DC Langmuir probe need to be swept with about 10 Hz. These two factors make it possible to use DC Langmuir probe, because to measure low current with high frequency is not possible. We review problems which raises for the ionosphere measurement by small satellite, and propose one solution to avoid these problems to accomplish accurate measurements. The data which have been used here are the contribution of three students, G. S. Jiang, W. H. Chen, and Y. W. Hsu, Plasma and Space Science Center, National Cheng Kung University,Taiwan.

Keywords: microsatellite, Dc Langmuir probe, surface area, contamination

Japan Geoscience Union Meeting 2014
(28 April - 02 May 2014 at Pacifico YOKOHAMA, Kanagawa, Japan)

PCG11-02 Room:421 Time:April 28 10:15-10:30

Canadian Instrument Participation in Japanese Space Science Mission: A Retrospective Look

YAU, Andrew[1*]

[1]University of Calgary

Canada has participated in a number of Japanese space science satellite and sounding rocket missions by contributing scientific instruments and participating in related science investigations since the 1980s, including the Akebono (EXOS-D) and Nozomi (Planet-B) satellite and the SS520-2, S520-23, and S520-26 sounding rocket missions. We review the experience of this participation, including the resulting scientific benefits and the lessons learned.

Keywords: space instrument, space plasma, satellite

Japan Geoscience Union Meeting 2014
(28 April - 02 May 2014 at Pacifico YOKOHAMA, Kanagawa, Japan)

PCG11-03 Room:421 Time:April 28 11:00-11:15

Development of Miniaturized Plasma Wave Receiver using ASIC

ZUSHI, Takahiro[1*] ; HANGYO, Kensuke[1] ; ONISHI, Keisuke[1] ; KOJIMA, Hirotsugu[1] ; YAMAKAWA, Hiroshi[1]

[1]Research Institute for Sustainable for Humanosphere

Plasma waves are an important physical phenomenon for understanding the electromagnetic environments in space. The plasma wave receiver is roughly divided into two types: a waveform receiver and a spectrum analyzer. Spectrum analyzer provides the frequency spectrums with low noises and high frequency resolution. On the other hand, waveform receiver provides the waveform. Though the waveform has more noise than the spectrum provided by the spectrum analyzer, only the waveform has phase information of a plasma wave. Thus it play a complementary role. However, these plasma wave receivers occupy a large amount of space because of its analog circuits, so a late scientific satellite has only a kind of plasma wave receiver. We have developed miniaturized waveform capture (WFC), a kind of waveform receiver, and sweep frequency analyzer (SFA), a kind of spectrum analyzer, using ASIC (Application Specific Integrated Circuit). We realized 6ch WFC in a chip of 5 mm x 5 mm. We execute experiment expose this chip to radiation. We find that though radiation influence WFC component, especially switched capacitor filter, our WFC fit for the space radiation environment. The SFA has fine frequency resolution, but its time resolution is poor. We propose a new kind of SFA combined with FFT. It has an improved time resolution without losing time resolution. We have developed analog circuits in the new SFA using ASIC technology. Furthermore, we propose the multipoint plasma wave observation system that consisted of some sensor probes using these miniaturized plasma wave receiver. We plan the sounding rocket experiment for performance test of this sensor probe.

Japan Geoscience Union Meeting 2014
(28 April - 02 May 2014 at Pacifico YOKOHAMA, Kanagawa, Japan)

PCG11-04 Room:421 Time:April 28 11:15-11:30

Development of a wide-field X-ray imaging spectrometer for solar system exploration

EZOE, Yuichiro[1*]

[1]Tokyo Metropolitan University

We present our development of a wide-field X-ray imaging spectrometer for solar system exploration. In the past decade or so, various types of X-ray emission have been discovered in the solar system (Bhardwaj et al., 2007, Planet. Space, Sci., Ezoe et al., 2011, Adv. Space, Res.). These X-rays are often associated with energetic particles in planetary magnetosphere and neutrals in planetary atmosphere and cometary coma. Therefore, X-ray observations of solar system objects will lead to better understanding of solar system environments and astrophysical phenomena.

For this purpose, we are developing a wide-field X-ray imaging spectrometer for future exploration missions such as GEO-X (Ezoe et al. 2014, Space Sci. Symposium) and JMO (Sasaki et al. 2011, EPSC-DPS). This instrument is composed of an ultra light-weight X-ray telescope and a low-power radiation-hard semiconductor pixel sensor. The telescope covers a wide field of view of ~4 deg in diameter in 0.3–2 keV with the angular resolution of <5 arcmin. It uses sidewalls of etched holes through thin 4-inch silicon wafers for X-ray mirrors (Ezoe et al., 2010, Mircosys. Tehc.). The detector covers a wide area of ~20 x 20 mm^2 with a ~300 x 300 um^2 pixel. It is an active pixel sensor developed by MPE and PNsensor (Strueder et al., 2010, SPIE). Compared to X-ray CCDs, this type is more radiation hard and allows higher frame time less than 1 ms. This instrument can satisfy stringent resource constraints in the exploration missions. The mass, size, and power are estimated to be ~10 kg, ~30 cm cubic, and ~10 W, respectively. Multiple units of this instrument are considered for GEO-X to achieve a wider field of view, while one unit will meet science requirements of JMO. In this presentation, we will describe design, fabrication, and performance of the instrument components and future prospects.

Keywords: X-ray, imaging spectroscopy, Earth’s magnetosphere, Jupiter, Mars

Japan Geoscience Union Meeting 2014
(28 April - 02 May 2014 at Pacifico YOKOHAMA, Kanagawa, Japan)

PCG11-05 Room:421 Time:April 28 11:30-11:45

ENA Imaging On board the DESTINY Mission

BRANDT, Pontus[1*] ; MITCHELL, Donald[1] ; WESTLAKE, Joseph[1] ; KEIKA, Kunihiro[2]

[1]The Johns Hopkins University Applied Physics Laboratory, [2]Solar-Terrestrial Environment Laboratory, Nagoya University

Energetic Neutral Atom (ENA) imaging is a technique that enables remote imaging of space plasma and neutral clouds. Several current space-borne missions including Cassini, IMAGE, TWINS, Chandrayaan-1, IBEX, and several future missions such as JUICE make use of ENA imaging to investigate magnetospheric plasma acceleration and evolution; structure and acceleration mechanisms in the boundary between the heliosphere and the interstellar medium; and surface and atmosphere interactions (terrestrial upper atmosphere, terrestrial moon, the Galilean moons, and Titan).

Demonstration and Experiment for Space Technology and INterplanetary voYage (DESTINY; See Kawakatsu et al., this conference) is an innovative technology demonstration mission that is being proposed to JAXA with a low-thrust increase of the apogee of an equatorial orbit, followed by a lunar swing-by, and finally an insertion in to a halo orbit around the Sun-Earth L2 point. This trajectory provides a historical opportunity to perform ENA imaging of the two following compelling targets.

- **The terrestrial magnetosphere:** the equatorial vantage point will offer the first compound view of how ions flow out from the polar ionospheres, , plasma stagnation at the sub-solar magnetopause, ion energization in the plasmasheet out to about 20 R_E and the subsequent heating and earthward transport that forms the terrestrial ring current.

- **The boundary between the heliosphere and the interstellar medium:** the NASA/IBEX and Cassini missions have revealed a global pattern and possibly dynamics that are believed to originate from ions charge exchanging in the heliosheath. A multitude of compelling science questions have arisen from the combined analysis of these two data sets that have demonstrated that ENA imaging is perhaps the only tool capable of remotely probing the global structure and acceleration processes in this important region.

The key to observing these targets in a new light that goes beyond previous missions is the ability to image with high angular and energy resolution, with a wide field of view (FOV) that can image large portions of the regions simultaneously. In this presentation we discuss a concept of an ENA camera to perform imaging from DESTINY. The ENA camera design is capable of imaging ENAs in the $\leq$1keV - 100 keV range with an angular resolution down to 2 degrees and an energy resolution down to 20%. The current design has a FOV of 120x90 degrees, which dramatically increases the duty cycle over single-telescope detectors on spinning platforms.

Japan Geoscience Union Meeting 2014
(28 April - 02 May 2014 at Pacifico YOKOHAMA, Kanagawa, Japan)

PCG11-06 Room:421 Time:April 28 11:45-12:00

A compact, broad-beam, low-energy, LED-based, UV photoelectron source for the calibration of plasma analysers.

BEDINGTON, Robert[1*] ; SAITO, Yoshifumi[1]

[1]Solar System Science Division, Institute of Space and Astronautical Science, JAXA

Electrostatic electron analyser instruments are used to make in-situ measurements of space plasmas and are typically designed to detect electrons with energies from a few eV to a few tens of keV. To make optimal use of such instruments, a complete calibration is performed in a laboratory vacuum chamber before flight. An electron source and a moveable stage are used so that the instrument response can be characterised at every relevant electron energy and beam direction. For an ideal calibration, the source should be a uniform, collimated electron beam of controllable energy and flux, which is sufficiently broad in diameter to cover the entrance aperture of the electron analyser instrument being tested.

Various sources are used for such purposes, including radioactive beta-emitters and thermionic emission guns — although the former have fixed flux and are broad-band in energy, and the latter are expensive and produce only a narrow beam with limited energy ranges and limited dynamical control. To produce a broad, uniform, highly-controllable, long-lifetime, monoenergetic beam, UV photoelectron sources are generally preferable. These consist of a UV light source which illuminates a photocathode causing it to release photoelectrons. These electrons, which are released with negligible kinetic energy, are accelerated toward a high transmission grid by an electric field. The source can thus be as wide as the grid and the photocathode, as spatially uniform as the light that falls on the photocathode, and as collimated and monoenergetic as the photocathode and grid are flat and parallel (and thus the E field uniform). The electron flux can be adjusted by adjusting the UV lamp intensity, and the electron energy can be varied by adjusting the strength of the grid-photocathode E-field.

Traditionally the UV photons are created using gas discharge lamps (e.g. mercury, xenon, deuterium), however these typically have poor dynamical control, can create large amounts of background light and are bulky and inefficient. In recent years however, advances in solid-state technologies have enabled increasingly powerful, efficient and affordable LEDs of various UV wavelengths. Accordingly this has enabled compact, low-power, UV-stimulated electron sources that can have intensities that vary between 10 to 10^{-9} electrons cm^{-2} s^{-1}.

To meet the requirements for calibrating the electron analysers for the SCOPE (cross Scale COupling in Plasma universE) mission, a 9cm beam diameter, UV photoelectron source of this nature has been built and is being tested. Weighing approximately 1.5kg (excluding power supplies) and consisting of rugged, low cost components it can be mounted inside the vacuum chamber with great flexibility, including on a motorised translation stage.

The SCOPE mission requires several FESA (Fast Electron energy Spectrum Analyser) instruments for 10eV to 30keV electrons and several EISA (Electron Ion Spectrum Analyser) instruments for 10eV to 20keV electrons and ions. The first duty of the new electron source is the testing of prototype developments for the EISA instrument: namely measuring the electron transmission properties of carbon foil and assessing the secondary electron emission performance of candidate dynode materials

Keywords: Electron energy analyzer, Plasma spectrometer, Particle source, Ultra-violet photoelectron, Calibration, UV LED

Japan Geoscience Union Meeting 2014
(28 April - 02 May 2014 at Pacifico YOKOHAMA, Kanagawa, Japan)

PCG11-07 Room:421 Time:April 28 12:00-12:15

Characterization of Exoplanets with High Contrast Instruments

KAWAHARA, Hajime[1*]

[1]Department of Earth and Planetary Science, The University of Tokyo

Small exoplanets in the habitable zone (HZ) have been recently discovered by Kepler spacecraft and by ground-based radial velocity surveys. Now one of most interesting issues in this field is how to characterize them. In this presentation, I review our approaches to develop the instruments of direct imaging for the Thirty Meter Telescope (TMT) and other ground-based telescopes. These instruments aim to detect exoplanets in the HZ around late-type stars. I show that the search for the oxygen 1.27 micron bands as a biomarker is promising with the ground-based direct imaging (Kawahara+12 ApJ). I also show that the combination of extreme adaptive optics and coronaraphs for the direct imaging is also valuable for other characterization of exoplanets, for instance, for detection of exoplanetary molecules in close-in planets.

Keywords: exoplanets, terrestrial planets, direct imaging, biomarker

Japan Geoscience Union Meeting 2014
(28 April - 02 May 2014 at Pacifico YOKOHAMA, Kanagawa, Japan)

PCG11-08 Room:421 Time:April 28 12:15-12:30

Development of geocoronal Hydrogen Lyman Alpha Imaging CAmera (LAICA)

SATO, Masaki[1*] ; KAMEDA, Shingo[1] ; YOSHIKAWA, Ichiro[2] ; TAGUCHI, Makoto[1] ; FUNASE, Ryu[2] ; KAWAKATSU, Yasuhiro[3]

[1]Rikkyo University, [2]University of Tokyo, [3]JAXA

Hydrogen and helium atoms are the main constituents of the outermost region of the earth's atmosphere. These atoms resonantly scatter solar ultraviolet radiation causing an ultraviolet glow in this region, called geocorona. Hydrogen Lyman alpha radiation (121.567 nm) is the brightest. To date, various observations of the geocorona have been made. The geocorona comprises three main particle populations: ballistic, escaping, and satellite. Escaping particles are present at all altitudes, and they become particularly dominant at higher altitudes. In previous observations, the geocorona was identified to extend to an altitude of about 20R_E. The geocoronal distribution reveals asymmetries from day to night, dawn to dusk, and north to south. Recently, abrupt temporary increases (from 6% to 17%) in the total number of hydrogen atoms in the spherical shell from a geocentric distance of 3R_E to 8R_E have been recorded during several observed geomagnetic storms.

Past exploration of the geocorona has mainly been obtained from earth orbiters. Therefore, several low altitude (˜8R_E) observations have been made. On the other hand, in order to obtain the geocoronal distribution at high altitude, it is necessary to observe the geocorona from the outside in. However, there have been very few such observations (only Mariner 5, Apollo 16, and Nozomi). Among them, only Apollo 16 obtained an image. However, the observational FOV was about 10R_E.

In this study, we are developing a LAICA (geocoronal hydrogen Lyman Alpha Imaging CAmera) which will go onboard the very small deep space explorer PROCYON that will escape the earth and navigate interplanetary space. From such an explorer, our equipment can perform wide FOV (more than 25R_E) imaging of the geocoronal distribution. The first observation will be conducted one week after the launch for a period of one or two weeks. Subsequently, observations will continue for about three months. These observations will be conducted in higher temporal resolutions than that obtained from earth orbiters. The prototype of the LAICA has now been manufactured for testing and verification. And the flight model will have been completed by May. This presentation will show the development status.

Keywords: geocorona, Lyman alpha line, exosphere, earth's atmosphere

Japan Geoscience Union Meeting 2014
(28 April - 02 May 2014 at Pacifico YOKOHAMA, Kanagawa, Japan)

PCG11-P01 Room:Poster Time:April 28 18:15-19:30

Effects of finite electrode area ratio on Langmuir probe measurement

CHEN, Wen-hao[1*] ; JIANG, Guo-hsiang[1] ; HSU, Yu-wei[1] ; FANG, Hui-kuan[3] ; OYAMA, Koichiro[2] ; CHENG, Chio[2]

[1]Institute of Space and Plasma Sciences, National Cheng Kung University, [2]Plasma and Space Science Center, National Cheng Kung University, [3]Department of Physics, National Cheng Kung University

Langmuir probe(LP) is a widely used instrument for measuring electron density and temperature on satellites and rockets. Recently pico- and nano- satellites have become more popular, when the surface area of satellite is similar to the probe, the effects on LP measurement due to limited satellite surface area need to be considered, and these effects may cause LP measurement inaccurate. We have investigated the effect of satellite surface area, satellite and probe contamination and LP sweeping frequency in laboratory. Also we have found that the satellite and probe voltage will decrease when a large quantity of electrons are attracted by probe voltage and the contamination effect of satellite surface becomes major.

In summary, a solution to these problems is suggested.

Keywords: Langmuir probe, finite electrode area ratio, electrode surface contamination, pico/nano-satellite, electron temperature, electron density

Japan Geoscience Union Meeting 2014
(28 April - 02 May 2014 at Pacifico YOKOHAMA, Kanagawa, Japan)

PCG11-P02 Room:Poster Time:April 28 18:15-19:30

Development of Electron Temperature and Density Probe (TeNeP) for Nano- and Micro-satellites -II

JIANG, Guo-siang[1*] ; CHEN, Wen-hao[1] ; HSU, Yu-wei[1] ; OYAMA, Koichiro[2] ; CHENG, Chio[2]

[1]Institute of Space and Plasma Sciences, National Cheng Kung University, [2]Plasma and Space Science Center, National Cheng Kung University

The nano/micro-satellite becomes popular for the study of near earth environment. To measure the electron temperature (T_e) and electron density (N_e) in the ionosphere, we have developed the Electron Temperature and Density Probe (TeNeP). The TeNeP measures T_e and N_e based on principles of electron temperature probe (ETP) and planar impedance probe (IP). By combining systems of ETP and IP, T_e and N_e can be measured by one single probe. The TeNeP system has advantages not only as being small, light weighted and low power consumption that fulfills the needs of instruments onboard nano/micro-satellites. It also overcomes problems associated with electrode surface contamination and satellite/probe surface area ratio for DC Langmuir probes.

Keywords: Electron Temperature and Density Probe, nano/micro-satellite, Electron Temperature, Electron Density, electrode surface contamination, satellite/probe area ratio

Japan Geoscience Union Meeting 2014
(28 April - 02 May 2014 at Pacifico YOKOHAMA, Kanagawa, Japan)

PCG11-P03 Room:Poster Time:April 28 18:15-19:30

Development of the small probe system to measure plasma wave for the sounding rocket experiment

ONISHI, Keisuke[1*] ; ZUSHI, Takahiro[1] ; KOJIMA, Hirotsugu[1] ; YAMAKAWA, Hiroshi[1]

[1]Research Institute for Sustainable Humanosphere, Kyoto University

Plasma filling the space is very rarefied. Ions and electrons in space plasma don’t exchange their kinetic energy through their collision but through plasma waves. Hence observing plasma wave is essential for measuring space electromagnetic environment. We propose the multipoint plasma wave observation system that consisted of some sensor probes.

The present paper shows the achievements in designing the small sensor probe system which is dedicated to the sounding rocket experiment. The experiment is performance test of the small sensor probe which measures the standard wave in outer space. The necessary components for the small sensor probe are Li-Ion battery, wireless LAN device, plasma wave receiver, A/D converter, and CPU. All of them should be installed in the cubic body with an edge of 10 cm. Therefore, we chose one-chip microcomputers as wireless LAN device, A/D converter, and CPU. The wave receiver is miniaturized by designing the analog ASIC (Application Specific Integrated Circuit).

The wave receiver has the function of observing electromagnetic waves in the frequency up to 100 kHz and we want to take three-axis data at the same time. So, we should design A/D converter which has three simultaneous sampling and sampling frequency over 200 kHz to fulfill the sampling theorem.

We also designed other necessary systems, such as attitude sensor and wireless communication system with the sounding rocket.

Keywords: Space plasma, Plasama wave, Small sensor probe, Sounding rocket

Japan Geoscience Union Meeting 2014
(28 April - 02 May 2014 at Pacifico YOKOHAMA, Kanagawa, Japan)

PCG11-P04 Room:Poster Time:April 28 18:15-19:30

Plasma properties of the space plasma operation chamber at NCKU in Taiwan

FANG, Hui-kuan[1*] ; HSU, Yu-wei[2] ; CHEN, Wen-hao[2] ; JIANG, Guo-hsiang[2] ; OYAMA, Koichiro[3] ; CHENG, Chio[3]

[1]Department of Physics, National Cheng Kung University, [2]Institute of Space and Plasma Sciences, National Cheng Kung University, [3]Plasma and Space Science Center, National Cheng Kung University

The space plasma operation chamber (SPOC), a research facility designed to calibrate and test satellite/rocket-borne instruments and study space plasma processes, is constructed at NCKU in 2009. It is a cylindrical chamber of 2m in diameter and 3m in length. Plasma is produced by two back-diffusion type sources installed at the center of both chamber sides. The sources produce ions of controllable drifting energy from a few ten to several hundred eV and density up to 10^6 cm^{-3}. These ions are neutralized by thermal electrons emitted from Nickel cathodes, and collide with neutral molecules in the chamber of pressure ~2.2×10^{-4} Torr, and a plasma environment with ion temperature ~300K and electron temperature ~1000-3000K is formed in the chamber. This paper presents measurement results of a retarding potential analyzer (RPA), an electron temperature and density probe (TeNeP) and a Langmuir probe installed on the 2-axis moving system in SPOC. The thermal and beam component ion energy distributions at different distances from the ion source and the electron temperature/density spatial distributions in the SPOC will be presented. The collision process of ions with neutral molecules will also be discussed.

Keywords: Plasma properties, space plasma operation chamber, back-diffusion plasma source, retarding potential analyzer, electron temperature and density probe, Langmuir probe

Japan Geoscience Union Meeting 2014
(28 April - 02 May 2014 at Pacifico YOKOHAMA, Kanagawa, Japan)

PCG11-P05 Room:Poster Time:April 28 18:15-19:30

Construction of a calibration system for developing space-borne particle analyzers

ITO, Fumihiro[1*] ; HIRAHARA, Masafumi[1] ; SHIMOYAMA, Manabu[1] ; HAYASHI, Ayuko[1] ; ISHIGURO, Keisuke[1] ; KOGISO, Shun[1]

[1]Solar-Terrestrial Environment Laboratory, Nagoya University

To study physical phenomena in the terrestrial/planetary ionosphere and magnetosphere, it is essential to consider effects of ionized particles and neutral particles which influence each other. For detailed investigations, in-situ observations by spacecraft are required. So we have been developing space-borne particle analyzers for planetary atmospheres with new technologies. As developing these analyzers, it is necessary to construct an appropriate calibration system for them.

For the calibration, we set the analyzer in a vacuum chamber, and irradiate an ion beam towards it, and investigate its response. We have already been constructing a calibration system (ion beam line) which can irradiate an ion beam of which energy per charge range is from 10keV/charge to 150keV/charge. It is necessary, however, for the system to irradiate a suprathermal ion beam of several tens eV/charge. Particularly the system provides the other species of atomic ion beams: H^+, He^+, O^+, N^+, Ar^+, over the energy per charge range from 10eV/charge to 10keV/charge in addition to the other species of molecular ions like $N_2{}^+$, $O_2{}^+$, $CO_2{}^+$. We have been constructed a new beam line which can irradiate an ion beam of which energy per charge range is from 10eV/charge to 10keV/charge. Eventually, we will construct a calibration system which can control each beam line integratedly. In this paper, we report the development of the suprathermal ion beam line.

The suprathermal ion beam line is mainly composed of six parts: (a) ion source, (b) electromagnetic ion mass spectrometer, (c) beam expander, (d) main acceleration, (e) vacuum chamber, (f) multi-axial turntable. In the ion source, introduced gases form a gas cylinder are ionized by thermal electrons emitted from filaments. The ionized particles are initially accelerated and discriminated by the electromagnetic ion mass spectrometer. The discriminated ion beam is expanded by electrostatic 2D raster scanning, and is parallelized through the deceleration and acceleration in the beam expander. The ion beam is accelerated or decelerated for the specific energy in the main acceleration. The analyzer is set on the turntable in the chamber. Incident angles of the beam are controlled by changing the elevation and azimuth of the turntable system. We can control the beam property to change parameters: (1) thermal electrons flux and its acceleration voltage, (2) pre-acceleration voltage for ionized particles, (3) strength of the magnetic field of the electromagnet, (4) raster scanning and parallelized electric field for enlarging the beam cross-section uniformly, (5) main acceleration/deceleration voltage, (6) elevation and azimuth of the turntable system. We have also been developing a system which can control them centrally and remotely by using a computer. As interfaces, we use wireless LAN, RS-232, and USB and make programs with LabVIEW. We have added a monitoring and alert system for multipoint vacuum components.

So far, we have constructed the system expect for the turntable system and can irradiate a specific energy beam which is expanded and parallelized sufficiently. We set up a MCP measurement system to measure the beam intensity and cross-section profile. We will present the updated status of calibration system and the beam properties in this paper.

Keywords: calibration system, ion beam line, suprathermal ion beam, particles analyzer, magnetic ion mass spectrometer, remote control

Japan Geoscience Union Meeting 2014
(28 April - 02 May 2014 at Pacifico YOKOHAMA, Kanagawa, Japan)

PCG11-P06 Room:Poster Time:April 28 18:15-19:30

Verification of engineering models of medium energy particle analysers for ERG

KASAHARA, Satoshi[1*] ; ASAMURA, Kazushi[1] ; MITANI, Takefumi[1] ; TAKASHIMA, Takeshi[1] ; HIRAHARA, Masafumi[2] ; SHIMOYAMA, Manabu[2] ; YOKOTA, Shoichiro[1]

[1]ISAS, [2]Nagoya University

ERG (Exploration of energization and Radiation in Geospace) is a geospace exploration spacecraft, which is planned to be launched in FY2015. The mission goal is to understand the radiation belt dynamics especially during space storms. The key of this mission is the observations of electrons and ions in medium-energy range (10-200 keV), since these particles excite various electromagnetic waves (e.g., EMIC waves, magnetosonic waves, and whistler waves), which are believed to play significant roles in the relativistic electron acceleration and loss. Engineering models (EMs) of medium energy electron analyser and ion mass spectrometer have been developed and their performances and tolerances are tested. We report the results of these verification tests on EMs.

Keywords: Geospace exploration spacecraft ERG, medium energy ion, medium energy electron

Japan Geoscience Union Meeting 2014
(28 April - 02 May 2014 at Pacifico YOKOHAMA, Kanagawa, Japan)

PCG11-P07 Room:Poster Time:April 28 18:15-19:30

The results in the initial operation of the Neutral Mass and Velocity Spectrometer (NMS) onboard the CASSIOPE satellite

KURIHARA, Junichi[1*] ; HAYAKAWA, Hajime[2] ; KOIZUMI-KURIHARA, Yoshiko[2]

[1]Graduate School of Science, Hokkaido Univeristy, [2]The Institute of Space and Astronautical Science/Japan Aerospace Exploration Agency

We report on the results in the initial operation of the Neutral Mass and Velocity Spectrometer (NMS) instrument that is one of the Enhanced Polar Outflow Probe (e-POP) mission payloads onboard the CASSIOPE satellite. The scientific objective of the e-POP mission is to explore the escape of plasma from the polar ionosphere and the escape of neutral particles from the upper atmosphere and their interactions. The NMS instrument is expected to contribute toward a quantitative understanding of occurrence morphology of neutral particles with non-thermal velocity distributions. Therefore, NMS was developed based on a new principle, which is different from previous satellite-borne neutral mass spectrometers. The NMS instrument has an entrance aperture for incoming neutral particles is perpendicular to the ram direction of the satellite in order to take in neutral particles using the satellite velocity of 7-8 km/s. The NMS instrument consists of three parts: an ionization part, a detection part, and data processing part. The ionization part has an electrostatic thermionic electron gun to ionize the neutral particles by the electron beam. In the detection part, the ionized neutral particles are perpendicularly accelerated by the electric field for the Time of Flight (TOF) mass spectrometry, and the two-dimensional positions are detected with a Microchannel Plate (MCP) and a resistive anode. The two-dimensional position detection provides the relative velocities of neutral particles with a certain mass and the original velocity distribution is derived by subtracting the satellite velocity from the relative velocities.

In the initial operation of the satellite, though the NMS instrument had nothing wrong in the status, it was found that charged particles a few orders of magnitude more than expected were detected if the electron gun was off. At present, we suppose this can be caused by the incident neutral particles ionized by collisions with internal surfaces of the instrument. The influence of the collision in the velocity distribution measurement and the results of the analysis in the routine operation are discussed in this paper.

Keywords: neutral mass spectrometer, atmospheric escape, non-thermal velocity distribution

Japan Geoscience Union Meeting 2014
(28 April - 02 May 2014 at Pacifico YOKOHAMA, Kanagawa, Japan)

PCG11-P08 Room:Poster Time:April 28 18:15-19:30

Development and evaluation of the drive system of InSb imager mounted on infrared cameras for Jovian aurora

NOGUCHI, Eriko[1*] ; KOTANI, Koji[2] ; SAKANOI, Takeshi[1] ; KAGITANI, Masato[1] ; ICHIKAWA, Takashi[3]

[1]Geophys., Graduate School of Science, Tohoku Univ., [2]Electronics, Graduate School of Engineering, Tohoku Univ., [3]Astronomy, Graduate School of Science, Tohoku Univ.

In Tohoku University, infrared observation system is being developed for self-owned 60cm telescope. The purpose of this research is to develop a driving system of a Focal Plane Array (FPA) mounted on both an infrared camera and Echelle spectrometer and to evaluate observation possibility for various specific objects by establishing a method to determine adequate operating conditions based on detailed evaluation and analysis of a FPA.

First, from the previous researches, we estimated the required S/N to reveal the variation of some specific Jovian objects. In the case of H3+ aurora, the required S/N and the limit imaging time are 15 and 15s, respectively. For H2 aurora, they are 5 and 1200s. For equatorial temperature field, they are 5 and 7200s. Based on these, we showed the noise indicator, is composed of an upper limit of read noise and leakage current of FPA to realize the required S/N, considering the emission from a telescope and terrestrial atmosphere, and object.

Next, based on the driving mechanism of the FPA: CRC463(Raytheon) used in this research, we revealed that adequate bias is under -3.0V:Vdet, and over -4.0V :Vdduc. In this condition, Full Well(FW) is increased from 0.02V to 0.4V when bias(Vdet-Vdduc) is set at 0.6V, and we succeeded in the imaging of halogen lamp. And, we made improvements as follows.1. Increasing of conductivity of thermal path in the IR camera. This successfully decreased the temperature near FPA from 45K to 20K, resulting in the decrease of both the leakage current from 17,145e/s to 200e/s and the read noise from 453e$_{rms}$ to 320e$_{rms}$.2. Verifying the specific problem on CRC463, and we suggested new driving sequence based on frame to frame control. This resulted in the decrease in the read noise (to 200e$_{rms}$). This made it possible to precisely evaluate the performance of this system.3. Improving bias circuit in FPA driving system. The noise in output was reduced, resulting in the decrease of read noise (to 90e$_{rms}$).

Thanks to the above, it became possible to evaluate the performance parameters of FPA by Photon Transfer Curve method. As the result, in the case of 0.6V bias, DSNU and PRNU were evaluated as 38 ‰ and 16 ‰, respectively. In addition, leakage current, FW and system gain were 200e/s, 133,000e, and 10.9e/DN. We confirmed that the quantum efficiency is 0.85. We also evaluated the NEDT. With a 2.3μm filter and incident flux of 400K of blackbody, the NEDT reaches 45mK, is the equivalent performance compared to the third generation FPAs. As well, the performance parameters of our system other than the leakage current are equivalent to those of the NASA's IRTF system using the same FPA.

And, we evaluated the bias dependences on FW, leakage current and system gain. Using the results, we established the method to determine the adequate bias setting to realize the maximum S/N for specific object. As a result, following estimations were obtained. Using this FPA driving system, H3+ aurora can be observed at the maximum S/N=30 when the bias and exposure time are set at 0.5V and 15s. In the case of H2 aurora, the maximum S/N is 3.14 after binning, when the bias and imaging time are 0.4V and 1200s, respectively. Obtained S/N is below the requirement. It is needed to decrease leakage current under 81e/s. The case of temperature field, the maximum S/N is 52.7 with accumulating 28times, when total imaging time is 7200s, and the bias is set at 0.4V. To decrease accumulating times, bias should be set at 0.9V. If the leakage current will be under 100e/s, the S/N will be over 40 with an accumulation.

In summary, we developed FPA driving system for IR observation instrument mounted on telescope of Tohoku University for planetary observation. We evaluated the performance in detail, and developed the method to determine the adequate bias conditions for each observational object. Decreasing the leakage current is the remaining issue since it is two orders of magnitude larger than the FPA ' s specification.

Keywords: Focal plane array drive system, IR telescope of Tohoku Univ., long-term observation for planet, NASA IRTF

Japan Geoscience Union Meeting 2014
(28 April - 02 May 2014 at Pacifico YOKOHAMA, Kanagawa, Japan)

PCG11-P09 Room:Poster Time:April 28 18:15-19:30

A study for candidate scientific instruments for DESTINY

IWATA, Takahiro[1*] ; KAWAKATSU, Yasuhiro[1]

[1]Institute of Space and Astronautical Science, JAXA

DESTINY (Demonstration and Experiment of Space Technology for Interplanetary Voyage) aims to demonstrate new technologies of high energy orbit insertion, large scale ion engine, ultra light-mass solar panel, etc., which will be useful for deep-space mission by Epsilon launch vehicles. DESTINY has possibility to equip scientific mission instruments when system design makes the margin of the resource. DESTINY can conduct scientific observations for a half to one year on the Halo orbit of solar-terrestrial Lagrange 2 (L2) point. If conditions permit, DESTINY will leave L2 Halo orbit, and transfer to the next destination. Potential scientific topics include in-situ observation and remote sensing from L2 for, such as, plasma, energetic particles, and the magnetosphere in the plasma sheet of terrestrial magnetosphere. It is considered to be useful for the pilot observations for future infrared, gamma-ray, and cosmic-ray space astronomical telescope. It is probable to observe and monitor Near Earth Objects (NEO), inter-planetary and inter-stellar dust. It is also valuable to observe ultra-violet and X-ray emission from planetary phenomena. The mass allocated for the instruments is, however, currently estimated as in the range of between a few and ten kilograms. DESTINY will play roles as pilot experiments for these full-scale observations.

Keywords: Epsilon Rocket, DESTINY, Lagrange point

Japan Geoscience Union Meeting 2014
(28 April - 02 May 2014 at Pacifico YOKOHAMA, Kanagawa, Japan)

PCG11-P10 Room:Poster Time:April 28 18:15-19:30

BepiColombo Euro-Japan Joint mission to Mercury: MMO Project Status update

HAYAKAWA, Hajime[1*] ; MAEJIMA, Hironori[1] ; BEPICOLOMBO, Project team[1]

[1]ISAS/JAXA

BepiColombo is a ESA-JAXA joint mission to Mercury with the aim to understand the process of planetary formation and evolution in the hottest part of the proto-planetary nebula as well as to understand similarities and differences between the magnetospheres of Mercury and Earth.

The baseline mission consists of two spacecraft, i.e. the Mercury Planetary Orbiter (MPO) and the Mercury Magnetospheric Orbiter (MMO). JAXA is responsible for the development and operation of MMO, while ESA is responsible for the development and operation of MPO as well as the launch, transport, and the insertion of two spacecraft into their dedicated orbits.

MMO is designed as a spin-stabilized spacecraft to be placed in a 400 km x 12000 km polar orbit. The spacecraft will accommodate instruments mostly dedicated to the study of the magnetic field, waves, and particles near Mercury. While MPO is designed as a 3-axis stabilized spacecraft to be placed in a 400km x 1500 km polar orbit. Both spacecraft will be in same orbital plane.

Critical Design Review(CDR) for MMO project is completed in November 2011 while ESA Spacecraft CDR is completed in Novemver 2013. MMO stand alone FM AIV is started from September 2012 and expected to be finished on this autumn. MMO FM will be transported to ESA/ESTEC to attend stack level (MCS) final AIV. BepiColombo is expected to be launched in 2016 summer.

10th BepiColombo science working team (SWT) meeting, which discusses science related matters, was held on September 2013 at Lapland. In this paper, we will report the latest information of BepiColommbo MMO project status.

Keywords: Mercury, Planetary Exploration, International Collaboration

Japan Geoscience Union Meeting 2014
(28 April - 02 May 2014 at Pacifico YOKOHAMA, Kanagawa, Japan)

PCG11-P11 Room:Poster Time:April 28 18:15-19:30

Magnetic Cleanliness of BepiColombo MMO

MATSUOKA, Ayako[1*] ; NAKAZAWA, Satoru[2]

[1]ISAS/JAXA, [2]JSPEC/JAXA

In the terrestrial planets, Earth and Mercury has the intrinsic dipole magnetic field. The Mercury magnetic moment is relatively smaller than that of Earth; the magnetic field intensity on the Mercury surface is about 1 percent of that on the earth surface. Therefore the Mercury magnetospheric condition is significantly affected by the variation in the solar wind, and varies with the short period. The magnetic field around Mercury and its nature has been studied by MESSENGER which was launched by NASA and arrived at Mercury in 2011. However, because the magnetic field around Mercury is summation of the intrinsic and external origin, and MESSENGER always has the perigee in the north hemisphere, the Mercury intrinsic magnetic moment has not been determined accurately. BepiColombo is planed to be launched in 2016 and arrive at Mercury in January 2024. It consists of two satellites, MMO built by JAXA, and MPO by ESA, which will observe together the magnetic field around Mercury. BepiColombo has advantages to determine the accurate magnetic moment, which is one of the major scientific target of the BepiColombo project. The orbit shape is not biased, and the measurement at two locations enables to separate the intrinsic field and the external contribution. For the accurate measurement of the magnetic field, it is very important to suppress the magnetic noise generated by the components installed on the satellite. In the phase of the development of the satellite, the design of the every component was examined not to cause the magnetic noise which would degrade the magnetic field measurement. During the manufacturing period, components were controlled not to be magnetized. The means of the magnetic cleanliness of MMO and the result of the system EMC test, where the magnetic moment of MMO was measured, are reported.

Keywords: Mercury, magnetic field

Japan Geoscience Union Meeting 2014
(28 April - 02 May 2014 at Pacifico YOKOHAMA, Kanagawa, Japan)

PCG38-01 Room:423 Time:May 1 09:00-09:15

Surface zonal flows induced by thermal convection in rapidly rotating thin spherical shells

SASAKI, Youhei[1*] ; TAKEHIRO, Shin-ichi[2] ; ISHIOKA, Keiichi[3] ; NAKAJIMA, Kensuke[4] ; HAYASHI, Yoshi-yuki[5]

[1]Department of Mathematics, Kyoto University, [2]Research Institute for Mathematical Sciences, Kyoto University, [3]Department of Earth and Planetary Sciences, Kyoto University, [4]Department of Earth and Planetary Sciences, Kyushu University, [5]Department of Earth and Planetary Sciences, Kobe University

Surface flows of Jupiter and Saturn are characterized by the broad prograde zonal jets around the equator and the narrow alternating zonal jets in mid- and high-latitudes. It is not yet clear whether those surface jets are the result of fluid motions in the ”shallow” weather layer, or they are produced by convective motions in the ”deep” region. ”Shallow” models consider atmospheric motions driven by the solar differential heating and the intrinsic heat flow from the deeper region under the assumption of hydrostatic balance in the vertical direction as a result of the thin atmospheric layer compared with the radius of the planet. These models can produce narrow alternating jets in mid- and high-latitudes, while the equatorial jets are not necessarily prograde. On the other hand, ”deep” models, which describe thermal convection in rapidly rotating spherical shells whose thickness is comparable to the radius of the planet, can produce equatorial prograde flows easily, while it seems to be difficult to generate alternating jets in mid- and high-latitudes.

Recently, Heimpel and Aurnou (2007) proposed thin spherical shell models and show that the equatorial prograde zonal jets and alternating zonal jets in mid- and high-latitudes can be produced simultaneously when the Rayleigh number is sufficiently large and convection becomes active even inside the tangent cylinder. However, they assume eight-fold symmetry in the longitudinal direction and calculate fluid motion only in the one-eighth sector of the whole spherical shell. Such artificial limitation of the computational domain may influence on the structure of the global flow field. For example, zonal flows may not develop efficiently due to the insufficient upward cascade of two-dimensional turbulence, or stability of mean zonal flows may change with the domain size in the longitudinal direction. In the present study, we perform numerical simulations of thermal convection in the whole thin spherical shell domain while coarse spatial resolution and slow rotation rate compared to Heimpel and Aurnou (2007) are used due to the limit of computational resources.

We consider Boussinesq fluid in a spherical shell rotating with constant angular velocity. The non-dimensionalized governing equations consist of equations of continuity, motion, and temperature. The non-dimensional parameters appearing in the governing equations, the Prandtl number, the Ekman number, the modified Rayleigh number, and the radius ratio, are fixed to 0.1, 10^{-4}, 0.05, and 0.75, respectively. The initial condition of the velocity field is state of rest and that of the temperature field is conductive state with random temperature perturbations. After time integration for 35000 rotation period, kinetic energy is saturated and statistically steady state seems to establish. Obtained velocity field satisfies Taylor-Proudman theorem; it is almost uniform in the direction of the rotation axis. An equatorial prograde surface zonal jet emerges in the region outside the tangent cylinder. In the inside of the tangent cylinder, the surface zonal flows are retrograde, but eastward spike features appear near the tangent cylinder in low latitudes. Correspondingly, coherent small scale convective motions exist in these latitudinal zones. It is expected that these convective motions excite topographic Rossby waves which remove westward angular momentum from these zones, producing eastward spike features. This mechanism may explain the origin of the strong thin jet at about 25 degrees north observed on the surface of Jupiter.

Acknowledgement : Numerical computations were carried out on the Earth Simulator (ES2) at the Japan Agency for Marine Earth Science and Technology.

Reference : Heimpel, M., Aurnou, J. (2007) Icarus, 187, 540–557.

Keywords: atmospheres of the gas giant planets, banded structure, equatorial prograde jet, Rossby waves, Jupiter, Saturn

Japan Geoscience Union Meeting 2014
(28 April - 02 May 2014 at Pacifico YOKOHAMA, Kanagawa, Japan)

PCG38-02 Room:423 Time:May 1 09:15-09:30

Numerical modeling of Cloud-level Convection in Venus Atmosphere

SUGIYAMA, Ko-ichiro[1*] ; KAWABATA, Takuya[2] ; ODAKA, Masatsugu[2] ; NAKAJIMA, Kensuke[2] ; ISHIWATARI, Masaki[3]

[1]ISAS/JAXA, [2]Department of Cosmosciences, Graduate School of Science, Hokkaido University, [3]Graduate school of Science, Kobe University

Cellular convection has long been thought to occur in the cloud layer of Venus, because some evidences for convection are obtained from radio occultation and spacecrafts data. However, the convective structure in the cloud layer is still unclear. Some numerical studies are performed to examine convective structure of the cloud layer (Baker et al., 1998, 2000, Imamura et al., 2014), but the domain of the model atmosphere in their numerical experiment is two-dimensional. In this presentation, we perform three-dimensional numerical calculation of convection using the same settings of Baker et al. (1998) in order to investigate a possible three-dimensional structure of convection in the cloud layer in statistically steady state.

The numerical model used in this paper is a cloud resolving model that is mainly used to simulate moist convection in Jupiter's atmosphere (Sugiyama et al., 2009, 2011, 2014), but condensation and chemical reaction are not considered in this experiment. The same sub-grid turbulence and radiation processes of Baker et al. (1998) are included in our model. The settings of the experiment are also based on those of Baker et al. (1998). In these settings, the altitudes of the lower and upper boundaries are 40 km and 60 km levels, respectively, and the layer between 48 km level and 55 km level is almost neutral.

The vertical motion obtained in our numerical experiment is characterized by wide, weak, warm updrafts and narrow, strong, cold downdrafts. This qualitative characteristic of convective motion is consistent with that obtained in Baker et al. (1998). The maximum velocity of downdrafts is about 10 m/s, while the mean vertical velocity is about 3 m/s. The downdrafts are driven by the cooling caused by the turbulent diffusion above the neutral layer and thermal flux at the upper boundary. The horizontal cell size is about 20 km, which is somewhat smaller than that of observed typical cloud-top cells in ultraviolet images; the sizes of the observed cells are typically 100-200 km and in some cases a few tens of kilometers across.

Keywords: Venus atmosphere, convection, numerical modeling

Japan Geoscience Union Meeting 2014
(28 April - 02 May 2014 at Pacifico YOKOHAMA, Kanagawa, Japan)

PCG38-03 Room:423 Time:May 1 09:30-09:45

Convectively-generated gravity waves on Mars and their influence on the upper atmosphere

WATANABE, Ayuka[1] ; IMAMURA, Takeshi[2*] ; MAEJIMA, Yasumitsu[3]

[1]Department of Earth and Planetary Science, The University of Tokyo, [2]Institute of Space and Astronautical Science, Japan Aerospace Exploration Agency, [3]Meteorological Research Institute, Japan Meteorological Agency

Gravity waves in the Martian atmosphere have been identified through various observations. The sources of the waves are still unclear, although topographically-generated gravity waves have been studied using regional models and incorporated into Mars GCMs with parameterizations. Here we investigate convective generation of gravity waves on Mars using a two-dimensional regional model based on the non-hydrostatic meteorological model CReSS. The heating source of the convection model is considered a horizontally-uniform heating of the atmosphere near the surface by sunlight and a localized heating caused by absorption of sunlight by dust clouds. The results show that tntense convection is generated as a result of a thin atmosphere, leading to generation of short-period, large-phase velocity (both in horizontal and vertical) waves. Such waves can reach high altitudes without serious dissipation; the horizontal wavelengths and the amplitudes of the gravity waves reproduced in the lower thermosphere are consistent with the density fluctuations measured during aerobraking experiments. The waves attain saturation amplitudes above ˜80 km altitude.

We further investigated the properties of vertical propagation and dissipation in the thermosphere using linear wave solutions based on the wave parameters observed in the convection experiment. Gravity waves reaching the thermosphere are damped by molecular diffusion and heat the atmosphere. The vertical profile of the heating rate shows two maxima: the lower one is located near the altitude where the amplitude peaks, and is generated by the sensible heat flux divergence, and the upper one is generated by the viscous dissipation of kinetic energy. These heating rates are comparable to other dominant processes such as EUV heating.

Keywords: Mars, gravity wave, convection

Japan Geoscience Union Meeting 2014
(28 April - 02 May 2014 at Pacifico YOKOHAMA, Kanagawa, Japan)

PCG38-04 Room:423 Time:May 1 09:45-10:00

A proposal of Martian dust devil observation by combination with eletromagnetic and acoustic wave measurements

YAMAMOTO, Masa-yuki[1*] ; TAKAHASHI, Yukihiro[2] ; ISHISAKA, Keigo[3] ; SATO, Mitsuteru[2] ; OGOHARA, Kazunori[4] ; KAMOGAWA, Masashi[5] ; MIYAMOTO, Hideaki[6] ; ABE, Takumi[7]

[1]Kochi University of Technology, [2]Hokkaido University, [3]Toyama Prefectural University, [4]University of Shiga Prefecture, [5]Tokyo Gakugei University, [6]The University Museum, The University of Tokyo, [7]Institute of Space and Astronautical Science, Japan Aerospace Exploration Agency

Mars 2020 rover is planned to launch by NASA in 2020, as the almost same package of the Mars Science Laboratory (named Curiosity after its successful landing in August 2012). The announcement of opportunity (AO) for scientific/technology payloads to be onboard the NASA Mars 2020 rover was called for to the scientists community in world wide in September 2013. Here, we introduce our proposed instrument designed for electromagnetic (EM) and acoustic wave (AW) measurements that have never been operated on Mars.

Low-frequency EM and AW are important for monitoring atmospheric events because of their long-distant propagating characteristics more than 1000 km. Electrical discharges could be a hazard for instruments and future human activities on Mars, hence it should be treated as one of the strategic knowledge gaps (SKGs) for future missions. Our concept is that combining EM and AW measurements, precise distance information of dust storms and/or dust devils can be obtained by using two independent velocities of light (c) and sound (Cs) because discharges could be generated by electro-static processes in low-pressure dusty atmosphere and the process also generates shock waves in acoustic/infrasonic pressure wave range. Moreover, wind roaring sound, shock waves by meteors entries, and operational sounds by rover itself will be recorded as the world first ”Martian sound.”

Our EM and AW detection system consists of antennae, microphones, and common receiver circuits with on-board software. For E-field detection, a legacy monopole of 10 cm will be used as a vertical antenna. Two orthogonal loop antennae should be applied for B-field with direction-finding system. However, instead of pop-up devices, these 3 antennae will be compressed into a fixed 10 cm cubic antenna to be equipped on rover surface. Although a legacy receiver circuit can be used, we can minimize it into a postcard size by applying a newly-developed chip device. Analyses of EM and AW for monitoring discharges can be operated by on-board software to reduce data volume. Similar software is used in GLIMS operated on JEM-Kibo/ISS, where only the most significant events will be sent to the Earth in priority basis.

EM sensing in the Martian atmosphere is significant for the future human exploration on Mars. Although the environment on Martian surface is too severe to survive even in fair climate condition, human activities on Mars is obviously dangerous especially when it is under the storm-like condition. Thus, dust devils on Martian surface are significant for the future human exploration, especially, electrostatic discharge events could be serious hazards for astronauts as well as for Martian base facilities. However, the EM condition on the Martian surface has never been measured in detail. Hence, we consider the remote-sensing of the dust devils and discharge events from a single site on Mars with simple sensors could be a potential instrumentation.

Here, as a proposal to the NASA 2020 AO, we introduce one of the most promising remote-sensing methods for dust devils and discharge events by using a combination of EM and AW. According to its rarefied atmospheric pressure condition on Martian surface, about 1/100 of the Earth’s surface, dust particles can easily be flown up by surface wind then could effectively produce charged particles by convection. Based on previous studies on the Earth, such charged particles possibly produce discharge events. Drastic changes in EM fields can be observed even at far-distant observatory, more than 1000 km away from the exact coordinates of discharges. AW also could be a remote-sensing method when there exists the atmosphere. Especially, low frequency AW less than 1 Hz can propagate for long distance more than 100 km even in the rarefied atmosphere. If we use two independent velocities of light (for EM) and sound (for AW), we can identify source coordinates of every discharge events within a few tenth km.

Keywords: Mars, electromagnetic wave, acoustic wave, discharge, dust devil, lander

Japan Geoscience Union Meeting 2014
(28 April - 02 May 2014 at Pacifico YOKOHAMA, Kanagawa, Japan)

PCG38-05 Room:423 Time:May 1 10:00-10:15

Observation of a few months temporal variability of UV brightness in Venus with Pirka telescope

IMAI, Masataka[1*] ; TAKAHASHI, Yukihiro[1] ; WATANABE, Shigeto[1] ; WATANABE, Makoto[1]

[1]Department of Cosmosciences, Graduate School of Science, Hokkaido University

The superrotation, which is a phenomenon that Venusian atmosphere moves westward at a velocity 60 times faster than the planetary rotation, is a unique atmospheric system of Venus. There are several theories to explain what drive the superrotation, but it is still unknown. Yamamoto and Tanaka (1997) suggested that the Kelvin wave in equator and the Rossby wave in mid-latitude, which propagating at an altitude of 70 km or higher, play an important role in the driving of the superrotation. They also suggested that the Kelvin and Rossby wave forms the Y-feature when they balanced. The Y-feature is the bright and dark pattern in UV range, and it has a planetary scale. From the Pioneer Venus spacecraft observation, it was revealed that the propagation and the distribution of UV features cause variation in several time scales [Del Genio and Rossow, 1982, 1990], but it has not been understood which dynamical processes determine these time scales. In our study, we focused on about 2-month brightness variation. That variation seems to be strongly associated with the Rossby wave because there is inverse correlation between low-latitude and mid-latitude, suggesting the existence of quasi-barotropic eddy. After the Pioneer Venus mission, there were no further observations to reveal the mechanism of the 2-month variation.

In this study, we observed the Venusian UV brightness variation as a function of latitude and time. We carried out the ground-based observations with Multi-Spectral Imager (MSI) onboard the Pirka telescope. The Pirka 1.6 m telescope, owned and operated by the graduate school of science in Hokkaido University, is primarily dedicated to the observations of solar planets. Using this system, we can monitor the planetary scale UV-features ($\sim$ 5,000 km) in Venus atmosphere over 8 hours in a day at 365 nm wavelength. In 2013, we carried out about 2 months total observations from mid-Aug. to mid-Nov.

There was a problem to estimate the absolute brightness variation because we observed Venus in the daytime and the correction of the extinction of the Earth's atmosphere had some difficulty. To investigate the brightness variation, we perform additional procedure for each image that we normalize the brightness in each latitudinal band with the mean brightness in 70^{o}N-70^{o}S area. Our results showed two types of UV feature. One showed the strong periodicity in both of equatorial region and mid-latitude and it also had the symmetric structure between northern and southern hemisphere. The other one did not show the strong periodicity and had the symmetric structure. We suppose that the Y-feature does not always exist and the balance of the Kelvin and Rossby wave might be lost when the periodicity and the symmetry disappear. From our observations, it seems to take more than 2 months to return from the asymmetric phase to symmetric phase. Additionally, we found that 2-month variation of brightness in each latitudinal band showed weak inverse correlation between both hemispheres like a seesaw. Such inverse correlation was not seen in the past Pioneer Venus observation. In this paper, we discuss the dynamical state of Venus during our observations and show further observation plans.

Keywords: Venus, Pirka telescope, superrotation, Y-feature

Japan Geoscience Union Meeting 2014
(28 April - 02 May 2014 at Pacifico YOKOHAMA, Kanagawa, Japan)

PCG38-06 Room:423 Time:May 1 10:15-10:30

Spatiotemporal variations of brightness temperatures in the middle atmosphere of Venus revealed by Subaru/COMICS

SATO, Takao M.[1*] ; SAGAWA, Hideo[2] ; KOUYAMA, Toru[3] ; IMAMURA, Takeshi[1] ; SATOH, Takehiko[1]

[1]Institute of Space and Astronautical Science, Japan Aerospace Exploration Agency, [2]National Institute of Information and Communications Technology, [3]National Institute of Advanced Industrial Science and Technology

The middle atmosphere (60-100 km altitudes) of Venus plays an important role in determining its own environment. Venus is completely shrouded by a curtain of dense clouds (50-70 km) with total optical thickness of 20-40 at visible wavelengths. The upper sulfuric acid (H_2SO_4) clouds reflect ˜76% of the incident solar radiation back to space (Crisp and Titov, 1997). More than 70% of the solar energy absorbed by Venus is deposited at altitudes higher than 64 km mainly due to absorption of unknown UV absorbers mixed in the upper cloud (Tomasko et al., 1980, 1985). This horizontally and vertically unusual heating in the cloud layer excites the thermal tides, which are the key process to understand the atmospheric super-rotation. In order to elucidate this mysterious atmospheric phenomenon, it is fundamental to investigate horizontal and vertical thermal structure in the middle atmosphere.

We conducted Venus observations at three mid-infrared wavelengths (8.66, 11.34, and 12.84 micron) with the Cooled Mid-Infrared Camera and Spectrometer (COMICS), mounted on the 8.2-m Subaru Telescope, during the period of October 25-29, 2007 (UT). Thermal radiations at these wavelengths (brightness temperature: 230-240 K) are most sensitive to altitudes of ˜70 km. The angular diameter of Venus and the solar phase angle (Earth-Venus-Sun angle) at the observation period were ˜25 arcsec and ˜90 deg (i.e., both the dayside and nightside hemispheres were observed), respectively. The spatial resolution of the observed images, which was determined by astronomical seeing, was ˜200 km for the sub-observer point. This was the first time that such high spatially-resolved images had been obtained at mid-infrared wavelengths (Mitsuyama et al., 2008).

From images at 8.66 micron, we obtained three important findings. First, the brightness temperatures at cloud top altitudes (˜70 km) in north high-latitudes seemed to be synchronized with those in south ones during the period, which implies that the rotational speeds of them were nearly identical in both high-latitudes. Such atmospheric synchronization has not been reported by any previous mid-infrared ground-based (Diner et al., 1982; Orton et al., 1991) and spacecraft (Taylor et al., 1980; Zasova et al., 2007) observations mainly because of low spatial resolution and tilt of Venus' north pole toward the Earth, and of restricted distribution of sounding, respectively. Second, the center-to-limb curves (dayside and nightside) showed a day-night asymmetry across the morning terminator except that those on October 25 were nearly symmetric. The magnitude of this asymmetry was variable from one day to the next. Such day-night asymmetric features would result from the differences of temperature and/or cloud optical thickness. Finally, there were some streaky and patchy patterns in the whole disk after high-pass filtering. These patterns, typical amplitude of which was ˜0.5 K, varied from day to day. It is worth noting that streaky patterns obtained on October 28 were similar to a well-known horizontal Y-shape structure seen in UV. The above three findings were commonly seen at the other wavelengths.

In this talk, we show the observational results and discuss what kind of atmospheric parameters are responsible for the anomalous features of planetary scale center-to-limb curves through radiative transfer calculations.

Keywords: Venus, middle atmosphere, ground-based observation, atmospheric synchronization, center-to-limb curve, small-scale streaky and patchy patterns

Japan Geoscience Union Meeting 2014
(28 April - 02 May 2014 at Pacifico YOKOHAMA, Kanagawa, Japan)

PCG38-07 Room:423 Time:May 1 10:30-10:45

Energy spectra of atmospheric motions simulated by a high-resolution general circulation model of Venus

KASHIMURA, Hiroki[1*] ; SUGIMOTO, Norihiko[2] ; TAKAGI, Masahiro[3] ; OHFUCHI, Wataru[4] ; ENOMOTO, Takeshi[5] ; TAKAHASHI, Yoshiyuki O.[6] ; HAYASHI, Yoshi-yuki[6]

[1]ISAS, [2]Keio Univ., [3]Kyoto Sangyo Univ., [4]JAMSTEC, [5]DPRI, Kyoto Univ., [6]CPS/Kobe Univ.

The dynamics of the Venus atmosphere is unclear because of the lack of observational data. Many researchers have developed General Circulation models (GCM) for the Venus atmosphere and have attempted to simulate atmospheric motions of Venus. Because the planetary rotation period of Venus is much longer than the Earth, long-term integrations are needed for the solution to achieve a statistically steady state. Therefore, the simulations have been performed by low-resolution ($\sim$ T21; i.e., about 5.6 deg x 5.6 deg grids) models. We have developed a simplified Venus version of the AFES (Atmospheric GCM for the Earth Simulator) (Sugimoto et al. 2012) and performed a very high-resolution simulation. In this paper, we report and discuss kinetic energy spectra obtained from the high-resolution simulation.

The dynamical core of AFES is descretized by the spectral method in horizontal. The model resolution is T159 (i.e., about 0.75 deg x 0.75 deg grids) and L120 (Δz is about 1 km). In the model, the atmosphere is dry and forced by the solar heating with the diurnal change and Newtonian cooling that relaxes the temperature to the zonally uniform basic temperature which has a virtual static stability of Venus with almost neutral layers. To prevent numerical instability, the biharmonic hyper-diffusion is included with 0.01 days of e-folding time for the truncation wavenumber. The coefficient of the vertical eddy diffusion is 0.15 m^2 s^{-1}. A sponge layer is set above 80 km to prevent the reflection of waves. The dry convective adjustment scheme is used to avoid statically unstable state. A fast zonal wind in a solid-body rotation and the temperature field that balances (gradient wind balance) with the zonal wind are given as the initial state. Time-integrations are performed until the solution achieves a statistically steady state.

We calculate the horizontal kinetic energy per unit mass per unit wavenumber from the spectral coefficients of the vertical vorticity and horizontal diffusion (Koshyk & Hamilton 2001). The energy decreases by –5/3 power law in a range from wavenumber 4 to 45. Both in lower and higher wavenumber sides, the energy shows higher decreasing rate.

A feature of the energy spectral of aircraft observations (Nastrom & Gage 1985) and high-resolution GCM calculation of the Earth (Takahashi et al. 2006) is that the energy decreases by –3 power law in low-wavenumber range (n $<$80) and by –5/3 power law in higher range. Terasaki et al. (2011) have reported that the –3 power law in synoptic scale is due to Rossby waves and the –5/3 power law in the mesoscales is due to gravity waves. The energy spectrum that we have obtained shows –5/3 power law in the wavenumber range lower than the Earth cases. This implies that the gravity waves may dominant even in scales of several thousand kilometers in the Venus atmosphere. A reason for the Rossby wave not being dominant in these scales may be the slow planetary rotation. The effect of the hyper-diffusion may appear in the range near the truncation wavenumber.

[Acknowledgement] This study was conducted under the joint research project of the Earth Simulator Center with title “Simulations of Atmospheric General Circulations of Earth-like Planets by AFES.”

Keywords: Venus atmosphere, general circulation model, high-resolution, kinetic energy spectra

Japan Geoscience Union Meeting 2014
(28 April - 02 May 2014 at Pacifico YOKOHAMA, Kanagawa, Japan)

PCG38-08 Room:423 Time:May 1 11:00-11:15

Microphysical properties of Venusian upper hazes observed with an Imaging-Polarimetry system " HOPS "

ENOMOTO, Takayuki[1*] ; SATOH, Takehiko[2] ; NAKATANI, Yoshikazu[3] ; SATO, Takao M.[1] ; HOSOUCHI, Mayu[4] ; NAKAKUSHI, Takashi[5]

[1]SOKENDAI, [2]ISAS/JAXA, [3]Kyoto University, [4]University of Tokyo, [5]Wakayama University

The high albedo of Venus is due to optically very thick main cloud deck which covers the whole planet. The small particles (hazes) which were distributed above the main cloud deck were discovered by the observations from Pioneer Venus Orbiter (PVO) which arrived at Venus in December 1978. Kawabata et al. [1980] found, from the data of Orbiter Cloud Photopolarimeter (OCPP) onboard PVO, that abundant sub-micrometer sized particles " hazes " were distributed above the main cloud deck mostly in polar regions. The optical thickness of the haze layer was reported to reduce during the PVO mission period [Sato et al., 1996]. Coincidently, decrease of the SO_2 abundance was also reported [Esposito, 1985]. After the PVO mission, however, the variation of the optical depth of the hazes has not been studied, so it is not clear what this correlation means for the generation and maintenance of hazes and whether a similar correlation between them exist today. Our study provides the latest information about the microphysical properties of hazes by ground-based monitoring observations which have not been done since PVO.

To monitor the distribution of the Venusian upper hazes, we developed an imaging-polarimetry system " HOPS " (Hida Optical Polarimetry System) and performed observations by attaching it to the 65cm refracting telescope at Hida Observatory of Kyoto University. As HOPS provides spatially resolved polarization map, polarization in an arbitrary area can later be obtained just by summing up the corresponding pixels for comparison with previous measurements. This is the biggest advantage of imaging polarimetry against the aperture measurements. HOPS is a " two beam type " polarimetry instrument which enables high accurate measurements against variable atmospheric conditions. The effect of variable atmospheric transparency, non-uniformity of sensitivities over the CCD pixels and different throughputs of two beams can be corrected through arithmetic operations in image processing.

The observations were carried out at solar phase angles around 39deg. (Jul., 2013), 56deg. (Aug., 2013), 58deg. (Oct., 2012), 85deg. (Aug., 2012) and 129 deg. (May, 2012) at 4 selective wave lengths 438nm (B), 546nm (G), 650nm (R) and 930nm (IR); G and IR data can be compared with similar wavelength data of PVO/OCPP. We averaged observed degree of linear polarization over the polar regions (latitudes higher than 60 deg.) and compared with the report of PVO. A clear difference is seen in IR data. The neutral point of our data is found to be at around 75 deg. while the point of PVO/OCPP is around 40 deg. This difference may indicate the different situation of the distribution and size parameters of hazes.

To analyze the obtained polarization data, we developed a radiative transfer calculation code using Adding?Doubling method with the Stokes parameters fully treated [de Haan et al., 1987, Hovenier et al., 2004]. It is possible to analyze three wavelengths IR, R, and G neglecting the Rayleigh scattering effect because Rayleigh scattering cross-sections for IR, R G and B are about 0.21, 0.083, 0.041, 0.0096μm^2 while Mie scattering cross-sections for a main cloud particle are the order of 7μm^2. We treated haze particle effective radius r_{eff} and optical depth τ_h as free parameters, respectively. The effective variance of hazes was fixed to 0.18 and parameters for main cloud layer were taken from Hansen and Hovenier [1974]. Single scattering albedos were assumed to be 1 for both haze and cloud layers. The resultant parameters for northern and southern polar region are r_{eff} = 0.22, 0.20μm, τ_h = 0.09, 0.05 at IR, respectively. The optical depth is smaller compared with the initial observations of PVO τ_h = 0.25 but comparable with those observed during the declining phase. Such declination of the abundance of SO_2 is also observed by Venus Express orbiter [Marcq et al., 2012], so our results are consistent with the report of the correlation with it.

Keywords: Venus, Hazes, Imaging-Polarimetry, Radiative transfer analysis

Japan Geoscience Union Meeting 2014
(28 April - 02 May 2014 at Pacifico YOKOHAMA, Kanagawa, Japan)

PCG38-09 Room:423 Time:May 1 11:15-11:30

Estimation of wind at the cloud top of Venus

IKEGAWA, Shinichi[1*] ; TAKESHI, Horinouchi[2]

[1]Graduate School of Environmental Science, Hokkaido University, [2]Faculty of Environmental Earth Science, Hokkaido University

A number of theories have been proposed to explain the formation of the super-rotation in the Venus atmosphere. Among them, we focused on the Gierasch mechanism. To validate the mechanism, it is required to investigate the horizontal momentum transport by eddies with an accuracy sufficient to resolve the eddies with scales smaller than several thousand kilometers. In this study, we used the ultraviolet images from Venus Monitoring Camera (VMC) onboard ESA's Venus Express. The VMC data have some random and coherent noises, so the simple cross-correlation methods used in previous studies do not necessarily provide an high accuracy. Here, we suggest a new and robust method to estimate wind velocity vectors accurately by using multiple images, thereby reducing the effect of noises. The accuracy of its results is estimated statistically. The results are also examined from the dynamical point of views. Contrary to conventional expectation, the magnitude of horizontal wind divergence has similar magnitude to its rotation on the horizontal scale of several thousand kilometers. It is discussed how the results are explained.

Keywords: Venus, super-rotation, estimation of wind

Japan Geoscience Union Meeting 2014
(28 April - 02 May 2014 at Pacifico YOKOHAMA, Kanagawa, Japan)

PCG38-10 Room:423 Time:May 1 11:30-11:45

Studying the Venusian atmosphere on the 2012 transit of Venus

KANAO, Miho[1*] ; NAKAMURA, Masato[1] ; SHIMIZU, Toshifumi[1] ; IMAMURA, Takeshi[1]

[1]ISAS/JAXA

The solar satellite Hinode observed the transit of Venus on June 5-6th 2012. The solar optical telescope (SOT) observed the dark Venus disk against the bright solar surface. The images were acquired continuously for the wavelength of 396.8, 430.5 450.4, 555.0, 668.4 nm with unprecedented spatial scale (∼0.3 arcsec).

The purpose is the derivation of the latitudinal and vertical distribution of the cloud particle, SO2 and SO from the transmittance for considering the global dynamics. We calculated the transmittance normalized by the unattenuated solar intensity after the data correction processes including the removal of the solar limn darkening and the calibration for the plate scale.

The altitude as the transmittance of 0.5 (∼90 km) in the Venus atmosphere has the slant toward the equator. The difference is 9.1 km in the evening and 6.1 km in the morning. In the equatorial region (latitude $\leq$ 40 degree), the fluctuation of the altitude is observed. The amplitude for the wavelength shorter than 400 nm is a few times larger than that of 430.5 nm. We would show the consideration to explain the longitudinal distribution of the altitude of the Venus disk.

Keywords: planetary atmosphere, the transit of Venus

Japan Geoscience Union Meeting 2014
(28 April - 02 May 2014 at Pacifico YOKOHAMA, Kanagawa, Japan)

PCG38-11 Room:423 Time:May 1 11:45-12:00

Millimeter Wave Band Monitoring of Venusian and Martian Middle Atmosphere with SPART Telescope

MAEZAWA, Hiroyuki[1*] ; IKEDA, Yoshinori[1] ; OSAKI, Shigeki[1] ; HORIUCHI, Kouske[1] ; KIRIDOSHI, Ryosuke[1] ; TANEKURA, Naruaki[1] ; SAGAWA, Hideo[3] ; NISHIMURA, Atsushi[1] ; OHNISHI, Toshikazu[1] ; TOKUMARU, Munetoshi[2] ; KONDOU, Syusaki[2] ; MIZUNO, Akira[2] ; KANZAWA, Tomio[4] ; HANDA, Kazuyuki[4] ; IWASHITA, Hiroyuki[4] ; MAEKAWA, Jun[4] ; OYA, Masaaki[4] ; KUNO, Nario[4]

[1]Osaka Prefecture University, [2]STEL Nagoya University, [3]NiCT, [4]Nobeyama Radio Observatory

To understand the influences of the activities of the central star on the middle atmospheres of the surrounding terrestrial planets, we have performed millimeter-wave-band monitoring of the atmospheres of Venus and Mars by using a 10-m radio telescope called SPART (solar planetary atmosphere research telescope). The telescope employs highly sensitive superconducting SIS mixer receivers in the 100- and 200-GHz bands for the front-end and a commercially available FFT spectrometer (1-GHz bandwidth and 67-kHz resolution) for the back-end. Millimeter-wave-band heterodyne sensing is a powerful technique that can be utilized to trace the abundance and vertical distribution of minor constituents in a planetary middle atmosphere.

In 2011, we began observations of the middle atmospheres of Venus and Mars in the 100-GHz band. In 2012, the telescope had problems with the azimuth gear, motor, and synchro-to-digital converter unit, which resulted in a pause in telescope operation. In 2013, we repaired these problems and resumed the substantive operation test. We are currently restarting double-band full remote monitoring of the spectral lines of minor constituents such as ^{12}CO J=2-1 at 230 GHz, ^{13}CO J=2-1 at 220 GHz, and ^{12}CO J=1-0 at 115 GHz toward Venus and Mars. This season, the apparent diameter of Venus is greater than the beam size at the 200-GHz band (35 arcsec.). We adopted position switching and on-the-fly modes for 100- and 200-GHz-band observations, respectively. The latter two-dimensional mapping allows us to cover the entire disk of Venus. The retrieved CO abundance variation is compared with the data of high-energy particles, X-rays, solar wind velocity/density, and other measured parameters. The data are associated with flare, coronal mass ejection, and solar proton events.

In this conference, the current status of the SPART project and the millimeter-wave-band monitoring will be presented.

Keywords: planet, solar activity, radio telescope, heterodyne spectroscopy, middle atmosphere, remote sensing

Japan Geoscience Union Meeting 2014
(28 April - 02 May 2014 at Pacifico YOKOHAMA, Kanagawa, Japan)

PCG38-12 Room:423 Time:May 1 12:00-12:15

Observation of a wave structure of stratospheric haze in Jupiter's polar regions by the ground based telescope

GOUDA, Yuya[1*] ; TAKAHASHI, Yukihiro[1] ; WATANABE, Makoto[1]

[1]Department of Cosmosciences, Graduate School of Science, Hokkaido University

Stratospheric haze formed by aerosol particles covers both polar regions in Jupiter. It has been reported based on the imaging using a methane band filter at 889 nm that the stratospheric haze can be measured. They show bright cap structures covering polar regions and the edge of the cap shows a wave structure spreading in longitudinal direction. This structure can be seen more clearly in the Jupiter's south pole than the north pole, and wave is clear at a latitude of about 67 S [Sanchez-Lavega, 2008].

Jupiter's polar areas have been investigated by the Hubble Space Telescope (HST) from 1994 to 1999 and the Cassini ISS in 2000. This wave structure is known to exist for several years in Jupiter's both polar regions. These observations suggested that this wave structure is caused by planetary Rossby waves because this wave structure presents for a longer period and moves westward relative to the background flow. However, the origin and mechanism keeping to this wave structure, the vertical structure of the wave, change of the propagation velocity of the wave in the short time scale, and north-south asymmetry of the wave structure are unclear so far, because of lack of the observations in short time scale (monthly scale). We have carried out the monthly monitoring of Jupiter from 2011 to 2014 with the 1.6 m Pirka telescope of Hokkaido University.

In this paper, we show results of our observations of the wave structure in Jupiter's polar region. We found a north-south asymmetry of the wave structure in the polar areas. The wave structure at 67 N spread to 42 N in the northern hemisphere, however it does not so in the southern one. In addition, we found that the wave structure has varied in the vertical direction a bit between altitude of 361 mbar and 750 mbar.

Keywords: Jupiter, haze, ground-based observation, Rossby wave

Japan Geoscience Union Meeting 2014
(28 April - 02 May 2014 at Pacifico YOKOHAMA, Kanagawa, Japan)

PCG38-13 Room:423 Time:May 1 12:15-12:30

Observing Jupiter with an infrared camera NIIHAMA

SATOH, Takehiko[1*] ; YONEDA, Mizuki[2] ; KAGITANI, Masato[2] ; KUHN, Jeff[3]

[1]Japan Aerospace Exploration Agency, [2]Tohoku University, [3]University of Hawaii

An infrared camera, NIIHAMA (1024x1024 pixels, PtSi array sensor), is attached to the SOLAR-C telescope (45-cm diameter off-axis Gregorian reflector) atop Haleakara in December 2013 and is now observing Jupiter.

NIIHAMA's 6-position wheel houses Dark, J, H, K, 3.4-micron (for Jupiter's H_3^+ aurora) and 2.26-micron (for Venus night-side IR emission) filters. The primary target of this project is to monitor the brightness of Jupiter's aurora simultaneously with SPRINT-A/HISAKI and other telescopes. However, due to smaller aperture of telescope, rather low quantum efficiency of PtSi sensor, etc., Jupiter's aurora has not yet been imaged so far. On the other hand, the satellite Io while in Jupiter's shadow was observed in K band, and the night-side IR emission of Venus was successfully imaged in 2.26-micron filter. We report the result of first-light observations and also discuss improvement and observing plans in near future.

Keywords: Infrared camera, Jupiter, aurora, Io, Venus, Haleakala

Japan Geoscience Union Meeting 2014
(28 April - 02 May 2014 at Pacifico YOKOHAMA, Kanagawa, Japan)

PCG38-14 Room:423 Time:May 1 12:30-12:45

Self-driven auroral acceleration process at Jupiter captured by continuous monitoring of Hisaki satellite with HST

KIMURA, Tomoki[1*] ; TAO, Chihiro[3] ; BADMAN, Sarah[2] ; YOSHIOKA, Kazuo[1] ; MURAKAMI, Go[1] ; YAMAZAKI, Atsushi[1] ; TSUCHIYA, Fuminori[4] ; FUJIMOTO, Masaki[1]

[1]JAXA/ISAS, [2]Lancaster University, [3]IRAP, Fance, [4]Tohoku University

Two possible drivers have been proposed for planetary auroral acceleration processes: magnetosphere-solar wind interaction referred to as an 'external driver' and shear flow of magnetospheric plasma around a planet referred to as an 'internal driver'. Recent observations of Jupiter's aurora indicated significant responses of auroral intensity and morphology to the solar wind. These results are suggestive of the 'external driver' for Jupiter. On the other hand, there have not been reported dynamics of the 'internal driver' for Jupiter yet which should be essential because of Jupiter's fast rotation and internal plasma source Io. Here we firstly report dynamics of the 'internal driver' based on long-term continuous observation of extreme ultraviolet (EUV) aurora by Hisaki satellite. The long-term variations in EUV aurora are compared with solar wind extrapolated from Earth's orbit by numerical simulation. We found dramatical brightening and decay of EUV aurora during the solar wind quiet period. The brightening occurs once every a few days followed by sudden decay with a timescale less than a half of rotation (˜5 hours), which is significantly faster than the solar wind daily variations. Highly-resolved auroral imaging by Hubble Space Telescope captured expansion of diffuse aurora down to latitudes of Io's footprint aurora during the brightening. These observations are indicative of hot plasma deeply injected into the inner magnetosphere around Io's orbit independently from the solar wind, followed by rapid energy dissipation through auroral emissions and possibly other radiation and/or chemical processes.

Keywords: Hisaki satellite, Hubble Space Telescope, Jupiter, aurora

Japan Geoscience Union Meeting 2014
(28 April - 02 May 2014 at Pacifico YOKOHAMA, Kanagawa, Japan)

PCG38-15 Room:423 Time:May 1 14:15-14:30

Characteristics of O+ velocity distributions at Venus and ion acceleration mechanisms: ASPERA-4 observations

MASUNAGA, Kei[1*] ; FUTAANA, Yoshifumi[2] ; TERADA, Naoki[3]

[1]STEL, Nagoya Univ., [2]Swedish Institute of Space Physics, [3]Grad. Sch. of Sci., Tohoku Univ.

O^+ ion velocity distributions for high energy O^+ beams ($>$100 eV) around Venus are statistically studied. The study shows that O^+ acceleration is controlled by the local convection electric field produced by the local proton and local magnetic field. In the magnetosheath, velocity distributions show a trend that perpendicular velocity component shifts from initial phase of the ring distribution to the local proton velocity. This indicates that gyro motions of the pickup ion immediately collapse after pickup and the ions are incorporated into the local proton flow. The pickup ions only escape through the $+E_L$ hemisphere. In the dayside induced magnetosphere in the $+E_L$ hemisphere, measurements show a scattered velocity distribution of O^+. This velocity distribution has two ion components depending on whether their gyro radius is larger or not than the scale of the induced magnetosphere. For O^+ ions with small gyro radius ($<$500 km), the O^+ velocity distribution appears on the middle phase of the ring distribution. On the other hand for the O^+ ions with a large gyro radius ($>$500 km), the O^+ velocity distribution is similar to the one in the magnetosheath. This means that in the induced magnetosphere two types of ions are mixed up: pickup ions subject to the E x B drift and ions moving with the local proton bulk velocity. Since both ion components flow tailward, they are convected toward the nightside. In the nightside of the induced magneto- sphere, velocity distribution shows initial and last phase of the ring distributions and parallel beam (3D ring distribution). This suggests that ion pickup occurs at the center of the plasma sheet. There is no evidence of an electric potential in the plasma sheet because the O^+ parallel beam velocity is larger than the parallel velocity component of the local proton. Our result suggests that the local convection condition is rather important to discuss ion acceleration mechanisms at Venus than the solar wind condition.

Keywords: Venus, ion escape, ion acceleration, Venus Express, ASPERA

Japan Geoscience Union Meeting 2014
(28 April - 02 May 2014 at Pacifico YOKOHAMA, Kanagawa, Japan)

PCG38-16 Room:423 Time:May 1 14:30-14:45

Characteristics of boundary layer between the magnetosheath and Martian ionosphere during solar wind penetration events

MATSUNAGA, Kazunari[1*] ; SEKI, Kanako[1] ; HARA, Takuya[1] ; BRAIN, David A.[2] ; LUNDIN, Rickard[3] ; FUTAANA, Yoshifumi[4] ; BARABASH, Stas[4]

[1]Solar-Terrestrial Environment Laboratory, Nagoya University, [2]Laboratory for Atmospheric and Space Physics (LASP), University of Colorado at Boulder, [3]Space Physics Swedish Institute of Space Physics (IRF), Umea, Sweden, [4]Space Physics Swedish Institute of Space Physics (IRF), Kiruna, Sweden

Deceleration of the solar wind due to the mass loading by planetary heavy ions forms the magnetic pile-up region around unmagnetized planets such as Mars and Venus. The Martian magnetic pile-up region diverts shocked solar wind plasma around the planet at altitudes typically in excess of 800 km [e.g., Vignes et al., 2000]. Mars Global Surveyor (MGS) measurements have shown, on one hand, that shocked solar wind (magnetosheath) plasma occasionally penetrates into much lower altitudes ($\sim$400km) [e.g., Brain et al., 2005; Crider et al., 2005]. Our previous statistical study of these solar wind penetration events using MGS magnetic field and electron observations revealed that both solar wind dynamic pressure (Psw) and the orientation of the interplanetary magnetic field (IMF) control the occurrence of the events. However, MGS cannot observe the solar wind regions due to its orbital design.

In this study, we focused on the simultaneous observation of the penetration events by MGS and Mars Express (MEX). MEX possess the ion mass analyzer (IMA) and electron spectrometer (ELS), which are parts of plasma packages of ASPERA-3. MEX partly observed the solar wind region, since the orbit of MEX is elliptical orbit. We can thus obtain the solar wind density and velocity from MEX data. Among the simultaneous observation data by MEX and MGS, we identified 46 simultaneous observation events of the solar wind penetration. We divided the 46 events into the low Psw ($\leq\sim$4nPa) and high Psw ($\geq\sim$4nPa) events. The solar wind penetration event on January 20, 2005 is observed during the high Psw periods, while the event on February 20, 2005 is during the low Psw periods. We investigated characteristics of the boundary layers between the magnetosheath and the ionosphere. We found that the electron flux shows a gradual decrease in the boundary in the high Psw event. On the one hand, intermittent appearance of both the magnetosheath plasma and the ionosphere plasma in the boundary is during the low Psw event. The signature of the boundary layer resembles with the K-H instability signature seen in LLBL (low-latitude boundary layer) in the Earth's magnetotail [e.g., Hasegawa et al., 2006]. We also report the results of statistical analysis of 46 simultaneous observation events.

Keywords: Mars, Ionospheres, Induced magnetosphere, Solar wind, Unmagnetized planet

Japan Geoscience Union Meeting 2014
(28 April - 02 May 2014 at Pacifico YOKOHAMA, Kanagawa, Japan)

PCG38-17 Room:423 Time:May 1 14:45-15:00

Effects of ion-ion collisions on vertical distribution of CO2+ in Martian ionosphere based on multi-fluid MHD simulation

KOYAMA, Kyohei[1*] ; SEKI, Kanako[1] ; TERADA, Naoki[2] ; TERADA, Kaori[2]

[1]Solar-Terrestrial Environment Laboratory, NAGOYA University, [2]Graduate School of Science, Tohoku University

Comparison of the mass fraction of CO2 and N2 with regard to the total mass of each terrestrial planet suggests importance of the atmospheric escape to space in Martian atmospheric evolution [Chassefiere et al., 2006]. It has been considered that heavy CO_2^+ ions are difficult to escape based on known atmospheric escape processes. Observations of a large amount of CO_2^+ ion escape by the Mars Express thus challenged the existing escape processes. Vertical distribution of CO_2^+ density in the ionosphere is one of important factors that determine the rate of CO_2^+ escape. Chemical reactions in ionosphere have been implemented in previous studies using multi-species MHD simulations [e.g., Ma et al., 2004; Terada et al., 2009]. The velocity difference between ion fluid cannot be reproduced by the multi-species MHD approximation. On one hand, the importance of vertical transport in the upper ionosphere (>300km altitude) was pointed out by some ionospheric models [Fox and Hac, 2009]. Multi-fluid MHD code [e.g., Najib et al., 2011] can solve such ion-species dependent velocity.

In this study, we developed a multi-fluid MHD simulation code. Our code includes ion-ion collisions in order to investigate their effects on the vertical distribution of CO_2^+ density in the Martian ionosphere. Three cases of the simulation runs are carried out: Multi-fluid MHD with ion-ion collision (Case1), multi-fluid MHD without ion-ion collision (Case2), and all ion species have the same vertical velocity corresponding to multi-species approximation (Case3). We compared the results after each simulation run reached to a quasi-steady state. The CO_2^+ density at altitude 460 km were turned out to be 82, 190, and 11 cm^{-3}, respectively for the Cases 1-3. The results suggest that inclusion of ion-ion collision is important to reproduce the realistic CO_2^+ transport from lower to upper ionosphere.

Keywords: Mars, ionosphere, Atmospheric escape, Multi-fluid MHD

Japan Geoscience Union Meeting 2014
(28 April - 02 May 2014 at Pacifico YOKOHAMA, Kanagawa, Japan)

PCG38-18 Room:423 Time:May 1 15:00-15:15

Temporal variability of exospheric sodium density

KAMEDA, Shingo[1*] ; FUSEGAWA, Ayaka[1] ; KAGITANI, Masato[2] ; YONEDA, Mizuki[2]

[1]Rikkyo University, [2]Tohoku University

Mercury's atmosphere is very thin and it is also called "surface-bounded exosphere". In the detected species, e.g., H, He, O, Na, Mg, K, and Ca, Na emission (NaD) is the brightest and has been most frequently observed. Solar-photon-stimulated desorption, sputtering by impacting solar particles, and meteoroid vaporization are considered to be the source processes of Mercury's sodium. However, the primary process among these three processes is unclear as yet. The resonance scattering constitutes exospheric emission. The NaD emission is well suited for study by ground-based observations because of its high intensity. Past observations have shown that the temporal variation and north-south asymmetry of intensity of sodium emission.

We have observed Mercury sodium exosphere at the Haleakala Observatory in Hawaii since April 2011. The observations were performed using a 40 cm Schmidt-Cassegrain telescope, a high-dispersion spectrograph, and a CCD camera. We determined the temporal variation of the sodium density using the observational data. It is possible that the temporal variation of the sodium density is caused by variation of solar wind magnetic field if solar wind ion sputtering is the primary source process of Mercury exosphere. To verify this assumption, we checked the temporal variation of solar wind magnetic field observed by MESSENGER, and then we compared these variations with our observational result.

In this presentation, we show our observational results and discuss the dominant source process.

Japan Geoscience Union Meeting 2014
(28 April - 02 May 2014 at Pacifico YOKOHAMA, Kanagawa, Japan)

PCG38-19 Room:423 Time:May 1 15:15-15:30

Study of heavy ion dynamics in the Mercury's magnetosphere with offset dipole

YAGI, Manabu[1*] ; SEKI, Kanako[2] ; MATSUMOTO, Yosuke[3] ; DELCOURT, Dominique[4] ; LEBLANC, Francois[4]

[1]Tohoku Univ., [2]Nagoya Univ., [3]Chiba Univ., [4]CNRS

From Mariner 10 and MESSENGER observations, Mercury's magnetosphere is thought to be a miniature of the Earth's magnetosphere. While these two magnetospheres have several characteristics in common, some critical differences are also evident. First, there is no atmospheric layer, but only tenuous exosphere. Second, the kinetic effects of heavy ions might not be negligible because Mercury's magnetosphere is relatively small compared to the large Larmor radii. Trajectory tracings is one of the dominant methods to estimate the kinetic effect of heavy ions which originate the exosphere, though the results of the simulation are quite sensitive to the electric and magnetic field. Hence, it is important to provide a realistic field model in the trajectory tracings. In order to construct a large scale structure, we developed a MHD simulation code, and adopted to the global simulation of Mercury's magnetosphere. We performed four solar wind conditions of the northward IMF, and the results showed that the global configurations such as the location of magnetopause depend heavily on the dynamic pressure, while the solar wind electric field contributes little to the magnetospheric configuration. On the other hand, the results of statistical trajectory tracings of exospheric sodium ions depend not only on the dynamic pressure but also on the solar wind electric field. In the results, we identified two efficient acceleration processes and formation of the 'sodium ring' which is formed by the accelerated ions drifting around the planet by magnetic gradient of the dipole field. When the solar wind dynamic pressure is low, acceleration by magnetospheric convection is efficient in the vicinity of Mercury. When the dynamic pressure is high, entry of the accelerated ions picked-up in the magnetosheath into the magnetosphere becomes dominant. The entry point of sodium ions changes due to the variation of the solar wind electric field, which causes a difference in the sodium ring's shape for the same solar wind dynamic pressure cases. Recent observation by MESSENGER revealed the weaker dipole field of Mercury than the past estimation based on Mariner 10 as well as large offset of dipole which could change the global configuration of Mercury's magnetosphere and behavior of sodium ions. In the presentation, we will also discuss the ongoing simulation including the above configuration of intrinsic magnetic field of Mercury especially focus on how will this affect the acceleration mechanisms.

Keywords: Mercury's magnetosphere, test particle simulation, MHD simulation

Japan Geoscience Union Meeting 2014
(28 April - 02 May 2014 at Pacifico YOKOHAMA, Kanagawa, Japan)

PCG38-20 Room:423 Time:May 1 15:30-15:45

Structure and time variability of Io plasma torus observed by EXCEED onboard the HISAKI satellite

TSUCHIYA, Fuminori[1*] ; YOSHIKAWA, Ichiro[2] ; YOSHIOKA, Kazuo[3] ; KIMURA, Tomoki[3] ; YAMAZAKI, Atsushi[3] ; MURAKAMI, Go[3] ; KAGITANI, Masato[1] ; TERADA, Naoki[1] ; KASABA, Yasumasa[1] ; SAKANOI, Takeshi[1]

[1]Tohoku University, [2]The University of Tokyo, [3]ISAS/JAXA

Spatial distribution and time variability of emission lines of sulfur ions in Io plasma torus (IPT) measured by EUV spectrograph (EXCEED) onboard the HISAKI satellite are presented. The satellite has been launched on 14 Sep. 2013 and begun regular observation of IPT and Jupiter's UV aurora since middle of Dec. and it will continue until the end of Feb. A wide slit whose designed field of view (FOV) is 400 x 140 arcsec was chosen to measure both radial and latitudinal distributions of IPT. Jupiter's north aurora was guided at the center of FOV and its spectrum was simultaneously observed. Averaged spatial distribution of sulfur emission lines is consistent with previous observations. Looking at the time variability of IPT, new features were found from the EXCEED observation. The most surprising one is periodic variation synchronized with Io's orbital period. The variations in dawn and dusk sides were out-of-phase, suggesting the bright region is co-rotating with Io. The amplitude of the periodic variation is larger than those of well-known Jupiter's rotation periodicities in shorter wavelength and becomes smaller as increasing wavelength. The wavelength dependence suggests significant electron heating and/or hot electron production processes associated with Io. Another noticeable feature is long-term change in dawn-dusk asymmetry of the emission intensity which had not been reported so far. The asymmetry has been assumed to be a proxy of large scale dawn-to-dusk electric field generated in Jovian magnetotail and the origin of the variation observed will be discussed in detail. Sporadic change in the emission intensity of IPT associated with the aurora brightening event is expected to investigate in detail with the EXCEED observation to reveal energy transport process between inner and middle/outer magnetospheres. The expected event has not been detected so far and further continuous observation will be expected to resolve this issue.

Japan Geoscience Union Meeting 2014
(28 April - 02 May 2014 at Pacifico YOKOHAMA, Kanagawa, Japan)

PCG38-21 Room:423 Time:May 1 15:45-16:00

Plasma dynamics of Io plasma torus seen from the EXCEED

YOSHIOKA, Kazuo[1*] ; MURAKAMI, Go[1] ; KIMURA, Tomoki[1] ; YAMAZAKI, Atsushi[1] ; TSUCHIYA, Fuminori[2] ; KAGITANI, Masato[2] ; YOSHIKAWA, Ichiro[3]

[1]Institute of Space and Astronautical Science, Japan Aerospace Exploration Agency, [2]Planetary Plasma and Atmospheric Research Center, Graduate School of Science, Tohoku University, [3]The University of Tokyo

Major ions in Io plasma torus have many allowed transition lines in the EUV and their radiation easily escapes to become observable from outside the region. In other words, Jovian inner magnetosphere is able to be monitored by the EUV spectral observation remotely. Moreover, with the atomic database which provides the cross sections to the ambient electron, transition probabilities, and these temperature dependence, EUV observations can be a very important diagnostic of ion densities, electron density, and its temperature.

The EUV spectroscope EXCEED on the Hisaki spacecraft has started to observe the Jovian magnetosphere from the Earth orbit since the end of 2013. The spacecraft is dedicated for the solar system planets so that all the observation window is spared for planetary science. The spectral range is from 52 to 148 nm and its resolution is 0.3 nm with one of the narrowest slit. The field of view is 400 arc-seconds which corresponds to around 18 RJ. Therefore, it can observe whole region of Io plasma torus at one time. Moreover, it can achieve better spatial resolution than 1 RJ. It is the first time to get a whole spectral images of Io plasma torus in the EUV with such a high performance instrument. In this presentation, we will show the first results of EXCEED observation with its high spectral resolution slit for Io plasma torus.

Keywords: EUV, Io plasma torus, Jovian magnetosphere, Hisaki, EXCEED

Japan Geoscience Union Meeting 2014
(28 April - 02 May 2014 at Pacifico YOKOHAMA, Kanagawa, Japan)

PCG38-22 Room:423 Time:May 1 16:15-16:30

Dust-plasma interaction in Saturn's inner magnetosphere and its magnetosphere-ionosphere coupling

SAKAI, Shotaro[1*] ; WATANABE, Shigeto[1]

[1]Dep. Cosmosciences, Hokkaido University

We investigated the magnetosphere-ionosphere coupling with a dust-plasma interaction in Saturn's inner magnetosphere by using a modeling of ionosphere and inner magnetosphere. From our previous model, it was revealed that the magnetospheric ion velocity was significantly reduced by the electric fields generated by the ion-dust collisions when the dust density is high and the thickness of dust distribution is large. It was consistent with observations when the dust density is larger than ~10^5 m^{-3} for ionospheric conductivity of 1 S. An average electron density of Saturn's ionosphere obtained from radio occultations by Cassini spacecraft was ~10^{10} m^{-3} at 2000 km where density had a peak and gradually decreased with the increasing altitude. The density was ~10^8 m^{-3} at 10000 km. Plasma densities calculated by models also were similar to the observations and the topside temperature is ~650 K. However, electron densities from those models were calculated at the altitudes below 4000 km.

We estimated the ionospheric Pedersen conductivity from the plasma densities, and the plasma temperatures and velocities by using a magnetohydrodynamics model. We used the magnetospheric plasma temperature, which was 2 eV, as a boundary condition to investigate the magnetospheric influences. The plasma density was about 10^9 m^{-3} at the altitude of 1200 km, and it decreased to about 10^7 m^{-3} at the altitude of 10000 km. Below 10000 km altitudes the light ion has the upward velocity, while heavy ions have zero or downward velocity at low altitudes. This might be due to the difference of mass. The electron temperature increased to 20000 K at the altitude of 10000 km due to the heat flow from the inner magnetosphere. The electron temperature was about 2000 K at the altitude of 1000 km, and the collision and joule heating were contributing to the temperature below 2000 km. The peak density changed between about 10^8 and 10^{10} m^{-3} during one Saturn's day, and the electron density decreased with increasing the altitude. On the other hand, the electron temperature didn't depend on the local time. The Pedersen conductivity was the maximum 0.77 S on day time and the minimum 0.30 S on dawn time. The Pedersen conductivity strongly depends on the ionospheric plasma density.

We estimated the magnetospheric ion velocity by using the calculated conductivity. The Pedersen conductivity was the largest value at L = 3 and it decreased with the increase of the distance from Saturn. The conductivity changed in local time. The maximum was on the day time and the minimum was on the dawn time. The calculated ion velocity decreases from the co-rotation speed outside 3.5 R_S. The ion velocity was 60-80% of the co-rotation speed in the inner magnetosphere. The ion velocity was smaller than the co-rotation speed since the magnetospheric electric field is smaller than the co-rotational electric field when the current due to the ion-dust collision flows in the inner magnetosphere. The ion velocity strongly depended on the local time since the conductivity also depended on the local time. It is suggested that the dispersion of the observed speeds could show the dependence of local time. The ion velocity is fast during the solar irradiation since the Pedersen conductivity is large, while it becomes slow after the sunset because of the small conductivity.

The magnetosphere-ionosphere coupling is significantly important for the dust-plasma interaction. It is impossible to understand the dust-plasma interaction in Saturn's inner magnetosphere without understanding of the Saturn's ionosphere, since the magnetosphere and ionosphere is intimately-connected.

Keywords: Saturn, Dust-plasma interaction, Magnetosphere-ionosphere coupling, Dusty plasma

Japan Geoscience Union Meeting 2014
(28 April - 02 May 2014 at Pacifico YOKOHAMA, Kanagawa, Japan)

PCG38-23 Room:423 Time:May 1 16:30-16:45

Relation between Kronian magnetospheric convection and auroral emission from MHD simulation with solar wind data observe

FUKAZAWA, Keiichiro[1*] ; WALKER, Raymond J.[2] ; ERIKSSON, Stefan[3]

[1]Research Institute for Information Technology, Kyushu University, [2]UCLA, IGPP, [3]Laboratory for Atmospheric and Space Physics, University of Colorado at Boulder

In a series of our simulation studies we have reported that vortices formed at Saturn's dawn magnetopause in simulations when IMF was northward. We interpreted these vortices as resulting from the Kelvin Helmholtz (K-H) instability. In addition, thanks to the recent developments of computer performance, we have been able to perform the high resolution global MHD simulations of the Kronian magnetosphere. In these simulations we obtained the signature of the field-aligned currents from the K-H vortices in Saturn's auroral ionosphere and found small patchy regions of upward field-aligned current which may be related to auroral emissions. These patchy aurorae resembling our results have been reported from Cassini observations.

In our previous simulations we used the constant and simple solar wind conditions to understand the basic behavior of Kronian magnetosphere. In this study we have used Cassini observations of the solar wind upstream of Saturn to drive a simulation. Using these solar wind data we simulated the Kronian magnetosphere from 2008-02-12/14:00:31 to 2008-02-13/01:59:31 when the Hubble Space Telescope (HST) observed the Kronian UV auroral emissions. In these solar wind conditions there are several enhancement of the solar wind dynamic pressure (shock) and polarity reversal in the IMF components.

From these simulation the shape and convection of Kronian magnetosphere dynamically changed according to the variation of dynamic pressure and IMF directions. As the results, layered convection formed between the corotation region and magnetopause. Furthermore these convection interacted each other, then the large vortex configurations appeared. The calculated configuration of field aligned currents from the simulation also showed the layered and patchy distributions. In addition the upward field aligned current appeared in the dawn side mainly which resembles the configuration of auroral emission by HST.

Japan Geoscience Union Meeting 2014
(28 April - 02 May 2014 at Pacifico YOKOHAMA, Kanagawa, Japan)

PCG38-24 Room:423 Time:May 1 16:45-17:00

Study of dynamics of the Jovian magnetosphere-II: energy transportation process to the inner magnetosphere

MIZUGUCHI, Takahiro[1*] ; MISAWA, Hiroaki[1] ; TSUCHIYA, Fuminori[1] ; OBARA, Takahiro[1] ; KASAHARA, Satoshi[2]

[1]Planetary Plasma and Atmospheric Research Center, Graduate School of Science, Tohoku University, [2]Institute of Space and Astronautical Science/ Japan Aerospace Exploration Agency

We have researched response of the Jovian inner magnetosphere to the substorm-like event which occurred in the night side of the middle/outer magnetosphere. The transport of magnetic flux tube is one of important issues in the global dynamics of the Jovian magnetosphere [Kivelson et al., 2005]. The magnetic flux tubes are carried outward from the Io plasma torus with the slowly outflowing plasma. As they move outward, alternative flux tubes should be returned to the torus through rapid inflow of lower-dense flux tubes. Goal of this study is to reveal the role of the substorm-like event in the transport of magnetic flux tube in the Jovian magnetosphere.

In this study, substorm-like events were identified by using the in-situ observation data obtained by the Plasma Wave Subsystems (PWS), Energetic Particle Detector (EPD) and Magnetometer (MAG) onboard the Galileo orbiter. X-lines where the substorm-like events are thought to start were located at around 60-80 RJ [Woch et al., 2002]. Narrowband KilOMetric radiation (nKOM) which was remotely observed by PWS was used to find response of the inner magnetosphere to the substorm-like event. The source of nKOM is suggested to be located at the outer edge of the Io torus (8-10 RJ) (Reiner et al., 1993).

In the preceding studies, Louarn et al. (2001) reported nKOM correlated with inward flow burst during Jovian substorm-like event reported by Woch et al.(1998) and Krupp et al.(1998). The report implies that the generation mechanism of nKOM relate with the return of magnetic flux tube to inner magnetosphere. However, it has not been revealed well yet how inner and outer magnetospheres couple each other during substorm-like event.

On the other hand, Dubyagin et al.(2011) reported about deeply penetrating flow burst at the terrestrial magnetosphere. They reported that an inward flow burst penetrated into the inner magnetosphere when its entropy was less than that of the inner magnetosphere, while flow burst did not penetrated when its entropy was larger than that of the inner magnetosphere.

We have analyzed Jupiter's several inward flow events which are expected to relate with tail reconnection and nKOM radiation by using the data obtained by Galileo. We also have applied Dubyagin's entropy analysis method to Jupiter's cases in order to reveal that how reconnection event at the outer magnetosphere couple with the inner magnetosphere.

In this presentation, we will show preliminary results on relations of Jovian substorm-like event and phenomena of inner magnetosphere.

Keywords: Jovian magnetosphere, magnetospheric dynamics, substorm, plasma density, Galileo, nKOM

Japan Geoscience Union Meeting 2014
(28 April - 02 May 2014 at Pacifico YOKOHAMA, Kanagawa, Japan)

PCG38-25 Room:423 Time:May 1 17:00-17:15

Jupiter's decametric Io-C modulation lanes observed by LWA1 (2)

IMAI, Kazumasa[1*] ; SHIMANOUCHI, Yoshiaki[1] ; CLARKE, Tracy[2] ; HIGGINS, Charles A.[3] ; IMAI, Masafumi[4]

[1]Kochi National College of Technology, [2]Naval Research Laboratory, [3]Middle Tennessee State University, [4]Kyoto University

The Long Wavelength Array (LWA) is a low-frequency radio telescope designed to produce high-sensitivity, high-resolution images in the frequency range of 10-88 MHz. The Long Wavelength Array Station 1 (LWA1) is the first LWA station completed in April 2011, and is located near the VLA site in New Mexico, USA. LWA1 consists of a 256 element array, operating as a single-station telescope. Each LWA1 beam provides dual orthogonal linear polarizations such that it is possible to reconstruct the full Stokes parameters for each tuning. The first Jupiter radio observation using LWA1 was made by Tracy Clarke (PI) from December, 2011. The initial analyses of Io-A/C, Io-B, and Io-D event, show many spectral features such as S-bursts, narrow-band events (N-bursts), as well as modulation lanes and Faraday lanes.

The modulation lanes in Jupiter's decametric radiation, which were discovered by Riihimaa [1968], are groups of sloping parallel strips of alternately increased and decreased intensity in the dynamic spectral plots. We present LWA1 observations of modulations lanes detected across a Jovian decametric Io-C burst that contains both right hand circular and left hand circular emission. The modulation lanes cross both handedness of polarization, suggesting that the emissions may be coming from the same hemisphere. These results add important information regarding the emission mechanism of Jupiter's decametric emissions.

Keywords: Jupiter radio, decametric wave, modulation lane, radio source, radio emission mechanism, LWA1

Japan Geoscience Union Meeting 2014
(28 April - 02 May 2014 at Pacifico YOKOHAMA, Kanagawa, Japan)

PCG38-26 Room:423 Time:May 1 17:15-17:30

Observations of Polarization of Auroral Kilometric Radiation by KAGUYA and its Lunar Occultations

HASHIMOTO, Kozo[1*] ; GOTO, Yoshitaka[2] ; UDA, Kazuaki[2] ; KASAHARA, Yoshiya[2] ; ONO, Takayuki[3]

[1]Professor Emeritus, Kyoto University, [2]Kanazawa University, [3]Tohoku University

In KAGUYA (SELENE) LRS[1], WFC-H[2] observes wave spectra in 1kHz-1,000kHz and various plasma waves like Auroral Kilometric Radiation (AKR), electron plasma waves, and broadband electrostatic waves have been observed. This system can observe wave polarizations by two pairs of dipole antennas. We have analyzed the AKR polarizations.

Kaguya moves behind the Moon every rotation. The occultations of AKR radiated from the Earth occur. Such occultation observation by the 32 channel burst receiver of lunar orbiter RAE2 was reported in [3,4]. The polarizations were not measured then. The polarization of AKR is defined with respect to the magnetic field from a view point of plasma waves. On the other hand, the polarization is observed with respect to the propagation direction. Both polarizations depend on the source hemisphere. When only one hemisphere can be seen due to the occultation, the source hemisphere is identified and the polarization can be measured correctly. This result is also useful when both hemispheres are seen after the occultation. We show the results and their interpretations.

References

[1] T. Ono, A. Kumamoto, Y. Kasahara, Y. Yamaguchi, A. Yamaji, T. Kobayashi, S. Oshigami, H. Nakagawa, Y. Goto, K. Hashimoto, Y. Omura, T. Imacahi, H. Matsumoto, and H. Oya, The Lunar Radar Sounder (LRS) Onboard the KAGUYA (SELENE) Spacecraft, The Kaguya Mission to the Moon (Guest Editors: A. Matsuoka, C.T. Russell), Space Science Reviews, 154, Nos. 1-4, 145-192, DOI:10.1007/s11214-010-9673-8, 2010

[2] Y. Kasahara, Y. Goto, K. Hashimoto, T. Imachi, A. Kumamoto, T. Ono, and H. Matsumoto, Plasma Wave Observation Using Waveform Capture in the Lunar Radar Sounder on board the SELENE Spacecraft, Earth, Planets and Space, 60, 341-351, 2008.

[3] J.K. Alexander and M.L. Kaiser, Terrestrial Kilometric Radiation 1. Spatical Structure Studies, J. Geophys. Res., 81, 5948-5956, 1976

[4] J.K. Alexander and M.L. Kaiser, Terrestrial Kilometric Radiation 2. Emission From the Magnetospheric Cusp and Dayside Magnetosheath. J. Geophys. Res., 82, 98-104, 1977

Keywords: AKR, Polarization, Occultation, KAGUYA, Moon

Japan Geoscience Union Meeting 2014
(28 April - 02 May 2014 at Pacifico YOKOHAMA, Kanagawa, Japan)

PCG38-P01 Room:Poster Time:May 1 18:15-19:30

Study of the Venus' upper haze

TAKAGI, Seiko[1*] ; ARNAUD, Mahieux[2] ; VALERIE, Wilquet[2] ; ANNCARINE, Vandaele[2] ; IWAGAMI, Naomoto[1]

[1]Graduate School of Science,the Univ. of Tokyo, [2]Belgian Institute for Space Aeronomy

Venus is completely shrouded by a thick cloud deck floating at 45 – 70 km. The major material of the cloud deck is thought to be H_2SO_4 – H_2O droplets. The upper haze on Venus lies above the cloud layer surrounding the planet, ranging from the top of the cloud ($\sim$70 km) up to as high as 90 km. The upper haze particles with an effective radius of $\sim$0.25 μm was suggested from Pioneer Venus Orbiter (PV) measurements. The particles were most likely composed of sulfuric acid in terms of refractive index $\sim$1.45. The haze vertical optical thickness in the polar region at 365 nm was found to be 0.8 above the main cloud of 1 μm particles by PV measurements. By comparison, the optical thickness of the haze above the main cloud at low latitudes was found to be 0.06 [Kawabata et al., 1980]. Knibbe et al. (1998) and Braak et al. (2002) observed a gradual decrease of the haze particle column density during the PV mission. Braak et al. (2002) reported a correlation between the decrease of SO_2 abundance [Esposito et al., 1988; Na et al., 1990] and that of the polar haze optical thickness. However, it is unclear how haze are produced and composition of haze.

The upper layer detected (above the clouds) is characterized by a SO_2 mixing ratio increase with altitude from 85 to 105 km [Belyaev et al., 2012]. It shows a new source of SO_2 at high altitude. One possible source of SO_2 in the upper haze layer could be photo-dissociation of H_2SO_4 vapor resulting from evaporation of acid aerosol droplets. However, recent upper limit of H_2SO_4 from sub-mm ground-based observation makes this theory less likely [Sandor et al., 2012]. The cause of the phenomena given above is still controversial.

The Solar Occultation at InfraRed (SOIR) on board Venus Express (ESA) is designed to measure the atmospheric transmission at high altitudes (70 – 220 km) in the IR (2.2 – 4.3 μm) with high resolution by solar occultation. The SOIR data obtained in 2006 – 2009 are analyzed to examine the upper haze at altitude above 90 km. Vertical and latitudinal distribution of haze extinction, optical thickness and mixing ratio are calculated in using SOIR data statistically. Extinctions and optical thickness at low latitude are two times thicker than those of high latitude. One of the notable results is that mixing ratios increase at altitude above 90 km at both high and low latitudes. It is speculated that sources of haze are transported upward from under altitude 90 km and haze is produced at high altitude. From comparison with the vertical distributions of SO and SO_2 mixing ratios reported by Belyaev et al. (2012), it is speculated about the correlation between sulfuric compound and haze.

Keywords: Venus, upper haze, Venus Express, SOIR, cloud

Japan Geoscience Union Meeting 2014
(28 April - 02 May 2014 at Pacifico YOKOHAMA, Kanagawa, Japan)

PCG38-P02 Room:Poster Time:May 1 18:15-19:30

Observation of CO2-ice cloud in the Martian mesosphere by using PFS onboard Mars Express

SATO, Yuki[1*] ; KASABA, Yasumasa[1] ; MARCO, Giuranna[2] ; AOKI, Shohei[1] ; NAKAGAWA, Hiromu[1] ; KURODA, Takeshi[3]

[1]Planetary Atmosphere , TOHOKU University, [2]IAPS,INAF,Italy, [3]Planetary Plasma and Atmospheric Research Center , TOHOKU University

Almost all of constituent of martian atmosphere is CO2 (95%). It condenses at very high altitude (60˜100km) and become cloud. CO2-ice cloud have been observed by many instrument , but it was difficult to clearly judge whether observed cloud is made of CO2 or not. However OMEGA, visible and near-infrared imaging spectrometer onboard Mars Express, have provided the first spectroscopic identification of a cloud as being composed of CO2 (Montmessin et al, 2007) CO2-ice cloud has characteristic spectral feature emission peak at 4.26μm. Recent study reported that CO2-ice cloud distributes around equator in spring equinox to early summer and mid latitude in local autumn. (Maattanen et al,2010 , Montmessin et al,2007 2006, Clancy et al 2007) However, it is not clear about cloud feature (particle size or opacity).

We try to observe CO2-ice cloud using high spectral resolution instrument PFS, infrared fourier spectrometer onboard Mars Express. Strong point of PFS is that spectral resolution is ten times greater than that of OMEGA and We can see spectral feature of CO2-ice cloud (spike at 4.26μm) more clearly. Another point is that PFS and OMEGA observe almost the same point , so two instruments can observe CO2-ice cloud at the same time. For the first step, we check the data where OMEGA observed CO2-ice cloud (10 orbits) and found CO2-ice cloud like feature all of the 10 orbits. However emission peak appears at shorter wavelength (at 4.25 μm) . In order to judge whether this signal is real or not, we compared PFS spectra and OMEGA spectra observed at the same point. When PFS observe signal at 4.25μm , OMEGA also show strong signal at 4.26μm ,so we can say PFS signal is real. In some orbit, PFS observed different signal from that of OMEGA. It is double spike feature at 4.25μm and 4.28μm which OMEGA can not resolve. It is possible that double peak feature shows different cloud feature, for example, particle size.Now we are trying radiative transfer model and discuss how cloud spectral feature changes when we changes cloud parameter (size distribution, altitude, cloud opacity).

Keywords: Mars, CO2-ice cloud

Japan Geoscience Union Meeting 2014
(28 April - 02 May 2014 at Pacifico YOKOHAMA, Kanagawa, Japan)

PCG38-P03 Room:Poster Time:May 1 18:15-19:30

Numerical Modeling of Moist Convection in Giant planets

SUGIYAMA, Ko-ichiro[1*] ; NAKAJIMA, Kensuke[3] ; ODAKA, Masatsugu[2] ; KURAMOTO, Kiyoshi[2] ; HAYASHI, Yoshi-yuki[4]

[1]ISAS/JAXA, [2]Graduate school of Science, Kobe University, [3]Department of Cosmosciences, Graduate School of Science, Hokkaido University, [4]Graduate school of Science, Kobe University

It is now widely accepted that moist convection is a common phenomenon in giant planets atmosphere. The moist convection is thought to play an important role in determining the mean vertical structure of the atmosphere; the mean vertical profiles of temperature, condensed components, and condensible gases in the moist convection layer is thought to be maintained by the statistical contribution of a large number of clouds driven by internal and radiative heating/cooling over multiple cloud life cycles. However, the averaged structure of the giant planets atmosphere and its relationship to moist convection remain unclear. For the purpose of investigating the above problem, we developed a cloud resolving model and investigated a possible structure of moist convection layer in Jupiter ′ s atmosphere with using the model (Sugiyama et al., 2009, 2011, 2014). In this presentation, we perform two-dimensional calculations of moist convection and demonstrate a possible structure in the atmospheres of Saturn, Uranus, and Neptune.

The basic equation of the model is based on quasi-compressible system (Klemp and Wilhelmson, 1978). The cloud microphysics is implemented by using the terrestrial warm rain bulk parameterization that is used in Nakajima et al. (2000). We simplify the radiative process, instead of calculating it by the use of a radiative transfer model. The model atmosphere is subject to an externally given body cooling that is a substitute for radiative cooling. Because the vertical profile of net radiative heating is not observed in giant planets except Jupiter, the layer between 2 bar level and the tropopause, which corresponds to the observed cooling layer in Jupiter, is cooled. The body cooling rate is set to be 100 times larger than that observed in Jupiter ′ s atmosphere in order to save the CPU time required to achieve statistically steady states of the model atmosphere.

The domain extends 960 km in the horizontal direction. The vertical domains are 400 km for Saturn case and 600 km for Uranus case and Neptune case, which are based on the one-dimensional thermodynamical calculation (Sugiyama et al., 2006). The spatial resolution is 2 km in both the horizontal and the vertical directions. The temperature and pressure at the lower boundary is also based on the thermodynamical calculation. The initial temperature profile follows adiabatic from lower boundary to tropopause and is constant above the tropopause. The abundances of condensable gases used in the each calculation are taken at 0.1, 1, 3, and 10 times solar.

The results obtained in Saturn case with 1 times solar abundance of condensible gases are discussed below; the results of other planets and the dependency on the abundances of condensable gases will be demonstrated at the meeting. The major characteristic of vertical motion in the moist convection layer obtained in Saturn case is that downdrafts are stronger than updrafts; this characteristic is obviously different from that obtained in Jupiter case (Sugiyama et al., 2009). Sugiyama et al. (2009) demonstrates that the vertical motion in the moist convection layer of Jupiter is characterized by narrow, strong, cloudy updrafts and wide, weak, dry downdrafts. On the other hand, the characteristics of mean vertical structure are consistent with those obtained in Jupiter case. Due to the active transport associated with convection, considerable amounts of H_2O and NH_4SH cloud particles exist above the NH_3 condensation level, while the mixing ratios of all condensible gases decrease with height from the H_2O condensation level. The stable layer associated with the H_2O condensation level acts as a fairly strong barrier for vertical convective motion; the vertical profile of root mean square of vertical velocity has local minimum at this level.

Keywords: atmosphere of giant planets, moist convection, numerical modeling, cloud resolution model

Japan Geoscience Union Meeting 2014
(28 April - 02 May 2014 at Pacifico YOKOHAMA, Kanagawa, Japan)

PCG38-P04 Room:Poster Time:May 1 18:15-19:30

Two dimensional numerical study on Venusian gravity waves by using mesoscale model

ANDO, Hiroki[1*] ; SUGIYAMA, Ko-ichiro[1] ; IMAMURA, Takeshi[1] ; ODAKA, Masatsugu[2] ; NAKAJIMA, Kensuke[3]

[1]ISAS/JAXA, [2]Hokkaido University, [3]Kyusyu University

Recently Venusian gravity waves are often observed. For example, Airglow measurements of O_2 found the gravity waves with horizontal wavelength of ∼100 km at 110 km altitude. UV images also detect gravity waves with the horizontal wavelength of 60-150 km at the cloud top level (70 km altitude). However, only a specific altitudes can be observed in these measurements, thus it is difficult to examine the propagation characteristics and momentum flux of waves. Radio occultation measurements also detect upward propagating waves from the vertical temperature profiles within the altitude range of 65-90 km and suggests that waves with the vertical wavelength of 5-10 km are dominant by the spectral analysis. However, horizontal resolution in this measurement is ∼200 km, then small scale gravity waves cannot be observed. Therefore, it is difficult to understand how these gravity waves have their influence on the Venusian atmosphere.

In this study we developed a new Venusian mesoscale model and examined the propagation characteristic of the waves. In the model, we simulated the generation and propagation of the waves including the convective motion in the Venusian cloud layer. We will make a presentation about the initial analysis results.

Keywords: Venus atmosphere, Gravity waves, Numerical study

Japan Geoscience Union Meeting 2014
(28 April - 02 May 2014 at Pacifico YOKOHAMA, Kanagawa, Japan)

PCG38-P05 Room:Poster Time:May 1 18:15-19:30

Temporal variations of Venus O2 night airglow using IRTF/CSHELL

OHTSUKI, Shoko[1*] ; IWAGAMI, Naomoto[2] ; ROBERT, Severine[3] ; SAGAWA, Hideo[4] ; KOUYAMA, Toru[5] ; SATO, Takao M.[6]

[1]Senshu University, [2]University of Tokyo, [3]Belgian Institute for Space Aeronomy, [4]National Institute of Information and Communications Technology, [5]Information Technology Research Institute, [6]Institute of Space and Astronautical Science, Japan Aerospace Exploration Agency

Venus 1.27-micron O_2 night airglow is the indicator of the general circulation at about 95 km in Venus. Recent observations reported that the airglow emission showed the temporal variations with a period of a few hours and days [e.g. Ohtsuki et al., 2008; Gerard et al., 2008]. Such variations may be caused by the upward momentum transport and fluctuations by atmospheric waves. In recent years, the importance of planetary-scale waves on the general circulation of the Venus atmosphere has been recognized. Forbes and Konopliv [2007] suggested the propagation of planetary-scale waves originated in the cloud deck into the upper atmosphere. However, effects of planetary-scale waves on the Venus upper atmosphere have not been investigated yet.

We conducted 5-days monitoring observation of the airglow to detect the planetary-scale waves with IRTF/CSHELL from 11-15 July 2012, 3 and 5 February 2014. The 1.27-micron O_2 night airglow in the Venus atmosphere can pass through the Earth's atmosphere with a help of the Doppler shift. We obtained spectral image cubes at the wavelength of R-branch of the airglow band, which includes several rotational lines. In order to cover spectral information continuously, a slit drifted across Venus' nightside disk. The spatial resolution of the image is governed by seeing. The typical seeing was 0.6" to 1.5" in our observing run and corresponds to 200-450km at the center of Venus' disk. Under such conduction, we may detect airglow structures of small scales due to atmospheric waves; this is smaller than the region of enhanced airglow having a horizontal scale of ˜3000km. We can also derive the hemispherical distribution of the rotational temperature. To coincide with our observations, SOIR/Venus Express stellar occultations were conducted. We can try to compare our horizontal temperature map and vertical temperature profile from SOIR data.

In this presentation, we will show temporal variation of the airglow distributions in July 2012 and report a preliminary result of our new observations in February 2014.

Japan Geoscience Union Meeting 2014
(28 April - 02 May 2014 at Pacifico YOKOHAMA, Kanagawa, Japan)

PCG38-P06 Room:Poster Time:May 1 18:15-19:30

Observing plan for planetary atmosphere using IR heterodyne spectroscopy in 2014

NAKAGAWA, Hiromu[1*] ; AOKI, Shohei[1] ; KASABA, Yasumasa[1] ; MURATA, Isao[1] ; SAGAWA, Hideo[2]

[1]Tohoku University, [2]National Institute of Information and Communications Technology

We propose a new developed infrared heterodyne instrument, called Mid-Infrared LAser Heterodyne Instrument (MILAHI), for our dedicated telescope at the top of Mt. Haleakala, Hawaii. It addresses the key physical/meteorological parameters, such as the atmospheric temperature profiles, abundance profiles of the atmospheric compositions and their isotopes, and wind velocity. The observational sensitivity of MILAHI is discussed in this paper. The scientific target of MILAHI is to understand highly variable phenomena in the planetary atmospheres. The nature of atmospheric activity in various time-scale will be investigated by continuous monitoring with our dedicated telescope, in order to increase our understanding of planetary atmospheric dynamics, photochemistry, and meteorology. New measurements with high spatial/spectral resolutions constrain the three-dimensional distributions of temperature and compositions. The D/H and other isotopic ratios, diagnostic of the terrestrial atmosphere evolution, will be accurately measured in H_2O and CO_2. The atmospheric chemistry will be studied by monitoring O_3, H_2O_2, H_2O, and HDO. Mapping of the H_2O isotopes reveal the mechanism of complex interaction between regolith-aerosols-atmosphere-polar caps on Mars. Direct measurements of wind velocity and temperature allow the first monitoring of the middle atmosphere oscillations to investigate the effects of the gravity waves from the lower atmosphere on the upper atmosphere for various seasons and dust loadings. A number of organics molecule bands in the mid-infrared regime will be accurately measured in planetary/cometary/stellar atmospheres. In addition to these interconnected objectives, serendipitous searches with our advantage of dedicated use for astronomical/atmospheric transient events which occur at frequent and unpredictable intervals (e.g. dust storm) will enhance our knowledge of the composition and dynamics of the astronomical sources.

Keywords: infrared spectroscopy, heterodyne, laser, observation, planetary atmosphere, isotopes

Japan Geoscience Union Meeting 2014
(28 April - 02 May 2014 at Pacifico YOKOHAMA, Kanagawa, Japan)

PCG38-P07 Room:Poster Time:May 1 18:15-19:30

Visual Orbit Design for the Next Mars Exploration Mission

OGURA, Satoshi[1] ; KAWAKATSU, Yasuhiro[1] ; MATSUOKA, Ayako[1] ; TAGUCHI, Makoto[2*]

[1]ISAS/JAXA, [2]Rikkyo University

In December, 2011, the working group concerned with the Japanese next Mars exploration mission began to study the use of orbiters to investigate the mechanisms of carbon dioxide and water escape from the Martian atmosphere, and the role played by the solar wind. This will be the successor to the first Japanese mission to Mars involving the NOZOMI spacecraft, and two different orbiters will be deployed around the planet. Orbiter-A will carry out in-situ observations of electric and magnetic fields, particles, plasma and the atmosphere at an altitude of about 100 km above the Martian surface. Orbiter-B will capture images of the escaping atmosphere and monitor solar-wind conditions. The mission life will be a Mars year. This paper describes a visual method for determining the orbits of both spacecraft, and presents examples of possible orbits.

The orbital constraints proposed by the working group are as follows.

Orbital constraints for Orbiter-A

A1. The periapsis altitude is around 150 km.

A2. The apoapsis altitude is between 5000 and 7000 km.

A3. The period during which periapsis occurs on the dayside of the planet is more than two thirds of the mission life.

Orbital constraints for Orbiter-B

B1. The apoapsis altitude is about 4-6 R_M.

B2. The period during which the orbiter is exposed to the solar wind is more than three quarters of the mission life.

B3. The period during which the orbiter can image the local time zone of 12-15 h at the planetary limb is more than three quarters of the mission life.

Orbital constraints for combined observations by both orbiters

C1. The number of times during which Orbiter-B is exposed to the solar wind and can also image Orbiter-A, whose solar zenith angle and altitude are less than 60 deg and about 300-800 km, respectively, is more than one hundred during the mission life.

C2. When C1 is satisfied, the angle between the line-of-sight of the imager onboard Orbiter-B and the velocity vector of Orbiter-A is within 90 ± 20 deg.

The orbital elements are obtained by solving the Lagrange planetary equations for a two-body boundary-value problem, taking only the J2 perturbation into account. Constraint A3 is chosen as an example for explaining the visual method of orbital design. The orbiter's longitude of ascending node and argument of periapsis in a Mars-Sun fixed coordinate system are taken as design variables, and the orbital constraint is used as an evaluation function. A contour map for a period in which periapsis occurs on the dayside is plotted in a coordinate system in which the longitude of ascending node and argument of periapsis are the X and Y axes, respectively. A mission profile is placed on the map, along which the changes in the longitude of ascending node and argument of periapsis during the mission period are plotted. The mission profile can be placed at anywhere on the map, since its shape can be kept almost constant by selecting an initial position determined by the position and direction of the spacecraft during Mars orbit insertion. By looking at the map, it then becomes easy to identify an appropriate initial point for the mission profile that maximizes the period during which periapsis occurs on the dayside.

By the method described above, it is possible to visually determine rough values for the longitude of ascending node and argument of periapsis that are suitable for the mission. This technique is also applicable to the general design of orbits around a planet by choosing a coordinate system appropriate for the given orbital constraints.

Keywords: atmospheric escape of Mars, Mars orbiter

Japan Geoscience Union Meeting 2014
(28 April - 02 May 2014 at Pacifico YOKOHAMA, Kanagawa, Japan)

PCG38-P08 Room:Poster Time:May 1 18:15-19:30

A Circumpolar Stratospheric Telescope for Observations of Planets ? FUJIN

MAEDA, Atsunori[1*] ; TAGUTI, Makoto[1] ; YOSIDA, Kazuya[2] ; SAKAMOTO, Yuji[2] ; NAKANO, Toshihiko[2] ; SHOJI, Yasuhiro[3] ; TAKAHASHI, Yukihiro[4] ; NAKAMOTO, Jumpei[4] ; IMAI, Masataka[4] ; WATANABE, Makoto[4] ; GODA, Yuki[5]

[1]College of Science, Rikkyo University, [2]Graduate School of engineering, Tohoku University, [3]JAXA/ISAS, [4]Graduate School of Science, Hokkaido University, [5]School of Science, Hokkaido University

It is important to conduct long-term continuous observations of time-dependent events in planetary atmospheres and plasmaspheres. The aim of the FUJIN project is to carry out continuous observations of planets using a telescope that is lifted by a balloon to the polar stratosphere. The FUJIN-1 experiment was organized at Taiki Aerospace Research Field in Taiki-cho, Hokkaido, Japan, from May to June 2013, but the experiment was canceled due to a failure found in the balloon operation system provided by JAXA. However, the results of various prelaunch ground tests clearly established the feasibility of the experiment.

We have recently begun organizing the FUJIN-2 experiment, in which scientific observations of planets will be conducted in the Arctic. Wind speed in the stratosphere is very low during April and May. The FUJIN-2 experiment will be conducted during this period in 2015 at ESRANGE in Kiruna, Sweden, since this is when Venus will be in the most favorable position for observations. The gondola will be recovered somewhere in the Scandinavian peninsula after one or two days of continuous observations.

In summer, an eastern circumpolar wind is dominant in the stratosphere. If a balloon is flown under these conditions, it will take a week to fly from Kiruna to Alaska and more than two weeks for it to fly back to Scandinavia along a constant-latitude path around the Earth. We are currently organizing another experiment (FUJIN-3) involving such a circumpolar flight that will be conducted in 2017 or later. The system used in FUJIN-2 will also be used for FUJIN-3, but with the inclusion of a high-sensitivity CCD camera and a liquid-crystal tunable filter. Venus, Jupiter, and Mercury will be the planets of interest for FUJIN-3. Moreover, a next-generation stratospheric telescope with a meter-class aperture, a mobile gondola to approach the center of the polar vortex, and a super-pressure balloon for year-round observations are being studied to upgrade the FUJIN system for future use.

Keywords: Circumpolar, Stratospheric, Telescope, Venus, FUJIN-project

Japan Geoscience Union Meeting 2014
(28 April - 02 May 2014 at Pacifico YOKOHAMA, Kanagawa, Japan)

PCG38-P09 Room:Poster Time:May 1 18:15-19:30

Study of fast resistive magnetic reconnection in the upper atmosphere of Venus

SAKAMOTO, Hitoshi[1*] ; TERADA, Naoki[1]

[1]Graduate School of Science, Tohoku University

Although Venus has no intrinsic magnetic field, magnetic field exists in the upper atmosphere through the interaction of the solar wind. In the dayside ionosphere of Venus, small magnetic rope-like structures called 'flux ropes'were often observed when solar wind dynamic pressure was low. Pioneer Venus Orbiter (PVO) observed flux ropes on more than 40% of the orbits passing through the dayside lower ionosphere, and founds its occurrence rate maximizes at altitude170km [Elphic et al., 1983].

So far some models to generate flux ropes have been proposed (K-H instability [Wolff et al., 1980], nonlinearity associated with the Hall effect [Kleeorin et al., 1994]), but the generation mechanism is not yet understood. In this study, we propose a new model to generate flux ropes based on recently proposed fast resistive magnetic reconnection [Loureiro et al., 2007]. This fast resistive reconnection occurs in a very long Sweet-Parker (SP) current sheet. The growth rate in the linear stage is proportional to the one-quarter power of the Lundquist number, and the current sheet is unstable under the condition that the Lundquist number is more than 10 to the power of 4. According to MHD simulation results [Samtaney et al., 2009], a chain of plasmoids is formed after reconnection at many points in the current sheet. Such a chain structure is similar to flux ropes. In the dayside ionosphere of Venus, a very long current sheet can form, where the fast resistive magnetic reconnection occur. Therefore, we considered a model to generate flux ropes through the formation of a very long current sheet and subsequent fast resistive reconnection in the dayside ionosphere of Venus, and then examined its applicability. The outline of the generation model we propose in this study is as follows: First, the interplanetary magnetic field (IMF) carried by the solar wind penetrates into the dayside lower ionosphere when solar wind dynamic pressure is high. Then, the field reversal structure resulting from an IMF turning penetrates there, and a very long SP current sheet is created. Finally, flux ropes are generated through the fast resistive reconnection in the current sheet.

In order to examine the applicability of our model, we estimated the altitude profiles of the Lundquist number, the growth rate of the fast resistive reconnection, and the SP current sheets thickness by using the result of a hybrid simulation in the upper atmosphere of Venus [Terada et al., 2002]. From the profiles, we chose the altitudes corresponding to specific Lundquist numbers, and we consider that the fast resistive reconnection can occur if the following conditions are satisfied at the chosen altitudes. First one is that the fast resistive reconnection can grow sufficiently. Second one is that the SP current sheet thickness is larger than the observed flux rope radius [Elphic et al., 1983]. Consequently, we found that our model is applicable between near 170 km altitude (Lundquist number is 10 to the power of 5 at this altitude) and near 230 km altitude (Lundquist number is 10 to the power of 6 at this altitude). We will show the result of MHD simulation performed with the parameters at these applicable altitudes.

Keywords: reconnection, ionosphere, Venus

Japan Geoscience Union Meeting 2014
(28 April - 02 May 2014 at Pacifico YOKOHAMA, Kanagawa, Japan)

PCG38-P10 Room:Poster Time:May 1 18:15-19:30

Estimation of the ion acceleration in the Ganymede polar magnetosphere by the Galileo spacecraft observation

WATANABE, Shinya[1*] ; KATOH, Yuto[1] ; KUMAMOTO, Atsushi[1] ; ONO, Takayuki[1] ; KURTH, William S.[2] ; HOSPODARSKY, George[2]

[1]Department of Geophysics, Graduate School of Science, Tohoku University, [2]Department of Physics and Astronomy, University of Iowa Iowa City, Iowa, USA.

Ganymede is one of the Jovian moons and is known as the only satellite that has an intrinsic magnetic field [Gurnett et al., 1996]. Since Ganymede is located in the Jovian magnetosphere, corotating magnetospheric plasma always blows toward Ganymede's magnetosphere [e.g. Kivelson et al., 1998]. Since the spatial scale of Ganymede's magnetosphere is comparable to the Larmor radius of magnetospheric ions, the characteristic plasma environment around Ganymede is formed due to the interaction between Ganymede's magnetosphere and Jovian magnetospheric plasma. Although previous studies discussed the morphology of Ganymede's magnetosphere and its plasma environment, most of them are still unknown and understanding of the interaction is necessary to reveal processes occurring in Ganymede's magnetosphere.

In the present study, we discuss the plasma environment observed in Ganymede's polar region by the Galileo spacecraft. First, we have identified Upper-Hybrid Resonance (UHR) frequency by the Plasma Wave Subsystem (PWS) and have analyzed the electron density at the point of observation. We have analyzed four Ganymede encounters including those on orbits G01 and G02 which have been analyzed in the previous study. Since the most dominant ion in Ganymede's magnetosphere is O+ [Vasyliunas and Eviatar, 2000], we assumed that the O+ density equals the electron density. Based on the results of this analysis, we have plotted the distribution of O+ density in the altitude range from 264 km to 5262 km and have revealed that the number density decreases rapidly with distance from Ganymede. Next, we have discussed the ion outflow from Ganymede's polar region. Based on the obtained distribution, we have found that the density distribution can be expressed by r^-5.98, where r is the distance from Ganymede. Assuming that the flux is conserved along the path of the ion outflow and that the cross section of the flux tube of outflow is proportional to r^2 and r^3, we have estimated that the ion velocity reaches 17.3 km/s and 14.5 km/s, respectively, at the distance of 500 km from Ganymede. This result is consistent with the previous study which suggested the outflow O+ velocity is 18 km/s from observations of the Galileo PLS instrument [Vasyliunas and Eviatar, 2000]. We also discuss candidate mechanisms for the ion outflow from Ganymede's polar region and report the current status of a simulation code which we are developing so as to discuss the outflow process quantitatively.

Keywords: Ganymede, magnetosphere, outflow, acceleration

Japan Geoscience Union Meeting 2014
(28 April - 02 May 2014 at Pacifico YOKOHAMA, Kanagawa, Japan)

PCG38-P11 Room:Poster Time:May 1 18:15-19:30

In-flight calibration of HISAKI/EXCEED by stellar observations

MURAKAMI, Go[1*] ; YOSHIOKA, Kazuo[1] ; YAMAZAKI, Atsushi[1] ; KIMURA, Tomoki[1] ; TSUCHIYA, Fuminori[2] ; KAGITANI, Masato[2] ; YOSHIKAWA, Ichiro[3]

[1]ISAS/JAXA, [2]Tohoku University, [3]The University of Tokyo

The extreme ultraviolet (EUV) telescope EXCEED (Extreme Ultraviolet Spectroscope for Exospheric Dynamics) onboard the Japan's small satellite HISAKI (SPRINT-A) will be launched in August 2013. The EXCEED instrument will observe tenuous gases and plasmas around the planets in the solar system (e.g., Mercury, Venus, Mars, Jupiter, and Saturn). One of the primary observation targets is Jupiter, whose magnetospheric plasma dynamics is dominated by planetary rotation. In the EUV range, a number of emission lines originate from plasmas distributed in Jupiter's inner magnetosphere. The EXCEED instrument is designed to have a wavelength range of 52-148 nm with a spectral resolution of 0.3-1.0 nm. The spectrograph slits have a field of view of 400 x 140 arc-seconds (maximum), and the attitude fluctuations are stabilized within 5 arc-seconds. The optics of the instrument consists of a primary mirror with a diameter of 20cm, a laminar type grating, and an EUV detector using microchannel plates (MCPs). The surfaces of the primary mirror and the grating are coated with CVD-SiC.

After the launch of the HISAKI satellite and the initial check out of the instrument for 2 months, we performed in-orbit calibrations of the EXCEED instrument by stellar observations. We observed the standard stars GD71, HZ2, and FEIGE110, and measured the absolute sensitivity and the spatial resolution of the EXCEED instrument. As a result, the absolute sensitivity was ˜1-2 cm^2 and the spatial resolution was ˜16 arc-seconds. In this presentation, we report the overview and initial results of the in-orbit calibration of EXCEED.

Keywords: HISAKI, EXCEED, EUV

Japan Geoscience Union Meeting 2014
(28 April - 02 May 2014 at Pacifico YOKOHAMA, Kanagawa, Japan)

PCG38-P12 Room:Poster Time:May 1 18:15-19:30

Coordinated observation of Io plasma torus using Hisaki/EXCEED and gourd-based telescopes

KAGITANI, Masato[1*] ; ANDREW, Steffl[2] ; BADMAN, Sarah[3]

[1]Tohoku university, [2]Southwest Research Institute, [3]University of Leicester

EXCEED is an EUV spectrograph onboard an earth-orbiting space telescope, Hisaki(SPRINT-A). One of the primal mission goal of Hisaki/EXCEED is to reveal radial transport of mass and energy in the Jovian magnetosphere. At the begging of January 2014, intense campaign observations of Jovian aurora and Io plasma torus were made using Hisaki/EXCEED, Hubble Space Telescope and other ground-based telescopes covering wavelength range from EUV through IR. We will present results of spectroscopic observation of Io plasma torus using the R.C. spectrograph attached to Kitt-Peak 4-meter telescope and an Echelle spectrograph attached to Haleakala 40-cm telescope.

The 4-meter R.C. Spectrograph was set up covering 550nm through 800nm which could successfully detect NaD (589nm), SIII 631.2nm, SII 671.6/673.1nm, and OII 731.9/733.0nm as well. A field-of-view was 98 arcseconds along the slit and the slit center was pointed at the dawn or dusk edge of the centrifugal equator. We could get 54 spectra from the observation during January 4th through 10th, 2014.

The Haleakala spectrograph is a high-resolution echelle spectrograh with an integrated field unit (IFU) which enables to capture 2-d distribution of [SII] 671.6/673.1nm emission with spectral resolution of 67000 over a field-of-view of 41” by 61”. The 40-cm telescope was observing Io plasma torus all over the night during the observing campaign period.

Based on preliminary analysis of the EUV spectrum from EXCEED/Hisaki, visible spectrum from Kitt-Peak 4-meter and Haleakala 40-cm, emission peaks of SIII and OII was located outward compared to the SII emission peak which is consistent with results from previous studies. More accurate analysis including pointing calibration and flux calibration are ongoing, the result will be presented at the meeting.

Keywords: Hisaki/EXCEED, Io plasma torus

Japan Geoscience Union Meeting 2014
(28 April - 02 May 2014 at Pacifico YOKOHAMA, Kanagawa, Japan)

PCG38-P13 Room:Poster Time:May 1 18:15-19:30

Coordinated observation of Jupiter thermosphere and radiation belt in January 2014

KITA, Hajime[1*] ; MISAWA, Hiroaki[1] ; TSUCHIYA, Fuminori[1] ; FUJISAWA, Shota[1] ; SAKANOI, Takeshi[1] ; KASABA, Yasumasa[1]

[1]Tohoku Univ.

In order to evaluate the solar UV/EUV heating effect on the Jovian radiation belt, we made coordinated observations for both temperature of the Jovian thermosphere using an infrared telescope and synchrotron radiation from the radiation belt (JSR) using a radio interferometer. JSR is the most effective probe for the dynamics of the Jovian radiation belt through remote sensing from the Earth. Recent intensive observations for JSR reveal short term variations of JSR with the time scale of days to weeks, but their causalities are not understood well. It is theoretically expected that the Jovian thermosphere is heated by solar UV/EUV radiation, and planetary atmospheric neutral wind is driven by solar UV/EUV heating. Then, induced dynamo electric field is mapped into the radiation belt and induces radial diffusion. From this scenario, the total flux density of JSR is expected to correlate with the solar UV/EUV flux.

Previous studies confirmed that the total flux density of JSR varied corresponding to the solar UV/EUV variations though it is unclear whether the temperature of the Jovian thermosphere actually varied during this event. The purpose of this study is to confirm whether sufficient solar UV/EUV heating occurs on the Jovian thermosphere and it actually causes variations of JSR total flux density. We made coordinated observations of the NASA Infra-Red Telescope Facility (IRTF) and the Giant Metrewave Radio Telescope (GMRT). From the infrared spectroscopic observations, we measured thermospheric temperature of H_3^+ ion. From the radio interferometer, we measured the total flux density and brightness distribution of JSR.

The IRTF is a 3 m infrared telescope located in Mauna Kea, Hawaii. The IRTF observations were made on Jan 3, 8, and 13 in 2014. We used the high spectral resolution spectrometer, CSHELL, and observed H_3^+ 3.9530 microns emission (Q(1,0)) and 3.4547 microns doublet emission (R(4,3) and R(4,4)). We assumed local thermodynamic equilibrium at the equatorial region and calculated thermospheric temperature from the two emission line ratio. The GMRT is a large radio interferometer located in India. The GMRT observations were made from Dec 31 to Jan 16 with a few days interval. The typical duration of observation time was 2 hours per day, and the observation frequency was 235 and 610 MHz. During this period, the SOHO satellite showed that the solar EUV flux increased from Dec 26, reached at the maximum flux on Jan 8, and then decreased to Jan 16. A preliminary analysis of the IRTF data showed that the temperature increased from Jan 3 to Jan 8, and decreased from Jan 8 to Jan 13. This is the first result that shows the temperature response of Jovian upper atmosphere to the solar UV/EUV heating. We will also introduce analyzed results of the GMRT data and discuss the relationship between Jovian thermosphere and radiation belt.

Keywords: Jupiter, thermosphere, radiation belt, infrared observation, radio interferometer

Japan Geoscience Union Meeting 2014
(28 April - 02 May 2014 at Pacifico YOKOHAMA, Kanagawa, Japan)

PCG38-P14 Room:Poster Time:May 1 18:15-19:30

Data analysis of Jupiter's decametric radio emission observed by LWA1

SHIMANOUCHI, Yoshiaki[1*] ; IMAI, Kazumasa[1] ; CLARKE, Tracy[2] ; HIGGINS, Charles A.[3] ; IMAI, Masafumi[4]

[1]Kochi National College of Technology, [2]Naval Research Laboratory, [3]Middle Tennessee State University, [4]Kyoto University

We present new results in the study of Jupiter's decametric emission obtained using the newly commissioned Long Wavelength Array Station 1 (LWA1). The LWA1 is a low frequency radio array operating in the frequency band between 10 and 88 MHz. The array consists of 256 dual polarization dipole stands, and observations are possible with up to four simultaneous beams, each of which has two independent tuning frequencies. The LWA1 is well suited to studying details of Jovian phenomena due to its high sensitivity as well as high time and frequency resolution over a wide bandwidth. We present LWA1 observations and the developed data analysis software by using IDL. The observed Io-C dynamic spectrum on March 10, 2012 shows the modulation lanes of both left and right hand polarization components share the same lane structure. It indicates that the both left and right hand Io-C radiations are emitted from the southern hemisphere. And the locations of the radio sources along the Jupiter's magnetic field should be very close.

Keywords: Jupiter radio, decametric wave, data analysis, radio source, radio emission mechanism, LWA1

Japan Geoscience Union Meeting 2014
(28 April - 02 May 2014 at Pacifico YOKOHAMA, Kanagawa, Japan)

PCG38-P15 Room:Poster Time:May 1 18:15-19:30

Long Term Variations of Jupiter's Auroral Radio Emissions - II

MISAWA, Hiroaki[1*] ; YONEDA, Mizuki[2] ; MORIOKA, Akira[1] ; TSUCHIYA, Fuminori[1] ; MIZUGUCHI, Takahiro[1]

[1]PPARC, Tohoku Univ., [2]PPARC, Tohoku Univ. / IFA, Univ. Hawaii

It is known that Jupiter's auroral radio emission (hereafter JAR) shows long term variations with the time scale of about a decade. The variations were first considered to be initiated by the solar activities in 1960's, however, longer term analyses in 1970's showed the variations relate with the Jovicentric declination of the earth (De). So far, their plausible causalities are considered to be brought by 1) De relating to amount of reachable rays to the earth, and 2) the geocentric declination of Jupiter relating to incidence angle of the radio wave to the terrestrial ionosphere. However, considering solar cycle dependence on the terrestrial auroral radio activity (e.g. Kumamoto et al., 2003), the solar activity control may not be negligible for the long term variations. Furthermore, we have not known well long term relationship between JAR and Jupiter's substorm-like process which may be controlled by Io's volcanic activity.

In order to assess the previously proposed causalities and the other effects, we have investigated occurrence features of JAR using the radio wave data observed outside the terrestrial ionosphere; i.e., by the WIND satellite after 1995. We have derived year-scale occurrence probabilities for 0.7 - 14 MHz around Jupiter's occultation periods, where the frequency range includes both Jupiter's decameter and hectometer radio emissions (so-called DAM and HOM, respectively). As the result, the yearly-scale occurrence probabilities show almost monotonous decrease from 1995 to 2005, then gradual increase after 2005, but change to somewhat complex nature with increase and decrease after 2009. The tendency is roughly similar for DAM and HOM, and also quite roughly similar for Io-related and non-Io-related DAMs. On the other hand, the JAR variation features do not seem to correspond to individual variation of De, solar activity and solar wind, but seem to somewhat correlate with those of Iogenic gas luminosity. These results imply that multiple causalities and/or Jupiter's internal process(es) control the long term variations.

Acknowledgements: We would greatly appreciate M. Kaiser and the WIND/WAVES team for providing the radio wave data.

Keywords: Jupiter, auroral radio emission, long term variation, Io's volcanic activity, Iogenic gas

Japan Geoscience Union Meeting 2014
(28 April - 02 May 2014 at Pacifico YOKOHAMA, Kanagawa, Japan)

AAS01-01 Room:423 Time:April 30 09:00-09:20

Analysis of the PWV variations observed by a hyper-dense network of GNSS receivers prior to localized rainfall

IWAKI, Yuya[1] ; REALINI, Eugenio[1] ; TSUDA, Toshitaka[1*] ; SATO, Kazutoshi[1] ; OIGAWA, Masanori[1]

[1]RISH, Kyoto University

Sudden and localized heavy rainfall events are posing increasing danger to urban areas, not only for the generation of floods, but also for the possibility to trigger landslides and damage crucial infrastructures. Numerical weather prediction models need to be supported by observations with sufficiently high spatial resolution, in order to be able to successfully forecast such localized precipitation events. To this aim, a crucial parameter to be monitored is the amount of precipitable water vapor (PWV), as well as its spatial distribution over the area of interest, and its variation over time. The Global Positioning System (GPS), which is one of the Global Navigation Satellite Systems (GNSS) currently available, has been increasingly used not only for positioning, but also for the remote sensing of physical parameters useful in Earth sciences. The PWV, or integrated amount of water vapor along the zenith direction, can be estimated by GPS (or GNSS) meteorology, which is a method that associates the amount of water vapor to the tropospheric delays which affect the signals of positioning satellites.

We deployed a dual-frequency (DF) GNSS network around Uji campus of Kyoto University, Japan, with inter-station distances of about 1-2 km. By using this network, we built a basic system to observe PWV fluctuations occurring within a small horizontal scale (less than 10 km), which are then analyzed to identify possible precursors of local torrential rain. Results from two observation campaigns (executed in the summer of 2011 and 2012) to retrieve and study GPS-derived PWV showed that its difference from other meteorological instruments was at most 2 mm in RMSE. We analyzed the variations of PWV detected when localized heavy rain was observed on July 9 and 25, 2012. Both the averaged value and the variance of PWV among GNSS stations increased before a nearby meteorological radar detected the rain clouds. In the latter case, the relative value of PWV among stations was larger than 5 mm.

For turning this system into practical use, e.g. for supporting a heavy rain early warning system, real-time satellite orbit and clock products are required. To estimate and correct the error of predicted satellite clock information, we used stations from the existing nation-wide GPS network in Japan (GEONET), with long baselines (˜100 km). The difference between the real-time PWV and that obtained in post-processing by means of precise orbit and clock products was 1.5 mm in RMSE.

Furthermore, the cost-effective deployment of hyper-dense GNSS networks over urban areas would benefit from the usage of inexpensive single-frequency (SF) receivers. We implemented and tested a software application that estimates and interpolates the ionospheric delay from DF stations surrounding the hyper-dense network, in order to compensate SF observations for the effect of the ionosphere, according to a method called SEID (Satellite-specific Epoch-differenced Ionospheric Delay), which was originally developed at the GFZ in Potsdam, Germany. By applying SEID for SF PWV retrieval, the error in terms of PWV with respect to the DF solution was about 1.6 mm in RMSE. The PWV horizontal distribution obtained by SF analysis with this model could detect localized PWV inhomogeneity emerging prior to a rainfall which occurred within a small horizontal scale (less than 10 km).

Keywords: GNSS, GPS, PWV, precipitation, tropospheric delay, ionospheric delay

Japan Geoscience Union Meeting 2014
(28 April - 02 May 2014 at Pacifico YOKOHAMA, Kanagawa, Japan)

AAS01-02 Room:423 Time:April 30 09:20-09:35

PWV retrieval by radiosondes and GPS receivers in Indonesia: spatial and time variations associated to rain events

REALINI, Eugenio[1] ; SATO, Kazutoshi[2] ; TSUDA, Toshitaka[1*] ; SUSILO, .[3] ; MANIK, Timbul[4]

[1]RISH, Kyoto University, Japan, [2]RISH, Kyoto University, Japan - now at JAXA, Japan, [3]Indonesian Geospatial Information Agency (BIG), Indonesia, [4]National Institute of Aeronautics and Space (LAPAN), Indonesia

Flooding due to local convective rain is a serious problem in the urban area of Jakarta, Indonesia. However, accurate prediction of local heavy rainfall events by means of current mesoscale numerical prediction models is difficult, partly because of lacking meteorological observations in Indonesia. Spatial and time variations of water vapor over a given area are expected to increase before precipitation occurs, due to the accumulation of water vapor in the lower troposphere, followed by convective instability. A means to reliably and continuously monitor Precipitable Water Vapor (PWV) is needed in order to detect such variations before the formation of rain clouds. GPS meteorology, i.e. the retrieval of PWV above a GPS station of known coordinates, is a useful technique to achieve this objective. The GPS signal delay induced by tropospheric refractivity is related to the amount of water vapor along the slant path between each satellite and the receiver antenna, therefore each fixed GPS station can be effectively employed as a sensor that continuously monitors the PWV with high temporal resolution (down to few seconds). By deploying multiple GPS stations that concurrently estimate the amount of PWV at different locations within an area of interest, one can evaluate the spatial and time fluctuations of the water vapor field, and investigate their relation to rain events.

We conducted a PWV observation campaign from 23 July to 5 August 2010 by using five GPS receivers installed at four different locations in Jakarta and Bogor, on Java island, Indonesia. Radiosondes were launched three to four times a day, from a site co-located with two of the receivers, in order to validate the GPS-derived PWV data. The validation resulted in a root mean square error of 2-3 mm. The influence of atmospheric pressure and temperature on GPS-derived PWV can be significant, therefore it was evaluated by referring to ground pressure and temperature measured by weather stations, and radiosonde temperature profiles. A regular semi-diurnal pressure oscillation was observed, showing an amplitude ranging from 3 to 5 hPa, which corresponds to 1.1-1.8 mm in PWV. A temperature inversion layer was observed in the radiosonde profiles during the night, which resulted in an error of about 0.5 mm in the retrieved PWV.

During the campaign, there was a passage of precipitation clouds over western Java, moving southwestward from the Equator towards the Indian Ocean, from 26 to 29 July. A second precipitation event, with localized rain clouds near Bogor, occurred on 2 August. Both events were observed also by a C-band Doppler Radar, operated in Serpong by the Japan Agency for Marine-Earth Science and Technology (JAMSTEC) as part of the HARIMAU project. The highest value of GPS-derived PWV (about 68 mm) was observed on 27 July, coinciding with the first rainfall event. Spatial and time variations in the estimated PWV between the four sites were enhanced before both the analyzed rainfall events, on 27 July and 2 August. We thus suggest the possibility that the spatial and time inhomogeneity of PWV detected by a network of GPS receivers could be used to support the prediction of rainfall events.

Keywords: PWV, GPS, precipitation, Indonesia

Japan Geoscience Union Meeting 2014
(28 April - 02 May 2014 at Pacifico YOKOHAMA, Kanagawa, Japan)

AAS01-03 Room:423 Time:April 30 09:35-09:55

A Dense Observation of the Tokyo Metropolitan Area Convective Study for Extreme Weather Resilient Cities (TOMACS)

SHOJI, Yoshinori[1*]

[1]Meteorological Research Institute

It is recognized that large cities with populations of several million people are inherently vulnerable to severe weather, such as torrential rainfall, lightning, and tornados. An increase in the occurrence of torrential rainfall and strong typhoons, which can be caused by global warming, can cause extensive damage to large cities (Ishihara, 2013). The number of days with thunderstorms has been increasing in Tokyo in recent years, and the requirement of an advanced monitoring and forecasting system for extreme weather is becoming greater.

An unprecedented dense observation campaign and relevant modeling and societal studies have been conducted since April 2010 by the National Research Institute for Earth Science and Disaster Prevention (NIED), Meteorological Research Institute (MRI), and more than 25 national institutions and universities in Japan that target local high-impact weather (LHIW) in the Tokyo metropolitan area. The objectives of the project, the Tokyo Metropolitan Area Convection Study for Extreme Weather Resilient Cities (TOMACS), include the 1) elucidation of the mechanism of LHIW in urban areas (e.g., local torrential rain, flash flood, strong wind, lightening), 2) improvement of nowcasting and forecasting techniques of LHIW, and 3) the implementation of high resolution weather information to end-users through social experiments.

One of the unique features of TOMACS is the utilization of dense meteorological instruments in the Tokyo Metropolitan area, which is one of the most urbanized areas in the world. Their objectives are to target the tropospheric environment, boundary layer, initiation of convections and the lifecycles of thunderstorms. For the study of the mechanism of LHIW, data are used from the advanced observational instruments owned by participating organizations (including X-band and C-band polarimetric radars, a Ku-band fast scanning radar, Doppler lidars, microwave radiometers, a network of Global Positioning Systems (GPS), radiosondes and unmanned aerial vehicles), which are currently deployed in the Tokyo metropolitan area in addition to the operational observation networks of the Japan Meteorological Agency (JMA) and the Ministry of Land, Infrastructure, Transport and Tourism (MILT) of Japan. The intensive operational period (IOP) of the observations was set to the summers of 2011, 2012 and 2013.

During the IOP, several LHIW events occurred and have been energetically studied. In this topic, we briefly overview the necessity of this study, observation system, and results obtained so far.

Keywords: Mesoscale Meteorology, Dense Observation, Climate Change, Extreme Weather

Japan Geoscience Union Meeting 2014
(28 April - 02 May 2014 at Pacifico YOKOHAMA, Kanagawa, Japan)

AAS01-04 Room:423 Time:April 30 09:55-10:10

A case study on the local front prior to the cumulonimbus cloud and the verification of JMA-NHM simulation

NAGUMO, Nobuhiro[1*] ; YAMADA, Yoshinori[1] ; KAWABATA, Takuya[1] ; SATO, Eiichi[1]

[1]Meteorological Research Institute

The local fronts observed over the Kanto plain on July 23, 2013 have been analyzed that is the origin of the isolated cumulonimbus cloud in Tokyo metropolitan area and verified numerical simulation by JMA-NHM.

The local fronts and cumulonimbus cloud formation have been examined based on the data from dense observation network around Kanto plain including Doppler radar for Airport Weather (DRAW) at Haneda, Doppler lidar installed in Tokyo Institute of Technology (Ookayama Campus) and surface meteorological data by Japan Meteorological Agency (JMA). The verification of numerical simulation was based on the results of 500 m horizontal resolution of Japan Meteorological Agency Non-Hydrostatic Model (JMA-NHM). As the initial and boundary data, JMA Meso-analysis data of 15 UTC July 22, 2013 have been adopted. The first simulations have been done with 5 km resolution covering East Japan and then nesting of 1 km and 500 m resolution have been done covering a large part of Kanto Plain. The simulation of 500 m resolution has been analyzed for 10 hours from 02UTC July 22, 2013 and the boundary process is based on Deardorff (1980).

The formation of cumulonimbus clouds in Kanto plain is often explained by the convergence of southerly wind and easterly wind. The southerly warm moist wind flows from Sagami Bay and Tokyo Bay by high pressure system in the south of Japan or sea breeze. The easterly wind flows from Kashima Bay. However, in one case of on July 23, it was found that the trigger of cumulonimbus was convergence with two different directions of sea breeze fronts and in addition gust front also plays an important role. The daytime sea breeze front is formed along the Sagami and Tokyo Bay, has entered inland at 1 m/s approximately. Several isolated cumulonimbus clouds have been formed in the rear of sea breeze front and some of them have been lost later, to form a gust front. The spread speed of gust front was about 3 m/s. The sea breeze front that was located in front of the gust front turned the direction to northwest. This sea breeze front and original northeast direction of front from Tokyo Bay have formed the convergence over Tokyo metropolitan area.

On the other hand, numerical simulations have predicted the strong rainfall in the Kanto plain but not all precipitation have been expressed. Comparing JMA-NHM 500 m resolution simulation with DRAW at Haneda, the horizontal distribution of sea breeze front was close to the position of real position. The simulations also have expressed the isolated cumulonimbus rear of sea breeze front. But the gust front spreading was small to the real one.

Doppler lidar had identified the horizontal and vertical structure of these fronts. The simulated structure by JMA-NHM can be compared with Observation. The knowledge of the representation of simulation leads to improve forecast accuracy. We would like to go on to investigate the similarities or difference between simulation and observation of these front structures.

Keywords: convective cloud, local front, numerical simulation

Japan Geoscience Union Meeting 2014
(28 April - 02 May 2014 at Pacifico YOKOHAMA, Kanagawa, Japan)

AAS01-05 Room:423 Time:April 30 10:10-10:25

Numerical simulations using WRF model for reproducing localized delay signals derived from InSAR

KINOSHITA, Youhei[1*] ; FURUYA, Masato[1]

[1]Natural History Sciences, Hokkaido University

For elucidating the mechanism of meso-scale phenomena involving a phase change of water molecule, water vapor is one of the most important but poorly understood parameter in meteorology. Recently, the Global Navigation Satellite System (GNSS) are routinely used to provide near-real-time estimates of PWV (Foster et al., 2005) and to assimilate routine weather forecasts (e.g. Nakamura et al., 2004). However, the limitation using GNSS atmospheric delay for meteorology is its spatial resolution, for example about 20 km for the Japanese GNSS network (GEONET). Interferometric Synthetic Aperture Radar (InSAR) phase signals, which can detect surface deformations with high-spatial resolution, are affected by earth's atmosphere like GNSS. Therefore, InSAR can detect water vapor distribution with high spatial resolution without any surface deformation signals or other errors and thus is potentially useful for meteorological applications. In previous studies, Hanssen et al. (1999) showed the coincidence between water vapor signals detected by InSAR and spatial distributions of rainfall echo detected by a weather radar (WR), indicating the possibility of InSAR as a water vapor sensor. Kinoshita et al. (2013) showed the water vapor distribution during the heavy rain event using ALOS/PALSAR emergency observation data. They conducted the estimation of the three-dimensional (3D) water vapor distribution and performed numerical simulations by means of the Weather Research and Forecast (WRF) model, which could reproduce a convective system observed as a localized signal in the InSAR image. However, there were still few cases detecting localized water vapor signals with InSAR and few studies using InSAR for meteorological applications.

In our past presentations, we reported several case studies detecting localized water vapor signals associated with deep convective systems with InSAR derived from ALOS/PALSAR data (Kinoshita et al., JpGU 2013), some of which reached over 20 cm in the line-of-sight direction within 10 km square. Observed locations of these interferograms are at Niigata (two cases), Shizuoka, Kyoto, Saga and Miyazaki. These signals are equivalent to about 21 mm in the precipitable water vapor, and are higher than that around each signal. Each signal located at the very location of high rainfall intensity in the WR data, and is regarded as including few ionospheric effects because of the use of PALSAR data with descending orbit. Such localized signals strongly suggest the existence of developed convective systems at SAR observation time. However, it is difficult to elucidate mechanisms of phenomena that caused these localized signals.

In this study, we will perform numerical simulations using the WRF model for the purpose of investigate mechanisms of these phenomena and compare simulation results with derived InSAR data. At the presentation, we will show these results and discuss them.

Keywords: InSAR, Water vapor, WRF, Propagation delay, Numerical simulation

Japan Geoscience Union Meeting 2014
(28 April - 02 May 2014 at Pacifico YOKOHAMA, Kanagawa, Japan)

AAS01-06 Room:423 Time:April 30 10:25-10:45

Development and Observation of the Phased Array Radar at X band

USHIO, Tomoo[1*] ; SHIGEHARU, Shimamura[1] ; KIKUCHI, Hiroshi[1] ; WU, Ting[1] ; MEGA, Tomoaki[1] ; MIZUTANI, Fumihiko[2] ; WADA, Masakazu[2] ; SATOH, Shinsuke[3] ; IGUCHI, Toshio[3]

[1]Osaka University, [2]Toshiba, [3]NICT

A new Phased Array Radar (PAR) system for meteorological application has been developed by Toshiba Corporation and Osaka University under a grant of NICT, and installed in Osaka University, Japan last year. It is now well known that rapidly evolving severe weather phenomena (e.g., microbursts, severe thunderstorms, tornadoes) are a threat to our lives particularly in a densely populated area and the number of such phenomena tends to increase as a result of the global warming. Over the past decade, mechanically rotating radar systems at the C-band or S-band have been proved to be effective for weather surveillance especially in a wide area more than 100 km in range. However, rapidly evolving weather phenomena have temporal and spatial scales comparable to the resolution limit (-10 min. and -500m) of typical S-band or C-band radar systems, and cannot be fully resolved with these radar systems. In order to understand the fundamental process and dynamics of such fast changing weather phenomena, volumetric observations with both high temporal and spatial resolution are required. The phased array radar system developed has the unique capability of scanning the whole sky with 100m and 10 to 30 second resolution up to 60 km. The system adopts the digital beam forming technique for elevation scanning and mechanically rotates the array antenna in azimuth direction within 10 to 30 seconds. The radar transmits a broad beam of several degrees with 24 antenna elements and receives the back scattered signal with 128 elements digitizing at each elements. Then by digitally forming the beam in the signal processor, the fast scanning is realized. After the installation of the PAR system in Osaka University, the initial observation campaign was conducted in Osaka urban area with Ku-band Broad Band Radar (BBR) network, C-band weather radar, and lightning location system. The initial comparison with C band radar system shows that the developed PAR system can observe the behavior of the thunderstorm structure in much more detail than any other radar system. The observed high temporal resolution images of the severe thunderstorm are introduced, showing the potential capabilities of the PAR system. The correlation coefficient of the reflectivity in PAR with C band radar ranges from 0.6 to 0.9 as a function of the distance from the PAR.

Although the phased array radar system using the digital beam forming technique can estimate the 3 dimensional structure of the precipitation system within 10 to 30 seconds with 100 meter resolution, the observation results also shows the received signal was seriously contaminated by the relatively high received power from ground clutter and strong precipitation echoes through the side lobes of the transmitting beam. To avoid this problem, a beam forming technique using the MMSE (Minimum Mean Square Error) formulation was proposed and tested. This approach can adaptively mitigate the masking interference that results from the standard digital beam forming method in the vicinity of ground clutter and strong precipitation area. The proposed method is compared with the standard beam forming technique by applying to the huge raw IF signal data digitized at each 128 antenna elements. The results show that the proposed technique can correctly estimate the precipitation echo within a few dB even in the presence of a strong ground clutter that is more than 20 dB higher than the precipitation echo with 15 pulse repetition number. The MMSE based technique is shown to be superior to the standard DBF scenarios under the small number of pulse repetitions to achieve the rapid scanning.

Keywords: Phased Array Radar, Precipitation

Japan Geoscience Union Meeting 2014
(28 April - 02 May 2014 at Pacifico YOKOHAMA, Kanagawa, Japan)

AAS01-07 Room:423 Time:April 30 11:00-11:15

Descending reflectivity core analysis by Ku-band radar

SATO, Eiichi[1*] ; KUSUNOKI, Kenichi[1] ; FUJIWARA, Chusei[1] ; SAITO, Sadao[1] ; SHOJI, Yoshinori[1]

[1]Meteorological Research Institute

In order to observe extreme weather such as localized heavy rainfall, tornado etc., we installed a Ku-band radar in Musashino-shi, Tokyo in 2011. Since the radar can create a 3D volume scan per minute, we expect that the data observed by the radar will contribute to understanding mechanisms of such phenomena.

In our research, we defined a cell as an area whose reflectivity is $\geq$ 25dBZ, and a core as a reflectivity peak in the cell. The procedures of the cell/core detection are as follows: 1) conversion from rθ data to xyz data, 2) cell detection by binarization and labeling, and 3) core detection by method of steepest descent(ascent).

In this presentation, results of an automatic cell/core detection algorithm will be shown.

Keywords: descending reflectivity core, Ku-band radar, fast scan radar, extreme weather

Japan Geoscience Union Meeting 2014
(28 April - 02 May 2014 at Pacifico YOKOHAMA, Kanagawa, Japan)

AAS01-08 Room:423 Time:April 30 11:15-11:30

Influence of urban heat excess on heavy rain environment

SUGAWARA, Hirofumi[1*] ; SEINO, Naoko[2] ; ODA, Ryoko[3]

[1]National Defense Academy, [2]Meteorological Research Institute, [3]Chiba Institute of Technology

There are several observed fact that cities give influence on the precipitation, or cumulus generation. However the mechanism of urban influence on precipitation is not clarified. There would be three physical processes. Buildings could form updraft through a roughness effect. Much heat excess from cars, air conditioners and asphalt roads could also form updraft. Urban aerosol can be a condensation nuclei and gives chance to form cloud, however too much nuclei should suppress cloud droplets growing.

This study focuses on the heat effect. We measured surface sensible heat flux in urban, suburban and rural areas, and evaluated the urban heat excess quantitatively. The resulted heat excess amount was used to in calculation of atmospheric stability index.

In the heat flux measurement, the eddy correlation method which should be the most reliable way of heat flux measurement was used at the rural and suburban site. At urban site, we used the scintillation method which has a advantage of larger scale of measurement (km scale) than that of the eddy correlation method (100 m scale). The reason for taking scintillation method at urban site is severe heterogeneity in urban area. Urban area is mosaic of buildings, roads, parks, bare soil on the school ground field, and sometimes rivers or channels. Scintillation method enable us to measure the area-averaged heat flux in the urban heterogeneity. We used a modified scintillation method which takes into account of surface unevenness by the buildings. We operated measurement site for three years and analyzed a hourly composite of 50 fine days in July. As a result, urban heat flux is largest followed by suburban and rural. The difference between urban and rural was 140 Wm-2 at noon time.

We evaluated CAPE index for each site. We used simple 1D model to calculate the change of temperature profile by the surface flux. The morning initial condition to calculate daytime growing of mixed layer was acquired from the sonde observation. We adopted same initial profile for urban, suburban and rural, and give observed surface heat flux for each. This way of analysis evaluates thermal influence of land-use on CAPE index. The CAPE at 1500 LST is largest in cities and the difference between rural and city is 15%.

Keywords: heat island, urban climate

Japan Geoscience Union Meeting 2014
(28 April - 02 May 2014 at Pacifico YOKOHAMA, Kanagawa, Japan)

AAS01-09 Room:423 Time:April 30 11:30-11:50

OROGRAPHIC PRECIPITATION OBSERVATION IN JEJU ISLABD, KOREA (2012-2013)

LEE, Dong-in[1*]

[1]Department of Environmental Atmospheric Sciences, Pukyong National University

In summer monsoon season, a Korean Peninsula is influenced by several weather phenomena such as the Changma-front, typhoon, strong low pressure, and local heavy precipitation. Especially, the orography plays an important role in controlling the cloud formation, amount and precipitation distribution. To find out the precipitation development mechanism by orographic effect, we performed the intensive field observation around Mt. Halla in Jeju island (33.21 N and 126.32 E, width 78 km and length 35 km) which is located at the southern part of Korea with JNU (Jeju National University), KNU (Kyungpook National University), IJU (Inje University), KMA (Korea Meteorological Administration), and NIMR (National Institute of Meteorological Research). We installed and arranged the observational instruments such as, AWS, radiosonde (including mobile sonde and ship sonde), Parsivel, 2DVD, ultrasonic anemometer, and raingauge along the altitudes in Jeju island. Each disdrometer sites were located in straight line considering topography between two S-band Doppler radars. We analyzed synoptic condition by NCEP/NCAR reanalysis data and kinematic characteristics of precipitation by dual Doppler radar analysis using S-band radars in KMA.

In 2012 case, the Changma-front was located in the northern part of the Jeju island and the precipitation system passed from the southwest to the northeast. The accumulated precipitation (31.7 mm) was recorded at the site PR4 which was placed in the highest (H: 975 m). During the passage of precipitation, the south westerly wind ($>$12 m s^{-1}) with warm and humid air and the cold (lower layer) and warm advection (upper layer) were observed. From the microphysical analyses, PR2 (windward side, H: 571 m) and PR6 (leeward side, H: 324 m) sites indicated high rain rate about 60 to 75 mm hr^{-1} by orographic effect.

In 2013 case, the Changma-front located in the center of Jeju island and precipitation system passed from the southwest to northeast. The warm advection in lower layer and cold advection in upper layer were observed by radiosonde analyses, relatively. Strong southwesterly winds were blown with moist environment in surface layer. By the wind field analysis, convergence in west and divergence in east were existed and updraft in Jeju island and downdraft in ocean area, relatively. High number concentration at PR4, 5 and PR8 were shown with small size raindrops (less than 2 mm), however large size raindrops (lager than 6 mm) were distributed at PR7(northeast in island) and PR9(southwest in island).

Keywords: Orographic precipitation, intensive field observation, Jeju island

Japan Geoscience Union Meeting 2014
(28 April - 02 May 2014 at Pacifico YOKOHAMA, Kanagawa, Japan)

AAS01-10 Room:423 Time:April 30 11:50-12:05

Characteristics of distribution and preceding surface conditions of cumulonimbus clouds appeared on Kofu Basin on a calm

SANO, Tetsuya[1*] ; SUETSUGI, Tadashi[1] ; OISHI, Satoru[2]

[1]International Reserch Center for River Basin Environment, University of Yamanashi, [2]Research Center for Urban Safety and Security, Kobe University

On a calm summer day, cumulonimbus clouds often appear on complex terrains with the thermal induced local circulations. The appearance of such cumulonimbus clouds on a basin is not so frequent ordinarily. Once a cumulonimbus cloud appears on a basin, it often brings much rainfall in a short time, which becomes triggers of weather related disaster in urban city on a basin. However, the characteristics of the generation of cumulonimbus clouds on a basin and the conditions in a basin preceding the generation of them have not been known enough. In this study, for the example of above situation, we analyze the distribution of the appearance of cumulonimbus clouds on Kofu Basin and the conditions in Kofu Basin preceding the appearance of them.

The days of the appearances of cumulonimbus clouds on Kofu basin in a calm day confirmed by the observation of X-MP radar of University of Yamanashi (UYR) were 8 days out of 1 July to 30 September on 2012. Although the number of the events was limited, they brought large rainfall amount of 20 to 30 mm in an hour. The positions of the appearance concentrated from center to eastern side on Kofu Basin.

Before the appearance, south-southwesterly (SSW-ly) and southeasterly (SE-ly) surface wind was measured on western and eastern sides on Kofu Basin, respectively. When SSW-ly or SE-ly wind expanded to reach Kofu city that locates center of Kofu Basin, surface equivalent potential temperature (θe) increased. From The meso-scale objective analyzed data of Japan Meteorology Agency (JMA-MANAL) shows strong south-component wind with high-θe toward Kofu Basin from Suruga Bay through a valley connecting Suruga Bay to Kofu basin at the level of about 900 hPa. At the eastern side of Kofu Basin, strong east-component wind with high-θe crossing the mountains on the eastern side was appeared. Then, the south-component wind and the east-component wind formed horizontal convergence on Kofu basin. So, we consider that, the winds entering from the outer side of Kofu Basin, conditional instability intensified and horizontal convergence formed in Kofu Basin, which played a role as trigger of precipitating cell on Kofu Basin.

Keywords: Cumulonimbus cloud, Kofu Basin, Conditions preceding the appearance of a cumulonimbus cloud

Japan Geoscience Union Meeting 2014
(28 April - 02 May 2014 at Pacifico YOKOHAMA, Kanagawa, Japan)

AAS01-11 Room:423 Time:April 30 12:05-12:25

Transition to resilience to extreme weather ,high-resolution monitoring and international synergies

SCHERTZER, Daniel[1*] ; MAKI, Masayuki[2] ; TCHIGUIRINSKAIA, Ioulia[1]

[1]Ecole des Ponts ParisTech, U. Paris Est, [2]Research and Education Center for Natural Hazards, Kagoshima U.

Transition from high vulnerability to extreme weather to resilience is a major challenge for megacities in response to two main drivers: urban sprawling and climate change. The functioning of cities, particularly the large ones, should be observed, understood, simulated and monitored on much larger ranges of scales than usually done. This requires at first observations of many geophysical fields with an unprecedented resolution to achieve high-resolution monitoring. However, this also require an advanced understanding/modeling of the nonlocal interactions between large and small scales, e.g. between weather and climate scales.

Finally, this pleads in favor of methodological approaches across scales, rather than over very limited ranges of scales. Such methodologies aim in fact to quotient out non trivial symmetries and therefore should enable us to dig out the relevant information from otherwise under-exploited big data.

Such approaches have been often invoked, but barely achieved because they correspond to formidable tasks that require an unprecedented development of international cooperation on both advanced technologies and methodologies. We will illustrate these questions with examples of research and innovation programs on flood resilience which seem rather complementary across national boundaries but require nevertheless much stronger international synergies.

Keywords: extreme weather, cities, resilience, high-resolution, synergies, international

Japan Geoscience Union Meeting 2014
(28 April - 02 May 2014 at Pacifico YOKOHAMA, Kanagawa, Japan)

AAS01-12 Room:423 Time:April 30 12:25-12:40

The effect of scaling anisotropy on weather extremes

FITTON, George[1*] ; TCHIGUIRINSKAIA, Ioulia[1] ; SCHERTZER, Daniel[1]

[1]Universite Paris Est, Ecole des Ponts ParisTech, LEESU, 6-8 avenue B. Pascal, Cite Descartes, 7745

Predicting extreme weather events in and around cities is far from straight forward. Even in a stable and unbounded atmosphere, crude numerical approximations of the Navier-Stokes equations are required for reasonable computation times. Hence, numerical simulations of the weather in and around cities become even more complex, and therefore require much coarser space and time scales to model both the macro weather and the complex boundary conditions created by buildings and other urban structures. Such models will severely underestimate extremes due to the necessary truncation of scales to deal with these additional complexities.

While progress in numerical simulation depends on the next fastest processor, measurement techniques on the other hand are becoming rapidly more and sophisticated. There appears however to be a gap forming in the ability to utilise the enormous datasets produced from new measurement techniques. This seems mainly due to outdated statistical methods that are used to make sense of these overwhelming databases.

In this study we propose a method, based on the structure function, that allows one to easily estimate the Levy index α of the wind. We show that due to the complex nature of a three-dimensional wind a rotated frame of reference is necessary in order to obtain a universal multifractal structure function exponent. We show that the angular dependency of the scaling exponent results in either an increase or decrease in dimension. This increase or decrease in dimension causes a first or second-order phase transition respectively. The kind of phase-transition that occurs is directly related to the generation of extremes of the wind.

The combination of this kind of analysis with the advancements in measurement techniques that are coming to light should allow for the better prediction of extreme weather events in and around cities.

Keywords: Extremes, Weather, Universal Multifractals, Wind, Anisotropy, Scaling

Japan Geoscience Union Meeting 2014
(28 April - 02 May 2014 at Pacifico YOKOHAMA, Kanagawa, Japan)

AAS01-13 Room:423 Time:April 30 14:15-14:30

The Impacts of extreme weather on urban water bodies

MEZEMATE, Yacine[1*] ; FITTON, George[1] ; TCHIGUIRINSKAIA, Ioulia[1] ; SCHERTZER, Daniel[1] ; BONHOMME, Celine[1] ; SOULIGNAC, Frederic[1] ; LEMAIRE, Bruno[1] ; VINCON LEITE, Brigitte[1]

[1]Universite Paris Est, Ecole des Ponts ParisTech, LEESU, Marne La Vallee, France

In the event of heavy rainfall, large amounts of storm water will carry roof runoff pollutants into urban lakes. This kind of discharge not only changes the dynamics of the lake (i.e. the mixing processes that occur) but also complicates ones ability to predict pollutant concentrations. Being able to quantify these changes in pollutant during and after extreme weather events is important for water quality management.

In the interest of understanding the impact of extreme weather events on water bodies, we set-up an Acoustic Doppler Current Profiler (ADCP) next to a storm water discharge point at the bottom of a shallow urban lake in Creteil, a region in Paris.

The ADCP is particularly useful for analysing the turbulent boundary-layer (TBL) during these extreme weather events as it is able to measure the 3D velocity, in 127 vertical cells, over 3 meters. This is a unique situation compared to the atmospheric boundary-layer where profilers are typically coarsely spaced in the vertical.

To analyse the TBL dynamics we look only at the scaling properties of the velocity field. If the velocity is scaling the log-log plot of the energy spectra will be linear in wavenumber (or frequency). The slope of the log-log plot of the spectra gives the spectral scaling exponent. Performing the analysis we find a spectral exponent close to -1. Dimensional arguments suggest that this exponent occurs when the energy flux becomes dependent on the friction velocity instead of the length scale; likely a result of the strong inflow during extreme rainfall events. The ADCP data allows us to observe a smooth transition from a free stream turbulent regime (-5/3) to a bounded-turbulent exponent (-1) through depth.

This kind of analysis suggests the possibility for a general scaling model of the TBL that can be used to predict the mixing of pollutants during and after extreme weather events.

Keywords: Urban Lake, Turbulence, Extreme Weather, Boundary-Layer

Japan Geoscience Union Meeting 2014
(28 April - 02 May 2014 at Pacifico YOKOHAMA, Kanagawa, Japan)

AAS01-14 Room:423 Time:April 30 14:30-14:45

Statistical Analysis of Large Drop Occurrence and Its Effect on Drop Size Distribution

JUNG, Sung-a[1*] ; MAKI, Masayuki[2] ; LEE, Dong-in[1] ; KIM, Ji-hyeon[3] ; TSUCHIYA, Shyuichi[4]

[1]Pukyong National University, Korea, [2]Kagoshima University, Japan, [3]Weather Radar Center, Korea, [4]National Institute for Land and Infrastructure Management, Japan

A large data set of raindrop size distribution (DSD) measured by 2-Dimensional Video Distrometer (2DVD) on 12 locations in Japan is analyzed using the truncated modified gamma DSD model and the normalized gamma DSD model. The present study seeks to: 1) explore the general properties of DSD observed at Kanto, Hokuriku, Nagoya, Kinki and Kyushu in Japan; 2) find the governing parameters of DSD models in different geographycal and seasonal regime; 3) statistics of big drops occurrence and instrinsic shape of the DSD with extremely large drops; 4) find relationships between DSD parameters such as the shape and slope parameters, the generalized intercept parameter and volume-weighted mean diameter, and etc. The present study on stratistical analysis of DSD provide us information which is nesessary to understand big drop microphysics and precipitation.

Keywords: large drop, DSD, 2DVD

Japan Geoscience Union Meeting 2014
(28 April - 02 May 2014 at Pacifico YOKOHAMA, Kanagawa, Japan)

AAS01-15 Room:423 Time:April 30 14:45-15:00

A Social Experiments on Disaster Prevention by Using of the Advanced Weather Information

NAKATANI, Tsuyoshi[1*] ; SHOJI, Yoshinori[2] ; MISUMI, Ryohei[1] ; NAKAMURA, Isao[3] ; MAKI, Masayuki[4]

[1]National Research Institute for Earth Science and Disaster Prevention, [2]Dept. of Meteorological Satellite and Observation System Research, Meteorological Research Institute, [3]Toyo Univ., Faculty of Sociology, [4]ERCPD, Kagoshima Univ.

The National Research Institute for Earth Science and Disaster Prevention has been carried out the research project on Tokyo Metropolitan Area Convection Sturdy for Extreme Weather Resilient Cities(TOMACS) in cooperation with 25 research agencies, researchers of more than 100 people and disaster management personnel of local governments. In this project we have been working on the following three research subjects.

(1) Studies on extreme weather with dense meteorological observations
(2) Development of the extreme weather early detection and prediction system
(3) Social experiments on extreme weather resilient cities

The study fields by the social experiment are Rescue Services (Tokyo Fire Department), Risk management(Edogawa ward,Yokohama city, Fujisawa city, Minamiashigara city), Infrastructure(JR East,JR Central, Obayashi) and Education and life(Toyo univ., The Certified and Accredited Meteorologists of Japan). In the social experiments, the each participated institutions have studied on the effective use of advanced weather information into disaster prevention according to their purposes.

The objective of social experiments are to enable the continous use of advanced weather information through the fixing of the monitoring and prediction system of extreme weather.

And also to discuss the problems and issues revealed in the course of social experiment, and to summarize as creating resilient city in extreme weather towards relevant government ministries and agencies, local government, the general population.

In this paper, overview of the social experiments is briefly explained and issues for continue use of advanced weather information are reported through the reference to the case of Edogawa-Ward where the X-band MP radar rainfall information is providing to residents. Finally this project is supported by the Japan Science and Technology Agency and Ministry of Education, Culture, Sports, Science and Technology.

Keywords: Extreme weather, Disaster prevention, Social experiment

Japan Geoscience Union Meeting 2014
(28 April - 02 May 2014 at Pacifico YOKOHAMA, Kanagawa, Japan)

AAS01-P01 Room:Poster Time:April 30 18:15-19:30

Analysis of meso-gamma-scale convection in tropical regions using GPS meteorology

MATSUDA, Takafumi[1*]

[1]Graduate School of Science, Kyoto University

In tropical regions such as Indonesia, strong wind with severe shower called squall occurs frequently, and has a large impact on residents in a rainy season. To predict accurately local heavy rain (occurring in a short time and in the range of a few km) is difficult today. Therefore, it is important to understand generation and development mechanism of the meso-γ-scale convection that leads to locally heavy rain.

”GPS meteorology” is a method to obtain the ”atmospheric information” such as water vapor from atmospheric delay of radio waves based on a satellite ”positioning error”. We can estimate precipitable water vapor (PWV: integrated amount of water vapor along the zenith direction) with a high time resolution by using this method. Occurrence of rainfall associated with the meso-γ-scale convection has good correlation with the spatial non-uniformity and temporal variation of PWV estimated by the GPS meteorology technique (GPS-PWV).

The purpose of this study is to find out the generation mechanism of meso-γ-scale convection in the tropics by focusing on the GPS-PWV.

We analyzed GPS-PWV, radiosonde and rainfall data obtained from the campaign which was conducted during the rainy season of 2013 in Bandung, Indonesia.

We carried out accuracy validation of GPS-PWV by analyzing the radiosonde data. As a result, the rainfall data showed that precipitation occurred often in the late afternoon together with an increase of PWV. Furthermore, we found the daily cycle of PWV showing minimum and maximum values in the morning and late afternoon, respectively. In addition, there is a difference in an altitude of more than 1000 m in each observation point. The difference has a severe influence on GPS-PWV. Therefore, it is need to correct altitude difference effect.

Keywords: GPS meteorology, local heavy rain, meso-gamma-scale convection, tropical regions, Indonesia

Japan Geoscience Union Meeting 2014
(28 April - 02 May 2014 at Pacifico YOKOHAMA, Kanagawa, Japan)

AAS01-P02 Room:Poster Time:April 30 18:15-19:30

Development of high resolution spatio-temporal precipitation data using a network of polarimetric X-band radars in Japan

KIM, Yu-ra[1*] ; LEE, Dong-in[1] ; JEONG, Jong-hoon[1] ; MAKI, Masayuki[2]

[1]Department of Environmental Atmospheric Sciences, Pukyong National University, [2]Department of Research and Education Center for Natural Hazards, Kagoshima University

Localized convective precipitation develops rapidly in a very short time and is conducive to extreme local rainfall amount. The X-band polarimetric radar is useful to analyze the convective precipitation because it can provide us polarimetric radar parameters which are useful to understand microphysical process in the precipitation. However, the radar observation has some limitations in detecting initial stage of rapidly developing convective cell; the radar volume scan strategy adopted in operational radar is 5 minute interval which is not enough for measuring rapidly developing convective precipitation. To detect the early stage of convective cell, we developed the algorithm which is based on the interpolation method both in space and time. The algorithm reproduces higher resolution spatio-temporal volumetric data using the operational network of four X-band polarimetric radars. The mosaic of multiple radars could be benefit for increased sampling into a certain volume. In addition, different scan strategy at each radar also improve spatio-temporal resolution. The algorithm is applied to radar data of convective precipitations observed in Kanto area in 2012. The new volumetric data can recognize more detail about echo which developed rapidly and detect the first appearance of convective echo at upper layer. Early detection of convective precipitation at upper layer can be useful for nowcasting or very short-term forecasting.

Keywords: convective cell, X-band polarimetric radar, high resolution precipitation data

Japan Geoscience Union Meeting 2014
(28 April - 02 May 2014 at Pacifico YOKOHAMA, Kanagawa, Japan)

AAS01-P03 Room:Poster Time:April 30 18:15-19:30

An Ensemble Nowcasting of Rainfall over the Kanto Region, Japan

P.C., Shakti[1*] ; MISUMI, Ryohei[1] ; NAKATANI, Tsuyoshi[1] ; MAKI, Masayuki[2] ; SEED, Alan[3]

[1]National Research Institute for Earth Science and Disaster Prevention(NIED), Tsukuba, Japan, [2]Kagoshima University, Kagoshima, Japan, [3]Bureau of Meteorology, Melbourne, Australia

Every year weather-related disasters: extreme rainfall, landslides and flooding destroy livelihoods and damage economics somewhere on the planet. Recently, number of flash flooding is believed to be increasing specially in urban areas. It has being a great challenge to forecast flood warning and urban drainage management. Nowcasting of rainfall (very short-range forecasting) is an important tool to minimize or manage all these weather-related disasters since precipitation is the main input. Common practice to forecast heavy precipitation for hydrological application varies from 0-6 hr and there are different kinds of nowcasting based on different method.

Nowcasting of rainfall comprises the detailed description of the current weather along with forecasts obtained by extrapolation for a different time period ahead. In this study, we focus on ensemble nowcasting of rainfall. It refers to the fact that many forecasts are produced, with the rainfall areas moving at slightly different speeds, and with the small rainfall features represented by slightly different random statistics. By comparing these different nowcasting of rainfall, the forecaster can decide how likely a particular weather event will be. It gives a much better idea of what weather events may occur at a particular time. Short Term Ensemble Prediction System (STEPS), one of the most advanced Quantitative Precipitation Forecast (QPF) systems currently available is considered for nowcasting of rainfall. Japan Meteorological Agency (JMA) and X-band multi-parameter (MP) radar data were considered to produce an ensemble nowcasting of rainfall. First, JMA radar rainfall data of Kanto region was fixed to check the performance of STEPS. Skill scores showed that STEPS can give a good forecast for less than one hour. However, more uncertainties can be seen during the starting and ending of rain event. High resolution of data (MP data) also used in the STEPS under the default condition. Overall, an ensemble nowcasting of rainfall seems close with real time data, which could be interesting to use them in hydrological model.

Keywords: nowcasting, ensemble, weather radar, extreme rainfall, STEPS, hydrological model

Japan Geoscience Union Meeting 2014
(28 April - 02 May 2014 at Pacifico YOKOHAMA, Kanagawa, Japan)

AAS01-P04 Room:Poster Time:April 30 18:15-19:30

X-band polarimetric radar and C-band conventional radar composite rainfall map with high spatio-temporal resolution

MAKI, Masayuki[1*] ; HIRANO, Kohin[2] ; P.C., Shakti[2] ; SCHERTZER, Daniel[3]

[1]Kagoshima University, [2]NIED, [3]Ecole des Ponts ParisTech, U. Paris-Est

Radar with shorter wavelength such as the X-band (3-cm) wavelength has several advantages compared to C- and S-band radar. First, X-band wavelength radar has high sensitivity of the specific differential phase of the rain rate. Second, it is possible to achieve finer spatial resolution more economically; for example, X-band wavelength radar can achieve a 1 degree beam width with a 2 m diameter parabolic antenna, while S-band needs a 7 m diameter antenna to achieve the same beam width. Third, due to advantage number two, X-band radar is easier to setup in mountainous areas, and at lower cost compared to S- and C-band wavelength radar. In Japan, success in the detection of torrential rainfall that occurred in Tokyo in 2008 triggered the deployment of 35 operational X-band polarimetric radars in major urban cities by MLIT. This radar network named XRAIN provides rainfall information with high spatio-temporal resolution. In US, the X-band polarimetric radar network is constructed in Dallas Fort Worth, which is a research and innovation network linking academic researchers, local stakeholders, and industry to address water issues as they relate to urban sustainability. In Europe, The project named RAINGAIN is ongoing to improve fine-scale measurement and prediction of rainfall and to enhance urban pluvial flood prediction. Activities include the implementation and use of advanced radar technologies (X Band) in Leuven, London, Paris, and Rotterdam. Although X-band polarimetric radar has the advantages mentioned above and used in hydrological applications, there are essential disadvantages. First, the maximum range is shorter than that of C-band and S-band radar; maximum ranges of 200km or 300km are easily obtained in case of C- and S- band radar, while that of X-band radar is limited to 30km-60km. Second, signal extinction area which is defined as the area where the received signal is below the receiver noise level occurs behind heavy rainfall areas. These disadvantages will be a fatal flaw when extremely heavy rainfalls occur. Authors have experience that the maximum observation range of X-band radar was shorter than 3km when heavy rainfall passed over the radar site. The present paper aims to develop an algorithm to overcome these disadvantages. The method is based on the C-band and X-band radar composite map which attains the 1 minute time resolution and 250m spatial resolution by the interpolation method. The algorithm is applied to the heavy rainfall case observed on 12-14 July, 2012 in northern Kyusyu, Japan. The algorithm is validated with surface raingauge network: the composite radar rainfall estimation agreed well with raingauge data.

Keywords: polarimetric radar, X-band, precipitation, high resolution, MP radar

Japan Geoscience Union Meeting 2014
(28 April - 02 May 2014 at Pacifico YOKOHAMA, Kanagawa, Japan)

AAS02-01 Room:314 Time:April 29 09:00-09:30

Entropic Balance Theory and Variational Field Lagrangian Formalism

SASAKI, Yoshi kazu[1*]

[1]University of Oklahoma

The entropic balance theory has been applied with outstanding results to explain many important aspects of tornadic phenomena. The entropic balance theory was originally developed in variational formalism with Lagrangian appropriate for supercell storm and tornadic phenomena. The entropic balance theory shares the same foundation as, symbolically called with keywords, ”variational field Lagrangian formalism” in short ”variational formalism”. It is broadly used in inmodern physics, not only in classical mechanics, with Lagrangian density and action designed for each physical problem properly. The Clebsch transformation (equation) was developed in the classical variational formalism, but has not been used because of the unobservable and non-meteorological Lagrange multiplier.

The Lagrange multipliers appeared in the Clebsch transformation are analogous to the mathematical vector potential (and gauge field) of the theoretically found Aharonov-Bohm effect . Its experimental verification has been difficult and has not been made until two decades later. The Lagrange multipliers in the Clebsch transformation seem similar to the vector potential and gauge of electromagnetic field and in advanced physics disciplines.

The entropic balance condition is thus developed from the Clebsch transformation, changing the unobservable non-meteorological Lagrange multiplier to observable meteorological rotational flow velocity with entropy and making it applicable to tornadic phenomena.

Japan Geoscience Union Meeting 2014
(28 April - 02 May 2014 at Pacifico YOKOHAMA, Kanagawa, Japan)

AAS02-02 Room:314 Time:April 29 09:30-09:45

Deterministic predictability of the most probable state and reformulation of variational data assimilation

TSUYUKI, Tadashi[1*]

[1]Meteorological Research Institute

Four-dimensional variational data assimilation (4DVar) and ensemble Kalman filter (EnKF) have been widely used for data assimilation in meteorology and oceanography. Since prior probability density functions (PDFs) used in 4DVar and EnKF are usually assumed to be Gaussian, those two methods may not work well for a strongly nonlinear system. Thus data assimilation with nonlinear systems or non-Gaussian PDFs is a challenge in geophysics. Theoretical study of the two methods for nonlinear systems may be expected to provide insight for further advancement of data assimilation. The present study addresses this issue by reformulating variational data assimilation.

A necessary condition for deterministic predictability may be that the forecast state starting from the most probable state at an initial time remains close to the most probable state at a forecast time. It is found from the Liouville equation that if the trace of the Jacobian matrix of a deterministic nonlinear system does not depend on the state variables (hereafter referred to as the trace condition), the mode of a PDF of the state variables evolves according to the governing equations of the system. A condition for the forecast state to be close to the mode of the PDF is derived under an assumption of small prediction error for general deterministic nonlinear systems. This condition depends on the sensitivity of the trace to an initial condition, the size of initial condition error, and the length of forecast lead time.

Since the dynamical cores of numerical models of the atmosphere and the ocean are based on fluid dynamics, it is interesting to examine whether the governing equations of fluid dynamics satisfy the trace condition. The trace of the Jacobian matrix is calculated for finite-dimensional analogs of several Eulerian equations of ideal fluids. It is readily found that the trace condition generally holds for unbounded fluids under periodic boundary conditions. It is shown that the trace condition also holds for the quasigeostrophic equations with rigid boundaries, the Boussinesq approximation with rigid boundaries, and the shallow water equations on a sphere, by expanding the state variables in eigenfunctions of the Laplacian operator or the curl operator. The shallow water equations in a channel and compressible fluid with top and bottom boundaries do not satisfy the trace condition due to divergence at the boundaries.

A new formulation of variational data assimilation is presented for deterministic nonlinear systems that satisfy the trace condition. Though the cost function in the new formulation takes the same form as the conventional one, it makes clear an advantage of 4DVar over EnKF. If the trace condition holds, the forecast state starting from the mode of the posterior PDF at the last analysis time is the mode of the prior PDF. In the new formulation, the logarithm of the prior PDF is expanded around the forecast state, and covariance globalization is introduced to take into account the global distribution of the prior PDF that may be non-Gaussian. A feasible method for the covariance globalization may be to replace the local covariance matrix at the mode with a forecast error covariance matrix taken from EnKF. It is proved that a non-Gaussian prior PDF that evolves according to the Liouville equation is implicitly used for assimilating observational data in 4DVar. Results from an assimilation experiment with a toy model suggest that 4DVar thus formulated outperforms EnKF if the global minimum of the cost function is found.

Finally, it is pointed out that enough observational data are necessary for variational data assimilation to work well for a deterministic nonlinear system that does not satisfy the trace condition. Otherwise, EnKF and ensemble prediction may be a better choice for data assimilation and prediction of the system.

Keywords: variational data assimilation, deterministic predictability, non-Gaussianity

Japan Geoscience Union Meeting 2014
(28 April - 02 May 2014 at Pacifico YOKOHAMA, Kanagawa, Japan)

AAS02-03 Room:314 Time:April 29 09:45-10:00

Modal analysis of near-bank velocity profiles in a tidal river.

WELLS, John[1*] ; PHAN, Tuy[1] ; NGUYEN, Linh V.[1] ; SUSUKI, Yoshihiko[2] ; BONNER, James[3] ; ISLAM, Mohammad S.[3] ; KIRKEY, William D.[3]

[1]Ritsumeikan University, [2]Kyoto University, [3]Clarkson University

We apply two decompositions to long-beam velocities of a 600 kHz 3-beam Horizontal Acoustic Doppler Current Profiler (HADCP) at West Point on the Hudson River Estuary, so as to efficiently characterize the spatiotemporal variation of near-bank velocity. One main motivation is to test statistical tools with which to benchmark computations. The HADCP is deployed next to the USGS gauging station at West Point, some 100 km upriver from Manhattan, on the inner bank downstream of a sharp bend and its associated 40 m deep trough. We analyzed a time series of 1-minute averages from October 2011, out to 80 meters from the bank with 1 m bins.

The first decomposition we apply is Principal Component Analysis. The PCA generates an optimally convergent set of spatial eigenfunctions or ”principal components” (PC), with which are associated temporally-varying amplitudes called ”temporal coefficients”. The first principal component captures more than 96.3% of the variance in velocity measured along the three HADCP beams, while the second PC captures about 2%. There appears an asymmetry between ebb and flood, as seen clearly from a phase plot of the temporal coefficient of the first PC versus that of the second.

The second is Fourier-based Koopman Mode Decomposition, i.e. decomposition into harmonic averages of the measurement vector. KMD associates a spatial structure with each of a series of temporal frequencies. For Oct 2011, the semidiurnal mode captured 74.33% of the variance. KMD also quantifies the phase lags at different distances from the river bank (and between normal and tangential velocity). Phase lags of tangential velocity between 10 and 80 m from the bank were about 1 hour for the semidiurnal mode, and 2 hours for the first (with a period of about 6 hours.), and this difference grew to a factor of four when considering flow within 10 m.

Keywords: principal component analysis, Koopman mode decomposition, ebb-flood asymmetry

Japan Geoscience Union Meeting 2014
(28 April - 02 May 2014 at Pacifico YOKOHAMA, Kanagawa, Japan)

AAS02-04 Room:314 Time:April 29 10:00-10:15

Pathways of the North Pacific Intermediate Water identified through the tangent linear and adjoint codes of an OGCM

FUJII, Yosuke[1*] ; NAKANO, Toshiya[2] ; USUI, Norihisa[1] ; MATSUMOTO, Satoshi[2] ; TSUJINO, Hiroyuki[1] ; KAMACHI, Masafumi[1]

[1]Meteorological Research Institute, [2]Japan Meteorological Agency

We develops a strategy of tracing a target water mass, and applies it for analyzing the pathway of the North Pacific Intermediate Water (NPIW) from the subarctic gyre to the northwestern part of the subtropical gyre south of Japan in a simulation of an ocean general circulation model. This strategy estimates the pathway of the water mass that travels from an origin to a destination area during a specific period using a conservation property concerning tangent linear and adjoint models. In our analysis, a large fraction of the low salinity origin water mass of NPIW initially comes from the Okhotsk and Bering Seas, meets at the southeastern side of the Kuril Islands, and is advected to the Mixed Water Region (MWR) by the Oyashio current. It then enters into the Kuroshio Extension (KE) around the first KE ridge, and is advected eastward by the KE current. It, however, deviates southward from the KE axis around 158E over the Shatsky Rise, or around 170E on the western side of the Emperor Seamount Chain, and enters into the subtropical gyre. It is finally transported westward by the recirculation flow. This pathway corresponds well to the shortcut route of NPIW from MWR to the region south of Japan inferred from the analysis of the long-term freshening trend of NPIW observation.

Keywords: Adjoint, Sensitivity analysis, North Pacific Intermediate Water, Kuroshio Extension, Oyashio

Japan Geoscience Union Meeting 2014
(28 April - 02 May 2014 at Pacifico YOKOHAMA, Kanagawa, Japan)

AAS02-05 Room:314 Time:April 29 10:15-10:30

Optimization of nested ocean circulation model by four dimensional variational data assimilation system

WAKAMATSU, Tsuyoshi[1*] ; ISHIKAWA, Yoichi[1]

[1]Japan Agency for Marine-Earth Science and Technology

Optimization of a regional ocean circulation model by a data assimilation system is achieved by estimating optimal initial condition and external forcing terms which include boundary values. In a nested regional data assimilation system, extracting maximum information from optimized outer model through these control variables is crucial to obtain optimal performance of the nested regional data assimilation system and many schemes were proposed in the atmospheric and oceanic data assimilation studies. In this presentation, the optimization schemes of a nested atmosphere and ocean circulation model by four dimensional variation data assimilation system are summarized in a unified framework. Their performance will be analyzed using observability matrix of a variational data assimilation system constructed on regional ocean circulation model surrounding Japan islands.

Keywords: data assimilation, regional ocean circulation model

Japan Geoscience Union Meeting 2014
(28 April - 02 May 2014 at Pacifico YOKOHAMA, Kanagawa, Japan)

AAS02-06 Room:314 Time:April 29 10:30-10:45

Estimated State of Ocean for Climate Research by Using a 4 Dimensional Variatinal approach

MASUDA, Shuhei[1*] ; DOI, Toshimasa[1] ; OSAFUNE, Satoshi[1] ; SUGIURA, Nozomi[1] ; ISHIKAWA, Yoichi[1] ; FUKUDA, Kazuyo[1]

[1]JAMSTEC

A 4-dimensional variational data assimilation system has been used to better define the 50-year global ocean state estimation for climate research. The synthesis of available observations and general circulation model with a pelagic ecosystem model based on nitrogen cycle yields a dynamically self-consistent dataset. Obtained ocean state estimation possibly has greater information than do models or data alone. In our 4D-VAR approach, optimized 4-dimensional analysis fields are sought by minimizing a cost function on the basis of adjoint method for physical parameters and Green's function approach for biogeochemical ones. The assimilated elements are temperature and salinity based on EN3 dataset provided by Met Office Hadley Centre, sea surface height anomaly form AVISO, nitrate from WOA05, and chlorophyll-a from WOA98 and SeaWiFS. We here present the properties of the analysis fields and some results of climate study by using this state estimation named ESTOC. This report implies that our synthesis scheme as a dynamical interpolation for sparse observations including bio-geochemical parameters is possibly promising and useful for " Integrated Earth System Analyses " .

Keywords: data assimilation, ocean, climate change

Japan Geoscience Union Meeting 2014
(28 April - 02 May 2014 at Pacifico YOKOHAMA, Kanagawa, Japan)

AAS02-07 Room:314 Time:April 29 11:00-11:20

Data assimilation for ocean and climate study

ISHIKAWA, Yoichi[1*] ; NISIKAWA, Shiro[1] ; MASUDA, Shuhei[1] ; TOYODA, Takahiro[2] ; SUGIURA, Nozomi[1] ; WAKAMATSU, Tsuyohi[1] ; NISIKAWA, Haruka[1] ; SASAKI, Yuji[1] ; IGARASHI, Hiromichi[1] ; TANAKA, Yusuke[1] ; AWAJI, Toshiyuki[3]

[1]JAPAN Agency for Marine-Earth Science and Technology, [2]Meteorological Research Institute, [3]Kyoto University

The data assimilation systems have been developed for the initialization of the numerical weather forecasting, and applied for other fields in recent studies. In the area of ocean and climate research, there are several interesting studies to utilize the advantage of the many aspects of the data assimilation, in addition to the ”ocean weather forecasting”.

The atmosphere-ocean coupled data assimilation system using variational adjoint method is one of the unique systems, which is developed in JAMSTEC. The target of this system is the variability of seasonal to inter-annual scale so that the integrated dataset of the observation both in atmosphere and ocean are derived using variational adjoint method. The remarkable feature of the system is that the bulk coefficients are estimated as well as the initial condition of the oceanic fields since the lower boundary condition of the atmospheric model are very important for seasonal to inter-annual time scale. Recently, the marine ecosystem model are embedded into this system and seasonal forecasting not only for physical fields but also for biogeochemical fields are carried out.

For oceanic long-term reanalysis dataset, the interesting data assimilation systems are developed using variational adjoint method (Masuda et al., 2010). In this data assimilation system, strong constraint conditions are applied for entire assimilation period over 50 years, so that the derived dataset are consistent with the dynamics in ocean general circulation model. This means that the derived dataset satisfies the conservation rules and suitable for the 4-dimensional analysis of the heat and water fluxes. This advantage is also suitable for the analysis of the oceanic tracers and useful for the biogeochemical studies.

The data assimilation system for the marine ecosystem model is also notable issues. Since it is difficult to identify the optimal parameters in the marine ecosystem model, the parameter estimation studies are widely used. The realistic fields of the biogeochemical variables are successfully obtained by parameter estimation (Toyoda et al., 2013).

Japan Geoscience Union Meeting 2014
(28 April - 02 May 2014 at Pacifico YOKOHAMA, Kanagawa, Japan)

AAS02-08 Room:314 Time:April 29 11:20-11:35

Development of an ensemble-based data assimilation system with a coupled atmosphere-ocean GCM

KOMORI, Nobumasa[1*] ; ENOMOTO, Takeshi[2] ; MIYOSHI, Takemasa[3] ; YAMAZAKI, Akira[1] ; TAGUCHI, Bunmei[1]

[1]Earth Simulator Center, JAMSTEC, [2]Disaster Prevention Research Institute, Kyoto University, [3]RIKEN Advanced Institute for Computational Science

To enhance the capability of the local ensemble transform Kalman filter (LETKF) with the Atmospheric general circulation model (GCM) for the Earth Simulator (AFES), a new system has been developed by replacing AFES with the Coupled atmosphere-ocean GCM for the Earth Simulator (CFES). An initial test of the prototype of the CFES-LETKF system has been completed successfully, assimilating atmospheric observational data (NCEP PREPBUFR archived at UCAR) every 6 hours to update the atmospheric variables, whereas the oceanic variables are kept unchanged throughout the assimilation procedure.

An experimental retrospective analysis-forecast cycle with the coupled system (CLERA-A) starts on August 1, 2008, and the atmospheric initial conditions (63 members) are taken from the second generation of AFES-LETKF experimental ensemble reanalysis (ALERA2). The ALERA2 analyses are also used as forcing of stand-alone 63-member ensemble simulations with the Ocean GCM for the Earth Simulator (EnOFES), from which the oceanic initial conditions for the CLERA-A are taken.

The ensemble spread of SST is larger in CLERA-A than in EnOFES, suggesting positive feedback between the ocean and the atmosphere. Although SST in CLERA-A suffers from the common biases among many coupled GCMs, the ensemble spreads of air temperature and specific humidity in the lower troposphere are larger in CLERA-A than in ALERA2. Thus replacement of AFES with CFES successfully contributes to mitigate an underestimation of the ensemble spread near the surface resulting from the single boundary condition for all ensemble members and the lack of atmosphere-ocean interaction.

In addition, the basin-scale structure of surface and subsurface ocean temperature in the tropical Pacific is well reconstructed from the ensemble correlation in CLERA-A but not in EnOFES. This suggests that use of a coupled GCM rather than an oceanic GCM could be important even for oceanic analysis with an ensemble-based data assimilation system.

Japan Geoscience Union Meeting 2014
(28 April - 02 May 2014 at Pacifico YOKOHAMA, Kanagawa, Japan)

AAS02-09 Room:314 Time:April 29 11:35-11:50

Data assimilation experiment of water vapor data derived from a hyper-dense GNSS network using a nested LETKF system

OIGAWA, Masanori[1*] ; TSUDA, Toshitaka[1] ; REALINI, Eugenio[1] ; IWAKI, Yuya[1] ; SEKO, Hiromu[2] ; SHOJI, Yoshinori[2] ; SATO, Kazutoshi[3]

[1]Research Institute for Sustainable Humanosphere (RISH), Kyoto University, [2]Meteorological Research Institute (MRI), Japan Meteorological Agency (JMA), [3]Japan Aerospace Exploration Agency (JAXA)

Data assimilation of observation data with high spatial and temporal resolutions within a numerical weather prediction model is important, in order to provide it with accurate and detailed initial conditions, which generally result in improved forecast accuracy for localized heavy rainfall. Assimilation of water vapor data is especially important because water vapor has a powerful effect on the initiation and development of cumulonimbus clouds. Many assimilation studies reported on the significant and positive impact of assimilating GNSS (Global Navigation Satellite System) derived PWV (Precipitable Water Vapor) data, i.e. the vertically integrated water vapor amount, on the modification of the initial distributions of water vapor, as well as on the forecast accuracy of localized heavy rainfall. The Japan Meteorological Agency (JMA) routinely assimilates PWV data derived from the nationwide GNSS observation network (GEONET) operated by the Geospatial Information Authority of Japan (GSI), which has a horizontal resolution of about 20 km. It is expected, however, that the assimilation of PWV data with higher spatial resolution will be needed as the horizontal resolution of numerical models becomes higher. Therefore, we investigated the assimilation impact of high resolution PWV observations derived from a hyper-dense GNSS network with a horizontal resolution of about 1 km, which we installed near Uji campus of Kyoto University (Sato et al., 2013).

The data assimilation carried out in this report is based on a two-way nested Local Ensemble Transform Kalman Filter (LETKF) system (Seko et al., 2013). Experiments were performed involving a heavy rainfall event that occurred on 14 August 2012, which brought about 260 mm of accumulated rain amount in 6 hours. First, GEONET-derived PWV data were assimilated into an outer model, with horizontal resolution of 15 km. The analysis window and assimilation interval of this first experiment were 6 hours and 1 hour, respectively. Next, PWV data derived from the hyper-dense GNSS network were assimilated into an inner model, with horizontal resolution of 1.875 km. The analysis window and assimilation interval of this second experiment were 1 hour and 10 minutes, respectively. Surface observations and upper atmospheric sounding data used in operational analyses by JMA were also assimilated in both the experiments.

In an experiment without assimilation of any PWV data, the location of the reproduced rainfall region was shifted, and the precipitation intensity was lower, compared with the observation result. When GEONET-derived PWV were assimilated into the outer model and no PWV data were assimilated into the inner model, the location of the simulated rainfall system was improved, although there was no modification in precipitation intensity. When PWV derived from the hyper-dense GNSS network was assimilated into the inner model together with the assimilation of GEONET-derived PWV into the outer model, the precipitation intensity was also modified in addition to the modification of rainfall system location.

These results suggest the usefulness of assimilating high spatial resolution PWV data for heavy rainfall forecast. In the future, we are planning to investigate how the assimilation impact of high resolution PWV data will change depending on the number of observation points of the hyper-dense GNSS network. In this talk, assimilation results of slant water vapor data will also be reported, which is the accumulated water vapor amount along ray paths of radio signals from a receiver to GNSS satellites.

Keywords: Data assimilation, local heavy rainfall, Hyper-dense GNSS observation, nested LETKF

Japan Geoscience Union Meeting 2014
(28 April - 02 May 2014 at Pacifico YOKOHAMA, Kanagawa, Japan)

AAS02-10 Room:314 Time:April 29 11:50-12:05

Data assimilation experiments of tropical cyclones with the NHM-LETKF

KUNII, Masaru[1*]

[1]Meteorological Research Institute

Intensity forecast of tropical cyclones (TCs) has still been a challenging task whereas TC track forecasts have constantly improved over the past several decades owing to advances in numerical weather prediction models as well as observational capabilities. This is partly due to the difficulties in TC initialization because TCs occur and remain almost throughout their existence over the ocean, where observational data have generally been scarce. In this study, TCVital observations are assimilated with an ensemble Kalman filtering, and their impacts are estimated by comparing with the conventional bogus assimilation scheme.

Keywords: data assimilation, ensemble Kalman ffilter, tropical cyclone

Japan Geoscience Union Meeting 2014
(28 April - 02 May 2014 at Pacifico YOKOHAMA, Kanagawa, Japan)

AAS02-11 Room:314 Time:April 29 12:05-12:20

Tropical cyclone forecast using a hybrid EnKF-4DVar system

ITO, Kosuke[1*] ; KUNII, Masaru[2] ; KAWABATA, Takuya[2] ; SAITO, Kazuo[2] ; HONDA, Yuki[3]

[1]JAMSTEC, [2]MRI, [3]JMA

Analysis increment is dependent on the prescribed background error covariance **B** in addition to innovation and model dynamics that describes the development of perturbations. Traditionally, **B** is assumed to be static in time according to so-called NMC method. Following this method, the differences between pairs of forecasts valid at the same time, but having different lead times, are taken to represent the background error. While **B** in NMC method approximates the climatological background error covariance, recent studies have shown that the forecast skill of 4DVar is further enhanced by making flow-dependent **B** out of the perturbations in the ensemble-Kalman filter (EnKF) (Buehner et al. 2010). This system is referred to as Hybrid EnKF-4DVar. We have developed the meso Hybrid-4DVar system based on the meso 4DVar system (JNoVA) in the Japan Meteorological Agency since the improvements is thought to be more pronounced for severe impact weather such as tropical cyclones and heavy rainfall. In this presentation, we present a preliminary result for a forecast of tropical cyclone Talas (2011). Figure 1 shows the analysis increment of horizontal wind in the conventional 4DVar and hybrid EnKF-4DVar. The first guess of the zonal wind is overplotted. It shows a pseudo observation of wind field near the center of the tropical cyclone yields the analysis increment of a pair of cyclonic and anti-cyclonic circulations. It corresponds to a vortex displacement in the hybrid EnKF-4DVar system. In contrast, the analysis increment does not fit the structure of the tropical cyclone when using **B** based on the NMC method. It suggests that the hybrid EnKF-4DVar system reproduces the reasonable analysis increment with a little information.

Keywords: data assimilation, tropical cyclone, 4DVar, ensemble Kalman filter

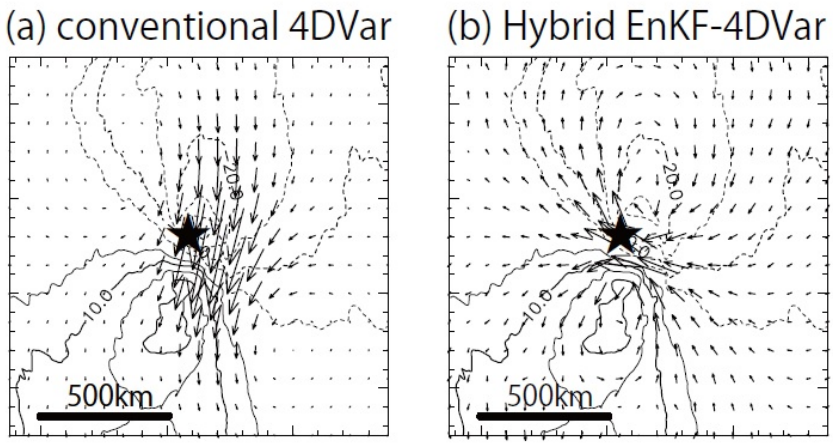

Japan Geoscience Union Meeting 2014
(28 April - 02 May 2014 at Pacifico YOKOHAMA, Kanagawa, Japan)

AAS02-12 Room:314 Time:April 29 12:20-12:35

Dual-Scale Neighboring Ensemble Variational Assimilation for a Cloud-Resolving Model

AONASHI, Kazumasa[1*]

[1]Meteorological Research Institute, Japan Meteorological Agency

1. Introduction

The purpose of the present study is to develop an Ensemble-based Variational Assimilation (EnVA) scheme with sampling error damping method for the Cloud-Resolving Model (CRM). This is because, in ensemble-based assimilation schemes for CRMs, sampling error is serious, in particular, for precipitation-related variables (precipitation rate, vertical wind speed) because they are confined in rainy areas.

2. Dual-Scale Neighboring Ensemble Variational Assimilation method

Based on the CRM ensemble forecast error analyses for various precipitation cases, we developed the sampling error damping method that consisted of a Neighboring Ensemble (NE) method and a dual scale separation of NE. The NE method approximated the forecast error correlation using NE members within a reduced-grid box (5 x 5 grids in the present study) based on the spectral localization assumption. In the dual scale separation, we divided the NE forecast error into large-scale portions (13 x 13 grid averages in the present study) and small-scale deviations so as to reflect the horizontal scale differences in forecast error between precipitation-related variables and others.

In order to introduce the sampling error damping method to the three-dimensional EnVA, we assumed that the EnVA analysis increments were subject to the dual scale NE forecast error subspace. In addition, we introduced a vertical reduce approximation using the primary Singular Value Decomposition (SVD) modes of the vertical cross correlation of the dual scale NE forecast error. Since the SVD modes were mutually independent, the three-dimensional cost function of EnVA resulted in that for the horizontal component of the analysis increment of the each SVD mode. Then, we horizontally diagonalized the background term of the cost function using the horizontal correlation of the NE forecast error. We used the conjugate gradient scheme to solve the nonlinear minimization of the cost function, and obtained the optimal analysis increment for the ensemble mean. Then, we calculated the analysis increments for ensemble members with the analysis error covariance at the reduced grids.

3. Results of OSSEs

In order to examine the EnVA scheme, we performed OSSEs for several meteorological disturbance cases. The results show that the NE method was successful in producing plausible analyses of precipitation-related variables from the simulated surface precipitation even for grid points where less than 20 % of the ensemble members forecasted precipitation, and that the dual scale separation of NE made spatial scale changes in analysis increments in correspondence with precipitation rates. The EnVA scheme was also successful in retrieving precipitation flags and precipitation profiles from the simulated multi-channel microwave brightness temperatures that were non-linear functions of various precipitation-related variables.

Keywords: Ensemble-based variational data assimilation, Neighboring ensemble, Dual-scale separation, GPM, GCOM, microwave imager

Japan Geoscience Union Meeting 2014
(28 April - 02 May 2014 at Pacifico YOKOHAMA, Kanagawa, Japan)

AAS02-P01 Room:Poster Time:April 29 18:15-19:30

Decadal climate prediction using 4D-VAR data assimilation approach

MOCHIZUKI, Takashi[1*] ; ISHIKAWA, Yoichi[1] ; MASUDA, Shuhei[1] ; AWAJI, Toshiyuki[2]

[1]JAMSTEC, [2]Kyoto University

It is very recently that decadal climate prediction experiments have been carried out with initialization. As a first step in decadal prediction, simple initialization approaches have usually been used so far, particularly focusing on ocean states. An advanced initialization technique is a pressing concern toward further enhancing the decadal predictability by obtaining suitable atmospheric and oceanic initial conditions that are compatible with both the model and observations. Here, by employing a 4D-VAR data assimilation approach to initialize the atmosphere-ocean coupled climate model, we attempt to perform ensembles of decadal hindcast experiments in line with the CMIP5 protocol. We perform full-field initialization rather than anomaly initialization and assimilate the atmospheric states together with the ocean states. We can validate the predictive skills in the atmosphere and ocean temperature hindcasts in some areas and, roughly speaking, the spatial patterns of the hindcast skills are similar to those of the multi-model ensembles of the CMIP5 decadal hindcasts. While our assimilation system has been developed originally for the purpose of seasonal-to-interannual climate simulations and we use 9-month assimilation window in these experiments, the hindcast results suggest that the atmosphere and ocean states associated with low-frequency variations beyond annual timescales can also be effectively initialized through the iterations of the forward and backward runs of the 4D-VAR data assimilation.

Keywords: decadal prediction, climate prediction, global warming, data assimilation, 4D-VAR

Japan Geoscience Union Meeting 2014
(28 April - 02 May 2014 at Pacifico YOKOHAMA, Kanagawa, Japan)

AAS02-P02 Room:Poster Time:April 29 18:15-19:30

Assimilation of TRMM-PR bright band heights

ENOMOTO, Takeshi[1*] ; YAMAMOTO, Munehisa[2]

[1]Disaster Prevention Research Institute, Kyoto University, [2]Graduate School of Science, Kyoto University

Bright band heights in TRMM PR 2A23 are assimilated as temperature observations. Bright bands are strong radio echo from the melting layer. Bright band heights are located several hundred m below the 0C isotherms (Harris et al. 2000). In the TRMM PR algorithms (Awaka et al 2009), bright band heights are computed as the nadir projection of the distance between the satellite and the Earth ellipsoid minus the distance between the bright band peaks. Although the 0C isotherms from reanalysis or operational analysis are required in detection of bright bands, bright band heights are direct observations. Because bright band heights are valuable information to complement sparse direct measurements over ocean, the analysis can be improve when assimilated. Satellite radiances are mainly used in cloud-free area and assimilation of water substances are not straightforward. By contrast, because bright bands are associated with stratiform clouds, bright band heights are easily assimilated as conventional data over cloudy regions.

The data assimilation system ALEDAS2 (Enomoto et al. 2013) used in this study is composed of the atmospheric general circulation model for the Earth Simulator (AFES) and the local ensemble transform Kalman filter (LETKF). The resolution of the model is T119L48 (1 degree horizontally and 48 levels vertically) and the ensemble size is 63. ALERA2 produced with this system is regarded as the control. Bright band observations are processed as follows. First, each record is regarded as a 0C temperature observation at 500 m above the bright band height. Second, in order to avoid excessive horizontal correlations and computational load, super-observations are produced by the average of observations within 0.5 degree radius linearly weighted with the distance and converted to the LETKF input format in the 1 h window.

The number of the original bright band heights in January 2010 is 2572986 and that of the super-observations is 61905. The super-observations are widely distributed in the tropics and subtropics between 35S and 35N. In the Northern Hemisphere bright bands are clustered along the 30N over ocean, indicating bright bands due to stratiform associated with cyclones along the storm track (Yamamoto et al. 2006). A few bright bands are detected in the horse latitudes between the equator and 25N. In the Southern Hemisphere bright bands are distributed in the tropical and subtropical convergence zones. ALEDAS2 uses the 7 h data window for each analysis time every 6 h. The number of temperature observations increases by a few percent in synoptic hours of 0 and 12 UTC, but by a factor of 1.5 or 2 at 6 and 18 UTC.

In a preliminary experiment from 0 UTC 3 January for 4 d, the analysis ensemble spread, a measure of the analysis error, is reduced by 0.51 Pa and 0.94 Pa over the globe and in the Souther Hemisphere (35S–0), respectively at 0 UTC 7 January. The root mean square of the analysis increment increases by 2.4 % and 5.9 % in the global domain and in the Souther Hemisphere (35S–0).

Keywords: melting layer, satellite data assimilation in cloudy area, observing-system experiment

Japan Geoscience Union Meeting 2014
(28 April - 02 May 2014 at Pacifico YOKOHAMA, Kanagawa, Japan)

AAS21-01 Room:313 Time:April 30 09:00-09:15

A Study on the Structure of Instability in the Mesosphere Using a High Resolution General Circulation Model

SATO, Kaoru[1] ; MASUDA, Akihiro[1*] ; OKAMOTO, Kota[1]

[1]Dept Earth & Planetary Sci., The University of Tokyo

It is well known that in the winter mesosphere, a necessary condition of barotropic and/or baroclinic instability, i.e., negative latitudinal gradient of potential vorticity (PV), is frequently satisfied. This study examines dynamical mechanism of the formation of such instability condition in boreal winter using high-resolution general circulation model data. This model does not include gravity wave (GW) parameterizations and hence all GWs are resolved, allowing us to analyze GWs directly. This is a strong advantage of our study because GWs are quite important for the momentum budget in the mesosphere. First, the 2-d TEM analysis was made. It is shown that the negative PV gradient is regarded as an enhanced PV maximum. This maximum is due to the poleward shift of the westerly jet in associated with strong EP-flux divergence caused by planetary waves from the troposphere. Strong GW drag slightly above the westerly jet shifts poleward as well, which can be understood by a selective GW-filtering mechanism. It seems that this GW-drag shift induces strong upwelling in the middle latitudes and adiabatically cools the middle mesosphere. Resultant enhanced static stability is the main cause of the PV maximum in the upper mesosphere. Because of the dominance of planetary waves during this event, this process may not be zonally uniform. Thus, the 3-d analysis was made using recent theoretical formula by Kinoshita and Sato (2013). As expected, the GW drag is distributed depending on the longitude. The zonal structure of PV maximum is consistent with the GW drag distribution. An interesting fact is that the spatial distribution of GW drag is not largely correlated with that of the zonal wind at the same level but highly correlated with that in the stratosphere. This result indicates that the mesosphere reflects the zonal structure of the stratosphere via the selective GW filtering.

Japan Geoscience Union Meeting 2014
(28 April - 02 May 2014 at Pacifico YOKOHAMA, Kanagawa, Japan)

AAS21-02 Room:313 Time:April 30 09:15-09:30

Dynamical mechanism of multiple tropopause structure observed over Syowa Station

SHIBUYA, Ryosuke[1*] ; SATO, Kaoru[1]

[1]Department of Earth and Planetary Science, Graduate School of Science, The University of Tokyo

Multiple tropopauses which are determined following the definition by the World Meteorological Organization (WMO) were detected in winter at Syowa Station (69.0S, 39.6E). It is shown that the multiple tropopause structures were observed along with a descent of the first (i.e., lowest) tropopause five times in the autumn period from 1 April and 16 May 2013. A detailed analysis using data from the PANSY radar and radiosonde observations was performed for a typical case in 8-11.

The mechanism of the multiple tropopause structure was analyzed using the PANSY radar and radiosonde observations. It is shown that the multiple tropopause structure was regarded as strong temperature fluctuations with a vertical length of about 3 km. Moreover, it is seen that the temperature fluctuations were out of phase with vertical wind fluctuations observed by the PANSY radar by 90o. This feature is consistent with the linear inertia-gravity wave theory. Thus, it is likely that the multiple tropopause structure above the first tropopause was due to the temperature fluctuations associated with an inertia-gravity waves (IGW) having a vertical length of about 3 km. The hodograph analysis also indicates that the multiple tropopause structure above the first tropopause is due to a monochromatic IGW.

To examine the dynamical mechanism and there-dimensional structure of this phenomenon, a numerical simulation was performed by NICAM without using any gravity wave parameterization. The model simulation period is from 0000 UTC 7 April 2013 to 0000 UTC 12 April 2013.

A close look at the time-height cross section of the zonal wind velocity and the static stability over Syowa Station indicates that the multiple tropopause structures together with the descent of the first tropopauses and associated wind disturbances were successfully simulated. A polar front jet strongly meanders in the time period from 8 April to 10 April and a tropopause folding structure is developed near Syowa Station. This means that the descent of the first tropopause was likely caused by the passage of a developing tropopause folding over Syowa Station. The IGW parameters were also consistent with those estimated by the hodograph analysis using the PANSY radar data.

Next, possible sources of the IGWs observed over Syowa Station were examined using data from the NICAM simulation. As a result, it was shown that wave packets observed over Syowa Station include gravity waves both excited by the steep topographic effect and the spontaneous adjustment process.

This mechanism is quite different from mechanisms which previous studies examined in the monsoon region or midlatitude, which is closely related to stratosphere-troposphere exchange (e.g. Randel et al. 2007). It is suggested this enable us to interpret a part of a significant seasonal sensitivity in the poles discussed by Anel et al. (2008). The static stability in the winter lower stratosphere in the Antarctic is particularly weaker than in other latitudes (Gettleman et al., 2011). It is likely because ozone heating is absent due to polar night. Based on the radiosonde observations, Tomikawa et al. (2009) also shows that the static stability in the lower stratosphere over Syowa Station is minimized in April through July. Temperature fluctuations associated with gravity waves are observed as fluctuations of the static stability. Thus, when the background static stability is sufficiently weak such as in the polar lower stratosphere, the temperature fluctuations associated with gravity waves can make local minima of the static stability which are detected as thermal tropopauses. Therefore, it is likely that multiple tropopause events due to IGWs are considered to occur frequently in the Arctic / Atarctic region in winter.

Keywords: Tropopause, Multiple tropopause, Gravity wave

Japan Geoscience Union Meeting 2014
(28 April - 02 May 2014 at Pacifico YOKOHAMA, Kanagawa, Japan)

AAS21-03 Room:313 Time:April 30 09:30-09:45

Tropical non-migrating tides appearing in a high vertical resolution GCM

SAKAZAKI, Takatoshi[1*] ; SATO, Kaoru[2] ; KAWATANI, Yoshio[3] ; WATANABE, Shingo[3]

[1]Research Institute for Sustainable Humanosphere, Kyoto University, [2]Graduate School of Science, The University of Tokyo, [3]JAMSTEC

Atmospheric tides are global scale waves with periods that are harmonics of a solar day. They are primarily excited in the troposphere and the stratosphere, and then, propagate upward. Tides are generally classified into two components: migrating (Sun-synchronous) and non-migrating (non-Sun-synchronous) tides. Although migrating tides were examined by many previous studies, a much fewer studies considered non-migrating tides particularly in the troposphere and the stratosphere. The purpose of this study is to reveal the horizontal and vertical structure of non-migrating tides and its seasonal variations in the region from the troposphere to the mesosphere, as well as to clarify the underlying physical processes.

In this study, data from a high-resolution (T213L256) global spectral climate model (Watanabe et al., 2008) are analyzed. This model covers quite a wide height range from the ground surface to the upper mesosphere (80 km in altitude), enabling us to investigate the full tidal coupling between the lower and upper atmosphere. Also, the vertical resolution is ˜300 m in the vertical, which is almost sufficient to simulate realistic propagation and momentum deposition of gravity waves including tides. We compared the model data with data from COSMIC GPS-RO measurements and TIMED/SABER satellite measurements, and confirmed that the model captures the observed characteristics at least qualitatively.

In the model data, we clearly see that non-migrating tides are mainly excited over the two large continents: over Africa and South America. The excited tides are propagating three-dimensionally like internal inertia-gravity waves. During the propagation, tides with small wavenumbers are filtered out by background zonal wind (e.g., stratospheric semiannual oscillation (SAO)). Thus, both excitation and filtering processes are important for understanding the tidal variability.

Keywords: nonmigrating tides, KANTO, SABER, COSMIC

Japan Geoscience Union Meeting 2014
(28 April - 02 May 2014 at Pacifico YOKOHAMA, Kanagawa, Japan)

AAS21-04 Room:313 Time:April 30 09:45-10:00

Stratospheric Geoengineering

WATANABE, Shingo[1*]

[1]Japan Agency for Marine-Earth Science and Technology

Overview of stratospheric geoengineering simulations proposed by GeoMIP (Geoengineering Model Intercomparison Project) will be presented with emphasis on impact of anthropogenic stratospheric aerosols on stratospheric ozone and surface UV.

Keywords: geoengineering, stratosphere, aerosol

Japan Geoscience Union Meeting 2014
(28 April - 02 May 2014 at Pacifico YOKOHAMA, Kanagawa, Japan)

AAS21-05 Room:313 Time:April 30 10:00-10:15

Influence of topography onto the temperature variation around the tropical tropopause layer

KUBOKAWA, Hiroyasu[1*] ; FUJIWARA, Masatomo[2] ; NASUNO, Tomoe[3] ; MIURA, Hiroaki[4] ; YAMAMOTO, Masayuki[5] ; SATOH, Masaki[1]

[1]Atmosphere Ocean Research Institute, The University of Tokyo, [2]Faculty of Environmental Earth Science, Hokkaido University, [3]Japan Agency for Marine-Earth Science and Technology, [4]Department of Earth and Planetary Science, Graduate School of Science, The University of Tokyo, [5]Research Institute for Sustainable Humanosphere, Kyoto University

The tropical tropopause layer (TTL) is a region where the tropospheric air passes through before entering the stratosphere. Since this region is very cold, the air from the troposphere is dehydrated around here. It is known the Kelvin wave around the TTL affects the big temperature variation and strong dehydration. We investigated the temperature variations around the TTL using the Nonhydrostatic Icosahedral Atmospheric Model (NICAM) on December 2006 (Miura et al. 2007). We found that the temperature variations associated with Kelvin waves are very large over the mountain regions. The amplitude is about 2-times larger than that over the ocean even on the same latitude. We think this result would be a new scientific discovery from simulations or finding of unknown biases of simulations. In this study, we investigate the influence of the topography on the temperature variations around the TTL using the NICAM, re-analysis, satellite, and radiosonde data. We used the Constellation Observing System for Meteorology, Ionosphere, and Climate (COSMIC) data as a satellite data in December, January and February from 2006 to 2010 in order to investigate the temperature variations. The large temperature variations (standard deviation) were found over the mountain regions. This result satisfies the 90% statistical significance level, but the number of data samples is a few. We investigated some reanalysis data having different horizontal resolutions. The standard deviations of the TTL temperature near mountains became large as the horizontal resolution of the model became high. We checked a reanalysis data of the Year of Tropical Convection (YOTC) data from ECMWF with a horizontal resolution of 0.125 degree. When Kelvin waves passed through over the Western Pacific, the amplitude of temperature was large about 2 K over the mountain regions. The power spectrum in the mountains between 7 days and 12 days was actually larger comparing with the ocean. We compared the two local radiosonde data in Jambi and Kototabang (near mountains region). We found that there was no clear difference of temperature variation. Although the temperature variations at Kototabang were slightly large, it is associated with local diurnal variations but not the wave activities. In this study, we found large temperature variation over the mountain in the observational data and numerical models. We would discuss present results and the possibility of this work.

Japan Geoscience Union Meeting 2014
(28 April - 02 May 2014 at Pacifico YOKOHAMA, Kanagawa, Japan)

AAS21-06 Room:313 Time:April 30 10:15-10:30

Constructing the Middle-Atmosphere Version of Non-hydrostatic Global Atmospheric Model NICAM

KODAMA, Chihiro[1*] ; NASUNO, Tomoe[1] ; WATANABE, Shingo[1] ; KUBOKAWA, Hiroyasu[2] ; SATOH, Masaki[2]

[1]Japan Agency for Marine-Earth Science and Technology, [2]University of Tokyo

Atmospheric gravity wave, which is generated by topography, convective activity, frontal system, jet, and/or so on, affects the formation of the basic state in the troposphere and middle atmosphere through wave convergence. It is difficult for a GCM (general circulation model) to explicitly simulate processes of generation, propagation and convergence of the gravity wave, and gravity wave drag scheme is often used in such a model. Watanabe et al. [2008] successfully simulated realistic gravity wave and basic state of the middle atmosphere using high resolution GCM (60 km in horizon and 300 m in vertical) without gravity wave drag scheme. However, propagation characteristics of the gravity wave cannot be appropriately simulated by the GCM based on the hydrostatic system, since dispersion relationship of the gravity wave is different between the hydrostatic and non-hydrostatic system. In addition, GCM cannot explicitly simulate convection, which is one of the source of the gravity wave.

We are constructing the middle-atmosphere version of the non-hydrostatic global atmospheric model, NICAM (Non-hydrostatic Icosahedral Atmospheric Model). Horizontal resolution of the NICAM is 220 km, 56 km, or 14 km. We adopt hybrid-z∗system as a vertical coordinate, in which the horizontal surface is almost flat in the middle atmosphere. Vertical level is located up to 80 km with the uniform interval in the middle atmosphere; the vertical interval is 2 km (61 layers), 1 km (91 layers), 500 m (162 layers), or 300 m (261 layers). We do not use gravity wave drag scheme and cumulus convection scheme. Other configurations are almost same as those in the standard NICAM, which is mainly used for the tropospheric research.

In this presentation, we will show initial results of the performance in the reproducibility of the basic state. Overall, zonal mean structure of the temperature and zonal wind are well simulated in both the troposphere and the middle atmosphere. Though axis of the polar night jet is biased poleward, it is somewhat improved as the vertical resolution is increased. Higher vertical resolution also brings better performance in the strength of the easterly jet in the summer hemisphere and in the QBO-like structure in the tropical lower stratosphere. In the winter hemisphere, cold bias is found around the pole in the upper stratosphere and the mesosphere, and too strong polar night jet is found. At present, the simulation tends to be numerically more unstable as the horizontal and/or vertical resolutions are increased. We will show the above points and wake up debate about the potential of the non-hydrostatic atmospheric model for future research of the whole atmosphere.

Keywords: nonhydrostatic global atmospheric model, atmospheric gravity wave, middle atmosphere, tropical convection

Japan Geoscience Union Meeting 2014
(28 April - 02 May 2014 at Pacifico YOKOHAMA, Kanagawa, Japan)

AAS21-07 Room:313 Time:April 30 11:00-11:15

Physical interpretation on the mechanisms of spontaneous gravity wave radiation using the renormalization group method

YASUDA, Yuki[1*] ; SATO, Kaoru[1] ; SUGIMOTO, Norihiko[2]

[1]Department of Earth and Planetary Science, Graduate School of Science, The University of Tokyo, [2]Department of Physics, Keio University

Gravity waves (GWs) are categorized into orographic ones and non-orographic ones. The mechanisms for non-orographic GW radiation are not clear, because the dynamics is quite nonlinear and complicated unlike orographic GWs. Recently it has been revealed that GWs are spontaneously radiated from an approximately-balanced flow, especially in the jet/front systems (e.g., O ' Sullivan and Dunkerton 1995). The balanced adjustment theory proposed by Plougonven and Zhang (2007) is considered to be the most likely to describe the spontaneous radiation. However, their theory does not give physical interpretations on GW sources and radiation mechanisms. In this study, we derived a new theory and made physical interpretations.

Using the renormalization group (RG) method (Chen et al. 1996), which is a singular perturbation method, the interaction between the vortical flow and the Doppler-shifted GWs which both have slow time-scales is formulated for the hydrostatic Boussinesq equations on the f plane. In general, the RG method enables us to extract slowly-varying components systematically and naturally from the system containing multiple timescale motions. The derived time evolution equations (RG equations, referred to as RGEs) describe the spontaneous radiation of GWs from the components slaved to the vortical flow through a quasi-resonance together with the GW radiation reaction on the large-scale vortical flow. The quasi-resonance occurs when the space and time scales of slaved components are comparable to those of GWs (quasi-resonance condition).

The RGEs are validated using numerical simulations of the vortex dipole by Japan Meteorological Agency Nonhydrostatic Model. The flow near the dipole center is quite strong due to the confluence, which is similar to a localized jet stream in the atmosphere. GW distribution obtained by the RGE integration accords well with the numerical simulation. This result supports the validity of our theory.

The main GW sources in the vortex dipole can be classified into two groups by using the RGEs. The GW sources in the first group are the slaved components produced by the horizontal divergence of acceleration of the vortical flow near the dipole center (Fig. A). The acceleration can be regarded as the sum of Coriolis and pressure gradient forces. This fact indicates that the GW sources express the horizontal compression of fluid. The horizontal compression can produce vertical motion, which radiates GWs when its space and time scales satisfy the quasi-resonance condition. This radiation mechanism corresponds to the velocity-variation mechanism proposed by Viúdez (2007).

The slaved component in the other group is mainly produced by the vortical flow over the deformed potential temperature surfaces (Fig. B). The deformation of potential temperature surfaces can be attributed to the Bernoulli effect due to the strong vortical flow near the dipole center. The vortical flow over the deformed potential surfaces can produce vertical motion, which radiates GWs when its space and time scales satisfy the quasi-resonance condition. In other words, the deformed potential temperature surfaces act like a mountain as in the radiation process of orographic GWs. This radiation mechanism corresponds to the mountain-wave-like mechanism proposed by McIntyre (2009).

Keywords: gravity wave, jet stream, spontaneous radiation, renormalization, wave, singular perturbation method

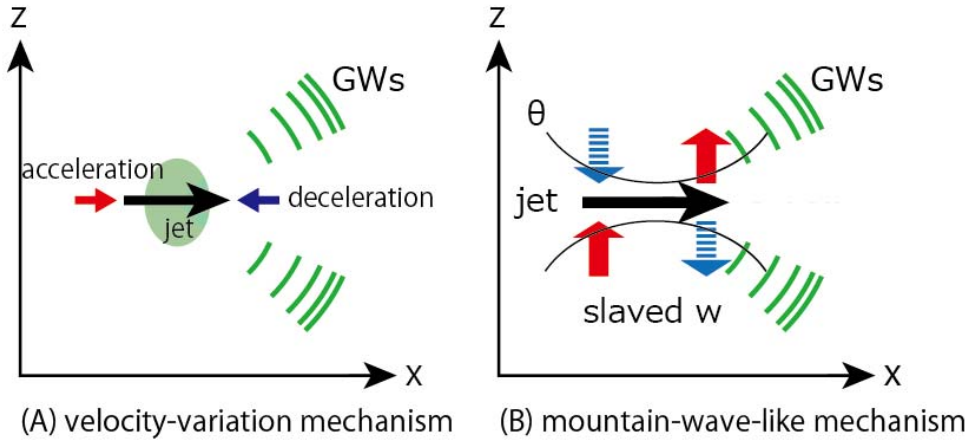

(A) velocity-variation mechanism (B) mountain-wave-like mechanism

Japan Geoscience Union Meeting 2014
(28 April - 02 May 2014 at Pacifico YOKOHAMA, Kanagawa, Japan)

AAS21-08 Room:313 Time:April 30 11:15-11:30

QBO-like oscillation in a radiative-convective equilibrium state obtained with a two-dimensional moist convection model

YODEN, Shigeo[1*] ; BUI, Hoang-hai[2] ; NISHIMOTO, Eriko[1]

[1]Division of Earth and Planetary Sciences, Graduate School of Science, Kyoto University, [2]Hanoi University of Science

Quasi-Biennial Oscillation (QBO) is a prominent internal variations in the equatorial stratosphere due to the interactions between a mean zonal wind and waves that propagate upward in the stratosphere. Over two decades ago, Held et al. (1993) investigated radiative-convective equilibrium states with a two-dimensional explicit moist convection model and obtained a QBO-like oscillation. Their model contains the fundamental dynamical processes of the QBO, though it is a highly-idealized two-dimensional model for a periodic domain without Coriolis effects. In this study, we re-examine the QBO-like oscillation found by H93 with a long enough integration period over two years, by using Advanced Research WRF Modeling System. We also investigate the sensitivity of the QBO-like oscillation in regards of different factors such as domain size, resolution and boundary conditions (e.g., prescribed zonal wind at the top and sea surface temperature).

The control experiment has a similar configuration to that of Held et al.; 640km domain width with a resolution of 5km, 130 vertical levels up to 26km. Convective parameterization is turned off in all simulations and only a cloud microphysics scheme is used. Other physics options are standard ones for short- and long-wave radiations, surface fluxes, planetary boundary layer, turbulence and diffusion, and Rayleigh damping near the top boundary. After spin up, the mean zonal wind shows a clear QBO-like oscillation with a period of 120.6 days. Unlike the observed QBO, the oscillation has a clear signal in the troposphere, in which moist convections dominate and gravity waves are generated. Such convectively generated gravity waves propagate into the stratosphere to produce the QBO-like oscillation in the stratosphere. On the other hand, intensity and propagation of organized convective systems, including zonal mean precipitation, are modulated in accordance with the oscillation of mean zonal wind in the troposphere.

Keywords: QBO, radiative-convective equilibrium, wave-mean flow interaction, two-dimensional moist convection model, stratosphere-troposphere dynamical coupling

Japan Geoscience Union Meeting 2014
(28 April - 02 May 2014 at Pacifico YOKOHAMA, Kanagawa, Japan)

AAS21-09 Room:313 Time:April 30 11:30-11:45

Interannual changes of the semiannual oscillation induced by stratospheric sudden warming events

OHATA, Tsuyoshi[1*] ; IIDA, Chihiro[1] ; HIROOKA, Toshihiko[3] ; EGUCHI, Nawo[2]

[1]Graduate School of Science, Kyushu University, [2]Research Institute for Applied Mechanics, Kyushu University, [3]Faculty of Science, Kyushu University

The semiannual oscillation (SAO) is observed in circulation changes in the equatorial middle atmosphere, which consist of two separate maxima centered near the stratopause (SSAO) and the upper mesosphere (MSAO) with an approximate out-of-phase relathionship between the two [e.g., Andrews et al., 1987]. The SSAO has eastely and westerly maxima at solstices and equinoxes, respectively, while the MSAO shows an out-of-phase change with the SSAO. It is known that somewhat different consideration must be made between the SSAO and the MSAO for their forcing mechanisms, and it seems to be also true of their interannual changes. In this study, we make global gridpoint data for geopotential and temperature fields up to the mesopause level derived from Aura MLS data, to make dynamical analyses for equatorial zonal wind and temperature changes since August 2004 to present. It is found that the strength of both the SSAO and MSAO might be modulated by stratospheric sudden warming (SSW) events in boreal winter solstices. In the equatorial regions, enhanced poleward flows of the residual meridional circulation associated with SSW events lead to temperature perturbations consisting of a cooling in the stratosphere and a warming in the mesosphere. Such temperature perturbations may bring about opposite changes in the SSAO and the MSAO through the thermal wind balance at the equator, leading to their amplifications.

Keywords: semiannual oscillation, stratospheric sudden warming, MLS data

Japan Geoscience Union Meeting 2014
(28 April - 02 May 2014 at Pacifico YOKOHAMA, Kanagawa, Japan)

AAS21-10 Room:313 Time:April 30 11:45-12:00

Recent variability and zonal asymmetry in upper troposphere and lower stratosphere observed with GPS radio occultation m

MEHTA, Sanjay[1*] ; TSUDA, Toshitaka[1] ; FUJIWARA, Masatomo[2] ; SCHMIDT, Torsten[3] ; VERNIER, Jean-paul[4]

[1]Research Institute for Sustainable Humanosphere (RISH), Kyoto University, Japan, [2]Faculty of Environmental Earth Science, Hokkaido University, Japan, [3]GFZ German Research Centre for Geosciences, Potsdam, Germany, [4]NASA Langley Research Center, Hampton, VA 23666, USA.

Tropical upper troposphere and lower stratosphere (UTLS) variability and zonal asymmetry are explored using global positioning system radio occultation (GPS-RO) measurements. GPS-RO offers global monitoring of fine structures of the UTLS temperature variability. GPS-RO continuous measurements from CHAMP (2001-2006) and COSMIC (2006-2013) for about 13 years allows us to study the interannual variability, trends (over the last decade) and its fine zonal structures. The warming of UTLS temperatures between 100 and 50 hPa, warming of tropopause and decrease in its height have been observed over the last decade. The possible reasons for such changes linking to the recent moderate volcanic eruptions and dynamical changes involving changes in sea surface temperature and Brewer Dobson circulation will discussed. The variability and structure observed in GPS-RO will be compared with existing conventional radiosonde and reanalysis datasets.

Keywords: UTLS Temperature, Zonal Assymetry, GPS Radio Occultation, Moderate Volcanic Eruptions, Dynamical Changes

Japan Geoscience Union Meeting 2014
(28 April - 02 May 2014 at Pacifico YOKOHAMA, Kanagawa, Japan)

AAS21-11 Room:313 Time:April 30 12:00-12:15

The role of the mid-latitude oceanic front in the ozone-induced climate change in the Southern Hemisphere

OGAWA, Fumiaki[1] ; OMRANI, Nour-eddine[2] ; NISHII, Kazuaki[1*] ; NAKAMURA, Hisashi[1] ; KEENLYSIDE, Noel[3]

[1]RCAST, University of Tokyo, [2]GEOMAR, University of Kiel, [3]Geophysical Institute, University of Bergen

The Southern Hemisphere Annular Mode (SAM) is the dominant mode of low-frequency atmospheric variability in the extratropical Southern Hemisphere, exerting substantial impacts on regional distributions of temperature and precipitation. Its multi-decadal trend in the troposphere observed in late 20th century has been related to the lower-stratospheric changes induced by the ozone depletion. Known as a manifestation of meridional shift of the eddy-driven polar-front jet (PFJ), which is collocated with the storm-track, the SAM variability may be sensitive to the near-surface baroclinicity associated with the midlatitude oceanic frontal zone.

In the present study, aqua-planet atmospheric general circulation model experiments are conducted with two different zonally symmetric profiles of sea-surface temperature (SST) whose frontal gradient in midlatitudes is retained or eliminated. A comparison of the tropospheric response to the assigned stratospheric ozone depletion between the two SST profiles reveals critical importance of the frontal SST gradient for the intensified stratospheric polar vortex, which is due to the ozone depletion, in triggering and keeping positive phase of the tropospheric SAM in late spring through summer.

We also reveal that the SAM trend in late 20th century simulated in CMIP3/5 models is sensitive to the position and intensity of the mid-latitude oceanic frontal zone. Specifically, a model that simulates the zonal-mean frontal zone at higher latitude tends to simulate the maximum positive trends in the zonal-mean westerlies and midlatitude precipitation also at higher latitudes than another model with the oceanic frontal zone at lower latitude. This relationship is more obvious in a subset of the models with the relatively strong oceanic fronts.

Keywords: Ozone hole, Annular mode, Oceanic front

Japan Geoscience Union Meeting 2014
(28 April - 02 May 2014 at Pacifico YOKOHAMA, Kanagawa, Japan)

AAS21-12 Room:313 Time:April 30 12:15-12:30

Global response to the major volcanic eruptions in 9 reanalysis datasets

FUJIWARA, Masatomo[1*] ; HIBINO, Takashi[1] ; MEHTA, Sanjay[2] ; GRAY, Lesley[3] ; MITCHELL, Daniel[3] ; ANSTEY, James[3]

[1]EES, Hokkaido Univ., [2]RISH, Kyoto Univ., [3]Oxford Univ.

The global climate response to the eruptions of Mount Agung in 1963, El Chichón in 1982 and Mount Pinatubo in 1991 is investigated using 9 reanalysis datasets (ERA-40, ERA-Interim, JRA-25/JCDAS, JRA-55, MERRA, NCEP/NCAR, NCEP/DOE, NCEP-CFSR, and 20CR). Multiple linear regression is applied to the zonal and monthly mean time series of key dynamical variables by considering the components of linear trends, seasonal variations, the Quasi-Biennial Oscillation (QBO), solar cycle, and El Nino Southern Oscillation (ENSO). The residuals are used to define the volcanic signals. Latitude-altitude distributions of the volcanic signals and of the regression coefficients are compared and discussed among the different reanalyses. In response to the Mount Pinatubo eruption most reanalyses show statistically significant negative and positive temperature anomalies in the tropical troposphere and in the tropical lower stratosphere, respectively. The signals are similar for the El Chichón eruption, with a statistically insignificant tropospheric response. The response to the Mount Agung eruption is asymmetric about the equator with significant warming in the Southern Hemisphere midlatitude upper troposphere to lower stratosphere. This work is a contribution to the SPARC Reanalysis Intercomparison Project (S-RIP).

Keywords: volcanic eruption, climate, reanalysis, stratosphere, troposphere

Japan Geoscience Union Meeting 2014
(28 April - 02 May 2014 at Pacifico YOKOHAMA, Kanagawa, Japan)

AAS21-13 Room:313 Time:April 30 12:30-12:45

Simulation of stratospheric aerosol changes after the Pinatubo eruption

SEKIYA, Takashi[1*] ; SUDO, Kengo[1]

[1]Graduate School of Environmental Studies, Nagoya University

An explosive volcanic eruption can inject a large amount of SO_2 into the stratosphere, which is oxidized to form sulfate aerosol. Such aerosol has an impact on the Earth's radiative budget by enhancing back-scattering of the solar radiation, and causes stratospheric ozone depletion through heterogeneous chemical reactions. This study investigates spatiotemporal changes in the volcanic aerosol after the 1991 Pinatubo eruption. We particularly focus on impacts of (1) heating due to volcanic ash, (2) injection height, and (3) temporal evolution of the aerosol radius, on transport and distribution of the volcanic aerosol. We conducted a control simulation and three sensitivity simulations using the MIROC-ESM-CHEM chemistry — climate model. In the control simulation, 20 Mt of the SO_2 and 30 Mt of the ash were injected into the altitudes between 16 km and 18 km over the Mt. Pinatubo on June 15th 1991. The radius of stratospheric sulfate aerosol is prescribed by the data estimated from SAGE II in the control simulation. The first sensitivity simulation injected only the SO_2 into the altitudes between 16 km and 18 km. The second sensitivity simulation injected the SO_2 into the altitudes between 17 km and 26 km. In the third sensitivity simulation, the radius of the sulfate aerosol was fixed to 0.08 μm. The control simulation reproduced a general feature of the observed aerosol optical depth (AOD) derived from SAGE II and AVHRR, although the simulated residence time of the aerosol is longer than the observed one. The sensitivity simulations show the following: (1) heating due to the ash causes an anomalous upward and equatorward transport of the volcanic aerosol during 4 — 5 days after the eruption, (2) the SO_2 injection into the altitudes of 17 — 26 km does not represent the anomalous transport due to the heating which is caused by long-wave absorption of the ash , (3) the temporal evolution of the aerosol radius slightly facilitates the removal of the aerosol from the stratosphere.

Keywords: stratospheric aerosol, volcanic eruption, chemistry-climate model

Japan Geoscience Union Meeting 2014
(28 April - 02 May 2014 at Pacifico YOKOHAMA, Kanagawa, Japan)

AAS21-14 Room:313 Time:April 30 14:15-14:30

Recent Results for Middle Atmospheric Sciences using Data from SMILES

SHIOTANI, Masato[1*]

[1]Research Institute for Sustainable Humanosphere, Kyoto University

The Superconducting Submillimeter-Wave Limb-Emission Sounder (SMILES) aboard the Japanese Experiment Module (JEM) of the International Space Station (ISS) made atmospheric measurements of minor species in the stratosphere and mesosphere for about six months from October 2009 to April 2010. Data for scientific community are now provided from DARTS (Data ARchives and Transmission System) of ISAS/JAXA (http://darts.isas.jaxa.jp/iss/smiles/). In this talk, we will present recent results from the SMILES measurements in association with middle atmospheric chemistry and dynamics. The main topics to be highlighted are as follows.

[Diurnal ozone variations in the stratosphere] The SMILES observations have revealed the global pattern of diurnal ozone variations throughout the stratosphere. The peak-to-peak difference in the stratospheric ozone mixing ratio reaches 8% over the course of a day, suggesting careful consideration when merging ozone data from different satellite measurements (Sakazaki et al., 2013).

[Ozonesonde bias suggested from comparisons with SMILES] The SMILES ozone data have been extensively compared with other satellite data sources (Imai et al., 2013a). Further comparisons of SMILES ozone profiles with those from ozonesondes show that the agreement was generally good, but at low latitudes the SMILES ozone data showed larger values than those at middle and high latitudes. To explain this bias, we examined an issue of the ozonesonde's response time, and found a negative bias in ozonesonde measurements more than 7% at 20 km in the equatorial latitude (Imai et al., 2013b).

[Mesospheric ozone variations during the solar eclipse] During the annular solar eclipse on 15 January 2010, SMILES successfully captured temporal changes in ozone concentration. We found that in the lower mesosphere ozone amounts get closer to the normal nighttime average, and the mechanism is detailed with use of an atmospheric chemistry box model (Imai et al., 2014).

Keywords: Middle Atmosphere, Ozone, Satellite Observation

Japan Geoscience Union Meeting 2014
(28 April - 02 May 2014 at Pacifico YOKOHAMA, Kanagawa, Japan)

AAS21-15 Room:313 Time:April 30 14:30-14:45

Stratospheric ClO observation by JEM/SMILES

SUZUKI, Makoto[1*] ; MANAGO, Naohiro[2] ; MITSUDA, Chihiro[3] ; IMAI, Koji[1] ; OZEKI, Hiroyuki[4] ; SAKAZAKI, Takatoshi[5] ; SHIOTANI, Masato[5]

[1]JAXA/ISAS, [2]Chiba U./CEReS, [3]Fujitsu FIP.Corporation, [4]Faculty of Science, Toho University, [5]Kyoto U./RISH

SMILES operated on the ISS from Oct. 12, 2009 to Apr. 21, 2010. Since the detector (Superconductor-Insulator-Superconductor: SIS mixer) was cooled down to 4K, SMILES showed system noise figure, Tsys ˜250K, or spectral noise floor ˜0.4K, which gave one order better signal to noise ratio compared to previous sub-mm observations from space (Aura/MLS and Odin/SMR).

Aura/MLS have been measuring ClO with a 0.1 ppbv precision at 25-50km altitude. Theoretical precision of SMILES has been reported to be about 0.01 pptv at 30 km. This value can be verified from bin-width of histogram of nighttime ClO, which should be almost zero below 35km at the background atmosphere. We obtained actual bin-width, or ClO random error, to be 0.015 pptv, which is slightly larger than the theoretical value. It has been estimated that

the additional random error might come from IFOV pointing error, a priori pressure error, or baseline fitting error.

In tropical region (N10-S10), difference between day and night profiles was 792 pptv at 25km. This result agreed quite well with reproductive calculated value (nearby 80 pptv) by using Chemical Transport Model (SD-WACCM). On the other hand, in middle latitude (N30-50) during Mar. 13-25, 2010, SMILES value were 712 pptv at 22km, and 352 pptv at 19 km. These value were significantly larger that reported as 10 pptv by airplane and balloon observation in 1986. SMILES mid-latitude value is about 3-7 times higher than the past observation, however, agrees with reproductive calculated value like as tropical region. These discrepancy in the mid-latitude between SMILES and past observation can be explained partly by the historical increase of total Clx from 2.4 pptv in 1968 to the present value, ˜3.0 ppbv.

Keywords: Chlorine monoxide, Stratosphere, International Space Station, submm, ozone, SMILES

Japan Geoscience Union Meeting 2014
(28 April - 02 May 2014 at Pacifico YOKOHAMA, Kanagawa, Japan)

AAS21-16 Room:313 Time:April 30 14:45-15:00

Correlation between O_3 and HCl in the lower stratosphere as observed by SMILES

SUGITA, Takafumi[1*] ; KASAI, Yasuko[2] ; TERAO, Yukio[1] ; HAYASHIDA, Sachiko[3] ; SAGAWA, Hideo[2] ; SUZUKI, Makoto[4] ; SHIOTANI, Masato[5]

[1]NIES, [2]NICT, [3]Nara Women's Univ., [4]JAXA, [5]Kyoto Univ.

Ozone (O_3) in the upper troposphere (UT) has an effect on radiative forcing. One of poorly constrained source of tropospheric O_3 is the stratosphere. Marcy et al. (Science, 2004) have suggested that measurements of HCl in the UT can be used to calculate how much O_3 was transported from the lower stratosphere (LS). Using the correlation between O_3 and HCl in the LS, a fraction of the source of the stratosphere has been quantified from measurements in the UT. To perform such a study, it is important to establish the O_3/HCl correlations in the LS. Here, we will present the O_3/HCl correlations as observed by the Superconducting Submillimeter-Wave Limb-Emission Sounder (SMILES) on board the International Space Station (ISS) (Kikuchi et al., JGR, 2010). We first focus on latitudes between 30^{o}S and 66^{o}S in periods of November 2009, February 2010, and April 2010, when SMILES mainly covered the Southern Hemisphere (S.H.). Both the slope and intercept of the O_3/HCl correlation in the S.H. Feb. are larger than those in Nov. (outside the Antarctic vortex). This is probably due to mixing of air inside and outside the Antarctic vortex, where the enhanced HCl values were observed only inside the vortex (The break-up of the vortex occurred in Dec. 2009 in the LS). Then, hemispheric contrasts in spring and fall will also be presented. In the S.H. Nov. (late spring), the slope is larger than that in the N.H. Apr. (30-66^{o}N). Also, in the S.H. Apr. (fall), the slope is larger than that in the N.H. Oct. (30-66^{o}N). Although, the reason for these larger slopes in the S.H. is not known, the O_3/HCl correlations obtained from SMILES give recent references for the mid to high latitude LS in both the hemispheres.

Keywords: SMILES, ISS, ozone, chlorine

Japan Geoscience Union Meeting 2014
(28 April - 02 May 2014 at Pacifico YOKOHAMA, Kanagawa, Japan)

AAS21-17 Room:313 Time:April 30 15:00-15:15

Reincrease of total columns of HCl and HF observed with FTIR at Tsukuba

MURATA, Isao[1*] ; NAKAJIMA, Hideaki[2] ; MORINO, Isamu[2] ; AKIYOSHI, Hideharu[2]

[1]Graduate School of Environmental Studies, Tohoku University, [2]National Institute for Environmental Studies

The vertical column densities of HCl and HF have been observed with high-resolution Fourier transform spectrometer at Tsukuba, Japan since 1998. SFIT1 spectral fitting program was used to derive the vertical column densities.

HCl and HF are the reservoir species of Chlorine and Fluorine, respectively. Chlorofluorocarbons are the main sources of both of them.

Daily averaged HCl column increased from 1999 to 2001, decreased from 2003 to 2006 and again increased after 2007. Daily averaged HF column increased from 1999 to 2002, level off from 2003 to 2006 and again increased after 2007. The trend fitting shows -1.8%/yr (2001-2006) and +1.0%/yr (2007-2013) for HCl, and +0.3%/yr (2001-2006) and +2.5%/yr (2007-2013) for HF.

The reason why HCl and HF increase again has not been investigated yet but this increase may lead to the delay of ozone recovery. One possible reason is the change of atmospheric circulation. Simulation result of chemical transport model with observed meteorological data (ERA-interim) shows stop of decrease of HCl at around 2008 while the result without observed meteorological data shows continuous decrease. Another possible reason is the increase in emissions of HCFCs and HFCs which increased the input of Cl and F to the stratosphere but there is no observational evidence.

Keywords: FTIR, Trace Species, CFCs

Japan Geoscience Union Meeting 2014
(28 April - 02 May 2014 at Pacifico YOKOHAMA, Kanagawa, Japan)

AAS21-18 Room:313 Time:April 30 15:15-15:30

The impact of altitude mis-estimation caused by Vaisala RS80 pressure bias on ozone and temperature profile data

INAI, Yoichi[1*] ; SHIOTANI, Masato[1] ; FUJIWARA, Masatomo[2] ; HASEBE, Fumio[2]

[1]RISH, Kyoto Univ., [2]EES, Hokkaido Univ.

Non-biased meteorological data are necessary for studies for detecting long-term climate change. Vaisala RS80 radiosonde is widely used for operational and scientific observations. It has been known, however, that the RS80 has pressure bias. The pressure bias affects height information of the profile in a traditional way where the geometric height (or geopotential height in some cases) is calculated from the hydrostatics equation. In addition, the pressure measurements affect the mixing ratio values of any chemical species because the calculation needs air pressure value. The RS80 pressure bias is estimated to be -0.3 $\pm$0.2 hPa, -0.4 $\pm$0.1 hPa, and -0.4 $\pm$0.1 hPa (1σ) at 20 km, 25 km, and 30 km, respectively from the observations using RS80 together with global positioning system (GPS) sensor in the Soundings of Ozone and Water in the Equatorial Region (SOWER) project during from December 2004 to January 2010. Since ozone mixing ratio and temperature are also measured simultaneously, the impact of the mis-estimated altitude on observed profiles of ozone and temperature was evaluated. The net biases of -1.3 $\pm$1.4%, -0.5 $\pm$0.7%, and 3.1 $\pm$1.9% (1σ) at 20 km, 25 km, and 30 km, respectively for ozone mixing ratio and that of -0.1 $\pm$0.2 K, -0.2 $\pm$0.3 K, and -0.4 $\pm$0.7 K (1σ) at 20 km, 25 km, and 30 km, respectively for temperature are estimated as impacts from RS80 pressure bias. Those ozone and temperature biases can result in artificial variation in the long-term meteorological records when there is a radiosonde change from or to RS80. Especially, sign-reversed biases of ozone and temperature appear as artificial variations when the instrument is changed from RS80 to non-pressure-biased radiosonde (for example GPS sonde).

Keywords: sonde observation, observational bias, stratospheric ozone, stratospheric temperature, stratospheric long-term variation

Japan Geoscience Union Meeting 2014
(28 April - 02 May 2014 at Pacifico YOKOHAMA, Kanagawa, Japan)

AAS21-19 Room:313 Time:April 30 15:30-15:45

Total ozone reduction over Rio Gallegos (Argentina) in November 2009 simulated by MIROC3.2 Chemical Transport Model

AKIYOSHI, Hideharu[1*] ; KADOWAKI, Masanao[1] ; NAKAMURA, Haruna[2] ; SUGITA, Takafumi[1] ; NAKAMURA, Tetsu[3] ; MIZUNO, Akira[4]

[1]NIES, [2]Fujitsu FIP, [3]Arctic Environment Research Center, NIPR, [4]STEL, Nagoya University

de Laat et al. (Geophys. Res. Lett., 2010) reported three weeks of reduced total ozone columns over the southern tip of South America in November 2009. The duration of the low total ozone was unusual for the regions. Ozone vertical profile measurements at Rio Gallegos, Argentina (51S, 69W) by ozone LIDAR suggest that the isentropic surfaces of 675K and 475K over Rio Gallegos was inside the Antarctic polar vortex around 13-14 November and 22-23 November respectively thus the low total ozone lasted for three weeks (Wolfram et al, 5th SPARC General Assembly, Queenstown, New Zealand, 2014). MIROC 3.2 Chemical Transport Model with a horizontal resolution of T42 (corresponding to 2.8 degree by 2.8 degree in grids) simulates this long term reduced total ozone over Rio Gallegos. The dynamical and chemical fields around the Antarctica in November 2009 are analyzed. Investigations of these fields for the other past years and comparisons with those in 2009 will be performed.

Keywords: Argentina, ozone hole, CTM, polar vortex, SATREPS, November 2009

Japan Geoscience Union Meeting 2014
(28 April - 02 May 2014 at Pacifico YOKOHAMA, Kanagawa, Japan)

AAS21-20 Room:313 Time:April 30 15:45-16:00

Relationship between total ozone and wave activities in Antarctic region

KADOWAKI, Masanao[1*] ; AKIYOSHI, Hideharu[1] ; YAMASHITA, Yousuke[1] ; NAKAMURA, Tetsu[2]

[1]National Institute for Environmental Studies, [2]Arctic Environment Research Center, National Institute of Polar Research

It is well known that the formation, development and inter-annual variation of the ozone hole are related to the dynamics in winter polar stratosphere. Stratospheric sudden warming was detected in the Southern Hemisphere in 2002 for the first time and then the ozone hole area (defined by the area inside 220DU) was reduced to less than 5 million square kilometers. A similar reduction of ozone hole was also simulated by CCSR/NIES CCM with CCMVal-REF2 scenario, in which the wave number 2 was unusually developed.

These suggest a possibility that ozone hole may suddenly be reduced in a specific year by the dynamics in the future, apart from the effect of the decrease in chlorine and bromine concentration in the atmosphere due to the halogen regulation. Thus, in order to speculate ozone hole trend and the variability in the course of the long-term climate change of the future, it is needed to clarify the relationship between wave activity and ozone hole in the past. Relationships among the ozone hole indices (maximum ozone hole area and minimum total ozone), wave activity and temperature in the Southern Hemisphere were investigated using observation data and chemical transport model output.

Keywords: stratospheric ozone, dynamics, chemical transport model

Japan Geoscience Union Meeting 2014
(28 April - 02 May 2014 at Pacifico YOKOHAMA, Kanagawa, Japan)

AAS21-P01 Room:Poster Time:April 30 18:15-19:30

Interannual and intraseasonal variability of gravity waves revealed from high resolution AIRS observations

TSUCHIYA, Chikara[1] ; SATO, Kaoru[1*] ; ALEXANDER, M. joan[2] ; HOFFMANN, Lars[3]

[1]University of Tokyo, [2]NorthWest Research Associates, [3]Forschungszentrum Juelich

An analysis was made of high-resolution temperature data from satellite onboard Atmospheric Infrared Sounder (AIRS) over eight years from 2003/2004 to 2010/2011 to examine gravity wave (GW) characteristics around an altitude of 40 km in terms of the interannual and intraseasonal variability in austral summer (DJF). AIRS is a nadir-view instrument and sensitive to the temperature fluctuations with vertical wavelengths greater than 15 km. The S-transform was applied to the data series in both cross-track or along-track directions to estimate GW characteristics. First, the DJF-mean time series of GW amplitudes and precipitation were regressed to the sea surface temperature time series in NINO.3 region. It is shown that both GW amplitudes and precipitation are large to the northeast (southwest) of the South Pacific convergence zone (SPCZ) in the El Nino (La Nina) phase. Second, the intraseasonal variation of GWs were examined in terms of the Madden-Julian Oscillation (MJO). Ten-day-mean time series was examined as a function of the longitude for GW amplitudes and precipitation that were averaged over the latitudes of 0-20S. Large GW amplitudes are observed in association with the eastward migrating precipitation of MJO, which is more clearly described by a regression to the Real-time Multivariate MJO Index. Another interesting finding is that the GW amplitudes are significantly weak when the zonal wind at 100 hPa is eastward regardless of the precipitation amount. These results suggest that the interannual and intraseasonal variations of GWs in the subtropical middle stratosphere are modified largely by ENSO and MJO through the precipitation as GW sources and the zonal wind around the tropopause regulating GW vertical propagation.

Keywords: gravity waves, ENSO, MJO, QBO

Japan Geoscience Union Meeting 2014
(28 April - 02 May 2014 at Pacifico YOKOHAMA, Kanagawa, Japan)

AAS21-P02 Room:Poster Time:April 30 18:15-19:30

Balloon-borne observations of lower stratospheric water vapor at the Antarctic Syowa Station

TOMIKAWA, Yoshihiro[1*] ; SATO, Kaoru[2] ; TSUTSUMI, Masaki[1] ; NAKAMURA, Takuji[1] ; HIRASAWA, Naohiko[1]

[1]National Institute of Polar Research, [2]The University of Tokyo

A variation of water vapor in the lower stratosphere has a large radiative forcing. It is considered that increase and decrease of lower stratospheric water vapor before and after 2000, respectively, altered the surface temperature trend by up to 30% in each period. However, since the water vapor content abruptly changes with height around the tropopause, it is hard to capture its variation exactly by satellite observations with a low vertical resolution. Many in-situ (i.e., balloon-borne and aircraft) observations with a high vertical resolution have been performed in low and middle latitudes, but few in the polar region. At the Antarctic Syowa Station (69.0S, 39.6E), three balloon-borne cryogenic frost-point hygrometer observations were performed in 2013 by the 54th Japanese Antarctic Research Expedition (JARE54), so that high precision and high vertical resolution data up to about a 25km altitude were obtained successfully. In this paper, a preliminary result of these observations is presented, and it will be discussed how important it is to continue the water vapor observation at Syowa Station.

Keywords: water vapor, sonde, Antarctic, lower stratosphere

Japan Geoscience Union Meeting 2014
(28 April - 02 May 2014 at Pacifico YOKOHAMA, Kanagawa, Japan)

AAS21-P03 Room:Poster Time:April 30 18:15-19:30

Three dimensional structure of planetary wave activity from tropical to extratropical regions in ENSO

KINOSHITA, Takenari[1*] ; SATO, Kaoru[2] ; HITCHMAN, Matthew, H.[3]

[1]Ntnl. Inst. of Information Comm. Tech., Japan, [2]Graduate School of Science, The University of Tokyo, [3]University of Wisconsin, Madison

It is kwon that the distribution of extratropical column ozone is modulated with El Nino Southern Oscillation (ENSO) (Hitchman and Rogal 2010a, b). This modulation is recognized as the 10 ˜20 day-scale responses including ”Tropical convective outflow into the upper troposphere and lower stratosphere”, ”amplification of subtropical anticyclone associated with transport of low potential vorticity” and ”modulated synoptic scale disturbances in extratropical regions”. On the other hand, it is suggested that planetary scale disturbances influence the distribution of extratropical column ozone. However, this is yet to be identified. The present study examines the modulation of planetary wave activity associated with ENSO from upper troposphere to stratosphere using the formulae describing wave-mean interaction in three dimensions and analytical techniques derived by Kinoshita and Sato (2013a, 2013b) , Sato et al. (2013).

First, we use the ERA-Interim reanalysis data and focus from August to October. Based on the Ocean Nino Index by NOAA, 1991, 1997, 2002, 2004, 2006, 2009 are selected as El Nino seasons and 1998, 1999, 2000, 2007 are selected as La Nina seasons. The Planetary scale disturbances are defined as the waves with zonal wavenumbers 1 ˜3 and periods more than 30 days.

We calculated the three dimensional wave activity flux and its divergences associated with the planetary scale disturbances. The results show that the planetary wave activity is amplified around Asian monsoon regions in La Nina seasons and the planetary wave propagates from tropical upper troposphere to polar stratosphere. The planetary wave activity in El Nino seasons is weak in this region. On the other hand, in the eastern pacific regions, the planetary wave activity in El Nino seasons is amplified and the planetary wave propagates from tropical upper troposphere to polar stratosphere, while the activity in La Nina seasons is weak. It is suggested that the source of tropospheric planetary waves is different between tropical and polar regions in both seasons. We plan to calculate the three dimensional material transport associated with the planetary waves and compare the transport and that associated with the mechanism shown by Hitchman and Rogal (2010a, b).

Keywords: middle atmosphere, planetary wave, wave activity flux, residual mean circulation

Japan Geoscience Union Meeting 2014
(28 April - 02 May 2014 at Pacifico YOKOHAMA, Kanagawa, Japan)

AAS21-P04 Room:Poster Time:April 30 18:15-19:30

A study of Antarctic ozone variation by using FORMOSAT-3/COSMIC observation

HSIAO, Chun-chieh[1] ; LIU, Jann-yenq[1*] ; YU, Shiann-jeng[1]

[1]National Space Organization

The Formosa Satellite 3, also named as the Constellation Observing System for Meteorology, Ionosphere, and Climate (abbreviated as FORMOSAT-3/COSMIC, F3/C), is a constellation of six micro-satellites, designed to monitor weather and space weather. The constellation was launched into an initial circular low-Earth orbit at an altitude of 512 km on 15 April 2006. The six micro-satellites have deployed to six mission obits at around 800 km altitude with 30-degrees separation in longitude for evenly distributed global coverage. The major payload onboard F3/C, GPS occultation experiment (GOX) instrument daily provides more than 2000 soundings of atmospheric vertical temperature profile. By binning radio occultation observations, the three-dimensional temperature structure can be obtained to monitor Antarctic temperature variation. Real-time measurements of vertical temperature structures over the Antarctic region are important for monitoring the formation of polar stratospheric clouds (PSCs) which is a critical factor in the ozone variation. On the other hand, the Ozone Monitoring Instrument (OMI) in the Aura mission observes for total ozone and other atmospheric parameters related to ozone chemistry and climate. The instrument observes Earth's backscattered radiation with a wide-field telescope feeding two imaging grating spectrometers. In this work, more than 5 years observation will be used to make a quantitative comparison of ozone and atmospheric temperature variation in Antarctic.

Keywords: FORMOSAT 3/COSMIC, ozone, Antarctic

Japan Geoscience Union Meeting 2014
(28 April - 02 May 2014 at Pacifico YOKOHAMA, Kanagawa, Japan)

AAS21-P05 Room:Poster Time:April 30 18:15-19:30

Interannual variations of stratospheric water vapor in microwave limb sounding observations and climate model simulation

KAWATANI, Yoshio[1*] ; JAE, Lee[3] ; HAMILTON, Kevin[2]

[1]JAMSTEC, [2]University of Maryland, [3]IPRC, Univ. Hawaii

Using the almost decade-long record of water vapor (H2O) measurements now available from the Microwave Limb Sounder (MLS) instrument on the NASA AURA satellite, the time-height structure of interannual variations in H2O content are investigated. The interannual anomalies display upward propagation below about 10 hPa in a manner analogous to the seasonal tape recorder, but at higher levels the anomalies in H2O appear to propagate downward. An explanation for this effect is sought by examining stratospheric water vapor in simulations of a fine horizontal and vertical resolution (T106L72) version of the MIROC-AGCM. This model is notable for its rather realistic simulation of the quasi-biennial oscillation (QBO) in the tropical stratosphere. The interannual anomlies in simulated stratospheric H2O display a similar propagation as seen in the MLS data. Further analysis shows that the upward propagation in the lower stratosphere is related to the mean advection of interannual water content anomalies induced by the QBO at the tropopause, while the downward propagation is due to the advection of the mean vertical gradient of water content by QBO's interannual fluctuations in the vertical wind. This conclusion is supported by additional experiments run with a modified MIROC that had a significantly different the mean vertical H2O gradient in the middle and upper stratosphere. Also analyzed are global warming simulations in both the MIROC model and in several other global models included in the recent Coupled Model Intercomparison Project 5 (CMIP5). The upward propagating interannual H2O variations are projected to become weaker in all these models because of a weakened QBO amplitude in the lowermost stratosphere.

Keywords: quasi-biennial oscillation

Japan Geoscience Union Meeting 2014
(28 April - 02 May 2014 at Pacifico YOKOHAMA, Kanagawa, Japan)

AAS21-P06 Room:Poster Time:April 30 18:15-19:30

Basic characteristics of forecast skill variations in JMA 1-month hindcast experiments

TAGUCHI, Masakazu[1*]

[1]Aichi University of Education

This study investigates basic characteristics of stratospheric predictability in the Northern Hemisphere using 1-month hindcast (HC) experiment data of the Japan Meteorological Agency for 1979-2009. We describe characteristics of forecast properties of spread, error (root mean square error), and anomaly correlation, contrasting the stratosphere and troposphere for different seasons, as well as explore the so-called spread-skill relationship for the winter stratosphere. We also examine the role of stratospheric sudden warmings (SSWs) in variations in the forecast skills. Our results show that for lead times shorter than about 10 to 15 days, the forecast skills of the HC data are higher on average and more variable in the stratosphere than in the troposphere especially for Northern winter. This is reflected in larger average and variability in predictable time limit, or characteristic time scale of useful predictions, for the winter stratosphere. We also reveal that the spread-skill relationship for the Northern winter stratosphere is characterized by the existence of notable outliers from their expected linear distribution; the outliers have markedly large errors, or low skills, for given spreads. Most of the outliers are contributed by HC sets initialized before observed major SSWs. Such HC data fail to reproduce the strength and/or shape of the stratospheric polar vortex including both onset and recovery phases of SSWs. The HC data tend to yield too strong vortex and shorter-than-average predictable limit.

Japan Geoscience Union Meeting 2014
(28 April - 02 May 2014 at Pacifico YOKOHAMA, Kanagawa, Japan)

AAS22-01 Room:511 Time:April 30 16:15-16:30

Impacts of the Arctic ozone depletion on Japan observed with FTIR

HASHIMOTO, Yuki[1] ; MURATA, Isao[1*] ; NAKAJIMA, Hideaki[2] ; NAGAHAMA, Yoshihiro[2] ; MORINO, Isamu[2] ; NAGAHAMA, Tomoo[3]

[1]Graduate School of Environmental Studies, Tohoku University, [2]National Institute for Environmental Studies, [3]Solar Terrestrial Environment Laboratory, Nagoya University

The ozone depletion occurs not only in the Antarctic but also in the Arctic. A record Arctic ozone depletion which was comparable to the Antarctic ozone depletion occurred in 2011. The ozone depletion itself occurs inside the polar vortex. But the airmass from the inside of the polar vortex is spread to mid-latitude in spring after its breakup. The purpose of this study is to quantify the impact of Arctic ozone depletion on mid-latitude by comparing the amounts of ozone in mid-latitude airmasses before and after the breakup of the polar vortex.

Vertical profiles of O_3, HF and N_2O have been retrieved from infrared spectra observed with Fourier transform infrared spectrometers (FTIR) at Tsukuba and Rikubetsu using the SFIT2 spectral fitting program. Spectra observed from 2006 to 2013 for Tsukuba and from 1997 to 2008 for Rikubetsu were used in this analysis.

HF and N_2O can be used as a tracer of the transport, because they are chemically stable species in the lower stratosphere. O_3 and HF (or N_2O) usually show a high correlation in the lower stratosphere because both species are stable. But the correlation will be changed when ozone is chemically perturbed. Therefore, we examined the correlations of mixing ratios between O_3 and HF (or N_2O) in the mid-latitude airmasses before and after the breakup and determined the chemical loss amount of ozone at the observational sites.

Some chemical ozone losses were found at the altitudes of 19 km and 21 km from O_3-HF correlation. Chemical losses in total ozone were also found from O_3-HF correlation and O_3-N_2O correlation. Then, these observed chemical loss amounts of ozone were compared with the total chemical loss amounts of ozone in the Arctic derived from Japanese Meteorological Agency [2012], Pommereau et al. [2013] and Rex et al. [2013].

Positive correlations were found between the observed chemical loss amounts of ozone at the altitude of 21 km for Tsukuba and at the altitude of 19 km for Rikubetsu and the total chemical loss amounts of ozone in the Arctic. Observed chemical losses in total ozone for both Tsukuba and Rikubetsu also showed positive correlation with the total chemical loss amounts of ozone in the Arctic.

The half-maximum total ozone loss amounts of 15 DU for Tsukba and 20 DU for Rikubetsu were estimated from the correlations, which result in the increases of 6 % and 7% of UV radiation, respectively.

Keywords: FTIR, Arctic ozone depletion, mid-latitude

Japan Geoscience Union Meeting 2014
(28 April - 02 May 2014 at Pacifico YOKOHAMA, Kanagawa, Japan)

AAS22-02 Room:511 Time:April 30 16:30-16:45

The first observation of ozone enhancement in the lowermost atmosphere over China from a spaceborne ultraviolet spectrom

HAYASHIDA, Sachiko[1*] ; YURIKO, Keyamura[1]

[1]Faculty of Science, Nara Women's University

This is the first report of observation from space using ultraviolet radiance for significant enhancement of ozone in the lowermost altitudes (0 to about 3000 m) over East and Central China. The recent retrieval products of the Ozone Monitoring Instrument (OMI) onboard EOS/Aura satellite revealed the spatiotemporal variation of the ozone distribution in the lowermost troposphere [Liu et al., ACP, 2010]. The ozone enhancement over East and Central China was clear in June and July every year, associated with enhancement of CO observed from Measurements Of Pollution In The Troposphere (MOPITT) and hotspots taken from MODerate resolution Imaging Spectroradiometer (MODIS). It suggests that considerable part of the enhancement can be attributed to the emissions of ozone precursors from residue burning after harvesting winter wheat in this area. Ozone enhancement was also observed in autumn and early winter over East and Central China every year, sometimes not accompanied by signals of burning, It implies that CO emissions from industrial activity, automobiles and coal burning for heating would affect on ozone production rather than biomass burning in winter.

Acknowledgments

This is a joint study with Dr. Xiong Liu and Dr. Kelly Chance at Harvard-Smithsonian Center for Astrophysics.This study was supported by GRENE-ei program.

Keywords: tropospheric ozone, satellite observation, ultraviolet radiation, atmospheric pollution

Japan Geoscience Union Meeting 2014
(28 April - 02 May 2014 at Pacifico YOKOHAMA, Kanagawa, Japan)

AAS22-03 Room:511 Time:April 30 16:45-17:00

The validity of the estimation of ozone origin by sectoral air mass classification verified with tracer-tagging simulati

NAGASHIMA, Tatsuya[1*] ; IKEDA, Ayaka[2] ; SUDO, Kengo[3] ; HAYASHIDA, Sachiko[2]

[1]Natinal Institute for Environmental Studies, [2]Nara Women's University, [3]Nagoya Univiersity

The air quality in East Asia has changed rapidly in recent years, especially region-wide transboundary air pollution is the main issue in the atmospheric environment in this region. Therefore, the solution to this issue is of great importance today in East Asia, and the scientific understanding of the structure about this region-wide scale air pollution is necessary. The sectoral air mass classification method has been used to estimate the origin of air pollutants in East Asia, and demonstrated the characteristics of air mass with different origins and extended the understanding of the structure of air pollution. However, this method has a problem to erroneously estimate the origin of air pollutant due to the simpleness of the method. Here, we validate of the estimation of ozone origin by sectoral air mass classification by using the tracer-tagging simulation done by a global chemical transport model (CTM). The analysis suggested that the origin of ozone estimated by these two different methods (sectoral air mass classification and tracer-tagging) generally agreed with each other in the warm season, but the two differ significantly in the cold season. The results suggested that the sectoral air mass classification method should consider the different threshold of residence time to separate the air mass into different origins.

Japan Geoscience Union Meeting 2014
(28 April - 02 May 2014 at Pacifico YOKOHAMA, Kanagawa, Japan)

AAS22-04 Room:511 Time:April 30 17:00-17:15

Long-term MAX-DOAS network observations of NO2 in Russia and Asia: comparisons with OMI satellite observations

KANAYA, Yugo[1*] ; IRIE, Hitoshi[2] ; TAKASHIMA, Hisahiro[3] ; IWABUCHI, Hironobu[4] ; AKIMOTO, Hajime[5] ; SUDO, Kengo[6] ; GU, Myojeong[7] ; CHONG, Jihyo[7] ; KIM, Young-joon[7] ; LEE, Hanlim[7] ; LI, Ang[8] ; SI, Fuqi[8] ; XU, Jin[8] ; XIE, Pinhua[8] ; LIU, Wenqing[8] ; DZHOLA, Anatoly[9] ; POSTYLYAKOV, Oleg[9] ; IVANOV, Victor[10] ; GRECHKO, Evgeny[9] ; TERPUGOVA, Svetlana[11] ; PANCHENKO, Mikhail[11]

[1]JAMSTEC, [2]Chiba University, [3]Fukuoka University, [4]Tohoku University, [5]Asia Center for Air Pollution Research, [6]Nagoya University, [7]Gwangju Institute of Science and Technology (GIST), [8]Anhui Institute of Optics and Fine Mechanics, Chinese Academy of Sciences, [9]A. M. Obukhov Institute of Atmospheric Physics, Russian Academy of Sciences, [10]Belarusian State University, [11]V. E. Zuev Institute of Atmospheric Optics, Siberian Branch of the Russian Academy of Sciences

We conducted long-term network observations using standardized Multi-Axis Differential optical absorption spectroscopy (MAX-DOAS) instruments in Russia and ASia (MADRAS) from 2007 onwards. At seven locations (Cape Hedo, Fukue, and Yokosuka in Japan, Hefei in China, Gwangju in Korea, and Tomsk and Zvenigorod in Russia) with different levels of pollution, we obtained 80,927 retrievals of tropospheric NO2 vertical column density (TropoNO2VCD) and aerosol optical depth (AOD). This large data set was used to analyze NO2 climatology systematically, including temporal variations from the seasonal to the diurnal scale. The results were compared with Ozone Monitoring Instrument (OMI) satellite observations and global model simulations. Two NO2 retrievals of OMI satellite data (NASA ver. 2.1 and Dutch OMI NO2 (DOMINO) ver. 2.0) generally showed close correlations with those derived from MAX-DOAS observations, but had low biases of ˜50%. The bias was distinct when NO2 was abundantly present near the surface and when the AOD was high, suggesting that the aerosol shielding effect could be important, especially for clean sites where the difference could not be attributed to the spatial inhomogeneity. Except for constant biases, the satellite observations showed nearly perfect seasonal agreement with MAX-DOAS observations, suggesting that the analysis of seasonal features of the satellite data were robust. A global chemical transport model, MIROC-ESM-CHEM, was validated for the first time with respect to background NO2 column densities during summer at Cape Hedo and Fukue in the clean marine atmosphere.

Keywords: Nitrogen dioxide, MAX-DOAS, Satellite data validation, temporal variation

Japan Geoscience Union Meeting 2014
(28 April - 02 May 2014 at Pacifico YOKOHAMA, Kanagawa, Japan)

AAS22-05 Room:511 Time:April 30 17:15-17:30

Temporal variations of aerosol, glyoxal, and formaldehyde retrieved by MAX-DOAS based on detailed error analysis

IRIE, Hitoshi[1*] ; CHIN, Sei[1] ; NI, Wentao[1] ; NAKAYAMA, Tomoki[2] ; YAMAZAKI, Akihiro[3] ; TAMIO, Takamura[1] ; KHATRI, Pradeep[1]

[1]Chiba University, [2]Nagoya University, [3]Meteorological Research Institute

The degradation of volatile organic compounds (VOCs) results in the formation of ozone (O_3) and secondary organic aerosols (SOA) in the troposphere. This process consists of the oxidation of VOCs by hydroxyl radical (OH), O_3, and nitrate radical (NO_3). Detailed understanding of the VOC degradation mechanism is challenged by the co-existence of vast variety of VOC species in the atmosphere. However, investigations on ubiquitous oxidation intermediates, e.g., formaldehyde (HCHO) and glyoxal (CHOCHO), can help us to test and improve the current knowledge of the VOC sources and degradation pathways.

We installed one ground-based Multi-Axis Differential Optical Absorption Spectroscopy (MAX-DOAS) system in Meteorological Research Institute (MRI) located at Tsukuba, Japan (36.06N, 130.13E) in June 2010. In addition, two more systems were installed in Chiba University at Chiba, Japan (35.63N, 140.10E) in June and December 2012, respectively. Since then, we have retrieved lower-tropospheric vertical profile information for eight components; aerosol extinction coefficients at two wavelengths, 357 and 476 nm, and NO_2, HCHO, CHOCHO, H_2O, SO_2, and O_3 concentrations. For a detailed evaluation for the aerosol retrieval, which is a key step in the MAX-DOAS eight-component retrieval, simultaneous aerosol observations with the Cavity Ring-Down Spectroscopy (CRDS) and the sky radiometer were conducted at Tsukuba on October 5-18, 2010 and September 7-18, 2012. At Chiba, in addition to the comparison with sky radiometer data, a self-consistency test was performed by comparing results obtained from two MAX-DOAS systems operated at the same place. Through these detailed evaluations, our retrieval method was improved significantly, attaining excellent agreement with CRDS and sky radiometer data. On the basis of these efforts, seasonal and diurnal temporal variations in HCHO and CHOCHO concentrations retrieved from our MAX-DOAS system are discussed in this talk.

Keywords: CHOCHO, HCHO, MAX-DOAS, CRDS, sky radiometer

Japan Geoscience Union Meeting 2014
(28 April - 02 May 2014 at Pacifico YOKOHAMA, Kanagawa, Japan)

AAS22-06 Room:511 Time:April 30 17:30-17:45

Development of an angle-resolved polar nephelometer and its application to non-spherical particles

NAKAGAWA, Maho[1*] ; SASAGO, Hiroshi[1] ; NAKAYAMA, Tomoki[1] ; MATSUMI, Yutaka[1] ; UEDA, Sayako[1]

[1]Solar-Terrestrial Environment Laboratory, Nagoya University

Angular distribution of scattering is one of the important optical properties contributing to the radiation balance in the Earth's atmosphere. Therefore,accurate description of the single-scattering properties of aerosol particles is required. In addition, the angular distribution of scattering of individual aerosol particle provides useful information to determine its size, shape, and refractive index of particles.

We are developing a new polar nephelometer, which can measure angular distribution of the optical light scattered by an individual particle. Laser light at 532 nm from a 300 mW YAG laser was used as light source. The laser beam intersects with a stream of aerosol particles introduced with a sheath flow using a double pipe. There are 21 photodiode detectors arrayed in each plane, totaling 42.Detector apertures were placed to limit sensing angles and minimize background light scattered from walls.

In this system, angular distributions of scattering for an incident light polarized parallel and perpendicular to the scattering plane were measured simultaneously. In the experiments, particles were atomized using a nebulizer and dried using a diffusion dryer. Then, size of particle was selected using a Differential Mobility Analyzer (DMA) and Aerosol Particle Mass Analyzer (APM) and introduced into the polar nephelometer.

The performance of the system was tested by measuring angular distributions of scattering by gaseous molecules (HFC-134 and CO2) and spherical particles. Polystyrene latex sphere is non-light absorpbing spherical particle, while nigrosine are light-absorbing spherical particle. The measured scattering angular distribution was compared with the simulation result calculated from the Mie scattering theory considering detection efficiency and of scattering angle range of each detector.

As a result, the scattering angular distributions could be reproduced by the simulation results for PSL particles with diameters between 150 and 900 nm. The scattering angular distributions for nigrosine particles, were in good agreement with the theoretical curve calculated using a literature refractive index value, $n = 1.63 + 0.24\,i$. This result suggests that light absorbing particles is distinguishable by the scattering angle distribution measurement.

In order to examine the influence of the difference of the shape, we also performed measurements of the scattering angle distributions of non-spherical particles such as sodium chloride and soot particles. In the presentation, capabilities of the system to determine the shape and refractive index of particle will also be discussed.

Japan Geoscience Union Meeting 2014
(28 April - 02 May 2014 at Pacifico YOKOHAMA, Kanagawa, Japan)

AAS22-07 Room:511 Time:April 30 17:45-18:00

Lidar With Multiple Field-Of-View Receiver To Determine Aerosol Size-Distribution

LIU, Yutong[1*] ; YABUKI, Masanori[1] ; TSUDA, Toshitaka[1]

[1]Research Institute for Sustainable Humanosphere, Kyoto University

Knowledge of aerosol size distribution is essential for human health studies, because small particles are able to penetrate lung tissues, thus increasing the risk of bronchitis or of lung diseases. Optical remote sensing techniques such as lidar are effective for monitoring aerosols with high temporal and spatial variations. Aerosol instruments that use light with UV, VIS, and near-IR wavelengths have been used to effectively detect particles with diameters comparable to the wavelength. However, to quantitatively estimate the shape of the particle number-size distribution, more information is required with respect to small particles in the size range of sub-micrometer and below.

Conventional lidar employs very small field-of-view (FOV) for profiling aerosol distribution, and thus simply detects single scatter in the direction opposite to that of incident light. Multiple scattered signals are influenced not only by aerosol distribution along the laser path, but also by the size of aerosols. In this study, depolarization UV lidar with a multiple FOV receiver was used for detecting such multiple scattering effects in order to obtain more quantitative information concerning particle-size distribution. Considering the advantage of high scattering cross section for small particles, we employ a UV laser of 266 nm or 355 nm. A program-controlled mechanical FOV selector is used for a receiver system that can change the FOV from 0.1 mrad to 12.4 mrad. In the presentation, we introduce a retrieval method for aerosol size distribution using this feature and show preliminary results from field measurements by the multiple FOV lidar.

Keywords: Lidar, Aerosol

Japan Geoscience Union Meeting 2014
(28 April - 02 May 2014 at Pacifico YOKOHAMA, Kanagawa, Japan)

AAS22-08 Room:511 Time:May 1 09:00-09:15

Retrieval of decadal record on the deposition of particulate refractory carbon urban and remote sites in Japan

KANEYASU, Naoki[1*] ; MATSUMOTO, Kiyoshi[2] ; YAMAGUCHI, Takashi[3] ; AKIYAMA, Masayuki[3] ; NOGUCHI, Izumi[3] ; MURAO, Naoto[4] ; NISHIMOTO, Shunya[4] ; FUNAKI, Daisuke[5] ; TAKAKI, Satoshi[5]

[1]National Institute of Advanced Industrial Science and Technology, [2]University of Yamanashi, [3]Hokkaido Research Organization, [4]Graduate School of Engineering, Hokkaido University, [5]Shimane Prefectural Institute of Public Health and Environment Science

The atmospheric concentration of refractory carbonaceous aerosol (black carbon, or elemental carbon) concentration are used for the evaluation of their direct radiative forcing. In addition, the deposition of such light absorbing substances on the snow or ice surface will result in the increase of the positive radiative forcing at the surface level. Long-term record of deposition for such relative inert substances is expected to reflect the change in the regional emission strength.

However, the reported measurements of deposition to the ground surface are scarce. We thus have conducted the retrieval of decadal record on the deposition of refractory carbon at two sites in the northern Japan (Rishiri Island: a remote site, and Sapporo City: an urban site). At these sites, the environmental monitoring division of local government have been measurering the total deposition of water-soluble aerosol components in the collected water by use of deposition gauges. To remove insoluble particles from the collected water placed beneath the funnel, a membrane pre-filter is placed at the bottom of the funnel of these deposition gauges. Such pre-filters were stored for more than 18 years for Sapporo site. These can be regarded as the long-term record of the deposited water-insoluble aerosol components in the past, as those in ice-core samples collected in glaciers.

We re-suspend these water-insoluble components into the aqueous phase by dissolving the membrane filter (mixed cellulose acetate) by an organic solvent and re-filter the suspended particles through quartz fiber filters for the analysis of TOT refractory carbon. Before dissolved into organic solvent, carbonate in soil dust particles were removed by the 2N HCl with heat. Collection efficacy of quartz fiber filters were corrected by the amount of retained particulate carbon on the first and second filters placed in series.

The deposition flux of TOT-EC is lager in Sapporo, while that in Rishiri showed a large seasonal variation, in general. In Sapporo, the flux decreased greatly in 2010s compared to those in 1990s, probably due to the introduction of regulations for diesel exhaust emission in 2000s. In addition, the deposition sample has been collected in Oki Island since 2013 spring. The preliminary result for this site will also be shown in the presentation.

Keywords: black carbon, deposition flux, decadal record, forest fire, long-range transport, diesel-powered vehicle exhaust

Japan Geoscience Union Meeting 2014
(28 April - 02 May 2014 at Pacifico YOKOHAMA, Kanagawa, Japan)

AAS22-09 Room:511 Time:May 1 09:15-09:30

The main controlling factor of black carbon mass concentration in rainwater during 2010-2013 summer in East Asia

MORI, Tatsuhiro[1*] ; OHATA, Sho[1] ; KONDO, Yutaka[1] ; MOTEKI, Nobuhiro[1] ; MATSUI, Hitoshi[2] ; IWASAKI, Aya[3] ; TOMOYOSE, Nobutaka[3] ; KADENA, Hisashi[3]

[1]Department of Earth and Planetary Science, Graduate School of Science, University of Tokyo, Japan, [2]Japan Agency for Marine-Earth Science and Technology, Tokyo, Japan, [3]Okinawa Prefectural Institute of Health and Environment

Black carbon (BC) particles are emitted into the atmosphere by incomplete combustion processes, and removed by precipitation. The measurements of BC mass concentration in rainwater improve the quantitative understanding of BC loss because wet deposition is the major sink of BC. We measured BC mass concentration in the air (M_{BC}) and in rainwater (C_{BC}) simultaneously at Cape Hedo on Okinawa Island, Japan, in the East China Sea, from April 2010 to March 2013 in order to understand C_{BC} in each rain event during 2010-2013 summer. The rainwater is collected by an automated wet-only sampler during a 24 period. Photo-absorption photometer with heated inlet (COSMOS) is used to measure M_{BC}. C_{BC} was measured by a system consisting of an ultrasonic nebulizer and a Single Soot Photometer (SP2).

It is often heavy rain by cumulonimbus cloud during summer in East Asia, so that M_{BC} an hour before raining is expected to be related to C_{BC}. However, the correlation between M_{BC} and C_{BC} in all rain events during 2010-2013 summer is not agreed (r^2 = 0.12). Then, we extracted the heavy rain events, which had positive convective available potential energy (CAPE). These extraction was performed with the National Centers for Environmental Prediction (NCEP) Final (FNL) Operational Global Analysis data every 6 hours. This result was that C_{BC} was correlated with M_{BC} (r^2 = 0.47).

In order to investigate if C_{BC} (Estimated C_{BC}) is explained with M_{BC} and the liquid water content, Estimated C_{BC} is verified by comparing the observed C_{BC}. The liquid water content is maximum at the equilibrium level (EL) by the condensation process theoretically if the total water mixing ratio is conserved in the air parcel. If BC in the parcel is active as cloud condensation nuclei (CCN) at lifted condensation level and removed by precipitation at EL, the equation of Estimated C_{BC} at EL is represented as Estimated C_{BC}=M_{BC}/(m_v∗WCR). m_v is the water vapor content an hour before raining at the ground level. Water condensation ratio (WCR) is the mass ratio of liquid water content to water vapor content, which is calculated with the NCEP reanalysis data. Compared with the observed C_{BC}, Estimated C_{BC} is correlated with the observed C_{BC} well (r^2 = 0.68). It suggests that Estimated C_{BC} is correctly represented as C_{BC} with M_{BC} and the most liquid water content at EL. The observed C_{BC} is three times higher than Estimated C_{BC} because the cloud droplets including BC particles might be collected during falling down.

Keywords: Black Carbon, wet deposition

Japan Geoscience Union Meeting 2014
(28 April - 02 May 2014 at Pacifico YOKOHAMA, Kanagawa, Japan)

AAS22-10 Room:511 Time:May 1 09:30-09:45

Number size distribution of ambient aerosols at Cape Hedo, Okinawa and Fukue Island, Nagasaki

MIYOSHI, Takao[1*] ; TAKAMI, Akinori[1] ; IREI, Satoshi[1]

[1]NIES

[**Introduction**]

Recent drastic economical growth in the East Asian region has caused large emission of anthropogenic pollutants to the atmosphere. Some aerosols act as cloud condensation nuclei (CCN) and influence the global climate. There was a report that the higher ratio of inorganic aerosol to the sum of inorganic and organic aerosol and the larger particle size resulted in the higher ratio of CCN to condensation nuclei at the same water vapor supersaturation.

We have conducted field studies for chemical compositions of ambient aerosols at some locations in the East Asian region. In this work, measurement results of number size distribution of aerosols, which potentially influences cloud formation, are presented. Obtained data at two locations were analyzed for better understanding the spatial distribution of aerosol size in the region.

[**Observation**]

The number concentration was measured at Cape Hedo, Okinawa (lat 26.9^{o}N, long 128.3^{o}E) from 15 to 22 February 2012 and at Fukue Island, Nagasaki (lat 32.8^{o}N, long 128.7^{o}E) from 15 to 28 February 2013 using a Wide-Range Particle Spectrometer (WPS, MSP Corp.), which has a capability to measure a wide particle size range. The WPS consists of two main parts: a combination of a Differential Mobility Analyzer (DMA) and a Condensation Particle Counter (CPC) for particle measurement from 5 to 350 nm (or from 10 to 500 nm) and a Laser Particle Spectrometer (LPS) for measurement from 350 to 10000 nm.

Simultaneously, chemical compositions of ambient aerosols (ammonium, nitrate, sulfate, chloride and organics) were measured by a Quadrupole Aerosol Mass Spectrometers (Q-AMS, Aerodyne Research, Inc.) at Cape Hedo and an Aerosol Chemical Speciation Monitor (ACSM, Aerodyne Research, Inc.) at Fukue Island. At Fukue Island only, sulfur dioxide concentrations were also measured by an SO_2 analyzer (Model 43i, Nippon Thermo Co., Ltd.). Sulfur dioxide concentrations at Cape Hedo were monitored at Hedo Acid Deposition Monitoring Station (Ministry of the Environment).

[**Results and Discussion**]

The size distributions at Cape Hedo consistently had two peaks at 50 nm and 200 nm. On the other hand, those at Fukue Island varied. There were two peaks at 50 nm and 150 nm after 0:00 a.m. JST on 23 February 2013. Ambient aerosols at 150 nm were largest among the particles which were measured at Fukue Island. There was one peak at 15-25 nm after 12:00 p.m. JST on 24 February 2013 when the number concentration was over 100000 #/cm^3. The concentration was also high on 16 and 25 February 2013. The growth of nucleation mode particles was observed from noon to night of each day. We believed that these cases were new particle formation (NPF) events. Such a case was not observed at Cape Hedo.

The molar ratio of sulfur dioxide to the sum of sulfur dioxide and sulfate was studied at both monitoring sites during the observation period by a WPS. When NPF events occurred at Fukue Island, the ratio increased over 80%. On the other hand, the ratio at Cape Hedo was at most 60% even on 17 February 2012 when the transport time of air masses from China according to back trajectory analyses (NOAA HYSPLIT) was approximately one day. The transport time was as long as that to Fukue Island. It was inferred that enough gases such as sulfur dioxide to cause NPF were around Fukue Island and semi-volatile vapors which were newly generated by photochemical reactions condensed on pre-existing particles because the concentrations of gases were low and those of aerosols such as sulfate were high around Cape Hedo.

Keywords: Number size distribution, East Asia, Wide-range particle spectrometer (WPS), New particle formation

Japan Geoscience Union Meeting 2014
(28 April - 02 May 2014 at Pacifico YOKOHAMA, Kanagawa, Japan)

AAS22-11 Room:511 Time:May 1 09:45-10:00

Continuous measurement of organic nitrates at Suzu, the Noto peninsula

SADANAGA, Yasuhiro[1*] ; TAKAJI, Ryo[1] ; ISHIYAMA, Ayana[1] ; MATSUKI, Atsushi[2] ; SATO, Keiichi[3] ; OSADA, Kazuo[4] ; BANDOW, Hiroshi[1]

[1]Osaka Prefecture University, [2]Kanazawa University, [3]Asia Center for Air Pollution Research, [4]Nagoya University

Peroxyacyl nitrates (PANs) and alkyl nitrates (ANs) act as one of the reservoirs of nitrogen oxides (NO_x) in the atmosphere. Since their lifetime is longer than that of NO_x, they can be transported over a long-distance and would be important as trans-boundary pollutants. In this research, continuous measurement system of total PANs and ANs in the troposphere has been developed by using a thermal dissociation / cavity attenuated phase shift spectroscopy (TD/CAPS) method. Both PANs and ANs are thermally decomposed to produce NO_2 and then NO_2 is measured by CAPS method. This system can observe PANs and ANs with high time resolution while this system cannot separate constituents of PANs and ANs. Total PANs and ANs can be measured separately by setting up decomposition lines at different temperatures.

Continuous field observations of PANs and ANs concentrations have been being carried out at NOTOGRO (NOTO Ground-based Research Observatory) supersite in Suzu, Noto Peninsula, since November 2012. NO_x, NO_y, total inorganic nitrate ($T.NO_3$), O_3 and CO concentrations have also been being observed at NOTOGRO.

NOy concentrations were in agreement with the sum of observed NO_y components (= NO_x + $T.NO_3$ + PANs + ANs) regardless of seasons. NO_x fractions were the highest in NO_y constituents. $T.NO_3$ fractions were small in winter and increased in spring. Opposite tendencies were observed for PANs fractions. These reflect that wet deposition of $T.NO_3$ is promoted in winter and temperature increasing accelerates decomposition of PANs.

Seasonal variations of both PANs and ANs concentrations showed spring maximum and summer minimum. From winter to spring, both PANs and ANs concentrations from Korea-China air mass origin were higher than those from the other air mass origins. On the other hand, both PANs and ANs concentrations were independent of air mass origins from spring to summer. These indicate that PANs and ANs concentrations in winter and spring are governed by long-range transport and local photochemical productions of PANs and ANs are relatively important from spring to summer. In addition, PANs and ANs diurnal variations being high and low in the daytime and nighttime, respectively, in spring and summer also imply the local photochemical productions of PANs and ANs.

Keywords: Organic nitrates, Total odd nitrogen species, Long-range transport

Japan Geoscience Union Meeting 2014
(28 April - 02 May 2014 at Pacifico YOKOHAMA, Kanagawa, Japan)

AAS22-12 Room:511 Time:May 1 10:00-10:15

Light absorption and morphological properties of soot-containing particle mixed with sulfate observed at Noto Peninsula

UEDA, Sayako[1*] ; NAKAYAMA, Tomoki[1] ; MATSUMI, Yutaka[1] ; TAKETANI, Fumikazu[2] ; ADACHI, Kouji[3] ; MATSUKI, Atsushi[4] ; IWAMOTO, Yoko[4] ; SADANAGA, Yasuhiro[5]

[1]STEL, Nagoya University, [2]JAMSTEC, [3]Meteorological Research Institute, [4]Kanazawa University, [5]Osaka Prefecture University

Black carbon (BC) in atmospheric soot particle is known as strongly absorber of visible spectrum solar radiation in the atmosphere. The coating materials on soot particle can enhance the magnitude of light absorption by the soot-containing particles, according to the coating conditions including composition, amount and morphology. Several studies have indicated that the estimation by assuming core-shell shaped particle and simple composition tends to estimate larger than that for the real soot-containing particles (Adachi et al., 2010; Lack and Cappa, 2010; Cappa et al., 2012). To elucidate the enhancement of light absorption of aged soot-containing particles and their relation with the individual particle condition, we made an observation for continental outflow at Noto Peninsula, Kanazawa, Japan, in spring 2013.

Atmospheric observations were conducted at NOTO Ground-base Research Observatory (NOTOGRO) in Suzu City, Kanazawa, Japan from April 17 to May 14 in 2014. Absorption and scattering coefficients at 405, 532, and 781 nm, and soot mass concentrations of PM1 particles were measured using the photoacoustic soot photometer (DMT, PASS-3) and a single-particle soot photometer (DMT, SP2), after passing through diffusion dryers and one of the heaters controlled at 25, 300, and 400 deg C every 10 min. Aerosol samples were collected using two-stage cascade impactors (50% cutoff diameters of the two stages were 1.5 um and 0.3 um) on carbon-coated nitrocellulose (collodion) films for individual analysis using a transmission electron microscope (TEM). Elemental compositions of individual particles were analysed for particles on second stage using an energy-dispersive X-ray spectrometer (EDS) used along with the TEM. Mixing states between non-volatile chain-like soot and volatile materials to high-density electron beam were identified by comparing photograph before and after EDS analysis.

Increase in BC light absorption due to coating was estimated by comparing absorption coefficients at 781 nm with and without heating (300 deg C). The increase in BC light absorption on average was 23$\pm$25%. The maximum values of the increase in BC light absorption ($>$40%) were observed in air mass condition that derived from around Shanghai across the East China Sea, based on backward air mass trajectory analysis. In the TEM sample obtained at the air mass, most of soot were found as internally-mixed particles, which were well-embeded into round-shaped sulphate. On the other hand, increase in light absorption estimated at 405 nm was usually less than that at 781 nm over the entire observation period. Particularly the increase in light absorption at 405 nm tended to be negative under air mass derived from around Japan or the Korean Peninsula. Because absorption at 405 nm is more affected from OC, the negative values might to be attributed to formation of brown carbon in thermo denuder. In TEM sample obtained when the increase in light absorption were negative at 405 nm and $<$25% at 781 nm, most of soot were also internally-mixed particles with sulphate. The differences with sample of air mass from Shanghai were that many soot-containing particles were irregular shape, and that carbonaceous residues other than soot were found in particles after irradiation of high electron beam. Our results suggest that the variation of increase in BC light absorption were attributed to morphology and mixing state with OC of internally mixed soot-containing particles.

Adachi, K. et al., J. Geophys. Res., 115, D15206 (2010)
Lack, D. A. and Cappa, C. D., Atmos. Chem. Phys., 10, 4207-4220 (2010)
Cappa, C. D. et al., Science, 337, 1078-1081 (2012)

Keywords: Aerosol optical properties, Ambient measurement, Black carbon, electron microscope, Lensing effect

Japan Geoscience Union Meeting 2014
(28 April - 02 May 2014 at Pacifico YOKOHAMA, Kanagawa, Japan)

AAS22-13 Room:511 Time:May 1 10:15-10:30

Mixing states of summer time aerosol particles in Noto peninsula

YAMADA, Reina[1*] ; KAMIGUCHI, Yusuke[1] ; KINOUCHI, Kento[2] ; IWAMOTO, Yoko[3] ; UEDA, Sayako[4] ; ADACHI, Kouji[5] ; MATSUKI, Atsushi[3]

[1]College of Science and Engineering, Kanazawa University, [2]Graduate School of Natural Science and Technology, Kanazawa University, [3]Institute of Nature and Environmental Technology, Kanazawa University, [4]Solar-Terrestrial Environment Laboratory, Nagoya University, [5]Meteorological Research Institute

Mixing state is one of the factors that determine the characteristic of aerosol particles, and it is important for evaluating their climatic impact. Until recently, summer time aerosol particles in the remote region of central Japan didn ' t attract much attention since human influence was considered minimal during the season. However, our measurement in the last few years showed that particle number concentrations in summer time were the highest in all seasons. In order to understand the characteristics of the summer time aerosols, we analyzed composition and mixing state of individual particles using transmission electron microscopy (TEM) coupled to energy dispersive W-ray spectrometer (EDX). We conducted quasi-daily sampling at research facility NOTOGRO (NOTO Ground-based Research Observatory) situated at tip of the Noto peninsula from 9th, Jun to 23rd, August. Samples collected during episodes of high aerosol loadings were selected and analyzed. Winds tend to transport air-mass from the Pacific Ocean to the sampling site in summer. However, we found that there were some other flow patterns including flow from the continent of Asia, associated with the high aerosol concentrations. Major composition of particles differed depending on the flow patterns. In addition, many particles were internally mixed, and organics were predominant in smaller diameter range, while sulfates were predominant in larger diameter range. Above results showed that, depending e.g. on the difference of the flow patterns, mixing state of aerosols observed in high concentrations in summer exhibit high temporal variability, and such mixing state are often unevenly distributed among different particle sizes.

Keywords: atmospheric aerosols, mixing state, organic aerosol particles, sulfate aerosol particles

Japan Geoscience Union Meeting 2014
(28 April - 02 May 2014 at Pacifico YOKOHAMA, Kanagawa, Japan)

AAS22-14 Room:511 Time:May 1 10:30-10:45

Observation of new particle formation event at Noto peninsula

KAGAMI, Sara[1*] ; MATSUKI, Atsushi[2] ; IWAMOTO, Yoko[2] ; KINOUCHI, Kento[3]

[1]College of Science and Engineering, Kanazawa University, [2]Institute of Nature and Environmental Technology, Kanazawa University, [3]Graduate School of Natural Science and Technology, Kanazawa University

New Particle Formation (NPF) of atmospheric aerosol particle is an important production process which increases the number concentration of the aerosol particles that would act as Cloud Condensation Nuclei and potentially affect the global climate. The measurement of number size distribution of atmospheric aerosol particles was conducted at the atmospheric observation site, NOTOGRO in Noto peninsula, from October 2012 to September 2013. We identified NPF events throughout the measurement period and this is the first year-round observation reported on the NPF events from coastal region of the Sea of Japan. NPF events tended to occur when Condensation Sink (CS) was relatively low. CS is a measure of the amount of preexisting particle concentration and depends on the particle size distribution. Comparing with meteorological parameters, NPF events were concentrated in daytime, which suggests interaction with solar radiation. However, precipitation preceding the event tended to trigger NPF events by lowering CS (i.e. preexisting particle concentration) especially in winter and summer. On the other hand, NPF events observed in autumn and spring tended to concentrate on days with particularly low relative humidity. Above results suggested that, the conditions favorable for the NPF event is closely related to the seasonal climatic features of the measurement region, that is, the winter monsoon in winter, the rainy season and typhoon in summer and anticyclones in autumn and spring.

Keywords: atmospheric aerosol, new particle formation, condensation sink, precipitation, seasonal variation

Japan Geoscience Union Meeting 2014
(28 April - 02 May 2014 at Pacifico YOKOHAMA, Kanagawa, Japan)

AAS22-15 Room:511 Time:May 1 11:00-11:15

Origin of atmospheric gaseous mercury using the Hg/CO ratio in pollution plume observed at Mt. Fuji Weather Station

NAGAFUCHI, Osamu[1*] ; YOKOTA, Kuriko[2] ; KATO, Syungo[3] ; OSAKA, Ken'ichi[1] ; NAKAZAWA, Koyomi[1] ; KOGA, Masaru[1] ; HISHIDA, Naoko[1] ; NISHIDA, Yuki[1]

[1]the University of Shiga Prefecture, [2]Toyohashi university of technology, [3]Tokyo Metropolitan University

Mercury (Hg) is a global pollutant, which is dispersed worldwide mainly is gaseous elemental form via long-range atmospheric transport. Due to the increasing fossil fuel consumptions and industrial emissions, Asia now contributes more than 50% of the global anthropogenic Hg emission with China being the largest atmospheric Hg emitter. Previous studies have demonstrated that the trans-Pacific Asian Hg export could impact North America. Therefore, we would like to study its transport mechanism in the free troposphere by monitoring atmospheric Hg concentrations at high elevation site in Japan. The sampling site is at the summit of Mt. Fuji Weather Station, which is 3,777 m above sea level.

Gaseous mercury and particulate mercury in the atmosphere were separately collected by using a mercury sampler developed by Kagaya et. al., (2007). A quartz filter (Palflex2000, Tokyo Dylec) was attached at the tip of a mercury absorbing tube in which amalgamated gold was impregnated, and the air was aspirated by an air pump through the filter and the mercury absorbing tube at a rate of 0.5L/min. Particulate mercury was filtered by the quartz filter and gaseous mercury was absorbed by the amalgamated gold in the tube. Both particulate and gaseous mercury were analyzed by an atomic absorbance spectrophotometer (Nippon Instruments, MA-2000) after vaporization by heating.

The mercury sampler was set in a place 5m or more away from the building at summit of Mt. Fuji (N35.21'.38", E138.43'39"). The sampling was performed from 11 to 18 August, 2008. The filer and the absorbing tube were changed with 12-24 hour-intervals.

Atmospheric mercury concentrations observed at summit of Mt. Fuji and Japan. High concentrations of both gaseous and particulate mercuries were observed at the summit of Mt. Fuji. Swartzendruber et al. reported the gaseous and particulate mercury concentrations in the free troposphere at the Mt. Bachelor as 1.54 and 0.0043 ng/m^3, respectively. Hans R. Friedli et al reported that gaseous elemental mercury were found in industrial plumes exiting China, Korea, and Japan ˜6.3ng/ m^3, ˜3ng/ m^3 and ˜3ng/ m^3, respectively. The higher atmospheric mercury concentrations at the summit of Mt. Fuji may imply that there is a specific pollution source in the East Asia. Because from the result of the back trajectory calculation, the air mass came from the China during this observation periods.

Japan Geoscience Union Meeting 2014
(28 April - 02 May 2014 at Pacifico YOKOHAMA, Kanagawa, Japan)

AAS22-16 Room:511 Time:May 1 11:15-11:30

Clarification of lead (Pb) species and its formation mechanisms in coarse and fine aerosol particles using X-ray absorpt

SAKATA, Kohei[1*] ; SAKAGUCHI, Aya[1] ; TANIMIZU, Masaharu[2] ; TAKAHASHI, Yoshio[1]

[1]Graduate school of Science, Hiroshima University, [2]JAMSTEC

There are very few studies on chemical speciation and atmospheric chemistry of trace elements. Among the trace elements in the aerosol particles, lead(Pb) has long been measured due to the toxicity of this element. The measurement of Pb isotope ratios in aerosol particles has also been employed as a powerful tracer for air-mass transportation because Pb isotope ratios differ significantly depending on the emission area/source. However the speciation of Pb has not been clarified, although their solubility is important to estimate the health effects for human/animal body. Furthermore, Pb in the aerosol particle is the dominant source of Pb, which is used as oceanic circulation tracer, in the surface seawater. Thus, the speciation of Pb in the aerosol particle is one of the important issue. In this study, we attempted to determine the Pb species in aerosol samples using X-ray absorption fine structure (XAFS) analysis.

Size-fractionated aerosol particles were collected by a high-volume aerosol sampler with cascade impactor at Higashi-Hiroshima. Lead LIII-edge (absorption edge: 13.04 keV) X-ray absorption near-edge structure (XANES) spectra were recorded on SPring-8 on BL01B1 and at KEK PF-AR on NW10A to identify the Pb species. The analyzed sample-sets of size-fractionated aerosol particles are follows: Spring (Asian dust event), summer (two sample sets), fall, and winter (transboundary pollution event).

Lead species in size-fractionated aerosol particles are different between fine and coarse aerosol particles. In the fine aerosol particles, the dominant Pb species were two or three components, $PbSO_4$, $Pb(NO_3)_2$ and PbC_2O_4, in all seasons. That is, the seasonal variation of Pb species in the fine aerosol was not found. It is because the Pb species in the fine aerosol particles are formed by uniform chemical reaction with H_2SO_4, HNO_3 and oxalic acid in droplet through a year. Pb species in the coarse aerosol particles, except for on Asian dust event, were $2PbCO_3$-$Pb(OH)_2$, $Pb(NO_3)_2$ and PbC_2O_4. These $2PbCO_3$-$Pb(OH)_2$ and partial PbC_2O_4 were derived from road dust, and $Pb(NO_3)_2$ in coarse aerosol particles was formed by chemical reactions with HNO_3 on the surface of the particle. In Asian dust event, the coarse aerosol particles showed PbSiO3 as major Pb species, although other species, $2PbCO_3$-$Pb(OH)_2$ and PbC_2O_4, were also obtained. Thus we could found the clear seasonal variation in the coarse aerosol particles. These results will be able to estimate the accurate estimation of Pb solubility to the surface seawater.

Japan Geoscience Union Meeting 2014
(28 April - 02 May 2014 at Pacifico YOKOHAMA, Kanagawa, Japan)

AAS22-17 Room:511 Time:May 1 11:30-11:45

Methyl chloride in the upper troposphere observed by CARIBIC: large-scale distributions and Asian summer monsoon outflow

UMEZAWA, Taku[1*] ; K. BAKER, Angela[1] ; ORAM, David[2] ; SAUVAGE, Carina[1] ; O'SULLIVAN, Debbie[2] ; RAUTHE-SCHOECH, Armin[1] ; A. MONTZKA, Stephen[3] ; ZAHN, Andreas[4] ; A.M. BRENNINKMEIJER, Carl[1]

[1]Max Planck Institute for Chemistry, [2]National Centre for Atmospheric Science, School of Environmental Sciences, University of East Anglia, [3]Earth System Research Laboratory, NOAA, [4]Institute for Meteorology and Climate Research, Karlsruhe Institute of Technology

CARIBIC is a flying observatory onboard a Lufthansa A340-600 aircraft that observes various atmospheric compounds at almost monthly intervals. In this study, we present spatial and temporal variations of methyl chloride (CH_3Cl) in the upper troposphere (UT) observed mainly by CARIBIC for the years 2005-2011. The CH_3Cl mixing ratio in the UT over Europe was higher than that observed at a European surface baseline station throughout the year, indicative of a persistent positive vertical gradient at NH mid latitudes. A series of flights over Africa and South Asia show that CH_3Cl mixing ratios increase toward tropical latitudes, and the observed UT CH_3Cl level over these two regions and the Atlantic was higher than that measured at remote surface sites. Strong emissions of CH_3Cl in the tropics combined with meridional air transport through the UT may explain such vertical and latitudinal gradients. Comparisons with carbon monoxide (CO) data indicate that non-combustion sources in the tropics dominantly contribute to forming the latitudinal gradient of CH_3Cl in the UT. We also observed elevated mixing ratios of CH_3Cl and CO in air influenced by biomass burning in South America and Africa, and the emission ratios derived for CH_3Cl to CO in those regions agree with previous observations. In contrast, correlations indicate a high CH_3Cl to CO ratio of 2.9 ± 0.5 ppt ppb^{-1} in the Asian summer monsoon anticyclone and domestic biofuel emissions in South Asia are inferred to be responsible. We estimated the CH_3Cl emission in South Asia to be 134 ± 23 Gg Cl yr^{-1}, which is higher than a previous estimate due to the higher CH_3Cl to CO ratio observed in this study.

Keywords: CARIBIC, aircraft observation, methyl chloride, upper troposphere

Japan Geoscience Union Meeting 2014
(28 April - 02 May 2014 at Pacifico YOKOHAMA, Kanagawa, Japan)

AAS22-18 Room:511 Time:May 1 11:45-12:00

Flattening of the equatorial bulge of annual mean APO observed in the Western Pacific during the 09/10 El Nino event

TOHJIMA, Yasunori[1*] ; MUKAI, Hitoshi[1] ; MACHIDA, Toshinobu[1] ; TERAO, Yukio[1] ; NOJIRI, Yukihiro[1]

[1]National Institute for Environmental Studies

A tracer known as **a**tmospheric **p**otential **o**xygen ($APO=O_2+1.1xCO_2$) has been proved to be useful to study air-sea gas exchange. Although both atmospheric CO_2 and O_2 concentrations are affected from the air-sea and air-land gas exchanges, APO mainly reflect the air-sea gas exchange because APO is invariant with respect to the land biotic gas exchanges (-1.1 in the definition represents the molar land biotic $-O_2$:C exchange ratio). To investigate the spatio-temporal variations in the APO over the Pacific region, we have been observing the atmospheric CO_2 and O_2 concentrations onboard commercial cargo ships sailing between Japan and US/Canada and Australia/New Zealand since December 2001. Our previous studies based on the shipboard flask measurements for 7-year period (2002-2008) revealed that the average latitudinal distribution of the annual-mean APO in the Western Pacific (from 40 deg. S to 50 deg. N) show a maximum near the equator and decreasing trends toward the mid-latitude in both hemisphere (Tohjima et al, 2012). This latitudinal distribution of the annual-mean APO is mainly attributed to the latitudinal differences in the air-sea gas exchange: outgassing fluxes around the equator and ingassing fluxes in the mid and high latitude. In the previous study, the equatorial bulge was robust and always observed during the 7-year period. However, the equatorial bulge disappeared and the latitudinal distribution was flattened especially in the Southern Hemisphere during the period from July 2009 to June 2010, when the most recent El Nino event occurred. Simulated APO based on an atmospheric transport model (NIES99) driven by a set of climatological oceanic O_2 and CO_2 fluxes also shows suppression of the equatorial bulge during El Nino periods, indicating that the atmospheric transport substantially contributes to the inter-annual change in the latitudinal distribution of the annual-mean APO. The simulated APO, however, cannot fully reconstruct the flattening of APO in the Southern Hemisphere. Thus, the suppression of the Eastern Pacific upwelling during the El Nino period might reduce O_2 and/or CO_2 outgassing around the equatorial ocean.

Keywords: atmospheric potential oxygen, APO, air-sea gas exchange, El Nino, Tropical western Pacific ocean

Japan Geoscience Union Meeting 2014
(28 April - 02 May 2014 at Pacifico YOKOHAMA, Kanagawa, Japan)

AAS22-19 Room:511 Time:May 1 12:00-12:15

Separation of gross primary production and ecosystem respiration of a Japanese forest using atmospheric O2/N2 ratio

ISHIDOYA, Shigeyuki[1*] ; MURAYAMA, Shohei[1] ; KONDO, Hiroaki[1] ; SAIGUSA, Nobuko[2] ; KISHIMOTO, Ayaka[3] ; YAMAMOTO, Susumu[1]

[1]National Institute of Advanced Industrial Science and Technology (AIST), [2]National Institute for Environmental Studies, [3]National Institute for Agro-Environmental Sciences (NIAES)

The atmospheric O2/N2 ratio (δ(O2/N2)) has been observed globally since the early 1990s to elucidate the global CO2 budget (e.g. Manning and Keeling, 2006). To apply this method, the global average terrestrial biospheric O2:CO2 molar exchange ratio is needed. Keeling (1988) estimated the - O2:CO2 exchange ratio (hereafter referred to as ER) of 1.05 by surveying the results from various elemental abundance studies. Severinghaus (1995) revised the ER to be 1.10±0.05, which has been used for the global average terrestrial biospheric ER in recent studies. However, Seibt et al. (2004) and Ishidoya et al. (2013) observed the ER values associated with respiration and photosynthesis in forests and reported that the ER for net turbulent O2 and CO2 fluxes between the forest ecosystem and the atmosphere above the canopy (hereafter referred to as ER_F) could be different from 1.1 significantly, based on one-box canopy O2/CO2 budget model analyses. Moreover, the ER_F reported by Seibt et al. (2004) is quite different from that by Ishidoya et al. (2013); the former is larger than 1.1 and the latter is smaller than 1.0 under the condition of uptake of CO2 from the atmosphere to a forest. Therefore, direct observation of the ER_F at various forests is expected to validate the global average terrestrial biospheric ER. In addition, such the observation of the ER_F will lead to estimate the gross primary production (GPP) and the ecosystem respiration (RE) of the forest separately.

In this study, we present the average daily mean ER_F at Takayama deciduous broadleaf forest site in central Japan (36○09′ N, 137○25′ E, 1420 m a.s.l.; designated as TKY in the Asia Flux site code database) for the period May 24 – August 28, 2013, observed firstly based on an aerodynamic method (Yamamoto et al., 1999). The observed average daily mean ER_F is 0.79±0.08, which is not only smaller than 1.0 as predicted by Ishidoya et al. (2013) but also significantly smaller than the assumed global average terrestrial biospheric ER (1.10±0.05). We also separate the average daily mean NEP for the corresponding period observed by the eddy covariance method (Saigusa et al., 2005) into average daily mean GPP and RE, by using the observed average daily mean ER_F in this study as well as the ER_A (the ER for GPP) and ER_R (the ER for RE) at TKY reported by Ishidoya et al. (2013). Then, the separated average daily mean RE is compared with that estimated from an empirical function of air temperature (Saigusa et al., 2005) and the soil CO2 efflux observed using soil chamber experiments (Mo et al., 2005), to discuss the validity of the observed ER_F and its implication to the forest and global carbon cycle (Ishidoya et al., in manuscript in prep.).

Reference

Ishidoya, S., Murayama, S., Takamura, C., Kondo, H., Saigusa, N., Goto, D., Morimoto, S., Aoki, N., Aoki, S., Nakazawa, T. (2013) O2:CO2 exchange ratios in a cool temperate deciduous forest ecosystem of central Japan. Tellus 65B, 21120, http://dx.doi.org/10.3402/tellusb.v65i0.21120.

Keywords: atmospheric O2/N2 ratio, O2:CO2 exchange ratio between a forest and the atmosphere, gross primary production, ecosystem respiration, forest carbon cycle

Japan Geoscience Union Meeting 2014
(28 April - 02 May 2014 at Pacifico YOKOHAMA, Kanagawa, Japan)

AAS22-20 Room:511 Time:May 1 12:15-12:30

Seasonal changes of greenhouse gases in the upper troposphere/lower stratosphere observed by commercial airliner

SAWA, Yousuke[1*] ; MACHIDA, Toshinobu[2] ; MATSUEDA, Hidekazu[1] ; NIWA, Yosuke[1] ; TSUBOI, Kazuhiro[1] ; MURAYAMA, Shohei[3] ; MORIMOTO, Shinji[4] ; AOKI, Shuji[4]

[1]Meteorological Research Institute, [2]National Institute for Enviromental Studies, [3]National Institute of Advanced Industrial Science and Technology, [4]Tohoku University

Atmospheric mixing ratios of greenhouse gases at about 11 km altitude were analyzed from monthly air sampling aboard commercial airliner during the flights between Europe and Japan from April 2012 to August 2013. Compared to the subtropic, higher CH4 and SF6 mixing ratios, similar values of N2O, and larger seasonal changes of CO2 were found in the upper troposphere. CH4, N2O and SF6 in the lower stratosphere, above the tropopause up to 30 K in potential temperature, showed simultaneous increases from June to October, and faster decreases at higher altitudes from January to March. Mean age of the air in the lower stratosphere was estimated based on SF6 mixing ratios to be about 2 years in late spring and 1 year in autumn, suggesting stronger influences on the mixing ratios in the stratosphere from troposphere in summer.

Keywords: Atmospheric Chemistry, Greenhouse Gas, Upper Troposphere/Lower Stratosphere

Japan Geoscience Union Meeting 2014
(28 April - 02 May 2014 at Pacifico YOKOHAMA, Kanagawa, Japan)

AAS22-21 Room:511 Time:May 1 12:30-12:45

Long-term changes of CH4 concentration and its carbon isotopic ratio in the lower stratosphere over Japan

SUGAWARA, Satoshi[1*] ; MORIMOTO, Shinji[2] ; UMEZAWA, Taku[3] ; AOKI, Shuji[2] ; NAKAZAWA, Takakiyo[2] ; ISHIDOYA, Shigeyuki[4] ; TOYODA, Sakae[5] ; HONDA, Hideyuki[6]

[1]Miyagi Univ. of Education, [2]CAOS, Tohoku Univ., [3]Max Planck Institute for Chemistry, [4]AIST, [5]Tokyo Institute of Technology, [6]ISAS/JAXA

It is expected that d13C of CH4 provides us with useful information not only about CH4 emissions from biogenic and abiogenic sources but also about its oxidation process in the atmosphere. Therefore, measurements of d13C have been carried out for the major CH4 sources as well as for the background atmosphere. However, the measurements are still insufficient for elucidating the CH4 cycle on the earth's surface. In the stratosphere, CH4 is destroyed by reactions with OH, O(1D) and Cl atom. These destruction processes play an important role in the stratospheric chemistry, but the respective contributions to the CH4 loss and their temporal changes have not been yet well understood quantitatively. Measurements of the isotopic ratios of the stratospheric CH4 are one of the most promising methods to detect possible change of the CH4 destruction processes in the stratosphere on the basis of the different isotopic fractionations occurring in the different reactions. However, only a few measurements have been made so far, due mainly to difficulty of collecting air samples in the stratosphere. Systematic collections of stratospheric air samples have been carried out over Japan since 1985 using a balloon-borne cryogenic sampler. We analyzed the air samples collected in the period of 1994-2010 for concentrations of CH4, N2O, CO2 and SF6, and d13C of CH4. In this study, we report the preliminary results of the long-term change of d13C of CH4 in the stratosphere. Almost linear and compact relationships between CH4 and N2O concentrations were found for the all observations in the different years. CH4 concentration and d13C also showed compact relationships in the lower stratosphere, although those in the mid-stratosphere were less correlated. The tight correlations between CH4 and N2O in spite of the different destruction processes suggest that the ratio of both destruction rates has been kept as almost constant during the transport process in the stratosphere. It is well known that tropospheric CH4 and N2O have been secularly increasing in the recent decades. Such increasing trends should have been propagated into the stratosphere, and the compact relationships between the stratospheric CH4 and N2O would change depending on their increase rates. To elucidate an inter-annual changes of the stratospheric CH4 and its d13C, we employed N2O-loss, instead of the N2O concentration, as an indicator of how the chemical reactions have proceeded during the stratospheric transport. The N2O-loss was calculated as a concentration difference between the tropical troposphere and the stratosphere by considering the mean age of air estimated from CO2 and SF6 concentrations. This procedure eliminates the effect of the secular N2O increase from the relationships between CH4 and N2O, and enables us to detect possible change in the stratospheric CH4. As a result, we found that the CH4 concentration increased at a rate of 4.5+-0.9 ppbv/year in the lower stratosphere during 16 years. This increase rate is consistent with those observed in the troposphere. The same technique was applied to the correlations between CH4 concentration and d13C, and we found no significant changes of d13C in the lower stratosphere. Considering the fact that d13C in the troposphere also does not show a clear trend in a recent decade, our result implies that the relative contributions of the CH4 destruction processes have been unchanged in the lower stratosphere over the observed period.

Keywords: stratospheric methane, carbon isotopic ratio

Japan Geoscience Union Meeting 2014
(28 April - 02 May 2014 at Pacifico YOKOHAMA, Kanagawa, Japan)

AAS22-22 Room:511 Time:May 1 14:15-14:30

Laboratory biomass burning experiments to investigate the dependence of emissions of volatile organic compounds on burni

INOMATA, Satoshi[1*] ; TANIMOTO, Hiroshi[1] ; PAN, Xiaole[2] ; TAKETANI, Fumikazu[2] ; KOMAZAKI, Yuichi[2] ; MIYAKAWA, Takuma[2] ; KANAYA, Yugo[2]

[1]NIES, [2]JAMSTEC

Biomass burning is one of major sources of primary fine carbonaceous aerosols and organic compounds.[1] A field observation campaign in a rural area of the Yangtze River Delta, China, was carried out during the harvest season in June of 2010 and air masses of open crop residue burning were frequently observed. It was found that the emission ratios of elemental carbon (EC) and organic carbon (OC) to CO were enhanced during the biomass burning episodes compared with those in urban pollution.[2] In addition, oxygenated volatile organic compounds were predominantly emitted during the biomass burning.[3] To investigate the emission properties of aerosols and organic compounds under controlled conditions, we carried out biomass burning experiments in the laboratory. Two types of crop residues, wheat straws and oilseed rapes, which were actually burned during the campaign, were used as the sample. We will mainly show the dependence of the emission ratios of volatile organic compounds to CO on burning conditions and compare with the field observation.

References
1) Akagi et al., Atmos. Chem. Phys. 11, 4039-4072, 2011.
2) Pan et al., J. Geophys. Res. 117, D22304, 2012.
3) Kudo et al., submitted to J. Geophys. Res., 2013.

Keywords: Biomass burning, Volatile organic compounds, Crop residue, Combustion efficiency, PTR-MS, SP2

Japan Geoscience Union Meeting 2014
(28 April - 02 May 2014 at Pacifico YOKOHAMA, Kanagawa, Japan)

AAS22-23 Room:511 Time:May 1 14:30-14:45

Impact of VOC emission from gasoline cars on ozone formation

HIROYUKI, Yamada[1*] ; INOMATA, Satoshi[2] ; TANIMOTO, Hiroshi[2]

[1]National Traffic Safety and Environment Laboratory, [2]National Institute for Environmental Studies

Ozone has been known that it was produced by the atmospheric reactions of volatile organic compounds (VOC) and NOx. The impact of VOC on ozone formation varies species by species. Thus, to evaluate the ozone formation in atmosphere, discussion based of ozone formation potential (OFP) is important.

This study discussed VOC emission from gasoline vehicle with OFP. Usually it is though that main source of VOC from vehicles were tailpipe emissions, however our former study suggested that main source from gasoline cars is not tailpipe emissions but evaporative emissions. So in this study, addition to tailpipe emissions, OFP of evaporative emissions were measured.

Keywords: ozone, ozone formation potential, evaporative emissions, gasoline cars, tailpipe emissions

Japan Geoscience Union Meeting 2014
(28 April - 02 May 2014 at Pacifico YOKOHAMA, Kanagawa, Japan)

AAS22-24 Room:511 Time:May 1 14:45-15:00

Improvement of measurement system for organic nitrates produced in the mixture of VOC, NOx and O3

MATSUMOTO, Jun[1*]

[1]Faculty of Human Sciences, Waseda University

Organic nitrates, ONs, are important as an intermediate of secondary organic aerosols (SOAs). Additionally, the branching ratio between ONs and NO2 formation after the reactions of NO with peroxy radicals (RO2) are critical for tropospheric ozone formation. In this study, laboratory experiments were conducted for the reaction of VOCs/O3/NO mixture. After the reactor, total ONs were monitored by the thermal-desorption laser-induced fluorescence (TD-LIF) technique. At this time, an improved glass double-tube flow reactor was constructed. The inner tube (Pyrex, O.D. 10 mm, I.D. 8 mm) was for the O3 flow, and the outer (Pyrex, O.D. 150 mm, I.D. 143 mm, length 500 mm) was for the additional flow (VOC sample and NO) to reduce the wall loss of ozone at the edges of reactor. As a result, after the improvement of the reactor and its conditions, the sensitivity of formed ONs was three times as large as the previous system. The sensitivity was defined as the slope of the regression line between VOC concentration and ONs increment. Observed sensitivities for isoprene and limonene were 0.00085 and 0.013 ppbv/ppbv, respectively. Sensitivity for limonene was 15 times as large as that for isoprene. Meanwhile, the reaction rate constant of limonene with ozone is 16 times larger than that of isoprene with ozone. It was experimentally indicated that the initial reaction of VOCs with ozone be critical for production of organic nitrates. It was also confirmed that measurements of ONs produced in the mixture of VOC, NOx and O3 was promising. As a next step, RO2 productivity of initial reactions (VOC+O3) and branching ratio between ONs and NO2 formation will be explored to clarify characteristics of ONs production in detail.

Acknowledgements: This work has been supported financially by a Grant-in-Aid for Scientific Research (No. 24651014), from the Ministry of Education, Culture, Sports, Science and Technology (MEXT) of the Japanese Government.

Keywords: Nitrogen oxides, Volatile organic compounds, Tropospheric ozone, Organic nitrates, Laboratory experiments, Gas phase reactions

Japan Geoscience Union Meeting 2014
(28 April - 02 May 2014 at Pacifico YOKOHAMA, Kanagawa, Japan)

AAS22-25 Room:511 Time:May 1 15:00-15:15

Humidity dependence of extinction coefficients of secondary organic aerosols and its relation with chemical properties

NAKAYAMA, Tomoki[1*] ; MATSUMI, Yutaka[1] ; SATO, Kei[2] ; IMAMURA, Takashi[2]

[1]Solar-Terrestrial Environment Laboratory, Nagoya University, [2]National Institute for Environmental Studies

Atmospheric aerosols scatter and absorb solar radiation, thereby influencing the Earth's radiation balance. Light extinction is the sum of scattering and absorption. The aerosol extinction coefficient depends on chemical composition, particle size, shape and mixing sate in addition to wavelength of light. The uptake of water by aerosol particles can change extinction coefficients by changing size and refractive index of particles. Therefore, the detailed understanding of the relative humidity (RH) dependence of the extinction coefficients is important to estimate the impact of aerosols on radiation balance. However, the RH dependence of optical properties for secondary organic aerosol (SOA) has not been studied in detail.

In this work, we have determined the RH dependence of extinction coefficients of the SOAs generated during (1) the photooxidation of toluene in the presence of NO_x and (2) the ozonolysis of α-pinene. The SOAs were generated in a 6 m_3 teflon coated stainless-steel chamber in the absence of seed particles. The RH dependence of aerosol extinction coefficients at 532 nm was measured using a custom-made cavity ring-down spectrometer (CRDS). The CRDS has two measurement cells, in which the RH were controlled at $<$10% and 80%, respectively. The size distributions and chemical compositions of the SOAs were also measured using a scanning mobility particle sizer (SMPS, TSI) and a time of flight aerosol mass spectrometer (ToF-AMS, Aerodyne), respectively.

The ratio of extinction coefficients measured under high RH condition (RH=80%) to those measured under dry condition, F(RH), were compared with the relative abundance of the ion signal m/z=44 measured by the ToF-AMS to total organic signal, f_{44}. The f_{44} factor is known as a maker of oxygenated species such as organic di-acids, poly-acids, oxo-acids, hydroxy-acids, and acyl peroxides. Small RH dependence of extinction coefficients was found for the α-pinene-SOA with F(RH) of about 1.05, but the F(RH) values for the toluene-SOA were increase up to 1.4-1.6 with increasing the f_{44}. Interestingly, the relationship between F(RH) and f_{44} for the toluene-SOAs did not depend on the initial NO_x concentrations. Our results suggest that the increase in hygroscopicity due to oxidation of the SOAs mainly contributes to the observed RH dependence of extinction coefficients for the toluene-SOA.

Keywords: Secondary organic aerosol (SOA), Optical property, Humidity dependence, Chemical property, Climate change

Japan Geoscience Union Meeting 2014
(28 April - 02 May 2014 at Pacifico YOKOHAMA, Kanagawa, Japan)

AAS22-26 Room:511 Time:May 1 15:15-15:30

Insoluble metal-oxalate complexes in the atmosphere: its stability and global cooling effect

YAMAKAWA, Yoshiaki[1*] ; SAKATA, Kohei[1] ; MIYAHARA, Aya[1] ; MIYAMOTO, Chihiro[2] ; SAKAGUCHI, Aya[1] ; TAKAHASHI, Yoshio[1]

[1]Department of Earth and Planetary Systems Science, Graduate School of Science, Hiroshima University, [2]Department of Science, Hiroshima University

Aerosols have cooling effect on the earth, which is divided into direct and indirect effects. The direct effect is reflection of sunlight directly by aerosols, whereas the indirect effect is the reflection by clouds formed by the aid of aerosols working as cloud condensation nuclei (CCN). Oxalic acid is a main component of secondary organic aerosols and abundant in the atmosphere, which is formed by degradation of organic matters with longer carbon chain such as cyclic olefin. Oxalic acid is hygroscopic, which can work as CCN with indirect cooling effect. It has been estimated that the degree of cooling effect by the aerosols are equal to that of the warming effect of carbon dioxide (CO_2). However, there is large uncertainty in the estimation. In addition, it is suggested that oxalic acid may form insoluble metal-oxalate complexes and does not have the indirect cooling effect. Therefore, it is important to re-evaluate the cooling effect of aerosols for precise prediction of global warming. Although dicarboxylic acid including oxalic acid is decomposed into CO_2 by photolysis, oxalic acid is more abundant than the other dicarboxylic acids. It is possible that oxalic acid can be stabilized by forming metal-oxalate complexes. This study was aimed (i) to measure the concentration of metal-oxalate complexes in the atmosphere to contribute to precise prediction of global warming and (ii) to measure the half-life time to evaluate the stability of metal-oxalate complexes during photoreaction.

Size-fractionated aerosol samples were collected at Higashi-Hiroshima in winter (Dec., 2012-Jan., 2013), spring (April, 2013), and summer (July-Aug., 2013). The ratio of oxalic acid and total metal-oxalate complexes was estimated based on the X-ray absorption fine structure (XAFS) spectroscopy for zinc (Zn), lead (Pb), and calcium (Ca). Photolysis experiments were conducted by ultraviolet ray for oxalic acid, Zn complex, and magnesium (Mg) complex, while absorption spectra were measured to evaluate photoreactivity.

As a result, metal-oxalate complexes were found in finer particles. There was a positive correlation between the ratio of oxalate/nitrate and ratio of metal-oxalate complexes/total oxalate species. Therefore, it is considered that metal-oxalate complexes are formed by relative increase of oxalate for nitrate. Although concentration of total oxalate species was largest, the ratio of metal-oxalate complexes/total oxalate species was smallest in summer. Concentration of total oxalate species was higher than that of metal ions (Zn^{2+}, Pb^{2+}, and Ca^{2+}). Therefore, it is considered that the ratio of metal-oxalate complexes is smallest in summer.

This ratio was about 30% to 50% for each sample through the year. This result showed that the cooling effect of oxalic acid may be smaller than previous estimation.

As a result of photolysis experiments, half-life time of oxalic acid, Mg complex, and Zn complex is 19 min, 71 min, and 172 min, respectively. This result showed that photoreactivity of oxalic acid was decreased by forming metal-oxalate complexes. Compared to absorption spectra between oxalic acid and metal-oxalate complexes, absorbance was decreased by forming metal-oxalate complexes. Therefore, it is considered that the increase of half-life time may be caused by the decrease of absorbance by forming metal-oxalate complexes.

Keywords: Aerosol, Metal-Oxalate Complex, Global Cooling Effect, Photoreactivity, X-ray Absorption Fine Structure Spectroscopy

Japan Geoscience Union Meeting 2014
(28 April - 02 May 2014 at Pacifico YOKOHAMA, Kanagawa, Japan)

AAS22-27 Room:511 Time:May 1 15:30-15:45

Volatility basis-set approach simulation of organic aerosol formation in East Asia

MATSUI, Hitoshi[1*] ; KOIKE, Makoto[2] ; KONDO, Yutaka[2] ; TAKAMI, Akinori[3] ; KANAYA, Yugo[1] ; TAKIGAWA, Masayuki[1]

[1]Japan Agency for Marine-Earth Science and Technology, [2]University of Tokyo, [3]National Institute for Environmental Studies

Organic aerosol (OA) accounts for a significant mass fraction of the submicron aerosols in the atmosphere, and it influences the Earth's climate either directly (by scattering/absorbing of solar radiation) or indirectly (by modifying cloud microphysical properties). Recent studies show that secondary OA accounts for a large fraction of OA globally. However, as secondary OA formation processes are very complicated, estimates of the secondary OA burden in the atmosphere and its impact on climate and human health remain highly uncertain compared with those of other aerosols such as inorganic species.

In this study, OA simulations using the volatility basis-set approach were made for East Asia and its outflow region. Model simulations were evaluated through comparisons with OA measured by aerosol mass spectrometers in and around Tokyo (at Komaba and Kisai in summer 2003 and 2004) and over the outflow region in East Asia (at Fukue and Hedo in spring 2009). The simulations with aging processes of organic vapors reasonably well reproduced mass concentrations, temporal variations, and formation efficiency of observed OA at all sites. As OA mass was severely underestimated in the simulations without the aging processes, the oxidations of organic vapors are essential for reasonable OA simulations over East Asia. By considering the aging processes, simulated OA concentrations considerably increased from 0.24 to 1.28 μg/m^3 in the boundary layer over the whole of East Asia. OA formed from the interaction of anthropogenic and biogenic sources was also enhanced by the aging processes. The fraction of controllable OA was estimated to be 87 % of total OA over the whole of East Asia, showing that most of the OA in our simulations formed anthropogenically (controllable). A large portion of biogenic secondary OA (78 % of biogenic secondary OA) formed through the influence of anthropogenic sources. The high fraction of controllable OA in our simulations is likely because anthropogenic emissions are dominant over East Asia and OA formation is enhanced by anthropogenic sources and their aging processes. Both the amounts (from 0.18 to 1.12 μg/m^3) and the fraction (from 75 % to 87 %) of controllable OA were increased by aging processes of organic vapors over East Asia.

Keywords: aerosol, organic aerosol, regional three-dimensional model, anthropogenic-biogenic interaction, East Asia, volatility basis-set

Japan Geoscience Union Meeting 2014
(28 April - 02 May 2014 at Pacifico YOKOHAMA, Kanagawa, Japan)

AAS22-28 Room:511 Time:May 1 15:45-16:00

Impacts of BVOCs changes on global atmospheric chemistry: off-line coupling of CHASER and VISIT

SUDO, Kengo[1*] ; ITO, Akihiko[2]

[1]Graduate School of Environmental Studies, Nagoya University, [2]National Institute of Environmental Studies

Biogenic volatile organic compound (BVOC) is one of important factors to control global atmospheric environment and climate change, affecting tropospheric chemistry which involves ozone production/loss, OH radical abundance (atmospheric oxidizing power), and global production of secondary organic aerosols (SOA). Emissions of BVOCs are basically determined by land ecosystem processes, but also tightly linked to climate factors (such as temperature and precipitation), atmospheric CO2 concentration, and deposition of nitrogen species. Therefore, a modelling framework to couple atmospheric chemistry with land ecosystem is needed for considering BVOCs changes and associated impacts. In this study, coupled simulation of global atmospheric chemistry and terrestrial ecosystem has been developed by combining atmospheric chemistry model CHASER (Sudo et al., 2002, 2007) and land ecosystem/trace gas emission model VISIT (Ito et al., 2008). The CHASER model, also developed in the framework of the MIROC earth system model (MIROC-ESM-CHEM), simulates detailed chemistry in the troposphere and stratosphere with an on-line aerosol simulation including SOA production. The VISIT model calculates terrestrial emissions of CO_2, CH_4, N_2O, and BVOCs. This paper focuses on isoprene as a proxy of BVOCs, and discusses the impacts of the past isoprene emission changes on global atmospheric chemistry using the CHASER model constrained with off-line input from the VISIT simulation. VISIT calculates an increase in global isoprene emissions from 420 to 520 TgC a^{-1} (24%) from the first half of the 20th century to 2011. As a response to this emission change, CHASER simulated a ˜2% increase in global ozone production causing ˜4% increases in ozone concentration in the tropical middle-upper troposphere. The model also showed that OH decreases by 5-10% in the most of NH due to the isoprene emission change, resulting in 2-4% decreases of CO in NH. Also, SOA is largely increased by more than 30% in the major part of the troposphere (especially in the tropics).

Keywords: biogenic VOCs, chemistry climate model, land ecosystem model, secondary organic aerosol, atmosphere-land interaction

Japan Geoscience Union Meeting 2014
(28 April - 02 May 2014 at Pacifico YOKOHAMA, Kanagawa, Japan)

AAS22-P01 Room:Poster Time:May 1 18:15-19:30

Emission of iodine molecule and iodine monoxide from frozen solutions containing iodide ion

OKUMURA, Masanori[1] ; YABUSHITA, Akihiro[1*]

[1]Kyoto University

Iodine oxides are receiving increasing attention in atmospheric chemistry, because it may contribute to ozone depletion and atmospheric particle formation in polar region. Iodine monoxide(IO) generates from the reaction of iodine atom with ozone. Iodine atoms may be formed by photolysis of iodine(I_2) or volatile iodocarbons, the main source of which is oceanic biogenic production. Emission processes from inorganic source are also being proposed, but they are so far unexplained. Iodine compounds were found above, below and within the sea ice of the Weddell Sea, and these measurements show the Weddell Sea as an iodine hotspot. But, the calculated fluxes from biological production of iodocarbons are too small to explain the observed atmospheric IO, and the modelled I_2 is also smaller than the observed I_2. This observation suggests there is an unidentified iodine source. One of the candidates is presumably an inorganic source. In this work, we studied the surface reaction between gaseous ozone and a frozen sodium iodide solution by using cavity ring-down spectroscopy to detect gaseous products, iodine, I_2(g) and an iodine monoxide radical, IO(g).

The I_2(g) and IO(g) emissions were observed during ozonolysis of liquid and frozen NaI aqueous solutions. The concentrations of NaI were typically 1 and 5 mM. The concentrations of flowing O_3(g) were (0.5-4.2)$\times 10^{15}$ molecules cm^{-3}. The observed products concentrations were $\sim 10^{11}$ molecules cm^{-3} for IO(g) and $\sim 10^{14}$ molecules cm^{-3} for I_2(g). The peak of I_2(g) emission was markedly enhanced on a frozen NaI aqueous solution more than that on a liquid at pH 2. The peak of IO(g) emission was also enhanced on a frozen solution under the same condition. The physical structures of the ice substrates supposedly play an important role in this enhancement. Iodide anions are expected to be excluded from ice matrix during freezing. This exclusion process leads to the formation of concentrated iodide anions at the air-ice interface. In fact, sea ice contains brine microchannels that permit transport of reactants over large distances. It was found that the amounts of I_2(g) and IO(g) produced depend on [NaI], I_2(g) production is markedly enhanced at pH $<$4, and I_2(g) emission is decreased with decreasing temperature of a frozen NaI solution. Acidification of the brine by atmospheric trace acids could potentially lead to low pH. These results imply that a surface reaction between gaseous ozone and frozen iodide could be responsible for the inorganic source of iodine.

Keywords: iodine, iodine monoxide, ice, ozone, heterogeneous reaction, cavity ring-down spectroscopy

Japan Geoscience Union Meeting 2014
(28 April - 02 May 2014 at Pacifico YOKOHAMA, Kanagawa, Japan)

AAS22-P02 Room:Poster Time:May 1 18:15-19:30

Speciation of S and Ca species in aerosols with its relations to global cooling effects and processes of chemical reacti

MIYAMOTO, Chihiro[1*] ; YAMAKAWA, Yoshiaki[2] ; SAKATA, Kohei[2] ; MIYAHARA, Aya[2] ; SAKAGUCHI, Aya[2] ; SUGA, Hiroki[2] ; TAKEICHI, Yasuo[3] ; ONO, Kanta[3] ; TAKAHASHI, Yoshio[2]

[1]Faculty of Science, Hiroshima Univercity, [2]Graduate School of Science, Hiroshima Univercity, [3]Photon Factory, KEK

Speciation of particles in aerosols is necessary to interpret what effects each species in the aerosols can have on environment. For example, global cooling effect by aerosols influences earth's climatic change (IPCC, 2007). In particular, sulfate aerosols are known to cool the earth by forming cloud condensation nuclei (CCN) because of their high hygroscopicity, which induces indirect cooling effect. Because the hygroscopicity differs depending on the species, sulfate speciation in aerosols is important for the determination of the magnitude of the indirect cooling effect.

In this study, major ion concentrations in aerosol samples were measured by ion-chromatograpy. In addition, chemical species of calcium and sulfur in the each aerosol sample were determined using X-ray absorption near-edge structure (XANES) measured at BL-9A in Photon Factory, KEK. The speciation analyses can have some implications on the influence on the environment and the processes of chemical reaction of aerosols collected during several periods, such as (a) dust (Kosa) period (March 4-9, 2013), (b) the period with high PM2.5 concentration (Jan. 31-Feb. 1, 2013), and (c) the periods before and after (a) and (b).

Major ion concentration data showed that Ca^{2+} , which is originated from soil, and NO_3^- and SO_4^{2-}, which were from human activities, increased in the period (a) compared with those in the periods before and after the period (a). On the other hand, SO_4^{2-} and NH_4^+, which were emitted from human activities, increased in the period (b). In the period (a), it is considered that species originated from acids such as sulfate and nitrate which were incorporated into the particles increased in the samples whose aerodynamic diameter is over 1.0 um, because they have reacted with $CaCO_3$ which was increased by Kosa event. In addition, from the fitting of XANES spectra, it was found that gypsum with low hygroscopicity were the main sulfur species in the period (a), whereas NH_4HSO_4, $(NH_4)_2SO_4$, and hydrated sulfate with high hygroscopicity were main sulfur species in the period (b). Therefore, it is considered that when the concentration of PM2.5 increases, the indirect cooling effect can be large due to the large fraction of NH_4HSO_4, $(NH_4)_2SO_4$, and hydrated sulfat. On the other hand, the indirect cooling effect by sulfate aerosols can be smaller during the dust period due to the formation of non-hygroscopic gypsum by high amount of calcite in the atmosphere.

Using the results of calcium and sulfur speciation both in the bulk and at the surface by fluorescence and conversion-electron yield detection, respectively, in the XANES analyses, we can discuss how chemical reactions occur at the surface of aerosol particles in each period. The abundance ratios of gypsum, $CaCO_3$, and $Ca(NO_3)_2$ were different at the surface and the bulk. As a result, it was concluded that calcium species changes from gypsum, $Ca(NO_3)_2$, to $CaCO_3$ from the surface to the core of the calcite particle. This results showed that (i) sulfuric acid from the atmosphere forms insoluble gypsum at the surface of calcite, (ii) $Ca(NO_3)_2$, formed as a result of the reaction of nitric acid and calcite, exists in the middle part, and (iii) unreacted $CaCO_3$ remains in the core of the particle.

Keywords: aerosol, XANES, sulfate, grobal cooling effect

Japan Geoscience Union Meeting 2014
(28 April - 02 May 2014 at Pacifico YOKOHAMA, Kanagawa, Japan)

AAS22-P03 Room:Poster Time:May 1 18:15-19:30

Properties of Fe-containing particles and structure of mineral particles in the mountain, urban, and marine atmosphere

MIKI, Yusuke[1*] ; UEDA, Sayako[2] ; MIURA, Kazuhiko[1] ; KATO, Hiroki[1] ; FURUTANI, Hiroshi[3] ; UEMATSU, Mitsuo[3]

[1]Tokyo University of Science, [2]Nagoya University, [3]University of Tokyo

Atmospheric aerosol particles play an important role in global material cycles and global climate by acting as an agent which transports materials over long distances. Iron (Fe) is an essential element for marine phytoplankton growth especially in high nutrient and low chlorophyll (HNLC) area. Long-range transportation of atmospheric aerosols from the continent and subsequent deposition is an important process to supply Fe to the ocean. The dry and wet depositions of aerosol particles depend on the particle size and the mixing states with water-soluble materials. In order to study the properties of Fe-containing particles and modification of individual particles, we collected aerosol particles at the top of Mt. Fuji, at Kagurazaka, Tokyo, and on the ship over the mid-latitude western North Pacific Ocean during the KH-12-1 (EqPOS) Leg 2 cruise of the R/V Hakuho Maru. We collected aerosol particles with a low pressure impactor. Collected particles were analyzed using a transmission electron microscopy (TEM) with a water dialysis method and an energy-dispersive X-ray (EDX) analysis. We chose the samples which were collected in the long-range transportation events from the continent on the basis of 5-day backward air trajectory analysis, number size distribution of aerosols measured by an optical particle counter (OPC), and the results of the TEM-EDX analysis.

Water-insoluble materials such as mineral dusts and industrial anthropogenic metals are main sources of Fe. This study focused on water-insoluble materials and performed the EDX analysis. In each sample, most of water-insoluble materials were internally mixed with water-soluble materials (internal mixed particles). The volume percent of the water-soluble materials in the mixed particles on a marine sample was higher than that of other samples, indicating that water-insoluble materials as well as Fe-containing particles were mixed with water-soluble materials during transportation.

Structures of some mineral particles were verified using the focused-ion-beam (FIB) technique. Particles larger than 5 μm collected on the Ti-plate were sliced into 200 nm in thickness. We performed selected-area electron diffraction (SAED) on the cross section of the sliced particles. On the basis of the diffraction patterns and EDX results, structures of the mineral particles were verified. $CaCl_2$ was found on the surface of the particle and bounded on $CaCO_3$, suggesting that $CO_3{}^{2-}$ was replaced by Cl^- ($CaCO_3$ + 2HCl $\longrightarrow$ $CaCl_2$ + CO_2 + H_2O). Fe was included in the particle. There is a possibility that changing insoluble $CaCO_3$ to soluble $CaCl_2$ changes the ability of cloud nuclei and/or ice nuclei and the solubility of Fe.

Keywords: aerosol, Fe, water-soluble materials, water-insoluble materials, long-range transportation

Japan Geoscience Union Meeting 2014
(28 April - 02 May 2014 at Pacifico YOKOHAMA, Kanagawa, Japan)

AAS22-P04 Room:Poster Time:May 1 18:15-19:30

Source of atmospheric lead in Omura City, west Japan, tied to the source of mineral particles

SAITOH, Yu[1*] ; UMEZAWA, Yu[2] ; KAWAMOTO, Kazuaki[2] ; TANIMIZU, Masaharu[3] ; ISHIKAWA, Tsuyoshi[3]

[1]Center for Advanced Marine Core Research, Kochi University, [2]Graduate School of Fisheries Science and Environmental Studies, Nagasaki University, [3]Kochi Institute for Core Sample Research, JAMSTEC

Lead is one of the major environmental pollutants, which seriously harms human body. Atmospheric lead concentration has been suppressed in Japan after the forbiddance of leaded gasoline in 1970s. However, the cross-border air pollution is getting unable to disregard with industrial development in neighboring countries. Identifying the source of aerosol particles is essential in painting a precise picture of the cross-border air pollution. The northern part of the Kyushu Island is the most affected area of the cross-border pollution in Japan due to closeness to the continent. We conducted isotopic analysis of aerosol particle samples corrected with high temporal resolution, once per a few days, from June 2011 to August 2012 in Omura City in the north Kyushu. Pb isotope ratios of 1M-HCl soluble component (”leachate”) of the corrected particles indicate the direct source of anthropogenic lead, while Sr-Nd isotope ratios of the residual mineral component digested by concentrated HF-HNO_3 (”slilicate”) indicate the source area of the mineral particles. High resolution sampling allowed us to distinguish the sources much more sensitively than commonly adopted monthly order sampling.

Sr-Nd isotope ratios of silicates indicate that the main source area of mineral particles changes seasonally. They have local origin in summer, while they are derived from deserts in mid-west China in fall and winter, and those in west China in spring (Figure A). Pb isotope ratios of leachates are distinct when the source of mineral particles is the mid-west China (Figure B). The values suggest the influence of the Chinese lead ore deposits. On the other hand, Pb isotope ratios of leachates are indistinguishable between samples of local origin and those originated from west China. An additional character of samples of west China origin is high amount of Pb in leachate relative to that of mineral component. Anthropogenic lead may be easier to be entrained to wind when the mineral particles comes from mid-west China because the wind trajectory should be much lower in altitude than when particles come from further distant west China. Cross-border atmospheric Pb pollution is suggested more serious in fall and winter when wind trajectory is low than in spring when the westerly transports vast amount of mineral particles known as ”Kosa” from the deserts in west China.

Keywords: dust, anthropogenic lead, PM10, Sr isotope ratio, Nd isotope ratio, Pb isotope ratio

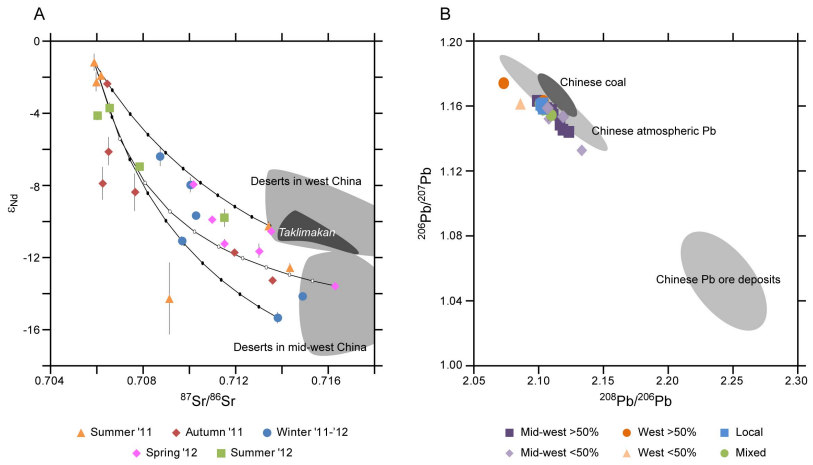

Japan Geoscience Union Meeting 2014
(28 April - 02 May 2014 at Pacifico YOKOHAMA, Kanagawa, Japan)

AAS22-P05 Room:Poster Time:May 1 18:15-19:30

Difference of composition and mixed state of dust particles by height

KAMIGUCHI, Yusuke[1*] ; IWAMOTO, Yoko[2] ; IWATA, Ayumi[3] ; HARA, Kazutaka[2] ; KINOUCHI, Kento[3] ; MAKI, Teruya[1] ; KOBAYASHI, Fumihisa[1] ; KAKIKAWA, Makiko[2] ; MATSUKI, Atsusi[2]

[1]College of Science and Engineering, Kanazawa University, [2]Institute of Nature and Environmental Technology, Kanazawa University, [3]Graduate School of Natural Science and Technology, Kanazawa University

Continental Asia has been recognized as one of the most important sources of atmospheric dust particles. Many investigators have pointed out the importance of the atmospheric processing of dust particles in the course of long-range transport. Such processing can potentially change their radiative properties and their ability to act as cloud condensation nuclei. Three major factors that govern the processing of dust particles are dust mineral composition, relative humidity and concentration of acidic gas species. These factors are considered to be closely related with the height at which dust particles are transported. However, there has been no report so far on the direct comparison of the morphology and chemical composition of individual dust particles in the free troposphere and in the planetary boundary layer in the event of a same dust outbreak.

The helicopter was employed as the airborne platform in this study. Aerosol particles were directly collected by aerosol impactor over Hakui city, Isikawa, Japan (36.9 N, 136.7 E) on March 19, 2013. Then, Dust event was observed western Japan by Japan Meteorological Agency. Morphology and elemental composition of the collected particles were later examined on individual basis under SEM-EDX (Scanning Electron Microscope equipped with Energy Dispersive X-ray spectrometry).

Atmospherically processed dust particles (with apparent morphological modification) were hardly found in the free troposphere. On the other hand, large fraction of dust particles was found modified in the planetary boundary layer, showing spherical outline. High proportion of Calcium and Magnesium were detected from the modified particles. Also, dust particles collected in the planetary boundary layer contained Sulfur in higher abundance.

It is suggested that the atmospheric conditions in the free troposphere are less favorable for the dust particles to be modified than in the planetary boundary layer, because the vertical supply of acidic gases and water vapor into free troposphere is generally limited by the temperature inversion layer.

Keywords: mineral dust, free troposphere, planetary boundary layer, SEM–EDX

Japan Geoscience Union Meeting 2014
(28 April - 02 May 2014 at Pacifico YOKOHAMA, Kanagawa, Japan)

AAS22-P06 Room:Poster Time:May 1 18:15-19:30

Demonstration test of atmosphere sampling system using combination of solar and fuel battery at Western part of Yakushim

NAGAFUCHI, Osamu[1*] ; YOKOTA, Kuriko[2] ; OSAKA, Kenichi[1] ; NAKAZAWA, Koyomi[1] ; TEZUKA, Kenshi[3]

[1]the University of Shiga prefecture, [2]Toyohashi University of Technology, [3]YOCA

We have measured PM 2.5 using soler panel and fuel cell system at Southern area of Yakushima island Japan.

In order to clarify the long-range transport of atmospheric pollutants in the East Asian regions, we have challenged the continuous observation at a mountainous area without the commercial power. Although, we are considered to be better the system with a solar battery, the pump was sometimes stopped for the brownout cause by the lack of insolation. Thereupon, we make an attempt the continuous observation of atmospheric pollutants using the combination of the solar and fuel battery. And thus we achieve the continuous observation of the atmospheric pollutants. Consequently, we will report new monitoring system.

Japan Geoscience Union Meeting 2014
(28 April - 02 May 2014 at Pacifico YOKOHAMA, Kanagawa, Japan)

AAS22-P07 Room:Poster Time:May 1 18:15-19:30

Development of a method to measure the hygroscopicity of black carbon-containing particles

OHATA, Sho[1*] ; MOTEKI, Nobuhiro[1] ; SCHWARZ, Joshua P.[2] ; KONDO, Yutaka[1]

[1]Department of Earth and Planetary Science, Graduate School of Science, The University of Tokyo, [2]Earth System Research Laboratory, National Oceanic and Atmospheric Administration

Black carbon (BC) aerosols are generated by the combustion of fossil fuels and biomass. During transport in the atmosphere, BC particles acquire ”coating materials” through the condensation of semi-volatile gaseous components, and coagulation with the other aerosols. Freshly emitted BC particles are generally hydrophobic, so the hygroscopicity of BC-containing particles is largely controlled by the composition and amount of coating materials. Although measurement of the hygroscopicity of ambient BC-containing particles is important to understand their cloud condensation nuclei activity and optical properties, measurement data are still quite limited (McMeeking et al, 2011; Liu et al. 2013). In this study, we present a modified single particle soot photometer (SP2) as a humidified-SP2 (hSP2), which quantifies the BC mass and the amount of coating material within individual aerosol particles, under controlled relative humidity (RH), by detecting both the laser-induced incandescence emitted and laser light scattered from each BC-containing particle. High time-resolved measurements of growth factor (GF: the ratio of wet particle diameter to dry diameter) and hygroscopicity parameter κ for BC-containing particles can be achieved by combining an aerosol particle mass analyzer (APM) or a standard SP2 with the newly developed hSP2.

We have tested the hSP2 in the laboratory using both homogeneous ammonium sulfate, and internally mixed particles of BC (fullerene soot) and ammonium sulfate. These particles were dried and classified by an APM and subsequently measured by the hSP2 between 60% and 90% RH. We assumed a core-shell geometry for the BC-containing particles, and took account of the reduction in refractive index of the coating materials due to their hygroscopic growth. Measured GFs of the laboratory-generated BC-containing particles agreed with GFs predicted by κ-Köhler theory to within measurement uncertainty, demonstrating the applicability of the hSP2 for ambient measurements.

Keywords: black carbon, hygroscopicity

Japan Geoscience Union Meeting 2014
(28 April - 02 May 2014 at Pacifico YOKOHAMA, Kanagawa, Japan)

AAS22-P08 Room:Poster Time:May 1 18:15-19:30

An Empirical Correction Factor for Filter-based Photo-absorption Black Carbon Measurements

IRWIN, Martin[1*] ; KONDO, Yutaka[1] ; MOTEKI, Nobuhiro[1]

[1]The University of Tokyo

Long-term observations of black carbon (BC) aerosol provide important information regarding seasonal variations, emission source attribution, and regional distribution & transport. Filter-based BC measurement techniques such as the Continuous Soot Monitoring System (COSMOS) are particularly well suited to this application, due to their relative robustness and reliability. However, caution is required when determining the threshold transmittance, Tr_{thresh} (proportional to the time interval between filter changes), in order to ensure that acceptable measurement accuracy is maintained throughout the sampling period. We present a new, empirically derived transmittance-dependent correction factor used to interpret the response characteristics of filter-based aerosol absorption measurements performed by COSMOS. Simultaneous measurements of ambient BC aerosol mass (M_{BC}) were conducted in Tokyo, Japan, using two identical COSMOS instruments operated with different threshold transmittance, Tr_{thresh}, values, of 0.95 and 0.6. The derived values for M_{BC} were consistently underestimated by the COSMOS operating at lower Tr_{thresh}, as a function of decreasing filter transmittance. The 1-hour averaged values of M_{BC} were underestimated by around 10 %, incorporating measurements across the entire range of filter transmittance (1 - 0.6), with a maximum underestimation at around 17 % immediately preceding filter advancement (i.e. $Tr = \sim 0.60$), and a minimum of $\sim$1 % immediately following filter advancement (i.e. $Tr = \sim 1$). An empirical second-order correction factor was derived from these ambient measurements, and was applied to M_{BC} as a function of filter transmittance, resolving the instruments to within 2 %.

Furthermore, the operational performance of COSMOS was tested for a new quartz fibre filter (HEPA). A comparison of different filter types demonstrated a systematic overestimation of M_{BC} of around 6 - 8 % when using HEPA filters. A sensitivity study of a radiative transfer model indicated that this enhanced absorption was primarily a result of the increased thickness of the HEPA filter.

Keywords: aerosol, black carbon, filter-based measurements, absorption

Japan Geoscience Union Meeting 2014
(28 April - 02 May 2014 at Pacifico YOKOHAMA, Kanagawa, Japan)

AAS22-P09 Room:Poster Time:May 1 18:15-19:30

Ship-borne measurements of black carbon aerosols over northwestern Pacific and Bering Sea

MIYAKAWA, Takuma[1*] ; KANAYA, Yugo[1] ; TAKETANI, Fumikazu[1] ; PAN, Xiaole[1] ; KOMAZAKI, Yuichi[1]

[1]Japan Agency Marine-Earth Science and Technology

Black carbon (BC) aerosol can strongly absorb the solar radiation and act as cloud condensation nuclei depending on the mixing state. Therefore, BC abundance and mixing state are key physicochemical properties to estimate the radiative impacts of BC aerosols [1]. Measurements of BC aerosols over the area where BC concentrations are very low are still limited because of the lack of high-sensitivity analytical methods. Single Particles Soot Photometer (SP2), which has been developed by Droplet Measurement, Inc., allows us to quantify the BC mass of single BC-containing particle and measure the BC number/mass concentration even in ultra-clean air [2]. Here we report the concentrations and mixing state of BC-containing particles observed using a SP2 on the research vessel *Mirai* during the research cruise over the northwestern Pacific and Bering Sea (MR13-05 cruise, 8/12-26, 2013).

BC mass concentrations over the sea near Japan ($<145^0$E) were elevated to $\sim$200 ng m^{-3}, whereas they were less than $\sim$40 ng m^{-3} over the northwestern Pacific and Bering Sea. Mixing states as a function of BC-containing particles deduced from SP2 raw data were categorized into three types; bare/thinly coated (type1), thickly coated (type2), and non-core-shell (type3) BC. Over the northwestern Pacific and Bering Sea, the number fractions of type1-BC were ~ 0.13, whereas those of type2-BC were as high as 0.8. We also found the minor but significant presence of type3-BC ($\sim$4%) over the remote ocean.

References
[1] Bond et al., J. Geophys. Res., 118, 5380-5552, doi:10.1002/jgrd.50171, 2013.
[2] Schwarz et al., Geophys. Res. Lett., 37, L18812, doi:10.1029/2010GL044372, 2010.

Keywords: Black carbon, Mixing state, Laser Induced Incandscence, Ship-borne measurement, Marine atmosphere

Japan Geoscience Union Meeting 2014
(28 April - 02 May 2014 at Pacifico YOKOHAMA, Kanagawa, Japan)

AAS22-P10 Room:Poster Time:May 1 18:15-19:30

High-m/z ion signal to total mass signal ratios measured for secondary organic aerosol using aerosol mass spectrometer

SATO, Kei[1*] ; FUJITANI, Yuji[1] ; TANABE, Kiyoshi[1] ; MORINO, Yu[1] ; FUSHIMI, Akihiro[1] ; TAKAMI, Akinori[1] ; IMAMURA, Takashi[1] ; HIKIDA, Toshihide[2] ; SHIMONO, Akio[2]

[1]NIES, [2]Shoreline Science Inc.

A volatility basis-set (VBS) model in which oligomerizations are taken into account has recently been tested for further improvements of conventional VBS models.[1)] In order to study the oligomerization rates during secondary organic aerosol (SOA) formation and the ratio of high-*m/z* ion to total SOA mass spectrum ion signal, SOA particles produced during laboratory chamber experiments were analyzed by using an Aerodyne aerosol mass spectrometer (AMS). Photooxidation of α-pinene, isoprene, toluene, and 1,3,5-trimethylbenzene (TMB) was investigated in the presence of NO_x. Ozonolysis of α-pinene and isoprene was also studied. A stainless steel tube was used as a collection tube for AMS. A mass spectrum measured for organic aerosol (OA) in the region *m/z* = 10 – 675 was divided into seven mass regions; the total signal of each mass region was studied as a function of time. Increase in the signal intensity was observed with increasing of the OA level in a region *m/z* <500. The oligomer signals increased up to substantial levels within one hour after nucleation. After substantial amounts of oligomers were produced, the ratio of the total signal of each mass region to total OA signal was constant. Next, the ratio of total mass signal in the region *m/z* $>m_1$ to total OA mass signal, ϕ, was determined:

ϕ = OA (*m/z* $>m_1$)/OA(total),
$m_1 = n\ m_C$ (OM/OC),

where n is the number of carbon atoms in SOA precursor, m_C is the carbon atomic mass, and OM/OC is organic matter to organic carbon mass ratio measured by AMS. The m_1 values of α-pinene, isoprene, toluene, and TMB were determined to be 217, 147, 180, and 204, respectively. We assumed that a contribution from monomer signals is low in a region *m/z* $>m_1$. Signals measured by electron ionization of AMS contain both the fragment and parent ions of organic compounds. Note that the value, ϕ, is an index of oligomer to total SOA ratio, but does not represent an absolute value of that ratio. The ϕ value of SOA from the same precursor decreased with increasing of SOA mass loading (Fig. 1), showing that oligomer formation is suppressed under high mass loading conditions. In a region 10 – 100 μg m^{-3}, the ϕ value of toluene SOA was the highest, whereas that of α-pinene SOA was the lowest. No apparent effect of oxidation method (photooxidation or ozonolysis) was observed.

Acknowledgements: This work was supported by Grant-in-Aid for Scientific Research of Japan Society for the Promotion of Science (No. 25340021, FY2013 – 2015) and Cross-Center Collaborative Research Fund of NIES (No. 1214AO001, FY2012 – 2014).

References: [1)] Trump and Donahue, Oligomer formation within secondary organic aerosol: equilibrium and dynamic considerations. *Atmos. Chem. Phys. Discuss.*, **13**, 24605 – 24634 (2013).

Keywords: secondary organic aerosol, oligomerizations, aerosol mass spectrometer, aerosol mass loading, chemical structure

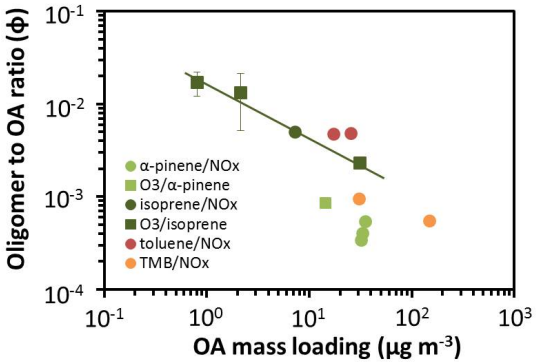

Fig. 1. Effects of OA mass loading on the oligomer to OA signal ratio (ϕ).

Japan Geoscience Union Meeting 2014
(28 April - 02 May 2014 at Pacifico YOKOHAMA, Kanagawa, Japan)

AAS22-P11 Room:Poster Time:May 1 18:15-19:30

Controlling factors of aerosol size distribution over East Asia

HASHIOKA, Hideaki[1*] ; SHIBANO, Yuki[1] ; MOTEKI, Nobuhiro[1] ; KITA, Kazuyuki[2] ; MATSUI, Hitoshi[3] ; KOIKE, Makoto[1] ; KONDO, Yutaka[1]

[1]Department of Earth and Planetary Science, Graduate School of Science, University of Tokyo, Japan, [2]Faculty of Science, Ibaraki University, Mito, Japan, [3]Japan Agency for Marine-Earth Science and Technology, Tokyo, Japan

Aerosol is known for its direct and indirect effects on climate, with both effects having a larger uncertainty than other radiative forcing elements, such as carbon dioxide. Investigating ambient aerosol size distributions is an important factor in estimating radiative forcing effects, as aerosol size is a major contributing factor to both the aerosol direct and indirect effects.

Ambient aerosol size and spatial distributions are controlled by various processes; e.g. new particle formation, coagulation, transportation, and wet deposition. For this reason, in situ measurements and analyses based on such processes are essential. However, results from measurements with high time resolution and low detection limits (e.g. of aerosol diameter) are rare. In this research, we introduce measurements of the aerosol size distribution over East Asia using the ultra high sensitivity aerosol spectrometer (UHSAS), and have tried to analyze the results based on wet removal processes.

The UHSAS is an optical particle counter. With its 2 types of photon diode and its efficiency in collecting scattering light, the UHSAS can obtain measurements of aerosol diameter in a wide range (about 70 to 1500 nm). We improved the hardware and software of the UHSAS specifically for use in aircraft measurements, to improve time resolution data and the instrumental precision of measurements of aerosol number concentration and size distribution (assuming spherical particles with refractive index 1.52). In addition, we have installed a robust mass-flow controlling system to deal with the significant changes in pressure associated with aircraft measurements. Scattering light signals obtained from photon diodes are saved to an external storage medium, which aids us in distinguishing signal from noise. We also present results showing the successful estimation of the optics inside UHSAS, in order to obtain highly precise diameter information using known standard particles.

The aerosol radiative forcing in East Asia (A-Force 2013W) aircraft campaign was conducted from late February to early March. We obtained air samples in real time from a forward facing inlet outside of the aircraft, Air was sampled by a variety of instruments including the UHSAS in real-time from a forward facing inlet outside of the aircraft. Data from the UHSAS showed good consistency with other instruments. During the campaign, the mean size distribution shifted to smaller diameters with increasing altitude. The transport efficiency (TE) of BC, which describes the degree of the wet removal of BC (calculated from the carbon monoxide mixing ratio and BC mass concentration), also decreased with increasing altitude (i.e. strong wet removal tendency for higher altitude). As the TE became smaller, the mean size distribution also shifted to smaller diameters, independent of altitude. This shows that the TE is the dominant factor controlling the aerosol size distribution, rather than absolute altitude. When the TE is smaller, the size distribution shifted to smaller diameters; this is the first observation of the size-dependent wet removal of general aerosols based on Köhler theory. This dynamic state of aerosol size distribution observed by the UHSAS surely contributes to quantitative understanding of aerosol direct and indirect effects on climate.

Keywords: aerosol, size distribution, wet removal process, black carbon, transport efficiency, UHSAS

Japan Geoscience Union Meeting 2014
(28 April - 02 May 2014 at Pacifico YOKOHAMA, Kanagawa, Japan)

AAS22-P12 Room:Poster Time:May 1 18:15-19:30

Vertical profiles of aerosol size distribution in small forest within a western suburb of Tokyo

YABUKI, Masanori[1*] ; TAKAHASHI, Kenshi[1] ; TSUDA, Toshitaka[1] ; MATSUDA, Kazuhide[2]

[1]Research Institute for Sustainable Humanosphere, Kyoto University, [2]Tokyo University of Agriculture and Technology

Forests interact in a complex manner with the atmosphere by acting as sinks for many atmospheric pollutants and trace gases, and by emitting biogenic volatile organic compounds into the air. These constituents influence the atmospheric chemistry and composition, including aerosols related to cloud condensation nuclei (CCN). Aerosol chemical and physical properties vary both temporally and spatially owing to various atmospheric processes (e.g., scavenging, nucleation, evaporation, and condensation) during the dispersion and transportation of air mass within and above forest canopies.

In this paper, we report on the field observations conducted from a 30-m-high tower in a small forest at the Field Museum Tama Hills, an experimental forest of the Tokyo University of Agriculture and Technology, located in a western suburb of Tokyo, between July 27 and August 3, 2013. At this site, atmospheric aerosols were expected to include the particles both from natural and anthropogenic sources. Using five sampling inlets placed at altitudes ranging from 8 m to 30 m, we conducted altitude-resolved measurements of particle number size distributions in the size range of 10-5000 nm. Herein, we present an outline of the observation systems, as well as the preliminary results of variability of sub-micrometer and nano particles within and above the forest canopy.

Keywords: Aerosol, Size distribution, Vertical distribution, Forest canopy

Japan Geoscience Union Meeting 2014
(28 April - 02 May 2014 at Pacifico YOKOHAMA, Kanagawa, Japan)

AAS22-P13 Room:Poster Time:May 1 18:15-19:30

Measurement of fluorescent particles over the western Pacific

TAKETANI, Fumikazu[1*] ; PAN, Xiaole[1] ; MIYAKAWA, Takuma[1] ; KOMAZAKI, Yuichi[1] ; KANAYA, Yugo[1] ; MATSUMOTO, Kazuhiko[1] ; HONDA, Makio[1]

[1]JAMSTEC

Recently, fluorescence from suspended single particles has been employed to identify and classify the certain types of organic/biological particles. Bioaerosols, including bacteria and other particles derived from living organisms, may explain large unidentified fraction of organic aerosols and play important roles in the cloud formation. In this study, we employed a single-particle fluorescence sensor, WIBS-4, to understand the abundance of bioaerosol particles over the western Pacific.

We conducted ambient air measurements over the western Pacific at July 2011, 2012, and 2013 by R/V MIRAI cruise. In order to avoid analyzing the particles emitted by ship's funnel, we eliminated the data by the wind direction. In the cruises, the bioaerosol particles based on fluorescent pattern were in the range of 0.1-2 particles/cc over the western Pacific. In the presentation, we will compare ocean surface chlorophyll data with detected fluorescence particles.

Keywords: aerosol particles, fluorescence

Japan Geoscience Union Meeting 2014
(28 April - 02 May 2014 at Pacifico YOKOHAMA, Kanagawa, Japan)

AAS22-P14 Room:Poster Time:May 1 18:15-19:30

Impact of the Kuroshio warm SST on low altitude clouds: Numerical model simulation with smoothed SST

ASANO, Naruhiko[1*] ; KOIKE, Makoto[1] ; MATSUI, Hitoshi[2] ; NAKAMURA, Hisashi[3]

[1]University of Tokyo, [2]Japan Agency for Marine-Earth Science and Technology, [3]RCAST, University of Tokyo

Along the Kuroshio ocean current, high sea surface temperature (SST) is maintained even in winter and a steep SST gradient is formed across the current. In winter and spring, cold northwesterly air often flows from the Asia continent into the East China Sea. Once this cold air reaches the Kuroshio warm current, a large temperature contrast between sea surface and surface air (SAT) causes the marine boundary layer unstable and affect low altitude cloud formation. The northwesterly wind also transports a large amount of anthropogenic aerosols to East China Sea. These aerosols work as cloud condensation nuclei (CCN) and they affect microphysical properties of clouds. Because the marine boundary layer stability affects aerosol activation to form cloud particles, the large contrast between SST and SAT over the Kuroshio can also affect the aerosol-cloud interaction as proposed by Koike et al. [2012].

In order to assess the impact of Kuroshio warm SST on low clouds, we made WRF model calculations for a period between 21 Mar and 30 Apr 2009. In addition to the control calculation, we made sensitivity calculations, in which artificially smoothed SST was given for a lower boundary condition. In this smoothed SST, the SST gradually decreases toward higher latitudes and the maximum along the Kuroshio current no longer exists.

In the control calculation, the monthly mean cloud fraction (frequency of cloud occurrence in April 2009) was high in the south of Kuroshio and had a steep north-south gradient, corresponding to the SST steep gradient. A monthly mean liquid water pass (LWP) was large along Kuroshio and small in East China Sea, although it enhanced when cyclones passed. As compared with the control calculation, both the cloud fraction and LWP decreased over the Kuroshio in smoothed-SST calculations, and their north-south gradients became gentler.

LWP differences between control and sensitivity calculations varied depending on the wind direction. In northerly wind conditions, the LWP decreased in warmer frank (downwind) of a SST front. Under calm and horizontally homogeneous wind conditions, water vapor transport convergence was relatively small over the Kuroshio and column-integrated water vapor increased mainly by evaporation from the sea surface. In such case, LWP decreased on the Kuroshio in sensitivity calculation. This suggests that warm SST associated with Kuroshio enhances the evaporation and contributes to increase LWP of low clouds.

Keywords: low clouds, Kuroshio

Japan Geoscience Union Meeting 2014
(28 April - 02 May 2014 at Pacifico YOKOHAMA, Kanagawa, Japan)

AAS22-P15 Room:Poster Time:May 1 18:15-19:30

Measurement of the hygroscopic growth factor distributions of aerosol particles and the mass spectra of single particles

KAWANA, Kaori[1*] ; NAKAYAMA, Tomoki[2] ; MOCHIDA, Michihiro[1]

[1]Graduate School of Environmental Studies, Nagoya University, [2]Solar-Terrestrial Environmental Laboratory, Nagoya University

Hygroscopicity is a property that relates to the lifetime, chemical reactivity and cloud condensation nucleus activity of atmospheric aerosol particles. The amount of water retained by the particles as a function of relative humidity (RH) is governed by the phase state and chemical composition. In this study, hygroscopic growth factor distributions of atmospheric aerosol particles and mass spectra of single particles selected by the growth factors were measured using a combination of hygroscopicity tandem differential mobility analyzer (HTDMA) and a high resolution time-of-flight aerosol mass spectrometer (AMS) in Nagoya.

The observation of urban aerosols was performed on Higashiyama campus of Nagoya University in June and July, 2013. After aerosols were passed through PM1 cyclone and dried in diffusion driers, 300 nm particles were selected in the first DMA of the HTDMA. The growth factor distributions of the particles were measured under humidified conditions (setting RH: 37%, 65%, and 87%). The measurements were performed in both humidification and dehumidification modes. The mass spectra of single particles with specific hygroscopic growth factors *g* (1.0 at setting RH of 37%; 1.0, 1.1, and 1.25 at setting RH of 65%; 1.0 and 1.5 at setting RH of 87%) were measured using the AMS. The size distributions of aerosol particles were measured separately. The concentrations of organic carbon and elemental carbon in parts of the study period were also obtained.

In the humidification mode, the averages of the growth factor distributions at setting RH of 37% and 65% did not show substantial hygroscopic growth in terms of mean *g* (1.00 and 1.02, respectively), and those at setting RH of 87% showed large mean *g* (1.48). In the dehumidification mode, mean *g* of the averages of the growth factor distributions at setting RH of 37% and 65% (1.07 and 1.18, respectively) were substantially larger than those in the humidification mode, suggesting the presence of metastable-state aqueous solutions in the particles. At setting RH of 87%, the mean *g* in the dehumidification mode was large (1.44) as in the case of the humidification mode. The mass spectra of single particles with specific *g* were extracted from the obtained data; the number of these spectra was 349.

Keywords: hygroscopicity, single particle

Japan Geoscience Union Meeting 2014
(28 April - 02 May 2014 at Pacifico YOKOHAMA, Kanagawa, Japan)

AAS22-P16 Room:Poster Time:May 1 18:15-19:30

CCN activity of aerosol and its relation to air mass origins: an analysis based on year-round observation at Noto, Japan

IWAMOTO, Yoko[1*] ; KINOUCHI, Kento[2] ; MATSUKI, Atsushi[1]

[1]Institute of Nature and Environmental Technology, Kanazawa University, [2]Graduate School of Natural Science and Technology, Kanazawa University

Atmospheric aerosols play an important role in controlling the earth ' s radiation balance and/or the hydrological system by acting as cloud condensation nuclei (CCN). For a quantitative evaluation of CCN characteristics in the East Asia, CCN activity of atmospheric aerosols in submicrometer size range were measured at Noto Ground-based Research Observatory (NOTOGRO), located at the tip of Noto peninsula, facing the Sea of Japan. The observation was conducted from October 2012 to September 2013, to investigate the seasonal variability in CCN activity of the atmospheric aerosols.

CCN efficiency spectra, where CCN number fraction is plotted against the diameter of aerosols, were obtained at four different supersaturation (SS) conditions (0.1%, 0.2%, 0.5% and 0.8%) by using a scanning mobility CCN analysis (SMCA) system (Moore et al., 2010). Hygroscopicity parameters kappa (Petters and Kreidenweis, 2007), which depends on the chemical composition of aerosols, were estimated through analyses of the CCN spectra. The bulk chemical composition of non-refractory submicrometer-sized aerosols was also measured by an aerosol chemical speciation monitor (ACSM). Seven-days backward trajectories at the height of 500 m above the sea level were calculated by using NOAA/HYSPLIT4 model.

The CCN activation diameters of the atmospheric aerosols were clearly larger than those of pure ammonium sulfate throughout the year. The mean kappa values ranged between those of pure ammonium sulfate (0.61) and several pure organic compounds (0 to 0.25). These evidences suggest that the atmospheric aerosols were mixture of ammonium sulfate and organics. The bulk chemical composition derived by ACSM also showed that organics, sulfate and ammonium were three major components throughout the observation period. The contribution of organics to the CCN activity of the atmospheric aerosols observed in this study was more apparent than those obtained in the previous studies in the East Asia. As most of the previous CCN studies in East Asia were conducted in the season significantly affected by Asian outflow of pollutants, current numerical models might overestimate CCN concentrations in the East Asia.

The mean kappa values were 0.30, 0.26, and 0.18 during the spring, autumn and summer, respectively. The difference in kappa values among the seasons might be caused by difference in air mass origin. Air masses to the NOTOGRO site came mainly from NW across the Sea of Japan during the autumn and spring, whereas air masses of Pacific origin, those passed over the Japan islands, prevailed in the summer. Relatively high kappa values were observed under the influence of continental polluted air masses with high sulfate concentration. On the other hand, organic aerosols derived by photochemical oxidation were dominant in summer, resulted in low kappa values. The variation in kappa values of organics with air mass origins will also be discussed.

References

Petters and Kreidenweis (2007), *Atmos. Chem. Phys.*, 7, 1961-1971.
Moore et al. (2010), *Aerosol Sci. Tech.*, 44, 861-871.

Keywords: atmospheric aerosol, cloud condensation nuclei, organic aerosol, hygroscopicity parameter, East Asia

Japan Geoscience Union Meeting 2014
(28 April - 02 May 2014 at Pacifico YOKOHAMA, Kanagawa, Japan)

AAS22-P17 Room:Poster Time:May 1 18:15-19:30

Long-term observation of initial droplet growth of activated CCN at Noto peninsula, Japan

KINOUCHI, Kento[1*] ; IWAMOTO, Yoko[2] ; KAGAMI, Sara[3] ; MATSUKI, Atsushi[2]

[1]Graduate School of Natural Science & Technology, Kanazawa university, [2]Institute of Nature and Environmental Technology, Kanazawa university, [3]College of Science and Engineering, Kanazawa university

Atmospheric aerosols affect the climate indirectly by changing optical property and lifetime of clouds through their ability to act as cloud condensation nuclei (CCN). Size of cloud droplets is an important factor to consider in the climate predictions because it can influence cloud albedo and frequency of precipitation. Important factors controlling the growth of cloud droplets are; 1. water vapor supersaturation (SS), 2. CCN size and 3. CCN chemical composition. Chemical composition of aerosols is a very important factor controlling the initial droplets growth. Recent studies indicate that there is high mass fraction of organics in the CCN relevant particles, and the droplet growth kinetics following the activation of such organic containing CCN is not fully understood.

East Asia is regarded as one of the most aerosol (hence CCN) dense regions in the world, but long-term monitoring of CCN properties in this region is relatively scarce. In this study, we conducted in-site and year-round measurement of CCN activity of submicron aerosols and related cloud droplet growth kinetics at NOTOGRO (acronym for NOTO Ground-based Research Observatory) located Suzu city, Noto Peninsula. A CCN counter (CCNC, CCN-100, DMT) was operated at four different super-saturation conditions (SS=0.1%, 0.2%, 0.5%, 0.8%). The diameters of cloud droplets activated from ambient aerosols ($D_{ambient}$) were compared to those activated from ammonium sulfate (D_{AS}) which is regarded as representative inorganic CCN. In order to identify factors that can potentially influence the initial cloud droplet growth, simultaneously measured chemical composition of aerosols with an Aerosol Chemical Speciation Monitor (ACSM, Aerodyne Inc.).

The measurement result showed that $D_{ambient}$ was not significantly difference from D_{AS} under higher SS conditions (i.e. SS=0.5% and 0.8%) throughout all seasons. However, there are periods that droplet growth was inhibited under lower SS conditions (i.e. SS=0.1% and 0.2%) especially during spring and autumn. Therefore, it was suggested that droplet growth under lower SS condition was more sensitive to other factors (other than SS). Based on the ACSM results, chemical composition of CCN was mainly contributed by various organics, ammonium and sulfate during the entire measurement period. The periods with limited droplet growth coincided with the periods with high organic mass fraction, and the negative correlation was found between the cloud droplets' diameters and organic mass fraction within atmospheric aerosols in CCN relevant sizes. On the other hand, we did not observe significant fluctuation in the cloud droplet diameters in winter. The measurement site is under the strong influence of winter monsoon especially during winter and the chemical species comprising CCN that are carried to the site may be considerably different from other seasons.

Keywords: cloud condensation nuclei, cloud droplet, chemical composition

Japan Geoscience Union Meeting 2014
(28 April - 02 May 2014 at Pacifico YOKOHAMA, Kanagawa, Japan)

AAS22-P18 Room:Poster Time:May 1 18:15-19:30

Seasonal variations of peroxyacyl nitrates and alkyl nitrates concentration at Suzu, the Noto Peninsula

ISHIYAMA, Ayana[1*] ; TAKAJI, Ryo[1] ; SADANAGA, Yasuhiro[1] ; MATSUKI, Atsushi[2] ; SATO, Keiichi[3] ; OSADA, Kazuo[4] ; BANDOW, Hiroshi[1]

[1]Osaka Prefecture University, [2]Kanazawa University, [3]Asia Center for Air Pollution Research, [4]Nagoya University

NO_x emissions have been increasing in East Asia with recent remarkable economic progress. NO_x has relatively short lifetime and NO_x concentrations are governed by local NO_x emissions. On the other hand, descendant photochemical products of NO_x such as $T.NO_3$ (the sum of gaseous nitric acid and particulate nitrates), PANs (peroxyacyl nitrates) and ANs (alkyl nitrates) have longer lifetime than NO_x, so that they can be transported over a long-distance. In order to understand influences of the cross-border pollution, it is important to clarify the long-range transport of $T.NO_3$, PANs, and ANs.

We have been continuously observing several pollutants at NOTOGRO (Noto Ground-based Research Observatory) supersite in Suzu, the Noto Peninsula. NOTOGRO is located at 37.45N and 137.36E. NO_x were determined by an LED photolytic converter / NO-O_3 chemiluminescence method. NO_y and $T.NO_3$ were observed by a scrubber difference / NO-O_3 chemiluminescence method. CO was monitored by a non-dispersive infrared photometer. PANs and ANs were measured by a thermal dissociation / cavity attenuated phase shift spectroscopy method.

In this presentation, observational results and discussion from December, 2012 to July, 2013 are described, focusing on seasonal variations of PANs and ANs. The air mass origins arriving at Suzu were classified into the following four groups, Russia and North China (RC), Korea and Middle China (KC) and Japan (JP) and Sea (S) using backward trajectory analyses. From winter to spring, both PANs and ANs concentrations from KC were higher than those from the other air mass origins. From spring to summer, their concentrations were independent of air mass origins.

From winter to spring, the lifetimes of PANs and ANs are long because of low temperature and weak solar radiation. In addition, their in-situ photochemical generation rates are low, so that PANs and ANs concentrations in this season are governed by long-range transport. From spring to summer, the lifetimes of PANs and ANs become shorter and their photochemical production rates become higher, that is, local photochemical productions of PANs and ANs are relatively important. Diurnal variations of PANs and ANs also support these concentration variation factors. From winter to spring, no diurnal variations were observed. Meanwhile, PANs and ANs concentrations began to be higher and lower in the daytime and nighttime, respectively, from spring to summer.

Keywords: peroxyacyl nitrates and alkyl nitrates, long-range transport, seasonal variation

Japan Geoscience Union Meeting 2014
(28 April - 02 May 2014 at Pacifico YOKOHAMA, Kanagawa, Japan)

AAS22-P19 Room:Poster Time:May 1 18:15-19:30

Development of a continuous measurement system of PANs and alkyl nitrates in the atmosphere and observations at Suzu, th

TAKAJI, Ryo[1*] ; ISHIYAMA, Ayana[1] ; SADANAGA, Yasuhiro[1] ; MATSUKI, Atsushi[2] ; SATO, Keiichi[3] ; OSADA, Kazuo[4] ; BANDOW, Hiroshi[1]

[1]Osaka Prefecture University, [2]Kanazawa University, [3]Asia Center for Air Pollution Research, [4]Nagoya University

Peroxyacyl nitrates (PANs) and alkyl nitrates (ANs) are generated in the atmosphere by oxidation of NO_x in the presence of solar ultraviolet. They have a comparatively long lifetime, and are important as transboundary air pollutants. On the other hand, PANs and ANs act as the reservoirs of NO_x. In order to clarify transboundary pollution of nitrogen oxides, comprehensive measurements of total odd nitrogen species (NO_y), including PANs and ANs, are required. In this research, a continuous measurement system of total PANs and ANs has been developed by a thermal dissociation / cavity attenuated phase shift spectroscopy (TD/CAPS) method.

This instrument consists of heated quartz tubes to decompose PANs and ANs into NO_2, and a CAPS-NO_2 analyzer. This system has three intake lines; NO_2, PANs and ANs lines. The NO_2 line equip of a quartz tube without heating. The PANs and ANs line equip quartz tubes heated at 433 K and 633 K, respectively for thermally decomposing them into NO_2. Concentrations of NO_2, NO_2 + PANs and NO_2 + PANs + ANs can be obtained from the NO_2, PANs and ANs lines, respectively. These concentrations are sequentially measured by switching solenoid valves and then NO_2, PANs and ANs concentrations are obtained. Since a part of HNO_3 is pyrolyzed in the ANs line, annular denuder coated with NaCl to remove HNO_3 is set before the heated quartz tube in the ANs line. The decomposition efficiencies of PANs and ANs were calibrated to be 100 and 95%, respectively, for all kinds of PANs and ANs examined.

Continuous field observations of PANs and ANs have been being performed at NOTOGRO (Noto ground-based Research observatory) supersite in Suzu, the Noto Peninsula, since November 2012. Continuous measurements of NO_x, NO_y, T.NO_3 (the sum of gaseous nitric acid and particulate nitrate) O_3, and CO have also been being conducted. NO_y concentrations were in agreement with the sum of observed NO_y components (= NO_x + T.NO_3 + PANs + ANs) regardless of seasons. NO_x fractions were the highest in NO_y constituents. Fractions of T.NO_3 in January and February were lower than those in other months. This reflects that wet deposition of T.NO_3 would be accelerated in winter due to snowfall. On the other hand, PANs fractions in spring and summer were smaller than those in winter. This suggests that temperature increasing promotes decomposition of PANs.

Keywords: peroxyacyl nitrates (PANs), alkyl nitrates, total odd nitrogen species, cavity attenuated phase shift spectroscopy

Japan Geoscience Union Meeting 2014
(28 April - 02 May 2014 at Pacifico YOKOHAMA, Kanagawa, Japan)

AAS22-P20 Room:Poster Time:May 1 18:15-19:30

On-line measurements of multiple alkanes by chemical ionization mass spectrometry using NO^+ as the reagent ion

INOMATA, Satoshi[1*] ; TANIMOTO, Hiroshi[1] ; YAMADA, Hiroyuki[2]

[1]NIES, [2]NTSEL

Proton transfer reaction mass spectrometry (PTR-MS) is a technique that allows for fast and sensitive measurement of volatile organic compounds (VOCs) at trace levels in air. Proton transfer is an example of chemical ionization: it enables soft ionization of chemical species that have a proton affinity (PA) higher than that of the reagent species (i.e., water):

H_3O^+ + VOC ->VOC?H^+ + H_2O (1)

Unlike gas chromatography, PTR-MS does not require any sample treatment such as drying and/or preconcentration, which makes possible quantitative measurement of alkenes (except ethylene), aromatics, and even oxygenated VOCs. However, the proton transfer in reaction (1) does not occur for alkanes because they have lower PAs than water. Very recently, a method to measure C_{12}-C_{18} alkanes using PTR-MS was demonstrated. They were, however, detected by a series of fragment ions with formula C_nH_{2n+1} and were detected not individually, but as an ensemble.

Reactions of alkanes with NO^+ have been investigated by selected ion flow tube mass spectrometry (SIFT-MS). It was reported that hydride ion transfer is a major channel in the reaction of alkanes (RH) with NO^+.

NO^+ + RH ->R^+ + HNO (2)

Recently, the PTR-MS instrument has been combined with switchable reagent ion capability, which allows for easy and fast switching between H_3O^+ and NO^+ (proton-transfer-reaction *plus* switchable reagent ion mass spectrometry (PTR + SRI-MS)).

In the present study, the detection properties of alkanes by PTR + SRI-MS are investigated. We confirmed that alkanes (RH) were usually detected as R^+ by PTR + SRI-MS using NO^+ as the reagent ion and detection sensitivities were comparable to those of aromatics observed by H_3O^+ ionization. We also demonstrated time-resolved measurements of C_4-C{16} alkanes in automotive exhaust during the Japanese JC08 transient cycle. It can be concluded that sensitive on-line measurement of multiple alkanes is possible by PTR + SRI-MS using NO^+ as the reagent ion.

Keywords: PTR-MS, alkane, NO^+ chemical ionization, Gasoline vehicle, Diesel vehicle, Exhaust gas

Japan Geoscience Union Meeting 2014
(28 April - 02 May 2014 at Pacifico YOKOHAMA, Kanagawa, Japan)

AAS22-P21 Room:Poster Time:May 1 18:15-19:30

Observation of formaldehyde and glyoxal variations by MAX-DOAS in Chiba and Tsukuba in 2013

CHIN, Sei[1*] ; NI, Wentao[1] ; IRIE, Hitoshi[1]

[1]Chiba university

BVOCs (Biogenic Volatile Organic Compounds) are plant-released organic chemicals that are volatile in air at normal ambient temperature and pressure. Reactions of BVOC in the atmosphere have a great influence on the OH abundance in the atmosphere. In addition, the reactions lead to the formation of ozone, which is not only adversely affecting plants and human health but also acting as a greenhouse gas. Furthermore, part of the products from the oxidation reaction of BVOCs forms aerosols, which play a critical role in cloud formation processes and radiation balance. Thus, BVOCs are deeply related with climate and air quality surrounding us. Recently, formaldehyde and glyoxal are recognized as important indicators of oxidations of BVOCs. However, their observations have been limited. In this study, we use the data got from MAX-DOAS to analysis the diurnal variation, seasonal variation of formaldehyde and glyoxal for the first time. And then we try to find the reason or the factors which makes the variations.

Figure1 shows the data of glyoxal concentration observed in China during 2013. To know the diurnal and seasonal variation, we calculated the average value of every hour in each month. We found the clearly pattern that the concentration of glyoxal is high during the day and summer. At noon of the summer, the concentration of glyoxal was increased to more than 0.105ppbv. We also found the same pattern in Tsukuba. In this study, we observed glyoxal and formaldehyde in the same time, and organize the data of Chiba and Tsukuba in 2013 and try to find the reason of the variation.

Keywords: Formaldehyde, Glyoxal, MAX-DOAS, diurnal variation, seasonal variation

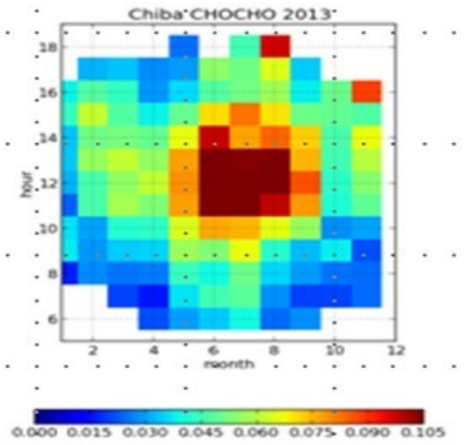

Japan Geoscience Union Meeting 2014
(28 April - 02 May 2014 at Pacifico YOKOHAMA, Kanagawa, Japan)

AAS22-P22 Room:Poster Time:May 1 18:15-19:30

Development of a direct measurement system of photochemical ozone production rate in the troposphere

KAWASAKI, Shio[1*] ; SADANAGA, Yasuhiro[1] ; TANAKA, Yuki[1] ; KAJII, Yoshizumi[2] ; BANDOW, Hiroshi[1]

[1]Osaka Prefecture University, [2]Kyoto University

Recently, ozone concentrations in the troposphere have been rising in spite of a steady decrease in concentrations of ozone precursors such as NO_x and volatile organic compounds. Photochemical production processes of ozone are non-linear to concentrations of ozone precursors. In addition, ozone concentration variations are influenced by meteorological factors such as transport and deposition processes as well as photochemistry. It is useful that the meteorological and photochemical factors could be divided to discuss ozone concentration variations. In order to discuss only "photochemical" factors for ozone production, a direct measurement system of photochemical ozone production rate has been developed.

Ambient air is introduced into "reaction" and "reference" chambers. The reaction and reference chambers (171-mm inner diameter and 500-mm length) are made of quartz and Pyrex, respectively. Inner walls of both the chambers are coated with Teflon to avoid wall loss of ozone. An outer wall of the reference chamber is coated with a UV-cut film (50%-cutoff wavelength of 405 nm). In the reaction chamber, photochemical reactions proceed to generate ozone. On the other hand, ozone is not produced photochemically in the reference chamber. Air passed from the reaction and reference chambers is introduced into "NO-reaction" tubes to covert O_3 to NO_2 in the presence of a high concentration of NO, and then the air is introduced into an NO_2 measurement system by a laser-induced fluorescence technique. Increment of ozone (ΔO_3) is defined by the difference of NO_2 concentrations derived from the reaction chamber and those from reference chamber. The ozone production rate is obtained by dividing ΔO_3 by a mean residence time of air in the reaction chamber (τ). In this system, O_3 concentrations are not directly measured but NO_2 concentrations converted by the reaction of O_3 with excess NO are observed. This is because the photostationary states between NO_x and O_3 are different between in the reaction and reference chambers, and ozone concentrations vary apparently. The sum of ozone and NO_2 concentrations (abbreviated as PO) are kept in the different photostationary states, so that this instrument measures production rates of PO instead of those of ozone practically.

Important parameters in this system are (1) ultraviolet transmittance of the reaction and reference chambers, (2) τ, and (3) conversion efficiency of O_3 to NO_2 in the NO-reaction tube. For (1), we measured solar spectra at inside and outside of the chambers using a spectroradiometer. Almost a hundred % of solar UV was transmitted into the reaction chamber. A wall of the reference chamber cut off solar UV adequately. For (2), about 10 ppmv of pulsed NO_2 was added into the reaction chamber and temporal variations of LIF signals were measured. τ was calculated to be 22.1 ± 0.5 min using the temporal variation the signals. For (3), quantitative conversions of O_3 up to 160 ppbv by NO in the NO-reaction tube were confirmed under the excess NO condition 0.97 ppmv.

Keywords: photochemical ozone, direct measurement of ozone production rate, laser-induced fluorescence

Japan Geoscience Union Meeting 2014
(28 April - 02 May 2014 at Pacifico YOKOHAMA, Kanagawa, Japan)

AAS22-P23 Room:Poster Time:May 1 18:15-19:30

Transbounday ozone pollution from China to Japan; a case study

YURIKO, Keyamura[1*] ; HAYASHIDA, Sachiko[1]

[1]Faculty of Science, Nara Woman's University

These days, high concentrations of atmospheric ozone are often observed at the ground and/or in the lower troposphere over Japan, and transboundary ozone pollution from China would be one the possibility.

In this study we sampled highly concentrated ozone events observed at the ground and in the lower troposphere, and calculated backward trajectories hourly from the observation sites and compared the trajectories with the ozone map obtained by satellite measurement. The ozone lidar used here is the MRL (Meteorological Research Laboratory) ozone lidar [Nakazato et al.,Applied Optics, 2007], which has short wavelengths in UV and thus continuous day-and-night measurements are possible. We also utilized the surface ozone monitoring network organized by Ministry of Environment.

The ozone distribution maps at the lower troposphere were obtained by OMI ozone product provided by Liu et al.[ACP, 2010]. They retrieved ozone profiles from the ground up to about 60 km into 24 layers among which 3 layers are in the troposphere. The lowermost layer (24th layer) is corresponding to 0 ˜about 3 km.

From analysis mentioned above, we found some cases indicating clear evidence of transboundary pollution from China to Korea and Japan.

This study was supported by a Grant - in - Aid from the Green Network of Excellence, Environmental Information(GRENE - ei) program. And OMI data were provided by Dr. X.Liu and Dr. K.Chance, and Ozone - liar data were provided by Dr. M.Nakazato.

Keywords: troposphere, ozone, trajectory, transport, China

Japan Geoscience Union Meeting 2014
(28 April - 02 May 2014 at Pacifico YOKOHAMA, Kanagawa, Japan)

AAS22-P24 Room:Poster Time:May 1 18:15-19:30

Validation observation for the derivation of lower tropospheric ozone by remote sensing

YANAKA, Fumiya[1*] ; KITA, Kazuyuki[2] ; YAMAGUCHI, Yuuki[1] ; FUKUJU, Tabito[1] ; ITABASHI, Ryohei[1] ; KINASE, Takeshi[1] ; IRIE, Hitoshi[3] ; NOGUCHI, Katsuyuki[4] ; NAKAYAMA, Tomoki[5] ; MATSUMI, Yutaka[5] ; NAGAI, Tomohiro[6] ; SAKAI, Tetsu[6] ; ZAIZEN, Yuji[6] ; MORINO, Isamu[7] ; UCINO, Osamu[7] ; INOUE, Makoto[7] ; TANAKA, Tomoaki[8]

[1]Graduate School of Science and Engineering, Ibaraki University, [2]College of Science, Ibaraki University, [3]Center for Environmental Remote Sensing, Chiba University, [4]Faculty of Science, Nara Women's University, [5]Solar-Terrestrial Environment Laboratory, Nagoya University, [6]Meteorological Research Institute, [7]National Institute for Environmental Studies, [8]NASA Ames Research Center

The lower tropospheric ozone is a major component of photochemical oxidant which causes photochemical smog, adversely affecting human health and vegetation when it comes to high concentration. Therefore knowing their behavior as air pollution is an important. In recent years, contrary to the reduction of lower tropospheric ozone precursor gases, their amount is increasing. It has been suggested that the long-range transport of the lower tropospheric ozone from Asian Continent affects air quality in Japan and other wide areas. Remote sensing from a satellite is effective to observe such extensive/transboundary air pollution. However it has been quite difficult to measure the lower tropospheric ozone from satellite.

We have proposed that it can be evaluated with simultaneous measurement of solar backscattering spectra in the ultraviolet(UV) and visible(Vis) regions. Because the atmospheric Rayleigh scattering cross-section is much larger in UV than that in Vis, lower tropospheric light path length of the solar scattered radiation observed from space is significantly different in these two wavelength regions. This difference of light path enables us to detect the lower tropospheric ozone by the simultaneous measurement of UV and Vis solar backscattered spectra from space.

For the validation of this technique, we carried out aircraft experiments to validate this method over Tsukuba on 10th and 13rd September 2012. UV and Vis backscatter spectra were measured with two spectroscopes (Maya2000pro, Ocean Optics, USA) at two altitudes 2500 ft (760 m) and 25000 ft (7600 m). Simultaneously, ozone profile was measured with ozone monitors on-board the aircraft, with ozonesonde launched near Tsukuba, and the tropopheric ozone lidar. Because aerosol scattering may significantly affect the evaluation of the lower tropospheric ozone amount, in situ aerosol observation with the CRDS, PSAP, and PASS instruments and the lidar observation were carried out in the Meteorological Research Institute. From the aircraft, we observed solar scattered radiation from zenith, nadir and 20 degree oblique directions in ultraviolet(300 - 380nm wavelength) and visible(400 - 700nm wavelength) spectral range. Because the surface reflected light greatly contribute to the scattered light from nadir, especially in the visible spectral range, for accurately estimation of the ozone amount, it is particularly important to understand the surface reflection spectrum. In this experiment, ground reflection spectra at different surface conditions such as rice paddy, forest, urban, farm areas and so on were measured at a low altitude of 2500ft (760m). It is necessary to consider the effect of scattering near the aircraft to estimate the surface reflected light. We estimated it with SCIATRAN (Rozanov et al., 2005). Results of these observations will be presented at this session.

Keywords: Remote Sensing, Lower tropospheric ozone

Japan Geoscience Union Meeting 2014
(28 April - 02 May 2014 at Pacifico YOKOHAMA, Kanagawa, Japan)

AAS22-P25 Room:Poster Time:May 1 18:15-19:30

The Relationship between CO Concentration and Biomass Burning over the North China Plain

KAYABA, Satoko[1*] ; HAYASHIDA, Sachiko[1] ; ONO, Akiko[1]

[1]Faculty of Science, Nara Women's University

Carbon monoxide (CO) controls the greenhouse gasses (e.g., CH4, O3) indirectly through a chemical reactions. Therefore, CO is regarded as an indirect-greenhouse gas and thus it is important to understand its spatiotemporal variation.

Wang et al.,[JGR, 2002] suggested that the open crop residue burning in June over the North China Plain affects on CO concentration, and it was confirmed by field campaign at Mt.Tai and investigated by model simulations [Kanaya et al.,2013 and reference therein]. Besides, the recent rapid industrialization in China brought significant increase in emission of CO [Ohara et al., ACP, 2007].

In this study, we analyzed the relationship between fire outbreak and CO concentration over the North China Plain by using satellite data. The CO data are taken from Measurement Of Pollution In The Troposphere (MOPITT). We used the Version 5 product. The fires detected by satellite observations are expressed as the hotspot numbers that are derived from the MODIS thermal anomaly product [Takeuchi and Yasuoka, 2006], using the algorithm by [Giglio et al.RSE,2003]. Here we used the hotspot numbers as proxy of the fire detection index.

CO concentration in June increases accompanied by a large number of the hotspot counts, which is consistent as previous studies. On the other hand, CO concentration gradually increases in fall and winter with only few hotspot numbers. It implies that CO emissions are possibly from industrial activity, automobiles and coal burning for heating rather than biomass burning in fall and winter. In addition, the year-to-year variability of CO concentration in June and in fall and winter was different.

This study was supported by a Grant-in-Aid from the Green Network of Excellence, Environmental Information (GRENE-ei) program.

Japan Geoscience Union Meeting 2014
(28 April - 02 May 2014 at Pacifico YOKOHAMA, Kanagawa, Japan)

AAS22-P26 Room:Poster Time:May 1 18:15-19:30

Development of Atmospheric Environmental Risk Management System in Chile and Argentina

MIZUNO, Akira[1*] ; SUGIMOTO, Nobuo[2] ; NAGAHAMA, Tomoo[1] ; OHYAMA, Hirofumi[1] ; NAKAJIMA, Tac[1] ; SUGITA, Takafumi[2] ; AKIYOSHI, Hideharu[2] ; NAKANE, Hideaki[3] ; YAMAGISHI, Hisao[4] ; OGAWA, Hideo[5]

[1]Solar-Terrestrial Environment Laboratory, Nagoya University, [2]National Institute for Environmental Studies, [3]Kochi University of Technology, [4]National Institute of Polar Research, [5]Osaka Prefecture University

We started an international collaboration project on research of ozone/UV and aerosol in South America since 2013. This project is supported by Japan Science and Technology Agency (JST) and Japan International Cooperation Agency (JICA) under SATREPS program. The counterpart institutions are CEILAP (Laser Application Research Center) in Argentina and Magellan University in Chile. The major aims of this project are (1) to construct new aerosol lidar network in Chile and Argentina, (2) to consolidate the ozone monitoring capability at the South Patagonian Atmospheric Observatory (OAPA , 52S, 69W) in Rio Gallegos at the southern end of the South American continent. The new aerosol lidar network consists of 9 lidars. Six of them are Raman lidars and the other 3 are high-resolution lidars with an iodine filter. Eight lidars are distributed over Argentine territory to observe volcanic ashes from volcanos in Andes, Patagonian dust, and black carbon from Bolivia and Brazil. From the observatory in Rio Gallegos, we will make comprehensive observations of ozone by using a DIfferential Absorption Lidar (DIAL), millimeter-wave spectral radiometer, brewer spectrometer, and so on. In addition to the consolidation of observing network, we will develop data analysis and data distribution system to deliver the data to the relevant organizations in the both countries.

In the presentation, we will introduce the overview of this project and present a progress report after the first year.

Keywords: Aerosol, Ozonehole, Lidar, Millimeter-wave spectroscopy, International cooperation, Contribution to society

Japan Geoscience Union Meeting 2014
(28 April - 02 May 2014 at Pacifico YOKOHAMA, Kanagawa, Japan)

AAS22-P27 Room:Poster Time:May 1 18:15-19:30

Observations of horizontal distributions of air pollutants by MAX-DOAS

NI, Wentao[1*] ; IRIE, Hitoshi[1] ; CHEN, Cheng[1] ; TAKAMURA, Tamio[1] ; KHATRI, Pradeep[1]

[1]Chiba University

In June 2012 we set up a MAX-DOAS device in Chiba University and continuous observations have been conducted since then. The MAX-DOAS method measures the spectra of scattered sunlight in ultraviolet and visible regions at various elevation angles. By analyzing the measured spectra with a radiative transfer model and an inversion method, vertical distributions of aerosol and gas and their column amounts can be retrieved (Irie et al., 2008,2009, Vlemmix, 2010). In this study, firstly, we compared the aerosol optical depth measured by the MAX-DOAS to that measured by the sky radiometer. We found the consistency of differences between MAX-DOAS and sky radiometer AOD values are within 30%.Secondly, we set up two MAX-DOAS devices (machine No.1 and No.2) for simultaneous observations at the same place. For both devices, the wavelength regions of 460-490nm and338-370nm were analyzed with the DOAS method to derive the differential slant column densities (DSCDs) of O4.In order to quantify the effect of the systematic offset of the elevation angle in O4 DSCDs, we have biased the offset of elevation angles by +-0.5,+-1.0 degrees. Comparisons such as correlation analysis etc. show that the effect is insignificant as there is only 20% differences found in the O4 DSCD comparisons between two devices. Based on such a detailed error evaluation, since December 2013, we have directed the machine No.1 to north and No.2 to west to perform quantitative observations of horizontal-distribution of aerosols. Results will be discussed in this work.

Keywords: MAX-DOAS, Elevation angle offset, vertical profile, tropospheric column amount, differential slant column density

Japan Geoscience Union Meeting 2014
(28 April - 02 May 2014 at Pacifico YOKOHAMA, Kanagawa, Japan)

AAS22-P28 Room:Poster Time:May 1 18:15-19:30

Validation of GOSAT SWIR xCH4 using TCCON and Airborne Measurements

IWASAKI, Chisa[1*] ; HAYASHIDA, Sachiko[1] ; ONO, Akiko[1] ; MACHIDA, Toshinobu[2]

[1]Faculty of Science, Nara Women's University, [2]NIES

As methane (CH_4) is one of the most important Short-Lived Climate Pollutants (SLCPs), global monitoring of atmospheric CH_4 with enough accuracy is expected to estimate its sources and sinks. For measurements of global distribution of CO_2 and CH_4 concentration from space, the Greenhouse gases Observing SATellite (GOSAT) was launched in 2009, and has continued measurements up to the present. However, cloud interferes satellite observation. To understand CH_4 emission from a cloudy region, the selection of an adequate criterion of cloud screening, and validation of data quality are necessary.

In this study, we validate the GOSAT CH_4 products of the column-averaged dry-air mole fractions (xCH_4) derived from Short-Wavelength InfraRed (SWIR) radiation by comparing them with data of Total Carbon Column Observing Network (TCCON). Yoshida et al. (AMT, 2013) had already carried out the validation for the NIES product, but we extended the period and involved more TCCON sites; Yoshida et al. (2013) used data observed at the 13 TCCON sites from June, 2009 to December, 2012 and we used data at the 17 TCCON sites from June, 2009 to August, 2013. We found that the average difference between TCCON and GOSAT for the whole period is -6.0 $\pm$ 16.1 ppbv.

We also examined the appropriate cloud screening for xCH_4 product from RemoTeC-MACC. The product was obtained by using the "proxy method" by which we can obtain more data under cloudy conditions. In this study, we also tried to compare GOSAT data with aircraft measurements over Siberia and other areas.

Acknowledgements

This research was supported by the Environment Research and Technology Development Fund of the Ministry of the Environment, Japan (A1202). The RemoTeC-MACC product was provided by Dr. Andre Butz (IMK-ASF, Karlsruhe Institute of Technology; KIT).

Keywords: GOSAT, validation, methane, cloud screening, aircraft

Japan Geoscience Union Meeting 2014
(28 April - 02 May 2014 at Pacifico YOKOHAMA, Kanagawa, Japan)

AAS22-P29 Room:Poster Time:May 1 18:15-19:30

Variations of tropospheric methane over Japan during 1988-2010

UMEZAWA, Taku[1*] ; GOTO, Daisuke[1] ; AOKI, Shuji[1] ; ISHIJIMA, Kentaro[2] ; PATRA, Prabir[2] ; SUGAWARA, Satoshi[3] ; MORIMOTO, Shinji[1] ; NAKAZAWA, Takakiyo[1]

[1]Center for Atmospheric and Oceanic Studies, Graduate School of Science, Tohoku University, [2]Research Institute for Global Change, JAMSTEC, Yokohama, Japan, [3]Miyaigi University of Education, Sendai, Japan

Mixing ratios of greenhouse gases and related trace gases have been measured using chartered and commercial aircraft in the lower to upper troposphere (LT and UT) over Japan by Tohoku University. We present variations of CH_4 during 1988-2010. The analysis is aided by simulation results using an atmospheric chemistry transport model (i.e. ACTM). Tropospheric CH_4 over Japan shows altitude-dependent interannual and seasonal variations, reflecting differences in air mass origins at different altitudes. The long-term trend and interannual variation of CH_4 in the LT are consistent with previous reports of measurements at surface baseline stations in the northern hemisphere. However, those in the UT show excursions from those in the LT. In the UT, CH_4 mixing ratios show seasonal maximum in August due to efficient transport of air masses influenced by continental CH_4 sources, while LT CH_4 reaches its seasonal minimum during summer due to seasonally maximum chemical loss. Vertical profiles of the CH_4 mixing ratios also vary with season, reflecting the altitude-dependent seasonal cycles. In summer, transport of CH_4-rich air from Asian regions elevates UT CH_4 levels, forming the uniform vertical profile above the mid troposphere. On the other hand, CH_4 decreases nearly monotonically with altitude in winter-spring. The ACTM simulations with different emission scenarios reproduce general features of the tropospheric CH_4 variations over Japan. Tagged tracer simulations using the ACTM indicate substantial contributions of CH_4 sources in South Asia and East Asia to the summertime high CH_4 values observed in the UT. This suggests that our observation data over Japan are highly valuable for capturing CH_4 emission signals, particularly from the Asian continent.

Keywords: aircraft observation, methane, troposphere, over Japan

Japan Geoscience Union Meeting 2014
(28 April - 02 May 2014 at Pacifico YOKOHAMA, Kanagawa, Japan)

AAS22-P30 Room:Poster Time:May 1 18:15-19:30

Measurement of CO2 stable isotope ratio by mid-inferred laser absorption spectrometry; analysis of CO2 cycle in urban

YUBA, Akie[1*] ; TAKAHASHI, Kenshi[2] ; NAKAYAMA, Tomoki[1] ; MATSUMI, Yutaka[1]

[1]Solar-terrestrial environment laboratory, Nagoya university, [2]Research Institute for Sustainable Humanosphere, Kyoto University

CO_2 concentration has been increasing from the range of 275 ppmv (parts per million by volume) to 285 ppmv in the previous industrial period to about 400 ppmv in 2013. IPCC reported that CO_2 has the most effective on the positive radiative force. The insight of CO_2 emission and absorption flux helps us to estimate the variation of radiative forcing and atmospheric environment. CO_2 concentration changed with the anthropogenic and biogenic emission and absorption. The stable isotope ratio of CO_2 (δ^{13}C and δ^{18}O) is associated with the CO_2 source such as combustion and biogenic respiration. The contribution of each CO_2 source in the urban area was estimated by using the stable isotope ratio of CO_2.

We conducted the continuous measurement for CO_2 concentration and stable isotope ratio of CO_2 using the mid-inferred absorption spectrometry which can obtain CO_2 concentration and its isotope ratio with high time resolution. The water vapor and stable isotope ratios of water vapor (δD and δ^{18}O-H_2O) were measured to show the relationship between H_2O and CO_2 due to the isotopic exchange reaction. CO and NO_x concentrations were obtained as a tracer of anthropogenic emission. The measurement was conducted for two weeks in summer and winter. The seasonal variation of CO_2 source was shown according to the comparison of CO_2 concentration and stable isotope ratio. Especially, we focused on the contribution of biogenic process to CO_2 concentration variation in the urban area.

CO_2 concentration and stable isotope ratio of CO_2 in the summer showed the diurnal variation. On the other hand, those in the winter had no diurnal variation. CO_2 concentration variation in the winter was correlated with CO concentration variation. These results suppose that CO_2 concentration variation in the winter was mainly dominated by the anthropogenic emission and that in the summer was related with biogenic process as well as anthropogenic emission. We will discuss the relationship between stable isotope ratio and meteorological condition or water vapor isotope ratio to identify the detail of CO_2 source.

Keywords: CO2 stable isotope ratio, Urban area, CO2 cycle, mid-interred laser absorption spectrometory

Japan Geoscience Union Meeting 2014
(28 April - 02 May 2014 at Pacifico YOKOHAMA, Kanagawa, Japan)

AAS22-P31 Room:Poster Time:May 1 18:15-19:30

Temporal and spatial variations of Radon-222 in the western North Pacific

TSUBOI, Kazuhiro[1*] ; MATSUEDA, Hidekazu[1] ; SAWA, Yousuke[1] ; NIWA, Yosuke[1] ; MURAYAMA, Shohei[2]

[1]Meteorological Research Institute, [2]National Institute of Advanced Industrial Science and Technology

A new compact radon measuring system has been developed for high-resolution observation of low-level radon-222 (Rn) for the remote sites, in collaboration with the MRI and AIST. The Rn measuring system was installed at 4 stations of Minamitorishima (MNM), Yonagunijima (YON), Chichijima (CCJ) and Ryori (RYO) operated by Japan Meteorological Agency (JMA) since 2007 . The Rn measurements clearly show that distinct seasonal variations as well as frequent episodic events with Rn enhancement peaks on a synoptic scale are successfully captured at all 4 stations. Although the seasonal cycles depended on the stations, significant correlations between the Rn and other trace gases were found for the most of the synoptic-scale events, indicating a large impact of widespread pollutions from the East-Asian countries on the regional air quality over the western North Pacific.

Keywords: Radon

Japan Geoscience Union Meeting 2014
(28 April - 02 May 2014 at Pacifico YOKOHAMA, Kanagawa, Japan)

AAS23-01 Room:424 Time:April 28 10:00-10:15

Estimation of Several Kilometer Scale PWV Distribution using GNSS Slant Path Delay for Monitoring of Cumulus Convection

SHOJI, Yoshinori[1*]

[1]Meteorological Research Institute

A procedure for estimating precipitable water vapor (PWV) distribution around each ground-based station of the global navigation satellite system (GNSS) on a scale of several kilometers is presented. This procedure utilizes the difference between zenith total delay above a GNSS station and zenith mapped slant path delay (SPD). By assuming an exponential distribution for the horizontal water vapor gradient, this difference can be used to estimate the PWV gradient in each SPD direction. Shoji (2013) proposed the WVI index, which is defined as the standard deviation of the PWV_{SPD}. The retrieved PWV gradient in this study can be regarded as another utilization of PWV_{SPD}. In the WVI index, ray path direction data is not utilized. The PWV gradient proposed in this paper utilizes both the deviation of PWVSPD and information on its direction.

The procedure was tested for an estimation of the PWV variation associated with the parent storm of an F3 Fujita scale tornado that occurred in Ibaraki prefecture on May 6, 2012. Differential reflectivity observed by a dual-polarimetric radar showed the existence of a developed parent cloud approximately 1 h before the tornado occurred. A high-resolution numerical weather model simulation showed the existence of a strong PWV gradient around the parent cloud, made evident by the co-existence of a strong updraft and downdraft within an approximately 5-km radius. The PWV gradient calculated using the GNSS observation network with an average spacing of approximately 17 km could not detect such a small-scale, strong PWV gradient. The PWV gradient estimated using the proposed procedure revealed a strong PWV gradient and its enhancement. In this case, higher order inhomogeneity component of each SPD played a critical role.

However, the gradient was weaker than the NWP simulation. This might be partly because of the insufficient observation density. Horizontal scale of the higher order inhomogeneity component of each SPD is about several kilometers and we adopt distance cutoff of 5 km. In order to analyze several kilometer scale PWV distribution, we need denser GNSS network with at least 10 km horizontal spacing. Another possible reason for the weaker gradient may be insufficient and inhomogeneous coverage of GPS satellites. As of 2012, carrier waves transmitted from six to twelve GPS satellites could be observed simultaneously at each GNSS site in Japan. This might be insufficient for estimating the water vapor gradient in all directions. Also, we need to carefully check the quality of each SPD. In this study, following Shoji (2013), the effects of the satellite clock error and multipath (reflected wave) are tried to eliminate. However it is difficult to distinguish atmospheric signal with those noises, especially under local severe weather.

The number of GNSSs has been increasing. As of December 2013, 24 satellites of the Russian GLONASS are in operation. The European Union's GNSS (Galileo) is in the experimental phase and China is also developing an independent GNSS system named COMPASS. Furthermore, a number of space-based augmentation systems (e.g., Japan's QZSS) and regional navigation satellite systems (e.g. the Indian Regional Navigation Satellite System, or IRNSS) will contribute further satellites and signals to the multi-constellation GNSS. In the next step of this study, we will assess the impact of the increased number of SPDs on multi-GNSS.

Keywords: Mesoscale meteorology, Watervapor, Global Navigation Satellite System

Japan Geoscience Union Meeting 2014
(28 April - 02 May 2014 at Pacifico YOKOHAMA, Kanagawa, Japan)

AAS23-02 Room:424 Time:April 28 10:15-10:30

Numerical Simulation on Retrieval of Meso-gamma Scale PWV Distribution with the Quasi-Zenith Satellite System (QZSS)

OIGAWA, Masanori[1*] ; REALINI, Eugenio[1] ; SEKO, Hiromu[2] ; TSUDA, Toshitaka[1]

[1]Research Institute for Sustainable Humanosphere (RISH), Kyoto University, [2]Meteorological Research Institute (MRI), Japan Meteorological Agency (JMA)

A simulation study was conducted to investigate the retrieval of meso-gamma scale Precipitable Water Vapor (PWV) distribution with QZSS, using the output of a non-hydrostatic numerical weather prediction model. The evaluation was performed on PWV values obtained by simulating three different methods: using all GPS satellites above an elevation angle higher than 10 degree (PWVG) (conventional GPS meteorology method), using only the QZSS satellite at highest elevation (PWVQ) and using only the GPS satellite at highest elevation (PWVHG).

The RMSEs of PWVG, PWVQ and PWVHG were compared, assuming the vertically integrated water vapor amount of the model as true PWV. As a result, the RMSEs of PWVG, PWVQ and PWVHG were 2.78, 0.13 and 0.59 mm, respectively, 5 minutes before the rainfall. The PWVHG time series had a large discontinuity (~2 mm) when the GPS satellite at the highest elevation changed, whereas that of the PWVQ time series was small, because the elevation angle at which the replacement of the highest elevation QZSS satellite occurs is much higher. The standard deviation of PWVQ was smaller than those of PWVG and PWVHG, which vary largely depending on the GPS satellites geometry.

When the spatial distributions of PWVG and PWVQ were compared to the meso-gamma scale distribution of the reference PWV, PWVG smoothed out the PWV fluctuations whereas PWVQ captured them well, due to the higher spatial resolution achievable by using only high-elevation slant paths. These results suggest that meso-gamma scale water vapor fluctuations associated with a thunderstorm can be retrieved by using a dense GNSS receiver network and analyzing PWV derived from a single high elevation GNSS satellite. In this paper we focus on QZSS, as this constellation is especially promising in this context since it is going to provide nearly continuous PWV observations also as its highest satellite changes, contrary to using highest satellites from multiple GNSS constellations.

Keywords: precipitable water vapor, Quasi-Zenith Satellite System, thunderstorm, non-hydrostatic model

Japan Geoscience Union Meeting 2014
(28 April - 02 May 2014 at Pacifico YOKOHAMA, Kanagawa, Japan)

AAS23-03 Room:424 Time:April 28 10:30-10:45

Data assimilation experiments of refractivity distribution observed by an operational Doppler Radar of JMA

SEKO, Hiromu[1*] ; SATO, Eiichi[2] ; SAKANASHI, Takanori[3]

[1]Meteorological Research Institute, JAMSTEC, [2]Meteorological Research Institute, [3]Japan Meteorological Agency

Because low-level convergence of water vapor generates the convections, accuracy of local heavy rainfall forecasts is expected to be improved when horizontal distribution of low-level water vapor is observed. We focused on radio waves of Doppler Radars that are returned from fixed structures. Because the radio waves are delayed by water vapor while passing atmosphere, we can estimate refractivity, which is a function of temperature and water vapor, from the delay of radio waves. If radio waves of many Doppler Radars that have been deployed in Japan are used in producing initial conditions of numerical forecasts, the forecast accuracy of thunderstorms is expected to be improved through improvement of water vapor fields by using this technique.

In this presentation, temporal variations of refractivity observed by Tokyo Radar and the impacts of refractivity on the rainfall forecasts will be presented.

Acknowledgements:

This study was supported by ”Grants-in-Aid for Scientific Research: Establishment of estimation methods of water vapor from Radar phase data reflected from fixed structures” and ”Projection of Planet Earth Variations for Mitigating Natural Disasters (Field 3)” in ”Strategic Programs for Innovative Research (SPIRE)”.

Keywords: Doppler Radar, Refractivity, Water vapor, Data assimilation

Japan Geoscience Union Meeting 2014
(28 April - 02 May 2014 at Pacifico YOKOHAMA, Kanagawa, Japan)

AAS23-04 Room:424 Time:April 28 11:00-11:15

Overview and future strategy of docomo Environmental Sensor Network(ESN)

TSUBOYA, Hisakazu[1*] ; HIGASHI, Kuniaki[2] ; FURUMOTO, Jun-ichi[2]

[1]Division of life support business promossion,NTT DOCOMO Corporation, [2]Research Institute for Sustainable Humanosphere, Kyoto University

NTT docomo had launched a nation-wide and hyper-dense network for the measurement of both weather and environmental element since 2008 and provide them as new information contents to the markets. Its realtime data could be applied to various industrial issues, namely hazard prediction, agriculture, and medical&healthcare. docomo make the new network infrastructure more sophisticated and is planning to expand its sensor stations, which has been set only to its radio base stations up to now, to any customers who need to measure their own environment.

Japan Geoscience Union Meeting 2014
(28 April - 02 May 2014 at Pacifico YOKOHAMA, Kanagawa, Japan)

AAS23-05 Room:424 Time:April 28 11:15-11:30

High Dense Ground Observation Network ”POTEKA” in Gunma, Japan

MAEDA, Ryota[1*] ; YOSHIKURA, Tomomi[1] ; KURE, Hirotaka[1] ; YADA, Takuya[1] ; MORITA, Toshiaki[1] ; IWASAKI, Hiroyuki[2]

[1]Meisei Electric co., ltd., [2]Faculty of Education, Gunma University

Meisei developed compact weather sensor (POTEKA Sta.) and cloud data-transfer system (POTEKA Lab.) to achieve high dense observation network. ”POTEKA” stands for ”Point Tenki Kansoku”. POTEKA project has been demonstrated the validity for the use of disaster prevention, health and medical care, teaching material, agriculture and energy management, and comfortable living environment in cooperation with local companies and education board since August 2013.

POTEKA Sta. measures wide range of meteorological and environmental variables such as temperature, relative humidity, pressure, sunlight, and rain detection with a one minute resolution. This low-cost weather sensor enables us to achieve finer-meshed or higher density weather observation system economically. Finer-meshed and more extensive data collected are easily accessible through ordinal Web sites (PC, Tablets, etc.) without any special software.

Spatio-temporal high dense observation network (total 55 stations, 1.5˜4km-mesh) was installed in Isesaki city, Gunma, Japan. Observation with elementary/junior high school and convenience store (SAVE ON) are performed at 14 stations and 41 stations, respectively, which spatially captured local surface weather phenomenon (fig. 1).

This paper presents some examples including 1. local distribution of surface temperature around Isesaki, 2. preventing heat stroke at school, and 3. school education for class and research.

Acknowledgments: The authors would like to thank SANDEN Corporation, SAVE ON, and Board of Education of Isesaki city for support POTEKA project.

Keywords: dense, big data, instrument, network, observation

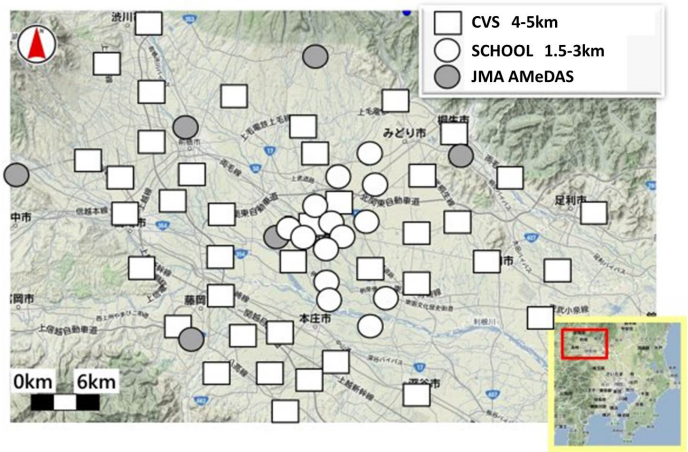

Japan Geoscience Union Meeting 2014
(28 April - 02 May 2014 at Pacifico YOKOHAMA, Kanagawa, Japan)

AAS23-06 Room:424 Time:April 28 11:30-11:45

Observation of downburst in Takasaki and Maebashi city, Gunma on 11 August 2013

NOROSE, Keiko[1*] ; KOBAYASHI, Fumiaki[1] ; KURE, Hirotaka[2] ; MORITA, Toshiaki[2]

[1]National Defense Academy, [2]Meisei Electric

On the evening of 11 August 2013, a severe thunderstorm passed over the Takasaki and Maebashi city, Gunma prefecture, and produced gusty wind damages. The change of surface weather elements was recorded by dense observation network POTEKA when gust occurred. In this study, we follow the development and propagation of gust-front and downburst through the analysis of features of the pressure field observed by POTEKA. The result of this analysis reveals that the reason of gust caused damages in Maebashi city is downburst.

Japan Geoscience Union Meeting 2014
(28 April - 02 May 2014 at Pacifico YOKOHAMA, Kanagawa, Japan)

AAS23-07 Room:424 Time:April 28 11:45-12:00

Helicopter-borne thermocamera measurements of surface temperatures in downtown Tokyo -Comparison of 2013 with 2007-

TSUNEMATSU, Nobumitsu[1*] ; YOKOYAMA, Hitoshi[1] ; HONJO, Tsuyoshi[3] ; ICHIHASHI, Arata[1] ; ANDO, Haruo[1] ; MATSUMOTO, Futoshi[1] ; SETO, Yoshihito[2]

[1]Tokyo Metropolitan Research Institute for Environmental Protection, [2]Chiba University, [3]Tokyo Metropolitan Research Institute for Environmental Protection/Tokyo Metropolitan University

Annual mean air temperatures in downtown Tokyo have increased about 3 degrees Celsius in the past 100 years due to global warming and urban heat island. The frequency of heat stroke outbreaks in Tokyo tends to increase in recent years. The Tokyo metropolitan research institute for Environmental Protection has therefore investigated the current situation of the temperature rises in Tokyo through the monitoring of urban heat island. This can contribute to verification of measure effects on urban heat island.

As part of the investigations, we performed helicopter-borne infrared thermocamera measurements of surface temperatures in downtown Tokyo (mainly an Otemachi-Marunouchi-Yurakucho area) on two different extremely hot days, Aug. 19, 2013 (hereafter, HTM13) and Aug. 7, 2007 (HTM07). The measurements were carried out in the daytime (12-13 local time) and the nighttime (20-22 local time), using a Robinson R22 helicopter with a longwave (8-14um) infrared thermocamera (TS7302) developed at NEC Avio Infrared Technologies Co., Ltd. An altitude of the helicopter flight was 610 m. The daytime air temperatures on those days reached 32-33 degrees Celsius although southerly sea breezes prevailed in the area. Compared with the HTM07 case, a higher air temperature condition was predominant prior to HTM13.

Results of analyses of data from the thermocamera-derived images (a 2 m ground resolution) show that surface temperatures obtained from HTM13 are relatively large in the greater part of the area, compared with HTM07 (refer to a figure shown below), whereas, smaller surface temperatures can be recognized in redevelopment areas where new buildings have been constructed after 2007. (Note that the emissivity of each surface material can influence it.) Also, the thermocamera-derived images projected on Google Earth show higher surface temperatures on intersections.

In addition, we would like to show geographical distributions of the observed surface temperatures in the nighttime, differences between the daytime and nighttime surface temperatures, and a relationship between surface temperatures and sky view factors.

Keywords: Helicopter-borne measurements, thermocamera, surface temperature, downtown Tokyo, verification of measure effects on urban heat island, extremely hot days

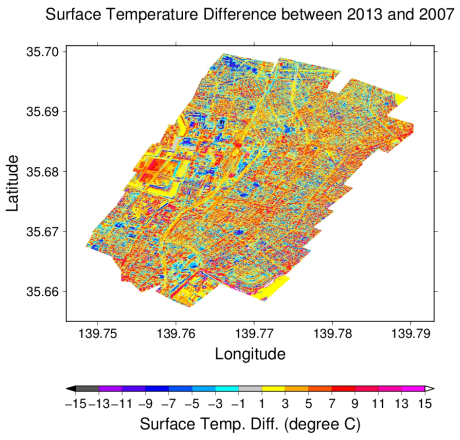

Japan Geoscience Union Meeting 2014
(28 April - 02 May 2014 at Pacifico YOKOHAMA, Kanagawa, Japan)

AAS23-08 Room:424 Time:April 28 12:00-12:15

How Does A Typhoon Affect The Local Downslope Wind Hirodo-Kaze In Japan?

FUDEYASU, Hironori[1*] ; KIYOHARA, Yasutomo[2] ; OHASHI, Yukitaka[3] ; KUWAGATA, Tsuneo[4] ; MORIYAMA, Fumiaki[1]

[1]Yokohama National University, [2]The Certified and Accredited Meteorologists of Japan, Japan, [3]Okayama University of Science, Japan, [4]National Institute for Agro-Environmental Sciences, Japan

The Hirodo-kaze is one of the well-known strong local winds in Japan. Hirodo-kaze occurs at the southern base of Mt. Nagi (1240 m) in the northeastern Okayama Prefecture, when the lower-troposphere synoptic wind is strong northerly in association with a typhoon. Previous studies have described the mechanisms that force downslope winds and large-amplitude mountain waves. However, descriptions of the effect of temporal changes in the large-scale environment on the severe downslope wind are not enough. The purpose of present study is to examine the forcing mechanisms during a Hirodo-kaze and the effects of typhoons on the occurrence of a Hirodo-kaze.

The Hirodo-kaze that occurred in association with Typhoon Pabuk was investigated as a case study. At 06 UTC on 21 August 2001, when Pabuk was located over the sea about 80 km southwest of the Kii peninsula, strong surface winds related to the cyclonic circulation of Pabuk were observed in Shikoku and Kinki districts. Relatively weak northerlies prevailed in Chugoku district far from Pabuk, but a strong northerly was observed at the station located in the lee of Mt. Nagi, about 5 km south of the crest of Mt. Nagi, namely Hirodo-kaze.

The mesoscale model, MM5, successfully reproduces the major features of the observed Hirodo-kaze and Typhoon Pabuk. During the Hirodo-kaze, the severe downslope winds in the transitional flow develop in the lower troposphere below the mean-state critical layer. The Hirodo-kaze is closely linked to the strong wind region accompanying the severe downslope winds. After the cessation of the Hirodo-kaze, distinct mountain waves dominate in the lower troposphere where the Scorer parameter decreases with height. The region of strong wind retreat windward as the Hirodo-kaze ceases. Temporal changes in the characteristics of mountain waves in the lee of Mt. Nagi are primarily attributed to the changes in the large-scale environmental winds due to the movement of Typhoon Pabuk.

The effects of intense typhoons on the occurrence of the Hirodo-kaze were also investigated statistically using data using European Center for Medium Range Weather Forecast 40?year re?analysis data (ERA-40). According to the several reports of Okayama meteorological station, twelve Hirodo-kaze events occurred between 1989 and 2001. During these events, strong lower-tropospheric northerlies were overlain by middle-tropospheric southerlies. These favorable conditions occur only as an intense typhoon moves over the sea southwest of Kii peninsula. Thus, the intense typhoon that moves over the sea southwest of the Kii peninsula creates favorable environmental conditions that support the occurrence of the Hirodo-kaze.

Keywords: typhoon, local downslope wind, MM5

Japan Geoscience Union Meeting 2014
(28 April - 02 May 2014 at Pacifico YOKOHAMA, Kanagawa, Japan)

AAS23-09 Room:424 Time:April 28 12:15-12:40

Observation and application of the Phased Array Radar

USHIO, Tomoo[1*] ; WU, Ting[1] ; KIKUCHI, Hiroshi[1] ; SHIMAMURA, Shigeharu[1] ; MEGA, Tomoaki[1] ; MIZUTANI, Fumihiko[2] ; WADA, Masakazu[2] ; IGUCHI, Toshio[3] ; SATOH, Shinsuke[3] ; TAKAHASHI, Nobuhiro[3]

[1]Osaka University, [2]Toshiba, [3]NICT

The phased array radar system which was installed in 2012 in Osaka University has the unique capability of scanning the whole sky with 100m and 10 to 30 second resolution up to 60 km. The system adopts the digital beam forming technique for elevation scanning and mechanically rotates the array antenna in azimuth direction within 10 to 30 seconds. The radar transmits a broad beam of several degrees with 24 antenna elements and receives the back scattered signal with 128 elements digitizing at each elements. Then by digitally forming the beam in the signal processor, the fast scanning is realized. After the installation of the PAR system in Osaka University, the continuous operation has been done and succeeded in getting several hazardous rain fall events with lightning locations. The data for these events captured by the Phased Array Radar shows the unique capability of the high resolution weather radar. In this presentation, over view of the Phased Array Radar is firstly given, and after that observation results and future direction of the Phased Array Radar Network with polarimetric capability is shown.

Keywords: Radar, Phased Array, Precipitation

Japan Geoscience Union Meeting 2014
(28 April - 02 May 2014 at Pacifico YOKOHAMA, Kanagawa, Japan)

AAS23-10 Room:424 Time:April 28 14:15-14:30

Statistical analyses on the characteristics of heavy rainfall events

TSUGUTI, Hiroshige[1*] ; KATO, Teruyuki[1]

[1]Meteorological Research Institute

In this study, to clarify general characteristics of heavy rainfall events in Japan, we have conducted various statistical analyses on them.

For the warm seasons (April - November) from 1995 to 2009, we objectively extracted heavy rainfall events occurring in Japan by using Radar-Raingauge analyzed rainfall dataset produced by the Japan Meteorological Agency. As a result, 386 events were extracted. Over 75 % of all events occurred during three months of July, August, and September, and many events were distributed around the coastal areas of the Pacific Ocean in Kyushu, Shikoku, Kinki, and Tokai regions. Synoptic weather conditions causing the heavy rainfall events were clarified, and consequently the pattern associated with typhoons or tropical cyclones was the most predominant, which accounted for 32.4 % of all events. Then, stationary fronts, remote precipitation of typhoons or tropical cyclones, and low depressions accounted for 21.2 %, 17.9 %, and 14.2 %, respectively. The classification for the shape of the precipitation systems causing the heavy rainfall events showed that the most predominant system was ”band-shaped”, which accounted for 43.5 % of all events.

The environmental fields of heavy rainfall events ($>$130 mm/3hr) were statistically analyzed using the Japanese 55-year reanalysis data (JRA-55). Characteristics of them were elucidated by comparing the environmental fields of moderate rainfall events (10-30 mm/3hr). In July (the late Baiu season) in Kyushu region, the low-level equivalent potential temperature and water vapor flux in the vicinity of Kyushu Island were significantly larger in heavy rainfall events than in moderate ones, and the atmospheric stability became more unstable in heavy rainfall events. Furthermore, to distinguish heavy rainfall events from moderate ones, the combination of two elements of low-level water vapor flux and atmospheric stability was more effective than the unique usage of each element.

Keywords: heavy rainfall, statistical analysis

Japan Geoscience Union Meeting 2014
(28 April - 02 May 2014 at Pacifico YOKOHAMA, Kanagawa, Japan)

AAS23-11 Room:424 Time:April 28 14:30-14:55

MRI Rapid-Scan and Super-Resolution Observations in severe storms: Recent Progress and Future Plans

KENICHI, Kusunoki[1*] ; INOUE, Hanako[1] ; YOSHIDA, Satoru[1] ; KATO, Rhohei[2] ; FUJIWARA, Chusei[3]

[1]Meteorological Research Institute, [2]Alpha-denshi Co., Ltd., [3]East Japan Railway Company

In this presentation, we will introduce the recent progress, present examples, and future plans of rapid-scan and super-resolution observations in severe storms of the Meteorological Research Institute (MRI).

1. A linear array of pressure and wind sensors for high resolution in situ measurements in winter tornadoes

In order to improve our understanding of near-surface tornadic features, we developed a linear array of wind and pressure sensors (LAWPS) for high resolution in situ measurements in winter tornado cores. The pressure and wind sensors were deployed along a 1.2km-long linear array that is located parallel to and about 100m from the shoreline. Wind data are obtained using 12 two- dimensional fast-response ultrasonic anemometers placed at a height of 5 m at intervals of 100 m. Pressure data are obtained using 25 barometers placed at a height of 50cm at intervals of 50m. The pressure ports are designed and loaded to the barometers to reduce the dynamic pressure associated with wind and turbulence. In this presentation, the system overview and the measurement technique will be described, as well as some examples of actual winter tornado observations of the system and X-band Doppler radar simultaneously.

2. An X-band phased array Doppler radar for the research of severe storms

Many severe storms evolve on time scales shorter than that resolved by conventional mechanically scanning radar systems. MRI has a new project of development of severe storm observations and detections from a phased array radar. The azimuth scan is similar to the conventional scan with a mechanically rotating antenna and at a variable rate between 1- 6 rpm. 128 slotted waveguide array elements fixed above the antenna panel produce transmit beam and an electronic elevation scanning will be performed. With the electronic elevation and mechanical azimuth scanning, the radar can observe the entire sky in less than a minute. Such high temporal resolution sampling will be expected to provide a realistic structure of rapidly evolving storm. In this presentation, some basic characteristics of the radar and a brief description of future tasks for detection and prediction of severe storms will be presented.

Keywords: tornado, rapid-scan and super-resolution observations, phased array radar

Japan Geoscience Union Meeting 2014
(28 April - 02 May 2014 at Pacifico YOKOHAMA, Kanagawa, Japan)

AAS23-12 Room:424 Time:April 28 14:55-15:20

Fine radar echo structure revealed by a high scanning and high-range-resolution X-band marine radar

FUJIYOSHI, Yasushi[1*]

[1]Inst. Low Temp. Sci., Hokkaido Univ.

We used an X-band (9410 MHz) marine radar (KODEN Co., Ltd.), which is not powerful and not very sensitive (its peak transmitted power is 25 kW and minimum detection power is -90 dbm); however, the radar has a high range resolution (15 m). Although its antenna usually rotates horizontally to detect ships, we changed the rotation direction of the slot antenna (2 m in length) from horizontal to vertical (Range Elevation Indicator-scan), and recorded every 2 s. We deployed this radar at various places. We will report very interesting phenomena that are firstly detected by this high-scanning and high-resolution radar.

Keywords: marine radar, fine structure of radar echo, precipitating cloud, angel echo, gravity current head

Japan Geoscience Union Meeting 2014
(28 April - 02 May 2014 at Pacifico YOKOHAMA, Kanagawa, Japan)

AAS23-13 Room:424 Time:April 28 15:20-15:35

Applications of weather radar network in private companies

TESHIBA, Michihiro[1*]

[1]Weathernews Inc.

Recently, various weather radars have been developed not only with novel functions of observation, but with low cost. As a result, each private companies can deploy their own weather radars and make a radar network. In the US, for example, local TV stations have their weather radars and the current situation is analyzed through their radars' data. However, in Japan weather radars have not been deployed yet. In this paper I would like to introduce the Weathernews (WNI)'s weather radar network in Japan and we would discuss future work in order to expand this type of network in Japan.

Keywords: weather radar, radar network, private company

Japan Geoscience Union Meeting 2014
(28 April - 02 May 2014 at Pacifico YOKOHAMA, Kanagawa, Japan)

AAS23-14 Room:424 Time:April 28 15:35-15:50

Temporal Variation of Close-Proximity Soundings within a Significant Tornadic Supercell Environment

ARAKI, Kentaro[1*] ; ISHIMOTO, Hiroshi[1] ; MURAKAMI, Masataka[1] ; TAJIRI, Takuya[1]

[1]Meteorological Research Institute

We examined proximity soundings at intervals of a few minutes and at distances of less than 20 km from a significant tornadic (SIGTOR) supercell that occurred on 6 May 2012 in Japan. We used a 1-dimensional variational (1DVAR) technique that combined the observations of a ground-based microwave radiometer with outputs from a numerical model. Based on the results of the 1DVAR, several supercell and tornado forecast parameters were calculated and compared with values typical of SIGTOR supercell environments in the United States. One and a half hours before the occurrence of the tornado, the value of convective available potential energy increased significantly to about 1000 J kg^{-1}, a value that is smaller than the typical value in the United States. Low-level vertical wind shear and some composite parameters attained maximum values at the time when the distance to the supercell was the smallest. The vertical wind shear parameters and some composite parameters indicated that the environment fell into the SIGTOR supercell category. This result shows that the thermodynamic environments became unstable before the approach of the supercell, and the low-level vertical wind shear changed locally near the supercell.

Keywords: tornado, supercell, microwave radiometer, 1DVAR

Japan Geoscience Union Meeting 2014
(28 April - 02 May 2014 at Pacifico YOKOHAMA, Kanagawa, Japan)

AAS23-15 Room:424 Time:April 28 15:50-16:05

Data Assimilation experiment of Tsukuba tornado on May 6, 2012 using MRI Doppler Radar data

YOKOTA, Sho[1*] ; KUNII, Masaru[1] ; SEKO, Hiromu[2]

[1]Meteorological Research Institute, [2]Meteorological Research Institute/JAMSTEC

A strong tornado with F3 scale caused serious damage in Tsukuba city on May 6, 2012. This tornado was generated at the southern tip of a precipitation area, which was moving northeastward over the Kanto Plain. Besides the Tsukuba tornado, two tornadoes were observed a few ten kilometers north of the Tsukuba tornado. The lower vortex associated with the Tsukuba tornado, as well as its precipitation area, was well captured by the Doppler Radar of the Meteorological Research Institute (MRI), because the Tsukuba tornado passed 15 km north of the MRI. However, data assimilation experiments using the high-resolution data, such as Radar data, have not been performed yet. In this study, Doppler wind data observed by the MRI-Radar were assimilated with an ensemble Kalman filter so as to evaluate the impact of the assimilation of Doppler wind.

In this experiment, a Nested Local Ensemble Transform Kalman Filter (Nested- LETKF) system, with 12 ensemble members, was used. In Outer-LETKF (horizontal grid interval: 15 km), hourly operational observation data used in the Japan Meteorological Agency (JMA) operational model were assimilated with 6 hour intervals. In Inner-LETKF (horizontal grid interval: 1.875 km), data obtained every 10 minutes was assimilated with 1 hour intervals. To assess the impact of the Doppler wind observations, we basically performed two experiments. The ”CTL” experiment used conventional observations, that is, the original settings of the Nested-LETKF. The other ”VR” experiment assimilated the Doppler wind data observed by MRI-Radar additionally in Inner-LETKF, while all other settings were the same as CTL. After the data assimilation experiments, downscaling ensemble experiments (horizontal grid interval: 350m) were carried out by using the analyses and 12 perturbations of each CTL and VR at 10:00 JST on May 6, 2012 as initial conditions.

In the downscaling ensemble experiments, two vortices were formed although three vortices were actually observed. The southern vortex in VR was stronger and passed about 2 km closer to the observed tornado than that in CTL. To clarify those differences, we focused on Storm Relative Helicity (SReH) and low level humidity (Low-Qv) at 10:00 JST. The SReH and Low-Qv were compared to the maximum velocity of the Tsukuba tornado vortex (Vmax) and to the latitude where the vortex existed when it passed 140E (L140), using the analyses and 12 perturbations of VR. As a result, Vmax had a positive correlation to SReH in and south of the precipitation area. It also had a positive correlation to the Low-Qv in the south of the precipitation area, and in the south of the genesis point of the vortices. In fact, Low-Qv in the south of the genesis point of vortices in VR was increased by the assimilation of Doppler wind. On the other hand, L140 had a negative correlation with Low-Qv in the south of the precipitation area. It shows that the precipitation area was elongated in the meridian directions and that the vortex was generated further to the south if humidity was higher in the south of the precipitation area.

The wind speed and location of the vortex had correlations with SReH in and south of the precipitation area. They also had correlations with Low-Qv in the south of the precipitation area and in the south of the genesis point of vortices. Therefore, proper correction of these values by data assimilation is important to better reproduce the vortex.

Acknowledgements:

The authors thank the members of the second Laboratory, Meteorological Satellite and Observation System Research Department, MRI for providing the Doppler radar data. This study was supported by ”Projection of Planet Earth Variations for Mitigating Natural Disasters (Field 3)” in ”Strategic Programs for Innovative Research (SPIRE)” and ”Tokyo Metropolitan Area Convection Study for Extreme Weather Resilient Cities (TOMACS)”.

Keywords: data assimilation, tornado, Doppler Radar

Japan Geoscience Union Meeting 2014
(28 April - 02 May 2014 at Pacifico YOKOHAMA, Kanagawa, Japan)

AAS23-16 Room:424 Time:April 28 16:15-16:40

Development of Phased Array Weather Radar and Doppler Lidar Network Fusion Data System

SATOH, Shinsuke[1*] ; YASUI, Motoaki[1] ; MAENO, Hideo[1] ; HANADO, Hiroshi[1] ; TAKAHASHI, Nobuhiro[1] ; IWAI, Hironori[1] ; KAWAMURA, Seiji[1] ; KOJIMA, Shoichiro[1] ; AMAGAI, Jun[1] ; TANAKA, Kenji[1] ; OCHIAI, Satoshi[1] ; KUBOTA, Minoru[1] ; IGUCHI, Toshio[1]

[1]National Institute of Information and Communications Technology

At National Institute of Information and Communications Technology (NICT), we promote advanced research and development of remote sensing technology, to reduce the damage of severe weather disasters caused by localized heavy rainfalls or tornadoes. An industry-academia-government team consisting of Toshiba, Osaka University, and NICT developed one-dimensional phased array weather radar (PAWR) that it is possible to seamless 3D observation in 10 ? 30 seconds. In May 2012, we installed PAWR at Osaka University Suita Campus, and started test observation. From the observation, a first echo appeared in an isolated cumulonimbus cloud was falling to the ground for about 10 minutes. In order to predict the generation point of the cumulonimbus cloud, we need other data which includes wind fields before cloud generation, distributions of water vapor and aerosol, and so on. For that reason, we develop a sensor fusion system with PAWR, Doppler lidar, and others. We install the systems to both NICT Advanced ICT Research Institute (Iwaoka, Nishi-ku, Kobe, Hyogo) and NICT Okinawa Electromagnetic Technology Center (Onna, Kunigami, Okinawa), and install the network data system to NICT headquarters (Koganei, Tokyo).

The sensor fusion system consists of the PAWR antenna in a radome installed on the roof of a 20 m tower, Doppler lidar (Leosphere 400s) on the deck at the height of 15 m of the tower, microwave radiometer to measure water vapor, and sky-radiometer to measure aerosol. Also, temperature, humidity, wind speed components (u, v, w), pressure, rainfall amount, radiation budget, and cloud images (4 directions and whole sky) are measured. All sensors are connected by network for remote operation and automatic data acquisition. The observation data are transferred in real-time through the fast network lines (JGN-X) from Kobe and Okinawa to Koganei for data processing to make a composite map, and so on. The processing data are displayed on a big 4K display TV, and are published using a web server.

We will start test observation after the system completion in March, 2014. At NICT, we also promote research and development of network data system using advanced ICT for big-data processing, transfer, visualization. We give this system a nickname of PANDA: **P**hased **A**rray weather radar and Doppler lidar **N**etwork fusion **DA**ta system, and will publish the data from http://panda.nict.go.jp/.

Keywords: phased array weather radar, Doppler lidar, network data system, remote sensing, localized heavy rainfall

Japan Geoscience Union Meeting 2014
(28 April - 02 May 2014 at Pacifico YOKOHAMA, Kanagawa, Japan)

AAS23-17 Room:424 Time:April 28 16:40-16:55

Campaign Observation at Keihanshin Area for Detecting Convection Genesis

YAMAGUCHI, Kosei[1*] ; NAKAKITA, Eiichi[1]

[1]Disaster Prevention Research Institute

In 2008, around 50 people who enjoyed sunny days along the riverside were flushed away by a sudden flash flood in a small river channel (Toga River) in Kobe urban area of Japan. This extreme event was a combinational result of steep basin slope, paved urban area, and severely localized heavy rainfall, which is more frequent happening in the recent summer of Japan. There are many short and steep rivers passing through urban areas in Japan, and the most of riverside along these rivers are used as a public open place. Because of the steep basin slope and the paved urban area, only short time of the localized heavy rainfall, such as 30 minutes of rainfall with 50mm/hr of intensity, can cause very dangerous situation in urban areas as in the Toga River case.

In order to prevent such flash flood damages, it is very necessary to detect the rain-cells, which may develop to sever storm, as soon as possible and to alert people to evacuate from riverfront before the severe events occur. In this study, we develop a detection technique for the early stage of rain-cell as the first cell aloft (hereafter, baby-cell) in the middle atmospheric layers before it generates heavy rainfall on the ground. The early detection technique is utilizing the 3-D volume scanning data from X-band Multi Parameter radars (X-MP radars), which are equipped near to the most urban area in Japan recently. In our recent study using the 3-D volume scanning information from the X-MP radars, we have successfully developed an algorithm (1) to detect newly generated baby-cells, (2) to identify dangerous level of the baby-cells, and (3) to trace the movement of the baby-cells.

In the developed algorithm, firstly, the detection of newly generated baby-cells is based on the information of 3-D volume scanning data with very fine resolution of the X-MP radars. Secondly, the identification of the dangerous level, whether the detected baby-cells will grow up to heavy rainfall on the ground, is evaluated with the information of vorticity of the baby-cells based on the Doppler velocity information from the radars. Finally, the tracking of the baby-cells is based on the conventional cell tracking scheme. The preliminary test of the algorithm shows that especially, the identification of the developing baby-cells with the vorticity information is very powerful, and most of baby-cells in the early stage of heavy rainfall events were successfully identified. In detail, all the 19 developing baby-cells under our surveillance were successfully detected, and there was only one false alarm (forecasted as a heavy rainfall event, but it was not).

In our presentation, upgraded performance index of our proposed algorithm will be introduced based on various rainfall events happened in Kyoto and Osaka area, Japan. In addition to improving this practical early detection algorithm for localized heavy rainfall events in urban area, we are conducting newly designed observation combination in Kansai area with numerous sensors and equipments as shown in figure to identify the mechanism of the localized heavy rainfall events in urban area, such as Osaka, Kobe and Kyoto. It is definitely our mission to realize a next-generation operational observation network with different types of sensors for earlier detection and/or prediction of generating storm from the stage of air plume and/or cloud. Presentation partly includes current situation and future plan of a plot type field experiment with X-band- polarimetric radar, Ku-band cloud radar, Lider, and X-band phased array radar.

Keywords: Radar, Lidar, Videosonde, Urban Meteorology

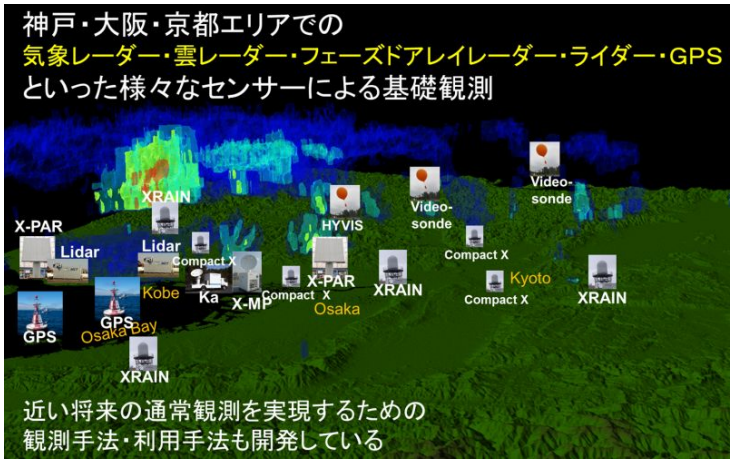

Japan Geoscience Union Meeting 2014
(28 April - 02 May 2014 at Pacifico YOKOHAMA, Kanagawa, Japan)

AAS23-18 Room:424 Time:April 28 16:55-17:10

Analysis of fine-scale airflows over complex topography by super-high-resolution numerical model

TAKEMI, Tetsuya[1*]

[1]Disaster Prevention Research Institute, Kyoto University

With the increase in computational resources, mesoscale meteorological simulations with the grid spacing on the order of 100 m have been conducted not only in idealized studies but also in studies that deal with real cases. In real cases, the benefits from such high-resolution simulations are considered to be better representations of surface topography such as complex terrains and complex distribution of man-made structures. In this presentation, we will demonstrate how fine-scale airflows over complex topography such as terrains and urban districts are represented in numerical simulations of local-scale wind fields under real meteorological settings. Some of the case studies of high wind events are described. For the numerical simulations of specific weather events, we use the Weather Research and Forecasting (WRF) model by downscaling from kilometer-scales to 100-meter-scales with the use of nesting capability. Further downscaling from 100-meter-scales down to 10-meters or higher requires the explicit representation of not only complex terrains but also buildings and structures. For this purpose, we developed an approach to couple a mesoscale meteorological model (i.e., the WRF model) and a computational fluid dynamics (CFD) model (Nakayama et al. 2012). A large-eddy simulation model for airflows over urban geometries (Nakayama et al. 2011) is employed as a CFD model. A unique feature of the present coupling approach, an improved version of the perturbation recycling method of Mayor et al. (2002), is to generate turbulence due to urban-like roughness obstacles with the meteorological effects produced by the mesoscale model being retained. The basic idea of this coupling approach and a case study for a high wind event in the downtown district of Tokyo are demonstrated. Furthermore, some other applications of the present approach for airflow simulations over complex topography including airflows over complex terrain of Fukushima during March 2011 will be briefly introduced.

Keywords: High-resolution numerical model, airflows over complex topography, mesoscale meteorological model, large-eddy simulation

Japan Geoscience Union Meeting 2014
(28 April - 02 May 2014 at Pacifico YOKOHAMA, Kanagawa, Japan)

AAS23-P01 Room:Poster Time:April 28 18:15-19:30

A study on an atmospheric propagation delay estimation method using a fixed radio source

INAKA, Shigeru[1*] ; FURUMOTO, Jun-ichi[1] ; SEKO, Hiromu[2] ; TSUDA, Toshitaka[1] ; HASHIGUCHI, Hiroyuki[1] ; ISHIHARA, Masahito[3]

[1]Research Institute of Sustainable Humanosphere, Kyoto University, [2]Meteorological Research Institute, [3]Education unit for Adaptation to Extreme Weather Conditons and Resilient Society, Kyoto University

This study aims to develop a new method to observe water vapor horizontal distribution using a side-lobe emission of the 1.3 GHz-band wind profiling radar (WPR). The phase delay of the received side-lobe emission is mainly due to the refractive index fluctuation along the propagation path. In the atmospheric boundary layer, the temporal and spatial non-uniformity of water vapor determines the refractive index fluctuation. Main scope of the study is to extract humidity information from the atmospheric phase delay of side-lobe emission from a WPR. Horizontal humidity distribution can be derived by the data assimilation into numerical prediction model.

The receiver system and data analysis algorithm were developed. A software radio, USRP N200 with an RX daughter board was employed to detect side-lobe emission received by an antenna. A Rubidium frequency standard and a 1 pps signal source of GPS receiver were used for accurate estimation of phase delay variation. The frequency stability of a crystal oscillator, which is generally employed for a reference frequency source of WPR, is insufficient for the accurate estimation. We proposed a new method to compensate the frequency uncertainty of WPR by using data of the additional receiver nearby the WPR site.

IQ data detected by USRP B210 which is controled by GNURadio, an open source software. By using GNURadio the system will be low cost.The program written in IDL language extracts the temporal variation of the phase delay from the received IQ signal. In order to achieve good performance even in low SNR conditions, we developed an algorithm using STFT (Short-term Fourier transformation) aiming to remove noise in undesired frequency range.

The developed system is promising to derive humidity information from side-lobe emission from various WPRs such as the operational WPR network in Japan (WINDAS (WInd profiler Network and Data Acquisition System)).

Keywords: Wind Profiling Radar, estimation of horizontal humidity distribution, non-hydrostatic forecast model, software radio, side-lobe, propagation delay

Japan Geoscience Union Meeting 2014
(28 April - 02 May 2014 at Pacifico YOKOHAMA, Kanagawa, Japan)

AAS23-P02 Room:Poster Time:April 28 18:15-19:30

Development of a 266 nm Raman lidar for profiling atmospheric water vapor

UESUGI, Takuma[1*] ; YABUKI, Masanori[1] ; LIU, Yutong[1] ; TSUDA, Toshitaka[1]

[1]Research Institute for Sustainable Humanosphere

It is projected that localized extreme weather events could increase due to the effects of global warming, resulting in severe weather disasters, such as a torrential rain, floods, and so on. Understanding water vapor's behavior in the atmosphere is essential to understand a fundamental mechanism of these weather events. Therefore, continuous monitoring system to measure the atmospheric water vapor with good spatio-temporal resolution is required. We have developed several water vapor Raman lidar systems employing the laser wavelengths of 355 and 532 nm. However, the signal-to-noise ratio of the Raman lidar strongly depends on the sky background because of the detection of the weak inelastic scattering of light by molecules. Therefore, these systems were mainly used during nighttime.

Hence, we have newly developed a water vapor Raman lidar using a quadrupled Nd:YAG laser at a wavelength of 266 nm. This wavelength is in the ultraviolet (UV) range below 300 nm known as the "solar-blind" region, because practically all radiation at these wavelengths is absorbed by the ozone layer in the stratosphere. It has the advantage of having no daytime solar background radiation in the system. The lidar is equipped with a 25 cm receiving telescope and is used for measuring the light separated into an elastic backscatter signal and vibrational Raman signals of nitrogen and water vapor at wavelengths of 266.1, 283.6, and 294.6 nm, respectively. This system can be used for continuous water vapor measurements in the lower troposphere. This study introduces the design of the UV lidar system and shows the preliminary results of water vapor profiles.

Japan Geoscience Union Meeting 2014
(28 April - 02 May 2014 at Pacifico YOKOHAMA, Kanagawa, Japan)

AAS23-P03 Room:Poster Time:April 28 18:15-19:30

About the approach and the progress of the DoCoMo environmental sensor network

KANO, Kayo[1*] ; MIYAJIMA, Akiko[1] ; KIKKAWA, Yoshiaki[1] ; TSUBOYA, Hisakazu[1] ; HIGASHI, Kuniaki[2] ; FURUMOTO, Jun-ichi[2]

[1]Division of life support business promossion,NTT DOCOMO Corporation, [2]Research Institute for Sustainable Humanosphere, Kyoto University

Since 2008, the automated meteorological observation network has been developed by NTT DOCOMO corporation and a total of 4,000 stations are operating now.

The hyper-dense wind measurement network was constructed through the industrial-academical corporation between NTT DOCOMO and Kyoto University, which enables us to elucidate the detailed characteristics of strong downslope windstorm, Hira Oroshi, blowing down in the West coast of the Lake Biwa.

This paper discussed the outline of our activities and fruitful results will be discussed in detail.

Keywords: Environmental Sensor Network

Japan Geoscience Union Meeting 2014
(28 April - 02 May 2014 at Pacifico YOKOHAMA, Kanagawa, Japan)

AAS23-P04 Room:Poster Time:April 28 18:15-19:30

Surface Pressure Distributions of Downburst and Tornado captured by High Dense Ground Observation Network ”POTEKA”

SATO, Kae[1*] ; KURE, Hirotaka[1] ; YADA, Takuya[1] ; MAEDA, Ryota[1] ; KOJIMA, Shinya[1] ; MORITA, Toshiaki[1] ; IWASAKI, Hiroyuki[2]

[1]Meisei Electric Co. Ltd., [2]Faculty of Education, Gunma University

Meisei developed low-cost compact weather sensor (POTEKA Sta., hereinafter referred to as the POTEKA), which can measure temperature, relative humidity, pressure, sunlight, and rain detection per one minute and achieve higher density weather observation system economically. We installed economical and high dense ground observation network (total 55 stations, 1.5˜4 km-mesh) in Gunma, Japan. This paper presents observation of wind gust phenomena around Takasaki city and Maebashi city on 11 August 2013 and tornado in Midori city on 16 September 2013.

Pressure jumps of 1-2 hPa were recorded at POTEKA with one minute resolution, indicating that the temporal high pressure was caused by downburst downflow. Beside, two pressure jump can be found at some stations. The first and second jumps are coincided with gust fronts and down flow of downburst, respectively (Discrimination between downburst and gust-front by the surface dense observation network POTEKA).

In the September 16, tornado occurred in Typhoon passes, and blackout occurred at 2:20(JST). At the point from 1.2km away, surface pressure was decreasing 3hPa in 3 minutes at 1.6km blackout area away (Fig.)

Local weather observation network consisting of POTEKA succeeded in capturing the change of surface pressure caused by gust wind phenomena with unprecedented spatio-temporal resolution, which enables us not only to distinguish between gust fronts and downbursts but also to detect such wind phenomena earlier. The observation network is going to continue in the future to data accumulation.

Acknowledgments: The authors would like to thank SANDEN Corporation, SAVE ON, and Board of Education of Isesaki city for support POTEKA project.

Keywords: High Dence observation network, Downburst, Tornado

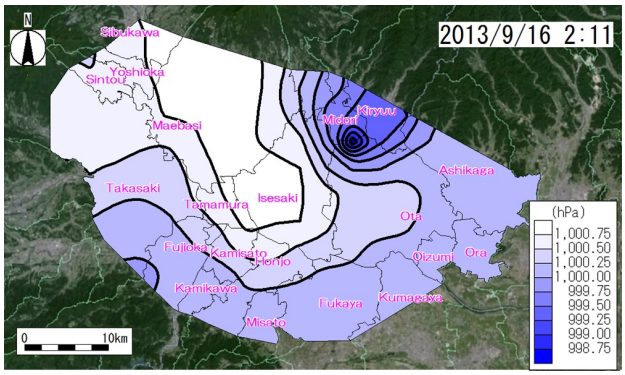

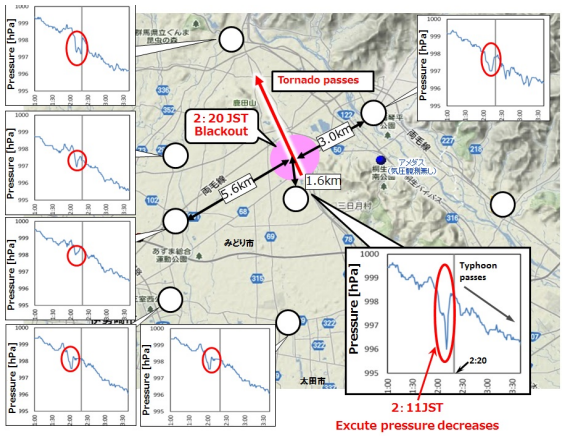

Japan Geoscience Union Meeting 2014
(28 April - 02 May 2014 at Pacifico YOKOHAMA, Kanagawa, Japan)

AAS23-P05 Room:Poster Time:April 28 18:15-19:30

A sensibity study on the role of the urban land surface scheme for a regional climate model, NHRCM

SHIDO, Fumitake[1*] ; AOYAGI, Toshinori[1] ; SEINO, Naoko[1] ; SASAKI, Hidetaka[1]

[1]Meteorological Research Institute, Japan Meteorological Agency

The conditions of land surfaces give large impacts on surface air temperature, via the dynamical and thermal energy exchanging. In order to forecast the physical quantities, such as momentum, heat, and vapor fluxes from the land surface, we have selected a sophisticated vegetation scheme of the SiB (Simple Biosphere) as the land surface scheme of the MRI's NHRCM (Non-Hydrostatic Regional Climate Model). Recently, as model-resolution became higher up to several kilo-meter, non-vegetation but urbanized grids had appeared, and these grids were treated as dried bare ground on the SiB to express the so-called urban deserts. But, in these grids, reproducibility of the climatology seemed to be insufficient. Therefore, we need to apply the new scheme to improve the representation of radiation and heat budgets in such urban area. For that purpose, we developed a new scheme for urban land surface to applied to a regional climate model. This new scheme is called SPUC (Square Prism Urban Canopy, Aoyagi and Seino 2011).

In this study, we applied SiB and SPUC scheme to the 4km-resolution NHRCM, executed present climate simulations, and compared outputs with observational data of JMA(Japan Meteorological Agency). The target area was Kanto-Koshin region including Tokyo metropolitan area. As initial and boundary condition, we used the JMA's RANAL (Regional analysis) dataset (20km resolution), which was downscaled once by NHRCM10km with SiB scheme for all grid. The 10km resolution dataset was also downscaled by NHRCM4km. We executed the 4km experiments, using SiB scheme for all land grids (NHRCM-SiB), and using both SiB for natural surface grids and SPUC for urban surface grids (NHRCM-SPUC).Time integration was continuously executed for about 5 years from August 1st, 2001 to September 1st, 2006.

The result of the experiment using SiB scheme had negative bias(about -1.3 ^{o}C) in the surface temperature in the Tokyo metropolitan area. By using SPUC scheme, this negative bias changed to positive(+1.55 ^{o}C). Although the bias remains, the correlation factor between the simulation and observation was improved from 0.73 (NHRCM-SiB) to 0.86 (NHRCM-SPUC). This improvement implies that NHRCM-SPUC had the better reproducibility on horizontal distribution of air temperature. On the other hand, the difference was hardly seen in total amount of precipitation in five years.

This research is supported by SOUSEI program of MEXT, Japan.

Keywords: regional climate, land surface, downscaling, urban canopy

Japan Geoscience Union Meeting 2014
(28 April - 02 May 2014 at Pacifico YOKOHAMA, Kanagawa, Japan)

AAS23-P06 Room:Poster Time:April 28 18:15-19:30

Temporal and spatial characteristics of gust ratio in the

SAKAMOTO, Hiroto[1*] ; HIGASHI, Kuniaki[1] ; MATSUI, Kazuyuki[2] ; KANO, Kayo[3] ; TSUBOYA, Hisakazu[3] ; FURUMOTO, Jun-ichi[1] ; HASHIGUCHI, Hiroyuki[1]

[1]Research Institute for Sustainable Humanosphere, [2]Environmental Education Working Group in Biwako Region, [3]NTT DOCOMO Corporation

Localized downslope wind often causes severe disasters, although the dynamics of these severe phenomena has not fully elucidated due to their small temporal and spatial scale. The damage by downslope wind is strongly determined by the instantaneous maximum wind speed. Since the numerical model can derive averaged wind speed along time and space determined by the model resolution. The classical analogous theory points out that the gust ratio, which is defined as the ratio of maximum wind velocity to the averaged wind velocity, becomes a constant value (1.5-2.0), depends only on the roughness length of surface condition.

In the actual atmosphere with the horizontal inhomogeneity, the gust ratio may varies with time even at the same location. The sophisticated modeling of gust ratio beyond the simple constant model is very important for the forecasting of gust damage. The detailed characteristics of gust ratio was investigated by the data of hyper-dense surface observation network in the Hira Oroshi region. The temporal and spatial characteristics of gust ratio and future prospective to install our algorithm into the numerical prediction models are discussed in the presentation.

Japan Geoscience Union Meeting 2014
(28 April - 02 May 2014 at Pacifico YOKOHAMA, Kanagawa, Japan)

AAS23-P07 Room:Poster Time:April 28 18:15-19:30

An traial of direct monitoring of turbulence intensity by using the balloon-borne high-resolution temperature sensor

FURUMOTO, Jun-ichi[1*] ; SHIMIZU, Kensaku[2] ; KAI, Kohei[2] ; HIGASHI, Kuniaki[1] ; HASHIGUCHI, Hiroyuki[1]

[1]Research Institute for Sustainable Humanosphere, [2]Meisei Electric Corporation

The fine tungsten wire (10 um diameter) temperature sensor, whose response time is 5/1000sec on surface and 40/1000sec at around 30km altitude, were employed to detect turbulence intensities. For the temperture data at the sampling frequency of 16Hz were used for the tuebulence detection. The comtamination of the wake of the ballon should be carefully removed from the original data before the analysis of turbulence.

We are developing the new method to extract temperature purtarvation by turbulence at the vertical wavelength shorter than the effects of pendular movement of radiosondes.

The preliminary results show very promissing to detect turbulence intensities to compare with echo intensity of atmosphere radar.

The detailed scheme and first results are discussed in the presentation.

Japan Geoscience Union Meeting 2014
(28 April - 02 May 2014 at Pacifico YOKOHAMA, Kanagawa, Japan)

AAS23-P08 Room:Poster Time:April 28 18:15-19:30

High resolution numerical study of migrating strong downslope wind ”Hira-Oroshi” in Japan

HIGASHI, Kuniaki[1*] ; FURUMOTO, Jun-ichi[1] ; HASHIGUCHI, Hiroyuki[1]

[1]Research Institute for Sustainable Humanosphere Kyoto University

This paper studied the generation mechanism of a unique downslope wind in the west coast of Lake Biwa, Shiga, Japan. This strong downslope wind, feared as ”Hira-Oroshi” for millennial years shows the narrow gust of a few kilometers in the various location within 10 km width area. This feature cannot be explained by the conventional mechanism of previous studies: the location of downslope wind is strongly restricted by the location of valley in mountain range. Due to such distinct characteristic, the numerical prediction of this gust wind is too inaccurate to use operationally.

Considering strong demands to the prediction of this gust wind, this study aims to elucidate the mechanism via very fine numerical forecast model with the horizontal resolution of 50 m. The results successfully represented the narrow gust wind structure in the edge of the mountain range. The spots of gust wind due to complicated topographical structure is also seen in the simulation results, although the gust wind speed changes with the larger scale wind direction and speed. Because the stagnant region due to the breaking of the mountain wave is widely extended in the leeward of the mountain range in the free atmosphere (˜1 km), the location of the gust wind looks to be determined by the detailed topographic structure of the mountain range and the a kilometer-scale eddies over the Lake Biwa.

The simulation results suggested these synergy effects determined the gust generation and its location. The unveiled behavior of the gust wind is also beneficial to the improvement of the gust prediction.

Keywords: High resolution numerical simulation, Downslope wind, Local wind

Japan Geoscience Union Meeting 2014
(28 April - 02 May 2014 at Pacifico YOKOHAMA, Kanagawa, Japan)

AOS24-01 Room:311 Time:April 30 15:15-15:30

Modeling of marine biogeochemical and ecosystem in Japan: future perspective and review during the last 20 years

YAMANAKA, Yasuhiro[1*]

[1]Faculty of Earth Environmental Science, Hokkaido University

The first global 3-D marine biogeochemical modeling was developed by Bacastow and Maier-Reimer(1990), and marine ecosystem model was developed by Fasham(1993) as pioneer works, such as Yamanaka and Tajika (1996) and Kawamiya et al.(2000) in Japan. Around 2000, most of marine biogeochemical models have the explicit ecosystem components as well as ecosystem model with focusing short-termed changes in nutrient concentration and pCO2 associated with spring bloom in sub-arctic regions. And representation of iron cycle was an important issue for both modeling, and trial of coupling between climate and carbon cycles was also started.

Everybody wish to develop the ultimate model explicitly and detailed representing hundreds, thousands, millions of plankton and nekton groups. As the first step, Plankton Functional Types (PFTs) models dealing with relatively small number of plankton and nutrient were introduced (e.g., Le Quere, 2005; Kishi et al., 2007). We have two directions as future model developments for marine biological cycles and marine ecosystem. Former focuses on grouping of phytoplankton having large energy (material) flow, and latter focuses on grouping of zooplankton having the linkage to higher trophic levels such as fish as wood web. If both two directions were covered by the almighty model, we would need unlimited number of prognostic values as plankton number multiplied by elemental components (and grazing-grazed relations proportional to square of plankton numbers). Therefore, model developing along two directions are separated necessarily. We are easily focusing on number of prognostic values as a discussion of model complexity (e.g., Friedrichs et al., 2007). But, we do not forget important improvements leaded by studying individual process and trade-off problem between parameters. For example, recent studies discussed formulation using affinity instead of half saturation constant as classical Michaelis-Menten fomula, unrestricted nutrient uptake optimized by the parameter of restricted nutrient, and different impacts by the global warming between these formulations (Smith and Yamanaka, 2007; Smith et al., 2009). Many people are interesting in another type of models relevant to biodiversity are recently developed (Follows, 2007)

I would like to mention another view such as developing researcher community developing biogeochemical cycles and ecosystem model. Pioneers for marine biogeochemical modeling launched Ocean Carbon cycle Model Intercomparison Project (OCMIP). Studies are leaded by the pioneers at earlier periods but by young researchers relevant to OCMIP around the end of Phase 2. It goes without say that they are the present world-leading scientists in this academic field (such as Le Quere, Follows, Gruber etc.). MARine Ecosystem Model Intercomparison Project (MAREMIP) as going project is designed based on OCMIP experiences, and next generations figure just in this field. I should mention other groups. I think developing NEMURO, a marine ecosystem model, in North Pacific marine Science Organization (PICES) as another good international collaboration. As for formulating specific processes such as trade-off problem, North Germany group are leading. Finally, I would like to express my wish that next generation in Japan friendly and positively get chance to lead international research projects one of world-leading scientists with their beautiful lives. This is based on my cancelled invited talk in the last year.

Keywords: marine biogeochemical cycles, marine ecosystem, modeling, international research project, OCMIP, MAREMIP

Japan Geoscience Union Meeting 2014
(28 April - 02 May 2014 at Pacifico YOKOHAMA, Kanagawa, Japan)

AOS24-02 Room:311 Time:April 30 15:30-15:45

Modeling fish production in the ocean: impacts on biogeochemical cycles and ecosystem service evaluation

ITOH, Sachihiko[1*] ; ITO, Shin-ichi[2]

[1]Atmosphere and Ocean Research Institute, The University of Tokyo, [2]Tohoku Nationarl Fisheries Research Institute, Fisheries Research Agency

Marine organisms play fundamental roles in biogeochemical cycles in the ocean. Ecosystem models formulating chemical and biological processes relevant to these organisms and materials have been developed in the past few decades, enabling quantitative evaluation of biological production, carbon and nutrient cycles, and their impact on the climate system. However, many of these models consider trophic levels up to zooplankton. Although much of storage and flux of carbon and nutrients are observed in the lower trophic levels, which is a good reason to focus on this level, importance of higher trophic levels has been increasingly recognized. Here, we review modeling studies incorporating higher trophic levels than zooplankton, especially focusing on fish production models. There are two major motivations developing the fish production model. The first one is that lower trophic level models with zooplankton as the highest trophic level are sometimes controlled too strongly by parameterized zooplankton mortality terms. Although parameterization of mortality terms is needed unless the model contains the apex predator (trophic closure), inclusion of planktivorous fish components does decrease the arbitrariness of the biogeochemical cycle in the model. The second reason to develop fish production models, the more classical reason than the first one, is based on the fact that fish stocks themselves have been major food resources for human societies. In this context, some recent models do not only include commercially important large piscivorous fishes but also consider fishing fleets. Increasing concern for the conservations of marine mammals and sea birds also enhances the model development. There are two different streams of the fish modeling at present: size-based and species-based approaches. We review their advantages and limitations and discuss future improvements of preferable frameworks of the higher trophic models.

Keywords: fish production model, trophic closure, fisheries resources

Japan Geoscience Union Meeting 2014
(28 April - 02 May 2014 at Pacifico YOKOHAMA, Kanagawa, Japan)

AOS24-03 Room:311 Time:April 30 15:45-16:00

The iron budget in ocean surface waters in the 20th and 21st centuries: projections by the Community Earth System Model

MISUMI, Kazuhiro[1*] ; LINDSAY, Keith[2] ; MOORE, Keith[3] ; DONEY, Scott[4] ; BRYAN, Frank[2] ; TSUMUNE, Daisuke[1] ; YOSHIDA, Yoshikatsu[1]

[1]Central Research Institute of Electric Power Industry, [2]National Center for Atmospheric Research, [3]University of California at Irvine, [4]Woods Hole Oceanographic Institution

We investigated the simulated iron budget in ocean surface waters in the 1990s and 2090s using the Community Earth System Model version 1 and the Representative Concentration Pathway 8.5 future CO_2 emission scenario. We assumed that exogenous iron inputs did not change during the whole simulation period; thus, iron budget changes were attributed solely to changes in ocean circulation and mixing in response to projected global warming, and the resulting impacts on marine biogeochemistry. The model simulated the major features of ocean circulation and dissolved iron distribution for the present climate. Detailed iron budget analysis revealed that roughly 70 % of the iron supplied to surface waters in high-nutrient, low-chlorophyll (HNLC) regions is contributed by ocean circulation and mixing processes, but the dominant supply mechanism differed by region: upwelling in the eastern equatorial Pacific and vertical mixing in the Southern Ocean. For the 2090s, our model projected an increased iron supply to HNLC waters, even though enhanced stratification was predicted to reduce iron entrainment from deeper waters. This unexpected result is attributed largely to changes in gyre-scale circulations that intensified the advective supply of iron to HNLC waters. The simulated primary and export production in the 2090s decreased globally by 6 and 13 %, respectively, whereas in the HNLC regions, they increased by 11 and 6 %, respectively. Roughly half of the elevated production could be attributed to the intensified iron supply. The projected ocean circulation and mixing changes are consistent with recent observations of responses to the warming climate and with other Coupled Model Intercomparison Project model projections. We conclude that future ocean circulation has the potential to increase iron supply to HNLC waters and will potentially buffer future reductions in ocean productivity.

Japan Geoscience Union Meeting 2014
(28 April - 02 May 2014 at Pacifico YOKOHAMA, Kanagawa, Japan)

AOS24-04 Room:311 Time:April 30 16:15-16:30

Response of phytoplankton community structure to global warming

HASHIOKA, Taketo[1*] ; HIRATA, Takafumi[2] ; CHIBA, Sanae[1] ; YAMANAKA, Yasuhiro[2]

[1]JAMSTEC, [2]Hokkaido Univ.

In recent studies using high-performance liquid chromatography (HPLC) pigment data, empirical relationships between total chl-a concentration and a phytoplankton size/PFT fraction on a global scale are shown. For example, a fraction of diatoms increases with total chl-a concentration. The same tendencies can be seen in the most of the hindcast experiments by current PFT models of MARine Ecosystem Model Intercomparison Project (MAREMIP) and Coupled Model Intercomparison Project Phase5 (CMIP5) although the reproduced absolute values of a phytoplankton fraction still has large uncertainties. Then, two different mechanisms can be expected as potential responses of phytoplankton community to global warming. One is a possibility that the phytoplankton community structure (i.e., relationships between a phytoplankton fraction and total chl-a concentration) can be significantly changed by changes in ecosystem dynamics under global warming condition (e.g., changes in grazing pass/strength, decomposition/mortality/respiration rate and phytoplankton stoichiometry). Another possibility is that the plankton community shifts to the other stable states associated with changes in total chl-a concentration (e.g., by decrease/increase in nutrient supply to the surface ocean by changes in stratification) while maintaining the current relationship between a phytoplankton fraction and total chl-a concentration. To clarify impacts of both effects, we analyzed model results of future simulation, which was conducted by CMIP5 and MAREMIP under the RCP8.5 emission scenario. PFT model more than half showed that relationships between phytoplankton composition and total chl-a concentration are stable against environmental changes associated with global warming. In these model results, changes in phytoplankton composition are mainly caused by plankton community shifts associated with changes in total chl-a concentration. This result suggests the possibility that current empirical relationships obtained by HPLC would be maintained in a future environment. Based on this hypothesis, we project a potential future community structure of phytoplankton using a multi-model ensemble mean of future changes in total chl-a concentration with the empirical relationship of HPLC. Some other models projected large changes in the community structure in specific regions and seasons. These results also suggest potentially important mechanisms, regions and seasons.

Keywords: Phytoplankton, Community structure, Global warming

Japan Geoscience Union Meeting 2014
(28 April - 02 May 2014 at Pacifico YOKOHAMA, Kanagawa, Japan)

AOS24-05 Room:311 Time:April 30 16:30-16:45

Introduction to our on-going development of an adaptive model for plankton communities in the North Pacific

SMITH, S. Ian[1*] ; YOSHIKAWA, Chisato[1] ; SASAI, Yoshikazu[1]

[1]RIGC, JAMSTEC, [2]CREST, JST

This presentation will introduce our on-going efforts, as part of a CREST project funded by JST, to develop a new prototype model to represent the biodiversity and adaptive capacity of lower-trophic ecosystems in the North Pacific. The ultimate goal is to develop a computationally efficient representation of the community-level interactions of the producers (phytoplankton) and consumers (zooplankton) with each other and with the marine environment. This of course includes the adaptive response of plankton communities to changing environmental conditions, and later potential feedbacks, including for example the impact of plankton communities on controlling nutrient concentrations. We will present the size-based model of phytoplankton communities that is already under development and one scientific result already obtained, regarding the size-scaling of growth parameters, as commonly applied in large-scale models, in terms of the more commonly measured parameters for nutrient uptake kinetics. This scaling relationship provides a basis for consistently incorporating observed allometries into models based on Monod growth kinetics. This new simplified model of phytoplankton communities accounts for biodiversity via size-scaling of phytoplankton traits and for flexibility of the C:N ratio of biomass.

Fig. 1. Traits, which define how organisms respond to environmental conditions, have evolved subject to inescapable biophysical constraints. Thus have arisen trade-offs in competitive ability under different conditions, here illustrated for typical small phytoplankton adapted to low-nutrient, high-light conditions, which have high affinity (α), low maximum uptake rates (V_{max}) and relatively less allocation to chlorophyll/light harvesting ability, vs. large phytoplankton adapted to high-nutrient, low-light conditions, which have low α, high V_{max}, and relatively more allocation to chlorophyll/light harvesting ability. Maximum growth rate (μ_{max}) is constrained by the opportunity cost of allocating resources to the various processes necessary to support growth.

Keywords: plankton, ecosystem, model, traits, trade-offs, adaptive

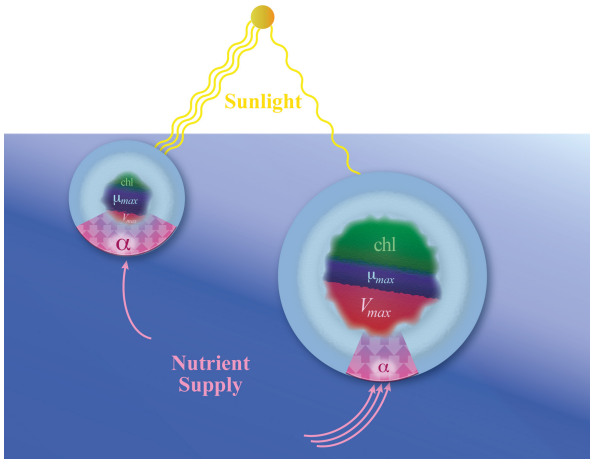

Japan Geoscience Union Meeting 2014
(28 April - 02 May 2014 at Pacifico YOKOHAMA, Kanagawa, Japan)

AOS24-06 Room:311 Time:April 30 16:45-17:00

Exploring mechanisms of phytoplankton coexistence using a marine ecosystem model with eddy-resolving resolution

MASUDA, Yoshio[1*] ; YAMANAKA, Yasuhiro[1] ; NAKANO, Hideyuki[2]

[1]Hokkaido University, [2]Meteorological Research Institute, Japan

Observational studies estimate that there are over 70,000 phytoplankton species. Various mechanisms which enable phytoplankton coexistence are proposed. Niche segregation are inspected under pelagic environment, using a numerical model. Since we considered that variation of pelagic environment resulted in mesoscale eddies plays an important role on phytoplankton diversity, an eddy-resolving model is employed. Based on NEMUEO and MEM, we developed a marine ecosystem model which can express a few hundred phytoplankton species and combined it to a physical oceanic model, MRI.com. The physical field represents idealized subpolar and subtropical gyres in a rectangular model domain of 30 by 30 degrees. To explore niche segregation, we seeded 240 phytoplankton species which have different trait for temperature, light and nutrient. After 10 years integration, 31 species are survived. In the subpolar (subtropical) region, species favorable high (low) nutrient condition are survived. Segregation with temperature is also confirmed.

Keywords: Phytoplankton diversity, Marine ecosystem model, Mesoscale eddy

Japan Geoscience Union Meeting 2014
(28 April - 02 May 2014 at Pacifico YOKOHAMA, Kanagawa, Japan)

AOS24-07 Room:311 Time:April 30 17:00-17:15

Numerical analysis of the influences of the meso-zooplankton mortality

YOSHIE, Naoki[1*] ; TOMITA, Kazuyuki[1] ; OKUNISHI, Takeshi[2] ; ITO, Shin-ichi[2]

[1]Center for Marine Environmental Studies, Ehime University, [2]Tohoku National Fisheries Research Institute, Fisheries Research Agency

In recent years, marine lower-trophic level ecosystem consisting of phytoplankton and zooplankton has been seriously affected by the various environmental changes due to the climate changes and the human activities. The quantitative assessment of the lower-trophic level ecosystem changes with the environmental changes is important for the human beings in the world. This is because the lower-trophic level ecosystem changes closely links to the fisheries resources and the global carbon cycles. For example, copepod which is one of the meso-zooplankton in the lower-trophic level ecosystem is main food for the fishes of good-catch such as Japanese saury and anchovy. Copepod also exports a huge amount of organic carbon from the surface water to the deep water in the ocean by the seasonal vertical migration to around 1000m depth and the rapid sinking fecal pellet. We have been developing a plankton functional types (PFTs) model which explicitly calculates each functional group of organisms such as copepod above. In particular, we developed a PFTs model eNEMURO (4-Nutrient, 4-Phytoplankton, 4-Zooplankton, 4-Detritous), which was an extend version of NEMURO [a standard lower-trophic-level marine ecosystem model of PICES (The North Pacific Science Organization)] by introducing the microbial food web and the phosphorous cycles and dividing diatoms to two compartments according to temperature dependency. eNEMURO successfully reproduced the spatio-temporal variations in the lower-trophic level ecosystem around Japan. In this study, we investigated the influences of the meso-zooplankton mortality which was little known from the filed observations and the laboratory experiments on the lower-trophic level ecosystem. We conducted the sensitivity analysis of two parameters of the meso-zooplankton mortality in eNEMURO in five regions with different types of the lower-trophic level ecosystem around Japan. Model result shows that the increase of the meso-zooplankton mortality associated with water temperature rising has large impacts on the nutrients concentrations, the biomasses of phytoplankton and zooplankton, especially in the regions with the high temperature. We also introduce results from the biological parameters optimization of eNEMURO using the genetic algorithm method.

Japan Geoscience Union Meeting 2014
(28 April - 02 May 2014 at Pacifico YOKOHAMA, Kanagawa, Japan)

AOS24-08 Room:311 Time:April 30 17:15-17:30

A benthic-pelagic coupled ecosystem model to clarify nutrient cycles in coastal areas

TATENO, Satoshi[1*] ; HATA, Kyoko[1] ; NAGAO, Kentaro[1]

[1]IDEA Consultans, Inc.

In many enclosed coastal seas in japan, coastal environment have changed due to increase of nutrient loading and land development after 1960s. This caused loss of material cycles balance, generation of red tides, anoxic conditions and hydrogen sulfide.Water quality has been gradually improved because of some policies such as water quality standard and water pollution control law, but the loss of balance remains in many areas. It is because various factor such as benthic system, fishery industry and the open sea of the areas affect it.

We developed a benthic-pelagic coupled ecosystem model to clarify the role and the contribution of them. The model also included important factors for the coastal environment as dissolved oxygen, oyster and eelgrass.

It was developed for Mitsu Bay area in the western part of Seto Inland Sea. In this area, oyster culture distribute widely. Model results indicated the most important factor for the material cycles was advection from out of the area. Nutrient load had lower impact than advection and oyster. Anoxic water did not appear but the oyster culture caused accumulation of organic matter on the sediment under oyster rafts and hydrogen sulfide production. It was suggested that control of it is important for improve the material circulation and keep it in balance.

Keywords: Marine Ecosystem Model, Marine Material Cycles

Japan Geoscience Union Meeting 2014
(28 April - 02 May 2014 at Pacifico YOKOHAMA, Kanagawa, Japan)

AOS24-09 Room:311 Time:April 30 17:30-17:45

A challenge to investigate environmental factors which determine spawning migration variability of small pelagic.

ITO, Shin-ichi[1*] ; OHNO, Sohsuke[1] ; OKUNISHI, Takeshi[1] ; SUYAMA, Satoshi[1] ; NAKAGAMI, Masayasu[1] ; AMBE, Daisuke[1] ; KAMEDA, Takahiko[1] ; KAKEHI, Shigeho[1]

[1]Fisheries Research Agency

In recent years, lower trophic ecosystem models, which represent phyto and zoo-plankton, have been coupled to fish growth-migration models. These coupled models enable to elucidate fish response to climate variability. However, mechanisms of fish migration has not been well clarified. Especially the mechanisms of spawning migration, by which spawner fish can home on to their spawning grounds, are one of the most difficult behavior to represent by a numerical model. Using realistic initial and boundary condition, an Euler-type model of Pacific saury was applied to investigate environmental factors which determine spawning migration variability. The initial distribution of Pacific saury was defined by synoptic surface trawl surveys and satellite derived environmental conditions were used as forcing; sea surface temperature (SST), prey density estimated from surface chl-a concentration and surface current speed. Growth of Pacific saury was calculated by a fish bioenergetics model (NEMURO.FISH). A fitness algorithm was applied for feeding migration in which the fish are assumed to be moving towards a place with optimal growth condition. A larvae fitness algorithm was applied for spawning migration in which the spawning fish moves to a place of the optimal growth of larvae. For spawning migration, westward migration was added to reproduce realistic spawning grounds around Japan Islands. Strength of the westward migration was adjusted to realize observed variability of saury migration to fishing grounds. The adjusted westward migration variability showed high correlation with basin wide SST in the North Pacific. This result suggested a strong influence of climate to fish spawning migration.

Keywords: ecosystem model, fish growth-migration model, Pacific saury, ocean environment

Japan Geoscience Union Meeting 2014
(28 April - 02 May 2014 at Pacifico YOKOHAMA, Kanagawa, Japan)

AOS24-P01 Room:Poster Time:April 30 18:15-19:30

Impacts of global warming on fisheries estimated from climate models: An application to Japanese scallops in Hokkaido

SHIBANO, Ryota[1*] ; FUJII, Masahiko[1] ; YAMANAKA, Yasuhiro[1] ; YAMANO, Hiroya[2] ; TAKAO, Shintaro[1]

[1]Faculty of Env. Earth Sci., Hokkaido Univ., [2]NIES

Climate change such as global warming is considered to affect marine ecosystem. For example, rise in seawater temperature in future may change distributions of marine species. We estimated the impacts of global warming on Japanese scallop, *Mizuhopecten yessoensis*, in Hokkaido. Japanese scallops are important target species for Japanese fisheries resources. Combining sea surface temperature output obtained from climate models and simplified indices that express distribution of Japanese scallops, we estimated suitable domains for Japanese scallop fisheries. We found rise in water temperature from 1990 to 2100 has an impact to aquaculture industries of Japanese scallops across Hokkaido. This study suggests a simplified method to estimate distributions of coastal marine species and the importance of observed data in the future projection.

Keywords: Global warming, Fishries resources, Japanese scallop, CMIP5

Japan Geoscience Union Meeting 2014
(28 April - 02 May 2014 at Pacifico YOKOHAMA, Kanagawa, Japan)

AHW07-01 Room:511 Time:April 29 09:00-09:15

Interannual variations and its control factors of evapotranspiration in a temperate Japanese cypress forest

TSURUTA, Kenji[1*] ; KOSUGI, Yoshiko[1] ; TAKANASHI, Satoru[2] ; TANI, Makoto[1]

[1]Graduate School of Agriculture, Kyoto University, [2]Forestry and Forest Products Research Institute

1.Introduction

Evapotranspiration from forests is a major factor affecting water yield and therefore water resources. Understanding the long-term impacts of variations of meteorological factors on variability of evapotranspiration is important, especially in the context of current and future climate change. Long-term continuous measurements of evapotranspiration using the eddy covariance method provide an opportunity to examine the response of forest ecosystem processes to climate change. We quantified the interannual variations of evapotranspiration, and examined its control factors using the multi layer model.

2.Material and methods

Observations were made in the Kiryu Experimental Watershed in the south of Shiga Prefecture, central Japan. The forest around the watershed comprises mainly 50-year-old Japanese cypress forest. A meteorological observation tower is located in the watershed. The fluxes of momentum, sensible heat, latent heat, and CO2 were measured using eddy covariance methods at a tower height of 28.5 m. Precipitation was observed at the open site.

We used the multi layer model to clarify the control factors of interannual variations of evapotranspiration. The model contained sub-models that calculated the gas exchange processes, including H2O and CO2 exchanges of leaves and the ground surface. This multi layer model simulates the above-canopy fluxes based on vertical profiles of meteorological factors. This model requires the above-canopy environmental variables as the input data. The parameters representing leaf gas exchange characteristics are determined by leaf gas exchange measurements. We used 7 years of eddy covariance data (from January 2001 to December 2007) in this study.

3.Results and discussion

Annual evapotranspiration for the seven years ranged between 715 (2001) and 780 mm (2004) with the average of 743 mm. Maximum interannual fluctuation in evapotranspiration was 75 mm.

Diurnal, seasonal, and interannual variations of evapotranspiration for the seven years were reproduced by a model simulation. This indicates that the model structure and parameterization are validated.

We calculated the components of evapotranspiration such as transpiration, evaporation, and soil evaporation. Each component shows interannual variations relating to meteorological factors. Wet years such as 2001 and 2002 had small annual evaporation and large annual transpiration. Dry years such as 2003 and 2006 had large annual evaporation and small annual transpiration. Both annual evaporation and transpiration were relatively large in 2004. Annual soil evaporation was slightly smaller than evaporation and transpiration. Interannual fluctuations in soil evaporation were also small compared with evaporation and transpiration.

We examined seasonal variations of evapotranspiration for the contrasting two years; 2004 and 2003 with maximum and minimum annual evapotranspiration simulated, respectively. The deviations of evapotranspiration for the two years were large in summer from June to August. Transpiration increased with vapor pressure deficit and solar radiation. Transpiration was relatively small in 2003, which had low vapor pressure deficit and solar radiation in the summer. Transpiration was relatively large in 2004, which had high vapor pressure deficit and solar radiation in the summer. Soil evaporation for the two years showed the similar seasonal variations with transpiration. Seasonal variations of evaporation were the similar to those of precipitation.

Each component of evapotranspiration showed different responses to the meteorological factors seasonally and annually. Interannual variations of evapotranspiration were almost explained by those of meteorological factors.

Keywords: Evapotranspiration, Interannual variation, Eddy covariance, Multi layer model, Japanese cypress forest

Japan Geoscience Union Meeting 2014
(28 April - 02 May 2014 at Pacifico YOKOHAMA, Kanagawa, Japan)

AHW07-02 Room:511 Time:April 29 09:15-09:30

Evapotranspiration and water use efficiency on a coniferous planted forest watershed in south western Japan

SHIMIZU, Takanori[1*] ; TAMAI, Koji[1] ; KUMAGAI, Tomo'omi[2] ; ISHIZUKA, Shigehiro[3] ; OHTANI, Yoshikazu[1] ; SHIMIZU, Akira[3]

[1]Forestry and Forest Products Research Institute, [2]Hydrospheric Atmospheric Research Center, Nagoya University, [3]Kyushu Research Center, Forestry and Forest Products Research Institute

Japanese cedar (*Cryptmeria japonica* D. Don) and Japanese cypress (*Chamaecyparis obtusa* Endl.) are the most popular planted species in Japan. These species cover about 20% of the land surface of the country. On a mountainous topography which is common in Japan, Japanese cedar was usually planted from valleys to lower hillsides with relatively wet and fertile soils, while Japanese cypress was planted on the drier and more nutrient poor ridge areas. Accordingly, evapotranspiration (ET) and carbon assimilation may be variable in the two species.

We applied multiple methods to estimate ET from a planted forest watershed located in Kyushu Island, south western part of Japan. The watershed existed on mountainous terrain, and the right bank was mainly covered with well-grown Japanese cedar while the larger part of the left bank was covered with relatively less-grown Japanese cypress. We applied the eddy covariance method, using an observation tower built in the center of the watershed. The eddy covariance data were experimentally divided to two sectors by wind direction, right bank side and left bank side of the watershed, and the lack of data for each wind sector were interpolated by the mutual imputation method. The analysis period in this study is 2007-2008. Within the period, the rainfall interception loss (I_c) and sap-flux density were also measured in Japanese cedar plots, and the lower canopy ET was estimated by a model. From the eddy covariance result, ET from the left bank side was estimated as 85% of that from the right bank side in the period. Compared the right bank side ET with the combination of I_c, upper- and lower-canopy ET, the difference in annual total ET was about 1% when global solar radiation (S_d) was greater than 0, which assured the accuracy of the eddy covariance method even over the complex terrain.

As for carbon assimilation, we simultaneously measured CO_2 flux and CO_2 concentration profile by using the observation tower. Based on the measurements, we can estimate the CO_2 exchange between the forest and atmosphere through the similar procedure to ET. Thus in this study, we will estimate the carbon budged and calculate the water use efficiency of the whole ecosystem of the watershed and of the both bank sides. From the tentative result obtained at present, the average NEE of the left bank side was 87% to that of the right bank side, in the daytime ($S_d > 0$) in 2007-2008. From the value and the aforementioned ET ratio (0.85), the water use efficiency of the both bank sides were might be almost the same as each other. In the presentation, we will discuss about the detail, considering the respired CO_2 in the nighttime and the rainfall interception in the Japanese cypress plot.

Keywords: Planted coniferous forest stand, Growth difference, Water vapor flux, Carbon dioxide flux, Water use efficiency

Japan Geoscience Union Meeting 2014
(28 April - 02 May 2014 at Pacifico YOKOHAMA, Kanagawa, Japan)

AHW07-03 Room:511 Time:April 29 09:30-09:48

Water budget and the consequent canopy duration period in a teak plantation in a dry tropical region

TANAKA, Katsunori[1*]

[1]Japan Agency for Marine-Earth Science and Technology

A soil-plant-air continuum multilayer model was used to numerically simulate canopy net assimilation (A_n), evapotranspiration (ET), and soil moisture in a deciduous teak plantation in a dry tropical climate of northern Thailand to examine the influence of soil drought on A_n. The timings of leaf flush and the end of the canopy duration period (CDP) were also investigated from the perspective of the temporal positive carbon gain. Two numerical experiments with different seasonal patterns of leaf area index (LAI) were carried out using above-canopy hydrometeorological data as input data. The first experiment involved seasonally varying LAI estimated based on time-series of radiative transmittance through the canopy, and the second experiment applied an annually constant LAI. The first simulation captured the measured seasonal changes in soil surface moisture; the simulated transpiration agreed with seasonal changes in heat pulse velocity, corresponding to the water use of individual trees, and the simulated An became slightly negative. However, in the second simulation, A_n became negative in the dry season because the decline in stomatal conductance due to severe soil drought limited the assimilation, and the simultaneous increase in leaf temperature increased dark respiration. Thus, these experiments revealed that the leaflessness in the dry season is reasonable for carbon gain and emphasized the unfavorable soil water status for carbon gain in the dry season. Examining the duration of positive A_n (DPA) in the second simulation showed that the start of the longest DPA (LDPA) in a year approached the timing of leaf flush in the teak plantation after the spring equinox. On the other hand, the end appeared earlier than that of all CDPs. This result is consistent with the sap flow stopping earlier than the complete leaf fall, implying that the carbon assimilation period ends before the completion of defoliation. The model sensitivity analysis in the second simulation suggests that a smaller LAI and slower maximum rate of carboxylation likely extend the LDPA because soil water from the surface to rooting depth is maintained longer at levels adequate for carbon gain by decreased canopy transpiration. The experiments also suggest that lower soil hydraulic conductivity and deeper rooting depth can postpone the end of the LDPA by increasing soil water retention and the soil water capacity, respectively. These hypotheses will be verified based on observations.

Keywords: canopy dyration period, carbon gain, dry tropical region, soil-plant-air continuum system, teak plantation, water budget

Japan Geoscience Union Meeting 2014
(28 April - 02 May 2014 at Pacifico YOKOHAMA, Kanagawa, Japan)

AHW07-04 Room:511 Time:April 29 09:48-10:03

Influence of canopy interception on the recovery in water balance after clear-cutting at a small headwater catchment

ODA, Tomoki[1*] ; EGUSA, Tomohiro[1] ; OHTE, Nobuhito[1] ; HOTTA, Norifumi[2] ; TANAKA, Nobuaki[3] ; GREEN, Mark[4] ; SUZUKI, Masakazu[1]

[1]Graduate School of Agricultural and Life Sciences, The University of Tokyo, [2]Faculty of Life and Environmental Sciences, University of Tsukuba, [3]Ecohydrology Research Institute, The University of Tokyo Forests, Graduate School of Agricultural an, [4]Center for the Environment, Plymouth State University

The impact of forest disturbance on stream runoff has been well studied using the paired catchment approach, usually finding increased stream runoff following forest disturbance due to the decline of transpiration and canopy interception. However the recovery processes of transpiration and interception have rarely been directly observed under a recovering forest, therefore mechanisms behind recovery time of stream runoff following forest cutting is still not well understood. The objective of this study is to evaluate the contribution of interception to the change of stream runoff after forest cutting. This study was conducted in a pair of small headwater catchments, where one catchment was clear-cut in 1999 and planted with the same species in 2000. Annual runoff increased 200 to 300 mm/yr after forest cutting and the higher runoff remains 12 years after cutting. Interception ratio in the clear-cut catchment were lower than 10 % of precipitation in 2007, 2011 and 2012, and those in the control catchment were 20 to 24 % of precipitation. The mean annual interception was still around 300 mm/yr smaller in the young forest compared to the mature forest, although canopy cover and LAI were similar. These results suggested that the recovery of interception rate is an important controlling factor for the recovery of stream runoff after forest cutting, and not only canopy structure, but also the microclimate condition above the canopy of young forest could be also important factors affecting interception.

Keywords: forest cutting, water balance, canopy interception, headwater catchment

Japan Geoscience Union Meeting 2014
(28 April - 02 May 2014 at Pacifico YOKOHAMA, Kanagawa, Japan)

AHW07-05 Room:511 Time:April 29 10:03-10:18

Changes in interannual variability of runoff in a conifer and deciduous hardwood mixed forested watershed

NOGUCHI, Shoji[1*] ; MURAKAMI, Wataru[1] ; TANI, Makoto[2]

[1]Forestry and Forest Product Research Institute, [2]Graduate School of Agriculture, Kyoto University

The National Forest Management conducts forest management in National Forests for the fulfillment of multi functional roles of forest including long-term wood production management. On the other hand, there are few studies that evaluated the runoff characteristics including a state of the forest for a long term. This study was conducted within the Kamabuchi No1 experimental watershed (3.06ha) in North part of Japan. Hydrological observation has been continued in cold snowy region since 1939. It is the longest record in this region in Japan. The site is covered with Natural hardwood forest (ex. Fagus crenata, Quercus mongolica var. grosseserrata and Quercus serrata) and coniferous plantation forest (Cryptomeria japonica and Chamaecyparis obtuse) which planted around 1912 to 1916. Surficial geology is tuff and shaletic tuff of the Tertiary period and soils are clay loam. Meteorological observation was conducted Yamagata experimental forests located to 800m from the watershed to the northeast. A 71-year record (1939-2010) of the precipitation and runoff was used for an analysis of the flow-duration curve. Tree (DBH ≥ 6cm) census in the watershed was also conducted at 5 times (1942, 1950, 1957, 1979, 2008). The tree volume of Chamaecyparis obtuse is a regular tendency and the tree volume of Cryptomeria japonica linearly increased. Stem volume of oak trees has increased remarkably from 1942 to 1979 but there was a close tendency of an increase in 2008 because mortality of oak trees occurred in the watershed. Based on 5 times tree census, positive linear relationship was found between tree volume and age of stand. While the proportion of plentiful runoff has shown a tendency to decrease over long term, those of ordinary, low and scanty runoffs have tended to increase with increasing the tree volume.

Keywords: duration curve, cold snowy region, long term hydrological observation, runoff characteristics

Japan Geoscience Union Meeting 2014
(28 April - 02 May 2014 at Pacifico YOKOHAMA, Kanagawa, Japan)

AHW07-06 Room:511 Time:April 29 10:18-10:33

Is there any general rainfall-runoff response function in mountainous catchments?

UCHIDA, Taro[1*] ; ASANO, Yuko[2] ; KANBARA, Jun'ichi[1] ; TOMOMURA, Mitsuhidde[3]

[1]National Institute for Land and Infrastructure Management, [2]University of Tokyo, [3]Meteorological Engnieering Center

Clarifying rainfall-runoff response function in mountainous catchments is one of key issues for flood and sediment disaster prediction, management of aquatic environment, water supply and so on. So, rainfall-runoff response function in mountainous catchments has been debated in more than several decades. A variety of studies, observation, modeling, theoretical studies etc., has been conducted. Many noble efforts have been conducted for clarifying complex systems in catchment hydrology through intensive observations. These observations were effective for documentation of the idiosyncrasies of each catchment environments. However, it has been difficult to derive general rainfall-runoff response function from these basin-centric approaches. So, several researchers emphasized the importance of intercomparison so as to better see first order controls of hydrologic responses. Except for several exceptions, intercomparisons for rainfall-runoff responses in many catchments are still limited. Thus, still it is very hard to predict rainfall-runoff response function at ungauged basin.

Thus, we compiled rainfall and stream flow data for around 150 catchments in Japan. We focused relatively small catchment (<100 km2) and a variety of geological, topographical and climatic conditions. We removed catchments where strongly affected human activities, such as urbanized catchment etc., from our intercomparison.

In this study, we randomly sampled 10 storms, i.e., total rainfall amounts were large than 50 mm, for each catchment and calculated three indices, peak specific discharge, peak lag time and direct runoff ratio, to characterize rainfall-runoff response. Also, we defined rainfall-runoff responses using three reservoirs model. We parameterized all of catchments using four storms data using SCE-UA method and validated these parameters using other four storms data. Then, we tested the roles of rainfall condition, climate, geology and topography on rainfall-runoff responses. We used multiple regression analysis to define first order controls of rainfall-runoff responses.

We found large variability in rainfall-runoff responses and it is hard to define general response patterns. While, through multiple regression analysis, we found several interesting results, as follow;

-Climatic conditions affected peak specific discharge and direct runoff ratio, suggesting that climate might give impacts on hydrological characteristics soil and bedrock.

-Geology, such as type of rocks and geological age, gave impacts on rainfall-runoff responses, but effects of geology were not so large, although many study focused on rock-controls on hydrology.

-Flowpath length, calculated by DEM, was one of important topographic parameters for describing rainfall-runoff responses.

Keywords: headwater catchment, rainfall-runoff response, database, multiple regression analysis

Japan Geoscience Union Meeting 2014
(28 April - 02 May 2014 at Pacifico YOKOHAMA, Kanagawa, Japan)

AHW07-07 Room:511 Time:April 29 11:03-11:18

A method of generating virtual drainage-basin by introducing models of slope/stream evolution

NAKAKITA, Eiichi[1*]

[1]Eiichi Nakakita

A method of generating virtual drainage basin to understand relationship among characteristics of geomorphic distribution, rainfall distribution, and runoff distribution was developed. Here the concept of generating virtual drainage-basin is that the drainage-basins are generated at random under some physically based conditions on the basin form. The method is an improvement of Nakakita and Matsuda (2007). They proposed the method of generating virtual drainage-basin based on erosional developing model of channel network by Horton (1945). For the improvement, mathematical models of evolution of slopes and streams were introduced into the methodology. As a result, we achieved to introduce the concept of time into the generating virtual drainage-basin model.

Keywords: drainage basin, landform evolution, channel network, slope evolution, longitudinal profile

Japan Geoscience Union Meeting 2014
(28 April - 02 May 2014 at Pacifico YOKOHAMA, Kanagawa, Japan)

AHW07-08 Room:511 Time:April 29 11:18-11:36

Rock control, denuded hillslope and discharge system in warm humid regions

IIDA, Tomoyuki[1*]

[1]Center for Research in Isotopes and Environmental Dynamics, University of Tsukuba

Under humid and warm regions as Japan, a stable discharge system of seepage water in hillslope is maintained by not only geophysical structures(soil and weathered layer) but also biological system such as forest. From long term point of view, topography, soil, ecosystem and water discharge system play hydro-geomorphological interactions directly or indirectly to one another. In the discharge system, both macro and micro pores of soil layer or weathered bedrock play especially important roll, which controls the permeability and storage capacity under the ground. Among them, natural pipes consisting of continuous macro pores play a roll in the water discharge during a heavy rainfall event. The capillary water stored in micro pore can be used by trees in dry season. These macro pores and micro pores are made by physical and chemical weathering processes. However, biological weathering is the most important for the development of these pores in soil. Forest ecosystems can evolve a matured soil system from soil particles in order to adjust a suitable environment for their own lives. Because the tree root system needs not only water but also enough air, an efficient discharge system may be created as one of the most important environment. This discharge system changes as follows according to the rainfall conditions.

1) In the case of usual storms: The discharge system is stable and it can discharge successfully the seepage water.

2) In the case of unusual heavy storms: The slope failure may occurs due to increasing of water pressure when the water table of throughflow, rises or the pipe-discharge system becomes plugged and partially destroyed. However, this system is recovered with the recovery of forest and soil. This can be called a healty feedback. The humid and warm climate suitable for forest contributes much to these recovery. Therefore, this feedback can contol the expansion of a denuded area made by a slope failure and a wide denuded area may not been naturally developed.

3) In the case of unusual heavy storms in bare lands created by severe human activities: In this case, especially in granite area or the Tertiary area, an unhealty feedback acts because the critical threshold of healty feedback is exceeded. Then, the bare land expands rapidly throughout a mountain area. It is almost impossible for forest and soil to be recovered naturally. Human afforestation work is necessary. Such hillslopes were founded in the wide area of Japan till the second half of 20th century. There is no stable discharge system in such bare hillslopes. Consequently, frequent occurrence of overland flow surface flows caused severe floods and soil hazard.

The discharge system seems to be made as a part of hillslope development. The geological character of the bedrock and the climate (rainfall and temperature) play an important roll in making of the discharge system. This system can be considered as one of the effects of rock control.

Keywords: hillslope hydrogy, discharge system, rock control, bare land, ground structure, hydro-geomorphological interaction

Japan Geoscience Union Meeting 2014
(28 April - 02 May 2014 at Pacifico YOKOHAMA, Kanagawa, Japan)

AHW07-09 Room:511 Time:April 29 11:36-11:51

The making method of two dimensional distribution map of the collapse prevention force with tree survey

ATSUJI, Makoto[1*] ; KITAHARA, Hikaru[2] ; ONO, Hiroshi[2]

[1]Graduate School of Agriculture, Shinshu University, [2]Faculty of Agriculture, Shinshu University

The collapse prevention force of the forest root system is a grand total of the pulling out resistance of each root per vertical cross section ($1m^2$) of soil layer. The pulling out resistance of root (T,N) shows a following equation using root diameter (D,mm) , $T=aD^{1.6}$, varies in the coefficient by a tree class. The quantity of root system is distributed concentrically from the tree center and decreases for distance from tree exponentially.

Here I propose the two dimensional distribution map of the collapse prevention force with only the ground information of tree survey, breast height diameters and distribution of trees.

I performed an investigation that each in 3 Hinoki artificial plantation stand and 1 natural broadleaf forest, and made a two dimensional distribution map of the collapse prevention based on the tree positioning and the diameter of trees at breast-height. And I compared which I got by investigating every tree and compared the outcome of maps and the actual measurement that I dug a trench. As a result, the estimated values and the actual values did not exactly match, however a very meaningful relation was seen in both value within 1% of the risk ratio.

Furthermore, I applied this method and estimated a chronological order change of the collapse prevention force. Because the data required for estimating the ability of collapse prevention are only positioning of the trees and diameter measurement at trees breast-height, I can even estimate a change in the result after thinning, by using it in conjunction with the growth prediction by the density management curve.

Keywords: root system, collapse prevention forse, artificial plantation, natural forest, two dimensional distribution map

Japan Geoscience Union Meeting 2014
(28 April - 02 May 2014 at Pacifico YOKOHAMA, Kanagawa, Japan)

AHW07-10 Room:511 Time:April 29 11:51-12:06

The growth-collapse simulation method of soil depth in which the effect of vegetation was taken into consideration

KUROKAWA, Ushio[1*]

[1]Kyushu Research Center, FFPRI

The impact accompanying the transition of the watershed conditions in a forest appears under the structurally development process of a triplex in which time scales differ; geographical feature is formed by a tubercle and erosion of a mountain, the soil which supports and grows up in the root system of a vegetation repeats a collapse and a renature, the forest grows and withers. Without understanding this process, the runoff impact evaluation of watershed conditions cannot occur. We paid our attention to the collapse process in which a soil grows up again, after the soil was supported by the root of the forest, grew up and collapsed with progress of a temporal. And the development method of the longterm soil growth simulation was considered.

This method is computed for every mesh. The following routines perform the compute process of geomorphic development. First, the amount of growths of the soil stratum in the fixed period in each mesh is computed. The amount of developments of the soil depth used the equation of the following which Heimsath et al. (1999) proposed.

Soil Production(m/million year)=77×exp(-0.024×Soil Depth)

The soil depth after a fixed period is computed by applying to the initial soil depth of each mesh the value calculated by the equation. Slope stability is computed using the soil depth set up newly. It is considered by the equation that the mesh by which the safety factor was computed or less with one is that to which the collapse occurred. After setting the value of the soil depth in the mesh to 0, the altitude data after a collapse and a soil depth are re-calculated. A prolonged soil development simulation is computed by repeating the predetermined number of these processes. The simulation was computed at the place which many shallow landslides caused by heavy rainfall. The initial soil depth in the mesh which the collapse caused by the heavy rain was set to 0, and the mesh which has not collapsed was set to 1 m. And, the soil layer assumed the condition of being completely saturated by the heavy rain. In addition, the effective soil internal angle was 32 degrees, effective soil cohesion was 0.01 kPa, unit weight of the moist soil was 17.64 kN/m^3, and unit weight of water was 9.8 kN/m^3. The effect of the vegetation was included in the simulation as the cohesion.

As results of the simulation, It was confirmed that the soil layer which collapsed with progress of the temporal is recovered. Moreover, when a vegetation does not exist, the probability that a soil layer will repeat a collapse becomes high, but when a vegetation exists, a soil layer does not collapse but is recovered early.

Keywords: soil depth, geographical feature, vegetation, simulation method

Japan Geoscience Union Meeting 2014
(28 April - 02 May 2014 at Pacifico YOKOHAMA, Kanagawa, Japan)

AHW07-11 Room:511 Time:April 29 12:06-12:30

Limits of Soil Production and the Couplings with Hillslope Hydrology

HEIMSATH, Arjun[1*]

[1]School of Earth and Space Exploration, Arizona State University

Rocky mountain ranges are broken down to sediment that is ultimately removed to the sea. Tectonic forces continually push mountains up, while physical and chemical processes continually transform bedrock to sediment and move it down. This simple sounding cycle is thought to regulate global climate over long timescales, while also responding to climate forcing itself, although the causal direction remain a mystery despite decades of sleuthing. Similarly mysterious are the connections between mechanisms of sediment production and the responses of watersheds to changes driven by humans, climate, or tectonics.

To address some of the potential connections between sediment production and hillslope hydrology, I focus here on soil mantled and steeply sloped landscapes from around the world, some thought to be at a critical threshold of soil cover. Observations reveal that even in the most rapidly eroding landscape there are significant areas mantled with soil that fit the conceptual framework of a physically mobile layer derived from the underlying parent material with some locally-derived organic content. The extent and persistence of such soils depends on the long-term balance between soil production and erosion despite the perceived discrepancy between high erosion and low soil production rates. I present cosmogenic Be-10-derived soil production and erosion rates that show that soil production increases with catchment-averaged erosion, suggesting a feedback that enhances soil-cover persistence, even in threshold landscapes. I also show that a process transistion to landslide-dominated erosion results in thinner, patchier soils and rockier topography, but find that there is no sudden transition to bedrock landscapes. The landslide modeling is combined with a detailed quantification of bedrock exposure for these steep, mountainous landscapes.

To conclude, I draw an important conclusion connecting the physical processes producing and transporting soil and the chemical processes weathering the parent material by measuring parent material strength across three different field settings. Parent material strength is observed to increase with overlying soil thickness and, therefore, the weathered extent of the saprolite. Soil production rates, thus, decrease with increasing parent material competence. These observation highlight the importance of quantifying hillslope hydrologic processes where such multi-facted measurements are made.

Keywords: Soil erosion, Soil production, Critical Zone, Weathering, Hillslope hydrology, Saprolite

Japan Geoscience Union Meeting 2014
(28 April - 02 May 2014 at Pacifico YOKOHAMA, Kanagawa, Japan)

AHW07-12 Room:511 Time:April 29 12:30-12:45

Soil production functions and soil layer mobility in Japanese mountainous catchments underlain by granitoid rocks

MATSUSHI, Yuki[1*] ; MATSUZAKI, Hiroyuki[2]

[1]DPRI, Kyoto University, [2]MALT, The University of Tokyo

Soil-mantled hillslopes cover a major area of mountainous catchments in humid temperate regions. The soil layer on hillslopes is maintained by a balance between soil production and transport especially at hill noses, while the soil accumulated in hollows is eventually removed by a rainfall-induced shallow landslide. The rates of soil production and soil creep pace the growth of soil thickness at a hollow and thus determine the return period of landsliding. The soil layer buffers rainfall infiltration into hillslopes and hence controls subsurface runoff system in a catchment. Hydro-geomorphological evolution of a catchment results from the interaction between long-term soil layer development and short-term rainfall runoff processes. The quantification of soil dynamics on hillslopes is thus critical in understanding present-day hydrological condition of a catchment and for geomorphological landslide hazard mitigation.

The uppermost part of decomposed bedrock (saprolite) gradually disintegrates to form the mobile soil layer, which achieves to a steady-state thickness reflecting sediment budget at a soil column. The saprolite-to-soil conversion rate beneath a soil column decreases with increasing thickness of the soil layer, which is called as soil production function (SPF). Soil particles apart from the saprolite move downslope by soil creep at a rate controlled by slope gradient, biological activity and soil thickness. Evaluation of SPF as well as the soil layer mobility is essential when we simulate soil dynamics on a hillslope. SPF can be determined from concentration of terrestrial cosmogenic nuclides at uppermost part of saprolite, while soil layer mobility can be estimated by soil thickness survey by digging pits on a nose-hollow pair of hillslopes. We present examples of SPFs in Japanese mountainous catchment underlain by granitic rocks, and demonstrate results of simulation of soil development to map potential sites of shallow landslide and to assess volume of sediment that may yield at a catastrophic landslide event by heavy rainfall.

Keywords: soil production function, terrestrial cosmogenic nuclides, sediment transport, shallow landslide, landscape evolution

Japan Geoscience Union Meeting 2014
(28 April - 02 May 2014 at Pacifico YOKOHAMA, Kanagawa, Japan)

AHW07-13 Room:511 Time:April 29 14:15-14:30

Interrelation between hillslope soil moisture and stream flow in a Paleozoic sedimentary rock watershed

HOSODA, Ikuhiro[1*]

[1]Kansai Research Center, FFPRI

It is well known that geology is one of influential factors on river regime. In the Paleozoic sedimentary rocks area in Japan, hydrographs are characterized by low base flow and spiky peak flow. To clarify the reasons of such characteristics occur, observation focused on hillslope soil moisture condition was conducted in the gauged Tatsunokuchi-yama Minami-tani watershed (34 ^{o} 42 ' N, 133 ^{o} 58 ' E, 50-257 m, 23 ha) underlain by Paleozoic sedimentary rocks. The watershed is covered with primarily *Quercus serrata* dominant mixed forest, and partly *Chamaecyparis obtusa* stands planted in 1970s. Annual precipitation is about 1200 mm with little snowfall.

Ground water levels (GWL) and soil moisture were continuously measured in and around boreholes in a concave slope in the middle reach. Deeper than 0.3 m from ground surface, a thick fractured and weathered bed rock layer extends down to about 10 m at upper slope, and about 16 m at mid-slope. Below the weathered bed rock layer, boring core was relatively unweathered. But conspicuous cracks were obviously seemed to perform as water flow pathway because the surface of crack was dyed. Low coefficients of permeability which ranged from 2^{-8} to 1^{-6} m/s were measured by in situ test in the boreholes.

In the mid-slope, GWL appeared about 15 to 17.5 m in depth from ground surface when surface soil layer was more than field moisture capacity. Although GWL greatly respond to about over 40 mm rainfall events, direct flow rate did not simply increased. In a little antecedent rainfall condition, GWL rising was detected only at the lower slope. Depending on increase of antecedent rainfall, fluctuations of GWL at the mid-slope and the upper slope became obvious, and also direct flow rate went up. The greater amount of rainfall including antecedent rainfall was brought, the more GWL rising belated to stream flow peak observed. The greater intensity of rainfall leads quick rising of stream flow, but it was not effective for GWL rising. According to the stream water quality, rain water component increased when intense rain was brought, subsequently ground water component increased for the duration of rainfall event.

It is realized that water movement is having macroscopic interrelation in the space from upper slope to stream channel. Its complexity would be derived from large soil moisture change by rainfall amount and vegetation activity in the thick weathered bed rock layer in the hillslope as water flow pathways. And it is considered that since the permeability of subsoil is low, stream flow respond by spiky peak against intense rainfall.

Keywords: permeability, soil water pF, ground water, Seto inland sea climate, Tatsunokuchi-yama

Japan Geoscience Union Meeting 2014
(28 April - 02 May 2014 at Pacifico YOKOHAMA, Kanagawa, Japan)

AHW07-14 Room:511 Time:April 29 14:30-14:45

Variability of the chemistry of streamwater and bedrock groundwater at a weathered granite mountain, Japan

FUJIMOTO, Masamitsu[1*] ; KOSUGI, Ken'ichirou[2] ; MASAOKA, Naoya[2] ; BANBA, Naoki[1] ; UEDA, Ryuya[1] ; SAKAI, Yasuhiro[1] ; FUKAGAWA, Ryouichi[2] ; TANI, Makoto[1]

[1]Ritsumeikan University, [2]Kyoto University

Introduction

Previous studies have noted that bedrock groundwater is one of the important factors influencing stream discharge and streamwater chemistry. However, most previous studies were conducted not by direct measurement of bedrock groundwater but by using indirect methods, such as solute tracers and water budget analysis. Thus, the movement and chemical characteristics of bedrock groundwater remain incompletely understood based on direct measurements of bedrock groundwater. To better understand the dynamics of bedrock groundwater, we investigated groundwater table movement and water chemistry of bedrock groundwater using dense borehole wells at a small catchment in a mountainous area.

Methods

The study was performed at the Fudoji Experimental Watershed located in the Tanakami Mountains in the southeastern part of Shiga Prefecture, central Japan. Precipitation was monitored using tipping-bucket rain gauges, and discharges were observed at eight small catchments, ranging in area from 0.1 to 2.3 ha. Seven small catchments (subcatchments) were included in the largest catchment (2.3 ha), within which we installed 61 borehole wells. The water table of bedrock groundwater was then observed at these borehole wells. Rainwater, streamwater from the small catchments and bedrock groundwater from the borehole wells were sampled, and the concentrations of major ions and SiO_2 as well as the water stable-isotope ratios $d^{18}O$ and dD were measured in the Graduate School of Agriculture, Kyoto University.

Results and Discussion

The results of the analysis of the groundwater table of bedrock groundwater indicated that there were several fluctuating characteristics and that these characteristics of groundwater table change had locality. At the area having higher altitude in the ridge, the bedrock groundwater-table changes were gradual but the ranges of fluctuation were larger than those of the lower wells. At the lower-altitude points, although the bedrock groundwater table responded rapidly, the ranges of fluctuation of the groundwater table were small relative to those of the higher points. Some areas responded only to peak rainfall over a short time. Based on the groundwater flux analysis, bedrock groundwater moves across the surface divide. A catchment inflowed by a neighboring catchment showed a high specific discharge. Additionally, the direction of groundwater movement changed during rainfall events, and such changes were similar for rainfall events of the same size.

The relationships among chemistries derived from the chemical weathering of bedrock indicated that although the weathering processes were similar in the catchment, the weathering level varied among the borehole wells. The chemistries of bedrock groundwater at each catchment and of streamwater at each catchment showed large variability. The concentrations of Na^{+} and Ca^{2+} had local characteristics, but no clear characteristics were observed among other bedrock groundwater components. The chemical concentrations of bedrock groundwater were higher than those of streamwater. We chose borehole wells that may contribute directly to the stream based on the direction of groundwater movement by an analysis of groundwater flux and distance from the borehole wells, and noticed that there were also large gaps between the chemistries of streamwater and bedrock groundwater. These results indicate that complex processes of chemical dynamics occur in the weathered bedrock and from the weathered bedrock to the stream.

Keywords: weatherd bedrock, densely bore holes, chemical variability, bedrock groundwater

Japan Geoscience Union Meeting 2014
(28 April - 02 May 2014 at Pacifico YOKOHAMA, Kanagawa, Japan)

AHW07-15 Room:511 Time:April 29 14:45-15:00

Mean residence time and hydrochemistry of bedrock groundwater aquifer in a Granite mountain

KATSUYAMA, Masanori[1*] ; KOSUGI, Ken'ichiro[2] ; TANI, Makoto[2]

[1]Center for the Promotion of Interdisciplinary Education and Research, Kyoto University, [2]Graduate School of Agriculture, Kyoto University

Bedrock groundwater dynamics is one of the latest frontier of hillslope- and catchment hydrology. Although it relate to water resources as well as sediment disasters, only few studies have accessed directly with boreholes to bedrock groundwater aquifer because of, for example, high costs. In this context, tracer approach is effective to clarify the bedrock groundwater dynamics and water pathways within deeper layers of mountains. We have been keeping on monitoring of the chemical and isotopic compositions of bedrock groundwater and streamwater in Kiryu Experimental Watershed (KEW), Japan since 2003. We set up a nested observation system; a hillslope plot (AP, 0.024ha), a subcatchment (A catchment, 0.086ha), and whole of KEW (K catchment, 5.99ha), and monthly sampled the streamwater of K and A, the outflow from AP, which occurs as saturated throughflow on the soil-bedrock interface during rainstorms, and groundwater in the soil sediment. Moreover, we excavated the bedrock and installed some tension lysimeters at 0.1, 0.2, 0.4, and 0.8 m deep and boreholes at 12, 15, and 20 m deep below bedrock surface, and sampled them. The stream flow from K and A were perennial. The SiO2 and Na+ concentrations increased along with the infiltration process. On the other hand, the NO3- concentration was highest at the surface soil water, and removed along with the infiltration process. The concentrations of both solutes in the streamwater from A and K were intermediate between the concentrations in the surface soil water and bedrock groundwater. These facts mean that the streamwater is the mixture of shallow soil water and deep groundwater. The mean residence times calculated by delta 18O variations were about 4 or 5 months in the groundwater in the soil sediment and in the shallow (<0.8m) bedrock groundwaters, about 50 months in 12- and 15 m deep, and about 120 months in 20 m deep, respectively. That in the streamwater in A was estimated as about 30 months. Thus, the MRT in 20 m deep groundwater is quite different from the others. The relationship between the MRTs and the solute concentrations were different in each solute; for SiO2, the concentration increased as a saturation curve, and it increased as linearly for Na+. It exponentially decreased for NO3-. The streamwater chemistries in A were on these curves. Therefore, the solute concentrations can be described as functions of MRTs. These results suggest that a part of the bedrock groundwater can contribute to the stream from the shallower layers. The fact that the stream flow is perennial in this subcatchment A means that plentiful supply of groundwater from the relatively shallow bedrock layers exist. On the other hand, other part of the bedrock groundwater infiltrate deeply and less contribute to the stream in this small subcatchment; we have to consider whether the deeply infiltrated groundwater may contribute at the outlet of K catchment. Moreover, as the deeper bedrock groundwater have especially long residence time, we have to keep long-term monitoring to understand the dynamics and roles of this groundwater to hydrological and hydrochemical processes, because it will be a key of spatio-temporal scaling of these processes, as well as the water yield function of forests.

Keywords: Bedrock groundwater, Tracer, Mean residence time, granite catchment

Japan Geoscience Union Meeting 2014
(28 April - 02 May 2014 at Pacifico YOKOHAMA, Kanagawa, Japan)

AHW07-16 Room:511 Time:April 29 15:00-15:24

Hydrological change at the catchment scale: The need to address both velocity and celerity

MCDONNELL, Jeffrey[1*]

[1]Global Institute for Water Security, University of Saskatchewan CANADA

Water quantity and quality response to climate- and land use change are difficult to predict. Much of this relates to the complexities of water flow paths and our inability to relate measureable catchment properties to measureable hydrologic response metrics. To date, most work has focused on rainfall-runoff response — that is, the celerity component of change. Here I present new work from 15 headwater catchments, (0.1 to 100 km^2) in the Oregon Cascades and Oregon Coast Range in the USA, aimed at quantifying both celerity and flow velocities (i.e. particle transport through the system). I illustrate this velocity component through stable isotope analysis of runoff components and the mean transit time and residence time analysis of surface water and groundwater, respectively. Results show that despite very similar rainfall-runoff determined celerities, these systems have distinctly different tracer velocities, where transit time of headwater streamflow is 1-3 years in the catchments draining the Western Cascade mountains and 3-11 years in the streams draining the Coast Range mountains. More importantly, the scaling of surface water mean residence time in the Cascades is linked to internal topographic structure of individual sub-catchments whereas Coast Range sites show no evidence of this; and streamwater residence times scale linearly with catchment area. I discuss the implications of these celerity-velocity differences for catchment-scale climate- and landuse change effects in the USA Pacific Northwest and for more general efforts like the IAHS Panta Rhei initiative.

Keywords: Hillslope, Rainfall-runoff, Stable isotope, Climate change, Landuse, Groundwater

Japan Geoscience Union Meeting 2014
(28 April - 02 May 2014 at Pacifico YOKOHAMA, Kanagawa, Japan)

AHW07-17 Room:511 Time:April 29 15:24-15:39

Toward understanding causal interrelationships between stormflow and erosion processes in a steep zero-order basin

TANI, Makoto[1*]

[1]Graduate School of Agriculture, Kyoto University

Stormflow generation and soil-erosion process on a steep zero-order basin have close interdependencies though their timescales are far different. This study pays attention to a difference in interdependences of stormflow and erosion processes between a near-ridge nose and a concave hollow within a zero-order basin.

Due to strong erosional forces in an active tectonic region, soil moves down by the gravity force throughout the basin. In a convex nose near the ridgeline, soil moves gradually by diffusive processes, and the curvature of bedrock surface controls the soil depth (Heimsath, Geomorphology 27, 1999). On the other hand, in a concave hollow, soil layer suddenly collapses as a landslide and a long-term soil-layer evolution at a timescale of 10^2 - 10^4 years continues unless a landslide occurs (Tsukamoto et al., IAHS Publ. 137, 1982). In the nose, the soil layer may move downslope with vegetation on it without disturbances. The recovery of soil layer after a landslide occurrence in a hollow is supported by the soil supply from the nose by the diffusive movement. The diffusive process near nose and the recovery process near hollow are closely related each other.

In order to ensure these processes, saturation excess overland flow should be suppressed both in a nose and a hollow because it is a trigger of landslide initiation. We can assume that the drainage capacity through pipe-like preferential paths (McDonnell, Water Resour. Res. 26, 1990) plays an important role in the suppression.

One hydrological analysis for addressing the assumption is attempted from estimating the expansion of stormflow contribution areas from rainfall-runoff responses in a small catchment. In the wet conditions when most of all the rainfall contributes to the stormflow, a hydraulic continuum under a quasi steady state is created and a single tank model can well simulate rainfall-runoff responses (Tani: Hydrol. Earth Syst. Sci., 17, 2013). This simple characteristic was utilized to estimate the contribution-area expansion with rainfall increases inversely from the runoff responses.

Results show that except a short dry period at the beginning of a storm, the waveform transmission of rainfall to runoff was simulated well by the same model parameters of our tank model though the contribution area only increased. This result suggests the waveform transmission was originated mainly from the vertical water movement instead of the downslope subsurface flow or the overland flow. As suggested from a conceptualized model (Montgomery and Dietrich, Water Resour. Res. 38, 2002), rainwater may be confined within the soil layer due to a large drainage capacity of the pipe-like preferential paths. This strongly encourages the soil-layer evolution process against strong erosional forces not only in a nose but also in a hollow.

Runoff and erosional processes are certainly linked, and collecting field evidences is expected. In addition, however, reanalyzing the existing hydrological data may also provide a new interesting finding from the linking point of view.

Keywords: erosion, hillslope hydrology, soil-layer evolution, stormflow, variable contribution area, zero-order basin

Japan Geoscience Union Meeting 2014
(28 April - 02 May 2014 at Pacifico YOKOHAMA, Kanagawa, Japan)

AHW07-18 Room:511 Time:April 29 15:39-16:00

Interaction between bedrock groundwater and surface-hydrological and geomorphological processes in mountainous headwater

KOSUGI, Ken'ichirou[1*] ; FUJIMOTO, Masamitsu[2] ; YAMAKAWA, Yosuke[3] ; MASAOKA, Naoya[1] ; ITOKAZU, Tetsushi[1]

[1]Kyoto Univ., [2]Ritsumeikan Univ., [3]Tsukuba Univ.

Enormous landslides with deep slipping surfaces, which are likely to be triggered by the huge storms expected with climate change, can be one of the major geomorphological processes in the temperate climate zone. This study focuses on groundwater in mountainous headwater regions as a potential cause of such landslides. Recent hydrological studies have revealed that large amounts of rainwater infiltrate into bedrock, suggesting the possibility that steep mountains could contain greater amounts of groundwater than previously thought. The decline in groundwater levels due to water harvesting should be effective for the prevention of landslides. At the same time, the exploitation of groundwater resources in mountainous regions may contribute to establish a sustainable supply of safe water; that is, groundwater in mountainous regions is of better quality and less vulnerable to pollution because human activities are limited in the source areas. Thus, the exploitation of groundwater resources in mountainous regions should produce a win?win situation that achieves both disaster mitigation and a sustainable water supply. This study investigates hydrological methods for observing and analyzing quantitative and qualitative signals in mountain streams that can be used for detecting groundwater dynamics in steep mountains. Such hydrological methods are effectively combined with geophysical surveys.

In the steep Rokko mountain range of central Japan, which consists of granite and has been greatly affected by diastrophic activities, discharge hydrographs are characterized by significant amount of baseflow. In order to elucidate contributions of bedrock groundwater to the hydrograph formation, long-term hydrological observations were conducted by using bedrock wells with depths of 7-78 m drilled at 31 points within a 2.1-ha headwater catchment in the Rokko mountain range. Results indicated a fairly regionalized distribution of bedrock groundwater; that is, upper, middle, and lower aquifers were present. We observed large differences in water level among the aquifers, instead of a gradual and continuous decline in water level. Discharge hydrograph from the catchment was notably characterized by gentle and significant variations in base flow and exhibited triple-peak responses. Flashy first peaks occurred just after rainfall peaks, while the second peaks lagged behind the rainfall peaks by a few days. Broad peaks in the base-flow discharge corresponded to the third peaks, which occurred once or twice in each hydrological year. The triple-peak discharge responses were explained by three types of water pathways: the first peak was caused by the peak in soil mantle groundwater around the outlet of the watershed; the second peak was caused by the first peak in the lower aquifer, which was fed by vertical rainwater infiltration; and the third peak was caused by the second peak in the lower aquifer, resulting from an increased lateral water supply from the middle aquifer. The middle aquifer was recharged by vertical infiltration through weathered bedrock and lateral flow from the upper aquifer. Because of its broad regional expanse and large capacity, the middle aquifer had a dominant effect on formation of the discharge hydrograph. Thus, this study has demonstrated how discharge from the steep headwater catchment is dominated by complex flow systems within bedrock groundwater; the spatial expanse of bedrock aquifers and interaction among aquifers are key factors.

Keywords: enormous landslide, geomorphological processes, headwater catchment, bedrock groundwater, water resources

Japan Geoscience Union Meeting 2014
(28 April - 02 May 2014 at Pacifico YOKOHAMA, Kanagawa, Japan)

AHW07-P01 Room:Poster Time:April 29 18:15-19:30

Evaluation of transpiration in a mature stand of Japanese cedar in Kanto region, Japan

IIDA, Shin'ichi[1*] ; SHIMIZU, Takanori[1] ; TAMAI, Koji[1]

[1]Department of Soil and Water Conservation, Forestry and Forest Products Research Institute

Forests cover about 70% of land area of Japan, and Japanese cedar (*Cryptomeria japonica*) occupies about 20% of total forested area. To understand the hydrologic cycle in Japan, we need measurements conducted in forested area, especially for the most representative species of Japanese cedar. Recently, the water balance of a stand of Japanese cedar has been made clear quantitatively by using eddy-covariance method and sap flow technique in Kyushu Island, south-western part of Japan (Kumagai et al., 2014; Shimizu et al., submitted). However, although Japanese cedar is most representative species in Japan, very few studies have been carried out in other part of the country. Based on the sap flow technique, we started to evaluate the amount of transpiration of a stand of Japanese cedar located in Kanto region, in the central part of Japan. In this paper, we show the relationship between outermost sap flow (Q_{0-20}) and single-tree transpiration (Q), tree-size parameter affecting Q, and correlation between stand transpiration (TR) and meteorological factors.

We conducted measurements in a mature stand of Japanese cedar, whose age is 61, within Tsukuba Experimental Watershed located in southern part of Mt. Tsukuba, Japan. Tree density is 1115 trees/ha, and annual mean leaf area index measured with LAI-2000 (LI-COR, USA) is 3.6. We set an observation plot in a Japanese cedar stand, and measured sap flux densities for all trees of the plot, 13 trees, with Granier method (Granier, 1985). Based on the wood core sampling with an increment borer, we determined the width of sapwood for 13 trees. Japanese cedar has white zone, in which water movement stops, in the sapwood area. We injected acid fuchsin into stem, and distinguished colored area as sapwood. The length of Granier sensor was 20 mm: in case that the width of sapwood was more than 20 mm, additional sensors were inserted into the sapwood at the depths from 20 to 40 mm and 40 to 60 mm. The sap flow at each depth is calculated as the product between the sapwood area corresponding to the depth and measured sap flux density. Q is finally obtained as total sum of sap flow of all depths. We calculated TR as the sum of Q of 13 trees divided by the area of the plot. On the meteorological tower, air temperature, humidity and net radiation were measured. Analyses are performed in the period from August to November, 2013.

The value of $Q/(Q_{0-20})$ had positive linear relationship with canopy projection area unshaded by other trees (CPA_{TH}). This trend implied that the contribution of Q_{0-20} to Q is small for trees having good light condition. Q had positive linear correlation with diameter at breast height (R^2=0.62), however, the higher correlation (R^2=0.70) was found between Q and CPA_{TH}. In this stand, CPA_{TH} is probably important factor affecting distribution of sap flow within the stem and tree-to-tree difference in Q. On the other hand, through the analysis period, TR had high positive correlation with equilibrium evaporation (R^2=0.83), but had lower correlation (R^2=0.39) with vapor pressure deficit (D). Focused on the summer period from August to September, we found higher correlation between TR and D (R^2=0.74). Thus, in summer, the driving energy of transpiration is mainly D due to the large aerodynamic conductance at the stand. However, the correlation between TR and D became small in the autumn. This stand is located in the north-facing slope, and has very high contrast in meteorological condition between summer and autumn. The different relationship between TR and D probably implies that plant physiological response of Japanese cedar in summer is different from that in autumn.

Cited paper
Granier 1985. Ann. Sci. For. 42: 193-200.
Kumagai et al. 2014. J. Hydrol. 508: 66-76.
Shimizu et al. Submitted for publication.

Keywords: Japanese cedar, sap flow, transpiration, tree-size parameter, vapor pressure deficit

Japan Geoscience Union Meeting 2014
(28 April - 02 May 2014 at Pacifico YOKOHAMA, Kanagawa, Japan)

AHW07-P02 Room:Poster Time:April 29 18:15-19:30

SURFACE RUNOFF ESTIMATION BASED ON TOTAL RAINFALL-TOTAL LOSS RAINFALL RELATIONSHIP FOR CATCHMENTS IN ISHIKARI RIVER

SUPRABA, Intan[1*] ; YAMADA, Tomohito J.[2]

[1]Member of JSCE, M.Sc., Doctoral Student, Graduate School of Engineering, Hokkaido University, [2]2Member of JSCE, PhD., Associate Professor, Faculty of Engineering, Hokkaido University

One of the main objectives of research in hydrology is to improve the accuracy of surface runoff estimation for enhancing flood prediction. Rain water falling to the ground surface will infiltrate into the soil and the excess rainfall will be surface runoff. The infiltrated water is defined as loss rainfall and loss rainfall is subtracted from total rainfall (actual rainfall intensity) to obtain the surface runoff (excess rainfall intensity). The non-linearity of surface runoff phenomena in the mountainous basins based on universal lumped kinematic wave model has been studied. Current study about total rainfall-total loss rainfall relationship by using tanh fitting curve has been conducted for 65 catchments located in 27 prefectures in Japan. Hourly rainfall and hourly runoff observation data for 10 years during summer time is used as required input data. Runoff parameters in the tanh function represented by *a* and *b* parameters are utilized to estimate effective rainfall based on water holding capacity theory. The purpose of this study is to estimate surface runoff by using effective rainfall for semi-ungauged river basins at the upper catchments area in Ishikari River Basin, Hokkaido Island, Japan. The obtained results are compared to the observation data for validation purpose.

Keywords: Surface Runoff, Flood Prediction, Total Rainfall-Total Loss Rainfall, Water Holding Capacity Theory

Japan Geoscience Union Meeting 2014
(28 April - 02 May 2014 at Pacifico YOKOHAMA, Kanagawa, Japan)

AHW07-P03 Room:Poster Time:April 29 18:15-19:30

Integrate simulated annealing algorithm and WASH123D to develop an automatic identification system for Chuoshui River in

CHANG, Ya-chi[1*] ; WANG, Yu-chi[1] ; CHEN, Cheng-hsin[2]

[1]Associate Researcher, Taiwan Typhoon and Flood Research Institute, NARL, Taiwan, [2]Assistant Researcher, Taiwan Typhoon and Flood Research Institute, NARL, Taiwan

Taiwan is located in the subtropical areas and often suffers from typhoons and heavy rains. In order to reduce the threat caused by typhoon, it is necessary to accurately estimate the water level of a river for flood disaster prevention and mitigation. Hydraulic analysis of a river is important in river management planning and engineering design. The identification of hydraulic parameter has huge impact on the water level estimation of a river during the hydraulic analysis. Manning ′ s roughness coefficient is usually used to describe a river ′ s surface roughness and sinuosity in hydraulic modeling. This coefficient is usually determined empirically in the past, which is tedious and time-consuming. Therefore, the optimization algorithms become an effective tool for engineers to select the Manning ′ s roughness coefficient.

The concept of simulated annealing algorithm (SA) is based on an analogy to crystallization process of the physical annealing from a high temperature state. Since SA has the Metropolis mechanism to escape local optimum trap, it has been applied to various types of optimization problems. In addition, the hydraulic model plays a crucial role for flood simulation and the WASH123D, an integrated multi-media, multi-processes and physics-based computational model suitable for various spatial-temporal scale, is selected in this study to simulate the water level. The purpose of this study is to integrate SA and WASH123D to develop a system for automatically identifying the optimal Manning ′ s roughness coefficients of the reach according to the given upstream and downstream boundary conditions of the river. Firstly, the cross sections and related hydrological data of the river are collected for flood hydrograph simulation in WASH123D and make sure the model can be executed for the reasonable range of the Manning ′ s roughness coefficient. Then, the system incorporates SA with WASH123D to identify the optimal Manning ′ s roughness coefficient according to the objective function for minimizing the difference between observed and simulated water level. The system is applied to the Chuoshui River in Taiwan. Flood in two typhoon events is simulated and the flood hydrograph is analyzed in this study to find the optimal Manning ′ s roughness coefficient. Results demonstrate that the system proposed in this study has feasibility to automatically identify the Manning ′ s coefficient.

Keywords: Simulated annealing algorithm, WASH123D, Manning's roughness coefficient, Automatic identification system

Japan Geoscience Union Meeting 2014
(28 April - 02 May 2014 at Pacifico YOKOHAMA, Kanagawa, Japan)

AHW07-P04 Room:Poster Time:April 29 18:15-19:30

Groundwater levels and qualities in megacities of Korea

YUN, Sang woong[1*] ; JEON, Woo-hyun[1] ; LEE, Jin-yong[1]

[1]Department of Geology, Kangwon National University, Republic of Korea

This study was conducted to evaluate the groundwater levels and groundwater qualities in six metropolitan cities (Seoul, Busan, Daegu, Incheon, Daejeon and Ulsan) of Korea. For this purpose, we collected the groundwater level data of 2001-2011 from the Korean National Groundwater Monitoring Stations in the cities and semi-annual groundwater quality data analyzed by the Korean Ministry of Environment for the same period. Using these collected data, we analyzed the change in the water levels in and outskirt of the cities and in groundwater qualities in the cities. The groundwater levels in the outskirt were generally higher (0.84-15.66 m bgs), compared with those in the central part of the city (3.89-75.16 m bgs), and well responded with the seasonal rainfall (higher in the summer but lower in the winter). However, the groundwater levels in the central part of the city were largely affected by pavement, deep underground building such as subway, and artificial pumping, not by the seasonal effect. The six metropolitan cities showed ranges of 0-507 mg/L and 0-22,000 mg/L for NO_3-N and coliform, respectively. In addition, groundwater contamination with TCE (0.00-4.50 mg/L), PCE (0.00-0.48 mg/L) and 1.1.1 TCA (0.00-0.11 mg/L) was also found. The groundwater contamination with these contaminants was relatively severe especially in Seoul and Busan, which may be attributed to their high densities of populations and industrial facilities. This research was supported by Basic Science Research Program through the National Research Foundation of Korea (NRF) funded by the Ministry of Education (NRF-2011-0007232).

Keywords: groundwater levels, qualities, metropolitan cities, contaminants, Korea

Japan Geoscience Union Meeting 2014
(28 April - 02 May 2014 at Pacifico YOKOHAMA, Kanagawa, Japan)

AHW07-P05 Room:Poster Time:April 29 18:15-19:30

Variation in groundwater-stream water interaction with season: focus on water level, temperature and chemistry

JEON, Woo-hyun[1*] ; YUN, Sang woong[1] ; LEE, Jin-yong[1]

[1]Department of Geology, Kangwon National University, Republic of Korea

This study was conducted to reveal seasonal variations of the groundwater and stream water interaction in Gangwon province of Korea using analyses of measured water levels, water temperature and water chemistry from August to November of 2013. For measuring the water levels in the hyporheic zone, four piezometers (IYGW-1˜4) were installed at depths of 0.830˜1.565 m below stream bed, perpendicular to stream flow direction and the stream level was also measured at IYSW-1. The water level and water temperature were measured every hour using an automatic logger (DIVER). In addition, nearby groundwater, hyporheic water and stream water were collected for ion and stable isotope analyses in the wet (September) and dry seasons (November) along with field measurements of pH, EC, DO and ORP. The water levels of the piezometers generally increased with rainfall, and they were lower than the stream water level in September, indicating a losing stream, but the former was higher than the latter in November, indicating a gaining stream. The reversal of the heads occurred at October 10. The stream water temperature (IYSW-1), directly affected by the surrounding air, was between 0.9˜22.9 ℃ with a large fluctuation. However, the hyporheic water (IYGW-4; 1.565 m depth) showed a small range of 13.2˜17.8 ℃. The water temperature at IYGW-4 was lower than those of the other piezometers but the reversal of the water temperatures also occurred at October, like the water levels. The groundwater, hyporheic water and stream waters were all classified as Ca-HCO_3 type by Piper diagram, which is indicative of effect of ambient air. The EC of IYGW-4 was the highest (136.7 μS/cm), indicating relatively higher influence of the groundwater. This research was supported by Basic Science Research Program through the National Research Foundation of Korea (NRF) funded by the Ministry of Education (NRF-2011-0007232).

Keywords: hyporheic zone, interaction, groundwater, piezometer, Korea

Japan Geoscience Union Meeting 2014
(28 April - 02 May 2014 at Pacifico YOKOHAMA, Kanagawa, Japan)

AHW07-P06 Room:Poster Time:April 29 18:15-19:30

Change of groundwater condition by operation of geothermal heat pump

PARK, Youngyun[1] ; MOK, Jong-koo[2] ; PARK, Yu-chul[2] ; LEE, Jin-yong[1*]

[1]Department of Geology, Kangwon National University, Republic of Korea, [2]Department of Geophysics, Kangwon National University, Republic of Korea

This study was conducted to evaluate the influence of open loop geothermal cooling and heating system (OLGCHS) and closed loop geothermal cooling and heating system (CLGCHS) on temperature and water level of local groundwater. For this study, groundwater temperature and level were measured daily using level logger at two sites where OLGCHS and CLGCHS are installed for approximately 30 months. In OLGCHS, fluctuation of groundwater temperature was similar to seasonal variation of ambient air temperature. However, this is not attributed to influence of air temperature. The groundwater temperature was fluctuated according the load of OLGCHS. The groundwater temperature was largely changed by operation of OLGCHS in summer compared to those in winter. These results represent that load of OLGCHS in summer is larger than that in winter. The groundwater levels were mainly controlled by precipitation and were slightly influenced by operation of OLGCHS. In CLGCHS, the groundwater temperature and level did not affected by operation of CLGCHS. The groundwater temperature was changed with 3^{o}C. The groundwater level was mainly influenced by precipitation because groundwater is not used directly in CLGCHS. In addition, response of groundwater level for precipitation was slower than those at OLGCHS because of difference of hydraulic conductivity. These results show that groundwater temperature and level did not significantly changed by OLGCHS and CLGCHS. However, it is necessary that long-term monitoring of groundwater temperature and level at sites, where OLGCHS and CLGCHS are installed, because OLGCHS and CLGCHS can affect the hydrological properties of aquifer with scale and type of use of geothermal energy. This work is supported by the Energy Efficiency and Resources of the Korea Institute of Energy Technology Evaluation and Planning (KETEP) grant funded by the Korea government Ministry of Knowledge Economy (No.20123040110010) and by the Korean Ministry of Environment under ”The GAIA project (No. 171-101-011)”.

Keywords: open loop geothermal cooling and heating system, closed loop geothermal cooling and heating system, time series analysis, groundwater level, groundwater temperature, Korea

Japan Geoscience Union Meeting 2014
(28 April - 02 May 2014 at Pacifico YOKOHAMA, Kanagawa, Japan)

AHW07-P07 Room:Poster Time:April 29 18:15-19:30

Impact of ground source heat pumps operation on groundwater condition

KIM, Namju[1*] ; PARK, Youngyun[1] ; JEON, Woo-hyun[1] ; YUN, Sang woong[1] ; LEE, Jin-yong[1]

[1]1Department of Geology, Kangwon National University, Republic of Korea, [2]Geo Engineering Co. Ltd

This study was conducted to summarize status of installation of open loop geothermal cooling and heating system (OLGCHS) and to evaluate impact caused by its operation on groundwater condition. In this study, six facilities where OLGCHS is installed were considered. Groundwater is directly used in OLGCHS. The facilities considered in this study have been operated over two years. Groundwater temperature ranged from 6.0 to 24.2oC. Water temperature of natural groundwater and groundwater used to operating of OLGCHS showed difference of 5 to 9oC. pH and EC ranged from 7.5 to 9.1 and from 138 to 465 uS/cm, respectively. pH and EC of natural groundwater and groundwater used to operating of OLGCHS did not show significant difference. All groundwater meet Korean standard of water quality for domestic purpose In addition, saturation indexes of most major dissolved components except H4SiO4 showed lower than 1. These results represent undersaturated condition and that there are no minerals which can be precipitated from groundwater used in OLGCHS. Consequently, impact of ground source heat pumps operation on groundwater condition do not observed. However, these monitoring have been conducted continuously because contamination by ground source heat pumps operation can occur in any time. This work is supported by the Energy Efficiency and Resources of the Korea Institute of Energy Technology Evaluation and Planning (KETEP) grant funded by the Korea government Ministry of Knowledge Economy (No.20123040110010).

Keywords: Heat pump, groundwater, ground source

Japan Geoscience Union Meeting 2014
(28 April - 02 May 2014 at Pacifico YOKOHAMA, Kanagawa, Japan)

AHW07-P08 Room:Poster Time:April 29 18:15-19:30

Change of the stream discharge process affected by the rainstorm magnitude in the small headwater catchment

KUDO, Keishi[1*] ; SHIMADA, Jun[1] ; TANAKA, Nobuhiro[2]

[1]Kumamoto University, [2]Kumamoto prefecture office

Recently, because rainstorm characteristics such as total and peak rainfall is increasing along with global warming, a lot of disaster as flood and landslide has been occurring in many areas worldwide. This change might engender changes in the water resource of a particular area. Therefore, this study was conducted for the two component hydrograph separation using EC value during rainstorm event between July 2012 and November 2013 in two small adjacent forest and grassland catchments at the headwaters of the western foot of Mt. Aso, Kumamoto prefecture, southwestern Japan, aims to understand the relationship between the groundwater discharge ratio and rainstorm magnitude. EC values of the stream water were recorded at 10-min interval at each Parshall flume using EC logger. We compared our results and data which we summarized, with published literature (Onda et al.,2006; Ichiyanagi and Kato, 1998; Ichiyanagi et al.,1994; Iwagami et al.,2010; Ohrui et al.,1992; Katsuyama et al.,2000; Katsuyama et al.,2001).

We observed 18 rainstorm events of varied magnitude in which total rainfall range from 9 mm to 727 mm and peak rainfall range from 5 mm/h to 94 mm/h. As a result, we reaffirmed that the groundwater discharge ratio decreased due to increase total rainfall and peak rainfall for small rainstorm event where total and peak rainfall were less than 200 mm and 20 mm/h respectively, and agreed with previous studies. The total discharge also increased in conjunction with an increase of ”new water” component. However; increasing of groundwater discharge ratio was observed for large rainstorm event where total and peak rainfall were larger than 200 mm and 20 mm/h, respectively. In this case, the total discharge increased in conjunction with an increase of ”old water” component. Therefore, we found that the rainstorm magnitude has an impact on the formation of the peak stream discharge during rainstorm. The peak stream discharge phenomena from catchment can be classified into two stages based on previous literature and our present studies. In the first stage, stream discharge is dominated by the old water before rainstorm, but the old water component of stream discharge decrease gradually with an increase of rainstorm magnitude. As the total rainfall reach 200 mm, most of stream discharge is dominated by the new water. Under larger rainstorm events, additional stream discharge increased in conjunction with an increase of ”old water” component (the second stage).

Keywords: Two component hydrograph separation, Stream discharge process, Rainstorm magnitude, Groundwater discharge

Japan Geoscience Union Meeting 2014
(28 April - 02 May 2014 at Pacifico YOKOHAMA, Kanagawa, Japan)

AHW07-P09 Room:Poster Time:April 29 18:15-19:30

General discussion on insight into change and evolution in hydrology

TANI, Makoto[1*]

[1]Graduate School of Agriculture, Kyoto University

Fluctuations in the water and chemical cycles icluding floods, droughts, and water-quality impacts are influeced by long-term changes and/or evolutions in catchment properties and climate conditions. For example, to predict stormflow responses only from the cachment topography is difficult because the runoff mechanism is strongly controlled by bedrock-weathering and soil-evolution processes.

Such a concept of change and evolution is raised by IAHS, called 'Panta Rhei,' as its decadal intiaitive from 2013 following PUB (Predictions in ungauges basins), and the international disscussions have started.

In paralle with this activity, we are now conducting a project on dependences of rainfall-runoff responses on a temporally-nested structure of topographic, soil, and vegetation developments under the JSPS budget from 2011 to 2015.

In this session, presentaions addressing effects of natural changes and their interactions on the water and chemical cycles are encouraged, and chaneges originated from human influences including the disturbances and managements are also welcomed.

Keywords: general discussion

Japan Geoscience Union Meeting 2014
(28 April - 02 May 2014 at Pacifico YOKOHAMA, Kanagawa, Japan)

AHW25-01 Room:414 Time:May 2 09:00-09:15

Radon Concentration around Tachikawa Active Fault

TSUNOMORI, Fumiaki[1*]

[1]Graduate School of Science, University of Tokyo

Characteristics of a radon concentration distribution around the Tachikawa active fault will be focused in this report.

According to the Headquarters for Earthquake Research Promotion, occurrence potentials of earthquake in active faults in Japan were updated after the Tohoku Earthquake (March 11, 2011). The report denotes the potential of the Tachikawa active fault while next 30 years was increased from 0.5-2% to 0.9-2%. In order to monitor a state change of the fault system by groundwater analysis, we have been surveying water qualities of spring water and hot-spring water.

Our survey of shallow spring waters around the fault in 2012 revealed that the radon concentration of shallow groundwater was affected by a cultivation process of groundwater on the ground surface around the northwest area of the Tama district. Therefore the shallow groundwater around the fault is not appropriate to get information on the state change of the fault. Our survey of deep hot-spring water around the fault in 2013 indicated the good relation between the radon concentration distribution and the location of the fault. The nearer the location of the hot-springs to the fault is, the higher the radon concentration becomes. Therefore the deep groundwater around the fault is useful to monitor the state change of the fault.

Keywords: Grounwater, Hot Spring, Radon, Active Fault

Japan Geoscience Union Meeting 2014
(28 April - 02 May 2014 at Pacifico YOKOHAMA, Kanagawa, Japan)

AHW25-02 Room:414 Time:May 2 09:15-09:30

Reconstruction of summer precipitation during last two millennia in central Japan by tree-ring oxygen isotope ratios

NAKATSUKA, Takeshi[1*] ; SANO, Masaki[1] ; XU, Chenxi[1] ; OHISHI, Kyohei[2] ; SAKAMOTO, Minoru[3] ; NAKAO, Nanae[4] ; YOKOYAMA, Misao[5] ; HIGAMI, Noboru[6] ; MITSUTANI, Takumi[7]

[1]Research Institute for Humanity and Nature, [2]Grad. Sch. Env. Studies, Nagoya Univ., [3]National Museum of Japanese History, [4]Musashi University, [5]Grad. Sch. Agriculture, Kyoto Univ., [6]Aichi Pref. Center for Archaeol. Operations, [7]Nara Nat. Res. Inst. Cultural Properties

Introduction

To establish long-term plans of flood control by river management and/or water supply by dam construction, it is necessary to predict future change in precipitation due to global warming. Because precipitation can change at various time scales, it is important to understand the statistical probability of giant flood occurring once a century or millennium. However, due to the shortage of hydrological and meteorological records, it has been difficult to understand statistical characteristics of precipitation in very long time scales. Recently, we have found that tree-ring cellulose oxygen isotope ratios (d18O) record summer precipitation in the corresponding years very precisely and started reconstructions of long term summer precipitation changes in annual time resolution all over Asia monsoon area. Here, we present the two millennial data of summer precipitation in central Japan based on the tree-ring d18O of Hinoki cypress samples obtained from various periods and discuss its meanings in historical hydrology.

Fundamental of precipitation reconstruction

Because cellulose is produced from carbohydrate originally photosynthesized in leaf, its d18O records changes in leaf water d18O. Leaf water d18O is controlled by two meteorological factors, precipitation d18O and relative humidity. It is positively correlated with precipitation d18O and negatively correlated with relative humidity due to the transpiration process. Because there are negative correlation between rain amount and precipitation d18O (amount effect) and positive correlation between rain amount and relative humidity, we can finally realize that there is distinct negative correlation between rain amount in growing season and tree-ring cellulose d18O.

Tree ring samples for long d18O time series

Because trees can seldom live more than several hundred years, we must collect many tree-ring samples during various periods to establish reliable time series of tree-ring d18O beyond last two millennia, not only from living trees, but also from old architectures, archaeological remains, tree logs buried by landslides and so on. Tree-ring samples of Japanese cypress were collected from a certain wide area in central Japan, where we can find consistent tree-ring d18O variations among different trees at different sites and combine many d18O time series, according to the consistent d18O patterns, to establish statistically reliable two millennia length of tree-ring d18O time series.

Application to historical hydrology

The time series of tree-ring d18O was first compared with various meteorological, historical and archaeological evidences on summer precipitation in Japanese history, including modern instrumental meteorological records, summer rainfall amounts quantitatively reconstructed from early modern diary weather notes, medieval documentary records on notorious flood and drought, and pit-house number in lowland plains of ancient Japan, and it was demonstrated that the tree-ring d18O coincides those records very well and successfully reconstruct past change in summer precipitation irrespective of reconstructed periods. However, the tree-ring d18O of Japanese cypress has a distinct age effect where it decreases gradually during its all life time, so that we cannot extract real precipitation trends more than 200 years periodicity from the cypress data. By comparing the tree-ring d18O time series with historical flood records in various rivers in central Japan, we found that there are very good coincidences in decadal time scale before 11th century, but the relation becomes diverse in 18th century, so that good coincidence disappeared in highly developed area where artificial flood control and/or excess logging might have influenced river hydrology. The summer precipitation records based on tree-ring d18O are useful to elucidate both of natural variability and human responses on the historical precipitation changes.

Keywords: two millennia, precipitation, central Japan, tree ring d18O

Japan Geoscience Union Meeting 2014
(28 April - 02 May 2014 at Pacifico YOKOHAMA, Kanagawa, Japan)

AHW25-03 Room:414 Time:May 2 09:30-09:45

Water vapor origins in all over Japan in winter simulated by the regional isotope circulation model

TANOUE, Masahiro[1*] ; ICHIYANAGI, Kimpei[1] ; YOSHIMURA, Kei[2] ; SHIMADA, Jun[1]

[1]Graduate School of Science and Technology, Kumamoto University, [2]Atmosphere and Sea Research Institute and Institute of Industrial Science, University of Tokyo

In this paper, water vapor origins in all over Japan in winter were simulated by using a regional isotope circulation model with stable isotopes in water (δ^{18}O and δD). Precipitation and stable isotopes were simulated for the period between December to February in 2001 — 2010, spatial distributions of them were reproduced observations well. Simulated daily sea-level pressure patterns were divided into two types: winter monsoon (WM) type and extratropical cyclone (EC) type. In the WM type, precipitation rate was high and low along the Japan Sea side and the Pacific Ocean side, respectively. Spatial distribution of δ^{18}O in precipitation was recognized the latitude effect (values decrease with increasing latitude) on the Pacific Ocean and the Japan Sea. Spatial distributions of d-excess (=δD-8$\times\delta^{18}$O) in precipitation and evaporation were above 16 ‰ around Japan, those were extreme high (above 22 ‰) especially on the Pacific Ocean and the Japan Sea. Simulated water vapor evaporated from the Japan Sea was predominant in all over Japan in the WM type without southwestern islands of Japan. Interestingly, a portion of this moisture moved eastward to the Pacific Ocean, however, the moisture was not contributed to total amount of precipitation along the Pacific Ocean side because it was little precipitation. In contrast, precipitation rate was high in all over Japan in the EC type. Spatial distribution of δ^{18}O in precipitation was recognized the latitude effect on the Pacific Ocean and the Japan Sea and the amount effect (values decrease with increasing precipitation amount) across Japan. Spatial distributions of d-excess in precipitation and evaporation were below 14 ‰ around Japan without the western part of the East China Sea. Simulated water vapor evaporated from the Pacific Ocean was predominant in all over Japan. Comparing δ^{18}O and d-excess in precipitation between the WM type and the EC type, those were 2 ‰ and 8 ‰ higher along the Japan Sea side in the WM type than in the EC type, respectively.

Keywords: stable isotopes in precipitation, water vapor origins, regional isotope circulation model, in all over Japan

Japan Geoscience Union Meeting 2014
(28 April - 02 May 2014 at Pacifico YOKOHAMA, Kanagawa, Japan)

AHW25-04 Room:414 Time:May 2 09:45-10:00

Preliminary results of the stable isotopes in precipitation throughout Japan observed in 2013

ICHIYANAGI, Kimpei[1*] ; TANOUE, Masahiro[2]

[1]Isotope Mapping Working Group, JAHS, [2]Kumamoto University

Stable isotopes in precipitation are used for a proxy of climate change, which is related with temperature or precipitation amount. By using the atmospheric general circulation model with stable isotopes in water, water vapor origins (where the water vapor evaporated from?) can be estimated to determine the air mass transportation process. There are a lot of studies to observe stable isotopes in precipitation at only one or a few places in Japan. Tanoue et al. (2013) revealed seasonal variation and spatial distribution of stable isotopes in precipitation over Japan from the previous observational data at about 50 stations. However, spatial and temporal variations of stable isotopes in precipitation across Japan are still unknown, because a specific site and an observation period are different among the previous studies. Intensive observation of stable isotopes in precipitation over the whole Japan is required during the same period.

The Isotope Mapping Working Group of Japanese Society of Hydrological Sciences was conducted intensive observation of stable isotopes in precipitation throughout the year in 2013 (IOP2013). More than 2,000 precipitation samples are already collected at about 50 stations, and are analyzing its stable isotopic ratios by the Isotope Ratio Mass Spectrometer (Delta-V, Thermo Scientific) in Kumamoto University. Stable isotopic ratios in precipitation across Japan will be considered the relationships with locations (i.e. latitude, altitude, and distance from the coastline) and meteorological elements (i.e. temperature, precipitation amount, winds, specific humidity). Also, water vapor origins are estimated by using atmospheric general circulation model with stable water isotopes. Finally, the equations to reproduce stable isotopic ratios in precipitation at a specific place in Japan will be determined by its location and/or meteorological elements. It's a useful for the paleo-climate change as a proxy data of temperature and/or precipitation amount in the past.

In this study, we present the preliminary result of the IOP2013.

Keywords: Stable isotopes in precipitation, d-excess, Japan, IOP2013

Japan Geoscience Union Meeting 2014
(28 April - 02 May 2014 at Pacifico YOKOHAMA, Kanagawa, Japan)

AHW25-05 Room:414 Time:May 2 10:00-10:15

Tracking phosphorus sources and cycling in freshwater: stable isotope approach

CID, Abigail[1*] ; SONG, Uhram[1] ; TAYASU, Ichiro[1] ; OKANO, Jun-ichi[1] ; TOGASHI, Hiroyuki[2] ; ISHIKAWA, Naoto F.[5] ; MURAKAMI, Aya[1] ; HAYASHI, Takuya[4] ; IWATA, Tomoya[4] ; OSAKA, Ken-ichi[3] ; NAKANO, Shin-ichi[1] ; OKUDA, Noboru[1]

[1]Ctr Ecol Res, Kyoto Univ, [2]Field Sci Educ Res Ctr, Kyoto Univ, [3]Univ Shiga Pref, [4]Dept Ecol Syst Engineer, Univ Yamanashi, [5]JAMSTEC

Stable isotope technique is increasingly used to provide ecological information to understand biological cycling and tracking environmental pollutants. The technique used for tracing phosphorus (P) in water is primarily based on the possibility of distinguishing the different P inorganic sources by phosphate oxygen isotopic signatures ($\delta^{18}O_p$) [1]. To date, there are only few studies to examine P cycling on watershed scales using the phosphate oxygen isotope analysis.

Here we aim to characterize individual $\delta^{18}O_p$ signatures of water, natural sources and potential anthropogenic sources in the Yasu River, the largest tributary river in the Lake Biwa Watershed. Special attention was paid to identify primary sources of P loadings in the Yasu River, associating with the land use pattern in its each catchment.

Materials & Methods

We collected river waters from 19 sites across the mainstream of Yasu River and its branches, whose catchment areas greatly vary in land use pattern. We also gathered water samples from 8 sewage treatment plants, 2 agricultural waste water plants and one livestock farm as point sources of anthropogenic P. We regarded phosphate fertilizers and sewage treatment plant waste waters as indicators for agricultural and domestic non-point P sources, respectively. We also collected sand from the riverbed of 5 headwaters as natural P sources. The sand samples were acid extracted to desorb dissolved inorganic phosphates [2]. These samples were treated with magnesium-induced coprecipitation (MagIC) method for phosphate extraction and then converted to silver phosphate after purification through the sequence of resin separation and precipitation [1,3]. We determined $\delta^{18}O_p$ for each of these silver phosphate samples using a thermal conversion elemental analyzer coupled to a continuous flow isotope ratio mass spectrometer via a helium stream.

We constructed an isotopic mixing model to estimate the relative contribution of individual P sources in each catchment.

Results & Discussion

A wide range of $\delta^{18}O_p$ in river water was detected. This indicates that this technique is a promising tool to trace P sources in the watershed ecosystems.

The isotopic mixing model showed that urban land use accounted for spatial variation in the relative contribution of domestic P loadings though there were some uncertainty in the model simulation.

[1] Young et al. (2009) Environ. Sci. Technol, 43:14, 5190-5196
[2] Tamburini et al. ni et al. (2010) Eur J Soil Sci, 61, 1025-1032
[3] McLaughlin et al. (2004) Limnol. Oceanogr. : Methods 2, 204-212

Keywords: Biological recycling, Eutrophication, Land use, Non-point phosphorus loading, Phosphate oxygen isotope analysis

Japan Geoscience Union Meeting 2014
(28 April - 02 May 2014 at Pacifico YOKOHAMA, Kanagawa, Japan)

AHW25-06 Room:414 Time:May 2 10:15-10:30

Stable isotopic map of spring water and surface water in the Shirakami Mountains, Japan

AMITA, Kazuhiro[1*] ; MIURA, Takuya[1] ; HAYASHI, Takeshi[2]

[1]Department of Earth Science & Technology Faculty of Engineering and Resource Science Akita Universit, [2]Faculty of Education and Human Studies, Akita University

The Shirakami Mountains is the general name given to an extensive mountainous region of 130,000 hectares ranging from the southwest of Aomori to the northwest of Akita prefecture. Within this area are 16,971 hectares of land, enclosing virgin forests of Japanese beech, which were registered as a world heritage region in December 1993. However, environmental impact by acid rain at the Shirakami Mountains is becoming an issue these days. Acid rain deposits nitrates that can lead to increases in nitrogen in forests. So we have studied about the chemical and isotopic compositions of river and spring waters in the Shirakami Mountains area, to clarify origin and geochemical characteristics since 2011.

The result of the investigation was that delta-18O and delta-D of water samples showed -8.8 to -11.5 permil and -48.8 to -64.8 permil, respectively. Stable isotope composition of the samples roughly resemble those of meteoric water (delta-D = 8delta-18O+20), thereby indicating that these are local meteoric water. The least-squares regression line for all data is: delta-D = 5.7delta-18O + 1.7 (R2 = 0.88). On the other hand, the regression line calculated with data from NW-part is: delta-D = 6.0delta-18O + 0.5(R2 = 0.98). Characteristics of two regression line suggest that these water origin were brought by rain from different air mass, respectively.

Keywords: The Shirakami Mountains, Stable isotope map

Japan Geoscience Union Meeting 2014
(28 April - 02 May 2014 at Pacifico YOKOHAMA, Kanagawa, Japan)

AHW25-07 Room:414 Time:May 2 10:30-10:45

Source of spring water and nitrate in northern foot of Mt.Fuji

NAKAMURA, Takashi[1*] ; HASEGAWA, Tatsuya[2] ; YAMAMOTO, Shinya[2] ; UCHIYAMA, Takashi[2]

[1]ICRE, University of Yamanashi, [2]Yamanashi institute of environmental Sciences

Water chemistry of spring water in Northern foot of Mt. Fuji is discussed with special reference to its source of water and nitrate. Monthly spring water and river water samples were collected from 8 springs and 7 locations of the 3 rivers, from June 2013 to January 2014. Land use of the study area are urban located about <1000m, forest distributed >1000m and forest limit is about 2500m. The oxygen isotope range of all spring water samples shows temporal variation (>1.0 permil), which suggests the possibility of the water changes of groundwater water recharge elevation. The nitrate-nitrogen concentration ranges from 0.2 to 1.8 mg/L and from 0.1 to 2.2 mg/L in river water and spring water samples respectively. Similarly, nitrate-nitrogen isotope values ranges from 2.7 to 9.9 permil and 1.4 to 10.4 permil in river water samples and spring water samples respectively. Although nitrate concentration was low, nitrogen isotope values overlaps with forest soil nitrogen and sewage or manure nitrogen. This trend suggests that the recharge elevation of the spring water might spread across a wide area. This presentation will discuss about recharge processes of the spring water including temporal variation of the isotopic values and water quality.

Keywords: Mt.Fuji, spring water, oxygen and hydrogen isotopes in water, nitrogen and oxygen isotopes in nitrate

Japan Geoscience Union Meeting 2014
(28 April - 02 May 2014 at Pacifico YOKOHAMA, Kanagawa, Japan)

AHW25-08 Room:414 Time:May 2 11:00-11:15

Spatial distribution of vanadium concentrations and water isotopes in lake bottom water from Lake Kawaguchi

YAMAMOTO, Shinya[1*] ; HASEGAWA, Tatsuya[1] ; YOSHIZAWA, Kazuya[2] ; NAKAMURA, Takashi[3] ; UCHIYAMA, Takashi[1]

[1]Yamanashi Institute of Environmental Sciences, [2]Yamanashi Institute for Public Health, [3]International Research Center for River Basin Environment, University of Yamanashi

Spatial distribution of vanadium concentrations was examined in bottom water from Lake Kawaguchi, on the northern foot of Mt. Fuji, in order to test the hypothesis that the water outflow from underwater springs in Lake Kawaguchi could affect the vanadium concentrations of lake water. The samples were collected from the east lake basin and the Funatsu lake basin on July 14-August 2, 2005, and from the west lake basin on November 1 and October 31, 2013. Vanadium concentrations in the bottom water from Lake Kawaguchi range from 0.66 μg/L to 3.18 μg/L. Because vanadium concentration in precipitation is generally $<$0.1 μg/L, the variations are most likely attributed to the dilution of the lake water due to precipitation, and/or the input of water masses with high vanadium content. Although the concentrations of vanadium are significantly lower than those in the groundwater of the Mount Fuji, we found a relatively vanadium-enriched water mass along the southern coast of the west lake basin, off coast of Higashiken lava flow from Mount Fuji. The area matches well with the potential location of underwater springs in Lake Kawaguchi, and the lack of any riverine input around the area suggests that a water mass with relatively high vanadium concentration is likely provided from underwater springs that are located in off coast of the basaltic lava flow of Mount Fuji. We also plan to discuss the source of underwater springs based on stable water isotope ratios in the presentation.

Keywords: Kawaguchiko, vanadium, stable water isotopes, Mount Fuji

Japan Geoscience Union Meeting 2014
(28 April - 02 May 2014 at Pacifico YOKOHAMA, Kanagawa, Japan)

AHW25-09 Room:414 Time:May 2 11:15-11:30

Contribution of volcanic gas to spring waters in the Mt. Yotei.

KUSANO, Yukiko[1*] ; YASUHARA, Masaya[2] ; ASAI, Kazuyoshi[3] ; INAMURA, Akihiko[2] ; TAKAHASHI, A., hiroshi[2] ; MORIKAWA, Noritoshi[2]

[1]The University of Tokyo, [2]Geological Survey of Japan, AIST, [3]Geo science Laboratory Co. Ltd.

The Mt. Yotei is a stratovolcano in southwest Hokkaido with an altitude of 1893 m. There are a lot of springs in the foot of the mountain and most of these are found from the altitude of 200 to 260 m. This elevation is consistent with that of boundary between volcanic rocks of the volcano and basement consists of tuff and pumice. Northern, eastern, and southern slopes of the mountain are covered by pyroclastic fall and reworked deposits of that, while the western slope is covered by lava erupted from summit and parasitic volcanos in western slope (Katsui, 1956).

It is revealed that springs in eastern and southern slopes tend to show lager discharge and lower dissolved components, while those in the western slope tend to show smaller discharge and higher dissolved components (Yamaguchi and Sato, 1971; Yamaguchi, 1972; Tsurumaki, 1989). Because of higher HCO_3^- and free CO_2 gas concentrations and higher temperature of springs in the western slope, addition of volcanic gas to those is estimated (Yamaguchi and Sato, 1971; Tsurumaki, 1989). However, contribution of volcanic gas to groundwater has not been evident. In this study, contribution of volcanic gas to spring waters will be discussed based on dissolved components and isotopic compositions.

Spring water samples were collected on August 2013, and were analyzed for major dissolved components, isotopic compositions (δD, δ^{18}O, δ^{13}C, ^{3}He/^{4}He), and groundwater-age indices (CFCs and SF_6). Dissolved components of spring waters are Ca-HCO_3 type or Na-HCO_3 type. Spring waters in the western slope tend to show higher HCO_3^- and free CO_2 gas concentrations. These results are consistent with those of previous studies. δ^{13}C of dissolved inorganic carbon (DIC) in spring waters in eastern and southern slopes are -21.7 to -17.7 ‰, while those of the western slope are -18.1 to -3.0 ‰. This result suggests that spring waters in western slope contain DIC of which origin is different from that contained in springs in eastern and southern slopes. Dissolution of marine carbonates is unlikely because groundwater flow in volcanic rocks. Relationship between δ^{13}C and inverses of concentrations of total carbon are plotted in mixing zone of volcanic CO_2 and soil CO_2, and spring water showing higher δ^{13}C and total carbon concentration were correspond to higher contribution of volcanic CO_2. These results suggest that spring waters in western slope showed higher δ^{13}C and total carbon concentrations because of addition of volcanic CO_2. δD and δ^{18}O of spring waters are plotted along the meteoric water line (GSJ, undisclosed data), suggesting contribution of magmatic water is quite small. Effect of parasitic volcanos in the wastern slopes is suggested by Yamaguchi and Sato (1971) as a possible factor for higher contribution of volcanic gas to springs in the western slope. Further discussions based on dissolved components, isotopic compositions, and groundwater-age indices will be performed to reveal relationship between contribution of volcanic gas and groundwater flow system.

References

Katsui, Y., 1956. Explanatory text of geological map of Japan, scale 1: 50,000, Rusutsu, appendix, Geological Curvey of Hokkaido, p14.

Tsurumaki, M., Journal of Groundwater Hydrology, 31, 3, 165-173.

Yamashita, K. and Sato, I., 1971. Report of of spring water survey in the Mt. Yotei, Geological Survey of Hokkaido, p27.

Yamashita, K., 1972. Journal of Geography, 81, 5, 4-20.

Japan Geoscience Union Meeting 2014
(28 April - 02 May 2014 at Pacifico YOKOHAMA, Kanagawa, Japan)

AHW25-10 Room:414 Time:May 2 11:30-11:45

Estimation of recharge elevation and residence time for springs in Mt. Yotei

ASAI, Kazuyoshi[1*] ; YASUHARA, Masaya[2] ; KUSANO, Yukiko[3] ; INAMURA, Akihiko[2] ; MORIKAWA, Noritoshi[2] ; TAKAHASHI, Hiroshi[2]

[1]Geo science laboratry, [2]AIST, [3]University of Tokyo

Mt Yotei is a stratovolcano located on southwestern part of the Hokkaido. 17 springs with flow rate over 20 L/s distribute on the foot of the volcano body. We used the multi tracer method to estimate the recharge elevation and the residence time for the springs. Water samples were collected from 14 springs at August 2013, and were measured in stable isotope, Tritium, CFCs and SF6. In this presentation, we discuss the relationships between the scale of groundwater flow system and the hydrogeology of volcano body, based on the recharge elevation and the residence time for springs.

Keywords: Mt. Yotei, spring, recharge elevation, residence time, transient tracer

Japan Geoscience Union Meeting 2014
(28 April - 02 May 2014 at Pacifico YOKOHAMA, Kanagawa, Japan)

AHW25-11 Room:414 Time:May 2 11:45-12:00

Isotope characteristics of groundwater in and around Mt. Sambe, an active volcano in western Japan

YASUHARA, Masaya[1*] ; SUZUKI, Hidekazu[2] ; ASAI, Kazuyoshi[3] ; INAMURA, Akihiko[1] ; YAMAMOTO, Atsushi[4] ; MORIKAWA, Noritoshi[1] ; TAKAHASHI, Hiroshi[1] ; TAKAHASHI, Masaaki[1] ; KAZAHAYA, Kohei[1] ; KITAOKA, Koichi[5]

[1]Geological Survey of Japan, AIST, [2]Komazawa University, [3]Geo Science Laboratory, [4]Kinki University, [5]Okayama Univeristy of Science

A study using a coupled hydrological and geochemical (water chemistry, δD·δ^{18}O, δ^{13}C, and helium isotope) approach is in progress to elucidate the groundwater system in and around Mt. Sambe, a 1126-m high active volcano located in western Japan. Groundwater in its south to east flanks proved to be characterized by high δ^{13}C values (in the range between -9 - -5 ‰ δ^{13}C) as well as an elevated concentration of total carbon compared to those in other flanks. These observations clearly indicate an admixture of magmatic fluid into shallow groundwater of the south to east flanks, being also in accordance with its water chemistry with an increased chloride ion concentration.

Keywords: active volcano, groundwater, water chemistry, isotopes, volcanic fluid

Japan Geoscience Union Meeting 2014
(28 April - 02 May 2014 at Pacifico YOKOHAMA, Kanagawa, Japan)

AHW25-12 Room:414 Time:May 2 12:00-12:15

Origin of the high-chloride groundwater in the central part of the Kanto Plain from the viewpoint of noble gas hydrology

MORIKAWA, Noritoshi[1*] ; YASUHARA, Masaya[1] ; HAYASHI, Takeshi[2] ; MIYAKOSHI, Akinobu[1] ; INAMURA, Akihiko[1] ; TAKAKASHI, Masaaki[1] ; NAKAMA, Atsuko[1]

[1]Gelological Survey of Japan, AIST, [2]Akita University

There exist three regions in the Kanto plain, central Japan, whose artesian groundwater is characterized by a high Cl^- concentration: 1) central parts of the Kanto plain (Saitama Prefecture), 2) south-east parts of Gunma Prefecture), 3) floodplains and deluvial uplands along the lower reaches of Kokai and Tone rivers (Ibaraki and Chiba Prefectures).

As for that in the central parts of the Kanto plain, confined groundwater with a high Cl^- concentration of up to 216 mg/l is obtained from the productive boreholes of 200-430 m depth. The area of Cl^--rich groundwater, spreading from the northwest to southeast, corresponds with the so-called Motoarakawa tectonic zone (ca. 10 km wide by 35 km long) bounded by the fault on its longer sides. The $^{36}Cl/Cl$ results of these high chloride groundwaters imply that admixture of meteoric water and sea water in the period of the Shimosueyoshi transgression (peak period at around 125,000 yrs. BP) is likely to account for its elevated Cl^- concentration (Yasuhara et al., 2011). Morikawa et al (2006) conducted dissolved noble gas analyses for the groundwaters in the Motoarakawa tectonic zone. The results of helium isotopes are as follows; (1) there is a tendency of high ^4He concentration in the groundwaters inside the tectonic zone, (2) helium isotopic ratios ($^3He/^4He$) are relatively homogeneous with an end member of 0.8-1.1 x 10^{-6}. Helium-4 concentration show clear positive correlation with chloride concentration. Combined with this correlation and characteristics of helium isotopic ratio, it is inferred that the groundwater from the tectonic zone is a mixture of meteoric water and high chloride saline water bearing with high 4He or is stagnant old groundwater and that the groundwater flow system is distinct from those from outside of the tectonic zone.

In this study, we investigated the noble gas in the deeper groundwaters (hot springs) around the Motoarakawa tectonic belt and the high-chloride groundwaters from south-east parts of Gunma Prefecture to elucidate the origin of water and chrolide component in the central parts of the Kanto plain. Low $^3He/^4He$ ratios in the hot springs indicate that there is no interconnectivity between the high chloride groundwater and hotspring water around the Motoawakawa tectonic zone. In contrast, both $^3He/^4He$ ratio and correlative ^4He and Cl concentration in the high-chrolide groundwaters from south-east parts of Gunma Prefecture are similar to those in the groundwaters in the Motoarakawa tectonic zone.

Keywords: Kanto Plain, groundwater, chloride ion, Noble Gas, Helium isotope

Japan Geoscience Union Meeting 2014
(28 April - 02 May 2014 at Pacifico YOKOHAMA, Kanagawa, Japan)

AHW25-13 Room:414 Time:May 2 12:15-12:30

Geochemical study of hot spring waters and gases in Jozankei area, Hokkaido, northern Japan

TAKAHASHI, Masaaki[1*] ; KAZAHAYA, Kohei[1] ; SASAKI, Munetake[1] ; MORIKAWA, Noritoshi[1] ; TAKAHASHI, Hiroshi[1]

[1]Geological Survey of Japan, AIST

Jozankei hot spring area is located in the western part of Sapporo city, Hokkaido, northern Japan. In this area, hot spring waters >85 degree C. are springing out from the entire Toyohira river volley. Total discharge rate of hot spring waters is about 10 tons/min and the ”heat energy index” is rank V (Fukutomi, 1965). Hydrogen and oxygen isotopic study clarified that the major origin of hot spring water is local meteoric water (Matsubaya et al., 1978)

To understand the other origin of Jozankei hot spring, analyses of chemical compositions, hydrogen and oxygen isotope ratios were carried out for hot spring waters from Jozankei area and its adjacent area. From the good correlation among chloride ion content, oxygen and hydrogen isotope ratio of hot spring waters in Jozankei area, it is clarified that one of the end member of hot spring waters of Jozankei area is originated from magmatic fluid and chemical composition of magmatic fluid is 3-5 NaCl wt%.

(References) Fukutomi(1961)J.Fac.Sci.Hokkaido Univ.Ser.VII, 315-330; Matsybaya et al.(1978)Papers of the Institute for Thermal Spring Research, Okayama Univ., 47, 55-67.

Keywords: Jozankei, magmatic fluid, hydrogen and oxygen isotopic ratio

Japan Geoscience Union Meeting 2014
(28 April - 02 May 2014 at Pacifico YOKOHAMA, Kanagawa, Japan)

AHW25-14 Room:414 Time:May 2 12:30-12:45

Genesis of Kashio brine: slab-derived fluid

KAZAHAYA, Kohei[1*] ; TAKAHASHI, Hiroshi[1] ; MORIKAWA, Noritoshi[1] ; OHWADA, Michiko[1] ; INAMURA, Akihiko[1] ; YASUHARA, Masaya[1] ; TAKAHASHI, Masaaki[1]

[1]Geological survey of Japan, AIST

In this study, we show the results obtained be investigation of a very saline spring named Kashio brine, central Japan and discuss its genesis and cause of chemical and isotopic features. The brine water is spouting out through the cracks of metamorphic rocks close to Median Tectonic Line (MTL) at 700m asl. The Cl concentration of water is greater than that of the seawater with ^{18}O-shifted isotopic composition. The brine is thought to originate from slab-derived fluid with the chemical and isotopic composition of water like the Arima hot spring, in spite of its low temperature and CO_2-less features. The cause of this chemical character might be explained by a reaction with ultramafic rocks existed close to Kashio area which causes high pH condition to deposit all the CO_2 as $CaCO_3$. The low temperature may be interpreted by the low upwelling rate because of the low $^3He/^4He$ ratio (lower than 2Ra) due to the addition of crustal 4He. The amount of NaCl is finally supplied to the river and is estimated to be 2000kg/day.

Keywords: Kashio brine, isotopic ratio, flow rate, slab-derived fluid

Japan Geoscience Union Meeting 2014
(28 April - 02 May 2014 at Pacifico YOKOHAMA, Kanagawa, Japan)

AHW25-P01 Room:Poster Time:May 2 16:15-17:30

GC/C/IRMS as a tool to evaluate the degradation of chlorinated organic compounds in groundwater

YONEYAMA, Yuki[1*] ; ARAI, Yohei[2] ; NAKAMURA, Takashi[1] ; KAZAMA, Futaba[1]

[1]ICRE, UNIVERSITY OF YAMANASHI, [2]Hitachi Plant Services Co.,Ltd

The in-situ remediation techniques by microbial activity are used for reduction of chlorinated organic compounds in polluted groundwater. However, the evaluation of microbial activity for decomposition of chlorinated organic compounds is not clear by only the concentration analysis. So, we focus on the usage of the stable carbon isotope analysis of chlorinated organic compounds such as trichloroethylene (TCE), and its daughter products; cis-dichloroethylene (cis-DCE) and vinyl chloride (VC).

The stable carbon isotope ratio (δ^{13}C) of these organic compounds were analyzed by a GC (Agilent : 7890A) coupled to an isotope ratio mass spectrometer(SerCon : 20-22) with combustion interface (SerCon : GC-CP) (GC/C/IRMS). The system was equipped with a purge-and-trap concentrator (GL science : AQUA PT 5000J PLUS) connected to the GC. In the δ^{13}C value measurement, the measurement limit was usually 200ng-C, and standard deviation in TCE, cis-DCE and VC were $\pm$0.08, $\pm$0.37, $\pm$0.11 permil, respectively.

Groundwater samples were collected at polluted site with and without bioremediation treatment.

In samples from without treatment site, even the concentration decreasing were detected, the δ^{13}C values of TCE are almost same as original one. On the other hands, δ^{13}C values of not only TCE but also the daughter products increase with a decrease in concentration of TCE. These results show the usefulness of GC/C/IRMS for distinguishing the reason of concentration reduction by in-situ microbial activity of decomposition of these organic pollutants from physical factors such as dilution, diffusion, and adsorption.

Keywords: GC/C/IRMS, chlorinated organic compounds, biodegradation

Japan Geoscience Union Meeting 2014
(28 April - 02 May 2014 at Pacifico YOKOHAMA, Kanagawa, Japan)

AHW25-P02 Room:Poster Time:May 2 16:15-17:30

Isotope characteristic of rain water and atmospheric vapor in Hiratsuka, Japan

TAKAGI, Kenta[1*] ; OOKI, Seigo[2] ; OHBA, Takeshi[2]

[1]Course of Chemistry, Graduate School of Science, Tokai University, [2]Course of Chemistry, School of Science, Tokai University

Introduction

The stable isotope ratios of hydrogen and oxygen in meteoric water (δD and δ^{18}O) are affected by geological and climatic conditions. Global meteoric water line (GMWL) describes the average isotopic compositions in the world. According to Craig (1961), the relationship between δD and δ^{18}O was expressed as

$\delta D=8\delta^{18}O+10$ (1)

However those intercept are not always 10 in each area. In Japan, the meteoric water originates in both Pacific Ocean and Japan Sea. The effects of two seas vary due seasonally. The isotope ratio of atmospheric vapor is important for study of atmospheric circulation, however, the number of published paper is not so much. In this study, we investigate the d-excess (d=δD -8δ^{18}O) of rain water and atmospheric vapor in Hiratsuka, Japan.

Sampling methods

Samples were collected on the roof of a No.17 building at Shonan campus, Tokai University from May to December 2013. Rain water samples were collected based on a method described by Negrel et al. (2011) and Yoshimura (2002). The collection duration was days or hours in scale. Rain water samples were percolated through 0.2 μm filter, and kept into a 100 ml low-density polyethylene bottle. Atmospheric vapor samples were collected through a trap cooled with ethanol and dry ice mixture. Samples were 42 of rain water and 11 of atmospheric vapor. δD and δ^{18}O of samples were measured by a Cavity Ring-Down Spectrometer analyzer (model L2120-I from PICARRO). Some data of rain water, which were sampled several times in a day, were processed to be the average value.

Results and discussion

Rain water shows a wide variation in δD and δ^{18}O from -86.4 to +6.2 ‰ and -12.6 to -2.6 ‰, respectively. Atmospheric vapor shows a variation from -223.5 to -98.6 ‰ and -31.2 to -14.7 ‰, respectively. The δD-δ^{18}O relationship of rain water gives a regression line: $\delta D=9.2\delta^{18}O+24.0$ (R^2=0.95) and that of atmospheric vapor gives a regression line: $\delta D=7.3\delta^{18}O+7.9$ (R^2=0.96). The d-excess values show a variation from 4.4 ‰ to 33.2 ‰. In Japan, origin of meteoric water affects to d-excess (Waseda and Nakai, 1983). In case of Pacific Ocean, d-excess is low (10$\geq$d). In case of Japan Sea, d-excess is high (20$\leq$d). In this study, the d-excess was low in summer when southern winds were blown from Pacific Ocean as the seasonal wind, and that value was high in winter when northern winds were blown from Japan Sea. Samples of atmospheric vapor show also this trend. Suggesting that atmospheric vapor is influenced by the same effect of meteoric water. The meteoric water line of rain samples was affected by d-excess which reflects variations of moisture sources, which is the reason why the slope of this line would be bigger than GMWL.

Keywords: rain water, isotope

Japan Geoscience Union Meeting 2014
(28 April - 02 May 2014 at Pacifico YOKOHAMA, Kanagawa, Japan)

AHW25-P03 Room:Poster Time:May 2 16:15-17:30

Exploring the sources of sulfur ion deposition and runoff in forest watersheds on the northern side of Lake Biwa

NAKAZAWA, Koyomi[1*] ; HORIE, Seigo[1] ; NAGAFUCHI, Osamu[1] ; OSAKA, Ken'ichi[1] ; NISHIMURA, Takuro[1]

[1]The University of Shiga Pref.

To clarify the sources of sulfur ions in precipitation and runoff from forest watersheds, bulk deposition and stream water samples were collected within the small Kutsuki and Surumi forest watersheds on the northern side of the Lake Biwa basin, central Japan. Samples were analyzed for major ions and δ34S. Continuous monitoring from 1990 to 2010 showed that the average SO_4^{2-}concentration in stream water samples was 1.62 $\pm$0.31 (0.76, 3.58) mg l^{-1}at Kutsuki and 6.59 $\pm$1.54 (3.68, 16.1) mg l^{-1}at Surumi (t-test, $p<0.01$). However, the average SO_4^{2-}concentration in bulk deposition samples was similar in both watersheds: 2.15 $\pm$ 1.31 (SD) mg l^{-1}(range, 0.202-10.2 mg l^{-1}) at Kutsuki and 2.24 $\pm$ 1.29 mg l^{-1}(0.350?6.07 mg l^{-1}at Surumi (t-test, $p>0.05$). The δ34S values in bulk deposition samples fluctuated from +8.86 to +9.14 ‰ at Kutsuki and from +9.87 to +11.1 ‰ at Surumi, whereas non-sea salt (nss-) δ34S in stream water samples varied from +6.89 to +12.0 ‰ and from ?4.64 to +5.11 ‰ , respectively (t-test, $p<0.01$). It is said that the δ34S values in coal products from northern China varied from -3 to -1 ‰ and Japanese oil varied from +5 to + 18 ‰ .

Our findings suggest that the difference in the ability of canopies in the watersheds to catch SO_4^{2-}dry deposition is the reason for the significant difference in nss- δ34S values in stream water samples. The more open canopy in the Kutsuki watershed consists of young conifers and deciduous broadleaf trees, whereas the canopy in the Surumi watershed consists of mature conifer trees at a high density. Therefore, it appears that the Kutsuki watershed was only affected by SO_4^{2-}deposition from the Asian continent.There were not any domestic air pollution sources on the north side of Kutsuki. In contrast, the dense canopy of the Surumi watershed was affected by local SO_4^{2-}pollution sources of national roads which were located 1 km northwest from Kutsuki, rather than continental sources. Overall, this investigation suggests that the difference in stream water SO_4^{2-}concentrations in both watersheds is caused by the canopy differences.

Japan Geoscience Union Meeting 2014
(28 April - 02 May 2014 at Pacifico YOKOHAMA, Kanagawa, Japan)

AHW25-P04 Room:Poster Time:May 2 16:15-17:30

Geochemical and isotope systematics of Asahi and Yoshii rivers

KAMEI, Takahiro[1] ; YAMASHITA, Katsuyuki[1*] ; OONISHI, Ayaka[2] ; KURIHARA, Yoko[2] ; CHIBA, Hitoshi[1] ; NAKANO, Takanori[3]

[1]Graduate School of Natural Science and Technology, Okayama University, [2]Faculty of Science, Okayama University, [3]Research Institute for Humanity and Nature

We have undertaken a detailed geochemical and isotopic analysis of water samples collected from the Asahi and Yoshii rivers of the Okayama Prefecture, Japan. More than 300 samples were collected from the rivers and their tributaries during March 2011 to January 2014. In several locations, samples were collected periodically in order to monitor the long-term fluctuation of the geochemical properties. All samples were filtered with 0.2 μm filter prior to the analyses for major dissolved constituents (F, Cl, NO_3, SO_4, Br, PO_4, Ca, Mg, Na, K), trace elements and O-H-Sr-S isotopes.

Based on the results obtained so far, we have constructed a high-resolution geochemical map of the rivers covering central to eastern Okayama Prefecture. The map shows that the concentrations of most major dissolved constituents, as well as the O-H-Sr isotope ratios changes systematically from the upstream towards the downstream. For example, the deuterium excess (DE) is generally high in the upstream ($>$20) and gradually decreases towards the downstream ($<$12). This difference in the DE exceeds the seasonal variation observed in locations where the long-term monitoring was conducted. Thus, the regional change in the DE is interpreted to be the result of different air mass contributing to the meteoric water of different locations.

The Ca, Sr, and Ba concentrations are generally low in the upstream and gradually increase towards the downstream. The $^{87}Sr/^{86}Sr$ also changes from approximately ˜0.705 and ˜0.706 in the headwaters of the Asahi and Yoshii rivers, respectively, to ˜0.708 in the areas close to the Seto inland sea. The shift in the Sr isotope ratio seems to correlate well with the change in the ages of the rocks exposed in the river basin. This implies that these variations are likely related to the water-rock interactions.

The concentrations of other important dissolved constituents such as the NO_3 and SO_4 tend to increase abruptly in the densely populated regions. This is also accompanied by a shift in the S isotopic composition. These variations may reflect a change in the degree of human influence such as breakdown of fertilizers used for agricultural activities.

Keywords: Geochemical map, Asahi River, Yoshii River

Japan Geoscience Union Meeting 2014
(28 April - 02 May 2014 at Pacifico YOKOHAMA, Kanagawa, Japan)

AHW25-P05 Room:Poster Time:May 2 16:15-17:30

Chracteristics of groundwater discharge around western foot of Mt.Chokai

ASAI, Kazumi[1*] ; ASAI, Kazuyoshi[1] ; HAYASHI, Takeshi[2] ; KUSANO, Yukiko[3] ; MOGI, Katsuro[3] ; YASUHARA, Masaya[4] ; MORIKAWA, Noritoshi[4] ; TAKAHASHI, Hiroshi[4]

[1]GEO-SCIENCE LABORATORY, [2]Akita university, [3]University of Tokyo, [4]AIST

To clarify the total discharge rate of the submarine spring from Mt. Chokai, base-flow observation was conducted on 15 streams around western foot of Mt. Chokai at the end of January 2014. In this presentation, based on the distribution of specific discharge rate, we discuss the characteristics of the groundwater discharge and the hydrological balance in this area.

Keywords: Mt.Chokai, submarine spring, base-flow, hydrological balance, groundwater age

Japan Geoscience Union Meeting 2014
(28 April - 02 May 2014 at Pacifico YOKOHAMA, Kanagawa, Japan)

AHW25-P06 Room:Poster Time:May 2 16:15-17:30

Estimation of groundwater recharge area at the south foot of Mt. Bandai using the observation data in 2013

YABUSAKI, Shiho[1*]

[1]Faculty of Symbiotic Systems Science, Fukushima University

The Mt. Bandai (1,816 m a.s.l.) which is an active volcano of the Quaternary period is located at Fukushima prefecture. Because of the geological characteristics in the volcanic area, it is estimated the groundwater recharge is large around Mt. Bandai. The groundwater and spring water around Mt. Bandai is used as the source of the public tap water, so it is important to comprehend the groundwater flow and groundwater recharge ratio at Mt. Bandai. To make clear the groundwater flow systems at Mt. Bandai, the investigation was carried out.

The EC value is under 10 mS/m and water quality indicates the Ca-HCO_3 type at most points in the south slope of Mt. Bandai. The oxygen isotopic ratios ($\delta^{18}O$) are -11.1 to -10.8 ‰ (Site 1) and -11.2 to -11.1 ‰ (Site 2), and hydrogen isotopic ratios (δD) are -67 to -65 ‰ (Site 1) and -68 to -67 ‰ (Site 2). The altitude effect is recognized in these areas. The average recharge area (altitude) in the south slope at Mt. Bandai is estimated from 1,150 to 1,270 m (Site 1) and from 1,360 to 1,420 m (Site 2). These recharge area (altitude) in the south slope is lower rather than the north and west slopes. In future, the investigation at more low altitude area (about 520 to 550 m) will be carried out, and estimate the groundwater flow in the south slope at Mt. Bandai.

Keywords: Mt. Bandai, recharge area, spring water, water quality, stable isotopes

Japan Geoscience Union Meeting 2014
(28 April - 02 May 2014 at Pacifico YOKOHAMA, Kanagawa, Japan)

AHW26-01 Room:424 Time:May 1 14:15-14:30

Future Projection of flow regime and water quality in Arakawa river basin

ISHIDAIRA, Hiroshi[1*]

[1]Interdisciplinary Graduate School of Medicine and Engineering

The research project of Core Research for Evolutional Science and Technology (CREST): ”Development of well-balanced urban water use systems adapted for climate change” (PI: Hiroaki FURUMAI, Univ. of Tokyo, Research area: Innovative Technology and System for Sustainable Water Use) have been conducted from 2009.

The objectives of this project are 1) to reexamine the current urban water use system, and 2) to propose a new urban water use system adaptive to the future climate change. In the new system, each water resource is properly allocated to each water use by considering the balance between supply potential of various water resources and demand. The information on available amount and detailed quality of water resources should be evaluated.

For the implementation of the project, 5 sub-groups were organized:
(1) Watershed Water Resources group
(2) Urban Rainwater Management and Use group
(3) Urban Groundwater Management and Use group
(4) Water Quality Assessment group
(5) Urban Water Use Design group

In this presentation, activities of Watershed Water Resources group (and collaborative work with Urban Groundwater Management and Use group) will be presented.

Keywords: climate change, water resources

Japan Geoscience Union Meeting 2014
(28 April - 02 May 2014 at Pacifico YOKOHAMA, Kanagawa, Japan)

AHW26-02 Room:424 Time:May 1 14:30-14:45

Cl- concentration in pore water beneath Tokyo bay area, Urayasu, Chiba Japan

YOSHIDA, Takeshi[1*] ; KAZAOKA, Osamu[1]

[1]Research Institute of Enviornmental Geology, Chiba

We investigated Chloride concentration of Holocene and latest Pleistocene in Urayasu city, Chiba Japan. As a result of analysis, Chloride concentration of Holocene in this area is affected by flushing of rain and groudwater flow from Pleistocene.

Keywords: Alluvium, Profile of Cl- concentration, basal topography

Japan Geoscience Union Meeting 2014
(28 April - 02 May 2014 at Pacifico YOKOHAMA, Kanagawa, Japan)

AHW26-03 Room:424 Time:May 1 14:45-15:00

An isotopic study on the origins of sulfate ion in shallow urban groundwater of the Musashino Plateau, Tokyo, Japan

YASUHARA, Masaya[1*] ; HAYASHI, Takeshi[2] ; NAKAMURA, Takashi[3] ; INAMURA, Akihiko[1] ; ASAI, Kazuyoshi[4]

[1]Geological Survey of Japan, AIST, [2]Akita University, [3]University of Yamanashi, [4]Geo Science Laboratory

Shallow groundwater in the highly-urbanized Shakujii-gawa River basin on the Musashino Plateau, Tokyo, Japan shows a remarkable spatial variability of its sulfate ion concentration in the range between 7-135 mg/L. The average sulfate ion concentration is 35mg/L, 36mg/L, 33mg/L, 21mg/L, 19mg/L, and 28mg/L in Kita Ward, Itabashi Ward, Toshima Ward, Nerima Ward, Nishi-Tokyo City, and Kodaira City, respectively, indicating higher concentration in the lower reaches of the river where urbanization has started earlier and progressed more rapidly than its upper reaches. To discuss possible origins of sulfate ion in groundwater, a hydrologic study using stable isotope of sulfur was carried out in 2012 to 2013. Although a limited number of samples, higher sulfur isotope measurements (+10.5 and +10.6 per mil delta-34S for Toshima and Kita Wards, respectively) suggest contribution of leaking sewage from aging, deteriorated sewer pipes, accounting for an elevated sulfate ion concentration in the lower reaches of the river.

Keywords: urban groundwater, central Tokyo, shallow groundwater, sulfate ion, sulfur isotope

Japan Geoscience Union Meeting 2014
(28 April - 02 May 2014 at Pacifico YOKOHAMA, Kanagawa, Japan)

AHW26-04 Room:424 Time:May 1 15:00-15:15

PPCPs polution in an urban watershed in Musashino upland, Tokyo

HAYASHI, Takeshi[1*] ; YASUHARA, Masaya[2] ; NAKAMURA, Takashi[3]

[1]Faculty of Education and Human Studies, Akita university, [2]Geological Survey of Japan, AIST, [3]ICRE, University of Yamanashi

Human activities discharge various chemical substances to water environment in urban area around the world. Some substances are concerned to affect health of human and aquatic organism because these substances are hardly decomposed not only in natural environment but also water treatment plant. We study on shallow groundwater environment in Musashino upland, Tokyo to evaluate sources and recharge processes of groundwater and present state of groundwater pollution by domestic wastewater (e.g. Hayashi et al., 2012; Nakamura et al., 2013; Yasuhara et al., 2013). Based on the result of our previous research, we newly collected water samples of river water and shallow unconfined groundwater in the watershed and measured PPCPs components. Three samples of river water were taken from two rivers: a natural river mainly recharged by groundwater and an artificial river recharged by treated waste water. 15 groundwater samples were collected from private wells that were distributed in the water shed of the natural river. A for PPCPs, 78 substances were measured by semi-quantitative analysis and another six substances (amantadine, caffeine, carbamazepine, crotamiton, ibuprofen, N,N-diethyl-m-toluamide) were measured quantitatively.

As for river water samples, 19 substances from semi-quantitative analysis and six substances from quantitative analysis were detected in the artificial river, and three substances from semi-quantitative analysis and five substances from quantitative analysis were detected in the natural river. On the other hand, only one substance from semi-quantitative analysis and four substances (amantadine, carbamazepine, crotamiton, N,N-diethyl-m-toluamide) from quantitative analysis were detected in groundwater samples in both peri-urban upstream area and urbanized downstream area.

We present present characteristics of PPCPs components and spatial distribution in the study area.

Keywords: Musashino upland, urban river, shallow groundwater, pollution, PPCPs

Japan Geoscience Union Meeting 2014
(28 April - 02 May 2014 at Pacifico YOKOHAMA, Kanagawa, Japan)

AHW26-05 Room:424 Time:May 1 15:15-15:30

Title: Household water treatment for the removal of contaminants in groundwaters in Hanoi, Vietnam

DO, Thuan an[1] ; TAKIZAWA, Satoshi[1*] ; KURODA, Keisuke[1] ; HAYASHI, Takeshi[2] ; TRAN, Viet nga[3]

[1]The University of Tokyo, [2]Akita University, [3]University of Civil Engineering, Hanoi

Between 2000 and 2025, the urban population in Vietnam is expected to double from 19 million to 40 million. Therefore, urbanization and increasing water demand is one of the most important challenges in Vietnam, especially in Hanoi. At present, Hanoi city relies on groundwater as a main source of water supply, but it is going to shift to the surface water as the demand increases in the near future. However, variation of rainfall, dam construction in the upstream of the Red River and climate change in the near future make the surface water unreliable water source for water supply in Hanoi City. As the extension of water supply coverage is slow, many households still rely on groundwater as their drinking water sources. However, groundwater is contaminated by ammonia, arsenic, iron, bacteria and others. In order to obtain clean drinking and cooking water many households use point-of-use (POU) treatment devices including sand filters, ceramic filters, reverse-osmosis filters, and UV irradiation.

To identify the impact of POU usage to water consumption and water quality, a survey of POU usage in 170 households in six communes in Hanoi was carried out in 2012 and 2013 Water samples were also taken to investigate the treatment efficiency of those POUs. As a result of the household survey, it was found that many households in rural and suburban areas have multiple water sources and use them for different purposes, while the urban households use only piped water supply. The result indicated that between 18% and 76% of the households in these communes used POU water treatment devices, of which RO devices accounted for 58%. Groundwater was contaminated by arsenic (max 0.3 mg/L), ammonia (max. 26 mg/L), and manganese (max. 3 mg/L). Although most of the arsenic was As(III) form in groundwater, it was oxidized to As(V) in the sand filters. Thus, RO filtration was found quite effective in removal of arsenic from groundwaters.

Keywords: ammonia, arsenic, household water treatment, MDGs, reverse osmosis device, safe drinking water

Japan Geoscience Union Meeting 2014
(28 April - 02 May 2014 at Pacifico YOKOHAMA, Kanagawa, Japan)

AHW26-06 Room:424 Time:May 1 15:30-15:45

Prevention of heavy metals release from natural soil

SUMIKURA, Mitsuhiro[1] ; ASADA, Motoyuki[1*] ; TASAKI, Masaharu[1] ; SERIZAWA, Sadayoshi[1]

[1]Shimizu Corporation

In marine silts of bay areas, or volcanic ash rocks of mountainous areas, heavy metals derived from natural soils or rocks, such as lead or arsenic have become a problem. In this paper, prevention of arsenic release from soils is reported using laboratory tests results.

Japan Geoscience Union Meeting 2014
(28 April - 02 May 2014 at Pacifico YOKOHAMA, Kanagawa, Japan)

AHW26-07 Room:424 Time:May 1 15:45-16:00

Recent surface displacement in Bangkok associated with groundwater recovery

ISHITSUKA, Kazuya[1*] ; FUKUSHIMA, Yo[2] ; TSUJI, Takeshi[3] ; YAMADA, Yasuhiro[1] ; MATSUOKA, Toshifumi[1]

[1]Graduate School of Engineering, Kyoto University, [2]Office of Research Promotion, Tohoku University, [3]International Institute for Carbon-Neutral Energy Research (I2CNER), Kyushu University

In many cities in the world, groundwater level decrease and subsequent land subsidence has been observed associated with groundwater pumping. Bangkok, the capital city of Thailand, is also one of the cities that had been suffered from land subsidence due to groundwater extraction. Since 1960s, groundwater has been extracted for commercial and personal use. Subsequently, the cumulative subsidence of about 1 m has been reported. Recently, Thailand government has implemented several measures to regulate groundwater use, and groundwater level recovery has been reported.

In this study, we used persistent scatterer SAR interferometry (PS-InSAR) analysis, which is the method to process a series of SAR data equipped on repeat-pass satellite, to estimate ground displacement in Bangkok from November 2007 to December 2010. Since SAR data is acquired by satellite, PS-InSAR analysis has an advantage for mapping displacement pattern in wide area with high spatial density.

As a result, we estimated ground uplift with the rate of about 1 cm/year. The secular uplift has decayed over time, and can be modeled by exponential function of time. Since the groundwater recovery has been observed in areas where uplift was estimated, this uplift is likely associated with groundwater recovery. Moreover, we also estimated seasonal displacement correlated with the cycle of precipitation in eastside of Bangkok.

Keywords: groundwater recovery, surface displacement, Bangkok, persistent scatterer SAR interferometry

Japan Geoscience Union Meeting 2014
(28 April - 02 May 2014 at Pacifico YOKOHAMA, Kanagawa, Japan)

AHW26-08 Room:424 Time:May 1 16:15-16:30

The Use of Isotopic Technique to the Assessment of River Recharge to the Depleted Ground Water Systems in Dhaka, Banglad

NAHAR, Mst. shamsun[1*] ; ZHANG, Jing[1]

[1]University of Toyama, Department of Environmental Biology and Chemistry

Surveys of groundwater quality across Dhaka demonstrate the impact of intensive groundwater abstraction, which has led to invasion of the Dupi Tila aquifer by lower quality water in parts of the city. Groundwater chemical/isotopic monitoring is capable of discriminating between the effects of induced recharge from the polluted River Buriganga and of enhanced vertical leakage through the Madhupur Clay in contaminated urban areas. Over-exploitation of the aquifer has led to a progressive decline in water levels. The resulting cone of depression is thought likely to be causing the infiltration of polluted surface water. Stable isotopic techniques were used to characterize the hydrogeology and water sources the Dupi Tila aquifer beneath Dhaka. An interpretation of the linear δ^{18}O versus δ^{2}H relationship as a simple two-member mixing series between river water and recent meteoric recharge suggests that all groundwater in the lower Dupi Tila aquifer of Dhaka contains at least 30% river water.

Environmental isotope distributions approaches identify the polluted River Buriganga as the main threat to groundwater quality, indicating priorities for monitoring and aquifer protection.

Keywords: Ground Water, Dupi Tila Aquifer, Isotopic Technique, Dhaka

Japan Geoscience Union Meeting 2014
(28 April - 02 May 2014 at Pacifico YOKOHAMA, Kanagawa, Japan)

AHW26-09 Room:424 Time:May 1 16:30-16:45

Groundwater Level and Flow Rate Model and Barometric Response of Water Level of Well at Otomeyama Park in Shinjuku Ward

TAKANO, Yuki[1*] ; YOSHIMURA, Kei[2] ; MURAKAMI, Michio[3] ; UEMURA, Takeshi[4]

[1]Dept. of Earth and Planetary Phys., Univ. Tokyo, [2]Atmosphere and Ocean Research Institute, Univ. Tokyo, [3]Institute of Industrial Science, Univ. Tokyo, [4]Kaijo Junior and Senior High school

Spring at Otomeyama Park in Shinjuku Ward is one of the 57 Great Springs of Tokyo, Japan. Recently, decreasing of the spring water quantity at Otomeyama Park has been at issue. In order to figure out long-term variations of the spring water quantity, the flow rate and the groundwater level have been continuously observed by Kaijo Earth Science Club since 2011. In this paper, we report the results of the examination concerning the groundwater level variation and the model, which can express the groundwater level and the flow rate simultaneously.

Otomeyama Park is located at Ochiai escarpment on the eastern part of Musashino plateau. The stratum near Otomeyama park are Kanto loam layer, Shimosueyoshi loam layer (tuffaceous clay layer), Musashino gravel layer, Tokyo layer (sand layer or clay layer) and Tokyo gravel layer from the top. Sato et al. (2013) estimated that the aquifer of the spring water is Musashino gravel layer and the catchment area is about 10-100 ha. The spring water finally joins Kanda River through the water way in the park.

Based on the flow rate observation at Otomeyama Park for more than one year, the arithmetic mean flow rate was about 20 L/min. The flow rate intensely responded to precipitation. The flow rate increased from 4 L/min to 50 L/min in 35 hours at the rainfall event in April 2-3, 2012, whose total amount of rainfall was 118 mm.

The water level of wells were observed at three stations: well No.1 (at Otomeyama park), well No.2 (at Otomeyama park) and Mejiro well (at Shinjuku Ward, 0.5 km to the north from Otomeyama park). The water level of the wells was calculated by subtracting atmospheric pressure from the water pressure in aquifer. The aquifer of well No.1 is Musashino gravel layer and is confined, while the aquifer of well No.2 is Tokyo gravel layer and is confined. The aquifer of Mejiro well is Kanto loam layer and is unconfined.

Semidiurnal fluctuation of water level was observed at well No.1 and No.2. The daily composites of water level of well No.1 in dry periods showed that the atmospheric pressure was at its top at about 9 a.m. and 9 p.m. (JST) in Tokyo by atmospheric tide, while the water level of well fluctuated anti-phase to atmospheric pressure. This barometric response caused by balancing the water level variation of well with atmospheric loading when pore pressure of aquifer is not affected by atmospheric loading (Rojstaczer, 1988). This is attributed to three reasons for the barometric response of water level of well No.1. The mouse of the well is open, so that barometric fluctuation is directly transferred to the water surface in the well. Since the well diameter is 51mm, small water exchange between the well and the aquifer can change the water level in the well. Simosueyoshi loam layer above the aquifer is difficult to infiltrate atmospheric pressure. In contrast, the water level of Mejiro well was not responded to atmospheric load, since there is no air-barrier layer above Kanto loam layer.

Better performance model is needed to figure out long-term variations of the spring water quantity. Sato et al. (2013) predicted flow rate from precipitation using two-tank model, but the model did not utilize groundwater level. We developed a model, which express both flow rate and groundwater level. Our model was based on three-tank model. The first tank of the model represents intermediate flow. The second tank infiltrates water into the third tank but does not have side outlet. The third tank corresponds to the groundwater level. The model parameters were estimated for the flow rate and the water level of Mejiro well by means of SCE-UA method (Duan et al., 1993). In the simulation, the model accurately reproduced the observed value.

Keywords: spring water, groundwater level, tank model, barometric response, atmospheric tides

Japan Geoscience Union Meeting 2014
(28 April - 02 May 2014 at Pacifico YOKOHAMA, Kanagawa, Japan)

AHW26-10 Room:424 Time:May 1 16:45-17:00

The Seasonal variation of the amount of flowing artesian well springwater in the Ashigara Plain, Kanagawa Prefecture.

MIYASHITA, Yuji[1*]

[1]Hot Springs Res. Insti. of Kanagawa Pref.

Introduction

Many of cities are located in the alluvial plain of an area along the shore for our country which is an island country. In the alluvial plain, the confined groundwater cultivated in an upside fan or mountain area is used as the source of industrial water, or a source of tap water with river water. Overuse of groundwater in the city region in period of high economic growth caused groundwater obstacles, such as ground subsidence as one of the seven typical pollution and depleted of springwater.

Also in the flowing artesian well area from which is distributed in the Ashigara plain in the western area of Kanagawa prefecture decline has been reported after the 1960s. Moreover, the investigation in 2011 showed that there were 1,000 or more flowing artesian wells in the whole Ashigara plain. Furthermore, it turned out that about 50,000 tons per day of from the whole artesian wells . However, although relation with the irrigation to a paddy field is pointed out about the seasonal variation of the amount of the springwater from flowing artesian wells, there are many questions about details.

So, in this study, investigation over one year was conducted about the flowing artesian well springwater distributed in the Ashigara plain, and seasonal variation of the amount of springwater which gushes from a flowing artesian well was clarified.

Results of an investigation and consideration

Investigation conducted one investigation per month for 205 flowing artesian wells for June, 2013 to one year, and performed measurement of the amount of natural flows, water temperature, electrical conductivity, pH, and dissolved ion concentration. Since the amount of natural flows measured at 205 points had the large variation in the amount of natural flows for every point, it standard scoreized the amount of natural flows of every month, and grouped by cluster analysis for every point where the change pattern of the amount of natural flows was alike.

As a result, the change pattern of the amount of natural flows was able to be classified into ”the type corresponding to an irrigation term” which increases to the irrigation term to a paddy field, and ”the type corresponding to un- irrigation term ” with which a remarkable changing trend is not seen through every year. Moreover, many flowing artesian wells on the west side of the Sakawa river of ”the type corresponding to an irrigation term” classified according to the above-mentioned method were distributed, and ”the type corresponding to un-irrigation term” was mostly distributed on the east side of the Sakawa river.

Keywords: flowing artesian well, Ashigara Plain, amount of flowing artesian well springwater, seasonal variation, irrigation to a paddy field

Japan Geoscience Union Meeting 2014
(28 April - 02 May 2014 at Pacifico YOKOHAMA, Kanagawa, Japan)

AHW26-P01 Room:Poster Time:May 1 18:15-19:30

Three-dimensional mapping of geochemical and isotopic characteristics of groundwater beneath the Osaka Plain

SHINTANI, Tsuyoshi[1*] ; MASUDA, Harue[1] ; FUCHIDA, Shigeshi[1] ; EVEN, Emilie[1] ; MORIKAWA, Noritoshi[2] ; YASUHARA, Masaya[2] ; NAKANO, Takanori[3]

[1]Graduate school of science,Osaka city University, [2]National Institute of Advanced Industrial Science and Technology, [3]Research Institute for Humanity and Nature

Osaka Basin, which is a large Quaternary sedimentary basin beneath the Osaka Plain, is a large reservoir of groundwater resources. The uptake of groundwater has been strictly regulated since 1960 to avoid land subsidence, which actively occurred in the period of rapid economic growth. Although the land subsidence has stopped since 1970s because of the regulation, it became a threat again due to start of uptake of groundwater for private water supplies after 2000 ' s. Excess groundwater uptake from 100 to 300 m depths for those purposes would squeeze porewater from impermeable marine clay layers causing subsidence again.

In this study, groundwaters were mainly sampled from the wells >100 m depths, and stable hydrogen and oxygen isotope ratios and major chemical components were determined to estimate origins of water. Combining the results of our and previous studies, overall picture of three-dimensional mapping of groundwater geochemistry was drawn to discuss the groundwater flow system and the relationship to the land subsidence.

In the coastal region below sea level, seawater invaded into the groundwater aquifers <100 m depth. Stable isotope ratios of the groundwater at >100m of this area(δ^2H:-50 ‰~ -60 ‰,δ^{18}O:-8 ‰~ -9 ‰) is smaller than those of groundwater at <100m(δ^2H:-40 ‰~ -50 ‰,δ^{18}O:-6 ‰~ -7 ‰). Especially low isotope ratios of the groundwaters, of which chemistry was diluted Na-HCO3 type, from the lowland west of Uemachi plateau suggest squeezing the pore water from clay layers.

In the same area, high electric conductivity and Na-Cl type chemistry indicates seawater invasion into the groundwater aquifers <100 m depth. Uemachi Fault works as recharging path for the groundwater aquifers <100 m along the western edge of Uemachi plateau. However, the recharge is not enough to fill the aquifer >200 m apart from the fault. These observations indicate that the aquifers in the aquifers beneath western lowland of Osaka Plain have not been recovered by newly recharged groundwater.

Keywords: groundwater, isotope

Japan Geoscience Union Meeting 2014
(28 April - 02 May 2014 at Pacifico YOKOHAMA, Kanagawa, Japan)

AHW26-P02 Room:Poster Time:May 1 18:15-19:30

Source of nitrate in shallow groundwater in the Shakujii river catchment, central Tokyo, Japan

NAKAMURA, Takashi[1*] ; HAYASHI, Takeshi[2] ; YASUHARA, Masaya[3]

[1]ICRE, University of Yamanashi, [2]Akita University, [3]Geological survey of Japan, AIST

Water chemistry of shallow groundwater in the Shakujii river catchment in the downtown Tokyo is discussed with special reference to its nitrate and chloride concentrations. The catchment is divided into the highly urbanized lower reaches (Toshima, Kita and Itabashi Wards) and the upper reaches which have been urbanized to a lesser extent (Nerima Ward, and Nishi-Tokyo and Kodaira Cities). Shallow groundwater samples were collected from 28 wells of less than 10m deep at October 2012 and October 2013. Groundwater aquifer is in the Kanto loam layer and/or underlying stream terrace gravels. The nitrate-nitrogen concentration had wide ranges (from 0.1 to 13.6mg/l). The total coliform was detected from all shallow groundwater samples. The nitrate nitrogen isotope ranges from 5.6 to 12.3 permil, which overlaps fertilized soil and wastewater nitrogen. Moreover, End-member mixing analysis using hydrogen and oxygen isotope values revealed spatial distribution in the contribution ratios of the local precipitation and domestic water (sewage and tap). The concentration of nitrate nitrogen and total coliform was increasing along with contribution ratios of precipitation in shallow groundwater, except some samples that has high nitrogen isotope and chloride concentration. This trend suggests that the nitrate source in this area is not only from sewage leakage. It also needs to consider the loading of the nitrogen fertilizer to shallow groundwater by the precipitation infiltration.

Keywords: tokyo, urban, groundwater, nitrate nitrogen and oxygen isotopes

Japan Geoscience Union Meeting 2014
(28 April - 02 May 2014 at Pacifico YOKOHAMA, Kanagawa, Japan)

AHW27-01 Room:424 Time:May 1 09:00-09:15

Underground structure and groundwater flow in Saijo plain

RYOTA, Ochi[1*] ; TANAKA, Kazuhiro[2] ; SUZUKI, Koichi[3] ; TOKUMASU, Minoru[4]

[1]Yamaguchi University, [2]Yamaguchi University, [3]Central Research Institute of Electric Power Industry, [4]Saijyo City Hall

Many flowing wells are excavated in the Saijo plain,Saijo-shi,Ehime Prefecture, which have been made use for supplying an industrial and agricultural water.

Objectives of the study is to investigate the underground structure and groundwater flow in the Saijo plain and to discuss about the relationship between geological structure and groundwater flow by CSA-MT geophysical exploration and groundwater geochemistry.The study area is composed of the late Cretaceous Izumi Group and Holocene sediments.CSA-MT method was applied to obtain the two dimensional resistivity distribution about 2 km long and 500 m deep along 3 lines with north-south direction in the Saijo Plain.As a result,the Okamura fault that displaces the Holocene and the Izumi Group with east-west strike was detected in the southern part of the area.The newly named Kita-Saijo fault that displaces the Holocene sediments with west-east strike was detected in north of the area,displacing the Kikai-Akahoya tephra (K-Ah) bed erupted at 6 Ka.River waters are penetrated from the Kamo river to the Holocene sediments in the Saijo Plain and flow on the paleo-seawater with low resistivity.Some of them were penetrated under the impermeable layer composed of silt and clay and interrupted by impermeable layer 2 m thick disturbed by the Saijo-Kita fault.Consequently,penetrated groundwater is pressurized by impermeable layer and fault.Then,pressurized groundwater erupts at the flowing wells named Uchinuki.

Keywords: flowing wells, CSA-MT method, groundwater flow, underground structure

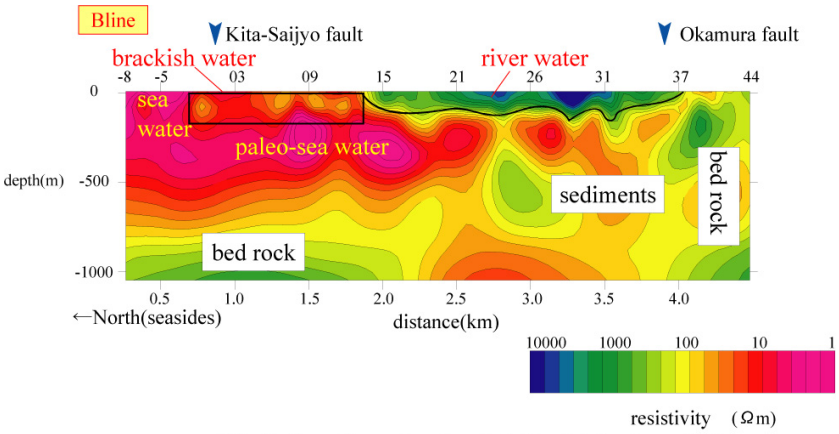

(Fig.1) .two dimensional resistivity distribution of Bline

Japan Geoscience Union Meeting 2014
(28 April - 02 May 2014 at Pacifico YOKOHAMA, Kanagawa, Japan)

AHW27-02 Room:424 Time:May 1 09:15-09:30

The subsurface distribution of saltwater and freshwater in the Nakano-shima island, by electromagnetic exploration

KUSANO, Yukiko[1*] ; SUZUKI, Koichi[2] ; TOKUNAGA, Tomochika[1]

[1]The University of Tokyo, [2]CRIEPI

Groundwater recharged during the last glacial period is revealed to remain in coastal aquifers and sub-seafloor formations, and it has been interpreted that the low-permeability formations have delayed the intrusion of saltwater into sub-seafloor formations (e.g. Groen et al., 2000). Thus, the effects of long-term sea-level change should be taken into account to better understand the groundwater flow system in coastal areas.

The Nakano-shima island, Oki-Dozen, is a volcanic island on a continental shelf. Because the island is situated on the continental shelf, the seafloor around the islands was most likely widely exposed during the last glacial period, and hence the distribution of salt/fresh water in subsurface is estimated to have been affected by the sea-level change after the Last Glacial Maximum. According to a well-drilling report of a hot spring well in the island, groundwater of which Cl concentration corresponds to 20% of sea water was obtained when the well reached to 320 m deep, and groundwater of which Cl concentration corresponds to 5% of sea water was obtained when the construction was completed (screen depth: 560 - 866 m). In addition, the hot spring water taken from the screen depth is suggested to be recharged in colder climate than present based on the stable isotopic ratios of water, dissolved components, and groundwater-age indices (Kusano et al., in press). These results suggest that the groundwater containing higher salinity exists in shallower than 320 m deep, and that the groundwater containing lower salinity and recharged in colder climate exists in deeper formations. In this study, electromagnetic exploration using CSAMT method was conducted to reveal the distribution of salt/fresh water beneath the island.

A 2.5 km-long measurement section for the electromagnetic exploration was set, along which the hot spring well exists, in east-west direction. Measurement points were placed at about 100 m intervals. Measured apparent resistivity data were used to obtain a two dimensional resistivity structure along the measurement line by two-dimensional inversion scheme developed by Uchida and Ogawa (1993). For better interpreting the resistivity structure in the island, volcanic and sedimentary rock samples obtained from the island were used to measure the bulk resistivity as a function of salinity of the pore water.

The result of two-dimensional inversion showed the higher resistivity zone from the surface to about 100 m depth, a continuous lower resistivity zone throughout the section in between 100 and 200 m depth, higher resistivity zone below, and lower resistivity zone further below, i.e., existence of four distinct resistivity zones. Resistivity values in between 100 and 200 m depth and those in the deepest zone were consistent with bulk rock resistivities saturated with higher salinity water. The results are consistent with the fact that groundwater with higher salinity was obtained when the well reached to 320 m depth and that groundwater with lower salinity was obtained after the well reached to 866 m depth. The obtained resistivity structure might suggest that fresh groundwater recharged in the last glacial period remains in the subsurface of the island, and salt water was intruded into the 100-200 m deep zone after transgression.

References

Groen, J. et al., 2000. J. Hydrol. 234, 1-20.
Kusano, Y. et al., in press, J. Hydrol.
Uchida, T. and Ogawa, Y. 1993. Geological Survey of Japan Open-File Report, 205.

AHW27-02 Room:424 Time:May 1 09:15-09:30

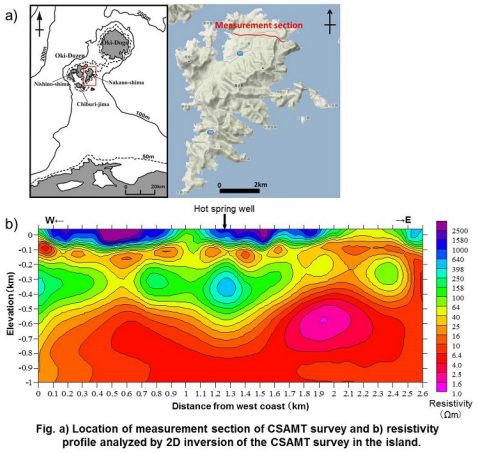

Fig. a) Location of measurement section of CSAMT survey and b) resistivity profile analyzed by 2D inversion of the CSAMT survey in the island.

Japan Geoscience Union Meeting 2014
(28 April - 02 May 2014 at Pacifico YOKOHAMA, Kanagawa, Japan)

AHW27-03 Room:424 Time:May 1 09:30-09:45

The method of an estimation of underground parameters of a geyser induced by boiling using the dynamical model

KAGAMI, Hiroyuki[1*]

[1]Nagoya College

We have proposed a static model, a dynamical model and a modified dynamical model of a geyser induced by gas inflow based on observation and model experiments of it and have also proposed a combined model combining above two models. And numerical simulations of the modified dynamical model or the combined model reappear spouting dynamics of a geyser induced by gas inflow and it becomes possible that parameters (volume of the underground space, depth of spouting hole and so on) under a geyser are estimated through comparison between results of numerical simulation and those of observation. Moreover we proposed a dynamical model which assumed more than two underground gas supply sources by extension of above-mentioned usual dynamical model. As a result, irregular spouting dynamics of a geyser induced by gas inflow could also be reappeared by the modified model. As a result, spouting mechanism of all kinds of geysers induced by gas inflow has been clarified.

However, in general, geysers are classified into two types dependent on inducer. That is, one is a geyser induced by inflow of gas and the other is a geyser induced by boiling. The latter is more popular and many ones exist all over the world. Though qualitative spouting models of a geyser induced by boiling have been proposed, its dynamics has not been discussed sufficiently. Therefore, then we derived a dynamical model of a geyser induced by boiling applying the above-mentioned dynamical model of a geyser induced by inflow of gas. Then we tried to estimate time derivation of spouting rate of a geyser induced by boiling through numerical simulations. Using the model we can estimate underground parameters of a geyser induced by boiling by comparison of results of numerical simulation of the model and those of observation of a geyser induced by boiling.

In this presentation, after we review above-mentioned models of a geyser induced by gas inflow and one induced by boiling in outline, we explain the method of an estimation of underground parameters of a geyser induced by boiling using the dynamical model.

Japan Geoscience Union Meeting 2014
(28 April - 02 May 2014 at Pacifico YOKOHAMA, Kanagawa, Japan)

AHW27-04 Room:424 Time:May 1 09:45-10:00

Rapid alkalization in Lake Inawashiro: implications for future changes in the carbonate system of terrestrial waters

MANAKA, Takuya[1*] ; USHIE, Hiroyuki[1] ; ARAOKA, Daisuke[1] ; INAMURA, Akihiko[2] ; SUZUKI, Atsushi[2] ; KAWAHATA, Hodaka[1]

[1]Atmosphere and Ocean Research Institute, The University of Tokyo, [2]National Institute of Advanced Industrial Science and Technology

The global carbon cycle, one of the important biogeochemical cycles controlling the surface environment of the Earth, has been greatly affected by human activity. Anthropogenic nutrient loading from urban sewage and agricultural runoff has caused eutrophication of aquatic systems. The impact of this eutrophication and consequent photosynthetic activity on CO_2 exchange between freshwater systems and the atmosphere is unclear. In this study, we focused on how nutrient loading to lakes affects their carbonate system. Here, we report results of surveys of lakes in Japan at different stages of eutrophication. Alkalization due to photosynthetic activity and decreases in PCO_2 had occurred in eutrophic lakes (e.g., Lake Kasumigaura), whereas in an acidotrophic lake (Lake Inawashiro) that was impacted by volcanic hot springs, nutrient loading was changing the pH and carbon cycling. When the influence of volcanic activity was stronger in the past in Lake Inawashiro, precipitation of volcanic-derived iron and aluminum had removed nutrients by co-precipitation. During the last three decades, volcanic activity has weakened and the lake water has become alkalized. We inferred that this rapid alkalization did not result just from the reduction in acid inputs but was also strongly affected by increased photosynthetic activity during this period. Human activities affect many lakes in the world. These lakes may play an important part in the global carbon cycle through their influence on CO_2 exchange between freshwater and the atmosphere. Biogeochemical changes and processes in these systems have important implications for future changes in aquatic carbonate systems on land.

Keywords: the global carbon cycle, lake, alkalization, nutrient, PCO2

Japan Geoscience Union Meeting 2014
(28 April - 02 May 2014 at Pacifico YOKOHAMA, Kanagawa, Japan)

AHW27-05 Room:424 Time:May 1 10:00-10:15

Variation of ?carbon isotope signatures of particulate organic matter in the Kuzuryu River system in Japan

NAGAO, Seiya[1*] ; KANAMORI, Masaki[2] ; ARAMAKI, Takahumi[3] ; OCHIAI, Shinya[1] ; YAMAMOTO, Masayoshi[1]

[1]LLRL, INET, Kanazawa University, [2]Grad. School of NST, Kanazawa University, [3]National Institute for Environmental Studies

Radioactive and stable isotopes of carbon (^{14}C and ^{13}C) can serve as powerful tools for identifying sources and estimating turnover times of organic matter in aquatic systems. This study discussed with the transport of particulate organic matter in the rivers from a river system with different watershed condition using carbon isotopic signatures.

The Kuzuryu River system is located in Fukui Prefecture in the central part of Japan and consists of a main river, Kuzuryu River and a main tributary of the Hino River. River research was conducted at a fixed station in the Hino River (Fukatani site) and the Kuzuryu River (Nakatsuno site) during June-October in 2010. Suspended solid samples were collected from 130-140 L of river waters using continuous centrifugation. Prior to analysis, inorganic carbonates were removed by adding 0.1 M HCl solution, rinsing with Milli-Qwater, and drying again. Stable carbon isotopic ratio of a sample and the VPDB standard used for normalization were made by analyzing sub-samples of CO_2 gas generated during graphite production using a triple collector mass spectrometer with precision of $\pm$ 0.2 ‰ as the $\delta^{13}C$ value. Radiocarbons were determined using accelerator mass spectrometry at the Japan Atomic Energy Agency. Radiocarbon values were reported as $\triangle^{14}C$ corrected for sample $\delta^{13}C$ with absolute error of less than 10 ‰.

$\delta^{13}C$ of organic matter in riverine suspended solids has -26.3 to -24.0 ‰ for the Kuzuryu River and -27.0 to -26.1 ‰ for the Hino River. The $\triangle^{14}C$ vales of the Kuzuryu and Hino samples are -168 to -87 ‰ and -209 to -143 ‰, respectively. The $\triangle^{14}C$ values of Hino River depleted in $\triangle^{14}C$ rather than the Kuzuryu River. The averaged TOC/TN ratio is 9.1 $\pm$ 1.1 for the Kuzuryu and 8.2 $\pm$ 1.1 for the Hino. There is a positive correlation with the $\triangle^{14}C$ vales and water discharge. These results indicate that the differences in POM character may be explained by the differences in watershed conditions and controlled by water discharge.

Keywords: POC, carbon isotopes, river waters, migration, water discharge

Japan Geoscience Union Meeting 2014
(28 April - 02 May 2014 at Pacifico YOKOHAMA, Kanagawa, Japan)

AHW27-06 Room:424 Time:May 1 10:15-10:30

Age dating of spring water, groundwater and stream water in mountainous watersheds using multi-tracer approach

IKEDA, Hayato[1*] ; TSUJIMURA, Maki[2] ; KATSUYAMA, Masanori[3] ; NAGANO, Ryuhei[4]

[1]College of Geoscience, School of Life and Environmental Sciences, University of Tsukuba, [2]Faculty of Life and Environmental Sciencies, University of Tsukuba, [3]Inter-Graduate School Unit for Sustainable Development and Survivable, Kyoto University, [4]Graduate School of Agriculture, Kyoto University

This study aims at estimation of mean residence time (MRT), to reveal the spatial distribution using multi-tracer approach in mountainous catchment, and to make clear relationship between hydrological characteristics and the variation of the residence time. First, we conducted field survey and sampling in Kiryu Experimental Watershed, in southern Shiga, in June, August and October, 2013 and analyze major dissolved inorganic ions, SiO_2, chlorofluorocarbons (CFCs) and stable isotopes (SI). Second, we estimated MRT using CFCs. We also evaluate MRT using seasonal variation of SI of rainfall, groundwater and stream water that collected monthly from 2008 to 2012.

The MRT of stream water and groundwater were estimated to be ranging from approximately 2.8 to 4.4 years by using SI as tracers. The MRT of spring water and groundwater were estimated to be ranging from 1.5 to 8.5 years and 15 to 23 years, given a water temperature as recharge temperature using CFCs. The relationship between Na^+ concentration and MRT based on CFCs suggested that short MRT that provided from decrease trend in atmospheric CFCs concentration is appropriate.

The MRT of water by CFCs ranged from 1.5 to 8.5 years, whereas that by SI ranged from 2.8 to 4.4 years in this catchment. This result conforms that of previous studies using SI, however the MRT by CFCs shows larger value range because CFCs represent time resolution information. In addition, the MRT varies in time and space due to mixing of different subsurface flow with different MRT and flow path.

Keywords: multi-tracer approach, mean residence time, stable isotope, chlorofluorocarbons

Japan Geoscience Union Meeting 2014
(28 April - 02 May 2014 at Pacifico YOKOHAMA, Kanagawa, Japan)

AHW27-07 Room:424 Time:May 1 10:30-10:45

Sources and recharge process of groundwater in sub-urban area of Hanoi city, Viet Nam

HAYASHI, Takeshi[1*] ; KURODA, Keisuke[2] ; AN, Do thuan[2] ; TAKIZAWA, Satoshi[2] ; NGA, Tran thi viet[3]

[1]Faculty of Education and Human Studies, Akita university, [2]School of Engineering, the University of Tokyo, [3]Hanoi University of Civil Engineering

Water demand in Hanoi city, the capital of Viet Nam, has been increased with recent rapid urbanization. Although high concentration of Arsenic is contained, groundwater is one of important water resources in this city. Groundwater abstraction has induced depletion of groundwater levels in major aquifers (Holocene shallower aquifer and Pleistocene deeper aquifer) not only in the central area but also sub-urban areas. On the other hand, urbanization reduces the surface water areas such as ponds, rivers and canals, and paddy fields. We focus on the interaction between surface water and groundwater to clarify water cycle and solute transport process in Hanoi area for sustainable water resource management. We are carrying out regular measurement of geochemical properties of surface water and groundwater, monitoring of groundwater levels in the major aquifers, and evaluation of groundwater age in some sub-urban villages.

The result of our previous study shows the surface water with evaporation process is a major source of groundwater in the study area. From the result of the regular measurement of surface and ground water and monitoring of groundwater levels in the shallower aquifer (unconfined condition), we found seasonal change of groundwater levels and geochemical properties of groundwater related with fluctuation of rainfall between rainy season and dry season. Also, seasonal change of geochemical properties was delayed several months to that of groundwater levels. This difference suggested the relatively slow infiltration of surface water with evaporation process into the shallower aquifer. On the other hand, result of CFCs and SF6 measurement showed apparent groundwater age in the shallower aquifer of the study area is several decades. These results may suggest groundwater abstractions enhance water cycle in the study area.

Keywords: Hanoi city, groundwater recharge process, fluctuation of groundwater level, isotopes, groundwater age

Japan Geoscience Union Meeting 2014
(28 April - 02 May 2014 at Pacifico YOKOHAMA, Kanagawa, Japan)

AHW27-08 Room:424 Time:May 1 11:00-11:15

Long-term trends of climate variability in upper Dong Nai river basin in Vietnam

TRUONG, Nguyen cung que[1*] ; KONDOH, Akihiko[2]

[1]Department of Earth Sciences, Graduate School of Science, Chiba University, [2]Center for Environmental Remote Sensing, Chiba University

According to a report of the Intergovernmental Panel on Climate Change (IPCC) and last studies, Vietnam is considered as one of the most countries affected by climate change. That are in the sea level rises (SLR) 1 m scenarios, about 10-12% of Vietnam's population are directly impacted and the country will lose up to 10% of GDP. With the combination of SLR and an increase in precipitation in the rainy season, there is a possibility of a serious impact on low-lying coastal area and leads to flooding of up to 40,000 km2 of the coastal delta and 90% of the Mekong River delta. It is also expected that temperatures will rise more significantly in the plateau region. Dong Nai river basin is located in the Southern Vietnam along with the Mekong River, that have supplied the major water resources of southern. Dong Nai river originates from the plateau of the Southeastern, through the Tri An reservoir, a major power generating dam of southern Vietnam, in the lower area it mixed with the tributaries of the Mekong Delta downstream and after that flows to East sea.

In the state which continues of changes on water resources Mekong river due to climate change, controversy about the potential impact of sediment transport and river flows downstream due to the cascade hydroelectric power plant system or dam construction on the upper Mekong basin, because of Dong Nai river basin is a water resources that can controlled by Vietnam, it is considered that is necessary to analyses change in hydrological regime due to climate variability and adaptation to that changes. The purpose of this study is detecting long-term changes in the climate data and runoff due to climate change in the Dong Nai river basin.

As hydrological information of the target basin, the Dong Nai river basin, last 20 years (form 1992 to 2011) data which observed by National Center for Hydro-Meteorological Forecasting (NCHMF), Department of Natural Resources and Environment (DONRE) of each region, Tri An hydroelectric power plant management office were analyzed by Empirical Mode Decomposition (EMD) to detected a long-term change in rainfall, temperature, potential evapotranspiration and runoff at the basin outlet (inflow of Tri An reservoir). EMD has recently been pioneered by Huang et al. for adaptively representing nonstationary time-series data as sums of zero-mean amplitude modulation frequency modulation components. The components, called intrinsic mode functions (IMFs), allow the calculation of a meaningful multicomponent instantaneous frequency.

The results show that trend of rainfall and temperature slightly increase, but the trend of potential evapotranspiration and runoff decrease in the last two decades within the basin. In the comparison with the results of Mekong River Commission or World Bank research on Climate change in Vietnam, we similarly conclude that rainfall and temperature tend to increase. It is considered change in land cover and land use within the basin is one of the causes of the downward trend of runoff. This is planning on the next study.

Keywords: Dong Nai river basin, climate variability, empirical mode decomposition, EMD

Japan Geoscience Union Meeting 2014
(28 April - 02 May 2014 at Pacifico YOKOHAMA, Kanagawa, Japan)

AHW27-09 Room:424 Time:May 1 11:15-11:30

A consideration of sustainable grazing over Mongolia, as point of view of recent climate change and vegetation responses

KAWAKAMI, Satoshi[1] ; HIGUCHI, Atsushi[2*]

[1]HP Japan, [2]CEReS Chiba University

We will present two topics. One is winter extreme-cold-events (ECE) detected by JRA-25/JCDAS reanalysis object dataset over Mongolia. Since 2000's ECE frequently occurred rather than 1990's, closely linking with synoptic scale circulation change in mid-high latitude. Such synoptic scale circulation change triggered by changing area of sea-ice over Barents Sea. Second topic is vegetation reaction process revealed by satellites observation. We used MODIS spectral reflectance dataset boarded on Terra/Aqua platform. Also we used two vegetation indices: One is major vegetation index, NDVI, the other is Green-Red ratio Vegetation Index (GRVI). NDVI is applied as proxy index of biomass, GRVI is regarded as proxy of biodiversity index. Based on matrix field of NDVI and GRVI, we define the recover status (2012) from herbaceous degradation in 2009. We found that faster recovered areas were located in the foot-fill. More detailed (e.g. degradation process period) analysis will be show in presentation.

Keywords: Mongolia, grazing, extreme colod events, NDVI, GRVI

Japan Geoscience Union Meeting 2014
(28 April - 02 May 2014 at Pacifico YOKOHAMA, Kanagawa, Japan)

AHW27-10 Room:424 Time:May 1 11:30-11:45

Effect of snow depth on hydrology of highland marshes - Analysis of PALSAR/ALOS data at Kiritappu, Sarobetsu and Oze -

IGARASHI, Masatoshi[1] ; HISADA, Yasuhiro[1] ; DEMURA, Hirohide[1] ; OGAWA, Yoshiko[1*] ; SOBUE, Shinichi[1]

[1]Univ. of Aizu, [2]RESTEC

It is basically very difficult to monitor the hydrological environment of highland marsh with snow in winter. We lastly reported that the most famous highland marshes Oze keeps a largest amount of liquid water body under the thick snow layer (more than 2 m) in midwinter based on our analysis of PALSAR/ALOS data, a kind of L-band radar. We concluded that such liquid water would be squeezed out from peat layers by the load of heavy snow and not the meltwater. In this presentation, we show our new analysis results at Kiritappu and Sarobetsu, both of which are highland marshes locating in Hokkaido, where it snows a lot but not as much as Oze in winter. The PALSAR/ALOS data is used again. This time we find almost no liquid water body in midwinter and recognize the singularity of Oze. We try to evaluate the effect of snow depth, peat depth on hydrology of highland marshes in winter.

Keywords: highland marsh, hydrology, PALSAR, remote sensing, snow, peat

Japan Geoscience Union Meeting 2014
(28 April - 02 May 2014 at Pacifico YOKOHAMA, Kanagawa, Japan)

AHW27-11 Room:424 Time:May 1 11:45-12:00

Modeling of hydrological temporal-spatial data by a universal model

KUZUHA, Yasuhisa[1*] ; ARAKI, Daisuke[1] ; SAITOH, Hanako[2] ; GOMI, Chieko[3] ; SENDA, Makiko[4]

[1]Graduate School of Bioresources, Mie University, [2]Faculty of Bioresources, Mie University, [3]Aichi Prefectural Government, [4]Kyoto Koka Women's University / Osaka Seikei University / Osaka Seikei College

We propose "the universal model" which generates hydrological temporal or spatial data. First a white noise is generetaed ,then the white noise is filterd by a specific filter and data are generated. If a field is fractal, log-log-linear-filter(ω vs.P(ω)) is used (Lavall*é*e, 2008). If a field is modeled by e-model (Gomi and Kuzuha, 2013), an exponential filter is used. We examined rainfall time series, spatial rainfall filelds, time series of ion concentration in river water, and ion concentration in tap water. As a result, those data were modeled by the universal model.

Gomi, C. and Y. Kuzuha(2013), Simulation of a Daily Precipitation Time Series Using a Stochastic Model with Filtering, Open Journal of Modern Hydrology, DOI: 10.4236/ojmh.2013.34025

Lavall*é*e, D.(2008), On the Random Nature of Earthquake Sources and Ground Motions: A United Theory, Advances in Geophysics, Vol. 50, 2008, pp. 427-461.

Keywords: fractal, hydrological temporal-spatial data, filtering, universal model, e-model

Japan Geoscience Union Meeting 2014
(28 April - 02 May 2014 at Pacifico YOKOHAMA, Kanagawa, Japan)

AHW27-P01 Room:Poster Time:May 1 18:15-19:30

Characteristics on groundwater salinization in a downstream area of dam reservoir, a coastal region of NorthEast Tunisia

UCHIDA, Chisato[1*] ; KAWACHI, Atsushi[2] ; TSUJIMURA, Maki[2] ; SHIBAYAMA, Naoyuki[1] ; ZIADI, Amira[3] ; TARHOUNI, Jamira[3]

[1]Graduate School of Life and Environmental Sciences, University of Tsukuba, [2]Faculty of Life and Environmental Sciences, University of Tsukuba, [3]National Institute of Agronomy in Tunisia

This study tried to characterize salinization processes of coastal shallow groundwater in a downstream are of dam reservoir, based on field investigation and chemical water analyses in order to indicate positive effects of dam reservoir on prevention of the groundwater salinization or seawater intrusion. Thus, focusing on two neighboring watersheds: Lebna and Chiba watersheds located in Korba aquifer (North-East Tunisia), the field investigation was carried out at 72 locations in June 2013, then water samples were collected at the 63 locations.

At first groundwater table contour map was drawn using investigated groundwater level data, and the groundwater flow was estimated. From the chemical analyses, spatial distributions of dissolved inorganic ions' concentrations, and stable hydrogen and oxygen isotopic compositions were obtained. Then, the seawater ratio in the groundwater samples were calculated using mass balance equation of chloride concentration under assumption chloride was derived from seawater. Using the seawater ratio, a theoretical concentration of each parameter were estimated, and differences between the analytical and theoretical concentrations were obtained. Additionally saturation indices were calculated based on chemical equilibration theory. Moreover, multivariable analyses: Cluster Analysis (CA) and Principal Component Analysis (PCA), were conducted to classify the groundwater salinization process and to determine the important parameters associated with the process.

As a result, the groundwater level (GWL) in the downstream of Lebna dam reservoir was higher than the sea level, while the GWL in Chiba watershed was lower than the sea level. The lowest point is about -10 m above sea level. According to seawater ratios and stable isotopic compositions, the study area were categorized into the following three types: (i) high seawater ratio, (ii) low seawater ratio and low isotopic compositions, and (iii) low seawater ratio and high isotopic compositions. On the other hand, CA results showed the study area were categorized into 5 clusters, and the PCA showed the following three phenomena were main reasons for the 5 clusters: (a) seawater ratio in groundwater, (b) inverse cation exchange by reaction between seawater and clay minerals, and (c) directly or indirectly groundwater recharge from Lebna dam reservoir. Moreover, considering totally the three types (i), (ii), (iii), three phenomena (a), (b), (c), and groundwater level, the study area could finally be divided into 3 areas A, B, C which have different characteristics on groundwater salinization

Area A is located around Lebna dam reservoir, in which groundwater level is higher than sea level and the stable isotopic compositions are relatively higher. High groundwater level is probably sustained by the direct recharge from the reservoir, or by infiltration of the irrigation water from the reservoir in the farm land. Area B is located near shoreline, in which groundwater level ranges 0 to -4 m above sea level, and high seawater ratio and high concentration of each dissolved ion are observed. The groundwater in this area has high concentrations of sodium and chloride (derived from seawater) and calcium (derived from inverse cation exchange) due to seawater intrusion. Area C is located in inland area of Chiba watershed, in which groundwater level is lower than -4 m above sea level. There should be three groundwater flows: from Area A, and the upstream of Chiba watershed with fresh groundwater derived from precipitation, and from Area B with saline water, especially high concentration of calcium. Therefore, the groundwater in this area probably consists of the three different origin waters.

Keywords: seawater intrusion, dam reservoir, dissolved inorganic ions, stable hydrogen and oxygen isotopic compositions, mass balance, multivariable analyses

Japan Geoscience Union Meeting 2014
(28 April - 02 May 2014 at Pacifico YOKOHAMA, Kanagawa, Japan)

AHW27-P02 Room:Poster Time:May 1 18:15-19:30

Geochemical features of groundwaters around the southern Itoigawa-Shizuoka tectonic line, western Kofu Basin

YAGUCHI, Muga[1*] ; MURAMATSU, Yoich[2] ; CHIBA, Hitoshi[3] ; OKUMURA, Fumiaki[4] ; YAMAMURO, Masumi[1]

[1]Gra.Shc.,The Univ.Tokyo, [2]Fac.Sci. and Tech.,Tokyo Univ.Sci., [3]Fac.Sci.,Okayama Univ., [4]Japex R.C.

Over the last few decades, drilling of thermal wells for hot spring bathing purposes were performed extensively on a deep aquifer at the depths more than 1000m in the non-volcanic area of Japan. Around the southern part of Itoigawa-Shizuoka Tectonic Line (ISTL), western Kofu Basin of central Honshu, many numbers of ground waters from drilled wells have been used for hot spring bathing. Some of these waters have high salinity, up to more than sea water salinity level, but their genesis and the formation mechanism of water quality have not been clarified previously. In this study, chemical and isotopic compositions of hydrogen (D/H), oxygen ($^{18}O/^{16}O$) and sulfur ($^{34}S/^{32}S$) of several ground water samples from, such as, natural spring and drilled wells around the southern part of ISTL, western Kofu Basin were analyzed in order to discuss the origin of waters and the formation mechanisms of water quality.

Temperature of the samples was up to 48.8 ℃, and the pH is between 6.4 and 9.7. The waters were subdivided into a Ca-HCO_3 type, Ca·Mg-HCO_3 type, Na·Ca-HCO_3 type, Na-HCO_3 type, Ca-SO_4 type, Na-Cl·HCO_3 type, and Na-Cl type. Among these, Na-Cl type was the most dominant water quality and maximum Cl concentration of the samples was up to about 23000 mg/L.

Due to plot of Na and Cl concentration of groundwaters were distributed along with mixing line between rain water and sea water, Na-Cl type water, which is dominant water quality type in the study area were appears to be derived from mixing of rain water and sea water end-members. δD and δ^{18}O plot of the low salinity waters were distributed along with the Global Meteoric Water Line, supporting that the low salinity end-member is originated from rain water. However, δD and δ^{18}O values of the waters which have high salinity (more than sea water salinity) were low compared with modern seawater values. The Mg/Cl and SO_4/Cl ratio of these high salinity waters were very low compared with modern sea water, whereas the Ca/Cl ratio is higher than modern sea water. These chemical and isotopic characteristics of the sample waters indicate that the high salinity end-member of the study area is altered sea water.

Keywords: Itoigawa-Shizuoka tectonic line, deep fluid, water quality, formation mechanism

Japan Geoscience Union Meeting 2014
(28 April - 02 May 2014 at Pacifico YOKOHAMA, Kanagawa, Japan)

AHW27-P03 Room:Poster Time:May 1 18:15-19:30

A Study on the Origin of a Spring in Tottori Sand Dunes using various geophysical and hydrological methods

SHIOZAKI, Ichiro[1*] ; KAWAI, Takayuki[2] ; NOGUCHI, Tatsuya[1] ; SAITO, Tadaomi[3]

[1]Graduate School of Engineering, Tottori University, [2]Research Institute for Natural Hazards and Disaster Recovery, Niigata University, [3]Faculty of Agriculture, Tottori University

There is an oasis that changes its appearance depending on the season in the depression south of Umanose (horseback), which is a symbol of the undulations of Tottori Sand Dunes. This oasis is not always visible. It disappears during the summer. The influent that constantly flows over the ground surface into the oasis depression forms Shirinashigawa River when oasis is gone, as the inflow water permeates into the sand or evaporates. By what mechanism does this oasis appear and disappear? That is, where does this influent come from and where does it go? This question about the oasis spring has been a scientific interest for a long time. For example, there have been a proposal that the rainwater from rain in the sand dunes became groundwater, some of which formed a spring and appeared on ground surface again(Akagi, 1991), a proposal that the rainwater permeating into the sand dunes with low water-holding property accumulated as groundwater near the impermeable stratum of the bedrock or volcanic ash layer with low water permeability and formed spring (Natural Parks Beautification and Management Foundation, 1995), and a recent study that investigated the relevance of oasis formation and the changes in water level in Tanegaike which is located south of the sand dunes (Hoshimi, 2009).

To answer this question, that is, to search for the origin of the spring in sand dunes (oasis), this study was conducted on the subsurface structure and circulation of groundwater in Tottori Sand Dunes. We estimated the subsurface structure of Sand Dunes and obtained basic data on groundwater existence, mode of its flow, the base structure of sand dunes using various nondestructive geophysical exploration methods, and tried to elucidate the origin of the oasis spring and the quantitative rise and fall mechanism also incorporating hydrological methods. While the specific methodologies used here will be described in a later section, we applied electrical resistivity imaging method, 1 m-depth geothermal prospecting, self-potential method, tremor probing and gravity probing to estimate the former subsurface structure and introduced continuous water level observation on oasis and analysis of evaporation quantity, groundwater level survey in oasis and its proximity, and analysis on stable isotope ratio of oasis spring water and water sampled from Tanegaike for the latter. For the former application, we conducted a GPS survey using a differential method so that we could understand the positions of observation points and grasp the overall topography of the sand dune area. For the latter application, we conducted a survey using total station to grasp the microtopography of the oasis area and its proximity.

As a result, we reached a conclusion as described below regarding the subsurface structure of Tottori Sand Dunes and the origin of the spring in sand dunes (oasis). “ Rainwater permeates into the sand dunes and form groundwater. A part of it is lead to the aquifer mainly formed on the volcanic ash layer (as perched water) and flows into the oasis spring. Then, the oasis spring flows into the sea through underground of Umanose. There is no simultaneous or direct relevance between oasis spring and the water in Tanegaike. We found association between the overall groundwater distribution in Tottori Sand Dunes area (sand dunes for sightseeing) and the undulations of the bedrock structure estimated by the subsurface structure analysis. ” It is surmised that this study verified these things from quantitative observation values including subsurface structure, changes in water level, changes in isotopes and so forth of sand dunes had significance of its own. This article will report on the basic scientific background, an outline of the study, the results of multiple surveys and their interpretation, and an overall summary of them.

Keywords: Tottori sand dunes, underground water, geophysical exploration methods

Japan Geoscience Union Meeting 2014
(28 April - 02 May 2014 at Pacifico YOKOHAMA, Kanagawa, Japan)

AHW28-01 Room:314 Time:April 30 09:00-09:15

Spatial distribution and transport of phosphorus in a hillslop profile in Ichikawa City, Chiba Prefecture, Japan

PIAO, Jingqiu[1*] ; TANG, Changyuan[1] ; ZHANG, Han[1] ; SAKO, Yoko[1]

[1]Graduate School of Horticulture, Chiba University

Transport of phosphorus (P) in subsoil is presumed to be minor in comparison to transport in topsoil. Three Soil columns that located at upland (agriculture land), hillslope and forest (background) were sampled in Ichikawa City (35.76^{o}N, 139.97^{o}E), Chiba Prefecture, Japan. Contents of the total P (STP), organic P (OP) and inorganic P (IP) were determined to assess the spatial distribution, origin and transport pathways of P in the soil of unsaturated zone. In unsaturated zone soil texture is in a sequence surface layer (SF), Kanto loam layer (LO), Joso clay layer (CY) and Narita sand layer (SA) of the upper part of slope profile and SF, the secondary deposited loam layer (SE), clayey sand layer (MI) and SA of the down part of slope profile. Soil samples were obtained from the slope profile at four sites (A, B, C, D). LO, CY and SA is covered the forest soil profile.

In forest soil, the contents of STP, OP and IP were 30-163 mg/kg, 5-63 mg/kg and 19-103 mg/kg, respectively. There averages in different layers were in the order: LO >CY >SA, respectively. In hillslop, the contents of STP, OP and IP were 42-1723 mg/kg, 20-1229 mg/kg and 18-839 mg/kg, respectively. The average in different layers were in the order: SF (1564 mg/kg) >SE (1349 mg/kg) >LO (494 mg/kg) >MI (492 mg/kg) >SA (91 mg/kg) >CY (69 mg/kg). There were similar changing trends between OP, IP and STP with the average in different layers. And the contents of OP were not higher than IP content in most layers, however, more than twice in SF and SE. Ratios of OP/STP in SF and SE were 63% and 64% which were similar with the ratios in topsoil of upland profile. Therefore, it is supposed that P in topsoil of hillslope was transported from upland by runoff and soil erosion. In addition, the average ratios of OP in LO, CY, MI and SA were 30-52%, lower than the average in SF and SEin hillslope profile.

STP contents of subsoil in hillslope were much higher than forest. It is assumed that there was external phosphorus loading on the subsoil in slop profile. The results indicated that P transported form the surface soil to subsoil. Moreover, there was an accumulation on the soil above CY which the depth is 2.8-3.4m than upper LO of A site. The CY is supposed to block the P transport along the profile. In SE, there was no obvious change of site B and C, showing that the soil of SE may be in saturation status of the P adsorption. And STP contents of MI and SA were lower than SE. It means there was no a great phosphorus accumulation on MI and SA. So P could transport toward to deeper stratum with soil water flow. Finally, P would be likely to enter the groundwater.

The results indicated that the contents of STP, OP and IP varied greatly in different stratum. And this study inferred that two P transport pathways. One was P transports as particulate form by surface runoff, soil erosion in the topsoil. The other one was P transports with the infiltration of soil water as soluble phosphate in the unsaturated zone. And P is likely to enter the groundwater, and would be moved towards wetland with groundwater flow, affect the ecological environment finally.

Keywords: phosphorus, spatial distribution, transport, hillslop profile

Japan Geoscience Union Meeting 2014
(28 April - 02 May 2014 at Pacifico YOKOHAMA, Kanagawa, Japan)

AHW28-02 Room:314 Time:April 30 09:15-09:30

Nitrogen budget of a headwater wetland

LI, Xing[1*] ; TANG, Changyuan[1] ; HAN, Zhiwei[1] ; CAO, Yingjie[1] ; PIAO, Jingqiu[1]

[1]Graduate School of Horticulture, Chiba University

As human activities continue to alter the global nitrogen cycle, understanding of the impact of increased nitrogen loading to freshwater systems is becoming more and more important. The study area is a typical headwater wetland, located at Ichikawa City (35.76oN, 139.97oE), Chiba Prefecture, Japan. The wetland valley is U-shaped with an elevation of about 16 m above sea level. The wetland receives discharge (both groundwater and overland flow) from an adjacent upland (elevation 26-31m) area with vegetation consisting of mostly pear orchard. A stream flowing through the wetland valley is recharged by spring water and groundwater in the wetland. Average flow rate of the stream all around a year is 21.7 L S-1 at the export of the wetland. The wetland is with surface area of 48000 m2, corresponding to 4.7% of the watershed. The uplands are covered by pear orchard, whereas the lowland is wetland. The average nitrate load is 501.9 mg S-1 at export of stream and average dissolved N2O load is 151.9 ug S-1 at export around a year. Ammonia and nitrite were nearly undeletable in the upland groundwater stream water in this study.

For the upland, annual nitrogen inputs refer to the sum of fertilizer application and atmospheric deposition, whereas the outputs refer to root absorption, N2O emission from soil surface and leaching of nitrogen. Nitrogen fertilizer is 346 kg ha-1yr-1 which is relative high to other studies. Annual average N deposition by precipitation over Japan was from 7 to 10 kg ha-1yr-1(with a mean value of 8.5 kg ha-1yr-1) during the past few decades (Hara, 1995). The composition in leaching nitrogen is only nitrate and the leached nitrate is 202 kg ha-1 yr-1in upland. The annual N2O emission was 5.77 kg ha-1 from the upland area.

For the wetland, annual nitrogen inputs refer to the sum of nitrate leaching from upland and atmospheric deposition of wetland. Annual nitrogen outputs refer to the sum of export by stream, and gas emission. The wetland receives 20652 kg-N yr-1 from atmospheric deposition and groundwater which recharge from agricultural upland. The nitrogen exports by stream were 15359.8 kg yr-1. The measured emission of N2O was 61.6 kg yr-1 and the calculated emission of N2 was 5218.6 kg yr-1. As a result, our estimate of N retention for the wetland watershed was 26.5%. Valigura (1996) and Whitall and Paerl (2001) estimated that N retention in urban watersheds ranges from 25% to 95%, with a best estimate of 40%. From the view of literature, the nitrate-nitrogen retention by mass was extremely low in this study. It is assumed that the high loading of nitrogen is a limit factor of nitrogen retention in wetland. The reason that the low percentage of nitrate-nitrogen retention may due to the extremely high load of nitrate input of groundwater (430 g-N m-2yr-1 or 4300 kg ha-1 yr-1). However, the nitrate-nitrogen retention was 110 g-N m-2yr-1 which is much higher than that (39 g-N m-2yr-1 and 46 g-N m-2yr-1) in study of William J. Mitsch (2005) and reach the retention level of constructed wetland.

Direct emission factor EF1 was 0.017 which is higher both than the default values of IPCC 1996 and 2006, but was still in agreement with the range of uncertainty. Indirect emission factor EF5-g was 0.003 which is much lower than the default value of IPCC 1996, whereas it was agreement with the default value of IPCC 2006. EF5-g value in this study was also consistent with the result of (0.0025) another study in Japan (Sawamoto, 2005). Ratio of dissolved N2O and NO3- in groundwater ranged from 0.00026 to 0.0157, with an average value of 0.0025. Using 0.0025 as the EF5-g value would revise the estimation of the indirect emission from this wetland, resulting of 51.5 kg yr-1. The measured emission of wetland was 61.5 kg yr -1 which is the same order of magnitude with calculated value, indicating that the method advised by IPCC could reasonable predict the indirect emission of wetland.

Keywords: nitrogen budget, dissolved N2O, wetland

Japan Geoscience Union Meeting 2014
(28 April - 02 May 2014 at Pacifico YOKOHAMA, Kanagawa, Japan)

AHW28-03 Room:314 Time:April 30 09:30-09:45

Influence of the Noboribetsu hydrothermal systems on surrounding water regions

OCHIAI, Yasuhiro[1*] ; CHIKITA, Kazuhisa[1]

[1]Division of Earth and Planetary Dynamics, Department of Natural History Sciences, Faculty of Science

A variety of hydrothermal systems exist in the Noboribetsu area, Hokkaido, which produces neutral to acidic hot springs. The high δD and δO^{18} values for the hot springs suggest that they originate from magmatic water (Matsubadani et al., 1977). Also, this area, including Lake Kuttara next to Noboribetsu, exhibits high geothermal gradient of 90 ℃/km (Matsubadani et al. 2011). However, a short knowledge of the geological structure makes us difficult to discuss the whole hydrothermal systems. In this research, water and heat budgets of a boiling pond, downstream of the Ohyunuma Pond, were estimated by monitoring water temperature. As a result, the heat fluxes from the bottom of the pond were estimated at 2,482 W/m^2 and 3,360 W/m^2 for two periods. Meanwhile, water temperature of Lake Kuttara was measured vertically and continuously at the deepest point. Using the data of a TCTD profiler, the heat flux at the bottom was estimated at 1.01 W/m^2, suggesting hot water input to the bottom. Henceforth, we will explore the relations between the bottom thermal variations and Noboribetsu geothermal activity.

Keywords: Noboribetsu hot spring, Lake Kuttara, Heat budget, Heat flux, Hydrothermal system

Japan Geoscience Union Meeting 2014
(28 April - 02 May 2014 at Pacifico YOKOHAMA, Kanagawa, Japan)

AHW28-04 Room:314 Time:April 30 09:45-10:00

Nitrogen and phosphorus export to watershed from Water-Conservation Forest

KAWABE, Ryosuke[1*] ; TANJI, Kazunori[2] ; OKAMURA, Masato[3]

[1]Faculty of Policy Management Keio University, [2]Faculty of Environment and Information Studies Keio University, [3]Graduate school of Media and Governance Keio University

The purposes of this study are to estimate and validate water contamination of Total nitrogen(T-N) and Total phosphorus(T-P) from forest as runoff, in order to discuss policy measures for controlling non-point source loads. The study area is Doshi village in Yamanashi Pref . Total population of the are is 1,884, forest area is 7,468ha, 4,594ha of whole region is designated as Water-Conservation Forest for Yokohama City. Rest 2,823ha is private forest area for forestry.

The Water-Conservation Forest has been done thining by Yokohama Waterworks Bureau, but private forest, especially coniferous plantation area has been hardly done thining because of the decline of forestry. Therefore it is great concern that decreasing of water supply, declining quality of drinking water by increasing of sediment discharge and non-point source loads from the forest. A mean inflow at Doshi reservoir is 6.7(?/sec), Water transfer to other reservoirs from Doshi reservoir reached 3.0(?/sec), as a result of them water discharge to downstream is 3.7(?/sec). Consequently, increase of non-point source loads of nitrogen and phosphorus influence on water quality of reservoir such as Sagami reservoir and Miyagase reservoir.

Non-point source load of forest depends on surface run-off volume. To take account of this difference InVEST model (P.Kareiva et,al., 2011) is adopted for estimation of non-point source loads. Equations are shown (1)-(3):

$EXPx = EAFx * polx \prod(1-Ey)$ (1)
$EAFx = \log \Sigma Yu / \log \sum Yw$ (2)
$Yx = \sum(1-AETx/Px)Ax$ (3)

Where EXPx is non-point source loading value at pixelx, polx is the export coefficient at pixel x, y is a pixel of the upper reaches of pixel x. u means all grids located upstream of x, w means a basin including x and y. We used the export coefficients at the Fuji river basin(S.Shrestha et. al.,2007) as polx value. E_y is nutrient retention coefficient. Because of calculating E_y by comparing with result of L-Q equation, E_y is set to be equal zero. EAFx is the hydrologic sensitivity score at the pixel x which is calculated as (2). Y_x is the water yield at pixel x. P_x is the annual precipitation. AETx is the annual actual evapotranspiration on pixel x. A_x is the area on pixel x.

In addition, we made two L-Q equations to explain relation of Total Nitrogen and water discharge., Total phosphorus and water discharge based on the observed water discharge from 1956 to 2012, and water quality from 1991 to 2012.

As a result, when nutrient retention coefficient is zero, non-point source loads of nitrogen is 251.5(t/yr) and that of phosphorus is 5.9(t/yr). In these result, artificial load s of nitrogen such as household is 1.8(t/yr) and that of phosphorus is 0.1(t/yr). These results show that non-point source loads come from forest area. Results of L-Q equation are $TN=0.791*Q^{0.0616}$,(R2:0.8374), $TP=0.00762*Q^{0.0238}+0.004$. Using these L-Q equations non-point loads are 192.3(t/yr) in T-N, 2.4(t/yr) in T-P.

In conclusion, the difference of nitrogen between result of InVEST model and L-Q equation is 59.0(t/yr) 23.5%, that of phosphorus is 3.5(t/yr) 59.3%. These difference due to amount of nutrient retention functions of forest area. It is also cleared that discharge of run-off are concentrated in valleys. Therefore, we conclude that it is important and necessary that forests in valleys are managed by appropriate thining.

Keywords: Water-Conservation Forest, Non-point sources, Nitrogen, Phophorus, L-Q Equation

Japan Geoscience Union Meeting 2014
(28 April - 02 May 2014 at Pacifico YOKOHAMA, Kanagawa, Japan)

AHW28-05 Room:314 Time:April 30 10:00-10:15

Estimation of hourly nitrogen flux in a suburban watershed using SWAT model

SHIMIZU, Yuta[1*] ; ONODERA, Shin-ichi[2] ; MATSUMORI, Kenji[3]

[1]NARO/WARC JSPS-PD, [2]Graduate School of Integrated Arts and Sciences, Hiroshima University, [3]NARO/WARC

The objective of this study is to estimate hourly nitrogen flux from a suburban watershed, using Soil Water Assessment Tool (SWAT). SWAT, which is a model developed by USDA-ARS and Texas A&M University, is a river basin-scale model to simulate the quality and quantity of surface and ground water. The model is widely used in assessing soil erosion prevention and control, non-point source pollution control and regional management in watersheds because one of the reason is that it can estimate reasonable result even if data is limited. However it is not suit for estimation of nitrogen flux in flood condition because the time step of the model is basically calculated in daily. On the other hands, the model has an option for hourly estimation of runoff if sub-daily precipitation data are inputted. So we tried to estimate hourly nitrogen flux in Takaya watershed located on Hiroshima prefecture using the option. Monthly water quality data in ordinary condition and hourly data in flood condition which are observed by authors ' group were used for validation. A result show that although the reproductively of hourly runoff was slightly decreased than daily estimation in validation period, estimated runoff peaks were fitted to observed. It was found that improvement of the model for hourly estimation of nitrogen flux, however, the result of the estimation was almost acceptable.

Keywords: Nitrogen flux, Hourly estimation, SWAT model, suburban watershed

Japan Geoscience Union Meeting 2014
(28 April - 02 May 2014 at Pacifico YOKOHAMA, Kanagawa, Japan)

AHW28-06 Room:314 Time:April 30 10:15-10:30

Trace elements fluxes and budgets in two forest watersheds

ITOH, Yuko[1*] ; KOBAYASHI, Masahiro[1] ; SHINOMIYA, Yoshiki[2]

[1]FFPRI, [2]FFPRI, Tohoku

Atmospheric deposition supplies some nutrients to forest ecosystem, serving as a source of reactive nitrogen, sulfur and the trace elements.

The objective of this study was to compare the behavior of four trace elements (Rb, Cs, Sr, Ba) in forest soil profiles in two forest sites: the Tsukuba experimental forest watershed and the Katsura experimental forest watershed.

Keywords: forest watershed, Rb, Cs, Sr, Ba

Japan Geoscience Union Meeting 2014
(28 April - 02 May 2014 at Pacifico YOKOHAMA, Kanagawa, Japan)

AHW28-07 Room:314 Time:April 30 10:30-10:45

The percolation mechanism in a forested drainage basin: The Oikamanai River basin

MIYAMOTO, Takuto[1*] ; CHIKITA, Kazuhisa[2] ; IWASAKA, Wataru[1] ; HOSSAIN, Md motaleb[1]

[1]Graduate School of Science, Hokkaido University, [2]Faculty of Science, Hokkaido University

The rainwater movement in soils of high permeability is important to know how river runoffs are produced, and how sediment and nutrient are additionally loaded. In this study, we focus on runoff processes in the forested Oikamanai river basin, Tokachi Hokkaido. The catchment area is 62.6km2, consisting of 88.3% forest and 10.6% farmland (mostly, grassland). Surface geology of the basin is mostly Miocene conglomerate, sandstone and mudstone. These are distributed on the hillslope or in mountainous regions. Farmlands are developed on the Holocene flood plane deposits. The Miocene sedimentary rocks are supposed to be highly permeable. We set a soil moisture profiler (4 channels) at each of forested area and grassland, and calculated the amount (mm) of percolation in the rainfall events (total rainfall of more than 50mm). As a result, the amount of percolation is near to total rainfall amount, and the ratio of the percolation amount to runoff height at a gauging station was low at ca. 12% in the forested area and ca. 19% at grassland. These low values suggest that the groundwater recharge to the deep zone is great because of the high permeability of the bedrock with many faults. Meanwhile, there is a soil layer of low permeability at depths of more than 20cm at grassland. Hence, it is suggested that saturated throughflow is more active than in forested area during the rainfall events. We set one more observation point near the upstream end of farmland. We will quantitatively estimate the farmland's contribution to water discharge and nutrient load by their comparison between the upper and lower observation points.

Keywords: percolation, soil moisture profiler, nutrient, river

Japan Geoscience Union Meeting 2014
(28 April - 02 May 2014 at Pacifico YOKOHAMA, Kanagawa, Japan)

AHW28-08 Room:314 Time:April 30 11:00-11:15

The radioactivity of cesium in stream water during base flow from a small watershed in forested headwaters

SHINOMIYA, Yoshiki[1*] ; KOBAYASHI, Masahiro[2] ; TAMAI, Koji[2] ; OHNUKI, Yasuhiro[2] ; ITOH, Yuko[2] ; SHIMIZU, Takanori[2] ; IIDA, Shin'ichi[2] ; NOBUHIRO, Tatsuhiko[3] ; SAWANO, Shinji[2] ; TSUBOYAMA, Yoshio[2] ; HIRUTA, Toshihide[4]

[1]Tohoku Res. Ctr, For. and For. Prod. Res. Inst., [2]For. and For. Prod. Res. Inst., [3]Hokkaido Res. Ctr., For. and For. Prod. Res. Inst., [4]Fukushima Pref. For. Res. Ctr.

The radiocaesium was released by the accident in Fukushima Dai-ichi nuclear power plant. Although the woodland is thought to have strong tendency to maintain radiocaesium within a forest ecosystem, the very small amount of radiocaesium flows downwards through stream water. As stream water was used for agriculture and transported nutrient materials to river and lake. Therefore, radiocaesium discharged from headwaters may influence the ecosystem in river and lake or agriculture, like rice crop. In this time, we report the radioactivity of cesium in stream water during base flow from a small catchment in forested headwaters, Fukushima Prefecture.

The investigation was carried out in a small catchment (drainage area 1.2 ha) in the Tadano experimental forest of the Fukushima Prefecture forestry research center in Koriyama city, Fukushima Prefecture (Annual rainfall 1163 mm and mean air temperature 12.1 ℃; the elevation 358 to 409 m, and the relief 0.42). The geology is a sedimentary rock (sandstone and tuff). As for the vegetation, the deciduous broad-leaved species such as Quercus serratas exists together with the Japanese red pine woods in the Cryptomeria japonica and the Chamaecyparis obtusa plantation (about the 48 years old). The runoff was observed by setting up the v-notched weir and the water level gauge in the catchment end. Stream water was collected twice a month (volume; about 10L) near the weir. The radiocaesium was divided to particulate and dissolved fractions by filtration (Glass fiber filter, 0.7um). Dissolved cesium-137 was measured after concentration by extraction disk(Sumitomo 3M, Empore Raddisk Cesium)

Based on results obtained from June 2012 to March 2013, the radioactivity of cesium-137 tended to be higher in summer and lower in winter. In January and February, the radioactivity of cesium-137 was not detected, but it began increasing in March. There is a possibility that variation in the radioactivity of dissolved cesium-137 has a relation with the decomposition of organic matter according to the temperature elevation. The change in radioactivity of particulate cesium-137 was almost same way as dissolved cesium-137. This is because the discharge of suspended solid was increasing during high flow and because suspended solid concentration kept low while a catchment was covered by snow.

Keywords: radiocaesium, baseflow, streamwater, forest

Japan Geoscience Union Meeting 2014
(28 April - 02 May 2014 at Pacifico YOKOHAMA, Kanagawa, Japan)

AHW28-09 Room:314 Time:April 30 11:15-11:30

Contribution of suspended solids to the migration of radiocaesium in forests

KOBAYASHI, Masahiro[1*] ; SHINOMIYA, Yoshiki[2] ; OHNUKI, Yasuhiro[2] ; HIRUTA, Toshihide[3]

[1]Forestry and Forest Products Research Institute, [2]Tohoku Reseach Center, Forestry and Forest Products Research Institute, [3]Fukushima Prefectural Forestry Research Centre

A wide area of forested land in eastern Japan was seriously contaminated by radiocaesium after the accident of the Fukushima Daiichi Nuclear Power Plant. In the contaminated forests, radiocaesium first trapped at the canopy and the litter layer has migrated to the mineral soil as throughfall (TF) and litter leachate (LL). TF and LL often contain suspended solids (SS) which are thought to transport the radiocaesium. The objective of this study is to clarify the contribution of the SS to the migration of radiocaesium in forests.

Throughfall (TF) and litter leachate (LL) were collected in forested slopes in Ibaraki and Fukushima prefectures. The concentration of Cs-137 of the water samples were measured by germanium detectors before and after filtration using membrane filters with pore size of 0.45 micrometer.

The concentrations of Cs-137 of the TF collected in the Ibaraki site (evergreen coniferous forest) in March and April 2011 were 14 - 60 Bq/L. In this period, the most of Cs-137 was detected as dissolved. Then the total concentration (dissolved + SS) of Cs-137 decreased and the proportion of Cs-137 in SS increased. The total concentration temporarily exceeded 20 Bq/L in the following summer season and the most of Cs-137 was detected from SS. The temporal increase in the radiocaesium in SS also observed in LL. The similar patterns of the concentration change of Cs-137 in summer observed in TF and LL at the evergreen coniferous forest and the deciduous forest in Fukushima. In winter, the total concentration of Cs-137 decreased and the migration rate also decreased. From these results, it was confirmed that the contribution of SS to the migration of radiocaesium as TF and LL in forests increased during summer.

Keywords: Radiocaesium, Forest, Migration, Suspended solid

Japan Geoscience Union Meeting 2014
(28 April - 02 May 2014 at Pacifico YOKOHAMA, Kanagawa, Japan)

AHW28-10 Room:314 Time:April 30 11:30-11:45

Water and radiocesium balance in several paddy fields in Fukushima

YOSHIKAWA, Seiko[1*] ; EGUCHI, Sadao[1] ; ITAHASHI, Sunao[1] ; IGURA, Masato[1] ; KIHOU, Nobuharu[1] ; FUJIMURA, Shigeto[2] ; SAITO, Takashi[3] ; FUJIHARA, Hideshi[1] ; KOHYAMA, Kazunori[1] ; YAMAGUCHI, Noriko[1] ; OHKOSHI, Satoru[3]

[1]National Institute for Agro-environmental Sciences, [2]National Agriculture and Food Research Organization, [3]Fukushima Agricultural Technology Centre

1. Introduction

By the released radionuclides from the Fukushima nuclear disaster in March, 2011, brown rice harvested at a 0.2% of paddy fields exceeded the provisional regulation value in 2011 in Fukushima. Water and radiocesium balance was studied in 3 paddy fields at different geographical sites in Fukushima to estimate radionuclides contamination in brown rice and to develope models for predicting radionuclides dynamics at watershed scale.

2. Monitoring and measurements

Field monitoring has been conducted in the following three paddy fields in Fukushima since spring in 2012. ; (1) a reorganized paddy field facing to forest in one side (clayey soil), (2) mountainous terraced paddy field surrounded by forest in three sides (sandy soil), (3) mountainous terraced paddy field surrounded by forest in three sides (organic soil). Water levels and turbidity of irrigation and drainage water in paddy fields and precipitation have been measured continuously. Water infiltration rates were measured several times during rice cultivation period in (2) and (3) fields. Water samples have been collected once a month for atmospheric precipitation, irrigation, surface drainage, subsurface pipe drainage, and seepage water on a ridge between terraced paddy fields. A membrane filter (0.025μm) was used to suspended solid (SS) and filtrate samples. The radiocesium concentrations were determined by Ge semiconductor detector after drying the SS and filtrate samples, respectively. Rice which was grown experimentally was harvested and measured its radiocesium concentrations by each part. Based on the relationship between turbidity and radiocesium concentrations, and flow rates of irrigation and drainage water, radiocesium concentration in rice plant, in/out flows of radiocesium in paddy fields were estimated for the monitoring period of one year (23rd May, 2012 ˜27th May, 2013). Radiocesium in/out flows induced by heavy rainfalls of 50˜150 mm by in July and October in 2013 were also estimated.

3. Results and Discussions

Monitored precipitation was about 800,900 and 1000mm,the estimated flow-in water (irrigation(+flow-in from spring which could be measured)) was about 300, 1300 and 3300 mm, the estimated flow-out water (surface drainage) was about 600mm, 1000mm and 7700mm for the one year in the (1), (2) and (3) field, respectively. Continuous spring-out of water was observed from side slope of the upper field in (2) and (3) fields. Infiltration and spring-out were almost same level in the surface in (2) field, however, averagely about 4 mm/day of spring-out was measured from the surface of (3) field during rice cultivation period. Furthermore, water flow-in and flow-out on the soil surface under snow and/or ice was observed in winter even in the latter part of January. Therefore, larger amount of water in/out flows were gained in the mountainous paddy fields (2) and (3) in comparison with common paddy fields located in flat areas like (1) field. Radiocesium concentrations of water samples, mainly taken at usual meteorological conditions, were 0.1-0.31 Bq/L for irrigation water, 0.02-1.4 Bq/L for surface drainage, 0.2-0.9 Bq/L for atmospheric precipitation, and 0.01-0.03 Bq/L for pype drainage. Most of the radiocesium was existent in the SS. Radiocesium inflow by irrigation, inflow by atmospheric precipitation, outflow by surface drainage, and carryout by rice harvest were 10^2, 10^2, and 10^3, and 10^2 Bq/m^2 orders in the 3 fields for the one year, respectively. Radiocesium net flow in the 3 fields for the one year was estimated to be outflow of 0.2%, 0.2%, and 0.7% to the amount of radiocesium in soil, respectively. Most of outflows of SS and radiosecium occurred at events such as puddling, transplanting, midsummer drainage, drainage, and heavy rain etc.. The heavy rainfalls in July and October in 2013 induced large amount of SS and radiocesium outflows.

Keywords: radiocesium, water balance, mountainous paddy field, suspended solid

Japan Geoscience Union Meeting 2014
(28 April - 02 May 2014 at Pacifico YOKOHAMA, Kanagawa, Japan)

AHW28-11 Room:314 Time:April 30 11:45-12:00

The characteristics of sediment load from a coastal forested drainage basin and their agents (2)

CHIKITA, Kazuhisa[1*] ; IWASAKA, Wataru[2] ; HOSSAIN, Md motaleb[2] ; MIYAMOTO, Takuto[2]

[1]Faculty of Science, Hokkaido University, [2]Graduate School of Science, Hokkaido University

Some of the five coastal lagoons in the Tokachi region of southeastern Hokkaido, open a few times per year to the Pacific Ocean. The openings affects water quality and deposits in the marine coastal region by discharging the lagoon water offshore. The Oikamanai River is a main river flowing into the Oikamanai Lagoon. The river basin is almost forested (ca. 88 % in area), from which the discharge and sediment load build up the ecosystem of the lagoon and its back marsh. In order to explore how the suspended sediment discharges into the Oikamanai Lagoon, we obtained hourly time series of discharge, Q (m3/s), and suspended sediment concentration, C (mg/L), in the upper Oikamanai River. As a result, it was found that, following the sediment availability (sediment amount to be eroded), the precedent type (peak C temporally precedes peak Q), synchronous type (two peaks synchronously appear) and antecedent type (peak Q precedes peak C) appear on the Q vs. C diagrams for sequential rainfall runoffs. The river-suspended sediment often originates from the river channels and/or basin slope. Hence, In order to judge the criterion for sediment erosion in the river channel and basin slope, the extended Shields diagram was applied to lognormal subpopulations separated for cumulative grain size distributions of river-bed sediment and basin soils.

Keywords: forested catchment, sediment load, precedent tyep, antecedent type, land collapse

Japan Geoscience Union Meeting 2014
(28 April - 02 May 2014 at Pacifico YOKOHAMA, Kanagawa, Japan)

AHW28-12 Room:314 Time:April 30 12:00-12:15

Changes of mineral composition and load of suspended materials in the Saru River, Hokkaido before and after 2003

IRINO, Tomohisa[1*] ; NAKADA, Satoshi[2] ; IKEHARA, Ken[3] ; YAMASHITA, Youhei[1] ; SEKI, Osamu[1] ; NAGAO, Seiya[4]

[1]Hokkaido University, [2]Kyoto University, [3]Institute of Geology and Geoinformation, National Institute of Advanced Industrial Science and Techn, [4]Kanazawa University

Supply of detrital material from river can affect the continuity, sedimentation rate, and composition of marine sediments deposited in front of the river system, which is controlled by the relief, weathering rate, and precipitation of the hinterland. In spite of the small drainage area, the small rapid rivers in the island arc located under warm humid climatic condition supply a huge amount of detrital materials to the surrounding seas. In addition, sediment transports tend to be concentrated during flooding events. In order to understand the depositional history and utilized it for paleo-climate reconstruction, it is necessary to study a mechanism of suspension generation and controlling factor of its composition.

We conducted a field survey during 2005-2011 in the Hidaka area in Hokkaido, Japan, to evaluate the influence of the flooding mud to marine sediments, promoted by the typhoon precipitation in August, 2003. We selected the Saru River as our target, and conducted the river water sampling and turbidity measurements along the main stream and a major branch called Nukabira River. Water samples were taken from the surface of flow center of each stream and stored in plastic bottles. The collected water was filtered through Millipore filter with 0.4 um opening and the suspended particles were collected and weighed in the laboratory. Mineral composition of the collected suspended materials on the filter was measured using an X-ray diffraction analysis (XRD).

Distribution of the turbidity in the Saru River drainage shows that high turbid water is localized only to the Nukabira River and others are relatively clear. The turbidity seems to be supplied only from one local source. Mineral composition of the suspended material in the Nukabira River does not contain serpentine, while the upper main stream before the junction with the Nukabira River contain serpentine. The suspended material in the lower main stream is also characterized by the lack of serpentine because of higher contribution from the Nukabira River. The surface sediment at the mouth of the Saru River also shows the same character. We also examined the mineral composition of marine surface sediments supplied as flood mud during the typhoon event in August, 2003. The flood mud contains the major amount of serpentine, which was not expected from the mass budget of suspended materials from the upper main stream and the Nukabira River under usual condition.

In order to estimate the suspension loads from the upper main stream and the Nukabira River, we compared the water discharge and suspension loads and established the rating curve for each tributary. Water discharge data for the main stream was available from the Water Information System of the Ministry of Land, Infrastructure and Transport, Japan. However, since the database contains too many missing data for the Nukabira River after 2008, we calculated the water discharge for this branch using the Hydrometeorological and multi-Runoff Utility Model (Nakada et al., 2012). As a result, the rating curve of the upper main stream is steeper than that of the Nukabira River, and the suspension load of the upper main stream could be larger than the Nukabira River at the water discharge of $>$300 m3/s. Therefore, the Nukabira River transports 5-10 times more suspended materials than the main stream during the usual discharge, which is reversed during the flooding situation.

Keywords: river suspended material, Saru River, Typhoon Etau, mineral composition

Japan Geoscience Union Meeting 2014
(28 April - 02 May 2014 at Pacifico YOKOHAMA, Kanagawa, Japan)

AHW28-13 Room:314 Time:April 30 12:15-12:30

Estimation of Sediment discharge with distributed USLE and L-Q Equation in Water-Conservation Forest

NAKASHIMA, Ryoichiro[2*] ; TANJI, Kazunori[2] ; OKAMURA, Masato[3]

[1]Faculty of Policy Management Keio University, [2]Faculty of Environment and Information Studies Keio University, [3]Graduate school of Media and Governance Keio University

The purpose of this study is to estimate and validate sediment discharge from forest area for providing water resources in order to discuss policy measures for controlling sediment discharge. The study area is Doshi village in Yamanashi Pref. Its population is 1,884, forest area is 7,468ha, 4,594ha of whole region is designated as forest area preserved for provision of water resource for Yokohama City. Rest 2,824ha is private forest area for forestry. The forest area preserved for provision of water resource has been done thining by Yokohama Water Bureau, nowadays the private forests are seldom do because of a decline of forestry. Therefore, it is concerned that the degradation of provision of water resources, the increase of sediment discharges volume.

To estimate the sediment discharge, we adopted USLE (Universal Soil Loss Equation) model. It considers 5 factors, R (the rainfall erosivity index), K (the soil erodibility factor), LS (the slope length-gradient factor), C (the cover-management factor) and P (The support practice factor).

We converted and integrated sets of data such as forest management plan in Doshi village, soil texture map, precipitation data analyzed by radar-AMeDAS and others to the proper dataset for utilizing GIS. The output data shows sediment discharge in 60 sub-watershed (Max:1,000ha) and in distributed 25m^2 grid. In addition, we tried to estimate more detailed information which is related to the land information, such as slope degree, land use and land cover.

Next, to validate the estimated result, we calculated the annual SS flux derived from L-Q equation, which makes correlation between the water discharge and SS density data. They were observed from 1955 to 2012 at the Doshi reservoir located down-stream of Doshi River. Based on the LQ equation, we estimated the annual sediment discharge.

As a result of evaluation with USLE, sediment discharge per year is valued 97,820 (t/yr). On the other hand, SS flux estimated 400(t/yr) [SS=1.732Q0.0238(R2=0.3223)] and sediment deposition in the reservoir is 62,500(t/yr) with LQ equation. It is known that SS load from households are valued 1.8(t /yr). Therefore the anthropogenic loads is not dominant factor in this area.

The result of USLE does not mean exported sedimentation to observation station. This indicates potential of sediment loss in each grid and their summation in total grid. The reason why sediment loss value decay in runoff process is considered to be the function of sediment retention of each grid. On the other hand, there are three dominant factors of sediment runoff from forest area.

First, more sediment runoff come from natural forest area than coniferous area. Second, more sediment runoff come from abandoned coniferous plantation area. Third, Slope factor is main reason of sediment export.

The results suggests that 1st sediment retention of in this area is able to retain 27% of total sediment discharge in this region, 2nd dominant sediment supply come from natural forest and abandoned coniferous plantation area, preservation measures to control sediment discharge are prioritize forest management in steep area.

Keywords: Water Conservation Forest, Sediment Discharge, Universal Soil Loss Equation, LQ equation

Japan Geoscience Union Meeting 2014
(28 April - 02 May 2014 at Pacifico YOKOHAMA, Kanagawa, Japan)

AHW28-14 Room:314 Time:April 30 12:30-12:45

Sediment loading processes in a tectonic and forested catchment: field observations and modelling

HOSSAIN, Md motaleb[1*] ; CHIKITA, Kazuhisa[2] ; MIYAMOTO, Takuto[1]

[1]Graduate School of Science, Hokkaido University, [2]Faculty of Science, Hokkaido University

Exploring fluvial sedimentary processes on catchment scale is useful for studies on the forest management, material cycle and ecosystem of short time scale and topographic evolution of long scale. The fluvial transportation of sediment is also related to sedimentation, material cycle and ecosystem in coastal regions. A considerable portion of suspended sediment discharging into a costal lagoon, the Oikamani Lagoon, Tokachi, Hokkaido annually is contributed by the forested Oikamanai River catchment with many tectonic faults. It is important to find out the sediment source in such forested catchments. Here, we have tried to find how sediment load occurs by rainfall and snowmelt runoffs in the forested (ca. 90% area) catchment. Grain size and mineralogy of catchment soil and stream sediment, survey techniques, and turbidimeters provide the information that allows us to understand fluvial sedimentary processes and the sediment source and its availability. Here, a semi-distributed model, ArcSWAT2012, was applied to time series of discharge and sediment load, which were obtained in 2011 to 2013. In ArcSWAT2012, the total basin area (62.48 km^2) was divided into 3 sub-basins, as subbasin into hydrological response unit (HRU) based on soil type, land use and slope classes that allow a high level of spatial detail simulation. In this study we have used the data of discharge, Q (m^3/s), suspended sediment concentration (SSC; C, mg/L) and sediment load, L (kg/s) of April 2011 to October 2013, weather data of 2008 to 2013, and soil data. Discharge and sediment load simulations by SWAT2012 offer reasonable results. The simulations of sediment load time series and hysteresis analysis indicate that most of the sediment input is coming from sub-basin 2, especially, from its basin slope.

Keywords: tectonic, forested, sediment load, SWAT, hysteresis

Japan Geoscience Union Meeting 2014
(28 April - 02 May 2014 at Pacifico YOKOHAMA, Kanagawa, Japan)

AHW28-15 Room:314 Time:April 30 14:15-14:30

Interaction properties between river and groundwater with assessment of oxygen isotope ratio and nutrient concentration

MARUYAMA, Yutaka[1*] ; ONODERA, Shin-ichi[1] ; SAITO, Mitsuyo[2] ; KITAOKA, Koichi[3]

[1]Graduate School of Integrated Arts and Sciences, Hiroshima University, [2]Graduate School of Environmental and Life Science, Okayama University, [3]Department of Applied Science, Okayama University of Science

In the alluvial fan, there are many palaeo-channels which are composed of more permeable media like gravel and sand, and many springs and wells on those have been useful for human life as well as ecosystem. These type of the springs have the different waveforms of the seasonal thermal variation from those of the river or air which is the thermal source. In detail, the phase shifting and amplitude declining are confirmed in springs. In this research, we examine to confirm the thermal waveforms in the river and springs and to estimate the horizontal bypass flow velocities in palaeo-channels around the river in the alluvial fan. The study areas are Asahi river springs in Okayama prefecture of western Japan. At the springs of Asahi River, the temperature data was collected 1 week interval. The temperature data of Asahi River springs was analyzed, assuming the subsurface water flow only through the bypath as the one-dimensional advection-diffusion equation and heat flux from the ground surface depends on the temperature gradient between the aquifer and the upper layer. The analytical solution of this equation was verified by parameter fittings with the data.

The Darcy velocity of subsurface flow was estimated about 1.3 m/day. The distribution of one-dimensional subsurface temperature in the alluvial fan was simulated that thermal conductive flux from the river exponentially decreased. The flux was mainly controlled by the advection process. In addition, the heat flux from the ground surface varied spatially from the rivers depends on the variation of the heat gradient. Especially, the flux was about 0 at several sites where heat gradient decreased.

Keywords: Surface water-groundwater interaction, Oxygen-18 isotope, Nutrient concentration, Temperature, Alluvial fan

Japan Geoscience Union Meeting 2014
(28 April - 02 May 2014 at Pacifico YOKOHAMA, Kanagawa, Japan)

AHW28-16 Room:314 Time:April 30 14:30-14:45

Surface water ? groundwater interaction and its effect on nutrient transport; the example in Hachiro-gata

ONODERA, Shin-ichi[1*] ; SAITO, Mitsuyo[2] ; HAYAKAWA, Atsushi[3] ; JIN, Guangzhe[1] ; MARUYAMA, Yutaka[1]

[1]Hiroshima University, [2]Okayama University, [3]Akita Prefecture University

We examined to confirm the surface water-groundwater interaction in Hachiro-gata of Akita prefecture and nutrient transport with the water flow. Hachiro-gata have decreased since 1960s. The reclamation land touches mainly at the east and south side to Hachiro-gata. The height of the reclamation land is lower than the lake water level. Water flow in the underground between the lake and land would have the stable direction from the lake to the land. Because the eutrophication often occurs in Hachiro-gata lake, the nutrient would accumulate in sediment. We installed three piezometers at the bankside of the lake and reclamation land, respectively. The water levels were monitored from September to December in 2013 and water samples were collected in September and December in 2013. We confirmed water flow from the lake to the land with the gradient of from 0.05 to 0.1. In addition, DOC and nutrient concentrations of groundwater were higher in the land than in the lake and lake water. The lake water has recently eutrophic condition, and so many organic matter originated from phytoplankton are deposited. The porewater in the lake bottom near the bank had the high nutrient and DOC concentrations. Based on this research, we can make a hypothesis of nutrient conversion from the lake to the land with groundwater flow.

Keywords: surfacewater, groundwater, interaction, nutrient, Hachiro-gata

Japan Geoscience Union Meeting 2014
(28 April - 02 May 2014 at Pacifico YOKOHAMA, Kanagawa, Japan)

AHW28-17 Room:314 Time:April 30 14:45-15:00

Identification of flow system, sources and behaviors of major anion in a typical soil water-groundwater continuum hillsl

CAO, Yingjie[1*] ; TANG, Changyuan[1] ; LI, Xing[1] ; KANG, Zhiwei[1] ; PIAO, Jingqiu[1]

[1]Graduate School of Horticulture, Chiba University

1 Introduction

In the hydrological system, headwater catchments are source areas for water, nutrients, sediment, and biota for larger steams (Sidle et al., 2000). Unsaturated zone is an important pathway for nutrition leaching in headwater where baseflow dominates (Costa et al., 2002), and the leach pattern is mainly controlled by soil texture and corresponding hydraulic properties. In this study, an intensive study including soil physics investigation, long-term monitoring about the soil water and groundwater hydrochemistry and sources identification of nitrogen by nitrogen isotope are conducted to describe the conceptual soil water-groundwater flow system and discuss the factors controlling the local groundwater hydrochemistry.

2 Study area

The study area is a typical headwater catchment in Ichikawa City (35.76oN, 139.97oE), Chiba Prefecture, Japan (reference). The annual average precipitation is 1,316mm, with the maximum monthly precipitation of 226.5mm/month in study area. The annual average temperature is 15.6 oC while the highest temperature of 31.2 oC occurring in August.

3 Result

From the surface, there are sandy loam (0-1 m), loam (1-2.5 m), clay loam (2.5-3.2 m) and sandy clay (3.2-4.5 m). The porosity shows slight increases from 0.68 at the surface to 0.78 at depth of 4.3m. Due to the occurrence of the Joso clay underlying the loam, the Ks of layer below 3.2 m in depth about two orders lower than the loam and sandy loam. The vertical profile of θr changes little with an average of 0.30.

The average background values for Cl-, NO3- and SO42- were 17.64 mg/L, 0.33 mg/L and 1.52 mg/L, respectively. At the pear orchard, Cl-, NO3- and SO42- concentrations increased dramatically due to anthropogenic inputs of fertilizers. The average concentrations of Cl-, NO3- and SO42- were 32mg/L, 233 mg/L and 85 mg/L, respectively. The concentrations of Cl-, NO3- and SO42- in groundwater of the valley in average are 35.17 mg/L, 129.67 mg/L and 2.39 mg/L, respectively.

4 Discussion

Base on the soil texture of the cross section A-A, there are three flows, interflow along the slope (I), local groundwater flow (LG) and regional groundwater flow (RG), and all of them finally dischage to the valley wetland. In average, the groundwater discharging to the valley at S4 is consisted of waters from LG (43%), RG (56%) and I (less than 1%). Mixing ratios also show seasonal variations. In winter, the ratio of RG with an average of 68% is larger than LG (32% in average), which implies that lateral discharge of groundwater is the dominant factor controlling the groundwater flow in the wetland. While in summer, the contribution of LG becomes higher, and the ratio of LG has exceeded that of RG in May and July, showing the strength of recharge from the upland to LG.

5 Conclusion

An intensive study including both hydrochemical monitoring and numerical simulation are applied to discriminate pollutants sources, evaluate pollutants behaviors and predict long-term effect of soil pollution to local groundwater.

Base on the soil texture and physics investigation, three runoff components interflow (I), local groundwater flow (LG) and regional groundwater flow (RG), are discriminated in the hillslope soil water-groundwater flow system. Two anthropogenic pollutants NO3- and SO42-, which have been approved keep conservation in both soil groundwater according to isotope and redox analysis, are treated as traces to separate these components. And it is found that in average, about 43% of groundwater comes from local groundwater recharge (LG) and 56% comes from regional groundwater recharge (RG). The ratio of interflow (I) only takes up smaller than 1%.

Reference

Sidle, R.C. et al., 2000. Stormflow generation in steep forested headwaters: a linked hydrogeomorphic paradigm. Hydrological Processes, 14(3): 369-385.

Costa, J.L. et al., 2002. Nitrate contamination of a rural aquifer and accumulation in the unsaturated zone. Agricultural water management, 57(1): 33-47.

Japan Geoscience Union Meeting 2014
(28 April - 02 May 2014 at Pacifico YOKOHAMA, Kanagawa, Japan)

AHW28-18 Room:314 Time:April 30 15:00-15:15

Contrasting vertical phosphorus profiles in sediment of Hachirogata ; considering water flow effect

JIN, Guangzhe[1*] ; ONODERA, Shin-ichi[1] ; OTA, Yuki[1] ; SATOU, Takaharu[1] ; SAITO, Mitsuyo[2] ; HAYAKAWA, Atsushi[3] ; ARITOMI, Daiki[1]

[1]Hiroshima University Graduate School of Integrated Arts and Sciences, [2]Graduate School of Environmental and Life Science, Okayama University, [3]Faculty of Bioresource Sciences, Akita Prefectural University

Coastal shallow lake sediment play an important role in the lake eutrophication process, it should be considered important sinks and sources of phosphorus. The accumulation and regeneration of sediment nutrients would be affected by some hydrological process. Lake Hachirogata is a shallow eutrophic lake located in north of Akita City. It used to be the second largest brackish water lake in Japan before the land reclamation project finished in 1977. A salt water barrier has been constructed at the outlet of the regulating reservoir through which water is discharged intermittently out to the Japan Sea. There probably exists the water flow from lake water into sediment due to the lower altitude of the farmland than lake water level after the land reclamation project. We would like to research on the sediment phosphorus accumulation and its activities base on the sediment phosphorus profiles, in consideration of the water flow effects. In order to better understand the possible change on lake phosphorus cycle by land reclamation.

Two core sediment samples were collected by piston core sampler (7-8 cm diameter), in east and west part of the lake (core HL-1 represents the core samples near river mouth area, core HL-2 represents the core samples which was collected near land reclamation area) during the investigations in September 2013. Samples were sliced at 1cm interval then centrifuged for extracting pore water soon after sampling, pore water nutrient and chlorine ion were determined in the laboratory with a spectrophotometer. The advanced SEDEX methods was used in sediment phosphorus fractionation.

Our results shows different pore water Cl^- and nutrient patterns between two locations. In HL-1 core, it shows an increasing trend of Cl^- from around 50mg/L at surface to around 500mg/L at bottom, however in HL-2 this profile shows relatively a constant range around 40mg/L. Both the DTP and DTN concentrations from the HL-1 core showed an increasing trend towards bottom, and they shows relatively constant and low in the HL-2 core, respectively. In sediment P fractionations, Iron bounded P comprise the main phosphorus species in HL-2 core, which comprises 42-72% of total phosphorus. this value is 15-28% in HL-1. Based on the dating information calculated by ^{210}Pb, it shows a larger sediment accumulation rate in HL-2 than HL-1 but with higher phosphorus burial trend in HL-1.

The sediment pore water profile shows significant change after the land reclamation project. Due to the enclosing of the sluice gate decades before, the changing from saline environment to freshwater could reflected by gradually decreasing trend of Cl^- profile towards current in HL-1. The pore water DTN DTP molar ratio shows large variations in HL-1 core. In HL-2, the low Cl^- and DTP in HL-2 provides an evidence that the diluting and transporting pore water phosphorus by water flow from lake into the sediment. On the other hand, it shows high sedimentation accumulation rate and sediment P accumulation rate in HL-2 core site, both at about 3.5 times of the HL-1 core. The supplying of relatively oxic lake water in into pore water may inhibit the iron bounded phosphorus releasing from sediment, decrease and average the mineralization process in sediment, this change in sediment could also be reflected by high phosphorus content, high phosphorus activities in HL-2 core. The increasing in sediment nutrient may be resulted from filtration by water flow into sediment, enhancing the sediment accumulation. Large mobile phosphorus trapped in sediment may increase the phosphorus releasing risk and intensify the algal bloom in Lake Hachirogata. Due to the high sediment phosphorus content and high activities in core HL-2, it would also be a considerable pollutant resources brought by water flow into coastal groundwater. The detailed results on sediment phosphorus property would be described in the presentation.

Keywords: Lake Hachirogata, sediment, pore water, phosphorus fractionation, water flow, land reclamation

Japan Geoscience Union Meeting 2014
(28 April - 02 May 2014 at Pacifico YOKOHAMA, Kanagawa, Japan)

AHW28-19 Room:314 Time:April 30 15:15-15:30

Effect of DO fluctuation on the manganese cycle around the sediment water interface in bottom of the Lake Biwa

ITAI, Takaako[1*] ; HYOBU, Yuika[1] ; CHIKAOKA, Kosuke[1] ; MORISHITA, Yohei[1] ; SHIN, Yoshiki[1] ; KUMAGAI, Michio[3] ; NAKANO, Shin-ichi[2] ; TANABE, Shinsuke[1]

[1]Center for Marine Environmental Studies (CMES), Ehime University, [2]Center for Ecological Research (CER), Kyoto University, [3]Ritsumeikan University Research Center for Biwako Sigma

Enrichment of Mn and As in the surface of sediment has been reported from various lakes in the world. This enrichment is generally caused by the precipitation/adsorption of MnO_2 and arsenate after upward diffusion of Mn^{2+} and arsenite. Lake Biwa is a typical example, in which clear enrichments of Mn and As within thin surface enriched layer (<2 cm) of sediment were observed. However, progressive hypoxia recently reported from the lake can induce release of these elements into water column (Yoshimizu et al. 2010, Itai et al. 2012). In order to reveal the dynamics of Mn and As in the lake bottom, we made geochemical survey through determination and speciation of Mn and As in sediment, porewater and lake bottom water. According to our estimation, total Mn and As in the enriched layer of Lake Biwa was roughly 10000 and 240 tons, respectively (Itai et al., 2012). These amounts are ca. 1800 and 12 times respectively higher than the inventory of these elements in Lake water, suggesting that releasing a portion of Mn and As from enriched layer can be a cause of large increase of these in lake water. The speciation of Mn and As in sediment determined by X-ray absorption fine structure (XAFS) indicated that predominant species of Mn from surface to 2 cm depth was MnO_2 while divalent Mn, likely ionic form, was predominant below enriched layer. Similar to Mn, oxidation state of As was gradually changed with depth, i.e., arsenate was predominant in surface, then arsenite and As in sulfide becomes predominant toward deep. These results suggested that Mn and As in enriched layer should be reduced when DO level in lake bottom becomes lower. The flux of Mn and As from the lake sediment to water column estimated by porewater profile were 3400 - 16000 and 400 - 1800 mg m^{-2} $year^{-1}$, respectively. The fluxes were higher in deeper part of the lake in which sediment character was more reducing than shallower part. With progressive hypoxia, this flux should increase. The monthly monitoring of DO and Mn level in lake water suggested that Mn level in water above 1 m of the lake floor increased from August to December with the highest level was ca. 100 times higher than the baseline level. This trend is consistent with the gradual decrease of DO during thermal stratification period. In the bottom water, the threshold DO level where apparent Mn release started was estimated to be 5-6 mgO_2/L. This value is higher compare to the inter-annual DO minimum ever reported (<4 mgO_2/L). If 40% of Mn released from enriched layer then completely mixed in whole lake, the Mn level becomes 0.6 mg/L which corresponds to lethal levels of some crustaceans and insects. Although such an extreme situation is unlikely, continuous monitoring Mn and As levels is important to safeguard the lake ecosystem and food supply.

Keywords: Lake Biwa, dissolved oxygen, manganese, arsenic, pore water, speciation

Japan Geoscience Union Meeting 2014
(28 April - 02 May 2014 at Pacifico YOKOHAMA, Kanagawa, Japan)

AHW28-20 Room:314 Time:April 30 15:30-15:45

Current status of the research on the phosphorus dynamics in the coastal groundwater discharge area

SAITO, Mitsuyo[1*] ; ONODERA, Shin-ichi[2]

[1]Okayama Univ., [2]Hiroshima Univ.

A large fraction of phosphorus (P) in groundwater generally exists as the dissolved form which is more efficiently used in nutrient cycle and ecosystem than the suspended form. It suggests phosphorus transport by groundwater discharge (e.g. SGD: Submarine Groundwater Discharge) significantly effects on the coastal ecosystem. In the paper, we aimed to review the previous researches related on phosphorus dynamics in the coastal groundwater discharge area and discuss on the future prospects on it.

Japan Geoscience Union Meeting 2014
(28 April - 02 May 2014 at Pacifico YOKOHAMA, Kanagawa, Japan)

AHW28-21 Room:314 Time:April 30 15:45-16:00

Distribution and sources of uranium in Okinawan rivers, Japan

MOCHIZUKI, Akihito[1*] ; HOSODA, Ko[1] ; SUGIYAMA, Masahito[1]

[1]Graduate School of Human and Environmental Studies, Kyoto University

We measured natural background concentrations of dissolved U in 194 Japanese rivers and the highest concentrations were observed in two Okinawan rivers in the limestone region, the Hija and Kokuba Rivers (Mochizuki and Sugiyama, 2012). However, the U concentrations in the earth's surface of their drainage areas are relatively low and therefore the mechanisms of U supply to these rivers are of interest. In this study, we determined U concentrations as well as major chemical compositions in 17 Okinawan rivers and estimated the sources of U supplied to these rivers.

The major chemical compositions of the rivers in the northeastern region of the island were the Na-Cl or Na-HCO_3 types, while those in the southwestern region were the Ca-HCO_3 type. The Ca-HCO_3-type composition is derived from the dissolution of limestone, which is widely distributed in the southwestern region. The U concentrations in rivers were much higher in the southwestern region (32 - 3500 ng/L) than in the northeastern region (5.6 - 18 ng/L).

In the 11 rivers with Ca-HCO_3-type compositions, the limestone-derived fraction of U was estimated using the concentration ratio of U/Ca in the limestone and the Ca concentration derived from limestone. The U concentrations were almost explained by the simple dissolution of limestone in 6 rivers, but this mechanism could not account for the concentrations in 5 rivers with higher U levels (710 - 3500 ng/L). These results suggest that the U in these 5 rivers is supplied by other mechanisms, such as selective dissolution of U from rocks in the drainage areas by carbonate ions.

Keywords: Uranium, Okinawan rivers, Limestone

Japan Geoscience Union Meeting 2014
(28 April - 02 May 2014 at Pacifico YOKOHAMA, Kanagawa, Japan)

AHW28-22 Room:314 Time:April 30 16:15-16:30

Longtime behavior (<50 yr) of Groundwater Quality with Dissolution of a Ryukyu-limestone Aquifer in Okinawa Island

NAKAYA, Shinji[1*] ; YASUMOTO, Jun[2] ; PHAN MIN, Ha[1] ; AOKI, Hideto[1] ; NAKANO, Takuji[2]

[1]Shinshu University, [2]The University of Ryukyu

Dissolution of a terrestrial limestone layer by chemical weathering is one of the most important factors affecting the carbon cycle and the transport of calcium from the land to the ocean. Residence times of sulfur hexafluoride (SF_6) and chlorofluorocarbons (CFCs), as well as their chemical composition in the groundwater, were investigated to estimate the longtime behavior of field dissolution of the Ryukyu-limestone aquifer on Okinawa Island, Japan. The Ca, (HCO_3+SO_4) and Pco_2 increase with groundwater residence time. The field dissolution of Ca was estimated to be 0.090 mM(Ca)/L/yr, with groundwater Ca ranging from 1.75 to 4.0 mM/L. The increase observed in groundwater alkalinity and SO_4 over time (0.170 meq(HCO_3+SO_4)/L/yr; 16 to 34 yr) implies that the groundwater acts as a CO_2 sink through chemical weathering of the Ryukyu-limestone aquifer when groundwater CO_2 (gas) concentrations range from 1.0% to 4.5%(logPco_2=-2 ˜-1.35 atom). The (Ca + Mg) content of groundwater was also affected by groundwater alkalinity (HCO_3), SO_4 and NO_3 derived from fertilizers used on Okinawa Island. These findings imply that the influence of fertilizer and the high partial pressure of groundwater CO_2 on the dissolution of Ryukyu-limestone aquifer may not be negligible. pH decreases with dissolution of the Ryukyu-limestone aquifer.

Keywords: Groundwater, Limestone, Dissolution, Residence time, Sulfur hexafluoride, Okinawa Island

Japan Geoscience Union Meeting 2014
(28 April - 02 May 2014 at Pacifico YOKOHAMA, Kanagawa, Japan)

AHW28-23 Room:314 Time:April 30 16:30-16:45

Rapid procedure for d15N and d18O determination and identifying nitrate sources in agricultural watershed

YADA, Saeko[1*] ; NAKAJIMA, Yasuhiro[1] ; UNO, Hikaru[1] ; ITAHASHI, Sunao[1] ; ASADA, Kei[1] ; YOSHIKAWA, Seiko[1] ; EGUCHI, Sadao[1]

[1]National Institute for Agro-Environmental Sciences

The natural abundance of nitrogen (δ^{15}N) and oxygen isotopes (δ^{18}O) of nitrate (NO_3^-) can be a powerful tool to discriminate the source of NO_3^- in agricultural watersheds. This dual isotopic approach has been used successfully to evaluate the denitrification process in an upland vegetable-field dominant watershed. Recently, determination of δ^{15}N and δ^{18}O of NO_3^- has been updated using a autosampler for automatic analysis. In this study, we developed a further time-saving procedure, which advanced the time-event efficiency by controlling sample traps and 6-port valves. Moreover, the procedure was used to identify sources of riverwater NO_3^- in a rice paddy watershed in Tsukuba, Japan, where the irrigationwater was supplied from out of the watershed.

The δ^{15}N and δ^{18}O values were determined by isotope-ratio mass spectrometry (IRMS) after converting NO_3^- to N_2O gas using the denitrifier method. We conducted sample purge and determination at the same time. Our developed procedure doubled the sample throughput, saving the amount of He carrier gas and liquid N_2. It also engaged the versatile utility of IRMS, since changeover of equipment was not required. This rapid procedure can be applied to other trace gas analysis, which require cryofocus e.g. CO_2, and will contribute for GWG dynamics studies.

Using the developed procedure, we identified principal sources of NO_3^- in mainstream riverwater of the watershed. The δ^{15}N — δ^{18}O relationship during irrigation period indicated that NO_3^- in mainstream riverwater were mainly provided from mountainstream and irrigationwater, and that significant effects of denitrification on the decrease in NO_3^- concentration were locally limited at some irrigationwaters and drainagewaters in the watershed.

Keywords: agriculture, irrigation, IRMS, nitrate, stable isotope, watershed

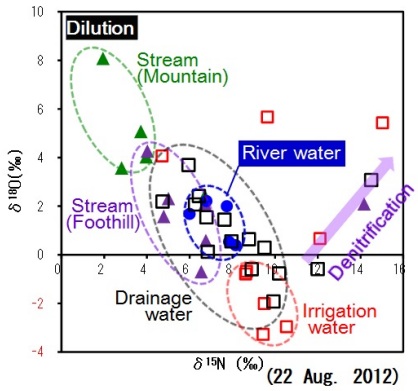

Fig.1 Identifying sources of riverwater nitrate using δ^{15}N and δ^{18}O values in an irrigated rice paddy watershed.

Japan Geoscience Union Meeting 2014
(28 April - 02 May 2014 at Pacifico YOKOHAMA, Kanagawa, Japan)

AHW28-24 Room:314 Time:April 30 16:45-17:00

Study on Effect of Rainfall Distribution and Rainfall Intensity on Discharge at The Concentration Point of The Basin

YOSHIMI, Kazuhiro[1*] ; WANG, Chao-wen[1] ; YAMADA, Tadashi[2]

[1]Graduate School of Science and Engineering, Chuo University, [2]Department of Civil and Environmental Engineering, Chuo University

In resent years, the damage caused by flood comes obvious because of unprecedented record-breaking rainfall event or largest recorded rainfall. Because of this situation, river planning starts to be looked at again in Japan. For example, it has been reported by MLIT (Ministry of Land, Infrastructure, Transport and Tourism) that even if total rainfall is the same when the rainfall distribution differs in a basin, the discharge at a reference point may differ (refer to MLIT). In other words, it is necessary to innovate a new intellection considering the difference of rainfall distribution when creating river planning.

This study aims to clarify the relation between rainfall distribution in a target basin and peak discharge at a reference point. The authors therefore verified how the peak discharge at a basing point responds to rainfall distribution at an intended basin. Moreover, the authors examine the impact on discharge at a reference point if rainfall intensity increases or decreases in a basin.

A target basin of this study is *Tone* upper river basin. In addition, largest recorded flood of this basin is Kathleen typhoon which 3-days accumulated rainfall is about 320mm(refer to document of Japan Society of Civil Engineers) in the basin. First, the authors separated the target basin into 4 parts (refer to document of Science Council of Japan). Then, we did runoff analysis for a number of rainfall distributions using this typhoon event as basic rainfall pattern. The conditions of this calculation are, first, average rainfall of *Tone* upper river basin is the same in every rainfall distribution. Secondly, soil condition and geotechnical condition do not change in every case. After that, we compared every peak discharge at the reference point. Moreover, the authors also did runoff analysis using a number of average-rainfall over watershed 0.8, 0.9, 1.1, 1.2 times as much as basic rainfall event. And then, we compared the peak discharge in the same way.

In consequence, the authors indicated that peak discharge at the point of reference was about from 20800m^3/s to 23800m^3/s in which case rainfall distribution differs. These range of values is $\pm$7% in contrast with basic design flood of *Tone* river. In particular, the peak discharge of the reference point becomes 22000m^3/s or more in which case heavy rainfall intensity occurred in a watershed nearby the point. Furthermore, it was found that the range of values of peak discharge grows wider as average-rainfall over watershed builds in intensity. Therefore, flood exceeding the designed level is necessary to be defined newly and exactly in *Tone* upper river basin.

Keywords: rainfall distribution, runoff analysis, peak discharge, average-rainfall over watershed

Japan Geoscience Union Meeting 2014
(28 April - 02 May 2014 at Pacifico YOKOHAMA, Kanagawa, Japan)

AHW28-25 Room:314 Time:April 30 17:00-17:15

Increasing Water Level in the Vietnamese Mekong Delta

FUJIHARA, Yoichi[1*] ; HOSHIKAWA, Keisuke[2] ; FUJII, Hideto[3] ; YOKOYAMA, Shigeki[3] ; NAGANO, Takanori[4] ; KOTERA, Akihiko[4]

[1]Ishikawa Prefectural University, [2]Kyoto University, [3]Japan International Research Center for Agricultural Sciences, [4]Kobe University

The Mekong Delta is highly susceptible to the impacts of flood, sea level rise, and land subsidence. We considered three factors that could have increased the water level: (1) decrease in flood mitigation functions due to dyke constructions, (2) sea level rise, and (3) land subsidence. We used daily maximum water level, daily minimum water level, and daily water level data. We analyzed data of 21 stations from 1987 to 2006. First, we classified the Delta into two groups; one area is dominated by flows from the upstream, while the other is dominated by the tide. Moreover, we obtained the trend of annual maximum and minimum water levels. Regarding land use, we used the NDVI to estimate the area of dyke construction and the area of the flood plain. It is found that (1) the constructed area of the dyke does not coincide with the area of water level increase, (2) the area with the water level increase correlates with the area with the minimum water level increase. The area with the minimum water level increase is located in the tide dominated zone, indicating that the increase in the maximum water level is caused by the relative increase of sea level.

Furthermore, we examined the trend of sea level rise, and detected a 2.4 mm/year sea level rise. The average of the minimum water level increase was 7.3 mm/year, and therefore, 4.9 mm/year must be the subsidence. In addition, we eliminated the trend of the increasing water level and reconstructed the data without sea level rise and subsidence. We estimated the probabilistic value of water level using the reconstructed data set, and estimated the probability of 100-year water level using the current data set. As a result, the 100-year probabilistic water level in the reconstructed data becomes 21.2-year water level in the current.

Keywords: Mekong delta, Increasing water level, Flood, Sea level rise, Land subsidence, Dyke

Japan Geoscience Union Meeting 2014
(28 April - 02 May 2014 at Pacifico YOKOHAMA, Kanagawa, Japan)

AHW28-P01 Room:Poster Time:April 30 18:15-19:30

Applicability of EUROSEM for surface runoff in forested slope plain

IKEDA, Hideshi[1*] ; WAKAMATSU, Takashi[1] ; NAKAYA, Ko[1] ; ABE, Seiya[1]

[1]Central Research Institute of Electric Power Industry

Sediment yield in agricultural area has been environmental and economic problems in many countries. In order to restrain sediment yield and to conserve water resource, scientific watershed managements are required in many watersheds. In USDA (United State Department of Agriculture), USLE model (Universal Soil Loss Equation) was developed and applied to many sites. USLE model is empirical model, and requires long term observation data. Then, physical based models, such as WEPP (Water Erosion Prediction Project) and EUROSEM (EUROpean Soil Erosion Model), were developed and applied to watersheds where long-term observation had not been conducted.

In some Japanese forest, forest management, such as thinning, has not been conducted fitly in these years. In poorly managed forest area, sediment yield with surface runoff has occurred and supplied suspended solids into stream, reservoir and coastal area. However, in forested watersheds, application of these models has not been conducted frequently, and it is required to validate and apply these models based on observation of meteorology, forestry, pedology and hydrology.

EUROSEM model is one of the useful tools for evaluation of sediment yield in forested area. In this study, hydrological applicability of EUROSEM is discussed. EUROSEM is a prediction model for sediment yield, which was developed by European Union in 1990s. It consists of hydrological and sediment sub-models, those are physical-based process models in non-steady state. EUROSEM has been applied to agricultural areas in Europe and China, for example in watershed of Three Gorge dam, Yangtze River. On the other hand, it is not applied to Japanese forest area frequently, where sediment yield is reported recently.

In Central Research Institute of Electric Power Industry (CRIEPI), we have been conducting observation for sediment yield since June 2010 in Akagi testing center, located in north Kanto plain. The observation system consists of 3 sites, one open field and two forest stands. For open field, precipitation was observed using Laser Precipitation Monitor (LPM,THEIS, FRG) consequently. For in two forest stands, vegetation, meteorology and hydrology survey were conducted. In vegetation survey, canopy analyzing and forest floor survey were conducted in every months. In meteorology survey, precipitation was observed using LPM consequently. In hydrology survey, surface runoff was observed in experimental area with 2m length and 0.5m width using tipping gauge continuously. Soil moisture and temperature were observed in every 10 minutes in experimental area.

In these two forest stands, EUROSEM hydrological sub - model was applied in 35 storm events, and siumlated surface runoff was validated based on observed data. EUROSEM hydrological sub model was applied to 10 storm events in previous study and appeared to simulate surface runoff for storm events with rainfall intensity between 2.0 - 5.0mm / 10mim. In this study, surface runoff was simulated well in storm events with rainfall intensity larger than 5.0mm/10min using infiltration rates lower than those in laboratory experiments.

Keywords: Forest, Surface Runoff, Sediment Yoelds, Prediction Method, EUROSEM, Storm - Runoff

Japan Geoscience Union Meeting 2014
(28 April - 02 May 2014 at Pacifico YOKOHAMA, Kanagawa, Japan)

AHW28-P02 Room:Poster Time:April 30 18:15-19:30

Distribution of trace elements in 3 small rivers and the surrounding geology in the North Osaka prefecture, Japan

EVEN, Emilie[1*] ; NOJIMA, Aki[1] ; MASUDA, Harue[1]

[1]Department of Geosciences, Osaka City University, Japan

The Rivers Yono, Ibaraki and Minoh, that are tributaries of the River Yodo in the northern part of the Osaka prefecture, Japan, flow across the Paleozoic-Mesozoic sedimentary formations and the Ibaraki granitic complex. Waters from these rivers have been used for domestic purposes and some trace metals have been reported in concentrations above the environmental standard limits. Previous studies have shown that the sedimentary rocks were the sources of trace metals, especially arsenic, whereas the granitic sequence of quartz diorite, granodiorite and adamellite is believed to be the source of rare earth elements (REEs). In addition to track back of the origin of these trace elements, the transportation phases and the geochemical budget of trace metals along the river flow are examined as a first step to set up a simple transportation model. Here are presented first results.

Results showed that the geochemical patterns of riverbed sediments matched the distribution of the source rocks. The geochemistry of trace elements in river water is likely controlled by the weathering of riverbed sediments. River sediments from sandstone and quartz diorite contained high amount of trace elements and yielded high concentrations of trace metals in river water but low concentrations of REEs. Comparatively, river sediments originated from adamellite contain lower amounts of trace elements but river waters flowing across this formation showed to have the highest concentrations of REEs. O/H isotopic ratio in river water pointed at the meteoritic origin of the water in the upper reaches of rivers and the contribution of groundwater in the lower reaches. The fractionation of trace elements regarding the different size pools of total concentration, 0.45μm and 0.22μm filtration showed that most of the trace elements were transported within the $<$0.22μm phase. Temperature of river water seems to influence the concentrations of elements, as concentrations increased with increasing temperature throughout the year. The role of organic matter (likely as colloidal carriers) is limited since an inverse relationship was observed. Water mixing calculation with major and trace elements yielded accurate geochemical budget model ($<$5% error), where as redox sensitive species induce large errors of $>$15%, even on few meters distance along the flow path.

Keywords: Rare Earth Elements, River Water, Source rock, Trace Metals, Transportation

Japan Geoscience Union Meeting 2014
(28 April - 02 May 2014 at Pacifico YOKOHAMA, Kanagawa, Japan)

AHW28-P03 Room:Poster Time:April 30 18:15-19:30

Seasonal variation in oxygen stable isotopic ratio and nitrate concentration in a mountain agricultural watershed

ARITOMI, Daiki[1*] ; ONODERA, Shin-ichi[1] ; SAITO, Mitsuyo[2] ; MARUYAMA, Yutaka[1] ; JIN, Guangzhe[1] ; ONISHI, Koki[3]

[1]Hiroshima University, [2]Okayama University, [3]Fukken Co., Ltd.

We aimed to examine the groundwater flow and seasonal variation of NO3–N in coastal aquifer of a granite catchment considering the contribution of bedrock groundwater and denitrification processes.

Japan Geoscience Union Meeting 2014
(28 April - 02 May 2014 at Pacifico YOKOHAMA, Kanagawa, Japan)

AHW28-P04 Room:Poster Time:April 30 18:15-19:30

An Overview of Recent Hydrological Models for Estimating Phosphorus flux

SHIMIZU, Yuta[1*] ; ONODERA, Shin-ichi[2] ; SAITO, Mitsuyo[3]

[1]NARO/WARC JSPS-PD, [2]Graduate School of Integrated Arts and Sciences, Hiroshima University, [3]Graduate School of Environmental and Life Science, Okayama University

Phosphorus which derived from forest, agricultural area and urban is discharged to river stream via surface runoff and drainages. There is a time lag from ”inflowing to river channel” to ”outflowing to coastal area” because most of transported phosphorus is retained in river channel due to physical, chemical and biological processes. Previous studies about material balance in watersheds show that total amount of phosphorus emission is not correspond to total amount of discharged phosphorus. This is because of phosphorus retention in watersheds. So it is necessary to understand about phosphorus retention processes for estimation of phosphorus transportation. In recent years, distributed hydrological models are used to estimate phosphorus transportation. Most of these models are developed in western countries, and have been improved its accuracy of estimation of sediment and water quality. The objective of this study is to review phosphorus retention process in watersheds and model description for understanding model limitation for phosphorus transportation.

Keywords: Hydrological Model, Phosphorus, Material transport, Watershed

Japan Geoscience Union Meeting 2014
(28 April - 02 May 2014 at Pacifico YOKOHAMA, Kanagawa, Japan)

AHW28-P05 Room:Poster Time:April 30 18:15-19:30

Water pollution and arsenic behavior in the Red River, North of Vietnam

INOUE, Ryo[1*]

[1]graduate school of science,Osaka City

Water pollution and arsenic behavior in the Red River, northern Vietnam.

Inoue,R1.Shinntani,T1.Masuda,H1.Yonezawa,G1.Truong Xuanluang2.Hang Do Thi2.
(1 Osaka City University, 2 Hanoi University of Mining Geology)

The Red River, flowing through the northern part of Vietnam, is originated in Yunnan, China and running parallel to the Hoang Lien Son mountain range. Arsenic pollution of groundwater has been a serious problem in rural area located on the Red River delta. The sources of arsenic must be carried to the aquifer through the river, although transportation processes are not well understood. In this study, arsenic transportation process through Red River was studied from the analytical results of river water, suspended particles, river-bed sediments which were collected in the Vietnam territory. In addition, general situation and the cause of the river water pollution was considered.

Total dissolved ions of river water sample is 5.0meq/L in Lao Cai located at the upper most stream in Vietnam, 2.4meq/L in Bao Ha and 2.1meq/L in Yen Bai at middle-stream, and 3.4meq/L in Hanoi at downstream. Low concentration of dissolved solids between Lao Cai and Hanoi is due to the inflow of the surface water from Hoang Lien Son mountain range. Such an inflow is clear from the lower oxygen and hydrogen isotope ratio of river water than those of main channel waters. δ18O: -9.9∼-10.0 ‰ and δ2H: -69 ‰ in Lao Cai. δ18O: -12.9∼-13.0 ‰ and δ2H: -91∼-92 ‰ in the branch channel in Hoang Lien Son mountain range, and δ18O:-11.6∼-11.9 ‰ and δ2H:-82∼-84 ‰ in Bao Ha and Yen Bai at middle-stream. Branch channel water in Hoang Lien Son mountain range diluted the dissolved salts and pollutants such as As and Pb. Arsenic is transported as dissolved components (∼60%) and adsorbed components (∼40%) in the river.

Arsenic concentration has clearly positive correlation to the XRD intensity of smectite. Weak positive correlation between arsenic and kaolinite was also found. However, there is no relationships between arsenic and iron, indicating that the arsenic doesn ' t behave with iron oxyhydroxides in the river. And, smectite found only in suspended particles sample of Red River main channel water, thus, the arsenic is transported with clay minerals in the Red River.

Keywords: arsenic, Red River, Vietnam, Isotope

Japan Geoscience Union Meeting 2014
(28 April - 02 May 2014 at Pacifico YOKOHAMA, Kanagawa, Japan)

AHW28-P06 Room:Poster Time:April 30 18:15-19:30

Estimation of water balance in a coastal agricultural catchment using SWAT and HYDRUS Model.

JIN, Guangzhe[1*] ; SHIMIZU, Yuta[2] ; ONODERA, Shin-ichi[1] ; SAITO, Mitsuyo[3] ; MATSUMORI, Kenji[2]

[1]Hiroshima University Graduate School of Integrated Arts and Sciences, [2]National Agriculture and Food Research Organization, Western Region Agricultural Research Center, [3]Graduate School of Environmental and Life Science, Okayama University

Quantify the rate of ground water recharge and clarify the water balance in watersheds is basic and important for efficient ground water resource management. It is particularly important in regions with little rain which face with the risk of water shortage. However, the rate of aquifer recharge is one of the most difficult factors to evaluate. Especially, the former method of groundwater recharge estimation, are normally subject to large uncertainties and easily to cause errors. Recently, there are several attempting for estimation of groundwater recharge using distributed hydrological models in the world.

The Soil and Water Assessment Tool (SWAT) Model is one of a physically based and quasi-distributed continuous time hydrological model used to estimate water budget in previous researches around the world. SWAT Model has been implemented for watershed hydrology related issues such as estimation of surface water flow and groundwater recharge rate. We could more specific testify the groundwater flux combined SWAT Model with HYDRUS Model which is a software package for simulating water, heat, and solute movement in two- and three-dimensional variably saturated media. The objective of this research is to estimate water balance and to clarify the groundwater recharge parameter in an agricultural catchment in the Seto Inland Sea, using the SWAT Model, and to estimate the groundwater flow using the HYDRUS Model.

The study site is located on the southern part of Ikuchi Island, which is one of the islands in central Seto Inland Sea. The orange groves cover approximately 50% of the total catchment area. Due to the small annual precipitation (approx.1000mm/y) with large inter-annual variation, Ikuchi Island is facing a risk of water shortage in the serious dry year.

As input to SWAT Model, topographic data (10 m grid), soil map (1/25000), land use map (1/25000) and weather information were used to build and calculate the SWAT Model. Evaporation was estimated by the Penman-Monteith method. Simulation time periods is 2000-2013, including warm up period of 2000-2003 and calibration period of 2003-2004. The calibration was conducted using the Sequential Uncertainty Fitting (SUFI2). The reproducibility of daily discharge in calibration period by the model was found to be acceptable (NSE=0.69, RSR=0.56, PBIAS%=18, R^2=0.75). Amount of groundwater recharge is accounted as the water discharge into aquifer except the flows which are eventually discharged from aquifer, such as return flows into river and amount of water moving into the vadose zone.

The result shows spatial difference in groundwater recharge rate. About 10 times higher groundwater recharge rate was found in middle and downstream areas. While middle and downstream area are indicated the main groundwater recharge area, upstream is small recharge rate due to steep slope. Groundwater recharge shows smaller volume than river discharge, it comprise about 17% of total precipitation in annual average consideration. From the comparison of water balance calculation, it is found that both of river discharge and groundwater recharge fluctuated in high precipitation year of 2011 (1,527mm), low precipitation year of 2005 (781mm) compared to average balance. In high precipitation year, groundwater recharge rate increased about 6 times than in low precipitation year, the increasing of river discharge is at about 2.5 times.

Consequently, it was confirmed that spatial and temporal variation of groundwater recharge rate in long term. And we could estimate the long term water balance base on these information. However, it is noted that this result may include some uncertainty and chance to improve. Seat model could not reflect the groundwater flow, simulated with HYDRUS Model on the groundwater flow could provide us with the groundwater data. In the presentation, more detailed data cover long time periods and results testifying groundwater level variation with HYDRUS Model will be displayed.

Keywords: Ikuchi Island, SWAT Model, HYDRUS Model, groundwater recharge rate, water balance

Japan Geoscience Union Meeting 2014
(28 April - 02 May 2014 at Pacifico YOKOHAMA, Kanagawa, Japan)

AHW28-P07 Room:Poster Time:April 30 18:15-19:30

Seasonal variation in nutrient dynamics in the tidal zone of Yamato river

ONODERA, Shin-ichi[1*] ; SAITO, Mitsuyo[2] ; SHIMIZU, Yuta[3] ; MARUYAMA, Yutaka[1] ; MIYAOKA, Kunihide[4] ; JIN, Guangzhe[1] ; ARITOMI, Daiki[1]

[1]Hiroshima University, [2]Okayama University, [3]NORO, [4]Mie University

In coastal megacities, sever groundwater depression and water pollution occurred. These impacts affected to river environment change. Especially, the river mouth area has been deposited the polluted matters. These areas have characteristics of water level fluctuation which causes river water-groundwater interaction and the associated change in dynamics of nutrients. However, these effects on the nutrient transport in tidal reaches and nutrient load to the sea have not been fully evaluated in previous studies. Therefore, we aimed to clarify the nutrient dynamics with the river water-groundwater interaction in the tidal river of Osaka metropolitan city. We conducted the field survey from the river mouth to the 7km upstream area of Yamato River, which has a length of 68km and a watershed area of 1070 km2. In addition, model simulations were also conducted. Spatial variations in radon (222Rn) concentrations and the difference of hydraulic potential between river waters and the pore waters suggest that the groundwater discharges to the river channel in the upstream area. In contrast, river water seeped into the groundwater in the river mouth area. It may be caused by the lowering of groundwater level associated with the excess abstraction of groundwater in the urban area. The spatial and temporal variations in nutrient concentrations indicate that nitrate-nitrogen (NO3-N) concentrations changed temporally and it negative correlated with dissolved organic nitrogen (DON) concentrations. Inorganic phosphorous (PO4-P) concentrations showed the increasing trend with the increase of the river water level. Based on the mass balance, nutrient reproduction from the river bed was suggested in tidal reach during a summer, especially phosphorus was large.

Keywords: seasonal variation, nutrient dynamics, tidal river, polution, phosphorus

Japan Geoscience Union Meeting 2014
(28 April - 02 May 2014 at Pacifico YOKOHAMA, Kanagawa, Japan)

AHW28-P08 Room:Poster Time:April 30 18:15-19:30

Examination on the classification and ecological index of ponds based on the stability of stratification

OKUBO, Kenji[1*] ; SAITO, Mitsuyo[1] ; TAKAGI, Shinya[1] ; ONODERA, Shin-ichi[2] ; MARUYAMA, Yutaka[2] ; JIN, Guangzhe[2] ; ARITOMI, Daiki[2] ; SHIMIZU, Yuta[3]

[1]Okayama Univ., [2]Hiroshima Univ., [3]JSPS PD, NARO/WARC

We aimed to examine on the classification and ecological index of the small ponds based on the stability of stratification. The seasonal variation of the stratification was examined using the monitoring data of water temperature in multiple depths in the 4 different ponds located on an island which is highly influenced by agricultural activity. DO, fluorescence, nutrients data were used for the evaluation of ecosystem condition.

∗This research is supported by the Grants-in-Aid for Scientific Research (A) (No. 25241028, Shin-ichi Onodera).

Japan Geoscience Union Meeting 2014
(28 April - 02 May 2014 at Pacifico YOKOHAMA, Kanagawa, Japan)

AHW28-P09 Room:Poster Time:April 30 18:15-19:30

Rock magnetic profiles of sediment cores in Hachirogata : effect of a land reclamation

OTA, Yuki[1*] ; SATO, Takaharu[1] ; ONODERA, Shin-ichi[1] ; JIN, Guangzhe[1] ; SAITO, Mitsuyo[2] ; HAYAKAWA, Atsushi[3]

[1]Graduate School of Integrated and Arts Sciences, Hiroshima University, [2]Graduate School of Environmental and Life Science, Okayama University, [3]Faculty of Bioresource Sciences, Akita Prefectural University

We examined the influence of land reclamation on rock magnetic profiles in Lake Hachirogata. In this lake, all flowing rivers exist on an east side and a large reclamation land touch at west and north sides. Two sediment core samples were collected at the eastern central (HL-1) and northwestern bankside (HL-2) sites in this lake in September 2013, using the 1m piston core sampler (7-8 cm diameter). HL-1 was 77cm and HL-2 was 78cm.

Keywords: Lake Hachirogata, sediment, rock magnetism, land reclamation

Japan Geoscience Union Meeting 2014
(28 April - 02 May 2014 at Pacifico YOKOHAMA, Kanagawa, Japan)

AHW28-P10 Room:Poster Time:April 30 18:15-19:30

Spatial distribution of radon (222-Rn) and radium (226-Ra, 228Ra) in the coastal seawater of Seto Inland Sea and its con

SAITO, Mitsuyo[1*] ; ONODERA, Shin-ichi[2] ; OHTA, Tomoko[3] ; GUO, Xinyu[4] ; TAKEOKA, Hidetaka[4] ; ONISHI, Hidejiro[4] ; KUBOTA, Takumi[5]

[1]Okayama Univ., [2]Hiroshima Univ., [3]Hokkaido Univ., [4]CMES, Ehime Univ., [5]KURRI, Kyoto Univ.

Previous studies have revealed that submarine groundwater discharge (SGD) is one of the important pathways for nutrients and the other dissolved materials from terrestrial area to the marine environment. For the evaluation of the effect of SGD, the timescale of nutrient transport in the coastal area derived by SGD such as residence time is important as well as nutrient flux by SGD. Radioactive isotopes of radon (222-Rn) and radium (226-Rn, 228-Ra) are one of the useful tracers for the evaluation of SGD and residence time of water mass in the coastal area. The objective of the study is to examine the spatial variation of 222-Rn and 226-Rn, 228-Ra in the coastal seawater of the central part of Seto Inland Sea and its controlling factors. The study area is southwestern part of the Hiuchi-Nada with the area of approximately 30 km $\times$ 13 km. Relatively high concentrations of 222-Rn, 226-Rn and 228-Ra were detected in the southern part of the study area. These results suggest the effect of SGD from seafloor.

$*$This research was supported by the KWEF research grant program by Kurita Water and Environment Foundation (No. 24254, Mitsuyo Saito) and cooperative research project in KURRI, Kyoto University (No. 2434, Shin-ichi Onodera) in 2012.

Japan Geoscience Union Meeting 2014
(28 April - 02 May 2014 at Pacifico YOKOHAMA, Kanagawa, Japan)

AHW28-P11 Room:Poster Time:April 30 18:15-19:30

Arsenic distribution in porewater and coexisting sediments of Kumano Basin, Nankai Trough

YOSHINISHI, Haruka[1*]

[1]Osaka City University

Arsenic contamination of groundwater is a serious problem in the world, especially in the deltas along large rivers originated from Himalayas such as Bangladesh and West Bengal, India. Sulfide minerals including pyrite in shales is one of the candidates of source minerals causing arsenic contamination. However, the mechanism of arsenic concentration in sedimentary rocks has not been well understood. In this study, arsenic behavior in the porewater and host sediments was determined to understand the fixing process of arsenic during early stage of diagenesis in modern marine sediments.

Porewaters and squeezed cakes were sampled at three sites (C0002, C0021, C0022) in the Nankai trough by IODP, Expedition 338. The sediments from Site C0002 is composed hemipelagic mud of distal turbidites, those from Site C0021 of mass transport deposits (MTDs), Site C0022 is dilled at right above the megasplay fault, and highly fractured zone, likely related to the megasplay faulting was found at 100 mbsf (meters below seafloor).

Arsenic concentration of the porewaters at Site C0002 was constant 0-1.1μM at 200-300 mbsf, and it increased with depth to 3μM in 300-400mbsf. The highest concentration (3μM) was recorded at 400 mbsf, and the concentration decreased below that depth. In C0021, arsenic concentration of the porewaters is 0.2μM on an average at 0-160 mbsf and give no relationship to the depths. It increased quickly to 1.2μM down to 200 mbsf. In C0022, arsenic concentration is 0.3μM on average at 0-100mbsf. The highest concentration (1.5μM) was observed at 130-160mbsf, and then drastically decreased to 200 mbsf. Arsenic concentration became constant below that depth.

Arsenic concentration of sediments is 40-120μM at 300-500 mbsf in Site C0002, 40-90μM at 100-150mbsf in Site C0022. The arsenic concentration is varied without relationship to the depth.

Mineral composition determined by XRD showed that the all sediments analyzed were dominated by quartz, feldspars, micas, calcites, smectite, and chlorite/ kaolinite. Hornblende and pyrite were occasionally observed.

Compared to the major chemical composition determined onboard, arsenic concentration of porewater correlated to pH, Fe, Pb, and Mn. It is suggested that the arsenic was accumulated in the sediments via coprecipitation with iron hydroxides/oxides at the sea floor, similar to many trace heavy metals, and was released intio the porewater by desorption under reducing environment, or by decomposition of iron hydroxides/oxides. After that, arsenic may be fixed into pyrite with depth, however, the fixing mechanism of arsenic in the deep is not clear at present.

Keywords: Arcenic, Nankai Trough, IODP

Japan Geoscience Union Meeting 2014
(28 April - 02 May 2014 at Pacifico YOKOHAMA, Kanagawa, Japan)

AHW28-P12 Room:Poster Time:April 30 18:15-19:30

Research on dissolved inorganic phosphorus concentrations forming process in a forested mountainous stream

TAKEDA, Manami[1*] ; OHTE, Nobuhito[1] ; EGUSA, Tomohiro[1] ; SUZUKI, Masakazu[1]

[1]Department of Forest Science Graduate School of Agricultural and Life Sciences

Since the ecosystems of river, lake, and ocean are supported by P supply from terrestrial area, it is important to understand the mechanisms behind the P discharge from the catchments through the aquatic system. It has generally been considered that loss of P from a forested area through a headwater stream is small, because it is preserved tightly within forested ecosystem. It has previously been reported that heavy rainfalls lead to a large P loss from forested catchments, and major fractions of exported P is particulate form absorbed onto soil particles. Therefore, many studies have focused on particulate P load during high flow condition. However, it has been still poorly understood about the controlling mechanisms of sources and transport of dissolved inorganic phosphorus (DIP), which is directly available for organisms. In order to explain the controlling mechanisms of DIP discharge, we conducted field investigations on the DIP dynamics through the elemental hydrological processes in the hill slopes of a headwater catchment, and illustrated the spatial distribution of DIP concentrations of the stream network in meso-scale catchment.

The study site was Fukuroyamasawa experimental watershed located in The University of Tokyo Chiba Forest and Inokawa watershed including Fukuroyamasawa. The size of Fukuroyamasawa is 1 ha, and that of the Inokawa watershed is 503 ha. Through fall water, stem flow water, litter layer infiltration water, soil water, groundwater and stream water were sampled once every two weeks from August 2013 to November 2013. Rainwater was collected at the meteorological station located near by Fukuroyamasawa. In Inokawa watershed, flow observation and stream water sampling at the point with various watershed area on low-flow period in September 2013 and December 2013. The samples were filtered by 0.45 micrometer membrane filters immediately after the sampling. Then DIP was analyzed using molybdenum blue (ascorbic acid) absorptiometry.

The average DIP concentration of rainwater was 0.2 micromol / L during the observation period. That of through fall, stem flow and litter layer infiltration water were 0.9, 1.7 and 10.9 micromol / L respectively. DIP concentration felt remarkably with soil layer passage, and the average DIP concentration of soil water, groundwater and steram water was 0.6 micromol /L. DIP concentration in Inokawa stream water ranged from minimum limit of determination, 0.1 micromol /L, or less to 9.2 micromol / L. When we investigated the relation between DIP concentration and a contributory area, DIP concentration differed in about 2 km2 or less, and it increased at the larger than 2 km2 as the contributory area became large. There was a strong positive correlation between DIP concentration and EC.

In Fukuroyamasawa, it was shown that DIP added during canopy passage was almost absorbed in the soil layer at particles, and was removed from the water, and hardly contributing to the outflow to a mountain stream. EC is an index for underwater dissolved matter concentration, and it turns out that the amount of the dissolved matter concentration of mineral origin is shown at Inokawa watershed. Therefore, the relationship of DIP concentration and EC has suggested that mountain stream underwater DIP mainly originates in bedrock weathering, and that the spatial distribution of DIP concentration is determined with the contribution of a groundwater course which passes bedrock.

Keywords: Dissolved Inorganic Phosphorus (DIP), forested mountainous stream, spatial distribution, catchment area

Japan Geoscience Union Meeting 2014
(28 April - 02 May 2014 at Pacifico YOKOHAMA, Kanagawa, Japan)

AHW28-P13 Room:Poster Time:April 30 18:15-19:30

Mixing of river water as deduced from major component concentration, Sr and S isotopic ratios in Tama River, Akita.

WAKASA, Sachi[1*] ; ISHIYAMA, Daizo[2] ; MATSUBAYA, Osamu[3] ; SATO, Hinako[2] ; SHIN, Kicheol[4] ; NAKANO, Takanori[4]

[1]Center for Geo-Environmental Science, Akita Unisity, [2]Faculty of International Resource Sciences, Akita University, [3]Emeritus professor, Akita University, [4]Research Institute for Humanity and Nature

The acidic high temperature hot spring discharged from the Tamagawa hot spring (Ohbuki) into the Tama River system through the Shibukuro creek is still acidic downstream. The acidity of the Ohbuki hot spring water is neutralized using limestone before it discharges into the Shibukuro creek. In this study, geochemical signatures of mixing between Tama River and its tributaries were deduced from concentration of major chemical components, Sr and S isotopic ratios. The Ohbuki hot spring water has high concentration of chloride and sulfate. The δ^{34}S of sulfate is the highest (δ^{34}S = 31.8 ‰) in the watershed. Due to the neutralization, the concentration of calcium, strontium and strontium isotopic ratio increases (^{87}Sr/^{86}Sr = 0.7068). The mixing rate of water flowing out from the neutralization facility is about 20% and 8% before and after the confluence of Shibukuro and Tama Rivers, respectively. The concentration of the major chemical components decreases gradually downstream and is almost similar to other tributaries in the Tama and Omono Rivers system. The pH of the water also decreases from 3 to neutral (about 7). The strontium isotopic ratios of 0.7040, 0.7068 and 0.7049-0.7062 for the Ohbuki, the neutralization facility and tributaries of the Tama River respectively, reflect the geology of the catchment area. A two component mixing phenomena is observed in the Tama River and its tributaries based on the major chemical components. However, the two component mixing relationship is not clearly distinct with the Sr isotope ratios. The δ^{34}S of sulfate in the Ohbuki thermal water (+31.8 ‰) and Tawa River (+6.6 – +8.8 ‰) near the confluence of the Tama and Omono Rivers supported the two component mixing relationship observed from the major chemical component. The results observed in this study are used to interpret the mixing mechanisms operating between the Tama River and its tributaries.

Keywords: Mixing of river water, Akita, Concentration of major chemical components, Strontium isotopic ratio, Sulfur isotopic ratio

Japan Geoscience Union Meeting 2014
(28 April - 02 May 2014 at Pacifico YOKOHAMA, Kanagawa, Japan)

AHW28-P14 Room:Poster Time:April 30 18:15-19:30

Feature of distribution of radioactive cesium in irrigation canal

KUBOTA, Tomijiro[1*] ; TARUYA, Hiroyuki[1] ; TANAKA, Yoshikazu[1] ; HAMADA, Koji[1]

[1]National Institute for Rural Engineering, NARO

The purpose of this study is to clarify distributive characteristics of a radioactive cesium in the irrigation canal by examining the radioactive cesium contained in the bottom sediment along the canal from its intake to the downstream. One of the millrace located in Fukushima Prefecture was selected as a case for investigation, and the distribution of the amount of the sedimentation, the concentration of radioactive cesium in the bottom sediment, and the air dose rate were examined. The sandy deposit was seen in the upstream of the canal, and those concentration of radioactivities Cs were comparatively low with 1-5kBq kg^{-1}. On the other hand, relatively high concentration of radioactivity Cs was seen in the downstream of canal, and was within 3-28kBqkg^{-1}. The air dose rate in the waterway were relatively low because of the influence of ponding, relatively high air dose rate were seen in the place where the depositional surface had been exposed.

Keywords: radioactive cesium, irrigation canal, sediment, air dose rate

Japan Geoscience Union Meeting 2014
(28 April - 02 May 2014 at Pacifico YOKOHAMA, Kanagawa, Japan)

AHW28-P15 Room:Poster Time:April 30 18:15-19:30

Current status of the groundwater use in an island of the Seto Inland Sea: a case study of Ikuchijima-island

TANIGUCHI, Tomomasa[1*] ; ONODERA, Shin-ichi[2] ; TAKAHASHI, Hidehiro[3] ; SAITO, Mitsuyo[4] ; SHIMIZU, Yuta[5]

[1]Faculty of Humanities, Law and Economics, Mie University, [2]Graduate School of Integrated and Arts Sciences, Hiroshima University, [3]NARO Western Region Agricultural Research Center, [4]Graduate School of Environmental and Life Science, Okayama University, [5]NARO Western Region Agricultural Research Center, JSPS PD

The study is aimed to examine the current status of the groundwater use in an island of the Seto Inland Sea, southern Japan. This area is characterized by high risk of drought with low annual rainfall and limited water resource. We conducted face-to-face surveys in the form of a multiple-choice questionnaire in two areas (districts of Miyabara and Hayashi) with different main resource of agricultural water in Ikuchijima-island, Onomichi-City. Citrus farms such as orange, lemon etc. are widely cultivated in both areas.

The rate of households having domestic well is about 74% in Miyabara district, and is about 62% in Hayashi district. The main purposes of groundwater use are watering in garden and car wash in both areas. About 20% of respondents answered that groundwater resource is not enough for the agricultural use in the dry season. It indicates the groundwater is regarded as one of the important water resource in the island. Averaged daily domestic use of groundwater per household are estimated to be 361L/day and 271L/day in Miyabara and Hayashi, respectively.

∗This research is supported by the Grants-in-Aid for Scientific Research (A) (No. 25241028, Shin-ichi Onodera).

Japan Geoscience Union Meeting 2014
(28 April - 02 May 2014 at Pacifico YOKOHAMA, Kanagawa, Japan)

AHW29-01 Room:314 Time:May 2 14:15-14:30

Evaluating the impact of disturbances on the carbon balance of forest ecosystems in Hokkaido by using data and model: fr

HIRATA, Ryuichi[1*] ; ITO, Akihiko[1] ; TAKAGI, Kentaro[2] ; HIRANO, Takashi[3] ; SAIGUSA, Nobuko[1]

[1]National Institute for Environmental Studies, [2]Field Science Center for Northern Biosphere, Hokkaido University, [3]Research Faculty of Agriculture, Hokkaido University

Changes in carbon flux and storage in forest ecosystems are influenced by climate at various temporal and spatial scales, whereas carbon flux and storage are affected instantaneously and heterogeneously by artificial and natural disturbances at the local scale. Disturbance events such as forest fire, damage by insects, and forest harvest drastically change NEP and carbon storage. In this study, we address the effect of disturbance on carbon balance based on two scale; one is site scale and another is local scale.

First, we performed a baseline simulation of carbon dynamics and compared these values with those observed across a wide range of stand ages (old mixed forest and young and middle-aged larch forests). By taking into account seasonal variation in the understory leaf area index, simulated net ecosystem production (NEP), gross primary production, ecosystem respiration, and biomass for the three types of forests were consistent with observed values.

We compared two cases of simulations concerning the carbon balance: one taking account of spatial distribution of disturbance-induced forest age derived from forest inventory data (disturbance case) and another ignoring the disturbance impact (non-disturbance case). NEP was gradually and spatially changed ranging from 0 to 1 t C/ha/y depending on meteorological conditions such as temperature or solar radiation. On the other hand, in the case of disturbance, large NEP ranging from 3 to 5 t C/ha/y were distributed patchwise like hotspots, because forest age of these spots ranging from 20 to 100 years old and then younger than those of the non-disturbance case. In the 1970s, wood harvest and tree planting were intensively conducted in Hokkaido. In the disturbance case during this period, there were many hotspots which show negative NEP.

Keywords: process-based ecosystem model, eddy covariance method

Japan Geoscience Union Meeting 2014
(28 April - 02 May 2014 at Pacifico YOKOHAMA, Kanagawa, Japan)

AHW29-02 Room:314 Time:May 2 14:30-14:45

Examining initialization procedures of terrestrial carbon cycle models

ITO, Akihiko[1*]

[1]National Institute for Environmental Studies

It has been realized that long-term trends in model simulation is affected by initialization procedure. In terrestrial carbon cycle models, insufficient stabilization can result in artificial trends (lingering sink or source in CO2 flux) in the simulated carbon budget, making it difficult to interpret simulation results and make comparison with observational data. Conventionally, an equilibrium state of terrestrial carbon budget has been obtained through iterative calculations using an appropriate forcing data. This spinning-up method requires high computational cost, typically, at over 90% of total computational cost. On the other hand, terrestrial modeling has another problem related to initialization; actual ecosystems are not always at steady state due to disturbance and environmental change. As a result, different model groups adopt different initialization procedures, raising some problems in inter-model comparison. In this study, I examined how an alternative initialization method (semi-analytical solution) works in a terrestrial carbon cycle model and is effective to reduce computational cost in comparison with the conventional spinning-up. I discuss possibility of better initialization procedures, in terms of idealism, realism, and generality, not only with model researchers but also with filed researchers.

Keywords: terrestrial ecosystem model, initialization, carbon budget

Japan Geoscience Union Meeting 2014
(28 April - 02 May 2014 at Pacifico YOKOHAMA, Kanagawa, Japan)

AHW29-03 Room:314 Time:May 2 14:45-15:00

Interannual variation of carbon allocation in a cool-temperate deciduous forest from 1999 to 2006

KONDO, Masayuki[1*] ; ICHII, Kazuhito[2] ; UEYAMA, Masahito[3]

[1]Faculty of Symbiotic Systems Science, Fukushima University, [2]Japan Agency for Marine-Earth Science and Technology, [3]Graduate School of Life and Environmental Sciences, Osaka Prefecture University

Carbon allocation is the key factor controlling the dynamics of carbon cycle. It determines partitioning of assimilated carbohydrate to components of vegetation, leaves, woody organs, and fine roots. To analyze seasonal and annual scale carbon allocation of forest ecosystems, it is conventional to use the mass-balance approach, which combine individual estimations of flux and biometric observations such as gross primary production, ecosystem respiration, soil respiration, net ecosystem production, leaf and tree biomass, litterfall, and soil organic carbon considering appropriate balances with each components. However, it is often the case that an attribution of fine roots was not fully assessed because it is required significant effort to monitor its dynamics in a long term. Pulse labelling technique allows directly measure allocation of assimilated carbon from foliage to belowground in various tree species. This approach provides detailed aspects of allocation dynamics, but assessing labelled carbohydrate allocated to fine roots is still challenging. Absence of allocation to fine roots limits our knowledge about mechanism of carbon allocation because net primary productivity of fine root (frNPP) potentially account for one-third of the annual total NPP. To compensate limited observation, a model-data integration technique would be a useful tool, in which a process-based biosphere model combined with multi-year biometric observations to inversely estimate plausible allocation to fine roots.

This study investigated the interannual variability of carbon allocation of a cool-temperate forest in the Takayama Forest Research Site, Japan. The multi-year biometric observations are available for most of carbon cycle components at the Takayama site (e.g., woody tissue net primary productivity (wNPP), foliage NPP (fNPP), aboveground and belowground woody biomasses, litterfall, recruitment, and mortality) except fine root NPP (frNPP); only one year data of frNPP is available for 2000?2001. To compensate the limited frNPP measurement, we calculated frNPP from 1999-2006 by a model-data integration technique. In the process of calculation, unnecessary freedom in the simulation of a process-based ecosystem model, Biome-BGC, was constrained as much as possible with multiple biometric observations at the Takayama site. With the observed components of allocation (fNPP and wNPP) in conjunction with the modeled frNPP, we characterized the internnual variability of carbon allocation at the Takayama site by focusing two aspects: (1) allocation priority among leaves, woody components, and fine roots, and (2) controlling climate factors for these allocation components.

Acknowledgments

This research was supported by the Environment Research and Technology Development Fund (RFa-1201) of the Ministry of the Environment of Japan.

Keywords: Allocation, ecosystem modelling

Japan Geoscience Union Meeting 2014
(28 April - 02 May 2014 at Pacifico YOKOHAMA, Kanagawa, Japan)

AHW29-04 Room:314 Time:May 2 15:00-15:15

Net nitrogen input through the atmospheric deposition and irrigation water at a paddy field in central Japan

HAYASHI, Kentaro[1*] ; ONO, Keisuke[1] ; TOKIDA, Takeshi[1] ; NAKAMURA, Hirofumi[2] ; HASEGAWA, Toshihiro[1]

[1]Natl. Inst. Agro-Environ. Sci., [2]Taiyo Keiki

The aim of the present study was to evaluate the net nitrogen input through the atmospheric deposition and irrigation water at a paddy field for single cropping of paddy rice in central Japan, where the wet deposition and exchanges of gases and particles (as the difference between the dry deposition and emissions) were measured for the atmospheric deposition. Target species of reactive nitrogen (Nr) were ammonium (NH_4^+) and nitrate (NO_3^-) for the wet deposition, ammonia (NH_3), nitric acid (HNO_3), and nitrous acid (HNO_2) as gases and particulate ammonium (pNH_4) and nitrate (pNO_3) as particles for the atmosphere-rice paddy exchange, and NH_4^+, NO_3^-, and organic nitrogen (OrgN) for the irrigation water.

Monitoring of those processes were conducted for three years from September 2010 to September 2013 at a paddy field in central Japan which was devoted for an experimental site of free-air CO_2 enrichment (FACE). Rainwater samples were collected weekly and the wet deposition was calculated using the Nr concentration and the collected volume of water. The air concentrations of Nr were measured using a filter-pack method at two heights of 6 m and 2 m above the ground surface on a weekly mean basis with day/night separation. A filter-pack consisted of five filter holders to collect the target Nr. The diffusion velocity was calculated using the micrometeorological and eddy covariance data in half-hourly basis and then the weekly-mean values in the daytime and nighttime were calculated. The exchange fluxes were expressed as the product of the difference in air concentration between the two heights multiplied by the diffusion velocity. Cumulative exchange fluxes were also calculated based on the weekly mean exchange fluxes. The flow rate and quality of irrigation water was monitored in the cropping seasons in 2011, 2012, and 2013 at a bay in the paddy field. Each of two inlets and one outlet at the bay was equipped with a flow gaging weir and the water flow was measured continuously. Water was sampled at the weirs every week in principle and the concentrations of Nr were measured, where OrgN was calculated as the difference between the total nitrogen and the sum of NH_4^+ and NO_3^-. The inflow and outflow of Nr by irrigation were then calculated using the flow rate and concentration data.

Annual wet deposition of Nr was 9.5, 8.6, and 5.9 kg N ha^{-1} yr^{-1} for the first, second, and third years, respectively, where NH_4^+ and NO_3^- showed similar contributions quantitatively. In addition, the contribution of OrgN was negligible in the wet deposition. Annual exchanges of Nr between the paddy field and the atmosphere were estimated to around 2-3 kg N ha^{-1} yr^{-1}, where a certain extent of the dry deposition was counterbalanced by the emissions. Ammonia was the most dominant Nr among the target species in the atmosphere. Ammonia also showed the largest dry deposition among Nr; however, a large part of which was canceled by the emissions of NH_3 from the paddy field. The differences between the inflow and outflow for the irrigation water were 10.7, 8.8, and 6.7 kg N ha^{-1} yr^{-1} for the first, second, and third years, respectively, where OrgN accounted for 30-40% of Nr. In total, the net input of Nr to the paddy field through the atmospheric deposition and irrigation water was estimated to approximately 20 kg N ha^{-1} yr^{-1} which corresponds to approximately 30% of a standard application rate of nitrogen fertilizers in this area. However, it is desired that the following processes are also incorporated to complete the evaluation of the nitrogen balance: the biological nitrogen fixation and the dry deposition of nitrogen oxides (nitrogen monoxide and nitrogen dioxide) as inputs; and the denitrification (nitrogen monoxide, nitrous oxide, and dinitrogen) and the leaching of Nr to the groundwater as outputs.

Keywords: reactive nitrogen, nitrogen balance, atmospheric deposition, emission, irrigation, rice paddy field

Japan Geoscience Union Meeting 2014
(28 April - 02 May 2014 at Pacifico YOKOHAMA, Kanagawa, Japan)

AHW29-05 Room:314 Time:May 2 15:15-15:30

The variations of ORP in the paddy soil and effects on the methane emission from a periodically irrigated paddy field.

YAGI, Kenta[1] ; WAKIKUROMARU, Naoki[1] ; IWATA, Toru[1*]

[1]Graduate school of Environmental and Life Sciense, Okayama University

Oxidation-Reduction Potential (ORP) in the paddy soil was measured during rice cultivaled season at a periadically irrigated paddy field, and some effects on the methane flux from the paddy soil was investigated. ORP showed rapid decrease when irrigation water was introduced in the paddy field, and lower ORP was shown under the longer flooded condition. From the seasonal-term point of view, lower ORP was shown in later rice season. ORP was suitably modeled as a function of irrigation time. During an irrigation period for four days, higher methane emissions were shown under lower OPR conditions. From the seasonal-term point of view, however, no significant relationship between ORP and methane fluxes. It is suggested that seasonal change of methane flux is affected by seasonal changes of soil temperature and the growth level of rice plants.

Keywords: Rice Paddy, Methane, soil, Oxidation-Reduction Potential

Japan Geoscience Union Meeting 2014
(28 April - 02 May 2014 at Pacifico YOKOHAMA, Kanagawa, Japan)

AHW29-06 Room:314 Time:May 2 15:30-15:45

Carbon emission by open burning from a paddy field and decomposition of the residual biomass in the paddy soil

OKADA, Kazuya[1] ; ONO, Keisuke[2] ; IWATA, Toru[1*]

[1]Graduate school of Environmental and Life Sciense, Okayama University, [2]National Institute for Agro-Environmental Sciences

Twice sampling surveys of residual biomass above ground surface were conducted before and after the open burning, and carbon contents compared for the estimation of carbon emission by the burning. It is suggested that about 43% of carbon contents of above-ground rice plant was yield out as grain by the harvest, and about 30% of carbon emitted as CO2 by burning. Coarse Organice Matter (COM) in the paddy soil of a single-crop rice field was sampled on a regular schedule for three years. The carbon emission from the COM decomposition of residual biomass was estimated by analyzing of the variations in carbon content of COM. Decrease in COM was accelerated at the warming season between April and June, but it was resisted during rice cultivated season. It is estimated that 70% of COM was decomposed after a year.

Keywords: Organic Carbon, Rice Paddy, Soil, Decomposition, Carbon Dioxide

Japan Geoscience Union Meeting 2014
(28 April - 02 May 2014 at Pacifico YOKOHAMA, Kanagawa, Japan)

AHW29-07 Room:314 Time:May 2 15:45-16:00

Continuous measurement of forest floor CO2 fluxes in a larch forest on the base of Mount Fuji

TERAMOTO, Munemasa[1*] ; LIANG, Naishen[1] ; ZENG, Jiye[1] ; IDE, Reiko[1] ; SAIGUSA, Nobuko[1] ; TAKAHASHI, Yoshiyuki[1]

[1]Center for Global Environmental Research, National Institute for Environmental Studies

Carbon fluxes of forest floor are thought to be important part of forest carbon dynamics. Multi-channel automated chamber system was installed to a larch forest site on the base of Mount Fuji in 2006 for continuous measurement of forest floor CO_2 fluxes. We prepared soil chambers for measuring soil respiration (Rs) and heterotrophic respiration (Rh). Root trenching was applied to separate Rs and Rh. Net ecosystem exchange (NEE) on the forest floor was measured with plant chambers. In 2013, the average efflux of CO_2 was 2.24, 1.81 and 2.11 μmol CO_2 m^{-2} s^{-1} in Rs, Rh and NEE, respectively. Root respiration was estimated to occupy 80.7% of Rs. Plants of forest floor was suggested to absorb about 5.9% of CO_2 in Rs, and it meant that the amount of carbon fixed by those plants was relatively low. There was little rain in summer time (July-August), and forest floor CO_2 fluxes were decreased due to decreased soil moisture. Q_{10} was 2.49 and 2.87 in Rs and Rh, respectively. Soil respiration was estimated to be 8.48 tC ha^{-1} yr^{-1}, and the forest floor was seen as 7.98 tC ha^{-1} yr^{-1} carbon source.

Keywords: soil respiration, chamber, forest floor plants, photosynthesis

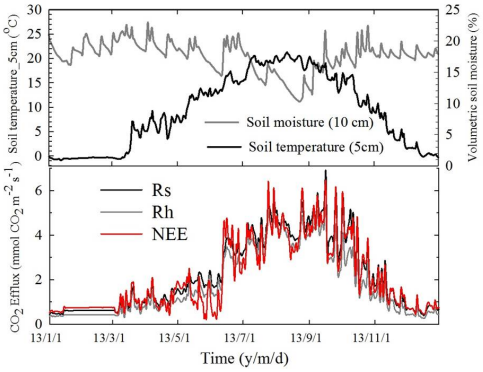

Fig 1. Seasonal variation of soil temperature, soil moisture and CO_2 efflux of each fluxes in 2013.

Japan Geoscience Union Meeting 2014
(28 April - 02 May 2014 at Pacifico YOKOHAMA, Kanagawa, Japan)

AHW29-08 Room:314 Time:May 2 16:15-16:30

Change in carbon dioxide absorption by a deciduous broadleaf forest due to the 2004 typhoon disturbance

MIZOGUCHI, Yasuko[1*] ; YAMANOI, Katsumi[1] ; UTSUGI, Hajime[1] ; TOBITA, Hiroyuki[1]

[1]Forestry and Forest Products Research Institute

Natural disturbances occur in forests at various scales and frequencies. It has an impact on the amount of carbon dioxide (CO_2) absorption by a forest. In Japan, large-scale disturbance often occurs in forests due to damage caused by strong winds of a typhoon. The 18th typhoon passing in 2004 brought about large-scale damage to forests, mainly in Iburi and Ishikari districts of Hokkaido. The Hitsujigaoka experimental forest (Sapporo forest meteorology research site, SAP) located in the southeastern area of Sapporo also suffered large-scale damage. An investigation related to CO_2 absorption, including flux observation, was conducted before the typhoon disturbance. After a 1-year interruption of the investigation due to facility damage by the typhoon, flux observation was reinitiated. To study the process of regeneration in the forest, the fallen trees were left into site. We report the results of a long-term observation of flux and biomass.

According to flux observation data, the annual carbon budget changed to negative after the disturbance. At present, carbon release is continuing. The supply of a lot of dead trees has caused a large amount of decomposition, which has lead to 1.5-fold heavy increases in ecosystem respiration. Meanwhile, average annual GPP from 2007 to 2012 decreased 5% compared with that before the typhoon.

Yearly maximum LAI including both trees and dwarf bamboo estimated by the attenuation rate of photosynthetically active radiation and the biomass survey was approximately 7 before the disturbance. It decreased to 4 in the following year and increased thereafter. It has been approximately 5.5 since 2007. The main source of total LAI recovery is the LAI of dwarf bamboo, which increased 2-fold. The amount of biomass of trees decreased to 70% after the typhoon, while that of dwarf bamboo increased 1.5-fold. However, biomass of bamboo was approximately 10% of that of trees. Therefore, dwarf bamboo did not fill in gaps due to a decrease in biomass of trees.

Photosynthetic increase due to dwarf bamboo partially compensated for photosynthetic decrease due to trees, and ecosystem respiration increased due to the increase in dead trees. As a result, the forest became the carbon source. To change the status of the forest from the carbon source to a carbon sink, it is necessary for carbon release to decrease with the advancing decomposition of dead trees.

Keywords: deciduous broadleaf forest, dwarf bamboo, CO_2 flux, disturbance

Japan Geoscience Union Meeting 2014
(28 April - 02 May 2014 at Pacifico YOKOHAMA, Kanagawa, Japan)

AHW29-09 Room:314 Time:May 2 16:30-16:45

Evapotranspiration of tropical peat ecosystems

HIRANO, Takashi[1*] ; KUSIN, Kitso[2] ; LIMIN, Suwido[2] ; OSAKI, Mitsuru[1]

[1]Research Faculty of Agriculture, Hokkaido University, [2]University of Palangkaraya

In Southeast Asia, mainly in Indonesia and Malaysia, peatland is widely distributed, coexisting with swamp forest, over an area of 2.48×10^5 km^2 and accumulates 11-14% of global peat carbon (Page *et al*., 2011). The peatland, however, has been rapidly degraded by deforestation and drainage. As a result, the proportion of forest cover in the peatlands of Peninsular Malaysia, Sumatra and Borneo fell from 77% to 36% from 1990 to 2010 (Miettinen *et al*., 2012). Such human pressures made the huge peat carbon pool vulnerable and raised the risk for the pool to be a large carbon source to the atmosphere chiefly because of peat fires and lowered groundwater level (GWL). The carbon balance of peatland is chiefly controlled by local hydrology, which determines saturation or unsaturation of surface peat. Under unsaturation conditions, peat is aerated, and its soil organic compounds are easily oxidized into carbon dioxide (CO_2). Therefore, drainage to lower GWL necessarily enhances oxidative peat decomposition and its resultant CO_2 emissions. Because tropical peatland is typically ombrotrophic, GWL varies according to residuals (storage change) between precipitation as input and evapotranspiration (ET) and runoff as output. Although precipitation can be also affected by large-scale deforestation, ET and runoff are directly affected by deforestation and drainage, respectively. To predict GWL under human pressures and assess the carbon balance of tropical peatland, therefore, it is crucial to quantify ET and elucidate the effects of disturbances on ET.

We have measured fluxes of sensible heat and latent heat using the eddy covariance technique and determined ET and energy balance at three sites within 15 km on tropical peatlands near Palangkaraya, Central Kalimantan, Indonesia (Hirano *et al*., 2012). The sites are different in disturbance degree: a relatively intact peat swamp forest with little drainage (UF), a heavily drained swamp forest (DF) and a drained burnt swamp forest (DB). Here we show the results of field measurement for four to six years between 2002 and 2009, including El Nino and La Nina events and discuss the effects of disturbances on the energy balance and ET of tropical peat swamp forest.

Because of energy imbalance (84 to 91% on an annual basis), ET was adjusted to close energy balance on a daily basis. Mean annual ET (±1 standard deviation) for the four years from 2004 to 2008 was 1636 ± 53, 1553 ± 117 and 1374 ± 75 mm y^{-1}, respectively, for the UF, DF and DB sites, which account for 67, 64 and 56% of mean annual precipitation of 2435 mm y^{-1}, respectively. Annual ET of the DB site was significantly smaller than those of the other sites, mainly owing to less transpiration due to few trees. This fact indicates that more water is lost by surface and groundwater runoff in the DB site. In addition, annual ET showed a positive linear relationship with annually mean GWL at each site. This significant linearity suggests that annually mean GWL is a robust indicator to assess the annual balances of carbon and water in tropical peat ecosystems (Hirano *et al*., 2012).

Keywords: disturbance, drainage, eddy flux, energy balance, fire

Japan Geoscience Union Meeting 2014
(28 April - 02 May 2014 at Pacifico YOKOHAMA, Kanagawa, Japan)

AHW29-10 Room:314 Time:May 2 16:45-17:00

Withering of Japanese oak by sulfuric acid of an air pollutant. and prevention from withering by charcoal

OMORI, Teiko[1*] ; YOSHIIKE, Yuzo[2] ; OKAMURA, Shinobu[3] ; IWASAKI, Masato[4]

[1]Teiko Omori, [2]Yuzo Yoshiike, [3]Shinobu Okamura, [4]Masato iwasaki

The sulfuric acid which generates by the combustion of a fossil fuel is carried by wind and adheres to trees and only water evaporates and the sulfuric acid concentrates and accumulates.Sulfuric acid is dropped on the root of a tree by rain and it acidi?es the soil.The metal ingredient in the soil becomes a soluble compound.The eluted metal ion is absorbed by trees and it combines with phosphoric acid.The trees become shortage of phosphoric acid and decay.If the tannin contained in Japanese oak combines with metal ion it becomes harmless to insect.Withering of trees originates in acidi?cations of soil.Charcoal can neutralize the acidi?ed soil.The results of an investigation are explained on the basis of consideration from chemical standpoint.

Keywords: air pollutant, charcoal, withering of pine, withering of Japanese oa, tannin, phosphoric acid

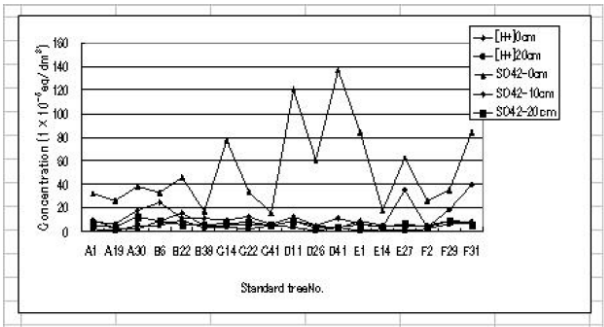

sampling: Kanayama,Onuma,Fukusima 10.10.2011
Measuring method :10g/ dried soil + 25g/water,
Filtration after 60minutes, $[H^+]$/pH meter, SO_4^{2-}/Ion chromatography
The relation of the hydrogen ion and sulfuric acid ion concentration in soil (1×10^{-5} eq/dm^3)

Japan Geoscience Union Meeting 2014
(28 April - 02 May 2014 at Pacifico YOKOHAMA, Kanagawa, Japan)

ACC31-01 Room:312 Time:April 29 09:00-09:15

Chemical dynamics of snow in the Japanese Alps region

KURAMOTO, Takayuki[1*] ; SASAKI, Akihiko[1] ; SUZUKI, Keisuke[1]

[1]IMS, Shinshu University

The Japanese Alps region is one of the heaviest snowy regions in Japan. In this area, winter precipitation is observed mainly two patterns such as winter monsoon pattern and low pressure pattern. Therefore, the chemical characteristics of the snowpack are different by snowfall types. In this study we aimed to clarify chemical dynamics of snowpack in the Japanese Alps region. We conducted a snow pit studies in the Japanese Alps region. We collected snow samples at the large flat place without obstruct by trees and the impact of human activities. The samples were melted, then pH, electric conductivity and major ions (Na^+, K^+, Mg^{2+}, Ca^{2+}, Cl^-, $NO_3{}^-$ and $SO_4{}^{2-}$) were analyzed in clean room. The Na^+ concentration correlates well with Cl^- concentration. These ions are considered to be sea-salt components. On the other hand, $SO_4{}^{2-}$ concentrations included non-sea-salt components.

Japan Geoscience Union Meeting 2014
(28 April - 02 May 2014 at Pacifico YOKOHAMA, Kanagawa, Japan)

ACC31-02 Room:312 Time:April 29 09:15-09:30

Change for chemical compornent of rime ice in two decades

NAGAFUCHI, Osamu[1*] ; YOKOTA, Kuriko[2] ; NAKAZAWA, Koyomi[1] ; HISHIDA, Naoko[1] ; IKEDA, Keisuke[1]

[1]the University of Shiga Prefecture, [2]Toyohashi University of Technology

Rime-ice and snow samples were collected at mountainous sites in Kyushu Island, Japan during from 1991 to 2014, and both soluble and insoluble substances in the melted rime-ice were analyzed by ion chromatography, inductively coupled plasma-mass spectrometry (ICP/MS) and analytical electron microscopy, in order to find the change of composition ratio of atmospheric pollutants cause by East Asian region. Although N/S ratio in rime-ice ranged from 0.1 to 0.3 in 1990's, recent year this ratio increased about 1.0. This phenomenon indicates that the composition of atmospheric pollutants changed during two decades in Eat Asian Continent.

Japan Geoscience Union Meeting 2014
(28 April - 02 May 2014 at Pacifico YOKOHAMA, Kanagawa, Japan)

ACC31-03 Room:312 Time:April 29 09:30-09:45

Variations in chemical composition of suface ice and meltwater on Svalbard glaciers

KONNO, Yudai[1*] ; TAKEUCHI, Nozomu[1]

[1]Graduate School of Science, Chiba University

Snow and ice on glaciers usually contain small amounts of various soluble substances. These chemical substances were supplied through the atmosphere, rain, and snow. Chemical substances in glacier surface ice and melting water are important to understand atmospheric circulation, material cycle and the ecology of glacial microbes. We analyzed the major soluble ions of surface ice, melt water, and fresh snow for three glaciers (Austre Broggerbreen, Midtre Lovenbreen, and Pedersenbreen) in the northwestern part of Svalbard in the melting season of 2013.

The concentrations of all of the solutes were low generally, but the compositions varied among the samples. Based on the significant correlation on the concentration of each samples, the solutes could be classified into 3 groups: Group A (Cl^-, SO_4^{2-}, Na^+),B (Mg^{2+}, Ca^{2+}), and C (NO_3^-, NH_4^+, K^+). They are likely to be derived from different sources. Group A solutes are probably sea salt origin, and Group B solutes are terrestrial dust origin, and Group C are anthropogenic or other unknown origin.

The altitudinal distribition of the concentration on Austre Broggerbreen showed that Groupe A (sea salt) solutes varied significantly although Group B (dust) solutes did not. Group A solutes were particularly higher in the higher area of the glacier. This variation can not be explained by distance from sea. It is probably due to supply from snow area remaining upper part of the glacier.

The chemical composition of the melting water was generally similar to those of the ice at the same site. However, some of the solutes (K^+ and SO_4^{2-}) were more abundant in meltwater than glacier ice at specific locations. This is probably due to supply from upper part of the glacier.

Keywords: Svalbard, glacier, chemical composition, sea salt

Japan Geoscience Union Meeting 2014
(28 April - 02 May 2014 at Pacifico YOKOHAMA, Kanagawa, Japan)

ACC31-04 Room:312 Time:April 29 09:45-10:00

Interannual variability of total SWE obtained by snow surveys in the Tuul river basin, Mongolia, from 2002 until 2013

SUGIURA, Konosuke[1*] ; KADOTA, Tsutomu[2] ; IIJIMA, Yoshihiro[2] ; KONYA, Keiko[2] ; ZHANG, Yinsheng[3] ; ISHIKAWA, Mamoru[4] ; YAMAZAKI, Takeshi[5] ; PUREVDAGVA, Khalzan[6] ; DAVAA, Gombo[6] ; OHATA, Tetsuo[2]

[1]University of Toyama/JAMSTEC, [2]JAMSTEC, [3]Institute of Tibetan Plateau Research, Chinese Academy of Science, [4]Hokkaido University, [5]Tohoku University, [6]Institute of Meteorology, Hydrology, and Environment, Mongolia

It is necessary for the southern limit of snow cover and the semi-arid region to be supplied with sustainable water. Mongolia is located in the southern limit and the semi-arid region. The capital, Ulaanbaatar, lies in a valley on the Tuul River. In order to investigate the actual conditions of snow water equivalent (SWE) in the upper Tuul River as water resources, the snow survey in the upper Tuul River has been carried out from 2002 to 2013. We have observed in each February when it will be the maximum amount of SWE. The snow water equivalent was estimated using a cylindrical snow sampler with 0.005-m^2 area. The total amount of SWE in the upper Tuul River basin was estimated using a global digital elevation model (DEM) with a horizontal grid spacing of 30 arc seconds (GTOP30) and a relationship between altitude and SWE. The main results obtained are shown below. The amount change of SWE in the upper Tuul River basin fluctuates over multiple years. The range of fluctuation was $0.25 \pm 0.07 km^3$. It was not necessarily fluctuating in monotone. The steep rise of the amount of SWE in the upper Tuul River basin coincides with increasing air temperature and snowfall roughly.

Keywords: snow water equivalent, snow cover, water resources, water cycle, Mongolia

Japan Geoscience Union Meeting 2014
(28 April - 02 May 2014 at Pacifico YOKOHAMA, Kanagawa, Japan)

ACC31-P01 Room:Poster Time:April 29 14:00-15:15

Identifyig the ice thickness of five perennial snow patches in the Tateyama Mountains based on GPR soundings

FUKUI, Kotaro[1*] ; IIDA, Hajime[1]

[1]Tateyama Caldera Sabo Museum

We carried out ground penetrating radar (GPR) soundings in the Kuranosuke, the Hamaguri-yuki, the Tsurugisawa, the Chojiro and the Ikenotan-migimata perennial snow patches in the Tateyama Mountains, the northern Japanese Alps since 2012. The Kuranosuke and the Ikenotan-migimata perennial snow patches had large ice masses (>30 m in thickness). We had measured the surface flows of both ice masses since 2011. The maximum surface flows of the Ikenotan-migimata and the Kuranosuke perennial snow patches were about 2 m a^{-1} and 0.14 m a^{-1}, respectively. Thus, we regard the both snow patches as active glaciers.

The Hamaguri-yuki, the Tsurugisawa and the Chojiro perennial snow patch had thin ice masses (<20 m in thickness). It is possible that these ice masses are not flowing at the present time. Thus, we guess that these snow patches are glacierets rather than active glaciers.

Keywords: glacier, perennial snow patch, Mt. Tateyama, Mt. Tsurugi, GPR

Japan Geoscience Union Meeting 2014
(28 April - 02 May 2014 at Pacifico YOKOHAMA, Kanagawa, Japan)

ACC31-P02 Room:Poster Time:April 29 14:00-15:15

Studies on internal structure of active glacier in the Tateyama Mountains

IIDA, Hajime[1*] ; FUKUI, Kotaro[1]

[1]Tateyama Caldera Sabo Museum

In 2013, we carried out 20 m depth boring in the Sannomado Glacier (2000 m above sea level), in the Tateyama Mountains, the northern Japanese Alps. The 20 m core was analyzed paying attention to the structure of firn and ice.The following observations were carried out;

(i) stratigraphic observation of snow layer and glacier ice.
(ii) measurement of density profi1e.
(iii) measurement of grain shape and profile of grain size.
(iv) observation of elongation of air bubbles.

The internal structure of the Sannomado Glacier was characterized by obvious boundary between firn and ice. At the depth of 5m, there was a distinct dirt layer formed in the last autumn. Above this dirt layer, firn transformed into ice abruptly and the density curve showed a discontinuity to 850kg/m^3. The temperature of the snow and ice measured in the borehole was 0 ℃ throughout the layer. Spouting water was found in the borehole, indicating an aquifer in the glacier. From these results, such a rapid transformation process from snow to ice in this glacier will be discussed.

The grain size gradually increased with depth and elongation of air bubbles was shown below 15m which suggests internal flow of the glacier.

Keywords: glacier, perennial snow patch, Mt. Tateyama, Mt. Tsurugi, boring

Japan Geoscience Union Meeting 2014
(28 April - 02 May 2014 at Pacifico YOKOHAMA, Kanagawa, Japan)

ACC31-P03 Room:Poster Time:April 29 14:00-15:15

Contribution ratio of glacier discharge to the river water in Mongolian Altai

KONYA, Keiko[1*] ; KADOTA, Tsutomu[1] ; DAVAA, Gombo[2] ; PURVDAGVA, Kalzan[2]

[1]JAMSTEC, [2]IMHE, Mongolia

The discharge from glaciers is an important theme for arid regions like Mongolia. The water from glaciers are accounted for the important water resources in Mongolia where little water is supplied from precipitation. It is to be revealed that how much water is available from the glaciers. In this study, we estimate how much water is available in the present states and in the future by analyzing water chemistry and water quantity.

We have measured the discharge, water temperature, electric conductivity (EC), pH, dD, d18O of the river at the beginning, middle and end of the melt season of the glacier. The contribution rate of the melt water to the river water were estimated by the two methods; A) discharge and EC, B) glacier melt rate.

The contribution rate was estimated to be 20-50 % of the flow. The future change of the contribution rate was estimated by method B with the temperature warming rate in the future estimated by the climate models in Mongolia. The results show that the river water is supposed to be increasing in next some decades and decreasing in next century. The snow melt water to the river is also need to be taken into account.

Keywords: glacier, glacier discharge, temperature warming, water resources, Mongolia, climate change

Japan Geoscience Union Meeting 2014
(28 April - 02 May 2014 at Pacifico YOKOHAMA, Kanagawa, Japan)

ACC31-P04 Room:Poster Time:April 29 14:00-15:15

Comparison of surrounding land features on the glacier terminal areas in the Himalayas derived from DEM

SUZUKI, Ryohei[1*]

[1]none

Radiation field on the surface of mountain glaciers is reported to be controlled by the surrounding land features and does not distribute uniformly. Net radiation, which is obtained as a result of radiation budget, has been reported as an important factor to melt the ice surface of glaciers in the Himalayas by the previous studies. On the other hand, the lower areas of many glaciers in the south area of Himalayas are covered with debris that has variety of thermal properties, which corresponds to the one of the factor to cause the spatial variety of ice melt rates fields. Considering the surrounding land form features in the radiation field is probably required for estimating thermal properties on the debris-covered glaciers accurately. However, in-situ observation of those phenomena cannot be conducted mainly due to the difficulties of accessibility to the Himalayas. Thus, application of satellite remote sensing techniques is a powerful tool as an alternate method.

This study focuses on the Lunana region, Bhutan, which corresponds to the target area where in-situ observation has been carried out since 2002, as a case study to estimate the influence of surrounding land features around the lower glacier areas on their radiation field. I calculated a distribution of azimuth and zenith angles from each target point (pixel) on the lower glacier areas to each direction to the skylines with an approximate method to derive surrounding land feature; the value 1 corresponds to the full sky view and it decreases to 0 with the decrease of openness. My first result, which was derived from 8 directions for each pixel with the limit of about 4.5 km far from the point as a line of sight, shows it ranges from 0.7 to 0.9 regarding the three glaciers; Thorthormi, Lugge and Lugge Ⅱ.

Because these values depend on the method to move the line of sight on the DEM, in other words, the method for processing the raster image as well as the accuracy of both elevations and horizontal positions, I would also like to present the other experimental results that were calculated with some different conditions to discuss the influence of the surrounding land form on the radiation field in the Himalayas.

Keywords: Digital Elevation Model (DEM), image processing, glacier melt rate, radiation budget, mountain glaciers, Himalayas

Japan Geoscience Union Meeting 2014
(28 April - 02 May 2014 at Pacifico YOKOHAMA, Kanagawa, Japan)

ACC31-P05 Room:Poster Time:April 29 14:00-15:15

Glacier lake and glacier lake outburst floods in Tien Shan and Ladakh Range

NARAMA, Chiyuki[1*] ; KAZEHARE, Saiga[1] ; YAMAMOTO, Minako[1] ; UKITA, Jinro[1] ; IKEDA, Naho[2] ; TADONO, Takeo[3]

[1]Niigata University, Department of Environmental Science, [2]Tohoku University, Institute for Disaster Reconstruction and Regeneration Research, [3]JAXA

As a result of recent glacier melting, present glacier lakes develop rapidly at glacier fronts in Tien Shan Mountains, Central Asia and Ladakh Range, Indian Himalayas. Although glacier lakes in the Tien Shan and Ladakh Range are small, compared to those in the eastern Himalayas (Bhutan and eastern Nepal), several GLOFs in the past have caused fatalities and serious damage to infrastructure and crops. With recent changes in the development of glacier lakes in these mountain regions, floods are becoming an increasing threat to local residents. However, the current status of glacier lakes is poorly characterized in this region. In this study, we researched glacier lakes in the Tien Shan Mountains and Ladakh Range using high-resolution ALOS/PRISM-AVNIR-2 images taken in 2007-2010. In addition, we report the characteristic of glacier lake and glacier lake outburst floods (GLOFs) in Tien Shan, using investigation of the appearance of glacier lake and GLOFs in the past.

We examined about 1600 glacier lakes ($>$0.001 km^2) in the Tien Shan. Although glacier lakes are distributed throughout the Tien Shan Mountains, regional differences in their number and size are large. Larger glacier lakes are found in the Teskey and Ili-Kungoy regions, whereas most small glacier lakes occupy other mountain ranges (4000-5000 m asl), such as the Pskem, Talas, and Kyrgyz Ala-Too ranges. In seven mountainous regions, many present-day glacier lakes have appeared since the 1980s. Glaciers in these mountain regions are most glacier shrinkage area in Tien Shan over the 30 years, and these glacier lakes appeared after glacier shrinkage area. We report our results in detail in JpGU meeting.

Keywords: glacier lake, glacier lake outburst floods, small-size glacier lake region, Tien Shan, Ladakh Range

Japan Geoscience Union Meeting 2014
(28 April - 02 May 2014 at Pacifico YOKOHAMA, Kanagawa, Japan)

ACC31-P06 Room:Poster Time:April 29 14:00-15:15

Chemical Composition on the surface in the Urumqi No.1 glacier, Tien Shan, China

WAKABAYASHI, Kozue[1] ; TAKEUCHI, Nozomu[1*] ; TANAKA, Sota[1] ; AMEMIYA, Shun[1]

[1]Graduate School of Science, Chiba University

Various chemical solutes are deposited in snow and ice on glaciers. Such solutes are usually washed out of glaciers during melting season. However, concentration and composition on snow and ice during melting season are little known. The solutes are important to understand microbes living on the glacier surface since chemical conditions affect their growth. In this study, we analyzed chemical compositions of ice surface in the melting season on Urumqi glacier No.1, Tien Shan Mountains in central Asia. Results showed that calcium ion was dominanted more than 60% in all of the area on the glacier. This indicates that the chemical composition on the melting glacial surface is greatly affected by dust from desert in this region. Total concentration of nigrogen solutes (ammonium) was highest in the middle part of the glacier. Measurements of chlorophyll a concentration revealed that it was also maximal in the middle of the glacier. The altitudinal variation of solutes may affect the algal community and biomass on the glacier.

Keywords: chemical composition, glacier

Japan Geoscience Union Meeting 2014
(28 April - 02 May 2014 at Pacifico YOKOHAMA, Kanagawa, Japan)

ACC32-01 Room:419 Time:April 29 14:15-14:30

Digital-image processing to analyze grain size variation in ice core from Gregoriev Ice Cap, Kyrgyz Tien Shan

MATSUHASHI, Yuta[1*] ; FUJITA, Koji[1] ; TAKEUCHI, Nozomu[2] ; VLADIMIR B, Aizen[3]

[1]Nagoya University, [2]Chiba University, [3]University of Idaho

It is known that impurities in ice core (etc. dust from continental) prevent grain growth rate at high-latitude regions. On the other hand, the effect of impurities for grain growth is not understood for ice cores retrieved from mid-low latitude glaciers, despite of higher dust concentration. This study aims to reveal relation between dust and grain size in an ice core drilled at Gregoriev Ice Cap, Kyrgyz Tien Siam in 2007.

We made thin sections which are reduced to thickness of 0.4mm. Three different images were taken by changing angle of crossed polarizers (0 deg, 30 deg, 60 deg). Changing controlled contrast and RGB, we converted the images into binary. Grain boundaries are then able to be picked by digital image-processing. This process made efficient extracting boundary and obtain area of grain using binary images.

We will present detailed procedures and preliminary results of comparison with dust concentration along the ice core.

Keywords: ice core, grain size, Grigoriev ice cap

Japan Geoscience Union Meeting 2014
(28 April - 02 May 2014 at Pacifico YOKOHAMA, Kanagawa, Japan)

ACC32-02 Room:419 Time:April 29 14:30-14:45

Post-depositional alteration of major ions under different accumulation environment in Antarctica

HOSHINA, Yu[1*] ; FUJITA, Koji[1] ; IIZUKA, Yoshinori[2] ; MOTOYAMA, Hideaki[3]

[1]Nagoya University, [2]Institute of Low Temperature Science, Hokkaido University, [3]National Institute of Polar Research

Major soluble ions and water stable isotopes are important for reconstructing paleo-environment and atmosphere circulation. It is also known that ion and isotope signals are modified after deposition if firn or ice core samples are analyzed at high temporal resolution such as seasonal scale. In inland Antarctica, we revealed that low accumulation rates have resulted in significant post-depositional modification of ions and isotopes due to long time exposure of snow near the surface.

We further investigated relation between major ion concentration and accumulation rate using a several snow pits and firn cores taken from east and west Antarctica. To exclude the geographical factor (east or west), we analyzed correlations with ions against oxygen stable isotope. Correlations of sea salt against oxygen stable isotope are gradually changed from no correlations under higher accumulation sites near coast to more negative correlations under dry environment in inland. On the other hand, correlations of MSA (methanesulfonic acid) against oxygen stable isotope rapidly are changed from positive to negative correlations at 100 kg m^{-2} a^{-1} of accumulation sites. Those different trends suggest different mechanisms of post-depositional modification for these ion species.

Keywords: Antarctica, ice core

Japan Geoscience Union Meeting 2014
(28 April - 02 May 2014 at Pacifico YOKOHAMA, Kanagawa, Japan)

ACC32-03 Room:419 Time:April 29 14:45-15:00

Greenland temperature variability over the past 2000 years inferred from NGRIP and GISP2 ice cores

KOBASHI, Takuro[1*] ; GOTO-AZUMA, Kumiko[1] ; KAWAMURA, Kenji[1] ; VINTHER, Bo[2] ; BLUNIER, Thomas[2] ; BOX, Jason[3] ; BUIZERT, Christo[4] ; MUTO, Atsuhiro[5] ; WHITE, James[6]

[1]National Institute of Polar Reseaerch, [2]Copenhagen University, [3]Geological Survey of Denmark and Greenland, [4]Oregon State University, [5]Pennsylvania state University, [6]University of Colorado at Boulder

We reconstructed Greenland temperature change for the past 2000 years using argon and nitrogen isotopes in trapped air in NGRIP and GISP2 ice cores. To identify true variability of temperature, we also applied various methods such as borehole temperature inversion, Monte Carlo inversion of borehole temperature, oxygen isotopes of ice, forward and inverse methods for argon and nitrogen isotopes with borehole temperatures. We will present the results of analyses and implications.

Keywords: Greenland, temperature, ice core, GISP2, NGRIP, 2000 years

Japan Geoscience Union Meeting 2014
(28 April - 02 May 2014 at Pacifico YOKOHAMA, Kanagawa, Japan)

ACC32-04 Room:419 Time:April 29 15:00-15:15

Greenland temperature variations in the last millennium climate simulation

YOSHIMORI, Masakazu[1*] ; ABE-OUCHI, Ayako[1]

[1]Atmosphere and Ocean Research Institute, The University of Tokyo

A series of climate simulations of the last millennium are conducted using the MIROC climate model. These include a simulation under volcanic-only, solar-only, or total forcings. Sensitivity experiments using different strength of volcanic and solar forcings are also conducted. With these dataset, we analyze the factors that influence Greenland temperature variations during the last millennium. Attention is paid to the effect of different external forcings and changes in the atmosphere and ocean circulations such as the North Atlantic Oscillation and the Atlantic meridional overturning circulation.

Japan Geoscience Union Meeting 2014
(28 April - 02 May 2014 at Pacifico YOKOHAMA, Kanagawa, Japan)

ACC32-05 Room:419 Time:April 29 15:15-15:30

The variation of the Arctic cryosphere in the Last Millennium simulation using MIROC and MIROC-ESM

SUEYOSHI, Tetsuo[1*] ; OHGAITO, Rumi[1] ; YOSHIMORI, Masakazu[2] ; HAJIMA, Tomohiro[1] ; ABE, Manabu[4] ; O'ISHI, Ryouta[4] ; OKAJIMA, Hideki[1] ; SAITO, Fuyuki[1] ; WATANABE, Shingo[1] ; KAWAMIYA, Michio[1] ; ABE-OUCHI, Ayako[2]

[1]Japan Agency for Marine-Earth Science and Technology, [2]Atmosphere and Ocean Research Institute, University of Tokyo, [3]National Institute for Environmental Studies, [4]National Institute of Polar Research

In this study, we analyze the result of Last Millennium (LM) Experiment using GCM and ESM, to verify the response of the cryosphere to the hundereds-year-scale climate change. In addition to the sensitivity analysis between the forcing conditions, comparison with existing climate/paleoclimate data. The period of the LM experiment covers the Little Ice Age and Medieval Climate Anomaly, and responses of the cryosphere during those periods are of interest.

The models used in this study are the Atmosphere-Land-Ocean General Circulation Model MIROC and the Earth System Model MIROC-ESM. Resolution of atmosphere/land components are T42 (ca 2.8o) in horizontal, 80 layers in vertical. Ocean component has a resolution of 1.4o (longitude) by variable 0.56?1.4o (latitude) in the horizontal and 44 levels in the vertical. As an ESM, MIROC-ESM has a carbon-cycle components for the land and ocean ecosystems. Setup of the experiments follow the protocol of model inter-comparison CMIP5/PMIP3.

As preliminary results, temporal variations in surface air temperature, snow amount, and snow/rain ratio for Siberia region was analyzed. Winter warming during 20th century is clear. Signatures are shown in rise of February Temperarure, decrease in snow amount, increase in runoff during spring. Ratio of Snow fall / Precipitation is sensitive to the temperature, which may caused the above-mentioned trends in snow.

Keywords: paleoclimate, climate modelling, Last Millennium, cryosphere, climate change

Japan Geoscience Union Meeting 2014
(28 April - 02 May 2014 at Pacifico YOKOHAMA, Kanagawa, Japan)

ACC32-06 Room:419 Time:April 29 15:30-15:45

A long-term ^{10}Be record from Dome Fuji ice core and cosmic-ray stratigraphy

HORIUCHI, Kazuho[1*] ; SUGUCHI, Shota[1] ; SUDA, Kensuke[1] ; UCHIDA, Tomoko[2] ; AZE, Takahiro[3] ; YOKOYAMA, Yusuke[4] ; MURAMATSU, Yasuyuki[5] ; MATSUZAKI, Hiroyuki[6] ; MOTOYAMA, Hideaki[7]

[1]Graduate School of Science and Technology, Hirosaki University, [2]Institute of Geology and Paleontology, Tohoku University, [3]Graduate School of Science and Engineering, Tokyo Institute of Technology, [4]Atmosphere and Ocean Research Institute, The University of Tokyo, [5]Faculty of Science, Gakushuin University, [6]Graduate School of Engineering, The University of Toky, [7]National Institute of Polar Research

Cosmogenic nuclides (^{10}Be, ^{14}C, ^{26}Al, ^{36}Cl) in paleoenvironmental archives serve as a proxy indicator of the paleointensity of cosmic ray, controlled largely by the strength of the solar/geomagnetic fields. Here, we present a millennial record of cosmogenic ^{10}Be covering the past 300 kyr and obtained from ice cores drilled at the Dome Fuji station (77^{o}19'S, 39^{o}42'E), inland East Antarctica. A number of specific increases in ^{10}Be were observed in this record and were connected semi-quantitatively to those in the cosmic-ray intensity caused by geomagnetic excursions during the last 300 kyr. These features can be used as stratigraphic time-markers for synchronization of not only Antarctic ice cores but also various paleoenvironmental archives such as deep-sea sediments

Japan Geoscience Union Meeting 2014
(28 April - 02 May 2014 at Pacifico YOKOHAMA, Kanagawa, Japan)

ACC32-07 Room:419 Time:April 29 15:45-16:00

Age synchronization between an Antarctic ice core and Northern Hemisphere marine cores: with special focus on MIS 11

KAWAMURA, Kenji[1*] ; AOKI, Shuji[2] ; NAKAZAWA, Takakiyo[2] ; ABE-OUCHI, Ayako[3] ; SAITO, Fuyuki[4]

[1]National Institute of Polar Research, [2]Tohoku University, [3]University of Tokyo, [4]JAMSTEC

Investigation of the roles of different forcings (e.g. orbital variations and greenhouse gases) on climate and sea level requires a paleoclimate chronology with high accuracy. Such a chronology for the past 360 ky was constructed through orbital tuning of O2/N2 ratio of trapped air in the Dome Fuji and Vostok ice cores with local summer insolation (Kawamura et al., 2007). We extend the O2/N2 chronology back to ˜500 kyr by analyzing the second Dome Fuji ice core, and find the duration of 11 ka, 5 ka, 9 ka, and 20 ka for MIS 5e, 7e, 9e and 11c interglacial periods in Antarctica, with similar variations in atmospheric CO2. The termination timings are consistent with the rising phase of Northern Hemisphere summer insolation.

Marine sediment cores from northern North Atlantic contain millennial-scale signatures in various proxy records (e.g. SST, IRD), including abrupt climatic shifts and bipolar seesaw. Based on the bipolar correlation of millennial-scale events, it is possible to transfer our accurate chronology to marine cores from the North Atlantic. As a first attempt, we correlate the planktonic d18O and IRD records from the marine core ODP 980 with the ice-core d18O and CH4 around MIS 11. We find that the durations of interglacial plateaus of planktonic d18O (proxy for sea surface environments) and benthic d18O (proxy for ice volume and deep-sea temperature) for MIS 11c are 20 and 15 ka, respectively, which are significantly shorter than originally suggested. These durations are similar to that of Antarctic climate and atmospheric CO2. However, the onsets of interglacial levels in ODP980 for MIS 11 are significantly later than those in Antarctic d18O and atmospheric CO2 (by as much as ˜10 ka), suggesting very long duration (more than one precession cycle) for the complete deglaciation and northern high-latitude warming for Termination V. Atmospheric CO2 may have been the critical forcing for this termination. The long duration of Termination V is consistent with our new ice sheet simulations (extended from the work of Abe-Ouchi et al., 2013) in which an ice-sheet/climate model is forced by insolation and CO2 variations. In the presentation, comparisons for other interglacial periods will also be reported.

Keywords: Antarctic ice core, Marine core, Chronology, Glacial-interglacial cycles

Japan Geoscience Union Meeting 2014
(28 April - 02 May 2014 at Pacifico YOKOHAMA, Kanagawa, Japan)

ACC32-08 Room:419 Time:April 29 16:15-16:30

What is the major factor which control global climate in the ice age?

KUMON, Fujio[1*]

[1]Faculty of Science, Shinshu University

The author and his co-workers have been analyzed total organic carbon (TOC) and total nitrogen (TN) contents of the various lake and marine sediment cores. The temporal changes of TOC show quasi-periodic fluctuation patterns similar to LR04 marine oxygen isotope curve and delta 18O profile of NGRIP ice core. Among the several long records of TOC in and around the Japanese islands, the TOC record from the Japan Sea is the most excellent one, and can be correlated precisely with the NGRIP record both on the orbital- and millennial time-scale in the ice ages.

This intimate relationship of climate is confirmed between Greenland and the Japanese islands. The good concordance of climate change can be explained by a hypothesis that extension of ice sheets in the Arctic region is major factor to control global climate not only in orbital-time scale but also in millennium-time scale.

Keywords: organic carbon content, climate change, ice sheet, Japan Sea sediment, Milankovich hypothesis, pinge-purge model

Japan Geoscience Union Meeting 2014
(28 April - 02 May 2014 at Pacifico YOKOHAMA, Kanagawa, Japan)

ACC32-09 Room:419 Time:April 29 16:30-16:45

The influence of glacial ice sheet on Atlantic Meridional Overturning Circulation through atmospheric circulation change

SHERRIFF-TADANO, Sam[1*] ; ABE-OUCHI, Ayako[1] ; YOSHIMORI, Masakazu[1] ; CHAN, Wing-le[1]

[1]Atmosphere and Ocean Research Institute, University of Tokyo

In glacial period, huge ice sheet covered the North America and the Northern Europe. Also, the Antarctica Ice sheet had expanded and increased its altitude. It is well known that these ice sheets (hereafter glacial ice sheets) have large influence on climate, for example atmospheric circulation, surface air temperature, and sea surface temperature. On the other hand, recent studies showed that wind stress changes play a crucial role on the AMOC under glacial climate. Moreover, increasing evidence suggests that glacial ice sheets have large influence on the Atlantic Meridional Overturning Circulation (AMOC). However the process how the ice sheets cause such a large impact on the AMOC is yet fully understood. Thus, in this study, we aim to reveal the detailed process of the ice sheet affecting the AMOC through atmospheric circulation change.

Commonly, the Atmosphere-Ocean General Circulation Model (AOGCM) is used to assess the influence of the ice sheet on the AMOC. However, as the atmospheric general circulation model (AGCM) and ocean general circulation model (OGCM) interacts in this model, the wind change as well as other process affect the AMOC. Therefore, it is difficult to divide each effect. Using the AGCM and the OGCM separately can overcome this problem because in this manner, they do not interact and the wind stress or other process can be treated as a boundary condition for the OGCM. This method consists of 2 steps. First, by using the AGCM, the effect of glacial ice sheets on the surface wind stress are evaluated by adding glacial ice sheets as a boundary condition. Second, by using the wind stress result as a boundary condition for the OGCM, the influence of the wind stress change on AMOC is estimated. In addition, by analyzing the results from each model, the underlying mechanism is explored.

As a result, glacial ice sheets largely intensified the AMOC under glacial climate. It was also found that the wind stress change at North Atlantic was important, thus glacial ice sheets at northern hemisphere were important. On the other hand, the AMOC was hardly influenced by wind stress change at Southern Ocean, which is mainly induced by the change in the Antarctica Ice sheet. Therefore change in the Antarctica Ice sheet had small impact on AMOC through surface wind stress change.

By analyzing the results from the AGCM and OGCM, it revealed that two processes were crucial; first, the strengthening of the northward salt transport, which resulted from enhanced westerly due to the North America Ice sheet. Second, the northward sea ice transport due to the southerly wind at Norwegian Sea forced by the Northern Europe Ice sheet. These two processes were found to drastically intensify the AMOC through affecting the sea ice distribution and shifting the NADW formation region.

Keywords: Ice sheet, Glacial climate, AMOC, wind stress

Japan Geoscience Union Meeting 2014
(28 April - 02 May 2014 at Pacifico YOKOHAMA, Kanagawa, Japan)

ACC32-10 Room:419 Time:April 29 16:45-17:00

Reconstruction of paleo-vegetation distribution by using an atmosphere ocean coupled GCM and a DGVM

O'ISHI, Ryouta[1*] ; CHAN, Wing-le[2] ; ABE-OUCHI, Ayako[2]

[1]National Institute of Polar Research, [2]Atmosphere and Ocean Research Institute, the University of Tokyo, [3]JAMSTEC

" The replacement of Neanderthals by Modern Humans has been considered to have occurred during 60,000-30,000 BP, which is also characterized by millennial scale climate change known as the Dansgaard?Oeschger events. The distribution of Neanderthals and Modern Humans during this period suggests correlation with that of paleo-vegetation and animals. This relation reflects the difference between the adaptabilities of Neanderthals and Modern Humans to environmental changes by way of their ability to hunt animals as food resources. Hence, it is important for the RNMH project to predict distribution of fauna, flora and climate change during this period. When estimating fauna distribution of the past, it is necessary to evaluate the changes in flora and thus changes in climate of the past. This can be directly achieved by examining data from sediment proxies, e.g. pollen records and isotopes. However, the availability of such proxies to reproduce the distribution of flora and climate changes is limited.

In the present study, we tried to reconstruct the vegetation distribution across North Africa, the Mediterranean and Europe during 60,000-30,000 BP from the results of a paleo-climate reconstruction by using a general circulation model as input for a dynamical global vegetation model. GCMs consume huge amounts of computational resources and so experiments are usually run using lower resolution models whose grid sizes are not sufficiently small for anthropological studies. In this study, we developed an " anomaly procedure " in order to incorporate features from both a high-resolution model and paleoclimate information. As a result of this new method, we successfully obtained a high-resolution vegetation distribution for a specific period of the past. However, it is not yet clear how these results can be validated against paleovegetation records. We need further discussions on how the appropriate paleoclimate can be reproduced by the GCM and how the vegetation model results can make a robust contribution toward the RNMH project.

Keywords: D-O cycle, Paleoclomate, Paleovegetation, Modeling

Japan Geoscience Union Meeting 2014
(28 April - 02 May 2014 at Pacifico YOKOHAMA, Kanagawa, Japan)

ACC32-11 Room:419 Time:April 29 17:00-17:15

Arctic amplification and the Greenland ice sheet at the Last Interglacial: the role of vegetation feedback

ABE-OUCHI, Ayako[1*] ; O'ISHI, Ryouta[1] ; TAKAHASHI, Kunio[2] ; SAITO, Fuyuki[2]

[1]University of Tokyo AORI, [2]JAMSTEC

We calculated the climatic conditions, mass balance and the transient volume of the Greenland ice sheet in the last interglacial period using the atmosphere slab-ocean vegetation general circulation model ASVGCM MIROC-LPJ and IciES ice sheet model. Taking into account the vegetation feedback, the annual mean temperature anomaly increases from +1 K to +2 K, and of summer temperature anomaly from +4 K to +6 K in central Greenland. This is close to the +5 K at NGRIP and +8 K at NEEM as inferred from ice core isotope data, which takes into account that summer precipitation contributes more to oxygen isotope values{reference}. The vegetation feedback, also increases precipitation by 20% averaged over the entire ice sheet and by 30 % in northwestern Greenland. The combination of the sea ice-temperature feedback and the vegetation feedback amplifies both the temperature and precipitation changes in the Eemian.

The increased ablation caused by high temperatures in central Greenland is partly compensated by the increased precipitation. The ice volume loss of Greenland in the Eemian compares to present day amounts to 1 to 2.5 meters sea level equivalent depending on the inferred present day reference climate and model parameters, such as lapse rate. The spatial pattern of increased temperature and increased precipitation is supported by the fact, that the modeled Eemian Greenalnd ice sheet covers all locations of ice core cites (GRIP/GISP, NGRIP, NEEM and Dye3), for which the existence of Eemian ice is confirmed. The reconstructed sea level elevations in the Eemian range from 6 to 9 m{references} above present day sea level. Thus, our results imply that the larger part of the difference in sea level between Eemian and present day stems from the Antarctica ice sheet.

Japan Geoscience Union Meeting 2014
(28 April - 02 May 2014 at Pacifico YOKOHAMA, Kanagawa, Japan)

ACC32-12 Room:419 Time:April 29 17:15-17:30

Sensitivity of Greenland ice sheet to climatic parameters during the last interglacial

TAKAHASHI, Kunio[1*] ; ABE-OUCHI, Ayako[2] ; SAITO, Fuyuki[1] ; O'ISHI, Ryouta[3]

[1]Japan Agency for Marine-Earth Science and Technology, [2]Atmosphere Ocean Research Institute, University of Tokyo, [3]National Institute of Polar research

In the last interglacial (LIG), sea level was 5 to 9 m above present, including contribution from Antarctica. Whole melting of the Greenland ice sheet (GIS) can contribute to the global sea-level rise of up to 7 m. It is important source of sea-level change. In the previous IPCC report in 2007 (IPCC AR4), estimates the GIS contribution to sea-level change during LIG range between 4 to 6 m. New IPCC AR5 points out that based on ice-sheet model simulations consistent with elevation changes derived form a new Greenland ice core, the Greenland ice sheet *very likely* contributed between 1.4 to 4.3 m sea level equivalent.

In this study, we present numerical experiments of GIS from 140 ka to 110 ka by using anomaly approach (present-day climate + perturbation obtained from MIROC-AGCM simulations including dynamic vegetation). We focus on the influence of the climatic parameters such as AMOC or northern hemisphere ice sheets. Our results are consistent with IPCC AR5. Considering of transient response to transient climate change are important to moderate ice melting. Several uncertainties remain however, such as the reference climate condition (influence melt from south, north or both?). and related the ice sheet model itself, more numerical studies are required.

Keywords: Last interglacial, Greenland, Ice sheet, Sea-level

Japan Geoscience Union Meeting 2014
(28 April - 02 May 2014 at Pacifico YOKOHAMA, Kanagawa, Japan)

ACC32-13 Room:419 Time:April 29 17:30-17:45

Sea-level changes and crustal deformations in Greenland based on the loading histories derived from 3D ice sheet model

OKUNO, Jun'ichi[1*] ; SAITO, Fuyuki[2] ; ABE-OUCHI, Ayako[3] ; TAKAHASHI, Kunio[2]

[1]NIPR, [2]JAMSTEC, [3]AORI, Univ. Tokyo

We study the implications of a recently published ice sheet history in Northern hemisphere and Greenland ice sheet, derived from the 3D thermo-mechanical ice sheet model (Ice Sheet for Integrated Earth system Studies: IcIES developed by Abe-Ouchi et al. 2013). To characterize the effects of this glaciologically consistent ice sheet history, we examine the time-variations of various geophysical quantities in response to the ice and water mass redistributions. They include vertical uplift and subsidence, global patterns of sea-level change, and regional sea-level variations along the coasts of Greenland. Relative sea-level (RSL) changes in response to past ice and water load variations are obtained solving the sea-level equation, which accounts for the crustal deformation due to glacio-isostatic adjustment (GIA). In this study, we report the predictions of RSL and geodetic signals in Greenland induced by GIA process based on the glaciologically and climatologically consistent ice loading history. And also, we show the temporal and spatial characteristics of predicted geophysical signals in Greenland in comparison with these observations. We expect that using the ice sheet histories derived from IcIES as input in GIA model may put better constraints on postglacial rebound and current rates of crustal deformation.

Keywords: Greenland ice sheet, relative sea-level change, crustal deformation, isostasy

Japan Geoscience Union Meeting 2014
(28 April - 02 May 2014 at Pacifico YOKOHAMA, Kanagawa, Japan)

ACC32-P01 Room:Poster Time:April 29 18:15-19:30

Chemical compositions of non-volatile particles in NEEM (Greenland) ice core over the last 100,000 years

OYABU, Ikumi[1*] ; IIZUKA, Yoshinori[2] ; KARLIN, Torbjorn[3] ; FUKUI, Manabu[2] ; HANSSON, Margareta[3]

[1]Graduate school of Environmental Science, Hokkaido University, [2]Institute of Low Temperature Science, [3]Department of Physical Geograohy and Quaternary Geology, Stockholm University, Sweden

The polar ice cores provide us with information of past atmospheric aerosols. Soluble aerosols in polar ice cores are well discussed by using proxies of ion concentration/flux, however, there are few studies about chemical compositions of soluble aerosols in ice cores. Using a sublimation method, we show differences in the compositions of non-volatile aerosols over the last 100,000 years in the NEEM ice core, which was drilled during 2008?2012 on the northwest ridge line of Greenland ice sheet (77 ′ 27 ″ N, 51 ′ 03 ″ W).

A total of 86 samples were distributed from NEEM ice core sections from 220 to 2195 m, which covers from late Holocene to Dansgaard-Oeschger event 24. Non-volatile particles were extracted from the ice by sublimation system [Iizuka et al., 2009]. Constituent elements of each non-volatile particle were measured by a scanning electron micro scope and energy dispersive X-ray spectroscopy. We made a classification of non-volatile particles into insoluble dust, soluble sulfate salts and soluble chloride salts as following; if Si found in a particle, we regard the particle as dust (Silicates); if S found, we regard the particle as sulfate; if Cl found, we regard the particle as chloride salt. For the sulfate salt, we did further classification that a particle containing Ca and S are assumed as CaSO4, Na and S are Na2SO4, Mg and S are MgSO4, K and S are K2SO4, the residual sulfate particles are " the other sulfate salt (other-S) " . In the same way, for chloride salts, we assumed NaCl, CaCl2, MgCl2, KCl and the other chloride salt (other-Cl).

The number ratio of soluble salts to total particles is 9±6 % during Dansgaard?Oeschger (DO) events. In Last Glacial Maximum (LGM), the ratio decreased in 3±2%. In Bolling-Allerod (BA), ratio of soluble salts slightly increased (10±5%). In Younger Dryas (YD), the ratio decreased again (6±3%). After Holocene, the ratio increased (16±10 %). In summary, more than 90 % of particles contain insoluble dust during the cold stages. These ratios suggest that during cold periods, insoluble dust concentration is higher contribution to total non-volatile particles than that in warm periods.

We examined chemical characteristics of non-volatile particles by dividing into 7 climatic stages (Late Holocene; LH, Early Holocene; EH, YD, BA, LGM, DO events-warm; DO-W and DO events-cold; DO-C). The 7 stages can be sorted into 2 types; interglacial-type (LH, EH and BA) and glacial-type (YD, LGM, DO-W and DO-C). For the interglacial-type, number of Na-containing particles is larger than that of Ca-containing particles (Na:Ca = 4:3). On the other hand, for the glacial-type, number of Ca-containing particles is larger than that of Na-containing particles (Na:Ca = 5:9). Ca-containing particles is suggested to mainly comes from terrestrial materials and Na-containing particles is mainly comes from sea-salt [Steffense et al., 1997]. Our results of the ratio of Ca and Na particles may be explained by not only absolute concentration of dust and sea-salt but also relative valance of those concentrations. In the three interglacial-type, the ratio of other-S and other-Cl, those are sulfate and chloride salts without Na, Mg, K, nor Ca, during the LH are relatively higher than the other stages. Since NH4+ concentration increased due to increasing of vegetation area and biological activity by warming in LH [Fuhrer and Legrand, 1997], other-S and ?Cl might be ammonium sulfate and ammonium chloride, respectively. Focusing on Ca-particles more in detail in the four glacial-type, number of Ca-containing particles without S and Cl is higher in LGM (11%) and DO-C (12%) than that in YD (6%) and DO-W (7%). Since the X-ray spectroscopy cannot detect carbon, the Ca-containing particles may be CaCO3 in the LGM and DO-C because CaCO3 was founded during the LGM by single particle measurement in the GRIP (Greenland) ice core [Sakurai et al., 2009].

Keywords: ice core, aerosol, paleo climate, greenland, ice sheet, NEEM

Japan Geoscience Union Meeting 2014
(28 April - 02 May 2014 at Pacifico YOKOHAMA, Kanagawa, Japan)

ACC32-P02 Room:Poster Time:April 29 18:15-19:30

Modelling the climate and the terrestrial carbon cycle for the last millennia

ABE-OUCHI, Ayako[1*] ; O'ISHI, Ryouta[1] ; YOSHIMORI, Masakazu[1]

[1]University of Tokyo AORI

Climate-induced changes in the terrestrial biosphere and the ocean modulate the release and uptake of carbon dioxide and this, in turn, alters atmospheric composition and influences the climate. This is known as the climate-carbon cycle feedback. The Coupled Carbon Cycle Climate Model Intercomparison Project (C4MIP), using models of the ?terrestrial and ocean carbon cycles inside ocean-atmosphere general circulation models, has shown that the carbon cycle-climate feedback appears to be positive BUT there is great uncertainty about the magnitude. It is important to know the magnitude of this feedback because it affects the amount of carbon dioxide that can be emitted in the future in order to stabilize the concentration of CO2 at a given level. There are projects attempting to reduce these uncertainties through systematic evaluation of carbon cycle models against observations of the contemporary carbon cycle. An alternative approach is to use knowledge about past variations in climate and CO2 to provide additional constraints. Here we therefore work on the last millennium (LM) climate-carbon modeling and examine the factors that contribute to atmospheric CO2 change. Ice core is the only proxy that provides the CO2 content in detail for the last millennium and it shows up to 10ppm change around the Little Ice Age and during the LM. Several LM experiments by AOGCM are used to drive the terrestrial carbon cycle model LPJ. We investigate the role of external forcing of climate such as volcano and solar forcing as well as that of internal variability of climate in an unforced experiment of decadal to centennial time scale. We show that the CO2 changes in the same order of magnitude in the unforced experiment as in the forced experiment.

Japan Geoscience Union Meeting 2014
(28 April - 02 May 2014 at Pacifico YOKOHAMA, Kanagawa, Japan)

AGE03-01 Room:213 Time:April 30 10:00-10:15

Concentration and Potential Mobility of Trace Metals in Surface Sediment of the North Pacific Ocean By BCR Sequential

ANDREAS, Roy[1*] ; ZHANG, Jing[1]

[1]Graduated school of science and engineeringUniversity of Toyama

Metals can accumulated in sediment, sludge and soil may therefore pose an environmental problem concerning possible metal transfer from sediment to the aquatic system and including them in the food chain. European Community Bureau of Reference (BCR)sequential methods commonly used to trace metals in the sediment or soil samples and can be provide information about bio-availability, mobility or toxicity which are basically depend on the chemical bonding between metals and solid phases of the samples.

Geochemical fractionation of Cadmium (Cd), Lead (Pb), Cobalt (Co), Zinc (Zn), Iron (Fe) and Manganese (Mn) in sediment of the North Pacific Ocean were determined using four-stages of modified BCR sequential extraction methods combination with ICP-MS. Also the contamination factors and risk assessment code effects on surface sediment samples are discussed.

The mean contents of the trace metals in surface sediment of the North Pacific Ocean were: Cd: 0.00; Pb: 13.94; Mn: 2732.94; Fe: 29795.10; Co: 22.16; and Zn:76.75 $\mu g.g^{-1}$, allowing to arrange the trace metals concentration from higher to lower were in the following order: Fe › Mn › Zn › Co › Pb › Cd. Pb was distributed in three fractions (acid soluble, reducible, and residual). Mn and Co were found in a group with mainly reducible fraction, while Fe and Zn were mainly in residual fraction. The high contamination factor was obtained for Mn and Co in the sediment samples, while the lowest was found for Fe. The result showed non risk for Fe, Co, Pb and Cd, while low risk is indicated for Mn and Zn at all stations.

Keywords: trace metals, BCR sequential extraction, North Pacific Ocean

Japan Geoscience Union Meeting 2014
(28 April - 02 May 2014 at Pacifico YOKOHAMA, Kanagawa, Japan)

AGE03-02 Room:213 Time:April 30 10:15-10:30

Leaching Properties of Naturally Occurring Heavy Metals from the Soils around Abandoned Metal Mines

ZHANG, Ming[1*] ; HOSHINO, Mihoko[1] ; HARA, Junko[1] ; SUGITA, Hajime[1] ; YOSHIKAWA, Miho[2] ; IMOTO, Yukari[1]

[1]AIST, [2]Chemical Grouting Co., LTD

The major threats to human health from heavy metals are associated with exposure to lead, cadmium, mercury, chromium, arsenic, as well as selenium, fluorine and boron. The effects of such heavy metals on human health have been extensively studies and officially reviewed by international organizations such as the WHO and heavy metal pollutions have been regulated by national environmental standards and/or laws such as the Soil Contamination Countermeasures Act in Japan.

Leaching of naturally occurring heavy metals from the soils around abandoned metal mines into surrounding water systems, either groundwater or surface water systems, is one of the major pathways of exposure. Therefore, understanding the leaching properties of toxic heavy metals from naturally polluted soils is of fundamentally importance for managing abandoned metal mines, excavated rocks discharged from tunneling and/or selecting a pertinent countermeasure against pollution when it is necessary.

In this study, soil samples taken from the surroundings of abandoned metal mines in Tochigi, Miyagi, Yamagata, Akita and Iwate prefectures in Kanto and Tohoku regions were collected and analyzed. The samples contained multiple heavy metals such as lead, arsenic and chromium. Standard leaching test and sequential leaching test considering different forms of contaminants, such as trivalent and pentavalent arsenics, and trivalent and hexavalent chromiums, together with X-ray Fluorescence Analysis (XRF), X-ray diffraction analysis (XRD) and Cation Exchange Capacity (CEC) tests were performed. This presentation illustrates the details of the above experimental study, discusses the relationships among leaching properties, and chemical and mineral compositions, indicates the difficulties associated with remediation of naturally polluted sites, and emphasizes the importance of risk-based countermeasures against naturally occurring heavy metals.

Keywords: Naturally occurring, Heavy metals, Leaching properties, Mineral composition, Bulk concentration

Japan Geoscience Union Meeting 2014
(28 April - 02 May 2014 at Pacifico YOKOHAMA, Kanagawa, Japan)

AGE03-03 Room:213 Time:April 30 10:30-10:45

Self-potential inversion for the estimation of hydraulic conductivity in the presence of unsaturated zone

OZAKI, Yusuke[1*] ; MIKADA, Hitoshi[1] ; GOTO, Tada-nori[1] ; TAKEKAWA, Junichi[1]

[1]Graduate School of Engineering, Kyoto University

Self-potential (SP) is the electrical potential naturally generated in and on the earth. The positive electrical charge in the diffuse layer of the electrical double layer is conveyed by the groundwater flow. The electrical potential is generated when the groundwater flow through the porous medium. This electrical potential directly reflects on the Darcy velocity in the porous material, and therefore the hydraulic conductivity can be estimated from the SP data. The hydraulic conductivity has non-linear characteristics as functions of the water saturation, and so does SP. These features suggest that the effect of the unsaturated zone should be considered for much quantitative analysis of SP. However, the dependency of the SP on the water saturation makes the development of inversion difficult. We solved this problem with the adjoint state method for the calculation of the sensitivity matrix that could save the calculation time. The characteristic of water saturation in SP based on Van-Genuichen model is adapted to our inversion. We applied our inversion to a synthetic SP profile to test the performance of our inversion scheme to compare the results with and without the consideration to unsaturated zone. When the effects of the unsaturated zone are not considered, the value of estimated hydraulic conductivity is underestimated. On the other hands, more accurate image could be derived from the inversion with the consideration to the unsaturated zone. Therefore, our inversion technique would allow us to obtain the accurate hydraulic conductivity structure from SP data at the ground surface, although the SP is affected by the distribution of saturation.

Keywords: Self potential, Inversion, Hydraulic conductivity, Unsaturated zone

Japan Geoscience Union Meeting 2014
(28 April - 02 May 2014 at Pacifico YOKOHAMA, Kanagawa, Japan)

AGE03-04 Room:213 Time:April 30 11:00-11:25

Root Water Uptake and Soil Water Storage in a Karst Savanna on the Edwards Plateau, Texas, USA

TOKUMOTO, Ieyasu[1*]

[1]Arid Land Research Center, Tottori University

Woody plants, especially Ashe juniper (Juniperus ashei) and honey mesquite (Prosopis glandulosa), are encroaching into a karst savanna on the Edwards Plateau in central Texas. However, their impact on hydrology is unclear because of high variability in soil depth and uncertainties about shallow and deep root contributions to water uptake in rocky soil overlying bedrock or other substrates that limit water storage capacity and root growth, and create high spatial variability in plant available water. This complex below-ground structure, while not uncommon, has of not been adequately characterized by most hydrological models. We evaluated root water uptake and water storage in the karst of the Edwards Plateau, at a typical savanna site with ˜50% woody cover, mainly Ashe juniper (Juniperus ashei) and honey mesquite (Prosopis glandulosa). Water content profiles to a depth of 1.6 m were measured by neutron thermalization and time domain reflectometry at 36 locations in a 25-by-25 m grid (5 m node spacing). Bulk density profiles were measured by gamma densitometry. Temporal changes in water storage were compared with eddy covariance measurements of evapotranspiration (ET) to evaluate relative amounts of ET originating from root water uptake at various depths. Water storage capacity in the measurement grid ranged from 185 to 401 mm, and coupled with heterogeneous distribution of trees created high spatial variability in root water uptake. Water uptake was higher beneath trees than beneath grass, in part because tree roots were able to extract water from regions of the root zone with high rock density. On average, 81% of the water uptake occurred from the upper 1 m of the profile with the greatest uptake occurring at depths of 0.4 to 0.8 m. An estimated 10% of the uptake occurred from below the maximum measurement depth of 1.6 m. While this result confirms the hypothesis that trees on rocky substrates take up water from greater depths compared to similar ecosystems on soil, it also refutes the view that trees in karst regions have greater access to groundwater.

Keywords: Root water uptake, Karst, Evapotranspiration, Spatial variability

Japan Geoscience Union Meeting 2014
(28 April - 02 May 2014 at Pacifico YOKOHAMA, Kanagawa, Japan)

AGE03-05 Room:213 Time:April 30 11:25-11:50

Estimation of Water Flux in Andisol with a Penta-Needle Heat Pulse Probe

SAKAI, Masaru[1*] ; KONDO, Naho[1] ; JONES, Scott[2]

[1]Graduate school of Bioresources, Mie University, [2]Department of Plants, Soils, and Climate, Utah State University

The potential for using heat pulse probes for estimating soil water flux as well as soil thermal properties has received more attention this past decade. Although many studies were carried out to validate water flux estimation using heat pulse probes in sandy soils, few studies were reported for other soils. The purpose of this study was to estimate water fluxes in an aggregated Andisol using a heat pulse probe, and investigate the applicability with hydrodynamic dispersion in a soil.

The Penta-needle heat pulse probe, which has a central heater needle surrounded by two pairs of orthogonally arranged thermistors, was used to estimate two directional water flux. Steady-state saturated water flow and unit-gradient unsaturated water flow experiments were conducted in Mie Andisol. To achieve saturated conditions, the Andisol was packed in the column with a bulk density of 0.85 g/cm^3 and afterward it was saturated by applying water from column bottom. A glass filter was located at the bottom of the column. $CaCl_2$ solutions were applied from the top of the column at fixed rates using a peristaltic pump, and outflows from the bottom were measured by a scale. The flow rates were decreased stepwise from fast (around 350 cm/day) to slow rates (around 5 cm/day). Using faster flow steps, steady state saturated water flows were developed. Steady state conditions for unit-gradient - unsaturated water flow were developed by controlling suction at the column bottom, in which water contents were uniform and water flowed by gravity. At each flow steps, heat pulse measurements were conducted, and the influent solution concentrations were changed to obtain breakthrough curves (BTCs) by measuring soil electrical conductivities with four-probe salinity sensors. Water fluxes were estimated by applying an analytical solution to temperature rise data. Dispersivities were determined by applying the convection-dispersion equation to BTCs. Each experiment, including packing soil and water flow testing, were repeated a few times.

In saturated conditions, water fluxes estimated by the heat pulse probe agreed well with independently measured water fluxes in one experiment and underestimations were found in two cases. For unsaturated conditions, estimated water fluxes agreed well with actual fluxes even in the experiment with disagreement in saturated conditions. The flux estimation errors were compared with dispersivities which can be interpreted as the scale of water flow spreading from mean displacement position. Large estimation errors were found for experiments with large dispersivities (λ >1.5 cm), while errors were relatively small for conditions with smaller dispersivities both in saturated and unsaturated water flows. Generally, dispersivity values in aggregated Andisol is larger in saturated condition than in unsaturated condition. The experimental results in this study indicates that the applicability of heat pulse probe to aggregated soils potentially results in better water flux estimation in unsaturated conditions.

Keywords: soil water flux, heat pulse probe, Andisol, dispersivity

Japan Geoscience Union Meeting 2014
(28 April - 02 May 2014 at Pacifico YOKOHAMA, Kanagawa, Japan)

AGE03-06 Room:213 Time:April 30 11:50-12:05

Geostatistical Interpolation of Thermal Properties of Boring Core Samples

MUTO, Hirou[1*] ; SAITO, Hirotaka[1]

[1]Tokyo University of Agriculture and Technology, [2]CREST, JST

Ground source heat pump systems (GSHP) that use ground or groundwater as a heat source can achieve much higher coefficient of performance (COP) than conventional air source heat pump systems. Although use of GSHP systems has been rapidly increasing worldwide, environmental impacts by GSHP systems have not been fully investigated. To rigorously assess GSHP impact on the subsurface environment, instead of relying on ”effective” properties, ground thermal properties including thermal conductivity and heat capacity need to be accurately characterized.

A geostatistical least-square interpolation method, known as kriging, has been used to characterize the spatial distribution of soil (or ground) physical (both hydrological and thermal) properties in one, two, and three dimensional domains. Kriging can estimate not only the values of an attribute at un-sampled locations accounting for spatial correlations between variables but also their uncertainties in terms of an error variance. Ordinary kriging (OK) which estimates unknown value as a linear combination of neighboring observations is one of the most commonly used kriging estimators. A secondary variable which is spatially cross-correlated with the primary variable can be used to reduce the estimation variance for the primary variable. Such method is known as cokriging. Ordinary cokriging (OCK) is one of the most commonly used cokriging estimator. The objective of this study was to compare OK and OCK in terms of estimating soil thermal properties along 50-m boreholes through the cross validation. Water content and sand content, which are relatively easy to measur, were used as the secondary attributes in cokriging.

In this study, undisturbed boring core samples were collected from two 50-m long boreholes at the campus of Tokyo University of Agriculture and Technology in Tokyo. Volumetric heat capacity (HC), thermal conductivity (TC), gravimetric water content (WC) and volumetric sand content (SC) were measured every 10-20 cm along the cores. The impact of sampling intensity on prediction errors were investigated by drawing random subsets of increasing size and using them to predict thermal properties at the remaining locations (jackknife approach). Then, subsets of N data were selected randomly or randomly per 10-m depth from the entire data set. For both sampling approaches, 50 different random subsets were selected to account for sampling fluctuations. Thermal properties at the remaining locations were then predicted.

This study showed that increasing the size of the subset leads to smaller mean absolute error. It was also found that kriging with random subsets per every 10-m depth yields lower mean absolute error than that with random subsets. Prediction errrors by OCK were smaller than those by OK when the sampling intensity was the same.

Keywords: thermal conductivity, kriging, cokriging, sampling intensity, prediction error

Japan Geoscience Union Meeting 2014
(28 April - 02 May 2014 at Pacifico YOKOHAMA, Kanagawa, Japan)

AGE03-07 Room:213 Time:April 30 12:05-12:20

Evaluation of Tangential Model Parameters with Respect to Various Soil Types

THIAM, Magatt[1*] ; KOHGO, Yuji[2] ; SAITO, Hirotaka[3]

[1]PhD Student, United Graduate School of Agriculture, Tokyo University of Agriculture and Technology, [2]IEAS, Graduate School of Agriculture, Tokyo University of Agriculture and Technology, [3]Department of Ecoregion Science, Tokyo University of Agriculture and Technology

Usage of Tangential model (Kohgo, 1995) for Soil Water Retention Curves (SWRCs) fitting requires knowing its parameters which are the numerical values of the coordinates of 3 tree points that are selected on the SWRC obtained from an experiment. Performing such an operation might be time consuming and may also lead to errors in the parameter estimation. This study aims to estimate these parameters and investigate possible relations between the parameters and some basic soil properties. SWRCs data and their corresponding hydraulic and physical properties were taken from the Unsaturated Soil Hydraulic Properties Database (UNSODA). The selected data consisted of 458 soils; among them: sand, sandy loams, loamy sands, sandy clay loams, silty loams, silty clay loams and silty clays. These SWRCs were fitted to Tangential model using nonlinear regression analysis with solver, the in-built Microsoft Excel tool. The iteration procedure, in solver, was the Generalized Reduced Gradient method. Results showed that the model performed well. The sum of the squared residuals (SSR) varied between 0.00011 and 0.2114 for sand and sandy soils, while it ranged between 0.021 and 0.00017 for all the others. Highest SSR values were noted with coarse sandy soils while the lower SSR values were noted with materials of finer structure. This suggests that this model is more adapted to fine structured soils. An attempt is being made in order to predict the Tangential model parameters, through multiple linear regression analysis, by using the soil bulk density values, saturated volumetric water content and the soil grain size distribution data.

Keywords: soil water retention curves, simulation, UNSODA, parametric model, fitting

Japan Geoscience Union Meeting 2014
(28 April - 02 May 2014 at Pacifico YOKOHAMA, Kanagawa, Japan)

AGE03-P01 Room:Poster Time:April 30 14:00-15:15

Quantification of soil pollution concentration of plating metals by bioassay using luminous bacteria

SUGITA, Hajime[1*] ; KOMAI, Takeshi[2] ; HARA, Junko[1] ; IMOTO, Yukari[1] ; ZHANG, Ming[1]

[1]National Institute of Advanced Industrial Science and Technology (AIST), [2]Tohoku University

Cd, Cr(6+), Pb, As and CN are substances which closely related to metal plating. These are regulated as Class II Specified Chemical Substances by Soil Contamination Countermeasures Act. However, many other plating metals have not been subject to this law. Some heavy metals, which are used as plating metals, may be harmful to the human body if taken in excess. They must be also assessed risk in the same way as a Class II Specified Chemical Substances.

On the other hand, there is a bioassay using luminous bacteria as one of the acute toxicity evaluation test on hazardous substances. Since there is normally correlation between the concentration of hazardous substances and the intensity of the acute toxicity, it may be possible to estimate the concentration of harmful substances from the intensity of the acute toxic effects.

Focusing on Fe, Ni, Cu, Zn, Ag and Sn which are widely used as common plating metals, in this study, systematic bioassay tests using luminous bacteria (Vibrio fischeri) were performed. Based on the data obtained in the experiments, quantification of the correlation between the concentration of the plating metals and the intensity of the acute toxicity was attempted.

Keywords: Soil contamination, Plating metal, Bioassay, Luminous bacteria, Quantification

Japan Geoscience Union Meeting 2014
(28 April - 02 May 2014 at Pacifico YOKOHAMA, Kanagawa, Japan)

AGE03-P02 Room:Poster Time:April 30 14:00-15:15

Effects of in-situ, long-term thermal loading on groundwater quality in marine sediments of Arakawa Lowland, Japan

SAITO, Takeshi[1*] ; UEKI, Takashi[1] ; HAMAMOTO, Shoichiro[2] ; MOLDRUP, Per[3] ; OHKUBO, Satoshi[1] ; KAWAMOTO, Ken[1] ; KOMATSU, Toshiko[1]

[1]Saitama University / CREST, JST, [2]The University of Tokyo / CREST, JST, [3]Aalborg University / CREST, JST

Subsurface temperature increase (”subsurface warming”) has been documented below many large cities worldwide. The observed subsurface temperature increase has shown close relations with surface warming effects due to global warming and urbanization. Recently, ground source heat pump (GSHP) systems have become popular as a renewable energy technology for space cooling and heating. Operation of GSHP systems for space cooling discharges waste heat into the subsurface environment and, thus, induces additional subsurface temperature increase. However, any potentially negative impacts of GSHP-induced temperature increase on the subsurface environment have not been studied in detail. The objective of this study was therefore to investigate the effects of in-situ, long-term thermal loading on groundwater quality.

A GSHP system was installed in a 50-m deep borehole with a corresponding 50-m long U-tube heat exchanger at the campus of Saitama University in the Arakawa Lowland, Japan. Four groundwater monitoring wells were installed in a marine sand sediment aquifer (around 17-m depth) at 1-m (W1), 2-m (W2), 5-m (W5), and 10-m (W10) distance from the U-tube. At each monitoring well, temperature detectors were placed in 10 depths at approximately 5-m interval, and the subsurface temperature was monitored before and during thermal loading. For the thermal loading, approximately 40 ℃ water was circulated inside the U-tube heat exchanger for 13 months, and groundwater was frequently sampled from all four monitoring wells every 1 to 2 weeks. A wide spectrum of chemical properties (including pH, EC, DO, ORP ”oxidation-reduction potential”, dissolved gases, dissolved organic carbon, inorganic ions, and trace elements) were measured to characterize groundwater quality.

The subsurface temperature at the nearest monitoring well (W1) increased gradually with approximately 8 ℃ from 17 ℃ (base-line) to 25 ℃ during 13 months of thermal loading. In contrast, at the farthest monitoring well (W10), there was no significant change in subsurface temperature, and W10 was therefore selected as a reference (non-temperature affected) monitoring well. A number of chemical components in the groundwater, including boron and potassium, increased markedly at W1 compared to W10. Since marine sediments typically contain high concentrations of chemical components including boron and potassium, the observed increase in groundwater concentration is likely due to thermally-induced dissolution and/or desorption from the marine sediment. The possible mechanisms behind the observed concentration increases will be discussed.

Keywords: subsurface temperature, thermal pollution, long-term thermal loading, GSHP, marine sediment, groundwater quality

Japan Geoscience Union Meeting 2014
(28 April - 02 May 2014 at Pacifico YOKOHAMA, Kanagawa, Japan)

AGE03-P03 Room:Poster Time:April 30 14:00-15:15

Characterization of water repellency parameters in soil water repellency characteristic curves for JP and NZ soils

WIJEWARDANA, Senani[1*] ; KAWAMOTO, Ken[1] ; MULLER, Karin[2] ; CLOTHIER, Brent[3] ; HIRADATE, Syuntaro[4] ; KOMATSU, Toshiko[1] ; MOLDRUP, Per[5]

[1]Graduate School of Science and Engineering, Saitama University, Japan, [2]Plant & Food Research Institute, Ruakura Research Centre, New Zealand, [3]Plant & Food Research Institute, Palmerston North, New Zealand, [4]Biodiversity Division, National Institute for Agro-Environmental Sciences (NIAES) Japan, [5]Department of Civil Engineering, Aalborg University, Denmark

Soil water repellency (SWR) is the phenomenon where soil does not wet when water is applied to its surface. Characterization of water repellency in natural soil is very important to understand the soil hydrological processes, surface flow and infiltration rates. Objectives of this study were (i) to characterize SWR using molarity of ethanol droplet (MED) test, sessile drop method (SDM) and water drop penetration time (WDPT) test, and (ii) to identify the relationships between the determined SWR parameters and soil organic carbon (SOC) contents. Soil samples were collected from different soil depths of representative Andosols and Cambisols in Japan (Nishigo, Hiruzen and Nikko; all sites under forest) and New Zealand (Ngahinapouri, Wahihora and Whatawhata; all sites under pasture). The soil-water contact angle was directly measured using SDM, and indirectly derived from MED and WDPT measurements. All the A horizons of the Japanese soils showed water repellency, and the New Zealand soils were also water repellent at all depths except the Ngahinapouri, B horizon. Then, soil water repellency characteristic curves (SWRCCs) were obtained for water repellent (WR) soils, i.e., soil-water contact angle / degree of WR as a function of the volumetric water content (θ). Three WR parameters were determined from the SWRCCs. They are (i) the integrated areas below a SWRCC, $S_{WR(}\theta), (ii) the soil water content at maximum (\theta_{WR-Max})$ and (iii) minimum (θ_{WR-Min}) WR. Further, WR parameters were studied with soil organic carbon (SOC) contents. These relationships were agreed well with recently published work of Kawamoto *et al*. (2007) and Karunarathna *et al*. (2010). The SOC contents of New Zealand soils varied between 1.4% (WR) to 12.1% (WR), for the Japanese soils they ranged between 2.6% (Non-WR) and 26.3% (WR). Although the Japanese soils had high SOC contents in >10 cm depths, they were not WR (for Nikko >5 cm depth-Not WR). Therefore, further studies are needed to assess SWR as affected by SOC.

Keywords: soil water repellency characteristic curve, water repellency parameters, soil organic carbon

Japan Geoscience Union Meeting 2014
(28 April - 02 May 2014 at Pacifico YOKOHAMA, Kanagawa, Japan)

AGE03-P04 Room:Poster Time:April 30 14:00-15:15

A result of Cs redistribution in a forest soil after FNP-I accident.

NISHIMURA, Taku[1*]

[1]The University of Tokyo

Cesium is a large atom which does not likely to hydrate. Similar to potassium and ammonium cation it prefers to site at siloxane ditrigonal cavity of silica sheet of phyllosilicates. Cesium is strongly, almost irreversibly, captured at frayed edge site of layered clay particles. These facts may make partition coefficient of cesium to be very large. The large partition coefficient may produce larger retardation of cesium transport with percolating water. At the same time large partition coefficient may cause enhance in migration of Cs with moving colloids. A comparison of Cs content distribution of near surface soil of between cleared forestry and a forestry with 5cm litter layer in Iitate village, Fukushima suggested organic colloids could be a transporter of Cs at litter covered forest. Soil total carbon content as well as C/N ratio had relation with soil Cs content. A depth where soil had higher organic carbon and lower C/N ratio tended to show high Cs content.

Keywords: Cs, forest, soil organic matter, colloids

Japan Geoscience Union Meeting 2014
(28 April - 02 May 2014 at Pacifico YOKOHAMA, Kanagawa, Japan)

AGE03-P05 Room:Poster Time:April 30 14:00-15:15

Observation of Pore Structure for Differently Compacted Landfill Final Cover Soils Using Microfocus X-ray CT

BANIYA, Arjun[1*] ; KOIKE, Takuya[1] ; WATANABE, Kai[2] ; HAMAMOTO, Shoichiro[3] ; KAWAMOTO, Ken[1]

[1]Graduate School of Science and Engineering, Saitama University, Japan, [2]Department of Civil and Environmental Engineering Saitama University, Japan, [3]Graduate School of Agricultural and life Sciences, University of Tokyo, Japan, [4]Institute of Environmental Science and Technology, Saitama university, Japan

The final cover soil on a solid waste landfill consists of many layers of materials and is highly compacted. It is used to prevent rain/surface water infiltration in to the waste layer. On the otherhand, the landfill site has a significant emission source of greenhouse gases. Gas and mass transport in soils occurs through the soil pore network, which is highly affected by soil physical properties including compaction, particle size, moisture content and total porosity. However, there are a limited number of studies on visualization and quantification of soil pore network for highly compacted soil like final cover soil. The objectives of this study were setting of microfocus X-ray Computed tomography (CT) for scanning landfill final cover soils in conjunction with 3-D image analysis techniques and analyzing the soil pore structure parameters. In this study, soil samples were collected from landfill site in Saitama prefecture, Japan. Soil pore structure was analyzed using micro focus X-ray CT (Shimadazu inspeXio SMX-90CT, Shimadzu Corporation) for air dried final cover soil samples of particle size (d$\leq$2mm) with different dry densities 1.4, 1.55 and 1.65 gcm^{-3} by a hand compaction. The tested soil texture was silty sand. The scanned images were taken by the micro focus X-ray CT. Then, by the use of software VGStudio MAX, they were reconstructed in 3-D images. Finally, using software of EXFact analysis they were analyzed to obtain pore structure parameters such as pore size distribution, coordination number, specific area and pore-network tortuosity. For determining suitable scanned images for soil pore structure and network, several scanning conditions for the microfocus X-ray CT have been tested i.e. different combinations of voxel size (10, 30 and 50 μmm), scan number, view number, field of view(FOV), region of interest(ROI), and percent of interior pore for pore structure analysis. Base on the results from the tested conditions, we will propose a suitable condition on the microfocus X-ray CT scanning for macropore network (typically, effective pore diameter $>$100 μmm) in differently compacted final cover soils.

Keywords: Microfocus X-ray Computed Tomography (CT), Pore network and structure, Final cover soil

Japan Geoscience Union Meeting 2014
(28 April - 02 May 2014 at Pacifico YOKOHAMA, Kanagawa, Japan)

AGE03-P06 Room:Poster Time:April 30 14:00-15:15

Consolidation characteristics of landfilling waste samples in Japan: Effects of waste compositions and various mixing pr

IQBAL, Muhammad rashid[1*] ; OOHATA, Hiroyuki[1]

[1]Graduate School of Science and Engineering, Saitama University, Japan, [2]Graduate School of Agricultural and Life Sciences, the University of Tokyo, Japan, [3]Institute for Environmental Science and Technology, Saitama University, Japan, [4]Center for Material Cycles and Waste Management Research, NIES, Japan

Solid waste materials are highly heterogeneous depending on various waste compositions, making it difficult to understand their consolidation characteristics. The purpose of study is to find out effects of waste compositions and mixing proportions on the consolidation characteristics of compacted solid waste materials. In this study, totally 6 different waste materials, un-burnable domestic waste, un-burnable industrial waste, incineration ash, crushed concrete, organic sludge and inorganic sludge, were used as tested materials.

By using the standard proctor test, compaction curves and maximum dry bulk densities were determined for each sample. Compaction results showed that maximum dry bulk densities of the Incineration ash (1.65 g/cm3) and crushed concrete (1.45g/cm3) were higher than the inorganic sludge (0.90 g/cm3) and organic sludge (0.742 g/cm3) respectively. The maximum dry bulk densities for mixed sample of inorganic sludge, concrete and incineration ash were larger than each independent waste sample. In especial, the maximum dry bulk density for the mixed sample with ratio 1:1:1 (dry mass basis) was 1.48 times larger than that for inorganic sludge.

Consolidation tests were carried out for selected pre-compacted waste samples with degree of compaction higher than 90 % after the compaction tests. For the consolidation tests, oedometer test apparatus which dimension of 10 cm diameter and 10 cm height was used for the waste materials with particle size larger than 2mm. Results of each independent sample showed that the coefficient of consolidation (Cv) for crushed concrete and incineration ash was higher than organic and inorganic sludge wastes while compressibility of un-burnable industrial waste was higher than the other materials due to a presence of compressible material. As the mixing ratio of crushed concrete in the mixed samples increased, the compression index (Cc) decreased. When the inorganic sludge and crushed concrete are mixed with the ratio 1:3, the Cc value of the mixed sample decreased up to 75% as compared to the one for only inorganic sludge. In addition, by mixing the inorganic sludge with the crushed concrete, the Cv values for mixed samples increased in the order of 10^{1}~10^{2}. Effect of mixed proportion of the various wastes on consolidation parameters will be further investigated.

Keywords: Compaction, Consolidation, Sludge, landfill

Japan Geoscience Union Meeting 2014
(28 April - 02 May 2014 at Pacifico YOKOHAMA, Kanagawa, Japan)

AGE03-P07 Room:Poster Time:April 30 14:00-15:15

Remediation of a Tsunami affected saline and sodic soil by calsium carbonate and rice straw

ISHIBASHI, Sakuya[1*] ; NISHIMURA, Taku[1] ; HAMAMOTO, Shoichiro[1] ; IMOTO, Hiromi[1]

[1]Graduate School of Agricultural and Life Sciences, The University of Tokyo

Japanese government recommends leaching of soluble salts as well as adding calcium amendments for remediating saline and sodic soil after Tsunami by the earthquake on March 11, 2011,. Application of calcium carbonate ($CaCO_3$) is recommended for soils having pH lower than 6 and calcium sulfate ($CaSO_4$) is that for pH higher than 6. However, since $CaCO_3$ has low solubility to water, it has not been often used in reclamation of sodic soils (Shainberg et al, 1989).

Solubility of CaCO3 is controlled by CO_2-H_2O-$CaCO_3$ equilibrium in water. The concentration of calcium ion in $CaCO_3$ solution is affected by CO_2 concentration (partial pressure) of air phase. The higher partial pressure of CO_2 causes the higher concentration of Ca^{2+}. In general, addition of organic matter may enhance soil respiration and increase partial pressure of CO_2 in soil. This might potentially enhance solubility of $CaCO_3$ and increase Ca^{2+} concentration in soil solution.

Increase in Ca^{2+} concentration in soil decreases exchangeable sodium percentage (ESP) of the soil. Lower ESP may inhibit soil dispersion and help to keep aggregation. Stability of aggregates has a role on soil permeability, and it affects efficiency of leaching practice.

Objective of this study was to investigate the effect of changes in partial pressure of CO_2 by organic matter decomposition on dissolution of $CaCO_3$, and subsequent Na^+-Ca^{2+} ion exchange of a Tsunami affected soil.

Soil was collected at a former paddy field at Terashima, Miyagi, Japan, where was damaged by Tsunami at the Great East Japan Earthquake. EC (1:5) of the soil was 5.2dS m^{-1}. The soil was mixed with rice straw and/or $CaCO_3$, and then packed into plastic columns of an inner diameter of 8.5cm and 20cm-high with the bulk density of 0.95g cm^{-3}. Amount of rice straw and $CaCO_3$ application was 10t ha^{-1} and 1t ha^{-1}, respectively. The soil columns were incubated for 23 days. During the incubation, 18mm of water was supplied for each three days. The temperature inside and around the columns, and soil water pressure were continuously monitored. The CO_2 concentration in soil air phase was measured at 5-days interval.

After the incubation, the columns were leached by 4 pore volumes of 4mmol L^{-1} KCl solution with. The leachate was collected for further analysis of EC, pH and concentration of cations. After the leaching, the soil columns were separated to 3cm thick layers. Each 3cm thick soil sample was used to measure EC, pH, soluble cations, and exchangeable cations of the soil.

In average, soil CO_2 concentration inside the column was high under the rice straw treatment regardless of $CaCO_3$ application. The CO_2 concentration rose at the periodical water application, and gradually decreased with time. Rise in CO_2 concentration could be due to the enhanced organic matter decomposition and the restricted CO_2 diffusion by higher soil water content following the water application.

Exchangeable cations of the column soil were measured after the leaching. Exchangeable Ca^{2+} slightly increased at whole layer of the four treatment. Increase in exchangeable K^+ coincided with decrease in exchangeable Na^+, suggesting ion exchange between Na^+ and K^+ was a dominant reaction during the leaching.

In this experiment, the effect of organic matter and $CaCO_3$ application on remediation of the Tsunami affected saline and sodic soil was not clear. With fluctuating soil water content, soil CO_2 concentration was not always high during the column incubation experiment. It is expected that depression of soil CO_2 concentration with decrease in soil moisture after water application could not enhance dissolution of applied $CaCO_3$.

Keywords: Tsunami affected soil, saline and sodic soil, rice straw, calcium carbonate

Japan Geoscience Union Meeting 2014
(28 April - 02 May 2014 at Pacifico YOKOHAMA, Kanagawa, Japan)

AGE03-P08 Room:Poster Time:April 30 14:00-15:15

Enhancing Radioactive Fallout Removal from the Surface Soils by using artficial macropore transport system

SATO, Naoki[1*] ; MIYAMOTO, Tamami[2] ; MORI, Yasushi[1] ; INAO, Eiko[3] ; NOBORIO, Kousuke[4]

[1]Faculty of Environmental Science and Technology,Okayama University, [2]Graduate School of Environmental and Life Science,Okayama University, [3]Miyagi Prefectural Institute of Agriculture and Horticulture, [4]Faculty of Agriculture,Meiji Unversity

Fukushima nuclear power plant damaged by the East Japan Great Earthquake caused radioactive fallout around the Tohoku-region. Because radioactive fallout was positively charged,it was reported to be absorbed to soil surface. Surface soil scraper and deep plowing would be,therefore effective for the removal of radioactive materials. However,these techniques were available for flat and wide area like school yard or farm land.

in many orchards,fruit absorbed radioactive Cesium, which indicated radioactive fallout did not immediately absorb to soil surface but stayed as exchangeable ion for a while and was absorbed by plant root. therefore the technique for sloped land is also needed for better management for radioactive fallout.

we applied artificial macropores to effectively remove radioactive fallout from the surface soil. artificial macropore filled with bamboo fiber was made in siol(Field:d=1 length=50cm,Lab:d=0.6cm,length=20cm). Zeolite was placed at the bottom of the macropores(Field:50cm,Lab:20cm)to absorb transported Cesium.Four treatments were prepared for field experiments,such as macropore with ammounium sulfate,no macropore and no macropore with ammonium sulfate. In the lab experiments, Potassium was used for safety reason and a 400mm artficial rainfall was applied for one month. Results showed artificial macropore effectively transported radioactive Cesium/Potassium to deeper profile. In the lab experiment, artificial ,macropore successfully delivered Potassium to deeper profile while no radioactive Cesium was observed from the drainage water.

Keywords: Macropore, Degraded Soils, Radioactive Substance

Japan Geoscience Union Meeting 2014
(28 April - 02 May 2014 at Pacifico YOKOHAMA, Kanagawa, Japan)

AGE03-P09 Room:Poster Time:April 30 14:00-15:15

A Design of Artificial Macropore for Improving Infiltration Process in Degraded Soils

SAKIKAWA, Kazuki[1*] ; MORI, Yasushi[1] ; SUETSUGU, Atsushi[1]

[1]Okayama university

Soil is largest carbon storage body in all terrestrial medium such as vegetation and the atmosphere. However, these days, soils could not show its function as water storage layer or culture medium for plant, because of climate change or rough management. In this study, artificial macropores are introduced in soils for purposing enhancing infiltration without cultivation. Fibrous material was inserted so that it reinforced the macropore structure. Moreover, capillary force caused by fibers drag the surface water into the deeper soil prior to saturation. Capillary force caused by fabric introduced vertical transport, while micropore(matrix) enhanced horizontal flow. It makes it possible effective infiltration than empty macropores. In the experiment, an ideal design of artificial macropore was searched. The density of fibrous material was altered as 0.2 0.3 0.5 g/100cm3-soil. Artificial rainfall of 2 (weak rain) and 20 (stormy rain) mm h-1 were applied on the soil column (D=5cm, H=30cm). Results showed that retention curve has gradually changed as we changed the density of fibrous material. Thus, the capillary force was effectively created according to the densities surface water was effectively collected by dense artificial macropore when weak rainfall was applied, while stormy rain was effectively drained by light artificial macropore.

Keywords: macropore, soil degradation

Japan Geoscience Union Meeting 2014
(28 April - 02 May 2014 at Pacifico YOKOHAMA, Kanagawa, Japan)

AGE03-P10 Room:Poster Time:April 30 14:00-15:15

Artificial Macropore installation effect on organic matter storage at a degraded land.

MORIWAKE, Shuichi[1*] ; MORI, Yasushi[1] ; SUETSUGU, Atsushi[1]

[1]Okayama University

At ill-drained lands, heavy rain would cause erosion which enhances degradation process much faster.According to our previous study, artificial macropore successfully enhanced vertical infiltration and increased organic matter contents. However,there was a concern that infiltrated fresh soil water transported nutrient and oxygen at the same time, resulting decomposition of the organic matter.

In this experiment,we prepared sandy soil column(D=50mm,H=300mm)with Cellulose, for which artificial rainfall of 210mL with nutrients (N,P,K)were applied on the surface soils. Then columns were placed at 30 oC constant temperature room to enhance organic matter decomposition. In order to observe structural difference for carbon storage,three treatments were prepared such as, cultivation,artificial macropore and control,respectively.

Results showed that evaporation was significant for cultivation column, which meant traditional agricultural practice had disadvantage for conservation of soil water conservation. On the other hand,artificial macropore column showed similar evaporation rate for control column in spite of their well-drained structure.Affected by water content,vertical profiles for carbon contents were different for three treatments. Standard deviations for vertical profiles were small for control column,and larger for macropore column and cultivation column.

Keywords: Artificial Macropore, degraded land

Japan Geoscience Union Meeting 2014
(28 April - 02 May 2014 at Pacifico YOKOHAMA, Kanagawa, Japan)

AGE03-P11 Room:Poster Time:April 30 14:00-15:15

Modelling of Critical Loads for Heavy Metals in Terrestrial Ecosystem in Slovenia

SVETINA VEDER, Marta[1*]

[1]RCE, marta.svetina@rce.si

In Slovenia a modelling application of As, Cd, Co, Cr, Cu, Hg, Mo, Ni, Pb and Zn critical loads in soil were performed. The calculation in the Salek Valley involved 30 research areas in the town Velenje area on a 500 x 500 m grid, where the chemical analyses of precipitation and soil were made.

The aim was application of theoretical models for determination the maximum critical levels of heavy metals in terrestrial ecosystem with empirical data. The basis for calculation was an effect-based approach, which limits are based on adverse effects on the ecosystem and the heavy metal concentrations should stay below those limits. As receptor was used a human health trough the eco toxicological risks with use of ground water for drinking water and/or consume crops that are grown on the soil. The simple model based on dynamic mass balance of heavy metals in soil was used for calculation. It was estimated that the critical time well illustrates the acute danger of soil pollution and is recommended as the draft estimation of actual condition in soil which could be valued with few data.

Two different soil conditions at the actual atmospheric input were used in calculation: unpleasant and average. The unpleasant condition was simulated for the surface soil to depth of 5 cm, and the advanced to soil depth of 20 cm and density of 1.500 kg/m3. The critical time for both conditions is calculated for As, Cd, Co, Cr, Cu, Hg, Mo, Ni, Pb, Zn. The comparison between heavy metals indicates high accumulation of As and Hg, and thus their quit fast approach to the critical loads. In second rang of atmospheric input are Cd, Pb and Zn which are accumulated much slowly, followed by Mo, Ni, and Co, and the slowest progress make Cr. The estimated periods to reach the permitted Slovene limits in surface soil are calculated for As, Hg 100, Cd 140, Pb 230, Zn 350, Cu 830, Mo 1.700, Ni 1.800, Co 1.900, and for Cr 6.000 years.

Keywords: heavy metals, soil, contamination, modelling

Japan Geoscience Union Meeting 2014
(28 April - 02 May 2014 at Pacifico YOKOHAMA, Kanagawa, Japan)

AGE03-P12 Room:Poster Time:April 30 14:00-15:15

Predicting soil moisture in arable land under climate change with soil-profile physical properties database

KATO, Chihiro[1*] ; NISHIMURA, Taku[2]

[1]Faculty of Agriculture and Life Science, Hirosaki University, [2]Graduate school of Agricultural and Life Sciences, the University of Tokyo

Soil is foundation of agriculture and ecosystems. Soil physical condition such as soil moisture and temperature directly and indirectly affects yields and quality of crop production. Therefore predicting soil moisture of arable lands under climate change is important and valuable for yield prediction and adaptation under climate change. For predicting soil moisture condition of agricultural lands in arbitrary areas, use of soil database and datasets of General Circulation Model (GCM) projections should be useful since physical properties of soils and meteorological condition vary with location. Most of available GCM projections have spatial and temporal resolution of 100 km and a month. However, using GCM projections as input data for soil moisture and temperature prediction, temporal and spatial scale of the input data is favorable to be small since effective surface soil layer of agricultural production is generally shallow. In this study we investigated possibility of predicting soil moisture of arable lands in arbitrary areas with local-scale (approximately 20km×20km) daily GCM projection dataset " ELPIS-JP " (Iizumi et al., 2012) and the agricultural soil-profile physical properties database, Japan, " Solphy " (Eguchi et al., 2010).

In this study, soybean fields of Yoshioka and Ookubo, which are located in neighbors (approximately 2 ~ 3km), in Toyama city were chosen as experimental sites and scenario studies were done for predicting soil moisture condition with HYDRUS model (Simunek et al., 2008) under climate change in the future (2071 ~ 2090). Soil physical properties of each site were determined with water retention data in the SolphyJ database by using RETC program (Yates et al., 1992). Before the scenario studies, validation of HYDRUS model and soil physical properties which are obtained with SolphyJ database was conducted by comparing observed and simulated soil moisture of the Yoshioka field. The projection of MIROC-hires 3.2 A1B scenario was chosen among 26 (10 GCMs × 3 Special Report of Emission Scenario) ELPIS-JP scenario datasets. For preparing input data for numerical simulation of soil water movement, daily ELPIS-JP datasets were temporally downscaled to hourly or minutes scale by using weather generator " CLIGEN " (Nicks et al., 1995)

Simulated results suggested that the duration of excess soil moisture condition following heavy rainfall events are more likely at Ookubo than Yoshioka even though they are located in neighbors and have similar soil textures. Increase in surface runoff fluxes is possible to be larger in Ookubo than in Yoshioka as well. These results imply that even in a small watershed it is important to consider soil spatial distribution in predicting effects of climate change on agricultural production. Also, combination of temporally downscaled GCM projection dataset and agricultural soil-profile physical properties database may be useful for predicting soil moisture in arbitrary areas.

References: Eguchi et al., 2011, Proceedings of Annual Meeting of JSDIRE, 302-303; Iizumi et al., 2012, Phil. Trans. R. Soc. A, 370, 1121-1139; Nicks et al., 1995, NSERL Report ♯10, pp.2.1-2.22.; Simunek et al., 2008, Vadose Zone J. 7, 587-600; Yates et al., 1992, Soil Sci. Soc. Am. J, 56, 347-354

Keywords: Climate change, Soil moisture, Numerical simulation, SolphyJ, ELPIS-JP

Japan Geoscience Union Meeting 2014
(28 April - 02 May 2014 at Pacifico YOKOHAMA, Kanagawa, Japan)

AGE03-P13 Room:Poster Time:April 30 14:00-15:15

A Case Study of Combining Geophysics Prospecting Techniques to a Soil Contaminated Site

WANG, Tzu-pin[1*] ; CHEN, Chien-chih[1] ; DONG, Tien-hsing[4] ; CHEN, Yi-chieh[3] ; LIU, Hsin-chang[2] ; LIN, Chih-ping[5] ; HUNG, Hao-chun[6] ; HO, Ching-jen[6]

[1]Dep. of Earth Sciences and Graduate Institute of Geophysics, National Central University, Taiwan, [2]Disaster Reduction Research Center, Chien Hsin University of Science and Technology, Taiwan, [3]Geophysical Technology and Engineering Co.,Ltd. R.O.C, [4]Apollo Technology Co.,Ltd. R.O.C., [5]D.P.W.E. National Chiao Tung University, Taiwan, [6]Environmental Protection Administration, Taiwan

This study utilizes a combination methods of Electrical Reisitivity Tomography (ERT), Ground Penetrating Radar (GPR), and Horizontal Loop Electromagnetic (HLEM) to examine a heavy-metal contaminated site before and after the remediation. It was a processed sludge tacking site of a smelting plant. The sludge is homogeneous red, and the main pollutants are chromium, arsenic and lead. The plant has been closed for more than twenty years. At the time when it was shut down, instead of removing the stacked sludge and underground structures (tank), the site was leveled directly and planted with lawns. Now, it is difficult to know the distribution of the sludge, the depth of its cover, and the correct location of the underground structures.

The pre-remediation investigation conducted with the application of geophysical prospecting techniques found that the HLEM could efficiently define the distribution of sludge efficiently, and ERT could be used to detect the thickness of the sludge and the location of the underground structures, but GPR results failed to meet expectations which may due to a significant attenuation of electromagnetic energy caused by the nature of the sludge. The post-remediation examination shows obvious different morphologies of the site than it was before the remediation. The results can be used to assess the effectiveness of remediation, and to check if any sludge remains.

Keywords: ERT, GPR, EM, pollution

Japan Geoscience Union Meeting 2014
(28 April - 02 May 2014 at Pacifico YOKOHAMA, Kanagawa, Japan)

AGE03-P14 Room:Poster Time:April 30 14:00-15:15

Cs migration to rice crop from soil after stripping the contaminated top soil at Iitate Village in Fukushima Prefecture.

NISHIWAKI, Junko[1*] ; ASAGI, Naomi[1] ; KOMATSUZAKI, Masakazu[1] ; MIZOGUCHI, Masaru[2] ; NOBORIO, Kosuke[3]

[1]College of Agriculture, Ibaraki University, [2]Graduate school of Agricultural and Life Sciences, The University of Tokyo, [3]School of Agriculture, Meiji University

Iitate Village is at about 40 km northwest from a Fukushima Daiichi nuclear power plant. An agricultural fertile layer in agricultural fields was contaminated by radionuclides, e.g., 134-Cs, 137-Cs, and 90-Sr, just after the accident of the Fukushima Daiichi Nuclear Power Plant in 2011. The decontamination work is an important subject for villagers to return to a village and live there again. Three decontamination methods are proposed by a Ministry of Agriculture, Forestry and Fisheries. They are 1) Stripping the top soil off, 2) Removal of fine particles after soil and water mixing, and 3) Tillage reversal. By the report of the Ministry of Agriculture, Forestry, and Fishery, 90% of radioactive contaminant has been removed by the method of stripping the contaminated top soil off. In this time, we examine the Cs migration to rice crop from soil after stripping the contaminated top soil off.

We used ˜4∗20 m paddy field at Iitate Village in Fukushima Prefecture. At first we decontaminated the site using the method of stripping 5 cm top soil off. After that potassium chloride (KCl) was put in all area as basal fertilizer on June 8, 2013. We comparted the area and made three kinds of treatments such as (1) mixed with rice straw that was harvested last year here, (2) only decontaminated, and (3) mixed with farmyard manure, and transplanted rice crop (rice cultivar is hitomebore) on June 9, 2013. We had sampled top soils at three points from each plot twice a month and the 134-Cs, 137-Cs, and 40-K concentration in soils were analyzed using a Ge semiconductor detector. The concentration of 134-Cs, 137-Cs, and 40-K in rice crop was analyzed by a NaI scintillation counter after harvest.

As a result, 134-Cs is about half of 137-Cs. Since the half-life of 34-Cs is two years, it has become approximately a half. Changes of Cs and K concentrations in soil were not observed during a rice cultivation period. The concentrations of radionuclides in mixed rice crop were 572.93±8.05 Bq/kg-dry / Cs-134, 1089.35±11.41 Bq/kg-dry/ Cs-137, and 127.29±27.59 Bq/kg-dry/ K-40. Although these values were comparatively high, soil did not show the high dose. The reason of that would be the volume of mixed rice straw was small and migration of caesium from the rice straw to the soil was hardly happened. The soil dose mixed with manure had been high through the whole cropping period. It might be the original manure dose was high, but the analysis of the manure has not completed yet. The concentration of radionuclides in rice crop below a detection limit of the NaI scintillation counter and it is below the regulation value defined in our country.

Keywords: stripping top soil off, rice crop, caesium

Japan Geoscience Union Meeting 2014
(28 April - 02 May 2014 at Pacifico YOKOHAMA, Kanagawa, Japan)

AGE03-P15 Room:Poster Time:April 30 14:00-15:15

Nitrogen removal and effect of chemical oxygen demand on removal of nitrogen in Coir Fiber Biofilm Treatment System

DHARMARATHNE, Nirmala kumuduni[1*] ; SATO, Naofumi[3] ; KAWAMOTO, Ken[1] ; TAKAHIRO, Koide[2] ; SATO, Hiroyasu[4] ; TANAKA, Norio[1]

[1]Graduate School of Science and Engineering, Saitama University, Japan, [2]Institute of Environmental science and Technology,Saitama University,Japan, [3]Kokusai Kogyo Co., Ltd, [4]Graduate School of Frontier Sciences, University of Tokyo,Japan

Biological treatment is the most useful process to remove nitrogen from water and wastewater. In this process, ammonium is first oxidized to nitrate by aerobic autotrophic nitrifying microorganisms. Nitrate is then reduced to nitrogen gas by heterotrophic denitrifying bacteria under anoxic conditions. Oxygen and organic carbon must be supplied to act as electron acceptor in nitrification and electron donor in denitrification. This study has carried out microcosm experiments in the laboratory for evaluating wastewater treatment mechanism and efficiency in the Coir Fiber Biofilm Treatment System (COTS). Coconut fiber was used to encourage the development of contaminant-degrading biofilms. A string of coconut-fiber (0.2-m length) was used as a biofilm support media and experiments were carried out using synthetic wastewater. The string of coconut-fiber was put inside the treatment container (0.012-m3 volume) with two conditions: low fiber density (LFD; single string per a container) and high fiber density (HFD; two strings per a container). As a control condition, a blank container without a coconut-fiber string was also used in the experiment. The flow rate is about 870 cm3/day (two-weeks retention time)

The inflow ammonium nitrogen concentration was 500 mg/l- 640 mg/l and the average nitrate nitrogen concentration in influent was 5.9 mg/l- 6.5 mg/l (low nitrate nitrogen loading rate). Dissolved Oxygen (DO) value of the treatment tanks were range between 0-0.3 mg/l. DO concentration in LFD and HFD treatment tanks were slightly lower than the inflow and blank tank during the whole experimental period. The maximum ammonium nitrogen removal efficiency was recorded in the 14 days of startup. It was approximately 45% and 30% in HFD and LFD treatment tank respectively. After that, ammonium nitrogen removal efficiency shows the slightly decreasing trend over the time. The maximum nitrate nitrogen removal was observed for 70 days of operation. It was around 90% and 72% in HFD and LFD tank respectively. Over the duration of the experiment, very low concentrations of Nitrite Nitrogen were observed and it was below 1 mg/l. low nitrite nitrogen is evident that the oxygen limited anaerobic nitrification-denitrification process leads to removal of ammonium nitrogen in this system. This process involves two-step as partial nitrification and Anammox. One of the most critical parameters of the nitrification process is the influent chemical oxygen demand (COD), because it directly influences the growth competition between autotrophic and heterotrophic microorganism population. The average inflow COD concentration in influent was 18300 mg/l- 19800 mg/l. Ammonium nitrogen removal efficiency decreased with the increasing of COD removal efficiency in both LFD and HFD treatment tanks. So there is a negative relationship between organic carbon concentration and biological ammonia removal. High organic loading can result in decreased nitrification due to faster growing heterotrophic bacteria dominating the surface of the biofilm, and leads to oxygen limitations for the nitrifying bacteria growing deeper inside the biofilm. As considering the results obtained from the microcosm system it can be conclude that partial nitrification and the subsequent anaerobic ammonium oxidation (Anammox) are the major process associated with the removal of ammonium nitrogen. This process is a shortcut biological nitrogen removal without increasing nitrite and nitrate concentration in the system. At the same time treatment tank with HFD always tend to eliminate significant amount of ammonium nitrogen than the LFD tank. Difference between results in HFD and LFD treatment tank indicating that surface provided for growth of biofilms is a major factor for improving biodegradation rates. COTS has effect on remove nitrate nitrogen effectively at low nitrate loading rate from the wastewater.

Keywords: Coir Fiber, Biofilm, Nitrogen removal, Chemical Oxygen Demand

Japan Geoscience Union Meeting 2014
(28 April - 02 May 2014 at Pacifico YOKOHAMA, Kanagawa, Japan)

AGE03-P16 Room:Poster Time:April 30 14:00-15:15

Estimation of water film thickness in geological media based on electric double layer interactions

NISHIYAMA, Naoki[1*] ; YOKOYAMA, Tadashi[1]

[1]Department of Earth and Space Science, Osaka University

Water film plays an important role in mineral-water interactions and mass transport in geological media under water-unsaturated conditions (Nishiyama and Yokoyama, 2013, Geochim. Cosmochim. Acta). To quantify such reactive-transport in water film, the understanding of the properties of water film is essential. Water film is retained on grain surfaces due to the action of electric double layer force associated with the compression of diffuse layers developed from mineral-water and water-air interfaces. In this study, we focused on the thickness of water film and developed a model to estimate the thickness taking into consideration the effect of ion concentration, pH, and electric double layers overlapping.

The surface charge density and electric potential at mineral-water and water-air interfaces depend on the amount of adsorption-desorption of proton and ions. When two diffuse layers developed from the opposite interfaces overlap, the concentration of ions in diffuse layers changes and consequently the adsorption-desorption reactions at the interfaces achieve a new equilibrium state. To take into account this process, we used a triple-layer model and a double-layer model to numerically solve the Poisson-Boltzmann equation describing the ion distribution in diffuse layer between the interfaces. We considered water film on quartz grains and calculated water film thickness as a function of pH and ion concentration. The results show that water film thickens with decreasing ion concentration and increasing pH. The model presented in this study allows film thickness to be estimated as a function of mineral type, ion concentration, and pH. Such model would be useful for considering the reactive-transport under unsaturated conditions including the geological storage of carbon dioxide and soil formation.

Keywords: water film, electric double layer, unsaturated zone

Japan Geoscience Union Meeting 2014
(28 April - 02 May 2014 at Pacifico YOKOHAMA, Kanagawa, Japan)

ACG04-01 Room:413 Time:May 1 14:20-14:40

Coastline as triple boundary among atmosphere, ocean and earth

YAMANAKA, Manabu D.[1*]

[1]JAMSTEC/Kobe U

Coastline is the boundary between ocean and land (earth beyond the sea level), and the liquid-solid heat contrast there produces monsoon or sea-land breeze circulation responding revolution (annual) and rotation (diurnal) periodicity of solar heating. The coastline is also the intersection between ocean surface and bottom, and its location is determined by water budget and erosion-orogeny balance. Furthermore, the coastline is the most active ecological (and also anthropogenic) zone. Based on these geoscientific meanings of coastline, we discuss climatological characteristics of land-sea coexisting planet such as earth.

Keywords: atmosphere-ocean-land interaction, monsoon and local circulation interaction

Japan Geoscience Union Meeting 2014
(28 April - 02 May 2014 at Pacifico YOKOHAMA, Kanagawa, Japan)

ACG04-02 Room:413 Time:May 1 14:40-14:55

Cold surge event observed by the research vessele Hakuho-maru over the Pacific in December 2012

OGINO, Shin-ya[1*] ; WU, Peiming[1] ; HATTORI, Miki[1] ; ENDO, Nobuhiko[1] ; KUBOTA, Hisayuki[1] ; INOUE, Tomoshige[1] ; MATSUMOTO, Jun[1]

[1]JAMSTEC, [2]Graduate School of Science, Kobe University, [3]Tokyo Metropolitan University

1. Introduction

A cold surge from the Siberian High is the typical phenomenon of the Asian winter-monsoon that sometimes reaches the southeast Asian regions, such as Philippines and the Indochina Peninsula, across the Pacific and resulted in heavy rainfall there. Airmass transformation is one of the key processes for this phenomenon. However, the quantitative evaluation based on the observation has not yet been done so far. We succeeded in observing a cold surge event by radiosondes from the research vessel over the Philippines Sea in the end of December 2012. The preliminary results are reported in this paper.

2. Observation and data

We conducted radiosonde observations on board the research vessel ”Hakuho-maru” during December 21, 2012 and January 4, 2013. Figure 1 shows the observation points and the launch time of the radiosondes. We launched radiosondes with 6-hour or 12-hour intervals during 23 to 24 December between 21N and 29N along the cruise from north to south. At the southernmost point (21N, 133E), we further carried out the fixed-point observation of 3-hour intervals for about 1.5 days during 24 to 25 December.

3. Synoptic fields

The cold surge from the Siberian High was intensified during December 20 to 26. Northwesterly winds were intensified around Japan and the northeasterly was strengthened in the Pacific Ocean and the Philippine Sea. Convections were activated over the Philippines, and the precipitation also became strong in the coastal area. The cyclonic disturbance propagated westward near the equatorial region over the western Pacific. The easterly flow at the northern edge of the disturbance and the northeasterly by the cold surge formed convergence zone over the offshore of Philippines.

4. Results

Latitude-height section of potential temperature and water vapor mixing ratio obtained by the moving observation during 23 to 24 December revealed the cold air intrusion was observed in the lower layer from the surface to 2 km height. The stable layer was formed at the top of the cold air intrusion (about 2 km height). The temperature and humidity were higher in the southern area. Time-height section of potential temperature and water vapor mixing ratio obtained by the fixed-point observation during 24 to 25 December showed that the stable layer around 2 km height were gradually intensified and that below the stable layer both the potential temperature and the water vapor mixing ratio had the uniform vertical distributions, which is consistent with the well-mixed layer during the cold surge event. The transition to such a typical mixed-layer structure was captured by high temporal resolution observation.

With the help of the operational radiosonde data at Minami-daitojima and at Chichijima, we performed a thermodynamic energy budget analysis and evaluated the transfer of thermodynamic energy between the atmosphere and the ocean. The result indicates that the amount of the energy transfer from the ocean to the atmosphere was even large over the Pacific remote from the Eurasian continent and compares with the one that observed near-continent area over the East China Sea by the AMTEX project (Ninomiya, 1975, JMSJ). The effect of the energy transfer to the precipitation over the Philippine area will be discussed.

Acknowledgement

We would like to thank Dr. Hodaka Kawahata (The University of Tokyo), Mr. Katsura Kameo (The University of Tokyo), Mr. Ei Hatakeyama (Marine Works Japan LTD) and all the crews of Hakuho-maru for their great help with conducting the radiosonde observation on board the research vessel. We wish to express our gratitude in Drs. Kaoru Sato (The University of Tokyo), Naohiko Hirasawa and Yoshihiro Tomikawa (National Institute of Polar Research) for permitting us to use their launch

device. Part of this study is supported by The Green Network of Excellence (GRENE) program of the Japanese Ministry of Education, Culture, Sports, Science and Technology.

Keywords: cold surge, air-sea interaction

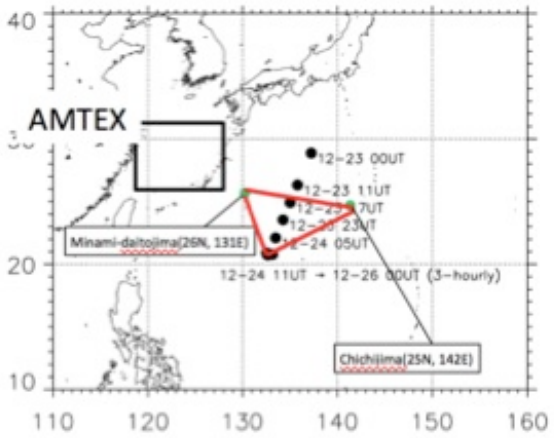

Japan Geoscience Union Meeting 2014
(28 April - 02 May 2014 at Pacifico YOKOHAMA, Kanagawa, Japan)

ACG04-03 Room:413 Time:May 1 14:55-15:10

Lightning climatology around Jakarta, Indonesia, based on 13-years SYNOP observation and GSMaP rainfall data

MORI, Shuichi[1*] ; ARBAIN, Ardhi[2] ; SYAMSUDIN, Fadli[2] ; YAMASHITA, Kozo[3] ; TAKAHASHI, Yukihiro[4] ; YAMANAKA, Manabu D.[5]

[1]JAMSTEC, [2]BPPT, Indonesia, [3]Dept.Electrical Engineering, Salesian Polytechnic, [4]Department of Cosmosciences, Graduate School of Science, Hokkaido University, [5]JAMSTEC/Graduate School of Science, Kobe University

Operational observation in Indonesia, where has much amount of active convections under the tropical maritime climate with high atmospheric and sea surface temperatures and abundant water vapor supply, showed more than 100-200 days of lightning a year and more than 10 times/km2/year of lightning density. Developed convective systems with lightning (thunderstorms) often generates severe mesoscale phenomena of heavy rainfall, gusty wind, and tornados, as well as lightning strikes at the ground. Indeed, much amount and kinds of serious damages caused by thunderstorms have been reported in Indonesia, e.g., massive blackout and serious damage on electrical devices in urban areas, and forest fires and burn-out of high voltage power lines in rural regions. Although Virts et al. (2013a, 2013b) clearly documented lightning climatology over Indonesia based on TRMM LIS and the World Wide Lightning Location Network (WWLLN) observations, temporal and spatial distributions of lightning activity and their dynamics have not been examined in detail because ground-based radar and lightning locating observations are not well organized and satellite observations have deficiencies in their spatial resolution and sampling frequency.

We started three years (JFY2013-2015) program to study lightning activity mainly over Jakarta, where is the capital megacity in Indonesia and has much risk to be damaged seriously by thunderstorms especially in the social sector, to clarify its characteristics from both the points of precipitation climatological and mesoscale meteorological views based on three approaches as follows: 1) statistical analyses for lightning activity by using operational surface observation and TRMM satellite, 2) case studies on environmental conditions for severe thunderstorms based on a C-band radar and surface observation data already obtained, and 3) campaign observation by using X-band dual-polarimetric radar, VLF receiver network, and hydrometeor video soundings.

We examined 13-years SYNOP data for statistical analysis of lightning activity around Jakarta and its relation to rainfall variation based on GSMaP data as the first step. Seasonal variation of lightning frequency shows two peaks in April and November, which correspond to periods just before and after the peak of the rainy season in February around Jakarta, at most of the stations over the inland region. However, these peaks are not clearly shown at stations close to the coastline of Java Sea and one peak in February is more predominant. Because previous studies (e.g, Hattori et al. 2011, Wu et al 2007) suggested the cross equatorial northerly surge (CENS) intensify local convection around Jakarta in the boreal winter season, the effect of CENS to generate thunderstorms was limited only along the coastal region but not for inland in February. Intraseasonal variation of lightning activity based on MJO index clearly shows a major peak in the MJO phases 3 (eastern Indian Ocean) and minor one in phase 7 (western Pacific). It suggested the lightning activity was intensified at the leading and trailing edges of MJO large scale disturbance which is consistent with previous studies (e.g., Morita et al. 2006). Whereas, GSMaP data show a peak of rainfall around Jakarta in the phase 3 at the same time of lightning peak, though the previous studies showed the rainfall was peaked in the phases 4-5 (maritime continent).

We plan to examine lightning characteristics more focused around Jakarta and its relation to rainfall quantitatively by adapting the rain-yields per flash (RPF) (Williams et al 1992, Takayabu 2006) and the other parameters. More than 15-years TRMM LIS and PR data shall be used in our future study as well as Asia VLF network (AVON) and WWLLN datasets.

Keywords: lightning & thunderstorm, convective diurnal variation, Indonesian maritime continent

Japan Geoscience Union Meeting 2014
(28 April - 02 May 2014 at Pacifico YOKOHAMA, Kanagawa, Japan)

ACG04-04 Room:413 Time:May 1 15:10-15:25

Interannual variability of rainy seasons onset over the eastern Indochina Peninsula

NGUYEN-LE, Dzung[1] ; MATSUMOTO, Jun[1*] ; NGO-DUC, Thanh[2]

[1]Tokyo Metropolitan University, [2]Vietnam National University

The onset dates of rainy seasons over eastern Indochina Peninsula (8.5o-23.5oN, 100o-110oE) for individual years from 1958 to 2007 were objectively determined by the principal component of two first dominant empirical orthogonal (EOF) modes of the precipitation data. It is found that onset of summer rainy season (SRS), which is described by the EOF1, is in 6 May on the average, with a standard deviation of 13 days. Meanwhile, the autumn rainy season (ARS) indicated by the EOF2 has the climatological onset and standard deviation is 16 Sep and 12 days, respectively. The SRS starts simultaneously with the eastward shift of the Western North Pacific sub-tropical high (WPSH) and the evolution of summer monsoon westerlies. On the contrary, the retreat of summer monsoon over northern and central Indochina in boreal autumn indeed signifies the onset of ARS. The relationship between the onset and intraseasonal variations (ISVs): the 30?60-day (30?60DV) and the 10?20-day variation (10?20DV), are identified.

The results also insisted that ENSO has considerable influence on the onset of rainy season in the Indochina. In general, La Nina (EL Nino) years with warm (cold) sea surface temperature (SST) anomalies in the western Pacific and cold (warm) SST anomalies in the central?eastern Pacific in the preceding winter-spring have early (late) SRS onset. For an early onset year, the equatorial easterly winds are observed be stronger. Strong convective activities also occur over the southern Indochina Peninsula and the SCS in the preceding winter and spring. Whereas, the early onset of ARS is likely related to El Nino years with weaken equatorial easterly winds. It could be explained by the earlier retreat of westerlies monsoon and farther westward extension of the WPSH. Finally, the differences of ISV between early-late onset years of two rainy seasons are also discussed.

Keywords: monsoon onset, interannual variation, Indochina Peninsula, sub-tropical high, summer monsoon

Japan Geoscience Union Meeting 2014
(28 April - 02 May 2014 at Pacifico YOKOHAMA, Kanagawa, Japan)

ACG04-05 Room:413 Time:May 1 15:25-15:40

How did North Atlantic Oscillation (NAO) cause drought in northwestern China at the multi-decadal to centennial scales?

LEE, Harry[1*]

[1]The University of Hong Kong

North Atlantic Oscillation (NAO) plays an important role in the Northern Hemisphere climate system. Although there is growing interest in the connection between NAO and precipitation change in China, there are few studies concerning that connection in northwestern China. Based on fine-grained historical drought disaster records and NAO proxies, we explored quantitatively their possible connection in northwestern China over the past millennium at the multi-decadal to centennial timescales. Statistical results show that NAO and drought disaster were negatively correlated, as positive modes of NAO caused northward-displaced, stronger-than average mid-latitude Westerlies with an enhanced latitudinal water vapor gradient into the central Asian drylands, resulting in reduced drought frequency and intensity in northwestern China. But, their correlation was out-of-phase during the Little Ice Age because of the southward shifting of monsoon, Westerlies, and the East Asian Jet Stream brought by long-term land surface cooling. As it has been indicated that the precipitation in northwestern China is also determined by El Nino-Southern Oscillation and North Atlantic sea surface and air temperature aside from NAO, further studies are needed to evaluate their individual roles and combined impacts upon the drought disaster there.

Keywords: NAO, Precipitation, Drought, Northwestern China

Japan Geoscience Union Meeting 2014
(28 April - 02 May 2014 at Pacifico YOKOHAMA, Kanagawa, Japan)

ACG04-06 Room:413 Time:May 1 15:40-15:55

Identifying Precipitation Sources in Northern Mongolia using Back Trajectory Analysis

KOIKE, Yuriko[1] ; ASANUMA, Jun[2*] ; DAVAA, G.[3]

[1]Graduate school of Life and Environmental Sciences, University of Tsukuba, Japan, [2]Center for Research in Isotopes and Environmental Dtnamics, University of Tsukuba, Japan, [3]National Agency for Monitoring for Environment and Meteorology, Mongolia

Prediction of precipitation variability and understanding of its mechanisms are essential in Northern Asia [Yatagai and Yasunari, 1994]. The objective of this study is to investigate linkages between the interannual variability of precipitation sources and that of precipitation amount in this area.

For this purpose, a back-trajectory model [Merrill et al., 1986] of atmospheric water vapor was developed and applied to the rainfall during the warm season from 2003 to 2009 at semi-arid grassland Kherlenbayan-Ulaan (KBU) in northern Mongolia, where an air parcel is tagged with the ambient potential temperature where it is precipitated, and is tracked adiabatically above the planetary boundary layer (PBL). When a parcel is tracked back into the PBL, its potential temperature is adjusted to the value at the top of PBL. In addition, diffusion process of water vapor evaporated from the ground surface into the atmosphere and the altitude raindrops are formed are calculated using the Monte Carlo simulation [Dirmeyer and Brubaker, 1999]. The model uses JRA-25/JCDAS [Onogi et al., 2007] reanalysis data set with 6hour intervals.

The results show that the major precipitation sources of rainwater at KBU are the local area of Mongolia and the central and the western Asia. Water vapor evaporated from the local area of Mongolia is approximately 20% of the total summer precipitation, and this ratio is particularly higher in Mongolia in compared with the other area on the globe [Dirmeyer et al., 2009]. This result consists with Yatagai and Yasunari, [1995] which suggested that the variability of precipitation in the arid areas in the northeastern Asia has higher correlation with the local atmospheric circulation, and Sato et al., [2007]. Moreover, this paper clearly exhibits that this ratio is fairly constant over the years in spite that the total precipitation varies.

Moreover, it was found that water vapor supply from the central and the western Asia is approximately 30% of the total summer precipitation at the target point, and therefore, the central and the western Asia may explain a major portion of the summer total precipitation.

In addition, the year 2003 and 2004 were found to here, anomalous relation. It is discovered that larger precipitation in the autumn of 2003 [Hirata et al., 2008] was followed by the increased contribution of the local evaporation to the precipitation in the following 2004. Shinoda et al., [2011] claimed that the cold season climate with low evapotranspiration and strong soil freezing acts to prolong the decay time scale of autumn soil moisture anomalies to the next spring over the eastern part of Mongolia. Therefore, it is considered that soil moisture at the local region in the autumn may be preserved during the winter up to the next spring and contribute to precipitation in summer in northern Mongolia.

Japan Geoscience Union Meeting 2014
(28 April - 02 May 2014 at Pacifico YOKOHAMA, Kanagawa, Japan)

ACG04-07 Room:413 Time:May 1 16:15-16:35

Philippine summer monsoon onset -Intensive observation PALAU2013 and data rescue for 109 years-

KUBOTA, Hisayuki[1*] ; SHIROOKA, Ryuichi[1] ; MATSUMOTO, Jun[2] ; CAYANAN, Esperanza[3] ; HILARIO, Flaviana[3]

[1]Japan Agency for Marine-Earth Science and Technology, [2]Tokyo Metropolitan University, [3]Philippine Atmospheric, Geophysical and Astronomical Services Administration

The Philippines is an archipelago country which is located in the western side of tropical western Pacific. There are distinct summer monsoon in the western side and winter monsoon in the eastern side of the country. This study focuses on the onset of summer monsoon in the western Philippines during May to July. Intensive observation of Pacific Area Long-term Atmospheric observation for Understanding of climate change (PALAU2013) was conducted by launching additional upper-air observation in Cebu, Laoag, and Puerto Princesa during May to August 2013. We captured the onset of summer monsoon in June 10, 2013. Low level strong southwesterly wind associated with moistening air was penetrated in the central Philippines during the onset. We compared the behavior of Philippines summer monsoon onset when there was no continuous upper-air observation in reanalysis data. The recovery of historical station back to 1903 called 'Data rescue' was performed using Monthly Bulletins of Philippine Weather Bureau from 1903 to 1940. We created rainfall dataset in the Philippines from 1903 to 2012 by connecting recovered data and PAGASA station data. Summer monsoon onset was defined by using 8 station rainfall data in the western Philippines. The onset date becomes earlier after 1990s and tends to occur in middle May. Early onsets were also seen in early 20th century.

Keywords: Philippines, monsoon onset, data rescue, Asian summer monsoon

Japan Geoscience Union Meeting 2014
(28 April - 02 May 2014 at Pacifico YOKOHAMA, Kanagawa, Japan)

ACG04-08 Room:413 Time:May 1 16:35-16:50

Relationships between heavy rainfall in East/Southeast Asia and track, intensity, duration patterns of tropical cyclones

ISERI, Yoshihiko[1*] ; KANAE, Shinjiro[1]

[1]Graduate School of Science and Engineering, Tokyo Institute of Technology

Tropical cyclones (TCs) have considerable impacts to many areas in East/Southeast Asia. For instance, TCs accompanied with heavy precipitation could cause floods, and the strong winds of TC also could induce huge damages on their track and surrounding environment. In addition, Intergovernmental Panel on Climate Change (IPCC) 5th assessment report mentions possible increasing of both global mean tropical cyclone maximum wind speed and rain rates. Thereby, it would be very important to deepen our understanding on the relation between TCs and their impacts to local climate in East/Southeast Asia.

This study aims to extract observed TC patterns by employing a nonlinear classification method, and also examine relations between extracted TC patterns and heavy rainfall in East/Southeast Asian cities. The classification method used in this study is the self-organizing maps (SOM). The SOM has been recently used in climate science and have shown significant performance for analysis of high dimensional climate data.

In this study, we utilized the TC data provided by JTWC (Joint Typhoon Warning Center). The data period used in this study is 62 years from 1951-2012. Then, we extracted longitude, latitude, maximum sustained wind speed, and duration from TC genesis in order to make input for the SOM. Consequently, each TC is represented as 39 dimension vector, and total 1,837 TCs are utilized as input for the clustering by the SOM. We set the map size of the SOM as 3x3 hexagonal grids.

By the SOM algorithm, total 1,837 TCs were classified in nine nodes (i.e. nine patterns). As a result, several distinguishable TC patterns were extracted by the SOM, according to their track, intensity and duration. Then, we extracted the TCs classified in each pattern, and subsequently examined relations between the extracted TC patterns and rainfall at 21 meteorological stations in East/Southeast Asian cities. Our analysis confirmed clustering method is quite useful in identifying TC properties. The result also suggested extracted TC patterns are highly related with heavy rainfall in some of the target cities.

Acknowledgments: This research was supported by the Environment Research and Technology Development Fund (S-10) of the Ministry of the Environment, Japan and the Research Program on Climate Change Adaptation (RECCA) of the Ministry of Education, Culture, Sports, Science and Technology, Japan.

Keywords: typhoon, western North Pacific, heavy rainfall, Self-Organizing Maps

Japan Geoscience Union Meeting 2014
(28 April - 02 May 2014 at Pacifico YOKOHAMA, Kanagawa, Japan)

ACG04-09 Room:413 Time:May 1 16:50-17:05

Application of pseudo global warming method and dynamic downscaling for typhoons approaching to Japan

TANIGUCHI, Kenji[1*] ; HOSOI, Mari[2]

[1]Faculty of Environmental Design, Kanazawa University, [2]School of Environmental Design, Kanazawa University

Results of global warming experiments indicate that an intensity of typhoon will be magnified in future climate. In this study, reproductive simulation of typhoons which approach to Japan are made. At the same time, pseudo global warming conditions are composed of a reanalysis product and multiple global warming experiments. Then, numerical simulations using the pseudo global warming conditions were conducted for each actual typhoon and variations of typhoons in future climate were investigated by comparing the reproductive simulation and the runs with pseudo global warming conditions. Results of a typhoon in summer showed significant variations in tracks. When a track deflects eastward, a typhoon goes over the ocean and its center pressure remarkably decreases. In addition, wind speed around the typhoon increases very much. Geopotential height in lower troposphere showed lower anomaly over the Pacific Ocean. Decreasing Pacific high is thought to be a cause of the change in typhoon tracks. In another typhoon in summer, although variations in tracks and center pressure were smaller, total precipitation in the typhoon increased in future. However, another typhoon in summer showed decreasing precipitation with small variation in tracks and center pressure. Results for another typhoon in autumn showed smaller variation in tracks and center pressures, and total precipitation increases in results of future climate. Such characteristics in future variations were found in other typhoons in autumn. On the other hand, hourly precipitations were not necessarily increased in future climate both in summer and autumn. These results indicate that extremely strong rainfall does not necessarily occur in short time, but modestly strong rainfall continues longer time. Even if no significant variation in center pressure, or intensity is similar to current climate, precipitation will increase in future climate.

Keywords: global warming, typhoon, numerical weather prediction, downscaling

Japan Geoscience Union Meeting 2014
(28 April - 02 May 2014 at Pacifico YOKOHAMA, Kanagawa, Japan)

ACG04-10 Room:413 Time:May 1 17:05-17:20

Assessment of GSMaP satellite rainfall products in Asian monsoon region

KAMIMERA, Hideyuki[1*] ; NABESAKA, Seishi[1] ; SYAMSUDIN, Fadli[2] ; NGO-DUC, Thanh[3] ; LE VIET, Xe[4] ; HERNANDO, Hilton T.[5] ; MATSUMOTO, Jun[6] ; USHIO, Tomoo[7] ; IWAMI, Yoichi[1]

[1]International Centre for Water Hazard and Risk Management, Japan, [2]Agency for the Assessment and Application of Technology, Indonesia, [3]Vietnam National University at Ha Noi, Vietnam, [4]National Hydro-Meteorological Service, Vietnam, [5]Philippine Atmospheric, Geophysical and Astronomical Services Administration, the Philippines, [6]Tokyo Metropolitan University, Japan, also at Japan Agency for Marine-Earth Science and Technology, [7]Osaka University, Japan

Satellite rainfall products provide the spatial and temporal distribution of rainfall estimates over the ungauged regions where no ground-based measurements with rain gauges and/or meteorological radars are available. For the regions, the satellite products have special importance in, for example, hydrological and agricultural applications such as flood forecasting/warning and water resources management. The Global Satellite Mapping of Precipitation (GSMaP) products have high resolution in space and time (0.1 deg. and 1 h); besides the near-real-time version of GSMaP opens to the public within four hours after measurements. They are thus highly expected to be in operational use in many countries and regions. There are the problems in accuracy and precision of the products due to the limitations on measuring principles, time intervals of sampling and others. However, the above-mentioned strengths of the products are considerable. Therefore, the performance of the GSMaP products needs to be investigated in various areas for the appropriate and effective use; moreover, through the investigation, it can be expected that the knowledge useful for improving the performance will be obtained. The present study investigates the performance of two GSMaP products, GSMaP_MVK and GSMaP_Gauge (a gauge-adjusted GSMaP_MVK), in the four river basins located from the tropics to mid-latitudes in the Asian monsoon region, including: the Solo Basin (16,100 km^2) in Jawa, Indonesia; the Thu Bon – Vu Gia Basin (10,350 km^2) in central Vietnam; the Pampanga Basin (9,759 km^2) in Luzon, the Philippines; and the Tone Basin (16,840 km^2), Japan. The study is ongoing and intermediate results mainly for the Solo and Thu Bon – Vu Gia river basins are discussed at this session.

Keywords: Asian monsoon, precipitation, satellite

Japan Geoscience Union Meeting 2014
(28 April - 02 May 2014 at Pacifico YOKOHAMA, Kanagawa, Japan)

ACG04-11 Room:413 Time:May 1 17:20-17:35

INTERIOR FLOOD DAMAGE IN JAPAN: PRESENT AND FUTURE

BHATTARAI, Rajan[1*] ; YOSHIMURA, Kei[1] ; KIGUCHI, Mashasi[1] ; NODA, Keigo[1] ; NAKAMURA, Shinichiro[1] ; OKI, Taikan[1]

[1]Depart. of Civil Engineering, The University of Tokyo

The assessment of flood risk and its future prediction under anthropogenic climate change are important to policy makers for future preparedness and adaptation planning. Almost all countries in the world including major cities suffer from flood damage every year due to large exposed population and property. The intensity of damage amount varies as per the level of their preparedness. The case of Japan is also similar, having about 100 billion yen annual damage due to interior flood. Flood losses are increasing more rapidly during late 20c and is expected to increase in future too. Another major factor contributes to future climate events like floods and its losses will be anthropogenic climate change. But due to lack of robust analytical framework to estimate future losses and lack of long term damage data; future projections of flood loss still have many uncertainties.

Most studies regarding flood damage assessment have been done for river flood which always excludes interior flood damage usually caused by rainfall inside city area due to poor or insufficient drainage facilities. Also some extreme events corresponding to large return period is usually taken for damage assessment, which always exclude the damages caused by high frequency events, but reported as equal as an extreme event. In this study, we present a robust methodology for interior flood damage assessment exclusively; taking all daily rainfall events into account and its application to future climate.

We use recorded historical daily damage data in Japan that was archived in Ministry of Land, Infrastructure, Transport and Tourism (MLIT) of Government of Japan to produce functions namely damage occurrence probability function and damage cost function. Our statistical approach gives the probability of damage following every daily rainfall event and thereby the annual damage as a function of rainfall, population density, topographical slope, and gross domestic product. Our results for Japan show reasonable agreement with area-averaged annual national damage for period 1993?2002 in calibration and 2003-2009 in validation. The flexibility of this method leads to future projection of interior flood damage in Japan.

Multiple climate models in different resolution with different convective schemes, sea surface temperature (SSTs) and future climate scenarios to predict the future interior flood damage amount in monetary term are being used. For Japan, we use high resolution Meteorological Research Institute (MRI) atmospheric general circulation models (MRI-AGCM) for present and future precipitation. The precipitation parameters are calculated from 1979-2009 in present and 2075-2099 in future using MRI-AGCM with two mesh sizes (20 km and 60 km) and three different convective schemes (Yoshimura Scheme, Arakawa-Schubert scheme & Kain-Fritsch scheme) which give multi-physics ensemble. The future sea surface temperature (SST) is as per the multi-model ensemble mean change of CMIP3 and CMIP5 with A1B and RCP8.5 scenario respectively. Moreover to consider uncertainty of future SST due to geographical SST distribution, three different clusters SST are also taken for future damage assessment.

Initial results for annual average interior flood damage in Japan shows 13.25% increase in average for future [2083- 2099] from the base period [1993-2009] for A1B scenario and 10.08 % increase for RCP8.5 scenario. The range of future estimate of average annual interior flood damage for A1B scenario is 68.17 billion yen to 117.81 billion yen and for RCP8.5 scenario, it is 78.93 billion yen to 119.06 billion yen in 2005 price. Another important notice in the result is future largest annual damage in A1B scenario seems quite same as present largest annual damage, but for RCP8.5, some year shows the largest damage will double than the present.

We will add different models and CMIP5 results and will describe more features of future interior flood damage in our presentation.

Keywords: interior flood damage, damage occurrence probability, damage cost function, preparedness, economic losses, climate change

Japan Geoscience Union Meeting 2014
(28 April - 02 May 2014 at Pacifico YOKOHAMA, Kanagawa, Japan)

ACG04-12 Room:413 Time:May 1 17:35-17:50

Application of performance metrics to climate models to project future river discharge in the Chao Phraya River basin

WATANABE, Satoshi[1*] ; HIRABAYASHI, Yukiko[1] ; KANAE, Shinjiro[2]

[1]the University of Tokyo, [2]Tokyo Institute of Technology

Future river discharge in the Chao Phraya River basin was projected, taking into account the performance of multiple General Circulation Models (GCMs). Future hydrological simulations using outputs from multiple GCMs are important for assessing the uncertainty in the projections. In addition, consideration of the spread of GCM projections should be included in the analysis to appropriately evaluate extremes, as there can be significant differences among projections. This study, therefore, developed a bias-corrected dataset for multiple GCMs outputs and a performance metrics to evaluate each GCM in order to project future river discharge more appropriately.

To develop a bias-corrected future climate dataset, an advanced bias correction method is applied, in which the trend of variables from the reference to the projection period is preserved. Then, future river discharge was projected by the H08 hydrological model. The newly developed future climate dataset enabled us to conduct a projection that considered the spread of projection derived from multiple GCMs.

Several metrics to evaluate the performance of each GCM to reproduce monsoon precipitation were proposed to estimate performance-based projection because evaluation of GCM performance in simulating monsoon behavior is important for projecting future discharge in the Chao Phraya River basin. This study was performed to investigate the effects of performance metrics and to estimate the spread of projections derived from the differences in multiple performance metrics.

Multiple future projections using available GCM outputs were conducted in the Chao Phraya River basin and multiple weighted ensemble means were obtained using the proposed multiple metrics related to monsoon precipitation. We compared the projected results obtained and discuss the characteristics of each projection. The performance-based projections indicated that the future river discharge in September is increased by 60%?90% of the retrospective simulation. Our results highlight the importance of appropriate evaluation for the performance of GCMs.

Keywords: Climate Change, River discharge

Japan Geoscience Union Meeting 2014
(28 April - 02 May 2014 at Pacifico YOKOHAMA, Kanagawa, Japan)

ACG04-P01 Room:Poster Time:May 1 18:15-19:30

Variation of the South China Sea Summer Monsoon onset

IMAKAWA, Shin[1*] ; HIGUCHI, Atsushi[2]

[1]Graduate School of Science, Chiba University, [2]CEReS, Chiba University

In this study, we reveal factors of variation of the South China Sea Summer Monsoon(SCSSM) onset. The study area of South China Sea(SCS) is 5-15N, 110-120E. We use the data set of JRA-25/JCDAS, and, calculate the SCSSM onset date for 30 years, 1979-2008, defined as the zonal wind. In Kajikawa and Wang(2012), the authors point out an advance in the SCSSM onset date around 1993/94. Then, we divide the 30 years into 2 groups , before 1993(Prior) and after 1994(Later). Moreover, we pick out the advanced and delayed onset date for 3 years in each groups, after all, classify 30 years into 4 groups(Prior-Advanced, Prior-Delayed, Later-Advanced, Later-Delayed).

Focusing on time-changes of Sea Surface Temperature(SST), it is difference between Prior groups(P-A, P-D) and Later groups(L-A, L-D) for SST over the Philippine Sea(PS: 0-15N, 125-140E). The SST for Prior is higher about 0.5 degrees than that for Later. On the other hand, over the SCS, the SST is higher Advanced groups(P-A, L-A) than Delayed groups(A-D, L-D). This is reason why the strength of meridional surface wind over the SCS before April. Therefore, an effect of the SST to the SCSSM onset date is difference between over the SCS and over the PS. The SST over the SCS affect the annual variation of the SCSSM onset, and, the SST over the PS affect the 93/94 change.

The SCSSM onset is affected by a warming of the Tibetan Plateau(TP: 30-35N, 80-100E) too. In Ueda and Yasunari(1998), they reveal that the onset of summer monsoon over the Bay of Bengal and the SCS coincide with a time of rapidly increase in the thermal contrast the TP and surrounding ocean. We calculate the warming over the TP by a difference of geopotential height between 200hPa and 500hPa. Comparing the time-change of warming in 4 groups, we examine the difference of the period of rapidly warming over the TP in each groups. It is consider a relation between variation of the SCSSM onset and variation of the warming over the TP.

Then, we compare the anomaly of SCSSM onset date defined by the zonal wind, the anomaly of a time of rapidly warming over the TP, and, the anomaly of SST contrast between over the SCS and over the PS in April. As a results, the annual variation of SCSSM onset correlate clearly with the variation of the warming over the TP. Moreover, the low(high) SST difference in over the SCS and over the PS and the advanced(delayed) warming over the TP cause the advanced(delayed) SCSSM onset date.

Keywords: Asia, monsoon

Japan Geoscience Union Meeting 2014
(28 April - 02 May 2014 at Pacifico YOKOHAMA, Kanagawa, Japan)

ACG04-P02 Room:Poster Time:May 1 18:15-19:30

Recent changes in heavy precipitation occurrences along the eastern coast of the Indochina Peninsula

FUKUTOMI, Yoshiki[1*] ; WU, Peiming[1] ; MATSUMOTO, Jun[2]

[1]JAMSTEC, [2]Tokyo Metropolitan University

Long-term changes of the frequency of heavy precipitation occurrence along the eastern coast of the Indochina Peninsula were analyzed using daily data from six Vietnamese meteorological stations for the period September–November of 1961–2010. The heavy precipitation days were defined by the 50 and 100 mm/day threshold values. The frequency of the coastal heavy precipitation days were decomposed into tropical cyclone (TC)-induced heavy precipitation days and non-TC heavy precipitation days, and their contribution to a recent increase in the coastal precipitation was examined. Over the 50-yr period, heavy precipitation occurrence indices show a significant increasing trend that is linked to an increasing trend in seasonal amount of the coastal precipitation. A rapid increase in the coastal heavy precipitation days was found from the mid-1990s through the 2000s. This marked increase is basically due to non-TC heavy precipitation events, suggesting that TC passages do not play a role in the recent increase in the seasonal precipitation amount and the heavy precipitation events. A role of tropical synoptic-scale disturbances (TSDs) as non-developing disturbances for TC formation in the non-TC heavy precipitation events was also explored. About 70% of the non-TC heavy precipitation events are associated with TSDs originated from the western North Pacific–South China Sea region. TSD passages are responsible for the recent increase in non-TC heavy precipitation events.

Keywords: heavy precipitation, synoptic-scale disturbances, Indochina Peninsula

Japan Geoscience Union Meeting 2014
(28 April - 02 May 2014 at Pacifico YOKOHAMA, Kanagawa, Japan)

ACG04-P03 Room:Poster Time:May 1 18:15-19:30

Climatology of explosively developing extratropical cyclones over the Kurosio Front

NAGAI, Masaki[1*] ; HIGUCHI, Atsushi[2]

[1]Graduate School of Science, Chiba University, [2]CEReS, Chiba University

When the East Asian winter monsoon is strong, the explosive cyclone activity tends to concentrate in the Kurosio Current(Yoshiike and Kawamura,2009). It is important to understand the relationship between the heat supply from the Kurosio extension region and the development process of cyclones. The purpose of this research is to reveal meteorological and oceanic environments that can provide deferences of the cyclone path or the rapid development.

Composite analysis for cyclones developed over the westerly(TypeW_P) or easterly(TypeE_P) Kurosio extension region was conducted. The Result suggests the existence of mesoscale circulation over the Sea of Japan is important to northwardly path of the TypeW_P cyclone. In addition, before the maximum deepning of the TypeW_P cyclone, latant heat flux clearly increased at the Kurosio extention region. It was result of easterly winds, to blow in front of a warm front of cyclone. The Kurosio extension region, which was meander north and south direction, responded to the winds. These results not appear in composite analysis for the TypeE_P cyclone. The influence on weather of Kanto region are also investegated. the results show the TypeW_P cyclone tend to provide heavy rain or snow, and the TypeE_P cyclones provide severe winds on that region. These results show the important contribution of water vapour provided from the Kurosio extension region to the TypeW_P cyclone. We conducted more composite analysis for that cyclones. Composite analysis at the cyclone center revealed some difference in advection of water vapour. The water vapor flux, blow from southeast quadrant to cyclone center, was more stronger in the TypeE_P, but The precipitable water that extend to south of cyclones was greater in the TypeW_P. As the result of strong water vapor advection, development of the TypeE_P cyclone was assisted. On the other hand, more humidity air masses cotributed to development of the TypeW_P cyclone. These experiments were conducted for cyclones that developed over the westerly or Easterly Subarctic frontal zone of the northwstern Atrantic(TypeW_A and TypeE_A, respectively). But no clear difference appeared in low-level environment associated with the TypeW_A or the TypeE_A cyclone. These results suggests that the deferences of low-level fields associated with the difference of the maximum deepning position are particular phenomenon in the Kurosio extention resion. In addition, the contribution of water vapour advection to the cyclone center was stronger for cyclones developed over the kurosio extension region.

Keywords: Explosively developing extratropical cyclone, East Asian winter monsoon

Japan Geoscience Union Meeting 2014
(28 April - 02 May 2014 at Pacifico YOKOHAMA, Kanagawa, Japan)

ACG04-P04 Room:Poster Time:May 1 18:15-19:30

Variability of GPS precipitable water vapor over the northeast Bangladesh

MURATA, Fumie[1*] ; TABEI, Takao[1] ; TERAO, Toru[2] ; HAYASHI, Taiichi[3] ; CHOUDHURY, S. A.[4]

[1]Kochi University, [2]Kagawa University, [3]Kyoto University, [4]Bangladesh Meteorological Department

Precipitable water vapor (PWV) derived from Global Positioning System (GPS) which were installed in the northeast Bangladesh was analyzed for different seasons. A GPS utilized for the analysis of pre-monsoon (May 2011) was installed at Sylhet. Two GPS utilized for the analysis of monsoon (July 2007) and winter seasons(December 2007) were installed by UNAVCO at Jamalpur and Jaflong. The simultaneous observation with GPS and radiosondes were conducted in May 2011. The PWV derived from GPS was well corresponded with that derived from radiosondes. A sharp PWV increase frequently observed during the passage of severe storms during the pre-monsoon season. The active and break monsoon periods in July 2007 showed average PWV of 67 mm and 62 mm, respectively. Severe flood occurred over Sylhet area during the active period. The PWV in the winter season showed 10-15-day periodicity in PWV between 15 mm in minimum and 25 mm in maximum. The amplitude of diurnal variation was larger in the break monsoon period than the active monsoon period. The nocturnal maximum and early afternoon minimum were remarkable in the diurnal variation of PWV in the monsoon period. The amplitude of diurnal variation was also large in winter. The phase in the diurnal variation was different in the two GPS stations. The PWV was increase on 12-18 LT at Jaflong, but the PWV had minimum on the same period of time at Jamalpur.

Keywords: GPS precipitable water, Bangladesh, Intraseasonal variation, Diurnal variation

Japan Geoscience Union Meeting 2014
(28 April - 02 May 2014 at Pacifico YOKOHAMA, Kanagawa, Japan)

ACG04-P05 Room:Poster Time:May 1 18:15-19:30

Distributed hydrological model simulation on the diurnal-cycle of Ciliwung River basin

SULISTYOWATI, Reni[1*] ; HAPSARI, Ratih indri[2] ; MORI, Shuichi[3] ; SYAMSUDIN, Fadli[4] ; OISHI, Satoru[1] ; YAMANAKA, Manabu D.[1]

[1]Kobe University, [2]State Polytechnic of Malang, [3]JAMSTEC, [4]BPPT

A systematic diurnal-cycle of water level is persistently generated over Ciliwung River basin during the Intensive Observational Period of HARIMAU2010 (15 January to 15 February 2010). It is almost uniquely explained by diurnal-cycle of rainfall observed with weather radar (C-band Doppler Radar) over Jakarta and surrounding area.

In this study, we have shown a simulation of the diurnal cycle of Ciliwung River water level by distributed hydrological model (the CDRMV3 model). Using the CDR rainfall data, river discharge is simulated both for short period and one-month period in two station, i.e. Manggarai (downstream outlet) and Katulampa (upstream outlet), and verified by comparing with the observation discharge from those two station.

Further improvement of the simulation scheme for the diurnal-cycle rainfall is also discussed.

Keywords: Diurnal-cycle, Weather radar, Distributed hydrological model, Rainfall, Runoff

Japan Geoscience Union Meeting 2014
(28 April - 02 May 2014 at Pacifico YOKOHAMA, Kanagawa, Japan)

ACG05-01 Room:211 Time:April 30 09:00-09:20

Introduction of the SCOSTEP's VarSITI program - Variability of the Sun and Its Terrestrial Impact

SHIOKAWA, Kazuo[1*] ; GEORGIEVA, Katya[2]

[1]Solar-Terrestrial Environment Laboratory, Nagoya University, [2]Space Research and Technologies Institute, Bulgarian Academy of Sciences

The Scientific Committee on Solar Terrestrial Physics (SCOSTEP) is an interdisciplinary body of the International Council for Science (ICSU) to run international interdisciplinary scientific programs and promotes solar-terrestrial physics research. The last solar minimum in 2008-2009 and the current solar maximum of sunspot cycle 24 show much lower activities compared with the previous two solar cycles 22 and 23. The scientists in the solar-terrestrial physics are watching very low solar activities and their consequences on Earth, which have never been observed since modern scientific measurements become available. The SCOSTEP program "Variability of the Sun and Its Terrestrial Impact (VarSITI)" (2014-2018) will focus on this particular low solar activity and their consequences on Earth, for various times scales from the order of thousands years to milliseconds, and for various locations and their connections from the solar interior to the Earth's atmosphere. In order to elucidate various sun-earth connections, we encourage communication between solar scientists (solar interior, sun, and the heliosphere) and geospace scientists (magnetosphere, ionosphere, and atmosphere). Campaign observations will be promoted for particular interval in collaboration with relevant satellite and ground-based missions as well as modeling efforts. Four scientific projects will be carried out in VarSITI as (1) Solar Evolution and Extrema (SEE), (2) International Study of Earth-Affecting Solar Transients (ISEST/Minimax24), (3) Specification and Prediction of the Coupled Inner-Magnetospheric Environment (SPeCIMEN), and (4) Role Of the Sun and the Middle atmosphere/thermosphere/ionosphere In Climate (ROSMIC). In this presentation we introduce the VarSITI program and its four projects to promote interdisciplinary studies among different fields.

Keywords: VarSITI, solar activity, climate change, atmosphere, magnetosphere and ionosphere, heliosphere

Japan Geoscience Union Meeting 2014
(28 April - 02 May 2014 at Pacifico YOKOHAMA, Kanagawa, Japan)

ACG05-02 Room:211 Time:April 30 09:20-09:35

California Nino/Nina in boreal summer

YUAN, Chaoxia[1*] ; YAMAGATA, Toshio[1]

[1]APL, JAMSTEC

Anomalous warming/cooling in the coastal ocean off Baja and Alta California has attracted broad attention due to its significant impacts on the coastal marine ecosystem. The anomalous warming/cooling has been attributed, especially in boreal winter, to the remote forcing of the tropical El Nino/Southern Oscillation (ENSO) through both oceanic and atmospheric teleconnections and/or the ENSO-independent basin-wide atmospheric circulation anomalies in mid-latitudes. In the present study, we show for the first time the existence of coastal air-sea coupled phenomenon in the coastal ocean off Baja and Alta California in boreal summer. An initial decrease/increase in the southward alongshore surface winds along the coast weakens/strengthens the coastal upwelling and raises/lowers the coastal sea surface temperatures (SSTs) through oceanic mixed-layer processes. The resultant coastal warming/cooling, in turn, heats/cools the overlying atmosphere anomalously, decreases/increases the atmospheric pressure in the lower troposphere, generates an anomalous cross-shore pressure gradient, and thus reinforces or maintains the alongshore surface wind anomalies. The air-sea coupled phenomenon is analogous to the well-known ENSO in the tropical Pacific but with much smaller time and space scales, and referred to as California Nino/Nina (CAN) after the pioneer work that describe the warming events in the coastal ocean off Baja and Alta California as California El Nino.

Keywords: California Nino/Nina, coastal air-sea interaction

Japan Geoscience Union Meeting 2014
(28 April - 02 May 2014 at Pacifico YOKOHAMA, Kanagawa, Japan)

ACG05-03 Room:211 Time:April 30 09:35-09:50

River discharges, ocean circulation and material transport in Japanese coastal waters: simulation with JCOPE ocean model

VARLAMOV, Sergey[1*] ; MIYAZAWA, Yasumasa[1] ; YAMASHIKI, Yosuke[2] ; SASAKI, Toshiaki[2]

[1]Japan Agency for Marine-Earth Science and Technlogy, [2]Graduate School of Advanced Integrated Studies in Human Survivability, Kyoto University

The total volume of fresh water discharged by rivers into the word ocean is incompatible with the total mass of ocean waters; however these discharges contribute significantly into formation of fresher coastal waters and details of coastal ocean circulation.

This impact is not local, and supports presence of lower salinity waters in wide coastal areas along Japanese coast. In an absence of rivers in ocean model for appropriate reproducibility of ocean surface salinity it is often required to apply salinity restoration approach. Additionally, rivers could bring to ocean surface-floating, suspended and dissolved substances, some of which are hazardous, like radioactive materials initially dropped on the ground following such disasters as Fukushima Dai-Ichi nuclear power plant accident. These could be washed to rivers by strong rainfalls.

Method of counting inflow of fresh water from rivers as horizontal fluxes to the designated model cells is used. Demonstrated are direct impacts of rivers on formation of fresher waters along the coast of Japan and some cases of induced by discharges local ocean circulation patterns near the river mouth locations. A preliminary experiment when the model utilizes the hourly information on the amount of river discharges demonstrates an importance of such approach for the correct simulation of transport processes in extreme conditions like the typhoon-induced precipitations that often take place in Japan and East Asia. For achieving of this capacity, we are looking for utilization of simple land waters hydrological models for main river basins that could transfer the detailed meteorological precipitation forecast information into the approximate forecasts of river discharges.

Keywords: river discharge, ocean circulation, river-ocean interaction, coastal ocean processes

Japan Geoscience Union Meeting 2014
(28 April - 02 May 2014 at Pacifico YOKOHAMA, Kanagawa, Japan)

ACG05-04 Room:211 Time:April 30 09:50-10:05

A spike-like input of perfluoroalkyl substances into the Western North Pacific from the Japanese Coast associated with t

MIYAZAWA, Yasumasa[1*] ; YAMASHITA, Nobuyoshi[2] ; TANIYASU, Sachi[2] ; YAMAZAKI, Eriko[2] ; GUO, Xinyu[3] ; VARLAMOV, Sergey[1] ; MIYAMA, Toru[1]

[1]Japan Agency for Marine-Earth Science and Technology, [2]National Institute of Advanced Industrial Science and Technology, [3]Ehime University

The recent great earthquake of magnitude 9.0 on 11 March 2011 followed by TSUNAMI and fire in Japan has resulted in serious environmental problems in and around Japan. A huge amount of materials has been discharged into the ocean after the tremendous flood damage by TSUNAMI. A research group of the National Institute of Advanced Industrial Science and Technology has sampled the perfluoroalkyl substances (PFAs), which are chemical materials included in the industrial products, in the Western North Pacific for past a few years. They found some evidences showing an abrupt increase of the PFAs concentration east of Japan in 2011 after the great earthquake. To confirm the anomalous input of two typical PFAs (PFOA and PFOS) from the Japanese coast into the ocean, we conducted a series of chemical tracer simulations using an eddy-resolving ocean reanalysis product, JCOPE2, by assuming the oceanic dispersion of the PFAs dissolved in sea water mainly driven by the ocean current. Comparison of the simulation results with the observation actually indicates a spike-like input of PFOA into the Western North Pacific after the great earthquake; however, the simulations could not well explain the observed distribution of PFOS, suggesting some differences in the oceanic dispersion processes between PFOA and PFOS. We discuss estimates of the total emission amounts of PFOA and PFOS based on a simple process representing the TSUNAMI effect on the emission from the land.

Keywords: perfluoroalkyl substances, the great earthquake 0311, oceanic dispersion, Tsunami, oceanic observation, numerical simulation

Japan Geoscience Union Meeting 2014
(28 April - 02 May 2014 at Pacifico YOKOHAMA, Kanagawa, Japan)

ACG05-05 Room:211 Time:April 30 10:05-10:20

Super high resolution experiments of torrential rainfall events with the K super computer

OIZUMI, Tsutao[1*] ; KURODA, Tohru[1] ; SAITO, Kazuo[2]

[1]Japan Agency for Marine-Earth Science and Technology, [2]Meteorological Research Institute / JAMSTEC

In Japan, localized torrential rainfalls sometimes cause severe disasters which impact on the society. (e.g., the urban flash flood disaster at the Toga-gawa River in Kobe in July 2008, and the debris flow disaster in Izu Ohshima Island in 2013). In these events, the precipitation amountswere very different in the small areas, and they were likely strongly affected by geographical features. In the Kobe event case, about 70 % of the initial flow of the flash flood is from the urban area that covers only about 30 % of the entire catchment area (14 square kilo meters). In the Izu Ohoshima case, two meteorological observation stations are in the northern part and the middle part (near the damaged area) in the island, and the distance between the two stations is only 4 km. However, the quantity of observed precipitation in the middle in island was about twice as much as north.

To understand these phenomena, high resolution (several hundred meter scale resolution) numerical weather simulation is necessary. Super high resolution experiments have been made by previous studies such as tornado for limited domains, however, a numerical weather simulation with wide domain is very few due to limitation of the computational resources. We conduct super high resolution numerical weather experiments for Japan area with the K computer and JMA nonhydrostatic model.

Keywords: Numerical weather prediction model, JMA-NHM, Kei super computer

Japan Geoscience Union Meeting 2014
(28 April - 02 May 2014 at Pacifico YOKOHAMA, Kanagawa, Japan)

ACG05-06 Room:211 Time:April 30 10:20-10:35

Interannual variability of Kuroshio nitrate flux and transport along western boundary in the North Pacific

SASAI, Yoshikazu[1*] ; SASAKI, Hideharu[1] ; NONAKA, Masami[1]

[1]JAMSTEC

An eddy-resolving coupled physical-biological ocean model has been employed to examine the interannual variability of nitrate flux and transport mechanism by the Kuroshio during 1995-2012. The Kuroshio provides an advective flux of nitrate carried in subsurface waters, redistributing nitrate from the tropics to the mid-latitude. Some observed data capture the nitrate flux and transport in the subsurface layers by the Kuroshio. The maximum nitrate flux core appears about 400 m depth in the East China Sea, and the nitrate transport by the Kuroshio had a mean of 170 kmol s-1. The model reproduces the maximum nitrate flux core in the subsurface layer from the Luzon strait to the Kuroshio Extension with the downstream. Along the vertical section of east side of Taiwan (24N), west side of Okinawa (28N), south of Kagoshima (130E), the time series of nitrate flux, volume transport, and nitrate concentration show the interannual variation. The variability of nitrate flux is strongly correlated with the variability of Kuroshio volume transport, but the nitrate concentration shows the increasing trend between 1995 and 2008. This trend may be related to the variability of nitrate concentration in the upstream of Kuroshio.

Keywords: Nitrate transport, Kuroshio, Interannul variability, High-resolution ocean physical-biological model

Japan Geoscience Union Meeting 2014
(28 April - 02 May 2014 at Pacifico YOKOHAMA, Kanagawa, Japan)

ACG05-07 Room:211 Time:April 30 11:00-11:20

High Resolution, Terrain Independent Radiation Mapping

SCOTT, Thomas[1*]

[1]Interface Analysis Centre School of Physics University of Bristol

The University of Bristol has developed a terrain-independent, wide area radiation mapping system using an UAV (Unmanned Aerial Vehicle). At the heart of the system is a micro computer, carried by a semi-autonomous multi-rotor copter (drone), combining data from a lightweight gamma spectrometer, laser range finder, and GPS, to geospatially map radioactive anomalies.

Aerial vehicles can be purpose built, according to range/flight time required, payload/sensing strategy and operational environment. For example, an unmanned vehicle could be tailored for mapping over both land and sea areas, where it could land in the sea at different locations to make water based gamma measurements. The system is also adaptable for use on ground vehicles, or handheld, walking surveys.

Information is streamed in real-time, providing high resolution detail on source isotopes, intensity and location of the radiation anomaly. More than just a flying Geiger counter, the system can differentiate between natural and man-made anomalies - such as types of nuclear fuel, radioactive waste or spent munitions.

This is all achieved from a safe distance, keeping people and manned aircraft away from hazardous environments.

Examples of uses include;

∗Rapid disaster response monitoring of nuclear events, providing real-time data on spread, source and intensity. This could range from site incidents to terrorist events.

∗Routine monitoring of nuclear sites (internally and externally), mining operations and oil and gas facilities.

∗Nuclear plants - new build: site survey and characterisation of pre and post construction and monitoring during plant life time.

∗Environmental monitoring for site decommissioning.

∗Environmental monitoring of war zones for spent depleted uranium munitions.

∗Homeland security and nuclear material detection.

The instrument securely transmits the location, identity and intensity of radionuclide contamination to a remote operator or base station. Sub metre resolution is attainable by flying slowly, even to the point of a fixed hover, relatively close to the ground.

It can be operated manually, using traditional radio-controls or semi autonomously via programmed GPS waypoints. Grid lines are used to create survey routes that provide detailed geographical coverage of a designated area. Programming can include automated landing and take-off, such that the device can gather long exposure spectra of the region of interest.

Japan Geoscience Union Meeting 2014
(28 April - 02 May 2014 at Pacifico YOKOHAMA, Kanagawa, Japan)

ACG05-08 Room:211 Time:April 30 11:20-11:35

Heat budget analysis on cooling events associated with typhoon passages in Seto Inland Sea, Japan

UCHIYAMA, Yusuke[1*] ; NISHII, Tatsuya[1]

[1]Graduate School of Engineering, Kobe University

Typhoons alter coastal oceans significantly through several mechanisms including the enhanced vertical mixing through increased surface wind and waves, resulting in extensive cooling of the upper oceans. In the present study, we investigate impacts of typhoon passages with a detailed ocean modeling in particular on the temperature structure in Seto Inland Sea, the largest semi-enclosed estuary in Japan. We develop a synoptic, double nested downscaling ROMS model (Shchepetkin and McWilliams, 2005; 2008) forced by the assimilative JCOPES oceanic reanalysis (Miyazawa *et al*., 2009) and JMA GPV-MSM atmospheric reanalysis for the surface momentum, heat and radiation fluxes by exploiting a bulk formula developed for COAMPS. The horizontal grid refinement occurs from 1/12 degree (JCOPE2) to 2 km (ROMS-L1) and to 600 m (ROMS-L2), where the L2 model running for about two years (2012-2013) is our test bed for the comprehensive heat budget analysis. The persistent clockwise estuarine circulation and the eastward-flowing Kuroshio are key features that cause the overall circulations of the estuary.

In the fall 2012, SST is found to decrease about two degrees for a two-week period during three consecutive typhoons passing nearby. The first EOF mode of the modeled SST corresponds to the seasonal cooling along with mixed-layer deepening, whereas the effects of the typhoons appear in higher modes. Kuroshio interacts with the topography to form standing cyclonic cold-core eddies as extracted in the second mode, resulting in intermittent eastward cold-water transport beyond the headlands. The third and forth modes jointly represent cold water formation associated with storm-driven coastal upwelling that propagates with the estuarine circulation. Similar EOF modes are detected in the SST during the fall 2013 when two typhoons attacked the study area.

In the falls in 2012 and 2013 after the mid September when a series of typhoons pass by the estuary, the heat budget analysis exhibits that the net heat flux at surface becomes negative to induce prominent surface cooling and cold-water formation in the upper ocean. Whereas divergence of the horizontal advective heat flux is crucial in the daily-averaged heat budget, the surface net heat flux is essential to long-term temperature variation. Latent heat flux is found to play a primary role in the negative net surface flux as well as decrease of downward shortwave (solar) radiation. Unstable lowest atmospheric planetary boundary layer leads to pronounced changes in the latent heat flux in response to surface wind and abrupt decrease of the near-surface humidity after the typhoon passages.

Keywords: typhoon, estuary, heat budget analysis, EOF analysis, ROMS

Japan Geoscience Union Meeting 2014
(28 April - 02 May 2014 at Pacifico YOKOHAMA, Kanagawa, Japan)

ACG05-09 Room:211 Time:April 30 11:35-11:50

Development of a hydro-ocean coupled model

KIDA, Shinichiro[1*] ; YAMASHIKI, Yosuke[2]

[1]Japan Agency for Marine-Earth Science and Technology, [2]Kyoto University

A new hydro-oceanic coupled model is developed for examining the basic dynamics of river-ocean interaction in estuary zones during high water discharge events. These high frequency and vigorous events are not reproduced in climatological river transport data sets that are often used in ocean circulation models. The new hydro-oceanic model is based on an isopycnal layer model. It treats continental and oceanic water with separate layers but allows dynamical interaction between the two. Mixing between the two layers occurs through a Richardson number criterion. When the model is forced with Radar-Rain gauge analyzed precipitation data around eastern Japan, the model simulates the river discharge of Abukuma river basin that is analogous to observations. The abrupt changes in the water mass transport at upstream and downstream locations are well captured, showing its applicability for hydrological basin analysis. Freshwater plumes that hug along the oceanic coasts are also well captured. We find the model, based on single dynamical core, useful for both hydrological catchment and estuary mixing zone and can be used for examining the impact of weather related events.

Keywords: Ocean model, Hydrological model

Japan Geoscience Union Meeting 2014
(28 April - 02 May 2014 at Pacifico YOKOHAMA, Kanagawa, Japan)

ACG05-10 Room:211 Time:April 30 11:50-12:05

FIELD OBSERVATION ON PHYSICAL CHARACTERISTICS OF ABUKUMA RIVER ESTUARY IN SENDAI BAY

YAMASHIKI, Yosuke[1*] ; PRATAMA, Adhiraga[3] ; VARLAMOV, Sergey[4] ; MIYAZAWA, Yasumasa[4] ; YAMAZAKI, Hideo[5] ; ISHIDA, Masanobu[5] ; NIWA, Yoshihiro[6]

[1]GSAIS, Kyoto University, [2]Application Laboratory, JAMSTEC, [3]GSE, Kyoto University, [4]RCGC, JAMSTEC, [5]Kinki University, [6]EPS, The University of Tokyo

Higher amount of radiocaesium transport from Abukuma river into Pacific Ocean, especially during the extreme events, has already estimated. The current study aims to clarify the following: i)to survey estuary mixing processes during freshwater and turbidity intrusion from Abukuma river mouth, largest river basin affected fallout, where annual radiocaesium flux reached 10 Terabecquerel during our observation in 2011-2012; ii) To identify bottom-sediment contamination along the river mouth by sediment sampling. Field observation was conducted both in March 18 and September 2-3 in 2013 in Sendai Bay. Vertical temperature and turbidity, together with the salinity field are observed using fishing vessel. We analyzed also vertical velocity profile using ADCP to identify the current movement of the bay. The velocity fields in Sendai Bay of the observation date are illustrated using JCOPE2 program.Figures 1 illustrates observation points, vertical salinity, turbidity and temperature field in each points, and vertical velocity profile observed in 18 March 2013 . The eastward surface current was observed in each transection line. At near bottom of the sea, westward current was observed, indicating estuary circulation. Southward surface current was observed in most of latitudinal section, weak northward bottom current was also found Freshwater intrusion was observed on some of the stations in transection A which is located near the mouth of Abukuma River.In most of the station, turbidity peak was observed in near bottom of the sea, except in some station in transection A where the peak of turbidity was found in surface similar to the location of freshwater intrusion. Higher concentration of radiocaesium in the bottom sediment near the Abukuma river mouth is observed where fine argilliferous soil are found, much higher than that in surrounded area, giving important evidence of radiocaesium in particulate form supplied from Abukuma River. Peaks of turbidity near the river mouth were found at slightly lower position than the freshwater-saline boundary at stations 1 and 3 (March 20), implying that the occurrence of coagulation of suspended particulate matter through mixing with saline water, supporting the observed concentration found in (1).

Keywords: Abukuma river, Coastal zone, Estuary circulation, Mixing zone, Radiocaesium

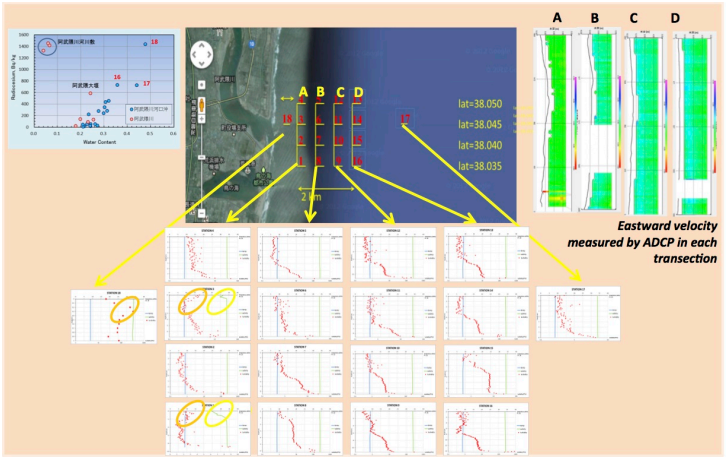

Japan Geoscience Union Meeting 2014
(28 April - 02 May 2014 at Pacifico YOKOHAMA, Kanagawa, Japan)

ACG05-11 Room:211 Time:April 30 12:05-12:25

Development of Satellite data manipulator for geography analysis

NAKANO, Fujio[1*]

[1]Japan Aerospace Exploration Agency, [2]Kyoto University

Development of Satellite data manipulator for geography analysis

ALOS (Advanced Land Observing Satellite: common name ”Daichi”) carried the sensor PRISM which can observe earth surface in high accuracy, and enabled acquisition of DSM (Digital Surface Model) data. By utilizing the data acquired by such an advanced sensor, it becomes possible to display high-precision three-dimensional satellite data. Using satellite data as three dimensions means expansion of the utilization range, and it can expect unprecedented multi-functionalization. Furthermore, three-dimensional satellite data was displayed on iPad interlocked with GPS in various satellite data including ALOS data, and ”Geo-Sim” which can be used also in area without communication environment was developed. Thereby, the generating situation of a mudflow or the ancient coastline is reproduced by CG, and the matching operation on-site becomes possible.

Keywords: ALOS, AVNIR-2, PRISM/DSM, DEM, Geo-Sim

Fig.1. Manipulation of 3D data on iPad display

Japan Geoscience Union Meeting 2014
(28 April - 02 May 2014 at Pacifico YOKOHAMA, Kanagawa, Japan)

ACG05-P01 Room:Poster Time:April 30 18:15-19:30

Land-Ocean Mutual Interaction: Sediment Transportation Processes in Coastal Zone Induced by Abukuma River Mouth Runoff

TROSELJ, Josko[1*] ; YAMASHIKI, Yosuke[2] ; TAKARA, Kaoru[3]

[1]Graduate School of Engineering, Kyoto University, [2]Graduate School of Advanced Integrated Studies in Human Survivability, Kyoto University, [3]Disaster Prevention Research Institute, Kyoto University

1. Introduction

Modeling of a contact zone between a river coming from potentially contaminated basin and an ocean is especially sensitive case for Land-Ocean coupling interaction due to significant risk of major environmental disaster which can occur in the case of contamination of the coastal zone. Therefore, it is of great importance to study and develop integrated modeling approach to comprehend the complex interaction processes in the contact zone in order to minimize disaster risk potential, which can consequently cause undesirable social and economical costs.

2. Objectives

The focus of this study is to promote relevant numerical simulation on Land-Ocean coupling modeling approach applicable for the bay and estuary zone affected by river inflow and associated sediment transportation from the Abukuma river basin in Japan. By conducting several field observations, we found interesting and unusual temporal and spatial distribution of radionuclides within the coastal zone near the river mouth. Sediment transportation processes which have led to the distribution as well as influence of near-shore bathymetry to sediment dispersion are of close interest for the study. Calculation was conducted by simulating stages and conditions for mechanisms of sediment transport in the coastal zone, from initial deposition onto river bed to final deposition onto ocean floor, with special focus on processes which are occurring during high water periods.

3. Model Description

The modeling approach has been studied by combining river mouth runoff boundary conditions by using Lagrangian particle tracking model for simulating sediment transportation, with coupled atmosphere-ocean-land model (MSSG model, JAMSTEC) which used fine resolution grid, and associated downscaling techniques for oceanic boundary conditions (JCOPE2 model, JAMSTEC) which used coarse resolution grid. We have simulated two different cases, at first circulation of ocean itself in non-equilibrium quasi stationary state, where its dynamics was induced only by its own temperature and salinity data differences among adjacent cells, and at second response of the ocean circulation to inflow from the river outlet, simulated under various boundary conditions and external effects.

ETOPO1, 1 Arc Minute Global Relief Model was chosen as initial database for bathymetry data, while World Ocean Atlas 2005 database was chosen as initial 3D database for temperature, salinity, pressure, and velocity field data. Incompressive Navier-Stokes equation and Yin-Yang grid were used in the calculation of the flow field.

4. Conclusions and follow up

The study is continuous part of the PhD study of the first author, so the results are about to be improved as the course will continue. So far, results neither confirmed nor denied the hypothesis that near-shore bathymetry may have important role in spatial dispersion of radionuclides, so the question still remains open and subject for discussion. Our assumption is that using fine resolution grid within the contact zone between two different fluids should give us better insight into the problem, while simultaneously proper downscaling of outer oceanic boundary conditions and proper coupling with sediment transportation model are needed to be done in order to maintain satisfactory level of simulated physics of processes during the calculation. In follow up of the study, we will try to simulate hydrograph based water wave rather than constant inflow from the river mouth, as well as try to put ocean side into initial dynamic state rather than non-equilibrium quasi stationary state. Also, more focus will be aimed to the physical processes behind mechanisms of radionuclide transportation from the basin towards the river mouth.

Acknowledgements

Dr. Shinichiro Kida, executive supervisor, JAMSTEC
Dr. Keiko Takahashi, MSSG program director, JAMSTEC
Monbukagakusho (MEXT) scholarship, GCOE-HSE program

Keywords: River-ocean interaction, Integrated atmosphere-land-ocean model, Sediment transportation of radionuclides, Lagrangian particle tracking model, Near-shore bathymetry influence

Japan Geoscience Union Meeting 2014
(28 April - 02 May 2014 at Pacifico YOKOHAMA, Kanagawa, Japan)

ACG05-P02 Room:Poster Time:April 30 18:15-19:30

modelling of radiocesium movement in catchment area of abukuma river, japan

PRATAMA, Mochamad adhiraga[1*] ; YAMASHIKI, Yosuke[2] ; YONEDA, Minoru[1]

[1]Department of Environmental Engineering, Kyoto University, [2]Graduate School of Advanced Integrated Studies in Human Survivability, Kyoto University

The great earthquake on March of 2011 followed by tsunami caused Fukushima Dai-ichi reactor meltdown which led to explosion and emission of radioactive substances into environment. As a result, Abukuma River, one of the most important rivers in Japan and its catchment area, received up to 2.25 x 10^6 Bq/m^2 of radiocesium. Previous study found that 80-90% of radiocesium influx to Abukuma River was in particulate form and it was estimated that 10 TBq of the radionuclide was released into the end point of the river, coastal sea of Sendai Bay. A lot of models of radionuclides movement had been developed, however just few models that account solid wash off process in catchment area . This study tried to simulate the influx of radiocesium into Abukuma River from its catchment area by modifying MOIRA model with addition on solid transport which was calculated with SWAT model. Deposition of the radiocesium was used as an input of the model. Then after, fixation process into surface ground, liquid wash-off by surface run off, and solid wash off by erosion are the mechanisms which govern the dynamic of the radiocesium in this model. The result at the model shows an agreement compared to the observed data. With R^2 value of 0.8 showed that the model could explain seasonal variability of observed data. However, as several uncertainties were observed such as quantification of storm effect and decontamination activities, further study to optimize and improve the result of the model is deemed necessary

Keywords: model, influx, radiocesium, Abukuma River

Japan Geoscience Union Meeting 2014
(28 April - 02 May 2014 at Pacifico YOKOHAMA, Kanagawa, Japan)

ACG05-P03 Room:Poster Time:April 30 18:15-19:30

A Study of Contribution of ”Nanohana Project” and Agricultural restoration in Sukagawa, Fukushima, Japan

KIMURA, Naoko[1*]

[1]GSGES, Kyoto University

This paper explores for what and to what extent ”Nanohana Project” contributes to restoration in Sukagawa, Fukushima Prefecture, Japan. Since the huge earthquake and tsunami occurred in March 2011, agricultural fields in these cities have been suffering damages caused by radionuclides classified as nuclear-fission products from the Fukushima No.1 Nuclear Power Plant (Tokyo Electricity Power Company (TEPCO)) due to the accident. Agricultural field restoration, especially decontamination of radionuclides from the soil, is one of the most important issues to be tackled for local farmers. This research reviews literatures regarding and conducted an interview to an agricultural production corporation in Sukagawa in order to grasp what initiatives has been taken to reduce radionuclides in their products as well as to fight to bad rumors among general public. ”Nanohana Project” has been implemented with local stakeholders in Sukagawa since 2007. They grow Nanohana (rapeseed flower or colza, Brassica Napus) and produce Biodiesel fuel (BDF) from seeds as well as biogas (BG) out of the pomace (leaves and stems after producing BDF), and they use the BDF and BG in the local area. The Nanohana absorbs some radionuclides in the soil in its growing process, and there was attention to it after disaster, however some scientific researches found that the absorption amount is limited and may not be a remedy itself for decontamination of radionuclides. Nevertheless, ”Nanohana Project” has been ongoing and the network is expanding in Sukagawa. This paper discusses contribution of ”Nanohana Project” and initiatives by an agricultural production corporation for restoration through qualitative analysis of interview and some key figures in order to speculate the Project’s possible roles for future reconstruction in the region.

Keywords: Nanohana, decontamination, restoration, agricultural production corporation, Sukagawa

Japan Geoscience Union Meeting 2014
(28 April - 02 May 2014 at Pacifico YOKOHAMA, Kanagawa, Japan)

ACG05-P04 Room:Poster Time:April 30 18:15-19:30

The relationship between monthly and yearly trend of Ammonia and SS loading at Rhine River and land use change

TERAMOTO, Tomoko[1] ; YAMASHIKI, Yosuke[2*] ; TAKARA, Kaoru[3]

[1]Department of Environmental Engineering Graduate School of Engineering Kyoto University, [2]Graduate School of Advanced Integrated Studies in Human Survivability Kyoto University, [3]Disaster Prevention Research Institute, Kyoto University

Rhine River is the international river, which flows through several countries, so it is important to know and maintain the water quality. To estimate the gross loading to the marine environment is necessary for assessment of the current status of the coastal zone, especially for the water quality of Bays and Estuary zone.

In this study, we estimate Ammonia SS loading at Rhine River by using GEMS/Water (Global Environment Monitoring System/ Water) Dataset and GRDC (Global Runoff Data Centre) Dataset.

The procedure of this research is three steps. First, we have used the set of discharge data obtained from GRDC to be used for the loading estimation based on the observed data. Second, the locations of GEMS/Water and GRDC station have been compared to identify appropriate station to set the calculation loading. Finally, we have multiplied concentration and discharge to get the loading.

The characteristics land use of Rhine River basin has been analyzed using the Global Land Cover Characterization dataset prepared by USGS.

For land use change of Rhine River basin has been analyzed by using landsat5 and landsat7 images.

The concentration and loading results show seven things :(1) From December to February, Ammonia concentration was higher than other months. (2) From January to march, Ammonia loading was higher than other months. (3) Ammonia concentration was gradually decreasing except through1983 to 1987. (4) Ammonia loading was decreasing and the number suddenly dropped at 1989 (5) SS concentration was stable through 1979 to 1994 except 1983, 1984 and 1995. (6) From December to February SS loading was higher than other months. (7) SS loading was gradually decreasing and the number suddenly dropped at 1989.

The Rhine river watershed is mainly forest and grassland by analyzing land use from USGS data. This land use affects water quality

Keywords: Water Quality, loading, land use, Rhine River

Japan Geoscience Union Meeting 2014
(28 April - 02 May 2014 at Pacifico YOKOHAMA, Kanagawa, Japan)

ACG06-01 Room:315 Time:April 28 16:15-16:38

NASA Earth Science and Applications

FREILICH, Michael[1*]

[1]Director, Earth Science Div. NASA Headquarters

Earth is a complex, dynamic system we do not yet fully understand. The Earth system, like the human body, comprises diverse components that interact in complex ways. We need to understand the Earth's atmosphere, lithosphere, hydrosphere, cryosphere, and biosphere as a single connected system. Our planet is changing on all spatial and temporal scales. The purpose of NASA's Earth science program is to develop a scientific understanding of Earth's system and its response to natural or human-induced changes, and to improve prediction of climate, weather, and natural hazards. A major component of NASA's Earth Science Division is a coordinated series of satellite and airborne missions for long-term global observations of the land surface, biosphere, solid Earth, atmosphere, and oceans. This coordinated approach enables an improved understanding of the Earth as an integrated system.

Over the coming decades, NASA and the Agency's research partners will continue to pioneer the use of both spaceborne and aircraft measurements to characterize, understand, and predict variability and trends in Earth's system for both research and applications. NASA Earth System Science conducts and sponsors research, collects new observations, develops technologies and extends science and technology education to learners of all ages. We work closely with our global partners in government, industry, and the public to enhance economic security, and environmental stewardship, benefiting society in many tangible ways. We conduct and sponsor research to answer fundamental science questions about the changes we see in climate, weather, and natural hazards, and deliver sound science that helps decision-makers make informed decisions. We inspire the next generation of explorers by providing opportunities for learners of all ages to investigate the Earth system using unique NASA resources, and our Earth System research is strengthening science, technology, engineering and mathematics education nationwide.

Japan Geoscience Union Meeting 2014
(28 April - 02 May 2014 at Pacifico YOKOHAMA, Kanagawa, Japan)

ACG06-02 Room:315 Time:April 28 16:38-17:00

JAXA's Earth Observation Missions

NAKAMURA, Kenji[1*] ; FUKUDA, Toru[2]

[1]Earth Observation Research Center, Japan Aerospace Exploration Agency/Dokkyo University, [2]Earth Observation Research Center, Japan Aerospace Exploration Agency

The Japan Aerospace Exploration Agency (JAXA) is promoting the Earth observation from space. JAXA is now operating GOSAT (the Green House Gases Observing Satellite) and GCOM-W1 (the Global Change Observation Mission 1st-Water). The GOSAT mission is a joint effort of JAXA, the National Institute for Environmental Studies (NIES) and the Ministry of the Environment (MOE). GOSAT has been launched in January 2009, and is equipped with the Fourier Transform Spectrometer and the Cloud Aerosol Imager providing global distribution of carbon dioxide and methane with seasonal changes. GCOM-W1 was launched in May 2012 for global water cycle observation and has the AMSR-2 (Advanced Microwave Scanning Radiometer 2). AMSR-2 follows the design of AMSR which was aboard ADEOS-2 satellite, but with improvements in antenna size and onboard calibration, etc. JAXA is also operating the Precipitation Radar (PR) aboard the TRMM (Tropical Rainfall Measuring Mission) satellite and Advanced Microwave Scanning Radiometer (AMSR-E) aboard Aqua satellite of the National Aeronautics and Space Administration (NASA). TRMM is a joint venture of JAXA and NASA. The TRMM satellite was launched in 1997 and is still in operation. The Precipitation Radar (PR) aboard the TRMM satellite is the first spaceborne radar dedicated for precipitation observation developed by JAXA and the National Institute of Information and Communications Technology, Japan (NICT). The data from PR for more than 16 years contributed much for better understanding the precipitation system climatology over tropical and subtropical regions. The Global Precipitation Measurement (GPM) which is led by JAXA and NASA with international collaboration is a multi-satellite system dedicated for the global precipitation observation. The core satellite of GPM will be launched by JAXA at the end of February 2014. JAXA has developed the dual-wavelength radar (DPR) with NICT for the GPM core satellite. DPR will observe rain including solid precipitation with better accuracy than TRMM PR. The ALOS-2 (Advanced Lang Observing Satellite-2) which is equipped with an L-band Synthetic Aperture Radar (PALSAR) is scheduled to launch in 2014. ALOS-2 is a follow-on mission from ALOS contributing to cartography, disaster monitoring, resource survey, etc. EarthCARE for cloud and aerosol observation is a collaboration mission with the European Space Agency (ESA). JAXA has developed a W-band Cloud Profiling Radar (CPR) with NICT for EarthCARE. CPR has high sensitivity to clouds with Doppler function. Using the Doppler function CPR can measure the vertical movement of clouds which is important to understand the cloudy systems. JAXA is also developing GCOM-C1 (the Global Change Observation Mission 1st-Climate) which is for surface and atmospheric measurements related to the carbon cycle and radiation budget. An SGLI (Second Generation Global Imager) will be aboard the satellite. JAXA is also studying future sensors including small sensors for the International Space Station (ISS).

Keywords: Earth observation, satellite, remote sensing

Japan Geoscience Union Meeting 2014
(28 April - 02 May 2014 at Pacifico YOKOHAMA, Kanagawa, Japan)

ACG06-03 Room:315 Time:April 28 17:00-17:15

Greenhouse gas observation by GOSAT during its five-year nominal operation period

YOKOTA, Tatsuya[1*] ; KIKUCHI, Nobuhiro[1] ; YOSHIDA, Yukio[1] ; BRIL, Andrey[1] ; OSHCHEPKOV, Sergey[1] ; INOUE, Makoto[1] ; MORINO, Isamu[1] ; UCHINO, Osamu[1] ; KIM, Heon-sook[1] ; TAKAGI, Hiroshi[1] ; SAITO, Makoto[1] ; MAKSYUTOV, Shamil[1] ; YUKI, Akira[1] ; KANEKON, Sayaka[1] ; KAWAZOE, Fumie[1] ; AJIRO, Masataka[1]

[1]National Institute for Environmental Studies

The Greenhouse gases Observing SATellite (GOSAT) recently completed its planned nominal operation period of five years on 23 January 2014, and it now entered the phase of extended operation. During the past five years, almost all of the GOSAT standard data products were opened to general users. These data products are publicly available and can be obtained through the GOSAT User Interface Gateway (GUIG, http://www.data.gosat.nies.go.jp/). From the spectral data that GOSAT collected, the concentrations of major greenhouse gases (GHGs), namely carbon dioxide (CO_2) and methane (CH_4), were retrieved, and their precisions are now at the level of much less than 1%. These concentration data are used to estimate the monthly surface fluxes of CO_2 and CH_4 on sub-continental and ocean-basin scales. The data are also utilized to monitor GHGs' temporal and spatial changes. Various reports on the results of GOSAT data analysis have appeared in peer-reviewed journals so far. The topics reported include the detection of large GHG point sources and anomalies in the inter-annual trend of CO_2 uptake by terrestrial biosphere.

In this presentation, we will summarize the five-year-long GHG observation by GOSAT and present the global distributions of the GHG concentrations and the surface flux estimates. Also, we will touch on the current status of researches conducted within the framework of the GOSAT Research Announcement.

Keywords: greenhouse gases, carbon dioxide, methane, column concentration, flux, GOSAT

Japan Geoscience Union Meeting 2014
(28 April - 02 May 2014 at Pacifico YOKOHAMA, Kanagawa, Japan)

ACG06-04 Room:315 Time:April 28 17:15-17:30

The NASA Orbiting Carbon Observatory - 2 (OCO-2), the next step in CO2 measurements from space

CRISP, David[1*]

[1]Jet Propulsion Laboratory, Caltech

Global, space-based remote sensing observations of atmospheric carbon dioxide (CO_2) and methane (CH_4) hold substantial promise for future, long-term monitoring of these important greenhouse gases. These measurements will complement those from the existing ground based greenhouse gas monitoring network with increased spatial coverage and sampling resolution. The principle challenge for this approach is the high precision and accuracy needed to resolve the small (<0.3 percent) variations in the background distributions of these gases associated with their emission sources and natural sinks. The European Space Agency (ESA) EnviSat SCIAMACHY and Japanese Greenhouse Gases Observing Satellite (GOSAT) TANSO-FTS were the first two space-based sensors designed to return high resolution spectra of the reflected sunlight in molecular oxygen (O_2), CO_2, and CH_4 bands at near-infrared wavelengths. These spectra are being analyzed to yield spatially resolved estimates of the column-averaged CO_2 and CH_4 dry air mole fractions (X_{CO2}, X_{CH4}) over the sunlit hemisphere. The availability of these data has already enabled substantial improvements in instrument calibration techniques, remote sensing retrieval algorithms, and data validation techniques. However, sensors with greater sensitivity, coverage, and resolution are needed to implement the space-based segment of a global greenhouse gas monitoring system.

In July of 2014, these space-based greenhouse gas pathfinders will be joined by the NASA Orbiting Carbon Observatory-2 (OCO-2). This satellite will fly at the front of the 705-km Afternoon Constellation (A-Train), along an orbit track aligned with the ground footprints of the CloudSat radar and CALIPSO lidar. Its 3-channel, imaging, grating spectrometer has been optimized to record high resolution spectra of reflected sunlight in the 765 nm O_2 A-band and in the 1610 and 2060 nm CO_2 bands. Coincident O_2 and CO_2 spectra are combined into soundings that are analyzed with a full-physics retrieval algorithm to yield estimates of X_{CO2} with accuracies exceeding 0.3 percent over most of the Earth. The OCO-2 spectrometer will collect up to 1 million of these soundings each day along a narrow ground track as it flies over the sunlit hemisphere. Between 20 and 30% of these soundings are expected to be sufficiently cloud free to yield full-column estimates of X_{CO2}. Even with these assets, OCO-2 is still only a research satellite, designed to validate a space-based CO_2 measurement approach. A coordinated network of satellites with similar capabilities will be needed to discriminate and quantify the CO_2 emissions from fossil fuel combustion, land use practices, and other human activities in the presence of the much larger CO_2 fluxes associated with the natural carbon cycle.

Keywords: Carbon Dioxide, Greenhouse Gases, Remote Sensing, Orbiting Carbon Observatory - 2

Japan Geoscience Union Meeting 2014
(28 April - 02 May 2014 at Pacifico YOKOHAMA, Kanagawa, Japan)

ACG06-05 Room:315 Time:April 28 17:30-17:45

NIES GOSAT-2 Project

MATSUNAGA, Tsuneo[1*] ; MORINO, Isamu[1] ; YOSHIDA, Yukio[1] ; SAITO, Makoto[1]

[1]National Institute for Environmental Studies

GOSAT-2, a successor of Greenhouse Gases Observation Satellite (GOSAT), is currently being developed by Ministry of the Environment, Japan Aerospace Exploration Agency, and National Institute for Environmental Studies (NIES). Its target launch year is FY2018.

In the presentation, the schedule of NIES GOSAT-2 project will be introduced.

Keywords: GOSAT, GOSAT-2, satellite, greenhouse gas

Japan Geoscience Union Meeting 2014
(28 April - 02 May 2014 at Pacifico YOKOHAMA, Kanagawa, Japan)

ACG06-06 Room:315 Time:April 28 17:45-18:00

Development of a 3D solar induced chlorophyll fluorescence simulator for satellite fluorescence observation

KOBAYASHI, Hideki[1*] ; NAGAI, Shin[1] ; INOUE, Tomoharu[1] ; ICHII, Kazuhito[1]

[1]Japan Agency for Marine-Earth Science and Technology

Recent studies show that the vegetation canopy scale chlorophyll fluorescence can be observed from satellite, such as GOSAT and OCO-2, using Fraunhofer lines (e.g. Frankenberg et al., 2011). Satellite-based fluorescence can be used to infer the photosynthetic capacity of plant canopy. To understand how the canopy scale bidirectional fluorescence observations are related to three-dimensional fluorescence distribution within a plant canopy, it is necessary to evaluate canopy scale fluorescence emission using a detail plant canopy radiative transfer model. In this study, we developed a three-dimensional plant canopy radiative transfer model that can simulate the bidirectional chlorophyll fluorescence radiance. This modeling was based on the 3D radiative transfer model, forest light environmental simulator (FLiES) (Kobayashi and Iwabuchi, 2008). FLiES is a Monte Carlo ray-tracing model to simulate radiative field in shortwave (solar domain) and long-wave (thermal infrared) radiation in 3D landscape. To realize individual tree crown shapes, the original FLiES model used geometric objects such as cone, cylinder, and spheroid. Recently, FLiES has been extending to utilize voxel-based tree crown datasets, which are favorable to LiDAR based tree crown data sets. In this presentation, we show the current status of the development of the 3D chlorophyll fluorescence simulator.

Keywords: GOSAT, plant canopy radiative transfer model, chlorophyll fluorescence, GPP

Japan Geoscience Union Meeting 2014
(28 April - 02 May 2014 at Pacifico YOKOHAMA, Kanagawa, Japan)

ACG06-07 Room:315 Time:April 29 09:00-09:15

Orbital checkout status of the DPR on the GPM core spacecraft

KOJIMA, Masahiro[1*] ; FURUKAWA, Kinji[1] ; MIURA, Takeshi[1] ; HYAKUSOKU, Yasutoshi[1] ; KAI, Hiroki[1] ; ISHIKIRI, Takayuki[1] ; IGUCHI, Toshio[2] ; HANADO, Hiroshi[2] ; NAKAGAWA, Katsuhiro[2] ; OKUMURA, Minoru[3]

[1]Japan Aerospace Exploration Agency, [2]National Institute of Information and Communications Technology, [3]NEC TOSHIBA Space systems

The Dual-frequency Precipitation Radar (DPR) on the Global Precipitation Measurement (GPM) core satellite was developed by Japan Aerospace Exploration Agency (JAXA) and National Institute of Information and Communications Technology (NICT). The GPM is a follow-on mission of the Tropical Rainfall Measuring Mission (TRMM). The objectives of the GPM mission are to observe global precipitation more frequently and accurately than TRMM. The frequent precipitation measurement about every three hours will be achieved by some constellation satellites with microwave radiometers (MWRs) or microwave sounders (MWSs), which will be developed by various countries. The accurate measurement of precipitation in mid-high latitudes will be achieved by the DPR. The GPM core satellite is a joint product of National Aeronautics and Space Administration (NASA), JAXA and NICT. NASA developed the satellite bus and the GPM microwave radiometer (GMI), and JAXA and NICT developed the DPR. JAXA and NICT developed the DPR through procurement. The contract for DPR was awarded to NEC TOSHIBA Space Systems, Ltd.

The configuration of precipitation measurement using an active radar and a passive radiometer is similar to TRMM. The major difference is that DPR is used in GPM instead of the precipitation radar (PR) in TRMM. The inclination of the core satellite is 65 degrees, and the flight altitude is about 407 km. The non-sun-synchronous circular orbit is necessary for measuring the diurnal change of rainfall similarly to TRMM. The DPR consists of two radars, which are Ku-band (13.6 GHz) precipitation radar (KuPR) and Ka-band (35.5 GHz) precipitation radar (KaPR). The objectives of the DPR are

(1) to provide three-dimensional precipitation structure including snowfall over both ocean and land,
(2) to improve the sensitivity and accuracy of precipitation measurement,
(3) to calibrate the estimated precipitation amount by MWRs and MWSs on the constellation satellites.

The DPR consists of Ku-band (13.6 GHz) precipitation radar (KuPR) and Ka-band (35.5 GHz) precipitation radar (KaPR). The KuPR unit will measure 2.6m X 2.4m X 0.7m in size. The KaPR unit will measure 1.3m X 1.5m X 0.8m in size. Both KuPR and KaPR have almost the same design as TRMM PR. The DPR system design and performance were verified through the development test and the proto flight test. DPR has handed over to NASA and integration of the DPR to the GPM core spacecraft have completed in May 2012. GPM core spacecraft satellite system test has completed in November 2013. The results of the satellite system test concerning to the DPR satisfied system requirements.

GPM core observatory was shipped to Tanegashima Space Center, JAPAN and Launch Site Operations has started on November 2013 and GPM core observatory will be launched in February 2014. DPR orbital check out will be started in March 2014 and it will be completed in April 2014. The orbital check out status of DPR will be reported .

Keywords: GPM, DPR

Japan Geoscience Union Meeting 2014
(28 April - 02 May 2014 at Pacifico YOKOHAMA, Kanagawa, Japan)

ACG06-08 Room:315 Time:April 29 09:15-09:30

Status of the Japanese Global Precipitation Measurement (GPM) Research Project

OKI, Riko[1*] ; KACHI, Misako[1] ; KUBOTA, Takuji[1] ; MASAKI, Takeshi[1] ; KANEKO, Yuki[1] ; FURUKAWA, Kinji[1] ; TAKAYABU, Yukari[3] ; IGUCHI, Toshio[2] ; NAKAMURA, Kenji[4]

[1]JAXA, [2]NICT, [3]University of Tokyo, [4]Dokkyo University

The Global Precipitation Measurement (GPM) mission is a satellite program led by Japan and the U.S., to measure the global distribution of precipitation accurately in a sufficient frequency so that the information provided by this program can drastically improve hydrological predictions, climate modeling, and understanding of water cycles. The GPM Core Observatory carries the Dual-frequency Precipitation Radar (DPR) developed by Japan Aerospace Exploration Agency (JAXA) and the National Institute of Information and Communications Technology (NICT), and the GPM Microwave Imager (GMI) developed by the National Aeronautics and Space Administration (NASA). The frequent precipitation measurement about every three hours will be achieved by constellation satellites with microwave radiometers or microwave sounders, which will be developed by international partners. JAXA also provides the Global Change Observation Mission (GCOM) 1st ? Water (GCOM-W1) named ”SHIZUKU,” launched on May 18, 2012, as one of constellation satellites.

The Japanese GPM research project conducts scientific activities on algorithm development, ground validation, application research including production of research products. In addition to those activities, we promote collaboration studies in Japan and Asian countries, and seek potential users of satellite precipitation products. JAXA develops the DPR Level 1 algorithm, and the NASA-JAXA Joint Algorithm Team develops the DPR Level 2 and DPR-GMI combined Level2 algorithms. JAXA also develops the Global Rainfall Map algorithm, which is a new version of the Global Satellite Mapping of Precipitation (GSMaP), as one of national products to distribute hourly and 0.1-degree horizontal resolution rainfall map. In the GPM era, the GSMaP algorithm will be improved by refining rainfall retrievals over land, considered the orographic rainfall effects, added the rain gauge corrected rainfall product. In the future, information from the Dual-frequency Precipitation Radar (DPR) will be compiled as a database to improve the retrieval accuracy of weak rainfall in mid-to-high latitudes.

The GPM Core Observatory is scheduled to be launched from the JAXA Takengashima Space Center by the H-IIA F23 rocket around 3:07 a.m. thru 5:07 a.m. (JST) on February 28 (Fri.,) 2014. After the initial checkout (about 2-month,) calibration and validation of the DPR, GMI and other products will be implemented toward the public release of all products to general users. Data release date is currently scheduled to be 6-month after the launch.

Keywords: GPM, DPR, GSMaP, ground validation

Japan Geoscience Union Meeting 2014
(28 April - 02 May 2014 at Pacifico YOKOHAMA, Kanagawa, Japan)

ACG06-09 Room:315 Time:April 29 09:30-09:45

Initial validation results of Dual-frequency Precipitation Radar on Global Precipitation Measurement Core Observatory

KUBOTA, Takuji[1*] ; IGUCHI, Toshio[2] ; SETO, Shinta[3] ; AWAKA, Jun[4] ; URITA, Shinji[5] ; YOSHIDA, Naofumi[5] ; OKI, Riko[1]

[1]Japan Aerospace Exploration Agency, [2]National Institute of Information and Communications Technology, [3]Nagasaki University, [4]Tokai University, [5]Remote Sensing Technology Center of Japan

The Global Precipitation Measurement (GPM) Mission consists of a Tropical Rainfall Measuring Mission (TRMM)-like non-sun-synchronous orbiting satellite (GPM Core Observatory) and a constellation of satellites carrying microwave radiometer instruments. The GPM Core Observatory, which will be launched in 28 February 2014, carries the Dual-frequency Precipitation Radar (DPR) developed by the Japan Aerospace Exploration Agency (JAXA) and the National Institute of Information and Communications Technology (NICT). The DPR consists of two radars; Ku-band (13.6 GHz) precipitation radar (KuPR) and Ka-band (35.55 GHz) radar (KaPR). The DPR is expected to advance precipitation science by expanding the coverage of observations to higher latitudes than those obtained by the TRMM Precipitation Radar (PR), by measuring snow and light rain via high-sensitivity observations from the KaPR, and by providing drop size distribution (DSD) information based on the differential scattering properties of the two frequencies. For operational productions of precipitation datasets, it is necessary to develop computationally efficient, fast-processing DPR Level-2 (L2) algorithms that can provide estimated precipitation rates, radar reflectivity factors, and precipitation information, such as the DSD and precipitation type. The L2 algorithms have been developed by the DPR Algorithm Development Team under the NASA-JAXA Joint Algorithm Team.

Before the launch of the GPM Core Observatory, synthetic DPR Level-1 (L1) data are needed as a test bed for the DPR L2 algorithms. In this work, we use data simulated from the TRMM/PR. The primary advantage is that measured Ku-band data from the TRMM/PR, obtained under a wide variety of meteorological conditions, forms the basis of the simulation. As such, the results can be compared directly to the standard TRMM/PR retrievals. Thus, ”at-launch” codes of DPR precipitation algorithms, which will be used in GPM ground systems at launch, were evaluated using synthetic data based upon the TRMM/PR data. Results from the codes (Version 4.20131010) of the KuPR-only, KaPR-only, and DPR algorithms were compared with ”true values” calculated based upon drop size distributions assumed in the synthetic data and standard results from the TRMM algorithms at an altitude of 2 km over the ocean. The results indicate that the total precipitation amounts during April 2011 from the KuPR and DPR algorithms are similar to the true values, while the estimates from the KaPR data are underestimated. By analysis results, the underestimation of the KaPR can be caused by a problem in the attenuation correction method. This was verified by the improved codes (Version 4.20131129), and so this problem has been resolved in the latest version.

After the launch, calibration and validation of the DPR products will be implemented toward the public release of all products to general users. Data release date is currently scheduled to be 6-month after the launch. In this work, we introduce initial validation results of the DPR-L2 product, mainly based upon comparisons of the TRMM/PR product.

Keywords: Global Precipitation Measurement, Dual-frequency Precipitation Radar, algorithm, validation

Japan Geoscience Union Meeting 2014
(28 April - 02 May 2014 at Pacifico YOKOHAMA, Kanagawa, Japan)

ACG06-10 Room:315 Time:April 29 09:45-10:00

Expectations for the Global Precipitation Measurements for Precipitation Sciences

TAKAYABU, Yukari[1*] ; OKI, Riko[2] ; IGUCHI, Toshio[3] ; AONASHI, Kazumasa[4] ; KACHI, Misako[2] ; KUBOTA, Takuji[2] ; HAMADA, Atsushi[1] ; TAKAHASHI, Nobuhiro[3] ; NAKAMURA, Kenji[5]

[1]The University of Tokyo, [2]Japan Aerospace Exploration Agency, [3]National Institute of Information and Communications Technology, [4]Meteorological Research Institute, Japan Meteorological Agency, [5]Dokkyo University

Three dimensional precipitation data observed with Ku (13.8GHz) band Precipitation Radar (PR) on board the Tropical Rainfall Measurement Mission (TRMM) satellite have enabled us to discover various precipitation characteristics over the tropics and subtropics between 36N and 36S. Precipitation system regimes are estimated with precipitation characteristics. The multiple instrument observations of TRMM have also made us quantify the discrepancies between TRMM Microwave Imager (TMI) vs. PR estimated rainfall, and provided us with opportunities to investigate various approaches to improve the rainfall retrieval algorithms.

With the launch of the GPM/DPR, scheduled in February 2014, dual band measurements from space with Ku (13.6GHz) and Ka (35.5GHz) band frequencies will be started. Increasing information of the drop size distributions with DPR should improve the accuracy of precipitation profile structures, which are essential to study precipitation characteristics. GPM/DPR will provide excellent cross calibrations for constellation microwave observations to construct better mapping of precipitation from 65N to 65S, which covers 91% of the earth surface. Weak rainfall measurements will enable us better energy budget calculations after all, as well as more precise examinations of rainfall system lifecycles. We can also expect reexamination and further improvements of TRMM PR rainfall products by comparing Ku-band retrievals with DPR retrievals.

Three dimensional satellite measurement of precipitation at mid-to-high latitudes is a completely new scientific experiment. Since the precipitation systems there are very different from those in the tropics and subtropics, we can certainly expect further scientific discoveries to improve our knowledge of precipitation characteristics with thorough observations from the satellite. Using this outcomes, we also expect to provide useful knowledge to improve the numerical models for weather predictions and climate projections.

Keywords: GPM, DPR, Precipitation Science, TRMM, precipitation characteristics, satellite constellation

Japan Geoscience Union Meeting 2014
(28 April - 02 May 2014 at Pacifico YOKOHAMA, Kanagawa, Japan)

ACG06-11 Room:315 Time:April 29 10:00-10:15

The Global Precipitation Measurement (GPM) Mission: Advancing precipitation measurement for science and society

KIRSCHBAUM, Dalia[1*]

[1]NASA Goddard Space Flight Center

Too much or too little rain can serve as a tipping point for triggering catastrophic flooding and landslides or widespread drought. Knowing when, where and how much rain is falling globally is vital to understanding how vulnerable areas may be more or less impacted by these disasters. Global Precipitation Measurement (GPM) is an international satellite mission to provide next-generation observations of rain and snow worldwide every three hours. The foundation of the GPM mission is the Core Observatory satellite provided by NASA and JAXA. This satellite, launching in early 2014, carries advanced instruments that will set a new standard for precipitation measurements from space. The Core satellite will measure rain and snow using two science instruments: the GPM Microwave Imager (GMI) and the Dual-frequency Precipitation Radar (DPR). The GMI captures precipitation intensities and horizontal patterns, while the DPR provides insights into the three dimensional structure of precipitating particles. Together these two instruments provide a database of measurements against which other partner satellites' microwave observations can be meaningfully compared and combined to make a global precipitation dataset.

Data collected from the Core satellite serves as a reference standard that will unify precipitation measurements from research and operational satellites launched by a consortium of GPM partners in the United States, Japan, France, India, and Europe. The GPM constellation of satellites can observe precipitation over the entire globe within 3 hours of acquisition. The GPM mission will help advance our understanding of Earth's water and energy cycles, improve the forecasting of extreme events that cause natural disasters, and extend current capabilities of using satellite precipitation information to directly benefit society.

Japan Geoscience Union Meeting 2014
(28 April - 02 May 2014 at Pacifico YOKOHAMA, Kanagawa, Japan)

ACG06-12 Room:315 Time:April 29 10:15-10:30

Development of attenuation correction method for GPM/DPR

SETO, Shinta[1*] ; IGUCHI, Toshio[2]

[1]Graduate School of Engineering, Nagasaki University, [2]National Institute for Information and Communications Technology

A new attenuation correction method is developed for the Dual-frequency Precipitation Radar (DPR) on the core satellite of the Global Precipitation Measurement (GPM) mission. Hitschfeld and Bordan's attenuation correction method (HB method) assumes relation between the specific attenuation k and the effective radar reflectivity factor Z_e (k-Ze relation) as $k=aZ_e^b$. The new method is based on HB method, but k-Ze relation is modified as $k=eaZ_e^b$ by using dual-frequency ratio of Z_e (DFR) and surface reference technique (SRT). Therefore, the new method is called HB-DFR-SRT method (H-D-S method in short). While the authors' previous attenuation correction method called HB-DFR method (H-D method in short) results in underestimation of precipitation rates for heavy precipitation, H-D-S method and its improved version try to correct the negative bias by means of SRT. When only single-frequency measurement is available, H-D-S method can be easily switched to HB-SRT method (H-S method in short), which is similar to the attenuation correction method used in the TRMM/PR standard algorithm.

The attenuation correction methods are tested with a simple synthetic dataset of DPR. As long as SRT gives the prefect estimates of path integrated attenuation (PIA) and the parameters of k-Ze relation (a and b) are given properly so that e could be vertically constant, H-S method is much better than the dual-frequency methods. In reality, SRT has error and we cannot give the parameters of k-Ze relation properly so that e should be vertically variable. Tests with SRT error and vertical variation of e show that H-D method is better than H-S method for weak precipitation but H-S method is better than H-D method for heavy precipitation. It is because SRT is unreliable for weak precipitation and DFR is unreliable for heavy precipitation. H-D-S method shows not the best but stable results for both weak and heavy precipitation, and it may work well for medium precipitation. Quantitative evaluation should be done with real measurement dataset of DPR.

Keywords: DPR, GPM, attenuation correction

Japan Geoscience Union Meeting 2014
(28 April - 02 May 2014 at Pacifico YOKOHAMA, Kanagawa, Japan)

ACG06-13 Room:315 Time:April 29 10:30-10:45

Analysis of rain characteristics by using CloudSat and TRMM/PR

TAKAHASHI, Nobuhiro[1*]

[1]National Institute of Information and Communications Technology

Spaceborne cloud/precipitation radars are suitable for understanding the global climate (especially precipitation in this study) that means both the average figure of the Earth climate and the local climate in the global climate. In terms of precipitation climatology, major parameters are the precipitation amount and its diurnal/seasonal changes as well as the drop size information that is a kind of proxy of the precipitation processes such as warm/cold rain. The purpose of this study is to develop the climate map of precipitation by using CloudSat that equips W-band (94 GHz) radar and TRMM/PR that equips Ku-band (13.8 GHz) radar; rain amount is estimated by the TRMM/PR level 2 product (2A25) and the drop size information is obtained by combining the CloudSat and TRMM/PR. The basic idea of the analysis method is to compare the histograms of radar reflectivity factor (Z) at near-surface range bin at the overlapping Z range (weak to moderate rain echo). Because the both satellites have different orbit, only the statistical approach is available. Since the different Mie scattering effect appears for the different frequency and drop size, the Z value of rainfall is different between w- and Ku-band radar observations and it reflects the difference in the histograms of w- and Ku-band. Based on these characteristics, drop size information is estimated by comparing the histograms. In this study, median diameter (D0) is estimated. For the comparison of the estimation, D0 is estimated by TRMM/PR only.

Climate data are created in 10 x 10 degrees in latitude and longitude boxes and each box consists of the unconditional and conditional rain rate (the former corresponds the rain amount) and D0 (median diameter) both from the CloudSat-TRMM/PR combined analysis and TRMM/PR-only analysis for every seasons (DJF, MAM, JJA, and SON), diurnal cycle (night time/day time orbit) and over land or ocean.

The results show that the general characteristic of global maps of D0 through the year and local time is apparent land-ocean contrast; larger D0 appears over land and smaller D0 appears over ocean except for relatively small D0 over southeastern Asia to China. Also, relatively larger D0 appears in tropical area and mid latitude summer. Diurnal change of D0 can be seen by comparing the day/night time D0; D0 is larger in the night time over ocean while day time D0 is larger over land. Tropical Ocean shows smaller seasonal change, while larger changes are seen over mid-latitude area. Comparison of the two estimates of D0 between CloudSat-TRMM/PR combined estimation and TRMM/PR-only estimation.

Since the Dual-frequency Precipitation Radar (DPR) onboard Global Precipitation Measurement (GPM) core satellite, which is launched in February 2014, can estimate the drop size distribution (DSD), the approach in this study can be useful of evaluation of the algorithm for DSD estimation.

Keywords: rain, drop size distribution, CloudSat, TRMM

Japan Geoscience Union Meeting 2014
(28 April - 02 May 2014 at Pacifico YOKOHAMA, Kanagawa, Japan)

ACG06-14 Room:315 Time:April 29 11:00-11:15

Characteristic differences between the heaviest rainfall and the strongest convection

HAMADA, Atsushi[1*] ; TAKAYABU, Yukari[1]

[1]Atmosphere and Ocean Research Institute, The University of Tokyo

Regional and seasonal differences in the rain characteristics between rain-rate and convection extreme events are examined using 11-yr measurements from the Precipitation Radar (PR) onboard the Tropical Rainfall Measuring Mission (TRMM) satellite. After defining a rainfall event as a set of contiguous rainy pixels of TRMM PR measurements, three different types of regional extreme rainfall events are defined, using the maximum values of near-surface rainfall rate (NSR) and 30-dBZ echo top height (ETH30) in rainfall event; Rainfall events of which the maximum NSR is within top 0.1% at a grid but the ETH30 is not are defined as R-only extreme events, those of which the maximum ETH30 is within top 0.1% but the NSR is not are defined as H-only extreme events, and those of which both of the maximum NSR and maximum ETH30 are within top 0.1% are defined as RH extreme events. This is done on a local basis with 2.5 x 2.5 degree horizontal resolution to examine regional extreme events.

It is shown that the fractional occurrence of RH extreme events are less than 30% in most regions, indicating that only a few dozen percent of convection extremes are related to rain rate extremes. There are robust differences in echo profiles, rainfall characteristics, and local environments between R-only and H-only extreme events. These characteristic differences are basically independent on region and season, except for their seasonal occurrence. R-only extreme events exhibit lower echo-top height than H-only extremes, linear downward increase of radar reflectivity (Ze) below freezing level, and sharp upward decrease of Ze in 5-7 km, whereas H-only extreme events exhibit slight downward decrease of Ze below freezing level. R-only extreme events are almost in phase with mean monthly rainfall, while H-only extremes tend to peak slightly out of phase with rainy season. Local environments related to R-only extremes are less convectively unstable, wetter in the low-middle troposphere, and larger moisture flux convergence in the lowermost troposphere, compared with those related to H-only extremes. The features related to R-only extreme events imply a dominance of warm-rain process.

Keywords: precipitation, extreme event, TRMM

Japan Geoscience Union Meeting 2014
(28 April - 02 May 2014 at Pacifico YOKOHAMA, Kanagawa, Japan)

ACG06-15 Room:315 Time:April 29 11:15-11:30

The next-generation GSMaP MWI precipitation retrieval algorithm

AONASHI, Kazumasa[1*]

[1]Meteorological Research Institute Japan Meteorological Agency

1. Introduction

The current GSMaP Microwave Imager (MWI) precipitation retrieval algorithm degrades retrieval accuracy for weak precipitation areas where MWI brightness temperatures (TBs) are sensitive to physical variables other than precipitation. In order to address this issue, we have been developing a new algorithm that retrieves the physical variables including precipitation from MWI TBs. The basic idea of this algorithm is to derive the statistically optimal values of the physical variables, based on Bayes's theorem (Elsaessar and Kummerow 2008, Boukabara et.al 2011). We adopted an ensemble-based variational method (EnVA) for deriving the optimal values from MWI TBs that are non-linear functions of the physical variables. The retrieval algorithm consists of the precipitation detection part and the retrieval part for physical variables in precipitation areas. In this presentation, we will report the precipitation detection part.

2. Precipitation detection part

In the precipitation detection part, we chose surface temperature (Ts), sea surface wind speed (SWS), precipitable water content (PWC), and cloud liquid water content (CLWC) as the over-sea control variables, Ts and surface emissivity (Es) as the over-land control variables, assuming no precipitation.

The EnVA employed forecasts of a cloud-resolving model (CRM) as the first guess of the physical variables, and estimated the first guess error covariance from CRM ensemble forecast. The EnVA calculated innovations and post-fit residuals of MWI TBs that were then used for the precipitation detection.

Keywords: GSMaP, MWI, GPM, GCOMW, precipitation retrieval

Japan Geoscience Union Meeting 2014
(28 April - 02 May 2014 at Pacifico YOKOHAMA, Kanagawa, Japan)

ACG06-16 Room:315 Time:April 29 11:30-11:45

Gage Adjusted Global Satellite Mapping of Precipitation (GSMaP Gauge)

MEGA, Tomoaki[1*] ; USHIO, Tomoo[1] ; KUBOTA, Takuji[2] ; KACHI, Misako[2] ; AONASHI, Kazumasa[2] ; SHIGE, Shoichi[4]

[1]Graduate School of Engineering, Osaka University, [2]Japan Aerospace Exploration Agency, [3]Meteorological Research Institute, [4]Graduate School of Science, Kyoto University

Fresh water is one of the most important resources for human. Precipitation is the main source of fresh water. Precipitation is also heating atmosphere by latent heat and one of important energy transport mechanism of atmosphere. Knowledge of world precipitation activity is important information for not only human activity, but also earth science.

Passive Microwave Radiometer (PMR) is a small and low power consumption sensor, thus many space-borne PMRs observe precipitation from low earth orbit. Space-born PMR provides uniform quality and stable observation data all over the world. PMR have become the precipital sensors for global precipitation retrieval, since these emission and scattering signals have a more direct relationship with precipitation rates than infrared radiometer (IR). The Global Satellite Mapping of Precipitation (GSMaP) project is developing PMR algorithm to provide global precipitation map with space-born PMRs. The GSMaP's goal is to develop the algorithm of high precision and eventually to produce a global precipitation map with high temporal (one hour) and special resolution (0.1 degree). PMR swathes, however, do not cover all surface in one hour. Therefore, it is necessary to utilize a gap-filling technique to generate precipitation maps with high temporal resolution. GSMaP derives Moving Vector (MV) from two successive IR images. GSMaP algorithm interpolates precipitation between gaps when PMRs overpass successive swath with MV by Kalman-filter. GSMaP algorithm now produces 0.1-grid-resolution precipitation map every one hour. Some evaluations, however, show the tendency of underestimation compared to some ground based observations, because PMR precipitation estimation over land has difficulty due to emission variability in surface. Rain gauge provides reliable data, and a rain gauge collects precipitation for certain period at a fixed location. PMR observes signals from precipitation instantaneously. We are developing the GSMaP gauge adjusted product (GSMaP Gauge). The GSMaP Gauge algorithm fits the GSMaP precipitation map to NOAA Climate Prediction Center (CPC) global rain gauge data set. The CPC data set is provided daily with low resolution (0.5-grid-degree). Quality of the CPC data set is not uniform (Quality of gauge-based analysis depends on density of rain gauge). We fill the gap of the precipitation estimation between the satellite and rain gauge attributable to the retrieval difficulty, the spatial and temporal resolution difference. The GSMaP Gauge succeeded to reduce the under estimation of the GSMaP algorithm. In this presentation, we introduce the GSMaP Gauge and its performance.

Keywords: Precipitation, Satellite observations, Microwave observations, Remote sensing

Japan Geoscience Union Meeting 2014
(28 April - 02 May 2014 at Pacifico YOKOHAMA, Kanagawa, Japan)

ACG06-17 Room:315 Time:April 29 11:45-12:00

Current Status of the Products of AMSR2 on GCOM-W1 Satellite

OKI, Taikan[1*] ; KACHI, Misako[2] ; NAOKI, Kazuhiro[2] ; HORI, Masahiro[2] ; MAEDA, Takashi[2] ; IMAOKA, Keiji[2]

[1]Institute of Industrial Science, The University of Tokyo, [2]Earth Observation Research Center, Japan Aerospace Exploration Agency

The Advanced Microwave Scanning Radiometer 2 (AMSR2), on board the first generation satellite of Global Change Observation Mission - Water (GCOM-W1 or ”SHIZUKU”) satellite, is multi-frequency, total-power microwave radiometer system with dual polarization channels for all frequency bands. The GCOM-W1 satellite was launched on May 18, 2012 (JST), and has started scientific observation since July 3, 2012. After the calibration and validation phase, which confirmed that all the pre-defined release accuracies are satisfied, the AMSR2 bright temperature product (Level 1) and geophysical parameter product (Level 2) were released to public since January 2013 and May 2013, respectively.

Monitoring and validation of the AMSR2 geophysical parameters have been continued for further improvements of the observation accuracy in future algorithms. For example, the precipitation product is validated by comparing with the Precipitation Radar (PR) on board the Tropical Rainfall Measuring Mission (TRMM) satellite, and relative errors were 48% over ocean and 88 % over land for the period from September 1, 2012 to August 31, 2013.

Quality control (QC) of in-situ data is also improved for the better validation. New QC method for buoy data, which is used in the validation of the sea surface temperature (SST) and sea surface wind speed products, is introduced to remove unreliable in-situ observation data from comparisons, including overlap check, movement speed check, comparison with numerical model, and statistical check by Bayes’ theorem. Those efforts will contribute to improve the algorithm for future version-up.

The AMSR2 standard products have been distributed through the GCOM-W1 Data Providing Service (https://gcom-w1.jaxa.jp/), and quick look of the products, browse images of all AMSR2 brightness temperatures and geophysical parameters are available at the JAXA Satellite Monitoring for Environmental Studies (JASMES) for Water Cycle (http://kuroshio.eorc.jaxa.jp/JASMES/WC.html).

Keywords: earth observation, hydrologic cycles, geophysical products, validation, data distribution

Japan Geoscience Union Meeting 2014
(28 April - 02 May 2014 at Pacifico YOKOHAMA, Kanagawa, Japan)

ACG06-18 Room:315 Time:April 29 12:00-12:15

Applications of ocean surface wind direction signals in microwave imager observation for atmospheric humidity analysis

KAZUMORI, Masahiro[1*]

[1]Japan Meteorological Agency

An empirical relative wind direction (RWD) model function was developed to represent azimuthal variations of oceanic microwave brightness temperatures of vertical and horizontal polarizations. The RWD model function was based on measurements of observed brightness temperature from the Advanced Microwave Scanning Radiometer and wind vector from SeaWinds, both on board the Advanced Earth Observing Satellite - II, and Special Sensor Microwave Imager Sounder (SSMIS) first guess departure and wind vector data in European Centre for Medium-Range Weather Forecasts (ECMWF) Integrated Forecasting System. The model function was introduced to a microwave ocean emissivity model; a FAST microwave Emissivity Model (FASTEM) in a radiative transfer model for satellite radiance assimilation. Performances of the RWD model function were much more realistic than present azimuthal model functions in FASTEM for low wind speed and high frequency channels.

An assimilation experiment using the RWD model function was performed in the ECMWF system. The experiment demonstrated reductions of first guess departure biases arising from modelling of the azimuthal variations in areas of high wind speed and low variability of wind direction. For example, bias reductions in ascending and descending SSMIS 19 GHz vertical polarized brightness temperature in Somali jet at the Arabian Sea were approximately 0.6 K and 0.7 K. The bias reductions were found for all assimilated microwave imager channels in a wide wind speed range. Moreover, analysis increments of specific humidity in the lower troposphere were reduced (e.g., 0.3 g kg^{-1} reduction at 1000 hPa in the Somali jet). We found improvements of relative humidity and temperature in short-range forecasts in the lower troposphere. The experiment results clearly showed the importance of modelling the azimuthal variation of emissivity for assimilation of microwave imager observations. The RWD model function should be included in the radiative transfer model used in the microwave radiance assimilation observation operator.

Japan Geoscience Union Meeting 2014
(28 April - 02 May 2014 at Pacifico YOKOHAMA, Kanagawa, Japan)

ACG06-19 Room:315 Time:April 29 12:15-12:30

Polar Research using Satellite Microwave Remote Sencing

ENOMOTO, Hiroyuki[1*] ; ALIMASI, Nuerasimuguli[1] ; SURDYK, Sylviane[1] ; FUJITA, Shuji[1] ; YABUKI, Hironori[2] ; SUGIMURA, Takeshi[1] ; SUGIYAMA, Shin[3] ; HOLMRUND, Per[4] ; INGVANDER, Susanne[4]

[1]National Institute of Polar Research, [2]JAMSTEC, [3]Hokkaido University ILTS, [4]Stockholm University

Satellite Microwave remote sensing is the powerful tool to investigate polar regions. The data enables monitoring and surveying ice sheet, sea ice,snow cover conditions for large scale and continuous monitoring in the changing climate, and , and studying their changing mechanisms. Satellite passive microwave observation has almost 30-years long data set which contribute climatological study. The recent GCOM-W data is useful for more precise investigations.

For the Arctic study, GRENE Arctic climate research project(2011-2016) has started by integrating Japanese scientific activities. satellite microwave data is very important to this project since satellite data expands availability of site data to large area and long term. The Arctic project enhances interdisciplinal study and collaboration between modelling and observation. Multi-discipilinaly information and scale-upping by satellite is very important.

Keywords: Polar region, Arctic, Antarctic, Cryosphere, satelllite, Mirowave

Japan Geoscience Union Meeting 2014
(28 April - 02 May 2014 at Pacifico YOKOHAMA, Kanagawa, Japan)

ACG06-20 Room:315 Time:April 29 12:30-12:45

Sea-ice production in Antarctic coastal polynyas estimated using AMSR-E data

NIHASHI, Sohey[1*] ; OHSHIMA, Kay I.[2]

[1]Department of Mechanical Engineering, Tomakomai National College of Technolog, [2]Institute of Low Temperature Science, Hokkaido University

Coastal polynyas are newly-forming sea-ice areas formed by divergent ice drift due to prevailing winds and/or ocean currents. In coastal polynyas, huge amounts of heat flux from the ocean to the atmosphere occur because the heat insulation effect of sea-ice is greatly reduced in the case of thin ice, and accordingly sea ice is formed actively. Dense water formed in Antarctic coastal polynyas with the intense sea-ice production is a major source of Antarctic Bottom Water, which is a key player in the global climate system.

In this study, an algorithm for estimating daily thin ice thickness is developed based on a relationship between polarization ratios (PR) of AMSR-E brightness temperatures (TBs) and thermal ice thickness. The TBs at 89 GHz and 36.5 GHz are used. The thermal ice thickness is based on heat flux calculation using ice surface temperatures derived from satellite thermal infrared images. We used cloud-free MODIS images.

In the Antarctic Ocean, landfast sea-ice (fast ice), which is stationary sea ice attached to coastal features such as grounded icebergs, is formed along the coast. Antarctic coastal polynyas tend to be formed adjacent to fast ice. The AMSR-E ice thickness algorithm possibly mis-classifies fast ice as thin ice, because the PR values of thin ice and fast ice are similar. Thus, also the fast ice detection algorithm is developed. Monthly fast ice extent is detected based on microwave characteristics that the horizontally- and vertically-polarized TBs of fast ice tend to be lower than those of thin ice and are similar to those of ice sheet close to the coast.

The spatial resolution of AMSR-E is about 6.25 km, and the pixel density is four times higher than that of SSM/I which has been used in previous studies. This advantage is critical for the coincident detection and monitoring of coastal polynyas and fast ice because their areal extent is fairly small (tens to a hundred kms at most). The accuracy of the created AMSR-E dataset is validated from comparisons with backscatter images acquired by ASAR on Envisat.

Sea-ice production in Antarctic coastal polynyas is estimated based on heat flux calculation using the AMSR-E dataset. For the estimation, it is assumed that heat from the ocean below is negligible and that all of the heat loss to the atmosphere goes towards freezing. The sea-ice production estimated using the AMSR-E data has been improved from the SSM/I ice production because of the finer spatial resolution. First, the AMSR-E data can better resolve the high production area close to the coast. Second, false sea-ice production in the fast ice pixels mis-included by SSM/I is corrected because AMSR-E can detect fast ice that cannot be resolved by SSM/I. In fact, the total sea-ice production in each polynya by AMSR-E does not change much from the SSM/I ice production for many polynyas because these two effects of opposite direction compensate for each other. The AMSR-E dataset presented in this study would give the boundary/validation data of sea-ice production and fast ice for modeling studies.

Keywords: AMSR-E, Antarctic Ocean, Coastal polynyas, Sea-ice production, Antarctic Bottom Water

Japan Geoscience Union Meeting 2014
(28 April - 02 May 2014 at Pacifico YOKOHAMA, Kanagawa, Japan)

ACG06-21 Room:315 Time:April 29 14:15-14:30

A proposal of mission combining active and passive microwave sensors and its applications for global water cycle

EBUCHI, Naoto[1*]

[1]Hokkaido University

A mission carrying active and passive microwave sensors is proposed to monitor the global water cycle and air-sea coupling. The passive microwave sensor will be a successor of AMSR2 on GCOM-W2, which was launched by JAXA on 12 May 2012. Channels to observe solid precipitation will also be added to AMSR2. The active sensor will be a scatterometer at operated at Ku- and Ka-bands. The Ka-band scatterometer can measure vector wind fields near the coasts with higher spatial resolution than the Ku-band scatterometer, which is similar to SeaWinds on QuikSCAT and ADEOS-II and OSCAT on Oceansat-2. Merits of the combination of the active and passive microwave sensors will be discussed in aspects of sensor and science synergisms. The microwave radiometer contributes to improve accuracy of vector wind measurements by the scatterometer under rain conditions. The wind direction provided by the scatterometer improves accuracy of the SST, water vapor and precipitation measured by the radiometer. The science synergy includes applications for studies of monsoon, tropical cyclones, air-sea coupling in various scales, global and regional water cycles, sea ice, soil moisture and snow over land.

Keywords: remote sensing, microwave radiometer, microwave scatterometer, water cycle, air-sea interaction

Japan Geoscience Union Meeting 2014
(28 April - 02 May 2014 at Pacifico YOKOHAMA, Kanagawa, Japan)

ACG06-22 Room:315 Time:April 29 14:30-14:45

Upwelling events at the western African coast related to atmospheric structures: An analysis with satellite observations

DESBIOLLES, Fabien[1*] ; BLANKE, Bruno[1] ; BENTAMY, Abderrahim[2]

[1]Laboratoire de Physique des Oceans (LPO), UMR 6523 CNRS-Ifremer-IRD-UBO, Brest, France, [2]Laboratoire d'Oceanographie Spatiale (LOS), IFREMER, centre de Brest, France

Satellite scatterometers provide continuously valuable surface wind speed and direction estimates over the global ocean on a regular grid both in space and time. The Level 3 data derived from the Advanced Scatterometer (ASCAT), available at $1/4^o$ spatial resolution (hereafter AS25), and Quick Scatterometer (QuikSCAT), available on $1/2^o$ and $1/4^o$ horizontal grids (QS50 and QS25 respectively), are studied at regional scales in both the Benguela and Canary upwelling systems. They are compared to the European Center for Medium-Range Weather Forecast surface wind analysis, with insight into their intrinsic and effective spatial resolutions. In the coastal band, the finest spatial patterns are found in the QS25 winds and are O(75km). This demonstrates the sensitivity of the high-resolution satellite-derived winds to coastal processes related to sea surface temperature (SST) perturbations and land-sea transition. More specifically, mesoscale coupling processes between SST and winds play a leading part in structuring the wind stress curl in both the Canary and Benguela upwelling systems. These processes act especially over the upwelling extension zone (O(100km) off the coast). Next, short-lived upwelling episodes (SUEs) calculated from SST anomalies are defined consistently with the QS25 effective resolution. These cold events refer to local, short-lived perturbations that add to seasonal upwelling variability. We characterize concomitant atmospheric synoptic conditions for SUEs identified at chosen latitudes and highlight two subregions in both upwelling systems, with contrasted patterns for the alongshore wind stress component and curl. The complexity of the latter patterns is closely linked to local, short-term SST variability. Closer to the shore, wind stress curl patterns derived from QS25 are only loosely related to SST/wind interactions and, as a working hypothesis, can also be associated with orographic effects that may play an important role in cooling processes. The derivation of a realistic coastal wind drop-off from satellite observations is an almost impossible task, first because a blind zone at the coast, second because the horizontal scales of pure orographic effects (a few tens of kilometers) are finer than the effective resolution of the satellite-derived product (˜75km). However, an alternative assessment can be given by evaluating the ocean response to contrasted coastal wind profiles. Numerical sensitivity experiments show that the imbalance between Ekman transport and Ekman pumping has an impact on ocean dynamics: a reduction of the wind in the QS25 forcing, partly induced by orography, contributes to SST cooling.

Keywords: scatterometry, upwelling dynamics, SST/Wind Interactions, orography effects, air-sea coupling

Japan Geoscience Union Meeting 2014
(28 April - 02 May 2014 at Pacifico YOKOHAMA, Kanagawa, Japan)

ACG06-23 Room:315 Time:April 29 14:45-15:00

The GNSS Ocean Winds and AIS Mission, An Earth Science and Marine Safety Satellite Constellation

ROSE, Randall[1*] ; GLEASON, Scott[1] ; RUF, Christopher[2] ; KITAZAWA, Yukihito[3] ; TANIMOTO, Kazuo[4]

[1]Southwest Research Institute, [2]University of Michigan, [3]IHI Corporation, [4]Meisei Electric Co., Ltd.

Recent developments in electronics and nano-satellite technologies combined with modeling techniques developed over the past 20 years have enabled a new class of remote wave and wind sensing capabilities that offer markedly improved performance over existing observatories while opening avenues to new applications. Most existing space borne ocean wind observatories operate in the C and Ku-bands which obscures key information about the ocean and the global climate. Using GNSS-based bi-static scatterometry performed by a constellation of nano-satellites, ocean wave and wind data can be provided with unprecedented temporal resolution and spatial coverage across the full dynamic range of ocean wind speeds in all precipitating conditions.

The NASA Cyclone Global Navigation Satellite System (CYGNSS) is a space borne mission being developed to study tropical cyclone inner core processes. CYGNSS consists of 8 GPS bi-static radar receivers to be deployed on separate nano-satellites in October 2016. It is anticipated that numerous additional Earth science applications can also benefit from the cost effective high spatial and temporal sampling capabilities of GNSS remote sensing. These applications include monitoring of rough and dangerous sea states, global observations of sea ice cover and extent, meso-scale ocean circulation studies, and near surface soil moisture observations.

The Automatic Identification System (AIS) is a maritime system used for global identification and tracking of ships. It is proposed as part of the GNSS Ocean Winds and AIS (GOWA) nano-satellite constellation concept to combine and improve upon the GNSS remote sensing capability of CYGNSS with a space based AIS system. GOWA will be capable of monitoring both the ocean roughness and the locations of ship traffic at the same time. This will result in both an increase in maritime safety and valuable Earth science measurements of ocean winds, sea ice and land surfaces.

This presentation will present a summary of the CYGNSS mission and plans for future instrument development to increase the number of science observations. The goal of this development is to enable the GOWA mission being proposed for Japanese science and maritime safety applications.

Keywords: GNSS, Earth Science, Remote Sensing, Satellites, GPS

Japan Geoscience Union Meeting 2014
(28 April - 02 May 2014 at Pacifico YOKOHAMA, Kanagawa, Japan)

ACG06-24 Room:315 Time:April 29 15:00-15:15

Development of Cloud Profiling Radar (CPR) for Earth Clouds, Aerosols and Radiation Explorer (EarthCARE) mission

SEKI, Yoshihiro[1*] ; TOMITA, Eiichi[1] ; KIMURA, Toshiyoshi[1] ; NAKATSUKA, Hirotaka[1] ; AIDA, Yoshihisa[1] ; OKADA, Kazuyuki[1] ; IIDE, Yoshiya[1] ; KADOSAKI, Gaku[1] ; TAKAHASHI, Nobuhiro[2] ; OHNO, Yuichi[2] ; HORIE, Hiroaki[2] ; SATO, Kenji[2]

[1]Japan Aerospace Exploration Agency, [2]National Institute of Information and Communications Technology

Earth Clouds, Aerosols and Radiation Explorer (EarthCARE) is a Japanese-European collaborative Earth observation satellite mission aimed to deepen understanding of the interaction process between clouds and aerosols and its effects on the Earth's radiation. The outcome of this mission is expected to improve accuracy of the Global Climate Change prediction.

The EarthCARE spacecraft, which weighs approximately 2,250kg and goes along a Sun-Synchronous 400km-hight orbit around the Earth, accommodates four instruments which are to observe the Earth's clouds, aerosols and radiation. The observation data acquired simultaneously by the four sensors will be processed into a variety of synergy products including vertical profiles of clouds and aerosols, microscopic cloud parameters, radiation fluxes and so on. As one of those observatories, the Cloud Profiling Radar (CPR), which has a 2.5m-diameter main reflector and W-band 1.5kW transmitter and receiver, is the world's first space-borne Doppler cloud radar jointly developed by the Japan Aerospace Exploration Agency (JAXA) and the National Institute of Information and Communications Technology (NICT), which provides vertical velocity as well as vertical structure inside clouds. The other payloads on the satellite are the Atmospheric Lidar (ATLID) for vertical structure measurement of clouds and aerosols, the Multi-Spectral Imager (MSI) for horizontal distribution measurement of clouds and aerosols, and the Broad-Band Radiometer (BBR) for measurement of radiation fluxes at top of the atmosphere. ATLID, MSI, BBR and the base-platform of the spacecraft are developed by the European Space Agency (ESA).

In Japan, the critical design review of the CPR has been completed in 2013 and CPR proto-flight model is currently being manufactured, integrated, and tested. After handed-over to ESA, the CPR will be installed onto the EarthCARE satellite together with the other instruments, tested, transported to Guiana Space Center in Kourou, French Guiana and launched by a Soyuz launcher in JFY2016.

Keywords: Cloud, Aerosol, Radiation, EarthCARE, CPR, Cloud Profiling Radar

Japan Geoscience Union Meeting 2014
(28 April - 02 May 2014 at Pacifico YOKOHAMA, Kanagawa, Japan)

ACG06-25 Room:315 Time:April 29 15:15-15:30

Shortwave direct aerosol radiative forcing using CALIOP and MODIS measurements

OIKAWA, Eiji[1*] ; NAKAJIMA, Teruyuki[1] ; WINKER, David[2]

[1]AORI, University of Tokyo, [2]NASA Langley Research Center

The aerosol direct effect occurs by direct scattering and absorption of solar and thermal radiation. Shortwave direct aerosol radiative forcing (SWDARF) under clear-sky condition is estimated about 5 Wm^{-2} from satellite retrievals and model simulations [e.g., *Yu et al*., 2006]. Simultaneous observations of aerosols and clouds are, however, very limited to validate the estimation of SWDARF under cloudy-sky condition. In 2006, the CALIPSO (Cloud-Aerosol Lidar and Infrared Pathfinder Satellite Observations) satellite was launched with the space-borne lidar, CALIOP (Cloud-Aerosol Lidar with Orthogonal Polarization). This enabled us to get data of the vertical distribution of aerosols and clouds all over the world. *Oikawa et al.* [2013] estimated SWDARF under clear-sky, cloudy-sky, and all-sky conditions using CALIOP Version 2 data and MODIS (Moderate resolution Imaging Spectrometer) data. They investigated four scenarios for evaluating the SWDARF: clear-sky, the case that aerosols exist above clouds (above-cloud case), the case that aerosols exist below high-level clouds (below-cloud case), and the case that aerosols are not detected by CALIOP in cloudy-sky condition. The cloudy-sky SWDARF is, then, estimated by the latter three scenarios. The all-sky SWDARF is the combination of clear-sky and cloudy-sky SWDARF weighted by the cloud occurrence.

We calculated SWDARF from 2007 to 2009 using CALIOP Level 2 Cloud and Aerosol Layer Products Version 2 (V2) and Version 3 (V3) with the method of *Oikawa et al.* [2013]. The procedure of daytime calibration, cloud screening, and aerosol-cloud classification are improved in the V3 algorithms [*Powell et al*., 2010; *Vaughan et al*., 2010; *Liu et al*., 2010]; therefore, the distributions of aerosols and clouds are significantly changed from V2 data. Compared V3 data with V2 data, the total cloud fraction and occurrence probability of above-cloud case decrease. In clear-sky condition, marine aerosols increase and single scattering albedo (SSA) of total aerosols increases over the ocean. In cloudy-sky condition, smoke and polluted dust decrease. Annual zonal averages of SWDARF from 60^oS to 60^oN under clear-sky, cloudy-sky, and all-sky are -2.85, -0.16, and -0.78 Wm^{-2} for V2 data and -3.70, -1.07, and -2.02 Wm^{-2} for V3 data. It indicates that SWDARF largely depends on the retrieval and classification algorithms of aerosols and clouds.

Previous studies reported that the aerosol absorption above clouds cause the underestimation of cloud optical thickness (COT) in the satellite retrievals [*Haywood et al*., 2004; *Coddington et al*., 2010]. We, therefore, have a plan to examine the effect on SWDARF from underestimation of COT.

Keywords: aerosol, radiative forcing, DARF, CALIPSO, CALIOP

Japan Geoscience Union Meeting 2014
(28 April - 02 May 2014 at Pacifico YOKOHAMA, Kanagawa, Japan)

ACG06-26 Room:315 Time:April 29 15:30-15:45

A new method for estimating biases in multi-spectral cloud parameter retrievals caused by cloud horizontal inhomogeneity

NAGAO, Takashi[1*] ; NAKAJIMA, Takashi[1]

[1]Tokai University

Clouds play an important role in terrestrial atmospheric dynamics, thermodynamics, and radiative transfer and are key elements of the water and energy cycles. Modification of cloud properties, lifetime, and amount by indirect aerosol effects has an effect on radiative forcing in the climate. Cloud observations using satellite-borne multispectral imagers (e.g. Aqua/MODIS, GCOM-C/SGLI and EarthCARE/MSI) provide data sets useful for understanding cloud characteristics and their distributions on a global scale. Previous studies, however, pointed out that cloud parameters (e.g. cloud optical thickness, cloud particle effective radius and cloud top temperature) retrieved from multispectral measurements were significantly impacted by vertical and horizontal inhomogeneities of clouds, bimodal particle size distributions in drizzling clouds, and three-dimensional radiative transfer. In this study, we suggest a new method for estimating bias in multi-spectral-retrieved cloud parameters caused by cloud horizontal inhomogeneity. The impact of cloud horizontal inhomogeneity is considered as a key for interpreting discrepancies between cloud parameters from satellite observations and in-situ measurements or numerical cloud models. The estimation method considers the bias as the combination of the following two impacts: One is the impact of clear-contamination in cloud pixel, which is parameterized by cloud-fraction. The other is the impact of subpixel scale variance of cloud properties (but no clear-contamination), which is parameterized by variance of multi-spectral radiances in sub-pixels, and based on error propagation theory. We evaluate the method by using high-spatial resolution measurements of Landsat 8. Additionally, to apply the method to several multi-spectral imagers (e.g. MODIS, GCOM-C/SGLI and EarthCARE/MSI), we also investigate co-variance matrices of adjacent pixels or sub-pixels obtained from different IFOVs because the accuracy of the method depends on the accuracy of the co-variance matrix.

Japan Geoscience Union Meeting 2014
(28 April - 02 May 2014 at Pacifico YOKOHAMA, Kanagawa, Japan)

ACG06-27 Room:315 Time:April 29 15:45-16:00

A study of the earth radiation budget using a 3D Monte-Carlo radiative transfer code (2)

OKATA, Megumi[1*] ; NAKAJIMA, Teruyuki[1]

[1]University of Tokyo, Atmosphere and Ocean Research Institute

The purpose of this study is to evaluate the earth radiation budget when data are available from satellite-borne active sensors, i.e. cloud profiling radar (CPR) and lidar, and a multi-spectral imager (MSI) in the project of the Earth Explore/EarthCARE mission. The scientific requirement of the evaluation accuracy is less than 10 Wm-2 for the upward broadband radiative flux for the instantaneous 10kmx10km footprint of CPR (EarthCARE, 2006). For this purpose, we first developed forward and backward 3D Monte Carlo radiative transfer codes called MCsatr that treat a broadband solar flux calculation including thermal infrared emission calculation by k-distribution parameters of Sekiguchi and Nakajima (2008). We have developed Forward and Backward Monte Carlo radiative transfer codes, and we have also developed both of two types for deciding optical mean path by extinction transmittance and scattering transmittance for Forward Monte Carlo radiative transfer code.

In evaluation system, 3D extinction coefficient fields are constructed by two methods: 1) the Minimum Information Deviation Profiling Method (MIDPM) (Barker and Donovan et. al., 2011) and 2) numerical simulation by bin-spectral non-hydrostatic cloud model. In the MIDPM, we first construct a library of pair of observed vertical profiles from active sensors and collocated imager products at the nadir footprint, i.e. spectral imager radiances, cloud optical thickness (COT), effective particle radius (RE) and cloud top temperature (Tc). We select a best matched active sensor-derived vertical profiles from the library for each of off-nadir pixels of the imager where active sensor-derived vertical profile is not available, by minimizing the deviation between library imager parameters and those at the pixel, to construct the 3D cloud field. We applied this method to data of Cloudsat/CPR and AQUA/MODIS for a case of summer stratus cloud of California coast on July 2, 2007.

The second construction of 3D cloud systems is performed by numerical simulation of Californian summer stratus clouds using an non-hyderostatic atmospheric model coupled with a bin-spectral cloud microphysics model based on the NHM+ACBM model (Iguchi et al., 2008; Sato et al., 2009, 2011). Most inner region of a three-fold nesting system is an area of 30km∗30km∗1.5km with horizontal (vertical) grid spacing of 100m (20m) and 300m (20m). Two different cell systems were simulated for small and large cloud condensation nuclei (CCN) concentration. The area mean cloud optical thickness, $<$COT$>$, and standard deviation are 3.0 and 4.3 for pristine case and 8.5 and 7.4 for polluted case.

We then re-calculated the solar radiation field by two types of Fowrad MCstar. We compared flux reflectivities of the 3D atmospheres with those by Plane Parallel Approximation (PPA) and Independent Pixel Approximation (IPA) (Cahalan et al., 1994). As expected, the reflectivity difference between 3D and PPA clouds increases with increasing COT horizontal variability of the 3D clouds. The reflectivity difference between 3D and PPA reaches 0.078 at maximum, which is equivalent to a solar radiative flux error of 70 Wm-2.

On the other hand, the IPA result between the two cases are significantly different. We infer this difference is caused by difference in the spatial characteristic size of inhomogeneity. The mean extinction of the cloud system is of 5 to 8 km-1, so that the kilometer-size clouds in the satellite case are optically dense enough to be approximated by IPA. The difference is less than 0.010 in reflectivity or 10 Wm-2 in upward flux. On the other hand, the model simulation case is optically thin to be approximated by IPA. The error reaches 0.07 at maximum by pristine case. A future work is needed to correct this significant error utilizing the 3D structure of the cloud system.

Keywords: 3D radiative transfer, MIDPM, Monte Carlo

Japan Geoscience Union Meeting 2014
(28 April - 02 May 2014 at Pacifico YOKOHAMA, Kanagawa, Japan)

ACG06-28 Room:315 Time:April 29 16:15-16:30

Synergistic use of the geostationary and the polar orbit satellites for surveying the cloud evolution process: plan

NAKAJIMA, Takashi[1*] ; NAGAO, Takashi[1] ; LETU, Husi[1]

[1]Tokai University

The use of spaceborne radar and imager aboard the CloudSat, Aqua, EarthCARE, GCOM-C1, and the 3rd generation geostationary satellites for investigating cloud evolution process, is suggested. These satellites have been in orbit or will be launched in the middle of 2010-era and contribute for observing aerosols, clouds on the earth system. Since aerosols and clouds exert an important influence on the planet water and energy balances, more understanding of their lifecycle is required. Optical thickness and particle size of clouds are primal information for estimating the cloud evolution process. These parameters are retrieved from multi-spectral imageries obtained from space-borne satellite sensors. Recently, active sensors, such as the CloudSat cloud profiling radar (CPR) and the CALIPSO Lidar present a new epoch of aerosol and cloud observation with the purpose of revealing transition of particles, from cloud condensation nuclei to rain droplets via cloud and drizzle particles. They observe vertical cross section of the cloud system along the satellite footprint. As follow on the CloudSat / CALIPSO, the EarthCARE that has both active and passive sensors is planed by JAXA, NICT, and ESA collaboration. Doppler capability of the EarthCARE CPR will reveals vertical motion of cloud particles. Moreover, the 3rd generation geostationary weather satellite will appear in 2015 and observe aerosol and cloud system in every 10 or 2.5 minutes. Therefore, it is expected that the combined use of polar orbital passive/active sensors and geostationary satellites reveal details of cloud evolution process, statistically and dynamically. In this presentation, we introduce recent progresses of aerosol and cloud observations from satellites, showing the multi-sensor views of cloud growth process obtained from an active radar (CPR) and a passive imager (MODIS).

Keywords: Cloud evolution, Satellite, GCOM, EarthCARE

Japan Geoscience Union Meeting 2014
(28 April - 02 May 2014 at Pacifico YOKOHAMA, Kanagawa, Japan)

ACG06-29 Room:315 Time:April 29 16:30-16:45

Retrieval algorithm for aerosols based on GCOM-C1/SGLI

SANO, Itaru[1*] ; MUKAI, Sonoyo[1] ; NAKATA, Makiko[1] ; HOLBEN, Brent[2] ; DUBOVIK, Oleg[3] ; KOKHANOVSKY, Alexander[4]

[1]Kinki University, [2]NASA/GSFC, [3]Lille University, [4]EUMETSAT

It is known that atmospheric aerosols have valuable information in many research fields. However estimation of aerosol direct and indirect effects on climate changes in the 5th report of IPCC still involves large uncertainty due to lack of precise aerosol properties.

JAXA (Japanese space agency) is developing the GCOM-C (Global change observing mission?climate) satellite series, which are expected to provide us new aerosol information as well as geo-physical parameters for thirteen years after launch. The first of GCOM-C series will carry the SGLI (second generation global imager) sensor which observes total radiance from near UV to thermal infrared wavelengths including polarization measurements at red and near IR. This work intends to develop an efficient algorithm for aerosol retrieval based on this polarization information to be given by GCOM-C1/SGLI.

Keywords: Aerosol, SGLI, GCOM-C

Japan Geoscience Union Meeting 2014
(28 April - 02 May 2014 at Pacifico YOKOHAMA, Kanagawa, Japan)

ACG06-30 Room:315 Time:April 29 16:45-17:00

Ocean primary production algorithm for the GCOM-C1/SGLI

HIRAWAKE, Toru[1*] ; FUTSUKI, Ryosuke[1] ; SHINMYO, Katuhito[1] ; TAKAO, Shintaro[2] ; FUJIWARA, Amane[3] ; SAITOH, Sei-ichi[1]

[1]Faculty/Graduate School of Fisheries Sciences, Hokkaido University, [2]Faculty of Environmental Earth Science, Hokkaido University, [3]National Institute of Polar Research

One of the objectives of second-generation global imager (SGLI) on the earth observation satellite, Global Change Observation Mission 1st-Climate (GCOM-C1) is to understand the global carbon cycle. Therefore, estimation of column integrated daily net primary production (PP_{eu}) as carbon assimilation by photosynthesis of phytoplankton in the ocean is essential for the objective of SGLI/GCOM-C1 project. Most of the algorithms developed in the past used chlorophyll *a* (chl *a*) concentration. However, estimation of chl *a* concentration from satellite data has uncertainty due to the effect of pigment packaging that leads to underestimation, and the interference of colored dissolved organic matter (CDOM) which leads to overestimation. Another uncertainty is derivation of photosynthetic rate of phytoplankton. Although the vertically generalized productivity model (VGPM) which is one of the frequently used algorithms expressed the maximal photosynthetic rate (${P^B}_{opt}$) as a function of sea surface temperature (SST), the SST derived ${P^B}_{opt}$ had large error, particularly in the polar waters. Furthermore, discussion on the effect of global warming to primary productivity in the ocean using satellite data is facilitated, if the photosynthetic rate is an independent parameter on the SST.

To reduce these issues, light absorption coefficient of phytoplankton (a_{ph}) was used in the algorithm for SGLI/GCOM-C1; product of ${P^B}_{opt}$ and chl *a* in the VGPM, which means productivity at the depth with the maximal photosynthetic rate within a water column, was expressed by photosynthetic available radiation (PAR) absorbed in phytoplankton. In situ primary production and optical data to develop the algorithm were measured in the North Pacific, Japan Sea, East China Sea, Southern Ocean, Chukchi Sea (Arctic Ocean), Bering Sea. Additional datasets of the Bermuda Atlantic Time-series Study (BATS), Hawaii Ocean Time-series (HOT) and The California Cooperative Oceanic Fisheries Investigations (CalCOFI) were also obtained for the development and validation of the algorithm. Accuracy in the estimation of product of ${P^B}_{opt}$ and chl *a* (P_{opt}) and PP_{eu} were fairly well and estimated values from the new algorithms almost satisfied a factor of 2 of the values measured in situ. If accurate value of aph is derived from SGLI data, global estimation of PP_{eu} without the issues of pigments packaging, CDOM and SST are expected.

Keywords: primary production, phytoplankton, absorption coefficient, GCOM-C, SGLI

Japan Geoscience Union Meeting 2014
(28 April - 02 May 2014 at Pacifico YOKOHAMA, Kanagawa, Japan)

ACG06-31 Room:315 Time:April 29 17:00-17:15

Global snow and ice cover observations using GCOM-C1/SGLI for studying climate changes

HORI, Masahiro[1*] ; AOKI, Teruo[2] ; STAMNES, Knut[3] ; TANIKAWA, Tomonori[1] ; KUCHIKI, Katsuyuki[2] ; LI, Wei[3] ; CHEN, Nan[3]

[1]Japan Aerospace Exploration Agency, [2]Meteorological Research Institute, [3]Stevens Institute of Technology

The ”Global Change Observation Mission-Climate” (GCOM-C) is a project of Japan Aerospace Exploration Agency (JAXA) for the global observation of the Earth environment. The GCOM-C is a part of the JAXA’s GCOM mission which consists of two satellite series, GCOM-C and GCOM-W (Water). GCOM-C carries a multi-spectral optical radiometer named Second Generation Global Imager (SGLI), which will have special features of wide spectral coverage from 380 nm to 12 micrometer, a high spatial resolution of 250m, a field of view exceeding 1000km, two-direction simultaneous observation, and polarization observation. The GCOM-C mission aims to improve our knowledge on the global carbon cycle and radiation budget through high-accuracy observation of global vegetation, ocean color, temperature, cloud, aerosol, and snow and ice. As for the cryosphere observation, not only snow and ice cover extent but also snow physical parameters are retrieved from SGLI data such as snow grain sizes at shallow layers, temperature, and mass fraction of impurity mixed in snow layer and so on. These snow physical parameters are important factors that determine spectral albedo and radiation budget at the snow surface. Thus it is essential to monitor those parameters from space in order to better understand snow metamorphosis and melting process and also to study the response of snow and sea-ice cover extent in the Polar Regions to a climate forcing such as global warming. In addition, one of important objectives of the GCOM mission is to monitor long-term trend of the geophysical parameters for understanding the mechanism of earth’s climate system. For this purpose, the data from GCOM series satellites are not enough. Thus, JAXA launched a website named ”JAXA Satellite Monitoring for Environmental Studies (JASMES)” for semi-near real-time monitoring of earth’s environmental variables. Through this website JASMES provides users with not only satellite datasets (flat binary) but also information on the current status of the climate variables such as solar radiation reaching the earth’s surface (photosynthetically available radiation: PAR), snow and cloud cover, dryness of vegetation (water stress trend), wild fire and so on. MODIS data since February 2000 are currently processed for this analysis but SGLI data will be used after the launch of GCOM-C. Furthermore, the data from Advanced Very High Resolution Radiometer (AVHRR) onboard polar orbiting satellites operated by the National Oceanic and Atmospheric Administration (NOAA) since 1978 are also under preparation toward establishing a half-century long datasets of remote sensing after the success of the GCOM mission. This presentation will summarize the SGLI cryospheric products and validation plans, and also briefly introduce the JASMES dataset.

Keywords: Snow Cover, Snow Grain Size, Snow Impurity, Surface Temperature, Remote Sensing, Climate

Japan Geoscience Union Meeting 2014
(28 April - 02 May 2014 at Pacifico YOKOHAMA, Kanagawa, Japan)

ACG06-32 Room:315 Time:April 29 17:15-17:30

Development of GCOM-C1 land surface reflectance product

MURAKAMI, Hiroshi[1*]

[1]JAXA, Earth Observation Research Center

Land-surface reflectance (RSRF) product is one of the essential products of Global Change Observation Mission-Climate 1/ Global Imager (GCOM-C1/SGLI; to be launched in JFY 2016); it is an input of other land algorithms, such as Leaf Area Index (LAI) and land cover classification (LCC), and will be used for surface albedo in the radiation budget, and used as the background of aerosol and cloud estimation. RSRF is estimated by subtracting scattering and absorption of an atmospheric molecule and aerosol from the top-of-atmosphere (TOA) radiance in cloud-free areas observed by the satellite (i.e., atmospheric correction). However, in order to extract the information on aerosols from the TOA radiation, it is necessary to know the information on land surface used as a background beforehand.

Experiential assumption and a candidate model about the spectral characteristic of aerosol and surface reflectance are often used in the presumption. Since the presumption can influence the output results, it is necessary to accumulate the knowledge of the various spectral characteristics and to perform suitable selection. Change of RSRF by the sun and the satellite geometries (BRDF) should be modeled when we preset the land-surface reflectance, because the satellite observes targets from a specific direction.

Candidate models of aerosol in the atmospheric correction (size distribution and vertical distribution, refractive index, etc.) may be able to be consistent with ones in the traditional aerosol-estimation algorithms which use candidate models as well. Since RSRF is used as a background of aerosol estimation, the consistency will be important for the product evaluation and accuracy improvement. There are groups which study aerosol properties by ground observation network, SKYNET, AERONET, etc., their regional characterization, spectral reflectance of the land surface, and observation and modeling (canopy radiation transfer) of the BRDF in the GCOM-C1 science team. The GCOM-C1 science team held a mini-workshop in summer of 2012, and decided that JAXA develops the land-surface atmospheric correction algorithm step by step by integrating their results . We confirmed importance of the consistency with the algorithms, such as LCC, LAI, albedo, etc., which use the estimated RSRF and BRDF.

We plan to develop the algorithm based on the existing knowledge (i.e., a traditional algorithm) for the at-launch version. Gas absorption of SGLI bands by water vapor, ozone, oxygen, and NO2 will be considered by using objective analysis data or Climatology. The surface elevation will be corrected by using objective-analysis sea-level pressure data and high-spatial resolution digital elevation data, DEM. Influence of surface slope will be reduced by using surface normal vector calculated by the DEM and solar vector. GCOM-C1/SGLI has an near-ultra violet (NUV) 380nm band, which will be used for the presumption of surface reflectance in the GCOM-C1 atmospheric correction, because reflectance and its directionality is generally small in the NUV and blue wavelengths. The presumption of the NUV band uses vegetation and land-cover information assumed from near infrared (NIR) and short-wave infrared (SWIR) reflectance, which are not so much affected by aerosols, and RSRF in the previous days by assuming temporal change of RSRF is generally smaller than the change of the atmosphere.

For the future algorithm version after the satellite launch, we expect to improve the presumption by knowledge from the canopy radiation transfer, LCC and vegetation phenology, adopt new aerosol estimation schemes, or use results of the aerosol-transport model to find the optimal aerosol models. SGLI has a polarization radiometer which observes the Stokes vector of red and NIR bands with 45-deg along-track slant view. It may be able to improve atmospheric correction accuracy after accumulation of surface BRDF and polarization knowledge in the future.

Keywords: GCOM-C1, SGLI, land surface reflectance, atmospheric correction

Japan Geoscience Union Meeting 2014
(28 April - 02 May 2014 at Pacifico YOKOHAMA, Kanagawa, Japan)

ACG06-33 Room:315 Time:April 29 17:30-17:45

Assessing the variations of the Alaskan tundra vegetation using MODIS NDVI 250-m imagery

SETIAWAN, Yudi[1*] ; KUSHIDA, Keiji[1]

[1]College of Bioresource Sci., Nihon Univ. Japan

Improving the understanding of Alaskan tundra vegetation using remote sensing data is a challenging task due to a general lack of consistency and coverage from historical and existing platforms. Furthermore, it should be essential for many aspects of global environmental change research.

Vegetation dynamics of the land surface is an integrated reflection of the vegetation and physical and chemical factors that shape the environment of a given land area and determinants for overall biological diversity patterns. In this paper, we demonstrate an approach for displaying detailed information of the Alaskan tundra ecosystem from the vegetation dynamics point of view. We assumed that locations displaying similar temporal vegetation patterns are inferred to have a similar vegetation and/or environment characteristics. Differences among land cover types as reflected in temporal profiles of NDVI are caused by differences in vegetation type composition and/or in their densities, and their responses to local environmental conditions, consequently, the use of long time-series NDVI will capture such different patterns in seasonal growth cycles.

The clustering method yields sets of clusters, which each cluster represents a significant different NDVI pattern at detailed information in the land cover type. However, the complexity and enormous amount of time-series NDVI datasets may lead to the difficulty of obtaining the actual number of clusters in this study. Therefore, to provide maximum effectiveness of the clustering algorithm, we first consider the number of clusters 15 which correspond to the number of dominant physiognomy of Alaska tundra ecosystem (Raynold et al., 2005). The number of clusters was then evaluated based on a statistical measurement of how separate that pattern is to patterns in its own cluster compared to patterns in other clusters. This separability analysis was applied to discriminate among high detailed significant patterns that were theoretically defined to portray the specific characteristics of each land cover type.

Keywords: Vegetation dynamics, Tundra vegetation, Alaska, MODIS

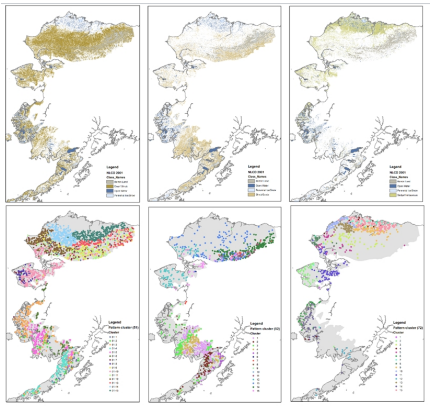

Figure 1. Three-dominant land cover classes of NLCD 2001 in Alaskan tundra: a) dwarf shrub, b) shrub/scrub, and c) sedge/herbaceous. Distribution of the 15-clusters for: d) dwarf shrub, e) shrub/scrub and f) sedge/herbaceous

Japan Geoscience Union Meeting 2014
(28 April - 02 May 2014 at Pacifico YOKOHAMA, Kanagawa, Japan)

ACG06-P01 Room:Poster Time:April 29 18:15-19:30

Detection of regional extent of permafrost thawing and waterlog damage area in boreal forest in eastern Siberia during w

IIJIMA, Yoshihiro[1*] ; ABE, Konomi[2] ; ISE, Hajime[2] ; MASUZAWA, Tadashi[2]

[1]JAMSTEC, [2]Regional Environmental Planning Inc.

Wet climate with largely increased in rainfall during summer and snow accumulation during winter had perennially continued since 2004 in eastern Siberia. Soil moisture in the active layer had been rapidly increased corresponding with thawing permafrost near the surface during following years. The perennially water-logged active layer furthermore exacerbated the boreal forest habitat, namely withered and dead forests widely extended in this region. In the present study, we have attempted to extract the region of degraded boreal (larch) forest based on the analysis of satellite data (ALOS-AVNIR2 and PALSAR) in the left and right banks of the central Lena River Basin near Yakutsk, along with expansion of the water-logged forest floor in relation to permafrost degradation.

Keywords: ALOS, permafrost, wet climate, boreal forest, degradation, eastern Siberia

Japan Geoscience Union Meeting 2014
(28 April - 02 May 2014 at Pacifico YOKOHAMA, Kanagawa, Japan)

ACG06-P02 Room:Poster Time:April 29 18:15-19:30

A potential map of precipitation area using the geostationary meteorological satellite for the GSMaP

HIROSE, Hitoshi[1*] ; HIGUCHI, Atsushi[1] ; USHIO, Tomoo[2] ; MEGA, Tomoaki[2] ; YAMAMOTO, Munehisa[3] ; SHIGE, Shoichi[3] ; SATOMURA, Takehiko[3] ; HAMADA, Atsushi[4]

[1]Center for Environmental Remote Sensing, Chiba University., [2]Division of Electric and Information Engineering, Osaka University., [3]Division of Earth and Planetary Science, Graduate School of Science, Kyoto University., [4]Atmosphere and Ocean Research Institute, Tokyo University.

The Global Satellite Mapping of Precipitation (GSMaP) produces accurate precipitation data with high time and spatial resolution (per 1hour, 0.1 degree) by utilizing the satellite microwave radiometer. At the time and place which all microwave radiometer satellites are not available, the GSMaP estimates where the precipitation area observed before that time will moves by using a cloud moving vector retrieved from the infrared brightness temperature (IR Tb) observed by the geostationary meteorological satellite (GMS) (GSMaP_MVK, GSMaP_NRT; v5.222.1). However this method has some possibility of missing the convective precipitation which develops quickly (Ushio et al. 2009), and uses only IR1 channel (10.5˜11.5μm) of the GMS observation to calculate the cloud moving vector. Therefore, this study made more accurate data of estimated precipitation area by using multi-channel GMS observation, called potential map, and then improved the accuracy of GSMaP_MVK and GSMaP_NRT precipitation areas by utilizing the potential map.

As a precipitation area index of the GMS, we used difference of the Tb between IR1 channel and water vapor (WV) channel (6.5˜7.0μm). This index is based on the assumption which a deep convective cloud with precipitation probably occurs at the area with a small Tb difference of IR1 and WV (Ohsawa et al. 2001). Moreover since almost all of geostationary satellites have the IR1 and WV channel, the index is available globally on a long-term basis. We used near surface rain observed by the precipitation radar of the Tropical Rainfall Measurement Mission (TRMM) (PR; 2A25, V7) and the rainfall intensity retrieved from ground-based precipitation radar of Japan Meteorological Agency (JMA) as the truth of the precipitation area and converted the Tb of the GMS to the probability of precipitation with simultaneous observation between the GMS and the precipitation radar.

At first we compared the precipitation area obtained from the GSMaP and the precipitation radar, and found that the GSMaP_MVK overestimated the precipitation area over the ocean without the microwave observation. And therefore we tried to identify the area which the GSMaP precipitation was less than 1.0 mm per hour and the possibility of precipitation obtained of the potential map was less than 15 % as non-precipitation area. As the result the threat score of the GSMaP_MVK precipitation detection was improved from 0.37 to 0.41 over the ocean without the microwave observation. As it is considered that the threat score of GSMaP_MVK with the microwave observation is 0.45, this improvement is regarded as significant. On the other hand, the GSMaP_NRT underestimated the precipitation area over the land and coast without the microwave observation. And then we identified the area which the potential map was more than 40 % as precipitation area. As the result the threat score of the GSMaP_NRT was much improved from 0.27 to 0.34 over the land and coast without the microwave observation. In these areas and conditions, we can expect that the GSMaP estimates the precipitation area more accurately by utilizing the potential map.

Keywords: microwave radiometer, GSMaP, GMS, precipitation radar, high time resolusion, mid-high latitude

Japan Geoscience Union Meeting 2014
(28 April - 02 May 2014 at Pacifico YOKOHAMA, Kanagawa, Japan)

ACG06-P03 Room:Poster Time:April 29 18:15-19:30

A study of multi-pixel and multi-parameter satellite remote sensing for aerosol properties

HASHIMOTO, Makiko[1*] ; MORIMOTO, Shotaro[1] ; TAKENAKA, Hideaki[1] ; NAKAJIMA, Teruyuki[1]

[1]AORI, the University of Tokyo

We have developed a new satellite remote sensing algorithm to retrieve the aerosol optical characteristics using multi-pixel information of satellite imagers. In this algorithm, the inversion method is a combination of the MAP method (Maximum a posteriori method, Rodgers, 2000) and the Phillips-Twomey method (Phillips, 1962; Twomey, 1963) as a smoothing constraint for the state vector. Retrieved parameters in our algorithm are aerosol optical properties, such as aerosol optical thickness (AOT) of fine mode, sea salt, and dust particles, a volume soot fraction in fine mode particles, and ground surface albedo of each observed wavelength. We simultaneously retrieve all the parameters that characterize pixels in each of horizontal sub-domains consisting the target area. Then we successively apply the retrieval method to all the sub-domains in the target area.

We conducted numerical tests for the retrieval of aerosol properties and ground surface albedo for GOSAT/CAI imager data to test the algorithm for the land area. The result of the experiment showed that AOTs of fine mode and dust particles, soot fraction and ground surface albedo are successfully retrieved within absolute. We discuss the accuracy of the algorithm for various land surface types. Our future work is to extend the algorithm for analysis of AGEOS-II/GLI and GCOM/C-SGLI data.

Keywords: GCOM/C-SGLI, Aerosol, Satellite remote-sensing

Japan Geoscience Union Meeting 2014
(28 April - 02 May 2014 at Pacifico YOKOHAMA, Kanagawa, Japan)

ACG06-P04 Room:Poster Time:April 29 18:15-19:30

Estimation of Phytoplankton Group-Specific Primary Production in Kuroshio Waters Using Ocean Colour Remote Sensing

HIRATA, Takafumi[1*] ; SUGIE, Koji[1] ; SUZUKI, Koji[1] ; SAITOH, Hiroaki[2]

[1]Faculty of Environmental Earth Science, Hokkaido University, [2]Tohoku National Fisheries Research Institute, Fisheries Research Agency

The ocean is a major sink of carbon dioxide released into the atmosphere. Phytoplankton conducting primary production plays a significant role on temporal and spatial variability in the absorption of the carbon. Also phytoplankton transfers carbon to higher trophic levels in a marine ecosystem, and the carbon pathways to the higher trophic levels affect vulnerability of food web, or the ecosystem, against external forcings. Tremendous efforts to measure primary productivity of the total phytoplankton community in the global oceans have been made historically. On the other hand, measurements of primary productivity of individual phytoplankton groups composing of the total community are relatively sparse. This is partly due to methodological difficulties to differentiate such productivity of individual groups in situ, on top of practical circumstance that in situ observation requiring ship time is usually expensive. Therefore, it is of great interest if satellite remote sensing can overcome these problems, given that a number of earth observation satellites have been and will be launched. Especially, it is a great advantage of satellite observation that one can hindcast primary productivity of individual phytoplankton groups using historical remote sensing data, once a remote sensing methodology/algorithm is developed. In this presentation, we show a primitive result of development of such methodology to estimate primary productivity of diatoms and haptophytes in Kuroshio waters using ocean colour remote sensing.

Keywords: Ocean Colour, Satellite Observation, Phytoplankton, Primary Production

Japan Geoscience Union Meeting 2014
(28 April - 02 May 2014 at Pacifico YOKOHAMA, Kanagawa, Japan)

ACG06-P05 Room:Poster Time:April 29 18:15-19:30

NICT Calibration and Validation experiment for DPR/GPM

NAKAGAWA, Katsuhiro[1*] ; HANADO, Hiroshi[1] ; KAWAMURA, Seiji[1] ; IWAI, Hironori[1] ; TAKAHASHI, Nobuhiro[1] ; IGUCHI, Toshio[1]

[1]National Institute of Information and Communications Technology

The GPM core satellite is scheduled to be launched on February 28, 2014. It carries the Dual-Frequency Precipitation Radar (DPR) developed by Japan Aerospace Exploration Agency (JAXA) and National Institute of Information and Communications Technology (NICT), which consists of two radars: Ku-band precipitation radar (KuPR, 13.6 GHz) and Ka-band radar (KaPR, 35.5 GHz). NICT is planning the GPM/DPR onboard calibration experiment at NICT Koganei. The beam matching of two radars will be evaluated. NICT is also planning the post-launch ground validation (product validation) experiment at two locations, NICT Kobe (NICT Advanced ICT Research Institute) and NICT Okinawa (Okinawa Electromagnetic Technology Center). NICT is developing two X-band phased array radars (PANDA: Phased Array radar Network DAta system) and will install at NICT Kobe and Okinawa. PANDA can scan three-dimensionally in thirty seconds. We can compare the radar directly and simultaneously. At NICT Okinawa, the C-band polarimetric Doppler radar (COBRA) is also installed. The differential reflectivity (ZDR) can be used to validate the rain drop size distribution parameter (D_0). The cross-correlation coefficient (ρHV) can be used to validate the melting layer flag. Using the ground-based rain drop size measurements, the two-dimensional Video disdtrometer (2DVD), Joss-type disdrometer, and Laser Optical disdrometr (Parsivel), and so on, the characteristics of DSD itself are analyzed and the k-Z relationship is estimated for evaluation and improvement of the GPM/DPR algorithm.

Keywords: GPM, DPR, Beam maching, Ground Validation, PANDA (Phased Array radar Network DAta system), COBRA

Japan Geoscience Union Meeting 2014
(28 April - 02 May 2014 at Pacifico YOKOHAMA, Kanagawa, Japan)

ACG06-P06 Room:Poster Time:April 29 18:15-19:30

Ground-based Validation of GPM/DPR

KANEKO, Yuki[1*] ; OKI, Riko[1] ; NAKAGAWA, Katsuhiro[2] ; NAKAMURA, Kenji[3]

[1]Japan Aerospace Exploration Agency (JAXA), [2]National Institute of Information and Communications Technology, [3]Faculty of Economics, Dokkyo University

The Global Precipitation Measurement (GPM) mission is an expanded follow-on mission to TRMM (Tropical Rainfall Measuring Mission) and GPM core satellite carries dual frequency precipitation radar (DPR) and GPM Microwave Imager on board. The DPR is expected to advance precipitation science by expanding the coverage of observations to higher latitudes than those of the TRMM/PR, measuring snow and light rain by the KaPR, and providing drop size distribution information based on the differential attenuation of echoes at two frequencies. After launch of GPM core satellite JAXA will perform evaluation of DPR L2 products, for example, precipitation rate, measured radar reflectivity, and drop size distribution. Those physical values will be compared with ground-based observations. This poster presentation will show the preliminary report of DPR evaluation comparison between DPR products and ground-based instruments during the first 2 months after launch, including a ground-based Ka-band radar system.

Keywords: GPM, DPR, validation

Japan Geoscience Union Meeting 2014
(28 April - 02 May 2014 at Pacifico YOKOHAMA, Kanagawa, Japan)

ACG06-P07 Room:Poster Time:April 29 18:15-19:30

Optimal choice of surface reflectance and aerosol types for Multi-Spectral Imager on board EarthCARE

FUKUDA, Satoru[1*] ; NAKAJIMA, Teruyuki[2] ; TAKENAKA, Hideaki[2]

[1]Japan Aerospace Exploration Agency, [2]Atmosphere and Ocean Research Institute, The University of Tokyo

EarthCARE is a satellite which will be launched in 2016. EarhtCARE is a joint mission between Europe and Japan. Four instruments such as CPR, ATLID, MSI and BBR will be equipped. MSI is a multi-spectral imager, and the purpose of it is to get the horizontal structure of aerosol and cloud. We are developing the aerosol retrieval algorithm for MSI. MSI aerosol products are consists of optical thickness over land, optical thickness over ocean, and Angstrom Exponent over ocean. Over ocean we implement two channel method with 0.68 um and 0.86 um (Higurashi and Nakajima, 1999) and we retrieve optical thickness and Angstrom Exponent. Over land we estimate the surface reflectance at 0.68 um from longer wavelength. Kaufman et al (1997) used 2.2 um to estimate the surface reflectance at 0.68 um. In this study we tried to use 1.6 um to estimate the surface reflectance at 0.68 um. This is because there is a possibility to get better estimation than to use 2.2 um and we can use this method for sensors which don't equip 2.2 um such as GOSAT/TANSO-CAI or CAI2. We have made a scatter plot of the reflectance between 0.68 um and 1.6 um. As reflectance data set, we used AERONET data of 0.68 um and GOSAT/TANSO-CAI's reflectance data of 1.6 um. We found that there are some correlations between these two reflectances when we classified by NDVI. The correlation is larger when the NDVI is large. The error induced by this parameterization is calculated. The standard error is 0.009 when 0.5 <NDVI <0.7, and the standard error is 0.007 when 0.7 <NDVI. We also calculated the error as aerosol optical thickness. The error as aerosol optical thickness at 0.5 um is 0.18 when 0.5 <NDVI <0.7, and that is 0.14 when 0.7 <NDVI. We will also develop aerosol models for each area by use of cluster method and linear classifier method.

Keywords: aerosol, remote sensing, EarthCARE

Japan Geoscience Union Meeting 2014
(28 April - 02 May 2014 at Pacifico YOKOHAMA, Kanagawa, Japan)

ACG06-P08 Room:Poster Time:April 29 18:15-19:30

Helicopter-borne observation with portable microwave radiometer in the Southern Ocean and the Sea of Okhotsk

TAMURA, Takeshi[1*] ; OHSHIMA, Keiichiro[2] ; LIESER, Jan[3] ; TOYOTA, Takenobu[2] ; TATEYAMA, Kazutaka[4] ; NOMURA, Daiki[2] ; NAKATA, Kazuki[2] ; FRASER, Alex[2] ; JANSEN, Peter[3] ; NEWBERY, Kym[3] ; MASSOM, Robert[3] ; USHIO, Shuki[1]

[1]National Institute of Polar Research, [2]Institute of Low Temperature Science, [3]ACE CRC, [4]Kitami Institute of Technology

It has been recently recognized that sea ice production in the polar regions is controlled by the thin sea ice area with thickness of less than 0.2 m. Spatial distribution of thin ice area and its variability are important information to better understand the reduction of the sea ice covered region in a changing climate environment. We have developed a thin ice thickness algorithm for satellite passive microwave data of the Advanced Microwave Scanning Radiometer-EOS (AMSR-E) and Special Sensor Microwave Imager (SSM/I). Although the microwave skin depth of bare sea ice is about several cm at most, microwave brightness temperatures correlate with the surface salinity (brine volume fraction), which is sensitive to thin ice thickness. Here, we present in-situ observations using a helicopter-borne portable passive microwave radiometer that has the same specifications as the satellite AMSR-E and AMSR-II sensors (36 GHz-vertical and -horizontal channels), to validate and improve our thin ice thickness algorithm. This study estimates the relationship between the microwave brightness temperatures (both satellite and helicopter-borne portable sensors) and in-situ observations of sea ice thickness.

We present data from two airborne missions, one in early austral spring 2012 during the Sea Ice Physics and Ecosystem eXperiment (SIPEX-2) of the Australian Antarctic Program in East Antarctica, and one from the Sea of Okhotsk in mid-winter 2009. These microwave data are compared with the satellite AMSR-E and AMSR-II data and ice thickness estimated from Moderate-Resolution Imaging Spectroradiometer (MODIS) data, helicopter-borne IR sensor data, and ship-borne downward looking camera data. High-resolution airborne microwave brightness temperatures show good agreement with low AMSR-E and AMSR-II brightness temperatures, despite the significant resolution mismatch. In the thin ice region, the polarization ratio of 36 GHz vertical and horizontal temperatures (PR-36) is found to be well correlated with ice thickness, supporting the validity of the AMSR-E thin ice algorithm which was developed previously by our group. We also discuss the microwave characteristics of fast versus pack ice, with a view to improving a satellite fast ice detection algorithm.

Keywords: passive microwave, heli-borne portable radiometer, thin ice region, in-situ validation, Southern Ocean, Sea of Okhotsk

Japan Geoscience Union Meeting 2014
(28 April - 02 May 2014 at Pacifico YOKOHAMA, Kanagawa, Japan)

ACG33-01 Room:418 Time:April 28 15:15-15:30

Diatom analysis on the late Pleistocene Takano Formation, Nagano, Japan

NAGAYASU, Koichi[1*] ; OTANI, Hiromi[3] ; KUMON, Fujio[2]

[1]Interdisciplinary Graduate School of Science and Technology, Shinshu University, [2]Department of Environmental Sciences, Faculty of Science, Shinshu University, [3]Faculty of Science, Shinshu University

Diatom analysis has been performed at a 0.5 m interval for a sediment core of 53.88 m length from the late Pleistocene Takano Formation. According to the age-model proposed by Tawara et al. (2006), this core can covers from 170 ka to 40 ka in age and analysis interval correspond to about 1500 years.

From 170 ka to 140 ka, benthoic diatoms such as *Achnanthes* spp. and *Staurosira* spp. are dominant, and diatom abundance is very low (lower than 1.0×10^8valves/g). After 140 ka, planktonic diatoms such as *Cyclotella radiosa*, *Aulacoseira ambigua*, *Cyclotella stelligera*, *Aulacoseira alpigena* are dominant. From 140 ka to 130 ka, *C. radiosa* is dominant, and diatom abundance is low (1.6 - 6.9×10^8 valves/g). From 130 ka to 115 ka, *Aul. alpigena* is dominant, and diatom abundance is high (over 10×10^8 valves/g). From 115 ka to 100 ka, *C. stelligera* is dominant, and diatom abundance varies largely (0.1 - 38.2×10^8 valves/g). From 100 ka to 70 ka, *C. radiosa* is dominant, and diatom abundance is abundant, between 3.2×10^8 valves/g and 56×10^8 valves/g. From 70 ka to 40 ka, *C. radiosa* and *Aul. alpigena* are dominant, and diatom abundance is low, fluctuating a little between 0.9×10^8 valves/g and 20×10^8 valves/g.

These results are compared with the diatoms analysis of the sediment cores from Lake Biwa. After 140 ka, planktonic diatoms are dominant in the Takano Formation, and the diatom assemblage changes synchronously between Takano Formation and Lake Biwa.

Japan Geoscience Union Meeting 2014
(28 April - 02 May 2014 at Pacifico YOKOHAMA, Kanagawa, Japan)

ACG33-02 Room:418 Time:April 28 15:30-15:45

Is small Abies mariesii forest in Pseudo-Alpine Zone spreading? :Case study in the Akitakomagatake

KONNO, Asaka[1*]

[1]Miyagi University of Education,MA

Pseudo-Alpine Zone composed of Sasa and shrubs occupies on subalpine zone of mountain along the Sea of Japan in eastern Japan. It is considered that heavy snowfall on those mountains prevents coniferous trees from growing and consequently Pseudo-Alpine Zone exists. But there is Pseudo-Alpine Zone in the part of the Ou Backbone Range which is less snowfall than mountains along the Sea of Japan. On Akitakomagatake, the one of mountains which has Pseudo-Alpine Zone, small Abies mariesii forests are scattered.

This landscape has been hitherto considered that spreading Abies mariesii forest which finally results in matured coniferous forest on the basis of pollen analysis. Perpose of this study is discussing whether small Abies mariesii forest is spreading or not in terms of tree distribution and local environment.

As the result, Abies mariesii seeding is distributed only within the small Abies mariesii forest, not in surrounding Sasa kurilensis and Fagus crenata.In addition, soil moisture is higher in the small Abies mariesii forest than in the surrounding vegetation. These results suggest that the small Abies mariesii forest is not spreading but just being established on appropriate site.

Keywords: Abies mariesii forest, Pseudo-Alpine Zone, Spreading range, Soil moisture

Japan Geoscience Union Meeting 2014
(28 April - 02 May 2014 at Pacifico YOKOHAMA, Kanagawa, Japan)

ACG33-03 Room:418 Time:April 28 15:45-16:00

The chemical characteristics of spring and river water in Kamikochi at the Japanese Alps

KURAMOTO, Takayuki[1*] ; SASAKI, Akihiko[1] ; SUZUKI, Keisuke[1]

[1]IMS, Shinshu University

There are much spring waters in the Azusa River which flows through Kamikochi. These spring waters form the branch of the Azusa River. Spring water shows the characteristics reflecting an underground water flow. Therefore, in order to understand the water cycle of Kamikochi, it is important to understand the formation mechanism of spring water. The purpose of this study is to clarify the chemical characteristics of spring and river water in Kamikochi. We set up the thermometer in five places of a basin for the measuring of spring and river water temperature. The water samples were collected in water temperature measuring site and Azusa River. The pH, electric conductivity, major ions (Na^+, K^+, Mg^{2+}, Ca^{2+}, Cl^-, $NO_3{}^-$ and $SO_4{}^{2-}$), and stable isotope of water were analyzed with the pH meter, conductivity meter, ion chromatographs, and isotopic water analyzer, respectively. In addition, $HCO_3{}^-$ concentration was measured using the sulfuric acid titration method. At almost observation points, the temperatures of spring and river water showed seasonal change. However, only one site did not have change of spring water temperature through a whole year.

Japan Geoscience Union Meeting 2014
(28 April - 02 May 2014 at Pacifico YOKOHAMA, Kanagawa, Japan)

ACG33-04 Room:418 Time:April 28 16:15-16:30

Geo-environmental changes after the fire on the alpine slopes of Mount Shirouma-dake, northern Japanese Alps

SASAKI, Akihiko[1*] ; KARIYA, Yoshihiko[2] ; IKEDA, Atsushi[3] ; SUZUKI, Keisuke[1]

[1]IMS, Shinshu Univ., [2]Senshu Univ., [3]Tsukuba Univ

This is the continuous study to clarify the geo-environmental changes on the post-fire alpine slopes of Mount Shirouma-dake in the Northern Japanese Alps. The fire occurred at May 9, 2009 on the alpine slopes of Mount Shirouma-dake, and the fire spread to the Pinus pumila communities and grasslands. Although the grass had a little damage by the fire, the Pinus pumila received nearly impact of the fire. In the Pinus pumila communities where the leaf burnt, forest floor is exposed and become easy to be affected by atmospheric condition such as rain, wind, snow, and etc.

First, we illustrated a map of micro-landforms, based on geomorphological fieldworks. We observed these micro-landforms repeatedly for four years after the fire. As the results of the observation, it is clear that remarkable changes of these micro-landforms have not occurred but some litters on the forest-floor in the Pinus pumila communities are flushed out to surroundings. The litter layer on the forest-floor in the Pinus pumila communities were 3-4 cm thick in August of 2011, but it became 1-2 cm thick in September of 2013. The Pinus pumila communities established on the slopes consists of angular and sub-angular gravel with openwork texture, which are covered by thin soil layer. Therefore, it is necessary to pay attention to soil erosion following the outflow of the litter.

In addition, we observe the ground temperature and soil moisture, under the fired Pinus pumila communities and the no fired Pinus pumila communities after the fire, to find influence of the fire. The ground temperature sensors were installed into at 1 cm, 10 cm, and 40 cm depth. The soil moisture sensors were installed into at 1 cm and 10 cm depth. The 1 cm depth of the soil on the post-fire slopes, diurnal freeze-thaw cycles occurred in October and November of 2011 and 2012, but it had not occurred in 2009 and 2010. In addition, the period of seasonal frost at 10 cm and 40 cm depth on the post-fire slopes are extended for two weeks. These thermal condition changes are triggered by decrease in the thickness of the litter layer on the fired Pinus pumila communities.

Japan Geoscience Union Meeting 2014
(28 April - 02 May 2014 at Pacifico YOKOHAMA, Kanagawa, Japan)

ACG33-05 Room:418 Time:April 28 16:30-16:45

Combining time-lapse photography and multisensor data logging to monitor slope dynamics in the southern Japanese Alps

MATSUOKA, Norikazu[1*]

[1]University of Tsukuba

Onsite time-lapse photography (TLP) is applied to visual monitoring of soil movements and rockfalls in an alpine zone (Mt. Ainodake area) of the southern Japanese Alps. The time-series images greatly improve understanding of slope processes in remote, seasonally inaccessible areas. TLP detects the timing of slope movements at a high time resolution. Stereographic view of successive images displays 3D slope dynamics that indicates the location and magnitude of displacement. When combined with sensor-based data logging, TLP allows more reliable evaluation of thresholds (environmental controls) for slope movements. This presentation demonstrates (1) how visual information improves the interpretation of both slow progressive soil movements (frost creep) and rapid temporary movements (rill erosion and rockfalls) and (2) how highly active is slope dynamics in the southern Japanese Alps that experience deep seasonal frost in winter and heavy rain storms in summer.

Continuous monitoring of a painted line drawn on a debris lobe highlights biannual shallow soil movements, mostly derived from diurnal frost heave by needle ice or shallow ice lens formation and approximated by the potential frost creep. The surface velocity shows a small interannual variation mainly reflecting snow conditions, but an extraordinary velocity is recorded once per decade. This is due to episodic rill erosion released when the topmost frozen soil is rapidly thawed and super-saturated by intensive rainfall during seasonal thawing periods.

Year-round TLP images of a rockslide scarp allows evaluation of the timing and magnitude of rockfalls at different scales. Close-up images of color-painted quadrangles (50 cm square) indicates centimeter- to decimeter-scale spalling events. Spalling activity reach a maximum at the beginning of seasonal thawing, when the rockwall experiences both diurnal freeze-thaw alternations within the outermost 20 cm and progressive warming of the still-frozen substrate. Stereographic view of successive images also identifies block-scale rockfalls. Such an event occurred between 16 h on 7 July and 8 h on 8 July 2011, triggered by nocturnal rainfall (total 33 mm).

Keywords: time-lapse photography, field monitoring, rockfalls, solifluction, periglacial, Japanese Alps

Japan Geoscience Union Meeting 2014
(28 April - 02 May 2014 at Pacifico YOKOHAMA, Kanagawa, Japan)

ACG33-06 Room:418 Time:April 28 16:45-17:00

Evaluation of long-term variability of rainfall-runoff properties in forested alpine catchment

KOJIMA, Toshiharu[1*] ; ZAINAL, Edwina[2] ; OHASHI, Keisuke[3] ; SHINODA, Seirou[4]

[1]River Basin Research Center, Gifu University, [2]Graduate School of Engineering, Gifu University, [3]Faculty of Engineering, Gifu University, [4]Information and Multimedia Center, Gifu University

The water conservation function of forest, so-called ”Green Dam” in Japan, is recognized as one of the important forest’s functions. However it is often miss-understood by general public such as ”sponge theory”. Water balance in forested catchment is not clear because of its complexity by many hydro processes. The authors investigate the long-term variability of rainfall-runoff properties by forest growth and climate changes in the Gamansawa catchment (3 km^2), Nakatsudawa, Gifu, Japan. The study area has long-term hydrological data acquired by Gifu prefecture and Forestry Agency, Japan from 1984 to 2007. Main forest types are cypress(67%), cider(4%), broad-leaves forest(20%) and so on. The long-term tendency of forest variation is investigated by satellite image analysis with Landsat/MSS, TM and Terra/ASTER images acquired from 1984 to 2010. The mean NDVI over the study area are increasing. Therefore the forest should be growing in the research period. The authors investigate the trend of event based discharge rates f (=total direct discharge at the event / total rainfall at the event). The hydrological data is divided to many rainfall events and event based discharge rates are evaluated. The event based discharge rates are on a slightly decreasing trend with df/dt = -0.006 [y^{-1}]. Moreover the long-term hydrological data is divided to four periods and apply to the 4-layer tank model in order to evaluate the variation of hydrological properties in the study area. We assumed that the long-term variation in forest property is mostly surface soil layer such as soil layer thickness and lateral permeability. Vertical permeability depends on bed rock cracks should not so much increase. Based on this assumption, the model parameter of the bottom hole, which is related to infiltration to aquifer, is fixed. The model parameters of the second and lower tanks are also fixed. And the variability of the model parameters of side holes of the first tank, which are related to direct discharge, is investigated. We obtained the results as the model parameters of the side holes have the tendency of decrease as 0.9 to 0.7[d^{-1}], during the research period. Next, using these model parameters, the test rainfall events are simulated and the following results were obtained. 1) The peak discharge volume is decreased. 2) The event based discharge rates f are decreased as 0.6 to 0.5. This trend is the almost same as the mentioned event based discharge rates with long-term hydrological data analysis. These results suggest the flood mitigation function is increased during this period. On the other hand, although the model parameter of the bottom hole is fixed, total infiltration volume to lower tanks and base flow are increased. This result suggests that water conservation to aquifer also increase without increasing of vertical permeability such as bed cracks. It can be explained as follows. Consider a simple tank has one side hole and one bottom hole. The discharge from the side hole q [mm/d] is defined as $q = ah$, where h [mm] is the storage depth of the tank, a [d^{-1}] is the side hole size. The infiltration from the bottom hole i [mm/d] is defined as $i = bh$, where b [d^{-1}] is the bottom hole size. The time variation of h is defined as $dh/dt = q - i$. We obtain the total infiltration volume I as $I = bC/(a+b)$, where C is a constant of integration. By the above equation, when a is decreased with fixed b, total infiltration is increased. Therefore, it is suggested that increasing of water conservation can be explained with lateral permeability depend on forest growth. Moreover, we simulated two cases about evapotranspiration. First case is considered evapotranspiration with Hammon equation, and second is not considered. Hammon equation estimates probability evapotranspiration based on air temperature and daylight time. The results with two cases are the almost same. It is suggested that influence of climate changes have less effect than other factors.

Keywords: water conservation function, climate change, percolation, tank model

Japan Geoscience Union Meeting 2014
(28 April - 02 May 2014 at Pacifico YOKOHAMA, Kanagawa, Japan)

ACG33-07 Room:418 Time:April 28 17:00-17:15

Canopy photosynthetic and soil respiratory responses to rising temperature in a cool-temperate deciduous forest

MURAOKA, Hiroyuki[1*] ; NOH, Namjin[1] ; NAGAO, Ayaka[1] ; SAITOH, Taku M.[1] ; KURIBAYASHI, Masatoshi[1] ; NODA, Hibiki M.[2] ; ITO, Akihiko[2] ; NAGAI, Shin[3] ; NAKAJI, Tatsuro[4] ; HIURA, Tsutom[4]

[1]Gifu University, [2]National Institute of Environmental Studies, [3]JAMSTEC, [4]Hokkaido University

Prediction of possible influences of global warming on terrestrial ecosystem structure and functions is one of an urgent research tasks in environmental sciences. This paper overviews our challenging research by open-field warming experiments on forest canopy photosynthetic productivity and on soil respiration in a cool-temperate deciduous broadleaf forest at Takayama AsiaFlux and JaLTER site, located on a mountainous landscape in central Japan. Canopy warming experiment is conducted by three open-top canopy chambers (OTCC) on branches of a mature tree of Quercus crispula, one of the dominant canopy species in the forest. The OTCC increased mean daytime air temperature by about 2 degree-C, with midday maximum of about 5 degree-C throughout the growing seasons. Soil warming treatment, with 3 degree-C higher than the control area, was made by installing electric heating cables below the soil surface.

Warming treatment at the canopy-top led (1) expansion of canopy photosynthetically active season in about 10 days by 3-5 days earlier leaf budbreak and expansion and about 5 days delay of leaf senescence, and (2) slightly higher chlorophyll content and photosynthetic capacity of oak leaves. Warming treatment of forest soil showed (1) higher soil respiration throughout the seasons, resulting in 15% higher CO2 efflux from the soil during the growing season, but (2) the temperature response of soil respiration acclimated to the higher temperature condition characterized by lower slope of the response curve. We also examined the possible effects of growing period length on forest canopy and understory vegetation ecosystem CO2 budget under future climate conditions by using canopy-phenology ecosystem carbon cycling combined model. Our simulation indicated that annual total ecosystem GPP, RE and NEP was greater under the future condition than under the current condition by 9-12 %, 9-13% and 12-17%.

Our study demonstrates that open-field warming experiments provide us with useful and insightful knowledge on the ecophysiological responses of both canopy and soil processes to rising temperature, and their critical roles in predicting future changes of forest carbon cycle processes in cool-temperate region in Japan where ecosystem structure, functions and services are subjected to influence of the climate change.

Keywords: global warming, forest, photosynthesis, soil respiration, phenology

Japan Geoscience Union Meeting 2014
(28 April - 02 May 2014 at Pacifico YOKOHAMA, Kanagawa, Japan)

ACG33-08 Room:418 Time:April 28 17:15-17:30

Effects of Open-top Chamber on Soil Oribatid Mites (Acari:Oribatida) at Mt. Kisokoma-gatake

FUKUYAMA, Kenji[1*] ; NAKAMURA, Hiroshi[1] ; KOBAYASHI, Hajime[1] ; TANAKA, Kenta[2]

[1]Faculty of Agriculture, Shinshu University, [2]Sugadaira Montane Research Center, University of Tsukuba

INTRODUCTION

Forest limit ecosystem on high mountains was one of the most vulnerable ecosystems against global warming. We investigated effects of artificial warming using an open-top chamber on forest limit ecosystem (2600m in elevation) of Mt. Kiso-komagatake, Chuo-alps, Nagano, central of Japan. Oribatid mites were useful environmental bio-indicator because they distribute most of all terrestrial soil habitats. Therefore, oribatid fauna were compared between artificial warming sites and control site in the study area. We investigate vertical distribution concerned with elevation of oribatid fauna from 2600m to 1250m. On the other hand, Mortality of oribatid species was investigated under different temperature in incubator.

METHOD

Research sites of vertical distribution were established at 1250m, 1700m, 1900m and 2100m above sea level in Nishikoma Station of Shinshu University. We selected two plots (coniferous forest and broad leaved forest) in each elevation site. Five soil samples were randomly corrected using core sampler (100cc) 5cm depth on 26 July 2012. Oribatid mites were corrected using the Tullgren funnel on same day. Additionally, two soil samples (about 400cc) were corrected at 1250m, 1400m, 1700m, 1800m, 1900m, 2000m, 2100m, 2200m and 2600m above sea level on 28 Aug. 2012.

Nine open-top-chambers (1m X 1m, about 2m in height) were established at 2650m above sea level near Mt. Shogigasira. Two soil samples (100cc, 5cm depth) were corrected using core sampler from each open-top-chamber on 20 Sept. 2013. Also two soil samples were corrected from control site close to each open-top-chamber. Two soil samples were set on one Tullgren funnel in laboratory on same day.

Soil samples (about 5000cc) were corrected from 2100m and 1250m above sea level in Nishikoma station of Shinshu University on 17 July 2013 and each soil sample was softly stirred by hand in laboratory and was divided in 15 nonwoven fabric bags (400cc). Each bag was set in unglazed pottery (11cm in diameter). Five potteries were incubated in incubator under 10 degrees centigrade, 20 degrees centigrade and 30 degrees centigrade from 17 July to 12 Aug. 2013.

RESULTS and DISCUSSION

Results of investigation of vertical distribution show that *Cyrtozetes* sp., *Tectocepheus velatus* and *Phthiracarus japonicus* positively increased their population densities correlated with elevation, and especially, *Cyrtozetes* was only found upper from 1900m above sea level.

Results of comparative study using the open-top-chamber show that *Cyrtozetes* and *Phthiracarus* in the open-top-chamber were significantly decreased instead of *Ghilarobizetes* significantly increased.

These results suggest that *Cyrtozetes* and *Phthiracarus* are good indicators for global warming monitoring in high mountain ecosystem.

On the other hand, mortality rate of *Cyrtozetes* and *Phthiracarus* were not affected by temperature from result of incubation one month after. The reason of no affection of temperature on *Cyrtozetes* is probably its long life cycle. More studies will be needed about it.

Keywords: oribatid mites, vertical distribution, global warming, bio-indicator, Cyrtozetes

Japan Geoscience Union Meeting 2014
(28 April - 02 May 2014 at Pacifico YOKOHAMA, Kanagawa, Japan)

ACG33-09 Room:418 Time:April 28 17:30-17:45

The parametric estimation of the amount of CO2 to be stored as HWP of the wooden house, based on the each of tree specie

TAKAMURA, Hideki[1*] ; ASANO, Yoshiharu[1]

[1]Faculty of Engineering, Shinshu University and Institute of Mountain Science, Shinshu University

In the term of the handling of wood in Kyoto Protocol, it has been considered to release carbon accumulated in growing stage immediately into atmosphere at the time of cutting down from forest in the first commitment period. In the second commitment period, it has been considered to fix carbon while it is used as harvest wood products (HWP), and to release carbon into atmosphere at discarded stage. The main utilization of domestic wood is to build wooden house domestically, and it has an important role as a carbon pool of HWP. However, the rate of utilization of domestic wood has been continued to decrease. In order to take concrete strategy to measure rate of increase in utilization of domestic wood in the future, it is important to estimate present amount of utilization by each of tree species and the amount of prospect for increased use in the future.

Future estimation of carbon pool by HWP for all over the country was studied in the past research. In the estimation for all over the country, national total gross floor space, the number of new constructions per year, the number of households, the amount of average for wood utilization are used as basic date, it has not been estimated by each of tree species. Therefore, in order to estimate target amount of increased utilization for each of tree species, it is urgent issue to make calculation flow based on area characteristic by using the amount of tree species used in each material by region, and the amount of carbon stock (hereinafter called carbon balance) for each of tree species by region.

In this study, it was investigated that estimation method of the amount of utilization by each of tree species and the amount of carbon stock which is applicable to wood statistics and all prefectures. Estimation, which is for Nagano, of the amount of utilization for each of tree species and the amount of carbon stock was conducted by using carbon balance for each of tree species in Nagano which was revealed by Yamagata et al. in the past research, and the rate of utilization for each of tree species which was surveyed by Nagano Prefecture.

As a result of estimation, it revealed that the amount of carbon stock would decrease with a peak of 380,000 [t-C] in 2021 (Heisei 33). From the increase in the total gross floor space in the whole area of Nagano by the increase in the average of gross floor space per house, the amount of carbon stock indicated an upward trend until 2021. However, the amount of carbon stock declined by the decrease in the number of new constructions per year and increase in the number of losses of existing houses in 2022 and later. In this research, we conducted the estimation of the case in which 60% of domestic wood utilization that Forestry Agency advocated as a measure against decrease in the amount of carbon stock was achieved. As a result of having changed the domestic wood utilization up to 60% in 2011 and later, the decrease in the amount of carbon stock was not seen until 2038 (Heisei 50).

The estimation revealed necessity to increase supply of domestic wood approximately 50,000m3 per year to achieve 60% of utilization rate for domestic wood. There is sufficient amount of accumulated forest resources in Nagano, however, it is necessary to secure supply capacity. Ido et al. pointed out that it is difficult to adjust the cut of timber from forest since it is difficult to show demand prospect. For this issue, the estimation of this study is very useful and contributes to increase distribution of domestic wood by feeding back the estimation result to supply side. Since there is a distribution of domestic wood between prefectures, it is necessary to estimate by the method of this study in other prefectures. It is important to create road map which raises rate of utilization of domestic wood by planning and grasping the wood distribution of the whole country by obtaining each demand prospect in the future.

Keywords: Kyoto Protocol, HWP, wooden house, carbon stock, domestic wood

Japan Geoscience Union Meeting 2014
(28 April - 02 May 2014 at Pacifico YOKOHAMA, Kanagawa, Japan)

ACG33-P01 Room:Poster Time:April 28 18:15-19:30

Snow patches of Japanese Alps last until late autumn 2013 and their past variations

ASAHI, Katsuhiko[1*]

[1]Institute of Mountain Science, Shinshu University

Variations in glaciers are visible indicators of climate change, especially in mountain region. In Japan, snow patch can be an alternate indicator since glaciers, long years, were not recognized in the Japanese Alps. One characteristic of the Japanese Alps is their extensive distribution of snow patch last until late autumn. A snow patch inventory for this mountain is urgently required, not only for monitoring snow patch variations but also to evaluate water reservoir in the region. Limited number of studies has attempted to complete snow patch atlas in Japan. As a step in this direction, the author has produced an inventory of snow patch lasts before winter 2013 at the entire area of the Japanese Alps. This study addresses the results of snow patch mapping 2013.

The work of compiling a perennial snow patch inventory for the Japanese Alps initially involved oblique aerial photographs taken from a charter flight throughout the Japanese Alps. These photographs were interpreted using a stereoscope. The photographs were taken on 7th and 10th October 2013. The planimetric outline of each perennial snow patch was manually delimited and drawn on 1:25 000 scale topographical maps and successfully compiled the complete set of snow patch inventory of the Japanese Alps in 2013. Then inventory of 2013 thus compiled reveals 579 snow patches with a total surface area of 3.66 km^2. The year 2013 distribution was much extensive rather than that of usual years. The lowest snow patch termini appeared at the altitude of 1070 m on Mt. Inu of the northern Japanese Alps and the southernmost was 35 ^{o} 40 $'$ 30.5 $''$ at Mt. Kita of the southern Japanese Alps. The largest one was the area of 0.184km^2 on Mt. Karamatsu of the Northern Japanese Alps. Ca. 80% of them locate east-facing slopes, where leeward side against winter prevailing NW wind. Latitudinal profile of the terminus altitudes of snow patches shows northward gradients. Winter northwesterly blown from the Siberian High, collecting vapor from warm current on the Sea of Japan, bring orographic heavy snowfall to the northern part of the Japanese Alps. Thereafter, peculiar snow patch distribution last before winter is likely to be a ruling by maldistribution of snowfall in winter.

In the same area, the inventory of 1976/77, compiled by the vertical aerial photograph interpretation, counts 264 with the area of 2.48 km^2. Major distribution concentrated in Mts. Tsurugi and Tateyama, central part of the Northern Japanese Alps. The total area in this mountains were 0.78, 0.77, 0.58, 0.84 km^2 in 1969, 1977, 2009, and 2013, respectively. Snowfall amount in winter and the snow patch area fluctuate largely year-by-year. However, the area fluctuation limits within a range of 30% the total area.

Keywords: Year 2013, Perennial snow patch, Japanese Alps, Snow patch inventory, Aerial photograph

Japan Geoscience Union Meeting 2014
(28 April - 02 May 2014 at Pacifico YOKOHAMA, Kanagawa, Japan)

ACG33-P02 Room:Poster Time:April 28 18:15-19:30

Effects of forest harvesting on winter microcrimate and sedmiment movements in mountainous area

IMAIZUMI, Fumitoshi[1*] ; NISHII, Ryoko[2] ; UENO, Kenichi[2] ; KUROBE, Kousei[3]

[1]Graduate Shool of Agriculture, Shizuoka University, [2]Faculty of Life and Environmental Sciences, University of Tsukuba, [3]Graduate School of Life and Environmental Sciences, University of Tsukuba

Activities of periglacial processes are controlled by the hillslope microclimate (i.e., air and ground temperatures, ground water content) that is highly affected by land cover conditions. Thus, forest harvesting in periglacial areas possibly affects activities of sediment movement (i.e., soil creep, dry ravel) by changing the microclimate of hillslopes. Knowledge on the effect of forest harvesting on sediment movement are needed to protect aquatic ecosystems as well as to develop better mitigation measures for preventing sediment disasters. We also observed difference in the microclimate as well as sediment movement between harvested and non-harvested artificial forests in a periglacial area. The field observation was conducted in Ikawa University Forest, University of Tsukuba, in southern Japanese Alps. In this region, air temperature frequently rises above and falls below 0 degree in winter. Forest harvesting changed both temperature and water condition of hillslopes; diurnal fluctuations in the ground surface temperature in the harvested area (about 15 degree) were much larger than that in the non-harvested area (about 3 degree). In the period without rainfall, water content ratio of soil in the harvested area was lower than that in the non-harvested area. Difference in the freezing and thawing frequency between the harvested and the non-harvested area was also observed by interval cameras. In the period without snow cover, diurnal frost heave was observed almost everyday in the harvested area. In contrast, diurnal frost heave in the non-harvested was observed only several times in one winter. Consequently, forest harvesting changes both microclimate and activities of periglacial processes. Meanwhile, the volume of sediment captured by sediment traps was not clearly different between the harvested and the non-harvested areas. In the harvested area, we found that a large volume of sediment was captured by litters and branches of harvested trees left on the hillslopes. Therefore sediment supply rate from harvested area may be also affected by other factors, such as existence of litters and branches on the ground surface.

Keywords: freeze-thawing, sediment movement, soil creep, frost heave, dry ravel, forst harvesting

Japan Geoscience Union Meeting 2014
(28 April - 02 May 2014 at Pacifico YOKOHAMA, Kanagawa, Japan)

ACG33-P03 Room:Poster Time:April 28 18:15-19:30

Spatial and temporal changes in soil respiration in an old-growth forest on the slope of Mt Hakusan

OHTSUKA, Toshiyuki[1*] ; SUCHEWABORIPONT, Vilanee[1] ; IIMURA, Yasuo[2] ; YOSHITAKE, Shinpei[1]

[1]Gifu University, River basin research center, [2]University of Shiga Prefecture, School of Environmental Science

Structure and function of cool-temperate beech forests have been dramatically altered by disturbance. Especially in old-growth forests, canopy disturbance has important influences on the structure and organization of forest communities. As a result, the complexity of forest structure affects the spatial difference in micro-environmental factors such as soil temperature and soil water content. Therefore, the spatial and temporal changes in soil respiration were studied using soda lime in 1-ha study site, and automated open-close chamber using IRGA (AOCC method) in canopy and gap areas in 2013 in an old-growth beech forest, Mt Hakusan. The spatial pattern with the different vegetation and micro-environmental factors showed the high efflux in canopy and the low efflux in gap. All soil effluxes increased from spring (Jun.-Jul.) to summer (Aug.), and then decreased in autumn (Sep.-Nov.). The seasonal pattern showed the hysteresis loop that soil respiration in spring was greater than that at the same temperature in autumn. Diel soil efflux was greatly controlled by soil temperature but a diel lag between soil respiration and soil temperature led to diurnal hysteresis loop in some season.

Keywords: Soil respiration, cool-temperate region, old-growth forests, carbon cycling, beech forests

Japan Geoscience Union Meeting 2014
(28 April - 02 May 2014 at Pacifico YOKOHAMA, Kanagawa, Japan)

ACG33-P04 Room:Poster Time:April 28 18:15-19:30

Spatial distribution of soil microbial characteristics in a cool-temperate deciduous broad-leaved forest in Takayama

YOSHITAKE, Shinpei[1*] ; YOSHITAKE, Ayako[1] ; IIMURA, Yasuo[2] ; OHTSUKA, Toshiyuki[1]

[1]Gifu University, River Basin Research Center, [2]The University of Siga Prefecture, School of Environmental Science

1. Introduction

Heterotrophic microorganisms have an important role in nutrients cycling and soil formation through the organic matter decomposition. Therefore, it is important to clarify the spatiotemporal variation in quantitative and qualitative characteristics of soil microbial community and the factor(s) affecting such spatiotemporal variation in considering the matter cycling. Takayama Field Station of Gifu University has studied carbon cycling in a cool-temperate deciduous forest for long term and have clarified that various ecological processes such as soil respiration showed significant spatiotemporal variation. However, the information of soil microbial community is largely limited and especially, the spatial variation of microbial characteristics and factors affecting it still remain unclear. Then, we aimed to describe the spatial distribution of microbial characteristics and clarify the relationships between spatial distribution and environmental factors.

2. Materials and Methods

Our study site was cool-temperate deciduous broad-leaved forest on the northwestern slope of Mt. Norikura, central Japan. The site was dominated by oak (*Quercus crispula*) and birch (*Betula ermanii*, *B. Platyphylla*) and the forest floor is covered with a dense dwarf bamboo (*Sasa senaninsis*) community. A permanent plot of 1 ha was set on a west-facing slope and 100 subplots (each 10 m$\times$10 m) are distributed along five microtopographic type: ridge (30), northern slope (25), valley bottom (19), southern slope (19) and western slope (7) (Fig.1). Litter (L layer) and mineral soil (0-5 cm of A layer) samples were collected from 100 subquadrat on early May 2013. Some soil properties (e.g., water content, pH, NH_4^+-N, NO_3^--N) were determined. Microbial respiration rate from mineral soil sample was determined by open-flow method with infrared gas analyzer in laboratory condition.

3. Results, Discussion and future plan

Average value of microbial respiration rate per gram soil was significantly differed among five topographic types (one-way ANOVA, P <0.01) and that in ridge (3.6$\pm$0.81 μg CO_2-C g^{-1} h^{-1}) was significantly higher than that in valley bottom (2.9$\pm$0.78 μg CO_2-C g^{-1} h^{-1}) (Tukey-Kramer test, P <0.05). In this poster presentation, the effects of topography on microbial respiration rate will be discussed based on the differences in environmental factors such as soil water content, litter amount, and soil carbon and nitrogen contents. In addition, soil microbial biomass and community structure will be determined for collected mineral soil samples by phospholipid fatty acid (PLFA) analysis in near future and spatial distribution of microbial biomass, community structure, and respiration activity (respiration rate per biomass) will be clarified.

Keywords: a cool-temperate deciduous broad-leaved forest, soil microbial community, microtopography, microbial respiration rate

Japan Geoscience Union Meeting 2014
(28 April - 02 May 2014 at Pacifico YOKOHAMA, Kanagawa, Japan)

ACG33-P05 Room:Poster Time:April 28 18:15-19:30

Global pattern of gene flow in plant species along altitudinal gradients on mountains

HIRAO, Akira[1*]

[1]Sugadaira Montane Research Center, University of Tsukuba

Several studies on mountain plants with wide-altitudinal distributions have found significant genetic differentiation and structuring among populations along altitudinal gradients. In most of the studies, however, the level of genetic differentiation was not highly remarkable. This is somewhat counterintuitive, since one would expect that mountainous species often exhibit heterogenous environments and phenological differences along altitudinal gradients, which should be forces driving genetic differentiation. Understanding how gene flow corresponds with altitudinal gradients can inform process of the genetic structuring. I reviewed published studies to categorize global patterns of gene flow in mountainous plant species. These outcomes can depend on 1) isolation by distance, 2) mobility within similar altitudes, and 3) mobility among dissimilar altitudes, and imply evolutionary processes of the plant populations on mountains.

Keywords: altitudinal gradients, gene flow, genetic differentiation, plants

Japan Geoscience Union Meeting 2014
(28 April - 02 May 2014 at Pacifico YOKOHAMA, Kanagawa, Japan)

ACG34-01 Room:213 Time:May 1 14:15-14:45

Frontier of using stable water isotopic information in studies on land-ecological, hydrological, and atmospheric process

YOSHIMURA, Kei[1*]

[1]Atmosphere and Ocean Research Institute, The University of Tokyo

In this study, it was clearly shown that vapor isotope data retrieved by satellite sensors or in situ monitoring networks have the potential to constrain the atmospheric fields. The results of this study can be applied in two directions. The first direction is a better analysis skill in current weather forecasting systems. Though our understanding of the atmosphere is improving, understanding the hydrological cycles of the mid- to upper troposphere and lower stratosphere in association with convective clouds remains difficult. Because it is apparent that water vapor isotopic information has unique characteristics with regard to the atmospheric hydrological cycle and technical improvements in satellite and in situ instruments are occurring rapidly, this direction is indeed quite promising. The second direction, regarding proxy data assimilation, is even more challenging and is significant in several disciplines. In the past, we lacked direct measurements of the Earth and were forced to rely on proxy data. Interpretation of proxy data is important but can be over-simplified. By using data assimilation for proxy data, an objective analysis of the past (specifically before the nineteenth century) can be achieved without simplifying the empirical relationship between proxy data and climate/environment information. Although there are many technical and theoretical obstacles in both directions, the authors strongly believe that scientific benefits can be achieved.

Keywords: stable water isotope ratio, data assimilation, hydrologic cycle, climate proxy, climate reanalysis, spectroscopic analysis

Japan Geoscience Union Meeting 2014
(28 April - 02 May 2014 at Pacifico YOKOHAMA, Kanagawa, Japan)

ACG34-02 Room:213 Time:May 1 14:45-15:15

Significance of hyper spectral solar radiation observation

KUME, Atsushi[1*] ; AKITSU, Tomoko[2] ; NASAHARA, Kenlo[2]

[1]Ashoro Research Forest, Kyushu University, [2]Faculty of Life and Environmental Sciences, University of Tsukuba

Land plants exhibit relatively weak absorbance of green light at around 550 nm, for reasons which remain elusive. Most research, however, has assumed that the solar radiation spectrum can be averaged without considering the spectral dynamics. The relations between the spectrum of incident radiation and light-harvesting pigments of organisms are crucial to understanding photosynthesis and light use efficiency. Although several light-harvesting pigments exist, most land plants use specific light harvesting chlorophylls, Chl a and Chl b, and carotenoids. Wavelengths longer than 700 nm or shorter than 400 nm are scarcely absorbed by chlorophylls, and cannot be used for photosynthesis. Radiation within the 400 to 700 nm waveband is defined as photosynthetically active radiation (PAR). However, chlorophylls do not absorb photons in the PAR waveband evenly. Only a few per cent of relative absorbance occurs in the green region (500 to 600 nm), nevertheless the photosynthetic quantum yields are equivalent to those from blue and red light.

Incident PAR comprises two main components, direct PAR (PARdir), which arrives directly from the sun, and diffuse PAR (PARdif), which is sunlight scattered by sky and clouds. These components are characterized by large differences in light quantity, directional characteristics and spectral quality. PARdir is highly directional and its energy can be concentrated and localized on a surface. PARdif is non-directional and its incident energy is well-averaged across a surface, allowing it to penetrate deeper into canopies. Consequently, PARdir and PARdif play different roles in the photosynthetic process both at the scale of individual leaves and of canopies. Most research, however, has assumed that the solar radiation spectrum can be averaged without considering the spectral and directional dynamics.

We had developed a precise solar tracking device for detecting direct and diffuse radiation. Direct and diffuse radiations were measured separately by two grating spectroradiometers (MS700, EKO Instruments Co. Ltd., Tokyo, Japan) fixed to sun trackers (STR-22G-S, EKO Instruments Co. Ltd.) equipped with a collimation tube (angle of view 5 degrees) for measurement of PARdir, and a shadow ball for measurement of PARdif.

Analyzing the relative absorption spectra of chlorophyll, we found that Chl a does not absorb direct solar radiation, while diffuse solar radiation is efficiently up-taken by Chl b. The spectrum of diffuse solar radiation is almost fixed with a peak wavelength (λmax) around 460 nm. However, that of direct solar radiation shifts from a broad peak with λmax around 700 nm towards a narrower peak around 540 nm, as solar zenith angle decreases. The absorption spectrum of Chl a lies outside the strongest energy regions of direct solar radiation. The λmax of the Chl b absorption spectrum matches that of diffuse solar radiation; therefore, Chl b can absorb the most energetic parts of this radiation. The spectral differences between direct and diffuse solar radiation elucidate the meaning of slight spectral differences in pigments for terrestrial organisms.

Strong light is known to enhance accumulation of carotenoids. We found that β-carotene consistently absorbed more energy per photon than other pigments, indicating that it effectively filters (i.e. accepts) the 350-500 nm waveband, independently of PAR class.

Overall, the spectral differences between PARdir and PARdif, as well as the steady λmax of PARdif, exert multiple effects on terrestrial organisms and may be effective drivers of diversification in pigment distribution and function. Further spectral-directional radiation observation at various sites is needed to reveal the effects of the dynamics of incident solar radiation on the terrestrial ecosystem.

Keywords: spectroradiomater, direct solar radiation, diffuse sky radiation, photosynthesis, spectral light use efficiency, PAR

Japan Geoscience Union Meeting 2014
(28 April - 02 May 2014 at Pacifico YOKOHAMA, Kanagawa, Japan)

ACG34-03 Room:213 Time:May 1 15:15-15:30

Simultaneous Estimation of Hydrologic and Ecologic Parameters in an Eco-Hydrological Model Assimilating Microwave Signal

SAWADA, Yohei[1*] ; KOIKE, Toshio[1]

[1]School of Engineering, the University of Tokyo

To improve the skill of reproducing land-atmosphere interactions in weather, seasonal, and climate prediction systems, it is necessary to simulate correctly and simultaneously the surface soil moisture (SSM) and terrestrial biomass in land surface models. Despite the performance of hydrological and ecosystem models depends highly on parameter calibration, a method for parameter estimation in ungauged areas has yet to be established. We develop an auto-calibration system that can simultaneously estimate both hydrological and ecological parameters by assimilating a microwave signal that is sensitive to both SSM and terrestrial biomass. This system comprises a hydrological model that has a physically based, sophisticated soil hydrology scheme, a dynamic vegetation model that can estimate vegetation growth and senescence, and a radiative transfer model that can convert land surface condition into brightness temperatures in the microwave region. By assimilating microwave signals from the Advanced Microwave Scanning Radiometer for Earth Observing System, the system simultaneously optimizes the parameters of these models. We test this approach at three in situ observation sites under different hydroclimatic conditions. Estimated SSM and leaf area index (LAI) exhibit good agreement with ground in situ observed SSM and satellite observed LAI, respectively. The root mean square error of SSM and LAI at all sites, estimated by the model with optimized parameters, is much less than that estimated by the model with default parameters. Using microwave satellite brightness temperature data sets, this system offers the potential to calibrate parameters of both hydrological and ecosystem models globally. This global-scale and automated parameter optimization system may contribute to many other research activities related to land surface, hydrological, and ecosystem modelling although the global-scale applicability of this approach should be investigated as a future work.

Keywords: Eco-hydrological model, passive microwave remote sensing, parameter optimization, data assimilation

Japan Geoscience Union Meeting 2014
(28 April - 02 May 2014 at Pacifico YOKOHAMA, Kanagawa, Japan)

ACG34-04 Room:213 Time:May 1 15:30-15:45

Changes of permafrost environment and the response to the long term climate change

SUEYOSHI, Tetsuo[1*] ; SAITO, Kazuyuki[1] ; ISHIKAWA, Mamoru[2] ; HARADA, Koichiro[3] ; IWAHANA, Go[4]

[1]Japan Agency for Marine-Earth Science and Technology, [2]Hokkaido University, [3]Miyagi University, [4]University of Alaska

Permafrost is soil and sediment that is frozen more than two consecutive years, most of which is located in high latitudes. Ground ice is not always present, as may be in the case of nonporous bedrock, but it frequently occurs and it may be in amounts exceeding the potential hydraulic saturation of the ground material. Permafrost accounts for 0.022% of total water and exists in 24% of exposed land in the Northern Hemisphere.

permafrost contains 1700 billion tons of organic material equaling almost half of all organic material in all soils. This pool was built up over thousands of years and is only slowly degraded under the cold conditions in the Arctic.

Most of the permafrost existing today formed during cold glacial periods, and has persisted through warmer interglacial periods, including the Holocene. The time scale of the thermal process is different depending on the depth (i.e. distance from the ground surface) and the soil thermal properties, while the vegetation processes such as accumulation of organic material have yet different time scales.

In this presentation, we discuss those complex character of permafrost and show the outlook on the future research needs, showing an example study on the relationship between permafrost distribution and long-term climate change.

Keywords: Permafrost, climate change, ground ice, Carbon Cycle

Japan Geoscience Union Meeting 2014
(28 April - 02 May 2014 at Pacifico YOKOHAMA, Kanagawa, Japan)

ACG34-05 Room:213 Time:May 1 15:45-16:00

Impacts of representation of stomatal conductance on vegetation distribution and functions under changing climate

SATO, Hisashi[1*] ; KUMAGAI, Tomo'omi[2] ; KATUL, Gabriel[3]

[1]RIGC, JAMSTEC, [2]HyARC, Nagoya University, [3]Duke University

Stomata reponce is under control of light intensity, CO2 concentration, vapor pressure deficit, leaf water potential. For describing stomatal responses to such environmental factors, several empirical and semi-empirical models have been developed. How these models response to the changing environmental is an important issue, because between 80% and 90% of the total evapotranspiration from the land surface is caused by transpiration, and the process consumes almost half of the solar energy absorbed by the ground (Jasechko et al. 2013).

Here, we examined how representation of stomatal conductance pose impact on the forecast of geographical distribution of vegetation and its functions (i.e. carbon and water fluxes) under the forecasted climatic condition during the 21st century. We studied the African continent, because Africa is a useful target for assessing changes in vegetation due to climate change. The distribution of African vegetation is primarily regulated by soil moisture availability and thus is tightly coupled with climatic variability. For our study, we employed a dynamic vegetation model SEIB-DGVM. Our previous study shows that the model reproduced geographical distributions of the continent's biomes, annual gross primary productivity (GPP), and biomass over the African continent under current climatic conditions (Sato et al. 2012).

References

Jasechko S, Sharp ZD, Gibson JJ, Birks SJ, Yi Y & Fawcett PJ (2013) Terrestrial water fluxes dominated by transpiration. Nature 496.

Kumagai, T., Katul, G. G., Porporato, A., Saitoh, T. M., Ohashi, M., Ichie, T. and Suzuki, M. (2004) Carbon and water cycling in a Bornean tropical rainforest under current and future climate scenarios. Advances in Water Resources, 27(12), P1135-1150.

Sato H & Ise T (2012) Effect of plant dynamic processes on African vegetation responses to climate change: Analysis using the spatially explicit individual-based dynamic global vegetation model (SEIB-DGVM). Journal of Geophysical Research-Biogeosciences 117.

Keywords: Stomatal Conductance, Hydrological Cycle, Carbon Cycle, Dynamic Global Vegetation Models, Global Warming, Africa

Japan Geoscience Union Meeting 2014
(28 April - 02 May 2014 at Pacifico YOKOHAMA, Kanagawa, Japan)

ACG34-06 Room:213 Time:May 1 16:15-16:30

Overview for terrestrial model intercomparison project in Arctic

MIYAZAKI, Shin[1*] ; SAITO, Kazuyuki[2] ; YAMAZAKI, Takeshi[4] ; ISE, Takeshi[3] ; MORI, Junko[1] ; ARAKIDA, Hazuki[5] ; HAJIMA, Tomohiro[2] ; HOSAKA, Masahiro[6] ; IIJIMA, Yoshihiro[2] ; ITO, Akihiko[7] ; MATSUURA, Yojiro[8] ; NIWANO, Masashi[6] ; O'ISHI, Ryouta[1] ; OHTA, Takeshi[9] ; PARK, Hotaek[2] ; SATO, Atsushi[10] ; SUEYOSHI, Tetsuo[2] ; SUGIMOTO, Atsuko[11] ; SUZUKI, Rikie[2] ; YAMAGUCHI, Satoru[10] ; YOSHIMURA, Kei[12]

[1]National Polar Research Institute, [2]Japan Agency for Marine-Earth Science and Technology, [3]Tohoku University, [4]University of Hyogo, [5]RIKEN, [6]Metorological Research Institute, [7]National Institute for Environmental Studies, [8]Forestry and Forest Products Research Institute, [9]Nagoya University, [10]National Research Institute for Earth Science and Disaster Prevention, [11]Hokkaido University, [12]The University of Tokyo

1. Introduction

The goals of the modeling group in the terrestrial research project of the GRENE Arctic Climate Change Research Project (GRENE-TEA) are to a) feed to the CGCM research project for the possible improvement of the physical and ecological processes for the Arctic terrestrial modeling (excl. glaciers and ice sheets) in the extant terrestrial schemes in the coupled global climate models (CGCMs), and b) lay the foundations of the future-generation Arctic terrestrial model development. To achieve these goals we are to conduct a model intercomparison project among the participating models, in which we will utilize the GRENE-TEA site observations data (stage 1) and GCM outputs (stage 2) for driving and validating the models. This project (GTMIP) is designated to 1) enhance communications and understanding of the "mind and hands" between the modeling and field scientists, 2) assess the uncertainty and variations stemmed from the model implementation/designation, and the variability due to climatic and historical conditions among the Arctic sites.

2. Data and models for GTMIP

At the stage 1, we will create data for forcing and validating the terrestrial model based on the extant and/or new observation data at GRENE-TEA sites to evaluate the inter-model and inter-site variations. However, the observation data are prone to missing or lack of the necessary variables or parameters to drive the model. Therefore, we create continuous forcing data (Ver. 0) taken from the reanalysis product (i.e. NCEP/NCAR) with the bias correction using the CRU data at the nearest grid to the GRENE-TEA sites. Then, it is merged with the observation data to create site-fit continuous data (Ver. 1) for each GRENE-TEA site (Fairbanks in Alaska, Yakutsk, Tiksi, Tura and Chokurdakh in Russia, Kevo in Finland). These data will be open at Arctic Data Archive System (https://ads.nipr.ac.jp/index.html).

The GTMIP participating models include a land surface model (MATSIRO, 2LM, CHANGE, HAL), a material cycle model (VISIT), a terrestrial ecological model (STEM-NOAHbgc), a dynamic vegetation model (SEIB-DGVM), a regional climate model (WRF), physical snow models (SNOWPACK, SMAP), and a permafrost model (FROST). The models enabled to couple with the CGCMs and regional climate model (RCM) consist of the 70% of the all participating models.

3. Results

The Ver. 0 data was compared with site observations near Fairbanks, Alaska, USA, to evaluate its reliability. The daily mean air temperature was well-reconstructed but the diurnal variation was underestimated. The total annual precipitation was close to the observed, but summer (DOY150-250) rain tended clumpy.

The observed ground temperature (Tg) at near surface showed the zero-curtain, while the simulated Tg failed to produce the zero-curtain except for 2LM. The 2LM reproduced the observed snow depth well while the CHANGE and MATSIRO-r showed later start and end of snow cover with lower snow depth than observed. The sensible heat flux was the dominant component of the energy budget in the simulation by 2LM. The daily net ecosystem exchange (NEE) simulated by CHANGE showed the large carbon uptake in summer. The annual gross primary production (GPP) simulated by CHANGE increased during 1988 to 2011. The simulated GPP by SEIB-DGVM using Tg by MATSIRO-r was similar to the GPP using air temperature. The wood biomass and grass biomass simulated by SEIB-DGVM using air temperature and Tg by MATSIRO-r was similar while it was lower when calculated using Tg by MATSIRO-c. The soil organic matter (SOM) simulated by SEIB-DGVM using MATSIRO-r was largest among the SOM using air temperature and Tg by MATSIRO-c.

Keywords: Arctic, Terrestrial model, Snow cover, Permafrost

Japan Geoscience Union Meeting 2014
(28 April - 02 May 2014 at Pacifico YOKOHAMA, Kanagawa, Japan)

ACG34-07 Room:213 Time:May 1 16:30-16:45

The assessments of projection uncertainties of global C budget in ISI-MIP study

NISHINA, Kazuya[1*] ; ITO, Akihiko[1] ; KATO, Etsushi[1] ; YOKOHATA, Tokuta[1] ; ISI-MIP, Team[2]

[1]National Institute for Environmental Studies, [2]ISI-MIP team

Global net primary production (NPP), vegetation biomass carbon (VegC), and soil organic carbon (SOC) changes estimated by six global vegetation models (GVMs) obtained from an Inter-Sectoral Impact Model Intercomparison Project study were examined. Simulation results were obtained using five global climate models (GCMs) forced with four Representative Concentration Pathway (RCP) scenarios. To clarify which component (emission scenarios, climate projections, or global vegetation models) contributes the most to uncertainties in projected global terrestrial C cycling by 2100, we applied analysis of variance (ANOVA) and wavelet clustering to 70 projected simulation sets. ANOVA revealed that the main sources of uncertainty are different among variables and depend on the projection period. We determined that in the global SOC and VegC projections, GVMs dominate uncertainties (90% and 60%, respectively) rather than climate driving scenarios, i.e., RCPs and GCMs. The clustering wavelet spectra of VegC and SOC time series data could identify more specific characterization of simulations in each GVM. Our study suggests that the improvement of GVMs is a priority concern for reduction of total uncertainties in projected C cycling for climate impact assessments.

Keywords: Model inter-comparison, Global carbon cycle, Uncertainties, RCP, GCM

Japan Geoscience Union Meeting 2014
(28 April - 02 May 2014 at Pacifico YOKOHAMA, Kanagawa, Japan)

ACG34-P01 Room:Poster Time:May 1 18:15-19:30

An aerosol correction algorithm to improve the GOSAT TANSO-CAI NDVI product

KIKUCHI, Nobuhiro[1*] ; YOKOTA, Tatsuya[1]

[1]National Institute for Environmental Studies

The Cloud and Aerosol Imager TANSO-CAI (CAI), onboard the Greenhouse gases Observing SATellite (GOSAT), is equipped with 4 spectral bands of 380, 674, 86,0 and 1600 nanometers (Band 1-4). The main purpose of CAI is to assist the Fourier Transform Spectrometer TANSO-FTS in retrieving accurately the column amount of carbon dioxide and methane by detecting and characterizing clouds and aerosols in FTS footprints. CAI is also designed to monitor the variation of global vegetation indices, and the CAI Normalized Difference Vegetation Index (NDVI) product has already been released.

Since GOSAT is orbiting with a three-day recurrence, CAI observes the same location from the same direction once in every three days. Unlike the MODIS NDVI product, this makes it difficult to correct the effects of Bidirectional Reflection Distribution Function (BRDF) on the CAI NDVI product, but it has a potential capability to detect changes in vegetation with shorter time scale. In the current version, the CAI NDVI is calculated from 30 days composite of the minimum reflectance to minimize contamination of clouds and aerosols, and the effect of aerosols is not explicitly corrected. The goal of this study is to develop an aerosol correction algorithm that can be applied to the CAI NDVI.

Due to the relatively limited number of spectral bands of CAI, we take an approach slightly different from so-called the Kaufmann method or the minimum reflectance method in developing our aerosol correction algorithm. Since the number of observables is four, which are TOA reflectance at bands 1-4, the maximum number of retrieved parameters is also four. We choose optical thickness of fine mode aerosols and coarse mode aerosols, surface reflectance at band 3 and band 4 as retrieved parameters. We assumed that surface reflectance at band 1 and band 2 is expressed as a function of surface reflectance at band 3 and band4. The parameterization of band 1 and band 2 surface reflectance is done by utilizing the CAI minimum reflectance product. We do not expect that this parameterization is rigorously valid in pixel-wise. Therefore, we do not determine aerosol optical thickness for every pixel, but for 10x10 pixels (5x5 km in horizontal scale). Moreover, we do not use all TOA reflectance of 10x10=100 pixels, but select the darkest 10 pixels. Then, the number of observables is 40, and the number of retrieved parameters is 22, which can be determined by least-square fitting.

Left panel of the figure shows optical thickness of fine mode aerosol over souse-east part of Australia on October 20th, 2013. Currently, aerosol optical thickness is not retrieved for pixels with TOA reflectance greater than 0.2 at band 4. Right panel of the figure demonstrates the effect of aerosols on NDVI by comparing NDVI with and without aerosol correction. We can see that the frequency distribution of NDVI is shifted by about 0.1 as a result of aerosol correction, which is consistent with the result of Vermote et al. (2002).

Keywords: vegetation index, retrieval method, GOSAT

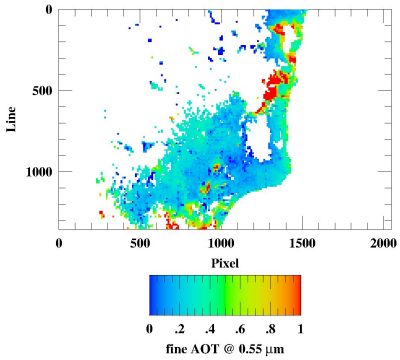

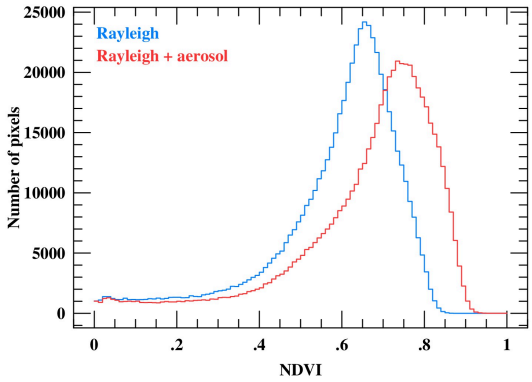

Japan Geoscience Union Meeting 2014
(28 April - 02 May 2014 at Pacifico YOKOHAMA, Kanagawa, Japan)

ACG34-P02 Room:Poster Time:May 1 18:15-19:30

Effects of water stresses due to climate change on production and dynamics of tree community in tropical rain forests

FUJII, Shinjiro[1*] ; SATO, Hisashi[2] ; KUMAGAI, Tomo'omi[1]

[1]Hydrospheric Atmospheric Research Center, Nagoya University, [2]Graduate School of Environmental Studies, Nagoya University

Recently, climate changes caused by the El Nino-Southern Oscillation have been reported to result in the widespread death of trees due to droughts in many parts of the world. Strong reductions in tree growth and litterfall production occurred during the record-hot 1997/98 El Nino. Tropical regions receive strong solar radiation, and tropical vegetation shows a strong feedback effect to carbon sequestration, water circulation, and climate formation. In addition, tropical forests are important ecosystems, and they act as a huge carbon sink because they accumulate 40-50% of land vegetation carbon of the Earth. In a biological community such as a tropical forest that consists of various species, response to changes in the physical environment depends on the operating functional group. A dynamic change in a particular functional group that plays a signi?cant role in the biological community may in?uence the structure and ecosystem functions of the tropical forests. The aim of this study is to predict the impact of drought on matter production and tree community dynamics in tropical rain forests by using a spatially explicit individual-based biogeochemical model developed for predicting vegetation dynamics in response to climate change at the global level, such as global warming (SEIB-DGVM). In the model simulation, applying stochastic rainfall model with the meteorological data, including the 1997/98 El Nino, of the tropical rain forests of Sumatra Island in Malaysia that were measured in 1997-2009, the rainfall experiments were performed by operating some parameters related to daily precipitation and frequency of rainfall events. Based on the experiment results, the turn of production with the amount of tree growth and death, and tree mortality dynamics in the tropical rain forests for 200 years were verified.

Keywords: drought, water stress, El Nino, tropical rain forests, matter production, SEIB-DGVM

Japan Geoscience Union Meeting 2014
(28 April - 02 May 2014 at Pacifico YOKOHAMA, Kanagawa, Japan)

ACG34-P03 Room:Poster Time:May 1 18:15-19:30

Modeling Interactions between Vegetation and Aeolian Processes

BANZRAGCH, Nandintsetseg[1*] ; SHINODA, Masato[1] ; SHAO, Yaping[2]

[1]Arid Land Research Center, Tottori University, [2]Institute for Geophysics and Meteorology

The sustainability of temperate grassland (TGs) ecosystems is determined by the feedbacks between climate, vegetation and human activities, in which Aeolian processes play a key role. Current existing dust models do not have sufficient capability in simulating vegetation growth and decay effects that play a major role in TG aeolian processes. In this study, we purposed to couple the DAYCENT, a vegetation-growth and nutrient-cycle model (the most prominent biogeochemical model), with QF2003, a wind-erosion model. The DAYCENT-QF2003 modeling system enables an examination of the feedbacks between grassland-grazing and aeolian processes. This approach is a completely new approach. First, we assessed the DAYCENT for its capability to provide estimations of vegetation dynamics under different grazing conditions in order to incorporate into the QF2003. DAYCENT was parameterized with the field experiment data (soil physical/chemical properties, vegetation and grazing) at the Bayan-Unjuul (BU) site in 2010-2012. BU is located in north of the most frequent dust outbreak region in Mongolia. Results showed that the DAYCENT could simulate realistically vegetation growth-decay, nutrient-cycle and the effect of grazing on grasslands, which are the factors controlling dust outbreaks in TGs. Then, the DAYCENT model was coupled into the QF2003 wind-erosion scheme. We conducted the numerical test of the coupled DAYCENT-QF2003 model to predict dust flux. With the initial results, we have demonstrated the potential of the DAYCENT-QF2003 coupled model. Therefore, the integrated DAYCENT-QF2003 modeling system will provide a useful tool for an early warning system and the future projection of dust events over dust source areas in TGs region.

Keywords: Temperate grassland, dust, vegetation, model

Japan Geoscience Union Meeting 2014
(28 April - 02 May 2014 at Pacifico YOKOHAMA, Kanagawa, Japan)

ACG35-01 Room:421 Time:April 28 14:15-14:30

Effects of water and dissolved material exchanges between land and ocean on coastal ecosystem and fishery resources

TANIGUCHI, Makoto[1*]

[1]Research Institute for Humanity and Nature

There are two pathways of water and dissolved materials from land to the ocean. The first one is river discharge and another is invisible submarine groundwater discharge (SGD). Many studies show the importance of SGD on coastal ecosystem and fishery resources. SGD is evaluated by using seepage meters and piezometers at local point scale, radon and strontium isotopes as tracers in bay scale to identify the origin of the fresh water, which is river water or groundwater. Another method is resistivity measurement which can tell us the salinity of the pore water in the sea bed near the coastal zone.

SGD observed by seepage meter and Rn concentration of the coastal seawater has a positive relationship over the world with different geology, geomorphology, and hydro-meteorological conditions. All SGD studies show that there are two components in SGD, one is fresh SGD and another is recirculated SGD. It is important for understanding coastal ecosystem and fishery resources to evaluate the ratios and processes of fresh SGD which is driven by hydrological condition in land, and recirculated SGD which is driven by oceanographic conditions in the sea.

In this study, SGD studies by using seepage meter and radon measurements over the world are reviewed to evaluate the physical and chemical factors which drive SGD and material transports by SGD, and the effects of SGD on the distribution of the fishery resources such as shell distributions in the coastal zone. River discharge is a main linkage between land and ocean through water and dissolved material transports, however it has huge temporal changes. On the other hands, the amount of SGD itself is not much but continuous contribution by SGD with constant temperature and nutrient discharges make stable physical, chemical, then biological conditions such as sea grass (Zostera bed).

Keywords: submarine groundwater discharge, coastal ecosystem, coastal fishery resources, nutrients, seepage, radon

Japan Geoscience Union Meeting 2014
(28 April - 02 May 2014 at Pacifico YOKOHAMA, Kanagawa, Japan)

ACG35-02 Room:421 Time:April 28 14:30-14:50

The effect of freshwater input from rivers on the ecosystem in coastal waters

KASAI, Akihide[1*]

[1]Field Science Education and Research Center, Kyoto University

High production in coastal areas is supposed to be supported by large organic and inorganic inputs from rivers. Therefore, excessive reduction of nutrient loads from rivers would decrease nutrient concentrations in coastal areas. This manifests in poor growth of seaweeds, which has been observed in Seto Inland Sea in recent years. However, primary production in coastal areas is not only supported by terrestrial nutrients, but also external nutrients derived from ocean and regenerated nutrients formed in hypoxic water at the bottom. Evaluation of the contribution of each source of dissolved inorganic nitrogen (DIN) to phytoplankton production in Ise Bay revealed that DIN consumption by phytoplankton exceeds the DIN supply from rivers and ocean. This indicates that a large amount of primary production depends on regenerated DIN within the bay rather than on newly supplied DIN, although the ratio of consumption to external supply differs seasonally. We have to pay more attention to the behavior of each source of nutrients for future managements of coastal waters.

The effect of the freshwater input from rivers on coastal areas is not only the nutrient supply, but also the formation of estuarine circulation, which plays an important role in coastal ecosystems. Since the flux of water by the estuarine circulation is considerably larger than the river discharge, it has large effects on the material transport and biological production in estuaries and bays. For example, larvae of temperate seabass do not distribute in the surface, but in the middle layer, and thus the landward flow effectively transports larvae to coastal areas from the spawning grounds in the offshore. Therefore, the year-to-year variation in the amount of juveniles in the coastal area shows that the survival of juveniles improves in the years when the river discharge increases.

Keywords: coastal ecosystem, estuarine circulation, freshwater, nutrients

Japan Geoscience Union Meeting 2014
(28 April - 02 May 2014 at Pacifico YOKOHAMA, Kanagawa, Japan)

ACG35-03 Room:421 Time:April 28 14:50-15:10

Possible effects of submarine groundwater on biodiversity and fishery production in coastal ecosystems

SHOJI, Jun[1*] ; SUGIMOTO, Ryo[2] ; TOMINAGA, Osamu[2] ; KOBYASHI, Shiho[3] ; YAMADA, Makoto[4] ; TANIGUCHI, Makoto[4]

[1]Hiroshima University, [2]Fukui Prefectural University, [3]Kyoto University, [4]Research Institute for Humanity and Nature

Economic values of the ecosystem services of coastal ecosystems have been evaluated as among the highest of those the world's ecosystems. Recently more attentions have been paid on the mechanisms how the freshwater contribute to the high productivity and species diversity of the coastal ecosystems. In the present paper, previous researches that focused on effects of freshwater input from the land on productivity and species diversity of fishery resources in the coastal ecosystems are reviewed. In addition, results from recent surveys conducted in order to examine the possible effects of river water and submarine groundwater on productivity and species diversity of fishery resources are introduced.

Relationship between river discharge and recruitment of several estuarine-dependent fish species (flatfish, seabass and clupeid) have been reported in the world. Among these fish species, the mechanisms how river discharge promotes survival during the early life stages and recruitment of Morone fishes (striped bass and white perch) have been well studied. Larval survival rate is high and recruitment of 1-year-old fish is successful in years with high precipitation in these species. High freshwater discharge has been reported to increase availability of prey for the larvae, decrease predation through affecting predator species composition and biomass, then increase the growth and survival during the larval stage.

In a previous paper, on the other hand, low salinity zone has been reported to be one of the ecosystems where biodiversity is the lowest among the world's aquatic ecosystems. High fluctuation in salinity and tidal level within a relatively small spatial and temporal scale could be stressful for a variety of animal species. Recently high abundance of juveniles of several flatfish species were observed in low salinity zones nearby an estuary in the coastal waters of Japan. Species diversity of fishes was higher in a seagrass bed where freshwater supply from the land through submarine groundwater was expected compared to the surrounding areas. These observations suggest that low salinity condition does not always decrease diversity of fish species in coastal ecosystems. Future research plan to investigate the mechanism how the freshwater input from the land contributes to the high productivity and species diversity in the coastal ecosystems will be introduced.

Keywords: water-food NEXUS, fishery production, species diversity, submarine groundwater

Japan Geoscience Union Meeting 2014
(28 April - 02 May 2014 at Pacifico YOKOHAMA, Kanagawa, Japan)

ACG35-04 Room:421 Time:April 28 15:10-15:25

Evaluation of nitrogen dynamics in the Yodo River estuary using stable isotopes

SUGIMOTO, Ryo[1*] ; KASAI, Akihide[2]

[1]Faculty of Marine Biosciences, Fukui Prefectural University, [2]Field Science Education and Research Center, Kyoto University

The increase in human population in coastal watersheds has increased the delivery of nitrogen from the land to coastal environments. Accelerated nitrogen cycles in coastal environments have led to an increase in hypoxic waters and instances of harmful algal blooms. Physical and biogeochemical processes within estuaries generally regulate nitrogen fluxes from land to sea. The estuaries of major rivers on the continents are thought to be sites of massive nitrogen losses. However, function of estuaries to nitrogen transfer must vary according to each estuarine hydrology and biogeochemistry. A large amount of terrestrial nitrogen empties into Osaka Bay head from the Yodo River. Although the estuary would have a crucial role in modifying nitrogen fluxes, its function to nitrogen transfer is still unclear. In this presentation, we will report the seasonal difference of nitrogen dynamics along the longitudinal section from the estuary to the head of Osaka Bay.

Keywords: nitrogen, stable isotopes, estuarine circulation, eutrophication, regeneration

Japan Geoscience Union Meeting 2014
(28 April - 02 May 2014 at Pacifico YOKOHAMA, Kanagawa, Japan)

ACG35-05 Room:421 Time:April 28 15:25-15:40

Factors of the temporal variation of marine phytoplankton at Yodo River estuary

HAYASHI, Mitsuru[1*] ; KOGA, Ryuraro[1] ; FUJII, Tomoyasu[2] ; YAMAMOTO, Keigo[3]

[1]Kobe Univ., [2]Nara University of Education, [3]Marine Fisheries Research Center, Osaka Prefecture

Red tides of *Alexandrium tamarense* have occurred in the estuary of the Yodo River in Japan in 2007, 2011 and 2013. *A. tamarense* is marine phytoplankton and causes shellfish poisoning. We have made in-situ observation in April 2-3 2012, and analyzed the temporal variation of marine phytoplankton by using the numerical ecosystem model. CTD and ADCP observation and water sampling ware carried out linked to the tidal change. Nutrient and chl.a concentration and cell density of *A. tamarense* were analyzed. *A. tamarense* was a few in this year. Typical estuary circulation which seawater run up to upstream in the surface layer and fresh water go down to the sea in the bottom layer. Therefore the estuary which have 2800m length was divided to three layers, 0-0.5m, 0.5-1.5m and 1.5m-bottom. The thickness of the bottom layer is changed with the tidal change. Nutrient, phytoplankton, the dissolved organic matter and the particulate mutter are in each layer, and the bio-chemical process between the forms, photosynthesis, mortality, decomposition and so on, are formulated. Then the temporal variations of each morphology and *A. tamarense*. Diurnal migration, salt limitation and utilization of organic matter for the photosynthesis and mortality by low salinity were considered in the bio-chemical process of *A. tamarense*. The temporal variations of phytoplankton in each layer were almost reproduced. Marine phytoplankton in the Yodo River estuary were not produced hardly and were supplied from the ocen. Phytoplankton which cannot swim by oneself is almost floated by the horizontal advection, it is the estuary circulation. But only 27% of *A. tamarense* transported from the ocean in the bottom layer go through upstream. 36% of it returned to the ocean in the middle and surface layers, and other 36% die in the surface layer. Weak estuary circulation is effective to limit the transport upstream of *A. tamarense* in Yodo River estuary.

Keywords: Yodo River, Estuary, Numerical ecosystem model, Phytoplankton, Alexandrium tamarense

Japan Geoscience Union Meeting 2014
(28 April - 02 May 2014 at Pacifico YOKOHAMA, Kanagawa, Japan)

ACG35-06 Room:421 Time:April 28 15:40-15:55

Utilization of terrestrial organic matter by marine benthic polychaetes in estuarine eosystem

SATO, Takahisa[1] ; SUGIMOTO, Ryo[2] ; YOKOYAMA, Yoshihiro[2] ; TOMINAGA, Osamu[2*]

[1]Yamagata prefectural fisheries high school, [2]Fukui prefectural university

In semi-enclosed bays, terrestrial plants transported by river have become a major constituent of estuary sediment. Since it is difficult for marine organisms to digest the terrestrial plants which mainly contains the non-living refractory cellulosic matrics, few studies have been taken into account the role played by the terrestrial particulate organic matter(tPOM) in enhancing the productivity of the coastal biotic community. However, the important role of tPOM as the food source for marine benthic organisms has been recognized in estuarine environments. In the present study, we examined the δ^{13}C, δ^{15}N values and cellulase activity of the several species of polychaetes to elucidate the contribution of terrestrial plants to benthic biological production in small semi-enclosed Bay. Polychaete annelids were collected at estuary of the Kita and Minami River in semi-enclosed Obama Bay, the Sea of Japan from August 2007 to June 2010. The carbon and nitrogen stable isotope ratios of polychaetes were analyzed. Cellulase activity analyses were assayed by using carboxymethyl cellulose (CMC) plate assay. The δ^{13}C values of deposit or suspension feeding polychaetes were lower than the δ^{13}C value of POM but higher than the terrestrial plants. The δ^{13}C and δ^{15}N values of carnivores-feeding polychaetes were higher than those polychaetes. Cellulase activities was found in many deposit or suspension feeding polychaetes but also carnivorous feeding polychaetes. On the other hand, the polychaete species with lower isotope signature did not show cellulase activities. The polychaetes which showed cellulase activity were abundant through the four seasons in estuary. These results suggest that many polychaetes can decomposition and assimilation the terrestrial plants.

Keywords: terrestrial plants, cellulase,, semi-enclosed bay, polychaetes

Japan Geoscience Union Meeting 2014
(28 April - 02 May 2014 at Pacifico YOKOHAMA, Kanagawa, Japan)

ACG35-07 Room:421 Time:April 28 16:15-16:30

The origin of submarine groundwater discharge in the coastal zone of Hiji, Oita prefecture

YAMADA, Makoto[1*] ; OHSAWA, Shinji[2] ; MISHIMA, Taketoshi[2] ; ABE, Yutaka[1] ; TANIGUCHI, Makoto[1]

[1]Research Institute for Humanity and Nature, [2]BGRL, Institute for Geothermal Sciences, Kyoto University

It is said that groundwater discharge from the seabed of the coastal zone of Hiji, Oita prefecture. The marbled sole which lives around this submarine groundwater discharge is called a " Shirosita Karei " , and is loved by the local people. From ancient times, the local people have believed that this Shirosita Karei grows because of submarine groundwater discharge. However, regarding the relevance of the ecology of a marbled sole and submarine groundwater discharge, it is not clear that this is the case. Moreover, although it is clear that there is submarine groundwater discharge, there is almost no information about the origin and dissolved component. Kono and Tagawa (1996) conducted an analysis of the major dissolved components of groundwater of this land area, and a vertical distribution investigation of the electric conductivity of the ocean. As a result, it has suggested the possibility that submarine groundwater discharge is the confined groundwater recharged in the mountain area. However, in that report, they said that they were not able to identify a recharge area clearly by this research. Because of that, we sampled the spring water of the land area, the spring water of a salt water mixture discharged in a seashore area, and a sea water sample, in order to conduct hydrological research using the stable isotope of water in this area and to clarify the flow process of submarine groundwater discharge. The recharge elevation of the spring water of this land area was assumed using the recharge-water line (Ohsawa et al., 2009) made using the data of the Beppu area of the southwest part of this research region. As a result, it became clear that the recharge area of most spring water is at an elevation of 200 m or more. Regarding fresh water and salt water mixture, the mixed rate of sea water and fresh water was calculated using electric conductivity, and the isotopic ratio of the original fresh water was computed using the mixed rate. As a result, it became clear that the recharge elevation of the fresh water mixed in sea water is near 300 m. Moreover, as a result of extracting the terrestrial environment of this area, the area with an elevation of 200 m or more is mainly forest, and there was a boundary between the forest area and plains near an elevation of 200 m. It became clear from these results that the origin of the submarine groundwater discharge in the coastal zone of Hiji is the water recharged in the forest area of the mountain slope, and that the water moves under the plain and is discharged at the sea bed.

Keywords: Submarine groundwater discharge, Stable isotope, recharge area, Hiji

Japan Geoscience Union Meeting 2014
(28 April - 02 May 2014 at Pacifico YOKOHAMA, Kanagawa, Japan)

ACG35-08 Room:421 Time:April 28 16:30-16:45

Location estimation of submarine groundwater discharge from Mt. Fuji in Suruga Bay

MURANAKA, Yasuhide[1*] ; KAMITANI, Takafumi[1] ; WATANABE, Masayuki[1] ; ONO, Masahiko[2] ; MARUI, Atsunao[2]

[1]Shizuoka Institute of Environment and Hygiene, [2]National Institute of Advanced Industrial Science and Technology

Around the foot of Mt. Fuji, the main flow passages of groundwater are thought to be in the Younger Fuji volcano, which consists of the pervious basaltic lavas in new volcanic stage. Especially, the Fujikawa-kako fault zone, which stretches south to north in the southwestern side of Mt. Fuji, has a potentially effect on the local groundwater flow system into Suruga Bay. Therefore, precipitation at Mt. Fuji have been considered to be discharging partly from seabed in Suruga Bay and making a great impact on the biological production at the coastal sea area.

For the purpose of contribution to make sense of the rich coastal ecosystem in Suruga Bay, we conducted a survey for submarine groundwater discharge (SGD) in Oku-Suruga Bay: from the mouth of the Fuji River, at which the fault is found, to Tagonoura, where the lavas of the Younger Fuji volcano are distributed from 100 to 200 m below sea level. We are trying to estimate some locations of SGD from the condition of seabed and geological structure by using the side scan sonar and the sub-bottom profiler. We also use a remotely operated vehicle (ROV) for photographing for the image of the extrapolated spring points. In this presentation, we introduce our works noted above.

Keywords: submarine groundwater discharge (SGD), Mt. Fuji, Suruga Bay, side scan sonar, remotely operated vehicle (ROV)

Japan Geoscience Union Meeting 2014
(28 April - 02 May 2014 at Pacifico YOKOHAMA, Kanagawa, Japan)

ACG35-09 Room:421 Time:April 28 16:45-17:00

Evaluation of submarine groundwater discharge in Suruga Bay by using radon 222

ONO, Masahiko[1*] ; MARUI, Atsunao[1]

[1]National Institute of Advanced Industrial Science and Technology

Submarine groundwater discharge (SGD) in coastal area has been recognized as an important pathway for material transport from land to ocean. SGD has been widely studied throughout the world and it is expected as ubiquitous phenomenon in coastal zone.

Suruga Bay is adjacent to the southern foot of Mt. Fuji where the permeable lava flow deposits and the active groundwater flow system exist. Therefore, large amount of groundwater input is expected at the coastal area in Suruga Bay. It is also expected that SGD has a significant effect for marine products in this area.

To evaluate submarine groundwater discharge in this area, we applied continuous radon measurement and sampled coastal water for chemical analysis. We will introduce these results in this presentation.

Keywords: Rn-222, Submarine groundwater discharge, Suruga Bay

Japan Geoscience Union Meeting 2014
(28 April - 02 May 2014 at Pacifico YOKOHAMA, Kanagawa, Japan)

ACG35-10 Room:421 Time:April 28 17:00-17:15

Estimating submarine groundwater discharge in Obama Bay, Japan, using 222Rn mass balance model

HONDA, Hisami[1*] ; SUGIMOTO, Ryo[1] ; KOBAYASHI, Shiho[2] ; TAHARA, Daisuke[1] ; TOMINAGA, Osamu[1] ; TANIGUCHI, Makoto[3]

[1]Fukui Prefectural University, [2]Kyoto University, [3]Research Institute for Humanity and Nature

Recently, a number of studies have shown that submarine groundwater discharge (SGD) is even more important than surface runoffs in terms of nutrient transport and can drive primary production in coastal seas. Obama Bay is semi-enclosed bay in central Japan. In spring, phytoplankton blooms in the bottom layer around 2 km offshore from the river mouth. Aquifer distribution in the Obama plain and our previous observation of low salinity water around the bottom layer suggests that unconfined groundwater discharges induce this phytoplankton bloom. However, quantitative contribution of groundwater discharge to the coastal ecosystem has not been well evaluated in Obama Bay. In this study, we estimated the input of freshwater and nutrients via SGD into Obama Bay using mass balance model of radon (^{222}Rn) and salinity. As a result, the volume of SGD into the bay was estimated to be 0.05-0.80$\times 10^6$ m^3 d^{-1} during February 2013 to November 2013. Especially, the fraction of SGD in total freshwater flux in summer reached to 44%, because river water discharge decreased drastically. The nutrient fluxes from SGD were approximately 84%, 210% and 28% of riverine fluxes dissolved inorganic nitrogen (DIN), dissolved inorganic phosphorous (DIP) and dissolved inorganic silicate (DSi), respectively.

Keywords: Submarine groundwater discharge, 222Rn mass balance, Obama Bay

Japan Geoscience Union Meeting 2014
(28 April - 02 May 2014 at Pacifico YOKOHAMA, Kanagawa, Japan)

ACG35-11 Room:421 Time:April 28 17:15-17:30

A study of primary production in plankton blooms driven by riverine inputs

HOSHIBA, Yasuhiro[1*] ; YAMANAKA, Yasuhiro[1]

[1]Faculty of Env. Earth Science, Hokkaido University

Rivers transport nutrients and suspended sediment matter (SSM) as well as fresh water from land to coastal regions, where the biological productivity is high. In the coastal area, the buoyancy of fresh water leads to the formation of horizontal anticyclonic gyres and vertical circulations, which affect the variation of biological production such as plankton blooms. However, the primary production caused by the three-dimensional dynamics have not been quantitatively discussed, and observations can hardly capture the daily temporal variations of phytoplankton blooms. We developed an ocean general circulation model (OGCM) including a simple ecosystem model, to investigate the three-dimensional and temporal changes in phytoplankton blooms caused by riverine input such as flooding.

We first conducted ideal setting-simulations. The distribution patterns of nutrients and phytoplankton differ significantly from that of fresh water. The phytoplankton maxima shift from the downstream (right-hand side of the river mouth) to the upstream regions (left-hand side of the river mouth). The shift from the downstream to the upstream region (D-U Shift) is categorized by the different nitrate origins: (1) river-originated nitrate (RO-nitrate) is dominant in the downstream region; (2) subsurface-originated nitrate (SO-nitrate) is dominant in the upstream region, and is transported by upwelling associated with vertical circulation and horizontal anticyclonic gyre; and (3) regenerated nitrate (R-nitrate) is dominant in the upstream region. The total primary production in phytoplankton blooms is maintained not only by RO-nitrate but also by SO-nitrate that is larger than the river-originated.

Next, we conducted a realistic simulation and a few ideal setting-simulations. The phytoplankton maxima shift toward the left-hand side of the river mouth during the early time, but the shift does not keep going to the left-hand side all the time. This is because much SO-nitrate does not come from the subsurface to the surface layer after the middle simulated time, due to weak upwelling forced by vertical circulation in the left-hand side. The gentle angle of bottom slope weaken the vertical circulation and SO-nitrate supply from the subsurface, and the NPP is small.

It is natural that D-U Shift of phytoplankton maxima often occurs in the real situation like Ishikari Bay when high riverine input such as flooding. The conclusion that the shift is categorized into three stages by the different nitrate origins, RO-, SO- and R- nitrates in turn depends on the bottom slope angle and the way of inputs and the amounts of fresh water and nutrients. Bottom slope angle and the way of fresh water input change the behaviour of plumes, nutrient supply from the subsurface with the change of vertical circulation, and the rate of regeneration.

Keywords: coastal ocean, biogeochemical cycles, 3-D modeling, riverine input, phytoplankton bloom, nutrient supply

Japan Geoscience Union Meeting 2014
(28 April - 02 May 2014 at Pacifico YOKOHAMA, Kanagawa, Japan)

ACG35-12 Room:421 Time:April 28 17:30-17:45

Clarification of relationship between nutrient loading and biological productivity in coastal area by ecosystem model

ABE, Masami[1*] ; TATENO, Satoshi[1] ; NAGAO, Kentaro[1] ; HATA, Kyoko[1]

[1]IDEA Consultants, Inc.

Recently, the total volume control of COD loading from continental areas to coastal areas that is generally regarded as a barometer of eutrophication produce an effect for water quality improvement. On the other hands, the reduction in biological productivity caused by concentration reduction of nutrient was pointed out. We face the limit of control policies due to build the suitable interaction between continental areas and coastal areas.

Due to understand the interaction between nutrients loading and biological productivity, the investigation how nutrients provide any biological populations and fish catch is effective. The circulation pathway of nutrients is complex web of interactions, for example, relationship between among biological populations (prey-predator relationship, competitive relationship et. al.) or indirect interaction web (extinction of predator caused by anoxic water, et. al.). The ecosystem response to decrease or increase in nutrient loading is complex.

In this report, we apply ecosystem-model which include fishery product (laver culture, clam) to around Kako-river (*Harima-nada*, *Seto-Inland-Sea*, *Japan*). We quantified responses of material circulation to decrease or increase in continental loading by using this model. The biological productivity is responding to decrease or increase in nutrient loading is varying with the structure of material circulation networks.

Keywords: ecosystem model, nutrient loading, material circulation, productivity, Harima-Nada

Japan Geoscience Union Meeting 2014
(28 April - 02 May 2014 at Pacifico YOKOHAMA, Kanagawa, Japan)

ACG35-13 Room:421 Time:April 28 17:45-18:00

Construction of the comprehensive aquatic model of the Ise Bay watershed

ONISHI, Takeo[1*] ; SUGIMOTO, Ryo[2] ; AOKI, Kazuhiro[3] ; SOMURA, Hiroaki[4] ; YOSHINO, Jun[5] ; HIRAMATSU, Ken[1]

[1]Faculty of Applied Biological Sciences, [2]Faculty of Marine Bioscience, Fukui Prefectural University, [3]National Research Institute of Fisheries Science, [4]Faculty of Life and Environmental Science, Shimane University, [5]Faculty of Engineering, Gifu University

Though Integrated Water Resource Management (IWRM) is recognized as an important philosophy for consistent management through terrestrial area to oceans in 1990s', lack of scientific prove and grounds is one of the essential obstacles to implement the philosophy into actual policy making processes. To enhance and enrich scientific basis of IWRM, objective evaluation of change of terrestrial area impacts on oceanic environment is essential. Thus, we are conducting to construct a comprehensive aquatic model which combines water, material, and ecosystem models throughout terrestrial area, rivers, and ocean. The study site is the Ise Bay and its catchment area. Our model is targeting at carbon, nitrogen, and phosphorous for material, and low trophic levels for ecosystems. In addition, model development is based on the philosophy that promotes a model to be opened for public.

The model structure is that combination of hydrological model, river model, oceanic model, and ecosystem model. For about hydrological model, PnET-BGC is used for natural vegetation, SWAT model for agricultural lands, and the tank model for domestic water outflow from urban area. For about river model flow model, one-dimensional open channel model using kinematic wave method is utilized. For ecosystem model, NPZD model was implemented into aquatic systems. And, for ocean model, ROMS was used. In addition, dam operational rules were included to consider the impacts of dams on river discharge regimes. Calibration and validation period was from 2000 to 2010. Simulation time step was 1 day, and spatial resolution of driving force (weather data) of the model was 2km. ASTER-GDEM is utilized for DEM, National Land Numerical Information for vegetation, and Basic Land Classification Survey for soil and geological data. The result showed that while river discharge was relatively good, the level of water quality was not acceptable. One of the possible reasons of this discrepancy was the incomplete implementation of agricultural water use. Moreover, since coupling with ocean model is not yet realized, thus, improvement of terrestrial model, coupling of terrestrial and ocean model, and sensitivity analysis is further required.

Keywords: Integrated Water Resource Management, Landuse change, Eutrophication, Hypoxia, Ise Bay

Japan Geoscience Union Meeting 2014
(28 April - 02 May 2014 at Pacifico YOKOHAMA, Kanagawa, Japan)

ACG35-P01 Room:Poster Time:April 28 18:15-19:30

Spatiotemporal distribution of organic matter buried in estuarine seagrass meadows

WATANABE, Kenta[1*] ; KUWAE, Tomohiro[1]

[1]Port and Airport Research Institute

Blue Carbon, captured and sequestrated by marine organisms, has attracted attention as one of the major sink of atmospheric carbon dioxide. One of the important process for carbon sequestration is burial of organic carbon into sediments. The burial rate of organic carbon is higher in estuaries and seagrass meadows than open oceans. A large amount of terrestrial carbon flows into shallow coastal systems, consequently being buried in the sediment. Also nutrient inflows elevate autochthonous organic matter production in the systems. Therefore, various organic matter compositions, having different origin and bioavailability, are mixed in shallow waters. In this study, we investigate the quality and quantity of organic matter buried in an estuarine seagrass meadow using elemental and isotopic techniques and ^{14}C dating.

Our study site, the Furen Lagoon, is located at the high latitude in Japan. The Furen lagoon is eutrophic due to riverine inflows. Seagrass meadows occupy 67 % of the total area of the lagoon. We collected core samples (about 2 m) in the lagoon along the salinity gradient. TOC (total organic carbon) and TN (total nitrogen), as well as carbon and nitrogen isotopic signatures were analyzed along the depth. Also Δ ^{14}C was analyzed for dating. In the low salinity zone, δ^{13}C was low and C/N ratio was high, indicating that terrestrial organic matter was dominant. These signatures were relatively stable with sediment depth, showing that terrestrial organic matter would have been buried for thousands years. Within the seagrass meadow, δ^{13}C and δ^{15}N were relatively high, indicating that the contribution of autochthonous organic matter (phytoplankton and seagrass) to TOC would increase in the presence of vegetation. δ^{13}C fluctuated with sediment depth in the seagrass meadow, showing that the contribution of terrestrial organic matter fluctuated temporally. These results suggest that the lagoon can be the long-term sink of carbon due to autochthonous production and deposition of terrestrial organic carbon.

Keywords: carbon sequestration, blue carbon, estuary, seagrass meadows, stable isotope, 14C dating

Japan Geoscience Union Meeting 2014
(28 April - 02 May 2014 at Pacifico YOKOHAMA, Kanagawa, Japan)

ACG35-P02 Room:Poster Time:April 28 18:15-19:30

Influences of submarine ground water discharge (SGD) on biogeochemical properties in coastal sea

KOBAYASHI, Shiho[1*] ; SUGIMOTO, Ryo[2] ; HONDA, Hisami[2] ; MIYATA, Yoji[1] ; TOMINAGA, Osamu[2] ; TAHARA, Daisuke[2] ; TANIGUCHI, Makoto[3]

[1]Kyoto University, [2]Fukui Prefectural University, [3]Research Institute for Humanity and Nature

Submarine groundwater discharge (SGD) often influences on biogeochemical properties in coastal seas. We have estimated the flux of SGD using seepage meter and compared it with 222Rn, chlorophyll and nutrients concentrations at a fixed point in Obama Bay for a month

Keywords: submarine groundwater discharge, costal ecosystem, land-ocean interaction

Japan Geoscience Union Meeting 2014
(28 April - 02 May 2014 at Pacifico YOKOHAMA, Kanagawa, Japan)

ACG35-P03 Room:Poster Time:April 28 18:15-19:30

Development of simultaneous monitoring method of submarine groundwater discharge and primary production in coastal seas

SUGIMOTO, Ryo[1*] ; OHKOUCHI, Masaki[1] ; HONDA, Hisami[1] ; SHOJI, Jun[2] ; OHSAWA, Shinji[3] ; TANIGUCHI, Makoto[4]

[1]Fukui Prefectural University, [2]Hiroshima University, [3]Kyoto University, [4]Research Institute for Humanity and Nature

In recent years, a number of studies have shown that submarine groundwater discharge is an alternative nutrient pathway and can drive primary production in coastal seas. However, very little is known about quantitative relationship between input of groundwater and response of primary production, because both processes are temporally variable. Recent technological advances (i.e., automation) have increased our ability to assess submarine groundwater discharge in coastal ecosystems using natural tracers such as radon-222 (^{222}Rn). Simultaneous monitoring of ^{222}Rn with indicators of primary production such as pCO_2 and/or chlorophyll-a would allow us to grasp the nexus of both processes. Therefore, automated radon and CO_2 gas analyzer were connected in series and a closed air loop was established with gas equilibration devices to examine the nexus between submarine groundwater discharge and primary production. In this presentation, we will report the results of simultaneous monitoring of ^{222}Rn and pCO_2 with other parameters in several coastal environments.

Keywords: simultaneous monitoring, submarine groundwater discharge, primary production, coastal seas

Japan Geoscience Union Meeting 2014
(28 April - 02 May 2014 at Pacifico YOKOHAMA, Kanagawa, Japan)

ACG35-P04 Room:Poster Time:April 28 18:15-19:30

Local scale assessment of submarine groundwater discharge in coastal seas (Beppu, Obama and Otuchi Bay)

HISAMI, Honda[1*] ; SUGIMOTO, Ryo[1] ; TOMINAGA, Osamu[1] ; KOBAYASHI, Shiho[2] ; MIYATA, Youji[2] ; ONO, Masahiko[3] ; OHSAWA, Shinji[4] ; TANIGUCHI, Makoto[5]

[1]Faculty of Marine Bioscience, Fukui Prefectural University, [2]Field Science Education and Research Center, Kyoto University, [3]National Institute of Advanced Science and Technology, [4]Institute for Geothermal Sciences, Kyoto University, [5]Research Institute for Humanity and Nature

Submarine groundwater discharge (SGD) is important as a major pathway for freshwater and nutrients loads from land to ocean. Various natural tracers of SGD have been applied to quantify local to regional SGD fluxes. Radon-222 (^{222}Rn) is a naturally occurring radioactive gas that is typically 2-3 orders of magnitude higher in groundwater than surface waters. Therefore, it is a powerful tracer of groundwater inputs to oceans. We have applied the continuous ^{222}Rn monitoring survey to three local scale coasts (Beppu Bay, Obama Bay and Otsuchi Bay), which have large amounts of groundwater resources in each watershed. As a result, spatial distributions of ^{222}Rn and other parameters displayed not only influence of submarine groundwater discharge but also possibility of submarine hotspring discharge.

Keywords: submarine groundwater discharge, 222Rn, land-ocean interaction

Japan Geoscience Union Meeting 2014
(28 April - 02 May 2014 at Pacifico YOKOHAMA, Kanagawa, Japan)

ACG35-P05 Room:Poster Time:April 28 18:15-19:30

Stable isotope compositions of dissolved inorganic carbon and water under the seabed of the coastal zone

YAMADA, Makoto[1*] ; SUGIMOTO, Ryo[2] ; OKOCHI, Masaki[2] ; HONDA, Hisami[2] ; KOBAYASHI, Shiho[3] ; ABE, Yutaka[1] ; TANIGUCHI, Makoto[1]

[1]Research Institute for Humanity and Nature, [2]Fukui Prefectural University, [3]Kyoto University

Groundwater often discharges from the seabed of the coastal zone. Such groundwater is called " submarine groundwater discharge (SGD) ". Mostly, SGD is the water which not fresh water but sea water and fresh water mixed. Although it is assumed that mixture has occurred under the seabed, there is almost no information about the behavior of water and dissolved component under the seabed such as the mixed process, zone of influence of sea water, and the behavior of the dissolved component from the land area. In order to clarify the behavior of water and dissolved component under the seabed of the coastal zone, we conducted the sampling of the water under the seabed of Obama Bay, Fukui prefecture. The stable carbon isotope ratio of dissolved inorganic carbon (DIC) was lower than that of sea water, and higher than that of groundwater which sampled from well near the seashore. The results show that not only mixture of water but mixture of DIC has occurred under the seabed. In the future, in order to comprehend the extent of the impact of sea water, it is necessary to research vertical distribution of the stable isotope composition under the seabed.

Keywords: submarine groundwater discharge, water stable isotope, carbon stable isotope, dissolved inorganic carbon

Japan Geoscience Union Meeting 2014
(28 April - 02 May 2014 at Pacifico YOKOHAMA, Kanagawa, Japan)

ACG36-01 Room:311 Time:April 29 14:15-14:30

Catastrophic reduction of sea-ice in the Arctic Ocean - its impact on the marine ecosystems in the polar region-

HARADA, Naomi[1*] ; KIMOTO, Katsunori[1] ; ONODERA, Jonaotaro[1] ; WATANABE, Eiji[1] ; HONDA, Makio[1] ; KISHI, Michio[1] ; KIKUCHI, Takashi[1] ; TANAKA, Yuichiro[2] ; SATOH, Manami[3] ; ITOH, Fumihiro[3] ; SHIRAIWA, Yoshihiro[3] ; MATSUNO, Kohei[4] ; YAMAGUCHI, Atsushi[5]

[1]JAMSTEC, [2]AIST, [3]Univ. of Tsukuba, [4]NIPR, [5]Hokkaido Univ.

The sea-ice in the Arctic Ocean has dramatically reduced during the past decade. The drastic sea-ice reduction would cause a complicated and difficulty to understand the perspective on marine ecosystem surrounding the Arctic Ocean, because disadvantage phenomena such as ocean acidification and advantage phenomena such as improving light condition for primary producers, respectively, are simultaneously progressing. We have investigated the response of marine organisms caused by catastrophic sea ice reduction in the Chukchi Sea and Northwind abyssal plain at where the sea ice reduction has progressed most seriously in the Arctic Ocean. The aims of our study are No.1 to understand temporal changes in primary production, No.2 to understand the physiological response of marine phyto and zooplanktons having carbonate tests on warming or freshening associated with sea ice melting, No.3 to develop a new model for marine ecosystems in the Arctic Ocean, to reproduce the primary production by using the model and to understand the response of marine ecosystems on the environmental changes caused by rapid sea-ice reduction. In this presentation, we will show an overview of this project composed of three sub-themes, Observation, Culturing, and Modeling. For the observation, we will show a seasonal change in biogenic components flux obtained at the Northwind abyssal plain by a year round time series sediment trap system and seasonal change in dissolution of pteropod tests due to the seasonal change in the ocean acidification. We will also show the potential mechanism of high biogenic fluxes found in the beginning of the sea-ice season using the original Arctic Ocean ecosystem model. For the culture experiment, the physiological response of Emiliania huxleyi, coccolithophorid strain on the environmental changes caused by sea-ice melting will be presented.

Keywords: Arctic Ocean, Biogenic particle, Eddy, Ocean acidification, Coccolithophorid

Japan Geoscience Union Meeting 2014
(28 April - 02 May 2014 at Pacifico YOKOHAMA, Kanagawa, Japan)

ACG36-02 Room:311 Time:April 29 14:30-14:45

Hindcast simulation of the ice and circulation in the Arctic Ocean for 1978-2012: An application of AO-FVCOM.

CHEN, Changsheng[1*] ; ZHANG, Yu[1] ; PROSHUTINSKY, Andrey[2] ; BEARDSLEY, Robert[2] ; LAI, Zhigang[3] ; GAO, Guoping[4]

[1]School of Marine Science, University of Massachusetts, USA, [2]Department of Physical Oceanography, Woods Hole Oceanographic Institution, USA, [3]School of Marine Sciences, Sun Yet-Sen University, China, [4]International Center for Marine Studies, Shanghai Ocean University, China

A high-resolution, unstructured-grid, finite-volume ice-ocean fully coupled model system, named AO-FVCOM, has been developed for the Arctic Ocean. The governing equations are cast in a generalized terrain-following coordinate system with spatially variable vertical distribution in the vertical and are discretized using flexible non-overlapped triangular grids in the horizontal. This model system includes a) an unstructured grid version of the Los Alamos sea ice model Community Ice CodE (UG-CICE), b) hydrostatic and non-hydrostatic dynamics (NH-FVCOM); c) an unstructured-grid version of the Simulating Wave Nearshore model (SWAN) (named SWAVE), d) 3-D wet/dry point treatment, which can simulate flooding/draining processes in estuaries and wetlands; e) 4-D nudging, OI and Kalman Filters data assimilation algorithms; f) the mass conservative nesting module to integrate multi-domain FVCOM domains; and g) the MPI parallelized visualization tool ViSiT, which allows users to monitor model performance during the simulation and post-process the model output data. An updated version of AO-FVCOM is capable of simulating the ice imbedded in the ocean.

AO-FVCOM is a regional model nested with Global-FVCOM. Two version of AO-FVCOM were configured with a finest horizontal resolution of 300 m and 2 km for the Arctic Ocean, respectively. The 2-km version has run for a period of 1978-2012. Without data assimilation, the model was capable of reproducing the seasonal and interannual variability of the ice coverage area in the Arctic and also significant drops of the ice coverage in 2007 and 2012. The 35-year simulation results for the circulation and water transport are being validated with comparison to field measurement data. The influence of the model resolution on water transport through the Canadian Archipelago has been also examined over seasonal and interannual scales, and an example of the water transport through Nares Strait will be presented.

Keywords: Arctic Ocean Modeling, Global-FVCOM, Arctic-FVCOM, Multi-domain nesting, 35 year Arctic simulation, Ice-Current Interaction

Japan Geoscience Union Meeting 2014
(28 April - 02 May 2014 at Pacifico YOKOHAMA, Kanagawa, Japan)

ACG36-03 Room:311 Time:April 29 14:45-15:00

Changes in the Western Arctic Biogeochemistry over the Last Three Decades: a Modeling Perspective.

SPITZ, Yvette H.[1*]

[1]Oregon State University, CEOAS, Corvallis OR 97331, USA

Over the last three decades, the Western Arctic Ocean (WAO) seasonal and permanent sea ice have experienced significant changes, with the summer sea ice extent still shrinking to record low levels and the permanent ice thickness being greatly reduced. Thus, the WAO circulation (e.g. intensification of the Beaufort Gyre), the oceanic heat content and biogeochemistry are directly impacted. We use the coupled pan-arctic Biology/Ice/Ocean Modeling and Assimilation System (BIOMAS) to investigate changes in the physical system, nutrient fluxes and productivity of the planktonic ecosystem between 1988 and 2011. Model simulations show that an earlier phytoplankton bloom and a slight increase in its biomass in general characterize the WAO. The largest response in the secondary producers is seen as an increase in the magnitude of the microzooplankton biomass as well as in the duration of its growing season. Primary productivity while increasing on average over the WAO shows some decrease in the Beaufort Gyre due to its intensification. Under ice blooms such as the one observed during the ICESCAPE (NASA funded program) in July 2011 are also intensified. This research was done in collaboration with colleagues from University of Washington (Dr M. Steele and Dr. J. Zhang), Woods Hole Oceanographic Institution (Dr. C. Ashjian) and University of Rhode Island (Dr. R. Campbell).

Keywords: Arctic, Modeling, Primary Productivity, Climate Change, Food Web

Japan Geoscience Union Meeting 2014
(28 April - 02 May 2014 at Pacifico YOKOHAMA, Kanagawa, Japan)

ACG36-04 Room:311 Time:April 29 15:00-15:15

Relationship of Primary Productivity in Northwind Abyssal Plain with Beaufort Gyre Variation

WATANABE, Eiji[1*] ; ONODERA, Jonaotaro[1] ; HARADA, Naomi[1] ; TERUI, Takeshi[2] ; KISHI, Michio[3]

[1]Japan Agency for Marine-Earth Science and Technology, [2]National Institute of Polar Research, [3]Hokkaido University

The western Arctic marine ecosystem was addressed using a combination year-round mooring observation and multiple numerical models. Our previous studies have revealed eddy-induced biological pump from the Chukchi shelf region to the southern Canada Basin. Whereas this system caused an early-winter peak of sinking flux of Particulate Organic Nitrogen (PON), we then focused on summertime ecological processes. The sediment trap measurements in the Northwind Abyssal Plain (NAP: 75N, 162W) of the western Arctic Ocean captured a maximum diatom flux with dominance of sea ice species in summer 2011. However, the particle fluxes in summer 2012 were considerably suppressed probably due to extension of oligotrophic Beaufort Gyre water to the NAP area. To examine interannual variability in ocean circulation around the target region, the decadal experiment from 1979 to 2012 was performed using the pan-Arctic ice-ocean model COCO. A virtual passive tracer provided inside the Canada Basin certainly suggested that the Beaufort Gyre direction switched southwestward (toward Station NAP) during the early period of 2012. In addition, the three-box lower-trophic model with sea ice species was applied under physical environments at Station NAP to assess an impact of nutrient deficiency on primary production in 2012. Finally, we plan to discuss how to improve existent problems of Arctic marine ecosystem model.

Keywords: Arctic marine ecosystem model, ice algae, oligotrophic water

Japan Geoscience Union Meeting 2014
(28 April - 02 May 2014 at Pacifico YOKOHAMA, Kanagawa, Japan)

ACG36-05 Room:311 Time:April 29 15:15-15:30

Estimating potential habitat for chum salmon (Oncorhynchus keta) in the Western Arctic using a bioenergetics model coupl

KISHI, Michio[1*] ; YOON, Seokjin[1] ; WATANABE, Eiji[1]

[1]Hokkaido University

Chum salmon (*Oncorhynchus keta*) are distributed widely in the Northern Pacific and are an important commercial fisheries resource in North Pacific countries. Chum salmon can be divided into North American and Asian groups, and the Asian groups can be divided further into Japanese and Russian groups, which show different migration routes. Japanese and Russian chum salmon stocks are predominant in the Bering Sea during summer and fall. However, recently, several studies reported different tendency. Higher densities of chum salmon were observed within the vicinity of the Bering Strait and the Chukchi Sea than the eastern Bering Sea on September 2007 and alike Japanese chum salmon migrated to northern areas in the Bering Sea on August 2009. Sea surface temperature in the Arctic marginal seas has increased since the mid-1960s, especially since 2000. We speculated that SST increase affect to salmon northing directly. Therefore, we focused on chum salmon migrating northward to the Western Arctic. We estimated the potential habitat for chum salmon in the Western Arctic using a bioenergetics model coupled with a three-dimensional lower trophic ecosystem model (3-D NEMURO). The model domain contained the entire Chukchi Sea and the southern area of the Canada Basin. The horizontal resolution was about 2.5 km, and there were 25 vertical levels (surface to 4000 m). We assumed chum salmon move to a depth where the growth rate is the maximum within 100 m, because chum salmon migrate vertically to below 100 m depth for controlling their body temperature and searching for prey. The model was run for nine months from March to November 2003, thus representing the entire months chum salmon are distributed in the Bering Sea from June to November. In the bioenergetics model, the growth rate of an individual chum salmon was calculated as a function of water temperature, salinity, and prey density, which were obtained from the 3-D NEMURO model results. We calculated the growth rates of chum salmon of 100 gWW to 4000 gWW and defined 'Potential habitat' as 'an area where chum salmon can grow up (i.e., the growth rate is positive)'. The potential habitat reflected the warm and nutrient-rich Pacific water inflowing from the Bering Strait. That was restricted to the southwestern Alaskan coast on June and expanded to the Chukchi Sea and along the Alaskan northwestern coast from July to September and reduced from October. The main limiting factor was the water temperature on June and November and the prey density on July to October. For global warming scenario, we used the modeled monthly water temperature anomaly between 2005 and 2095 under the IPCC SRES-A1B scenario. Under the global warming scenario, the potential habitat for chum salmon increased during early summer and autumn due to the water temperature increase, whereas during summer the potential habitat for smaller chum salmon increased but that for larger chum salmon decreased because the water temperature exceeded the optimal condition, especially in the southern Chukchi Shelf and near the Bering Strait. The water temperature limitation was relaxed with a water temperature increase on June and November, but regionally the water temperature was the main limiting factor during summer.

Keywords: Arctic, marine ecosystem model, Chum salmon

Japan Geoscience Union Meeting 2014
(28 April - 02 May 2014 at Pacifico YOKOHAMA, Kanagawa, Japan)

ACG36-06 Room:311 Time:April 29 15:30-15:45

Seasonal changes in zooplankton swimmer and faecal pellets collected using a sediment trap in the western Arctic Ocean

MATSUNO, Kohei[1*] ; YAMAGUCHI, Atsushi[2] ; FUJIWARA, Amane[1] ; ONODERA, Jonaotaro[3] ; WATANABE, Eiji[3] ; HARADA, Naomi[3] ; KIKUCHI, Takashi[3]

[1]National Institute of Polar Research, [2]Hokkaido University, Graduate School of Fisheries Sciences, [3]Japan Agency for Marine-Earth Science and Technology

Most studies on zooplankton community in the Arctic Ocean have been performed on the basis of net-collected samples. However, seasonal sea ice coverage in this area prevents the accurate evaluation of their seasonal changes. To overcome these challenges, analysis on zooplankton swimmers collected using a moored sediment trap is a powerful tool. In the present study, we analysed the seasonal changes in zooplankton swimmers and faecal pellets collected using a sediment trap moored at the Northwind Abyssal Plain in the western Arctic Ocean.

Samples were collected using a sediment trap moored at 184-260 m at St. NAPt (75N, 162W, bottom depth: 1975 m) in 10-15 day intervals from October 4, 2010 to September 18, 2012. The sample cups were filled with 5% buffered formalin seawater. After the trap was retrieved, a total of 52 samples were gently sieved using a 1-mm mesh, and a fine-size fraction ($<$1 mm) of each sample was filtered using a membrane filter and subsequently weighed. Next, the total mass flux (mg DM m^{-2} day^{-1}) was evaluated. Zooplankton faecal pellets were then quantified in an aliquot of the fine-size fraction, according to four morphological types (oval shape, cylinder shape, spherical shape and brown oval shape). On the basis of both the size fraction samples ($<$1 mm and $\geq$ 1 mm), species identification and enumeration of zooplankton were performed under a dissecting microscope. Furthermore, cluster analysis by Bray-Curtis similarity using the connected unweighted pair group method and the arithmetic mean was performed on the zooplankton flux data (ind. m^{-2} day^{-1}). To identify the species most responsible for the similarity between zooplankton communities, SIMPER analyses were performed on the flux data.

In addition, satellite data were obtained, which revealed the sea ice coverage period (November-June), open water period (August-October), and high chlorophyll a period (August-October). The total mass flux ranged from 0.1-263.3 mg DM m^{-2} day^{-1}, and its peaks occurred in November, which corresponded to the onset of sea ice coverage. In the faecal pellets, oval shaped and spherical shaped morphologies were predominant, and resulted in a total pellet number of 60% and 30%, respectively. With regards to the specific characteristics of the faecal pellets, the brown oval shape occurred only in the open water period (July-August) and their maximum composition during this period reached 80%. The zooplankton flux ranged from 35 to 739 ind. m^{-2} day^{-1} and was significantly higher in September-November compared with other periods (p $<$0.0001, one-way ANOVA). In addition, poecilostomatoid copepods were numerically the most dominant taxa (annual mean$\pm$1sd: 69$\pm$18%). For seasonal dominant taxa, bivalve larvae were found in October-November (53%), and barnacle larvae were abundant in August 2011 (33%) but were not present in 2012. Cluster analysis on the zooplankton flux identified five zooplankton community groups. The occurrence of each group clearly showed seasonality, and alterations in their timings corresponded with the timing of the onset or offset of ice coverage or seasonal changes in daylight hours.

On-board experiments demonstrated that the brown-oval-shaped faecal pellets might be egested by amphipods. Furthermore, the high brown-oval-shaped faecal pellets found during the open water period (July-August) might reflect the massive feeding activity of amphipods. For zooplankton swimmers, seasonal abundant bivalve and barnacle larvae may be transported from a shallower region (e.g., the Chukchi Sea). The annual change in occurrence of barnacle larvae (present in 2011, but not in 2012) may be caused by the annual changes in water mass formation in the upper layer of the St. NAPt.

Keywords: western Arctic Ocean, sediment trap, zooplankton community, faecal pellets

Japan Geoscience Union Meeting 2014
(28 April - 02 May 2014 at Pacifico YOKOHAMA, Kanagawa, Japan)

ACG36-07 Room:311 Time:April 29 15:45-16:00

Volume, heat and freshwater fluxes of Pacific Water through the Barrow Canyon in the Arctic Ocean

ITOH, Motoyo[1*] ; KIKUCHI, Takashi[1] ; NISHINO, Shigeto[1]

[1]JAMSTEC

Interest in Pacific Water flowing from the Bering Strait into the Arctic Ocean has increased markedly in recent years, because of warming and increasing of Pacific Water inflow. Barrow Canyon, in the northeast Chukchi Sea, is a major conduit for Pacific Water to enter the interior Arctic basins. Our study focuses on the quantitative estimate of volume, heat and freshwater fluxes through Barrow Canyon by mooring observations with hydrographic surveys. We conducted year-round mooring observations at one station from 2000 to 2001 and at three stations from 2001 to 2013 in the mouth of Barrow Canyon. The annual mean volume, heat and freshwater fluxes through Barrow Canyon were 0.49 Sv, 2.25 TW and 31 mSv, respectively. Annual averaged volume and freshwater fluxes though Barrow Canyon in recent years from 2010 to 2013 were lower than the 2000-2008 averages, mainly due to strong northerly wind. In contrast, heat flux for the period 2010-2013 was higher than the 2000-2008 average. It tended to be three highest maximum in 2007, 2010 and 2012, when summer sea ice extent extraordinary retreats in the Arctic Ocean, mainly because of the warming of Pacific Summer Water. Heat fluxes observed in these years were 3-4 times larger than that observed in summer 1993. It is sufficient to melt 1-m-thick ice over an area of 360,000 km^2, which is equivalent to the total land area of Japan. The heat possibly contributes to both sea-ice melt in summer and a decrease in sea-ice formation during winter because this water typically subsides just below the surface mixed layer in the Canada Basin.

Keywords: Arctic Ocean, Pacific Water, Heat flux, Sea ice extent

Japan Geoscience Union Meeting 2014
(28 April - 02 May 2014 at Pacifico YOKOHAMA, Kanagawa, Japan)

ACG36-08 Room:311 Time:April 29 16:15-16:30

Water masses transporting process from the Bering Sea to the Arctic Ocean revealed from multiple chemical tracers

JIANG, Kai[1*] ; ZHANG, Jing[2]

[1]Graduate School of Science and Engineering for Education, University of Toyama, [2]Graduate School of Science and Engineering for Research, University of Toyama

The Arctic Ocean is tightly connected to the Pacific Ocean through the only oceanic gateway Bering Strait. Water, heat, nutrients, and other substances inflowing via water masses exchanges affect the marine environment in the Arctic Ocean. In recent decades, the Arctic Ocean has changed dramatically, especially the rapid reduction of sea ice. The changing of water masses through the Bering Strait is thought to be one of the main reasons. Thus, focusing on the process of water masses transporting will contribute to understanding and forecasting the marine environment in the Arctic Ocean. In this research, stable oxygen isotopes, salinity and rare earth elements (REEs) are used to reveal the water masses transporting process from Bering Sea to the Chukchi Sea, which data comes from the Oshoro-Maru C255 cruise during 14June ? 07 August 2013. 182 water samples of δ^{18}O from 31 stations were analyzed by IR-MS (Isotope Ratio Mass Spectrometry). The δ^{18}O composition and salinity are used to separate the different water sources based that river water is highly depleted in δ^{18}O relative to marine waters as well as to sea-ice. Rare earth elements in the sediments from 8 stations were also analyzed by the method of BCR sequential extraction procedure which partitions the elements in sediments among various forms. It aims to trace the material sources, reflecting the water masses transporting process indirectly. The investigations show that in the Bering Sea, δ^{18}O value is around -2 ‰ in the surface increasing to -0.8 ‰ in the bottom water, closed to the δ^{18}O value of Pacific Ocean water, indicating that the up layer water is obviously affected by freshwater. In the Bering Strait, δ^{18}O value is similar in the whole water column, around -1.3 ‰, consistent with salinity, which means that the water is well mixed in the Bering Strait (East side of Bering Strait). In the Chukchi Sea, δ^{18}O value is also affected by sea ice melt water. REEs data shows that different fraction of sediment has different sources, most part of sediments originally come from land, after charged into ocean, they combine with particles or substance under different marine environment.

Keywords: Arctic Ocean, water mass, oxygen isotope, rare earth element

Japan Geoscience Union Meeting 2014
(28 April - 02 May 2014 at Pacifico YOKOHAMA, Kanagawa, Japan)

ACG36-09 Room:311 Time:April 29 16:30-16:45

Influence of the Gulf Stream on the Barents Sea ice retreat and Eurasian coldness

SATO, Kazutoshi[1*] ; INOUE, Jun[2] ; WATANABE, Masahiro[3]

[1]The Graduate University for Advanced Studies, [2]National Institute of Polar Research, [3]Atmosphere and Ocean Research Institute, University of Tokyo

Abnormal winter sea-ice retreat over the Barents Sea has been considered as a leading clue to the recent midlatitude severe winters. Barents Sea is considered as a hot spot for the rapid Arctic climate change due to the intense air-sea interaction induced by the sea-ice decrease; however, the underlying mechanisms remain uncertain, in particular causal relation of sea-ice retreat and atmospheric forcing and response. To understand this causality, we selected typical cases, defined as averaged warm and averaged cold years of December using the NCEP Climate Forecast System Reanalysis (CFSR). The composite analysis, revealed that anticyclonic anomaly is obvious over the northwestern Eurasia. The western Barents Sea and Sbarvard locates at the strong pressure gradient zone, prevailing southerly winds. Over the Barents Sea, the difference in daily mean air temperature between warm and cold winters is more than 10^{o}C, suggesting that warm advection prevails during warm years. Therefore, during warm years, decrease in sea-ice cover is induced by southerly warm advection. The positive anomalies of precipitation from the southeast of Greenland to Barents Sea and negative anomalies of them from Nordic Sea to western Eurasia means the poleward shift of cyclone tracks, suggesting that the moisture transport is also changed poleward. Because the cyclones tend to shift poleward in less sea ice year over the Barents Sea, it is natural that the snow depth over the sea ice near the Fram Strait shows a positive anomaly during warm winters. Here we show that the poleward shift of sea surface temperature over the Gulf Stream, where is situated upstream from the Barents Sea, modifies the horizontal distribution of tropospheric condensational heating resulted from change in convection over the warm current, likely acting as a bridge to the Barents Sea by forcing planetary waves. This remote atmospheric response modifies cyclone tracks poleward, resulting in anomalous warm advection over the Barents Sea sector.

Keywords: Gulf Stream, Arctic, Barents Sea, Eurasian coldness

Japan Geoscience Union Meeting 2014
(28 April - 02 May 2014 at Pacifico YOKOHAMA, Kanagawa, Japan)

ACG36-10 Room:311 Time:April 29 16:45-17:00

Study of interannual variability of the atmospheric water cycle in the Arctic circumpolar region

ISHIGE, Takaya[1] ; HIYAMA, Tetsuya[2*] ; FUJINAMI, Hatsuki[3]

[1]Graduate School of Environmental Studies, Nagoya University, [2]Research Institute for Humanity and Nature, [3]Hydrospheric Atmospheric Research Center, Nagoya University

The thawing depth (active layer depth) in late summer drastically deepened and the soil moisture increased from 2005 to 2008 in the middle of the Lena River Basin. This was partly due to the high rainfall in late summer, as well as the high snowfall in winter. Subsequently, permafrost-forest degradations and waterlogging has been detected in the region. To clarify whether high precipitation occurred in the past in this region, we investigate the atmospheric water cycle and water budget using archived precipitation (PREC/L) and atmospheric re-analysis data (JRA-25, JRA-55). Previous studies revealed a negative correlation in the summer atmospheric circulation pattern between the Lena and Ob River Basins. However, little is known about the atmospheric water cycles in the Arctic circumpolar region, including the Mackenzie River Basin. Hence we analyzed the interannual variability of the atmospheric water cycle in the Arctic circumpolar region, comparing the three large North Eurasian river basins (Lena, Yenisei, and Ob) and the Mackenzie river basin. The analyzed results are as follows.

1) In the highest five-year summer net precipitation in the Lena River basin during the period 1958 to 2012, significant cyclonic deviation was present from the Barents Sea towards the region across from the Yenisei and Lena. The deviation distribution of the height field and the water vapor flux from the west to the Lena river basin were significantly increased, so as to form a positive deviation of net precipitation.

2) A significant enhancement of cyclonic circulation was detected from 2005 to 2008 on the Eurasian side of the Arctic Ocean. However, anticyclones appeared over Mongolia. These probably increased the atmospheric moisture convergence over the Lena River Basin in this period.

3) A significant positive trend in the summer precipitation and the summer net precipitation appeared after 1995 between the Lena and Yenisei River Basins. On the contrary, the negative trends between the Lena and the Ob River Basins became unclear from 1993.

Keywords: summer precipitation, summer net precipitation, Lena River Basin, Arctic cyclone

Japan Geoscience Union Meeting 2014
(28 April - 02 May 2014 at Pacifico YOKOHAMA, Kanagawa, Japan)

ACG36-11 Room:311 Time:April 29 17:00-17:15

Evaluation of Large-scale Surface Wetness Variations in Northern High Latitudes During 1980-2010

TAKATA, Kumiko[1*] ; XU, Jianqing[2] ; HARA, Masayuki[2] ; NOZAWA, Toru[3]

[1]NIPR/NIES/JAMSTEC, [2]JAMSTEC, [3]Okayama University

Large-scale surface wetness is evaluated by a wetness index (WI), calculated from GPCC precipitation divided by potential evaporation (Ep) using ERA interim data during 1980-2010. The climatological distribution of annual WI agrees with that of surface soil moisture (SSM) in ERA interim. Annomalies of annual WI also have strong relation with that of SSM in each region; the correlation coefficient between SSM and WI is higher than that between SSM and precipitation. Therefore WI corresponds to SSM for climatology and year-to-year variations.

The linear trends of WI, Ep and precipitation are calculated, with an attempt to decompose the factors of WI trend into those of Ep and precipitations. In high latitudes of Eurasia and eastern Canada, the increasing precipitation trends are canceled by the increasing Ep trends, resulting in little WI trends. In central Asia, western North America and Alaska, the decreasing precipitation trends and the increasing Ep trends lead to the decreasing WI trends. The precipitation variations dominate the WI variations in most regions. For example in Alaska, the decreasing precipitation trend contributes 72% to the decreasing WI trend and the increasing Ep trend does 27%. On the other hand, there are some regions where the Ep trend is important for the WI trend. For example in monsoon Asia, the precipitation trend is small and contributes only 3% to the decreasing WI trend, while the increasing Ep trend does 99%.

Consequently, it is shown that WI corresponds to surface soil moisture and indicates surface wet/dry conditions, and that the contributions of precipitation and Ep to its trends are quantified. Further analyses will be applied to the outputs of global climate models (GCMs) to evaluate reproducibilities of the surface energy-water balances in those GCMs.

Keywords: surface wetness, large-scale variations, reanalysis data

Japan Geoscience Union Meeting 2014
(28 April - 02 May 2014 at Pacifico YOKOHAMA, Kanagawa, Japan)

ACG36-12 Room:311 Time:April 29 17:15-17:30

Multidisciplinary in situ and satellite observations for accurate detection of phenology in sub- and Arctic ecosystems

NAGAI, Shin[1*] ; TEI, Shunsuke[2] ; KOBAYASHI, Hideki[1] ; IKAWA, Hiroki[4] ; NAKAI, Taro[3] ; KIM, Yongwon[4] ; SUZUKI, Rikie[1] ; SUGIMOTO, Atsuko[2]

[1]Research Institute for Global Change, Japan Agency for Marine-Earth Science and Technology, [2]Graduate School of Env.Science / Faculty of Env.Earth Science Hokkaido University, [3]Hydrospheric Atmospheric Research Center, Nagoya University, [4]International Arctic Research Center, University of Alaska Fairbanks

To accurately evaluate the spatio-temporal variability of ecosystem functions and service in sub- and Arctic regions under rapid meteorological and climate changes, global, long-term, and comprehensive phenological observations are required. Towards this aim, satellite remote-sensing is useful to detect the spatio-temporal variability of plant phenology such as the timing of start (SGS) and end of growing season (EGS). However, from the in situ ecological research viewpoint, the satellite remote-sensing has not been sufficiently tested and validated by ground-truthing. Here, (1) we performed daily field observations with time-lapse digital cameras in boreal forests in Alaska and Siberia; (2) we examined the relationship between satellite-observed vegetation indices and plant phenology; and (3) we evaluated the spatio-temporal variability of the timing of SGS and EGS in sub- and Arctic regions by using MODIS Terra and Aqua-observed green-red vegetation index (GRVI). We found that (1) satellite-observed vegetation indices (i.e. NDVI, EVI, and GRVI) mainly detected the plant phenology of forest floor in sparse forests; (2) large year-to-year variability of the timing of SGS was detected in eastern Siberia and western Ural Mountains, while that of EGS was not clearly detected; and (3) in contrast, large year-to-year variability of the timing of EGS was detected in western Alaska, which is mainly covered by tundra vegetation, while that of SGS was not clearly detected.

Keywords: phenology, remote sensing, terrestrial ecosystem, Siberia, Alaska, ground-truthing

Japan Geoscience Union Meeting 2014
(28 April - 02 May 2014 at Pacifico YOKOHAMA, Kanagawa, Japan)

ACG36-13 Room:311 Time:April 29 17:30-17:45

Estimate of permafrost organic carbon balance in Alaskan boreal and tundra ecosystems using natural radiocarbon tracer

KONDO, Miyuki[1*] ; UCHIDA, Masao[1] ; UTSUMI, Motoo[2] ; IWAHANA, Go[3] ; YOSHIKAWA, Kenji[3] ; IWATA, Hiroki[4] ; HARAZONO, Yoshinobu[3] ; NAKAI, Taro[5] ; TANABE, Kiyoshi[1] ; SHIBATA, Yasuyuki[1]

[1]National Institute for Environmental Studies, [2]University of Tsukuba, [3]University of Alaska, Fairbanks, [4]Kyoto University, [5]Nagoya University

The high-latitude regions, where a serious warming is expected, currently store large amounts of soil organic carbon in active-layer soils and permafrost, accounting for nearly half of the global belowground organic carbon pool. Despite the importance of these regions in the present carbon cycle, the soil C fluxes and budget are still only poorly known. Here, we use radiocarbon as the tool for quantifying the C balance of the inputs and decomposition in tundra and boreal soil. We evaluated the C inputs (I) and decomposition rates (k, inverse of turnover time) and net C accumulation (CA), using ^{14}C approaches.

Tundra and boreal soils show different patterns of depth distribution and C storage. Cumulative organic carbon stocks in boreal forest are 5.3 and 19.2 kgCm^{-2}, in surface organic layer (0-25 cm), and deep organic and mineral layers (25-70 cm), respectively. Large annual C input (0.25 kgCm^{-2} yr^{-1}) and relatively slow decomposition (27 years) lead to rapid CA (0.05 kgCm^{-2} yr^{-1}) in surface organic layer in boreal forest. Deep organic and mineral layers including near-surface permafrost show slower rate of input (0.03 kgCm^{-2} yr^{-1}) and turnover (617 years) and CA about 20 times slower (0.003 kgCm^{-2} yr^{-1}) than surface organic layer. Decomposition organic matter (Rh), which in accord with C losses from both surface and subsurface layers, was 0.23 kgCm^{-2}yr^{-1}. This value agreed well with Rh (0.23 kgCm^{-2} yr^{-1}) simulated by process-based models that simulate the biogeochemical and hydrologic cycle, where Rh averaged 45% of ecosystem respiration and 59% of soil respiration.

In contrast, large amount of SOC (36.4 kg m^{-2}) have accumulated over millennia (turnover time: 4540 yrs) below the thin organic layer in tundra. The CA of mineral layer and permafrost is close to zero (0.003 kgCm^{-2} yr^{-1}), and Rh is 0.008 kgCm^{-2} yr^{-1}. Our radiocarbon data show that the most SOC in tundra soil was mode of stabilizing OC by permafrost and steady-state SOC stocks under current C balance.

Japan Geoscience Union Meeting 2014
(28 April - 02 May 2014 at Pacifico YOKOHAMA, Kanagawa, Japan)

ACG36-14 Room:311 Time:April 29 17:45-18:00

Large-Scale Forest Fires in Alaska: Weather Conditions in 2004 and 2005

HAYASAKA, Hiroshi[1*]

[1]Graduate School of Hokkaido University

In Alaska, large-scale forest fires mainly occurred in the boreal forest of the Interior (area roughly around 400 x 800 km) in 2004 and 2005. Number of large-scale forest fires (burnt area more than 500km^2) were 17 in 2004 and 12 in 2005. These large-scale forest fires boosted up burnt areas 26,000km^2 in 2004 and 18,800km^2 in 2005. Their areas were largest and third largest among the past 58 years from 1956 to 2013.

In order to evaluate large-scale forest fires in both years, statistical analysis for the fire data in the past 58 years was carried out. As a result, annual average burnt area was 3,480 km^2, and the coefficients of standard deviation (sigma) were +4.25 for 2004 and +2.88 for 2004. In the background of these large standard deviation coefficients, only 11-year could show large burnt area of more than 6,000km^2, and burnt area of other 47-year were less than 5,000km^2. In addition to this trend, the occurrence of fire year with burnt area more than 6,000 km^2 was once per decade from the 1950s to the 1980's. But from the 1990's, fire year tended to occur more frequently. That is, they were 1957 (2nd largest), 1969 (6th), 1977 (7th), 1988 (8th), and these frequencies were once per decade. However, from the 1990s, fire years occurred in 1990 (4th largest), 1997 (9th), and 1991 (11th). From the 2000s, four fire years observed in 2004 (largest), 2005 (3rd largest), 2009 (5th), and 2002 (10th). The frequent occurrence trend of such fire year may be suggesting close relationship with the rapid reduction of sea ice in the Arctic Ocean under a rapid climate change.

From the comprehensive analysis in this paper, largest burnt areas in 2004 happened under the condition made by ridge extended from Canada lasted about three month from June to August. The very severe fires observed in August 2005 occurred along with the movement of the high pressure system from the Gulf of Alaska to the Beaufort Sea.

Keywords: Forest Fire, Hotspot, Climate Change, Lightning, Jet Stream, Sea ice

Japan Geoscience Union Meeting 2014
(28 April - 02 May 2014 at Pacifico YOKOHAMA, Kanagawa, Japan)

ACG36-15 Room:311 Time:April 30 09:00-09:15

Detection and attribution of changes in arctic ecosystems and atmospheric CO2

PATRA, Prabir[1*] ; KOBAYASHI, Hideki[1] ; SAEKI, Tazu[1]

[1]RIGC/JAMSTEC

Atmospheric CO_2 responds to terrestrial ecosystem activity widely from sub-hourly to decadal time scales primarily due to photosynthesis, weather and climate variations. The measurements of CO_2 thus consist of source signals from anthropogenic as well as natural ecosystem activities convolved with atmospheric transport. Since the records of CO_2 concentration in ambient air at monthly or finer time resolution began in the late 1950s, the seasonal ecosystem dynamics has enhanced significantly in the recent years (Graven et al., 2013). We further analyse the relative contributions of fossil fuel emissions and atmospheric transport on the CO_2 at a greater number of surface measurement sites since the 1980s using the CCSR/NIES/FRCGC atmospheric general circulation model (AGCM)-based chemistry transport model (ACTM). Our results suggest the trends in fossil fuel emissions and transport have detectable contribution to the CO_2 seasonal cycle chances at the sites in northern tropics to mid-latitudes, and that the seasonal cycle increase in the arctic region is governed mainly by the terrestrial ecosystem.

To attribute causes for the recent changes in carbon cycle dynamics we have chosen the period of 1999-2011, which is covered by high quality process oriented ecosystem parameters from remote sensing and atmospheric CO_2 measurements at the largest network of sites for flux inversion. Our analysis suggests that the early greening by several days in the Alaskan tundra region closely correlated with the amplitude of CO_2 seasonal cycle at Point Barrow, Alaska. But no clear trend in the greening onset is detectable at semi-arid grasslands near Ulaanbaatar, Mongolia, except for the closely coupled interannual variations in greening onset time and CO_2 seasonal cycle amplitude. We estimated CO_2 fluxes from 84-regions of the globe at monthly time intervals using measurements from about 100 sites. The terrestrial CO2 fluxes are estimated after removing the effects of fossil fuel emissions and oceanic fluxes in measured CO_2 concentrations. We find the carbon exchange of the Alaska region of our inversion is increased both for the seasonal cycle amplitude and net annual uptake over the period of 2002-2011.

Our results have large implications for developing the future and validating the present earth system models for studying climate-carbon-biosphere interactions.

Keywords: CO2 seasonal cycle, Ecosystem phenology, Arctic environment

Japan Geoscience Union Meeting 2014
(28 April - 02 May 2014 at Pacifico YOKOHAMA, Kanagawa, Japan)

ACG36-16 Room:311 Time:April 30 09:15-09:30

Epoch difference of water cycles in eastern and western Siberia

OSHIMA, Kazuhiro[1*] ; OGATA, Koto[2] ; PARK, Hotaek[1] ; TACHIBANA, Yoshihiro[2]

[1]Japan Agency for Marine-Earth Science and Technology, [2]Mie University

Among all the rivers flowing into the Arctic Ocean, the three great Siberian rivers; Lena, Yenisei and Ob, are the three largest in terms of water discharge (R), and they are a large source of freshwater. We examined the relationship of long-term water cycle variability between eastern and western Siberia on the basis of net precipitation (P-E) estimated from an atmospheric reanalysis, and Rs from observations at the river months and from a reconstruction based on tree rings.

The relationship of summer (P-E)s between the Lena and Ob Rivers is different in the first half and the second half of the past three decades. During 1980s to mid-90s, the (P-E)s have a strong negative correlation. These variations were affected by the east-west seesaw pattern of moisture flux. These results are consistent with Fukutomi et al. (2003). The decomposition analysis revealed that the stationary component of moisture flux dominates the seesaw pattern during the period. After mid-1990s, the correlation of the (P-E)s between the Lena and Ob becomes weak. During mid-1990s to 2000s, the P-E over the Lena was affected by cyclonic moisture flux over the basin. In addition to the stationary component, the transient component of moisture flux also affects the P-E variation in this period.

Long-term records revealed that the Rs of the Lena and Ob Rivers have moderate or weak positive correlations and strong negative correlations before the 1980s. Interestingly, the correlations tend to be distributed in the negative side. It implies that the east-west seesaw pattern frequently appear over Siberia. In conclusion, the moisture transport processes over Siberia are different in each era and they result in the different variability of the Rs and (P-E)s of the Lena and Ob Rivers.

Keywords: Siberian rivers, moisture transport process, net precipitation, river discharge, interannual variation, long-term variability

Japan Geoscience Union Meeting 2014
(28 April - 02 May 2014 at Pacifico YOKOHAMA, Kanagawa, Japan)

ACG36-17 Room:311 Time:April 30 09:30-09:45

The Structure Change of Arctic Cyclones on Cyclone Phase Space

AIZAWA, Takuro[1*] ; TANAKA, Hiroshi[2]

[1]Life and Environmental Sciences, University of Tsukuba, [2]Center for Computational Sciences, University of Tsukuba

In this study, we investigated the structure change of the Arctic cyclone’s life cycle on a cyclone phase space.

Keywords: Arctic cyclone, Structure change, Cyclone phase space

Japan Geoscience Union Meeting 2014
(28 April - 02 May 2014 at Pacifico YOKOHAMA, Kanagawa, Japan)

ACG36-18 Room:311 Time:April 30 09:45-10:00

A negative phase shift of winter AO/NAO due to the recent Arctic sea ice reduction in late autumn

NAKAMURA, Tetsu[1*] ; YAMAZAKI, Koji[1] ; IWAMOTO, Katsushi[1] ; HONDA, Meiji[2] ; UKITA, Jinro[2] ; MIYOSHI, Yasunobu[3] ; OGAWA, Yasunobu[1]

[1]National Institute of Polar Research, [2]Niigata University, [3]Kyushu University

Attribution of the long-term changes in the wintertime Arctic Oscillation (AO)/North Atlantic Oscillation (NAO) to the recent Arctic sea ice reduction is studied. Observations using ERA interim reanalysis and Merged Hadley/OI-SST show that small (large) sea ice area in summer to autumn leads the negative (positive) phase of AO in early winter and NAO in late winter. Relationship with winter AO/NAO is the strongest with the sea ice variability in November rather than September. To separate influences of sea ice variability and sea surface temperature (SST) anomalies, sensitivity experiments are performed with atmospheric general circulation model (AGCM for Earth Simulator, AFES4.1), in which observed changes (anomalies of 2005-2009 from 1979-1983) of the sea ice and SST are prescribed. The Arctic ice reduction generates the negative AO/NAO pattern that brings cold winter in mid-latitude continental regions. Both SST anomalies in the tropics and mid-/high-latitudes mask the continental cooling. Model-based analysis reveals that stationary Rossby wave response to the ice reduction in Barents Sea induces anomalous meridional circulation corresponding to the negative AO. The ice reduction increases (decreases) a frequency of the large negative (positive) AO occurrence about a twice (half). The anomalous meridional circulation warms the Arctic and cools the mid-latitudes. This provides additional Arctic heating about 25% of heat release due to the ice reduction. As a response to ice reduction, transient eddy activity over northern Eurasia is reduced and the change in the eddy damps the stationary responses.

Keywords: Arctic sea ice loss, Arctic Oscillation, long-term changes

Japan Geoscience Union Meeting 2014
(28 April - 02 May 2014 at Pacifico YOKOHAMA, Kanagawa, Japan)

ACG36-19 Room:311 Time:April 30 10:00-10:15

Cross spectral analysis of the AO index using the AOI equation

TANAKA, Hiroshi[1*]

[1]CCS, University of Tsukuba, [2]Life and Environmental Science, University of Tsukuba

Arctic Oscillation (AO) is explained as an atmospheric dynamical eigenmode. There is an argument, however, that the AO is a statistical illusion by the EOF analysis. Tanaka and Matsueda (2005) showed AO mode as the most unstable standing mode in the barotropic atmosphere. In addition to the zero frequency of the mode, the growth rate becomes also zero for adequate frictional force and interaction with transient eddies. Such a mode can be amplified resonantly by quasi-situational forcing. This idea of the AO is called singular eigenmode theory. For the problem of missing correlation in surface pressure between the Pacific and Atlantic is explained by Suzuki and Tanaka (2007) by analyzing barotropic height instead of the surface pressure. The barotropic height indicates significant correlation between the two regions. The missing correlation is thus explained by the baroclinic component of the atmosphere. We support the singular eigenmode theory, but a further analysis is required by the data analysis of the AO index. In this study we derived an equation called AOI equation from the definition of the AOI differentiated with respect to time, and substituting the primitive equation. According to the analysis result of the NCEP/NCAR reanalysis for 62 years of data, it is found that the AOI time series is proportional to the linear term of the AOI equation. The nonlinear term and external forcing term indicate inverse correlation with the AOI, which tend to damp the AOI to the normal. The fact that the linear term of the primitive equation is proportional to the AO structure, i.e., $L*x = a*x$ implies that the AO is an eigensolution of the dynamical system. The present study supports the singular eigenmode theory from the data analysis using the AOI equation.

Keywords: Arctic Oscillation, Global warming, Low-frequency variability, Singular eigenmode theory, Normal mode, Barotropic instability

Japan Geoscience Union Meeting 2014
(28 April - 02 May 2014 at Pacifico YOKOHAMA, Kanagawa, Japan)

ACG36-20 Room:311 Time:April 30 10:15-10:30

Cryospheric studies using satellite data in the GRENE Arctic Project

ENOMOTO, Hiroyuki[1*] ; ALIMASI, Nuerasimuguli[1] ; KAMEDA, Takao[2] ; YABUKI, Hironori[3] ; TAKESHI, Sugimura[1]

[1]National Institute of Polar Research, [2]Kitami institute of Technology, [3]JAMSTEC

GRENE Arctic Climate Research project aims to establish interdisciplinary collaborations of different scientific area. The GRENE project constructed the Arctic Data archive System (ADS) at NIPR to support this researching frame. ADS stores the field data obtained by the project, satellite data by collaboration with JAXA and modelling output from climate models. This presentation introduces activity of data archiving in GRENE Arctic project and ADS for multiple studies.

This study investigates cryospheric change using satellite data stored in the ADS and other satellite programs.

Keywords: Arctic, Cryosphere, Satellite, data archive

Japan Geoscience Union Meeting 2014
(28 April - 02 May 2014 at Pacifico YOKOHAMA, Kanagawa, Japan)

ACG36-21 Room:311 Time:April 30 10:30-10:45

Recent changes of satellite-derived snow grain size and glacial microbial activities in Greenland ice sheet

AOKI, Teruo[1*] ; KUCHIKI, Katsuyuki[1] ; NIWANO, Masashi[1] ; TANIKAWA, Tomonori[2] ; HORI, Masahiro[2] ; SHIMADA, Rigen[3] ; TAKEUCHI, Nozomu[3] ; STAMNES, Knut[4] ; LI, Wei[4]

[1]Meteorological Research Institute, [2]Japan Aerospace Exploration Agency, [3]Chiba University, [4]Steven Institute of Technology

Snow surface albedo strongly depends on snow grain size and mass concentration of light absorbing impurities. These snow parameters are uncertain factors for the recent drastic snow and ice meltings in the Arctic. Particularly, Greenland ice sheet (GrIS) is presently undergoing drastic changes. In 2012 a record melting event of surface snow/ice occurred over the GrIS. When air temperature increases, snow grain size is also increased by accelerating the snow metamorphism and thus the albedo is reduced (positive albedo feedback). This process is mainly dominant in the accumulation areas. On the other hand, the bare ice area is extended by snow melting on ice associate with air temperature raise in ablation areas. It is recently reported that wide bare-ice areas in GrIS are covered with glacial microbes whose albedos are lower than that of blue ice surface. This albedo reduction effect is also another positive albedo feedback effect by glacial microbes. To examin these feedback effects by snow grain growth and glacial microbial activities in conjunction with air temperature increase, we retrieved snow grain size and glacial microbe concentration from Moderate Resolution Imaging Spectroradiometer (MODIS) data. The employed algorithm is based on a look-up table method for bidirectional reflectance distribution function at the top of the atmosphere as functions of snow grain size, snow impurity (soot) concentration, solar and satellite geometry. The employed satellite channels are 0.46, 0.86, 1.24, and 1.64 μm. Since the snow impurity concentrations in accumulation area are the same or lower level of the detection limit of soot concentration in GrIS, we use this retrieval result as an indicator of microbial activities in bear ice areas. The monthly averages of snow grain size and snow impurity concentration from 2000 to 2013 in GrIS derived from Terra/MODIS revealed the following facts. (1) The areas of large grain size changed year by year. (2) There is no constant increasing trend, but the larger values were observed in recent years (2009-2012) and especially for 2012 the remarkable increase in whole Greenland. (3) Larger snow grain size and high impurity concentration, which indicate the areas of high glacial microbial activities, are distributed in coastal regions of GrIS in June (mainly in southern part), July and August. These parameters in colder summer of 2013 than the recent several years, were almost the same as those in 2000.

Keywords: Greenland, snow grain size, glacial microbe, albedo, satellite remote sensing, MODIS

Japan Geoscience Union Meeting 2014
(28 April - 02 May 2014 at Pacifico YOKOHAMA, Kanagawa, Japan)

ACG36-22 Room:311 Time:April 30 11:00-11:15

Acceleration and deceleration of ice thickness variations in Greenland from ICESat laser altimetry (2003-2009)

MATSUO, Koji[1*] ; FUKUDA, Yoichi[1] ; SUZUKI, Kazuyoshi[2]

[1]Graduate school of Science, Kyoto University, [2]JAMSTEC

The laser altimeter mission ICESat, launched by NASA in January 2003, measures the Earth's surface elevation with a precision of several cm. ICESat has performed campaign observation of about 90 days a year between September 2003 and October 2009. The spatial resolution of the measurement in Greenland is about 20 km in average. In this study, we analyze acceleration/deceleration of ice thickness variations in Greenland from ICESat elevation data. We employ Plane fitting method (e.g. Zwally et al., 2011) to correct topographic effect coming from gaps of repeat-track paths, and fit the time-series of surface elevation variations with a linear combination of linear and quadratic terms by least-squares method at every 700m interval. The quadratic trend signal thus extracted represents accelerated/decelerated variations.

The obtained linear variation suggests significant ice thinning trend in southeastern and western Greenland. Their thinning rates attain to about 1.5-2 m/yr. On the other hands, inland area shows ice thickening trend with a rate of 0.3 m/yr. Assuming the firn density as 700 kg/m^3 in ice thinning area and 300 kg/m^3 in ice thickening area, we obtain the total ice loss rate of about -200 Gt/yr, which is equivalent to about 0.55 mm/yr sea level rise. This agrees well with GRACE gravimetric estimate.

Next we focus on the quadratic variation. Western Greenland shows significant negative quadratic variations, suggesting acceleration of ice thinning rate. Such trend is particularly noticeable in Jakobshavn glacier and Qaanaaq area. On the other hands, southern Greenland shows different behaviors: negative quadratic variations (accelerated ice thinning) in Helheim glacier and Kangerdlugssuag glacier, and positive quadratic variations (decelerated ice thinning) in other coastal area. We speculate that accelerated ice thinning in the above outlet glaciers reflects recent global warming, while decelerated ice thinning in other coastal area of southern Greenland does anomalous precipitation of Arctic Oscillation with positive phase during the winter of 2007-2008.

Keywords: Greenland, Ice thickness variation, Climate change, Space geodesy, ICESat, GRACE

Japan Geoscience Union Meeting 2014
(28 April - 02 May 2014 at Pacifico YOKOHAMA, Kanagawa, Japan)

ACG36-23 Room:311 Time:April 30 11:15-11:30

Sensitivity of Response of Greenland Ice Sheet to Global Warming on Surface Mass Balance and Initialization methods

SAITO, Fuyuki[1*] ; ABE-OUCHI, Ayako[2] ; TAKAHASHI, Kunio[1]

[1]JAMSTEC, [2]AORI, Univ. of Tokyo

We present a series of numerical experiments of Greenland ice sheet under global warming condition using Ice sheet model for Integrated Earth system Studies (IcIES).
In this study, influence on the simulation from the difference in the method to compute the surface mass balance is focused.
Typically, ice sheet simulation is driven by a *reference-anomaly* method, in which the surface temperature and/or the accumulation are decomposed into the reference terms (e.g., observation), the anomaly (e.g., climate scenario from climate models).
Then the surface melting is computed using parameterization such as positive degree-day (PDD) method with the temperature.
These decomposed terms have own uncertainties, which may influence the ice-sheet simulation.
In this study, impact of these properties to the present-day control case, as well as the response under uniform warming condition are discussed, which is thought be a useful and basic information of the property/sensitivity of the Greenland ice sheet.

In addition, several initialization methods (free spin-up, fixed-topography spin-up, etc) are applied to IcIES in order to evaluate the influence of the error in the present-day simulated topography to the short-term response of Greenland ice sheet.

Keywords: Greenland ice sheet, Ice-sheet model

Japan Geoscience Union Meeting 2014
(28 April - 02 May 2014 at Pacifico YOKOHAMA, Kanagawa, Japan)

ACG36-24 Room:311 Time:April 30 11:30-11:45

Ice thickness change of Bowdoin Gletscher, northwestern Greenland

TSUTAKI, Shun[1*] ; SUGIYAMA, Shin[2] ; SAKAKIBARA, Daiki[2] ; SAWAGAKI, Takanobu[3] ; MARUYAMA, Mihiro[2]

[1]Arctic Environmental Research Center, National Institute of Polar Research, [2]Institute of Low Temperature Science, Hokkaido University, [3]Faculty of Environmental Earth Science, Hokkaido University

Ice discharge from calving glaciers in the Greenland ice sheet (GrIS) has recently increased through the acceleration of glaciers, and this increase plays an important role in the ice volume change of GrIS and sea level rise. Previous studies have used remote-sensing (RS) data to assess surface lowering of calving glaciers in GrIS. However, because of the remoteness of these glaciers, relatively few field data are available on the surface elevation change. Consequently, RS data have been used without calibration with filed data. The accuracy of such studies relies on digital elevation models (DEMs) derived from satellite data.

In this study, surface elevation was measured along longitudinal and three transverse profiles in Bowdoin Gletscher (77^{o}41'18"N, 68^{o}29'47"W) in July 2013. DEMs of Bowdoin Gletscher in August 20, 2007 and September 4, 2010 were generated by Advanced Land Observing Satellite (ALOS) Panchromatic remote-sensing Instrument for Stereo Mapping (PRISM) images with a 50 m grid mesh, and calibrated using field data. Mean surface elevation change along the field survey profiles were -16.3$\pm$4.0 m (5.3 m yr^{-1}) in 2007-2010 and -10.8$\pm$4.0 m (-3.8 m yr^{-1}) in 2007-2013. Surface elevation change along the lower most transverse profile (800 m from the calving front) was more negative than those along the other profiles in the upper reaches. Surface lowering rate at all profiles has decreased from 2007-2010 to 2010-2013.

Keywords: Calving glacier, Greenland

Japan Geoscience Union Meeting 2014
(28 April - 02 May 2014 at Pacifico YOKOHAMA, Kanagawa, Japan)

ACG36-25 Room:311 Time:April 30 11:45-12:00

Estimation of glacier motions at Svalbard, NovayaZemlya with ALOS/PALSAR

KONUMA, Yoshiki[1*] ; FURUYA, Masato[2]

[1]Department of Natural Sciences History, Hokkaido University, [2]Department of Natural Sciences History Hokkaido University

While the Greenland Ice Sheet's mass loss is equivalent to 0.6mm/yr sea level rise, a half of them is attributed to the changes in glacier dynamics (Broeke et al., 2009). Namely, surface velocities of many glaciers in Greenland have increased in the recent decade (Moon et al., 2012). We thus wonder if glacier velocities outside Greenland have also increased or not.

Svalbard and NovayaZemlya are arctic islands located at 78 degrees north and 74 degrees north, respectively, and have many glaciers. Stozzi et al. (2008) estimated glacier motions in these islands with SAR in 1990s. However, there are not any studies with SAR in recent decade.

We examined Duvebreen glacier in Svalbard and Vize Glacier in NovayaZemlya. In this study, we used PALSAR derived by the ALOS satellite launched from Japan. The PALSAR data were acquired 10 times at Duvebreen glacier from July 2007 to October 2010, 13 times at Vize Glacier from February 2007 to December 2010. We compared the result with 1990s velocity in previous study.

Accordingly, two glaciers in Svalbard and NovayaZemlya speeded up from 1990s. This result suggests that velocity of other arctic glaciers increase as Greenland's glaciers.

Keywords: svalbard, novaya zemlya, glacier, alos, duvebreen, vize glacier

Japan Geoscience Union Meeting 2014
(28 April - 02 May 2014 at Pacifico YOKOHAMA, Kanagawa, Japan)

ACG36-26 Room:311 Time:April 30 12:00-12:15

Snow impurity concentration and snow grain size measured in Ny-Alesund, Svalbard

KUCHIKI, Katsuyuki[1*] ; AOKI, Teruo[1] ; NIWANO, Masashi[1] ; SHIOBARA, Masataka[2] ; GOTO-AZUMA, Kumiko[2]

[1]Meteorological Research Institute, [2]National Institute of Polar Research

Mass concentration of light absorbing impurities in snow and snow grain size are important parameters controlling snow albedo. An increase in light absorbing impurities such as black carbon (BC) reduces the visible albedo and that in snow grain size reduces the near-infrared albedo. To monitor these snow physical parameters and evaluate those effects on snow albedo in the Arctic, we have measured the snow parameters using a ground-based spectral radiometer system for albedo and flux (GSAF) in Ny-Alesund, Svalbard (78^{o}55'N, 11^{o}55'E). The BC concentration in snow and snow grain sizes in the topmost and subsurface layers were retrieved from spectral albedos measured using the GSAF from March to June, 2013. Furthermore, the retrieved snow parameters were validated by comparing with in-situ measurements based on snow pit work and snow sampling in April, 2013. The collected snow samples were filtrated, and then elemental carbon (EC), organic carbon (OC) and dust concentrations in snow were measured by filter weighing and thermal optical analysis.

The snow depth gradually increased up to 40 cm during the polar night from late October to late February. It maintained around 40 cm until the middle of May, and then rapidly decreased to 0 cm in early June. The BC concentrations retrieved from the GSAF varied little during March to June with about 110 and 40 ppbw for external and internal mixture models employed in the retrieval algorithm, respectively. The in-situ measured EC, OC and dust concentrations were 8-35, 32-190 and 570-3180, respectively. The BC-equivalent concentrations estimated from the light absorbing effects of both EC and dust were 18-43 ppbw, which agreed with the GSAF-derived BC concentrations using the internal mixture model. The topmost layer snow grain radius retrieved from the GSAF were varied within the range 30-300 μm until the middle of May, then increased more than 1000 μm with the snow melting. The snow grain sizes in the subsurface layer were generally larger than those in the topmost layer, which was consistent with the in-situ measurement. We estimated the possible albedo reduction by snow impurities using a physically based snow albedo model with the GSAF-derived snow parameters. The albedo reduction was enhanced to -0.038 during snow melting period after the mid-May, compared with -0.027 before the mid-May, mainly due to the increase in snow grain size.

Keywords: light absorbing snow impurity, black carbon, dust, snow grain size, Ny-Alesund

Japan Geoscience Union Meeting 2014
(28 April - 02 May 2014 at Pacifico YOKOHAMA, Kanagawa, Japan)

ACG36-27 Room:311 Time:April 30 12:15-12:30

New developments of Arctic Data archive System(ADS)

YABUKI, Hironori[1*] ; SUGIMURA, Takeshi[2]

[1]Japan Agency for Marine-Earth Science and Technology, [2]National Institute of Polar Research

Arctic is the region where the global warming is mostly amplificated, and the atmosphere/ ocean/ cryosphere/ land system is changing. Active promotion of Arctic environmental research, it is large and responsible for observational data. Promotion of Arctic research in Japan, has not been subjected to independent in their respective fields.

In the National Institute of Polar Research, perform the integration and sharing of data across a multi-disciplinary such as atmosphere, ocean, snow and ice, land, ecosystem, model, for the purpose of cooperation and integration across disciplines, we build a Arctic Data archive System (ADS).

Arctic Data archive System (ADS), to promote the mutual use of the data across a multi-disciplinary to collect and share data sets, such as observational data, satellite data, numerical experiment data. Through these data sets, clarify of actual conditions and processes of climate change on the Arctic region, and further contribute to assessment of the impact of global warming in the Arctic environmental change, to improve the future prediction accuracy.

ADS developed the the online visualization system (VISION) of grid data (a satellite and model simulation), which observational researcher was not good. This VISION which can easily visualize special change can become effective for not only the understanding of the phenomenon but also the design of the observation for an observational researcher.

Keywords: Arctic, Environment, Global Warming, ADS, Visualization, VISION

Japan Geoscience Union Meeting 2014
(28 April - 02 May 2014 at Pacifico YOKOHAMA, Kanagawa, Japan)

ACG36-28 Room:311 Time:April 30 12:30-12:45

Recent advance in discussions on the Arctic Environmental Studies

ENOMOTO, Hiroyuki[1*] ; OHATA, Tetsuo[2]

[1]National Institute of Polar research, [2]JAMSTEC

This presentation introduces rescent activities of the discussion on Arctic environmental studies. There are many national and international discussions on the Arctic study. Japan Consortium for Arctic Environmental Research (JCAR) has started discussions on thefuture study plan. IASC and ICARP-III discusses on the enhancement of present and future Arctic research and coordinations.

Keywords: Arctic, Environmetal study, planning

Japan Geoscience Union Meeting 2014
(28 April - 02 May 2014 at Pacifico YOKOHAMA, Kanagawa, Japan)

ACG36-P01 Room:Poster Time:April 30 18:15-19:30

Sea ice and ocean primary production and phenology in the Arctic Ocean

JIN, Meibing[1*]

[1]International Arctic Research Center, University of Alaska Fairbanks

In the Arctic Ocean, both phytoplankton and sea ice algae are important contributors to primary production and the arctic food web. We use a coupled ice algal and pelagic ecosystem model embedded in the global physical model POP-CICE (Parallel Ocean Program- Los Alamos Sea Ice Model) to study the ecosystem response to climate changes. The model results showed a mean seasonal cycle of ice algal production from March to May and subsequent ocean production from May to September in the Arctic. The ice algal production, although smaller than that of the ocean, is of ecological importance as a food source for higher trophic levels during the long arctic winter before ice melt. The simulated mean open-ocean upper 100m primary production within the Arctic Circle was 413 Tg C/yrin the years 1998 to 2006, close to the remote sensing derived estimate of 419 Tg C /yr but with higher interannual variations. The mean sea ice algal production in the Northern Hemisphere from 1998 to 2007 was 21.3 Tg C/yr, which is in the range of multi-observational estimations of 9 to 73 Tg C/yr based on in situ measurements. Arctic organisms are adapted to the strong seasonality of environmental forcing. Climate warming causes shrinking ice coverage and earlier ice retreat in the Arctic, which is likely to change the timing of primary production. Using a synthesis of available satellite observation data and the coupled ice-ocean ecosystem model, we found that, over a large portion of the Arctic marginal seas, the timing variability of ice retreat at a specific location has a strong impact on the timing variability of pelagic phytoplankton peaks but weak or no impact on the timing of ice-algae blooms in those regions. The model predicts latitudinal and regional differences in the timing of ice algae biomass peak (varying from April to May) and the time lags between ice algae and pelagic phytoplankton peaks (varying from 45 to 90 days). The correlation between the time lag and ice retreat is significant in areas where ice retreat has no significant impact on ice-algae peak timing, suggesting that changes in pelagic phytoplankton peak timing control the variability of time lags. Phenological variability of primary production is likely to have consequences for higher trophic levels, particularly for the zooplankton grazers, whose main food source is composed of the dually pulsed algae production of the Arctic.

Keywords: Arctic Ocean, primary production, phenology, sea ice algae, phytoplankton

Japan Geoscience Union Meeting 2014
(28 April - 02 May 2014 at Pacifico YOKOHAMA, Kanagawa, Japan)

ACG36-P02 Room:Poster Time:April 30 18:15-19:30

The effect of meteorological condition on energy and carbon budget on taiga-tundra boundary in North-eastern Siberia

MIYAZAKI, Shin[1*] ; TEI, Shunsuke[1] ; BRAGIN, Ivan[4] ; SUZUKI, Rikie[2] ; TAKANO, Shinya[3] ; SHINGUBARA, Ryo[3] ; MOROZUMI, Tomoki[3] ; SUGIMOTO, Atsuko[3] ; MAXIMOV, Trofim[5]

[1]National Institute of Polar Research,, [2]Japan Agency for Marine-Earth Science and Technology, [3]Hokkaido University, [4]FarEast Geological Institute, FE RAS, [5]nstitute for Biological Problems of Cryolithozone SD RAS

1. Introduction

In Arctic, temperature has increased almost twice the global average rate in the past 100 years. We aim to clarify the land-atmosphere interaction over the boundary between taiga and tundra in northeastern Siberia, where the climate change effect might be remarkable. We have started the energy, water and carbon fluxes observation as well as hydro-meteorological observation in northeastern Siberia, Sakha Republic, Russia in June 2013.

2. Material and methods

Our observation site is located at Kodack site (70.564 N, 148.267E, altitude 7m) about 100km south from East Siberian Sea in Arctic Ocean near Chokurdakh city in the North-Eastern Siberia, Sakha Republic, Russia. The Kodack site is belong to Indigirka river basin (drainage area: 324,244km^2) which flow to the East Siberian Sea. The annual air temperature and precipitation are -13.4 deg. C and 200mm respectively (1979-2008, Baseline Meteorological Data in Siberia (BMDS) Ver.5.0, Yabuki et al., 2011). The surface is covered by snow except July and August and the maximum snow depth is 40cm in April. In this region, the permafrost exits and the active layer depth ranges from 25cm to 40cm (van der Molen et al., 2007). The topography at the site consists of higher mounds and lower wet lands, where the difference of the height are about 50cm. At the higher mound, the shrubs and larches are dominant, while the sphagnum are prevailing at the lower wet land. The meteorological and flux observation has been carried out over the mound area.

The air temperature, relative humidity, wind speed and direction, air pressure, precipitation were observed at 1.5m height. The incoming and outgoing shortwave and longwave radiation were observed by 4-compnent radiometer at 1.37m height. The soil heat flux was observed by heat flux plate at 0.05m depth. The soil temperature was observed by platinum sensor at depths of 0.025, 0.05, 0.225, 0.425, and 0.625 m. The soil moisture was observed by capacitance sensor and frequency domain reflectometry sensor at depths of 0.035, 0.145, 0.335, and 0.535 m. The energy and carbon fluxes were calculated by the eddy covariance method from the observed values of the sonic anemo-thermometer at 2.55m height.

3. Results

The analysis results from 23 June to 27 October 2013 will be shown. The daily mean air temperature and relative humidity varied from 0.5 to 21.9 deg. C and from 53.9 to 90.0%, respectively. The total precipitation was 29.5 mm, and the maximum daily precipitation was 9 mm?day-1. The daily mean wind speed varied from 1.3 to 6.1 m s^{-1}. There was clear relationship between the daily mean air temperature and wind direction. When the wind direction was northerly (southerly), the air temperature was low (high). The soil temperature (Ts) at surface varied from 2.8 to 10.8 deg. C while Ts at deeper than 0.425 m kept below 0 deg. C, which implies the frozen soil. The Ts at depth of 0.225m increased from -0.4 to 1.8 deg. C. The soil water content (SWC) was higher than 50% in surface layer of wet land while SWC at dry mound was lower than 11%. The net radiation varied from 50 to 200 W m^{-2} and soil heat flux varied from 11 to 40 W m^{-2}. The daily mean latent heat flux (average during analysis period: 39 W m^{-2} was little higher than the daily mean sensible heat flux (26 W m^{-2}). The daily mean net ecosystem exchange (NEE) on 24 and 26 June was 0.32 and 0.41 g C m^{-2} day^{-1}, respectively, which implies the carbon was released from the surface to the atmosphere while the NEE of the other days was negative value which implies the carbon was uptaken from the atmosphere. The accumulated NEE during analysis period was about -64 g C m^{-2} day^{-1}, which was smaller uptake than the value observed at tundra (-92g C m^{-2} day^{-1}; van der Molen et al., 2007). As our observation was started about half month after the start of growing season (late May), further analysis using the next year observation is necessary.

Keywords: Taiga-Tundra boundary, Siberia, Energy and carbon budget

Japan Geoscience Union Meeting 2014
(28 April - 02 May 2014 at Pacifico YOKOHAMA, Kanagawa, Japan)

ACG36-P03 Room:Poster Time:April 30 18:15-19:30

Year to year variations in larch growth and their controlling factors in taiga-tundra boundary ecosystem, NE Siberia

LIANG, Maochang[1*] ; TEI, Shunsuke[1] ; SUGIMOTO, Atsuko[2] ; MAXIMOV, Trofim C.[3] ; KIYASHKO, Sergey[4] ; VELIVETSKAYA, Tatiana A.[5] ; IGNATIEV, Alexander V.[5]

[1]Graduate School of Environmental Sci. Hokkaido Univ., [2]Faculty of Environmental Earth Sci. Hokkaido Univ., [3]Inst. Biological Problems of Cryolithozone, SBRAS, Yakutsk, Russia, [4]Far East Inst. of Marine Biology, FEB RAS, Vladivostok, Russia, [5]Far East Inst. of Geological, FEB RAS, Vladivostok, Russia

Eastern Eurasia is covered by permafrost which is the largest and the deepest in the world. In its arctic region of lowland of Indigirka River, taiga-tundra boundary ecosystem covers the area. For better understanding of this boundary ecosystem, it is important to understand controlling factors on the growth of larch trees which is the dominate tree species of taiga. Larch growth can vary spatially and temporally. In spatial variation, we found that high soil moisture influences mortality of the larch trees and N availability explains differences in trees ability of C assimilation among the sites. To know the controlling factors on temporal variation of larch growth, we conducted field measurements on photosynthesis, needle nitrogen (N) content, needle mass and isotopic ratios in larch needle and stem in every summer from 2009 to 2013 at four sites in the Indigirka River Basin, near Chokurdakh (70^{o}37'N,147^{o}53'E), northeastern Siberia.

There was no seasonal variation in needle mass during the growing season after needles were fully open, while needle N content showed seasonality. Needle N content in the year positively correlated with July air temperature and stem δ^{13}C and following year needle δ^{13}C. These results indicates that, in the year with higher July air temperature, more N was allocated to needle and larch trees exhibited higher photosynthetic rate and photosynthetic C used for needle production was one year delayed. Higher air temperature in the year possibly indicates higher solar radiation based on positive correlation between July temperature and sun hours. Therefore, it can be said that larch growth shows strong dependence on solar radiation. In terms of temperature itself, we found higher temperature could limit photosynthetic rate. In addition, wet event, occurred at some sites in 2011 and 2012, caused low photosynthetic rate and low needle N content in 2012, and higher needle δ^{13}C in 2012 and 2013. These results indicate that high soil moisture could limit larch photosynthesis and reduce N uptake and cause stomata closure as well.

Our observational results indicate that solar radiation is one of the most important controlling factors on larch growth, and high soil moisture and high temperature can limit larch growth.

Keywords: Carbon and nitrogen isotopes, Needle N content, Photosynthesis, Air temperature and solar radiation, Soil moisture, Vegetation change

Japan Geoscience Union Meeting 2014
(28 April - 02 May 2014 at Pacifico YOKOHAMA, Kanagawa, Japan)

ACG36-P04 Room:Poster Time:April 30 18:15-19:30

Spacial distribution of vegetation at taiga-tundra boundary ecosystem in eastern Siberia

MOROZUMI, Tomoki[1*] ; BRAGIN, Ivan[5] ; STAROSTIN, Egor[6] ; SHINGUBARA, Ryo[1] ; TEI, Shunsuke[2] ; TAKANO, Shinya[1] ; MIYAZAKI, Shin[2] ; MAXIMOV, Trofim C.[7] ; SUGIMOTO, Atsuko[3]

[1]Hokkaido University Graduate School of Environmental Science, [2]National Institute of Polar Research, Arctic Environment Research Center, [3]Hokkaido University Faculity of Environment Earth Science, [4]Japan Agency for Marine-Earth Science and Technology, Research Institute for Global Change, [5]Far East Geological Institute, Far Eastern Branch Russian Academy of Science, [6]North-Eastern Federal University, [7]Institute for Biological Problems of Cryolithozone, Siberian Branch of Russian Academy of Sciences

Vegetation types, species compositions were observed with physical environment such as micro topography and soil moisture at taiga-tundra boundary ecosystem in lowland of Indigirka river in north eastern Siberia near Chokurdahk village(70^oN,148^oE)in July 2012 and 2013. There are 4 types of plant communities: driest Tree mound(*Larix gmelnii* etc.), Shrub(*Betula nana* etc.), Sphagnum(*Sphagnum* sp. etc.), wettest Hollow(*Eriophorum angustifolium* etc.). Large area is also covered by Willow(*Salix udensis* etc.) along the river. Soil moisture is the most important factor controlling vegetation and other biogeochemical cycles, such as methane emission. Thus, it is necessary to make a vegetation map with a classification as a key for estimating methane emission.

The objective of this study is classify land cover vegetation using remote sensing approach on satellite images and photographs. In remote sensing approach we used high resolution satellite multispectral image(GeoEye-1, WorldView-2) and aerial photo by radio-control helicopter. Supervised classification was conducted for spacial distribution of vegetation based on aerial photos. This vegetation map will be used for upscaling of biogeochemical cycle process such as greenhouse gases.

Keywords: Taiga-Tundra boundary, vegetation map, remote sensing, Siberia

Japan Geoscience Union Meeting 2014
(28 April - 02 May 2014 at Pacifico YOKOHAMA, Kanagawa, Japan)

ACG36-P05 Room:Poster Time:April 30 18:15-19:30

Satellite observation of cryospheric change using Arctic Data archive System (ADS)

ALIMASI, Nuerasimuguli[1*] ; ENOMOTO, Hiroyuki[1] ; YABUKI, Hironori[3] ; SUGIMURA, Takeshi[1] ; KAMEDA, Takao[2]

[1]National Institute of Polar Research, [2]Kitami Institute of Technology, [3]JAMSTEC

Arctic Data archive System (ADS) has been constructed in the GRENE Arctic Climate Research project. ADS is useful for quick look of data and visualizing satellite data in the Arctic. The decline of sea ice area in the Arctic influences on the environment and industrial activities in the coastal region and people's life. Satellite microwave data since 1978 was archived in ADS. They are SMMR, SSM/I, AMSR, AMSR-E and AMSR2. These data sets enable to analyze more than 35-years time series of snow conditions, sea ice conditions in the Arctic.

The data is available for all-weather, even during the polar night season. The data enables climatological analysis for more than 30-years time spanThis study demonstrates ADS capabilities for long-time monitoring and snow and ice conditions.

Keywords: Arctic, Cryosphere, Satellite, Data archive

Japan Geoscience Union Meeting 2014
(28 April - 02 May 2014 at Pacifico YOKOHAMA, Kanagawa, Japan)

ACG36-P06 Room:Poster Time:April 30 18:15-19:30

Age of the Pacific Winter Water in the Canada Basin estimated from SF6

OGIWARA, Yusuke[1*] ; KAWAI, Michiyo[2]

[1]Tokyo University of Marine Science and Technology, [2]Tokyo University of Marine Science and Technology

In the Pacific sector of the Arctic Ocean, Pacific Winter Water (PWW) distributes between 100m and 200m depths. Because the PWW has high nutrient concentrations and low pH, its spreading pathway has implications on primary production and ocean acidification in the Arctic Ocean. In this study, we have observed distribution of SF6, a transient tracer alternative to CFCs, in order to trace newly formed PWW into the Canada Basin.

Sampling was carried out in summer of 2013 on the CCGS Louis S. St-Laurent. Seawater at the core of PWW (salinity = 33.1) were collected in Niskin bottles and then transferred into custom-made glass bottles. Samples were kept at low temperature and brought back to Japan. Concentrations of SF_6 in seawater samples were determined by an ECD-GC following the method described in Bullister and Wisegarver (2008).

Results show that younger PWW distributes at the periphery of the Beaufort Gyre, a major anticyclonic circulation in Canada Basin. The age of PWW estimated from SF_6 was 13∼15 years in the center of the gyre, whereas age was 6∼9 years around the gyre. From the distributions of SF_6 age, dissolved oxygen and nutrients, it is suggested that there is a pathway of PWW from the Siberian shelves or slopes into the northeastern Canada Basin.

Keywords: arctic ocean, time transit tracer, SF6, ocean circulation

Japan Geoscience Union Meeting 2014
(28 April - 02 May 2014 at Pacifico YOKOHAMA, Kanagawa, Japan)

ACG36-P07 Room:Poster Time:April 30 18:15-19:30

Mineralization Rate of Soil Organic Carbon at the Lowland of Indigirka River in Northeastern Siberia

SHINGUBARA, Ryo[1*] ; TANABE, Shinichi[2] ; TAKANO, Shinya[1] ; BRAGIN, Ivan[3] ; MURASE, Jun[4] ; TEI, Shunsuke[5] ; MAXIMOV, Trofim C.[6] ; SUGIMOTO, Atsuko[7]

[1]Grad. School of Env. Sci., Hokkaido Univ., [2]School of Sci., Hokkaido Univ., [3]Far East Geological Inst. FEB RAS, Vladivostok, Russia, [4]Grad. School of Bioagr. Sci., Nagoya Univ., [5]National Inst. of Polar Research, [6]Inst. for Biol. Problems of Cryolithozone SB RAS, Yakutsk, Russia, [7]Faculty of Earth Env. Sci., Hokkaido Univ.

The Arctic has a large amount of organic carbon accumulated in the soil. If the enhanced warming under the Anctic amplification leads to higher soil temperature or deepening of the active layer, emission of greenhouse gases, i.e. CO_2 and CH_4 can increase. The decomposition rate of organic matter, which is an important factor of CO_2 and CH_4 emission, depends not only on the quantity of organic matter, but also on that quality. In this work, surface soils from the lowland of Indigirka river in Northeastern Siberia were incubated at constant temperatures (5, 10 ℃) to evaluate the production rates of CH_4 and CO_2 and to know the degradability of the soil organic matter.

The study site is around Chokurdakh (70.62 N, 147.90 E) located in the continuous permafrost of Eastern Siberia and situated in the boundary of tundra and taiga. Surface soil layers (ca. 10-60 cm deep) were sampled at 7 points of a drier mound with larch trees and of wetter areas with sedges and *Sphagnum spp.*. Besides thawed layers (10, 20, 30 cm deep) sampled in July were incubated at Chokurdakh for 8 days anaerobically, frozen soil layers sampled in the early summer of June (13-62 cm) were incubated in Japan for 34-42 days both anaerobically and aerobically. These soils include the active layer (ca. 20-50 cm) and the top of the permafrost of this region.

CH_4 production was not detected in the mound soils while CO_2 production was, suggesting areas with dry condition have few methanogens and will not produce CH_4 even if they turn into anaerobic condition. On the other hand, soils from wet areas produced CH_4 (0-0.88 μmol (g dry soil)$^{-1}$ day^{-1}) and the production as well as that of CO_2 was more active at the shallower layers, representing larger amount of labile organic matter. The rate of CH_4 production at 10 ℃ were found to be 0.9-1.1 times of that at 5 ℃ in the shallower layers (ca. 10-40 cm), while 1.9-3.3 times in the deeper layers (32-45 cm). It indicates that the temperature dependency of CH_4 production is higher in the middle to the bottom of the active layer than in the top layer.

Keywords: methane, carbon dioxide, incubation experiment, Eastern Siberia, taiga-tundra boundary, stable isotope ratio

Japan Geoscience Union Meeting 2014
(28 April - 02 May 2014 at Pacifico YOKOHAMA, Kanagawa, Japan)

ACG36-P08 Room:Poster Time:April 30 18:15-19:30

Accurate snowfall measurement at Yakutsk, Russia

HIRASAWA, Naohiko[1*] ; SUGIURA, Konosuke[2] ; HOSAKA, Masahiro[3] ; MAXIMOV, Trofim[4]

[1]National Institute of Polar Research, [2]Center for Far Eastern Studies, University of Toyama, [3]Meteorological Research Institute, [4]Institute for Biological Problems of Chryolithozone

In association with global warming, the water cycle in the atmosphere also changes for every climatic region on the globe. In polar regions, change in snowfall turns in change in distribution of snow surface and snow cover period, which will drive the ice-albedo feedback process. In order to know the present condition of the water cycle of polar regions and to study the trajectory of the polar climate systems in future, we have to observe not only air property such as temperature but also hydrological property such as snowfall amount, snow depth and so.

In spite of the development in accurate measurements for air temperature, pressure, wind speed and direction, the accuracy of snowfall measurement is not sufficiently high. While heated raingauge is currently generally deployed all over the world, the capture rate of snow particles falls together with wind speed, e.g., around 0.5 of the rate at 5 m/s. It means we measure only a half of the true value of snowfall amount at 5 m/s. This effect has been known for long time as wind loss. Evaporation loss also is more important in the polar regions than the other regions because many snowfall events have the smaller amounts in the total and lower snowfall rates according to the lower-temperature condition in the polar regions. Now, the accurate measurement of snowfall amount is one of the top issues in polar climate science.

The purpose of this study is to measure the accurate snowfall amount in the Arctic region. Moreover, based upon the results, we intend to correct other data which are measured in other region and in past years and also contribute to improve climate model by provideing accurate snowfall data. This study deploys a disdrometer, which measures diameter and fall velocity for each particle and out put the statistics minutely. It is not affected by wind loss and evaporation loss. This presentation shows a snowfall event observed at Yakutsk in early winter of 2013/14.

Keywords: Yakutsk, Snowfall, Disdrometer

Japan Geoscience Union Meeting 2014
(28 April - 02 May 2014 at Pacifico YOKOHAMA, Kanagawa, Japan)

ACG36-P09 Room:Poster Time:April 30 18:15-19:30

Continuous measurements of the atmospheric O2/N2 ratio at Ny-Alesund, Svalbard

GOTO, Daisuke[1*] ; MORIMOTO, Shinji[2] ; AOKI, Shuji[2] ; NAKAZAWA, Takakiyo[2] ; MURAYAMA, Shohei[3]

[1]National Institute of Polar Research, [2]Graduate School of Science, Tohoku University, [3]National Institute of Advanced Industrial Science and Technology

Simultaneous observations of atmospheric O_2 (defined as O_2/N_2 ratio) and CO_2 concentrations provide valuable information about the global carbon cycle. For a better understanding of the global carbon cycle, several laboratories have developed precise measurement systems for the O_2/N_2 ratio and carried out systematic observations since the early 1990s. To elucidate the variations of the atmospheric O_2/N_2 ratio in detail and to contribute to a better understanding of the role of Arctic region on the regional and global carbon cycle, we developed a continuous measurement system using a differential fuel-cell O_2 analyzer, and then initiated systematic observation at Ny-Ålesund, Svalbard in November 2012, which is the first continuous observation in the Arctic region. The system is equipped with NDIR analyzer to measure CO_2 concentration simultaneously. The analytical precisions of O_2/N_2 ratio and CO_2 are estimated to be $\pm$1.4 per meg and $\pm$0.03 ppmv, respectively. Here, we will present observational results of the first year.

The O_2/N_2 ratio observed at Ny-Ålesund shows a clear seasonal cycle with peak-to-peak amplitude of about 120 per meg, which reaches a minimum in late March to early April and a maximum in August. On the other hand, the CO_2 concentration varies seasonally in opposite phase with the O_2/N_2 ratio, showing the amplitude of 16 ppm. Short-term variations on time scales of several hours to several days are also clearly seen. In winter, it is often observed that the O_2/N_2 ratio sharply declines in a short time, accompanied by an increase in the CO_2 concentration, and the low values last for several hours or days. The O_2:CO_2 exchange ratio defined as the slope of a linear regression line between the measured values of O_2/N_2 ratio and CO_2 range between -1.6 and -1.5 ppm/ppm, which are close to the average O_2:CO_2 exchange ratio expected from fossil fuel burning in Europe. The results of backward trajectory analysis indicated that the air masses arrived at Ny-Ålesund during the periods when such short-term variations were observed passed near or over Scandinavian Peninsula. Therefore, such a decline in the O_2/N_2 ratio is ascribed to transport of urban air influenced by human activities in Europe. In spring to summer, irregular fluctuations of O_2/N_2 ratio are often observed. The amplitude of such fluctuations reaches 50-60 per meg (corresponding to about 10-13 ppm). Similar fluctuations of CO_2 are also found in opposite phase with O_2/N_2 ratio. However, their amplitudes are 5 ppmv at most. The comparison of backward trajectories of air parcels with the distributions of marine biotic net primary production suggests that such fluctuations of O_2/N_2 ratio are closely related to O_2 emission due to marine biological activity near Norwegian Sea.

Keywords: atmospheric O2, carbon cycle, O2:CO2 exchange ratio, air-sea O2 flux

Japan Geoscience Union Meeting 2014
(28 April - 02 May 2014 at Pacifico YOKOHAMA, Kanagawa, Japan)

ACG36-P10 Room:Poster Time:April 30 18:15-19:30

Geographical variations in formation process of cryoconite granules on Arctic glaciers

FUJISAWA, Yuta[1*] ; TAKEUCHI, Nozomu[1] ; NAGATSUKA, Naoko[2] ; UETAKE, Jun[2] ; MIYAIRI, Masaya[1]

[1]Graduate School of Science, Chiba University, [2]National Institute of Polar Research

The dark colored impurities deposited on the glacier ice are called cryoconite. Cryoconite is consisted of mineral particles, organic matter and microbes, including snow algae, cyanobacteria and bacteria. They usually form small spherical aggregates known as cryoconite granules. The spherical shape is maintained by filamentous cyanobacteria. The satellite images of Greenland ice sheet revealed that the dark colored bare ice surface has expanded recently and may have a big impact on the melting of ice. The darkening may be due to increase of cryoconite on the surface. Therefore, the understanding of the structure and formation process of the cryoconite granules is important for studies of the influence on the glacier ecosystem and mass balance of glaciers. In this study, we analyzed the structure and characteristics of cryoconite granules on Arctic glaciers and we clarified the differences in the formation process with the glaciers.

We analyzed the cryoconite samples collected on the northwestern part of the Greenland ice sheet, the Longyearbreen glacier of the Svalbard, the Suntar-Khayata glacier of the Siberia, the Gulkana glacier of the Alaska. We observed the cryoconite granules using a microscope in order to clarify the characteristic of the composition, the granule size. Furthermore, to observe inner structures, thin sections of cryoconite granules were made.

Microscopy of cryoconite granules revealed that their size and coloration differed among the glaciers. The size of granules was the largest for Svalbard followed by Siberia, Alaska, and Greenland. The coloration of cryoconite granules was brown for Svalbard, black for Siveria, gray for Alaska, and black to brown for Greenland. Cross section of the granules also showed the disticnct features. The granules from Greenland had mostly subgranules inside. The granules from Svalbard had some concentric layers of dense organic matter. The granules from Siberia had a large mineral particle inside. The granules from Alaska had no specific inner structure. These differences of cryoconite granules may reflect physical and/or chemical conditions of each glacier.

Japan Geoscience Union Meeting 2014
(28 April - 02 May 2014 at Pacifico YOKOHAMA, Kanagawa, Japan)

ACG36-P11 Room:Poster Time:April 30 18:15-19:30

Development of a Palsa along the Denali Highway, Alaska

IWAHANA, Go[1*] ; UCHIDA, Masao[2] ; KONDO, Miyuki[2] ; YOSHIKAWA, Kenji[1] ; LARRY, Hinzman[1]

[1]University of Alaska Fairbanks, [2]National Institute for Environmental Studies

Palsa is a peaty permafrost mound distributing in continuous and discontinuous permafrost zones. Main mechanism of the development the mounds is frost heave by ice segregation of peat or mineral soil material. Upper part of palsa usually consists of peat and lower part of a core of alternating layer of segregated ice and mineral soil material. History of paleo-environment around the period of last glacial retrieve in surrounding area can be inferred from analysis of palsa cores and stratigraphy. Our target palsa was located along the Denali Highway, Alaska, and the mound was truncated during highway construction in 1957. The outcrop of palsa have been eroded away from the highway line about 20m partly exposing the internal structure. This permafrost mound was firstly introduced as palsa by Pewe in 1983, and from dating of basal peat, deglaciation of this area occurred at least about 10500 year BP. History of palsa development and environment change was reconstructed from results of analysis from 6.5m core and ground temperature.

Keywords: Alaska, Denali Highway, Palsa

Japan Geoscience Union Meeting 2014
(28 April - 02 May 2014 at Pacifico YOKOHAMA, Kanagawa, Japan)

ACG36-P12 Room:Poster Time:April 30 18:15-19:30

Sr-Nd isotopic ratios of mineral dust in Arctic snow

NAGATSUKA, Naoko[1*] ; OGAWA, Yoshimi[1] ; GOTO-AZUMA, Kumiko[1] ; SUGIURA, Konosuke[2] ; ENOMOTO, Hiroyuki[1] ; YAMADA, Hironobu[1] ; NAKANO, Takanori[3]

[1]NIPR, [2]Toyama University, [3]RIHN

Snow and ice on glaciers contain various atmospheric depositions, such as soot and mineral dusts. These light-absorbing impurities can reduce surface albedo and affect melting of glaciers. Thus, it is important to understand how these impurities were supplied on glaciers.

Stable isotopic ratios of Sr and Nd provide a means of identifying sources of substances and can use for the dusts in snow because it requires low samples for analysis. In this study, we analyzed Sr and Nd isotopic ratio of the mineral dusts collected from snow in several Arctic regions (Mongol, Alaska, and Greenland).

The Sr and Nd isotopic ratios of mineral dusts in Arctic snow showed geographical variations among the sampling sites. The ratios of dust collected from snow in Mongol showed higher Sr and lower Nd values, while those of Greenland were higher Sr and lower Nd values, and were close to the ratios that have been reported in loess, desert sand, soil, or moraine around each region. This result indicates that mineral dusts in snow on the two sampling sites were mainly derived from surrounding regions. On the other hand, the isotopic ratios of dust in snow of Alaska were close to those of deserts in Kazakhstan and Taklamakan Desert, suggesting that the mineral dusts originated from such further deserts were likely to be long-range transported to Alaska.

Keywords: Sr-Nd isotopic ratio, mineral dust in snow, Arctic region

Japan Geoscience Union Meeting 2014
(28 April - 02 May 2014 at Pacifico YOKOHAMA, Kanagawa, Japan)

ACG36-P13 Room:Poster Time:April 30 18:15-19:30

Intercomparison of Arctic atmospheric reanalysis data: Deriving observation-based forcing data for terrestrial models

MORI, Junko[1*] ; SAITO, Kazuyuki[2] ; MIYAZAKI, Shin[1] ; SUEYOSHI, Tetsuo[2] ; IIJIMA, Yoshihiro[2] ; HAJIMA, Tomohiro[2]

[1]National Institute of Polar Research, [2]Japan Agency for Marine-Earth Science and Technology

The goals of the modeling group in the terrestrial research project of the GRENE Arctic Climate Change Research Project (GRENE-TEA) are to a) feed to the CGCM research project for the possible improvement of the physical and ecological processes for the Arctic terrestrial modeling (excl. glaciers and ice sheets) in the extant terrestrial schemes in the coupled global climate models (CGCMs), and b) lay the foundations of the future-generation Arctic terrestrial model development.

In GTMIP (GRENE-TEA Model Intercomparison Project), we utilize the GRENE-TEA site observations to drive and validate the participating models. However, the observation data are prone to missing or lack of the necessary variables or parameters to drive the model. Therefore, we create continuous forcing data in the following manner: First, we create 30-year hourly time series (version 0; v0) of 7 meteorological components from the closest point data of the reanalysis products (a model-based dataset for the sub-monthly variations, and the observation-based CRU for the monthly). Then, v0 is merged with the observation data to create site-fit continuous data (v1) for each GRENE-TEA site. Use of this v1 expects to reduce the systematic biases in the input data in comparing the model outputs with the site observations, to delineate the variations among the models.

So far several atmospheric reanalysis datasets, for example NCEP-NCAR or JRA-55 are available as model input data. In this study, six atmospheric reanalysis datasets are compared in terms of the climatic reproducibility in the region north of 60^{o}N to select the one to be used for constructing the v0 data. The compared datasets are ERA Interim, JRA-55, MERRA, NCEP/NCAR Reanalysis 1, NCEP-DOE Reanalysis 2, and NCEP-CFSR. The CRU dataset is used as a representative of the ground-level observations. We take air temperature at 2m high and precipitation as the key parameters representing the climate condition.

Keywords: Arctic region, Terrestrial model, Reanalysis dataset

Japan Geoscience Union Meeting 2014
(28 April - 02 May 2014 at Pacifico YOKOHAMA, Kanagawa, Japan)

ACG36-P14 Room:Poster Time:April 30 18:15-19:30

Automatic measurement of gas emission/uptake of Alaskan permafrost soils

YONEMURA, Seiichiro[1] ; UCHIDA, Masao[2] ; KONDO, Miyuki[2*]

[1]NIAES, [2]NIES

The release of carbon from the decomposition of organic matters in permafrost soils are very important for the acceleration of global watming . We applied our dynamic system to Alaskan soils and measured temperature dependence of gas (CO2, CH4, N2O, NO, H2, CO) emission/uptake. The Four core samples were placed on petri-dishes which were put into chambers where temperature was controlled. CO2 emission from soils showed variations different from sample to sample. Even at -5C, CO2 emissions were observed. From the time series of CO2 emission rates, we estimated Q10 values. Q10 values were similar between 5-15C and 15 and 25C. Some soils also temperature-dependently emit NO, CO and N2O.

Keywords: permafrost soil, Alaska, CO2, NO, laboratory experiment

Japan Geoscience Union Meeting 2014
(28 April - 02 May 2014 at Pacifico YOKOHAMA, Kanagawa, Japan)

ACG36-P15 Room:Poster Time:April 30 18:15-19:30

Simulating effects of natural fire disturbance on soil carbon storage of boreal forest and tundra ecosystems in Alaska

WANG, Xin[1*] ; YOKOZAWA, Masayuki[2] ; ARAKIDA, Hazuki[3] ; MORI, Kensuke[4] ; ISE, Takeshi[5] ; KONDO, Miyuki[6] ; UCHIDA, Masao[6] ; KUSHIDA, Keiji[7] ; TODA, Motomu[1]

[1]Department of Environmental Dynamics and Management, Graduate School of Biosphere Science, Hiroshima, [2]Department of Mathematical and Systems Engineering, Graduate School of Engineering, Shizuoka Univers, [3]Riken Kobe Branch, Kobe, [4]Department of Geomatics Engineering, University of Calgary, [5]Graduate School of Simulation Studies, University of Hyogo, [6]Center for Environment Measurement and Analysis, National Institute for Environmental Studies, [7]College of Bioresource Sciences, Nihon University

Boreal forest and tundra are the major ecosystems in the northern high latitudes and represent one of the largest reservoirs of carbon over terrestrial ecosystems in the world. Most of the carbon is stored in permafrost where frozen organic matter is protected from decomposition due to biotic activity in the underlying soil. The surface humus layers that should work as the protective layers insulate the permafrost soil far away from the effect of climate warming. Hence, the removal of protective layers by natural fire episodes increases the vulnerability of permafrost to thaw, and the carbon stored in permafrost to decomposition under climate warming in the near future. To elucidate effects of fire severity and temperature sensitivity on the soil carbon storage of boreal forest and tundra ecosystems in Alaska, we conducted simulations using the Physical and Biogeochemical Soil organic carbon Dynamics Model (PB-SDM), which consists of meteorologically-relevant land surface model and soil organic carbon dynamics model. The PB-SDM model of fire severity, designed from the analysis of the field observations, describes the effects of fire characteristics in frequency and size on the reduction of the soil organic layer. The simulation captured realistic annual variations in soil organic carbon storage and thickness in boreal forest and tundra ecosystems individually by finding optimal model parameters in terms of the frequency and size of fire events and temperature sensitivity. The result reveals that our model can be used for predicting soil carbon storage in boreal forest and tundra ecosystems at regional scales where fire regimes play a key role in the soil organic carbon storage as affected by climate warming.

Keywords: High-latitude soil, fire severity, Soil organic carbon, boreal forest, tundra

Japan Geoscience Union Meeting 2014
(28 April - 02 May 2014 at Pacifico YOKOHAMA, Kanagawa, Japan)

ACG36-P16 Room:Poster Time:April 30 18:15-19:30

Methane Oxidation Potential of Arctic Wetland Soil of a Taiga-Tundra Ecotone in Northeastern Siberia

MURASE, Jun[1*] ; SUGIMOTO, Atsuko[2] ; SHINGUBARA, Ryo[3] ; MAXIMOV, Trofim C.[4]

[1]Grad. Sch. Bioagr. Sci., Nagoya Univ., [2]Fac. Earth Environ. Sci., Hokkaido Univ., [3]Grad. Sch. Environ. Sci., Hokkaido Univ., [4]Inst. Biol. Problems of Cryolithozone

Arctic wetlands are significant sources of atmospheric methane and the observed accelerated warming of the arctic causes increased methane formation in water-saturated tundra soil with deepened permafrost thawing. Methane oxidation is regarded as the key process to regulate methane emission from wetlands. In this study we determined the potential methane oxidation rate of the wetland soils of a Taiga-Tundra transition zone in Northeastern Siberia with special reference of the spatial heterogeneity and response to environmental parameters. The surface peat soil samples (0-10 cm) were collected in the summer of 2012 and 2013 from depressions that were covered with tussocks of sedges and Sphagnum spp. and mounds vegetated with moss and larch trees. The potential methane oxidation rate was estimated by a bottle incubation experiment in which homogenized soil samples were incubated with methane at the initial concentration of 0.5-0.8 %v/v. Soil samples from the mounds showed no detectable methane oxidation, whilst the soils collected from depressions exhibited active methane oxidation with no lag. The potential methane oxidation rates at 15 oC were of 270 and 190 nmol h^{-1} g^{-1} dw in the moss- and sedge-dominated zones, respectively. Methane oxidation was active over the depths including the water-saturated anoxic layers, suggesting the resilience of methane oxidizing bacteria. The maximum methane oxidation rate was recorded in the layer above the water-saturated layer: the surface (0-2cm) layer in the sedge-dominated zone and in the middle (4-6 cm) layer in the moss-dominated zone. Temperature-dependent methane oxidation was observed at the range of temperature from 0 to 15 oC. The estimated threshold temperature of methane oxidation was -4 to -11 oC, which suggested methane oxidation at subzero temperatures. Treatment with inorganic nutrients and black carbon did not affect the potential methane oxidation rate.

Keywords: Methane oxidation, tundra, peat

Japan Geoscience Union Meeting 2014
(28 April - 02 May 2014 at Pacifico YOKOHAMA, Kanagawa, Japan)

ACG36-P17 Room:Poster Time:April 30 18:15-19:30

Online visualization tool ”VISION” on Arctic Data archive System (ADS)

SUGIMURA, Takeshi[1*] ; YABUKI, Hironori[2]

[1]National Institute of Polar Research, [2]Japan Agency for Marine-Earth Science and Technology

We are constructing an online archive system of data about Arctic research that many researchers and institutes have collected, which is named ADS (Arctic Date archive System). We aim at that the many researchers specializing in the various fields of the Arctic research - such as atmosphere, ocean, land, physical and chemical analysis and computer simulation, etc - can become to mutually use their data across their own fields through our data archive. For this purpose, it is necessary for us not only to manage data systematically, but to build the system where researchers can easily grasp the contents of the data archive.

However, it is difficult to exactly understand contents of the data that others made. The researchers try to understand the contents of the data of their own fields and succeed in many cases. But it is not easy for them even to judge the contents of the data out of their fields. Therefore, we developed GUI-based online data visualization application named “ VISION ”, which all the researchers engaged in the Arctic research can easily operate. It can be expected that “ VISION ” facilitates an understanding the data of the various fields of the Arctic research among the researchers, then the researchers become also use the data out of their own fields.

We will introduce a structure and function of “ VISION ” and demonstrate an operation of this system.

Keywords: online visualization, satellite data, SSMI, AMSR

Japan Geoscience Union Meeting 2014
(28 April - 02 May 2014 at Pacifico YOKOHAMA, Kanagawa, Japan)

ACG36-P18 Room:Poster Time:April 30 18:15-19:30

Shrinking glaciers in Suntar Khayata, east Siberia

KADOTA, Tsutomu[1*] ; SHIRAKAWA, Tatsuo[2] ; KUSAKA, Ryo[2] ; TAKAHASHI, Shuhei[2] ; GALANIN, Andrey[3] ; FEDOROV, Alexander[3] ; ENOMOTO, Hiroyuki[4] ; OHATA, Tetsuo[1] ; YABUKI, Hironori[1]

[1]Japan Agency for Marine-Earth Science and Technology, [2]Kitami Institute of Technology, [3]Melnikov Permafrost Institute, [4]National Institute of Polar Research

Introduction

Since Northern Hemisphere high latitude regions are noticeable trend of global warming and climate change, appearance of its impact is interest. Northeastern Eurasia is area of blank of observational research. One of a few regions studied in the past is Suntar Khayata in east Siberia, where Russian scientists carried out wide range of study during IGY (1957-1959).

Study area

Suntar Khayata region, located in the latitudes between 62and 63 degree north and in the longitudes between 140.7 and 142 degree east, forms a divide between the Arctic Sea and the Sea of Okhotsk. Oymyakon depression, known as the cold pole in the Northern Hemisphere, is located to the northeast. Glacier inventory of this region was prepared based on the aerial photographs taken in 1944-1947 (Koreisha, 1963). Total number and area of glaciers were 205 and 206.28 km^2. Three glacierized region are recognized, namely Northern massif, Central massif and Southern massif. The highest elevation of each massif is 2959 m, 2933 m and 2944 m.

Glaciers observed are No. 29 to 33 in Northern massif including No. 31 which was intensively studied during IGY.

Observation

We carried out glaciological observations such as mass balance (stake method), ice thickness measurement (radio-echo soundings), and topographic survey (DGPS) in July/August in 2012 and 2013. Automatic weather stations were also set on/around the glaciers.

Results

Glacier-wide mass balance in 2012/2013 was -1.04 m w.e. for a glacier complex (Glaciers No. 29, 30 and 31). This value shows more negative state than those in 1957-1959.

We generated DEMs of surface and bed of the Glacier No. 31 using ice thicknesses obtained by radio-echo soundings and surface elevations by GPS survey, then we estimated the volume of the glacier to be 0.20 km^3 (area: 3.02 km^2, mean thickness: 62 m). Ice thicknesses in its tongue reduced by 110-60 m (terminus to upstream) since 1957.

Based on multi-temporal aerial and satellite imagery, 18 investigated glaciers reduced in area by approximately 36% from 1945 to 2011.

Concluding remark

Summer (July-August) air temperature observed on the glacier in 2012 and 2013 were higher than those in 1957-1959, which brought about more negative mass balance than those in 1957-1959. Superimposed ice formation was also very limited in 2012/2013. This resulted in disappearance of accumulation area. Reconstruction of long-term mass balance history is present target.

Acknowledgement

This study has been jointly carried out by JAMSTEC (Northern Cryosphere Research Program) and GRENE Arctic Climate Change Research Project (The role of arctic cryosphere in global change).

Keywords: glacier, Siberia, Suntar Khayata, shrink

Japan Geoscience Union Meeting 2014
(28 April - 02 May 2014 at Pacifico YOKOHAMA, Kanagawa, Japan)

ACG36-P19 Room:Poster Time:April 30 18:15-19:30

Effect of snow depth on pan-Arctic permafrost thermal regimes

PARK, Hotaek[1*] ; FEDOROV, Alexander[2] ; WALSH, John[3]

[1]JAMSTEC, [2]Melnikov Permafrost Institute, Yakutsk, Russia, [3]International Arctic Research Center, University of Alaska Fairbanks

This study quantitatively evaluated how insulation by snow depth (SND) affected the soil thermal regime and permafrost degradation in the pan-Arctic area, and more generally defined the characteristics of soil temperature (T_{SOIL}) and SND from 1901-2009. This was achieved through experiments performed with the land surface model CHANGE, to assess sensitivity to winter precipitation as well as air temperature. Simulated T_{SOIL}, active layer thickness (ALT), and SND were generally comparable with in-situ or satellite observations at large scales and over long periods. Northernmost regions had snow that remained relatively stable and in a thicker state during the past four decades, generating greater increases in the T_{SOIL}. Changes in SND have led to changes in the thermal state of the underlying soil, which is strongly dependent on both the magnitude and the timing of changes in snowfall. Simulations of the period 2001-2009 revealed significant differences in the extent of near-surface permafrost, ranging from 15.6 to 18.7 million km^2. This spread was the result of differences in the model$'$s treatment of meteorology. Permafrost loss was greater when SND increased in the autumn rather than in the winter, due to insulation of the soil from the early cooling. Simulations revealed that T_{SOIL} tended to increase over most of the pan-Arctic from 1901-2009, and this increase was significant in northern regions, especially in northeastern Siberia where SND is responsible for 50% or more of the changes in TSOIL at a depth of 3.6 m. In the same region, ALT also increased at a rate of approximately 2.3 cm per decade. The most sensitive response of ALT to changes in SND appeared in the southern boundary regions of permafrost, in contrast to permafrost temperatures within the 60^o-80^oN region, which were more sensitive to changes in the SND. Finally, the modeling performed in this study suggests that snow cover contributes to the warming of permafrost in northern regions and could play a more important role under conditions of future Arctic warming.

Keywords: active layer thickness, land surface model, permafrost, snow depth, soil temperature

Japan Geoscience Union Meeting 2014
(28 April - 02 May 2014 at Pacifico YOKOHAMA, Kanagawa, Japan)

ACG36-P20 Room:Poster Time:April 30 18:15-19:30

Fixed-point observation of diatom biocoenosis and water mass condition in the northern Chukchi Sea during September 2013

ONODERA, Jonaotaro[1*] ; NISHINO, Shigeto[1]

[1]JAMSTEC-RIGC

In order to estimate the relationship between diatom flora and water mass condition in the northern Chukchi Sea, fixed-point ocean observation was conducted at Station 41 (72.45N, 168.24W, 56 m water depth) by R/V Mirai (Cruise MR13-06) in 10-25 September 2013. The optical equipment named ”Multi-wave length excitation fluorescence photometer (Multi-Exciter)” was applied with CTD observation for the estimation of chlorophyll concentration in each major phytoplankton groups (diatom, green algae, and blue algae). Chlorophyll concentration gradually increased with the weakening of summer stratification by intensified sea-surface wind. The Multi-Exciter showed the clear increase of diatom in upper water column, which were also suggested by size-fractionated analysis of chlorophyll concentration and microscopic observation by scanning electron microscope and light microscope. However, the increase of diatom cell abundance was minor compared to the increase of total chlorophyll concentration. The dominance of large diatom genus *Proboscia* and the increased chlorophyll concentration in one diatom cell were the main causes on the increase of total chlorophyll concentration. The 3-6 fold increase of chlorophyll concentration within 6 hours was rarely observed around chlorophyll maximum layer during the middle observation period, which is probably explained by not only improved habitat environment for diatom but also movement of water masses such as lateral input of high chlorophyll waters.

Keywords: Arctic Ocean, Chukchi Sea, diatom, excitation fluorescence, chlorophyll concentration

Japan Geoscience Union Meeting 2014
(28 April - 02 May 2014 at Pacifico YOKOHAMA, Kanagawa, Japan)

ACG36-P21 Room:Poster Time:April 30 18:15-19:30

Reconstruction of paleoenvironmental changes in the Chukchi Borderland over the last 15.5kyr

UCHIDA, Masao[1] ; KUMATA, Hidetoshi[2] ; KONDO, Miyuki[1*] ; RELLA, Stephan[1] ; SHIBAHARA, Akihiko[3] ; AMANO, Chie[4] ; UTSUMI, Motoo[5]

[1]National Institute for Environmental Studies, [2]Tokyo University of Pharmacy and Life Sciences, [3]National Institute of Advanced Industrial Science and Technology, [4]Toyo University, [5]University of Tsukuba

Knowledge on past variability of sedimentary organic carbon in the Arctic Ocean is important to assess natural carbon cycling and transport processes related to global climate changes. However, the late Pleistocene oceanographic history of the Arctic is still poorly understood. In the present study we show sedimentary records of organic carbon(TOC, δ13C), CaCO3, benthic and planktonic foraminiferal δ18O, BIT index for terrestrial organic carbon input, IP25 for sea ice condition, and the coarse grain size fraction. The 8m length sediment core was retrieved in the northern Northwind Ridge in the far western Arctic Ocean, during the MR08-05 cruise by R/V Mirai. An age model based on oxygen isotope stratigraphy, radiocarbon dating and lithological constraints suggests that the core records paleoenvironmental changes of the last 155 kyr. In this conference, we discuss presented millennial scales records of glacial erosion, intermediate water and/or surface water and sea ice variabilities during cold/warm episodes of the last two glacial interglacial cycles in the light of ice sheet and ocean-atmosphere dynamics.

Japan Geoscience Union Meeting 2014
(28 April - 02 May 2014 at Pacifico YOKOHAMA, Kanagawa, Japan)

ACG37-01 Room:423 Time:April 28 11:00-11:25

What the recent international field campaign in and around the Indian Ocean has advanced our knowledge of the MJO?

YONEYAMA, Kunio[1*]

[1]JAMSTEC

A coordinated international field experiment with special focus on the convective initiation mechanism study of the Madden-Julian Oscillation (MJO) took place in and around the central equatorial Indian Ocean from October 2011 through January 2012. This campaign consisted of several projects including CINDY2011 (Cooperative Indian Ocean experiment on intraseasonal variability in the Year 2011), DYNAMO (Dynamics of the MJO), AMIE (Atmospheric Radiation Measurement program - MJO Investigating Experiment), and LASP (Littoral Air-Sea Process). More than 70 institutes/universities from 16 countries joined the campaign. During a four-month intensive observing period from October through January, three MJO events were observed. It is worth noting that while it is clear to identify three events (late October, late November, and late December) from the time-longitude cross section of outgoing long-wave radiation data along the equator, the most popular MJO identification method - Real-time multivariate MJO Index introduced by Wheeler and Hendon (2004) - could not capture the December event.

While the vertical stepwise moistening which was trapped around trade inversion and 0degC level were confirmed from the equatorial sounding data as previously reported, it was emphasized that lateral transport of moisture and dry air from the Southern Hemisphere as well as westward-propagating disturbances from the Indonesian Maritime Continent were also keys. Several topics from published works during past 2 years after the campaign will also be introduced to indicate what we expected and what are not.

Keywords: Madden-Julian Oscillation, CINDY2011

Japan Geoscience Union Meeting 2014
(28 April - 02 May 2014 at Pacifico YOKOHAMA, Kanagawa, Japan)

ACG37-02 Room:423 Time:April 28 11:25-11:40

Mesoscale Convective Complex Activities over Indian Ocean and Their Effects on Convections Over Sumatera Island

-, Trismidianto[1*] ; HADI, Tri wahyu[2] ; KODAMA, Yasu-masa[1]

[1]Meteorological Laboratory, Graduate School of Science and Technology, Hirosaki University, [2]Departement of Earth Sciences, Faculty of Earth Sciences and Technology, Institut Teknologi Bandung

Effects of Mesoscale Convective Complexes (MCC) over Indian Ocean on convections over Sumatera Island have been investigated using Multi-functional Transport SATellite (MTSAT) infrared (IR1) imageries, Tropical Rainfall Measuring Mission (TRMM) rainfall data and Cross-Calibrated Multi-Platform (CCMP) surface wind data of 10-year period (2000-2009). Occurrences of MCC were identified using an algorithm that combines criteria of cloud coverage, eccentricity, and cloud lifetime. This study begins with a case study on 16 to 17 August 2005 and 27 to 28 October 2007 to show the evolution of MCC, we found the development phase of MCC was accompanied by surface wind convergence, while wind divergence was clearly seen below decaying MCC. Following the decay of MCC, convective activities were observed in the surrounding regions by the presence of a new convective cell around the MCC, indicating the role of cold pool mechanism. The new convective cell was generated from cold pool affect convective clouds in the surrounding area and propagate to over Sumatra Island so causing extreme rainfall over Sumatra.

The correlation between MCC and convection over Sumatera was further investigated by performing composite analysis using more samples of MCC events. During the 10-year period, about a number of 553 MCC events have been identified over Indian Ocean. However, it is of interest to that MCC events tend to occur with significantly higher frequency during the monsoon transition season of March- April-May (MAM) period. Available data suggest that the life cycle of MCC over Indian Ocean is about 12 to 15 hours. Results of composite analyses confirmed that the MCC have significant influence on the development of cloud convection over Sumatera Island by means of cold pool propagation mechanism. This seems to imply that weather observations over the western Indian Ocean are crucial for rainfall prediction in Sumatera regions.

Keywords: Cold Pool, MCC, Convection, Rainfall

Japan Geoscience Union Meeting 2014
(28 April - 02 May 2014 at Pacifico YOKOHAMA, Kanagawa, Japan)

ACG37-03 Room:423 Time:April 28 11:40-11:55

Observed moisture variations associated with shallow convection

BELLENGER, Hugo[1*] ; KATSUMATA, Masaki[1] ; YONEYAMA, Kunio[1] ; NISHIZAWA, Tomoaki[2] ; YASUNAGA, Kazuaki[3] ; SHIROOKA, Ryuichi[1]

[1]JAMSTEC, [2]NIES, [3]University of Toyama

The variability of tropospheric moisture is a key feature of tropical climate. In particular, the importance of moisture variations due to convective transport is still to be quantified on a variety of spatial and temporal scales. For instance, there is a debate on the importance of moisture convective transport in preconditioning the atmosphere prior to deep convection development associated with the Madden–Julian Oscillation (MJO). We use here high frequency observations of humidity and convection in the Indian Ocean by lidars and radars on board the R/V Mirai during the CINDY/DYNAMO campaign. Significant moisture variations on the scale of few hours are observed within the first first kilometers of the atmosphere in association with shallow convective and congestus clouds. We then compare these local tendencies with large–scale ones and discuss the potential importance of convective transport by convection in the moisture budget during the transition from convectively suppressed to convectively active periods.

Keywords: Convection, moisture, MJO, CINDY/DYNAMO, preconditionning, observation

Japan Geoscience Union Meeting 2014
(28 April - 02 May 2014 at Pacifico YOKOHAMA, Kanagawa, Japan)

ACG37-04 Room:423 Time:April 28 11:55-12:10

In-situ observed detailed temperature profile in surface 10-meter layer over the tropical western Pacific

KATSUMATA, Masaki[1*] ; BELLENGER, Hugo[1] ; YONEYAMA, Kunio[1]

[1]JAMSTEC

The oceanic thermal stratification in the first meters impacts significantly the energy exchanges between the atmosphere and the ocean by modulating the skin Sea Surface Temperature (SST). A thermistor chain was deployed from a research vessel to continuously measure the temperature profile in the ocean first 10 meters during 17 days in June 2013 in the tropical western Pacific (12N-135E). A clear diurnal cycle was captured with daytime warming in the first meters of the ocean that gradually decrease and deepened during the evening. In addition, a 0.5K-cooling event of the first meter with duration of about 3 hours was also captured during the passage of precipitating cloud system. By utilizing meteorological data from on-board instruments, we asses the relative importance of precipitation and accompanying cold pool in this cooling event.

Japan Geoscience Union Meeting 2014
(28 April - 02 May 2014 at Pacifico YOKOHAMA, Kanagawa, Japan)

ACG37-05 Room:423 Time:April 28 12:10-12:25

Abrupt cooling associated with the oceanic Rossby wave and lateral advection during CINDY2011

SEIKI, Ayako[1*] ; KATSUMATA, Masaki[1] ; HORII, Takanori[1] ; HASEGAWA, Takuya[1] ; RICHARDS, Kelvin J.[2] ; YONEYAMA, Kunio[1] ; SHIROOKA, Ryuichi[1]

[1]Japan Agency for Marine-Earth Science and Technology, [2]University of Hawaii

The cooperative Indian Ocean experiment on intraseasonal variability in the Year 2011 (CINDY2011) was conducted to capture atmospheric and oceanic characteristics of the Madden-Julian Oscillation (MJO) in the central Indian Ocean from late 2011 to early 2012. During CINDY2011, the research vessel (R/V) MIRAI stayed at 8 ^{o} S, 80.5 ^{o} E for two months during the special observing period (SOP). Intraseasonal convection associated with the MJO was organized in the central Indian Ocean in late October and late November during the SOP. In the middle of November, both sea surface temperature (SST) and mixed layer temperature decreased suddenly when cold low salinity water intruded into the upper layer around the R/V MIRAI. This intrusion was accompanied by a surface current change from southwestward to westward/west-northwestward associated with the passage of the annual oceanic downwelling Rossby wave. The mixed layer heat budget analysis shows that horizontal advection plays an important role in the abrupt cooling whereas the net surface heat flux cannot account for the cooling. This is an interesting result because the associated downwelling Rossby wave is usually considered to increase SST through a reduction of entrainment cooling. In addition, for the second MJO event convection was activated around 20 November over the central north and equatorial Indian Ocean but not in the south. It is suggested that the cooler surface waters (as seen at the location of the R/V MIRAI) tended to suppress the initial atmospheric convection, resulting in the lagged convective onset in the end of November over the central south Indian Ocean.

Keywords: CINDY2011, abrupt cooling, Indian Ocean

Japan Geoscience Union Meeting 2014
(28 April - 02 May 2014 at Pacifico YOKOHAMA, Kanagawa, Japan)

ACG37-06 Room:423 Time:April 28 14:15-14:30

Modulation of Equatorial Turbulence by Tropical Instability Waves

INOUE, Ryuichiro[1*] ; LIEN, Ren-chieh[2] ; MOUM, James[3] ; PEREZ, Renellys[4] ; GREGG, Mike[2]

[1]JAMSTEC, [2]University of Washington, [3]Oregon State University, [4]University of Miami

Strong modulation of turbulent mixing by a westward propagating Tropical Instability Wave (TIW) was observed during October and November 2008 on the equator at 140^{o}W in the stratified shear layer between the equatorial undercurrent (EUC) and the surface mixed layer. At these depths, the unique deep diurnal-cycle mixing in the stratified layer under the equatorial cold tongue was observed with nighttime turbulent mixing a factor of 10 greater than during daytime. The turbulent kinetic energy dissipation rate, ϵ, was O(10^{-6})Wkg^{-1}, and the turbulent heat flux was ˜500 Wm^{-2}, at least 5-10 times greater than previously observed at the central equatorial Pacific. Turbulence mixing varied significantly during the four distinct phases of the meridional flow associated with the TIW: steady northward (˜0.6 ms^{-1}), northward-to-southward transition, steady southward (˜-0.6 ms^{-1}), and southward-to-northward transition. During the northward-to-southward transition, we observed the largest values of reduced shear squared (Sh^2?4N^2), where Sh^2 is the total shear squared and N^2 the buoyancy frequency squared, the thickest nighttime surface mixed layer, the deepest penetration of the deep-cycle turbulence, and the largest turbulent heat flux and largest integrated ϵ in the deep-cycle layer. During steady southward flow, the depth of the bases of the nighttime surface mixed layer and of the deep-cycle layer were shallowest. For the first time, a 50-m-thick layer of strong turbulence was observed immediately above the EUC core during the northward-to-southward and steady southward phases. The average ϵ exceeded 10-^{6} Wkg^{-1}, the eddy diffusivity was ˜10^{-3} m^{2}s^{-1}, and the turbulent heat flux was ˜500 Wm^{-2}. It is likely that to accurately parameterize mixing in the central equatorial Pacific, numerical models must properly simulate not only the enhancement of mixing associated with TIWs but also the variability of mixing within individual TIWs. In this talk, some results from the extensive (from November 2008 to February 2009) mooring data set, comparisons with a general circulation model, and details of mixing events will also be shown.

Japan Geoscience Union Meeting 2014
(28 April - 02 May 2014 at Pacifico YOKOHAMA, Kanagawa, Japan)

ACG37-07 Room:423 Time:April 28 14:30-14:45

Air-sea interaction over the northern edge of the Pacific wam pool

HASEGAWA, Takuya[1*] ; NAGANO, Akira[1] ; HATTORI, Miki[1] ; INOUE, Tomoshige[1] ; KUBOTA, Hisayuki[1]

[1]JAMSTEC

Abstract is written in Japanese.

Keywords: norhtern edege of the Pacific warm pool, air-sea interaction, multi-scale temporal-spatial variability

Japan Geoscience Union Meeting 2014
(28 April - 02 May 2014 at Pacifico YOKOHAMA, Kanagawa, Japan)

ACG37-08 Room:423 Time:April 28 14:45-15:00

Why is initialization of heat content anomalies in the tropical Indian Ocean difficult in a CGCM with SST-nudging?

KOHYAMA, Tsubasa[1] ; TOZUKA, Tomoki[2*]

[1]University of Washington, [2]The University of Tokyo

We have evaluated oceanic initial conditions in the tropical Indian and Pacific Oceans prepared by a coupled general circulation model (CGCM) with a sea surface temperature (SST)-nudging scheme. It is shown that the heat content anomalies in the upper 150 m are generated extremely well in the Pacific even though only the SST data is incorporated. In contrast, the upper ocean heat content anomalies produced by the model have negative correlation coefficients over vast areas of the tropical Indian Ocean. We propose that this is due to a difference in the SST-outgoing longwave radiation (OLR) relationship between the Indian and Pacific Oceans; the use of SST-nudging generally assumes that correlation coefficients between SST and OLR are negative, but this is not necessarily true. The correlation coefficients between SST and OLR anomalies are negative in the central to eastern equatorial Pacific, and this feature is well reproduced in the model. As a result, equatorial zonal wind anomalies are well captured by the model, and forced equatorial Kelvin and Rossby waves are accurately reproduced. On the other hand, the model cannot capture the observed positive correlation coefficients in the eastern equatorial Indian Ocean, particularly from January to April. As a result, equatorial zonal wind anomalies tend to have an opposite sign and induce equatorial Kelvin and Rossby waves with a wrong sign. The positive correlation between SST and OLR is an outcome of remote influence, but this is more difficult to simulate in an atmospheric general circulation model (AGCM) and a CGCM with strong SST nudging, in which local air-sea interaction is not explicitly allowed. Since the results presented in this study is based on a single model, it will be interesting to check skills of other models in initializing the upper ocean heat content with an SST-nudging scheme.

Keywords: Tropical Indian Ocean, Ocean-atmosphere coupled model, SST-OLR relationship, Upper ocean heat content, SST-nudging

Japan Geoscience Union Meeting 2014
(28 April - 02 May 2014 at Pacifico YOKOHAMA, Kanagawa, Japan)

ACG37-09 Room:423 Time:April 28 15:00-15:15

Two flavors of the Indian Ocean Dipole

ENDO, Satoru[1*] ; TOZUKA, Tomoki[1]

[1]Graduate School of Science, The University of Tokyo

The Indian Ocean Dipole (IOD) is known as a climate mode in the tropical Indian Ocean accompanied by negative (positive) sea surface temperature (SST) anomalies over the eastern (western) pole and easterly wind anomalies along the equator during its positive phase. However, the western pole of the IOD is not always covered by positive SST anomalies throughout the region. For this reason, the IOD is further classified into two types in this study based on SST anomalies in the western pole. The first type is close to the canonical IOD with negative (positive) SST anomalies in the eastern (central to western) tropical Indian Ocean. The second type, on the other hand, is associated with negative SST anomalies in the eastern and western tropical Indian Ocean and positive SST anomalies in the central tropical Indian Ocean. Based on a composite analysis, it is found that easterly wind anomalies reach the east coast of Africa in the first type, and as a result, positive rainfall anomalies are observed over East Africa. Also, due to the basin-wide easterly wind anomalies, the first type is accompanied by strong sea surface height (SSH) and thermocline depth anomalies. In contrast, zonal wind anomalies converge in the central tropical Indian Ocean in the second type, and no significant precipitation anomalies are found over East Africa. Also, only weak SSH and thermocline depth anomalies are seen during the second type, because equatorial downwelling anomalies induced by westerly wind anomalies in the west are counteracted by equatorial upwelling anomalies caused by easterly wind anomalies in the east. Due to the above difference in oceanic anomalies, the first type is stronger and lasts longer than the second type.

Japan Geoscience Union Meeting 2014
(28 April - 02 May 2014 at Pacifico YOKOHAMA, Kanagawa, Japan)

ACG37-10 Room:423 Time:April 28 15:15-15:30

Evolution and mechanism of the positive Indian Ocean Dipole event in 2012

TANIZAKI, Chiho[1*] ; TOZUKA, Tomoki[1]

[1]Graduate School of Science, The University of Tokyo

Evolution and mechanism of a peculiar positive Indian Ocean Dipole (IOD) event that occurred in 2012 are examined. In contrast to the normal IOD event, which starts to develop in late boreal spring, peaks in fall, and decays in winter, the 2012 IOD event was initiated in July, peaked in August, and decayed quickly in fall. Although the normal IOD event is associated with shallower thermocline in the eastern equatorial Indian Ocean, it was deeper than normal in 2012 and this may have delayed the onset of the IOD in this year. For quantitative discussions, mixed layer temperature balance of the eastern pole of the IOD is calculated using outputs from an ocean general circulation model. In agreement with past studies, negative sea surface temperature anomalies in the eastern pole are generated mainly owing to anomalous cooling by the vertical terms (i.e. entrainment and turbulent vertical diffusion) during the normal IOD. However, anomalous cooling by the surface heat flux term played the dominant role in the development of the eastern pole in 2012, and the vertical terms opposed the anomalous cooling. The anomalous cooling by the surface heat flux term is due to stronger cooling by latent heat flux. Also, warming of the surface mixed layer by the climatological shortwave radiation was suppressed owing to deeper mixed layer.

Japan Geoscience Union Meeting 2014
(28 April - 02 May 2014 at Pacifico YOKOHAMA, Kanagawa, Japan)

ACG37-11 Room:423 Time:April 28 15:30-15:45

Interannual Variability in SST off Bangladesh

NAGURA, Motoki[1*] ; TERAO, Toru[2] ; HASHIZUME, Masahiro[3]

[1]JAMSTEC, [2]Kagawa University, [3]Nagasaki University

Oceanic variability off Bangladesh is one of the environmental factors which can impact on the local community. For example, Hashizume et al. (2011) pointed out that the number of cholera patients increases in Dhaka, which is populated by 15 million people and the largest city in Bangladesh, when sea surface temperature (SST) off Bangladesh rises. This study examines interannual SST variability in the coastal regions off Bangladesh, which has not attracted much attention in climate sciences so far. We detect a significant interannual SST variability off Bangladesh in two different satellite datasets (NOAA OI SST and TMI SST) and a high-resolution ocean general circulation model driven by a reanalysis dataset. The SST variability is trapped near the coast, amounts to 0.5 to 1.0 degrees Celsius in magnitude, and peaks in the boreal winter. The two observational datasets and the model results show consistency in the spatial and temporal patterns of SST variability, which gives credibility to the detected phenomenon. A statistical analysis shows that SST off Bangladesh tends to be high in the year next to El Nino and in the year of negative Indian Ocean Dipole events, suggesting those climate modes as possible drivers. We are conducting a mixed layer heat budget analysis using the model output, a preliminary result of which shows that a thick barrier layer caused by the freshwater supply from the Ganges plays a role in the generation of the SST variability. Details of the mixed layer heat budget analysis will be reported in the meeting.

Japan Geoscience Union Meeting 2014
(28 April - 02 May 2014 at Pacifico YOKOHAMA, Kanagawa, Japan)

ACG37-12 Room:423 Time:April 28 15:45-16:00

A drastic change in predictability of precipitation off the west coast of Australia after late 1990s

DOI, Takeshi[1*] ; BEHERA, Swadhin[1] ; YAMAGATA, Toshio[1]

[1]JAMSTEC APL

Global warming and natural decadal variability after late 1990s strongly warm the coastal ocean off West Australia, which drastically changed climate dynamics there. The warm ocean drives precipitation locally there after the late 1990s, while the local atmospheric variability or the remotely forced atmospheric bridges mainly controlled the local precipitaiton variability before that. By virtue of that, precipitation predictability off West Australia on a seasonal time scale is also drastically changed after late 1990s; austral summer precipitation off West Australia is significantly predictable 5 months ahead after late 1990s, while there is no predictability of that in 1980s and early 1990s. Although the high prediction skill of precipitation off West Australia is useful for its early warning to extreme events and reducing their damages, the extreme event itself might increase due to global warming and decadal climate variability through a local air-sea feedback.

Keywords: Seasonal prediction, Precipitation, Ningaloo Nino

Japan Geoscience Union Meeting 2014
(28 April - 02 May 2014 at Pacifico YOKOHAMA, Kanagawa, Japan)

ACG37-13 Room:423 Time:April 28 16:15-16:35

Interdecadal Amplitude Modulation of ENSO and its Impacts on TPDV

OGATA, Tomomichi[1*]

[1]Faculty of Life and Environmental Sciences, University of Tsukuba

ENSO is a major climate mode in the tropical Pacific, and its interdecadal variabilities in ENSO characteristics (e.g. amplitude, propagation, period) are investigated as responses to background mean state change. On the other hand, tropical Pacific decadal variability (TPDV) is known as a major decadal-interdecadal variability, and coupled-GCM has revealed that ENSO also acts to TPDV. This study shows that the GFDL coupled-GCM (GFDL-CM2.1) also captures significant relationship between ENSO amplitude modulation and TPDV in interdecadal timescale. Furthermore, importance of ENSO rectification on TPDV is investigated by OGCM sensitivity experiments.

Keywords: air-sea interaction, tropical ocean, ENSO

Japan Geoscience Union Meeting 2014
(28 April - 02 May 2014 at Pacifico YOKOHAMA, Kanagawa, Japan)

ACG37-14 Room:423 Time:April 28 16:35-16:50

The role of interaction between the Pacific and the north Atlantic Oceans in the prediction of ENSO

YAMAZAKI, Kuniko[1] ; IMADA, Yukiko[1*] ; WATANABE, Masahiro[1]

[1]Atmosphere and Ocean Research Institute, the University of Tokyo

Observational and climate modelling studies indicate a close link between the north tropical Atlantic (NTA) sea surface temperature anomalies (SSTA) and the El Nino-Southern Oscillation (ENSO). An El Nino peak in boreal winter is followed by a warming of the NTA SSTA in the subsequent spring, which in turn leads to a La Nina in the following autumn/winter. Using the seasonal prediction system based on the atmosphere and ocean general circulation model (AOGCM) MIROC5, we conducted an ensemble of hindcast experiments from 1979 to present, in which the transition from El Nino to La Nina in 1997-1998 was successfully predicted. We also conducted a series of accompanying sensitivity experiments targeted at the transition event in 1997-1998, in which the NTA or equatorial Pacific air-sea interactions were decoupled. We found that NTA SSTA plays an important role in increasing the skill in predicting the following La Nina event. We also found that the preceding particularly-large El Nino SSTA and the associated atmospheric bridge are essential for the generation of NTA SSTA of the observed magnitude.

References

Ham, Y.-G., J.-S. Kug, J.-Y. Park, and F.-F. Jin, 2013: Sea surface temperature in the north tropical Atlantic as a trigger for El Nino/Sourthern Oscillation events, Nature Geoscience, 6, 112-116.

Keywords: ENSO, the north tropical Atlantic climate variability, seasonal prediction, atmosphere and ocean general circulation model

Japan Geoscience Union Meeting 2014
(28 April - 02 May 2014 at Pacifico YOKOHAMA, Kanagawa, Japan)

ACG37-15 Room:423 Time:April 28 16:50-17:05

Important factors for long-term change in ENSO transitivity

OHBA, Masamichi[1*]

[1]CRIEPI

El Nino and La Nina exhibit significant asymmetry in their duration. El Nino tends to turn rapidly into La Nina after the mature, while La Nina tends to persist for up to 2 years. Reconstructed historical sea surface temperatures (SST) show a significantly increase in the intensity of El Nino-Southern Oscillation (ENSO) asymmetry, particularly El Nino transitivity, during the last six decades. Atmospheric observational data have shown that the relationship between El Nino and surface zonal wind anomalies over the equatorial Western Pacific (WP) has strengthened, and anomalous WP easterlies have appeared after the 1970s climate regime shift. To investigate the dependency of ENSO transitivity on its amplitude, a suite of idealized experiments using an atmospheric general circulation model (AGCM) is performed by imposing historical SST and 12 different ENSO-related SST anomalies exhibiting equal spatiotemporal distribution but different amplitude. Our AGCM experiments show strong nonlinearity in the WP zonal wind against the amplitude of the warm phase.

Keywords: Sea surface temperature, Pacific Ocean, El Nino/Southern Oscillation, Indian Ocean

Japan Geoscience Union Meeting 2014
(28 April - 02 May 2014 at Pacifico YOKOHAMA, Kanagawa, Japan)

ACG37-16 Room:423 Time:April 28 17:05-17:20

Temporal variations of Mascarene High in austral summer and their causes, and influences on the SST field

OHISHI, Shun[1*] ; SUGIMOTO, Shusaku[1] ; HANAWA, Kimio[1]

[1]Department of Geophysics, Graduate School of Science, Tohoku University

Changes in intensity and longitudinal/latitudinal position of Mascarene High (MH) in austral summer (November-January) from 1951 to 2012 are investigated using NCEP-NCAR reanalysis dataset. We define the MH intensity and longitudinal/latitudinal position as sea level pressure (SLP) maximum within a region of [40E-120E, 50S-10S]. The intensity has an interannual variation on a dominant timescale of 3-4 years. The pressure variations associated with the intensity show annular and equivalent barotropic structures throughout the troposphere, which are similar to Southern Annular Mode (SAM). The intensity time series shows a significant correlation with the SAM index. Therefore, it is suggested that the MH intensity variation results from the SAM. The MH longitudinal position also shows an interannual variation on a dominant timescale of 5-6 years and the time series has no significant correlation with the intensity time series. The SLP anomalies associated with the longitudinal variation represent a dipole pattern, whose centers of action are located off the western Australia (WA) and off the south-eastern Madagascar Island (SEMI). The geopotential height anomalies in these regions have different vertical structures; those off the WA are confined from the sea surface to the middle troposphere, while those off the SEMI are distributed throughout the troposphere. In addition, the SLP anomalies averaged within these regions show no significant correlation. It is indicated that the SLP variations off WA are associated with El Nino Southern Oscillation (ENSO). On the other hand, the SLP changes off the SEMI have no relationship with the large-scale atmospheric variations such as SAM and ENSO.

The MH intensity variation forms southwest-northeast dipole pattern of sea surface temperature (SST) field, which resembles the Indian Ocean Subtropical Dipole (IOSD) pattern. In addition, the MH longitudinal changes also show the dipole pattern, which is shifted westward by 10 degrees in longitude compared to the SST pattern associated with the intensity variation. The correlations between the MH variations and IOSD index show significant values (0.39 for intensity and -0.57 for longitudinal position). Therefore, it is suggested that both the changes in the intensity and the longitudinal position cause the IOSD.

Keywords: Mascarene High, Indian Ocean Subtropical Dipole, El Nino Southern Oscillation, Southern Annular Mode

Japan Geoscience Union Meeting 2014
(28 April - 02 May 2014 at Pacifico YOKOHAMA, Kanagawa, Japan)

ACG37-17 Room:423 Time:April 28 17:20-17:35

Role of tropical SST variability in the generation of subtropical dipoles

MORIOKA, Yushi[1*] ; MASSON, Sebastien[2] ; TERRAY, Pascal[2] ; PRODHOMME, Chloe[2] ; BEHERA, Swadhin[3] ; MASUMOTO, Yukio[4]

[1]JAMSTEC / RIGC, [2]LOCEAN-IPSL, Universite Pierre et Marie Curie, [3]JAMSTEC / APL, [4]Graduate School of Science, The University of Tokyo

Interannual variations of Sea Surface Temperature (SST) in the midlatitudes of the Southern Hemisphere play an important role in the rainfall variability over the surrounding countries by modulating synoptic-scale atmospheric disturbances. These are frequently associated with a northeast-southwest oriented dipole of positive and negative SST anomalies in each oceanic basin, referred to as a subtropical dipole. This study investigates the role of tropical SST variability on the generation of subtropical dipoles by conducting SST-nudging experiments using a coupled general circulation model. In the experiments where the simulated SST in each tropical basin is nudged to the climatology of the observed SST, the subtropical dipoles tend to occur as frequently as the case in which the simulated SST is allowed to freely interact with the atmosphere. It is found that without the tropical SST variability, the zonally elongated atmospheric mode in the mid-high latitudes, called the Antarctic Oscillation (AAO), becomes dominant and the stationary Rossby waves related to the AAO induce the SLP anomalies in the midlatitudes, which, in turn, generate the subtropical dipoles. These results suggest that the tropical SST variability may not be necessary for generating the subtropical dipoles, and hence provide a useful insight into the important role of the AAO in the midlatitude climate variability.

Japan Geoscience Union Meeting 2014
(28 April - 02 May 2014 at Pacifico YOKOHAMA, Kanagawa, Japan)

ACG37-18 Room:423 Time:April 28 17:35-17:50

Mechanism of long-term change in the Indian Ocean subtropical dipole mode

YAMAGAMI, Yoko[1*] ; TOZUKA, Tomoki[1]

[1]Department of Earth and Planetary Science, Graduate School of Science, The University of Tokyo

The Indian Ocean subtropical dipole (IOSD) is a climate mode in the Southern Indian Ocean associated with negative sea surface temperature (SST) anomalies in the southeastern tropical Indian Ocean and positive SST anomalies in the southwestern part of the southern Indian Ocean during its positive phase. In this study, the long-term change in the IOSD is investigated for the first time using observational data and outputs from an ocean general circulation model. It is found that the frequency of the IOSD has become higher in the recent decade because of a decreasing trend in the mixed layer depth (MLD) over the southwestern pole in January and February. Positive (Negative) SST anomalies associated with the IOSD are generated when the mixed layer becomes anomalously shallow (deep) and the warming of the mixed layer by the climatological shortwave radiation is enhanced (suppressed). The thinner mixed layer in the recent decade amplifies this effect and even weak atmospheric forcing may trigger the IOSD. Based on a diagnosis of the Monin-Obukhov depth, we show that an increasing trend of surface heat flux is the cause of the decreasing trend in the MLD. On the other hand, it is found that the amplitude of the IOSD has become smaller. This is because the IOSD generally starts to develop in December, but the thicker mixed layer in December in the recent decade is unfavorable for its development. Also, the thinner mixed layer in January and February amplifies the negative feedback processes that damp the SST anomalies, as well as the positive effect on generating the SST anomalies. Since no long-term change in atmospheric forcing corresponding to that in the IOSD is observed, the long-term change in the MLD is essential in that of the IOSD.

Japan Geoscience Union Meeting 2014
(28 April - 02 May 2014 at Pacifico YOKOHAMA, Kanagawa, Japan)

ACG37-P01 Room:Poster Time:April 28 18:15-19:30

Multiscale Interactions In The Genesis Of Tropical Cyclone Observed In PALAU2013

YOSHIOKA, Hiroaki[1*] ; FUDEYASU, Hironori[1] ; KATSUMATA, Masaki[2] ; YOKOI, Satoru[2] ; TSUJINO, Satoki[3] ; MASUDA, Ayumi[1]

[1]Yokohama National University Graduate School, [2]Japan Agency for Marine-Earth Science and Technology, [3]Hydrospheric Atmospheric Research Center, Nagoya University

To understand the formation of a tropical cyclone (TC), has long been a captivating subject at the frontier of science and remains challenging because of the complex multi-scale interactions involved. During the genesis stage, sustained convective activities, which may stem from a variety of processes in a favorable environment, develop into a surface mesoscale or synoptic vortex. The mesoscale processes in the genesis stage have been the least understood aspect of the lifecycle of a TC. Although the climatological large-scale conditions favorable for TC genesis have been well known since Gray (1968, 1979), the interactions between the large-scale conditions and mesoscale processes have been poorly understood. The main purpose of this study is to conduct a detailed analysis on the multiscale interactions involved in the cyclogenesis based on observational data and numerical simulations.

The Japan Agency for Marine-Earth Science and Technology (JAMSTEC) conducted a field project named the Pacific Area Long-Term Atmospheric Observation for Understanding of Climate Change (PALAU2013) over the northwest Pacific Ocean. In this project, a sounding and radar network was deployed over the ocean during the early summer of 2013. During PALAU2013, the four initial disturbances growing tropical depression (TD) or tropical storm (TS) were observed. This study focused on the disturbances, growing TS (T1304) in association with the temporal changes in large-scale environment. We analyzed re-analysis data (JMA-GSM data), observational data during PALAU2013, and simulation results using WRF-ARW. The radiosondes were launched every 3h on the R/V Mirai and every 6h at Koror and Yap. The Doppler radar was installed on this sip, collected volume-scan every 10 and 7.5 min.

Initial disturbances which occurred at (3N, 175W) in 03UTC June 10, 2013, passed through the observation point R/V MIRAI MR13-03 at (12N, 135E), grew T1304 in 00UTC June 18. The disturbance was developing along the convergence region between the trade easterlies and monsoonal westerlies. Results of radiosonde show that potential temperature was higher in the middle and upper troposphere and CAPE increased as disturbances approached. Moreover, the zonal wind component of the lower troposphere changed to the strong easterly, corresponding to the meridional wind component of the troposphere also changed to the south from the north. The temporal variation of the radar-echo area during the convections showed the organization of convective clouds to form the intense cyclones.

Keywords: Tropical storm, Tropical depression, Tropics, Doppler radar, WRF

Japan Geoscience Union Meeting 2014
(28 April - 02 May 2014 at Pacifico YOKOHAMA, Kanagawa, Japan)

ACG37-P02 Room:Poster Time:April 28 18:15-19:30

Seasonality of boreal winter MJO and its relation to SST variability

SUEMATSU, Tamaki[1*] ; MIURA, Hiroaki[1]

[1]Graduate School of Science University of Tokyo

Madden-Julian Oscillation (MJO) is a prominent intraseasonal variability in the tropics, which is characterized by eastward moving large-scale convective system along the equator. Overall seasonality of MJO paths has been recognized to be eastward during boreal winter and north-eastward during boreal summer. However, analysis of satellite data of NOAA Interpolated Outgoing Longwave Radiation (OLR) from 1982-2012 suggests that there is a notable variability in MJO paths just within boreal winter season. The paths of MJOs were observed to make a notable shift southward from about 10 ^{o} N to 10 ^{o} S from September to April, often with an event passing over the equator during November to December. Structural differences were also recognized between MJOs taking northern paths (northern MJO) and southern paths (southern MJO), with northern MJOs consisting of smaller convective components and being accompanied by more westward propagating components. Using weekly NOAA Optimum Interpolated Sea Surface Temperature (SST) data of the same time period, this shift in the paths of MJOs is further analyzed in relation to variability in SST distribution. Temporal changes in zonal SST gradient of MJO occurring regions, and equatorial asymmetry of SST distribution were evaluated. The result was suggestive of effective influence of positive zonal SST gradient from equatorial Indian Ocean to equatorial Western Pacific on the existence of MJO, and that equatorial asymmetry of SST distribution may be playing a part in the shift of the MJO paths.

Keywords: MJO, SST variability, intraseasonal variability

Japan Geoscience Union Meeting 2014
(28 April - 02 May 2014 at Pacifico YOKOHAMA, Kanagawa, Japan)

ACG37-P03 Room:Poster Time:April 28 18:15-19:30

Seasonal Variations of the Mascarene High and Related Changes in Jetstreams and a Stormtrack

MIYAMOTO, Ayumu[1*] ; NAKAMURA, Hisashi[1] ; MIYASAKA, Takafumi[1]

[1]RCAST, University of Tokyo

The subtropical high in the Southern Indian Ocean, called the Mascarene high, is an integral part of the climate system there, influencing not only weather conditions in the surrounding regions but also the oceanic state. The present study examines the mechanisms for the seasonal variations of the Mascarene high. The high resides over the eastern portion of the basin in summer, while it shifts westward in winter toward the Agulhas storm-track core in strengthening. This large seasonal displacement is a distinct feature of the Mascarene High from other subtropical highs. Our analysis reveals that, while low-level thermal contrasts between the Australian continent and southeastern Indian Ocean is important for the formation of the high in summer, its wintertime formation is owing primarily to eddy-feedback forcing due to the seasonally-enhanced storm-track activity that is maintained in the presence of pronounced SST gradient along the Agulhas Return Current. In winter, the mid-tropospheric subsidence over the surface high is associated with upper-tropospheric convergence of the cross-equatorial divergent flow, indicative of a connection between the high and the Asian summer monsoon. From the viewpoint of vorticity budget, the cyclonic tendency by the upper-level convergence is balanced with the westerly advection of the anti-cyclonic vorticity. While the converging upper-tropospheric flux of Rossby wave activity from lower and higher latitudes acts to reinforce the high in winter, the high itself acts as a source of the climatological-mean planetary waves with the net local divergence of the flux, which is suggestive of the importance of the high even on the hemispheric scale.

Keywords: subtropical high, Indian Ocean, Agulhas Return Current, SST front, jetstream, stormtrack

Japan Geoscience Union Meeting 2014
(28 April - 02 May 2014 at Pacifico YOKOHAMA, Kanagawa, Japan)

ACG37-P04 Room:Poster Time:April 28 18:15-19:30

Decadal variabilities in the Pacific and Atlantic Oceans and frequency of hot summers over the Northern Hemisphere

KAMAE, Youichi[1*] ; SHIOGAMA, Hideo[1] ; WATANABE, Masahiro[2] ; KIMOTO, Masahide[2]

[1]National Institute for Environmental Studies, [2]Atmosphere and Ocean Research Institute, the University of Tokyo

Mean temperature increase over the Northern Hemisphere (NH) land areas during warm seasons enhances frequency of extreme warm events (e.g. Russian heat wave in 2010; 1). Human influences on Earth's climate have been detected in observational records since the late 20th century. During the past 15 years, the increase in global surface air temperature (SAT) has slowed (called hiatus; 2) whereas observations show a continuous increase in summertime (June-July-August, JJA) land-mean SAT and the frequency of hot summers over the NH land areas. This discrepancy represents that some other factors except global sea surface temperature (SST) can influence on the increasing frequency of hot summers. The recent phase shifts of the decadal and multidecadal SST variabilities in the Pacific and Atlantic Oceans could have influenced the mean SAT and extreme events over the land.

For attributing the recent increase in NH hot summers, we performed three sets of ensemble simulations for 1949-2011 using an atmospheric general circulation model (AGCM). An ensemble driven by prescribed observed SST, sea-ice concentration, and radiative forcing agents, reproduces well the observed SAT time series over the NH land. Simulated anomalies can be decomposed into three components: anthropogenic influence via SST increase (ASST); direct effect of anthropogenic forcing including GHG radiative forcing (ADIR); and natural climate forcing and internal SST variability (NAT). The decomposition is made by conducting two additional ensemble, one with prescribed GHGs at the pre-industrial level and the other similar to the SST run but without human induced components in SST and sea ice have been removed.

The model simulates well 1) the long-term increase of the frequency of hot summers and 2) the recent increase during the hiatus period. Both ASST and ADIR contribute to 1). Particularly, the ADIR effect is the dominant factor for the middle and high latitude land areas, consistent with earlier studies presenting the ADIR effects for increase in mean land SAT during warm seasons (3, 4). In contrast, the NAT effect is essential for 2). The recent SST variabilities in the Pacific and Atlantic Oceans are characterized by the negative phase of PDO and the positive phase of AMO. Atmospheric teleconnection patterns associated with these SST variabilities result in low SAT over the Canada and high SAT over the United State middle latitude. In addition, the warm SST in the North Atlantic Ocean and the Mediterranean Sea contribute to high SAT over the Europe.

The recent decadal and multidecadal variabilities in the Pacific and Atlantic Oceans contribute to the increase in land SAT and frequency of hot summers over the NH middle latitude despite the recent climate hiatus. In the recent future, global and regional frequencies of hot summers can be influenced largely by phase shifts of decadal and multidecadal SST variabilities in the Pacific and Atlantic Oceans.

References

[1] Watanabe, M., H. Shiogama, Y. Imada, M. Mori, M. Ishii, and M. Kimoto, 2013: Event attribution of the August 2010 Russian heat wave. SOLA, 9, 64-67, doi:10.2151/sola.2013-015.

[2] Watanabe, M., Y. Kamae, M. Yoshimori, A. Oka, M. Sato, M. Ishii, T. Mochizuki, and M. Kimoto, 2013: Strengthening of ocean heat uptake efficiency associated with the recent climate hiatus. Geophys. Res. Lett., 40, 3175-3179.

[3] Kamae, Y., and M. Watanabe, 2013: Tropospheric adjustment to increasing CO2: its timescale and the role of land-sea contrast. Clim. Dyn., 41, 3007-3024.

[4] Kamae, Y., M. Watanabe, M. Kimoto, and H. Shiogama: Summertime land-sea thermal contrast and atmospheric circulation over East Asia in a warming climate. Part II: Importance of CO2-induced continental warming. Clim. Dyn., in revision.

Keywords: global warming, hot summer, heat wave, PDO, AMO

Japan Geoscience Union Meeting 2014
(28 April - 02 May 2014 at Pacifico YOKOHAMA, Kanagawa, Japan)

ACG37-P05 Room:Poster Time:April 28 18:15-19:30

Zonal Momentum Budget Along the Equator in the Indian Ocean from a High Resolution Ocean General Circulation Model

NAGURA, Motoki[1*] ; MCPHADEN, Michael j[2]

[1]JAMSTEC, [2]NOAA

This study examines the zonal momentum budget along the equator in the Indian Ocean, with emphasis on the Wyrtki Jets in a high-resolution ocean general circulation model. The Wyrtki Jets are wind-driven eastward flows in the upper 100 m of the equatorial Indian Ocean that appear typically twice per year during the monsoon transitions in boreal spring and fall. Our results indicate significant contributions from zonal, meridional and vertical advection of zonal momentum, with the dominant contribution coming from zonal momentum advection. These results contrast with those from previous idealized wind-forced model experiments that emphasized the importance of vertical momentum advection. The extra eastward force caused by zonal momentum advection reinforces eastward wind stress, resulting in swifter jets in the eastern basin than in the western basin. Another consequence of these nonlinearities is that, annually averaged, zonal currents in the upper thermocline flow against the zonal pressure gradient rather than down gradient. Thus, there is no mean subsurface undercurrent flowing against the surface winds in the Indian Ocean as there is in the Pacific and Atlantic Oceans. These results indicate that proper simulation of the mean and the semi-annual zonal flows along the equator in the Indian Ocean, including their climatically relevant impacts on the mass and heat balance of the region, requires accurate representation of nonlinearities that derive from a broad range of interacting time and space scales.

Japan Geoscience Union Meeting 2014
(28 April - 02 May 2014 at Pacifico YOKOHAMA, Kanagawa, Japan)

ACG38-01 Room:213 Time:April 28 09:00-09:15

Development of a visualization and download system for dataset of ocean state estimation

FUKUDA, Kazuyo[1*] ; SAITO, Hideaki[1] ; ISHIKAWA, Yoichi[1] ; MASUDA, Shuhei[1] ; SUGIURA, Nozomi[1] ; ISHIGURO, Shun[1] ; SONODA, Akira[1]

[1]JAMSTEC

In order to promote the use of a dataset of ocean state estimation useful for climate research, a data visualization and download system called ”Estimated State of Global Ocean for Climate Research (ESTOC) [1]” has been developed. The dataset contains 3- or 2-dimensional grid data of eight physical parameters such as potential temperature and salinity, and five geochemical parameters such as nitrate and phytoplankton. It covers the 53-year period from 1957 to 2009, and consists of 6996 NetCDF files of 55 gigabytes. We have considered the functions required for the system based on the assumption that the main users of the dataset are researchers not only in climatology but also in ocean ecosystem science and fisheries science.

Quick look of the data can be carried out under the conditions specified by users in the visualization page. Contour lines or vector arrows are drawn on a base map. Users can zoom in an area of the map that they are interested in, and change display color with color tables. Animations of the estimated ocean state can also be played easily. The data at users’specified location on the map can be displayed as a graph of time series, vertical profile, latitude-depth or longitude-depth sections. Furthermore, the displayed map and graph can be downloaded as png or jpeg image files.

Logged-in users are able to download a data file of the map being displayed in the visualization page, and also able to download multiple files in the download page. The following two download methods are available. One is the normal download via web browser. The other is the sending an e-mail describing a download URL to user’s registered e-mail address to use the wget command. The download state of data files is recorded in the log files for the system administrator. It will be used for improvement of data dissemination service in this system in the future.

URL
[1] http://www.godac.jamstec.go.jp/estoc/e/

Japan Geoscience Union Meeting 2014
(28 April - 02 May 2014 at Pacifico YOKOHAMA, Kanagawa, Japan)

ACG38-02 Room:213 Time:April 28 09:15-09:30

Development of Wide-area Observation Monitoring System and Data Crawling System for Global Earth Observation

MURATA, Ken T.[1*] ; NAGATSUMA, Tsutomu[1] ; YAMAMOTO, Kazunori[1] ; WATANABE, Hidenobu[1] ; UKAWA, Kentaro[2] ; MURANAGA, Kazuya[2] ; YUTAKA, Suzuki[2]

[1]NICT, [2]Systems Engineering Consultants Co., LTD.

This paper is to propose a cloud system for data-intensive science, which has been developed at NICT (National Institute of Information and Communications Technology), Japan. The NICT science cloud is one of the cloud systems for scientists who are going to carry out their research works.

The science cloud is not for simple uses. Many functions are expected to the science cloud; such as data standardization, data collection and crawling, large and distributed data storage system, security and reliability, database and meta-database, data stewardship, long-term data preservation, data rescue and preservation, data mining, parallel processing, data publication and provision, semantic web, 3D and 4D visualization, out-reach and in-reach, and capacity buildings.

In the present talk, we introduce two types of tools for global data collection (crawling) and data transfer. The former is to collect observation data files from a variety of data server public on the Internet. The latter is to manage observation systems at observatories over the world. Data file transfer, monitoring servers and networks and system recovery are easily carried out using this system.

Japan Geoscience Union Meeting 2014
(28 April - 02 May 2014 at Pacifico YOKOHAMA, Kanagawa, Japan)

ACG38-03 Room:213 Time:April 28 09:30-09:45

WCRP/AMY data archive and data release on the DIAS

TAMAGAWA, Katsunori[1*] ; OHTA, Tetsu[1] ; IKOMA, Eiji[1] ; KINUTANI, Hiroko[1] ; OYANAGI, Misa[1] ; MATSUMOTO, Jun[2] ; KITSUREGAWA, Masaru[3] ; KOIKE, Toshio[4]

[1]EDITORIA, The University of Tokyo, [2]Dept. of Geography, Tokyo Metropolitan University, [3]IIS, The University of Tokyo, [4]Dept.Civil Eng., The University of Tokyo

The purpose of this presentation is to introduce World Climate Research Programme (WCRP)/Asian Monsoon Years (AMY) data archiving and opening status along with its data uploading, data quality control, and metadata registration systems on the Data Integration and Analysis System (DIAS).

DIAS was launched in 2006 as a part of the Earth Observation and ocean Exploration System that provides cooperative opportunities for constructing data archives, and developing data integration and analysis functions (http://www.editoria.u-tokyo.ac.jp/projects/dias/).

The goal of WCRP/AMY is to improve Asian monsoon prediction for societal benefits through coordinated efforts and to promote a better understanding on Asian monsoon variability and predictability. Under the framework of the WCRP/AMY the various kinds of in-situ data have been archived among 21 different international projects. (http://www.wcrp-amy.org/). The basic for the WCRP/AMY collaborative framework is the mutual consensus among the participating countries, international organizations, individual participants, and their partner projects. It that defines the data sharing and exchange policies and is responsible for the data management.

Keywords: DIAS, WCRP/AMY, in-situ data, Water Cycle, Asian Monsoon

Japan Geoscience Union Meeting 2014
(28 April - 02 May 2014 at Pacifico YOKOHAMA, Kanagawa, Japan)

ACG38-04 Room:213 Time:April 28 09:45-10:00

VDVGE: Volume Data Visualizer for Google Earth

KAWAHARA, Shintaro[1*] ; SUGIYAMA, Tooru[1] ; ARAKI, Fumiaki[1] ; TAKAHASHI, Keiko[1]

[1]JAMSTEC

Software to visualize volume data that is called VDVGE (Volume Data Visualizer for Google Earth) has been developed. VDVGE visualizes a four-dimensional scalar data, and exports it to KML and COLLADA which are suitable format to Google Earth. Currently, VDVGE are used not only visualization of simulation data, also visualization of observed data, such as meteorological radar and meteorological satellites. In the presentation, the development status of VDVGE is introduced. Application examples of the recent will be also introduced.

Keywords: Google Earth, Volume visualization, Software development

Japan Geoscience Union Meeting 2014
(28 April - 02 May 2014 at Pacifico YOKOHAMA, Kanagawa, Japan)

ACG38-05 Room:213 Time:April 28 10:00-10:15

Introduction of the UndearwayCTD observation: A new instrument of oceanography

HASEGAWA, Takuya[1*] ; YOKOI, Satoru[1] ; MOTEKI, Qoosaku[1] ; KATSUMATA, Masaki[1] ; UEKI, Iwao[1] ; ANDO, Kentaro[1] ; YONEYAMA, Kunio[1]

[1]JAMSTEC

Abstract is written in Japanese.

Keywords: In-situ observation in the upper-ocean, UnderwayCTD

Japan Geoscience Union Meeting 2014
(28 April - 02 May 2014 at Pacifico YOKOHAMA, Kanagawa, Japan)

ACG38-06 Room:213 Time:April 28 10:15-10:30

Development of a satellite land and cloud data assimilation system coupled with WRF, and its application to Kanto area

SETO, Rie[1*] ; RASMY, Mohamed[1] ; KOIKE, Toshio[1]

[1]Department of Civil Engineering, the University of Tokyo

For flood prediction and optimized dam control, it is crucial to predict whether a rain area will be over the river basin or not after few hours, and this needs very fine prediction of time and space distribution. For system development focusing on the ‘location‘ of rain areas, it is effective to introduce the information of cloud distribution from the observations into the model as initial conditions. Clouds can be observed by microwave remote sensing by satellite. But it is not easy to observe the cloud over the land from the satellite because emissivity of clouds is so week compared to that of land surface.

In order to observe cloud over the land, we at first have to adequately represent the heterogeneity of land state, especially soil moisture distribution, which has large effect on emissivity of the land, and estimate the surface emissivity, then remove it as background information for cloud observation. Therefore, we developed a satellite-based land and cloud data assimilation system coupled with the Weather Research and Forecasting Model (CALDAS-WRF) and applied it to the Kanto area.

The CALDAS-WRF includes Simple Biosphere model version 2 (SiB2) as a land surface driver, radiative transfer models for soil and atmosphere as observation operators, and Ensemble Kalman Filter (EnKF) and 1DVAR as assimilation algorithms for land and cloud, respectively.

The CALDAS-WRF first initializes the whole system, integrates the WRF and the SiB2 repeatedly until observations are available, and then assimilates the soil moisture heterogeneity, using passive microwave brightness temperature (Tb) at lower frequency, which has a high sensitivity to soil moisture. Then the CALDAS-WRF assimilates cloud over the land, using Tb at higher frequency, which is sensitive to cloud, and optimized emissivity of land as a background information.

We applied the CALDAS-WRF to the Kanto area, and the system effectively assimilated information of clouds and largely improved the representation of cloud distribution. Precipitation areas were also reproduced in the correct locations and consistent atmospheric fields were generated around the cloud areas through dynamical and physical processes in the atmospheric model. However the precipitation amount and duration were not enough, which will be the next target of our development.

Keywords: cloud, soil moisture, satellite microwave data assimilation, Kanto area, heavy rain prediction

Japan Geoscience Union Meeting 2014
(28 April - 02 May 2014 at Pacifico YOKOHAMA, Kanagawa, Japan)

ACG38-07 Room:213 Time:April 28 10:30-10:45

Atmosphere-Ocean coupled regional modeling for dynamical downscaling of current and future climates

YOSHIMURA, Kei[1*] ; HAM, Suryun[1] ; LI, Haiqin[2]

[1]Atmosphere and Ocean Research Institute, The University of Tokyo, [2]Center for Ocean-Atmospheric Prediction Studies, Florida State University

We have developed regional downscaling system of the Regional Spectral Model for the atmosphere and the Regional Ocean Modeling System (RSM-ROMS) to improve the downscaling simulation accuracy of particularly coastal area, and we have achieved a dynamical downscale of the climate model simulation for 20th and 21st century forced by SST and atmospheric state from the global Community Climate System Model version 3.0 (CCSM3) for California area. The results indicate that the surface air temperature rise was decreased over San Francisco Bay area due to the effect of uplifting current at the Pacific coast. The projected change of extreme warm events is quite different between the coupled and uncoupled downscaling experiments, with the former projecting a more moderate change. The projected future change in precipitation is not significantly different between coupled and uncoupled downscaling. Both the coupled and uncoupled downscaling integrations predict increased onshore sea breeze change in summer daytime and reduced offshore land breeze change in summer nighttime along the coast from the Bay area to Point Conception. Compared to the simulation of present climate, the coupled and uncoupled downscaling experiments predict 17.5 % and 27.5 % fewer Catalina eddy hours in future climate respectively. Similar framework was applied for East Asian region, and preliminary results show quite significant change in surface temperature and precipitation field due to having dynamically predicted fine scale ocean currents. Particularly in summer to fall, when Kuroshio Current direction and prevailing surface wind direction are about opposite, coastal subsidence occurs so that it warms the coastal air temperature. This feature is opposite from the California's case, and potentially indicating the possible underestimation of warming. We will further investigate the detail of the influence of regional atmosphere-ocean coupling in the presentation, as well as the impact of fresh water input from the terrestrial runoff.

Keywords: Atmosphere-Ocean coupled regional model, coastal uplifting current, regional climate projection, dynamical downscaling

Japan Geoscience Union Meeting 2014
(28 April - 02 May 2014 at Pacifico YOKOHAMA, Kanagawa, Japan)

ACG38-08 Room:213 Time:April 28 11:00-11:15

What can we find with the ensemble atmospheric reanalysis: ALERA2? -New aspect of the MJO-

MOTEKI, Qoosaku[1*]

[1]JAMSTEC

An ensemble atmospheric reanalysis ALERA2 is now open to public for the period of 2003-2013. New aspect of the MJO with the ensemble spread of the ALERA2 will be introduced.

Keywords: ALERA, ensemble, reanalysis, MJO

Japan Geoscience Union Meeting 2014
(28 April - 02 May 2014 at Pacifico YOKOHAMA, Kanagawa, Japan)

ACG38-09 Room:213 Time:April 28 11:15-11:30

Climate Change Signal Represented in Reanalyses

KAMAHORI, Hirotaka[1*]

[1]Meteorological Research Institute

Since NOAA/NCEP competed the first atmospheric reanalysis NCEP/NCAR, 20 years are passed. During these 20 years, many reanalyses NCEP/DOE, ERA-15, ERA-40, JRA-25 MERRA, CFSR, and ERA-Interim were released. Last year, JRA-55 was completed as the third generation reanalysis.

Now a day, the atmospheric reanalyses are widely utilized as fundamental database of pseudo observations in meteorology as well as in in various research fields. However, their adaptation to the climate change studies have not been advanced very much, because of less temporal S/N ratio in reanalyses products. That is, present available reanalyses include large artificial variations compared with natural variations in real atmosphere. Since the first reanalysis NCEP/NCAR, all reanalysis assumes the frozen data assimilation system in order to avoid artificial variations accompanying with changes of the system. We expected the homogeneous products with the frozen systems, but there are many artificial changes in the products different from the change of the real atmosphere, due to the change of the observation systems. As the largest artificial change, it should be noted that the large gaps in the products characteristics were introduced due to introduction of geosynchronous satellites around 1979. These artificial variations in the products make difficult to adapt them to climate change studies. On the other hand, continuous efforts have been made to reduce the artificial variation and make the products applicable to the climate change studies. For examples, bias correction techniques for satellite and upper air observations that are input data in the data assimilation system, are developed and adapted in recent reanalyses. As a result, homogeneity of reanalysis products is largely improved, and we become to be able to extract the signals of climate change from the products. Of course, degrees of availability of the climate change signals in the products largely depend on the variables. Here, I introduce specific examples of the application possibilities of the products for the climate change studies.

Keywords: Climate Change, Reanalysis, Data Assimilation, Observation

Japan Geoscience Union Meeting 2014
(28 April - 02 May 2014 at Pacifico YOKOHAMA, Kanagawa, Japan)

ACG38-P01 Room:Poster Time:April 28 18:15-19:30

The data release of Earth observation project data products considering data provider's policies by DIAS

KINUTANI, Hiroko[1*] ; SHIMIZU, Toshiyuki[2] ; LI, Jiyi[2] ; NAKAHARA, Yoko[2] ; YOSHIKAWA, Masatoshi[2] ; KITSUREGAWA, Masaru[3] ; KOIKE, Toshio[1]

[1]The University of Tokyo, [2]Kyoto University, [3]The University of Tokyo, National Institute of Informatics

Our project, DIAS (Data Integration and Analysis System) started in 2006, has a purpose of constructing data infrastructure that can integrate earth observation data, numerical model outputs, and socio-economic data effectively. DIAS also has a purpose to create knowledge enabling us to solve earth environment problems and to generate socio-economic benefits. From October 2010, we have released data of DIAS with Document-metadata, describing about dataset in English and Japanese. Anyone can use the DIAS data discovery system by accessing http://dias-dss.tkl.iis.u-tokyo.ac.jp/ddc/, and can download data files of 195 datasets through the system.

The data in DIAS is classified into 4 categories:

1) Numerical simulation outputs for the purpose of research,
2) Satellite data for the purpose of research,
3) Datasets created by DIAS researchers,
4) Datasets created at related projects supported by DIAS.

Newly released datasets are **NIES CGER Ochiishi Monitoring Station Greenhouse Gases Data**, **NIES CGER Tomakomai Energy, Water, CO2 Flux, Spectral Radiation, Vegetational Index Data**, **Atmosphere and ocean carbon dioxide monitoring using volunteer observing ship (Pyxis) servicing between Japan and West Coast**, **The Japanese 55-year Reanalysis (JRA-55)**, **GRENE-City Tsunami archive**, **AGURAM Ground Information Database** and Asian Monsoon Year projects data products.

Data provider to release datasets from DIAS should create the document metadata (both in English and Japanese) that describes the dataset.Data provider should write a policy concerning the data in order to notify to data user in it. In addition to data policy of data provider, project policy of a project that became the background of the data creation, and DIAS data policy are included in the document metadata. If conflicting terms are written among the data policies, we have determined the priority of data policy; the order is data provider, project and DIAS.

The data policy of DIAS is as follows:

1. With regard to Data policy, if there is any data policy indicated by the data provider, that policy always has priority over this DIAS data policy.
2. DIAS data sets are to be used only for scientific research or educational purposes. Commercial use and exploitation of DIAS data sets are prohibited
3. Any modification or change of the original DIAS data sets is prohibited.
4. Any Re-export or transfer of the original data sets to a third party is prohibited.
5. The origin of DIAS data being used for any publication of scientific results must be acknowledged and referenced in the publication, with the *quotation* given below as an acknowledgement.
6. Whenever DIAS data sets are used for publication of scientific results, the author(s) shall send a copy of the respective publication, preferably in an electronic form or in a separate printed version, to the DIAS CONTACTS as indicated

Data policy of DIAS may use as the basis for data providers to create their own data policy.

In addition, the data download system developed by DIAS has 4 level access controls to the data for users' data downloading.

1) Registered users are able to download.
2) In addition to 1), after agreement of data policy, users are able to download.
3) In addition to 2), after sending a use application through the system to the data provider and approval is obtained, users are able to download.
4) In addition to 2), after users have negotiated individually with the data provider and approval is obtained, users are able to download.

By considering the data policy of data provider in this way, we are trying to improve the reliability of DIAS data repositories and DIAS data release.

Keywords: DIAS, Earth Observation data, Satellite data, Model output data, In-situ data, data policy

Japan Geoscience Union Meeting 2014
(28 April - 02 May 2014 at Pacifico YOKOHAMA, Kanagawa, Japan)

ACG38-P02 Room:Poster Time:April 28 18:15-19:30

Development of a basic common library (SCALE) for future HPC and datasets created by the library

SATO, Yousuke[1*] ; NISHIZAWA, Seiya[1] ; YASHIRO, Hisashi[1] ; MIYAMOTO, Yoshiaki[1] ; TOMITA, Hirofumi[1]

[1]RIKEN Advanced Institute for Computational Science

A basic Common library named Scalable Computing for Advanced library and Environment (SCALE) is now being developed at RIKEN, Advanced Institute for Computational Science (AICS). The library is developed to solve the problems that come from the sophistication of numerical models and the recent trend of high performance computing (HCP). The library is downloadable from the web site of RIKEN, AICS (http://scale.aics.riken.jp/). The license of the SCALE is based on BSD 2 license.

SCALE-Large Eddy Simulation (LES) is now available as a component of the SCALE library. The SCALE-LES is based on fully compressible system, and it uses vertically explicit and horizontally explicit (HE-VE) scheme. Even ordered central differential schemes (2nd ordered central differential scheme for the terms relating to the density, 4th ordered central differential scheme for the other terms) are applied for spatial discretization. The 3rd ordered Runge-Kutta scheme is applied for the temporal discretization. Physical components implemented in the SCALE-LES are turbulent scheme, a radiation scheme, cloud microphysical schemes (1-moment bulk, 2-moment bulk, and spectral bin scheme), and surface flux model. The aerosol model, chemical transport model, urban canopy model will be implemented near future.

In future, the SCALE library will be extended to regional model with nesting system, global model. As well as the atmospheric component, the SCALE will be extended to the entire targets for numerical simulation (e.g. ocean, biosphere, molecular dynamics, or so).

We will introduce some examples of the results obtained from the SCALE-LES and some datasets. We aim to share and discuss about not only the model results but also the problem when we treat the big data (e.g. data handling, visualization or so) with the participants regardless of their background.

Japan Geoscience Union Meeting 2014
(28 April - 02 May 2014 at Pacifico YOKOHAMA, Kanagawa, Japan)

ACG38-P03 Room:Poster Time:April 28 18:15-19:30

Japan mosaic land-cover 0.01 degrees raster dataset

HIGUCHI, Atsushi[1*] ; KAWAKAMI, Satoshi[2] ; MURAKAMI, Akinobu[3] ; MASUTOMI, Yuji[4] ; TAKAMI, Akinori[5]

[1]CEReS, Chiba University, [2]HP Japan, [3]University of Tsukuba, [4]Center for Environmental Science in Saitama, [5]NIES

As one of basic information for numerical weather simulation, land-cover and land-use dataset is essential for initial condition. In Japan, MILT published land-cover information as tile and vector files. We mosaicked tile vector files into one raster (gridded) file dataset over Japan. Such mosaicked raster files are available for 1976, 1987, 1991, 1997 and 2009. We also made convert programs from original land-cover flag (number) into typical land surface model (SiB and SiB2) land-cover flag. We also try to explain how to utilize these dataset for the assessment of urban-green to reduce heat island without use of urban canopy model within the poster session core-time. To make the dataset, SALSA project under RECCA/MEXT supports our activity.

Keywords: land use, land numerical mesh, Japan mosaic, raster data

Japan Geoscience Union Meeting 2014
(28 April - 02 May 2014 at Pacifico YOKOHAMA, Kanagawa, Japan)

ACG38-P04 Room:Poster Time:April 28 18:15-19:30

Meteorological observations for the purpose of educational use in Nagata ward, Kobe

FUKUSHIMA, Azusa[1*] ; OTSUKA, Shigeaki[1]

[1]Faculty of Humanities and Sciences, Kobe Gakuin University

Weather and climate are the units in science or geography classes in elementary and junior high school. Recently, many data have archived on the Internet by the individuals or scientific groups other than JMA with the spread of the meteorological instruments. However, if a teacher who is working at a public school hopes to do constructive class with some practical works using the meteorological data, he has to spend for hours and hours preparing. For example, he has to choose a case day to learn the unit in effective way, and he has to prepare the data that it can be used in his students easily. Therefore we considered that if a provider prepares some support measures for using the data, the teacher might be easy to introduce the meteorological dataset into his class as a course material. In this study, we report an approach to the educational use of a meteorological dataset observed at the Nagata center of the Center for Area Research and Development, Kobe Gakuin University from 2011.

The Nagata center of the Center for Area Research and Development was established in 2010. It is located in the former buildings of the Futaba elementary school in Nagata ward, Kobe-shi. The instruments for the observation of the meteorology and seismology were installed on summer of 2011. The elements of meteorological observation are air temperature, wind speed and direction, relative humidity, rainfall, net solar radiation, ultraviolet A and B, and pressure. The elements for the seismology are seismic intensity, seismic wave, groundwater level, and underground water temperature. The observation data is automatically saved as daily reports, monthly reports, and annual reports. The daily reports are available on our website to the registered users. The data can be used only for the educational and research purposes.

Observation site is located in the urban area between Shin-Nagata station (JR line) and the port of Nagata. It is at a distance of about 7km southwest of Kobe Local Meteorological Observatory. JMA Akashi AMeDAS station is in Futami coastal area of Harima-Nada. Nagata is the side of Osaka Bay and is located in the south of Rokko-Awaji fault zone. If the observation data used in conjunction with the data of Kobe Local Meteorological Observatory, it can be carried out a research of urban heat island and sea and land breezes at the regional scale. A practical training of the meteorological observation or the tour of equipment at the Nagata center is also possible.

The data that observed in near at hand can be used to understand local scale weather and climate as a course material in the school. Furthermore, it is possible to feed the geographic and the temporal sense of the weather phenomenon by comparing the data of several weather stations including Nagata.

Keywords: Meteorological and Seismological Data, Earth Science Education, Nagata ward, Kobe

Japan Geoscience Union Meeting 2014
(28 April - 02 May 2014 at Pacifico YOKOHAMA, Kanagawa, Japan)

ACG38-P05 Room:Poster Time:April 28 18:15-19:30

Study of tropospheric tomography for water vapor distribution with Neural Network

HIROKI, Akimitsu[1*] ; HATTORI, Katsumi[1] ; HIROOKA, Shinji[1]

[1]Graduate School of Science, Chiba University

Many meteorological disasters such as landslides with torrential rain have been reported. Monitoring and a prediction of the precipitation activity are very important to mitigate these disasters. However, in the developing countries such as Indonesia and the Philippines, the observation with the radars is difficult in the present conditions due to the cost and the maintenance. The water vapor tomography using a GPS and/or broadband satellite is considered to be effective for the precipitation monitoring system instead of the radars in the above countries.

When the rain cloud bringing the damage of a heavy rain and the thunderstorm is developing, there is an apparent flow of the water vapor from the neighborhood. It is possible that the GPS can detect the flow and distribution of water vapor. Therefore, in this study, we develop a water vapor tomography from GPS and AMeDAS data using algorithm of residual minimization learning neural network (RMTNN). The numerical simulation demonstrates a capacity of the developed method, that is, the reconstructed image can show the transient changes and the inverse layer in given water vapor distributions. The details will be shown at our presentation.

Keywords: tomography, water vapor, GPS

Japan Geoscience Union Meeting 2014
(28 April - 02 May 2014 at Pacifico YOKOHAMA, Kanagawa, Japan)

HGG01-01 Room:424 Time:April 29 14:15-14:30

Influence of existing scenery in an on-site forest environment in terms of Subjective Appraisal, Restorativeness, Affect

TAKAYAMA, Norimasa[1*] ; FUJIWARA, Akio[2] ; SAITO, Haruo[2] ; HORIUCHI, Masahiro[3]

[1]Forestry and Forest Products Research Institute, [2]The University of Tokyo Forests, [3]Yamanashi Institute of Environmental Sciences

INTRODUCTION

Many stressors of urban life are increasingly driving humans to seek some form of stress relief (Frumkin, 2001). Natural environments, including typical urban parks and natural, secondary or artificial man-made forests are generally associated with stronger positive health effects compared with urban environments (Velarde, Fry & Tveit, 2007). For instance, natural scenes bring higher tranquility and a reduced feeling of danger compared to urban scenes (Herzog & Chernick, 2000), while outdoor recreation in a green environment has been shown to relieve stress among urban inhabitants (Li et al., 2008), hence the evidence to date seems to indicate the positive health effect of a natural setting. However, the question of how the existence of scenery as a sight stimulus produces a psychological effect in an on-site forest environment and to what extent remain unclear.

Therefore, during this research conducted in an on-site forest environment (a mixed forest including Larch, Giant dogwood), we set out our research purpose, namely to clarify the psychological healing effect of forest scenery as visual stimuli on respondents.

METHOD

With eleven male and four female adult respondents respectively, we conducted a viewing experiment to investigate the appraisal (Semantic differential method; abbreviated to SDM; 25-paired adjectives), the affect (Positive And Negative Affect Schedule; abbreviated to PANAS; 16-queries), subjective restorative quality (Restorative Outcome Scale; abbreviated to ROS; 6-queries) and degree of attention restoration (Perceived Restorativeness Scale; abbreviated to PRS; 26-queries) using four types of research questionnaires. The viewing experiment was conducted in the forest inside the Forest Therapeutic Research Institute (Fuji Iyashi-no-mori Institute) and managed by the University of Tokyo Forests in early May 2013. The experiments were conducted one-by-one during fine weather throughout the experimental period (four days). Each respondent was given respectively from the opening session (with well-managed forest scenery) to the closing session (forest scenery covered by tarpaulin) or vice versa to eliminate any order effect.

RESULT AND CONSIDERATION

Consequently, in terms of the comparison of appraisal, the opening session saw scores higher than the closing session for many measurement indexes and the degrees of score difference were cleared. Conversely, it became clear that a difference would emerge in both the opening and closing sessions, even if it was a measurement index not corresponding to visual senses but directly to other senses. Finally, based on the result of multiple regression analysis, it emerged that the basic links between them included aspects of difference and commonality for the integrated index appraisal such as likableness, comfort, beauty and sense of security when comparing the opening and closing of the forest landscape respectively, and this was an appraisal of concrete environmental factors which resulted in such differences and commonality. Furthermore, in terms of afect, even though neither a positive nor negative affect could be confirmed from statistical interaction when comparing the opening and closing sessions, there was a statistical decline (reduction) in the before (pre-viewing experiment) compared to after (post-viewing experiment). As for the quality of subjective restorative, the interaction between the opening-closing and before - after sessions was confirmed as well as individual statistical differences when comparing before and after in the opening session and opening and closing sessions in the after session sequentially. Regarding the degree of attention restoration, subsequent results of the opening-closing comparison clarified that the criteria of run away, fascination, scope and compatibility were statistically higher in the opening rather than closing session.

Keywords: Attention restoration theory, Positive affect, Negative affect, Subjective restorative outcome, Appralsal, Forest therapy

Japan Geoscience Union Meeting 2014
(28 April - 02 May 2014 at Pacifico YOKOHAMA, Kanagawa, Japan)

HGG01-02 Room:424 Time:April 29 14:30-14:45

Evaluation of Landscape Conservation at Green Space on Campus Based on the Level of Willingness to Work

TAKASE, Yui[1*] ; FURUYA, Katsunori[1]

[1]Graduate School of Horticulture, Chiba University

1. Introduction

A university campus with a large-scale green space is precious access to green for the residents in the surrounding vicinity. However, very often only a very low budget is granted for management of green space on university campuses in Japan. Volunteer activities among students are expected for management of the landscape and maintenance of those green spaces on campus. In this study, landscape conservation of green space on campus has been evaluated, based on the level of students' willingness to work.

2. Study Methods

Matsudo Campus of Chiba University in Japan has been selected as a subject. The total area of this campus is 15 hectares, and 13.7 of which counts for green space. A survey was conducted in July, 2013, with students who belong to the Faculty of Horticulture at Chiba University. The number of respondents was 77. The following four items were surveyed: 1) Attribute of respondents (gender, participation experience in green space conservation activities, and willingness to participate), 2) future vision of green space on campus from nature experiences, 3) ecosystem services expected from green space on campus, and 4) desired participation hours to spare for green space conservation activities.

3. Results and Considerations

Regarding respondents' attributes, the number of valid responses was 59, with 35 males (59%) and 24 females (41%). The number of people who have participation experience in green space conservation activities counted 27 (46%). The number of those who are willing to participate in those activities was 48 (81%).

With regard to the future vision of green space on campus, an free answer question was provided and 65 valid responses were obtained. The two most common opinions were as following: 1) "Increasing of nature experience events" (19 respondents, 29%), and 2) "Increasing of facilities such as restrooms, benches, gathering area, and lighting" (19 respondents, 29%). The next most significant answer was "Better management of gardens and woods" (15 respondents, 23%).

The next topic about ecosystem services expected from green space on campus was captured from 59 valid responses. Approximately 90% of them had certain expectations from ecological services related to green space on campus: examples, "to create beautiful landscape in the area" and "space where people can enjoy nature".

Finally, as for the number of participation days to spare for conservation activities on Matsudo campus, 59 students provided valid answers. The average number of days that they are willing to participate is 14.2. Since the participation hours per day had been specified and presented as four hours, the average hours figure is 56.8, converted from the number of days. The grand total of days willing to spare among all valid respondents counted 841 days. Next, the number of desired days to spare was computed for each activity location within the campus. "Ohisama Garden", which is a flower garden managed mainly by students' initiatives earned the highest number of days among all the campus locations. Thirty-five respondents (59%) are willing to spare time here with an average of 6.4 days, which totals 225 days. On the other hand, traditional garden is the most popular in terms of the number of respondents who are willing to spare time. Forty respondents (68%) indicated their interest in sparing time in the traditional garden. The average counted 4.8 days, which totals 191 days. While the main reason of the location choice for Ohisama Garden was "interest in the activities" (14 respondents), the one for the traditional garden was "to acquire knowledge and know-how" (12 respondents).

4. Conclusion

In this study, students' willingness to participate in landscape conservation was clarified by gauging their willingness to work. In doing so, the specific number of days and the available labor in scenery maintenance have been drawn.

Keywords: Willingness to Work, Landscape Conservation, Green Space on Campus

Table. Result of the number of participation days to spare for conservation activities on Matsudo campus

Traditional Garden	Ohisama Garden	Bamboo Grove	Around School Grounds	Sloping Forest	Other
					
Average of days 4.7 days	Average of days 6.4 days	Average of days 3.4 days	Average of days 3.2 days	Average of days 4.9 days	Average of days 4.8 days
Number of Respondents 40 (68%)	Number of Respondents 35 (59%)	Number of Respondents 36 (61%)	Number of Respondents 20 (34%)	Number of Respondents 32 (54%)	Number of Respondents 16 (27%)

Japan Geoscience Union Meeting 2014
(28 April - 02 May 2014 at Pacifico YOKOHAMA, Kanagawa, Japan)

HGG01-03 Room:424 Time:April 29 14:45-15:00

Landscape Evaluation Method by Visitor-Employed Photography with Usage of Cellphones - Case Study of Mount Gwanak, Korea

MIZUUCHI, Yusuke[1*] ; SON, Yonghoon[2] ; KANG, Moonseok[2] ; FURUYA, Katsunori[1]

[1]Graduate School of Horticulture, Chiba University, [2]Graduate School of Environmental Studies, Seoul National University

1. Introduction

For spatial planning and designing such as natural parks, it is important to understand how users percept and evaluate landscapes. The relationship between viewpoints and a viewing object has been regarded important in the landscape perception model which has been studied in Landscape architecture, Geography and some sciences. One of the study methods to understand such landscape perception uses a camera called Visitor-Employed Photography (VEP), and this method is considered effective in extracting visual images of a space. However, while existing VEP is effective in understanding viewing objects, it still has shortcomings. It requires interviews and descriptions separately in order to extract viewpoints. Therefore, in order to develop a study method of landscape perception to overcome these limitations, we conducted experiments to get viewpoints by using the GPS function of cellphones which visitors to the sites possess for their daily usage.

2. Outline of the experiment

A research was conducted with 60 subjects, and the trail of Mount Gwanak in the suburbs of Seoul, Korea, was selected as a site. This location is designated as Urban Eco-Park. The subjects were instructed to use their own cellphones and take photos of landscapes which subjects evaluate. They were also instructed that Geotag must be attached to the photos. In addition, geographic information of the subject's action was simultaneously collected by GPS logging application of their cellphones. Following this activity, a questionnaire survey about subject's profile was conducted. From the collected photos and spatial characteristics of Mount Gwanak, we analyzed landscape objects which are appreciated by the visitors.

3. Results

1,119 photos were collected from 60 respondents. Among these, the redundant photos of the same composition taken by the same subject (121 photos) were eliminated. In addition, geographic information were not available from 6 subjects, hence theirs (99 photos) were also eliminated. Further eliminated were the other photos with geographic information errors (45 photos), and the remaining 842 photos were used for analysis. These photos were categorized based on the viewing objects and viewing distance. As a result, based on the trail as a viewpoint, the photos of landscapes within the woods counted most with 120 photos. Panoramic views (105 photos) and closer shots of the space with a river as a main subject were also common. We analyzed the collected geographic information with the Kernel density estimation, and identified the viewpoints of visitor's preference (Fig. 1). This result was combined with the categorized viewing subjects for further analysis, and it was found that photo shooting density tends to be high at the following locations: 1) panoramic view, and the rock and the building at the mountain top in the surrounding area of the mountain top (Fig. 1.1), 2) the touching points of the trail and the river (Fig. 1.2 and 1.3), and 3) locations with a temple (Fig. 1.4)

4. Conclusion

In this research, landscapes within the woods, panoramic views, and river views from the trail are highly appreciated at Mount Gwanak. While panoramic views and river landscapes were concentrated in certain locations, there was no spatial tendency detected with the landscapes within the woods. From the questionnaire survey, 42 respondents (70%) responded comfortable. Eighteen (30%) responded not comfortable; and among those, two (3.3%) were about GPS and others were about the course. Thus, the load of study method itself can be considered light. As described above, this study method can be useful as a future development of a landscape perception research method. It enables visual extraction of viewpoints and viewing objects as shown in this research. Furthermore, this method can be applicable to international comparative studies to identify cultural differences in landscape recognition.

Keywords: landscape evaluation, GPS, GIS, Visitor Employed Photography

HGG01-03 Room:424 Time:April 29 14:45-15:00

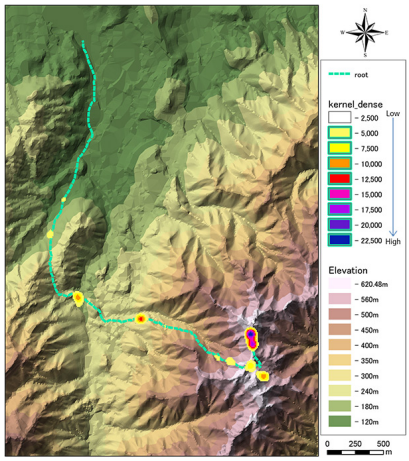

Japan Geoscience Union Meeting 2014
(28 April - 02 May 2014 at Pacifico YOKOHAMA, Kanagawa, Japan)

HGG01-04 Room:424 Time:April 29 15:00-15:30

Comparison of natural landscape appreciation between Russia and Japan: landscape exoticism evaluation

PETROVA, Elena[1*] ; MIRONOV, Yury[2] ; AOKI, Yoji[3] ; MATSUSHIMA, Hajime[4] ; EBINE, Satoshi[4] ; FURUYA, Katsunori[5] ; PETROVA, Anastasia[6] ; TAKAYAMA, Norimasa[7] ; UEDA, Hirofumi[8]

[1]Lomonosov Moscow State University, Faculty of Geography, [2]Vernadsky State Geological Museum of the Russian Academy of Sciences, [3]Haiku International Association, [4]Research Faculty of Agriculture, Hokkaido University, [5]Graduate School of Horticulture, [6]Institute for Oriental Studies of the Russian Academy of Sciences, [7]Forestry and Forest Products Research Institute in Japan, [8]School of Design, Sapporo City University

People belonging to different cultures differ by their landscape preferences due to a number of ethno-cultural features as well as historical, social, and environmental factors. It is very important to reveal and consider these differences. The purpose of this study is to compare perception, visual and emotional evaluation of natural landscapes in Russia and Japan, that are situated so close to each other and share a common border, but differ so greatly in cultural aspects, while both have deep-rooted traditions of landscape appreciation. We have interviewed respondents in university centres of Russia (Moscow in Central Russia, Irkutsk in East Siberia, and Petropavlovsk-Kamchatsky in Far East) and Japan (Sapporo, Chiba, and Miyazaki); metropolitan areas of both countries and two outermost areas, which differ most strongly in their natural environment, were represented. Young respondents (17 to 30 years old men and women) have taken part in the survey. During the interview, each respondent received the same set of 70 photos of natural landscape. For evaluating the exoticism, we asked respondents to use the 3-point scale, on which exotic landscape got a mark ”+1” and usual landscape - ”-1”. When respondents could not decide between these categories, they were suggested to use an average value ”0”. Data obtained were analyzed using elementary and multivariate statistical methods.

Exoticism is very important parameter in landscape appreciation and evaluation. As we have learned during the interview, respondents consider attractive landscape as beautiful and comfortable not only for a long-term stay, but for living in. Exotic landscape is ”unfamiliar” to respondents; even if it were unsightly, it would be interesting to look at, at least once. Therefore, when assessing attractiveness of landscape, respondents focus primarily on their aesthetic feelings, but in the evaluation of exoticism dominates their educational interest to an unknown. As we revealed, practically no correlation exists between Russian and Japanese respondents to evaluate exotic landscapes (R = 0.26). The majority of Russian respondents evaluate mountain landscapes, waterfalls, and see coasts as the most exotic, but forests, rivers, and treeless plains as the most usual. At the same time, coastal areas are usual and treeless plains are exotic for the Japanese. All the other types of landscapes vary considerably in their exoticism degree for Japanese respondents. All groups of Japanese respondents assess the exoticism of landscapes virtually identical (the correlation coefficients between their scores are: R = 0.90-0.96), while the groups of Russian respondents show some differences.

To discover the ethno-cultural aspect, we compare the survey data from Kamchatka to that from Hokkaido, which are similar in terms of natural conditions. In their assessments of the exotic landscapes residents of Kamchatka are closer to the representatives of their culture, living in fundamentally different environmental conditions, than to the representatives of the Japanese culture, living in a similar environment. At the same time, Kamchatka respondents evaluate some of exotic landscapes virtually identical to the estimates of Japanese respondents and very different to those of Russian respondents from other regions. This applies to seacoasts and mountain landscapes that are both the most remarkable and most similar elements of natural environment of Kamchatka and Japan. Thus, if all respondents evaluate the attractiveness of landscapes almost equally, which may indicate the existence of universal human concepts of their aesthetics, then when assessing the exoticism, important role play both ethno-cultural differences and features of natural environment where the respondents live or that they have experience to communicate with. For Russian respondents the most exotic landscapes are also the most attractive, although we cannot see such a tendency for Japanese respondents.

Keywords: landscape appreciation comparison between Russia and Japan, visual and emotional evaluation of natural landscapes, exotic landscape, attractive landscape, ethno-cultural differences, features of natural environment

Japan Geoscience Union Meeting 2014
(28 April - 02 May 2014 at Pacifico YOKOHAMA, Kanagawa, Japan)

HGG01-05 Room:424 Time:April 29 15:30-15:45

Exploring reasons for residents use and appreciation of informal urban greenspace in Sapporo and Brisbane

RUPPRECHT, Christoph[1*]

[1]Environmental Futures Research Institute, [2]School of Environment, Griffith Univ.

Informal urban greenspaces (IGS), such as vacant lots, street verges and river banks are an important new topic in urban recreation and landscape studies. At last year's JpGU 2013 I showed that residents in Sapporo (Japan) and Brisbane (Australia) use and appreciated IGS as adults and during their childhood. But two important questions remained: (1) What role does IGS play for residents in comparison to formal green space, such as parks?, and (2) Why do residents in Brisbane evaluate IGS more positively than in Sapporo? This presentation reports preliminary answers to these questions.

To examine the first question, I used a GIS analysis to compare the amount of formal greenspace within 500m of the sites where the questionnaire on IGS use and perception was distributed to Sapporo and Brisbane residents. A negative correlation between formal greenspace area and IGS use would imply residents indeed use IGS as a substitute for parks. But the results showed no correlation. This suggests residents deliberately choose to use IGS. IGS therefore plays a unique role in residents' recreation - different from formal greenspace.

But why did residents in Sapporo feel IGS made their daily life both better and worse, while residents in Brisbane felt IGS had a mostly positive impact on their daily life? Looking for potential reasons for this difference in IGS appreciation, I measured IGS quantity, accessibility and vegetation structure in both cities. The type of IGS (e.g. lot, street verge, brownfield, railway, gap space, powerline, waterside etc.) was determined using a IGS typology. Accessibility of IGS was categorized in three levels: accessible, partially accessible and not accessible. Vegetation structure was recorded by measuring coverage of four strata: tree, bush, herb and ground cover.

The results show IGS makes up a surprisingly large percentage of city land use in both cities (˜5% of total surveyed land use), but there were differences in the amount of IGS types and vegetation structure. We analysed the questionnaire data and field survey data, and found these different IGS types and vegetation structure could explain why residents evaluate IGS differently. Understanding how residents appreciate IGS may in turn help us to unlock the potential of IGS for recreation.

Keywords: urban geography, recreation, wildscape, urban planning, naturalness, spontaneous vegetation

Japan Geoscience Union Meeting 2014
(28 April - 02 May 2014 at Pacifico YOKOHAMA, Kanagawa, Japan)

HGG01-P01 Room:Poster Time:April 29 18:15-19:30

A review of English papers on psychological evaluation of landscape from 2009 to 2013

AOKI, Yoji[1*]

[1]Open University of Japan

This paper reviews interesting studies on landscape evaluation in terms of psychological tests referred in Landscape and Urban Planning, Landscape Research, J. of Environmental Psychology, Environment and Behavior, J. of Environmental Management and some other scientific journal from 2009 to 2013. Until 2005, I reviewed various experiments of landscape evaluation in the papers of Review Articles (Aoki 1999, Aoki 2006, and Aoki 2007). During recent 5 years, more works were published compared to the decade of last report. So I tried to summaries them according to the key subjects of the former papers, i.e. (1) clarifications of landscape phenomena, (2) respondents' attributes, (3) landscape appreciation, (4) sampling of landscapes and presentation, and (5) predictive models of psychological response and applications in physical planning.

(1) Clarifications of landscape phenomena (Table1)

The first proposal of the explanation of the landscape appreciation was proposed by J. Appleton (1975). The detail mechanisms of the appreciations were not explained because of the complicated reaction system of human brain (Thiel 1997). This hard situation was discussed by the advanced brain system endowed to human being (Bourassa 1991). We already got the tool to measure the activities in the brain, but the clarification of the landscape phenomena will take more time because of the complicity of the landscape appreciation (Aoki 2008).

In recent 5 years, the childhood and adolescence to feel at home was examined (Adevi and Grahn 2012).

(2) Respondents' attributes (Table 2, 3)

Two kinds of attributes e.g. identities of human group and personality were reported.

For the former, mountain tribe Sherpa (Beza 2010) and Nigeria children (Falk and Balling 2010) were investigated.

For the latter, the attribute of tourists was increased and sibling was newly investigated (Howley et al. 2012).

The meaning of sampling through internet was yet under consideration.

(3) Landscape appreciation (Table 4)

Preference has popularly used in recent years. Willingness to pay became popular in this field. SD method was yet used in the appreciation.

Other appraisals, e.g. feeling at home (Adevi and Grahn 2012), familiarity (Dobbe 2013) and photo location (Sugimoto 2013) were used.

(4) Landscape sampling and presentation (Table 5, 6)

In the landscape sampled, new ideas; transportation (Bernasconi et al. 2009), Mt Everest (Beza 2010), fire prone (Islas and Vergara 2012), seasonal change (Eroglu et al. 2012) were tried.

As for the presentation method, on-site visits was increasing and use of GPS (Sugimoto 2013) became popular by the development of mobile phone.

(5) Predictive model and planning (Table 7, 8)

As for the predictive model, biodiversity (Jungels et al. 2013) and flow of stream (Pflueger et al. 2010) were tried.

Proposal for planning were offered in terms of mapping (Ribeiro et al 2013, Schirpke et al. 2013).

Reference

Aoki, Y. 1999 Review Article: trends in the study of the psychological evaluation of landscape, Landscape Research 24(1), 85-94.

Aoki, Y. A. 2006 Historical review on landscape studies in term of psychological evaluation, Landscape planning for Russia: results and prospects 37-46.

Aoki, Y. 2007 Recent trends of English papers on the psychological evaluation of landscape, J. of Environmental Information Science 35(5), 181-188.

Aoki, Y. 2008 Scientific evaluation of landscape, Seasonal publication Environmental Research 148, 120-126.

Appleton, J. 1975 The Experience of Landscape, London. Wiley.

Bourassa, S.C. 1991 The Aesthetics of Landscape, London: Belhaven Press.

Thiel, P. 1997 People, Paths and Purposes, Seattle, WA: University of Washington Press.

Keywords: landscape appreciation, English papers, 200-2013, review

Japan Geoscience Union Meeting 2014
(28 April - 02 May 2014 at Pacifico YOKOHAMA, Kanagawa, Japan)

HGG01-P02 Room:Poster Time:April 29 18:15-19:30

Comparison of Races in Terms of Images of Landscapes in Fiji Using Image Sketches

KOSUGE, Takashi[1*] ; FURUYA, Katsunori[1] ; VERMA, Mukesh[2]

[1]Graduate School of Horticulture, Chiba University, [2]Hard, Social Sciences, Fiji National

Methods

This research was intended to clarify the difference in imaging of forests between Fijian and Indian residents based on the SKETCH SURVEY. We administered the sketch survey to Fijian residents during our stay in the Republic of Fiji from August to December, 2013. The survey was carried out through interviews, and 158 respondents gave their answers. In the survey, the respondents were asked to describe forests in keywords, sentences or sketches. 1) Firstly, the respondents entered several keywords related to FORESTS in Fiji based on their own idea. 2) Secondly, they described the image of FORESTS in sentences consisting of about 100 words. 3) Lastly, they drew simple sketches of the image of FORESTS. In the process of analysis, the number of elements depicted in the sketches was counted in order to review their imaging of forests. Furthermore, the space structures of the sketches drawn by the respondents were divided into four categories in total: the near view, intermediate view and distant view based on the distance between the landscapes and the drawers, and the downward view depicted from high view points. For analysis of the differences in the races, Mann Whitney U test was used.

Considerations and Research results

1,504 elements were sampled from the sketches drawn by all the 158 respondents, and that is to say 9.5 elements were sampled from one sketch on an average. These 1,504 elements were classified into 73 categories. When the appearance rate of the elements in the 158 respondents sketches was calculated, the appearance rate of mountains was highest (82%), followed by trees (69%), the sun (63%), palm trees(58%), houses (51%), oceans (47%), rivers (44%), woods (42%), birds (35%), villages (34%) and clouds (32%). In many of their sketches, not only nature elements such as mountains, trees and the sun but also familiar elements such as palm trees, houses and oceans were depicted. In some of the Fijian residents sketches, palm trees extending in the tropical zone with a background of mountains were depicted. Furthermore, houses, villages and other elements were simultaneously depicted in the natural landscapes, and it seems that nature is closely linked to their daily lives. Concerning space structures of the sketches, the rate of the distant view was highest (59%), followed by the downward view (18%), near view (13%) and intermediate view (8%).

Regarding the differences in the percentage of the answers between the races, 76% of Fijian respondents and 54% of Indian respondents associated forests with nature, and here a significant difference was found ($p<.05$). Furthermore, 24% of Fijians and 44% of Indians associated forests with farming villages, and here a significant difference was also found ($p<.05$). It may be possible that Fijians regard forests as a factor of nature, while on the other hand Indians consider forests as a factor of not only nature but also farming villages.

Differences between the races were checked in each of the 73 categories, and significant differences were detected with only six categories of them. The categories in which significant differences in the percentage of the answers between the races were detected were palm trees (50%, 74%), the sun with expression (19%, 34%), grass fields (34%, 12%), sugar canes (7%, 20%), plains (1% of Fijians, 10% of Indians) and hotels (0%, 8%). The analysis of the depictions in the sketches showed that Fijians tend to depict nature-related objects elaborately and Indians tend to depict plants and other similar objects more elaborately than Fijians.

Concerning space structures of the sketches, 55% of Fijians 55% of Fijians and 68% of Indians drew distant-view sketches, and there was a tendency that both races preferred the distant view. In some of the sketches, there was a range of mountains from which waterfalls and rivers flew into the sea, and in some of the sketches trees, tropical palm trees and artifacts such as houses and villages were depicted.

Keywords: Image Sketches, Landscape, Comparison of Races, Republic of Fiji

Japan Geoscience Union Meeting 2014
(28 April - 02 May 2014 at Pacifico YOKOHAMA, Kanagawa, Japan)

HGG01-P03 Room:Poster Time:April 29 18:15-19:30

A Comparative Study on Landscape Cognition Between Japanese who have been in New Zealand(NZ) and who have not been to NZ

HORIUCHI, Kana[1*] ; FURUYA, Katsunori[1]

[1]Graduate School of Horticulture, Chiba University

Introduction

NZ is almost same size and has same climate, temperate zone and subtropical zone, with Japan. Though a lot of Japanese have immigrated to or lived on long term in NZ, few Japanese knows NZ well because the long distance between both countries might be bottleneck for flow of people. Thus, the objective of this study is to clarify differences of landscape recognition of Japanese who have been in NZ and Japanese who have never been to NZ.

Methods

69 landscape photos taken in both countries (35photos from Japan, 34photos from NZ) were categorized to the group of coast, waterfall, river, forest, wetland, mountain, and lake. Respondents were asked to select three photos each for characteristic landscape image of NZ and Japan. Then, they were asked to write down the three keywords each about the landscape image of both countries. Respondents were the group of 25 Japanese people who have been in NZ (NJG), the group of 42 Japanese people who have never been to NZ (JPG), and the group of 12 New Zealander people (NZG).

Result

Firstly, the most selected photo as the characteristic landscape image of Japan among all groups was the photo of Mt.Fuji with Ashinoko lake and shrine gate (NJG76.0%, JPG74.0%, NZG50.0%). Also, second top photo was Mt.Fuji's one. The different result was shown on third top photo. NJG chose the photo of Mt.Fuji with forest (32.0%), JPG chose the photo of creek (28.7%), NZG chose the photo of waterfall with autumn leaves (16.7%), and the photo of forest with lingering snow (16.7%).The creek's photo selected by JPG was recognized as Japanese landscape though taken in NZ.

For the characteristic landscape image of NZ, there was not the photo selected intensively such as Mt. Fuji one. However, the most selected photo was common among all groups. That was the photo of lighthouse on cape surrounded by ocean (NJG36.0%, JPG40.5%, NZG16.7%). As Second top photo, NJG chose the lake on volcano with volcanic steam (24.0%). JPG selected the solid magma in volcanic crater (23.8%) and the lake (23.8%). These two photos might be chosen as the characteristic landscape image of NZ because those are unfamiliar sceneries in Japan. In NZG, it was hard to find out the characteristic scenery because the groups of selected photos were decentral.

For keywords about the landscape image (KLI), noun showing plants and landscape, noun showing animals, noun showing color, adjective indicating impression, and proper noun were answered. As KLI of NZ, FOREST, MOUNTAIN or HILL was answered 29.6% as total. And GREEN, DYNAMIC or BROAD was answered 22.2 % for each in NJG. People would have the image of landscape that broad and dynamic mountain and hill are spread in NZ. On the other hand, JPG answered BROAD(35.0%), MEADOW and GRASSLAND(27.5%), SKY(25.0%), WILD(25.0%) as KLI. Though it also shows broad image, JPG would have the image of broad glass land instead of mountain or hill.

It revealed the difference of landscape cognition between NJG and JPG. There was not obvious difference on the photo selecting exercise. However, JPG recognized the photo taken at NZ as Japanese landscape photo. For KLI, JPG indicated broad glass land, and NJG shown the landscape consisted of broad forest and mountain.

Keywords: Japan, New Zealand, Landscape Cognition, Landscape

HGG01-P03 Room:Poster Time:April 29 18:15-19:30

Japan Geoscience Union Meeting 2014
(28 April - 02 May 2014 at Pacifico YOKOHAMA, Kanagawa, Japan)

HGG01-P04 Room:Poster Time:April 29 18:15-19:30

Analysis of Scenery Transition and Residents' Opinion in Dalai Lake Nature Reserve

HAN, Guorong[1*] ; FURUYA, Katsunori[1]

[1]Graduate School of Horticulture, Chiba University

Introduction

Grassland scenery has been diminishing in Inner Mongolia in People's Republic of China. It is said that increase in farmland and desertification of grasslands are the cause of diminishing grasslands. This is a serious issue for the Mongolians who make a living from pasturing. In this research, Dalai Lake Nature Reserve, which is located in the Hulunbuir Grasslands has been selected as a study subject. The objective is to clarify the transition of the scenery in the nature reserve by extracting scenery factors in relation to usual lives of the residents in the area.

Study Methods

An opinion research was conducted between the end of December, 2013 and the middle of January, 2014. The survey subjects were the residents who are nomadic in the grasslands of Dalai Lake Nature Reserve. Interviews were conducted and 409 responses were obtained. In this research, demographics of the respondents and the composition factors of grassland scenery in Dalai Lake Nature Reserve were confirmed. The composition factors of grassland scenery were studied in three different time frames: 10 years ago, present, and future vision (for example, 10 years later). For this research of scenery composition factors, 25 factors had been obtained from the initial literature research, and typical factors had been pre-selected among those for multiple choice questions. Multiple answers were accepted for this question, and an open answer section was also provided. Responses to the grasslands management which local residents would expect were also obtained. A chi-square test was applied to statistical analysis.

Results

Scenery factors of Dalai Lake Nature Reserve obtained from literature research included; 1) natural scenery such as lake, river, swamp, wild animals, and wild vegetation, 2) cultural landscape like Mongolian gels, and 3) factors which developed along with economic development, including electricity, mining and building.

The demographics of respondents showed that residents within the nature reserve counted 236; therefore, the number of the effective responses has been determined as 236. The average age of the respondents was 41.1 years old. These respondents include 170 Mongolians (72%), the Hans (23%), and the Evenk (5%).The following factors are the ones that all effective respondents selected as typical scenery composition factors of 10 years ago: wild animals, wild vegetation, grasslands, and river, whereas 99%selected lake, sandy soil, and livestock. Only1%selected railroad, ger camp, signboard, tourism facilities, and camping car. Next, the following factors are the ones that all effective respondents selected as current factors: village, railroad, sandy soil, and livestock, while 232(98%) selected roads and electric lines. Following these, 229(97%) selected mining field. The factor mentioned by the least respondents was wild animal with 54respondents (23%).Lastly, in the question of future scenery composition factors, the following ones are those that all respondents selected: wild vegetation, grasslands, livestock, and river. Road was selected by 233 respondents (98%), and lake by 227 (96%). A small number of respondents selected mining field (41 respondents, 17%) and electric wire (50 respondents, 21%).Comparing the scenery composition factors of 10 years ago and those of current, natural scenery factors decreased from 93% to 60%. On the other hand, future natural scenery factors counted 87%.

In terms of grasslands management which residents would expect, major responses were as following: 1) maintain status-quo (103 respondents, 44%), unplanned succession(79 respondents, 34%), and reinforce management (51 respondents, 22%).

Conclusion

This study clarified the scenery which residents in the nature reserve area have in mind and specified it in three different time frames: 10 years ago, present, and future vision (approximately 10 years later). Grasslands management which residents would expect has been also captured.

Keywords: Dalai Lake Nature Reserve, Scenery Transition, Resident, Scenery factors, Opinion, Grasslands

HGG01-P04 Room:Poster Time:April 29 18:15-19:30

Dalai Lake Reserve

Japan Geoscience Union Meeting 2014
(28 April - 02 May 2014 at Pacifico YOKOHAMA, Kanagawa, Japan)

HGG01-P05 Room:Poster Time:April 29 18:15-19:30

Research on Comparison of Races in Terms of Evaluation of Natural Landscapes in the Republic of Fiji

KOSUGE, Takashi[1*] ; FURUYA, Katsunori[1] ; VERMA, Mukesh[2]

[1]Graduate School of Horticulture, Chiba University, [2]Hard, Social Sciences, Fiji National

Methods

1) after collecting Natural landscape photos of Japan and Fiji national countries, Fiji 33 photos and Japan 39 phots of WATERFALL, FOREST, SEASHORE, RIVER, FARMLAND, SWAMP, MOUNTAIN, and LAKE were selected from each country, which sum up to a total of 72 photos, 2) these photos were categorized in groups by 141 a citizens and each group was labeled with a name, 3) the same students evaluated these photos according to preference (5-scale) and exoticism (3-scale), and 4) they were asked to select three photos which they believe to represent the unique characteristics of the Fiji, so that landscape that exhibit the unique characteristics of each ethnic can be extracted. I stayed in Fiji August-December 2013. And A research was run among the Fiji residents during stay. I used a investigation by interview. Then answers were collected from 141 respondents. Cluster analysis (Ward's method, squared Euclidean distance, 3) was applied for the analysis of photo categories, and Mann-Whitney U Test was applied for the analysis between ethnic groups.

Considerations and Research results

Firstly, the difference in classification of the pictures of SWANP was observed between the two races. Fijians classified SWANP and FOREST into different groups, and they included SWANP in the category of RIVER. On the other hand, some Indians included SWANP in the category of FOREST and some included SWANP in the group of RIVER.

Secondly, regarding classification of LAKE, both Fijians and Indians classified LAKE into the same group as SEASHORE. In Fiji, where the percentage of water area in the land is extremely low, there is a possibility that LAKE are not recognized as such. Regarding classification of SEASHORE, both races divide BEACHE into two broad categories: landscapes of sandy BEACHE where there are only a few rocks and trees, and rocky BEACHE where rocks and reefs are common.

In the analysis of preference, significant differences were detected with the six pictures. Five of the six pictures were landscapes of Fiji, and one of them was a landscape of Japan. Furthermore, in the analysis of exoticism, significant differences were seen with the four pictures. Three of the four pictures were landscapes of Fiji, and one of them was a landscape of Japan. Concerning preference of the pictures of the landscapes of Fiji, the value of Fijians is 4.06 higher than that of Indians. Regarding selection of the pictures typical of Fiji, there was a variance between Fijian and Indian residents. Fijians selected the pictures of FARMLAND (21 %), MOUNTAIN (17 %) and SEASHORE (17 %), while on the other hand Indians chose the pictures of SEASHORE (44 %), RIVER (14 %) and SWANP (12 %). The reason for Fijians' choice may be that they think fields of taro, which is the staple food in Fiji, and mountains extending into villages as traditional landscapes of Fiji. On the other hand, the reason for Indians' selection may be that they associate landscapes of BEACHE with a scattering of resort spots in Fiji.

Fijians' preference was in the order of WATERFALL (4.43), LAKE (4.41), RIVER (4.14) and SEASHORE (4.09), and Indians' preference was in the order of WATERFALL (4.41), LAKE (4.33), SEASHORE (4.08) and RIVER (4.02). That is to say, both races preferred the pictures of waterfront landscapes. Particularly, the pictures of SEASHORE may be considered as familiar landscapes of Fiji. Most of the pictures of WATERFALL and LAKE were from Japan, and they are unfamiliar sights in Fiji and considered as exotic landscapes (the pictures of Japanese landscapes). However, the pictures of SWANP were not very much preferred compared to other pictures of waterfronts. There was not much big difference in preference between Fijians and Indians excluding the six pictures with which significant differences were detected. However, there was a difference in that Fijians preferred traditional landscapes whereas Indians preferred landscapes of seashores.

Keywords: Landscape evaluation, Republic of Fiji, Fijians, Indians, Comparison

HGG01-P05 Room:Poster Time:April 29 18:15-19:30

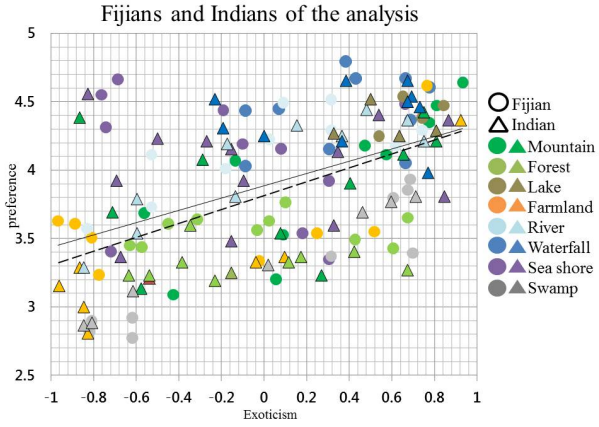

Japan Geoscience Union Meeting 2014
(28 April - 02 May 2014 at Pacifico YOKOHAMA, Kanagawa, Japan)

HGG01-P06 Room:Poster Time:April 29 18:15-19:30

Study on natural amenities in off-limits area: imagination of virtual activities received from landscape

MIZUKAMI, Shogo[1*]

[1]Department of Public Policy, School of Sociology, Bukkyo University

Introduction

In urban areas, there is little space that has been kept natural although it is now recognized that natural elements such as green space, water features or wildlife habitat, etc. increase the value of an environment. However, human influences on natural habitats interfere with restoring natural spaces to their original condition.

It is difficult to maintain such green space and limit its availability to people. In fact, it is often the case that areas with a high level of undisturbed natural habitats are off-limits areas.

For example, storm-water reservoirs for flood control in urban areas are off-limits, concrete-covered, fenced-in spaces. However, a variety of wild fauna and flora manage to make their habitats in some reservoirs. In other words, reservoirs are an example of artificial yet informal urban green spaces, where spontaneous wild vegetation grows. However, clearly reservoirs were not planned as natural spaces.

Although these spaces are off limits, people can enjoy a view of natural growth from the wall of the reservoirs. On the other hand, due to the physical boundary, people cannot get in touch with natural elements due to perceptual constraints.

Viewing such restricted areas has a beneficial effect as a solution for symbiosis with nature because human development and natural preservation are opposed to each other.

This study clarifies people's impressions of the spontaneous and wild vegetation in reservoirs. Moreover, this study considers the affordance research for environment afford prevision of behavior to perceiver as seen in the case of flying stone. Flying stone is a concrete block put into a river bed. This paper presents a new way for people to virtually take part in nature-friendly activities. This study explains how imaginary contact with nature by viewing spontaneous vegetation in off-limits, informal urban green space creates satisfaction.

Methods

Research Questionnaire 1

In a Tokyo suburb, 108 reservoirs were selected for this study. We surveyed shapes, size, location, and surrounding environment and explored possibilities of whether the space was a beautiful landscape and from what perspective.

We conducted an awareness survey regarding environment and landscape with 88 residents living around three reservoirs. Correlative relationship was applied to analyze the relationship between question items.

Research Questionnaire 2

Another study was conducted in Kyoto with 175 university students who responded to questions about the image of flying stones on the Kamogawa River. Responses were given as free descriptions. A text mining approach was applied to analyze symbolic representations for water-friendly activities.

Results and Considerations

The results show that most of the reservoirs were concaved and had good views of open space. Therefore, reservoirs have a high potentiality to be urban green space, where people can view spontaneous natural habitats. Reservoirs are artificially made. The results also showed vegetation succession has possibilities for creating transient esthetic appraisal. However, questionnaire results showed that residents who lived around reservoirs feel that the naturally occurring vegetation is not beautiful.

The results of affordance research were as follows. Flying stones provide an image of physical behavior. for getting across a river or playing in the water. The image is a trigger for the imagination of virtual water-friendly activities. Symbolic representation of environmental signatures is a device that affords imaginary familiarity with environmental elements.

Keeping a view of nature in off-limit green spaces leads to an imaginary sense of familiarity with nature.

Symbiosis with nature increases the value of an environment in urban. Image of nature-friendly activities have a commonality of body. Therefore, symbolic representations for nature-friendly activities have a functional role as a landscape appraisal standard.

Keywords: off-limits area, amenity of nature, symbol of water-familiar, affordance

Japan Geoscience Union Meeting 2014
(28 April - 02 May 2014 at Pacifico YOKOHAMA, Kanagawa, Japan)

HGG01-P07 Room:Poster Time:April 29 18:15-19:30

The questionnaire was consisted with two main part, survey about figure of the coastal mindscape and individual backgrou

MATSUSHIMA, Hajime[1*]

[1]Research Faculty of Agriculture, Hokkaido University

In this study, the image of coastal landscape as the mindscape were compared between Japanese university students and Russian university students by the questionnaire survey.

The questionnaire survey were conducted to 24 university students of Irkutsk city as Russian university students and 73 university students in Sapporo city as Japanese university students.

Furthermore, 12 Russian students who studied in the university in Sapporo city were added as Russian students in Japan.

The questionnaire was consisted with two main part, survey about figure of the coastal mindscape and individual background of respondents. As a result, the sandy beach and sea were the major component of mindscape. Because most respondents enjoyed sea bathing as recreational use, it was guessed that the viewpoint from the beach were dominated and inland area, like coastal dune, was not described.

On the other hand, Russian university students described more emotional words as beautiful, calm, bright, etc. in addition to major components.

There was no difference in a drawn composition type, but Russian university students described more natural components, mainly coastal plants, than Japanese. About the shore protection, the Russian student did not image in particular it at all.

Keywords: mindsape, coastal landscape, figure, drawing method, Japan, Russia

Japan Geoscience Union Meeting 2014
(28 April - 02 May 2014 at Pacifico YOKOHAMA, Kanagawa, Japan)

HGG01-P08 Room:Poster Time:April 29 18:15-19:30

Landscape Appreciation on Green Passages with Waterway in Edogawa Ward, Tokyo

SADO, Susumu[1*] ; FURUYA, Katsunori[1]

[1]Graduate School of Horticulture, Chiba University

Introduction

Edogawa Ward equipped itself with the first water nature park in Japan in 1974, and sterilized purified water has been utilized in this park. By 1996, water nature parks with natural water had been also established with considerations for ecosystem. The focus of this study is inhabitation of living creatures and human usage in relation to differences between purified water and natural water. The objective of this study was determined to clarify the following three points at two green passages in Edogawa Ward: 1) impressions among the users, 2) behavior of users, and 3) inhabitation of living creatures. Comparing the aquatic life, more variety of living creatures was identified in natural water, and fewer in purified water.

Study Methods

First, an opinion survey about impressions of green passages was conducted among the green passage users. A survey questionnaire was directly handed out to 288 users on the 24th and the 28th of July and the 4th of August, 2013. The following four items were tested in this study: 1) if they like it, 2) if they feel good, 3) if the water is clean, and 4) if there are many living creatures. Following this questionnaire, a behavioral study was executed in order to compare the results of the opinion survey and the actual usage of green passages. This behavioral study was administered between 10:00 and 14:00 on the 25th and the 31st of July, 2013. The subjects of this research were fish, crustacean, reptiles (turtles), and amphibians (frogs). This research was conducted between 9:00 and 17:00 on the 17th, the 18th, and the 31st of July, 2013. The research area of the green passage was segmented into 27 sections.

Results

The impression survey concluded that over 98% of the users had favorable impressions of both green passages from the results of two questions: *if they like it* and *if they feel good*. As for the question *if there are many living creatures*, 74.5% responded *very many* or *many* in the green passage with many natural water streams. Although the difference is small, relatively smaller figure of 65.6% responded *very many* or *many* in the one with purified water streams.

The behavioral study result showed that the most popular usage among the eight categories was *playing with water* with over 25% of usage. The result was same with both green passages. Similar tendencies were detected with both passages with other activities which followed the most popular *playing with water*: *resting*, *walking*, and *exercising*, in order of popularity.

The inhabitation research confirmed 14 kinds of aquatic habitat on the green passage with natural water, and nine kinds on the one with purified water. Among the confirmed aquatic habitat, reptiles and amphibians such as the Chinese three-keeled pond turtles, Mississippi common sliders, and Japanese toads were observed on the green passage with natural water; however, they were not found on the green passage with purified water. In addition, the average number of creatures per 100 meters counted 14.7 on the green passage with natural water, but the figure on the green passage with purified water counted only 7.0. More than double the difference was detected between the two.

Considerations

Based on the research results of the two green passages, the difference in the inhabitation situation has been clarified. However, there were no significant differences detected in users impressions of the scenery and in their behavior. From these results, it can be inferred that the differences in aquatic habitat on the green passage does not have a significant influence on users impressions with the scenery or on their behavior. Futures researches on other factors such as vegetation and surrounding environment of a green passage, including grass and woods, shall further clarify favorability of sceneries and user behaviors.

Keywords: Edogawa ward, green passage, appreciation, impression, usage, creature

HGG01-P08 Room:Poster Time:April 29 18:15-19:30

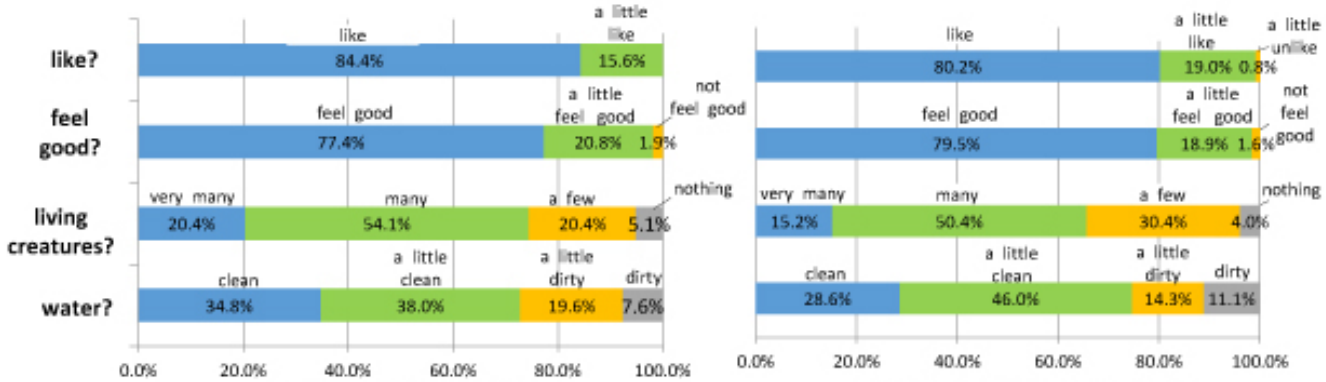

The inpression of two green passages

Japan Geoscience Union Meeting 2014
(28 April - 02 May 2014 at Pacifico YOKOHAMA, Kanagawa, Japan)

HGG21-01 Room:421 Time:April 29 16:15-16:30

The Development of Large-scale Upland Farming and Farmland Use in Hokkaido : A Case Study of Otofuke Town

SASAKI, Toru[1*]

[1]Sapporo Gakuin University

Japanese agriculture falls into a decline. Especially, farmland resources very important as a factor of production are decreasing. From 1961 to 2010, farmlands decreased by 25% in Japan. On the other hand, in Hokkaido, farmland is not decreasing so much.

This presentation tries to explain the characteristics of large-scale upland farming and condition of farmland use in Otofuke town.

Keywords: Farmland use, Upland crops, Wheat, Large-scale Farming, Otofuke Town

Japan Geoscience Union Meeting 2014
(28 April - 02 May 2014 at Pacifico YOKOHAMA, Kanagawa, Japan)

HGG21-02 Room:421 Time:April 29 16:30-16:45

Change of forest use and current state of coppice forest in Nenoshiroishi near Sendai

MATSUBAYASHI, Takeshi[1*] ; KANO, Arika[2] ; UCHIGASAKI, Aya[3]

[1]Tohoku Fukushi University, [2]Resarch Student, Miyagi University of Education, [3]East Japan Railway Company

Coppice forest had been repeatedly felled in an interval of about 15 to 30 years in order to produce and provide fuel wood and charcoal. A charcoal production worker produced 1,500kg of the charcoal in the winter of 2009-2010 in Nenoshiroishi near Sendai. The felled area is approximately 800 square meters. The amount of production of charcoal was approximately 3,000,000kg per year in Nenoshiroishi in the 1930s, therefore the felled area is calculated approximately 1.6 square kilometers per year at that time. After the fuel revolution in the late 1950s and the early 1960s, felled area rapidly decreases, and trees have grown to large sized. In recent years, mass mortality of oak trees has been expanding rapidly in Nenoshiroishi. Growth of the tree is considered to one of the causes of mass mortality of oak trees.

Keywords: coppice forest, forest use, mass mortality of oak trees, Sendai

Japan Geoscience Union Meeting 2014
(28 April - 02 May 2014 at Pacifico YOKOHAMA, Kanagawa, Japan)

HGG21-03 Room:421 Time:April 29 16:45-17:00

Utilization of local resources in agricultural cooperatives in Inner Mongolia,China

SEKINE, Ryohei[1*] ; SASAKI, Toru[2] ; SUDE, Siqin[3]

[1]Tohoku University, [2]Sapporo Gakuin University, [3]Inner Mongolia University

This study considers about the regional action mainly on the sales of dried beef established with agricultural cooperative modality in Xilingol League, Inner Mongolia Autonomous Region, China that it lived by mainly in live stock farming before 1990s. Agricultural cooperative in China is a new co-operative association institutionalized from 2007 as a position improving local economy. Dried beef is winter excellent products in this area. The agricultural cooperative targeted in this study produces dried beef by oneself, and sells it by oneself at the store established in Xilinhot City that is local metropolis of Xilingol League.It is administered by 25 households live in Bulgan County.They got an adjunct to 300,000 yuan from the government in 2009 to establish this cooperative. This study discusse about the business processes after the establishment of this cooperative and the relations with local resources.

Japan Geoscience Union Meeting 2014
(28 April - 02 May 2014 at Pacifico YOKOHAMA, Kanagawa, Japan)

HGG21-04 Room:421 Time:April 29 17:00-17:15

Placing sediment budgets in the socio-economic context for management of sedimentation in Lake Inle, Myanmar

FURUICHI, Takahisa[1*] ; WASSON, Robert[2]

[1]Department of Science, IT, Innovation and Arts, Queensland Government, Australia, [2]National University of Singapore, Singapore

In soil erosion and sedimentation research in developing countries, scientists are expected to be better involved in quantifying mechanisms and rates of sediment movement and objectively demonstrating their impacts. Soil erosion and sedimentation in the ca. 3,800km^2 Lake Inle catchment, Myanmar have been of both local and national concern given the significance of the lake to the economy, environment, and culture. Sediment budgets that include a focus on different sedimentation rates in various sink environments around and in the lake were constructed for this lake catchment. The sediment budgets showed that deltas stored more than half of the sediment transported to the lake area, and that, despite the relatively smaller storage mass, the highest specific storage was found at river mouths. Socio-economic assessment identified diverse perspectives on impacts of sedimentation. Of those perspectives, increasing difficulty in water transportation was recognized as a common, significant problem among stakeholders. Proposals for management of sedimentation therefore emphasize that a priority should be given to controlling sedimentation at river mouths.

<Reference>
Furuichi,T., Wasson, R.J., 2011. Placing sediment budgets in the socio-economic context for management of sedimentation in Lake Inle, Myanmar (Burma). In: *Sediment Problems and Sediment Management in Asian River Basins* (ed. Walling, D.E.), IAHS Red Book 349, 103-113.

Keywords: sedimentation, sediment budget, socio-economic assessment, Lake Inle, Myanmar

Japan Geoscience Union Meeting 2014
(28 April - 02 May 2014 at Pacifico YOKOHAMA, Kanagawa, Japan)

HGG21-05 Room:421 Time:April 29 17:15-17:30

Regional Governance of Forest and its Fringe - case of South India -

KIMOTO, Koichi[1*] ; S., Arun das[2]

[1]Hiroshima Jogakuin University, [2]University of Mysore

In recent years, on a global scale, forest issues are being ”organized”. The ”facts” of a serious deforestation and ”needs” of appropriate protection, as the international public opinion, becomes the general framework of forest policy in each country and region, and under the framework various policies have been implemented. In the late of the 1980s, it may be said that the short turn from the timber-oriented forest government to the community based forest management and governance is a beginning of such a trend. Since the 1990s, many of research such as various case studies of the present situation of forest, a critique of forest policies and foreign aids, and theoretical studies including the commons theory, have been accumulated.

In India, Joint Forest Management (JFM) which was launched at the beginning of 1990s has been showing a certain ”recovery” in the forest rate. However, since the late 1990s, various problems such as land acquisition and competition and the human ? wildlife conflict spout out. Indeed, under the JFM program, we might be able to recognize the results of certain ”improvement” in both the macro level of forest rate recovery and micro level of participatory activities in village. On the other hand, it has been overlooked the issues related with the forest ”region” including the forest and its fringe areas. The success of forest policy, so to speak, has dug out the forest ”region” issues.

Even if the community based forest management will be developed continuously, the problem of the forest ”region” must be considered with a peculiar frame of its own. As the forest ”purification” by the setting of ”National Park” and an enclosing of legal and/or physical, the doughnut-shaped chaotic area around the forest appears like sprawling phenomenon in the sub-urban area.

In this study, we are trying to overview of the problems in the forest ”region” based on our field survey in Karnataka, India.

Keywords: Protected Areas (PAs), National Park, Region, Governance, India

Japan Geoscience Union Meeting 2014
(28 April - 02 May 2014 at Pacifico YOKOHAMA, Kanagawa, Japan)

HGG21-06 Room:421 Time:April 29 17:30-17:45

Hydrologic Environment in Rangwa Caldera on Lake Victoria, West Kenya

OTSUKI, Yoshinori[1*] ; UEDA, Gen[2]

[1]Graduate School of Science, Tohoku Univ., [2]Graduate School of Environmental Studies, Tohoku Univ.

In this presentation, we discuss on the hydrologic and physical geographic environment of sustainable settlements in the Rangwa Caldera, situated on the coast of the Lake Victoria, west Kenya.

Japan Geoscience Union Meeting 2014
(28 April - 02 May 2014 at Pacifico YOKOHAMA, Kanagawa, Japan)

HGG21-P01 Room:Poster Time:April 29 18:15-19:30

Borehole use and management in agro-silvo-fishery settlements around Lake Victoria, Kenya: water use rules

UEDA, Gen[1*] ; OTSUKI, Yoshinori[2]

[1]Graduate School of Environmental Studies, Tohoku University, [2]Graduate School of Science, Tohoku University

This study is an interim report on the use and management of boreholes, whose importance as a domestic water source becomes greater as one goes far from Lake Victoria, in the sub-area (former Suba District) of Homa Bay County, Nyanza Province, Kenya. As for one of the boreholes outlined in 2013, the water level rose during the rainy season, the daily change in the water level corresponded to control by the water users' association, and not all member households could fetch water within the daily stipulated time table. Water use of this particular borehole was on the "first come, first served" basis, and it alternated between one queue for those who transported water with a donkey and the other queue for those carrying by human power. Individual boreholes scattered in the research area had a variety of "queueing system" rules reflecting different geographical and other conditions. The water use rule of each borehole can be seen as a historical product of people's attempt to level off inequality in water use in each settlement. It is indispensable for a better understanding of sustainable water use and livelihood security to investigate such rules.

Keywords: water resources, rule, Kenya, Tropical Africa

Japan Geoscience Union Meeting 2014
(28 April - 02 May 2014 at Pacifico YOKOHAMA, Kanagawa, Japan)

HGG21-P02 Room:Poster Time:April 29 18:15-19:30

Pig raising frontiers in Tropical Africa: Changing small and medium sized piggeries and their regional system in Kenya

UEDA, Gen[1*]

[1]Graduate School of Environmental Studies, Tohoku University

Although Eastern and Southern African regions have experienced dramatic growth in the pig raising industry since the early 1990s, its enterprise reality has not yet been well researched. This study takes Nyeri County, Central Province and Homa Bay County, Nyanza Province, both in Kenya, as examples of ”pig raising frontiers” in Tropical Africa where pigs are introduced as new livestock. It examines changing entrepreneurial activities that small- and medium-sized pig raisers have performed since their beginning, particularly between 2009 and 2012. Zero-grazing is affected by increasing feed prices, and free ranging/scavenging in urban and peri-urban areas causes crop damages and hygienic problems. These are pointed out as the main reasons which stimulate shift among breeding, fattening and integrated production in an enterprise, and which even trigger withdrawal from pig husbandry. The study also illuminates locational conditions and the regional system of rural and urban pig raising, all of which influence the change in the economic sector. Since the frontier experiences constitute a variety of trial and error, and changes, in achieving a success, their cases suggest potential factors that may promote distribution and sustainability of pig husbandry in Tropical Africa as a quick means to supply food and alleviate poverty.

Keywords: pig husbundry, small and medium sized producers, Kenya, Tropical Africa

Japan Geoscience Union Meeting 2014
(28 April - 02 May 2014 at Pacifico YOKOHAMA, Kanagawa, Japan)

HGG21-P03 Room:Poster Time:April 29 18:15-19:30

The value of coral and its change in Kushimoto, southern Kii Peninsula

SAKITA, Seishiro[1*]

[1]Graduate School of Environmental Studies, Nagoya University

In the tropical and subtropical regions, coral is given the status important as one of the symbolic living things of the marine environment. Especially, in the consideration of resource use, coral is generally treated as a physiographic factor which provides a coral reef ecosystem and is often related to local fishing. Meanwhile, the use of coral itself has been seldom brought up for discussion.

Kushimoto is one of the regions in Wakayama Prefecture, and is located in the southernmost end in Kii Peninsula. Owing to the influence of the Kuroshio Current, the subtropical marine biota, typified by coral assemblages, has been produced in the western coastal waters of Kushimoto, and some local residents who lived in the area have collected and used coral as resources. In Kushimoto, coral was usually collected by gathering the casted corpses on the littoral zone, and sometimes by skin diving. Mainly, people has used coral as a material of slaked lime to make mortar, or for processing as a souvenir thing. The scale of these productions was not much extensive, but the use of coral in Kushimoto has been practiced and continued in relation to other local resource uses. For instance, to make mortar, other materials which were collected or produced in the region, such as seaweed and whale oil, were also used with slaked lime made from coral. And when making slaked lime, old timber and thinnings were used as fuel at the sequence of calcination.

Such collection and use of coral in Kushimoto were at least continued until 1970s, and then, these activities have been completely abandoned now. Instead, since the designation of some parts of the coastal area in Kushiomoto as a national park in 1970, the coral and coastal environments have become an object of conservation. Therefore, a collection and use of the coral which inhabits the coastal waters of Kushimoto have been forbidden. And also, following such a increasing of the evaluation to the coral as an important factor of the marine environment, it brings an expectation of the value of coral as tourist attractions.

Besides, in recent years, the temperature of the nearshore waters in Kushimoto tends to rise notably, and it brings about the increase of a number of species and cover degree of coral which inhabits the coastal waters of Kushimoto. Given this situation, the increase in coral has a negative effect on regional fishery. On the other hand, large amounts of corallivorous organisms such as *Acanthaster planci* and *Drupella* spp. have been caused a problem for the conservation of coral since 2000s. Thus, the conditions of natural and social environments which surround the coral inhabits the coastal waters of Kushimoto have been constantly changing.

In this presentation, I would like to show the structure of resource use focusing on coral once formed in Kushimoto, and examine how the value of coral has been changed up to the present to consider the relationship between coral and people.

Keywords: coral, natural resource use, marine environmental conservation, Kushimoto

Japan Geoscience Union Meeting 2014
(28 April - 02 May 2014 at Pacifico YOKOHAMA, Kanagawa, Japan)

HGM02-01 Room:422 Time:April 30 14:15-14:30

PALEO-ENVIRONMENTAL HISTORY AND KOSA (DUST AND SAND STORM) FLUCTUATION AT ARID - SEMI-ARID REGIONS IN EAST ASIA

KASHIMA, Kaoru[1*]

[1]Department of Earth and Planetary Sciences, Faculty of Sciences, Kyushu University

There are two methods to monitor environmental changes and desertification at arid and semiarid regions. The first one is the short-term monitoring, and examined the changes during several years or decades by meteorological, hydrological, geophysical and geochemical observations. The second one is the long-term monitoring, and presumed changes of environment during hundreds or thousands years using geologic and geographical methods. Although a lot of expeditions have reported short-term changes, the reports for long-term environmental changes have been limited because it takes a lot of efforts to take efficient samples to presume in detail environmental histories.

Department of Earth and Planetary Sciences, Kyushu University has started international research project to make long-term monitoring of desertification in East Asia to correspond with the East Asian Environmental Problems Project of Kyushu University. In cooperation with Mongolian Academy of Sciences, National University of Mongolia, Xinjiang University in China, the filed surveys have been done to obtain samples for long-term monitoring at lakes, ponds and marshes in Mongolia and north western China using geological and geographical methods. Our researches presumed long-range (about hundreds or thousands years) changes of the lowering of lake levels and under grand water levels, the reducing of forest areas and the expanding of deserts in those regions. The desertification has been accelerated in these two hundred years in both regions.

Keywords: Xinjiang Uyghur, Climatic changes, Desertification, Mongolia, The Global Warming, KOSA (Dust and Sand Strom)

Japan Geoscience Union Meeting 2014
(28 April - 02 May 2014 at Pacifico YOKOHAMA, Kanagawa, Japan)

HGM02-02 Room:422 Time:April 30 14:30-14:45

Visualization of liquefied layers using GPR in Watarase flood plain, central Kanto

SETO, Masayuki[1*] ; ICHIKAWA, Minami[2] ; KITAZAWA, Toshiyuki[2] ; NAKAMURA, Yosuke[1] ; TAMURA, Toshikazu[2]

[1]Fukushima University, [2]Rissho University

At the Watarase flood plain, central Kanto, there were many cracks and sand mounds caused by liquefaction in 11, Mar 2011. Various liquefaction models have been proposed based on a profile observation of the old liquefaction and experiment. This study tried visualization of liquefied underground layers. We carried out boring investigations and GPR explorations in Watarase flood plain. Core samples show typical lower river deposits. There was loosely-deposited sandy layer near the groundwater level which was 2m deep. We traced liquefied layers using GPR (Ground Penetrating Rader) which can display the reflection profile about 5m deep with frequency of 250 MHz. By the comparison of core records with GPR images, we confirmed that GPR image is applicable to the distinction of sand, sandy clay and clay layers. Moreover, we found sharply shaped reflection patterns in sandy layers near 200cm deep. Width and height of the pattern is 0.5-2.5m and 0.2-0.95m respectively. Interval of sharp-shaped reflection patterns are 1-20m. The interval is related between the GPR survey line and the location of deformed layer. We considered that these sharp shaped reflection patterns were shown liquefied sandy layers. GPR is thus available for the visualization of the invisible liquefied layers.

Keywords: GPR, Liquifaction, 3.11 Mega quake

Japan Geoscience Union Meeting 2014
(28 April - 02 May 2014 at Pacifico YOKOHAMA, Kanagawa, Japan)

HGM02-03 Room:422 Time:April 30 14:45-15:00

Coastal geomorphology as a proxy of large paleothrust earthquakes along the Andaman Trench

ANDRADE, Vanessa[1*] ; RAJENDRAN, Kusala[1] ; RAJENDRAN, C. P.[2]

[1]Indian Institute of Science, Bangalore., [2]JNCASR, Bangalore.

Estimating hazards from earthquakes and tsunamis along subduction zones is of significance to coastal communities. Here, we discuss the coastal geomorphology of selected sites in the Andaman Islands, which lie within the rupture zone of the 2004 Sumatra-Andaman earthquake. As part of the near-source region, these islands witnessed considerable geomorphic changes, both before and after the 2004 earthquake, which may be related to the maturity of a megathrust subduction zone earthquake cycle. Assuming that these geomorphic landforms are properly preserved and attributed to the right sources, it is possible to build the history of large paleothrust earthquakes for the Andaman Islands. Given that these landforms are a result of similar processes through time, our sites are broadly divided as regions that subsided or were uplifted in 2004.

At Hut Bay and Interview Island, uplifted coralline terraces were mapped, as were stream inlets that cut through the newly-formed as well as older terraces. Samples collected from these locations include wood pieces from trees embedded in the stream bank, shells from pebble-rich layers along the exposed bank as well as coral fragments from the terraces themselves. At Port Blair, large stretches of land subsided in 2004. While several farmlands remain inundated beneath the present-day tidal-line, several mangroves trees died in situ, their roots being preserved in the shallow subsurface. Along a steam bank, a similar root horizon was identified 1m below the present day surface which was sampled at multiple locations. Additionally, a shell sample was collected from within the paleo root-zone.

The ages of these samples were estimated using AMS radiocarbon dating, and they cluster at AD 1100, AD 1500, and AD 1900. Though these geomorphic landforms may be the result of other coastal processes, either regional or global, we believe that these ages, with corroborating evidence from several studies in the Andaman Islands and from coastlines in Sri Lanka, mainland India, Sumatra, and Thailand are representative of large earthquakes in recent history, some of may have been tsunamigenic.

Keywords: 2004 Sumatra-Andaman earthquake, Coastal geomorphology, Andaman Islands, Uplifted terraces, Subsided lowlands, Paleothrust earthquakes

Japan Geoscience Union Meeting 2014
(28 April - 02 May 2014 at Pacifico YOKOHAMA, Kanagawa, Japan)

HGM02-04 Room:422 Time:April 30 15:00-15:15

Volumetric changes of various rocks during weathering and their geologic significance

CHIGIRA, Masahiro[1*] ; NAKATA, Eiji[2] ; OOYAMA, Takahiro[2]

[1]Disaster Prevention Research Institute, Kyoto University, [2]Central Research Institute of Electric Power Industry

A rock volume may change during weathering, which would have various importance in earth surface processes. However, little is known on the volumetric change. We summarize our research results of various rock types and refer to it's geomorphological importance. Basic idea is so-called isocon concept, which assumes immobile chemical elements during weathering and calculate a volume change from density and chemistry of rock before and after weathering (Grant, 1986). We assume TiO2 is the immobile element.

Granitic rocks:

Volumetric change may be different between granite and granodiorite/quartz diorite. White et al. (2002) reported that granodiorite and quartz diorite are isovolumetric during weathering. Chigira (2002) reported that granite expands 50% during weathering, which is consistent with Folk and Patton (1982) who estimated the volume change from the inflection of a pegmatite vein in a weathering zone. These expansions lead to spheroidal weathering or micro-sheeting.

Sandstone:

Matsuzawa (2008) studied the weathering of sandstone of the Cretaceous Izumi Formation in Ehime and estimated 20-30% expansion during weathering, which closed joint openings.

Mudstone:

Calculation from the data of Chigira (1988) for the Quaternary Haizume Formation in Niigata suggested that mudstone expanded 10-30% during weathering in the upper part of the dissolved zone. Such expansion may facilitate downslope soil creep.

Vapor-phase crystallized tuff:

Calculation from the data of Chigira et al. (2002) for vapor-phase crystallized tuff of the Shirakawa ignimbrite in Fukushima suggested it's weathering was isovolumetric except for the topmost part, in which fabric collapsed and the rock shrank.

Tuff breccia:

We studied the weathering of tuff breccia of the Miocene Tomari Formation in Aomori, which suggested that it occurred with 20-50% expansion. So-called active faults in the Higashidori nuclear power plant site are apparent active faults made by rock expansion during weathering.

Chigira , M. 1988. J. Japan Geol. Soc. 94, 419-431. Chigira, M., Nakamoto, M., and Nakata, E., 2002. Engineering Geology 66, 111-125. Folk, R.L., and Patton, E.B., 1982. Zeitschrift fur Geomorphologie N. F. Bd 26, 17-32. Matsuzawa, M. 2008, Master thesis of Kyoto University. Grant, J.A., 1986. Economic Geology, 81, 1976-1982. White, A.F., 2002. Chemical Geology 190, 69-89.

Keywords: weathering, volumetric change, active fault

Japan Geoscience Union Meeting 2014
(28 April - 02 May 2014 at Pacifico YOKOHAMA, Kanagawa, Japan)

HGM02-05 Room:422 Time:April 30 15:15-15:30

Use of rock properties in classification of weathering grades: A Sri Lankan case study

UDAGEDARA, Dashan T.[1*] ; OGUCHI, Chiaki T.[2]

[1]Graduate School of Science and Engineering, Saitama University, [2]GRIS, Saitama University

Rocks utilised for the Samanalawewa project, have undergone severe weathering after they were excavated late 90's. The rate of weathering is incomparably high with respect to the normal soil formation processes. Different weathering grades of rocks that were used as construction materials, foundation materials and road aggregates are found in the project area. Consequently, they have been threatening to the sustainability of the project. The access adit and rip-rap zone of the dam are vulnerable to damage owing to the rapid weathering. Even though charnockite, marble, biotite and garnet granulitic gneisses were utilized for the project, only pyrite-sillimanite-garnet gneiss has shown extensive weathering. The rapid weathering of this rock is being observed since the commissioning of the project. Rocks were subjected to a petrographic study under the optical microscope. Point load strength, slake durability, loss on ignition and water content tests were employed to distinguish weathering grades. Water-rock interaction was experimented to study the pyrite oxidation. Comparatively to charnockite and marble, pyrite-sillimanite-garnet gneiss is weaker according to point load strength and slake durability indices. Rock strength and chemical properties illustrates that the weathering process takes place at a rapid and a normal stages. It is mainly observed on set of weathering. Corroded grains boundaries and decayed minerals in the rock are consequences of weathering induced by the acidic water generated by pyrite oxidation. The abundance of pyrite in pyrite-sillimanite-garnet gneiss is uneven. Thus, different weathering grades of the rock can be seen over the study area. Extensive fractures, which might be generated during tectonic activities or during excavations, facilitate better interaction with the atmosphere. It also effectively reduces the strength of the rock. It is another reason for differential weathering.

Keywords: Point load strength index, Rapid rock weathering, Loss on ignition, Samanalawewa project, Pyrite oxidation, Pyrite-sillimanite-garnet gneiss

Japan Geoscience Union Meeting 2014
(28 April - 02 May 2014 at Pacifico YOKOHAMA, Kanagawa, Japan)

HGM02-06 Room:422 Time:April 30 15:30-15:45

Experimental Study on Deterioration and Durability of Bicks due to Salts

NGUYEN, Thi hai duong[1] ; OGUCHI, Chiaki T.[2*]

[1]Graduate School of Science and Engineering, [2]GRIS. Saitama University

In Vietnam, heavy construction materials such as bricks are often used because there are many floods. However, the deterioration due to weathering has been found at general houses and historic brick buildings. To investigate deterioration of bricks used in these buildings, the present study performed salt weathering experiments using 6 bricks produced in Vietnam, Japan and China; red brick (RD), beige brick (BG), Vietnam brick (VN), amber brick (AB), brown brick (BR) and refractory brick (RF). These bricks were cut into cylindrical with a size of 3.5 cm in diameter and 7.0 cm in height. After examined rock properties such as physical, mechanical chemical and mineralogical characteristics, two types of salt weathering experiments were performed under 15-35 ℃ and 20 ℃ atmosphere. The saline solutions used in this study are 4%-Na_2SO_4, 8%-Na_2SO_4, 10%?Na2CO3. Results of the experiments show that the deterioration mechanism of bricks is explained that 1) when the salt is absorbed and crystallizes inside brick, micropores of brick are extended by crystal expansion pressure and make cracks, 2) strength of the brick increases slightly by salt crystallization, but decreases gradually by salt deliquescence, and 3) with repeating of 1) and 2), bricks will be damaged. Even chemical and the mineralogical characteristics are almost equal except for BG, physical and mechanical characteristics are deferent, which controls durabilities of these bricks.

Keywords: salt weathering, brick, Vietnum, experiment, durability factor, salt susceptibility index

Japan Geoscience Union Meeting 2014
(28 April - 02 May 2014 at Pacifico YOKOHAMA, Kanagawa, Japan)

HGM02-P01 Room:Poster Time:April 30 18:15-19:30

Channel migration processes observed in 2013 in the upper reaches of the Azusa River, central Japan

SHIMAZU, Hiroshi[1*]

[1]Rissho University

The upper reaches of the River Azusa in central Japan is a braided gravel-bed river running down Japan Alps. They are characterized by frequent landform changes occurring in the riverbed. This area is located in the high conservation area in the Chubu-Sangaku national park and thus physical processes of river are preserved. This study is the first step to clarify the fluvial processes of a braided gravel-bed river during a flood event.

The geomorphological maps of the observation site were made by the Research Group for Natural History in Kamikochi in every summer from 1994. These maps recorded annual landform changes of the riverbed. Sediment transport and/or major landform changes, such as channel migration, occurred once or twice in several years in severe heavy rain events more than 120 millimeters per day during the snowmelt flooding season in late May and/or the rainy season in June and July.

Interval shooting cameras were set up in 2011. These have taken the images of the riverbed and recorded the condition in every 15 or 20 minutes since 3 July 2011, only in the daylight and twilight. Channel migration in the observation area during the flood event was recorded on 19 June 2013, 166 millimeters of daily rainfall. The rain event began at night of 18 June. Water level began to rise early in the morning of 19 June. The heavy rainfall more than 13 millimeters per hour was recorded from 3 a.m. to 5 a.m. and from 7 a.m. to 9 a.m. The river was above bank-full stage at 12:00 a.m. and this condition continued until night. Highest water level was recorded at 16:15. Although water overflowed on gravel bars and shallow branching channels were formed before the bank-full stage, the landform of the main channel was still in the same condition. Changes of patterns of the water surface and movement of woody debris flowing downstream show that during the bank-full stage the channel landform changed and the main channel was migrated. The channel migration was not caused by lateral shifting with lateral erosion. Channels were buried and new channels were excavated tracing the shallow branching channels.

Keywords: channel migration, geomorphic process, braided river, flood, interval shooting camera, Azusa River

Japan Geoscience Union Meeting 2014
(28 April - 02 May 2014 at Pacifico YOKOHAMA, Kanagawa, Japan)

HGM02-P02 Room:Poster Time:April 30 18:15-19:30

Risk evaluation of steep slope failure using a slope angle and mean curvature

NISHI, Hayata[1] ; OGUCHI, Chiaki T.[2*]

[1]Civil and Engineering Department, [2]GRIS. Saitama University

According to the previous techniques for the evaluation of slope failures, only steep slopes are taken into account. However, the influence of earthquakes on slope failures has not been considered on the hazard map delivered by local government. After the Great East Japan Earthquake occurred in 2011, Necessity for considering earthquakes on to slope failure evaluation is increasing. Therefore, the present study focused on risk evaluation of steep slope failures caused by earthquakes. Within various techniques, a technique proposed by National Institute for Land and Infrastructure Management, was adopted in this study. With comparing manual and GIS calculations to obtain the parameters of slope angle and mean curvature, the degree of the risk was evaluated. The target slope is Mt. Shinobu, in Fukushima Prefecture. After examination , it is resulted in that the evaluation using GIS is useful as well.

Keywords: Slope failure, Risk evaluation

Japan Geoscience Union Meeting 2014
(28 April - 02 May 2014 at Pacifico YOKOHAMA, Kanagawa, Japan)

HGM22-01 Room:422 Time:April 30 09:00-09:15

Limit of mountain growth in the development of experimental landforms

OUCHI, Shunji[1*]

[1]Faculty of Science and Engineering, Chuo University

A series of experiments with rainfall-erosion and uplift of various rates, in which a square (60×60 cm) mound of a mixture of fine sand and kaolinite is uplifted at a constant rate under the artificial mist-type rainfall, suggests the existence of threshold uplift rates. In the run with the uplift rate below the lower threshold, drainage networks develop as the surface is slowly uplifted. The erosion is exclusively fluvial and no high slope develops. When the uplift rate becomes higher than this lower threshold, uplift exceeds erosion on the divides of drainage basins, which developed with fluvial erosion, and hills grow and slope processes start working. The divides grow into low mountain ridges with the uplift and slope failures become dominant. When the relief grows high enough, large landslides occur concentratedly. The average height and relief lower with the landslides, but the ridges soon grow again with the uplift till the next concentration of large landslides, and this process proceeds repeatedly. Uplift and erosion seems to become balanced to keep average height and relief roughly constant and landscapes similar. Assuming the existence of the critical slope controlled by the strength of mound-forming material and the rainfall intensity, the experimental landform is considered to reach a dynamic equilibrium condition at a certain relief regardless of the uplift rate. However, when the uplift rate is in the range between the lower and the upper thresholds, both relief and average height become higher with the uplift at higher rate. A simple equilibrium or steady state seems difficult to be expected with the critical slope. Although the maximum slope in a 1 cm grid becomes higher than 80 degree in all runs, considering that the angle of repose of dried mound-forming material is about 34 degree, it is rather difficult to take this maximum slope as the critical slope. The observation of the experiment suggests that large landslides require triggering events to occur, and without triggering events slopes can grow higher. Large landslides often occur when the rainfall is resumed after halting the rainfall for the measurement. This resumption of rainfall can be the major triggering event in the experiment. The interval of measurement is not exactly constant but does not vary so much among runs. As far as the resumption of rainfall after the measurement is the major triggering event, hills can grow higher with the uplift at higher rate. Moreover, fluvial processes can work more with the uplift at lower rate to widen valleys and therefore increase the area of lower slope. Average slope, relief, maximum height, and average height all become lower. In this way experimental landforms can have average height and relief corresponding to the uplift rate. This condition may be called quasi steady state. When the uplift rate is higher than the upper threshold, on the other hand, relief grows to the limit determined by the width of deposition area. In this case further increase in uplift rate cannot increase the height or relief any more, and this condition apparently does not agree with the condition of equilibrium.

Erosion rate is considered to increase with average slope, and some people pointed out that the relation is nonlinear. In the experiments the average value of the highest slope in a 1 cm grid shows similar linear increase with relief regardless of the uplift rate, but they become to show no clear relationship after relief reaches about 60 mm when landslides become dominated in the landform change process. Erosion rate also increase linearly with average slope first, but it becomes almost constant after the dominance of large landslides in the process of landform development. The relation between erosion rate and average slope seems necessary to be reconsidered with taking uplift rate into account.

Keywords: rainfall-erosion experiment, limit of mountain growth, threshold uplift rate, critical slope, landslides

Japan Geoscience Union Meeting 2014
(28 April - 02 May 2014 at Pacifico YOKOHAMA, Kanagawa, Japan)

HGM22-02 Room:422 Time:April 30 09:15-09:30

Evolution of river profile of experimental mountain building

OGAMI, Takashi[1*] ; OUCHI, Shunji[1]

[1]College of Science and Engineering, Chuo University

River profiles and their evolution during mountain building are investigated and the characteristics of river profile under mountain steady-states are examined by rainfall-erosion experiments under various uplift rate. Miniature landforms are developed with constant uplifting of sand-block (mixture of fine sand and kaolinite) and artificial rainfall. Four experiments are operated under the uplift rate of 0.2 mm/h, 0.5mm/h, 1.2 mm/h and 5.0 mm/h. Based on landform measurement, 1 cm grid elevation models are constructed. Streams are generated by basin analysis with the elevation models.

Relationship between the slope of channel (S) and the catchment area (A) are examined. Plots of log S and log A (S-A plots) show convex, linear and slightly concave forms as mountain building progress. In the mountain steady-states, the S-A plots show slightly concave forms, and the forms are stable until end of uplifting. It is deduced that S-A plots become linear forms if they are at steady-state by stream-power incision model. But our result shows that S-A plots under steady-state shows slightly concave forms, expressing that channel slopes at downstream becomes relatively steep than those deduced by the model. This situation should be result of downstream increasing sediment flux, which is important factor of graded river but neglected by the traditional stream-power incision models.

Keywords: rainfall-erosion experiment, uplift, river profile, equilibrium, sediment flux

Japan Geoscience Union Meeting 2014
(28 April - 02 May 2014 at Pacifico YOKOHAMA, Kanagawa, Japan)

HGM22-03 Room:422 Time:April 30 09:30-09:45

Experimental study of the effect of partial uplift on river channels

NAKAUCHI, Takuya[1] ; ENDO, Noritaka[1*]

[1]Kanazawa Univ.

Flume experiments were conducted to examine the effects of uplift on river channels in which the uplift area was restricted to the middle reaches. Experimental landform was evolved by exerting fine water mist on the slope consisting of a mixture of fine sand and clay, and the uplift was realized by jacking up the partial area of the flume bottom. The conventional idea that the occurrence of water gaps was determined by the balance between rates of uplift and downward erosion is true locally. The rate of down erosion is, however, variable due to the change of channel paths in the meso-scale. The avoidance of flowing in the uplift area tends to cause a new confluence and higher stream power producing larger erosion rate. A confluence makes the possibility of forming water gap high. The avoidance of the uplift area, however, does not always induce a confluence, in which the water gap is not generated.

Keywords: river channel, uplift, laboratory experiments

Japan Geoscience Union Meeting 2014
(28 April - 02 May 2014 at Pacifico YOKOHAMA, Kanagawa, Japan)

HGM22-04 Room:422 Time:April 30 09:45-10:00

Current status and issues of grain-size analysis using a digital image method and a laser diffraction method for sedimen

NANAYAMA, Futoshi[1*] ; FURUKAWA, Ryuta[1]

[1]Geological Survey of Japan, AIST

Grain size measurement is the most fundamental physical information in evaluating the characteristics of various materials, the analytical technology. These are JIS standardized clearly by the association of powder process industry and engineering, Japan. In geomorphological field, we are carried out the grain size analysis of volcanic ash, mud, sand, and gravel using in combination of settling tube method, laser diffraction scattering method (LD), sieve classification method and the precipitation method in generally. According to currently technology, it is possible that the LD of each company to measure the particles of a wide range of 10nm to 3mm in a short period. However, we believe that a technical problem for analyzing nature sediments still now because these are not a powder of industrial products with same physical properties.

For example, we know a large scattered light intensity can be achieved in the shorter wavelength of the incident light because it is confirmed by measurement of the fine particles of submicron order, strength is not enough laser light. Moreover backscatter increases depending on the shape of non-spherical particles, tend to shift the fine particle side is confirmed grain size. Further, when using an algorithm for determining the particle size by inverse calculation using the Mie theory, it is necessary to set the user side of the value of the absorption coefficient and the particle refractive index.

This assumption is a very annoying problem for the user.

Recently, the particle size measurement in the field of powder technology, the development of new analytical instruments using digital image analysis method has been increasing. In this method, it is acquired the two-dimensional image of the particle is first digitally imaged by pixel division using the CCD camera and divided into two sub-methods, static (JIS Z 8827-1:2008; ISO 13322-1) and dynamic (JIS Z 8827-2:2010; ISO 13322-2). The methods may be used either, a process that takes as a digital image the particles, the statistical processing on a personal computer is the same.

Analysis method using a digital image of a single particle is clear, it is easy to be trusted from the user side. In addition, the use of the digital image, various particle shape parameter as well as information about the particle size distribution and the particle size of each definition different, for example, can be analyzed at the same time the value aspect ratio, elongation, circularity, HS circularity, convexity, solidity, etc.. Further, it is possible to obtain also the physical properties such as transmittance and intensity. We believe that it is analyzed in conjunction with the particle size measurement result data on physical properties and particle shape these, and becoming a new standard for particle size analysis in the future.

The present study includes the result of ”Research and Development of Margin Assessment Methodology of Decay Heat Removal Function against External Hazards” entrusted to Japan Atomic Energy Agency by the Ministry of Education, Culture, Sports, Science and Technology of Japan (MEXT).

Keywords: laser diffraction method, digital image method, sediment, grain-size analysis, current status, issues

Japan Geoscience Union Meeting 2014
(28 April - 02 May 2014 at Pacifico YOKOHAMA, Kanagawa, Japan)

HGM22-05 Room:422 Time:April 30 10:00-10:15

Causes of gravel-sand distribution in upstream part of the river revealed from changes in lithology and form of detritus

UTSUGAWA, Takako[1*] ; SHIRAI, Masaaki[1]

[1]Department of Geography, Tokyo Metropolitan University

Downstream fining of fluvial clastic sediments has been generally attributed to two processes, ”hydraulic sorting” and ”sand grains production”, the former is that finer grains are transported farther than coarser grains, while the latter implies crushing and abrasion of gravels. In this study, we investigated that how the two processes operate on this tendency along the tributary of Watarase River, the major branch of the Tone River on the basis of field survey and measurement of finer grains (4 to 0.5 mm in diameter). Lithological composition of each grain size fraction from cobble to coarse-grained sand (128-0.5 mm in diameter) with 1 ϕ (phi scale) intervals and roundness were obtained with digital microscope.

Changes in lithological composition of cobble – pebble, granule and very coarse sand fractions are not explained only with ”hydraulic sorting” of clastic grains. It implies that crushing and abrasion of gravel – very coarse sand fractions and consequent ”sand grains production” occur at the studied area.

Whereas, coarse sand fraction (1-0.5 mm) shows remarkable features that (i) change in lithological composition along the tributary was not recognized and (ii) grains become rounded in downstream direction. These facts suggest that abrasion of the grains occur dominantly than crushing in coarse sand fraction and ”sand grain production” may not be efficient to grains smaller than coarse sand. Therefore, it will be important to research the distribution of coarse sand and finer grains in bed material along the river in order to reveal the transition from ”producing process” to ”sorting process”, erosion – transport processes of clastic sediments and a development of sedimentological geomorphology along the river.

References

Frings, R. 2011. Journal of Sedimentary Research 81 : 52-63.
Kodama, Y. 1994. Journal of Sedimentary Research A64(1) : 68-75.

Keywords: gravel, sand, crush-abrasion, lithological component, roundness, tributary of Watarase River

Japan Geoscience Union Meeting 2014
(28 April - 02 May 2014 at Pacifico YOKOHAMA, Kanagawa, Japan)

HGM22-06 Room:422 Time:April 30 10:15-10:30

Earth-surface processes on the basis of instrumental observations in Takidani-ike lake-catchment system, central Japan

ITONO, Taeko[1*] ; KASHIWAYA, Kenji[1] ; OCHIAI, Shinya[1]

[1]Kanazawa University

Lacustrine sediments contain both high-resolution regional environmental records and global information in lake-catchment systems. They are also of great use for reconstructing short-term environmental changes (precipitation, water discharge, etc.) and understanding earth-surface processes (erosion, transportation, sedimentation) in the lake-catchment system.

Process understanding is essential for clarifying causal relations in earth surface phenomena and proper interpretation of sediment information. Instrumental observation (monitoring) is of great use for the process understanding. This study deals with the instrumental observation for a small pond-catchment system (Takidani-ike) near Kanazawa University. The pond is storage reservoir. It is used for agricultural irrigation in summer. Therefore the water level shows highly fluctuation. Our observation consists of sediment sampling with trap, water level measurement, temperature measurement, and precipitation measurement. Observation in Takidani-ike using sediment trap has continued since June 2000.

Observational and analytical results for Takidani-ike show that; the sedimentation rate (both monthly and seasonal sedimentation) is expressed as a function of two factors; precipitation intensity (external factor) and water level change (system factor, closely related to size of erosible area). The correlation for the seasonal relationship is better than one for the monthly relationship, suggesting that reservoir effect in the catchment should be considered. The results also show that mineral grain size may be used as proxies for sedimentation rate.

Keywords: lake-catchment system, earth-surface process, pond sediment, sedimentation rate

Japan Geoscience Union Meeting 2014
(28 April - 02 May 2014 at Pacifico YOKOHAMA, Kanagawa, Japan)

HGM22-07 Room:422 Time:April 30 10:30-10:45

Characteristics and production processes of coastal huge blocks in the Miyako Island

SHIMAZU, Hiroshi[1*] ; SETO, Masayuki[2]

[1]Rissho University, [2]Fukushima University

There are many coastal huge blocks in the Miyako Island. Some were brought from the sea bottom by tsunamis. Most of others were made by landslides of the coastal cliffs. Previous studies showed the dynamics of the production of such huge blocks from the coastal cliffs of Ryukyu limestone. Development of notches formed near the sea level and vertical cracks on the surface of the marine terraces near the cliffs caused the instability of the rock mass and finally it were torn into coastal huge blocks. This process indicates that the height of the cliff relates the block form and size. However there are large variety of form and size of coastal blocks in Miyako Island. Although smaller blocks are distributed in front of the higher cliff in the Boraga beach, huge blocks with vegetated top are distributed in front of the 20 meters high cliff in Higashi-hennazaki. This Study aims to describe the characteristics and distribution of coastal blocs and discuss production processes of the blocks.

In the Miyako Island the Ryukyu limestone covers the semi-consolidated sandstone or mudstone called the Shimajiri formations. These are unconformable. The Ryukyu limestone is hard and permeable rock and the Shimajiri formations are soft and impermeable rocks. These two layers outcrop on the cliffs and their boundary usually occurs high above the sea level. Groundwater springs or seeps from the boundary on the cliff. The water erodes the Shimajiri formations along the boundary. This process causes the notch-like form at the boundary. At the Braga beach the height of the cliff is more than 40 meters and the boundary of the layers, where groundwater springs, locates 14-20 meters high above the sea level. Development of the notch-like form caused instability of the limestone layer. And then the layer collapsed and produced limestone blocks. They rolled down to the beach breaking into smaller blocks. At the Aragusuku and Urasoko fishing port coasts the blocks were produced by same process. At the Higashi-hennazaki the boundary locates several meters above the sea level. Groundwater sapping forms notch-like form at the boundary. At the Shimajiri coast the Ryukyu limestone appears on all the cliff. A notch was formed at the sea level by the wave process. On these type of coasts the limestone cliffs were torn into huge blocks. The blocks with vegetation on the top of them were deposited along the coast.

Keywords: huge block, geomorphic process, coastal cliff, spring, Ryukyu limestone, Miyako Island

Japan Geoscience Union Meeting 2014
(28 April - 02 May 2014 at Pacifico YOKOHAMA, Kanagawa, Japan)

HGM22-08 Room:422 Time:April 30 11:00-11:15

Late Quarternary tectonic development at the northeastern margin of Tibet revealed by 10Be and 26Al

SHIRAHAMA, Yoshiki[1*] ; MIYAIRI, Yosuke[2] ; HE, Honglin[3] ; FU, Bihong[4] ; KANO, Ken-ichi[5] ; ECHIGO, Tomoo[6] ; YOKOYAMA, Yusuke[2] ; IKEDA, Yasutaka[1]

[1]Department of Earth and Planetary Science, Graduate School of Science, The University of Tokyo, [2]Atmosphere and Ocean Research Institute, The University of Tokyo, [3]Institute of Geology, China Earthquake Administration, [4]Institute of Geology and Geophysics, Chinese Academy of Sciences (IGGCAS), [5]Faculty of Science, Shizuoka University, [6]Geo-Research Institute

Tibetan Plateau has been growing up due to collision between the Indian and Eurasian plates and expanding its area laterally by invading marginal forelands and making them involved into deformation. The mechanism of expansion at the northeastern margin of the plateau is still a subject of much debate due to the scarcity of tectonic researches. In the Kumkol Basin at the northeastern margin of the plateau we made detailed geomorphological mapping using satellite images, and revealed that there is a huge anticlinorium that consists of many thrusts and folds covered with significantly deformed fluvial or fluvio-glacial fans or terraces along the Pitileke River. The development and deformation rate of the anticlinorium would give an important clue to understanding the growth mechanism of the plateau. In order to estimate the deformation rate, we dated depositional surfaces by surface exposure dating by using cosmogenic radionuclides (CRNs), such as ^{10}Be or ^{26}Al. Field investigations were conducted in 2011 and 2013, and mainly pebbles of vein quartz were collected at 22 points on the surface of fans and terraces. Depth-profile samples were collected also from 3-m deep sections at two points; each depth profile of ^{10}Be and ^{26}Al concentrations were analyzed for the exposure age, erosion rate, and inheritance by the Monte Calro simulation. In addition, grain-by-grain CRN concentrations were measured for surface samples from two points to estimate the origin of sediments. Following three inferences were obtained: (1) the sediments of the lower part of terraces and the present river contain reworked sediments; (2) depositional processes and erosion processes are strengthened in the glacial and interglacial period, respectively; (3) the upper-most two steps of terraces were formed before the MIS6 and in the transition period from MIS6 to MIS5, respectively.

Keywords: Tibetan Plateau, Qaidam Basin, tectonic landform, surface exposure dating

Japan Geoscience Union Meeting 2014
(28 April - 02 May 2014 at Pacifico YOKOHAMA, Kanagawa, Japan)

HGM22-09 Room:422 Time:April 30 11:15-11:30

Longitudinal distribution of incision rates in the Oshika Gorge, Tottori prefecture using terrestrial cosmogenic 10Be:

WATAKABE, Takuma[1*] ; KODAMA, Yoshinori[2] ; MATSUSHI, Yuki[3] ; MATSUZAKI, Hiroyuki[4]

[1]Graduate School of Regional Sciences, Tottori University, [2]Faculty of Regional Sciences, Tottori University, [3]Disaster Prevention Research Institute, Kyoto University, [4]School of Engineering The University of Tokyo

We determined longitudinal changes of incision rates in the 3 km long Oshika Gorge, Tottori prefecture, Western Japan, by exposure dating of a series of granitic strath terraces using terrestrial cosmogenic 10Be. Thereby we discuss development of a waterfall sequence zone and an incised meander zone. The bedrock of the gorge consists of granite. We collected 24 granite samples from surface of erosional terraces. The oldest exposure age of a strath terrace was 50.2 kyr (relative height from river-bed is 11.0 m) and the youngest exposure age was 1.2 kyr (relative height is 1.2 m). Incision rates in the Oshika Gorge varied from 0.24 mm/yr to 1.40 mm/yr. Those of step-pool sequence zones and large boulder scatter zones were about 0.64˜1.40 mm/yr, which showed increasing tendency toward downstream. Those of the waterfall-pool sequence zone were 0.24˜0.57 mm/yr, which showed rapid increase toward downstream. This means that gradient of the waterfall-pool sequence zone has been under increasing conditions in these c.a.50 kyr, resulting from river-bed roughness increase according to waterfall-pool growth. The incised meander zone is located just upstream adjacent to the waterfall-pool sequence zone. Incision rate of the incised meander zone was 0.36 mm/yr, which was slower than that of step-pool sequence zones and faster than that of the waterfall-pool sequence zone. In this reach, alternate gravel bars were developed because of lower gradient and as a result, lateral migration of the river occurred and the incised meander zone was developed.

Keywords: bedrock river, incision rate, cosmogenic nuclide 10Be, waterfall-pool sequence, incised meander zone

Japan Geoscience Union Meeting 2014
(28 April - 02 May 2014 at Pacifico YOKOHAMA, Kanagawa, Japan)

HGM22-10 Room:422 Time:April 30 11:30-11:45

Basin-averaged erosion rates of Yakushima using cosmogenic 10Be in river sediments

SHIROYA, Kazuyo[1*] ; MATSUSHI, Yuki[2] ; MATSUZAKI, Hiroyuki[3]

[1]Geological Survey of Japan, AIST, [2]Disaster Prevention Research Institute, Kyoto University, [3]Department of Nuclear Engineering and Management, School of Engineering, The University of Tokyo

Quantitative understanding of erosion rates under several geomorphic and geological settings is important to discuss the process of erosion. We investigated basin-averaged erosion rates from cosmogenic ^{10}Be in quartz grains from river sediments in Yakushima. Erosion rates in Yakushima are relatively low within a similar range to those in regions of several times lower rainfall than Yakushima. This finding suggests that rainfall is not necessarily a causal factor of landform evolution. In this presentation, we focus on a pattern of hillslope erosion and a process of landform evolution in Yakushima.

This research project has been conductedas the regulatory supporting research funded by the Secretariat of Nuclear Regulation Authority (Secretariat of NRA), Japan.

Keywords: Yakushima, Basin-averaged erosion rate, precipitation, cosmogenic Be-10

Japan Geoscience Union Meeting 2014
(28 April - 02 May 2014 at Pacifico YOKOHAMA, Kanagawa, Japan)

HGM22-11 Room:422 Time:April 30 11:45-12:00

Temporal variation of Kurobe River Sediments revealed by TL and ESR signals in quartz

YOSHIDA, Msanori[1*] ; TOYODA, Shin[1] ; NINAGAWA, Kiyotaka[1] ; TAKADA, Masashi[2] ; SHIMADA, Aiko[3]

[1]Department of Applied Physics, Faculty of Science, Okayama University of Science, [2]Department of Geography, Nara Women's University, [3]Application Support Team, JEOL RESONANCE Inc

While the ESR signals of the E1' center in quartz was used to investigate the origin of the loess in MIS 1 and 2 (Toyoda and Naruse, 2002) and of the sediments in the Sea of Japan (Nagashima et al., 2007). Shimada (2008) showed that TLCI (thermoluminescence color image) may be useful for similar qualitative study on river sediments. In the present study, the wavelength-temperature two dimensional thermoluminescence measurement was employed, together with the ESR measurements, to investigate the temporal change of these characteristics observed in fluvial sediments of the Kurobe river.

Eight sediment samples were collected from the present river bed along the Kurobe River in 2012 and 14 samples in 2013. They were sieved into two grain size fractions of 500-250μm, 250-75μm. Quartz grains were extracted using chemicals, heavy liquid, and an isodynamic magnetic separator. The obtained quartz grains were heated at 300 degree Celsius for 1 hour to erase the inherited signals. Each sample was then separated into 9 subsample aliquots for gamma ray irradiation up to 2640 Gy, which are for ESR measurements. Other aliquots for TL measurement were given a dose of 809 or 857 Gy with wrapping the tubes with Al foil in order to keep the samples in the dark.

TL measurements were performed by using the two dimensional TL apparatus. We measure the TL emission spectra during heating up to 450 degree Celsius. Red emission (538 to 658 nm) was observed between 140 and 250 degree Celsius (Low Red) and 290 and 370 degree Celsius (High Red) and Blue emission (379 to 538 nm) was between 103 and 211 degree Celsius (Blue). The integrated counts were taken as the intensities of the red and blue emissions. The results of ESR measurements will be given in the presentation together with the TL results.

Keywords: ESR, TL(thermiluminescence)

Japan Geoscience Union Meeting 2014
(28 April - 02 May 2014 at Pacifico YOKOHAMA, Kanagawa, Japan)

HGM22-12 Room:422 Time:April 30 12:00-12:15

Distribution pattern and formation processes of potholes in Oshika, Tottori: role of pothole on river incision processes

KODAMA, Yoshinori[1*] ; INOUE, Yuuki[2]

[1]Fac.of Regional Sciences, Tottori-Univ., [2]Under Graduate, Fac.of Regional Sciences, Tottori-Univ.

Potholes on the Oshika River bed near Takaganma, Misasa-Town, Tottori, Western Japan were surveyed. Surrounding terrace development revealed that there potholes were formed within 3,600 years. Plan view survey illustrated a line distribution pattern of potholes, resulting from longitudinal vortices generated in flood flows. Longitudinal profiles (Fig.) showed that bottom levels of potholes were close to or towards to those of the present river bed. In general, potholes have a role of effective drilling erosion on a hard bedrock elinimation with few sediment loads in the river incision processes.

Keywords: potholes, potohole developing processes, line distribution, river incision processes, balloon photoes, The Oshika River, Tottori, Japan

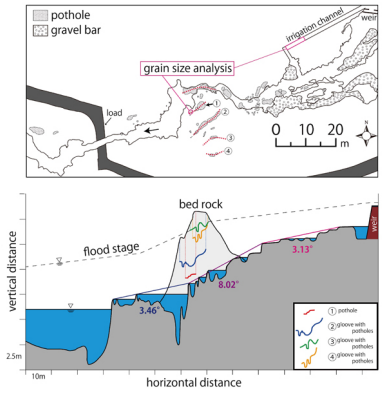

Fig. Plan view and long profiles of Takaganma-Potholes, Misasa Town, Tottori Pref., Japan

Japan Geoscience Union Meeting 2014
(28 April - 02 May 2014 at Pacifico YOKOHAMA, Kanagawa, Japan)

HGM22-P01 Room:Poster Time:April 30 18:15-19:30

Accumulation patterns of in-channel modern deposits in the lower Stung Sen River

NAGUMO, Naoko[1*] ; SUGAI, Toshihiko[2] ; KUBO, Sumiko[3] ; OKAZUMI, Toshio[1]

[1]ICHARM, PWRI, [2]Graduate School of Frontier Sciences, University of Tokyo, [3]School of Education, Waseda University

The Stung Sen River flows down the central region of Cambodia, is the main tributary in the Tonle Sap drainage basin. It develops fluvial lowland in its downstream and the longitudinal profile is very flat, with the slope of less than 0.1 ‰. Monsoonal precipitation provides seasonal flood every year in the fluvial lowland and cyclic water level changes of the Tonle Sap Lake about 8 m in the river mouth, therefore the river seems to change sediment transportation processes in each season. While meander scrolls formed by channel migration and back marsh are found in the floodplain throughout the year (Nagumo et al., 2013), four types of channel bars are recognized within the river channel about 10 m lower than back marsh during dry season. Outcrop observations at concave type channel bars revealed the alternate layers of reverse-graded sand and mud layers, and inserted plastic pieces with date stamps indicated that the deposits are quite new and have been partly replaced to reflect flow regime changes of the river. Such sedimentary structures suggest that minute fluctuations of water level and discharge control bar construction, and would be important source to understand recent flood history and patterns.

Keywords: fluvial lowland, meander, monsoon, water level fluctuation, Lake Tonle Sap, Cambodia

Japan Geoscience Union Meeting 2014
(28 April - 02 May 2014 at Pacifico YOKOHAMA, Kanagawa, Japan)

HGM22-P02 Room:Poster Time:April 30 18:15-19:30

Development of Strandplain Ridges Group in the Kujukuri Coastal Plain by LiDAR DEMs

OOI, Shinzou[1*] ; NANAYAMA, Futoshi[2] ; NAKASHIMA, Rei[2]

[1]GSI/AIST, [2]AIST

The DEM data based on an Airborne laser survey was fixed recently, and it became possible also in the Kujuukuri Coastal plain to use this DEM data. Then, this DEM data analyzed the microtopography of the plain. And the development of the Kujuukuri Coastal plain, especially the north-south difference were considered.

Keywords: Kujukuri Coastal Plain, Strandplain ridge, LiDAR DEMs

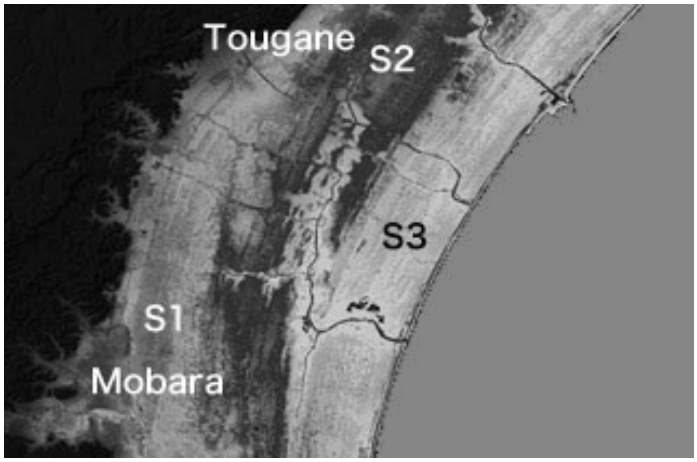

Japan Geoscience Union Meeting 2014
(28 April - 02 May 2014 at Pacifico YOKOHAMA, Kanagawa, Japan)

HGM22-P03 Room:Poster Time:April 30 18:15-19:30

Controlling factor on evolution of late Pleistocene to Holocene sequences in Nara Basin

HORI, Kazuaki[1*] ; ITO, Nobuaki[1] ; TAKADA, Masashi[2]

[1]Department of Geography, Graduate School of Environmental Studies, Nagoya University, [2]Department of History, Sociology and Geography, Faculty of Letters, Nara Women's University

Many researches on late Pleistocene to Holocene sequences (Chuseki-so) have been carried out in coastal lowlands. In contrast, stratigraphy and evolution of alluvial plain located above the coastal lowlands is less well known. We focus on Nara Basin to clarify stratigraphy and evolution of alluvial plain.

Two borehole cores (MK1, MK2) were taken at Matsukasa, Yamatokoriyama city located in the middle part of the basin. Sedimentary facies analysis and AMS radiocarbon dating were performed. Stratigraphy of late Pleistocene and Holocene deposits was built by analyzing existing borehole columns and radiocarbon ages. Additionally, an incised valley formed beneath the Kawachi Plain located near the Old Yamato river mouth during the sea-level lowstand was reconstructed by analyzing existing borehole logs. Sediment accumulation rate of the basin mainly during the last two millennia was estimated from depth of remains shown in archaeological reports published by Archaeological Institute of Kashihara, Nara prefecture.

Radiocarbon ages obtained from the cores suggest that thickness of Holocene deposits is less than approximately 3 m and they have mainly accumulated after 2,000 cal BP. The timing is not related to sea-level change of Osaka Bay. Sea-level change would affect change of river-bed gradient at Kawachi Plain near the river mouth. However, Kamenose narrow segment in Ikoma Mountain is located between Kawachi Plain and Nara Basin and is composed of Cretaoeous and Neogene igneous rock. Rock hardness may have resulted in small incision rate of the river bed at the segment, and influence of the sea-level change above the segment was little.

Geological section of Nara Basin shows thickness of Holocene deposits on south area is larger than that of north area. Discharge and drainage area of south district are ca. 2.3 times larger than those of north district. This may be related to the difference in thickness of Holocene deposits.

Depth of remains during the era of Yayoi to Kamakura suggests that increase in sedimentation rate occurred after Asuka era. Existing pollen analysis results indicate that second growth forest probably influenced by human activity had already occurred in and around the basin at Kofun era. Therefore, it is possible that artificial effects in the basin caused increase in sediment production and influenced formation of late Pleistocene to Holocene sequences in Nara Basin.

Keywords: Late Pleistocene to Holocene sequences, inland basin, borehole log, Nara Basin

Japan Geoscience Union Meeting 2014
(28 April - 02 May 2014 at Pacifico YOKOHAMA, Kanagawa, Japan)

HGM22-P04 Room:Poster Time:April 30 18:15-19:30

Quantitave Evaluation of Microtopography in the Riverside Land of the Mizunashigawa River, Japan

OGURA, Takuro[1*] ; AOKI, Tatsuto[2]

[1]School of Humanities, Kanazawa University., [2]School of Regional Development Studies, Kanazawa University.

This research did the quantitative assessment of how the amount of encroachment changed and microtopography change in the outside area of the new dike, which modify the land, of Mizunashi River. The origin of this river is the mount Unzen which is well known of its eruption in 1990. This area is unique because of the artificial preparation of the soil; its base-level of erosion was reset. Thus, this area cannot be discussed by the usual landform evolution, but quantitative assessment.

The result of the research showed that the effect of the change can be divided into 4 periods. There was no large-scale debris flows and erosion of the lateral had progressed with the formation of the micro watercourse network in the 7 years since the 1998.

vdebris flows in the riverside land stabilized as the result of the terrain became stable in 2005.

There were debris flows that occurred intensively in a short period while 2005 to 2008. They were large enough to cause the outflow of the vegetation of the surface layer. As a result of these debris flows, the lateral erosion changed to the downward erosion. After those debris flows, the passage was fixed.

There was a rapid recover of the flora in 2011. This increased the stability of the outside area of the bank.

Overview of the area

It has been more than 20 years since the Heisei eruption; however, a light rain amount of about 20 ˜30mm rainfall time can cause debris flows in the Mizunashi River. To minimize the damage of the volcanic disaster, constructions for the erosion control are still continuing.

Results and the research method

Calculation of bare land ratio by GIS

Putting the base-level of the erosion to the 1998, as the time lapses the ratio of the bare land decrease. For instance the bare land area was 91.62[%] in 2003, but in 2005 it became 50.32[%]. However, the ratio of the 2008 was 58.66[%] and after 2008 the ratio is repeating a micro increase and decrease.

Calculation of the flow path extending ratio

The calculation is about the the ratio of the flow path extending of the same waterway since 2008. The result of the calculation shows the quantitative assessment of the immobilization of the channel. This is shown by the result of the 2008, 2011 and 2013, in these three years the ratios are 1.11 and 1.10.

Measure of the erosional cross section and local observation

The survey date show the width of gully is 8.27[m]. This is approximately equal to the size of the width and gully erosion in the upper reaches. This date can be seen in the report of 2011 by the Unzen reconstruction office. Calculating the average erosion speed (v) from the base level of erosion and the maximum deepening speed (Mv) from the maximum depth of erosion, the results are v=4.66[cm/year] and Mv=20.6[cm/year]. These results show two things. First, the lateral erosion has the bigger scale than that of lower erosion. Second, the direction of the erosion changed recently from horizontal to down.

Keywords: geomorphological process, gully erosion, debris flow, GIS, Unzen Volcano

Japan Geoscience Union Meeting 2014
(28 April - 02 May 2014 at Pacifico YOKOHAMA, Kanagawa, Japan)

HGM22-P05 Room:Poster Time:April 30 18:15-19:30

Timing of sediment discharge events on a welded tuff slope in Chugoku Mountains, Japan

WAKATSUKI, Tsuyoshi[1*] ; YAMADA, Ryuji[1]

[1]National Research Institute for Earth Science and Disaster Prevention

Many slope disasters were occurred by a heavy rain on July 28, 2013 in Yamaguchi and Shimane Prefectures. In particular, a number of shallow slope failures and debris flows occurred on mountain slopes underlain by rhyolite-dacite welded tuff in the Tsuwano Town, Shimane Prefecture and the adjacent Ato District, Yamaguchi City. The debris flows eroded the sidewalls and the riverbed of the flow channel, and outcrops of deposits accumulated by sediment discharge events older than 2013 appeared intermittently. From five outcrops along two channels, we collected 11 chip samples of the woods that may have buried and died at the time of the sedimentation. We performed 14C dating of them, and the calendar-calibrated radiocarbon ages showed a 0.6 - 52 Ka BP. Sedimentary structures suggest that these ages correspond to the occurrence time of debris flows and slope failures in the past.

Keywords: 14C dating, debris flow, slope failure, soil slip

Japan Geoscience Union Meeting 2014
(28 April - 02 May 2014 at Pacifico YOKOHAMA, Kanagawa, Japan)

HGM22-P06 Room:Poster Time:April 30 18:15-19:30

The characteristic of roots distribution on the slopes in Izu-Oshima where landslides were occurred by Typhoon No.26

MURAKAMI, Wataru[1*] ; OGAWA, Akiho[1] ; OGAWA, Yasuhiro[1] ; DAIMRU, Hiromu[1]

[1]FFPRI

Large-scale landslides were occurred in Izu-Oshima by Typhoon No.26 on October 16, 2013. By the urgent investigation after the disaster, it is reported that the landslides were occurred in the part within about 1m from the slope surface and the few rhizomes were on the slip surface. We surveyed the distribution of the fallen trees (species, height, the root depth, and the extensions (widths) of the roots) on the slope near the landslide. The surveyed fallen trees were a lot of *Eurya japonica*, and were the order of *Ilex crenata var.hachijoensis*, *Prunus lannesiana var. speciosa*, and *Camellia japonica*. Most of the surveyed fallen trees were about 5-7m in height, and the high one was 10m or less. The root depth of most fallen trees was 60-80cm; however, the root depth had the difference by the tree species. The Camellia japonica and the Prunus lannesiana var. speciosa had comparatively deep roots. On the other hand, the Eurya japonica and the Ilex crenata var.hachijoensis tended to be distributed shallowly the root systems. As a factor to which the root systems are not deeply distributed, a peculiar properties of soil situation of the volcano is pointed out. In this survey, the difference of characteristics of the tree species on the surveyed slopes was guessed as a cause, too.

Keywords: Izu-Oshima, Typhoon No.26, landslide, roots distribution

Japan Geoscience Union Meeting 2014
(28 April - 02 May 2014 at Pacifico YOKOHAMA, Kanagawa, Japan)

HGM22-P07 Room:Poster Time:April 30 18:15-19:30

Verification of incision rate estimation baseed on the geomorphological history of river terraces in Kaligandaki, Nepal

YOSHIDA, Takahiro[1*] ; SUGANUMA, Yusuke[2] ; MAEMOKU, Hideaki[3]

[1]The Guraduate University for Advanced Studies, [2]National Institute of polar rearch, [3]Housei unversity

The Himalaya is the highest mountains of the world. To estimate long-term (1 ˜100 kyers) uplift history of the Himalaya, erosion rates of the incised river have been used with presuppose of dynamic equilibrium between tectonics and aggradations. This estimation is based on the correlations of the river terraces, however, depositional processes of the terraces usually have not been described in detail.

The Kaligandaki is the one of the longest river across the Nepal Himalaya. The long-term uplift history of the Himaraya has been estimated from the distribution of Holocene and Pleistocene terraces along the Kaligandaki river. In this study, we carried out the detailed geomorphological and sedimentological survey at the upper and middle part of the Kaligandaki River to verify the correlations of the river terraces. The fluvial terraces at the upper part of the Kaligandaki river is thought to be originated to the local sediment supply from three phases of the glacial events, although the middle part of the terraces are fluvial sediment. This indicates that correlations of the river terraces along the Kaligandaki river is not suitable for the estimations of incision rate and uplift history of the Himalaya.

Keywords: Himaraya, Geomorphology, Kaligandaki, Fuluvial terrace

Japan Geoscience Union Meeting 2014
(28 April - 02 May 2014 at Pacifico YOKOHAMA, Kanagawa, Japan)

HGM22-P08 Room:Poster Time:April 30 18:15-19:30

Field measurements on the reduction of wave height on a fringing reef: A study from the Miibaru coast, Okinawa Island

TAKEISHI, Yu[1*] ; AOKI, Hisashi[2] ; MAEKADO, Akira[3] ; HIROSE, Takashi[3]

[1]Graduate School of Humanities and Social Sciences, University of the Ryukyus, [2]Faculty of Business Administration, Daito Bunka University, [3]Faculty of Law and Letters, University of the Ryukyus

To investigate the relationship between reduction of wave height on a fringing reef and the water depth at the reef edge, field measurements were carried out on Miibaru coast with a fringing reef in Okinawa Island, Japan. The ratio of the shore break height (the height of final breaking waves near the shoreline) to the wave height at the reef edge, H_b/H', which denotes the degree of the reduction of wave height on a reef, was found to decrease with decreasing water depth at the reef edge. This result indicates that the reduction of wave height on a reef is greatly controlled by water depth on a fringing reef.

Keywords: Reduction of wave height, Coral reef, Fringing reef, Water depth, Okinawa Island

Japan Geoscience Union Meeting 2014
(28 April - 02 May 2014 at Pacifico YOKOHAMA, Kanagawa, Japan)

HGM22-P09 Room:Poster Time:April 30 18:15-19:30

Experiments on Salt Weathering in Cold Environments : Effects of Dissolved Salts on Frost Shattering

SATO, Masato[1*] ; HATTANJI, Tsuyoshi[2]

[1]Graduate School of Life and Environmental Sciences, University of Tsukuba, [2]Faculty of Life and Environmental Sciences, University of Tsukuba

Weathering experiment was carried out to investigate the effects of dissolved salts on frost shattering using four types of rocks (two tuffs, one sandstone and one andesite) and three types of salt solutions (sodium chloride, sodium sulphate and magnesium sulphate). Cubic specimens with a side of 5 cm in length were immersed in saturated salt solution of NaCl, Na_2SO_4, $MgSO_4$ or distilled water for 72h. After immersion, the specimens were covered with foil and subjected to up to 80 freeze-thaw cycles in a cold chamber where the temperature ranges from -30 ℃ to 10 ℃ within twenty four hours.

Freezing points of salt solutions were decreased by dissolved salts. In particular, the saturated solution of NaCl did not freeze under -25 ℃. The liner strain on the surface of specimens was measured with strain gauge during freeze-thaw cycle. The specimens immersed in salt solutions showed greater freezing strain than those immersed in distilled water. Specimens with $MgSO_4$ solution produced the large strain. In most cases, the strain strongly correlated with Weathering Susceptibility Index (WSI). The decreasing rates of the longitudinal wave velocity and the Equotip hardness value during freeze-thaw cycles also correlated with WSI.

Keywords: salt weathering, frost shattering, cold environments, freezing strain, laboratory experiment

Japan Geoscience Union Meeting 2014
(28 April - 02 May 2014 at Pacifico YOKOHAMA, Kanagawa, Japan)

HGM22-P10 Room:Poster Time:April 30 18:15-19:30

The volume expansion of pyroclastic rocks by the crystal growth of Halloysite at the Higashidoori

NAKATA, Eiji[1*] ; OOYAMA, Takahiro[1] ; TORIGOE, Yuji[2] ; MIWA, Tadashi[2] ; CHIGIRA, Masahiro[3]

[1]Central Research Institute of Electric Power Industry, [2]Tohoku Electric Power Co., Inc., [3]Disaster Prevention Research Institute Kyoto University

We find the ground deformation by volume expansion of pyroclastic rocks at the Higashidoori Nuclear power station site. The Tomari formation is strongly altered by light brown colored weathering with halloysite crystallization. The Tomari formation mainly consists of lappili tuff including andesitic lava. The Gamanosawa formation is laid on the Tomari formation consists of alternated sandstone, mudstone, conglomerate and tuff layers. These stratum are covered by the middle terraces deposit including the Toya tephra: 110 ka and Towada red tephra: 80 ka. Towada red tephra in the middle terrace deposit is not deformed on this site.

The convex deformation is formed absorbing the water of montmollironite in fault zone (clay rich zone). Strongly weathered surface rocks of the Tomari and Gamanosawa formation are also deformed toward upper parts around fault zone. This deformation is also formed regardless of fault zone.

Montmollironite distributes at the deeper area (the Tomari formation) which consists of weakly weathered rocks. Halloysite crystallized from montmollironite at shallow area. Plagioclase disappers with the crystallization of halloysite by XRD results. Halloysite which formed tube shapes covered the all over the materials are changed the shape to aggregation of fan shapes by SEM observation. Halloysite crystals increases a distance of the space between minerals under the micro scopic observation.

To assume that Ti is immobile elements with weathering in the rock, the volume of weathered rocks (lapilli tuff: the Tomari formation) increases in 1.3 to 1.5 times to compare with fresh rocks.

Montmollironite crystallizes the surface of minerals at first. After crystallization of montmollironite, halloysite crystallizes on the montoollironite to be affected by weathering at shallow depth.

Crystal growth of halloysite causes the volume expansion of rock and the deformation of ground surface.The old faults plane and joints slip as the appearance reverse faults by crystal growth at this site.

Keywords: Halloysite, Volume expansion, Higashidoori

Japan Geoscience Union Meeting 2014
(28 April - 02 May 2014 at Pacifico YOKOHAMA, Kanagawa, Japan)

HQR23-01 Room:414 Time:May 1 09:00-09:15

Characteristics and Development Processes of Wetlands on Landslide Masses in Hachimantai Volcanic Group, NE Japan

SASAKI, Natsuki[1*] ; SUGAI, Toshihiko[1]

[1]the University of Tokyo

Wetlands are widely distributed in the mountainous regions in Japan, and are subject to protection and conservation because of their beautiful landscapes and their peculiar biota. Considering not only their climate and hydrological conditions but also their geomorphological conditions is necessary to characterize development processes and environmental responses of wetlands. In tectonically active and warm humid regions like Japan, landslides are one of the most important factors for mountain development. Recently the role of landslides creating biodiversity and landscape diversity has been much attracted attention in the field of ecology and geomorphology(Geertsema *et al*., 2007). This study focuses on wetlands as one of the representative landform units composing landslides and presents their characteristics and development processes in Hachimantai volcanic groups which have been deformed by many landslides. 'Wetlands' generally includes various types of water-rich conditions. In this study, as their primary components we focuses on 'bogs' and 'ponds', and define 'bogs' as grasslands in moisture conditions.

Hachimantai volcanic group stands in Ohu backbone range and is composed of some Quaternary complex basaltic or andesitic stratovolcanoes. Their bodies are being collapsed by landslides characterized by a variety of body size and structures: some have deformed into several numbers of sliding blocks. Wetlands occur in almost all large scale landslide bodies. Its climate is categorized in Japan Sea side climate pattern as heavy-snow.

We investigated the characteristics of wetlands using remote sensing images and digital elevation models and analyzed the relationship with landforms by GIS. Then we reconstructed the development process of typical wetlands located both in and out of the landslide masses by the analyses of the sediment including ^{14}C dating, tephra identification, carbon content measuring and grain size analysis.

On landslide masses 33.2 % (185 of the 599 in total) wetlands stood and area rate was 63.7 %. Most wetlands out of landslides stood on the volcanic original surface along the ridge line of Ohu mountain range or some were in the craters of Hachimantai volcano. The formers are the small bogs formed by meteoric-water (snow) cultivation in the nivation hollows. On the other hand, those on the landslide masses scattered widely. Large landslide masses frequently had ponds cultivated by ground water in the large and deep depressions along the scarps and in the small ones among pressure ridges.

In Oyachi, a wetland in a landslide, black mud and organic sand and silt (representing for bog and forest), sand and gravel (disturbance), clay and silt (pond) and peat (bog) deposited from their bottoms. Wetlands typically develop under the stable circumstance from ponds to bogs, and finally to forests. In the case of Oyachi, at BC 4000-3500 the bog changed to the pond, the former developmental stage, probably because the landslide activity formed the dam, and then it developed to the bog with stabilization of the slopes and the water discharge. On the other hand, the development process of Okuno-maki, a wetland out of landslides, were probably directly affected by climate changes. Diminishing erosion along with decreasing snow accumulation in the nivation hollow and warming of melt season climate toward the Medieval Warm Period enabled to be the bog. In contrast, landslide activities and denudation of landslide masses control the developmental stages of wetlands. Consequently, various ages and types of wetlands are presumed to coexist in humid mountains with large landslide masses.

Reference

Geertsema *et al*. (2007): Influence of landslides on biophysical diversity -A perspective from British Columbia. *Geomorphology* 89, 55-69.

Keywords: wetland, landslide, development process, Hachimantai

Japan Geoscience Union Meeting 2014
(28 April - 02 May 2014 at Pacifico YOKOHAMA, Kanagawa, Japan)

HQR23-02 Room:414 Time:May 1 09:15-09:30

Comparison between two chronological methods - in situ TCN and WRT applied to periglacial landforms in Kiso Mountains

ENDO, Ryo[1*] ; SUGAI, Toshihiko[1] ; EZURE, Yasuhide[1] ; MATSUZAKI, Hiroyuki[1] ; MATSUSHI, Yuki[2]

[1]The University of Tokyo, [2]Kyoto University

A lot of types of chronological methods have been suggested in the field of earth science. Chronological methods are classified into absolute dating methods and relative dating methods. Absolute dating methods contain isotopic age or tree-ring chronology for example, and they provide the age as numerical values. Otherwise, relative dating methods are the methods which detect the time series of the formation of geomorphology or deposition. However, they cannot fix the age without the absolute age data (Watanabe, 1990).

Two chronological methods - in situ Terrestrial Cosmogenic Nuclides (TCN) and weathering-rind thickness (WRT) -are subjected. These two methods are especially effective in high mountain areas as it is difficult to find radiocarbon samples or key tephra layers (Aoki, 1994). These two methods were compared using terminal moraines in the cirques (Aoki, 2000). However, this comparison is not made in other mountainous terrains, and it is made in Kiso Mountain Range in this study.

In order to compare these two methods, samples were taken from multiple ridges in the eastern part of Mt Kisokomagatake, and Shirabidaira. Six samples were taken from 3 ridges and 2 depressions of triple ridges, and one sample from Shirabidaira. In order to obtain the exact formation age, we selected the bedrock or the oldest boulder filling the depression and collected their surface layer of 4 cm or less in thickness

Each sample is divided in two, one for TCN and the other for WRT.

10Be exposure dating method is subjected as TCN. The samples are chemically preprocessed and at MALT (Micro Analysis Laboratory, Tandem Accelerator), University of Tokyo. The exposure age is calculated by means of the formula as follows(∗)

$T=-1/\lambda \ln\{(1-\lambda N/P)\}$ (∗)

T: Exposure Age [yr] λ:Decay constant [1/yr] N: Number of isotopes [atoms/g] P: Production rate of isotopes [atoms/(g • yr)]

Weathering-rind is a discolored part of rocks. It is formed due to oxidation or hydration. Though the age is nearly in portion to WRT, its correlation depends on the rock type, sampling point and so on. In this study, samples were cut so that the weathering-rind can be observed as clearly as possible.

In 7 samples, radioactive ages are in either late Pleistocene or Holocene. Weathering-rind was observed and detected for 5 samples. There is a positive correlation between WRT and the exposure age. The primary regression equation is as follows : WRT [mm] = 0.367 × (Exposure age [kyr]) + 1.16. The correlation coefficient is about 0.85. This suggests that in order to get the exposure age of multiple ridges, WRT is also an effective method to a certain extent. Therefore, mean weathering rate (= 0.367 mm/kyr) can be gained by calculating a primary regression line that shows the relationship of the WRT and the exposure age. This weathering rate is the same in the order of magnitude as that (= 0.283 mm/kyr) estimated from Seki and Koizumi (1992).

Keywords: In-situ Terrestrial Cosmic Nuclides, Weathering-rind Thickness, Periglacial landforms, Kiso Mountain Range

Japan Geoscience Union Meeting 2014
(28 April - 02 May 2014 at Pacifico YOKOHAMA, Kanagawa, Japan)

HQR23-03 Room:414 Time:May 1 09:30-09:45

Tree-line change since the Last Glacial from the pollen profile at the Hiroppara peat bog, central Japan

YOSHIDA, Akihiro[1*]

[1]Center for Obsidian and Lithic Studies, Meiji University

To better understand the interaction between the human and environment in past period, this study reconstructed vegetation history and climate change since the late Pleistocene at the Hirropara peat bog (1,400m a.s.l.), central Japan, from the pollen and micro-charcoal profiles at HB-1A cores. Arboreal pollen assemblages and influx of the cores indicated the vegetation history and climate change since the Last Glacial Maximum as follows; 1) ca. 30,000˜19,000 cal BP, grassland and wasteland distributed due to decreasing the tree-line; 2) ca. 19,000 cal BP, around the site was covered with a mixed forest of boreal conifers and cool-temperate deciduous, because the tree-line passed the altitude of site; 3) ca. 16,000 cal BP, Betula forest expanded; 4) ca. 12,000 cal BP, a cool temperate deciduous broad-leaved forest consisting of *Quercus* subgen. *Lepidobalanus* and *Carpinus* was distributed; 5) ca. 4,000 cal BP, temperate conifer such as Taxaceae-Cupressaseae, Tsuga, and Abies increased; 6) secondary forest of *Pinus densiflora* and *Larix kaempferi* plantation increased in ca. 500 and 100 cal BP, respectively. It is highly possible that the tree-line change impacted strongly the human activities since the Last Glacial Maximum.

Keywords: pollen analysis, vegetation history, tree-line, obsidian, prehistoric age, central Japan

Japan Geoscience Union Meeting 2014
(28 April - 02 May 2014 at Pacifico YOKOHAMA, Kanagawa, Japan)

HQR23-04 Room:414 Time:May 1 09:45-10:00

Vertical crustal movements along the Japanese coastlines inferred from the Quaternary and recent sea-level changes

OKUNO, Jun'ichi[1*] ; NAKADA, Masao[2] ; ISHII, Masayoshi[3] ; MIURA, Hideki[1]

[1]NIPR, [2]Faculty of Sciences, Kyushu University, [3]MRI

Observed relative sea-level (RSL) changes during the past 130 kyr are mainly caused by change of ocean volume, tectonic crustal movement and glacio-hydro isostatic adjustment (GIA) of the Earth in response to the redistribution of ice and water loads. Here we examine the tectonic crustal movements along the Japanese coastlines on three typical timescales (50 yr, 6 kyr and 125 kyr) based on several sea-level observations and their predictions due to GIA process and recent melting of mountain glaciers and both polar ice sheets. We use the observations of RSL based on tide gauge and Holocene RSL observations and the altitudes of marine terraces formed at the last interglacial (LIG) phase at about 125 kyr. The rates on a timescale of 50 yr are derived from tide gauge data, thermosteric sea-level changes due to thermal expansion of the oceans and predictions due to the GIA for the last deglaciation and also recent melting of the mountain glaciers and both polar ice sheets. Those for 6 kyr and 125 kyr are based on the RSL observations and the predictions by GIA modeling, considering uncertainties for temporal changes in eustatic sea-level for the mid- to late-Holocene and LIG phase. The inferred rates for 50 yr are significantly different from those for 125 kyr in most sites, particularly for sites along the coastline from eastern Hokkaido to northeastern Japan, Shikoku and south Kyushu facing the Pacific Ocean. In these regions, the rates for 125 kyr and 50 yr are positive (uplift) and negative (subsidence), respectively. Also, the observed RSL changes at 6 kyr BP are consistent with the inferred RSL changes using the rates for 125 kyr and GIA-predictions in many sites, but inconsistent with those for 50 yr in most sites except for a few sites. These results suggest that the rates on a timescale of 50 yr are not representative of the tectonic crustal movements for timescales longer than 6 kyr in most sites along the Japanese coastlines. The inferred rates on these timescales may be useful in discussing the recurrence of megathrust earthquake with its interval of about 1 kyr like the 2011 off the Pacific coast of Tohoku Earthquake.

Keywords: crustal deformation, sea-level change, Quaternary, tide gauge, thermometric sea-level

Japan Geoscience Union Meeting 2014
(28 April - 02 May 2014 at Pacifico YOKOHAMA, Kanagawa, Japan)

HQR23-05 Room:414 Time:May 1 10:00-10:15

Prehistoric human activity around the Hiroppara wetland, central Japan: a case study in and around the obsidian sources

HASHIZUME, Jun[1*] ; SHIMADA, Kazutaka[2] ; SUDA, Yoshimitsu[1] ; ONO, Akira[1]

[1]Center for Obsidian and Lithic Studies, Meiji University, [2]Meiji University Museum

The Hiroppara wetland is located about 1.5 km to the north of Wada-toge, a well known obsidian source 1,400 m above sea level. Many prehistoric sites and geological obsidian sources are scattered around this area.

Through general surveys and small-scale excavations conducted by the former Wada Board of Education between 1989 and 1991, several prehistoric sites were identified around the wetland. In 2011, the Center for Obsidian and Lithic Studies (COLS), Meiji University began a new research project on this wetland and the prehistoric sites around it. Our research goal is to reveal the relationship between human activities in and around the obsidian sources and paleoenvironmental changes during the late Late Pleistocene (Upper Palaeolithic) to the Early Holocene (Incipient to Early Jomon period). This presentation is a preliminary report of our research, with a particular focus on the results of our archaeological excavations.

On the basis of results of previous surveys and our observations of the topographical features around the wetland, we distinguished the archaeological landscape around the wetland into seven sites, which we numbered from I to VII. The COLS has set up an excavation area 1 (EA-1) at site I and excavation area 2 (EA-2) at site II.

Excavations at EA-1, the Hiroppara I site, and EA-2, the Hiroppara II site, have revealed the following:

1. EA-1

1) This site yields evidence of an Early Upper Palaeolithic lithic industry from layer 6 (under the Aira-Tn tephra).

2) The latter part of the Late Upper Palaeolithic industry, represented in layers 2b and 3, primarily features bifacial points with a blade core.

3) Incipient to Early Jomon period assemblages are found in layers 2a and 2b.

2. EA-2

1) The early part of the Early Upper Palaeolithic industry, from layers 4a and 4b, yields an ”obsidian concentration” characterized by a dense lithic concentration in a small area mainly composed of large lithics. Layers 4a and 4b contain the Aira-Tn tephra and a ground-edge stone ax made from tremolite rock.

2) The latter part of the Late Upper Palaeolithic industry, from layer 3, appears to be a knife-shaped tool industry using a developed blade technique.

3) Jomon pottery of the early part of the Initial Jomon with pebble concentrations and a pit, arrowheads, and cobble tools.

These new findings expand the scope of information about multilayered prehistoric occupations at the Hiroppara I and II sites. In addition, it has allowed us to extract a significant amount of information on prehistoric human behavior with specific regard to exploitation, transportation and consumption of obsidian during the late Late Pleistocene to the Early Holocene. However, these issues require further study.

Keywords: Obsidian sources, Central Japan, Hiroppara wetland, Hiroppara site group, Jomon period, Upper Palaeolithic

Japan Geoscience Union Meeting 2014
(28 April - 02 May 2014 at Pacifico YOKOHAMA, Kanagawa, Japan)

HQR23-06 Room:414 Time:May 1 10:15-10:30

Prehistoric obsidian exploitation in the Central Highlands obsidian sources and excavations of the Hiroppara site group

SHIMADA, Kazutaka[1*]

[1]Meiji University Museum

The Center for Obsidian and Lithic Studies, Meiji University (COLS) has conducted archaeological and palaeoenvironmental excavations at the Hiroppara wetland and prehistoric site group (sites I and II) located 1,400m of the Kirigamine mountains in Nagawa Town, Nagano Prefecture, Japan. This paper presents a review of the Central Highlands obsidian source area where Hiroppara is located and its circumstances of prehistory, and preliminary results of Hiroppara excavations. Many sites assigned to the Upper Palaeolithic and the Jomon periods have been discovered in and around the Central Highlands. The site distribution of both periods shows distinctive patterns. The Upper Palaeolithic sites concentrate in relatively high-altitudinal zone over 1,000m close to the obsidian sources, while the Jomon sites shows dense-distribution on the hill slopes in low-altitudinal zone below 1,000m. This ebb and flow pattern reflects historical changes between the Upper Palaeolithic and the Jomon periods in the technology of obsidian acquisition, the way of land-use in the source area, the group organization, and the obsidian circulation system. The emergence of an obsidian mining site in the initial Jomon is one of representatives of those changes in the relationship between humans and obsidian. Data for archaeological chronology and changes in palaeoenvironment in the Central Highlands, however, are less accumulated than other areas, resulting in insufficient explanation for changes in human activities in and around obsidian sources. Multidisciplinary research on the Hiroppara wetland and site group provide us with a useful set of data concerning archaeological and palaeoenvironmental changes that represents a limited narrow area. The excavations of Hiroppara by COLS have been conducted three times in 2011, 2012, and 2013. The excavations at sites I and II have unearthed several cultural layers ranging from the Early and Late Upper Palaeolithic to the earliest Jomon. Palaeoenvironmental data during the late MIS 3 and the early Holocene have been obtained from microfossil analyses on the peat cores from the Hiroppara wetland. Though further analyses and integration on obtained data are still required, the Hiroppra wetland and site group will allow us to make an explanatory model for relationships between prehistoric humans and palaeoenvironmemt in and around obsidian sources of the Central Highlands.

Keywords: the Upper Palaeolithic, the Jomon, the Central Highlands, obsidian sources, the Hiroppara wetland, microfossil analysis

Japan Geoscience Union Meeting 2014
(28 April - 02 May 2014 at Pacifico YOKOHAMA, Kanagawa, Japan)

HQR23-07 Room:414 Time:May 1 10:30-10:45

Discovery of fresh water diatom from aeolian sediments in the conical pit structure in the Arsanjan area, south Iran

HISADA, Ken-ichiro[1*] ; TSUNEKI, Akira[2] ; CHIBA, Takashi[1]

[1]Graduate School of Life and Envionmental Sciences, University of Tsukuba, [2]Graduate School of Humanities and Social Sciences, University of Tsukuba

It is well known that the life of ancient people was greatly influenced by various natural conditions, such as climate, topography, and geology. In particular, geology is not only important as a source of raw material for stone tools and residence construction material, but also as a provider of groundwater and mineral resources. Furthermore, soil is generated from weathered bedrocks, and soil is a key influence on vegetation. Thus, when ancient people considered the natural conditions for first settlement locations, geology would have been a crucial factor in these conditions. The present paper offers a preliminary examination of interaction of the humankind - Iranian Zagros Mountains.

One of the most important discoveries among the humankind studies was the existence of many Middle Paleolithic and Epi-Paleolithic cave sites in the Arsanjan area, south Iran. One of the caves, named A5-3 (Qar-e Tang Sikan), produced a large amount of Middle to Epi-Paleolithic stone implements. Thus the Arsanjan area is one of the most suitable areas for the study of human evolution and cultural transition from the Middle/Late Paleolithic to the Epi-Paleolithic/Neolithic periods. This means that the investigation of this area can possibly provide opportunity for the better understanding of the evolution of modern Homo sapiens and of the interface of geology-archaeology.

We accomplished the trench survey recently. The results of B3 trench survey (4 X 4 m square) at A5-3 (Qar-e Tang Sikan) are as follows (Hisada and Tsuneki, 2013). The culture layers are divided into ten layers. Layers 1 to 3 correspond with Late Paleolithic to Proto Neolithic. Six samples from layers 2 and 3 indicate approximate 36,000 BP. Layers 4 to 10 are included into Middle Paleolithic culture layers. It is noteworthy that structure 3 was discovered from layer 7. Structure 3 presents a circular from on plan, 1 m in long axis and 0.7 m in short axis. In profile, it is conical and depth is about 50 m. Cave limestone bedrock is used as a bottom wall of the conical shape, and concrete-like harden wall with pebbles and clays is used as the other one. The concrete-like wall might be built after cutting soil surface. The filling of the conical shape structure is light orange color clay, 50 cm in thickness. This clay presents a bimodal pattern, 5 phi and 11 phi in grain size analysis, and consists of quarts, muscovite and hydroxylapatite. The color of the clay is characteristics (10YR7/6, 6/6 etc) and conspicuous from other soil. Based on the color and clay-seized sediments, it can be concluded that they are aeolian sediments. This conical structure may be intended to be a water-reserved place keeping water oozed from the limestone wall (Hisada and Tsuneki, 2013). Thus, the clay might be deposited in this conical pit, 50 cm deep. This laying down at the pit seems to be prevented from erosion and transportation because the pit was full of water. Very recently, it is clarified that clay bed yields diatom, Pinnularia spp.. This genus indicates a living in fresh water (Watanabe et al., 2005). The ages for layer 7 are inferred before 51,000 BP, because layer 5 is dated as 50±2Ka and the ages for the boundary between layers 6 and 7 are 51±2Ka based on the photoluminescence measurement (Ito, in pers. comm.).

Keywords: West Asia, Paleolithic ages, Iran, water-reserved place

Japan Geoscience Union Meeting 2014
(28 April - 02 May 2014 at Pacifico YOKOHAMA, Kanagawa, Japan)

HQR23-08 Room:414 Time:May 1 11:00-11:15

Quantitative detection of event deposits in the piston core of Beppu Bay, central Kyushu, Japan

YAMADA, Keitaro[1*] ; TAKEMURA, Keiji[2] ; KUWAE, Michinobu[3] ; IKEHARA, Ken[4] ; YAMAMOTO, Masanobu[5]

[1]Division of Earth and Planetary Sciences, Graduate School of Science, Kyoto University, [2]Beppu Geothermal Research laboratory Institute for Geothermal Science, Kyoto University, [3]Center for Marine Enviromental Studies, Ehime University, [4]Institute of Geology and Geoinformation, AIST, [5]Faculty of Enviromental Earth Science, Hokkaido University

Particle transportation and deposition is repeated by various phenomena to be caused by constant cycle of water and atmosphere (non-event) and sudden phenomenon (event) such as earthquake, volcanic eruption, flood, and a stratum is formed. Therefore we can know paleo-disaster or climate change from the stratum. In addition, because the deposit caused by event (event deposits; Shiki, 1998) supplied a lot at a time, it is very important for solving formation process of the stratum. In recent years, due to analysis technique development high resolution/precision study in sedimentology is increasing (Katsuta *et al*., 2007). For this reason, details of the sedimentation mechanism and the environmental change are more clearly, but on the other hand influence of development on age models and various analyses is actualized. Therefore clear distinction of event and non-event is one of the important problems.

In Beppu Bay, the detailed age model to omit major events was constructed by Kuwae *et al*.(2012). Event deposits were identified by sighting based on facies, CT images, magnetic susceptibility and wet bulk density. This method can identify event deposits seamlessly, but it is a problem to depend on the personal experience and to have difficult to quantitative detection. Therefore we tried quantitative detection of event deposits by the statistical method and compared the detection result and the sighting result in Kuwae *et al*.(2012). The BP09-3 core (about 9.3 m long) using this study which was used in Kuwae *et al*.(2012) was obtained at the deepest place in the head of Beppu Bay.

Generally, because the source and sedimentation process of event deposits are greatly different from non-event deposits, chemical composition, particle composition or other profiles have difference. Therefore, in this study, we defined event deposits as " the sediment which has significantly different composition or physical properties ", we tied the quantitative detection of the event sediment using test for outliers. Analysis data are particle composition of very fine sand which sampled every 2 cm from the core, and we used MSD method (Wada, 2010) which is the robust and multivariate method for test. As a result, 47 events were detected. The detected event in this study and the sighing event in Kuwae *et al*.(2012) are relatively congruent, so it is thought that detective method using this study is useful for quantitative detection of event deposits. However, there are problems that 1) one is not to be able to detect minute event sediments enough and 2) the other is difficult to recognize the border of event deposit and non-event deposit. Because the event layer which was not able to detect is thin relative to sampling interval, it is thought that event layer was diluted by non-event deposits. Because there is no a meaningful difference in composition of the neighborhood of border, clear border detection using only test for outliers is difficult. It is necessary to evaluate and reflect event attenuation (vertical change) and preservation potential to solve these problems.

Keywords: Beppu Bay, Event deposits, Quantitative detection, Particle composition

Japan Geoscience Union Meeting 2014
(28 April - 02 May 2014 at Pacifico YOKOHAMA, Kanagawa, Japan)

HQR23-P01 Room:Poster Time:May 1 18:15-19:30

Paleolithic human activity and summer temperature recorded in oxygen isotope of Semisulcospira from Sakitari-do archeolo

FUJITA, Hikaru[1] ; SONE, Tomomi[1] ; KANO, Akihiro[1*] ; OKUMURA, Tomoyo[2] ; FUJITA, Masaki[3] ; YAMASAKI, Shinji[3] ; KATAGIRI, Chiaki[3]

[1]SCS Kyushu University, [2]JAMSTEC, [3]Okinawa Pref. Mus. & Art Mus.

Sakitari-do archeological site is located in Gyokusen-do cave system in Nanjyo City, Okinawa Prefecture. Since 2009, this site has yielded important remains including a 12.4-ka-old human canine (Yamasaki et al., 2012). One of the noticeable animal remains is Eriocheir crub. Large and uniform size of the forceps indicates individuals of autumn season when this crub grows into an adult. Paleolithic people may have stayed in this cave during autumn and eaten Eriocheir crub.

In order to examine this hypothesis, this study focuses on Semisulcospira shell that was excavated together with Eriocheir. Semisulcospira is a freshwater gastropod that grows spiral shell. It is known that change in the water temperature was recorded in oxygen isotope of a series of samples collected along the spiral growth axis (Kano et al., 2008). If the Paleolithic people ate the gastropod, the oxygen isotopic value of the outermost sample indicates when it was taken. We analyzed the gastropod shell from two Paleolithic layers (19 ka and 12.4 ka) of the Sakitari-do site, as well as modern Semisulcospira collected a stream 5 km east from the site in late November 2013.

Paleolithic specimens from the Sakitari-do often exhibit a sign-shaped oxygen isotopic curve. Amplitude of the change is ˜2 permil that corresponds to ˜8 degree temperature change under stable water isotopic composition. More importantly, the outermost value locates on an autumn position in many specimens, which support the hypothesis based on Eriocheir remains. In contrast, the modern Semisulcospira specimens that lack the sign-shaped pattern were young individuals that born in early summer. They recorded temperature change from summer to November. Comparing the summer oxygen values, the modern specimens are 1-1.5 permil lower than the Paleolithic specimens. If the oxygen isotopic value has been constant, it can be evaluated that the Paleolithic summer water was 4-6 degree cooler than the modern summer water.

Kano, A., Suzuki, S., Hori, M. (2008) Information recorded in oxygen isotopic profiles of freshwater gastropod Semisulcospira livertina. Ann. Bull Hiroshima Univ. Taishaku-do site Research Center. 22, 47-61.

Yamasaki, S., Fujita, M., Katagiri, C., Kunikida, D., Matsuura, S., Suwa, G., Oshiro, I. (2012) Excavations (2009?2011) at Sakitari-do cave site, Nanjo city, Okinawa prefecture ?a new Late Pleistocene paleoanthropological site- Anthropological Science (Japanese Series), 120, 121-134.

Keywords: Paleolithic age, oxygen isotope, Okinawa

Japan Geoscience Union Meeting 2014
(28 April - 02 May 2014 at Pacifico YOKOHAMA, Kanagawa, Japan)

HQR23-P02 Room:Poster Time:May 1 18:15-19:30

Environmental changes of prehistoric culture of the Ryukyu, reconstructed by sedimentological studies of Haneji-naikai.

GOTANDA, Katsuya[1*] ; YAMADA, Kazuyoshi[2] ; HARAGUCHI, Tsuyoshi[3] ; SETO, Koji[4] ; HAYASHIDA, Akira[5] ; YONENOBU, Hitoshi[6]

[1]Faculty of Policy Informatics, Chiba Univeristy of Commerce, [2]School of Human Sciences, Waseda University, [3]Department of Geosciences, Graduate School of Science, Osaka City University, [4]Research Center for Coastal Lagoon Environments, Shimane Univeristy, [5]Department of Environmental Systems Science, Doshisha University, [6]Graduate School of Education, Naruto University of Education

The beginning of agriculture in Ryukyu Islands goes back to the 10th-12th century (Takamiya and Itoh, 2011). Land clearing for farm lands accelerated soil discharge into water systems in Ryukyu Islands due to heavy rain in summer. In a closed bay, finer-grained clastics can remain sub-merged for long periods, causing adverse effects in fishery.

In this study we will report on the analytical results for sediment cores recovered from Haneji-naikai. Haneji-naikai is a bay closed by the Yagachi and Okubu Islands. Its maximum water depth is 10 m with the area is 10km^2. The Nasata river flows into the Haneji-naikai. In 2010 and 2012, 3-m and 24-m long sediment cores were recovered from the center of the bay. These were used to reconstruct the past environmental changes and human activities. The latter longer cores consisted of clay and silt with shell fragments from the surface up to the 16-m depth, while he lower part was composed of gravels. The radiocarbon dates of terrestrial plant flagments were 2880+/-40, 4210+/-30 6150+/-40 and 31680+/-220 at the depths of 7.42 m, 10.78 m, 14.84 m and 23.90 m, respectively. The cores were subsampled at an interval of 2.3 cm to analyze carbon, nitrogen and sulfur (CNS) contents, magnetic susceptibility and visible color reflectance. It is considered that the Haneji-naikai was dried up around 30000 yr BP probably due to marine regression. The changes in TOC, TN and TS were recognized from 4m in depth, showing drastic decreased from 4m in depth. This suggests that the deforestation induced by agricultural activities have begun since 1000 yr BP in this region.

Keywords: Haneji-naikai, CNS analysis, Magnetic Susceptibility, Human activity, Ryukyu Islands

Japan Geoscience Union Meeting 2014
(28 April - 02 May 2014 at Pacifico YOKOHAMA, Kanagawa, Japan)

HQR23-P03 Room:Poster Time:May 1 18:15-19:30

Paleoenvironments analysis for the past 50 ka based on TOC and TN of the sediment cores INW2012-1 and -2,Lake Inawashiro

WATANABE, Kei[1*] ; NAGAHASHI, Yoshitaka[2] ; HIROSE, Kotaro[3] ; KUMON, Fujio[4]

[1]Graduate School of Science, Shinshu University, [2]Faculty of Symbiotic Systems Science, Fukushima University, [3]Graduate School of Systems and Technology, Fukushima University, [4]Department of Environmental Sciences, Faculty of Science, Shinshu University

The total organic carbon (TOC) and total nitrogen (TN) were measured at 2 cm interval for the long sediment cores (INW2012-1, INW2012-2) taken from a central site of 90 m depth in Lake Inawashiro in Fukushima Prefecture. Depth-age relationship has been established based on six 14C data, and the bottom of the drilled core, about 28 m, is estimated as old as 48 ka. Sampleinterval is 50 to100 years.

The compilation of information on lithology, TOC and TN concentrations, C/N ratio and water contents of INW2012-1 and -2 enable us to reveal the paleoenvironments of Lake Inawashiro from the early stage to the present with high temporal resolution. Deep condition of Lake Inawashiro started 42,000 years ago and then the lake has been constantly deep until now.Temporal change of TOC concentration of Lake Inawashiro shows the quasi-periodical fluctuation similar to the marine isotope curve known as LR04, and corresponds well to that of TOC concentration of Lake Nojiri in Nagano Prefecture. Vegetation change revealed at theYanohara, moor in Fukushima Prefecture corresponds with the TOC fluctuation of TOC in the lake. Therefore, Temporal change of the TOC concentration in Lake Inawashiro seems to be controlled mainly by climate, probably temperature, and can be one of the useful paleoclimate records in the Tohoku region, Japan.

Keywords: Lake Inawashiro, TOC, TN, C/N, paleoenvironments, paleoclimate

Japan Geoscience Union Meeting 2014
(28 April - 02 May 2014 at Pacifico YOKOHAMA, Kanagawa, Japan)

HQR23-P04 Room:Poster Time:May 1 18:15-19:30

Environmental Changes based on the variations of the grain size distributions of MD179 cores, off Joetsu, Sea of Japan

TAKIZAWA, Michiru[1*] ; SUGAI, Toshihiko[2] ; MATSUMOTO, Ryo[3]

[1]Graduate School of Frontier Sciences, University of Tokyo (current PASCO Corporation), [2]Graduate School of Frontier Sciences, University of Tokyo, [3]Gas Hydrate Research Laboratory, Organization for the strategic Coordination ,Meiji University

1.Introduction

Climate change during the Quaternary period experienced a 10,000year?glacial?interglacial cycle. This cycle has an influence on land formation. In Japan, the sea level changes, in coastal areas, and the variations of precipitations, at up stream and middle stream areas, change the riverbeds. Thus the marks from climate changes are expected to be archived around the rivers. However, the long term and continuous records hardly remain on the land, due to weathering and erosion. On the other hand, owing to the more stable environment, the continuous records are expected to remain on the seafloor(Tada et al., 1999). In this study, to reconstruct the correlation between the land formations and climate changes, the variations of the grain size distributions during past 130 ka on the East marginal area of Sea of Japan was revealed.

2.Study Area and Methods

There are a lot of Paleoenvironmental records concerning the Sea of Japan. In this study, 3 cores, which were sampled during the MD179 cruise in the Umitaka Spur and the Unnamed ridge off Joetsu, are used and the variations of grain size distributions of these cores were revealed. The Umitaka Spur is located in the continental slope. Moreover the sedimentation rate off Joetsu is very rapid (Nakamura et al., 2013; Ishihama, et al., in press) and the supply from the island arc is active (Freie et al., 2009). The supply from the Tateyama Mountains has the highest amount in Japan. So the of these supply are speculated to contribute to the sediment off Joetsu.

In this study the age models of these cores are constructed by using tephrochronology, radiocarbon dating, oxygen isotope ratio of foraminifer (Ishihama et al., in press) and additional data from tephra and radiocarbon dating. The organic matters in 485 samples from the 3 cores were removed by 10%H2O2. Then the grain size distributions of these are analyzed by using SALD3000S (Laser diffraction particle size analyzer).

3.Result

The sediments off Joetsu are composed mainly of suspended load. The coarser sediments that contain little fine sand existed during the interglacial age. The variations of the median grain sizes off Joetsu have a similar pattern to the glacial cycles.

In general, it is assumed that the grain sizes of seafloor sediments become smaller as it gets farther from the land. Nevertheless, in this area, the variations in the size of the sediment supplied from land driven by the glacial cycles, have a large influence on the grain sizes of sediments in the study area, because of (1) the active supply from the rivers and (2) the narrow continental shelf.

However, in the case of the rapid rise in sea level, for example after LGM, the formation of alluviums in coastal zone is speculated to have an influence on the size of the sediment in study area.

References

Freire, A. F. M. et al. (2009) Journal of the Sedimentological Society of Japan, 68:117-128.
Ishihama, et al. (in press) Journal of Asian Earth Sciences.
Kashiwaya (1989) Journal of Geography, 98:725-730.
Nakamura, Y. et al. (2013) Journal of the Japanese Association for Petroleum Technology, 78:79-91.
Tada, R. et al. (1999) Paleoceanography, 14:236-247.

Keywords: Seafloor cores on MD179, Umitaka Spur, grain size analysis, Last Interglacial Age

Japan Geoscience Union Meeting 2014
(28 April - 02 May 2014 at Pacifico YOKOHAMA, Kanagawa, Japan)

HQR23-P05 Room:Poster Time:May 1 18:15-19:30

Developing process of the erosional landform and the developmental mechanism of slope failure in Shirasu area

IGARASHI, Ryusuke[1*] ; SUGAI, Toshihiko[1] ; IMURA, Ryusuke[2]

[1]Graduate School of Frontier Sciences, The University of Tokyo, [2]Graduate School of Science and Engineering, Kagoshima University

Pyroclastic flow deposits are distributed throughout Japan, dotting the country's landscape. In Kagoshima Prefecture, in particular, the cliff overlain by " Shirasu " deposits has undergone repeated slope failures during a period of several decades, which is an extremely short timeframe for such activity (Tsukamoto, 1993). Ito pyroclastic flow deposits are part of a huge pyroclastic flow that occurred approximately 29,000 years ago (Machida and Arai, 2003); these deposits span an area of approximately 90 km from Aira Caldera, which was the source of Shirasu deposits (Yokoyama, 2000). Although the stratigraphic relationship between the erosional landform and the Shirasu deposits of volcanic ash and gravel layers is important, little research has been conducted on this topic. Among the current and the former incised valleys engraving Shirasu plateau, an ancient fossil valley has been identified; however, the factors contributing to the ceasing of its growth remain unknown (Yokoyama, 2000). This study examined the relationship between the developmental mechanism of slope failure and the long-term development process of the erosional landform in the Shirasu distribution area to clarify the region's geomorphological evolution. In this presentation, we focus on the Satsuma Peninsula, which includes a part of the Shirasu plateau in northern area. In the peninsula, ancient shallowly incised valleys remain on the plateau, while the current deeply incised valleys have been dissecting the plateau. A landform classification map was made by interpretation of color aerial photograph in 1975 and by analysis of samples obtained from the plateau cliff that developed through erosion-denudation processes such as slope failure and erosion of Shirasu by running water; strength measurements were performed with a Schmidt hammer.

The valley width decreases rapidly from the main stream valley to the tributary valley and in the current incised valley, from downstream to upstream corresponding to the high-density distribution of failures in this site. The failure substance can be easily transported downstream because the " Shirasu " rapidly changes fine sand and silt after the failure. The failure at the valley wall slope has likely been continued by the valley width expansion of the current incised valley. Incision can be estimated from the beginning edge of the downstream side of the original Shirasu located in the place that is near to the East China Sea of the Satsuma Peninsula west, and has progressed in the upstream side gradually. This is probably because that the attitude of the Shirasu deposition surface is low, and the incised valley bottom is close to the base level of erosion, which has been almost stable during the last 7ka.

It is considered that lateral erosion of current incised valleys has continued during the time whereby failure has occurred in the vicinity of the lower end of the incised valley wall. From a long-term perspective, it can be said that the failure potential is high for current incised valleys dominated by width enlargement processes.

Keywords: Shirasu, Slope Failure, Records, Geomorphological Development, Southern Kyushu

Japan Geoscience Union Meeting 2014
(28 April - 02 May 2014 at Pacifico YOKOHAMA, Kanagawa, Japan)

HQR23-P06 Room:Poster Time:May 1 18:15-19:30

Total organic carbon fluctuation from the lake sediments in central Japan during the past 200 ka

KIGOSHI, Tomohiko[1*] ; KUMON, Fujio[2] ; TAWARA, Takaharu[3]

[1]Interdisciplinary Graduate School of Science and Technology, Shinshu University, [2]Faculty of Science, Shinshu University, [3]Wakayama Prefectural Government

Lake sediment is a useful recorder of paleoclimate in the mid-latitude regions. However, the life span of a lake is shorter than that of the marine sediments or polar ice sheets in the most cases. Furthermore, a general condition of a lake may be disturbed by an accidental event. Then, we try to combine a climate proxy of total organic carbon (TOC) records from several lake sediments central Japan, and have compiled an average TOC in the past 200 ka which may correspond to the regional climate change.

Used data include Lake Biwa (BIW07-5, 6 core: 0-50 ka, BIW08-B core: 0-200 ka), Lake Nojiri (NJ88+NJ95 core: 0-72 ka), Takano Formation (TKN-2004: 38-160 ka). The time resolutions in those data are between 20-100 years. TOC data of the six sediment cores were normalized as dividing a data by standard deviation. Their fluctuation curves of the normalized TOC were matched by the method of Lisiecki and Lisiecki (2002). Then the matched normalized data were interpolated at 100-year interval by polynomial interpolation method.

The compiled TOC fluctuation in central Japan is well correspond to the D18O curves of the marine sediments (LR04) and the Greenland ice core (NGRIP) respectively both in the orbital and millennial time scales. In late MIS (marine isotope stage) 7 and MIS 1, the compiled TOC values are generally high. In MIS 6, 4 and 2, the TOC values are generally low, and their temporal fluctuation is not so large. The compiled TOC in MIS 5 is characterized by large fluctuation in orbital scale. In contrast, the compiled TOC in MIS 3 shows many peaks which correspond with the repetition of cold stadials and warm interstadials, known as D-O cycle.

This result suggests that the normalized TOC may be a useful proxy of paleoclimate for the past 200 ka, which can be correlated with other sediments or climate records by the many marker tephra beds in central Japan.

Keywords: Total organic carbon, past 200 ka, central Japan

Japan Geoscience Union Meeting 2014
(28 April - 02 May 2014 at Pacifico YOKOHAMA, Kanagawa, Japan)

HQR23-P07 Room:Poster Time:May 1 18:15-19:30

Morphosis of the Oyster shell bed and Diatom assemblage in Tokyo bay

NOGUCHI, Marie[1*] ; ENDO, Kunihiko[2] ; KASHIMA, Kaoru[1]

[1]Kyushu University, [2]Nihon University

Recently, oyster shell beds and reefs have been found in various places in Tokyo bay. Six shell bed types can be recognized on the basis of their lithology (YOKOYAMA et.al., 2004). Topographic and paleogeographic changes closely related to the Holocene Jomon Transgression, have been investigated by reconstructing the migration of oyster shell beds, which are good markers of paleoshorelines, throughout the wide inner bay during the rising stage of sea-level. However, ecology of benthos and diatom assemblages is not clear about oyster shell bed types(Endo et.al.,2013). This study describes taphonomic processes of the oyster reefs well exposed in Tokyo bay, Sanbanze. The oyster reefs of Sanbanze have grown up during about 5 years. The growth of oyster reefs was rapid but nowadays it is reduced due to change of oyster environment as consequences of Torrential rain and Typhoon. We started to do research 5 years ago in Sanbanze. We are making a report on oyster shell bed types and ecology of diatom assemblage in this area.

Keywords: Tokyo bay, oyster shell bed, diatom

Japan Geoscience Union Meeting 2014
(28 April - 02 May 2014 at Pacifico YOKOHAMA, Kanagawa, Japan)

HQR23-P08 Room:Poster Time:May 1 18:15-19:30

A possibility of influence of deposition in dam-lake to deep marine environments around the Japanese Islands

SHIRAI, Masaaki[1*] ; OMURA, Akiko[2] ; HAYASHIZAKI, Ryo[1] ; UTSUGAWA, Takako[1]

[1]Tokyo Metropolitan University, [2]University of Tokyo

It is well known that dams construction on river caused decrease in sediment supply and serious coastal erosion. While, taking into account similarity of grain size, deposition in dam-lake may also cause decrease in deep marine hemi-pelagic depositional rate. Mass accumulation rate (MAR) during ca. 100 years around the Japanese Islands were estimated with Pb-210 radioactivity concentration.

Core samples were obtained with multiple corer (core length <60 cm) on the R/V Tansei-maru from off the Enshu, Kumano and Niigata regions in the central Japan. Subsamples sliced with 1 or 2 cm thick were dried, crushed and measured by an ORTEC High Purity Ge gamma spectrometer housed in the Department of Geography, Tokyo Metropolitan University with a 48 hour counting. MAR was estimated from Pb-210 radioactivity concentration and dry bulk density of other subsamples measured with the Shimadzu Accupyc 130 gas pycnometer housed in Atmosphere and Ocean Research Institute, the University of Tokyo.

In the off Enshu area, MAR of two core samples obtained from small basin on the outer ridge-Nankai Trough slope (ca. 2500 m water depth) were estimated for this study. Although one core did not show change in MAR, the other core showed decrease in MAR around 1930-1940. In the off Kumano area, MAR of two core samples obtained from bottom of the Kumano Trough (ca. 2100 m water depth) were estimated. Both core showed decrease in MAR around 1940-1960. In the off Niigata area, MAR of a core sample obtained from bottom of submarine canyon on the SE slope to the Mogami Trough (ca. 400 m water depth) was estimated. The core showed decrease in MAR around 1960-1970.

Although estimated ages of decrease in MAR have considerable error, it is remarkable that decrease in MAR was estimated from all the studied areas. Contemporaneity of decrease in MAR and dams construction and similarity of the grain size between hemipelagic sediment and dam sediment suggest that deposition in dam-lake may influence sediment supply to deep marine hemipelagic environment.

Keywords: dam, hemipelagi deposits, mass accumulation rate

Japan Geoscience Union Meeting 2014
(28 April - 02 May 2014 at Pacifico YOKOHAMA, Kanagawa, Japan)

HQR24-01 Room:313 Time:May 1 14:15-14:30

Seismic history of the last 5500 years reconstructed from the topographic development of the Furen-ko barrier system

NANAYAMA, Futoshi[1*] ; SHIGENO, Kiyoyuki[2] ; HASEGAWA, Takeshi[3] ; WATANABE, Kazuaki[1] ; ISHIWATA, Kazuto[5] ; IKEDA, Yasuo[4] ; UCHIDA, Yasuhito[6]

[1]Geological Survey of Japan, AIST, [2]Meiji Consultants Ltd., [3]Ibaraki University, [4]Kushiro Branch, Hokkaido University of Education, [5]Betsukai Museum, [6]Geological Survey of Hokkaido, HRO

There are some active barrier (island) systems in eastern Hokkaido. Since 2011, we have been investigating the Hashirikotan barrier spits in the northern part of Furenko barrier system facing the Sea of Okhotsk/ Nemuro Strait because five branches of spits (BR1-BR5) are clearly observed. According to GPS topographic survey, GPR exploration, hand drilling survey, grain size analysis, AMS 14C dating and tephra chronology, we already got some important geomorphological results as bellows.

As a first point, the Furenko barrier system has been established since 5.5 ka, and there were two lagoon-expanding stages at 5.2 and 4.0 ka estimated by volcanic ashes, Ma-e and Ma-d from Mashu volcano. As a second point, the youngest BR5 has occurred after the 17th century and BR4 caused by the last seismic up rifting in the 17th century because it was covered with two historical volcanic ash layers, Ta-a and Ko-c2 from Tarumai and Komagatake volcanoes. BR2 caused by the seismic up rifting in the 9th century because it was covered with B-Tm from Baitoushan volcano in AD 929. BR3 and BR1 were undated clearly, but we are able to assume that BR3 rifted in the 12-13th century and BR2 rifted at 4.0 ka. These two BRs were covered with large eolian dune layers just after emerging each BR.

Since 2003, it was clearly that the great earthquakes (Mw8.5˜) have been occurred at an interval of 500 years along the southern Kuril subduction zone. Especially coastal area raised almost 1 or 2m just after the great earthquakes due to the post-seismic displacements. But conversely land subsidence has been continuing at a rate 8.5mm/year since the 17th century until now. We express that geomorphological evolution of the Furenko barrier system has been controlled by the seismotectonics along the southern Kuril subduction zone.

This work was supported by JSPS KAKENHI Grant Number 23540539.

Keywords: Lake Furen-ko, barrier spit, topographic development, Nemuro Strait, sea-level change, seismic history

Japan Geoscience Union Meeting 2014
(28 April - 02 May 2014 at Pacifico YOKOHAMA, Kanagawa, Japan)

HQR24-02 Room:313 Time:May 1 14:30-14:45

Late Quaternary tephras and basin fill sediments under Ukinuman, Murayama city in the north part of Yamagata basin, Nort

SUZUKI, Takehiko[1*] ; KASAHARA, Amao[1] ; YAGI, Hiroshi[2] ; IMAIZUMI, Toshifumi[3] ; YOSHIDA, Akihiro[4]

[1]Tokyo Metropolitan University, [2]Yamagata University, [3]Tohoku University, [4]Meiji University

Yamagata basin, one of the tectonic basins aligning along the west part of Ou Backbone Range, Northeast Japan Arc, exists between hills and mountains. Active faults concentrate along the west margin of the Yamagata basin. In the north part of the basin where more active faults were recognized than the south part of the basin, not only marginal faults bordering hills and mountains but also isolated faults in central part of the basin were recognized by Yagi et al. (2001). In order to establish the history of fault activity and landform development in the basin, chronological and sedimentological studies on the basin fill sediments beneath the ground surface is necessary. In this study, an all-core boring (MR-13-1) with a depth of 101.00 m was carried out at Ukinuma (81.40 m a.s.l.), Murayama City, Yamagata Prefecture in October to November, 2013. Preliminary results are as follows.

Stratigraphy

Fine sediments dominate less than 64.60 m in depth, composing of silt to organic silt except three sand and gravel layers with thickness of $<$1.65 m. Sediments between 64.60 and 101.00 m in depth consist of an alternation of silt, sands, and gravels. Depths of tephras already identified are 3.34-3.47 m, 35.34 m, and 75.86-76.24 m.

Tephra

A gray to white ash-fall deposit with a depth of 3.34-3.47 m contains hornblende (n_2=1.670-1.673) and orthopyroxene (gamma=1.709-1.714). Refractive indices of glass shards is n=1.499-1.500. These characteristic properties show that this ash is correlative to Hijiori-Obanazawa Tephra (Hj-O, 11-12 ka; Machida & Arai 2003).

A thin white vitric tephra (4 mm in thickness) at 35.34 m in depth characterized by bubble-wall to stripe types of glass shards (n=1.496-1.500; SiO_2: 78.44 wt.%, Al_2O_3: 12.05 wt.%, CaO: 1.08 wt.%, FeO: 1.12 wt.%, K_2O: 3.21 wt.%, Na_2O: 3.40 wt.%) (containing a small mount of quartz) is correlated to Kikai-Tozurahara Tephra (K-Tz, 95 ka; Machida & Arai 2003).

An ash-fall deposit with a depth of 74.86-75.17 m was detected. This tephra contains orthopyroxene (gamma=1.724-1.730), quartz, and sponge to fiber types of glass shards (n=1.498-1.502), and is possibly originated from volcano in the vicinity.

In presentation, chemical compositions of glass shards in tephras mentioned above and ages by carbon 14 dating will be reported.

Keywords: Yamagata basin, Underground geology, Tephra, Late Quaternary, Boring core

Japan Geoscience Union Meeting 2014
(28 April - 02 May 2014 at Pacifico YOKOHAMA, Kanagawa, Japan)

HQR24-03 Room:313 Time:May 1 14:45-15:00

Late Quaternary tephras and basin fill sediments under northeast part of Yonezawa basin, Northeast Japan

KASAHARA, Amao[1*] ; SUZUKI, Takehiko[2] ; KITAMURA, Akihisa[2] ; KATO, Shinji[4]

[1]Graduate student, Tokyo Metropolitan University, [2]Tokyo Metropolitan University, [3]Shizuoka University, [4]NEXCO East

We report tephras distributed under the northeastern part of the Yonezawa Basin, in the southern part of the Northeast Japan Arc.The Yonezawa Basin is the one of the inland tectonic basins along the backarc side of the Ou Backbone Mountains. There is a wetland which delimited by the small fans in the southern and western margins and by the mountains in the northern and eastern margins around the Lake Hakuryu in the northeastern part of the Yonezawa Basin, which called Oyachi (Yoshida, 1955). We observed two cores, B7-1-2 and B7-1-14, both drilled at Fukanuma , Takahata Town at the southern margin of the wetland. Both core obtained at distance of about 200 m, and about 90 m long.

Both B7-1-2 and B7-1-14 cores have well developed peat deposit. Silt and peat deposit contains about 1-20 cm thick thin sand layers repeatedly. Well sorted granule thin layers and pebble thin layers which contains max 4 cm in diameter are observed at the middle and lower part of the sediments, but poorly lateral continuities. In addition, both cores are not drilled through the Quaternary deposit under the Yonezawa Basin.

In the B7-1-2 core, Numazawa-Kanayama tephra (Nm-KN; 62-65 ka: Suzuki and Soda, 1994) is in 31.59-31.655 m depth, Aso-4 tephra (Aso-4; *ca.* 87 ka: Aoki et al. 2008) is in 44.16-44.23 m depth as a blocky form, and two-pyroxene crystalline ash (B7-1-2L) is in 79.14-79.16 m depth, are observed.

In the B7-1-14 core, Nm-KN is in 27.33-27.34 m depth, two-pyroxene crystalline ash (B7-1-14E) is in 75.47-75.485 m depth, and glassy ash contains babble-wall type of glass shards (B7-1-14G) is in 83.97-84.07 m depth, are observed. Furthermore, a beige ash patch observed in 39.385-39.39 m depth would correlate to Ontake-Nagawa tephra (On-NG; 85.1 ka: Nagahashi et al., 2007).

We could not observed a AT bed in the both cores, however, we detected babble-wall type of glass shards from correlate to AT in the gray silt bed in 21.62-21.63 m depth between a peaty silt bed in the B7-1-2B core (not sequential sampled). In addition, B7-1-2L and B7-1-14E are correlate to each other because of its height above sea level and petrographic features.

It is concluded that height above sea level of Nm-KN and B7-1-2L/B7-1-14E indicate sediments in the both cores deposited almost horizontal form. Deposition rate simply calculated and estimated from age and depth of Aso-4 in the B7-1-2 core is about 0.5 m/kyr, which shows slightly larger value than 0.22-0.35 m/kyr (Suzuki et al., 2013) based on tephrochronology obtained in the Aizu Basin to the south of the Yonezawa Basin recently. This deposition rate is generally reconciling rate if it is assumed that deposition rate of the Yonezawa Basin floor depends on the activity of the Yonezawa Basin Western Margin Fault which slip rate is 0.4-0.5 m/kyr.

Keywords: Yonezawa basin, Underground geology, tephra, Late Quaternary, Boring core

Japan Geoscience Union Meeting 2014
(28 April - 02 May 2014 at Pacifico YOKOHAMA, Kanagawa, Japan)

HQR24-04 Room:313 Time:May 1 15:00-15:15

The age of the Inubou Group in the Choshi district, Chiba Prefecture, Japan, based on tephra correlation

TAMURA, Itoko[1*] ; YAMAZAKI, Haruo[1] ; MIZUNO, Kiyohide[2]

[1]Dep. Geography, Tokyo Metropolitan Univ., [2]AIST, GSJ

Numerous widespread tephra layers of late Pleistocene and Holocene age have been known since the early 1970s and greatly contribute to paleoenvironmental reconstruction in the Japan islands and adjacent seas. This study has identified a new widespread tephra using the trace element composition of volcanic glass determined by ICP-AES analysis and the stratigraphy.

In1 tephra is found at lowest part of the Naarai Formation in the Inubou Group, Choshi district, Chiba Prefecture, accumulated during Pliocene to Early Pleistocene. Ikg1 tephra is found in upper Ikego Formation in the Miura Group, Kanagawa Prefecture, accumulated during Pliocene. B25 tephra is found at Horinouchi Formation in the Kakegawa Group, Shizuoka Prefecture, accumulated during Pliocene to Early Pleistocene.

In1, Ikg1 and B25 tephras are white and fine grain. The thickness of these deposits range from cm(Ikg1) to 22cm(B25). These tephras mainly consist of glass shards of bubble-wall type. The glass shards of these are poor in K_2O ($<$2 %) and La ($<$15 ppm) and rich in Y($>$40 ppm), which give low La/Y (about 0.3) and high Ba/La (about 30). These characteristic chemical compositions of glass in tephras erupted from the Tohoku area (Mizuno, 2001).

The age of In1 tephra is estimated at about older than 3 Ma based tephrochronology in Choshi area (Tamura et al.,2007). The age of Ikg1 is estimated at about older 3.1Ma based biostratigraphy and magnetostratigraphy (Utsunomiya et al, 2012 and Utsunomiya, 2013). The B25 tephra is estimated at about older 2.9Ma based on tephrochronology (Tomita and Kurokawa, 1999 and Kurokawa and Tomita, 2000).

This tephra correlation indicates that the age at lowest part of the Inubou Group is estimated older than 3.1 Ma.

Keywords: Plio-Pleistocene, Tephra correlation, Inubou Group, Depositional age, Marker Tephra

Japan Geoscience Union Meeting 2014
(28 April - 02 May 2014 at Pacifico YOKOHAMA, Kanagawa, Japan)

HQR24-05 Room:313 Time:May 1 15:15-15:30

Underground electrical resistivity and soil water content on the surface around former river channel of Tone River

NAKANO, Takayuki[1*] ; KOARAI, Mamoru[1]

[1]GSI of Japan

Land liquefaction occurred in a land reclaimed water area such as former river channel induced by the 2011 off the Pacific coast of Tohoku Earthquake. The land liquefaction was a biased distribution even in former river channel. We assumed that groundwater level and/or shape of former river bed (depth of former river) have a significant influence though the factor of this phenomenon is various. Therefore, we conducted electrical prospecting (2-D electrical resistivity prospecting) on former river channel of Tone River around Kozaki Town, Chiba Prefecture, to estimate a distribution of groundwater level and/or shape of former river bed from underground distribution of electrical resistivity. In addition, we considered a relationship between underground distribution of electrical resistivity and soil water content on the surface by measuring soil water content on the surface along the electrical prospecting line. In this survey area, there are data of layer profiles (trench survey profiles) and boring core stratigraphes by the National Institute of Advanced Industrial Science and Technology (AIST) and the Chiba Prefectural Environmental Research Center (CERC) (Mizuno et al., 2013; Miyaji et al., 2013).

Electrical prospecting was performed by the pole-pole array in 280m length, electrode intervals of 1m and until 15m deep. Measurement of soil water content was performed by volumetric soil water content sensor (by the method of responding to changes in the apparent dielectric constant) and weight water content sensor (by alternating current two electrode method). These measurements of soil water content were performed intervals of 10m on the electrical prospecting line, and three times in each measurement points and each sensors. We used these average values.

Electrical resistivity profile indicated clearly difference between reclaimed soil in the former river channel with relative high electrical resistivity (more than 20-30 ohm-m) zone and a ground out of former river channel with relative low electrical resistivity (less than 20-30 ohm-m) zone. The position where the boundary of these zones reaches near the surface was correspondent with a boundary of land liquefaction (sand volcano) area by the 2011 off the Pacific coast of Tohoku Earthquake. It is possible that the underground distribution of electrical resistivity is affected by a soil property more than soil water content. Distribution of groundwater level was unclear though it was estimated to be 1.5m in depth from that usual electrical resistivity of saturated sand is 80-100 ohm-m (The Japanese Geotechnical Society, 2003). As a groundwater level near this survey area by the boring survey (Mizuno et al., 2013) was 0.7m in depth, it is possible that electrical resistivity near the groundwater level is higher than 80-100 ohm-m.

As a result of compared the soil water content on the surface with the electrical resistivity beneath the surface, there was a correlation that weight water content is low in a high electrical resistivity. However, there was not a correlation between volumetric soil water content and electrical resistivity. Also, it was not able to confirm the relationship between soil water content and groundwater level because of the groundwater level was not able to estimate from the distribution of electrical resistivity.

This result indicated a detection of the shape of former river bed and a correlation between the soil water content on the surface and the electrical resistivity beneath the surface. We would like to find out an index with land liquefaction in former river channel due to perform a ground penetrating radar survey in the same field.

Keywords: former river channel of Tone River, Kozaki Town, electrical prospecting, distribution of electrical resistivity, soil water content

Japan Geoscience Union Meeting 2014
(28 April - 02 May 2014 at Pacifico YOKOHAMA, Kanagawa, Japan)

HQR24-06 Room:313 Time:May 1 16:15-16:30

Geological survey for liquefaction-fluidization phenomena: damage and survey by PD-CPT

KAMEYAMA, Shun[1*] ; KAZAOKA, Osamu[1] ; SHIGENO, Kiyoyuki[2] ; SUZUKI, Yoshiyuki[2] ; FUKUMA, Tetsu[3] ; MORISAKI, Masaaki[1] ; YOSHIDA, Takeshi[1] ; KAGAWA, Atsushi[1] ; SAKAI, Yutaka[1] ; KIMURA, Michio[1] ; OGURA, Takayuki[1]

[1]Research Institute of Environmental Geology, Chiba, [2]Meiji Consultant Co., Ltd, [3]ACE Sisui Kogyo Co.,Ltd

2011 off the Pacific coast of Tohoku Earthquake and the aftershock brought heavy damage in the various places in East Japan. At a public high school in Mihama ward, Chiba city, remarkable liquefaction - fluidization phenomena occurred in a part of the bicycle place. Sand spouted out the surface of the ground and the ground level sank partially 30 - 40cm height.

In the part that the level of the ground surface changed, we investigated portable dynamic cone penetration test every 1.5 - 2m densely horizontally.

As a result of investigation by portable dynamic cone penetration test, the situation of the subsidence of the ground surface and relations with geological structure became clear.

We can grasp the hardness of the layer in exact depth by portable dynamic cone penetration test, but it is only hardness. We cannot confirm a particle size and the sedimentation structure of the stratum by portable dynamic cone penetration test.

It becomes the high investigation into precision more by comparing geological survey with portable dynamic cone penetration test. Because stratum sample may expand and contract when we pull up stratum in geological survey, this is because it can correct depth by comparing it with the result of portable dynamic cone penetration test.

Keywords: Liquefaction-Fluidization, The 2011 off the Pacific coast of Tohoku Earthquake, Chiba city, Man-made Strata, Geological survey, Portable Dynamic Cone Penetration Test

Japan Geoscience Union Meeting 2014
(28 April - 02 May 2014 at Pacifico YOKOHAMA, Kanagawa, Japan)

HQR24-07 Room:313 Time:May 1 16:30-16:45

Geological survey for liquefaction-fluidization phenomena: New method of geological survey by new ACE liner

SHIGENO, Kiyoyuki[1*] ; SUZUKI, Yoshiyuki[1] ; FUKUMA, Tetsu[2] ; KAZAOKA, Osamu[3] ; KAMEYAMA, Shun[3] ; MORISAKI, Masaaki[3] ; YOSHIDA, Takeshi[3] ; KAGAWA, Atsushi[3] ; SAKAI, Yutaka[3] ; KIMURA, Michio[3] ; OGURA, Takayuki[3]

[1]Meiji Consultant Co., Ltd, [2]ACE Sisui Kogyo Co.,Ltd, [3]Research Institute of Environmental Geology, Chiba

Thinking about origin by collecting the stratum in the alluvial lowland that is the main living surface of us is very important. Liquidizing-fluidizing phenomenon occurs mainly in man-made strata distribution area in Chiba Prefecture, surface subsidence local area of more than 50cm occurs in the Tohoku-Pacific Ocean Earthquake in 2011. As one of the causes liquidizing-fluidizing, greater potential impact of geological structure of the deep alluvium and man-made strata of shallow has become high (Kazaoka et al., 2012). This improved ACE liner ((Japanese patent application No.3669495) in order to clarify the mechanism and certification of liquidizing-fluidizing point in the layer , and man-made strata deeper and man-made strata that has been soil filled with the dredged sand in shallow underground in this study because it was able to taken the state of the oriented and non-disturbing, observe various structures of the layer, and reports a research method.

Survey results, as well Geoslicer (Nakata et al., 1997) and, without having to be re-liquefaction during drilling the sand hard cohesive soil soft to subsurface 8m, new ACE liner became recoverable in undisturbed sample. Survey results, as well Geoslicer (Nakata et al., 1997) and, without having to be re-liquefaction during drilling the sand hard cohesive soil soft to subsurface 8m, new ACE liner became recoverable in undisturbed sample. On the other hand, there is the core shrinks during drilling and fall of the sand layer at the bottom device to prevent falling of the sample does not operate, loose sand layer is dehydrated deformation during press-fitting part. I believe you require improved by updating technology and experience accumulated in the future.

Keywords: Liquefaction-Fluidization, The 2011 off the Pacific coast of Tohoku, Chiba city, Man-made Strata, Geological survey, ACE liner

Japan Geoscience Union Meeting 2014
(28 April - 02 May 2014 at Pacifico YOKOHAMA, Kanagawa, Japan)

HQR24-08 Room:313 Time:May 1 16:45-17:00

Geological survey for liquefaction-fluidization phenomena: Geological cross section of man-made strata and mechanism

KAZAOKA, Osamu[1*] ; KAMEYAMA, Shun[1] ; MORISAKI, Masaaki[1] ; SHIGENO, Kiyoyuki[2] ; SUZUKI, Yoshiyuki[2] ; KAGAWA, Atsushi[1] ; YOSHIDA, Takeshi[1] ; KIMURA, Mitsuo[1] ; SAKAI, Yutaka[1] ; OGURA, Takayuki[1]

[1]Research Institute of Environmental Geology, Chiba, [2]Meiji Consultante Co., Ltd

Terrible liquefaction-fluidization phenomena happened partially with subsidence, 10-50 m width and 20-100 m length, less than 1m height in northern Tokyo bay reclaimed land on the 3011 off the Pacific coast of Tohoku Earthquake. Large amount of sand and groundwater spouted out in the terrible subsided parts. But there are little subsidence and jetted sand outside of the terrible subsided part (RIEGC, 2011).

Continuous box core samples from surface to 5-7 m depth could be taken at the each 3-5 m length from little subsided part to terrible subsided part in Chiba city. Detailed litho-stratigraphy and liquefaction-fluidization parts were studied on the continuous box core samples and large relief peel on the core samples. These data indicate as follows.

1. The thickness of man-made strata is 5-7 m. The thickness increases to subsided part.

2. Man-made strata is composed of Dumped Association, Upper Filling Association and Lower Filling Association. Two Filling Associations were made by sand pump method from bottom sediments in the Tokyo bay. Upper Filling Association consists of lowermost, lower, upper and uppermost bandle.

3. Litho-facies of each man-made strata is as follows.

Dumped Association: This association is composed of 1.5-2.2 m thick sandy silt to silty fine sand layers with siltstone brocks and rock gravels. Sand dike with yellowish brown sand and gray sand distribute rarely

Uppermost Bandle of Upper Filling Association: this bandle is composed of 0.2-0.8 m thick yellowish brown laminated fine-medium sand layers. Upper part of this bandle lost primary sedimentary structures and loose. The base of this bandle consists of laminated coarse-very coarse sandy shell fragment layers.

Upper Bandle of Upper Filling Association: This bandle is composed of 0.4-1.8 m thick gray medium sand layers. Shell fragment layers often interbeded in this sand layers. The sand layers lost primary sedimentary structures and very loose.

Lower Bandle of Upper Filling Association: This bandle is composed of 0-1.8 m thick gray silt layers. Lower part of the silt layer sometimes show slump structures.

Lowermost Bandle of Upper Filling Association: This bandle is composed of 0.7-1.8 m thick gray shelly medium sand layers. Shell fragment layers often interbedded in the shelly sand laters. Top of this bandle consists of loose medium sand without primary sedimentary structures. The medium sand injected in the upper silt layers.

Lower Filling Association: This association is composed of 0.5-3.5 m thick yellowish gray laminated relatively dence matrix free good sorted fine-medium sand layers. This association may deposited removed filling sand by wave action on shoreface.

4. Liquefaction-fluidization parts are in man-made strata, top of the lowermost bandle, upper bandle and uppermost bandle of the Upper Filling Association.

5. Subsidence part distribute in thin part of lower bandle and thick part of upper bandle of the Upper Filling Association. The aboves show that subsidence concern with the liquefaction-fluidization part of the upper bandle of Upper Filling Association.

Keywords: Liquefaction-Fluidization, The 2011 off the Pacific coast of Tohoku Earthquake, Tokyo bay reclaimed land, Man-made Strata, Geological survey by continuous box core, Mechanism

Japan Geoscience Union Meeting 2014
(28 April - 02 May 2014 at Pacifico YOKOHAMA, Kanagawa, Japan)

HQR24-P01 Room:Poster Time:May 1 18:15-19:30

Revised stratigraphy of the upper Quaternary in Yufutsu Plain and Shikotsu Pyroclastic flow upland, central Hokkaido

KOMATSUBARA, Junko[1*] ; KOMATSUBARA, Taku[1] ; TANABE, Susumu[1] ; HONGO, Misao[2] ; UEKI, Takeyuki[3] ; NAKASHIMA, Rei[1] ; ISHIHARA, Takeshi[1]

[1]AIST, [2]Alps Technical Research laboratory Co. Ltd., [3]Chiba Institute of Science

Upper Quaternary stratigraphy in Yufutsu Plain and Shikotsu Pyroclastic Flow Upland, southern Hokkaido is revised based on review of previous studies and three boring core analysis, which includes sedimentary facies, pollen, diatom, shell assemblages and paleomagnetic analysis.

Active folds have been assumed beneath Yufutsu Plain and Shikotsu Pyroclastic Flow Upland because they are located south-west of the active faults along the eastern margin of the Ishikari Lowland, but neither displacement rare nor continuity of the folds has been specified. The detailed stratigraphy of the Shikotsu Pyroclastic Flow Upland is unknown due to lack of boring surveys for stratigraphic research. To establish subsurface stratigraphy in Yufutsu Plain and Shikotsu Pyroclastic Flow Upland to specify the fold activity, we take three boring cores (BT1, YF1 and CT1). BT1 and YF1 are 4.25 km apart along the coastline, the former is on the Yufutsu anticline axis and the latter is on the west side of the axis. CT1 is in the center of the upland.

In BT1 core we found two characteristic units: First unit is estimated as MIS11 for its abundant *Fagus* pollen, and second unit is estimated as MIS7 for its marine strata which yields cool temperature pollen assemblages. CT1 core is composed MIS7 marine deposits, MIS6 conglomerate, and MIS5 marine deposits. Two unidentified tephra layers found in MIS7 marine deposits in CT1 core may be traceable upto the north of the Shikotsu Pyroclastic Flow Upland.

Keywords: Ishikari lowland, Yufutsu plain, boring survey, Quaternary stratigraphy, Pleistocene

Japan Geoscience Union Meeting 2014
(28 April - 02 May 2014 at Pacifico YOKOHAMA, Kanagawa, Japan)

HQR24-P02 Room:Poster Time:May 1 18:15-19:30

Geological overview of the Mobara District: Quadrangle Series, 1:50000, GSJ/AIST

NANAYAMA, Futoshi[1*] ; NAKAZATO, Hiroomi[2] ; OOI, Shinzou[3] ; NAKASHIMA, Rei[1]

[1]Geological Survey of Japan, AIST, [2]NARO, [3]GSI

Between 2010 and 2014, geological and geomorphological research for the Quadrangle Series, 1:50000 of the Mobara district was performed by Geological Survey of Japan, AIST. In this poster presentation, we presents the proto version of geological map due to have opinions from everyone.

The Mobara district is located in the northeastern part of Boso Peninsula of the Kanto region. The district partly includes the Pacific Ocean in the eastern district. The land area is geomorphological divided into hills, diluvia uplands, river terraces, alluvial lowlands and Kujyukuri strand plane. The hills and uplands occupy the southwestern to western and northwestern part of the district, respectively. The hills constitute parts of the Kazusa Hills and the uplands are parts of the Shimosa Uplands. River terraces and alluvial lowlands are distributed along Ichinomiya River, Isumi River and Murata River. The Murata River runs through the northwestern district flows into the Tokyo Bay. On the other hand, the Ichinomiya River runs through the central district eastward into the Pacific Ocean. Also the Isumi River runs through the southern district eastward into the Pacific Ocean.

In the Mobara district, there are mainly two stratigraphic units, the lower to middle Pleistocene Kazusa Group and the middle to upper Pleistocene Shimosa Group, trending northeast to southwest and gently dipping northwest. Furthermore Upper Pleistocene terrace deposits with Kanto Loam, Holocene terrace deposits and alluvial deposits arc mostly distributed along the Ichinomi, Isumi and Murata Rivers.

The Kazusa Group is divided into seven formations, Otadai, Umegase, Kokumoto, Kakinokidai, Chonan, Kasamori and Kongochi Formations. These were conformably deposited upward the continuous change of the sedimentary environments from the lower bathyal through upper bathyal to inner shelf.

Keywords: Chiba Prefecture, Mobara District, Quadrangle Series, 1:50000, GSJ/AIST, Geology, Geomorphology, overview

Japan Geoscience Union Meeting 2014
(28 April - 02 May 2014 at Pacifico YOKOHAMA, Kanagawa, Japan)

HQR24-P03 Room:Poster Time:May 1 18:15-19:30

Subsurface geology of the Shimizu Loland and the Miho Peninsula along the northern Suruga Bay, central Japan

ISHIHARA, Takeshi[1*] ; MIZUNO, Kiyohide[1]

[1]Geological Survey of Japan, AIST

We conducted the drilling survey, core analysis, and boring data analysis to clarify the subsurface geologic structure of the the Shimizu Loland and the Miho Peninsula, the Shizuoka Prefecture, central Japan. GS-MMB-1 was drilled in the northern Miho Peninsula. GS-MMB-1 is composed of the gravely layer, sandy and muddy layer with burrows and shell fragments, and gravely layer in ascending order.

In the Shimizu Lowland, a buried incised valley is along the right bank of the Tomoe River. The basal altitude of the incised valley appears to be decrease upstream, suggesting that coastal area of the Shimizu Lowland has been relatively uplifting.

Keywords: Shimizu Loland, Miho Peninsula, Subsurface geology, Boring survey

Japan Geoscience Union Meeting 2014
(28 April - 02 May 2014 at Pacifico YOKOHAMA, Kanagawa, Japan)

HQR24-P04 Room:Poster Time:May 1 18:15-19:30

Reconstruction of tectonic movements using ravinement surfaces: A case study for the subsurface geology of the Osaka

SAKURAI, Minao[1*] ; MASUDA, Fujio[2]

[1]Graduate School of Science and Engineering, Doshisha University, [2]Facluty of the Science and Engineering, Doshisha University

Ravinement surfaces are produced when the sea floor is eroded into a flat surface by the action of waves or tides during a marine transgression. They are preserved in the transgressive deposits as a sharp erosion surface. In a geological cross section across the ancient shoreline, primary ravinement surfaces appear as a subhorizontal line slightly dipping toward the sea. In a cross section, comparing successive ravinement surfaces deformed by tectonic movement allows for the reconstruction of relative tectonic movement. For example, when successive ravinement surfaces are parallel, the entire region has subsided or uplifted uniformly. However, when the lower ravinement surface dips more steeply than the upper ravinement surface, this indicates differential subsidence. With sufficient data, ravinement surfaces can be used to reconstruct the deformation history of an area in three dimensions. Furthermore, because many ravinement surfaces in Quaternary sediments are associated with transgressions related to glacio-eustatic sea level changes, the age of the surfaces can determined and used to estimate the rate of the tectonism.We used the reconstruction of tectonic movement derived from ravinement surfaces to reconstruct the shallow subsurface geologic structures of the Osaka Plain, an intra-arc basin in the Japan island arc. For this study, we constructed cross sections from drill hole data extracted from a civil engineering drilling database. Our study revealed that, in different areas of the Osaka Plain, the land had been uplifted and differentially subsided toward the sea; a relatively large uplift occurred near a flexure zone, and the rate of the tilting of an anticline was constant.

Keywords: ravinement surface, tectonic movement, intra-arc basin, Quaternary, drilling database

Japan Geoscience Union Meeting 2014
(28 April - 02 May 2014 at Pacifico YOKOHAMA, Kanagawa, Japan)

HSC03-01 Room:312 Time:April 30 09:00-09:15

Effects of the offshore barrier against the 2011 Tohoku Earthquake Tsunami and related Recovery Process

MORI, Nobuhito[1*] ; WILLIAM, Pringle[1] ; YONEYAMA, Nozomu[1]

[1]Disaster Prevention Research Institute, Kyoto University

In this study, the effectiveness of an offshore breakwater for the 2011 off the Pacific Coast of Tohoku Earthquake Tsunami was examined by two-dimensional (2D), quasi three-dimensional (quasi-3D) and three-dimensional (3D) numerical models. First, both 3D numerical models were applied to the behavior of tsunami inundation for Kamaishi Bay in Iwate Prefecture where an offshore deep-water breakwater was installed against an assumed tsunami before 2011. The numerical results indicate 20% error of maximum inundation height compared with the post-event tsunami survey on the land. It is found that the offshore breakwater significantly reduced the tsunami height on the land. The reduction of tsunami height on the land gave about 30% tax revenue in comparison with similar locations with or without breakwater. Based on the results the construction and or rebuilding of damaged offshore breakwaters can be considered as a viable option against tsunami particularly in vulnerable areas

Keywords: tsunami, offshore barrier, disaster reduction, recovery

Japan Geoscience Union Meeting 2014
(28 April - 02 May 2014 at Pacifico YOKOHAMA, Kanagawa, Japan)

HSC03-02 Room:312 Time:April 30 09:15-09:30

The Agri-Reconstruction Project and Rapeseed Project for Restoring Tsunami-Salt-Damaged Farmland after the GEJE

NAKAI, Yutaka[1*] ; NISHIO, Takeshi[1] ; KITASHIBA, Hiroyasu[1] ; NANJO, Masami[1] ; SAITO, Masanori[1] ; ITO, Toyoaki[1] ; OMURA, Michiaki[1] ; ABE, Miyuki[1] ; OGUSHI, Yukie[1]

[1]Tohoku Univ, Grad School Agricultural Sci.

The Graduate School of Agricultural Science, Tohoku University, launched an Agri-Reconstruction Project in 2011 immediately after the March 11 Great East Japan Earthquake disaster, and this continues to date. The project's objective is to support the agricultural, forestry and fisheries reconstruction process in the tsunami disaster area. The activities have been implemented through more than 40 research projects along the Tohoku region including the Rapeseed Project for Restoring Tsunami-Salt-Damaged Farmland.

Immediately after the disaster, damaged farmlands were surveyed and salt-tolerant rapeseed varieties from Brassicaceae and related species were used to restore the soil. The plants came from the gene bank developed at the Graduate School of Agricultural Science, and were planted on damaged farmland in Sendai, Iwanuma and Higashi Matsushima cities. The varieties used to restore the soil depended on the specific damage.

As part of the project, the production and sale of edible as well as fuel oil obtained from rapeseed plants was organized in coordination with the Miyagi Prefecture Sendai City government, a number of private companies and other partners. This enterprise continues to date.

Besides using the salt-tolerant varieties of Brassicaceae plants in tsunami-damaged fields they are also used overseas in the rehabilitation of salt-damaged farmlands.

Keywords: earthquake, tsunami, reconstruction, rapeseed, salt damage

Japan Geoscience Union Meeting 2014
(28 April - 02 May 2014 at Pacifico YOKOHAMA, Kanagawa, Japan)

HSC03-03 Room:312 Time:April 30 09:30-09:45

Evacuation response of fishermen during the 2011 Great East Japan Tsunami and present recovery status

SUPPASRI, Anawat[1*] ; YASUDA, Mari[1] ; ABE, Yoshi[1] ; FUKUTANI, Yo[1] ; IMAMURA, Fumihiko[1]

[1]International Research Institute of Disaster Science (IRIDeS), Tohoku University

The 2011 Great East Japan tsunami severely damaged or destroyed most of the fishing ports and facilities along the Sanriku coast. Fishing boats can be considered as the most important thing for fishermen as their activities are mostly depending on their boats. By getting out offshore to protect their boats from tsunamis is a custom in Japan but this is considered as a risky action. Interviews with fishermen were conducted to investigate their evacuation response, experience and opinion of the recovery status after the 2011 tsunami. We found that most of fishermen who did not decide to get out offshore but evacuated to high ground was although felt deploring in losing their boats but in all cases, they believed that their own lives are the most important. Knowing about tsunami characteristic of fishing port is also important. Tsunami generally arrives the Sanriku areas as fast as 30 min because of the deep sea and short distance from the earthquake epicenter. By this reason, boats can reach to the safety zone of 50 m sea depth very soon as well. However, boats in Sendai Plain will need about one hour to the deep sea. For the recovery, all of the villages are still facing problems resulting from land subsidence when the ports are partly submerged during high tide. In addition, land ownership is another issue that delays any recovery process as local governments need their permissions before doing any kind of construction. Although there are some small differences in detail, they have decided to move the entire community to high ground. Local residents feel that constructing high seawalls are unnecessary because there will be no more houses on the low part of the land and the local governments are trying to solve these problems neutrally.

Keywords: 2011 Great East Japan tsunami, Tsunami evacuation, Fishing port

Japan Geoscience Union Meeting 2014
(28 April - 02 May 2014 at Pacifico YOKOHAMA, Kanagawa, Japan)

HSC03-04 Room:312 Time:April 30 09:45-10:00

A method to determine the area of tsunami inundation level 1 and level 2 for pre- and post-disaster situation

MUHARI, Abdul[1*] ; IMAI, Kentaro[1] ; SUGAWARA, Daisuke[1] ; IMAMURA, Fumihiko[1]

[1]IRIDeS, Tohoku University

After the 2011 tsunami, a new approach in the land use planning is introduced and starting to be applied in some areas in Japan. An area that is likely to be affected by the high frequency, but low impact tsunamis -calling as Level 1. It will be used in a separated function in an area that is likely to be affected by low frequency but high impact tsunamis -calling as Level 2. The countermeasures adopted in both areas are different as well. The physical structures will be improved to minimize the effects of the medium-to-low tsunamis to human as well as prosperies in the area of tsunami Level 1. In the area of tsunami Level 2, the coverage of flooded area is much wider. Thus, evacuation facilities and education are the major efforts to save lives. This study aims to address the process on how we can distinguish the boundary between area Level 1 and Level 2. We firstly exercise the use of numerical simulations to establish the framework in assigning area Level 1 and Level 2 at a post-disaster area. Next, we examine the possibility to apply similar techniques in a pre-disaster area. We demonstrate that distinguishing areas of tsunami inundation Level 1 and Level 2 is not only important for the reconstruction in the post-disaster areas, but also necessary to mitigate the future tsunamis in pre-disaster areas.

Keywords: Tsunami inundation area Level1, Tsunami inundation area Level2, numerical simulation, GIS modeling

Japan Geoscience Union Meeting 2014
(28 April - 02 May 2014 at Pacifico YOKOHAMA, Kanagawa, Japan)

HSC03-05 Room:312 Time:April 30 10:00-10:15

Advanced researches of Earthquakes and Tsunamis -Towards disaster mitigation on Earthquakes and Tsunamis-

KANEDA, Yoshiyuki[1*] ; KAWAGUCHI, Katsuyoshi[1] ; ARAKI, Eiichiro[1] ; MATSUMOTO, Hiroyuki[1] ; NAKAMURA, Takeshi[1] ; KAMIYA, Shinichiro[1] ; ARIYOSHI, Keisuke[1] ; HORI, Takane[1] ; HYODO, Mamoru[1] ; TAKAHASHI, Narumi[1] ; BABA, Toshitaka[1] ; NAKANO, Masaru[1] ; CHOI, Jin-kyu[1] ; NISHIDA, Shuhei[1]

[1]Japan Agency for Marine-Earth Science and Technology

Based on lessons learned from the 2011 East Japan Earthquake/Tsunami, we recognized the importance of real time monitoring of these natural hazards. As a real time monitoring system, DONET1 was already deployed and DONET2 is being developed constructing the dense ocean floor networks around the Nankai trough Southwestern Japan. DONET observatories detected offshore tsunamis 15 minutes earlier than onshore stations at the 2011 East Japan Earthquake, and provided the significant information of the tsunami amplification process between off shore and on shore. Using these systems, we can detect not only early earthquakes and tsunamis but also low frequency tremors, slow earthquakes and micro earthquakes in the inter-seismic or pre-seismic stage, which provide useful information for the estimation of seismic stage. As the conclusion, the integration of the real time monitoring data and advanced simulations such as the recurrence cycle of mega thrust earthquakes, tsunami inundation, seismic response on buildings/cities and evacuation, is the very important methodology towards future disaster mitigation programs and related measures. We will explain disaster mitigation researches on earthquakes and tsunamis around the Nankai trough.

Japan Geoscience Union Meeting 2014
(28 April - 02 May 2014 at Pacifico YOKOHAMA, Kanagawa, Japan)

HSC03-06 Room:312 Time:April 30 10:15-10:30

Sociocultural and Economic Aspects in Restoration after Tsunami Hit: Minamisanriku, Miyagi, Japan

KIMURA, Naoko[1*]

[1]GSGES, Kyoto University

This research discusses sociocultural and economic aspects through description of initiatives taken by local people and organizations in Utatsu area, Minamisanriku, Miyagi Prefecture, for reconstruction after the Great East Japan Earthquake and huge tsunami hit in March 2011. Utatsu is located on the coast of Isatomae-Bay, the Pacific Ocean. The key industry of town is fishery, however, the number of people involved in fishery has decreased since 1990, and the town also has issue related to aging of population year by year. Like any afflicted people by huge tsunami induced by the earthquake, Utatsu residents had to move to another area located higher hillside and start to rebuild their life. This research focuses on two initiatives: a painting-art project and *miso* factory (*miso* is fermented soybean paste, a traditional preservative food in Japan) managed by local housewives. Interviews were conducted to some key stakeholders of those initiatives, and its results were qualitatively analyzed. The interview revealed some positive changes in mind among participants, especially young generation, as well as problems and obstacles long-deep rooted in the local socio-economic structure of the area, for example, mental conflicts between communities, concerns to influence of radionuclides from Nuclear Power Plant accident in Fukushima. The research concludes with a view regarding a possible way forward to their sound rebuilding and reconstruction.

Keywords: tsunami, reconstruction, community, sociocultural and economic aspects, Minamisanriku

Japan Geoscience Union Meeting 2014
(28 April - 02 May 2014 at Pacifico YOKOHAMA, Kanagawa, Japan)

HSC03-07 Room:312 Time:April 30 10:30-10:45

Living with Natural Hazards; Tsunami

SANTIAGO-FANDINO, Vicente[1*]

[1]Independent Environmental Advisor

Tsunamis are a common natural hazard originated by earthquakes, landslides, volcanic eruptions and even meteorological conditions. These events have hit coastal areas particularly along the Pacific Ocean (Rim of Fire), Eastern Mediterranean Sea and the northern part of the Indian Ocean resulting in large impacts to the environment and coastal settlements.

Adaptation by organisms and ecosystems after being hit by tsunamis follow nature's processes for adaptation to the new realities, which also applies in the case of mankind but in this case intelligence, reasoning and complex social structures makes the process more complex reflecting in turn in how the restoration and reconstruction process may develop and its success.

Efforts made to reconstruct and restore impacted areas have proven to be very complicated and controversial oftentimes, this mainly due to differences of opinion on the approaches to be taken and decision-making processes added to the societal aspects. Moreover, lack of direct and effective participation of impacted communities, sectorial and top dawn decision-making further exacerbates the debate resulting in reducing trust by the locals, diminished resilience and increases emigration amongst other aspects.

Tsunamis are complex natural events requiring the integration of sound research and knowledge, the same is required to understand local communities where traditions, customs and societal components are crucial before decision making. Living in Tsunami exposed areas call for building trust with authorities as well as developing early warning and disaster prevention policies, appropriate defence systems and mechanisms, provision of education and awareness raising as well as the understanding of the affected communities needs, capabilities as well as their customs and traditions together with their living environment. Proactive and integrative policies rather than sectorial and reactive top dawn ones bring all these elements together whereby strengthening local communities, increasing resilience and allowing the reconstruction and restoration process to be effective and successful.

Japan Geoscience Union Meeting 2014
(28 April - 02 May 2014 at Pacifico YOKOHAMA, Kanagawa, Japan)

HSC04-01 Room:315 Time:May 2 16:15-16:30

Local community and Tsunami-lesson from 2011 eastern Japan mega earthquake

HARUYAMA, Shigeko[1*]

[1]Mie University

The coastal plain facing Pacific Ocean in north-eastern Japan was suffered by Tsunami and mega-earthquake at 2011 Easter Japan Mega-Earthquake. Still now, the regional planners are preparing for appropriate resuscitation or reconstruction for mitigation in the disaster-stricken areas. In this study, the authors tried to clarify local community activity for disaster prevention at the moment of Mega-earthquake occurrence and Tsunami intrusion. The lower Abukuma river basin and coastal and fluvial landforms comparing with former Tsunami intrusion referred to historical records on this site and local communities based on different landform units of the lower Abukuma river basin were selected for analysis to avoid disaster risk level using questionnaire survey. The local community activities were designed by strong leadership of community, former experience of disaster, preparedness of evacuation drill, work sheering experience of community building up social capital in each region. The land use pattern and recent land use change processes in this study area are analyzed and the rapid land use change dealing with urbanization is another trigger of disaster risk level enlargement under the disaster. The future disaster prevention work and disaster mitigation planning should be argued with local community social capital.

Keywords: Tsunami, Local community, landform

Japan Geoscience Union Meeting 2014
(28 April - 02 May 2014 at Pacifico YOKOHAMA, Kanagawa, Japan)

HSC04-02 Room:315 Time:May 2 16:30-16:45

Fluvial Environmental Changes of the Ayeyarwady Delta: Case Study for Nyaungdon Borecore Area

KAY THWE, Hlaing[1*] ; SHIGEKO, Haruyama[2] ; AYE, Maung maung[3]

[1]Researcher, Graduate School of Bioresources, Mie University, [2]Professor, Graduate School of Bioresources, Mie University, [3]Professor, Department of Geography, University of Yangon

The Ayeyarwady River is one of the largest rivers in Myanmar and drains an area of 85,534 km2. The study area is mainly located in the central part of deltaic of the Ayeyarwady River belonging to Nyaungdon Township, Ayeyarwady Region.The main purpose of this study is to clarify geomorphologic land classification mapping and fluvial features of the Ayeyarwady River Delta derived from aerial photos, Landsat +ETM7 Global Digital Elevation Model Version 2 with GIS and RS linkage and to check long term natural environmental restoration of the lower Ayeyarwady River at Nyaungdon drilling point in Ayeyarwady Region. The volume of sediment deposited rate and discharge rate should be accumulated rapidly before Holocene period because we could clarify with the results of 14C dating of the organic materials including each layer and all core drilling samples, concept of paleo-geography and geomorphologic evolution, landform development of the study area.

Keywords: Ayeyarwady River Delta, Geomorphologic land classification map, sedimentary facies, drilling bole core, discharge, radiocarbon age

Japan Geoscience Union Meeting 2014
(28 April - 02 May 2014 at Pacifico YOKOHAMA, Kanagawa, Japan)

HSC04-03 Room:315 Time:May 2 16:45-17:00

The Impact of Joint Forest Management on Household Income and Forest Condition: The Case of Madhya Pradesh, India

SAKURAI, Takeshi[1*] ; ISAKA, Masashi[2]

[1]Institute of Economic Research, Hitotsubashi University, [2]Graduate School of Economics, Hitotsubashi University

Joint Forest Management (JFM) is a benefit-sharing scheme between rural households and the state government. Rural households are the user of forest resources for their livelihood, such as grazing, fuel woods, wild foods, etc., while the state government is the owner of the forest land and trees in the forest and makes revenue from the sales of forest resource such as timber, medicinal plants, etc. In the past, the state government used to protect the state forest from rural households, but the protection had been becoming more costly due to the increasing population and as a result forest resources had been depleted. JFM scheme was formally introduced by the central government in 1988 to provide rural households with incentive for forest management by benefit sharing, and each state government adopted JFM since then. Under JFM scheme, rural households have to regulate their use of forest resources for their livelihood and they are promised to will a significant share (e.g. 50%) of timber sales revenue.

Although JFM has been implemented for almost 20 years in most states in India, its impact on the welfare of rural households and forest condition has rarely investigated quantitatively. Thus, the objective of this paper is to tackle this remaining question. This paper utilizes a two-year panel data of 360 households and the satellite images of forest around their residential places. The panel data were collected in 1998 and 2008 in 60 villages spread over 6 districts in Madhya Pradesh.

Our analyses show that JFM neither increased nor decreased household income per capita although household income per capita increased significantly during the 10 year period investigated. It implies that the restriction of forest use did not have any negative effect on the welfare of rural households, but that the benefit sharing was not realized or did not increase household income. The latter is consistent with the fact that most timber trees are still immature to harvest. On the other hand, forest condition was improved during the 10 year period in villages where JFM was implemented. The improvement of forest resources is considered to be caused by forest protection from grazing and tree plantation as part of JFM activities. In conclusion, the state government has benefited from JFM, while rural households have not benefited from JFM although they have not decreased their welfare at least in the short-run.

Keywords: joint forest management, impact assessment, panel data, household income, forest condition, India

Japan Geoscience Union Meeting 2014
(28 April - 02 May 2014 at Pacifico YOKOHAMA, Kanagawa, Japan)

HSC04-04 Room:315 Time:May 2 17:00-17:15

Forming the Inter-mediate Region between Urban and Rural in India - a case of Mysore city, Karnataka -

SUNDERRAJ, Arun das[1] ; KIMOTO, Koichi[2] ; R., Umakanth[1] ; HR, Vishwanatha[1*]

[1]University of Mysore, [2]Hiroshima Jogakuin University

The fragmentation of agricultural land due to inheritance and partial selling has put the farming community into marginal farmers. A marginal farmer owning less than one acre of land, losses complete livelihood from his land. He becomes a partial non agriculture worker along with his farming occupation. Ultimately, leading to permanent change in occupation. In the later period he disowns the farming activity and migrates to the fringe of the nearby city. The CBD pressure on fringe begins as ripples from the city towards fringe. Consequence of this the fringe pressure ripples towards the farming and forest land. This has vice versa effect from Rural to Urban Fringe. The rural pressure which emanates from outer country land towards city mounts up its pressure on Fringe.

This paper discusses about the process of expanding cities, its pressure on fringe, the rural farming land, shifting occupation and bouncing effect towards city. A fast growing city like Mysore city bounded by farming land of Mysore and Chamaraja districts is a good example to explain the situation of many cities of India which are experiencing similar process and bouncing effect.

Keywords: Inter-mediate Region, Land Use and Cover Changes, Population Pressure, Urban - Rural, India

Japan Geoscience Union Meeting 2014
(28 April - 02 May 2014 at Pacifico YOKOHAMA, Kanagawa, Japan)

HSC04-05 Room:315 Time:May 2 17:15-17:30

Time-serial trend of built-up area of China - A preliminary consideration of statistical data

DOI, Haruhiro[1*]

[1]Faculty of Education and Welfare Sciences, Oita University

The research group of SLUAS (Research project of ”Towards Sustainable Land Use in Asia” Grant-in-Aid for Scientific Research(S) 2009-2013, Yukio Himiyama) has executed several research field trips in various regions of China. The author fortunately has chance to join the field trips and to observe several land-use conditions and land-use changes on the way. As a result of those research field trips, the author confirmed that the built-up area remarkably expanded by fast growing economy of big cities in the coastal area such as Beijing and in those cities not only the industrial development but also the housing development and shopping malls are developed actively in the suburban area. On the other hand, the author also felt that the cities in the inland area, however, it is late comparatively its economic growth from the coastal region, a built-up area growth is generated recently by the industrial and housing developments in the high rise apartment building etc. The present study intends to confirm such a personal impression about recent built-up area growth of China by using statistical material.

The objectives of the research are as follows. First object is to confirm time serial feature of the built-up area expansion. Second is to analyse the relation between the built-up area expansion and population scale. Third is to confirm regional difference of built-up area expansion by using regional division in China. And forth is to consider factors or the background of the built-up area expansion. So the author analyses the relations among built-up area expansion, a population increase, and GDP indexes. Findings concerning obtaining by these objectives are beneficial to estimate how a spatial expansion of the China city will become in the future.

The author set up hypothesis obtaining by the research are as follows. One is that built-up area expands according to a population increase and economic growth of a city. Second is that structural change of an economic condition of a city such as secondary industry and tertiary industry is reflecting its expansion of built-up area of a city. Third is that the growth wave of a city spreads from the coastal region to the inland area.

Keywords: built-up area, population, regional division, economic structure

Japan Geoscience Union Meeting 2014
(28 April - 02 May 2014 at Pacifico YOKOHAMA, Kanagawa, Japan)

HSC04-06 Room:315 Time:May 2 17:30-17:45

Study on the relationship between human activities. natural environment of food production in Xinjiang

XIAOKAITI, Aji[1*] ; KONDOH, Akihiko[2]

[1]Graduate School of Sciences, Chiba University, [2]CEReS, Chiba University

Maintaining the food production force is a basic condition for ensuring the food security in Xinjiang Uygur Autonomous Region. In this study, We have carried out the factors analysis from both sides of the natural and social factors on food production in Xinjiang, using the unit area production volume as the main indicator of food production. In order to understand the temporal change of the unit area production volume in Xinjiang at first, We extracted the unit area production volume data from the Statistical yearbook in Xinjiang, and analyzed the secular change of food production in Xinjiang. The result shows that the unit area production volume had been growing steadily over the 1990-2003, but shows an unstable state since 2004, and has been reduced in 2008; In order to understand the spatial variation of the unit area production volume, We have created a difference image using GIS technique, between 2008 when the unit area production volume reduced, and 2003 when the unit area production volume had been continued growth to analysis the regional changes of food production. It shows that the regions which the unit area production volume decreased are distributed more in the area of the north and east of Xinjiang in 2008 comparison to 2003.

In order to understand the change factor of food production, the analysis has been done on the causes of changes in food production in Xinjiang, by extracting the data of the chemical fertilizer that was used for the food production, irrigation area, agricultural machinery and the rural electricity from the statistical yearbook, The result shows that the effective irrigation rate in Xinjiang after 2005 was reduced by the loss of irrigation facilities and equipments, and it is confirmed that these area are substantially matches to the region in which the unit area production volume decreasing. The data of the agricultural production material price, commodity retail price, agricultural products purchase price are also used for the same analysis, It was estimated that the rise of agricultural production material prices, has become a factor in reduction of food production indirectly through reduced production cost in 2008 that unit area production volume was reduced.

On its outer, using the TRMMB343 precipitation data and CRU TS3.21 temperature data, analyzed the natural factors of food production change. It shows that the trend of precipitation in decline, and the reduction position matches well with the area of unit area production volume are decreased. However, it is suspected that both of human activities and natural factors have been the impact jointly to the changes in food production in Xinjiang.

Keywords: Xinjiang Uygur Autonomous Region, Food production, Human activities, Natural environmen, GIS

Japan Geoscience Union Meeting 2014
(28 April - 02 May 2014 at Pacifico YOKOHAMA, Kanagawa, Japan)

HSC04-07 Room:315 Time:May 2 17:45-18:00

Framing Land Use Sustainability Research in Future Earth Context

HIMIYAMA, Yukio[1*]

[1]Hokkaido University of Education

The Future Earth Initial Design issued late in 2013 emphasizes the importance of land use research related with sustainability. What are written about land use are not particularly new to land-use specialists, but what is significant is that land use is considered as a priority concern of Future Earth. The paper discusses how to frame land use sustainability research in Future Earth Context based on the achievements and experiences of IGU-LUCC (International Geographical Union Commission on Land Use/Cover Change), GLP (Global Land Project), SLUAS (Towards Sustainable Land Use in Asia Project) and others.

Keywords: Future Earth, land use, GLP, IHDP, IGU-LUCC

Japan Geoscience Union Meeting 2014
(28 April - 02 May 2014 at Pacifico YOKOHAMA, Kanagawa, Japan)

HSC04-P01 Room:Poster Time:May 2 16:15-17:30

RIHN Archives - for transdisciplinary research on global environmental studies

YASUTOMI, Natsuko[1*] ; SEKINO, Tatsuki[1]

[1]Research Institute for Humanity and Nature

Research Institute for Humanity and Nature (RIHN) solicits, develops, hosts, and funds fixed-term research projects on pressing areas of interaction between humanity and nature. RIHN promotes coordinated, problem-centered, context-specific, and multi-dimensional science. RIHN projects can last from three to five years; they are always multidisciplinary and employ multiple methodologies, and they are supposed to offer solutions to the problems under study.

RIHN undertake an important task to accumulate their research products on transdisciplinary global environmental studies and resources for successors since almost all researchers leave RIHN after the end of their project.

”RIHN Archives” was developed in 2008 in order to accumulate and charge research products of RIHN research projects. It contains metadata of publications, reports, posters, handsouts and movies of seminars, evaluations, obtained data, maps, and so on. RIHN Archives database is open to public.

”RIHN Archives” itself is the record of transdisciplinary studies held in RIHN. Moreover, RIHN research projects have been conducted on objectives which should contribute to Future Earth. RIHN Archives must play an important role on planning new feasible studies to design futurable earth.

Keywords: global environmental studies, interdisciplinary research, outreach

Japan Geoscience Union Meeting 2014
(28 April - 02 May 2014 at Pacifico YOKOHAMA, Kanagawa, Japan)

HSC25-01 Room:421 Time:April 30 09:00-09:15

The reconstruction 2014 present circumstances after The 2011 TOHOKU Great Eaerthquake disaster

NISHIZAWA, Masaru[1*]

[1]none

1. Suggest the collective bargaining with the authorities concerned with the important matter.
2. I am hoping the youth for a marked conception to our country.
3. Suggest the building serves both as a residence and a place of refuge.

Keywords: The 2011 TOHOKU Great Earthquake Disaster, The building serves both as a residence and refuge, youth, Reconstruction

Japan Geoscience Union Meeting 2014
(28 April - 02 May 2014 at Pacifico YOKOHAMA, Kanagawa, Japan)

HSC25-02 Room:421 Time:April 30 09:15-09:30

Application of Information on Seasonal Landscapes for Landcover Classification by Satellite Data

KUROKI, Takahito[1*]

[1]Fukuoka Univ. of Edu.

We cannot ignore the influence of seasonal landscapes in landcover classification by Satellite data. Therefore in the analysis, we always have to select the data acquired in the best season for available landcover classification. The seasonal landscape change is also caused by human activities as well as natural conditions. The higher the resolution of the data used for classification, the influence on the landscape by human activity increases in the results. Considering human activity on the classification, it seems that we cannot obtain the realistic image for natural conditions. We do not have much interest in the influence of classification of natural conditions induced by landcover classification based on human activity and the countermeasure. In this study, seasonal landcover classifications based on human activity are analyzed in Aso volcano with remarkable seasonal change of landscape every year. Then, the accuracy is confirmed by such as sign of human activity that can be identified in the classified images. Finally, I discuss on the influence of the classification to that of natural conditions in the volcano and show a countermeasure for the problem in the classification. We used four ALOS data acquired in spring 2010, summer 2006, autumn 2007 and winter 2007 for the classification. The study area was classified into 6 items such as green grass, withered grass, forest, arable land, urban area, open burning area by the supervised maximum likelihood classification.

On the landcover classified maps of all seasons, similar distribution patterns were observed on forest of caldera wall and piedmont of central cone, and on arable land and urban area of caldera floor. On the other hand, distribution of different items was shown in crater rim and mountainside of central cone every season. They are green grass in September, green grass, arable land and withered grass in November, withered grass in February, green grass, withered grass and open burning area in April. On the classified maps, the large seasonal landscape changes at the grassland in crater rim and mountainside of central cone can be understood. From the interpretation of these changes, signs of human activity of boundary of management association for grassland, such as firebreak of open burning were identified clearly. However, this classification work could not induce appropriate classified images that represent the natural conditions in the volcano at the summit area and crater lake area of central cone, dissected valley of lava dome and past slope failure area in caldera wall. At the summit area of central cone, I selected the seasonal image that is easy to represent the distribution for each class of natural conditions. The items in the image were reclassified into the classes of natural conditions and the values of the power of 10 were given to them. Finally, I obtained the realistic landcover classification image at the volcanic area from the overlay analysis by using the reclassified images. Consequently, I clarified in this study that landcover classification representing the characteristics of natural conditions can be performed with high accuracy by using the information of seasonal landscapes based on human activities.

Keywords: Aso volcano, landcover classification, ALOS, seasonal change, natural condition

Japan Geoscience Union Meeting 2014
(28 April - 02 May 2014 at Pacifico YOKOHAMA, Kanagawa, Japan)

HSC25-03 Room:421 Time:April 30 09:30-09:45

Disaster information gathering depend on the geographic characteristics zone using geospatial information

KOARAI, Mamoru[1*]

[1]GSI of Japan

In order to build a national land equipped with resilience, it is important to advance environmental preservation, land conservation and development which performed geographic division summarized the area where the geographic characteristics is similar. The author tried to classify into the about one hundred geographic characteristics zones of Central Japan for disaster prevention.

Geographic characteristics classification from the viewpoint of the disaster prevention was carried out by the following method. First, it classified into mountain, hill, volcano, plateau and lowland by landform classification. Next, about mountain, hill and volcano, it subdivided according to geology. About plain, it subdivided according to the ratio of plateau and lowland. High-risk areas, such as slope collapse, landslide, liquefaction and collapse of volcanic bodies, were extracted from the analysis of geospatial information, including DEMs, geological maps, landslide distribution maps, landform classification maps, etc.

In this presentation, the author will discuss how to use the geographic characteristics zone for emergency assistance at early stage. It is necessary to consider the disaster information gathering according to the difference of disaster characteristics on each geographic characteristics zone. The most important issue in mountain area is grasping of an isolated colony, and detection of an isolated colony is possible by overlay of slope collapse expected area and road network information. In the viewpoint of a catastrophic secondary disaster, extraction of the flooding area by a landslide dam is very important. Satellite SAR and airborne SAR ware effective method in the case of deep collapses by the typhoon heavy rain of Kii Peninsula in 2011. In the disaster information gathering in early stages of a plain area, tsunami damage is very important. Satellite SAR was effective method for the detection and monitoring of the tsunami flooding area in the case of the Great East Japan Earthquake. From the viewpoint which carries out emergency assistance at early stage, the extraction of the heavy damaged area is required. The development of automatic classification technology about spill zone, failure zone and flood zone using polarization SAR is required.

Keywords: geoigraphic characteristics zone, geospatial information, disaster information gathering, emergency assistance at early stage, synthetic aperture radar

Japan Geoscience Union Meeting 2014
(28 April - 02 May 2014 at Pacifico YOKOHAMA, Kanagawa, Japan)

HSC25-04 Room:421 Time:April 30 09:45-10:00

Towards detailed tsunami hazard assessment for specific regions

HIRATA, Kenji[1*] ; FUJIWARA, Hiroyuki[1] ; NAKAMURA, Hiromitsu[1] ; OSADA, Masaki[1] ; OHSUMI, Tsuneo[1] ; MORIKAWA, Nobuyuki[1] ; KAWAI, Shin'ichi[1] ; AOI, Shin[1] ; YAMAMOTO, Naotaka[1] ; MURASHIMA, Yoichi[2] ; MURATA, Yasuhiro[2] ; INOUE, Takuya[2] ; SAITO, Ryu[2] ; MATSUYAMA, Hisanori[3] ; TOYAMA, Nobuhiko[3] ; KITOH, Tadashi[3] ; AKIYAMA, Shi'ichi[4] ; KORENAGA, Mariko[4] ; ABE, Yuta[4] ; HASHIMOTO, Norihiko[4]

[1]NIED, [2]KKC, [3]OYO, [4]CTC

NIED began research projects regarding tsunami hazard assessment (THA) in Japan to support various kind of measures against possible tsunami attacks in future by sectors such as local governments, life-line companies, etc after the national tragedy caused by the 11st March 2011 Tohoku earthquake (Mw9.0) (Fujiwara et al., 2013, JpGU). One of the research projects is a research of probabilistic tsunami hazard assessments (PTHA) in which we consider all of possible tsunamis that may affect coastal regions in future. The research of PTHA consists of two subjects; (1) nation-wide probabilistic tsunami hazard assessment (NWPTHA) (Hirata et al., 2014, JpGU) and (2) detailed probabilistic tsunami hazard assessment for specific regions (DPTHASR). We briefly show outlines of (2) here.

The objective of DPTHASR is to bridge the gap between probabilistic tsunami hazard assessment and local measures for disaster prevention in city-scale. In the research and development process of DPTHASR, we are planning to conduct several kinds of tsunami inundation assessment for specific regions by using tsunami propagation and inundation simulations based on a non-linear long wave equation with staggered leap-flog, finite difference method (FDM) over a nesting grid system with the minimum grid size of 10 meters. As for presentation tools of DPTHASR, we are planning to present (a) inundation flow depth hazard curve (excess probability) at specified point and (b) probabilistic spatial distribution of inundation flow depth as well as we are also planning to investigate development of (c) probabilistic inundation flow velocity assessment that is closely related to tsunami destructive force against buildings, etc. and that can be directly applied to risk assessments. As the first attempt in researches regarding DPTHASR, we are investigating a probabilistic method of depth flow assessment in which both of probabilistic assessment for inundation flow depth distribution and inundation flow hazard curves (excess probability) are presented (Saito et al. 2014, JpGU).

For a high-precision forecast of inundation phenomena based on tsunami run-up calculation in DPTHASR, it is the most important to use fine and precise topographic data with detailed information on breakwaters and seawalls in coastal region and riversides. We make effort to collect these information and will have to investigate relationship between inundation flow assessment and destruction conditions of coastal infrastructures in near future. The Ministry of Land, Infrastructure, Transport and Tourism (MLIT) of Japanese Government recommends users for tsunami runup calculation to basically use high-precision topographic data acquired with airborne laser scanning (MLIT, 2012, Guideline for tsunami inundation forecasting). The Geospatial Information Authority of Japan (GSI) is progressively releasing the precise coastal topographic data acquired with airborne laser scanning. DPTHASR will be advanced using processed data, converted for tsunami simulation, created from high-precision topographic data acquired with airborne laser scanning by GSI.

Keywords: tsunami, hazard assessment, runup, probability, local tsunami forecast, utilization

Japan Geoscience Union Meeting 2014
(28 April - 02 May 2014 at Pacifico YOKOHAMA, Kanagawa, Japan)

HSC25-05 Room:421 Time:April 30 10:00-10:15

Evacuation passage from Tunami-map exercise with inhabitants

FURUTA, Noboru[1*] ; CHUJYO, Yoshiteru[1] ; KOBAYASHI, Ikunori[1] ; KAWASE, Kumiko[2]

[1]Tokushima Bunri Univ., [2]Ehime Univ.

At the time of the south seas earthquake occurrence, the security of the refuge course is necessary. The investigation area is Shiwagi, Minami-cho, Tokushima. We identified the evacuation route as local inhabitants in students. We had you tell local people a number and the location of the person requiring nursing care. A person requiring nursing care is an elderly person, an infant, a person with a physical disability.

Keywords: Evacuation, tunami, DIG, ?obstruction, GIS

Japan Geoscience Union Meeting 2014
(28 April - 02 May 2014 at Pacifico YOKOHAMA, Kanagawa, Japan)

HSC25-06 Room:421 Time:April 30 11:00-11:15

The Significance of Partnership and Participatory Sharing of Geospatial Information through crisis mapping in Izu-Oshima

SETO, Toshikazu[1*]

[1]Center for Spatial Information Science, the University of Tokyo

1. Introduction

Various platforms enable online-based plotting of disaster information map using reviews and other social networking services (SNS). Examples Ushahidi has been noted since the Great East Japan Earthquake for its usefulness in promoting rapid situational awareness in disaster areas. This platform also is used OpenStreetMap (OSM), a free mapping project used to generate background maps. Indeed, as regards natural disasters that occurred in Japan after year of the Great East Japan Earthquake, simplified versions of information sharing sites have been established by volunteers, such as Crowdmap. Meanwhile, during the onslaught of Typhoon Wipha last October 2013, information sharing by volunteers progressed smoothly using the rapid launch of Crowdmap.

However, the method of geospatial information gathering in the event of a crisis as a means of quickly relaying information in and out of disaster areas, as typified by crisis mapping using Ushahidi, is not fully and properly utilized in Japan.This study examines the role of information sharing and the development of geospatial information on the Web related to disaster response.

2. Sharing of geospatial information by participatory mapping in Izu-Oshima

To promote Izu-Oshima tourism around the Geopark with the aid of information technology, Izu-Oshima Tourist Association and other groups held the Hackathon and Mapping Party in January 2013. In this event, a detailed map created or developed smartphone applications for leisure by about 30 cooperating participants composed of OSM developers and mappers, as well as local residents involved in geopark's tour guide.

3. Cooperation with other organizations and launch of crisis mapping during the occurrence of Typhoon Wipha

After the event in January 2013, participants continue to engage in exchanges through a Facebook group, including participants of the island nature tour guide. For instance, users in Tokyo, who tuned in to the news regarding the occurrence of heavy rain and landslides brought by typhoon Wipha last October 16, intensified their information collection and uploaded data on the Web site very quickly. Twitter accounts with high reliability, such as that of "Izu-Oshima's disaster prevention", published information picked up by disaster prevention radio stations.

In another case, the Red Relief Image Map made by Asia Air Survey and slant ortho-photo data gathered by emergency shooting by some survey companies provided as a possible WMS layer through "e-com map" of the Research Institute for Earth Science and Disaster Prevention and Geoserver of the Code for Japan community. Such geospatial information can serve as the basic data for the estimation of location information, in which Crowdmap helps screen information via SNS features. As such, the number of page views of Crowdmap reached 12,000, and 248 reports are posted on Crowdmap in about a month after the disaster. In addition, as information transfer throughout and mapping of the disaster area had become a major issue, it was reported in local as well as analog information of paper maps, such as the large-format guide to the Great East Japan Earthquake by the Nature and Tourism Association staff.

4. Conclusions

In Japan, crisis mapping that fully utilizes the Web, such as online maps, has come to be carried out quickly and serve as a source of understanding and cooperation between volunteers and various organizations. In this context, the need for information gathering and sharing at a high public degree in the initial disaster stage is recognized, triggered by the events of the Great East Japan Earthquake. In addition, even in areas where information technology and geospatial information have not been as highly developed compared with Izu-Oshima, the cases covered in this study revealed that stakeholders could work together through workshops to build a relationship aimed at advancing information sharing development.

Keywords: crisis mapping, crowdsourcing, Ushahidi, volunteered geographic information, Izu-Oshima island

Japan Geoscience Union Meeting 2014
(28 April - 02 May 2014 at Pacifico YOKOHAMA, Kanagawa, Japan)

HSC25-07 Room:421 Time:April 30 11:15-11:30

Study of natural disasters and terrain of Izu Oshima with Red Relief Image Map

CHIBA, Tatsuro[1*]

[1]Asia Air Survey Co., Ltd.

Introduction

In recent years , advances in LiDAR technology , detailed topographic data with high accuracy by eliminating the influence of the tree is now obtained. The contour by aerial photogrammetry so far , terrain under the trees is due to the estimation of operator that assumes the tree height , the difference of the laser measurement was evident . However, it is to express in scale in which it is easy to utilization of the whole picture microtopography measurement such results is difficult. Also shaded contour plot also altitude tints Figures it was not appropriate. I ivented red relief image map method at the time of terrain reconnaissance of Aokigahara-Jukai of Mount Fuji in 2002. After that I've been used to field survey and interpretation of volcanic terrain around the country .

red relief image map

The more red than at steep slope , as bright as ridge , expressed the darker the valley , red relief image map is a some false color image of certain ortho . Since the state overlapping the topographic map , without the use of specialized equipment , it is possible to obtain a natural three-dimensional feeling in one piece , a combination of a red relief image map and LiDAR DEM and revolutionized the field survey.

terrain of Izu-Oshima

Also in Izu-Oshima , LiDAR DEM were detected, H24 by Tokyo,H25 by Tokyo ,H18 by GSI has been carried out . In addition , as the foundation map information 5mDEM, measurement results of H24 have been published from the GSI.

This section shows a red relief image map of Izu-Oshima , we describe the features of the volcanic terrain that can be read from there .

Izu-Oshima , there is a caldera in the center , Mt central cone is located in the center . Mt shows the terrain of tuff cone crater is large in proportion to size , but I'm repeating the activity in which the bottom of the crater of the central vertical hole moves up and down , to overflow the lava . The eruption occurred at 1950-51 and 1986 in recent years . In addition, in the Izu-Oshima , fissure eruption many distribution on the outside of the caldera , C fissure eruption in 1986 . It has been estimated that there is a fissure of Y5 drained the lava flow the steep slopes on the east side of Motomachi , but the exact location has not been clearly covered in trees . The red relief image map by the laser measurement of H18, Y5 fissure is visible clear , although confirmation has been difficult by many trees . After that , the field survey of the collapse can be accomplished by the typhoon disaster of October 2013 , it was confirmed to be Y5 fissure .

Features of the terrain of the surface slope collapse

The typhoon of October 16, 2013 , a large debris flow disaster occurs at the Motomachi Kandachi area of Izu-Oshima . Wake of this disaster was the collapse of the surface layer of volcanic ash on the slopes , and this slope are crossed by Y5 fissure, debris flow was flowing down over the Motomachi lava flowed from there . For the valley of this lava flow is very shallow , became the disaster spill debris flow can not swallow . In addition, I describe the characteristics of the micro-topography in the poster .

Keywords: izu-ooshima, DEM, red relief image map, lava flow, LiDAR, surface failure

Japan Geoscience Union Meeting 2014
(28 April - 02 May 2014 at Pacifico YOKOHAMA, Kanagawa, Japan)

HSC25-08 Room:421 Time:April 30 11:30-11:45

Debris flow by Tyhoon Wipha and creating maps with flow accumulation

SAWANO, Nobuhiro[1*]

[1]Kanazawa Seiryo University

1.Typhoon Wipha

2. Flow accumulation

3. A case of Izu Oshima

4. Web Publication

5. Summary

Keywords: Typhoon Wipha, Debris flow, Flow accumulation, Web publishing, Geoserver

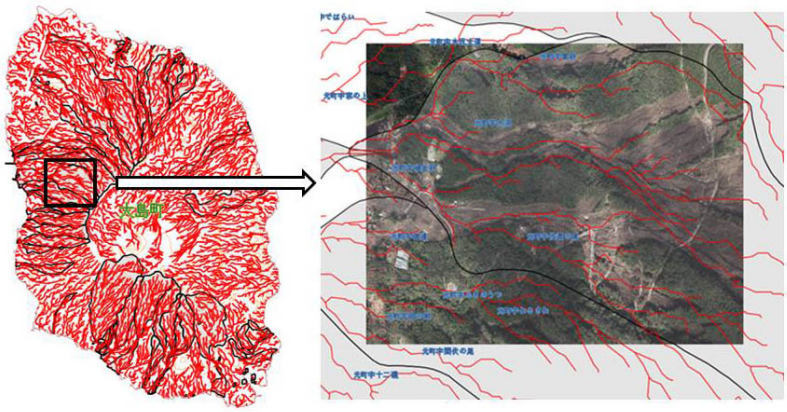

Japan Geoscience Union Meeting 2014
(28 April - 02 May 2014 at Pacifico YOKOHAMA, Kanagawa, Japan)

HSC25-09 Room:421 Time:April 30 11:45-12:00

The effort of prompt information-gathering - crisis response to damages by Typhoon Wipha (2013) on Izu Oshima island

UCHIYAMA, Shoichiro[1*] ; SUZUKI, Hinako[1] ; USUDA, Yuichiro[1]

[1]National Research Institute for Earth Science and Disaster Prevention (NIED)

Disaster Information Laboratory (DIL) at National Research Institute for Earth Science and Disaster Prevention (NIED) integrates information provided related organizations and release to public in case of hazard strikes. This paper shows the effort of prompt information-gathering as crisis response by NIED at Izu-Oshima devastated by the typhoon Wipha in 2013.

Keywords: crisis response, information-gathering, structure from motion (SfM), typhoon Wipha in 2013, Izu-oshima

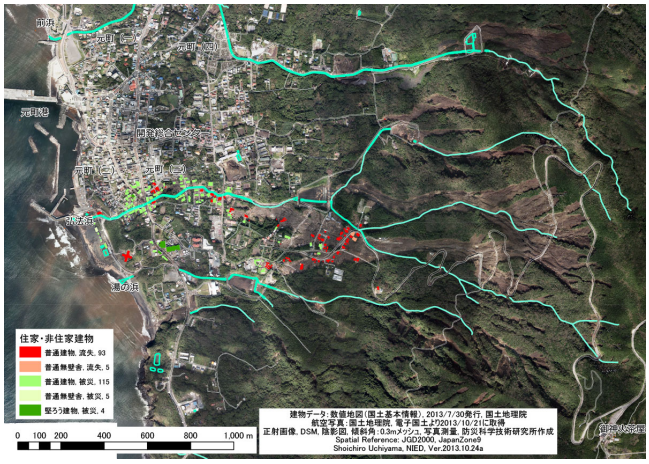

Japan Geoscience Union Meeting 2014
(28 April - 02 May 2014 at Pacifico YOKOHAMA, Kanagawa, Japan)

HSC25-10 Room:421 Time:April 30 12:00-12:15

Role of the cloud based GIS for disaster management system at Emergency Operation Center

GOTO, Shintaro[1*] ; SAWANO, Nobuhiro[2] ; SAKAI, Toshikazu[1]

[1]Department of Environmental Systems Faculty of GEO-Environmental Science Rissho University, [2]Kanazawa Seiryo University

The cloud-based GIS center with the assumption that on the basis of the lessons learned in disaster information logistic support of the Great East Japan Earthquake 2011, ICS is introduced at the provincial level, to function under ICS concepts in the field Saitama Prefecture. The object of the invention is to organize the features and to operate by implementing it.

For this purpose, the contents of this study are as follows;

1. Study of cloud-based GIS data management perspective for the basic system

2. Application to the COP(Common Operational Picture) and the study of the utilization by the cloud of electronic results

3. Demonstration and calibration in collaborative disaster drill applying the ICS

Keywords: GIS, Incident Command System, Common Operational Pucture, Information Management Process, Emergency Management Center

Japan Geoscience Union Meeting 2014
(28 April - 02 May 2014 at Pacifico YOKOHAMA, Kanagawa, Japan)

HSC25-11 Room:421 Time:April 30 12:15-12:30

Micro - Landform Mapping and Applications in Hilly Area Using LIDAR Data

BORJIGIN, Habura[1*] ; GOTO, Shintaro[2]

[1]National Institute for Environmental Studies Center for Regional Environmental Research, [2]Rissho University Department of Environmental Systems Faculty of GEO-Environmental Science

The objective of this study is to develop the information to be provided for natural regeneration by investigating the relationship between Micro-Landform and vegetation in hilly area of Higashi-matsuyama City in Saitama Pref. The Micro-Landform was classified based on the conversion line of the slope angle derived from DEM (digital elevation model) generated from LIDAR (Laser Imaging Detection And Ranging). Furthermore, we summarized the classification situation of each Micro-Landform by every tree measurement. Finally, the relationship between vegetation and Micro-Landform in the study area was detected by analyzing the relationship between the summarized situation of Micro-Landform and the woody life type corresponding to the Micro-Landform classification using TWINSPAN.

Keywords: LIDAR data, Micro-Landform, Vegetation, TWINSPAN

Japan Geoscience Union Meeting 2014
(28 April - 02 May 2014 at Pacifico YOKOHAMA, Kanagawa, Japan)

HSC25-12 Room:421 Time:April 30 12:30-12:45

An influence of roadway on occurrence of slope failure and debris flow of the Izu-Oshima Typhoon Wipha (1326) disaster

SHIRAI, Masaaki[1*] ; WATANABE, Makiko[1]

[1]Tokyo Metropolitan University

Vast slope collapse took place and debris flows struck the Motomachi-town foot of western slope of the Izu-Oshima Island on early morning 16, Oct. 2013. Field survey on the collapsed slope by *TMU Group for Izu-Oshima Typhoon Wipha (1326) Disaster Survey* was carried out 4 to 6, Dec. 2013.

One of the major concerns of the authors was an influence of roadway built after 1986 eruption on occurrence of 2013 slope collapse. Results of the survey are summarized as follows, (a) Collapse points originated from downslope side of the roadway (type-A collapse) were located on ridges and adjacent to collapse points originated from upslope side of the roadway (type-B collapse). (b) A large amount of debris of fallen tree which would have been transported by mud flow on the road was observed around the type-A collapse points. (c) A 1-0.5 m thick surface soil mass with tree and its dense roots was peeled from base of the retaining wall at the other small collapse. An appearance of the base of the retaining wall at the small collapse is similar with base of the retaining wall at type-A collapse.

Taking account into these results (a) to (c), it is inferred that type-A collapse would have occurred according to the following scenario, (1) rainwater and mud flow from type-B collapse flowed on the roadway, (2) around the curve on the ridge, rainwater/muddy water fell down from road surface to retaining wall and (3) surface soil mass (1-0.5 m thick) with dense tree roots and trunks was saturated by water and peeled from base of the retaining wall. Consequently, we conclude that the roadway was not a primary factor but secondary factor of the slope collapse, which expanded collapse area in this case.

Keywords: slope failure, Izu-Oshima, Typhoon Wipha (1326), roadway

Japan Geoscience Union Meeting 2014
(28 April - 02 May 2014 at Pacifico YOKOHAMA, Kanagawa, Japan)

HSC25-P01 Room:Poster Time:April 30 18:15-19:30

Reexamination of the 1960 Chilean tsunami disasters at the northern part of Amami Oshima island, Kagoshima Prefecture

IMURA, Ryusuke[1*] ; ZAIZEN, Yui[2] ; KUSAHARA, Hitomi[2] ; TOMIYASU, Kosuke[2]

[1]Graduate School of Science and Engineering, Kagoshima University, [2]Faculty of Science, Kagoshima University

We've interviewed about the Chilean tsunami disasters of 1960 at the northern part of Amami Oshima island. Results of our investigation suggest that the 1960 Chilean tsunami heights exceeding 3-4 m were observed in the almost coastlines of the northen part of Amami Oshima island.

Keywords: Amami Oshima, 1960 Chilean tsunami, tsunami disasters

Japan Geoscience Union Meeting 2014
(28 April - 02 May 2014 at Pacifico YOKOHAMA, Kanagawa, Japan)

HSC25-P02 Room:Poster Time:April 30 18:15-19:30

Utilization of the natural hazard database by NIED - a case of utilization at Typhoon Wipha (2013) on Izu Oshima island

SUZUKI, Hinako[1*] ; UCHIYAMA, Shoichiro[1] ; USUDA, Yuichiro[1]

[1]National Research Institute for Earth Science and Disaster Prevention (NIED)

This study introduces a case study on utilization of natural hazard database by NIED for extracting historical hazard events on Izu Oshima island suffering Typhoon Wipha in 2013. This powerful typhoon attacked on Motomachi area, and caused large-scale landslides. We searched the historical hazard events in this place from the natural hazard database to investigate relation between hazard this time and old events. Keywords for searching the database were ”typhoon”, ”heavy rain” and ”landslide”. As a result, seven events were found between 1925 and present, and typhoon Ida in 1958 was a particularly massive scale. The typhoon Ida that caused large landslide in Motomachi area, which was devastated again by Typhoon Wipha, was named ”Kanogawa typhoon” in Japan. Through these unification processes, we found two problems in our database:

1) No records about typhoon, heavy rain, and landslide before 1925 in this area
2) Little information about the date and time of occurrence and the extent

We will enrich these event records and information.

Keywords: natural hazard database, utilization, typhoon Wipha in 2013, Izu-oshima

Japan Geoscience Union Meeting 2014
(28 April - 02 May 2014 at Pacifico YOKOHAMA, Kanagawa, Japan)

HSC25-P03 Room:Poster Time:April 30 18:15-19:30

A new methodology to assess the impacts of precipitation change on flood risk in Tokyo 23 ward Area

HIRANO, Junpei[1*] ; DAIRAKU, Koji[1]

[1]National Research Institute for Earth Science and Disaster Prevention

n this study, we attempted to develop a new methodology for flood risk assessment in the Tokyo metropolitan area by considering the effect of precipitation change. By comparing the statistical distribution of the daily precipitation frequency for the whole study period, and those for flood occurrence days, we found that the distributions of the precipitation frequency for the flood occurrence days are corresponding to those for the whole study period. These results indicate that we can estimate flood damage based on frequency of daily precipitation. Based on these results, we estimated the flood damage for Tokyo based on distribution of daily precipitation frequency. We then created a flood-risk curve that represents the relationship between damage and exceeding probability of a flood. By comparing the newly developed flood-risk curve, based on the precipitation frequency, with those in the previous studies, we indicated that a newly developed flood-risk curve could evaluate the potential flood risk in Tokyo with high accuracy.

Keywords: Flood risk, Precipitation change, Risk curve, Tokyo metropolitan area

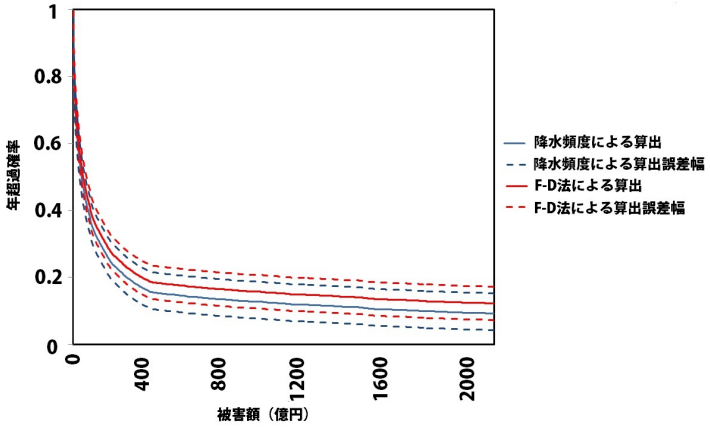

Japan Geoscience Union Meeting 2014
(28 April - 02 May 2014 at Pacifico YOKOHAMA, Kanagawa, Japan)

HSC25-P04 Room:Poster Time:April 30 18:15-19:30

Map Drilling of Disaster Prevention by Voluntary Group - An Example at Nasu Volcanic Area

FUKUSHIMA, Tamio[1] ; TAKAMORI, Shouji[3] ; INABA, Shigeru[4] ; NAKAMURA, Yoichi[2*] ; NASU, Local governmnet[5]

[1]National Association For Diaster Prevention, [2]Utusunomiya University, [3]Promotion Council of Distric Continuity Management, [4]Disaster Prevention Qualiged Counselor in Tochigi, [5]Manucipal Governmnet of Nasu Town

A map drilling of volcanic disaster prevention by voluntary groups: An Example at Nasu volcanic area was hold in the area of Nasu active volcano. This evacuation drilling at Nasu municipal government for voluntary groups of town people was supported by National Association for Disaster Prevention, Promotion Council of District Continuity Management, and Disaster Prevention Quailed Counselor in Tochigi. This project was managed financially to perform for last two fiscal years between 2012 and 2013. As a result, present drilling was very effective, especially for community people living near active Nasu volcano, in order to learn evacuation managements at the future volcanic emergency.

Keywords: Disaster Prevention, Map Drilling, Volcanic Diaster, Active Volcano, Eruption, Voluntary Group

Japan Geoscience Union Meeting 2014
(28 April - 02 May 2014 at Pacifico YOKOHAMA, Kanagawa, Japan)

HSC25-P05 Room:Poster Time:April 30 18:15-19:30

Disaster risk reduction workshop utilizing GIS and Saba-meshi: A practice of the Department of Geography, Oita Univ.

KOYAMA, Takushi[1*] ; DOI, Haruhiro[1] ; MORIMATSU, Maya[2] ; UCHIYAMA, Shoichiro[3]

[1]Department of Geography, Oita University, [2]Nihon Suido Consultants Co. Ltd., [3]NIED

The Department of Geography at Oita University held a disaster risk reduction workshop on November 3, 2013, for schoolchildren and their parents (A total number of participant was fifty one). The purpose of the event was to motivate the schoolchildren and their parents to aware of a disaster prevention and reduction in their daily life. The event consisted of the following two experiences: drawing a map using a geographic information system (GIS), and cooking rice using two 350ml aluminum cans and three 1L milk cartons (Survival *Meshitaki*). Survival *Meshitaki* is called *Saba-meshi* for short, and it is material for teaching about disaster prevention through practical experience.

After the event, the participants were requested to respond the questionnaires in order to evaluate the event. The results of the questionnaire showed that we received high evaluations from many participants on the experiences offered at the event. Therefore, we were able to raise the participants' awareness of disaster prevention and disaster reduction.

Furthermore, thirteen university students, who intend to become schoolteachers, participated the event as assistant staffs. They acquired in advance the fundamental skills of GIS and *Saba-meshi* by a preliminary training workshop. These are useful skills in the field of school education. The event, in conclusion, has given the participants and the students intending to be schoolteachers' very effective experiences and practical knowledge respectively and the experience-based event such as this workshop is worth to be held repeatedly.

Keywords: Geographic Information System, Saba-meshi, Disaster risk reduction workshop, The 2011 off the Pacific coast of Tohoku Earthquake, Students intending school teachers, Oita Prefecture

Japan Geoscience Union Meeting 2014
(28 April - 02 May 2014 at Pacifico YOKOHAMA, Kanagawa, Japan)

HSC25-P06 Room:Poster Time:April 30 18:15-19:30

Liquefaction occurrence ratio and geomorphic conditions in the inland area caused by the Great East Japan Earthquake

AOYAMA, Masafumi[1*]

[1]Japan Map Center

The area ratio of liquefied sites in the inland area caused by the 2011 off the Pacific coast of Tohoku Earthquake was estimated from the field survey and Google Earth images interpretation. In the Tone River lowland, the occurrence of liquefaction concentrated in the former river channel and pond, and the area ratio of liquefied sites is about 23%. The ground consisting of younger landfill age is more susceptible to liquefaction than that created by the older ones. Area ratio of Liquefied sites in the Tone River lowland is larger than the Osaki plain, Miyagi Prefecture. In the Osaki plain, the area of former river channels and ponds buried by loose sandy soils is less than the Tone River lowland.

Keywords: liquefaction, geomorphic classification, former river channel and pond, landfill age, 2011 off the Pacific coast of Tohoku Earthquake

Japan Geoscience Union Meeting 2014
(28 April - 02 May 2014 at Pacifico YOKOHAMA, Kanagawa, Japan)

HSC25-P07 Room:Poster Time:April 30 18:15-19:30

Problems on the disaster mitigation plan of the elementally and junior high school - a case study of Ishikawa Prefecture

AOKI, Tatsuto[1*] ; HAYASHI, Kiyomi[1]

[1]School of Regional Development Studies, Kanazawa Universiy

.

Keywords: Elementally and junior high school, Manual for disaser mitigaion, Hazard Map, Evacuation

Japan Geoscience Union Meeting 2014
(28 April - 02 May 2014 at Pacifico YOKOHAMA, Kanagawa, Japan)

HSC25-P08 Room:Poster Time:April 30 18:15-19:30

Tsunami hazard inventory survey of utilize for municipalities

OHSUMI, Tsuneo[1*] ; NAKAMURA, Hiromitsu[1] ; HIRATA, Kenji[1] ; OSADA, Masaki[1] ; FUJIWARA, Hiroyuki[1]

[1]National Research Institute for Earth Science and Disaster Prevention

A tsunami hazard inventory is important for tsunami disaster mitigation due to earthquakes, and also for a Tsunami hazard assessments. The tsunami hazard assessments project for Japan was started since 2012 by NIED (Fujiwara, *et al.,* 2013, Hirata, *et al.,* 2014). We performed inventory survey on utilization of the tsunami hazard assessments to Ibaraki and Chiba prefectures, which damaged municipalities of the tsunami during the 2011 off the Pacific Coast of Tohoku Earthquake. First stage, we surveyed the crisis management departments of the Ibaraki and Chiba Prefectures. Second stage, we surveyed 10 municipalities of Ibaraki prefecture and 18 municipalities of Chiba prefecture. Tsunami hazard inventory was carried out with a description of the Tsunami hazard assessments as the introduction. To discuss the possibility of the use of the municipality of tsunami hazard assessments current status and Issues of tsunami measures, organize the opinion and negative opinion aggressive to report the problem extraction.

Keywords: tsunami, hazard, public disclosure, disaster mitigation, probabilistic

Japan Geoscience Union Meeting 2014
(28 April - 02 May 2014 at Pacifico YOKOHAMA, Kanagawa, Japan)

HSC25-P09 Room:Poster Time:April 30 18:15-19:30

Reconstruction of paleo earthquake intensity

INOUCHI, Yoshio[1*] ; OKUMURA, Yuka[2] ; NAMEKI, Katsuhiko[3]

[1]Faculty of Human Sciences, Waseda University, [2]School of fHuman Sciences, Waseda university, [3]Graduate School of Human Sciences, Waseda University

Many drastic earthquakes have been occurred historically in Japan. In order to reduce damages caused by those earthquakes, data concerning frequency, magnitude and influenced areas of each earthquake are inevitable. Here, we report measuring method of paleo intensity of historic earthquakes at arbitrary selected stations based on empirical formulas. Based on data regarding position of epicenter and magnitude of each paleo earthquake, intensity of paleo earthquake at arbitrary site is estimated. At the beginning, these data were used to recognize earthquake triggered turbidites at several lakes. The results show that lower threshold of triggering turbidites are 45gal in Lake Biwa and 79gal in Lake Inawashiro, respectively. Usage of this kind of method will enable us to reconstruct paleo earthquake data which have no written record.

Keywords: paleo earthquake, intensity of quake, sediment

Japan Geoscience Union Meeting 2014
(28 April - 02 May 2014 at Pacifico YOKOHAMA, Kanagawa, Japan)

HSC25-P10 Room:Poster Time:April 30 18:15-19:30

An overview on current status of public disclosure for tsunami hazard information in and around Japan

OSADA, Masaki[1*] ; NAKAMURA, Hiromitsu[1] ; HIRATA, Kenji[1] ; OHSUMI, Tsuneo[1] ; FUJIWARA, Hiroyuki[1]

[1]National Research Institute for Earth Science and Disaster Prevention

A probabilistic tsunami hazard assessment research work is currently conducting by the National Research Institute for Earth Science and Disaster Prevention (NIED) (Fujiwara et al, 2013, Hirata et al., 2014). It is well recognized that output from such assessment should be transferred to the public as understandable and utilizable informations in various stages on hazard prevention works. From this point of view, as part of this project, we make a brief survey on how and what sort of hazard informations local residents are receiving from administrative authorities or agencies in and around Japan. Survey is focused on hazard map which is reachable through internet. In this paper, results are summarized in two categories, 1) type of maps and 2) distribution methods. Category 1 is able to divide into four subgroup; 1a is due to tsunami height map at shore (ex. Australia), 1b is tsunami inundation depth map which are based on the simulations on worst, most probable case, or probabilistic case (ex. most of Japanese prefectures, Indonesia, Oregon and Washington, USA), 1c is tsunami evacuation map in which zones to be quit are shown according to the warning level (Wellington, NZ, Oregon and Hawaii, USA), and 1d tsunami regulation map which prohibits (Oregon, USA). These maps are based on probabilistic or deterministic assessment outputs. Tsunami hazard informations are available mainly in style of the poster (downloadable in PDF format) although Web mapping (ex. Hawaii, USA) or GIS format (ex. Australia) can be found. Later seem to urge a user to secondary or further utilization. This survey suggests that it should be to provide tsunami hazard assessment results in various ways of presentations which meet user’s purposes.

Keywords: tsunami, hazard information, disclosure, hazard map, utilization

Japan Geoscience Union Meeting 2014
(28 April - 02 May 2014 at Pacifico YOKOHAMA, Kanagawa, Japan)

HDS05-01 Room:415 Time:April 29 09:00-09:15

Pore water pressure in slopes composed of multi-layer geological structure

IMAIZUMI, Fumitoshi[1*] ; MIYAMOTO, Kuniaki[2]

[1]Graduate School of Agriculture, Shizuoka University, [2]Faculty of Life and Environmental Sciences, University of Tsukuba

Increasing in pore water pressure in the slopes during heavy rainfall events is considered as an important factor induceing landslides. Sliding surface of many of these landslides locates on the boundary between different rock/soil strata. We need to know spatial distribution of the pore water pressure in slopes composed of multi-layer geological structure in order to explain occurrence mechanism of these landslides. Many of prior studies generally analyzed slope stability under condition that the pore water pressure is same as the hydrostatic pressure. These studies ignored influence of depth profile of hydraulic parameters on magnitude of the pore water pressure. We, therefore, tried to understand spatial distribution of the pore water pressure on the basis of the continuity equation and equation of motion for seepage flow in two-dimensional slopes with multi-layer soil structure. Our study clarified that the water velocity as well as the depth profile of the pore water pressure are affected by depth profile of the hydraulic conductivity in the saturated zone. Pore water pressure agrees with hydrostatic pressure in case that the saturated zone develops on the impermeable soil layer. Meanwhile, pore water pressure is smaller than hydrostatic pressure in case that bottom of the saturated zone contacts with unsaturated zone. In this case, magnitude of the pore water pressure depends on the difference in the hydraulic conductivity between upper and lower layers. In addition, pore water pressure is highest at a layer boundary. Our analysis results agree with the general landslide characteristic that the sliding surface locates on a layer boundary.

Keywords: landslide, pore water pressure, multi-layer soil structure, seepage flow

Japan Geoscience Union Meeting 2014
(28 April - 02 May 2014 at Pacifico YOKOHAMA, Kanagawa, Japan)

HDS05-02 Room:415 Time:April 29 09:15-09:30

Landsliding phenomenon under abnormal weather conditions: a case study

WANG, Gonghui[1*] ; SUEMINE, Akira[1] ; MATSUURA, Sumio[1] ; ARAIBA, Kiminori[2]

[1]Disaster Prevention Research Institute, Kyoto University, [2]National Research Institute of Fire and Disaster

To examine the initiation and movement mechanisms of landslides occurring during abnormal weather conditions, we have been monitoring a landslide on Nisenotani area in Miyazaki Prefecture, Japan. The monitoring items include the weather conditions (rainfall and air pressure), moisture content of surficial soil layers, groundwater table, and displacements (by means of borehole wire extensometer, surficial extensometer, and total station). Cracks appeared on the slope after a heavy rainfall and borehole investigation revealed that this landslide is a large compound one, consisted of several sub-blocks. Our dense monitoring is performed on a small block of the toe part, and our results showed that: (1) landsliding was initiated by a heavy rainfall, but was not less affected by small rainfall; (2) landsliding varies with air-tide; (3) lower part of the sliding sub-block had been continuously compressed; (4) the sliding surface and the compressed soil layer had been effectively identified by means of a surface-wave technique.

Keywords: Abnormal weather, air pressure, Rainfall, landsliding, groundwater table

Japan Geoscience Union Meeting 2014
(28 April - 02 May 2014 at Pacifico YOKOHAMA, Kanagawa, Japan)

HDS05-03 Room:415 Time:April 29 09:30-09:45

Extreme Rainfall Effect on Slope Hazards along Mountain Roadway

WANG, Chao-wen[1*] ; YOSHIMI, Kazuhiro[1] ; YAMADA, Tadashi[1]

[1]Graduated School of Science and Engineering, Chuo University

Due to the global climate changes, the scale and frequency of natural disasters are more difficult to predict and measure. Extreme rainfall often brings astonishing amount of water and causes very serious damage in the mountain areas. And for different environment conditions, the slope hazards induced by rainfall would be different like geology, topography or location. Therefore in this research, the authors considered the elevations, slope aspect, slope gradient and geology to compare and analysis the rainfall effect on slope hazards by using the historic landslides records. And the major method of rainfall analysis is the snake line model that is using dual-indexes of rainfall- short term rainfall intensities and accumulated rainfall data. Short term rainfall intensities mean hourly rainfall, 3 hourly rolling rainfall, 6 hourly rainfall and so on. The most important of these rainfall analyses are trying to find some regulars in occurrence of slope hazards. Furthermore, the authors also collected different hazard types in order to try to get the rainfall characteristics of different disasters. In this research, the authors used the Da-Jia River upstream region (Taiwan) as the case study. In this region, over than half area the slope gradient is larger than 55%. Through the results of the analyses, the authors get some important conclusions. Firstly, in the environment conditions, the effects of slope gradient, elevation, and geology are obvious. Secondly, the effect of slope aspect is according to the rainfall events. Finally, in extreme rainfall events, the trend of occurrence time in different hazards can be observed. According to the above conclusions, it can be effective to make decisions to prevent disasters and reduce lost.

Keywords: Landslides, Rainfall

Japan Geoscience Union Meeting 2014
(28 April - 02 May 2014 at Pacifico YOKOHAMA, Kanagawa, Japan)

HDS05-04 Room:415 Time:April 29 09:45-10:05

Shallow Landslide Susceptibility Mapping for Selected Areas in the Philippines Severely Affected by Super Typhoon Haiyan

RABONZA, Maricar[2*] ; FELIX, Raquel[1] ; ORTIZ, Iris jill[1] ; ALEJANDRINO, Ian kaye[2] ; AQUINO, Dakila[2] ; ECO, Rodrigo narod[1] ; LAGMAY, Alfredo mahar francisco[2]

[1]University of the Philippines Diliman, [2]Nationwide Operational Assessment of Hazards, Department of Science and Technology

Super Typhoon Haiyan, considered as one of the most powerful storms recorded in 2013, devastated the central Philippines region on 8 November 2013. In its wake, Haiyan left 6,190 fatalities, 28,626 injured and 1,785 missing, as well as damage amounting to more than USD 823 million. To mitigate damage from similar events in the future, it is imperative to characterize hazards associated with tropical cyclones such as those brought by Haiyan, with detailed studies of storm surges, landslides and floods. Although strong winds and powerful storm surges up 15-17 feet were the primary causes of damage, landslides studies are also vital in the rehabilitation of typhoon damaged areas. Cities and municipalities of Leyte (7,246.7 sq. km) and Samar (13,121 sq. km) provinces, the heaviest cities area during the onslaught of Haiyan, require detailed and up-to-date hazard maps for their rebuilding and disaster mitigation programs. In order to delineate areas susceptible to rainfall-induced shallow landslides and generate a worst-case scenario hazard map of the two provinces, Stability INdex MAPping (SINMAP) software was used over a 5-meter-resolution Interferometric Synthetic Aperture Radar (IFSAR)-derived digital elevation model (DEM) grid. SINMAP has as its theoretical basis in the infinite plane slope stability model. Topographic, soil-strength and hydrologic parameters (cohesion, angle of friction, bulk density and hydraulic conductivity) were used for each pixel of a given DEM grid to compute for the corresponding factor of safety. The landslide maps generated using SINMAP are found to be highly consistent with the landslide inventory derived from high-resolution satellite imagery dated 2003 to 2013. The landslide susceptibility classification found in the landslide hazard maps are useful to identify no-build, areas that can be built upon but with slope intervention and monitoring as well as places that are safe from shallow landslides. These maps complement the debris flow and structurally-controlled landslide hazard maps that are also being prepared for rebuilding Haiyan‘s devastated areas.

Keywords: Natural Hazards, Landslide, Hazard Mapping

Japan Geoscience Union Meeting 2014
(28 April - 02 May 2014 at Pacifico YOKOHAMA, Kanagawa, Japan)

HDS05-05 Room:415 Time:April 29 10:05-10:20

Calculation of Shallow-Landslide Rainfall Threshold for Libon, Albay, Philippines Using TRIGRS

ALEJANDRINO, Ian kaye[1*] ; ALEMANIA, Maneka kristia[1] ; AQUINO, Dakila[1] ; ECO, Rodrigo narod[1]

[1]DOST Project NOAH

In a rainfall event caused by a cold front and a low pressure area during the 14th until the 21st of February 2008, the Albay province experienced several landslides with $4.6 million in damages to infrastructure alone. Aside from delineating areas that are highly susceptible to landslide, it is important to determine shallow-rainfall threshold aid in the development of an early warning system. The study area was carried out on an area in Libon town in Albay with approximately 1000 residents living near the high hazard area. Using TRIGRS software (Transient Rainfall Infiltration and Grid-based Regional Slope-stability analysis), 6 different sustained rainfall intensities with the duration of 24 hours were simulated to a 5-meter resolution IFSAR (Interferometric Synthetic Aperture Radar)-derived DEM (Digital Elevation Model). Topographic, soil strength, and hydrologic parameters were assigned to each pixel of the given DEM grid to compute for the factor of safety using the theory on Infinite Plane Slope Stability to produce a shallow-landslide susceptibility map. The values of the different rainfall intensities were selected to represent different rainfall events equal (1.26mm/hr), less than (.5 and 1mm/hr) and greater than (1.5, 2.73, 7.5 mm/hr) the infiltration rate of the soil. After comparison, there were no observed differences in the hourly variation of the Factor of Safety Maps for 1.26 mm/hr and greater intensities. The rainfall threshold determined to be 4.5 to 5mm of effective accumulated rainfall on which the pixels that failed (FS$<$1) matched the landslide inventory from 2003-2014 and the shallow-landslide hazard map. This study shows that in determining rainfall thresholds for shallow landslides the effective infiltration rate and hydraulic diffusivity of the soil serves as factors on how fast the slope reaches instability during a rainfall event. The results of this study may be treated as the worst case possible due to the sustained intensities and may be further improved through simulations using data of actual rainfall events, considering varying rainfall intensities and durations.

Keywords: Landslide, Shallow, Rainfall, GIS, Albay, Philippines

Japan Geoscience Union Meeting 2014
(28 April - 02 May 2014 at Pacifico YOKOHAMA, Kanagawa, Japan)

HDS05-06 Room:415 Time:April 29 10:20-10:35

Sensitivity of the initiation of debris flow to initial soil moisture

HU, Wei[1*] ; XU, Qiang[1] ; WANG, Gonghui[2] ; VAN ASCH, T.w.j.[3] ; HICHER, Pierre-yves[4]

[1]State Key Laboratory of Geo-Hazard Prevention and Geo-Environment Protection, Chengdu University of, [2]Disaster Prevention Research Institute, Kyoto University, Japan, [3]Faculty of Geosciences, Utrecht University, Heidelberglaan 2, 3584 CS, The Netherlands, [4]LUNAM University, Ecole Centrale de Nantes, CNRS UMR 6183, France

The initiation of debris flows is commonly attributed either to fluidization as a result of rainfall induced landslides or to gully erosion induced by concentrated run-offs. A series of flume tests have been performed to show how the initial soil moisture influences the initiation of debris flows. At the start of each experiment, surface run-off was generated over loose granular deposits, triggering debris flows. These experimental debris flows enacted different scenarios according to the small variations among the initial soil moistures. In the loose granular deposits with initial soil moistures ranging from 1% to 5%, most run off water could infiltrate and trigger a landslide, which accelerated within one second to speed over 1 ms-1 and then transformed into a debris flow. In the same soil deposits with initial moistures >5% or <1%, the debris flow was initiated by slow gully erosion with episodic events of damming and breaching due to small-scale landslides occurring on the side-slopes of the erosion valley. The slope failures were not triggered by positive pore pressure but by a decrease in suction due to the wetting of the soil. This suction decrease in initially unsaturated slopes explains why the transformation of these slope failures into debris flows are due not only to an increase of pore pressure leading to soil liquefaction, which is one of the expected triggering mechanisms, but also to a loss of the cohesive strength of the soil.

Keywords: debris flow, soil moisture, initiation

Japan Geoscience Union Meeting 2014
(28 April - 02 May 2014 at Pacifico YOKOHAMA, Kanagawa, Japan)

HDS05-07 Room:415 Time:April 29 11:00-11:15

Gully development on flows and deep-seated slides in the Mangaoporo catchment, North Island, New Zealand

PARKNER, Thomas[1*]

[1]College of Geoscience, University of Tsukuba

Mass movements and gully erosion are widespread phenomena in many steep, erosion prone catchments. Understanding gully erosion on unstable slopes is important for the management of slopes as well as for management of river systems, as large quantities of sediment are supplied by gully erosion directly into river systems causing off-site damage.

The development of gullies on unstable slopes is not well understood. In this study gully development on slopes affected by mass movements was analysed in 14 headwater catchments of the Mangaoporo catchment, North Island, New Zealand. Bedrock consists of Cretaceous-aged, highly crushed and sheared mudstones and sandstones. Deforestation by European settlers at the beginning of the 20th century for pastoral farming was followed by reforestation for wood production from the 1980s. Sequential aerial photographs from 1939 to 2005 were interpreted to map mass movements and the development of gullies. Digital elevation models were extracted from aerial photography using ERDAS to assess the applicability of the commonly applied topographic threshold approach for gully incision.

Flows of varying depth occurred in all catchments underlain by mudstone, while the catchment consisting of alternations of mudstone and sandstone were affected by deep seated sliding and secondary shallow sliding. Deep (few meters to 15m) gullies were located at the toe of mass movement bodies. Such gullies developed oversteepened sidewalls, which in turn initiate extensive mass movements at the gully walls. Shallow (about 1 -2m deep), hundreds meter long gully arms extended upslope. Topographical changes by active flows and slides caused stream capture or gully destruction. Cracks and scraps functioned as incision pathways.

The topographic threshold approach is not appropriate for unstable slopes, as the mass movement topography exhibits irregular drainage pattern and gully incision depends on the morphology of mass movements. New approaches need to be developed for gully incision on unstable slopes to understand the spatial and temporal variability of incision dynamics on unstable slopes.

Keywords: gully erosion, flow, slide, New Zealand

Japan Geoscience Union Meeting 2014
(28 April - 02 May 2014 at Pacifico YOKOHAMA, Kanagawa, Japan)

HDS05-08 Room:415 Time:April 29 11:15-11:35

Quantifying the seismic response of slopes: observed and modelled amplification from the Port Hills of Christchurch

MASSEY, Chris[1*] ; KAISER, Anna[1] ; HOLDEN, Caroline[1]

[1]GNS Science

ABSTRACT: Before the Christchurch 2010/11 earthquake sequence the influence of site effects on landslide triggering during earthquakes was reported in many studies, but evaluating these effects has been difficult through lack of high-resolution data, especially the lack of local ground motion instrumental observations. As a result of the Christchurch 2010/11 earthquake sequence we now have high temporal and spatial resolution data, including subsurface geotechnical and geophysical information that allows quantification of the amplification relationships between the near surface geology, topography and seismic inputs.

This paper presents preliminary results on site effects in the Port Hills of Christchurch caused by near surface material impedance contrasts and slope morphology. Results from small scale temporary arrays installed on several of the large rock slopes that failed repeatedly during the earthquakes suggest amplification factors of up to 300% of peak ground acceleration when compared to free field rock outcrop peak ground accelerations. These are corroborated not only by two dimensional seismic site response analyses using synthetic earthquake motions as inputs to the models but also by comparing recorded ground motions from borehole and surface seismometers.

Based on these findings it is apparent that particular slope shapes and material contrasts can significantly amplify peak ground accelerations during earthquakes. At present in New Zealand such amplification effects are not routinely taken into account when designing earthworks or structures on slopes or in landslide risk assessments.

Keywords: Earthquake induced landslides, topographic amplification, earthquake hazards

Japan Geoscience Union Meeting 2014
(28 April - 02 May 2014 at Pacifico YOKOHAMA, Kanagawa, Japan)

HDS05-09 Room:415 Time:April 29 11:35-11:55

Distribution loess landslides triggered by the 1920 Haiyuan earthquake and their formation mechanisms

HUANG, Runqiu[1*] ; PEI, Xiangjun[1] ; HAN, Xiangsen[1] ; ZHANG, Xiaochao[1]

[1]Chengdu University of Technology

The 1920 Haiyuan Earthquake (M=8.5) is one of the strongest earthquakes in Chinese modern history, and directly resulted in more than 200,000 people dead. The Earthquake induced a large number of landslides. Among them, we investigated 544 landslides in the meizoseismal area, and found that the distributions of the landslides are mainly concentrated in the southeastern part of the seismogenic fault, but the relationship with the NW-trending seismogenic fault is not noticeable. Further investigation indicated that such distribution is mainly controlled by two types of factors. One is the nearly SN-trending secondary faults concealed under the loess cover. The other one is the thickness of the loess. The landslide is more intensive in those areas with thicker loess and the density of the landslides decreases with the decreasing in the loess thickness, while landslides occurring in the bedrocks are very rare.

Investigation shows that the sliding surface of a large number of loess landslides is extremely gentle with the apparent friction angle ranging between 8 -11 degrees. Liquefaction phenomenon was found on a large number of areas in loess tableland along both sides of the river in the meizoseismal area. This is likely one main reason for the occurrence of landslides with very gentle sliding surface angle. Laboratory testing of undisturbed loess of these regions indicated that the sand content ranges from 3% to 15%, silt content is about 65% - 85%, clay content between 10% - 20%, and thus this kind of soil belongs to silt. But the sand content showed uneven distribution and high sand content occurred in local area. Dynamic triaxial tests showed the saturated loess could suffer from liquefaction failure.

However, there existed a large number of low angle slip surface, large runout and high mobility loess landslides in the slope zone with low underground water level. Loess is characterized by large pores with high compressibility and low strength. Scanning electron microscopy revealed that cement of loess particles were dispersed particulate, distributed discontinuously attached to the particle surface or accumulated at the point of the contact in the skeleton, the adhesive strength is very low. The earthquake occurred in December of that year’s winter. Due to very low water content of loess, relatively dry shallow loess easily shattered and collapsed under strong shaking of extreme earthquake. Therefore this caused occurrence of the high-speed and long runout landslide.

Finally, we conclude that because of the special geological characteristics of loess, there are more than two types of landslide mechanism: one is the liquefaction occurring on the loess layer affected by the groundwater level; the other one is the collapse of loess structure under strong earthquake.

Japan Geoscience Union Meeting 2014
(28 April - 02 May 2014 at Pacifico YOKOHAMA, Kanagawa, Japan)

HDS05-10 Room:415 Time:April 29 11:55-12:10

Geomorphological and Geological Features of The Collapsing Landslides Induced by The 2009 Padang Earthquake.

NAKANO, Maho[1*] ; CHIGIRA, Masahiro[2]

[1]CTI Engineering Co., Ltd., [2]Disaster Prevention Research Institute, Kyoto University

The Mw7.6 Padang earthquake in 2009 attacked the northwest of Sumatra, Indonesia, and triggered many landslides, which killed at least 130 people at one village. We made satellite image interpretations, field investigations, and laboratory tests to identify the geomorphological and geological features of these landslides. As a result, we found that the number of landslides was 159, materials that slid were pumice fall deposits, and their sliding surface was made within the base of the pumice layer where pumice grains were mixed with underlying lahar and heavily weathered. These landslides had the following characteristics: 1) they occurred in the areas with pumice beds with $>$3 m thickness, which was controlled by the distance from their source; 2) the pumice fall deposits had a slope-parallel layering, which had been cut at the foots of slopes; and 3) the mixed layer at the base of the pumice beds was heavily weathered to be clayey materials with abundant halloysite.

We made an isopach map of the pumice fall deposits, which is so-called Qhpt and believed to be from Maninjau Caldera. The isopach contours, however, showed that Qhpt is from Tandikat Volcano, and that landslides occurred in clusters in the areas with pumice beds thicker than 3.5 m.

Qhpt beds had slope-parallel bedding, but they were undercut by subsequent river incision. Interpretations of stereoscopic satellite images and field surveys showed that there are four terraces along the Magung River, and Qhpt covers widely distributed higher terraces (Lh) of lahar younger than 80 ka and middle terraces (Lm) but are cut by lower terraces (Ll1 and Ll2) as well as small nearby tributary gullies. This undercutting likely reduced the support of Qhpt beds from downslope.

The mixed layers, in which sliding surfaces were formed, were heavily weathered and very weak; weaker than the main Qhpt above and the lahar below. XRD analyses showed that pumice grains of the main part of Qhpt scarcely had halloysite but pumice grains and weathered lahar in the mixed layers were rich in halloysite. The formation of halloysite could be attributed to the interaction between the materials of the mixed layers and the water coming through Qhpt beds; water, which gets Si and other chemical components from the volcanic glass of pumice, may become stagnant in the mixed layers because they are much less permeable than the Qhpt beds above. This would be a preferable condition of halloysite formation.

Infinite slope stability analysis using geotechnical parameters, pumice bed thickness, and slope angles, which we obtained, suggested that landslides with sliding surfaces within the mixed layers could be triggered by the shaking of the 2009 Padang earthquake. The natural water contents of the materials of the mixed layers exceeded their liquid limits, which suggests that they would behave like a liquid after remolding.

The geological history, which is volcanic eruption, weathering, and undercutting by river incision as stated above, is typical in tropical volcanic areas. That means we can make a hazard map of such a catastrophic landslide induced by earthquakes on the basis of geological development.

Keywords: 2009 Padang earthquake, Halloysite, Collapsing landslide, pumice fall deposits, weathering

Japan Geoscience Union Meeting 2014
(28 April - 02 May 2014 at Pacifico YOKOHAMA, Kanagawa, Japan)

HDS05-11 Room:415 Time:April 29 12:10-12:25

The seismic signals from the model slope failure and erosion tests

FENG, Zheng-yi[1*] ; YU, Chia-cheng[1]

[1]National Chung Hsing University, Taiwan, ROC

High intensity rainfalls in mountainous areas often induce floods. The floods could erode riverbank slopes and cause them to landslide. This study selected Landao Creek of Huisun Experimental Forest (Nantou, Taiwan) as the in-situ test site for the model slope failure and erosion tests. We built a large size model soil slope and an artificial landslide dam in Landao Creek for the tests. The Nengau agricultural channel at the upstream of Landao Creek was setup to control the inflow to Landao Creek. Therefore, the artificial landslide dam were overtopped when the retention space were full by the inflow water. Consequently, the dam breached and caused the model soil slope to be eroded by the flooding water. The model soil slope failed partially due to the erosion and generated seismic signals during the slope materials sliding down. We installed of several accelerometers sensor on the model soil slope to collect seismic signals generated. We present two test results in this study. The seismic signals were analyzed using the Hilbert-Huang Transform for time-frequency spectrograms. We explored the characteristics of seismic signals due to the model soil slope sliding and the flooding. In addition, we can use the time-frequency spectrograms to identify the timings when the model slope slid repeatedly.

Keywords: Landslide, slope, erosion, seismic signal, flood, dam

Japan Geoscience Union Meeting 2014
(28 April - 02 May 2014 at Pacifico YOKOHAMA, Kanagawa, Japan)

HDS05-12 Room:415 Time:April 29 12:25-12:40

Characteristics of the slope failures in Izu-Oshima Island on Oct. 16, 2013, inferred from seismic waveform records

DOI, Issei[1*] ; KAMAI, Toshitaka[1] ; WANG, Gonghui[1] ; MORITA, Yuichi[2]

[1]DPRI, Kyoto Univ., [2]ERI, Univ. of Tokyo

On Oct. 16, 2013, large-scale slope failure took place due to extreme rainfall in Izu-Oshima Island in Japan. The precipitation reached over 90 mm per hour from 1:00 to 5:00 before and during the period when the failures took place. Through geological surveys by us and Natural Disaster Research Council, piping holes were observed on the collapsed slopes, which suggested that the ground water spouted due to high water pressure. It is important to grasp the detailed behaviors of water and sediment movement in order to reduce the slope disaster in the volcanic regions.

Signals of failures and their related sediment movements were recorded many times by several seismometers installed around by Oshima Volcano Observatory of ERI, Univ. of Tokyo. The seismic signals were observed almost at the same time at several stations. Four major signals were detected from 2:00-3:00, while at least a few tens were observed from 3:00-5:00. These signals had unclear initial phases and long (several minutes) durations. The amplitudes increased almost at the same time at the beginning among the stations, while the times when they attained the maximum values were earlier at the stations located in the upper side of the slope. These facts indicate that the vibrations were firstly generated in the upper side of the slope, then moving toward the downside.

Acknowledgments: We used meteorological data recorded by JMA.

Keywords: slope failure, seismic waveform, sediment movement

Japan Geoscience Union Meeting 2014
(28 April - 02 May 2014 at Pacifico YOKOHAMA, Kanagawa, Japan)

HDS05-13 Room:415 Time:April 29 14:15-14:35

Friction law of gouges from monotonic and cyclic shear tests - implications for rockslide triggered by earthquakes

DONG, Jia-jyun[1*] ; TETSUHIRO, Togo[2] ; LAI, Jun-rong[1] ; YANG, Che-ming[1] ; LEE, Chyi-tyi[1] ; SHIMAMOTO, Toshihiko[2]

[1]Graduate Institute of Applied Geology, National Central University, Taiwan, [2]State Key Laboratory of Earthquake Dynamics, Institute of geology, China Earthquake Administration

The differences of soil strength under static and dynamic loading have been well recognized. This study utilized rotary shear apparatus to elucidate the friction coefficient of gouge materials under monotonic and cyclic shearing conditions. A rigid block model incorporating the velocity/displacement dependent friction law from monotonic tests was adopted to simulate the dynamic shearing behavior. Basically, the friction coefficient under maximum shearing velocity was well depicted. However, the friction coefficient under zero velocity for dynamic shearing tests was overestimated. A frequency factor, which taking the healing effect into account, was successfully incorporated into the friction law to simulate the variation of the friction coefficient under dynamic loading condition. The modify friction law with consideration of the cyclic shearing frequency was used to evaluate the triggering of a dip slope rockslide during earthquake. It is illustrated that the cyclic shear induced from the earthquake is critical for the initiation of large scale rockslide. The influence of seismic loading on earthquake-triggered rockslide can thus be evaluated quantitatively.

Keywords: monotonic and cyclic shear, velocity and displacement dependent, friction coefficient, rotary shear test, gouge, earthquake triggered rockslide

Japan Geoscience Union Meeting 2014
(28 April - 02 May 2014 at Pacifico YOKOHAMA, Kanagawa, Japan)

HDS05-14 Room:415 Time:April 29 14:35-14:50

Fast Shear Behaviour of Granular Material and Rapid Landsliding Phenomena

JIANG, Yao[1*] ; WANG, Gonghui[2] ; KAMAI, Toshitaka[2]

[1]Graudate School of Science, Kyoto University, [2]Disaster Prevention Research Institute, Kyoto University

Many rapid landsliding events are normally catastrophic in which granular masses flow with extremely low friction. In order to prevent and mitigate the disaster, it is essential to better understand their mechanisms of initiation, motion and deposition. Although a great deal of research and attention has been focused on the unusual physical features for rapid landsliding events, the dependence of frictional properties on particle characteristics and test conditions has not yet been clearly understood. In the present research, we performed a set of experimental studies to examine the grain-scale frictional properties. We used two kinds of glass beads to examine how particle size affected the strength and stability of granular materials by employing a large ring-shear, and sheared the samples by changing the shear rate from 0.1 to 100 mm/s under different normal stresses (50, 100, 200, 400 kPa). It was found that the influence of shear rate on the residual shear strength for glass beads was negligible, while the stress fluctuation was observed for different particle sizes. Three distinct spectral peaks were identified in the frequency spectra for the two glass beads by utilizing Discrete Fourier Transform (DFT) method. According to the frequency spectra, we found that the stress fluctuation of glass beads was closely related to the particle size. Then we analyzed the role of particle size in the fast shear behaviour of granular materials and their relationship to the rapid landsliding behavior of rock avalanche.

Keywords: fast shear behavior, rapid landsliding, glass beads, particle size, shear rate, stress fluctuation

Japan Geoscience Union Meeting 2014
(28 April - 02 May 2014 at Pacifico YOKOHAMA, Kanagawa, Japan)

HDS05-15 Room:415 Time:April 29 14:50-15:05

Changes in particle size distribution of clayey material at a catastrophic landslide base

TSOU, Ching-ying[1*] ; CHIGIRA, Masahiro[1] ; FENG, Zhengyi[2] ; HIGUCHI, Kohei[3]

[1]Disaster Prevention Research Institute, Kyoto University, Uji, Japan, [2]Department of Soil and Water Conservation, National Chung Hsing University, [3]Department of Civil Engineering, National Cheng Kung University

In August 2009, a catastrophic rockslide avalanche was initiated by a cumulative rainfall of 1676.5 mm by Typhoon Morakot in the southern mountainous region of Taiwan. The landslide occurred on slopes extending from head scarp to the opposite riverside with a fall height of 830 m and generated the runout distance of 3.2 km long. The mobility of the landslide was high, indicating by its low apparent friction angle of 14 degrees and velocity of 70 to 120 km hr^{-1} in 95 s. The landslide claimed more than 400 people dead and missing when the village of Shiaolin was destroyed directly in the path of the landslide. We found clayey material in many locations at the base of the landslide deposits. Two samples S1 and S2 and one sample D1 of clayey material were respectively collected from the base of the remaining debris in the lower part of source area and the base of the deposits in the depositional area. Their mineralogy and particle size distribution were analyzed using an X-ray diffractometer (Rigaku Gaigerflex RAD IIB) and a laser diffraction particle size analyzer (Shimadzu, SALD-3100), respectively. The X-ray analysis indicates that the samples are the same material, in terms of texture and mineralogy, consisting of illite, chlorite, quartz, feldspar, and calcite. Besides, particle size analysis shows that samples S1 and S2 of the source area had two particle size modes at 15 μm and 50 – 100 μm, and sample D1 of the depositional area had one mode at 15 μm. This difference between the samples may reflect pulverization during movement of the material from the source area to the depositional area. The overall particle size distribution is narrower in sample D1, and the mean grain size (D_{50}) decreased from 11.03 μm in sample S2 to around 8.96 μm in sample D1. Sample S1 has larger amounts of finer fractions than do samples S2 and D1, and its distribution curve has a flattened top in comparison with the other two samples, which could be attributed to intense shearing between bedrock and debris. The results suggest that the clayey material at the landslide base and the increasing fine-grained content of the clayey material during shearing are assumed to have a significant impact on its long, rapid movement.

Keywords: rockslide avalanche, high mobility, clayey material, particle size distribution

Japan Geoscience Union Meeting 2014
(28 April - 02 May 2014 at Pacifico YOKOHAMA, Kanagawa, Japan)

HDS05-16 Room:415 Time:April 29 15:05-15:20

Application of TCP-InSAR technique for the Deep-Seated landslides detection and monitoring at Cingjing village, Taiwan

LIU, Shouheng[1] ; LIN, Chingweei[1] ; CHEN, Roufei[2*] ; ZHANG, Lei[3]

[1]Department of Earth Sciences, National Cheng Kung University, Taiwan, [2]Department of Geology, Chinese Culture University, Taiwan, [3]Department of Land surveying and Geo-informatics, Hong-Kong polytechnic university, Hong-Kong

Taiwan located at an active mountain belt and subtropical climate environment, severe gigantic landslide that have caused considerable damages commonly occurred in mountainous areas. After the 2009 Hsiaolin landslide that caused 450 casualties, how to identify potential sites of Deep-Seated landslides, evaluate their activity and susceptibility become an important issue. In the past few years, our research team has processed many slope failures that have caused considerable damages by using airborne LiDAR Digital Elevation Model (DEM), and implemented related analyses for the goal of deep-seated landslide. Cingjing village located at Centre Taiwan is well known as one of the three high altitude agriculture area in mountainous regions. In this study, we using TCP-InSAR interfermotry from ALOS/PALSAR images to detect and monitoring the landslide activity and its susceptibility of deep-seated deformation over a large area. The method obtains more ground deformation information than other InSAR approaches, providing more comprehensive analytical results for the slope related hazard studies. Our TCP-InSAR result shows a significant subsidence pattern around the Cingjing area. Comparing the surface deformation data and the field investigation records, several imperceptible deep-seated landslide locations are found and the boundaries can be identified as well as the spatial distribution of instability to them. The deposition pattern also implies different landslide development types on the slopes. This case study shows the great potential of TCP-InSAR evaluating the slope activities and deformation in the vegetated mountain area. Combined with topography signatures from high resolution digital elevation model data, it will be an effective way to determine the stability of slopes and potential hazard locations over a large area.

Keywords: Deep-Seated landslides, TCP-InSAR technique, Airborne LiDAR, Cingjing village

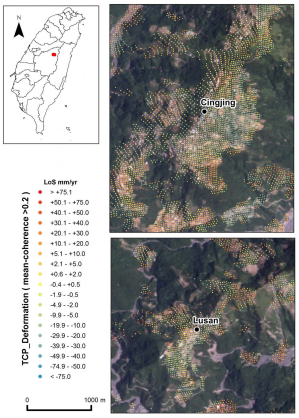

Japan Geoscience Union Meeting 2014
(28 April - 02 May 2014 at Pacifico YOKOHAMA, Kanagawa, Japan)

HDS05-17 Room:415 Time:April 29 15:20-15:35

Preceding topographic features of catastrophic landslides in an accretion complex in the Kii Mountains

CHIGIRA, Masahiro[1*] ; MATSUSHI, Yuki[1] ; TSOU, Ching-ying[1] ; HIRAISHI, Narumi[2]

[1]Disaster Prevention Research Institute, Kyoto University, [2]previously Fukada Geological Institute

Slope movements is one of the major processes of denudation as well as erosion and transportation by rivers or glaciers, and many slope movements themselves are induced by river or glacier erosion. We investigated the linkage of river erosion, deep-seated gravitational slope deformation, and catastrophic landslides in the Kii Mountains Japan, where occurred tens of catastrophic large landslides during 1889 Totsukawa typhoon and 2011 typhoon Talas. The consequent fatalities were 168 and 56, respectively. The Kii Mountains is underlain by the Cretaceous to Neogene Shimanto accretional complex in large areas and has paleosurface remnants in higher elevations. The paleosurfaces have been newly incised by rivers, of which the Kumano River catchment occupies the central part of the Kii Mountains. The new incision of the Kumano River proceeded with the upstream propagation of knickpoints, which developed well-defined convex slope breaks on interfluve slopes. High-resolution DEMs clearly delineated deep-seated gravitational slope deformations, which are characterized by scarps, linear depressions, and bulges, aligned along the convex slope breaks, suggesting that they were induced by gravitational instability induced by the erosion undercutting. The catastrophic landslides during the 1889 Totsukawa typhoon and 2011 typhoon Talas occurred had been preceded by deep-seated gravitational slope deformation on newly incised inner valley slopes. Most of the landslides had sliding surfaces along undulating minor faults, probably thrusts, which might have made rock bridges when shearing along preferably oriented parts of the faults occurred. Catastrophic slop failure may occur when those rock bridges are finally fractured.

Keywords: gravitational slope deformation, landslide, accretion complex

Japan Geoscience Union Meeting 2014
(28 April - 02 May 2014 at Pacifico YOKOHAMA, Kanagawa, Japan)

HDS05-18 Room:415 Time:April 29 15:35-15:50

Recognition of large scaled deep-seated landslides using high resolution topography and case studies in Taiwan

HO, Dia jie[1*] ; LIN, Ching-weei[2]

[1](1)Disaster Prevention Research Center National Cheng Kung University, [2](2)Department of Earth Sciences National Cheng Kung University Tainan Taiwan

High resolution topography and topographic characteristics of large scale deep-seated landslides (landslide area >10 ha) are used to interpret large scale deep-seated landslides in an area of 4980.8 km2 and a total number of 1607 potential large scale deep-seated landslides are recognized. The results show that main distribution of potential large scale deep-seated landslides in Kao-Ping River watershed is near structural lineaments and both sides of the river.

Two cases discussed in the study are on the right bank of Baolai River in Baolai, Kaohsiung City and on the left bank of Luliao River in Yanping Township, Taitung County. Typhoon Trami (08/20˜08/22), Typhoon Kong-Rey (08/27˜08/29) and Typhoon Usagi (09/19˜09/22) are main typhoon events of 2013.

Potential landslide area, average slope angle and main lithology of case I is 96.6 ha, 31.1? and argillite. GPS data show a maximum horizontal displacement of 27.6 cm to southwest and a maximum subsidence of 20.5 cm after Typhoon Trami and Typhoon Komg-Rey. Surface extensometer data show the extension amount of 8 cm and 5 cm after three typhoon events. Potential landslide area, average slope angle and main lithology of case II is 6.4 ha, 32.5? and slate. A landslide with an area of 2 ha happened in the range of case II after Typhoon Usagi. These two cases indicate that rainfall and riverbank erosion are important factors on triggering large scale landslides.

Keywords: deep-seated landslides, GPS

Japan Geoscience Union Meeting 2014
(28 April - 02 May 2014 at Pacifico YOKOHAMA, Kanagawa, Japan)

HDS05-P01 Room:Poster Time:April 29 18:15-19:30

The Assessment of Landslide Displacements Using Digital Photogrammetry and Numerical Analysis

CHANG, Kuang-tsung[1] ; LIN, Chun-te[1*] ; SU, Miau-bin[2] ; CHENG, Min-chieh[1]

[1]Department of Soil and Water Conservation, National Chung Hsing University, Taichung 402, Taiwan., [2]Department of Civil Engineering , National Chung Hsing University, Taichung 402, Taiwan

Instead of comparing remote sensing images between before and after a landslide event, this study compares aerial photographs over the years with the velocities of surface movements of landslide to evaluate the feasibility of aerial photographs as a monitoring tool. Before the total collapse of the slope of Freeway No.3, there were signs showing sliding of the slope, but no equipment was set up for monitoring. We use GIS to discriminate aerial photographs of different years to evaluate the displacements of specific objects or marks. From 2002 to 2004, the average displacement was 49.5cm, and the average displacement rate was 23.7cm/yr; from 2004 to 2007, the average displacement was 22.5cm, and the average displacement rate was 7.3cm/yr.

According to time-dependent creep behavior, the primary creep might have occurred from the beginning of the excavation in 1998 to 2004. And the secondary creep was from 2004 to 2007, so the velocity was comparatively lower than the previous stage. As for the tertiary creep, the displacement rate might rise since 2007 till the total collapse in 2010. The software Plaxis 2D based on the finite element method will be used to analyze the displacement process of the slope. The numerical model is set up according to the digital terrain model (DTM) of the slope. The numerical results will be calibrated with the results of the digital photogrammetry. We expect to obtain the creep behavior of the slope such as the slope strength reduction with time and the changes of surface displacement rate with time.

Keywords: digital photogrammetry, Freeway No.3 landslide, displacement rate, creep

Japan Geoscience Union Meeting 2014
(28 April - 02 May 2014 at Pacifico YOKOHAMA, Kanagawa, Japan)

HDS05-P02 Room:Poster Time:April 29 18:15-19:30

Deformation Analysis of the Pliocene-Pleistocene Sedimentary Rocks Mountain using Lidar Data

ASAHINA, Toshihiro[1*]

[1]PASCO CORPORATION

1.Introduction

Be a topic for the deformation of the Shimanto Supergroup in the Oigawa River basin and in the Kii Peninsula in many cases. How deformation of sedimentary rocks of the Pliocene to Pleistocene age strata earlier age and lower strength than the Shimanto Supergroup is in progress, I report on the basis of the analysis result of airborne Lidar data. The study area is the mountain in Tsunan of Niigata Prefecture around located on the border between Nagano and Niigata Prefecture. Geologically, the study area is located in the south side of the Matsunoyama dome and the Uonuma formation of Pliocene to Pleistocene age is widely distributed.

2.Mountain block geology and geomorphology

The northwestern part of Tsunan is a steep mountain of 1100m altitude from 200m, where the Uonuma formation, being of sand, silt, alternating beds of silt and sand, massive silt and volcanic rocks, is distributed. The investigation mountain has a monoclinic structure facing the Shinanogawa River on geological structure, which the Uonuma formation dips 40 degrees from 15 degrees SE generally and shows a monotonic spread to the whole.

In this area, a number of landslides have occurred, but at the time of the earthquake in northern Nagano Prefecture (March 12 2011, M6.7, depth: 8km, epicenter: Sakae village in Nagano Prefecture), the large plane slip presumed to be caused by this earthquake has occurred.

3.Lidar data

An airborne Lidar survey was conducted on May 14, 2013 for the morphological analysis of the northwest mountain of Tunan. Lidar measurement was carried out in the range of about 30km2 by ALS60 system. The Lidar point data were interpolated using a natural neighbor method on a grid with 1.0m spacing.

In order to understand the characteristics of the mountain deformation, I analyzed the mountain terrain in the following procedure.

1)Analysis 1

a.Classification of slope gradient (a grid with 5.0m spacing),b.Extraction of the cells of 40 degrees from 15 degrees slope gradient,c.Analysis of surface structure,d.Extraction of bedding surface slopes that is likely to cause a slip

2)Analysis 2

a.Image analysis,b.Extraction of linear deformation terrain , such as a lineation or an edge,c.Extraction of deformation terrain surface, such as a depression zone,d.Integrated analysis of analysis 1 and 2

4.Discussion

The GIS analysis of the cells obtained by the process of Lidar data and GIS processing has revealed that the slopes which are considered to bedding plane are found very widely in the mountain. Furthermore, based on the morphological features obtained, the two mountain blocks with a trace of a slip plane as the bedding planes were extracted. These mountain slopes have a characteristic of both showing a bedding plane sliding surface morphology on the terrain surface and the irregular linear trough. The largest linear trough is running diagonally across the hillside slope, and its extension reaches 600m from 550m. The thickness of the terrain block forming a linear trough is about 10m from 6m maximum. These morphological features suggest that the bedding surface played a major role in events that may have caused the extensive deformation and collapse of the edifice. The above is a morphological characteristic that is not found in such the Shimanto Supergroup.

These are important key points in extracting mountain deformation due to the bedding slip.

5.Conclusions

By the analysis of Lidar data, it has been confirmed the distribution of distinctive slopes to suggest that the edifice extensive deformation has occurred in the past in this area.

6.References

Takeuchi, K., et al. (2000) Geology of the Matsunoyama Onsen District. With Geological Sheet Map at 1:50,000, Geol. Surv. Japan, 76p. (in Japanese with English abstract 5p.).

Yanagisawa, Y. et al. (2001) Geology of the Iiyama district. With Geological Sheet Map at 1:50,000, Geol. Surv. Japan, 144p. (in Japanese with English abstract 6p.).

Keywords: Lidar, surface morphology, bedding plane slip, line trough, edifice deformation

Japan Geoscience Union Meeting 2014
(28 April - 02 May 2014 at Pacifico YOKOHAMA, Kanagawa, Japan)

HDS05-P03 Room:Poster Time:April 29 18:15-19:30

Interaction between river bed condition and debris flow in Ichino-sawa subwatershed of Ohya-kuzure landslide, Japan

TSUNETAKA, Haruka[1*] ; HOTTA, Norifumi[1] ; IMAIZUMI, Fumitoshi[2] ; HAYAKAWA, Yuichi S.[3]

[1]Life and Environmental Sciences, University of Tsukuba, [2]Graduate School of Agriculture, Shizuoka University, [3]Center for Spatial Information Science, The University of Tokyo

In recent years, there has been significant concern about large-scale sediment movements, such as deep-seated landslides, that are expected to occur more intensively due to changes in rainfall patterns. These landslides not only induce immediate sediment disasters downstream but also produce a large amount of unstable sediment that is transported gradually following the landslide. Most of the unstable sediment residing in a deep-seated landslide area is first discharged as debris-flow forms. Thus, after the occurrence of landslides, debris flows have a long-term affect on the watershed regime through their impact power, riverbed aggradation, and the production of turbid water, among other effects.

To facilitate better prediction of debris flows from landslide areas, this study investigated the interactions among topographic conditions, bed-material conditions, and debris flow events in a headwater catchment where a deep-seated landslide had occurred.

The study site was the Ichino-sawa subwatershed in the Ohya-kuzure basin, Shizuoka Prefecture, Japan. The basin experienced a deep-seated landslide about 300 years ago and is currently actively yielding sediment with a clear annual cycle. During the winter season, sediment moves from the hillslope to the channel bed because of freeze?thaw activity and weathering. In the summer season, the deposited sediment is discharged incrementally by debris flows related to storm events.

Topographical surveying and grain-size analysis were carried out several times between November 2011 and November 2013. Point cloud data were acquired during the topographical surveying, using a ground-based laser scanner, and used to create a high-resolution digital elevation model. Grain-size analysis was conducted in the upper, middle, and lower parts of the study site. A line-grid method was employed for the in situ analysis, and the fine particle fraction was determined by sieving the sampled materials. Debris flow occurrences were also being monitored in the same period by a sensor-triggered video camera. Rainfall was observed during the summer season for comparison with debris flow occurrence and magnitude.

Several debris flows with different magnitudes were observed during the study period. Although rainfall events in the early spring season altered bed inclination, the thickness of deposited sediment, and the grain-size distribution of the bed material, more significant changes were detected after the debris flows. While the initial grain-size distribution in early spring was roughly identical over the study site, the subsequent grain-size distribution changed differently, according to location. The source, transport, and deposition areas of the debris flows were different among different rainfall events, resulting in different transitions in geomorphic conditions at different locations. The lower part of the study site changed from a source area to a deposition area through the summer season.

A comparison of the topographic conditions, bed-material conditions, and debris flow events indicated that, in addition to the conditions of the triggering rainfall, topographic and bed-material conditions affected debris flow occurrence and magnitude. These interactions could be observed in the deep-seated landslide area, where a substantial and continuous supply of sediment prevents stabilization of the channel bed through exposure of bedrock or by armoring of bed materials.

Thus, to predict the long-term impact of large landslides, it is necessary to assess the subsequent debris-flow discharge considering the sediment dynamics and changes in topographic and bed-material conditions in the landslide area.

Keywords: debris flow, deep-seated landslide, topographic condition, grain size distribution

Japan Geoscience Union Meeting 2014
(28 April - 02 May 2014 at Pacifico YOKOHAMA, Kanagawa, Japan)

HDS05-P04 Room:Poster Time:April 29 18:15-19:30

Deep seated landslides along the geological structure in Chishan River Watershed,southern Taiwan

LIAO, Chi-yueh[1*] ; LIN, Ching-weei[2]

[1]) Disaster Prevention Research Center National Cheng Kung University, [2]Department of Earth Sciences National Cheng Kung University Tainan Taiwan

Landslide is the common nature hazard in Taiwan. The Typhoon Morakot in 2009 brought huge precipitation and induced severe hazards in south-central and eastern Taiwan. Except the landslides, debris flow and flooding hazards induced by Typhoon Morakot, the large scaled deep seated landslides deserve more attention because they may cause the destructive disaster.

The Chishan River watershed which covered 750 km2 is selected as study area. The study area is mainly compose of meta-morphic and sedimentary rocks. Within the study area, 313 sites greater than 10 ha with sliding topographic features of deep seated landslide such as crown main escarpment, down slope scarp ,and lateral cracks are recognized from LiDAR derived 1 m resolution DEM, and we noticed the distribution of these sites is close to the structure in our study area. In order to know the influence of structure in the development of deep seated landslides, landslide density are calculated. The landslide density decreases with increasing distance and there are 79% of. deep seated landslides developed along the structure with a 1km buffer zone. The Result indicates that deformation zone associated structure is crucial in the development of deep seated landslides in the study area.

Keywords: Chishan River watershed, deep seated landslides, geological structure

Japan Geoscience Union Meeting 2014
(28 April - 02 May 2014 at Pacifico YOKOHAMA, Kanagawa, Japan)

HDS06-01 Room:422 Time:May 2 09:00-09:25

Natural-technological disasters of recent years in Japan and Russia: social and economic consequences

PETROVA, Elena[1*]

[1]Lomonosov Moscow State University

During the last decade, natural hazards impacts on people, the environment, urban and industrial areas, infrastructure and other technological systems were increasing, causing large social, environmental and economic damages in many countries. The number and severity of natural-technological accidents and disasters were also increasing all over the world, because of these impacts. The term ”natural-technological” applies to an accident (disaster) in the technosphere (including industrial plants, power stations, transport, infrastructure facilities, communication lines, etc.) triggered by any natural process or phenomenon. Their growth is accounted for: 1) by observed increasing in frequency and intensity of various natural hazardous events; 2) by much more complicated structure and complexity of modern technological systems and facilities exposed to natural hazards, and 3) by increasing advancement of economic activities and population into the regions at natural risk. The most severe consequences for people and the environment have the so-called Natech-accidents, which are accompanying by release of dangerous substances (like chemicals or oil), and accidents at nuclear power stations.

One of the most large-scaled natural-technological disasters having enormous social, environmental and economic consequences occurred on March 11, 2011 in Japan due to a massive 9.0-magnitude earthquake off the northeast coast of Honshu Island, which triggered a more than 30-meter tsunami. The disaster not only caused a large direct and indirect damage to the people (about 20 thousand fatalities) and economy of the country (more than $500 billion), but also influenced on regional, national and international development reaching a truly global scale. It clearly demonstrated high vulnerability of a human society and modern technosphere to natural disasters; even in a country like Japan that is highly developed and well-prepared to natural risks. A distinctive feature of events, such as of the 2011 Tohoku earthquake, is their multihazard and synergistic nature, as a disaster spawns a secondary disaster that increases the impact on people and technosphere, resulting in simultaneous occurrences of numerous technospherical accidents. The secondary effects of natural-technological accidents can be even much more serious, such as at ”Fukushima-1” nuclear power plant. These impacts are the more severe the higher are the population density and concentration of industrial facilities and infrastructure (especially hazardous and vulnerable objects) in disaster-affected areas. In addition, all rapid reaction forces and resources tend to be primarily fighting natural disaster; it limits the capability to eliminate secondary technological impacts, especially in those situations when transport facilities and required infrastructure are destroyed, and economic communications are broken.

The lessons of the Tohoku disaster should be taken into consideration while placing, constructing and operating nuclear power plants and other high-risk facilities. It is necessary to consider carefully possible intensity and frequency of all potential impacts, including natural hazards.

In Russia, natural-technological disasters with catastrophic consequences occur not so often. However, their possibility should be taken into account, especially in the economic development of areas at high natural risk, which is, for example, the Far Eastern region exposed to earthquakes, tsunamis, volcanic eruptions, floods, strong winds, storms, heavy rain- and snowfalls and other natural hazards. The most severe damages caused the Sakhalin earthquake in 1995, which was the most destructive in the Russian history. Severe social and economic consequences cause floods, for example, the flood in the autumn 2013. Natural-technological risk to the regions of Russia was evaluated using a database that was created by the author.

Keywords: natural hazards impacts, social and economic consequences, natural-technological risk, natural-technological disaster

Japan Geoscience Union Meeting 2014
(28 April - 02 May 2014 at Pacifico YOKOHAMA, Kanagawa, Japan)

HDS06-02 Room:422 Time:May 2 09:25-09:50

The Egyptian Tempest Stele: an Example of Ancient Natural Disaster

PETROVA, Anastasia[1*]

[1]Institute of Oriental Studies, Russian Academy of Sciences

Some Ancient Egyptian texts tell us about violent storms and rains. One of the most impressive ancient accounts of natural disasters is the so-called Tempest stele (1550 BC), which describes a very destructive storm happened under Ahmose I, the king of Egypt's 18 dynasty. The upper portion of the stele describes the catastrophe. Many essential details are given, such as the specific noise, overall darkness etc. Numerous houses were washed into the river; temples, tombs and pyramids were badly damaged. The main features of the storm can be highlighted: torrential rain; darkness; and loud noise, probably caused by a thunder or a wind, or both. It evidently occasioned large-scale flooding, property damage, and loss of life. After describing the events, the stele gives account of the restoration works made by the king to repair the damages made by this great disaster. There are Egyptologists who believe the stele to be propaganda put out by the pharaoh, the "tempest" being the depredations of officials of the embattled seventeenth dynasty of Egypt drawing upon the financial resources of the temples during the escalating conflict with the Hyksos. To my opinion, we don't have sufficient grounds to deny that the storm took place in reality. Nevertheless, the Tempest Stele actually is a political propaganda, because the main purpose of the erection of the stele was to draw attention to the role of the king in coping with the disaster. Traditionally, the king was responsible for maintaining maat (a cosmic order as opposed to chaos), and this responsibility included protection from natural disasters. The main point of the specific political context of the Ahmose I's times was the struggle of what would become the 18th Dynasty to establish its rule in opposition to the Hyksos. This effort required success on two levels: the human and the divine, which meant what would be classified as the natural world today. To simply liberate the land from Hyksos rule was a necessary but not sufficient step to legitimate one's rule. The king also needed to demonstrate divine blessing meaning that the cosmic order of the natural world had been restored as well as the political world had been. The storm commemorated by the Tempest stele is not the only example of heavy storms in Egypt. It seems that hazards of that kind were more common than we now believe. What makes the Ahmose stele unique is the description of the details of such a severe catastrophe, which go beyond what is usually experienced by a regular storm and therefore might be the oldest description of a natural hazard. The catastrophe described in the Ahmose I's Tempest Stele can be considered one of the most ancient examples of natural disasters, which caused a huge impact on the society. This is also a significant example of a political propaganda, reflecting the situation when government uses a catastrophe and its consequences to its own benefit.

Keywords: natural disaster, social impact, history of disasters, ancient egypt

Japan Geoscience Union Meeting 2014
(28 April - 02 May 2014 at Pacifico YOKOHAMA, Kanagawa, Japan)

HDS06-03 Room:422 Time:May 2 09:50-10:05

Relationship between social and natural disasters

VIKULINA, Marina[1*] ; VIKULIN, Alexander[2] ; SEMENETS, Nikolai[3]

[1]Research scintist, Faculty of Geography, Lomonosov Moscow State University, Russia, [2]Senior Research Fellow, Institute of Volcanology and Seismology, Russia, [3]Acting general director, Research and Production Company " EKOS ", Moscow, Russia

The problem of reducing the damage caused by geodynamic and social disasters is a high priority and urgent task facing the humanity. The vivid examples of the earthquake in Japan in March 2011 that generated a new kind of threat ? the radiation pollution, and the events in the Arabic world that began in the same year, are dramatic evidences. By the middle of this century, the damage from such disastrous events is supposed to exceed the combined GDP of all countries of the world. The authors have developed the first database to include the largest geodynamic and social phenomena that occurred on Earth before 2005. We suggest the following phenomenological model based on the database (uniform with respect to the quantitative classification). All disasters are classified by size using a single logarithmic scale suggested by Rodkin and Shebalin in 1993. The base consists of 2000 disasters. The following phenomenological model is proposed: 1. The scale of disasters does not decrease with time. (Earthquakes in China in 1556 and 1976; the tsunami after the Sumatra earthquake in 2004, which can be compared in regards to the level of consequences only with the World Flood or a series of floods that occurred approximately 13000 years BP). 2. There were a minimal number of disasters in the 15th century; during which there were not a single disaster with J = I and II; from that time the number of such disasters gradually increases; in the 20th century there were 20. 3.The number of disasters is characterized by cycles, which are a few thousand years long; the available longterm measurements confirm this (for example, the overflow of the Nile observed over more than 5000 years or deformations of the Earth surface in the last few thousand years based on the geodynamic, seismotectonic, and paleoseismic data). 4. Natural and social disasters together are distributed uniformly in time, while only natural and only social disasters are distributed nonuniformly, i.e. disasters group.

5. The proportion of the social disasters has a tendency to increase in time, which confirms the viewpoint of V.I. Vernadskii about the constantly increasing role of humans and society in the noosphere. It was shown that natural and social disasters are interrelated. The Earth from the point of view of the disaster theory evolves according to the definite laws of the unique bio-socio-geodynamics. The investigation and understanding of the nature of this mechanism that "mixes the disasters" will allow us in the future to formulate a scientific hypothesis and/or a law on the basis of the phenomenological model that we suggest in this work and use it in the system of expert global process management. In the aspects of modern methods of studying of the global disasters, the authors suggest an approach to understanding global disasters based on modern data. The global disaster is an event damage from which cannot be liquidated by the joint resource. Irreversible process of death of a modern civilization can become a consequence of a global disaster.

Keywords: geodynamics, society, magnitude of disaster, interaction of disasters, impact of society

Japan Geoscience Union Meeting 2014
(28 April - 02 May 2014 at Pacifico YOKOHAMA, Kanagawa, Japan)

HDS06-04 Room:422 Time:May 2 10:05-10:20

The numerical model of natural hazards development in the environment stressed by opposing forces

KUDIN, Valery[1*]

[1]Lomonosov Moscow State University, Faculty of Geography

Natural hazards include earthquakes, tsunami, volcanic eruptions, floods, etc. The time of appearance of such significant events within hundreds of years can be considered as random. In most cases, the dangers' amplitudes are not amenable to prediction, i.e. their size is also random. From the mathematical point of view, the deposition of natural hazards is described by exponential dependence, which is connected with the involvement of the own "mass" of danger. In the presence of opposing forces in a first approximation, these processes are described by the Verhulst equation. It is a particular variant ($Q<0$, $A=L$) of the total autonomous differential equations of the 2nd order for the function x(t) on time t, i.e. $dx/dt=N+L*x+Q*x*x$, where N,L,Q are constants of equation with initial conditions t(n) and x(n).

The complete solution of this equation with arbitrary initial conditions has bulky appearance, although the logistic curve reflects it qualitatively quite well. However, these solutions allow us to reveal a violation of the principle of stability of numerical solutions of the logistic equation $x(n+1)=x(n)*(1+a*(1-x(n)))$, where $a=A*(t(n+1)-t(n))$, when the derivative dx/dt is replaced by the value for $(x(n+1)-x(n))/(t(n+1)-t(n))$.

It is shown that the instability of the processes with the opposing factors invoked by jumps of initial conditions on consecutive segments. For certain values of the parameters of the differential equation associated with capacity of the stressed environment, both volatile and deterministic modes of development of the variable x(t), normalized to unit, can be formed. An example of the Verhulst model with parameter A shows the dependence of the solutions x(t) at time intervals t(n+1)-t(n) and tabular values of x(n) and different a jumps of initial conditions. Negative inclinations of dependency associated with the tabular values x(n) are shown. Thus, there appears a situation, which leads to the release of the variable x from the corridor, normalized per unit, of sustainable values. For each a-case, the changes in the structure of x(t) in time look diverse and complex.

Therefore, the numerical logistic equation can be taken as a numerical model for the development of natural hazards in the geographical environment, characterized by capacity (option a) of a tension of opposing factors.

Keywords: natural hazards, model, numeric equations, stability

Japan Geoscience Union Meeting 2014
(28 April - 02 May 2014 at Pacifico YOKOHAMA, Kanagawa, Japan)

HDS06-P01 Room:Poster Time:May 2 16:15-17:30

Studies on the understanding of haiku composed by earthquake disaster of East Japan on 11. 3. 2011

AOKI, Yoji[1*]

[1]Student of Open University of Japan, [2]Member of Kuramae Hiku Club, [3]Translator of Haiku International Association, [4]Professor of Aomori University

Studies on the understanding of haiku composed by earthquake disaster of East Japan on 11. 3. 2011

Aoki, Yoji (student of Open University of Japan), Chida Sosuke (Kurame Haiku Club), Jambor Kinuko (translator of Haiku International Association) and Hitoshi Fujita (Professor of Aomori University)

The damage of the Fukushima nuclear power plant and the East Japan big earthquake, the east part of Japan received big impact on the March 11, 2011. Many haiku poet composed haiku poems to the impact of the nuclear power plant accident and the earthquake disasters. Of these haiku what was published in the magazine, 234 haiku on the home page were to be used in the data. Copies of haiku were shown to 19 people of the general public and the poet, and we asked whether they can understand them, or they are impressed by them. 2354 haiku was chosen in total. 124 haiku was chosen average.

10.1 average people, understand of haiku and the distribution of the two-peaked mountain with 8 and 13 people was observed. Haiku understood by more than half of people were relatively large and 132 (56.4%), so it was found that haiku is yet the useful means of communication of mind for the Japanese today. As for the impressive haiku, it has the maximum value in 0 and at 1.4 person average, and decreases the distribution of people. 91 (38.8%) haiku were impressed by more than two people. To convey the emotion equally to many people, it showed difficulties. Taking the correlation of the number of people impressed with the number of people evaluated, it showed weak association of 0.515. The results suggested that haiku could be understood by a lot of people, but could give the impression variously.

According to the evaluation method in the Haiku Society, one point in haiku which was able to understand, to give two points to haiku that was impressed, we calculated the total score. Correlation of the number of people understood and the people impressed indicates 0.731, the stronger association was obtained. This is a result of the score added points. As it was not a very strong connection, so the individual differences affect the evaluation of haiku.

By the principal component analysis in the factors respondents, six-axis was obtained with eigen value greater than 1.0. This indicates that there are many different preferences in the evaluation by the respondents. The axis with maximum eigen value has the largest explanatory power, and showed the severity of the evaluation. We estimate 5-axis remaining as the evaluator's preferences for haiku.

The highest scored Haiku observed 2 haiku of 20 points.

(1) Mud certification of graduation, mud portrait digging under the debris by Tsunami (Sinogo SONE)

(2) Finding my mother in turning disaster's debris, light snow falling (Minu KASHIWABARA)

(3) Children crying bright hopes for their future a graduation ceremony (Nagahiko KAMIGORI)

(1) described the scenery that the photographs of deceased persons and the certification of diploma by deceased became muddy by the tsunami, people are digging them after the disaster in the damaged areas.

(2) described the scenery that light snow was falling, while people are removing the disaster debris of earthquake to find their mother of missing, at the neighborhood home.

(3) was praying for the pupil who were singing the graduation song with full of tears to be lighten

We thought that both of them were touched deeply by sadness.

Reference

Haiku: http://blog.goo.ne.jp/humon007/e/fcc6b3e8f8dc3ca1cbc6a2177d6d0637

Acknowledgments: Cooperation was obtained from Kuramae Haiku Club (Tokyo Institute of Technology) and Blue Ridge Haiku Association (Roanoke City, Virginia) for the investigation of haiku. The Haiku used in this study was introduced by the site.

Keywords: earthquake disaster of East Japan on 11. 3. 2011, haiku poet, understandings and deep impressions

Japan Geoscience Union Meeting 2014
(28 April - 02 May 2014 at Pacifico YOKOHAMA, Kanagawa, Japan)

HDS06-P02 Room:Poster Time:May 2 16:15-17:30

Hazard Mapping of Structurally Controlled Landslides in Leyte, Philippines Using High Resolution Digital Elevation Model

MONTALBO, Kristina rochelle[1*] ; LUZON, Paul kenneth[1] ; LAGMAY, Alfredo mahar francisco[1]

[1]Nationwide Operational Assessment of Hazards, Department of Science and Technology, Philippines, [2]National Institute of Geological Sciences, University of the Philippines, Diliman, Quezon City, Ph

Structurally controlled landslides are one of the most destructive natural hazards that have occurred in the Philippines. The 2006 Guinsaugon Landslide, which was produced by the displacement of the Philippine fault, is a classic example of such hazard that took more than 1,000 lives and displaced more than 19,000 residents in the municipality of St. Bernard, Southern Leyte. Frequent monitoring and assessment should be done across the Philippine archipelago. The purpose of this study is to locate structurally controlled landslide prone areas with the aid of Coltop3D, Matterocking and Conefall using a high resolution digital elevation model (5 m resolution Interferometric Synthetic Aperture Radar images). The study area is set in the municipality of Ormoc, Leyte where the Philippine fault also cuts through and trending northwest. Discontinuity sets were identified using Coltop3D software that simulates a 3D model of the digital elevation model showing the dip and dip direction of different discontinuities. Lineation analysis and rose diagrams were made to verify the discontinuity sets in the area. Matterocking computes and estimates the locations where rock instabilities can occur according to the identified discontinuity sets that may allow sliding. Conefall was then used to compute and estimate the potential rockslide extent. Results show that the area has zones of potential rockslides with generated simulation of rockslide propagation extent. There is a high probability of landslides in Ormoc area where continuous monitoring of such danger zones should be done.

Keywords: structurally controlled landslides, geohazard, philippine fault, discontinuities, landslide mapping, structures

Japan Geoscience Union Meeting 2014
(28 April - 02 May 2014 at Pacifico YOKOHAMA, Kanagawa, Japan)

HDS06-P03 Room:Poster Time:May 2 16:15-17:30

Developing Automatic Delineation of Alluvial Fans for Rapid Hazard Assessment in Aurora Province, Philippines

ORTIZ, Iris jill[1*] ; AQUINO, Dakila[1] ; NORINI, Gianluca[3] ; SALVOSA, Sheena[1] ; LLANES, Francesca[1] ; GALANG, Jan albert macario[1] ; ECO, Narod[1] ; VELEZ, Maria clara zuluaga[4] ; LAGMAY, Alfredo mahar[1]

[1]Nationwide Operational Assessment of Hazards, Department of Science and Technology, [2]2National Institute of Geological Sciences, University of the Philippines, Diliman, Quezon City, Phi, [3]Istituto per la Dinamica dei Processi Ambientali, Consiglio Nazionale delle Ricerche, Italia, [4]Universita degli Studi di Napoli Federico II, Napoli, Italy

On Nov. 14, 2004, flashfloods from Subsob River struck Barangay(village) Paltic in Dingalan, Aurora Province around 4 a.m. when most residents were asleep - leaving hundreds homeless and 135 people dead. The series of floods caused by Violeta, Winnie, and Yoyong until December 2004 killed at least 300 people in Dingalan, Aurora alone. Mud buried 300 houses and residents were forced to stay on rooftops or seek higher ground. Because of these incidents, measures were devised to improve available geohazard maps to raise public awareness about landslides, debris flows and alluvial fans. This study developed a method to rapidly identify alluvial fans, thereby, hastening geohazard mapping in the region. Alluvial fans are fan shaped geologic formations deposited from tributaries from a mountainous terrain which flows out from the sudden break of a slope. Intense rainfall increases the discharge of sediments and water on these areas which could induce disastrous events such as flooding and debris flows. In this study, manual and automated methods in delineating fans in Aurora Province were compared. Manual delineation of alluvial fan boundaries were done through the contour lines generated from the 10-meter synthetic aperture radar (SAR)-derived digital elevation model (DEM). However, manual mapping of alluvial fan boundary which makes use of topographic interpretation of geomorphic features is subjective and time consuming. Biases were addressed by the second method by including factors such as 1) fan area of slope ranging from 1 to 8 degrees, 2) contributing stream networks from fan apex to fan toe , and 3) the fan potential lateral extent within the buffer zones based on the relief of the sediment source area in the GIS-based model. The outputs were compared with the manually delineated fans. Manual delineation identified 14 alluvial apex of 14 alluvial fans in 6 municipalities affecting 36 barangays . On the other hand, automated method identified 183 apex of 126 alluvial fans in 7 municipalities affecting 105 barangays. Although greater number of fans and wider fan area were identified using the automated method, manual delineation is still needed to check the results especially in volcanic regions. In addition, inactive alluvial fans are not accounted by the automated method.

Keywords: alluvial fan, natural hazard mapping, geohazard, GIS, Aurora, Philippines

Japan Geoscience Union Meeting 2014
(28 April - 02 May 2014 at Pacifico YOKOHAMA, Kanagawa, Japan)

HDS06-P04 Room:Poster Time:May 2 16:15-17:30

Strong Explosive Eruptions of Kamchatkan Volcanoes in 2013

GIRINA, Olga[1*] ; MANEVICH, Alexander[1] ; MELNIKOV, Dmitry[1] ; NUZHDAEV, Anton[1] ; DEMYANCHUK, Yury[1] ; PETROVA, Elena[2]

[1]Institute of Volcanology and Seismology FEB RAS, KVERT, [2]Lomonosov Moscow State University, Geographical faculty

There are 30 active volcanoes in the Kamchatka, and three of them (Sheveluch, Klyuchevskoy, and Karymsky) continuously active. In 2013, two of the Kamchatkan volcanoes ? Sheveluch and Klyuchevskoy - had strong explosive eruptions.

Powerful explosive eruption of volcanoes is the most dangerous for aircraft because in a few hours or days in the atmosphere and the stratosphere can produce about several cubic kilometers of volcanic ash and aerosols. Ash plumes and the clouds, depending on the power of the eruption, the strength and wind speed, can travel thousands of kilometers from the volcano for several days, remaining hazardous to aircraft.

The eruptive activity of Sheveluch Volcano began since 1980 (growth of the lava dome) and is continuing at present. Strong explosive events of the volcano occurred in 2013: on June 26, on October 18, and on December 03: ash plumes rose up to 10 km a.s.l. and extended about 200-400 km, respectively, to the south-west, south-southeast, and north of the volcano. A form of pyroclastic flow deposits with run-out 12 km accompanied these explosive eruptions. Ashfalls occurred at Klyuchi Village (on June 26) and Ivashka Village (on December 03). Activity of the volcano was dangerous to international and local aviation.

Klyuchevskoy volcano had two eruptions in 2013: moderate Strombolian explosive eruption from October 14, 2012, till January 15, 2013; and strong Strombolian-Vulcanian explosive and effusive eruption from August 15, 2013, till December 20, 2013. There were four lava flows to effuse on the north-west, west and south-western volcanic flanks. Probably a flank eruption began at the pass between Klyuchevskoy volcano and Kamen volcano on October 06. Culmination of strong Vulcanian explosive activity of the volcano occurred on October 15-20: ash column rose up to 10-12 km a.s.l. and ash plumes extended to the different directions of the volcano according to cyclonic activity in the this area. Phreatic ash plumes on the fronts of lava flows rose up to 5 km a.s.l. Weak ash falls were noted at Klyuchi Village on October 09 and 13, and Mayskoe Village on October 16. Activity of the volcano was dangerous to international and local aviation.

Keywords: explosive eruption, volcano, Kamchatka, Sheveluch, Klyuchevskoy

Japan Geoscience Union Meeting 2014
(28 April - 02 May 2014 at Pacifico YOKOHAMA, Kanagawa, Japan)

HDS27-01 Room:418 Time:May 1 09:00-09:15

Magnitude of the Solomon Tsunami of February 6, 2013

HATORI, Tokutaro[1*]

[1]nome

The great earthquake occurred on February 6, 2013 at the junction of Solomon and New Hebrides trenches (10.738S, 165.138E, 28.7km depth, M8.0, USGS). Moderate tsunami was widely observed in the Pacific zone (WC/ATWC, NOAA, JMA). The tsunami killed 10 persons and 590 houses destroyed at Nendo Is.(Santa Cruz Is.) located near the source region. The estimated source lies 250km length toward E-W direction. Judging from the attenuation of tsunami height with distance, tsunami magnitude is determined to be m=2 that the grade is the mean value for earthquake magnitude. For tsunami magnitude, semi-amplitudes of the following regions are relatively large: 20cm at Crescent City, California, 18cm at Maui, Hawaii, 17-19cm in Galapagos and Coquimbo, South America and 40cm at Hachijo Is., 19cm at Chichijima ,Japan. The pattern of amplitude distribution is similar to other Solomon-Vanuatu tsunamis.

Keywords: Solomon Tsunami, Tsunami magnitude, February 6, 2013, Tsunami source, amplitude deviation

Japan Geoscience Union Meeting 2014
(28 April - 02 May 2014 at Pacifico YOKOHAMA, Kanagawa, Japan)

HDS27-02 Room:418 Time:May 1 09:15-09:30

Arrival times of reflected waves and the maximum phases of tsunami?the 1993 Hokkaido Nansei-oki Tsunami

ABE, Kuniaki[1*] ; OKADA, Masami[2] ; HAYASHI, Yutaka[3]

[1]none, [2]MRI, [3]MRI

Tsunami maximum phases are frequently attained by reflected waves. Arrivals of reflected waves were studied in relation with arrivals of maximum phases. Arrival times of reflected waves are calculated from combination of refraction diagrams of direct wave and arbitral reflected wave. The arrivals are recognized in coincidence between the prediction and the observation. Under this circumstance travel times of first and maximum waves were obtained for the 1993 Hokkaido Nansei-oki Tsunami and predicted travel times of reflected wave from Russia, Korea and double reflected waves from Honshu and Korea are plotted in figure 1. As the result arrivals of maximum phases are classified into three groups. First one, the direct wave from the source, is earlier arrivals before the reflected wave from Russia. Second one is a group found between arrival times from Russia and Korea. This is recognized as reflected wave from arbitral coast of Eurasia continent. Third group is one found at arrival times shorter than those of the double reflection. This group is interpreted from double reflections from coast near the source and Korea.

Keywords: Tsunami, maximum phase, late arrival, reflected wave, 1993 Tsunami

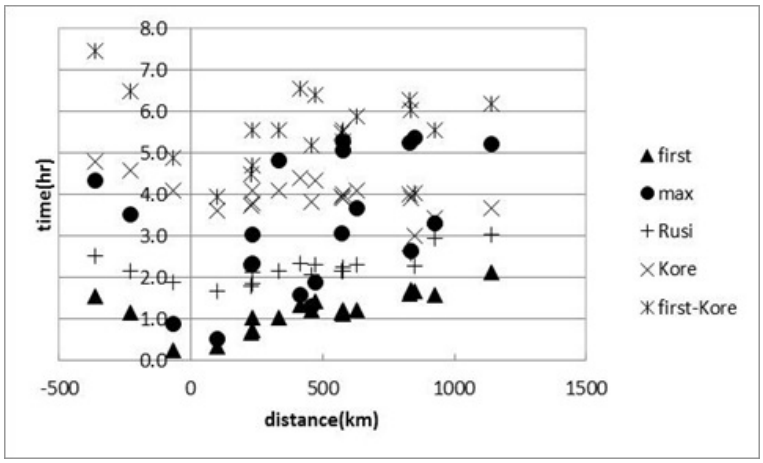

Japan Geoscience Union Meeting 2014
(28 April - 02 May 2014 at Pacifico YOKOHAMA, Kanagawa, Japan)

HDS27-03 Room:418 Time:May 1 09:30-09:45

Quantitative comparison of the 2011 Tohoku earthquake and past tsunami heights

SATAKE, Kenji[1*] ; TSUJI, Yoshinobu[2] ; HARADA, Tomoya[3] ; ISHIBE, Takeo[1] ; NISHIYAMA, Akihito[1] ; KUSUMOTO, Satoshi[4]

[1]Earthquake Research Institute, the University of Tokyo, [2]ERI, the University of Tokyo, Now at Fukada Geological Institute, [3]CIDIR/ERI, the University of Tokyo, [4]ERI, the University of Tokyo, Now at Dia Consultants

The tsunami heights from the 2011 Tohoku earthquake were on the average 1.5 times the 1896 Meiji Sanriku tsunami, 3 times the 1933 Showa Sanriku tsunami, 4 times the 1960 Chilean tsunami, and 14 times the 2010 Chilean tsunami along the Sanriku coast. The Sanriku coast is a typical ria coast, a sawtooth-shaped irregular coastal shape, and the local variation of tsunami heights is very significant. We carefully selected the sites where the past measurement points are known, and comparisons were made at the same villages or small-scaled bays (roughly a km scale).

Along the Sanriku coast, the median value of 1896/2011 tsunami height ratio at 83 measurement points is 0.69, and a correlation coefficient is 0.34. The median 1933/2011 ratio at 94 points is 0.33 with a correlation coefficient of 0.47. The 2011 tsunami was higher along the southern Sanriku coast (Miyagi prefecture). In the central Sanriku coast (Iwate prefecture), the 2011 tsunami was 1.2 times the 1896 tsunami and 2 times the 1933 tsunami. The comparison was made at 98 points for the 1960 tsunami with a median ratio of 0.25, and at 12 points for the 2010 tsunami with a median ratio of 0.07. The correlation coefficients are lower, 0.17 and 0.14 for the 1960 and 2010 Chilean tsunamis, than the past Sanriku tsunamis. All the Sanriku tsunamis (1896, 1933 and 2011) had different earthquake source area and types, but the tsunami height distributions were similar, indicating that the tsunami heights are more sensitive to the local topography for the near-field tsunamis. The lower correlation with the Chilean tsunami may be due to the fact the dominant period of incoming tsunami was more than twice longer for the trans-Pacific tsunamis.

Comparisons with the two Chilean tsunamis were also made on the Ibaraki and Chiba coasts. The tsunami heights were compared at 24 points for the 1960 tsunami and 14 points for the 2010 tsunami. The median 1960/2011 ratio is 0.62, while the median 2010/2011 ratio is 0.28. The correlation coefficients with the 2011 tsunami heights are higher, 0.63 and 0.41 for the 1960 and 2010 Chilean tsunamis. The high correlation may be due to general decrease of tsunami heights toward south, and the fact that the tsunamis were locally high near peninsula such as Asahi city in Chiba prefecture.

We used the 2011 tsunami heights at 120 points measured and reported by Tsuji et al. (2011 BERI); the 1896 tsunami heights reported by Yamana, Iki and Matsuo, the 1933 heights by Matsuo, Kunitomi and ERI, the 1960 heights by Comm. Field Investigation and Japan Meteorological Survey, and the 2010 heights by Tsuji et al. and Imai et al. The full data and reference are given in Tsuji et al. (Pageoph in press).

Keywords: The 2011 Tohoku earthquake, tsunami, 1896 Sanriku tsunami, 1933 Sanriku tsunami, 1960 Chile tsunami, 2010 Chile tsunami

Japan Geoscience Union Meeting 2014
(28 April - 02 May 2014 at Pacifico YOKOHAMA, Kanagawa, Japan)

HDS27-04 Room:418 Time:May 1 09:45-10:00

Tsunami reflected from Chilean coast and observed in Japan - the 2011 off Tohoku Tsunami

OKADA, Masami[1*] ; ABE, Kuniaki[2] ; HAYASHI, Yutaka[1]

[1]MRI, JMA, [2]None

We identified reflected waves from Chilean coast at Kushimoto and Owase tide stations in Japan on the 2011 off Tohoku Tsunami. It is based on amplitude increases at predicted travel times. The travel times were calculated by using the tide gage records of the 2011 tsunami at Talcuano in Chile and those of the 1960 Chilean Tsunami observed at Kushimoto and Owase. For the latter we noticed reflected waves from Chilean coast and obtained the travel times between Chile and Japan. Then, two phases of large amplitude of the 2011 tsunami observed at Talcuano were selected, and travel times of 46.7, 47.9 hrs for Kushimoto and of 48.1, 49.3 hrs for Owase were estimated. Amplitude increases at the predicted times were recognized in both tide stations. Waveforms and predicted travel times are shown in Fig.1. The identification is supported by amplitude increases at almost same travel times for two different tide stations.

Keywords: tsunami, Chile, Japan, reflected wave, 2011 tsunami

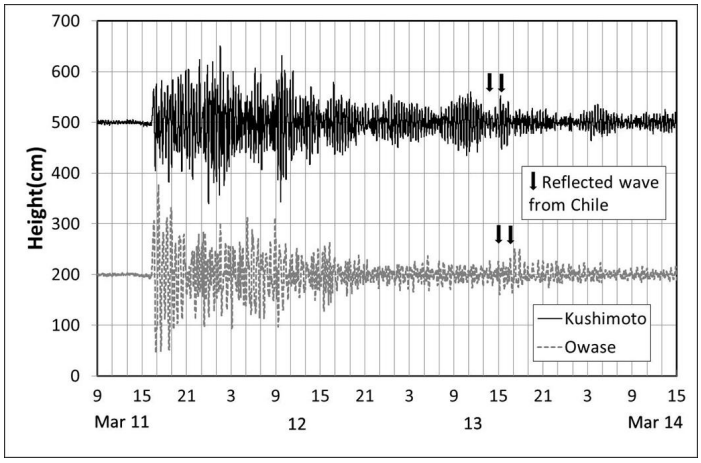

Japan Geoscience Union Meeting 2014
(28 April - 02 May 2014 at Pacifico YOKOHAMA, Kanagawa, Japan)

HDS27-05 Room:418 Time:May 1 10:00-10:15

Disaster Warning System in Thailand through Enterprise Engineering Perspective

LEELAWAT, Natt[1*] ; SUPPASRI, Anawat[2] ; IMAMURA, Fumihiko[2]

[1]Tokyo Institute of Technology, [2]Tohoku University

Introduction

Identify, assess and monitor disaster risks and enhance early warning has been set as one of the five priority areas of action in the Hyogo Framework for Action 2005-2015. This study is a part of our research project on disaster warning process management analysis as well as Leelawat et al. (2013).

Enterprise Engineering & DEMO

Enterprise engineering is an interdisciplinary field focusing on investigating of each aspect of the enterprise, including a business process, information flow, and organizational structure (Dietz, 2006). While most of the current modeling tools (e.g., BPMN) cannot achieve the enterprise engineering principles, *Design and Engineering Methodology for Organizations (DEMO)* (Dietz, 2006; Perinforma, 2012), an enterprise engineering and business process modeling language, has capability to demonstrate the validity of some principles (Dietz & Hoogervorst, 2012). Thus, DEMO has been selected in this study.

Data Collection

(Primary and Secondary) Data collection took place during Aug.-Dec. 2013. The face-to-face interviews with the acting Director of National Disaster Warning Center (NDWC) of Thailand and the Director of the Seismological Bureau, Thai Meteorological Department (TMD) were conducted in Sep. 2013 through the semi-structured style interviews, together with the observation.

Findings and Discussion

There are 2 main actual players in the Thai warning system as mentioned. The case has been analyzed by DEMO. According to Perinforma (2012), the *Organization Construction Diagram (OCD)* and *Transaction Product Table (TPT)* have been created to show the compact form of the system. DEMO shows its capability to express the sketch of the organization, together with some interesting issues.

First, we can understand the authority and responsibility from OCD and TPT. It can be seen that announcement decision is authorized to only NDWC (i.e., one actual warning announcer). It is a good practice because it does not create the confusion that may occur from many announcing sources.

Second, through the TPT, we can see the chain of warning message announcement, from monitoring information to seismological information. It means that the duty of declaring seismological disaster and declaring warning is separated to different actor roles which in turn increase the performance because each executor can focus on their responsibility works and increase the accuracy since the seismological information has been confirmed by the initiator.

Third, by comparing with Japanese case, it can be seen that the warning system in Japan is mainly executed by one organization (i.e., JMA) while Thai case contains 2 main organizations plus other 4 monitoring organizations regarding to the aspect of information. One reason is probably from the different government hierarchical structures which separated the expertise into each departments (in different ministries) in Thai case.

Acknowledgements

The study was supported by the ACEEES and the Risk Solutions 2013 project of Tokyo Tech. The authors would like to acknowledge Capt. Song Ekmahachai (acting Director of NDWC), Mr. Burin Wechbunthing (Director of Seismological Bureau), Prof. Junichi Iijima (Tokyo Tech), and Dr. Jing Tang for their advice and support.

References

Dietz, J. L. G. (2006). *Enterprise Ontology - Theory and Methodology*. Heidelberg: Springer-Verlag.

Dietz, J. L. G., & Hoogervorst, J. A. P. (2012). The Principles of Enterprise Engineering. In *Advances in Enterprise Engineering VI* (pp. 15-30). Heidelberg: Springer Berlin Heidelberg.

Leelawat, N., Suppasri, A., & Imamura, F. (2013). Analyzing the essence of the disaster warning system in Japan. In *Proceedings of the Second International Education Forum on Environment and Energy Science 2013*.

Perinforma, A. P. C. (2012). *The Essence of Organisation Version 1.2*. South Holland: Sapio.

Keywords: Design and Engineering Methodology for Organizations, Disaster Management, Enterprise Engineering, Thailand, Tsunami, Warning System

Japan Geoscience Union Meeting 2014
(28 April - 02 May 2014 at Pacifico YOKOHAMA, Kanagawa, Japan)

HDS27-06 Room:418 Time:May 1 10:15-10:30

A methodology for near-field tsunami inundation forecasting and its application to the 2011 Tohoku tsunami

GUSMAN, Aditya[1*] ; TANIOKA, Yuichiro[1]

[1]Institute of Seismology and Volcanology, Hokkaido University

We develop a new methodology for near-field tsunami inundation forecasting (NearTIF). This method required site-specific pre-computed tsunami inundation and pre-computed tsunami waveform database. Information about tsunami source of an event is required as an input for the method to work. By this method, we will not attempt to obtain a reliable earthquake source model for an event. Instead, any available information about tsunami source such as earthquake moment magnitude, earthquake fault model, or tsunami source model will be used. After information about the tsunami source is obtained, tsunami waveforms at near-shore points can be simulated in real-time during an event. Simulating tsunami waveforms by solving the linear shallow water equation on low-resolution bathymetric data does not take long time, therefore it is suitable to be used in real-time. By using root mean square analysis, a scenario that gives the most similar tsunami waveforms in the database is selected as the best-fit site-specific scenario. Then the corresponding pre-computed tsunami inundation of the best scenario is selected as the tsunami inundation forecast.

The pre-computed tsunami database is built from thrust earthquake scenarios of simple rectangular fault models with moment magnitude ranged from Mw 8.0 to 9.0. We arrange a total of 56 reference points along the subduction zone off the east coast of Honshu, Japan as the center top of the fault planes. The points are grouped into four depth categories of shallowest, upper intermediate, lower intermediate, and deepest plate interface. The earthquake scenarios for each depth category have moment magnitude range of Mw 8.0 to 9.0, Mw 8.0 to 8.9, Mw 8.0 to 8.8, and Mw 8.0 to 8.7, respectively, from the shallowest to the deepest plate interface, making a total of 532 scenarios.

Sites are chosen based on their coastal geomorphology (i.e. bay, lagoon, isthmus) or location of coastal community. Virtual observation points at which tsunami waveforms is computed are placed strategically near-shore, around a bay at depth of deeper than 30 or 50 m depending on the bathymetry.

We test the algorithm to hindcast tsunami inundation along the Sanriku coast that was generated by the 2011 Tohoku earthquake. To produce accurate tsunami inundation map, accurate information about tsunami source is required. We used source models for the 2011 Tohoku earthquake previously estimated from GPS, W phase, or offshore tsunami waveform data. These source models could be available before tsunami hits the shore. The forecasting algorithm is capable of providing a tsunami inundation map that is similar to that obtained by numerical forward modeling, but with remarkably faster speed. Using a regular laptop computer, the time required to forecast tsunami inundation in coastal sites from the Sendai Plain to Miyako City is approximately 3 min after information about the tsunami source is obtained. We found that the tsunami inundation forecasts from the GPS (5 min), W phase (5 min and 10 min) fault models, and tsunami source model (35 min) are reliable for tsunami early warning purposes and considerably similar to the observation. This method can be used to develop a future tsunami forecasting systems with a capability of providing tsunami inundation forecasts in the near field locations.

Keywords: near-field tsunami inundation forecast, pre-computed tsunami database, tsunami early warning

Japan Geoscience Union Meeting 2014
(28 April - 02 May 2014 at Pacifico YOKOHAMA, Kanagawa, Japan)

HDS27-07 Room:418 Time:May 1 11:00-11:15

An offshore type of GPS tsunami meter using QZSS and ETS-VIII satellites

TERADA, Yukihiro[1*] ; HASHIMOTO, Gousei[2] ; MOTOHASHI, Osamu[2] ; YAMAMOTO, Shinichi[3] ; WADA, Akira[4] ; KATO, Teruyuki[5]

[1]Kochi National College of Technology, [2]Japan Aerospace Exploration Agency, [3]National Institute of Information and Communications Technology, [4]Hitachi Zosen Corporation, [5]The University of Tokyo

A new tsunami observation system has been developed, which employs the GPS technology to detect a tsunami before it reaches the coast. The GPS antenna attached on the top of a buoy floating at the sea surface is one of the important apparatus in this system. The estimated positions of the antenna includes not only tsunami but also all kinds of sea surface changes including wind waves, tides etc. The low pass and high pass filters are used for detection of tsunami. After a series of preliminary experimental studies, the operation-oriented experiments were conducted at two offshore sites. These results showed that a GPS buoy was useful to early detection of tsunami. And the Ministry of Land, Infrastructure, Transport and Tourism has established the GPS buoy system for monitoring sea waves with fifteen GPS buoys along the Pacific coast and Japan sea coast since the year of 2008. These system succeeded to detect the tsunami of the 2011 off the Pacific coast of Tohoku Earthquake.

Currently, the GPS buoy system uses RTK (Real Time Kinematic) method which requires land base for precise positioning of the buoy. This limits the distance of the buoy from the coast at most 20km. There are two problems to be conquered, one is the precise GPS positioning and the other is the data transmission methods. The algorithm of PVD (Point precise Variance Detection) method and PPP-AR (Precise Point Positioning method with Ambiguity Resolution) method are successfully under examination in the Muroto GPS buoy. Also, the satellite communication system using QZSS (Quasi-Zenith Satellite System) and ETS-VIII (Engineering Test Satellite VIII) were introduced for this GPS tsunami observation system experimentally.

Keywords: QZSS, ETS-VIII, GPS Tsunami Meter, PVD, PPP-AR

Japan Geoscience Union Meeting 2014
(28 April - 02 May 2014 at Pacifico YOKOHAMA, Kanagawa, Japan)

HDS27-08 Room:418 Time:May 1 11:15-11:30

Long-term deployment of Wave Glider for a real-time tsunami monitoring system using the Vector Tsunameter

HAMANO, Yozo[1*] ; SUGIOKA, Hiroko[1] ; TOH, Hiroaki[2]

[1]JAMSTEC, [2]Kyoto University

We have been developing a real-time tsunami monitoring system by using the Vector Tsunameter(VTM), in which we use an unmanned surface vehicle called Wave Glider, manufactured by Liquid Robotics Inc. The WG, equipped with both an acoustic and a satellite communication modems, can be used to transmit data messages from the VTM to shore. In order to investigate the feasibility for this type of station-keeping operation, we made a long-term deployment of the WG at sea area. We deployed the WG on September 22, 2013 at 38 14.99N, 143 35.13E, water depth = 3420.1 m. We set 6 waypoints along a circle (200m in diameter) centered at the above position, so that the WG trace the watch circle. The experiment had been continued until the WG was caught by a drift net and delivered to the Kesennuma port on December 6,2013.

The 75-days deployment of WG gives valuable information on the performance of the WG. As for the feasibility of WG for the station-keeping operation, two problems become apparent. During the experiment, the WG sporadically escaped from the watch circle and drifted away following the ambient water current, and it returned to the circle after several days of trip. Four excursions occurred during the first 50 days, and the total of the excursion period is 20 days. For monitoring slow activities such as crustal deformation, this performance is acceptable. However, some improvements are required for monitoring the short period signals such as tsunami. The other problem is the reduction of speed over water occurred after about 2 months operation. In the middle of November, the speed abruptly decreased to less than 0.5 knots and remains low until the end of the experiment.

Based on the detailed analyses of the navigation data sets and inspection of the WG, we conclude that the twist of the umbilical cable, which connects the surface float to the sub-surface glider, triggered both the excursion and the speed reduction. The small size of the watch circle and the short distance between the waypoints (about 100 m) are main cause of the twist. The short distance causes large and frequent changes of glider heading. Since the float can not follow the abrupt changes of heading, differential rotation of the glider relative to the float arises and enhances the twist of the cable. This twist of the cable increases water drag to the WG, and the stress of the cable due to the twist inhibit the rotation of the WG. These effects reduce the movability of WG, and the speed reduction start the drift of WG following the ambient current motion. The twist of the cable mainly occurs while the WG follows the path along the watch circle. On the other hand, during the excursions, glider heading is fixed and rewinding of the cable was observed. This rewinding reduces the drag force to the WG and assist the WG in returning to its home circle.

Extreme reduction of the speed is observed after 2 months of deployments. Inspection of the WG right after the recovery indicates that the propulsion system of the sub-glider had been working well until the end of the experiment, whereas the float suffered by the biofouling of eboshi-gai (goose barnacle). The biofouling seems responsible for the speed reduction, but theoretical estimate suggests that the hydrodynamic drag due to the biofouling is not sufficient to explain the observed speed reduction. The twist of the cable and the biofouling both contribute to the speed reduction. These analyses suggest larger size of the watch circle may improve or solve the present two problems of the excursion and the speed reduction.

Keywords: tsunami, tsunameter, real-time observation, seafloor observatio

Japan Geoscience Union Meeting 2014
(28 April - 02 May 2014 at Pacifico YOKOHAMA, Kanagawa, Japan)

HDS27-09 Room:418 Time:May 1 11:30-11:45

Enhancement of GEONET Real-time Analysis System for Covering over Japan

YAHAGI, Toshihiro[1*] ; MIYAGAWA, Kohei[1] ; KAWAMOTO, Satoshi[1] ; OSHIMA, Kennichi[1] ; YAMAGUCHI, Kazunori[1] ; MURAMATSU, Hiroki[1] ; OHTA, Yusaku[2] ; DEMACHI, Tomotsugu[2] ; MIURA, Satoshi[2] ; HINO, Ryota[2] ; SAIDA, Yuichi[3] ; DOUKE, Yuki[3]

[1]Geospatial Information Authority of Japan, [2]Graduate School of Science, Tohoku University, [3]Hitachi Zosen Corporation

Geospatial Information Authority of Japan (GSI) has been operating a continuous GNSS observation network system, known as GEONET (GNSS Earth Observation Network System), since 1994. Currently, GEONET consists of approximately 1,300 nationwide GNSS stations and its analysis center. Each station collects GNSS data with 1Hz sampling and those data are transmitted to the analysis center in real-time. GSI offers the observation data to the public in order to support various types of public surveys in Japan and precise positioning services using GNSS.

In the field of disaster prevention or mitigation, GEONET also plays very important roles by monitoring crustal deformation occurred by such as earthquakes or volcanic activities. In addition, after the 2011 off the Pacific coast of Tohoku Earthquake (Mw9.0), it is pointed out by a governmental committee that GEONET should be utilized for tsunami early warning by offering a first realistic estimation of moment magnitude (Mw) after large earthquakes. It is based on the fact that GNSS real-time positioning generally has big advantages in estimating moment magnitude (Mw) of the large earthquakes compared to short-period seismometers in terms of avoiding underestimation problem.

Since then GSI has been developing a new GEONET real-time analysis system, named REGARD (Real-time GEONET Analysis System for Rapid Deformation Monitoring), jointly with Tohoku University. It is designed for estimating permanent displacement field and Mw of giant earthquakes and notify the results in real-time. First, the GEONET data are processed by RTKLIB ver.2.4.1 (Takasu, 2011) for real-time GNSS positioning. We adopt both 'RAPiD' technique (Ohta et al., 2012) and the Early Earthquake Warning (EEW) information (Kamigaichi et al., 2009) for automated detection process of permanent displacements. Once the displacements are detected, corresponding fault source model is immediately estimated and the system sends the results to registered addresses by e-mail.

GSI launched its prototype system in April 2012 with 143 stations covering mainly Tohoku region and also has been evaluating its performances using archived data of some past earthquakes. We verified that the system successfully could estimate appropriate Mw values just after a couple of minutes in case of large events (e.g. Mw8.9 in the 2011 Tohoku earthquake), whereas it hardly detect proper values if the size of earthquake is less than Mw7.5. Based on the results and performances of the prototype system, we upgraded REGARD in 2013 for covering all over Japan by using most GEONET stations and enhancing its redundancy by carrying out two independent processing in parallel. This new system was launched in April 2014.

We present the evaluation results of the prototype system and introduce the upgraded REGARD including future plans focusing on exploiting to tsunami warning.

Keywords: GEONET, RTK-GPS, Real-time

Japan Geoscience Union Meeting 2014
(28 April - 02 May 2014 at Pacifico YOKOHAMA, Kanagawa, Japan)

HDS27-10 Room:418 Time:May 1 11:45-12:00

Tsunami inundation modeling of the 2011 Tohoku tsunami using the source estimated from the offshore tsunami records

BABA, Toshitaka[1*] ; TAKAHASHI, Narumi[1] ; KANEDA, Yoshiyuki[1]

[1]JAMSTEC

As the number of offshore tsunami stations comes up, it is becoming possible to estimate tsunami source in real time by exclusively using offshore tsunami information. The issue we would like to discuss in this study is how accurate is it in terms of coastal tsunami prediction? In order to investigate this, we performed a tsunami inundation modelling of the 2011 Tohoku tsunami and compared with the tsunami field survey. We used the Saito et al. (2011) source model inverted from the offshore tsunami waveforms alone, although it was not a real-time solution, in the numerical simulation. The nonlinear Boussinesq equations were solved for the tsunami propagation because tsunami soliton fission was observed during the 2011 tsunami, which is split short-period waves around tsunami crest caused by combination of wave nonlinearity and dispersion. We also applied a variable nested algorithm which allows the spatial resolution of the study region to be easily increased. The finest grid spacing was set to be 2/9 arcsec (about 5m). The three dimensional shape of buildings and structures from lidar measurements were directly embedded on the digital elevation model to include the effect of them on tsunami inundation. Our dispersive tsunami code (JAGURS) was fully parallelized with MPI and OpenMP libraries so that the large scale dispersive modeling could be implemented within realistic computation time. According to Aida (1978), the geometric mean K and geometric standard deviation k was used to evaluate the reproducibility of the numerical simulation. For our numerical simulation results, the K and k were calculated to be 0.97 and 1.27, respectively. These values satisfy the adequacy criteria for tsunami numerical modeling established by the Japan Society of Civil Engineers (2002) ($0.95 < K < 1.05$, $k < 1.45$). Accordingly, the present study showed the reliability of the tsunami prediction procedure that uses tsunami sources obtained with the offshore tsunami records alone.

Keywords: 2011 Tohoku tsunami, Nonlinear dispersive theory, Simulation

Japan Geoscience Union Meeting 2014
(28 April - 02 May 2014 at Pacifico YOKOHAMA, Kanagawa, Japan)

HDS27-11 Room:418 Time:May 1 12:00-12:15

Real-time tsunami simulation and visualization system using rapid CMT solutions in Southeast Asia

INAZU, Daisuke[1*] ; SAITO, Tatsuhiko[1] ; KUMAGAI, Hiroyuki[2] ; PULIDO, Nelson[1] ; FUKUYAMA, Eiichi[1]

[1]NIED, [2]Nagoya University

Southeast Asia, especially Indonesia and Philippines, is one of the most seismically active region in the world. NIED carries out real-time estimation of moment tensors of earthquakes and maintains a CMT catalogue in this region using the SWIFT system (Nakano et al. 2008), as well as waveform data from dense broadband regional seismic networks in Indonesia and Philippines, under a cooperative research with BMKG (Indonesia), PHIVOLCS (Philippines), and GFZ (Germany). Developing a rapid forecast/hindcast system of the tsunami is also necessary in particular for the tsunamigenic earthquakes.

We have been constructing an automated system for the tsunami simulation (Inazu et al. 2013 SSJ meeting). The current version of the system conducts simulations and visualizations of the followings procedures (1-4). The tsunami simulation is numerically carried out with a finite difference scheme from an initial condition given by a rectangular fault model.

1) Estimate a CMT solution by the SWIFT system.

2) Calculate the width, length, and slip amount of the rectangular fault model from Mw using an empirical scaling law. We here employ two scaling laws for the sake of evaluation of the uncertainties among the tsunami simulation results. Two parameters with small/large slip amount (or large/small rupture area) are then obtained for an estimated Mw.

3) Two fault mechanisms are obtained based on the double couple solutions, and then we expect four scenarios of the initial tsunami conditions. The seafloor deformation or initial tsunami condition are calculated by the Okada's (1985) theory for each scenario.

4) Carry out numerical simulations for the respective scenarios. We visualize the regional tsunami height distribution and the time series of the tsunami height at selected sites around the epicenter. The visualization is carried out in parallel to the simulation for an integral time interval. The maximum tsunami heights are displayed on a regional map and on coastal areas as well in parallel to the simulation.

We will present typical graphical outputs produced by the above procedures for several tsunami events.

Keywords: CMT, Tsunami, Rapid analysis

Japan Geoscience Union Meeting 2014
(28 April - 02 May 2014 at Pacifico YOKOHAMA, Kanagawa, Japan)

HDS27-12 Room:418 Time:May 1 12:15-12:30

Proper scoring systems with definite connections to information values of tsunami warnings

HAYASHI, Yutaka[1*]

[1]Meteorological Research Institute

Necessary conditions which newly introduced method can improve forecast are, existing proper scoring system, and that the new method marks better score than the present method do. Up to now, these scoring system have never applied to tsunami warning system.

Some scoring rules being applied widely to binary forecasts in weather forecasting, such as having precipitation or not, have close connections to change of utility for users. These scores are based on assumption that all user know their cost to make counter measures (C) and loss in case of no counter measure (L). When the forecast says the event will occur, and all users are assumed to make counter measures. In addition, a simple probability density distribution of U(-C)/U(-L) is assumed for cost-loss model, where U is the utility function. In general, a score is calculated by using a targeted dataset, e.g., a fixed period of time, and frequencies: occurrence of targeted phenomena is forecasted and observed (hit: N_a), forecasted but not occurred (false alarm N_b), not forecasted but occurred (misdetection: N_c), and not forecasted and not occurred (hit: N_d). For example, equitable threat score (ETS $\equiv$ (N_a-K)/(N_a+N_b+N_c-K), where K $\equiv$ (N_a+N_b)(N_a+N_c)/(N_a+N_b+N_c+N_d)) is one of their scoring system.

In this paper, suitable scoring rules for tsunami warnings are derived by considering the characteristics of tsunami warnings and following assumptions.

(1) Scores can be defined without N_d, because counting N_d does not make sense for tsunami warning.

(2) In case of tsunami warning, users of forecasts can select actions to take a counter measure or not. In case of no warning, users do not take a counter measure. Change of utilities are U(-C) and U(-L) for taking a counter measure and for when a phenomenon happens without a counter measure, respectively.

(3) All users know the fault alarm ratio (FAR $\equiv$ N_b/(N_a+N_b)) of the warning, their utilities for each condition (U(-C), U(-L)), and then their rational decision-making choose the option so that their expectation of utility (E_x(U)) become maximum. Here, if U(-L)/U(-C) <FAR/(1-FAR) is satisfied, not taking a counter measure is the more reasonable decision. According to this assumption, larger the FAR is, larger the cost-loss ratio is, warning become easier to be ignored.

(4) Assuming three types of probability density functions on x=U(-C)/U(-L). a) Uniform model: f(x)=1, b) Low-cost model: f(x)=2-2x, and (c) High-cost model: f(x)=2x for the range of 0 $\leq$ x $\leq$ 1.

(5) The scores are set to be proportional to the information value of the warning. Here, $\triangle$U can be calculated as the integral corresponding to each distribution of (4) and utilities of selected actions at the N_a+N_b warnings based on the rational decision-making described in (3). Besides, if there were not for warning system, users should have lose utility as much as -U(-L) at every event. Then, V $\equiv$-ΔU/((N_a+N_c)U(-L)).

Scores corresponding to models a)-c) in (4) are derived as follows.

a) V=$N_a{}^2$/(2(N_a+N_b)(N_a+N_c)). For good warning which satisfies both $N_a \gg N_b$ and $N_a \gg N_c$, the score can be approximated to V $\fallingdotseq$ CSI/2, where CSI $\equiv$ N_a/(N_a+N_b+N_c) is threat score or critical success index.

b) V=(2/3)(1-FAR)(1-M)(1+M/2), where M $\equiv$ N_c/(N_a+N_c) is missing ratio. For warnings with few misdetection which satisfies Nc $\ll$ Na, the score can be approximated to be V $\fallingdotseq$ (2/3)(1-FAR)(1-M/2).

(c) V=(1-FAR)^2(1-M)/3.

The proper score system thus changes according to the cost-loss ratio, which have close relation to preparedness. It is necessary to choose suitable forecast method using proper scoring system which is corresponding to a social structure. In the meeting, the author would like to discuss also on the problem for the practical application of the scoring systems.

Keywords: binary forecast, cost-loss model, expected-utility theory, rational decision-making, score

Japan Geoscience Union Meeting 2014
(28 April - 02 May 2014 at Pacifico YOKOHAMA, Kanagawa, Japan)

HDS27-13 Room:418 Time:May 1 12:30-12:45

Tsunami height distribution of the 1843 Tenpo Nemuro-oki earthquake

TSUJI, Yoshinobu[1*] ; HORIE, Takehito[2] ; HASHIMOTO, Keisuke[2] ; SASAKI, Takayuki[2] ; MABUCHI, Yukio[3] ; OKADA, Kiyohiro[3] ; KUROYANAGI, Yousuke[3] ; OOIE, Takayuki[3] ; KURIMOTO, Masashi[3] ; KINAMI, Takahiro[4] ; IMAMURA, Fumihiko[5]

[1]Fukada Geolog. Inst., [2]Alpha Hydraulic Eng.Consultant, [3]Pacific Consultant, [4]Kubiki Techno., [5]IRIDeS, Tohoku Univ.

A large earthquake occurred in the sea area east offing Nenuro, Hokkaido at 6 AM, April 25, 1843 and is called Tenpo Nenuro-Oki earthquake whose magnitude is estimated at M7.5. A tsunami was accompanied with this earthquake, and hit the Pacific coast of Hokkaido and the east coast of Sanriku district, the north part of Honshu. Historical documents which record the tsunami were published by Musha (1941) and ERI, university of Tokyo(1984). It is recorded in the diary kept by a priest of Kokutaiji Temple at Akkeshi town, Kushiro district, Hokkaido that the Akkeshi branch office of the Tokugawa Government and huts of Ainu race were swept away in the residential area around the temple, and in Muko-Gishi area, north opposite coast of Akkeshi all houses were washed away and 34 Ainu people were killed. The official report written by an officer at Kushiro described that one hut and one barn were swept away at Betsufuto, about 36 kilometers east of Kushiro, and 2 houses were swept away at Atoega village. Documents written by the local meteorological observatory of Namuro described that 50 houses village were swept away at Hanasaki, about 8 kilometers south west of Nemuro Town, and survived people moved their residences to Honioi village about 6 kilometers north of Hanasaki. In this official report also it was recorded that a boy called Yamamoto Koshichi was lived on the coast of Notsuke peninsula. He experienced the tsunami there when he was 12 years old. He mentioned that the wave was divided into two waves in the offing of Notsuke coast, and the bigger wave hit the south coast of Shiretoko Peninsula. On the basis of those records, we conducted field survey for three times, and obtained the distribution of the tsunami height as the figure. The authors of the present study wish to express their thanks to JNES for its financial support in promoting our research.

Keywords: historical earthquake, historical tsunami, Hokkaido, Nemuro, Kushiro, Kuril trench

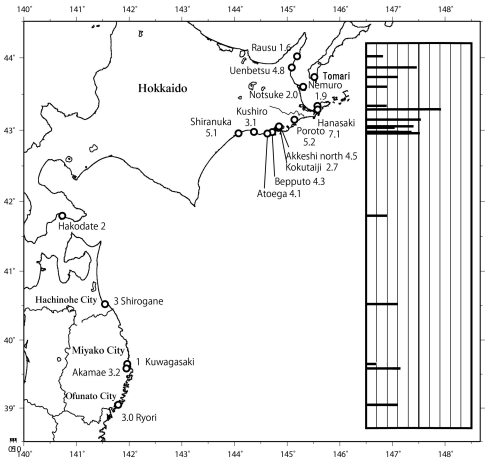

Japan Geoscience Union Meeting 2014
(28 April - 02 May 2014 at Pacifico YOKOHAMA, Kanagawa, Japan)

HDS27-14 Room:418 Time:May 1 14:15-14:30

A new calculation method for seabed displacement due to fault slip by boundary integration

AKIYAMA, Shinichi[1*] ; FUJIWARA, Hiroyuki[2] ; HASHIMOTO, Norihiko[1]

[1]CTC, [2]NIED

In tsunami simulation, initial water level of tsunami is often considered to be equal to vertical displacement of seabed generated by a source fault slip. Exact solution for displacement due to rectangular fault slip in elastic half space (Okada, 1985) has been generally applied to calculate the seabed displacement.

In order to calculate the displacement due to the source fault which has irregular form using this solution, the source fault should be modeled by patching many rectangular small faults along the irregular surface. As a result, the source-fault model has portions in which the rectangular small faults are overlapped each other or not covered the fault surface. Then, calculated displacement from the fault model is overestimated near the overlapped area or underestimated near the uncovered area. This kind of displacement discontinuity is not negligible when the fault is located near the seabed, while it is negligible in the case that it is far from the seabed. Therefore, a new technique to take the irregular form into consideration accurately is required to solve the above problem.

Under such a background, we developed a new method to calculate displacement of seabed due to slip of the source fault using boundary integration. It is well known that deformation of the medium due to a fault slip is represented by the boundary integration for the medium surface and the fault surface by applying Green's theorem to the governing equation. Considering the seabed as an elastic half space, it can also be expressed only with the boundary integration for the fault surface. Calculating the boundary integration numerically, we introduce the linear element which is used by Boundary Element Method (BEM) into the proposed method to guarantee continuity of the displacement. However the numerical integration based on Gauss quadrature formulae at the point near the fault surface is broken down by the influence of singularity of Green's function. We apply the Projection and Angular & Radial Transformation (PART) method (Hayami and Brebbia, 1988) to the proposed method to evaluate the effect of the singularity accurately. We will present formulation, validation, verification and application of this method.

This research was carried out as part of Tsunami Hazard Assessment for Japan by National Research Institute for Earth Science and Disaster Prevention (NIED).

Reference

Okada, Y. (1985) Surface deformation due to shear and tensile faults in a half-space, Bull. Seism. Soc. Am., 75, 1435-1154.

Hayami, K. and Brebbia, C.A. (1988) Quadrature methods for singular and nearly singular integrals in 3-D boundary element method, (Invited paper), Proc. 10th Int. Conf. on Boundary Elements, Southampton, Computational Mechanics Publication with Springer-Verlag, Vol. 1, pp. 237-264.

Keywords: seabed displacement, fault slip, numerical calculation, boundary integration, singularity of Green's function, PART method

Japan Geoscience Union Meeting 2014
(28 April - 02 May 2014 at Pacifico YOKOHAMA, Kanagawa, Japan)

HDS27-15 Room:418 Time:May 1 14:30-14:45

Inundation hazard mapping toward probabilistic tsunami hazard assessment

SAITO, Ryu[1*] ; FUJIWARA, Hiroyuki[2] ; HIRATA, Kenji[2] ; MURASHIMA, Youichi[1] ; MURATA, Yasuhiro[1] ; INOUE, Takuya[1] ; AKIYAMA, Shinichi[3] ; ABE, Yuta[3] ; MATSUYAMA, Hisanori[4] ; TOHYAMA, Nobuhiko[4]

[1]KOKUSAI KOGYO CO., LTD. (KKC), [2]National Research Institute for Earth Science and Disaster Prevention (NIED), [3]ITOCHU Techno-Solutions Corporation (CTC), [4]OYO Corporation

A method to obtain probabilistic hazard information on tsunami run-up and inundation area is described in this study, as part of the probabilistic tsunami hazard assessment research work [NIED]. A tsunami hazard assessment has been conducted to estimate frequency of exceedance wave height at several monitoring sites along coastal region, and to be useful for the study of coastal vulnerability, based on results from a tsunami simulation with an earthquake scenario and occurrence probability. Although the main target of a tsunami hazard assessment has contributed to quantify risk in critical infrastructure facilities, inundation hazard information for urban and river regions are also important. In a study of a probabilistic tsunami hazard assessment for Japan, tsunami exceedance wave height in coastal region is probabilistically derived from numerical modelling of tsunami sources available. However, horizontal resolutions in the model is only 50 m of minimum in a land region due to computational cost constrained by tsunami simulation for Japan, which is not enough resolution to assess inundation hazard mapping on a urban area. A detailed inundation hazard assessment is expected as a result of implementing smaller grid size than 50 m.

Here we provides a technical note for estimation of inundation hazard mapping resulted from a simulation run at horizontal resolution 10 m, and show their results at Rikuzentakata, one of example. A horizontal distribution of the probabilistic inundation is calculated from hazard curves on every grid cells in inundation area. Earthquake scenarios are set by many tsunami sources and occurrence frequencies around Japan trench. An annual exceedance probability of inundation when reaching threshold is calculated from tsunami sources and occurrence probability of the earthquake scenarios. This describes the benefit of tsunami inundation hazard mapping. We could successfully show this point clearly for the first time.

Keywords: Tsunami hazard, Tsunami inundation, Probability, Hazard curve

Japan Geoscience Union Meeting 2014
(28 April - 02 May 2014 at Pacifico YOKOHAMA, Kanagawa, Japan)

HDS27-16 Room:418 Time:May 1 14:45-15:00

Uncertainty for sunami hazard caused by heterogeneous slip on the characterized source model

ABE, Yuta[1*] ; HASHIMOTO, Norihiko[1] ; KORENAGA, Mariko[1] ; FUJIMOTO, Keisuke[1] ; AKIYAMA, Shinichi[1] ; FUJIWARA, Hiroyuki[2] ; HIRATA, Kenji[2]

[1]ITOCHU Techno-Solutions Corporation, [2]National Research Institute for Earth Science and Disaster Prevention

In preparation for probabilistic tsunami hazard assessment for the whole of Japan, we discuss uncertainty for tsunami heights due to a difference in slip distribution of source models.

In the process of probabilictic tsunami hazard assessment, tsunami heights at assessment points are estimated by numerical simulations. We calculate crustal deformations from source models, which are assumed as initial sea surface displacements, and then simulate tsunami propagations till tsunamis arrive in coastal sites. A simulation result changes depending on fault parameters of a source model such as magnitude, location, dip, strike, rake and slip distribution. Therefore, tsunami hazard includes uncertainties due to variability of fault parameters.

For the cases of subduction-zone earthquakes, focal mechanism is thought to be subject to a plate boundary in the characterized tsunami source model defined by probabilistic tsunami hazard assessment for the whole of Japan (Toyama et al., 2014, JpGU). On the other hand, magnitude, location and slip distribution are thought to have large varieties and their variabilities will create a large difference in tsunami height distributions. We therefore take account of the variabilities by calculating a number of source models with the different fault parameters. In this study, we give a qualitative verification for the variation in tsunami height due to slip distribution for the purpose of simplifying the hazard assessment process by using a probabilistic model for the uncertainty due to slip distribution. We examine a parameter study for several models with different slip distributions using two topography models, an uniform water depth model and a real ocean floor topography model. As the result, there is little to distinguish of geometric standard deviations between the two topography models, the values are 0.09 at a maximum.

This study was performed as a part of research for ”Tsunami hazard assessment for the whole of Japan” in NIED.

Keywords: Tsunami, Probabilistic Hazard Assessment, Characterized tsunami source model, heterogeneous slip distribution

Japan Geoscience Union Meeting 2014
(28 April - 02 May 2014 at Pacifico YOKOHAMA, Kanagawa, Japan)

HDS27-17 Room:418 Time:May 1 15:00-15:15

Large slip area in characterized Tsunami source model toward Tsunami Hazard assessment

KORENAGA, Mariko[1*] ; AKIYAMA, Shinichi[1] ; ABE, Yuta[1] ; HASHIMOTO, Norihiko[1] ; HIRATA, Kenji[2] ; FUJIWARA, Hiroyuki[2] ; MATSUYAMA, Hisanori[3] ; MURASHIMA, Yoichi[4]

[1]CTC, [2]NIED, [3]OYO, [4]KKC

In previously deterministic Tsunami hazard assessment, it had been ordinary method in setting tsunami source model that it is accountable for signature of historical tsunami events. Therefore it is difficult to evaluate of tsunami risk for future events unascertained focal area or magnitude and so on. On the other hand, in probabilistic tsunami hazard assessment, it ' s necessary to be designed for all potentially tsunamigenic earthquakes considering target region in principle, in planning phase of modeling of elastic fault parameter (Toyama et al., 2014,JPGU). For our purpose, on setting for characterized tsunami source model for probabilistic tsunami hazard, it is essential to characterize tsunami source model and include the statistical variability. We focused on the " heterogeneous slip distribution " of tsunami source, and studied on how to setting area ratio of large slip.

According to the distribution of the fault plane slip obtained from the wave source inversion studies of the 2011 off the Pacific coast of Tohoku Earthquake (2011 Tohoku tsunami), the ratio of large slip area is said to have contributed significantly to the tsunami wave height, the ratio of the area is much the same.

Therefore, in this study, we analyzed the ratio of seismic moment by unit area regardless of the assumed size of the fault element to all mean of seismic moment. As a result from inversion models of 2011 Tohoku tsunami source and other magnitude of 9 level source, three stage characterized modeling is required, it was found that the model which accounts for 30% of the total area of 2 times the average slip, and 10% of the total area of 4 times the average slip is appropriate. And two stage characterized model for magnitude 8 level sources, its large slip (twice the average) region accounts for 30%. Comparing the maximum coast wave heights simulated using characterized model above with a detailed inversion fault model, we verified that the former covering the latter.

This study was conducted by a part of research project in NIED for tsunami hazard assessment for the whole of Japan.

Keywords: tsunami, probabilistic hazard assessment, characterized fault model, heterogeneous slip distribution

Japan Geoscience Union Meeting 2014
(28 April - 02 May 2014 at Pacifico YOKOHAMA, Kanagawa, Japan)

HDS27-P01 Room:Poster Time:May 1 18:15-19:30

Large tsunami remote observations from high altitude using the induced magnetic field of tsunami.

TATEHATA, Hidee[1*] ; HAMANO, Yozo[2]

[1]JMA, [2]JAMSTEC

On The 2011 off the Pacific coast of Tohoku Earthquake, massive tsunamis more than 10m attacked it in the wide range of Ibaraki from Aomori coast area. The tsunami warnings were not only sufficient but also no observation result of the tsunami, it was a big problem. The other side, at the Chichijima geomagnetic observation point had observed the tsunami induced magnetic field

As a result of example analysis for a past tsunami on Chichijima islands, the signal of the induced magnetic field was able to detect almost more than 1m tsunamis. The observation of the tsunami by the tsunami induced field has a weak point that sensitivity and a point of S/N ratio, but has a characteristic of the remote observation unlike the observation by tide gauges. If a geomagnetism sensor was installed in the hill of the Sanriku coast as a huge tsunami meter, they endured a massive tsunami and might continue observation without being destroyed.

We introduce the wave pattern of the prospective induced field of the tsunami and some character, if a sort of electromagnetic huge tsunami meter had been installed in the Sanriku coast.

Keywords: tsunami, Huge tsunami meter, induced magnetic effect

Japan Geoscience Union Meeting 2014
(28 April - 02 May 2014 at Pacifico YOKOHAMA, Kanagawa, Japan)

HDS27-P02 Room:Poster Time:May 1 18:15-19:30

Tsunami spectral analysis in and around Tokyo Bay

TAKIGAWA, Akira[1*] ; MUROTANI, Satoko[1] ; HEIDARZADEH, Mohammad[1] ; WU, Yifei[1] ; SATAKE, Kenji[1]

[1]Earthquake Research Institute, University of Tokyo

Coastal areas in the Kanto region have been damaged by large tsunamis in the past. The reported tsunami heights from the 1923 M7.9 Kanto earthquake show a great difference between in and around Tokyo Bay. Attenuation of tsunami heights was observed at the mouth of the bay. For example, tsunami heights were less than 1.0 m inside the bay at Shinagawa, Funabashi, and Chiba, although they were 3.0-10.0 m outside the bay (Hatori et al., 1973, ERI special publication).

On the other hand, the tsunams from the 2011 Mw 9.0 Tohoku earthquake did not experience such attenuation. For example, tsunami heights were 1.46 and 2.84 m inside the bay at Tokyo and Funabashi respectively, although they were 1.45 and 1.60 m outside the bay at Tateyama and Kyonan (Sasaki et al., 2012, CEJ).

It is important to know why this difference occurs, when estimating tsunami damage to the metropolitan area for future earthquakes. Therefore we conducted spectral analysis of tsunami waveform obtained by numerical simulations, and found that the dominant wave period in the bay is different for each earthquake. It is around 100 min for the Kanto earthquake tsunami and around 70 min for the Tohoku one. We inferred that the 100 min period may result from the normal mode of Tokyo bay (Aida, 1996, Zisin) and the 70 min period from the normal mode of Sagami Bay (Imai et al., 2011, SSJ meeting). In future, we will examine the relation between these different periods and tsunami behaviors.

Keywords: Tsunami, Spectral analysis, Tokyo Bay, 1923 Kanto earthquake, 2011 Tohoku earthquake

Japan Geoscience Union Meeting 2014
(28 April - 02 May 2014 at Pacifico YOKOHAMA, Kanagawa, Japan)

HDS27-P03 Room:Poster Time:May 1 18:15-19:30

Wave period dependence of the tsunami energy decay based on observation: In the case of the 2011 Tohoku-oki Earthquake

TANOBE, Atsushi[1*] ; IMAI, Kentaro[2] ; HAYASHI, Yutaka[3] ; IMAMURA, Fumihiko[2]

[1]Graduate School of Engineering, Tohoku University, [2]IRIDeS, Tohoku University, [3]Meteorological Research Institute

1. Introduction

2011 Tohoku-oki Earthquake caused serious damage. In the case of such a giant earthquake, transportation network suffer serious damage. Therefore ensuring sea route safety as the relief course is important for smooth relief and restoration activity. It is important that realize the decay process of tsunami to early ensure the security of the sea route. On the other hand, there is no clear and scientific standard to judge tsunami convergence (Hayashi et al., 2010).

In this study, we use the 2011 Tohoku-oki Earthquake tsunami wave form and show the characteristic of the tsunami decay process by the connection with time of the moving root mean square amplitude maximum onset and tsunami arrival time. And we paid attention to period, intended to clarify the characteristic of each decrement process.

2. Analysis

We targeted for analysis 20 points chose from observed tsunami wave form in the 2011 Tohoku-oki Earthquake that located in the Japanese Islands Pacific on shore and off shore station (observed by Japan Meteorological Agency, NOWPHAS, Geospatial Information Authority of Japan).

It is obvious that long sampling intervals can lead to a marked distortion of the wave properties (Rabinovich et al., 2011). We unified the sampling intervals for 30 sec and High-frequency filtering was used to remove sea level variations associated with synoptic atmospheric activity. We used the maximum of the moving root mean square amplitude to normalize the observed wave because of tsunami amplitude different from every observation point. After the Normalized process we analyzed that wave form.

Because the tsunami includes wave of various periods, and suggested decay process is different every period (Rabinovich et al., 2013). So we used band-pass 2-16 min, 16-32 min, 32-64 min, and 64-128 min filter to divide tsunami every periods. I calculated the moving root mean square amplitude and we analyzed it with a method of Hayashi et al. (2010) to define a decay coefficient.

In this study, t is the elapsed time from shock, M(t) is moving root mean square amplitude at t, Mmax is maximum of the M(t), Tm is time of onset Mmax, Tt is time of the first wave′s maximum observed, TL is differences between Tm and Tt, k is proportional constant every observation point, e is Napier's constant, τ is decay time. τ mean time required for the average amplitude being decay to 1/e .

As a result of analyzed, the tsunami decrement process of each observation point is characterized by the longer period wave that attenuate later and shorter period wave that maximum wave late for arrival.

3. Conclusion

In this study, we used the tsunami wave pattern at the 2011 Tohoku-oki Earthquake and analyzed it. I discussion a factor to characterize a decay process of the tsunami energy, and get the following result.

(1)Regardless of on shore or off shore, equilateral correlation has τ and Tt, and on shore points tends to get longer than τ.

(2)For a wider tendency, tsunamis indicates that shorter period waves attenuate much faster than longer period waves in a short period.

(3)Some observation point have a long TL about less than 32 min period.

Acknowledgments

This work was partly supported by JSPS KAKENHI Grant No.24310132.

And I gratefully acknowledge the following organizations for providing with records for the 2011 tsunami: observed by Japan Meteorological Agency, NOWPHAS, Geospatial Information Authority of Japan

Keywords: tsunami, decay, decay time, period

Japan Geoscience Union Meeting 2014
(28 April - 02 May 2014 at Pacifico YOKOHAMA, Kanagawa, Japan)

HDS27-P04 Room:Poster Time:May 1 18:15-19:30

Oscillations starting immediately after the 2011 Tohoku earthquake in Japan Sea

MUROTANI, Satoko[1*] ; IWAI, Maki[2] ; SATAKE, Kenji[1]

[1]ERI, the Univ. of Tokyo, [2]Yokohama City Univ.

The tsunamis from the March 11, 2011 Tohoku earthquake were recorded in the Japan Sea. At some tide gauge stations along the Japan Sea coast of Honshu and the Russian coast, sea surface disturbances were observed immediately after the earthquake, followed by tsunami propagated through the Tsugaru Strait between Honshu and Hokkaido. Using tsunami numerical computations from seafloor displacements including the effect of the horizontal displacement and seafloor slope, the oscillations starting immediately after the origin time were reproduced. We interpret that these tsunami forerunners were generated from horizontal motion of seafloor slopes in the Japan Sea.

The tsunami forerunners were particularly remarkable at Awashima (JCG), Sado, Noto Toyama and Fukaura (JMA) tide gauge stations along the Japan Sea coast of Honshu and at Rudnaya Pristan, Preobrazhenie, and Nakhodka stations along the Russian coast of Primorye (Shevchenko et al., 2013: Pageoph). The 2011 tsunami originated in the Pacific Ocean would pass the Tsugaru Strait 1.5 hours after the earthquake. It indicates that these forerunners were different from the tsunami originated in the Pacific Ocean.

We made the tsunami numerical computation to reproduce these forerunners from seafloor displacements in the Pacific Ocean and Japan Sea. We used the source model of Satake et al. (2013, BSSA). According to Tanioka and Satake (1996, GRL), if the ocean bottom contains steep slopes or steps, the effect of the horizontal displacement of ocean bottom cannot be neglected. Computation including this effect showed the oscillations starting immediately after the origin time. However, the short-period components about a few minutes are not well reproduced. Use of finer bathymetry grid than we used (30' and 5') may better reproduce the short-period components of the Japanese tide gauge stations. Seismograms at nearby stations suggest that some of the short-period components may be the seismic ground motion. When we applied low-pass filter to the observed waveforms, the agreement between the observed and synthetic waveforms on tide gauges became better.

Because the Russian stations are about 500 km away from the source area, we also computed the synthetic tsunami waveforms from seafloor displacements computed on the spherical Earth model (Sun et al., 2009: Geophys. J. Int.). However, the computed waveforms from the spherical models are not very different from those computed on Cartesian coordinate system. It is necessary to compute the tsunami waveforms using the finer grid including the shape of the bay.

Keywords: the 2011 Tohoku earthquake, the 2011 Tohoku tsunami, Japan Sea, seafloor displacement

Japan Geoscience Union Meeting 2014
(28 April - 02 May 2014 at Pacifico YOKOHAMA, Kanagawa, Japan)

HDS27-P05 Room:Poster Time:May 1 18:15-19:30

The 24 September 2013 tsunami in the Makran region, northwestern Indian Ocean

HEIDARZADEH, Mohammad[1] ; SATAKE, Kenji[1*]

[1]Earthquake Research Institute (ERI), The University of Tokyo

Tsunami waves were observed in the northwestern Indian Ocean following the Mw 7.7 Pakistan inland earthquake on 24 September 2013. We analyze eleven tide gauge records as well as one DART record of this tsunami and perform numerical modeling of tsunami. The tsunami registered a maximum wave height of 109 cm in Qurayat tide gauge station (Oman). Spectral analysis showed that the most governing period of the tsunami waves was around 12 min though wavelet analysis showed that parts of the tsunami energy were partitioned into other period bands of 7 and 16 min. Distribution of aftershocks in the region showed that all of them were located inland indicating that the tsunami was generated by submarine geological phenomena triggered by the earthquake. Tsunami backward ray tracing showed that the tsunami source was possibly located at offshore Jiwani (Pakistan) and the tsunami was most likely generated immediately after the main shock. Tsunami modeling assuming a pile-up structure at the location of the new island was not successful in reproducing the observed sea level records. A landslide source with a length of about 15-20 km, a thickness of 100-150 m located at 61.72^{o}E and 24.60^{o}N seems capable of fairly reproducing the observed sea level records. This event was the second tsunami recorded in the Makran region since 1945, and may be evidence for hazards from landslide-generated waves following seismic activities.

Keywords: Northwestern Indian Ocean, Tsunami, Makran subduction zone, Landslide, Spectral analysis, Numerical modeling

Japan Geoscience Union Meeting 2014
(28 April - 02 May 2014 at Pacifico YOKOHAMA, Kanagawa, Japan)

HDS27-P06 Room:Poster Time:May 1 18:15-19:30

Pre-computed Tsunami Database with Additional Slip Near to the Trench for Tsunami Early Warning in Southern Java

SUNENDAR, Haris[1*] ; TANIOKA, Yuichiro[1] ; GUSMAN, Aditya[1] ; LATIEF, Hamzah[2]

[1]Institute of Seismology and Volcanology, Hokkaido University, [2]Bandung Institute of Technology

We build tsunami database based on simple fault model scenarios for the Java trench subduction zone. We have 480 points along the subduction zone with distance between each other of 20 arc-min. This points are used as the center of simple fault model scenarios. Each point is the center of several fault models with different moment magnitudes.We used a magnitude to fault length and width scaling relationship for the fault model scenario. The moment magnitudes for the fault model scenarios are from Mw 6.3 to Mw 9.0 with interval of 0.3. The fault depth parameter is also a variable for the fault model scenario. We used depth between 10 km to 60 km with interval of 10 km.

From each fault model scenario we simulate tsunami propagation by solving the linear shallow water equations. We used bathymetry data based on Indonesian navy chart and GEBCO bathymetric dataset. The grid size for the tsunami simulation is 1 arc-min. The pre-computed maximum tsunami heights and tsunami arrival time at every point along the coast are stored in a database.

If a real earthquake occur at any location in the forecasting domain then the pre-computed tsunami heights from 16 scenarios are retrieved from the database. Theses 16 scenarios are those that are surrounding the actual hypocenter and each of the scenario has the closest higher or closest lower magnitude to the actual one. Then the tsunami heights from these scenarios are used in interpolation methods to get the tsunami height forecast. The tsunami heights from two scenarios with a same hypocenter and different moment magnitudes are interpolated by logarithmic interpolation. Then the tsunami heights with different depths and different epicenters are interpolated using linear interpolation and bilinear interpolation, respectively. The the interpolated tsunami heights is group into district administrative regions, then the maximum height for each administrative region is selected. The selected tsunami heights are categorized into three different warning levels. These levels are tsunami smaller than 0.5 m, between 0.5 m to 3 m, and larger than 3 m.

We apply this method to forecast the tsunami generated by the 1994 East Java earthquake. The 1994 earthquake is classify as a tsunami earthquake (Newman and Okal, 1998; Pollet and Kanamori, 2000). The earthquake moment magnitude was estimated to be Mw 7.6 (Abercrombie et al., 2001), Mw 7.8 (Bilek et al., 2006; USGS), Mw 7.9 (Pollet and Kanamori, 2000). Our result shows that the forecasted tsunami heights underestimate the actual tsunami heights. One of the main cause could be the fact that we used simple fault model scenarios which sizes were estimated from scaling relationship of magnitude to fault dimension of regular earthquake but not tsunami earthquake. Previous studies shows tsunami earthquake may generate large slip near the trench (Tanioka and Satake, 1996; Satake et al., 2013). Therefore to obtain a more accurate forecast, the fault model scenarios near the trench should represent fault model for tsunami earthquake event.

Keywords: pre-computed tsunami database, tsunami earthquake, tsunami early warning

Japan Geoscience Union Meeting 2014
(28 April - 02 May 2014 at Pacifico YOKOHAMA, Kanagawa, Japan)

HDS27-P07 Room:Poster Time:May 1 18:15-19:30

Simulation of tsunami inundation from future megathrust earthquake scenarios of Central Peru

MAS, Erick[1*] ; ADRIANO, Bruno[2] ; PULIDO, Nelson[3] ; KOSHIMURA, Shunichi[1]

[1]International Research Institute of Disaster Science, IRIDeS, Tohoku University, [2]Graduate School of Engineering, Tohoku University, [3]National Research Institute for Earth Science and Disaster Prevention, NIED

Great tsunami events like the 2011 Great East Japan Earthquake and Tsunami might occur around the world in the future. In particular at areas of the Pacific Rim or the Andaman Sea as history has confirmed. In this study we will focus on the central coast of Peru on the western Pacific. The earthquake history of Peru accounts for many devastating tsunami disasters in the past (1555, 1586, 1609, 1630, 1655, 1678, 1687, 1746). The potential damage to national infrastructure exposed in Callao and Lima could yield to a heavy economical breakdown in Peru. It is of great importance to assess and estimate the future tsunami inundation scenarios in order to grasp the extent of possible damage and the severity of it. Consequently, this study evaluates the tsunami hazard and the related features of inundation at the central coast areas of Peru based on possible megathrust earthquakes.

The source model we used in this study (Mw = 8.90) was obtained from results of the interseismic coupling distribution in subduction areas using GPS monitoring data as well as historical earthquake recurrence information (Pulido et al., 2011). This slip model was used to generate twelve additional slip scenarios for strong ground motion simulation, by adding spatially correlated short-wavelength slip heterogeneities (Pulido et al., 2012).

Here, we used these thirteen scenarios to evaluate the tsunami hazard of Callao area in Peru. From results of strong ground motion simulations Pulido et al. (2012) reported that the slip scenario with the deepest along strike slip average (Mw = 8.86) was the worst case scenario for strong ground motion in Lima-Callao area. On the other hand, in this study the slip model with the largest peak slip (Mw = 8.87) yielded the highest tsunami inundation and maximum velocity near shore. Such differences on maximum scenarios for peak ground acceleration and tsunami height reveals the importance of a comprehensive assessment of earthquake and tsunami hazard in order to provide plausible worst case scenarios of strong ground motion and tsunami inundation.

Acknowledgments

This study was carried out under the framework of the SATREPS project ”Enhancement of Earthquake and Tsunami Disaster Mitigation Technology in Peru, project sponsored by the Japan International Cooperation Agency (JICA) and the Japan Science and Technology Agency (JST). Our appreciation goes to the Ministry of Education, Culture, Sports, Science and Technology (MEXT), National Research Institute for Earth Science and Disaster Prevention (NIED) and the International Research Institute of Disaster Science (IRIDeS), Tohoku University for their support.

References

Pulido, N., Tavera, H., Aguilar, Z., Chlieh, M., Calderon, D., Sekiguchi, T., Nakai, S., and Yamazaki, F. (2012). Estimation of slip scenarios of mega-thrust earthquakes and strong motion simulations for Central Andes , Peru realizations (poster S33A-2505). In *American Geoscience Union Fall Meeting 2012*, number section III, pages 1?2, San Francisco, California, USA.

Pulido, N., Tavera, H., Perfettini, H., Chlieh, M., Aguilar, Z., Aoi, S., Nakai, S., and Yamazaki, F. (2011). Estimation of Slip Scenarios for Megathrust Earthquakes: A Case Study for Peru. In *4th IASPEI/IAEE International Symposium*, pages 1?6, Santa Barbara, CA, USA.

Keywords: megathrust earthquake, megatsunami, numerical simulation, tsunami Peru, scenarios

Japan Geoscience Union Meeting 2014
(28 April - 02 May 2014 at Pacifico YOKOHAMA, Kanagawa, Japan)

HDS27-P08 Room:Poster Time:May 1 18:15-19:30

Identification of submarine landslide tsunami sources: A probabilistic approach for the Gulf of Mexico

SHIGIHARA, Yoshinori[1*] ; HORRILLO, Juan[2]

[1]National Defense Academy, [2]Texas A&M University at Galveston

The devastating consequences of recent tsunami events in Indonesia (2004), Japan (2011) have changed the perception about tsunami potential and have prompted a scientific response in assessing the tsunami hazard in regions even though an apparent low-risk or/and lack of complete historical tsunami record exists. Although a great uncertainty exists regarding the return period of large-scale tsunami events in the Gulf of Mexico (GOM), geological and historical evidences indicate that the most likely tsunami hazard could come from a submarine landslide triggered by a moderate earthquake. Under these circumstances, the assessment of the tsunami hazard in the region could be better accomplished by means of a probabilistic approach to include the uncertainty in the hazard analysis and thus to identify tsunami sources.

This study aims to customize for the GOM an existing probabilistic methodology to determine landslide-tsunami sources associated with return periods. The Monte Carlo Simulation (MCS) technique is employed to determine the uncertainty related to location/water-depth and landslide dimension based on normal/lognormal distributions obtained from observed data. Along fixed transects over the continental slope of the GOM, slide angle of failure, soil properties and seismic peak horizontal accelerations (PHA) are determined by publicly available data. These parameter values are used to perform slope stability analyses in randomly generated translational submarine mass failure (SMF) obtained from the MCS technique. Once the translational SMF is identified as tsunamigenic for a given recurrence rate, a preliminary tsunami amplitude can be estimated by using empirical formulations. Thus, the annual probability of a tsunamigenic SMF is determined by the joint probability with the annual PHA.

By using the probabilistic approach we identified tsunami sources associated with return periods from few thousands to 10,000 years for each fixed transects defined over the continental slope of the GOM.

Keywords: tsunami, submarine landslide, the Monte Carlo Simulation

Japan Geoscience Union Meeting 2014
(28 April - 02 May 2014 at Pacifico YOKOHAMA, Kanagawa, Japan)

HDS27-P09 Room:Poster Time:May 1 18:15-19:30

A stochastic analysis and an uncertainty assessment of tsunami wave height using a random source parameter model

FUKUTANI, Yo[1*] ; SUPPASRI, Anawat[1] ; IMAMURA, Fumihiko[1]

[1]International Research Institute of Disaster Science, Tohoku University

In this paper, we conducted a stochastic tsunami hazard assessment including various uncertainties using a logic tree with targeting a region of the 3.11 Tohoku earthquake and investigated how heterogeneous slip faults generated by CRSP (Correlated Random Source Parameter) model influence the stochastic tsunami hazard assessment. In the assessment, observed tsunami wave height 6.7m in the 3.11 Tohoku Earthquake corresponded to 1112 year (0.50 fractile point), 1129 year (simple average) and 490 year (0.95 fractile point) for return period. Next, we investigated an influence that the number of slip patterns has on the results of the assessment. While the number of slip patterns had little impact on the results of the stochastic assessment in cases which a target wave height was comparatively low (2.0m), the return period at each fractile point was overestimated in case of 3 slip patterns and 5 patterns than 1 pattern when a target wave height was comparatively high (6.7m or 10.0m). We can conclude that the number of slip patterns had a great impact on the stochastic assessment depending on the target wave height. To clarify the uncertainties of tsunami wave height, we defined a 90 percent confidence interval and a coefficient of variation as indexes which can quantify the uncertainties of tsunami wave height. Basically, the 90 percent confidence interval had high value where the wave height at each fractile point was high. In addition, we confirmed that changing of maximum wave height due to changing of the asperity location in the assuming fault had a great impact on the coefficient of variations in the offshore point of the Ibaraki coast. The coefficient of variation in the offshore point of peninsula located in ria shoreline of the Iwate coast was comparatively higher than a result in closed-off section of bay located in ria coast. This result indicates an effect due to a characteristic topography in ria coast.

Keywords: probabilistic tsunami hazard assessment, uncertainty analysis, rogic tree, CRSP model

Japan Geoscience Union Meeting 2014
(28 April - 02 May 2014 at Pacifico YOKOHAMA, Kanagawa, Japan)

HDS28-01 Room:312 Time:May 1 16:15-16:30

Seismic and tsunami fragility of industries, revealed by the 2011 Tohoku-oki earthquake

KUWAHARA, Yasuto[1*] ; HASEGAWA, Isao[1] ; YOSHIMI, Masayuki[1] ; NAMEGAYA, Yuichi[1] ; HORIKAWA, Haruo[1] ; NAKAI, Misato[1] ; MASUDA, Satoru[2]

[1]AIST, GSJ, [2]Graduate school of Economics and Management, Tohoku University.

We have developed seismic and tsunami fragility curves of industries by using damage data of industrial companies, estimated strong motions and estimated tsunami heights of the 2011 Tohoku-oki earthquake. The damage data were obtained from 7,019 industrial companies through inquiry surveys by the Regional Innovation Research Center of Tohoku University. As a damage level indicator for each company, we introduced a ratio of an economical damage of physical fixed assets excluding lands to previous balance of the physical fixed assets. The estimated strong motions of the 2011 Tohoku-oki earthquake at all the sites of the companies were from the database of the so-called QuiQuake system (Quick estimation system for shaking maps triggered by observation records) operated by the National Institute of Advanced Industrial Science and Technology (AIST). It is noted that the estimated data were obtained by taking account of seismic local site effects and the actually observed ones. The tsunami height data at each site of the company were obtained by interpolating the confirmed data compiled by the 2011 Tohoku Earthquake Tsunami Joint Survey Group (2013). It is found that a frequency-damage level distribution for each seismic intensity is well correlated with a binominal distribution where the only parameter characterizing the distribution is an average value of the damage levels in each seismic intensity. The tsunami fragilities are also obtained as a function of the tsunami height in the same way. These fragility curves can be useful not only to estimate economic damages for future huge earthquakes, but also to rapidly assess the damage just after earthquakes.

Keywords: Seismic, Tsunami, fragility curve, industry, the 2011 Tohoku-oki earthquake

Japan Geoscience Union Meeting 2014
(28 April - 02 May 2014 at Pacifico YOKOHAMA, Kanagawa, Japan)

HDS28-02 Room:312 Time:May 1 16:30-16:45

Compiling the source area data of large earthquakes occurred in Pacific Rim

ISHIKAWA, Yuzo[1*]

[1]Y. Ishikawa

The locations of hypocenters were usually plotted by some symbols. This way leads to misunderstand that the earthquake source is the point source. It was caused by the earthquake catalog of which location data were given as a point.

Now, the earthquake source are given by the area obtained by the one month aftershock distributions. Events of which magnitude are larger than 8.0 from 1970, using PDE earthquake catalog. Some large events were added in 20 century. The source areas of large earthquakes occurred in Pacific Rim were digitized.

Keywords: source area, large earthquake, Pacific Rim

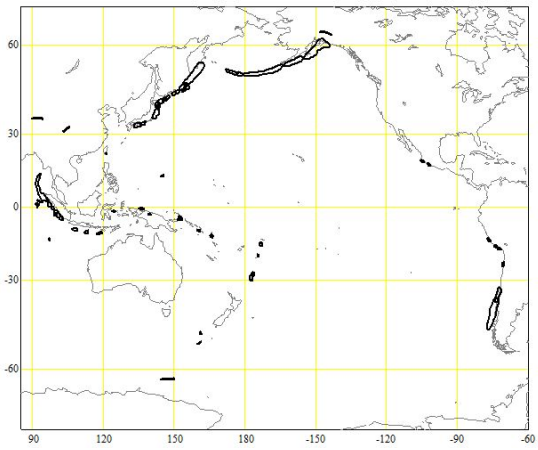

Japan Geoscience Union Meeting 2014
(28 April - 02 May 2014 at Pacifico YOKOHAMA, Kanagawa, Japan)

HDS28-03 Room:312 Time:May 1 16:45-17:00

A set of characterized earthquake fault models for the probabilistic tsunami hazard assessment in Japan

TOYAMA, Nobuhiko[1*] ; HIRATA, Kenji[1] ; FUJIWARA, Hiroyuki[1] ; NAKAMURA, Hiromitsu[1] ; MORIKAWA, Nobuyuki[1] ; OSADA, Masaki[1] ; MATSUYAMA, Hisanori[2] ; KITO, Tadashi[2]

[1]NIED, [2]OYO CORPORATION

A set of characterized earthquake fault models are necessary for nation-wide probabilistic tsunami hazard assessment in Japan (Fujiwara et al., 2013; Hirata et al., 2014). It should include all possible earthquakes in future and should take into account various types of uncertainty.

In general, origins of tsunamis include a volcano, a landslide as well as an earthquake, but as the first step we focus on tsunamis that are caused by only earthquakes occurring near Japanese Islands. We introduce our strategy to construct a set of earthquake fault models for tsunami hazard assessment in Japan, showing examples of earthquake fault models along the Japan Trench.

The ”Long-term Evaluation of earthquakes from Sanriku-oki to Boso-oki region (2nd edition)” (2011/11/25) by the Headquarters for Earthquake Research Promotion(HERP), Japanese government, defined 8 seismogenic segments along the Japan Trench. Based on these segmentations, we classify tsunamigenic earthquakes into 7 categories as follows; 1)”March 11, 2011 Tohoku earthquake-type” earthquakes, 2) maximum-sized class earthquakes, 3) other large-sized earthquakes, 4) earthquakes occurring in any single segment which HERP assessed its possible magnitude and/or location with recurrence interval, 5) tsunami earthquakes, 6) intra-plate earthquakes with normal faulting, and 7) moderated-sized earthquakes (HERP called this type ”earthquakes which we cannot expect its magnitude and size”). HERP assessed earthquake potentials only in categories 1), 4), 5), and 6). To enhance the entirety of tsunami hazard assessment, we newly add the categories 2), 3) and 7), though no previous earthquakes in categories 2), 3), and 7) are known yet. We place earthquake fault on the upper boundary of the subducting Pacific Plate except earthquakes of the category 6).

Seismic moment, Mo, to a characterized earthquake fault model, is determined by an empirical scaling relation between Mo and fault area, S. To determine the empirical relation we first make a list of tsunamigenic earthquakes from the data base of ”Size of tsunamis around Japan for 1498-2006” (http://wwweic.eri.u-tokyo.ac.jp/tsunamiMt.html) by Abe. Next we assign Mo and S to listed tsunamigenic earthquakes, referring in previous studies (Sato et al.,1989) and then derive an empirical Mo-S scaling relation for tsunamigenic earthquakes occurred in the area of the Pacific ocean side. There are some previous studies suggesting that rigidity is depth dependent, but we use a constant value of $5*10^{10}$(N/m^2) as rigidity.

We introduce inhomogeneity in earthquake fault slip to define ”large slip area (LSA)” and ”extremely large slip area (ELSA)” by following a characterized ratio of high-slip area to entire fault area (Korenaga et al., 2014). For great earthquakes of Mw $>$˜8.4, LSA is allowed to be located 3 patterns for along-trench direction and 3 patterns for trench-normal direction, thus total of 9 basic configurations, for each characterized earthquake fault model. ELSA can be allowed to be located along the upper edge in a LSA when the LSA is located adjoined the trench axis. For large earthquakes with the magnitudes less than ˜8.3, that is the category 7), we consider only a LSA at the center of the entire fault area. In this case, variability of possible LSA location is taken into account by introducing an uncertainty value of possible LSA location in process of tsunami hazard curve calculation.

A set of characterized earthquake fault models that we place along the Japan Trench, spans from Mw 7.0 to 9.4 at every 0.1 or 0.2 magnitude intervals. Total number of the models along the Japan Trench reaches more than 1800. It takes whole three months to complete non-linear tsunami simulations for all characterized earthquake fault models.

This study was done as a part of ”Tsunami hazard assessment project for Japan”in NIED.

Keywords: tsunami hazard assessment, probability, characterized earthquake fault model

Japan Geoscience Union Meeting 2014
(28 April - 02 May 2014 at Pacifico YOKOHAMA, Kanagawa, Japan)

HDS28-04 Room:312 Time:May 1 17:00-17:15

Tsunami hazard assessment project in Japan

HIRATA, Kenji[1*] ; FUJIWARA, Hiroyuki[1] ; NAKAMURA, Hiromitsu[1] ; OSADA, Masaki[1] ; OHSUMI, Tsuneo[1] ; MORIKAWA, Nobuyuki[1] ; KAWAI, Shin'ichi[1] ; AOI, Shin[1] ; YAMAMOTO, Naotaka[1] ; MATSUYAMA, Hisanori[2] ; TOYAMA, Nobuhiko[2] ; KITOH, Tadashi[2] ; MURASHIMA, Yoichi[3] ; MURATA, Yasuhiro[3] ; INOUE, Takuya[3] ; SAITO, Ryu[3] ; AKIYAMA, Shi'ichi[4] ; KORENAGA, Mariko[4] ; ABE, Yuta[4] ; HASHIMOTO, Norihiko[4]

[1]NIED, [2]OYO, [3]KKC, [4]CTC

Tsunami hazard assessment (THA) is the most important information to take effective measures against possible tsunami attacks in future. After the national tragedy caused by the 11st March 2011 Tohoku earthquake (Mw9.0), NIED started a research project regarding TSA in Japan to support various kind of measures by sectors such as local governments, life-line companies, etc (Fujiwara et al., 2013, JpGU). Our research project consists of two components; (A) a research of probabilistic tsunami hazard assessments (PTHA) in which we consider all of possible tsunamis that may affect coastal regions in future and (B) a research to forecast coastal tsunami heights and inundation flow depths based on specified earthquake scenarios.

In the research (A) of PTHA, we began working on subjects of (1) nation-wide probabilistic tsunami hazard assessment (NW-PTHA) and (2) detailed probabilistic tsunami hazard assessment for a specific region (DPTHASR). Outlines of (1) NWPTHA are as follows; (i) we consider all of possible earthquakes in future including earthquakes that the Headquarters for Earthquake Research Promotion (HERP), Japanese Government, already assed. (ii) We construct a set of simplified earthquake fault models, called ″ characterized earthquake fault models (CEFMs) ″ , for all of the earthquakes mentioned above by following prescribed rules (Toyama et al., 2014, JpGU; Korenaga et al., 2014, JpGU). (iii) We solve a non-linear long wave equation, using staggered leap-flog, finite difference method (FDM), including inundation calculation as coastal boundary condition, over a nesting grid system with the minimum grid size of 50 meters, to calculate tsunamis for each of initial water surface distributions (under research for initial water surface calculation by Akiyama et al., 2014, JpGU) generated from a large number of the CEFMs. (iv) Finally we integrate information about coastal tsunami heights from the numerous CEFMs to get nation-wide tsunami hazard curves, defining excess probability, for coastal tsunami heights, incorporating uncertainties inherent in tsunami forward calculation and earthquake fault slip heterogeneity (Abe et al., 2014, JpGU). In the present step we are revising a prototype of NWPTHA in the case where possible tsunami sources are located along the Japan Trench as well as we are constructing a set of CEFMs in the case where possible tsunami sources are located along the Nankai Trough.

As for the research of (2) DPTHASR, we are going to develop new methods to assess inundation probability and inundation time, etc., through tsunami inundation simulations for a set of CEFMs using the same FDM over a nesting grid system with the minimum grid size of 10 meters including information of seawalls and breakwaters. Some of results from DPTHASR will be represented in a similar format of ″ Karte ″ (medical chart) to help understandings of tsunami hazard information by residents. In the present step, we are constructing a new method to assess probabilistic inundation depth distribution along with calculation of hazard curves for inundation depth at specified points on land (Saito et al., 2014, JpGU).

In the research (B), we are planning to construct a deterministic method to forecast coastal tsunami heights, inundation area and depth, etc. in specified sites in the scenarios that possible maximum-sized tsunamis strike there. These deterministic forecasts should be examined through comparisons with tsunami deposits distribution, historical materials, and instrument records.

Also, we are making a lot of effort to utilize probabilistic and deterministic tsunami hazard information by investigating actual usages of domestic/oversea tsunami hazard information (Osada et al.,2014, JpGU) and by investigating opinions and ideas from persons-in-charge of measures by local governments for tsunami disasters thorough questionnaire surveys with direct interviews (Ohsumi et al., 2014, JpGU).

This work partially functions to support activities of HERP.

Keywords: tsunami, hazard assessment, probability, scenario-type tsunami forecast, hazard map, utilization

Japan Geoscience Union Meeting 2014
(28 April - 02 May 2014 at Pacifico YOKOHAMA, Kanagawa, Japan)

HDS28-05 Room:312 Time:May 1 17:15-17:30

G-EVER Earthquake and Volcanic Eruption Risk Management Activities and Asia-Pacific Region Hazard Mapping Project

TAKARADA, Shinji[1*] ; ISHIKAWA, Yuzo[1] ; BANDIBAS, Joel[1] ; G-EVER, Promotion team[1]

[1]Geological Survey of Japan, AIST

The Asia-Pacific Region Global Earthquake and Volcanic Eruption Risk Management (G-EVER) Consortium among the geo-hazard research institutes in the Asia-Pacific region was established in 2012. G-EVER aims to formulate strategies to reduce the risks caused by earthquakes, tsunamis and volcanic eruptions worldwide. The First Workshop on Asia-Pacific Region Global Earthquake and Volcanic Eruption Risk Management (G-EVER1) was held in Tsukuba, Japan from February 22 to 24, 2012. During the workshop, the G-EVER1 accord was approved by the participants. The Accord consists of 10 recommendations such as; enhancing collaboration, sharing of resources, and making information of the risks of earthquakes and volcanic eruptions freely available and understandable. The G-EVER Hub website was setup to promote the exchange of information and knowledge about volcanic and seismic hazards among Asia-Pacific countries. Establishing or endorsing standards on data sharing and analytical methods is important to promote data and analyses results sharing. The major activities of G-EVER include participation in global risk reduction efforts such as the Integrated Research on Disaster Risk (IRDR) Program, Global Earthquake Model (GEM) and Global Volcanic Model (GVM). The 2nd G-EVER International Symposium and the 1st IUGS&SCJ International Workshop on Natural Hazards was held in Sendai, Tohoku Japan on October 19-20, 2013. We endorsed Sendai Agreement during the symposium (http://g-ever.org/en/sendai/). Several G-EVER Working Groups and projects were proposed such as; (1) Risk mitigation of large-scale earthquakes WG, (2) Risk mitigation of large-scale volcanic eruptions WG, (3) Next-generation volcanic hazard assessment WG, and (4) Asia-Pacific region earthquake and volcanic hazard mapping project.

The Asia-Pacific region earthquake and volcanic hazard mapping project aims to make an advanced online information system that provides past and recent earthquake and volcanic eruption information (e.g. age, location, scale, affected areas and fatalities) and risk assessment tools for earthquake and volcanic eruption hazards. A printed map will also be published as the new version of the Eastern Asia Geological Hazard Map of the Commission for the Geological Map of the World (CGMW). The online hazard mapping system will provide useful information about earthquake and volcanic hazards in an interactive and user-friendly interface. Past and recent large-scale earthquakes and volcanic eruptions, tsunami inundation areas, and active faults distributions will be shown on the map. Links to major earthquakes and volcanic eruptions databases will be available in the system. The earthquake and volcanic eruption hazard mapping project will be implemented with the cooperation of major research institutes and organization in the Asia-Pacific region such as PHIVOLCS, CVGHM, GNS Science, EOS, USGS and CCOP.

Keywords: Earthquake, Volcano, Risk, Hazard, Hazard Map, Asia Pacific

Japan Geoscience Union Meeting 2014
(28 April - 02 May 2014 at Pacifico YOKOHAMA, Kanagawa, Japan)

HDS28-06 Room:312 Time:May 1 17:30-17:45

Observing Schumann Resonance by demodulating High Frequency Waves

CAO, Bingxia[1*] ; ZHOU, Hongjuan[1]

[1]Harbin Institute of Technology at Weihai

The limited dimensions of the Earth cause the waveguide between the surface of the Earth and the conductive ionosphere to act as a resonant cavity for electromagnetic waves in the ELF band so that Schumann Resonance (SR)occurs there. It has been suggested that SR may be used to monitor global temperature variations. SR has been used to study the lower ionosphere on Earth and suggested as one way to explore the lower ionosphere on celestial bodies. A new field of interest using SR is related to short-term earthquake prediction. The manmade noises in the ELF band was a problem for observing. A new way to observe SR based on cross-modulation in the low ionosphere is discussed.

The effect of cross-modulation was established by Yampolski et al. between SR and HF signals experimentally. The HF signals called Round-the-world signals (RWS) and large antenna arrays of the radio telescope UTR-2 were used. But the problem is whether the SR can be seen only with a simple antenna. If the answer is yes, we have a new measurement method for SR.

The HF-SR multiple mode nonlinear interaction theory is researched based on the basic theory model established. In the multiple interaction mode theory, the modulation depth is affected by electromagnetic wave phase in the nonlinear effect. Before the experiment, a lot of simulation experiments and theoretical research are carried out , including Schumann Resonance global distribution simulation and multi-mode interaction of HF-SR theory etc.. One simpler half wave cross dipole antenna is used to receive the time service signal of China called BPM. And in the demodulation spectrum of BPM, the first 4 order resonance peaks of the SR are obtained successfully, respectively on 7.5Hz, 14Hz, 20Hz and 26Hz.

The electric field distributions and phase variations of the firse 3 order peaks of Schumann Resonance in the earth ionosphere cavity are obtained through a series of SR distributed simulation experiments. The result shows that in the same phase region, the phase of SR only depends on time. At the same time all the points have the same vibration phase. Two points have 180 degree difference phase after a phase mutation point.

The actual multi interaction mode effect between RWS and SR is uncertain. It may change with the propagation conditions. The modulation depth can not be increased significantly in the multiple interaction effects of HF wave and SR propagate around the globe. The main reason is the high frequency wave goes through the the phase jump points of Schumann Resonance. The final depth of modulation in the Yampolski experiment is about 07-3.5 times to the modulation depth of single interaction.

RWS goes through around the earth. But the modulation depth of of RWS and SR nonlinear effect is not significantly far greater than that of 1 jump value because of the path length growth.

Using the RWS signal, greater modulation than short reception, for example, 1 hop, can be obtained. But due to the SR wave distribution in the earth ionosphere cavity, the value is less than the direct summation of each modulation results. That is to say, high frequency electromagnetic wave propagates around the earth for nearly a circle. It is modulation result with SR dose not significantly increase compared with that of the obtained by ionospheric reflection arrive at the receiving station.

According to the new theory of HF-SR interaction, a receiving station was established. The system receives the BPM time service signals from the National Time Service Center in PuCheng, 1160 km away from the receiver. The carrier frequency is 10 MHz. By demodulating the BPM signal, the first 4 order peaks of SR are obtained. Maybe it is a new way for SR observing.

Keywords: earth ionosphere cavity, Schumann Resonance, nonlinear effect, high frequency wave

HDS28-06 Room:312 Time:May 1 17:30-17:45

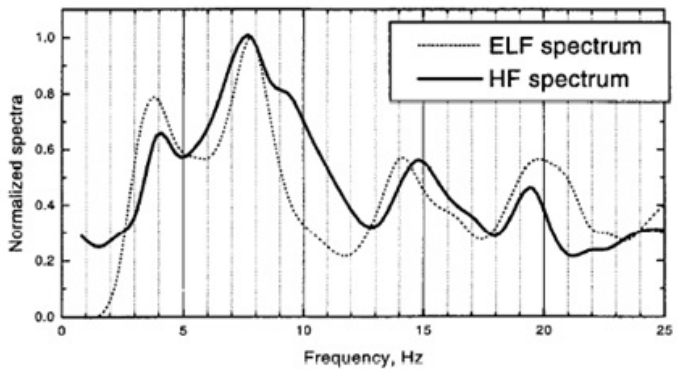

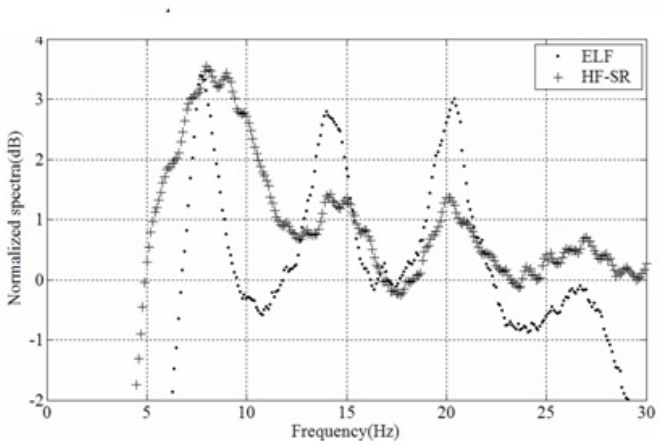

Japan Geoscience Union Meeting 2014
(28 April - 02 May 2014 at Pacifico YOKOHAMA, Kanagawa, Japan)

HDS28-P01 Room:Poster Time:May 1 18:15-19:30

Influence of mircotopography in lowland to tsunami disaster of 2011 Tohoku Earthquake

IKARI, Kazuya[1*] ; NARAMA, Chiyuki[2]

[1]Graduate School of Science & Technology, Niigata University, [2]Faculty of Science, Niigata University

The earthquake (magnitude 9.0) on Mar 11, 2011 in Tohoku, Japan triggered the terrible destructive tsunami, striking the eastern coastal region of Japan. Although residents in valley bottom plain of the Sanriku Coast (ria coast) have a refuge area around hills, residents in Sendai Plain (meander plain of lowland) had to go to inland in order to escape tsunami. The lowland such as Sendai Plain is very vulnerable to tsunami. However, Building damages differed among the Sendai Plain. This study evaluated the influence of landform in lowland of Sendai Plain to tsunami disaster.

The Sendai plain is meander plain of lowland (0-3m asl.), including beach ridges and inter-ridge march of ridged beach plain, and natural levees along present and mender scars.Three beach ridges are developed along the coast. Relative height of present beach ridge is 3-5m, and inner two beach ridges are 1-2m.

We classified three damage-categories (flow out, destroy, and remain) to individual buildings in tsunami inundation area of the Sendai Plain, based on interpretation of aerial-photographs on 2011 and Google Earth satellite image 2012.In addition, we made a GIS data of utility pole, flattened tide protection forest, driftwood, tsunami scratch in Sendai Plain, to know flow directions of tsunami and distribution of woods.

Building damages in the Sendai plain show >80% of buildings flowed out within 1km area from the coast. Remaining buildings are located on ridged beaches with 1-2m high. Driftwood and rubble had stopped on the near side of beach ridges and highway embankment. Tsunami flow was concentrated in the inter-ridge march or small stream channels. Around the Abukuma River, buildings under cut slope received tsunami damage, and slip-off slope side was safety. In lowland plain, we clarified microtopography with 1-2m relative height reduced tsunami damages around inland side area (>1km) from the coast.

Keywords: 2011 Tohoku Earthquake, tsunami, Sendai Pliain, lowland, mircotopography, aerial-photographs

Japan Geoscience Union Meeting 2014
(28 April - 02 May 2014 at Pacifico YOKOHAMA, Kanagawa, Japan)

HDS28-P02 Room:Poster Time:May 1 18:15-19:30

Eruptive Sequence of Rinjani Caldera, 13th Century, Lombok, Indonesia

FURUKAWA, Ryuta[1*] ; TAKADA, Akira[1] ; NASUTION, Asnawir[2] ; TAUFIQURROHMAN, Roni[3]

[1]Geological Survey of Japan, AIST, [2]Institute Technology of Bandung, [3]Center for Volcanology and Geological Hazard Mitigation

Rinjani Volcanic Complex located at northern part Lombok Island is centered by a large stratovolcano, Rinjani volcano, which is the volume of 100 km^3 and 3726m high (Nasution et al., 2003). A caldera of 6x8 km in diameter lies western side of the summit formed at mid-13th century (Nasution et al., 2010; Lavigne et al., 2013). Sequence of the caldera forming eruption is reconstructed from original stratigraphy of eruptive deposits and consists of 6 phases with no prominent time interval between them. Phase 1 is a small phreatic eruption produced thin ash fall bed only occurrs proximal of the summit. Phase 2 is large plinian eruption dipersed pumice lapilli to western side and extending to adjacent islands. Pumice lapilli become finer and lithic fragments increase upward in the fall bed. Phase 3 is defined by widely extending pyroclastic flow deposit consists of vaguely bedded unsorted ash with subordinating rounded pumice lapilli. Its thickness varies from several to 50 cm especially thickens local topographic depression and eroding underlying pumice fall bed. This deposit extends more than 50 km from the probable source and reached Gili Island isolated by ocean suggesting extremely dilute pyroclastic flow possibly caused by plinian eruption column collapse from high altitude. Phase 4 is unstable plinian eruption implied by graded pumice lapilli bed intercalated by multiple thin ash beds. Phase 5 is characterized by enormous pyroclastic flow effusion resulting thick and massive pumiceous lapilli tuffs extending more than 30 km from the source. Proximally fines depleted lithic breccia including andesite lavas and minor amount of granodiorite are interbedded with massive pumiceous lapilli tuff. Thickly stratified lapilli tuff beds exposes along the coastline suggest the pyroclastic flow caused the secondary explosions and formed littral cone at the ocean entry. Phase 6 is last plinian eruption dispersed pumice fall of limited extent which is smaller than preceding plinian phases 2 and 4. Petrological analysis shows magma composition changes between phase 3 and 4 suggesting formation of new vent or widening pre-existing vent eventually causes the caldera formation.

Keywords: volcano, caldera, pyroclastic flow, Indonesia, ash, icecore

Japan Geoscience Union Meeting 2014
(28 April - 02 May 2014 at Pacifico YOKOHAMA, Kanagawa, Japan)

HDS29-01 Room:415 Time:April 28 11:00-11:15

Holocene rock avalanche phenomena from the upper Okumatashirodani Basin, Kamikochi Valley, northern Japanese Alps

KARIYA, Yoshihiko[1*] ; MATSUSHI, Yuki[2] ; HARAYAMA, Satoru[3] ; MATSUZAKI, Hiroyuki[4]

[1]Senshu University, [2]Kyoto University, [3]Shinshu University, [4]University of Tokyo

Hummocks and a minor ridge both of which have been considered to be moraines are present on alluvial fans near the Shinmurabashi Bridge, Tokusawa Area of Kamikochi Valley in the Hida Mountains. A series of geomorphological, lithological, and chronological studies of these landforms and their forming materials revealed that hummocks and a minor ridge were formed by two different rock avalanches that occurred on the steep east face of Kitahotaka-dake north ridge about 3000 m ASL and ran into valley floor near the Shinmurabashi Bridge. A terrestrial cosmogenic nuclide dating method of igneous rocks comprising hummocks and a minor ridge showed that hummocks were formed during 6.0-7.9 ^{10}Be ka and a ridge was during 0.8-1.1 ^{10}Be ka.

Keywords: landslide, in-situ terrestrial cosmogenic nuclide dating, Hida Mountains

Japan Geoscience Union Meeting 2014
(28 April - 02 May 2014 at Pacifico YOKOHAMA, Kanagawa, Japan)

HDS29-02 Room:415 Time:April 28 11:15-11:30

Rock failure of welded tuff in Sounkyo valley, Hokkaido, on September 2013

ISHIMARU, Satoshi[1*] ; TAJIKA, Jun[1] ; WATANABE, Tatsuya[1] ; ISHIKAWA, Isao[2] ; SHIMURA, Kazuo[3]

[1]Geological Survey of Hokkaido, [2]Hokkaido Government, [3]Shin Engineering Consultants

A rock failure occurred at the left valley side of the Ishikari River in Sounkyo, Hokkaido, on 8th September 2013. Although Route 39 runs along the Ishikari River, rocks did not reach on the road, because the road is 170m distance from the collapse slope in the other side of the Ishikari River. However, the rock debris buried a part of the river, and formed a 200m-long flooding area at the upper reach. The type of this rock failure is a rock slide to a debris avalanche with high velocity flow.

Paleogene shale of the Hidaka Supergroup is overlain by Sounkyo welded tuff at the valley wall. Sounkyo welded tuff consists of two facies. The lower is a soft non-welded part, and the upper is a welded part with developed columnar or platy joints. Sounkyo valley has been formed by erosion of the pyroclastic flow deposits (30Ka), Sounkyo welded tuff, from Ohachidaira Caldera by the Ishikari River. In consequence, steep cliffs have developed in the valley. At the collapse point, only the uppermost 30m of the slope is steep cliff, but the lower 140m is about 40 degree. According to air photo interpretation, the surface with gently roughness profile develops on the 40 degree slope. This shows talus deposits as past collapse debris overlie the slope.

The area of the slope failure, erosional and depositional area, is 190m in height, 90-100m in width, and 365m in length. The equivalent coefficient of friction is 0.52. The volume of the collapse is more than 33,000m^3. Sounkyou welded tuff is exposed on the upper slope with 90m height, and the debris of the collapse covers on the lower slope with 95m height. A debris slump, 45m height and 20m width, is locates on the lower center part of the debris slope. A part of the past talus deposits is exposed by this debris slump. The Hidaka Supergroup shale is covered with talus deposits. Springs from the piping halls eroded the gullies in talus, and the talus deposits were wet state at the investigation of two days after the failure.

The debris from the collapse slope was spread in lobe-shapes over the valley flat. Arcuate ridges and troughs, 1-2m high, shaped concentric half circles in the center axes of the main lobe. This suggests flow-type mass movement. The debris is distributed on 130m in length and 120m in width of the valley flat. The most of the debris is grayish white welded tuff, and the pale reddish welded tuff originated from the uppermost slope is distributed around the ridges. Shale of the Hidaka super group is rare. The squeeze of the mixture of the soil deposits, composed of woods and organic matters, and volcanic ash is distributed in front of the ridges and in gaps in the troughs. This was dragged from the base of the moving body of the collapse, and played a role in a flow layer, matrix facies, of debris avalanche. The talus deposits would be fluidized. The debris would run with high velocity at the front part of the depositional area. According to the estimating equation (Sceidegger, 1973), using the equivalent coefficient of friction, the velocity is estimated by 38m/s at the foot of the slope.

The rock failure was occurred by the bellow mechanism. Rock slide was occurred near the boundary, the Hidaka Soupergroup shale and the non-welded part of the tuff, and the upper slope broke down. Ground water concentrates in the permeable layer of the non-welded tuff on the impermeable layer of the shale. Because the pyroclastic flow, the Sounkyo Welded Tuff, buried the former valley slope of the Hidaka Soupergroup shale in 30,000 years ago, the boundary is incline toward the river, and also the structure of the tuff is incline. This rock failure was occurred at the instability slope, which consisted of soft non-welded tuff with concentrated groundwater beneath heavy welded tuff. The columnar joints, the collapse surface, at the uppermost of the slope have opened before the rock failure, because moss grows on the joint surface.

Keywords: rock failure, welded tuff, rock slide, debris avalanche

Japan Geoscience Union Meeting 2014
(28 April - 02 May 2014 at Pacifico YOKOHAMA, Kanagawa, Japan)

HDS29-03 Room:415 Time:April 28 11:30-11:45

Geologic causes of Akatani rockslide induced by heavy rain with typhoon Talas (1112)

NAGATA, Hidehisa[1*] ; YOKOYAMA, Shunji[2] ; INOKUCHI, Takashi[3] ; KATO, Hironori[4] ; KIMURA, Katsumi[5]

[1]Fu Sui Do co. ltd., [2]Kochi Univ., [3]NIED, [4]Aratani Civil Eng. Consultants, [5]AIST

Heavy rain by the Typhoon Talas in 2011 triggered many landslides at Kii Peninsula. The Akatani rockslide in Gojo City, Nara Prefecture is one of the largest landslides, which has dimensions of 500 m wide, 1100 m long, about 80-100 m deep, and 10 million cubic meters in volume. Geologic causes of the rockslide were investigated.

Geology of the Akatani rockslide is composed of mudstone and sandstone of the Miyama Complex of the Shimanto Belt. Not only bedding plane, but also fault planes and joint planes formed in various stages are weak planes related to the rockslide. The average attitude of the bedding planes tends to dip steeply northward while varying. However, there are low-angle dip slip faults nearly parallel or daylight to the slope surface. These are considered to be out-of-sequence thrusts, because they obliquely intersect bedding plane and some of them subdivided the Miyama Complex into several tectonic units. The rupture surface is not smooth curved but rough. This was the combined fragile planes including faults subparallel to the slope. It is similar to the other landslides in the Shimanto Belt that simple slide along bedding planes did not occur.

Japan Geoscience Union Meeting 2014
(28 April - 02 May 2014 at Pacifico YOKOHAMA, Kanagawa, Japan)

HDS29-04 Room:415 Time:April 28 11:45-12:00

Development history of sagging around Kanmuriyama Pass, Gifu-Fukui prefecture boundary

KOJIMA, Satoru[1*] ; NIWA, Ryota[1] ; KANEDA, Heitaro[2] ; IKEDA, Akiko[3] ; NAKAMURA, Toshio[3] ; OHTANI, Tomoyuki[1]

[1]Department of Civil Engineering, Gifu University, [2]Department of Earth Sciences, Chiba University, [3]Center for Chronological Research, Nagoya University

Recently sagging landforms like double ridges and uphill-facing scarps attract attention as precursors of large-scale landslides. Many types of large- and small-scale saggings have been ubiquitously found in the Japanese mountainous regions by the analyses of detailed topographic maps made by LiDAR survey. Their development histories and processes, however, are unclear. We report the results of field and chronological researches on saggings in the Kanmuriyama Pass area, Gifu-Fukui prefecture boundary. Since the lithology and age of sediments accumulated in the linear depression between the double ridges east of the Kanmuriyama Pass were reported in the last meeting, those on the uphill-facing scarps west of the pass will be presented in the meeting this year.

Four rows of uphill-facing scarps parallel to the slope are recognized on the south side of the prefecture boundary ridge about 2 km west of the Kanmuriyama Pass. The sediments accumulated in the linear depressions were collected and analyzed by the hand-auger boring and pit survey. Lithological characteristics of these sediments are common and they are composed of, in descending order, 1) carbonaceous mud/leaf litter mixture, 2) dark gray mud, 3) light gray mud, and 4) orange-color conglomeratic mud. This lithology is also similar to that of the sediments between the double ridges east of the Kanmuriyama Pass. The sediments in the first, second and third depressions from the top include Kikai-Akahoya tephra (K-Ah) about 7.3 ka or have peaks of volcanic glass contents of this tephra. The horizons of the tephra, however, are recognized in the different lithologies; the sedimentary environment about 7.3 ka varied with the depression. The ages of the tephra and the AMS-^{14}C ages of wood fragments embedded in the sediments indicate that the sedimentation rates of the dark and light gray mud members are about 0.08 mm/year, and several times slower than those of the upper carbonaceous mud/leaf litter mixture member. The depressions and uphill-facing scarps formed about several tens of thousand years ago on the basis of the estimation of the thickness of sediments and the extrapolation of the sedimentation rate of the mud formations.

Keywords: sagging, landslide, Gifu, Fukui, Kanmuriyama

Japan Geoscience Union Meeting 2014
(28 April - 02 May 2014 at Pacifico YOKOHAMA, Kanagawa, Japan)

HDS29-05 Room:415 Time:April 28 12:00-12:15

Detection of pre movements of landslide or deep collapse using InSAR and LiDAR

KOARAI, Mamoru[1*] ; NAKANO, Takayuki[1] ; TODA, Kenichiro[2] ; DAIMARU, Hiromu[3]

[1]GSI of Japan, [2]Nagano Prefecture Forestry Reserch Center, [3]Forestry and Forest Products Research Institute

It is possible to detect pre movements of landslide or deep collapse using SAR interferometry technology. As previous studies, there are example of the Shimegake Landslide on the foot of Mt. Gassan, Yamagata Prefecture and the Ohkamizawa Landslide in Higashi-naruse Village, Akita Prefecture. In this research, the usefulness of the monitoring methodology which combined SAR interferometry and LiDAR data will be verified for the monitoring of region where the deep collapse will occurred. This research is supported by the Grants-in-Aid for Scientific Research (No.22500994). The main verification fields are Nagano Prefecture and Shizuoka Prefecture. The used InSAR imageries are analyzed by Geodetic Department, the Geospatial Information Authority of Japan, using the data of PALSAR which is L band SAR of the earth observation satellite ”Daichi” (ALOS).

Near the Kuchisakamoto Landslide of Shizuoka Prefecture, a change significant by InSAR imagery in the autumn of 2008 and the autumn of 2009 had occurred, and about 6-7 cm deformation to the LOS direction was observed in one month and a half of 2009. In field survey, the authors checked that the large landslide had occurred between November, 2012 and June, 2013 (Nakano et al., 2013; Koarai et al., 2013).

In west side of Sakamaki hot spring of Nagano Prefecture, about 6-7 cm deformation to the LOS direction was observed in InSAR imagery of one year from 2008 to 2009, and large collapse occurred in September, 2011. In LiDAR data imagery taken before the collapse occurred, it is possible to detect linear depression behind collapse slope.

In this presentation, the authors report many case of pre movement of landslide detected by field survey or LiDAR data in the areas where InSAR imageries show small deformation in Nagano Prefecture.

Fig.1 InSAR imagery of west side of Sakamaki hot spring (2008/07/20-2009/09/07) and sloop deformation detected in field survey

Keywords: deep collapse, landslide, InSAR, LiDAR, Nagano Prefecture

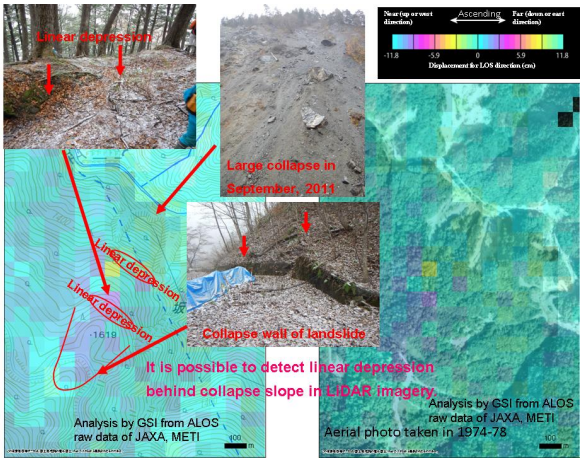

Japan Geoscience Union Meeting 2014
(28 April - 02 May 2014 at Pacifico YOKOHAMA, Kanagawa, Japan)

HDS29-06 Room:415 Time:April 28 12:15-12:30

Prediction and stability evaluation of potential sites of deep-seated catastrophic landslide

CHIGIRA, Masahiro[1*] ; SAKASHIMA, Toshihiko[2] ; FUNAYAMA, Atsushi[2] ; MINAGAWA, Jun[2] ; SHIBUYA, Kenichi[3]

[1]Disaster Prevention Research Institute, Kyoto University, [2]Pacific Consultants Co. Ltd, [3]Aero Asahi Corporation

Chigira (2009) and Chigira et al. (2013) analyzed geological structures and topographic features of deep-seated catastrophic landslides induced by rainstorms in accretion complexes of the southwest outer belt of Japan, and found that those landslides had been preceded by gravitational slope deformation typified by small scarps along their future crowns, which could be a clue to predict potential sites of catastrophic deep-seated landslide. This paper summarizes the methodology of potential site prediction and stability evaluation of catastrophic landslides, including stratified rocks in addition to broken beds and mixed rocks in accretion complexes.

In order to extract potential sites of catastrophic landslide, we need to judge whether deep-seated gravitational slope deformation may develop to catastrophic failure or not, considering possible structures of gravitational slope deformation on a certain geologic background. We examined the relationships among morphological expression of gravitational slope deformation, geologic body, geological structure, and deformation mechanisms, then took account of upslope and downslope conditions, and finally tried to evaluate the probability of catastrophic failure with the help of our experience of previous catastrophic landslides.

Irregularly shaped bumpy slope:

This is typically made when incipient sliding zones are being made in a rock body with complex discontinuities like broken beds or mixed rocks. Only this topography does not suggest the high probability of catastrophic failure, but additional eye-brow shaped small scarps and failures in the lower part of a slope may suggest high probability.

Linear depressions and wrinkles:

Symmetric alignment of linear depressions on both sides of a ridge suggests lateral spreading with the settlement of the ridge top, which does not likely develop to catastrophic failure.

Linear depressions and wrinkles developed on one side of a ridge are made flexural toppling of steeply dipping foliations of bedding or cleavage. This type is self-stabilizing deformation, but when downslope-facing eye-brow scarps are made and lower part of the slope is failed, catastrophic failure likely occur. Ridge-top depressions, when connected to steps and to a hollow on the side margin of a deformed area, catastrophic failure also likely occur.

Large head scarps or ridge top depressions:

These topographies on an under-dip cataclinal slope suggest buckling deformation, which may be stable when a competent rock layer exists or deformation extent is less, but when the deformation progresses further and lower slope is failed, the probability of catastrophic failure becomes high.

Large head scarps or ridge top depressions on an over-dip cataclinal slope suggest sliding in a strict sense with mature and continuous sliding zones. Such a landslide may continue slow movement without catastrophic failure, but when the foot is cut by failure, it may develop to catastrophic failure.

References

Chigira, M., 2009. September 2005 rain-induced catastrophic rockslides on slopes affected by deep-seated gravitational deformations, Kyushu, southern Japan. . Engineering Geology, 108, 1-15.

Chigira, M., Tsou, C.-Y., Matsushi, Y., Hiraishi, N., Matsuzawa, M., 2013. Topographic precursors and geological structures of deep-seated catastrophic landslides caused by Typhoon Talas. Geomorphology, 201, 479-493.

Keywords: deep-seated catastrophic landslide, gravitational slope deformation, site prediction, susceptibility evaluation

Japan Geoscience Union Meeting 2014
(28 April - 02 May 2014 at Pacifico YOKOHAMA, Kanagawa, Japan)

HDS29-07 Room:415 Time:April 28 12:30-12:45

Estimation of the slip-surface of landslide using electromagnetic approaches at Nishiikawa, Japan

YMAZAKI, Tomohiro[1*] ; HATTORI, Katsumi[1] ; YOSHINO, Chie[1] ; HAN, Peng[1] ; KANEDA, Heitaro[1] ; SAKAI, Hideo[2] ; TSUKADA, Noriko[3] ; TERAJIMA, Tomomi[4] ; SUEMINE, Akira[4]

[1]Graduate school of science, Chiba University, [2]Graduate School of Science and Engineering for Education (Science) , Toyama University, [3]Faculty of Science, Toyama University, [4]The Disaster Prevention Research Institute(DPRI), Kyoto University

Landslide is one of the severe disasters triggered by rainfalls or earthquakes. Recently, landslides tend to increase by global-warming. Therefore, exploration into behavior of landslide becomes more important disaster prevention.

In order to explore landslide's behavior, we verified if there is slip-surface or not using magnetic approaches. In previous research, we had selected a test slope at Nishiikawa, Tokushima and we had performed electrical resistivity exploration and core-sampling. The core-sampling results indicate that there exists the structure which corresponds to slip surface. To verify this result, anisotropy in magnetic susceptibility (AMS) and natural residual magnetization (NRM) of samples that include that structure and periphery of it were measured. AMS result showed that slip-surface region provides the oblate ellipsoid characteristics, which was consistent with the developmental mechanism of slip-surface during sliding. And result of NRM indicated that magnetic minerals in slip-surface region oriented certain direction. This describes that magnetic minerals was able to move in saturated region and then were oriented to direction of earth magnetism.

These studies showed the possibility to identify slip-surface using rock magnetic approach. However, we found necessity of consideration of core-sampling technique to estimate the direction of slip using this approach because samples had rotated during core-sampling.

The details will be provided in the presentation.

Keywords: landslide, anisotropy in magnetic susceptibility, natural residual magnetization

Japan Geoscience Union Meeting 2014
(28 April - 02 May 2014 at Pacifico YOKOHAMA, Kanagawa, Japan)

HDS29-P01 Room:Poster Time:April 28 18:15-19:30

Dendrochronology of a fossil log from the dammed lake deposit by Dondokosawa rock avalanche, the Southern Japanese Alps

KARIYA, Yoshihiko[1*] ; MITSUTANI, Takumi[2] ; INOUE, Kimio[3]

[1]Senshu University, [2]Nara National Research Institute for Cultural Properties, [3]Sabo Frontier Foundation

Large-scale rock avalanche deposits (Dondokosawa rock avalanche deposits; DRAD, V=1.9×10^7 m^3) are present in the east side of Mount Jizo, the Akaishi Range. The age of DRAD has been determined by a ^{14}C-method as AD780-870 or as AD778-793 (with help of wiggle matching). However, precise age determination of DRAD is further required as the some uncertainties remain in the previous age data. Therefore, we performed dendrochronology of a fossil wood log of Japanese cypress (*Chamaecyparis obtusa*) with 226 tree rings and bark obtained from the dammed lake deposits formed by DRAD. As a result, the fluctuation pattern of tree ring width of the sample log (DDK-A) clearly coincided with the pattern during a period from AD662 to AD887 of the 2705-year-long standard curve (705BC-AD2000) established from some tree ring samples of Japanese cypress. Statistical analysis showed that a degree of agreement between DDK-A's tree ring curve and the standard curve (t) is 7.9. Generally, it can be judged that there is high agreement between two tree ring patterns when t-value is more than 3.5. We also observed cell structures of the outermost tree ring for determining the kill season of DDK-A. The early wood ring was completely formed and the late wood ring was almost invisible. Therefore we concluded that DDK-A was dead in the late summer of AD887.

The old Japanese documents *Nihon-Sandai-Jitsuroku* and *Fuso-Ryakki* described the mega earthquake(M 8-8.5) , the *Goki-Shichido* earthquake, in AD887 August. This earthquake was considered to occur along the Suruga and Nankai Troughs off central Japan. Slope movement related to DRAD would be caused by this historical earthquake.

Keywords: dendrochronology, large landslide, Gokishichido earthquake, Akaishi Range

Japan Geoscience Union Meeting 2014
(28 April - 02 May 2014 at Pacifico YOKOHAMA, Kanagawa, Japan)

HDS29-P02 Room:Poster Time:April 28 18:15-19:30

Occurrence of large landslides in past 40 years and sediment supply in the southern Japanese Alps

NISHII, Ryoko[1*] ; IMAIZUMI, Fumitoshi[2]

[1]University of Tsukuba, [2]Shizuoka University

Many large landslides are distributed in the southern Japanese Alps which consists of high relief and steep slopes. A lot of sediments deposited in dams suggest that sediments are produced actively in upper streams. To evaluate the sediment supply from landslides, this study addressed the mapping of landslides (>10000 m^2) in Ooi River and Hayakawa River (total area is 862 km^2) using aerial photographs and orthophotographs in 1970s and 2000s (partly including 2010s). In addition, we computed the volume of sediment supply in several large landslides based on the difference between DEMs from LiDAR data in multiple shooting periods. One hundred eighty landslides were extracted from photographs in 2000s to 2010s. The comparison between the distribution maps of landslides in 1970s and 2000s indicated that an initial large landslide (>100000 m^2) had not occurred since 1970s. In contrast, some landslides had enlarged gradually. Erosion rate computed from LiDAR data indicated the order of 10^{-1} to 10^{-2} m yr^{-1}. Such erosion rate suggests that the bare grounds after landslides are important as sediment supply area.

Keywords: large landslide, sediment supply, aerial photograph, GIS, the Southern Japanese Alps

Japan Geoscience Union Meeting 2014
(28 April - 02 May 2014 at Pacifico YOKOHAMA, Kanagawa, Japan)

HDS29-P03 Room:Poster Time:April 28 18:15-19:30

Cause and age of the Yabusawa Gravel in the northern foot of Mount Senjo, the Akaishi Range, Japan: a reappraisal

KUROSAWA, Hiroshi[1*] ; KARIYA, Yoshihiko[2] ; MATSUSHI, Yuki[3] ; MATSUZAKI, Hiroyuki[4]

[1]Graduate School of Senshu University, [2]Senshu University, [3]Kyoto University, [4]University of Tokyo

The Yabusawa gravel (YG) consists of poorly-sorted thick angular clasts of sand stone, mud stone, and hornfels, forming a geomorphic feature like fluvial terraces along Yabusawa River from Mount Senjo. The previous authors had considered that YG was of glaciofluvial or large landslide origin. However, there is no clear consensus as to the origin and age of YG. We therefore carried out new analysis of geology, geomorphology, and geochronology of YG. The following results were obtained. On the outcrop walls of YG, rock clasts clearly exhibit jigsaw crack structures, although specific sedimentary facies reflecting fluvial processes such as lamination and imbrication are not observed at all. A lithotype of rock clasts in YG is almost restricted to single geology at a given outcrop locality. Surficial topography of YG has hummocks and levee-like terrain. Terrestrial cosmogenic nuclide dating of sandstone fragments obtained from three localities apart from each other gave 10.3-8.4 ka, 10.0-8.1 ka, and 9.4-7.6 ka (in ^{10}Be scale). On the basis of these facts, we concluded that YG was produced by catastrophic rock slide (rock avalanche) in the early Holocene as single event. Although the previous authors stressed degradation of mountain permafrost for landslide occurrence, we invite attention to paleoearthquakes caused by nearby active faults or convergent plate margins as well as early Holocene pluvial climate and long-term gravitational rock deformation. A multidisciplinary study for better understanding of basic factors, onset triggers, kinematic behavior of landslide is further required

Keywords: Shimanto group, Rock avalanche, Terrestrial cosmogenic nuclides, Holocene

Japan Geoscience Union Meeting 2014
(28 April - 02 May 2014 at Pacifico YOKOHAMA, Kanagawa, Japan)

HDS29-P04 Room:Poster Time:April 28 18:15-19:30

Gravitational rock deformation since the late Pleistocene on the Hounose-dendeiro Ridge, the southern Kanto Mountains

SAWABE, Koichiro[1*] ; KARIYA, Yoshihiko[2] ; SHIMIZU, Chosei[3]

[1]Graduate School, Senshu University, [2]Senshu University, [3]Komazawa University

We describe the geology and geomorphology related to gravitational rock deformation on the Hounose-denndeiro Ridge(HB), the upper Tama River Basin. HB is a broad ridge line 200 to 300 m wide running from northwest to southeast, and its altitudinal range spans from 1050 m to 1180 m ASL. The bedrock geology of HB is Cretaceous sedimentary rocks of Shimanto Group that generally show NE-SE strike and east dip at 60 to 80 degrees.

Linear depressions and step-like slopes both parallel to HB are present on and around the ridge-top. Depth and length of depressions are usually less than 20 m and several tens to hundreds meters in many cases. Features of valley bulging with downhill-facing scarp and gentle slopes are also found from valley side slopes immediately below ridge-top linear depressions and step-like slopes . In the area of gravitational slope deformation where bulging features occur, rock deformation caused by toppling and buckling can be observed.

We recovered sediment drill cores in the linear depressions on HB (P1 and P2). The bottom of surficial humic soil gave 4.1-4.3 cal ka (P1, -64 cm) and 9.5-9.8 cal ka (P2, -162 cm). Also a vitric ash layer Aira-Tanzawa (30 ka) was found from -153 cm (P1) and -325 cm (P2). In addition, a patch of pumice grain of Ontake-Ina (93 ka) was discovered at -709 cm of P2. These facts indicate that linear depressions as depositional sinks on HB were already formed before 30 ka at P1 and before 93 ka at P2.

Keywords: Shimanto Group, Linear depression, Toppling, Buckling, Tephra, 14C age

Japan Geoscience Union Meeting 2014
(28 April - 02 May 2014 at Pacifico YOKOHAMA, Kanagawa, Japan)

HDS29-P05 Room:Poster Time:April 28 18:15-19:30

Relief, bell-shape and distortion indexes as critical topography of creep deformation due to mountain gravity

YAGI, Hiroshi[1*] ; HAYASHI, Kazunari[2] ; IMAIZUMI, Fumitoshi[3] ; SATO, Go[4] ; HIGAKI, Daisuke[5]

[1]Fac. Art, Science & Education, Yamagata University, [2]Okuyama Boring Co.,Ltd., [3]Fac. Agriculture, Shizuoka University, [4]Teikyo-Heisei University, [5]Fac. Agriculture & Life Sciences, Hirosaki University

1.Introduction

Double ridges or up-hill facing scarplets distributed on mountain ridge in high relief are known as indicators that mountain bodies are undergoing gravitational creep deformation and as signs of landslide in large scale. However, such micro topographies on ridges in Japan Alps has developed since 30 ka before. That is presumably attributed to one of the para-glacial phenomena. Trench study in Southern Japan Alps clarified that they have intermittently developed in a time scale of 10000 year and the last event, but a slight deformation occurred about 500-600 years ago. It is quite gradual movement. Consequently dense distribution of the up-hill facing scarplets is not always a pre-causious sign of sudden collapse of the mountain body in near future, though the earthquake occurs near the mountains. Other causative factors are required to induce landslide for hazard susceptibility mapping. We analyzed topographic features of mountain around Mt Shichmenzan and Ooyakuzure, which locate along the marginal mountains in Shizuoka Pref, and where huge co-seismic landslides occurred in 17th and 18th century, using DEM of 10m grid scale and more precise scale.

2.Topographic feature of mountain collapsed by earthquakes

Mountain ridges around Mt. Shichimenzan and Ooyakuzure show gentle and round and are fringed by distinct break of slopes. Mountain profiles of high contrast between steep lower slope and gentle ridge ridge tops are similar to a bell-shaped mountains of high relief. In another word, the bell-shaped profile is one kind of the concavity in ridge profiles.

3.Critical topography of creep deformation

Dense distribution of uphill facing scarplets are observed along the main ridges of the study area by aerial photograph interpretation. However, co-seismic landslides occurred only at Mt. Shichimenzan and Ooyakuzure. We analyzed relief of ridges, considering those of the surrounding slopes and ridge scale over the study area. We call it the relief index. Also we analyzed degree of bell-shape, weighting the area of convex part of the profile. These two indexes are highly scored around Mt. Shichimenzan and Ooyakuzure, but not so high along the main ridge from Mt. Yambushi-toge to Mt Dainichi-toge where the uphill facing scarplets are densely distributed. These are considered as very convenient indexes to know the high susceptibility of landslide induced by earthquake. And distortion index that is calculated ratio of total length of up-hill facing scarplets to a original slope length is also introduced as critical topography of creep deformation due to mountain gravity.

Keywords: gravitational creep, critical topography, relief index, bell-shape index, distortion index, large scale landslide

Japan Geoscience Union Meeting 2014
(28 April - 02 May 2014 at Pacifico YOKOHAMA, Kanagawa, Japan)

HDS29-P06 Room:Poster Time:April 28 18:15-19:30

Development of Lake Shibire and its geomorphological relationship with landslides in Misaka Mountains, central Japan

SUZUKI, Terumi[1*] ; KARIYA, Yoshihiko[2] ; KUROSAWA, Hiroshi[1]

[1]Graduate School of Senshu Univ., [2]Senshu Univ.

Geomorphological classification mapping and geological investigation were carried out to reconstruct the development of Lake Shibire (890 m ASL, max depth 9.5 m, perimeter 1.2 km) in Yamanashi Prefecture. Lake Shibire was formed on a closed depression of the hilly mound with antislopes that was produced by landslide on the steep slopes adjacent to the lake. Other smaller landslide bodies were also identified next to Lake Shibire. Lacustrine deposits with plant macro fossils and a thin vitric ash layer (Aira-Tanzawa, 30 cal ka) were discovered from the side slope of a small channel close to Lake Shibire. Radiocarbon age of a plant macro fossil sampled from the bottom of the lacustrine deposits was 47-46 cal ka. The paleo Lake Shibire was likely to consist of independent two or more basins in the late Pleistocene and only one basin has survived to the present-day Lake Shibire. It is also likely that a single basin was decoupled into two or more basins due to occupation of landslide masses caused by secondary landslide activities adjacent to the basins, and only the certain basin linked to the present-day Lake Shibire has endured.

Keywords: landslide, lacustrine deposit, Aira-Tanzawa tephra, 14C dating, late Pleistocene

Japan Geoscience Union Meeting 2014
(28 April - 02 May 2014 at Pacifico YOKOHAMA, Kanagawa, Japan)

HDS29-P07 Room:Poster Time:April 28 18:15-19:30

Geological implication of the lahar disaster by Typhoon Wipha on October 16, 2013 in Izu Oshima Volcano

KOYAMA, Masato[1*] ; SUZUKI, Yusuke[2]

[1]CIREN, Shizuoka University, [2]Izu Peninsula Geopark Promotion Council

Heavy rain (over 800mm per 24 hours) triggered by Typhoon Wipha on October 16, 2013, caused many slope failures and associated lahars in the western part of Izu Oshima Volcano, Japan. Tephrostratigraphic study revealed a mechanism of the slope failures and history of similar lahars for the past 700 years. Seven fallout ash or scoria layers, which were ejected during the 7 eruptions since the early 14th century, are distributed in the study area. These tephra layers are interbedded with eolian dust (loess) layers, each of which was deposited during a 10-200 years dormant period. Stratigraphic horizons of the slope failures concentrated at the boundaries between ashes and underlying loess layers. This means that more permeable ash layers were saturated with rainwater and slid down along the upper surface of less permeable loess layers. We newly found that three lahars (Lahar A, B, and C) occurred in historic time. Lahar A and B are correlated to the disaster documents of 1856 (or 1932) and of the late 16th century, respectively. Lahar C overlies directly on the Y5.2 scoria and associated Motomachi Lava and thus occurred in the early-middle 14th century.

Keywords: Izu Oshima, volcano, eruptive history, lahar, Typhoon Wipha (2013), slope failure

Japan Geoscience Union Meeting 2014
(28 April - 02 May 2014 at Pacifico YOKOHAMA, Kanagawa, Japan)

HDS29-P08 Room:Poster Time:April 28 18:15-19:30

Preliminary report on the landslides, Oct. 2013, Izu-Oshima Volcanic island, central Japan: Shallow landslide, landforms

SUZUKI, Takehiko[1*] ; TMU GROUP FOR, Izu-oshima typhoon wipha (1326) disaster[1]

[1]Tokyo Metropolitan University

Before dawn of 16th October 2013, the heavy rain associated with Typhoon Wipha (1326) caused landslides disaster in Izu-oshima volcanic island, 120 km south of Tokyo. Many shallow landslides occurred on the west slope of the Younger edifice of Pre-caldera volcano, facing Moto-machi Town. Several reports (e.g. Ministry of Land, Infrastructure, Transport and Tourism; http://www.mlit.go.jp/river/sabo/h25_typhoon26/izuooshimagaiyou131112.pdf) have suggested that the distribution of the landslides overlap the area of lava flow effused 14 Centuries (AD1338?). For examine this relation between landslides and the geomorphological and geological conditions, we preliminary surveyed shallow landslides, landforms and geology along the Gojinka Sky Line on the slope of the Younger edifice of Pre-caldera volcano, 7th and 8th of December and 4th to 6th of January. In presentation, we will report results of field survey for shallow landslides, landforms and geology in detail.

Keywords: Izu-Oshima, Typhoon Wipha (1326), Shallow landslide, Fall-out tephra, Lava flow

Japan Geoscience Union Meeting 2014
(28 April - 02 May 2014 at Pacifico YOKOHAMA, Kanagawa, Japan)

HDS29-P09 Room:Poster Time:April 28 18:15-19:30

Landslides of granite porphyry induced by Typhoon Talas 2011 around Mt. Myoho at Nachikatsuura, Wakayama, Japan

HIRATA, Yasuto[1*] ; CHIGIRA, Masahiro[2]

[1]Department of Geophysics, Graduate School of Science Kyoto University, [2]Disaster Prevention Research Institute, Kyoto University

Typhoon Talas brought heavy rain in Kii Peninsula, Japan on September 2-5, 2011, causing a large number of rock-avalanches and debris flows in the southeastern part of Kii Peninsula. We mapped the landslide scars on aerial photographs at the scale of 1:20000, made rainfall distribution maps by using the rainfall data analyzed by radar-AMeDAS, and compared position of landslides with rainfall distribution and the geological map by Geological Survey of Japan. The result shows that almost all of the landslides occurred in both over 80 mm/h of rainfall zone and Kumano granite porphyry area. In order to clarify the geological topographical background of the landslides, we also made field investigation around Mt. Myoho at Nachikatsuura, Wakayama Prefecture, where the landslide disaster concentrated.

The field investigation showed that the landslides had different attributes at inside area of granite porphyry mass and at the edge of the mass. Mt. Myoho consists of the Kumano granite porphyry around the top and the Kumano group (sedimentary rock) of Miocene age which occupies at the lower part of surrounding slope and below plain land. Slope is gentle around the top and gets steeper from the surrounding slope break, and eventually becomes gentle again below the boundary between granite porphyry and the Kumano group. The granite porphyry shows typical spheroidal weathering with corestones in the surface layer of gentler slope. The corestones were included in deposits caused by the landslides. Accordingly, landslides within granite porphyry area had scarps at the slope breaks, where weathered and/or reworked material of granite porphyry seemed to have collapsed. At landslides near the boundary between granite porphyry and the Kumano group, the shale of the Kumano group was altered to dark gray clay. Talus deposit of the saprolite and corestones on the clay seemed to have collapsed there.

We estimated volumes of some rock-avalanches around Mt. Myoho to be range from 10^2 to 5×10^5 cubic meters, and their equivalent friction coefficients were 0.20-0.46 on the basis of positions from the rock-avalanches and following debris flows plotted on topographical maps at the scale of 1:25000. These landslides of granite porphyry were similar to those of granite in Hiroshima Prefecture induced by heavy rain on June 1999 in terms of volume and equivalent friction coefficient. In the case of weathered granite in Hiroshima, however, corestones were formed slightly and it was a different type of landslide that saprolite collapsed and transformed into debris flows.

Keywords: landslides, Typhoon Talas, granite porphyry, Nachi Katsuura

Japan Geoscience Union Meeting 2014
(28 April - 02 May 2014 at Pacifico YOKOHAMA, Kanagawa, Japan)

HDS29-P10 Room:Poster Time:April 28 18:15-19:30

Interpretation of landslides triggered by 1944 Tonankai earthquake around Owase City using U.S. military aerial photos

SATO, Hiroshi, P.[1*]

[1]Japan Map Center

Shallow landslides were interpreted around Owase City, Mie Prefecture using U.S. military aerial photographs (1/16,000 in scale) taken on 7 December 1944, just three days after Tonankai earthquake (M7.9). It is thought that some of landslides were triggered by the earthquake. Result of the interpretation will be reported.

Keywords: landslide, slope failure, Tonankai, earthquake, U.S. military, reconnaissance

Japan Geoscience Union Meeting 2014
(28 April - 02 May 2014 at Pacifico YOKOHAMA, Kanagawa, Japan)

HDS29-P11 Room:Poster Time:April 28 18:15-19:30

Long-traveling conditions for the rock-on-snow landslide: insights from the field and lab evidence

YAMASAKI, Shintaro[1*] ; KAWAGUCHI, Takayuki[1] ; NAKAMURA, Dai[1] ; YAMASHITA, Satoshi[1] ; SHIRAKAWA, Tatsuo[1] ; HAS, Baator[2]

[1]Kitami Institute of Technology, [2]Asia Air Survey Co., Ltd.

On March 12, 2011, the M 6.6 earthquake hit the typical deep snow area of Niigata and Nagano prefectures. This earthquake (2011 north Nagano Earthquake) induced a lot of landslides, and some of them travelled on snow moving long distance. We are studying that type of landslides which named rock-on-snow landslide by field observations and lab experiments. The rock-on-snow rock avalanche differs from other conventional earthquake-induced landslides because of high mobility, and slash avalanche because water before the event does not drive rocks. Then its high mobility is important to consider earthquake disaster prevention for deep snow area.

The physical properties of snow under the moving mass could affect long-travelling property. We investigated the Tatsunokuchi landslide induced by the earthquake and found temporal liquefaction zone which lay between landsliding mass and autochthonous snow (Yamasaki et al., 2013). The condition of snow getting liquefaction depends on temperature and pressure. Snow also has effect of friction reducing as skiing. However, all rock-on-snow landslides including small rock falls on snow do not travel long-distance, rather most of them stop shorter distance from the origin than normal rock falls. Thus, condition of the long-travelling could be limited. We conducted lab experiments that miniature rock fragments slides on snow slope which tilt angle is 20 degrees, the width is 20 cm and the length is 300 cm, and then we try to understand basic properties of relation between rock and snow and processes during the sliding. The results and our field observations gave us insights to understand larger phenomena.

Reference

Yamasaki, S. Nagata, H. and Kawaguchi, T., Long-traveling landslides in deep snow conditions induced by the 2011 Nagano Prefecture earthquake, Japan, Landslides, 2013 Online available.

Keywords: landslide, snow, earthquake, avalanche, debris avalanche

Japan Geoscience Union Meeting 2014
(28 April - 02 May 2014 at Pacifico YOKOHAMA, Kanagawa, Japan)

HDS29-P12 Room:Poster Time:April 28 18:15-19:30

Definition of the database fields for landslide hazard database by NIED

UCHIYAMA, Shoichiro[1*] ; YAMADA, Ryuji[1] ; ISHIKAWA, Haruna[2] ; SUZUKI, Hinako[1] ; USUDA, Yuichiro[1]

[1]National Research Institute for Earth Science and Disaster Prevention (NIED), [2]Advantechnololy Corporation

The history of natural hazard at a certain place is greatly related to the current risk there. It provides indispensable information to the hazard and the risk assessment. The Research Institute for Earth Science and Disaster Prevention (NIED) is building a comprehensive database of natural hazard events over the historical period in Japan, and distributing these information with Web API. Such a hazard event database is, however, no more than an index with a limited amount of information about the reality. Therefore, especially for the large natural hazards that had big social impacts, it is important to provide specific databases classified with types of hazards such as earthquake, volcano, storm, flood, slope, snow and ice disasters. We discuss about the database for slope disasters in particular here.

Keywords: landslide hazard database, database field, definition of fields

Japan Geoscience Union Meeting 2014
(28 April - 02 May 2014 at Pacifico YOKOHAMA, Kanagawa, Japan)

HDS30-01 Room:511 Time:April 29 16:15-16:30

Submarine mass-transport deposits of the Paleogene Muroto Formation in the Kuromi coastal region, Kochi Prefecture

IKAWA, Yu[1] ; TONAI, Satoshi[1*] ; SHIBATA, Tadahiro[2]

[1]Faculty of Science, Kochi University, [2]Muroto Geopark Promotion Committee

We report stratigraphy and geologic structures of ancient mass-transport deposits exposed as a nearly 2 km continuous outcrop of the Kuromi coastal region, Shikoku Island, Japan to provide detailed information on internal structures of mass-transport deposits and their relationships with encasing sediments. It is allowing important considerations on triggering mechanisms and transport/depositional process of mass-transport deposits.

The mass-transport deposits studied here are in the Upper Eocene to Lower Oligocene Muroto Formation which is a part of the Paleogene Shimanto accretionary complex. The Muroto Formation, about 650 m thick in this area, consists of six lithofacies. These units are thick-bedded mudstone, thin-bedded very fine grained sandstone and mudstone, thin- to medium-bedded fine sandstone and mudstone, thick-bedded sandstone, folded thin-bedded sandstone and mudstone, and chaotic deposits. These sediments are interpreted as a deep-sea channel-levee system with occurrence of submarine landslides.

A field-based study of the Muroto Formation reveals that folded thin-bedded sandstone and mudstone and chaotic deposits are made up of at least two distinct mass-transport deposits, the larger of which reaches thickness of more than 270 m. Fold hinges in these mass-transport deposits are uniformly orientated and parallel to the host bedding. Axial planes in these mass-transport deposits show a girdle-like distribution which are perpendicular to the host bedding. These patterns of fold orientations show that the style of their transport is mainly flow and partly is turbulent flow including broken detrital blocks. These characters show that huge mass-transport deposits may be often formed on plate convergent margins and involved in accretionary prism.

Keywords: submarine mass-transport deposit, accretionary complex, Shimanto belt, Paleogene

Japan Geoscience Union Meeting 2014
(28 April - 02 May 2014 at Pacifico YOKOHAMA, Kanagawa, Japan)

HDS30-02 Room:511 Time:April 29 16:30-16:45

Feature of slump and associated structure observed at Daini-Atsumi knoll, the gas production test site from gas-hydrate

SUZUKI, Kiyofumi[1*] ; TAKAYAMA, Tokujiro[1] ; SANADA, Yoshinori[2] ; FUJII, Tetsuya[1]

[1]JOGMEC/TRC, [2]Japan Agency for Marine-Earth Science and Technology

The Daini-Atsumi knoll became famous as the first offshore gas production test site from methane hydrate-bearing marine sediments, is one of outer ridges along northeast Nankai trough, near central Japan. Several slumps were found on seismic sections around Daini-Atsumi knoll. Fortunately, several wells had been penetrating slump deposits and logging data were measured. As a result of seismic profile observations, a strong negative-impedance seismic reflector (NISR) was found in the turbidite sequence beneath the slump deposits. A seismic reflector containing the NISR has good continuity with variable reflectivity from a bottom-simulating reflector (BSR) sequence; that is, the NISR does not indicate a slump basement or the boundary of a chaotic unit. Nevertheless, very normal thin-layer turbidites were found at the depth of NISR from LWD measurement and coring, however, fluid data could indicate difference between upper slump unit and beneath turbidites unit. It implies that NISR does not mean pressured fluid but some fluid stagnation.

Acknowledgement
This research is conducted as a part of MH21 research and the authors would like to express their sincere appreciation to MH21 and the Ministry of Economy, Trade and Industry for disclosure permission for this research.

Keywords: Slump, 3D seismic profile, LWD, Over-consolidate, Gas hydrate, Low impedance

Japan Geoscience Union Meeting 2014
(28 April - 02 May 2014 at Pacifico YOKOHAMA, Kanagawa, Japan)

HDS30-03 Room:511 Time:April 29 16:45-17:00

Role of slump deposits in a high-methane-flux gentle continental slope

MORITA, Sumito[1*]

[1]AIST-GREEN

A great number of submarine landslide deposits (slump deposits) are known to be buried in Pliocene and the upper formations in northern part of Sanrikuoki Basin (Morita et al., 2011). The slump deposits are mainly made up of imbricated thrust sheets of stacked sedimentary layers which were peeled off from ancient bottom surface. The slump deposits often show dimmed facies as an acoustic characteristic and have dewatering structure from the slip surface, and sometimes have gas chimney at the roof of the slump deposits. These indicate that the slump deposits are strongly related to natural gas in formation water. A key to grasp the nature of the slump deposits is likely in a comparison with a result of previous scientific drilling. Site C9001 is a drill site which was operated by D/V CHIKYU in this survey area (Higuchi et al., 2009). By the result of the expedition, the sedimentary basin is mostly composed of mud and few thin ash and sand layers. The sediments are normal and the parts judged as mass transport deposits (MTD) by visual core description are very limited even in the depth domain interpreted as slump deposits in seismic data. However, methane detected in head space gas and methane hydrate bearing sediments recovery were reported only in the slump deposits domain interpreted in the seismic data. Previous reports with respect to MTD indicate that MTDs generally have the nature as seal where the beds have higher shear strength and density due to compaction. Nevertheless, the nature of the slump deposits in the Sanrikuoki Basin is opposite to those of the other MTDs, and may indicate as if reservoir. The difference of the natures is maybe caused by the environment of very gentle continental slope where the slumping has repeated. There is a hint of it in the fact that slump deposits in the survey area avoided fatal collapse by sliding on the very gentle slope and basically formed the imbrication of block-supported structure.

Keywords: submarine landslide, mass transport deposits, slump, Sanrikuoki Basin, CHIKYU, methane hydrate

Japan Geoscience Union Meeting 2014
(28 April - 02 May 2014 at Pacifico YOKOHAMA, Kanagawa, Japan)

HDS30-04 Room:511 Time:April 29 17:00-17:15

Liquefaction-induced water-film mechanism in submarine slide

KOKUSHO, Takaji[1*]

[1]Kokusho Takaji

As one of possible mechanisms of seismically triggered submarine slides in cohesionless sandy & gravelly deposits, void redistribution or water film effect seems to be deeply involved (Kokusho, 1999, 2000). In this view, fine soil sublayers sandwiched in coarse grain deposits are considered to play a key role in flow failure. The formation of water films between liquefied sand and overlying lower-permeability seams has been observed under level ground conditions in a number of model tests. Fig. 1 shows a typical example of water film formed beneath a thin silt seam sandwiched in a uniform horizontal sand layer. It has also demonstrated that water film can be generated not only in sands beneath silt seam but also in gravels beneath smaller permeability sands (Kokusho & Kojima 2002). Visit http//:www.civil.chuo-u.ac.jp/lab/doshitu/index.html for video images of the model tests.

For sloping ground conditions it has been demonstrated, based on model shake table tests, that the water film plays an important role in post-earthquake large lateral flow in liquefied ground. Fig.2 shows typical test results where clean fine sand was rained in water to make saturated sand slope shown in (d) in a transparent soil box (Kokusho 2003). Fig.2(a) indicates a case of a uniform sand model where small flow deformation occurs mostly during shaking. The locations of markers in the model are shown in (d) with the same symbols. If a silt seam shown with chain-dotted arc is sandwiched in the uniform sand, a larger flow deformation above the arc occurs not only during but also after shaking as indicated in (b). These results in (a) and (b) are for the input acceleration of 0.31 G. Interestingly, for weaker input acceleration of 0.18G given to the same model in (c), much larger post-shaking flow than (b) occurs, while only minimal deformation takes place during shaking. In these tests, very thin water film can be observed beneath the silt arc.

A basic question may arise that sand which can be so dilative if sheared under a low confining stress may absorb ambient excess pore water and hence block the water film development. It can be pointed out, however, based on the comparative observation of the cases with and without a silt seam that a water film formed beneath the seam serves as a shear stress isolator which prevents deeper soils developing shear strain and positive dilatancy (Kokusho, 2000). Consequently, sand can experience large shear strain beneath the silt seam without suffering from the dilatancy effect, whereas it stops moving after the end of shaking if the sand is uniform.

Another shaking table tests has shown that a soil mass slides even on a very gently inclined water film, which breaks at weak points of the overlying sublayer, triggering the boiling failure in the sand above and a mud avalanche of the upper layer (Kokusho 1999, 2000). For video images of these model tests, visit http//:www.civil.chuo-u.ac.jp/lab/doshitu/index.html.

If water films are formed continuously, they will tremendously reduce the residual strength down to zero if sliding occurs all the way through a continuous water film. Kabasawa and Kokusho (2003) quantified the residual shear resistance exerted during the delayed flow along a water film in the model tests. The result shown in Fig.3 indicates that the residual strength along the water film is almost independent of sand density and other test parameters and remains around 20% that of the uniform sand. Considering that soil deposits are naturally stratified with sandwiched low permeability seams, it seems quite reasonable to identify the water film effect as a major mechanism for seismically induced submarine slides in gently sloped sandy or gravelly sea-bed near coastal areas.

Thus, liquefaction may be highly responsible in earthquake-induced submarine slides, particularly in near-shore sites where the seabed is composed of liquefiable loose sand or gravel.

Keywords: seismic liquefaction, water film, time delay, permeability

Japan Geoscience Union Meeting 2014
(28 April - 02 May 2014 at Pacifico YOKOHAMA, Kanagawa, Japan)

HDS30-05 Room:511 Time:April 29 17:15-17:30

Factors controlling submarine landslide occurrence: Lessons learned from plate-boundary decollement zones

UJIIE, Kohtaro[1*]

[1]University of Tsukuba

Most submarine slopes are inherently stable. However, once submarine landslide generated, it could induce destruction of seabed infrastructure and tsunamis. The factors controlling submarine landslide occurrence remain poorly understood, mainly because there has been very limited access to slip surface of landslide. Initiation and evolution of plate-boundary decollements in subduction zones may be useful to understand the location of slip surfaces and the slip behavior of submarine landslides. Here, I review decollement processes in subduction zones, which have been revealed from deep ocean drilling in the last 20 years. The decollements develop along (1) weak, smectite-rich layers, (2) the zones of elevated pore pressure, and (3) the mechanical boundary between cemented and non-cemented intervals. These results provide important implications for submarine landslide occurrence. The slip surfaces may localize along an interval of smectite-rich lithology. Such smectite-rich lithology could link to the increased volcanic activity as smectite is commonly derived from alteration of volcanic ash/tuff. The permeability contrast in slope sediments could also play an important role on the development of slip surfaces. The rapid sedimentation of coarse-grained sediments onto fine-grained, argillaceous sediments may cause the generation of elevated pore pressure, which in turn facilitates the onset of submarine landslide. The trap of the hydrate-derived fluid beneath the low permeability sediment may also cause the development of overpressure. The slope sediments may contain the cementation boundary (e.g., opal-A to opal-CT reaction) particularly when geothermal gradient is high. In such case, the submarine landslides may generate along the surface bounding different cementation states.

Japan Geoscience Union Meeting 2014
(28 April - 02 May 2014 at Pacifico YOKOHAMA, Kanagawa, Japan)

HDS30-06 Room:511 Time:April 29 17:30-17:45

Flow dynamics of Nankai Trough submarine landslide inferred from internal deformation using magnetic fabric

KANAMATSU, Toshiya[1*] ; KAWAMURA, Kiichiro[2] ; KITAMURA, Yujin[3] ; NOVAK, Beth[4] ; STRASSER, Michael[5]

[1]Japan Agency for Marine-Earth Science and Technology, [2]Graduate School of Sciences and Engineers, Yamaguchi University, [3]Department of Earth and Environmental Sciences, Graduate School of Science and Engineering, Kagoshim, [4]Department of Geology Western Washington University, [5]Geological Institute, Seiss Federal Insitute of Technology ETH Zurich

Submarine landslide deposits in one of the most active subduction zone was investigated by Integrated Ocean Drilling Program (IODP) Expedition 333 as ”Nankai Trough Submarine Landslides History” (NanTroSLIDE). The expedition recovered a Pleistocene to Holocene sequence of stacked mass-transport deposits (MTDs) within a slope on the footwall of the megasplay fault at Site C0018, Nankai Trough SW Japan (Strasser et al., 2012). A series of MTDs interbeded with coherent intervals were recovered from the upper 190-meter at C0018 site. We present results of detail fabric analysis using drilled succession of buried mass transport deposits in the slope of Nankai Trough in order to investigate rheology of mass transportation in the subduction zone. Despise very limited lithological information of core research, AMS is proved useful tool to identify MTD deformation and recognize depositional process of MTD (Kitamura et al., 2013, Noback et al., 2013).

Magnetic fabric patterns reveal inhomogeneity within each MTD unit indicating a different compaction and shear occurred during flowing and subsequent deposition (MTD2, MTD3, MTD5). Magnetic fabric in upper interval of each unit generally indicates vertical compression. On the other hand lower interval involve magnetic fabrics showing effect of shear. In the largest MTD (MTD6), a distribution of magnetic foliations images tightly folded strata. Using available paleomagnetic data the shear directions are reoriented, and two different directions are obtained in term of MTD flow directions. It is considered that such variation in flow types and directions derived from the results occurred in responding to a change of slope environment controlled by the tectonic evolution of Nankai accretionary wedge. Through such analysis we can improve our understanding for submarine landslide formation in the active margin.

Keywords: submarine landslide, NanTroSLIDE, IODP, Nankai Trough

Japan Geoscience Union Meeting 2014
(28 April - 02 May 2014 at Pacifico YOKOHAMA, Kanagawa, Japan)

HDS30-07 Room:511 Time:April 29 17:45-18:00

Potential tsunamigenic submarine landslides in active margins

KAWAMURA, Kiichiro[1*] ; JAN SVERRE, Laberg[2] ; KANAMATSU, Toshiya[3]

[1]Yamaguchi Univerisity, [2]University of Tromso, [3]JAMSTEC

A review of modern, historical and submarine landslides from the geological record shows that landslides in active continental margins can generate tsunamis. The tsunamis may damage coastal and seabed infrastructure and so represent an important element of marine geohazards research due to their potentially significant impacts on society. The primary trigger mechanism of tsunamis in this type of setting was thought to be earthquake activity; however, there are also a number of alternative hypotheses regarding the likely initiation mechanism including the generation of submarine landslides. In this paper, we briefly review the geological features and trigger mechanisms of tsunamigenic submarine landslides on active margins. Large tsunamigenic submarine landslides appear to occur mostly on margins characterized by non-accretion. These observations has implications for tsunami warning systems as the Japanese system does not consider the scenario of tsunami excitation by submarine landslides

Keywords: tsunamigenic submarine landslide, tsunami earthquake, tectonic erosion, Japan trench, the 2011 Tohoku-Oki earthquake

Japan Geoscience Union Meeting 2014
(28 April - 02 May 2014 at Pacifico YOKOHAMA, Kanagawa, Japan)

HDS30-P01 Room:Poster Time:April 29 18:15-19:30

Temporal changes of internal stresses and pore pressures of a large-scale submarine debris flow

OTSUBO, Makoto[1*] ; NARUSE, Hajime[2] ; MIYAKAWA, Ayumu[1]

[1]Geological Survey of Japan, AIST, [2]Graduate School of Science, Kyoto University

Mass-transport deposits are major components of depositional systems in the deep sea environments. These deposits usually are composed of muddy chaotic deposits, and are expected to conduct as permeability seals over channel deposits. These mass transport deposits appear as transparent layers on seismic data and chaotic intervals in cores (e.g., Weimer, 1991). Regardless of their common occurrence and distinctive geometry, the dynamics of subaqueous mass transport processes (debris flows) are not well known. It is great difficult to observe directly a subaqueous debris flow.

Naruse and Otsubo (2011) documented quantitatively the internal structures of a mass-transport deposit in the Akkeshi Formation, from the middle part of the Cretaceous-Paleocene Nemuro Group, Japan. The paleostress analysis using meso-scale faults (Yamaji, 2000) of a large-scale mass-transport deposit revealed that the flow experienced two different stress fields: (1) a vertical uni-axial compressional stress field with the sigma1-axes oriented normal to the bedding surface (Phase I) and (2) horizontal tri-axial compressional stress fields with the sigma1-axes oriented parallel to paleocurrent direction (Phase II) (Naruse and Otsubo, 2011).

We examined the temporal changes of internal stresses and pore fluid pressures in a submarine mass transport from the relationships between the principal stresses axes and attitude of fault planes in the mass transports deposits in the Akkeshi Formation. We used 22 fault data and stresses of two Phases in a mass transport deposits. We attribute fault variations to the degree of fault overpressure acting on faults to estimate the pore fluid pressure ratio in the submarine mass-transport deposits. The theory can be explained using the Mohr circles. The inferred internal stresses results imply that the stress fields of Phase I are created by a radial spreading of the flow during its downcurrent movement, while the stress fields of Phase II result from compression during deposition on the basin plain (Naruse and Otsubo, 2011). The increase of pore fluid pressure ratio from Phases I to II represents that the pore fluid pressures have been recognized as playing an important role in the occurrence of the faults in Phase II. On the subdivided Phase II, pore fluid pressure ratio increases until Phase IIa and decreases after Phase IIb while sigma-hmax increases during Phase II.

References:

Naruse, H., and, Otsubo, M. (2011) Heterogeneity of Internal Structures in a Mass-transport Deposit, Upper Cretaceous to Paleocene Akkeshi Formation, Hokkaido Island, Northern Japan. SEPM Special Publication, 96, 279-290.

Weimer, P. (1991) Seismic facies, characteristics and variations in channel evolution, Mississippi Fan (Plio-Pleistocene), Gulf of Mexico, in Weimer, P., and Link, M.H., eds., Seismic Facies and Sedimentary Processes of Submarine Fans and Turbidite Systems, New York, Springer, 323-347.

Yamaji, A. (2000) The multiple inverse method: a new technique to separate stresses from heterogeneous fault-slip data. Journal of Structural Geology, 22, 441-452.

Keywords: stress, pore pressure, meso-scale fault, mass-transport, debris flow, land slide

Japan Geoscience Union Meeting 2014
(28 April - 02 May 2014 at Pacifico YOKOHAMA, Kanagawa, Japan)

HRE31-01 Room:419 Time:May 2 09:30-09:45

CCS-geoengineering: the only one reasonable climate geoengineering technology at present

KOIDE, Hitoshi[1*]

[1]Climate Change Geosystem

The climate geoengineering is already inevitable to avoid imminent global climate disasters. Even extreamly cautious approach is not enough for any grand-scale practices of climate geoengineering as we never understand the complex global climate system exactly. However, modern human beings have unintentionally done the global-scale climate geoengineering that increases the atmospheric CO2 level with the wide-spread massive burning of fossil fuels.

The CCS-geoengineering in the broad sense includes the CO2 capture and sequestration, CO2 capture and CO2-EOR/EGR, air capture and sequestration, air capture and CO2-EOR/EGR and also underground microbial CO2 recycling. The CCS-geoengineering only reduces the artificial emission of CO2 into the atmosphere or suck the excessive CO2 from the atmosphere. The CCS-geoengineering is a naturally safe geoengineering technology as the CCS-geoengineering restore the atmosphere only toward the natural CO2 level minimizing untoward effects.

Keywords: geoengineering, CCS, atmosphere, EOR, recycling, global warming

Japan Geoscience Union Meeting 2014
(28 April - 02 May 2014 at Pacifico YOKOHAMA, Kanagawa, Japan)

HRE31-02 Room:419 Time:May 2 09:45-10:00

The influence of measurement methods on evaluation of threshold pressures

KAMEYA, Hiroshi[1] ; ONO, Masaki[1*]

[1]Oyo Corporation

In site selection process for the geological sequestration of greenhouse gas, threshold pressures should be evaluated as sealing efficiency of a seal layer. Threshold pressure means the minimum gas injection pressure over which constant gas flow will occur through a sealing layer. For evaluating threshold pressure, strictly conditioned tests to reproduce in-situ stress, fluid pressure, temperature and type of injected gas will sometimes be planned. On the contrary, easy evaluation by simple method will sometimes be planned by estimating capillary pressure curves from pore size distributions and surface tensions. The former will provide more strict evaluations of threshold pressures but this process will be limited by using a particular test apparatus. So, researches for comparing the test results from some methods to verify the accuracy of each test have been studied. In the research on CO2 geological sequestration, three methods are usually used; i.e. (1) threshold pressure test using supercritical CO2, (2) threshold pressure test using N2 gas, (3) threshold pressure estimation from a mercury intrusion test result. In abroad, some researcher report that the results from different methods are consistent considering the surface tensions of relevant fluid system, but others say that the results are inconsistent because of the sample preparation process or anisotropy of samples. Also, there are only few studies in Japan. The authors conducted three kinds of tests using domestic and foreign sedimentary samples (mudstones and sandstones) and examined the consistencies of their results.

Comparing the results using supercritical CO2 and N2 gas, the threshold pressures might be consistent considering the surface tensions in relevant fluid systems. However, there are some inconsistencies with the anisotropic young sediments which could not be reused because of their low solidification. On the other hand, the threshold pressures from mercury intrusion tests with estimation are almost equal to or a little lower than those from N2 threshold pressure tests. This discrepancy may be caused by the anisotropy or shrinkage during drying process.

In Japan, the candidate of seal formation will be thought as not only massive mudstones but also alternated layers of mudstones and sandstones. In latter case, a limit number of strictly conditioned tests should be compensated by sufficient number of lower quality test results. So, the approach in this study will be important in future site selection process.

Keywords: threshold pressure, seal layer, sealing efficiency

Japan Geoscience Union Meeting 2014
(28 April - 02 May 2014 at Pacifico YOKOHAMA, Kanagawa, Japan)

HRE31-03 Room:419 Time:May 2 10:00-10:15

Evaluation of permeabily fault related damage zone in sandstone from a viewpoint of microstructure

SATO, Minoru[1*] ; TAKEMURA, Takato[2] ; TAKAHASHI, Manabu[3] ; ANMA, Ryo[1]

[1]Tsukuba University, [2]Nihon University, [3]National Institute of Advanced Industrial Science and Technology

It is known that strengthened fragmentation is often observed in damage zones along the fault planes. Studying permeability of faults and damage zones is important because they control fluid migration in subsurface environment (e.g. oil migration and reservoir development, carbon dioxide storage, methane hydrate development). Field and laboratory permeability test have shown that permeability within shear bands, fault gouge or cataclasite is lower than of wall rocks (Zhang and Tullis. 1998), and permeability of damage zones is higher than wall rocks (Fowles and Burley. 1994). The authors compared permeabilities of the wall rocks and damaged zones and their relation to the changes in porosity and pore-size distribution obtained by mercury porosimetry.

The sample was chosen from sandstones from the Nichinan Formation. We conducted shear test on cylindrical sample 90mm in diameter and 180mm long to develop damaged zones in the sample. Cylindrical sample of 50mm in diameter and 25mm long were then cored from the 90mm sample, that intersected the shear plane and damages zones at right angle. The permeability tests were conducted on the cored sample using transient pulse method (Brace et al. 1968) at effective confining pressures 5 and 10MPa. We calculated permeability by Hsieh method (Hsieh et al. 1981) that considered the specific storage value of sample and apparatus. Porosity and pore-size distribution were measured using mercury porosimetry on 10mm cube samples taken from 0 to 10mm, 10 to 20mm, 20 to 30mm, 30 to 40mm from the shear plane.

The permeability of the intact wall rock was 9.40×10^{-9}m/s at 5MPa effective confining pressure, and 2.52×10^{-9}m/s at 10MPa. Permeability of damaged zones were 1.41×10^{-8}m/s at 5MPa effective confining pressure, and 2.70×10^{-9}m/s at 10MPa. Porosity of the intact wall rock was 7.9% and the pore size was dominantly ˜0.1 micro meter. Along the damaged zone, the frequency of 0.1 micro meter pore decreased and that of 0.5 to 10 micro meter pore increased with decreasing distance from the shear plane. On the other hand the porosity of the damaged zones was 5% in average and no clear correlation was observed between the distance from the shear plane and porosity. We suggest that pore structure was affected by micro-fractures or rearrangement of grains from the porosity reduction in the damaged zone samples; nevertheless permeability of the damaged zone samples is higher than that of wall rock samples.

Keywords: permeability, permeability test, mercury porosimetry, pore-size distribution, shear test

Japan Geoscience Union Meeting 2014
(28 April - 02 May 2014 at Pacifico YOKOHAMA, Kanagawa, Japan)

HRE31-04 Room:419 Time:May 2 10:15-10:30

Injection-induced seismicity: insights gained from laboratory AE study using sedimentary rocks

LEI, Xinglin[1*] ; LI, Xiaying[2] ; LI, Qi[2]

[1]Geological Survey of Japan, AIST, Japan, [2]Institute of Rock and Soil Mechanics, Chinese Academy of Science

Injection-induced seismicity associated with applications, in which fluids are intensively pressed into deep formations such as Enhanced Geothermal System (EGS), fracking shale gas, geological sequence of CO2, have attracted growing attentions. Motivated by the desire to better understand the mechanism of damaging events so that they can be avoided or mitigated, we have started an integrated study on rock fracturing and fault reactivation in multiscales. In the present paper, we present some preliminary results of an ongoing experimental study utilizing acoustic emission technique in laboratory. Samples of typical sedimentary rocks collected from Sichuan basin, China, where a number of injection-induced seismic swarms with sizable earthquakes ranging up to M4˜5 have been observed in some gas/oil reservoirs. Since most injection-induced earthquakes are located in sedimentary formations of a wide range of lithology and depth, the fracturing behaviors of such rocks are thus important. In order to investigate the role of over pressured fluid in triggering fault instability, the authors carried out two rock fracture tests under tri-axial compression in laboratory. Detailed space-time distribution of acoustic emission due to microcracking was used to examine pre-failure damages and failure behaviors. Our experimental results demonstrate that dolomitic limestone, shale, and porous sandstone from the Sichuan basin show both brittle and ductile fracturing behaviors depending on a number of factors, including drainage condition and confining pressure.

Keywords: Acoustic emission (AE), Microfracture, Rock fracture, Injection-induced earthquake, Sedimentary rocks

Japan Geoscience Union Meeting 2014
(28 April - 02 May 2014 at Pacifico YOKOHAMA, Kanagawa, Japan)

HRE31-05 Room:419 Time:May 2 10:30-10:45

Geochemical reproduction of deep water related to Matsushiro earthquake swarm for TOUGH-FLAC simulation

OKUYAMA, Yasuko[1*] ; FUNATSU, Takahiro[1] ; FUJII, Takashi[1]

[1]Institute for Geo-Resources and Environment, AIST

A technique of fluid flow ? rock mechanics couple simulation is attracting attentions in the research on CO2 geological storage (CGS) as a promising tool to assess stress conditions in reservoir and caprock associated with CO2 injection. The assessment is important in CGS to set conditions for sustainable injection that does not cause dynamic responses of underground rock mass such as plastic deformation, minor fracturing, re-activation of small faults and so on. AIST is conducting a study using TOUGH-FLAC simulator developed by LBNL, USA, to numerically simulate the 1965-1967 Matsushiro earthquake swarm as a natural analogue of dynamic leakage of stored CO2 associated with fault re-activation. The study using natural data was chosen as the basic data on ground motions and recognizable seismicity would never be obtained in actual CGS demonstration sites because the dynamic responses of rock mass must not occur in the demonstration. The objective of this natural analogue study is to customize the simulator applicable to Japanese CGS sites having bedrocks composed of so-called ”soft rock”.

It is necessary for fluid flow ? rock mechanics coupled simulation to give salinity of formation water in a geologic model as an initial condition. In the case of Matsushiro simulation, the salinity of injected water is also necessary since the Matsushiro earthquake swarm is considered to be caused by a forcible intrusion of saline water beneath the Marsushiro area. The salinity of initial formation water is determined from water geochemistry on several deep wells obtained in the survey during 2010-2011. The salinity of input water is newly estimated based on the similar dataset combined with hydrogen and oxygen isotopic ratios. The hydrogen and oxygen isotopic ratios of well water fall on a line having a gentle slope as compared to the meteoric water line (MWL), a similar relation reported by Yoshida et al. (2002). The extension of this line presents a field of ”andesitic water” by Guggenheim (1992). Assuming that the deep water caused the earthquake swarm has isotopic characteristics of the minimum of ”andesitic water”, the ratio of dilution of the deepest well water was determined from the isotopic ratios of the ”andesitic water” and of the shallow ground water on the MWL. The geochemistry of the deep water caused the earthquake swarm was then determined by using the dilution ratio and the compositions of the deepest well water. The salinity of the deep water caused the earthquake swarm is found to be comparable to present sea water. The salinity is about 7 times higher than that assumed in the previous study of TOUGH-FLAC modeling of the Mtaushiro earthquake swam (Cappa et al., 2009). Similarly, the concentration of HCO3 is estimated by using well water data. The estimated amount of CO2-related soluble species indicates that the initial deep water was oversaturated with respect to CO2 at the postulated temperatures and pressures of Matsushiro simulation.

Keywords: CO2 geological storage, Matsushiro earthquake swarm, natural analogue, dynamic leakage, TOUGH-FLAC, salinity

Japan Geoscience Union Meeting 2014
(28 April - 02 May 2014 at Pacifico YOKOHAMA, Kanagawa, Japan)

HRE31-06 Room:419 Time:May 2 11:00-11:15

Seismic monitoring at the commercial-scale CO2 geological storage site, Cranfield, U.S (Part 3)

TAKAGISHI, Makiko[1*] ; HASHIMOTO, Tsutomu[1] ; HORIKAWA, Shigeo[2] ; KUSUNOSE, Kinichiro[3] ; XUE, Ziqiu[1]

[1]RITE, [2]Suncoh Consultants Co., Ltd., [3]AIST

Public concerns about felt seismic events induced by fluid injection have been raised recently. These felt events have magnitudes of more than $M_L 3$ and occur in the area where seismicity not active. The induced seismic events were triggered due to the pressure changes at the reservoir. CO_2 geological storage, a kind of the fluid injection activities, is regarded as a key potential technology to mitigate greenhouse gas emission. Since this technology involves long-term and large amount of CO_2 injection, some researchers warm that CO_2 geological storage would trigger felt seismicities at the site. Passive seismic monitoring is conducted at CCS sites around the world since 2000's. A few of the sites reported occurrences of seismic events related to CO_2 injection and these events were unfelt with small magnitudes. To ensure the safety against induced seismicity and obtaining public acceptance, seismic monitoring is necessary for operating CCS project, especially for countries with high seismicity such as Japan.

RITE has performed a long-term seismic monitoring at the commercial-scale CO_2 injection site in the U.S. to elucidate the relation between CO_2 injection and occurrences of seismic events collaborating with Lawrence Berkeley National laboratory (LBNL) and Bureau of Economic Geology, University of Texas at Austin (BEG) since 2011. Seismic monitoring is conducted at the Cranfield oilfield, Mississippi. This oilfield is the CO_2-EOR field and a million tonnes of CO2 is annually injected into the Cretaceous sandstone reservoir (porosity 20 ˜30%, permeability for 10 ˜200mD) at the depth of about 3,100m. A total of more than four million tonnes of CO_2 have stored as of January 2013. We composed a circle seismic monitoring array deploying 6-3component of seismometers at the depth of 100m in a 3km radius.

We have monitored seismicities more than two years now, but we have recorded no seismic events at the Cranfield site. The recorded of vertical components of waveforms were examined by semi-automated processing and visual judgments for the entire monitoring of period, and the triggered signals were all identified as artificial noises, noises due to weather changes such as lighting or strong wind, and distant earthquakes.

In this presentation, we discuss why seismic events were not recorded at the Cranfield site. We estimated minimum detectable magnitudes of our monitoring array by means of theoretical calculations based on discrete wavenumber integration method which concerned geological properties from surface to the reservoir. We confirmed that the array could detect seismic events with more than Mw0.4 at the hypocentral distance of 3.2 km. We also discuss the question in terms of pressure changes at the reservoir and other studies conducted at the Cranfield site.

Acknowledgements: This study was funded by Ministry of Economy, Trade and Industry (METI) as a part of the 'safety evaluation technology development projects carbon dioxide capture and storage'.

Keywords: CO_2geological storage, Seismic monitoring, fluid injection

Japan Geoscience Union Meeting 2014
(28 April - 02 May 2014 at Pacifico YOKOHAMA, Kanagawa, Japan)

HRE31-07 Room:419 Time:May 2 11:15-11:30

Risk Assessment Study of Bio-CCS (2)

TANAKA, Atsuko[1*] ; SAKAMOTO, Yasuhide[1] ; HIGASHINO, Haruyuki[1] ; SUZUMURA, Masahiro[1] ; KANO, Yuki[1] ; MAYUMI, Daisuke[1] ; YUJI, Nishi[1] ; NAKAO, Shinsuke[1]

[1]National Institute of Advanced Industrial Science and Technology (AIST)

Among in-situ geo-microbes within depleted oil/gas reservoir, there are some species those generate methane gas from residual oil. Mayumi et.al (2013) identified some methanogens in depleted oil reservoir, those generate more methane gas when they are cultivated in higher CO2 partial pressure environment than in CO2 poor environment. CO2 acts as a catalyst in the reaction. If we maintain preferable conditions for methanogenesis archaea during geological CCS, we will be able to abate greenhouse gas emission and produce natural gas as natural energy resource at the same time. We named the technology concept as 'Bio-CCS'. Assuming Bio-CCS site, CO2 is injected from a well for to abate greenhouse gas emission and cultivate methanogenic geo-microbes, and CH4 is produced from another well. The procedure is similar to the Enhanced Oil/Gas Recovery (EOR/EGR) operation, but in Bio-CCS, the target is generation and production of methane out of depleted oil/gas reservoir during CO2 abatement. We are evaluating the basic practicability of Bio-CCS. In our project, while biologists are identifying the most effective cultivating conditions for methanogenic archaea, geologists, environmental scientists and system scientists are evaluating feasibilities of the technology concept. To evaluate total feasibility of Bio-CCS concept, we are estimating: CH4 generation volume, environmental impact along with life cycle of injection well, and risk-benefit balance of the Bio-CCS. For that purpose, we assumed two conceptual sites of Bio-CCS: One is depleted oil field and the other one is depleted gas field. In our presentation, we will introduce methodologies and interim results of our feasibility study on Bio-CCS.

Keywords: CO2 Geological Storage, CCS, Methanogenesis, Feasibility study, Risk assessment, Methane gas

Japan Geoscience Union Meeting 2014
(28 April - 02 May 2014 at Pacifico YOKOHAMA, Kanagawa, Japan)

HRE31-08 Room:419 Time:May 2 11:30-11:45

Horizontal wells placement optimization for CO2 geological storage in confined aquifers subjected to brine recycling

VILCAEZ, Javier[1*] ; LI, Hualong[1] ; SATO, Kozo[1]

[1]Graduate School of Engineering, The University of Tokyo

Geological storage of CO_2 has potential of mitigating CO_2 emissions into the atmosphere. CO_2 in geological formations can be trapped through solubility, residual, mineral, and structural trapping mechanisms. Of these trapping mechanisms structural trapping is likely to be the least secure because CO_2 accumulated at the cap-rock can potentially leak through pressure-induced fractures in the cap-rock.

In order to maximize the trapping of CO_2 and at the same time prevent the leakage of CO_2, placement of injection and production wells were optimized in a saline aquifer subjected to brine recycling under the constraint of a fixed maximum bottomhole pressure which corresponds to the breakthrough pressure of the cap-rock. Contrary to previous well placement optimization studies, in this study the target geological formation is a confined saline aquifer, permeability is heterogonous (10 - 100 md), and wells for CO_2 and brine injection are horizontal. TOUGH2-ECO2N and an iterative Latin hypercube sampling optimization method were employed for the multiphase flow and optimization calculations, respectively. Optimization variables included the locations of two CO_2 injection wells and one brine production well, as well as the injection rate of CO_2. The total volume of the geological model is 20 km $\times$ 20 km $\times$ 0.1 km which has 4 layers initially containing only brine at a temperature of 40 ℃ and pressure of 10 MPa at the top layer. Simulations were performed for 30 years of CO_2 injection at rates of 5 - 20 kg/s, and 10 years of brine production and/or recycling. The two injection wells for brine recycling were located above the two CO_2 injection wells.

Optimizations of wells placement were performed for two scenarios: 1) injection of CO_2 without brine recycling, and 2) injection of CO_2 with brine recycling. Our optimization results indicate that placing brine injection wells above CO_2 injection wells in conjunction with equal fractions of brine recycling and CO_2 injection to each well leads to highest amounts of dissolution and residual trapping of CO_2. The trapping of CO_2 was improved by 5.4% with brine recycling in comparison to the trapping of CO_2 obtained without recycling (13.26 Mt). Although CO_2 was confirmed to be produced along with brine from production wells located near the injection wells, placement of the production well has shown to have little to no affect on the trapping of CO_2 under the given conditions. With regard to the optimal placement of injection wells, 3 and 6 potential areas were clearly identified for scenario 1 and 2, respectively. It is theorized that heterogeneous permeability formations may have multiple local optima; however this is yet to be confirmed.

Keywords: CO2 geological storage, Well placement, Brine recycling, Optimization

Japan Geoscience Union Meeting 2014
(28 April - 02 May 2014 at Pacifico YOKOHAMA, Kanagawa, Japan)

HRE31-09 Room:419 Time:May 2 11:45-12:00

Reservoir Rocks of CO2 Micro-Bubble Storage (CMS) and its Dissolution Characteristics

SUZUKI, Kenichirou[1*] ; MIYOSHI, Satoshi[1] ; HITOMI, Takashi[1] ; OKUZAWA, Koichi[1] ; MIIDA, Hideaki[2] ; YUKI, Noriyuki[2]

[1]Obayashi Corporation, [2]Engineering Advancement Association of Japan (ENAA)

Among many different portfolios in the CCS technology, CO2 micro-bubble storage (CMS) system that stores CO2 by injection in the gas phase and dissolution at shallower depths has been proposed. Basic concept of CMS is the replacement of underground water with CO2 dissolved water. CO2 is stored safely once it is dissolved and there is low leakage risk because of residual micro-bubbles having little buoyancy forces. CO2 dissolved in water is weakly acidic and can react with the minerals in the surrounding rocks. It is well-known that acidic solution is neutralized by rocks as it soaks into the ground, however the ability of neutralization is not completely estimated.

In this paper, in order to estimate the ability of rocks to neutralize CO2 micro-bubble dissolved water, two types of dissolution experiments of rocks were carried out using crashed and column specimens of sedimentary rock such as limestone, sandstone, and tuff. A batch type dissolution experiment in which rock samples were treated with the solution of CO2 dissolved in pure water using micro-bubble under CO2 partial pressure 0.0003 atm. And a flow-through type dissolution experiment was carried out using limestone samples for over 40 days in order to investigate the change of pore structure between before and after experiment. From these experimental results, the dissolution rate and the ability of neutralization of reservoir rocks were discussed.

Japan Geoscience Union Meeting 2014
(28 April - 02 May 2014 at Pacifico YOKOHAMA, Kanagawa, Japan)

HRE31-10 Room:419 Time:May 2 12:00-12:15

Dawsonite synthesis/dissolution experiment under the relevant condition of CO_2 underground storage

TAKAYA, Yutaro[1] ; NAKAMURA, Kentaro[2*] ; KATO, Yasuhiro[1]

[1]Frontier Research center for Energy and Resoueces (FRCER), Graduate School of Engineering, Universit, [2]Department of Systems Innovation, Graduate School of Engineering, University of Tokyo

Geochemical trapping is a mechanism for defining the longer-term security of CO_2 underground storage. Especially, mineral trapping improves the storage security by the transformation reaction of injected CO_2 (liquid or supercritical phase) to carbonate minerals.

Recently, several studies based on the computer simulation predicted the formations of dawsonite ($NaAlCO_3$ $(OH)_2$) as an initial phase of mineral trapping and that dawsonite may play important role for the storage security in the early stage of CO_2 storage. However, it has not been reported the formation of dawsonite in the experiments under the relevant condition of the CO_2 underground storage to date and the problem "whether dawsonite will be formed in the CO_2 reservoir and will contribute the improvement of the CO_2 storage security" is still remaining.

In this study, therefore, we conduct the synthesis/dissolution experiments of dawsonite under the CO_2 reservoir condition and discuss the formation/preservation condition of dawsonite. We further discuss the possibility of dawsonite formation in the CO_2 reservoir based on our experimental results.

Keywords: CO_2 underground storage, mineral trapping, dawsonite

Japan Geoscience Union Meeting 2014
(28 April - 02 May 2014 at Pacifico YOKOHAMA, Kanagawa, Japan)

HRE31-11 Room:419 Time:May 2 12:15-12:30

Liquid carbon dioxide storage beneath man-made hydrate-seal layers

OHSUMI, Takashi[1*] ; SHIDAHARA, Takumi[2]

[1]School of Science, Tokai University, [2]NEWJEC Inc.

The findings by Sakai *et al.* (1990) that carbon dioxide (CO_2) hydrate occurs on the Okinawa Trough seafloor of 1,335m in depth and at a temperature of 3.8^{o}C stimulated the research on how to isolate the anthropogenic CO_2 from the atmosphere. Various offshore sites under the CO_2-hydrate stable conditions, *i.e.* above 4.4MPa and below 10^{o}C, are found in the Japan Archipelago. Above all, there are ten or more places where from the coastline the ERD well can make a direct access to the sub-seabed under the CO_2-hydrate stable conditions (Ohsumi, 2012). Sakai *et al.* postulated that CO_2 hydrate fills in the pore of the sediment right beneath the sea bottom, which can be explained by the fact that the density of $CO_2 \bullet nH_2O$ as calculated to be 1.07 ~ 1.04 g cm^{-3} corresponding to n = 7 ~ 8, is larger than that of the bottom seawater, and hence the even thin hydrate layer functions as a barrier for the underlain fluid (its estimated density is 0.92 g cm^{-3}) composed mainly of liquid CO_2 tending to leak to the bottom waters.

Koide *et al.* (1997) pointed out that the formation of CO_2 hydrate in pores and gaps, in rocks and sediments, could almost completely block the migration of fluid. CO_2 that is injected into a deep reservoir would migrate upward into cooler aquifers and eventually form a CO_2 hydrate cap. Numerous engineering studies thereafter were targeted at how such a sealing layer can be created in the CO_2 storage site. It should be noted that CO_2 hydrate exposed to the open bottom water will be dissolved easily even under the low-temperature, high-pressure stable conditions. Nevertheless, in his examination on how underwater pavement operation could realize the CO_2-hydrate storage beneath seabed, Ohsumi (2012) illustrated that a 1-m thick sediment layer would be enough to serve as an effective barrier. Since the solute CO_2 diffusion in sediment pores between the hydrate layer and the sea-bottom is rate-limiting, the seepage flux of CO_2 would be below 0.1 kgCO_2 m^{-2} per year.

There is an offshore steep slope to the Sagami Trough at the north-east coast of the Izu-Oshima Island. A 440-m isobath is near to the shoreline (the nearest point is 1.1 km offshore) and hence due to the fact that the sea bottom temperature will not exceed 10^{o}C throughout the year, the CO_2-hydrate stable conditions spread over the offshore bottom and its sub-seabed. The offshore geology consists of ”old volcano” bodies, several hundred thousand years of age, of which volcanism is probably similar to the present volcano of the Izu-Oshima Island. Hence, we can suppose that it is composed of alternating layers of basalt lava and pyroclastic rocks. When the pores of horizontally permeable layers are filled with CO_2 hydrate, the underlain formations can hold the liquid CO_2 for storage. Ikegawa *et al.* (2012) proposed the injection method of CO_2-in-water emulsion applicable to the sedimentary layers for the purpose of enhanced recovery of methane hydrate. By their method, while avoiding hydrate blockage in the horizontal pore space flow, as shown in Figure we might be able to create the effective CO_2-hydrate seal layers with a large area coverage. A horizontal coverage of the supposed storage site could be 5×1 km. When storage layers with 200-m effective thickness are selected, 10% of the effective pore volume ratio for liquid CO_2 storage gives 100 million tCO_2 as an attractive storage potential.

Ikegawa, Y *et al.* (2012) *CRIEPI Report* N11024 (in Japanese with English abstract); Koide *et al.* (1997) *Energy* **22**(2/3) 279-283; Ohsumi, T (2012) The 23rd Ocean Engineering Symposium (in Japanese with English abstract); Ohsumi,T (2013) *2013 Fall meeting Programme and Abstracts* (in Japanese) 152-154; Sakai *et al.* (1990) *Science* **248,** 1093-1096.

Keywords: man-made seal layer, CCS, hydrate seal, Izu-Oshima Island, Extended Reach Drilling, CO2-in-water emulsion

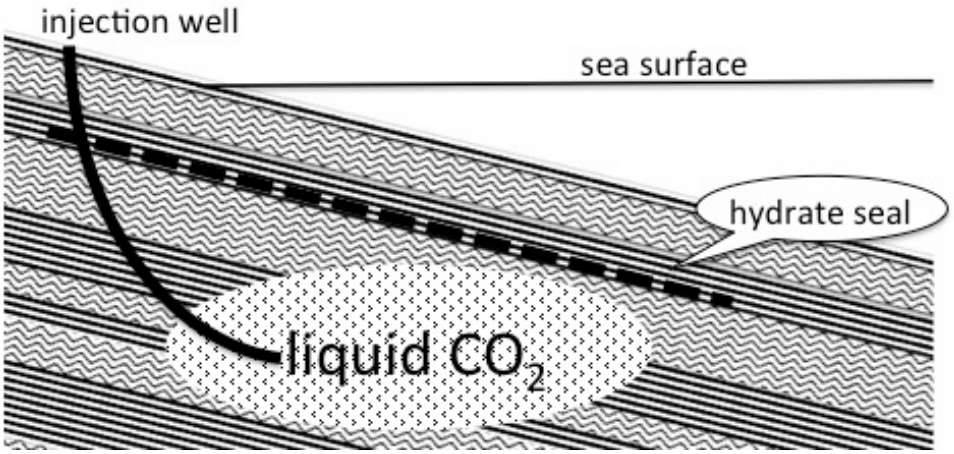

Japan Geoscience Union Meeting 2014
(28 April - 02 May 2014 at Pacifico YOKOHAMA, Kanagawa, Japan)

HRE31-P01 Room:Poster Time:May 2 16:15-17:30

Use of sodium polytungstate as an X-ray contrast agent to reduce beam hardening in hydrogeological experiments

NAKASHIMA, Yoshito[1*]

[1]AIST

Iodine is conventionally used as a contrast agent in hydrogeological experiments using polychromatic X-ray computed tomography (CT) to monitor multi-phase Darcy flow in porous geological media. Undesirable beam hardening artifacts, however, make the quantitative analysis of the obtained CT images difficult. CT imaging of porous sand packs saturated with iodine and tungsten-bearing aqueous solutions, respectively, was performed using a medical CT scanner. The result (Fig. 1) shows that sodium polytungstate ($Na_6H_2W_{12}O_{40}$) significantly reduced the beam hardening compared with potassium iodide (KI). This result is due to the location of the K absorption edge of tungsten, which is nearer to the peak of the polychromatic X-ray source spectrum than that of iodine. As sodium polytungstate is chemically stable and less toxic than other heavy element bearing compounds, we recommend it as a promising contrast agent for hydrogeological CT experiments.

Acknowledgements:
The medical CT experiment was performed under the cooperative research program of Center for Advanced Marine Core Research (CMCR), Kochi University (13B034) with the support of JAMSTEC.

References:
Nakashima, Y. and Nakano, T. (2012) Analytical Sciences, 28, 1133-1138. http://dx.doi.org/10.2116/analsci.28.1133
Nakashima, Y. (2013) Journal of Hydrology and Hydromechanics, 61, 347-351. http://dx.doi.org/10.2478/johh-2013-0043
Nakashima, Y. and Nakano, T. (2014) Journal of X-Ray Science and Technology, 22, 91-103. http://dx.doi.org/10.3233/XST-130411

Keywords: beam hardening, contrast agent, Darcy flow, porous media, multi-phase flow, relative permeability

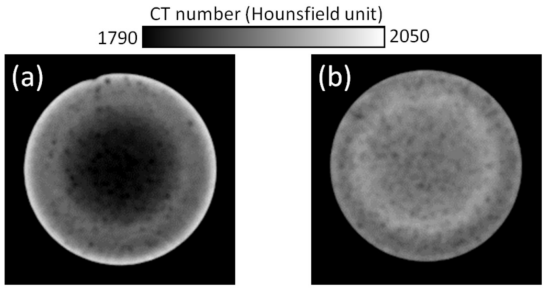

Fig. 1. Two-dimensional CT slices of homogeneous sand pack samples (diameter, 56 mm) saturated with a heavy-element-bearing fluid. Each image dimension is 210^2 voxels = 66^2 mm^2. The image for KI 9.16 wt.% (a) shows marked beam hardening compared with $Na_6H_2W_{12}O_{40}$ 8.80 wt.% (b). Numerous dark spots are small bubbles.

Japan Geoscience Union Meeting 2014
(28 April - 02 May 2014 at Pacifico YOKOHAMA, Kanagawa, Japan)

HRE31-P02 Room:Poster Time:May 2 16:15-17:30

Gravity monitoring at the Farnsworth CO2-EOR site, TX

SUGIHARA, Mituhiko[1*] ; NAWA, Kazunari[1] ; SOMA, Nobukazu[1] ; ISHIDO, Tsuneo[1] ; MIYAKAWA, Ayumu[1] ; TANAKA, Akiko[1] ; NISHI, Yuji[1]

[1]AIST

Time-lapse gravity measurements with a combination of absolute and relative observation array will reduce uncertainties caused by regional gravity variations. The technique is called hybrid gravity measurement. By adding continuous measurement with a superconducting gravimeter (SG) to the hybrid system we are applying the super-hybrid gravity monitoring at the Farnsworth unit (FWU) in TX along with SWP. We started baseline measurement in January 2013. Using SG and barometric data at FWU, we obtained average gravity-atmosphere admittances. The observed admittances during storms can be far from the mean admittance. We often observed several outstanding responses to atmospheric pressure changes. Comparing with precipitation, soil moisture and atmospheric pressure the residuals were attributed to hydrologic components and/or local atmosphere admittance. Several circular irrigation systems work at FWU. At each system water is pumped from a nearby well to the center of the system. The process will result in the redistribution of mass which may result in gravity signals. Basically the booms rotate to cover the circular field over an approximately three day cycle during agricultural season, however the exact watering pattern varies from field to field. We have tried to monitor the watering effects.

This research is funded and supported by Ministry of Economy, Trade and Industry (METI).

Keywords: Fansworth, CO2-EOR, gravity monitoring, superconducting gravimeter

Japan Geoscience Union Meeting 2014
(28 April - 02 May 2014 at Pacifico YOKOHAMA, Kanagawa, Japan)

HTT07-01 Room:422 Time:April 28 09:00-09:15

Analysis of topographical characteristics of flooded areas for constructing simple warning system of pluvial flooding

SATO, Rina[1*] ; OGUCHI, Takashi[2]

[1]Graduate School of Frontier Science, The University of Tokyo, [2]CSIS, The University of Tokyo

Pluvial flooding is a major disaster in Japanese urban areas. Physical models are often used for assessing pluvial flood risk, but the models are complex. Therefore, this study aims to analyze topographical characteristics of flooded areas in the 23 wards of Tokyo as the basis for constructing a simple warning system. At first, we extracted four factors as topographical characteristics: depression depth, catchment volume, elevation difference and slope using a digital elevation model (DEM) for the whole study area, but there were some problems when the methods were simply applied to the DEM. Accordingly, we extracted the factors only for roads, and then compared the obtained values for flooded and non-flooded areas. According to t-test, there were significant differences between the two types of areas for all factors. However, similar values sometimes occur for these areas, indicating that not only topography but also rainfall and drainage systems should be analyzed in future work.

Keywords: pluvial flooding, topographical characteristics, road, DEM, GIS

Japan Geoscience Union Meeting 2014
(28 April - 02 May 2014 at Pacifico YOKOHAMA, Kanagawa, Japan)

HTT07-02 Room:422 Time:April 28 09:15-09:30

Effect of the definition of a single rainfall event on the rainfall threshold of mass movements

CHEN, Chiwen[1*] ; OGUCHI, Takashi[1]

[1]Department of Natural Environment Studies, The University of Tokyo

This study analyzes mass movements caused by rainstorm and typhoon events in Taiwan during 2006 to 2012. Data for 263 mass movement events were collected from the reports of the Soil and Water Conservation Bureau of Taiwan, including 172 landslides and 107 debris flows caused by nine frontal rainstorm events and 15 typhoon events. After checking the location of each event, we compiled relevant rainfall data by interpolating data from the surrounding rain gauges. This approach is useful to analyze rainfall conditions for the events and discuss the mechanism of the rainfall-induced mass movements. This study uses two different definitions of a single rainfall event in relation to the triggering of mass movements. One is defined as a period from the time when hourly rainfall becomes greater than 4 mm to the time when the hourly rainfall becomes less than 4 mm for the next six consecutive hours. The other is defined as a period delimited by a non-rainfall period of more than 24 h. These two definitions gave significantly different results concerning the rainfall condition of mass movements. The first definition represents higher rainfall intensity, shorter duration and less cumulative rainfall. The second definition represents lower intensity, longer duration and more cumulative rainfall. We also used the rainfall intensity-duration (*I-D*) relationship from these two definitions to establish two *I-D* thresholds of mass movements in Taiwan. Comparing the thresholds from this study to those for Taiwan and Japan from previous studies, we found that the definition of a single rainfall event and the number of data are two important factors affecting the rainfall threshold of mass movements.

Keywords: mass movements, rainfall event, landslides, debris flows, I-D threshold

Japan Geoscience Union Meeting 2014
(28 April - 02 May 2014 at Pacifico YOKOHAMA, Kanagawa, Japan)

HTT07-03 Room:422 Time:April 28 09:30-09:45

Implementation of Random Forest in landslide susceptibility study, a case study of the Tokamachi area, Niigata, Japan

PAUDEL, Uttam[1*] ; OGUCHI, Takashi[2]

[1]Graduate School of Frontier Sciences, The University of Tokyo, [2]Center for Spatial Information Science, The University of Tokyo

Random Forest (RF), a bagged trees ensemble, is widely appreciated for its superiority amongst classification algorithms and is popular in various fields of data mining. However, the application of RF in susceptibility analysis of landslide hazard remains very limited. This study highlights the results of such an attempt. The study area was selected on the basis of landslide density distribution. A density map of landslide distribution in Japan was prepared from the landslide inventory provided by the National Research Institute for Earth Science and Disaster Prevention (NIED). The Tokamachi area in Niigata Prefecture has a very high density of events and was thence selected for this study. Seven topographic factors (aspect, curvature, drainage density, elevation, plan curvature, profile curvature, and slope) derived from the 10 m DEM obtained by the Geospatial Information Authority of Japan (GSI) were used for the analysis. The classification data concern 9747 landslide events and 20685 randomly generated instances from the areas with no landslides. Unlike the values of a centroid used in many other studies, each landslide event in the classification data was represented by a mean of values of the respective factors in each landslide feature. Information gain for each factor was also evaluated and it was found that the profile curvature is the most effective factor in classifying landslides in the area, whereas elevation is the least effective. A 10-fold cross validation of the RF model with 200 trees resulted in an 'out of bag error' of 0.1443, an accuracy of 85.87%, and an ROC area of 0.926. These results suggest the suitability of RF in susceptibility analysis, the stability of which can be further strengthened with an increase of factors and the number of trees.

Keywords: Landslide susceptibility, GIS, Machine learning, Random Forest

Japan Geoscience Union Meeting 2014
(28 April - 02 May 2014 at Pacifico YOKOHAMA, Kanagawa, Japan)

HTT07-04 Room:422 Time:April 28 09:45-10:00

Viewshed analysis of the trails in SriPada mountain area in Sri Lanka

SIRIWARDANA, Halgamage malinda[1*]

[1]University of Tsukuba

Each year about 3 millions of people climb SriPada Mountain. The trail system around SriPada in the Peak Wilderness has been used over centuries in good harmony. According to local people, there used to be 18 trails to reach the top of SriPada Mountain. Some of those trails were rarely used and thus getting vanished over time. This research focuses on analyzing Viewshed and the flow of people alone some of the trails.

Japan Geoscience Union Meeting 2014
(28 April - 02 May 2014 at Pacifico YOKOHAMA, Kanagawa, Japan)

HTT07-05 Room:422 Time:April 28 10:00-10:15

Geospatial analysis of deforestation factors in central Cambodia after 2000s

MATSUURA, Toshiya[1*] ; MIYAMOTO, Asako[1] ; KURASHIMA, Takayuki[1] ; SANO, Makoto[2] ; CHANN, Sophal[3] ; PAK, Chealy[3] ; LENG, Chivin[3]

[1]FFPRI, [2]Forestry Agency, [3]Forestry Administration Cambodia

Reducing emissions from deforestation and forest degradation; and the role of conservation, sustainable management of forests and enhancement of forest carbon stocks in developing countries (REDD-plus) have attracted interest in Southeast Asian countries where deforestation has been a serious issue. To estimate future deforestation, the REDD-plus requires analyses of trends in land cover changes and the effects of various factors including infrastructure development, national policies and natural environment such as topographic conditions. This study analyzed the spatial characteristics and important factors of recent deforestation by taking eastern Kompong Thom, central Cambodia as an example.

We used three periods (i.e., 2002, 2006, 2010) of forest cover maps produced by Cambodian Forestry Administration (FA) and an object-based image analysis map made from Landsat 8 imagery taken in January 2014. We examined three types of geographic factors, namely, (1) distances from roads, rivers/water bodies, settlements, and forest edges (2) terrain features, e.g., gradient and relative slope position generated from 90-m SRTM DEM, and (3) zoning categories such as forest concession, economic land concession (ELC), community forestry and protected forest, in order to clarify the trend and explanatory variables of deforestation. All the spatial data were converted into 90 m resolution raster. A generalized linear model (GLM) with logit link function (i.e., logistic regression) was then used to analyze the effect of each factor on deforestation.

Between 2002 and 2006, deforestation mainly occurred in canceled forest concessions. During the period 2006-2010, this trend of deforestation accelerated particularly in and around the newly designated ELCs for rubber plantation. After 2010, deforestation further increased due to the development of small-scale agriculture by local farmers in addition to the newly designated ELCs. Factors consistently selected during the study periods with negative effects were “ forest concession ” and “ distance from forest edge ” . These indicate that deforestation occurred more readily in the canceled forest concessions and closer to forest edges. The magnitude of the effect of “ distance from roads ” has become smaller, indicating that recent deforestation occurred more in the forest interior. Gradient had a negative effect, highlighting the difficulties in farming on slopes. Community forestry and the protected forest established by the FA from the late 2000s also had negative effects on deforestation, indicating that these zoning have their value for forest conservation.

Keywords: REDD-plus, land use/cover change, generalized linear model, GIS

Japan Geoscience Union Meeting 2014
(28 April - 02 May 2014 at Pacifico YOKOHAMA, Kanagawa, Japan)

HTT07-06 Room:422 Time:April 28 10:15-10:30

ENSEMBLE-CELLULAR AUTOMATA (CA) MODELS FOR IMPROVING FOREST COVER CHANGE SIMULATION

KAMUSOKO, Courage[1*]

[1]Asia Air Survey Co., Ltd

Reliable spatial simulation models are a prequisite for understanding temporal and spatial forest cover changes. However, spatial simulation models require accurate transition potential maps, which represent the probability of change from one forest cover class to another. Previous studies have shown that conventional methods such as logistic regression, weights-of-evidence and neural networks fail to adequately model forest cover transition potential. The objectives of this study are to: (1) evaluate the performance of adaboost (AB) and random forests (RF) algorithms for computing transition potential maps, and (2) simulate forest cover changes using the computed transition potential maps and cellular automata (CA) model. Our results show that adaboost-CA and random forest-CA models produced better simulation accuracy than logistic regression/ weights of evidence-CA models. These results provide valuable insights, which can be used to improve transition potential modeling and forest cover change simulation in complex landscapes.

Keywords: Adaboost, Random forests, Cellular automata, Transition potential, Forest cover changes

Japan Geoscience Union Meeting 2014
(28 April - 02 May 2014 at Pacifico YOKOHAMA, Kanagawa, Japan)

HTT07-07 Room:422 Time:April 28 10:30-10:45

Capacity building initiative for satellite data utilization for evaluation of environmental degradation using FOSS4G

IWASAKI, Nobusuke[1*] ; MORI, Toru[3] ; HESHIKI, Kanetaka[3] ; KAYAMA, Yoichi[4] ; FURUHASHI, Taichi[5] ; MASUMOTO, Shinji[2] ; YONEZAWA, Go[2] ; YOSHIDA, Daisuke[2] ; RAGHAVAN, Venkatesh[2]

[1]National Institute for Agro-Environmental Sciences, [2]Osaka City University, [3]Orkney Inc., [4]Aero Asahi corp., [5]MAPconcierge

Recently, satellite image data become more and more easily accessible. For example, NASA provide MODIS and LANDSAT data as Open Data. ESA will provide Sentinel data free and open access for any user. In addition, GIS data will also become accessible under the influence of the global trend of promoting Open Data. In such circumstance, a demands for utilizing satellite images and GIS also have been growing steadily and widely. But, it is still complicated to get original satellite data and how to deal with it for for the non-specialist, such as public employees.

Under such circumstances, Ministry of Education, Culture, Sports, Science and Technology in Japan (MEXT) has considered the plan of removing the barriers on satellite data usage. From 2009 to 2014, we have taken part in this project, and have strived to overcome this problem through the following three points.

1. Developing the Free & Open Source Software for Geospatial (FOSS4G) tools, such as GRASS, QGIS, GDAL/OGR and Proj.4.
2. Making tutorial about processing and analyzing the satellite data with FOSS4G tools.
3. Constructing the e-learning contents of satellite data usage and conducting outreach activity and capacity building in not only Japan but also developing countries.

(cf. http://www.osgeo.jp/foss4g-mext)

In first three years, main targets of our project were Japanese and novice user. We translate QGIS and GRASS GIS menu and manuals into Japanese and improve such FOSS4G tools to adapt Japanese data format and projection. Also, basic and advanced the tutorials for satellite data utilization were published as e-book and e-learning system including video tutorials.

The software and knowledge base have been rapidly improved by our works. These achievements are anticipated to expand base of satellite data users and to create a new utilization scene for space derived products. One of the effective results from this project was shown in actions against the Tohoku Earthquake in 2011. Many people could collaborate on that software base and offered ortho-image of Tohoku region (i.e. Iwasaki et al. 2011, GISA-Japan).

Based on previous result, we are started next project to develop an evaluation system for environmental degradation based on above GRASS and QGIS. In the project we use Global Map (http://www.iscgm.org/cgi-bin/fswiki/wiki.cgi) as a fundamental information for evaluating environment. The project had started from 2102 and focused on natural hazard and environmental degradation, especially in developing countries. We will report the status and progress of the project.

Keywords: FOSS4G, Satellite data, Capacity building

Japan Geoscience Union Meeting 2014
(28 April - 02 May 2014 at Pacifico YOKOHAMA, Kanagawa, Japan)

HTT07-08 Room:422 Time:April 28 11:00-11:15

Assessment of Natural Landscape Resources for Tourism Development in Hangzhou, China

ZHAO, Wenqi[1*]

[1]University of Tsukuba

This study aims to establish criteria based on various factors and then provide comprehensive assessment to the value of main natural landscape resources in Hangzhou, China. Twenty-two attractions in Hangzhou are selected to be the research objects of this study. Also, eight factors are selected as the criteria of this study, which are general scientific value, rarity, aesthetic value, integrity, scale, popularity, transportation and hotels. The model of Analytic Hierarchy Process(AHP) is utilized in this study to determine the weights of the 8 factors.

In order to collect the root data for determining AHP weights, a questionnaire form was sent out to 12 experts. The other data for measuring the 8 factors are collected from the previous papers, census and reports, the websites and pamphlets of the attractions, Google earth, and also collected by questionnaire survey to the public and doing fieldwork. ArcGIS is a supplementary tool for making evaluation with spatial distribution, especially being used when measuring the factors of transportation and hotels. After evaluating the attractions with abstract scores, rank the scores of the 22 attractions and see the spatial distribution with the map.

Hangzhou's natural landscape resources are mainly categorized into volcanic rock, Karst landform, granite, scenery with hills and waters, waterfall scenery, lakes, wetland and rivers. As the result of the assessment, 9 of the 22 attractions comprehensively have high value, and 10 of them have medium value, and the left 3 have low value. Hangzhou is originally famous for the West Lake, however, after the research it is learnt that the west region of Lin'an city also has abundant natural landscape resources with remarkable value, where should be paid more attention in the future development and preservation. As the suggestion to the future, it is better to construct more nature preserves and Geoparks in Hangzhou.

Keywords: Hangzhou, tourism, natural landscape resources, AHP, evaluation

Japan Geoscience Union Meeting 2014
(28 April - 02 May 2014 at Pacifico YOKOHAMA, Kanagawa, Japan)

HTT07-09 Room:422 Time:April 28 11:15-11:30

Tsunami Vertical Evacuation Sites: A Case Study of Shizuoka City

VOULGARIS, Gerasimos[1*]

[1]University of Tsukuba, Graduate School of Life and Environmental Sciences

The City of Shizuoka directly faces the Nankai Trough which has given two M8.1 earthquakes in modern history (1944 and 1946), which were tsunamigenic. After the great Tohoku earthquake the Japanese government updated its worst case scenario for a tsunami from the Nankai trough, which is expected to have a maximum run-up of 34m. This study aims to use GIS in order to locate vertical evacuation sites in the City of Shizuoka within the existing urban structure, and to assess their potential in supporting the population for immediate evacuation under an extreme 34m run-up tsunami event. This study is still in its initial phase, however, spatial analysis of the current designated evacuation locations in the city indicates that under extreme circumstances only a very small minority of sites would remain if such an extreme tsunami were to happen. Therefore, there is an apparent need to investigate for new evacuation sites that will be suitable even under a tsunami of great magnitude.

Keywords: Tsunami, Vertical Evacuation, Shizuoka City, GIS

Japan Geoscience Union Meeting 2014
(28 April - 02 May 2014 at Pacifico YOKOHAMA, Kanagawa, Japan)

HTT07-10 Room:422 Time:April 28 11:30-11:45

Spatial Analysis of Urban Accidents; A Case Study of Tehran,Iran

HAJI MIRZA AGHASI, Niloofar[1*]

[1]The University of Tsukuba. Spatial Information Science Division

Road accidents may be seen as discrete promote events, localized in space and time. The most important objective of the study was to identify the spatial pattern of urban accidents in Tehran city in order to finding the causes and consequences as well as the temporal and spatial variation of accidents. Based on spatio-temporal data analysis method, this paper aims to analyse traffic accidents data in time and space. The spatial relationship between time of daily activities which generate trips and urban traffic accidents is examined and applied to Tehran for 2010˜2011.

The research was based on different primary and secondary data sources, which include locations of accidents and many rich attribute such as date, reason, kind, etc. Questionnaires were distributed to 600 drivers in the study area in order to gather data about drivers' knowledge, beliefs, attitude and behaviours. GIS software was used in this study and different maps were made using GIS Arc view 10.2. Tehran urban accidents point by point data with different attributes was collected from Police Department of Islamic republic of Iran, Tehran. These rich accident data were used as source of information and data analysis. The study considered different factors in urban traffic accidents. These include environmental, human and cultural factors, etc. this study stated that the concentration of educational, commercial and cultural activities that make large number of urban trips and road usage and traffic volume in peak hour and road type are among the main causes of the urban accidents in Tehran city. The spatial distribution and variation of Tehran's urban accidents indicated those accident occurrences are highly concentrated along the residential, primary, and secondary roads as well as dense in highways and freeways. This study also shows the relations ship between the occurrences of accidents with peak hours of the day. Highways and freeways are the most dangerous road type in road type variation in Tehran city. And the key reason of accidents in these road types is high speed. High occurrences of urban accidents were caused by culture and behaviour of not only drivers but also all users of the roads. It has been recommended that the improvement of knowledge and culture by education through the public Medias and the rules for offenders must be reissue soon.

Keywords: GIS, Urban Traffic Accidents, Peak time, Road Type

Japan Geoscience Union Meeting 2014
(28 April - 02 May 2014 at Pacifico YOKOHAMA, Kanagawa, Japan)

HTT07-11 Room:422 Time:April 28 11:45-12:00

Historical changes in land price formation factors over 100 years in Kyoto, Japan: comparison of the land price distribu

AOKI, Kazuto[1*] ; TAKEDA, Koji[2] ; YANO, Keiji[3] ; NAKAYA, Tomoki[3]

[1]Research Center for Disaster Mitigation of Urban Cultural Heritage, Ritsumeikan University, [2]PASCO CORPORATION, [3]Ritsumeikan University

The land price formation factor is an index, which shows the social economy situation of the time.

Although a large number of studies have been made on evaluating land price formation factors which show socio-economic situations, most of the studies have been cross-sectional analysis focusing on specific factors, such as zoning, road width and accessibility to public transportation. Little attention has been paid to historical changes of land price formation in a long-term perspective, mainly because of the lack of historical data representing land price distribution in the past. Fortunately, the Kyoto cadastral map made in 1912 was digitized to create the historical GIS database containing detailed land price information for each land parcel by the GIS research team at Ritsumeikan University. It should be noted that the city has not received large-scale disasters and war damages since the age of the cadastral map. We can thus investigate historical changes of the city without effects of such large-scale disasters. Comparing the current land price distribution with that in early 20th century in the city of Kyoto, we examine historical changes in the geographical factors of land price formations reflecting changes in urban physical and social formations of the city. With the aid of GIS-based mapping and overlay analysis, we mainly argue on the effects of the changes in urban formation on land price distributions over 100 years in the city.

The land price formation factors of quantitative getting are road width and distance from the train station is easy.However, quantitative getting of ambiguous land price formation factor represented by downtown property is difficult.In this study, for the understanding of land price formation factor of 100 years ago, take advantage of old photographs.

Keywords: Kyoto cadastral map, land price formation factor, old map

Japan Geoscience Union Meeting 2014
(28 April - 02 May 2014 at Pacifico YOKOHAMA, Kanagawa, Japan)

HTT07-12 Room:422 Time:April 28 12:00-12:15

Spatio-Temporal Analysis of Bicycle Commuting Behavior in the Greater Tokyo Area Using a Micro-Scale Persontrip Database

GREGER, Konstantin[1*] ; MURAYAMA, Yuji[1]

[1]University of Tsukuba, Division of Spatial Information Science

Compared to other nations, the share of motorized individual traffic in the daily commuting flows in Japan is rather low. Instead, the share of railway transportation is significantly higher. In addition, this generates feeding traffic from homes and workplaces to and from the stations, which is done mostly on foot or by bike. This holds especially true for highly urbanized areas, such as the Greater Tokyo Metropolitan Area with its 34 million inhabitants, which we use as a study area in this paper.

Here we investigate the role and structure of the use of bicycles in the course of commuting traffic. This paper provides a thorough spatio-temporal analysis of bicycle behavior, since we analyze how bicycles are used in the daily commutes, by whom, and where. We investigate how bicycles are integrated in the commuting process and what spatial factors determine the use of bicycles.

For this paper we employ a massive micro scale person trip database provided by the Center for Spatial Information Science at the University of Tokyo. It contains sociodemographic data about approximately 600,000 sample individuals, as well as information about the purpose of each of their trips, their chosen means of transportation (e.g. car, bus, bike, etc.) and their location in 1-minute steps over all 24 hours of one sample day.

As the scientific discourse about bicycle traffic in Japan is scarce, we hope to be able to contribute by this study and provide valuable insights into this important mode of transportation.

Keywords: bicycle, big data, commuting, gis, japan, tokyo

Japan Geoscience Union Meeting 2014
(28 April - 02 May 2014 at Pacifico YOKOHAMA, Kanagawa, Japan)

HTT07-13 Room:422 Time:April 28 12:15-12:30

Geospatial analysis of land changes in the megacities of Southeast Asia

ESTOQUE, Ronald[1] ; MURAYAMA, Yuji[1*]

[1]Graduate School of Life and Environmental Sciences, University of Tsukuba, Japan

The advancements of remote sensing and geographic information systems technologies enable us to monitor land changes at various spatial and temporal scales, and analyze the implications of such changes from different perspectives. This study assesses the spatiotemporal patterns of land changes in the megacities of Southeast Asia, namely Bangkok (Thailand), Jakarta (Indonesia) and Manila (the Philippines). The goal is to gain better understanding on the land transformation process in each megacity, which may be useful from the perspective of sustainable landscape and urban planning. Remote sensing data were used to develop land cover maps for the megacities across three epochs, i.e. t1-1990, t2-2000 and t3-2010. A hybrid classification method that integrates pixel-based and object-based techniques was employed in land cover classification. Transition matrices for the two time intervals (t1-t2 and t2-t3) were computed and geospatial tools and techniques were applied in order to reveal the spatiotemporal patterns of land changes in each megacity. The implications of the findings for future landscape and urban planning in relation to the sustainable development of the three megacities are explored.

Keywords: GIS, Remote sensing, Land change, Urbanization, Megacities, Southeast Asia

Japan Geoscience Union Meeting 2014
(28 April - 02 May 2014 at Pacifico YOKOHAMA, Kanagawa, Japan)

HTT07-P01 Room:Poster Time:April 28 18:15-19:30

Spatial analysis of archaeological sites and landforms in Kayseri, central Turkey using multiscale topographic data

HAYAKAWA, Yuichi S.[1*] ; OBANAWA, Hiroyuki[2] ; NARUHASHI, Ryutaro[3] ; YOSHIDA, Hidetsugu[4] ; ZAIKI, Masumi[5] ; KONTANI, Ryoichi[6] ; SUDO, Hiroshi[7] ; ODAKA, Takahiro[8] ; YAMAGUCHI, Yuji[9] ; KULAKOGLU, Fikri[10]

[1]Center for Spatial Information Science, The University of Tokyo, [2]Center for Environmental Remote Sensing, Chiba University, [3]Earthquake Research Institute, University of Tokyo, [4]Department of Geography, Meiji University, [5]Faculty of Economics, Seikei University, [6]Notre Dame Seishin University, [7]Okayama Orient Museum, [8]Waseda University, [9]Okayama University, [10]Ankara University

Human habitat and cultural activities had been significantly influenced by natural environments including landforms in the prehistoric periods. Assessment of such relationships between palaeoenvironment and artificial remains is therefore crucial in understanding the historic development. Here we examine the nature-human interactive system in the ancient period of Kayseri region, central Anatolia Highland in Turkey, in terms of spatial analysis of the distribution of landforms and archaeological settlements, targeting mainly the period from B.C. 3000 to A.D.100. We perform geospatial analyses based on several topographic data including topographic maps, satellite-based remote sensing (10 m DEM derived from PRISM sensor images on ALOS), ground-based laser rangefinder measurement with global navigation satellite system (LRF + GNSS) and ground-based structure from motion multi-view stereo photogrammetry (SfM-MVS). The topographic data at different levels of scales provides both regional- and local-scale views of landform conditions, landform classifications, and detailed characteristics of settlements. Certain effects of gradual and sudden changes in palaeoenvironment on human activities are detected, and potential of natural disasters in the study area is also discussed.

Keywords: geoarchaeology, landform classification, digital elevation models, structure from motion

Japan Geoscience Union Meeting 2014
(28 April - 02 May 2014 at Pacifico YOKOHAMA, Kanagawa, Japan)

HTT08-01 Room:415 Time:April 29 16:15-16:30

Estimation of ground displacements by Geomorphic Image Analysis, using multi-temporal LiDAR DEM

MUKOYAMA, Sakae[1*] ; HOMMA, Shin'ichi[1]

[1]Kokusai Kogyo Co., Ltd.

In the previous study, authors developed the new method which applies the technique of image matching analysis with high resolution DEM over difference times, to estimate the minute ground displacement of less than 1m order quantitatively and easily (Mukoyama et al., 2009 and Mukoyama, 2011). The present study shows the results of subsequent case studies to measure crustal movement, earthquake fault displacements, and the movement of landslides. Additionally we will show the results of comparative verification with some field observations by GNSS stations.

There are two approaches for the calculation of ground displacements from geomorphic point cloud data which is acquirable by temporal high-resolution LiDAR survey. Iterative Closest Point (ICP) is the method for 3D-matching by iterative calculation to find the positions which minimize the difference of coordinate values between paired points in the search area. The other approach is the combined methods of 2D-image measurement for estimation of horizontal component and point cloud calculation for vertical component. These two approaches share common process for finding the best position to minimize the difference between points belong the small search window in the temporal data. For this study, we applied the latter approach which is based on the technique of digital image matching analysis using geomorphic image made from grid data of digital elevation model (DEM).

In this method, the existing Particle Image Velocimetry (PIV) algorithm was used for the 2-dimentional image matching. And orthographic slope angle image was used as measurable digital geomorphic image. Although PIV method has been developed generally for fluid analysis, grayscale gradient slope angle image is suitable for PIV analysis as it utilizes the validity of random distribution image of particles in fluid. In order to estimate vertical displacements, the vertical component is available by interpolation of the elevation values of DEM around endpoints of the calculated vector.

In recent study, above-mentioned method was applied to measure ground displacement due to the Great Japan Earthquake in 2011. In the region where liquefaction had damaged the reclaimed land, 10-50cm of lateral displacements were observed in some divided small areas, and seaward deformation of sheet-pile revetment by lateral movement was also observed at the spot on the seaside. After the earthquake, northern part of Japanese Islands moved eastward 6m or less. Verification analysis was conducted in order to compare between the results of Geomorphic Image matching Analysis and GPS observations in the region where temporal LiDAR data and GPS station data was available. Generally both of the results were corresponding with a high correlativity. In the additional study, verification analysis of landslide movement was conducted with GPS observation data; and both of the results were corresponding well with small error range.

The displacement measurement technique by high-definition digital geomorphic image made from high-resolution point cloud survey is effective and simple method, which has the accuracy of about 1/10 pixels or more. It is thought that this method is practicable for measurement of the movement of landslides, earthquake faults, etc.

References

Mukoyama, S., Nishimura, T., Asada, N. (2009) JpGU Meeting 2009 Abstract, Y167-004
Mukoyama, S. (2011) Journal of Mountain Science, Vol. 8, No. 2, pp. 239-245

Keywords: DEM, LiDAR, DEMs of Difference, image matching analysis

Japan Geoscience Union Meeting 2014
(28 April - 02 May 2014 at Pacifico YOKOHAMA, Kanagawa, Japan)

HTT08-02 Room:415 Time:April 29 16:30-16:45

Landslide surface deformation detection by Iwate-Miyagi Nairiku earthquake using 2.5D analysis on SAR interferometry

SATO, Hiroshi, P.[1*] ; MIYAHARA, Basara[2]

[1]Japan Map Center, [2]Geospatial Infomation Authority of Japan

We have already reported landslide surface deformation by 2008 Iwate-Miyagi Nairiku earthquake using Synthetic Aperture Radar interferometry (InSAR) images. In this study, to detect the landslide surface deformation quantitatively in the SE area of Mt.Kurikoma, report the result of 2.5D analysis on the images (i.e., combination of the images observed from ascending and descending orbits).

Keywords: SAR, interferometry, earthquake, landslide, 2.5D analysis

Japan Geoscience Union Meeting 2014
(28 April - 02 May 2014 at Pacifico YOKOHAMA, Kanagawa, Japan)

HTT08-03 Room:415 Time:April 29 16:45-17:00

Evaluation of topographic measurements using UAV- and ground-based SfM and TLS: A case study at a rocky coast bench

HAYAKAWA, Yuichi S.[1*] ; OBANAWA, Hiroyuki[2] ; SAITO, Hitoshi[3]

[1]Center for Spatial Information Science, The University of Tokyo, [2]Center for Environmental Remote Sensing, Chiba University, [3]College of Economics, Kanto Gakuin University

Recent advances in measurement methodologies of high-resolution topographic data, including terrestrial laser scanning (TLS), structure from motion photogrammetry (SfM) on unmanned aerial vehicle (UAV) and ground-based SfM, enabled detailed investigations of land surface morphology in terms of morphometry and processes. Although such advanced methodologies are becoming widely applied in geomorphological studies, the nature of such data including error estimates needs to be carefully assessed when being applied in geomorphological researches. In this study we examine similarities and differences among three methods for the topographic data acquisition at a local scale (˜100 m): UAV-SfM, ground-based SfM and TLS. The study site is a coastal bench at Aburatsubo in Miura Peninsula, central Japan, which suffers from intermittent uplift by large earthquakes such as the 1923 Kanto earthquake (M 7.9). UAV-based SfM was performed from higher altitude (ca. 30 m) to lower (ca. 10 m) using a quadcopter on which a digital camera with single-focus lens is mounted. We also used a digital camera mounted on a 4-m long pole for ground-based SfM. TLS measurement was carried out using a short-range scanner from 6 scan positions. Also, coordinates of three benchmarks on ground that are commonly used in all the methods were measured using global navigation satellite system (GNSS) capable of receiving dual radiowaves and post-processing based on career-phase correction with an accuracy of centimeters. The comparisons of the point clouds and digital elevation models (DEMs) obtained by three different methods indicate that 1) SfM-based data shows good accuracies in and around, but significant discrepancies outside of the benchmarks, 2) TLS sometimes give significant lack of data in shadow areas, and 3) data quality of SfM partly depends on the altitude of its platform (either UAV and pole). These characteristics we assessed will give insights into the selection of appropriate methodology for different purposes of geomorphological surveys.

Keywords: rocky coast, structure from motion, terrestrial laser scanning, point cloud, digital elevation model, accuracy

Japan Geoscience Union Meeting 2014
(28 April - 02 May 2014 at Pacifico YOKOHAMA, Kanagawa, Japan)

HTT08-04 Room:415 Time:April 29 17:00-17:15

Comparative analysis of knickpoint extraction using semi-automatic and automatic methods

ZAHRA, Tuba[1*] ; PAUDEL, Uttam[1] ; HAYAKAWA, Yuichi S.[2] ; OGUCHI, Takashi[2]

[1]Graduate School of Frontier Science, The University of Tokyo, [2]Center for Spatial Information Science

Extraction of knickpoints (or knickzones) from a DEM has gained immense significance in studies of fluvial erosion and/or slope failures because of their geomorphological significance. Previously, knickpoint extraction from a DEM included a vector-based semi-automatic, but somewhat tedious and time-consuming data processing because GIS and spreadsheet software were separately used. Raster-based Python scripting, developed in our study and deployed in the form of a toolset, can automate the processes making the extraction of knickpoints automatically, fast and user friendly. Both the methods are based on the assumption that the slope gradient along a bedrock river changes with change in measurement length and any locally steep segment of the riverbed may then be considered a knickpoint. The relative steepness index R_d or the rate of decrease of gradient along the measurement length is calculated by solving a linear regression equation, $G_d = ad + b$ where, G_d (m m^{-1}) is the stream gradient at a point and d (m) is the measure distance, while a and b are coefficients and $-a$ is regarded as R_d which means the rate of gradient decrease with increasing d. In the former method G_d is measured at the mid-point of a segment of variable length d along longitudinal stream profiles where; $G_d = (e_1 - e_2) / d$ where, e_1 and e_2 are elevations at both ends of the segment, thereby analyzing both the upstream and the downstream segments along a stream. The automated Python processing, however, follows a slightly different approach from the one previously used and thus requires a comparative analysis of the two prior to its future use. The methods differ in the calculation of the stream gradient G_d; the former employs both the upstream and downstream elevations $d/2$ apart, whereas the latter uses the elevation at the point and d downstream. In this study, the Python toolset has been applied to a 10-m DEM of a mountainous region near Mount Ontake in the Northern Japanese Alps. The results were then compared and validated with the previous method. In order to study the fluvial characteristics of the knickpoints, analysis were confined only to the stream locations, the results of which provide insights into morphological developments of the watersheds.

Keywords: automatic extraction, DEM, knickpoints, Python

Japan Geoscience Union Meeting 2014
(28 April - 02 May 2014 at Pacifico YOKOHAMA, Kanagawa, Japan)

HTT08-P01 Room:Poster Time:April 29 18:15-19:30

Structure from motion and multiview stereo (SfM-MVS) in geomorphometry

UCHIYAMA, Shoichiro[1*] ; INOUE, Hiroshi[1] ; SUZUKI, Hinako[1]

[1]National Research Institute for Earth Science and Disaster Prevention (NIED)

Software that unifies structure from motion (SfM) and multiview stereo (MVS) is currently in use. Hence, the construction of three-dimensional models and digital elevation models (DEMs) has been readily achieved at low cost using PCs. Both SfM and MVS are technologies developed in the computer vision field. SfM refers to the process of estimating three-dimensional structures from two-dimensional images. MVS generates three-dimensional models as point clouds. Digital cameras images or aerial photos are used in the calculations and three-dimensional models are produced. To date, DEMs are derived by conventional photogrammetry or LiDAR. However, photogrammetry requires special software, experience, and extensive manual measurement of ground control points (GCPs); furthermore, LiDAR is expensive. To use SfM?MVS in geomorphometry, data accuracy is an issue as well as the precision of GCPs; issues that have attracted the attention of many researchers. In this study, we discuss three examples of the application of SfM?MVS to geomorphometry.

First, we present the case of a detailed topographic map in Izu-Oshima, Tokyo, where a large-scale slope failure occurred before dawn on October 16, 2013, owing to the heavy rains of Wipha typhoon. To obtain a detailed DEM of the damaged slope, we took vertical photographs by UAV and generated a DEM by using SfM?MVS. As a result, we produced a topographic map with a 0.5 m contour interval. The topography was well reproduced and well compared to the LiDAR map with a resolution of 5 m provided by the Geographical Survey Institute.

Second, we created a topographic map using a vertical movie taken by UAV and SfM?MVS processing. A movie has few total pixels per picture compared with a still picture. A 4K-resolution movie has approximately 8 million pixels, whereas a high-definition (HD) movie has approximately 2 million. Moreover, because of lens distortion corrections when a wide-angle lens is used, the pixels that can be used in the calculations decrease. However, there is noise owing to compression compared with a still picture. Thus, the results are not as good as time-lapse photography using still pictures. UAV has also the risk of crashing, thus, it is wise not to use expensive equipment. Cheap cameras without time-lapse function are also available for SfM?MVS. Moreover, old video data can be used to obtain DEMs.

Finally, third, we obtained DEMs from scanning aerial photos. In Japan, the aerial photo archives are currently exceeding 1 million sheets. Therefore, if accurate DEMs are obtained from aerial photos, comparisons are possible and changes over time can be identified. We examined color aerial photographs taken in 1978 and 2012 at downstream area of Nakama River, Iriomote island, Okinawa Prefecture. The aerial photos comprised scans of 23-cm one-side analog photographs (1978) and digital aviation camera data (2012). The data were scanned at a resolution of approximately 1,270 dpi and the total number of pixels per image was approximately 120 million pixels. The resolution of the digital aviation camera photographs was 9,920 x 14,430 pixels. We also processed them by using SfM?MVS and we obtained DEMs with ground resolution of 0.3 m. We used the processed photographs to evaluate the vegetation damage caused by the 2006 and 2007 typhoons.

We show that SfM?MVS can be used in geomorphometry taking advantage of archived records. We anticipate that this methodology will be used more in the future.

Keywords: Structure from Motion (SfM), multi-view stereo (MVS), geomorphometry, topographic map, movie, aerial photograph

HTT08-P01 Room:Poster Time:April 29 18:15-19:30

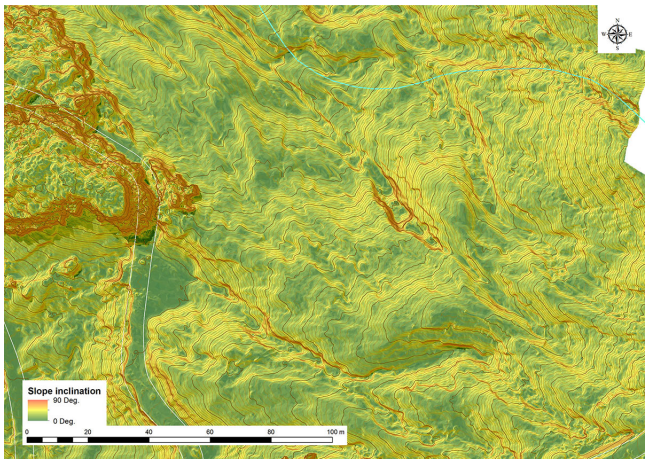

Japan Geoscience Union Meeting 2014
(28 April - 02 May 2014 at Pacifico YOKOHAMA, Kanagawa, Japan)

HTT08-P02 Room:Poster Time:April 29 18:15-19:30

Terrestrial laser scanning approach on quantification of weathering depth of sandstone blocks in a coastal environment

AOKI, Hisashi[2] ; HAYAKAWA, Yuichi S.[1*]

[1]Faculty of Business Administration, Daito Bunka University, [2]Center for Spatial Information Science, The University of Tokyo

Weathering in a coastal environment often causes degradation of artificial constructions if they are composed of weathering-prone materials including natural rocks and cements. Conservations of the vulnerability of such construction materials to weathering processes are thus important for their maintenance. Point to point, or cross-sectional measurements using scale bars have often been effective in describing the degree of weathering of such materials. However, accurate measurements of the amount of weathering in terms of areas and volumes have not often been performed due to the limitation in the measurement method for detailed, three-dimensional surface morphology. Here we demonstrate terrestrial laser scanning to describe three-dimensional surficial morphology of a weathered material: sandstone blocks used for masonry piers of bridge on a shore platform at Aoshima, Miyazaki in western Japan. The blocks have suffered from salt weathering above the sea level since the construction of the bridge in 1951. Weathering-induced depressions of sandstone blocks well develop in the spray zone. Our approach revealed sub-centimeter scale morphology of the block surfaces, as well as weathering depths and volumes of each block. Spatial distribution of the amount of weathering was also examined with regard to the sea level and the rock surface hardness. Continuous measurement of such detailed morphology will be necessary to clarify the contemporary rates of weathering therein.

Keywords: Weathering, Sandstone, TLS, Rock strength

Japan Geoscience Union Meeting 2014
(28 April - 02 May 2014 at Pacifico YOKOHAMA, Kanagawa, Japan)

HTT32-01 Room:422 Time:May 2 11:00-11:15

Simple technique of PM2.5 measurement in Higashi-Hiroshima city using a portable particle counter

OSHIME, Azusa[1*] ; SAKUNO, Yuji[2]

[1]Graduate School of Engineering, Hiroshima University, [2]Institute of Engineering, Hiroshima University

In recent years, we are anxious about the trans-boundary air pollution by PM2.5. Therefore the development of various measurement, monitoring methods is demanded.It was begun the full-time monitoring in Hiroshima from FY.2012. It is only ten places at the end of May, 2013 to measure PM2.5 among 39 places of atmosphere measurement station in the prefecture. In addition, because there is not the PM2.5 measurement station in Higashi-Hiroshima city that population continues increasing, we did not understand the situation of PM2.5. Therefore, in this study, a technique to measure PM2.5 with a relatively cheap portable particle counter (PPC) was considered. At first each particle size (the number of each particle more than diameter 0.3, 0.5, 0.7, 1.0, 2.0, 5.0μm) included in the atmosphere was measured using PPC (KR-12A, RION Ltd.) near Inokuchi Elementary School station (34.37268 degrees N, 132.38475 degrees E) that was one of the observation stations of Atmospheric Environmental Regional Observation System (AEROS) in order to estimate PM2.5 from PPC. All 11 data set measured was used on May 25, June 8, June 22, August 3. The number of the particles less than 2.5μm (C2.5) was calculated by the relationship between cumulative particle number (CPN) and particle size. After having aspirated the atmosphere of 1L per 1 measurement, CPN of each particle size is measured by the scattering intensity of the semiconductor laser at 790nm. On the other hand, CPN for 195 days from March, 2013 to April, 2014 were observed to check PM2.5 in Higashi-Hiroshima. On the other hand, CPN were measured for 195 days (only on weekdays) from March, 2013 to April, 2014 to check PM2.5 in the city. Statistically high correlation was observed the relationship between CPN (total count of all particle size) and the in-situ PM2.5 in Inokuchi station. The measurement limit of PM2.5 and the estimation error (RMSE) were 4.1-12.8μg/m3. The environmental standards of PM2.5 in our country are 35μg/m3 by one-day average now. Therefore, the measurement limit by this method is judged to be a value quite lower than these standard values. This simple technique can be used enough as how for it to be careful of PM2.5 at least. Moreover, as a result of creating the time series variation diagram of PM2.5 in Higashi-Hiroshima using this observation method, the percentage which exceeds environmental standards in Higashi-Hiroshima was about 16%. Moreover, the season when the probability which exceeds the standard is the highest was in August.

Keywords: PM2.5, atmosphere, monitoring, parcicle counter

Japan Geoscience Union Meeting 2014
(28 April - 02 May 2014 at Pacifico YOKOHAMA, Kanagawa, Japan)

HTT32-02 Room:422 Time:May 2 11:15-11:30

Examination of the green space index by using CO2 concentration at ibaraki prefecture

ISHII, Kenta[1*] ; IMAI, Yukako[2] ; KANZAWA, Masanori[3] ; KUWAHARA, Yuji[4]

[1]Depertment of Urban and Civil Engineering, Ibaraki University, [2]Graduate School of Science and Engineering, Ibaraki University, [3]U-DOM co., Ltd., [4]Center for Water Environment Studies, Ibaraki University

The objective of this study is to propose the correction method and evaluation index of CO_2 concentration data which is observed in human living sphere, Ibaraki prefecture. Since, sensor drift arise in the process of long-term continuous duty, it is important to correction process by using standard reference gas. However, sensor drift time are different in each sensor and installation location, so, it is conducted the laboratory experiment and observation data analysis to grasp the action of CO_2 sensor. The results of this study were as follows: 1) It was proposed that the correction method for observation data which is combined linear transformation. 2) It was verified of the correction effect focused on the time variation and spatial distribution of CO_2 concentration.

Keywords: CO2 concentration, fixed point observation, living environment sphere, the green space index

Japan Geoscience Union Meeting 2014
(28 April - 02 May 2014 at Pacifico YOKOHAMA, Kanagawa, Japan)

HTT32-03 Room:422 Time:May 2 11:30-11:45

Estimation for water surface temperature distribution in Lake Shinji and Lake Nakaumi using Landsat-8 TIRS data

SAKUNO, Yuji[1*]

[1]Institute of Engineering, Hiroshima University

Lake Shinji and Lake Nakaumi are brackish water lakes with the rich biological resources represented by Corbicula japonica. However, the abrupt increase of blue-green algae or the spontaneous expand of aquatic macrophytes are anxious about the influence on such a biological resources of the lake in recent years. Therefore, various monitoring methodology for the elucidation of those generating mechanisms is examined. The satellite remote sensing is expected as a leading monitoring tool. Especially water temperature is important as most fundamental physical parameter. On the other hand, the Landsat-8 in the field of satellite remote sensing on February 11, 2013 was launched by NASA/USGS. This satellite has been continuing observation with 16 diurnal periodicity. The thermal infrared sensor (spatial resolution of 100 m) called TIRS (Thermal Infrared Sensor) with the multiple-spectrum sensor at visible and near- infrared bands with a spatial resolution of 30 m called OLI is carried in this satellite. Since high quantization (12 bits) and 2 band of TIR are realized as compared with conventional Landsat-7, more highly precise WT distribution estimation is expected. So, in this paper, to develop the surface water temperature (SWT) estimation by MCSST (Multi Channel Sea Surface Temperature) algorithm in these lakes using TIRS sensor and the accuracy was checked. Moreover, the SWT distribution characteristic in these lakes was considered using the proposed algorithm. The satellite data used is ten scenes from April to December, 2013. The Landsat-8 TIRS Leve l 1 product data was downloaded through the Internet site ”Earth Exploler.” The average value of 3x3 pixels of Band10 (10.6 - 11.2 μm) and Band11 (11.5 - 12.5 μm) in these lakes was extracted from the obtained satellite data. The data was changed into brightness temperature (BT). On the other hand, the SWT data at 1.0 meters under water was obtained from the Water Information System of Ministry of Land, Infrastructure and Transport. Moreover, MCSST (Multi Channel Sea Surface Temperature) which can reduce the air effect using two bands at thermal infrared for WST estimation from TIRS data was adopted. 19 datasets in the center of these lakes were used for development of MCSST. Three datasets acquired to the Yonago Bay were used for validation. WST estimation accuracy is expressed by average (bias) and standard deviation (error) of the residual substance of in-situ WST and satellite estimation WST. The WST accuracy using the single band algorithm of TIRS Band 10 and Band 11 was [bias: 1.3 oC, error: 1.7 oC] and [bias: 0.9 oC and error: 2.4 oC], respectively. On the other hand, the WST accuracy by the MC method was calculated with [bias: 1.3 oC, error: 0.6 oC]. The WST difference of the 3 data validated in Yonago Bay was an average of 1oC. Noise Equivalent Differential Temperature (NEdeltaT) of TIRS sensor, The estimation accuracy of NOAA AVHRR in Mutsu Bay using the MCSST method is considered that this result is an appropriate numerical value from their being 0.4K (= 0.4 oC) (Irons et al, 2012) and about 0.5±0.2oC, respectively. The WST map in these lakes was created using the proposed MCSST type. As for the WST in Lake Shinji lake in this period, it was checked through every year from these figures that a surface water temperature difference is about 3-5oC in the range of 5-30oC. Moreover, in the mouth of a river of Hii River and Shintate River which are located in the Shinji Kosai shore especially in a summer, the low-wash temperature pattern resulting from inflow of river water was observed.

Keywords: satellite, remote sensing, water temperature, lake

Japan Geoscience Union Meeting 2014
(28 April - 02 May 2014 at Pacifico YOKOHAMA, Kanagawa, Japan)

HTT32-04 Room:422 Time:May 2 11:45-12:00

Feasibility Study for the Estimation of the Chlrophyll-a Using ASTER Data in an Eutrophic Lake, Sri Lanka

DAHANAYAKA, D.d.g.l.[1*] ; TONOOKA, Hideyuki[1] ; WIJEYARATNE, M.j.s.[2] ; MINATO, Atsushi[1] ; OZAWA, Satoru[1]

[1]Graduate School of Science & Engineering, Ibaraki University, [2]Department of Zoology, University of Kelaniya

The objective of this study is to evaluate the performance of the previously proposed band ratio approach in estimating Chl-a in Bolgoda Lake, Sri Lanka as a representative example of Case II waters. Lake is located at western province in an area with lot of industries and also with some agricultural activities. Considerable amount of industrial effluents are discharged into it. Illegal filling and also encroachment has occurred in the recent past. This study focused on to determine the trends in eutrophication via Chl-a changes during the recent past, make predictions and recommend mitigatory measures and suggest precautionary measures to restore the environment. From March to December 2013, water samples at 5 points of Lake were collected once per month parallel to ASTER overpass and Chl-a of each sample was measured using a laboratory spectrophotometer. Cloud-free ASTER scenes acquired over Lake under clear sky conditions were selected during 2000 to 2013 for Chl-a estimation and trend analysis. All the ASTER images were atmospherically corrected using FLAASH and in-situ Chl-a data on Lake were regressively analyzed with atmospherically corrected three ASTER VNIR band ratios such as B1/B2 of the same date. Finally, the regression equation of the band ratio with highest correlation (B1/B2; R^2 = 0.78) was used to develop algorithm for generation of 15-m resolution Chl-a distribution maps using atmospherically corrected time series satellite imageries in day by day basis. This method applied for ASTER band 1/2 ratio due to Chl-a is positively correlated with the green band reflectance and negatively correlated with the red band reflectance. Therefore, the reflectance ratio of green and red bands becomes a robust parameter to estimate the Chl-a content. According to the ASTER based Chl-a distribution maps it is clearly evident that eutrophication of the Bolgoda Lake has been gradually increased from 2005-2011. Further, results showed that there were significant eutrophic conditions throughout the year 2013 in several parts of the Lake and considerable spatial heterogeneity with higher concentrations being recorded water stagnant areas and in water adjacent to freshwater outlets. It is clear that Bolgoda Lake is apparently a disposal site of various discharges of factories in addition to poor drainage and sewage systems present in this area. Highly unplanned urbanization and absolutely lack of adequate waste disposal management facilities in industries close to Lake have resulted in pollution of water. If the present trend of waste disposal and unplanned urbanization continue, they would create enormous environmental problems in future. Results of the present study showed that information from satellite remote sensing can play a useful role in determining the changes in Chl-a related to eutrophication in Bolgoda Lake and in the development of time series Chl-a distribution maps. Such information is important for the future predictions, development and management of this area as well as in the conservation of biodiversity. Therefore we recommend incorporation with this technique for routine monitoring of water quality using multi satellite data such as ASTER in inland water bodies like Bolgoda Lake in the future.

Keywords: Chlorophyll-a, Remote Sensing, ASTER, Sri Lanka, Bolgoda Lake

Japan Geoscience Union Meeting 2014
(28 April - 02 May 2014 at Pacifico YOKOHAMA, Kanagawa, Japan)

HTT32-05 Room:422 Time:May 2 12:00-12:15

Study on the information visualization aimed at maintenance and utilization of local resources

ISHIUCHI, Teppei[1*]

[1]Akashi National College of Technology

In recent years, the problems of loss of sense of community and increase of indifferent residents, dilution of human relationships in the neighborhood, by dilution of a sense of belonging to the community, such as the moral decline is happening at local areas. Therefore, It become difficult for precisely corresponds to such changes alone to public administration ? driven. Target area of this study is Akashi city. This area has many rich rural environment and ponds, wooded area, waterway as remnant of village forest. And half of the residents of the town Uozumi-cho are a migrant.

In these areas, in order to promote community development befitting UOZUMI town, on an understanding of the digging up the history and culture of various regions, it is possible to stare life in the current region is important in the future. And, it is leading to a chance to foster protect the charm of a familiar town to residents themselves living in the town. Further, in order to form a hometown, it is necessary to dig the local resources, reaffirming residents share a town appeal. In this study, we dug up local resources existing in Uozumi-cho, and visualized as maps using the GPS positioning system. Finally, in order to convey to posterity the presence of valuable community resources, this study is proposed that the residents to re-recognize the appeal of the region by using a map.

Keywords: local resources, hometown, GPS, visualization

Japan Geoscience Union Meeting 2014
(28 April - 02 May 2014 at Pacifico YOKOHAMA, Kanagawa, Japan)

HTT32-06 Room:422 Time:May 2 12:15-12:30

Examination of land cover change region presumption method by using coherence value

SEKINE, Daiki[1*] ; YUKI, Sohei[2] ; KUWAHARA, Yuji[3]

[1]Depertment of Urban and Civil Engineering, Ibaraki University, [2]Graduate School of Science and Engineering, Ibaraki University, [3]Center for Water Environment Studies, Ibaraki University

In recent years, many natural disasters have occurred because of abnormal climate. In a time like this, use of satellite data is advantageous to observation of the disaster region for a wide area. However, in order that photo sensor data may tend to be subject to the influence of atmospheric, synthetic opening data attracts attention. And, this research examined coherence data among the information generated from the Synthetic Aperture Radar data. The results of the research are as follows: 1)The coherence value of a vegetation region is low. This result is expressing that the growth environment of vegetation differs for every year. 2)The coherence value of a city area is high.

Keywords: land cover change, SAR, coherence value, land cover classification map, PALSAR

Japan Geoscience Union Meeting 2014
(28 April - 02 May 2014 at Pacifico YOKOHAMA, Kanagawa, Japan)

HTT32-07 Room:422 Time:May 2 12:30-12:45

A Technique for High-performance Data Processing of Satellite Observation Data via NICT Science Cloud

MURATA, Ken T.[1*] ; KASAI, Yasuko[1] ; SATO, Shinsuke[1] ; ISHII, Shoken[1] ; WATANABE, Hidenobu[1] ; UKAWA, Kentaro[2] ; MURANAGA, Kazuya[2] ; YUTAKA, Suzuki[2] ; YAMAMOTO, Kazunori[1] ; TATEBE, Osamu[3] ; TANAKA, Masahiro[3] ; KIMURA, Eizen[4]

[1]Natl. Inst. of Info. and Communications Technology, [2]Systems Engineering Consultants Co., LTD., [3]University of Tsukuba, [4]Ehime University

It is said that data-intensive/data-centric science is the fourth paradigm of science after observation/experiment, theory and computer simulation. The NICT science cloud is one of the cloud systems for scientists who are going to carry out their research works for their big-data science. The science cloud is not for simple uses: Many functions are expected to the science cloud; such as data standardization, data collection and crawling, large and distributed data storage system, security and reliability, database and meta-database, data stewardship, long-term data preservation, data rescue and preservation, data mining, parallel processing, data publication and provision, semantic web, 3D and 4D visualization, out-reach and in-reach, and capacity buildings.

The present talk is focused on the topics of applications of the NICT Science Cloud to environment sensing research works. There are three applications to be introduced: (1) real-time data processing and visualization of 3D Doppler radar, (2) GOSAT CH4 data processing for global mapping, and (3) high-performance simulation of the ISOSIM-L (Integrated Satellite Observation SIMulator for a spaceborne coherent Doppler lidar) for wind measurement from space. These three projects are started and carried out in the NICT. With help of the NICT Science Cloud, they show progressive development to either larger-scale studies or more practical uses.

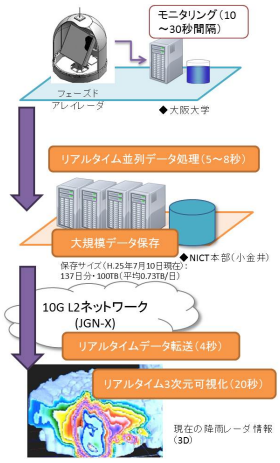

Japan Geoscience Union Meeting 2014
(28 April - 02 May 2014 at Pacifico YOKOHAMA, Kanagawa, Japan)

HTT32-08 Room:422 Time:May 2 14:15-14:30

Investigation of geographical feature and vegetation using for planting plan of the coastal zone at Tuvalu

KUWAHARA, Yuji[1*] ; SATO, Daisaku[2] ; HIROMUNE, Yokoki[3] ; FUJITA, Masafumi[4]

[1]Center for Water Environment Studies, Ibaraki University, [2]Dept. of Architectural, Civil and Environmental Engineering, Tokyo Denki Univrsity, [3]Dept. of Urban and Civil Engineering, Ibaraki University, [4]Dept. of Urban and Civil Engineering, Ibaraki University

The objective of this study is to investigate the geographical feature of coastal vegetation growing in Funafuti Atoll, Tuvalu. In order to maintain the living environment of the South Pacific islands countries, sea-level rise is a serious problem. Thus, in this study, analyzed was the relation of land cover of shoreline area and hinterland by using aerial photograph (1984) and satellite image (2004). Then, geographical feature conditions of the coastal vegetation growing under natural condition were surveyed, and it was found that the coastal vegetation was growing in the altitude between 1.1m - 2.2m at Fongafale-island, Funafuti atoll.

Japan Geoscience Union Meeting 2014
(28 April - 02 May 2014 at Pacifico YOKOHAMA, Kanagawa, Japan)

HTT32-09 Room:422 Time:May 2 14:30-14:45

Factor analysis and vegetation change in China Inner Mongolia through Satellite Remote Sensing

BUHE, Baoyin[1*] ; KONDOH, Akihiko[1]

[1]Center for Environmental Remote Sensing, Chiba University

In this study, the spatial and temporal vegetation cover change of the Inner Mongolia Autonomous Region was analyzed by using the time series satellite SPOT VEGETATION dataset from 1999 to 2012. The vegetation change trend was analyzed by the Normalized Difference Vegetation Index (NDVI), and the result was estimated by the Mann-Kendall rank statistic method. Annual maximum vegetation biomass can respond well with maximum NDVI change trend and annual vegetation product approximately similar with total amount of NDVI trend. Vegetation index has closely correlation with annual precipitation. The results revealed that the vegetation status of Inner Mongolia was affected significantly by the precipitation. Due to the benefit of return farmland to grassland and forestry policy such as forestation, cultivation of the arable land and increase the irrigation area, the vegetation in the southeast and middle south of Inner Mongolia significantly increased. In the northeast of Inner Mongolia, due to the global warming and wetland development the forestry growing period become longer that exactly reflect the vegetation cover increasing phenomenon . The vegetation distributed in middle-west of Inner Mongolia has decreasing trend and desert area was continuously extending within 14 years.

Keywords: Inner Mongolia, Desertification, Vegetation change, Mann-Kendall rank statistic, SPOT VEGETATION

Japan Geoscience Union Meeting 2014
(28 April - 02 May 2014 at Pacifico YOKOHAMA, Kanagawa, Japan)

HTT32-10 Room:422 Time:May 2 14:45-15:00

Study on the Spatial Analysis of River Flooding in the Amur River Basin

YOU, Qin[1*] ; KONDOH, Akihiko[2] ; HARADA, Ippei[3]

[1]Graduate School of Science,Chiba University, [2]Center for Environmental Remote Sensing, Chiba University, [3]GIS Laboratory, Tokyo University of Information Sciences

Amur River is flowing through the border of China and Russia, and pour into the sea of Okhotsk. There are three plains in the Amur River basin, China famous commercialized food producing area of the Sanjiang Plain and the Songneng Plain are two of them. In order to develop the arable land in recent years, the land cover change and destroyed natural environment made the floods to be easily happened which be concerned. On the other hand, the drainage area of Amur River is 2.05 millions km^2, it is a problem for satellite observation in spatial, and for extracting the flood information when there are clouds in the sky, the microwave image is used, but it will be expensive in the area of Amur River basin. So the analysis of river flooding will be the challenge. In this study, in order to understand the flooded situation of the Amur River basin, we used high temporal resolution satellite image to extract the two big floods of 1998 and 2013 by the spectral absorption characteristics of the water. We understood that there are different courses in twice flooded, and at the downstream of Amur River where is well to flooding, because of the wetland be changed and topography relief bring about drain off water difficulty.

Keywords: Near-infrared, MODIS, AVHRR, SRTM, Spectrum Character

Japan Geoscience Union Meeting 2014
(28 April - 02 May 2014 at Pacifico YOKOHAMA, Kanagawa, Japan)

HTT32-P01 Room:Poster Time:May 2 16:15-17:30

A preliminary study on using MODIS NDVI time series for monitoring abandoned farmlands in mountainous areas

SAKUMA, Asahi[1*] ; SHIMAZAKI, Hiroto[1]

[1]Kisarazu National College of Technology

This study preliminary evaluated the feasibility of Normalized Difference Vegetation Index (NDVI) time series for monitoring abandoned farmlands in mountainous areas in Chiba prefecture. NDVI time series was derived from 8-day composite of MODIS Surface-Reflectance Product (MOD09) for the period from 2003 to 2013. The noise component in NDVI time series, which was induced mainly by cloud contamination and atmospheric variability, was reduced with the method based on Savitzky-Golay filter. The refined NDVI time series was then decomposed into trend, seasonal, and reminder components. A simple linear regression model was fitted to the trend component of each pixel, and model parameters (i.e., intercept and slope) estimated were considered to be candidate features to find the occurrence of abandoned farmlands in the pixel area. This idea was based on the assumption that (1) overall NDVI in mountainous areas would be higher than that in other areas because of relatively-dense vegetation; and that (2) NDVI in specific seasons would have differences between farmlands and abandoned farmlands due to the effect of cropping activity. Classification performance was measured with the area under the receiver operating characteristic (ROC) curve (AUC). The results showed that the model parameters were poor (AUC=0.6) in terms of classification performance. Further efforts are needed to evaluate the feasibility of NDVI time series for detecting abandoned farmlands in mountainous areas.

Japan Geoscience Union Meeting 2014
(28 April - 02 May 2014 at Pacifico YOKOHAMA, Kanagawa, Japan)

HTT33-01 Room:211 Time:May 2 09:15-09:30

Visual Surveillance of Natural Geography by means of UAV

HASEGAWA, Hitoshi[1*] ; ISOGAI, Tatsuhiro[1] ; ONO, Isamu[1]

[1]Kokushikan University

Unmanned aerial vehicle (UAV) systems can lead to major advances in physical geography. We have obtained a high-resolution digital aerial photographs using UAV (Unmanned Aerial Vehicle). UAV can make an automatic flight under the GPS control and take aerial photographs repeatedly with the same flight route. In this study, UAV was flying at 50 to 100m altitude. We have taken aerial photographs at coral reefs ,mangrove forests and the trench site of active fault. The high-resolution aerial photographs, a detailed classification map could be created, and it would also allow the extraction of dynamical topographic and vegetation development temporal changes.

Keywords: UAV, High-resolution digital aerial Pjotograh, Proximal Remote Sensing Method

Japan Geoscience Union Meeting 2014
(28 April - 02 May 2014 at Pacifico YOKOHAMA, Kanagawa, Japan)

HTT33-02 Room:211 Time:May 2 09:30-09:45

The acquisition of geospatial information by small UAV

TANAKA, Kei[1*] ; KONDOH, Akihiko[2]

[1]Japan Map Center, [2]Center for Environmental Remote Sensing, Chiba University

The recent advances of MEMS devices(GPS, gyro and acceleration sensor) has made possible low-cost and miniaturization. Thereby, multi-copter mounted with these sensors have appeared.That it requires a high level of technology and knowledge in the handling of RC traditional helicopter,beginners to steer is difficult.To enable even beginners to get easily geospatial information of high-resolution by multicopter.

In this study, we examined method of acquiring geospatial information(orthophoto, DSM, NDVI, and temperature distribution) by using small UAV.

Keywords: UAV (Unmanned Aerial Vehicle), SfM (Structure from Motion), DSM, orthophoto, NDVI, temperature distribution

Japan Geoscience Union Meeting 2014
(28 April - 02 May 2014 at Pacifico YOKOHAMA, Kanagawa, Japan)

HTT33-03 Room:211 Time:May 2 09:45-10:00

UAV application and possibility for disaster prevention.

SAITOU, Osamu[1*] ; KUWAHARA, Yuji[1]

[1]Center for Disaster Prevention and Security, IBARAKI University

Videos of the tsunami taken from the airplane conveyed the horror of the recent great disaster which attacked the various places in eastern Japan, the Great East Japan Earthquake of 2011. Numerous engineers and researchers were shocked by the images. Moreover, many real-time movies and images of this disaster exist. Especially in the past several years, other disasters caused by extreme weather because of our changing climate, such as heavy typhoons, rain cataracts, flurries, and tornadoes, also cause widespread destruction. When these disasters or earthquakes occur, rapid situational assessment is crucially important, but it is difficult because transportation systems including roads and railways often shut down under those circumstances. Therefore, a monitoring system that provides information immediately when a disaster occurs is required. When a disaster occurs, monitoring from an airplane or satellite is effective but such systems are not easy to use. This study examines the possibility of disaster monitoring systems using uncrewed aerial vehicles (UAV).

Keywords: UAV, sensor network, sensor, disaster prevention

Japan Geoscience Union Meeting 2014
(28 April - 02 May 2014 at Pacifico YOKOHAMA, Kanagawa, Japan)

HTT33-04 Room:211 Time:May 2 10:00-10:15

Proximity air measurement of the radiation by unmanned small helicopter

KAJIWARA, Koji[1*] ; HONDA, Yoshiaki[1]

[1]Center for Environmental Remote Sensing, Chiba Univ.

The decontamination work of the radioactive material which dispersed in the accident of Fukushima nuclear power plant accompanying the Great East Japan Earthquake, is continuing to residential area, cultivated land, etc.

However, the still high dose is measured in the forest region.

It is a question whether safety can be guaranteed or not, even if it performs the roof of a house or building, and decontamination of only soil, when a forest is in living environment.

The radiation measuring instrument which enabled it to adjust the distance to the target for measurement with the winch attached to the small unmanned helicopter in this research is used, the dose of a tree crown from the position close to about 100m has been measured, and it was shown that field dose measurement in the forest is possible.

Moreover, even if it was the decontaminated place, it checked that a space dose in case it approaches and a forest exists changed with altitudes.

Keywords: UAV, Radiation Measurement, Forest Canopy

Japan Geoscience Union Meeting 2014
(28 April - 02 May 2014 at Pacifico YOKOHAMA, Kanagawa, Japan)

HTT33-05 Room:211 Time:May 2 10:15-10:30

Generating three-dimensional models by a software that unifies SfM and multiview stereo (MVS)

UCHIYAMA, Shoichiro[1*]

[1]National Research Institute for Earth Science and Disaster Prevention (NIED)

In recent years, the software which unified Structure from Motion (SfM) and multi-view stereo (MVS) was developed. By this, construction of three-dimensional models and its Digital elevation models (DEMs) can be achieved with PC at easy and low cost. This paper shows a method for generating three-dimensional models by using with a SfM-MVS software and images captured by a handheld camera or an UAV's.

Keywords: structure from motion (SfM), three-dimensional model, digital surface model (DSM), unmanned aerial vehicle (UAV), geomorphometry, image acquisition for calculation

Japan Geoscience Union Meeting 2014
(28 April - 02 May 2014 at Pacifico YOKOHAMA, Kanagawa, Japan)

HTT33-06 Room:211 Time:May 2 10:30-10:45

Safety measures for multicopter aerial photo survey

INOUE, Hiroshi[1*] ; UCHIYAMA, Shoichiro[1] ; SUZUKI, Hinako[1]

[1]National Research Institute for Earth Science and Disaster Prevention(NIED)

Low-altitude aerial photographing using multicopters, radio-controlled multi-rotor helicopters, became easy for everybody because of their recent technical advancement and price declines of the equipment. The technology will become popular rapidly as one of the methodologies of field surveys. Multicopters, however, can crash into the ground. We have experienced crash or near-crash accidents through our surveys and test flights in the past. The causes are sometimes a simple pilot error, loss of a propeller, unexpected strong wind, and out of battery, and are sometimes unclear, like GPS signal loss and barometer error, and their combinations. The crashes could have made serious injuries if the multicopters hit humans judging from the damage to the equipment we experienced.

The measures we take are careful pre-examination of the flight plan, making propeller guards, knowing battery capacity-flight time characteristics, monitoring battery voltage during the flight, regular maintenance of the batteries, pre-flight equipment checks, acceleration and compass calibrations, communication between the pilot and copilot, full utilization of autonomous flight, training of manual control for emergency, and following the safety check list.

Multicopter survey could cause problems to the society if accidents occur often as the result of popularization. If the usage becomes too strictly regulated, we may limit or even lose the large potential of applying the multicopter technology to our field survey. We therefore need to establish the safety measures to be obeyed, and share experiences of accidents for wider recognition of its potential danger, clarify individual causes, in order to strengthen the measures. Compliance to the aviation and wireless communication laws and regulations are indisputable. We also have to buy an insurance to compensate the possible damage caused by an accident.

Japan Geoscience Union Meeting 2014
(28 April - 02 May 2014 at Pacifico YOKOHAMA, Kanagawa, Japan)

HTT33-P01 Room:Poster Time:May 2 16:15-17:30

Mapping active faults by using small unmanned aerial vehicle and structure from motion: a case study on Midori fault

UCHIYAMA, Shoichiro[1*] ; NAKATA, Takashi[2] ; INOUE, Hiroshi[1] ; KUMAHARA, Yasuhiro[2] ; SUGITA, Satoru[3] ; GOTO, Hideaki[2] ; IZUTSU, Jun[3] ; FUKUI, Hiromichi[3] ; SUZUKI, Hinako[1] ; TANIGUCHI, Kaoru[4]

[1]National Research Institute for Earth Science and Disaster Prevention, [2]Hiroshima University, [3]Chubu University, [4]National Institute of Advanced Industrial Science and Technology

We photographed the geomorphometry of the Midori fault scarp formed by the 1891 Nobi earthquake in Motosu city, Gifu Prefecture (Japan) by using a multirotor radio control helicopter as a small unmanned aerial vehicle (sUAV), and we analysed these images. A digital surface model (DSM) of 0.09 m mesh and an orthophoto with a resolution of 0.03 m were generated from these images by PhotoScan software produced by structure from motion (SfM). A topographic map with 1 m interval contours and a cross-section profile were processed using a DSM produced by ArcGIS. We expect that the new technology will be applied to tectonic landform survey and geomorphology research. In addition, our results should help to ensure flight safety and compliance with the law.

Keywords: structure from motion (SfM), small unmanned aerial vehicle (sUAV), digital surface model (DSM), orthophoto, geomorphometry, midori fault scarp

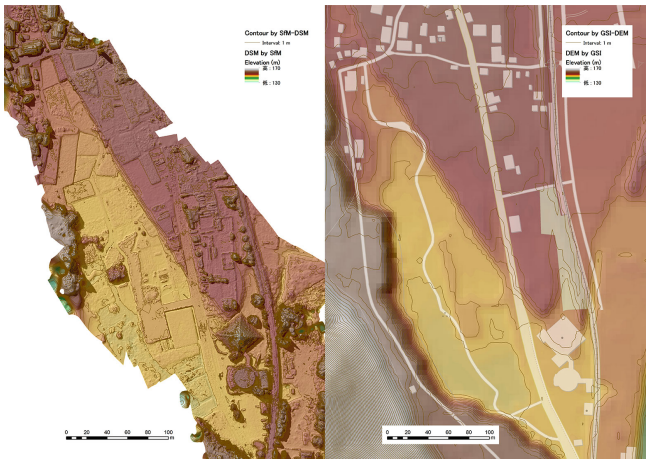

Japan Geoscience Union Meeting 2014
(28 April - 02 May 2014 at Pacifico YOKOHAMA, Kanagawa, Japan)

HTT33-P02 Room:Poster Time:May 2 16:15-17:30

Generating an orthophoto from SfM calculation with the low-quality air photographs taken in the 1964 Niigata earthquake

SUZUKI, Hinako[1*] ; UCHIYAMA, Shoichiro[1]

[1]National Research Institute for Earth Science and Disaster Prevention (NIED)

This study shows that generating the orthophoto from low quality aerial photographs using structure from motion (SfM).National Research Institute for Earth Science and Disaster Prevention (NIED) is archiving a lot of old aerial photographs and its original roll films. However, some films are deteriorating. One of them is the 1964 Niigata earthquake's film.This deteriorated photographs were taken 50 years ago, nevertheless, the result of SfM calculating were sufficient quality and generated orthophoto with 0.2 m resolution.As a result, low quality aerial photographs are available to utilize for SfM.

Keywords: structure from motion (SfM), low quality aerial photograph, 1964 Niigata earthquake, ground control point (GCP), orthophoto

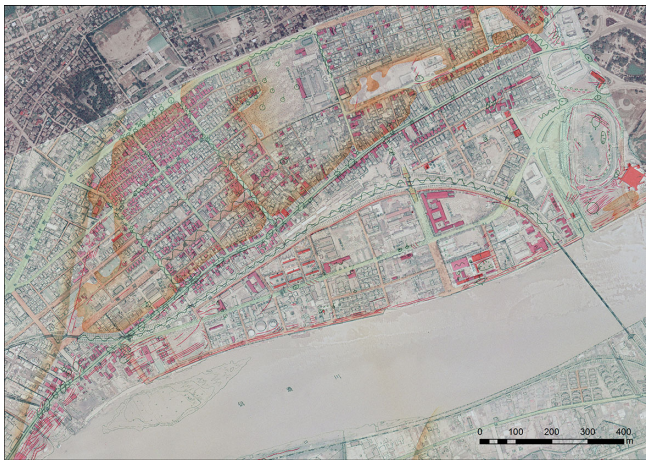

Japan Geoscience Union Meeting 2014
(28 April - 02 May 2014 at Pacifico YOKOHAMA, Kanagawa, Japan)

HTT33-P03 Room:Poster Time:May 2 16:15-17:30

Mapping of the fault scarp formed during the 2013 Bohol earthquake by small UAV

NAKATA, Takashi[1*] ; INOUE, Hiroshi[2] ; CAHULOGAN, Mabee[3] ; RIVERA, Danikko[3] ; LIM, Robjunelieaaa[3] ; POGAY, Cathy[3]

[1]Hiroshima University Professor Emeritus, [2]NIED, [3]PHIVOLCS

A 5km-long surface fault rupture appeared during 2013 Bohol earthquake (M 7.1) in the Philippine. We took low-altitude air-photos of the ruptures using a small UAV, and made 3D images and contour maps by SfM software. This survey method is a low-cost, easy and effective method for mapping for quick respond field work for unexpected large earthquake damage especially in remote areas in under developing countries.

Keywords: UAV, SfM photogrammetry, earthquake fault, 2013 Bohol earthquake

Japan Geoscience Union Meeting 2014
(28 April - 02 May 2014 at Pacifico YOKOHAMA, Kanagawa, Japan)

HTT33-P04 Room:Poster Time:May 2 16:15-17:30

Multicopter Aerial Photo Survey of Building Damages by 2013 Bohol Eearthquake in the Philippines

INOUE, Hiroshi[1*] ; HANAZATO, Toshikazu[2] ; IMAI, Hiroshi[1] ; MELOSANTOS, Arnold[3] ; ALCONES, Ponzch[3] ; SORIANO, Karl vincent[3]

[1]National Research Institute for Earth Science and Disaster Prevention(NIED), [2]Mie University, [3]Philippine Institute for Volcanology and Seismology(PHIVOLCS)

We demonstrate the effectiveness of multicopter aerial photographing for recording earthquake damages of low to medium-rise buildings. M7.2 shallow inland earthquake occured on Bohol Island in the Philippines on October 15, 2013, which caused thousands of building damages and more than 200 casualties in the western part of the island. Post- earthquake surveys by PHIVOLCS showed the maximum earthquake intensity in Tagbilaran city near the epicentral area was VII in Philippines Eearthquake Intensity Scale, which is equivalent to VI in JMA intensity scale. We visited the island three weeks after the earthquake, to make the damage survey focusing on church buildings using a multicopter. We also carried out aerial photogrammetric survey of the surface rupture of the earthquake fault and the coastal uplift(Nakata et al., JpGU 2014) and the landslide damage of chocolate hill, a distinguishing morphology on the island.

A number of stone masonry churches founded in the 16th century in the Spanish colony times were damaged by the earthquake. The existing building of Baclayon Church, which was constructed in 1727 and known as the oldest church in the Philippines, lost the upper half of the bell tower and the whole front wall of the cathedral. Loboc Church and the adjoined museum in the Loboc city lost most of the side walls except their lower part. Maribojoc Church in the west and Clarin Church in the north of the island collapsed completely. Notable damages are also on non-structural masonry walls confined by RC columns and beams of public buildings, such as Sagbayan city hall and Tubigon city hall.

We used a small and easy-to-fly multicopter named DJI Phantom and a high-resolution and compact digital camera GoPro Hero3 Black Edition for the aerial photographing. We attached the camera facing obliquely down and manually controlled the copter in GPS stabilized mode. We used a FPV (First Person's View) system FatShark Telepoter V3 for watching the camera view. Photos were taken continuously in 2 seconds interval, while the copter was flying around the subjects. We limited the duration of each flight to five minutes and attached propeller guards to the rotors in order to reduce the possible dangers by crash as much as possible because people's activities in the areas around the churches were normal. We had no accident during the survey. We found that FPV is very useful in building damage survey because it can reduce the risk to crash to the building when taking photos, while it is difficult to know the distance from the copter to the subject in manual control from the ground.

The left figure shows the multicopter aerial photos of the damaged Baclayon Church. We can observe the fracture surfaces of the upper structure and its inside which are invisible from the ground. Aerial photographing using multicopter right after an earthquake is an efficient tool to easily get full picture of the damage even when approaching from the ground around a building is difficult. We then processed about 50 aerial photos using an SfM (Structure from Motion) software PhotoScan to reconstruct the 3-D model of the bell tower as shown in the right figure. The techniques enable modeling fractures of buildings and their analyses. The 3-D models are also valuable as digital architectural remains of disasters. Aerial photogrammetry using multicopter and SfM is easier than 3-D measurement using laser scanner. Creating a miniature of damaged building from the digital model using 3-D printer will also be useful for planning repairs and earthquake resistant design of buildings.

HTT33-P04 Room:Poster Time:May 2 16:15-17:30

Japan Geoscience Union Meeting 2014
(28 April - 02 May 2014 at Pacifico YOKOHAMA, Kanagawa, Japan)

HTT33-P05 Room:Poster Time:May 2 16:15-17:30

Production of vegetation/landcover and dose rate maps by small helicopter and UAV

KONDOH, Akihiko[1*] ; HONDA, Yoshiaki[1] ; KAJIWARA, Koji[1] ; NORO, Naoki[2] ; TAKARA, Yohei[2] ; ANDO, Fuminori[2] ; FUJIMORI, Takahiro[2] ; NONAMI, Kenzo[3] ; YAMAGUCHI, Hidetoshi[4]

[1]Center for Environmental Remote Sensing, Chiba University, [2]EBA JAPAN CO.,LTD., [3]Graduate School of Engineering, Chiba University, [4]SWR CO.,LTD.

The most essential and important information for restoration of the area contaminated by radioactive materials is dose rate and landcover map. The map should cover the SATOYAMA watershed with several hundreds to several kilometers scale, because the life in mountain village depend on water and material cycles in SATOYAMA watersheds and mode of deposition is strongly affected by vegetation type such as deciduous broad-leaved or evergreen coniferous forests. However, large scale maps on present vegetation and dose rate distribution are not available at present, so our team attempts to create vegetation/landcover map and dose rate distribution map by using UAV(Unmanned Areal Vehicle).

Manned helicopter (Robinson R44), radio controlled gasoline engined helicopter (YAMAHA/RMAX), and radio controlled electric multicopter (Minisurveyer MS-06L) are used as platform of dose rate measuring system. Dose rate is measured by radiation detector module (C12137-01, Hamamatsu Photonics) controlled by small laptop computer.

Hyperspectral camera (NH-7, Eba-Japan Co.,Ltd.) and video camera are installed on manned and unmanned helicopter to map precise vegetation and landcover map. In hyperspectral camera operation, both pushbroom and still images are taken. Motion video is captured to get still images, and mosaicked to ortho-areal photo.

Field campaign are carried out two times during August and November in 2013, and various photographing modes three-dimensional dose rate mapping, and dose rate on various landcover such as forest canopy are attempted.

The campaign reveals the feasibility of low-cost, on-demand photographing and dose rate survey buy using UAV. Next subject is implementation to the actual scene. We plan to continue dose rate survey in Yamakiya district, Kawamata Town in Fukushima Prefecture.

Keywords: nuclear disaster, dose rate measurement, UAV, hyperspectral camera, Yamakiya District, FUKUSHIMA

Japan Geoscience Union Meeting 2014
(28 April - 02 May 2014 at Pacifico YOKOHAMA, Kanagawa, Japan)

HTT34-01 Room:422 Time:April 28 14:15-14:30

Airborne LiDAR bathymetry survey in Japanese Pacifc coast in 2013

MATSUNAGA, Tsuneo[1] ; ISHIGURO, Satoshi[1*] ; YAMANO, Hiroya[1] ; OGUMA, Hiroyuki[1]

[1]National Institute for Environmental Studies

In 2013, Airborne lidar bathymetry survey in Japanese Pacific coast was planned and partially conducted at several selected-sites.

The objective of this survey is to acquire detailed bathymetry data in Japanese Pacific coast which are important for Tsunami simulation as well as monitoring of coastal environment and ecosystem heaviliy damaged by the Great East Japan Earthquake occurred in March 2011.

An airborne lidar bathymetry system, Fugro LADS Mk. III, was brought to Japan for the first time in October 2012. Data acquisition flights over several coastal areas in Hokkaido, Tohoku, Mie, and Tokushima were conducted in November and December, 2012, and remaining areas in Tohoku and Izu were conducted in September and October, 2013. Obtained data are currently being calibrated and evaluated.

In this presentation, the outline of the survey including instrument specifications, mapping areas, and the survey schedule as well as lidar data acquired will be presented.

Keywords: Airborne LiDAR

Japan Geoscience Union Meeting 2014
(28 April - 02 May 2014 at Pacifico YOKOHAMA, Kanagawa, Japan)

HTT34-02 Room:422 Time:April 28 14:30-14:45

Identification of sidewalk steepness from LIDAR data for Tsukuba University campus bicycle riders

MURAYAMA, Yuji[1] ; LWIN, Koko[1] ; ZHOU, Yifei[1*]

[1]Graduate School of Life and Environmental Sciences, University of Tsukuba

(1) Motivation

Bicycles are the most prominent travelling mode in many universities. Measurement of safety factors for sidewalk bicycle riders is essential for university authorities in order to concern public safety and to improve campus facility management information system. Information of sidewalk steepness is useful for daily bicycle riders inside the university campus in order to prevent unnecessary accidents while they are riding, especially at night.

(2) Data and Methods

In this study, we used very fine scale Light Detection And Ranging LIDAR data to identify the sidewalk steepness by integrating with Smart Field Data Collection System∗and deliver the information through Campus Web-GIS.

(3) Results

Based on our study, LIDAR data are much promising to detect sidewalk steepness in open spaces. However, the accuracy was reduced in some areas where the sidewalk covered with trees and bridges. Intensive field investigations are required to correct them. We built a *Smart Field Data Collection System* to correct and modify the results by using Android smart phone application.

(4) Prospect

Identification of sidewalk steepness from LIDAR data is cost and time effective. Additional user friendly real-time Web-based GIS field data collection system to collect, store and modify the results by multiple users is a great benefit for data validating purposes.

(5) References

Yuji Murayama and Ko Ko Lwin, (2013). Smart Data Collection and Real-time Digital Cartography, IGU Kyoto Regional Conference 2013, August 4-9, Kyoto, Japan.

Keywords: Lidar, fieldwork, campusGIS

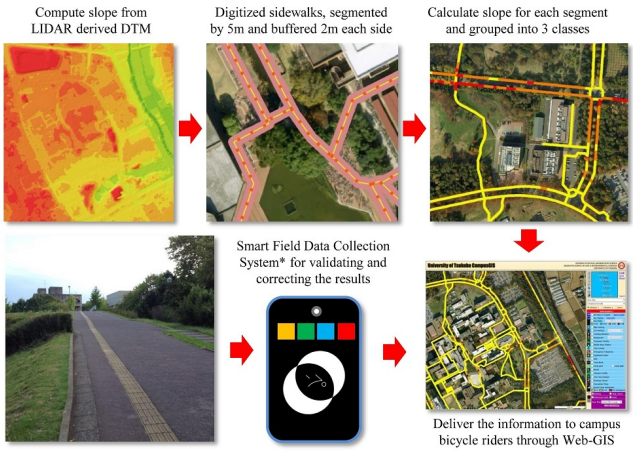

Japan Geoscience Union Meeting 2014
(28 April - 02 May 2014 at Pacifico YOKOHAMA, Kanagawa, Japan)

HTT34-03 Room:422 Time:April 28 14:45-15:00

The Buffer Zone Model of Natural Conservation Area

TANKA, Kazunari[1*] ; YOSHIKAWA, Shin[1]

[1]Osaka Institute of Technology

1. Introduction

In the Kii mountainous region in the south Kinki area, there are preserved beautiful forest and river. However, the area faces problems of sustaining local industries as number of successors was declining due to the decrease of birthrate which is the major problem of Japanese society. Especially the decline of population and competitiveness of local industries are serious problems.

The 'Sacred Sites and Pilgrimage Routes in the Kii Mountain Range' are registered under the World Heritage Site in July 2004. This is the second example of linear type World Heritage Site. The first Site was the 'Camino de Santiago', which means the 'Way of St. James' in northern Spain.

The buffer zone of the 'Sacred Sites and Pilgrimage Routes in the Kii Mountain Range' is set as fifty meters from the center of the trails for both sides. This fifty meters' buffer zone was set without theory in terms of conservation of the environment around the World Heritage registered area.

The core area of the 'Camino de Santiago' is linear type as well. It connects cultural monuments, cathedrals and beautiful nature sites in Spain and in France. The buffer zones of the area was set for thirty meters from the center of the trails for both sides. However, if considering the visibility of the Pyrenees mountainous areas, wider area should be covered as buffer zone. As there are no standard criteria for the buffer zone setting that the study aims to develop GIS, which can determine the appropriate buffer zone.

2. Purpose of Report

In this report, we tried two studies; one was to survey the visibility of forest with plants laser measurement device. Secondly, the study achieved the method to describe the forest model in digital format. As for the further step, we will analyze the relationship between the result of the survey and the model. Based on the data we obtained, we will try to make a model to set buffer zone for conservation area.

3. Analysis

The analyzed area of this report is Koyasan Cyoichi-michi trail in the 'Sacred Sites and Pilgrimage Routes in the Kii Mountain Range' World Heritage Site. We surveyed several points using 3D laser scanner. The points were determined based on the pre-survey by photo and conventional measured. The points we surveyed differ such as vegetation and geographical conditions. The typical vegetation was the cluster of plants of cryptomeria. On an average within the seventeen meters there were many obstacles, which disturb visibility (24.7%).

We also analyzed to application of the survey results to a model plantation area for the comparison. The artificial plantation model is created from the typical trunks of trees with locations and even distances, which make the model to be quantitative.

We set the viewpoint surface every one meters. We estimated that the visible area and invisible area can be determined by setting lines between human visions and trees within. It showed the difference between visible area and invisible area. The percentage of the transitivity of visibility is calculated based on the above results.

The model is set based on periodical growth of plants. The previous study indicated that statistically cryptomeria of forty to sixty years old is majority of plantation. We calculated the distances of transitivity (an average distance) based on the visible-invisible analysis using GIS system. Finally, we verified the results (photographs) at the actual sites.

4. Conclusion

The study found out the possibility of the method that make the model of the buffer zone related with real space. The model we established in this study can expect statistically reliable results from simple survey method and objective data. The study will fine-tune results in applying the detailed data. Simultaneously, we aim to develop criteria based on the differences of the part of trees, as well as other natural environment.

Keywords: buffer zone, world heritage, Sacred Sites and Pilgrimage Routes in the Kii Mountain Range, GIS

Japan Geoscience Union Meeting 2014
(28 April - 02 May 2014 at Pacifico YOKOHAMA, Kanagawa, Japan)

HTT34-04 Room:422 Time:April 28 15:00-15:15

Effects of the buffer models in the estimation of the spatial SPM distribution at the sky of the Yokohama city

YAMAKAWA, Junji[1*]

[1]Graduate School of Natural Science and Technology, Okayama University

In the estimation of the SPM distribution on successive region of interest from the concentrations observed at the observatories located in various places, the kriging method (Matheron, 1973) has been frequently employed. At the case, the universal kriging with auxiliary maps is used for minimize the variance of the estimation. In this study, two types of the auxiliary maps were used in the universal kriging estimation of the SPM concentration distribution. One of the map was a terrain map based on the DEM, and the other map is a buffer map generated from the buffer model based on the buffer distance from the coastline. However, if the region of interest is a wide area that includes a sea part and the land part, and if the observed values of SPM concentration at sea part have not been obtained, the validity of the estimated SPM distribution by the universal kriging may be affected by the used buffer models. Therefore, the effect of the buffer maps in the estimation of the SPM spatial distribution by a universal kriging was investigated in this study.

The SPM concentration data used in this study were published by the National Institute for Environmental Studies. The DEM data was extracted from the digital elevation models that have been published from the Geographical Survey Institute used with the FGDV application. The buffer model were created by the GIS applications based on the coastline data extracted from 1:200,000 Japan seamless geological map that was published from the Geological Survey of Japan. The coordinate projection method of all data were converted to Japan datum 2000 (JGD2000) to minimize the occurrence of error due to the difference of the projection method in geospatial computing. In the representation and geospatial statistical analysis of the data, the R language and its geospatial packages and, the Google earth and FOSS4G were used.

In this study, the observation points of the SPM concentration were present only on the land area and not present on the sea part. Moreover, the altitude of the sea part were all zero in the DEM data. Therefore, in the prediction by the universal kriging at the sea part, even if the variance of the prediction is small, the accuracy of the prediction may be lost at the relatively large buffer distances. So, some care may be required when the predicted distributions are used.

Keywords: GIS, Kriging, R-Language, FOSS4G, Google earth, JPGIS-GML-DEM

Japan Geoscience Union Meeting 2014
(28 April - 02 May 2014 at Pacifico YOKOHAMA, Kanagawa, Japan)

HTT34-05 Room:422 Time:April 28 15:15-15:30

Investigation of indoor positioning technology focused on signboard in railway station

SHIMIZU, Tomohiro[1*] ; YOSHIKAWA, Shin[2]

[1]Graduate School of Eng., OIT, [2]Faculty of Eng., OIT

The acquisition of the outdoor location information has become convenient and precise by the appearance and development of the satellite positioning technology. Recently, it has been more high precise positioning on a centimeter level by the launch of the quasi-zenith satellite in 2010. So, the various services utilizing the location information have been produced. In this way, the location information has become more important and essential as a kind of social infrastructures. Under such circumstances, the acquisition of location information in the indoor environment where the satellite radio wave cannot reach has been regarded important as a next step.

In this study, the authors are going to investigate an indoor positioning estimation technology focused on the railway station. In the railway station, the various needs, such as the advancement of amenities, the facilitation of pedestrian movement, the universal design associated with an aging society, the creation of a compact space appropriate for the population decline society and so on, have been required. In particular, the development of the railway station with multiple functions like business has been recently promoted in the metropolitan areas. So, the spatial structure of the railway station has been complicate because it has been required to play various daily roles for urban residents. And the precise acquisition of location information is more important in the indoor environment like the railway station which has much complexity in recent years. Therefore, the authors are going to investigate an indoor positioning estimation technology in the railway station space. Especially, the authors pay their attention to the signboards of important information indicating ”positional relations of the space” in the railway station.

First of all, the authors built the database of the sign system and the floor maps to estimate the indoor location. The authors built it with three-dimensional information including the display height in addition to the plane information by extracting the signboard from the photograph. Also, they built the attribute information like the size and direction of sign boards, and the type and number of pictograms in the database. So, they tried to estimate an indoor location by using the photograph. Actually, they extracted signboards in the photograph by using the image processing technology. After that, the rough location where the signboards were taken in photos can be grasped by matching the attribute information. It is necessary to set an area in each signboard. In this study, the authors set up ” the effective visual field range ” of signboard , because they assumed to take a photograph when the signboard is confirmed. Finally, they are going to estimate a detailed indoor location by using photogrammetry technology. For the purpose, it is necessary to orient the already known three points with coordinates. Therefore, in this study, the detailed location is estimated by using three-dimensional coordinates on four corners of the signboard in the database. This study could obtain certain results as an indoor positioning technology through the investigation of ”the extraction of a signboard from the photograph ”, ”the estimation of the area from effective visual field range” and ”the estimation of the point location by photogrammetry technology”.

In future, it is necessary to make an effort for the improvement of accuracy related to the technology used in this study. In addition, the authors have to build the system that can automatically estimate an indoor position from the photograph.

Keywords: railway station space, railway signboards, indoor positioning, image processing

Japan Geoscience Union Meeting 2014
(28 April - 02 May 2014 at Pacifico YOKOHAMA, Kanagawa, Japan)

HTT34-06 Room:422 Time:April 28 15:30-15:45

Handling non-aggregated person trip data with Web-GIS

MURAYAMA, Yuji[1*] ; LWIN, Koko[1] ; GREGER, Konstantin[1] ; ESTOQUE, Ronald[1] ; KUBO, Takafumi[1]

[1]Yuji Murayama

Understanding of human mobility from spatial perspective is important for urban transport planners, human geographers, social scientists and other spatial information users. Advances in geospatial data collection methods and communication devices, we can nowadays collect, store and integrate large amounts of data with GPS and GIS technologies, including mobile phone log data, real-time weather information, person flow data etc. However, handling of these Spatial Big Data require computational power and considerable period of time. Extraction of information from these Spatial Big Data is also challenging for end users in terms of time consuming and requires knowledge on spatial data handling and processing. Here we construct a Web-GIS to extract, visualize and analyze the Person Trip Survey (PTS) data by providing common GIS analytical functions to novice to expert users in timely manner.

Keywords: GIS, person trip, big data, spatial analysis, WebGIS, visualization

Japan Geoscience Union Meeting 2014
(28 April - 02 May 2014 at Pacifico YOKOHAMA, Kanagawa, Japan)

HTT34-07 Room:422 Time:April 28 15:45-16:00

The Process of Growth and Cityscape Transition in Modern Osaka

NISHIMOTO, Takahiro[1*] ; YOSHIKAWA, Shin[2] ; TANAKA, Kazunari[2]

[1]NEWJEC Inc., [2]Faculty of Eng.,OIT

Most of big cities in modern Japan had been growing up remarkably with modernization from the Meiji period. Especially, the structure of space has been changing dramatically throughout a revival development in the post-war and in the high economic growth period. As the result, it have been become difficult to see the cityscapes of the past which built up with the modernization. However, in recent years after the arrangement of urban infrastructure settled down, the community development or a tourism using the historical environment have been carried out, and the interest in history has been increasing. In other words, to keep the historical environment has been increasing importance as property of city. On the other hand, GIS becomes more familiar to us by geospatial information technology spreads rapidly in recent years, in the middle of a highly information-oriented society. Especially, the utilization GIS is effective for the historical research, because it can process long-term spatiotemporal information like transition analysis.

Osaka was prosperous as the Aqua Metropolis in Edo period, and has become the modern city crowded with public transport and high-rise buildings in Kansai area at present. In this study, the authors are trying to investigate the historical transition in Osaka with modernization by using geospatial information technology. And they are going to recognize again the existence of characteristics in urban space which formated and disappeared with modernization, and to aim at reconstructing the historical environment.

It becomes necessary to arrange the long-term change efficiently in the study of urban transition. Therefore the authors decided to use the topographical map for six terms in this study from the middle of Meiji period when the modernization began. The authors make the spatial data which the street and the wetlands from this topographical map. And they constructed the urban transition database by using both these data and the database which was already built the river and the railway in our laboratory. As a result of expressed urban transition, the authors grasped that Yodo River which was the most catchment area in the present was formed with repairing Nakatsu River in the late Meiji period. And, the Dohjima canal was dug in Umeda from the early Meiji until before the war, the authors thought that this area was different urban space from present day. Paying attention to the street, the right bank area of the old Yodo River focusing Umeda has been becoming earlier urbanization than the other areas. At the same time, the reconstruction of buildings in the built-up area repeated with modernization, and the authors found the possibility that a changing of the scene was taking place close to the old Yodo River. From these results, the authors direct their attention to Umeda and the old Yodo River basin, and tried to simulate of the cityscape transition using the three-dimensional models in this study.

A terrain model is important for constructing urban model. In this study, the terrain was created 140 kilometers square using digital elevation model (DEM) data based a knowledge of the precedent study. The features are created as landmarks and general houses using CAD/CG. The authors selected Osaka station of Umeda and the mint of the old Yodo River basin for landmarks. These are reconstructed in great detail basing historical materials. As a results of the simulation, the authors could visualized the landscape transition in Umeda and the old Yodo River basin with modernization.

As the result of this study, the authors clarified the historical transition in the part of Osaka by using GIS and CAD/CG. At the same time, they reconstructed the historical environment as property of Osaka. In the near future, they are going to construct the animation of the transition of Osaka for the communication tool by using created spatial data. And it is necessary for three-dimension models to improve the accuracy.

Keywords: modernization, cityscape transition, Umeda, old-Yodo River

Japan Geoscience Union Meeting 2014
(28 April - 02 May 2014 at Pacifico YOKOHAMA, Kanagawa, Japan)

HTT34-08 Room:422 Time:April 28 16:15-16:30

Landscape analysis of daimyo garden using photograph information

ONO, Yoichi[1*] ; YOSHIKAWA, Shin[2] ; TANKA, Kazunari[2]

[1]FUKKEN CO., LTD., [2]Faculty of Engineering, Osaka Institute of Technology

In recent years, social media in the information technology have been developed remarkably. The scenes at sightseeing are photographed, and the photos are accumulated as the personal spatio-temporal information in a non-structured state on the Internet. In this study, the authors analyze the landscape phenomenon by using personal photographs, the photos are accumulated on the Internet in daimyo gardens.

Specifically, they take photograph images and spatio-temporal information on site and they pay theirs attention to the both sides of the space and time, and analyze the data on using GIS. At first, they choose the case study area from daimyo gardens where many tourists visit at present. Then, they pay theirs attention to the flickr is a photograph community site, and they make a photograph information database and grasp the scene phenomenon by using it.

Among other things, the three famous gardens in Japan are Kairakuen, Kenrokuen, and Korakuen. And Riturin-park is a beautiful garden as well as the three famous gardens. In addition, there are sightseeing spots that many people visit at present. Then, they collected spatio-temporal information and photograph images taken by the visitors in the four gardens by using the flickr API. As a result, Kenrokuen was selected as the case study garden for analysis.

At first, they utilize the Exif information contained in the photographic image data. This metadata is the information of the camera itself, and various information including the F-number and the focus distance are recorded with the positioning data. The Exif information is the index recorded at the time of the photography. In this study, the authors grasp visual characteristics of Kenrokuen by using the focus distance and a photography direction.

Based on the positional information, they plotted the focus distance on GIS with conversion into the 35mm film camera. As a result, they were able to grasp the characteristic in the garden. First of all, around the Ume grove, an angle of view range is narrow and people look the fixed scenes. People watched the buds and the flowers of the plum closely. The second is around the Kotoji-torou area. This area is an angle of view range is wide, and photography is carried out of showed, using the plural focus distances.

Then, the analysis was focused on the photographic images, The photography position is not usually fixed and shows a variety of distribution for one object. Therefore, the authors grasp each viewpoint field by a directional distribution analysis. In this analysis, the point cloud are photography positions, so the standard deviation ellipse created by the analysis is regard as the photography viewpoint field.

First of all, they classify the photographs and create the photography viewpoint fields. As a result, it was revealed that the place, where plural viewpoints fields were overlapped, while people went round the gardens. So, in the sequence around the garden, the people do not watch an object in turn, and it is thought that the features were seen under the complicate influence. In addition, as they investigate the relationship between the subject and the viewpoint field individually, they found several characteristics from the positional relationship between the object and the shape of the standard deviation ellipse. So, they classified photography viewpoint field based on the analysis and grasped viewpoint field with four different characteristics. They grasp on landscape phenomenon in viewpoint field at minute time, and they were similar to expression of the camera work.

In this study, the authors grasped visual characteristics of the case study area by using the Exif information. In addition, they grasp each viewpoint field for every photography object, and was able to model the viewpoint field.

Keywords: daimyo garden, landscape, photograph information

Japan Geoscience Union Meeting 2014
(28 April - 02 May 2014 at Pacifico YOKOHAMA, Kanagawa, Japan)

HTT34-09 Room:422 Time:April 28 16:30-16:45

Spatial pattern of agriculture using GIS and small area statistics

MORIMOTO, Takehiro[1*]

[1]University of Tsukuba

The author used small area statistics of agriculture and composed grid square statistics to make spatial pattern of agriculture in the Kanto District of Japan using GIS. The grid square statistics is suitable for analyses in combination with other ready-made social and environmental grid-square statistics.

Japan Geoscience Union Meeting 2014
(28 April - 02 May 2014 at Pacifico YOKOHAMA, Kanagawa, Japan)

HTT34-10 Room:422 Time:April 28 16:45-17:00

GIS analysis of Australian urban social geography by using Census Table Builder Data designated by ABS

TSUTSUMI, Jun[1*]

[1]Graduate School of Life and Environmental Sciences, University of Tsukuba

A body of literature about multi-cultural aspects in Australia can be found in the fields of international politics, international relations and Australian history as well as Australian geography. Diverse origins of immigrants had a great impact on the changing structure of metropolitan areas in Australia. Based on some previous studies, non-English speaking immigrants, e.g. Greek and Italian in the 1960s, tended to live in the suburbs located 10-15 km apart from the Melbourne metropolitan core. These suburban areas were relatively " less convenient area " in terms of public transportation, but newly developed area supported strongly by motorization. New university, huge industrial parks, distribution centres and relocated suburban offices have been established in these newly developed areas. Immigrants in 1960s could only find affordable houses in these " new suburbs, " resulted in the expansion of the metropolitan area.

After 1990s and later, Australian cities are strongly affected by a " surge " of immigrants from Asian countries. They tended to live in the existed Asian communities located at the peripheries of the metropolitan area, much farther than " new suburbs. " Footscray in the west, Glen Waverley in the east and Springvale in the southeastern suburbs are typical examples of those communities.

In this paper, I focused on the changing structure of Sydney and Melbourne metropolitan areas in terms of diverse origins of immigrants. A GIS-based mapping with " table-builder data " distributed by Australian Bureau of Statistics was used to identify the process. This paper not only provides a methodological innovation but also a new and practical contribution to urban-social process studies.

Keywords: GIS, Australia, Urban area, Sydney, Melbourne, metropolitan area

Japan Geoscience Union Meeting 2014
(28 April - 02 May 2014 at Pacifico YOKOHAMA, Kanagawa, Japan)

HTT34-P01 Room:Poster Time:April 28 18:15-19:30

Land use change in the Loess Plateau of North-Shaanxi and East-Gansu Province, China

HARA, Yuta[1*]

[1]GSGES, Kyoto Univ.

The Loess Plateau in China has some problems about erosion, desertification and economical problems. Erosion has a major influence on agriculture, forestry and grazing, because it cut the cropland and ruin the ecosystem (Matsunaga 2013, Saito 2008a).

From the end of 1990s, the Conversion of cropland to forest and grassland, namely the afforestation project to steep slope, started by the Chinese government for deal with these problems. However, these are not only the fruits (Saito 2008b). The reason, the Loess Plateau has diversity about the environment and humanity due to extensive.

From 2000, there are many investigations about the Land use change in the Loess Plateau. They made the quantitative spread about the green land clear caused by the Conversion of cropland to forest and grassland in China. However the quantitative land use change in the wide area of the Loess Plateau is unknown, because the study areas of the investigations are each basin of the Yellow River. Their compared years are deferent. The compared years are 2 after 1980s.

This study cleared the land use change by remote sensing in North-Shaanxi and East-Gansu Province of the Loess Plateau. In addition, I made the division map based on the change of forest and grassland. Used satellite photos are Landsat/MSS, TM. I did supervised classification by Maximum likelihood estimation. Moreover I did logical disjunction operation using the ArcGIS.

The following results were obtained : 1. There are conflicting differences to changes of the forest in Huanglong Mountains and Ziwu Mountains. 2. There are differences about more than one degree of desertification in the adjacent area of Mu Us desert. 3. Since 1990s, there are conflicting differences to changes about desertification in the hilly-gullied loess region as administrative boundary of Gansu and Shaanxi province. Moreover I estimated the first factor due to local differences using the SRTM.

Keywords: the Loess Plateau, land use change, Landsat, ArcGIS

Japan Geoscience Union Meeting 2014
(28 April - 02 May 2014 at Pacifico YOKOHAMA, Kanagawa, Japan)

HTT34-P02 Room:Poster Time:April 28 18:15-19:30

Miniature LiDAR DEM data smoothing techniques and effects

KAMIHARA, Noriya[1*] ; SATOU, Takeharu[2]

[1]Eight-Japan Engineering Consaltants Inc., [2]Okayama University of Science, Faculty of Biosphere-Geosphere Science

Miniature LiDAR DEM data smoothing techniques and effects

Keywords: LiDAR DEM, Mass Mouvement, Laplacian, Convex

Japan Geoscience Union Meeting 2014
(28 April - 02 May 2014 at Pacifico YOKOHAMA, Kanagawa, Japan)

HTT35-01 Room:311 Time:May 1 09:00-09:15

Review of development of AMS in the past 30 years and future perspective

NAKAMURA, Toshio[1*]

[1]Center for Chronological Research, Nagoya University

One of the main aims of Quaternary research is to understand global environmental changes of the past and to predict the expected changes in the near future. To pursue this aim, high-resolution age estimation is particularly important. Dating methods so far used for Quaternary research can be classified into five categories: (1) age estimation based on the decay procedure of cosmogenic radioisotopes such as radiocarbon (14C) and 10Be, U-series nuclides and a K-Ar pair; (2) age estimation by cumulative dose from natural nuclear radiation and cosmic rays such as TL, OSL, ESR, FT dating methods; (3) age estimation with geological or geochemical evidences of prehistoric events such as paleomagnetic reversals or excursions, oxygen stable-isotope-ratio variations, tephra stratigraphy; (4) age estimation with paleontological records of prehistoric events such as diatom, pollen, nanno-plankton and shellfish assemblages, as well as semi-global fluctuations of tree ring width; (5) age estimation based on archeological evidences. These dating methods are selectively applied dependent on the characters of geological and archeological events to be analyzed. Among the radio-isotopic dating methods, 14C dating is most frequently used because of its applicability to many different types of Quaternary samples, as well as age range covered by this method (a few hundred to 50,000 yr BP).

Developments of accelerator mass spectrometry (AMS) have triggered a wide area of application in radiocarbon (14C) dating. The AMS system requires only 1mg of carbon in precise determination of 14C/12C and 13C/12C isotope ratios, and this advantage has broadened the applicability of 14C measurements. Nowadays, AMS contributes to almost all kinds of research that utilize 14C dating in archeology, cultural property science, geology, and those that employ 14C tracer in environmental sciences, medical sciences and even forensic studies.

For example, a Tandetron AMS system dedicated to 14C measurement was installed at Nagoya University, and its routine operation for 14C measurement was started in 1983 for the first time in Japan. In 1996, another AMS system (HVE-Model-4130-AMS) was purchased and has been used for high precision 14C measurements. By 30 minutes measurement of carbon isotopes repeated for consecutive three days for a sample, one-sigma uncertainty of +-17 to +-30 years is achieved. A reproducibility test for 2000-year-old archeological samples yielded a fluctuation error as small as +-11 years. We also have evaluated accuracy in our 14C measurements by participating in international 14C inter-comparison tests, and confirmed that our14C results were quite consistent with the consensus values by all the participants. After the critical tests, we are sure that our AMS system can be applicable to historical samples that require high precision as well as high accuracy 14C measurements.

Quite frequent applications of 14C dating with AMS to the Quaternary samples in the last bidecade are promoted by the following reasons: (1) a very small amount of carbon (about 1mg of carbon for the final target preparation) is required; (2) uncertainties of 14C ages are from +-17 to +-30 yr, mainly owing to the 14C counting statistics; (3) calibration of 14C age to the calendar age scale become quite popular, for 14C ages up to 50,000 cal BP; (4) marine reservoir effect on 14C age has been recognized and investigated recently, and a realistic correction for the effect is becoming possible partly.

Along with 14C, other cosmogenic radioisotopes such as 10Be, 26Al, 36Cl, 129I are also measured with AMS systems. We briefly describe history of development of domestic AMS groups as well as worldwide AMS groups, along with the research fields of AMS applications and future perspective.

Keywords: accelerator mass spectrometry, cosmogenic nuclides, radionuclide, age measurement, ion nuclide separation, ion particle counting

Japan Geoscience Union Meeting 2014
(28 April - 02 May 2014 at Pacifico YOKOHAMA, Kanagawa, Japan)

HTT35-02 Room:311 Time:May 1 09:15-09:30

Present status of YU-AMS

TOKANAI, Fuyuki[1*]

[1]Center for YU-AMS

Yamagata University (YU) installed an AMS (YU-AMS) system in the Kaminoyama Research Institute to meet the requirement of ^{14}C AMS for microdosing and medical studies as well as that of radiocarbon dating in the same facility. An automated graphitization line was also installed in the same research institute for sample preparation. This AMS system is the first AMS system installed in a university in north Japan (Tohoku-Hokkaido region). The facility also provides radiocarbon dating for samples from other universities, institutes and public organizations. Currently, we are planning to install a second new ion source and an automated graphitization line until March in 2014. In this paper, we describe the status of the YU-AMS system.

Keywords: AMS, microdose

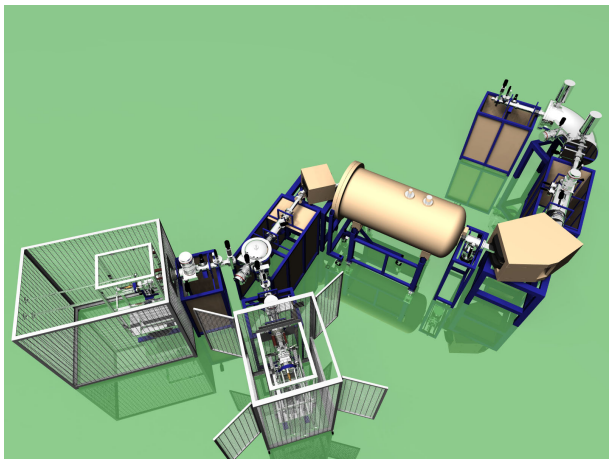

Japan Geoscience Union Meeting 2014
(28 April - 02 May 2014 at Pacifico YOKOHAMA, Kanagawa, Japan)

HTT35-03 Room:311 Time:May 1 09:30-09:45

Development of isobar suppression system using Laser in Accelerator mass spectrometry

MIYAKE, Yasuto[1*] ; MATSUZAKI, Hiroyuki[1] ; HASEGAWA, Shuichi[2]

[1]Department of Nuclear Engineering and Management, School of Engineering, The University of Tokyo, [2]Nuclear Professional School, The University of Tokyo

For Accelerator mass spectrometry (AMS), isobar separation is quite important to improve measurement accuracy and the background. In order to suppress isobar interference, gas-filled magnet or gas counter have been conventionally used [1,2]. Nuclides of interest are separated from isobars by interaction between ions and materials in these devices.

In the 1980s, Berkovits et al. tried to remove stable isobars before acceleration with laser light[3]. In this method, the difference of the electron affinity (EA) was utilized for isobar suppression. If the EA of the nuclide of interest is higher than the EA of the isobar nuclide, only negative isobar can be selectively neutralized by photodetachment with photons of energy, which is higher than the EA of isobar nuclide but lower than the EA of the nuclide of interest. Consequently, only nuclide of interest can be injected into the accelerator and isobar suppression can be effectively achieved. However, due to the limited laser performance, the laser-ion interaction time was too short to suppress isobar sufficiently at that time. Therefore, this technique has not been in practical use yet.

Recently, as laser improved in quality and the way to increase the laser-ion interaction time effectively was proposed, development of isobar suppression system is going on. For example, Liu et al. developed the RFQ ion cooler to slow ions [4]. This apparatus is filled with a buff gas and ions collide with gas molecules, which results in the deceleration of ions and the long interaction time. This photodetachment system can remove isobar interference in AMS measurements for nuclides, such as Cl-36 (EA=3.62eV) with S-36 (EA=2.08eV), Ni-59 (EA=1.156eV) with Co-59 (EA=0.661eV) [4]. Furthermore, even if the EA of the nuclide of interest is lower than the EA of the isobar nuclide, photodetachment could be useful by converting the nuclides into the molecular ions and reversing these electron affinities.

In order to make laser interact with ion beams effectively, the ion beam optics including the devices like the ion cooler should be optimized. This device will be installed after the electrostatic deflector or after the injection magnet in the beam line. In this study, as a preliminary step, optimization of the ion beam optics including some components to decelerate ion will be dicussed.

[1] H. Matsuzaki, Journal of the Vacuum Society of Japan, Volume 50, Issue 7, 467-474 (2008).

[2] T. Aze, H. Matsuzaki, H. Matsumura, H. Nagai, M. Fujimura, M. Noguchi, Y. Hongo. and Y. Yokoyama, Nucl. Instr. Meth. **B259**, 144-148 (2007).

[3] D. Berkovits, E.Boaretto, G. Hollos, W. Kutschera, R. Naaman, M. Paul, and Z. Vager, Nucl. Instr. Meth. **A281**, 663 (1989).

[4] Y. Liu, P. Andersson, J.R. Beene, O.Forstner, A. Galindo-Uribarri et al., Rev. Sci. Instr. **83**, 02A711 (2012).

Keywords: AMS, isobar, laser, photodetachment

Japan Geoscience Union Meeting 2014
(28 April - 02 May 2014 at Pacifico YOKOHAMA, Kanagawa, Japan)

HTT35-04 Room:311 Time:May 1 09:45-10:00

Development of C14-free laboratory animals.

KOBAYASHI, Koichi[1*] ; AMS, Dating group[1]

[1]Paleo Labo Co.,Ltd.

In the early stage of pharmaceutical researches, ^{14}C labeled chemicals with very high radioactivity are administrated to laboratory animals to study pharmacokinetics. However, when $^{14}C/^{12}C$ of the laboratory animals could be reduced, the radioactivity level of the chemicals is expected to be reduced lower. Also when ^{14}C-free (DC ; denoted as dead carbon) laboratory animals were developed, the radioactivity level for the study is expected to be reduced down by five orders of magnitude or lower by using AMS technique. That means that we need not the ^{14}C labeled chemicals but natural level chemicals for the study of pharmacokinetics. In this case, it is also expected that we can be free from the hazardous high radioactivity and from the strictly regulated troublesome laboratory to handle the high level radioactive materials.

In Dec. 2010, we started the project to produce ^{14}C-free lives as feed for the ^{14}C-free laboratory animals. This is a preliminary report on the project, and parts of the investigation were already reported at 13th Japanese Symposium on AMS (Kobayashi et al., 2011). Here will be also introduced some recent studies.

When lives were cultivated in DC surroundings they grow up inevitably to be DC lives. For example, photosynthetic lives like vegetables or some kinds of microbes with chloroplast like euglena (midorimushi ; in Japanese) can easily be DC lives when they were cultivated in DC surroundings.

For the first step, we cultivated some plants and euglena using ^{14}C free water set in a glove box that was filled with artificial air (N_2, O_2 and dead carbon CO_2 with proper concentration) irradiating with some artificial lights. ^{14}C concentrations in the plants and the microbes were measured by AMS. Since the modern carbon (natural carbon) CO_2 could not be perfectly removed from the air and the water and air tightness of the glove box system was also not perfect, the percentages of dead carbon to modern carbon (DC ratio) in the samples could not be higher than about 80 %.(Kobayashi et al., 2011a ; Kobayashi et al., 2011b)

While investigating the cause of the imperfect DC ratio, we got 96% DC Euglena by using a little different way. That is to use a small glass bowl with an airtight lid, in which were set CO_2 tablets, a small amount of chemical fertilizer and Euglena. From outside of the bowl, fluorescent lamps irradiated adequate amount of light to them. One or two months later, the euglena was carefully collected on glass filters in a glove box filled with DC air. $^{14}C/^{12}C$ of the euglena was measured by AMS and the ^{14}C concentration was 3.71 ± 0.02 pMC (percent Modern Carbon) which leads to DC ratio as 96% (Kobayashi et.al., 2012).

In order to make sure that mice really eat the euglena tablets, we fed the mice with euglena tablets which were mixed with chlorella powder by 20%. The tablet is on the market for people as a health food. After three months feeding on three mice, there were no large differences compared to the other three mice which were fed by ordinary food for comparison. The experiment concluded that mice will grow up healthy by eating the euglena tablet.

Those two above data show the possibility to realize the DC animals.

Recently, we have started to extend the project to realize for business, supported by a grant.

References:

Kobayashi, K. et al. (2011a), Production of ^{14}C-free plants and animals (in Japanese) ; Kobayashi, K. et al. (2011b), Production of ^{14}C-free plants and animals ; Kobayashi, K. et al. (2012), Production of dead carbon lives (in Japanese)

Keywords: Pharmacokinetics by AMS, C14-free lives, Euglena

Japan Geoscience Union Meeting 2014
(28 April - 02 May 2014 at Pacifico YOKOHAMA, Kanagawa, Japan)

HTT35-05 Room:311 Time:May 1 10:00-10:15

^{14}C measurement of the Southern Japanese tree by the AMS method for high-precision radiocarbon calibration

HAKOZAKI, Masataka[1*] ; NAKAMURA, Toshio[1]

[1]Center for Chronological Research, Nagoya University

Radiocarbon (^{14}C) dating method has contributed to the age determination of samples of the past 50,000 years in geology and archaeology. However, since ^{14}C date is not in agreement with the calendar year, the calibration using a dataset which consists of ^{14}C data of calendar year known samples is required for it. Moreover, since there is regional difference of ^{14}C concentration in the atmosphere (regional ^{14}C offset; Hogg et al. 2002), in order to be high-precision calibration, the dataset for each area needs to be established.

The Center for Chronological Research (CCR), Nagoya University has measured ^{14}C data of tree-rings of a Yaku cedar from the Southern Japan, in order to establish a calibration dataset for Japan. Previous measurement has shown that the cedar shows 14C date older than global standard calibration dataset IntCal13 (Reimer et al. 2013) in various times for the past 2000 years (Nakamura et al. 2013). This report shows the measurement result of the tree-rings formed in the 5th century.

Sample is a Japanese cedar from Yaku Island, Kagoshima prefecture (sample code: Yaku_A). Dendrochronological analysis with a master-chronology (Kimura unpublished) has carried out, and the calendar year of this sample is known. After exfoliating the annual rings of AD434-502 of a sample in one year respectively, only even-numbered years was measured (n = 35). The tandetron AMS II of CCR was used for this measurement. Measuring only even-numbered years in order to understand a whole tendency previously, it also measures the samples of odd-numbered years in the future.

Thirty five ^{14}C dates of tree-ring samples showed that it will be older than IntCal13 for an average of 28 $\pm$ 22 years, a maximum of 76 $\pm$ 21 years (in AD488). These ^{14}C dates were mostly located in the middle of IntCal13 and SHCal13 (the calibration dataset for the Southern Hemisphere; Hogg et al. 2013).

Since Yaku Island touch the northernmost end of the Intertropical Convergence Zone in a summer, it is thought that the Southern Hemisphere atmosphere with regularly low ^{14}C concentration is easy to be supplied (Nakamura et al. 2012). This measurement result might suggest that ^{14}C concentration in the atmosphere of the Japanese neighborhood fell in the 5th century, and the atmospheric supply from the Southern Hemisphere may have become strong. Sakamoto et al. (2013) measured the tree-ring samples in the 5th to 6th century of the Japanese cedar from Nagano Prefecture Central Japan, and they has reported that the data is older than a IntCal13. Our result harmonizes with the measurement result of the trees from Nagano, and this time can consider a possibility that the influence of the Southern Hemisphere atmosphere had reached to central Japan. From now on, the tree-rings of Yaku cedar in formed the 6th century will measure, and it will compare with the result of Sakamoto et al. (2013).

Keywords: radiocarbon calibration, regional ^{14}C offset, Southern Japan, tree-ring, Yaku cedar

Japan Geoscience Union Meeting 2014
(28 April - 02 May 2014 at Pacifico YOKOHAMA, Kanagawa, Japan)

HTT35-06 Room:311 Time:May 1 10:15-10:30

C-14 dating and geochemical analyses of the tsunami sediments in continuous soil deposits from Tohoku area, Japan

WATANABE, Takahiro[1*] ; HOSODA, Norihiro[1] ; TSUCHIYA, Noriyoshi[1] ; NAKAMURA, Toshio[2] ; YAMASAKI, Shin-ichi[1] ; NARA, Fumiko[1]

[1]Graduate School of Environmental Studies, Tohoku University, [2]Center for Chronological Research, Nagoya University

Past tsunami sediments preserved in continuous soil and lake sediments are crucial and unique clues to reconstruct the past tsunami invasion area. Generally, the tsunami sediments originated from sea floor, sandy beach and/or coastal land soils containing gravels, sands, muds, shells and microfossils. In particular, muddy tsunami sediments should be found to detect the limit of tsunami invasion areas, because relative small particles move to more inland area with tsunami in comparison with sand deposits. Additionally, dating of tsunami sediments is indispensable to refer for historical disaster events. Therefore, we have to make age models of continuous soil deposits with tsunami sediments and new techniques for detection of invisible muddy tsunami sediment in strata. In this study, we performed the nine radiocarbon measurements of plant residues in continuous soil deposits as well as geochemical characteristics of tsunami sediments. 2m-continuous soil deposits were taken by the handy geoslicer (Fukkenn co. ltd.) from the Pacific coast of Tohoku area in northeast Japan. The samples were composed of cultivated surface soils, peaty clay, silt and sub-rounded medium sands. The sandy deposits were found between the peaty clay layers. To show the sedimentary ages of sandy deposits, plant residues were taken from the sandy and peaty clay layers in the continuous soil sediments. The plant residues were washed with ultra pure water using ultra sonic cleaner to remove soil particles containing relative old carbon. Then, the samples were treated sequentially with 1.2M-HCl, 1.2M-NaOH and 1.2M-HCl at 60 degrees of Celsius for 3 hours. After neutralization and freeze-drying, the samples were combusted in evacuated quartz tubes. Then, the purified carbon dioxide was reduced to graphite using Hydrogen gas with iron catalysts. Radiocarbon measurements were performed by the Tandetron AMS system (Model-4130, HVEE) in Center for Chronological Research, Nagoya University. Total organic carbon contents of the plant residues were from 45.9 to 54.5 wt.% (50.4 wt.% in average) and stable carbon isotope ratios of the plant residues ranged between -26.7 and -30.1 permil (vs. PDB), which consist with those of modern terrestrial C3 plants. As a result of this study, part of the calibrated ages of plant residues taken from just above the sandy tsunami sediments was about 1000-1300 cal BP, and these ages were agreed well with those of the Jogan earthquake and tsunami in the Sendai plain.

Keywords: Radiocarbon dating, Tsunami deposits, Jogan tsunami, Geochemistry, EDXRF

Japan Geoscience Union Meeting 2014
(28 April - 02 May 2014 at Pacifico YOKOHAMA, Kanagawa, Japan)

HTT35-07 Room:311 Time:May 1 10:30-10:45

AMS radiocarbon dating of tephra layers on Adak Island, central Aleutian

OKUNO, Mitsuru[1*] ; NAKAMURA, Toshio[2]

[1]Fac. Sci., Fukuoka Univ., [2]CCR, Nagoya Univ.

The Holocene tephra layers distribute on Adak Island located in the central part of the Aleutian Islands. Radiocarbon (ˆ{14} C) age determination of charcoal fragments in the soil layer has been performed. Moreover, tephra is intercalated with sand layer of dune. Since sand dune has high depositional rate and low contamination of organic matter, a possibility of polluted charcoal sample from below and above tephra is low. Thus reliable age was able to be obtained by the AMS method to these small samples. We report those results.

Keywords: Adak Island, Holocene, tephra, radiocarbon date

Japan Geoscience Union Meeting 2014
(28 April - 02 May 2014 at Pacifico YOKOHAMA, Kanagawa, Japan)

HTT35-08 Room:311 Time:May 1 11:00-11:15

Radiocarbon dating of stalagmites from the Ryugashi Cave, Shizuoka

KATO, Tomomi[1] ; MINAMI, Masayo[2*] ; HORIKAWA, Keiji[3] ; NAKAMURA, Toshio[2]

[1]Graduate School of Environmental Studies, Nagoya University, [2]Center for Chronological Research, Nagoya University, [3]Graduate School of Science and Engineering for Research, University of Toyama

Stalagmites are cave deposits precipitated from drip water. Drip water consists of carbon derived from soil CO_2, which has atmospheric ^{14}C values in isotopic equilibrium with atmosphere, and carbonate-dissolved CO_2, which has ^{14}C-free (dead) carbon through interaction with cave host bedrock. As a result, drip water contains a percentage of dead carbon, which will make the ^{14}C ages of the stalagmite older. Therefore, a correction of the dead carbon fraction is needed for ^{14}C dating of stalagmites. In recent years, young stalagmites of 10-20 ka have been ^{14}C dated by comparing the ^{14}C on samples of known calendar age with the tree ring record of atmospheric ^{14}C during a period of overlap (Hoffmann *et al*., 2010; Southon *et al*., 2012). This procedure involves the implicit assumption that dead carbon fraction in stalagmite remained constant through its growth time. In this study, therefore, we examined dead carbon fraction in two stalagmites from the Ryugashi Cave in Hamamatsu, Shizuoka by investigating seasonal variation in ^{14}C concentrations of drop water coupled with soil CO_2, atmospheric CO_2, and host limestone, in order to reveal possibility of accurate and precise ^{14}C dating on stalagmite in Japan.

The drip water samples showed ^{14}C of 1130 BP to 980 BP and $\delta^{13}C$ of -10.1 ‰ to -9.1 ‰, which are lower in fall and winter, and higher in spring and summer, and have the annual means of ^{14}C of 1025±140 BP and $\delta^{13}C$ of -9.4±0.4 ‰. The RYGS12 stalagmite of 7 cm in length showed 945±30 BP at its top and 2150±40 BP at its bottom, and had a growth rate of about 60 μm/yr. The calibrated age of RYGS12 was estimated by comparing the ^{14}C with the IntCal13 calibration curve, resulting that the stalagmite had a constant dead carbon fraction through its growth time and gives ^{14}C ages of 1050 years older than the true age. The carbon isotopic fractionation between drip water and stalagmite was negligible. The results indicate that high-resolution ^{14}C measurement can be performed on stalagmites in the Ryugashi Cave.

The RYGS12 sample showed rapid decrease of $\delta^{13}C$ from -8.3 ‰ to -11.8 ‰ at around AD1450 The decrease suggests an increase of soil input to the stalagmite, since soil CO_2 has low $\delta^{13}C$ of -22.0 ‰. It is reported that there was a great earthquake of magnitude 8.6 (Meio earthquake) accompanied by a catastrophic tsunami in this study area in AD1498. Therefore, the $\delta^{13}C$ decrease might be caused by the Meio earthquake. In the presentation, we will present ^{14}C result on another stalagmite sample RYG08 of 30 cm in length.

Keywords: stalagmite, radiocarbon age, carbon isotope ratio, oxygen isotope ratio

Japan Geoscience Union Meeting 2014
(28 April - 02 May 2014 at Pacifico YOKOHAMA, Kanagawa, Japan)

HTT35-09 Room:311 Time:May 1 11:15-11:30

14C-based source apportionment of carbonaceous component in PM2.5 in Nagoya city

IKEMORI, Fumikazu[1*] ; YAMAGAMI, Makiko[2] ; HONJYO, Koji[3] ; NAKAMURA, Toshio[4]

[1]Graduate School of Environmental Studies, Nagoya University, Nagoya City Institute for Environmental, [2]Nagoya University, Nagoya City Institute for Environmental, [3]Graduate School of Environmental Studies, Nagoya University, [4]Center for Chronological Research, Nagoya University

The measurement of radiocarbon (14C) has been used to estimate the relative contributions of fossil and contemporary carbon sources in particulate matter throughout the world. In this study, we use 14C to provide quantitative estimates of carbon origin sources in Nagoya in April 2003 to March 2004. pMC and OC/EC showed similar seasonal variations and high values (range 39.8 to 68.4, 1.0 to 2.0; average 53.4, 1.5, respectively) in May and early June, whereas the values of pMC stayed relatively low values (range 28.3 to 41.9, 0.7 to 1.2; average 34.2, 1.0, respectively) after middle June. To estimate the source region of high pMC values, backward air mass trajectories were calculated during the sampling period in April to June. The air mass appeared to have passed through eastern Siberia when the pMC values showed high values in May and early June which also showed high values of OC/EC ratio and OC concentrations. In 2003, many researchers reported the influence of large forest burning in Siberia. This large forest burning occurred in spring to summer. The smoke from this forest burning had reached to Korea, Japan, and North America. The influences from the Siberian forest fires had an important implication for air quality over East Asian region. We conclude that high pMC values measured in spring are originated from large forest fires in Siberia and transported long distance.

Keywords: atmospheric aerosol, PM2.5, radiocarbon

Japan Geoscience Union Meeting 2014
(28 April - 02 May 2014 at Pacifico YOKOHAMA, Kanagawa, Japan)

HTT35-10 Room:311 Time:May 1 11:30-11:45

Decadal change in bomb-produced radiocarbon in the Pacific Ocean revealed by WHP repeat hydrography

KUMAMOTO, Yuichiro[1*] ; MURATA, Akihiko[1] ; KAWANO, Takeshi[1]

[1]Japan Agency for Marine-Earth Science Technology

Radiocarbon produced by nuclear weapon tests is one of ideal tracers for the air-sea gas exchange and ocean circulation. In the 2000s, radiocarbon in dissolved inorganic carbon was measured during revisit cruises along the WOCE (World Ocean Circulation Experiment) lines of P01 (47N approx., 2007), P03 (24N approx. 2005), P06 (32S approx., 2003), P10 (149E approx., 2005), P13N (165E approx., 2011), P14N/C (179E approx., 2007), P17N (135W approx., 2001), and P21 (17S approx., 2009) conducted in the 1990s in the Pacific Ocean. Comparison of radiocarbon data from the 1990s and 2000s revealed decadal changes of radiocarbon concentration in the thermocline, most of which were due to temporal changes in the bomb-produced radiocarbon. Vertical profiles and vertical-integrated inventories of the bomb radiocarbon in the subarctic and equatorial regions have not changed significantly. In the subtropical regions, radiocarbon decreased in upper thermocline from surface to about 500-m depth. In contrast, radiocarbon increased in lower thermocline from about 500-m to 1500-m depths. In the southern and northeastern subtropical regions, the two opposing directions in radiocarbon change resulted in small temporal changes of the total inventory of the bomb radiocarbon. On the other hand, the water column inventory significantly decreased in the northwestern subtropical region because the radiocarbon decrease in the upper thermocline was larger than the radiocarbon increase in the lower one. These decadal changes are primarily due to the meridional transport of the bomb radiocarbon from high latitude into temperate zone. The decrease in the vertical-integrated radiocarbon in the northwestern subtropical region implies that the turnover time of the thermocline circulation in the region is faster than those in the other subtropical regions in the Pacific Ocean. In addition the loss of the bomb-radiocarbon in the North Pacific Ocean could be explained by its transformation to the Indian Ocean via Indonesian Through Flow. This work was partially supported by Japan Society for the Promotion of Science (JSPS) KAKENHI Grant Number 18310017 and the Common-Use Facility Program of JAEA (2007A-F03, 2007B-F05, 2008A-F02, 2009A-F05, 2010A-F06, and 2011A-F04).

Keywords: bomb-produced radiocarbon, Pacific Ocean, ocean circulation

Japan Geoscience Union Meeting 2014
(28 April - 02 May 2014 at Pacifico YOKOHAMA, Kanagawa, Japan)

HTT35-11 Room:311 Time:May 1 11:45-12:00

Study on property of soil organic matter decomposition by global warming using radiocarbon

ARAMAKI, Takafumi[1*] ; LIANG, Naishen[1] ; TERAMOTO, Munemasa[1] ; TOMITA, Ayako[1]

[1]National Institute for Environmental Studies

Current research indicates that future atmospheric CO_2 concentration may be increased more than predicted value by furthering of soil organic matter decomposition due to global warming. The information on soil organic matter decomposition property in long-term warmer environment has not yet been obtained. We have carried out artificial soil warming experiment in six forest sites having different vegetation in Japan for long time. We planed vertical ^{14}C measurement of soil core at an even-green Japanese oak forest in Setonaikai region (Higashi-Hiroshima). A soil core was collected from both the soil warming and the control plot in December 2011, and was cut into 1cm layers in laboratory. Each sample was hydrolyzed with 1N HCl overnight to remove inorganic carbon in the sample, and then was analyzed particulate organic carbon (POC) and organic nitrogen (PON) by an elemental analyzer. For ^{14}C analysis by an accelerator mass spectrometer (AMS), soil samples adjusted to a weight of approximately 3mg-C were first converted to CO_2 gases by combustion with CuO and Ag foil at 900 ℃, and then purified cryogenically in a vacuum line. The CO_2 gas samples were reduced to graphite with H_2 gas over Fe powder. The $^{14}C/^{12}C$ ratios of the sample graphite were measured at the Tandetron AMS Facility in the Mutsu Office of the Japan Atomic Energy Agency. The ^{14}C results are expressed as $\Delta^{14}C$. The typical analytical error of the $\Delta^{14}C$ values was about $\pm$ 4 ‰ based on the 1σ value of the counting statistics.

Both of POC and PON weight percent in the soil were high above 3cm depth and decreased sharply with depth from 5cm to 15cm. Both of POC and PON of the soil warming plot were 20-30% lower than those of the control plot irrespective of depth above 15cm depth. The result indicates that the soil warming experiment was encouraged the microbial decomposition of soil organic matter up to comparatively deep layer. The $\Delta^{14}C$ profile of the warming plot was unique with a maximum (220 ‰) at 5cm depth, although the $\Delta^{14}C$ of the control plot was approximately constant from surface to 10cm depth. In terms of $\Delta^{14}C$ vertical profile above 10cm depth, although the $\Delta^{14}C$ of the warming plot above the 3cm depth having POC $>$15 wt% were lower than those of the control plot, the $\Delta^{14}C$ of the warming plot below the 3cm depth were obviously higher than those of the control plot. The results indicate that microbes selectively decomposed young POC at surface layer and old POC at intermediate layer by the soil warming experiment.

Keywords: soil carbon, radiocarbon, global warming, organic matter decomposition, forest soil

Japan Geoscience Union Meeting 2014
(28 April - 02 May 2014 at Pacifico YOKOHAMA, Kanagawa, Japan)

HTT35-12 Room:311 Time:May 1 12:00-12:15

Cosmogenic $^{36}Cl/^{10}Be$ ratio in the Antarctic ice core during the last deglaciation and early Holocene

SASA, Kimikazu[1*] ; KUROSUMI, Kazuna[1] ; SUEKI, Keisuke[1] ; TAKAHASHI, Tsutomu[1] ; MATSUSHI, Yuki[2] ; TOSAKI, Yuki[3] ; HORIUCHI, Kazuho[4] ; UCHIDA, Tomoko[5] ; MATSUZAKI, Hiroyuki[6] ; MOTOYAMA, Hideaki[7]

[1]University of Tsukuba, [2]Kyoto University, [3]National Institute of Advanced Industrial Science and Technology, [4]Hirosaki University, [5]Tohoku University, [6]The University of Tokyo, [7]National Institute of Polar Research

^{36}Cl is cosmogenic nuclide (half-life:301 kyr) produced mainly by a reaction of $^{40}Ar(p, n\alpha)^{36}Cl$ in the upper atmosphere. Cosmogenic nuclides fall on the Earth's surface at a rate depending on the nuclide production rates and hence reflecting the cosmic ray intensity. Therefore we can reconstruct fluctuations of cosmic ray intensity, by determining the past ^{36}Cl depositional flux. Such fluctuations of cosmic ray intensity may indicate paleo solar activity and/or variations in the Earth's geomagnetic field.

In this presentation, we report the results of cosmogenic ^{36}Cl measurements during 10.55 - 18.42 kyr b2k in the ice core drilled at the Dome Fuji station, Antarctica (Motoyama et al., 2007). ^{36}Cl in the ice was measured with the accelerator mass spectrometry (AMS) system at the University of Tsukuba (Sasa et al., 2010). The results show that ^{36}Cl conc. is 0.21 - 1.80 $\times$ 10^4 atoms g^{-1} and ^{36}Cl flux is 0.54 - 3.25 $\times$ 10^4 atoms cm^{-2} yr^{-1}. The variation of ^{36}Cl flux in early Holocene shows similar fluctuations of ^{10}Be flux in the same ice core. $^{36}Cl/^{10}Be$ is constant at 0.10 $\pm$ 0.01 in early Holocene. This means that this value can be used for radioactive age dating of the old ice core. $^{36}Cl/^{10}Be$ varies in the last deglaciation. It suggests that the decrease in $^{36}Cl/^{10}Be$ ratio is linked to climate change.

Keywords: $^{36}Cl/^{10}Be$, Cosmogenic nuclide, Accelerator Mass Spectrometry, Radiometric age determination, Ice core

Japan Geoscience Union Meeting 2014
(28 April - 02 May 2014 at Pacifico YOKOHAMA, Kanagawa, Japan)

HTT35-13 Room:311 Time:May 1 12:15-12:30

Correlation between the concentrations of cosmogenic Be-7, Be-10 in atmosphere and solar activities.

YAMAGATA, Takeyasu[1*] ; NARAZAKI, Yukinori[2] ; NAGAI, Hisao[1] ; MATSUZAKI, Hiroyuki[3]

[1]Collage of Humanities and Sciences, Nihon University, [2]Fukuoka Institute of Health and Environmental Science, [3]School of Engineering, the University of Tokyo

The concentrations of ^{7}Be and ^{10}Be were investigated at Dazaifu, Fukuoka (1998-2002), Hachijo-Island (2002-2005) and Tokyo (2002-2008) during 1998 to 2008. The seasonal variations were same each year; high concentrations and high isotopic ratios of ^{10}Be/^{7}Be that was caused by strong stratosphere-troposphere exchange (STE) were appeared in February to June, and various concentrations but constant ^{10}Be/^{7}Be by vertical convection in troposphere were appeared in July to December. The concentrations were reconstructed by the box model formula. The parameters of the mean residence time and STE intensities, and period, were constant. The amplitudes of production rate were higher than the amplitude of cosmic ray neutron flux observed at Moscow near earth's surface by a factor of 4. Since the neutron flux amplitude at polar region that was little influenced by geomagnetic field was only 10% higher than Moscow, the high amplitudes of production rate were assumed that caused by changing of energy spectrum of galactic cosmic ray.

Keywords: Accelerator mass spectrometry, Cosmogenic nuclide, atmosphere, aerosol

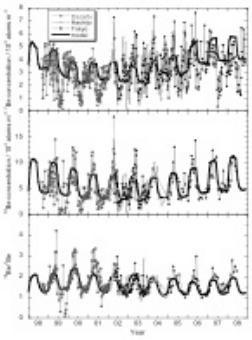

Fig. 1 The decadal variations of ^{7}Be, ^{10}Be concentration and ^{10}Be/^{7}Be in the atmosphere in Dazaifu, Hachijo-Island and Tokyo during 1998 to 2008.

Japan Geoscience Union Meeting 2014
(28 April - 02 May 2014 at Pacifico YOKOHAMA, Kanagawa, Japan)

HTT35-14 Room:311 Time:May 1 12:30-12:45

Distributions of radionuclides Cl-36 and I-129 in surface soils before Fukushima accident

SUEKI, Keisuke[1*] ; KITAGAWA, Jun-ichi[2] ; SASA, Kimikazu[1] ; TAKAHASHI, Tsutomu[1] ; MATSUKURA, Masumi[1] ; KINOSHITA, Norikazu[3] ; TOSAKI, Yuki[4] ; MATSUSHI, Yuki[5] ; MATSUZAKI, Hiroyuki[6]

[1]University of Tsukuba, [2]High energy acclerator research organization, [3]Shimizu corporation, [4]The National Institute of Advanced Industrial Science and Technology, [5]Kyoto University, [6]The University of Tokyo

The long-lived radionuclides ^{36}Cl and ^{129}I are generated by the nuclear tests or interaction with cosmic rays. They have descended to ground or sea level surface, and they have remained ground surface afterward. We have measured amount of ^{36}Cl and ^{129}I by accelerator mass spectrometry (AMS) before nuclear accident at the Fukushima No. 1 nuclear power plant.

We have collected surface soil samples from the Sea of Japan to the Pacific Ocean at the equal-latitude cross-sectional areas (37 ^{o} 20' N - 37 ^{o} 30' N) in the south Tohoku, Japan. Inorganic chlorine in soil developed an improved leaching process that uses diluted HNO3 as an extractant, activated carbon to remove organic matters without decomposition, and H_2O_2 to remove residual organic matters. After leaching from soils, the AgCl samples for AMS-target made from the obtained solutions at ordinary treatment. Isotopic ratios of ^{36}Cl/Cl were determined by AMS at Tandem Accelerator Complex, University of Tsukuba. Preparation of Iodine-129 target was following ordinary method. Isotopic ratios of ^{129}I/I were determined by accelerator mass spectrometry (AMS) at MALT, the University of Tokyo. Moreover, we determined ^{137}Cs concentrations by gamma spectroscopy and LOI (loss on ignition used by an electric furnace) which related to the amount of the organic matter in soil.

We obtained the distributions of radionuclides ^{36}Cl and ^{129}I in surface soils. The measured ^{36}Cl/Cl ratios of 34 surface soil samples which were about 0-10 cm in depth from 6 sites at the equal-latitude cross-sectional areas were between 0.1 x 10^{-13} and 4.1 x 10^{-13}. It was shown that the ^{36}Cl/Cl ratios are lower at both sea sides. The concentrations of ^{129}I and ^{129}I/I ratios in surface soil (0-10 cm) at 28 points were determined to be 0.18 - 1.13 mBq/kg and 4.3 x 10^{-9} - 11.7 x 10^{-9}, respectively.

The depth profiles of ^{36}Cl/Cl, ^{129}I and ^{137}Cs were examined that the difference of distribution. The concentrations are higher at close surface in each nuclide. The results of ^{36}Cl/Cl profiles in soil cores up to 1 m long suggested that bomb-produced ^{36}Cl remains in uppermost sections, typically for ˜20 cm deep, in undisturbed soil layers. The observed close correlation between organic matter content and ^{36}Cl/Cl ratio implies that presence of biological activity contributes the retention of fallout ^{36}Cl in the surface zone. The concentration of ^{129}I is shown the highest in uppermost surface. It is thought that the influence of global fallout has been received until now. In both nuclides, a constant amount exists in deeper than 30 cm. The concentrations of ^{137}Cs are not detection in deeper than 40 cm. It is showed that ^{137}Cs was lower mobility in soils. Therefore, the sampling soils were not a disturbance.

Keywords: AMS, Cl-36, I-129, soil

Japan Geoscience Union Meeting 2014
(28 April - 02 May 2014 at Pacifico YOKOHAMA, Kanagawa, Japan)

HTT35-P01 Room:Poster Time:May 1 18:15-19:30

Geoscience studies using by AMS at JAEA-AMS-TONO in the Tono Geoscience Center of the Japan Atomic Energy Agency

KOKUBU, Yoko[1*] ; MATSUBARA, Akihiro[1] ; HANAKI, Tatsumi[1] ; YASUE, Ken-ichi[2] ; UMEDA, Koji[2]

[1]Tono Geoscience Center, Japan Atomic Energy Agency, [2]Geological Isolation Research and Department Directorate

The JAEA-AMS-TONO facility was established in 1997 at the Tono Geoscience Center, Japan Atomic Energy Agency (JAEA). Our AMS system is a versatile system based on a 5MV tandem Pelletron type accelerator (National Electrostatic Corporation, US) and has been made available for ^{14}C-, ^{10}Be- and ^{26}Al-AMSs. These multi-nuclide AMSs have been mainly applied to neotectonics and hydrogeology, in support of our research on geosphere stability applicable to the long-term isolation of high-level radioactive waste. Furthermore, the ^{14}C- and ^{10}Be-AMSs are used for geoscience, environmental science and archaeology by researchers of universities and other institutes under the JAEA's common-use facility program.

Major contribution of radiocarbon (^{14}C) dating through our ^{14}C-AMS to geoscience studies are as follows. Yasue *et al.* identified fault displacement and stratigraphic correlation of black soils based on ^{14}C ages (presented in this conference). They conducted ^{14}C dating of the black soil collected from a trench wall of the Atera Fault, Gifu. The results of ^{14}C date show that the soil age varies from 4,000 to 2,000 y with depth of the sampling points and the soil was deposited at approximately constant rate. Imaizumi *et al.* (2006) estimated the faulting age based on ^{14}C dating of soils at the Senya Fault in the Toen Fault Zone, Yokote Basin, Akita. It was found that the ages range between 1000 - 1300 y, indicating that the Senya Fault was caused by the Rikuu Earthquake in the year of 1896. Sasaki *et al.* (2006) studied local climate change in an inland basin. Pollen records and ^{14}C ages of sediments in Ohkute Basin, Gifu were used to reconstruct past climate change. The results suggested that the local climate has been warmer for the last 10000 yBP.

Since the fiscal year of 2013, the ^{10}Be-AMS has been routinely measured and used to study long-term erosion rates of weathered granitic soil surfaces using cosmogenic ^{10}Be depth profile under the joint research program with the National Institute of Advanced Industrial Science and Technology (AIST). Recently, we have started development of ^{26}Al-AMS. The system tuning and test measurement have been carried out for routine measurement. The development has so far done well and the routine measurements of the ^{26}Al-AMS will be started in near future. The ^{10}Be- and ^{26}Al-AMSs will be used to estimate the exposure age of basement rocks as well as the sedimentation rate and the assessment of volcaniclastic material ejected during volcanic eruptions.

Keywords: AMS, Dating, C-14, Be-10, Al-26

Japan Geoscience Union Meeting 2014
(28 April - 02 May 2014 at Pacifico YOKOHAMA, Kanagawa, Japan)

HTT35-P02 Room:Poster Time:May 1 18:15-19:30

Radiocarbon dating of charcoal by the ABOX-SC method

TOMIYAMA, Shinji[1*] ; MINAMI, Masayo[2] ; NAKAMURA, Toshio[2]

[1]Department of Earth and Environmental Sciences, Graduate School of Environmental Studies, Nagoya Uni, [2]Center for Chronological Research, Nagoya University

Charcoal is one of the most important samples for radiocarbon dating. It is necessary to remove contaminants from charcoal sample to obtain the reliable date. ABA (acid-base-acid) method is usually used for chemical pretreatment of charcoal: First, a sample is treated with HCl to remove carbonate contaminant. Next, the sample is treated with NaOH to remove organic contaminants derived from soil during burial. After then, the sample is treated with HCl again to remove absorbed atmospheric carbon dioxide during NaOH treatment. The residue is combusted with CuO at 850?C and graphitized to be 14C-dated.

However, the ABA treatment often cannot completely remove contaminants from poorly-preserved and/or old charcoals (>about 30 ka). Bird et al. (1999) showed that the ABOX-SC (acid-base-oxidation stepped combustion) method removes organic contaminants more efficiently than the ABA treatment. The age of the charcoal sample treated with the ABOX-SC was reported to be older than that of the charcoal sample treated with the ABA (Brock et al., 2010).

The ABOX-SC method consists of 3 step chemical pretreatments: HCl and NaOH treatments followed by K2Cr2O7-H2SO4 treatment in a sealed tube at 60?C for 20 hr (Brock et al., 2010). The mixed solution of K2Cr2O7 and H2SO4 removes organic contaminants effectively from charcoal samples, and can extract carbon fraction of oxidation resistant elemental carbon, OREC, which is resistant to oxidation and is less affected by contamination during burial (Bird et al., 1999). After the ABOX chemical treatment, the OREC is heated at 630?C with CuO for 2 hr to remove atmospheric CO2 contaminants adsorbed during sample treatment and contaminants remained after the ABOX treatment. Finally, the residue of OREC is oxidized completely into CO2 at 850?C for 1 hr, and the CO2 is graphitized to be 14C-dated.

In this study, we apply the ABOX-SC method to some charcoal samples of known age to measure 14C ages. The charcoal samples, which were excavated from Tang-e Sikan cave in Arsanjan city, Iran, have been dated at about 40 ka and 26 ka by the ABA method, and are considered to be attributed to Upper Paleolithic period. In this study, we confirm the age difference of Paleolithic charcoal samples by the two pretreatment methods of ABA and ABOX-SC.

Keywords: Radiocarbon, Charcoal, ABOX-SC method

Japan Geoscience Union Meeting 2014
(28 April - 02 May 2014 at Pacifico YOKOHAMA, Kanagawa, Japan)

HTT35-P03 Room:Poster Time:May 1 18:15-19:30

AMS radiocarbon dating of Japanese tree rings for regional calibration curve

SAKAMOTO, Minoru[1*] ; OZAKI, Hiromasa[2] ; IMAMURA, Mineo[1]

[1]National Museum of Japanese History / The Graduate School for Advanced Studies, [2]The University Museum, The University of Tokyo

Calibration of radiocarbon data can be achieved by comparison of measured radiocarbon age of samples with known calendar age. Tree rings that determined by dendrochronology are one of the important data set for calibration. IntCal13 calibration curve was launched mainly based on trees grown in the northern high latitude. These rings were sampled in ten years each at once to cancel the variation of solar activity, and to obtain sufficient sample size for conventional radiocarbon measurement as well. AMS radiocarbon dating can measure less than 1mg of carbon efficiently and is capable of date annual tree rings. Recent advance in accuracy of AMS radiocarbon measurement reveals that the resolution of IntCal may be insufficient for precise calibration. In particular, regional effect on the calibration curve had turned out to be a major problem. AMS radiocarbon dating of Japanese tree rings with actual age has been carried out to accomplish Japanese regional calibration curve. Tree ring preserves atmospheric ^{14}C concentration at that time, therefore the offset between radiocarbon age of Japanese tree ring and IntCal should indicate the inhomogeneity in the northen hemisphere.

Keywords: radiocarbon dating, tree ring, calibrated age, atmospheric inventory, regional effect

Japan Geoscience Union Meeting 2014
(28 April - 02 May 2014 at Pacifico YOKOHAMA, Kanagawa, Japan)

HTT35-P04 Room:Poster Time:May 1 18:15-19:30

Radiocarbon dating of archeological remains related with the 13th century Mongol Inversion to Japan

NAKAMURA, Toshio[1*]

[1]Center for Chronological Research, Nagoya University

The shallow sea floor off Takashima, Matsuura, Nagasaki Prefecture, has been investigated archeologically as a potential site where many Mongolian warships exist under the sea sediments. It is historically recorded that more than 4000 Mongolian warships were destroyed by a typhoon during the Mongol invasion to Japan in 1281. The underwater investigations have been performed since 1980, and a lot of archeological remains related with the invasion have been collected there. In 2006, we were allowed to get some archeological remains for 14C dating with AMS. The samples were fragments of palm-bark ropes, lacquer products, bamboo ropes and charred rice. 14C ages for the samples were all consistent with the age of Mongol invasion in 1281.

Recently a body of submerged wrecks most probably originated from Mongolian warship has been discovered in the 1m-deep horizon of the sea sediment off Takashima. During the survey of the new warship, shell samples were collected near the ship. Some shells were recognized to be hull-fouling species, which may have grown up on the bottom of Mongolian warship and preserved along with the broken ship in the sea sediment. We have conducted 14C dating for some shell samples and found out that shells belong to hull-fouling species showed 14C ages consistent with the time of Mongol Inversion. Some other shells not belonging to hull-fouling species showed younger or older dates as compared with the time of Mongol invasion.

Keywords: AMS 14C dating, historical remains, remains from submerged wrecks, Mongol invasion, shell of hull-fouling species

Japan Geoscience Union Meeting 2014
(28 April - 02 May 2014 at Pacifico YOKOHAMA, Kanagawa, Japan)

HTT35-P05 Room:Poster Time:May 1 18:15-19:30

AMS radiocarbon dating of peaty layers in Kimotsuki lowland, southern Kyushu

FUJIKI, Toshiyuki[1] ; OKUNO, Mitsuru[1*] ; NAKAMURA, Toshio[2] ; MORIWAKI, Hiroshi[3]

[1]ACRIFIS-EHAI, Fukuoka Univ., [2]CCR, Nagoya Univ., [3]Fac. Law, Econ. Human., Kagoshima Univ.

Since the middle Holocene, peaty layers have accumulated on the Kimotsuki lowland in south Kyushu, Japan. They can be applied radiocarbon (ˆ{14} C) wiggle-matching for establishing high-resolution chronology. Moreover, several tephra intercalated with the peat bed which originated from Kaimondake, Sakurajima, and the Kirishima volcanoes, and they can certify the reproducibility of ^{14} C dates. On the other hand, the age of the tephra by them can be determined correctly. We present here the results of AMS ^{14} C dating on the core sample, and report the age of each tephra determined from these dates.

Keywords: Kimotsuki lowland, peaty layer, tephra, radiocarbon date

Japan Geoscience Union Meeting 2014
(28 April - 02 May 2014 at Pacifico YOKOHAMA, Kanagawa, Japan)

HTT35-P06 Room:Poster Time:May 1 18:15-19:30

Offset in radiocarbon ages between shell and plant pairs in the Holocene sediments around the Korea

NAKANISHI, Toshimichi[1*] ; HONG, Wan[1] ; SUNG, Kisuk[1] ; SUNG, Kilho[1] ; NAKASHIMA, Rei[2]

[1]KIGAM, [2]AIST

Since 2009, a research project to evaluate the marine reservoir effects of the coastal sites of Korea has been progressed by KIGAM. Estimating the reservoir effect of this area is difficult because age-known marine samples obtained before AD 1950 are rare. In order to solve this problem, 61 sediment cores were collected with 1 m intervals by a percussion drilling tool from 52 coastal sites in the southern area of the Korean Peninsula. These drilling sites were roughly preselected by the interpretation of modern air photos of internet map services provided by the websites such as Daum and Google. Topographic maps in 1918-1926 with 1/50000 scale and old air photos were also used for the site selection. The length of each core was less than 5 m and the total length was 132 m. Based on analysis of lithology and mollusk assemblages, we selected marine shell and terrestrial plant pairs from same horizons. These samples were cleaned by physical and chemical pretreatments, and reduced by automatic graphitization system in KIGAM. The radiocarbon ages of the samples were measured by the AMS facility of KIGAM. This presentation will report about spatial and historical variation of radiocarbon marine reservoir effect around Korea.

Keywords: Radiocarbon dating, Marine reservoir effect, Coastal sediments, Korea

Japan Geoscience Union Meeting 2014
(28 April - 02 May 2014 at Pacifico YOKOHAMA, Kanagawa, Japan)

HTT35-P07 Room:Poster Time:May 1 18:15-19:30

Estimation for the growth rate of benthic biotic communities in Antarctic lakes

TANABE, Yukiko[1*] ; UCHIDA, Masaki[2] ; KONDO, Miyuki[3] ; UCHIDA, Masao[3]

[1]Waseda Institute for Advanced Study, Waseda University, [2]National Institute of Polar Research, [3]National Institute for Environmental Studies

Antarctica is an ice continent. It has one of the most extreme environments for life in the world. There are very little ice-free regions with life in it, so these regions are sometimes called polar oasis within the polar desert. The ice-free regions are scattered along the coastal regions and around mountainous peaks (Nunataks) in continental Antarctica or concentrated in Antarctic Peninsula in maritime Antarctica. The biota is simple due to lack of remarkable organisms at the top of food webs, and primary producers such as cyanobacteria, algae, lichens, mosses, heterotrophic microorganisms and metazoans dominate the sparse communities. A remarkable diversity of lakes exists in Antarctica, ranging from hypersaline with nearly 10 times the conductivity of seawater, to brackish and freshwater, sub-glacial, permanently ice-covered and seasonally ice-covered lakes. These lakes are unproductive with typical photosynthetic levels of 0.5 — 30 μg-C/L/day from phytoplankton. Phytoplankton cannot bloom and hardly survives in the water column during the best light-available summer around the Syowa region. This results from low annual levels of photosynthetically active radiation and ice cover that attenuate light into the water column or photo-inhibit photosynthetic systems due to continuous low temperatures and the lack of any significant input of inorganic nutrients. Despite such severe situations, one of the most productive ecosystems in continental Antarctica is found in freshwater lakes, where benthic microbes form thick mats, and aquatic mosses can flourish on the lakebeds of the Syowa region. These lakes were exposed by glacial retreat after the Last Glacial Maximum. The benthic mats consist of almost organisms, dominantly cyanobacteria, algae, and mosses in the lakes, because there are a little inorganic particles and organic matters inflow to the lakes from the water catchment, and as pointed out above, almost no phytoplankton in the water column. This negligible level of any sedimentation and turbulence situation is specific to Antarctica, which is suitable to estimate the growth rate of benthic biotic communities in fine-scale. We collected sediment cores from 17 freshwater lakes in S$\hat{o}$ya Coast on the south area of Syowa station, continental Antarctica during January-February in 2009 — 2010. The core samples were vertically sliced in each 1 cm as soon as possible after sampling in the field hut, and transported to Japan at -20 ℃. Then, we analyzed the samples by using an AMS (accelerator mass spectrometry), and estimated the growth rate of the benthic biotic mats in each Antarctic lake.

Keywords: sediment, AMS, lakes, Antarctic, growth rate

Japan Geoscience Union Meeting 2014
(28 April - 02 May 2014 at Pacifico YOKOHAMA, Kanagawa, Japan)

HTT35-P08 Room:Poster Time:May 1 18:15-19:30

Black SOM dynamics during reforestation of Japanese grassland

IIMURA, Yasuo[1*] ; UCHIDA, Masao[2] ; KONDO, Miyuki[2]

[1]School of Environmental Science, The University of Shiga Prefenture, [2]National Institute for Environmental Studies (NIES)

The dynamics of the polyaromatic structures of black humic acids (HAs), which are presumably derived from charred materials, are of significant interest for the global carbon cycle. However, the details of those dynamics are not yet well understood. We investigated differences in the degree of darkness (A600/C values), isotopic ratios (δ13C, δ15N, and Δ14C values), and 13C NMR spectra of size-separated black HAs extracted from Japanese volcanic ash soils in order to estimate the variations in the polyaromatic structures of black HAs during ca. 100 years of natural reforestation of Japanese pampas grassland. For several hundred years, all the study sites were managed similarly as grassland by burning. Subsequently, their management differed: at site G (Miscanthus sinensis: C4 plant), maintenance as of the time of this study was still performed by mowing, while at sites P (Pinus densiflora: C3 plant) and Q (Quercus crispula: C3 plant), maintenance was discontinued ca. 30 and 100 years ago, respectively. Thus, the sites range from grassland (site G) to coniferous forest (site P) to broad-leaved forest (site Q). For all HA size fractions at all sites, we found that δ13C values correlate positively with δ15N values, although the gradients are much lower for fractions of small to medium molecular size than for fractions of medium to large molecular size (denoted as lower-size and higher-size fractions, respectively). Overall, for the lower-size fractions, the contribution ratio of C4-plant-derived carbon shows a significant positive correlation with A600/C values and a negative correlation with Δ14C values, and their aromatic characteristics are greater than those of higher-size fractions within the same black HA. Furthermore, the relative proportion of lower-size fractions decreases with reforestation, especially from site P to Q. The δ13C values for all size fractions are similar for sites G and P, but are relatively low for site Q. The aryl C contents of the lower-size fractions are lower and the O-alkyl C contents and the aliphaticity (alkyl C:O-alkyl ratio) are clearly higher for sites P and Q than for site G. These results strongly suggest that stimulation of HA biodegradation might be achievable by continuous input of new plant litter during reforestation, even for lower-size HA polyaromatic structures, despite the fact that lower-size HAs biodegrade more slowly than higher-size HAs.

Keywords: land use, reforestation, soil organic matter, 14C

Japan Geoscience Union Meeting 2014
(28 April - 02 May 2014 at Pacifico YOKOHAMA, Kanagawa, Japan)

HTT35-P09 Room:Poster Time:May 1 18:15-19:30

Potential sink of soil organic carbon in a Japanese cool-temperate forest based on bomb radiocarbon based residence time

KONDO, Miyuki[1*] ; UCHIDA, Masao[1] ; OHTSUKA, Toshiyuki[2] ; MURAYAMA, Shohei[4] ; SHIRATO, Yasuhito[3] ; SHIBATA, Yasuyuki[1]

[1]National Institute for Environmental Studies, [2]Gifu University, [3]National Institute for Agro-Environmental Studies, [4]Environmental Management Technology

Functional roles of SOC pool for carbon dynamic remains almost unknown. In this study, residence time (RT) based on carbon and radiocarbon (14C) inventories, was f investigated in a Japanese temperate forest (Takayama) under Asian Monsoon climate, and the potential of soil carbon sequestration were also investigated. Soil organic matter was divided to two fractions as low density humified material (LOM) and high density mineral-associated material (HOM). Our results were thoroughly compared with those in a temperate forest (Harvard forest) conducted using a similar approach [Gaudinski et al., 2002]. The LOM was the major part of the SOC (76%) and its contribution was higher even in the deep layer. 14C contents of LOM in surface layer were similar to those of atmospheric CO2 and roots, whereas those in deep layer are significantly low (?14C <-200 per mil) as well as HOM fractions, although LOM fraction seems to consist of labile carbon. RTs for low density fractions as derived from their radiocarbon content are 53 ?330 yrs BP in surface layer and 1760 ?2780 years BP. Storage of SOC in our site was larger, irrespective of depths and differed considerably from that in Harvard forest. We also measured soil 14CO2 profile to determine the rate of CO2 production from heterotrophic respiration of two SOM fractions. The ?14C values of soil CO2 profile was constant down to 75 cm depth, which were close to those of atmospheric CO2 and fine roots, suggesting that most of soil CO2 is derived from recent photosynthetic fixed C. These results indicate that this forest might be higher sequestrating soil carbon as low density fractions semi-permanently, which is also concerned about instability of near future climate change.

Japan Geoscience Union Meeting 2014
(28 April - 02 May 2014 at Pacifico YOKOHAMA, Kanagawa, Japan)

HTT35-P10 Room:Poster Time:May 1 18:15-19:30

Source diagnosis of PAHs using compound class specific 14C analysis and Monte Carlo source appotionment at Kolkata canal

KUMATA, Hidetoshi[1*] ; UCHIDA, Masao[2] ; KONDO, Miyuki[2] ; SHIBATA, Yasuyuki[2] ; SAHA, Mahua[3] ; TAKADA, Hideshige[3]

[1]Tokyo Univ Pharm Life Sci, [2]NIES, [3]Tokyo Univ Agri Technol

Atmospheric polycyclic aromatic hydrocarbons (PAHs) originate mostly from incomplete combustion of carbon-based fuels. PAHs account for most (35-82%) of the total mutagenic activity of ambient aerosols. Reduction of air pollution by PAHs is essential for an effective air quality control, which requires reliable source apportionment. It has been reported that atmospheric pollution by PAHs in Indian megacities, such as Kolkata, Mumbai and Chennai, is comparable to the highest levels across the globe and Kolkata air exhibit the highest level among them. Also, our previous survey revealed that sediments from Kolkata city canals have the highest PAHs concentrations (i.e., 15.9±11.6 μg of $\sum$14-parent PAHs/g dw, n=12) among the 174 surface sediments from 8 tropical Asian countries.[1] Examining methylated-to parental PAHs ratios of three homologous series and C30-hopane/$\sum$PAHs ratios both in sediment samples and in probable source materials, the high level sedimentary PAHs were ascribed to those emitted from combustion sources. However, relative importances of combustion sources were not solved. The present study aimed to apportion sources of combustion to PAHs in highly contaminated sediments from Kolkata, India by using combined approaches of CCSRA technique, molecular fingerprinting and Monte Carlo source apportionment.

Furthermore, three- and four ring PAHs (MW178, 192, 202) in leftover extracts were harvested on PCGC and analyzed for 14C on AMS at NIES-TERRA, NIES (Tsukuba, Japan). PAHs isolated from Kolkata canal sediments showed mostly fossil carbon isotopic signatures, i.e., ^{14}C signal of PAHs with MW178, 202 and those with MW?228 were 10.6±0.1, 5.9±0.4, 7.6±0.5 pMC (KKNC), 8.4±0.5, 8.3±0.4, 8.5±0.3 pMC (KKSC). By using source end-members of MW202 and MW276 isomer pair ratios, Monte Carlo source apportionment[2] revealed that most of fossil-PAHs were derived from coal combustion, i.e., relative contributions (median) from coal and petroleum combutions were 50% and 11% in KKNC and 13% and 56% in KKSC.

1. Saha M. *et al., Mar. Pollut. Bull.*, **2009**, 58 (2), 189-200
2. Sheesley R.J. *et al., Atmos. Environ.*, **2011**, 45(23), 3874-3881

Keywords: compound class specific radio carbon analysis, PAHs, monte carlo simulation, molecular fingerpringing, source apportionment

Japan Geoscience Union Meeting 2014
(28 April - 02 May 2014 at Pacifico YOKOHAMA, Kanagawa, Japan)

HTT35-P11 Room:Poster Time:May 1 18:15-19:30

Accurate age estimation using ^{14}C in human teeth enamel.

KUNITA, Keisuke[1*] ; NAKAMURA, Toshio[2]

[1]Graduate School of Environmental Studies, Nagoya University, [2]Center for Chronological Reserch, Nagoya University

Radiocarbon (^{14}C) concentration in the atmosphere showed a stable value until 1955. However, as a result of the nuclear bomb testing, modern ^{14}C concentration in the atmosphere dramatically increased during late 1950s and early 1960s. These bomb-produced ^{14}C is then oxidized to form CO_2, and incorporated into plants by photosynthesis. Then, by eating plants or animals fed by these plants, the ^{14}C concentration in human body reflects the ^{14}C value of atmospheric CO_2 at a certain time. Recent studies insisted that these ^{14}C can play important role for forensic analysis, especially age estimation using ^{14}C in human teeth enamel.

Teeth enamel is such a harder part of the human body that they are hardly destroyed by a natural process. And, the most important is, there is no turnover of enamel after its formation has completed. Although there are previous works which estimate the birth year of individuals by using ^{14}C concentration in enamel, their samples are teeth from Swedish, Scottish and American people, and study areas are mainly at high latitudes of the northern hemisphere. The precision of age estimation using teeth enamel is determined by enamel formation time of teeth and atmospheric ^{14}C concentration in a certain area at a certain year. It is known that teeth formation time of Japanese is different from that of Caucasian. It has been found that ^{14}C concentration in the atmosphere indicates 5 different zones according to different peak ^{14}C concentration of the nuclear bomb testing. These zones are named NH zone1, NH zone2, NH zone3, SH zone3 and SH zone1-2 from north to south. The boundary between NH zone1 and NH zone2 is Ferrel cell - Hadley cell boundary. It is nearly located at 35 ^{o}N. So it means that previous works mainly focused on NH zone1 samples, not NH zone2 samples. One of NH zone2 samples, teeth enamels of Japanese have not studied sufficiently. The aim of this study is to clarify whether age estimation using teeth enamels of Japanese can determine the precise year of birth of individuals and to discuss the mechanism of carbon fixation of enamels or other parts of the teeth.

7 of 44 collected tooth samples have been analyzed. They are 5 third molars and 2 second molars. The year of birth of each individual is 1943, 1946, 1951, 1951, 1951 for third molars, and 1933 and 1959 for second molars. In order to get the estimated year of birth, a model age for enamel completion of Japanese was subtracted from the year given by the ^{14}C analysis of samples. The result shows that age estimation using teeth of Japanese gives precise age determination. Needless to say, taking account of the degree of individual variation and possibility of differences in local environment or in diet is important, however, this result seems to be uninfluenced by those effects. Larger number of, more and more various parts of teeth (for example, first molars, anteriors, such as early-completed teeth.) have to be analyzed.

To determine whether an individual is born before or after the peak of atmospheric ^{14}C concentration (in 1964, in NH zone2), root of teeth have to be analyzed. Since root completion age is some years after enamel completion age, it can be easily found that the sample age is whether rising or falling part of the atmospheric ^{14}C curve. We now are preparing for analysis of ^{14}C of root dentine collagen and root inorganic matter. Their results will give more compelling data, now discover what is waiting for you!!

Keywords: human tooth, enamel, ^{14}C, forensic science, nuclear bomb testing, age estimation

Japan Geoscience Union Meeting 2014
(28 April - 02 May 2014 at Pacifico YOKOHAMA, Kanagawa, Japan)

HTT35-P12 Room:Poster Time:May 1 18:15-19:30

Observations of atmospheric radiocarbon in carbon dioxide at Hateruma Island and Cape Ochi-ishi, Japan

TERAO, Yukio[1*] ; MUKAI, Hitoshi[1]

[1]Center for Global Environmental Research, National Institute for Environmental Studies

Atmospheric radiocarbon in carbon dioxide ($^{14}CO_2$) is a powerful tracer for understanding of carbon cycles, e.g. oceanic and biospheric CO_2 exchanges and CO_2 emissions from fossil fuel combustion. Observation sites for radiocarbon concentrations, $\triangle^{14}C$, are not many enough to evaluate the global and regional carbon flux. We present an analysis of trends, interannual variability (IAV) and seasonal cycle of $^{14}CO_2$ in background air from July 2004 to December 2012 at two NIES/CGER monitoring stations; Hateruma Island (HAT; latitude 24.06N, longitude 123.81E) and Cape Ochi-ishi (COI; latitude 43.16N, longitude 145.50E). The air samples were collected in 2 L Pyrex glass flasks. The sampling frequency was monthly. CO_2 was extracted from the whole air at NIES and CO2 samples were converted to graphite and analyzed ratios of $^{14}C/^{12}C$ by accelerator mass spectrometry (AMS, National Electrostatics Corp., 1.5SDH) at Paleo Labo Co., Ltd., Japan. Analytical precision in $\triangle^{14}C$ determined from statistical uncertainty (number of ^{14}C counts) was $\pm$1.7-2.0 ‰ for most samples. The repeatability of measurements using modern reference air was $\pm$1.9 ‰ . A decreasing trend in $\triangle^{14}C$ was -5 ‰ yr^{-1} in average but large IAV was observed at both stations: large decreases in 2007-2008 and in 2010-2011 (-8 to -9 ‰ yr^{-1}) and almost zero decrease in 2009. We also observed clear seasonal cycle of $\triangle^{14}C$. The peak-to-peak amplitudes in the seasonal cycle determined from the smooth curve fits were 7 ‰ at both stations and the maximum of $\triangle^{14}C$ appeared in July and the minimum in January at HAT, and the maximum in September and the minimum in May at COI. The differences in phase of $\triangle^{14}C$ seasonal cycle between HAT and COI suggested that the atmospheric $\triangle^{14}C$ at COI was influenced by CO_2 emitted from terrestrial biosphere.

Japan Geoscience Union Meeting 2014
(28 April - 02 May 2014 at Pacifico YOKOHAMA, Kanagawa, Japan)

HTT35-P13 Room:Poster Time:May 1 18:15-19:30

Radiocarbon based source apportioning of PM2.5 carbonaceous aerosols at Cape Hedo, Okinawa and Fukue island, Japan

UCHIDA, Masao[1] ; KONDO, Miyuki[1*] ; KANEYASU, Naoki[2] ; ARAKAKI, Takemitsu[3] ; HANDA, Daishi[3] ; KUMATA, Hidetoshi[4]

[1]National Institute for Environmental Studies, [2]National Institute of Advanced Industrial Science and Technology, [3]University of Ryukyus, [4]Tokyo University of Pharmacy and Life Sciences

Radiocarbon (14C) analysis of the carbonaceous aerosol allows an apportionment of fossil and non-fossil sources of air-borne particulate matter (PM). A chemical separation of total carbon (TC) into its sub-fractions organic carbon (OC) and elemental carbon (EC) refines this powerful technique, as OC and EC originate from different sources and undergo different processes in the atmosphere. Although 14C analysis of TC, EC and OC has recently gained increasing attention, Nowadays gigantic brownish haze from various burning and combustion processes is also blanketing India and surrounding land and oceans during the winter season. In China and surrounding countries, same kind of atmospheric pollution are widely observed and occurred as well. Additionally this soot-laden Brown Cloud is affecting South and East Asian climate as much or more than carbon dioxide and cause hundreds of thousands of premature deaths annually, yet its sources have been poorly understood. In this study, we investigated the contribution of continent derived aerosol to Japan. Aerosol samples with diameter of 2.5mm were collected at Fukue island, one of Goto islands and at the Cape Hedo is located at the northern end of Okinawa Island. The 14C contents of EC of PM2.5 aerosols collected from October, 2009 and May, 2010 including the Kosa event in Cape Hedo and Fukue were measured. The 14C content represents in the unit of pMC . Results of EC-14C in both sites were 25-30pMC in Cape Hedo and 18-44pMC in Fukue, respectively. These results mean that relative apportions of biomass burning and fossil fuel were 25-30% and 18-44% in Cape Hedo and 25-35% and 65-75% in Fukue, respectively. The observed variations of pMC in Cape Hedo during February and March were relatively smaller than those of Fukue, which was more than 20%. According to back trajectory analysis in this duration, because ca. 70% of air mass in both sites was derived from the continent. The aerosols particulate matter to be transferred to Cape Hedo from continent would be relatively smaller than those to Fukue. Our data of EC-14C obtained during the Kosa event showed the relatively higher contribution of biomass burning sources in Fukue although these interpretation need to consider variation of the magnitude and concentration of EC in both sites. In further study we need to investigate details of the source of EC during this period.

Keywords: Radiocarbon, PM2.5, aerosol, source apportioning

Japan Geoscience Union Meeting 2014
(28 April - 02 May 2014 at Pacifico YOKOHAMA, Kanagawa, Japan)

HTT35-P14 Room:Poster Time:May 1 18:15-19:30

Study on monitoring of volcanic activity using ^{129}I / ^{127}I ratios in crater lake and hot spring at Zao volcano

MATSUNAKA, Tetsuya[1*] ; SASA, Kimikazu[1] ; SUEKI, Keisuke[1] ; SHIBAYAMA, Nao[1] ; TAKAHASHI, Tsutomu[1] ; MATSUMURA, Masumi[1] ; SATOU, Yukihiko[1] ; MATSUZAKI, Hiroyuki[2] ; GOTO, Akio[3] ; WATANABE, Takahiro[3] ; TSUCHIYA, Noriyoshi[3] ; HIRANO, Nobuo[3] ; KIZAKI, Akihisa[3]

[1]University of Tsukuba, [2]The University of Tokyo, [3]Tohoku University

Volcanic tremors and mountain gradient changes have been detected at Zao volcano in Miyagi and Yamagata since January 2013, volcanic activity began to intensify although Zao volcano will not erupt immediately[1]. Since the water quality of crater lake are correlating with volcanism changes[2][3], basic water quality of crater lake and hot spring at Zao volcano have been studied by the group of Tohoku University from September 2013. As a part of this project, we are trying to monitor the volcanic activity using ^{129}I / ^{127}I ratios (atomic ratio of radioiodine and stable iodine) in crater lake and hot spring of Zao volcano.

Natural ^{129}I (half-life: 15.7 million year) are produced by nuclear spallation reaction of ^{129}Xe with cosmic ray in the atmosphere and spontaneous fission of ^{238}U in the geological layer. In the ocean, steady-state ^{129}I / ^{127}I ratio of the seawater is estimated to be 1.5×10^{-12}[4]. Sunken iodine by the ocean plate having lower ^{129}I / ^{127}I ratio (older ^{129}I age) compared to the steady-state ratio of seawater, are supplied to the atmosphere mainly via magmatic activity. In general, ^{129}I / ^{127}I ratio in hot spring water and brine water are used as indicator of origin and behavior of iodine in the water[5][6]. ^{129}I / ^{127}I ratio of hydrothermal at Zao volcano are considered to become lower by the supply of chronologically-old iodine in terms of global iodine cycle.

In September 2013, water samples of 2 L were collected from the surface of crater lake (Okama, diameter: 350 m, maximum depth: 35 m) located at 1,560 m in elevation and hot spring (Kamoshika Hot Spring) located at 1,230 m in elevation in the eastern side of Zao volcano. Water temperature and pH were measured on site. After water samples were filtered by 0.2 μm filter, ^{129}I / ^{127}I ratio were measured for the isotopic diluted water samples by adding carrier (^{127}I standard) at MALT, The University of Tokyo. ^{127}I concentrations were measured by ICP-MS, and original ^{129}I / ^{127}I ratio of water samples were estimated.

Water temperature and pH were 10.2 ℃ and 3.3 at Okama; 40.0 ℃ and 3.3 - 4.0 at Kamoshika Hot Spring. ^{129}I / ^{127}I ratios of Okama and Kamoshika Hot Spring were respectively, estimated to be $(1.5 \pm 0.4) \times 10^{-9}$ and $(0.78 \pm 0.2) \times 10^{-9}$, 500 - 1000 times higher than the steady-state ratio of sea water (1.5×10^{-12})[4]. Since ^{129}I / ^{127}I ratio of anthropogenic metric water were over 9.0×10^{-12}[7], surface water of Okama and Kamoshika Hot Spring water were very likely to be strong affected by the meteoric water including anthropogenic ^{129}I. For the monitoring of volcanic activity using ^{129}I / ^{127}I ratio, it is necessary to decide the site as few anthropogenic ^{129}I as possible through the measuring of ^{129}I / ^{127}I ratio of the Okama bottom water and some hot spring around Zao volcano. Continuous water quality survey of 1 - 2 times for Okama and 1 time per 1 - 2 months for hot springs are planned from June to November of this year.

[1] Japan Meteorological Agency (2013) Monthly Volcanic Activity Report.
[2] Ohba et al. (2000) Journal of Volcanology and Geothermal Research, 97, 329-346.
[3] Ohba et al. (2008) Journal of Volcanology and Geothermal Research, 178, 131-144.
[4] Moran et al. (1998) Chemical Geology, 152, 193-203.
[5] Snyder and Fehn (2002) Geochimica et Cosmochimica Acta, 66, 3827-3838.
[6] Muramatsu et al. (2001) Earth and Planetary Science Letter, 192, 583-593.
[7] Tomaru et al. (2007) Applied Geochemisty, 22, 676-691.

Keywords: Zao volcano, volcanic activity, crator lake, hot spring, ^{129}I / ^{127}I, AMS

Japan Geoscience Union Meeting 2014
(28 April - 02 May 2014 at Pacifico YOKOHAMA, Kanagawa, Japan)

HTT35-P15 Room:Poster Time:May 1 18:15-19:30

Speciation analysis of the Fukushima accident derived I-129 in the soil using sequential extraction method

HONDA, Maki[1*] ; MATSUZAKI, Hiroyuki[2] ; SAITOU, Takumi[3] ; NAGAI, Hisao[4]

[1]Graduate School of Integrated Basic Sciences, Nihon University, [2]Department of Nuclear Engineering and Management, School of Engineering, The University of Tokyo, [3]Nuclear Professional School, School of Engineering, The University of Tokyo, [4]College of Humanities and Sciences, Nihon University

In previous study, we investigated the depth profile of the accident derived ^{129}I ($T_{1/2}$ = 1.57x10^7 y) and downward migration speed in soils of near field of Fukushima Dai-ichi Nuclear Power Plant (FDNPP), including crop fields and man-made fields. ^{129}I in soil was measured by AMS and stable iodine (^{127}I) was measured by ICP-MS at MALT (Micro Analysis Laboratory, Tandem accelerator), The University of Tokyo. It was found that ^{129}I was concentrated near surface but distributed deeper compared with ^{137}Cs ($T_{1/2}$ = 30 y). From the estimation of relaxation length using depth profiles, the FDNPP derived ^{129}I move 0.6 cm/y downward and ^{137}Cs 0.3 cm/y for it. It was also found that ^{129}I seems to move downward more quickly than ^{137}Cs.

To investigate the adsorption mechanism and the elemental process of migration of the accident derived ^{129}I in soil, it is important to know what kind of component the ^{129}I combines with.

Recent studies on the X-ray absorption fine structure (XAFS), especially near edge structure (XANES), reported that the stable iodine (^{127}I) in soil existed as an organic component[1]. However, it had not yet been proved that it was also the case with the accident derived ^{129}I because it had been incorporated in the soil system only recently and the abundance of ^{129}I in soil was more than 8 orders of magnitude smaller than sub-ppm level stable iodine (^{127}I).

In this study a progressive sequential extraction method including the dialysis was newly developed to obtain only the iodine sticking to the soil organic component. The advantage of sequential extraction over other method is that stable iodine can be quantified by direct analysis of the fraction and ^{129}I can be quantified by AMS method of the fraction added with carrier. The fraction of the organic component for ^{127}I and ^{129}I can be evaluated respectively by comparing with the other fraction and/or with the total concentration obtained by the bulk analysis (e.g. by the pyrohydrolysis).

Repeatability is 20% for the water soluble, oxides and organic fraction, 10% for Exchangeable fraction and 50% Residue (mainly minerals).

The results show that 60% of the total ^{129}I are associated with oxides and 30% associated with organic matter in crop field soil. The former, the oxides bond iodine, it takes a form of iodate (IO_3^-) absorbed in amorphous oxides, especially goethite or delta-MnO_2. They are formation of monodentaten mononuclear outer-sphere species and bidentate, binuclear inner-sphere species [2]. The latter iodine are linked to organic carbon directly by a covalent bond.

[1] Y. S. Shimamoto et at., 2011, *Environ. Sci. Technol.*, **45**, pp2086-2092
[2] T. Nagata et al., 2010, *Geochim. Cosmochim. Acta.*, **74**, pp6000-6013

Japan Geoscience Union Meeting 2014
(28 April - 02 May 2014 at Pacifico YOKOHAMA, Kanagawa, Japan)

HCG36-01 Room:411 Time:April 29 15:15-15:30

Relationship between progress of borehole investigations and the geometric data of fractures at the crystalline rocks

ISHIBASHI, Masayuki[1*] ; SASAO, Eiji[1] ; NAKAJIMA, Makoto[2] ; ATSUMI, Hiroyuki[2] ; ONOE, Hironori[1] ; SAEGUSA, Hiromitsu[1] ; KAWABATA, Junichi[2] ; MASUMOTO, Kazuhiko[2] ; SENO, Shoji[2] ; IWANO, Keita[2]

[1]Japan Atomic Energy Agency, [2]Kajima Corporation Technical Research Institute Rock Mechanics and Hydrogeology Group

In order to evaluate deep geological environment for geological disposal of high level radioactive waste (HLW) and underground storage of liquefied petroleum gas, understanding of the geometry of water conducting features such as fractures is essential. Geometric data of fractures are obtained by borehole investigations. But, methodology to understand the geometry of fractures has not been established in terms of planning borehole investigation such as number and total length of boreholes. Thus, relationship between progress of borehole investigation and increase of the geometric data of fractures is studied.

In this study, discrete fracture network models with the size of 100×100×100m cube were used as virtual fractured rock mass, and virtual boreholes were drilled in the virtual rock mass. Five boreholes with the length of 100m each were located in four directions. One dimensional fracture intensity (as the number of fractures per unit length; P10) of virtual boreholes is calculated. The P10 is depending on the relationships borehole directions and fracture orientations. In addition, The P10 is become constant at each direction of borehole as investigations progressed.

These results suggest that in order to obtain the geometric data of fracture, the borehole investigation should be planned in consideration of distribution of the fracture orientations.

Keywords: Borehole investigation, DFN model, Methdology, Fracture intensity

Japan Geoscience Union Meeting 2014
(28 April - 02 May 2014 at Pacifico YOKOHAMA, Kanagawa, Japan)

HCG36-02 Room:411 Time:April 29 15:30-15:45

Characterization of the fracture zone on the basis of fracture spacing, case study at the Toki granite, central Japan

SASAO, Eiji[1*] ; ISHIBASHI, Masayuki[1]

[1]Japan Atomic Energy Agency

In order to evaluate deep geological environment for geological disposal of high level radioactive waste, understanding of the geometry of water conducting features such as fractures is essential. The fracture zones have been divided based on the fracture intensity that has been obtained deep boreholes. But fracture intensity could be changeable in different portion of the rock body. The method to divide the fracture zones based on fracture spacing is studied. In this study, cumulative frequency curve of fracture spacing based on fifteen deep borehole with the total length of ca.12,000 meters was used. Cumulative frequency curve shows that half of fracture spacing is lower than 1m. Thus, fracture could exist in fracture zones. The fractures with the dip of middle to high angle are needed to divide into fracture zones based on the fracture spacing. In the future, we will establish the methodology to divides the fracture zones coupled with spatial distribution of fracture spaces.

Keywords: fracture zone, fracture spacing, Toki granite

Japan Geoscience Union Meeting 2014
(28 April - 02 May 2014 at Pacifico YOKOHAMA, Kanagawa, Japan)

HCG36-03 Room:411 Time:April 29 15:45-16:00

Examination of realistic conceptual model of near-field process in HLW repository

YOSHIDA, Hidekazu[1*] ; KOJIMA, Keiji[2] ; OONISHI, Yuzo[3] ; TOCHIYAMA, Osamu[4] ; NISHIGAKI, Makoto[5] ; TOSAKA, Hiroyuki[6] ; SUGIHARA, Kozo[7] ; OGATA, Nobuhisa[7]

[1]Nagoya University, [2]Geospace Labo, [3]Kansai University, [4]Nuclear Safety Research Association, [5]Okayama University, [6]University of Tokyo, [7]Japan Atomic Energy Agency

Since 2000, data of deep underground has been accumulated through the URLs in-situ studies and related underground investigation. Based on these data, here we show the result on the examination of realistic conceptual model of near-field process in HLW repository.

Keywords: Geological Disposal of Radioactive Waste, Near filed processes

Japan Geoscience Union Meeting 2014
(28 April - 02 May 2014 at Pacifico YOKOHAMA, Kanagawa, Japan)

HCG36-04 Room:411 Time:April 29 16:15-16:30

An approach to establish information basis of Weathered zone for the Safety Assessment to HLW Disposal over long-term.

SHIMEMOTO, Hidenori[1*] ; WAKASUGI, Keiichiro[2] ; SHIBATA, Masahiro[2] ; YAMAGUCHI, Masaaki[2]

[1]Japan Atomic Energy Agency (*Present position: Mitsubishi Materials Techno Corporation), [2]Japan Atomic Energy Agency

The consideration of evolution on geological environment is required in the safety assessment of geological disposal for the high level radioactive waste (HLW). The HLW repository can be expected to come close to ground surface assuming a continuous uplift and erosion for a long-term period. Therefore, the consideration of shallow zone (weathered zone) environment is also required. Since the geological condition in the near-surface underground is different from that in the deep underground due to weathering, the basic information and understanding for the near-surface condition are essential for the scenario development. Therefore, information regarding weathered zone is surveyed and arranged based on available literatures.

As a result, 37data of depth (thickness) of weathered zone were extracted. Then the data distribution and these characteristics for the thickness of weathered zone were discussed. In order to understand the formation process of weathered zone, the relation between weathered zone and landform was also discussed and categorized into four patterns. The key factors which account for the patterns are also analyzed in a qualitative manner.

Regarding the geological property/condition in the weathered zone, although information on hydraulic and chemical conditions are very limited, information on tensile strength and porosity are available.

For the sake of condition setting for near-surface underground in the long-term safety assessment, continuous research and development for the characterization on weathered zone are important.

Keywords: HLW, Long-term, Safety Assessment, Weathered Zone, Landform, Geological Environmental Conditions

Japan Geoscience Union Meeting 2014
(28 April - 02 May 2014 at Pacifico YOKOHAMA, Kanagawa, Japan)

HCG36-05 Room:411 Time:April 29 16:30-16:45

A Bayesian approach to assess the probability of concealed active faults existing using helium isotope ratios

MARTIN, Andrew[1*] ; ISHIMARU, Tsuneari[2] ; UMEDA, Koji[2] ; ASAMORI, Koichi[2]

[1]NAGRA, [2]Tono Geoscience Center, JAEA

In Japan, numerous studies have been carried out to assess the stability of the geological environment including in particular, the spatio-temporal distribution of active faulting in the context of site selection of a radioactive waste repository and/or assessing the safety of current nuclear facilities etc. One key concern is the existance of active faults that do not show any surface rupture.

High He-3/He-4 ratios which tend to be found in volcanic regions have also been measured in non-volcanic regions. This has been attributed to degassing from the mantle with faults potentially acting as conduits (e.g., Kennedy et al., 1997). Studies carried out in the western Tottori district have shown the potential of using He-3/He-4 ratios as a means of providing indirect evidence of the existence of source fault(s) that caused the 6 Oct 2000 Tottori earthquake (Mw 6.8), but which had no apparent surface indication prior to the earthquake (Umeda and Ninomiya, 2009).

Here we introduce a new technique based on Bayesian inference in an effort to quantify this theory. In the Bayesian paradigm, we make *a priori* assumptions based on the tectonic setting of the study area as a starting point. 'Known' active faults are divided into equal distant fault segments. The *a prior* assumption here is that 'unknown' fault segments do not exist far from 'known' fault segments. It is also assumed that the probability of 'unknown' faults existing decreases with distance from the 'known' faults.

2D *a priori* probability distributions of unknown fault(s) existing are then calculated using kernel functions (Martin et al., 2003) centered over the known fault segments. A Cauchy probability density function (PDF) is assigned here conservatively as the *a priori* distribution in the first step so that probability is never zero.

In the second step, the method developed by Martin et al. (2004, 2012), is adapted to remap He-3/He-4 ratios into a PDF, called a likelihood function based on Kolmogorov-Smirnov statistical tests. The *a prior* PDF from the first step above is then combined with the likelihood PDF using Bayes's rule to produce a *a posteriori* PDF.

Carrying out the calculation using data from before the Tottori 2000 earthquake, the *a posterior* 2D probability maps showed increased probability of unknown active fault(s) existing in the region above the source zone of the 2000 earthquake. Thus, in the case of the Tottori region, the *a posterior* probabilities corraborate the theory that faults could be acting as conduits for mantle helium.

The potential of the methodology to incorporate other information such as gravity and crustal strain rates will also be presented and discussed.

References

Kennedy et al. (1997), Mantle fluids in the San Andreas fault system, California, *Science*, 278, 1278-1281.
Martin et al., (2003) *Acta Geophys*. 51, 271-289
Martin et al. (2004) *J. Geophys. Res*., 109, B10208, doi:10.1029/2004JB003201.
Umeda, K. and Ninomiya, A. (2009) *Geochem. Geophys. Geosys*., 10, Q08010, doi:10.1029/2009GC002501.
Martin A. J., Umeda K. and Ishimaru T. (2012) *InTech Pub*., doi:10.5772/51859

Keywords: Active fault, Bayesian, Helium isotope ratio

Japan Geoscience Union Meeting 2014
(28 April - 02 May 2014 at Pacifico YOKOHAMA, Kanagawa, Japan)

HCG36-06 Room:411 Time:April 29 16:45-17:00

An active shear zone, southwest Japan: electromagnetic geophysics and noble gas geochemistry

UMEDA, Koji[1*] ; ASAMORI, Koichi[1] ; MAKUUCHI, Ayumu[1] ; KOBORI, Kazuo[1]

[1]Japan Atomic Energy Agency

In 1997, the Kagoshima earthquake doublet with two Mw ˜6 strike-slip events struck 5 km and 48 days apart in southwest Japan, where an E-W trending discontinuity along 32 degree N latitude in GPS velocities across southern Kyushu Island is clearly defined, indicating a highly active left-lateral shear zone. However, there was no obvious prefaulting indication at surface (active fault) in relation to the shear zone. Three-dimensional inversion of magnetotelluric sounding data observed in the source region of the the earthquake doublet reveals a near-vertical conductive zone with a width of 20 km, extending down to the base of the crust and perhaps into the upper mantle. The prominent conductor corresponds to the western edge of the active shear zone. Elevated 3He/4He ratios of groundwaters sampled around the seismic source region suggest the emission of mantle-derived helium from the electrical conductor. The geophysical and geochemical observations provide significant evidence that the invasion of mantle fluids into the crust, driven by upwelling asthenosphere from the Okinawa trough, triggers off the notable left-lateral shear zone in the present-day subduction system. In addition, the conductive fluids enhance stress concentration in the seismogenic layers leading to mechanical failure of strong asperities, resulting in the occurrence of the 1997 earthquake doublet.

Keywords: 1997 Kagoshima earthquake doublet, active shear zone, magnetotelluric sounding, helium isotope

Japan Geoscience Union Meeting 2014
(28 April - 02 May 2014 at Pacifico YOKOHAMA, Kanagawa, Japan)

HCG36-07 Room:411 Time:April 29 17:00-17:15

Predominant process for transport of radiocaesium released by the TEPCO's Fukushima Daiichi Nuclear Power Plant Accident

NIIZATO, Tadafumi[1*] ; ISHII, Yasuo[1] ; ABE, Hironobu[1] ; WATANABE, Takayoshi[1] ; SASAKI, Yoshito[1]

[1]Fukushima Environmental Safety Center, Japan Atomic Energy Agency

Understanding the environmental dynamics of the radiocaesium (particularly Cs-134 and 137) released from the Fukushima Daiichi Nuclear Power Plant provides the firm foundation for a remediation of the Fukushima environment because it is the main radionuclide to radiological dose within the contaminated area. One of the main sources of radiocaesium under the current situation is a mountain forest, where the decontamination work has not been carried out as yet. Therefore, transport process, flux and chemical form of the radiocaesium flowing from the mountain forest are crucial issues for an evaluation of a radiation exposure, taking into a dynamics behavior of radiocaesium from the highest contaminated mountain forests down through the river to eventual deposition in the sea. This paper discusses the predominant process of the radiocaesium transport in the mountainous region, Fukushima, Japan.

The four investigation areas, which have different characteristics of vegetation, geomorphology and soil type, were selected in the Abukuma Mountain, eastern part of Fukushima. The soil samples were obtained from ridge, slope, and valley bottom in the areas by soil sampler and scraper plate to the depth about 40 cm and 20 cm, respectively. The observation plots, which have an area of 40 to 60 m2, for a monitoring of surface runoff and soil loss are also installed. The concentration of radiocaesium in the uppermost soil horizon is related to the geomorphological aspects, that is, the concentration trends to be higher in the depositional area than in the erosional area. Additionally, the radiocaesium concentration of solid phases (soil particles and fragmented organic materials) including in surface runoff is one to two orders of magnitude greater than that of a liquid phase (running water).

Therefore, predominant process of the radiocaesium transport is the surface runoff accompanied with a detachment of soil particles from the mountain slope.

Keywords: radiocaesium, environmental dynamics, mountain forest, nuclear accident, Fukushima

Japan Geoscience Union Meeting 2014
(28 April - 02 May 2014 at Pacifico YOKOHAMA, Kanagawa, Japan)

HCG36-08 Room:411 Time:April 29 17:15-17:30

Current State of the additional geological surveys of crush zones at the fast breeder prototype reactor ”Monju” site

ISHIMARU, Tsuneari[1*] ; SHIMADA, Koji[1] ; SASAKI, Akimichi[1] ; TANAKA, Yukumo[1] ; MIYAZAKI, Masashi[1] ; YASUE, Ken-ichi[1] ; NIWA, Masakazu[1] ; SUEOKA, Shigeru[1] ; UMEDA, Koji[1] ; IKEDA, Makinori[1]

[1]Japan Atomic Energy Agency (JAEA)

Background: In the fast breeder prototype reactor Monju of the Japan Atomic Energy Agency (JAEA), a report of the additional geological survey regarding the crushed zones at the Monju site was submitted to the Nuclear Regulation Authority (NRA) on April 30, 2013. The NRA instructed to develop a further additional research plan on September 25. Accordingly, JAEA compiled and submitted the plan on October 3, followed by a ”preliminary report” on November 29, and a ”complete report” in March 2014.

Overview of additional research: The instructions from the NRA of September 25, 2013 were as follows:

1. to implement the dating of materials within the crushed zones, to research the displacement markers, and to understand their formation age, etc.,in order to enhance understanding of the activity of crushed zones at the Monju site in the bedrock of the site investigation area; 2. to investigate the distribution of the fracture zones, the relationship of the sediment layer, and the depositional age of the sediment layer (14C dating, tephra analysis, etc.) for data expansion of the extended portion of the L-2 lineament located near the Monju site; and 3. to implement marine seismic surveys in the coastal sea area and geographical and geological surveys ofthe coast, etc., in order to understand the geological structure and activities of the coastal seabed in the extended portion of the Shiraki-nyuu active fault and the L-2 lineament.

JAEA developed a research plan in response to these instructions and conducted the stripping investigation over an expanded area, the additional detailed geographical and geological surveys around the mountains/terrace boundary, and the marine seismic surveys in the coastal waters.

Summary of findings: The basement rock of the northern Tsuruga peninsula where the Monju site is located is composed of the Late Cretaceous-Paleogene granite known as the Kojyaku granite. In the on-site investigation, the stripping area was extended in the northern direction of the longest fracture zone in the reactor building foundation rock. The fracture zones were grouped into 2 systems called α-system and β-system. We examined the cross-cuttingrelationships and displacementsof the fracture zonesand confirmed that the α-system was formed after the β-system. The α-system fracture zones are left-lateral faultsthat have mesh-like clay veinlets, and the width of the α-system fracture zones is several centimeters. The K-Ar ages of the basalt dyke displaced by the α-system fracture zones were about 19Ma. In addition, U-Pb and FT dating of apatite and zircon separated from the fracture zone materials and granite were conducted to reconstruct their thermal histories. The investigation results so far obtained were similar to the survey results of April 30, 2013, offering no clear evidence that the on-site crushed zones are of an active fault. It can be considered that these crushed zones are small-scale older (pre-Quaternary?) geological structures formed under the hydrothermal environment of the deep part before exposure of the granitic body. On the detailed geographical and geological surveys around mountainous/terrace boundary, no fracture zone along the strike of the boundary was observed. From the C-14 dating and tephra analysis of the depositional layer covering the granite, the distribution of sediments from about 40,000-50,000 years ago was confirmed in a few outcrops. The marine seismic surveys in the coastal waters were performed in conjunction with the bathymetric survey in December 2013. Currently, the data are being analyzed.

Upcoming: In order to further enhance the reliability of the investigation results and accumulate further data related to on-site geology and the underground, voluntary investigations are being conducted on a continuous basis. In addition, a basic study is also being carried out on the evaluation method of the activity of the fault zone not applicable to the overburden strata method.

Keywords: fast breeder reactor Monju, survey of crush zone, Kojyaku granite, Nuclear Regulation Authority

Japan Geoscience Union Meeting 2014
(28 April - 02 May 2014 at Pacifico YOKOHAMA, Kanagawa, Japan)

HCG36-P01 Room:Poster Time:April 29 18:15-19:30

The linearity of geographical features and a planation surface along the seashore around the fast breeder reactor Monju

SASAKI, Akimichi[1*] ; YASUE, Ken-ichi[1] ; SHIMADA, Koji[1] ; TATEISHI, Ryo[2] ; ISHIMARU, Tsuneari[1] ; TANAKA, Yukumo[1]

[1]Japan Atomic Energy Agency, [2]OYO Corporation

We have not only conducted a survey of crush zones near the reactor building in the fast breeder prototype reactor Monju site but also carried out geographical investigations such as terrace classification and lineament investigation around the site. This presentation reports the results of the geographical and geological survey on the linearity of geographical features and a planation surface along the seashore around the site.

1. An investigation into the linearity of the mountain/terrace boundary

It is estimated that the lineament of the NW-NNW direction, also called the L-2 lineament, exists to the south of the Monju site. Geographical and geological surveys by JAEA suggest that this lineament is highly likely to be a structural landform. The mountain/terrace boundary to the north of this lineament extends in a straight line-like form in the NW direction. During an expert meeting of the Nuclear Regulation Authority, it was suggested that an active fault might exist along this boundary. It was in response to this suggestion that we carried out the geographical and geological survey.

Geographical investigation: We carried out a terrace classification, field survey, and analysis of the survey data for regions around the mountain/terrace boundary. The mountain slope directly faces the sea; the slope of the present stream bed and terrace surfaces is comparatively steep in the investigation area. In the topographical map before artificial change, we can recognize that the stream makes the loosely curved dissected topography without winding greatly and that the mountain/terrace boundary is loosely curved similarly.

Geological survey: Outcrop investigation was conducted on the mountain/terrace boundary by paying attention to the existence of crush zones and the development style of the joints. In addition, we also estimated the age of the sedimentary layers.

The results clearly indicate that the joints are progressing mainly in the NW or the NE direction, and the comparatively hard granite is also distributed. Moreover, although crush zones were observed in some outcrops near the mountain/terrace boundary, we could not detect crush zones that continue in the same direction as the mountain/terrace boundary. In the outcrop near the northwestern end of the mountain/terrace boundary, it was observed that the covering layer, which was deposited after about 40,000-50,000 years ago and covers a crush zone, is not displaced.

The results of the above-mentioned geographical and geological survey suggest that the linearity of the mountain/terrace boundary has not originated from fault displacement.

2. An investigation into the linear coastline and planation surface along the seashore

A linear coastline extending in the NE direction can be seen around the Monju site. In addition, a planation surface is observed in parts along the seashore. We performed a geographical and geological survey to determine the origin of such a geographical feature and whether such a planation surface could exist elsewhere.

Geographical investigation: While carrying out the air photograph interpretation, the contour line maps and topographic profiles were created using a digital elevation map created from aviation laser survey data. As a result, except for one place which is present at an altitude of about 5 m, a geographical feature that can be recognized as a comparatively flat field was not observed.

Geological survey: We carried out an outcrop investigation that paid attention to the development of joints and searched for evidence that suggested the upheaval of land. The results suggest that the direction of the coastline and the direction of developing joints are similar. Moreover, we could not observe the remains of living things which suggest the possible upheaval of land.

Keywords: fast breeder reactor Monju, survey of crush zone, lineament

Japan Geoscience Union Meeting 2014
(28 April - 02 May 2014 at Pacifico YOKOHAMA, Kanagawa, Japan)

HCG36-P02 Room:Poster Time:April 29 18:15-19:30

On the turn determination of crush zone activity, a lesson from granitic basement rock holding the fast breeder reactor

SHIMADA, Koji[1*] ; TATEISHI, Ryo[2] ; ISHIMARU, Tsuneari[1] ; SASAKI, Akimichi[1] ; TANAKA, Yukumo[1] ; MIYAZAKI, Masashi[1] ; YASUE, Ken-ichi[1] ; NIWA, Masakazu[1] ; SUEOKA, Shigeru[1] ; UMEDA, Koji[1] ; IKEDA, Makinori[1]

[1]Japan Atomic Energy Agency, [2]OYO Co.

Activity evaluation of crush zones encountered in basement rock is an issue of the seismic safety assessment of nuclear plant and geological isolation of radioactive wastes. The selection of crush zone of which has been evaluated should be defined as the latest one by means of turn determination of crush zone activity based on stratigraphic or structural geological method. A lesson from granitic basement rock (Kojaku granite) holding the fast breeder reactor "Monju" is presented. The Kojaku Granite form the oval Tsuruga peninsula (ca. 8km in width) on the southeastern coast of the Sea of Japan and the age is 68.5±0.7Ma (Zircon U-Pb age).

1. Stratigraphy-oriented turn determination of crush zone activity.

(1.1) Turn determination using cover sediments

The age determination of undeformed cover sediments indicates the activity of crush zone older than the sediments. In the case of crush zones observed at separate outcrop, deformation of the same strata can be utilized for the turn determination.

Trenching evidence (with tephra chronological analyses) of the active Shiraki-Nyu fault near the Monju site indicate repeated activity after ca. 30ky strata (including AT-tephra). On the other hand, crush zones in the Monju site affect no deformation on the strata of identical age observed during the site construction. These data indicate the last movement of the latter is older than the active fault, and no movement in sympathy with the active faulting repeatedly during, at least, ca. 30ky.

(1.2) Turn determination using dyke, mineral and clay vein ("Dyke", hear after)

Undeformed dykes intersecting crush zones indicate that the movements of crush zones are older than the dyke formation. Age determination of the dyke constrain the latest age of the crush zone activity.

Excavation survey of basement rocks at the Monju site shows a basaltic dyke (ca. 19Ma, Plagioclase K-Ar age) cut by the crush zone (crush zone alpha-3 and alpha-4) indicate that the movements of these crush zones are later than the dyke formation.

2. Structural-oriented turn determination of crush zone activity

Intersecting relationship between crush zones indicate which of them is the latest one at least locally. This rule can be hold in the case of conjugate set, although they suggest the contemporaneous development in one tectonic stage. Conjugate relations should be judged from traditional Griffith-Coulomb failure criterion as well as the Maximum effective moment criterion(1). Despite of the development of remarkable clay rich zone, cross cutting crush zone with meso- and microstructures developed under the higher temperature and pressure indicate the movement of the clay rich zone is older.

Excavation survey of basement rocks at the Monju site shows conjugate like development of the crush zone beta and younger alpha-3 with 50-55 degrees between them. The crush zone beta is composed of clay rich vein. Along the crush zone arpha-3, drugged sigmoidal quartz veins, drugged biotite along shear layers and preferred orientation of quartzo-felspathic lenses composed of foliated cataclasite with P-Y-R_1 fabric are observed. These ductile features suggest that relatively higher temperature and pressure during the development of crush zone arpha-3. Hence, the crush zone beta is old structure.

These stratigraphic and structural evidences for the turn determination indicate that the activity of crush zone arpha-3 is the object of the evaluation.

(1)Zheng et al., 2004, Journal of Structural Geology, 26, 271-285.

Keywords: fast breeder reactor Monju, survey of crush zone, Kojaku granite

Japan Geoscience Union Meeting 2014
(28 April - 02 May 2014 at Pacifico YOKOHAMA, Kanagawa, Japan)

HCG36-P03 Room:Poster Time:April 29 18:15-19:30

Depth-dependent coseismic groundwater level changes by seismic ground motion of the 1999 Chi-Chi earthquake, Tiwan

HIGA, Mayumi[1*] ; NAKAMURA, Mamoru[2] ; KOIZUMI, Naoji[3] ; LAI, Wen-chi[4]

[1]Faculty of Science and Graduate School of Engineering and Science, University of the Ryukyus, [2]Faculty of Science, University of the Ryukyus, [3]Geological Survey of Japan, National Institute of Advanced Industrial Science and Technology, [4]Disaster Prevention Research Center, National Cheng Kung University, Taiwan

The coseismic water level change (Cw) has been reported (Montgomery and Manga, 2003; Koizumi, 2013). One of the causes of the Cw is crustal displacement (static strain change and vertical displacement etc.), and seismic ground motion(dynamic volumetric strain change and hydraulic conductivity change etc.)(Lee *et al*., 2002; Lai *et al*., 2004; Wang *et al*., 2001). The static strain change has been assumed as one of the main factor of the water level change from the comparison of water level change with static strain change in the earthquakes. However, the relation between water level change and static strain change doesn·t correspond clearly. Although the dynamic strain change by the ground motion would be more effective to the cause of Cw, the effect has not been known yet.

The Chi-Chi earthquake (Mw7.6) occurred in central Taiwan at 1:47 (local time) on September 21, 1999. The earthquake was the largest event which occurred recently in the inland of Taiwan. Since the both networks of strong motion seismometer (Lee *et al*, 1999) and water level monitoring system (Koizumi, 2001) are distributed densely around the source fault of the Chi-Chi earthquake, good seismic waveform and the data of Cw has been obtained.

For the previous study of Cw in the Chi-Chi earthquake, Wang *et al*.(2003) has been analyzed the relationship between Cw and seismic ground motion from the point of view of liquefaction at the shallow groundwater in the alluvial plain part. They showed that there is correlation between the spectrum velocity or acceleration and water level. However, they did not account much for the effects of the permeability or other characteristics in each aquifer although they analyzed the Cw of all wells at once. Since the hydrogeological conditions effects to the occurrence of liquefaction similar to the effect of ground motion, the effect for the hydrogeological conditions, that is the geological characteristics and permeability of aquifer in confined aquifer or unconfined aquifer, must be investigated.

We divided the aquifer to similar hydrogeological categories and examined the Cw response by the ground motion in each aquifer. We put target groundwater of two aquifer, the shallow aquifer 1(unconfined aquifer)and underlying aquifer 2(confined aquifer), and investigated whether there are the different character in those. I measured the degree of Cw. Therefore the wells observed Cw were 84 wells, fall wells were 14 wells in these wells. I used the observation wells with water level rises in the alluvial plain part, because the mechanism of water level change for water level fall is different. We investigated the relationship spectral response of seismic wave and groundwater level change, because spectral response can read the effect to the ground in comparison spectrum of normal. We calculated the response of Cw against the frequency of 1 Hz (high-frequency) and 0.1 Hz (low-frequency) to evaluate the groundwater level change as a function of frequency. We calculated the acceleration, velocity, and displacement spectral response of vertical, horizontal, and 3 components from acceleration waveform data. I investigated the correlation coefficient between spectrum and Cw in each aquifer. The result frequency band in those show different response was obtained. Correlation between the response spectrum and water level change in the high-frequency side (1 Hz) was higher in the aquifer considered unconfined aquifer, but the correlation in low-frequency side (0.1 Hz) was higher in the aquifer considered confined aquifer. In common to both aquifer, correlation between hydraulic conductivity and water level change showed strong positive correlation.

Keywords: Groundwater level changes, The 1999 Chi-Chi earthquake, Taiwan, Seismic ground motion

Japan Geoscience Union Meeting 2014
(28 April - 02 May 2014 at Pacifico YOKOHAMA, Kanagawa, Japan)

HCG36-P04 Room:Poster Time:April 29 18:15-19:30

Occurrence of faults and water conducting features at 350m gallery of the Horonobe URL project

HAYANO, Akira[1*] ; MATSUOKA, Toshiyuki[1] ; ISHII, Eiichi[1]

[1]Japan Atomic Energy Agency

In the Horonobe Underground Research Laboratory Project, methodology development for the investigation of geological structure in sedimentary rocks has been carried out through construction of underground facility. As part of the methodology development, hydrogeological models have been constructed and the geological structure associated with water-conducting features (WCFs) has been conceptualized on the basis of the surface-based investigations including geophysical survey, outcrop observation and borehole investigation. The horizontal gallery named ‘ 350m gallery ’ and having approximately 740m long in total has been excavated at a depth of 350m below the surface by January 2014. This study presents the predictive distribution of geological structures contributing to WCFs in 350m gallery based on the surface-based investigations and the characteristics of geological structures observed in 350m gallery.

Keywords: Hydrogeological model, Fault, Water-conducting feature

Japan Geoscience Union Meeting 2014
(28 April - 02 May 2014 at Pacifico YOKOHAMA, Kanagawa, Japan)

HCG36-P05 Room:Poster Time:April 29 18:15-19:30

Permeability variation in Toki granite and its relationships with crack structure and alteration processes

KUBO, Taiki[1*] ; MATSUDA, Norihiro[1] ; KASHIWAYA, Kouki[1] ; KOIKE, Katsuaki[1]

[1]Kyoto University

Understanding of physical and chemical properties of rock mass is essential to implement the geological disposal of the high level nuclear waste. Especially, extraction of highly permeable zone that acts as channel of fluid flow is required. In this study, permeability measurements of Toki granite were carried out to reveal the permeability variation in rock mass and to understand factors causing that. Image analysis was applied to disc-like specimens and thin sections of the granite, for quantitative characterization of crack structure. Additionally, fluorescent X-ray analysis (XRF) was carried out to obtain elemental compositions of granite cores showing various degrees of alteration and to consider the relationship of the permeability with the alteration degree.

Permeability was measured using the gas permeameter. The samples are cores collected from about 1 kilometer depth range boreholes in Tono area (Mizunami, Gifu, Japan) drilling by Japan Atomic Energy Agency (JAEA). Over 40 granite cores were sampled at 25-meter intervals ranging from 100 to 1000 meters depth to measure the permeability. Permeability was larger in the altered and fault zones. In addition, the anisotropy was appeared around the fault part and the permeability was enhanced along E-W direction. This direction is consistent with the fault strike, and thus the anisotropy of the permeability was presumably caused by the cracks developed in the fault movement.

Next, the crack structures were quantitatively characterized using an image analysis and compared with the permeability data to clarify their relationship. The specimens were impregnated with fluorescent resin and images were acquired to characterize the mesocrack structure using a fluorescent scanner equipped with ultraviolet ray source. Additionally, thin sections were made from the specimens and microphotographs for characterizing microcracks were taken with a stereomicroscope. Cracks were extracted from these images and length and direction of each crack were determined by the image analysis, following segmentation of crossing cracks. Positive correlation was observed between the permeability and cumulative crack length. These results suggest that cracks cause the permeability anisotropy and microcrack can be a factor controlling the permeability.

XRF was carried out to examine relationships between the permeability and the alteration processes of Toki granite. Positive correlations were recognized between the permeability and Ca concentration in the cores. Hydrothermal alteration of Toki granite is considered to follow three steps, 1) chloritization of biotite, 2) illitization of plagioclase, and 3) precipitation of calcite (Nishimoto and Yoshida, 2010). Considering that precipitation containing Ca is formed in the illitization of plagioclase, strong hydrothermal alteration presumably occurred in the altered and fractured zones that show relatively high Ca concentration. It implies that these zones were highly permeable as forming flow paths of hot water in the past. Although the fault-zone core had high permeability, its Ca concentration was relatively low. Fault movement caused development of fault gouge in addition to fracturing of granite. Permeability was enhanced by the fracturing, but the impermeable fault gouge occurred in the fault interfered circulation of hot water and addition of Ca precipitation.

These results suggest that fractured zone accompanying densely distributed microcracks and altered zone can be groundwater flow paths. Distribution of the highly permeable zones is essential to understand the hydrogeological structure.

Acknowledgement: We would like to express our sincere thanks to the co-researchers of Japan Atomic Energy Agency for their supports and many constructive comments for this study.

References

Nishimoto, S., Yoshida, H. (2010): Hydrothermal alteration of deep fractured granite: Effects of dissolution and precipitation, Lithos, vol. 115, pp. 153-162.

Keywords: fracture system, permeability, microcrack, altered zone, hydrogeological structure, Toki granite

Japan Geoscience Union Meeting 2014
(28 April - 02 May 2014 at Pacifico YOKOHAMA, Kanagawa, Japan)

HCG36-P06 Room:Poster Time:April 29 18:15-19:30

The relation between imaging of soil structure with GPR and depth profile of radioactive cesium

WATANABE, Takayoshi[1*] ; MITACHI, Katsuaki[1] ; ABE, Hironobu[1] ; NIIZATO, Tadafumi[1]

[1]Japan Atomic Energy Agency

Radionuclides such as radioactive cesium, now the main radiological contributor, were released in the environment by the Fukushima Dai-ichi nuclear power plant accident. The government and local governments have proceeded with decontamination plans to reduce dose rate in living spheres. But most areas of forests have been still contaminated. Japan Atomic Energy Agency initiated a project entitled 'Long-Term Assessment of Transport of Radioactive Contaminant in the Environment of Fukushima' (F-TRACE project) in November 2012. Main objective of this project is to implement a comprehensive system for predicting radioactive cesium transport in the future and the impact of various countermeasures by understanding transport of radioactive cesium from forests to living spheres and the sea through rivers and dams.

To understand radioactive cesium transport in forest, we have conducted forest investigation at Ogi district, Kawauchi Village and Yamakiya district, Kawamata Town, Fukushima Prefecture since December 2012. As a part of the investigation, we carried out geophysical exploration of soil structure with ground penetrating radar (GPR) with 100MHz and 500MHz radio wave.

In this presentation, we report correlation between imaging of soil structure obtained by GPR survey and depth profile of radioactive cesium in soil.

Keywords: ground penetrating radar, depth profile of radioactive cesium, F-TRACE project

Japan Geoscience Union Meeting 2014
(28 April - 02 May 2014 at Pacifico YOKOHAMA, Kanagawa, Japan)

HCG36-P07 Room:Poster Time:April 29 18:15-19:30

Current situation and improvement of methylene blue adsorption testing method for bentonite

HORIUCHI, Yu[1*] ; MIYOSHI, Youko[1] ; TAKAGI, Tetsuichi[1]

[1]Geological Survey of Japan

Large amount of bentonite will be required as shielding material for radioactive waste disposal from nuclear power plant and contaminated soil management of Fukushima disaster. The testing methods of bentonite performances are important in terms of the safety of the disposal facility. Methylene blue (MB) adsorption test, which has generally been used for determining either cation exchange capacities (CEC) or surface areas of bentonite, is one of the important testing methods. However, current testing method of MB adsorption is different for each company and it is difficult to compare the performance of bentonite products. Since the current standard testing methods, which are developed by JBAS in the 1970s, are obsolete already, it is necessary to renew the standard testing methods. Therefore, we are planning to propose new standard testing methods for bentonite as JIS, based on this study.

In this study, we interviewed 13 companies and conducted questionnaire about the details of the current MB adsorption testing method. As the result, 10 companies are currently doing MB adsorption test. Of the 10 companies, MB adsorption test based on conventional JBAS method is conducted in eight companies. In addition, four companies are using their own methods, such as colorimetric method which is not defined in the JBAS, including 2 companies using compound of JBAS and colorimetric methods. The tests based on conventional JBAS methods have variation among companies in terms of determining the end point, reagents and sample preparations. Short testing time and simple decision of end point were raised by several companies, as the reasons for using their own methods such as colorimetric method.

As consider in result of interview, the method which aims to propose in this study is required of eliminating the ambiguity of the conventional method, minimal use of consumables, and streamlining for time saving. At the same time, sufficient accuracy is required with this method for ensuring safety in waste disposal. In future, it needs to consider time of reaching adsorption equilibrium, and dispersion and adsorption properties of bentonite by different localities and conditions.

Keywords: bentonite

Japan Geoscience Union Meeting 2014
(28 April - 02 May 2014 at Pacifico YOKOHAMA, Kanagawa, Japan)

HCG37-01 Room:421 Time:April 30 14:15-14:30

The sedimentary process and distribution of tsunami deposits in coastal lakes: a flume experiment

YAMAGUCHI, Naofumi[1*] ; SEKIGUCHI, Tomohiro[2]

[1]Center for Water Environment Studies, Ibaraki University, [2]Center for Research in Isotopes and Environmental Dynamics, University of Tsukuba

A series of flume experiments were performed to examine the sedimentary process and distribution of tsunami deposits in coastal lakes. In the experimental program, a fixed slope of 1/20 and terrestrial area including a pool as a coastal lake were installed, and tsunami-like solitary wave was generated. The tsunami flow transported sediments from a sand bed placed on the slope, and deposited them on the terrestrial area. When the tsunami flow irrupted into the pool, hydraulic jump was occurred. In the area where the hydraulic jump made turbulence, little sediment deposited. Thus, the distribution of the tsunami deposits in the pool did not always show the thinning-landward trend in the present experimental series. The dependence of the amount of sediments on magnitude of tsunami waves was more pronounced in the pool than the land area.

Keywords: tsunami deposit, flume experiment, coastal lake

Japan Geoscience Union Meeting 2014
(28 April - 02 May 2014 at Pacifico YOKOHAMA, Kanagawa, Japan)

HCG37-02 Room:421 Time:April 30 14:30-14:45

Variations of terrigenous organic carbon content in flood and slope failure sediments

OMURA, Akiko[1*] ; IKEHARA, Ken[2] ; KATAYAMA, Hajime[2] ; USAMI, Kazuko[2] ; IRINO, Tomohisa[3] ; KUWAE, Michinobu[4] ; ASHI, Juichiro[5]

[1]JSPS Research Fellow, Univ.Tokyo, [2]IGG, AIST, [3]Hokkaido Univ., [4]Ehime Univ., [5]Univ. Tokyo

In this study, we analyzed the stable organic carbon isotope of sea floor sediments, which were deposited by the modern large floods with typhoon and the slope failure with earthquakes. Stratigraphic variations of terrigenous organic carbon content in the flood sediments were different from those of slope failure sediments.

Sediment cores KH-11-9-FB12 and FB14 were corrected from the deep-sea floor off the Kumano River mouth, which is located on the Kii Peninsula. The sediment cores contain flood-induced sediments by large typhoon in September, 2011, the largest 20^{th} century typhoon, and the large 19^{th} century Totsukawa flood (Ikehara et al.,2012). These flood-induced sediments have high terrigenous organic carbon content. The base of turbidite, which include wood fragments, has highest peak of terrigenous organic carbon content. On the other hand, terrigenous organic carbon content of the lower part of turbidite mud are lower than those of the middle and upper parts of turbidite mud. The stratigraphic variations of terrigenous organic carbon content is not recognized in the middle and upper parts of turbidite mud.

Sediment cores 95A and 104A were corrected from the shallow depression on shelf off the Saru River mouth, Hokkaido, in 2007. These cores contain the sediments by the severe flood with typhoon in August, 2003. The shallow depression on shelf, which is thought to be the old river path during lowstand of the last glacial age, was suitable for preservation of the flood-induced sediments (Katayama et al., 2007). The lower part of the turbidite mud has low terrigenous organic carbon content and the middle and upper parts have high terrigenous organic carbon content. The stratigraphic variations of terrigenous organic carbon content is not recognized in the middle and upper parts of turbidite mud. The turbidite mud off the Saru River mouth have same characteristics as those off the Kumano River mouth. These results suggest that the lower part of flood-induced sediments were formed by erosion and deposition of sea-floor sediments during the early stage of flood. The middle and upper parts were considered to be formed by continuous supply and deposition of terrigenous materials from river mouth during the flood.

The sediment core BP09-6 was corrected from the Beppu Bay. The sediment core contains the slope failure sediments by the large earthquake in 1596 (Keicho-Bungo earthquake; Kuwae et al., 2013). The slope failure sediments are characterized by upward decreasing of terrigenous organic carbon. This result suggests that the turbidity currents were caused by collapse of delta slope sediments, which contain both terrigenous and marine organic materials.

Stratigraphic variations of terrigenous organic carbon content might be important information, when we investigate the records of paleo natural disasters with sea-floor sediments.

References

Ikehara,K. et al., 2012, Unique 210-Pb and 137-Cs profiles in marine sediment cores sontaining recent event deposits off Kumano and Sanriku Japan. *2012 Annual Meeting of Geological Society of America*.

Katayama,H. et al., 2007, Distribution of surface sediments after the 2003 flood on the shelf off Hidaka, southern Hokkaido. *Bull. Geol. Surv. Japan*, 58, 189-199.

Kuwae,M. et al., 2013, Stratigraphy and wiggle-matching-based age-depth model of late Holocene marine sediments in Beppu Bay, southwest Japan. *Journal of Asian Earth Science*, 69, 133-148.

Keywords: turbidite mud, hemipelagites, organic carbon, natural disasters

Japan Geoscience Union Meeting 2014
(28 April - 02 May 2014 at Pacifico YOKOHAMA, Kanagawa, Japan)

HCG37-03 Room:421 Time:April 30 14:45-15:00

Quartzose sand and kaolinite-dominated mud derived from felsic plutonic rocks in intense weathering condition

YOSHIDA, Kohki[1*] ; HATANO, Nozomi[1] ; MORI, Saori[1] ; IRIE, Shiori[2] ; ADACHI, Yoshiko[3]

[1]Shinshu University, [2]Inpex Cooperation, [3]Center for Transdisciplinary Research, Niigata University

In the Upper Miocene - Early Pliocene time, Japanese island had a warm and subtropical climate. The mineralogical and chemical compositions of sand and mud of the Upper Miocene Tokiguchi Porcelain Clay and the Early Pliocene in the Kobiwako Group were examined for sedimentary petrography and geochemistry to clarify the influence of the warm climatic condition on sediment composition. Both sediments are considered to have been produced from felsic crystalline basement provenance. These sediments are characterized by the deposition in warm and humid climate on the basis of plant and diatom fossils.

The humid tropical climate produced quartz rich sand and kaolinite rich mud. The Upper Miocene sediments indicate that mafic silicates and feldspars were destroyed so that the sand rages from arkoses with plagioclase rich sand to subarkoses with dominant of K-feldspar. The Upper Miocene mud show kaolinitic clay mineral composition and aluminous chemical composition. In contrast, the Pliocene sand is arkosic to litharenitic with abundant of feldspars and accessory minerals. In the Pliocene mud, an increase in the relative abundance of smectite accompanies the breakdown of volcanic fragments and volcanic glass is detected.

The intense weathering, rare earth elements (REE) are concentrated in mud. The Miocene sand shows the REE concentration less than one of PAAS level, whereas the Miocene mud display similar level of concentration in PAAS. In many samples, the REE concentration is mostly by biotite and zircon evidenced by HREE concentration.

The intense weathering condition, such as high temperature with humidity, affects the sand and mud compositions with selective destruction of minerals and newly formation of clay minerals. The relative increase of HREE, which is mainly housed in durable minerals, and mineral assemblage of sand and mud probably provide quantitative estimation of weathering degree for the sediments derived from felsic plutonic rocks.

Keywords: Miocene, sand composition, mud composition, REE composition, weathering

Japan Geoscience Union Meeting 2014
(28 April - 02 May 2014 at Pacifico YOKOHAMA, Kanagawa, Japan)

HCG37-04 Room:421 Time:April 30 15:00-15:15

Depositional environment of the recent Yangtze Delta sediment deduced from the natural gamma-ray spectroscopy of YD13-G2

IRINO, Tomohisa[1*] ; WANG, Ke[1] ; SAITO, Keita[2] ; TADA, Ryuji[2] ; SUZUKI, Yoshiaki[2] ; KUBOKI, Yui[2] ; SUGISAKI, Saiko[2] ; ZHENG, Hongbo[3]

[1]Hokkaido University, [2]University of Tokyo, [3]Nanjing Normal University

The Yangtze River has transported approximately 500 mt/yr of sediments which formed a well-developed tide-dominated delta on its mouth during the Holocene high-stand. Sediment transport is dominant in rainy summer season or during flooding events, and the 40% is deposited in the estuary and the remaining sediments are transported offshore by tide forming a submerged delta or re-transported southward during stormy winter season. Due to these seasonally contrasted and event driven feature of sedimentation, spatial distribution of the accretion and erosion of the delta body is highly heterogeneous.

The Holocene subaqueous delta sediment has been also used as good sediment archives of the history of the Yangtze discharge and flooding due to its high sedimentation rate and good coverage of the Late Holocene. We also performed drilling of the delta sediment and collected two ˜30 m drilling cores and four gravity cores in order to reconstruct the flooding history and the associated change in the detrital provenance. The drilled site (YD-13) is located on clayey bottom with the water depth of 40 m. The top 10 m of the sediment core consists of homogeneous clay with rare sand patches, which could be formed during the Holocene high stand. One of the gravity core (YD13-G2) recovers the 140 cm of surface sediments, and we decided to examine the natural gamma-ray spectrum and stacking pattern of this gravity core at 1 cm resolution in order to stationarity of sedimentation.

Since Cs-137 was not detected from the YD13-G2 sediment, even the surface material was judged to be older than 1950. Pb-210 is detected from the top 50 cm interval, which suggests the near-surface sediments were deposited during these ˜100 yrs. However, the vertical profile of Pb-210 shows highly variable from zero to 25 Bq/kg with zigzag shape, which suggests repeated intercalation of old materials. Th-234 / K-40 and Ac-228 / K-40 ratios varies consistently suggesting some varieties in the provenance or grain size. Further examination is necessary to resolve potential event sedimentation and the apparent age of the related sediments.

Keywords: Yangtze Delta, Depositional environment, natural gamma-ray spectroscopy

Japan Geoscience Union Meeting 2014
(28 April - 02 May 2014 at Pacifico YOKOHAMA, Kanagawa, Japan)

HCG37-05 Room:421 Time:April 30 15:15-15:30

Provenance changes of Yangtze Delta core sediments and their implications for precipitation changes during the Holocene

WANG, Ke[1*] ; TADA, Ryuji[2] ; IRINO, Tomohisa[1] ; ZHENG, Hongbo[3] ; SUGISAKI, Saiko[2] ; SAITO, Keita[2] ; KUBOKI, Yui[2]

[1]Hokkaido Univ., [2]Univ. of Tokyo, [3]Nanjing Normal Univ.

Understanding the complex evolution of the natural environment in response to changes in climatic boundary conditions is a major challenge. Changes in frequency and magnitude of flooding of the Yangtze in association with the variations in East Asian Summer Monsoon (EASM) precipitation during the Holocene is one of such examples. The Yangtze River catchment is particularly sensitive to periodic flooding and droughts caused by temporal and spatial variations in the seasonal precipitation regime.

As a joint research project with Nanjing Normal University, we conducted Yangtze Delta drilling to reconstruct temporal and spatial changes in precipitation within the Yangtze River drainage during the Holocene. Core YD13-1 (31’02’ 59.9250” N, 122’50’00.2538” E) was recovered from Yangtze subaqueous delta at a water depth of 37 m, its penetration depth is 39.5 m, and probably covering the entire Holocene. The project focus on decadal/centennial-scale variability of river discharge and its provenance in the lower Yangtze reaches, deltaic system and East China Sea (ECS). It includes the study of the reconstruction of the flood history, the variability of fresh-water input and redistribution of Yangtze-derived sediments and Holocene floodplain development in these areas.

A new tool that use of electron spin resonance (ESR) signal intensity of the E1’ center and the crystallinity index (CI) of quartz is introduced to characterize the provenance of the Yangtze River Delta sediments, which were derived from various parts of the Yangtze River drainage, and its temporal changes that should have reflected the spatio-temporal changes in precipitation and flooding. The result will contribute to a more accurate understanding of the changes in spatial precipitation pattern associated with rapid climatic changes, of evolution of the lower Yangtze river-delta-shelf system, and of the environmental and climatic conditions under which the process took place. Our previous research result from the mudbelt core in ECS suggests possible scenarios for the response of the Yangtze catchment to the changes in monsoon intensity and extreme events. New analytical result of the provenance proxy for core sediments from Yangtze River Delta will be presented and possible scenario will be discussed.

Japan Geoscience Union Meeting 2014
(28 April - 02 May 2014 at Pacifico YOKOHAMA, Kanagawa, Japan)

HCG37-06 Room:421 Time:April 30 15:30-15:45

Estimating mixing ratio of the sediments from tributaries in the sediments from Yangtze River mouth

SAITO, Keita[1*] ; TADA, Ryuji[1] ; ZHENG, Hongbo[2] ; IRINO, Tomohisa[3] ; CHAO, Luo[4] ; MENGYING, He[4] ; WANG, Ke[3] ; SUZUKI, Yoshiaki[1]

[1]EPS, Univ. of Tokyo, [2]Nanjing Normal University, [3]Hokkaido University, [4]Nanjing University

Yangtze river is the largest river in eastern Asia. The rain front is accompanied with the development of summer monsoon, and moves within the Yangtze drainage, bringing heavy rain. Thus, the spatial fluctuation is also important for understanding the behavior of summer monsoon.

A paleoclimate record is needed for reconstructing the distribution of precipitation before metrological record. In Yangtze, over 95% of yielded sediment is suspended particle matter(SPM). The precipitation in drainage is proportional to water discharge, and water discharge is also proportional to suspended sediment concentration.

In this study, as a basis for reconstructing the past distribution of rain in Yangtze drainage, 1) analyze the ESR(Electron Spin Resonance) signal intensity of each tributary, 2) confirm that ESR values can explain the mixture of sediments in the mainstream, 3) discussing how large flood can be detected as a change of ESR values in the river mouth.

The sediments from major tributaries of Yangtze shows different ESR values each other. Using ESR values of each tributary as end members, the modern ESR value at rivermouth is estimated. The estimated value is consistent with the analyzed ESR value of sediments near rivermouth. So, ESR signal intensity can be used for estimating mixture of sediments.

We also calculated how large ESR value at rivermouth can change on the assumption that the flood occurs in specific tributaries. As a result, the flood can be detected as the change of ESR value at rivermouth when the sediment yield increases 5 times than usual.

Japan Geoscience Union Meeting 2014
(28 April - 02 May 2014 at Pacifico YOKOHAMA, Kanagawa, Japan)

HCG37-07 Room:421 Time:April 30 15:45-16:00

Evaluation of chemical weathering and sediment flux for several drainages within the Yangtze River basin

KUBOKI, Yui[1*] ; LUO, Chao[3] ; TADA, Ryuji[1] ; SAITO, Keita[1] ; ZHENG, Hongbo[2] ; IRINO, Tomohisa[4] ; HE, Mengying[3] ; WANG, Ke[4] ; SUZUKI, Yoshiaki[1]

[1]Department of Earth and Planetary Science, The University of Tokyo, [2]Nanjing Normal University, [3]Nanjing University, [4]Graduate School of Environmental Science, Hokkaido University

Chemical weathering is closely coupled with erosion and driving landscape evolution. Silicate weathering plays a major role of fixing atmospheric CO2 in the carbon cycle in time scales longer than 105 years. Therefore, quantitative estimation of chemical weathering rate and evaluation of its controlling factors are critical to understand its role on landscape evolution and controlling the carbon cycle on a long time scale. Researches on evaluating controlling factors of the weathering rates have been conducted using various methods and on various temporal and spatial scales, including theoretical approaches based on mineral dissolution experiments, empirical approaches based on analyses of river water, suspended material and sediments, and numerical modeling approaches to synthesize these data. Although empirical formulations of the chemical weathering and physical erosion rates specific to a certain river have been presented, processes of weathering and erosion should be considered together both from physical and chemical aspects in order to obtain more generalized formulas. Besides, in order to reconstruct the past processes of chemical weathering and erosion from the knowledge of the present processes, it is necessary to establish methods for reconstructing chemical vs physical weathering processes by using sediments which are the end products of weathering and erosion.

Toward the objective above, this study aims to explore the present processes of chemical weathering and erosion in the Yangtze River drainage as an example. Yangtze River is the longest river in Asia with the great water discharge and sediment flux. Hence, the river's role on material cycle on Earth's surface is significant. In addition, water and meteorological data are accumulated for long time period by many gauging stations and meteorological stations in the basin.

Mineral and chemical compositions of suspended particles and sediments as well as chemical composition of dissolved matter are analyzed for water samples and river bank sediments obtained from Yangtze River and its tributaries in the summer of 2011. Using these results, together with river discharge data and dissolved/suspended load concentrations, the fluxes for each element are calculated, and then the inputs from each watershed are obtained. Then, the relative contribution between chemical weathering and physical erosion is estimated. The calculation revealed that chemical weathering rate increases downstream but the relative contribution between chemical weathering and physical erosion in the uppermost part is the maximum in the upper, erosional part. In the lower, depositional part, dissolved carbonate is diluted after the main stream has merged with Poyang Lake, and then increased again toward the river mouth. The processes of chemical weathering and physical erosion in each watershed and their possible controlling factors will be discussed.

Japan Geoscience Union Meeting 2014
(28 April - 02 May 2014 at Pacifico YOKOHAMA, Kanagawa, Japan)

HCG37-08 Room:421 Time:April 30 16:15-16:30

Underwater topographic survey for inaccessible water areas, and its applications to submarine and sublake landslides

YAMASAKI, Shintaro[1*]

[1]Kitami Institute of Technology

Landslides, volcanoes, active faults and other hazard related topographies exist on the sea floor or lake bottoms. It is important to investigate them for assessing future hazard potential. But investigations for these underwater topographies are not so easy because it needs quite high cost, and its heavy weight equipment also requires a ship big enough to hold it. These days, dramatically advanced leisure-use fish finders enable us to investigate underwater topographic survey from shallow to several hundred meters deep. These fish finders are low cost and light weight, so can be equipped on inflatable rafts that is accessible into ultra shallow area of 0.5 - 20 m deep that is usually inaccessible for usual scientific research vessels. Thus the investigating method using the fish finder and an inflatable raft is more versatile than other technical ways. Some advanced fish finders have a side-scan sonar system that obtains 2D image of acoustic reflections, and it can identify bottom materials and underwater structures. Now we are trying to apply for studying submarine and sublake landslides in water areas that have not been surveyed. This presentation shows successful examples of our conducted investigations for the sublake landslides in Lake Kussharo and the 1923 Nebukawa landslide that a part of the landslide dived into the sea. These results have contributed the innovative discussion in generation of tsunamis on the lake, and revealed unknown submarine ruins that landslide devastated.

Keywords: fish finder, submarine landslide, underwater landslide, bathymetric survey, side-scan sonar

Japan Geoscience Union Meeting 2014
(28 April - 02 May 2014 at Pacifico YOKOHAMA, Kanagawa, Japan)

HCG37-09 Room:421 Time:April 30 16:30-16:45

Development of a monitoring system of bathymetric change and related sediment transport using optic fiber cables

YOSHIKAWA, Shuro[1*] ; SAKAGUCHI, Hide[1] ; AKUTAGAWA, Shinichi[2] ; MACHIJIMA, Yuichi[3] ; YUE, Zhao[3]

[1]JAMSTEC, [2]Kobe University, [3]LAZOC Inc.

A development of monitoring system is important for understanding more detailed process of the bathymetric change and sediment transport. At the nearshore zone, to monitor the nearshore features such as sand ripple migration, and the sediment suspension processes, optical back-scatter sensors (Downing et al., 1981), rotary sidescan sonar system (Traykovski et al., 1999), and sand ripple profiler (Masselink et al., 2007) were developed and used. Those systems can provide the very high-resolution morphological change and transportation, but not suitable for investigation of large-scale sediment erosion and deposition generated by high-energy waves in the surf zone. Where change in water depth is large (e.g. more than 1 m) in short span, the systems will be destroyed, lost, or submerged.

In the present study, we developed a new instrumentation for the monitoring of bathymetric change and related sediment transport in the high-energy shallow marine environment using optic fiber cables. The system consists mainly of four components: (1) an array of optical sediment sensors (OSSs); (2) a support structure (steel pipes); (3) an electronics unit that transmit and receive the LED through the optic fiber cables; and (4) a digital data acquisition system. The OSSs are mounted in a vertical steel pipe, 2 m long; and the spacing between the sensors is 10 cm. The steel pipe with OSSs was embedded to the seafloor at two places beneath a pier (427 m long) of Hazaki Oceanographical Research Station (HORS) owned by the Port and Airport Research Institute (PARI) at Sudahama Coast facing the Pacific Ocean, Japan. Both the electronics unit and the data acquisition system were installed in an observation room on the pier. In addition, those points of measurement are aligned perpendicular to the coastline in water depth approx. 4-5 m. Since active sediment transport that creates and deforms the longshore bar have been observed in this area (e.g., Kuriyama, 2010), detailed process of change in the cross section will be acquired by the present systems. In this presentation, we will show the system and data, and discuss those availability and future plan.

Acknowledgment: We would like to thank Dr. Satoshi Nakamura and Mr. Masayuki Banno belonging to the PARI for understanding and support of using the HORS, and MIKUNIYA Construction Co., Ltd. for installation work of the pipes. We wish to express our deep gratitude to the above-mentioned individuals and organizations.

Keywords: monitoring system, bathymetric change, sediment transport, optic fiber cable

Japan Geoscience Union Meeting 2014
(28 April - 02 May 2014 at Pacifico YOKOHAMA, Kanagawa, Japan)

HCG37-10 Room:421 Time:April 30 16:45-17:00

New insight of tsunami excitation mechanism and its recordable evidence in deep-sea

KAWAMURA, Kiichiro[1*]

[1]Yamaguchi University

Not yet

Keywords: Japan trench, 2011 Tohoku-Oki earthquake, Tsunami, Earthquake, Sediments, Submersible

Japan Geoscience Union Meeting 2014
(28 April - 02 May 2014 at Pacifico YOKOHAMA, Kanagawa, Japan)

HCG37-11 Room:421 Time:April 30 17:00-17:15

Deposition and preservation of fine-grained turbidites around the Japanese islands

IKEHARA, Ken[1*] ; USAMI, Kazuko[1] ; NISHIDA, Naohisa[1]

[1]Geological Survey of Japan, AIST

We will report the sedimentological characteristics of fine-grained turbidites occurred around the Japanese islands such as off Sanriku, off Kumano, Suraga Bay, Beppu Bay, Japan Trench and off Hidaka. Some of these are thought to be formed in relation to the slope failures by the earthquake-ground shaking. Sometimes, subaqueous debris flow deposits were observed below the fine-grained turbidites. Agitation of the shelf floor by the tsunami waves is another mechanism to create the fine-grained turbidites. Third mechanism is the hyperpycnal flows related to the flood events. Preservation potential of the fine-grained turbidites will be discussed based on the repeated surveys of surface sediments off Sanriku region after the 2011 Tohoku-oki earthquake and its related tsunami. Based on these observation, we will discuss on the depositional processes of the fine-grained turbidites and preferable setting to preserve them as the geological records.

Keywords: turbidite, earthquake, tsunami, preservation potential, sedimentary structure, depositional process

Japan Geoscience Union Meeting 2014
(28 April - 02 May 2014 at Pacifico YOKOHAMA, Kanagawa, Japan)

HCG37-P01 Room:Poster Time:April 30 18:15-19:30

Comparison between the Tidal Zone Deposits and the Terrace Deposits Emerged in the 1703 and 1923 Kanto Earthquakes

KIM, Haeng yoong[1*] ; MANNEN, Kazutaka[1] ; SASAGE, Kazuo[2] ; KUMAKI, Yohta[3] ; MATSUHIMA, Yoshiaki[4]

[1]Hot Springs Reserch Institute of Kanagwa Prefecture, [2]PASCO, [3]Senshu University, [4]Kangawa Prefecture Museum of Natural History

Recurrent giant earthquakes at the plate boundary along the Sagami Trough have been considered as one of the greatest thread of the Tokyo Metropolitan area. At the southwestern tip of the Miura Peninsula, in south of Tokyo, the tide gauge station records the coseismic uplift amount of 1.4 m and the interseismic subsidence amount of 0.3 m in and after 1923 earthquake, respectively. It is effective to reveal evidences of the past coseismic uplift to know the future earthquake.

Wave-cut benches which emerged in 1923 are widely distributed along the rocky coast. Higher wave-cut benches, good indicators of coseismic uplift prior to 1923, are also recognizable. It is, however, often difficult to spatially compare one another due to the erosion.

We investigated the distribution of the tidal-flat deposits and the 1923 wave-cut benches at two small bays in the southwestern and southern parts of the Peninsula. The aggradation of the coastline associated with the 1923 uplift was identified by the comparison between the 1:25,000 topographic maps before and after the 1923 earthquake. Observations of outcrops and drilling cores at the 1923-formed marine terrace showed that the tidal-flat deposits consist of shelly sand and gravels. The elevation of tidal-flat deposits indicates the coseismic uplift in 1923 and the interseismic subsidence after 1923. The uplift amount was estimated approximately 0.9 m and 2.1 m at the southwestern and southern parts of the Miura Peninsula, respectively. The uplift amount inferred from the tidal-flat deposits is concordant with that inferred by the wave-cut benches.

Keywords: Kanto Earthquake, Paleo-earthquake Record, Terrace Deposits, Tidal-flat Deposits

Japan Geoscience Union Meeting 2014
(28 April - 02 May 2014 at Pacifico YOKOHAMA, Kanagawa, Japan)

HCG37-P02 Room:Poster Time:April 30 18:15-19:30

The paleosols and topography of sedimentary basin relationships in the upper Miocene Clay deposit, central Japan

HATANO, Nozomi[1*] ; YOSHIDA, Kohki[2]

[1]Division of Science and Technology, Graduate School of Shinshu University, [2]Department of Geology, Faculty of Science, Shinshu University

The Tokiguchi Porcelain Clay Formation is fluvial deposit distributed in central Japan in middle to late Miocene period. The sedimentary facies analysises were carried out in this formation. Those studies, however, were insufficient to reconstruct fluvial environment, because the fluvial deposit essentially have been bounded by short hiatuses due to sub-aerial erosion and paleo-surface formation. In this study, therefore, we focused on paleosols so as to reconstruct the weathering environment during the hiatuses. In general, paleosol formation in the fluvial sediments also depends on the supply of detritus and drainage conditions. Consequently it is very useful to research paleosol features for reconstruction of the topography in the small sedimentary basin where Tokiguchi Porcelain Clay Formation was deposited.

The clay-dominated sediments, which are interpreted to have been deposited in small sedimentary basin within a radius of 2 kilometers, were examined in two mines, Hishiya and Nakayama mines, across Toki and Tajimi Cities in Gifu Prefecture. The sediments in Hishiya mine shows the deposition in proximal area of the sedimentary basin, whereas those in Nakayama mine displays the facies formed in marginal area of the basin. On the sedimentary facies analysis, 13 facies are recognized in the formation. The sedimentary facies associations indicate the deposition mainly in backswamp environment with minor channel incision. Furthermore the coarse-grained sediments which were deposited as channel-bar and levee deposits intercalating debris flow deposits, with high accumulation rate, were particularly deposited in the marginal area of the basin. In contrast, the fine-grained sediments which were deposited with low accumulation rate in lakes and swamps, were particularly distributed in the proximal area of the basin. For this result, the fluvial system with lakes and swamps was developed near mountain slope side. In the whole are of the basin, approximately 20 paleosol horizons were founded in the lake and swamp deposits within a thickness of approximately 30 meters. In the proximal of the basin, these paleosol horizons range sparser. These paleosol horizons, with various pedogenic features, such as root with approximately 150 centimeters length and trunk traces with approximately 50 centimeters wide, pedogenic concretions, ped structures and microfabric of clay minerals, are formed thickly and developed clearly. In addition to, abundant siderite nodules covered with bright clay are present in lake deposit in the proximal area of the basin.

As a result the characteristics of the sedimentary facies could depend on the sedimentation rate depending on variation of the distance from the rim of the sedimentary basin. Besides the characteristics of the paleosol features could be affected by the drainage conditions due to morphological variation related to the location in the sedimentary basin. The characteristics of the sedimentary facies and paleosol features, however, suggest the large change of water level in the whole sedimentary basin. Concretely the redox condition had shifted from reductive condition in lakes or swamps to oxic condition in bushy grounds. The plausible cause for this change of redox condition in the sedimentary basin could be responsible for water-level change which was frequently occurred by damming of rivers formed from debris flow deposition.

Keywords: paleosols, Miocene, terrestrial environment, Tokiguchi Porcelain Clay Formation, sedimentary facies analysis

Japan Geoscience Union Meeting 2014
(28 April - 02 May 2014 at Pacifico YOKOHAMA, Kanagawa, Japan)

HCG37-P03 Room:Poster Time:April 30 18:15-19:30

Applications of a method to detect varved sediments

SASAKI, Hana[1] ; ISHIHARA, Yoshiro[1*] ; SAITO-KATO, Megumi[2] ; KOMATSUBARA, Junko[3]

[1]Fukuoka University, [2]National Museum of Nature and Science, [3]Geological Survey of Japan / AIST

Studies of lacustrine deposits, especially on varved sediments, have further clarified the high-resolution record of paleoenvironments. Varved sediments are very useful for these studies because they are expected to contain annual records of depositional environments. In order to obtain annual records such as annual thickness, color tones, and chemical compositions, at the very least, it is necessary to detect the boundaries of annual bands. In addition, the detection and measurements should be reproducible.

Methods to measure boundaries of varved sediments are divided into two main categories: (1) measurment by visual judgment and (2) measurment by image analyses. The latter method uses photographs of the sediment, soft-X ray images, element maps, and so on. In order to detect boundaries, a threshold value, wavelet analysis, and wave analyses of the gray value of images have been previously used. While the visual judgment method has the disadvantages of human error and criteria, the image analysis method also has limitations as follows: one threshold value cannot be used for all locations in successive images; this method is dependent on the resolution of images, and it is affected by noise in the image-values.

In this study, we used a new method to detect the boundaries of banded deposits using the following procedure: (1) smooth the images, (2) calculate the inclination of ”gray-value map” of the images, (3) calculate a mid-value in one wavelength of the ”gray-value wave” in the map, and (4) detect a boundary as a point of the maximum inclination around the mid-value. The result obtained using this a method shows well-defined ”boundary map” of the bounded deposits, similar to the result obtained by visual judgment. Using this method, internal information, such as the transmittance value of soft-X ray in a lamina, can also digitized like a lamina thickness. Since a time-series of lamina thickness and internal information of the lamina can be calculated based on this method, lamina-by-lamina facies analysis, such as that performed for detection of flood deposits, can be employed in studying varved deposits automatically and quickly.

Keywords: varved sediments, image analysis, time-series, soft-X ray, diatomite

Japan Geoscience Union Meeting 2014
(28 April - 02 May 2014 at Pacifico YOKOHAMA, Kanagawa, Japan)

HCG37-P04 Room:Poster Time:April 30 18:15-19:30

Depositional cycle and flood and slope-failure events in an 8,000-yr varve of Pleistocene Hiruzenbara Formation, Japan

SASAKI, Hana[1*] ; ISHIHARA, Yoshiro[1] ; SAITO-KATO, Megumi[2] ; NARUSE, Hajime[3]

[1]Fukuoka University, [2]National Museum of Nature and Science, [3]Kyoto University

Paleoenvironmental changes can be reconsructed from varve deposits. The Middle Pleistocene Hiruzenbara Formation, which is distributed in the Hiruzen Highland, Maniwa city, Okayama Prefecture in Japan, is composed of mostly pure lacustrine diatomite that contains finely-laminated varves. From these varves, researchers have found decadal-scale depositional cycles that are thought to correspond to solar activities (Ishihara and Miyata, 1999), and intercalated flood- and slope-failure events have been detected. However, the relationship between the solar cycles and hydrogeological events remains unclear. In the present study, we sampled the finely laminated varves in the Hiruzenbara Formation, and obtained an 8,000-yr time-series of varve-thickness, gray-values for each lamina, variance of the gray-values, and deposits of flood- and slope-failure events using image analysis methods. Wavelet analysis and a fast Fourier transform (FFT) were applied to these time-series data to evaluate event-cyclicities.

In the time-series of varve-thickness, a long-term cyclicity of 1,000 - 2,000 yr was recognized. The upper parts of varves were light-green in color, and these were likely deposited during the winter season. Clear increases in thicknesses of the light-green parts were observed from the lower to upper parts of the analyzed section. Results from frequency analyses using the FFT and wavelet analysis of the time-series of varve-thickness data suggest that periods of 8 to 12 yr, 20 yr, and 30 to 35 yr dominate in this region. These periods were also found by Ishihara and Miyata (1999) and Masuda et al. (2004) in other sections of the formation. The periods in varves of 8 - 12 yr and around 20 yr correspond to solar activity, and a 35-yr periodicity of lake environmental change has been reported previously. In this study, however, these periods were not stable in the analyzed section, which is similar to the results obtained by Ishihara and Miyata (1999) and Masuda et al.(2004) who measured varve-thickness using a microscope.

One hundred-forty seven flood deposits were identified in the 8,000-yr record. Portions of the high-frequency parts and low-frequency parts were repeated in the analyzed section. Mean thickness of the flood beds was around 2 mm. Thirty-three deposits from slope failures were found in the section. These deposits were rare in the upper and lower most parts of the section, but were dominant in the lower part. There was no repetition of domination for the deposits that were observed during the flood events. Mean thickness of the slope-failure deposits was around 5.5 mm.

In the sections where flood deposits dominated, the mean varve-thickness tended to thinner without exception. In the upper part of the analyzed section, which lacked flood event signatures, the mean varve-thickness was generally greater. These trends suggest that climate conditions and the frequency of flood events might have affected the productivity of diatoms (thickness of the lamina). In addition, the periods detected by frequency analyses were not clear in the flood-deposit dominated sections. Results showing that dominations of slope-failure deposits were not related to the varve-thickness and the gray-values suggest that the slope-failure events were influenced by local phenomena related to lake development.

Keywords: Banded diatomite, Varve, Image analysis, flood deposit, slope-failure deposit, Solor activity

Japan Geoscience Union Meeting 2014
(28 April - 02 May 2014 at Pacifico YOKOHAMA, Kanagawa, Japan)

HCG37-P05 Room:Poster Time:April 30 18:15-19:30

Subsidence and a change of depositional environment by the 1662 Hyuganada earthquake in southern Miyazaki Plain

IKUTA, Masafumi[1*] ; SATO, Yoshiki[1] ; NIWA, Masakazu[1] ; KAMATAKI, Takanobu[2] ; KUROSAWA, Hideki[3] ; TAKATORI, Ryoichi[4]

[1]Japan Atomic Energy Agency, [2]Akita University, [3]OYO Corporation, [4]Chi-ken Sogo Consultants Co.,Ltd.

The Miyazaki Plain, southern Kyushu Island, have been damaged repeatedly by a number of great earthquakes (measured or estimated to be >M7-8) occurred in not only the Nankai trough but also the Hyuganada coastal region. A total of six great earthquakes happened in the Hyuganada coastal region in the range of AD1909 to 1984. Historical documents indicate such great earthquakes had also occurred in AD1662, 1769 and 1899. Furthermore, the great earthquakes in the Nankai trough, such as the 1707 Hoei Nankai earthquake and the 1946 Showa-Nankai earthquake, had also attacked the plain with terrible tsunamis (Usami *et al*., 2013).

Recently, the Nankai trough has received extensive attention as hypocenter of great earthquake attacking the Miyazaki Plain, because the Central Disaster Management Council (2012) proposed a new source model of the earthquakes including the Hyuganada coastal region. On the other hand, previous geological and seismological studies about past Hyuganada earthquakes are much less than the Nankai trough despite of their high seismic activity indicated by historical documents.

For example, historical documents shows that the 1662 Hyuganada earthquake brought about serious social and natural damages to the plain (Hatori, 1985). Especially, around the estuaries of the Oyodo-gawa River and the Kaeda-gawa River in southern area of the plain, the tsunami with about 4-5 m height and ˜1 m subsidence occurred. This coseismic subsidence made a coastal lagoon around the estuarine area of the Kaeda-gawa River (Shimayama region). After buried by riverine debris, this lagoon was reclaimed and became paddy fields (Miyazaki-city, 1978).

The purpose of our study is to clarify depositional changes around the Shimayama region including coseismic geomorphological change. A multiple geological borings were carried out in the study area. Depositional environments were reconstructed inferred from paleontological, geochemical analyses. Depositional ages of core sediments were estimated by radiocarbon ages. The surface geology was divided into four layers mainly (layer A, B, C and D) in ascending order. The layer A was composed of alternate layers of grayish sand and silt with many angular pumices and organic materials. The layer B consisted of alternate layers of gray or grayish brown mud and sand including numerous well-preserved molluscan fossils. The bottom of the layer B, which covered the layer A above ˜-1.5 m T.P. with 10 to 40 cm thick, was black or dark gray muddy fine sand with bioturbation including rip-up clasts, shell fragments and volcanic rocks with >1 mm diameter. The layer C was composed of gray silt with several thin layers of fine to medium sand and plant fragments. The layer D consisted of silt to fine sand layers and surface cultivated sediments with ˜20 cm thick overlying them.

Result of some analyses showed their quantitative differences corresponding to depositional facies. The main diatom components of the lower part of the layer A was fresh water benthic species such as *Cymbella turgidula* and *Gomphonema parvulum*, and the upper was few diatom fossil. On the other hand, the layer B showed abundance of brackish to marine water species such as *Cocconeis scutellum* and *Thalasionema nitzschioides*. In addition, absorbed water analysis of the core sediments showed that K, Ca, Na, Mg and SO_4^{2-} concentration, which are rich in sea water, were few in the layer A but increased drastically at the bottom of the layer B. And grain size and molluscan fossils species were also different between the layer A and B.

These results indicate that depositional environment changed drastically from fresh water marsh or shallow pond to tidal or inner bay. Depositional ages of the layer A, B and C were estimated from radiocarbon ages to be AD1445 to 1595, AD1549 to 1771 and AD1651 to 1771 respectively and suggest that the depositional environment between the layer A and B correlate to crustal deformation by the 1662 Hyuganada earthquake.

Keywords: Hyuganada earthquake, Miyazaki Plain, depositional environment

Japan Geoscience Union Meeting 2014
(28 April - 02 May 2014 at Pacifico YOKOHAMA, Kanagawa, Japan)

HCG38-01 Room:424 Time:April 29 11:00-11:15

Selected organisms for systems of life-support in closed bio-ecosystem, and the chemical circulation

TOMITA-YOKOTANI, Kaori[1*]

[1]University of Tsukuba

Living organisms on the earth have been evolved since its origin a long time ago. They equip several important functions affecting each other. Knowledge on those functions and interaction of the ecology is essential for secure design of a closed-ecosystem with limited number of living species under the harsh environments, such as space and deep sea or desert. The important elements related to the closed bio-ecosystem have to be discussed among the researchers, having each specialized field . Here, we will discuss the detail of species of several selected organisms for the closed bio-ecosystems and its chemical circulation.

Keywords: chemical circulation, closed bio-ecosystems

Japan Geoscience Union Meeting 2014
(28 April - 02 May 2014 at Pacifico YOKOHAMA, Kanagawa, Japan)

HCG38-02 Room:424 Time:April 29 11:15-11:30

Dry heat tolerance of the dry colony in *Nostoc* sp. HK-01 for useful usage in closed bio-ecosystems

KIMURA, Shunta[1*] ; KATOH, Hiroshi[2] ; SATO, Seigo[1] ; TOMITA-YOKOTANI, Kaori[1]

[1]University of Tsukuba, [2]Mie University

Closed bio-ecosystem as an artificial design requires the high flexibility and versatility system. As one of elements for all of introduced organisms, heat tolerance is important one such closed environment. *Nostoc* sp. HK-01 is one of terrestrial cyanobacterium having a high dry tolerance and it has several ability, photosynthesis, nitrogen fixation and usefulness as a food, it is thought that it can be used for bio-chemical circulation in a closed ecosystem, including space. Besides, a study on each tolerance predicted at the time of introduction to a closed bio-ecosystem is necessary. Therefore, as one of the tolerance that are intended to space environment, dry heat (100 ℃, 10 h) tolerance of dry colony in *Nostoc* sp. HK-01 has been investigated, but the detail function of them has not yet been elucidated. We focused on the extracellular polysaccharides (EPS) having the various tolerance, desiccation, low temperature, NaCl, and heavy particle beam. We will consider the function and useful usage of this cyanobacterum in closed bio-ecosysitems after the consideration of the results of contribution of the possibility that EPS improves dry heat tolerance under a dry condition.

Keywords: bio-chemical circulation, closed bio-ecosystem, cyanobacteria, dry heat tolerance, extracellular polysaccharides, *Nostoc* sp. HK-01

Japan Geoscience Union Meeting 2014
(28 April - 02 May 2014 at Pacifico YOKOHAMA, Kanagawa, Japan)

HCG38-03 Room:424 Time:April 29 11:30-11:45

Utilization of the terrestrial cyanobacteria

KATOH, Hiroshi[1*] ; YOKOSHIMA, Mika[2] ; KIMURA, Shunnta[2] ; FURUKAWA, Jun[2] ; TOMITA-YOKOTANI, Kaori[2] ; YAMAGUCHI, Yuji[3] ; TAKENAKA, Hiroyuki[3]

[1]Mie University, [2]University of Tsukuba, [3]MicroAlgae Corporation

The terrestrial, N_2 -fixing cyanobacterium, *Nostoc commune* has expected to utilize for agriculture, food and terraforming cause of its extracellular polysaccharide, desiccation tolerance and nitrogen fixation. Previously, the first author indicated that desiccation related genes were analyzed and the suggested that the genes were related to nitrogen fixation and metabolisms in *Nostoc*(*Anabaena*) sp. PCC 7120. In this report, we suggest possibility of agriculture, using the cyanobacterium. Further, we also found radioactive compounds accumulated *Nostoc commune* (cyanobacterium) in Fukushima, Japan after nuclear accident. Thus, it is investigated to remove radioactive compounds from soil by the cyanobacterium and showed to accumulate radioactive compounds using the cyanobacterium. We will discuss utilization of terrestrial cyanobacteria under closed environment.

Keywords: desiccation, terrestrial cyanobacteria, bioremediation, agriculture, decontamination

Japan Geoscience Union Meeting 2014
(28 April - 02 May 2014 at Pacifico YOKOHAMA, Kanagawa, Japan)

HCG38-04 Room:424 Time:April 29 11:45-12:00

Evaluation of functional components in selected organisms as food after cooking in closed bio-ecosystem

KIMURA, Yasuko[1*] ; KATOH, Hiroshi[2] ; CHIDA, Yukari[3] ; NITSU, Fumie[3] ; SATO, Seigo[3] ; TOMITA-YOKOTANI, Kaori[3]

[1]Jumonji University, [2]Mie University, [3]University of Tsukuba

We have been studying life-support in closed bio-ecosystem to provide food and oxygen for the habitation area in the sever environment. To select the species of organisms is very important matter because it is difficult to use all the species of creature for the system. We have been proposing the several species of organism as the candidate species. In this time, we have selected and show terrestrial cyanobacteria and tree that have a possibility as high contributed materials for the induction into the closed systems. Here, we will discuss about the changes of the functional components produced from each materials, after their cooking.

Keywords: Cyanobacteria, tree plant, food, closed bio-ecosystem

Japan Geoscience Union Meeting 2014
(28 April - 02 May 2014 at Pacifico YOKOHAMA, Kanagawa, Japan)

HCG38-05 Room:424 Time:April 29 12:00-12:15

Study of Closed Life Support System for Manned Space Exploration

SAKURAI, Masato[1*]

[1]JAXA

To further advance manned space exploration, a critical issue that must be addressed is recycling of resources, especially air revitalization and water reclamation. Japan is already a leader in terrestrial environmental technologies, and aims to apply this know-how to develop air and water recycling technologies for space applications. To support proposed post-ISS missions such as manned lunar or asteroid exploration and an Earth-Moon Lagrange point (EML1) space station, JAXA is developing an air revitalization system for an on-orbit demonstration on the International Space Station (ISS) early in the extended ISS operation period (2015-2020). The requirements for this technical demonstrator have been investigated and its specifications established. Regenerative life support functions include oxygen recovery from carbon dioxide using a combination of CO_2 reduction by a Sabatier process and O_2 generation by electrolysis. Each air and water re-vitalization subsystem is planned to be transported to the ISS separately by H-II Transfer Vehicle (HTV) launches in the Water Electrolysis This paper presents the air re-vitalization system developed by JAXA, and gives details of water electrolysis in microgravity.

A technical issue with space electrolysis systems is that gas-liquid separation is fundamentally different in a microgravity environment to its behavior in a gravity field. It is supposed that the electrode surface will become covered with generated gas. In microgravity, the gas will have to be removed using forced convection. A water/gas separator will be used to separate gas and water.

Keywords: Life Support System, Manned Space Expolaration, Air Re-vitalization, Microgravity, Closed System, Water Electrolysis

Japan Geoscience Union Meeting 2014
(28 April - 02 May 2014 at Pacifico YOKOHAMA, Kanagawa, Japan)

HCG38-06 Room:424 Time:April 29 12:15-12:30

Human body and oxygen

SHIMIZU, Tsuyoshi[1*]

[1]Shimizu Institute of Space Physiology, Suwa Maternity Clinic Hospital

We found recently that a mild hyperbaric condition with a mild hyper oxygen-concentration ,which was maintained in the special container called as Ishihara's original oxygen capsule, was effective to treat infertility women patients. This result did let us realize again an importance of oxygen for cells and tissues of human body . In space development effects of microgravity, space radiation and other various environmental factors have been extensively investigated and discussed, however we should also remember again that oxygen is the basic component to support our body in the space environment as well as on the earth. In this presentation I will summarize over again the meaning of presence of oxygen related to human body for future space development.

Keywords: oxygen, human body, space environment

Japan Geoscience Union Meeting 2014
(28 April - 02 May 2014 at Pacifico YOKOHAMA, Kanagawa, Japan)

HCG38-P01 Room:Poster Time:April 29 14:00-15:15

Growth of Hydrobryum puncticulatum(Yakushimakawagoromo) may be blocked by the increase of Melosira varians in Isso River

KITABUCHI, Hiroyuki[1*] ; NAGAFUCHI, Osamu[1] ; NAKAZAWA, Koyomi[1] ; YOKOTA, Kuriko[2] ; TETUKA, Kenshi[3] ; AYUKAWA, Kazuyasu[4] ; TANABE, Masahiro[5]

[1]The University of Shiga Prefecture, [2]Toyohashi University of Technology, [3]Yakutane-goyou Research Group, [4]Environmental System Co., Ltd, [5]Nikkaki Bios Co., Ltd

Hydrobryum puncticulatum (*Yakushimakawagoromo*), the national monument and endangered species are making their habitat only in Isso river of Yakushima. For the first time in our observation, the bloom of *Melosira varians* which is periphyton of diatom was observed to be covered over the *H.puncticulatum* from 2011. This impact for the *H.puncticulatum* is a serious concern .The purpose of this study is to clarify the cause of bloom of *M.varians*. We examined the annual variability of dissolved nutrient concentration which was most accessible to *M.varians*. As a result, there was no increase in concentration of NO_3-N, SiO_2-Si from 2009 to 2013. In addition, PO_4-P was much lower concentration(0.003 ± 0.001 mg/ l). Therefore, we assumed that there was no relationship between the bloom of *M.varians* and dissolved nutrient concentration in Isso river. Meanwhile, the floating mud which was deposited in the bottom of the river has been continued during dry-spell. Tachibana et al (1986) reported that an algae can intake the suspended nutrient same as dissolved nutrient. It suggests that the *M.varians* and *H.puncticulatum* can take suspended nutrient.

Keywords: Hydrobryum puncticulatum, periphyton, Yakushima, nutrient

Japan Geoscience Union Meeting 2014
(28 April - 02 May 2014 at Pacifico YOKOHAMA, Kanagawa, Japan)

HCG38-P02 Room:Poster Time:April 29 14:00-15:15

Environmental response in bacteria to an applied magnetic field

ABE, Makoto[1*] ; YAMANA, Masao[2] ; ABE, Tomoko[2]

[1]Graduate School of Science and Engineering,Graduate School of Tokyo Denki University, [2]School of Science and Engineering,Tokyo Denki University

Metabolic changes in living cells under various magnetic fields should be considered in closed-ecology on planets.

Magnetic fields may induce multiple effects in biological systems, including change in DNA replication or RNA transcription and modification of ion and protein flow across membranes. In recent years, influences of various electromagnetic fields on cell and organisms have been investigated by many researchers. However, the detailed mechanisms in the effects of magnetic field on organisms are still controversial.

In this study, we had focused on influences of the magnetic field on environmental microbes. Some bacteria susceptible to the applied magnetic field were isolated from the soil. To investigate expression changes of intracellular proteins involved in regulating cell growth by the applied magnetic field, cellular proteins in the bacteria cultured under the applied magnetic field were analyzed by SDS-polyacrylamide gel electrophoresis.

Keywords: Magnetic field, Bacteria, Growth curve

Japan Geoscience Union Meeting 2014
(28 April - 02 May 2014 at Pacifico YOKOHAMA, Kanagawa, Japan)

HCG38-P03 Room:Poster Time:April 29 14:00-15:15

Useful utilization in closed bio-ecosystems of *Nostoc* sp. HK-01 having the tolerance of gamma-ray

AJIOKA, Reiko[1*] ; KIMURA, Shunta[1] ; KATOH, Hiroshi[2] ; SATO, Seigo[1] ; TOMITA-YOKOTANI, Kaori[1]

[1]University of Tsukuba, [2]Mie University

Photosynthetic organisms contribute to the circulation of oxygen or carbon dioxide and utilization of foods as a induced organism in closed bio-ecosystems. A terrestrial cyanobacterium, *Nostoc* sp HK-01, having a high drought tolerance, photosynthetic organism, is one of candidate organisms that can be introduced into the closed environment. It has a possibility that HK-01 has also a high gamma-ray tolerance in according to the results from several reports related to the interaction of drought tolerance and gamma-ray tolerance. Here, we will show the several influences on the growth of HK-01 after the exposure of gamma-ray in the dry colony.

Keywords: closed bio-system, cyanobacteria, gamma-ray tolerance, *Nostoc* sp. HK-01, photosynthetic organism

Japan Geoscience Union Meeting 2014
(28 April - 02 May 2014 at Pacifico YOKOHAMA, Kanagawa, Japan)

SGD21-01 Room:413 Time:April 28 09:00-09:15

Long-baseline laser strainmeter in Kamioka

TAKAMORI, Akiteru[1*] ; ARAYA, Akito[1] ; MORII, Wataru[2] ; UCHIYAMA, Takashi[3] ; OHASHI, Masatake[3] ; TELADA, Souichi[4]

[1]Earthquake Research Institute, University of Tokyo, [2]Disaster Prevention Research Institute, Kyoto University, [3]Institute for Cosmic Ray Research, University of Tokyo, [4]National Institute for Advanced Industrial Science and Technology

In order to facilitate the gravitational-wave astronomy, ‘ KAGRA project ’ has been proceeding under international collaboration hosted by the Institute for Cosmic Ray Research of University of Tokyo. The authors are constructing a long-baseline laser strainmeter with a 1.5 km long baseline in the Kamioka underground site as the part of the project (left figure). It will be the longest baseline laser strainmeter in Japan, and one of the largest instruments worldwide. The longer baseline was opted to achieve the superior sensitivity for the ground strain, more than 10 times better than the currently available 100 m strainmeter. The better sensitivity is anticipated to enable more detailed studies in the ground deformation caused by the fault activities and the Earth ’ s free oscillations.

The basic design of the long-baseline strainmeter is adopted from the 100 m strainmeter, consists of the highly asymmetric Michelson interferometer using the Iodine-stabilized laser as the standard of length (right figure). Nevertheless, there are some technical challenges required due to the gigantic scale of the new instrument. The outline of the instrument and the status of R&D will be reported in this presentation.

Keywords: laser interferometer, strainmeter, Kamioka

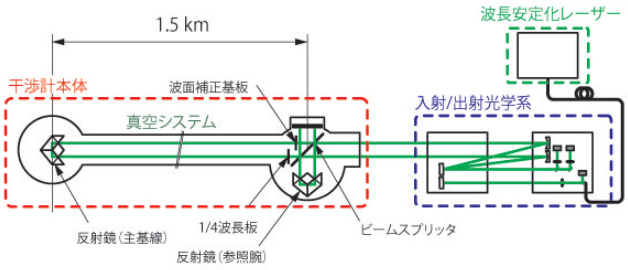

Japan Geoscience Union Meeting 2014
(28 April - 02 May 2014 at Pacifico YOKOHAMA, Kanagawa, Japan)

SGD21-02 Room:413 Time:April 28 09:15-09:30

Development of software for precise LLR data analysis, Part 2

NAGASAWA, Ryosuke[1*] ; OTSUBO, Toshimichi[2] ; SEKIDO, Mamoru[3] ; HANADA, Hideo[4]

[1]Graduate University for Advanced Studies, [2]Hitotsubashi University, [3]National Institute of Information and Communications Technology, [4]RISE Project Office, National Astronomical Observatory

We are developing new analysis software for precise determination of lunar orbital/rotational motion and tidal deformation using lunar laser ranging (LLR) observation data.

As the first step of the study, we construct an LLR observation model. This model consists of the lunar orbit and libration obtained from DE430 (provided by NASA JPL), and the other newest physical models compatible with IERS Conventions (2010) such as Earth orientation, solid Earth/Moon tides, and some factors affecting propagation delay. For the purpose of calculating these components precisely, we use the modules of the geodetic data analysis software ”c5++” (Otsubo et al., 2011). LLR observation data are provided as normal points. In this calculation, there are 3577 points distributed from June 1996 to July 2013, obtained at Apache Point, Grasse, Matera and McDonald. Comparing the observed and calculated one-way ranges, the mean and the standard deviation of the residuals are about 5.7 cm and 4.8 cm respectively.

The presentation contains the result of the above-mentioned modeling and comparison, and the current status of the software development.

Keywords: lunar laser ranging, analysis software, ephemeris

Japan Geoscience Union Meeting 2014
(28 April - 02 May 2014 at Pacifico YOKOHAMA, Kanagawa, Japan)

SGD21-03 Room:413 Time:April 28 09:30-09:45

Scale parameters of the Earth sensitive to the optical response of spherical SLR targets

OTSUBO, Toshimichi[1*] ; MATSUO, Koji[2] ; SHERWOOD, Robert a[3] ; APPLEBY, Graham m[3] ; NEUBERT, Reinhart[4]

[1]Hitotsubashi University, [2]Kyoto University, [3]NERC SGF Herstmonceux, UK, [4]GFZ Potsdam, Germany

Recent technology upgrades in SLR technique, especially driven by kHz laser ranging systems, make it possible to measure the station-satellite distance at mm precision. The optical response of a sphere-shaped SLR target has been one of the major error factors in measuring the two-way distance, and, following the study on AJISAI, LAGEOS and ETALON (Otsubo and Appleby, JGR, 2003), we look into relatively smaller targets, STARLETTE and its twin STELLA. Based on the detailed optical response simulation adjusted by the actual kHz laser ranging data obtained at Herstmonceux and Potsdam, it is calculated that the standard centre-of-mass correction value for STARLETTE is too small by 3 mm. The impact can be up to 0.5 ppb for the terrestrial reference frame scale and up to 1.7 ppb for the gravity constant (GM) of the Earth.

Long-term worldwide technology upgrades can have a systematic impact on the long-term trend of such scale parameters. As the intensity of photons received at a given detector is reduced, the detection point (timing) goes rearwards and the center-of-mass correction gets smaller as listed in Appleby and Otsubo (LW18, 2013). This can map a non-negligible drift especially in the GM parameter.

Keywords: space geodesy, satellite laser ranging, terrestrial reference frame

Japan Geoscience Union Meeting 2014
(28 April - 02 May 2014 at Pacifico YOKOHAMA, Kanagawa, Japan)

SGD21-04 Room:413 Time:April 28 09:45-10:00

VLBI application for Frequency Transfer and Development of GALA-V System (III)

SEKIDO, Mamoru[1*] ; TAKEFUJI, Kazuhiro[1] ; UJIHARA, Hideki[1] ; MIYAUCHI, Yuka[1] ; TSUTSUMI, Masanori[1] ; HASEGAWA, Shingo[1] ; HOBIGER, Thomas[1] ; ICHIKAWA, Ryuichi[1] ; KOYAMA, Yasuhiro[2]

[1]National Institute of Information and Communications Technology, Space-Time Standards Laboratory, [2]National Institute of Information and Communications Technology, International Relations Office

NICT is developing the frequency comparison technology using the VLBI as one of the remote frequency comparison technologies. The small broadband VLBI station, which is an important element of this project (Gala-V), is semi-compliant with the specification of the broadband geodetic VLBI system VGOS (VLBI2010 Global Observing System) specifications. Many VLBI observation stations compliant with the VGOS are under development several countries as an international standard specification for the next generation geodetic VLBI. Our Gala-V system is aimed for the comparison of the frequency standard, but of course this is useful for the geodetic observations too.

[broadband feeding development for large diameter antenna]
Most of the VGOS VLBI stations under development are adopting the special optical system so called ring-focus, That is because of wider beam width characteristic of wide frequency band (2-14GHz) feed, currently available. The receiver feed, that has sensitivity about 3 octaves of frequency, has generally wide beam angle, and therefore, existing Cassegrain reflector antenna is difficult to use it. We have been developing a new broadband feed for our 34m antenna. The first test feed become ready and it was mounted on the 34m diameter modified Cassegrain parabola in the end of 2013, and successfully we observed 6.7GHz, and 12.2 GHz emission line of the Methanol maser simultaneously.

[Zero redundant frequency array - Direct Sampler]
The Gala-V system, which is under the development at NICT, is designed to use four bands of the 1 GHz bandwidth with intervals of zero redundancy in the 2-14 GHz frequency range. This enables a fine delay resolution function without uncertainty (Ambiguity), and the precision of delay measurement could be improved by a one order higher than conventional.
In addition to a conventional analog frequency conversion method, we are experimentally adopting a method to acquire specific frequency band with a digital filter with a direct sampler, which acquires data without frequency conversion via a high-speed sampler. If a direct sampling method is established, system components and cost necessary for the system are simplified and reduced.

[development of the broadband signal composition technology]
The VGOS system is targeting to achieve high precision delay measurements by synthesizing 2-14 GHz broadband signal coherently. A new data processing software, which enables estimation of nonlinear phase change caused by the ionosphere and derivation of precise delay from the super broadband signal, and broadband stable phase calibration system are required.

Keywords: VLBI, VGOS, Frequency Comparison

Japan Geoscience Union Meeting 2014
(28 April - 02 May 2014 at Pacifico YOKOHAMA, Kanagawa, Japan)

SGD21-05 Room:413 Time:April 28 10:00-10:15

Ishioka VLBI Observing Facility - Telescope Completion and Setting up the System -

KURIHARA, Shinobu[1*] ; FUKUZAKI, Yoshihiro[1] ; KURODA, Jiro[1] ; KAWABATA, Ryoji[1] ; WAKASUGI, Takahiro[1]

[1]GSI of Japan

The Geospatial Information Authority of Japan (GSI) proceeded with construction of new VLBI station compliant with the next generation VLBI observing system (VGOS) promoted by the International VLBI Service for Geodesy and Astrometry (IVS). By March 2014, a VLBI telescope with a 13.2-m dish was completed in Ishioka, Ibaraki, now we are going on setting up and testing of the whole system from the telescope through data acquisition system toward. In this presentation I describe the completed VLBI observing facility and progress situation of its setting up and testing.

Keywords: IVS, VGOS

Japan Geoscience Union Meeting 2014
(28 April - 02 May 2014 at Pacifico YOKOHAMA, Kanagawa, Japan)

SGD21-06 Room:413 Time:April 28 10:15-10:30

Development of a new precise positioning technique using multi-GNSS signals

FURUYA, Tomoaki[1*] ; SAKAI, Kazuki[1] ; MANDOKORO, Motomu[1] ; TSUJI, Hiromichi[1] ; YAMAGUCHI, Kazunori[1] ; MIYAGAWA, Kohei[1] ; YAHAGI, Toshihiro[1] ; HATANAKA, Yuki[1] ; MUNEKANE, Hiroshi[1] ; KAWAMOTO, Satoshi[1]

[1]GSI of Japan

Geospatial Information Authority of Japan (GSI) is developing and standardizing new precise positioning techniques which deal with multiple GNSS constellations, GPS, QZSS, GLONASS, and Galileo, in order to mainly encourage effective surveys at places where are currently difficult to carry out them using only GPS satellites.

In FY 2013, we examined analysis methods to correct Inter System Bias for using single/double differences between GPS and other GNSS. We developed the new analysis software named GSILIB based on RTKLIB developed by Mr. T.Takasu. In addition, we obtained multi-GNSS data in eight cities and evaluated the effects and problems using multi-GNSS signals.

This presentation shows results of FY 2013 and future plans from FY 2014.

Keywords: GNSS, Geodetic survey, ISB

Japan Geoscience Union Meeting 2014
(28 April - 02 May 2014 at Pacifico YOKOHAMA, Kanagawa, Japan)

SGD21-07 Room:413 Time:April 28 10:30-10:45

Notes on the quality of GEONET coordinate solutions

IMAKIIRE, Tetsuro[1*] ; KAGAWA, Akira[1] ; HATANAKA, Yuki[1] ; MUNEKANE, Hiroshi[1]

[1]GSI of Japan

The routine solutions of geodetic coordinate of observation stations of GEONET, the continuous GNSS observation network operated by GSI, are fundamental data for the studies of crustal deformation and tectonics and widely utilized for a variety of purposes. As GEONET data is available freely, researchers can discuss the crustal deformation or tectonics without carrying out GNSS observation or baseline analysis. However, it should be noted that the coordinates provided by GEONET may include errors caused by various noise sources or factors, such as obstruction of observation signals by trees, multipath caused by site environment or um-modeled tropospheric noise. We present results of evaluation the effects of some of the error factors and introduce ways of examining the quality of coordinate solutions done for crustal deformation monitoring by GSI.

Keywords: GEONET, GNSS positioning, Data quality

Japan Geoscience Union Meeting 2014
(28 April - 02 May 2014 at Pacifico YOKOHAMA, Kanagawa, Japan)

SGD21-08 Room:413 Time:April 28 11:00-11:15

Positioning error estimation due to snow accumulation on GNSS antenna using winter experimental data

YOSHIHARA, Takayuki[1*] ; MOTOYOSHI, Hiroki[2] ; SATO, Takeshi[2] ; YAMAGUCHI, Satoru[2] ; SAITO, Susumu[1]

[1]Electronic Navigation Research Institute, [2]National Research Institute for Earth Science and Disaster Prevention

In research field of precise positioning using Global Navigation Satellite System (GNSS) such as GPS, it is well known that positioning error is caused by snow accumulation on GNSS antenna [1]. It is important to quantitatively evaluate the error taking account for shape of snow-cap and GPS satellite configuration, which are changing with time past. In this study, we performed two winter experiments in each winter of 2011/2012 and 2012/2013, which enabled us to quantitatively investigate reduction in receiving intensity and propagation delay due to snow accumulation on GNSS antenna. The experimental data was also able to use for positioning error estimation resulted by such effects. We installed a GPS antenna about 50 meters away from weather observational equipment, which measured pressure, temperature, humidity, wind direction and velocity, precipitation, snow depth, etc.), in observation field of Snow and Ice Research Center, National Research Institute for Earth Science and Disaster Prevention (NIED) in Nagaoka, Japan. To observe snow accumulation on GNSS antenna, a photograph of GNSS antenna was automatically took by an interval camera every 10 minutes during winter. To evaluate quantitative effects of snow accumulation on GPS signal measurement, we investigated drop events of snow-cap on GNSS antenna and analyzed gaps of rapid changes in both receiving intensity and carrier phase measurements[2]. Consequently, a snow-cap with a height of 40cm yielded reduction of several dB in receiving intensity (C/N0) and propagation delay of about 4 cm in slant range. We will show relationship between size of snow cap and positioning error based on the experimental data, including simulation analysis with range errors due to snow accumulation and satellite configuration. We will also show evaluation results to use water repellent paint on GNSS antenna radome for mitigation of snow accumulation.

References
[1] R. Jaldehag, J. Johansson, J. Davis and P. Elosegui, ”Geodesy using the Swedish permanent GPS network: Effects of snow accumulation on estimates of site positions”, Geophys. Res. Lett., vol.23, No. 13, pp.1601-1604, June 1996.
[2] T. Yoshihara, H. Motoyoshi, T. Sato, S. Yamaguchi and S. Saito, ”GAST-D integrity risks of snow accumulation on GBAS reference antennas and multipath effects due to snow-surface reflection”, Proc. ION ITM 2013, no.A1-5, pp.112-120, San Diego, CA, January 2013.

Keywords: GNSS, snow accumulation, positioning error, precise positioning, propagation delay, GPS

Japan Geoscience Union Meeting 2014
(28 April - 02 May 2014 at Pacifico YOKOHAMA, Kanagawa, Japan)

SGD21-09 Room:413 Time:April 28 11:15-11:30

Periodic displacement on continuous GPS observation in coastal area due to long term sea level elevation

OICHI, Kazuyoshi[1*]

[1]Hydrographic and Oceanographic Department, Japan Coast Guard

Since 1999, Hydrographic and Oceanographic Department carried out continuous GPS observation to survey the crustal deformation at the stations collocated with tidal stations or lighthouse etc. of Japan Coast Guard in south Kanto area. And precise positions in earth centered coordinates of these GPS stations are automatically determined by long baseline analysis from Simosato GPS station. Several stations show significant unexpected annual oscillation in its daily position series. On the other hand, hourly sea level data are available via Japan Oceanographic Data Center from tidal stations of Japan Coast Guard and Japan Meteorological Agency in this area. To eliminate annual oscillation from crustal deformation observation, correlation functions between daily precise position series of GPS stations and sea level height series of tidal stations are calculated. And I tried to evaluate an error from weight variation of sea water on precise GPS observations in coastal area.

Hydrographic and Oceanographic Department continuously observes 30 sec interval data at GPS stations in Izu islands area from 2002. And long baseline analysis from Simosato hydrographic observatory is performed with Bernese GPS Software and IGS final ephemerides. Calculated daily precise positions are utilized for crustal deformation monitoring. However, time series of calculated positions contains unexpected component other than crustal deformation. Particularly, Izu O-Shima station shows significant oscillation in a north-south direction. This oscillation is synchronous with four GPS stations of GSI in Izu O-Shima, and these show annual apparent cycle of expansion and contraction. Some oscillation of local load is suspected as cause of this deformation and move of sea water is considered as major component of these in coastal area. Analyzed positions of these stations are obtained as daily value, thus influence of major component of tide (diurnal or semidiurnal) is negligible, but long term component, for instance, annual change of sea level is inadequately considered. According to the sea level observations at adjacent tidal stations, annual oscillation of sea level shows its amplitude in tens of centimeters, thus long term component of sea water load change is expected as considerable.

To eliminate annual oscillation from GPS monitoring of crustal deformation, I tried to analyze strain caused by load change from sea level elevation. This analysis is performed with the time series of daily precise positions of four GPS stations: Izu O-Shima, Miyake Shima, Kozu Shima, Hachijo Shima, from 2002. Because of Miyake Shima, Kozu Shima and Hachijo Shima stations are collocated with tidal stations of JCG, correlation functions are calculated with time series of sea level in place of stations. And the Izu O-Shima station is collocated with lighthouse, thus analyzed with the Okada tidal station of JMA in Izu O-Shima.

Keywords: GPS, tidal observation, crustal deformation, sea level change, annual oscillation

Japan Geoscience Union Meeting 2014
(28 April - 02 May 2014 at Pacifico YOKOHAMA, Kanagawa, Japan)

SGD21-10 Room:413 Time:April 28 11:30-11:45

Seismic waves detected by 50Hz sampled GNSS observations

KATO, Teruyuki[1*] ; MIURA, Satoshi[2] ; IKUTA, Ryoya[3]

[1]Earthq. Res. Inst., the University of Tokyo, [2]Grad. Sch. Sci., Tohoku University, [3]Faculty of Science, Shizuoka University

Application of frequently sampled GNSS data is getting increasingly attractive research field, in particular, in the field of seismology (e.g., Larson et al.; 2003, Miyazaki et al., 2004; Yokota et al., 2009; Ohta et al., 2012). As most of GEONET (GNSS Observation NETwork) sites are now archiving 1Hz sampled data, such application research will be more active in the future. Analysis of ground shake may require higher frequency observation such as 5Hz, 10Hz or higher. However, it is known that amplitude and phase of observed ground displacements show fluctuations due to characteristics of data acquisition in the receiver electric circuits (e.g., Ebinuma and Kato, 2012). Thus, we need to be careful in applying such highly sampled GPS data for geoscientific researches.

We have used commercially available GNSS receivers to record 50Hz sampling to tackle above problems. We are introducing a record of ground shake due to an earthquake of 50Hz sampled data. We used three NetR8 (Trimble Co. Ltd.) GNSS receivers and they were established at Shizuoka University (Shizuoka Prefecture) since October 2011, Katono Elementary School (Fukushima Prefecture; KTNO) and Daido-higashi Elementary School (Ibaraki Prefecture; DDHG) since March 2012. We chose latter two locations as they are among the most active aftershock area due to 2011 Tohoku-Oki earthquake (Mw9.0).

About two weeks of 50Hz sampled data are stored in the internal memory of the receiver which are refreshed automatically in the receiver. Data at KTNO and DDHG are remotely archived through internet and data at Shizuoka University are downloaded manually, after a large earthquake occurred. Several data sets due to large earthquakes have been archived so far, all of which registered at least bigger than or equal to JMA Intensity 5- at nearby GPS sites. These data are analyzed using RTNet GPS software.

Among the archived data sets, a seismic wave was detected for the 2013 September 20 Fukushima-Hamadori earthquake, whose hypocentral parameters are as follows: latitude= N37.1deg, longitude=E140.7deg, depth=20km, M5.9, and the biggest JMA Intensity was 5+ at Iwaki, which is nearly immediately below the KTNO site. We used IGS final orbits and estimated the position of KTNO by putting the reference site at Daido-higashi (Baseline distance is about 106km to south) and Shizuoka University (Baseline length is about 308km to south east). Clear seismic wave was obtained for the baseline KTNO-DDHG for three components. Also, clear seismic wave was obtained for the baseline KTNO-Shizuoka Univ., though vertical component was not very clear, probably because the baseline distance was longer.

GNSS antennas at KTNO and DDHG sites are placed at the roof of the school buildings and at the roof of observation hut of Shizuoka University. Therefore, we may have to investigate the effects of swing of the building by comparing the record with nearby recorded strong motion. Moreover, the method of correction for amplitude and phase due to receiver characteristics should be investigated, which is left for future studies.

Keywords: GNSS, high-frequency sampling, GPS, GPS seismology, 50Hz

Japan Geoscience Union Meeting 2014
(28 April - 02 May 2014 at Pacifico YOKOHAMA, Kanagawa, Japan)

SGD21-11 Room:413 Time:April 28 11:45-12:00

Detection of eruption column by using the kinematic precise point positioning

OHTA, Yusaku[1*] ; IGUCHI, Masato[2] ; UEKI, Sadato[1] ; DEMACHI, Tomotsugu[1]

[1]RCPEVE, Tohoku University, [2]DPRI, Kyoto University

We investigate the ability of kinematic precise point positioning to detect volcanic plumes at Minami-dake of Sakurajima Volcano. In Houli$\acute{e}$ et al. [1], the authors processed the GPS data obtained during the eruption of Miyakejima volcano, occurred in 2000, and found anomalous values in the ionosphere-free linear combination of the L1 and L2 phase measurements (LC). They related these anomalous values to the path delay effects caused by the presence of a hot volcanic plume; by applying techniques of seismic tomography. Another test was carried out during the eruption of Mt. St. Helens on March 9, 2005, and again the GPS signal showed a clear signature of the volcanic plume presence [2].

In this study, we describe the July 24, 2012 activity at Minami-dake of Sakurajima Volcano. We analyzed the data from 18 continuous GPS stations (3 GEONET sites and 15 Kyoto University sites), which located on the volcano flanks. For the GPS analysis, we used GIPSY-OASIS II version 6.1.4 software [3]. We estimated the post-fit phase residual in the ionosphere-free linear combination for each pair of GPS satellites and ground stations for the detection of eruption column. We applied absolute IGS phase center corrections for satellite and receiver antennas. The wet zenith tropospheric delays and its gradient at all the GPS sites were estimated at all processing epochs (every 30 seconds) under the assumption of a random walk stochastic model. Firstly, we analyze the all of the GPS data in July 21, 22 and 23, 2012 for the reference. Obtained post-fit phase residual of the reference days showed the noise-level for the path delay effects caused by the volcanic plume. This reference post-fit phase residual contained many noise sources such as multipath effects, local atmospheric disturbance, and so on. The noise level of the post-fit phase residual strongly depends on the each GPS satellite and ground station pair. Finally, we analyzed the data of the July 24, 2012. The post-fit phase residual clearly shows large disturbance just after the eruption. For example, the phase residual between SVN34 satellite and GEONET 0720, which located in the east coast of Sakurajima, suddenly increased just after the eruption. The obtained residual amount reached 80mm. It is clearly larger than the noise level measured on the reference days. Furthermore, other GPS satellite and ground station pairs also clearly showed significant amounts of disturbance. These results suggest that the eruption column moved to the westward by the wind after the eruptive event.

[1] Houli$\acute{e}$ et al. GRL, 2005. [2] Houli$\acute{e}$ et al. Eos Trans, 2005. [3] Lichten and Border, JGR, 1987.

Japan Geoscience Union Meeting 2014
(28 April - 02 May 2014 at Pacifico YOKOHAMA, Kanagawa, Japan)

SGD21-12 Room:413 Time:April 28 12:00-12:15

Airport survey method for transition to the new CNS/ATM systems in east Mekong area

NAKAGAWA, Yuji[1*] ; OKADA, Kaoru[2] ; SHIMADA, Seiichi[3] ; SATOMURA, Mikio[3] ; SHINDE, Yohei[1] ; ITOH, Hirokazu[1] ; UKEI, Kazuyuki[1]

[1]Nippo Co.,Ltd., [2]Japan International Cooperation Agency, [3]NIED, [4]Hot Springs Res. Inst, Kanagawa Pref.

The project by the name of ”Capacity Development for Transition to the New CNS/ATM Systems in Cambodia, Lao PDR and Vietnam” (Jan.2011-Dec.2015) was officially announced by Japan International Corporation Agency (JICA) on April 2011, and Nippo got the order, after that we got the orders five times for two years. We would like to introduce the procedure of surveying airport coordinates.

The concept of New CNS/ATM System (Communication, Navigation and Surveillance/Air Traffic Management) utilizing satellite technologies was developed by International Civil Aviation Organization (ICAO) in 1991 for globally harmonized implementation in order to cope with the expected increase of air traffic. All the Contracting States of ICAO are required to move from the conventional air navigation systems to the New CNS/ATM Systems in accordance with ICAO Global Plan.

In order to shift air navigation from the ground-based facility use to the satellite use, it is essential to have accurate and updated data of latitude and longitude of airports and air navigation facilities based on WGS-84 coordinates as ICAO Standard. However, in Cambodia, Lao PDR and Vietnam it has not been made known whether airport survey has been conducted, applying long-baseline analysis by using International GNSS Services (IGS) points in accordance with ICAO WGS-84 Manuals (Doc9674 2nd edition).

The purpose of the project is transferring survey method and surveyed airport coordinates in accordance with WGS84 coordinate system.

Airport survey procedure and recommendation

1.Confirmation of required survey points and facilities

Runway ends, ILS, VOR/DME, control tower, TV antenna, etc.

2.Reconnaissance of Primary Airport Control Station (PACS) and Secondary Control Station (SACS). Installed two PACS survey markers near runway ends and seven or eight SACS survey markers at a regular distance.

3.Set up receivers at two PACS and one SACS and surveyed 24 hours at PACS for three days, at SACS for 1.5 hours simultaneously by differential GPS satellite surveying. (when prepared three receivers. if prepared four receivers, observe two PACS and two SACS simultaneously)

4.Install GPS receivers at other SACS points over lapping the base line on every session.

5.Install total station (TS) at every PACS and SACS and observe each other to verify the coordinates surveyed by GPS receivers.

6.Survey runway ends, radio navigation facilities (ILS, VOR/DME, etc.) and obstacles like control tower, big Buddha stature, tall building. If the obstacle cannot seen from coordinates known points PACS, SACS, set up receivers at PACS and auxiliary two points in the vicinity of the obstacle.

7.Determine the coordinates of PACS using long baseline analysis software (Bernese) by down loading ultra rapid orbit. Coordinates of SACS using short baseline analysis software.

8.Survey runway ends, radio navigation facility and obstacles by TS using SACS and PACS.

9.We surveyed a fiducial point which have x, y coordinates and above sea level height, and compared the result which obtained by Earth Gravitational Method (EGM) 2008 software in Cambodia. (The result of EGM2008 is higher than our survey by about 80cm, but we could not confirm the accuracy of the height of fiducial point.)

10.Lecture on how to choose the PACS and SACS location, how to use the long baseline software and how to maintenance the result data including process of calculation.

Keywords: WGS84, GPS, CNS/ATM, Airport coordinates, East Mekong area

Japan Geoscience Union Meeting 2014
(28 April - 02 May 2014 at Pacifico YOKOHAMA, Kanagawa, Japan)

SGD21-13 Room:413 Time:April 28 12:15-12:30

Vertical deformations revealed by laser scanning surveys in the Murono mud volcano

TAKAHASHI, Atsushi[1*] ; FUKUDA, Yoichi[1] ; KUSUMOTO, Shigekazu[2]

[1]Graduate School of Science, Kyoto University, [2]Department of Earth Science

In order to reveal the land surface deformation in the Murono mud volcano area located in Tokamachi city, Niigata prefecture, we have conducted the laser scanning surveys two times in June and October 2013, using TOPCON Imaging Station IS-301, which can obtain 3D point cloud data by the automatic laser scanning mode without reflector. In the same survey area, Toyama University has been conducting successive leveling surveys at 61 benchmarks so far. We also conducted the height measurements at the benchmarks using the precise ranging mode.

The obtained cloud data have been interpolated on regular grids for the two data sets, respectively, and the surface deformation has been calculated by comparing the gridded data. The obtained result showed a clear concentric uplift pattern in a part of the survey area. We thus modeled the uplift using the Mogi source model. The maximum amplitude estimated from the model was about 1.5 cm and it was almost coincident with the uplift obtained at the nearest benchmark. The result showed that the scanning mode was really beneficial to search for the spatial deformation pattern and the source of the deformation as well, even though its accuracy would be lower than the one of the precise ranging mode.

Keywords: LaserRangeFinder, LaserScanningSurvey, Mud Volcano, Vertical Deformation, Mogi Model

Japan Geoscience Union Meeting 2014
(28 April - 02 May 2014 at Pacifico YOKOHAMA, Kanagawa, Japan)

SGD21-14 Room:413 Time:April 28 12:30-12:45

Asymptotic solutions to the quasi-static spheroidal and toroidal deformation of the SNREI earth

OKUBO, Shuhei[1*] ; TAKAGI, Yu[1]

[1]Earthquake Research Institute, The University of Tokyo

Asympotic solutions to the quasi-static deformation of SNREI earth are essential to compute Green's functions, i.e., deformations due to a point load and a point dislocation. So far, only the surface deformations have been presented by previous authors. That is, internal stress/strain fields are not left uncalculated because of lack of asymptotic solutions to the internal deformation fields. In this talk, we present complete sets of spheroidal/toroidal deformations when spherical harmonic degree n increases to infinitiy.

Keywords: Internal elastic deformation, Green's function, SNREI earth, Asymptotic expansion

Japan Geoscience Union Meeting 2014
(28 April - 02 May 2014 at Pacifico YOKOHAMA, Kanagawa, Japan)

SGD21-P01 Room:Poster Time:April 28 18:15-19:30

Evaluation of uncertainty in distance measurement by GNSS surveying instrument and EDM

YOSHIDA, Shigeru[1*] ; SATO, Yudai[1]

[1]GSI of Japan

GSI has conducted research to establish traceability for distance measurement by GNSS surveying instrument to international standard. The international standard of distance is defined based on speed of light. In order to measure a distance based on the standard, it is necessary to use Electro-optical Distance Meter (EDM) for which the traceability to the standard is established. On the other hand, the traceability for GNSS surveying instrument used in various surveys is not established, because it is difficult and complex to estimate the uncertainty in distance measurement by the instrument. Therefore, we conducted an experiment to compare results of distance measurement by GNSS surveying instrument and EDM on a 2 km baseline.

Although the EDM measurement in this experiment should have been conducted indoors to reduce an affect of meteorological condition change, it was almost impossible to find an indoor 2 km baseline. We therefore divided an outdoor 2 km baseline into 10 short baselines and measured them by EDM. After that, the distance and uncertainty of the whole baseline were estimated from the results of measurements on the short baselines. The 2 km baseline was also measured by GNSS, and the estimated distance and uncertainty was compared to the results of EDM measurements.

The distances and uncertainties estimated by the measurements of EDM and GNSS survey instrument were 1,999.9828±0.0014 m and 1999.9828±0.006 m respectively. As a result of the experiment, we verified that the traceability for GNSS surveying instrument can be established on the 2 km baseline.

Keywords: GNSS surveying instrument, EDM, Uncertainty, Traceability

Japan Geoscience Union Meeting 2014
(28 April - 02 May 2014 at Pacifico YOKOHAMA, Kanagawa, Japan)

SGD21-P02 Room:Poster Time:April 28 18:15-19:30

Changes of E-W observed by the Quartz-tube Extensometer in the Matsushiro extending after the 2011 Tohoku Earthquake

HASHIMOTO, Tetsuo[1*] ; FUNAKOSHI, Minoru[1]

[1]Matsushiro Seismic Obsevatory JMA

We observed a coseismic step of 5.8×10^{-7} strain in the E-W direction by the quartz-tube extensometer at Matsushiro during the 2011off the Pacific coast of Tohoku earthquake. After that, an aftereffect of 0.4×10^{-7} strain continued extending in the E-W direction about 1 month. And more, the E-W extension has continued since October, 2011 and it becomes over 0.5×10^{-7} strain. Similar phenomena were observed by superconducting gravity meter in Matsushiro and Kamioka (Imanishi, personal communication). Therefore, we think that these data of the E-W extension indicate true crustal deformation.

Figure shows data of the quartz-tube extensometer, water-tube tiltmeter, thermometer, and the other points of the extensometer. The air temperature in the tunnel heated up 0.03 ℃ in this range. But the influence of the temperature change hardly caused the extension, because it is very small extension of 1.6×10^{-8} as 5.4×10^{-7} of the temperature response of the quartz-tube. And more, the tiltmeter and the other point data of the extensometer show a similar change, therefore, the change seems to be true. We can catch geophysical phenomena such as the seismic waves (not shown in the figure) of the 2011 off the Pacific coast of Tohoku earthquake, the coseismic step, the aftereffect and continuing extensive change by the one device. This extensive change may indicate a part of crustal upheaval in a geological meaning.

Acknowledgement: We thank Yuichi Imanishi Associate Professor of ERI for teaching us about the continuity of decreasing gravity by the superconducting gravity meters in Matsushiro and Kamioka after the Tohoku earthquake.

Keywords: extensometer, tiltmeter, aftereffect, the 2011 off the Pacfic coast of Tohoku Earthquake

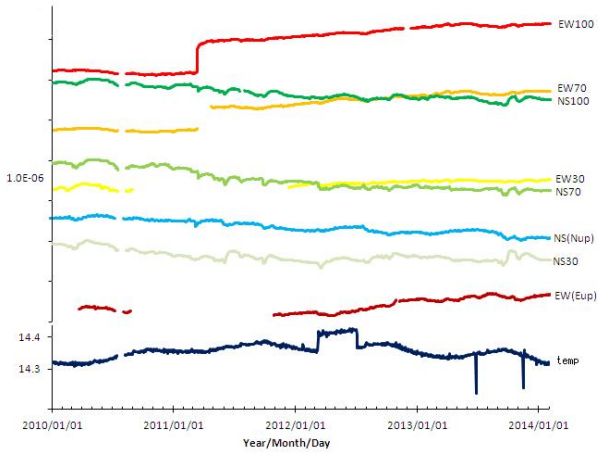

Japan Geoscience Union Meeting 2014
(28 April - 02 May 2014 at Pacifico YOKOHAMA, Kanagawa, Japan)

SGD21-P03 Room:Poster Time:April 28 18:15-19:30

Equqtorial flattening of the cylindrical outer core

KAKUTA, Chuichi[1*]

[1]none

Zhong et al.(2007),showed that the Africa supercontinent was formed after the Pangea(330Ma)in an initially by a spherical harmonic degree-1 form with the Pacific superplume. They suggested that the degree-1structure is responsible for supercontinent assembly with downwellings(Africa) and upwellings(Pacific).Recent studies show that light elements are transferred from the mantle to the outer core (OC) through the core-mantle boundary(CMB) and that the stably stratified layer are formed in the OC beneath the CMB. The stable layer shows the superadiabatic gradient, 1 Kkm-1 and its thermal conductivity is 150Wm-1K-1. The heat flux is over 100mWm-2.The heat flux of the mantle near the CMB is 100mWm-2 in the high temperature region (Perovskite) and 50mWm-2 in the low temperature region(Post-Perovskite). The heat flux flows into the low temperature region from the OC. We assume that the OC is a thin cylindrical rotating fluid around the rotating axis. The fluid shows a low frequency motion and the effects of flow pressure fluctuations on the density is ignored (Subseismic Approximation;Smylie and Rochester, 1981). The heat flux in the OC is expressed in the form of the exponential function of the central distance which decreases outward near the CMB. We derive the 1st order variations of the Potential. The azimuthal variation of the potential shows the variation of the equatorial flattening. The maximal value of its variation relative to the mean gravitational potential at the CMB is 1.1x10-5 (flattening). This value can be compared with the value of the equatorial flattening of the OC to be 6x10-6 obtained by Szeto and Xu(1997).

Keywords: thin cylindrical outer core, heat flux, heat flux in the mantle, potential, variation of potential, equatorial flattening of core

Japan Geoscience Union Meeting 2014
(28 April - 02 May 2014 at Pacifico YOKOHAMA, Kanagawa, Japan)

SGD21-P04 Room:Poster Time:April 28 18:15-19:30

A bias correction method for improving regularized solution in linear inverse ill conditioned models

SHEN, Yunzhong[1*] ; XU, Peiliang[2] ; LI, Bofeng[1]

[1]1. College of Surveying and Geo-infomatics, Tongji University, Shanghai 200092, P.R. China, [2]Disaster Prevention Research Institute, Kyoto University, Uji, Kyoto 611-0011, Japan

Geodetic downward continuation and inverse problems are often ill conditioned, and regularization is used for deriving stable and better solutions. However, the regularized estimates of parameters and residuals are well known to be biased. Theoretically the biases of the estimated parameters and residuals can only be computed with the true values of parameters. Since we do not know the true values of parameters in practice, we attempt to improve the regularized estimates by using the regularized estimates themselves to replace the true parameters for estimating the biases and then removing the computed biases from the regularized estimates. Furthermore the biases are also removed from the residuals, and then the variance of unit weight of the observation noises is estimated with the bias-reduced residuals. We derive the analytical conditions for bias correction and show that the bias-corrected regularization performs better than the ordinary regularization in terms of mean squared errors. However, for estimating the variance of unit weight, the biases still need to be full removed from the residuals. We then present the numerical examples of gravity downward continuation to demonstrate the performance of our bias correction method for improving regularized solution. The results show that our bias correction method can successfully reduce the absolute biases of the regularized estimates, and improve the accuracies with more than 5 per cent. Moreover, by removing the biases from the residuals, the derived variance of unit weight is almost unbiased.

Keywords: Linear ill-conditioned model, Regularization solution, Bias correction, Gravity downward continuation, Variance of unit weight

Japan Geoscience Union Meeting 2014
(28 April - 02 May 2014 at Pacifico YOKOHAMA, Kanagawa, Japan)

SGD22-01 Room:413 Time:May 1 09:00-09:15

Gravity observation using a superconducting gravimeter at Ishigakijima, Japan (part 3)

IMANISHI, Yuichi[1*] ; NAWA, Kazunari[2] ; TAMURA, Yoshiaki[3] ; IKEDA, Hiroshi[4] ; MIYAJI, Takeshi[3] ; TANAKA, Yoshiyuki[1]

[1]ERI, The University of Tokyo, [2]AIST, [3]NAOJ, [4]University of Tsukuba

About two years have passed since we started gravity observation by means of a superconducting gravimeter at the VERA Ishigakijima Station, National Astronomical Observatory Japan in 2012, with the main purpose of detecting possible gravity changes associated with the long-term slow slip events beneath the Yaeyama Islands. Up to now, we have experienced three times of events, which took place in May 2012, December 2012 and July 2013. For the two events in 2012, gravity changes possibly associated with the slow slip events were recorded. The July 2013 event was not well recorded because of the damages by the typhoon. In addition, an earthquake swarm near the Yaeyama Islands in April 2013 may have also influenced the observed gravity. The next slow event is expected to take place around February 2014. Modeling and interpretation of the data will be presented in the paper.

Keywords: superconducting gravimeter, slow slip, Ishigakijima

Japan Geoscience Union Meeting 2014
(28 April - 02 May 2014 at Pacifico YOKOHAMA, Kanagawa, Japan)

SGD22-02 Room:413 Time:May 1 09:15-09:30

Various drift rates of gPhone gravimeters obtained from short-term observations at geothermal fields

NAWA, Kazunari[1*] ; MIYAKAWA, Ayumu[1] ; SUGIHARA, Mituhiko[1]

[1]Geological Survey of Japan, AIST

We carried out short-term but continuous gravity observations using gPhone (spring type) gravimeters at geothermal fields. At hot spring area of Hachijojima, we obtained 1-4 months gravity data using several gPhone gravimeters at different sites and situations of the period between February 2011 and December 2012. Using the obtained data, we calculated and compared temporal variations of the drift rate. As a result, drift rates of gravimeters showed various characteristics according to location and elapsed time from installation. In many cases, it took about a month until initial drift stabilized, that is, dirift rate became quasi-constant. Even after stabilized, drift rate of gPhone gravimeters remained a few microGal/day (on the other hand, the nominal drift rate of iGrav superconducting gravimeter is 0.5 microGal/month), although the magnitude of the drift rates were considerabty smaller than several hundred microGal/day of CG-3M gravimeters. We will show the result of gPhone-133 replaced from Hachijojima to a geothermal power plant at Kyushu District in March 2013.

Keywords: relative gravimeter, temporal gravity change, Hachijojima, on-land observation

Japan Geoscience Union Meeting 2014
(28 April - 02 May 2014 at Pacifico YOKOHAMA, Kanagawa, Japan)

SGD22-03 Room:413 Time:May 1 09:30-09:45

Gravimetrical vertical array observation -the 2013 fiscal year-

TANAKA, Toshiyuki[1*] ; HONDA, Ryo[1]

[1]TRIES, ADEP

A vertical array of gravimeters (Mizunami Underground Laboratory; MIU) is quite rare in the world, and this method that suppresses rainfall responses and stacks signal from deep part of the crust can contribute to leveling up the potential of gravimetry (Tanaka et al., EPS, 2013). This time (Nov. 2013~Jan. 2014), we have succeeded in getting higher quality data than before with almost same configuration; namely, using two gPhone gravimeters (#130 on the ground, #90 at 300m under the ground). Though blasting for construction works had performed frequently during last year, we can detect sub-microGal responses of rainfall this time in the frequency band from hourly to daily. In the longer band, the sensor temperature of #130 is still shifting slightly, which can affect drifting rate. Here, we describe the four time-series data: data of belowground, (1); data on the ground, (2); sum of the two, (3); difference between the two, (4). We have finally got residual gravity values without tidal and atmospheric responses by using the BAYTAP-G (Tamura et al., 1991), with assuming of linear drift. When it rains, (1) should show gravity decrease, (2) should show gravity increase, (3) should offset the response, and (4) should superimpose the response. Because, only the main part of the Akeyo formation, which overlies an impervious layer from the surface to approximately 80m depth, responds to precipitation (e.g. Tanaka et al., Gcubed, 2006). Actually, we have observed such responses of rainfall. These depend on the way of rainfall; however, it seems that the amplitude of the response of (1) is slightly larger than (2). If so, the infinite slab assumption of a groundwater layer caused by rainfall is unsuitable for this gravimeter layout. On atmospheric correction, (1) and (2) should be almost same, (3) should superimpose, and (4) should offset the response. Actually, we have observed such responses and confirmed that (4) is one-tenth the atmospheric response of that of (1) or (2).

In the future, we will aim to accumulate high quality data, survey the habit of these two gravimeters (i.e. sensor drift, sensor temperature, and tilt response), and finally construct a vertical array including an absolute gravimeter.

Acknowledgements: This work is supported by a promotion grant for the establishment of the underground research facility of the Agency for Natural Resources and Energy, Minister of Economy, Trade and Industry. We thank the JAEA for the cooperation of observations (especially Mr. Y. Horiuchi) and our colleagues.

Keywords: continuous gravity measurement, gravimeter, inland water, rainfall, atmospheric correction, measuring method

Japan Geoscience Union Meeting 2014
(28 April - 02 May 2014 at Pacifico YOKOHAMA, Kanagawa, Japan)

SGD22-04 Room:413 Time:May 1 09:45-10:00

Huge uplift event of Iwoto: Estimation of gravity change based on the result of gravimeter calibration in Sapporo-Naha

OZAWA, Taku[1*] ; MIYAGI, Yosuke[1] ; UEDA, Hideki[1] ; NAGAI, Masashi[1] ; FUJITA, Eisuke[1]

[1]National Research Institute for Earth Science and Disaster Prevention

Ogasawara-Iwoto is the volcanic island located to 1200km south of Tokyo. It has a caldera with the diameter of 10km, and its central and southwestern part appears on the sea surface. One of characteristics for its volcanic activity is to have the large uplift rate, and National Research Institute for Earth Science and Disaster Prevention (NIED) has revealed occasional ×occurrence of huge uplift events and distribution of its crustal deformation (Ukawa et al., 2006). NIED started gravity survey from 1996, and Ukawa (2006) suggested involvement of magma in a huge uplift event. Though continuous subsidence had been observed from early 2003, it rapidly changed to uplift in mid-2006. Its uplift decelerated with time after 2007, but it rapidly re-accelerated in Feb. 2011. According to GNSS observation by NIED and GSI, the amount of uplift from re-acceleration to Apr. 2012 reached 2m. In late April of 2012, discolored water was found around Iwoto, and uplift activity slowed down after that. To investigate crustal deformation and gravity change associated with this event, we carried out GNSS campaign observation and gravity survey. We presented the result of GNSS campaign observation in fall meetings of the geodetic society of Japan and the volcanological society of Japan. We also presented preliminary result for gravity survey, but there was a problem on uncertainty for temporal change of scale factors of used gravimeters (Scintrex CG-3M #284 and #371). To estimate scale factors of their gravimeters, we carried out gravity survey between Sapporo and Naha. In this presentation, we show temporal change of scale factors revealed from this calibration and gravity change of Iwoto estimated using its result.

In gravimeter calibration, we measured gravities at NIED (Bosai-BS), GSI (Tsukuba-GS and Tsukuba-FGS), Haneda airport (Haneda-GS), Chitose airport (Chitose-GS), Hokkaido University (Sapporo-GS), and Okinawa Meteorological Observatory (Naha-GS and Naha-FGS). In estimation of relative gravity, we assumed that the drift rate was constant, and estimated gravities and the drift rate simultaneously. Then we estimated scale factors so that estimated gravities corresponded to those of JGSN96 (Geospatial Information Authority of Japan, Geodetic department, 1997). Since Sapporo-GS was moved to new benchmark, we used gravity measured by GSI. Estimated changes of scale factors from those in 2006 were $+2\times10^{-5}$ and -1×10^{-4} for #284 and #371, respectively. Temporal changes of scale factors are not orderly, and then obtained scale factor is different significantly from estimated value by the linear approximation. Therefore it indicates that consideration of temporal change of scale factor is important in survey of large gravity difference.

Estimating gravity at the benchmark in Iwoto (IWO101), estimated gravities from #284 and #371 were consistent within 0.027mGal, and its average was decrease of 0.734mGal from that in 2006. Uplift in this period was 3.05m, and then gravity change rate with respect to uplift was -0.241mGal/m. This gravity change rate is in good agreement with that for the 2001-2002 huge uplift event by Ukawa et al. (2006). This result suggests that the huge uplift event from 2006 has been caused by the magma with the similar density to that in the 2001-2002 event.

Acknowledgements. GNSS and gravity surveys were supported by JSDF. A part of survey and analysis for Iwoto was carried out by Ohba Co. Ltd. Gravity calibration was supported by GSI, Hokkaido University, and Okinawa Meteorological Observatory.

Keywords: Iwoto, gravity, scale factor, magma

Japan Geoscience Union Meeting 2014
(28 April - 02 May 2014 at Pacifico YOKOHAMA, Kanagawa, Japan)

SGD22-05 Room:413 Time:May 1 10:00-10:15

Absolute gravity measurements near the Sor-Rondane Mountains, Antarctica

FUKUDA, Yoichi[1*] ; AOYAMA, Yuichi[2] ; SUGANUMA, Yusuke[2] ; OKADA, Masaki[2] ; DOI, Koichiro[2]

[1]Graduate School of Science, Kyoto University, [2]National Institute of Polar Research

In order to detect the gravity changes due to ice sheet mass changes, Glacial Isostatic Adjustment (GIA) and other effects, we have conducted absolute gravity measurements at Princess Elisabeth Station (PES) near the Sor-Rondane Mountains, Antarctica, as part of the 55th Japanese Antarctic Research Expedition (JARE-55). In addition, the first absolute gravity measurements using a field absolute gravimeter have also been conducted on the Seal rock near the Asuka station, where the gravity reference point (No.26-01) established by JARE-26 is located.

The absolute gravimeters employed were FG5#210 and A10#017, and a relative gravimeter LaCoste #805 was also used for dg/dz measurements and gravity connections. Using DROMLAN (Dronning Maud Land Air Network), we moved to PES with the instruments via Novolazarevskaya from Cape Town in South Africa. The length of our stay in PES was for 18 days from Nov. 29 to Dec. 16, 2013. Belgian researchers have already conducted absolute gravity measurements using a FG5 in North Shelter (NS), a small observation hut built on an outcrop a few hundred meters apart from the main base of PES. One of the main purposes of this project is to monitor long-term gravity changes by means of successive absolute gravity measurements at the same gravity point in NS. Since NS has not enough space for adjusting the gravimeters before measurements, we borrow a room in the main base for the purpose and test measurements as well. We established a tentative gravity point in the room and compared the gravity values measured by A10 and FG5. The result showed the discrepancy was within 2 micro-Gals. This means that A10 was well calibrated. Unfortunately a crucial fault arose in the dropping chamber of the FG5, and it could not be recovered to the last. For this reason, the measurements in NS were carried out using A10. The gravity value on the reference point was calculated to be 982302155.21 micro-Gals with the measured dg/dz of -4.4529 micro-Gals/cm. Although the exact comparisons with the gravity values obtained by the Belgian team have not been completed yet, the gravity values seem to be in agreement within several micro-Gals. Therefore the temporal gravity change would be very small, even if it existed.

The gravity measurements on the Seal rock have been conducted on Dec. 5th and 6th. Since No.26-01 is located near the summit of the Seal rock, where strong wind blows constantly, it is very difficult to conduct absolute gravity measurements even using A10. Therefore a tentative gravity point was set up at the foot of Seal rock, and measurements with A10 were conducted at the point. Then gravity connection to No.26-01 was conducted with the LaCoste gravimeter. The gravity value thus obtained at No.26-01 was 982406.109 mgal with the accuracy of about 15 micro-Gals including the errors due to the gravity connection.

The gravity values of No.26-01 so far obtained were 982405.33mgal by JARE-26 (GSI, 2002), and 982402.817mgal by JARE-27 (Fukuda, 1986). The new value is 0.779 mgal and 3.292 mgal larger than those of JARE-26 and JARE-27, respectively. In JARE-27, two sets of LaCoste gravimeters were employed for the gravity connection between Seal rock and Syowa Station. Since a large discrepancy between the values obtained by two gravimeters was found, Fukuda (1986) applied a step correction of 3.765mGals to the suspected gravimeter. However, judging from the present result, the correction could be applied to the wrong gravimeter. If the correction was applied to the other gravimeter, the difference of 3.292 mgal was set to about 0.5mGals, and it would be likely as the accuracy of the gravity connection. The gravity value of No.26-01 has been used as a reference value for the gravity surveys so far conducted in the Sor-Rondane area. Therefore the revisions of those values should be required from now on.

Keywords: absolute gravity measurement, Sor-Rondane, Antarctica, ice sheet movement, gravity changes, gravity reference point

Japan Geoscience Union Meeting 2014
(28 April - 02 May 2014 at Pacifico YOKOHAMA, Kanagawa, Japan)

SGD22-06 Room:413 Time:May 1 10:15-10:30

Performance of the recoil-compensation mechanism used for a throw-up type absolute gravimeter

SAKAI, Hirotaka[1*] ; ARAYA, Akito[1] ; TSUBOKAWA, Tsuneya[2] ; EMANUELE, Biolcati[3]

[1]Earthquake Research Institute, University of Tokyo, [2]Shin-ei keisoku, [3]L'Istituto Nazionale di Ricerca Metrologica

Absolute gravimeters can measure gravity acceleration in the accuracy of 8 to 9 digits. They are accurate and useful for many applications, however the apparatus is too bulky and heavy. Therefore, in the field observation, their installation site is limited. As a result, for volcanic observations, a gravity value is usually measured by an absolute gravimeter at a reference point of foot, and then a gravity value of an observation point can be obtained from the gravity difference between a reference point and an observation point measured with a relative gravimeter; such a method is laborsome, and requires long time. Furthermore it is hazardous to approach the observation points when the volcano is active. This study is to minimize absolute gravimeter in order to improve these situations. The original point of our new apparatus is to incorporate a recoil-compensation mechanism to improve the measurement accuracy.

In the absolute gravity measurements, we adopted a rise-and-fall method, while conventional absolute gravimeters usually adopt a simple free-fall method. The simple free-fall method has several problems such as bulky mechanism to lift up a test mass, repeated measurements, and long time to take for the preparation. Hence, we developed a throw-up equipment that had no need for lifting up a test mass and could measure repeatedly. This enabled to minimize one of the biggest parts in the absolute gravimeter.

The equipment which we developed this time can throw up the test mass by 3mm in height simply by applying the signal to a piezoelectric element which is incorporated in the expansion mechanism. When the test mass was thrown up, it rotated by an anchoring effect and it may cause the error in the gravity measurement. We applied other piezoelectric elements which separate the stage from the test mass just before the test mass leaves the stage to cut off the anchoring force. At the end of 2012, we carried out a performance test of the throw-up equipment at Esashi Earth Tidal Station in Iwate. At Esashi, we replaced the free fall equipment of the existing absolute gravimeter with the throw-up equipment. As a result, the throw-up equipment was able to detect a gravity change of earth tides. The resolution of the gravity measurement δg was estimated to be 40μgal. However, the absolute gravity deviated from the value expected from the past measurements up to $\triangle$g= 3mgal. This big error was inferred from the recoil effect at the time of throw that induces vibration to the interferometer.

We developed the recoil compensation mechanism of the throw-up equipment to improve the measurement accuracy $\triangle$g. Specifically, we put the same piezoelectric element and the expansion mechanism on the other side of the baseplate to which the throw-up mechanism is attached. These expansion mechanisms move symmetric by applying the same signal to the piezos. When the test mass is thrown up, the counter mass fixed by springs is launched downward at the same time to compensate the recoil effect. We could observe the recoil reduction as much as 2.7% of peak acceleration without the compensation mechanism. After performing fine adjustment of the equipment, we plan to conduct gravity measurement by the same method to 2012, and the result and the development status will be reported.

Keywords: absolute gravimeter, throw-up equipment, miniaturization, recoil effect, compensation mechanism, gravity measurement

Japan Geoscience Union Meeting 2014
(28 April - 02 May 2014 at Pacifico YOKOHAMA, Kanagawa, Japan)

SGD22-07 Room:413 Time:May 1 10:30-10:45

Development of a laser-interferometric gravity-gradiometer and its trial operation on the volcanic island of Sakurajima

SHIOMI, Sachie[1*] ; KAGIYAMA, Tsuneomi[1]

[1]Aso Volcanological Laboratory, Kyoto University

We have been developing a laser-interferometric gravity-gradiometer for volcanological studies. The gravity gradiometer measures differential accelerations between two test masses that are in free fall at different heights. Because its detection principle is based on the differential measurements, measured values are insensitive to the motions of observation points. That is to say, the gravity gradiometer is expected to have a good resolution even when it were used on an accelerating vehicle, such as an airship, or in an active volcanic area. Therefore, the gravity gradiometer could be useful for, for example, resource explorations and studies on volcanic activities.

The gravity gradiometer, to be used on an airship, had been developed at the Institute for Cosmic Ray Research (ICRR) of the Tokyo University from 2009 to 2012. A prototype of the gravity gradiometer was built up and tested at the ICRR. Their laboratory test showed that its resolution of measuring vertical gravity gradients was about a few μGal/m in two second measurements. However, large unexplained disturbances were observed in longer term measurements. In order to understand the sources of the disturbances, the prototype was moved to the Aso Volcanological Laboratory (AVL) of the Kyoto University in July 2012. Since then, its further development, to be used at an observatory in a volcanic area, has been carried out at the AVL.

We will report the current status of the development for volcanological studies and results of trial measurements performed at the Sakurajima Volcanological Laboratory of the Kyoto University, on the volcanic island of Sakurajima, Kyusyu, Japan.

Keywords: gravity gradients

Japan Geoscience Union Meeting 2014
(28 April - 02 May 2014 at Pacifico YOKOHAMA, Kanagawa, Japan)

SGD22-08 Room:413 Time:May 1 11:00-11:15

The two components of postseismic gravity changes and their mechanisms

TANAKA, Yusaku[1*] ; HEKI, Kosuke[1]

[1]Graduate School of Science, Hokkaido University

The time series analysis of the gravity changes of the three Mw9-class mega-thrust earthquakes (2004 Sumatra-Andaman earthquake; 2010 Chile (Maule) earthquake; and 2011 Tohoku-oki earthquake) gives the strong possibility that the gravity observation separates postseismic phenomena. There are three sensors for earthquake observations: the first sensor is seismographs, the second sensor is GNSS (Global Navigation Satellite System) or SAR (Synthetic Aperture Rader), and the third sensor is the gravity observation. Seismographs cannot be used to catch the signal of postseismic phenomena because they do not shake the ground. GNSS like GPS (Global Positioning System) and SAR catch the signal of postseismic phenomena but they cannot separate those phenomena because the phenomena move the ground with the same polarities. However, the polarities to gravity changes of postseismic phenomena can be different each other. This suggests that the gravity can become the first sensor to catch the separated signals of postseismic phenomena.

GRACE (Gravity Recovery And Climate Experiment), which is the twin satellites launched in 2002 by NASA and keeps on observing the gravity field of the earth, gives the two-dimensional gravity data and the insight into phenomena under the ground when and after earthquakes occur. The results of time series analysis of postseismic gravity changes with GRACE data show that the gravity which decreases coseismically keeps on decreasing for a few months and increases for a longer period; the postseismic gravity changes have two components (short- and long-term gravity changes). This is a new discovery and this also suggests that the gravity observation gets the different postseimic phenomena with different polarities.

The mechanisms of coseismic gravity changes are well known but those of short- and long-term postseismic gravity changes are not clear completely. They are explained with afterslip and viscoelastic mantle relaxation to some extent but each of them has each problem.

Although the mechanisms of postseismic gravity changes have rooms to be discussed, the gravity observation can do what the seismographs, GNSS and SAR cannot do; the gravity observation separates the postseismic phenomena.

Japan Geoscience Union Meeting 2014
(28 April - 02 May 2014 at Pacifico YOKOHAMA, Kanagawa, Japan)

SGD22-09 Room:413 Time:May 1 11:15-11:30

High resolution mapping of ice mass trend in Greenland using GRACE GFZ solution

MATSUO, Koji[1*] ; FUKUDA, Yoichi[1]

[1]Graduate school of Science, Kyoto University

The gravity satellite mission GRACE has been measuring monthly variations of the Earth's gravity field since its launch in 2002. The GRACE data has updated from RL04 to RL05 in May 2012, and have been provided in the form of spherical harmonic (Stokes') coefficients with degree and order up to 60 (d/o60) from CSR and JPL. In addition, GFZ has provided Stokes coefficients with d/o90 as RL05a product in December 2013. In this study, we examine the measurement error of GFZ RL05a product (d/o90). Then we attempt to delineate a high resolution map of ice mass trend in Greenland by making use of the full Stokes' coefficients.

First, we examine the measurement error. Following the method of Wahr et al. (2006), we derive temporal and spatial variation of the measurement error from error variance matrix of GRACE data. The global average of RL05a error is about 100cm in equivalent water thickness. Because RL04 error is about 300cm, RL05a achieves triple the precision improvement. The temporal variation of error in global average is about 200 cm from January 2003 to July 2003, and reduces to about 100cm afterwards. The spatial distribution shows large error in equatorial region (about 130cm) and small error in polar region (about 40cm). Considering these results, it can be said that the quality of RL05a is especially high in polar region after August 2003.

Next, we derive ice mass trend in Greenland from GFZ RL05a (d/o90) product. Here we apply de-striping filter (Swenson and Wahr, 2006) to alleviate the noise. In addition, we employ spherical Slepian Basis (Harig and Simons, 2012) to extract ice mass trend in Greenland effectively. In doing so, we can successfully delineate a clear ice mass trend map with about 200 km spatial resolution, which is 1.5 times as high as before. We confirmed very good agreement with ICESat result.

Keywords: Satellite gravimetry, Greenland, Ice sheet mass variation, Space geodesy, GRACE, ICESat

Japan Geoscience Union Meeting 2014
(28 April - 02 May 2014 at Pacifico YOKOHAMA, Kanagawa, Japan)

SGD22-P01 Room:Poster Time:May 1 18:15-19:30

Establishment of GSIGEO2011 (Japanese geoid model)

KODAMA, Tokuro[1*] ; MIYAHARA, Basara[1] ; KAWAWA, Hiroshi[1] ; KUROISHI, Yuki[1]

[1]GSI of Japan

Geospatial Information Authority of Japan (GSI) established Japanese geoid model ”GSIGEO2000”. The model has enabled a translation from ellipsoidal heights to orthometric heights in GNSS survey for triangulation points, which are positional reference for surveys in Japan. As a result, the model greatly has contributed to realize efficient control point survey. In order to expand utilization field of geoid model to height determination of third-order benchmarks by GNSS satellite positioning, GSI has established new Japanese geoid model ”GSIGEO2011” and reported here.

GSIGEO2011 has established as a hybrid geoid model of a gravity geoid model and observed geoid height data. New Japanese gravity geoid model, JGEOID2008 (Kuroishi, 2009), is adopted as the base model, and least square collocation method is adopted to fit the model to observed geoid height data obtained at over 750 GNSS-based control stations all over Japan. In order to utilize for height determination of third-order benchmarks, residuals between the model and input observed geoid heights are set to 2cm in standard deviation. JGEOID2008 is greatly improved at reduction of local systematic errors which are contained in older gravity geoid models. Therefore, short wavelength components in geoid are well described and fit to observed data, and as a result, the accuracy of the hybrid model is improved.

The 2011 off the Pacific coast of Tohoku Earthquake caused huge crustal deformation in an wide area around eastern Japan. GSI urgently conducted control point surveys for restoration and opened the result for eastern Japan. GSI also conducted geoid surveys for GNSS-based control points which is located in an area experienced huge crustal deformation, and the results have been utilized for the input geoid heights data of GSIGEO2011. Therefore, GSIGEO2011 is consistent with the revised survey results in eastern Japan.

GSI has published newly established GSIGEO2011 and tired to realize height determination of third-order benchmarks by GNSS survey referring GNSS-based control points which have orthometric heights. This challenge is expected to drive further improvement in efficiency of survey procedure in Japan.

Keywords: GSIGEO2011, Geoid model, survey results

Japan Geoscience Union Meeting 2014
(28 April - 02 May 2014 at Pacifico YOKOHAMA, Kanagawa, Japan)

SGD22-P02 Room:Poster Time:May 1 18:15-19:30

The Japan Gravity Standardization Net 2013 (JGSN2013)

YOSHIDA, Kenji[1*]

[1]GSI of Japan

Geospatial Information Authority of Japan (GSI) have established new gravity standardization net, the Japan Gravity Standardization Net 2013 (JGSN2013), from the latest absolute and relative land gravity data which covers Japanese islands. GSI already established and published the Japan Gravity Standardization Net 1975 (JGSN75), which is consistent with the International Gravity Standardization Net 1971 (IGSN71). JGSN75 have been officially referred as Japanese gravity standard.

JGSN2013 have been established by combining gravity data obtained from primary-order absolute gravity survey and first-order relative gravity survey. In Tohoku area, at least one gravity survey was done for each gravity benchmark after the 2013 off the Pacific coast of Tohoku Earthquake. Therefore, the gravity survey data include gravity change caused by the earthquake.

JGSN2013, which is the second Japanese gravity standard net established by GSI, have achieved great improvement in accuracy and special coverage by adopting FG5 absolute gravity meter as an instrument, updating station coordinates to ITRF2008 and modifying tidal correction procedure to more consistent manner through all process. As a result, JGSN2013 have a capacity not only to contribute to monitoring of earth gravity filed, which is promoting by GGOS, but also to be registered to international absolute gravity database (AGrav), which is operated as a joint project by IAG IC-WG2.1 and IGFS. The establishment of JGSN2013 is reported in the paper.

Keywords: The Gravity Standardization Net, JGSN75, JGSN2013

Japan Geoscience Union Meeting 2014
(28 April - 02 May 2014 at Pacifico YOKOHAMA, Kanagawa, Japan)

SGD22-P03 Room:Poster Time:May 1 18:15-19:30

Calibration of the superconducting gravimeter iGrav10 by parallel observation with the absolute gravimeter FG5 #217

SUGIHARA, Mituhiko[1*] ; NAWA, Kazunari[1] ; MIYAKAWA, Ayumu[1]

[1]AIST

An iGrav superconducting gravimeter (SG) was re-installed in the Farnsworth field, TX for the purpose of studying the effects of CO2 injection at an enhanced oil recovery (EOR) site in December 2013. Usually the iGrav SG has an ultra-low drift of less than 0.5 microGal / month and a virtually constant scale factor. Empirically, the drift rate looks negligible using the TSoft program. However observed trend contains the drift-like component which is about 0.4 microGal / day. Strictly it is difficult to distinguish real gravity changes from time-varying instrumental drift. We made co-located measurements with the FG5 absolute gravimeter (AG) in middle of December 2013 and middle of January 2014. The gravity differences between the two periods was determined to be +1 +-2 microGal by the AG measurements, whereas -12 microGal by the SG measurements. The observed drift of the SG was much larger than the specified value, so that the SG was determined to be reset and is improved. Generally it takes at least six months to evaluate such low drift of less than 0.5 microGal / month using co-located measurements with AG. Another choice is parallel SG and SG measurements located in close proximity. We are planning such measurements at the Farnsworth site in 2014. This research is funded and supported by Ministry of Economy, Trade and Industry (METI).

Keywords: Superconducting gravimeter, iGrav, absolute gravimeter, FG5, parallel observation

Japan Geoscience Union Meeting 2014
(28 April - 02 May 2014 at Pacifico YOKOHAMA, Kanagawa, Japan)

SGD22-P04 Room:Poster Time:May 1 18:15-19:30

Densed gravity survey on the southeastern Kego fault system

NISHIJIMA, Jun[1*] ; FUJIMITSU, Yasuhiro[1]

[1]Faculty of Engineering, Kyushu University

The Kego fault system is one of the active fault located in Fukuoka city, southwestern Japan. We have conducted densed gravity survey on the southeastern Kego fault systems. One of the purposes of the survey is to reveal the location and detailed shape of the active fault syatem. We have measured gravity value at 721 points using Scintrex CG-3+ and CG-5 gravimeter. The measurement point interval was arranged as about several tens to hundreds meters. The measured gravity values were processed with a series of correction (height, drift, tidal, the free-air, the Bouguer and terrain) in order to obtain a gravity anomaly map. We determined the Bouguer density of 2.47 g/cm^3 using an objective Bayesian approach (Murata, 1993).

According to the gravity anomaly map of the Fukuoka City area that consists of not only our gravity data but also the gravity data of other institutions, the gravitational basement, which has a high density and affects to the gravity anomaly, is thought as Paleozoic Sangun metamorphic rocks and Cretaceous plutonic rocks (Sawara Granite, etc.) (Karakida et al., 1994). And a clear low gravity anomaly extension that has a strike of NW-SE is detected and coincides with the location of Kego Fault confirmed by a trenching survey (Shimoyama et al., 2005).

We will report the result of a three-dimensional analysis using GRAV3D ver. 3.0 (Li and Oldenburg, 1998).

Keywords: Densed gravity survey, active fault, gravity anomaly

Japan Geoscience Union Meeting 2014
(28 April - 02 May 2014 at Pacifico YOKOHAMA, Kanagawa, Japan)

SGD22-P05 Room:Poster Time:May 1 18:15-19:30

Crustal thickness deduced from a three-dimensional gravity modeling with seismic survey results

FUJIOKA, Yukari[1*] ; ISHIHARA, Takemi[2] ; OIKAWA, Mitsuhiro[1] ; KANEDA, Kentaro[1] ; NISHIZAWA, Azusa[1]

[1]Hydrographic and Oceanographic Department, Japan Coast Guard, [2]National Institute of Advanced Science and Technology

The Japan Coast Guard (JCG) has conducted multichannel seismic reflection and refraction surveys as part of the Continental Shelf Survey from 1983 through 2008 in the area from the northwest part of the Pacific plate to the Philippine Sea plate. On the other hand, it has also conducted marine gravity surveys in the same area and possesses enormous amount of gravity data. We calculate crustal density distribution by applying the three-dimensional gravity inversion method (Ishihara and Koda, 2007) using these data.

This method has performed in the following procedures: First, an initial density structure model constituting of seawater, sediment, crust and mantle is made by interpolation of seismic survey results with reference to a gravity distribution. Second, gravity anomalies are calculated using the initial model. Mantle Bouguer anomalies are calculated by subtracting a constant, which depends on the regional structure, from the differences between observed and calculated gravity anomalies. Finally, the Moho depths are obtained by inversion analysis to minimize the mantle Bouguer anomalies. We can estimate the crustal thickness distribution in this way.

It confirmed that the above method improves the initial model with the Moho depths due to velocity structure from refraction surveys, and that a more appropriate density structure model can be obtained.

In addition, it is necessary that whole structure depending on a sea area with the effects given by structure, such as a density and/or a thickness of sediment and/or lithosphere, should be considered if the effects of them are large. For example, in the case of the northwest part of Philippine plate, we found that the thickness of the lithosphere depending on its age strongly affects the result of the inversion. Therefore, we used the calculated gravity data after removal of variation for wave length than or equal to 400 km in order to remove effect given by the structure under crust.

We will report these revisions and the crustal thickness distribution in several sea areas. It is expected that gravity determination of the crustal thickness distribution in large sea area gives important clues on tectonic evolution of crust.

Keywords: gravity

Japan Geoscience Union Meeting 2014
(28 April - 02 May 2014 at Pacifico YOKOHAMA, Kanagawa, Japan)

SGD22-P06 Room:Poster Time:May 1 18:15-19:30

Estimation of the density structure beneath the Kanto Distinct, Japan, by 3-D gravity inversion

EDO, Tatsumi[1*] ; YAMAMOTO, Akihiko[1]

[1]Graduate School of Science and Engineering, Ehime University

We applied an improved gravity inversion technique by Bear et al. (1995) to rapidly invert Bouguer gravity data in Kanto District, Japan, for a 3-D density distribution as a source of the observed field. The technique estimates the density distribution within the source volume using a least-squares inverse solution that is obtained iteratively by singular value decomposition using orthogonal decomposition of matrices with sequential Householder transformations. The source volume is subdivided into a series of right rectangular prisms of specified size but of unknown density. This discretization allows the construction of a system of linear equations relating the observed gravity field to the unknown density distribution. Convergence of the solution to the system is tightly controlled by a damping parameter which may be varied at each iteration. Application to a gravity data set from Kanto District, Japan, has yielded a geologically reasonable result that agrees with published models derived from interpretation of gravity, magnetic, seismic, and drilling data.

Japan Geoscience Union Meeting 2014
(28 April - 02 May 2014 at Pacifico YOKOHAMA, Kanagawa, Japan)

SSS01-01 Room:419 Time:May 2 14:15-14:30

Collaboratory for the Study of Earthquake Predictability - Global Activities

SCHORLEMMER, Danijel[1*] ; GERSTENBERGER, Matt[2] ; HIRATA, Naoshi[3] ; JORDAN, Thomas[4] ; LIUKIS, Maria[4] ; MARZOCCHI, Warner[5] ; RHOADES, David[2] ; TSURUOKA, Hiroshi[3] ; WERNER, Maximilian[6] ; ZECHAR, Jeremy[7] ; CSEP WORKING GROUP, The[4]

[1]GFZ German Research Centre for Geosciences, 14473 Potsdam, Germany, [2]GNS Science, Avalon, Lower Hutt, New Zealand, [3]Earthquake Research Institute, University of Tokyo, Tokyo 113-0032, Japan, [4]Southern California Earthquake Center, University of Southern California, Los Angeles CA 90089, USA, [5]Istituto Nazionale di Geofisica e Vulcanologia, 00143 Roma, Italy, [6]School of Earth Sciences and Cabot Institute, University of Bristol, Bristol BS8 1RJ, UK, [7]Swiss Seismological Service, ETH Zurich, Zurich, Switzerland

The Collaboratory for the Study of Earthquake Predictability (CSEP) aims to improve our understanding about the physics and predictability of earthquakes through rigorous and prospective testing of earthquake forecast models. The system-science character of earthquake prediction research demands an open and collaborative structure for experimentation in a variety of fault systems and tectonic regions. CSEP Testing Centers in California, New Zealand, Japan, and Europe are being developed to provide adequate infrastructure for predictability research. CSEP is currently running prospective, automated evaluations of more than 350 models in various testing regions, e.g. California, New Zealand, Japan, Italy, and globally. We present the evolution of CSEP since its inception in 2007 and discuss results from several types of CSEP experiments. Finally, we describe how CSEP is expanding into other areas, including the testing of earthquake early warning systems, geodetic transient detectors, intensity prediction equations, ground-motion prediction models, and other types of hazard models.

Keywords: Earthquake forecasting, Seismic hazard, Statistical seismology, Earthquake statistics, Forecast testing

Japan Geoscience Union Meeting 2014
(28 April - 02 May 2014 at Pacifico YOKOHAMA, Kanagawa, Japan)

SSS01-02 Room:419 Time:May 2 14:30-14:45

One-day earthquake forecasting experiment in Japan after the 2011 Tohoku-oki earthquake

HIRATA, Naoshi[1] ; TSURUOKA, Hiroshi[1*]

[1]Earthquake Research Institute, the University of Tokyo

An experiment for earthquake predictability in Japan started in 2009 with a framework of CSEP. We have conducted one-day, three-month, one-year, and three-year forecasting experiments with three different regions of Japanese Islands; all Japan including sea area, main lands without sea area, and Kanto area(Nanjo et al., 2011; Tsuruoka et al., 2012). We currently have 160 modes for three regions and four periods.We conducted a retrospect one-day forecast of aftershocks of the 2011 Tohoku-oki earthquake showing that all proposed models failed in consistency tests immediately after the mainshock but in several days some of the models recovered its performance of forecasting (Nanjo et al., 2012).A current method for short-term forecasting has limitation of a period of one-day, which is arbitrarily determined. A shorter time period may be necessary for very intensive seismicity. Seismic activities in Japan have changed very much after the 2011 Tohoku-oki event, which brought us an idea that current forecasting models should be modified. We will present some new results of one-day forecasting experiments in Japan to discuss how to get information about real time earthquake hazard to mitigate earthquake risk. A new method to test performances of a model is also proposed.

Keywords: Earthquake forecasting, One-day forecasting, seimicity, Tohoku-okiearthquake, Statistical seismology

Japan Geoscience Union Meeting 2014
(28 April - 02 May 2014 at Pacifico YOKOHAMA, Kanagawa, Japan)

SSS01-03 Room:419 Time:May 2 14:45-15:00

Prospective evaluation of 3-month testing class of the CSEP-Japan earthquake forecasts

TSURUOKA, Hiroshi[1*] ; HIRATA, Naoshi[1]

[1]Earthquake Research Institute, University of Tokyo

Collaboratory for the Study of Earthquake Predictability (CSEP) is a global project of earthquake predictability research. The primary purposes of the CSEP is to develop a virtual, distributed laboratory. The final goal of this project is to investigate the intrinsic predictability of earthquake rupture mechanisms.

One major focus of the Japanese earthquake prediction research plan 2009-2013 is testable earthquake forecast models. So, the Earthquake Research Institute joined the CSEP and installed in an international collaboration a testing center as CSEP-Japan for rigorous evaluation of earthquake forecast models.

A total of 160 models were submitted from all over the world. And CSEP-Japan started the prospective experiments from 1 November 2009. The models are currently under test in 12 categories, with 3 testing regions and 4 testing classes of different time spans (1day, 3 month, 1 year and 3 years). We evaluate the performance of the models in the official suite of tests defined by the CSEP (L, M, N, S, R, T and W tests) against authorized catalogue compiled by Japan Meteorological Agency.

CSEP-Japan testing center has conducted over 6-12 rounds tests for 3-month testing classes including 2011 Tohoku-oki earthquake. We will discuss these results of evaluation test of the prospective experiments, and checked the performance of the earthquake models.

Keywords: CSEP, Earthquake Predictability, Seismicity

Japan Geoscience Union Meeting 2014
(28 April - 02 May 2014 at Pacifico YOKOHAMA, Kanagawa, Japan)

SSS01-04 Room:419 Time:May 2 15:00-15:15

Does using Coulomb stress change information create quantifiable improvements in earthquake forecast models?

GERSTENBERGER, Matt[1*] ; STEACY, Sandy[2] ; MARZOCCHI, Warner[2] ; RHOADES, David[1]

[1]GNS Science. 1 Fairway Drive, Avalon, Lower Hutt, New Zealand, [2]Environmental Sciences Research Institute, University of Ulster, Coleraine, N. Ireland, [3]Istituto Nazionale di Geofisica e Vulcanologia, Roma, Italy

The Darfield, New Zealand earthquake sequence has provided an interesting and active sequence for rigorous testing of earthquake forecast models that include Coulomb stress change information. Coulomb forecast models have long been discussed in the scientific literature as providing useful forecast information during aftershock sequences; however, a challenge that has limited our understanding of their ability is the difficulty in specifying such models so that they are prospective and unbiased. With the Darfield sequence we have the opportunity to use the Collaboratory for the Study of Earthquake Predictability (CSEP) earthquake forecast testing centre, that is already in operation in New Zealand, to develop Coulomb models in such a way. By taking advantage of archived data sets to provide all of the necessary inputs into the models, we are able to pseudo-prospectively test the models within the CSEP testing centre. An initial study by Steacy et al (2013) tested several models with Coulomb information. These models include a hybrid model with STEP (Gerstenberger, 2005), a rate-and-state based model, and several non-Coulomb models. Results of this study indicate that adding Coulomb information that was available 10-days after each main event, to a more traditional Omori-based model, provides a statistically improved forecast, even when attempting to test in an unbiased fashion. The experiment also highlighted significant differences when testing models retrospectively and pseudo-prospectively; these differences are driven by the reduced quality of data available to models in pseudo-prospective tests. Following this study, we are now implementing a larger experiment in collaboration with the European Union funded Strategies and Tools for Real Time Earthquake Risk Reduction (REAKT) project. In this experiment we are testing more than 20 Coulomb and non-Coulomb models within the NZ-CSEP testing centre. These models include hybrid statistical-Coulomb models and pure statistical and Coulomb models. We will discuss both experiments and their implications.

Keywords: Earthquake forecasting, New Zealand, CSEP, Coulomb, aftershock model, Christchurch

Japan Geoscience Union Meeting 2014
(28 April - 02 May 2014 at Pacifico YOKOHAMA, Kanagawa, Japan)

SSS01-05 Room:419 Time:May 2 15:15-15:30

Test of the argument for remote dynamic triggering by small mainshocks

PENG, Wei[1*]

[1]Wei Peng, [2]Shinji Toda

To understand earthquake interaction and forecast time-dependent seismic hazard, it is essential to determine whether static or dynamic stress change triggers most aftershocks and subsequent mainshocks. Felzer and Brodsky (2006) argued that the observed linear seismic density of small aftershocks with distance from small mainshocks is a product of the decay of seismic wave amplitude. They conclude that even small shocks can dynamically trigger remote earthquakes at distances more than ten source fault dimensions away. Richards-Dinger et al. (2010) counter-argue that the power law decay is an apparent product from independent aftershocks occurring along a large rupture zone or near-simultaneous occurrence in seismic swarms. To test the argument of Richards-Dinger et al. (2010), we use the Taiwanese earthquake catalog of the Central Weather Bureau Seismic Network, whose quality is as good as that in California and Japan. Further, we take an advantage of the absence of major inland earthquakes and significant swarms in the period, 2001-2011.

We follow the methodology of Felzer and Brodsky (2006) for selecting mainshocks using their declustering algorithm, and then seek all shocks that occurred within 5 minutes to make a diagram of linear aftershock density as a function of distance from mainshock. First we select as a mainshock any event that is not preceded by a larger shock within 3 days (t1) and 100 km, and that is not followed by a large shock within 12 hr (t2) and 100 km. The mainshocks and aftershocks are 2?M<3 and M?2 respectively. This yields 706 declustered mainshocks from the 110,157 candidate shocks, but the number of mainshock-aftershock pairs is just 56. We only find four pairs within 50 km distance range (the maximum considered by Felzer and Brodsky), which precludes any regression, while the others located further than 50 km are regarded as background. We then shorten the time period for both t1 and t2 to be 1.5 days and 0.25 days, which allows us to regress a power law slope of -1.16±0.45 for the 35 pairs within the 50-km distance range. The pairs are located mostly along the northern part of the Longitudinal Valley fault zone where small swarm activity and M~6 shocks often occur. We conclude that the much fewer ratios of mainshock-aftershock pairs in the Taiwanese catalog, in comparison to California and Japan, are due to lack of any large rupture and the absence of significant swarms in Taiwan, which supports the argument of Richards-Dingers et al. and renders the possibility that these small shocks are dynamically triggered untenable.

Japan Geoscience Union Meeting 2014
(28 April - 02 May 2014 at Pacifico YOKOHAMA, Kanagawa, Japan)

SSS01-06 Room:419 Time:May 2 15:30-15:45

Prediction performance of empirically defined foreshocks in the Izu region

MAEDA, Kenji[1*] ; HIROSE, Fuyuki[1]

[1]Meteorological Research Institute

1. Introduction

Foreshocks have been thought one of the most promising phenomena to predict large earthquakes. However, as the physical mechanism of foreshocks is not clarified yet, it is very difficult to distinguish them deterministically from background seismicity before a mainshock occurs. Therefore, empirical approach is one of the realistic ways to use foreshock activity as a precursor of a mainshock. We investigate probabilistic features of empirically defined foreshocks and search for the best parameters to define foreshocks which present relatively high performance to predict large earthquakes. Maeda (1996) and Maeda and Hirose (2012) proposed a foreshock definition which gives relatively high performance to predict large earthquakes along the Japan trench. In this study we basically apply the same method to the seismicity in the Izu region where swarm activities related with magma movements are frequently observed, and estimate the prediction performance based on empirically defined foreshock activities.

2. Method

The method to search for parameters for foreshocks that present high prediction performance consists of four steps. 1) To eliminate small aftershocks from the original data. 2) To define foreshock candidates as the activities that have number of Nf earthquakes with magnitude >= Mf during the period of Tf days in the segment of the size of D x D degree (latitude x longitude). 3) To set the alarm period of Ta days after a foreshock candidate during which a mainshock is expected to occur. 4) To search for the values of Tf, Mf, D, Nf, and Ta which give high prediction performance by the grid search method. The prediction performance is measured mainly by dAIC, which is defined as the difference of AIC for a stationary Poisson model and a model based on a foreshock activity, and additionally by alarm rate (AR: the fraction of mainshocks alarmed), truth rate (TR: the fraction of foreshock candidates followed by a mainshock), and probability gain (PG: the ratio of mainshock occurrence rate for predicted space-time to background occurrence rate).

3. Data and Results

By applying the above method to the earthquakes cataloged by JMA for the period of 1977 - 2013/06 in the Izu region (33.5N, 138.6E - 35.3N, 139.8E), we obtained the best parameters for foreshocks as Tf=3 days, Mf=3.0 D=0.2 degree, Nf=3, and Ta=5 days for the prediction of mainshocks with M>=5.0. The prediction performance is expressed as dAIC=473, AR=68% (=44/65), TR=23% (=46/196), and PG=225. We also confirmed that the distribution of interval time between foreshocks and mainshocks is better approximated by a power law like the modified Omori's aftershock distribution rather than an exponential distribution. The 26%(=20/77) of mainshocks that occurred within 5 days after the foreshocks have occurred within 4.8 hours after the foreshock. The distance distribution between foreshocks and mainshocks is also found to be better expressed by a power law. If we focus on the specific region of Off Ito (34.8N, 139.0E - 35.1N, 139.3E) where is one of the most active foreshock region, the prediction performance of the same foreshock definition measured by AR and TR, becomes as better as AR= 100% (=18/18) and TR= 37% (=15/41) with dAIC= 166, and PG= 105. As for the Off Ito region, the JMA have been operating an algorithm for predicting the swarm activity basing on the rate increase of volumetric strain observed near the region. When we compare the timing of issuing the prediction information about the swarm activity by the JMA with that of the occurrence of the foreshock defined above, we find that there is not much difference between them. This means that the foreshock activity in this region is strongly related to the crustal deformation before the mainshock.

Keywords: foreshocks, probabilistic prediction, prediction performance, alarm rate, truth rate, Izu region

Japan Geoscience Union Meeting 2014
(28 April - 02 May 2014 at Pacifico YOKOHAMA, Kanagawa, Japan)

SSS01-07 Room:419 Time:May 2 15:45-16:00

Foreshocks and short-term forecasting: comparisons between real seismicity and synthetic catalogs

OGATA, Yosihiko[1*]

[1]The Institute of Statistical Mathematics

Some of the statistical characteristics of foreshocks in the Japan Meteorological Agency (JMA) earthquake catalog are similar to those in synthetic catalogs simulated by the space-time epidemic-type aftershock sequence (ETAS) model or even the space-time nonhomogeneous Poisson process. However, they are quantitatively different from each other. Also, the information gain of a foreshock probability forecasting for real seismicity is significantly larger in comparison with that of synthetic catalogs. We discuss the reasons for such differences between the JMA and the synthetic catalogs.

Keywords: Foreshocks, short-term forecasting, JMA earthquake catalog, synthetic catalogs simulated by ETAS model, statistical characteristics of foreshocks, foreshock probability forecasting

Japan Geoscience Union Meeting 2014
(28 April - 02 May 2014 at Pacifico YOKOHAMA, Kanagawa, Japan)

SSS01-08 Room:419 Time:May 2 16:15-16:30

Modelling the effect of fault geometry on earthquake triggering

GUO, Yicun[2] ; ZHUANG, Jiancang[1*] ; ZHOU, Shiyong[2]

[1]Institute of Statistical Mathematics, [2]School of Earth and Space Sciences, Peking University

This study incorporates the rupture extensions of big earthquakes in the formulation of the Epidemic Type Aftershock Sequence model (ETAS) model, which is a point process model widely applied in the studies of spatiotemporal seismicity, rather than regarding every earthquake as a point in space and time. We apply the new model to the catalog from Sichuan province, China between 1990 and 2013, during which the Wenchuan Mw7.9 earthquake occurred in May 2008. Our results show that the modified model has better performance in both data fitting and aftershock simulation, confirming that the elliptical aftershock zone is caused by the superposition of isotropic triggering effects from each patch of the rapture extension. Also, using the technique of stochastic reconstruction, we found that the direct productivities of aftershocks from each patch on the mainshock fault are positively correlated to the slip distribution. We also confirm that the elliptical aftershock zone is caused by the superposition of isotropic triggering effects from each patch of the rapture extension.

Figure: (Left panel) Reconstruction results of aftershock productivity from each patch of Wenchuan mainshock fault based on the new ETAS model, which considers the rupture extension of large earthquakes instead of regarding all the earthquakes as point source. The values are in the logarithm scale. The Wechuan mainshock is marked by the black pentagon.
(Right panel) Contour image of the vertical component of the coseismic displacement distribution and isoseismal lines caused by Wenchuan mainshock.

Keywords: earthquake fault, ETAS model, earthquake forecast, aftershock

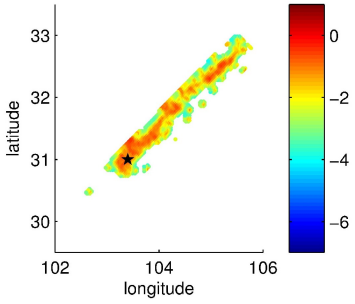

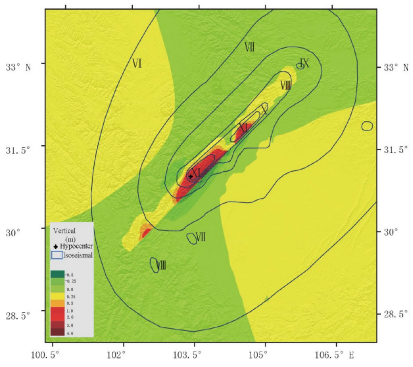

Japan Geoscience Union Meeting 2014
(28 April - 02 May 2014 at Pacifico YOKOHAMA, Kanagawa, Japan)

SSS01-09 Room:419 Time:May 2 16:30-16:45

History of network detection completeness in Japan

SCHORLEMMER, Danijel[1*] ; HIRATA, Naoshi[2] ; ISHIGAKI, Yuzo[3] ; NANJO, Kazuyoshi[2] ; TSURUOKA, Hiroshi[2] ; BEUTIN, Thomas[1] ; EUCHNER, Fabian[4]

[1]GFZ German Research Centre for Geosciences, 14473 Potsdam, Germany, [2]Earthquake Research Institute, University of Tokyo, Tokyo 113-0032, Japan, [3]Seismological and Volcanological Department, Japan Meteorological Agency, Tokyo 100-8122, Japan, [4]Institute of Geophysics, ETH Zurich, Zurich, Switzerland

An important characteristic of any seismic network is its detection completeness, which should be considered a function of space and time. Many researchers rely on robust estimates of detection completeness, especially when investigating statistical parameters of earthquake occurrence like earthquake rates. Contrary to traditional approaches, we do not estimate completeness using methods in which the completeness magnitude is defined as the deviation of the frequency-magnitude distribution from the linear Gutenberg-Richter relation. Here, we present a method based on empirical data only: phase data, station information, and the network-specific attenuation relation. For each station of the network we estimate a time-dependent distribution function describing the detection capability depending on magnitude and distance to the earthquake. For each point in time, maps of detection probabilities for certain magnitudes or overall completeness levels are compiled based on these distributions. Therefore, this method allows for inspection of station performances and their evolution as well as investigations on local detection probabilities even in regions without seismic activity.

We present a full history of network detection completeness for Japan and discuss details of this evolution. These results are compared with estimated completeness levels of other methods and with completeness levels in other regions of the World. We present scenario computations showing the impact of different possible network failures. All presented results are published on the CompletenessWeb (www.completenessweb.org) from which the user can download completeness data from all investigated regions, software codes for reproducing the results, and publication-ready and customizable figures.

Keywords: catalog completeness, earthquake recording, statistical seismology, earthquake statistics, earthquake forecasting, seismic hazard

Japan Geoscience Union Meeting 2014
(28 April - 02 May 2014 at Pacifico YOKOHAMA, Kanagawa, Japan)

SSS01-10 Room:419 Time:May 2 16:45-17:00

Collaboratory for the Study of Earthquake Predictability & Global Earthquake Model - Testing Center Software Development

BEUTIN, Thomas[1*] ; LIUKIS, Maria[2] ; MAECHLING, Philip[2] ; MAK, Sum[1] ; SCHORLEMMER, Danijel[1] ; YU, John[2]

[1]GFZ German Research Centre for Geosciences, 14473 Potsdam, Germany, [2]Southern California Earthquake Center, University of Southern California, Los Angeles CA 90089, USA

The Collaboratory for the Study of Earthquake Predictability (CSEP) aims to improve our understanding about the physics and predictability of earthquakes through rigorous and prospective testing of earthquake forecast models. CSEP operates four testing centers in California, New Zealand, Japan, and Europe running prospective, automated evaluations of more than 350 models. These testing centers are the technical infrastructure of CSEP and implement all procedures and protocols for rigorous testing and evaluation of earthquake prediction experiments. These experiments run in various testing regions and comprise forecast periods of one day to many years.

The CSEP testing center software system is the general infrastructure of all CSEP testing centers and is now being used for earthquake early warning systems, geodetic transient detectors, intensity prediction equations, and ground-motion prediction equations. We present the recent developments and introduce the structure of the software system.

Keywords: Earthquake forecasting, Seismic hazard, Statistical seismology, Earthquake statistics, Forecast testing, Software

Japan Geoscience Union Meeting 2014
(28 April - 02 May 2014 at Pacifico YOKOHAMA, Kanagawa, Japan)

SSS01-11 Room:419 Time:May 2 17:00-17:15

Lithospheric stress and deformation, and megathrust prediction

HONG, Tae-kyung[1*] ; LEE, Junhyung[1]

[1]Yonsei University, Department of Earth System Sciences, Seoul 120-749, South Korea

Lithospheres respond to stress load that is a major cause of earthquakes. Thus, understanding the lithospheric response before and during the megathrusts may allow us to find a way to predict megathrusts. We investigate the lithospheric responses for megathrusts with magnitudes greater than 8.7 since 2000 from precursory and coseismic events. The seismicity presents the cumulation or release of stress before and after megathrust, and discriminative spatial distribution of stress. Normal-faulting earthquakes were increased particularly around large slip regions at shallow depths after the megathrusts, which may be associated with lithospheric rebound and splay-fault development. The earthquake occurrence rate (b value) displays a characteristic slip-dependent feature. The earthquake occurrence rates were decreased with slip amount by forthcoming megathrust due to continuous accumulation of plate-driven stress and tectonic loading around the future rupture planes on slab

surface. The slip dependency of earthquake occurrence rates is enhanced with time until the occurrence of megathrust. The level of seismicity after megathrust is inversely proportional to that before megathrust, yielding the compatible average seismicity before and after megathrust over rupture regions regardless the slip amount of each subregion due to difference of accumulated stress depending the rock properties. It was also observed that the dynamic lithospheric response is highly associated with slip distribution on the rupture plane. Temporal changes of slip-amount-dependent b values are fitted well with an exponential function, suggesting an exponential increase of normal stress with time on locked region until the occurrence of megathrust.

Keywords: lithospheric stress, lithospheric deformation, megathrust, prediction, seismicity

Japan Geoscience Union Meeting 2014
(28 April - 02 May 2014 at Pacifico YOKOHAMA, Kanagawa, Japan)

SSS01-12 Room:419 Time:May 2 17:15-17:30

Global distribution of the earthquake-induced Schumann resonance anomalies

ZHOU, Hongjuan[1*] ; CAO, Bingxia[1] ; YU, Haiyan[1] ; QIAO, Xiaolin[1]

[1]Harbin Institute of Technology at Weihai, China

Schumann resonance (SR) is a global electromagnetic resonance phenomenon. Recently, SR anomalies before some earthquakes (EQs), which are considered to be concerned with the irregular disturbance of the lower ionosphere above the epicenters, are discovered. Although the examples are limited, we can see that the SR anomalies are usually different for different EQs. This paper concerns with the distinctions of SR anomalies observed at different locations for the same EQ, with the 2011 Magnitude 9.0 Tohoku-Oki EQ in Japan, before which significant SR anomalies have been observed in China, as an example.

Zhou et al. (2013) have found an anomalous SR affect observed at YS and AJ stations of China, associated with the Tohoku-Oki EQ. The anomalies were characterized by an increase in the intensity at frequencies from the first mode to the fourth mode in both magnetic field components, and the abnormal behaviors of the north-south magnetic field component primarily appeared at 0000-0900 UT 3 days prior to the main shock, about 2 h ahead of east-west magnetic field component. The above phenomena are shown in Figures 1 and 2. Figure 1 shows the deviations of the magnetic field amplitudes from the monthly averaged values observed at YS and QJ stations from 1 to 11 March 2011. Figure 2 shows the comparison of the amplitude differences of both magnetic fields on 8 March observed at YS station with 2 standard deviations which is calculated by the spectra over $\mp$15 days around 8 March, and the areas where the amplitudes are stronger than 2 standard deviations are marked with white. After the comparative analysis of the disturbed phenomena produced by the selected 10 sites shown in Figure 3 by numerical method with a locally EQ-induced disturbance model of the atmospheric conductivity in the day-night asymmetric Earth-ionosphere cavity, it is concluded that the SR anomalous phenomena before the Tohoku-Oki EQ have much to do with the excited sources located at South America and Asia marked with red circles in Figure 3.

Another 2 observing sites, with Sites 1 and 2 located at (N35^o, E137^o) and (N0^o, E110^o) respectively, are selected besides YS in order to compare the abnormal variations of SR magnetic fields observed at different locations under the same disturbance situation. The same simulation model and method as those in Zhou et al. (2013) are used, and the abnormal variations of both magnetic field spectra of SR observed at 3 sites are shown in Figures 4 and 5, with the source located at SA2 and AS4 as shown in Figure 3 respectively. It is obvious that the differences of the abnormal variations observed at different sites are distinct.

Further, Figures 6 and 7 show the global distributions of the anomalies for the first 3 modes of both SR magnetic field components under the excitation of the source SA2 and AS4 respectively. The color codes stand for the ratio of disturbed amplitude to the regular one, and the regions with green color represent the disturbed ratio lower than 1 and also include the possible nodal points which are the results of the simple model of point sources, while white to dark red colors represent the appearance of SR anomalies. It can be seen that the distribution of SR anomalies is very complicated, and is related to the relative locations of EQ epicenter, lightning currents and the observatories, and of course the EQ-induced disturbance of atmospheric conductivities.

The present simulations are done under the simple models of lightning and disturbed conductivity, which will be improved in the next studies.

Keywords: Schumann resonance, Tohoku-Oki earthquake, earthquake-induced Schumann resonance anomalies, day-night asymmetric Earth-ionosphere cavity

SSS01-12 Room:419 Time:May 2 17:15-17:30

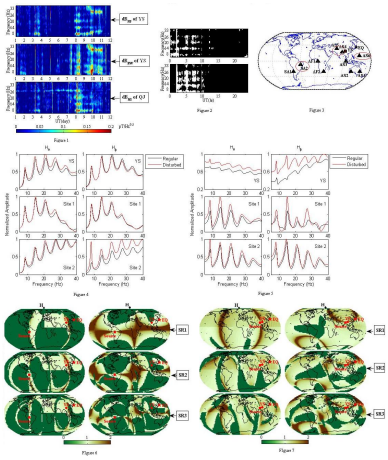

Japan Geoscience Union Meeting 2014
(28 April - 02 May 2014 at Pacifico YOKOHAMA, Kanagawa, Japan)

SSS23-01 Room:211 Time:May 1 09:00-09:15

Study on long strike-slip fault model with heterogeneous dynamic stress drops on asperities

OANA, Atsuko[1*] ; ISHII, Toru[1] ; DAN, Kazuo[1] ; FUJIWARA, Hiroyuki[2] ; MORIKAWA, Nobuyuki[2]

[1]Institute of Technology, Shimizu Corporation, [2]National Research Institute for Earth Science and Disaster Prevention

Oana *et al*. (2013) has established the long strike-slip fault model for a scenario earthquake along the Median Tectonic Line fault zone using the procedure for evaluating the fault parameters by Dan *et al*. (2011), and has simulated the strong ground motions. On that fault model, the dynamic stress drops on the asperities have been homogeneous. However, this is unnatural because the all stress drops on the asperities must be inhomogeneous in the actual earthquakes. How we consider the heterogeneity of the fault rupture is very important subject on the strong motion prediction, because the heterogeneity will have great effects on the spatial distribution of strong ground motions along a fault, especially along a very long fault. The uncertainty of the fault parameters also should be considered into the evaluation of the fault parameters.

In this study, for the strike-slip fault, the procedure for establishing the fault model which takes into account the heterogeneity of the dynamic stress drops on the asperities is examined, and then the spatial strong ground motions are simulated using the fault model based on the procedure. And also, some fault models with the uncertainty of the rupture starting point, the layout of the asperities, and the relationship between the asperity area and the dynamic stress drop on the asperity are established, and then the spatial strong ground motions are simulated using these fault models.

First, the procedure for establishing the fault model to give each asperity the heterogeneous dynamic stress drop is examined. Concretely, first, the probability density distribution of the stress drop is calculated based on the data of the stress drops on the strong motion generation areas of the past earthquakes by previous studies. And then, the procedure is proposed, that gives each asperity the dynamic stress drop corresponding to the frequency of the midpoint of the probability density distribution which is equally divided by the number of the asperity. Here, to satisfy the all relationships among the fault parameters of the asperity model is impossible. So we preceded satisfaction of the relationship formula of the seismic moment, and allowed an error between the obtained short period spectral level and the relationship formula of the short period spectral level. But the error became smaller than about 6 % of the short-period level of the fault model with the homogeneous dynamic stress drops on the asperities. As one of the ideas, we assumed that the relationship between the ratio of the asperity areas and the ratio of the dynamic stress drops on the asperities is random.

Next, for a scenario earthquake along the Median Tectonic Line fault zone, we established the long strike-slip fault model with the heterogeneous dynamic stress drops on the asperities based on the above proposed procedure, and also simulated the strong ground motions by the stochastic Green's function method. As a result, the deviation for the average of the attenuation relation by Si and Midorikawa (1999) of PGA became 0.20 and that of PGV became 0.16. Each deviation is smaller than 0.25, 0.23, which are derived from Si and Midorikawa (1999). It is concluded that this result is relevant, because the attenuation relation is based on a lot of observed records of various earthquakes and sites, while this study targets for the specific earthquake, the local pass, and the local site condition.

Finally, we examined the effect of the uncertainty of the source parameters for the strong ground motions. In the cases of the various rupture starting points, the deviation for the average of the attenuation relation of PGA became 0.23 and that of PGV became 0.21. In the cases of the various layouts of the asperities, those became 0.22 and 0.17, respectively. In the cases of the various relationships between the asperity area and the dynamic stress drop on the asperity, those bacame 0.20 and 0.17, respectively.

Keywords: Very long fault, Heterogeneity, Strong motion prediction

Japan Geoscience Union Meeting 2014
(28 April - 02 May 2014 at Pacifico YOKOHAMA, Kanagawa, Japan)

SSS23-02 Room:211 Time:May 1 09:15-09:30

Establishing procedure of evaluating fault parameters for predicting strong motions from intra-slab earthquakes with M8

ARAI, Kensuke[1*] ; DAN, Kazuo[1] ; ISHII, Toru[1] ; HANAMURA, Masaki[1] ; FUJIWARA, Hiroyuki[2] ; MORIKAWA, Nobuyuki[2]

[1]Shimizu Corporation, [2]National Research Institute for Earth Science and Disaster Prevention

For precise prediction of strong motions from intra-slab earthquakes, it is necessary to establish a new procedure of evaluating fault parameters based on the characteristics of intra-slab earthquakes. Although such studies had been conducted by Sasatani et al. (2006) and Dan et al. (2006), procedures of evaluating fault parameters were not fully validated by reproduction of the actual earthquake records. So, Arai et al. (2013) simulated the ground motions of the intra-slab earthquake that occurred off the coast of Miyagi Prefecture on April 7, 2011, and they pointed out the problem of existing procedures of evaluating fault parameters and suggested the ideas to overcome the problem. Hence, in this study, we simulated the ground motion of the intra-slab earthquakes with M8, the 1993 Kushiro-oki earthquake of January 15 (Mw 7.6) and the 1994 Hokkaido Toho-oki earthquake of October 4 (Mw 8.2), using the procedures of evaluating fault parameter proposed by Arai et al. (2013) and we pointed out the problem of the procedure.

In the case of the intra-slab earthquakes of the 1993 Kushiro-oki earthquake and the 1994 Hokkaido Toho-oki earthquake, there was a possibility that the results of evaluation of strong ground motions using the equation of the short period spectral level proposed by Sasatani et al. (2006) or Dan et al. (2006) became too small. So, we tried to use the procedures of evaluating fault parameter proposed by Arai et al. (2013). But, the fault model of the 1994 Hokkaido Toho-oki earthquake was unnatural because the short period spectral level of the earthquake estimated by Morikawa and Sasatani (2004) was too large. For this problem, we developed the new fault model using a method to reduce the fault area while increasing the short period spectral level. We also developed the fault model using a crack model.

We set fault models of the intra-slab earthquakes of the 1993 Kushiro-oki earthquake and the 1994 Hokkaido Toho-oki earthquake, which were derived from the relationships of intra-slab fault parameters by Sasatani et al. (2006), Dan et al. (2006), Arai et al. (2013), and the procedure developed here. And we also set the fault model using a crack model. By using these five fault models, we evaluated strong ground motions by the empirical Green's function method. As a result, in the case of the 1993 Kushiro-oki earthquake, ground motion evaluation results by using Sasatani et al. (2006) and Dan et al. (2006) were smaller than the actual records. On the other hand, ground motion evaluation results by using the Arai et al. (2013), the procedure developed here, and the procedure of using a crack model showed better agreements with the actual records. In the case of the 1994 Hokkaido Toho-oki earthquake, ground motion evaluation results by using Sasatani et al. (2006) and Dan et al. (2006) were smaller than the actual records. And ground motion evaluation results by using Arai et al. (2013), the procedure developed here, and the procedure of using a crack model were larger than the actual records especially in the period of 0.5 seconds or less. This may result from overestimation of the short period spectral level obtained by estimating the S-wave acceleration source spectrum by Morikawa and Sasatani (2004). Actually, the short period spectral level calculated from the fault parameters by Morikawa and Sasatani (2004) is smaller than the short period spectral level obtained by estimating the S-wave acceleration source spectrum. So, we will reconsider the short period spectral level of 1994 Hokkaido Toho-oki earthquake for setting fault models. In this study, we targeted the intra-slab earthquakes of the Pacific Ocean plate. The study on intra-slab earthquakes of the Philippine Sea Plate remains as a future subject.

Keywords: Intra-slab earthquakes, Strong motion prediction, Fault model

Japan Geoscience Union Meeting 2014
(28 April - 02 May 2014 at Pacifico YOKOHAMA, Kanagawa, Japan)

SSS23-03 Room:211 Time:May 1 09:30-09:45

Source effects of the intraslab and interplate earthquakes in Miyagi-ken-oki region based on spectral inversion

KASATANI, Naoya[1] ; KAKEHI, Yasumaro[1*]

[1]Faculty of Science, Kobe University

Previous studies showed that intraslab earthquakes generate stronger high-frequency waves than interplate earthquakes. For example, Satoh (2004) estimated the high-frequency levels of acceleration source spectra for seven intraslab earthquakes and four interplate earthquakes in Miyagi-ken-oki region. Their result showed the high-frequency level of intraslab earthquake is 3 to 4 times higher than that of interplate earthquake on the average. On the other hand, Katoh et al. (1999) estimated the excitation strength of high-frequency strong motions for intermediate-depth earthquakes based on the peak ground accelerations (PGA). Their result showed the focal depth is a key parameter controlling the PGA amplitudes rather than the difference of tectonic environments, such as intraslab or interplate earthquakes. Thus, the reason for the excitation strength of high-frequency waves of slab earthquake varies among studies, and this problem requires more precise investigation.

In this study, spectral inversion of NIED K-NET strong motion data is done to evaluate source effects of the intraslab and interplate earthquakes in Miyagi-ken-oki region. Then, seismic moments and corner frequencies are estimated from the evaluated source effects, and the high-frequency levels of the earthquakes are determined.

From the comparison between the intraslab and interplate earthquakes, the high-frequency levels of the former are 2 to 3 times higher than those of the latter. On the other hand, from the viewpoint of source depth, a clear trend is found that deeper earthquakes have higher high-frequency spectral levels. Here, it should be noted that the source depths of intraslab earthquakes are systematically larger than those of interplate earthquakes. Additionally, we find no significant difference between the spectral levels of intraslab and interplate earthquakes that have almost the same source depths. This is also seen for the difference between the spectral levels of upper-plane and lower-plane intraslab earthquakes.

Based on these results, we conclude (1) the trend that intraslab earthquakes have higher- high-frequency level than interplate earthquakes is apparent due to the fact that the former have systematically deeper source depths than the latter, and (2) the high-frequency level does not depend on the difference of tectonic environments, such as intraslab or interplate earthquakes, but on the source depth, and deeper earthquakes have higher high-frequency spectral levels. Difference of 4 times is seen between the high-frequency levels of deeper (˜80 km depth) and shallower (˜30 km depth) earthquakes for the depth difference of ˜50 km.

Finally, we pick up two factors, other than source-originated ones, that may effect the evaluation of the high-frequency level: effect of the waveform difference depending on source depth and depth-dependent Q-value structure. These effects are evaluated quantitatively, and we conclude that they cannot bring such biases as can change the above-mentioned trend of the high-frequency level. Thus, we have successfully enhanced the reliability of our interpretation that deeper earthquakes have higher high-frequency spectral levels.

Acknowledgments: The strong ground motion data recorded by K-NET, KiK-net, and F-net of National Institute of Earth Science and Disaster Prevention and the hypocenter data of the unified hypocenter catalogue by the Japan Meteorological Agency were used for the analysis.

Keywords: spectral inversion, high-frequency level, intraslab earthquake, interplate earthquake, focal depth

Japan Geoscience Union Meeting 2014
(28 April - 02 May 2014 at Pacifico YOKOHAMA, Kanagawa, Japan)

SSS23-04 Room:211 Time:May 1 09:45-10:00

Comparative study of the performance of source models for the 2011 Tohoku earthquake

NOZU, Atsushi[1*]

[1]Port and Airport Research Institute

The 2011 Tohoku, Japan, earthquake is obviously the first M9 earthquake which was recorded by dense strong motion networks such as K-NET, etc. Several source models have been proposed to explain strong ground motions from this earthquake. It is significantly important to evaluate the relative performance of these models, especially in the frequency of engineering importance. From engineering point of view, the most striking feature of strong ground motions of the Tohoku earthquake is the generation of strong-motion pulses in the frequency range from 0.2 to 1 Hz observed at many sites along the coast of Miyagi through Ibaraki Prefecture. It is significantly important to consider the generation of such pulses in the strong-motion prediction for mega earthquakes, especially when the prediction is aimed at seismic design of structures. To model strong motion pulses from the Tohoku earthquake, a source model including nine subevents with relatively small size (on the order of several kilometers) was developed (Nozu et al., 2012). The model is called the 'SPGA model'. On the other hand, several 'SMGA models' have been proposed for the same earthquake, in which larger subevents (on the order of several tens of kirometers) are considered. In this study, the errors between the synthetic and the observed ground motions are evaluated for each of these source models. The result clearly indicates that the SMGA model cannot reproduce strong ground motions in the frequency range from 0.2 to 1 Hz, which is characterized by strong-motion pulses. In this frequency range, the performance of the SPGA model is significantly better than the SMGA models. The SPGA model also reproduces the seismic intensity proposed by Sakai et al. (2002), which is in good agreement with the building damage. Based on such results, the author concludes that the SPGA model should be used to calculate strong ground motions for a future mega earthquake as long as the strong motion prediction is aimed at structural safety.

Keywords: mega earthquake, the Tohoku earthquake, source model, strong ground motion, SPGA model, SMGA model

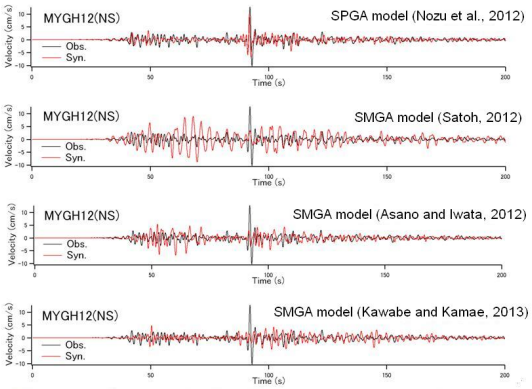

Observed (black) and synthetic (red) velocity waveforms (0.2 -1 Hz)
MYGH12, surface, NS

Japan Geoscience Union Meeting 2014
(28 April - 02 May 2014 at Pacifico YOKOHAMA, Kanagawa, Japan)

SSS23-05 Room:211 Time:May 1 10:00-10:15

A pseudo point-source model for off Miyagi intraslab earthquake on May 26, 2003

WAKAI, Atsushi[1*] ; NAGASAKA, Yosuke[1] ; NOZU, Atsushi[1]

[1]Port and Airport Research Institute

In a recent research, a pseudo point-source model, which is a simplified version of the conventional characterized source model, was proposed and it was verified that the source model can be applied to the 2011 Tohoku earthquake, Japan. In the source model, the spatio-temporal distribution of slip within each subevent is not modeled. Instead, the source spectrum associated with the rupture of each subevent is modeled. For the future application of the source model, it is important to investigate its applicability to other destructive earthquakes.

In this study, the off Miyagi intraslab earthquake on May 26, 2003 is taken as an example, and the applicability of the pseudo point-source model is investigated. It was revealed that the source model can reproduce the waveforms and the Fourier spectra at least as well as the conventional characterized source model.

Keywords: pseudo point-source model, intraslab earthquake, strong ground motion, the 2003 off Miyagi earthquake

Japan Geoscience Union Meeting 2014
(28 April - 02 May 2014 at Pacifico YOKOHAMA, Kanagawa, Japan)

SSS23-06 Room:211 Time:May 1 10:15-10:30

Strong ground motion simulation for the July 23, 2005 northwestern Chiba earthquake by pseudo point-source model

NAGASAKA, Yosuke[1*] ; NOZU, Atsushi[1] ; WAKAI, Atsushi[1]

[1]Port and Airport Research Institute

We propose a pseudo point-source model (Nozu, 2012) of the July 23, 2005 northwestern Chiba earthquake. The model is developed for the benchmark test (Hisada *et al*., 2013) in which various strong ground motion generation methods are compared.

In the pseudo point-source model, detailed spatiotemporal slip distributions within a subevent are not considered. Instead, the source spectrum associated with the rupture of each subevent is specified and it is assumed to follow the omega square model. This model has been applied for some earthquakes and shows good agreement with observations.

With this simplificationi, each subevent involves only six parameters, namely, longitude, altitude, depth, seismic moment, corner frequency and rupture time. In addition to these parameters, strike, dip and rake angles of the subevent are considered in this study in order to investigate the effect of radiation pattern while average value has been used in the previous studies. In this study, it is assumed that the theoretical radiation pattern becomes less evident with the increase of the hypocentral distance divided by the wavelength. This means that when the hypocentral distance is large of the wavelength is short, the radiation pattern is close to the average value rather than the theoretical value and vice versa. A new parameter Q_R is introduced to express this effect that determines how slowly the radiation pattern converges to the average.

The parameters for this particular earthquake are determined as follows. The hypocenter and the mechanism are from Koketsu and Miyake (2005). The seismic moment (=9.11×10^{17}Nm), the density (=3.2g/cm^3) and the S wave velocity (=4.46km/s) in the source region are from the F-net. The corner frequency (=0.75Hz) and Q_R(=10π) are determined so that the synthetic velocity waveforms and the Fourier spectra become consistent with the observations.

The site amplification factor for the K=net or KiK-net sites is from Nozu and Nagao (2005). For other sites (Building Research Institute and UR sites), the site amplification factors are newly determined by using the spectral ratio of the observed records between the target site and neighboring K=net or KiK-net stations. In terms of the Fourier phase information, we pick up 3 earthquakes before the main shock and chose the best one for each site.

As an example of the result, the synthetic Fourier spectra at 3 sites are compared with the observations (see the Figure).

Keywords: pseudo point-source model, benchmark test, the 2005 northwestern Chiba earthquake, radiation pattern, site amplification factor

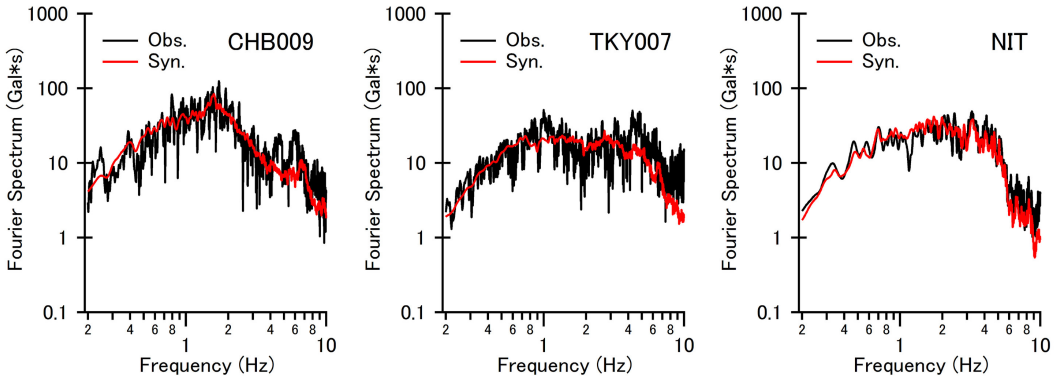

Comparison of acceleration fourier spectrum
(CHB009 and TKY007: K-NET station, NIT: BRI station)

Japan Geoscience Union Meeting 2014
(28 April - 02 May 2014 at Pacifico YOKOHAMA, Kanagawa, Japan)

SSS23-07 Room:211 Time:May 1 10:30-10:45

Three-dimensional grid modeling based on analysis of borehole data

KIMURA, Katsumi[1*] ; HANASHIMA, Yuki[2] ; NISHIYAMA, Shoichi[3] ; ISHIHARA, Yoshiro[4] ; SEKIGUCHI, Haruko[5]

[1]AIST, Geological Survey of Japan, [2]Smart Solution Corporation, [3]OYO Corporation, [4]Fukuoka University, [5]Kyoto University

The article presents a 3D geologic modeling method and applies it to build a subsurface 3D geologic model in the northern Tokyo and southern Nakagawa lowlands and the adjacent upland area. The modeling method, using borehole data for ground survey consists of (1) the surface modeling of the base of the Chuseki-so (the latest Pleistocene to Holocene incised-valley fill) , which has been improved by interpolating borehole data and (2) the 3D grid modeling of lithofacies and *N*-values constrained by the above surface model. The 3D grid model is very useful for not only geologic expression, but also the ground model of seismic response characteristics, because this can be converted to be S-wave velocity and density models.

Keywords: 3D model, ground, grid model, basal surface of the Chuseki-so, Tokyo lowland, borehole data

Japan Geoscience Union Meeting 2014
(28 April - 02 May 2014 at Pacifico YOKOHAMA, Kanagawa, Japan)

SSS23-08 Room:211 Time:May 1 11:00-11:15

Three-dimensional structure model for modeling strong motion around the Ryukyu arc

FUJIOKA, Akira[1] ; TAKENAKA, Hiroshi[2*] ; YAMADA, Nobuyuki[3] ; NAKAMURA, Takeshi[4] ; OKAMOTO, Taro[5] ; FUJIWARA, Hiroyuki[6]

[1]Kyushu Univ., [2]Okayama Univ., [3]Kyushu Univ. of Education, [4]JAMSTEC, [5]Tokyo Institute of Technology, [6]NIED

The Ryukyu Islands have frequently been damaged by large earthquakes and tsunamis since ancient times. For instance, in 1771, gigantic tsunamis are occurred from an earthquake and more than 12000 people died in Yaeyamya Islands. From the point of view of disaster prevention, it is also important to improve the precision of strong ground motion prediction. Here we build a 3D numerical structure model for modeling of strong ground motion, which includes land and ocean-bottom topographies and a seawater layer as well as subsurface structures of the arc side and the PHS slab, partially based on the J-SHIS model for near-surface structure (NIED) and a slab-top depth model of the PHS (Headquarters for Earthquake Research Promotion, Japan). We then try to improve the near-surface structure model in the islands using our original microtremor surveys. We also conduct numerical simulations of seismic motions for three sub-oceanic earthquakes occurring near the Amami Islands, Okinawa Island and Miyako Island to confirm the applicability of the constructed structure model and to check the improvement of the near-surface model.

Keywords: Ryukyu arc, strong motion, simulation

Japan Geoscience Union Meeting 2014
(28 April - 02 May 2014 at Pacifico YOKOHAMA, Kanagawa, Japan)

SSS23-09 Room:211 Time:May 1 11:15-11:30

3-D sedimentary layers model and simulation of seismic motions around the Tachikawa fault zone

SAGUCHI, Koichiro[1*] ; CHIMOTO, Kosuke[1] ; YAMANAKA, Hiroaki[1]

[1]Interdisciplinary Graduate School of Science and Engineering, Tokyo Institute of Technology

Tachikawa fault is one of the most activity faults in the western part of the Tokyo metropolitan area. Strong motion estimation is necessary to know the possible damage due to rupture of the fault considering effects of geological structure. However, a three-dimensional subsurface structural model is not well tuned in the vicinity of the fault.

In this study, we estimated a three-dimensional structure of deep sedimentary layers around the Tachikawa fault zone using Rayleigh wave phase velocity and horizontal-to-vertical spectrum obtained from microtremor explorations and receiver functions from the obtained records of the K-NET, KiK-net and SK-net. And we simulated seismic ground motions around the Tachikawa fault zone using the three-dimensional finite difference method to validate of a three-dimensional structure of deep sedimentary layers.

To accomplish it, we first conducted the array observations of microtremors at 12 sites around the Tachikawa fault. Rayleigh-wave phase velocity at periods from 0.5 to 5.0 seconds was estimated from a frequency-wave number spectral analysis of the microtremors. We next conducted the observations of microtremors at 268 sites on nine lines across the Tachikawa fault zone. Predominant periods of the H/V spectrum clearly indicated differences of subsurface structure across the Tachikawa fault.

Then, we conducted the joint inversion of the phase velocity and the receiver function to a P and S-wave velocity profile based on the simulated annealing method. P-wave velocities, S-wave velocities and thickness of individual layers are inverted very well, and the S-wave velocities of the inverted profile are 0.5, 0.9, 1.5, 2.4 and 3.2km/s. We constructed a three-dimensional structures of the deep sedimentary layers in this area from integrating the 1-D S-wave velocity profiles at all the stations. The basement depth at hanging-wall side of the Tachikawa fault is larger than that at foot-wall side with a difference of about 1.7km in the 3-D model.

Finally, we simulated seismic ground motions around the Tachikawa fault zone using the three-dimensional finite difference method considering three-dimensional velocity structure down to 50km. The results indicate that the maximum accelerations in simulated waveforms were similar to the observed one.

Keywords: Tachikawa fault zone, array microtremor exploration, Rayleigh wave phase velocity, 3-D sedimentary layers model, 3-Dfinite difference method

Japan Geoscience Union Meeting 2014
(28 April - 02 May 2014 at Pacifico YOKOHAMA, Kanagawa, Japan)

SSS23-10 Room:211 Time:May 1 11:30-11:45

DETERMINATION OF S-WAVE VELOCITY STRUCTURE BY MICROTREMOR ARRAY OBSERVATION IN TEKIRDAG AND ZEYTINBURNU (TURKEY)

KARAGOZ, Ozlem[1*] ; CITAK, Seckin ozgur[2] ; CHIMOTO, Kosuke[1] ; YAMANAKA, Hiroaki[1] ; OZEL, Oguz[3] ; YALCINKAYA, Esref[3] ; ZANEIH, Hussam[1] ; ASKAN GUNDOGAN, Aysegul[4] ; KAOURU, Kojima[1] ; TOMOHIRO, Tsuchiya[1] ; AKSAHIN, Behiye[3] ; ILKAY, Sena[3] ; SISMAN DERAN, Fatma[4]

[1]Interdisciplinary Graduate School of Science and Engineering, Tokyo Institute of Technology, [2]Japan Agency for Marine-Earth Science and Technology (JAMSTEC), [3]Istanbul University,Department of Geophysical Engineering, Turkey, [4]Middle East Technical Uni.,Dept .of Civil Engineering and Dept. of Earthquake Studies,Turkey

The use of environmental vibration recordings (microtremors) is cost effective and easily collected data for site characterization that is a component of microzonation mapping and has become very popular around the world in the last years.

Local site conditions have a major effect on the level of ground shaking. For this reason we carried out microtremor measurements by using circular small array configuration at twenty one locations in Tekirdag, four locations in Zeytinburnu and one location in Yesilkoy. In addition to eight large array measurements for estimating S-wave velocity structures of shallow deeper soil formations for site effect analysis. These sites were selected by considering the different geological units (i.e. recent landfill, clay stone, silt stone, alluvium, lime stone, sand) in the cities. We also collected data on five buildings in Tekirdag in order to understand dynamics properties of buildings.

We estimated the phase velocities of Rayleigh waves at each site from the vertical components of recorded microtremor data by using Spatial Autocorrelation (SPAC) method. Obtained phase velocity dispersion curves are varied from area to area. The obtained phase velocities range from 100 m/s to 750 m/s along the coastline in Tekirdag while, they range from 200 m/s to 500 m/s for Zeytinburnu area.

Genetic Simulated Annealing Algorithm technique was applied for inversion of phase velocities to estimate 1-D S-wave velocity structures beneath the sites. The inverted Vs profiles are not uniformed. The preliminarily results show that similar phase velocity changes have been seen at the low and the high periods on the different geological units along the parallel direction of the coastline. When we check the velocity changes from coastline toward the inland, we can see the different phase velocities on the different geological units.

Keywords: Microtremor, Spac, S-wave velocity, Tekirdag, Zeytinburnu, Turkey

Japan Geoscience Union Meeting 2014
(28 April - 02 May 2014 at Pacifico YOKOHAMA, Kanagawa, Japan)

SSS23-11 Room:211 Time:May 1 11:45-12:00

Characteristics of long-period strong ground motion in the Keihin-area during the 2011 Tohoku earthquake

UETAKE, Tomiichi[1*]

[1]Tokyo Electric Power Company

The velocity response spectra of 5% damping calculated from the observed data in the Keihin area during the 2011 Tohoku Earthquake had no significant peak at period of around 8 s and had peak over 100cm/s at period of around 3 s. The acceleration seismograms had spindle-shaped envelope and peak accelerations were recorded about 120 s after S-wave on-set. The maximum velocity response at period of around 3 s was recorded in the first half part of waveforms. It is important to realize the difference of wave propagation characteristics between in the first half part and the later part of the waveforms. In this article, the propagation characteristics of long-period strong ground motions during the 2011 Tohoku Earthquake were studied by semblance analysis using the data observed in the Keihin area.

Sixteen strong motion observatories in the Keihin area were used for array analysis. The major axis of the array area is about 18 km and minor axis is about 9km. Distance between adjacent observation points is from 0.6km to 5km. We performed semblance analysis using narrow-band pass filtered waveforms and evaluated the phase velocity for each time sections from the peak point of semblance in slowness plane. The center periods of the filters were 1, 2, 2.5, 3, 4, 5, 6, 7, 8, 9, 10, 12, 15 and 20 s. The length of time window for analysis was 20 s and the time windows were opened every 10 s in wave traces.

The peak semblance values were high for longer period waveforms and were lower value for short period waveforms. The value at period of 1 and 2s were lower than 0.5. The values calculated from large array data were lower than those from small array data. The semblance values in first part of waveform were high but the values in the later part show lower value. The phase velocities in first half part are over 3 km/s for all case. The phase velocities in later part were 1 to 2 km/s and showed the dispersion characteristics. The back azimuths of wave propagation in the first part indicated the epicenter direction but those in later part did not indicate constant direction especially in short period range.

To examine the relation between this dispersion characteristics and underground structure, we calculated phase velocities of surface waves using the underground structure model. The phase velocities evaluated in the first part were faster than phase velocity of the fundamental mode. The phase velocities evaluated for several last time windows in the later part coincided with the phase velocity of the fundamental mode. These characteristics are similar to the results from the data observed the Tokyo lowland area [Uetake (2013)].

Judging from the property of the acceleration waveform and a result of the semblance analysis, the waves caused large response in a period of 2-3 s were more likely to be a body wave not a surface wave of the fundamental mode.

The strong ground motion data used in this study were observed by TEPCO, K-NET of NIED, ERI, JMA, Tokyo Metropolitan office and Yokohama-City. I appreciate these organizations for making the data be available.

Keywords: Long-period strong ground motion, the 2011 Tohoku earthquake, Semblance analysis, Phase velocity, Keihin area

Japan Geoscience Union Meeting 2014
(28 April - 02 May 2014 at Pacifico YOKOHAMA, Kanagawa, Japan)

SSS23-12 Room:211 Time:May 1 12:00-12:15

Characteristics of Long-period Ground Motion in the Osaka Sedimentary Basin due to the 2011 Great Tohoku Earthquake

SATO, Kayoko[1*] ; IWATA, Tomotaka[1] ; ASANO, Kimiyuki[1] ; KUBO, Hisahiko[1] ; AOI, Shin[2]

[1]Disaster Prevention Research Institute, Kyoto University, [2]National Research Institute for Earth Science and Disaster Prevention

The 2011 great Tohoku earthquake (Mw 9.0) occurred on March 11, 2011, and the largest aftershock (Mw 7.7) occurred in the Ibaraki-oki region, adjacent to south boundary of the mainshock's source region. Long-period ground motions (2?10s) of large amplitude were observed in the Osaka sedimentary basin about 550-800km away from the source regions during both events. We collected the strong motion records in and around the Osaka basin and analyzed the long-period ground motions. The amplitude of horizontal components of the ground motion at the site-specific period is amplified at each sedimentary station and its duration is prolonged. The predominant period is around 7s in the bayside area inside the Osaka basin where the largest pSv among the stations inside the Osaka basin were observed. The pSvs at the bedrock sites surrounding the Osaka basin also have their peak values around 7s.

Then, we focus on the propagation characteristics from the source region to the Osaka basin. We compared the pSvs of 7s at the sedimentary stations in the Osaka basin with those in the Kanto basin. The maximum pSv among the Osaka basin is comparable to the maximum pSv among the Kanto basin whose fault distance is about 500km nearer than the Osaka basin. Moreover, the amplitude of observed pSvs is systematically larger than prediction from the empirical attenuation relationship by Kataoka et al. (2008) at non-sedimentary stations in the region between the Nobi and Osaka basins. The large long-period ground motions in the Osaka basin might be generated by the combination of propagation-path and basin effects.

Thus, we simulate ground motions due to the largest aftershock using the three-dimensional Finite Difference Method (GMS; Aoi and Fujiwara, 1999). The reason we use the largest aftershock is that this event has a relatively small rupture area and simple rupture process compared to the mainshock. The size of the model space is 730km (EW) x 330km (NS) x 100km (Vertical) including the source region and the Osaka basin. A three-dimensional velocity structure model based on the Japan Integrated Velocity Structure Model (Koketsu et al., 2008, 2012) is assumed. The minimum S-wave velocity is 350m/s and the grid spacing in the sedimentary layers is 200m for horizontal direction and 100m for vertical direction, respectively. The minimum effective period in this computation is 3s. We estimated a point source using the long-period ground motions (4-10s) at a station close to the source region (KiK-net CHBH14) and used it for our simulation.

We compared the synthetic and observed waveforms in the periods of 4-10s. As well as the observed ones, the amplitude of synthetic waveforms was amplified and the durations were prolonged at the sedimentary stations in the Kanto basin, the Nobi basin and the Osaka basin. The feature of the attenuation relations in the region between the Nobi basin and the Osaka basin was qualitatively reproduced. At the period of 7s, the amplitudes of synthetic waveforms were little underestimated in the Osaka basin.

Finally, we simulate the ground motion during the mainshock. The model space is 730km (EW) x 400km (NS) x 100km (Vertical). The grid interval and velocity structure model are same as those for the largest aftershock. We assume two point sources based on the two southern SMGAs of the four SMGAs estimated by Asano and Iwata (2012). As a result of the simulation, the synthetic waveforms reproduced the observed ones qualitatively. Therefore, we conclude that the large long-period ground motions in the Osaka basin during both events mainly resulted from the combination of those two SMGAs, propagation-path and basin effects.

ACKNOWLEDGEMENTS

We used strong motion data recorded by K-NET, KiK-net and F-net of NIED, CEORKA, BRI, JMA, and Osaka prefecture. GMS provided by NIED is used for the computation.

Japan Geoscience Union Meeting 2014
(28 April - 02 May 2014 at Pacifico YOKOHAMA, Kanagawa, Japan)

SSS23-13 Room:211 Time:May 1 12:15-12:30

Long-period ground motion evaluation for the Nankai Trough megathrust earthquakes

MAEDA, Takahiro[1*] ; MORIKAWA, Nobuyuki[1] ; AOI, Shin[1] ; FUJIWARA, Hiroyuki[1]

[1]NIED

We evaluate long-period ground motions associated with the Nankai Trough earthquakes (M8~9) in southwest Japan. Large interplate earthquakes occurring around the Nankai Trough have caused serious damages due to strong ground motions and tsunami. Such large interplate earthquake potentially causes damages to high-rise and large-scale structures due to long-period ground motions. The long-period ground motions are amplified particularly on sedimentary basins, where big cities have been established. Therefore it is important to evaluate long-period ground motions as well as strong motions and tsunami for the anticipated Nankai Trough earthquakes.

The long-period ground motions are evaluated by the finite difference method (FDM) using " characterized source models " and the 3-D underground structure model. The parameters of the characterized source model are determined based on a " recipe " for predicting strong ground motion [Earthquake Research Committee (ERC), 2009]. We construct various source models (more than 300 scenarios) assuming various possible source parameters, including rupture area, asperity configuration, and hypocenter location. Each source region is determined by " the long-term evaluation of earthquakes in the Nankai Trough " published by ERC. The asperity configuration and hypocenter location control the rupture directivity effects. These parameters are important because our preliminary simulations are strongly affected by the rupture directivity (Maeda et al., 2013). We apply the system called GMS (Ground Motion Simulator) for simulating the seismic wave propagation based on 3-D FDM scheme using discontinuous grids (Aoi and Fujiwara, 1999) to our study. The 3-D underground structure model used in the FD simulation is the Japan integrated velocity structure model (ERC, 2012).

We evaluate the long-period ground motions using the peak ground velocity (PGV) and velocity response spectra (Sv). The simulation shows a large variation of PGV and Sv at a site. The large variation is important to understand the seismic hazard. The variation at the Kanto region, an eastern extension of the source area, seems larger than those at the Nobi and Osaka regions. The scenarios with wider source area have larger PGV and Sv than those with smaller source area. The large number of simulations of this study allows us to select scenarios that correspond to representative (e.g. average and maximum) response spectra at each site.

Keywords: Nankai Trough, long-period ground motion, megathrust earthquake, hazard assessment, GMS

Japan Geoscience Union Meeting 2014
(28 April - 02 May 2014 at Pacifico YOKOHAMA, Kanagawa, Japan)

SSS23-14 Room:211 Time:May 1 12:30-12:45

Long-period ground motion evaluation for the Sagami Trough megathrust earthquakes

MORIKAWA, Nobuyuki[1*] ; MAEDA, Takahiro[1] ; IWAKI, Asako[1] ; IMAI, Ryuta[2] ; AOI, Shin[1] ; FUJIWARA, Hiroyuki[1]

[1]National Research Institute for Earth Science and Disaster Prevention, [2]Mizuho Information & Research Institute, Inc.

It is important to assess seismic hazard in consideration of uncertainty and occurrence frequency in order to mitigate disasters from future earthquake. Iwaki et al. (2013) examined the influence of the long-period ground motion on uncertainty of asperity (strong motion generation area) or hypocenter location, and the heterogeneity of rupture velocity or slip direction for megathrust earthquakes occurring at the Sagami Trough region. They showed that the asperity or hypocenter location largely affects to the amplitude and predominant period of simulated long-period ground motions. Based on their results, we simulate long-period ground motions by a large number of source models considering the uncertainty of asperity or hypocenter location, and we try to assess long-period ground motion due to megathrust earthquakes occurring at Sagami Trough by evaluating the simulation results statistically.

We set ten source regions containing Taisho and Genroku earthquakes by changing those from Iwaki et al. (2013) referring the model by Central Disaster Council (2013). The range of moment magnitude (Mw) is 7.9 to 8.6 and total number of source model is more than 150. We use a ”characteristic source model” and source parameters are evaluated by following the method in ”Recipe” by Headquarters of Earthquake Research Promotion of Japan. We use a velocity structure model by Earthquake Research Committee (2012) but we revise the topography of the Philippine Sea plate based on recent researches. The long-period ground motions are simulated using a 3D finite difference method with discontinuous grid coded by Aoi and Fujiwara (1999). As long-period-ground motion hazard assessment, we first calculate average and slightly large (i.e. +1 sigma; sigma is the standard deviation) amplitude of peak velocity and velocity response spectrum whose natural period is 5, 7 and 10 seconds respectively on engineering bedrock for every ten source region. And then we integrate them by assuming the ”weight” which corresponds to occurrence frequency of each source region.

Although a large number of source models are set up in this study, the uncertainty on the megathrust earthquake occurring at Sagami Trough cannot be covered completely. So it should be required to examine much source models. On the other hand, the source region of magnitude 8-class earthquake at Sagami Trough extends to beneath the metropolitan area. In addition, it is said that the occurrence of the magnitude 7-class earthquake, which does not take in this study, is imminent in southern Kanto region. It is necessary to advance broadband ground motion hazard assessment also including a short-period ground motion.

Keywords: long-period ground motion, seismic hazard assessment, Sagami Trough, megathrust earthquake, GMS

Japan Geoscience Union Meeting 2014
(28 April - 02 May 2014 at Pacifico YOKOHAMA, Kanagawa, Japan)

SSS23-15 Room:211 Time:May 1 14:15-14:30

Emplical ground motion model for long period motions and for long distance -Distance dependent geometrical spreading ter

MOTOKI, Kentaro[1*] ; KATO, Kenichi[1]

[1]Kobori Research Complex Inc.

The GMPEs have been proposed by Sato et al.(2012), Kataoka et al.(2008), and Yuzawa and Kudo(2011). For predictions of long period ground motions on Kanto Plain for the Nankai Trough mega earthquake, the proposed GMPEs cannot be adopted because of the deficiency of applicable distance ranges. In order to establish an adoptable GMPE for long distance, we investigate the distance dependent geometrical spreading term.

We used records for magnitude equal to or greater than 5.0 and distance less than 1000 km. The dataset used in this study is provided by F-net, because of high sensitivity for long period motions and continuous recordings. Since the F-net stations can be regarded as hard rock sites, the site term was not taken into account in the regression.

First, we use a constant geometrical spreading and anelastic attenuation for distance. The regression curve at the 20sec of period decays more slowly than the average of records in the short distance less than 100km, and decays more steeply than records in the longer distance. It implies that the GMPE with a constant geometrical spreading term may underestimate near the source region and in the longer distance.

In the long period range, the dominance of seismic wave changes from the body wave to the surface wave according to the travelling distance, and the slope of the geometrical spreading depends on distance. We will evaluate the geometrical spreading term in the separated distance range to reveal how the geometrical spreading changes.

Keywords: long period motions, long distance, geometrical spreading

Japan Geoscience Union Meeting 2014
(28 April - 02 May 2014 at Pacifico YOKOHAMA, Kanagawa, Japan)

SSS23-16 Room:211 Time:May 1 14:30-14:45

Long-Period Ground Motion Prediction Equations and Their Application to the Magnitude Estimation of Large Earthquakes

IBRAHIM, Rami[1*] ; SI, Hongjun[1] ; KOKETSU, Kazuki[1] ; MIYAKE, Hiroe[1]

[1]Earthq. Res. Inst., Univ. Tokyo

We developed long-period ground motion prediction equations (GMPEs) for peak ground velocities (PGVs) and peak ground displacements (PGDs) in a period range of 5-30 s. We only used strong motion data of KiK-net downhole stations located in layers of shear-wave velocities equal to or greater than 2000 m/s. We confirmed that the site effects due to surface geology for long-period PGVs and PGDs can be ignored at these observation stations. The dataset consists of 20 earthquakes of $6 \leq M_w \leq 9.1$ occurred in and around Japan. Two-stage regression analyses were carried out to derive the GMPEs. We fit the data with bilinear regression lines bending at M_w 7.5. Additional factors of focal depth and earthquake type were found to enhance the fitting with the observed data. Our developed long-period GMPEs predict the PGVs and PGDs of crustal earthquakes are larger than those of inter-plate and intra-plate earthquakes. The attenuation coefficients presented in the current study indicate that the long-period PGVs and PGDs increase by increasing depth.

We used the long-period GMPEs developed in this study to estimate the moment magnitude by fitting observed PGVs and PGDs at period range of 5-30 s with GMPEs. We estimated the magnitudes of the same 20 earthquakes and the 2013 Awaji Island earthquake (M_w 5.8) recorded by downhole accelerometers of KiK-net. The results are consistent with the moment magnitudes from the Global CMT project. The method is useful to estimate the magnitude of giant earthquakes such as the 2011 Tohoku earthquake (M_w 9.1). The proposed method can estimate the moment magnitude quickly if information of source area is available.

Keywords: long-period ground motion, ground motion prediction equation, moment magnitude, PGV, PGD

Japan Geoscience Union Meeting 2014
(28 April - 02 May 2014 at Pacifico YOKOHAMA, Kanagawa, Japan)

SSS23-17 Room:211 Time:May 1 14:45-15:00

Evaluation of random errors of displacements and velocities from strong motion records

XU, Peiliang[1]*

[1]Disaster Prevention Research Institute, Kyoto University

Strong motion accelerographs have been deployed worldwide to monitor the ground shaking of the Earth and the recorded accelerograms have been used to recover the velocities and displacements by integration. In spite of their fundamental importance in seismology and earthquake engineering, few works address the error estimates of the derived velocities and displacements. Although accelerographs have been used to compute velocity and displacement waveforms for more than 80 years, we show that no publications on error estimates of computed velocity and displacement waveforms are correct from the statistical point of view. We show that the error estimates of the velocities and displacements obtained from accelerograms in the earthquake literature approach to zero as the sampling interval of accelerographs tends to zero; those are erroneous from the statistical point of view. As a result, we present a set of formulae to correctly estimate the errors (or variances)of the integrated velocities and displacements from accelerograms. In addition, we also derive the covariances between the velocities and displacements.

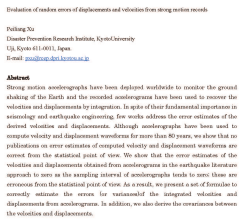
Evaluation of random errors of displacements and velocities from strong motion records

Peiliang Xu
Disaster Prevention Research Institute, Kyoto University
Uji, Kyoto 611-0011, Japan.
E-mail: pxu@rcep.dpri.kyoto-u.ac.jp

Abstract

Strong motion accelerographs have been deployed worldwide to monitor the ground shaking of the Earth and the recorded accelerograms have been used to recover the velocities and displacements by integration. In spite of their fundamental importance in seismology and earthquake engineering, few works address the error estimates of the derived velocities and displacements. Although accelerographs have been used to compute velocity and displacement waveforms for more than 80 years, we show that no publications on error estimates of computed velocity and displacement waveforms are correct from the statistical point of view. We show that the error estimates of the velocities and displacements obtained from accelerograms in the earthquake literature approach to zero as the sampling interval of accelerographs tends to zero; those are erroneous from the statistical point of view. As a result, we present a set of formulae to correctly estimate the errors (or variances)of the integrated velocities and displacements from accelerograms. In addition, we also derive the covariances between the velocities and displacements.

Japan Geoscience Union Meeting 2014
(28 April - 02 May 2014 at Pacifico YOKOHAMA, Kanagawa, Japan)

SSS23-18 Room:211 Time:May 1 15:00-15:15

Earthquake detection from strong ground motion observation network in Himalaya, India

MASUDA, Tetsu[1*] ; KOKETSU, Kazuki[1] ; TAKANO, Kiyoshi[2] ; FURUMURA, Takashi[2] ; OKI, Satoko[3] ; ITO, Takamori[3] ; CHADHA, Rajender kumar[4] ; SRINAGESH, Davuluri[4] ; SRINIVAS, Dakuri[4]

[1]Earthquake Research Institute, [2]University of Tokyo, [3]Keio University, [4]National Geophysical Research Institute

It is an important subject to establish the technical issues and environment of data acquisition and analysis of natural hazards for the disaster mitigation, the first aid and recovery planning. The Indo-Japanese collaborative project on 'Information Network for Natural Disaster Mitigation and Recovery' of 'Science and Technology Research Partnership Sustainable Development International Collaborative Research Program' supported by JST and JICA, Japan initiated strong ground motion observation, crustal movement measurement, and building vibration measurement in Indo-Gangetic plain and foot hills of Himalaya, India.

We started the strong ground motion observation network with deployment of broadband velocimeters and digital equipments at 26 sites near the seismic active region in Himalaya, India by October 2012. The continuous time history of ground motion is digitally recorded with high resolution. Because of the broadband response of the sensor and the high resolution of the recorder, it is expected that the long- period motions or weak ground motions from small local earthquakes and distant earthquakes will be recorded as well as the short-period strong ground motions. It is a necessary task for the seismic data analysis to detect earthquakes using continuous records from the network. In this paper, we present a method developed for fast and precise earthquake detection from continuous records of the network.

The stations of the network are located in the compounds of local schools. The ambient noise is not always low but it changes as well as contains abrupt increases. We developed a detection method with simple algorithm adequate for the noisy circumstances. We compared our detections with the earthquakes reported in the NEIC catalogue. Our results show that the network detected all earthquakes of magnitude 7 or more, more than 90% of magnitude 6.5 through 6.9, more than 50% of magnitude 6.0 through 6.4 regardless of epicentral distances, and more than 80% of magnitude 6 or more from epicentral distances less than 100 degrees.

Several local earthquakes with short S-P times which were not reported in the NEIC catalogue were also detected by the network. Local seismicity is an index of the stress status, and detection of local earthquakes is important to understand the stress distribution in a small region. The preliminary results show that the network will provide data from local and global earthquakes to study the local seismic activity in the Himalayan region, the propagation path effects from the source to the stations, amplification effects at sites, the physical process of the seismic source, and subsurface velocity structure.

Keywords: strong ground motion, observation, network, earthquake detection

Japan Geoscience Union Meeting 2014
(28 April - 02 May 2014 at Pacifico YOKOHAMA, Kanagawa, Japan)

SSS23-19 Room:211 Time:May 1 15:15-15:30

Liquefaction damage expansion caused by the generation of surface waves from base end section

NAKAI, Kentaro[1*] ; NODA, Toshihiro[1] ; MURASE, Kotaro[1] ; ASAOKA, Akira[2] ; SAWADA, Yoshihiro[2]

[1]School of Engineering, Nagoya University, [2]Association for the development of earthquake prediction

The 2011 off the Pacific coast of Tohoku Earthquake caused liquefaction to occur in reclaimed lands in Urayasu City and in other wide areas of reclaimed land along Tokyo Bay. One of the important characteristic of the observed liquefaction damage is that the level of liquefaction damage was nonuniform spatially, and the variation in the damage levels was large. The difference in damage levels in various parts has often been explained by the presence/absence of past ground improvement and by the difference in the dates of reclamation work. From the boring survey at Urayasu, thin layer of soft alluvial clay is located directly under the liquefiable layer on the inland side where liquefaction damage was small. However, the basement layer is inclining towards coast side and alluvial clay layer is increasing in thickness as approaching to the coast where liquefaction damage was severe. This paper examines the cause of extensive and nonuniform liquefaction damage observed in Urayasu City by focusing attention on the stratum inclination at the deeper part of the liquefiable layer with the use of 2D elasto-plastic seismic response analysis of the multi-layer ground. The analysis code employed in this report was the soil-water coupled finite deformation analysis code GEOASIA (Noda et al. 2008), which incorporates an elasto-plastic constitutive model (SYS Cam-clay model; Asaoka et al. 2002) that allows description of the behavior of soils ranging from sand through intermediate soils to clay under the same theoretical framework.

Fig.1 (a) illustrates the velocity vector distribution 50 sec after earthquake occurrence. Only the area around the sloped part is shown in this figure, and the scale in the vertical direction has been magnified by 2 times. Surface waves generate at the base end section of the inclination which shows orbit in a counterclockwise direction with ongoing wave propagation to the right-hand side. Excess pore water pressure ratio at the liquefiable layer is shown, superimposing the result of 1D analysis with same stratigraphic composition at the point. 2D analysis result shows liquefaction (excess pore water pressure ratio is greater than 0.95), even 1D analysis did not liquefy (Fig.1 (b)). In the case of 2D analysis, in addition to the magnitude, duration time of the oscillation increases in subsurface layer accompanied by the generation of surface waves (Fig.1 (c)). Excess pore water pressure ratio of 2D analysis continues to increase for a long period even after the primary earthquake motion. Fig.1 (d) illustrates the shear strain distribution 200 sec after earthquake occurrence. Although shear strains are small in the non-inclined horizontal strata, large strains are produced in the subsurface liquefiable layer. Furthermore, this strain distribution is nonuniform and localized even assuming homogeneous initial conditions for subsurface layer. The nonuniform, localized shear strain are due to the existence of the sloped boundary. In other words, in addition to the vertical component of seismic movement being generated by the stratum slope, multi-dimensional propagation is also exhibited because of complex reflection behavior in the diluvial layer. Moreover, in sloped layers such, the danger of liquefaction is increased compared with the one-dimensional model. The actual liquefaction damage observed in Urayasu City was heavy in the sloped stratum locations where midterm reclamation work had been executed. This behavior resembles the results of the analysis carried out here. The current analysis shows that even in the case of homogeneous geomaterials, stratigraphic nonhomogeneity results in large variations in ground deformation behavior and that such deformation becomes particularly large in sloped strata locations. These things cannot be taken into consideration in one-dimensional analysis and highlight the necessity of performing multi-dimensional effective stress analysis.

Keywords: liquefaction, stratum inclination, surface wave, effective stress analysis

SSS23-19 Room:211 Time:May 1 15:15-15:30

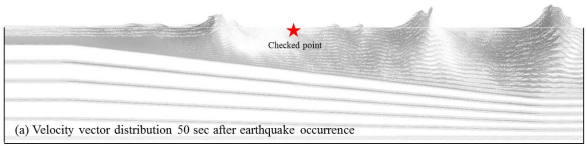

(a) Velocity vector distribution 50 sec after earthquake occurrence

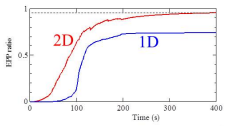

(b) Excess pore water change at checked point ★

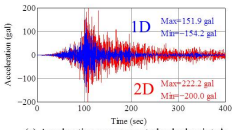

(c) Acceleration response at checked point ★

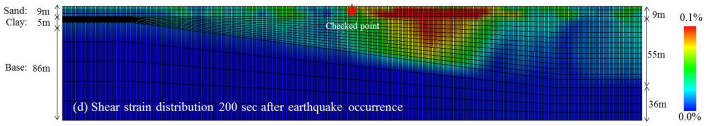

(d) Shear strain distribution 200 sec after earthquake occurrence

Japan Geoscience Union Meeting 2014
(28 April - 02 May 2014 at Pacifico YOKOHAMA, Kanagawa, Japan)

SSS23-20 Room:211 Time:May 1 15:30-15:45

Relationship between liquefaction occurrence ratio and strong ground motion duration for the 2011 off the Pacific coast

SENNA, Shigeki[1*] ; WAKAMATSU, Kazue[2] ; MATSUOKA, Masashi[3]

[1]NIED, [2]Kanto Gakuin University, [3]Tokyo Inst. Tech

In this study, We first reorganized the points of liquefaction in the 2011 off the Pacific coast of Tohoku Earthquake and plotted the number of liquefaction points in 250m mesh units, because many areas had not been investigated or were insufficiently investigated, as revealed in the information on liquefaction points disclosed and summarized by December 2011.

Next, using the reorganized liquefaction data, the seismic intensity were calculated and the 'real-time seismic intensity' noted by Kunugi et al.(2008) based on the waveforms recorded by seismographs of K-NET, KiK-net, the Meteorological Agency, and the municipalities and examined the effects of earthquake duration on liquefaction using the data on liquefaction points and the method of Matsuoka et al.(2011) to calculate the liquefaction occurrence, so that the liquefaction occurrence can be examined with consideration of the effect of the duration of seismic motion in the March 11 earthquake.

Keywords: Occurrence of liquefaction, Continuation time of strong ground, Geomorphologic classification, Fragility curve, Regional peculiarity

Japan Geoscience Union Meeting 2014
(28 April - 02 May 2014 at Pacifico YOKOHAMA, Kanagawa, Japan)

SSS23-21 Room:211 Time:May 1 15:45-16:00

The Wave Features Theory and Soliton

NISHIZAWA, Masaru[1*]

[1]none

1. The eye of Writers under the title “ The Great Kanto Earthquake (of 1923) ” correctly spotted, the demolished style difference between the large and small structure.
2. Fourier Spectrum of Earthquake Motion near the observatory forms The Normal Distribution (Gaussian Distribution). And The further near the observatory. And The Sharp shape of Normal distribution mean densely the frequency.

Keywords: Wave Features Theory, Soliton, KDV Equation, Nonlinear waves

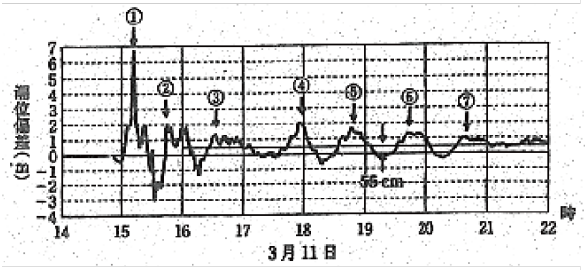

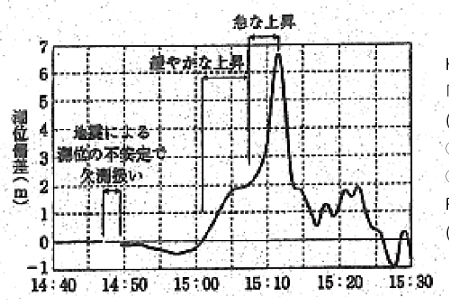

岩手県南部沖のＧＰＳ波浪形の記録（左）と最初の部分の拡大図（右）
国土交通省のデータをもとに作成

Kazuo OIKE
「Massive earthquake in Japan archipelago」
(Iwanami Library of Science 185, P10)
①: Soliton
②〜⑦: Break down of Solitary wave Solitons
Reference：Mikio HINO「流体力学」
(Asakura Publishing Co., Ltd. (1992))

Japan Geoscience Union Meeting 2014
(28 April - 02 May 2014 at Pacifico YOKOHAMA, Kanagawa, Japan)

SSS23-22 Room:211 Time:May 1 16:15-16:30

Seismic hazard karte : A Tool for distribution of seismic hazard information with Multi-index

AZUMA, Hiroki[1*] ; FUJIWARA, Hiroyuki[1]

[1]National Research Institute for Earth Science and Disaster Prevention

1. Overview of seismic hazard karte

NIED distributed the ”seismic hazard karte(chart)” in July, 2013. An ”seismic hazard karte” is what summarized the earthquake hazard information for every point, arbitrary places can be searched and the diagnosis of the earthquake hazard about the place can be drawn up. A result displays many indices, such as various foundation information, hazard curves, etc. about the danger of an earthquake, like the notice of a medical examination by the view format summarized to A41 sheet using many charts and graphs.

2. Purpose of Development

It was thought possible to spread the recognition to seismic hazard by using for the user itself the form of diagnosing a certain point with the connection as a starting point, from the investigation by HERP, the argument in a comprehensive sectional meeting, etc. Although the seismic hazard karte was dispatch fundamentally turned to the whole average citizen like other seismic hazard information, when it decomposed into use-cases, it assumed roughly dividing and being used in the following domains. For insurance and real estate, as customer-oriented service data. As the teaching materials which teach the tool for advancing a measure at a workshop or a home to the local resident engaged in disaster prevention educational persons concerned and disaster prevention, and the view of the seismic hazard information on the area. It developed by being that it is easy to carry out use, respectively conscious as a sample of the way of expressing a response using J-SHIS Web API which is open API, and designing to IT persons concerned and developers.

3. Distributed Result

There are many echoes from the exhibited beginning and it is thought that effect fixed as one of the how to show the seismic hazard information evaluated across the board by the country was achieved. Nothing new as contents have in the information offered as seismic hazard karte this time, and it is already J-SHIS seismic hazard station offered, was only visualized in a different form. However, receiving a karte ”it may be very intelligible. From the thing of having also let the family know who lives in the distance”as a positive thing, many reactions ”worth of the possessions affair of our company will be influenced and it will be troubled by it if such a thing comes out” were seen by the negative thing, like when the hazard information is released newly.

4.References.

Seismic hazard karte |http://www.j-shis.bosai.go.jp/labs/karte/ (Japanese only)
Manual |http://www.j-shis.bosai.go.jp/karte-manual (Japanese only)
Description |http://www.yullege.jp/?p=282 (Japanese only)
J-SHIS Web API |http://www.j-shis.bosai.go.jp/api-list (Japanese only)
Hiroki Azuma, Shinichi Kawai and Hiroyuki Fujiwara, 2013, Development of J-SHIS and Applications Using API, Journal of Disaster Research, Vol.8 No.5, 869-877.

Keywords: Seismic hazard, information tool

SSS23-22 Room:211 Time:May 1 16:15-16:30

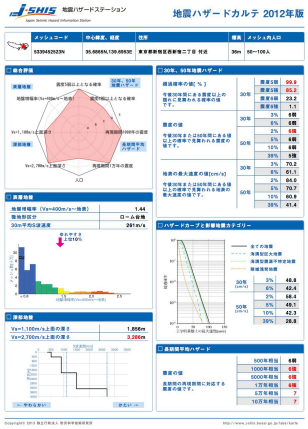

Japan Geoscience Union Meeting 2014
(28 April - 02 May 2014 at Pacifico YOKOHAMA, Kanagawa, Japan)

SSS23-23 Room:211 Time:May 1 16:30-16:45

JMA intensity distribution of the 1943 Tottori earthquake derived from immediately conducted questionnaire survey

NAKAMURA, Mariko[1] ; KAGAWA, Takao[2*] ; NOGUCHI, Tatsuya[2] ; NISHIDA, Ryohei[2]

[1]Okayama City Office, [2]Tottori University

Questionnaire surveys were conducted by university of Tokyo immediately after five disastrous earthquakes in 1940s to evaluate modified Mercalli (MM) intensity scale. The raw data of the surveys had been stored long time without following analyses. We have studied explanation of each item in the Questionnaire sheet and developed the relational expressions between MM and JMA intensity scales. Finally, we derived JMA intensities at 1935 sites in southwest Japan, and estimated JMA intensity distributions with almost same resolution as modern intensity observation network. The distribution map suggests radiation pattern of strike slip fault and effect of surface geology. The result is worth of basic information for earthquake disaster prevention.

Keywords: the 1943 Tottori earthquake, questionnaire survey, JMA intensity scale, modified Mercalli scale

Japan Geoscience Union Meeting 2014
(28 April - 02 May 2014 at Pacifico YOKOHAMA, Kanagawa, Japan)

SSS23-24 Room:211 Time:May 1 16:45-17:00

Mortality in the East Japan Great Earthquake (4) Infants and elderlies should always suffer heavy rate of deaths?

OHTA, Yutaka[1*] ; KOYAMA, Maki[2]

[1]TRIES, ADEP, [2]Engr. Fac. Kyoto Univ.

With the aim of clarifying age dependency of mortality in earthquakes we have been conducting a series of studies, just employing a simple division of number of deaths over population in age intervals of 5 or 10 years from area to area in devastated region. What we have found up to now is that there are 2 dominant types approximated by the capital U and J letters in English on the 2 dimensional coordinates of X axis as increasing ages and Y axis as mortality. In case of the 2011 East Japan earthquake, the age dependency in terms of J letter type dominates in most of devastated areas, which suggests that the mortality gets heavier with increasing ages but for infants it stays milder. Such result on age-dependency looks to be apart from our general recognition as infants are very much vulnerable in mortality at many disasters. The discrepancy requests further in-depth studies. In order to settle this issue we attempted two different approaches, that is, 1) comparing natural deaths of certain population with number of accidental deaths by an earthquake (Ozaki. 2012) and 2) introducing a way of evaluating the loss of life expectancy as an weighting factor inversely changing with increasing ages.

Consequently, we succeeded to make clear that infants are still very vulnerable in the meaning of bringing heavy rate of deaths.

Reference

Ozaki; kousei no shihyou, 59, 2012 (in Japanese)

Keywords: East Japan Earthquake, Mortality, Age-dependency, Life Expectqancy

Japan Geoscience Union Meeting 2014
(28 April - 02 May 2014 at Pacifico YOKOHAMA, Kanagawa, Japan)

SSS23-P01 Room:Poster Time:May 1 18:15-19:30

Disaster research in the Toyama Earthquake(1718)

SAKAMOTO, Masao[1*]

[1]Iida city Museum

1,Introduction

Of the destructive earthquakes recorded in Japan over the past approx.1600 years, the only one that caused widespread damage in the southern part of Nagano Prefecture was the Toyama Earthquake of 1718,which had its epicenter at Minamishinano Wada, Iida City. The Toyama Earthquake struck just after 2 pm on August 22, 1718 with a magnitude estimated at 7.0. This earthquake is considered to have occurred along the Median Tectonic Line.

2,Survey Results

I identified 35 places where disasters occurred in each prefecture of Nagano Gifu Shizuoka and Aichi. Among these places, a number of characteristic disaster examples are shown as follows.

(1)Minamishinano Wada,Iida City: Mt.Moriheizan located close to the epicenter of the earthquake, partially collapsed to form the elevated area called Deyama at its foot. A landslide pushing out from Oshidezawa dammed the Toyama River. **(2)Arakida, Anan Town:** The right bank of the Tenryu River is composed mostly of Neogene strata centered on sandstone and mudstone overlaying granite bedrock. The slope at the place called Kibishima collapsed due to the earthquake and dammed the Tenryu River. **(3)Furujo,Anan Town:** Geologically, this area consists of Neogene sandstone and mudstone. In the Furujo district, landslides occurred in 24 places, and fields with place names that are still in use today were damaged or destroyed in 33 places**.(4)Hisawa,Shimojo Village:** There is an oral tradition stating that the local people saw the collapsed state of mountainsides in the Ina and Akaishi Mountains from this district. **(5)Enshu Yokoyama Town** (Yokoyama Town, Tenryu Ward, Hamamatsu City, Shizuoka Prefecture): A document was found stating that the Tenryu River was stopped at a place called Enshu”Teuna”. Currently this place name is not used, but there is a place name ”Unna”, which is also along the Tenryu River, so it was presumed that this was where the river was dammed.

3,Discussion and Consideration

(1)What this survey shows: The distribution of the records concerning this earthquake disaster with its epicenter on the Median Tectonic Line in Minamishinano Wada, Iida City is quite one-sided. Records of damage were found only on the west side of a border marked by the Median Tectonic Line running roughly north-south. Because the Akaishi Mountains on the east side of the border had almost no inhabitants, no records of damage from the earthquake were left there. Also, over the course of the nearly three centuries that have passed since the earthquake occurred, the amount of documentary material has been greatly reduced as a result of natural and human causes. **(2)Geological specificity:** The disasters associated with this earthquake can be divided into three typs according to geological differences and the disaster distribution. The first type involved large-scale landslides and disasters occurring on basement granite. The second type constituted disasters occurring on Neogene strata centered on Anan Town. The third type of disaster occurred on Quaternary terrace gravels and alluvial fan gravels. **(3)Rrelation to the Hoei Earthquake:** In 1707, the Hoei Earthquake struck with an estimated magnitude of 8.6, making it one of the largest earthquakes in Japannese history. The Toyama Earthquake, which struck 11 years later, is considered to be an after-shock of the Hoei Earhquake.

Keywords: toyama earthquake, the year 1781, earthquake disaster, median tectonic line, hoei earthquake

Japan Geoscience Union Meeting 2014
(28 April - 02 May 2014 at Pacifico YOKOHAMA, Kanagawa, Japan)

SSS23-P02 Room:Poster Time:May 1 18:15-19:30

A discussion on improvement of calculation technique for questionnaire survey of seismic intensities

SAITO, Ryohei[2] ; YAMAMOTO, Hidekazu[1*] ; SAITO, Tsuyoshi[1]

[1]Faculty of Engineering, Iwate University, [2]GraduateSchool of Engineeing, Iwate University

We compared the seismic intensity from the average intensity with a 1km mesh obtained in the vicinity of the instrumental seismic intensity observation sites. Only in the case of the 2011 off the Pacific coast of Tohoku Earthquake, questionnaire seismic intensities were about 0.5 larger than the instrumental seismic intensities, however, in the cases of other earthquakes, the questionnaire ones were smaller than the instrumental ones. The differences between the instrumental seismic intensity and the questionnaire one are 0.1 to 0.2 at the sites where the instrumental seismic intensities indicate 6 weak. However, at the sites where the instrumental seismic intensities indicate 5 strong, the differences were more than 0.5. Results of the earthquakes of 2008 and 2003 show that the questionnaire seismic intensity is about 0.3 smaller than the instrumental one in the range of 5 weak to 5 strong. Therefore, we compare the method by Inoue et al.(1999) as another method capable in the larger seismic intensity range with the method by Ohta et al.(1998). Inoue et al.(1999) had pointed out that the questionnaire seismic intensity estimated by Ohta et al.(1998) were low in the middle seismic intensity range near about 4.5. They proposed a method capable in large seismic intensity range using the empirical formula to modify the difference without changing the calculating method of Ohta et al. (1979). When questionnaire seismic intensities were calculated using the empirical equation by Inoue et al.(1999), they showed a better correlation with the instrumental seismic intensity for other earthquakes except the 2011 off the Pacific coast of Tohoku Earthquake.

Keywords: Calculation technique for questionnaire seismic intensities, Instrumental Seismic Intensity, Large seismic intensity range

Japan Geoscience Union Meeting 2014
(28 April - 02 May 2014 at Pacifico YOKOHAMA, Kanagawa, Japan)

SSS23-P03 Room:Poster Time:May 1 18:15-19:30

SATREPS Project on Earthquake and Tsunami Disaster Mitigation in the Marmara Region and Disaster Education in Turkey

CITAK, Seckin ozgur[1*] ; KANEDA, Yoshiyuki[1] ; ERDIK, Mustafa[2] ; TAKAHASHI, Narumi[1] ; OZEL, Nurcan meral[2] ; HORI, Takane[1] ; HORI, Muneo[3] ; KUMAMOTO, Kunihiko[4] ; KALAFAT, Dogan[2] ; PINAR, Ali[2] ; OZEL, Oguz[5] ; YALCINER, Ahmet cevdet[6] ; NURLU, Murat[7] ; TAMIRCAN, Gulum[2] ; MIRZAOGLU, Mete[7] ; ARIYOSHI, Keisuke[1]

[1]Japan Agency for Marine-Earth Science and Technology (JAMSTEC), Japan, [2]Bogazici University, Kandilli Observatory and Earthquake Researches Institute (KOERI), Turkey, [3]University of Tokyo, Japan, [4]Edogawa University, Japan, [5]Istanbul University, Turkey, [6]Middle East Technical University, Turkey, [7]Disaster and Emergency Management Presidency (AFAD), Turkey

Since 1939, devastating earthquakes with magnitude greater than seven ruptured North Anatolian Fault (NAF) westward, starting from 1939 Erzincan (Ms=7.9) at the eastern Turkey and including the latest 1999 Izmit-Golcuk (Ms=7.4) and the Duzce (Ms=7.2) earthquakes in the eastern Marmara region. On the other hand, the west of the Sea of Marmara an Mw7.4 earthquake ruptured the NAF's Ganos segment in 1912. The only un-ruptured segments of the NAF in the last century are within the Sea of Marmara, and are identified as a "seismic gap" zone. The Sea of Marmara should be focused on through a multidisciplinary research and uncertainty in magnitude, epicenter, recurrence, fault segmentation, and their cross effects should be identified and characterized. To fill the necessity above, a comprehensive multidisciplinary research on earthquake and tsunami disaster mitigation in the Marmara region and disaster education in Turkey in the framework of Science and Technology Research Partnership for Sustainable Development (SATREPS) sponsored by Japan Science and Technology Agency (JST) and Japan International Cooperation Agency (JICA) has been started.

The project is composed of four research groups.

The first is "Earthquake Source Model research" group. Long-term OBS observation, Electromagnetic observation, Seafloor extensometer observation and Trench survey studies will be conducted in order to identify the detailed seismic zone, fault geometry, 3D Velocity structure and reliable crustal deformation beneath the Sea of Marmara.

The second is "Tsunami prediction based on earthquake cycle simulation research" group. In this group earthquake and tsunami occurrence scenarios will be proposed based on especially the research Group 1's outputs and current knowledge on NAF's seismic activities. The outputs will be used for the simulation of strong ground motion, developing of advanced hazard maps and a tsunami early warning system.

The third is "Seismic characterization and damage prediction research" group. This group focuses on modeling of 3D velocity structure, theoretical prediction of ground motion and evaluation of existing structures in the selected urban areas using research outputs of the other groups. Also there will be an attempted of making an urban area model for Istanbul using available data for this area, and to execute earthquake hazard and disaster simulation for various scenarios of a possible earthquake. Improved hazard maps and visual materials for disaster education are expected.

The fourth is "Disaster education using research result visuals from each research" group In group four, effective use of media in the dissemination of disaster information will be examined and disaster management planning through regional disaster prevention community will be encouraged. as well as, using the research visuals a disaster prevention education program will be conducted through media, web, local communities and schools.

Goals of the project are as follows,

1- To develop disaster mitigation policy and strategies based on multidisciplinary research activities.

2- To provide decision makers with newly found knowledge for its implementation to the current regulations.

3- To organize disaster education programs in order to increase disaster awareness in Turkey.

4- To contribute the evaluation of active fault studies in Japan.

Through the project, the research results will be integrated for disaster mitigation in The Marmara region and disaster education in Turkey. The details of SATREPS Japan-Turkey joint research project and latest achievements will be presented.

Keywords: sea bottom observation, earthquake disaster mitigation, tsunami disaster mitigation, disaster education, Turkey, SATREPS

Japan Geoscience Union Meeting 2014
(28 April - 02 May 2014 at Pacifico YOKOHAMA, Kanagawa, Japan)

SSS23-P04 Room:Poster Time:May 1 18:15-19:30

Fragility curves of buildings during the 2011 Tohoku Earthquake using the damage data in the northern Miyagi Prefecture

WU, Hao[1*] ; MASAKI, Kazuaki[2] ; IRIKURA, Kojiro[3] ; KURAHASHI, Susumu[3]

[1]Graduate School of Engineering, Aichi Institute of Technology, [2]Department of Urban Environment, Aichi Institute of Technology, [3]Disaster Prevention Research Center, Aichi Institute of Technology

Damage ratios in subdistricts of Osaki and Kurihara cities, northern of Miyagi Prefecture are obtained from the damage data provided by the local City Offices. Ground motions in these subdistricts are estimated by use of source model proposed by Kurahashi and Irikura (BSSA, 2013) and underground velocity structures identified from microtremor H/V spectral ratios. The estimated ground motion indices (PGA, PGV, I_{JMA}, and SI) are used to relate with the damage ratios to construct the fragility curves. It is found that the correlation in small subdistricts is improved, compared with that between the observed ground motion indices and corresponding damage ratios in a wider district.

In addition, we have added some microtremor measurement at plural sites inside each subdistrict, such as Furukawa, and Tajiri, in order to assess the representativeness of ground motions estimated at only one site for the entire subdistrict. We conducted such measurement at or near the preliminary schools inside the subdistricts. The ground motions during the mainshock are estimated with the identified velocity structures from the microtremor H/V spectra ratios. It is found that the variability of ground motions in the Furukawa subdistrict is relatively small. It suggests that the ground motions used for the fragility curves are representative for the entire subdistrict. In contrast, the variability of ground motions in Tajiri is relatively large. It may be caused by the limited numbers of preliminary schools with similar amplification factors.

Keywords: Fragility curve of buildings, microtremor H/V spectral ratio, underground velocity structure, representative of ground motions

Japan Geoscience Union Meeting 2014
(28 April - 02 May 2014 at Pacifico YOKOHAMA, Kanagawa, Japan)

SSS23-P05 Room:Poster Time:May 1 18:15-19:30

The earthquake vibration observation of the Yasuda auditorium using the IT Kyoshin seismometer

ITO, Takamori[1*] ; TAKANO, Kiyoshi[2]

[1]Keio University, [2]lll&ERI, The University of Tokyo

In order to reduce the seismic disaster, it seems to be the usefulness to investigate the seismic vibration of our familiar buildings such as housing, companies, schools, etc. in small earthquake, examine the weak point and improve the earthquake resistance of these building effectively. For this purpose, we devised IT strong motion seismometer as a new type self install strong motion seismometer.

With this IT Kyoshin seismometer, we continue the vibration observation of some buildings in University of Tokyo from 2006.

The repair work of the Yasuda auditorium will be carried out. We install the IT Kyoshin seismometer and will observe it to confirm an effect of the construction.

We used the high-performance sensor and, in addition to a low cost standard IT Kyoshin seismometer, observed it.

We finish observation before the construction and analyze data now.

After construction was completed, we install the IT Kyoshin seismometer again and are going to compare it.

Keywords: IT Kyoshin (Strong Motion) Seismometer, Structural Health Monitoring

Japan Geoscience Union Meeting 2014
(28 April - 02 May 2014 at Pacifico YOKOHAMA, Kanagawa, Japan)

SSS23-P06 Room:Poster Time:May 1 18:15-19:30

The effect of torsional and bending vibration on shear-wave velocity extracting from building response by seismic interf

WANG, Xin[1*] ; MOTOSAKA, Masato[1] ; MASAKI, Kazuaki[2] ; IRIKURA, Kojiro[3] ; HISADA, Yoshiaki[4]

[1]International Research Institute of Disaster Science,Tohoku University, [2]Department of Urban Environment, Aichi Institute of Technology, [3]Disaster Prevention Research Center, Aichi Institute of Technology, [4]Department of Architecture, Kogakuin University

Because shear-wave velocity correlates with the shear rigidity of buildings, the decrease of it is a indicator of the loss of stiffness, which is possibly caused by structural damage or degradation. Therefore, shear-wave velocity identification is intended for use in health monitoring of upper structures excluding the effect of soil-structure interaction. Shear-wave velocity can be extracted from tracing the propagation of a pulse from normalized cross-correlation of the motion between two points based on the view of response as the wave vertical propagation process. In this study, the reference point is the top of the building (virtual source) instead of the base (physical source) which results in the transfer function including the effect of rigid-body rocking. However, for high-rise and eccentric structures torsional motion and bending motion is inevitable. In practical measurement of horizontal motions with single sensors located on the side not the core of the building plane, it is unavoidable to record the torsional response which mixed with the shear-mode motions. Therefore, the effect of torsional response to shear-wave velocity extraction should be deliberated on to avoid erroneous use of the travel time of torsional wave instead of that of shear wave. Furthermore, the extraction of shear-wave propagation from building vibration generally in bending mode is valid or not should be examined.

In this study, firstly a 3D model with eccentricity is used to calculate the horizontal and vertical impulse response to analyze the effect of torsional and bending response to shear-wave velocity extraction. And the method to eliminate the effects of torsional and bending vibrations to obtain the shear-wave propagation with high resolution is presented. Secondly, a practical use of earthquake records measured in a high-rise building to examine the effect of torsional and bending vibration to shear-wave velocity extraction. Thirdly, velocities of shear wave, torsional wave, and bending wave are extracted separately to evaluate the changes of stiffness before and after the Tohoku earthquake for health monitoring.

Keywords: shear-wave velocity of buildings, deconvolution method, torsional response, seismic interferometry, system identification, Tohoku earthquake

Japan Geoscience Union Meeting 2014
(28 April - 02 May 2014 at Pacifico YOKOHAMA, Kanagawa, Japan)

SSS23-P07 Room:Poster Time:May 1 18:15-19:30

Global ”strong” ground motions from the 2013 Sea of Okhotsk great deep earthquake

KUGE, Keiko[1*]

[1]Dept. Geophsyics, Kyoto University

This study presents the characteristics of global ground motions caused by the Sea of Okhotsk deep earthquake (Mw8.3) of May 24, 2013. The earthquake occurred at a depth of 609 km in the subducting Pacific plate, and it is now the largest deep earthquake ever recorded. According to reports in NEIC, the earthquake was felt at very long distances in the world, including Dubai (˜76 degrees) and Moscow (˜58 degrees). In this study, by using global broadband seismic data from IRIS DMC, we examine ground motions from the earthquake. For the 1994 Bolivia deep earthquake (Mw8.3), which was formerly the largest and were felt in North America, the distant ground motions were examined by Anderson et al. (1995) from the perspective of strong motion seismology. Due to the location, the 2013 Sea of Okhotsk earthquake was recorded by a much better coverage of global stations, compared to the 1994 Bolivia earthquake. This study is an opportunity for exploring the distant ”strong” ground motions from the perspective of Anderson et al. (1995).

Peak ground accelerations (PGA) from the 2013 Sea of Okhotsk earthquake decrease as distance increases out to 120 degrees, and have a peak at a distance of approximately 140 degrees. The variation as a function of distance is similar to that of Anderson et al. (1995) for the 1994 Bolivia earthquake. The values of PGA are a few times larger than those from the Bolivia earthquake. At distances between 30 and 80 degrees, PGA are associated with vertical components of direct P waves, and the values of PGA are often in a range from 0.1 to 1 gal. Peak ground velocities (PGV) vary with distance in a similar way to PGA. The values of PGV at distances between 30 and 80 are lower than 0.1 cm/s.

Large PGA at distances between 30 and 80 degrees are observed in the Eurasian continent. The values of PGA in the western part of the continent are larger than those in the eastern part. Because this difference is also observed for PGA of P waves from an outer-rise shallow earthquake near the Kurile trench, it can be attributed to regional structure in the Eurasian continent. PGA from the 2013 deep earthquake are not low in the southern part of the continent, although from a deep earthquake beneath Sea of Okhotsk that has a different focal mechanism from that of the 2013 earthquake, PGA decrease toward the south as distance increases. The focal mechanism of the 2013 earthquake represents that the P wave radiation is the maximum along a ray toward Karachi, Pakistan. This P wave radiation can account for the observations of PGA in the southern part. Global ”strong” ground motions from the 2013 Sea of Okhotsk deep earthquake are thus likely to be affected by regional structure and P wave radiation, as suggested by Anderson et al. (1995).

Japan Geoscience Union Meeting 2014
(28 April - 02 May 2014 at Pacifico YOKOHAMA, Kanagawa, Japan)

SSS23-P08 Room:Poster Time:May 1 18:15-19:30

Relation between smallest microtremor amplitudes and largest seismic amplitudes observed at TRIES seismographic stations

TANAKA, Torao[1*] ; OKUBO, Makoto[2]

[1]Kyoto University Emeritus Professor, [2]Tono Research Institute of Earthquake Science

In 1999 TRIES, Tono Research Institute of Earthquake Science, started to establish an observation network of seismographic stations in Tono district, the eastern area of Gifu Prefecture, and completed a 10 stations network at the end of the year. The seismographic station TRIES was the first station, and 9 stations, TOGARI, ENA, MIZUNAMI, AKECHI, IWAMURA, NATAKI, MITAKE, TOKI and INUYAMA were established one by one. In order to investigate the correlation between the smallest spectral amplitudes of microseisms and largest seismic spectral amplitudes, we started spectral analysis of microtremors and seismic waves recorded on the same seismograms. By the discrete Fourier transform we calculated the spectral amplitudes and frequencies from the observed microtremors recorded just before the first arrival of seismic waves in the frequency range from 2.0 to 4.0 Hz. Similarly we calculated the spectral amplitudes and frequencies of seismic waves by the discrete Fourier transform in the frequency range from 2.0 to 4.0Hz. We calculated the ratios of the relative amplitudes of the smallest amplitude of microtremors and largest amplitude of seismic waves to those at the station TRIES. By taking the relative amplitudes of micro tremors and largest seismic amplitudes to those at TRIES we can extract the relative site effects caused by the ground soil to those at TRIES. Since the site effect at TRIES is small, the relative largest seismic amplitudes at TOGARI, for example to those at TRIES simply give multiples of the amplitude at TRIES, at each station. Preliminary results show that the smallest amplitude of microtremors will give the spectral amplitudes of the site effect that will amplify the incident seismic waves from the underlain basements.

Keywords: microtremor, seismic waves, discrete Fourier transform, ground soil, largest amplitude, site effect

Japan Geoscience Union Meeting 2014
(28 April - 02 May 2014 at Pacifico YOKOHAMA, Kanagawa, Japan)

SSS23-P09 Room:Poster Time:May 1 18:15-19:30

A study on model selection methods for ground-motion prediction equations using synthetic data

NODA, Akemi[1*] ; WU, Changjiang[2] ; SI, Hongjun[3] ; SAIJO, Yusuke[1] ; JIAO, Ning[1]

[1]Kozo Keikaku Engineering Inc., [2]Japan Nuclear Energy Safety Organization, [3]Earthquake Research Institute, University of Tokyo

Numerous ground motion prediction equations (GMPEs) have been proposed for the purpose of assessing seismic hazard. However, a critical problem is that how to select appropriate GMPEs for the application of GMPEs to practical engineering problems.

Recently some model selection methods for GMPEs that evaluate the agreement between observed and predicted data have been proposed. In present study, in order to check the properties of model selection methods, we compare the model selection methods by using artificial dataset generated by a known GMPE. As candidate model selection methods, we have chosen three methods, that is, analysis of root mean square residual (RMR), the log-likelihood method (LLH method, Scherbaum et al., 2009, BSSA) and the Euclidean distance-based ranking method (EDR method, Kale and Akkar, 2013, BSSA). The analysis of RMR is one of the simplest methods to evaluate the difference between observed data and medians of GMPE model. On the other hand, the LLH method quantifies the distance between observed data and GMPEs defined as probability density function (both of median and standard deviation), based on information-theoretic perspective. However, Kale and Akkar (2013) points out the problem that the LLH method may favor GMPEs with larger standard deviations. The EDR method considers not only ground-motion uncertainty of model through standard deviation, but also agreement between the median estimations of models and observed data trend (model bias).

First, we assumed a vertical strike-slip fault with moment magnitude 7.0. We randomly chose 200 sites, whose fault distances are up to 200km. Next, we calculated theoretical PGA and response spectral acceleration for 16 periods using ground motion prediction model of Chiou and Youngs (2008, Earthq. Spectra), which is referred to as CY08 hereafter. And, we generated three kinds of synthetic dataset by adding three types of random noise with (1) zero standard deviation, (2) standard deviation of CY08, and (3) twice the standard deviation of CY08, respectively.

We selected five candidate GMPEs, that is, CY08, Abrahamson and Silva (2008, Earthq. Spectra), Campbell and Bozorgnia (2008, Earthq. Spectra), Zhao et al. (2006, BSSA) and Kanno et al. (2006, BSSA), and ranked the performance of candidate GMPEs for each synthetic dataset. In analysis of RMR that does not account for standard deviations of the prediction models, CY08 is stably ranked the best performing model for all kinds of synthetic dataset. The LLH method basically ranked CY08 as the best performing model for synthetic dataset (1) and (2), but it favored GMPEs with larger standard deviations for synthetic dataset (3). It suggests that the standard deviation of model is emphasized more than the median when we apply the LLH method to poor quality data. In the EDR method, in principle, the parameter to measure the level of model bias of CY08 is not able to be calculated for synthetic dataset (1) that does not have random noise. For synthetic dataset (2) and (3), however, the EDR method ranked CY08 as the best performing model both in the point of view of model uncertainty and model bias.

Keywords: attenuation relationship, ground motion predicting equation, root mean square residual, the log-likelihood method, the Euclidean distance-based ranking method

Japan Geoscience Union Meeting 2014
(28 April - 02 May 2014 at Pacifico YOKOHAMA, Kanagawa, Japan)

SSS23-P10 Room:Poster Time:May 1 18:15-19:30

Seismic hazard assessment using a new ground motion prediction equation

MORIKAWA, Nobuyuki[1*] ; FUJIWARA, Hiroyuki[1] ; OKUMURA, Toshihiko[2] ; FUJIKAWA, Satoshi[2]

[1]National Research Institute for Earth Science and Disaster Prevention, [2]Shimizu Corporation

In the ”National Seismic Hazard Map for Japan” by Headquarters of Earthquake Research Promotion of Japan, seismic hazard is evaluated by the ground motion prediction equation (GMPE) of peak velocity by Si and Midorikawa (1999), and conversion from peak velocity to seismic intensity by using an experiential relation. It is indispensable that earthquakes of moment magnitude (Mw) 9 class take into consideration in the present seismic hazard evaluation. However Si and Midorikawa's (1999) equation is obtained from strong motion records of earthquake up to Mw 8.3. In this study we evaluate seismic hazard by using our new GMPE obtained by using strong-motion database including the records of the 2011 Tohoku earthquake and show the comparison it with the National Seismic Hazard Maps for Japan.

The target strong-motion parameters are peak velocity on an engineering bedrock (here, it is considered as the upper surface of Vs=400 m/s layer), and peak velocity and JMA seismic intensity on the ground. The value on the ground is calculated by using the amplification factor obtained from the average S-wave velocity up to 30 m depth based on the 250m-mesh national geomorphologic classification map.

First, we compare the ground motion distributions calculated from two GMPEs. Here we target following 6 assumed earthquake. (1) crustal earthquake on the Itoigawa-Shizuoka fault zone (Mw7.4), (2) crustal earthquake on the Muikamachi fault zone (Mw=6.6), (3) subduction-zone plate-boundary earthquake at Nankai Trough (Mw=9.1), (4) subduction-zone plate-boundary earthquake at Tokachi-oki reigion (Mw=8.1), (5) subduction-zone shallower intra-plate earthquake at Chishima trench region (Mw=8.2), and (6) subduction-zone deeper intra-plate earthquake at Chishima trench region (Mw=7.5). Amplification by the deep sediments layers can be obviously seen in our new result of peak velocity distribution. As the result, amplitude in our new result becomes larger in basin region and smaller in mountain region. On the other hand, the influence of the deep sediments is not so remarkable in result of JMA seismic intensity on the ground. The calculated value from our new GMPE is smaller in the distance area (in general 100 km or more) for subduction-zone earthquakes. Midorikawa and Ohtake (2002) pointed out that Si and Midorikawa's (1999) GMPE overestimates the peak values in distant region earthquake whose focal depth is deeper than 30 km. Our results are consistent with them.

Next, we compare the seismic hazard for the megathrust earthquake occurring at the Nankai Trough. Here we use the model in probabilistic seismic hazard maps by HERP (2013).

Moreover, we use the value of variance in the National Seismic Hazard Maps for Japan as it is. The hazard by our new GMPE decreases especially at the distant area as expected from comparison of above-mentioned strong-motion distribution. However, the decrease does not serve in Kanto and Osaka area where amplification by deep sediments is large. On the contrary, JMA seismic intensity is larger when exceedance of probability is lower at some points. This is considered that that the value of the set-up variation is not in agreement for JMA seismic intensity has influenced.

Keywords: seismic hazard assessment, grount motion prediction equation, variance of ground motion

Japan Geoscience Union Meeting 2014
(28 April - 02 May 2014 at Pacifico YOKOHAMA, Kanagawa, Japan)

SSS23-P11 Room:Poster Time:May 1 18:15-19:30

Ground amplification estimates based on very dense seismic array observation in Furukawa district, Osaki, Japan

GOTO, Hiroyuki[1*] ; MORIKAWA, Hitoshi[2] ; INATANI, Masayuki[1] ; OGURA, Yumiko[2] ; TOKUE, Satoshi[2] ; HAMASAKI, Shohei[2] ; ZHANG, Xinrui[2] ; SAKKRAWIT, Sripunyaphikhup[2] ; IWASAKI, Masahiro[3] ; ARAKI, Masayuki[4] ; SAWADA, Sumio[1] ; ZERVA, Aspasia[5]

[1]Kyoto University, [2]Tokyo Institute of Technology, [3]Osaki city, [4]aLab Co.Ltd, [5]Drexel University

On March 11, 2011, a huge earthquake hit the eastern part of mainland Japan. The earthquake caused a huge tsunami that killed more than ten thousand people. Structures were also severely damaged over the area of eastern Japan by the tsunami, ground motions, liquefaction, and so on. We focus on the Furukawa district of Osaki City, where severe residential damages occurred downtown. Ground motion records in the downtown area are available at two stations, MYG006 (K-NET) and JMA Furukawa (JMA). The damage level was different between the areas within several hundred meters from the MYG006 and JMA Furukawa stations, which are about 1km away from each other. The severe damages were concentrated within the area approximately 1x1km2 including the JMA station. This implies that the ground motion characteristics were not uniform in sub-kilometer scale, and the existing two stations are not enough to clarify the damage distribution (Goto and Morikawa, 2012).

In aftermath of the earthquake, we distributed dozens of low-cost seismometers, namely ITK sensor, around the area about 3x2km^2 in the Furukawa district (Goto et al., 2012). The observed data are sent to the remote server through internet connection in real time. The seismometers were installed beside the volunteers' houses. The volunteers can access the interactive information service, namely on-line viewer system. The observed PGA and PGV values show significant spatial variability that may be correlated to the structural damage caused by the major 2011 event.

We assumed one-dimensional horizontally-layered structure just beneath the stations and estimated ground structure by using the records based on the observation. The results indicate that the area where the severe damages were concentrated is related to the area with the thicker surface layers. The distribution is also indicated by the results obtained from gravity anomaly data.

References

Goto and Morikawa: Ground motion characteristics during the 2011 off the Pacific coast of Tohoku earthquake, Soils and Foundations, 52(5), 769-779, 2012.

Goto, Morikawa, Inatani, Ogura, Tokue, Zhang, Iwasaki, Araki, Sawada and Zerva: Very dense seismic array observations in Furukawa district, Japan, Seism. Res. Lett., 83(5), 765-774, 2012.

Keywords: Ground amplification, Furukawa district, Very dense seismic array observation

Japan Geoscience Union Meeting 2014
(28 April - 02 May 2014 at Pacifico YOKOHAMA, Kanagawa, Japan)

SSS23-P12 Room:Poster Time:May 1 18:15-19:30

Physics-based decomposition of ground amplification using ground transfer function expansion

GOTO, Hiroyuki[1*]

[1]DPRI, Kyoto University

Amplification of earthquake ground motions at actual deposit sites is an important factor to consider when assessing the risk of an earthquake disaster. In order to identify the amplification properties, several preprocessings such as the Fourier transform are required. I propose a series expansion of the amplification with simple ground transfer functions as a new preprocessing. I define a sequence of transfer functions based on a two-layered structure excluding an internal damping, and a function space spanned by the set of the functions. I mathematically prove that the function space is equal to L2 space. This indicates that all the functions belonging to L2 space, i.e., an arbitrary ground amplification, have a unique series expansion.

In practice, the expansion requires the observed ground amplification. It is directly observable from the spectral ratio of the Fourier spectra at the target site to that at a reference rock site (Goto et al., 2013). When the observations are available, the expansion is applicable even for the site response including a 3D basin effect as the preprocessing, whereas it requires a more precise investigation of what the extracted components physically means for the general cases.

I apply the series expansion to the physics-based decomposition of the amplification. The results indicate that the contribution from the given bases can be represented by the absolute value of their coefficients. The contribution may enable direct quantification of the similarity of models. This property potentially has wide applications, e.g., spatial interpolation of the amplifications from the sites where they are reliably determined, stochastic modeling of the amplification as a mixed state of the fundamental simple states, etc. The detailed application is currently under way.

References

Goto, H.: Series expansion of complex ground amplifications with a sequence of simple transfer functions, Earth. Engng. Struct. Dyn., submitted.

Goto, H., Kawamura, Y., Sawada, S. and Akazawa, T.: Direct estimation of near-surface damping based on normalized energy density, Geophys. J. Int., 194(1), 488-498, 2013.

Keywords: Ground amplification, Function expansion

Japan Geoscience Union Meeting 2014
(28 April - 02 May 2014 at Pacifico YOKOHAMA, Kanagawa, Japan)

SSS23-P13 Room:Poster Time:May 1 18:15-19:30

Case study on the wavefield in the 3D structure including sedimentary basin and the effect of source depth on it

ARISUE, Maho[1] ; KAKEHI, Yasumaro[1*]

[1]Faculty of Science, Kobe University

It is widely recognized that the existence of sedimentary layers has a great influence on the excitation of surface waves. During the 2011 Fukushima-ken shallow inland earthquake (Mw 5.5, depth = 10.6 km), long-period surface wave was observed at a station in the Niigata sedimentary basin, which is over 150 km away from the epicenter, and its duration reached over 100 s. Long-period surface wave was observed also during the 2012 Fukushima-ken-oki deep interplate earthquake (Mw 5.7, depth = 53 km) at the same station, and its duration reached ˜100 s. Thus, significant difference was not seen between the surface wave duration in the Niigata basin of these two earthquakes despite of large difference of their source depths. This seems inconsistent with the recognition that surface wave is more efficiently excited by shallower source.

This study investigates the effect of source depth on the seismic wave filed in the sedimentary basin based on the numerical simulation using finite difference method for shallow and deep sources. The calculation area is from off the Fukushima Prefecture to the Niigata basin, and the following three simulations are performed.

In the simulation 1, a simple structure model composed of circular homogeneous sedimentary basin and background two-dimensional structure, two cases of source depths: 5 km and 85 km, and source duration of 3 s are assumed. The result shows the duration of the surface wave in the sedimentary basin is ˜50 s for the both shallow and deep sources, and large difference is not seen the two different source depth cases. At the station prior to the basin, wave duration for the shallow source is ˜10 s longer than that for the deep source. This difference of 10 s is shorter than the long duration of 50 s in the sedimentary basin, and this can explain the result that large difference is not seen in the basin.

In the simulation 2, a simple structure model composed of circular homogeneous sedimentary basin and background two-dimensional structure, as in the simulation 1, is assumed, and the case study on the material property values of the homogeneous basin is done. Two cases of source depths: 5 km and 75 km, and source duration of 3 s are assumed. The result shows longer duration of seismic waves is seen in the basin for smaller value of S-wave velocity of the basin medium (˜125 s for Vs = 0.5km/s, ˜90 s for Vs = 1.0 km/s, and ˜40 s for Vs = 2.0 km/s). This is interpreted to be because of larger arrival time difference of S-wave and surface wave for smaller S-wave velocity of the basin.

In the simulation 3, realistic complex three-dimensional structure model is assumed both for the sedimentary basin and for the background structure. We use the three-dimensional model by Koketsu et al. (2012), two cases of source depths: 5 km and 75 km, and source duration of 3 s. Long wave duration of ˜90 s is obtained both for the shallow and deep sources. The maximum amplitude at the station is the sedimentary basin is ˜2 times (for the deep source) and ˜6 times (for the shallow source) larger than that at the station prior to the basin.

Comparing the result of the realistic three-dimensional model case (simulation 2) and that of the simple structure model case (simulation 2), more complex and more continuous wave-packet with long duration is seen in the basin in the former case than that in the latter case. On the other hand, siginificant difference is not seen in the amplitude and duration at the station prior to the basin, both for the shallow and deep sources. This result suggests the wavefield in the sedimentary basin is mainly affected by the basin structure itself, rather than the structure model of the path from the source to the basin.

Keywords: sedimentary basin, surface wave, numerical simulation, source depth

Japan Geoscience Union Meeting 2014
(28 April - 02 May 2014 at Pacifico YOKOHAMA, Kanagawa, Japan)

SSS23-P14 Room:Poster Time:May 1 18:15-19:30

Surface wave propagation in the large-scale sedimentary basin: distinct lateral variation of Love wave velocity around m

TAKEMURA, Shunsuke[1*] ; YOSHIMOTO, Kazuo[1]

[1]Yokohama City University

By detailed analysis of surface waves recorded at dense seismic arrays in Kanto, sudden change of Love wave velocity for frequency of 0.125-0.25 Hz is found at very narrow, 20 km by 20km, region of southern Saitama.

To clarify cause of such sudden change and characteristics of surface wave propagation in thick sediments, we conducted 3D FDM simulations of seismic wave propagation assuming various basement structure (interface between sediments and bedrock) or velocity structure models in the sediments. Our simulations demonstrated that propagation velocity of Love wave is mainly controlled by shallower velocity structure at depth less than 1.5 km, rather than deeper basement structure. Our results were supported by the analysis of sensitivity kernel of Love wave in the sediments.

We constructed S-wave velocity structure in the sediments of Kanto basin using interpolation technique from 14 boreholes VSP measurements and surface wave analysis in this study. To confirm validity of our modeling, we conducted 3D FDM simulations of seismic wave propagation using constructed velocity structure and compared simulation results with observation. Our simulation results well reproduced peak amplitude and propagation velocity of Love wave for frequency of 0.125-0.25 Hz. Our results indicates that realistic modeling of shallower velocity structure and impedance contrast at the sediments-bedrock interface is important for precise evaluation of long-period ground motion in thick sedimentary basin.

Acknowledgement

We acknowledge the National Research Institute for Earth Science and Disaster Prevention, Japan (NIED) for providing the K-NET/KiK-net waveform data. We also use strong motion data from SK-net. The computations were conducted on the Earth Simulator at the Japan Marine Science and Technology Center (JAMSTEC).

Keywords: long-period ground motion, basin structure, numerical simulation, surface wave

Japan Geoscience Union Meeting 2014
(28 April - 02 May 2014 at Pacifico YOKOHAMA, Kanagawa, Japan)

SSS23-P15 Room:Poster Time:May 1 18:15-19:30

Long-Period Ground Motion Simulation in the Kanto Basin with/without Accretionary Prism

GUO, Yujia[1*] ; KOKETSU, Kazuki[1] ; MIYAKE, Hiroe[1]

[1]Earthquake Research Institute, University of Tokyo

Large earthquakes in subduction zones generally excite long-period seismic waves. Once these waves enter into basins filled with thick sedimentary layers, they develop and result in largely-amplified long-period ground motions. Such long-period ground motions have caused damage to large-scale buildings during some earthquakes. For the 2003 Tokachi-oki earthquake (M_w 8.3), long-period ground motions with a dominant period of 7-8 seconds were observed in the city of Tomakomai, located on thick sedimentary layers and at a distance of about 250 km from source region. The long-period ground motions triggered the sloshing in many oil tanks, and two of them caught fire (Koketsu *et al.*, 2005). For the 2011 Tohoku earthquake (M_w 9.0), long-period ground motions were observed at a large distance from source region such as the Osaka and Kanto basins, where some tall buildings shook over about 10 minutes (JMA, 2011).

The large earthquakes along the Nankai trough which are expected to occur in the near future can generate long-period ground motions in the Osaka, Nobi and Kanto basins (Furumura *et al.*, 2008). Along the Nankai trough, a accretionary prism composed of soft materials with a thickness of several kilometers lies near the toe of the Eurasian plate. Such prism does not exist at the Japan or Kuril trench. For this reason, in evaluating the long-period ground motions during the large earthquake occurring along the Nankai trough, we should consider the additional effect of accretionary prism on seismic waves. Yamada and Iwata (2005) simulated long-period ground motions for the Kinki region, and concluded that the existence of accretionary prism reduces the amplitudes of direct S-waves and elongates long-period ground motions. In this study, we performed simulations of the long-period ground motions in the Kanto basin for the foreshock (M_w 7.1) of the 2004 off the Kii peninsula earthquake on 5 September at 19:07 (JST) in order to examine the effect of accretionary prism.

In the simulation, we assumed a point source. Except its depth, its source parameter and source time function were the same as those of Yamada and Iwata (2005). We located the source at a depth of about 16 km, which is slightly shallower than that of Yamada and Iwata (2005), to fit it to the depth of the subducting Philippine Sea plate. We used the Japan Integrated Velocity Structure Model (Koketsu *et al.*, 2008, 2012). We calculated long-period ground motions using the finite element method with voxel meshes (Ikegami *et al.*, 2008). The frequency range of the calculation was 0.05-0.3 Hz, and the time duration of synthetic waveforms was set to be six and a half minutes from the rupture starting time. Our simulation model covered an area of 564 km$\times$198 km and extended to a depth of 61 km. An absorbing boundary with a width of 54 km was also introduced outside the simulation model. According to the velocity structure, the model was discretized by variable voxel meshes with the smallest size of 175 m. We also assumed a velocity structure model without accretionary prism, where the S-wave velocity of accretionary prism (1.0 km/s) is replaced with 3.2 km/s. Then, we calculated waveforms in this model and compared them with those in the accretionary-prism model to examine the effect of accretionary prism.

Our simulation shows that, compared with the velocity structure model without accretionary prism, the long-period ground motions for the accretionary-prism model have smaller amplitudes for direct waves but larger ones for later phases. Our results are consistent with those by Yamada and Iwata (2005). In the accretionary-prism model, the waves trapped in the accretionary prism are continually converted to surface waves, and the incident surface waves to the Kanto basin propagate in the basin. We confirm that this process contributes to the reduction of direct waves and the amplification of later phases in the Kanto basin.

Keywords: Long-period ground motion, Accretionary prism, Nankai trough, Kanto basin

Japan Geoscience Union Meeting 2014
(28 April - 02 May 2014 at Pacifico YOKOHAMA, Kanagawa, Japan)

SSS23-P16 Room:Poster Time:May 1 18:15-19:30

Semblance analysis for the 2011 Tohoku earthquake using strong-motion and 1Hz GPS data

KUBO, Hisahiko[1*] ; IWATA, Tomotaka[1] ; ASANO, Kimiyuki[1]

[1]DPRI, Kyoto Univ.

Source inversion is well used for the analysis of the earthquake source-process. However in the source inversion some assumptions and constraint conditions are used and there are cases where the settings of these affect the result. On the other hand, array analysis can produce the direct image for the seismic-wave radiation. In this analysis, we investigate the seismic-wave radiation characteristics for the 2011 Tohoku earthquake with the semblance array analysis using strong-motion and 1Hz GPS data.

We use not only the strong-motion data recorded by K-NET, KiK-net, and F-net of NIED and JMA but also 1 Hz GPS data recorded by GEONET of GSI. Additional use of 1 Hz GPS data leads to increase the station density and therefore the number of the available arrays increased remarkably compared to previous work (Kubo & Kakehi, 2013). Except for F-net data, the strong-motion acceleration waveforms are integrated into velocity waveforms. 1Hz GPS data is converted into displacement waveforms using Kinematic PPP as implemented in RTKLIB Ver. 2.4.2 (Takasu, 2013) and they are differentiated into velocity waveforms. These waveforms are bandpass-filtered from 10s to 25s and resampled with a sampling interval of 0.1s. From the comparison of the observed velocity waveforms for the 2011 Tohoku earthquake at the GEONET and strong-motion stations which distance is less than 3 km, we confirmed that the waveform of 1Hz GPS data matches one of strong-motion data at above period-band.

We use the same method of the semblance analysis in Kubo & Kakehi (2013). In this method, we firstly assumed the fault surface model consisting of some subfaults. Then the semblance value for each subfault is calculated assuming spherical-wave incidence when the subfault is the seismic-wave radiation source, and these values are plotted on the fault surface. By doing this analysis with time shift, we can obtain temporal change of the seismic-waves radiation source on the fault surface. The incident waves are assumed to mainly consist of S-wave because the estimated apparent velocity through the semblance analysis assuming plane-wave incidence is approximately 4 km/s and it don ' t have the dispersion. As the velocity structure model for the calculation of the travel time, we use one-dimensional velocity structure model in Asano & Iwata (2012). In this analysis, we constructed nine arrays at Tohoku and Kanto regions, and estimated the snapshot of semblance images at each array for 250s after the synthetic S-wave onset, which is comparable to the rupture starting time. The time length for semblance calculation is 20s and the time shift is 10s. The semblance value is obtained by averaging the three semblance values of the three-component waveforms.

The semblance images at the arrays north of 39^{o}N are different from ones at the arrays south of 39^{o}N. The images at the former arrays demonstrate that the seismic waves were strongly radiated from off Miyagi up to approximately 150s and that then the seismic waves were continued to be weakly radiated from off Miyagi. On the other hand, the images at the latter arrays demonstrate that the duration time of the seismic-wave radiation from off Miyagi is approximately 100s, that subsequently the radiation source moved to off Fukushima and Ibaraki, and that its radiation continued up to approximately 180s. This image difference indicates that the seismic-wave radiation area for the 2011 Tohoku earthquake extended to south approximately 100s after the rupture start and that off Miyagi radiated the seismic-waves during long time (~200s). We will also investigate the spatial variation for the seismic-wave radiation source along dip direction.

[Acknowledgments] The strong-motion data recorded by K-NET, KiK-net, and F-net of NIED and JMA and the 1Hz GPS data recorded by GEONET of GSI were used for this analysis.

Keywords: The 2011 Tohoku earthquake, Seismic-wave radiation characteristics, Semblance analysis, Strong-motion data, 1Hz GPS data

Japan Geoscience Union Meeting 2014
(28 April - 02 May 2014 at Pacifico YOKOHAMA, Kanagawa, Japan)

SSS23-P17 Room:Poster Time:May 1 18:15-19:30

Stochastic green function considering 3-D Qs structure-Predicting ground motion of the 2011 Tohoku Earthquake-

NAKAMURA, Ryoichi[1*] ; UETAKE, Tomiichi[2] ; HIKIMA, Kazuhito[2]

[1]Tokyo Electric Power Services Co.,Ltd., [2]Tokyo Electric Power Company

We have developed a method to simulate strong ground motions by combining the stochastic green function (SGF) and 3-D attenuation effects.

The calculation procedures of our method are as follows.

(1) To give Source spectra for sub-fault events.

(2) To calculate basement spectra considering 3-D Qs structure.

(3) To calculate ground surface spectra by multiplication of the site factors to basement spectra.

(4) To make time history of ground motions using ground surface spectra and envelope function (Boore, 1983).

(5) To create main shock ground motion by superimposing the ground motions from sub-fault events considering lapse time: ex. fault ruptures. (Kamae et al.,1991)

In this study, we reproduced strong motions of the 2011 Tohoku Earthquake (M9) by using this method. The fault plane of the 2011 Tohoku Earthquake was divided into 10∗10∗10 element faults planes, and seismic moment of Mo=4E+25 Nm and stress drop 25 MPa are given to the elements uniformly. Target sites to evaluate are ground surfaces of the K-NET and the KiK-net observation stations. The 3-D Qs model and site amplification factors estimated by Nakamura (2009) were used in this study. To show validity of this method, we compared calculation results by using the 3-D Qs model with by a uniform Qs model; $Qs=100f^{1.00}$.

The standard deviation of the logarithmic residual of PGA from the 3-D Qs model is 0.224 and that from the uniform Qs model is 0.231 for the stations with PGA>100Gal and the values are 0.253 and 0.360 respectively for the stations with PGA>1Gal. The difference was more significant for longer epicenter distance area. The response spectra calculated from the uniform Qs model are underestimated in the long distance areas, ex. Kinki and Hokkaido, whereas the response spectra using the 3-D Qs model were well reproduced the observed ones. Seismic wave spreads in deeper part for longer distance travels without attenuating. It is necessary to consider the three-dimensional Qs structure in evaluating the ground motion distribution in a broad area.

We tried to use the complex source model with SMGA. The model with five SMGA segments (Kurahashi and Irikura, 2011)) was adopted for calculation. The waveforms calculated from the uniform source model are like spindle shape generally, but the waveforms from the SMGA model are divided into several wave groups of the corresponding to individual SMGA especially for observation points close to the source. The SMGA model could explain well the observed record shape.

Keywords: 3D attenuation structure, Stochastic green function, Qs, 2011 Tohoku earthquake, Depth dependence, Strong ground motion prediction

Japan Geoscience Union Meeting 2014
(28 April - 02 May 2014 at Pacifico YOKOHAMA, Kanagawa, Japan)

SSS23-P18 Room:Poster Time:May 1 18:15-19:30

Estimation of Strong Motion Generation Area during the 2008 Iwate-Miyagi Nairiku earthquake using broadband strong groun

KURAHASHI, Susumu[1*] ; IRIKURA, Kojiro[1]

[1]Aichi Institute of Technology

1.Introduction

The 2008 Iwate-Miyagi Nairiku earthquake was an Mw6.7 reverse-fault crustal earthquake that occurred at Iwate prefecture, Japan. Surface ruptures associated with the earthquake were found to distribute near the eastern edge of the southern part of the aftershock zone. Strong ground motions were observed at three stations very near the fault area in addition to the Kik-net and K-NET stations. It is important that strong motion generation areas are estimated using broad-band ground motions to find out the source mechanism generating low-frequency ground motions as well as high strong ground motions.

In this study, we attempt to determine the strong ground motion area (SMGA) of the 2008 Iwate-Miyagi Nairiku earthquake using the broad-band ground motions from the earthquake.

2. The previous studies of the source model for strong ground motions

We presented the SMGA model of this earthquake by forward modeling using the empirical Green's function method by Irikura (1986) in 2008 and 2013.

The model we presented in 2008 was determined to reproduce the observed waveforms around the fault area of the mainshock. We found the first SMGA was located coinciding with large slip area in the southern part of the fault plane obtained by several authors from the waveform inversion analyses using teleseismic body wave data. We clarified to require one more SMGA in the northern part from the hypocenter. However, we realized that the location and geometry of the fault plane we assumed are not so accurate enough according to the aftershock distribution determined from temporary aftershock observation network deployed just after the occurrence of the earthquake (Okada et al., 2012).

We reanalyzed the SMGA model in 2013 using the fault plane determined by the aftershock distribution from the high dense network. In particular, we attempted to simulate the strong ground motions at IWTH25 located very near the fault plane. We obtained one of the best-fitting SMGA models from which simulated and observed ground motions agreed well including the ground motions at a very-near-field station IWTH25. However, it shall be examined whether this model can explain the broad-band ground motions at other near-field stations.

3. Estimation of SMGAs for broadband strong ground motions

In this study, we try to estimate the SMGAs using not only the strong motion records at IWTH25 but other near-field stations, Aratozawa Dam. The observed records at Aratozawa Dam show distinctive strong-motions. This suggests that one of the SMGAs possibly exists near Aratozawa Dam site. On the other hands, the observed records at Aratozawa Dam may have near-field-terms because of very-near-fields from the source area. Therefore, in order to reproduce the mainshock waveform we need to use the empirical Green's functions including the near-field terms, that is ground motion records from an element earthquake occurring very near a source in the fault area. When there is no element earthquake satisfying the near-field condition mentioned above, we use the hybrid Green's functions that have low frequency motions theoretically simulated and high frequency motions empirically obtained. We have no aftershock records at the Aratozawa Dam sites. Therefore, we attempt to simulate the broad-band strong motions at Aratozawa Dam site using only numerically calculated Green's functions to precisely estimate the SMGAs.

Keywords: Iwate Miyagi Nairiku earthquake, Strong Motion Generation Area, broad-band Strong Ground Motion

Japan Geoscience Union Meeting 2014
(28 April - 02 May 2014 at Pacifico YOKOHAMA, Kanagawa, Japan)

SSS23-P19 Room:Poster Time:May 1 18:15-19:30

Source Model and Strong Ground Motion Simulation for the 2013 Northern Tochigi Prefecture, Japan, Earthquake

SOMEI, Kazuhiro[1*] ; MIYAKOSHI, Ken[1] ; IRIKURA, Kojiro[2]

[1]G.R.I., [2]A.I.T.

On February 25, 2013, an inland crustal earthquake (M_{JMA}6.4, Strike-slip type) occurred in the northern Tochigi prefecture, Japan. Strong ground motions with a peak acceleration of 1225 cm/s^2 and a peak velocity of 39 cm/s were recorded at one of the nearest strong motion stations, TCGH07, about 5 km away from the hypocenter. Maeda and Sasatani (2009) showed that a similar large ground motion of 1100cm/s^2, 75cm/s at HKD020 during the 2004 South Rumoi district, Hokkaido, Japan, inland crustal earthquake (M_{JMA}6.1, Dip slip type) is mainly attributable to the source effect, short distance from the strong motion generation area (SMGA) and the forward directivity effect. To investigate how large ground motions at TCGH07 from a source's point of view, we estimate the source model based on the two different approaches.

First, we employ the multi-time window linear waveform inversion method (Sekiguchi et al., 2000) by using the 15 strong motion waveforms (0.1-1.0Hz) recorded by K-NET, KiK-net near the source. A finite extent of the fault plane is assumed referring to the aftershock distribution and moment tensor solution determined by F-net. The fault plane is divided into 84 subfaults of 1.0 km $\times$ 1.0 km. The temporal moment release history from each subfault is expressed by a series of 6 smoothed ramp functions with a rise time of 0.6 sec separated by 0.3 sec. The first time window triggering velocity (FTWTV) was 2.4 km/s. The rise time and FTWTV are given by the smallest misfit solution. The weight of the spatio-temporal smoothing constraint value for inversion was determined based on Akaike's bayesian Information Criterion (ABIC). The velocity structure model for each strong motion station is improved by the downhill simplex method (Nelder and Mead, 1965) using the receiver function. The theoretical Green's function is calculated by using the discrete wavenumber integration method (Bouchon, 1981) with the reflection and transmission matrix (Kennett and Kerry, 1979). To validate the improved velocity structure models, we simulate the aftershock records with a point-source approximation.

The derived rupture model has a large slip area whose maximum slip of 0.98 m in the vicinity of the hypocenter. The rupture mainly propagated from the hypocenter toward the shallower northern part. Seismic moment of the estimated model is 6.67$\times$10^{17}Nm (M_w 5.8). From the contribution of the large slip area to the synthetic waveforms for TCGH07, we find both the SH-wave radiation pattern from the strike-slip fault source and the forward directivity effect toward TCGH07 mainly yield the large pulse velocity waveform (0.1-1.0 Hz) at TCGH07.

Second, the source model is constructed based on the forward simulations using the empirical Green's function method (Irikura.1986) in the frequency range 0.3-10 Hz. One rectangle SMGA is estimated to include the rupture start point, i.e., the hypocenter of the mainshock. The rupture of this SMGA mainly propagates from the hypocenter to shallow side for dip direction, and also propagates to the northward for strike direction. The obtained source model explains the observed acceleration, velocity, and displacement waveforms of this event in the broadband frequency range fairly well. As same as the result from waveform inversion (0.1-1.0 Hz), we also see the large pulse velocity waveform is caused by the forward directivity effect toward TCGH07.

Consequently, we concluded that the main factors generating large pulse velocity waveform at TCGH07 are as follows: 1) the SH-wave radiation pattern from the strike-slip fault source and 2) the forward directivity effect along dip direction toward TCGH07.

Keywords: The 2013 Northern Tochigi Prefecture, Japan, Earthquake, Waveform inversion, Empirical Green's function method, Source model, Strong ground motion simulation

Japan Geoscience Union Meeting 2014
(28 April - 02 May 2014 at Pacifico YOKOHAMA, Kanagawa, Japan)

SSS23-P20 Room:Poster Time:May 1 18:15-19:30

Source process of the Feb. 25, 2013 Tochigi Hokubu Earthquake (M 6.3) [2] -Analyses using Empirical Green's Functions-

HIKIMA, Kazuhito[1*]

[1]Tokyo Electric Power Company

INTRODUCTION

An M6.3 earthquake occurred in the northern part of Tochigi prefecture on February 25, 2013. A high acceleration strong motion, over 1 G, was observed at the TCGH07 (Kuriyama-west) of KiK-net, which is situated close to the source region. To explain the reason why such strong acceleration was observed, the author has made the studies using the source process analysis and spectral inversion method to separate site and path effects. However, in the source process inversion, it is difficult to calculate accurate theoretical Green's functions in good enough level, because of the difficulty of making accurate subsurface structures. Consequently, the degree of coincidence between observed and calculated waveforms was not so good.

To overcome such the drawbacks in the source process inversions, the author uses the observed waveforms from a small earthquake as empirical Green's functions (EGF) in this study.

FAULT MODEL and OUTLINE of ANALYSES

Tentative analyses are performed with same fault geometry with Hikima (2013, SSJ fall meeting). The fault model was made using the relocated hypocenters, determined by the DD method, and the F-net mechanism solution. The strike direction is NNW-SSE (165 degree in strike, 80 degree in dip). The fault plane is divided in 1km size for the inversion.

The source process is inverted by the multi time window analysis (Yoshida *et al*. (1996), Hikima (2012)). The velocity waveforms, filtered between 0.03 and 1.5Hz, are used in the inversion analyses. The waveforms at TCGH07 are not used in the inversion, because the station is too close from the fault plain. Only the transverse components are used in this study, to weight the S-wave portion of the waveforms. The waveforms from the Mw 4.0 foreshock, which occurred on 15:26, February 25, 2013, are used as EGFs.

RESULT

Tentative result shows a more concentrated slip distribution than the former results by the theoretical Green's functions (Hikima, 2013). The high moment release area is about 4km *3km. However, the image of the rupture, whose slip propagates to the north, is almost same as former results. The coincidence between observed and calculated waveforms in this study is fairly better than the result by theoretical Green's functions.

Only one result using single EGF has been explained in this abstract. However, many other small earthquakes, which will be candidates for EGFs, occurred in the source area. So the results using other EGFs will be shown and I will discuss the accuracy of resultant slip distributions at the time of the presentation.

Keywords: Source process, Crustal earthquake, Near source, Strong motion, 2013 Tochigi Hokubu earthquake

Japan Geoscience Union Meeting 2014
(28 April - 02 May 2014 at Pacifico YOKOHAMA, Kanagawa, Japan)

SSS23-P21 Room:Poster Time:May 1 18:15-19:30

Source rupture process of the 2011 Northern Nagano earthquake (Mj 6.7) based on strong-motion records

SHIBA, Yoshiaki[1*]

[1]CRIEPI

The slip distribution model of the March 12, 2011 Northern Nagano earthquake (M6.7) were estimated by assuming the multiple fault planes model based on the aftershock hypocenters detected from the high-dense seismometer array and the crustal deformation information derived by the interferometry synthetic aperture radar (InSAR). Since the strong-motion record with peak ground acceleration more than 700 gal was obtained at the K-NET station NIG023 near the main shock, it is important to investigate the geometrical relation between the strong motion generation area (SMGA) on the main shock fault and the observation station. Estimated source model displays the largest slip near the K-NET NIG023 and beneath the existing anticlinal structure. The reverse fault motion of this event is considered to contribute the growth of the anticline. On the other hand the secondary fault plane, which was recognized clearly from the crustal deformation data inferred from InSAR, released relatively small or negligible amount of the moment according to our examination. It might have been the deformation caused by the aftershock occurring just after the main shock.

Keywords: 2011 Northern Nagano earthquake, Source process, Strong ground motion, Inversion analysis, InSAR, Anticlinal structure

Japan Geoscience Union Meeting 2014
(28 April - 02 May 2014 at Pacifico YOKOHAMA, Kanagawa, Japan)

SSS24-01 Room:315 Time:May 1 15:15-15:30

Structural analysis of seismogenic fault of the 2013 Mw 5.8 Awaji Island earthquake, NW Japan

LIN, Aiming[1*] ; KATAYAMA, Shouichi[1] ; RAO, Gang[2] ; KUBOTA, Yasu'uchi[3]

[1]Department of Geophysics,Graduate School of Science, Kyoto University, [2]Department of Earth Sciences, Zhejiang University, China, [3]OYO Cooperation

The 2013 Mw 5.8 (Mj 6.3) Awaji Island earthquake occurred in the southwest Awaji Island, at 5:33, 13 April, 2013, ca.25 km southwest of the epicenter of the 1995 Mw 6.8 (Mj 7.2) Kobe earthquake, southwest Japan. Pre-existing geologic data and focal mechanism show that this earthquake was triggered by an unknown active fault with a thrusting-dominated mechanism at high-dip angle of >70 degree. Interpretations of aerial photographs and 3D perspective images, field investigations and structural analysis of fault rocks, reveal that: i) a new fault, called Yamada Fault here, striking NNW and dipping WSW at a high-angle of 86 degree was found along a topographic lineament developed along the geological boundary between the Mesozoic granitic rocks and the Late-Tertiary-Quaternary Osaka Group composed of interbeded sandstone and mudstone; ii) a main shear zone of the Yamada Fault consists of a fault core that includes a narrow fault gouge zone of <10 cm in width (generally 1˜5 cm), a fault breccia zone of <100 cm in width, and a damage zone of 10˜50 m in width that is composed of cataclastic rocks and fractures; iii) the foliations characterized by S-C fabrics developed in the shear zone indicate a dominantly thrusting sense, consistent with that revealed by the focal mechanism; and iv) co-seismic surface ruptures occurred locally along the Yamada Fault, which are composed of numerous short fissures ranging from centimeters to several meters in length and concentrated in a zone <5 m. Our findings show that the newly found Yamada Fault is a active fault that probably triggered the 2013 Mw 5.8 (Mj 6.3) Awaji Island earthquake. Therefore, it is necessary to reconstruct the fault model for studying the tectonic activity and paleoseismicity and to reassess the seismic hazard of the active faults for densely populated Awaji Island, northwest Japan.

Keywords: 2013 M 6.3 Awaji Island earthquake, seismogenic fault, active fault, Yamada Fault, S-C fabrics of fault rocks, fault damage zone

Japan Geoscience Union Meeting 2014
(28 April - 02 May 2014 at Pacifico YOKOHAMA, Kanagawa, Japan)

SSS24-02 Room:315 Time:May 1 15:30-15:45

Quasi-cylindrical seismic waveform modeling considering surface topography

TOYOKUNI, Genti[1*] ; TAKENAKA, Hiroshi[2] ; OKAMOTO, Taro[3] ; ZHAO, Dapeng[1]

[1]RCPEVE, Tohoku Univ., [2]Okayama Univ., [3]Tokyo Tech

An accurate and efficient modeling of regional seismic wave propagation can be achieved by the axisymmetric modeling using the cylindrical coordinates. It assumes the structural model as rotationally symmetric along the vertical axis including a seismic source, and then solves the 3-D wave equation in cylindrical coordinates only on a 2-D structural cross section (i.e., 2.5-D modeling). Therefore, this method can correctly model 3-D geometrical spreading effects and the pulse shape, with computation time and memory comparable to 2-D modeling.

On the other hand, application of the conventional purely axisymmetric approximation is difficult in practice because the structure along the measurement line of the seismic survey is rarely symmetric with respect to the source location. To overcome this difficulty, Takenaka et al. (2003) proposed a ”quasi-cylindrical approach”. They developed a numerical scheme for seismic exploration using the finite-difference method (FDM). The FDM scheme had then been improved to include an arbitrary moment-tensor point source and the anelastic attenuation for further realistic modeling (Toyokuni et al., 2013, AGU Fall meeting).

In this work, we extended the scheme to treat land and ocean-bottom topographies. We adopted the cell-based staggered-grid FDM, which places the normal-stress components at the center of a unit cell, and applies the 2nd-order FD approximation around the free surface or fluid-solid boundary (Okamoto & Takenaka, 2005; Takenaka et al., 2009; Nakamura et al., 2012). In the presentation, we will show an application of the scheme to the waveform modeling for the volcanic areas in Japan.

Keywords: seismic waveform, finite-difference method, topography, fluid-solid boundary

Japan Geoscience Union Meeting 2014
(28 April - 02 May 2014 at Pacifico YOKOHAMA, Kanagawa, Japan)

SSS24-03 Room:315 Time:May 1 16:15-16:30

Spatial distribution of aftershock decay property beneath Japan Trench

IKUTA, Ryoya[1*] ; KUWAHARA, Masanori[2] ; MURAKAMI, Hiroki[3]

[1]Graduate School of Science, Shizuoka University, [2]Center of Integrated Research and Education of Natural Hazards, Shizuoka University, [3]Faculty of Science, Shizuoka University

We analyzed the aftershock sequences for individual M6-9 class inter-plate earthquakes and intra-plate earthquakes in Japan Trench for the period between October 1997 and March 2013 using JMA hypocenter catalog (final solution). The purpose is to examine a spatial relationship between the slip zone by the M9 earthquake and activity of aftershock series before the M9 and to understand the mechanism of aftershock. We approximated time variation of the number of aftershock sequences for each earthquake by the modified Omori ' s Law. Each aftershock sequence was identified from its spatial and temporal distribution. K and P parameters of Omori ' s Law were obtained by fitting the logarithmic Time-Frequency graphs of the aftershock sequence by linear function. We analyzed aftershock sequences for 44 events and adopted 17 whose K values are larger than 10 as available results because the results with smaller K values than 10 had large uncertainties due to lack of data. The results showed negative correlation between P values and Mj of the mainshocks. Before and after the M9 earthquake, there was no significant change in the aftershock parameters. However, we found a depth-dependent spatial distribution of aftershock decay properly. In the plate boundary, the aftershock sequence lasts for longtime without significant decay in the deeper portion, in contrast that the aftershock decays quickly at the shallower portion. It is known that the deeper part of plate boundary tends to slip aseismically without earthquakes. Taking this slow slipping property into account, our result suggests that the inter-plate frictional property should be responsible to the delay and decay property of the aftershocks.

Keywords: Aftershocks, Modified Ohmori's Law, Tohoku-Oki earthquake, Seismicity

Japan Geoscience Union Meeting 2014
(28 April - 02 May 2014 at Pacifico YOKOHAMA, Kanagawa, Japan)

SSS24-04 Room:315 Time:May 1 16:30-16:45

Location of early aftershocks of the 2011 Tohoku-oki Earthquake using seismogram envelopes as templates

KOSUGA, Masahiro[1*] ; SAKAI, Yuuka[2]

[1]Graduate School of Sci. & Tech., Hirosaki Univ., [2]Fac. Sci. & Tech., Hirosaki Univ.

The location of early aftershocks is very important to estimate the initial size of mainshock fault, because the aftershock zone generally extends with time. However, the location of early aftershocks is often difficult due to the long-lasting coda wave of mainshock and successive occurrence of aftershocks. To overcome this situation, we developed a location method using seismogram envelopes as templates. During the process of location, we firstly calculate the cross-correlation coefficients between a continuous (target) and template envelopes, and obtain time series of station-averaged cross-correlations for all templates. We then search for templates (initial location) in the descending order of cross-correlations in a time window excluding the dead times around the previously detected events. The third process is the relative event location that accounts for the lag times between actual and template envelopes. We applied the method to the early aftershock sequence of the 2011 Off the Pacific Coast of Tohoku Earthquake (Mw = 9.0). In a time window of 30-minutes just after the mainshock, we could locate 22 events in 8 Hz band by using 96 templates recorded at 33 Hi-net stations. The number of located events by the JMA is 13. Though we should carefully examine the location of detected events, we conclude that the proposed detection method works adequately even just after the mainshock of large earthquake.

Acknowledgement: We thank the NIED for providing waveform data of Hi-net. This work was supported by JSPS KAKENHI Grant Number 23540487.

Keywords: early aftershocks, template, envelope, Off the Pacific Coast of Tohoku Earthquake

Japan Geoscience Union Meeting 2014
(28 April - 02 May 2014 at Pacifico YOKOHAMA, Kanagawa, Japan)

SSS24-05 Room:315 Time:May 1 16:45-17:00

Aftershock distribution in the northern source region of the 2011 Tohoku earthquake by long-term OBSs

SHINOHARA, Masanao[1*] ; YAMADA, Tomoaki[1] ; NAKAHIGASHI, Kazuo[2] ; MOCHIZUKI, Kimihiro[1] ; MACHIDA, Yuya[1] ; SHINBO, Takashi[3] ; MURAI, Yoshio[4] ; HINO, Ryota[5] ; ITO, Yoshihiro[6] ; SATO, Toshinori[7] ; UEHIRA, Kenji[3] ; YAKIWARA, Hiroshi[8] ; SHIOBARA, Hajime[1]

[1]ERI, Univ. of Tokyo, [2]Kobe Univ., [3]NIED, [4]Hokkaido Univ., [5]Tohoku Univ., [6]DPRI, [7]Chiba Univ., [8]Kagoshima Univ.

The 2011 Tohoku earthquake occurred at the plate boundary and many aftershocks followed. To obtain a precise aftershock distribution is important for understanding of mechanism of the earthquake generation. In order to study the aftershock activity, we carried out extensive sea floor aftershock observation using more than 100 ocean bottom seismometers just after the mainshock. Deployment and recovery of the OBS were repeated, and we obtained the data from OBSs just after the mainshock to the middle of September, 2011. A precise aftershock distribution for approximately three months in the whole source area, with an emphasis on depths of events, was obtained from the OBS data. In the southern source region, an aftershock distribution until September, 2011 was also estimated. Totally urgent OBS observations located 1210 aftershocks (Shinohara et al., 2011, 2012). After the urgent aftershock observation using short-term OBSs, we continued the observation using long-term OBSs to monitor seismic activities in the source area. We deployed 40 LT-OBSs in the whole source region in September 2011 and have completed recovery of the LT-OBSs until November, 2012. In this presentation, we concentrate seismic activities in the northern source region using the data from the urgent aftershock observation and long-term seafloor observation.

We selected events whose epicenter is located below the OBS network form the JMA earthquake catalog, and P and S-wave arrival times were picked from the OBS data. Hypocenters were estimated by a maximum-likelihood estimation technique with one dimensional velocity structures. Thickness of sedimentary layer changes at each OBS site was evaluated and the estimated travel times by the location program were adjusted. We will report precise seismic activities in the northern source region with spatial and temporal variation. From preliminary analysis, seismic activity in off-Miyagi region was still low until the end of the long-term observation.

Japan Geoscience Union Meeting 2014
(28 April - 02 May 2014 at Pacifico YOKOHAMA, Kanagawa, Japan)

SSS24-06 Room:315 Time:May 1 17:00-17:15

A boundary of stress-field orientation in northwestern area of the Kanto plain

YANO, Tomoko elizabeth[1*] ; TAKEDA, Tetsuya[1] ; SHIOMI, Katsuhiko[1]

[1]NIED

Kanto-Tokai area is particularly important in terms of seismic hazard and mitigating disaster since this area is having high potential to economic and social impacts. Despite the fact, the Kanto region is one of the most seismic active areas due to its complicated tectonics and has an active fault zone, containing Fukaya fault, in northwestern area of the Kanto plain, which has potential to the M8 class earthquake. Many studies and research projects have attempted to understand the seismic activity and stress field. However, reliable and high-resolution catalog is required for the detailed discussion.

We have launched Japan Unified High-resolution Relocated Catalog for Earthquakes (JUICE) project since 2013. Events were relocated using the Double-Difference method for high-resolution hypocenter location to estimate seismogenic layer thickness, to evaluate active faults, and to understand the tectonic processes in Japan. We have completed for the first version of Catalog in the region of Kanto-Tokai area for the shallow (>40 km) earthquakes between M0 and M6.5 from 2001 to 2012. Here, in this presentation, we introduce the result from JUICE focusing on the northwestern area of the Kanto plain that contains a sharp boundary in which pressure and tension axis dramatically change by 90 degrees.

The JUICE catalog clearly shows a band of seismicity from Izu peninsula to the north. This seismic band has a nearly constant width of about 50 km. The focal mechanisms show that strike and thrust type dominate throughout this seismic band continuously, though there exists a area where pressure and tension axis dramatically change within this seismic band. While this " area " has been already recognized (e.g. Suzuki, 1989), JUICE helps to draw a precise " line " as a stress-field orientation boundary where happened to be close to Fukaya fault.

Bouguer gravity anomaly and seismic exploration data imply structural changes at the stress-field orientation boundary. According to the Bouguer gravity anomaly (Komazawa, 2004), the boundary appears to be associated with the gravity-low zone. The gravity anomalies show a lineation that trends NW-SE, the same direction of the boundary. Seismic profile (Sato et al., 2003) displays changes in basement character showing the pattern of depression beneath Fukaya fault. The shape of depression corresponds to the pattern of seismicity beneath this area, and also the boundary sites beneath the lowest point of the depression.

It appears to split into different regimes at the stress-field orientation boundary. We conclude that it is possible to have major tectonic boundary underneath this northwestern area of the Kanto plain. Moreover, we suggest that Median tectonic line (MTL) is a major candidate underneath this area. MTL runs parallel to the island arc through southwest Japan and divides different geological structures into outer (the forearc side) and inner arc (the backarc side). The trace of MTL disappears on the eastern side of Itoigawa-Shizuoka tectonic line, but Takagi et al. (2006) found an evidence of inner arc materials in the core sample obtained around this area. Therefore we assume that MTL is buried underneath the boundary. This finding may eventually impact on the research relates to hazard of Kanto area.

Keywords: Seismicity and tectonics

Japan Geoscience Union Meeting 2014
(28 April - 02 May 2014 at Pacifico YOKOHAMA, Kanagawa, Japan)

SSS24-07 Room:315 Time:May 1 17:15-17:30

Estimating earthquake swarms in volcanic regions

KUMAZAWA, Takao[1*] ; OGATA, Yosihiko[1] ; KIMURA, Kazuhiro[2] ; MAEDA, Kenji[2] ; KOBAYASHI, Akio[2]

[1]The Institute of Statistical Mathematics, [2]Meteorological Research Institute

In the eastern Izu region, earthquake swarms have occurred repeatedly since 1978. These events are known to be triggered by magma intrusions, and the amount of magma intrusion is correlated with volumetric strain of the crust. We show the background seismicity rate is highly correlated with the volumetric strain in this region, with a short time delay. We then discuss the possibility to forecast the seismicity in volcanic regions.

To calculate the background seismicity rate, we used the epidemic-type aftershock sequence (ETAS) model extended for application to nonstationary seismic activity, introduced by Kumazawa & Ogata (2013). The time-dependent rates of both background seismicity and aftershock productivity in the ETAS model are optimally estimated from hypocenter data by Bayesian smoothing method. These rates can provide quantitative evidence for abrupt or gradual changes in shear stress and/or fault strength due to aseismic transient causes such as triggering by remote earthquakes, slow slips, or fluid intrusions within the region.

Keywords: ETAS model, Bayesian smoothing, earthquake swarm, volcanic region, Izu

Japan Geoscience Union Meeting 2014
(28 April - 02 May 2014 at Pacifico YOKOHAMA, Kanagawa, Japan)

SSS24-08 Room:315 Time:May 1 17:30-17:45

Source Characteristics and Coulomb Stress Change of the 19 May 2011 Mw 6.0 Simav-Kutahya Earthquake, Turkey

GORGUN, Ethem[1*]

[1]Department of Geophysical Engineering, Istanbul University

Abstract

On 2011 May 19, Simav district of Kutahya province in northwest Anatolia was hit by a moderate size (Mw=6.0) earthquake. Centroid moment tensors for 41 events with moment magnitudes (Mw) between 3.5 and 6.0 are computed by applying a waveform inversion method on data from the Kandilli Observatory and Earthquake Research Institute broadband seismic network. The time span of data covers the period between 2011 May 19 and 2011 August 22. The mainshock is a shallow focus normal event at a depth of 10 km. Focal depths of aftershocks range from 5 to 20 km. The seismic moment (Mo) of the mainshock is calculated $1.15x10^{18}$ Nm. The estimated rupture duration of the Simav mainshock is 30 s. The focal mechanisms of the aftershocks are mainly normal faulting with a variable strike-slip component. The geometry of focal mechanisms reveals a normal faulting regime with NE-SW trending direction of T-axis in the entire activated region. A stress tensor inversion of focal mechanism data is performed to acquire a more accurate picture of the Simav earthquake stress field. The stress tensor inversion results indicate a predominant normal stress regime with a NW-SE oriented maximum principal compressive stress. According to variance of the stress tensor inversion, to first order, the Simav earthquake area is characterized by a homogeneous intraplate stress field. Eventually, Coulomb stress analysis is performed to calculate the stress transfer and correlate it with the activated region. Positive lobes with stress more than 3 bars are obtained, indicating that these values are large enough to increase the Coulomb stress failure towards NW-SE direction.

Keywords: Aftershock, Coulomb Stress Analysis, Focal Mechanism, Simav earthquake, Stress tensor inversion, Western Anatolia

Japan Geoscience Union Meeting 2014
(28 April - 02 May 2014 at Pacifico YOKOHAMA, Kanagawa, Japan)

SSS24-09 Room:315 Time:May 1 17:45-18:00

The Great Kanto Earthquake (of 1923) and YOKOHAMA (1)

NISHIZAWA, Masaru[1*]

[1]none

1. The reinforced cocrete buildings has been complated the leadership factions after The Great Kanto Earthquake (of 1923).
2. The YOKOHAMA Civilization Colour Print was important mediums of the YOKOHAMA exoticim and cultures.

Keywords: The Great Kanto Earthquake (of 1923), Yokohama, Open a port, YOKOHAMA civilization color print, The reinforced concrete building

クライスチャーチの波形

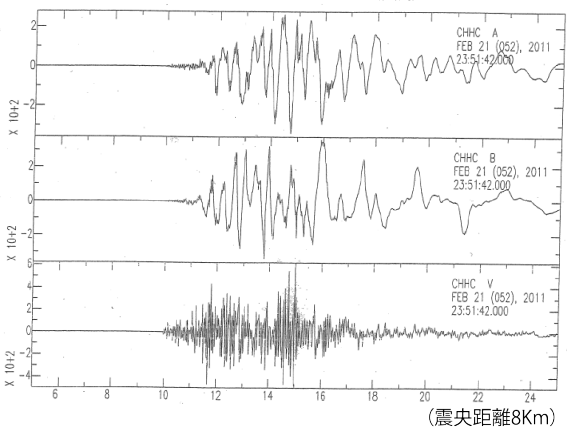

（震央距離8Km）

東西、南北の波の位相は逆転していることは
他と同じで、水平方向に建物に対して
回転力（又はねじれ）が生じることが判る。

主要動以後の波形は波うっていることは
他と同様。
しかし、上下動も多少は波うってはいるが、
東西、南北に比べると小さい。

Japan Geoscience Union Meeting 2014
(28 April - 02 May 2014 at Pacifico YOKOHAMA, Kanagawa, Japan)

SSS24-P01 Room:Poster Time:May 1 18:15-19:30

Seismic activity in eastern Japan and the source region after the 2011 off the Pacific coast of Tohoku earthquake

UOOCHI, Akiko[1] ; KUGE, Keiko[1*]

[1]Dept. Geophysics, Kyoto University

Changes of seismic activity in eastern Japan and the source region were shortly reported after the 2011 off the Pacific coast of Tohoku earthquake (Toda et al., 2011; Kato and Igarashi, 2012). To clarify subsequent changes, we investigated seismic activity in the wide region for two and a half years since the 2011 Tohoku earthquake.

We examined a region in a range of 33.4-42N and 136-145E. The region was divided into small squares with a size of 0.2 degree, and in each square, we computed seismicity rates. First, as the background seismicity, we computed the average number of earthquakes per a year, based on seismic activity for nine years before the 2011 earthquake. Then, to obtain seismicity rates after the 2011 earthquake, we counted the number of earthquake during two periods, respectively, and computed the ratios against the background seismicity. The two periods are 0-1 and 1.5-2.5 years after the 2011 earthquake. We used hypocenters determined by JMA. In regions where large inland earthquakes occurred before 2011, the background seismicity was computed from a period excluding aftershocks. Finally, by plotting the resultant seismicity rates in maps, we searched regions where seismic activity significantly changed. By the same method, we also examined seismicity rates of interplate earthquakes in the source region of the 2011 Tohoku earthquake, based on data selected from the F-net CMT catalog.

Our results show that when two and a half years passed since the 2011 earthquake, seismicity of interplate earthquakes had been lower than the background, throughout the source region of the 2011 Tohoku earthquake except for a region off Iwata. High seismic activities for a year since the 2011 earthquake were found in Iwaki, the middle and northern parts of Akita, the southern part of the Kanto region, and also in regions near active volcanos (Bandai, Nikko-Shirane, Kusatsu-Shirane, Naeba, and Fuji mountains). When two and a half years passed, seismicity in many regions of eastern Japan had been lower than the background, including the activities near Bandai, Naeba, and Fuji mountains. However, activities in Iwaki, the middle and northern parts of Akita, the southern part of the Kanto region, and near Nikko-Shirane and Kusatsu-Shirane mountains continued to be high.

Furthermore, we carefully examined seismic activity in the regions where we detected significant changes of seismic activity. In many regions of eastern Japan, we found that locations of earthquakes and focal mechanisms were changed before and after the 2011 Tohoku earthquake.

Using JMA hypocenters, we also attempted to apply the modified Omori's law for seismic activity after the 2011 earthquake in the regions with significant changes of seismic activity. The modified Omori's law could roughly model the changes of seismic activity in many regions, even when a region is inland, away from the source region. The Omori's regression parameter, p, was estimated in a range from 0.2 to 1.1. The values ranged between 0.2 and 1.1 in the regions where seismic activity has been high for 2.5 years, whereas they were between 0.8 and 1.1 where high seismic activity for the first 1 year decreased in 2.5 years since the 2011 earthquake. In the southern part of the Kanto region, the value of p (0.2) was extremely low, compared to the other regions, which implies that the seismic activity decays very slowly. In the regions near active volcanos, the values of p tended to be high. In the source region of the 2011 Tohoku earthquake, we estimated the values of p in three regions; a whole source region, an afterslip region, and a region excluding the afterslip region. The values ranged from 1.0 to 1.1, and there was no significant difference in the three regions.

Japan Geoscience Union Meeting 2014
(28 April - 02 May 2014 at Pacifico YOKOHAMA, Kanagawa, Japan)

SSS24-P02 Room:Poster Time:May 1 18:15-19:30

A statistical feature of anomalous seismic activity prior to large inland earthquakes in Japan

KAWAMURA, Masashi[1*] ; WU, Yi-hsuan[2] ; KUDO, Takeshi[3] ; CHEN, Chien-chih[2]

[1]Department of Geosciences, National Taiwan University, [2]Grad. Inst. of Geophysics, National Central University, Taiwan, [3]General Education Division, College of Engineering, Chubu University

To reveal the preparatory processes of large inland earthquakes, we systematically applied the pattern informatics (PI) method to earthquake data of Japan. We focused on 12 large earthquakes with magnitudes greater than M6.4 (based on the magnitude scale of the Japan Meteorological Agency) that occurred at depths shallower than 30 km between 2000 and 2010. We examined the relationship between the spatiotemporal locations of these large shallow earthquakes and the locations of PI hotspots, which correspond to grid cells of anomalous seismic activity during a designated time span. Based on a statistical test conducted using Molchan's error diagram, we investigated whether precursory anomalous seismic activity occurred in association with these large earthquakes and, if so, studied the characteristic time spans of such activity. Our results indicate that Japanese inland earthquakes with M $\geqq$ 6.4 are typically preceded by anomalous seismic activity in timescales of 8-10 years.

Keywords: pattern informatics, seismic quiescence, seismic activation, Molchan's error diagram, stress accumulation, inland earthquake

Japan Geoscience Union Meeting 2014
(28 April - 02 May 2014 at Pacifico YOKOHAMA, Kanagawa, Japan)

SSS24-P03 Room:Poster Time:May 1 18:15-19:30

Coulomb stress change inverted from the seismicity rate change in southern 2011 Tohoku earthquake's source region

TAKAHASHI, Go[1*] ; TSUMURA, Noriko[1]

[1]Graduate School of Science, Chiba University

By using the analysis of seismicity rate change, we estimated spatio-temporal evolution of Coulomb stress around the upper boundary of the Pacific plate (PAC) and Philippine Sea plate (PHS) in and around the southern edge of the rupture zone of the 2011 Pacific coast of Tohoku earthquake (Mw=9.0). We used hypocenter catalog of the Japan Meteorological Agency (JMA) for the period between 1998/1/1 and 2013/3/31. Estimated stress change became large just after the 2011 Tohoku earthquake in most of rupture zone. The large stress change estimated from the seismicity reached the southern outside of the contact zone of the PHS and the PAC, while this area is located at outside of the source fault of the 2011 Tohoku earthquake. Moreover, in the October 2011 Boso slow slip event (SSE) initiation area, stress change remained large value after the 2011 Tohoku earthquake.

To estimate the effect of the mainshock and largest aftershock in our inversion result, we calculated Coulomb stress change by simulating the mainshock, afterslip and Mw7.9 aftershock for the 2011 Tohoku earthquake in an elastic half space. From similarity between the result from seismicity rate change and result of forward modeling, most of the stress change pattern in and around mainshock rupture zone after the 2011 Tohoku earthquake might be explained by the effect of the 2011 Tohoku earthquake mainshock, afterslip and the largest aftershock. On the other hand, since the result from seismicity rate change didn't correspond to the result of forward modeling in the October 2011 SSE area, this region was possibly affected by other event or closeness to break strength.

Keywords: stress change, 2011 Tohoku earthquake, aftershock, slow slip

Japan Geoscience Union Meeting 2014
(28 April - 02 May 2014 at Pacifico YOKOHAMA, Kanagawa, Japan)

SSS24-P04 Room:Poster Time:May 1 18:15-19:30

Spatial distribution of earthquakes off the coast of Ibaraki and the Boso Peninsula after the 2011 Tohoku Earthquake

NAKAHIGASHI, Kazuo[1*] ; MACHIDA, Yuya[2] ; SHINBO, Takashi[7] ; YAMADA, Tomoaki[2] ; MOCHIZUKI, Kimihiro[2] ; SHIOBARA, Hajime[2] ; SHINOHARA, Masanao[2] ; MURAI, Yoshio[3] ; HINO, Ryota[4] ; AZUMA, Ryosuke[4] ; SUZUKI, Kensuke[8] ; KUBOTA, Tatsuya[4] ; HASEGAWA, Kazuya[4] ; SATO, Toshinori[5] ; TAKATA, Hiroyoshi[5] ; UEHIRA, Kenji[7] ; YAKIWARA, Hiroshi[6]

[1]Kobe Univ., [2]Earthquake Research Inst., [3]Hokkaido Univ., [4]Tohoku Univ., [5]Chiba Univ., [6]Kagoshima Univ., [7]National Research Institute for Earth Science and Disaster Prevention, [8]JAMSTEC

The 2011 off the Pacific coast of Tohoku Earthquake occurred on March 11, 2011, off shore of the northeast Japan region. Many aftershocks occurred following the mainshock. To obtain a precise aftershock activity is important for understanding the mechanism of earthquake generation, and the recovery of plate coupling at a ruptured plate boundary. In order to study the aftershock activity, we had deployed 66 long-term ocean bottom seismometers(LTOBS) off the coast of Ibaraki and the Boso Peninsula from October 2011 to November 2012.

For hypocenter determination, we selected 1606 events whose epicenter catalog which the Japan Meteorogical Agency for hypocenter determination.P- and S- wave arrival times were manually picked using the WIN system (Urave and Tsukada, 1991).Hypocenters were determined by the maximum-likelihood estimation technique (Hirata and Matsu·ura, 1987). The hypocenter location program used in this study is based one-dimensional structure with constant Vp/Vs ratio of 1.73. Because a sedimentary layer below the sea floor generally has a large Vp/Vs value, an adjustment of the station corrections is needed. To obtain the station correction, we used the following method. First, we located the hypocenter using the P- and S-wave arrival times with the assumed station correction values for the velocity structure used. The averaged differences between observed travel time and estimated travel times (O-C times) for each station were then calculated. The averaged O-C times were added to the previous station correction values, and the hypocenters were relocated. We repeated this procedure eleven times. After this procedure, the averaged O-C times were less than 0.1 s for both the P-wave and S-wavesWe estimated 458 hypocenter locations with an error of less than 5 km in the horizontal direction and less than 3 km in depth by using LTOBS data.

Most of the hypocenter locations have a depth shallower than 40km. The earthquakes form a plane dipping landward in the study area. Comparing the hypocenter locations with crustal structures obtained by active seismic studies (e.g. Miura et al., 2003). Many events occurred along the plate boundary. We also compared the hypocenter locations with aftershock distribution of the seismic observation conducted immediately after 2011 Tohoku Earthquake (Shinohara et al., 2012). Shinohara et al., (2012) reported that the low seismicity region has seen at the shallow part of the plate interface in the off-Fukushima. On the other hand, our results showed the seismicity is not low at the same region. This difference may reflect the change of stress fields at a ruptured plate boundary.

Japan Geoscience Union Meeting 2014
(28 April - 02 May 2014 at Pacifico YOKOHAMA, Kanagawa, Japan)

SSS24-P05 Room:Poster Time:May 1 18:15-19:30

Spatial distribution of earthquakes off the coast of Fukushima deduced from a one-year OBS observation in 2013

YAMADA, Tomoaki[1*] ; NAKAHIGASHI, Kazuo[2] ; SHINOHARA, Masanao[1] ; MOCHIZUKI, Kimihiro[1] ; SHIOBARA, Hajime[1]

[1]Earthquake Research Institute, Univ. of Tokyo, [2]Kobe Univ.

The 2011 Tohoku earthquake (M9.0) vastly changes stress field around the rupture zone, and many aftershocks and other related geophysical phenomenon such as geodetic movements have been observed. The seismicity not only keeps still high rate compared with that before the 2011 earthquake but is important to figure out the time-spacious distribution during the relaxation process for understanding the giant earthquake cycle. Many studies using ocean bottom seismometers (OBSs) [e.g. Shinohara et al,, 2011, Nakahigashi et al., this meeting] have been doing since soon after the 2011 Tohoku earthquake in order to obtain aftershock activity precisely. Here we show one of the studies at off the coast of Fukushima which is located on the southern edge of the rupture zone of the 2011 Tohoku earthquake. 12 short-period type [Lennartz 3Dlite] OBSs (SOBS) and 4 broadband type [Guralp CMG 3T] OBSs (BBOBSs) in Auguest 2012 were installed. 20 SOBSs and 4 BBOBSs attached with absolute pressure gauge [Paroscientific Model 8B] were added in November 2012. After one year continuous recording, 36 OBSs were recovered in November 2013. We selected characteristic 1,000 events in the vicinity of the OBS network based on a hypocenter catalog publish by the Japan Meteorological Agency, and extracted the events' data from all available OBS data after time corrections caused by each internal clock. Each P and S wave arrival times, P wave polarity and maximum amplitude were picked manually on a computer display using the WIN system [Urabe and Tsukuda, 1991]. We assumed one dimensional velocity structure that is modification of the result from an active source experiment close to our network, and applied time corrections every station which were estimated from differences from theoretical and observational travel times for removing ambiguity of the assumed structure. Then we adopted the maximum-likelihood estimation technique [Hirata and Matsu'ura, 1987] and calculated the hypocenters. Preliminary results show that intensive activity near the Japan trench can be seen while there was a quiet seismic zone between the trench zone and landward high activity zone.

Keywords: off Fukushima, Aftershock activity, Long-term OBS

Japan Geoscience Union Meeting 2014
(28 April - 02 May 2014 at Pacifico YOKOHAMA, Kanagawa, Japan)

SSS24-P06 Room:Poster Time:May 1 18:15-19:30

Relation between Seismicity and Stress Change Associated with Interplate Slips off Boso Peninsula: Part 2

HIROSE, Fuyuki[1*] ; MAEDA, Kenji[1]

[1]Meteorological Research Institute

Hirose & Maeda (2012, 2013, JpGU; 2013, SSJ) investigated a relation between temporal variation of seismicity rate or b-value of the G-R law (Gutenberg and Richter, 1944, BSSA) and stress change associated with slow slip events (SSEs) around Boso peninsula. For example, there are three characteristic stages about seismicity: (S-1) activation during SSE, (S-2) quiescence before 2002 and 2007 SSE, and (S-3) seismicity rate increases after 2007 SSE. On the other hand, b-value repeats a cycle as follows: (b-1) small during and just after SSE, (b-2) gradually increases up to the next SSE.

By considering the correlation of seismicity rate with stress increase and inverse correlation of b-value with stress obtained in laboratory experiments (Dieterich, 1994, JGR; Scholz, 1968, BSSA), they interpreted their result as follows: for (S-1, b-1) during SSE, the slip rate at the edge of SSE on the plate boundary where is seismically active becomes higher (We can confirm it from the distribution of slip deficit and SSE estimated by GNSS data). Then because a strain accumulation rate increases, the stressing rate increases. Thus, seismicity rate increases, and b-value decreases at the same time. On the other hand, for (S-2, b-2) in SSE interval, because the slip rate on the plate boundary becomes lower than that during SSE, the seismicity rate decreases, and b-value increases at the same time. For (S-3) seismicity rate increases after 2007 SSE, the distribution of slip deficit after 2007 SSE is not much different from that before SSE. When we consider a frame of Dieterich (1994), only steady slip rate should become higher without changing of slip deficit rate so that seismicity rate changes under this situation because slip deficit on the plate boundary is independent of the value of steady slip rate (Savage, 1983, JGR). That means the drop of the coupling rate on plate boundary (slip deficit rate / steady slip rate). Therefore, the temporal change of the seismicity and b-value is comprehensively consistent with the perturbation of the slip rate on the plate boundary.

By the way, Boso SSEs had occurred every 4-7 years, but the latest interval of occurrence has a shorter period because those occurred in the end of 2011 and early in 2014. It is considered that the shortening of interval is mainly caused by the influence of the 2011 off the Pacific Coast of Tohoku Earthquake (Mw9.0, hereinafter Tohoku earthquake). We extended data period and investigated whether the same characteristics as before are also seen for the 2014 SSE. As a result, it showed such the same characteristics that (S-1) activation during SSE, (S-3) seismicity rate increases after 2007 SSE, (b-1) small during and after SSE, and (b-2) gradually increase up to the next SSE. On the other hand, (S-2) quiescence before SSE was not recognized because the perturbation of stress caused by the Tohoku earthquake may affect the seismicity.

Keywords: Boso peninsula, slow slip event, b value, stress, temporal change

Japan Geoscience Union Meeting 2014
(28 April - 02 May 2014 at Pacifico YOKOHAMA, Kanagawa, Japan)

SSS24-P07 Room:Poster Time:May 1 18:15-19:30

Microseismicity around the Nankai trough south off the Kii Peninsula

YAMAZAKI, Akira[1*]

[1]Meteorological Research Institute

The seismicity around the Nankai trough axis and its southern area, south off the Kii Peninsula, was not well understood, because most previous ocean bottom seismograph observations had been performed at landward from the trough axis. In order to investigate the seismicity around the region, Meteorological Research Institute conducted ocean bottom seismograph observations at around the Nankai trough axis and its southern area from 2005 to 2008, cooperated with Seismology and Volcanology Department, Japan Meteorological Agency (JMA). We conducted four observations, which period was approximately three months, using about ten pop-up type ocean bottom seismographs. As a result, we could detect a microseismic activity, which were not listed in the earthquake catalogue by JMA, around the trough axis.

The features of the microseismic activity are as follows. The depth of the hypocenters distributes around 10km to 25km. Since the depth of hypocenters determined by JMA at the region distributes around 30km to 40km, the true depth of the earthquakes is considered about 20km shallower than that of the JMA. There is a clear lower limit plane of hypocenters, and little earthquakes occur deeper than 25km. As a general tendency, the microseismic distribution has south incline at seaward from the trough axis, north incline at landward. The distribution of the hypocenters is not uniform, and we can detect some seismic clusters, liner arrangements and several seismic gaps of the 20km to 30km in diameter. It seems that seismic segment structures are formed within the Philippine Sea plate.

In general, seismic activity around a trough axis is causes by bending of oceanic plate. Moreover, the activity is affected by somewhat change of interplate coupling status at subduction zone. For instance, it is pointed out that the focal mechanism at outer rise region changes from compressional to tensional tectonic field by occurrence of large interplate earthquakes at subduction zone. We propose a possibility that the temporal change of the microseismic activity around the Nankai trough axis reflects a temporal change of the plate motion or a somewhat change of plate coupling conditions.

Keywords: ocean bottom seismograph, Tonankai earthquake, Nankai earthquake, Nankai trough, microseismicity, Philippine Sea plate

Japan Geoscience Union Meeting 2014
(28 April - 02 May 2014 at Pacifico YOKOHAMA, Kanagawa, Japan)

SSS24-P08 Room:Poster Time:May 1 18:15-19:30

Repeating earthquake activity along the Izu-Bonin and Ryukyu trenches

HIBINO, Kota[1*] ; UCHIDA, Naoki[1] ; MATSUSHIMA, Takeshi[2] ; NAKAMURA, Wataru[1] ; MATSUZAWA, Toru[1]

[1]Graduate School of Science Tohoku University, [2]Faculty of Sciences,Kyushu University

There are several subduction systems near the Japanese islands. The 2011 Mw9.0 Tohoku-oki megathrust earthquake occurred at the northeastern Japan subduction zone and revealed a complementary relation between the slip areas for huge earthquakes and small repeating earthquakes (REs). Investigations of REs in other subduction zones and their comparison with Tohoku area are important for revealing generation mechanism of megathrust earthquakes.

We use seismograms from the High Sensitivity Seismograph Network (Hi-net) and Japan Meteorological Agency (JMA)'s permanent seismograph stations from 8 May 2003 to 31 December 2012. We detect RE along the Izu-Bonin and Ryukyu trenches, using similarity of seismogram pairs.

Although, Igarashi (2010) and Yamashita et al. (2012) have already examined RE activity in this region, we mainly follow the method of Uchida et al. (2010) to compare with the REs at Tohoku area. In the method, pair with coherence larger than 0.95 at multiple stations is considered to belong to a repeating earthquake group. We apply this method to the earthquakes along the Ryukyu trench. Along the Izu-Bonin trench, however, the signal-to-noise (S/N) ratios of the waveforms are not so good because of the limited seismic stations at sparsely distributed islands. Therefore, we adopt a coherence threshold of 0.8 and even if S/N ratios of the waveform are good at only one station, earthquake pairs that satisfy the threshold in multiple components are considered as candidates of REs along the Izu-Bonin trench.

Along the Ryukyu trench, we find RE distribution shows two dense bands parallel to the trench axis. This feature is similar to the northeastern Japan subduction zone. We consider the regions between the two bands of REs may have strong interplate locking as suggested at Tohoku.

Along the Izu-Bonin trench, in spite of the non-strict coherence threshold, we find much fewer REs than that in northeastern Japan. Our result suggests that REs are relatively rare along the Izu-Bonin trench and they mainly occur at the shallow part where the Pacific plate contacts with the crust of the Philippine Sea plate.

These varieties in the RE occurrences suggest different interplate locking patterns along these subduction systems.

Keywords: subdection zone, repeating earthquake, Izu-Bonin, Ryukyu, interplate locking

Japan Geoscience Union Meeting 2014
(28 April - 02 May 2014 at Pacifico YOKOHAMA, Kanagawa, Japan)

SSS24-P09 Room:Poster Time:May 1 18:15-19:30

Ocean bottom seismic observation in the Hikurangi subduction zone offshore the North Island of New Zealand

HAIJIMA, Daisuke[1*] ; MOCHIZUKI, Kimihiro[1] ; SHIOBARA, Hajime[1] ; YAMADA, Tomoaki[1] ; SHINOHARA, Masanao[1] ; HENRYS, Stuart[2] ; FRY, Bill[2] ; BANNISTER, Stephen[2]

[1]Earthquake Reserch Institute, University of Tokyo, [2]GNS Science

The Hikurangi Plateau which has ∼12 km thick crust subducts under the Australian plate
in the Hikurangi subduction zone offshore North Island, New Zealand. The plate interface is relatively shallow so that geometry of the plate interface has been revealed in detail by high quality seismic reflection data collected along dense profiles along the margin [Bell et al. 2010]. Distribution of interseismic plate-coupling has been estimated and series of slow slip events (SSEs) have been detected at around the lower limit of the coupling region due to recent installation of dense GPS network over the North Island. In the northern part, along-strike coupling region is narrow and the upper limit extends to near the trench axis and the lower limit is shallow at ˜15 km depth. Most of the region of strong interplate coupling is under the sea. We need to conduct seismic observation using ocean bottom seismometers (OBSs) to understand seismicity and hypocentral distribution in detail. SSEs occur at much shallower depth than other subduction zones.

We conducted a passive seismic observation using OBSs for the first time offshore Gisborne to reveal seismisity and low-frequency events accompanying SSEs. We deployed four OBSs in April 2012 and recovered all instruments after 11 months of observation. The northern two instruments were a broadband type and the other southern two were equipped with 1Hz seismometers. Although the recorder of one of the broadband type OBSs recorded only intermittently, good data were obtained from the others. An earthquake swarm occurred to the north of the array in September to November 2012. A large SSE occurred around the Hawke's Bay to the south of the array from mid-February 2013. At first we apply STA/LTA algorithm to this data to detect seismicity. The result shows seismicity was activated accompanying both the earthquake swarm and the SSE. We tried to determine the hypocenters of these events using 4 OBSs and some GeoNet onshore seismometers. We could detect more offshore events than are listed in the GeoNet catalogue owing to higher Signal-to-Noise ratios of the OBS data while most events occurred beneath the seafloor.

Keywords: seismicity, Hikurangi, OBS

Japan Geoscience Union Meeting 2014
(28 April - 02 May 2014 at Pacifico YOKOHAMA, Kanagawa, Japan)

SSS24-P10 Room:Poster Time:May 1 18:15-19:30

Greenland Ice Sheet Dynamics and Glacial Earthquake Activities

KANAO, Masaki[1*] ; TSUBOI, Seiji[2] ; TOYOKUNI, Genti[3] ; HIMEMO, Tetsuto[4] ; TONO, Yoko[2]

[1]National Institute of Polar Research, [2]Japan Agency for Marine-Earth Science and Technology, [3]Tohoku University, [4]Seikei University

The Greenland ice sheet and its response to climate change have potentially a great impact upon mankind, both through sea-level rise and modulation of fresh water input to the oceans. Monitoring a dynamic response of the Greenland ice sheet to climate change is a fundamental component of long-term observations in global science. Glacial earthquakes have been observed along the edges of Greenland with strong seasonality and increasing frequency in this 21st century by the data from Global Seismographic Network (GSN). During the period of 1993-2006, more than 200 glacial earthquakes were detected, but more than 95% have occurred on Greenland, with the remaining events in Antarctica. Greenland glacial earthquakes are considered to be closely associated with major outlet glaciers at the margins of the continental ice sheet. Temporal patterns of these earthquakes indicate a clear seasonal change and a significant increase in frequency after 2002. These patterns are positively correlated with seasonal hydrologic variations, significantly increased flow speeds, calving-front retreat, and thinning at many outlet glaciers. These long-period surface waves generated by glacial earthquakes are incompatible with standard earthquake models for tectonic stress release, but the amplitude and phase of the radiated waves can be explained by a landslide source model. The seismicity around Greenland including tectonic/volcanic events was investigated by applying a statistical model to the globally accumulated data. Calculated b values, the Magnitude-frequency-dependence parameter, indicated a slight increase from 0.7 to 0.8 in 1968-2007, implying that the seismicity including glacial events around Greenland become slightly higher during the last four decades. The detection, enumeration, and characterization of smaller glacial earthquakes were limited by the propagation distance to globally distributed stations of the GSN. Glacial earthquakes have been observed at stations within Greenland, but the coverage has been very sparse. In order to define the fine structure and detailed mechanisms of glacial earthquakes, a broadband, real-time network needs to be established throughout the ice sheet and perimeter. The International Polar Year (IPY 2007-2008) was a good opportunity to initiate the program with international collaboration. Then, the Greenland Ice Sheet Monitoring Network (GLISN) was initiated for the purpose of identifying the dynamic response of the Greenland ice sheet to climate change.

Keywords: Greenland, global warming, glacial earthquakes, broadband seismometer, monitoring

Japan Geoscience Union Meeting 2014
(28 April - 02 May 2014 at Pacifico YOKOHAMA, Kanagawa, Japan)

SSS25-01 Room:312 Time:May 2 14:15-14:30

Foreshock activity of the large-scale interplate earthquakes around Japan

TANAKA, Rika[1*] ; ORIHARA, Yoshiaki[1] ; KAMOGAWA, Masashi[1]

[1]Dpt. of Phys., Tokyo Gakugei Univ., [2]Earthquake Prediction Reserch Center, Tokai University

According to Bouchon et al. (Nature Geosci, 2013), they reported that the number of foreshocks increased towards the mainshock in the interplate earthquakes around North America and Japan. But, the foreshocks were much less frequent in the intraplate earthquakes. We investigate whether such a clear difference is really found between the interplate earthquakes and the intraplate earthquakes around Japan.

Keywords: Foreshocks, Interplate earthquakes, Accelerating seismicity

Japan Geoscience Union Meeting 2014
(28 April - 02 May 2014 at Pacifico YOKOHAMA, Kanagawa, Japan)

SSS25-02 Room:312 Time:May 2 14:30-14:45

Development of Acoustic Frequency Comb technology by ACROSS appropriate for active monitoring of the earthquake field

KUMAZAWA, Mineo[1*] ; HIGASHIHARA, Hiromichi[2] ; NAGAI, Toru[1]

[1]Nagoya University, [2]University of Tokyo

Acoustic Frequency Comb technology by utilizing ACROSS (Accurately Controlled Routinely Operated Signal System) has been developed since 1994 at Nagoya Univ. and Earthquake Research Institute at Univ. of Tokyo for the active monitoring method of the subsurface structures. It is now being operated routinely in several locations in Gifu, Aichi, Shizuoka, Hyogo and Kagoshima prefectures.

A group of earthquake seismologists wrote in a book"Science of Earthquake Prediction"(UT Press, 2007) as follows: Whereas ACROSS is an indispensable element for earthquake prediction works, there are problems in stability of the instrumentations, methods of data analysis, etc. To resolve the problems raised by them, our own research works are demanded rather than to complain or to criticize.

1..In the current ACROSS transmitters, single force vector F as frequency-modulated signal is generated by centrifugal force by rotation of a rather small mass M ($\sim$ 100 kg) with a displacement amplitude u as constrained by equation of motion;

$F = M\, d^2u/dt^2 = -\omega^2 (Mu)$

The centrifugal force thus generated is transmitted towards the Earth's interiors through a transmitting antenna named 'ground coupler', which is a steel-reinforced concrete block of several meters in size and $\sim$ 100 tons in weight. As specified by the formula above, transmitted force amplitude is proportional to frequency squared, so that signal transmission is difficult in the useful low frequency range. The previous transmitters designed are practically limited for the use above 5Hz. To extend the frequency to the lower span, we propose the use of a linear motion of larger inertia mass M, 100 $\sim$ 100000 times larger the current transmitter to reduce the frequency by a factor of 10 $\sim$ 100. This could be simply realized by utilizing a large ground coupler as an inertia mass. Quantitative examination of this approach is found to be promising, and we have started the works on the technical realization of this observation system.

2. Low frequency acoustic signal below 1 Hz is useful for the stationary monitoring system covering everything in the whole Japanese Islands, once we build a transmitter array consisting of several tens transmitting statins, since the signal is easily detected up to 100 km distance without any environmental pollution. Local dense array of the signal sensors would provide us with the accurate data set on the swarm of local eigen-modes within the frequency range of the transmitted signals. This approach is the frequency comb interferometry much potential than the seismic daylight interferometry commonly applied nowadays. To make the structural inversion of the data by frequency comb interferometry, we have developed a new forward method named PANW, in which wave equation as a differential equation is converted to arithmetic equation in frequency and wavenumber domain on the basis of the theory of generalized functions.

3. The combined use of observation data by frequency comb ACROSS transmitter array and the data analysis method of frequency comb interferometry by PANW theory is expected to provide us with a potential tool for the practical active monitoring methodology. The contemporary application most relevant is the safety evaluation of artificial constructions such as buildings, tunnels and so on in contact with their subsurface structures.

The prediction and/or control of the earthquakes and volcanic activities will come to be our sound research target after the accumulation of data, our experiences on the 'evolving structural sensitivity' of the materials and its detailed nature at the target zone. Additional essential factor is the associated experimental and theoretical studies on the structural sensitivity of polycrystalline materials containing hydroxyl ions under stress.

We note that the developmental works of this method have been continued for a long period of time by collaboration of so many research workers of a variety of disciplines.

Keywords: Acoustic Frequency Comb, ACROSS, Structure Estimation

Japan Geoscience Union Meeting 2014
(28 April - 02 May 2014 at Pacifico YOKOHAMA, Kanagawa, Japan)

SSS25-03 Room:312 Time:May 2 14:45-15:00

Earthquakes are directed to diversity: An arithmetic seismic activity model

FUJIWARA, Hiroyuki[1*]

[1]NIED

Seismic activity is diverse. If we use the methodology in which an earthquake generation process is decomposed into individual fundamental processes and they are integrated by assembling a detailed physical model in each process, initial conditions and boundary conditions to be determined become an enormous amount.Therefore, it is difficult to describe the earthquake generation process by finding the solution of one deterministic equation system. In the prediction of seismic activity that has been attempted in recent years, stochastic or statistical techniques have been used. In approaches of stochastic processes theory, characteristics of seismic activities are modeled as probability distributions which are estimated theoretically or empirically. One of the sample path of a stochastic process that is modeled corresponds to the value to be observed. Such an approach is effective to represent the statistical properties of the entire seismic activity, but it cannot be applied to analyze a depth nature of the individual sample path. In this study, we mathematically construct a specific sample path corresponding to the observed value. By showing that they satisfy the statistical nature of seismic activity, we propose seismic activity model based on the idea that different from the stochastic processes approach. A model is proposed for seismic activity due to ”number”.

We consider a correspondence between earthquakes and prime numbers. We parameterize occurrence time of earthquakes as the prime numbers and magnitude of earthquakes as the interval of prime numbers. Then we obtain a relationship similar to Gutenberg-Richter law. We call the model obtained by this correspondence as ”arithmetic seismic activity model”. In the ” arithmetic seismic activity model”, earthquake is equivalent to prime number of prime numbers distribution theory. Earthquake prediction is something equivalent to prediction of emergence of prime numbers. Earthquake is captured as a phenomenon that corresponds to changes in the energy level of the field. Using certain quantum system, we consider to model a field of earthquake occurrence. Considering the Hamiltonian of the field of earthquake occurrence, we set earthquake occurrence as an eigenvalue problem for the Hamiltonian. If we can show that the eigenvalue problem is associated with the zeta function, we can expect to explain the similarity between the distribution of the prime and seismic activity. At present, dynamical system can explain seismic field based on this concept is not known. On the other hand, trying to capture the zero distribution of the zeta function of Riemann in the relationship equivalent to the prime number distribution as an eigenvalue problem of the quantum dynamical system, research on the distribution of prime numbers is progressing. Distribution of prime numbers is related to limits of diversity of ”number”. Distribution of prime numbers is likely to be associated with critical phenomena. Earthquake can be interpreted as an critical phenomena. For this reason, it is considered that there is a similarity between the prime numbers and earthquakes.

Keywords: Number theory, Prime number, Gutenberg-Richter relation, Earthquake

Japan Geoscience Union Meeting 2014
(28 April - 02 May 2014 at Pacifico YOKOHAMA, Kanagawa, Japan)

SSS25-04 Room:312 Time:May 2 15:00-15:15

Comments on a Bayesian approach to earthquake probabilities of the Poisson model

IMOTO, Masajiro[1*] ; FUJIWARA, Hiroyuki[1]

[1]NIED

In making national seismic hazard maps for Japan, earthquake probabilities are estimated based on past seismicity with the Brownian passage time model and the Poisson process model. With a small number of past earthquakes, unreliable model parameters produce large uncertainties of estimated values. In the present paper, we discuss a Bayesian approach to the problem for the Poisson model. When n earthquakes were observed in period T_0, a Bayesian approach gives the probability that m earthquakes are observed in period T_1 in the form of a binomial distribution. We compared Bayesian probabilities with those obtained by the maximum likelihood estimate (MLE) for n less than 5 and found the following significant differences between them. 1) When T_1 is the average interval of the past earthquakes, Bayesian probabilities of at least one earthquake increase 3 to 12% over those of MLE. 2) For a somewhat smaller T_1 than that in 1), the differences become larger. The Bayesian approach presented here could be tested by a simulation study.

Keywords: Earthquake probability, Poisson model, Bayesian statistics, Seismic hazard maps for Japan, Kanto

Japan Geoscience Union Meeting 2014
(28 April - 02 May 2014 at Pacifico YOKOHAMA, Kanagawa, Japan)

SSS25-05 Room:312 Time:May 2 15:15-15:30

Long-term probability for large earthquake along the Nankai trough estimated from an incomplete catalog

OKADA, Masami[1*]

[1]MRI, JMA

The Earthquake Research Committee of Japan published a report (the second edition) on the long-term evaluation for great recurrent earthquake along the Nankai trough in May, 2013 and newly forecasted the probability for such event in coming 30 years to be 60 - 70%. The giant earthquake may be possible, and the report was socially paid attention to very much. In the calculation of probability the BPT, Brownian Passage Time, distribution model is used in which the distribution parameters estimated with the maximum likelihood method or the time predictable model are plug in directly to the formula of conditional probability. Those are estimated from a few data, but not considered about the bias and uncertainty in them.

The committee explained that an earthquake, the Keicho event (1605) may not occur along the Nankai trough and some qualifying earthquakes are probably missed from the current catalog. In this presentation I will introduce a Bayesian new method with non-informative prior distribution to the parameters in a lognormal distribution for calculating the probability for the coming event from an incomplete catalog, and show the result of about 23 % for the event in the forthcoming 30 years along the Nankai trough

Keywords: Nankai trough, recurrent earthquake, forecast, Bayesian approach, incompleteness of catalog

Japan Geoscience Union Meeting 2014
(28 April - 02 May 2014 at Pacifico YOKOHAMA, Kanagawa, Japan)

SSS25-06 Room:312 Time:May 2 15:30-15:45

Space- temporal stability of the seismic quiescence (4) -Relation of seismic quiescence area and the main shock

YOSHIKAWA, Sumio[1*] ; HAYASHIMOTO, Naoki[2] ; AKETAGAWA, Tamotsu[3]

[1]Meteorological Research Institute, [2]Meteorological Research Institute, [3]Japan Meterological Agency

We have been continuing investigation of seismic quiescence phenomena for the purpose of application to earthquake prediction. As a result of re-investigation of the cases for the earthquakes of M7 class in Japan, we found that the distance between the hypocenter of the main shock and the center of seismic quiescence area becomes large with the earthquake magnitude to occur in the detected cases. Based on this scaling law, detectable cases could be newly found in the non-detected ones in the previous investigation.

We applied the method of 'eMAP' which was developed by Aketagawa and Ito (2008) and Hayashimoto and Aketagawa (2010) for detection of the seismic quiescence. For the study we picked up 26 earthquakes that occurred from 1987 to 2011 with the magnitude larger than or equal to 6.7 and the intensity larger than or equal to five in Japan. There were 11 detected cases and 15 non-detected cases in the past investigation (Ota et al.(2009) and Yoshikawa (2012)). In the case of the 1995 Kobe earthquake, where seismic quiescence could not be detected by 'eMAP' in the past investigation, a clear seismic quiescence has been reported by the DPRI of Kyoto University (1995) and the Japan Meteorological Agency (1995). As a result of re-investigation of this case, it became possible to treat it as a detectable case if the following things were considered. Though we have considered as the necessary condition for the precursor that the phenomenon appears in and around the focal area before occurrence of the main shock, we could not recognize as a phenomenon to be connected directly with the main shock because a seismic quiescence appeared in Tamba region approximately 30km distant from the epicenter near the Akashi Channel. And any remarkable quiescence was not detected in the epicenter, since the average seismic activity before the earthquake was too low. It is necessary to make clear the condition to treat the quiescence as a precursor. Then as we re-examined the detected cases, we found that the distance between the epicenter of the main shock and the center of the quiescence area became large with the magnitude of the earthquake to occur. We have reported that there are scaling laws in the size of the quiescence area and the duration of quiescence against the magnitude (Yoshikawa et al., 2013). As the quiescence is supposed to occur in the stress reduction area caused by aseismic slip, the main shock should occur in the periphery of the quiescence area and it is quite natural that the distance between the epicenter and the center of the quiescent area becomes larger obeying the scaling law.

We re-examined other non-detection cases and found that the precursory seismic quiescence can be detected also in the 1987 eastern off Chiba earthquake, the 1994 far-off Sanriku earthquake, the 2000 western Tottori earthquake, and the 2004 south-east off Kii peninsula earthquakes. As a result of this, 16 cases can be considered as detected and 10 cases as not- detected for 26 cases in total.

Keywords: earthquake, quiescence, hypocenter

Japan Geoscience Union Meeting 2014
(28 April - 02 May 2014 at Pacifico YOKOHAMA, Kanagawa, Japan)

SSS25-07 Room:312 Time:May 2 15:45-16:00

Recent anomalous groundwater temperature and water level changes and impending great earthquakes at the Nankai trough

TSUKUDA, Tameshige[1*]

[1]Japan Women's Univ.

Earthquakes are generated by the anisotropic principal stress regime in the rock medium. In the preparing process of a large earthquake, the medium would be deformed generating regions of contraction and dilatation around the nucleus of the shearing stresses. According to a hydraulic model, pore fluid flow is driven upward to the ground surface through crack systems serving as flowing pipes by high pressure pumps at a deep spot. The change in the quantity of the upwelling hot water from deep underground causes a change of groundwater temperature(Tsukuda et al., 2005).

We have groundwater observation stations for temperature at 12 sites, and for water level at two in the Tokai and Nanki regions, central and southwest Japan, respectively, where are close to the so-called Tokai and Nakai earthquakes. High precision quartz thermometers are installed at Otomi (OT) in Yaizu City and Nakajima (NK) in Shizuoka City. At other stations, platinum resistance thermometers are installed. We use semiconductor pressure sensors for water level. At OT(Yaizu) in the Tokai region, the temperature has been monotonously increasing since the measurement started in 2003. The rate of increase has clearly fallen down since the end of 2012, suggesting weekning of the contraction in the rock medium. At NK(Shizuoka), 14km northeast of OT, the temperature data presented a precursory change from increasing to decreasing trend, one year before the 2009 Suruga-bay earthquake of M6.5 (Tsukuda, 2012). The decreasing rate after the earthquake became much higher than before and had continued till 2012. The temperature changed suddenly into increasing trend since May, 2013. The dilatation of the rock medium under Shizuoka recently changed into contraction. At stations HA and WA in Shionomisaki, Nanki region, Wakayama Prefecture. The long-term trend of the water level is rising, corresponding to the ground subsidence found by levelling and GNSS data (Kobayashi, 2013). The trend of temperature is similarly rising, suggesting contraction of the rock medium under Shionomisaki, the southernmost end of Honshu. At KZ(Kozagawa) in the Nanki region, the temperature is monotonously falling since the observation started in 2002. The decreasing rate is growing during recent two years, suggesting the dilatation turned to be intensified recently.

As mentioned above, the deformations of the rock medium are accelerated under the regions close to the source regions of the great erthquakes at the Nankai trough. For prediction studies for the impending great erthquakes, we should start to conduct detailed and multidisciplinary observations.

Keywords: dailatation, contraction, groundwater temperature, water level, precursor, earthquake prediction

Japan Geoscience Union Meeting 2014
(28 April - 02 May 2014 at Pacifico YOKOHAMA, Kanagawa, Japan)

SSS25-08 Room:312 Time:May 2 16:15-16:30

Two questions related to short- and long-term prediction of the so-called Tokai earthquake

GELLER, Robert J.[1*]

[1]UTokyo, Earth Planet. Sci.

In the 1970s there was widespread discussion suggesting that a large subduction zone earthquake was imminent in the Tokai district (the so-called ”Tokai earthquake”), but the ”Tokai earthquake hypothesis” was not stated in a testable form. About 40 years have passed, but no such event has occurred in Tokai. Under those circumstances it seems justifiable to conclude that the hypothesis has been falsified. That does not mean that Tokai is not at risk, just that the risk is not greater than other tectonically similar regions.

Under the Large Scale Earthquake Countermeasures Act (LECA), which was enacted in 1978, an organization for monitoring possible ”precursors” and issuing short-term alarms was established. But no reliable precursors have ever been found. LECA should therefore be repealed and the monitoring organization abolished.

Reference:
Geller, R.J., 1997, Earthquake prediction: a critical review, GJI, 131, 425-450.

Keywords: earthquake prediction, Tokai earthquake

Japan Geoscience Union Meeting 2014
(28 April - 02 May 2014 at Pacifico YOKOHAMA, Kanagawa, Japan)

SSS25-09 Room:312 Time:May 2 16:30-16:45

On the sea level changes before the 1946 Nankai earthquake on the Pacific coast of Shikoku, Japan

UMEDA, Yasuhiro[1*]

[1]Geological Survey of Japan, AIST

1. Introduction

The abnormal sea level changes before the 1946 Nankai earthquake (M8.0) were witnessed by the inhabitants, on the Pacific coast of Shikoku, Japan. From a few days before the main shock, irregular tides were witnessed. The fishing boats could not arrive at the ports, because of the low sea level. On the contrary, some boats could arrive at ports. We considered that the abnormal sea level changes were caused by the small tsunamis from a few days before the main shock. The period and amplitude of the small tsunamis seem to have been larger and shorter closer to main shock.

2. Period and amplitude of the sea level changes

At seven points in the Susaki bay, the sea level changes were observed from

2010 to 2011. The height of tsunami by the 2011 off the Pacific coast Tohoku earthquake was amplified 20 and 8 times compared to that of the Nankai trough of 2300m depth (JAMSTEC) and 100m depth, respectively. The periods of 30-40, 50 and 80 minutes of sea level changes were observed in either case of tsunami, storm or mild weather. The periods of 50 and 80 minutes would be characteristic periods of Tosa bay. We considered that the small tsunamis were generated in the Tosa bay before the 1946 Nankai earthquake.

3. Assumed sea level changes

The assumed sea level changes(f(t)) before the main shock were obtained by the summation of the sea level changes by long term crustal movements(Fl(t)), small tsunami(F0(t)) with the period of 50-80 minutes and astronomical tide(Ft(t)). That is, f(t) = Fl(t) + F0(t) + Ft(t). Fl(t) = a • ln(t) + D0 was adopted by Umeda and Itaba(2013). In view of the summaries by the testimony for the abnormal sea level changes, F0(t) was assumed as F0(t)= A • B(t)m[cos{ωln(t-tc) +ϕ}]. ω and ϕ is frequency and phase angle, respectively. A is the amplitude ratio at each fishing port when the amplitude of Susaki bay is 1.0. Assumed sea level f(t) is shown by solid line in figure. f(t) of Susaki bay is expressed well the witness testimonies, but that of Muroto is not expressed them. f(t) of Muroto will be improved by considering the short -term and small-scale crustal deformations just before the main shock in the Muroto region.

Keywords: 1946 Nankai earthquake, sea level change, witness testimony,

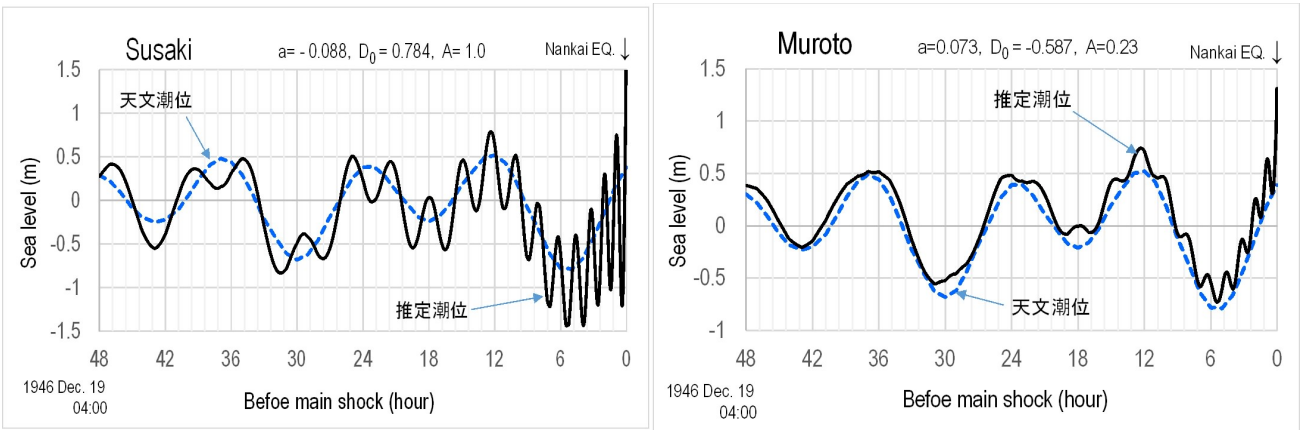

1946年南海地震の前に小規模な津波が発生していたとして，各地で推定される海水位の変化（黒の実線）と比較のための天文潮位（青の点線）

Japan Geoscience Union Meeting 2014
(28 April - 02 May 2014 at Pacifico YOKOHAMA, Kanagawa, Japan)

SSS25-10 Room:312 Time:May 2 16:45-17:00

Mechanism of generating electric fields just before earthquakes

TAKAHASHI, Kozo[1*]

[1]none

1. Precursory seismic electric fields

We consider that precursory seismic electric fields are generated by the mechanism as follows:(Refer to attached Figure):

(1) Before earthquakes, micro-cracks run in the source regions (Assumption), and into these cracks pore water pours.

(2) Uranium compounds, radium compounds and radon, which exist in crystal boundaries, dissolve into the pore water.

(3) The cracks connect the pore water and spring water, and the radio active materials appear on the surface of source regions.

(4) The radio active materials ionize the lower atmosphere above the source regions, and the electric conductivity increases there locally and temporarily.

(5) The ionization increases the current along the trace of cosmic shower between the surface and the ionosphere.

(6) As the current is pulsating, it radiates wide band radio-waves, which are observed as precursory seismic waves.

For the above mechanism the precursory micro-cracks are indispensable.

2. Mechanism generating the current between the surface and the ionosphere

The top of thunderclouds has the voltage up to about 100MV, so the electrons and negative ions flow into the clouds from the ionosphere. As a result, the ionosphere has a few MV. The mechanism, which increases the voltage at the cloud top, will be as follows:

(I) At middle latitudes, in the cloud lower than -10 deg. waterdrops become crystals, and they collide with each other. Then the water film on the smaller crystal, which is negatively charged, moves to the larger crystal, and makes the smaller crystal charged positive. The smaller crystals blow up to the cloud top and make it high voltage.(1)

(II) At low latitude, in the cloud no crystal will exist, but electric fields of about 1 kv/m exist, as other areas. So, waterdrops are polarized such as the top is negative and bottom is positive. When they collide, the negative part of smaller waterdrops, which have higher speed than the larger ones, neutralizes the positive charge of the larger waterdrops, and the smaller ones become positively charged and blow up to the cloud top, resulting the high voltage.

In the smoke billowing from volcanos, the lightning is observed. The tephra collide with each, other, and are charged by frictional electricity. By the same reason shown in (II), the charge is polarized and high voltage in the upper part of the cloud is generated. If this high voltage is observed, the explanation mentioned above will be considered to be valid.

References

(1) Kozo Takahashi: Mechanism of generating electromagnetic fields just before great earthquakes, Japan Geoscience Union Meeting 2011, S-SS024-13

(2) Kozo Takahashi: Mechanism of Generating The Earthquake Cloud just before Shallow Great Earthquakes, Japan Geoscience Union Meeting 2010, S-SS012-08

Keywords: precursory seismic electric fields, mechanism of generating thunder, thunder in middle-latitude, thunder in low-latitude, thunder in smoke of volcano

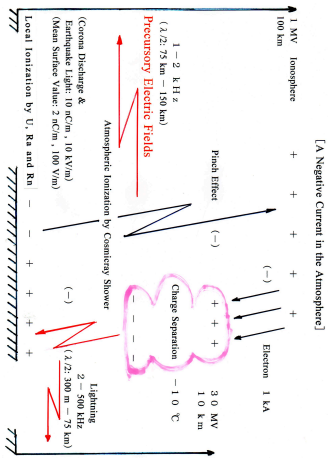

Japan Geoscience Union Meeting 2014
(28 April - 02 May 2014 at Pacifico YOKOHAMA, Kanagawa, Japan)

SSS26-01 Room:315 Time:April 30 15:45-16:00

Relationship between half-graben and high-velocities area at depths of 10 km 7

OISHI, Yukio[1*]

[1]Atelier Science

There are four oval shaped high velocities areas in Kanto Area .Two of them are in the southern part of Ibaraki prefecture. (after Matsubara Makoto 2005)

These two high velocities areas in Ibaraki prefecture gets larger, the deeper you see. At the depths of about 30km, this huge high velocities mass ,whose shape is donut, almost covers the southern part of Ibaraki prefecture and reaches at the depths of about 50km.

The western half of this huge high velocities area is on The Fourth Plate under Kanto; a part of Philippine Sea Plate(Toda Shinji 2005) at the depths of about 50km.

The eastern half of huge high velocities mass rides on the low velocities and low Poisson's ratio area, that is under beneath Lake Kasumigaura and the Southern of Lake Kasumigaura.(after Matsubara Makoto 2008)

This low velocities and low Poisson's ratio area faces subducting Pacific Plate at the depths of about 70 km.

Speaking of the low velocities and low Poisson's ratio area , the similar area exists in the asperity of M9 in 2011 off the Pacific Coast of Tohoku Earthquake; the upper part of the Pacific plate and also exists in Unzen in Nagasaki prefecture from the ground to the depths of about 30km.

I pointed out the possibility that the flexibility of the existence of the felsic rock or magma developed adherence of asperity of M9. (Ohishi Yukio 2013)

From the above it seems to be necessary to examine the possibility of the major earthquake outbreak underneath Lake Kasumigaura and the Southern Lake Kasumigaura at the depths of about from 50km to 70km.

There is another view that this low velocities area is not low Poisson's area but high Poisson's area (Nakajima Junichi 2008).

I want to wait for solution.

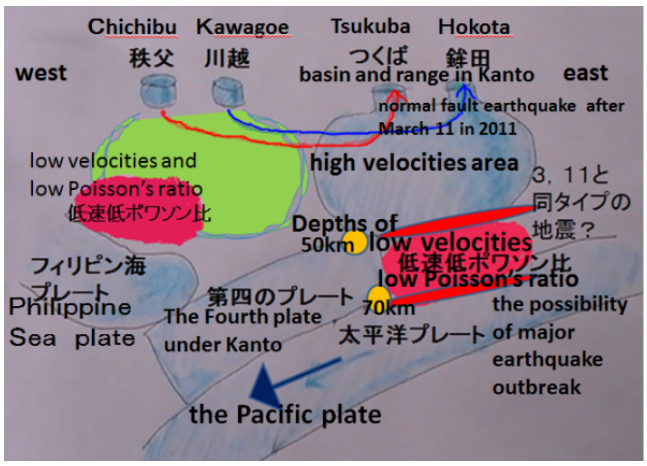

Japan Geoscience Union Meeting 2014
(28 April - 02 May 2014 at Pacifico YOKOHAMA, Kanagawa, Japan)

SSS26-02 Room:315 Time:April 30 16:15-16:30

Three-dimensional S-wave velocity structure beneath the Naruko volcanic area by ambient noise seismic interferometry

TAMURA, Jun[1*] ; OKADA, Tomomi[1] ; MATSUZAWA, Toru[1]

[1]RCPEV, Tohoku Univ.

The 2008 Iwate-Miyagi Nairiku earthquake (M7.2) occurred along a fault ranging from the south of Iwate to the north of Miyagi. The focal region of the earthquake is located in the proximity of four volcanoes: Yakeishi-dake, Mt. Kurikoma, Onikobe, and Naruko. To study the positional relationship between the fault and magmatic bodies beneath these volcanoes, several studies have been conducted. Okada et al., (2010) estimated the S-wave velocity structure up to a depth of 40 km from body-wave tomography, and revealed that aftershock regions are distributed escaping the low velocity zones beneath the volcanoes. This study attempts to elucidate the correlation between the shallow structure of the volcanic bodies and aftershock regions in detail, focusing on the Naruko volcano locating in the south of the focal region, by seismic interferometry using cross-correlation analysis from ambient noise. Seismic interferometry is a method based on the fact that a cross-correlation function calculated from particle-motion records at a pair of stations in a wave field is equivalent to a Green's function between the two stations.

In cross-correlation analysis, we used the vertical-component data recorded by an observation network, which is densely installed in the Naruko volcanic region. By spectrum and beamforming analysis, we identified the characteristic of noise dominating in 0.1-10 Hz. The main sources of the noise are due to ocean waves coming from the Pacific Ocean and the Sea of Japan. Targeting the low-frequency range in which surface waves are more dominant than body waves, cross-correlation functions are calculated for each observation day for each pair of stations, and then stacked for 18 months to obtain a Green's function with a high SN ratio. We extract group velocity dispersion curves of Rayleigh waves using the multiple filter technique proposed in Dziewonski et al., (1969). Rayleigh-wave velocity maps from the period of 3 to 10 seconds are then calculated by processing surface-wave tomography based on the method of Barmin et al. (2001). Finally, we estimate the 3-D S-wave velocity structure up to 10 km depth by S-wave velocity inversion.

The structure shows two significant low velocity anomalies in the northwest of Naruko and in the south of Onikobe Caldera between 3 and 4 km depth. These anomalies are presumably magmatic bodies or geothermal water. Compared with the distribution of aftershocks and the fault, we can see that aftershocks do not occur in the low velocity anomaly beneath the Naruko volcano, and aftershock activity stops immediately at the northeast part of the anomaly.

Keywords: seismic interferometry, cross-correlation analysis, ambient noise, tomography

Japan Geoscience Union Meeting 2014
(28 April - 02 May 2014 at Pacifico YOKOHAMA, Kanagawa, Japan)

SSS26-03 Room:315 Time:April 30 16:30-16:45

Three-dimensional velocity structures in the region between Hakone volcano and Tanzawa Mountains, central Japan

YUKUTAKE, Yohei[1*] ; HONDA, Ryou[1] ; HARADA, Masatake[1] ; SATOMURA, Mikio[1] ; MATSUBARA, Makoto[2]

[1]Hot Springs Research Institute of Kanagawa prefecture, [2]Earthquake Research Institute, National Research Institute for Earth Science and Disaster Prevention

Hakone volcano is located in the northern boundary zone of the Izu-Mariana volcanic arc in central Japan, where the Izu Peninsula on the Philippine-sea plate has been colliding into the Japan island arc. There has been fumarolic activity around the Owakudani area, and many intense swarm activities have occurred in the caldera of Hakone Volcano. Previous studies (e.g. Oki and Hirano, 1970; Yukutake et al., 2011) interpreted that the hydro thermal fluid derived from a deep-seated magma beneath Hakone volcano contributes to the occurrence of swarm earthquake. However, there is no evidence to show existence of the hydro thermal fluid and a deep-seated magma. To understand the mechanism of swarm earthquake occurrence and tectonic process around Izu-collision zone, we tried to estimate three-dimensional velocity structure in and around Hakone volcano, by using tomographic inversion of seismic wave velocity.

We used the data of 52 temporary stations installed in and around the caldera of Hakone volcano. We also used the data obtained by the permanent seismic station installed by Hot Springs Research Institute of Kanagawa prefecture, Earthquake Research Institute, National Research Institute for Earth Science and Disaster Prevention, and Japan Meteorological Agency. The double-difference tomography method (Zhang and Thurber, 2003) was applied to the present analysis.

Under Hakone volcano, low Vp and low Vs anomaly regions were estimated in the depth range from 6 km to 15 km. Within the low velocity zone, Vp/Vs is high (1.9) in the 10-15km depth, while that at the 6 km depth is relatively low (1.6). This result suggests that the deep-seated magma body is located in the high Vp/Vs region, and the low Vp/Vs region reflects the hydro thermal fluid or volatiles from the magma body. High Vp and high Vs regions were estimated under Tanzawa Mountains. The high velocity zone corresponds to a plutonic body of tonalite or hornblende gabbro. A low-velocity wedge was estimated between Tanzawa Mountains and Hakone volcano that corresponds to trough-filled deposits.

Keywords: Three-dimensional velocity structures, Hakone volcano, Tanzawa Mountains

Japan Geoscience Union Meeting 2014
(28 April - 02 May 2014 at Pacifico YOKOHAMA, Kanagawa, Japan)

SSS26-04 Room:315 Time:April 30 16:45-17:00

Continental Moho slanting upwards to the southeast beneath Kii Peninsula and middle layer earthquakes

SHIBUTANI, Takuo[1*] ; IMAI, Motohiro[1] ; HIRAHARA, Kazuro[2] ; NAKAO, Setsuro[1]

[1]DPRI, Kyoto Univ, [2]Science, Kyoto Univ

We carried out linear array seismic observations in Kii Peninsula from 2004 to 2013 in order to estimate the structure of the Philippine Sea slab and the surrounding area. We performed receiver function analyses for 14 cross-sections including four profile lines in the dipping direction of the slab and two lines in the perpendicular direction so far. We estimated three dimensional shapes of seismic velocity discontinuities such as the continental and oceanic Mohos and the upper surface of the oceanic crust. The results clearly showed that the slab top and the oceanic Moho are dipping northwestwards and that they correspond to the upper surfaces of the low and high velocity layers, respectively. Beneath northern to central Kinki the continental Moho spreads subhorizontally at 35 - 37 km deep, while beneath the Kii Peninsula it shallows southeastwards above the slab, reaching 20 km at the central part and 15 km at the southern shore.

Mizoue et al. (1983) analyzed data from permanent seismic stations which were being developed in the Kii Peninsula at that time, found that the travel time differences between the direct P waves and the Moho reflections or the Moho refractions propagating in the east - west direction became smaller from the northern part to the southern part of the peninsula, and suggested that the continental Moho slanted upwards to the south. They also found out earthquakes in the middle depth which were distinguished from both events in the upper crust and in the Philippine Sea slab, and called them as middle layer events. They pointed out that the middle layer events occurred around the slant continental Moho.

As mentioned above our receiver function analyses successfully estimated the three dimensional configuration of the continental Moho with a high accuracy. The results clearly showed that the middle layer events are located beneath the continental Moho shallowing southeastwards. Usually no earthquake occurs in the depth range equivalent to the lower crust. This is because crustal materials deform plastically at the depth and the strength of plastic flow becomes lower than that of brittle fracture. However, if the continental Moho shallows to the depth, the strength of plastic flow for mantle materials becomes larger than that of brittle fracture. This can be a cause of the middle layer events in the shallow mantle.

Keywords: continental Moho, middle layer earthquakes, Kii Peninsula, receiver function

Japan Geoscience Union Meeting 2014
(28 April - 02 May 2014 at Pacifico YOKOHAMA, Kanagawa, Japan)

SSS26-05 Room:315 Time:April 30 17:00-17:15

Seismic anisotropy within the subducting Philippine Sea slab beneath the central Japan

SHIOMI, Katsuhiko[1*]

[1]NIED

Subduction of the Philippine Sea slab (PHS) is caused recurrent megathrust earthquakes every 100 to 150 years. Knowledge of slab geometry has been increased by using the recently established dense seismograph networks, but anisotropic feature, which is related to the tectonic stress field and/or rock properties, within the slab is still unclear. To reveal depth-dependent anisotropic feature within the PHS by using teleseismic receiver functions (RFs), we select 100 stations located in the Kii Peninsula and Shikoku, southwest Japan. We choose teleseismic events (M>6.0) from October 2000 to November 2013 for RF analysis, and use seismograms with good S/N. Low-pass filters with fc = 1.0 and 1.5 Hz are applied to estimate RFs. To estimate the orientation of anisotropy symmetry axis at each station, we apply the harmonic expansion method to the RFs (Bianch *et al*., 2010; JGR). When we apply this method to the data, we focus at the Moho depth for the CCD stacking and use the seismic velocity model by Matsubara & Obara (2011; EPS).

In the depth range around the slab Moho, the plunge azimuths in the eastern Kii, central and western Shikoku are corresponds well to the dip direction of the slab Moho estimated from the radial RFs only (Shiomi *et al*., 2008; GJI). At the southern edge of the Kii Peninsula, the plunge azimuths are rotated to clock-wise from the result of Shiomi *et al*. (2008). When N-S directed anisotropic rock exists just above the Moho, this feature can be explained. In the oceanic crust, the plunge azimuths and anisotropic axes correspond well to the dip direction of the slab, and 4-lobed terms are dominant as the Moho deepens to 40 km. This feature is consistent with the NE-SW extension field estimated from the focal mechanisms of earthquakes occurred in the slab. Within the oceanic mantle, plunge azimuths and anisotropic axes are directed to E-W direction. This direction corresponds to the spreading direction of the subducting PHS beneath this area.

Keywords: Philippine Sea slab, Receiver function, Harmonic analysis, Seismic anisotropy

Japan Geoscience Union Meeting 2014
(28 April - 02 May 2014 at Pacifico YOKOHAMA, Kanagawa, Japan)

SSS26-06 Room:315 Time:April 30 17:15-17:30

The receiver function analysis at the area of the Nobi earthquake (II)

IIDAKA, Takashi[1*] ; IGARASHI, Toshihiro[1] ; KATO, Aitaro[1] ; IWASAKI, Takaya[1] ; JOINT SEISMIC OBSERVATIONS, At the area of nobi earthquake[1]

[1]ERI, Univ. of Tokyo

1) Introduction

The mechanism of the inland earthquakes is related to the concentration of the strain and accumulation of the stress. It is very important to know the relationship between the stress/strain and fault plane. The 1891 Nobi earthquake is one of the biggest inland earthquakes in Japan. The joint geophysical observations had been done at the area. Based on the results of the previous survey at the Atotsugawa fault region, we found that the lower crust structure and fluid were very important factors to the cause of the inland earthquake. In the Nobi earthquake area, the seismic tomography studies figured out the existence of a low velocity region beneath the fault. The low velocity region continues to the subducting Philippine Sea slab. It can be interpreted that the low velocity region is made by water, which was dehydrated from the subducting slab. It is expected that there is some close relationship between the inland earthquake and liquid released from the subducting slab. We did receiver function analysis at the faults area of the Nobi earthquake.

2) Data

The seismic network deployed by the Japanese University Group of the Joint Seismic Observations and the seismic stations belong to the Hi-net were used.

The earthquakes with the epicentral distances from 30 to 90 degs were used. The earthquakes occurred from Aug., 2002 to Mar. 10, 2011.

3) Results

It has been suggested that the configuration of the subducting Philippine Sea plate is distorted in the southwestern Japan region. We figured out the image of the subducting Philippine Sea plate using the receiver function analysis.

The cross sections along the longitude of 137.5^{o} E and 137^{o} E suggested the negative and positive receiver function boundaries. We can trace the negative and positive boundaries from shallower part to deeper part. The boundaries are interpreted as the upper boundary and oceanic Moho of the subducting Philippine Sea plate. It was found that the Philippine Sea plate is lying in a horizontal beneath Ise bay to Wakasa bay by the previous studies. Our receiver function results also support the result. We can obtain clear image of the crust and upper most mantle of the area using the spatially high dense seismic array deployed by the joint seismic observation.

Keywords: crust, mantle, Receiver function, Nobi earthquake

Japan Geoscience Union Meeting 2014
(28 April - 02 May 2014 at Pacifico YOKOHAMA, Kanagawa, Japan)

SSS26-07 Room:315 Time:April 30 17:30-17:45

P-wave velocity structure in the forearc region of the southwestern Nansei-Shoto (Ryukyu) Trench subduction zone

NISHIZAWA, Azusa[1*] ; KANEDA, Kentaro[1] ; OIKAWA, Mitsuhiro[1] ; FUJIOKA, Yukari[1] ; HORIUCHI, Daishi[1]

[1]Japan Coast Guard

We carried out five seismic lines across the southwestern Nansei-Shoto (Ryukyu) forearc region to elucidate variation in crustal structures along the trench. The seismic experiment consists of multichannel reflection seismic (MCS) profiling using 240 ch. and 3000 m long hydrophone streamer and wide-angle seismic refraction profiling using ocean bottom seismographs (OBSs) as receivers. We present the seismic structure related to the Philippine Sea plate subduction in the forearc region of the Nansei-Shoto island arc.

Thick materials with Vp less than 4 km/s characterize the accretionary wedge at the front of the forearc basin in the oblique subduction area to the southwest of 126 E. On the other hand, P-wave velocity structure beneath the high free-air gravity region in the forearc at 126-128 E reveals that materials with a high velocity of around 4.5 km/s ascend to 2-3 km beneath the seafloor. The subducting Okinawa-Luzon fracture zone was able to be clearly imaged not only in MCS profiles but also in the P-wave velocity distribution to the northeast of 126 E. We will discuss the relationship between the variation in the seismic structure and the characteristic of the regional seismicity.

Many OBSs on the forearc region recorded several reflection signals from the subducting Philippine Sea plate. We tried mapping these signals to estimate the position of the subducting plate.

Japan Geoscience Union Meeting 2014
(28 April - 02 May 2014 at Pacifico YOKOHAMA, Kanagawa, Japan)

SSS26-P01 Room:Poster Time:April 30 18:15-19:30

Spectral and spatial characteristics of the refined CRUST1.0 gravity field

TENZER, Robert[1*] ; CHEN, Wenjin[1]

[1]School of Geodesy and Geomatics, Wuhan University

We investigate the density structure of the oceanic and continental crust using the global crustal model CRUST1.0, which has been refined by incorporating additional global datasets of the topography/bathymetry (ETOPO1), the polar ice sheets (DTM2006.0 ice-thickness data) and the global geoid model (GOCO-03S). The analysis reveals that the average crustal density is 2830 kg/m^3, while it decreases to 2490 kg/m^3 when including the seawater. The average density of the oceanic crust (without the seawater) is 2860 kg/m^3, and the average continental crustal density (including the continental shelves) is 2790 kg/m^3. We further compile the gravity field quantities generated by the Earth crustal structures. The correlation analysis of results shows that the gravity field corrected for major known anomalous crustal density structures has a maximum (absolute) correlation with the Moho geometry. The Moho signature in these gravity data is seen mainly at the long-to-medium wavelengths. At higher frequencies, the Moho signature is weakening due to a noise in gravity data, which is mainly attributed to crustal model uncertainties. The Moho determination thus requires a combination of gravity and seismic data. In global studies, gravimetric methods can help improving seismic results, because (i) large parts of the world are not yet sufficiently covered by seismic surveys, and (i) global gravity models have a relatively high accuracy and resolution. In regional and local studies, the gravimetric Moho determination requires either a detailed crustal density model, or seismic data (for a combined gravity and seismic data inversion). We also demonstrate that the Earth long-wavelength gravity spectrum comprises not only the gravitational signal of deep mantle heterogeneities (including the core-mantle boundary zone), but also shallow crustal structures. Consequently, the application of spectral filtering in the gravimetric Moho determination will remove not only the gravitational signal of (unknown) mantle heterogeneities, but also the Moho signature at the long-wavelength gravity spectrum.

Keywords: correlation, crust, density, gravity, Moho

Japan Geoscience Union Meeting 2014
(28 April - 02 May 2014 at Pacifico YOKOHAMA, Kanagawa, Japan)

SSS26-P02 Room:Poster Time:April 30 18:15-19:30

Correction of Gravity Measurements Utilizing GSI Maps and its Application in the Southern part of Uemachi Fault Zone

RYOKI, Kunihiro[1*]

[1]Hyogo Polytechnic Center

1. Summary

In Earth science research with some field work, acquisitions of geolocation of the measurement point are essential. Particularly, it is a major burden that the latitude, longitude and altitude of the measurement points are obtained for the various corrections in gravity measurements. These pieces of information can be obtained by geodetic surveying or GNSS surveying in the field. Occasionally, topographic maps of large scale are substituted for these surveying.

On the other hand, the acquisition of geographic information, that has been digitized, into a numerical value has become possible on WWW in recent years. Web browsing service map of GSI, Geospatial Information Authority of Japan, which had been put to the test, was translated to the formal opening to the public on October 30, 2013. The new browsing service is ”GSI Maps” (GSI, 2013a). According to the Agreement of GSI Tile Use, it is to be able to take advantage of this service in the academic research (GSI, 2013b). Therefore, it is created that JavaScript applications give information on the measuring position by using GSI Tiles (GSI, 2013c). If combined with some mobile digital devices, information of geolocation is readily available even in the field.

When gravity measurements have been conducted, until now, the authors have been made the most use of the large-scale topographic map as the base map in the southern part of Uemachi Fault Zone. These results were mixed up to base on Tokyo Datum and Japanese Geodetic Sytem 2000. Therefore, they are integrated with the latter in this time.

2. Target area

Survey’s line of the target has integrated the results by Ryoki (2011), Ryoki and Nishitani (2013) and recent measurements. The length of the survey line is about 9,7 Km. The line lies from Yunagi-cho Izumiotsu to Ibukino Izumi and intersects the some faults included in Uemachi Fault Zone.

3. Acquisition of geographic information

Latitude, longitude and altitude of the measuring points were used numerical information provided by GSI. These elements obtained by constructing an HTML application. A JavaScript code has been created to revise some samples of GSI Tile. In general, for the purpose of protecting the system, the string is not transferred directly to the clipboard from a Web browser. However, there is a function to be transferred through JavaScript in the specific browser. On the other hand, in some browsers which not support such a function, the ZeroClipBoard library is possible to use to transfer the information (zeroclipboard.org, 2014). Numerical information, transferred to the clipboard, is edited in a spreadsheet application or in an editor software. In this study, an application which is used at indoor after measurement in situ is coded for a batch process. If operated in tablet devices instead to a field note book, numerical information is easily got in the measurement point. Numerical site information is used for various corrections and illustrated the gravity measurement point on the map.

4. Result

Formerly, in order to obtain numerical information related to the measurement point, latitude, longitude and altitude had been read using a digitizer from topographic map. But, if using the application proposed in this paper, time required for these operations could be significantly reduced. In particular, as it becomes a constant accuracy of the reading errors of the elevations which determined by GSI Maps, homogeneity of the data could be secured.

5. Challenges for the future

It is obvious that the application, which is proposed in this paper, ensures the homogeneity of data and improves the measurement efficiency in a variety of field research that includes geosciences. Development of the system for the operation of the tablet terminal is able to challenge, and it is an aim that an application of the terrain correction have been considered in the future.

Keywords: gravity structure, digital geographic information, JavaScript, Uemachi Fault, field research, efficiency of measurement

Japan Geoscience Union Meeting 2014
(28 April - 02 May 2014 at Pacifico YOKOHAMA, Kanagawa, Japan)

SSS26-P03 Room:Poster Time:April 30 18:15-19:30

The crustal structures of the subduction of the Philippine Sea Plate in the northern Nansei-Shoto trench

OIKAWA, Mitsuhiro[1*] ; NISHIZAWA, Azusa[1] ; KANEDA, Kentaro[1] ; FUJIOKA, Yukari[1] ; HORIUCHI, Daishi[1]

[1]Japan Coast Guard

Seismic characters of convergent plate boundaries are reflected in the heterogeneity in the structural evolution, the interior regime as well as external architecture (Kopp, 2013). At the north end of the Nansei-Shoto trench the Amami plateau, which is known as a remnant arc, is subducting, and this causes a landward concave of the subduction axis. The Nansei-Shoto trench was recognized that its seismicity is rather low, but in the past few years, new scientific researches indicated the possibility of a mega earthquake is not so much low. There are needs to grasp the Philippine Sea plate's topography and crustal structure around the sea area of the Amami plateau because they might be constraint conditions how the mega earthquake could happen.

Japan Coast Guard conducted two integrated seismic experiments that combine a wide-angle refraction survey and a multi-channel reflection survey. The first line (line ECr10) was conducted in 2009 and the second line (line ECr11) was carried out in 2012. ECr10 started from the west end of the Amami plateau to the north sea area to the Amami-O-Shima island. ECr11 started from the Kikai basin to the just south of the Yaku Shima Island. A depression on the Nansei-Shoto arc between two seismic lines is well known as a major tectonic boundary of the Nansei-Shoto arc.

The southern end of ECr10 is the west edge of the large Amami plateau. Uyeda(2005) said that there is a local bouguer low anomaly and this means the crust of the Amami plateau should be thicker than the normal oceanic crust. The past seismic survey (Nishizawa et. al., 2009, 2014) reveals that the thickness of the center Amami plateau is approximately 16km, which is obviously thicker than the normal oceanic. The southern end of ECr11 is located on the Kikai basin. The Kikai basin's bouguer anomaly is rather high, this means the possibility that the crust of the Kikai basin should be an oceanic crust. The seismic survey supports the high anomaly because of its thin crust. However the composition of the crust shows the horizontal heterogeneity of its crust and an identification of the middle crust (6.0 - 6.5 km/s layer) exists (Nishizawa et. al. 2009). These characters do not support that the basin is a typical oceanic crust.

We made a comparison of the structure on the Philippine plate between ECr10 and ECr11, by using the seismic surveys results and the precise bathymetric data collected by Japan Coast Guard. Regarding topography, we found many normal faults parallel to the trench direction. Especially there are more faults on the margin of the Amami plateau than of the Kikai Basin. As for crustal structures, the crust of the Amami plateau has a middle crust. The existence of middle crust is along with the past results but not only of the Amami plateau but also of Kikai basin. This means that the subducting margin of the Kikai basin might not be a typical oceanic crust.

Keywords: MCS, crustal structure, subduction, OBS

Japan Geoscience Union Meeting 2014
(28 April - 02 May 2014 at Pacifico YOKOHAMA, Kanagawa, Japan)

SSS26-P04 Room:Poster Time:April 30 18:15-19:30

Seismic structure beneath Kyushu island, Japan, inferred from S-wavevector receiver functions.

UEDA, Takuya[1*] ; TAKENAKA, Hiroshi[2] ; MURAKOSHI, Takumi[3] ; OKAMOTO, Taro[4]

[1]Kyushu Univ., [2]Okayama Univ., [3]National Defense Academy, [4]Tokyo Institute of Technology

The underground structure of Kyushu region is characterized by active subduction of the Philippine Sea plate (PHS) beneath the Eurasian plate and several active volcanos, for example, Aso, Kirishima, and Sakurajima volcanos along with the volcanic front, and Unzen volcano located Beppu-Shimabara graben. And also there are very thick sediments at several plains in Kyushu. Therefore the seismic structure beneath Kyushu Island is seemed to be very complicated and it is very important to understand the detailed structure, especially around Moho and the top of PHS. There are many previous researches on seismic structure beneath Kyushu Island. Travel time tomography method is very useful tool for imaging the subsurface structures. In the previous works, a lot of characteristic structures are identified by the tomography for example, low velocity structure beneath volcanic front.

Receiver function analysis is also very useful tool to image the seismic velocity structures. We apply it to image seismic structure on Kyushu area. In this study, we use teleseismic records from Hi-net and F-net seismic stations in Kyushu, which are supplies by the National Research Institute for Earth Science and Disaster Prevention.

If those seismic stations are located at the top or in the sedimentary layer, the records include strong effect of reverberation within the sedimentary layer, which makes the image of the structure unclear. To overcome this problem, we exploit the modified S-wavevector receiver functions (SWV-RFs). The SWV-RFs are derived by deconvoluting the upgoing S-wave component with the upgoing P-wave component of the records. For suppressing the sedimentary layer effect, we apply SWV-RFs for borehole records and move virtually the seismic sensor to the top of the basement layer, and calculate the SWV-RFs at that location [Takenaka and Murakoshi, 2010]. This method needs the structure model from the surface to the sensor location. We employ the Integrated Velocity Structure Model by the Headquarters for Earthquake Research Promotion. We take several cross sections in Kyushu Island to map the calculated SWV-RFs. We then interpret the continental Moho and low velocity regions in the mapped SWV-RFs. It can be seen that characteristic low velocity regions in mantle wedge, some of which may be related to magma. We also model some SWV-RF sections by the 2.5-D finite-difference method to confirm our imaging results.

Keywords: receiver function, crustal structure, top of plate, Kyushu region

Japan Geoscience Union Meeting 2014
(28 April - 02 May 2014 at Pacifico YOKOHAMA, Kanagawa, Japan)

SSS26-P05 Room:Poster Time:April 30 18:15-19:30

Seismic reflection survey at the Kego fault, Kyushu, Japan

MATSUMOTO, Satoshi[1*] ; SHIMIZU, Hiroshi[1] ; NAKAMOTO, Manami[2] ; MIYAZAKI, Masahiro[2] ; ABE, Susumu[3]

[1]Institute of Seismology and Volcanology, Kyushu Univ., [2]Faculty of Sciences, Kyushu University, [3]R&D Department, JGI, Inc

Kego fault is one of the active faults in Japan, which located Kyushu Island, Japan. The fault is composed of two major segments; the earthquake fault of the 2005 West-off Fukuoka prefecture earthquake and southeastern part running through central Fukuoka City. We performed reflection survey at the southeastern part of the fault in order to explore detailed structure of the fault. The experiment was carried out on the two profile. One was located at central part of Fukuoka city with length of 1 km for obtaining reflection section shallower than depth of 1 km. Another was for imaging heterogeneous structure in the seismogenic zone beneath the fault, which was deployed 35 km length across southeast end of the fault. After applying seismic reflection processing, we obtain reflection sections for two profiles. The gap of horizontal reflector was found around the depth of 0.6 km in the shallow seismic section at central Fukuoka, corresponding to the Kego fault. The hanging wall of the fault is western side of the fault as geological study suggested. The deep section at the southeastern part of the fault reveals that strong reflective layers exist in the seismogenic zone at the west of the fault. In addition, we found many reflectors at the lower crust beneath the whole area of the profile.

Keywords: Kego fault, seismic reflection survey

Japan Geoscience Union Meeting 2014
(28 April - 02 May 2014 at Pacifico YOKOHAMA, Kanagawa, Japan)

SSS26-P06 Room:Poster Time:April 30 18:15-19:30

P-wave heterogeneous structure around the Kego fault inferred from reflection analysis for seismic network data

KAMIZONO, Megumi[1*] ; MATSUMOTO, Satoshi[2] ; MIYAZAKI, Masahiro[1] ; NAKAMOTO, Manami[2] ; SHIMIZU, Hiroshi[2] ; ABE, Susumu[3]

[1]Department of Earth and Planetary Sciences, Graduate School of Sciences, Kyushu University, [2]Institute of Seismology and Volcanology, Faculty of Sciences, Kyushu University, [3]R&D Department, JGI, Inc.

The Kego fault is one of the active fault in Japan, running through the western margin of the Fukuoka plain. On March 20, 2005 the west off Fukuoka earthquake (M7.0) occurred at northwestern extension of the Kego fault. In order to evaluate the effect on the fault by the earthquake, crustal structure is basic information to model the fault condition. This study estimated the subsurface structure around the Kego fault from artificial source used in the reflection survey.

In the survey, vibrator tracks are used as seismic sources at 8 shot points. Sweep time of the source is 24 seconds and sweep frequency range is from 6 Hz to 30 Hz. We recorded the signal from the vibrators at seismic stations deployed by Kyushu University and NIED. Seismic reflection analysis was applied to the data for detecting reflectors beneath the CMP line located between the reflection profile and the station. As simplicity, we processed observed data on the assumption that basement is homogeneous.

We obtained seismic deapth sections at CMP lines for the seismic stations. Numerous refletors in the lower crust are found in the sections; therefore the lower crust is heterogeneous. The reflective zone in the lower crust is from the depth 20 to 32 km in the section, suggesting that the lower limit of the zone corresponds to the Moho discontinuity. Since the section imaged heterogeneous structure across the Kego fault, we compared characteristics of reflectivity between footwall and hanging walls of the fault. The structure of the superficial part is different depending on the place. At the some point CMP lines, there are reflector in the western side, however in the eastern side of the fault it is not so. This difference in reflectivity depends on the cross point between the CMP line and the fault. This suggests that there isn't clear difference in east and west of the fault at other point. Consequently, there might be variation of the structure along the strike of the Kego fault.

Keywords: Kego Fault, Seismic Reflection Profiling

Japan Geoscience Union Meeting 2014
(28 April - 02 May 2014 at Pacifico YOKOHAMA, Kanagawa, Japan)

SSS26-P07 Room:Poster Time:April 30 18:15-19:30

The seismic velocity structure in the Northern Kinki District using the dense seismic observation

KAIYA, Emi[1] ; KATAO, Hiroshi[1*] ; SHIBUTANI, Takuo[1] ; IIO, Yoshihisa[1] ; MIURA, Tsutomu[1]

[1]DPRI, Kyoto Univ.

Micro-seismicity in the Northern Kinki District is active. However we don not know the cause and the relation between these seismic activities and crustal structure or active faults around there clearly. In the Northern Kinki District, we are carrying out a dense array seismic observation using 83 temporal stations since 2008. The average station interval at the center of the Tamba plateau is about 5km, so we expect to know the seismic structure beneath this region with higher resolutions than that derived from the permanent stations.

In this study, we estimate high-resolution seismic velocity structure using data from these dense observations. Based on the results of 3D seismic velocity tomography, we discuss about relations between the seismic activities and other geophysical and geological features of this area.

Keywords: Tamba Plateau, Tomography, micro-earthquake, crustal fluid, dense observation, Manten Project

Japan Geoscience Union Meeting 2014
(28 April - 02 May 2014 at Pacifico YOKOHAMA, Kanagawa, Japan)

SSS26-P08 Room:Poster Time:April 30 18:15-19:30

Seismic attenuation beneath Tateyama volcano

IWATA, Koji[1*] ; KAWAKATA, Hironori[2] ; DOI, Issei[3]

[1]Ritsumeikan University, [2]Ritsumeikan University, [3]Disaster Prevention Research Institute

Tateyama volcano (Midagahara volcano) locates in southeast Toyama prefecture. Subsurface structures beneath active volcanoes have frequently been investigated using seismic attenuation (e.g., Oikawa et al., 1994: Sudo et al., 1996), and it was reported that there are strong attenuation regions beneath some active volcanoes. The volcanic activity of Tateyama volcano is quite low, and subsurface structure beneath the volcano has not been investigated in detail. Since Hi-net was developed by NIED, the attenuation structure of whole area of Japan has been estimated (e.g., Jin and Aki, 2005; Carcole and Sato, 2009). However, local structure beneath inactive volcanoes is still in question. In this study, we investigated the seismic attenuation beneath Tateyama volcano using seismograms obtained by Hi-net.

In this study, we used seismograms of five Hi-net stations near Tateyama volcano. The seismograms were selected so that epicentral distances from Tateyama volcano were 70 km˜140 km, the magnitudes of the earthquakes were larger than 2.5, focal depths were less than 30 km, and signal-to-noise ratios were sufficiently high.

At first, we focused on the two stations which locate opposite sides of Tateyama volcano each other, and compared seismograms whose epicenters were located almost along the line of Tateyama volcano and the two stations. For the seismograms which passed beneath the volcano, S-waves were more attenuated than P-wave. In detail, S-wave attenuation was pronounced in 4˜8Hz and 8˜16 Hz bands. This feature was seen in all seismograms from northwestern or southeastern sources. On the other hand, seismograms from northeastern or southwestern sources did not show such a feature. There should be a region that preferentially attenuated S-waves beneath Tateyama volcano, and the distribution is heterogeneous.

Also, it should be noted that S-waves passing beneath Tateyama volcano showed clear peak delay, which suggested that there was a region with high scattering attenuation beneath Tateyama volcano.

Keywords: seismic attenuation, volcano, spectral analysis

Japan Geoscience Union Meeting 2014
(28 April - 02 May 2014 at Pacifico YOKOHAMA, Kanagawa, Japan)

SSS26-P09 Room:Poster Time:April 30 18:15-19:30

Detailed velocity structure along the Nankai trough, off the Kii Peninsula, obtained from DONET data

NAKANO, Masaru[1*] ; NAKAMURA, Takeshi[1] ; TONEGAWA, Takashi[1] ; KANEDA, Yoshiyuki[1]

[1]JAMSTEC

Along the Nankai trough off southwestern Japan, the Philippine Sea (PHS) plate is subducting to the northwest below the Eurasian plate. Historically, mega-thrust earthquakes have occurred repeatedly along the Nankai trough (e.g., Ando, 1975). Future great earthquakes will cause serious and widespread damage in central and western Japan. The Japan Agency for Marine-Earth Science and Technology (JAMSTEC) installed a network of permanent ocean-bottom observation stations off the Kii Peninsula above the source region of the expected great earthquakes. This is known as the Dense Oceanfloor Network System for Earthquakes and Tsunamis (DONET). Previous studies (e.g. Nakano et al., 2014) revealed that the present seismic activity well overlaps the aftershock region of the sequence of 2004 off the Kii Peninsula earthquakes (M_{JMA} = 7.1, 7.4, and 6.5). The focal mechanisms of the earthquakes show that the axis of compressive stress in the PHS plate is oriented N?S, almost perpendicular to the direction of plate convergence, indicating a complex tectonic regime in this region. In this study, we investigate detailed seismic velocity structure in this region.

In this region, P-wave velocity (Vp) structure is well developed based on repeated seismic surveys, but S-wave velocity (Vs) structure is not well known. Therefore, we start from an initial layered velocity structure assuming Vs, and update it to well explain the travel-time of earthquakes, then obtain three-dimensional velocity structure described below.

1. Estimate average layered structure below the study area.

1.1. An initial layered structure of Vp is constructed referring to the result of seismic surveys. The Vp/Vs ratio of each layer is assumed considering oceanic structures. Using this structure, we determine the hypocenter distribution.

1.2. Using the travel-time and initial hypocenters, 3D velocity structure is computed by using the tomoDD program (Zhang and Thurber, 2003).

1.3. The 1D velocity structure is updated by averaging the velocity at each depth.

1.4. Hypocenters are re-calculated based on the updated velocity structure, and the procedures 1.2.-1.4. are repeated until the 1D velocity structure converges.

2. Construction of 3D velocity structure.

2.1. Initial 3D velocity structure representing the subducting plate and oceanic sedimentary layers is constructed based on the study of Nakamura et al. (2011). Vp is from the result in 1.

2.2. The Vp/Vs ratio of each layer is obtained by a grid search method, in which minimizes the residual between observed and calculated travel time.

2.3. Site correction is obtained for the best model.

3. Computation of detailed 3D velocity structure.

3.1 Using the velocity structure and hypocenter distribution obtained in 2. as the input, detailed 3D velocity structure is obtained by using tomoDD program. In the computation of travel time, the site correction obtained in 2.3. is included.

The obtained velocity structure shows that the velocity anomaly along the trough anomaly well corresponds to the earthquake distribution. In the oceanic crust, seismic activity corresponds to a region of low-velocity anomaly, while earthquake distribution corresponds to a high-velocity anomaly in the mantle. The obtained structure may help to understand the detailed structure in this region. However, since the used data is from earthquakes immediately below DONET, the resolution of tomography may not be good. We will investigate the resolution and dependence on the initial velocity structures in the future study.

Keywords: Nankai trough, Ocean-bottom seismic observations

Japan Geoscience Union Meeting 2014
(28 April - 02 May 2014 at Pacifico YOKOHAMA, Kanagawa, Japan)

SSS26-P10 Room:Poster Time:April 30 18:15-19:30

Mechanism of large crustal earthquakes in Kanto and Chubu: Influence of structural heterogeneities

FUJISAWA, Moeto[1*] ; ZHAO, Dapeng[1] ; TOYOKUNI, Genti[1] ; KITAGAWA, Hiroki[1] ; NISHIZONO, Yukihisa[2] ; INAKURA, Hirohito[2]

[1]RCPEV, Tohoku Univ., [2]West Japan Engineering Consultants, Inc.

Large inland crustal earthquakes often cause heavy damage to human society. Therefore it is very important to clarify the generation mechanism of the large crustal earthquakes for disaster reduction. It is considered that fluids dehydrated from the subducting Pacific and Philippine Sea slabs affect the nucleation of large crustal earthquakes under the Japan Islands (Zhao et al., 2010). In this study, we focus on the Kanto and Chubu regions, and investigated the cause of large crustal damaging earthquakes (M>6) (Usami et al., 2013; Utsu, 1999) by comparing the earthquake distribution with tomographic images of the crust and upper mantle.

We used high-quality arrival-time data of local earthquakes which occurred during June 3, 2002 to June 26, 2013 complied by the Japan Meteorological Agency (JMA) Unified Catalogue and those during June 3, 2002 to November 10, 2013 compiled by the Tohoku University Data Base. The local events were carefully selected based on the following criteria. (1) All the events were recorded by more than 20 seismic stations; (2) the uncertainty of hypocentral location is smaller than 4 km; (3) to keep a uniform distribution of hypocenter locations and avoid the event clustering, we divided the study area into small blocks (5 km $\times$ 5 km $\times$ 1 km), and selected only one event in each block that was recorded by the maximal number of seismic stations. As a result, our data set consists of 824,742 P-wave and 627,664 S-wave arrival times from 21,831 events recorded by 877 seismic stations in the study area. We applied the tomographic method of Zhao et al. (1992) to our data set. The grid interval is 0.20 deg. in the lateral direction and 15?30 km in depth, which is the resolution scale of the 3-D velocity model we obtained. The final root-mean-square ravel time residual is 0.287 s for the P-wave data and 0.424 s for the S-wave data.

Our results show significant velocity variations in the crust and upper mantle. The subducting Pacific and Philippine Sea slabs are imaged clearly as high-velocity zones. In contrast, low-velocity anomalies are revealed in the crust and mantle wedge beneath active arc volcanoes, which reflect the source of arc magmatism produced by slab dehydration and corner flow in the mantle wedge. Most of the large crustal earthquakes are located in or around the low-velocity zones in the crust and/or the uppermost mantle. These results suggest that the generation of large crustal earthquakes are affected or controlled by the structural heterogeneities. In particular, fluids play an important role in the nucleation of the large earthquakes.

References

Utsu, T., 1999. Seismic Activity. Univ. Tokyo Press.

Usami, T. et al., 2003. Catalogue of Damaging Earthquakes in Japan. Univ. Tokyo Press.

Zhao, D., A. Hasegawa, S. Horiuchi, 1992. Tomographic imaging of P and S wave velocity structure beneath northeastern Japan. J. Geophys. Res. 97, 19909-19928.

Zhao, D., M. Santosh, A. Yamada, 2010. Dissecting large earthquake in Japan: Role of arc magma and fluids. Island Arc 19, 4-16.

Keywords: seismic tomography, crustal fluid

Japan Geoscience Union Meeting 2014
(28 April - 02 May 2014 at Pacifico YOKOHAMA, Kanagawa, Japan)

SSS26-P11 Room:Poster Time:April 30 18:15-19:30

Seismic Reflection Surver around the Mouth of Fuji River

ITO, Shinobu[1*] ; YAMAGUCHI, Kazuo[1] ; IRITANI, Ryohei[1] ; YAMANAKA, Yoshiaki[2] ; ITO, Shun'ichiro[2] ; MURATA, Kazunori[2]

[1]GSJ, AIST, [2]Suncoh Consultants Co., Ltd

We conducted seismic reflection survey around the mouth of Fuji River in February 2014. Fujikawa-kako fault zone is identified around this area. Shimokawa et. al. (1996) conducted seismic reflection survey in this area, and identified the Iriyamase fault. Shizuoka Pref. (1996) also identified the Nakayama fault. Our purpose of the survey is that we understand structure around both the Iriyamase and the Nakayama fault in more detail than the previous studies. There are two seismic survey lines. A survey line FJK1 is located from the mouth of Fuji river toward Mukaida river along the coastline, and the length of the line is about 3.5km. A survey line FJK2 is located on the right bank of Fuji river and at about 2km north from the coastline, and cross over the Kambara Jishinyama. The length of FJK2 is a little bit longer than 1km. We used IVI Y2400 as seismic source. Sweep frequency for FJK1 and FJK2 is 10 to 100Hz and 10 to 120Hz, respectively. Sweep length is 12s, and record length is 16s for both lines. We used SG-10 (10Hz of natural frequency) and DSS-12 that is a distributed seismic data acquisition system. Temporal spread length of FJK1 is about 1km. We fixed the spread of FJK2. Geophones are set at intervals of 5 meters for both lines. Some events can be deduced as reflected waves in some samples of shot records for FJK1. However, we are afraid that they are produced by a bank. Soon, we are going to show detailed results.

Keywords: seismic reflection survey, Fuji River

Japan Geoscience Union Meeting 2014
(28 April - 02 May 2014 at Pacifico YOKOHAMA, Kanagawa, Japan)

SSS26-P12 Room:Poster Time:April 30 18:15-19:30

Depth variation of the P- and S-wave velocities in the Kanto sedimentary basin inferred from seismic interferometry

YOSHIMOTO, Kazuo[1*] ; SUGAWARA, Yuma[1] ; KAJIKAWA, Kengo[1] ; KOBAYASHI, Manabu[1] ; MASUDA, Kei[1] ; TAKEMURA, Shunsuke[1] ; HIRATA, Naoshi[2] ; SAKAI, Shin'ichi[2] ; SATO, Hiroshi[2] ; NAKAHARA, Hisashi[3]

[1]Nanobioscience, Yokohama City Univ, Yokohama, Japan, [2]ERI, Univ. of Tokyo, Tokyo, Japan, [3]Geophysics, Science, Tohoku Univ, Sendai, Japan

Information on the seismic velocity structure of the Kanto sedimentary basin is necessary for evaluating the strong and long-period ground motions in the Tokyo Metropolitan area for future large-to-great earthquakes. However, there are few studies on the depth variation of both P and S wave velocities of the sediment, except for the vertical seismic profiling (VSP) measurements at a limited number of deep boreholes. In this presentation, we will report the characteristics of the depth variation of both P and S wave velocities of the sediment on the basis of the seismic interferometry for P and S waves of local earthquakes.

Seismic waveforms of 160 local earthquakes recorded by the MeSO-net were analyzed in this study. The autocorrelation of vertical displacement waveform of P wave and SH displacement waveform from a single event were stacked over all events available at each station, respectively, to obtain the P- and S-wave reflection responses of the Kanto sedimentary basin. We successfully found clear P- and S-wave reflections from the bedrock (seismic basement) at 266 observation points. This result indicates that the P-wave seismic interferometry is effective for the exploration of deep sedimentary basin as well as S-wave interferometry. In our dada, two-way travel time between the free surface and the bedrock of P-wave and S-wave (hereafter Tp and Ts, respectively) ranges from 0.5 s to 4.0 s and 2.0 s to 8.0 s, respectively. A graph showing Tp-Ts relation reveals that the trend of its variation is very similar to that reported at Iwatsuki deep boreholes from VSP measurement, even though there is a large scatter of data. Our results indicate that the ratio of P-wave velocity and S-wave velocity of the sediment is approximately 4 at a shallow depth ($<$0.5 km) and decreases down to 2 or less at a deep depth ($>$2.0 km) in the Kanto sedimentary basin.

ACKNOWLEDGMENTS
Data provided by the MeSO-net is gratefully acknowledged. This research was partially supported by the Earthquake Research Institute, University of Tokyo.

Keywords: seismic interferometry, Kanto sedimentary basin, sedimentary structure, seismic velocity structure

Japan Geoscience Union Meeting 2014
(28 April - 02 May 2014 at Pacifico YOKOHAMA, Kanagawa, Japan)

SSS26-P13 Room:Poster Time:April 30 18:15-19:30

Seismic activity and attenuation structure in fukushima-yamagata prefectural border area

MIYAGKI, Keiichiro[1*] ; TSUMURA, Noriko[1]

[1]Faculty of Science, Chiba University

In Fukushima - Yamagata prefectural border area, seismicity suddenly became active after off the Pacific coast of Tohoku earthquake (here after we call it 2011 Tohoku earthquake). We estimated distribution and focal mechanisms of earthquakes that occurred in the time period before and after the 2011 Tohoku earthquake to clarify causes of the seismicity activation. We used seismograms which are observed at the Hi-net stations operated by National Research Institute for Earth Science and Disaster Prevention. Earthquakes with M ≧ 2.0 in the Hi-net catalogue from July 3 , 2002 to March 10 , 2011 and from April 1 , 2011 to August 31 , 2011 were analyzed in this study. As a result, hypocenters which occurred after the main shock were distributed into five clusters they were located at different region from those where earthquakes occurred before the main shock. It is known that there are active faults near the study area. A fault plane estimated from a northwestern cluster ' s hypocenters shows similar strike and dip of that of an active fault. Further, fault planes estimated from another clusters ' hypocenters seems to have a conjugate relationship with the fault plane of the active faults. In addition, we observed that hypocenters in some certain clusters moved to lateral and vertical direction with approximately constant speed. Most earthquakes have the thrust-type focal mechanisms during the study period. Q value is considered to be a sensitive parameter to temperature and existence of fluid in the crust. We estimated Qp/Qs value by taking velocity amplitude spectral ratio between P and S waves to evaluate the affection of magma or fluid to earthquake occurrence. We used 898 spectra of 152 earthquakes which were observed by 9 stations nearby source region to calculate average Qp/Qs value on the ray path by Takaoka et al. (2013) ' s method. As a result, ray paths from the hypocenters to stations within 20km showed high Qp/Qs values, while paths from the hypocenters to the far stations showed low Qp/Qs values. This result might indicate that high attenuation region exists in a shallow part nearby source region.

Keywords: Q value, attenuation, In Fukushima - Yamagata prefectural border area, seismicity, off the Pacific coast of Tohoku earthquake

Japan Geoscience Union Meeting 2014
(28 April - 02 May 2014 at Pacifico YOKOHAMA, Kanagawa, Japan)

SSS26-P14 Room:Poster Time:April 30 18:15-19:30

Crustal and upper mantle structure of East Antarctica, derived from broadband seismic deployments at the International P

KANAO, Masaki[1*] ; TSUBOI, Seiji[2]

[1]National Institute of Polar Research, [2]Japan Agency for Marine-Earth Science and Technology

Deployment of broadband seismic stations on the Antarctica continent have been an ambitious project to improve the spatial resolution of seismic data across the Antarctic Plate and surrounding regions. Several international collaborative programs were conducted in Antarctica during the International Polar Year (IPY 2007-2008). The Antarctica's GAmburtsev Province (AGAP; IPY #147), the GAmburtsev Mountain SEISmic experiment (GAMSEIS), a part of AGAP,, and the Polar Earth Observing Network (POLENET; IPY #185) were major contributions in establishing a geophysical network in Antarctica. The AGAP/GAMSEIS project was an internationally coordinated deployment of more than 30 broadband seismographs over the crest of the Gambursev Mountains (Dome-A), Dome-C and Dome-F area. The investigations provide detailed information on crustal thickness and mantle structure; provide key constraints on the origin of the Gamburtsev Mountains; and more broadly on the structure and evolution of the East Antarctic craton and subglacial environment. In addition to the PASSCAL observation system by USA, original coordinated systems were developed by Japan (at Dome-F (GM07) and GM06 stations), as well as by other groups in China and France. Regarding Japanese instrument system, the same sensor and data logger as used by US/PASSCAL were utilized, but the electric power supply system and enclosures were developed independently. Data were recorded in MiniSEED format, a commonly accepted international standard, to ease analysis. Logistical and staff support were provided by the US researchers and staff at AGAP-S camp in the installation of the Japanese stations GM06 and GM07. From GAMSEIS and POLENET data obtained, local and regional seismic signals associated with ice movements, oceanic loading, and local meteorological variations were recorded together with a significant number of teleseismic events. In this presentation, in addition to the Earth's interiors, we will demonstrate some of the remarkable seismic signals detected during IPY that illustrate the capabilities of broadband seismometers to study the sub-glacial environment, particularly at the margins of Antarctica. In future, monitoring stations inland ice plateau of Antarctic, such as Dome-F, firmly attribute a crucial role in the Federation of Digital Seismographic Network (FDSN) in southern high latitude.

Keywords: Antarctica, International Polar Year, crustal structure, broadband seismographs, international project

Japan Geoscience Union Meeting 2014
(28 April - 02 May 2014 at Pacifico YOKOHAMA, Kanagawa, Japan)

SSS26-P15 Room:Poster Time:April 30 18:15-19:30

Seismo-stratigraphy and structure of the Adventure Plateau (Sicily Channel): an example of old data recovery

CIVILE, Dario[2] ; ALP, Hakan[1*] ; LODOLO, Emanuale[2] ; CENTONZE, Jacques[2]

[1]Istanbul University Department of Geophysics, [2]Istituto Nazionale di Oceanografia e di Geofisica Sperimentale

We present here a seismo-stratigraphic and structural study of the Adventure Plateau, the north-westernmost sector of the Sicily Channel. This bank, where water depths do not generally exceed 150 m, is the shallowest part of the whole Sicily Channel, with relief which sometime rises up to less than 50 m. This analysis is based on a large set of multichannel seismic profiles and well information acquired mostly for commercial purposes in the 70s and 80s. Despite the general poor quality and consistency of the data used, it was possible to draw with sufficient detail the various seismo-stratigraphic sequences, calibrated with well information. The sedimentary sequence crossed by wells in the Adventure Plateau comprises deposits ranging from Triassic to Plio-Quaternary. A broad lithological distinction can be made between the sequences ranging from Triassic to Middle Miocene, predominantly carbonate, and the sequences ranging from Tortonian to Quaternary, predominantly siliciclastic. Moreover, we observe in the wells the presence of various hiatuses, particularly at the top of the Miocene and at the Early Jurassic. Three main structural domains have been identified within the Adventure Plateau: (a) a compressional belt in the N-W part of the bank, deformed during Middle-Late Miocene, and corresponding to the SW-trending offshore part of the Maghrebian Chain; (b) the Adventure foredeep of the Maghrebian Chain, located in the central part of the bank, and filled by over 2000 m of siliciclastic Late-Miocene to Quaternary deposits; (c) the Adventure foreland of the Maghrebian Chain, corresponding to the S-W part of the bank, affected from the Early Pliocene by a strong extensional phase associated to the Pantelleria Graben rifting. The eastern boundary of the Adventure Plateau is part of a broadly NS-trending, lithospheric-scale transfer zone which separates the Sicily Channel into two distinct sectors. This study shows the potential and capability of old data in areas where there is scarce geophysical knowledge. They represent an important source of information, especially for the shallow water areas of the Sicily Channel that are still poorly known in terms of geology and stratigraphy.

Keywords: Sicily Channel, Adventure Plateau, seismo-stratigraphy, synthetic seismograms, structural setting

Japan Geoscience Union Meeting 2014
(28 April - 02 May 2014 at Pacifico YOKOHAMA, Kanagawa, Japan)

SSS27-01 Room:411 Time:April 29 09:00-09:15

Possibility of timelapse survey by seismic interferometry in image domain

SHIRAISHI, Kazuya[1*]

[1]JGI, Inc.

(1) Seismic interferometry in image domain

Seismic interferometry (SI) is generally applied in a data domain by crosscorrelating the different seismic traces without information of media for a redatuming or a signal extraction. Then the synthesized virtual source records are processed for a subsurface imaging. The direct subsurface imaging of passive seismic data by interference of extrapolated wavefields based on an imaging condition can be recognized as a SI in the image domain. Although the image domain SI is based on the velocity model for wavefield extrapolation, the fact that both the passive observation data and the velocity model are required for the depth imaging is common in the data domain SI and the image domain SI.

In the SI in the image domain by combining with the principle of a reverse time migration (RTM), arbitrary time-windowed seismic record is propagated forwards from a receiver point which become a virtual source and the same time-windowed records are propagated backwards from other receiver points. If any multiple reflection waves between the surface and the reflection boundaries satisfy the imaging condition, the reflected energy will be focused on those points. Because the seismic records of all receivers in one passive observation are not independent each other, the wavefield extrapolations can be only once in forward and backward respectively. In the data domain SI, however, the forward and backward extrapolations are repeated over all receiver points in a final RTM, because the virtual source records synthesized by the crosscorrelation should be treated independently. Therefore, total computational cost of the image domain SI could be lower than the data domain SI.

(2) Applicability to a time-lapse study of passive

Passive seismic monitoring or time-lapse survey using permanent observation systems are one of recent research topics. Although high repeatability can be kept in the active seismic survey both on sources and receivers, any repeatability on sources is not guaranteed in the passive seismic survey. In this study, numerical simulation is demonstrated to evaluate the repeatability of the subsurface image and the possibility of extracting a small temporal velocity change by image domain SI with passive seismic data. In this simulation study, simple assumptions with an acoustic wavefield and a same mechanism for all sources are introduced. The passive seismic data for different condition of source distribution or/and velocity perturbation are synthesized, and then the image domain SI is applied for each data set. The repeatability of imaging and the possibility of extraction are measured by some repeatability indexes.

The passive observation records are synthesized using modified overthrust model of SEG/EAGE (15 km x 5 km) with 151 receivers on the surface due to independent 128 sources in the ground (Ricker wavelet with 10 Hz). The sources in the ground are randomly distributed for each model respectively. A velocity change with 10 percent decrease is added in an anticline structure around the center of the model with an elliptical shape (1 km x 0.1 km). A smoothed model from the true velocity model is commonly used for each RTM.

From the simulation study, the global images of the overthrust model are well reproduced in appearance for the different source distributions. However, the repeatability indexes show that the amplitude change due to the source distribution difference is too large to ignore even though the small velocity change can be extracted. Some additional techniques are required to extract only the velocity change without the influence due to the source distribution difference. In addition, there are other difficulties in a real data such as different source mechanism, elastic effects, and some kinds of noises.

Keywords: seismic interferometry, timelapse, reverse time migration

Japan Geoscience Union Meeting 2014
(28 April - 02 May 2014 at Pacifico YOKOHAMA, Kanagawa, Japan)

SSS27-02 Room:411 Time:April 29 09:15-09:30

Temporal changes of P and S wave velocities in NE Japan associated to the M9Tohoku-Oki earthquake from doublets analyses

PACHECO-VIVERO, Karim[1*] ; NISHIMURA, Takeshi[1] ; NAKAHARA, Hisashi[1]

[1]Geophysics, Science, Tohoku University

Application of seismic interferometry using ambient noise and coda waves of regional earthquakes have shown notable seismic wave velocity decreases associated with the occurrence of the M9.0 Tohoku-Oki earthquake. These analyses can be generally attributed to S-wave velocity changes at shallow structures because these waves are dominant in surface waves. On the other hand, analyses of doublets have also succeeded in detecting temporal changes of direct arrival times of P waves as well as those of S waves. Also, the seismic rays pass deeper portions. However as the medium changes by the M9 earthquake are widely observed in East Japan, it is difficult to separate the observed travel time differences into the effects of hypocenter parameters and the travel time differences caused by the change in the medium beneath the stations. In this study, therefore, we develop a new method to determine temporal changes of P and S wave velocities beneath stations by simultaneously determining hypocenter parameters of doublets. We relate travel time differences of doublets to site factors at each station and the differences of hypocenter parameters. We further give a constraint in which the sum of the differences in origin times of the doublets analyzed is set to be zero, since the doublets are considered to randomly occur. As a result, our inverse problem estimates the model parameters, namely the site factors for P and S waves at each station and the relative locations of hypocenters and origin times of the doublets. Seismic data at 454 stations of the Hi-net seismic network in East Japan are used. We analyze 35 doublets with magnitudes ranging from 3.7 to 4.7 and depths from 30 to 60 km located offshore in East Japan for the period from 2005 to 2013. The seismic data are band-pass filtered between 1-2 Hz and travel time differences of arrival times of P and S waves are measured by applying a cross-spectrum method. The inversion results show that hypocenters of doublets differ by about 0.05 km and 0.12 km at a maximum each other in the horizontal and vertical directions, respectively. Even when we change the data set of doublets, the relative hypocenter locations do not significantly change, which indicates our inversion method is stably determining the hypocenter parameters. For the site factors, we find significant delays of arrival times as large as 0.04 s for the S-waves and about 0.01 s for the P-waves. Time delays are observed mainly at stations located widely in Tohoku region between 37 and 40 degrees in latitude, which are west from the M9 fault zone. The observed spatial distributions of time delays seem not to be well matched with the regions strongly shaken, which are located mostly in the eastern area of Tohoku region, or the regions where seismic velocity reductions at shallow medium are detected from analyses of bore-hole and ground surface records. These discrepancies suggest that the time delays detected from doublets originate from different regions, maybe deeper portions beneath Tohoku region.

Keywords: Tohoku-Oki earthquake, Velocity change, Similar earthquakes, Direct P and S waves

Japan Geoscience Union Meeting 2014
(28 April - 02 May 2014 at Pacifico YOKOHAMA, Kanagawa, Japan)

SSS27-03 Room:411 Time:April 29 09:30-09:45

Estimation for seismic wave propagation property of soil structure based on seismic interferometry

SEIICHIRO, Kuroda[1*] ; MASUKAWA, Susumu[1] ; TAGASHIRA, Hidekazu[1]

[1]National Institute for Rural Engineering, NARO

Recently seismic interferometry was applied to estimation for seismic response of natural ground but also those of artificial structure like a building. We applied seismic interferometry concept for retrieval of seismic response of a model dike of soil structure like a fill dam. We employed deconvolution interferometry to estimate seismic response in time domain. From the waveforms obtained from deconvolution with the motion in the basement of a model dam, we estimate traveltimes of shear wave propagating through it and its mean velocity. Estimated velocity explain the normal mode of a model dike well. This approach can be applicable to monitor change in seismic response a dike caused by strong earthquakes or its internal water content change.

Keywords: Seismic interferomtetry, Soil Structure, Dam body, Dike, Shear velocity, Centrifuge test, Fill dam

Japan Geoscience Union Meeting 2014
(28 April - 02 May 2014 at Pacifico YOKOHAMA, Kanagawa, Japan)

SSS27-04 Room:411 Time:April 29 09:45-10:00

Temporal changes of auto-correlation functions associated with the volcanic activity in Hakone volcano, central Japan

YUKUTAKE, Yohei[1*] ; UENO, Tomotake[2] ; HONDA, Ryou[1] ; MIYAOKA, Kazuki[1] ; HARADA, Masatake[1] ; SATOMURA, Mikio[1]

[1]Hot Springs Research Institute of Kanagawa Prefecture, [2]National Research Institute for Earth Science and Disaster Prevention

Auto-correlation functions (ACFs) of ambient noise are thought to be a powerful tool for searching temporal change of crustal structure associated with strong ground motion, or volcanic activity. In this study, we investigated the velocity changes at Hakone volcano associated with an intense swarm activity.

Hakone volcano is located at the northern boundary zone of the Izu?Mariana volcanic arc in central Japan, Many intense periods of swarm activity have occurred in the caldera. It was noted, in last two decades, that seismic swarms were remarkably prevalent in 2001, 2006, 2008-2009, 2011 and 2013. During the swarm activities, except for that in 2011, crustal deformations related to volcanic activities were detected by the GNSS stations network in and around the caldera of Hakone volcano. In particular, remarkable tilt changes were also detected by the tiltmeters within the caldera in 2001 and 2013 activities. It is interpreted that the crustal deformation was caused by pressure from a Mogi point source or dike at a depth of 7 km and two shallow open cracks in the caldera (e.g. Daita et al., 2009; Harada et al., 2009).

To estimate the velocity changes associated with the 2013 activity, we used the continuous velocity waveforms recorded at the stations of Hot Springs Research Institute, National Research Institute for Earth Science and Disaster Prevention Hi-net, Japan Meteorological Agency in and around the caldera, in the period between January 2012 and December 2013. Filtered trace at the frequency band of 1-3 Hz was used to calculate autocorrelation by one-bit correlation technique. To obtain stable record of the one-day ACF, we stacked the ACFs for time intervals of one week. We obtained fluctuations of the velocity structure by using the stretching method (e.g. Wegler et al., 2009).

The velocity fluctuations at the stations in the caldera show a gradual decrease prior to the swarm activity. The velocity decreases at these stations are consistent with increases in base length detected by the GNSS stations around Hakone volcano. We also found that there was sudden velocity decrease at Owakudani station near fumarolic area just after the beginning of swarm activity and tilt changes. We interpreted the velocity decrease at these stations as a material change or a crustal deformation associated with the volcanic activity.

Keywords: auto-correlation functions, volcanic activity, Hakone volcano

Japan Geoscience Union Meeting 2014
(28 April - 02 May 2014 at Pacifico YOKOHAMA, Kanagawa, Japan)

SSS27-05 Room:411 Time:April 29 10:00-10:15

The roles of dispersion and nonlinear effects in the 2001 Tohoku-Oki earthquake tsunami

SAITO, Tatsuhiko[1*] ; INAZU, Daisuke[1]

[1]National Research Institute for Earth Science and Disaster Prevention

The present study aims to reveal the roles of the dispersion and the nonlinear effects in the 2011 Tohoku-Oki earthquake tsunami. Tsunami simulations were conducted based on the nonlinear dispersive equations with a high-resolution source model. The result successfully reproduced the waveforms recorded in both near shore and deep sea. The calculated inundation area showed a good coincidence with the actual inundation at the Sendai Plain, the widest inundation area during this event. Conducting sets of simulations using different equations, we obtained the followings insights. Although the dispersion was neglected in most studies, the maximum-amplitude distribution was significantly overestimated in the deep sea if the dispersion was not included. The waveform observed at the station in which the largest tsunami height (>2 m) recorded among deep-ocean stations also verified the necessity of the dispersion. It is well known that the nonlinear effects play an important role for the tsunami inside bays and harbors. Additionally, the nonlinear effects needed be considered for the accurate modeling of the later waves even at the offshore stations. In particular, including nonlinear terms rather than including the inundation was more important for the precise modeling of the waves reflected from the coast.

Keywords: tsunami, dispersion, nonlinear wave, the 2011 Tohoku-Oki earthquake

Japan Geoscience Union Meeting 2014
(28 April - 02 May 2014 at Pacifico YOKOHAMA, Kanagawa, Japan)

SSS27-06 Room:411 Time:April 29 10:15-10:30

Numerical simulation of tsunamis due to a landslide

YOSHIKAWA, Ryo[1*] ; KAKINUMA, Taro[1]

[1]Graduate School of Science and Engineering, Kagoshima University

Numerical simulation of tsunamis due to a landslide has been performed using a MPS method, where the water surface is indicated based on the spatial gradient of number density of particles. In comparison with the water surface displacements through hydraulic experiments, the calculation results are accurate when the inflow can be assumed as a fluid. The larger the initial potential energy of the inflow is, the larger the tsunami height becomes, although the tsunami height is not large when the initial position of inflow is below the water surface since the initial relative potential energy of the inflow is lower, as well as without impact of plunging. Due to the inflows of the assumed initial values for mass, shape, and velocity caused by a sector collapse of Sakurajima Island, the tsunami height shows more than ten meters in Kagoshima Bay.

Keywords: tsunami, landslide, sector collapse, MPS method

Japan Geoscience Union Meeting 2014
(28 April - 02 May 2014 at Pacifico YOKOHAMA, Kanagawa, Japan)

SSS27-07 Room:411 Time:April 29 11:00-11:15

Point spread functions for earthquake source imaging

NAKAHARA, Hisashi[1*] ; HANEY, Matthew[2]

[1]Graduate School of Science, Tohoku Univ., [2]U.S. Geological Survey

Recently, various methods such as back-projection method (e.g. Ishii et al., 2005), time-reversal (TR) method (e.g. Larmat et al. 2006), and hybrid back-projection (HBP) method (Yagi et al., 2012) have been proposed and applied for earthquake source studies in addition to kinematic waveform inversions (e.g. Hartzell and Heaton, 1983) . In addition, theoretical relationships among the methods have also been clarified (e.g. Kawakatsu and Montagner, 2008, Fukahata et al., 2013). In this study, we introduce the notion of the point spread function (PSF) into earthquake source imaging, and show that the PSF clarifies the meaning of the earthquake source inversions. Under ideal circumstances in which receivers continuously surround the source, the PSF can be interpreted with seismic interferometry.

Kinematic waveform inversion methods are now standard for earthquake source studies. The observation equations (or forward modeling equations) are based on the representation theorem. According to Claerbout (2001), imaging is defined to be the mathematical process of multiplying adjoint Green's functions with both sides of the observation equation. Fukahata et al. (2013) pointed out that the process is very close to the one used in the HBP method. The source image may be blurred and degraded due to uneven distributions and insufficient number of stations. The degree of blurring and degradation can be expressed by the PSF which is often used in optics. The PSF for the source imaging can be expressed by stacked cross correlations of Green's functions between two source points with respect to receivers on a surrounding surface. If distributions of sources and receivers are discretized, the observation equation can be formulated in matrix form. Source inversion is found to remove the effect of the PSF, but other source imaging methods suffer from the PSF.

Ideal circumstances are considered here to better clarify the meaning of the PSF. It is assumed that stations are continuously distributed so as to surround the source points. For this case, we use source-receiver reciprocity of Green's functions. Then, we can consider the following reciprocal configuration in which sources are surrounding two stations. The point spread function is expressed as the stacked cross correlations of waveforms between the two receivers with respect to the surrounding sources. This configuration is exactly the same as ones in seismic interferometry and therefore we can interpret the PSF based on seismic interferometry. For single-force sources, the PSF is found to be the imaginary part of the Green's function. This fact was already pointed out in terms of TR method (e.g. Fink, 2006). For moment-tensor sources, the PSF is shown to be the imaginary part of the spatial derivative of Green's function with respect to each coordinate of the two receivers. This is a novel finding of this study. It is also suggested that the source image is the integrated version of the true source process when the interpretation based on seismic interferometry strictly holds.

In summary, kinematic source inversion methods can remove the effect of the PSF, but other source imaging methods suffer from blurring and degradation by the PSF. As a result, careful weighting of data is necessary for the source imaging methods. For ideal cases in which receivers surround the sources, the PSF can be interpreted with seismic interferometry with the help of the source-receiver reciprocity of Green's functions. This study will contribute to better understanding of the meaning of source inversion methods.

Keywords: Earthquake source imaging, Point spread functions, Seismic interferometry

Japan Geoscience Union Meeting 2014
(28 April - 02 May 2014 at Pacifico YOKOHAMA, Kanagawa, Japan)

SSS27-08 Room:411 Time:April 29 11:15-11:30

Analysis and application of wave propagation process of sweep signals in attenuative media

MATSUSHIMA, Jun[1*]

[1]Graduate School of Engineering, The University of Tokyo

The sweep signal is the most extensively used land seismic exploration technique. In conventional data processing using sweep signals, a received trace is cross-correlated with source sweep to convert the extended sweep signal into a pulse signal. For attenuation estimation, a time window is often used to compute the frequencies of the direct-arrival waveforms. Uncorrelated sweep signals are useful in the discussion of harmonics simply because the uncorrelated data are one of the few situations in which we commonly input a nearly pure frequency into the earth. Our previous study proposed a method that enables accurate measurement of ultrasonic attenuation using sweep signals under the assumptions that velocity dispersion can be ignored and the quality factor (Q) is not dependent on frequency. This method is independent of the effect of windowing while the windowing effect underestimates the attenuation results due to a spectral leakage effect. In most cases, however, the presence of attenuation is accompanied by velocity dispersion because of causality. The presence of velocity dispersion causes attenuation to be disturbed, although the proposed method is not so sensitive to the presence of velocity dispersion. The present paper elucidates the wave propagation process of sweep signals in attenuative media with velocity dispersion to develop the method which can take the effect of dispersion into account. We obtain a time-scale representation of sweep signals by using the continuous wavelet transform method to perform a time-series analysis of a seismic trace that decomposes the trace into its respective amplitude and phase components in both the frequency and time domains.

Keywords: Seismic attenuation, velocity dispersion, sweep waveform

Japan Geoscience Union Meeting 2014
(28 April - 02 May 2014 at Pacifico YOKOHAMA, Kanagawa, Japan)

SSS27-09 Room:411 Time:April 29 11:30-11:45

3D numerical simulation of seismic wavefield in inhomogeneous rock samples

YOSHIMITSU, Nana[1*] ; FURUMURA, Takashi[1] ; MAEDA, Takuto[2]

[1]CIDIR/ERI, The Univ. of Tokyo, [2]ERI, The Univ. of Tokyo

We focus on expanding the applicability of the transmitted waveforms obtained at laboratory experiments to examine detailed medium structure with the aid of novel numerical simulations. For this purpose, we investigate the feature of elastic waveforms in a centimeter class rock sample based on a 3D finite difference method (FDM) simulation. Previously, there were a few ways to approach the later phase of transmitted waveform in a rock sample because the propagation process of the reflected and converted waves generated in a finite-sized rock sample were not figured out. If analyses with entire waveform including the later phases will be possible, it should bring more detailed information on internal medium structure of rock samples.

First, we obtain transmitted waveforms in laboratory with cylindrical Westerly granite sample which horizontal to vertical ratio is 1 : 2. A source transducer is put on the center of the side surface and step voltage is applied to it. Vibration on sample surface is recorded as velocity waveform by laser Doppler vibrometer.

Next, we prepare the simulation model that covers the size of the rock sample. The volume is discretized into 512 x 512 x 1024 grids with an interval of 100 μm. Assuming proportional relationship with X-ray absorption coefficient obtained from micro focus X-ray CT images of the rock sample, we set the density (2.5 - 3.1 g/cm^3), P wave velocity (5.0 - 6.0 km/s), and S wave velocity (2.8 - 3.5 km/s) on each grid. Then, 3D FDM numerical simulation is performed with a single point force which is the same movement with the source transducer of the experiment. Band pass filter with a cut-off frequency of 50 kHz to 2 MHz is applied to the obtained waveforms.

The wavefield obtained from the simulation show that the reflected (PP, SS, PPP, and SSS) and converted (PS, SP, and PPS) waves are generated at the boundary of the sample. As time progresses, waves reflected at the side boundary return to the source area, and waves reflected at the top of the sample propagate through the sample at same time. Thus, we confirmed that waves trapped in the closed medium generate a very complicated shape of the later part of waveforms. Scattering and conversion at mineral grains are also observed due to the heterogeneity of medium, while they have only a limited effect on the simulated waveform in this case.

Radial component of measured and simulated waveforms recorded in the same horizontal plane at the source position are compared. Each phase shape in entire simulated waveform is matched with measured waveform. Two large amplitude phases observed in the measured waveforms are revealed as direct P wave and reflected SS wave from the simulated waveforms. Complex waveform shapes after the arrival of SS wave are indicated to as multiple reflected and converted S waves at the round boundary of the sample.

Keywords: transmitted wave, reflected wave, rock sample, numerical simulation

Japan Geoscience Union Meeting 2014
(28 April - 02 May 2014 at Pacifico YOKOHAMA, Kanagawa, Japan)

SSS27-10 Room:411 Time:April 29 11:45-12:00

Curvilinear grid finite difference method simulation of seismic wave propagation for depth-dependent velocity structure

MAEDA, Takuto[1*]

[1]ERI, The University Tokyo

I propose curvilinear grid method on large-scale finite difference method (FDM) simulation of seismic wave propagation in depth-dependent structure. The FDM usually uses uniform-sized grid having spatial scale smaller than 6-10 of wavelength. Although it is quite straightforward method and is therefore suitable to large-scale parallel simulation, it is not economical to use homogeneous grid size under depth-dependent structure in regional scale because of wide dynamic range of wavelength. Low-velocity sediment requires fine scale grid, but such smaller grid size also requires very small time-stepping in deeper part to satisfy the stability condition of FDM. To deal with this problem, discontinuous-grid method (Aoi and Fujiwara, 1999; Lee et al., 2008) has been proposed. However, possible numerical instability at a discontinuous surface in the former method (Kristec and Moczo, 2010).

The curvilinear coordinate method can use any non-linear, non-orthogonal coordinate. The uniform-size numerical grid is used along the curved coordinate in the computation domain. On the other hand, we still uses the Cartesian coordinate for expressing physical quantities such as velocity vector and stress tensor. This method has been used to incorporate rough ground surface (e.g., Hestholm, 1999). However the recent study on staggered-grid FDM (e.g., Nakamura et al., 2012) suggest that the rough surface can be expressed by the fine-scale homogeneous grid. So, I use a coordinate whose grid-width gradually and smoothly increases with depth to make ratio between grid-size and wavelength nearly constant. My coordinate transform equation depends on vertical depth only, so that to make the computational loads in coordinate transformation and additional memory requirements relatively small. The rotated-grid staggered grid (RSG) scheme (Saenger et al., 2000) has been adopted to make central finite differentiation possible in all directions under the curvilinear coordinate.

As a test, we implemented this curvilinear coordinate FDM in 2D SH and P-SV systems, with using the Butterworth-shape grid-size increase function. This coordinate has a characteristic depth. Grid size linearly increases with depth at deeper than the characteristic depth. On the contrary, this curvilinear coordinate converges to the Cartesian at the shallow limit. This feature is preferable since one can connect the homogeneous Cartesian grid in the shallower portion to the curvilinear grid system without any boundary conditions. In the numerical experiments, I found that the method is effective and stable even for the coordinate system having large grid-size ratio of up to 10. Extension to the 3D model is quite straightforward, and it makes possible to perform broadband large-scale wave propagation simulations including slow sediment in medium-sized computers.

Keywords: seismic wave propagation, numerical simulation, finite difference method, curvilinear coordinate

Japan Geoscience Union Meeting 2014
(28 April - 02 May 2014 at Pacifico YOKOHAMA, Kanagawa, Japan)

SSS27-11 Room:411 Time:April 29 12:00-12:15

Waveform inversion of seismic reflection data and its application to fault structure survey

WATANABE, Toshiki[1*] ; KOBAYASHI, Masami[1] ; YAMAOKA, Koshun[1] ; ITO, Tanio[2] ; KANO, Ken-ichi[3] ; ABE, Susumu[4]

[1]Nagoya University, [2]Teikyo Heisei University, [3]Shizuoka University, [4]JGI, Inc.

Seismic waveform inversion (Tarantola, 1984) is a novel technique of imaging subsurface structures. It reconstructs a model of physical parameters that best explains waveforms of observed seismic data by incorporating a nonlinear least-squares inversion. Waveform inversion provides high-resolution model than that from traveltime tomography. Recent development of computational environment accelerates studies on practical application of the method to 2-D/3-D field data.

In this study, we investigate an application of the method, originally developed for crosswell seismic data, to reflection seismic data. The problems are (1) singular nature of sensitivity near sources and receivers at the surface, (2) attenuation of sensitivity in deeper part of the section, and (3) contamination of surface wave. We introduced a weight increasing with depth on the gradient, and near-offset trace mute to reduce the effects of the problems listed above. Using the synthetic waveform data numerically generated from a given structure model, we proved that a clear structure image was successfully retrieved after iteration.

Then, we applied the method to the field data of wide-angle reflection survey acquired in the Fujikawa-kako fault zone - ISTL seismic reflection survey conducted in 2012 (2012FIST)(Ito et al, 2013) to reveal the detailed structure of Omiya fault. Although the reconstructed velocity structure is consistent with the recent interpretation that the Omiya fault is a reverse fault, it was far from convergence due to the insufficient number of seismic sources used in the survey. Problems and requirements for future survey design will be discussed in the presentation.

Keywords: seismic reflection method, waveform inversion, fault structure, non-linear inversion

Japan Geoscience Union Meeting 2014
(28 April - 02 May 2014 at Pacifico YOKOHAMA, Kanagawa, Japan)

SSS27-12 Room:411 Time:April 29 12:15-12:30

Site amplification factor of the Hi-net stations

UENO, Tomotake[1*] ; SAITO, Tatsuhiko[1] ; SHIOMI, Katsuhiko[1]

[1]NIED

This study estimated site amplification factors of all the Hi-net stations. Employing the coda normalization method and analyzing more than one thousand earthquakes, we obtained the values of all Hi-net sites in the frequency bands of 0.6-1.0 Hz, 1-3 Hz, 2-4 Hz, 2-6 Hz, 4-8 Hz, 6-9Hz, and 8-12 Hz. The cite amplification factors were rather small showing that 90 % of the cite amplification factors ranged within 20 dB. The site amplification varies from station to station more largely with decreasing the frequency. A correlation between the site amplification factor and the S-wave velocity where the sensor is installed was recognized. The cite amplification factor decreases with increasing the S-wave velocity when the S-wave velocity is less than 1.5 km/s. When the S-wave velocity is larger than 1.5 km/s, the correlation disappears. Stations in southwest Japan show smaller site amplification factors, while stations in plains and around the volcanic front in the northeastern Honshu, Japan show larger site amplification factors.

Keywords: Hi-net, Site amplification factor

Japan Geoscience Union Meeting 2014
(28 April - 02 May 2014 at Pacifico YOKOHAMA, Kanagawa, Japan)

SSS27-13 Room:411 Time:April 29 12:30-12:45

Separating body and Rayleigh waves with cross terms of the cross-correlation tensor of ambient noise

TAKAGI, Ryota[1*] ; NAKAHARA, Hisashi[2] ; KONO, Toshio[1] ; OKADA, Tomomi[1]

[1]RCPEV, Graduate School of Sci., Tohoku Univ., [2]Geophysics, Graduate School of Sci., Tohoku Univ.

We develop a novel method to separate body and Rayleigh waves with the vertical-radial (ZR) and radial-vertical (RZ) components of the cross-correlation tensor of ambient noise. Furthermore, analyzing ambient noise records observed at a seismic array, we validate the method. For the separation, we utilize the difference in polarizations between the rectilinear P and the elliptic Rayleigh waves. Assuming the two-dimensional surface and three-dimensional body waves are the superposition of random uncorrelated plane waves, we derive two fundamental characteristics of the ZR and RZ correlations. One is that, between the ZR and RZ correlations, Rayleigh wave contributions have the opposite signs and P waves have the same signs. The other is that, for both ZR and RZ correlations, Rayleigh wave contributions are time-symmetric and P waves are time-antisymmetric. Accordingly, we can separate P and Rayleigh waves by just taking the sum and difference between ZR and RZ correlations and by just taking the time-symmetric and time-antisymmetric components. This method can be performed (1) without any knowledge of velocity structure, (2) using only two stations with three-component sensors on a ground surface, (3) even in the case of anisotropic wave incidence, and (4) with the quite simple procedure. We consider that the developed method can make better use of three-component observations of ambient noise for evaluating the cross-correlation tensor accurately, for improving deep velocity structure using both of extracted body and surface waves and, more fundamentally, for understanding the composition of ambient noise.

Keywords: ambient noise, seismic interferometry, cross-correlation function, wavefield separation, polarization, body and Rayleigh waves

Japan Geoscience Union Meeting 2014
(28 April - 02 May 2014 at Pacifico YOKOHAMA, Kanagawa, Japan)

SSS27-14 Room:411 Time:April 29 14:15-14:30

Study of high-frequency seismic wave propagation by active-source experiments

TANIMOTO, Toshiro[1*] ; OKAMOTO, Taro[2]

[1]University of California, Santa Barbara, [2]Department of Earth and Planetary Sciences, Tokyo Institute of Technology

Seismic wavefields generated by resonant shaking experiments of the Millikan Library, on the campus of California Institute Technology (Pasadena, California, USA), were analyzed. Because the resonant shaking frequencies are 1.12 Hz (the east-west direction) and 1.64 Hz (the north-south direction), this active-source experiment can provide opportunities for studying high-frequency seismic wave propagation in Southern California.

Two such experiments for each frequency were analyzed; for the north-south shaking experiments, the harmonic signals were observed up to distance 323 km in one experiment and up to 396 km in another experiment. For the east-west shaking (1.12 Hz), the maximum distance was 200 km but most observations were confined to less than 100 km.

Spectral amplitudes showed a systematic decaying trend with distance in all cases. Numerical simulations indicated that the predominant signals were surface waves. Assuming that all signals were surface waves, we obtained estimates for the parameter QU for surface waves where Q is the attenuation parameter and U is the group velocity (in km/s). There was, however, a major break in the amplitude-distance trend at a distance about 50 km; for data with distance less than 50 km, QU = 95 $\pm$16 , where U is in km/s. For data beyond 50 km, we obatined QU= 1454 $\pm$ 226. This change in trend must be related to the regions sampled by waves, as the shorter-distance data were dominated by paths in the Los Angeles basins while the longer-distance data did not contain paths in the basin structures.

Through cross correlations between MIK (station in the Millikan library) and a station in the regional network, phase information was also analyzed. For many stations, phase was stable for frequencies between 1.637 and 1.638 Hz which meant that phase is locked between MIK and a station. While it was not possible to estimate phase velocity, because the number of cycles cannot be resolved for high-frequency waves, a stacking approach for multiple-window data allowed us to estimate frequency derivative of phase and group velocity for 25 paths. Group velocity between MIK and network stations are mostly less than 2 km/s. For stations with distance less than 50 km, most group velocity results were about 0.5 km/s or less. Combined with the estimate for QU from the amplitude-distance data, Q is estimated to be 190 for distances less than 50 km. This estimate, however, contains uncertainty up to a factor of two as variations in group velocity estimates differ from station to station.

Keywords: Seismic wave propagation, Crustal structure, Active source experiment

Japan Geoscience Union Meeting 2014
(28 April - 02 May 2014 at Pacifico YOKOHAMA, Kanagawa, Japan)

SSS27-15 Room:411 Time:April 29 14:30-14:45

Estimations of seismological structure in the northwestern Pacific using OBS records: Approaches from >1 Hz component

TONEGAWA, Takashi[1*] ; FUKAO, Yoshio[1] ; FUJIE, Gou[1] ; TAKAHASHI, Tsutomu[1] ; KODAIRA, Shuichi[1] ; SUGIOKA, Hiroko[1] ; ITO, Aki[1]

[1]JAMSTEC

Tentative ocean bottom arrays using seismometer, hydrophone and pressure gauge have recently been deployed through many scientific projects all over the world. However, in Japan, a permanent ocean bottom monitoring system, called DONET, is now working, and dense cabled-OBSs (ocean bottom seismometers) have been constructed around the Japan Trench. It seems that, compared to other countries, such environments in Japan potentially give us some advantages for investigating the Earth ' s interior, seismic activity, and wavefields under the ocean. In order to easily kickoff the use of these records, it would be better to know characteristics of wavefields observed at seafloor.

A large amplitude in the frequency range of 0.07-0.5 Hz can be often seen in the spectrum of noise record observed at seafloor, which is known as microseisms that are generated by wind propagating sea surface. This large amplitude also emerges at land observation. At frequencies longer than 0.02 Hz in the spectrum observed at typical broadband OBS, the amplitude of infragravity wave is strong in the vertical component, and that of tilt effect is dominant in the horizontal component.

In this presentation, avoiding the use of such longer period components, we focus on shorter period components than 1 Hz of records observed at OBSs. We introduce what kind of analyses we can do hereafter with permanent OBS records, which is based on the use of records observed at tentative ocean bottom arrays. In particular, we will introduce ambient noise and receiver function analyses, in which short period components are mainly used.

Keywords: OBS records, short period components, receiver function, seismic interferometry

Japan Geoscience Union Meeting 2014
(28 April - 02 May 2014 at Pacifico YOKOHAMA, Kanagawa, Japan)

SSS27-P01 Room:Poster Time:April 29 18:15-19:30

Nonlinear radiation of hypocenter and prevision of earthquakes

KIKUCHI, Toshiaki[1*]

[1]National defence Academy

Hypocenter vibrations have been analyzed using the analysis method based on time reversal. The dynamic model of the hypocenter vibrations based on the results was advocated. In addition, the effectiveness of the dynamic model was confirmed. The activity regions in the hypocenter are presumed using the dynamic model here.

First, the outline of the dynamic model is described. The time-reversal process was executed to the P wave signals received at the observation stations for the earthquake that occurred in the central part of Suruga Bay in August, 2009, and the pulses formed at the position of the hypocenter, that is, time reversal pulse (TRP) was obtained. The TRP corresponds to an equivalent source to which the hypocenter emits. The obtained TRP provided clear orientation dependency. To clarify the origin of the azimuthal dependence, the frequency spectrum of the TRP to azimuth was obtained. The frequency spectrum was greatly changed by the azimuth. Then, the distribution of the maximum amplitude frequency to azimuth was obtained. As a result, the maximum amplitude frequency rises greatly as azimuth moves from west to east and it has descended afterwards. This frequency rise shows the local movement of sources by high speed. The moving direction converged in the direction of Nishiizunishi, Kawazu, and Ito.

The P waves received at these observation stations exhibited a unique behavior. The head part of the wave received in Nishiizunishi was expanded. However, there was no expansion in the head part in the waves received in Ito and Kawazu near Nishiizunishi.

The head's growing in this manner occurs when the progression rate of cracks in an active fault becomes near the velocity of propagation. The pressure that occurs due to the crack is added cumulatively by moving by high speed. That is, the parametric effect occurs in the active fault. Nishiizunishi is a specific point that reflects the feature of this earthquake.

As for the waveform of the aftershock that received at the specific observation station, the head part of the P waves expanded more than that of main shock. Similarly, the expansion of the head part was observed for the precursor earthquake that occurred before the main shock. The dynamic model of hypocenter vibrations has advocated from these results. The point where the narrow beam emitted from an active fault reaches the surface of the earth is called a parametric spot. The head of the pulse to which the head expands is called a parametric head. This model was verified about four earthquakes larger than M5 that occurred from 2012 to 2009 near Mt. Fuji. The effectiveness of the dynamic model was confirmed.

The dynamic model is consistently approved for precursors, a main shock, and aftershocks. Therefore, the dynamic model may be used for the prevision of earthquake.

The precursor earthquakes of the earthquake that occurred in the central part of Suruga Bay in August, 2009 are examined. The receiving waves that accompanied the parametric head in that were observed seven times. These represent evidence that the progress of the crack began to become a high speed in the active fault. Therefore, observing the seismic waves of a slight earthquake at the peculiar parametric spot and examining the change, may foresee a big earthquake afterwards.

Keywords: hypocenter vibrations, dynamic model, time reversal, prevision of earthquakes

Japan Geoscience Union Meeting 2014
(28 April - 02 May 2014 at Pacifico YOKOHAMA, Kanagawa, Japan)

SSS27-P02 Room:Poster Time:April 29 18:15-19:30

Frequency domain calculation of the seismic wavefield propagating along an ocean trench, with a constant Q attenuation

MITSUHASHI, Yuta[1*] ; FURUMURA, Mitsuko[2] ; MATSU'URA, Ritsuko S.[2] ; SHOJI, Masahiro[1]

[1]KKE, [2]ADEP

For shallow interplate earthquakes, large long-period later phases are frequently observed at long distance. Simulations using the finite difference, which we have performed, revealed an important effect of seawater on those later phases (e.g. Furumura et al., 2011).

However, attenuation $\exp(-\pi ft/Q)$ in the finite difference calculation is set to $\exp(-\pi ft/(Q_o f/f_o))$, meaning $Q/f=Q_o/f_o$ is set as a constant, where f_o is a target frequency of the calculation purpose, and Q_o is its corresponding attenuation factor, so it causes some problems especially for waves propagating for a long distance.

Then we calculated waves propagating in a 2.5D structure in the frequency domain with FEM to realize Q as a constant instead of Q/f, for both cases with and without seawater. We could confirm the important effect of seawater on later phases as well as the finite difference calculations. Calculated later phases have relative large amplitude for frequencies lower than f_o in the Q-constant model compared with the Q/f-constant model. It indicates necessity of estimation of difference between realistic Q and modeled one, when we use the finite difference method. In addition, the results reveal large later phases in the case with seawater, which are rarely seen in the calculated waveforms without seawater. It implies overestimation of magnitude of ocean earthquakes obtained from analysis of waves propagating through a long distance along and across an ocean trench, such as the 1911 off Kikai Island earthquake and the 1933 off Sanriku earthquake observed in Honshu.

Japan Geoscience Union Meeting 2014
(28 April - 02 May 2014 at Pacifico YOKOHAMA, Kanagawa, Japan)

SSS27-P03 Room:Poster Time:April 29 18:15-19:30

Development and extinction of long-period ground motion in thick sediments

TAKEMURA, Shunsuke[1*] ; YOSHIMOTO, Kazuo[1]

[1]Yokohama City University

To obtain better insights of long-period ground motion in thick sediments, which often cause severe damage of large-scale man-made structures, we analyzed horizontal seismograms recorded by dense strong motion networks in the complex large Kanto basin. We found distinct large amplitude long-period ground motion around northern Kanto, which is caused by Love wave excited at the northwestern edge of Kanto basin. Amplitude of Love wave significantly developed during propagation in thick (>3 km) sediments and then suddenly weakened at region where significant change of basin structure exists.

To clarify causes of such observations, we conducted 3D finite difference method (FDM) simulation of seismic wave propagation. In simulation, we assumed plane SH-wave incident into a realistic basin structure model embedded in a homogeneous half-space background structure, to focus characteristics of Love wave excited at the basin edge. Simulation result in a realistic basin model referred from JIVSM (Koketsu et al., 2008) well reproduced observed Love wave development around the northern Kanto. Another simulation in the model, which is limited to maximum bedrock depth of 3 km, shows no significant difference of simulated waveforms compared with the previous model. Thus, development of surface waves in thick sediments is mainly caused by the deepening of shallower low-velocity layers, rather than the depth variation of bedrock.

Acknowledgement

We acknowledge the National Research Institute for Earth Science and Disaster Prevention, Japan (NIED) for providing the K-NET/KiK-net waveform data. We also use strong motion data from SK-net.

Keywords: long-period ground motion, surface wave, kantou basin, basin structure, numerical simulation

Japan Geoscience Union Meeting 2014
(28 April - 02 May 2014 at Pacifico YOKOHAMA, Kanagawa, Japan)

SSS27-P04 Room:Poster Time:April 29 18:15-19:30

Receiver function travel time tomography

HIRAHARA, Kazuro[1*] ; YAMASAKI, Tomona[1] ; ABE, Yuki[1] ; SHIBUTANI, Takuo[2]

[1]Graduate School of Science, Kyoto University, [2]Disaster Prevention Research Institute, Kyoto University

Hirahara et al. (2006) proposed a method of Receiver Function (RF) Tomography which combines travel time tomography using travel times from local and teleseismic events with receiver function analyses. In the method, a 3-D P and S wave velocity structure is estimated together with the velocity discontinuity interfaces, where we add both data of the amplitudes and differential travel times of Ps converted phases in RFs employing Gaussian beam RF synthetics. We found, however, that it is difficult to match the amplitudes of Ps phases to estimate the velocity contrasts between velocity discontinuity interfaces with 2-D undulations.

.

Here, as a step toward RF Tomography, we are developing a method of RF Travel Time Tomography using only travel times of P and S waves from local and teleseismic events and P-Ps times of Ps converted phases obtained with the receiver function analyses. Abe et al. (2011) developed a method to estimate iteratively geometries of dipping seismic velocity discontinuities with high dipping angles of 30 to 70 degrees from common conversion point stacking of receiver functions, in which the multistage fast-marching method (de Kool et al., 2006) is applied to the ray tracing with refraction at dipping interfaces. The large amplitudes of RFs stacked in 3-D cells are interpreted to the Ps phases converted at the velocity discontinuity interfaces and the differential travel times P-Ps of the corresponding phases are additionally used for the travel time tomography of P and S waves from local and teleseismic events.

In this paper, we do not analyze the actual data but aim at developing the code of RF Travel Time Tomography based on the code of FMTOMO (Fast Marching Tomography) by Rawlinson (2007). First, for a 3-D heterogeneous structure with interfaces of a Moho and a subduction slab, we synthesize travel times of P and S waves from local and teleseismic events, and also Ps times converted at the Moho and the slab top and the oceanic Moho interfaces. Then we investigate the ability of retrieving the 3-D velocities and the undulation of the Moho and the dipping slab interfaces.

Keywords: Receiver function, Tomography, Ps convered wave, Travel time, Seismic velocity discontinuity interface

Japan Geoscience Union Meeting 2014
(28 April - 02 May 2014 at Pacifico YOKOHAMA, Kanagawa, Japan)

SSS27-P05 Room:Poster Time:April 29 18:15-19:30

Ocean acoustic Rayleigh wave persistently excited by earthquake signals

TONEGAWA, Takashi[1*] ; FUKAO, Yoshio[1] ; TAKAHASHI, Tsutomu[1] ; OBANA, Koichiro[1] ; KODAIRA, Shuichi[1] ; KANEDA, Yoshiyuki[1]

[1]JAMSTEC

In the interferometry, the wavefield propagating between two positions can be retrieved by correlating ambient noise recorded on the two positions. This approach is useful for applying to various kinds of wavefield, such as ultrasonic, acoustic (ocean acoustic), and also seismology. Off the Kii Peninsula, Japan, more than 150 short period (4.5 Hz) seismometers, in which hydrophone is also cosited, had been deployed for 2 months on 2012 by Japan Agency for Marine-Earth Science and Technology (JAMSTEC) as a part of " Research concerning Interaction Between the Tokai, Tonankai and Nankai Earthquakes " funded by Ministry of Education, Culture, Sports, Science and Technology, Japan. In this study, correlating ambient noise recorded on the hydrophones, we attempt to investigate characteristics of wavefield observed at seafloor.

The observation period is from Sep. 2012 to Dec. 2012. Station spacing is around 5 km. For 5 lines off the Kii Peninsula, the 30 - 40 seismometers are distributed at each line. Sampling interval is 200 Hz for both seismometer and hydrophone. The instruments are located at 100 - 4800 m in water depth. In the processing for the both records, we applied a bandpass filter of 1 - 3 Hz, replaced the amplitude to zero if it exceeds a value that was set in this study. We calculated cross correlation function (CCF) by using continuous records with a time length of 600 s, stacked the CCFs over the whole observation period.

We first aligned only CCFs using two stations with a separation distance of 5 km along lines off Kii Peninsula. As a result, we could detect strong signals in the CCFs that clearly show travel time variation as a function of water depth. The group velocity of the signal gradually changes from 1.3 km/s to 0.7 km/s at water depths from 2000 to 4000 m. In addition to the wave, a relatively weak signal with a group velocity of 1.4 - 1.5 km/s can be seen in the region at water depth of 4,000 m.

We investigated the wavefield by using a numerical simulation with finite difference technique. As a result, all of these signals can be explained by acoustic Rayleigh wave, which has the energy within not only the ocean but also sediment. A case in which vertical forces are located at subseafloor generated the acoustic Rayleigh wave well, and the CCFs using synthetic waveforms match well with the observed ones. However, another one in which vertical forces are located at sea surface failed to describe the observation. This means that the observed acoustic Rayleigh wave in background wavefield would be generated by earthquake signal, not signals due to microseisms. Moreover, we will show that the amplitude of the signals possibly correlates with seismicity distribution, which also supports that the signals are excited by earthquake signals.

Keywords: acoustic Rayleigh wave, ambient noise, correlation analysis

Japan Geoscience Union Meeting 2014
(28 April - 02 May 2014 at Pacifico YOKOHAMA, Kanagawa, Japan)

SSS27-P06 Room:Poster Time:April 29 18:15-19:30

Modeling inclined cracks in a 2-D finite difference grid

NASUNO, Arata[1] ; KAWAHARA, Jun[1*] ; SHIINA, Takahiro[2] ; OKAMOTO, Taro[3]

[1]Ibaraki University, [2]Tohoku University, [3]Tokyo Institute of Technology

Seismic scattering due to cracks are often numerically simulated using a boundary integral equation method (BIEM), a finite element method, or a finite difference method (FDM). Among others, the FDM has a great advantage in tractability, though having a limitation that it can treat rectangular grids only. Using the rotated staggered grid that they developed, Saenger et al. (2000, Wave Motion) modeled a crack or cavity as a gather of grid points with zero elastic constants. In contrast, Suzuki et al. (2006, 2013, Earth Planets Space) modeled a 2-D empty crack as a linear array of grid points with zero traction on the basis of a standard staggered grid (Virieux, 1984, 1986, Geophysics). Using this method, these authors successfully simulated seismic wave scattering due to cracks. However, they only treated cracks parallel to grid lines.

Here we extended the method of Suzuki et al. (2006) for modeling cracks with zero antiplane shear traction to the case of cracks inclined with respect to grid lines. Using the idea of the staircase approximation to irregular free surface (Ohminato and Chouet, 1997, Bull. Seis. Soc. Am.), we modeled an inclined crack as staircase-like arrayed grid points with zero antiplane shear traction within a staggered grid. We then simulated a plane harmonic SH wave obliquely incident on the crack until the resultant oscillation of the crack became stationary. We then measured the amplitude of displacement discontinuity along the crack. We also calculated the same displacement discontinuity using a frequency-domain BIEM (Murai et al., 1995, Geophys. J. Int.). It was confirmed that the both results were consistent, irrespective of the crack inclination angle, if the grid spacing was much smaller than the crack length and hence the staircase-shaped crack plane was sufficiently smooth. This implies the validity of the present method of modeling inclined cracks.

Acknowledgments: For the BIEM calculations, we used a code of Dr. Yoshio Murai (Hokkaido University), and used the computer systems of the Earthquake and Volcano Information Center of the Earthquake Research Institute, the University of Tokyo.

Keywords: finite difference method, crack, SH wave

Japan Geoscience Union Meeting 2014
(28 April - 02 May 2014 at Pacifico YOKOHAMA, Kanagawa, Japan)

SSS28-01 Room:312 Time:May 2 10:00-10:15

The recent movement and the future plans of the JMA EEW

NAKAMURA, Masaki[1*] ; KODERA, Yuki[1] ; TAMARIBUCHI, Koji[1] ; AIZAWA, Koji[1] ; OGAMI, Yoshie[1] ; HIRANO, Kazuyuki[1] ; YAMADA, Yasuyuki[1] ; SAKIHARA, Hirokazu[1] ; URATANI, Junpei[1] ; MORIMOTO, Masahiko[1]

[1]JMA

We sometimes reported our efforts to improve the JMA EEW system and we will make a presentation about the recent movement of the JMA EEW and the future plan to improve the system.

In the case of the 2011 off the Pacific Coast of Tohoku Earthquake (Mw9.0), the warning of the EEW was disseminated 30 s after the Mw9.0 event occurrence, which was 8 s after the first detection. The estimated magnitude was 7.2 at the time and the warning was issued only for Tohoku. We could provide the warning before the arrival of S-waves for all warning areas. However, the actual magnitude was 9.0 and the wide area was ruptured. The under estimate of the magnitude and the extent of the source region caused the under estimate of intensities. Especially, in Kanto, we observed 6-upper, but we could not provide the warning for the public. The warning was provided for the public only once, but the updated information was provided only to the limited users. We issued the EEW totally 15 times for the event. Finally the EEW estimated M8.1 105 s after the first detection. Moreover, aftershocks sometimes occurred simultaneously over the wide region. Then, the system became confused and did not always determine the hypocenter parameters correctly. In 49 days after the main shock to April 28, 2011, 70 EEWs were announced to the public, but actual observed intensities did not exceed 2 at any stations in 17 cases.

To overcome those problems, we will introduce the real-time pseudo seismic intensity by Kunugi et al. (2008), by which we will be able to monitor the extent of the strong motion field (the simplest version of Hoshiba, 2013) and to evaluate the calculated hypocenter parameter. The current JMA EEW system is based on the calculated hypocenter parameter. We have the idea of a hybrid method using the conventional method and the real-time intensities (Kotera et al, 2014). Furthermore, Tamaribuchi et al. (2014) developed a new method to classify multiple concurrent events for EEW. Their approach used the particle filter method and the method estimated location, origin time and magnitude in the probabilistic framework, using trigger time, maximum amplitude, epicentral distance and incident angle of the waveform for the likelihood function. We have a plan to use the method additionally.

Moreover, JMA began to provide long period ground motion information, using the observed waveform at each station, on JMA web site March, 2013 (Aizawa et al., 2014). We have just begun to investigate the long period ground motion forecast aiming at establishing an earthquake early warning for long period ground motion (Ogami et al., 2014).

References: Aizawa et al., 2014, the abstruct of this meeting. Hoshiba, 2013, DOI: 10.1002/jgrb.50119. Kotera et al., 2014, the abstruct of this meeting. Ogami et al., 2014, the abstruct of this meeting. Tamaribuchi et al., 2014, Zisin 2, submitted.

Keywords: EEW, long-period ground motion, JMA, seismic intensity, intensity scale on long-period ground motion, hypocenter determination

Japan Geoscience Union Meeting 2014
(28 April - 02 May 2014 at Pacifico YOKOHAMA, Kanagawa, Japan)

SSS28-02 Room:312 Time:May 2 10:15-10:30

Earthquake Early Warning system combined with real-time ground motion prediction

KODERA, Yuki[1*] ; YAMADA, Yasuyuki[1] ; HIRANO, Kazuyuki[1] ; MORIMOTO, Masahiko[1] ; HOSHIBA, Mitsuyuki[2] ; NAKAMURA, Masaki[1]

[1]Seismology and Volcanology Department, Japan Meteorological Agency, [2]Meteorological Research Institute

We introduce a hybrid method which is a combined method of the current JMA EEW system and the simplest version of real-time ground motion prediction method. We also report applications of the hybrid method to some cases in which the current JMA EEW system underestimates or overestimates seismic intensity.

The current JMA EEW system (the conventional method) forecasts seismic intensity on the basis of hypocenter parameters estimated from observed seismic waveform. When accurate hypocenter parameters are determined in an early phase, forecast values of seismic intensity in all areas are calculated quickly and long lead times are available in many areas. On the other hand, if estimated hypocenter parameters are inappropriate, the conventional method leads to underestimation or overestimation of forecast values of seismic intensity.

Hoshiba (2013) proposes real-time ground motion prediction method as a method of forecasting ground motion without the use of hypocenter parameters. The real-time ground motion prediction method predicts wave field directly from observed wave field by a boundary integral equation for displacement. This method is expected to robustly forecast accurate ground motion because it utilizes actual wave field information. Forecast of JMA seismic intensity based on the real-time ground motion prediction method can be performed easily by the following algorithm:

(1) Gather real-time pseudo seismic intensities (Kunugi et al., 2013) of observation stations within a radius R from a target station.

(2) Take the maximum value of the real-time pseudo seismic intensities as a forecasted seismic intensity of the target station.

This is the simplest version of real-time ground motion prediction method. The algorithm assumes that a ground motion which causes large seismic intensity propagates within a radius R without attenuation. In this method, a lead time tends to be short because the area where actual wave field information is available is limited to a radius R.

The conventional method and the simplest version of real-time ground motion prediction method have complementary features on earliness and robustness. Therefore, appropriate combination of these methods is expected to become a hybrid method which has both earliness and robustness. We propose a hybrid method as follows:

(1) Take the maximum forecasted value of two methods in ordinary circumstances.

(2) Reject a forecasted value of the conventional method when the conventional method is not consistent with the real-time ground motion prediction method.

We set input data as real-time pseudo seismic intensities of JMA observation stations, output data as forecasted values of seismic intensity meters in Japan and radius R as 30km and apply the hybrid method to some previous earthquake events. In the case of the 2011 off the Pacific coast of Tohoku Earthquake, whereas seismic intensity scales of Kanto region the conventional method estimates are more than one degree smaller than actual, the hybrid method estimates them appropriately with an accuracy of about one degree. In the case of multiple events on April 3, 2011, the hybrid method can avoid overestimation of seismic intensity the conventional method leads to by qualify control of estimated hypocenter parameters of the conventional method. In the case of an earthquake in the northern part of Tochigi prefecture on February 25, 2013, forecasted seismic intensities of the conventional method are one or two degrees larger than actual although the conventional method estimates hypocenter parameters appropriately. The hybrid method also overestimates seismic intensity in consequence of the overestimation of the conventional method.

Reference:
Hoshiba, M. (2013), *J. Geophys. Res. Solid Earth,* **118,** 1038-1050.
Kunugi, T., S. Aoi, H. Nakamura, W. Suzuki, N. Morikawa and H. Fujiwara (2013), *Zisin 2,* **65,** 223-230. (in Japanese)

Keywords: Earthquake Early Warning, Japan Meteorological Agency, seismic intensity

Japan Geoscience Union Meeting 2014
(28 April - 02 May 2014 at Pacifico YOKOHAMA, Kanagawa, Japan)

SSS28-03 Room:312 Time:May 2 10:30-10:45

Achievement of Faster and More Accurate Earthquake Early Warning System - Combining JMA and Hi-net data -

YAMADA, Masumi[1*] ; TAMARIBUCHI, Koji[2]

[1]DPRI Kyoto University, [2]JMA

Earthquake Early Warning systems (EEWS) are designed to quickly determine locations and magnitudes of earthquakes and then provide predictive warnings about the arrival time and amplitude of the strong shaking. Current JMA EEWS uses data from two seismic networks: JMA accelerometer network and NIED high sensitive seismometer network (Hi-net). Currently, these two datasets are processed in the different scheme and the results are merged to issue a warning. Combining these two datasets and processing in the same framework should improve the accuracy and speed of the warning.

In this study, we tried to develop a method to use these two dataset in the same framework. A major barrier to do this is that the instrument responses are different in these networks. Hi-net seismometers are velocity-type sensor with the corner frequency of 1Hz, which means that the response of long-period components underestimates ground motions. It also saturates for very large ground motions. We need a special care to use this Hi-net data in the same framework.

We applied time-domain recursive filters to correct instrumental response of Hi-net sensors and adjust them to the response of mechanical seismometers. We successfully developed a method to produce records with the same response to the JMA acceleration data. We evaluated the saturation of the Hi-net data with the data in 2 month after the Tohoku earthquake, and found the effect of saturation was minor. Therefore, we can use Hi-net data and JMA acceleration data in the same scheme theoretically. Speed of the warning improved by 3 seconds in the average for the inland earthquake by combining these two networks.

Keywords: earthquake early warning, Hi-net, saturation, instrument response

Japan Geoscience Union Meeting 2014
(28 April - 02 May 2014 at Pacifico YOKOHAMA, Kanagawa, Japan)

SSS28-04 Room:312 Time:May 2 11:00-11:15

Automatic arrival time picking compared to manual picking (6)

HORIUCHI, Shigeki[1*] ; HORIUCHI, Yuko[1] ; IIO, Yoshihisa[2] ; TAKADA, Youichiro[2] ; SAWADA, Yoshihiro[3] ; SEKINE, Shutaro[3] ; NAKAYAMA, Takashi[4] ; HIRAHARA, Satoshi[4] ; KONO, Toshio[4] ; NAKAJIMA, Jyunichi[4] ; OKADA, Tomomi[4] ; UMINO, Norihito[4] ; HASEGAWA, Akira[4] ; OBARA, Kazushige[5] ; KATO, Aitaro[5] ; NAKANO, Masaru[6] ; NAKAMURA, Takeshi[6] ; TAKAHASHI, Narumi[6]

[1]Home Seismometer Corporation, [2]Disaster Prevention Research Institute Kyoto University, [3]Association for the Development of Earthquake Prediction, [4]Research Center for Prediction of Earthquake and Volcanic Eruptions, [5]Earthquake Research Institute, The University of Tokyo, [6]Japan Agency for Marine-Earth Science and Technology

1. Introduction

Recent installation of many ocean bottom seismometers increases the number of P and S-wave arrival times to be measured. The number becomes more than the limit that we are able to conduct picking. We have started to develop an automatic system of hypocenter location which is able to locate hypocenter with accuracy compatible to manually picking. Our previous study introduced a method of using the evaluation equation composed of many parameters based on seismological knowledge about how to pick arrival times. We have showed that the method can pick reliable arrival times of P and S waves. We also have introduced the method of hypocenter location which is able to locate hypocenters even at a period of earthquake swarm. The method makes pseudo seismograms whose amplitude become large at P and S wave arrival times and locates hypocenter with applying the semblance technique to the pseudo seismograms. In this paper, we preset the accuracy of P and S wave picking by the automatic system.

2. Method

In general, the predominant frequency of S wave is lower than that of P wave. We added the data of time variations of predominant frequency for S wave picking. The predominant frequency is calculated by the similar manner of calculating τc, which is used widely to calculate magnitude in the EEW system. Firstly, we calculate differential and double differential of horizontal component observed seismograms as follows.

V (t) = (u(t)-u(t-dt))/dt

A (t) = (u(t)-2u(t-dt) + u(t+2dt))/dt2

Then we compute 0.1 second running mean of the absolute value of V(t),and A(t) and calculate the ratio of two running means. We get time variations in predominant frequency from the time change of the reciprocal value of the ratio, though it is required to multiply a constant value. We assume dt to be 0.02 seconds. We put values of time changes of predominant frequency in the evaluation equation, which is composed of many parameters showing characteristic of seismograms; correspond to the periods between the candidates of arrival times.

3. Results

1) Remarkable drop in predominant frequency are found in almost all seismographs at times of S wave arrivals, showing the effectiveness of its usage in the arrival time picking. Same drop is found at P wave arrivals but there are many cases of increase.

2) We copied all available continuous seismic waveform data in Japan for 24 hours on September 3, 2011, and computed hypocenter automatically. Our automatic system locates 1523 events and the number by JMA catalogue is 588 in the same period. The number of automatically picked P waves is 2.6 times larger than that of manually picking by JMA, and S wave 1.6 times larger.

3) We compared P and S wave arrival times picked automatically with those by manually picking. P and S wave time differences are 0.06 and 0.16 seconds, respectively. This value is close to the difference in a case when two operators conduct picking for the same data.

4) We compared origin times estimated by two closed stations both of which have P and S wave arrivals. We select all couple of two stations with station distance less than 30km and compared origin times estimated from P and S wave arrival times. The average origin time differences by the manually picked data and those by automatically are 0.26 and 0.27sec, respectively.

We can conclude from these comparisons that we already developed an automatic system compatible to manually picking.

Keywords: Hypocenter location, Automatic P and S wave picking, Evaluation equation, Senblance, Predominant frequency, compatible to manual picking

Japan Geoscience Union Meeting 2014
(28 April - 02 May 2014 at Pacifico YOKOHAMA, Kanagawa, Japan)

SSS28-05 Room:312 Time:May 2 11:15-11:30

Real-time site correction based on evaluating relative responses to common reference station for wide area network

AOKI, Shigeki[1*] ; HOSHIBA, Mitsuyuki[1]

[1]MRI, JMA

Hoshiba (2013a, JGR) proposed a method for prediction of ground motion based on real-time monitoring, in which hypocenter and M are not required. In this method, site amplification must be corrected in real-time manner. Aoki and Hoshiba (2013, AGU) designed the recursive filters for real-time site correction according to Hoshiba (2013b, BSSA), and predicted the JMA seismic intensity of a station by applying this filter to the observed record at the neighboring station, namely exchanging the site amplification factors with each other. In their experiments, in order to consider the effects of the source and propagation in the observed records at adjacent two sites to be identical, the events whose epicentral distances were greater than 100km were selected. Consequently, they show the accuracy of frequency-dependent site correction is better than that of frequency-independent correction using the scalar value, which indicates the average difference in observed intensities at both stations.

In this study, we regard the average spectral ratio, which can be evaluated from the strong motions simultaneously observed at adjacent two stations without the assumptions of attenuation function and source information, as the relative site amplification (RSF) between these two stations. The RSF between distant two stations are estimated by least squares method, combining RSFs of adjacent stations in the network which consists of adjacent station pairs in wide area (Ikeura and Kato, 2011, JAEE). The method is applied to JMA seismic intensity meter network and NIED strong motion seismograph network (K-net and KiK-net including borehole meters), and we can get the RSFs of the stations which almost cover Honshu and Shikoku islands to the common reference station (JMA Tokyo Chiyoda-ku).

The causal digital filters having similar amplitude property to the RSFs are designed according to Hoshiba (2013b, BSSA) and are applied to the waveforms observed in the 2011 Tohoku great earthquake and 2004 Chuetsu earthquake. Site-corrected waveforms can be regarded as the waveforms simulated observing on the sites having the same amplification factor as the reference station. We compare the distribution of seismic intensity with and without site correction. In the distribution of site-corrected intensity on the ground surface, small-scale heterogeneities found on the distribution without site correction vanish and the smooth attenuation of seismic intensity with distance becomes clearer. Before the site correction, the intensity observed in the borehole generally tends to become smaller than that on the ground surface. However the distributions of site-corrected intensities in the borehole are very similar to the distribution of site-corrected intensities on the ground surface. These results indicate that our site correction method applicable to real-time processing works well.

Acknowledgements: We make use of the recordings of NIED strong motion seismograph network (K-NET and KiK-net) and JMA seismic intensity meter network.

Keywords: Site amplification factor, Spectral ratio method, Real-time processing, Strong motion seismograph network in Japan, Prediction of the ground motion

Japan Geoscience Union Meeting 2014
(28 April - 02 May 2014 at Pacifico YOKOHAMA, Kanagawa, Japan)

SSS28-06 Room:312 Time:May 2 11:30-11:45

Real-time prediction of earthquake ground motion -application of data assimilation and its application to actual data-

HOSHIBA, Mitsuyuki[1*] ; AOKI, Shigeki[1]

[1]Meteorological Res. Inst., JMA

Aiming at improvement of prediction of seismic intensity in Earthquake Early Warning, we are investigating a new technique for real-time prediction of earthquake ground motion. We have proposed to use data assimilation technique for estimation of current wavefield of ground motion, and then predict future wavefield based on physics of wave propagation. In this presentation, we will show examples of application of the technique to the actual data, such as those from the 2011 Tohoku earthquake and the 2004 Mid-Niigata earthquake.

In the proposed technique, estimation of current wavefield is important. We correct site amplification factors using recursive filtering (Aoki and Hoshiba, 2014), apply band pass filter which is used for JMA seismic intensity (Kunugi et al., 2008), and then estimate envelope of 3-component vector summation of the filtered waveforms. We apply the data assimilation technique to the envelope and then estimate the spatial distribution of strength and propagation direction of ground motion.

The strength and the propagation direction are used as an initial condition, and then wave propagation is calculated. In this presentation, as the physics of wave propagation we will use Radiative Transfer Theory in which wave propagation is simulated by energy propagation based on high frequency approximation. The theory has been used for interpretation of seismogram envelope. We will indicate examples of predictions of 10 and 20s in this presentation.

For application to the 2011 Tohoku earthquake, this method reproduces the strong ground motion which were generated from multiple SMGA, and then propagated into many directions. Strong ground motion, generated at off Fukushima much later than the earthquake origin time, propagated into Kanto region, and then around Kofu and Nagoya. The prediction of 10 and 20s reflects the spatial distribution. In the conventional method based on hypocentral location and magnitude, it was not easy to predict the ground motion for the case of the late rupture.

For case of the 2004 Mid-Niigata earthquake, this method reproduces propagation of strong ground motion from repeated aftershocks. Especially at around epicenter region, strong ground motion repeatedly arrived even when the motion of earlier events still large. In the conventional method, the case of the repeated occurrence of aftershocks was not easy.

The proposed method is expected to be useful for improvement of prediction of seismic intensity in Earthquake Early Warning.

Keywords: Earthquake Early Warning, Data assimilation, Prediction of ground motion, Radiative transfer theory, 2011 Tohoku earthquake

Japan Geoscience Union Meeting 2014
(28 April - 02 May 2014 at Pacifico YOKOHAMA, Kanagawa, Japan)

SSS28-07 Room:312 Time:May 2 11:45-12:00

Investigation for earthquake early warnings of long-period ground motion

OGAMI, Yoshie[1*] ; AIZAWA, Koji[1] ; SAKIHARA, Hirokazu[1] ; URATANI, Junpei[1] ; NAKAMURA, Masaki[1]

[1]JMA

Sometimes seismic intensity cannot express difficulty of action and indoor situations in high rise buildings properly when severe long-period ground motion occurs. To notify people of such situations and facilitate effective countermeasures, JMA started to provide information on long-period ground motion from March 28th, 2013. And now, we are investigating for an earthquake early warning for long-period ground motion.

There are some techniques for prediction long-period ground motion, and we investigate attenuation relationships of response spectrum because it can calculate at any given seismic parameter and calculate fast.

We investigate following three relationships that they are used for governmental studies, we can get their coefficients and detail information on amplification factors, and they have different equation format or adjustment techniques.

-Sato et al.(2010) and Sato et al.(2012)
-Morikawa and Fujiwara(2013)
-Yokota et al.(2010)

We use earthquakes that earthquake early warnings were issued, their magnitudes are bigger than 5.5, and maximum seismic intensities are 3 or larger, and we calculate absolute velocity response spectrum for seismic parameters of each earthquake early warning information and JMA seismic catalog. Prediction points are JMA seismic stations, K-net stations and KiK-net stations, and prediction element is intensity scale of long-period ground motion.

As a result, every equation represent trend properly. Especially, the probability that intensity scales fall inside the error of +/- 1 is 70 to 80 percent when we use seismic parameters of JMA seismic catalog. But there is a tendency that prediction intensity scale is bigger than one of calculated from real wave form near the epicenter because we use the shortest distance from source faults to observation stations which depend on Mw. In addition, calculated results are affected accuracy of seismic parameters of earthquake early warnings. Therefore there is need to discussion when we issue prediction information and what information number we should use.

Keywords: long-period ground motion, JMA, EEW, attenuation relationship, response spectrum

Japan Geoscience Union Meeting 2014
(28 April - 02 May 2014 at Pacifico YOKOHAMA, Kanagawa, Japan)

SSS28-08 Room:312 Time:May 2 12:00-12:15

Updating of Earthquake Early Warning for Long-Period Ground Motions

IRIKURA, Kojiro[1*] ; KURAHASHI, Susumu[1]

[1]Aichi Institute of Technology

Introduction: In the present EEW systems developed by the JMA, Japan, hypocenter and magnitude of an earthquake are determined quickly, after which ground shaking strengths such as seismic intensity are predicted based on a ground motion prediction equation and then earthquake warning are sent to public when the seismic intensity are beyond 5-lower. This method might underestimate ground motions for large earthquakes with wide rupture area because source extent produces error in estimating distance from source to site and the effects of rupture directivity prediction are not taken into account. Another problem is that the magnitude and source distance cannot be determined before the rupture terminate. Therefore, lead times of prediction become smaller in disastrous regions as earthquakes become larger. Long-period strong motions related to damage of skyscrapers and large oil-storage tanks are generated only from large earthquakes.such as mega-thrust earthquakes. It takes very long time before the rupture terminates. A new idea applying the Kirchhoff-Fresnel boundary integral equation proposed by Hoshiba (2013) will solve the above problem by predicting ground motions at front stations where ground motions do not arrive yet without estimating the hypocenter and magnitude of an earthquake. We attempt to examine the applicability of the front detection method to prediction of long-period strong motions.

Methodology: Ground motion u(P,t) in the wavefield at location P and time t inside a close region is approximated as Kirchhoff-Fresnel Integral.

Equation (1)

In the above equation, u(r,t) is ground motion at a reference point on S and G(P-r,t) is the Green's function between a reference point r and a target point P. The above equation is available for the case where the wave length is much smaller than the spatial fluctuation of absolute amplitude of u(r, t) and G(P, t?t, r , 0), i.e. in high-frequency motions.

When the distance to the source is much larger than |P ? r|, plane wave incidence can be assumed locally around P. Then, u(P,t) is approximated as a convolution between G(P-r,t) and u(r,t).

Equation (2)

When the target point is almost aligned along a line connecting the source to the reference point, the crosscorrelation of u(P,t) and u(r,t) is approximated as follows.

Equation (3)

T(P,r, t) is the transfer function between the reference point and the target point. S(t) is defined as the autocorrelation of the source time function s(t).

Equation (4)

We can estimate the transfer function when the ground motions from some small earthquakes are obtained at the target point and at the reference point at the same time from (3). The autocorrelation function of the source time function of the small earthquake is estimated in advance, e.g. from the waveform inversion of the source process. When large earthquakes such as mega-thrust earthquakes happen in the subduction zone, we can evaluate long-period ground motions at sites where large shakings do not arrive yet using ground motions at stations already observed closer to the source and the transfer functions calculated in advance.

Keywords: Earthquake Early Warning, Long-Period Ground Motions, the applicability of the front detection method

$$u(\boldsymbol{P},t) = \int \frac{1}{v(\boldsymbol{r})} \cdot (\cos\theta + \cos\theta') \cdot G(\boldsymbol{P}-\boldsymbol{r},t) * \dot{u}(\boldsymbol{r},t) dS \quad (1)$$

$$u(\boldsymbol{P},t) = G(\boldsymbol{P},\boldsymbol{r},t) * u\left(\boldsymbol{r}, t - \frac{\boldsymbol{P}-\boldsymbol{r}}{v}\cos(\theta'-\theta)\right) \quad (2)$$

$$u(\boldsymbol{P},\boldsymbol{r}_0,t) * u(\boldsymbol{r},\boldsymbol{r}_0,-t) = T(\boldsymbol{P},\boldsymbol{r},t) * S(\boldsymbol{r}_0,t) \quad (3)$$

$$S(\boldsymbol{r}_0,t) = s(\boldsymbol{r}_0,t) * s(\boldsymbol{r}_0,-t) \quad (4)$$

Japan Geoscience Union Meeting 2014
(28 April - 02 May 2014 at Pacifico YOKOHAMA, Kanagawa, Japan)

SSS28-09 Room:312 Time:May 2 12:15-12:30

Current Status and Issues of the Broadcast Start Condition of Earthquake Early Warning

TAKANO, Kiyoshi[1*]

[1]III and ERI, the University of Tokyo

In-site broadcasting system is widely used as a means of transmitting of earthquake early warning. But about the current situation of the broadcast start condition, it is determined by the user who introduced it in consultation with providers. For example, if there is a hazardous material in the building, it will be broadcast starting at predicted seismic intensity 3 or more. On the other hand, in the building with no less hazardous materials, it will be broadcast starting at predicted seismic intensity lower 5 or more. The current situation of the broadcast start condition is as described above; the users have determined in consideration of the user environment.

The document, which serves as a reference in the broadcast start condition to determine appropriate, did not exist until the JMA had published guidelines in April 2011. In this guideline, in particular, for the case of in-site broadcasting towards an unspecified number of people, it has been recommended to broadcast suited to the alarm condition of earthquake early warning of JMA.

The alarm condition of earthquake early warning in JMA is, ”it is issued for areas predicted strong shaking (seismic intensity lower 5 or more) and for areas where seismic intensity 4 is predicted when if seismic wave were observed at more than two seismic stations and the seismic intensity was predicted to lower 5 or more”. And to match in this, mobile phone companies and commercial televisions have broadcast the earthquake early warning in areas where JMA issued an alarm.

At the beginning, we also have set the broadcast start condition of our in-site broadcasting system to match to this alarm condition in JMA. Furthermore, we have operated by setting the ”broadcast start condition for giant earthquakes” by using the combination of not only predicted seismic intensity but also predicted magnitude because from the fact that at the time of the Tohoku Giant Earthquake, the predicted seismic intensity at the alarm of earthquake early warning was much lower than the actual.

However in the period of one year from the start of the operation, there were three broadcasting occurred but in those case the real seismic intensity were 2 or 3 and as a result, these broadcasting became the excessive broadcast.

In this opportunity, I would like to report on the results of review for broadcast start condition of earthquake early warning. And I hope to discuss issues for better broadcast start condition and realizing it.

Keywords: Earthquake Early Warning, Broadcast Start Condition, Alarm Condition

Japan Geoscience Union Meeting 2014
(28 April - 02 May 2014 at Pacifico YOKOHAMA, Kanagawa, Japan)

SSS28-P01 Room:Poster Time:May 2 14:00-15:15

New-development of real-time seismic waveform viewing system feeding from DONET

TAKAESU, Morifumi[1*] ; HORIKAWA, Hiroki[1] ; SUEKI, Kentaro[1] ; TAKAHASHI, Narumi[1] ; SONODA, Akira[1] ; MIURA, Seiichi[1] ; TSUBOI, Seiji[1]

[1]Japan Agency for Marine-Earth Science and Technology

Jamstec-Ocean seismological database-Integrated byNetwork data (team JOIN) is started since 2012, with the purpose of developing an earthquake research information database through the integration of discrete database, such as real-time earthquake study and lithosphere structure research catalogue. JOIN is consist of three divisions, 1) seismological study using DONET (Dense Ocean-floor Network for Earthquake and Tsunamis) data, 2) sub-structural study for nankai-tonankai earthquake area, and 3) data-management and opent to public for oceanographic data acquired JAMSTEC equipment. These can lead not only scientific but practical outreach, consequently, disaster prevention of each local government.

We have developed web-based real-time monitoring system of strong motion and pressure sensor of DONET observatory network, this is user-friendly tool for servant service of disaster prevention department.

Trial operation with the monitoring system is undergoing for a few government close to nankai-tonankai area, aiming full-scale operation which will start from April 2014.

Technical summary of this system will be introduced.

Keywords: DONET, database, real-time trace view, outreach for local government

Japan Geoscience Union Meeting 2014
(28 April - 02 May 2014 at Pacifico YOKOHAMA, Kanagawa, Japan)

SSS28-P02 Room:Poster Time:May 2 14:00-15:15

Examination of the relative site amplification factor of OBS and their real-time correction: examples of Sagami Bay OBS

HAYASHIMOTO, Naoki[1*] ; HOSHIBA, Mitsuyuki[1]

[1]Meteorological Research Institute

Hoshiba (2013, JGR) proposed a method for real-time prediction of ground motion based on real-time monitoring as the next-generation EEW, in which detection of hypocenter and Magnitude are not required. In this method, site amplification is one of the important factors. Therefore, relative site amplification factor have been evaluated at KiK-net (Iwakiri and Hoshiba, 2011) and at JMA seismic intensity stations (Aoki and Hoshiba, 2013) in the frequency domain. Ocean Bottom Seismograph (OBS) will provide valuable information to grasp ground motion propagation from ocean area. However, it is necessary to correct the site amplification factor of OBS for applying real-time monitoring method. Hayashimoto and Hoshiba (2013, SSJ) reported relative site amplification factor of OBSs at Tonankai region (Tonankai OBS (JMA) and DONET (JAMSTEC)) as a preliminary result. In this study, we evaluate relative site amplification factor of Sagami Bay OBS (NIED, Eguchi *et al*., 1998, MGR) which is close to land stations, and examine the effects of real-time correction to predict ground motion of land station from OBS.

The averaged spectral ratio of a station-pair from many events can be regarded as the relative site factor when the hypocentral distances to station-pair are much larger than the distance of those stations. In this study, we use the waveform data from the Sagami Bay OBSs and adjacent land stations (K-NET and KiK-net, NIED), and select the dataset with the hypocentral distance which is greater than 100km. We compare Fourier spectra from the waveforms of S-wave portion (20s) on OBSs with those on adjacent land stations as the relative site factors. In examples of the relative site factors of OBSs to KNGH23 (KiK-net borehole station), the amplification factor of the horizontal component is greater than that of the vertical component for frequencies 1-10Hz. We conclude that the site effects of OBSs characterized by such a low velocity sediment layers causes those amplification factors.

In order to examine the effect of frequency-dependent relative site amplification factor, we compare the accuracies of predicted seismic intensity using the spectral ratio with those using the average of seismic intensity (frequency-independent factor). We design the causal digital filter (Hoshiba, 2013, BSSA) having similar amplitude property to relative site factor for the station pair. The filter parameters are estimated and applied for both horizontal and vertical components. And we use the real-time processing of seismic intensity (Kunugi *et al*., 2008, Zisin 2) to estimate seismic intensity from observed and predicted waveforms. Both of the techniques are applicable in real-time. We consider the RMS of residual between observed and predicted seismic intensities as the accuracy of site correction of each station pair. In the case of prediction of seismic intensities from OBSs data to land stations, the average RMS of frequency-dependent method are smaller than that of frequency-independent method. Similar results are also obtained at pairs of land station. These results indicate that the frequency-dependent site factor is crucial factor to predict seismic intensity from OBS data, and also show that OBS can be used as front stations in the method for prediction of ground motion based on the real-time monitoring.

Acknowledgments: Strong motion acceleration waveform data were obtained from K-NET and KiK-net of NIED.

Keywords: Earthquake Early Warning, Ocean Bottom Seismograph, Real-time prediction of ground motion, Site amplification factor

Japan Geoscience Union Meeting 2014
(28 April - 02 May 2014 at Pacifico YOKOHAMA, Kanagawa, Japan)

SSS28-P03 Room:Poster Time:May 2 14:00-15:15

Improvement of earthquake early warning system using the extrapolation of wavefield with apparent velocity and direction

SATO, Asuka[1*] ; YOMOGIDA, Kiyoshi[1]

[1]Global Seismology, Natural History Sciences, Graduate School of Science, Hokkaido University

The present early warning system in Japan utilizes the epicenter information preliminary estimated by P-wave arrival times at stations near an event. The present system is still not effective in the following cases, for example, (a) more than one earthquakes occur nearly simultaneously, (b) a deep event whose wave front propagates in a different manner from shallow ones, particularly with very high apparent velocity on the surface, and (c) a large event (M>8) whose finite fault area cannot be neglected. In order to deal with non-circular wave front expansion of these cases, we propose a new approach based on the extrapolation of the early observed wave field alone without determining an epicenter. The idea is similar to the migration method of exploration seismology. The conventional migration method utilizes the wave field on a given wavefront (e.g., Kirchhoff integral migration). In the early warning system, on the other hand, we can obtain the speed and direction of wave field expansion over the surface. Based on the standard representation theorem with a Green's function, we extrapolate wave field outwards or in the future with not only the observed waveform but also its spatial derivative (normal for the wavefront). This enhances the resolution and reliability in the extrapolated wave field in comparison with the conventional approach with the waveform only.

For the extrapolation of wave fields accurately and reliably, we need a reliable Green function in each case. Since the actual wave propagation of P or S waves is very complex or sensitive to details of 3-D velocity structure between a source to each target point on the surface, we shall consider it in a two dimensional manner only focusing on the practical use of the early warning system, that is, a wavefront propagates on the surface with an apparent velocity of P-wave. These apparent velocities vary for events of various depths in different regions. The velocity of shallow events in Hokkaido is about 7.1km/s while that in Nagano prefecture of central Honshuu island is about 5.5km/s. The velocity strongly depends on focal depth: 7.1km/s for the depth of 10km, and 8.9km/s for the depth 100km. The velocity also varies as a function of epicentral distance, particularly for a deep event. We make a table of apparent velocities in different depths, regions and epicenters so that we can pick up an appropriate Green function (apparent velocity) for the wave field extrapolation when an event takes place. We also explain how to estimate the apparent velocity and propagation direction with several early observed wave forms. One key to apply the wavefield extrapolation in the warning system is the good correlation among the seismograms that are observed early as input data. Nevertheless, correlations are generally poor in high-frequency (about 1Hz) seismograms recorded in Japan such as Hi-net data. To enhance the correlation of P waveforms among adjacent stations, we need to correct the site response of each station promptly. Using both shallow and deep events, we first estimated site effect as a function of frequency for Hi-net stations in Hokkaido. We used a rock site station (ONPH) as a reference station for site correction terms for other stations.

For deep earthquakes, a region of anomalous seismic intensity is seen in the Pacific Ocean side of Japan called 'abnormal seismic intensity' , due to a subducting Pacific plate of high velocity and small attenuation. For the earthquake of 590 km deep beneath Vladivostok on 18 February 2010, we examined the direction of P waves propagating in Japan. The apparent velocity is highly anisotropic: fast along the islands but slow perpendicular to them. It is about 7.5km/s in the Souya district in the north of Hokkaido while about 13km/s in the Hidaka district in the south. In our extrapolation scheme, we can model the amplification of wavesin terms of abnormal seismic intensity.

Keywords: earthquake early warning system, extrapolation of seismic wave field, migration, apparent velocity, site effect, abnormal seismic intensity

Japan Geoscience Union Meeting 2014
(28 April - 02 May 2014 at Pacifico YOKOHAMA, Kanagawa, Japan)

SSS28-P04 Room:Poster Time:May 2 14:00-15:15

Early forecasting of aftershocks from seismic energy release rate immediately after the mainshock

SAWAZAKI, Kaoru[1*] ; ENESCU, Bogdan[2]

[1]NIED, [2]University of Tsukuba

The detection completeness of earthquakes just after a large earthquake becomes very poor because their signals are overlapped each other in seismogram records and are hidden by the large amplitude of coda waves. Currently, the JMA starts to serve the aftershock forecasting at least 24 hrs after the mainshock because long lapse times are necessary before the catalog data becomes available for the forecasting with a certain reliability. Recently, Sawazaki and Enescu (under review) succeeded in estimating temporal change in energy release rate for the mainshock and the early aftershock sequence by using the Hi-net continuous records. In their method, the energy release is not determined for each discrete event, but is estimated as a continuous process like a source time function which sums up energies from all the earthquakes occurring at the same time. Therefore, theoretically there are no missing energies in the energy release rate even just after the mainshock. The estimated energy release rate follows a power-law temporal decay like the modified Omori law from about 40 s after the mainshock, and the deviation of the energy release rate with respect to the temporal regression curve distributes according to a power-law like the Gutenberg-Richter law. Since the current aftershock forecasting is conducted based on these two statistical laws, the energy release rate would be available for the early forecasting of the aftershocks.

We examine the statistical characteristics of energy release rate in the frequency range of 8-16 Hz for three crustal earthquakes took place in Japan. From the energy release rate obtained at the first 1 hr, 3 hrs, and 6 hrs after the mainshock, we estimate the number of energy release rate larger than 10^8 J/s (about M_W4/s) occurring within 24 hrs after the mainshock. For the 2008 Iwate-Miyagi Nairiku earthquake, the ratios of the estimated/observed numbers are 24/35, 12/20, and 20/10 for the forecasting at 1 hr, 3 hrs, and 6 hrs after the mainshock, respectively. Likewise, the ratios are 1524/223, 231/99, and 113/50 for the 2004 Niigata Chuetsu earthquake, and 17/59, 8/59, and 30/21 for the 2007 Niigata Chuetsu-oki earthquake. For the Niigata Chuetsu earthquake, M_J5.9, M_J5.8, and M_J6.3 aftershocks occurred in the first 1 hr, while there are no aftershocks larger than M_J5.5 in the lapse times from 1 to 24 hrs. For the Niigata Chuetsu-oki earthquake, there are no aftershocks larger than M_J5 in the first 3 hrs, while M_J5.7 aftershock occurred 5.4 hrs after the mainshock. Such large aftershocks and their secondary aftershocks may change the pattern of aftershock activity, and causes the over- and under-estimations in the forecasting.

Keywords: aftershocks, early forecasting, energy release rate, modified Omori law, Gutenberg-Richter law

Japan Geoscience Union Meeting 2014
(28 April - 02 May 2014 at Pacifico YOKOHAMA, Kanagawa, Japan)

SSS28-P05 Room:Poster Time:May 2 14:00-15:15

A method to remove non-seismic long-period pulses for improved estimations of automatic centroid moment tensor solutions

SAKAI, Takahide[1*] ; KUMAGAI, Hiroyuki[1] ; NAKANO, Masaru[2] ; MAEDA, Yuta[1] ; YAMASHINA, Tadashi[3] ; PULIDO, Nelson[4] ; INOUE, Hiroshi[4] ; MELOSANTOS, Arnold[5] ; FIGUEROA, Melquiades[5] ; PUNONGBAYAN, Jane[5] ; NARAG, Ishma[5]

[1]Nagoya University, [2]JAMSTEC, [3]Kochi University, [4]NIED, [5]PHIVOLCS

Non-seismic long-period pulse-like waveforms appear in broadband seismic records when P or S waves arrive (e.g., Delorey et al, Bull. Seism. Soc. Am., 2008). The pulse-like waveforms affect centroid moment tensor (CMT) solutions estimated from waveform inversion, but a method to remove those pulse-like waveforms yet to be established. Broadband seismograph networks were installed in the Philippine and Indonesia region to monitor earthquakes and tsunamis. The pulse-like waveforms appear in those network data frequently. Those data are used for automatic estimations of CMT solutions by SWIFT (Source estimates based on Waveform Inversion of Fourier Transformed seismograms), which was developed by Nakano et al. (Geophys.J.Int, 2008). SWIFT estimates both the CMT and moment function by the use of long-period (50-100 s) waveform data, but sometimes the long-period pulse-like waveforms affect SWIFT solutions. To monitor earthquakes and tsunamis, we have to estimate source parameters rapidly and adequately. In this study, we propose a simple and rapid method to remove long-period pulse-like waveforms from broadband seismic records.

Japan Geoscience Union Meeting 2014
(28 April - 02 May 2014 at Pacifico YOKOHAMA, Kanagawa, Japan)

SSS28-P06 Room:Poster Time:May 2 14:00-15:15

Japan Meteorological Agency information on long-period ground motion

AIZAWA, Koji[1*] ; OGAMI, Yoshie[1] ; URATANI, Junpei[1] ; SAKIHARA, Hirokazu[1] ; NAKAMURA, Masaki[1]

[1]Japan Meteorological Agency

An earthquake generates seismic waves with various periods, and earthquakes with larger magnitudes generate stronger long-period ground motions. When the natural period of a high-rise building is close to the predominant period of ground motion, resonance happens and the building is severely shaken longer than surface of the Earth. Today, more and more people spend time in high-rise buildings especially in metropolitan areas. If great earthquake occurs, many people in high-rise buildings will be affected by long-period ground motion.

To notify people of such situations and facilitate effective countermeasures, JMA started to provide information on long-period ground motion from March 28th, 2013. Based on questionnaires to tenants of high-rise buildings, it has become clear that difficulty of people's activities depends on the velocity of floor movement, and we classified the intensity of long-period ground motion into four on the basis of velocity. To get the classification, we use wave forms observed by JMA seismic intensity meters on the surface of the Earth which are automatically sent to the JMA system. To estimate shaking at higher floors from wave forms on the surface of the Earth, we simulate the shaking of buildings by absolute velocity response spectrum of the period between 1.5 and 8.0 seconds which causes a significant resonance of buildings with 45 meters or higher. The information is available on the JMA website, with various kinds of contents such as absolute velocity and acceleration response spectrum.

Keywords: long-period ground motion, strong motion

Japan Geoscience Union Meeting 2014
(28 April - 02 May 2014 at Pacifico YOKOHAMA, Kanagawa, Japan)

SSS28-P07 Room:Poster Time:May 2 14:00-15:15

Prediction of long-period ground motion intensity for earthquake early warning

DHAKAL, Yadab prasad[1*] ; KUNUGI, Takashi[1] ; SUZUKI, Wataru[1] ; AOI, Shin[1]

[1]National Research Institute for Earth Science and Disaster Prevention

The 2011 Mw 9.1 Tohoku-oki earthquake caused strong shakings of high rise buildings constructed on deep sedimentary basins in Japan. During the earthquake, many people got into difficulty with their movements inside the high rise buildings even on the Osaka basin located at distances as far as about 750 km from the epicentral area. Japan Meteorological Agency (JMA) has started to provide people with information on intensity of long-period ground motions based on the absolute velocity response spectra (1.6 to 7.8 s) of the observed records on the grounds (Aizawa et al., 2013). The intensity scale of long-period ground motions is classified into four: 1, 2, 3, and 4 having spectral values of 5 to 15 cm/s, 15 to 50 cm/s, 50 to 100 cm/s, and more than 100 cm/s, respectively. The spectra were computed at natural periods of 1.6 to 7.8 s using 5% of critical damping. The maximum value of the computed spectra among 1.6 to 7.8 s defines the class of intensity. We have recently constructed empirical prediction equations of absolute velocity response spectra in the period range of 1 to 10s aiming for earthquake early warning application (e.g., Dhakal et al., 2013). The equations use JMA displacement magnitude and hypocentral distance as basic parameters. Earthquakes having JMA magnitude 6.3 or larger and focal depths shallower than 50 km were used. One of the difficulties in empirical prediction of long-period ground motions is to effectively include the effects of local geological structure such as 3-D basin effects in the prediction equations. To simplify this problem, we obtained site correction factors at K-NET and KiK-net strong motion sites as the mean value of the logarithmic residuals. To make predictions possible at sites other than the strong motion observation sites, we derived correction coefficients based on the relationships between the average residuals and depths of deep sedimentary layers, which are available for whole Japan at Japan Seismic Hazard Information Station (J-SHIS). We found that the standard deviations are minimized by corrections using the depth of layer having Vs value of 1.4 km/s.

To define intensity at a site, we obtained the maximum value of the predicted spectra among T=1.6 to 7.8 s using the empirical prediction equations explained above. However, we found that the maximum predicted values were somewhat biased against the observed maximum values. Therefore, we applied an additional correction factor to the maximum predicted values to finally obtain the intensities. When a prediction equation was constructed using the maximum value of the observed spectra as the independent parameter, the additional correction factor was eliminated as the resulting residuals were normally distributed; also, the predicted intensities were almost identical to those obtained based on the regression analysis results for each natural period. In this study, we illustrate and discuss the application of empirical prediction equations for the prediction of JMA intensity of long-period ground motions for earthquake early warning application.

References

Aizawa K, Kawazoe Y, Uratani J, Sakihara H, Nakamura M (2013), Japan Meteorological Agency information on long-period ground motions, Abstract S41A-2410 presented at 2013 Fall Meeting, AGU, San Francisco, Calif., 9-13 Dec.

Dhakal Y P, Kunugi T, Suzuki W, Aoi S (2013), Attenuation relation of absolute velocity response spectra (1-10s) in Japan - a preliminary analysis. Proceedings: 2nd Intl Symp. on Earthq. Engg, Japan Assoc. of Earthq. Engg., Tokyo, Nov 11-12, vol 2, pp 39-48.

Keywords: Long-period ground motion intensity, Earthquake early warning, Absolute velocity response spectra, Attenuation relations

Japan Geoscience Union Meeting 2014
(28 April - 02 May 2014 at Pacifico YOKOHAMA, Kanagawa, Japan)

SSS28-P08 Room:Poster Time:May 2 14:00-15:15

Regional Earthquake Early Warning Applications in Marmara Region Based on KOERI Seismic Network

PINAR, Ali[1*] ; COMOGLU, Mustafa[1] ; ZULFIKAR, Can[1] ; TUNC, Suleyman[1] ; ERDIK, Mustafa[1]

[1]Bogazici University, Kandilli Observatory and Earthquake Research Institute, Istanbul, Turkey

KOERI (Kandilli Observatory and Earthquake Research Institute) operates a seismic network in Marmara Sea region (NW Turkey) consisting of 40 broadband and 30 strong motion inland and OBS stations which has a good topology for regional EEW studies. Data transmission between the remote stations and the base station at KOERI is provided both with satellite and fiber optic cable systems. The continuous on-line data from these stations is used to provide real time warning for emerging potentially disastrous earthquakes.

The Virtual Seismologist in SeisComP3 and the PRESTo regional EEW (earthquake early warning) softwares are the two regional EEW algorithms that have been recently setup at KOERI data center to generate the EEW sygnal. Onsite EEW application are underway for more than a decade.

The early warning sygnal is communicated to the appropriate servo shut-down systems of the receipent facilities, that automatically decide proper action based on the alarm level. Istanbul Gas Distribution Corporation (IGDAS) is one of the end users of the EEW signal. IGDAS, the primary natural gas provider in Istanbul, operates an extensive system 9,867 km of gas lines with 550 district regulators and 474,000 service boxes. State of-the-art protection systems automatically cut natural gas flow when breaks in the pipelines are detected. IGDAS uses a sophisticated SCADA (supervisory control and data acquisition) system to monitor the state-of-health of its pipeline network. This system provides real-time information about quantities related to pipeline monitoring, including input-output pressure, drawing information, positions of station and RTU (remote terminal unit) gates, slum shut mechanism status at 581 district regulator sites. The SCADA system of IGDAS receives the EEW signal from KOERI and decide the proper actions according to the previously specified ground acceleration levels. Presently, KOERI sends EEW signal to the SCADA system of IGDAS Natural Gas Network of Istanbul.

The EEW signal of KOERI is also transmitted to the serve shut down system of the Marmaray Rail Tube Tunnel and Commuter Rail Mass Transit System in Istanbul. The Marmaray system includes an undersea railway tunnel under the Bosphorus Strait. Several strong motion instruments are installed within the tunnel for taking measures against strong ground shaking and early warning purposes. This system is integrated with the KOERI EEW System. KOERI sends the EEW signal to the command center of Marmaray. Having received the signal, the command center put into action the previously defined measures. For example, the trains within the tunnel will be stopped at the nearest station, no access to the tunnel will be allowed to the trains approaching the tunnel, water protective caps will be closed to protect flood closing the connection between the onshore and offshore tunnels.

Keywords: EEW sygnal, Virtual Seismologist, PRESTo, end users, IGDAS, Marmaray

Japan Geoscience Union Meeting 2014
(28 April - 02 May 2014 at Pacifico YOKOHAMA, Kanagawa, Japan)

SSS29-01 Room:416 Time:April 28 14:15-14:30

Full moment tensor inversion for the 2013 Sea of Okhotsk deep earthquake

HARA, Tatsuhiko[1*] ; KAWAKATSU, Hitoshi[2]

[1]IISEE, BRI, [2]Earthquake Research Institute, The University of Tokyo

We performed full moment tensor inversion for the May 24, 2013 Sea of Okhotsk deep earthquake, which is the largest deep earthquake (the moment magnitude is 8.3 after the Global CMT solution). Following Kawakatsu (1991), we redefined the diagonal components of the moment tensor, and determined full six component moment tensors. In order to determine the isotropic component independently from the CLVD component, we analyzed long period signals in the period range between 550 and 1000 s following Kawakatsu (1996), and Hara et al. (1995, 1996). We retrieved VHZ channel broadband waveform data from the IRIS DMC. The duration of the time series is five hours. We used the Direct Solution Method (Hara et al., 1991, 1993) to calculate the Green's functions. We considered the 3-D velocity structures of model SAW24B16 (M*é*gnin and Romanowicz, 2000) and crust 2.0 (Bassin et al., 2000; http://igppweb.ucsd.edu/~gabi/rem.html) to calculate synthetic seismograms. We set spatial grids around the PDE hypocenter for possible centroid locations and temporal grids around the centroid time of the Global CMT solution for possible centroid times. We conducted linear moment tensor inversions for pairs of the spatial and temporal grids to investigate the dependence of solutions on centroid location and time. In the preliminary analysis, the isotropic components of the solutions with larger variance reductions and smaller correlation coefficients with the isotropic component and the other moment tensor components are in the range around 2 to 4 per cent (implosive) of the seismic moment of this event. This preliminary result is consistent with Okal (2013), who obtained the implosive isotropic component with about 2 per cent of the seismic moment by the analysis of the normal modes ${}_0S_0$ and ${}_1S_0$, although further evaluation on uncertainty of the estimates obtained in this study is required.

Keywords: deep earthquake, moment tensor, isotropic component

Japan Geoscience Union Meeting 2014
(28 April - 02 May 2014 at Pacifico YOKOHAMA, Kanagawa, Japan)

SSS29-02 Room:416 Time:April 28 14:30-14:45

Estimation of Radiated Seismic Energy from Teleseismic Body Waves

KIUCHI, Ryota[1*] ; MORI, James[1]

[1]Disaster Prevention Research Institute, Kyoto University

Radiated seismic energy is a fundamental parameter for understanding source physics. Using teleseismic P waves, Choy and McGarr (2002) reported that strike-slip earthquakes in the oceanic lithosphere have high apparent stress (rigidity multiplied by the ratio of radiated energy to seismic moment). However, that estimates may have a large variation, because of the large radiation pattern of nodal arrivals. Therefore, we improved that used method to better correct for radiation pattern. From our result, we find that the strike-slip earthquakes have apparent stress values that are 5 to 8 times higher than dip-slip earthquakes with the oceanic events having slightly higher values than continental events. In addition, using our improved methods, we can estimate the apparent stresses for strike-slip earthquakes with more reliability, since the error of radiated seismic energies becomes smaller.

Keywords: Radiated seismic energy, Apparent stress, Strike-slip earthquake

Japan Geoscience Union Meeting 2014
(28 April - 02 May 2014 at Pacifico YOKOHAMA, Kanagawa, Japan)

SSS29-03 Room:416 Time:April 28 14:45-15:00

Seismic energy estimation of repeating earthquake sequences offshore northeastern Japan

ARA, Masamichi[1*] ; IDE, Satoshi[1] ; UCHIDA, Naoki[2]

[1]The University of Tokyo, EPS, [2]Graduate school of science Tohoku university

Repeating earthquakes are thought to occur on locked patches, which represent almost time-independent irregularity on the plate interface, to catch up with stable slip on the surrounding interface. Thus, they produce spatial and temporal stress heterogeneity around the source area, which may control the spatial and temporal patterns of seismic energy of repeating earthquakes. We estimate seismic energy for many small to moderate repeating earthquakes that occurred offshore northeastern Japan, to understand the nature of stress heterogeneity and hidden structural irregularity.

Seismic energy reflects dynamic fault motion during an earthquake, while seismic moment is determined by the difference between the initial and final states of the fault. Seismic moment is determined relatively precisely using the low frequency limit of seismic spectra. In contrast, seismic energy has large errors because it is determined from the entire frequency range of seismic spectra, after correcting path and site effects which can be significant especially at high frequencies. Another problem is the size dependence of seismic energy, which has been a matter of debate for two decades in seismological community. A typical question is whether scaled energy (the ratio of seismic energy to moment) is dependent on seismic moment. These problems have to be alleviated to discuss the spatial and temporal variation of radiated seismic energy. Seismic energy must be estimated as precise as possible.

As mentioned, the most serious problem in estimating seismic energy is removing path and site effects. To avoid this problem, the present study adopts an empirical Green's function (EGF) method. We regard the ratio of seismic spectra as the ratio of source spectra, since the seismic spectra of co-located events observed at one station share the same path and site effects. We modify an EGF method with coda waves developed by Baltay et al. (2010), to rigorously evaluate the uncertainty in corner frequencies and the effects of noise.

This method is applied to several repeating earthquakes of magnitude ˜2 to 6 that occurred offshore northeastern Japan. We estimate seismic energy for a group of events by calculating the ratios of source spectra using S-coda waves in two horizontal components of Hi-net, National Research Institute for Earth Science and Disaster Prevention. The scaled energy is almost constant or slightly increasing with seismic moment. Nevertheless, the results are still tentative because the estimation of seismic energy is dependent on the assumption of source spectral model, such as the omega-square model, which have not been constrained well.

Japan Geoscience Union Meeting 2014
(28 April - 02 May 2014 at Pacifico YOKOHAMA, Kanagawa, Japan)

SSS29-04 Room:416 Time:April 28 15:00-15:15

Stress drop variations among small earthquakes in the Tohoku-oki region - implications for the 2011 megathrust event

UCHIDE, Takahiko[1*] ; SHEARER, Peter[2] ; IMANISHI, Kazutoshi[1]

[1]Geological Survey of Japan, AIST, [2]Scripps Institution of Oceanography, UC San Diego

It is important to assess the likely rupture characteristics of future megathrust earthquakes. One approach is to study the spatio-temporal variation of geophysical properties in active subduction zones. We explore this idea by examining stress drops of 1536 small earthquakes (Mw 3.0 - 4.5) shallower than 80 km in the Tohoku-oki region before the 2011 Tohoku-oki earthquake. We estimate stress drops using the spectral analysis method described by Shearer et al. [2006], which isolates source, path, and receiver terms and then applies an empirical Green's function (EGF) correction before computing corner frequencies and stress drops using the Madariaga [1976] model.

We find an overall increase in stress drop with depth, as well as lateral variations in stress drop along strike. Higher-than-average stress drops are found in East Aomori-oki and Miyagi-oki, whereas Sanriku-oki is a moderate stress-drop area. The high stress-drop zone in Miyagi-oki is located just south of the large slip area of the 2011 Tohoku-oki earthquake, and possibly acted as a barrier to further rupture propagation during the event. The Miyagi-oki high-stress-drop zone is located on west of the 1978 Miyagi-oki earthquake rupture area.

Stress drops of earthquakes in the large slip patch of the 2011 Tohoku-oki earthquake are comparable to the mainshock stress drop. Since studies [Hasegawa et al., 2011; Yagi and Fukahata, 2011] indicate that the 2011 Tohoku-oki earthquake released nearly all the stored shear stress, our findings suggest that small earthquakes prior to the mainshock also released a large fraction of the accumulated shear stress. Note that the absolute values of the stress drops of small earthquakes are not well constrained due to assumptions such as the choice of source models, whereas the relative values among the stress drops of small earthquakes are better resolved. Therefore the hypothesis of nearly complete stress drops for the small earthquakes needs to be confirmed by other approaches.

In addition, the frequency dependence of the seismic radiation observed during the mainshock, with proportionally higher frequencies coming from the deeper parts of the fault, mimics the depth dependence we see in small earthquakes in the same region.

These results imply that smaller pre-mainshock earthquakes can provide insights into the fault properties and consequent rupture processes of future megathrust earthquakes.

Keywords: The 2011 Tohoku-oki earthquake, Stress drop, Miyagi-oki, Spatial Heterogeneity of Fault Properties

Japan Geoscience Union Meeting 2014
(28 April - 02 May 2014 at Pacifico YOKOHAMA, Kanagawa, Japan)

SSS29-05 Room:416 Time:April 28 15:15-15:30

Broad-band source image for the 2011 Tohoku earthquake constructed by strong-motion data

KUBO, Hisahiko[1*] ; ASANO, Kimiyuki[1] ; IWATA, Tomotaka[1] ; AOI, Shin[2]

[1]DPRI, Kyoto Univ., [2]NIED

From the comparison between slip model using long-period (10s˜) seismic waves and excitation zones of short-period (0.1-10s) seismic waves, it has been suggested that the 2011 Tohoku earthquake (Mw9.1) has the period-dependent spatial variation on the seismic-wave radiation and this variation would be caused by the spatial difference of slip behavior on the plate boundary (e.g., Koper *et al.*, 2011; Lay *et al.*, 2012). However, their studies were based on the qualitative comparison of the results obtained by different methods, and the quantitative comparison between source models having different period-bands has not been made. Therefore, the construction of the source models at different period-bands by a common method is important to further understand the source characteristics of the 2011 Tohoku earthquake. Kubo et al. (2013, Fall Meeting of SSJ) estimated the spatiotemporal slip models for the 2011 Tohoku earthquake on three different period bands (10-25s, 25-50s, and 50-100s). In this study, we estimate the source models for the 2011 Tohoku earthquake on five continuously-different period bands (10-25s, 17-33s, 25-50s, 33-67s, and 50-100s) using strong-motion data, and construct broad-band source image for the 2011 Tohoku earthquake.

The spatiotemporal rupture history is estimated by the kinematic linear waveform inversion using multiple time windows (Hartzell & Heaton, 1983). The Green's functions are calculated by the 3D FDM (GMS; Aoi & Fujiwara, 1999) using a 3D velocity structure model, Japan Integrated Velocity Structure Model Version 1 (Koketsu *et al.*, 2012). Three components of velocity waveforms at 25 stations of K-NET, KiK-net, and F-net of NIED are used in this analysis. Using waveform records at the stations for the middle-size events which occurred in the source area of the 2011 Tohoku earthquake, we confirmed the adequacy 3D velocity structure model at the analyzed period-band.

The source image for the 2011 Tohoku earthquake on the period band of 10-100s is summarized as follows: (1) (1st) Deep rupture off Miyagi rupture at 0-60s toward down-dip mostly radiating relative short period (10-25s) seismic waves. (2) Shallow rupture off Miyagi at 45-90s toward up-dip with long duration radiating long period seismic wave. (3) (2nd) Deep rupture off Miyagi at 45-90s toward down-dip radiating long period (25-100s) seismic waves. The dominant-period difference in the seismic-wave radiation between twice deep ruptures off Miyagi may result from the mechanism that the second rupture is smoother than the first one because small-scale heterogeneities on the fault are removed by the first one. (4) Deep rupture off Fukushima at 90-135s.

The broad-band source model on the period band from 5-100s is under construction and we will report this.

[Acknowledgments] The strong-motion data recorded by K-NET, KiK-net, and F-net of NIED was used for this analysis.

Keywords: The 2011 Tohoku earthquake, Broad-band source image, Source models on different period bands, Source inversion, Strong-motion data

Japan Geoscience Union Meeting 2014
(28 April - 02 May 2014 at Pacifico YOKOHAMA, Kanagawa, Japan)

SSS29-06 Room:416 Time:April 28 15:30-15:45

Foreshocks implying slow slip transients leading to large earthquakes

KATO, Aitaro[1*] ; OBARA, Kazushige[1]

[1]ERI University of Tokyo

In the recent decades, a growing number of geophysical evidences has clarified that a major fault zone along plate interface hosts not only the unstable fast sliding during rupture of ordinary earthquake, but also slow slip transients without any seismic radiations. Because slow slip transients quasi-statically release the shear stress in the adjacent seismogenic regions, the slow slip transients may have caused stress loading on the nearby seismic patch and might play a role in a slow nucleation process leading to a large earthquake (Beroza and Ide, 2010; Bouchon et al., 2011; Kato et al., 2012). Therefore, it is quite important to reveal interplay between slow slip and unstable fast slip, in order to shed light on the nucleation process of large earthquake.

Here, we explored foreshock activities implying slow slip transients leading up to large earthquakes. We applied the matched filter technique to continuous waveform data around 10 days prior to the past large earthquakes in Japan (M >˜6.5), and created newly foreshock catalog for each sequence. We found out accelerating seismicity preceding some large earthquakes at plate interfaces and intraplate at time scales of days to hours. These foreshocks were located very close to the initiation point of each mainshock rupture. The increase in foreshock seismicity implies that a fault may begin to slowly slip before large earthquake, as like recognized in the foreshock sequence prior to the 2011 Tohoku-Oki earthquake.

Japan Geoscience Union Meeting 2014
(28 April - 02 May 2014 at Pacifico YOKOHAMA, Kanagawa, Japan)

SSS29-07 Room:416 Time:April 28 15:45-16:00

Similar Characteristics between the earthquake source process and Vere-Jones' Branching model

ZHUANG, Jiancang[1] ; WANG, Dun[2*]

[1]Institute of Statistical Mathematics, [2]Earthquake Research Institute, University of Tokyo

Vere-Jones' branching crack model was develop in 1970s. In this model, the earthquake source is regarded as the results of the total population of crack elements in a critical or near-critical branching process, where the crack does not propagate in a single continuous movement, but through a series of steps. At each step, each crack element simply terminates or generates several other crack elements nearby. Regarding the total number of steps (generation) as the duration time and the total number of crack elements as the total energy released, the following similarities are found between earthquake sources and this model:

1. The distribution of energies is asymptotically a Pareto distribution (power law) for the critical case, or a tapered Pareto distribution (tapered power law, Kagan distribution) for the subcritical case.
2. The duration time of ruptures has a tapered inverse power distribution.
3. The number of crack elements at each generation (time step) show similar patterns of earthquake source time functions.

Figure 1 (a) and (b): Plots of the numbers of crack elements at each time step in two simulation examples. (c): Distribution of half duration times in real earthquake catalog. (d): Distribution of duration times in synthetic catalogs.

Keywords: Branching process, Gutenberg-Richter Magnitude-Frequency Relation, Tapered Pareto distribution, Earthquake source

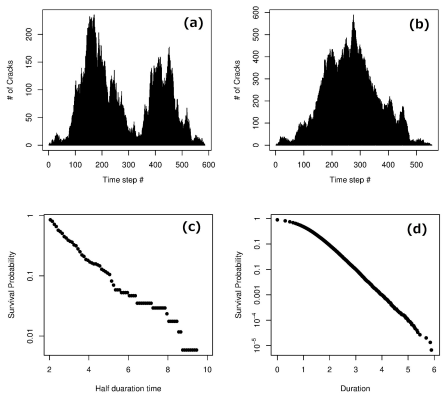

Japan Geoscience Union Meeting 2014
(28 April - 02 May 2014 at Pacifico YOKOHAMA, Kanagawa, Japan)

SSS29-08 Room:416 Time:April 28 16:15-16:30

Review on Source Type Diagrams

ASO, Naofumi[1*] ; OHTA, Kazuaki[1] ; IDE, Satoshi[1]

[1]Graduate School of Science, The University of Tokyo

Force system of earthquake is expressed by a symmetric moment tensor, assuming internal forces on a point source, and it has information of characteristic directions, source size, and source type. Although we often assume double couple as the source type, significant non-double-couple component including isotropic component is reported mainly for induced earthquakes or volcanic earthquakes. It is also known that combination of double couples may produce non-double-couple components. For discussion on source types, it is helpful to display them into some visual diagrams.

Since the information of source type has two degrees of freedom, it can be displayed on a two-dimensional flat plane. Although the diagram developed by Hudson et al. [1989] (HPR diagram) is popular, it is inconsistent with the concept of scalar moment [Aki and Richards, 2002]. This problem originates in the projection of a three-dimensional point (λ_1, λ_2, λ_3) on a cubic surface, where λ_1, λ_2, and λ_3 are eigenvalues of moment tensor.

Then, Chapman and Leaney [2012] developed a new diagram by combining spherical projection and stereographic projection (CL diagram). The spherical projection overcomes the problem of the HPR diagram, and the stereographic projection keeps areal density from a spherical surface to a flat plane. This diagram has an advantage that a straight line passing through the center corresponds to the mechanism obtained by combination of an arbitrary mechanism and a double couple, but the diagram is curved shape, and it does not suit for detailed discussions on non-double-couple component when the isotropic component is dominant.

In the present study, we developed another new rectangle diagram that overcomes difficulties of the HPR diagram and the CL diagram simultaneously (AOI diagram). After projecting (λ_1, λ_2, λ_3) on a spherical surface, we project it on a cylinder, keeping areal density. This diagram is an orthogonal system of the isotropic axis (the trajectory for varying isotropic component) and the deviatoric axis (the trajectory for varying deviatoric component while keeping its scalar moment). Since isotropic component represents the information from P-wave and deviatoric component represents the information from both P- and S-waves equivalently, the AOI diagram is consistent with the concept of seismogram analyses.

Since there is no source type diagram that is the best at everything, as well as map projection, it is important to use various diagrams taking account of their advantages and disadvantages. In the present study, we also provide examples of projecting a data set on different diagrams, and point out their apparent differences and important considerations.

Keywords: moment tensor, source type diagram, double couple, CLVD, isotropic deformation

Japan Geoscience Union Meeting 2014
(28 April - 02 May 2014 at Pacifico YOKOHAMA, Kanagawa, Japan)

SSS29-09 Room:416 Time:April 28 16:30-16:45

Stress concentration ahead of supershear rupture

FUKUYAMA, Eiichi[1*] ; XU, Shiqing[1] ; MIZOGUCHI, Kazuo[2] ; YAMASHITA, Futoshi[1]

[1]Nat'l Res. Inst. Earth Sci. Disas. Prev., [2]Centr. Res. Inst. Elect. Pow. Ind.

We report the shear strain field ahead of a supershear rupture. The strain data was obtained during the large-scale biaxial friction experiments conducted at NIED in March 2013. We conducted friction experiments using a pair of meter-scale gabbro rock specimens whose fault area was 1.5m x 0.1m. We applied 2.6MPa normal stress and loading velocity of 0.1mm/s. At the long side of the fault edge, which is parallel to the slip direction, 32 2-component semi-conductor strain gauges were installed at an interval of 50mm and 10mm off the fault. The data are conditioned by high frequency strain amplifiers (<0.5MHz) and continuously recorded at an interval of 1MHz with 16-bit resolution. Many stick slip events were observed and a unilateral rupture event was chosen in this analysis that propagated with supershear rupture velocity. By focusing at the rupture front, stress concentration was observed and sharp stress drop occurred immediately inside the rupture. We found that the stress concentration becomes mild as the rupture propagates and length of the stress concentration area becomes longer. This observation is quite interesting because the rupture propagates at a constant speed close to square root two times the shear wave velocity and thus a longer stress concentration region suggests more energy dissipation. We might speculate that such longer stress concentration area suggests longer plastic region ahead of the rupture (or longer cohesive distance). I.e. The cohesive zone length might be longer as the rupture propagates to maintain constant rupture velocity propagation.

Keywords: Earthquake rupture, Stress concentration, Supershear rupture

Japan Geoscience Union Meeting 2014
(28 April - 02 May 2014 at Pacifico YOKOHAMA, Kanagawa, Japan)

SSS29-10 Room:416 Time:April 28 16:45-17:00

Effects of normal stress on the evolution of AE activities and frictional properties of a fault

IIDA, Takuro[1] ; YABE, Yasuo[1*]

[1]Graduate School of Science, Tohoku University

To numerically investigate earthquake generations on a plate interface or a fault, we need to know their frictional properties. This study provides a clue to evaluate the frictional properties from spatio-temporal variations of such observations as seismicity and aseismic sliding on the interface of the fault.

We performed frictional sliding experiments using a rotary shear apparatus under a variety of normal stress from about 5 MPa to about 15 MPa. Stepwise change in the sliding rate was imposed to investigate rete dependences of AE activity and friction. Cumulative displacement up to 200 mm was achieved to elucidate their evolutions.

We confirmed similar evolutions of AE activities and friction to those shown by Yabe (2002). That is, the frictional property (rate dependence of friction) of the fault was first the velocity strengthening. The velocity strengthening became weak with an increase in the cumulative sliding. Then, the fault showed the frictional property of velocity weakening. Finally, the rate dependence of friction converged to a constant negative value, when the cumulative sliding reached a critical distance. The m-value of AE events increased with sliding, when the cumulative sliding distance was smaller than a critical distance. After the critical sliding distance, the m-value took a constant value. The critical sliding distances of the frictional property and the m-value were almost the same each other. The rate dependence of the m-value, which was negative under a small sliding distance, also converged to a constant value of about zero at the cumulative sliding distance.

The evolutions were quantitatively evaluated by applying an exponential-decay function to data that is similar to the function proposed by Wang and Scholz (1994) to express wear processes of a fault. The function well reproduced the experimental data, suggesting that AE activities and frictional properties evolved in association with the wear. The decay distances of evolutions of the AE activities and the frictional properties were equal to each other and in inverse proportion to the normal stress. The latter could be understood by taking into account that the larger the overlap volume of asperities on the fault, the larger the normal stress. Further, when the normal stress was increased, the velocity weakening became weak and the m-value was decreased.

These results imply that there exists interrelations among seismicity and frictional properties of the fault.

Keywords: frictioanl sliding, AE activity, frictional property, rotary shear, evolution, normal stress dependence

Japan Geoscience Union Meeting 2014
(28 April - 02 May 2014 at Pacifico YOKOHAMA, Kanagawa, Japan)

SSS29-P01 Room:Poster Time:April 28 18:15-19:30

Determination of the coefficients of Mhdd by a grid search approach

HARA, Tatsuhiko[1*]

[1]IISEE, BRI

Hara (2007) developed an empirical magnitude formula using durations of high frequency energy radiation and maximum displacement amplitudes using tele-seismic P waves. Recently, Hara (2013), who referred to this magnitude as M_{hdd}, tried to re-determine the coefficients of the formula using a larger dataset by a linear inversion. The M_{hdd} calculated by the proposed coefficients better agree with the moment magnitudes from the Global CMT catalog. However, there is slight epicentral distance dependence for their differences. In this study, in order to reduce this epicentral distance dependence, we performed a grid search to determine the coefficients of M_{hdd} by minimizing both the differences between M_{hdd} and moment magnitudes and the dependence of their differences on the epicentral distance. The dataset is the same as that of Hara (2013). The search ranges for each coefficient can be set reasonably based on the studies of Hara (2007) and Hara (2013). The preliminary result suggests that it is possible to reduce the epicentral distance dependence using the coefficients obtained by the grid search method.

Keywords: magnitude, high frequency energy radiation, Grid search method

Japan Geoscience Union Meeting 2014
(28 April - 02 May 2014 at Pacifico YOKOHAMA, Kanagawa, Japan)

SSS29-P02 Room:Poster Time:April 28 18:15-19:30

Wavelet domain inversion for examination of the frequency-dependent characteristics of the seismic wave radiation

SUZUKI, Wataru[1*] ; AOI, Shin[1] ; SEKIGUCHI, Haruko[2] ; KUNUGI, Takashi[1]

[1]NIED, [2]DPRI, Kyoto University/NIED

Frequency-dependent characteristics of the seismic wave radiation from earthquake sources are important subject for advancing the source physics and the strong-motion prediction. The 2011 Tohoku-Oki earthquake has exhibited particularly distinctive characteristics. The large slip is estimated in the shallow part of the fault from the low-frequency waveforms or geodetic data, whereas the source models derived from the analysis of the higher-frequency seismic data, such as the empirical Green's function modeling or backprojection method, suggest that the high-frequency waves were intensely radiated from the deeper portion. Our previous study (Suzuki et al., 2011) examined the contribution of the significant slip events to the waveform synthesis from the low-frequency waveform inversion results. We found that the sources of the very-low-frequency waves (<0.02 Hz) and higher-frequency waves seem different in the location even in the frequency band used in the waveform inversion. The examination on the frequency dependence in this previous study is somewhat indirect. We have therefore developed the source inversion method that utilizes the wavelet coefficients as the target to fit. This new method is based on the multi-time-window scheme and is linear inversion. The moment rate is directly related to the waveform in each octave band. We have first applied the developed method to 0.01-0.125 Hz strong-motion data of the largest aftershock of the Tohoku-Oki event that occurred in the off Ibaraki prefecture. The preliminary analysis does not suggest the clear frequency dependence for this Mw7.9 event in the analyzed frequency band. As future work, we will extend the analyzed frequency range and also apply to the Tohoku-Oki mainshock.

References:
Suzuki, W., S. Aoi, H. Sekiguchi, and T. Kunugi (2011): *Geophys. Res. Lett.*, **38**, L00G16.

Japan Geoscience Union Meeting 2014
(28 April - 02 May 2014 at Pacifico YOKOHAMA, Kanagawa, Japan)

SSS29-P03 Room:Poster Time:April 28 18:15-19:30

Tracing Rupture Process of the 2011 Tohoku M 9.0 Earthquake Using Small Seismic Arrays in China

XUELIN, Shen[1] ; WANG, Dun[2*]

[1]1.Key Laboratory of Earthquake Geodesy Institute of Seismology, China Earthquake Administration, [2]2.Earthquake Research Institute, The University of Tokyo

Back projection(BP) can trace rupture front of large earthquakes. It has been widely applied for better understanding rupture processes of recent large earthquakes. An important result/ouput from BP is rupture length, which roughly corresponds to the final size of earthquakes given geological environment. Thus it can be used for fast estimate of the size of large earthquakes for the purpose of tsunami warning and disaster evacuation.

Most studies were focused on using data recorded at distances of 30 to 85 degrees to epicenter, in which distance range the first coming wave is direct P wave which ensures a good resolution for the results from BP.

Here we applied several sub China array data to trace the rupture propagation of the Tohoku earthquake to investigate the effect of the other regional phases such as Pn. We tested the effects with seismograms recorded in sub arrays of China seismic array. The results suggest that the overall rupture length can be recovered, though there is some visible disconvergence, especially for those results derived from distant sub arrays.

Keywords: Back projection, Rupture Process, The 2011 Tohoku M 9.0 Earthquake, Small Seismic Arrays in China

Japan Geoscience Union Meeting 2014
(28 April - 02 May 2014 at Pacifico YOKOHAMA, Kanagawa, Japan)

SSS29-P04 Room:Poster Time:April 28 18:15-19:30

Waveform correlation analysis of small repeating earthquakes using high sampling-rate seismograms

HATAKEYAMA, Norishige[1*] ; UCHIDA, Naoki[1] ; MATSUZAWA, Toru[1] ; OKADA, Tomomi[1] ; NAKAJIMA, Junichi[1] ; MATSUSHIMA, Takeshi[2] ; KONO, Toshio[1] ; HIRAHARA, Satoshi[1] ; NAKAYAMA, Takashi[1] ; TOHOKU-EQ, Group for the aftershock observations[3]

[1]Graduate School of Science, Tohoku University, [2]Faculty of Sciences, Kyushu University, [3]Group for the aftershock observations of the 2011 Tohoku Earthquake

Repeating earthquake sequence is a series of earthquakes with nearly identical waveforms which occur at the same location repeatedly and they are thought to represent repeated ruptures of small asperities on a fault plane. Since there are many unknown features about asperities such as detailed structures, reproducibility and fluctuation of rupture patterns, it is very important to reveal such features to understand the generation process of interplate earthquakes.

Numerical simulations of the repeating earthquakes with rate- and state-dependent friction laws reveal that stress disturbance caused by postseismic slip of a large earthquake near the repeater can change rupture pattern of the repeater's asperity. Actually, some observations show systematic changes in the magnitudes of small repeating earthquakes immediately after large earthquakes. Such rupture pattern changes will make difference especially in high-frequency components of the waveforms. Therefore, in order to verify the rupture pattern changes of small repeating earthquakes, we have to perform detailed analysis on the differences in high-frequency components of the waveforms.

In this study, we performed 1 kHz sampling-rate seismograph observation at permanent borehole stations along Sanriku coast, Japan for the period from April to November 2011, immediately after the Tohoku-Oki earthquake. We investigate the waveform correlations of small repeating earthquakes using waveform data. We make a pair of earthquakes belonging to the same group of repeating earthquakes and calculate their coherences. The results show that in high-frequency band, there are both high-coherence pairs and low-coherence pairs even in the same repeating earthquake group, although all the pairs show high coherence in low-frequency band. Furthermore, frequency bands in which the coherences are low are nearly the same for all the pairs. These results suggest rupture pattern changes in the asperity.

We also find that earthquakes which show low coherence in high-frequency band for all the counterparts occur immediately after events in the vicinity of the repeater's asperity. This observation implies that rupture pattern changes in the asperity, which make difference in high-frequency components of the waveforms, are caused by stress disturbance due to the nearby earthquakes.

Keywords: repeating earthquake, asperity, high sampling-rate seismogram, waveform correlation analysis, Tohoku-Oki earthquake

Japan Geoscience Union Meeting 2014
(28 April - 02 May 2014 at Pacifico YOKOHAMA, Kanagawa, Japan)

SSS29-P05 Room:Poster Time:April 28 18:15-19:30

Study on the source process of the largest aftershock of 1923 Kanto earthquake

HONDA, Ryou[1*] ; KIMURA, Hisanori[2] ; KASAHARA, Keiji[3] ; YUKUTAKE, Yohei[1] ; HARADA, Masatake[1] ; DOKE, Ryosuke[1] ; MIYAOKA, Kazuki[1]

[1]Hot Springs Research Institute, [2]National Research Institute for Earth Science and Disaster Prevention, [3]Association for the Development of Earthquake Prediction

The largest aftershock of M7.5 (Takemura, 1994) occurred at off Boso Peninsula following the 1923 Kanto earthquake. Although the hypocenter have been estimated by previous studies (e.g., Takemura, 1994; Hamada et al, 2001), precise source process have not been estimated yet.

The source region of the largest aftershock is characterized by the region of seismic and aseismic phenomena associated with subduction motion of the Philippine Sea Plate, including slow slip events (SSEs), large backslip events, and repeating earthquakes. Kimura et al. (2009) estimated fault plane of the largest aftershock from geodetic data and they concluded that the fault plane lies within the region of large backslip and the large slip area of the Boso SSE. Estimation of the source process during the largest aftershock is, therefore, important to understand earthquake preparation process around the region.

We set three point sources on the fault plane estimated by Kimura et al. (2009); shallow part (S1), middle part (S2) and deep part (S3). We calculated synthetic seismograms and evaluated the cross correlations between the observed and the synthetic waveforms. We tested the nine hypocenter-asperity combinations using S1, S2 and S3. The combination with the highest value of the average cross correlation is regarded as the best model. We obtained the best score for combination of S2 (hypocenter) and S3 (asperity). This result shows that rupture started from S2 and propagated toward S3.

The observed data used in this study were provided by Kajima Corporation. We are grateful for their kind considerations.

Keywords: 1923 Kanto earthquake, the largest aftershock, source process

Japan Geoscience Union Meeting 2014
(28 April - 02 May 2014 at Pacifico YOKOHAMA, Kanagawa, Japan)

SSS29-P06 Room:Poster Time:April 28 18:15-19:30

Earthquake source process of the 2013 Santa Cruz earthquake and the tsunami

PARK, Sun-cheon[1*] ; KIM, Satbyul[2] ; LEE, Jun-whan[1]

[1]National Institute of Meteorological Research, Korea Meteorological Administration, [2]Pukyong University, South Korea

In order to understand the characteristics of large tsunamigenic earthquakes, we analyzed the earthquake source process of the 2013 Santa Cruz earthquake and simulated the tsunami. We first estimated the fault length of about 200 km using 3-day aftershock distribution and the source duration of about 110 sec using the duration of high-frequency energy radiation (Hara, 2007). From these results, we used the initial value of rupture velocity as 1.8 km/s for teleseismic waveform inversions. Teleseismic body wave inversion was carried out using the inversion package by Kikuchi and Kananmori (1991). Teleseismic P waveform data from 28 stations were used and band-pass filter of 0.005 ˜1 Hz was applied. Our best-fit solution indicated that the earthquake occurred on the northwesterly striking (strike = 290) and shallowly dipping (dip = 15) fault plane. Focal depth and rupture velocity were determined to be 23 km and 1.3 km/s, respectively. Moment magnitude of 7.8 was obtained showing somewhat smaller than the result of previous study (Lay et al., 2013). Slip distribution of the event showed roughly two patches of large slip, one around the hypocenter and the other to the southwest.

Using the slip distribution obtained by teleseismic waveform inversion, we calculated the surface deformations using formulas of Okada (1985) which would be assumed as the initial change of sea water by tsunami. Then tsunami simulation was carried out using Cornell Multi-grid Coupled Tsunami Model (COMCOT) code and 1 min-grid topographic data for water depth. Two DART buoy data were used to verify our simulation. In the presentation, we will discuss more details on the results of source process and tsunami simulation and compare them with the previous study.

Keywords: Santa Cruz, source process, tsunami

Japan Geoscience Union Meeting 2014
(28 April - 02 May 2014 at Pacifico YOKOHAMA, Kanagawa, Japan)

SSS29-P07 Room:Poster Time:April 28 18:15-19:30

Relationship between the source process of the 2013 Sea of Okhotsk deep earthquake and the thermal structure of the slab

ENDO, Suguru[1*] ; YAGI, Yuji[1] ; NAKAO, Atsushi[2]

[1]Univ.Tsukuba, [2]Tokyo Institute of Technology

Deep earthquakes occur at depths where, due to the high normal pressures and the prominence of plastic behavior caused by high temperatures, the brittle fracture is difficult to explain. As a consequence, the mechanism of deep earthquakes has been long standing challenge in Earth Science since the early twentieth century. Some mechanisms of deep earthquakes have been suggested and these mechanisms are sensitive to the thermal structure of slabs. Accordingly, the purpose of this study is (1) to infer the source process of the Sea of Okhotsk deep earthquake (Mw 8.3, depth 608.9 km) on 24 May 2013 (UTC) by using the Hybrid Back?projection (HBP) method (Yagi et al., 2012) and waveform inversion (Yagi and Fukahata, 2011) and (2) to elucidate the relationship the source process and the thermal structure in the Kurile slab.

We found that the reactivation of the rupture occurred near the hypocenter. This means that a stress concentration near the hypocenter overcomes the fault strength and reactivates rupture at the hypocenter (Gabriel et al., 2012). We investigated the relationships between our results and the thermal structure of the Kurile slab and found that (1) the main shock started to rupture from the outer portion of the slab (2) the source region of the earthquake extended in a temperature range between 740 ℃ and 990 ℃. This study does not clearly support transformational faulting as a mechanism for occurrence of the Sea of Okhotsk deep earthquake suggested by Zhan et al. (2013) because it is unlikely that metastable olivine exists all over the slab at the depth of the main shock.

Keywords: deep earthquake, HBP method, rupture reactivation

Japan Geoscience Union Meeting 2014
(28 April - 02 May 2014 at Pacifico YOKOHAMA, Kanagawa, Japan)

SSS29-P08 Room:Poster Time:April 28 18:15-19:30

Focal mechanisms of the triggered tremor beaneath the Hinagu fault zone, southwestern part of Japan

MIYAZAKI, Masahiro[1*] ; MATSUMOTO, Satoshi[2] ; SHIMIZU, Hiroshi[2]

[1]Grad. Sch. Sci., Kyushu Univ., [2]SEVO, Kyushu Univ.

Non-volcanic tremors induced by large amplitude surface wave have been detected all over the world. Most of them are located on and near the plate boundary (Miyazawa and Mori, 2005; Nadeau and Dolene, 2005) and few of them are near volcanoes (Obara, 2012). Chao and Obara (2012, SSJ) found the triggered tremor that located beneath the Hinagu active fault zone, western part of Kyushu Island, Japan. Miyazaki et al. (2013, SSJ) reported that the tremor occurred beneath the seismogenic zone.

In this study, we attempted to estimate focal mechanisms of the tremors triggered by the surface wave of the 2012 Sumatra earthquake. We use the method developed by Hirasawa (1966) that uses the S wave polarization angles. We eliminated the data with low Signal-to-Noise ratio because the angles of waves of tremors were sensitive to background noise.

As a result, we found that focal mechanisms of the triggered tremors were roughly consistent with regional stress field. They could provide constraint for investigating dynamic triggering process of the tremor.

Acknowledgement
We used the seismic data from Kyushu University, the Japan Meteorological Agency, the National Research Institute for Earth Science and Disaster Prevention and Kagoshima University.

Keywords: triggered tremor, focal mechanisms, Hinagu fault zone

Japan Geoscience Union Meeting 2014
(28 April - 02 May 2014 at Pacifico YOKOHAMA, Kanagawa, Japan)

SSS29-P09 Room:Poster Time:April 28 18:15-19:30

Spatio-Temporal Variation of Stress Drop Observed at Carthage Cotton Valley Gas Field, Texas

IIDA, Shuhei[1*] ; KIM, Ahyi[1]

[1]Yokohama City University

Understanding source characteristics of hydraulic fracturing induced microearthquakes is expected to provide a better understanding of the fracturing process and the influence of pre-existing structures controlling the distribution of events. Especially it is still controversial whether the events are associated with volumetric change or not. To address this question, we estimated the source parameters using the empirical Greens function analysis.

Keywords: Stress Drop, Hydraulic Fracturing, Induced Seismicity, Pore Pressure

Japan Geoscience Union Meeting 2014
(28 April - 02 May 2014 at Pacifico YOKOHAMA, Kanagawa, Japan)

SSS29-P10 Room:Poster Time:April 28 18:15-19:30

Collapse of intraplate earthquake, Separation of accretionary wedge, and Rotation of plate by lateral-fault type

MASE, Hirofumi[1*]

[1]none

(Refer to the chart)

”Nankai Slab” that subduct from Nankai Trough forms the slope that turned to the northwest and is soaked to the thing that heads eastward. That edge shapes to receive resistance. And, ”Nankai Slab” receives the right turning force and weak places collapse. The part that is deeper than that place crawls up and the whole might rotate right. (A),intraplate earthquake of ”Nankai Slab”, and (B), lateral-fault type earthquake that the boundary with ”Tokai Slab” causes, are the Nankai Earthquake(EQ) and the To-Nankai EQ and the Tokai EQ.(this paragraph (1)(2))

Two huge cracks that seem that they relate to the right rotation exist if seafloor topography chart(3) is seen.

Crack(a):This crack starts from the place of about 10km to the east in Cape Daio and lengthens to the south. And, this crack gets to the trough. The trough projects to the south on the west side on the boundary of this place. I think that this crack slips when the upper plate(land side plate, accretionary wedge)

greatly moves on the lower plate ”Nankai Slab”.

Crack(b):This crack is shape of the character of Y off Lake Hamana and reach the trough. ”Nankai Slab” and ”Tokai Slab” are completely separate in the north from Lake Hamana(7). And, I think in the south this crack leads to the trough while touched. This crack is the one that this plasmotomy reached bottom of the sea and that slips when the whole of lower plate moves with the upper plate put.

Earthquake(B) is the one that Crack(b) slips. It can be said that that Crack(a) slips is intermediate of earthquake(A) and (B).

Dr. Yamanaka proposed in 2004 large and clear source model of the 1944 To-Nankai EQ that eastern edge within the range gets to Omaezaki(4).

That large area of slip is equal to the area of Crack(a) and (b). The 1944 EQ was not only earthquake(A) and everything might have happened. I composed the source process by earthquake(A),(B) and Crack(a),(b) referring to Dr. Yamanaka’s (interplate earthquake) source process.

1.Earthquake(A) occurred, and it spread in the direction of northeast along the slab-contour. 2.Separation of the accretionary wedge spread to the southeast and it reached the trough. 3.The separation spread along the trough first and spread along Crack(a) next. 4.(Rotation of upper plate) Crack(a) slipped because the separation was large-scale. 5.(Rotation of lower plate) Crack(b) slipped and earthquake(B) occurred because the environment was in order. The stress occurred in the vicinity of the trough. 6.The Mikawa EQ occurred because of the influence of 4,5. 7.The 2004 EQ occurred and the stress of 5 was absorbed.

Reference literature

(1)Hirofumi MASE(2009)/SSJ2009/P3-64
http://jglobal.jst.go.jp/detail.php?JGLOBAL_ID=200902239527416838
(2)Hirofumi MASE(2010)/JpGU2010/SSS027-P10
http://www2.jpgu.org/meeting/2010_disc2/program/S-SS027.html
(3)JHOD,JCG/Seafloor Topography of the Plate Boundaries
http://www1.kaiho.mlit.go.jp/jishin/sokuryo_E/sokuryo_E.html
(4)Yoshiko YAMANAKA(2004)/Source rupture processes of the 1944 Tonankai earthquake and the 1945 Mikawa earthquake/ERI U-Tokyo
http://www.eri.u-tokyo.ac.jp/sanchu/report/Tonankai_Mikawa.pdf
(7)Nagoya Univ./Structure of the Subducting Philippine Sea Slab/ http://www.seis.nagoya-u.ac.jp/SEIS/slab/slab-j.html

Japan Geoscience Union Meeting 2014
(28 April - 02 May 2014 at Pacifico YOKOHAMA, Kanagawa, Japan)

SSS29-P10 Room:Poster Time:April 28 18:15-19:30

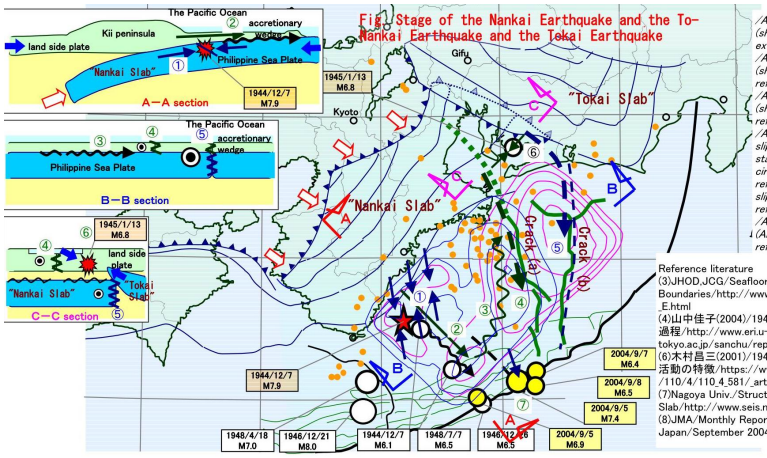

/About sea bottom (shape line) extracted from (3)/
/About "Nankai Slab" (shape line, contour) referable to (6)/
/About "Tokai Slab" (shape line, contour) referable to (7)/
/About the 1944 To-Nankai EQ slip distribution contour(pink line), rupture-starting point(red star), aftershocks(orange circle) referable to (4)Fig.1
slip snap-shot contour(45sec.blue line) referable to (4)Fig.3/
/About information on earthquake (All not mentioned specially) referable to (8)/

Reference literature
(3)JHOD,JCG/Seafloor Topography of the Plate Boundaries/http://www1.kaiho.mlit.go.jp/jishin/sokuryo_E/sokuryo_E.html
(4)山中佳子(2004)/1944年東南海地震と1945年三河地震の震源過程/http://www.eri.u-tokyo.ac.jp/sanchu/report/Tonankai_Mikawa.pdf,(図1,図3)
(6)木村昌三(2001)/1946年南海地震に関係する四国における地震活動の特徴/https://www.jstage.jst.go.jp/article/jgeography1889/110/4/110_4_581/_article/-char/ja/,(図2)
(7)Nagoya Univ./Structure of the Subducting Philippine Sea Slab/http://www.seis.nagoya-u.ac.jp/SEIS/slab/slab-j.html
(8)JMA/Monthly Report on Earthquakes and Volcanoes in Japan/September 2004/特集2(図7－1)他

Japan Geoscience Union Meeting 2014
(28 April - 02 May 2014 at Pacifico YOKOHAMA, Kanagawa, Japan)

SSS30-01 Room:Main Hall Time:April 28 09:30-09:45

Long-term seismic quiescence and activation anomalies preceding to the 2004 Sumatra and the 2005 Nias earthquakes

KATSUMATA, Kei[1*]

[1]Inst. Seismology and Volcanology, Hokkaido University

I find long-term precursory seismic quiescence and activation anomalies before the 2004 Sumatra (M_w9.1) and the 2005 Nias (M_w8.6) earthquakes. An earthquake catalog created by International Seismological Center is analyzed between 1964 and 2004, including 1153 earthquakes shallower than 100 km with the body wave magnitude of $5.0 \leq M \leq 6.0$. A detailed analysis of the earthquake catalog using a gridding technique (ZMAP) shows that the 2004 Sumatra and the 2005 Nias earthquakes are preceded by not only a seismic quiescence anomaly started in December 1987, but also a seismic activation anomaly started in July 1989. The quiescence and activation areas are located very closely each other between 2S and 6N, which cover the area around the rupture initiation point of the 2004 Sumatra earthquake and the whole area ruptured by the 2005 Nias earthquake. The observed spatial pattern of quiescence and activation can be explained by stress perturbation due to a long-term slow slip event located on the two main shock faults, which is predicted by a numerical simulation [*Kato et al.,* 1997].

Kato, N., M. Ohtake, and T. Hirasawa (1997), Possible mechanism of precursory seismic quiescence: Regional stress relaxation due to preseismic sliding, Pure Appl. Geophys., 150, 249-267.

Keywords: The 2004 Sumatra earthquake, The 2005 Nias earthquake, seismic quiescence, seismic activation, ZMAP, ISC

Japan Geoscience Union Meeting 2014
(28 April - 02 May 2014 at Pacifico YOKOHAMA, Kanagawa, Japan)

SSS30-02 Room:Main Hall Time:April 28 09:45-10:00

Spatial heterogeneity of the frictional property on the Pacific plate off south-east of Hokkaido, Japan

SAITO, Yu[1] ; YAMADA, Takuji[1*] ; TANIOKA, Yuichiro[1]

[1]ISV, Hokkaido Univ.

The stress drop is an indicator of the difference of the shear strength and the dynamic frictional stress. We analyzed 330 middle-size earthquakes to investigate the spatial heterogeneity of the frictional property on the Pacific plate off south-east of Hokkaido.

Large earthquakes have been occurring repeatedly off south-east of Hokkaido, Japan, where the Pacific Plate subducts beneath the Okhotsk Plate in the north-west direction. For example, the 2003 Tokachi-oki earthquake (Mw8.0) recently took place in the region in 2003. Yamanaka and Kikuchi (2003) analyzed the slip distribution of the earthquake and concluded that the area with a large slip during the 2003 earthquake was mostly overlapped with the area of the 1952 Tokachi-oki earthquake. Miyazaki *et al*. (2004) reported that a notable afterslip was observed at adjacent areas to the coseismic rupture zone of the 2003 earthquake, which suggests that there would be significant heterogeneities of strength, stress and frictional properties on the surface of the Pacific Plate in the region. In addition, some previous studies suggest that the region with a large slip in large earthquakes permanently have large difference of strength and the dynamic frictional stress level and that it would be able to predict large slip areas by analyzing the stress drop of small earthquakes (e.g. Allmann and Shearer, 2007 and Yamada *et al*., 2010).

We estimated stress drops of 330 earthquakes ($4.2 \leq M \leq 5.0$), using S-coda waves of Hi-net data. The 330 earthquakes were the ones that occurred from June, 2002 to December, 2012 off south-east of Hokkaido, Japan, with the latitude from 40.5N to 43.5N and the longitude from 141.0E to 146.5E. First we selected the closest earthquakes with magnitudes between 3.0 and 3.2 to individual 330 earthquakes as empirical Green's functions. We then calculated source spectral ratio of the 330 pairs of interested earthquakes and EGFs by deconvolving the spectra of S-coda waves. We finally estimated corner frequencies of earthquakes from the source spectral ratios by assuming the omega-squared model of Boatwright (1978) and calculated stress drops of the earthquakes by using the model of Madariaga (1976). The estimated values of stress drop range from 3.0×10ˆ(-1) MPa to 2.0×10ˆ(2) MPa independent of the seismic moment. Figure shows the spatial distribution of estimated stress drops.

We found spatial difference of estimated values. The average value of stress drop in the afterslip area at the 2003 Tokachi-oki earthquake, where the small displacement was observed, was 1.2 MPa. On the other hand, the value in the source area of the 2004 Kushiro-oki earthquake was 2.0 MPa. In addition, the average values of stress drops in the deeper and shallower parts of the source area of the 1973 Nemuro-oki earthquake were 1.0 MPa and 2.1 MPa, respectively, and the difference was statistically significant. These differences would reflect the spatial heterogeneity of the frictional property on the Pacific plate.

Acknowledgments: We used Hi-net waveform data (http://www.hinet.bosai.go.jp/) and the slip distribution of large earthquakes (EIC seismic note; http://www.eri.u-tokyo.ac.jp/sanchu/Seismo_Note/index.html)

Keywords: Pacific plate, Friction, Spatial heterogeneity, Stress drop

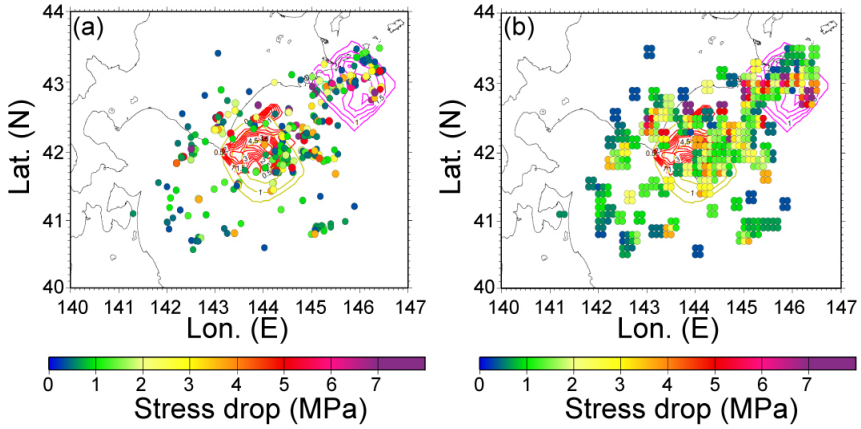

Fig. (a) Estimated stress drops of analyzed 330 middle-size earthquakes ($4.2 \leq M \leq 5.0$). Each circle shows the stress drop for each earthquake. Contours indicate slip distributions of past four large earthquakes off south-east of Hokkaido (EIC seismic note, http://www.eri.u-tokyo.ac.jp/sanchu/Seismo_Note/index.html). (b) Spatial pattern of the averaged stress drop. Individual circles indicate averaged values of stress drop for every 0.1 degree, which were calculated from the values of earthquakes in areas with 0.2 x 0.2 degrees.

Japan Geoscience Union Meeting 2014
(28 April - 02 May 2014 at Pacifico YOKOHAMA, Kanagawa, Japan)

SSS30-03 Room:Main Hall Time:April 28 10:00-10:15

Seismically inferred rupture process of the 2011 Tohoku-Oki earthquake by using 3D and 2.5D Green's tensor waveforms

OKAMOTO, Taro[1*] ; TAKENAKA, Hiroshi[2] ; HARA, Tatsuhiko[3] ; NAKAMURA, Takeshi[4] ; AOKI, Takayuki[5]

[1]Dep. Earth Planet. Sci., Tokyo Institute of Technology, [2]Dep. Earth System Sci. Okayama University, [3]IISEE, Building Research Institute, [4]Japan Agency for Marine-Earth Science and Technology, [5]GSIC, Tokyo Institute of Technology

The March 11, 2011 Tohoku-Oki earthquake (GCMT Mw9.1) generated strong ground motions and large tsunamis, and caused devastating damages in the northeastern Japan. The rupture process of this event provides important clues for understanding the geophysical condition of the generation of mega-thrust earthquakes and the mechanism of the excitation of the large tsunamis.

We analyze "seismic" rupture process of this event by using a non-linear full-waveform inversion method. We incorporate the effect of the near-source laterally heterogeneous structure on the synthetic Green's tensor waveforms because the analysis can result in erroneous solutions if the effect is not considered [1]. Also, in order to increase the resolution we use the teleseismic and the strong-motion seismograms jointly: the distribution of strong-motion station is one-sided and analysis with only the strong-motion records may result in reduced resolution near the trench axis [2]. For the teleseismic P-wave synthetics we use a 2.5-dimensional finite-difference method [3]. For the strong-motion synthetics we use a full three-dimensional finite-difference method that incorporates topography, oceanic water layer, three-dimensional heterogeneity and attenuation. Our simulation is accelerated by GPUs used in parallel [4]: we use the TSUBAME GPU supercomputer in Tokyo Institute of Technology.

In the previous study [5] we used only a single structure model (i.e., a single vertical slice of the 3D heterogeneous structure) to generate all the 2.5D Green's functions. In this paper we have updated the 2.5D structure models. That is, we extracted twenty-three vertical slices from the 3D structure model: each slice was (nearly) perpendicular to the trench axis and was taken along the nodes of the grid that formed the fault plane. By using these new models the 2.5D Green's functions and 3D Green's functions are now "consistent" with each other.

We computed Green's tensor synthetic waveforms for 31 teleseismic and 32 strong-motion components. We used 640 GPUs of the TSUBAME supercomputer for the calculation of each strong-motion synthetics. The inferred slip distribution has large slips near the JMA epicenter with the maximum slip of about 32 m. The amount of slips at the areas close to the trench axis is smaller than that of the land-ward area (i.e., near the JMA epicenter). Inversion results similar to these features have been obtained by previous study [2] but it is remarkable that our joint "seismic" inversion using 2.5D-teleseismic and 3D-strong-motion Green's tensor waveforms resulted in the solution with these features (i.e., land-ward large slips and trench-ward small slips). These features have important implications for tsunami studies because large slips near the trench axis are expected for large tsunamis. In order to verify the solution we will inspect the resolution by using simulations of inversion and the effect of the choice of the Green's tensor waveforms on the solutions.

[1] Okamoto and Takenaka, Earth Planets Space, 61, e17-e20, 2009.
[2] Yokota et al., Geophys. Res. Lett., 38, doi:10.1029/2011GL050098, 2011.
[3] Takenaka and Okamoto, in Seismic Waves, Research and Analysis, ed. K. Masaki, Intech, 2012.
[4] Okamoto et al, in GPU Solutions to Multi-scale Problems in Science and Engineering, ed. D.A. Yuen et al., Chapter 24, 375-389, Springer, 2013.
[5] Okamoto et al., Seismological Society of Japan, 2013 Fall Meeting, P1-62, Yokohama, Japan, October 7, 2013.

Keywords: Tohoku-Oki earthquake, rupture process, GPU computing, seismic waveforms

Japan Geoscience Union Meeting 2014
(28 April - 02 May 2014 at Pacifico YOKOHAMA, Kanagawa, Japan)

SSS30-04 Room:Main Hall Time:April 28 10:15-10:30

Seismic velocity and attenuation tomography of the source zone of the 2011 Tohoku-oki earthquake (Mw 9.0)

ZHAO, Dapeng[1*] ; LIU, Xin[1] ; HUANG, Zhouchuan[1]

[1]Tohoku University, Department of Geophysics

Detailed 3-D P and S wave velocity (Vp, Vs) and attenuation (Qp and Qs) tomography of the crust and upper mantle under the entire Northeast Japan arc from the Japan Trench to the Japan Sea coast is determined (Zhao et al., 2011; Huang and Zhao, 2013; Liu et al., 2014). The suboceanic earthquakes under the Pacific Ocean and the Japan Sea are used in this work and they are relocated precisely using sP depth phases. Vp and Vs tomography is determined using a large number of high-quality arrival times, whereas the Qp and Qs tomography is obtained using a large number of t∗data measured precisely from P and S wave spectra of local earthquakes. Our results reveal the high-V and high-Q subducting Pacific slab, and significant low-V and low-Q anomalies in the crust and mantle wedge under the volcanic front and the back-arc area. Large megathrust earthquakes (M >6.0) during 1900-2013 including the great 2011 Tohoku-oki earthquake (Mw 9.0) sequence are generally located in high-V and high-Q patches which are surrounded by low-V and low-Q anomalies in the megathrust zone. The high-V/high-Q patches in the megathrust zone generally exhibit large coseismic slips of megathrust earthquakes and large slip deficit on the plate interface. We think that these highV/high-Q patches represent asperities in the megathrust zone, whereas the low-V/low-Q anomalies reflect weakly coupled areas. These results suggest that structural heterogeneities in the megathrust zone control the interplate seismic coupling and the nucleation of megathrust earthquakes.

References

Huang, Z., D. Zhao (2013) Mechanism of the 2011 Tohoku-oki earthquake (Mw 9.0) and tsunami: Insight from seismic tomography. J. Asian Earth Sci. 70, 160-168.

Liu, X., D. Zhao, S. Li (2014) Seismic attenuation tomography of the Northeast Japan arc: Insight into the 2011 Tohoku earthquake (Mw 9.0) and subduction dynamics. J. Geophys. Res. 119, doi:10.1002/2013JB010591.

Zhao, D., Z. Huang, N. Umino, A. Hasegawa, H. Kanamori (2011) Structural heterogeneity in the megathrust zone and mechanism of the 2011 Tohoku-oki earthquake (Mw 9.0). Geophys. Res. Lett. 38, L17308.

Keywords: earthquakes, slab, fluids

Japan Geoscience Union Meeting 2014
(28 April - 02 May 2014 at Pacifico YOKOHAMA, Kanagawa, Japan)

SSS30-05 Room:Main Hall Time:April 28 10:30-10:45

A Study on Seismicity before and after the Tohoku Earthquake around its Southern Boundary Using Dense OBS Array Data

NAKATANI, Yukihiro[1*] ; MOCHIZUKI, Kimihiro[1] ; SHINOHARA, Masanao[1] ; YAMADA, Tomoaki[1] ; HINO, Ryota[2] ; ITO, Yoshihiro[3] ; MURAI, Yoshio[4] ; SATO, Toshinori[5]

[1]Earthquake Research Institute, The University of Tokyo, [2]International Research Institute of Disaster Science, Tohoku University, [3]Disaster Prevention Research Institute, Kyoto University, [4]Graduate School of Science, Hokkaido University, [5]Graduate School of Science, Chiba University

The southern boundary of the 2011 Tohoku earthquake, the source area of the largest aftershock, and a subducting seamount are located around off Ibaraki in the Japan Trench subduction zone. It is important to evaluate the spatial and temporal distribution of seismicity which provides key information about the seismic energy release. However, the seismicity is not well constrained due to a large distance offshore from the onshore network. Therefore, estimating seismic energy release off Ibaraki by using ocean-bottom seismometer (OBS) data is essential to understand the characteristics of the main shock rupture propagation. In this study, we estimated seismicity distribution around off Ibaraki region before and after the 2011 Tohoku earthquake using dense OBS array data.

It is difficult to apply methods that have been designed for on-land seismic stations due to the large ambient noise and effects of thick seafloor sediments. Furthermore, conventional manual picking is difficult because of the occurrence of many aftershocks. We therefore applied a semblance analysis to OBS waveform data with theoretical P-wave travel-time table obtained by the construction of an original 3-D P-wave velocity structure model.

To evaluate the validity of event identification and the accuracy of the epicenter distribution, I conducted comparisons of our epicenters with the JMA epicenters and synthetic tests using theoretical waveforms with several different sets of signal-to-noise ratio and focal depths.

As results of epicenter determination by the semblance analysis, we found that a lot of earthquakes occurred in the vicinity of the frontal region of the subducting seamount after the 2011 Tohoku earthquake. Next, there exists an along-strike density contrast of seismicity, and the inactive region possibly corresponds to the seismically quiet band previously revealed by a seismic observation. Furthermore, we applied the semblance analysis to OBS waveform immediately after the main shock and estimated the spatial and temporal transition of detailed seismicity. We found that the seismicity around the subducting seamount was activated after the largest aftershock rather than between the occurrences of the main shock and the largest aftershock. It puts constraints on the southern boundary of the 2011 Tohoku earthquake.

Keywords: dense OBS array data, seismicity, the southern boundary of the 2011 Tohoku earthquake

Japan Geoscience Union Meeting 2014
(28 April - 02 May 2014 at Pacifico YOKOHAMA, Kanagawa, Japan)

SSS30-06 Room:Main Hall Time:April 28 11:15-11:30

Large shallow slip during the 2011 Tohoku-Oki earthquake: New insights from JFAST and high-velocity friction experiments

UJIIE, Kohtaro[1*] ; TANAKA, Hanae[1] ; SAITO, Tsubasa[1] ; TSUTSUMI, Akito[2] ; MORI, James[2] ; KAMEDA, Jun[3]

[1]University of Tsukuba, [2]Kyoto University, [3]Hokkaido University

The Japan Trench Fast Drilling Project (JFAST), Integrated Ocean Drilling Program (IODP) Expeditions 343 and 343T were conducted to understand the coseismic deformation mechanisms and dynamics of large shallow slip during the 2011 Tohoku-Oki earthquake. The drill site is located at the toe of the frontal prism near the Japan Trench axis. Observations and analyses of recovered core samples as well as logging-while-drilling data indicate that the plate-boundary fault is highly localized in pelagic clay less than 5 m-thick. The smectite content in pelagic clay is ˜78%. The deformations in the plate-boundary fault are marked by distributed shear along anastomosing scaly foliations and localized slip along the boundary between red-brown and dark-brown scaly clays with different fabric orientations. On the microscopic scale, injection structures and mixing of clays of different colors without shear surfaces are observed along the localized slip zone, suggesting fluidization during the localized slip. High-velocity (1.3 meters per second) friction experiments on core samples taken from smectite-rich clay of the plate-boundary fault, show a small stress drop with very low peak and steady-state shear stress. The very low shear stress can be attributed to the abundance of smectite and thermal pressurization effects. Steady-state shear stress is independent of normal stress, and the microstructures after the experiments show evidence for fluidization. These features suggest that the fault material behaved like a fluid during high-velocity shearing due to thermal pressurization of pore fluid. Our results indicate that large shallow slip resulted from coseismic fault lubrication, and the similarity of microstructures between natural and experimental shear zones may represent the fluidization of fault material during earthquake faulting. Seismic slip could be promoted even in plate-boundary faults at shallow depths, as the slip propagates through the smectite-rich fault material.

Japan Geoscience Union Meeting 2014
(28 April - 02 May 2014 at Pacifico YOKOHAMA, Kanagawa, Japan)

SSS30-07 Room:Main Hall Time:April 28 11:30-11:45

Trace element and isotope characteristics of core samples from the Japan Trench Fast Drilling Project (JFAST)

ISHIKAWA, Tsuyoshi[1*] ; MATSUOKA, Jun[2] ; KAMEDA, Jun[3] ; MORI, James[4] ; CHESTER, Frederick[5]

[1]JAMSTEC, [2]Marine Works Japan Ltd., [3]Hokkaido University, [4]Kyoto University, [5]Texas A&M University

The Integrated Ocean Drilling Program (IODP) Expedition 343 drilled three holes through the plate boundary near the Japan Trench to investigate the cause of very large fault slip during the 2011 Tohoku-Oki earthquake. In this paper, we report trace element and Sr-Nd-Pb isotope compositions of core samples, including plate-boundary fault rocks, recovered from Hole C0019E.

The rocks in C0019E are lithologically subdivided into seven units (Chester et al., 2013): Units 1 to 3, wedge sediments of upper plate; Unit 4, plate-boundary fault; Units 5 to 7, sediments of lower plate. The clay-rich plate-boundary fault rocks (Unit 4) are characterized by elevated concentrations of rare earth elements (REE) and some refractory metals, and are distinct from any other JFAST samples in terms of trace element characteristics. Brown mudstones of the lower plate (Unit 5) show trace element characteristics (e.g. REE pattern) roughly similar to those of the upper plate sediments (Units 1 to 3), but they are still distinguishable from each other. Pelagic sediments in the lower plate (Unit 6) show highly varied trace element compositions with a large Ce anomaly. The Sr, Nd and Pb isotope data show variations that are essentially consistent with trace element characteristics observed for each unit.

The clear relationship observed between lithological units, trace element and isotope compositions and radiolarian ages of the JFAST samples provides a key for understanding the origin of the shallow fault zone of the Tohoku-Oki earthquake and the frontal wedge at the Japan Trench. Geochemical characteristics of the JFAST samples will be discussed along with those of sediments from DSDP site 436, which is a nearby input site, for elucidating the origin of the JFAST rocks and for evaluating coseismic/interseismic processes possibly recorded in the plate-boundary fault rocks.

Keywords: Earthquakes, Fault rocks, Trace elements, Isotopes, IODP

Japan Geoscience Union Meeting 2014
(28 April - 02 May 2014 at Pacifico YOKOHAMA, Kanagawa, Japan)

SSS30-08 Room:Main Hall Time:April 28 11:45-12:00

Paleomagnetic analyses of core samples from the plate-boundary thrust obtained during the IODP JFAST

MISHIMA, Toshiaki[1*] ; YANG, Tao[2] ; UJIIE, Kohtaro[3] ; KIRKPATRICK, James[4] ; CHESTER, Frederick[5] ; MOORE, Casey[6] ; ROWE, Christie[7] ; REGALLA, Christine[8] ; REMITTI, Francesca[9] ; KAMEDA, Jun[10] ; WOLFSON, Monica[11] ; BOSE, Santanu[12] ; ISHIKAWA, Tsuyoshi[13] ; TOY, Virginia[14]

[1]Osaka City University, [2]China Earthquake Administration, [3]University of Tsukuba, [4]Colorado State University, [5]Texas A&M University, [6]University of California Santa Cruz, [7]McGill University, [8]Pennsylvania State University, [9]Universita di Modena e Reggio Emilia largo, [10]Hokkaido University, [11]University of New Hampshire, [12]University of Calcutta, [13]JAMSTEC, [14]University of Otago

IODP Expedition 343, Japan Trench Fast Drilling Project (JFAST), drilled through the plate-boundary dècollement of the Japan Trench, where large slip occurred during the 11 March 2011 Tohoku-Oki Earthquake. In order to reconstruct the deformation of the sediments at the cm scale and less, we conducted paleomagnetic measurements of the core sample from the plate-boundary dècollement zone.

The plate-boundary core sample has a scaly fabric and is composed of bicolored clay layers with sharp contacts. We prepared slabs for thin sections across the contacts with typical dimensions of 3x3x5 cm^3 from the core sample. We measured remanent magnetization of 16 slabs. The slabs were subjected to natural remanent magnetization (NRM) measurements in 0.5-1 cm intervals and progressive alternating field demagnetization (AFD) up to 80 mT with a 2G755 pass-through superconducting rock magnetometer at Kochi University.

Typically, two paleomagnetic components were isolated during the AFD of slab samples up to 80 mT. One component (‘soft’ component) was demagnetized below 20-30 mT, and another component (‘hard’ component) was not demagnetized even up to 80 mT. For multiple slab samples cut from the same whole-round sample, the hard component generally has a consistent paleomagnetic direction. Contrastingly, the direction of the soft component is not so consistent between adjacent slabs, and even varies within a single slab.

The direction variation of the soft component possibly reflects the cm-scale rotation of competent phaccoids during deformation within the slab samples from the plate-boundary thrust zone. The consistency of the hard component directions implies that the hard component was remagnetization during/after the rotation, and was possibly carried by newly-formed magnetic minerals during the deformation.

Japan Geoscience Union Meeting 2014
(28 April - 02 May 2014 at Pacifico YOKOHAMA, Kanagawa, Japan)

SSS30-09 Room:Main Hall Time:April 28 12:00-12:15

Change of permeability caused by 2011 Tohoku earthquake detected from pore pressure monitoring

KINOSHITA, Chihiro[1*] ; KANO, Yasuyuki[2] ; ITO, Hisao[2]

[1]Graduate School of Science, Kyoto University, [2]DPRI

We have monitored pore and atmospheric pressures at the Kamioka mine in Gifu Prefecture, central Japan since 2005 to study relationship between groundwater and earthquake. Pore pressure decreased after the 2011 Tohoku earthquake (M9.0) occurred on 11 March 2011, which may be attributed to expansion of the crust west of the epicenter or a permeability increase. To evaluate rock permeability changes, we analyzed the Earth tide response of pore pressure before and after the earthquake. Pore pressure fluctuates associated with the meteorological effects, Earth tides and crustal deformation. We assumed that without the change of aquifer conditions tidal response of pore pressure is constant. We compared the tidal response before and after the event. We extracted amplitude and phase lag of M2 and O1 constituents from pore pressure by tidal analysis program, BAYTAP-G. These amplitudes decreased and phases changed after the earthquake. It was in accord with pore pressure decreases. We estimated the hydraulic diffusivity using the poroelastic theory and diffusion equation. If we assume that the poroelastic coefficient is constant, the hydraulic diffusivity increased from 8.9 to 65.0 m^2/s at the time of the Tohoku earthquake. We also analyzed data before and after the Noto Hanto Earthquake (M6.9) which occurred in the northwestern part of Ishikawa Prefecture, central Japan on 25 March, 2007. The epicentral distance of the Noto Hanto Earthquake from our observation site is 112 km. No hydraulic diffusivity change is detected. The causes of the hydraulic diffusivity change are potentially related to a static and/or dynamic stress change. In order to discuss the difference in hydraulic diffusivity change between the Tohoku and Noto Hanto earthquakes, we analyzed other earthquakes to relate the hydraulic diffusivity changes, and the amount of static and dynamic strain changes.

Keywords: hydraulic diffusivity, pore pressure, Earth tide

Japan Geoscience Union Meeting 2014
(28 April - 02 May 2014 at Pacifico YOKOHAMA, Kanagawa, Japan)

SSS30-10 Room:Main Hall Time:April 28 12:15-12:30

Enigmatic phase lead of pore pressure: 11+ years of ACORK monitoring at the frontal decollement of Nankai Trough

KINOSHITA, Masataka[1*] ; KANO, Yasuyuki[2]

[1]JAMSTEC, [2]Kyoto Univ. DPRI

For more than 11 years we have been conducting a continuous monitoring of downhole pore pressures at multiple sub-bottom intervals in ODP Holes 808I and 1173B situated landward and seaward of the deformation front in the Nankai Trough off Cape Muroto. We found that the pressure response to the semi-diurnal ocean tide (M2), both amplitude and phase, gradually change during the observed period. The M2 amplitudes at most depths in Hole 808I decay as their phase delay (up to 45 degrees), ONLY IF the amplitude is larger than ˜0.2 of that for the seafloor. On the other hand, we observe an anomalous phase LEAD (up to -40 degrees) if the relative amplitude is lea than ˜0.2. We hypothetize that the recorded pore pressure is a combination of two components; one with larger amplitudes and phase-delay and the other with small amplitude and phase-lead. The former can be interpreted as the decrease in formation compliance relative to that of the system, or as the decrease in hydraulic diffusivity around the sensors. The mechanism of the latter variation remain still enigmatic. Existence of gas-rich layer next to the sensor, as suggested by wang and Davis (1996), is difficult to generate such a large phase lead. The predicted earth tide at this site does not coincide with the observed phase. Thermal expansion/contraction caused by the flow within the casing, induced by tidal loading, may cause this phase shift, but a simple thermal/hydrological diffusion cannto explain both the amplitude and phase simultaneously. A complex process including some unknown mechanism may be in operating at Hole 808I.

Keywords: Nankai Trough, ACORK, ODP

Japan Geoscience Union Meeting 2014
(28 April - 02 May 2014 at Pacifico YOKOHAMA, Kanagawa, Japan)

SSS30-11 Room:Main Hall Time:April 28 14:15-14:30

The increase in missing waveform images of the F-net seismographs preceding the 2004 off Kii peninsula earthquake

SUE, Yoshiki[1*]

[1]No institution affiliation

1. Introduction

The F-net is a broadband seismograph network constituted of 73 STS-1 and 2 seismometers. Natural frequency of the seismometers is 120 seconds (STS-2) and longer, thus they can detect long-period ground motion. On its website, waveform images of the stations for a day or an hour are provided. The analyses on their file size have shown long-period vibrations (Sue, 2010).

2. Analysis

Variation recorded in waveform images may mean variation of ground motion. Thus operational status of the F-net is investigated. There are two sources on it.

a. Data acquisition trouble log: This is the formal information covering from instantaneous to long-lasting loss of data. Reasons for troubles are shown. While, update of the information is irregular.

b. Missing of waveform images: The website displays the message ”Waveform image does not exist”. It is surmised that this situation is caused by continuous loss of data exceeding 1 day (Daily plot) or 1 hour (Hourly plot). The reasons are not shown. While update of the information is regular.

So far, analyses on ”missing of waveform images” for the 2011 Tohoku earthquake (M=9) has been done (Sue, 2013). As a next step, the 2004 off Kii peninsula earthquake (M=7.4), which occurred on September 5, 2004 at the Nankai trough, is carried out. For details, for the period of about 3 months from June 1, 2004 to September 10, 2004, the F-net stations located in the area between Itoigawa - Shizuoka tectonic line and Okinawa island are investigated (The one in Noto peninsula is excluded).

3. Results

Fig. 1 shows the result. During June - first half of July, 2004, which is more than 1.5 month before the main shock, the most frequent number of the image-missing station is 1, and it was stable condition. From last half of July and later, the number varied.

On August 30 and 31, which are 6 and 5 days before the earthquake, there were large increases of the number. Further, arrangement of image-missing stations is mainly in southern part and east coast of the Kyushu island respectively.

On Sept. 4, which is the previous day of the main shock, there were 3 image-missing stations, located from Shikoku island to Kyushu island alongside the Nankai trough (Fig.2).

After the earthquake, number of image-missing station decreased to zero.

The major reasons for missing images are ”Network trouble” and ”Electric power supply trouble”.

4. Discussion

Number of F-net station with missing waveform images increases before an earthquake. The phenomena appear not only close to the epicenter, but wide area surrounding it. The phenomena are also observed at the 2011 Tohoku earthquake, thus they may usually appear before a large earthquake. Similar phenomena as shown in this paper might be observed at the anticipated Nankai trough earthquake.

Missing images of all 73 stations happened on 23 to 25 in July (Fig.1). Same phenomena appeared at the 2011 Tohoku earthquake, thus the phenomena may be a sign of unstableness of the F-net system.

It is assumed that increases of the missing waveform images preceding a big earthquake was because the F-net could not withstand possible long-period variation of the earth’s surface. ”Network trouble” and ”Electric power supply trouble” might be causes for such situation. Such phenomena are not observed for the Hi-net seismograph network, probably because of its characteristic (NF = 1 sec).

When the DONET (Dense Oceanfloor Network System for Earthquakes and Tsunamis) detects anomaly, malfunctioning of the F-net may appear at the same time or even earlier.

The area formed by the F-net stations with missing images may have certain relation with magnitude of the earthquake.

Acknowledgement

The author thanks NIED for using the data of the F-net.

References

Yoshiki Sue, 2010, SSJ Fall meeting, D31-12. (In Japanese)
Yoshiki Sue, 2013, The increase in missing waveform images of the F-net broadband seismograph network preceding the 2011 Tohoku earthquake, JpGU2013, S-SS30-P01.

Keywords: F-net, broadband, seismograph network, long period, waveform, Nankai trough

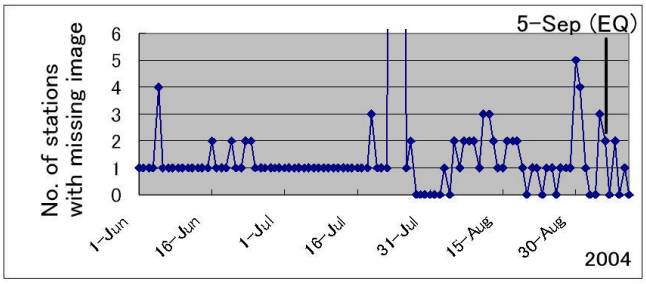

Fig.1. No. of stations with missing waveform images for June 1 to September 10, 2004. No. is 73 on July 23-25. Day is on UT.

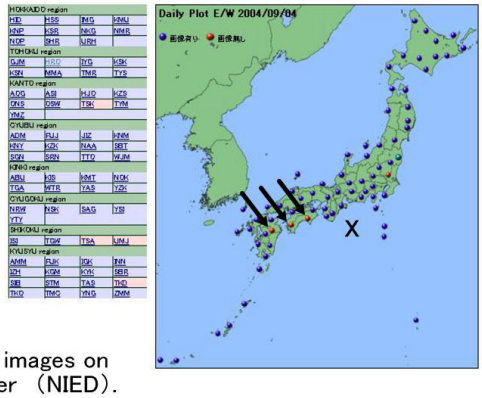

Fig.2. The staions with of missing waveform images on Spetember 4, 2004 (Arrow) and the epicenter (NIED).

Japan Geoscience Union Meeting 2014
(28 April - 02 May 2014 at Pacifico YOKOHAMA, Kanagawa, Japan)

SSS30-12 Room:Main Hall Time:April 28 14:30-14:45

Heat flow distribution along the Nankai Trough: Influence of the structure of the Shikoku Basin oceanic crust

YAMANO, Makoto[1*] ; KAWADA, Yoshifumi[1] ; GOTO, Shusaku[2] ; HAMAMOTO, Hideki[3]

[1]Earthq. Res. Inst., Univ. Tokyo, [2]Geol. Surv. Japan, AIST, [3]Center Environ. Sci. Saitama

The thermal structure of the Philippine Sea plate (Shikoku Basin) subducting along the Nankai Trough, one of the most important factors controlling the temperature structure around the plate interface, significantly affects physical/chemical processes in the seismogenic zone of subduction earthquakes. Surface heat flow observed on the floor of the Nankai Trough should reflect the thermal structure of the incoming Shikoku Basin. Previous surveys showed that heat flow on the trough floor is extremely high for the seafloor age between 135^{o}E and 136^{o}E (south of the Kii Peninsula), while it is comparable to the value expected from the age in the neighboring area to the east of 136^{o}E. The transition zone from high to normal heat flow lies in the vicinity of the rupture segmentation boundary between the 1944 Tonankai and the 1946 Nankai earthquakes, across which seismicity on the landward side of the trough significantly changes, implying influence of the temperature structure on subduction earthquake processes.

For further investigation of the along-strike variation in heat flow on the trough floor, we conducted heat flow measurements around the Nankai Trough off the Kii Peninsula and off Shikoku in 2011 to 2013. Most of the measurements were made in the area around 136^{o}E, where the high to normal heat flow transition occurs, and on the trough floor to the south of Shikoku, where the existing data were very sparse. 39 new heat flow data on the trough floor allowed us to delineate heat flow variation along the trough. A conspicuous change in heat flow distribution was found at around 136^{o}E. On the west of 136^{o}E, heat flow is extremely high and variable, ranging from 130 to 250 mW/m^2,while on the east of 136^{o}E, heat flow monotonously decreases eastward from 200 to 100 mW/m^2 in about 50 km with no appreciable scatter. On the trough floor south of Shikoku, west of 134.5^{o}E, no significant change was observed along the trough in spite of westward increase in the seafloor age.

The heat flow distribution described above appears to be correlated with the structure of the Shikoku Basin oceanic crust. The high and variable heat flow area between 134.5^{o}E and 136^{o}E corresponds to the youngest part of the Shikoku Basin which was formed by spreading in NE-SW direction, whereas the neighboring areas with less scattered heat flow, east of 136^{o}E and west of 134.5^{o}E are the older parts formed by E-W spreading. The thickness of the oceanic crust and the basement relief also change around 136^{o}E, in the vicinity of the heat flow transition boundary. Spinelli and Wang (2008) proposed a model for the high heat flow around 135^{o}E that vigorous pore fluid circulation in a permeable layer in the subducting oceanic crust efficiently transfers heat upward along the plate interface. We may infer that the permeability structure of the oceanic crust changes at the transform boundaries between the E-W and NE-SW spreading, which yields variations in vigor and/or pattern of pore fluid circulation, resulting in the contrasting heat flow distributions. Since heat transfer by fluid circulation in the subducting oceanic crust lowers the temperature of the plate interface, the along-strike variation in the trough floor heat flow could indicate corresponding variation in the temperature distribution in the seismogenic zone.

Keywords: Nankai Trough, heat flow, pore fluid, oceanic crust, temperature structure, seismogenic zone

Japan Geoscience Union Meeting 2014
(28 April - 02 May 2014 at Pacifico YOKOHAMA, Kanagawa, Japan)

SSS30-13 Room:Main Hall Time:April 28 14:45-15:00

Reevaluation of temperature at the updip limit of locked portion of Nankai megasplay, inferred from IODP Site C0002 tem

SUGIHARA, Takamitsu[1*] ; KINOSHITA, Masataka[2] ; ARAKI, Eiichiro[3] ; KIMURA, Toshinori[3] ; KYO, Masanori[1] ; NAMBA, Yasuhiro[1] ; KIDO, Yukari[1] ; SANADA, Yoshinori[1] ; MOE, Kyaw thu[1]

[1]CDEX/JAMSTEC, [2]KCC/JAMSTEC, [3]DONET/JAMSTEC

Temperature near the updip limit of the locked zone still has large uncertainties due to lack of knowledge about thermal and hydrological properties at depth.

In 2010, the first Long-Term Borehole Monitoring System was deployed at ˜900 m below sea floor (mbsf) above the updip limit of seismogenic fault zone in the Nankai Trough off Kumano (Site C0002).Four temperature records show that the effect of drilling diminished in less than 2 years and they all reached thermal equilibrium by 2012. From in-situ temperatures and thermal conductivities measured on core samples, the temperature and heat flow at 900 mbsf are determined as 37.9 ℃ and 56.1 mW/m2, respectively. This heat flow value is in excellent agreement with that from shallow borehole temperature corrected for rapid sedimentation in the Kumano Basin. We use these values to constrain the temperature below 900 mbsf to the mega-splay and plate boundary fault zones.

To extrapolate temperature downward, we use LWD bit resistivity data as a proxy for porosity and the thermal conductivity is modeled from this porosity using a geometrical mean model. Upon integration by the 1-D thermal conduction we included the radioactive heat and frictional heat production. Estimated temperature at the megasplay ranges between 132 to 149 ℃, depending on thermal conductivities and radioactive heat. It is significantly higher, by up to 40 ℃, than previous 2-D numerical model predictions that can account for the heat flow across the deformation front. The discrepancy may be explained either by increasing the effective frictional coefficients along the fault zones or by introducing a lateral fluid flow along the permeable layers somewhere in the sedimentary layer. Revision of 2-D simulation by introducing our new boundary conditions will also be useful. Ultimately, reaching the megasplay fault and in-situ temperature measurement in the drilled hole is required to understand seismogenesis in the Nankai subduction zone.

Keywords: Seismogenic zone, Nankai Trough, Megasplay fault, Thermal regime, IODP, NanTroSEIZE

Japan Geoscience Union Meeting 2014
(28 April - 02 May 2014 at Pacifico YOKOHAMA, Kanagawa, Japan)

SSS30-14 Room:Main Hall Time:April 28 15:00-15:15

Preliminary Scientific Results of IODP Expedition 348: Ultra-deep Riser Drilling into the Nankai Accretionary Prism

HIROSE, Takehiro[1*] ; TOBIN, Harold[2] ; SAFFER, Demian[3] ; TOCZKO, Sean[1] ; MAEDA, Lena[1] ; KUBO, Yusuke[1] ; EXPEDITION 348, Scientists[6]

[1]JAMSTEC, [2]University of Wisconsin-Madison, [3]Pennsylvania State University, [4]Chiba University, [5]The university of Tokyo, [6]IODP Expedition 348

The Nankai Trough Seismogenic Zone Experiment (NanTroSEIZE) is a multi-disciplinary scientific project designed to investigate fault mechanics and seismogenesis along subduction megathrusts through seismic imaging, direct sampling, in situ measurements, and long-term monitoring in conjunction with laboratory and numerical modeling studies. International Ocean Discovery Program (IODP) Expedition 348, the latest advance of the NanTroSEIZE project, started on 13 September 2013 and was completed on 29 January 2014. During Expedition 348, the drilling vessel *Chikyu* advanced the ultra-deep riser hole at Site C0002, located 80 km offshore of the Kii Peninsula, from a depth of 860 meters below sea floor (mbsf) to 3058.5 mbsf, the world record for the deepest scientific ocean drilling, and cased it for future deepening. The drilling operation successfully obtained data on formation physical properties from logging while drilling (LWD) tools, as well as from lithological analyses of cuttings and core from the interior of the active accretionary prism at the Nankai Trough. IODP Site C0002 is the currently only borehole to access the deep interior of an active convergent margin.

Preliminary scientific results of Expedition 348 include:

(1) Fine-grained turbiditic mudstones with coarser silty and sandy interbeds, exhibiting steep dips (between ˜60 and 90 degrees) are predominant in the prism down to ˜3000 mbsf. The biostratigraphic age of the sediments in the lowermost part of the hole is thought to be 9-11 Ma, with an assumed age of accretion of 3-5 Ma.

(2) Slickenlined surfaces, deformation bands and mineral veins are present throughout the drilled interval, while well-developed scaly clay fabrics are increasingly observed below ˜2200 mbsf. A substantial fault zone with well-developed foliation was successfully cored from the deep interior of the prism at ˜2205 mbsf.

(3) Porosity generally decreases from ˜60% to ˜20% from the seafloor to 3000 mbsf. However, physical properties including grain density, electrical conductivity and P-wave velocity suggest fairly homogeneous properties in the interior of the prism between ˜2000 and 3000 mbsf.

(4) Drilling mud gas analysis during the riser drilling indicates that a source of hydrocarbon gas shifts from microbial origin to thermogenic at around 1700-2300 mbsf.

Lithological and structural characterizations, the style of deformation, and downhole physical properties all indicate a complex structural evolution and will provide unprecedented insights into the mechanical state and behavior of the prism at depth.

Keywords: IODP, NanTroSEIZE, Nankai Trough, accretionary prism

Japan Geoscience Union Meeting 2014
(28 April - 02 May 2014 at Pacifico YOKOHAMA, Kanagawa, Japan)

SSS30-15 Room:Main Hall Time:April 28 15:15-15:30

Levels of frictional heat along deep to shallow parts of the megasplay fault : a Raman spectroscopic analyses of CM

MUKOYOSHI, Hideki[1*] ; HIRONO, Tetsuro[2] ; MASUMOTO, Hirokazu[2]

[1]Faculty of Education and Integrated Arts and Sciences, WASEDA University, [2]Department of Earth and Space Science, Graduate School of Science, Osaka University

Estimation of frictional heating of deep to shallow portion of ancient megasplay fault is important for understanding of weakening mechanism (e.g., thermal pressurization, melt lubrication) of present plate boundary fault and megasplay fault. In this study, we performed microstructural observation and Raman spectroscopic analyses of carbonaceous materials (CM) in the fault rock of 2.5-5.5 km depth of an ancient megasplay fault (an out-of sequence thrust in the Shimant accretionary complex) and 1-4 km depth of a thrust in the Emi group, Hota accretionary complex. We also conducted heating experiment of CM in host rock of these fault with anaerobic condition (rate of temperature increase: 20 K/min) in order to investigate the effects of fast heating rate like frictional heating during earthquake.

Raman spectrum of CM of both fault is similar to spectrum of 400∼600 ℃ heating experiment of CM. This result shows that both fault had heating history of 400∼600 ℃ by frictional heating. Further examination for effect of shearing to molecular stricter is needed for more detailed evaluation of frictional heating history.

Keywords: ancient megasplay fault, heating experiment

Japan Geoscience Union Meeting 2014
(28 April - 02 May 2014 at Pacifico YOKOHAMA, Kanagawa, Japan)

SSS30-16 Room:Main Hall Time:April 28 15:30-15:45

Upper plate geology controls the rupture area segmentation -A case study of the Nankai Trough

KIMURA, Gaku[1*] ; HASHIMOTO, Yoshitaka[2] ; KITAMURA, Yujin[3] ; YAMAGUCHI, Asuka[4] ; HAMAHASHI, Mari[1] ; KOGE, Hiroaki[1] ; MORITA, Sumito[5]

[1]Dept. Earth and Planetary Science, The University of Tokyo, [2]Kochi University, [3]Kagoshima University, [4]Atmosphere and Ocean Research Institute, The University of Tokyo, [5]AIST

What controls the earthquake rupture area of megathrust is one of the most fundamental questions in geodynamic research of subduction zone. In the case of the Nankai Trough, Japan, three major controlling factors have proposed so far, surface topography of the subducting plate like seamount, locally strong rigidity of upper plate due to igneous rock composition, andfriction property of the plate boundary megathrust including abnormal pore fluid pressure distribution. Such controlling factors are applicable to other subduction zone in general. For example, the topographic high like seamount is proposed to control the location of asperity due to stronger coupling. The topographic-high worked as an asperity contacts with upper plate and rupture could be propagated when the contact breaks. The topographic-high also works as a barrier in the difficult case to be broken. From the geological point of view, plate boundary megathrust in the seismogenic zone must be composed of fault rock in brittle regime because of its temperature range from ~150 ℃ to ~350 ℃, which is cooler than the temperature for the plastic deformation of quarts, feldspar and other rock forming minerals of oceanic crust except for clayey phyllosilicates. In this temperature range, tectonic melange like fault rock with highly pressurized interstitial fluid is expected. Seismic observation showing a reflector with intensive amplitude of negative reflection coefficient suggests a plate boundary fault layer with abnormal fluid pressure. The friction behavior of the fault rock and pore fluid effect is a recent main concern in the subduction zone. The third factor is the mechanical property of the upper plate for the plate boundary megathrust in subduction zone. It is used to treat that the upper plate is a mechanical uniform media saving the elastic energy for theseismic slip along the megathrust. The mechanical property of the upper plate changes for a geological long time scale due to the growth of accretionary prism or tectonic erosion. In addition to such subduction mode of accretion vs erosion, some peculiar tectonic events (e.g. change in convergent direction, some obstacle collision, spreading ridge collision and rapid magmatic accretion etc.) modify the mechanical property of the upper plate and its heterogeneity in space. In the case of the Nankai Trough, a pultonic body is situated beneath the place of epicenter and is suggested to have been functioned as an asperitiy of 1944 Tonankai and 1946Nankaido Earthquakes. We examined the on-land geology of the Shikoku island and the Kii Peninsula, SW Japan, basement structure and composition beneath the forearcKumano Basin on the basis of recent results of ocean drilling by IODP (Integrated Ocean Drilling Project) and other investigations to infer the geologic composition of the upper plate. As a result we conclude that the key geologic event was middle to late Miocene episodic and rapid growth of forearc crust, mainly due to the magmatic intrusion and extrusion. This event was casued by the eastward migration of the T-T-T triple junction. Such ancient event now controls therupture area of the great earthquake in the subduction zone.

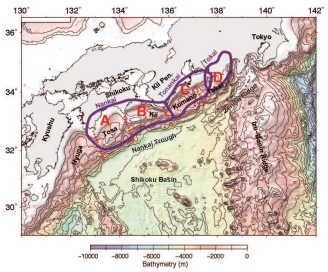

Japan Geoscience Union Meeting 2014
(28 April - 02 May 2014 at Pacifico YOKOHAMA, Kanagawa, Japan)

SSS30-17 Room:Main Hall Time:April 28 15:45-16:00

The research project on the extended Nankai seismogenic zones towards disaster mitigation of the mega-thrust earthquakes

KANEDA, Yoshiyuki[1*] ; FUKUWA, Nobuo[2] ; FURUMURA, Takashi[3]

[1]Japan Agency for Marine-Earth Science and Technology, [2]Nagoya University, [3]The University of Tokyo

The recurrence of Nankai trough mega thrust earthquakes and tsunamis are the very severe problem to Japan. Therefore, MEXT of Japanese government has implemented the research project during a period from FY2008 to 2012 to evaluate seismic linkage around the Nanakai trough mega thrust earthquake seismogenic zones. We have obtained many significant scientific results, such as the extended seismogenic zone, in this previous research project. In the 2013 fiscal year, a new project launched aiming mitigation of disaster caused by the Nankai trough earthquakes in the extended seismogenic zone. This new project is composed of three research fields which are the disaster mitigation research filed, observational research filed and the simulation research field. According to lessons learned from the 2011 East Japan Earthquake, the disaster mitigation research filed are progressing 5 sub-themes which are precise seismic hazard estimation, providing research results to local government/community for disaster measures, investigating recovery and revival methodologies based on social environmental changes, and constructing redundant hazard information database. The observational research field reveals structures of crust and plate, seismicity, and historical tsunami events in the Nankai trough. In the simulation research field, investigations will be conducted for recurrence cycle simulation of mega thrust earthquakes, data assimilation method that improves reliability of the simulation, seismic and tsunami wave simulations for disaster mitigation. We must surely progress each sub-theme at the beginning and finally integrate them for disaster mitigation around the extended Nankai trough sesimogenic zones. In this talk, we will introduce the outline of new project and the present progress.

Keywords: Nankai trough seismogenic zone, Seismic linkage, Disaster mitigation

Japan Geoscience Union Meeting 2014
(28 April - 02 May 2014 at Pacifico YOKOHAMA, Kanagawa, Japan)

SSS30-18 Room:Main Hall Time:April 28 16:15-16:30

Ogasawara Bending Slab and Mantle Convection

NIITSUMA, Nobuaki[1*]

[1]Inst. GeoSciences, Shizuoka Univ.

Ogasawara Slab is not only steeply dipping, but also, bending concentrically and reaching to bottom of upper mantle, which are shown with the hypocenters of 14 May 2013 M7.3 (619 km depth) and 7 February 1998 M6.4 (552 km depth).

Pacific Plate is spreading along East Pacific Rise, and subducting along Japanese Islands down to bottom of upper mantle as slab. If we consider the mass balance in upper mantle on Plate motion with accompaning beneath mantle, the mantle should convect from subduct area toward spreadin area.

The allover concentric bending within the upper mantle realizes overturn of the slab. The slab surface contacts with upper surface of lower mantle where upper mantle minerals change phase for higher pressure. The coldest slab surface in the upper mantle could not change the phase, and might float on the surface of lower mantle toward opposit direction of Plate motion. The return flow of the upper mantle, induced by the floating slab surface, might allow the high speed of the largest Pacific Plate motion.

Izu Slab, north extend of Ogasawara Slab, is bending concentrically above ca. 410km of depth and unbending blow the depth as flat slab. The geometry of the shape from Ogasawara Salb to Izu Salb should intercalate discontinuous part of the slab. Nishinoshima erupted in Nobember 2013 on the slab discontinuous part. The forcal mechanisms on the slab discontinuous part change before and after the East Japan Super Erthquake.

Keywords: Ogasawara Slab, Concentric Bending, Mantle Convection, Upper Mantle Bottom, Nishinoshima Eruption

Japan Geoscience Union Meeting 2014
(28 April - 02 May 2014 at Pacifico YOKOHAMA, Kanagawa, Japan)

SSS30-19 Room:Main Hall Time:April 28 16:30-16:45

Rectified tidal loading: Control on earthquakes manifested by deep tremors

IDE, Satoshi[1*] ; TANAKA, Yoshiyuki[2]

[1]Deptartment of Earth and Planetary Science, University of Tokyo, [2]Earthquake Research Institute, University of Tokyo

Earthquakes occur due to plate motion, but it remains unclear as to what controls the plate motion. A clue to this problem is provided by a recently discovered cluster of deep tectonic tremors or tiny earthquakes that are occurring in western Japan. Here we demonstrate that tremor activity is strongly correlated with tide levels observed at a nearby station. The correlation is interpreted as representing a nonlinear relationship between stress and slip, which is similar to the rate-dependent friction law. An empirical relationship and observed tide records explain the temporal changes in tremor activity over a period of nine years. The nonlinear fault rheology rectifies oscillating tidal stress and amplifies small changes in tidal amplitude. This mechanism of rectified tidal loading may control temporal changes in plate motion and earthquake occurrence. Remarkably, the background seismicity in the present study area matches the predicted tremor rate obtained from tidal observations over the past 50 years. This mechanism may also explain the weak periodicity of large earthquakes, and is likely to be helpful in probabilistic forecasting of future seismicity.

Keywords: tremor, tide, rectification, slow slip, seismicity, Nankai earthquakes

Japan Geoscience Union Meeting 2014
(28 April - 02 May 2014 at Pacifico YOKOHAMA, Kanagawa, Japan)

SSS30-20 Room:Main Hall Time:April 28 16:45-17:00

Structural mechanics model of plate-interface fracture at subduction zones

EGUCHI, Takao[1*]

[1]National Defense Academy, Japan

There are unidentified and unveiled properties concerning the physical process of greater inter-plate earthquakes at subduction zones. We, here, present a stochastic fracture model of the plate-interface with dynamic discrete interaction blocks. The stochastic treatment in this study is mainly based on structural mechanics. Here, in the four-dimensional point of view, regarded as significant long-wavelength components of the mechanical inter-plate coupling, we assign several discrete lattice-like blocks being connected each other on a hypothesized plate boundary system. The representative mechanical interaction vector (or tensor) for each discrete block should be variable on the plate boundary system. The total number of the discrete blocks and their nesting pattern should also vary with time during the long-term subduction process with intermittent greater seismic events.

Hereafter, we treat the inter-plate coupling at discrete blocks, using parameters such as failure probability *(Psf)* and safe probability *(Pss)* of the total system of the plate boundary. Here, $Psf + Pss = 1$.

The system fracture for the case of parallel connecting blocks is defined as the breakdown of all parallel blocks. Whereas, for the case of a series connecting block system, the system fracture is defined as the failure of one of the series block, or more. The system failure probability of a simple mechanical system being coupled in parallel N blocks is given as a product of $p(i)$ from $i = 1$ to $i = N$. Here, $p(i)$ is the failure probability of the *i-th* block of the system. For the case of a mechanical system connected in series N blocks, the system safe probability becomes a product of $\{1-p(i)\}$ from $i = 1$ to $i = N$. For a mechanical system composed of both parallel and series blocks, the system failure probability and system safe probability can be estimated with the above definition. Then, we assume that the inter-plate shear coupling of the plate-interface progresses only at discrete blocks of brittle fracture.

We consider two different configuration models for a two-by-four matrix *(2x4)* system of discrete coupling blocks, consist of four columns in the trench-parallel direction and two rows of deep side and a shallow side in the dip direction, as follows.

Configuration model A is a series-connected system of both the shallower parallel-connected column blocks and the deeper parallel-connected ones.

Configuration model B is a parallel-connected system of the four columns of the shallower and deeper rows being directly series-connected in the dip direction.

By setting the failure probability, $p(i,j)$, of *(i,j)-th* block, we can estimate the system failure probability *(Psf)* and system safe probability *(Pss)* for the configuration models, A and B. For the configuration models A and B, the system safe probability, *Pss(A)* and *Pss(B)* can be obtained. In the case of p(i,j) less than 0.5 for all blocks, *Pss(A)* becomes larger than *Pss(B)*, indicating that the configuration model A is safer than the model B. When the representative pattern of the inter-plate coupling changes from the configuration model A to B, or vice versa, we should carefully estimate the system probabilities.

We also demonstrated the detailed hypothetical expression form of p(i,j) by considering the effect of preceding larger seismic ruptures at blocks and the subsequent healing process, etc.

Keywords: subduction zone, inter-plate coupling, structural mechanics, system failure probability, system safe probability

Japan Geoscience Union Meeting 2014
(28 April - 02 May 2014 at Pacifico YOKOHAMA, Kanagawa, Japan)

SSS30-21 Room:Main Hall Time:April 28 17:00-17:15

Seismicity rate variations in subduction zones related to forearc topography

NISHIKAWA, Tomoaki[1*] ; IDE, Satoshi[1]

[1]Department of Earth and Planetary Science, University of Tokyo

There are clear variations in seismicity among subduction zones worldwide in terms of such as the frequency of earthquake occurrence and maximum earthquake magnitude. These variations have been attributed to differences in tectonic properties in subduction zones, such as relative plate velocity and subducting plate buoyancy. For example, Ide [2013] demonstrate proportionality between relative plate velocity and background seismicity rate — the frequency of seismic events excluding aftershocks. Given that earthquakes occur to release strain in the crust accumulated by relative plate motion, we can intuitively understand this proportionality.

The overriding plate is also an important control on earthquake occurrence in subduction zones. Seismological observations and studies of tectonics have suggested the relationship between forearc topography and frictional properties on the plate interface, such as interplate locking and pore fluid pressure. Given this relationship, variations in forearc topography may reflect differences in frictional properties on the plate interface among subduction zones worldwide. However the relation between forearc topography and variations in seismicity among subdcuction zones is still unclear. In this study, we compare forearc slope and background seismicity rate in subduction zones worldwide. The forearc slope is based on Smith and Sandwell [1997], and the background seismicity rate is estimated using the epidemic type aftershock sequence (ETAS) model [Ogata, 1988]. We show the correlation between forearc slope and background seismicity rate. Subduciton zones with steeper forearc slopes have higher seismicity rates. Furthermore, subduction zones that are outliers of the proportionality between relative plate velocity and background seismicity rate [Ide, 2013], such as Cascadia and South Chile trench, also appear to obey this correlation.

According to the critical taper theory [Davis et al., 1983; Dahlen, 1984], which explains the relationship between forearc topography and frictional properties on the plate interface, and sand box experiments [e.g., Gutscher et al., 1996], steep forearc slope is associated with high basal friction. When we take these studies into account, our results suggest that the seismicity rates are high in subduction zones with steep slopes and high basal friction. This can be explained by considering erosion and accretion processes and geometrical irregularities on the plate interface. Erosional margins tend to have steeper forearc slopes [Clift and Vanucchi, 2004]. Because of thin trench sediments in erosional subduciton zones, geometrical irregularities on the subducting plate are not smoothed. Such irregularities may cause high basal friction at the tip of the forearc wedge and steepen the forearc slope. In the seismogenic zone, these irregularities act as numerous small asperities, and these asperities result in many seismic events in the erosional subduction zone. In contrast, accretionary margins generally have gradual slopes. Thick trench sediments smooth subducted seafloor, and it results in low basal friction at the tip of the forearc wedge and the gradual forearc slope. The smoothed plate interface may act as one large asperity in the seismogenic zone, and fewer earthquakes occur in the accretionary subduction zone. Furthermore, these variations in number and size of asperities among subduction zones worldwide may cause differences in megathrust earthquake occurrence.

Our results reveal the relation between forearc topography and seismity, and suggest that the frequency of seismic events in subduction zones is controlled by not only the mechanical factors such as relative plate velocity and the strain accumulated in the crust, but also the material factors such as erosion and accretion processes, trench sediments, and geometrical irregularities on the plate interface.

Keywords: seismicity rate, subduction zone, forearc topography, erosion and accretion, asperity

Japan Geoscience Union Meeting 2014
(28 April - 02 May 2014 at Pacifico YOKOHAMA, Kanagawa, Japan)

SSS30-22 Room:Main Hall Time:April 28 17:15-17:30

Feasibility of acoustic monitoring of strength drop precursory to earthquake occurrence

KAME, Nobuki[1*] ; NAGATA, Kohei[2] ; NAKATANI, Masao[1] ; KUSAKABE, Tetsuya[1]

[1]Earthquake Res. Inst., Univ. of Tokyo, [2]Ministry of Education, Culture, Sports, Science and Technology

Rate- and state-dependent friction law (RSF), proposed on the basis of laboratory experiments, has been extensively applied to modeling of earthquake stick-slip cycles. A simple spring-slider model obeying RSF predicts a significant decrease of the frictional strength Phi (the state of contact) that is localized within a few years preceding the earthquake occurrence. On the other hand, recent laboratory experiments successfully monitored the history of the strength by simultaneously measuring P-wave transmissivity |T|across the frictional interface using a 1MHz transducer. This suggests a possibility of earthquake forecast by monitoring the strength of a natural fault by acoustic methods.

The present paper explores the feasibility of such monitoring in the field on the basis of the physics of RSF combined with the linear slip model (LSM) employed in the classical acoustic methodology for monitoring an imperfectly welded interface. The characteristic frequency f_c, around which |T|(or reflectivity |R|) has a good sensitivity to the interface strength, is shown to be proportional to the strength and inversely proportional to the representative scale of real contacts.For natural faults f_c is estimated to be 1 to 100Hz, which is practicable in the field. The changes of |T|and |R|depend on the ratio of the strength drop to the absolute strength level, the latter of which is not constrained by RSF simulations. Expected changes in wave amplitude in the preslip period would be several percent for strong faults and several tens percent for weak faults, which may be detectable by acoustic methods such as seismic reflection surveys.

Keywords: fault strength, earthquake cycle, rate- and state-dependent friction, precursor, linear slip model, acoustic monitoring

Japan Geoscience Union Meeting 2014
(28 April - 02 May 2014 at Pacifico YOKOHAMA, Kanagawa, Japan)

SSS30-23 Room:Main Hall Time:April 28 17:45-18:00

Semi-quatitative analysis of change in stress state in Chelung-pu Fault, Taiwan

HASHIMOTO, Yoshitaka[1*] ; TOBE, Kota[1] ; YEH, En-chao[2]

[1]Kochi Univerisity, [2]National Taiwan Normal University

Semi-quantitative stress state before and after earthquake in Chelung-pu fault, Taiwan

Stress change caused by earthquake is important to understand size and nature of an earthquake. Detailed waveforms of the 1999 Chi-Chi earthquake were taken along the Chelung-pu fault. In the aftermath of the earthquake, Taiwan Chelungu-pu Fault Drilling Project (TCDP) was conducted to take core with the seismogenic fault. In this study, we estimated paleo-stress condition semi-quantitatively using micro-fault inversion method and stress polygon. Then we discuss the relationship between spatial and temporal changes of stress with seismic cycles.

We used Multiple inversion method (MIM) (Yamaji, 2000) and k-means clustering (Otsubo et al., 2006) to estimate paleo-stress. As a result, we obtained four solutions of stress state (c1-c4) from TCDP core. To estimate the range of stress conditions we used stress polygons on the basis of the Anderson theory of faulting as used in Lin et al. (2007). We projected our paleo-stress orientations to the directions of SHmax, Shmin and SV. In addition to that, using stress ratio and a definition that SHmax is larger than Shmin, we can restrict the stress conditions for the paleo-stress in the stress polygons.

Two stress conditions (c1 and c3) were comparable with that from Lin et al. (2007) as a present state and post-seismic condition in normal stress regime. The range of stress condition for c2 is obviously higher than others, and the stress condition is in revere fault regime. The differences of stress condition possibly indicate the change in stress magnitude in the seismic cycle. Stress drops were estimated as -7.94˜2.60MPa for c1 and c2, and 2.71˜13.68MPa for c2 and c3. The calculated stress drop is comparable with estimated average stress drop from slip distribution in Chi-Chi earthquake (Ma et al. 2000).

Keywords: stress, micro-fault inversion, stress drop, Chelung-pu fault

Japan Geoscience Union Meeting 2014
(28 April - 02 May 2014 at Pacifico YOKOHAMA, Kanagawa, Japan)

SSS30-24 Room:Main Hall Time:April 29 14:15-14:30

Fluid transport property and diagenetic microstructure of chert in the Mino Belt

YAMAGUCHI, Asuka[1*] ; TANIKAWA, Wataru[2] ; KAMEDA, Jun[3] ; SHIMIZU, Mayuko[4] ; HAMADA, Yohei[5] ; KIMURA, Gaku[4]

[1]Atmosphere and Ocean Research Institute, the University of Tokyo, [2]JAMSTEC/Kochi, [3]Graduate School of Science, Hokkaido University, [4]Department of Earth and Planetary Science, the University of Tokyo, [5]JAMSTEC/IFREE

Pore fluid pressure along plate boundary megathrust is controlled by both fluid supply and fluid transport property, and it affects on faulting and earthquake mechanics. In the case of subduction zones where relatively old (older than 50 m.y. in age) oceanic plate subducts, oceanic crust is covered with thick pelagic siliceous sediments composed of diatomic and/or radiolarian oozes. In the Japan Trench, Kimura et al. (2012) pointed out that the volume of dehydrated fluid during silica diagenesis from opal-A to quartz through opal-CT is significant compared to that from clay mineral (smectite-illite) transition. However, fluid transport property of siliceous sediments has not been well-understood yet. In this study we conducted both permeability measurement and microstructural/microchemical observation of bedded chert from Inuyama-section in the Mino belt, Jurassic accretionary complex in Japan, as an on-land analog of subduction zone where old oceanic plate subducts.

Initial porosity of chert samples at atmospheric pressure is 0.4 to 2.2 %. Permeability was measured at room temperature under isostatic confining pressures of 5 to 120 MPa, by the steady state flow method with nitrogen gas as a pore fluid. Water permeability was then obtained by using Klinkenberg equation. At effective pressure of 5 MPa converted water permeability is 10^{-17} to 10^{-19} m^2, decreases with increasing effective pressure down to the ranges of 10^{-20} to10^{-21} m^2.

Optical and electron probe microanalyzer (EPMA) analyses show that chert is composed of radiolarian fossils filled with quartz and chalcedony, and red-colored matrix. Red matrix shows ˜95 wt.% of SiO_2, whereas >99 wt.% of SiO_2 are commonly observed from inside part of the radiolarian fossils. Such high concentration of SiO_2 within radiolarian fossils indicates that dissolved silica was precipitated into cavities maintained by radiolarian tests. This process would be related with silica diagenesis, occurring as dissolution-precipitation processes.

Silica mineral precipitation onto pore spaces would contribute to construct characteristic low porosity and permeability of chert. Our result shows that silica diagenesis works as not only a fluid source but also as a process for porosity/permeability reduction in convergent margins characterized by old subducting oceanic plate.

Keywords: subduction zone, diagenesis, permeability, chert

Japan Geoscience Union Meeting 2014
(28 April - 02 May 2014 at Pacifico YOKOHAMA, Kanagawa, Japan)

SSS30-25 Room:Main Hall Time:April 29 14:30-14:45

Mechanical properties of the shallow Nankai Trough accretionary sediments

KANAGAWA, Kyuichi[1*] ; TAKAHASHI, Miki[2] ; AZUMA, Shuhei[1] ; ITO, Hidenori[1] ; INOUE, Atsuyuki[1]

[1]Graduate School of Science, Chiba University, [2]Active Fault and Earthquake Research Center, Geological Survey of Japan

We report the results of triaxial compression and friction experiments of clayey mudstone, silty mudstone, sandstone and tuff samples, which are cored from the shallow (1000-1500 mbsf) Nankai Trough accretionary prism at IODP Sites C0002 and C0009, at room temperature, and confining pressures and pore water pressures close to their in situ conditions.

Triaxial compression experiments at these conditions and an axial displacement rate of 10 μm/s reveal that the failure strength is ≈300 MPa for a sandstone sample, ≈48 MPa for a tuff sample, ≈20 MPa for a silty mudstone sample, and ≈14 MPa for a clayey mudstone sample. The sandtone, tuff and silty mudstone samples failed relatively rapidly within 20 s, while the clayey mudstone sample failed slowly for ≈40 s. Another silty mudstone sample did not fail, and deformed ductilely at a strength of ≈15 MPa. The sandstone sample is strongly lithified by being cemented by calcite, which makes this sample's failure strength very high. The ductilely deformed silty mudstone sample seems not lithified enough to fail. A probable increase in pore pressure during compression of the clayey mudstone sample due to its low porosity (≈11 %) and permeability (≈10^{-19} m^2) in addition to its intrinsic weakness due to the abundance of clay minerals (≈42 wt%) likely makes this sample weak and promotes its slow failure. Such failure in clayey mudstone is a possible source for slow slip events observed in the shallow Nankai Trough accretionary prism.

Friction experiments at these conditions and axial displacement rates changed stepwise among 0.1, 1 and 10 μm/s reveal that frictional properties of these samples change systematically according to the content of clay minerals. The content of clay minerals is ≈6 wt% in the sandstone sample, ≈17 wt% in the tuff sample, 29-34 wt% in the silty mudstone samples, and ≈42 wt% in the clayey mudstone sample. Steady-state friction coefficient at the axial displacement rate of 1 μm/s decreases with increasing content of clay minerals, from 0.87 of the sandstone sample, through 0.71 of the tuff sample and 0.53-0.56 of the silty mudstone samples, to 0.25 of the clayey mudstone sample. Slip-dependent frictional behavior also changes from slip hardening to slip weakening with increasing content of clay minerals. Although all samples exhibit velocity-strengthening behavior upon stepwise changes in sliding velocity, the ratio of $(a - b)$ value to the velocity dependence of steady-state friction decreases with increasing content of clay minerals, which implies that the friction component decreases while the flow component increases accordingly. Thus, faulting in the shallow Nankai Trough accretionary prism is likely controlled by the content of clay minerals in sediments as well as in fault zones.

Keywords: Nankai Trough, accretionary sediments, failure properties, frictional properties

Japan Geoscience Union Meeting 2014
(28 April - 02 May 2014 at Pacifico YOKOHAMA, Kanagawa, Japan)

SSS30-26 Room:Main Hall Time:April 29 14:45-15:00

Velocity weakening behavior observed for friction of the shallow subduction zone fault material

TSUTSUMI, Akito[1*] ; NAMIKI, Yuka[1] ; NAKANO, Ryuji[1] ; KAWAI, Tomoaki[1]

[1]Division of Earth and Planetary Sciences, Graduate School of Science, Kyoto University

Recent observations of slow earthquakes along faults within shallow part of subduction zones, for example the very low frequency earthquakes at the Nankai Trough [Ito and Obara, 2006; Sugioka et al., 2012], has demonstrated that faulting there is slow yet seismic; suggesting that frictional velocity dependence along the fault at the shallow portion must be negative. However, previous experimental results have repeatedly shown that velocity dependence of the expected fault zone material is generally estimated to be positive. Here, we present our recent experimental results showing that velocity dependence of the friction of the shallow subduction zone faults are not necessarily be positive.

We have performed a series of rotary-shear large displacement (>150 mm) friction experiments on the following shallow fault simulating material: clayey fault material form the shallow megasplay fault zone within the Nankai accretionary prism, input pelagic siliceous to calcareous sediments to the Costa Rica subduction zone, and simulated artificial gouge of montmorillonite/quartz mixtures (20-40 wt% of montmorillonite). Experimental results reveal that these material do exhibit velocity weakening behavior at a range of velocities from 0.003-0.3 mm/s. Velocity weakening of these material is mostly characterized by a small degree of the friction velocity dependence (the absolute value of (a-b) is typically <0.005.

The SSEs are often described as conditionally stable sliding of faults [e.g., Shelly et al., 2006]. High pore fluid pressure could alter a velocity-weakening fault with a small value of (a-b) to conditionally stable regions by reducing the effective normal stress [Scholz, 1998]. The presented velocity weakening property with a small value of (a-b) could be responsible for generating shallow slow seismic slip events in subduction zones. Textural observation reveals the importance of studying effects of both the clay content and shear-induced deformation textures on the frictional velocity dependence.

Keywords: Nankai Trough, subduction zone, frictional velocity dependence, slow earthquakes

Japan Geoscience Union Meeting 2014
(28 April - 02 May 2014 at Pacifico YOKOHAMA, Kanagawa, Japan)

SSS30-27 Room:Main Hall Time:April 29 15:00-15:15

Frictional properties of simulated faults containing amorphous silica/calcite mixtures

NAMIKI, Yuka[1*] ; TSUTSUMI, Akito[1]

[1]Graduate School of Science, Kyoto University

Various seismic behaviors such as large earthquakes, episodic slow slip events, or silent earthquakes are observed in subduction zones. Knowledge of the frictional properties of input material to subduction zones would help to understand the complicated seismic behaviors. On the Cocos plate, which subducts beneath the Caribbean Plate at Middle America Trench offshore Costa Rica, input sediments containing clay, silty clay sediments and silicic to calcareous ooze were collected during the IODP expedition 334. We have been studying the frictional properties of the collected input material to the Costa Rica subduction zone. In order to better understand frictional processes of a fault in silicic to calcareous ooze, we have performed a series of friction experiments on a simulated fault gouge containing mixtures of amorphous silica and calcite.

Frictional experiments were performed at a constant slip velocity of v = 0.28 mm/s, and also under a velocity-stepping condition. The silicic to calcareous ooze sample showed the following characteristic behavior. The friction coefficients at 0.28 mm/s showed initial peaks at 0.4?0.6 and subsequent little decrease, followed by a gradual increase to attain a constant friction value at 0.6?0.8. The analogue gouge containing 40?80 wt% of calcite reproduced such frictional behavior well. The experimental samples of the input ooze material required only about 40 mm of displacement to attain constant steady-state friction level. However, the calcite/amorphous silica mixtures needed larger displacement to attain steady-state friction. Furthermore, the calcite/amorphous silica mixtures could not reproduce friction velocity dependence observed for the collected ooze samples. The result suggests the importance of studying effects of grain size distribution and the grain morphologies on the frictional properties of the silicic to calcareous ooze material.

Keywords: subduction zone, frictional experiment, CRISP

Japan Geoscience Union Meeting 2014
(28 April - 02 May 2014 at Pacifico YOKOHAMA, Kanagawa, Japan)

SSS30-28 Room:Main Hall Time:April 29 15:15-15:30

Effect of temperature on frictional behavior of smectite and illite: Implication for the updip limit for seismogenic zon

KUBO, Tatsuro[1*] ; KATAYAMA, Ikuo[1]

[1]Department of Earth and Planetary Systems Science, Hiroshima Univercity

Introduction: Along plate boundary subduction thrusts, the transformation of smectite to illite within fault gouge at temperatures of ˜150C is one of the key mineralogical changes thought to control the updip limit of seismicity. Saffer and Marone (2003) reported illite shale exhibited only velocity-strengthening behavior, opposite to the widely expected, potentially unstable velocity-weakening behavior of illite. They concluded transformation of smectite to illite is not responsible for the seismic-aseismic transition in the updip limit of subduction zones. However, their experiments were limited at room temperature although the updip limit of seismogenic zone is thermally controlled that occurs at temperature around 150oC. Therefore, in this study, we determined the effect of temperature of frictional properties of smectite and illite and discuss whether the smectite-illite transition accounts for the updip limit of seismogenic zone along subduction thrust.

Experimental methods: Frictional experiments were performed using a biaxial frictional testing machine at Hiroshima University. The powder materials of clays were placed on the simulated fault surface and two side blocks were placed together to produce a double-direct shear configuration. Normal stress was applied via a hydraulic ram on the side block with 15, 40, 60 MPa, and then, shear stress was applied by advancing the central block downward at a constant velocity. The sample assembly was heated by an external furnace up to 200oC that is monitored by thermocouples located close to the central block. Mechanical data were recorded continuously with a sampling rate of 10 Hz and the frictional coefficient was calculated from the shear force divided by the normal force assuming zero cohesion.

In the frictional experiments, we determined the velocity dependence of sliding friction, which is a key parameter for stable or unstable sliding (e.g., Dieterich, 1979). After steady-state sliding, the loading velocity of 3 μm/s was abruptly changed to 30 μm/s in each frictional experiments to determine the velocity dependence of these clay minerals. We calculated the velocity dependence of sliding friction as follow:

$$(a-b)=d\mu(d \ln V)$$

where a,b is the frictional parameter and V is sliding velocity. The velocity dependence is important to show seismic slip, in which negative values of (a-b) reflect velocity-weakening behavior, whereas positive values of (a-b) reflect velocity-strengthening behavior and thence stable (aseismic) sliding.

Results and Discussion: In comparison of steady-state fictional strength of clay minerals, the value of frictional strength of smectite is nearly half as large as that of illite. The effect of temperature on the frictional strength is rather weak, and the steady state friction is slightly increased at high temperatures. Our results suggest that the shear stress required to initiate sliding is much lower for smectite than illite, and smectite could not accumulate much strain energy.

The velocity dependence at room temperature shows always positive at normal stress higher than 40 MPa, which is similar to the results of Saffer and Marone (2003). However, at temperature of 200C, illite shows negative values of (a-b), suggesting that illite exhibits unstable velocity-weakening behavior. This results explains smectite is potentially aseismic for stable sliding at the subduction thrust, whereas illite becomes seismic due to a negative velocity dependence and unstable sliding at high temperatures. These experimental results indicate that the smectite-illite transition potentially account for the updip limit of seismogenic zone along subduction thrust, which is opposite to the previous results at room temperature.

Keywords: updip limit, smectite-illite transformation, effect of temperature, velocity dependence

Japan Geoscience Union Meeting 2014
(28 April - 02 May 2014 at Pacifico YOKOHAMA, Kanagawa, Japan)

SSS30-29 Room:Main Hall Time:April 29 15:30-15:45

Frictional properties of basalt-derived fault rocks and implications for subduction earthquakes

SAITO, Tsubasa[1*] ; UJIIE, Kohtaro[1] ; TSUTSUMI, Akito[2]

[1]Life and Env. Sci., Univ., Tsukuba, [2]Sci., Kyoto Univ.

Recent seismic reflection surveys in subduction zones such as Nankai Trough suggest that subduction earthquakes mostly occurred along the upper part of oceanic crust composed of basaltic rocks (e.g., Bangs et al., 2009). Hence, frictional properties of basalt appear to be keys for understanding earthquake nucleation and rupture propagation during subduction earthquakes, yet they remain poorly understood. In the Upper Shimanto accretionary complex of eastern Shikoku, basalt and tectonic melange are repeated by thrusts, representing duplex structure associated with underplating (Ikesawa et al., 2005). Underplating-related thrusts develop in basalt and consist of basalt-derived foliated cataclasite and ultracataclasite. Fluidization of comminuted material and mineralogical signatures of frictional heating were reported from a few centimeters-thick ultracataclasite (Ujiie et al., 2007; 2008; Kameda et al., 2011). We examined the frictional velocity dependence at slip rates of 0.0028-0.28 mm/s and high-velocity (1.3 m/s) frictional properties of disaggregated pillow basalt and basalt-derived foliated cataclasite and ultracataclasite. The samples from pillow basalt show velocity-weakening behavior, while those from foliated cataclasite and ultracataclasite exhibit velocity-strengthening behavior. All samples show slip weakening behavior during high-velocity friction experiments, with the samples from ultracataclasite marked by smaller stress drop, slip weakening distance, and fracture energy. The compositions of materials and preliminary microstructural observations suggest that velocity-weakening samples show lower clay content (21 wt.%) and grain-size reduction, while velocity-strengthening samples exhibit relatively high clay content (29-50 wt.%) and clay foliations. Our results suggest that earthquake nucleation likely occurs in subducting basalt, but slip tends to be stable when clays and clay fabrics are formed by hydrothermal alteration and shear deformation, respectively. The results of high-velocity friction tests suggest that earthquake rupture propagates easily through ultracataclasite rather than foliated cataclasite and pillow basalt, which is consistent with the fact that the geological evidence of earthquake faulting was found from the ultracataclasite.

Keywords: subduction earthquakes, basalt, frictional velocity dependence, high velocity friction

Japan Geoscience Union Meeting 2014
(28 April - 02 May 2014 at Pacifico YOKOHAMA, Kanagawa, Japan)

SSS30-30 Room:Main Hall Time:April 29 15:45-16:00

Amorphization of clay minerals by wet and dry grinding

FUJIMOTO, Koichiro[1*] ; FUKUCHI, Rina[2]

[1]Tokyo Gakugei University, [2]Tokyo University

Nanoparticles in fault zones are recently paid much attention since they give significant influences on the frictional properties (Ma et al., 2006). Nanoparticles are considered to be formed not only by mechanical grinding but also by mechanochemical processes. Amorphous nanoparticles were found in Iida-Matsukawa fault, Central Japan (Ozawa and Takizawa, 2007). It is well known that clay minerals are easily transformed into amorphous phase by mechanochemical processes. We conducted pulverization experiments of some clay minerals under both dry and wet conditions to clarify the characteristics of the pulverized materials and the mechanism of amorphization.

We used kaolinite saponite and sericite as starting materials. Pulverization experiments were conducted using planetary ball mill and characterization of run products were conducted by XRD, FT-IR, TG-DTA and FE-SEM. Three minerals were completely transformed into amorphous materials by dry grinding. XRD peaks were weakened but still remain after one day wet drying as for kaolinite and sericite. On the contrary, as for saponite, XRD peaks do not show remarkable change under wet condition. Probably amorphization rate is reduced because impact energy in the ball mill is decreased in the presence of water. Presence of interlayer water affects on the behavior of saponite.

Keywords: clay minerals, kaolinite, sericite, saponite, amorphous

Japan Geoscience Union Meeting 2014
(28 April - 02 May 2014 at Pacifico YOKOHAMA, Kanagawa, Japan)

SSS30-31 Room:Main Hall Time:April 29 16:15-16:30

Fluid inclusion as fossil fluid in seismogenic zone, trap mechanism and interpretations for fault science

SAKAGUCHI, Arito[1*] ; YANAGISAWA, Kazumichi[2]

[1]Yamaguchi Univ./JAMSTEC, [2]Kochi Univ.

A fluid inclusion, fluid-fill capsule within rigid crystal, preserves density and chemical composition of fluid in deep crust. This records pressure, temperature and other information of the fluid when the fluid trapped. Pore fluid pressure drop due to rapid fluid ejection along the fault was discussed in Kodiak accretionary complex (Vrolijk et al., 1988). CH4-H2O fluid inclusions are reported at pseudotachylyte bearing Nobeoka Thrust, Shimanto accretionary complex (Kondo et al., 2005). Thermal stretching of fluid inclusions due to seismic frictional heating were found at seismogenic Mugi Melange, Shimanto accretionary complex (Ujiie et al., 2008). Though fluid inclusion tells us fluid condition in deep crust, trapping mechanism within crystal is still uncertain. The fluid inclusion is one of crystallographic defect, but general size from sub-micron meter to several mm is much greater than crystal lattice. A crystal tend to growth without large defect, and it seems irregular process to be formed a fluid inclusion. The trap mechanism is significant to interpret the fluid inclusion data.

We succeeded to make artificial fluid inclusion in calcite during hydrothermal experiment. A calcite crystals are nucleated and grown with temperature decrease in autoclave. Fluid inclusions were never formed in simple cooling procedure, but many large fluid inclusions were found at the overgrowth zone formed by re-heating process. Surface condition of artificial calcite of re-heating and overgrowth process were observed using SEM. Etched pattern covers the surface of re-heated calcite crystal. Some depressions are wide shallow and others are small deep. Many growth steps were found on surface of over-growth calcite. The calcite surface may have been advanced with lateral motion of growth steps. This growth step covers most of the etched depressions except small deep one. These small deep depressions are surrounded by new grown surface and became increasingly deep. Some depressions may make large pore within overgrowth zone in this process.

This observation shows that the fluid inclusion were made during overgrowth after surface etching, and this requires temporary solubility change in crystal growth process. The fluid inclusions may record pore-fluid condition after the event of pressure, temperature and/or chemical change in deep crust.

Keywords: Fluid inclusion, trap mechanism, artificial calcite

Japan Geoscience Union Meeting 2014
(28 April - 02 May 2014 at Pacifico YOKOHAMA, Kanagawa, Japan)

SSS30-32 Room:Main Hall Time:April 29 16:30-16:45

New fluid flow mechanism at seismogenic depth in subduction zone

TAKE, Kotaro[1*]

[1]Dept. of Geosphere. Yamaguchi Univ.

Since pore fluid pressure may concern with seismogenesis, large amount of articles are published for fluid flow research, and -previous researches have been focused only crack flow in deep crust. In general, a pore between sedimentary grain decreases with depth, and fluid flows only within crack in deep crust. This study shows new fluid flow mechanism that doesn't depend on crack in the rocks. This produces new perspective of fluid flow of seismogenic depth in subduction zone.

The Shimanto accretionary complex at SW-Japan, formed at seismogenic depth suffers pressure solution deformation and generally includes brittle failure of web structure and crack-filled veins. The carbonate matrix is lacked in the sediments due to deposition below CCD.

Some sandstones in the late Cretaceous Nonokawa Formation, includes spotted carbonate deposit. This carbonate deposit occurs limited area less than several meters square within sandy layer without crack-filled vein. Microscopic observation shows following features as below.

The spotted carbonate minerals overprint with embayment structure in pressure-solution deformed sandy grains, and these are cut by web structure and crack-filled veins. The fluid may have dissolved the sandy grains, and carbonate minerals were deposited at latest stage of lithification process between pressure solution deformation and brittle failure. These occurrences suggest that fluid can flow with dissolution of rock-forming grains in rigid crust without crack.

Keywords: fluid flow, accretionary complex

Japan Geoscience Union Meeting 2014
(28 April - 02 May 2014 at Pacifico YOKOHAMA, Kanagawa, Japan)

SSS30-33 Room:Main Hall Time:April 29 16:45-17:00

Generation of high-temperature fluid and its spatial distribution in an ancient megasplay fault

MASUMOTO, Hirokazu[1*] ; HIRONO, Tetsuro[1] ; ISHIKAWA, Tsuyoshi[2] ; TANIKAWA, Wataru[2] ; MUKOYOSHI, Hideki[3]

[1]Department of Earth and Space Science, Graduate School of Science, Osaka University, [2]Kochi Institute for Core Sample Research, Japan Agency for Marine-Earth Science and Technology, [3]Faculty of Education and Integrated Arts and Sciences, Waseda University

An ancient megasplay fault outcrop is identified within Kure region of the Shimanto accretionary complex and has been formed at 2.5 – 5.5 km depth. Recent works show pseudotachylyte produced by frictional melt, fluid-rock interactions at high temperatures (>350 ℃) and enrichment of incompatible element concentrations on the fault. However, spatial distribution of pseudotachylyte and high-temperature fluid is not investigated. These informations are important to understand an earthquake is able to produce extensively high-temperature fluid and thermal pressurization. Accordingly, we performed deformation structures analysis and obtained 46 rock samples from the outcrop and analyzed these samples by vitrinite reflectance measurement, powder X-ray diffraction-RockJock mineral composition analyses and trace elements compositions measurement. Therefore, analyses of black gouge samples from the slip zone indicate fluid-rock interactions at high temperatures, whereas footwall sandstone samples that are close to fault gouge indicate enrichment of quartz and decrease of rare-earth element concentrations. These contrasts may be regarded as mobilization of elements derived from seepage of yielded high temperatures fluid within the slip zone.

Keywords: Nankai trough, megasplay fault, Shimanto accretionary complex, fault rocks, fluid-rock interactions, X-ray diffraction

Japan Geoscience Union Meeting 2014
(28 April - 02 May 2014 at Pacifico YOKOHAMA, Kanagawa, Japan)

SSS30-34 Room:Main Hall Time:April 29 17:00-17:15

Multiple damage zone system of an exhumed subduction zone megasplay fault

HAMAHASHI, Mari[1*] ; KAWASAKI, Ryoji[1] ; FUKUCHI, Rina[1] ; SAITO, Saneatsu[2] ; HASHIMOTO, Yoshitaka[3] ; HAMADA, Yohei[2] ; KITAMURA, Yujin[4] ; YAMAGUCHI, Asuka[1] ; KIMURA, Gaku[1]

[1]The University of Tokyo, [2]Japan Agency for Marine-Earth Science and Technology, [3]Kochi University, [4]Kagoshima University

More than 90% of the major earthquakes and tsunamis are known to occur at plate convergent margins, along plate boundary faults and megasplay faults. Investigating the mechanical properties and deformation patterns of these megathrusts are important to understand the generation of earthquakes and the dynamics on the subduction plate interface. Large displacement faults contribute to the reduction of steady-state strength at mid-crustal levels, and cause the frictional-viscous deformation at depth. As the candidate for such weak faults, foliated, phyllosilicate-rich fault rocks have been prevalently recognized in many tectonic settings. However, whether foliated fault rocks behave as weak structures in the longer terms and their roles in the strain localization and fault evolution, are poorly understood.

Exhumed fault zones are helpful to constrain fault strength and deformation process of foliated cataclasites formed at upper-midcrustal depths over geological time. One of the well-studied exhumed major fault zones in subduction settings is the Nobeoka Thrust, a fossilized megasplay fault in Kyushu Shimanto Belt, southwest Japan, which exposes foliated fault rocks that were formed under the temperature range of ~180-350 ℃ (Kondo et al., 2005). During the Nobeoka Thrust Drilling Project in 2011, core samples were retrieved containing both consolidated fault rocks and less consolidated, brecciated fault rocks, preserved from surface weathering and less likely to be drilling-induced. The core samples are expected to provide a different aspect on fault rock strength from previous geological studies on exposed, consolidated outcrops. In the current study, given the unique opportunity to determine the coexistence of cohesive and less cohesive fault rocks in a single fault system, we conduct macroscopic and microscopic structural observation and physical property measurements on the core samples, synthesizing with geophysical logs obtained from the drilling of the Nobeoka Thrust to characterize the damage zone architecture of the fault rocks formed in the frictional-viscous regime along the megasplay fault.

The hanging wall consists of the shale-dominant intervals of dense development of phyllitic cleavages, the sandstone-dominant intervals of disturbed foliations, and the damage zone above the fault core characterized by cataclastically broken phyllite with thick abundant sandstone blocks. The observed density of brittle fractures, breccias, and mineral veins is increased at the sandstone-dominant intervals and near the fault core, whereas brecciated and less brittle/ductile structures are abundant within the shale dominant intervals. The brittle deformation near the fault core may have caused the wearing away of the shale-rich zones by abrasion, and as a result, the sandstone-rich zones that have relatively larger strength, remained and deformed cataclastically near the fault core. On the other hand, the footwall in the drilled range consists of six sets of fracture zones, all of which include a ”brecciated zone” intensively broken in the center, sandwiched by a ”surrounding damage zone” with abundant cohesive faults, mineral veins, and sandstone blocks. The surrounding damage zone is characterized by the increase in fault and fractures with distance from the fault core, and interestingly associate with the increase in resistivity, P-wave velocity, and density and decrease in porosity. The deformation in the surrounding damage zone is inferred to occur in a strain-hardening manner, strengthening with distance from the fault core. Shear localization may initiate more easily in the sandstone-rich area later forming the surrounding damage zone, and eventually develop an intensively deformed fault core in the center. These insights would enable to reinterpret the deformation processes and weakening mechanisms that occur in foliated fault rocks along the megathrust in subduction zones.

Keywords: subduction zone, megasplay fault, physical property of rock, damage zone, structural observation, rock deformation

Japan Geoscience Union Meeting 2014
(28 April - 02 May 2014 at Pacifico YOKOHAMA, Kanagawa, Japan)

SSS30-35 Room:Main Hall Time:April 29 17:15-17:30

Damaged coasts of the tsunami of the Enpo Boso-Oki Earthquake of November 7, 1677

YANUMA, Takashi[1*] ; TSUJI, Yoshinobu[2] ; HIRAHATA, Takenori[1] ; MABUCHI, Yukio[3] ; OOIE, Takayuki[3] ; OKADA, Kiyohiro[3] ; IMAI, Kentaro[4] ; IWABUCHI, Yoko[5] ; IMAMURA, Fumihiko[4]

[1]Pasco., [2]Fukada Geolog. Inst., [3]Pacific Consultant, [4]IRIDeS, Tohoku Univ., [5]JNES

The Enpo Boso-Oki earthquake of November 7th, 1677 occurred in the sea area of the south east offing of Boso peninsula, Kanto district, Central Japan. The shaking of the earthquake was weak, and no damage occurred due to the shaking. The shaking was felt only on the Boso Peninsula and at Edo (Tokyo). Though the shaking was small, but a huge tsunami hit the coasts of Boso peninsula, and north to Iwanuma city about 20 kilometers south of Sendai. Detailed house and human damage was recorded in "Gyokuro-So", one of the fundamental chronologies of the Tokugawa Government. In Katsuura city on the coast of Boso Peninsula, at Kawazu, Sawakura, and at Shinga villages 47 houses were destroyed, and 7 people were killed in total. Inundation heights of the tsunami at those three villages are estimated at 8.0, 8.5 and 6.3 meters, respectively. At Onjuku fishery village, 30 houses were destroyed and 57 people were killed, and tsunami height was estimated at 9.7 meters. At Yasahido village, where total number of houses was about 30, 25 houses were swept away and 13 people were killed, and tsunami height was 12.8 meters. In Choshi city, sea water rushed into Obata Ike pond. We measure the height of the saddle point separating the pond from the open sea, and we found out that tsunami height was 13.5 meters there. The tsunami height at Iwaki City, Fukushima Prefecture was 4.8 to 6.9 meters. On Hachijo Island, about 300 kilometers south of Tokyo, the residential area of Yato behind Yaene port was flooded by sea water and the inundation height is estimated at about 10 meters. The tsunami wave affected west to Ise Bay, Nagoya City. At Utsumi port in Minamichita town about 25 ships were wrecked due to the tsunami. Tsunami also recorded at Owase city on the south east coast of Kii peninsula. The authors of the present study wish to express their thanks to JNES for its financial support in promoting our research.

Keywords: historical earthquake, historical tsunami, the 1677 Boso-Oki earthquake, metropolotan area, Ise bay, Kii peninsula

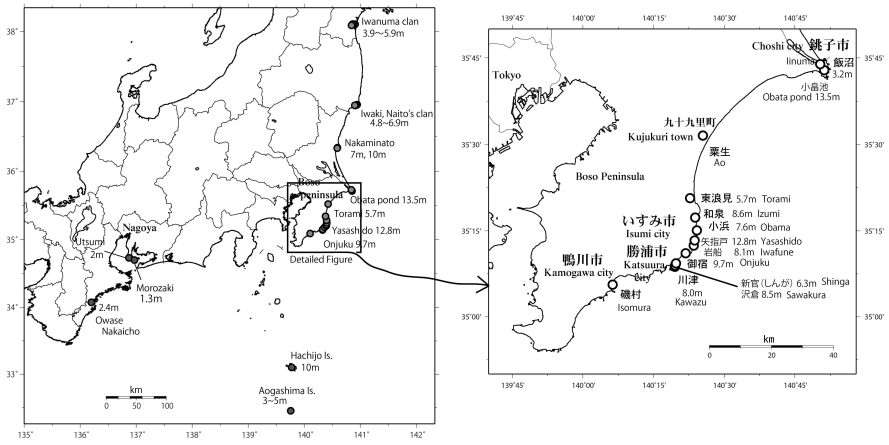

Japan Geoscience Union Meeting 2014
(28 April - 02 May 2014 at Pacifico YOKOHAMA, Kanagawa, Japan)

SSS30-36 Room:Main Hall Time:April 29 17:30-17:45

Crustal movement associated with the 1703 Genroku earthquake

NAKANISHI, Ichiro[1*]

[1]Dept. Geophysics Kyoto University

We analyzed historical documents on the 1703 Genroku earthquake to estimate the crustal movement associated with the earthquake in the Tokyo Bay area, central Japan.

Keywords: 1703 Genroku earthquake, Tokyo Bay, crustal movement

Japan Geoscience Union Meeting 2014
(28 April - 02 May 2014 at Pacifico YOKOHAMA, Kanagawa, Japan)

SSS30-37 Room:Main Hall Time:April 29 17:45-18:00

A Reproduction of 1707 Hoei Tsunami with long rupture duration, referring to 2011 East Japan Pacific Ocean Earthquake

MATSU'URA, Ritsuko S.[1*] ; ANJU, Akira[2] ; SHOJI, Masahiro[2]

[1]ADEP, ERC, [2]Kozo Keikaku Engineering Inc.

Hoei earthquake in 1707 was the largest earthquake in the Edo period that gave the tsunami damage to a wide area along the Pacific Ocean, from the Izu Peninsula to the Southwest Japan. It was assumed that in Hoei earthquake, the source areas of Ansei Tokai and Nankai earthquakes ruptured subsequently within a very short time [e.g. Usami (2003)], or the source areas of the two earthquakes of Ansei were broken at a time [e.g. Ishibashi (2004)]. However, the recent detailed study of historical records revealed that the crustal deformation and the seismic intensity distribution tell that the western and eastern margins of the Hoei source region did not overlap with the two earthquakes in Ansei [e.g. Matsu'ura (2012)]. Hoei earthquake was the exceptionally huge earthquake, which should be called "Western Japan Pacific Ocean Earthquake" in Edo period.

In order to explain very high tsunami of Hoei in the Western Japan, Aida (1981) set the doubled slip to the source area off the cape Ashizuri. Furumura et al. (2011) even expanded the source area further west towards Kyushu. However, their models cannot match the intensity distribution in Kyushu and arrival times of tsunami to villages along the east coast of Kyushu. We suspect that the commonly used tsunami simulation method does not work for a M9-class huge tsunami like Hoei. The theoretical calculation program of crustal deformation of a rectangular fault in a semi-infinite medium [e.g. Sato and Matsu'ura (1973)], which is widely used for the tsunami simulation, inevitably produces singular margins. When the source area was huge, the singularity should affect coastal areas. When the shallow part near the trench is included in the source area, using the same elastic constants as the deeper part should result in an unrealistic deformation solution for a tsunami simulation.

To avoid these limits to applications of the theory used, we put aside obtaining crustal deformation of the sea floor from a dislocation source model, and calculate tsunami from the model of sea floor upheaval and subsidence, which evolve in time. For a test, we first examine the case of the East Japan Pacific Ocean Earthquake of 2011. In order to avoid the detailed topography along coasts, we only used data from GPS buoys and pressure gauges located offshore. We used the ocean bottom upheaval and subsidence obtained by Saito et al. (2011) as the final crustal deformation of the 2011 huge quake. From the known epicenter, the deformation spreads gradually, with the intermittent of 20 seconds, which was observed by GPS as the stop of movement. Paying the attention for the physical plausibility, the movement starts when the rupture reaches, and continues moving until the rupture reaches the edge of a source area. Since the small smooth subsidence spreads over wide area around the major large upheaval area in Saito's model, most tsunami waveform features were reproduced only from the major upheaval area and the smaller upheaval zone protruding toward Japan Trench.

Then we did for Hoei tsunami. As the source of upheaval, we use the source region proposed by Matsu'ura et al. (2011). The topography in Hoei period, we stripped down claimed lands like the islands of Kansai International airport, and Tenpozan, which are apparently made after Hoei period. We also increased the depth of Sakai port, which had been buried by depositions carried by Yamato River since 1704. Examining tsunami for two cases of hypocenter, one at the east end of the source area near Zenisu, and the other at Kumano-nada, we realized that it is impossible to distinguish a hypocenter from limited tsunami information obtained for historical earthquakes. Even with our rough model, Hoei tsunami can go up to canals in Osaka and in the Lake Ryujin in Hazako, Oita. Our experience tells that we shall leverage the recent high power of ordinary computers for a tsunami simulation and molt to go beyond the 40-year-old theoretical crustal deformation.

Keywords: Hoei Earthquake in 1707, East Japan Pacific Ocean Earthquake in 2011, rectangular source fault model, huge tsunami, historical earthquakes

Japan Geoscience Union Meeting 2014
(28 April - 02 May 2014 at Pacifico YOKOHAMA, Kanagawa, Japan)

SSS30-P01 Room:Poster Time:April 29 18:15-19:30

Close examination of universality of matter off Miyagi that earthquakes advanced toward the east

MASE, Hirofumi[1*]

[1]none

I explained how the surrounding of the plate boundary is always compressed(1). I reproduced the Off-Miyagi by the easy experiment(2). I understood earthquakes off Miyagi gradually climbed the slope of the plate boundary. The head within range where small earthquakes occur advanced toward the east gradually and went beyond the hypocenter of 3.11 in November, 2010.(3)

Therefore, the model of off Miyagi is the following. The earthquake of M7 class occurs in several decades by one degree. In every case the hypocenter of it moves east. And, the rear side of it slips to a deep point. The moderate quake guides the earthquake of M7. And, the front of crack is formed. Slip-all-together occurs if the front of crack arrives at a proper place. The feature of this model is to be able to give the answer to the following three large problems at a time. (a)A lot of people think that it is generated repeatedly within the specific range. (b)The cause of the swerve that causes large slip in every case is not discovered. (c)Finally happening is that a shallow part is destroyed at a time.

I want to think about (IC)Off Iwate-Chubu,(IH)Off Iwate-Hokubu,(AT)Off Aomori-Toho,(TK)Off Tokachi referring to (MY)Off Miyagi(Fig.1). The 1968 Tokachi-oki earthquake and the 1994 Sanriku-Haruka-Oki earthquake occurred in (IH)(AT). The co-seismic slip distributions on the map of (4) is interesting. Though the rupture starting point and the main rupture zone can be understood of those relation of upper-lower part on slope, both are considerably away. This is a feature and it is necessary to be clarified. I interpret that a main rupture zone is the peak of slip nearest the trench. The 1968 earthquake has two large slip zone. The main rupture zone in the south is located in lower part of the main rupture zone of the 1994 earthquake on slope. I want to pay attention to that. I think the 1968 earthquake went with the earthquake that had to happen ahead of the 1994 earthquake. The earthquakes that occurred in the vicinity in the past(5) have the possibility that there were rupture zones in lower part of the 1968 earthquake or the earthquake that had to happen ahead of the 1994 earthquake on slope. Therefore, I think that (IH)(AT) walks on the road similar to (MY). And, that a shallow part can slips and timing is only waited for. We should think that the earthquake similarly climbs the slope also in region (TK).

Range (39N-40N,143E-144E) in region (IC) is the earthquake-prone zone of small and medium-sized earthquakes after 1923. It is seen that there are a lot of intraplate earthquakes(12). The lower plate always collapses due to the earthquakes and the material overflows up and accretionary wedge will be made. The upper plate relatively becomes long and swells because the lower plate shortens. And, the vicinity of the surface comes into a expansion field. And, steep cliffs are formed and fall because the upper plate surges to the trough. This will explain the geographical features of (IC) shown by (9) and the cause. The expansion field in the vicinity of the surface causes the occurrence of the lateral-fault type(10). The structure of the cliff where the sudden falls easily happen reacts sensitively to peripheral earthquakes. In addition, it has the possibility that is an efficient tsunami generator. This harmonizes with the result of (11).

Reference literature (Details are described to space in the drawing)

(1)MASE(2012) (2)MASE(2012) (3)MASE(2013) (4)NAGAI et al.(2000)/ERI U-Tokyo (5)Wikipedia (9)IZUMI et al.(2012)/JCG (10)NAKAJIMA(1974)/Hokkaido U. (11)ICHIHARA et al.(2013)/JAMSTEC (12)JMA/Monthly Report/June 2004

SSS30-P01 Room:Poster Time:April 29 18:15-19:30

参考文献
(1)Hirofumi MASE(2012)/The power to form and maintain oceanic basin and island arc /JpGU2012/SCG67-P06 http://www2.jpgu.org/meeting/2012/html5/session/S-CG67.html
(2)Hirofumi MASE(2012)/Materialization and Experiment of Model of Miyagi Prefecture offing on the 2011 Tohoku-Oki Earthquake/SSJ2012/P2-75 http://jglobal.jst.go.jp/detail.php?JGLOBAL_ID=201202271822634851
(3)Hirofumi MASE(2013)/Model that harmonizes with the rupture process of (Ide et al.2011) ～Relation between 3.11 and off-Miyagi-earthquakes～/JpGU2013/SSS28-P09 http://www2.jpgu.org/meeting/2013/session/S-SS28.html
(4)永井理子・菊地正幸・山中佳子(2000)/三陸における再来大地震の震源過程の比較研究 /東大震研/JpGU2000/Sa-005 Riko NAGAI, et al.(2000)/Comparative study on the asperities of large earthquakes in Sanriku region/ERI Univ. of Tokyo http://www.eri.u-tokyo.ac.jp/YOTIKYO/11seikahoukoku/koukai/r11.5fig1.JPG
(5)ウィキペディア(Wikipedia)「三陸沖北部地震/繰り返し発生する地震以外の地震」 http://ja.wikipedia.org/wiki/三陸沖北部地震
(6)佐竹健治・平田賢治・谷岡勇市郎・山木 滋(2004)/1952年・2003年十勝沖地震の津波波源の比較－1952年津波の再検討に基づいて－/産総研/SSJ2004年大会 http://unit.aist.go.jp/actfault-eq/seika/meeting/jishin2004/satake.html
(7)八木勇治(2004)/2003年9月26日十勝沖地震(Mjma 8.0)の破壊伝搬の様子EPS分/建築研 http://iisee.kenken.go.jp/staff/yagi/eq/Japan20030926/japan20030926-j.html
(8)山中・菊地(2003)/遠地実体波解析9月26日十勝沖地震(Mj8.0)/東大震研/EIC地震学ノートNo.139 http://www.eri.u-tokyo.ac.jp/sanchu/Seismo_Note/EIC_News/030926.html
(9)泉紀明・堀内大嗣・西澤あずさ・木戸ゆかり・中田高・後藤秀明・渡辺満久・鈴木康弘(2012)/150mグリッドDEMから作成した日本海溝付近の3D海底地形 /海保海洋情報部/研究報告第48号 Noriaki IZUMI, et al.(2012)/3D bathymetric image along the Japan Trench based on 150 meter grid DEM/JHOD,JCG http://www1.kaiho.mlit.go.jp/GIJUTSUKOKUSAI/KENKYU/report/rhr48/rhr48-tr10.pdf
(10)中島徹(1974)/ 1968年十勝沖地震の前後における発震機構の変化/北大/地球物理学研究報告 Tohoru NAKAJIMA(1974)/Spacial and Sequential Distribution of Focal Mechanisms before and after the Tokachi-Oki Earthquake of May/Hokkaido U. http://eprints.lib.hokudai.ac.jp/dspace/handle/2115/14044
(11)市原寛・浜野洋三・馬場聖至・笠谷貴史(2013)/東日本大震災で発生した津波が巨大化した原因となった場所を特定/海洋研究開発機構/2013年10月8日 Hiroshi ICHIHARA, et al.(2013)/Tsunami source of the 2011 Tohoku earthquake detected by an ocean-bottom magnetometer/JAMSTEC http://www.jamstec.go.jp/j/about/press_release/20131008_2/
(12)気象庁/地震・火山月報(防災編)/平成16年6月/6月12日岩手県沖の地震/震央分布図、断面図 JMA/Monthly Report on Earthquakes and Volcanoes in Japan/June 2004/6月12日岩手県沖の地震 http://www.seisvol.kishou.go.jp/eq/gaikyo/index.html#monthly (13)気象庁/地震・火山月報(防災編)/平成15年10月/特集1/図1-4, 平成17年8月/特集1/図8-1,等 http://www.seisvol.kishou.go.jp/eq/gaikyo/index.html#monthly

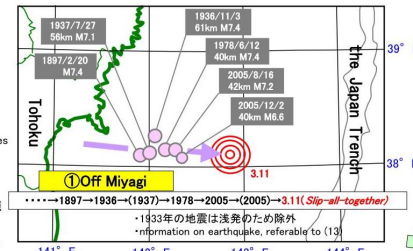

Fig.1 earthquakes climbed up (Off Miyagi)

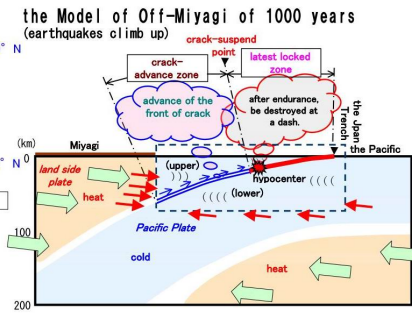

Fig.2 Model cross section intersecting squarely in the Trench and crossing over Miyagi

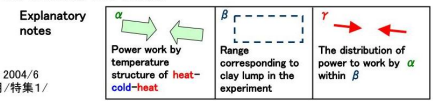

Japan Geoscience Union Meeting 2014
(28 April - 02 May 2014 at Pacifico YOKOHAMA, Kanagawa, Japan)

SSS30-P02 Room:Poster Time:April 29 18:15-19:30

Diversity of outer-rise earthquakes: As an example of the Off-Fukushima earthquake on 26 October 2013

YOMOGIDA, Kiyoshi[1*]

[1]Graduate School of Sciences, Hokkaido University

Earthquakes occurring in the outer-rise of a subducting plate are associated with the ruptures of the subduing plate itself, that is, intra-plate earthquakes. Such outer-rise earthquakes have been considered to excite much larger high-frequency than earthquakes in the plate boundary of the subducting and overriding plates, because the outer-rise earthquakes should break a lithospheric part where no peculiar weak zones exist.

A M7.1 earthquake occurred off the coast of Fukushima on 26 October 2013, which was probably associated with the 2011 great Tohoku-oki earthquake. We analyzed broadband seismic waveform data of this event recorded by F-net and other seismic networks. Compared with other large outer-rise earthquakes, the high-frequency component (>1Hz) of all the stations along the Pacific coast of eastern Japan is not abundant although slightly larger than plate-boundary earthquakes of low-angle thrust faulting. In contrast, there was the excitation of several impulsive wave packets of several seconds in period. Since only high-frequency waves are abundant at common stations for aftershocks of this outer-rise earthquake, the above features should not be originated by either propagation path or site effect.

Unlike the other outer-rise earthquakes, the rupture process of this earthquake was unique, relatively smooth with several strong patches on a rather homogeneous fault. The breakout of these patches should have been connected without any complex unbroken areas on the fault in the end, in order to explain the observed waveforms. Although we do not deny the break of a virgin (without any peculiar weak planes) lithosphere in this case, several distinguished large strong patches are likely to characterize the heterogeneity in the fault region of this outer-rise earthquake.

Among recent large outer-rise earthquakes along subduction zones near Japan, we have found another example similar to the Fukushima-oki earthquake: for the M7.0 outer-rise event on 14 March 2012 at the junction between Kuril Trench and Japan Trench, several impulsive waveforms with minor high-frequency waves. The state stress of this subducting Pacific plate should be very complex, which might lead to its non-standard rupture process. We shall need to investigate broadband frequency excitation patterns carefully for large outer-rise earthquakes.

In summary, there should be a wide variety of heterogeneities and/or stress state within a subducting lithosphere, which may be important to consider not only the source process of outer-rise earthquakes but also their tsunami generations.

Keywords: outer-rise earthquake, intra-plate earthquake, high frequency seismic waves, fault rupture, heterogeneity of oceanic lithosphere

Japan Geoscience Union Meeting 2014
(28 April - 02 May 2014 at Pacifico YOKOHAMA, Kanagawa, Japan)

SSS30-P03 Room:Poster Time:April 29 18:15-19:30

High resolution seismic profiling in the northern Japan Trench axis area

NAKAMURA, Yasuyuki[1*] ; KODAIRA, Shuichi[1] ; MIURA, Seiichi[1] ; YAMASHITA, Mikiya[1] ; FUJIE, Gou[1] ; SHIMOMURA, Norio[1] ; IWAMARU, Hikaru[1]

[1]Japan Agency for Marine-Earth Science and Technology

Marine geological and geophysical surveys and analysis of their results have revealed that the ruptured area of the 2011 Tohoku earthquake extended up to the vicinity of the trench axis along the plate boundary fault. To investigate the geological structure, especially the faults and the deformation of the sediments, we have conducted reflection seismic surveys in the trench axis area of the Japan Trench off Miyagi and Iwate prefectures. Three seismic cruises have been carried out in 2011 and 2013 along 81 E-W (dip) lines and 17 N-S (strike) lines. We have used 320 or 380 inch^3 cluster air guns and a 1200 m long streamer cable to obtain high resolution seismic data. Surveyed area covers the trench axis area along the trench strike from seaward of the hypocenter of the Tohoku earthquake around 38 N at south, to ˜40 N at north. Seismic profiles around 38 N show that the trench axis is located on a graben with sediments which have been deformed by reverse faulting. Similar deformation structure is observed around 40 N, but the trench axis is located on a horst not a graben there. The thickness of the incoming sediments on the Pacific plate typically ranges ˜0.3 ? 0.5 s in two way time, however it is reduced down to $<$0.2 s around 39.5 N where the basement of the oceanic crust shows higher relief and trench inner wall is significantly steep. The thickness variation of the incoming sediments can be traced seaward and corresponded with along strike variation of the structure in the outer rise. These high resolutions seismic data served for the site selection of the JFAST drilling project by IODP and also contributes to the JTRACK proposal for future drilling in the Japan Trench following success of the JFAST.

Japan Geoscience Union Meeting 2014
(28 April - 02 May 2014 at Pacifico YOKOHAMA, Kanagawa, Japan)

SSS30-P04 Room:Poster Time:April 29 18:15-19:30

Seismic surveys in the ruptured area of the 2011 Tohoku earthquake

NAKAMURA, Yasuyuki[1*] ; KODAIRA, Shuichi[1] ; KAIHO, Yuka[1] ; NO, Tetsuo[1] ; FUJIE, Gou[1] ; SATO, Takeshi[1] ; YAMAMOTO, Yojiro[1] ; KASAYA, Takafumi[1] ; OBANA, Koichiro[1] ; MIURA, Seiichi[1] ; TAKAHASHI, Narumi[1]

[1]Japan Agency for Marine-Earth Science and Technology

We have conducted seismic surveys in the ruptured area of the 2011 Tohoku earthquake off Miyagi prefecture in 2011 and 2013 using JAMSTEC's R/V Kairei. Three multi-channel reflection seismic (MCS) surveys were conducted in 2011 with R/V Kairei's 7800 inch^3 tuned air gun array and ˜6 km long streamer cable. The MCS profiles along 14 E-W (dip) lines and two N-S (strike) lines were acquired during these surveys. Another seismic survey was carried out in 2013 around the JFAST drill site along one dip line and two strike lines. Time migrated sections demonstrated characteristic structure in the Japan Trench subduction zone; the Pacific plate deformed by normal faults (horst and graben structure), frontal prism with seismically transparent or chaotic feature, strong landward dipping reflections corresponding to the backstop interface, "deep sea terrace" in the upper landward trench slope covered with younger sediments mainly deformed with normal faults. Our survey area covers ˜150 km in the trench strike direction around the epicenter area, which is rather small compared with the entire rupture zone (400 ? 500 km in the strike direction) of the Tohoku earthquake, however the structure is considerably variable from south to north. We have selected 6 dip lines, including the JFAST dip line, to apply pre-stack depth migration (PSDM). The PSDM sections provide higher quality profiles and interval velocity models in depth domain which are suitable for understanding the structural framework of the Japan Trench subduction zone. In 2013 survey, we also used four ocean bottom seismographs (OBSs) in addition to the MCS system. The P to S converted wave was clearly observed in the horizontal component seismograms, and the Vp/Vs in the sediment layer around the JFAST drill site was estimated at $>$4.5.

Japan Geoscience Union Meeting 2014
(28 April - 02 May 2014 at Pacifico YOKOHAMA, Kanagawa, Japan)

SSS30-P05 Room:Poster Time:April 29 18:15-19:30

Determination of Three Thermal Properties in Japan Trench Fast Drilling Project (JFAST)

LIN, Weiren[1*] ; TADAI, Osamu[2] ; FULTON, Patrick[3] ; HARRIS, Robert[4] ; TANIKAWA, Wataru[1] ; KINOSHITA, Masataka[1]

[1]Kochi Institute for Core Sample Research, Japan Agency for Marine-Earth Science and Technology, [2]Marin Works Japan LTD, [3]University of California, Santa Cruz, USA, [4]Oregon State University, USA

The 2011 Mw 9.0 Tohoku-oki earthquake produced a maximum coseismic slip of >50 m near the Japan Trench. Japan Trench Fast Drilling Project (JFAST) as the Integrated Ocean Drilling Program (IODP) Expedition 343 and 343T drilled through the plate boundary fault ruptured during the Tohoku-oki earthquake at site C0019 approximately one year after the earthquake. The most highlighted objective is to detect residual positive temperature anomaly induced by the coseismic frictional heat. To interpret measured temperature anomaly and to calculate coseismic shear stress on the ruptured fault from the temperature anomaly, the full three thermal properties (thermal conductivity, thermal diffusivity and specific heat; only two thermal properties among the three are independent) are necessary. We measured the three thermal properties using four whole round core samples retrieved from borehole C0019E at 177, 697, 802 and 828 mbsf (meter below seafloor), respectively by a transient plane heat source method (also called Hot Disk method). Independently with Hot Disk method, thermal conductivity were also measured by a line heat source method for 45 half core samples using a TEKA half-space probe onboard the D/V Chikyu and by a divided bar technique using 38 crushed core samples (particle samples) in onshore laboratory. The thermal conductivities determined independently by the three methods were consistent each other. Also, the Hot Disk measurements revealed very little anisotropy in thermal conductivity and thermal diffusivity.

Acknowledgments: This research used core samples provided by IODP. We thank all Expedition 343 and 343T scientists and the drilling and logging operation staff on board the D/V Chikyu during expedition 343 and 343T.

Keywords: Thermal Prpperty, JFAST, Thermal conductivity, Thermal diffusivity, Specific heat

Japan Geoscience Union Meeting 2014
(28 April - 02 May 2014 at Pacifico YOKOHAMA, Kanagawa, Japan)

SSS30-P06 Room:Poster Time:April 29 18:15-19:30

Modeling slow and seismic slips off Tohoku considering low to high speed friction behavior of the shallow plate boundary

SHIBAZAKI, Bunichiro[1*] ; IKARI, Matt[2] ; NODA, Hiroyuki[3]

[1]International Institute of Seismology and Earthquake Engineering, Building Research Institute, [2]Marum, Center for Marine Environmental Sciences, [3]Japan Agency for Marine-Earth Science and Technology

Ikari et al. (2013) examined low to high speed frictional properties of fault zone material from the shallow plate boundary in the Tohoku region obtained by the IODP Expedition 343 (JFAST). They found velocity-weakening frictional behavior at slip velocities slower than 10^{-6} m/s and velocity-strengthening at higher slip velocities. This frictional property is considered to be a mechanism that causes slow slip events and stress accumulation during the period between slow slip events. We investigate the effects of this frictional property on generation of slow slip events and megathrust events.

We use a rate- and state-dependent friction law with cut-off velocity to an evolution effect to represent this frictional behavior. Based on the experimental results (Ikari et al., 2013), we set the cut-off velocity at 10^{-6} m/s. We also consider dynamic weakening due to thermal pressurization at high slip velocity. We perform three-dimensional quasi-dynamic modeling of slip processes. Numerical results show the occurrence of slow slip events at intervals of several ten years at the shallow plate boundary. During the period between slow slip events, stress accumulation proceeds. When an earthquake nucleates at the deeper region, coseismic slip propagates into this region, which results in larger slip compared to the case where a simple velocity-strengthening friction law is considered.

Ito et al. (2012) detected slow slip events in the Japan subduction zone before the 2011 Tohoku-Oki earthquake. Shallow very low frequency earthquakes off Tohoku were detected by Matsuzawa et al. (2012). In addition, along the shallow plate boundary off Tokachi, sequential activity of very low frequency earthquakes occurs at intervals of several years (Asano et al., 2008). These observations suggest that the transitional friction behavior investigated by Ikari et al. (2013) occurs along the shallow plate boundary off Tohoku.

Keywords: off Tohoku, shallow plate boundary, low to high speed friction behavior, slow slip, seismic slip

Japan Geoscience Union Meeting 2014
(28 April - 02 May 2014 at Pacifico YOKOHAMA, Kanagawa, Japan)

SSS30-P07 Room:Poster Time:April 29 18:15-19:30

Friction properties beneath the frontal wedge near the Japan Trench: deduction from topographic variation

KOGE, Hiroaki[1*] ; KODAIRA, Shuichi[2] ; FUJIWARA, Toshiya[2] ; SASAKI, Tomoyuki[3] ; KAMEDA, Jun[7] ; KITAMURA, Yujin[6] ; HAMAHASHI, Mari[1] ; HAMADA, Yohei[4] ; YAMAGUCHI, Asuka[5] ; ASHI, Juichiro[5] ; KIMURA, Gaku[1]

[1]The University of Tokyo, [2]Institute for Research on Earth Evolution Japan Agency for Marine-Earth Science and Technology, [3]Ocean Engineering & Development Corporation, [4]Japan Agency for Marine-Earth Science and Technology, [5]Atomosphere and Ocean Research Institute, The University of Tokyo, [6]Kagoshima University, [7]Hokkaido University

The 2011 Tohoku-oki earthquake (Mw 9.0) produced a fault rupture, extending to the Japan Trench. Deformation and frictional properties beneath the forearc are the keys to elucidate this unusual event.

In this study, to obtain frictional properties (μ_b'; the coefficient of effective basal friction), we extracted shape-related parameters from the cross sections of the frontal wedge which are obtained from surveys across the trench that span sporadically along the axis of the Japan Trench. The following two methods were adopted for this study; Critical Taper Theory (CT) and Critical State Theory (CS). Both of the theories are based μ_b' From the Critical Taper Theory. Near latitude 36.1, the taper angles (slope angle + decollement dip angle) has been developed . A possible seamount subduction may differentiate this area. However, near the latitude 38.15 where the largest slip was reported with the 2011 earthquake, the taper angle has also been large without any seamounts. The calculated [or estimated] value of μ_b' in this area is larger than that of the other area, suggesting that the larger strain energy was accumulated in comparison with the other wedges.

From the Critical State Theory, the value of ω (angle between the basal decollement and backstop interface) becomes smaller toward the north. The results of CS show the increase of the ω associate with the increase of the μ_b', suggesting that strain energy is more stored toward the North.

Both results show that the μ_b' has decreased after the earthquake. The change in μ_b' may be due to the earthquake.

It is possible to know friction properties of before the earthquake and that of after the earthquake with bathymetry.

Keywords: Japan Trench, Critical Taper Theory

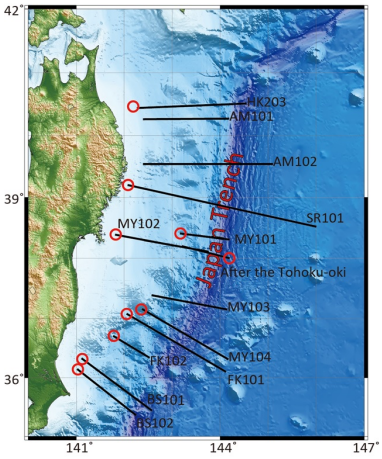

Japan Geoscience Union Meeting 2014
(28 April - 02 May 2014 at Pacifico YOKOHAMA, Kanagawa, Japan)

SSS30-P08 Room:Poster Time:April 29 18:15-19:30

Long-term crustal movement in the Rikuzentakata area, southern Sanriku coast, based on geomorphological/geological featu

NIWA, Yuichi[1*] ; TODA, Shinji[1]

[1]International Research Institute of Disaster Science, Tohoku University

In the northeast Japan forearc, strain rate estimated based on by geological feature is different from that by geodetic feature. Thus, marine terrace suggests that the Sanriku coast has uplifted at the rate of 1 mm/yr since the late Quaternary. On the other hand, this area has subsided at the maximum rate of 10 mm/yr during the past 100 years based on geodetic data. This disaccord indicates the possibility that the giant mega-thrust earthquake causes the Sanriku coast to uplift. However, the 2011 Tohoku-Oki Earthquake (Mw9.0) was accompanied by subsidence along the Sanriku coast. This fact led us to reexamine long-term crustal movement.

We conducted geomorphological/geological analyses in the Sanriku coast, especially the southern part of the coast, where long-term crustal movement is unknown because of lack of widely distributed Pleistocene marine terrace. In this presentation, we will report preliminary results of consideration of long-term crustal movement in the Rikuzentakata area, southern part of Sanriku coast.

Keywords: marine terrace, southern Sanriku coast, long-term crustal movement, alluvial plain

Japan Geoscience Union Meeting 2014
(28 April - 02 May 2014 at Pacifico YOKOHAMA, Kanagawa, Japan)

SSS30-P09 Room:Poster Time:April 29 18:15-19:30

Large-scale simulation of coseismic and postseismic crustal deformation using a high-fidelity finite element model

AGATA, Ryoichiro[1*] ; ICHIMURA, Tsuyoshi[1] ; HIRAHARA, Kazuro[2] ; HYODO, Mamoru[3] ; HORI, Takane[3] ; HORI, Muneo[1]

[1]The University of Tokyo, [2]Kyoto University, [3]Japan Agency for Marine-Earth Science and Technology

Postseismic crustal deformation of a subduction zone earthquake is an essential factor in such studies as interseismic slip deficit rates and stress-field change of the focal area of inland earthquakes. The viscoelastic behavior of the asthenosphere largely affects postseismic crustal deformation. Several studies have used analytical models or three-dimensional (3D) finite element (FE) method to simulate postseismic crustal deformation, considering the viscoelasticity. Yet because of the large computational cost, simulations using a realistic model of crustal structure have not been carried out, despite that detailed crustal data are available. Based on the technique of high performance computing, we performed large-scale finite element simulations using 3D FE models of higher-fidelity (High-fidelity model: HFM) to available crustal data. We used the data of JTOPO30, which was constructed in a 900 m resolution by MIRC (JTOPO30, 2003), for modeling the ground surface and CAMP standard model (Hashimoto et al. 2004) for the interplate boundaries. By using this data, we constructed a one-kilo-meter-resolution HFM with the size of 1700 x 2600 x 400 km, which includes the whole of the Japanese Islands. The model has 30km thick crust and the underlying viscoelastic mantle wedge, where the Philippine Sea and the Pacific plates are subducting beneath the Eurasian and the North American plates. Because the target area was large, we also took into consideration the curvature of the earth. We expect a large degrees-of-freedom in our HFM. Therefore, to compute the time history of the crustal deformation with such a large-scale model, we used the K computer, the fastest supercomputer in Japan.

In the session, we will show the simulation of the 200-year time history of postseismic crustal deformation using the HFM. In addition, by comparing the results of various sizes of temporal and spatial discretization, we will demonstrate that our method can compute the solution with discretization fine enough for numerical convergence.

Keywords: postseismic crustal deformation, high-fidelity finite element model of crustal structure, large-scale simulation

Japan Geoscience Union Meeting 2014
(28 April - 02 May 2014 at Pacifico YOKOHAMA, Kanagawa, Japan)

SSS30-P10 Room:Poster Time:April 29 18:15-19:30

Tsunami simulation in the Western Pacific Ocean and East China Sea from the hypothetical M9 Nankai earthquake models

HARADA, Tomoya[1*] ; SATAKE, Kenji[2] ; FURUMURA, Takashi[1]

[1]CIDIR/ERI, the University of Tokyo, [2]Earthquake Research Institute, the University of Tokyo

We computed tsunamis in the Western Pacific Ocean and East China Sea from the hypothetical models of the giant Nankai earthquake proposed by the Cabinet Office of Japanese government (2012). The maximum tsunami heights on the New Guinea coasts, Philippine Islands coasts, and Shanghai coasts in China are about 1.0-5.0 meters, 1.0-7.0 meters, and 0.5-2.0 meters, respectively. They are up to twice large as those computed from the 1707 Hoei earthquake (the largest earthquake along the Nankai trough in Japanese history). The simulation also shows that tsunami heights on the coasts in this area depend on the slip amounts on the Nankai fault.

Responding to the unexpected occurrence of the 2011 Tohoku earthquake, the Cabinet Office of Japanese government (2012) assumed 11 models of the giant Nanakai earthquake (Mw 9.1), computed tsunami heights along the Japanese coasts, and estimated the human and economic disasters. The tsunami heights exceed 10 m on the coasts of 13 prefectures, with a maximum height of 34.4 m.

Tsunamis from such a gigantic earthquake may impact the coasts in the Western Pacific Ocean and East China Sea. Harada and Satake (2012, AOGS; 2013, "Tsunami Events and Lessons Learned", Springer) performed numerical tsunami simulations in these oceans by using various fault models of the past Tokai and Nankai earthquakes.

In this study, we carried out the same simulations from the 11 fault models of the M9 Nankai earthquake. Tsunami propagations were computed by the finite-difference method for the non-linear long-wave equations with Corioli's force (Satake, 1995) in the area of 115-155 deg. E and 8 deg. S to 40 deg. N using the GEBCO 30-second bathymetry data. Initial tsunami heights computed by the Cabinet Office were used. A Manning's roughness coefficient of 0.025 $m^{-1/3}s$ was assumed for the friction and a computation time step of 1 s is used to satisfy the stability condition of the finite-difference method. We simulated tsunamis for 24 hours after the earthquakes.

We thank the Cabinet Office of Japanese government for providing the hypothetical models of the giant Nankai earthquake.

Keywords: sunami numerical simulation, Western Pacific Ocean, East China Sea, maximum tsunami heights, hypothetical M9 Nankai earthquake

Japan Geoscience Union Meeting 2014
(28 April - 02 May 2014 at Pacifico YOKOHAMA, Kanagawa, Japan)

SSS30-P11 Room:Poster Time:April 29 18:15-19:30

Stress concentration in the C0002 borehole of the NanTroSEIZE Project, Nankai Trough

WU, Hungyu[1*] ; KINOSHITA, Masataka[1] ; SAITO, Saneatsu[1] ; LIN, Weiren[1] ; SANADA, Yoshinori[1]

[1]Japan Agency for Marine-Earth Science and Technology

Wellbore instability is a major challenge for the engineer evaluating borehole and formation conditions. Instability is especially important to understand in areas with high stress variations, significant structure anisotropy, or pre-existing fracture systems. Borehole (in)stability is influenced by rock strength, structural properties, and near-field principal stresses. During drilling, the borehole conditions also impact borehole integrity. Factors that we can measure in the borehole during with logging while drilling (LWD) to understand these conditions include Mud Weight, mud loss, ROP (Rate of Penetration), RPM (Rotation Per Minute), WOB (Weight on Bit), and TORQ (Power swivel torque value). By observation the resistivity images, we can utilities the significant features under the interactions of effective stresses and formation.

We conducted stress analysis for Site C0002F of the Nankai Trough transect based on riser and riserless drilling data during IODP Expedition 338. Rock strength and basic physical properties, including velocity, density and porosity are obtained from core samples. The borehole shape, determined from LWD resistivity images, indicates that most of drilling occurred in stable environments, however, in a few instances the bottom hole assembly became stuck. We used our stress profile model to evaluate the mud weight required to drill a stable borehole for the measured rock strength and physical properties. Based on our analysis, we constrained the stress magnitude and possible orientation during IODP Expedition 338 by the drilling parameters. The enlargement and collapse in the borehole indicated that mud weight plays the essential role in the drilling.

Keywords: NanTroSEIZE, LWD, Breakout, Drilling, Borehole Instability

Japan Geoscience Union Meeting 2014
(28 April - 02 May 2014 at Pacifico YOKOHAMA, Kanagawa, Japan)

SSS30-P12 Room:Poster Time:April 29 18:15-19:30

Preliminary results of lithology examined during IODP Expedition 348 in the accretionary wedge of the Nankai Trough

FUKUCHI, Rina[1*] ; SCHLEICHER, Anja[2] ; MAIA, Ana[3] ; SONG, Chen[4] ; YANG, Kiho[5] ; EXPEDITION 348, Scientists[6]

[1]The University of Tokyo, [2]University of Michigan, [3]Cardiff University, [4]University of Missouri-Columbia, [5]Yonsei University, [6]IODP Expedition 348

International Ocean Discovery Program (IODP) Nankai Trough Seismogenic Zone Experiment (NanTroSEIZE) Expedition 348 took place from 13 September 2013 to 29 January 2014. This expedition was primarily designed to extend riser Hole C0002N to 3600 mbsf (in the event, C0002N sidetrack Hole C0002P was drilled to 3058.5 mbsf). We collected cuttings, core samples, mud gas, and logging data. Here we report the preliminary shipboard lithological results of IODP Expedition 348.

Four lithologic units were identified at Site C0002 based on geological and geochemical characteristics of core and cuttings samples: Unit II (475-512.5 mbsf in Hole C0002M), Unit III (875.5-975.5 mbsf in Hole C0002N), Unit IV (975.5-1665.5 mbsf in Hole C0002N), and Unit V (1665.5-2325.5 mbsf in Hole C0002N, and 1965.5-3058.5 mbsf in Hole C0002P).

Lithologic Unit II is dominated by fine-grained turbiditic deposits. Silty claystone is the main lithology, with subordinate fine-grained sandstone and sandy siltstone. Lithologic Unit III is dominated by silty claystone with trace amounts of very fine loose sand, containing common glauconite grains. Those units are interpreted to be the Kumano forearc basin sediments. Lithologic Unit IV is dominated by silty claystone, with sandstone as a minor lithology. Sandstone cuttings in this unit are generally very weakly consolidated, and occur as disaggregated loose sand. Lithologic Unit IV is divided into five subunits based on sand content and interpreted as the upper accretionary prism sediment. Lithologic Unit V is dominated by silty claystone. Fine-grained and moderately cemented sandstone was a minor component. In Hole C0002P, clay-size content in the silty claystone increases at the depth up to 2625.5 mbsf. The fine silty claystone becomes the dominant lithology from 2625.5 mbsf. This unit is possibly interpreted to be the trench or Shikoku Basin hemipelagic deposits.

Keywords: IODP Expedition 338, NanTroSEIZE, Site C0002

Japan Geoscience Union Meeting 2014
(28 April - 02 May 2014 at Pacifico YOKOHAMA, Kanagawa, Japan)

SSS30-P13 Room:Poster Time:April 29 18:15-19:30

Physical properties of Nankai accretionary prism sediments at Site C0002, IODP Expedition 348

KITAMURA, Manami[1*] ; KITAJIMA, Hiroko[2] ; HENRY, Pierre[3] ; VALDEZ, Robert[4] ; JOSH, Matthew[5] ; EXPEDITION 348, Scientists[6]

[1]Hiroshima Univerisity, [2]Geological Survey of Japan National Institute of Advanced Industrial Science and Technology, [3]Aix-Marseille University, [4]Pennsylvania State University, [5]The Commonwealth Scientific and Industrial Research Organization, [6]IODP Expedition 348

Integrated Ocean Drilling Program (IODP) Nankai Trough Seismogenic Zone Experiment (NanTroSEIZE) Expedition 348 focused on deepening the existing riser hole at Site C0002 to ˜3000 meters below seafloor (mbsf) to access the deep interior of the Miocene inner accretionary prism. This unique tectonic environment, which has never before been sampled in situ by ocean drilling, was characterized through riser drilling, logging while drilling (LWD), mud gas monitoring and sampling, and cuttings and core analysis. Shipboard physical properties measurements including moisture and density (MAD), electrical conductivity, P-wave, natural gamma ray, and magnetic susceptibility measurements were performed mainly on cuttings samples from 870.5 to 3058.5 mbsf, but also on core samples from 2163 and 2204 mbsf.

MAD measurements were conducted on seawater-washed cuttings (”bulk cuttings”) in two size fractions of >4 mm and 1-4 mm from 870.5 to 3058.5 mbsf, and hand-picked intact cuttings from the >4 mm size fractions within 1222.5-3058.5 mbsf interval. The bulk cuttings show grain density of 2.68 g/cm3 and 2.72 g/cm3, bulk density of 1.9 g/cm3 to 2.2 g/cm3, and porosity of 50% to 32%. Compared to the values on bulk cuttings, the intact cuttings show almost the same grain density (2.66-2.70 g/cm3), but higher bulk density (2.05-2.41 g/cm3) and lower porosity (37-18%), respectively. The grain density agreement suggests that the measurements on both bulk cuttings and intact cuttings are of good quality, and the differences in porosity and density are real, but the values from the bulk cuttings are affected strongly by artifacts of the drilling process. Thus, the bulk density and porosity data on handpicked cuttings are better representative of formation properties. Combined with the MAD measurements on hand-picked intact cuttings and discrete core samples from previous expeditions, porosity generally decreases from ˜60% to ˜20% from the seafloor to 3000 mbsf at Site C0002.

Electrical conductivity and P-wave velocity on discrete samples, which were prepared from both cuttings and core samples in the depth interval of 1745.5-3058.5 mbsf, range 0.15-0.9 S/m and 1.7-4.5 km/s, respectively. The electrical resistivity (a reciprocal of conductivity) on discrete samples is generally higher than the LWD resistivity data but the overall depth trends are similar. On the other hand, the P-wave velocity on discrete samples is lower than the LWD P-wave velocity between 2200 mbsf and 2600 mbsf, while the P-wave velocity on discrete samples and LWD P-wave velocity are in a closer agreement below 2600 mbsf. The electrical conductivity and P-wave velocity on discrete samples corrected for in-situ pressure and temperature will be presented.

The shipboard physical properties measurements on cuttings are very limited but can be useful with careful treatment and observation.

Keywords: IODP Expedition 348, NanTroSEIZE, accretionary prism

Japan Geoscience Union Meeting 2014
(28 April - 02 May 2014 at Pacifico YOKOHAMA, Kanagawa, Japan)

SSS30-P14 Room:Poster Time:April 29 18:15-19:30

Effects of frictional heating and comminution on coal maturation

FURUICHI, Hiroyuki[1*] ; UJIIE, Kohtaro[1] ; SAITO, Tsubasa[1] ; SAKAGUCHI, Arito[2] ; TSUTSUMI, Akito[3]

[1]Life and Env., Sci., Univ. Tsukuba, [2]Sci., Yamaguchi Univ., [3]Sci., Kyoto Univ.

The detection of friction heating on faults is crucial to estimate frictional heat during earthquakes. Recently, vitrinite reflectance (Ro) has been used to detect friction heating along faults. However, the factors controlling increase in Ro on faults remain poorly understood. Moreover, the application of the commonly used kinetic model to the estimation of temperature rise during short-lived thermal events such as frictional heating on faults has not been convinced. Here, we conducted friction experiments on a mixture of 95 wt% clay-rich material from the host rock of the megasplay fault gouge and 5 wt% coal grains from the forearc basin in the Nankai subduction zone at slip rates of 0.15 mm/s-1.3 m/s under dry (room humidity) and wet (water-saturated) conditions. After the experiments, we examined microstructures, Ro and size of coal grains and then compared with those obtained from in and around the megasplay fault gouge. The results show that Ro does not increase by rapid heating alone; grain-size reduction due to comminution is required for increase in Ro. The combination of comminution and heating is the most effective for increase in Ro, possibly due to enhanced mechanochemical reaction associated with an increase in surface area of coal grains. The application of the results to the Nankai megasplay fault gouge is that increased Ro in the fault gouge results from frictional heating and comminution, while that in adjacent to the gouge are mainly derived from comminution. The Ro calculated from the chemical kinetic model is higher than that measured after the experiments. Ro is an useful tool to detect past frictional heating on faults, but the estimation of temperature rise from Ro is problematic; the new kinetics model considering the effects of frictional heating and comminution is necessary to estimate amount of frictional heat.

Keywords: vitrinite reflectance, frictional heating, comminution, Nankai Trough

Japan Geoscience Union Meeting 2014
(28 April - 02 May 2014 at Pacifico YOKOHAMA, Kanagawa, Japan)

SSS30-P15 Room:Poster Time:April 29 18:15-19:30

Receiver function analysis using OBS data: modeling 3-D structure of the Philippine Sea plate off the Kii Peninsula

AKUHARA, Takeshi[1*] ; MOCHIZUKI, Kimihiro[1]

[1]Earthquake Research Institute, University of Tokyo

Megathrust earthquakes have repeatedly occurred beneath the southwestern Japan, on the subducting Philippine Sea plate, in cycles of 100-150 years [Ando, 1975]. The rupture boundary of the latest two megathrust earthquakes, the 1944 Tonankai and 1946 Nankai earthquakes, is located at the south of the Kii Peninsula. Although some structural heterogeneity was proposed as factors of the rupture boundary [Mochizuki et al., 1998; Kodaira et al., 2006], the question of why rupture propagation stops there is still open in light of our little knowledge about 3-D geometry of the subducting Philippine Sea plate at offshore region.

In this study, we aim to construct 3-D structure model of the subducting Philippine Sea plate by receiver function (RF) analysis, using data of ocean-bottom seismometers (OBSs) deployed from 2003 to 2007 off the Kii Peninsula [Mochizuki et al., 2010; Akuhara et al., 2013]. These OBSs have three-component velocity sensors with natural frequency of 1 Hz, and their orientations were determined in this study from particle motion of regional P-wave. The difficulty of our RF analysis using OBS data is summarized by the following two factors. The first is that noise is dominant within a low-frequency band (1 <Hz), the most stable band for estimating RFs. The second is that the number of teleseismic events is limited because of short observation periods and low S/N ratio.

To overcome these problems, we calculated RFs with the aid of multi-taper correlation (MTC) method [Park and Levin, 2000]. The method is resistant to spectral leakage and able to estimate frequency-dependent uncertainties for RF, which is suitable for noisy OBS data and for high-frequency analysis. We binned resultant RFs by back azimuths, and computed time-domain uncertainties of the RFs from the frequency-dependent uncertainties estimated by the MTC method, using jackknife resampling within each back azimuth bin [Leahy and Collins, 2009]. This uncertainty estimation makes the following phase identification more reliable, even though the number of teleseismic events is limited.

Our preliminary results show some coherent peaks throughout all back azimuth bins, whose amplitude is larger than one-sigma uncertainties. Some of them have moveout, implying existence of dipping layers, and have arrival times roughly corresponding to the depth of the slab mantle. Although more detailed identification process for these peaks is largely left for our future work, these peaks might be converted phases from the slab mantle.

Keywords: ocean-bottom seismometer, receiver function, subduction zone

Japan Geoscience Union Meeting 2014
(28 April - 02 May 2014 at Pacifico YOKOHAMA, Kanagawa, Japan)

SSS30-P16 Room:Poster Time:April 29 18:15-19:30

Three-dimensional velocity model for the Nankai Trough seismogenic zone based on structural studies

NAKANISHI, Ayako[1*] ; TAKAHASHI, Narumi[1] ; YAMAMOTO, Yojiro[1] ; TAKAHASHI, Tsutomu[1] ; OBANA, Koichiro[1] ; KODAIRA, Shuichi[1] ; KANEDA, Yoshiyuki[1]

[1]JAMSTEC

Coseismic rupture area of the great interplate earthquake concerned about its occurrence along the Nankai Trough presumed by government of Japan is now wider to the west, north and south than the former assumption. Although the new estimation is based on seafloor topography, source area of the past largest megathrust event, present seismic activity and so on, structural information has not always been enough reflected yet. In order to estimate precise coseismic rupture area of the Nankai megathrust earthquake, it is necessary to improve a physical model of the Nankai Trough seismogenic zone based on the geometry of the subducting plate and velocity structure model.

Japan Agency for Marine-Earth Science and Technology had conducted the large-scale high-resolution wide-angle and reflection seismic survey and long-term observation from off Kyushu to Tokai between 2008 and 2012. Layered velocity structure models are now obtained along grid two-dimensional seismic profiles from the Hyuga-nada to the Kii channel area. A three-dimensional seismic tomography using active and passive seismic data observed both land and ocean bottom stations had been also performed for the western Nankai Trough.

In this study, we constructed a three-dimensional velocity model of the Nankai Trough with the procedure as follows;

1) Sampling the velocity structural information along each seismic profile with interval of ˜1km in horizontal, and ˜100m in vertical directions

2) Preparing the geometry model of each interface included in layered models, e.g., basement, plate boundary, Moho, etc.

3) Setting minimum and maximum velocities of each layer based on the velocity models along two-dimensional seismic profiles

4) Interpolating sampled velocity information considering layered structure

(Landmark DecisionSpaceDesktop is used for constructing 3-D modeling)

Previously published layered models are also used to make up for insufficient structural information for the eastern Nankai Trough.

Reliability of the three-dimensional model was confirmed by comparing calculated travel-times with observed travel-times along each seismic profile. We will also try to evaluate the reliability of the model by comparing the hypocenter distribution using three-dimensional velocity model obtained in this study with that determined by three-dimensional seismic tomography using active and passive source data. We will plan to revise our 3D model with additional structural information and construct more precise and detailed model for the entire Nankai Trough area so that the model can be applied to more realistic numerical simulation.

This study is part of 'Research concerning Interaction Between the Tokai, Tonankai and Nankai Earthquakes (FY2008-2012)' funded by Ministry of Education, Culture, Sports, Science and Technology, Japan.

Japan Geoscience Union Meeting 2014
(28 April - 02 May 2014 at Pacifico YOKOHAMA, Kanagawa, Japan)

SSS30-P17 Room:Poster Time:April 29 18:15-19:30

Seismic observations off Kii Peninsula

YAMAMOTO, Yojiro[1*] ; TAKAHASHI, Tsutomu[1] ; KAIHO, Yuka[1] ; OBANA, Koichiro[1] ; NAKANISHI, Ayako[1] ; KODAIRA, Shuichi[1] ; KANEDA, Yoshiyuki[1]

[1]JAMSTEC

In the Nankai Trough subduction zone, megathrust earthquakes of M 8 class occur repeatedly. There are three main seismogenic segments (Tokai, Tonankai and Nankai earthquake regions), and these segments have ruptured sometimes simultaneously and sometimes individually. To understand the control factor of the seismic linkage among these segments and Hyuga-nada segments, Japan Agency for Marine-Earth Science and Technology has been carried out a series of wide-angle active source surveys and local seismic observations from 2008 to 2012, as a part of Research concerning Interaction Between the Tokai, Tonankai and Nankai Earthquakes' funded by Ministry of Education, Culture, Sports, Science and Technology, Japan. In this study, we show the results of two local seismic observations off Kii peninsula, the one is in the Kii channel and the other is in the Kumano-nada. The boundary of the Tonankai and Nankai segments is located in this region (Baba and Cummins, 2005), and the existence of the high velocity plutonic rock in the landward plate just beneath Shionomisaki is considered as the control factor of historical rupture variation (Kodaira et al., 2006). Japan Meteorological Agency (JMA) catalogue also indicates the spatial relationship between the seismic activity and seismogenic segments; shallow microseismicity seems to be more active in the Nankai region than in Tonankai region.

The observation in the Kii channel has been performed in FY2010 and was composed of 155 short-tern (about 1.5 months) ocean bottom seismographs (OBSs) and 19 long-term (about 10 months) OBSs. First, we relocated the JMA catalogue earthquakes by using three-dimensional velocity model obtained by active source surveys and adding the first arrival time data at OBSs. As a result, the earthquakes near the trough axis were generally relocated 10-20 km shallower than JMA location. Then, we attempt to detect the earthquakes by using long-term OBS records and found the active intraslab seismicity, especially in the up-dip part of the subducted seamount (Kodaira et al., 2000). The observation in the Kumano-nada has been performed in FY2011 and was composed of 150 short-tern (about 2.5 months) OBSs and 14 long-term (about 8 months) OBSs. Now we perform the first arrival picking of these data with the seismograph data of Dense oceanfloor network system for earthquakes and Tsunamis (DONET), according to the JMA catalogue earthquake list. We will show the preliminary results of hypocenter distribution in the Kumano-nada at the presentation.

Keywords: Nankai Trough, ocean bottom seismographic observation, seismicity

Japan Geoscience Union Meeting 2014
(28 April - 02 May 2014 at Pacifico YOKOHAMA, Kanagawa, Japan)

SSS30-P18 Room:Poster Time:April 29 18:15-19:30

Seismic observation and active-source seismic surveys on southern Ryukyu arc

TAKAHASHI, Tsutomu[1*] ; KAIHO, Yuka[1] ; ISHIHARA, Yasushi[1] ; YAMAMOTO, Yojiro[1] ; NAKANISHI, Ayako[1] ; OBANA, Koichiro[1] ; KODAIRA, Shuichi[1] ; KANEDA, Yoshiyuki[1]

[1]JAMSTEC

The Ryukyu arc is an island arc located on southeast of the Eurasian plate. The Philippine Sea plate is subducting northwestward at Ryukyu trench. Many large earthquakes (M7˜8) occurred on this arc, and some of them generated tsunamis. The 1771 Yaeyama earthquake (M7.4) caused a large tsunami of which a maximal height is 30m. For detailed examinations of fault rupture zones and mechanisms of large earthquakes in this arc, it is important to know the seismicity, lithospheric structures and plate geometry. In 2013, Japan Agency for Marine-Earth Science and Technology (JAMSTEC) launched a series of seismic observations and active-source seismic surveys at the Ryukyu arc as a part of research project funded by Ministry of Education, Culture, Sports, Science and Technology, Japan. In FY2013, we conducted refraction and reflection wide-angle seismic surveys and seismic observation on southern Ryukyu arc.

Active source seismic data were acquired on two survey lines. The one is a 480km-long line across the island arc from the south of Ryukyu trench to Okinawa trough. The other is a 100km-long line in Okinawa trough at northwest of Iriomote island. We conducted a refraction survey on the former survey line with 60 ocean bottom seismographs (OBS), and multichannel seismic reflection (MCS) surveys on both lines. Retrieved data shows clear wave trains propagating in the Philippine Sea plate and island arc. Normal faults in Okinawa trough were clearly observed in MCS data.

For seismic observation, we deployed 36 seismic stations including 30 OBSs and 6 onshore stations. All OBSs are equipped with short period geophones. Onshore stations are deployed at Miyako, Tarama, Ishigaki, Iriomote, Kuroshima and Hateruma islands. They are composed of broadband and/or 2Hz seismometers. We also retrieved seismic data from 60 OBSs that was deployed for the active source refraction survey. Observed seismic waves of small earthquakes show path dependences of waveforms that suggest spatial variations of random inhomogeneities and attenuation. For example, OBSs in Okinawa trough did not record clear S-wave for most of earthquakes. However, they observed clear S-wave and long-lasting coda waves for some shallow earthquakes occurred at north of Iriomote and Yonaguni islands. These waveforms suggest strong random inhomogeneities at the shallow part and high apparent attenuation (due to scattering and intrinsic attenuation) at deeper part underneath the Okinawa trough. In this presentation, we outline our observations and notable features of obtained data.

Japan Geoscience Union Meeting 2014
(28 April - 02 May 2014 at Pacifico YOKOHAMA, Kanagawa, Japan)

SSS30-P19 Room:Poster Time:April 29 18:15-19:30

A plate boundary earthquake model with consideration on submarine active faults

NAKATA, Takashi[1*] ; WATANABE, Mitsuhisa[2]

[1]Hiroshima University Professor Emeritus, [2]Toyo University

Active faults observed on seafloor along Japan Trench are resultants of repeated large earthquakes. We discuss on the relation between large earthquakes and their source faults based on a detailed active fault map along Japan Trench. Judging from the location and continuation of active faults in the earthquake source area, we consider that one of the extensive thrust faults which extends from off-Sanriku to off-Ibaraki for about 500km, is directly related to the source fault of the 2011 off the Pacific coast of Tohoku Earthquake.

The 2011 off the Pacific Coast of Tohoku Earthquake (Mw9.0) generated large tsunami with massive pulsating pattern of waves (Maeda et al. 2011). A leading hypothesis believed among many seismologists is that rupture of two extensive asperity patches surrounded by stable sliding area on the plate boundary generated the earthquake. One of the asperity patches in depth caused the strong motion and the other near the surface caused fault rupture along the axis of Japan Trench and generated gigantic tsunami. Large displacement ˜50m eastward and ˜7 to ˜10m upward was estimated from comparison of data obtained before and after the earthquake in 2004 and 2011 by multi-narrow beam bathymetric surveys across the trench (Fujiwara et al. 2011). Satake et al. (2011) explained the large tsunami height by simultaneous faulting on two different fault planes that fit with the above-mentioned asperities. Since most of the workers hypothesized without any doubt believed that the earthquake was caused by the fault ruptured up to the trench axis, existence of submarine active fault is rather overlooked so far. However, we consider the large displacement is due to landslide and do not find any extensive fault scarp on the trench axis.

We simulated pattern of seafloor deformation associated with the earthquake using a simple dislocation model for a single fault plane with uniform slip that dips 14 degree in depth and 33.6 degree beneath the tectonic bulge related to the extensive active fault. A result shows that an area of large uplift agrees more or less with the location of tectonic bulge with width of about 20km.

The record of tsunami first wave obtained by the GPS wave gage set on about 200m deep seafloor off Kamaishi on southern Sanriku Coast (Port and Airport Research Institute, 2011). The record suggests that after gradual sea-level rise of 2m during 6 minutes, acute sea-level rise of 4m took place within 4 minutes, and then sea-level abruptly dropped by 4m within 2 minutes. The length of pulsating tsunami wave is estimated about 17km from tsunami propagation velocity at 200m deep sea and total duration of pulsating pattern of tsunami, i.e. 7 minutes. This tsunami wave pattern resembles the pattern of seafloor deformation we calculated above.

We also simulate crustal movement and tsunami height along the Tohoku coast by an earthquake source fault model based the location of the submarine fault with fault-slip deduced from tectonic scarp height that is regarded as cumulative fault-slip. Our simulation explains the observed co-seismic subsidence and large tsunami height along the coast better than many other simulations based on various inversion models.

Based on these observations, we propose active fault model for plate boundary earthquake that large earthquakes are characteristically caused from submarine active faults in the island arc crust that overlap each other above the plate boundary in the narrow sense.

Keywords: plate boundary earthquake, asperity model, active fault model

Japan Geoscience Union Meeting 2014
(28 April - 02 May 2014 at Pacifico YOKOHAMA, Kanagawa, Japan)

SSS30-P20 Room:Poster Time:April 29 18:15-19:30

The last 6000 years record of tsunami events in the Kaniga-ike pond along the Nankai Trough

MATSUOKA, Hiromi[1*]

[1]Kochi Univ.

In order to reveal pre-historic record of Nankai Trough earthquakes, we collected 46 vibrocore samples from the Kaniga-ike pond. Stratigraphical study and radiocarbon dating of these samples revealed that sediment of Kaniga-ike pond recorded 17 tsunami events during the last 6000 years. These 17 events repeated almost constant intervals through 300 years. A 2000 years ago event formed remarkable thick tsunami sequence, and also shows an exclusive event in the past 6000 years.

Keywords: Nankai Trough, Tsunami sediment

Japan Geoscience Union Meeting 2014
(28 April - 02 May 2014 at Pacifico YOKOHAMA, Kanagawa, Japan)

SSS30-P21 Room:Poster Time:April 29 18:15-19:30

Estimate of the contact state of microcrack from the elastic wave velocity measurement

TAMAI, Hayata[1*] ; MUTO, Jun[1] ; NAGAHAMA, Hiroyuki[1] ; ISHIKAWA, Masahiro[2]

[1]Depertment of Geology, Graduate School of Science, Tohoku University, [2]Geological institute, Graduate School of Environment and Information Science, Yokohama National Univ

Birch (1960) studied about the relationship between the confining pressure and the elastic wave velocity. It was indicated that the elastic wave velocity increases with the increasing confining pressure because the microcrack is closed at high pressure. The velocity includes the effect of microcracks at low pressure. We must the elastic wave velocity without the effect of microcrack to know the elastic constants of a rock. To do that, it is necessary to know the process of closing microcracks and the contact state of microcrack.

The power-law relation between the elastic wave velocity and confining pressure is expressed with pressure exponent of μ (Kobayashi and Kozumi, 1976). They assume that the microcrack has single contact in this model. It is necessary to take account in multiple contacts because the microcracks of a rock have multiple contacts. We applied the single contact model to multiple contacts model with the previous study (Archard, 1953). The microcrack has the point contact, ball contact and plane contact when μ is 2/3, 3/5 and 1/2 respectively. The microcrack contacts plastically if μ is $<$1/2. We measured the elastic velocity of rocks with gas medium high pressure apparatus to discuss the effect of the confining pressure.

We measure the velocity with the pulse transmission technique. We set the assembly, composed of a sample between two metal jig pasted piezoelectric transducers, in the pressure vessel. The sample height is about 15-40 mm and diameter is 20 mm. The frequency of transmission wave is 2 MHz. We recorded it 10^{-9}s rate. We measured Vp and Vs of the gabbro and granite during pressurization and depressurization to a maximum confining pressure of 200 MPa. The velocity increased drastically with the increase in the confining pressure up to 100 MPa. When confining pressure is lower than about 100 MPa, μ of the gabbro and granite is about 2/3, indicating that the contact state of microcrack is point contact. However, under pressure higher than 100 MPa, μ becomes under 1/2, indicating that all microcracks are closed plastically in the experiment with gas medium high pressure apparatus. So the velocity at pressure higher than 100 MPa does not include the effect of microcracks. Furthermore, we estimated μ of several rocks from previous studies (Birch, 1960, Zimmer et al., 2002). Although μ depends on rock type at low pressure, it converges to values smaller than 1/2 at high pressure. This indicates that all microcracks are completely closed at high pressure and this result conforms to our experiment. If fluid exists in rocks, the value of μ is less than 1/2 even at low pressure. Therefore the microcrack with fluid acts as having plastic contact. We revealed the process of closing microcracks with the increasing confining pressure from the elastic wave velocity measurement.

Japan Geoscience Union Meeting 2014
(28 April - 02 May 2014 at Pacifico YOKOHAMA, Kanagawa, Japan)

SSS30-P22 Room:Poster Time:April 29 18:15-19:30

Frictional properties of the shallow Nankai Trough accretionary sediments

HOSHINO, Koki[1*] ; OOHASHI, Kiyokazu[2] ; KANAGAWA, Kyuichi[2]

[1]Faculty of Science, Chiba University, [2]Graduate School of Science, Chiba University

We have conducted friction experiments on sandstone, tuff, silty mudstone and clayey mudstone samples cored from the shallow Nankai Trough accretionary prism, using a triaxial apparatus recently installed at Chiba University, at a confining pressure of 37 MPa, a pore pressure of 29 MPa, a temperature of 42 degrees C, and an axial displacement rate of 1 micrometer/s. These pressure, pore pressure and temperature correspond to those supposed at the depth of 1 km below seafloor at IODP Site C0002. The results reveal that frictional properties of these samples change systematically according to the content of clay minerals, in particular of smectite. The content of clay minerals is 6.0 wt% in the sandstone sample, 17.2 wt% in the tuff sample, 34.1 wt% in the silty mudstone sample, and 42.0 wt% in the clayey mudstone sample. Except for the sandstone sample in which smectite is absent, smectite is the most abundant clay mineral in all the other samples, occupying 68-76 wt% of total clay minerals.

Steady-state friction coefficient decreases with increasing content of clay minerals, from 0.83 of the sandstone sample, through 0.74 of the tuff sample and 0.34 of the silty mudstone sample, to 0.27 of the clayey mudstone sample. Slip-dependent frictional behavior also changes according to the content of clay minerals; the sandstone sample exhibits slip hardening, while the other samples exhibit slip softening, which becomes more pronounced with increasing amount of clay minerals.

We will also report the velocity dependence of steady-state frictional strength at this condition as well as how frictional properties of these samples change at deeper conditions up to 5 km below seafloor.

Keywords: Nankai Trough, accretionary sediments, frictional properties

Japan Geoscience Union Meeting 2014
(28 April - 02 May 2014 at Pacifico YOKOHAMA, Kanagawa, Japan)

SSS30-P23 Room:Poster Time:April 29 18:15-19:30

Effects of shear displacement and fault zone structure on the frictional be havior of montmorillonite-quartz gouge

KAWAI, Tomoaki[1*] ; TSUTSUMI, Akito[1]

[1]Graduate School of Science,Kyoto University

Recent observation of the low frequency earthquakes in the shallow part of the Nankai subduction zone has demonstrated that faulting there is slow yet seismic; suggesting that frictional velocity dependence along the fault would be negative. However, in a widely accepted model, sediments there is expected to exhibit velocity-strengthening frictional behavior. We have reported that the fault material along the megasplay fault in the Nankai Trough exhibited both velocity-strengthening and velocity-weakening frictional behavior [Tsutsumi et al., 2011]. Fault zone structures may be important to understand why the samples exhibited different velocity dependence. In this study, we have conducted frictional experiments on artificial gouges composed of montmorillonite and quartz mixtures, in order to understand the relationship between the fault zone structures and velocity dependent frictional behavior.

We examined frictional behavior and fault zone structure of the artificial gouge samples composed of montmorillonite/quartz mixtures. All of the experiments were conducted under water-saturated conditions at 1 to 5MPa of normal stress, with shear displacement of 30 mm to 14 m, using a rotary-shear friction testing machine. Velocity step tests were conducted in a range of velocities from 0.003mm/s to 30 mm/s, in order to examine velocity dependent frictional behavior.

Results of these experiments reveal influences of normal stress and displacements on frictional behavior. Velocity weakening behavior was observed for the mixtures of montmorillonite/quartz = 20/80 and 40/60 wt%, respectively, at large displacement. In velocity-weakening samples, montmorillonite becomes to be finer-grained and is well mixed with quartz in the gouge layer after long shear displacements and at high normal stresses. These observation demonstrates that frictional behavior of the montmorillonite/quartz gouge changes with the development of the deformation structures. It is suggested that fault zone structure is one of the important factors of describing the frictional behavior along faults at the Nankai Trough.

Keywords: montmorillonite, frictional experiment, fault zone structure

Japan Geoscience Union Meeting 2014
(28 April - 02 May 2014 at Pacifico YOKOHAMA, Kanagawa, Japan)

SSS30-P24 Room:Poster Time:April 29 18:15-19:30

Friction constitutive properties of shallow subduction zone material as estimated from rotary shear friction experiments

NAKANO, Ryuji[1*] ; NAMIKI, Yuka[1] ; TSUTSUMI, Akito[1]

[1]Graduate School of Science, Kyoto University

In order to understand the dependence of constitutive parameters, a, b, and Dc, on slip velocity, V, we conducted experiments by using a rotary shear high velocity friction apparatus. Samples used in this work were collected from the Nankai accretionary prism, offshore from Kii Peninsula, Japan, at Site C0004 during Integrated Ocean Drilling Program (IODP) Expedition 316 [Expedition 316 Scientists, 2009; Tsutsumi *et al*., 2011], and from the Costa Rica subduction zone, Cocos Ridge, at Site U1381 during IODP Expedition 334 [Expedition 334 Scientists, 2012]. All of the samples from the Nankai accretionary prism are clayey silt, whereas those from Costa Rica can be divided into 2 groups with respect to their composition: one is clayey silt (hereinafter referred to as ”Costa Rica Unit I”), the other is silicic to calcareous ooze (”Costa Rica Unit II”). All experiments were carried out at 5 MPa normal stress and 0.0028-2.8 mm/sec slip velocity under wet condition (0.5 g samples with 0.5-0.9 ml distilled water). Moreover, we created a simulation program, which can estimate the values of constitutive parameters and system stiffness, k, with Levenberg-Marquardt method, supposing the spring-block model.

The results are summarized as the following: (1) a, b and/or Dc increase with slip velocity; (2) the values are the highest at V = 0.028-0.28 mm/sec; (3) the values are the lowest at V = 0.028-0.28 mm/sec. The reason is not clarified yet, but it is remarkable that, despite the composition, the result of the clayey megasplay fault material from the Nankai accretionary prism resembles the result of Costa Rica Unit II. This implies that, as expected, constitutive parameters depend on not only material but also other conditions. Another remarkable point to be noted is that the values of system stiffness of Costa Rica Unit I decrease by a factor of 10 when compared with the measured apparatus stiffness value. This implies that the mechanical property of the material of Costa Rica Unit I may be more flow-dominated than others. This implies that the mechanical property of the material of Costa Rica Unit I may be more flow-dominated than others. Considering that the samples of the Nankai accretionary prism and Costa Rica contain 20-30 wt%, 60-70 wt% clay, respectively, it is possible that total clay content reflects the gouge behaviour.

Keywords: friction, subduction zone, rate- and state- friction constitutive law, Nankai Trough, Costa Rica

Japan Geoscience Union Meeting 2014
(28 April - 02 May 2014 at Pacifico YOKOHAMA, Kanagawa, Japan)

SSS30-P25 Room:Poster Time:April 29 18:15-19:30

Physical properties of sediments in reference sites and Frontal prism off Costa Rica: IODP Expedition 344

SAIKI, Ayaka[1*] ; HASHIMOTO, Yoshitaka[1]

[1]Kochi University

Comparing physical properties in reference and frontal prism sites is key to understand dewatering and lithification processes in subduction zone. Furthermore, it can be evidence for identifying the location of decollement and the underthrusting materials into seismogenic depth. In this study, we examined the physical properties of sediments in reference sites and frontal prism site both from on-board data and from laboratory experiments for velocity and porosity measurements with variation of effective pressure. Finally, we converted on-board porosity to fluid pressure using laboratory experimental data for reference sites and frontal prism site.

We focused on reference sites, U1381 and U1414, and frontal prism site, U1412 in the Integrate Ocean Drilling Program Expedition 344 off Costarica. Laboratory experiments for velocity and porosity measurements were conducted with variation of effective pressure. We kept 1MPa of pore pressure and changed confining pressure stepwise to control effective pressure. We calculated in-situ effective pressure using sample depth, bulk density and assumption of hydrostatic pressure of pore pressure. We obtained velocity and porosity data by 5 steps up to the in-situ effective pressure and 5 steps more up to 10 times of the in-situ effective pressure. Porosity change during experiments was calculated using volume change in pore water volume. We assumed on-board porosity under atmospheric pressure condition. 4 samples from sites U1381 and U1414 were measured so far.

Porosity ranges from about 77% to about 53% during experiments. P-wave velocity ranges from about 1.4 to 1.6 km/s. Velocity-porosity relationships from on-board data and from laboratory experiments are comparable nicely and also represents a good agreement with global empirical model. Because both laboratory data and on-board data shows a similar trend in the velocity-porosity relationship except for data from U1381 Unit II, the physical properties of sediment except for sediments from U1381 Unit II is similar in velocity-porosity-effective pressure relationships. Therefore, the porosity-effective pressure can be applied on most of sediments, implying that we can convert the porosity to effective pressure using laboratory results. We estimated fluid pressure from on-board porosity with depth using porosity-effective pressure relationship obtained from laboratory experiments.

For U1381 Unit I, hydrostatic fluid pressure was estimated although the error was large. Because U1381 is located in reference site, the hydrostatic pressure is expected in U1381. On the other hand, for U1414, lower fluid pressure than hydrostatic pressure was estimated in ˜10m intervals in the upper part of Unit II. Hydrostatic pressure was estimated in other interval in U1414. Therefore, fluid pressure was recovered to hydrostatic pressure below the over-consolidated layer. In the over-consolidated layer, porosity decreases quickly with constant grain density, which is comparable with the over-consolidation state. Below the over-consolidated layer, porosity increases with decrease of grain density, although the hydrostatic pressure is estimated. In the interval with increase of porosity, because sediments possibly have different physical property, further laboratory experiments on the sediments are needed. Finally, for U1412, over-consolidated sediments were estimated, which may be due to quick dehydration by frontal accretion.

Keywords: IODP, subduction zone, physical property of sediment, elastic wave velocity, pore pressure

Japan Geoscience Union Meeting 2014
(28 April - 02 May 2014 at Pacifico YOKOHAMA, Kanagawa, Japan)

SSS30-P26 Room:Poster Time:April 29 18:15-19:30

A structural traverse across the Shimanto belt in western Shikoku, Japan

OOHASHI, Kiyokazu[1*] ; KANAGAWA, Kyuichi[1]

[1]Graduate School of Science, Chiba University

The Cretaceous and Tertiary Shimanto accretionary complex is largely characterized by imbricated thrust slices of trench-fill and ocean-floor sediments, and is thought as an ancient analog of the Nankai accretionary prism. Recent studies on a thermal structure and fault rock analysis for the Shimanto accretionary complex in the central and eastern Shikoku revealed that it has suffered earthquake faulting along the out-of-sequence thrusts associated with tectonic uplift. However, special distributions of thermal and tectonic structures are remaining unclear since those in the western part of Shikoku are poorly understood. In the presentation, we demonstrate the distributions and details of deformed rocks (e.g. melange and brittle faults), geological structure, and vitrinite reflectance across the Shimanto belt in western Shikoku.

Keywords: Shimanto accretionary complex, Out of sequence thrust, Melange, Vitrinite reflectance, Fault rocks

Japan Geoscience Union Meeting 2014
(28 April - 02 May 2014 at Pacifico YOKOHAMA, Kanagawa, Japan)

SSS30-P27 Room:Poster Time:April 29 18:15-19:30

Stress estimation of Kure OSTs, Shimanto accretionary complex

KOMETANI, Yusuke[1*]

[1]yamaguchiuniversity

Stress must be concentrated at front of seismogenic fault during rupture propagation. The level of this stress concentration depends on rupture propagation velocity, fault length, thickness of process zone and strength of host rock. However, few quantitative analysis was reported in natural fault due to difficulty of stress estimation. The calcite-twin piezometer, enables stress estimation from elastic rebounded rock, was proposed based on discrete element method simulation and tri-axial rock experiments (Sakaguchi et al., 2011).

The Shimanto accretionary complex is ancient subduction zone and some fossil seismogenic faults were reported.

Among them, pseudotachylyte bearing Kure OSTs cuts Cretaceous Shimotsui, Nonokawa Formation and Kure Melange. This Kure OSTs is composed of echelon formed small faults with thin damaged zone, and burial depth of the host rock is estimated as below 3 km in depth. We obtained three rock samples, applicable for calcite-twin piezometer. The highest value of estimated stress was approximately 420MPa. This is much higher value than the other seismogenic fault in Shimanto accretionary. The Okitsu Fault, formed deeper depth of approximately 4 km, have suffered lower stress of 350 MPa at fault center (Sakaguchi et al., 2011). This indicates that much higher stress was concentrated at shallow Kure OST than deep Okitsu Fault. We propose two models to make high stress at shallow portion. Long crack length from deep to surface causes high stress concentration at shallow portion. Other model causes high stress due to narrower fault zone than the Okitsu Fault. Stress may tend to concentrate at narrower process zone of Kure OSTs than wide process zone of Okitsu Fault.

Keywords: subduction zone, ancient seismogenic, calcite, twin density

Japan Geoscience Union Meeting 2014
(28 April - 02 May 2014 at Pacifico YOKOHAMA, Kanagawa, Japan)

SSS30-P28 Room:Poster Time:April 29 18:15-19:30

Paleostress analysis of a subduction zone megasplay fault - An example from the Nobeoka Thrust, Japan

KAWASAKI, Ryoji[1*] ; HAMAHASHI, Mari[1] ; FUKUCHI, Rina[1] ; HASHIMOTO, Yoshitaka[2] ; YAMAGUCHI, Asuka[3] ; KAMEDA, Jun[4] ; HAMADA, Yohei[5] ; KITAMURA, Yujin[6] ; OTSUBO, Makoto[7] ; KIMURA, Gaku[1]

[1]Dept. Earth and Planet. Sci., Univ. Tokyo, [2]Kochi Univ., [3]Atmosph. Ocean Res. Inst., Univ. Tokyo, [4]Hokkaido Univ., [5]Japan Agency for Marine-Earth Science and Technology, [6]Kagoshima Univ., [7]AIST, Geological Survey of Japan, Inst. Geology and Geoinformation

The megasplay faults in subduction zones, branching from plate boundary thrusts, are thought to have a potential to generate earthquakes and accompanying tsunamis. It is therefore important to understand the fault mechanism of megasplay faults for earthquakes and tsunamis occuring in subduction zones. Paleo-splay faults exposed on land often preserve clear deformation features of the seismogenic zone and provide information on the fault mechanisms at depth. One of the important informations that can be obtained from exhumed faults is paleo-stress field. Here we investigated the Nobeoka Thrust, a fossilized megasplay fault in the Shimanto Belt in Kyushu. The hanging wall is Eocene Kitagawa Group, composed of phyllitic shales. The footwall is Eocene to early Oligocene Hyuga Group, composed of foliated cataclasite originated from sandstone-shale melanges. The thrust has been active during the period of 48-40 Ma [Hara and Kimura, 2008]. The hanging- and the footwall have experienced maximum burial temperatures of approximately 320^{o}C and 250^{o}C, respectively [Kondo et al., 2005]. The existence of klippes apart from the Nobeoka Thrust shows that the Nobeoka Thrust is nearly horizontal in regional scale [Murata, 1991, 1995]. Kondo et al. (2005) described two orientations of slickensides from the outcrop, suggesting the existence of flexural gentle fold in kilometer scale. In addition to the previous studies focusing on outcrops, scientific drilling has performed in 2011 penetrated through the Nobeoka Thrust, and core samples and geophysical logging data are obtained. The cores provide important information for investigating geological features under the ground and have an advantage without surface weathering.

In this study, we analyzed paleo-stress from slip vectors on small faults observed in the cores. Small faults are expected to be less-reactivated. The number of small faults is much larger than that of large faults, accordingly, high statistical reliability is expected. Multiple inverse method (MIM; Yamaji, 2000; Otsubo and Yamaji, 2006) was applied to the small faults. K-means clustering (Otsubo et al. , 2006) was applied to stress tensors detected by the MIM for estimating optimal solutions. Preliminary results indicate the presence of solutions with three maximum horizontal stress axes: N85.24^{o}E, N30.07^{o}W and N65.47^{o}E. We examined the formation process of the Nobeoka Thrust based on the results and slickensides on the outcrop. Our results would provide potential insights to the fault evolution of a megasplay fault in subduction zone.

Keywords: Nobeoka Thrust Drilling Project, Subduction zone, Shimanto Belt, paleo-stress, Multiple inverse method

Japan Geoscience Union Meeting 2014
(28 April - 02 May 2014 at Pacifico YOKOHAMA, Kanagawa, Japan)

SSS30-P29 Room:Poster Time:April 29 18:15-19:30

3D micro structural observation of pseudotachylyte

HAMADA, Yohei[1*] ; KIMURA, Gaku[2] ; KAMEDA, Jun[3] ; YAMAGUCHI, Asuka[4] ; HAMAHASHI, Mari[2] ; KITAMURA, Yujin[5] ; FUKUCHI, Rina[2] ; KAWASAKI, Ryoji[2]

[1]Kochi institute for Core Sample Research, JAMSTEC, [2]Department of Earth and Planetary Science, The University of Tokyo, [3]Earth and Planetary System Science Department of Natural History Science, [4]Atomosphere and Ocean Research Institute, The University of Tokyo, [5]Department of Earth and Environmental Sciences,Graduate School of Science and Engineering Kagoshima

Pseudotachylyte, molten fault rock due to dynamic frictional heating, is a strong evidence of seismic fault slip [Sibson 1975]. Recent research reveals pseudotachylytes can be related with dynamic weakening mechanism such as melt lubrication [DiToro et al., 2006]. However, observations of internal structure of pseudotachylyte have been confined to 2D observations with optical-electron microscope. Here we performed X-ray 3D structural observation of natural pseudotachylyte developed close to the Nobeoka thrust which is a major Out of sequence thrust in fossil accretionary prism (Shimanto-belt).

The Nobeoka thrust located in Kyusyu Island, south west Japan, bounding northern and southern Shimanto belt of Cretaceous-Tertiary accretionary complex. The thrust is considered to have been active during 40-48Ma at seismogenic depth of ˜11kmbsf, experienced maximum temperature of which is 320 Cin the hanging wall and 250 C in the footwall. Thus, the Nobeoka thrust is examined that it was major OST in seismogenic zone of accretionary prism (Kondo et al., 2005; Hara and Kimura, 2008; Raimbourg et al., 2009). The pseudotachylyte bearing fault develops in the hanging wall of the Nobeoka thrust with 1 mm of width. Okamoto et al. (2007) reported that carbonate-matrix implosion breccia fill tensile cracks and inner periphery of the fault, interposing pseudotachylyte, based on optical microscopic observation. Though pseudotachylyte cut the implosion breccia, the fault jog consists only of the carbonate-matrix breccia. It may show the fault experienced dynamic pore water pressurizing accompanied by pseudotachylyte generation at its first frictional slip. Therefore, the fault is appropriate to structural investigation of dynamic fault weakening mechanism.

We performed structural observation of this pseudotachylyte with scanning electron-microscope and 3D X-ray microscope. In the electron microscopic observation, we found that fragments of host rock unevenly distributed in the pseudotachylyte. The number of fragments is larger at lower part (footwall-side) than within the center of the pseudotachylyte. We also found open cracks along the fragments arrangement. It is considered to be cooling crack generated due to rapid cooling of molten rock. The 3D x-ray microscopic observation was performed with cylinder sample of 8 mm diameter. The spatial resolution of the x-ray microscope is 1 micro meter, and detailed 3D fault structure was imaged. We focused four planes, A: lower plane of lower fault filling vein, A': lower plane of pseudotachylyte, B: upper plane of upper vein, B': upper plane of pseudotachylyte. The surfaces configurations were extracted and its roughness was evaluated as calculated average roughness, Ra (theta), in each direction. We found that Ra has minimum value in the same direction in each plane, and the lineation strongly develops at the lower planes (A, A').

From the above results, we discussed the faulting process as:

1) Start faulting. strain concentrated in the footwall side and pore pressure was raised at the part.
2) Hydraulic fracturing by high pore pressure, tensile cracks formation and fluid migration.
3) Strength (friction) recovery by draining and formation of pseudotachylyte.

Keywords: pseudotachylyte, 3D micro structure, surface roughness

Japan Geoscience Union Meeting 2014
(28 April - 02 May 2014 at Pacifico YOKOHAMA, Kanagawa, Japan)

SSS31-01 Room:502 Time:April 30 14:15-14:30

Basement structure beneath the Tokyo metropolitan area as revealed with the MDRS method

HORIKAWA, Haruo[1*] ; ABE, Shintaro[1] ; YAMAGUCHI, Kazuo[1] ; NODA, Katsuya[2] ; ABE, Susumu[2]

[1]AIST/GSJ, [2]JGI

We applied the multi-dip reflection surfaces (MDRS) method to seismic data originally acquired by the Tokyo Metropolitan Government, and successfully revealed the shape of basin floor and geological structure above the basin floor. The resultant seismic image is interpreted as rift geometry with imbricated normal faults. Moreover, the active Tachikawa fault seemingly has a high dip angle.

The Kanto region that includes the Tokyo Metropolitan area is located near the boundary between the northeastern Japan and the southwestern Japan, and has complicated tectonic history. Moreover, the region is covered with thick sediment of Neogene to Quaternary. Seismic profiling has contributed to revealing the structure such as concealed half-graben and tectonic history.

The MDRS method is an improvement on the common reflection surface stacking (CRS) method in that the MDRS method can deal with conflicting dipping events. The CRS method can detect subtle reflection events by stacking the data along a specific reflection surface. However, complex geological structure often yields a seismic wave field that contain events from various surfaces with different geometry, and the CRS method has difficulty in resolving such complicated reflection events. The MDRS method seeks subtle reflected events, repeatedly applying the CRS method with various sets of parameters that govern the character of reflection surfaces, and superimposes the derived seismic images with high values of semblance. Consequently, the MDRS method can provide a clear image of such complex geological structure.

Seismic data reprocessed in this study was acquired in the Tokyo metropolitan area. The seismic survey was conducted in order to clarify the depth of the top of pre-Neogene basement and the sedimentary structure above the basement. data processing with the conventional common mid-point stacking was performed in the original survey, and provided an image with vertical offset of the top of the basement that corresponds to the active Tachikawa fault, but it generated a poor image for the overall shape of the basin floor; we can only recognize that the basin floor is not flat.

On the contrary, the MDRS method successfully generated a clear image of the basin floor and the stratification of sediments just above the basin floor. The sediments are in a wedge shape, and contain reflectors with a fanning and upward shallowing of dips. The wedge-shaped sediments are aligned horizontally. We interpret this structure as rift system with imbricated normal faults. In fact, rift system has been recognized beneath the Kanto region that is believed to be formed during the Miocene associated with opening of the Sea of Japan. Moreover, we have newly found that the top of the basement extends further beneath the Tachikawa fault. This suggests that the Tachikawa fault has high dip angle.

Acknowledgement
The Civil Engineering Center of the Tokyo Metropolitan Government provided the seismic data reprocessed in this study.

Keywords: multi-dip reflection surfaces method, basement structure, seismic reflection survey, common reflection surface stacking

Japan Geoscience Union Meeting 2014
(28 April - 02 May 2014 at Pacifico YOKOHAMA, Kanagawa, Japan)

SSS31-02 Room:502 Time:April 30 14:30-14:45

Seismic velocity structure in Ou backbone range by using a dense seismic array

AOYAGI, Yasuhira[1*] ; KIMURA, Haruo[1]

[1]Central Research Institute of Electric Power Industry

Ou backbone range is a strain concentration zone with E-W contraction along NE Japan arc, hence forms one of the most active reverse-faulting zone in Japan. Some destructive earthquakes, such as the 1896 Rikuu earthquake (M7.2) and the 2008 Iwate-Miyagi nariku earthquake (M7.2), have occurred there for this century. Fault rupture of the 1896 Rikuu earthquake which occurred along the eastern margin of the Yokote Basin fault zone did not reach all over the fault zone but limited to its northern part. The purpose of this study is to find some crustal structures which could control a termination of fault rupture. In this presentation, we will discuss a property of seismic velocity structure which might terminate the fault rupture of some historical earthquakes based on seismic tomography using a dense arrayed micro-earthquake observation data.

Keywords: Ou backbone range, Seismic velocity structure, Rupture termination, Micro-earthquake observation, Seismic tomography

Japan Geoscience Union Meeting 2014
(28 April - 02 May 2014 at Pacifico YOKOHAMA, Kanagawa, Japan)

SSS31-03 Room:502 Time:April 30 14:45-15:00

Relation between the resistivity structure around Hakone volcano and seismicity induced by the 2011 Tohoku Earthquake

YOSHIMURA, Ryokei[1*] ; OGAWA, Yasuo[2] ; YUKUTAKE, Yohei[3] ; KANDA, Wataru[2] ; KOMORI, Shogo[4] ; GOTO, Tadanori[5] ; HONDA, Ryou[3] ; HARADA, Masatake[3] ; YAMAZAKI, Tomoya[1] ; KAMO, Masato[1] ; YASUDA, Yojiro[6] ; TANI, Masanori[5]

[1]DPRI, Kyoto University, [2]Volcanic Fluid Research Center, Tokyo Institute of Technology, [3]Hot Springs Research Institute of Kanagawa Prefecture, [4]Institute of Earth Sciences, Academia Sinica, [5]Graduate School of Engineering, Kyoto University, [6]Graduate School of Engineering, Tottori University

Seismicity around the Hakone volcano was activated just after the arrival of surface waves caused by the 2011 off the Pacific coast of Tohoku Earthquake. Most of these triggered earthquakes had similar distribution to prior occasional swarm activities. In order to image electrical properties around such seismic events, we carried out audio-frequency magnetotelluric (AMT) measurements at 39 sites in December 2011 (Yoshimura et al., 2012). In this study, we conducted 3D modeling of dense AMT (Yoshimura et al., 2012) and MT (Ogawa et al., 2012) data, to figure out electrical characteristics around the triggered seismicity. In spite of careful treatments for noise reduction, the effects of noise were still seen on the longer parts of the responses ($<$1 Hz) at the several measurement sites. Thus we determined to have use of the frequency range from 320 Hz to 1.02 Hz. The full components the impedance tensors at 51 sites in total were inverted using the code developed by Siripunvaraporn et al. [2005]. The model space consists of 64(x-)$\times$46(y-)$\times$36(z-direction; including 7 air layers) blocks. The minimum horizontal size of blocks was 400m$\times$400m. Significant characteristics of the obtained three-dimensional resistivity model are: (1) the most of the triggered earthquakes, which occurred shallower than a depth of 4km, seem to align along edges or areas just inside the relatively resistive block; (2) surface conductive blocks, in which there were very few earthquakes, were observed beneath not only fumarolic areas but geothermal non-active regions.

Keywords: magnetotellurics, three-dimensional resistivity structure, Hakone volcano, triggered earthquake

Japan Geoscience Union Meeting 2014
(28 April - 02 May 2014 at Pacifico YOKOHAMA, Kanagawa, Japan)

SSS31-04 Room:502 Time:April 30 15:00-15:15

Three-dimensional seismic velocity structure around the Neodani fault

NAKAJIMA, Junichi[1*] ; KATO, Aitaro[2] ; IWASAKI, Takaya[2] ; THE JAPANESE UNIVERSITY GROUP OF THE, Joint seismic observations at the are[3]

[1]Graduate School of Sci., Tohoku Univ., [2]ERI, Univ. of Tokyo, [3]The Japanese University Group of the Joint Seismic Observations at the Area of Nobi Earthquake

The joint research project started in 2007 to enhance our knowledge on the deep structure around the Neodani fault, along which the largest crustal earthquake, the Nobi earthquake (M8.0), occurred in 1891. As a part of the project, 73 seismograph stations were installed around the fault, resulting in a dense seismograph network with a spatial separation of ˜10 km.

We performed a travel-time tomography to reveal a detailed 3D velocity structure around the Neodani fault. The tomographic method of Zhao et al. (1992) was applied to arrival-time data of earthquakes (N=3027) that occurred from 2002 to January 2013. The total number of arrival-time data was 248,354 for P waves and 215,034 for S waves. Horizontal grid nodes spaced at intervals of 0.1 degrees were set in the study area and vertical grid nodes were set at intervals of 5?30.

The obtained results show interesting features in terms of heteroegensou structures beneath the source area of the Nobi earthquake.

1. The lower crust beneath the Nobi plain shows low Vp and Vs compared to surrounding areas.
2. A low Vp and Vs area is imaged continuously from the Philippine Sea slab and the mid crust beneath the Nobi earthquake.
3. The lower crust beneath the Neodani fault shows an along-fault variation in seismic velocities, with moderate- to high-velocity crust to the southeast and low-velocity crust to the northwest.

Japan Geoscience Union Meeting 2014
(28 April - 02 May 2014 at Pacifico YOKOHAMA, Kanagawa, Japan)

SSS31-05 Room:502 Time:April 30 15:15-15:30

Stress tensor inversion in the Nobi fault area, Central Honshu, Japan

KATSUMATA, Kei[1*] ; KOSUGA, Masahiro[2] ; KATAO, Hiroshi[3] ; YAMADA, Takuji[1] ; KATO, Aitaro[4] ; THE JAPANESE UNIVERSITY GROUP, The joint seismic observations[4]

[1]Inst. Seismo & Volcano, Hokkaido Univ., [2]Earthquake and Volcano Observatory, Graduate School of Science and Technology, Hirosaki University, [3]Research Center for Earthquake Prediction, Disaster Prevention Research Institute, Kyoto University, [4]Earthquake Research Institute, University of Tokyo

A stress tensor inversion method was applied to 702 focal mechanism solutions in the Nobi fault area, Central Honshu, Japan, which are obtained by using HASH (Hardebeck and Shearer, 2002) that is a method using a first motion polarity of P-wave as data. The study area, 35.3-36.1N and 136.0-137.0E, is gridded with 0.1 X 0.1 spacing in the east-west and north-south directions, respectively. The focal mechanisms are divided into three groups according to the depth of hypocenter: 2-7 km, 5-10km, and 8-13km. From each group the focal mechanisms are selected that the epicenters are located within a radius of 15 km centered at each grid. The SATSI is applied to the data at each group of depth, which is a stress tensor inversion method developed by Hardebeck and Michael (2006). The spatial pattern of stress is obtained at each depth: 2-7 km, 5-10km, and 8-13km. We find that (1) the maximum principal stress (σ_1) is oriented east-west direction almost all over the study area, and (2) the σ_1 direction rotates clockwise by some tens degrees around the Nobi fault.

Keywords: Nobi fault, joint seismic observations, focal mechanism, stress tensor inversion, inland earthquake, active fault

Japan Geoscience Union Meeting 2014
(28 April - 02 May 2014 at Pacifico YOKOHAMA, Kanagawa, Japan)

SSS31-06 Room:502 Time:April 30 15:30-15:45

Strain concentration zone recognized from GNSS data in the San-in region

NISHIMURA, Takuya[1*]

[1]Disaster Prevention Research Institute, Kyoto University

Introduction

In the San-in region, southwest Japan, there were many large earthquakes including the 1943 M7.2 Tottori and the 2000 M7.3 Western Tottori prefecture earthquakes in the shallow crust. It is well-known that an active zone of microseismicity exists parallel to the coastline of Sea of Japan. On the other hand, recent geodetic data acquired by the GEONET (GNSS Earth Observation Network) suggest that a rate of contemporary deformation is small in the Chugoku district including the San-in region (e.g., Sagiya *et al.*, 2000). We study a detailed pattern of crustal deformation using the GEONET data to clarify a relation between contemporary deformation and microseismicity.

Method

We used daily coordinates of the GEONET GNSS stations published by the Geospatial Information Authority of Japan (F3 solution). We fit a function of linear, annual, and semi-annual components to time-series of site coordinates relative to site 950462 (Fukue) to estimate secular site velocities. We also estimate strain distribution at grid points (Shen *et al.*, 1996) and in Delaunay triangles using the site velocities.

Result

We identify a concentration zone of deformation corresponding to the active zone of microseismicity in an eastern part of the San-in region during April 2005 and December 2009. Distribution of maximum shear strain rate shows that an eastern inland part of the Chugoku district has the lowest strain rate (10^{-8} yr^{-1}) in the Japanese Islands and that the high strain rate (10^{-7} yr^{-1}) is distributed in a band along the coast of Sea of Japan. High strain rate is also observed in a vicinity of the source area of the 2000 Western Tottori prefecture earthquake, which suggests postseismic deformation of the 2000 earthquake is still continuing.

Velocity profile across the active zone of microseismicity shows a velocity component parallel to the active zone (N80^{o}E) has an offset of 2 mm/yr in and around the active zone. Movements across the offset suggest a right-lateral strike slip, which is consistent with a typical focal mechanism of shallow crustal earthquakes in the zone. The 2011 Tohoku-oki earthquake affects crustal deformation in the San-in region. In a postseismic period from January 2012 to December 2013, the strain rate in the San-in region became twice as large as that before 2011.

The deformation can be roughly explained by a right-lateral block motion across the active zone of microseismicity. The used GNSS network is too sparse to estimate a locking depth of a fault between the blocks. A dense GPS array is necessary for more detailed analysis.

Concluding remarks

Analysis of the GEONET data identifies a strain concentration zone corresponding to the active zone of microseismicity along the coast of Sea of Japan in an eastern part of the San-in region. This zone with a width of ˜10 km accommodates right-lateral strike-slip movement of 2 mm/yr, which is concordant with a focal mechanism of shallow earthquakes. The observed strain rate doubled after the 2011 Tohoku-oki earthquake. More detailed distribution of deformation in the strain concentration zone is important to clarify the deformation mechanism. We need to study with both observation and model calculation.

Reference

Sagiya *et al*., PAGEOPH, 147, 2303-2322, 2000
Shen *et al.*, JGR, 101(B12), 27957-27980, 1996

Keywords: Crustal deformation, Strain concentration zone, GNSS, the San-in region

Japan Geoscience Union Meeting 2014
(28 April - 02 May 2014 at Pacifico YOKOHAMA, Kanagawa, Japan)

SSS31-07 Room:502 Time:April 30 16:15-16:30

HV frictional strength of wet Longmenshan fault gouge and its comparison with the temperature anomaly in WFSD drill hole

TOGO, Tetsuhiro[1*] ; SHIMAMOTO, Toshihiko[1] ; MA, Shengli[1] ; YAO, Lu[1]

[1]Institute of Geology, China Earthquake Adiministration

Estimation of frictional strength from temperature anomaly along coseismic fault in a drill hole after a large earthquake has received much attention recently (e.g., J-FAST project in Japan Trench after the Tohoku-oki earthquake. Surface ruptures more than 250 km long formed along existing Yingxiu-Beichuan fault, a major fault in the Longmenshan fault system, during the 2008 Wenchuan earthquake (Mw = 7.9). Drilling was conducted at Hongkou in Dujiangyan city, a western part of the fault, as a part of Wenchuan Earthquake Fault Scientific Drilling (WFSD). Temperature monitoring is an important task in the project, and WFSD-1 hole was drilled within one year after the earthquake (fastest drilled hole after a large earthquake in the world). Drilling revealed a large scale fault zone for the depth range of 580˜760 m, consisting of cataclasites (about 10 m wide), many thin fault gouge zones and fault breccia (Li et al., 2013, Tectonophysics). Temperature anomaly of only 0.15 degrees Centigrade was recognized at a depth of 590 m along a presumed coseismic slip zone (evidence for coseismic slip zone is not so strong though). Mori et al. (2010, AGU) report friction coefficient less than 0.03 from this temperature anomaly. This friction coefficient was even lower than low friction coefficients (typically 0.05˜0.2) at high slip rates, reported in the last two decades.

We have conducted wet gouge experiments on foliated fault gouge containing 25 wt% of water with Teflon sleeve at slip rates to 1.3 m/s and at normal stresses of 1.0˜4.8 MPa, and compared the results with those on dry gouge with room humidity. Sample was collected from the Hongkou outcrop (see Togo et al., 2011a, EQS), only several hundred meters from the WFSD-1 drill site. Wet gouge has peak friction coefficient of 0.1˜0.36 and steady-state friction coefficient of 0.03˜0.14, as compared with 0.65˜0.8 and 0.15˜0.2 for dry gouge (Togo et al., 2011b, EQS). Wet gouge is substantially weaker than dry gouge, but its frictional strength is still somewhat greater than expected from the near absence of temperature anomaly. However, normal stress expected at the depth of temperature anomaly is expected to be more than twice as high as those of our experiments (experiments could not be done at higher normal stresses due to gouge leak). Both peak and steady state friction coefficients of wet gouge tend to decrease by a power low with increasing normal stresses and the extrapolated steady state friction coefficient at the drilling depth reached from 0.028 to 0.022, which results are consistent with the result by Mori et al. (2010). Thus wet gouge has frictional strength fairly close to that expected from the temperature anomaly.

Wet and dry gouges have completely different deformation textures. Deformed dry gouge is characterized by ultrafine-grained slip zones (typically several to a few tens of microns thick) and weakly deformed gouge. Overlapped slip-zone structures are very common in sheared dry gouge. On the other hand, slight grain-size refinement occurs in wet gouge, and the whole wet gouge zone remains only weakly deformed. We consider that the build-up of pore pressure due to compaction induced and/or thermal pressurization separated grains and suppressed grain crushing in wet gouge.

Keywords: High-velocity friction experiment, Longmenshan fault, Wenchuan earthquake, Frictional heating, Bore hole temperature measurement

Japan Geoscience Union Meeting 2014
(28 April - 02 May 2014 at Pacifico YOKOHAMA, Kanagawa, Japan)

SSS31-08 Room:502 Time:April 30 16:30-16:45

Numerical simulation of shear bands formation in ground due to strike-slip fault

NODA, Toshihiro[1*] ; YAMADA, Shotaro[1] ; ASAOKA, Akira[2] ; SAWADA, Yoshihiro[2] ; KAWAI, Yuta[1]

[1]Nagoya University, [2]Association for the Development of Earthquake Prediction

When a strike-slip fault occurs, flower structures denoting petaloid patterns of shear bands appear inside the ground above the fault, and also the Riedel shear structures showing en-echelon shear bands appear on the surface of the ground. Ueda[1)] conducted model experiments accounting a strike-slip fault and showed evolution process of shear bands inside the model ground using X-ray CT scan system. Also, Sawada and Ueda[2)] numerically simulated evolution of flower structures etc., using a large-deformation analysis where an elasto-perfectly plastic model with the Mohr Coulomb failure criteria was used.

In this study, referring the research work by Sawada and Ueda[2)], evolution of shear bands was numerically investigated by using a soil-water coupled finite deformation analysis code ***GEOASIA***[3)] on which the SYS Cam-clay[4)] was mounted as an elasto-plastic soil model. In the analysis, since the rate-type equation of motion is precisely time-integrated, progressive failure will be analyzed as a nonlinear dynamic problem, and then generation and/or propagation of waves induced by shear bands formation[5)] will also naturally be developed in the analysis. The constitutive model used is capable of describing a wide variety of soils within the same theoretical framework. Here are shown numerical examples in which soil is taken as a non-coupled material with liquid.

First considered was a 3D FE mesh with one element in strike direction of a fault (i.e. y-direction) shown in Fig.1. The right-lateral strike-slip fault was assumed to be located below the three elements at the mid bottom of the ground. As for the boundary conditions, periodic boundary was taken directly above the fault on the x-z planes of the ground, and displacement was applied to the y-direction on the other parts of the x-z planes with a constant rate of 10^{-6}m/s on the opposite side across the fault. Also, x-z and y-z planes were frictionless. In this case, the ground exhibited localization of deformation and the shear bands grow from the bottom in a logarithmic spiral manner (“ flower structures ”). Then, the formation was attributed to plastic swelling behavior of soil element.

Next used were the other 3D meshes with forty elements in the strike direction (Fig.2) so as to investigate evolution of shear bands and effect of homogeneity/initial-imperfection in ground on the evolution. Here, as the boundary conditions, periodic boundary was assumed on the mutually opposite x-z planes and displacement was applied to the nodes located at the bottom with the same rate on the opposite side across the fault, while the same material constants were used. The imperfection was given to some elements directly above the fault by slightly altering a material constant of them. In the imperfection case, flower structures occurred inside the ground, thereafter Riedel shear structures appeared on the surface. The parts of the Riedel shear exhibited more significant upheavals than its surroundings. Furthermore, in the other numerical cases, angle between the Riedel shear and the strike varied with the different material constant.

1) Ueda K.(2003): Evolution of strike-slip fault systems and associated geomorphic structures: Model Test, CRIEPI Rep. No.U03021, in Japanese.

2) Sawada, M. & Ueda K.(2009): Numerical simulation for evaluation of structure zone distribution due to strike-slip fault, CRIEPI Rep.No.N08028, in Japanese.

3) Noda, T. et al.(2008): Soil-water coupled finite deformation analysis based on a rate-type equation of motion incorporating the SYS Cam-clay model, Soils and Foundations, 48(6), 771-790.

4) Asaoka, A.et al.(2002): An elasto-plastic description of two distinct volume change mechanisms of soils, Soils and Foundations, 42(5), 47-57.

5) Noda, T. et al.(2013): Acceleration generation due to strain localization of saturated clay specimen based on dynamic soil-water coupled finite deformation analysis, Soils and Foundations, 53(5), 653-670.

Keywords: strike-slip fault, shear bands, Riedel shear, flower structure, numerical analysis

SSS31-08 Room:502 Time:April 30 16:30-16:45

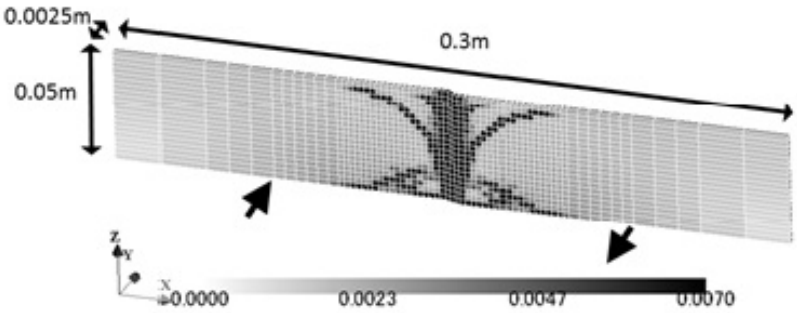

Fig.1. Occurrence of flower structure

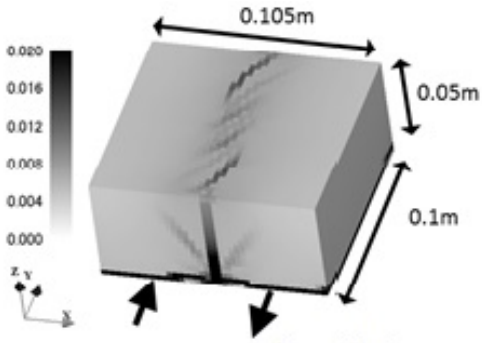

Fig.2. Occurrence of Riedel shear after flower structure, ground with initial material imperfection

Japan Geoscience Union Meeting 2014
(28 April - 02 May 2014 at Pacifico YOKOHAMA, Kanagawa, Japan)

SSS31-09 Room:502 Time:April 30 16:45-17:00

Spatially inhomogeneous stress field in the source area of the 2011 Fukushima Hamadori earthquake sequence

YOSHIDA, Keisuke[1*] ; HASEGAWA, Akira[1] ; OKADA, Tomomi[1]

[1]Research Center for Prediction of Earthquakes and Volcanic Eruptions, Tohoku University

After the 2011 great Tohoku-Oki earthquake, many earthquakes occurred near Iwaki, Fukushima Prefecture, including Mw6.8 event of April 11. This 2011 Fukushima Hamadori earthquake sequence is characterized by normal faulting, with T-axis oriented in the NW-SE, E-W and NE-SW directions for events in the northern, central and southern parts of the source area, respectively.

In order to understand the cause of such a remarkable spatial variation of focal mechanisms, we investigated the stress field in the source area of this earthquake sequence. First, we relocated hypocenters of events that occurred during the period from 1997 to 2012 by the double-difference location method. Relocated hypocenters show that events near the 3/19 Mw 5.8 earthquake in the southern area, those near the 3/23 Mw 5.7 earthquake in northern area and those near the 4/11 Mw 5.9 earthquake in central area are aligned along planes dipping westwards corresponding to one of nodal planes, respectively.

Then, we estimated the stress field in the source area of the sequence by a stress tensor inversion of focal mechanisms reported by the National Research Institute for Earth Science and Disaster Prevention and Japan Meteorological Agency. Results show that the stress field is very heterogeneous in space with normal fault stress regime after the occurrences of the main-shock of each part of the source area. In the northern, central, southern and east parts of the source area, the minimum principal stress ($\sigma 3$) axes are oriented in the NW-SE, E-W, NE-SW and NNE-SSW directions, respectively. As a whole, $\sigma 3$ axis shows the concentric circle-like distribution. In contrast, before the occurrence of the main-shock of each part, $\sigma 3$ axis is oriented homogeneously in space in the E-W direction.

This observation suggests the possibility that the remarkable heterogeneity in stress field is caused by the static stress change of large earthquakes. We estimated the static stress changes caused by the 2011 Fukushima Hamadori earthquake sequence. A slip model estimated by Hikima (2012) using strong motion waveforms was used for the Mw6.8 earthquake. Furthermore, we made fault models of the 3/19 Mw 5.7, 3/23 Mw 5.8 and 4/12 Mw 5.7 events using hypocenter locations and the scaling relation between moment magnitude, fault length, width and slip amount for estimating their static stress changes.

Spatial distribution of $\sigma 3$ axis direction of the static stress change is approximately the same as that of the observed stress field after the occurrences of the main-shock of each part of the source area. This strongly suggests that $\sigma 3$ axis rotated after the 2011 Fukushima Hamadori sequence and the stress magnitude in the focal area before the sequence was smaller than the static stress change ($<$˜several MPa). We estimated the differential stress magnitude assuming that the difference in the stress tensor before and after the earthquakes is equal to the static stress change associated with the large earthquakes. Estimated magnitude of the differential stress was $<$20 MPa.

Keywords: crustal stress, focal mechanism, weak fault

Japan Geoscience Union Meeting 2014
(28 April - 02 May 2014 at Pacifico YOKOHAMA, Kanagawa, Japan)

SSS31-10 Room:502 Time:April 30 17:00-17:15

To what degree can rocks become weak during deformation?: Fracturing-dissolution-mass transfer-precipitation creep

TAKESHITA, Toru[1*] ; OKAMOTO, Ayumi[1]

[1]Hokkaido University

The megaquake underneath the pacific ocean off the northeast Japan revealed important facts on crustal dynamics of the Japanese island. Among them, a new suggestion on the magnitude of differential stress in the crust is important. After the megaquake, peculiar earthquakes occurred in places, where earthquakes do not frequently occur. A typical example was an earthquake caused by normal faulting near the Iwaki-city, northeast Japan, where the stress field of a weak E-W compression was changed to that of an E-W extension. Based on the facts, Yoshida et al. (2012) estimated that the magnitude of differential stress was on the order of 1 MPa in upper crust. In this presentation, we will discuss the newly arising problems of crustal dynamics in Japanese islands, and also whether or not rocks can be deformed by such low differential stresses (i.e. *c.* 1 MPa), if this estimate of flow stresses is in fact correct.

We have been studying deformation processes and mechanisms in rocks at brittle ductile transition conditions, which seem to control the strength of upper crust, based on microstructural analyses in naturally deformed rocks. Deformation behaviors at the conditions of brittle-ductile conditions can be observed in metamorphic rocks formed at great depths, because these are elevated from ductile to brittle regions across the depth of brittle-ductile transition. For example, pervasive semi-brittle micro-faulting occurred in quartz schist from the Sambagawa metamorphic rocks at brittle ductile transition conditions. Here, although quartz layers were truncated by micro-faults, very-fine grained dynamically recrystallized quartz grains were also formed along them (i.e. micro-shear zone), suggesting components of ductile deformation. Further, very-fine-grained white mica was formed along the micro-faults, suggesting fluid percolation. With increasing deformation, the density of micro-faults increased, accompanied by the widening of micro-shear zones and associated decrease of the volume fraction of undeformed lenses. Perhaps, dissolution-precipitation creep dominated in micro-shear zones, having led to stress concentration in undeformed lenses, which were subsequently fractured. It is inferred that the rocks became softened with the increasing volume fraction of micro-shear zones.

Similarly, broken and displaced quartz detrital grains are observed in meta-sandstones deformed at brittle-ductile conditions from the Kamuikotan metamorphic rocks, northern Japan. Fibrous overgrowth of quartz occurred between the broken and displaced fragments of quartz, which appears as if these grains themselves restore the original shape. On the other hand, embayment occurred toward quartz grain sides at the boundary between quartz and white mica grains, suggesting dominant dissolution of quartz at this type of boundaries. Further, cataclasites formed along the Median Tectonic Line at the conditions of brittle-ductile conditions in the Cretaceous, and new minerals precipitated from fluids in the space created by fracturing and displacement of protolith forming minerals. The fracturing is accompanied by element migration via fluids, thus the degree increases with increasing degree of fracturing. In conclusion, deformation occurred by dissolution-mass transfer-precipitation assisted by fracturing under the conditions of brittle-ductile transition, by which significant weakening can be generated in rocks.

Keywords: differential stress in the upper part of crust, strain softening, micro-fracturing, dissolution, mass transfer, precipitation of minerals

Japan Geoscience Union Meeting 2014
(28 April - 02 May 2014 at Pacifico YOKOHAMA, Kanagawa, Japan)

SSS31-11 Room:502 Time:April 30 17:15-17:30

Detecting the stress condition at a fault from focal mechanism: application to the 2013 Awaji Island earthquake (M6.3)

MATSUMOTO, Satoshi[1*] ; KATAO, Hiroshi[2] ; IIO, Yoshihisa[2]

[1]Institute of Seismology and Volcanology, Kyushu Univ., [2]Disaster Prevention Research Institute, Kyoto Univ.

One of the approaches used to evaluate potential of an earthquake occurrence is the detection of stress concentration at an earthquake fault. Stress fields in stages for pre- and post-seismic event will be different from one another. However, this change cannot provide information regarding the potential for an earthquake to occur. Here, we propose a detection method for stress conditions that uses focal mechanism data. The condition can be defined both by background stress and by a moment tensor equivalent to the stress concentration. We apply this method to actual focal mechanism data from the Awaji Island earthquake (M6.3), Japan, and show the presence of stress concentration around the earthquake fault before the mainshock. In addition, the regional shear stress is shown to be ∼25 MPa in the area, implying that the stress level is still high, thus the potential for further seismicity in the area could be high.

Keywords: stress field, earthquake fault, focal mechanism

Japan Geoscience Union Meeting 2014
(28 April - 02 May 2014 at Pacifico YOKOHAMA, Kanagawa, Japan)

SSS31-12 Room:502 Time:April 30 17:30-17:45

A friction to flow constitutive law and its application to a two-dimensional modeling of earthquake cycles

SHIMAMOTO, Toshihiko[1*] ; NODA, Hiroyuki[2]

[1]Institute of Geology, China Earthquake Administration, [2]JAMSTEC

Establishment of a constitutive law from friction to high-temperature plastic flow has long been a task for solving problems such as modeling earthquakes and plate interactions. A linear combination of friction and flow laws disagrees with experimental data. Here we propose an empirical constitutive law that describes this transitional behavior with good agreements with experimental data on halite shear zones. A complete spectrum of properties including steady-state and transient behaviors can be predicted if friction and flow parameters are known. We show numerical models of seismic cycles of a fault across the lithosphere as an application. Our friction-to-flow law merges brittle-plastic Christmas-tree strength profiles of the lithosphere and rate-dependency fault models used for earthquake modeling on a unified basis. Conventionally strength profiles were drawn assuming a strain rate for the flow regime, but we emphasize that stress distribution evolves reflecting the fault behavior. Previous fault models are revised based on our earthquake modeling. Seismic fault motion is followed by fault creep in the transitional regime and this explains pseudotachylytes overprinted by mylonitic deformation, reported at various places in the world.

Keywords: Friction to flow constitutive law, Earthquake cycle modeling, Fault model, Lithosphere rheology, Mylonite, Pseudotachylite

Japan Geoscience Union Meeting 2014
(28 April - 02 May 2014 at Pacifico YOKOHAMA, Kanagawa, Japan)

SSS31-13 Room:502 Time:April 30 17:45-18:00

A consideration about computation of tectonic stress field for inland thrust earthquake

MIYATAKE, Takashi[1]*

[1]ERI, The Univ. of Tokyo

In the case of pure thrust earthquake, the driving stress system is expected to have been as shown in Fig.1a. The stress in this figure is tectonic stress; thus, the lithostatic pressure σ_V(=ρgh) must be added. The tectonic system (Fig. 1a) can be decomposed into two systems (Fig. 1b): A and B. The functional forms of σ_X and σ_Y are unknown. The assumption that that σ_X is uniform in system A causes almost uniform shear and normal stresses on the fault. Strength (peak stress) and dynamic friction can be estimated when σ_V (=ρgz) is added to the fault normal stress and the resultant normal stress is multiplied by static and dynamic frictional coefficients. Under these conditions, we found a large stress drop in the shallower parts and minimum strength excess at the free surface. This suggests that the earthquake rupture must have started at the surface and that the stress drop must have been the highest at the ground surface. These results can be avoided if the stress σ_X is assumed to increase with depth. The depth dependency is related to variations in elastic constants. The stress field in this region likely originated primarily from plate motions. Therefore, we selected the displacement boundary condition $u_X=u_0$, which correspondings to system A' in Fig. 1c. It should be noted that other displacement components were not fixed, but free stress conditions (except the σ_{xx} component) were imposed according. After solving the stress field imposing the above boundary condition, the resultant stress component σ_{xx} was added on the boundary of $x=\pm L_X$ as a further boundary condition. The solution is the same as the problem in which the boundary condition is imposed. Taking the linear elasticity into account, the target solution can be estimated by superposing solutions A and B in Fig. 1b. System A is equivalent to system A'. The effect of system B on fault normal and shear stress is expected to be negligible, because these stresses are exactly zero for a uniform structure. We estimated such effects in a heterogeneous structure by assuming that the value of σ_Y=σ_{yy} (z) on the boundary of $y=\pm L_y$ is the same as σ_{xx} (z) on the boundary of $x=\pm\pm L_x$. We found system B to exert little effect (less than 5%) on the stress components of σ_{zx}, σ_{xx}, and σ_{zz}. Thus, B had little effect on fault normal and shear stress on the fault plane, where σ_{xx} (z) is the averaged stress component along the y-axis on the corresponding boundaries. Based on the condition of thrust earthquake that $||\sigma_X|>|\sigma_Y|>|\sigma_Z|$(Fig. 1a), the above mentioned σ_{zx}, σ_{xx}, and σ_{zz} were overestimated in our study. Thus, we can ignore the effects of system B.

Keywords: inland earthquake, stress field

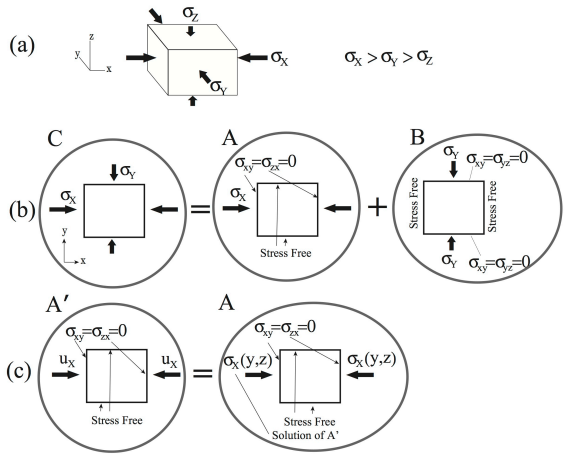

Japan Geoscience Union Meeting 2014
(28 April - 02 May 2014 at Pacifico YOKOHAMA, Kanagawa, Japan)

SSS31-P01 Room:Poster Time:April 30 18:15-19:30

Aftershock activity of the 2008 Iwate-Miyagi inland earthquake suppressed by stress shadow of the 2011 Tohoku earthquake

SUZUKI, Yuhei[1*] ; TODA, Shinji[2] ; YOSHIDA, Keisuke[1] ; OKADA, Tomomi[3]

[1]Department of Geophysics, Graduate school of Science, Tohoku university, [2]International Research Institute for Disaster Science, Tohoku university, [3]Research Center for Prediction of Earthquakes and Volcanic Eruptions, Tohoku university

The 2011 Tohoku-oki M9 earthquake has increased seismicity rates in many areas in eastern Japan. Several papers already sought the triggering mechanism to static stress change (Toda et al., GRL, 2011), dynamic stress change (Miyazawa et al., GRL, 2011) and pore fluid pressure change (Terakawa et al., EPSL, 2013). In contrast, areas where seismicity rate evidently dropped are restricted to the vicinity of the 2011 rupture zone (Kato & Igarashi, GRL, 2012), the 2004 Chuetsu aftershock zone (Hirose & Toda, SSJ fall meeting, 2011) and the 2008 Iwate-Miyagi inland earthquake aftershock zone (Suzuki & Toda, AGU fall meeting, 2013). Suzuki and Toda (2013) claim that the cause of seismic quiescence is Coulomb failure stress (CFF) decrease due to the 2011 event. However, a small quantity of focal mechanisms prevents them to confirm the mechanism.

In this study, we determine 4106 newly focal mechanisms in the area and develop a model to explain spatio-temporal seismic evolution. To estimate the focal mechanisms, we employ the method of Hardeback & Shearer (BSSA, 2002) using first motion of P-wave, provided by the campaign data by the Group for the Aftershock Observations of the 2008 Iwate-Miyagi inland Earthquake and Japan Nuclear Energy Safety Organization (JNES) in addition to the stationary data from Hi-net and F-net by NIED. Besides, we use F-net moment tensor solutions (VR?80%) and JMA focal mechanisms together with our estimates. Most of the focal mechanisms are strike-slip or thrust fault type and the distribution of ratio of strike-slip type to thrust type is spatially heterogeneous. We find several distinctive seismic clusters from all the distribution. Seismicity in two clusters in southern rupture zone of the 2008 event has been clearly decreased by the 2011 event. We calculate △CFF on all nodal planes as a proxy for background faults using a Tohoku-oki coseismic slip model given by Iinuma et al. (JGR, 2012) in an elastic half-space of Okada (BSSA, 1992). Apparent friction coefficient, μ' , is assumed to be 0.0, 0.4 or 0.8. In the case of μ' =0.0, 80% of △CFF resolved on all nodal planes are negative and over 50% △CFF are negative in the case of μ' =0.8. In the distinctive clusters mentioned above, ratios of the negative △CFF far exceed above overall average.

Seismic response to △CFF is formulated by Dieterich (JGR, 1994) based on the rate-and state-dependent friction law. The physics-based model can reproduce the empirical Omori's aftershock decay after a stress step controlled by several parameters. In this study, we estimate reference seismic rate from an average number of earthquakes from 2000 to the 2008 mainshock, △CFF associated with the 2008 mainshock, stressing rate, product of constitutive parameter and normal stress on a fault plane ($A\sigma$) estimated from the aftershocks occurred until the Tohoku-oki earthquake. Using these parameters, we calculate seismic time series from all the calculated △CFF by the Tohoku-oki earthquake, and then compare the observation with the average of all time-series curves. As a result, the models increase seismicity rate at the Tohoku-oki earthquake, which is inconsistent with the observation. We seek that reasons for mismatch between our model and observation to (i) the paucity of aftershock hypocenter data because of detectability decrease immediately after the Tohoku-oki earthquake, (ii) change in stressing rate due to the post-seismic deformation of the Tohoku-oki earthquake, (iii) reduction of friction coefficient due to fluid injection and/or pore pressure change on fault planes.

Acknowledgments. We are grateful to JMA and NIED for hypocenter list and fault plane solutions. We also thank the regional campaign data given by the Group for the Aftershock Observations of the 2008 Iwate-Miyagi inland Earthquake and JNES.

Keywords: induced earthquake, static Coulomb failure stress change, rate-and state-dependent friction law, seismic quiescence

Japan Geoscience Union Meeting 2014
(28 April - 02 May 2014 at Pacifico YOKOHAMA, Kanagawa, Japan)

SSS31-P02 Room:Poster Time:April 30 18:15-19:30

Improvement of gas medium triaxial apparatus derived from thermal fluid analysis

SAOMOTO, Hidetaka[1*] ; SHIGEMATSU, Norio[1]

[1]Active Fault and Earthquake Research Center, AIST

A huge amount of effort has used to be required for trial productions during the development of experimental apparatus. Since such trial productions generally consume vast time period and cost, the reduction of them is now a significant issue. Numerical modeling such as the finite element simulation (FE) is widely used to reduce them in various engineering fields.

Gas medium triaxial apparatus is widely used to determine the mechanical properties of rocks precisely at higher temperature. However, there has been a limitation for the use at the higher temperature in Japan due to the thermal design. In this presentation we plan to improve the gas-medium triaxial appratus derived from thermal fluid analysis based on the finite element simulation.

Here, the governing equations for thermal fluid analysis consist of the heat conduction equation, the Navier-Stokes equation and the equation of state. By solving those equations simultaneously, we obtain important physical quantities such as temperature distribution, fluid velocity field, delay of heating, etc. The knowledge derived from the computer simulations are: (1) The argon gas flow hardly has any relation with the temperature distribution on solid materials. (2) The temperatures of adiabatic materials placed near the heat sources are below the maximum operating temperature. (3)A large thermal gradient is observed close to the plastic O-ring.

Based on above results, we have attained valuable improvement policies such as replacement of meterials, improvement of radiation factor on the copper jig, etc.

Keywords: heat, fluid, Navier-Stokes, equation of state, gas medium triaxial apparatus

Japan Geoscience Union Meeting 2014
(28 April - 02 May 2014 at Pacifico YOKOHAMA, Kanagawa, Japan)

SSS31-P03 Room:Poster Time:April 30 18:15-19:30

The crustal structure beneath northern Mino region, central Japan revealed by seismic reflection survey

EMOTO, Tomoko[1*] ; TSUMURA, Noriko[1] ; FUJIWARA, Akira[2] ; ABE, Susumu[2] ; KOJIMA, Satoru[3] ; KANO, Ken-ichi[4] ; OMURA, Kentaro[5] ; TAKEDA, Tetsuya[5] ; ASANO, Youichi[5] ; OBARA, Kazushige[6] ; ITO, Tanio[7]

[1]Chiba University, [2]JGI, Inc., [3]Gifu University, [4]Shizuoka University, [5]NIED, [6]ERI, The University of Tokyo, [7]Teikyo-Heisei University

The Nobi earthquake, the largest inland earthquake in Japan, occurred in 1891 in northern Mino district, central Japan. In that region, most active faults run nearly parallel to the NW-SE trending hinge of megakink structure of the Mino belt (Kano et al., 1990). It is remarkable that the upper surface of the subducting Philippine Sea Plate (PSP) also shows a NW-SE trending broad anticlinal form whose axial zone is deeply situated almost below the hinge of the magakink. However we don't have sufficient information about seismic structure of whole crust and the uppermost mantle beneath this region to discuss influence of subducting plate on surface deformation.

To elucidate the seismic structure, a seismic reflection survey was carried out in October in 2009 (Komada et al.,2010). The survey line intersected at high angle with Neodani faults zone. We applied the seismic reflection method to the shot records of this survey and got seismic profiles of whole crust and the uppermost mantle.

We found reflectors having 2 s duration around 10 s two way travel time (TWT) in the seismic profiles. These waves occurred at TWT 9 - 11 s in the southwestern part of the study area, and at TWT 10 - 12 sec in the northeastern part. Applying depth conversion, the reflectors are located in the depth of 28 - 37km in the southwestern part, and of 32 - 39km in the northeastern part. We can clearly see that the depth of the reflection waves in the southwestern side of the Neodani fault zone are shallower than that in the northeastern side. Further the depth varies just beneath the Neodani fault zone. These feature correspond with the result of velocity analysis in the study area (Emoto et al., 2012).

Those reflection waves are interpreted as a lower crustal lamination by comparing with the result of previous seismic profiles. The geometry of laminated lower crust is consistent with the trend of the displacement on Nodani Fault Zone of Nobi earthquake. The fact might show that the difference of the reflectors depths between the southwestern and the northeastern side is caused by fault displacement and it might reach the whole crust. In southwestern part of study area, the depth of top boundary of the Philippine Sea plate (PSP) was estimated from travel time tomography in the previous studies. Its depth is equivalent in the lower limit of the lower crustal lamination. Then it might show that the crust of the land plate contacts on the subducting PHP beneath the northern Mino district.

Keywords: lower crust, Neodani fault, reflection seismic survey, Philippine Sea Plate, northern Mino region

Japan Geoscience Union Meeting 2014
(28 April - 02 May 2014 at Pacifico YOKOHAMA, Kanagawa, Japan)

SSS31-P04 Room:Poster Time:April 30 18:15-19:30

Temporary observation of micro earthquakes in the northern Ibaraki prefecture by using commercially-supplied IC recorder

SAITO, Keisuke[1*]

[1]KEISUKE SAITO, [2]KEI KATSUMATA

In case of estimate focal mechanism solutions by using P-wave first-motion polarity data, a dense seismic observation network is required. In this study we propose a new seismic observation system to record a P-wave first-motion polarity. The system consists of a seismometer with a vertical component that price is approximately ten thousand yen and a commercially-supplied IC recorder that price is approximately ten thousand yen. According to the specification of the IC recorder, the recordable frequency band is from 60 to 3400 Hz. We compare frequency characteristic of waveforms recorded in stations of National Research Institute for Earth Science and disaster Prevention (NIED Hi-net) and those recorded by using IC recorder. As a result we find that the IC recorder is able to record seismic waves that frequency band is from about 20 to 3400 Hz.

In this study, we conducted a temporary observation of micro-earthquakes for one month from August to September 2012 in the northern Ibaraki prefecture where many normal-faulting type events occur, and we addressed the effectiveness of the seismic observation system. The 29 seismic stations were deployed along a road so that it allows a deployment of many stations for a short time. After collecting the temporary stations, based on the P-wave first motion polarity, we estimated the focal-mechanisms by using HASH program (Hardebeck and Shearer, 2002). As a result, we obtain the 87 focal-mechanisms for micro-earthquakes occurred in the study area.

To test the accuracy of the focal mechanisms obtained in this study, we compared those with focal-mechanisms determined by Earthquake Research Institute, The University of Tokyo (ERI) temporary stations. We compared focal-mechanisms determined by ERI and Hi-net stations and focal-mechanisms determined by using IC recorder and Hi-net stations. We compare P axis and T axis for focal-mechanisms determined by ERI and Hi-net stations and determined by using IC recorder and Hi-net stations. As a result, nothing is difference of accuracy about focal-mechanisms between determined by ERI and Hi-net stations and determined by using IC recorder and Hi-net stations, because of P axis T axis has almost same distribution on the focal sphere. We conclude that focal mechanisms determined by using IC recorder stations has almost same accuracy as those determined by a traditional three component seismometer.

Japan Geoscience Union Meeting 2014
(28 April - 02 May 2014 at Pacifico YOKOHAMA, Kanagawa, Japan)

SSS31-P05 Room:Poster Time:April 30 18:15-19:30

Modeling the viscoelastic deformation of the NE Japan arc after the 2011 Tohoku-oki earthquake

SHIBAZAKI, Bunichiro[1*] ; NAKAI, Yoshihiko[1] ; MUTO, Jun[2] ; IINUMA, Takeshi[3]

[1]International Institute of Seismology and Earthquake Engineering, Building Research Institute, [2]Department of Earth Sciences, Tohoku University, [3]International Research Institute of Disaster Science, Tohoku University

The rheological structure of the Northeastern Japan arc crust and the upper mantle is heterogeneous along and transverse to the arc. Shibazaki et al. (2014) developed a model of the stress state of the Northeastern Japan island-arc crust using a finite element method with viscoelasticity and elastoplasticity. They reproduced several elongated low-stress regions transverse to the arc with viscous deformation that corresponds to hot fingers (high-temperature regions in the mantle wedge). The viscous relaxation process after the 2011 Tohoku-oki earthquake could be affected by the existence of low-viscosity regions caused by hot fingers. A three-dimensional (3D) finite element model was developed to investigate the viscoelastic deformation processes with heterogeneous viscosity distribution after the 2011 Tohoku-oki earthquake. The model considers the realistic crustal and mantle structures, viscoelasticity (Maxwell or Burgurs rheology), and coseismic fault slip distribution obtained by Iinuma et al. (2012). For simplicity, only the elastic crust and viscoelastic mantle structure were considered. The westward movement near the trench and eastward movement in the inland region due to viscoelastic relaxation were reproduced, which are consistent with the observations. We also consider the local low viscosity region in the Northeastern Japan arc crust. In this case, extensional viscous strain concentrates on this region. We report the numerical results that take into account the realistic 3D heterogeneous viscosity distribution in the crust and the upper mantle beneath the Northeastern Japan island arc.

Keywords: 2011Tohoku-oki earthquake, NE Japan arc, Viscoelastic deformation

Japan Geoscience Union Meeting 2014
(28 April - 02 May 2014 at Pacifico YOKOHAMA, Kanagawa, Japan)

SSS32-01 Room:315 Time:May 1 09:00-09:15

Rheological phenomena of Zebra fault in South Africa goldmine by the 2011 Tohoku earthquake's surface waves

OKUBO, Makoto[1*] ; OGASAWARA, Hiroshi[2] ; NAKAO, Shigeru[3] ; MURAKAMI, Osamu[2] ; ISHII, Hiroshi[1]

[1]TRIES, [2]Ritsumeikan Univ., [3]Kagoshima Univ.

The 2011 Tohoku earthquake was a huge earthquake. We can understand again its magnitude by large dynamic-strain observations. In general, fresh rock rupture will relieve 10^{-4} strains at the source. On the other hand the 3.11 had unleashed more than 10^{-5} dynamic strains to almost all of Japan. After these strain state changes, it activated seismic swarm events of Japan. On the other hand, more than 10^{-7} dynamic strains had been also observed at the South Africa Republics distant from 14,000 km epicenter. Ritsumeikan university takes initiative of the projects 'Grant-in-aid : Multidisciplinary monitoring of preparation and generation of earthquakes at M2 sources in South African gold mines' and 'SATREPS: Observational Studies in South African Mines to Mitigate Seismic Risks'. In the project, we can come, we can see, we can observe at proximity micro-seismicity and/or strain field at 1-3 km depths of gold mine.

In this study, we analyzed dynamic strain records of 'Cooke4' mine, which caused by the 2011 Tohoku earthquake. Although static strain changes may be disturbed by mining activity, dynamic strain variations such as teleseismic waves and surface waves have been recorded clearly. We have estimated the strain field variations vicinity of zebra fault from two strain meter combination, and we obtained the result that dilatational strain in the fault and shear strain of both size of fault have changed by passing through the seismic waves. In presentation, we will discuss inactive fault vibration caused by teleseismic waves.

Keywords: Surface waves, Zebra fault, Dynamic strain, SATREPS

Japan Geoscience Union Meeting 2014
(28 April - 02 May 2014 at Pacifico YOKOHAMA, Kanagawa, Japan)

SSS32-02 Room:315 Time:May 1 09:15-09:30

Relationship between ESR signal intensity and grain size distribution in shear zones within the Atotsugawa fault system

FANTONG, Emilia bi[1*] ; TAKEUCHI, Akira[1] ; KAMISHIMA, Toshio[1] ; DOKE, Ryosuke[2]

[1]Graduate School of Science and Engineering, University of Toyama, 3190 Gofuku, Toyama 930-8555., [2]Hot Spring Research Institute of Kanagawa Prefecture, 568 Iriuda, Odawara, Kanagawa 250-0031, Japan

Shear zones are zones of strong deformation within active faults and constitute significant sources of information on the seismogenic behavior of faults. The Atotsugawa fault system, which is in the Northern margin of the Hida Highland lies within a complex tectonic zone consisting of the Pacific plate, the Philippine Sea plate, the Amurian plate and the Okhotsk plate. This system consists of the Ushikubi fault, the Atotsugawa fault and the Mozumi-Sukenobe fault. The study of deformational fabrics and features within these shear zones can give more clarification on geodynamics of faults. Moreover, seismogenic behavior of a fault depends greatly on fault zone internal structure and fault rock constitutive properties. Although there are many studies on shear zone descriptions and deformational mechanisms, only few relate the description of cataclastic rocks (fault gouge) with Electron spin resonance (ESR) signals, which is based on the detection of paramagnetic defects in minerals produced by natural radiation that have accumulated for a long time and produces a characteristic signal detectable with an ESR spectrometer. By measuring the intensity of these trapped electrons, the rate of comminution and displacement of a fault can be clarified or envisaged. This study therefore focuses on the relationship between grain size distribution (sieve method) and ESR analysis, and rate of deformation with proximity to a slip plane.

Three shear zones from both the Atotsugawa and the Ushikubi fault were investigated. Sieve analysis and photomicrographs from thin sections revealed that grain size becomes coarser away from the slip plane (e.g. Fig.1a and Fig.2) indicating that the effect of displacement is more close to the slip plane. However, an irregular pattern in the grain size distribution was equally observed in some of the shear zones. This could be due to multiple phases of deformation. ESR analysis showed a decreasing trend in the intensity of signals toward the fault plane (Fig. 1b and Fig. 2) indicating that the rate of comminution was more intense towards the slip plane. However, the decreasing trend in ESR signal intensity with proximity to the slip plane was not observed in some of the shear zones probably due to multiple phase of deformation as indicated by the anatomizing faults in the shear zone II of the Ushikubi fault.

Results from ESR analysis suggest that samples closest to a slip plane will have low signal intensity than those further away while grain size distribution analyses indicates that samples closest to a slip plane become finer due to intensive crushing that is always associated with large displacement during fault activities.

Keywords: Active fault, Shear zones, ESR signal intensity, Grain size distribution, Atotsugawa fault system

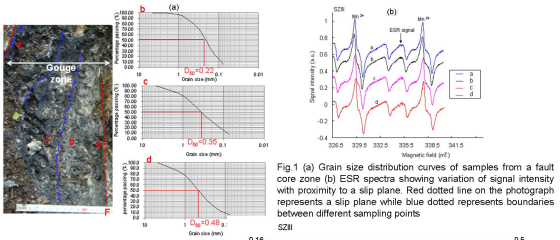

Fig.1 (a) Grain size distribution curves of samples from a fault core zone (b) ESR spectra showing variation of signal intensity with proximity to a slip plane. Red dotted line on the photograph represents a slip plane while blue dotted represents boundaries between different sampling points

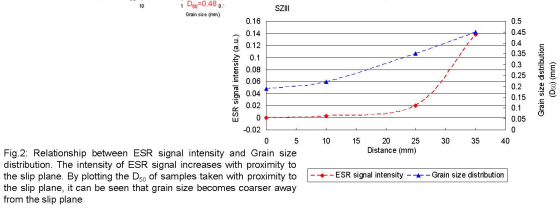

Fig.2: Relationship between ESR signal intensity and Grain size distribution. The intensity of ESR signal increases with proximity to the slip plane. By plotting the D_{50} of samples taken with proximity to the slip plane, it can be seen that grain size becomes coarser away from the slip plane

Japan Geoscience Union Meeting 2014
(28 April - 02 May 2014 at Pacifico YOKOHAMA, Kanagawa, Japan)

SSS32-03 Room:315 Time:May 1 09:30-09:45

Physico-chemo-mechanical processes in a slip zone during the 1999 Taiwan Chi-Chi earthquake

HIRONO, Tetsuro[1*] ; KAMEDA, Jun[2] ; KANDA, Hiroki[1] ; TANIKAWA, Wataru[3] ; ISHIKAWA, Tsuyoshi[3]

[1]Osaka Univ., [2]Hokkaido Univ., [3]JAMSTEC

To investigate the physicochemical processes of minerals during and after slip of the 1999 Taiwan Chi-Chi earthquake, we analyzed the mineral assemblages in the Chelungpu fault by using quantitative X-ray diffraction together with scanning and transmission electron microscope observations. In the primary slip zone, we found markedly low contents of quartz and clay minerals and large amounts of amorphous particles ranging in size from submicrometer to several tens of nanometers. Milling and heating experiments with host-rock samples indicated that these mineralogical changes are due to comminution and frictional heat during slip. Moreover, the changes may affect slip behavior through a mechanism such as thermal pressurization assisted by clay-mineral dehydration. In addition, preservation of a high amount of amorphous fine particles can potentially be used to identify the slip zone of the latest earthquake on not only the Chelungpu fault but also on other faults.

Keywords: mechanochemical, amorphous

Japan Geoscience Union Meeting 2014
(28 April - 02 May 2014 at Pacifico YOKOHAMA, Kanagawa, Japan)

SSS32-04 Room:315 Time:May 1 09:45-10:00

Characterization of carbonaceous materials in the Taiwan Chelungpu fault by micro FTIR-Raman spectroscopies

MAEKAWA, Yuka[1] ; HIRONO, Tetsuro[1*] ; YABUTA, Hikaru[1]

[1]Department of Earth and Space Science, Graduate School of Science, Osaka University

Coseismic slip during an earthquake induces frictional heating in fault zone. Determination of the temperature recorded in the fault is important for estimating the dynamic shear stress and displacement during the earthquake. Here we performed micro FTIR-Raman spectroscopic analyses of carbonaceous materials from the Taiwan Chelungpu fault, which slipped at the 1999 Chi-Chi earthquake. We also conducted heating experiments and friction experiments and analyzed by FTIR-Raman spectroscopies in order to investigate the effects of fast heating rate like frictional heating during earthquake. Based on the results of analyses, we discuss the capability as new temperature proxy during the earthquake.

Keywords: Taiwan Chi-Chi earthquake, carbonaceous materials, FTIR spectroscopy, Raman spectroscopy

Japan Geoscience Union Meeting 2014
(28 April - 02 May 2014 at Pacifico YOKOHAMA, Kanagawa, Japan)

SSS32-05 Room:315 Time:May 1 10:00-10:15

Frictional properties of ground dolerite gouges at low to high slip velocities

WADA, Jun-ichi[1] ; KITAJIMA, Hiroko[2] ; TAKAHASHI, Miki[2] ; OOHASHI, Kiyokazu[1] ; INOUE, Atsuyuki[1] ; KANAGAWA, Kyuichi[1*]

[1]Graduate School of Science, Chiba University, [2]Active Fault and Earthquake Research Center, Geological Survey of Japan

We investigated how frictional properties of ground dolerite gouges change according to grinding time. We have ground crushed and sieved grains (smaller than 500 microns) of dolerite using an automated agate mill for 10 minutes, and 6, 12, 24, 36, 48 and 60 hours. Quantitative XRD analyses indicate that amorphous phase is absent in the gouge ground for 10 minutes, but its amount increases up to 40 wt% with grinding time. Gouges ground for more than 6 hours contain abundant spherical grains composed of amorphous nano-particles. Such spherical grains are likely formed by accretion of amorphous nano-particles through their electrostatic attraction and moisture-induced binding, as accretionary lapilli. In fact, thermogravimetric analyses reveal that the amount of water adsorbed increases up to 14 wt% with grinding time in accordance with the amount of amorphous phase.

We have then conducted friction experiments on the ground dolerite gouges using a rotary shear apparatus at room temperature, a normal stress of 2 MPa, and constant slip velocities ranging from 20 micrometers/s to 1.3 m/s. At slip velocities slower than or equal to 1.3 cm/s, temperatures of gouges were lower than 70 degrees C, and steady-state friction coefficients range from 0.59 to 0.75, which tend to be higher for gouges with longer periods of grinding time at the same slip velocity. At the slip velocity of 4 cm/s, temperatures of gouges were over 100 degrees C, and steady-state friction coefficients range from 0.60 to 0.66, the difference of which among gouges with different periods of grinding time was relatively small. At slip velocities faster than or equal to 13 cm/s, however, temperatures of gouges reached higher than 180 degrees C, and steady-state friction coefficients dramatically decreased with increasing slip velocity. In addition, steady-state friction coefficients at the same slip velocity tend to be lower for gouges with longer periods of grinding time.

Such frictional properties of ground dolerite gouges depending on grinding time can be explained by the amount of water adsorbed in amorphous gouge. At slip velocities slower than or equal to 1.3 cm/s, temperatures of gouges were lower than 100 degrees C so that water adsorbed in amorphous gouge was retained. Thus, gouges ground for longer periods of time with larger amounts of adsorbed water likely became stronger in steady-state friction due to capillary bridging between amorphous gouge particles. At the slip velocity of 4 cm/s, temperatures of gouges became higher than 100 degrees C so that dehydration occurred from the amorphous gouge, which resulted in a small difference in steady-state friction among gouges with different periods of grinding time. At slip velocities faster than or equal to 13 cm/s, the moisture production rate from the dehydrated amorphous gouge was likely faster than its leak rate, which resulted in an increase in pore pressure in the gouge layer and hence a decrease in frictional strength. Thus, gouges ground for longer periods of time with larger amounts of adsorbed water became weaker in steady-state friction due to larger increases in pore pressure.

Keywords: dolerite, ground gouge, frictional properties, amorphous gouge, moisture adsorption

Japan Geoscience Union Meeting 2014
(28 April - 02 May 2014 at Pacifico YOKOHAMA, Kanagawa, Japan)

SSS32-06 Room:315 Time:May 1 10:15-10:30

Modelling of the postseismic deformation of the 2011 Tohoku Earthquake based on land and seafloor geodetic observations

IINUMA, Takeshi[1*] ; HINO, Ryota[1] ; KIDO, Motoyuki[1] ; SUN, Tianhaozhe[2] ; WANG, Kelin[3] ; OHTA, Yusaku[4] ; OSADA, Yukihito[1] ; FUJIMOTO, Hiromi[1] ; INAZU, Daisuke[5]

[1]International Research Institute of Disaster Science, Tohoku University, [2]Victoria University, [3]Geological Survey of Canada, [4]Graduate School of Science, Tohoku University, [5]National Research Institute for Earth Science and Disaster Prevention

On 11 March 2011, the 2011 off the Pacific coast of Tohoku Earthquake (M 9.0, hereafter Tohoku Earthquake) occurred on the plate boundary between the subducting Pacific and overriding continental plates. Terrestrial and seafloor geodetic observations on and around the Japanese Islands has been clearly detecting postseismic deformation associated with the Tohoku Earthquake, although three years have passed since the main shock. Iinuma et al. (2013, IAG Scientific Assembly) reported that just considering elastic response to the interplate coupling and postseismic slip on the plate boundary is insufficient to investigate the mechanical process of the postseismic deformation. We must take the inelastic deformation such as viscoelastic relaxation into account.

To tackle this problem, we estimated the displacement due to the viscoelastic relaxation by using a FEM model that includes subducting oceanic slab, difference of the viscosity between the continental and oceanic mantle, and high viscosity at the mantle wedge. The coseismic slip model based on the terrestrial and seafloor geodetic data (Iinuma et al., 2012) is used to initialize the viscoelastic relaxation process. After subtracting displacements due to the large aftershocks and viscoelastic relaxation from the original displacement time series data that are measured not only with the terrestrial GPS but also GPS/Acoustic ranging and vertical displacements observed by using Ocean bottom pressure gauges, we estimated the spatial and temporal evolution of the postseismic slip distribution on the plate interface by applying a time-dependent inversion method devised by Yagi and Kikuchi (2003).

The result of FEM calculation shows that westward displacements at seafloor sites are accounted for by viscoelastic relaxation process. However, eastward movements larger than the observed displacements at the most terrestrial GPS stations are predicted by means of the FEM model. Therefore, postseismic slip (or recovery of the interplate coupling) needs account for onshore westward displacement.

One of two areas where normal-fault-type slip distributes is estimated by applying the time dependent inversion analysis to the displacement time series as well as the result of the inversion when we assume a spherical layered structure to calculate the displacements due to the viscoelastic relaxation. But, the locations of the normal-faulting areas are different. When we use the layered structure, the area is mapped inside the main rupture area of the M9 main shock. On the other hand, normal-fault-type slip at a portion of the plate boundary deeper than the coseismic main rupture area is estimated when we calculate displacements due to the viscoelastic relaxation by means of our FEM model. Since such normal faulting areas can be regarded as the patches on the plate boundary where interplate coupling occur, it is essential to estimate the locations and rates of the slip accurately to consider the frictional character on the plate interface. Therefore we need reduce and exclude the dependency of the postseismic slip distribution with respect to the estimation of crustal deformation due to the viscoelastic relaxation. We will examine and improve rheological structure that is included in the FEM model, and will present results of further investigation at the meeting.

Keywords: The 2011 off the Pacific coast of Tohoku Earthquake, Postseismic deformation, Viscoelastic relaxation, Postseismic slip, GPS, Seafloor crustal deformation

Japan Geoscience Union Meeting 2014
(28 April - 02 May 2014 at Pacifico YOKOHAMA, Kanagawa, Japan)

SSS32-07 Room:315 Time:May 1 11:15-11:30

Scale dependency of rock friction strength revealed by large scale biaxial friction experiment

YAMASHITA, Futoshi[1*] ; FUKUYAMA, Eiichi[1] ; MIZOGUCHI, Kazuo[2] ; TAKIZAWA, Shigeru[3] ; KAWAKATA, Hironori[4]

[1]NIED, [2]CRIEPI, [3]Tsukuba Univ., [4]Ritsumeikan Univ.

In order to bridge a scale-gap between natural earthquakes (~10^3 m) and laboratory experiments (~10^{-2} m), we carried out biaxial friction experiments using meter-sized rock specimens. We used a pair of Indian gabbro, whose nominal contact area was 1.5×0.1 m^2. The experiments were conducted under conditions with loading velocities from 10^{-4} to 3×10^{-2} m/s and with normal stress of 1.3, 2.7 and 6.7 MPa. The normal and shear loads were measured with load cells. Hereafter, we refer the shear load divided by the normal load as the friction coefficient. It is well known that the rock friction has dependency on slip velocity at high slip velocity. We observed a similar tendency in the present experiments; the friction coefficient is almost constant (~0.75) at low loading velocities (10^{-4} to 10^{-3} m/s), whereas it falls suddenly at the loading velocity of 10^{-2} m/s approximately. This feature is consistent with the results using small rock specimens whose dimension is on the order of 10^{-2} m (e.g. Di Toro *et al*., 2011, Nature). It should be noted that the velocity weakening characteristics of rock friction is first confirmed on meter-sized rock. However, we found that the measured friction coefficients show weak dependency on normal stress, which suggests that the slip velocity is not a unique factor controlling the rock friction strength. On small sized rock specimens, dependency of the friction coefficient on work rate was reported; the friction coefficient is almost constant at low work rates, whereas it becomes smaller with approaching to natural conditions (e.g. Di Toro *et al*., 2011; Mizoguchi and Fukuyama, 2010, Int. J. Rock Mech. and Min. Sci.). We investigated this relationship using the present data, and found a sudden and clear reduction of the friction coefficient at the work rate higher than 10^{-2} MJ/m^2s. The clear dependency of the friction on the work rate indicates that the weakening property of rock friction is governed by the work rate rather than the slip velocity. Di Toro *et al*. (2011) suggested that the work rate is proportional to a rate of temperature increase on a fault and the heating causes various transitions of rock mineral properties, which leads to the frictional weakening. In the present experiments, similar mechanisms should work and weaken the fault strength. However, we found that the meter-sized rock friction starts to decrease at the work rate one order of magnitude lower than that of the small gabbro specimens. This difference may come from the heterogeneity of the shear stress on the fault. From the point of view, we calculated heterogeneous stress distribution on the simulated fault produced by the present apparatus, and then, we estimated the weakening property of macroscopic friction depending the work rate under the estimated stress condition. We further estimated the weakening property in the case that additional stress heterogeneity was given on the fault surface. The results reveal that stronger stress heterogeneity can make more decrease in the macroscopic friction, which suggests that the rock friction has scale dependency, because such spatial heterogeneity will become strong in larger scale.

Keywords: Rock friction, Biaxial friction experiment, Scale dependency, Work rate

Japan Geoscience Union Meeting 2014
(28 April - 02 May 2014 at Pacifico YOKOHAMA, Kanagawa, Japan)

SSS32-08 Room:315 Time:May 1 11:30-11:45

Graphite-bearing pseudotachylytes in metasediment: Implication for CO2 degassing by oxidation of graphite

NAKAMURA, Yoshihiro[1*] ; MADHUSOODHAN, Satish-kumar[2] ; TOYOSHIMA, Tsuyoshi[2]

[1]Graduate School of Science & Technology, Niigata University, [2]Department of Geology, Faculty of Science, Niigata University

Graphite in fault rocks has important role in controlling the redox states in COH fluid, and many researchers have pointed out that the behavior of fluid in pore water or hydrous minerals dramatically change the physical and chemical property of fault rocks. Recently, the CO_2 degassing, form possible biogenic sources, along the faults is monitored in various active faults (e.g. Lewickie and Brantley, 2000). It is expected that the behavior of graphite in fault rocks play a key role about the fluid composition and the physicochemical properties. Here we present a detailed analysis of graphite found in pseudotachylyte and discuss the relationship between graphite and fluid during earthquake activity.

Graphite-bearing pseudotachylyte in Hidaka metamorphic belt, Hokkaido, Japan was examined using SEM, EMPA, and XRD. In pseudotachylyte-bearing cataclasite, melt-induced textures such as biotite microlites, shell textures of Fe-oxide, flow textures, spherulites and vesicles in Fe-oxide are observed. On the basis of microtextures, mineral assemblages of melted and survived minerals, pseudotachylytes are divided into two types; Pst I and Pst II. The matrix of Pst I is composed of sanidine, hematite and vesicles in Fe-oxide, and plagioclase and quartz are remained. These observations suggest that they are solidified from silicate melts by dehydration of biotite at around 700 - 1150 degree Celsius based on the experimental data. In addition, we can also deduce the stability of biotite and graphite in silicate melts of Pst I from the reaction of biotite equilibria on the T-fO_2 plane at 200MPa based on the experimental data of graphite and biotite. Mineral assemblages of sanidine, hematite and volatile in vesicles are stable only in high fO_2 fields, suggesting fO_2 in the range of over 10^{-11} at around 700 degree Celsius by frictional melting of Pst I phase. In this phase, graphite in Pst I is unstable and will be converted to COH fluid in silicate pseudotachylyte melts. On the other hand, in Pst II matrix, these phyllosilicates but also quartz, plagioclase and apatite are found to be melted or have formed embayment textures, whereas only zircon has survived. These data indicate that the Pst II has formed at a peak temperature of around 1200 - 1400 degree Celsius by the breakdown of plagioclase, sulfide and apatite. The graphite content in Pst II decrease from 1.5 wt.% to 0.9 wt.% with increasing degree of frictional melting and alter the δ^{13}C values, which shows wide range of δ^{13}C values between -20.9 and -33.1 permil, when compared with the δ^{13}C values of graphite from associated fault rocks and host metamorphic rocks (-24.8 +/- 0.67 permil). These data suggest that the host graphite has been converted to the COH fluids and then a part of fluid deposited graphite are re-precipitated from COH fluid during isobaric cooling and other carbon expelled as COH fluid due to the oversaturated melt.

Thus it is evident that frictional melting and dehydration of sheet silicates during coseismic slip generates CO_2 gas by the oxidation of carbonaceous materials. During the transformation of cataclasite to pseudotachylyte the total carbon content has decreased by about 0.5 wt.%. Assuming a rock density of 2.7g / cm^3, the fusion of 10^{-3} m^3 (i.e. 1mm thickness $\times$ 1m^2 fault plane) of cataclasite into Pst II releases 50g of excess CO_2. The estimation of CO_2 degassing in this study is comparable to those reported by Famin et al. (2008). Thus, not only carbonates but also organic matters, including graphite and carbonaceous materials in crustal rocks, are potential to be a source of CO_2 by frictional melting, and the release of CO_2 into fault planes may drastically change the dynamic properties of flash fluid pressure and frictional properties of fault planes during seismic activity.

Reference: Famin. et al., 2008. EPSL, 265, 487?497. Lewicki. & Brantley., 2000. GRL, 27(1), 5?8.

Keywords: Graphite, Pseudotachylyte, Carbon isotopes, Frictional melting, CO2 degassing

Japan Geoscience Union Meeting 2014
(28 April - 02 May 2014 at Pacifico YOKOHAMA, Kanagawa, Japan)

SSS32-09 Room:315 Time:May 1 11:45-12:00

Nanograins and carbonaceous film on a fault surface: an example from a fossil megasplay fault in the subduction zone

KITAMURA, Yujin[1*] ; KIMURA, Gaku[2] ; KAMEDA, Jun[4] ; KOUKETSU, Yui[5] ; YAMAGUCHI, Asuka[6] ; KAGI, Hiroyuki[5] ; HAMAHASHI, Mari[2] ; FUKUCHI, Rina[2] ; HAMADA, Yohei[3] ; FUJIMOTO, Koichiro[7] ; HASHIMOTO, Yoshitaka[8] ; SAITO, Saneatsu[3] ; KAWASAKI, Ryoji[2] ; KOGE, Hiroaki[2] ; SHIMIZU, Mayuko[2] ; FUJII, Takenao[9]

[1]Dept. Earth and Environmental Sci., Kagoshima University, [2]Dept. Earth and Planet. Sci., University of Tokyo, [3]IFREE, JAMSTEC, [4]Dept. Nat. Hist. Sci., Grad. Sch. Sci., Hokkaido University, [5]Geochem. Research Center, University of Tokyo, [6]Atmosph. Ocean Research Institute, University of Tokyo, [7]Tokyo Gakugei University, [8]Kochi University, [9]SHIMADZU Corp.

Friction on the fault plane controls the behavior of faulting during seismic slip. Recent studies suggest that the frictional process on faults shows scale dependency. It is critically important to observe structures on the fault planes in various scales, especially in smaller scale in the sub-micron range. The roughness on fault planes has long been thought to hold fractal property, however, a recent work observed that a mirror fault plane, when examined up to nanometer-scale, does not obey self-affine roughness. Their observation revealed that the fault surface is coated by grains of several ten nanometers in diameter. In this abstract, we show a detailed observation of a glossy fault plane with striations sampled from drilled core of the Nobeoka Thrust taken by a scientific drilling project, the Nobeoka Thrust Drilling Project (NOBELL).

The NOBELL recovered cores with a total depth of 255 m penetrating the Nobeoka Thrust at 41 m below ground surface. The visual observation of the cores and the wireline log of the borehole clearly differentiate the hanging wall and the footwall. In this study, we analyzed a fault plane just below the Nobeoka Thrust main fault core on which gloss and striation develop using an integrated apparatus of Confocal Laser Scanning Microscope (CLSM) and Atomic Force Microscope (AFM). We also analyzed the sample surface applying Raman spectroscopy, Auger electron spectroscopy (AES) and organic component analysis using CHN coder (Yanaco MT-6).

The sample surface was imaged by the CLSM and AFM in various scale and its topography was obtained. The grains of several tens of nanometers in diameter were observed under the AFM image. This surface shows very flat surface with a hight difference of ˜80 nm in the imaged square ten micrometers on a side. The X-Z measurement by CLSM revealed an interface of around 1 micrometer below the surface. The interference fringe was observed at the rim of dark area. These facts suggest that the fault surfece is covered by a thin film approximately 1 micrometer thick. The result of the Raman spectrometry indicates that the glossy fault plane material is rich in carbon. The organic component analysis of handpicked samples reported carbon fraction. Applying the AES, we recognized carbonaceous material on the true surface.

In conclusion, the questioned sample here appears to have been polished with fault frictional process so intensely that the surface grains comminuted to sub-micrometers and then a thin carbonaceous film developed. Such nanoscale structure observations in combination with the geometrical fractal property and chemical and surface analysis could provide further details of dynamic weakening during seismic slip.

Keywords: Nobeoka Thrust Drilling Project, subduction zone, accretionary prism, Shimanto belt, fault weakening, fault mirror

Japan Geoscience Union Meeting 2014
(28 April - 02 May 2014 at Pacifico YOKOHAMA, Kanagawa, Japan)

SSS32-10 Room:315 Time:May 1 12:00-12:15

Dynamic backthrust branching: role of barriers, and implications

XU, Shiqing[1*] ; FUKUYAMA, Eiichi[1] ; BEN-ZION, Yehuda[2] ; AMPUERO, Jean-paul[3]

[1]NIED, [2]University of Southern California, [3]California Institute of Technology

Increasing evidence indicates that backthrusts may become active during or after megathrust ruptures in subduction zones, such as in Chile and Sumatra (Melnick et al., 2012; Singh et al., 2011). Previous studies of relevant mechanisms mainly focused on the interaction between forethrusts and the megathrust. Here we investigate through dynamic rupture simulations how backthrusts may be activated by megathrust ruptures in subduction zone environments. Assuming a single backthrust branch that is backward inclined to the compressional side of a continuous main fault, our results show that (1) fast speed and long propagation distance of the main rupture favor the activation of backthrust; (2) the outward propagation of the activated branch rupture interacts with the main fault mainly in the backward direction, while the tapered slip towards the branch end at the junction affects the main rupture behavior around the junction. We further assume an effective barrier for the main fault at the junction, motivated by the previous studies that barriers of various types (e.g. sharp fault bend, fault end, and transition region with increased basal friction) can also generate backthrusts during the long-term quasi-static process. Compared to the case without barrier, one prominent effect of the barrier is to arrest or delay the forward propagation of the main rupture, such that a resultant backward stress lobe as discussed in Xu and Ben-Zion (2013) can load the backthrust branch over a considerable time. This is particularly important for rupture activation along relatively immature backthrusts within sediments, where the nucleation time leading to the spontaneous propagation phase could be long, due to the large effective Dc, low frictional strength drop, or surface roughness. Indeed, our additional results confirm that the barrier model, although not always necessary, is more favorable for the activation of backthrusts with increased dynamic friction.

Our study has several implications: (i) it agrees with the quasi-static model based on the critical taper theory and limit analysis (Cubas et al., 2013) that an increase of basal friction towards the toe may statistically favor the activation of backthrusts near the up-dip limit of megathrust ruptures; (ii) there are also possibilities that backthrusts can still be activated by a propagating rupture, therefore the dynamic critical taper theory developed by Wang and Hu (2006) needs to be improved. In fact, not only the region near the up-dip limit of the seismogenic zone can be pushed into a critical state, successive region around the propagating rupture front within the seismogenic zone can also be temporarily stressed to failure and may even sustain a failure propagation along preexisting branches; (iii) it provides a specific example of compressional-side antithetic branching that can support the early speculation of fault behavior at junctions (King, 1986; Andrews, 1989).

Keywords: earthquake branching, friction of fault zones, fault barrier

Japan Geoscience Union Meeting 2014
(28 April - 02 May 2014 at Pacifico YOKOHAMA, Kanagawa, Japan)

SSS32-11 Room:315 Time:May 1 12:15-12:30

A possibility of a CM fault thermometer Part 1: Reflectances

OKAMOTO, Shiori[1] ; HOSHINO, Kenichi[2*]

[1]Fac. Sci., Hiroshima Univ., [2]Grad. Sch. Sci., Hiroshima Univ.

The chemical kinetics of thermal maturation (coalification) of carbonaceous matters (CMs) in the oil and gas windows was well investigated by Burnham and his coworkers (e.g., Braun and Burnham, 1987). Burnham and Sweeney (1989) and Sweeney and Burnham (1990) introduced an activation energy distribution model for their rate law of dehydration and degassing of CMs and presented the correlation between the reflectance of CM in oil (%Ro, in percent) and the extent of the reaction (F) calculated from the rate law. They also noted that the rate law can be applied for heating rates ranging from laboratory conditions (1C/week), igneous intrusions (1C/day), and geothermal systems (10C/100 yr) to burial diagenesis (1C/10 m.y.).

On the other hand, Huang (1996) demonstrated that %Ro increased after a few days heating experiments and estimated a power rate law with t (second) to the power of 0.078. Muirhead et al. (2012) also examined that R1 ratios of Raman spectra of CMs increased after a few tens-seconds pyrolysis and proposed a power rate law with the power depending on T (K). However, those power rate laws were obtained from the experiments with bare CM fragments extracted from rocks. The power rate laws may not be applied to CMs in rocks, since we confirmed that the R1 ratios of CMs on surfaces of heated rock samples are larger than those inside the samples (details will be shown in the following presentation, Part 2).

Chips of pelitic rocks collected from the Shimanto accretionary complex were heated in an Ar-purged capsule in an oven. Since the oven takes 18-21 minutes to achieve pre-set steady temperatures and a few minutes for cooling down after heating, the following heating durations are regarded as those of constant temperatures during heating runs. The chips were heated at temperatures, 300, 350, 450, 550, 600 and 750C for 2, 5, 13 and 34 minutes.

Reflectance measurements and Raman spectroscopic analyses were taken for CMs in the chips of which surfaces were scraped off before polishing. The reflectances in air (Ra, not in percent) of CMs of unheated and heated chips and standards (SiC, GGG, YAG, sapphire and spinel) were obtained by analyzing gradations of G color of 24 bit color microphotographs taken by a reflecting microscope.

Averages of Ra of CMs in two unheated chips are 0.093 and 0.106, while an average of measured %Ro of the former is 1.99 of which F (extent of reaction) calculated from the correlation of Sweeney and Burnham (1990) is 0.618. Ra values of CMs in chips heated below 450C show no significant difference with those in unheated ones. This is consistent with that F simulated along the T-t paths of the 300C, 350C and 450C for 34 minutes runs are 0.618, 0.618 and 0.622, respectively.

On the other hand, averages of Ra of CMs heated at 550C, 600C and 750C for 34 minutes are 0.121, 0.127 and 0.151, respectively, and their respective F values simulated are 0.742, 0.811 and 0.850. It is interesting that the averages of Ra for the runs at 750C for 2, 5 and 13 minutes are 1.47, 1.50 and 1.50, respectively. The all simulated F values for the last three runs are 0.850, the maximum extent of reaction of the rate law.

Although additional heating experiments of rocks with CMs of various initial maturities are needed, we may say from the above results that the CM fault thermometer is quite possible for high temperature faulting.

CM maturations due to heating indicated by Raman spectra will be shown in the following presentation (Part 2).

Keywords: carbonaceous matter, thermometer, fault, reflectance

Japan Geoscience Union Meeting 2014
(28 April - 02 May 2014 at Pacifico YOKOHAMA, Kanagawa, Japan)

SSS32-12 Room:315 Time:May 1 12:30-12:45

A possibility of a CM fault thermometer Part2: Raman spectra

OKAMOTO, Shiori[1*] ; KOUKETSU, Yui[2] ; SHIMIZU, Ichiko[3] ; HOSHINO, Kenichi[4]

[1]Fac. Sci., Hiroshima Univ., [2]Univ. Tokyo, Grad. Sch. Sci., [3]Univ. Tokyo, Grad. Sch. Sci., [4]Grad. Sch. Sci., Hiroshima Univ.

A possibility of a CM fault thermometer Part2: Raman spectra

OKAMOTO, Shiori, KOUKETSU, Yui, SHIMIZU, Ichiko, HOSHINO, Kenichi

Key words: carbonaceous matter, thermometer, fault, Raman spectra

Parameters of Raman spectra of carbonaceous matters (CMs) have been widely used to estimate geological temperatures (e.g., Beyssac et al., 2002). Huang (1996) and Muirhead et al. (2012) proposed empirical power rate laws for CM maturation represented by reflectances in oil (%Ro) and R1 ratios of Raman spectra, respectively, from pyrolysic experiments of bare CM fragments extracted from rocks and meteorites, respectively.

To investigate a possibility of a fault thermometer by thermal maturations of CMs indicated by their Raman spectra, we conducted heating experiments of pelitic rock samples taken from Aki Group of the Shimanto accretionary belt in Kochi Prefecture, whose diagenetic temperature is estimated as ˜180C by vitrinite reflectances (Kitamura et al., 2014). The samples were heated at temperatures, 300, 350, 450, 550, 600 and 750C for 2, 5, 13 and 34 minutes (see details in the previous presentation, Part 1).

It was indicated by comparing the spectra of CMs on surfaces of heated samples and those inside the sample that maturations of the former proceeded faster than the latter during heating. Therefore, in order to apply the thermal maturation of CM to a fault thermometer, it is needed to analyze CMs inside the samples.

It should be mentioned that micro-XRD analyses of CMs after the highest and longest heating run show no graphite peak. Hence, the maturation process during the present experiments is not graphitization but coalification.

Raman spectra of CMs show two major peaks, so-called G-band and D1-band peaks. Analytical results of the peaks indicate that certain parameters of Raman spectra of CMs remarkably vary even after low temperature (300 - 450C) heating runs, whereas reflectances of CMs do not increase (see Part 1). The positions of G-band peak (Gp) and D1-band peak (Dp) tend to shift toward higher wave numbers with increasing heating durations in the all temperature runs. However, they do not shift monotonically with heating temperatures. Their wave numbers increase with the heating temperatures up to 450C, then decrease at 550C, and again increase up to 750C.

Differences between Gp and Dp (Gp-Dp) also vary with heating temperatures and durations. Although they become smaller as the temperature is higher for the longest runs (34 minutes), this temperature dependency could not be seen for the other heating durations.

The ratio of intensity to full width at half maximum of the G-band peak (Gif) and that of the D1-band peak (Dif) decrease with increasing temperatures from 300C to 450C and from 550C to 750C, but increase from 450C to 550C. The both Gif and Dif do not show monotonic change with the heating durations.

As stated in the above, a simple indicator varying monotonically with heating temperatures and durations has not been found yet. However, we conceive that the sensitivities of the above indices of the Raman spectra to the thermal maturation of CM may show their potentials as a fault thermometer. Size dependencies of variations in some of the above indices with heating temperatures and durations and similarities of those of small-grained CMs and rims of large-grained ones also show a possibility to estimate both heating temperature and duration simultaneously by a size dependent thermometer, that is, a thermo-chronometer.

Keywords: carbonaceous matter, thermometer, fault, Raman spectra

Japan Geoscience Union Meeting 2014
(28 April - 02 May 2014 at Pacifico YOKOHAMA, Kanagawa, Japan)

SSS32-13 Room:315 Time:May 1 14:15-14:30

Mineral characteristics of the plate-boundary fault at the Japan Trench

KAMEDA, Jun[1*] ; SHIMIZU, Mayuko[2] ; UJIIE, Kohtaro[3] ; HIROSE, Takehiro[4] ; IKARI, Matt[5] ; REMITTI, Francesca[6] ; MORI, James[7] ; CHESTER, Frederick[8] ; KIMURA, Gaku[2]

[1]Hokkaido University, [2]University of Tokyo, [3]Tsukuba University, [4]JAMSTEC, [5]University of Bremen, [6]Universita di Modena, [7]kyoto University, [8]Texas A&M University

The rupture and slip of the 2011 Tohoku-oki earthquake (Mw9.0) propagated along the plate-boundary megathrust and caused a huge tsunami. In order to elucidate the physical mechanisms responsible for such unexpectedly large slip of the fault, the IODP Exp. 343, the Japan Trench Fast Drilling Project (JFAST) was carried out one year after the earthquake. It succeeded in recovery of material from the plate boundary shear zone. We have examined how mineralogical properties vary through a depth-section including the plate boundary fault rock.

At the drill site (C0019E) where the large fault slip (>50m) occurred, a plate boundary shear zone was identified around 820 mbsf. X-ray diffraction (XRD) analysis revealed that abundance of smectite is markedly higher within the fault (60?80 wt.%) than in the surrounding host rocks, suggesting the shear zone material had a low intrinsic friction coefficient. Laboratory experiments on these materials demonstrated very low frictional state under various sliding conditions (Ujiie et al., 2013; Ikari et al., submitted)

In comparison, we also examined the mineralogy of reference material recovered on the outer rise of the Japan Trench (Site 436) during DSDP Leg 56. XRD analyses on the continuous series of cores found a marked anomaly in smectite abundance in the topmost ~5m section in the pelagic clay layer. Such a mineralogical feature compares well to that observed in the JFAST cores, and the smectite-rich horizon in the incoming sediments is inferred to be the localized deformation zone (decollement) when it arrives at the Japan Trench.

Keywords: Japan Tnrech, smectite, pelagic clay, Tohoku-oki earthquake

Japan Geoscience Union Meeting 2014
(28 April - 02 May 2014 at Pacifico YOKOHAMA, Kanagawa, Japan)

SSS32-14 Room:315 Time:May 1 14:30-14:45

Shock compression experiment of olivine- Part 3: pulverization occurred before frictional melting

OBATA, Masaaki[1*] ; MASHIMO, Tsutomu[2] ; CHEN, Liliang[2] ; ANDO, Jun-ichi[3] ; YAMAMOTO, Takashi[3] ; UEDA, Tadamasa[1]

[1]Graduate School of Science, Kyoto University, [2]Institute of Pulsed Power Science, Kumamoto University, [3]Graduate School of Science, Hiroshima University

Seismic waves may be generated by a rapid slip accompanied by a rapid drop of shear stress at or near the rapture tip that propagates rapidly. It is an important subject of seismology to identify the material changes occurring at the fracture tip. The inferred slip weakening has been ascribed to (1) frictional melting and lubrication, (2) thermal pressurization, (3) flash heating and melting, (4) powder lubrication, and the combinations of those above. High-speed rotary shear friction apparatus has played important roles in formulating the above hypothesis in the past, but in these experiments fault planes are already prepared and the formation of new fault planes cannot be studied. Moreover normal pressure cannot exceed few tens of mega-Pascal because of the instrumental limitation.

We performed a series of shock compression experiments using a keyed powder gun at Kumamoto University in order to investigate the focal mechanics of deep earthquakes. We used a single crystal of forsterite (Fo 94; shaped in a diskette of diameter 12 mm and thickness 3 mm nearly perpendicular to the olivine c-axis). The olivine disk is mounted in a steel capsule. Flyer speed was 1.5 km/s; applied pressure, 31 GPa; and shock wave velocity, ca. 7 km/s; particle velocity, ca. 1 km/s. After the shock experiment the capsule is recovered from the gun and cut perpendicular to the disk plane and polished thin sections were prepared for optical, SEM an TEM observations.

Many shear planes were generated. Olivine shows wavy extinctions and locally cataclastic texture. Shear planes (i.e., fault) are typically sharp and show up to 0.5 mm displacement. The TEM observation of the fault wall where 'spongy material is attached' revealed that the wall has a zonal structure as follows. Well inside the wall are developed densely spaced and tangles [001] screw dislocations. Outer 2-5 micron zone is polycrystalline olivine of average grain size 200-300 nm. The outermost rim is an aggregate of semi-rounded small olivine particles (ca. 200 nm) mounted in a matrix of glass of olivine composition, indicating that melting of olivine occurred here. It is important to note that the same dislocation structure remained in these olivine nano-particles. It is inferred from these structure that polygonization and pulverization of olivine has occurred before melting began near the fault wall (within a few microns). Such pulverization is possible at running fracture tip, where stress and strain rate are the highest (Reches and Dewer, 2005). The whole process occurred in a short duration of the order of 0.5 microsecond. The fracturing was probably propelled by the rapid sweep of shock waves running through the sample in our experiment. Apart from the role of the shock waves, the situation is considered to be analogous to natural earthquakes. Present experimental result sheds light on the long-lasting controversy on the formation of pseudotachylytes.

Reference: Reches and Dewers (2005) Gouge formation by dynamic pulverization during erthquake rupture. EPSL 235, 361-374.

Keywords: shock compression experiment, olivine, frictional melting, pulverization, fault, earthquake

Japan Geoscience Union Meeting 2014
(28 April - 02 May 2014 at Pacifico YOKOHAMA, Kanagawa, Japan)

SSS32-15 Room:315 Time:May 1 14:45-15:00

High-velocity frictional behaviors of dolerite under controlled pore-water pressure

TOGO, Tetsuhiro[1*] ; SHIMAMOTO, Toshihiko[1] ; MA, Shenli[1] ; YAO, Lu[1]

[1]Institute of Geology, China Earthquake Adiministration

High-velocity friction experiments on rocks with or without gouge have been conducted mostly under dry conditions and demonstrated dramatic weakening of faults at high velocities (e.g., Di Toro et al., 2011, *Nature*). Recent experiments under wet conditions (e.g., Ujiie and Tsutsumi, 2010, *GRL*; Faulkner et al., 2011, *GRL*) revealed very different behaviors from those of dry faults, but those experiments were done under drained conditions. Experiments with controlled pore pressure Pp are definitely needed to determine mechanical properties of faults under fluid-rich environments such as those in subduction zones. Thus we have developed a pressure vessel that can be attached to our rotary-shear low to high-velocity friction apparatus (Marui Co Ltd., MIS-233-1-76). With a current specimen holder, friction experiments can be done on hollow-cylindrical specimens of 15 and 40 mm in inner and outer diameters, respectively, at controlled Pp to 35 MPa, at effective normal stresses of 3-9 MPa, and at slip rates of 60 mm/year to 2 m/s. An effective normal stress can be increased by about 10 times by replacing a 10 kN pneumatic actuator with a 100 kN hydraulic actuator. We report an outline of the experimental system and preliminary high-velocity experiments with controlled pore pressure on Shanxi dolerite.

High-velocity friction experiments were performed on hollow-cylindrical specimens of Shanxi dolerite at effective normal stresses of 0.13-1.07 MPa and at slip rates of 1, 10, 100 and 1000 mm/sec. Nitrogen gas and water were used of the pore fluid and compared the frictional behavior. In the N^2 tests an axial force was kept at 1 kN and the nitrogen gas pressure was increased in steps from 0 to 5 MPa to change an effective normal stress. In the wet tests the specimens were soaked in distilled water in the vessel and Pp was applied by nitrogen gas in a similar manner as in the dry tests. Nitrogen gas acted as buffer to prevent an abrupt change in the pore-water pressure during experiments. The steady-state friction coefficient of dry dolerite increased from 0.3-0.35 at 10 mm/s to 0.55-0.8 at 100 mm/s and then decreased down to 0.2-0.6 at 1000 mm/s. The results are quite similar to those of dry granite tested under similar conditions (Reches and Lockner, 2010, *Nature*). However, the steady-state friction coefficient of dolerite under a pore-water pressure decreased monotonically from 0.4-0.8 at 1 mm/s to 0.3˜0.5 at 1000 mm/s, and the strengthening from 10 to 100 mm/s disappeared with a pore-water pressure. We plan to conduct more experiments with controlled pore-water pressure and to do textural and material analysis of specimens to gain insight on the weakening mechanisms.

Keywords: High-velocity friction experiment, Pore-water pressure

Japan Geoscience Union Meeting 2014
(28 April - 02 May 2014 at Pacifico YOKOHAMA, Kanagawa, Japan)

SSS32-P01 Room:Poster Time:May 1 18:15-19:30

Re-evaluation of frictional heat recorded in the dark gouge of a megasplay fault at the Nankai Trough

MASUMOTO, Hirokazu[1*] ; HIRONO, Tetsuro[1] ; ISHIKAWA, Tsuyoshi[2] ; KAMEDA, Jun[3] ; YABUTA, Hikaru[1] ; MUKOYOSHI, Hideki[4]

[1]Department of Earth and Space Science, Graduate School of Science, Osaka University, [2]Kochi Institute for Core Sample Research, Japan Agency for Marine-Earth Science and Technology, [3]Graduate School of Science, Hokkaido University, [4]Faculty of Education and Integrated Arts and Sciences, Waseda University

Because a megasplay fault branching from the deep subduction boundary megathrust in the Nankai Trough is thought to be the source of large tsunamis associated with past Tonankai earthquakes, investigation of the heat signal due to frictional slip recorded in the fault is important for estimating the earthquake slip parameters. We performed X-ray diffraction and infrared spectroscopic analyses of a megasplay fault-rock sample and re-examined previously reported trace-element and isotope compositions, but observed no specific change related to high temperature (≥250 ℃). In addition, although a qualitative increase of the illite content in illite/smectite mixed-layer minerals within the slip-zone sample was previously reported, our kinetic evaluation of illitization, taking into consideration the coseismic temperature change due to frictional heating and heat conduction, revealed that the illitization reaction hardly progresses at temperatures under 250 ℃. Alternatively, we suggest that the illite content in mixed-layer minerals might increase progressively via a comminution – dissolution – recrystallization process during multiple past slips. Accurate assessment of the slip behavior of the megasplay fault could be efficiently obtained by drilling to penetrate the fault zone at a deeper depth of approximately 1.5 km, where records of high temperatures would be detectable.

Keywords: NanTroSEIZE, Tonankai earthquake, fluid-rock interactions, trace elements, X-ray diffraction, infrared spectroscopy

Japan Geoscience Union Meeting 2014
(28 April - 02 May 2014 at Pacifico YOKOHAMA, Kanagawa, Japan)

SSS32-P02 Room:Poster Time:May 1 18:15-19:30

Roughness of fault surfaces over a length-scale range from nano- to milimeters.

KISHIDA, Minori[1*] ; MIZOGUCHI, Kazuo[2] ; TAKAHASHI, Miki[3] ; HIROSE, Takehiro[4]

[1]Hiroshima University, [2]Central Research Institute of Electric Power Industry, [3]Geological Survey of Japan, AIST, [4]Kochi, JAMSTEC

Geometric complexities of faults are first-order effects that complicate the mechanics of earthquakes and faulting. Here we report on the topographic roughness measurements on two natural fault surfaces with a continuous length-scale range from 1 nm to 3 mm. The fault surfaces observed in this study include (1) the Corona Heights fault in the Castro Area of San Francisco, that has been studied mineralogical and microstructural in detail, and (2) the Itozawa fault in Fukushima prefecture, a normal fault moved just after the 2011 Off the Pacific Coast of Tohoku earthquake. Both fault surfaces exhibit shiny slickensides on which various length and width of slickenlines are observed.

In order to measure fault surface topography with a scale range from 1 nm to 3 mm, we performed line-measurements both parallel and perpendicular to the slickenlines using two scanner devices; a confocal whilte-light scanning microscope (measurable range: 0.15 ˜3000 μm) and a scanning probe microscope (1 ˜50000 nm). The topographic properties of the measured surfaces were expressed either as a Hurst exponent (H) which are calculated from power spectrum density (PSD) of topography data. As a result, the Corona Heights fault and the Itozawa fault exhibit a consistent geometrical property, a linear behavior on a log-log plot where axes are PSD and spatial length scale. A slope of the log-log plot, H, of the Corona Heights fault and the Itozawa fault shows H_N = 0.73 $\pm$0.010 perpendicular to the slickenslide and H_P = 0.81 $\pm$0.012 parallel to it, and H_N = 0.87 $\pm$0.013 and H_P = 0.94 $\pm$0.014, respectively. Smaller H_P than H_N is often reported, that interpreted as surface roughness in the slip direction becomes less pronounced selectively with progressive displacement (e.g., Sagy et al., 2007). Therefore, almost no difference between H_P and H_N in the observed fault surfaces could imply that both faults may be relatively immature due to less total displacement, or otherwise H_P and H_N are undifferentiated with displacement in the length-scale range from 1 nm to 3 mm. Candela et al., (2012) measured roughness of thirteen earthquake fault surfaces and suggested that the fault geometry can be expressed as a single geometrical description (i.e., single H) over a range of scales from 50 μm to 50 km. Our data, at least H_N = 0.81 perpendicular to the slickenlines, is consistent with their universal H_N = 0.81 $\pm$0.04 even for lower length-scale range. Hence, the geometric complexiity of fault surfaces in nature can be maintained over length-scales from nano- to kilometer and be described as the sigle Hurst exponent.

Keywords: fault surface, roughness, fractal, Hurst exponent

Japan Geoscience Union Meeting 2014
(28 April - 02 May 2014 at Pacifico YOKOHAMA, Kanagawa, Japan)

SSS32-P03 Room:Poster Time:May 1 18:15-19:30

Evolution of fluid transport property by diagenesis in basaltic rocks from the Shimanto belt, Southern Shikoku

TANIKAWA, Wataru[1*] ; YAMAGUCHI, Asuka[2] ; KAMEDA, Jun[3] ; TADAI, Osamu[4] ; HATAKEDA, Kentaro[4] ; KITAMURA, Manami[5]

[1]JAMSTEC/Kochi, [2]Atomosphere and Ocean Research Institute, The University of Tokyo, [3]Graduate School of Science, Hokkaido University, [4]Marine Works Japan Ltd., [5]Hiroshima University

Large slip displacement was observed at shallow portion of the plate boundary fault during 2011 Tohoku earthquake, and this slip has contributed to cause large tsunami. The large displacement was probably caused by dynamic fault weakening at shallow boundary fault, or reduction of fault strength at middle to deeper portion by pore pressure generation. Pore pressure can be generated by chemical dehydration, fluid influx from deeper crust or pore volume reduction associate with permeability reduction at a large subduction plate boundary. In this study, we investigate the change of fluid transport property for basalt during diagenesis process at Nankai Subduction zone.

We collected basalt brocks in the Cretaceous Shimanto accretionary complex of Japan from Okitsu-Kozurutsu site and Kure site in Kochi, Japan. Porosity and P-wave velocity of each basalt at atmospheric pressure are 1.4 % and 2.1%, and 6.4 km/s and 5.9km/s, respectively. We found a slight difference of S-wave velocity for basalts. Permeability was measured by using N2 gas as a pore fluid, and calculated by steady state gas flow method. Permeability was measured at room temperature and under confining pressure that were increased from 1 to 160 MPa in steps.

Gas permeability was decreased with an increase of differential pore pressure at a same confining pressure. This pore pressure dependence implies the Klinkenberg effect, therefore we converted gas permeability to water permeability using the Klinkenberg equation. We did not find a variation of permeability at the lowest effective pressure of 1MPa, and permeability shows from 10^{-15} to 10^{-16} m^2. Permeability in all basalts decreased with an increase of effective pressure, and reaches from 10^{-18} to 10^{-21} m^2. Basalt from Kure site shows the lowest permeability of 10^{-21} m^2 at 100 MPa, and permeability of basalt from Okitsu site shows the largest value of 3×10^{-19} m^2. Permeability reduction with an increase of effective pressure in most samples is described by the power law equation where exponent ranges from -2 to -3. The permeability reduction for the highest permeable basalt was expressed by the theoretical relation that is based on the Hertzian contact theory (Gangi, 1978). Fractures are apparently developed in this sample, therefore the reduction in permeability is influenced more by fracture asperity rather than pore structure.

The permeabilities of basalts in this study are smaller than permeability of basalt in fault zone at Okitsu site (Kato et al., 2004), Juan de Fuca and Tonga-Kermadec (Christensenan and Ramananantoandro, 1988). At present, we did not see clear relationship between the permeability and diagenesis. Most of basalt rock shows very low permeability, therefore they have higher potential to generate a pore pressure by dehydration reaction or influx from depth during subduction at Nankai Trough.

Keywords: permeability, fluid pressure, diagenesis, subduction zone, Nankai Trough earthquake, basalt

Japan Geoscience Union Meeting 2014
(28 April - 02 May 2014 at Pacifico YOKOHAMA, Kanagawa, Japan)

SSS32-P04 Room:Poster Time:May 1 18:15-19:30

Effects of thermal cracking on elastic wave velocities and Poisson's ratio of basalt, gabbro and granite

NISHIMURA, Kaya[1*] ; UEHARA, Shin-ichi[1] ; MIZOGUCHI, Kazuo[2]

[1]Faculty of science, Toho University, [2]Central Research Institute of Electric Power Industry

Marine seismic refraction studies have found that there are high Poisson's ratio regions (>0.35) in oceanic crust at subducting plate. Christensen (1984) performed laboratory measurements of compressional and shear wave velocities (Vp and Vs, respectively) of basalt, which is one of major rocks in oceanic crust, and estimated Poisson's ratio, and suggested that observed high Poisson's ratio can be explained by high pore pressure. This distribution of high pore pressure have been concerned because it should influence fault mechanism of plate boundary at subduction zones. Christensen (1984) used intact rock for the measurements. But there are probably dense cracks near faults in nature. Therefore, to investigate Vp, Vs and Poisson's ratio for fractured rock is important to evaluate distribution of high pore pressure regions by using seismic studies. This study reports the results of measurements of Vp and Vs, and estimations of Poisson's ratio for thermally cracked gabbro, basalt and granite, which are major rocks in oceanic crust and continental crust. Rock specimens were heated at 100 ℃, 300 ℃, 500 ℃ and 700 ℃ to thermally crack them. We performed measurements at atmospheric pressure and dry condition. We also measured Vp and Vs for water-saturated specimens of gabbro and basalt heated at 700 ℃, and compared the results with those under dry condition to investigate the effect of pore fluid on Vp and Vs.

As results, specimens heated at higher temperature tended to have slower Vp and Vs. Density of the specimens was also decreased as heating temperature was increased, and especially the density change was clear from 500 ℃ to 700 ℃. This imply that clack density of specimens was increased with increasing temperature, and this might be the reason why Vp and Vs were decreased. Poisson's ratios obtained in this study (0.05-0.25) were lower than the observed high Poisson's ratio. Vp and Vs for water-saturated specimens were generally faster than those for dried specimens, but output signals tended to be smaller and therefore improvements of the measurements systems and methods to analyze the signals should be necessary.

Keywords: Poisson's ratio, Elastic wave, High pore pressure, Basalt, Gabbro, Granite

Japan Geoscience Union Meeting 2014
(28 April - 02 May 2014 at Pacifico YOKOHAMA, Kanagawa, Japan)

SSS32-P05 Room:Poster Time:May 1 18:15-19:30

Frictional property of rocks in the Izu-Bonin-Mariana Forearc under high temperature and pressure conditions

HYODO, Geni[1*] ; TAKAHASHI, Miki[2] ; SAITO, Saneatsu[3] ; HIROSE, Takehiro[4]

[1]Department of Earth and Planetary Systems Science, Graduate School of Science, Hiroshima University, [2]Geological Survey of Japan-Advanced Industrial Science and Technology, [3]Japan Agency Marine-Earth Science and Technology, [4]Kochi Institute for Core Sample Research, Japan Agency Marine-Earth Science and Technology

The Kanto region lies atop of three tectonic plates: the North American Plate, the Pacific Plate, and the Philippine Sea Plate. In addition, the collision and subduction of the Izu-Bonin-Mariana (IBM) arc into the Kanto region results in a characteristic tectonic setting as compared with other convergent margins. Due to such complicated plate configuration, the different type of earthquakes including seismic slip (e.g., the Kanto earthquake) and aseismic creep (i.e., slow earthquake of Boso peninsula) occurs at the intra-plate and plate boundaries beneath the Kanto region. Moreover, the different type of events seems to take place side by side at almost same depth (probably nearly same P-T conditions). Although many factors including pore fluid pressure and fault topography can control earthquake generation, this study focus on frictional property of incoming materials to be subducted into the Kanto region in order to examine a hypothesis that the different types of slips arise from different input materials. Thus, we have performed friction experiments on rocks that constitute the IBM forearc using a high P-T gas medium apparatus at AIST.

We sampled five rocks (marl, boninite, andesite, sheared serpentinite and serpentinized dunite) recovered from the IBM forearc by Leg 125, Ocean Drilling Program (ODP Site 784, 786). The rocks were crushed and sieved into 10˜50 μm in grain size. Then, the rock powders were sandwiched between saw-cut alumina cylinders and sheared at temperature of 300^{o}C, confining pressure of 156MPa, pore pressure of 60MPa and axial displacement rates of 0.1 and 1 μm/s. The sheared serpentinite and serpentinized dunite exhibit steady-state friction of 0.55 and 0.35-0.41, respectively and their velocity dependence of friction is positive (velocity strengthening behavior). On the other hand, for marl, boninite and andesite, a periodic stick-slip behavior appears at 1 μm/s. However, contrary to a stick-slip behavior at room temperature in general, rise time of the stick-slip behaviors are quite long (3.9, 9.3 and 10.8 sec, respectively), that could be called as a “ slow stick-slip ” . Similar slow stick-behavior were observed in halite and serpentinite slipped at high temperatures (Noda and Shimamoto, 2010; Okazaki, 2013), but this is first time to recognize this unique slip behavior in sedimentary and igneous rocks. Although it is difficult to discuss the diverse slip behaviors observed at the Kanto region based on our limited experimental results, we will examine the conditions where the transition between stable and unstable sliding appears using the input materials and explore the generation mechanisms of earthquakes at the Kanto region.

Keywords: Friction, Izu-Bonin-Mariana Forearc (IBM), slow earthquake, stick-slip, earthquake

Japan Geoscience Union Meeting 2014
(28 April - 02 May 2014 at Pacifico YOKOHAMA, Kanagawa, Japan)

SSS32-P06 Room:Poster Time:May 1 18:15-19:30

Temperature-dependent frictional strength of dolerite in a nitrogen atmosphere and its relation to amorphous material

TANAKA, Nobuaki[1*] ; WADA, Jun-ichi[1] ; KANAGAWA, Kyuichi[1]

[1]Graduate School of Science, Chiba University

Noda et al. (2011, JGR) revealed by rotary shear experiments on dolerite at a normal stress of 1 MPa, a sliding velocity of 1 cm/s and controlled temperatures from room temperature to 1000 ℃, that its frictional strength has a negative correlation with the amount of amorphous phase in wear materials as well as a positive correlation with the amount of iron oxides which increases with increasing temperature by oxidation of the iron-bearing minerals. However, oxidation of iron-bearing minerals as observed in their experiments is unrealistic in fault zones at depths due to the paucity of oxygen there.

We therefore conducted rotary shear experiments on the same dolerite at the same normal stress, sliding velocity and temperature conditions with Noda et al. (2011) in a nitrogen atmosphere with the oxygen content of 0.1 %, and compared the results with those of Noda et al. (2011). We collected mechanical data during stable sliding of 20 m after the presliding of 100 m at each experimental condition. Sieved wear materials smaller than 250 μm were then used for quantitative X-ray diffraction analyses.

Steady-state friction coefficient was ~0.47 at room temperature and 200 ℃, ~0.7 at 400 and 600 ℃, and ~0.9 at 1000 ℃. Steady-state was not reached at 800 ℃ due to intense fracturing of samples. The amount of amorphous phase in wear materials shows a change with increasing temperature similar to that for experiments in the air (Noda et al., 2011); ~65 wt% at room temperature, ~70 wt % at 200 ℃, ~70 wt% at 400 ℃, ~45 wt% at 600 ℃, ~15 wt% at 800 ℃, and 0 wt% at 1000 ℃. In contrast, the amount of iron oxides does not show a noticeable change with increasing temperature.

Experiments by Noda et al. (2011) in the air showed a negative correlation between frictional strength and the amount of amorphous phase at temperatures lower than or equal to 800 ℃. Our experiments also show an overall tendency of increasing frictional strength and decreasing amount of amorphous phase with increasing temperature. However, steady-state friction coefficient differs by more than 0.2 between room temperature and 400 ℃, while the amount of amorphous phase differs by only ~5 wt% between these two temperatures. In addition, the amount of amorphous phase differs by ~15 wt% between 400 and 600 ℃, whereas steady-state friction coefficient is almost the same at these two temperatures. This implies lack of a direct relationship between frictional strength of dolerite and the amount of amorphous phase in wear materials. Study on what controls the temperature-dependent change in frictional strength of dolerite is now in progress.

Keywords: Dolerite, Frictional strength, Wear material, Nitrogen atmosphere, Rotary shear experiment

Japan Geoscience Union Meeting 2014
(28 April - 02 May 2014 at Pacifico YOKOHAMA, Kanagawa, Japan)

SSS32-P07 Room:Poster Time:May 1 18:15-19:30

Observation of 2-D rupture propagation for stick-slip events during large-scale biaxial frictional experiments

TSUCHIDA, Kotoyo[1*] ; KAWAKATA, Hironori[1] ; FUKUYAMA, Eiichi[2] ; YAMASHITA, Futoshi[2] ; MIZOGUCHI, Kazuo[3]

[1]Ritsumeikan University, [2]National Research Institute for Earth Science and Disaster Prevention, [3]Central Research Institute of Electric Power Industry

Pre-slip was expected to occur prior to large earthquakes, since a pre-slip model was proposed by Ohnaka and Kuwahara (1990) based on their rock frictional experiments. The pre-slip accelerates toward an unstable sliding event. However, such phenomena have never been clearly observed for natural earthquakes. Ohnaka and Kuwahara (1990) observed a 1-D strain distribution along a sample surface, and estimated the apparent rupture propagation speed. In addition, the fault was narrow, and the rupture growth might be affected by free surfaces at the edge of the sample, though the free surface effect is not so common for natural earthquakes. Therefore, we closely observed two-dimensional rupture propagation on a wider fault during rock frictional experiments.

We carried out meter-scale rock frictional experiments (Fukuyama *et al*., 2013), and investigated rupture propagation of stick-slip events and some of their characteristics, using AE (acoustic emission) and strain records. The fault consisted of an interface of two Indian gabbro blocks. Their width and height were 0.5 m, and the length of upper and lower blocks were 1.5 m and 2.0 m, respectively. The arrays of strain gauges and AE sensors were installed within the lower block in order to understand two-dimensional rupture propagation. Twenty four sets of AE sensors and biaxial strain gauges were attached 60 mm below the sliding surface at intervals of 150 mm parallel to the slip direction and at intervals of 75 mm perpendicular to the slip direction. We analyzed time series of strain and AE data, and found stick-slip events accompanied with slow and accelerating strain decrease that propagated at a speed much slower than elastic wave speed.

This study was supported by NIED research project ”Development of monitoring and forecasting technology for crustal activity” and JSPS KAKENHI Grant Number 23340131.

Keywords: stick-slip event, rupture propagation, large-scale biaxial frictional experiment

Japan Geoscience Union Meeting 2014
(28 April - 02 May 2014 at Pacifico YOKOHAMA, Kanagawa, Japan)

SSS32-P08 Room:Poster Time:May 1 18:15-19:30

The experimental study about frictional instability of fault gouges in terms of Rowe's energy ratio

HIRATA, Momoko[1*] ; MUTO, Jun[1] ; NAGAHAMA, Hiroyuki[1]

[1]Dept. Earth Science, Tohoku University

1. Introduction

The stress-dilatancy relationship for granular materials in a dense packing state was introduced by Rowe (1962). He used the energy ratio (K), which was the ratio of rate of energy dissipation in the direction of minimum principal stress to energy supply in that of maximum principal stress. According to the concept, K shall be a minimum and constant value (Rowe, 1962). However, there are many questions about the physical meaning of K. Therefore, the Rowe's low has not been applied much for fault mechanics until now. Nevertheless the stress-dilatancy relation is related to the onset of frictional instability, it has not been clear yet. So, we conducted friction experiments using simulated fault gouges in order to confirm whether Rowe's law can be applied to fault situation or not.

2. Methods

The friction experiments using simulated fault gouges were conducted in a gas-medium apparatus. The confining pressure was ranging from 140 to 180 MPa. We used a cylindrical gabbroic forcing blocks (20 mm in a diameter, 40 mm in a length, and cut by a 50 degree from their cylindrical axis) and quartz gouges were sandwiched by them. The sample sustained loading initially and holding at several values of axial stresses at 190, 450, 640 and 800 MPa. The strain rate was 10^{-3} /s. In order to measure strain, three strain gauges were glued onto a gouge layer through the Teflon jacket. Another one was placed to a forcing block in a vertical direction and far from a gouge layer. Data were recorded at 2 MHz.

3. Results and Discussion

From our friction experiments, we obtained K of gouges at different confining pressures. K is given by the ratio of rate of energy dissipation in σ_3 direction to energy supply in σ_1 direction, so it can be represented by the ratio of output energy to input one. We obtained strain of σ_3 direction from three strain gauges glued onto a gouge layer. Similarly, σ_1 and strain of σ_1 direction were obtained from another gauge. σ_3 was the confining pressure. Our results showed that the output energy was the linear function of input one. K increased with confining pressure and showed a certain constant value at each loading and holding stage. Moreover, the change in K was remarkable at the final loading stage. In other words, the output energy increased suddenly because gouge particles began to slip. So, the change in K is large under high stress, including just before unstable slip. It matched shear localization (e.g. Logan et al., 1992; Marone, 1998).

Because K is represented by a function of internal friction angle, we suggest that the change reflects the process of microstructural development. It implied that the statistical particle arrangements of gouges changed at each stress level. After gouges become a closest packing state at the peak stress, the grain size reduction (GSR) of gouges occurs leading to the development of shear structure. Under GSR occurrence, K became a new state. From previous study, it is known that the microstructural development has a close relation with frictional instability (e.g. Logan et al., 1992; Marone, 1998; Onuma et al., 2011). During progressive shear, the angle of R1-shear developed in gouges decreases with cumulative slip (Gu and Wong, 1994). Hence, the change in K, that is to say the change in internal friction angle must be connected with not only microstructural development but also frictional instability.

4. Summary

From our experiments using simulated fault gouges, we obtained relationships among microstructural development, frictional instability and energy ratio of it. We confirmed that the Rowe's law could be applied to simulated fault gouges. Therefore, we can assess frictional instability in terms of the energy ratio based on Rowe's law. Systematic laboratory observation provides better understanding on energetical or microstructural consideration on the shear localization and seismogenic process.

Keywords: frictional instability, simulated fault gouge, Rowe's minimum constant energy ratio, friction experiments

Japan Geoscience Union Meeting 2014
(28 April - 02 May 2014 at Pacifico YOKOHAMA, Kanagawa, Japan)

SSS32-P09 Room:Poster Time:May 1 18:15-19:30

Temporal evolution of slip event probability -Case study of slow slip off the Boso Peninsula and the Yaeyama Islands

MITSUI, Yuta[1*]

[1]Grad. Sci., Shizuoka Univ.

Spatially-isolated slip events (earthquakes and slow slip events) have occurred quasi-periodically especially at plate interfaces (e.g., Nadeau and McEvilly [1997], Matsuzawa et al. [2002], Rogers et al. [2003]). This fact suggests that the concept of simple elastic rebound at the plate interfaces is true at a certain level.

Of course, the recurrence intervals of the slip events have no periodicity in a strict sense. Probably it is because the slip events never repeat in the same pattern. Earthquakes with dynamic processes especially tend to have this trend. In fact, an earthquake event occurred beyond the expected period from the previous earthquake sequence (Bakun et al. [2005]). Moreover, seemingly spatially-isolated events can be strongly affected by nearby huge earthquakes (e.g., Uchida and Matsuzawa [2013]). Thus it is difficult to discuss the event recurrence quantitatively based on deterministic physical models. Reseacheres alternatively used probability distribution to evaluate the recurrence intervals.

When we examine the event recurrence by the probability distribution approach, one of the most important point is actual event probabilities at the time of event occurrences. There has been little discussion on this point. We address it, focusing on slow slip events with shorter recurrence intervals. We select the Boso-oki slow slip events (Hirose et al. [2012]) and the Yaeyama-oki slow slip events (Heki and Kataoka [2008]). The probability distribution of the event recurrence intervals is the Poisson distribution. We evaluate the event probability as the subtraction of cumulative probability of zero occurrence from 100%. The cumulative probability reverts back to 100% at the time of an event. The mean recurrence interval as a parameter of the Poisson distribution is the sample average from the forepassed events. The above settings allow us to calculate the temporal evolution of the event probabilities off the Boso Peninsula and the Yaeyama Islands. **We can validate the calculated results** by comparing with the actual event occurrences.

In the result off Yaeyama Islands, the event numbers that occurred at a stage with the smaller probability than 50% are five out of the total numbers twenty six. About 80% of the events occurred with the event probability $>$50%. Besides, off the Boso Islands, the event numbers during a stage of the smaller probability than 50% are two out of the total numbers five. The two events followed the 2011 Tohoku earthquake. This fact may reflect the effect of the stress perturbation due to the Tohoku earthquake, as suggested by Hirose et al. [2012]. In summary, few slow slip events occur with the event probability $<$50%, in the probability evaluation based on the Poisson distribution. We additionaly find that the event probability at the time of an event off the Yaeyama islands has increased gradually.

Keywords: Repeating slow slip event, Event probability, Statistical approach, Off Boso Peninsula, Off Yaeyama Islands

Japan Geoscience Union Meeting 2014
(28 April - 02 May 2014 at Pacifico YOKOHAMA, Kanagawa, Japan)

SSS32-P10 Room:Poster Time:May 1 18:15-19:30

Numerical modeling of concurrent occurrence of shallow very low frequency earthquakes and long-term slow slip events

MATSUZAWA, Takanori[1*] ; SHIBAZAKI, Bunichiro[2] ; OBARA, Kazushige[3] ; HIROSE, Hitoshi[4]

[1]National Research Institute for Earth Science and Disaster Prevention, [2]Building Research Institute, [3]Earthquake Research Institute, University of Tokyo, [4]Research Center for Urban Safety and Security, Kobe University

Concurrent occurrences of shallow very low frequency earthquakes (VLFEs) and long-term slow slip events (SSEs) are found in the Bungo channel (Hirose et al., 2010, Science). This region is located at the western rim of the area where a large slip of megathrust earthquake is expected. Thus, the understanding of such behaviors will help us to reveal the preparation process of megathrust earthquakes. We aim to numerically reproduce the concurrent slip at the shallow VLFE and the long-term SSE region.

In our numerical model, a subducting plate interface is modeled as a flat plane within a semi-finite elastic medium. Frictional stress on the plate interface is given by a rate- and state-dependent friction law with cut off velocities (e.g., Matsuzawa et al., 2010, JGR). To reproduce long-term SSEs, a region with a cutoff velocity of $10^{-6.5}$ m/s and low effective normal stress is assumed below the depth of 10 km. In terms of shallow VLFEs, result of rock experiments shows that velocity-weakening and strengthening behaviors are found at low and high slip velocity, respectively (Saito, et al., 2013, GRL). In addition, it is estimated that a radius of shallow VLFEs is 5-10km from seismic data analysis (Ito and Obara, 2006, GRL). Based on these results, we assume circular regions for VLFEs with a cutoff velocity of 10^{-4} m/s and a radius of 6 km. In addition, we pose a stable sliding region beside the long-term SSE region, as more stable sliding behavior is expected in the Hyuganada region where shallow VLFEs frequently occur even in the period without long-term SSEs. In this study, some cases are calculated to examine the effect of the distribution of frictional parameters. Model 1 is a model based on the above assumptions. Model 2 is a model without a stable sliding region beside the long-term SSE region. In Model 3, the top of the long-term SSE region is set to the depth of 18 km.

In the numerical results of these three models, recurring slip at shallow VLFE and long-term SSE regions are reproduced. Concurrent occurrence of shallow VLFEs and long-term SSEs are reproduced in Model 1 and 2, while the concurrent occurrence is not clear in Model 3. In addition, slip events at the VLFE region are also found during the period without long-term SSEs in Model 2, while most of slip events at the VLFE region are found with long-term SSEs in Model 1. Our results suggest that the top of the long-term SSE region are close to the VLFE region, and the model with stable sliding region beside the long-term SSE region (Model 1) is more preferable to reproduce observed results than the model with fully locked surrounding region (Model 2).

Keywords: very low frequency earthquake, slow slip event, numerical simulation, Bungo Channel

Japan Geoscience Union Meeting 2014
(28 April - 02 May 2014 at Pacifico YOKOHAMA, Kanagawa, Japan)

SSS33-01 Room:315 Time:April 30 09:00-09:15

Spatio-temporal afterslip distribution of the 2011 Tohoku-Oki earthquake considering visco-elastic response

SUZUKI, Syota[1] ; ITO, Takeo[1*] ; SATO, Kachishige[2] ; HYODO, Mamoru[3]

[1]Graduate School of Environmental Studies, Nagoya University, [2]Faculty of Education, Tokyo Gakugei University, [3]Japan Agency for Marine-Earth Science and Technology

1. Introduction

The 2011 off the Pacific coast of Tohoku Earthquake with a moment magnitude (Mw) of 9.0 occurred at 5:46 (UTC) on March 11, 2011 along the boundary between the subducting Pacific Plate and the overlying plate. Since large earthquake are likely to produce stress concentrations in neighboring region along the plate boundary, the mainshock might have been trigger afterslip. It is very important to determine the detail of spatio-temporal distribution of afterslip, in order to understand the characteristic of friction relationship on the plate boundary. In this study, we estimate spatio-temporal afterslip distribution using visco-elastic Green's function (GF).

2. Method

We make GF using 3D finite element method (FEM) with a grid model for the Hokkaido and Tohoku regions. The model space and assumed subsurface structure for the 3D-FEM have a dimension of 2600 km (in the ESE direction) x 1500 km (in the NNE direction) x 400 km (depth) and typical subsurface structure consist of four sub-regions, i.e., upper crust, lower crust, upper mantle, and Pacific plate. The numbers of node and cell of 3D-FEM mesh are 3,205,950 and 3,121,200, respectively. For the calculation, we use the Pylith version 1.9.0, which is designed for simulating lithospheric deformation. In order to estimate the distribution of afterslip, we assume subfaults on the plate interface in and around the co-seismic slip zone of the 2011 Tohoku-Oki event. In inversion, we impose the smoothness constraint on the slip distribution. We estimate co-seismic and spatio-temporal distributions at the same time, considering visco-elastic response, derived from GEONET and seafloor observations.

3. Results and discussion

We obtain the co- and post-seismic slip distributions. The maximum slip of the 2011 event is about 60 m close to the Japan Trench. Estimated afterslip distribution is complementary to co-seismic slip distribution and also historical source regions. Amount of afterslip is about 2m, and the cumulative seismic moment is 8.06, considering visco-elastic response during 2.5 years after event. In case of only considering elastic response, amount of after slip is about 4m. There is no slip off Fukushima prefecture only considering visco-elastic response. And, our result can explain seabottom observations. i.e., Miyagi-Oki1 site move to west about 38 cm during 2 years after event. The effect of visco-elastic response is too large. In inversion for afterslip distribution from geodetic data, it must be consider to visco-elastic response due to relaxation in upper mantle.

Keywords: Afterslip, Visco-elastic response, FEM

Japan Geoscience Union Meeting 2014
(28 April - 02 May 2014 at Pacifico YOKOHAMA, Kanagawa, Japan)

SSS33-02 Room:315 Time:April 30 09:15-09:30

Vertical displacement in Naruko Volcano area following the 2011 Tohoku earthquake deduced from precise leveling survey

TSUKAMOTO, Yuya[1*] ; SUGIYAMA, Kenichi[1] ; FUJITA, Wakana[1] ; WATANABE, Keitaro[1] ; WATANABE, Kosui[2] ; TAKAHATA, Akihiro[2] ; MATSUOKA, Moe[2] ; GOTO, Akio[3] ; OHTA, Yusaku[2]

[1]Fac. Sci., Tohoku University, [2]Grad. School Sci., Tohoku University, [3]CNEAS, Tohoku University

Large subsidence accompanied the 11 March 2011 Great East Japan Earthquake along the Pacific coast. GEONET data have indicated that the subsidence goes down westward (http://www.gsi.go.jp/common/000059956.pdf). In a summer field seminar by the Division of Earth and Planetary Material Science, Tohoku University, we made precise leveling survey for 10km on the second-order leveling route along the National Route 47 (from benchmark number 047-064 to 047-074; hereafter indicated as BM64, BM74 etc.) which locates along the east to west in Naruko area, Miyagi prefecture, to detect the vertical crustal deformation of this area. We performed the leveling twice (23-28 August, 2011 and 19-25 August, 2013) using bar-code leveling rods (Leica CPCL3) and an electronic digital level (Leica DNA03). By comparison with the data by Geospatial Information Authority of Japan in 2009, we acquired the change of difference in elevation at each benchmark against the westernmost BM64. We conducted round-trip survey between each benchmark and re-measured when the residual error did not meet the first-order leveling, except the segments between BM66 and BM68 in 2011 and between BM72 and BM74 in 2013 due to the fixed seminar schedule.

Contrary to our expectation before the leveling, we found all benchmarks subsided against BM64 and the degree of subsidence increases westward. At the 2011 leveling 5 months after the earthquake, benchmarks BM66, 68, 70, 72, and 74 subsided 13.0mm, 21.4mm, 81.7mm, 91.1mm and 113.9mm, respectively. This subsidence continued further with decreasing the amount, 8.5mm, 16.2mm, 23.7mm, 41.9mm and 46.2mm between 2011 and 2013, respectively. Obtained displacement pattern along the leveling survey between 2011 and 2013 is almost similar pattern with the 2009 and 2011 one.

Ozawa and Fujita (2013) and Takeda and Fukushima (2013) showed local depressions on some major volcanic areas in Tohoku region by In-SAR analysis. They explained the depressions by the east-west extension of hot and soft medium under the volcanoes. Our research route locates on one of that volcanic area and our leveling result is consistent with their previous studies. In contrast, their analysis just focused on the coseismic displacement. In our analysis, we found not only subsidence during the coseismic stage but also the subsidence in the postseismic stage. Particularly, it is worth noting that the subsidence increases remarkably between BM68 and BM70, which is inferred to cross the rim of Naruko caldera.

Acknowledgement
We appreciate Ryohei Kobayashi and Emi Hara who joined the leveling survey in 2011.

Keywords: Great East Japan Earthquake, Naruko caldera, precise leveling survey, subsidence

Japan Geoscience Union Meeting 2014
(28 April - 02 May 2014 at Pacifico YOKOHAMA, Kanagawa, Japan)

SSS33-03 Room:315 Time:April 30 09:30-09:45

Postseismic gravity changes after the 2011 Tohoku earthquake recorded by superconducting gravimeters

IMANISHI, Yuichi[1*] ; TAMURA, Yoshiaki[2] ; NAWA, Kazunari[3] ; IKEDA, Hiroshi[4]

[1]ERI, The University of Tokyo, [2]NAOJ, [3]AIST, [4]University of Tsukuba

Continuous gravity monitoring by means of superconducting gravimeters is revealing significant effects of the 2011 Tohoku Earthquake on surface gravity in Japan. Two stations of superconducting gravimeters, Matsushiro and Kamioka, both in the main island of Japan (Honshu), are indicating gravity decreases at similar rates of approximately 10 microgal per year after the 2011 event, and this trend is still going on. Since Matsushiro and Kamioka are relatively far from the earthquake source region (epicentral distances being 420 km and 490 km, respectively), the postseismic crustal uplifts of the stations recorded by GPS are too small to account for the observed gravity decreases. Therefore, the observed gravity changes are likely to reflect ongoing changes in the density of the earth material, maybe associated with a viscoelastic flow of the asthenosphere. Data from Mizusawa, another SG station in Honshu, will also be presented in the paper.

Keywords: superconducting gravimeter, 2011 Tohoku earthquake, postseismic gravity changes, viscoelasticity

Japan Geoscience Union Meeting 2014
(28 April - 02 May 2014 at Pacifico YOKOHAMA, Kanagawa, Japan)

SSS33-04 Room:315 Time:April 30 09:45-10:00

Pressure Source Model Inferred from Crustal Deformaton Preceeding Seismic Swarm in 2013 beneath Tarumae Volcano

KOSHIROMARU, Takuma[1] ; MURAKAMI, Makoto[1*]

[1]ISV, Hokkaido University

Tarumae-volcano is an active volcano with an altitude of 1,041 m located in the southwestern part of Hokkaido. In past 350 years, three major magmatic eruptions occurred, i.e. Plinian eruptions in 1667 and 1739 and dome forming eruption in 1909. Volcanic activity in recent years is restricted to gas emission or volcanic earthquake activity at the shallow part of the volcano. A spherical source model for inflation/deflation sequence is inferred at shallow depth beneath the summit dome by campaign GPS observations by the Meteorological Agency. No sign of crustal deformation is found at the deeper depth of the volcano by continuous GPS observation in a regional scale either by the Geographical Survey Institute nor the Meteorological Agency. Thus, until now, a crustal deformation which suggests fluid activity beneath the Tarumae-volcano at deeper depths had not been detected.

In July, 2013 swarm seismic activity started at the depths of between 2-5 km about 2 km to the west of summit dome. In addition a crustal deformation preceding the swarm was identified at several observation sites. The size of the change was at about 1 micro radian or micro strain level. Because the change appeared commonly at several stations around the volcano, it is highly likely that the strain and tilt change is resulting from a activity of a source at a depth beneath the volcano. A spherical inflation source was inferred from the observation data. The estimated position is at the m.s.l. depth of 4.2 km and about 1.3 km to the NNW of the summit horizontally with inflation volume of 3.4×10^5 m^3.

Since the position and time of activation of the source are close to those of seismic activity, it is likely that there is some geodynamic relationship between swarm seismicity and crustal deformation. In our presentation we also discuss possible relationship between them.

Keywords: Crustal Deformation, Active Volcano, Swarm Earthquake, Tarumae Volcano

Japan Geoscience Union Meeting 2014
(28 April - 02 May 2014 at Pacifico YOKOHAMA, Kanagawa, Japan)

SSS33-05 Room:315 Time:April 30 10:00-10:15

Campaign GPS for detection of the volcanic deformation on and around Mt.Meakan and Mt.Tokachi

WADA, Sayaka[1*] ; MORI, Hitoshi, Y.[1] ; OKUYAMA, Satoshi[1]

[1]Hokkaido University, Institute of Seismology and Volcanology

Mt. Meakan is an active volcano located in the eastern Hokkaido, Japan. It made phreatic eruptions in 1996, 1998, 2006 and 2008. Mt. Tokachi is one of the famous active volcanoes sits in the central Hokkaido. In the recent 100 years, three major magmatic eruptions took place in 1926, 1962 and 1988-1989.

In this presentation, we will discuss the results of the campaign GPS on and around Mt. Meakan and Mt. Tokachi. Each broad area GPS observation had begun at Mt. Meakan in 2006 and at Mt. Tokachi in 2007, respectively. The campaign GPS observations have made for several days to weeks in each year for Mt. Meakan at 8 sites, and that for Mt. Tokachi at 12 sites.

We used the data of our campaign observations after the 2008 eruption for Mt. Meakan and since 2007 for Mt. Tokachi. We also used the data of several sites operated by JMA (Japan Meteorological Agency) at the same time. Analyzing these data, annual movements at those points were estimated. These movements included deformations of the regional tectonic moving, and of the coseismic step of Tohoku-oki earthquake on March 11, 2011. For making corrections of these non-volcanic deformations, we used the continuous data of GEONET sites by Geospatial Information Authority of Japan (GSI) around the volcanoes. Using the GEONET data from 2007 to 2013, the regional tectonic and the seismic deformations were estimated by linear approximation in space. To elucidate the volcanic deformation, seasonal variations should be taken into consideration. The discussion about estimated volcanic deformation will be made, with the corrections about the regional deformation, the coseismic step and the after slip of 2011 Tohoku-oki earthquake, and the seasonal change.

Acknowledgements

In this study, JMA, Sapporo District Meteorological Observatory furnish their observation data to us. We would like to express our gratitude to them. Also, we used the data of GEONET sites of GSI with thanks.

Keywords: campaign GPS observation, volcanic crustal deformation, Mt. Tokachi, Mt. Meakan

Japan Geoscience Union Meeting 2014
(28 April - 02 May 2014 at Pacifico YOKOHAMA, Kanagawa, Japan)

SSS33-06 Room:315 Time:April 30 10:15-10:30

Crustal deformation associated with the unrest of Zao Volcano

MIURA, Satoshi[1*] ; NISHIMURA, Takeshi[1] ; OHTA, Yusaku[1] ; YAMAMOTO, Mare[1] ; DEMACHI, Tomotsugu[1] ; TACHIBANA, Kenji[1] ; OHMI, Katsuya[2] ; SHINOHARA, Eiichiro[2]

[1]Graduate School of Science, Tohoku University, [2]Sendai District Meteorological Observatory

Mt. Zao (1,841 m) is an active volcano located in northeastern Japan and having histories of phreatic or phreato-magmatic eruptions in the last 2 ka. Unrest of Zao volcano started in January, 2013 with a volcanic tremor (JMA, 2013) followed by activated seismicity mainly in the lower crust and very ?long-period seisimic events (VLP) up to today. Since the number of volcanological observatories within a distance of 10 kilometers from the volcano was limited at the time of beginning of the unrest; two continuous GPS sites and two sites equipped with borehole seismometers and tiltmeters, Tohoku University has built up 4 sites with broadband seismometers, 5 sites with continuous GPS, 1 site with shallow borehole tiltmeter, and 2 sites with a Proton magnetometer.

Using the new broadband network, we detected some VLPs with dominant period of about 10 sec, and revealed the source of the VLPs is located at a depth range of 2?4 km beneath the crater lake, from where the recent eruptions occurred since ˜600 years ago. There were, however, no significant surface phenomena such as steam explosion, ash effusion, and so on associated with the VLPs, except for precursory tilt signals about 5 minutes preceding a few major events.

We deployed dual-frequency GPS receivers at 5 new stations and the data are transmitted to the university using cellphone network for continuous observation (Demachi et al., 2011). The data are processed using the precise point positioning strategy (Zumberge et al., 1997) of GIPSY-OASIS II ver. 6.1.2 with IGS08 precise ephemerides and GMF mapping functions (GMF, Boehm et al., 2006). Since the wide area of northeastern Japan still suffers the long lasting postseismic deformation following the 2011 Tohoku-oki earthquake (M9.0), we try to extract volcanic deformation related to the unrest of the volcano using spatial and temporal filtering. Even though no distinct deformation has been recognized in the continuous GPS and tiltmeters at present, we may detect cm level variation of the shape of the mountain.

Reference

Boehm et al. (2006), GRL, 33, L07304, doi:10.1029/2005GL025546.
Demachi et al. (2011), Abstract for JpGU2011.
Japan Meteorological Agency (2013), http://www.seisvol.kishou.go.jp/tokyo/STOCK/kaisetsu/CCPVE/shiryo/127/127_no06_2.pdf
Zumberge et al. (1997), JGR, 102, 5005-5017.

Keywords: GPS, Ground Tilt, Volcanic deformation, Volcanic activity

Japan Geoscience Union Meeting 2014
(28 April - 02 May 2014 at Pacifico YOKOHAMA, Kanagawa, Japan)

SSS33-07 Room:315 Time:April 30 10:30-10:45

The acceleration episode of the back-arc rifting in the Izu-Bonin Arc possibly triggered by a remote earthquake in 2004

ARISA, Deasy[1*] ; HEKI, Kosuke[1]

[1]Department of Natural History Sciences, Faculty of Science, Hokkaido University

The Izu-Ogasawara (Bonin)-Mariana Island arc lies along the convergent boundary between the subducting Pacific plate (PA) and the overriding Philippine Sea plate (PH) in the western Pacific. Nishimura (2011) found that the back-arc rifting goes on behind the Izu arc by studying the horizontal velocities of GNSS stations on the Izu Islands. Here we show that this rifting has accelerated in 2004 using GNSS data at stations such as Aogashima, Hachijojima, Mikurajima, Shikinejima, and Nijima (we excluded stations in the Miyake Island because of the volcanic deformation).

The back-arc rifting behind the Izu islands can be seen as the increasing distance between stations in the Izu Islands (they are located to the east of the rifting axis) and stations located in the stable part of PH, e.g. Minami- and Kita-Daito islands. We found that their movement showed clear acceleration around the third quarter of 2004. Such an accelerated eastward movement could be interpreted not only as the acceleration of the back-arc rifting, but also as the trenchward movement of the arc due to a slow slip episode at the PH-PA boundary.

We first rule out the second possibility by constraining the onset time of the acceleration episode, and by correlating it with other inter-plate earthquakes in the PH-PA boundary. There was an inter-plate earthquake occurred on May 29, 2004 (M6.5) at the PA-PH boundary just to the south of the Boso-oki triple junction. However, the time series clearly lacked the jump which should mark the onset of the eastward slow movement. Moreover, the additional velocity vectors do not converge to the epicenter, and the onset time that minimizes the post-fit residual is significantly later than May. We therefore conclude that the accelerated eastward movement started in 2004 was not due to the afterslip of the interplate earthquake in May.

We found that the onset time coincides with the occurrence of the September 5, 2004, Kii-Hanto-oki, September 5, 2004, earthquake (M7.4), which occurred in the PH slab subducting at the Nankai Trough off the Kii Peninsula. We found that the accelerated movement vectors of these islands are almost parallel with each other, and perpendicular to the rift axis. We hypothesize that the seismic wave radiated from the epicenter of this earthquake dynamically triggered the acceleration of the back arc opening in the Izu Arc.

Keywords: GPS, GNSS, Izu-Bonin Arc, time series, back-arc opening, acceleration

Japan Geoscience Union Meeting 2014
(28 April - 02 May 2014 at Pacifico YOKOHAMA, Kanagawa, Japan)

SSS33-08 Room:315 Time:April 30 11:00-11:15

Subsurface structure and slip pattern of the Median Tectonic Line, SW Japan inferred from GPS displacement rate field

EDAGAWA, Nobuko[1] ; TABEI, Takao[1*] ; ICHITANI, Shozui[2] ; NAKAMURA, Yasuhiko[2]

[1]Fac. Science, Kochi Univ., [2]Grad. School Int. Arts Sciences, Kochi Univ.

The Median Tectonic Line (MTL) is the longest arc-parallel fault system in southwest Japan. Its right-lateral strike-slip motion is originated from oblique subduction of the Philippine Sea plate at the Nankai Trough, separating the Nankai forearc sliver (the outer zone) from the inner zone of southwest Japan. The deformation of the forearc sliver is characterized by interseismic contraction in the direction of the plate convergence (NW-SE) and long-term westward block movement along the MTL. In addition the MTL itself has a potential to generate a large inland earthquake in the future. Therefore it is important to understand subsurface structure and current slip/locking pattern of the MTL fault plane.

From dense GPS campaign measurements along a traverse line across the MTL, we have made it clear that a transition zone of the relative motion between the outer and inner zones is located 20-30 km north of the surface trace of the MTL (Tabei et al., 2002). To interpret the transition zone, we used a northward-dipping MTL fault plane which was revealed by seismic reflection survey (Ito et al., 1996) and assumed that its upper part was locked and a stationary right-lateral slip was occurring at depth. However, the concept of a pure strike-slip on an inclined fault plane seems somewhat unrealistic. In addition linear distribution of earthquakes aligned 20-30 km north and parallel to the MTL seems inconsistent to the hypothesis of the dipping MTL fault plane because most of them show a right-lateral slip on a nearly vertical fault plane. Unfortunately station distribution of the nationwide continuous GPS network is rather sparse in the north of the MTL because of the existence of the Seto Inland Sea. In this area we have deployed supplementary three GPS stations and collected continuous data since November 2010.

We propose a kinematic model of the transition zone. The model consists of several vertical right-lateral faults in a hanging wall above the northward-dipping MTL fault plane, which are close and parallel to each other. Distributed slip deficits on this parallel fault system may block the relative motion between the outer and inner zones and act as s broad shear zone as a whole. In this study we assume four parallel faults with different widths and depths from surface. Integrated displacement field from relative block motion and slip deficits on these faults is consistent with that derived from a strike-slip on an inclined fault.

We check the effect of the 2011 Tohoku-Oki earthquake on the deformation field of southwest Japan. We compare two displacement rate fields before (Jan. 2006 - Dec. 2009) and after (Mar. 2011 - July 2013) the earthquake. After the earthquake, additional wide-area displacements of 1-4 cm/yr trending to the source region (extension) have been superposed on the original compressional deformation field due to the subduction of the Philippine Sea plate. No significant change has been recognized in the latter.

Keywords: Median Tectonic Line, Nankai Trough, GPS, Deformation

Japan Geoscience Union Meeting 2014
(28 April - 02 May 2014 at Pacifico YOKOHAMA, Kanagawa, Japan)

SSS33-09 Room:315 Time:April 30 11:15-11:30

Continuous GPS observation in northern part of Nansei Islands

NAKAO, Shigeru[1*] ; YAKIWARA, Hiroshi[2] ; HIRANO, Shuichiro[2] ; GOTO, Kazuhiko[2]

[1]GSSE, Kagoshima Univ., [2]NOEV, Kagoshima Univ.

GEONET, which is a nationwide GPS observation in Japan cover on all over Japan. However, there is a GEONET site in Toshima-mura which is located in northern part of Nansei Islands. This region is defined the boundary between Northern and Central part of Ryukyu arc (Nishimura et al., 2004). It is not clear that where is the boundary because there is almost no GPS site. Goto (2013) concluded that the great earthquake occurred in 1911 is the interpolate event in this region. We set up the continuous GPS in islands of this region due to observe crustal deformation in this region.

In Akuseki Island (AKSK), Takarajima (TAKR) and Kuchinoshima (KCHI), continuous GPS (CGPS) observation started in March 2007, July 2007 and September 2010, respectively. CGPS set up on Gajyajima (GJYA) and Ujishima (UJIS), where is a deserted island, in May 2009. CGPS in Yokoatejima (YKAT) started in September 2013. Data is recorded at CGPS sites. Electric power system at GJYA, UJIS and YKAT is composed of batteries and photovoltaic cells.

Bernese GPS Software ver. 5.0 are used with IGS precise ephemerides and IERS rotation parameters. We also estimated tropospheric delays every hour and their horizontal gradients every six hours.

The short-term repeatabilites are from 1.6 to 3.0 mm in horizontal component and from 6.5 to 7.9 mm in vertical components. These observation is expected to make contribution to resolve rigid movement and crustal deformation in this region.

Japan Geoscience Union Meeting 2014
(28 April - 02 May 2014 at Pacifico YOKOHAMA, Kanagawa, Japan)

SSS33-10 Room:315 Time:April 30 11:30-11:45

The detection of crustal deformation associated with earthquake swarm in Tanzania observed by SAR

HIMEMATSU, Yuji[1*] ; FURUYA, Masato[1]

[1]Graduate School of Science, Hokkaido University

The East Africa Rift Valley is one of the divergent plate boundaries can be seen on the land surface. The area undergoes middle-class earthquakes and eruptions due to the existing faults and volcanoes.

An earthquake swarm occurred in the Northern Tanzania in July 2007 including the largest earthquake with Mw5.9 and lasted for approximately two months. According to the Global CMT solution, eight M>5 earthquakes occurred during the earthquake swarm and all of them were reported to be caused by normal fault. One week after the start of the swarm, an effusive eruption began at Mt. Oldoinyo Lengai located near the epicentral region, and a major ash eruption was observed by the time when swarm was terminated.

Biggs et al. (2009, 2013) also detected the crustal deformation associated with the earthquake swarm and Mt. Oldoinyo Lengai eruption, using mainly ENVISAT/ASAR C-band SAR data. In these interferograms, however, the ground displacements at some deforming areas were uncertain because of the difficult of phase-unwrapping. Also, these datasets were acquired only along the descending track, and the 3D deformation fields were unclear. Therefore, we used the L-band ALOS/PALSAR data obtained at both ascending and descending track to detect the detailed crustal deformation.

The purpose of this paper is to elucidate the mechanism of crustal deformation associated with the earthquake swarm in Tanzania in 2007 by interferometric synthetic aperture radar (InSAR).

By using InSAR data for ascending and descending track and the azimuth-offset data, we determined the 3D displacement. The results show a subsiding region along the NE-SW direction that are sandwiched by two horizontally deforming regions toward NW and SE directions. These spatial variation patterns are consistent with the expected direction, where the East Africa Rift Valley is expanding. In addition, the azimuth-offset data reveals slightly southward displacement in sediment area.

The ground at the subsiding region indicated ˜62 cm subsidence and ˜33 cm horizontal displacement toward SSE. The two-lobe pattern in eastern and western half each moved several centimeter upward and ˜50 cm in NW-SE direction horizontally.

In order to describe the ground displacement in detail, we estimated a fault source model assuming slip distribution in a homogeneous elastic half-space. Considering the complexity of the fault geometry, we derive a non-planar fault source model with triangular dislocation elements. Based on the result captured by InSAR and the observed area is in tension field, we propose two fault segments. The model indicates dip-slip and strike-slip displacement with maximum slip of about 1 m and 75 cm at 2-4 km depth.

Derived slip distribution can well explain the spatial variation pattern acquired by InSAR. The amount of moment release inferred from the model (Geodetic Moment: GM) exceeds that of the earthquake swarm (Seismic Moment: SM), and the ratio (SM/GM) is 37.2 percent. The ratio indicates that significant aseismic crustal deformation contributes to GM.

Some interferograms also detected the crustal deformation associated with Mt. Oldoinyo Lengai eruption during the earthquake swarm. We will also discuss the relationship between the earthquake swarm and the volcanic eruption of Mt. Oldoinyo Lengai.

Keywords: InSAR, Crutal deformation, East Africa rift valley, Earthquake swarm, Continental techtonics, Tanzania

Japan Geoscience Union Meeting 2014
(28 April - 02 May 2014 at Pacifico YOKOHAMA, Kanagawa, Japan)

SSS33-11 Room:315 Time:April 30 11:45-12:00

Coseismic Deformation Detected by SAR and Fault Source Modeling of the 2009 Cinchona Earthquake (Mw6.1), Costa Rica

UMEMURA, Shutaro[1*] ; FURUYA, Masato[1]

[1]Department of Natural History Sciences, Hokkaido University

A shallow earthquake with magnitude 6.1 (Mw) occurred in Costa Rica, Central America, on 8 January 2009. This earthquake, called Cinchona earthquake, accompanied with many landslides and caused around 20 fatalities. In the proximity of epicenter, there is the Angel-Vara Blanca fault that has a strike NNW-SSE. Montero et al. (2009) inferred the fault as the earthquake source fault. After 4 days of the earthquake occurrence, Poas volcano located 6 km to the west of the epicenter erupted (Volcanic Explosivity Index 1) after a quiescence of one year. This volcano had remained dormant for a decade after 1996 and became active since 2006. As the 1st step to study the possible relationship between earthquake and volcanic eruption, we detected the coseismic deformation by using the ALOS/PALSAR data and created fault models to explain the data.

In this study, we used ascending (path 162, frame 190) and descending (path 465, frame 3410) data of ALOS/PALSAR. To correct for the topography effect, we used the digital elevation model of ASTER GDEM. We analyzed the SAR data with GAMMA software. In the interferogram processing, we removed the atmospheric noise. We calculated the Green's function by triangular dislocation elements using Meade (2007) scripts.

The detected interferogram indicated that the maximum coseismic LOS (Line of Sight) changes were 20cm for ascending and 22cm for descending track, respectively. We derived the fault source model that could explain the LOS changes by trial-and-error approach. The estimated strike/dip angle of the fault were 133/65, and the rake angle at the center of fault was -163 degree. The difference of fault parameter from Angel-Vara Blanca fault suggested that the previously unknown fault worked. We calculated the pressure change caused by fault movement. This indicated positive change (compression) under the Poas volcano.

Keywords: InSAR, Coseismic Deformation, Fault Source Model, Costa Rica

Japan Geoscience Union Meeting 2014
(28 April - 02 May 2014 at Pacifico YOKOHAMA, Kanagawa, Japan)

SSS33-12 Room:315 Time:April 30 12:00-12:15

An acceleration event of creeping slip detected by precise leveling survey at the central part of the Longitudinal valle

MURASE, Masayuki[1] ; MATSUTA, Nobuhisa[2*] ; LIN, Cheng-hong[3] ; CHEN, Wen-shan[4] ; LIN, Jui-jen[3] ; NISHIKAWA, Yuka[4] ; WADA, Erika[1] ; KOIZUMI, Naoji[5]

[1]Department of Geosystem, College of Humanities and Sciences, NIHON University, [2]Graduate School of Environmental Studies, Nagoya University, [3]Institute of Earth Sciences, Academia Sinica, [4]National Taiwan University, [5]The National Institute of Advanced Industrial Science and Technology

Precise levelling surveys were conducted across the central Longitudinal Valley Fault, eastern Taiwan, to understand the deformation of the transition zone between the stable fault creep area and the locked area, which maybe correspond to an asperity. In order to investigate the surface relationship between the fault creep area and the geological condition of the transition zone, we established levelling routes in the Yuli, and Chike-san areas. The Yuli area forms the geological boundary of the Lichi Melange Formation, which is composed of chaotic mudstones containing numerous exotic blocks of various sizes and lithologies. Along the Yuli route, located on the Lichi Melange, an uplift rate of 30 mm/yr was detected during the period 2010-2013, suggesting that aseismic fault creep might be continuing with long-term stability. Along the Chike-san route, located on no Lichi Melange, a vertical deformation rate of 8 mm/yr, 40mm/yr, and 20mm/yr were detected in the period 2010-2011, 2011-2012, and 2012-2013, respectively.

The creep slip distribution was estimated by using a two-dimensional single-fault model proposed at Chike-san in the period 2012-2013. Large slip rates were estimated at 4-5 km of the fault plane. At the previous periods 2010-2011 and 2011-2012, relatively large slip rates were estimated at two parts of the fault plane-one at a depth of about 1.5 km and another at a depth of 4-5 km-. We believe that the acceleration event of creeping slip was continued at the depth of 4-5 km in the period 2012-2013. The northern limit of the stable creep area may be the Yuli area. The episodic creep event occurred in the transition zone between the stable fault creep area and the asperity area. The boundary between the stable creep area and the episodic creep area is consistent with the geological boundary of the Lichi Melange Formation.

Keywords: Taiwan, Longitudinal valley fault, precise leveling survey, aseismic creep motion

Japan Geoscience Union Meeting 2014
(28 April - 02 May 2014 at Pacifico YOKOHAMA, Kanagawa, Japan)

SSS33-13 Room:315 Time:April 30 12:15-12:30

Internal stress changes due to point dislocations in a spherical earth

TAKAGI, Yu[1*] ; OKUBO, Shuhei[1]

[1]Earthquake Research Institute, The University of Tokyo

A simple and complete theory about internal deformations due to point dislocations in a homogeneous half-space was proposed by Okada (1992). This theory has been used by many researches to estimate Coulomb stress changes due to an earthquake and has contributed to understanding of seismology. Although a homogeneous half-space is a first approximation of the earth, global deformation like broad stress changes due to a great earthquake have to be calculated in a more realistic earth model, spherically symmetric earth model. Sun and Okubo (1993) succeeded in calculating surface displacements and gravity changes due to point dislocations in a spherically symmetric earth model. However, internal stress changes and displacements have never been calculated because there exist some difficulties to realize the calculation in spite of early proposal of a fundamental method (Takeuchi and Saito, 1972). In this research, we propose a strategy to realize the calculation of internal deformations and present some computational results.

We shall

i) outline the strategy to calculate internal deformations,

ii) compare the stress changes in a homogeneous sphere with those in a half-space which were already solved and

iii) show the results in a stratified earth model such as PREM.

Our study shows that significant difference between a homogeneous sphere and a half-space model occurs when epicentral distance exceeds several hundreds kilometers. For example, epicentral distances at which difference of radial stress changes in two models reach 10% are 4, 5 and 6.5 degrees at observation depth at 10, 20 and 30, respectively (Figure). Angular distance of 4 degrees, which is 400km, roughly equals the length of fault that is thought to have slipped in the 2011 Tohoku-Oki earthquake.

Figure. Difference of radial normal stress changes due to a vertical-strike slip at depth of 32km in two models, a homogeneous sphere and a half-space.The horizontal axis is epicentral distance and vertical axis is difference between the two models in percentage. Red, green and blue points indicate observation depth of 10, 20 and 30km, respectively.

Keywords: internal stress change, spherically symmetric earth, point dislocation, stratification

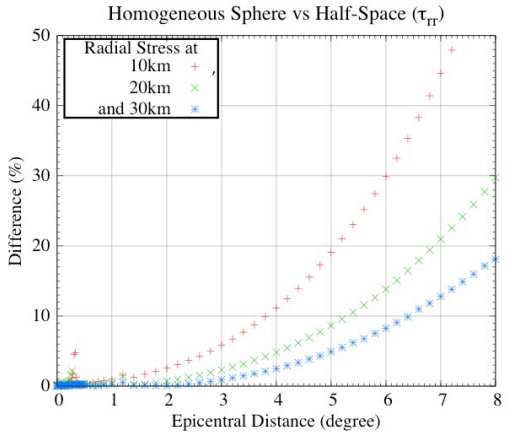

Japan Geoscience Union Meeting 2014
(28 April - 02 May 2014 at Pacifico YOKOHAMA, Kanagawa, Japan)

SSS33-14 Room:315 Time:April 30 14:15-14:30

Continuous measurements of ocean bottom crustal movements based on GPS-acoustic system using GPS buoy

IMADA, Naruyuki[1*] ; TERADA, Yukihiro[2] ; SAKAUE, Hiromu[3] ; TADOKORO, Keiichi[4] ; KATO, Teruyuki[5]

[1]Hitachi Zosen Corporation, [2]Kochi National College of Technology, [3]None, [4]Graduate School of Environmental Studies, Nagoya University, [5]Earthquake Research Institute, the University of Tokyo

We report the results of experiments of continuous measurements of ocean bottom crustal movements using GPS buoy and acoustic system.

We have developed a GPS buoy system for the early detection of tsunami. The system uses a buoy that is freely floating on the sea, tied to the sea bottom using an anchor, equipped with a GPS sensor at the top of the buoy. The system enables us to estimate the position of the buoy in a few centimeter accuracy.

On the other hand, Spiess (1985) and other researchers have developed the GPS-acoustic system for estimating the ocean bottom position in sub-decimeter accuracy. However, these systems have used owned or chartered vessels to measure the position of ocean surface, so that the measurements have been only intermittent. After the 2011 Tohoku-oki earthquake of Mw9.0, it has been recognized that continuous monitoring of ocean bottom crustal deformation is very important. Thus, we got an idea in that the GPS buoy could be used for the continuous monitoring of the ocean bottom crustal movements, if an acoustic system is equipped at the GPS buoy.

Based on this idea, we started experiments using our GPS buoy, which is located off Muroto Peninsula, western Japan, in the year of 2013. After a preliminary experiment in March 2013, we made an experimental observation from August to October of 2013. Three transponders were placed around the buoy and the equipment of sound sender/receiver at the side surface of the buoy. The water depth of the site is about 700meter and the ocean bottom transponders are placed so that the distances among these are in the same scale. We will report the results including noise characteristics of data, daily repeatability of estimated ocean bottom position, effects of swinging buoy, etc.

Currently, 15 GPS buoys have been established around the Japanese coasts. Augmentations of the acoustic system in these GPS buoy network will provide a powerful tool of monitoring ocean bottom crustal movements as well as tsunamis. Further requirements to GPS buoys are to be placed farther offshore, say, more than 100km from the coast. Recent developments of the GPS buoy system, including a newly developed algorithm, PPP-AR (precise point positioning with ambiguity resolution), clarified this requirements. However, still another problem of how data at the buoy placed far offshore is transmitted to land in real-time manner is still to be solved. For such problem of a newly designed high capacity data transmission system using a dedicated satellite system will be necessary. Our current experiment will provide an important data for designing a specification of such satellite system.

Spiess, IEEE Trans. Geosci. Remote Sens., 23, 502-510, 1985

Japan Geoscience Union Meeting 2014
(28 April - 02 May 2014 at Pacifico YOKOHAMA, Kanagawa, Japan)

SSS33-15 Room:315 Time:April 30 14:30-14:45

Movement of a fault arised by a pumping or a spring water and its understanding by poroelasticity -a case of NNW fault-

ISHII, Hiroshi[1*] ; ASAI, Yasuhiro[1]

[1]TRIES, ADEP

Tono Research Institute of Earthquake Science (TRIES) has developed a borehole stress meter for continuous observation and multi-component borehole instruments. At the present time about 15 borehole stations are in operation. We have investigated crustal movements and behavior of underground water by using data obtained from borehole observations. The depth of the deepest borehole is 1030 m.

Near TRIES, JAEA (Japan Atomic Energy Agency) is constructing deep boreholes with diameters of 4m and 6.5m. And depth is about 500m at the present time. The boreholes are 40m apart and connected by stages. NNW fault is running beside the 6.5m borehole. We are investigating a relationship between water flow and geophysical observations by using experiments of pumping water and spring water.

The main results obtained are as follows:

1. Water level of TGR350 borehole station decreases by pumping water and spring water. Data of the strain meters installed at 350m depth indicate right lateral movements of NNW fault.
2. Data of the strain meters installed at 350m depth indicate left lateral movements of NNW fault in case of recovery of water level.
3. Strain meters installed shallower depth (165m) and extensometers installed in sedimentary layer do not indicate such fault movements.
4. We have considered a mechanism explaining the phenomena by using poroelastic understanding.

We will present the details of observations and analyses.

Keywords: Deep borehole observation, Fault movement by spring and pumping water, Groundwater flow, Understand by poroelasticity, Continuously observable stressmeter

Japan Geoscience Union Meeting 2014
(28 April - 02 May 2014 at Pacifico YOKOHAMA, Kanagawa, Japan)

SSS33-16 Room:315 Time:April 30 14:45-15:00

Construction of Syobasama crustal activity observatory ?Installation of Ishii-type borehole stressmeter?

ASAI, Yasuhiro[1*] ; ISHII, Hiroshi[1]

[1]Tono Research Institute of Earthquake Science, Association for the Depvelopment of Earthquake Pred.

Large changes in the pore pressure in Toki granite have produced by the excavation of underground facilities of Mizunami Underground Research Laboratory (MIU) and drilling well for hydraulic tests in MIU (e.g. Asai and Ishii, JpGU2013). We have observed remarkable stress/strain/tilt variations associated with the pore pressure changes at borehole observation site TRIES, STG300 (on the north-east side of the fault), Togari(TGR350/TGR165), STG100, STG200 (south-west side), respectively within 500m of the MIU.

In this area the NNW trending sub-vertical (normal) fault is exists (e.g. JNC, 2003 and 2004). Pore pressure changes occurs in the south-west side of the fault, its impact were observed in water level/pressure record of the same side, and were also observed in stress, strain and tilt record. On the other hand, its impact were not seen in the water level/pressure record of the north-east side of the fault, but its impact were observed on stress, strain and tilt record. Pore pressure change occurs in the north-east side of the fault are similar to those of the south-east side. This observation results indicate that fault has impermeability and elastic deformation of the rock caused by pore pressure change extends over the fault.

In order to clarify the relationship of groundwater level changes to crustal strain changes at Syobasama observation site which is located approximately 1km northwest of MIU, Tono Research Institute of Earthquake Science has constructed the new borehole depth of 110 m and installation of Ishii-type borehole stress meters is scheduled in February 2014. We will present the details of construction of Syobasama observatory, and result of continuous stress observation with groundwater records.

Keywords: Pore pressure change, Elastic deformation, Mizunami Underground Research Laboratory, Ishii-type borehole stress meter

Japan Geoscience Union Meeting 2014
(28 April - 02 May 2014 at Pacifico YOKOHAMA, Kanagawa, Japan)

SSS33-P01 Room:Poster Time:April 30 18:15-19:30

Post-seismic crustal movements of the 11 April Mw6.6 Fukushima Hamadori earthquake based on GPS observations

HORI, Kayako[1*] ; AOKI, Yosuke[2] ; KATO, Teruyuki[2] ; MIYASHITA, Kaoru[1]

[1]Graduate School of Science, Ibaraki University, [2]Earthquake Research Institute , The University of Tokyo

Tohoku earthquake on March 11, 2011 (Mw9.0) was accompanied by a vigorous aftershock activity. One of the aftershocks occurred on April 11, 2011, nearby Iwaki city, Fukushima Prefecture, and was called as Fukushima-Hamadori earthquake (Mw6.6; Depth=5km). The focal mechanism of the earthquake was a normal fault. Co-seismic crustal movements due to the earthquake observed by GPS observation was amounted to about 30cm to northeast direction at Iwaki site.

Crustal deformations associated with the Fukushima-Hamadori earthquake is obtained by InSAR and the data were used to construct detailed fault slip models by the previous studies (Kobayashi et al.,2013 : Fukushima et al.,2013). However, it has not been possible to measure the postseismic deformations using the SAR because the ALOS satellite has terminated its operation in immediately after the Fukushima-Hamadori earthquake. Thus, the postseismic crustal movements has been observed only by the GPS observations. Therefore, we aim to elucidate the mechanism of postseismic deformations due to the Fukushima-Hamadori earthquake using the GPS data in this study.

In this study, it was assumed that postseismic crustal deformations were caused by a slip in the vicinity of the fault. We used earthquake fault geometries employed by previous studies (Kobayashi et al.,2013 : Fukushima et al.,2013). As the GPS data is including large postseismic displacements due to the main shock since the March 11, first, we removed the postseismic transient displacements from GPS data using a postseismic slip model of the main shock (Fukuda et al., 2013). The obtained residual displacements after April 11, 2011, are considered as postseismic displacements due to the Fukushima-Hamadori earthquake. We, then, estimated slip distribution on the fault plane based on the residual displacement field. We will discuss estimated results in our presentation.

Japan Geoscience Union Meeting 2014
(28 April - 02 May 2014 at Pacifico YOKOHAMA, Kanagawa, Japan)

SSS33-P02 Room:Poster Time:April 30 18:15-19:30

Coseismic slip distribution for the 2011 Tohoku-Oki earthquake with topographic corrections

GOSHIMA, Hitoshi[1*] ; MIYAZAKI, Shinichi[1]

[1]Graduate School of Science, Kyoto Univerisy

Seismological study (Ide et al., 2011) revealed that the rupture of the 2011 Tohoku-Oki earthquake extended to the Japan Trench (i.e. free surface). Since the depth of the trench is about 8km, it is not appropriate to use green functions for elastic half-space media as given by e.g., Okada (1992). When we employ green functions for the half-space, it is not possible to satisfy the following two conditions simultaneously; (1) the updip limit of the rupture is ˜8km deeper than the ground surface, and (2) the rupture extends to the free surface (i.e. the trench). If the condition (1) is satisfied, the rupture extends to ˜8km at depth, not to the free surface. On the other hand, if the condition (2) is satisfied, the depth of the trench must match to the ground surface. The maximum discrepancy in between predicted ground displacements for the condition (1) and (2) is 5% in horizontal, and 15% in vertical component. Thus, it may be important to take the topography into account in green functions.

In this study we applied the topographic correction on green functions as proposed by Williams and Wadge (2000). Segall (2010) suggests that this method is applicable to approximately incorporate the earth sphericity into green function for observation sites within about 600km from the dislocation. Combining those two corrections, we are able to calculate corrected green functions for spherical earth with topography. Although this method gives only approximate green functions, it helps us to investigate the dependence of green functions on topography and fault geometry.

Then we use the corrected green functions for the inversion of coseismic slip distribution for the 2011 Tohoku-Oki earthquake. In the invsersion we use the following data set: GEONET F3 solutions obtained by the Geospatial Information Authority of Japan (GSI), the ocean bottom deformation data by the Japan Cast Guard (Sato et al., 2011), and that of Tohoku University (Kido et al., 2011; Ito et al., 2011). Then the inversion result is compared with the half-space solutions.

Keywords: crustal deformation, the 2011 Tohoku-Oki earthquake, topography, sphere

Japan Geoscience Union Meeting 2014
(28 April - 02 May 2014 at Pacifico YOKOHAMA, Kanagawa, Japan)

SSS33-P03 Room:Poster Time:April 30 18:15-19:30

Secular change of permeability estimated by using the variations of groundwater discharge

MUKAI, Atsushi[1*] ; OTSUKA, Shigeaki[2]

[1]Faculty of Informatics, Nara Sangyo University, [2]Faculty of Humanities and Sciences, Kobe Gakuin University

Secular change of permeability causes the variation of the atmospheric pressure admittance of groundwater discharge. We estimated the permeability of the surrounding crust by using the groundwater discharge observed at Rokko-Takao station during 12 years from 2001 to 2012. The estimated secular change of permeability contained the short term variations for about a year as well as the gradual decrease. It is considered that the gradual decrease of permeability was caused by the closure of the cracks, which were opened in the 1995 Hyogoken Nanbu earthquake, due to the accumulation of mud and the crustal stress. On the other hand, the short term variations of permeability suggest the temporary re-open of the cracks due to the earthquake ground motions.

The Rokko-Takao station is located in Kobe, the southern Hyogo prefecture, and passes through the fracture zone of Manpukuji fault. At this station, the significant increase of groundwater discharge was observed just after the 1995 Hyogoken Nanbu earthquake (Fujimori et al., 1995). This suggested that the many cracks were opened in the fracture zone around the station by the ground motion of the earthquake. Mukai and Otsuka (2009) estimated the elastic properties by using the tidal strains observed at the station and reported that the Young's modulus of the surrounding crust showed the secular increase. This suggested that a part of cracks were closed by the crustal stress and the accumulation of mud and the strength of the fracture zone had been recovering.

Mukai and Otsuka (2013) estimated the variations of permeability due to the 2011 Tohoku earthquake by using the atmospheric pressure admittances of the groundwater discharge observed at the station under the assumption of one-dimensional model about groundwater migration. The permeability just after the earthquake increased by about 1.9 times just before the earthquake and decreased to the level about 1.3 times just before the earthquake in 10 months. This suggested that even the small ground motions due to the teleseismic waves could cause the outflow of the mud and the temporary re-open of the cracks in the fracture zone.

In this study, we estimated the secular change of permeability around the station during 12 years from 2001 to 2012 by using the procedure of Mukai and Otsuka (2013). The permeability estimated by using the atmospheric pressure admittances of the groundwater discharge showed the secular decrease by about 50% in 12 years. This result agrees to the secular increase of Young's modulus estimated by using the tidal strain and is considered that the gradual decrease of permeability was caused by the recovering of the fracture zone, in which the cracks were opened in the 1995 Hyogoken Nanbu earthquake.

Keywords: fracture zone, permeability, groundwater discharge, strain change

Japan Geoscience Union Meeting 2014
(28 April - 02 May 2014 at Pacifico YOKOHAMA, Kanagawa, Japan)

SSS33-P04 Room:Poster Time:April 30 18:15-19:30

Vertical crustal deformation in Boso Peninsula from 1966 to 2001 deduced from leveling and sea level data

KOBAYASHI, Akio[1*]

[1]Meteorological Research Institute

Leveling data and sea level data for the period from 1966 to 2001 in Boso Peninsula, Japan, were investigated to characterize unsteady vertical deformation. We estimated the steady vertical deformation rate at each GEONET GNSS station using the daily coordinates for the periods from January 1997 to January 2011 avoiding the period of the large earthquakes.

First-order leveling surveys have been conducted repeatedly every one or several years since 1966 in Boso Peninsula. We determined crustal displacements by comparing leveling data from successive surveys. We subtracted subduction-related steady component derived by the GNSS from the distribution of vertical crustal displacements during periods between leveling surveys. If any episodic events have not occurred, they should show little spatial variation around zero vertical displacement. Unsteady vertical deformation was not seen in the period from 1966 to 2001 except the land subsidence by pumping industrial water and natural gas brine.

Keywords: Boso Peninsula, crustal deformation, leveling, sea level

Japan Geoscience Union Meeting 2014
(28 April - 02 May 2014 at Pacifico YOKOHAMA, Kanagawa, Japan)

SSS33-P05 Room:Poster Time:April 30 18:15-19:30

2014 Boso slow slip

OZAWA, Shinzaburo[1*]

[1]Geospatial Information Authority of Japan

Introduction

The GPS network detected transient crustal deformation on the Boso peninsula in 1996, 2002, 2007, and 2011. The detected transient displacements subsided for approximately 10 days. Rupture process and slip area are similar among the past four Boso SSE. The recurrence intervals of Boso SSE are 6.4, 4.9, 4.2 years from 1996. Under this circumstance, the anticipated slow slip event started from January 1 2014. This recurrence interval of 2.2 years is the shortest one compared with the previous 4 slow slip events. In this research, we estimate spatio-temporal evolution of the 2014 Boso slow slip and compare it with those in 1996, 2002, 2007, 2011.

Data and analytical procedure

Trend and annual components which are estimated for the period between 2009 and 2011 are removed from the raw time series. The detrended crustal deformation in 2014 shows southeastward movments with 1 cm maximum movement in the Pacific coastal area.

We employed time dependent inversion to the detrended crustal deformation associated with the 2014 Boso SSEs. We used EW, NS, and UD components of crustal deformation at approximately 40 GPS sites relative to Yasato station. The plate geometry of the upper surface of the Philippine Sea plate is based on Nakajima and Hasegawa [2006]. The fault geometry is composed on the B-spline and slip on the fault is also composed of superposition of B-spline function. As a boundary condition, we set 0 slip on the edge of the fault geometry.

Results and Discussion

The results show that the slow slip started offshore of the Boso peninsula and expanded to the south over time. The estimated moment magnitudes are 6.4, while those area 6.4 in 1996, 6.5 in 2002, 6.5 in 2007 and 6.6 in 2011. The 2014 Boso SSE ruptured an area similar to those of the four Boso SSEs. The recurrence interval is 6.4 year from 1996 to 2002 events, 4.9 years from 2002 to 2007 events, 4.3 year from 2007 to 2011, and 2.2 years from 2011 to 2014 events. The five events do not seem to be slip predictable nor time predictable. Though the 2011 event shows the largest magnitude among four cases, recurrence interval from 2007 event is the shortest. We cannot rule out a possibility that the Tohoku earthquake may have affected the occurrence of the 2011 event. In fact, dCFF increased near the rupture area of the Boso peninsula from the Tohoku earthquake [Hirose et al. 2012]. However, it remains unclear the reason why recurrence interval change drastically from 4.2 to 2.2 years for the 2011 and 2014 events, since dCFF does not change so much from 2011 and 2014. Another interpretation of shortening of recurrence interval is based on a scenario proposed by several simuylation studies in which recurrence interval of slow slip events become shorter as occurrence of large earthquake nears. If this is the case, it is quite important to monitor crustal deformation on and around the Boso peininsula..

Keywords: Boso peninsula, slow slip

Japan Geoscience Union Meeting 2014
(28 April - 02 May 2014 at Pacifico YOKOHAMA, Kanagawa, Japan)

SSS33-P06 Room:Poster Time:April 30 18:15-19:30

Estimation of frictional parameters in afterslip areas by assimilating GPS data :The 2003 Tokachi-oki earthquake

KANO, Masayuki[1*] ; MIYAZAKI, Shinichi[2] ; ISHIKAWA, Yoichi[3] ; HIYOSHI, Yoshihisa[3] ; ITO, Kosuke[3] ; HIRAHARA, Kazuro[2]

[1]ERI, Tokyo Univ., [2]Kyoto University, [3]JAMSTEC

Seismological and geodetic observations have revealed that various aspects of fault slips are determined by frictional properties on the interface. Kano et al. (2013) developed an adjoint data assimilation method to estimate frictional parameters from synthetic in-situ slip velocity data and found by numerical experiments that all frictional parameters are constrained if both acceleration and deceleration phases are observed. Additionally, we found that synthetic surface displacement data also have the ability to constrain frictional parameters in the areas where slip is well resolved. Following their study, we then applied the method to an actual case of the 2003 Tokachi-oki earthquake. Given reasonable initial conditions of simulation variables, estimated frictional parameters are well constrained if two conditions above are satisfied. Our results imply that the adjoint method we developed is useful to investigate and understand fault frictional properties.

Keywords: afterslip, adjoint method, frictional parameters, GPS, earthquake cycle

Japan Geoscience Union Meeting 2014
(28 April - 02 May 2014 at Pacifico YOKOHAMA, Kanagawa, Japan)

SSS33-P07 Room:Poster Time:April 30 18:15-19:30

Crustal deformation of the northeastern margin of the Izu Collision Zone inferred from GPS observations

DOKE, Ryosuke[1*] ; HARADA, Masatake[1] ; SATOMURA, Mikio[1] ; MIYAOKA, Kazuki[1]

[1]Hot Springs Research Institute of Kanagawa Prefecture

Izu Collision Zone is characterized by the collision between Izu Peninsula and Tanzawa Mountains, and Philippine Sea Plate also subducts beside this zone. Because of these complicated plate geometries, a number of historical earthquakes occurred in the northeastern margin of this zone. Additionally, there are a lot of active faults in the marginal area of the collision zone.

It is important to describe the steady state of crustal deformation in the Izu Collision Zone, in order to clarify mechanisms of earthquakes occurring in this area. In this study, we examined crustal deformation of the northeastern margin of Izu Collision Zone by using the datasets of GEONET sites (coordinate F3) and our original GPS sites.

Based on the displacement velocity vector diagram and profile, we can point out the following characteristics of crustal deformation there.

1) Remarkable northward crustal displacement vectors were observed in the eastern area of the Kita-Izu fault zone.

2) A shear zone with North-South trend was detected in the area between Kita-Izu fault zone and Ashigara Plain. Width of its zone was estimated about 15-20 km. Average shear strain rate in this zone was about 0.47 micro-strain per year.

3) Such remarkable crustal displacement vectors were not observed in the western area of the Kita-Izu fault zone.

This shear zone may be a transition zone between the collision and the subduction blocks on the Philippine Sea Plate, caused by the displacement gap between the blocks.

Keywords: GPS, crustal deformation, Izu Collision Zone, Kita-Izu fault zone

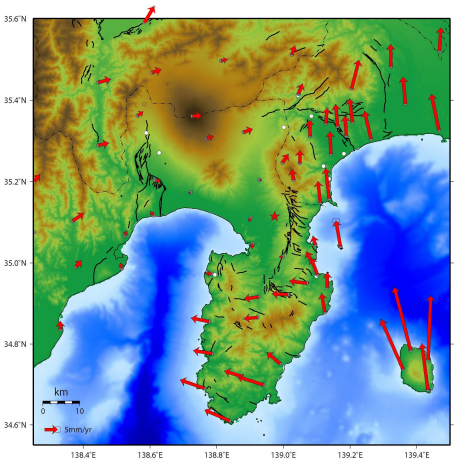

Japan Geoscience Union Meeting 2014
(28 April - 02 May 2014 at Pacifico YOKOHAMA, Kanagawa, Japan)

SSS33-P08 Room:Poster Time:April 30 18:15-19:30

The wind velocity correction of the precipitation to use for the rainfall correction of the volumetric strainmeter

KIMURA, Kazuhiro[1*]

[1]Meteorological Research Institute

The rainfall correction of the volumetric strainmeter has the sensitivity that can judge quality of the precipitation data.(Kimura et al., 2013) In the observation of the rain gauge, it is well known that a capture rate of the rainfall decline at the time of a strong wind. We try the ranfall correction of the volumetric strainmeter in consideration of wind velocity dependence. As a result, the strainmeters at the slope of the big mountain or near the river where had a long basin area is improved the rainfall correction. This is not influence of the capture rate of the rain gauges, it is caused by the fact that altitude dependence of the precipitation is remarkable as a strong wind.

For the rainfall correction of the crustal movement data such as the volumetric strainmeter, it is necessary to consider it about the rainfall at high altitudes in addition to the precipitation around the observation station.

Keywords: strainmeter, rainfall correction, wind velocity, altitude dependence of the precipitation

Japan Geoscience Union Meeting 2014
(28 April - 02 May 2014 at Pacifico YOKOHAMA, Kanagawa, Japan)

SSS33-P09 Room:Poster Time:April 30 18:15-19:30

The change except the sudden contraction of the Higashiizu staraimeter with the seismic activity east off Izu Peninsula

KIMURA, Kazuhiro[1*] ; KIMURA, Hisao[2]

[1]Meteorological Research Institute, [2]Japan Meteorological Agency

The sudden contraction strain change of the Higashiizu staraimeter with the seismic activity east off Izu Peninsula is well known. These changes were clear for anyone, but the Higashiizu staraimeter couldn't detect the long-term change that Murakami(2006) pointed out by the GNSS data until now. However we became able to remove the seasonal change by the rainfall from the strainmeter data by using the rainfall correction(Kimura et al., submitted). After reviewing the Higashiizu strainmeter data using the rainfall correction, this data detect the interesting change with the seismic activity east off Izu Peninsula.

Keywords: Strainmeter, seismic activity east off Izu Peninsula, Higashiizu

Japan Geoscience Union Meeting 2014
(28 April - 02 May 2014 at Pacifico YOKOHAMA, Kanagawa, Japan)

SSS33-P10 Room:Poster Time:April 30 18:15-19:30

Characteristic strain distribution following the 2011 Tohoku earthquake based on the kinematic PPP analysis

HIRATA, Yuichiro[1*] ; OHTA, Yusaku[1] ; OHZONO, Mako[2] ; MIURA, Satoshi[1]

[1]Gradual School of Science, Tohoku University, [2]Faculty of Science, Yamagata University

The 2011 off the Pacific coast of Tohoku Earthquake (March 11, 2011, M 9.0) generated widespread coseismic deformation. The slip on the plate boundary is larger than the 10 m in widely (e.g. [1]). Ohzono et al [2] found inhomogeneous strain distribution caused by the coseismic step of the 2011 Tohoku earthquake. They extracted the residual strain distribution, which is estimated by comparison between the expected coseismic displacement by a simple rectangular faults model and the observed coseismic displacement in the Tohoku area. Ozawa and Fujita [3] found the local deformation around the Akita-Komagatake, Kurikoma, Zao, Azuma, and Nasu volcanoes caused by the 2011 Tohoku earthquake based on the ALOS/PALSAR and GPS data. They suggested that the coseismic extensional deformation concentrates in the soft medium under a volcano and that this deformation has caused local deformation with subsidence based on the FEM modeling. These previous studies , however, used the daily coordinates time series of the GPS observation. Thus, these previous studies result might be contained early postseismic displacement following the 2011 Tohoku earthquake. Based on these backgrounds, we tried to extract the pure coseismic deformation by the kinematic Precise Point Positioning (kPPP) approach.

We estimated every 1 seconds coordinates time series of the 1,208 GEONET by the GIPSY-OASIS II software version 6.1.2. We defined the " pure " coseismic displacement, which is coordinate difference between just before the origin time and 600 seconds after the event. We averaged from 500 to 700 seconds after the event for eliminating short-term fluctuation of the time series. Based on the estimated " pure " coseismic displacement, we estimate the dilatation strain distribution by method of the [4]. We also estimated strain distribution in the early time period after the 2011 Tohoku earthquake, which estimated coordinate difference between coseismic displacement by the daily coordinate (e.g. difference between 10 to 12th March, 2011) and " pure " coseismic displacement by the kPPP analysis.

As a result, we found the characteristic local expansion in and around the Mt. Gassan, which located in Yamagata prefecture. We also found the characteristic contraction in and around Mt. Zao even though this obtained strain amount is smaller than the noise level determined by the kPPP time series. We also estimated strain distribution of early postseismic between mainshock and 15th March for the understanding the spatiotemporal development of strain distribution. The area of the expansion is clearly larger than the 12th March in and around the Mt. Gassan. Furthermore, the contraction area around the Mt. Zao clearly changed to expansion between just after the mainshock and 15th March.

In the presentation, we will discuss more detail characteristics and its interpretation of the obtained strain distribution.

[1] Iinuma et al., (JGR, 2012), [2] Ohzono et al., (EPS, 2012), [3] Ozawa and Fujita, (JGR, 2013), [4] Shen et al., (JGR, 1996)

Keywords: strain, 2011 Tohoku earthquake, postseismic deformation, kinematic PPP

Japan Geoscience Union Meeting 2014
(28 April - 02 May 2014 at Pacifico YOKOHAMA, Kanagawa, Japan)

SSS33-P11 Room:Poster Time:April 30 18:15-19:30

Convergence of the Philippine Sea Plate in Mindanao, the Philippines

NAKAMURA, Yasuhiko[1*] ; TABEI, Takao[2] ; OHKURA, Takahiro[3] ; KIMATA, Fumiaki[4] ; TERESITO C., Bacolol[5] ; ENDRA, Gunawan[6]

[1]Grad. School Int. Arts Sciences, Kochi Univ., [2]Fac. Science, Kochi Univ., [3]Aso Volcanological Laboratory, Kyoto Univ., [4]Tono Research Institute of Earthquake Science, [5]Philippine Institute of Volcanology and Seismology, [6]Grad. School of Environmental Studies, Nagoya Univ.

Tectonics of the Philippines Archipelago is characterized by westward subduction of the Philippine Sea plate at the Philippine Trench in the east (5.8 - 7.0 cm/yr), eastward subduction of the Sunda plate at the Manila Trench in the west (3.3 - 3.6 cm/yr), and left-lateral strike-slip movement of the Philippine fault inland. Under the SATREPS project ”Enhancement of earthquake and volcano monitoring and effective utilization of disaster mitigation information in the Philippines” we have conducted yearly GPS campaign measurements in the eastern part of Mindanao since March 2010. The main purpose of the observation is to make clear the plate locking distribution at the Philippine Trench and slip/locking pattern of the Philippine fault in order to estimate earthquake generation potential in Mindanao.

We occupied 15 sites in the eastern Mindanao and collected continuous data for successive three to six days on March 2010-2013. Collected data were processed with Bernese software ver.5.0 together with the data from global IGS station (PIMO near Manila) to obtain coordinates and displacement rates based on ITRF2008. The displacement rates were then converted to those with respect to the Sunda plate. Moreover we used previous displacement rate data obtained in the central and western Mindanao from the 1997-2003 campaign measurements to cover the whole of Mindanao.

The resulted displacement rate filed shows that west-northwest motions are dominant due to the convergence of the Philippine Sea plate from the east but their spatial decay with increasing distance from the trench is not significant. Even the full locking of the Philippine Trench plate interface down to the depth of 80 km can explain only 29 percent of the observed displacement rate at the maximum. Thus we need to introduce remarkable rigid block rotations to interpret the deformation pattern of Mindanao. As a result of the estimate of pole position and angular velocity of the block rotation, deformation field of Mindanao cannot be reproduced by a rotation of single block. Considering the Philippine fault as a block boundary, it is natural to introduce multiple blocks into Mindanao. Unfortunately current station coverage and density are not enough to resolve elastic deformation due to plate locking at the trench and rigid motions due to multiple block rotations.

Keywords: Philippine Trench, Philippine fault, GPS observation, Mindanao

Japan Geoscience Union Meeting 2014
(28 April - 02 May 2014 at Pacifico YOKOHAMA, Kanagawa, Japan)

SSS33-P12 Room:Poster Time:April 30 18:15-19:30

Slip deficit rate distribution and its temporal changes along the Japan islands

HIGUCHI, Shun[1*] ; KOKETSU, Kazuki[1] ; YOKOTA, Yusuke[2]

[1]Earthq. Res. Inst., [2]Japan Coast Guard

The Japan islands are located along several plate boundaries, where the oceanic plates are subducting beneath the continental plates. Due to this subduction, slip deficits are being generated and strain is being accumulated in coupled zones of the plate boundary so that many large earthquakes have occurred. Therefore, in order to reveal the generation mechanism of large earthquakes at the plate boundaries, it is necessary to clarify slip deficit rate distributions. In addition, as seen in long-term slow slip events, there are significant temporal changes in the slip deficit rate distributions. In this study, we determined the slip deficit rate distribution along the whole Japan islands for each year from 1996 to 2010 (the observation period of GEONET operated by GSI before the 2011 Tohoku earthquake) using the inversion method, and compared each other to investigate their temporal changes.

For calculating the deformation fields in Japan, we used the daily coordinates of F3 solutions. We obtained daily time series data considering the movements of the continental plates against reference frame and removing the offsets and postseismic effects due to nearby earthquakes. We then derived horizontal rate fields in Japan for each year by least-squares fittings. For reflecting the geometry of the plate boundaries, we used the plate model (Baba et al., 2005) incorporated in JIVSM (Koketsu et al., 2012). The Green's functions were calculated using the frequency-wavenumber method (Zhu and Rivera, 2002). We performed slip deficit inversions using the method of Yoshida et al. (1996).

The slip deficit rate distributions derived from the inversions were consistent with the previous study and the plate convergence rates. In addition, known long-term slow slip events were found in the temporal changes of the slip deficit rate distributions. Furthermore, we can see the temporal changes in the Hokkaido and Kanto regions, which suggest variations of plate coupling in these regions. The zones of large slip deficit rate in the distributions look corresponding to the source regions of past megathrust earthquakes. These correspondences are significant not only in Earth science but also in seismic hazard assessments.

Acknowledgement: We would like to thank Geographical Survey Institute for geodetic data recorded by GEONET.

Keywords: the Japan islands, crustal deformation, GPS, slip deficit, megathrust earthquake

Japan Geoscience Union Meeting 2014
(28 April - 02 May 2014 at Pacifico YOKOHAMA, Kanagawa, Japan)

SSS34-01 Room:502 Time:April 29 09:00-09:15

Height Distribution of the tsunami of the Ansei North Sanriku-Oki earthquake of August 23, 1856

TSUJI, Yoshinobu[1*] ; MABUCHI, Yukio[2] ; OKADA, Kiyohiro[2] ; KUROYANAGI, Yosuke[2] ; OOIE, Takayuki[2] ; KURIMOTO, Masashi[2] ; KINAMI, Takahiro[3] ; HORIE, Takehito[4] ; HASHIMOTO, Keisuke[4] ; SASAKI, Takayuki[4] ; IWABUCHI, Yoko[5] ; IMAI, Kentaro[6] ; IMAMURA, Fumihiko[6]

[1]Fukada Geolog. Inst., [2]Pacific Consultant, [3]Kubiki Techno., [4]Alpha Hydraulic Eng. Consultant, [5]JNES, [6]IRIDeS, Tohoku Univ.

A large earthquake occurred in the sea area between Aomori coast, most northern district of Honshu, and Hidaka coast, Hokkaido, on 23rd August, 1856 (3rd year of Ansei era) . This earthquake is a one of the series of the plate boundary earthquakes at the joint point of the Japan and the Kuril trenches, where the 1968 Tokachi-Oki earthquake occurred. The 1677 Enpo North Sanriku-Oki earthquake is considered also as the same typed one. The tsunami of the 1856 North Sanriku-Oki earthquake hit the coasts of Sanriku districts, the north east part of Honshu, and the pacific coast of Hokkaido. As the total number of victims of the tsunami was only 38 people in all, and it was considered not to be a large natural hazard. So it did not become a lecture for tsunami hazard in the time of the 1896 Great Meiji Sanriku tsunami. The diary kept by a priest of Kokutaiji Temple at Akkeshi in east Hokkaido records that human disturbance broke out there, and tsunami height was estimated at 2.0 m. At Saru-Kaisho office in Monbetsu town, Hidaka district, a strong tide came in front of the building of the office, where sea water rose up to the height of 11.2 meters. At Etomo village in Muroran city, sea water invaded into the residential area (height: 5.6m). On the pacific side of Hakodate peninsula, sea water flooded up to the fort of Tsugaru Clan ”Tsugaru-han Jin’ya” where the ground height is 8.6 m. At Same fishery port in the central area of Hachinohe city, residential area was flooded up to 7.3 meters height. At Kanehama village in Miyako city, which is located at the innermost point of the V-shaped bay, inundation height was 5.7 meters. As for the coasts of south part of Iwate Prefecture Tsuji et al.(1995) conducted survey. Together with this result,we have the distribution map of the tsunami height as the figure. The authors of the present study wish to express their thanks to JNES for its financial support in promoting our research.

Keywords: historical earthquake, historical tsunami, Sanriku coast, Hokkaido, Japan trench

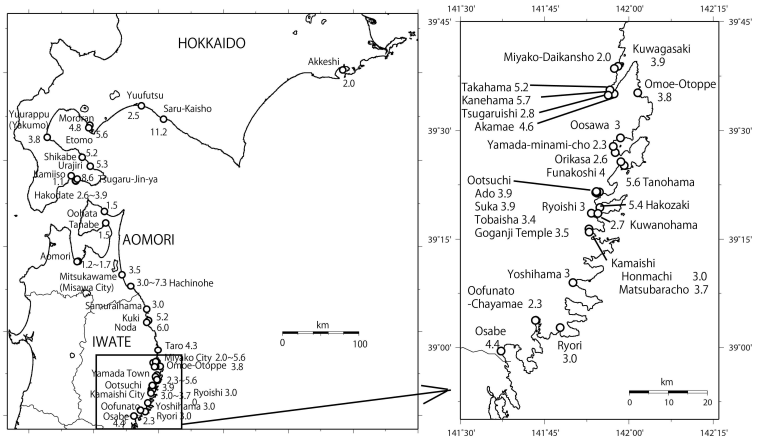

Japan Geoscience Union Meeting 2014
(28 April - 02 May 2014 at Pacifico YOKOHAMA, Kanagawa, Japan)

SSS34-02 Room:502 Time:April 29 09:15-09:30

Reexamination of 1945 Mikawa earthquake disaster (1) Detailed distribution of earthquake victims

KIMATA, Fumiaki[1*] ; MATSUTA, Nobuhisa[2]

[1]Tono Research Institute of Earthquake Science, Association for the Development of Earthquake Predict, [2]Earthquake and Volcano Research Center, Graduate School of Environmental Studies, Nagoya University

Iida (1978) organized the Mikawa earthquake disaster under the cooperation of Aichi prefecture, and clarify the whole picture of the disaster. However, he could not discuss the disaster in community level precisely. For example, 46% of 1200 houses were collapsed in Hukuji village, Hazu-gun in 1944 ToNankai earthquake, and additionally 67% of left 650 houses were also collapsed in 1945 Mikawa earthquakes one month later. The reason of strong damages in Hukuji is not discussed enough until now.

It is very important to make clear whole picture of the earthquake disaster in history and in near future as national government. As the earthquake disaster remains a rare event, detailed research of the historical earthquake disasters needful to understand the following disasters. In the presentation, we would like to discuss the disaster of the Mikawa earthquake in local community level.

1. Discussion on characteristic disaster based on earthquake victim distribution

Earthquake fault shaped S was appeared in the ground surface at the Mikawa earthquake. However recent researches of fault geomorphology and ground deformation based on geodesy point out two main faults striking with NNW-SSE direction, and an E-W striking fault is tear fault caused by slips on two faults. Additionally, dominant rupture should be occurred at Fukodu fault located in east. The total Mo estimated by ground deformation is the earthquake moment of 1.6x1019Nm(Mw6.7), and the third four of the released one is by slip of Fukodu fault. In our presentation, we discuss earthquake disaster with the local community level based on two N-S striking earthquake faults.

1) Katahara: compact cluster of dead located close to Fukodu fault

Katahara town of Hoi-gun (then-9300 people and 1887 houses) located just on Fukodu fault, lose 227 people and 319 completely destroyed houses (15.2% collapse rate). In the town, the damages are different in each street corner. Numbers of dead and completely destroyed houses within the town are shown as bar charts and color scale in 59 neighborhood blocks. The dead are limited in the narrow zone of 1 km wide along the earthquake fault. There are some communities with no collapsed house, which are located 1 km distance from the fault. Dead are corresponding to 73 % of completely-destroyed houses, and some blocks closing the fault show the rate over 90%. Precisely, people are attacked by strong seismic waves during the hours of sleep, and they had no time to evacuate to outsides from houses. There are many blocks to have no dead and no collapsed houses, which are locating more 1 km far from the fault.

2) Fukuji: Decentralized dead far from fault in river plain

On the one way, Fukuji village (then-673 houses), Hazu-gun locating 5 km southwestward from the Yokosuka Fault, one of main faults, lost 162-350 peoples and 400 houses completely. In one month before, the village also attacked by 1944 ToNankai earthquake, lost 21 people and 550 houses completely. They lost 1000 houses by earthquakes in 1200 houses for one month. The numbers of the dead are shown in each block in Fig.1B.

The dead distributions are obviously different with that in Katahara. They lost many people in almost all blocks in the village. The collapse rate of ToNankai earthquake is by far the worst in Aichi prefecture, because, second worst is 21.3% in Tomiki village, Chita-gun. The Fukuji village is just located in river plain with Yahagi and old-Yahagi rivers. An exist of thick alluvial formation caused the large damages in Fukuji.

The dead by Mikawa earthquake are caused by two reasons. One is there are very strong shaking at the blocks located immediately above the fault, and second is amplitude shaking by alluvial formation in river plain. The former is a case of Katahara and later is a case of Fukuji.

Keywords: Mikawa erathquake, Fukozu fault, Yokosuka fault, earthquake disaster, seismic victim, collapse rate

Japan Geoscience Union Meeting 2014
(28 April - 02 May 2014 at Pacifico YOKOHAMA, Kanagawa, Japan)

SSS34-03 Room:502 Time:April 29 09:30-09:45

Interpretation of an illegible old stone inscription by SfM image analysis at Itsukushima shrine, Nojimazaki

SUZUKI, Hinako[1*] ; UCHIYAMA, Shoichiro[1] ; INOUE, Hiroshi[1]

[1]National Research Institute for Earth Science and Disaster Prevention (NIED)

This study shows that interpretation the illegible old stone inscription by structure from motion (SfM) image analysis. The stone monument built in 1927 for memorial on the 1923 Taisho Kanto Earthquake, the inscribed capitals can hardly read. We captured 158 photographs on the surface of the stone, and processed by SfM to generate 3 D model of it. As a result, illegible capitals became clear on the 3 D model, so visible coated contamination removed by SfM. It is effective method to archive stone inscriptions.

Keywords: structure from motion (SfM), stone inscription, interpretation, historical natural hazard, Nojimazaki

Japan Geoscience Union Meeting 2014
(28 April - 02 May 2014 at Pacifico YOKOHAMA, Kanagawa, Japan)

SSS34-04 Room:502 Time:April 29 09:45-10:00

The Evidence of the Uplift associated with the Kanto Earthquakes inferred from the Marine Terrace in the Alluvial Valley

KIM, Haeng yoong[1*] ; MANNEN, Kazutaka[1] ; SASAGE, Kazuo[2] ; KUMAKI, Yohta[3] ; MATSUSHIMA, Yoshiaki[4]

[1]Hot Springs Research Institute of Kanagawa Prefecture, [2]PASCO, [3]Senshu University, [4]Kangawa Prefecture Museum of Natural History

Recurrent giant earthquakes at the plate boundary along the Sagami Trough have been considered as one of the greatest thread of the Tokyo Metropolitan area. At the southwestern tip of the Miura Peninsula, in south of Tokyo, the tide gauge station records the coseismic uplift amount of 1.4 m and the interseismic subsidence amount of 0.3 m in and after 1923 earthquake, respectively. It is effective to reveal evidences of the past coseismic uplift to know the future earthquake.

Wave-cut benches which emerged in 1923 are widely distributed along the rocky coast. Higher wave-cut benches, good indicators of coseismic uplift prior to 1923, are also recognizable. It is, however, often difficult to spatially compare one another due to the erosion.

We investigated the distribution of the tidal-flat deposits and the 1923 wave-cut benches at two small bays in the southwestern and southern parts of the Peninsula. The aggradation of the coastline associated with the 1923 uplift was identified by the comparison between the 1:25,000 topographic maps before and after the 1923 earthquake. Observations of outcrops and drilling cores at the 1923-formed marine terrace showed that the tidal-flat deposits consist of shelly sand and gravels. The elevation of tidal-flat deposits indicates the coseismic uplift in 1923 and the interseismic subsidence after 1923. The uplift amount was estimated approximately 0.9 m and 2.1 m at the southwestern and southern parts of the Miura Peninsula, respectively. The uplift amount inferred from the tidal-flat deposits is concordant with that inferred by the wave-cut benches.

Keywords: Kanto Earthquake, Paleo-earthquake Record, Alluvial Valley, Microlandform, Tide-zone Deposits, Miura Peninsula

Japan Geoscience Union Meeting 2014
(28 April - 02 May 2014 at Pacifico YOKOHAMA, Kanagawa, Japan)

SSS34-05 Room:502 Time:April 29 10:00-10:15

Coseismic uplifts of the southern Izu Peninsula and the coastal area of Shimizu Plain

KITAMURA, Akihisa[1*] ; KOBAYASHI, Konatsu[1] ; OHASHI, Yoko[2] ; YOKOYAMA, Yusuke[2] ; MIYAIRI, Yosuke[2]

[1]Shizuoka University, [2]The University of Tokyo

We examined coseismic uplift events in the coastal area of the Shimizu Plain, and at the southern end of the Izu Peninsula. On the basis of lithologies, fossil contents, and radiocarbon dating, we identified geological and paleontological evidence for abrupt changes in depositional environments related to coseismic uplift associated with the AD 1854 Ansei-Tokai earthquake. We estimated a maximum coseismic uplift of 1.2 m and post-earthquake gradual subsidence of ca. 0.6 m. Radiocarbon dating of the emerged sessile assemblages at the southern end of the Izu Peninsula, central Japan suggest that at least four coseismic uplift have occurred in the area, during 3387-2485 cal yr BP, AD 570?820, AD 1000?1270, and AD 1430?1660.

Keywords: Coseismic uplifts, southern Izu Peninsula, Shimizu Plain, Holocene, Ansei-Tokai earthquake

Japan Geoscience Union Meeting 2014
(28 April - 02 May 2014 at Pacifico YOKOHAMA, Kanagawa, Japan)

SSS34-06 Room:502 Time:April 29 10:15-10:30

Former shoreline height and Active Faulting around Obama Bay, Fukui, Central Japan

WATANABE, Mitsuhisa[1*]

[1]Toyo Univ.

I examined the distribution of marine terrace surface assigned to the oxygen isotope stage 5e along the coast around Obama Bay, Fukui Prefecture, central Japan. The marine surface is recognizable on the western and southern coast of Obama bay, which indicates only southwestern coast has progressively uplifted. There is no marine terrace surface along the NE coast of the bay. This strongly suggests that an active fault divides the bay just on the extension of the FO-A fault and the Kumagawa fault. The FO-B and FO-A fault are left-lateral active fault trending NW-SE direction. The Kumagawa fault trending WNW-SES direction display the same vertical displacement as them and SW hanging-wall uplift. These active faults composing of an extensive active fault ca. 65-km long across Obama bay displaying distinct trace jog close to the mouth of the bay (Nokogiri-zaki point). Height distribution of the former shoreline on the marine terrace surface shows the uplift pattern in this area. Comparing the uplift pattern with calculated displacement based on the dislocation theory, the fault model mentioned above explains the general features of the crustal deformation.

Keywords: marine terrace surface, former shoreline, submarine active fault, caclculated displacement, Obama bay

Japan Geoscience Union Meeting 2014
(28 April - 02 May 2014 at Pacifico YOKOHAMA, Kanagawa, Japan)

SSS34-07 Room:502 Time:April 29 11:00-11:15

Comparison of the fault zones of the fault activity terminated until the Early Pleistocene and the active fault

OHTANI, Tomoyuki[1*] ; KONO, Masahiro[1] ; KOJIMA, Satoru[1]

[1]Gifu Univ.

In the active fault surveys without younger sedimentary layers, it is desired that the new method is developed to assess the fault activity using the fault rocks in the basement rocks. To achieve this, it is important to understand the characteristic features of the fault zones not only active faults, but also the faults terminated their activity recently. We studied the fault zone of the Median Tectonic Line (MTL) in Yoshino, Nara, and compare its results with those of active faults.

The MTL is the active fault in the west of the central part of the Kii peninsula, in which the fault activity is terminated recently in the east. In this eastern area, Okada and Togo (2000) show the fault which terminated its activity until 300 ka in the active fault maps. Sangawa and Okada (1977) reported an exposure of fault zone that makes a border of the Early Pleistocene Shobudani Formation and the Cretaceous Izumi Group, and that is covered by the Middle Pleistocene Gojo Formation unconformably. Based on the sedimentary ages of their formation, the MTL in this area is terminated until 1 to 1.2 Ma. The fault exposure reported by Sangawa and Okada (1977) is covered by concrete presently, we studied the fault exposure 13 km east away from the previous exposure.

In this exposure, the fault gouge zone with ca. 1 m thickness strikes E-W. The Izumi formation is in the northern side of the fault zone, in which no exposure in the southern side. The Izumi Formation in this exposure is mainly mudstone. Bedding plane is subholizontal in the host rock, in which foliation is subvertical in cataclasite near the fault gouge. Composite planar fabric in foliated cataclasite indicates the uplift of the southern side.

The powder X-ray diffraction and X-ray fluorescence analyses were performed using the samples from this fault exposure. The results of the powder X-ray diffraction analysis shows disappearance of mica and formation of chlorite in the foliated cataclasite close to the fault gouge, and decomposition of plagioclase and formation of calcite in foliated cataclasite and fault gouge. The altered minerals indicate a remarkable alteration in foliated cataclasite rather than fault gouge. Smectite is not detected in fault gouge and cataclasite.

The results of the X-ray fluorescence analysis show the increase of TiO2, Al2O3, MgO, K2O and P2O5 toward the fault gouge and the decrease of CaO, Na2O and MnO in foliated cataclasite and fault gouge. The decrease is especially in foliated cataclasite rather than fault gouge.

The studied feature is compared by that of the active faults. In the active fault zone, the latest fault gouge is characterized by the formation of smectite and concentration of Mn. Smectite is the mineral formed under lower temperature. Mn deposits under the oxidized condition. These are consistent with recent near-surface condition of the active fault zone. The studied fault zone would be displaced in the deeper part because its activity has been terminated and present surface exposure should be exhumed from 1 to 1.2 Ma to present. Mn is difficult to concentrate in the deeper reduction condition.

Keywords: Early Pleistocene, fault zone, active fault

Japan Geoscience Union Meeting 2014
(28 April - 02 May 2014 at Pacifico YOKOHAMA, Kanagawa, Japan)

SSS34-08 Room:502 Time:April 29 11:15-11:30

Analysis for deformation structures, mineral composition, and elemental composition in the Atera fault

KATO, Naoki[1*] ; HIRONO, Tetsuro[1] ; ISHIKAWA, Tsuyoshi[2] ; KAMEDA, Jun[3] ; OHTANI, Tomoyuki[4]

[1]Department of Earth and Space Science, Graduate School of Science, Osaka University, [2]Kochi Institute for Core Sample Research, Japan Agency for Marine-Earth Science and Technology, [3]Department of Natural History Sciences, Graduate School of Science, Hokkaido University, [4]Department of Civil Engineering, Gifu University

The Atera fault is an active fault extended 70 km along southern — central Gifu Prefecture, Japan, which is considered to slip at 1586 Tensho earthquake based on the field outcrop and trenching survey by previous researches. However, the seismic slip behavior along the fault has been understood. In this study, we performed the field observation on the Tase outcrop of the Atera fault, microscopic observation, X-ray diffraction, trace element analysis by using ICP-MS for investigating the deformation structure, mineral assemblage, and geochemical anomaly in the Atera fault. We will present their preliminary results.

Keywords: Active fault, Fault gouge, Trace element

Japan Geoscience Union Meeting 2014
(28 April - 02 May 2014 at Pacifico YOKOHAMA, Kanagawa, Japan)

SSS34-09 Room:502 Time:April 29 11:30-11:45

Deformation simulations by the discrete element method controlling basement motions by the dislocation solutions

KUSUMOTO, Shigekazu[1*] ; ITOH, Yasuto[2]

[1]Grad. Sch. Sci. Eng. Res., Univ. Toyama, [2]Grad. Sch. Sci., Osaka Prefecture University

In previous studies on deformation of sedimentary layer due to fault motions within the basement by means of the discrete element modeling, the basement has been treated as rigid body. In this study, we attempted to control motions of the basement by dislocation analytical solutions based on the elasticity in order to discuss the deformation field of the sedimentary layer in connection with fault parameters.

As a result, we found tilt of deformed sedimentary layer which did not appear in the rigid basement model. And, shapes of deformed sedimentary layer around the fault tip were different from rigid basement model, and even in the elastic basement model it was shown that their shapes will be varied by the fault parameters selected in the modeling.

Since sedimentary layers deform by following to shape of deformed basement, and the basement controlled by the dislocation analytical solutions deforms by the fault parameters, it was shown that not only shape of deformed sedimentary layers but trishear and its propagation processes will be able to be discussed in connection with the fault parameters. In the future, we will accumulate some know-how on practical analyses method by applying our modeling procedure to interpretations of topography, geological structures and seismic survey data, and we would like to hasten quantitative discussions on tectonics and/or forming processes of geological structures.

Keywords: Discrete Element Method, Dislocation analytical solutions, Displacement of sedimantary layer, PFC

Japan Geoscience Union Meeting 2014
(28 April - 02 May 2014 at Pacifico YOKOHAMA, Kanagawa, Japan)

SSS34-10 Room:502 Time:April 29 11:45-12:00

The reproductive experiments of stratum deformation on the trench for the Kushibiki fault using numerical experiments

ANDO, Koichi[1*]

[1]Tokyo Metropolitan University Department of Geography

Introduction

The Quaternary regional stress field in eastern-central Japan tend to be east and west compaction force. Therefore, a number of thrust faults develop in this area. These faults sometimes indicate complex features, such as back thrusts or branches above 3 km depth.

It is considered that seismic waves are generated by fault activity below 3 km depth. Therefore, indirect earthquake surface faults which branch off from a earthquake source fault not generate seismic waves. Additionally, earthquake surface faults which directly connect to a earthquake source fault specify crustal movements around these faults. Therefore, we must distinguish between indirect earthquake surface faults and faults which directly connect to a earthquake source fault.

According to the approach of foam rubber models and dynamic lattice model simulations, it is known that a fault slip velocity accelerates toward a ground surface (e.g., Oglesby *et al.*, 2000; Ma and Hirakawa, 2013). According to numerical calculations which base on dynamic models, peak slip velocities of thrust faults with dip angles of 30-45 degree are 2.5-4.0 m/s (e.g., Oglesby *et al.*, 2000; Ma and Hirakawa, 2013). On the other hand, according to the numerical calculation, the peak slip velocity of the back thrust which was the indirect earthquake surface fault from the 2008 Iwate-Miyagi Nairiku earthquake in Japan was 0.05 m/s (Ando and Yamazaki, 2013). Therefore, we may be able to distinguish between indirect earthquake surface faults and faults which directly connect to a earthquake source fault, from peak slip velocities. Thus I estimated the peak slip velocity of the Kushibiki fault which is considered as indirect back thrust of the Fukaya fault, from numerical experiments.

Relation between the Kushibiki fault and the Fukaya fault

Sugiyama *et al.* (2009) described that the Kanto-heiya-hokuseien fault zone is active fault zone which intervenes between the Kanto mountain terrain and the Kanto plain with NW-SE strike. The Kanto-heiya-hokuseien fault zone which is SW dipping thrust consists chiefly of fault groups along the Fukaya fault and the Fukaya fault.

The Hirai-Kushibiki fault zone which is considered as back thrust of Fukaya fault except the Hirai fault, consists of the Hirai fault, the Kushibiki fault and Kamikawa fault. In addition, the Kushibiki fault is bedding fault of Neogene sediments which have a dip angle of about 20 degree (Sugiyama *et al.*, 2009b; Shintani *et al.*,2009).

Methods

In this study, I performed numerical experiments about stratum deformation by faulting of the Kushibiki fault, and these experiments were executed by SDSSC (Strata Deformation Simulation System using CIP method) Ver 4.09. The model which feeds into SDSSC is modeled by the stratigraphy, the dip angle and the unit displacements from drilling surveys (Sugiyama *et al.*, 2009b) and trenching study (Shintani *et al.*, 2009).

Numerical experiments were performed with taking into account the erosional vacuity and the sedimentation for stratum by the faulting at the trenching area, and the peak slip velocity was estimated by comparison between experimental results and trenching results.

I adopted CWFS (cohesion weakening and frictional strengthening) model (Hajiabdolmajid *et al.* 2002) as the deformation characteristic about the stratum.

Result and Discussion

I estimated the peak slip velocity of the the Kushibiki fault at 1-1.5 m/s. Therefore, this conclusion leads to the suggestion that the peak slip velocity of the indirect back thrust is slower than the thrust faults.

Achnowlegement

For this study, I have used the computer systems of the Earthquake and Volcano Information Center of the Earthquake Research Institute,the University of Tokyo.

Keywords: Kushibiki fault, earthquake surface faults, back thrust, fault slip velocity, numerical experiment, CIP method

Japan Geoscience Union Meeting 2014
(28 April - 02 May 2014 at Pacifico YOKOHAMA, Kanagawa, Japan)

SSS34-11 Room:502 Time:April 29 12:00-12:15

Spatial Variation on Recurrence-time Distribution of Paleoearthquakes and Its Influence for Long-term Forecast

NOMURA, Shunichi[1*] ; OGATA, Yosihiko[2]

[1]Graduate School of Information and Engineering, Tokyo Institute of Technology, [2]The Institute of Statistical Mathematics

The Earthquake Research Commitee (ERC) of Japan performs and publishes the long-term forecast of major paleoearthquakes in Japan. The ERC adopts renewal processes assuming that the recurrence intervals of paleoearthquakes are independently and identically distributed as the BPT (Brownian Passage Time) distribution. When applying this model, we need to estimate the mean and coefficient of variation (CV) on recurrence times. The estimation error in CV occationally affect so much on the long-term forecast. However, while the mean parameter can be estimated with a certain precision from only the number and approximate ages of historical activities,the estimates of CV parameter have quite large errors without plentiful and accurate data. So the ERC assumes a common estimate for all active faults in Japan to ensure a certain reliability for the estimate.But as the historical paleoseismic data are accumulated by investigations, some active faults show significantly large variation in recurrence times.

Renewal processes with the BPT distribution are based on an physical model that assumes a cyclic mechanism where stress on a fault surface is accumulated by tectonic forces until an earthquake occurs that releases the accumulated stress to a basal level. In this model, the mean recurrence time represents the rate of stress accumulation by tectonic motionand the CV implies the strength of stress perturbation caused by nearby seismicity. Therefore, these parameters are supposed to have regional trends as seen in the analysis of Nomura et al. (2011). In our study, we estimate the spatial variation of these parameters on the BPT distribution in Japanand apply it to the long-term forecast on the active faults with very few historical data. In addition, we compare our forecast with the forecast by the ERC to discuss the influence of parameter estimation on earthquake prediction.

Keywords: long-term forecast, BPT distribution, renewal process, coefficient of variation, spatial model

Japan Geoscience Union Meeting 2014
(28 April - 02 May 2014 at Pacifico YOKOHAMA, Kanagawa, Japan)

SSS34-12 Room:502 Time:April 29 14:15-14:30

Spatial distribution of faults and folds in the offshore extension of the western margin fault zone of the Takada plain

ABE, Shintaro[1*] ; ARAI, Ryoyu[2] ; OKAMURA, Yukinobu[1]

[1]AIST, [2]KGE.Co.,Ltd

We carried out a marine geological investigation on an offshore extension of the western margin fault zone of the Takada plain. The main purpose of this study is to clarify the total length of the fault zone and characterization of recent faulting. The western margin fault zone of the Takada plain is west dipping reverse fault, and the total length of this fault zone is 30 km from land to sea are based on the existing material.

We conducted 31 lines of high-resolution multichannel seismic reflection survey to recognize the detailed structure of the faults and folds. The reflection profiles depict the geological structure with extremely clear images.

The reflection profiles showed that the geological structure of the offshore area is characterized by the fold belt along the northern margin of the sedimentary basin that is formed in front of Takada plain. The shape of the fold is asymmetric weakly, and suggesting the fault related fold that has been deformed by west or north west dipping blind reverse fault as with land. This fault related fold zone is continuous to the Northern Kashiwazaki-oki Anticline from the Naoetsu-oki fault while changing asymmetry on the way. The North Kashiwazaki-oki Anticline is an active structure that has been pointed out the relevance of the source fault of the Chuetsu-oki earthquake.

Keywords: The western margin fault zone of the Takada plain, offshore, fault, fold, active structure, high-resolution seismic reflection survey

Japan Geoscience Union Meeting 2014
(28 April - 02 May 2014 at Pacifico YOKOHAMA, Kanagawa, Japan)

SSS34-13 Room:502 Time:April 29 14:30-14:45

Geologic structures and their activities around junction of main part and southern part of the active eastern boundary f

KOMATSUBARA, Taku[1*] ; SATO, Tomoyuki[1] ; KOU, Yoshihide[1] ; OZAKI, Masanori[1] ; KOMATSUBARA, Junko[1]

[1]Institute of Geology and Geoinformation, Advanced Industrial Science and Technology

A 130-km-long N-S trending active fold and thrust zone (eastern boundary fault zone of Ishikari lowland) occurs in the Ishikari lowland and off the Yufutsu plain. This fault system is one of the boundary faults between the Kuril arc and the Northeast Japan arc. This fault system consists of east-dipping thrusts accompanying with fault-related folds. This fault system is subdivided into two parts with gap and echelon arrangement around the Yufutsu plain. The main part is 72 km-long and its mean vertical displacement rate is larger than 0.4 m/ky since the late Pleistocene. The south part is 86-km-long and its mean vertical displacement rate is 0.2-0.3 m/ky since the late middle Pleistocene. The southern part of this fault zone includes discontinuous structures such as short-axis anticlines and short monocline in the terrestrial part. This discontinuity of geologic structure would be related to irregularity of basement rocks underlying the southern part of Ishikari Lowland.

Keywords: Eastern margin fault zone of Ishikari Lowland, fold and thrust belt, active fault, mean displacement rate, geographical information system

Japan Geoscience Union Meeting 2014
(28 April - 02 May 2014 at Pacifico YOKOHAMA, Kanagawa, Japan)

SSS34-14 Room:502 Time:April 29 14:45-15:00

Revisited most recent paleoearthquakes along the ISTL active fault system, central Japan

KONDO, Hisao[1*] ; TANIGUCHI, Kaoru[1] ; SUGITO, Nobuhiko[2]

[1]AIST AFERC, [2]Hosei University

The ISTL active fault system, central Japan, is well-known as one of the most hazardous fault systems based on the previously-reported paleoseismological works. Since the first paleoseismic trench survey was performed in 1980s, the number of paleoseismic sites becomes over 44 sites along the 150-km-long fault system, that is the highest density on active fault zone in Japan. In those studies, the timing of the most recent paleoearthquake had been reported around 1200 y.B.P., and the events had been longly estimated to be correlated with one muti-segment earthquake either 762 A.D. or 841 A.D. historical earthquakes. On the other hands, the recent result of geoslicer survey at the middle section of the ISTL indicate that the most recent event occurred around 2300 y.B.P., contradicting with the correlations with the historical earthquakes. Thus the most recent earthquakes on the ISTL is still ambiguous, therefore, we carried out systematic paleseismic surveys around the largest segment boundary, Lake Suwa segment boundary, at the middle of the ISTL active fault system. The Lake Suwa segment boundary is structural Quarternary basin formed by left fault step-over between left-lateral strike slip faults. At three paleoseismic sites inside of the Suwa basin, we revealed the most recent events occurred a few thousands years before ˜1200 y.B.P. and those are not correlatable with the historical earthquakes. These data indicate that the most recent earthquake along the ISTL did not rupture through the Lake Suwa segment boundary. In addition with this, the compiled timing of the most recent event along the entire the ISTL suggest that spatial clustering of the most recent earthquake. One large earthquake ruptured between the Kamishiro fault and the Gofukuji fault or possibly up to the Okaya fault, and another event ruptured between the Kamanashi-Yama faults and the Shimotsutaki fault. These two events will be correlated with either the 841 A.D. and the 762 A.D. earthquakes along with more reliable historical document surveys. Furthermore, this paleoseismic scenario during the most recent earthquake cycle do not deny the possibly that the larger multi-segment earthquake rupturing through the Lake Suwa segment boundary. In fact, paleoseismic event occurred between 2000 y.B.P. and 2300 y.B.P. was identified at the sites on the Gofukuji fault, the Okaya fault, and the Chino fault. Since those faults have left-lateral-strike slip component forming the pull-apart basin, the 2000-2300 y.B.P. event might have ruptured through the Lake Suwa segment boundary. To be testified this possibility, further investigation on the slip per event around the segment boundary is necessary.

Keywords: active fault, paleoearthquake, historical earthquake, ISTL active fault system

Japan Geoscience Union Meeting 2014
(28 April - 02 May 2014 at Pacifico YOKOHAMA, Kanagawa, Japan)

SSS34-15 Room:502 Time:April 29 15:00-15:15

High resolution seismic reflection profiling across the Kurehayama fault, Otokawa Line, central Japan

ISHIYAMA, Tatsuya[1*] ; KATO, Naoko[1] ; SATO, Hiroshi[1] ; KOSHIYA, Shin[2] ; TODA, Shigeru[3] ; KOBAYASHI, Kenta[4] ; TERUI, Kyoko[2] ; KONDO, Shiori[3] ; YAMAUCHI, Koichi[1] ; SHIORI, Abe[1]

[1]Earthquake Research Institute, University of Tokyo, [2]Department of Civil and Environmental Engineering, Faculty of Engineering, Iwate University, [3]Aichi Educational University, [4]Department of Geology, Faculty of Science, Niigata University

We collected and processed shallow high-resolution seismic reflection data in order to resolve shallow structures and to understand structural linkage between active faults and folds recognized at ground surface and deeper, complicated fold and thrust structures along the Kurehayama fault, Toyama Prefecture, central Japan. We deployed more than 800 seismic channels, 10-Hz geophones, and Enviro-Vib (IVI, Inc) as a seismic source along about 8-km-long seismic line. Common midpoint stacking by use of initial velocity analysis successfully illuminates subsurface geometries of active fault-related fold to 1.5 two-way time in time section and up to about 1.5 km in depth section. Detailed seismic reflection analyses including refraction and residual statics, migration, deconvolution, and time-space variant bandpass filters, and depth-conversion by use of stacking velocities enable to obtain subsurface depth section of these active structures.

Japan Geoscience Union Meeting 2014
(28 April - 02 May 2014 at Pacifico YOKOHAMA, Kanagawa, Japan)

SSS34-16 Room:502 Time:April 29 15:15-15:30

Active faults in and around the Yoshinogari Heritage

KAGOHARA, Kyoko[1*] ; YOSHIDA, Haruka[2] ; SOEDA, Yoshio[3] ; OKADA, Shinsuke[4] ; MATSUTA, Nobuhisa[5] ; TODA, Shigeru[6] ; IMAIZUMI, Toshifumi[7] ; NAGAOKA, Shinji[8]

[1]Facultu of Education, Yamaguchi University, [2]non, [3]West Japan Engineering Consultants,Inc., [4]International Research Institute of Disaster Science, Tohoku University, [5]Disaster Mitigation Research Center, Nagoya University, [6]Aichi University of Education, [7]Graduate school of Science, Tohoku University, [8]formerly Nagasaki University

The normal faults are distributed around the boundary line of between Saga Plain and Sefuri Mountains (The Research group for Active tectonics in Kyushu, 1989, etc.). Shimoyama (2010) suggested that this normal fault zone relatively uplift the north side block, based on the displacement of boundary between Aso-4 and Mitagawa Formation. According to the Regional evaluation of the active fault (Kyushu), the Headquarter of Earthquake Research Promotion evaluated that the normal fault zone (Saga Heiya Hokuen Fault Zone) can be traced about 22 km from Ogi City to Yoshinonogari Town, based on the feature of gravity anomaly and tectonic geomorphology. However, the distribution and activities of active fault are not understood well. Yoshinogari Heritage, one of the Japan's important heritages, is on a terrace that is formed by Aso-4 pyroclastic flow deposits. Many relics during the Paleolithic era and Early-modern era have been excavated from here. Especially, it is famous for moat-surrounded settlements of the Yayoi period. The prospered moat-surrounded settlements were abandoned in the late third century. In the Nara period, Kando (ancient road) and government agencies which extend to Hizen Province (Saga and Nagasaki Prefecture) from Dazaifu,were established in the northern Saga Plain including the Yoshinogari Heritage. Yoshinogari Heritage and surrounding areas are regions where the civilizations of the many periods remain. Therefore, in this area that records man's activity for a long time, it is expected that influences of fault activities on civilizations can be known. To clarify the time and spatial relationships between active faults and ruins, we described the distribution map on active faults and ruins in and around the Yoshinogari Heritage, based on interpretation of topography using large-scale maps, aerial photograph, 5m DEM and results of field and archaeological surveys, and also conducted several very shallow seismic reflection profiles across clear tectonic scarps.

Keywords: Normal fault zone, Saga Plain, Yoshinogari Heritage, DEM, Very shallow seismic reflection profiling

Japan Geoscience Union Meeting 2014
(28 April - 02 May 2014 at Pacifico YOKOHAMA, Kanagawa, Japan)

SSS34-17 Room:502 Time:April 29 15:30-15:45

Study on great palaeoearthquakes and the decline of the Sanxingdui and Jinsha civilizations, Sichuan basin, China

LIN, Aiming[1*] ; RAO, Gang[2] ; WANG, Maomao[1]

[1]Department of Geophysics, Graduate School of Science, Kyoto University, Kyoto 606-8502, Japan, [2]Department of Earth Sciences, Zhejiang University, Hangzhou 310027, China

The ruins of ancient civilizations damaged by large palaeoearthquakes, which have been reported worldwide, are often used as surface markers for Holocene tectonic and palaeoseismic events. Previous studies have demonstrated that recurring palaeoearthquakes have caused repeated soil liquefaction at the same site, leaving a record in both sediments and ancient ruins; such records can reveal a great deal about earthquakes that occurred prior to human-recorded observations or measurements5?10.

The Sanxingdui civilization, which developed on the Sichuan Plain, central China, during the Bronze Age (ca. 4800 years ago), flourished from ca. 4200 to ca. 3500 years ago until its sudden disappearance ca. 3200 years ago. Subsequently, the Jinsha civilization arose in the area around Chengdu city, ca. 40 km southwest of the Sanxingdui site, but it too suddenly disappeared ca. 2500?2200 years ago. It has been speculated that floods or regime changes might explain the collapse of both civilizations, but no solid evidence for such causes has so far been reported.

In this study, to search for a link between palaeoearthquakes and the abrupt unexplained falls of the Sanxingdui and Jinsha civilizations, we investigated the liquefaction induced by great palaeoearthquakes that occurred repeatedly in the past 5000 years on the Sichuan Plain, central China, in the region of the former Sanxingdui and Jiasha civilizations. Here, we present evidence that great palaeoearthquakes may have caused the collapse of both the Sanxingdui and Jinsha civilizations, as the cultures flourished in the periods during ca. 4200?3500 years and ca. 2800?2300 years ago, respectively, on an active fault zone of the Longmen Shan Thrust Belt (LSTB) that triggered the 2008 Mw 7.9 Wenchuan earthquake. Field observations, archaeological evidence, and radiocarbon dating reveal that at least four great palaeoearthquakes have induced liquefaction in wide areas around the Sanxingdui and Jinsha civilization sites during the past 5000 years, with an average recurrence interval of ca. 1000 years. We suggest that palaeoearthquakes occurring ca. 3300 and ca. 2200 years ago caused the fall and disappearance of the Sanxingdui and Jinsha civilizations, respectively, by causing extensive damage to infrastructure and manufacturing facilities, as well as numerous deaths.

Keywords: palaeoearthquake, Sanxingdui civilization, Jinsha civilization, Yangtze River civilization, Longmen-Shan Thrust Belt, Sichuan Basin

Japan Geoscience Union Meeting 2014
(28 April - 02 May 2014 at Pacifico YOKOHAMA, Kanagawa, Japan)

SSS34-18 Room:502 Time:April 29 15:45-16:00

Active thrusting beneath an alluvial terrace in the southern Longmen Shan range front, Sichuan basin, China

WANG, Maomao[1*] ; LIN, Aiming[1] ; JIA, Dong[2] ; SHAW, John[3]

[1]Department of Geophysics, Kyoto University, [2]Nanjing University, [3]Harvard University

The devastating 2008 Mw7.9 Wenchuan earthquake, China, demonstrates that the central and northern parts of the Longmen Shan are currently active. However, evidence for active faulting and folding in the southern Longmen Shan remains poorly documented. In this paper, we define the structural geometry, fault kinematics, and seismic hazard of the Qiongxi thrust fault system (QTF) along the southern Longmen Shan range front by integrating deep and shallow seismic reflection data and geomorphic observations. The QTF is a 50-km-long, N-S-trending set of faults and associated folds that exhibit geomorphic evidence of Quaternary surface deformation. Geomorphic observations and seismic reflection data reveal that these faults dip steeply to the east and merge at depth with a blind, west-dipping thrust ramp. The trend and reverse sense of slip along the QTF indicates that the structure accommodates east-west crustal shortening. Based on uplift of stratigraphic horizons across the fault zone, we define a late Pliocene to early Pleistocene fault slip rate of 0.2-0.3mm/yr, and a middle Pleistocene to present rate of 0.4-1.2 mm/yr on the west-dipping thrust ramp.. This ramp soles to a basal detachment in the Triassic section at a depth of 4.5-5.5 km. To the west, this detachment steps down onto a blind, northwest-dipping thrust termed the Range Front Thrust. A rupture of the QTF in combination with the Range Front Thrust could generate a Mw7.8 earthquake with averages displacement of 5.7m. This type of earthquake source poses significant hazards to the adjacent, highly populated Sichuan basin.

Japan Geoscience Union Meeting 2014
(28 April - 02 May 2014 at Pacifico YOKOHAMA, Kanagawa, Japan)

SSS34-P01 Room:Poster Time:April 29 18:15-19:30

Identification of Fault Displacement and Stratigraphic Correlation of Black Soils based on Radiocarbon Ages

YASUE, Ken-ichi[1*] ; HIROUCHI, Daisuke[2] ; SAITO-KOKUBU, Yoko[1] ; MATSUBARA, Akihiro[1] ; FURUSAWA, Akira[3]

[1]Japan Atomic Energy Agency, [2]Shinshu University, [3]Furusawa Geological Survey

In order to clarify the stratigraphic correlation around the fault and the timing of faulting event, we carried out radiocarbon dating of the black soil sampled from the trench wall of the Atera Fault. Black soils were sampled at an interval of 3-6 cm along the vertical direction on both the hanging wall and footwall located approximately 50 cm away from the fault plane. Sample preparation and radiocarbon dating were carried out in the JAEA-AMS-TONO of Tono Geoscience Center, JAEA. Calendar years were obtained by calibrating ^{14}C age using OxCal 4.2.3 (Bronk Ramsey, 2013) with IntCal13 atmospheric curve (Reimer et al., 2013).

The dating results show that the soil ages vary from 4,000 to 2,000 years with depth of the sampling points. Black soil was deposited at approximately constant rate each at both sides of the fault in 4,000-2,000 years ago. This indicates that the fault didn't move during this period. In the upper part, there is no variation in ages of black soils including the gravel with depth. This suggests that sedimentation rate was faster. One of the causes that the sedimentation rate around the fault suddenly changes is fault displacement. It is thought that this fault move in about 2,000 years ago. About this timing, it is necessary to consider in behavioral segments of the Atera Fault zone in detail.

In addition, we are going to present results of the volcanic ashes analysis and radiocarbon ages of the lower part.

Keywords: radiocarbon dating, C-14 age, black soil, Atera fault, timing of faulting event

Japan Geoscience Union Meeting 2014
(28 April - 02 May 2014 at Pacifico YOKOHAMA, Kanagawa, Japan)

SSS34-P02 Room:Poster Time:April 29 18:15-19:30

SEM observation on the active fault surface

TANAKA, Shiro[1*] ; KAMACHI, Takao[2] ; KANII, Takehiro[3] ; MIZOGUCHI, Kazuo[1] ; NAKATA, Eiji[1]

[1]CRIEPI, [2]KEPCO, [3]NEWJEC

SEM observation of the fault surface was attempted in order to clarify the feature of the fault plane of active fault. The sharp plane of cutting other structures in outcrop was judged to be the latest activity surface, and the block sampling of the latest surface was carried out. After identifying the continuity of the fault plane by observing the internal structure of the sample in detail using helical X-ray CT, the samples for SEM observation were prepared. As a result of observation on the latest activity surface with a stereomicroscope and a scanning electron microscope, the following features have been identified. (1) A slickenside and striations are observed on the latest fault surface. (2) The fault plane is formed of the crushed fine-grained particles, and the dumpling-like structure where fine-grained particle was covered with paste-like clay is observed as a feature. (3) Growth of euhedral minerals formed by diagenesis in deep such as illite and chlorite, were not observed on the latest fault surface.

Keywords: active fault, fault surface, clay minerals

Japan Geoscience Union Meeting 2014
(28 April - 02 May 2014 at Pacifico YOKOHAMA, Kanagawa, Japan)

SSS34-P03 Room:Poster Time:April 29 18:15-19:30

Examination of evaluation method for fault activity based on an observation of fault zone - 1. Selection of outcrops -

KAMETAKA, Masao[1*] ; OKAZAKI, Kazuhiko[1] ; NAKAYAMA, Kazuhiko[2] ; SESHIMO, Kazuyoshi[2] ; AOKI, Kazuhiro[2] ; TANAKA, Yoshihiro[2] ; SHIMADA, Koji[2] ; SHIMOGAMA, Kota[1] ; INADA, Noriyuki[1]

[1]Dia Consultants, [2]Japan Atomic Energy Agency

The activity of a fault is normally evaluated by observing the displacement/deformation of strata which cover the fault. However, it is difficult to evaluate the activity of a fault which exists only in the basement rock without any overlying strata. In such a case, the fault activity needs to be judged carefully through a comprehensive approach to geomorphology, geology and present/past stress fields. Items in analyzing a fault zone include observation of the fault plane, width of fracture zone, color, hardness, magnetic susceptibility, form of fractured material, mineral and chemical composition analysis, dating, etc. Since some of these items have uncertainties in quantification and reproducibility, a method for evaluating fault activity by analyzing the fault zone in the basement rock is yet to be established. The authors have been carried out the observation and analysis of the fault zone to establish more scientific method of evaluation of fault activity.

In order to do the survey of certain active fault, we should study the outcrop of fault which give a displacement/deformation to the overlying certainly younger formations, and should observe the extension of fault from the overlying formations to the basement rocks. On the other hand, in order to do the survey of the fault zone of certain non-active fault, we should study the outcrop of fault which is covered by the old enough formations from the evaluation point of view.

We selected the outcrops which fulfilled the above-mentioned conditions through literature, then we decided the study outcrops through geological survey. The study area are limited in granite-bearing area, because granite show generally homogeneous and simple structure, is widely distributed in land, and well documented about fault rocks.

Examples of outcrops of active fault are one of the Gosukebashi Fault (Loc. 5 of Maruyama et al., 1997, Active Fault Res.) and one of the Rokko Fault (Loc.1 of Maruyama and Lin, 2002, Tectonophysics) in the Rokko Mountains, southern Hyogo Prefecture.

The fault zone of the Gosukebashi Fault appears in the Rokko Granite at the upperstream of the Gosuke-Dam site. Sand and gravel beds are bounded with granitic fault zone in the upper part of the outcrop. The fault zone consists of thick fault gouge in black and brown color, foliated cataclasite and granitic cataclasite.

At the western Funasaka, the Rokko Granite is in contact with rhyolitic volcaniclastic rocks of the Arima Group and overlying gravel beds through the Rokko Fault. The fault zone of the granite are remarkably altered and composed of brown fault gouge, foliated cataclasite and granitic cataclasite. The fault zone of the rhyolite is composed of black Fe-Mn-bearing layer, rhyolitic cataclasite and damaged rhyolite.

An example of non-active fault was selected from the fault which does not effect the strata of higher terrace deposits. Higher terrace deposits surrounded by badlands of weathered granite are well developed around the Rokko Horai-kyo in the northern Rokko Mountains. The fault including relatively thick gouge which is overlain by the deposits was selected for this survey, and is named the Rokko Horai-kyo Fault. For keeping the safety against the rock fall, the survey has done in the lower extension of granitic slope from the unconformity. The fault zone appears in the weathered granite, and composed of brown gouge, with black Fe-bearing layer and cataclasite.

The observation of fault zone (evaluation of fault plane, in-situ measurements of color and hardness), striation analysis, observation of fault structure by slabs, sections and SEM samples, mineral composition (XRF) and chemical composition (ICP-MS) analysis, mechanical and physical tests were done at the fault zones of these 3 faults. In this paper, the outline of this study and the results of geological survey are described. The details of the observation results of fault zones are explained in another paper (Okazaki et al., 2014, Abst. JpGU).

Keywords: active fault, evaluation method of fault activity, Rokko Mountains, Gosukebashi Fault, Rokko Fault, fault zone

Japan Geoscience Union Meeting 2014
(28 April - 02 May 2014 at Pacifico YOKOHAMA, Kanagawa, Japan)

SSS34-P04 Room:Poster Time:April 29 18:15-19:30

Examination of evaluation method for fault activity based on an observation of fault zone - 2. in-situ experiments -

OKAZAKI, Kazuhiko[1] ; KAMETAKA, Masao[1*] ; NAKAYAMA, Kazuhiko[2] ; SESHIMO, Kazuyoshi[2] ; AOKI, Kazuhiro[2] ; TANAKA, Yoshihiro[2] ; SHIMADA, Koji[2] ; SUZUKI, Kazushige[1] ; SHIMOGAMA, Kota[1] ; INADA, Noriyuki[1]

[1]Dia Consultants, [2]Japan Atomic Energy Agency

In order to establish a method for evaluating fault activity based on observation and analysis of fault zone in the basement rock, a comparative study has been carried out at outcrops of active and non-active fault. Of the three outcrops selected in the Rokko Mountains situated in southern Hyogo Prefecture, two were of an active fault and one of non-active fault. They are: the outcrop of Gosukebashi Fault at the upperstream of Gosuke-Dam site (GSB) and the outcrop of Rokko Fault at the western Funasaka (FSW) for active fault, and the outcrop of Rokko Horai-kyo Fault overlain by higher terrace deposits (HRK) for non-active fault (Kametaka et al., 2014). This paper focuses on an evaluation method which is relatively brief and easily enforceable at the outcrops, and describes the suitability of making a morphological observation of the fault plane and conducting in-situ experiments on hardness and color.

Fault plane of the active fault seems to be well continued, smooth surface and cut the older texture of the fault zone. To describe these features objectively and quantitatively, we measure 1) the relationships between the fault plane and the older texture, 2) the continuity of the fault plane, 3) planarity of the fault plane, 4) semi-quantitative observation using guideline of ISRM (Rock Net Japan, 1985, ISRM Guidelines), 5) arithmetic average toughness based on the authorized photograph. The results indicate that the fault plane of GSB and FSW show good continuities and well cut the older texture, while that of HRK show discontinuous part and poorly cut the older texture. The planarity, surface roughness and waviness, of the fault plane are well in GSB and poor in HRK, and partly poor in FSW possibly caused by the texture of alteration. The fault plane in the basement rock show relatively better planarity than that between basement rock and gravel beds. The arithmetic average toughness leads quantitative evaluation of fault plane, though there are some soluble problems about forming of outcrops and recognition of fault plane.

It qualitatively said that the fault gouge of an active fault is possibly soft and that of a non-active fault gouge is possibly hard and consolidated (Kimura, 1981, Jour. Japan Soc. Eng. Geol.). To quantify the hardness of intrafault materials, in-situ experiment of needle penetration test has been done. The result indicates that the fault gouge of GSB, FSW and HRK show 0 kN/m2. The altered cataclasite and weathered granite (damaged granite) of rock surface even show low value, while they show higher value at 20 cm below the surface. On the other hand, the fault gouge of the underground indicates still low value.

Fault gouge of an active fault possibly show reductive color and that of a non-active fault possibly show oxidative color (Research Core for Deep Geological Environments, AIST, 2012, GSJ Open File Rep.). To quantify the color of intra-fault materials, color measurements (Lab color) were done by using portable soil color meter. The results indicates that the fault gouge of GSB show low a∗value and low-middle b∗value, that of FSW show high a∗value and very high b∗value, and that of HRK show low-middle a∗value and low-high b∗value. The fault rocks around the fault gouge show intermediate value between fault gouge and non-deformed granite, indicating color change associated with weathering pass of granite.

In this paper, we show the specific contents of each measurement, and discuss about the validities of evaluation methods of the fault activity.

Keywords: active fault, evaluation method of fault activity, Rokko Mountains, Gosukebashi Fault, Rokko Fault, fault zone

Japan Geoscience Union Meeting 2014
(28 April - 02 May 2014 at Pacifico YOKOHAMA, Kanagawa, Japan)

SSS34-P05 Room:Poster Time:April 29 18:15-19:30

Active faults and topographic surfaces on the stereoscopic topographic map

IMAIZUMI, Toshifumi[1*] ; MIYAUCHI, Takahiro[2] ; KAGOHARA, Kyoko[3] ; OKADA, Shinsuke[4] ; SHIRASAWA, Michio[5] ; YOKOYAMA, Ryuzo[5] ; SASAKI, Tatsuya[6]

[1]Graduated School of Science, Tohoku University, [2]Graduated School of Science, Chiba University, [3]Faculty of Education, Yamaguchi University, [4]International Research Institute of Disaster Science, Tohoku University, [5]Yokoyama Geo-Spatial Information Lab., [6]OYO Corporation, Database Business Department

Thematic topographic maps have developed by the progress in analysis using digital elevation model (DEM) and have made clear representation possible.

We made digital stereoscopic topographic maps in scale 1:25,000, by using 5m mesh DEM data arranged by Geospatial Information Authority of Japan (GSI) . These 3D maps have same information, mode, scale and interval 10m contour, comparing to Quadrangle topographic sheet map.

We demonstrated the overlapping active fault line (Nakata and Imaizumi, edit 2002) on these 3D maps, in order to easily interpretation of the location of fault line, fault feature, evidence of faulting and displacement of faulting from professional and educational viewpoints.

Keywords: Active fault, Topographic surface, Stereoscopic topographic map, Interpretation of topographic map

Japan Geoscience Union Meeting 2014
(28 April - 02 May 2014 at Pacifico YOKOHAMA, Kanagawa, Japan)

SSS34-P06 Room:Poster Time:April 29 18:15-19:30

Genetic algorithm-based displacement extraction technique for LiDAR dataset

SAOMOTO, Hidetaka[1*] ; MARUYAMA, Tadashi[1] ; KONDO, Hisao[1]

[1]Active Fault and Earthquake Research Center, AIST

Owing to recent progress of aerial survey with laser transmitting device, we can easily obtain detailed digital elevation model represented by point cloud data. This model is applicable to many purposes such as active fault detection, quantification of bluff lines, and extraction of ground displacement caused by an earthquake.

Although some methods for seismic displacement extraction from point cloud data have been proposed, we need more robust and powerful method in terms of noise immunity. In this study, we propose a new method based on the RBF (Radial Basis Function) interpolation and the GA (Genetic Algorithm) for the seismic dis-placement detection and then conduct a series of inquests including the parameter setting, the evaluation of noise resistance, and the comparison among four optimization techniques: GA, L-BFGS-B, Nelder-Mead, and COBYLA.

The results of considerations revealed that: (1) the size of unit for pattern matching should be set to 24 m square for the point cloud divided into 1 m grid; (2) the proposed method stably detect the correct dis-placement even under ill-posed condition; (3) the combination of the RBF and the GA is well suited for this problem because the objective function appearing in this study possesses extreme multimodality, suggesting that we should not use the optimization method based on gradient information.

Keywords: genetic algorithm, interpolation, LiDAR, displacement, optimization

Japan Geoscience Union Meeting 2014
(28 April - 02 May 2014 at Pacifico YOKOHAMA, Kanagawa, Japan)

SSS34-P07 Room:Poster Time:April 29 18:15-19:30

Geologic structures around the coastal area of the southern part of the active eastern boundary fault zone of Ishikari l

SATO, Tomoyuki[1*] ; KOMATSUBARA, Taku[1] ; KOU, Yoshihide[1]

[1]Institute of Geology and Geoinformation, Geological Survey of Japan, AIST

A 130-km-long N-S trending active fold and thrust zone (eastern boundary fault zone of Ishikari lowland) occurs in the Ishikari lowland and off the Yufutsu plain. This fault system is one of the boundary faults between the Kuril arc and the Northeast Japan arc. We surveyed around the coastal area of the Yufutsu plain based on the marine high-resolution seismic-survey and the database of land borehole cores. As a result, two active anticlines (Yufutsu anticline and Hamaatsuma anticline) were recognized. These anticlines can be correlated to the anticlines described as a part of the active eastern boundary fault zone of Ishikari lowland (AIST, 2007). The trand of the Yufutsu anticline was N-S despite The Headquarters for Earthquake Research Promotion reported the trend was NW-SE. The Hamaatsuma anticline continued to the Mukawaoki anticline and the southern end of the fault zone extend to the southern end of the Mukawaoki fault which is concerned to the Mukawaoki anticline.

AIST(2007)Activity survey of the eastern boundary fault zone of Ishikari lowland. Working papers. H18-8, 35p.
Headquarters for Earthquake Research Promotion(2010) Evaluation of the eastern boundary fault zone of Ishikari lowland (revised). 34p.

Keywords: Active eastern boundary fault zone of Ishikari lowland, Seismic survey, Quaternary, Hokkaido, Coastal area

Japan Geoscience Union Meeting 2014
(28 April - 02 May 2014 at Pacifico YOKOHAMA, Kanagawa, Japan)

SSS34-P08 Room:Poster Time:April 29 18:15-19:30

Seismic reflection survey across the northern part of the Western Boundary Fault Zone of the Yamagata Basin

OKADA, Shinsuke[1*] ; IMAIZUMI, Toshifumi[1] ; KAGOHARA, Kyoko[2] ; ECHIGO, Tomoo[3] ; YAGI, Hiroshi[4] ; MATSUBARA, Yoshikazu[5] ; MIWA, Atsushi[5] ; KOSAKA, Hideki[6]

[1]IRIDeS, Tohoku Univ., [2]Yamaguchi Univ., [3]Geo-Reaearch Institute, [4]Yamagata Univ., [5]OYO Corportion, [6]Kankyo Chishitsu Company Limited

The Western Boundary Fault Zone of the Yamagata Basin borders the western margin of the Yamagata basin and is traceable for about 60 km. In the northern part of this fault zone (from Sagae to Ooishida area), subpallarel traces of the active fault distribute in the western side of the basin. At the center of the basin, Kawashima-yama located as a tectonic bulge and its western side the Mogami river incise and meander in the fault zone. Along the eastern side of the Kawashima-yama, syncline is indicated as a frontal deformation by Ikeda (2002) and Imaizumi (2001).

To reveal the subsurface structure and tectonic evolution of this fault zone, we carried out two lines (Line A and Line B) of seismic reflection survey from September to October 2013. The Line A has a length of 4.11 km and started from Saigo area to Oomaki via. Kyouei bridge. The Line B has about 3.75 km length and started from Taruishi area to Goten along the Taruishi river. The source used in this survey was an Enviro Vib (IVI Inc.). Sweep length was 16 sec and sweep frequency range beginning at 10 Hz up to 120 Hz. The receiver was GS-20DX (natural frequency, 10 Hz; Geospace Inc.). The source and receiver spacing was 10m, with 192 ch geophones used for each recording. We selected the Geode (Geometrics) for the recording system and its sampling rate is 1 msec.

We thank to students of Tohoku University and Kanazawa University for their assistance in our survey. This work was supported by project research of the International Research Institute of Disaster Science (IRIDeS), Tohoku University.

[References]

Ikeda et al., 2002, Atras of Quaternary Thrust Fault in Japan, Univ. of Tokyo Press, 254pp.
Imaizumi et al., 2001, Active Fault Map in Urban Area, Geographical Survey Institute.

Keywords: active fault, seismic reflection survey, the Western Boundary Fault Zone of the Yamagata Basin, subsurface structure, Murayama City

Japan Geoscience Union Meeting 2014
(28 April - 02 May 2014 at Pacifico YOKOHAMA, Kanagawa, Japan)

SSS34-P09 Room:Poster Time:April 29 18:15-19:30

Very shallow seismic surveys of the Shionohira earthquake fault appeared at the Fukushima-ken Hamadori earthquake

YAMAGUCHI, Kazuo[1*] ; ITO, Shinobu[1] ; KANO, Naomi[1] ; YAMANAKA, Yoshiaki[2] ; ITO, Shunichiro[2]

[1]AIST,GSJ, [2]Suncoh consultant

In the southern part of the Fukushima-ken Hamadori area, seismicity increased after 2011 Tohoku earthquake and an M7.0 earthquake occurred on April 11th, 2011. Remarkable surface raptures appeared along active faults by this earthquake. We conducted very shallow seismic surveys to reveal subsurface structure of the surface rapture down to 20 m in depth.

The survey line is located along a road in the Shionohira of Iwaki city. The displacement of the surface rapture is 2m east-side-up and 0.4m left lateral at the cross point of the survey line. The road was fixed and flat at the survey time.

The survey menus were S-wave survey and P-wave survey. Survey instruments and specifications are as following. Seismic source: S-wave/SWG-5(Suncoh), P-wave/10kg hammer, receiver: S-wave/GS20DM(Oyo Geospace, 28Hz), P-wave/GS11D(OyoGeospace, 4.5Hz), recorder: DSS-12(Suncoh), line length: 191m, source interval: 1m, receiver interval: 1m, stack number: 1-5, spread: S-wave/192ch fixed, P-wave/96ch landstreamer. The data quality was good because of low traffic noise.

The data were processed by S-wave refraction, S-wave reflection, P-wave refraction and surface wave methods. S-wave tomography and P-wave tomography analyses were applied and confidence of resolution and dependency to primary model were estimated. P-wave data were processed by inversion of phase velocity dispersion and S-wave velocity structure was obtained. S-wave data was processed by CMP stacking method and time section, migrated section and depth section were obtained.

According to S-wave velocities by S-wave refraction and surface wave methods, velocity layers below 0.7 km/s is thick to the west of the fault and thin to the east of the fault. Strong reflector between sediments and basement is deep and continuous to the west of the fault, shallow and uneven to the east of the fault and steps are recognized around the fault. The basement rises between this step and 135m of the survey line. This corresponds to the part of high Bouguer anomaly of 0.06 mgal.

Keywords: Fukushima-ken Hamadori earthquake, Itozawa fault, Shionohira fault, subsurface structure, very shallow seismic survey

Japan Geoscience Union Meeting 2014
(28 April - 02 May 2014 at Pacifico YOKOHAMA, Kanagawa, Japan)

SSS34-P10 Room:Poster Time:April 29 18:15-19:30

Pit excavation along the Tachikawa fault at Sayama Shrine Site

ISHIYAMA, Tatsuya[1*] ; HIROUCHI, Daisuke[2] ; SATO, Hiroshi[1] ; SUZUKI, Takehiko[3] ; KOBAYASHI, Kenta[4] ; KORIYA, Yorihide[5] ; OMATA, Masashi[5] ; SHIBATA, Tsuyoshi[6]

[1]Earthquake Research Institute, University of Tokyo, [2]Department of Education, Shinshu University, [3]Faculty of Urban Environmental Sciences, Tokyo Metropolitan University, [4]Department of Geology, Faculty of Science, Niigata University, [5]Crearia, Inc., [6]Aero Photo Center

We excavated a 10-m-long, 2-m-deep pit across the hypothesized south-facing topographic scarp on along the Tachikawa fault. Preliminary results include clear evidence of accumulated, west-facing monoclonal folding of underlying conglomerates, predicted by the topographic scarp. Asymmetric ductile shear zone exposed on the bottom indicate nature of significant sinistral strike-slip component of faulting, rather than a simple reverse faulting. Future works include establishing stratigraphy based on radiocarbon dating and tephrostratigraphy.

Japan Geoscience Union Meeting 2014
(28 April - 02 May 2014 at Pacifico YOKOHAMA, Kanagawa, Japan)

SSS34-P11 Room:Poster Time:April 29 18:15-19:30

Geological structure interpreted from two boring cores beside the Tachikawa Fault Zone, Tokyo, NE Japan

SUZUKI, Takehiko[1*]

[1]Tokyo Metropolitan University

In order to clarify the accurate position and activity of the Tachikawa Fault Zone, which possibly cause an earthquake under Tokyo in future, survey on the Quaternary sediments with tephrochronological method is effective. We conducted an all-core boring (TC-12-1) survey at Enoki in Musashi-Murayama City in 2012, where a relative subsidence will be occurred at its activity. By this result, we pointed out the evidence of deformation in altitudes of Middle Pleistocene gravel bed base, and also found a tephra layers estimated its age to be at 1.63 Ma. In this study, an additional all-core boring (TC-13-1) survey in relative uplifting side was carried out. The following are preliminary report of TC-13-1 core survey. Site of all-core boring (TC-13-1) with the length of 90 m is ca. 300 m northwest of Tachikawa Fault Zone of which the altitude is 109.50 m. Sediment with a depth 0 to 28.65 m is composed of coarse gravels with diameters 3 to 10 cm (max. 20 cm). Upper part of this gravel bed is equivalent to the fluvial terrace deposits of Tachikawa 2 Surface, and lower one is most likely to be the gravel bed identified as Middle Pleistocene sediment in the survey of TC-12-1 in 2012. Altitude of the base of this gravel bed (80.85 m) is higher than that of TC-12-1 (71.97 m), suggesting the evidence of fault activity with uplifting of east side. Sediment with a depth 28.65 to 90.00 m is composed of the alternation of silt (mudstone), sands, and gravels, and is correlative to the Kazusa Group of Lower Pleistocene. Five cycles of sedimentation composed of upper consolidated silt to mudstone and lower gravel bed were recognized. Also. shell in mudstone of 67.15-68.00m in depth and tuffaceous mudstone layers were found. We will examine theses sediments in detail. This survey was financially supported by Ministry of Education, Science, Sports, and Culture (Intensive Survey and Observation on the Tachikawa Fault Zone).

Keywords: Tachikawa Fault Zone, Underground geology, Boring core, Musashi-murayama

Japan Geoscience Union Meeting 2014
(28 April - 02 May 2014 at Pacifico YOKOHAMA, Kanagawa, Japan)

SSS34-P12 Room:Poster Time:April 29 18:15-19:30

Examination of tectonics of the Shinano River basin, Niigata and Nagano prefectural border.

TAKAKUWA, Kensuke[1*]

[1]Department of Geology, Faculty of Science, Niigata University

In Niigata and Nagano, the trend of a general structure has a NNE-SSW strike called what is called the direction of Niigata. Moreover, it is thought that the trend of an active fault has the direction of Niigata similarly. However, the western Tokamachi fault belt continuous from Tokamachi city to Niigata and Nagano prefectural border contains in the south the Miyanohara fault which is an ENE-WSW strike(Headquarter of Earthquake Research Promotion 2010).

The Shinano River syncline which has in Tokamachi a NNE-SSW strike which exists in Shinano River and parallel being crooked in Tsunan-cho, and becoming an E-W trend.(Shimazu and Tateishi 1993. And Takeuchi et al 2000).

However, the exact position and a posture are not specified.

That is, it was not necessarily confirmed based on detailed investigation, the structure of the area is the direction.

The tectonics of the area has many questions as mentioned above. It inquired for the purpose of solving the tectonics of the area.

It was able to ask for the exact position of the Shinano Kawamuki slant continuous to a the area as a result of investigation. Moreover, Chikumagawa anticline and hokushin syncline was was newly authorized in the area.

Moreover, the sectional view over the Miyanohara fault in this research was compared with Sega (2012MS) in a Tokamachi basin west marginal fault belt. When done so, it turned out that the form of folding is alike. Therefore, it is thought that a Tokamachi basin west marginal fault belt and the Miyanohara fault are the same postures. Therefore, these connect and it is thought that the western Tokamachi fault belt is constituted. Moreover, the form of folding is alike also around hirataki. Therefore, the southernmost end of the western Tokamachi fault belt may be extended further west.

Furthermore, small fault method which used the Multiple Inverse Method was conducted. A result, it turned out that the small fault is recording two or more times of transcurrent fault type stress.

Horizontal gap stress is as conformable as the earthquake mechanism of aftershock of the northern Nagano earthquake in 2011,3,12.

Therefore, it is possible that Japan of those days was also placed by the same stress-ization as the present after the offing earthquake of the Tohoku earthquake.

Japan Geoscience Union Meeting 2014
(28 April - 02 May 2014 at Pacifico YOKOHAMA, Kanagawa, Japan)

SSS34-P13 Room:Poster Time:April 29 18:15-19:30

Tectonic geomorphology around the eastern piedmont of the Myoko volcano and their tectonic implications

TAJIKARA, Masayoshi[1*] ; MIZUMOTO, Tadaki[1] ; MATSUDA, Tokihiko[1] ; TSUTSUMI, Hiroyuki[2] ; GOTO, Hideaki[3] ; NAKATA, Takashi[3]

[1]ERC, ADEP, [2]Kyoto Univ., [3]Hiroshima Univ.

The Myoko volcano group is located in the south of Takada plain, and its eastern piedmont is intermontane trough (hereafter, referred as the Myoko trough) between the Nishi-kubiki Mountains and the Higashi-kubiki Hills. The Myoko trough is located from the south of the Takada plain to the north of the Nagano Basin. The Takada-heiya-toen fault, Takada-heiya-seien fault, and the Nagano-bonchi-seien fault are located along the eastern margin of the Takada plain, the western margin of the Takada Plain, and the western margin of the Nagano Basin, respectively (Nakata and Imaizumi, 2002). Based on detailed analysis of areal photographs, we newly mapped active faults and tectonic landforms in the Myoko trough. we describe evidences of recent activity and discuss the property of these tectonic landforms and their tectonic implications. Newly mapped active faults and tectonic landforms are distributed almost continuously from the southern edge of the Takada-heiya-toen-fault to around Fujisato village in the Shinano town. Based on these distributions, we judged that newly mapped active faults constitute a part of the Takada-heiya-toen fault, and that the length of the Takada-heiya-toen fault may be elongated from 26 km to max. 55 km. However, active faults in the Myoko trough and the Nagano-bonchi-seien fault are distributed in parallel at distance of 13-14 km. Therefore, these two faults may be converged at depth of 6-7 km, and the southern part of the Takada-heiya-toen fault may be a backthrust of the Nagano-bonchi-seien fault.

Keywords: Takada plain, active fault, air photo, Myoko volcano group, Takada-heiya-toen fault

Japan Geoscience Union Meeting 2014
(28 April - 02 May 2014 at Pacifico YOKOHAMA, Kanagawa, Japan)

SSS34-P14 Room:Poster Time:April 29 18:15-19:30

Investigating the role of the Itoigawa-Shizuoka tectonic line in the evolution of the Northern Fossa Magna rift basin

PANAYOTOPOULOS, Yannis[1*] ; HIRATA, Naoshi[1] ; SATO, Hiroshi[1] ; KATO, Aitaro[1] ; IMANISHI, Kazutoshi[2] ; KUWAHARA, Yasuto[2] ; CHO, Ikuo[2] ; TAKEDA, Tetsuya[3] ; ASANO, Youichi[3]

[1]Earthquake Research Institute, the University of Tokyo, [2]Geological Survey of Japan, AIST, [3]National Research Institute for Earth Science and Disaster Prevention

The Itoigawa-Shizuoka tectonic line (ISTL) fault system is considered to have one of the highest probabilities for a major inland earthquake occurrence in the whole of Japan. It is a complex fault system with the dip directions of the local fault segments changing from north to south between an east-dipping low-angle thrust fault, a strike slip fault and a west-dipping thrust fault. The tectonic relations between the different parts of the fault system and the surrounding geological units are yet to be fully explained. This study aims to reveal the juncture of the northern and central parts of the ISTL and investigate its contribution towards the shaping of the Northern Fossa Magna rift basin. We conducted 3 deployments of 1 or 2 linear arrays of seismic stations across the central and northern ISTL regions and observed local micro-earthquakes for a period of 3 years. Each deployment recorded continuous waveform data for approximately 3 months. Using arrival times of 1193 local earthquakes, we jointly determined earthquake locations and a 3D velocity model, applying the tomography method. We were able to image the regional crustal structures from the surface to a depth of 20 km with a spatial resolution of 5 km. Subsequently, we used the obtained 3D velocity model to relocate the background local seismicity from 2003 to 2009. The juncture of the northern and central parts of the ISTL was well constrained by our results. The depth extension of the northern parts of the ISTL fault segments follows the bottom of the Miocene Northern Fossa Magna rift basin (NFM) and forms an east-dipping low-angle fault. In contrast, the central parts of the ISTL fault segments are estimated to lie along the eastern boundary of the Matsumoto basin forming an oblique strike slip fault.

Keywords: Itoigawa-Shizuoka tectonic line, tomography

Japan Geoscience Union Meeting 2014
(28 April - 02 May 2014 at Pacifico YOKOHAMA, Kanagawa, Japan)

SSS34-P15 Room:Poster Time:April 29 18:15-19:30

Mapping of active faults in the area around the southern segment of the Itoigawa-Shizuoka Tectonic Line, central Japan

SANO, Mikako[1*] ; IIDA, Kenta[2] ; LIN, Aiming[1]

[1]Department of Geophysics,Graduate School of Science, Kyoto University, [2]Institute if Geosciences, Faculty of Science, Shizuoka University

It is well known that tectonic-related topographic features that develop around active faults record displacements during large-magnitude earthquakes, and that tectonic-related topographic studies are essential for developing a historic and/or paleoseismic perspective of the locations, magnitudes, recurrence intervals, and slip patterns of seismogenic faults. Therefore, it is important to recognize and identify active faults and tectonic-related topographic landform features for studying the present activity of active faults to assess the seismic hazard in a densely populated region.

This study focuses on the mapping of active faults in the area around the southern segment of the Itoigawa-Shizuoka Tectonic Line (ISTL), central Japan. Although previous studies have reported the presence of some active faults in this area, the detail distribution and geometric features of active faults are still unclear. In this study, we identified the active fault traces using perspective maps made from the digital elevation mode (DEM) data with 5-m-contours and stereo-examination of aerial photography and conducted field investigations. Interpretations of perspective topographic maps, field investigations, and structural analysis of fault zones reveal that i) many fault traces are newly found, which formed a deformation zone of up to ˜100-500 in width; ii) the active fault traces show more irregular shape than that previously reported, curved around boundary between the mountains and basin, indicating the lower dip-angle thrust fault structures; iii) the active faults developed along the southern sector of the ISTL are found to be extended to the south at least ˜25 km longer than that reported previously.

The findings of this study show that the detail mapping of the active faults can provide new insights to study the tectonic activity and fault nature of active faults and to reassess the seismic hazard for the densely populated area around the ISTL.

Keywords: active fault, fault mapping, Itoigawa-Shizuoka Tectonic Line (ISTL), fault trace, fault geometry, thrust fault

Japan Geoscience Union Meeting 2014
(28 April - 02 May 2014 at Pacifico YOKOHAMA, Kanagawa, Japan)

SSS34-P16 Room:Poster Time:April 29 18:15-19:30

ESR dating of the Shimotsuburai and Hoozan faults in the Itoigawa-Shizuoka Tectonic Line Active Fault System

FUKUCHI, Tatsuro[1*] ; TANAKA, Mami[1] ; KITTA, Takuto[1] ; IMAI, Noboru[2]

[1]University of Yamanashi, [2]AIST

The Shimotsuburai fault, which is located in the south part of the Itoigawa-Shizuoka Tectonic Line (ISTL) Active Fault System, displaces the lower terrace deposits formed at about 20 kaBP. The trenching survey at the Tozawa outcrop revealed that the latest fault movement occurred at 1,550 +or- 70 yBP - 2,350 +or- 60 yBP (Toda et al., 2000). Along the fault plane of the Shimotsuburai fault, black injection veins are distributed forming complex networks and a part of the black veins is injected into the fault gouge or lower terrace deposits. Kano et al. (2004) proposed that this black intrusion veins are crushing-originated pseudotachylyte formed at 30-40m or less in depth at the time of the latest fault movement. On the other hand, the Hoozan fault is distributed about 6km west of the Simotsuburai fault. At the Dondokozawa outcrop, fault gouge is hardly recognized besides cataclasite and mylonite. This suggests that the Hoozan fault may not have moved since its formation in Neogene to early Quaternary, and that the main activity of the ISTL may have shifted to the Simotsuburai fault (Koyama, 1990). The Gofukuji fault located at the northwest extension of the Hoozan and Shimotsuburai faults may cause a Magnitude 8-class large earthquake, and besides its activity may have increased after the 2011 Tohoku-oki earthquake (M9.0). When the Gofukuji fault moves in the future, it is unclear whether or not its southeast extension would also move operating together. It is important to exactly assess the activity of the Hoozan fault as well as the Shimotsuburai fault. We thus carried out XRD (X-ray diffraction) and ESR (electron spin resonance) dating of fault rocks collected from the Shimotsuburai and Hoozan faults.

As a result of XRD analysis, smectite is detected from the Shimotsuburai fault gouge at the Tozawa outcrop, and smectite and a chlorite/smectite (C/S) mixed layer mineral from the black injection vein just on the fault plane, while besides illite chlorite and C/S are respectively detected from the black and gray gouges of the Hoozan fault at the Ishiutoro-gawa outcrop. In general, the formation depth of clay minerals tends to increase in order of smectite, C/S, chlorite and illite. Therefore, the result from the XRD analysis suggests that the Hoozan fault was much more active at deeper positions. As a result of ESR dating, strong signals of the Al and Ti centers are detected from quartz in the Shimotsuburai fault gouge and black injection vein however these centers show the tendency of saturation implying that the resetting by frictional heating did not work. Since the Al and Ti centers can be completely reset at about 300-350 degree C (Fukuchi, 2004), the result from the ESR dating shows that the frictional heat temperature did not rise so much at the time of the latest fault movement. On the other hand, the quartet signals intrinsic to montmorillonite are detected from the gray gouge of the Hoozan fault, and give the age of 2.8-3.2 +or- 0.4 Ma. The chlorite/smectite mixed layer is considered to be formed at about 130-200 degree C (Yoshimura, 2001), so that its formation age may be estimated as 2.2-3.3 Ma assuming the upheaval rate of 2 mm/y and the geothermal gradient of 30 degree C/km. This formation age is consistent with the ESR age obtained from the gray gouge.

References

T. Fukuchi (2004) ESR dating of fault movement, Fukadaken Library 63, 45p.
K. Kano et al. (2004) J. Geol. Soc. Japan, 110, 779-790.
A. Koyama (1990) J. Geosci. Osaka City Univ. 33, 1-47.
S. Toda et al. (2000) Zishin (Bull. Seism. Soc. Japan), 52, 445-468.
T. Yoshimura (2001) Clay Minerals and Alteration, Chigakusosho 32, 293p.

Keywords: electron spin resonance, ESR dating, Itoigawa-Shizuoka Tectonic Line, active fault system, pseudotachylyte, clay mineral

Japan Geoscience Union Meeting 2014
(28 April - 02 May 2014 at Pacifico YOKOHAMA, Kanagawa, Japan)

SSS34-P17 Room:Poster Time:April 29 18:15-19:30

The SEM observation on the latest active fault plane - the Atera Fault, Tase, Gifu prefecture-

NAKATA, Eiji[1*] ; UETA, Keiichi[1] ; AIYAMA, Kotaro[2] ; SIGEMATSU, Yasumune[3] ; OTSUKA, Yoshiharu[3]

[1]Central Research Institute of Electric Power Industry, [2]Dia Consultants Co.,Ltd, [3]Kansai Electric Power Co.,Inc.

To evaluate of seismic activity of fault, we performed mineralogical and morphological studies by SEM on the latest fault plane of the Atera fault. On the results of SEM observation, authigenic minerals do not crystallize on the whole shear planes including the latest active fault plane.

Study area is outcrop along the Tase path, Gifu prefecture (Toda et al., 1994). Granitic rock (hanging wall) is thrusted on the late Quaternary sandy formation including a lot of conglomerate and humus soil layer. The Atera fault consists on gouge: 3 - 20 cm thickness.

There are two light grayish green gouge zones: 3 - 10 cm width each, including dark brownish gouge: about 3mm width. The sharpest share zone, which is straightly brownish gouge, distributes in the gouge of hanging wall side. This gouge continues under the humus soil (440y B.P. Toda et al., 1994). This sharp zone was confirmed by X ray CT observation collected mass samples from the outcrop. Another dark brownish gouge zone runs parallel in the light grayish green gouge zone distributed the footwall side, converged into the sharpest shear zone at the central parts of the outcrop. At the footwall side, clayish sandy sediments were intruded into the light grayish green gouge with ductile deformation toward the left direction.

SEM observation was performed for the whole shear planes to be able to identify. For the dark brownish gouge zone, the observation was performed for the bottom, top, and sharp plane. On the results, authigenic minerals do not crystallize on the whole planes. Clay mineral (smectite) aggregates to form small clay ball (0.2 micron diameter), which covered the small particles as the paste (Kamachi et al., 2014).

Column shape? minerals (halloysite?) only coexist with Mn, Fe elements in the brackish lens zone including rhyolite and hexagonal biotite originating the foundation rock mass of the footwall side.

The results of this study show that authigenic minerals crystallized under the a few hundred degrees (clay and zeolite) do not confirm on the Atera fault plane to active after about 8400y B.P.

Reference; Toda et al.,(1994)Zisin,47,(1994),73-77. Kamachi et al.,(2014)JpGU2014.

Keywords: Atera, fault, latest plane, SEM

Japan Geoscience Union Meeting 2014
(28 April - 02 May 2014 at Pacifico YOKOHAMA, Kanagawa, Japan)

SSS34-P18 Room:Poster Time:April 29 18:15-19:30

Sand boiling traces at the Netsuno ruin in Ishikawa Prefecture and the Morimto-Togashi fault zone

HIRAMATSU, Yoshihiro[1*] ; KOZAKA, Yutaka[2]

[1]Kanazawa Uiversity, [2]Hakusan Tedorigawa Geopark Promotion Council

Sand boiling traces detected at an archaeological site provides important information to reveal historical seismicity. In the Bunyudo ruins located at the central part of the Tedori-river fan, Hiramatsu and Kozaka (2013) detected sand boiling traces, which are the evidence of liquefaction, and discussed its relation to the activity of the Morimoto?Togashi fault zone. We report here sand boiling traces detected by an excavation survey of the Netsuno ruin, near the Bunyudo ruins, in 2013.

In the Netsuno ruin, we observe four sand boiling traces on the plane on which traces of vertical caves housing and Tsukikage wares of the late Yayoi period (1800-1900 years ago) were found. The sand boiling traces consist of ash gray sand with a diameter less than 1 mm. The largest trace has the maximum width of 20 cm and the length of about 2 m. This trace extends from a sand layer between a gravel layer and a silt layer located about 50 cm below the plane on which the traces are observed. Furthermore, this trace does not penetrate into a black soil layer above the plane that deposited from the late Yayoi period to the early Heian period. The observed traces are likely to have been covered by the black soil layer after the boiling on the ground surface at the time, implying that the formation age of the traces is from 1800-1900 to about 1100 years ago.

The Togashi fault is located near the Netsuno and the Bunyudo ruins, and, together with the Morimoto and the Nomachi faults, constitutes the Morimoto?Togashi fault zone of which a the total length is 26 km. No active fault has been reported around the Netsuno and the Bunyudo ruins. We, therefore, consider that the sand boil traces detected at these ruins are possibly formed by the activity of the Togashi fault or of the Morimoto?Togashi fault zone. An excavation survey at the Umeda area located at the northern part of the Morimoto fault revealed that a fault movement occurred about 1800-2000 years ago. A ruin where the surface displacement caused by the fault movement was observed is formed in the late Yayoi period. This period is the same as those of the Netsuno and the Bunyudo ruins. We, thus, conclude that the latest event of the Morimoto?Togashi fault zone is likely to be occurred 1800-1900 years ago.

Keywords: strong motion, the Morimto-Togashi fault zone, liquefaction, geopark

Japan Geoscience Union Meeting 2014
(28 April - 02 May 2014 at Pacifico YOKOHAMA, Kanagawa, Japan)

SSS34-P19 Room:Poster Time:April 29 18:15-19:30

Offshore active faults of the Mikata and Nosaka fault zones in Fukui Prefecture, revealed by high-resolution seismic pro

INOUE, Takahiko[1*] ; SUGIYAMA, Yuichi[1] ; SAKAMOTO, Izumi[2] ; TAKINO, Yoshiyuki[2] ; MURAKAMI, Fumitoshi[1] ; HOSOYA, Takashi[3] ; USAMI, Takuya[4]

[1]AIST, [2]Tokai University, [3]Corporation of Chuokaihatu, [4]Sogo Geophysical Exploration Co,Ltd

The Mikata and Nosaka fault zones are located in coastal and shallow sea area off Mihama, Fukui Prefecture. National Institute of Advanced Industrial Science and Technology (AIST) and Tokai University conducted, as part of MEXT 2013 nearshore active fault survey project, a high-resolution multi-channel seismic survey using Boomer and a 12-channel streamer cable, acoustic profiling survey using parametric sub-bottom profiler and shallow-sea drilling survey, in order to clarify distribution and activity of the Mikata and Nosaka fault zones. We present mainly about the results of the high-resolution multi-channel seismic survey.

The most remarkable reflection surface in the seismic profiles is the ravinement surface that truncated evenly the lower sediment. Holocene sediments cover this surface and the sediments become thinner toward offshore.

In seismic profiles across the fault zones, flexure-like deformation in the Holocene sediments continue in the N-S direction in the Mikata fault zone and in the NW-SE direction in the Nosaka fault zone along faults shown by Komatsubara et al. (2000). The deformation in the Holocene sediments has been growing by displacements of an underlying active fault. The vertical offset of the flexure on the ravinement surface is larger than those on other reflectors in the sediments covering the ravinement surface and these offsets decrease upward. This growing deformation indicates that faults are reactivated several times in the last 10000 years. At the Mikata fault zone, vertical displacement of ravinement surface is about 11 meters. Based on the formation age of the ravinement surface presumed by sea level change in the world, we estimate the mean vertical slip rate at about 0.9 m/ky. On the other hand, at the Nosaka fault zone, vertical displacement of the erosional surface is about 8 meters. We obtained core samples reaching to the erosional surface at the Nosaka fault zone. We will compare in detail the seismic profiles with sedimentation ages obtained from the cores, in order to estimate vertical slip rate of the Nosaka fault zone. Event history, latest event and slip rate of the Mikata and Nosaka fault zones are further examined, incorporated with advanced analysis of seismic survey data and core samples.

Keywords: Offshore active fault, the Mikata fault zone, the Nosaka fault zone, high-resolution seismic survey, Event history

Japan Geoscience Union Meeting 2014
(28 April - 02 May 2014 at Pacifico YOKOHAMA, Kanagawa, Japan)

SSS34-P20 Room:Poster Time:April 29 18:15-19:30

Offshore active fault survey ”Mikata fault and Nosaka fault zones”. Result of high-resolution stratigraphic survey.

YAGI, Masatoshi[1*] ; SAKAMOTO, Izumi[1] ; TAKINO, Yoshiyuki[1] ; FUJIMAKI, Mikio[2] ; TAJIMA, Tomoko[1] ; INOUE, Tomohito[1] ; SUGIYAMA, Yuichi[3] ; INOUE, Takuhiko[3]

[1]School of Marine Science and Technology, [2]COR, [3]Active Fault and Earthquake Research Center

The 26km long Mikata fault zone is extending from Kaminaka to Wakasa Bay. The fault zone consists of fault A, Hiruga fault, Mikata fault and Kuramitouge fault. The fault zone is estimated to cause M7.2 earthquakes (The Headquarters for Earthquake Research Promotion, 2002).

The 31km long Nosaka fault zone is extending from Nosaka Mountains to the Wakasa Bay. This fault zone consists of fault B, Nosaka fault and Nosaka southern fault. FaultB displaced the Holocene deposits and the vertical displacement rate is estimated to be about 0.8m/thousand years which are proposed by The Headquarters for Earthquake Research Promotion, 2002. Mikata fault and Nosaka fault zones show horizontal converges a single fault in the continental shelf.

Tokai University performed high-resolution stratigraphic survey to confirm a formation, distribution, and displacement of crust around the coastal area of the Mikata fault and Nosaka fault zones at Wakasa Bay in 2013. Transparent layer with poor internal reflection was observed as the surface layer in this survey area. This transparent layer is defined to as layer A. Layer A is ranges in thickness between 8 and 0 meter generally increase toward west. Displacement of the layer A is about 10m in most. Below layer A, sediments characterized by several reflections. First, we confirmed tilted reflection toward the Nosaka fault in the faults horizontal convergence section. Second, we confirmed progradation pattern reflection inclines to the offshore in the around Mikata fault.

Mikata fault and Nosaka fault are represented as a significant step in the seabed. The west side layer A is thicker than others. In the layer A, faults have not displaced surface sediments in this region. But several characteristic formations are which shows activities of fault has confirmed in sediments below layer A. The analysis still going on, the studies including the boring data will show more detail.

Keywords: Wakasa Bay, Mikata fault zone, Nosaka fault zone

Japan Geoscience Union Meeting 2014
(28 April - 02 May 2014 at Pacifico YOKOHAMA, Kanagawa, Japan)

SSS34-P21 Room:Poster Time:April 29 18:15-19:30

Drilling survey of the seaward extension of the Mikata and Nosaka fault zones off Mihama Town, Fukui Prefecture

SUGIYAMA, Yuichi[1*] ; INOUE, Takahiko[1] ; MURAKAMI, Fumitoshi[1] ; SAKAMOTO, Izumi[2] ; TAKINO, Yoshiyuki[2] ; NAGATA, Takahiro[3] ; HOSOYA, Takashi[4] ; USAMI, Takuya[5]

[1]AIST, [2]Tokai University, [3]Dia Consultants Co., Ltd., [4]Chuo Kaihatsu Corporation, [5]Sogo Geophysical Exploration Co., Ltd.

AIST and Tokai University conducted, as part of MEXT 2013 nearshore active fault survey project, high-resolution acoustic reflection surveys and shallow-sea drilling survey across the Mikata and Nosaka fault zones off Mihama Town, Fukui Prefecture. We present the major results of the drilling survey. For the N-S-trending Mikata reverse fault zone, a 4-m-deep core was extracted from the 51-m-deep sea bottom on the western (downthrown) side. For the NW-trending Nosaka strike-slip fault with a reverse component, 27m- and 12m-deep cores were obtained from the 12m-deep sea on the SW (downthrown) and NE (upthrown) sides, respectively. We compiled geologic columns at scale of 1: 10 and conducted magnetic susceptibility measurement, radiocarbon dating, volcanic ash analysis, and diatom and pollen analyses.

Regarding the Mikata fault zone, obtained radiocarbon ages are proportional to the depth, reaching 6,180 to 6,010 and 6,380 to 6,260 cal.yBP at a depth of 3.8m. The average sedimentation rate during the recent 6ky is calculated at 0.6 m/ky. Acoustic reflection surveys have revealed several continuous reflection surfaces displaced by the fault, including the probable base of the postglacial deposits. We are trying to identify faulting-event horizons, using height difference of each reflection surface across the fault. Because drilling survey was unable to determine the age of each reflection surface, we are making efforts to estimate them, extrapolating possible depth-age curves of the postglacial deposits.

The deposits extracted from the both sides of the Nosaka fault zone are divided into the following stratigraphic units based on lithofacies and radiocarbon ages: A1 (<ca.6ka), A2 (ca.6-7.3ka), A3 (ca.7.3-7.5ka), B1 and B2 (ca.7.5-8ka), C (ca.8-10ka) and D intercalating 30-ky-old AT tephra. A1 is subdivided into the upper part (<ca.4ka) and the lower part (ca.5.5-6ka). While the basal surface of B2 shows 5m height difference across the fault, that of the lower A1 represents 1.7m difference across the fault. The lower A1 also shows drastic change in thickness from 1.1 m on the downthrown side to 0.2 m on the upthrown side. These suggest that faulting occurred twice; in the periods post-C/pre-A (8-6ka) and post-lower A1/pre-upper A1(ca.5.5-4ka). Faulting history and slip per event are further examined, incorporated with analyses of acoustic reflection survey data.

Keywords: Mikata fault, Nosaka fault, active fault, acoustic reflection survey, sea drilling

Japan Geoscience Union Meeting 2014
(28 April - 02 May 2014 at Pacifico YOKOHAMA, Kanagawa, Japan)

SSS34-P22 Room:Poster Time:April 29 18:15-19:30

The fault gouge along the Ikoma active fault zone

MITAMURA, Keisuke[1*] ; OKUDAIRA, Takamoto[1] ; MITAMURA, Muneki[1]

[1]Graduate School of Science, Osaka City University

The characteristic of the topography of Middle Kinki is reflected as an alternation arrangement of a mountainous district and the basin of north-south characteristics. Ikoma mountains share the Osaka plain and the Nara Basin. The NNE-SSW-N-S trending Ikoma active fault zone is recognized as a high-angle reverse fault under the E-W compressional stress field in the Quaternary Japan. However, from the rock mechanics point of view, high-angle fault is favorable as normal fault formed under extensional stress regime. The high-angle reverse faults may be resulted from the reactivation of the high-angle normal faults (inversion tectonics). In this study, we examined some fault gouge zones along the Ikoma fault zone (Katano and Ikoma faults).

We found three fresh outcrops of mesoscopic fault zones developed along the Ikoma fault zone at Kuraji of Katano City, Kiyotaki of Shijonawate City and Iimoriyama of Shijonawate City. In these fault zones, fault gouge wit the width of 5-20 cm can be observed. We collected some oriented samples and made thin sections parallel to the striation and normal to the fault plane. In the samples, many dark seams develop parallel to the main fault plane (striation) to form a distinct foliation within the fault gouges. Many fragments with various sizes are observed and their long axis aligned oblique to the fault plane. The parts where edges of the fragments meet the dark seam the edges tends to be rounded, suggesting that the formation of the dark seam was associated with material transportation due to pressure solution. The fragments with high aspect ratios tend to align oblique to the fault plane, suggesting the rigid-body rotation caused by non-coaxial shear deformation. The asymmetric structures, i.e., preferential orientation of the long axis of fragments, drag folds and shear lenses indicate the top-down-sense-of-shear. Furthermore, fractal dimensions of the fragments in samples near the main fault plane are higher than in samples at the margin of the fault gouge.

Consequently, we found the lines of evidence indicative of normal fault movement in the fault gouges associated with the Ikoma active fault zone, suggesting that the N-S striking Ikoma fault zone is recognized as a high-angle reverse fault under the E-W compressional stress regime are of reactivation of the preexisting high-angle normal faults that may be formed under extensional stress field.

Keywords: Ikoma fault zone, active fault, tectonic inversion, fault gouge, internal structures, fracture zone

Japan Geoscience Union Meeting 2014
(28 April - 02 May 2014 at Pacifico YOKOHAMA, Kanagawa, Japan)

SSS34-P23 Room:Poster Time:April 29 18:15-19:30

Subsurface density structure in Southern Osaka Plain based on gravity and magnetic anomalies

INOUE, Naoto[1*] ; KITADA, Naoko[1] ; TAKEMURA, Keiji[2]

[1]Geo-Research Institute, [2]Beppu Geothermal Researh Laboratory, Institute for Geothermal Sciences, Graduate School of Science,

Geomorphological, geological and geophysical surveys have been carried out in the Osaka plain for the highly precise construction of a model to predict strong ground motion. In recent years, many seismic surveys were performed in the south of the plain. The outline of the basement configuration was estimated from the relationship between gravity anomaly and the depth of the basement. The depth of the basement inferred from the gravity anomaly was shallower than that from the seismic and micro tremor surveys at several points in the Osaka plain. The difference is considered the variation of density contrast due to some local distribution of the volcanic rocks. The magnetic anomaly indicates higher value at these points. The density structure was discussed from the gravity anomaly in consideration of the high magnetic anomaly area.

Keywords: gravity anomaly, magnetic anomaly, density structure, Osaka plain

Japan Geoscience Union Meeting 2014
(28 April - 02 May 2014 at Pacifico YOKOHAMA, Kanagawa, Japan)

SSS34-P24 Room:Poster Time:April 29 18:15-19:30

Age and horizontal offset of the latest faulting event on the Okamura fault of the MTL fault zone in central Shikoku

IKEDA, Michiharu[1*] ; GOTO, Hideaki[2] ; TSUTSUMI, Hiroyuki[3] ; KONDO, Hisao[4] ; NISHIZAKA, Naoki[5] ; OHNO, Yuki[5] ; TSUYUGUCHI, Koji[6] ; KOBAYASHI, Shuji[1]

[1]Shikoku Research Institute Inc., [2]Hiroshima University, [3]Kyoto University, [4]AIST/AFERC, [5]Shikoku Electoric Power Co. Inc., [6]Yonden Consultantsu Co. Inc.

In general, information about fault offsets along active faults is one of the important factors to estimate faulting behavior in seismogenic zones. However, it is challenging to determine the information about fault offsets. So far, the average slip-rate and the amount of a single-event offset are obtained only 30 and 6 points on the Median Tectonic Line active fault zone (MTLAFZ) in the Shikoku area (200 km-length), respectively (Tsutsumi and Goto, 2006).

We conducted a trench survey for the Okamura fault which is a part of the MTLAFZ in order to determine the latest faulting event age and the fault offset. The Okamura fault is distributed in a rage of 30 km on the central Shikoku. The survey point, Hagioi point, locates on a central part of the Okamura fault. The amount of the fault offset at the latest faulting event is estimated to be below 5.7 m (Tsutsumi et al., 1991). However, this is just one data about fault offset on the Okamura fault. Moreover, the latest event age of the Okamura fault has not been sufficiently constrained by some previous research results; 4-7th century (Okada et al., 1998), 1090-960 yBP (Ehime Prefecture, 1999) and after 16th century (Goto et al., 2001).

The main two results of this trench survey are as fallowing. The latest faulting event age is estimated to be after AD 1490, consisting with after 16th reported in Goto et al. (2001). Moreover, the amount of fault displacement at the latest faulting event is estimated to be below 7.5 m. This value is consistent with the trend of the surface offset information that the surface slip associated with the latest event is greater than 5 m between the Zunden and Okamura faults, and decrease gradually to the east and west.

In taking hypothetical consideration, the fault offset 7.5 m is greater than 5.7 m (Tsutsumi et al., 1991) at 5 km away from this survey site. The recurrence interval (938-1500 years) calculated on the basis of average slip rate (5-8 mm/y) and the fault offset 7.5 m is consistent with the value (1245-1620 years) from the paleoseismological data (Morino and Okada, 2002; Okada et al., 1998). Therefore, the survey result might indicate variety of fault offsets along the Okamura fault, however this fault offset 7.5 m contains estimation errors. Since the fault offset becoming larger toward the fault end is unreasonable, this survey site might not locate on near the end of the Okamura fault and but near the asperity region.

Keywords: latest faulting event age, fault offset, Median Tectonic Line active fault zone, Okamura fault

Japan Geoscience Union Meeting 2014
(28 April - 02 May 2014 at Pacifico YOKOHAMA, Kanagawa, Japan)

SSS34-P25 Room:Poster Time:April 29 18:15-19:30

Seafloor exploration at off Kochi Prefecture for coseismic subsidence during hysterical Nankai earthquakes

TANIKAWA, Wataru[1*] ; TOKUYAMA, Hidekazu[2] ; MURAYAMA, Masafumi[2] ; YAMAMOTO, Yuhji[2] ; EBIHARA, Shu[3]

[1]JAMSTEC/Kochi Kore Center, [2]Center for Advanced Marine Core Research , Kochi University, [3]Nippon Kaiyo ltd.

Paleoseismic trenching study and tsunami deposit analysis on land has been performed to understand the historical earthquakes and the scale of disasters caused by the earthquakes. Paleoseismic records are probably stored in seafloor sediments near the coast as well, though the seafloor researches were rarely performed.

In ancient documents, the great Hakuho Earthquake (684 A.D.), that had been classified a Nankai earthquake, had caused large subsidence near the coast and submerged a small village named "**Kuroda-gori**". In addition that, ancient artificial buildings and artifacts were found at off Kochi Prefecture from Aki city to Cape Ashizuri cape. However the relationship between the ancient foundation and the historical Nankai earthquake is not well understood.

Here, we investigate the seafloor foundation at off Kochi Prefecture based on marine seismic profiling and diving. We collect artifacts and sediment core samples from seafloors, and perform chemical and age analyses using them. We then evaluate the coseismic uplift and subsidence process and a magnitude scale of earthquake during paleo-Nankai earthquakes. We begin seafloor exploration at two sites, off-Tochi site and Nomi bay site in Kochi area. We introduce preliminary results of seafloor research on March 2014 and our future plan.

Acknowledgement
We appreciate the technical support by Nippon Kaiyo ltd..

Keywords: Hakuho earthquake, earthquake foundation, Nankai Trough earthquake, coseismic uplift and subsidence

Japan Geoscience Union Meeting 2014
(28 April - 02 May 2014 at Pacifico YOKOHAMA, Kanagawa, Japan)

SSS34-P26 Room:Poster Time:April 29 18:15-19:30

Fault activity of the Kokura-higashi fault and the Fukuchiyama fault zone in northern Kyushu Island, Japan

YOSHIOKA, Toshikazu[1*] ; TANIGUCHI, Kaoru[1] ; HOSOYA, Takashi[2] ; YAGI, Tatuya[2]

[1]Active Fault and Earthquake Research Center, AIST, [2]Chuo Kaihatsu Corporation

The Kokura-higashi fault is an active fault extending in NNE-SSW direction with west-side-up vertical displacement. The Fukuchiyama fault zone consists of the Tonda and Fukuchiyama faults extending in NNW-SSE direction with also west-side-up vertical displacement. Both are located in the northern Kyushu Island. The Earthquake Research Committee evaluated that the probability of the earthquake occurrence in the future on the Kokura-higashi fault and the Fukuchiyama fault zone are unknown or ambiguous because of the luck of paleoseismological data. We carried out a trench excavation study and boring surveys in four sites with total 20 cores on these faults.

A trench is excavated across a reverse scarplet along the estimated fault trace of the Tonda fault in the Fukuchiyama fault zone. On the trench wall, steeply inclined sandstone and mudstone of the Paleogene Ashiya Group and overlaid gravel and silt layers are cropped out. However, no clear fault is observed in between bedrocks and sediments.

Based on arrayed boring surveys at the Shii and Shindoji site on the Kokura-higashi fault, a few meters differences in depth of the bedrocks are recognized.

Faults are observed in the cores from the arrayed boring surveys at the Ikeda and Horita sites on the Fukuchiyama fault zone.

Keywords: Kokura-higashi fault, Fukuchiyama fault, Tonda fault, Fukuoka Prefecture, Kyushu Island, active fault

Japan Geoscience Union Meeting 2014
(28 April - 02 May 2014 at Pacifico YOKOHAMA, Kanagawa, Japan)

SSS34-P27 Room:Poster Time:April 29 18:15-19:30

Revised fault model of the 1771 Yaeyama tsunami, southwest Ryukyu

NAKAMURA, Mamoru[1*]

[1]Faculty of Science, Univ. Ryukyus

The 1771 Yaeyama tsunami (Meiwa tsunami) has been the largest and devastating tsunami in the Ryukyu Trench since about 300 years. The maximum runup height was about 30 m and 12000 people were dead by the tsunami. Although this tsunami is important for estimating the maximum tsunami in the Ryukyu Trench, the fault model has been unsolved. Then we estimated the source fault model of this tsunami.

(1) The maximum runup heights were 30 m near the southeast coast of Ishigaki Island, 15 m at Tarama Island, 15 m at Irabu Island, and 18 m at south coast of Miyako Island (Goto et al., 2011). The runup height at south coast of Miyako Island was estimated to 10.5 m from the old document ”Kyuyo”. However, folklore (Goto et al., 2011) and the inundation area estimated from the old document ”Otoegaki” (Kato, 1988) showed the runup height were about 20 m.

(2) Tarama Island is formed by the coral middle terrace at the height of 10-14 m. The tsunami reached at the villages (Nakasuji and Shiokawsa) which were located at the center-to-north of the Island. The estimated runup heights in these villages were about 15 m. Since the hill, whose height is 30 m, is located at the north of the villages, the tsunami will have inundated about 1.5-3.0 km from the south or east coast. Shimoji Island is also formed by the middle coral terrace at the height of 10-20 m. Although the Island was uninhabited at that time, the terrace was inundated by the tsunami, and the soil was stripped by the tsunami inundation, and cattle and domestic animals drown by the inundation (Shimajiri, 1988). These suggest that the wide area of the Tarama and Shimoji Island are inundated by the tsunami.

Using these data, we re-construct the fault model of this tsunami. We employed intraplate earthquake and landslide (Miyazawa et al., 2012), interplate earthquake (Nakamura, 2009), and splay fault (Hsu et al., 2013) models.

First, in the case of intraplate earthquake and landslide model, calculated runup heights were consistent with the observed ones. However, the calculated inundation area is limited within about 500 m from the shore at Tarama Island.

In the case of splay fault model, we set the western part of fault at the 125.5E based on Hsu et al. (2013). The calculated tsunami heights were smaller than the observed in the Ishigaki Island. The inundation area is limited within 500 m from the shore at Tarama Island.

Finally, we set the interplate earthquake model, which is revised the model of Nakamura (2009). We set the fault length, width, slip, and dip to 200 km, 70 km, 20 m, and 12 degrees, respectively (Mw8.6). In this case, the calculated runup heights were almost consistent with the observed ones except southeast coast of Ishigaki Island. The calculated inundation area is 1.5 km from the shore at Tarama Island. Then we added the local patch at the south of Ishigaki Island. The length, width, and slip of the patch is 40 km, 30 km, and 40 m (total Mw=8.7). Then we could reproduce the observed runup heights.

Keywords: tsunami, Ryukyu Trench, interplate earthquake, historical tsunami

Japan Geoscience Union Meeting 2014
(28 April - 02 May 2014 at Pacifico YOKOHAMA, Kanagawa, Japan)

SSS34-P28 Room:Poster Time:April 29 18:15-19:30

Systematical deflections and offsets of stream channels along the left-lateral strike-slip Kunlun Fault

YAN, Bing[1*] ; LIN, Aiming[2]

[1]Graduate School of Science and Technology, Shizuoka University, [2]Department of Geophysics, Graduate School of Science, Kyoto University

During the past two decades, the integration of geologic, geomorphic, seismic, and geophysical information has led to increased recognition and understanding of the tectonic significance of geomorphic features caused by strike-slip along active strike-slip faults. Tectonic landforms developed along active strike-slip faults are mainly characterized by systematic deflections and offsets of streams which are regarded as reliable displacement markers useful for reconstructing the long-term activity of active faults. It has been demonstrated that stream offsets have resulted from repeated large strike-slip earthquakes. The study of tectonic geomorphology will provide a new insight into the seismic activity, longevity and structural evolution of active strike-slip faults.

The Kunlun Fault is a typical active strike-slip fault zone extends for ˜1200 km in the northern Tibetan Plateau that has triggered the 2001 Mw 7.8 Kunlun great earthquake. In this study, we present evidence for the systematical sinistral deflection and/or offset of the stream channels and valleys of the upper Yellow River drainage along the eastern intramontane segment of ˜400 km of the fault zone. Topographic analysis of 3D perspective images constructed using Digital Elevation Model (DEM) data, high resolution Google Earth images and 15-m-resolution Landsat Enhanced Thematic Mapper (ETM+) images reveals the following: (i) various amounts of sinistral offset have accumulated on the tributary stream channels, valleys, and gullies of the upper Yellow River; (ii) the eastern intramontane segment of Kunlun fault accumulated sinistral offset amount for at least 12 km; (iii) the linear relationship between the between the accumulated offset amount and the upstream length from the deflected point to valley head of the stream involved can be reliable indicator of long-term slip rate.

The findings of this study support that the Kunlun Fault is a left-lateral strike-slip that partitions deformation into the eastward extrusion of the Tibetan Plateau to accommodate the continuing penetration of the Indian plate into the Eurasian plate.

Keywords: Kunlun Fault, left-lateral strike-slip fault, stream channel, systematical deflection, Tibetan Plateau, eastward extrusion

Japan Geoscience Union Meeting 2014
(28 April - 02 May 2014 at Pacifico YOKOHAMA, Kanagawa, Japan)

SSS35-01 Room:502 Time:May 2 14:15-14:35

On the generalization of the SPAC method and the development of a CCA method

CHO, Ikuo[1*]

[1]National Institute of Advanced Industrial Science and Technology

Introduction

Microtremor array methods refer to techniques for estimating subsurface velocity structures from the dispersion of Rayleigh-wave phase velocities obtained through array analysis of microtremors. Methods for analyzing Rayleigh-wave phase velocities include two major constituents: the spatial autocorrelation (SPAC) method [Aki, 1957] and the frequency-wave number spectral (FK) method [Capon, 1969]. SPAC method excels the FK method in the overall analysis efficiency, when account is taken of the requisite number of seismic sensors and the breadth of the wavelength ranges eligible for analysis [Okada, 2003]. The SPAC method, in addition, is intrinsically usable with a two-sensor seismic array [Aki, 1957], a potential that has received reappraisal during the past decade. Given this context, the SPAC method in recent years has not only come to be used more often, but has also seen progress in theoretical studies of its applicability.

Generalization of the SPAC method and the development of a CCA method

In our case, Cho et al. [2006] generalized the Aki's theory following Henstridge[1979], describing generic formulae to analyze a circular array of three-component microtermors on the basis of the theory of stationary random processes. The generic theory provided a basis for constructing various methods to efficiently analyze Rayleigh- and Love-wave phase velocities, Rayleigh-wave ellipticities, and power partition ratios of Rayleigh to Love waves. It also provided a theoretical foundation to examine applicability conditions and optimal observation durations for two-sensor SPAC methods.

The centerless circular array (CCA) method [Cho et al., 2004] represents one method on the basis of the generic theory to analyze phase velocity of Rayleigh waves. The CCA method is characterized, among other things, by its applicability to an array of three seismic sensors in irregular configuration. It is also characterized by superior analytic performance in long-wavelength ranges. Methods have been proposed to evaluate noise levels, which can negatively impact its analytic performance, in terms of signal-to-noise (SN) ratios and to compensate for the effects of noise.

In the first half of the presentation, the above history will be described after a simple explanation of the general features of microtremor array explorations.

Development of miniature array analyses for shallow surveys

In the second half, the situation on the miniature array analyses based on the CCA method will be reported. "Miniature array analyses" involves 15-min microtremor measurement sessions using very small seismic arrays, 1 m or less in radius, to obtain the dispersion of Rayleigh-wave phase velocities corresponding to depths of several tens of meters, and sometimes more than 100 m, beneath the surface. In addition to this feature, the analysis results are accompanied with quality control factors. In the last year, we dealt with the following problems so as to put the miniature array analysis into practical use: (i) What is an appropriate way to deal with analysis results of limited quality and dubious reliability in general? (ii) What is a better way to pursue the efficiency of surveys, including the step of estimating subsurface structures after the dispersion curve is obtained?

In the presentation, I will report the solution for this problem on the basis of the experience, the automatization of the analysis procedure (Cho et al., 2014; Senna et al., 2014), and a plan to release a new BIDO package (https://staff.aist.go.jp/ikuo-chou/bidodl.html) to draw 2D S-wave sections by miniature array analysis.

Acknowledgement The outcomes in the first half were obtained in the collaborative investigation with Dr. Taku Tada and Prof. Yuzo Shinozaki. Those in the second half were obtained in the collaborative investigation with Dr. Shigeki Senna and NIED, and through discussions with the members of the microtrmor working group.

Keywords: Microtremor, velocity structure, surface waves, phase velocity, exploration method, array

Japan Geoscience Union Meeting 2014
(28 April - 02 May 2014 at Pacifico YOKOHAMA, Kanagawa, Japan)

SSS35-02 Room:502 Time:May 2 14:35-14:50

Detection of Rayleigh wave and Love wave detection from microtremor array measurements

OHORI, Michihiro[1*] ; CITAK, Seckin[2] ; KUBO, Atsuki[3] ; OISHI, Yusuke[3] ; TAKAHASHI, Hirokazu[3] ; YAMASHINA, Tadashi[3]

[1]University of Fukui, [2]Japan Agency for Marine-Earth Science and Technology, [3]Kochi University

Microtremor array measurements are considered to be one of the most practical ways to explore the S-wave velocity structures for the seismic hazard evaluation. As seen in many articles (e.g. Horike, 1985), the Rayleigh-wave dispersive characteristics have been derived from vertical components to model the S-wave velocity structures. On the other hand, the detection of Love-waves from horizontal components seems to be limited in very few literatures (e.g. Yamamoto, 2000), because horizontal components of microtremors are composed of the Love-waves and the Rayleigh-waves and the separation of two different kinds of surface waves is usually considered to be difficult.

As representative methods to analyze the microtremoer array records, the FK spectral method proposed by Capon (1969) and the spatial autocorrelation (SPAC) method by Aki (1957) have been used. Both methods have been extended to treat three-component data and detect the Love-wave as well as the Rayleigh-wave: the FK spectral method by Saito (2007) and the SPAC method by Okada and Matsushima (1990) and Yamamoto (2000), respectively. It is considered to be significant to apply these extended methods to observed data in various test fields. In our previous study, we carried out microtremor array measurements at Takasu area in Kochi city, south-west Japan on November 2010. We used two circular arrays with radii of 50 m and 100 m simultaneously, and successfully detected dispersive characteristics of both Rayleigh-waves and Love-waves in a frequency range between 1.2 to 3.8 Hz (Ohori et al. 2013). In analyses of observed array records, we used two kinds of the FK spectral methods: Capon's technique (1969) applied to vertical component and Saito's one (2007) to horizontal components.

To make a better understanding about characteristics of microtremors for the targeted area and obtain surface wave dispersive characteristics in more higher frequency range (up to 6Hz), we additionally conducted a few smaller array measurements on March 2013, using 4 sets of three-component portable seismometers which compose a circular array with a radius varying step-by-step from 50 m to 25 m and 12.5 m. In our study, results from newly observed data are reported and discussed. Phase velocity results were obtained from FK spectral method for vertical and transverse components. We also applied the SPAC method (Yamamoto, 2000) and compared the estimated phase velocity results from the SPAC method with those from the FK spectral method. The SPAC method provided that the energy power ratio of Love-waves in horizontal components distributed within 40-70% in a frequency range between 1.4 to 6 Hz.

Keywords: microtremor array measurements, FK spectral method, SPAC method, Rayleigh-wave, Love-wave

Japan Geoscience Union Meeting 2014
(28 April - 02 May 2014 at Pacifico YOKOHAMA, Kanagawa, Japan)

SSS35-03 Room:502 Time:May 2 14:50-15:05

Estimating composition of ambient noise from three-component records at Tono array

TAKAGI, Ryota[1*] ; NAKAHARA, Hisashi[2] ; KONO, Toshio[1] ; OKADA, Tomomi[1]

[1]RCPEV, Graduate School of Sci., Tohoku Univ., [2]Geophysics, Graduate School of Sci., Tohoku Univ.

Ambient noise methods have become common tools to explore and monitor subsurface structure. However, effective uses of ambient noise should stand on the knowledge of a nature of ambient noise. In order to reveal the composition of ambient noise quantitatively, we extend the SPAC method to body wave incidence. Applying the extended SPAC method to the observation at Tono array, northeast Japan, we shows a good agreement between the theoretical cross spectra and the observed cross spectra. By fitting the theoretical cross spectra to the observed cross spectra, we estimated the composition ratio of Rayleigh, Love, and P waves. The characteristics of the composition ratio show a significant change at 1 Hz. While the P wave composition in total power is 5-15% and the lowest one below 1 Hz, the P wave composition suddenly increases above 1 Hz and reaches 50% and the highest one in those of the three wave modes. The change at 1 Hz is attributed to attenuation of high-frequency surface waves because the decay rate of the absolute value of power spectra of surface waves gets steeper around 1 Hz as compared with the constant decay of P wave. We also examine the temporal variation of the composition of ambient noise. Whereas power spectrum of each mode shows long-term and short-term temporal variations coincident with offshore significant wave height, the ratio between power spectra varies little with time. The constant composition ratio suggests that the mechanism and the source-receiver distance are stable in time. Accordingly, near coastal region is a possible region of the dominant source of the observed ambient noise. For applications of ambient noise, we should take account of the composition of ambient noise.

Keywords: ambient noise, SPAC, three-component array observation

Japan Geoscience Union Meeting 2014
(28 April - 02 May 2014 at Pacifico YOKOHAMA, Kanagawa, Japan)

SSS35-04 Room:502 Time:May 2 15:20-15:35

Toward Earthquake Ground Motion Prediction using the Onshore-Offshore Ambient Seismic Field in Subduction Zones

VIENS, Loic[1*] ; MIYAKE, Hiroe[1] ; KOKETSU, Kazuki[1]

[1]Earthquake Research Institute, University of Tokyo

Ground motion prediction is critical to evaluate the seismic hazard specially in high seismicity areas as Japan. A source of particular concern is the complex geological structures as sedimentary basins which can trap and amplify seismic waves. It has been proved by Prieto and Beroza (2008) that reliable phase and amplitude of the impulse response functions can be extracted by deconvolution of the ambient seismic field recorded by two on-land stations without any pre-processing. This approach has the great advantage to predict accurate ground motion of moderate earthquakes at periods longer than 4 s without the need of any external information about the velocity structure. However, this method allows only to recover relative, rather than absolute, amplitudes. To retrieve the corresponding Green's functions, impulse response amplitudes need to be calibrated using records of an earthquake which happened close to the "virtual" source. Moreover, as surface-to-surface Green's functions are extracted, some mismatches are observed between Green's functions and the earthquake records. This feature is due to the fact that depth and focal mechanism of the event are not taken into account. Despite of these disadvantages, accuracy of the predicted ground motion is high and such long-period ground motion investigation is critical to carried out seismic hazard assessment for high-rise buildings, bridges, or oil tank having long-period resonance. In this study, we use this technique in subduction zones to extract vertical-to-vertical component of the Green's functions between seismic stations located on the ocean bottom and on-land Hi-net stations. The target region is located in the Tokai/Tonankai areas where two submarine cable-based sea-bottom seismographic observation systems have been deployed by the Japan Meteorological Agency (JMA). We use one month of noisy data recorded in January 2013 to compute the Green's functions. The choice of these data is motivated by a strong signal-to-noise ratio of the causal part of the Green's functions during this period. We validate this approach by comparing computed Green's functions with offshore moderate earthquake (Mw ˜5) records in the Nobi sedimentary basin where the Nagoya city is located. As megathrust earthquakes are expected in this area, we extrapolate our results to predict magnitude Mw ˜6 or larger earthquake ground motions using the scaling law of seismic spectrum developed by Aki (1967). These results are finally compared to long-period ground motion prediction equations to evaluate their validity.

Keywords: Ground motion Prediction, Ambient seismic field, Subduction zones, Low frequency, Deconvolution

Japan Geoscience Union Meeting 2014
(28 April - 02 May 2014 at Pacifico YOKOHAMA, Kanagawa, Japan)

SSS35-05 Room:502 Time:May 2 15:38-15:57

Review of study on microtremors and application for subsurface structure modeling

SUZUKI, Haruhiko[1*]

[1]OYO

The study on microtremors start by Kanai(1954). In his study, the relation between the subsurface structural model and the predominant period.

The method of the spectral ratio of two sites are devises. The influences source and path is removed.

From the 1980s, using spectral ratio between horizontal and updown component the subsurface structural model was estimated(Arai and Tokimatsu,2005). They assumed the microtremor consists by surface waves. On the other hand Nakamura(1988) assumed the microtremor consists by the SH waves.

H/V spectral ratio is using earthquake damage assumption investigations. Using H/V spectral ratio and phase velocity of Rayleigh wave, R/V spectral ratio of earthquake ground motion, the subsurface structural model from several meter to several kilometer depth are estimated in the Kanto area.

Keywords: Microtremors, Spectral ratio, S-wave structural modeling

Japan Geoscience Union Meeting 2014
(28 April - 02 May 2014 at Pacifico YOKOHAMA, Kanagawa, Japan)

SSS35-06 Room:502 Time:May 2 16:15-16:30

Geological Interpretation of a Liquefied Area by 'i-Bido': A Case Study in Urayasu City, Japan (2)

SATO, Shinji[1*] ; HIGASHI, Masashi[2] ; HIGUCHI, Shigeo[3] ; INADA, Akira[3] ; ITO, Akihide[4] ; IWAMOTO, Hiroshi[5] ; KAMIKASEDA, Satoshi[6] ; KAWASAKI, Kenichi[7] ; KUSUNOKI, Keiko[8] ; SHINADA, Shoichi[2] ; SUENAGA, Kazuyuki[9] ; WATANABE, Takumi[3] ; SENNA, Shigeki[10] ; FUJIWARA, Hiroyuki[10]

[1]Chishirodai high school, [2]JAPEX, [3]No affiliation, [4]Chiba-kita High school, [5]Kanto Natural Gas Development Co., Ltd, [6]NTC Consaltants Co., Ltd., [7]Chiba-nishi High school, [8]Urayasu high school, [9]Earth System Science Co., Ltd., [10]NIED

The Great East Japan Earthquake that occurred in 2011 off the Pacific coast of Tohoku caused the formation of two long cracks (crack 1 and crack 2) at Urayasu High School in Chiba Prefecture, Japan. Iwamoto et al. (2014) classified the survey area into different parts by examining the reclamation history and found the following three areas: A, 'Kaimenka-tochi'∗; B, reclaimed land from dredged seabed deposits; and C, the embankment and its surrounding zone. Crack 1 was situated between areas A and B, and crack 2 was between areas B and C.

Based on the investigation, the authors conducted micro-tremor observations at the three reclaimed land areas and Alluvial area. These measurements were conducted to reveal the area's geophysical aspects and to extrapolate three-dimensional data of the subsurface geology from two-dimensional data. At each measurement position, the results of micro-tremor observation were analyzed to give H/V spectra and the relationship between the site's geology and physical data. Field measurements of micro-tremors were performed with JU310, which was designed by the National Research Institute for Earth Science and Disaster Prevention. Measurements and analysis were performed using the i-Bido system (Senna et al., 2011), named after the Japanese word for micro-tremor, which was designed by the same institute.

Analysis revealed that the micro-tremors in areas A, B, and C had clear peaks at 1 Hz or slightly higher. This result corresponds to the impedance ratio at the boundary between the Holocene and Pleistocene deposits. Additionally, the micro-tremors observed at area B, which contains land reclaimed in 1965-1971, had peaks from approximately 4-5 Hz. These peaks were not observed or were unclear in areas A and C. For both crack 1 and crack 2, the peak was clear on one side but not on the other. The interval across a crack was only a few meters; therefore, these peaks depend on the impedance ratio between the silt bed, which was reclaimed by dredging from the seafloor, and the Holocene deposits. Additionally, the Nd-value∗∗of the silt bed was 0, as determined by a survey of the subsurface geology.

The analytical results determined using i-Bido supported the physical aspect put forth by Iwamoto et al. (2014) as the reason and mechanism by which the two cracks formed. Each frequency peak also showed the individual geological unit in the reclaimed bed, further supporting Iwamoto et al. (2014). The i-Bido system was very useful for analysis of the relationship between the site's geology and physical characteristics and for extrapolation of three-dimensional data from two-dimensional data. The authors hope that the methods discussed here will aid the progress of disaster prevention.

∗'Kaimenka-tochi' means land below sea level literally. Before reclamation, it was located in front of seashore, and it was in the possession of the private owner. and was used to reed cultivation etc.

∗∗Nd-value is brought by Dynamic Cone Penetration Test, which has the following conditions: a slide hammer with a weight of 5kg falling through a distance of 50cm, and diameter of 2.5cm cone. The number(i.e. Nd-value) of blows needed for the cone to penetrate each 10cm is recorded.

Acknowledgements

The authors are very gratful to Mr. Toshio NAKAYAMA of visiting researcher of NIED, who supported them for using i-Bido system.

References:

Hiroshi IWAMOTO, Masashi HIGASHI, Shigeo HIGUCHI, Akira INADA, Akihide ITO, Satoshi KAMIKASEDA, Kenichi KAWASAKI, Keiko KUSUNOKI, Shinji SATO, Shoichi SHINADA, Kazuyuki SUENAGA, and Takumi WATANABE (2014) Recent Geological Interpretation of Liquefied Area: A Case Study in Urayasu City, Japan(1). Japan Geoscience Union Meeting 2014.

Shigeki Senna, Hiroki Azuma(NIED), Yuuko Murui(MSS Corp), and Hiroyuki Fujiwara(NIED) (2011) Development of microtremor survey of observation system i-bidou, etc. The 124 th SEGJ (Society of exploration geophysics of Japan) Conference. 346-348.

Keywords: liquefaction, crack, micro tremor, i-Bido, Urayasu, reclaimed land

SSS35-06 Room:502 Time:May 2 16:15-16:30

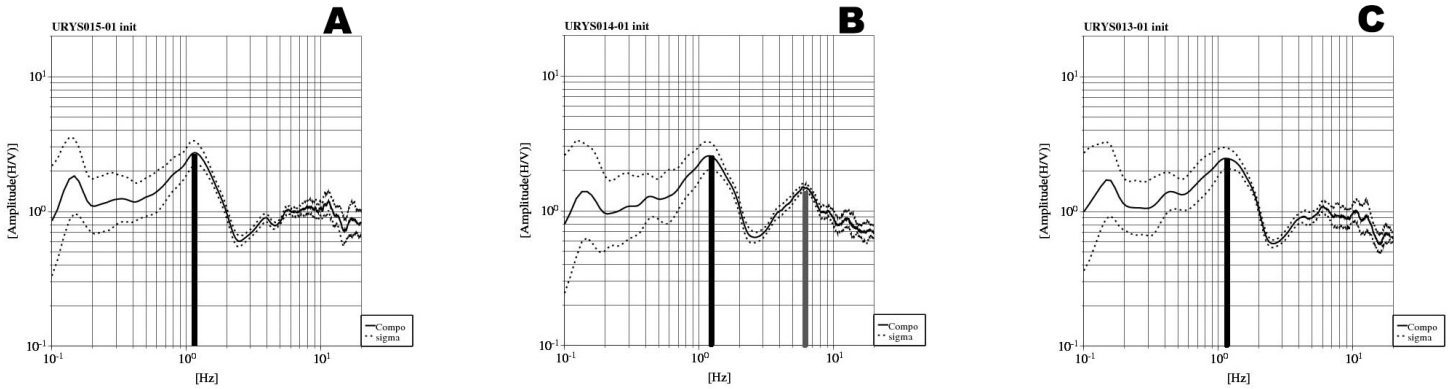

Fig.1 H/V Spectra of A, B, and C Areas

Japan Geoscience Union Meeting 2014
(28 April - 02 May 2014 at Pacifico YOKOHAMA, Kanagawa, Japan)

SSS35-07 Room:502 Time:May 2 16:30-16:45

H/V Spectral Ratios for Both Microtremors and Earthquake Motions and Interpretation based the Diffuse Field Theory

KAWASE, Hiroshi[1*] ; MATSUSHIMA, Shinichi[1]

[1]DPRI, Kyoto University

Horizontal-to-vertical spectral ratios (HVRs) of microtremors have been traditionally interpreted theoretically as representing the Rayleigh wave ellipticity or just utilized a convenient tool to extract predominant periods of ground. However, based on the diffuse field theory (Sanchez-Sesma et al., 2011) microtremor H/V spectral ratios (MHVRs) correspond to the square root of the ratio of the imaginary part of horizontal displacement for a horizontally applied unit harmonic load and the imaginary part of vertical displacement for a vertically applied unit load at the same position.

The same diffuse field concept leads us to derive a simple formula for earthquake HVRs (EHVRs), that is, the ratio of the horizontal motion on the surface for a vertical incidence of S wave divided by the vertical motion on the surface for a vertical incidence of P wave with a fixed coefficient depending on the bedrock wave velocity (Kawase et al., 2011). The difference of EHVRs from MHVRs comes from the fact that primary contribution of earthquake motions would be of plane body waves. Traditionally EHVRs are interpreted as the responses of inclined SV wave incidence only for their coherent S wave portions.

Before the advent of these compact theoretical solutions, EHVRs and MHVRs are either considered to be very similar/equivalent, or totally different in the previous studies. With these theoretical solutions we need to re-focus our attention on the difference of HVRs.

To that end we have compared HVRs at several dozens of strong motion stations in Japan. When we compared observed HVRs we found that EHVRs tend to be higher in general than the MHVRs, especially in higher frequencies than their fundamental peaks. As previously reported, their general shapes share the common features. Especially their fundamental peak and trough frequencies show quite a good match to each other. However, peaks in EHVRs in the higher frequency range would not always show up in MHVRs. When we calculated theoretical HVRs separately at these target sites, we found that the underground structures that are optimized for EHVRs would not explain perfectly MHVRs.

So we invert underground structures which can explain both EHVRs and MHVRs at the same time based on the different theoretical formula. Using the hybrid heuristic algorithm primarily based on the GA method with generation-dependent probability, we successfully obtain the detailed S-wave velocity structures for these investigated sites. The proposed method using HVRs is quite robust to obtain S-wave velocity structures that can be used quantitative simulation of strong motions at the target sites.

Keywords: microtremors, strong motion, diffuse-field theory

Japan Geoscience Union Meeting 2014
(28 April - 02 May 2014 at Pacifico YOKOHAMA, Kanagawa, Japan)

SSS35-08 Room:502 Time:May 2 16:45-17:00

The Effect of the Basin Edge to the Directional Dependent Horizontal-to-Vertical Spectral Ratios of Microtremors

MATSUSHIMA, Shinichi[1*] ; DE MARTIN, Florent[2] ; KAWASE, Hiroshi[1] ; FUKUOKA, Yuri[3] ; SANCHEZ-SESMA, Francisco[4]

[1]DPRI, Kyoto University, [2]Risk and Prevention Division, BRGM, [3]School of Engineering, Kyoto University, [4]Institute of Engineering, UNAM

Based on the diffuse field theory (Perton et al., 2009), Horizontal-to-Vertical (H/V) spectral ratios of microtremors (or ambient noise) correspond to the square root of the ratio of the imaginary part of horizontal displacement for a horizontally applied unit harmonic load, Im[G_{11}] and/or Im[G_{22}], and the imaginary part of vertical displacement for a vertically applied unit load, Im[G_{33}], where both the loads and receivers are at the same point on the free surface (Sanchez-Sesma et al., 2011). This theory can be applied to a site where the subsurface structure cannot be considered as sufficiently flat, horizontally layered (i.e., Im[G_{11}] /= Im[G_{22}]), and lateral heterogeneity exists, and the H/V spectral ratio of microtremors can be derived by the square root of the Im[G_{11}] and/or Im[G_{22}] and Im[G_{33}] (Matsushima et al., 2014).

The authors have shown that by using a numerical method such as the 3-D Spectral Element Method (SEM) (e.g., De Martin, 2011) to calculate the Green's functions from 3-D wave propagation analysis using a 2-D basin structure, it is possible to qualitatively simulate the significant directional dependency that can be seen in H/V spectral ratios of microtremors observed at sites on Uji campus, Kyoto University. The NS/UD has higher peak amplitude and EW/UD has higher peak frequency. The H/V spectral ratios derived from numerical analysis using Green's functions calculated for a simple 2-D basin model with one layer over bedrock show that the observed H/V spectral ratios are qualitatively simulated (Matsushima et al., 2014). Also, Matsushima et al. (2014) has shown that the shape of the H/V spectral ratio is distorted at sites close to the basin edge. This is an indication that if we observe microtremors at several sites close to the assumed basin edge, there may be possibility to identify the shape of the basin edge in detail.

In this study, we focus on the effect of the basin edge to the H/V spectral ratios and study the relation between the basin edge shape and the difference between NS/UD and EW/UD by simulating the H/V spectral ratios at sites close to the basin edge by numerical calculation. We consider a simple 2-D basin model with one layer over bedrock and change the shape of the basin edge. Also, we made micorotremor observation for two line arrays orthogonal to the 2-D basin in Uji and found that the observed H/V spectral ratios show the characteristics assumed from the numerical analysis.

From these results, we can see that the condition of the basin edge changes the H/V spectral ratios drastically at sites close to the basin edge. If we accumulate the relation between the shape and condition of the basin edge to the shape of the H/V spectral ratios in two orthogonal horizontal directions, we will be able to use the information from the observed H/V spectral ratios of microtremors to determine the basin edge shape.

References

Matsushima S, De Martin F, Hirokawa T, Kawase H, Sanchez-Sesma FJ (2014): The Effect of Lateral Heterogeneity on Horizontal-to-Vertical Spectral Ratio of Microtremors Inferred from Observation and Synthetics, Bulletin of the Seismological Society of America, 104(1):doi: 10.1785/0120120321

Perton M, Sanchez-Sesma FJ, Rodriguez-Castellanos A, Campillo M, Weaver RL (2009): Two Perspectives on Equipartition in Diffuse Elastic Fields in Three Dimensions, Journal of Acoustical Society of America, 126(3):1125-1130

Sanchez-Sesma, FJ., Rodriguez M, Iturraran-Viveros U, Luzon F, Campillo M, Margerin L, Garcia-Jerez A, Suarez M, Santoyo MA, Rodriguez-Castellanos A (2011): A theory for microtremor H/V spectral ratio: Application for a layered medium, Geophysical Journal International Express Letters, 186(1):221-225 doi: 10.1111/j.1365-246X.2011.05064.x

Keywords: Microtremor, H/V Spectral Ratio, Diffuse Field, Heterogeneity, Velocity Structure

Japan Geoscience Union Meeting 2014
(28 April - 02 May 2014 at Pacifico YOKOHAMA, Kanagawa, Japan)

SSS35-P01 Room:Poster Time:May 2 16:15-17:30

Sophistication of microtremor methods to survey shallow structures, PartI: Development of automatic reading algorithms

CHO, Ikuo[1*] ; SENNA, Shigeki[2] ; FUJIWARA, Hiroyuki[2]

[1]National Institute of Advanced Industrial Science and Technology, [2]National Research Institute for Earth Science and Disaster Prevention

We have been seeking an efficient way to maximize the potential of the microtremor methods for shallow surveys. It is considered that a practical approach has been gained in the observation by the development of portable seismometers (Senna, 2006, 2012) and by the finding of the full usability of the data obtained by a miniature array (radius $<$1 m), optionally together with a small irregular-shaped array (radius less than 10 m) consisting of three seismometers (Cho et al., 2013a).

As an efficient way to infer an S-wave velocity structure, we consider that a classical, simple profiling method (SPM), where a dispersion curve is directly converted into an S-wave velocity structure (e.g., Heukelom and Foster, 1960), is a good scheme from a view point of simplicity, thus, the balance between the efforts and the information to be extracted. It is true, however, that we frequently like to increase to resolution. Facing this dilemma, we suggested a simple tool ”H/V depth conversion” (Cho et al., 2013). We found that the use of an H/V depth conversion followed by a simplified inversion method (SIM) of Pelekis and Athanasopoulos (2011) can in fact increase the resolutions (e.g., Senna et al., 2013; Yoshida et al., 2013).

The current problem is to further promote the efficiency in the data processing procedure. A visual reading of analysis results, which we take at the current time, is time consuming to deal with a vast mount of microtremor data, now obtainable by a streamlined observational procedure. The reproducibility and biases constitute other kinds of problem of visual reading.

To address this problem, we invented the following automatic-reading algorithms. We applied them to observed data consisting of multiple arrays along a measurement line. As the results, natural images of two-dimensional S-wave velocity sections were obtained, not considerably different from the one obtained by visual readings (Senna et al., 2014).

Automatic readings of phase velocities

Let us suppose that multiple dispersion curves have been obtained by either multiple arrays or multiple analysis methods (i.e., nc-CCA, CCA, and SPAC methods) at a single observation point. In the first step, apply the following procedure to each dispersion curve. (i) Divide the frequency range used for analyses into equally-spaced intervals (bins) in a logarithmic scale. Take an average of phase-velocity data in each bin. (ii) Exclude the results from the analyses either when the wavelengths relative to an array radius lie out of the range defined a-priori for each method or when they exceeds the analysis limits having been evaluated by the use of an array with a sensor at the center point. Also, exclude the results when they seem to align in a line passing through the origin.

An automatic reading is obtained for each bin by averaging all values left after the procedure (ii). Readings are deleted, however, when they seem to align in a line passing through the origin.

Automatic readings of peak and troughs of an H/V spectrum

First, an H/V spectrum obtained at a single observation point, or an average spectrum if there are multiple spectra as a representative value, is smoothed using a spectral windows having a frequency-dependent window width. Peaks and troughs of the spectrum are searched from the lower side of the frequency range by using the derivatives. We search pairs of a peak and a trough to stabilize the analysis result: A pair is excluded from the reading results when the difference in either frequency or H/V ratio between a peak and trough is smaller than a threshold. Also, a pair is excluded when a peak (trough) value is smaller than that of an anterior peak (trough). The peak and trough of each pair, thus obtained, are used for the depth conversion, and the resulting depths are averaged to be the representative depth obtained by an automatic reading.

Keywords: Microtremor, velocity structure, surface waves, phase velocity, expolation method, array

SSS35-P01 Room:Poster Time:May 2 16:15-17:30

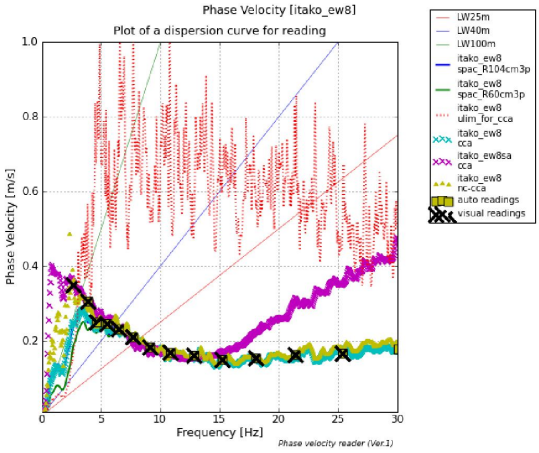

Japan Geoscience Union Meeting 2014
(28 April - 02 May 2014 at Pacifico YOKOHAMA, Kanagawa, Japan)

SSS35-P02 Room:Poster Time:May 2 16:15-17:30

Sophistication of microtremor methods to survey shallow structures, Part2 : Application of automatic reading algorithms

SENNA, Shigeki[1*] ; CHO, Ikuo[2] ; FUJIWARA, Hiroyuki[1]

[1]NIED, [2]AIST

We have been seeking an efficient way to maximize the potential of the microtremor methods for shallow surveys. It is considered that a practical approach has been gained in the observation by the development of portable seismometers (Senna, 2006, 2012) and by the finding of the full usability of the data obtainable by a miniature array (radius less than 1m), optionally together with a small irregular-shaped array (radius less than 10 m) consisting of three seismometers (Cho et al., 2013a).

As an efficient way to infer an S-wave velocity structure, we consider that a classical, simple profiling method (SPM), where a dispersion curve is directly converted into an S-wave velocity structure (e.g., Heukelom and Foster, 1960), is a good scheme from a view point of simplicity, thus, the balance between the efforts and the information to be extracted. It is true, however, that we frequently like to increase to resolution. Facing this dilemma, we suggested a simple tool 'H/V depth conversion' (Cho et al., 2013). We found that the use of an H/V depth conversion followed by a simplified inversion method (SIM) of Pelekis and Athanasopoulos (2011) can in fact increase the resolutions (e.g., Senna et al., 2013; Yoshida et al., 2013).

The current challenge is to further promote the efficiency in the data processing procedure. A visual reading of analysis results, which we take at the current time, is time consuming to deal with a vast mount of microtremor data, now obtainable by a streamlined observational procedure. The reproducibility and biases depending on analyst constitute other kinds of problem of visual reading.

To address this problem, Cho et al. (2014, thismeeting) invented automatic-reading algorithms. In this study we test their algorithm by applying it to observed data to compare the results with those obtained with visual readings. Our method of observation and analysis is described in the following.

1. Observation

Observation duration is set to 15 minutes irrespective of the array shape, where either miniature arrays with a radius of 60 cm or irregular-shaped arrays with radii about 3 to 10 m are used.

2. Automatic analyses and readings of phase velocities and H/V spectra

The selectin of the data portions and the spectral analysis are automatically executed by using the software BIDO. Cho et al. (2014)'s algorithms are used for automatic readings of phase velocities and H/V spectra.

3. Inferring 1D S-wave velocity structures and constructing 2D sections

A dispersion diagram, represented by the relation between the wavelength, L, and phase velocity, Vr, is converted into a 1D S-wave structure having the relation between the depth, D, and S-wave velocity, Vs, where relations Vs= Vr/0.92 and D=0.375L are used (SPM). The resulting 1D structures are spatially interpolated to obtain a 2D section, where H/V depth conversions are overdrawn.

The above procedure from 1 to 3 is fully automatically executed. Incidentally, this study include no examination on SIM because no automatic algorithm has been developed yet because of the robustness problem.

We applied the above procedure to microtermor data obtained along survey lines in four different areas with variable geological environments (e.g., Itako City, Hadano City, Kashiwa City, Urayasu City). As the results, natural views of 2D S-wave velocity sections are obtained in all cases, similar to those obtained by visual readings. Furthermore, resulting velocity sections are consistent with other kinds of subsurface structural data (i.e., geological sections, N-value distributions, the 3D soil model of Senna et al. (2013)). We consider that, needing further improvement, Cho et al. (2014)'s algorithms can provide us with acceptable results at the first stage of automating the analysis procedure.

Keywords: Microtremor, velocity structure, surface waves, phase velocity, array, underground structure model

Japan Geoscience Union Meeting 2014
(28 April - 02 May 2014 at Pacifico YOKOHAMA, Kanagawa, Japan)

SSS35-P03 Room:Poster Time:May 2 16:15-17:30

Future Initiatives of development of microtremor survey observation system

SENNA, Shigeki[1*] ; FUJIWARA, Hiroyuki[1]

[1]NIED

The microtremor observation has treated till today as physical investigation information, including the structure model creation for strong motion prediction of the researcher and engineer , etc.

If microtremor observation can observe easily and the observed data can be easily transmitted to a database with information on that observation point, it can expect that the number of collection of observational data will increase explosively in the future because an amateur can also observe, and the advancement of structural model and prediction of seismic strong motions will be attained by leaps and bounds.

It will become an unprecedented thing which leads to grasp of detailed damage distribution, and the improvement in accuracy of real-time earthquake information from the above.

Keywords: microtremor, survey observation system, cloud system, big data

Japan Geoscience Union Meeting 2014
(28 April - 02 May 2014 at Pacifico YOKOHAMA, Kanagawa, Japan)

SSS35-P04 Room:Poster Time:May 2 16:15-17:30

Estimation of phase velocity of Rayleigh wave using linear array

ZHANG, Xinrui[1*] ; MORIKAWA, Hitoshi[1]

[1]Tokyo Institute of Technology

Since the spatial autocorrelation (SPAC) method has been proposed by Aki (1957), the observation using a circular array of evenly spaced sensors and a central sensor becomes a commonly used measurement technique in the microtremor survey method (Okada, 2003). However, in practice, the strict arrangement of sensors required by the method is difficult to conduct because of the limit of real environment. In order to slacken the requirement of the arrangement, Chavez-Garcia et al. (2005) discussed the validity of performing the SPAC method with a linear array. However, the conclusion of this research is result-based and is not backed by theoretical demonstration. Aki's autocorrelation coefficient could be alternatively seen as the azimuthal average of CCFs (Okada, 2003; Shiraishi 2006). A CCF consists of the Bessel function and an error term which varies with the azimuth of sources. By taking the azimuthal average, the error term vanishes and direct J_0(kr) can be obtained. The discrete formula of the CCF offers the possibility of extending the original SPAC method. In this research, we develop the solution by controling the error term in CCF which can obtain directly the phase velocity instead of using records of sensors in a line instead of azimuthally arranged ones.

Under the assumption: 1) Only the fundamental mode is dominated. 2) Different sources are not correlated, the real part of discrete formula of CCF could be expressed as (Shiraishi, 2006). If we neglect the terms of order larger than 6, we can obtain:

$\mathrm{Re}(\gamma_{pq})=J_0(kr)-2J_2(kr)\sum\lambda_l\cos2\theta_l+2J_4(kr)\sum\lambda_l\cos4\theta_l$. It can be seen that there are only three unknown variables kr, $\sum\lambda_l\cos2\theta_l$ and $\sum\lambda_l\cos4\theta_l$. It is required of at least three sensors (3 different intervals) to solve the 3 unknown variables theoretically. The three sites need to be in a line to make the three CCFs share the same unknowns. Because of the coupling variables and non linear functions, we use the genetic algorithm and particle filter to solve out the optimum solution.

In order to comfirm the validity of this new theory preliminarily, the simple wavefield composed of unidirectional plane wave is used to examine the accuracy of estimating phase velocity obtained from a linear array with 3 sensors. The distances between adjacent sensors (r and 0.5r, r=30m) are set to be different so that we can have totally 3 different CCFs to solve out the optimum solution. Except for the analytical simulation, we also applied a field test to examine the availability of the new method. We have applied field test to comfirm the availability of the method. Observation was conducted on 23 October 2013 at the parking lot of Zoorasia Yokohama Zoological Gardens (ZRS) in Yokohama city of Japan. We deployed 7 seismometers (KVS-300, moving speedometer) constituting two linear arrays. The two linear arrays forms an angle of 60 degree so that the SPAC method could be applied for confirmation.

In the analytical simulation, we confirmed the availability of the new method. The sensitivity of CCF with respect to phase velocity depends on the direction of linear array. When the sensitivity is low, the estimation will be bad. Hence, it is better to use at least two linear arrays forming an angle (90 degree is the best). In the field test in Yokohama, we applied both the SPAC method and the new method using 7 speedometers. Both SPAC method and the new method show good match with the theoretical dispersion curve. The new method shows narrower effective scope and shows some unstablity in both low and high frequency range. Through both simulation and field test, the availability of the new method has been confirmed. This new method makes the arrangement of sensors easier which needs only two linear arrays with a non-strict angle. In the future, we will study more about improving the inversion technique and the application of linear array.

Keywords: SPAC method, linear array, coherence complex function, particle filter

Japan Geoscience Union Meeting 2014
(28 April - 02 May 2014 at Pacifico YOKOHAMA, Kanagawa, Japan)

SSS35-P05 Room:Poster Time:May 2 16:15-17:30

Estimation of Subsurface Structure using Microtremor Observation in Ogasawara Iwo-To Island

MURAKOSHI, Takumi[1*] ; KOMORI, Etsuro[1] ; SHIMADA, Masaki[1]

[1]National Defense Academy

Ogasawara Iwo-To island is an active volcanic island which is located on the southernmost part of Izu-Ogasawara arc. The microtermor obserbation was carried out during the period from December 18 to 21, 2013 in Ogasawara Iwo-To island. The microtremor measurements were performed at 54 sites as 3-component seismometers for horizontal-to-vertical spectral ratio (HVSR) analysis. The obtained HVSRs of microtremor are used to determine the dominant frequencies of vibration of the subsurface structures beneath several recording sites in Ogasawara Iwo-To island. The H/V peak period varies from 1.1 to 3.5 sec.

For using the SPAC method of microtremor, the circular-array microtremor data were recorded by 6 seismometers distributed along the circumferences of two circles as well as a seismometer deployed in the center at two sites in the center of the island. The phase velocities and the S-wave velocities of the subsurface structures down to a depth of several km were estimated at each site from the microtremor data by using the SPAC method.

Keywords: microtremor, Ogasawara Iwo-To Island, subsurface structure

Japan Geoscience Union Meeting 2014
(28 April - 02 May 2014 at Pacifico YOKOHAMA, Kanagawa, Japan)

SSS35-P06 Room:Poster Time:May 2 16:15-17:30

Determination of Subsurface Structure of the Mt. Daisen area in Tottori Prefecture by Microtremor and Gravity Survey

NOGUCHI, Tatsuya[1*] ; KAGAWA, Takao[1] ; YASUNAGA, Harunobu[1] ; ISHIGO, Masaharu[1] ; KOASAKA, Shuhei[1]

[1]Tottori Univ.

Earthquake damages occurred by the earthquake that occurred at the Middle West of Tottori in 1983 , 2002 and the 2000 Western Tottori earthquake in Mt.Daisen area of Tottori Prefecture. It is supposed that the damage influenced the subsurface structure. It is important that the information of subsurface structures is obtained for prediction of ground motion in the area. Microtremor and gravity surveys were carried out in the plains of the shore part and Mt.Daisen area. S-wave velocity models are obtained at the array observation 3 sites and predominant period distribution at 3-components observation newly. The gravity anomalies were obtained by gravity survey data newly.

Japan Geoscience Union Meeting 2014
(28 April - 02 May 2014 at Pacifico YOKOHAMA, Kanagawa, Japan)

SSS35-P07 Room:Poster Time:May 2 16:15-17:30

Estimation of inter-station Green's functions using microtremor array data

HAYASHIDA, Takumi[1*] ; YOSHIMI, Masayuki[2]

[1]International Institute of Seismology and Earthquake Engineering, BRI, [2]Geological Survey of Japan, AIST

The seismic interferometry technique is used to evaluate seismic velocity structure beneath two observation sites [e.g., Ma et al. (2008); Yamanaka et al. (2010); Asano et al. (2012); Hayashida et al. (2014)]. The technique can be applied under the assumptions of non-stationary and uniform distribution of microtremor (ambient noise) sources and it is important to investigate whether the data satisfy the conditions. The array observations of microtremor [Yoshimi et al. (2012)] were conducted at 13 sites in Niigata prefecture, Japan. The surveys were carried out for more than 10 days per site and each array consists of three equilateral triangular arrays whose radii range from several hundred meters to several kilometers. Here we used the data to estimate inter-station Green's functions with the seismic interferometry technique. The stacked cross-correlation functions (CCFs) of microtremor showed coherent and dispersive wave trains in frequency ranges between 0.4 and 1.0 Hz for the small array, 0.2 and 0.7 Hz for the middle array and 0.1 and 0.6 Hz for the large array. The wave trains derived for each array correspond well to each other regardless of azimuth angles, showing the effect from the abnormal microtremor source can be negligible in this study. We also calculated theoretical Green's functions from the estimated S wave velocity structures with the spatial autocorrelation (SPAC) method for each site, assuming 1D velocity structure. The agreements between the calculated Green's functions and the derived CCFs from the seismic interferometry are generally good, especially at lower frequencies. Our results suggest that a combination of velocity structure estimation with surface-wave phase velocity (conventional array methods) and velocity structure validation with Green's function (seismic interferometry technique) provides better estimations for S wave velocity structures.

Acknowledgements:
We used the microtremor array data observed in a research project funded and supported by Japan Nuclear Energy Safety Organization (JNES).

Keywords: microtremor, seismic interferometry, Green's function, group velocity, SPAC method

Japan Geoscience Union Meeting 2014
(28 April - 02 May 2014 at Pacifico YOKOHAMA, Kanagawa, Japan)

SSS35-P08 Room:Poster Time:May 2 16:15-17:30

Seismic basement structure estimated from seismic interferometry and microtremor analysis

KOIZUMI, Ryo[1] ; SAWADA, Akihiro[1] ; HIRAMATSU, Yoshihiro[1*] ; THE GROUP, Aftershock observation[2]

[1]Kanazawa Uiversity, [2]the group for the joint aftershock observations

Recently, seismic interferometry has been considered to be a powerful tool for subsurface structure survey. Seismic interferometry is a method that produces pseudo reflected waveform data by computing the autocorrelation function (ACF) of seismic waveform record. In this study, we estimate the seismic basement structure beneath the northwestern Noto Peninsula from seismic interferometry and microtremor analysis. We examine the reliability of seismic interferometry and microtremor analysis by comparing those results with the results from gravity anomalies and a reflection seismic survey (Sato et al., 2007) in this area.

For seismic interferometry, we use waveform data of the aftershocks of the 2007 Noto Hanto earthquake at 44 seismic stations which are located in the northwestern Noto Peninsula. We apply high-pass filter of 2 Hz to SH component of displacement waveform and set a time window of 10 s after the arrival of S wave to calculate ACF. We make the average ACF by stacking all ACFs at each station. For microtremor analysis, we performed microtremors observation at 44 points where the stations for the aftershock observation were located and calculate H/V spectrum at each station. We estimate the basement structure in the analyzed area by assuming two-layer structure from ACF and H/V spectrum.

For the ACF analysis, it is difficult to identify the dominant peak of ACF for most stations. Especially, we cannot estimate the basement depths where the basement depths estimated from the reflection seismic survey (Sato et al., 2007) are shallower than 100 m. Finally, we obtain the basement depths at 14 of 44 stations. On the other hand, for the microtremor analysis, we can estimate the basement depths at 35 of 44 points. This indicates that the seismic interferometry with ACF is not an effective approach to estimate the basement depths in the northwestern Noto Peninsula.

We compare the basement depths estimated from ACF, H/V spectrum and gravity anomaly each other. These estimates are approximately coincident each other and shows that the basement depth of the Kuwatsuka block is shallower than that of the Saruyama block. Coseismic uplift was observed in the Kuwatsuka block at the 2007 Noto Hanto earthquake. Therefore, the results of this study is coincident with the hypothesis that the activity of active faults on seafloor near the coast causes the uplift of the Kuwatsuka block and makes its basement depth shallower (Hiramatsu et al., 2008).

Acknowledgements: We are grateful to the group for the joint aftershock observations of the 2007 Noto Hanto Earthquake for the use of waveform data and to NIED for the use of the instrument of microtremor observation. We thank Dr. Shigeki Senna for helpful advice.

Keywords: auto correlation function, H/V spectrum, gravity anomaly, geological block structure, the Noto Peninsula

Japan Geoscience Union Meeting 2014
(28 April - 02 May 2014 at Pacifico YOKOHAMA, Kanagawa, Japan)

SSS35-P09 Room:Poster Time:May 2 16:15-17:30

Retrieval of Green's function in a 3D inhomogeneous medium with nonisotropic source distribution using interferometry

CHIMOTO, Kosuke[1*] ; YAMANAKA, Hiroaki[1]

[1]Tokyo Tech.

Seismic interferometry is known to retrieve Green's functions in an elastic homogeneous medium with isotropic source distribution (e.g., Wapenaar and Fokkema, 2006), and is applied to estimate velocity structures using long time series of ambient noises (e.g., Shapiro and Campillo, 2004). However, the realistic noise field might be an inelastic inhomogeneous medium with nonisotropic source distribution, and thus the reliability of retrieval of Green's functions using seismic interferometry should be examined.

We study on the reliability of seismic interferometry in a 3D inhomogeneous structure model of Kanto basin with nonisotropic source distribution. The numerical study on seismic interferometry was conducted by using 3D FDM. We cross correlated the surface responses at two sites with multiple surface sources. We used Yamanaka and Yamana (2006) for the 3D inhomogeneous model of Kanto basin. Nonisotropic source distribution was made by using sources located only on the sea area. We investigated the influence for the cross correlation functions by comparing with that in a homogeneous medium or isotropic source distribution.

In a case of homogeneous medium with isotropic source distribution, we see slight difference between the cross correlation function and Green's functions, but the surface wave component was well retrieved and surface wave velocity compares well with the Green's function. The slight difference might have been caused by the approximations in seismic interferometry (e.g., Kimman and Trampert, 2010). The cross correlation function showed symmetry for positive and negative lagtimes. In a case of homogeneous with nonisotropic source distribution, the cross correlation function shows asymmetry whose surface wave cannot be seen in positive lagtimes. However, the cross correlation functions in negative lagtime compares well with that retrieved with isotropic source distribution, and it showed good agreement in terms of group velocity. These indicate the influence of source distribution on seismic interferometry would be large as indicated in numerous studies (e.g., Tsai, 2010).

In a case of a 3D inhomogeneous model of Kanto basin, the cross correlation function showed asymmetry even with isotropic source distribution. That is, an inhomogeneity complicates wave propagations and then make apparent source distribution non-isotropic even with the isotropic case. Specifically, larger amplitudes in negative lagtimes than that in positive lagtimes indicate that eastern sources became large apparently. Considering the Kanto basin model, Kanto mountains located in western part and Pacific Ocean located in eastern part, where have thick sediment layers, the eastern sources would have excited surface wave significantly, which caused apparent nonisotropic source distribution. Due to asymmetry in the cross correlation function, it does not match with the Green's function. Group velocities also show asymmetry, however, they agrees to that of Green's function. In a case of a 3D inhomogeneous model with nonisotropic source distribution, the cross correlation function shows asymmetry and show less agreement with the Green's function. However, the group velocity shows agreement.

As a result, the retrieval of Green's function using seismic interferometry is strongly influenced by source distributions. Moreover, an inhomogeneity affect to source distribution, it would also be the problem. In a realistic case, therefore, to understand how much isotropy is satisfied is important. Because understanding the source isotropy is tough, it is important to examine the influence considering with realistic applications. However, on group velocity estimations as many applications, the reliability showed good in this study, suggesting the high possibility for reliable applications in seismic interferometry.

Keywords: Seismic interferometry, Green's function, inhomogeneous, isotropic source, 3D FDM

Japan Geoscience Union Meeting 2014
(28 April - 02 May 2014 at Pacifico YOKOHAMA, Kanagawa, Japan)

SSS35-P10 Room:Poster Time:May 2 16:15-17:30

Estimation of subsurface structure by high density microtremor observations in Kochi Plain

OISHI, Yusuke[1*] ; KUBO, Atsuki[2] ; TAKAHASHI, Hirokazu[3] ; YAMASHINA, Tadashi[2]

[1]Studies in Science, Graduate School of Integrated Arts and Sciences, Kochi University, [2]Kochi Earthquake Observatory, Faculty of Science, Kochi University, [3]Faculty of Science, Kochi University

Kochi Plain is located around source region of the great Nankai Earthquake. Strong ground motion is expected in this area, because soft subsoil is widely deposited in Kochi Plain. In this study, we investigate H/V spectra of microtremor in the Kochi Plain. Microtremor study with single station is cheaper, quick and easier way than sampling boring core. It is convenient to reveal horizontal variation of soil/basement structure. We append 213 measurements in addition to previous reported 1041 measurements (Oishi et al., JpGU 2013, SSS35-P02). In total 1254 measurements are used to H/V spectral analysis. Figure shows distribution map of dominant periods by H/V spectral analysis based on microtremor observations in Kochi Plain. In perspective, dominant periods of H/V spectra around northern Urado-Bay region are longer than other regions. According to soil/basement model using boring data, the bedrock depth at this region is especially deep but boring which reaches the bedrock is limited. In contrast, H/V spectral analysis is useful to grasp the extent of region with deep soil/basement boundary. Dominant periods of H/V spectra around western part of Kochi Plain are relatively shorter than Urado region. The damaged areas of the past 2 (1854 and 1946) Nankai Earthquakes match with areas where the dominant period is long and/or the amplification factor is large. High density observations in this region show clear local variations. These are not reflected on current hazard maps or seismic intensity estimation maps. Using H/V spectral analysis based on high density microtremor observation, we are detecting patterns of soil/basement structure which has not be grasped using only boring core data.

Acknowledgement: We thank to Tadashi Hara and Nobuaki Kitamura, Kochi University and NEWJEC Inc. for providing their data.

Keywords: microtremor, H/V spectral ratio, subsurface structure, Kochi Plain

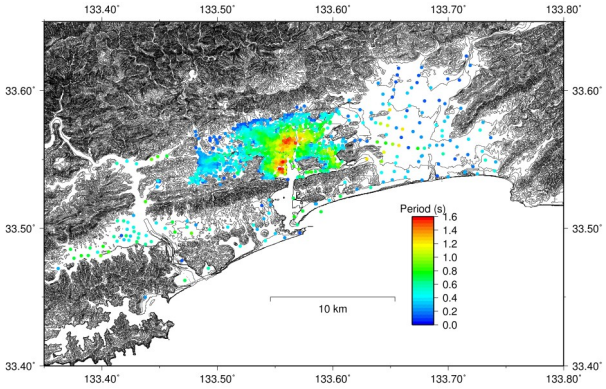

Japan Geoscience Union Meeting 2014
(28 April - 02 May 2014 at Pacifico YOKOHAMA, Kanagawa, Japan)

SSS35-P11 Room:Poster Time:May 2 16:15-17:30

Recent Geological Interpretation of A Liquefied Area: A Case Study in Urayasu City, Japan (1)

IWAMOTO, Hiroshi[1*] ; HIGASHI, Masashi[2] ; HIGUCHI, Shigeo[3] ; INADA, Akira[3] ; ITO, Akihide[4] ; KAMIKASEDA, Satoshi[5] ; KAWASAKI, Kenichi[6] ; KUSUNOKI, Keiko[7] ; SATO, Shinji[8] ; SHINADA, Shoichi[2] ; SUENAGA, Kazuyuki[9] ; WATANABE, Takumi[3]

[1]Kanto Natural Gas Development Co., Ltd, [2]JAPEX, [3]No affiliation, [4]Chiba-kita High School, [5]NTC Consaltants Co., Ltd., [6]Chiba-nishi High School, [7]Urayasu High School, [8]Chishirodai High School, [9]Earth System Science Co., Ltd.

At Urayasu High School (Urayasu City, Chiba Prefecture), where one of authors worked, the 2011 Great East Japan Earthquake caused the formation of two large open cracks from which large amounts of sand and water erupted as a result of soil liquefaction (Kusunoki et al., 2011). The objectives of this study were to investigate both the cause and the mechanism of this phenomenon. The site is located on reclaimed land, and a survey of the site's subsurface geology was carried out by hand auger boring and simple dynamic cone penetration testing to observe the stratigraphy of the reclaimed bed. Aerial photographs of the different stages of the reclamation were also used for analysis.

The survey area was the school grounds, which are located several hundred meters from the former seashore. Holocene deposits were situated at a depth of approximately 3-4 m. Two large open cracks formed in the ground: crack '1' in the NNE-SSW direction and crack '2' in the WNW-ESE direction. Beneath the cracks, we found row of piles from the original ground reclamation work. These rows of piles had been laid underground, and the reclaimed bed consisted of sand and silt. The cracks appeared to be due to the difference in vibrational characteristics between the opposite sides of each crack. Also, the facies of the reclaimed bed were notably different on the opposite sides of each crack. In the cross section of crack '2', the Nd-value∗was very large on the northeast side (Nekozane River side) but relatively smaller on the southwest side. In the cross section of crack '1', the facies of the reclaimed bed from approximately 2 m above to the top of the Holocene deposits were sandy on the western side relatively large Nd-value, but on eastern side mainly formed of silty material recorded almost 0.

Analysis was conducted using aerial photographs and revealed that both cracks '1' and crack '2' were located on the same discontinuity in the reclamation work history, both spatially and temporally. Therefore, the survey area contained three sections of reclaimed land demarcated by the two cracks. Moreover, a fourth section consisted of Holocene deposits. Chronologically, the survey area contained (a) 'Kaimenka-tochi' ∗∗(Urayasu City, 1985), (b) reclaimed land composed of sand and silt dredged from the seabed, and (c) the surrounding embankment. The reclamation process differed between areas (a) and (b). Area (b) was the widest and was typical of reclaimed land. Area (c), in contrast, was not constructed by dredging sand and silt from the seabed. Crack '1' was located between areas (b) and (c), and crack '2' was located between areas (a) and (b).

Therefore, the occurrence of these cracks seems attributable to discontinuities in the reclamation history. This case shows that recognizing the geological and historical processes of both the Holocene deposits and the reclaimed land is an important aspect of disaster prevention.

∗Nd-value is brought by Dynamic Cone Penetration Test, which has the following conditions: a slide hammer with a weight of 5kg falling through a distance of 50cm, and diameter of 2.5cm cone. The number(i.e. Nd-value) of blows needed for the cone to penetrate each 10cm is recorded.

∗∗'Kaimenka-tochi' means land below sea level literally. Before reclamation, it was located in front of seashore, and it was in the possession of the private owner. and was used to reed cultivation etc.

References

KUSUNOKI Keiko, HIGASHI Masashi, HIGUCHI Shigeo, INADA Akira, ITO Akihide, IWAMOTO Hiroshi, KAMIKASEDA Satoshi, KAWASAKI Ken-ichi, and SUENAGA Kazuyuki (2011)Ground Damage on Man-made Land caused by The 2011 off the Pacific coast of Tohoku Earthquake- Wooden Pile Lines indicate artificial land failure-, The 65 th Annual Meeting (Aomori) of the Association for the Geological Collaboration in Japan.

'History of Urayasu City'(1985). Urayasu City, 64-66.

Keywords: liquefaction, crack, dynamic cone penetration test, Urayasu, reclaimed land

Japan Geoscience Union Meeting 2014
(28 April - 02 May 2014 at Pacifico YOKOHAMA, Kanagawa, Japan)

SEM36-01 Room:413 Time:April 30 15:15-15:30

Development of analysis strategy for continuous total geomagnetic field data around Mt. Fuji

ABE, Satoshi[1*] ; MIYAHARA, Basara[1] ; MORISHITA, Hitoshi[1] ; KOBAYASHI, Katsuhiro[1] ; TOYOFUKU, Takashi[1] ; KOYAMA, Takao[2] ; OGAWA, Tsutomu[2]

[1]GSI of Japan, [2]Earthquake Research Institute, The University of Tokyo

Geospatial Information Authority of Japan (GSI) has conducted continuous total geomagnetic field observation at Fuji Yoshida observation station (FUJ), which is located the northeast mountainside of Mt. Fuji, and Fuji-City observation station (FJI), which is located at the southern bottom of Mt. Fuji, since 2000. These stations were established in order to enhance observation infrastructure to monitor low-frequency earthquakes underneath Mt. Fuji which had rapidly increased since October 2000. Additional continuous observation in the northwest mountainside of Mt. Fuji had also been started by utilizing electrical power and communication line of Remote GNSS Monitoring System (REGMOS) at Fuji Oniwa. Furthermore, Earthquake Research Institute, the University of Tokyo has conducted continuous total geomagnetic field observation at Fuji Yoshida (FJ1) and continuous geomagnetic observation at Yatsugatake (YAT). These data are also available and useful to monitor and understand geomagnetic variation around the Mt. Fuji.

Although GSI has been monitoring total geomagnetic field difference between the station at the bottom, FJI, and the stations at the mountainside, FUJ and REGMOS, it is almost impossible to identify variation truly caused by volcanic activities because total geomagnetic field around volcanoes can be fluctuated by both volcanic activities and locally unique geomagnetic variation as well as earth's main magnetic field and external magnetic field variation. Therefore, GSI tries to extract volcano-induced total geomagnetic field variation from the observation data around Mt. Fuji by principal component analysis, and develop monitoring strategy by principal component analysis of total geomagnetic fields around Mt. Fuji.

Keywords: Total geomagnetic filed, Mt.Fuji, principal component analysis

Japan Geoscience Union Meeting 2014
(28 April - 02 May 2014 at Pacifico YOKOHAMA, Kanagawa, Japan)

SEM36-02 Room:413 Time:April 30 15:30-15:45

Classification of tsunami dynamo phenomena in terms of ocean depths

MINAMI, Takuto[1*] ; TOH, Hiroaki[1]

[1]Graduate School of Science, Kyoto University

Conductive seawater moving in the geomagnetic main field drives an electromotive force and induces secondary electromagnetic (EM) fields. This effect is well known as ”oceanic dynamo effect” and has been investigated for many years, especially for low-frequency phenomena such as tides and steady oceanic flows. However, it was recently found that tsunamis are also significant sources of the oceanic dynamo effect. Toh et al. (2011) reported tsunami-induced EM field data observed at the northwest Pacific seafloor EM station (NWP) at the time of the 2006/2007 Krill tsunamigenic earthquakes. Ever since, many events associated with the oceanic dynamo effect by tsunamis, hereafter called ”tsunami dynamo effect”, have been reported (e.g., Manoj et al. 2011; Suetsugu et al., 2012; Ichihara et al., 2013). To explain the tsunami dynamo effect, most of the preceding studies adopted analytical approaches in the frequency domain (e.g., Tyler, 2005). However, it is difficult to understand how EM fields are generated by tsunami propagations, although analytical solutions are very useful and handy.

In order to understand the tsunami dynamo effect more physically, we compared analytical solutions and results of numerical simulations using solitary waves, and revealed that tsunami dynamo phenomena can be classified according to the influence of the diffusion term in the induction equation for the magnetic field. In tsunami dynamo phenomena, the ocean depth has a dominant influence on the diffusion term. When the ocean depth is shallow enough, the diffusion term is large and comparable with the source term, while the self-induction term is small. In this case, the self-induction effect cannot attenuate the magnetic field induced by the coupling of the oceanic flows (v) and the geomagnetic main field (F), namely $\mathbf{v}\times\mathbf{F}$. We can understand this case mostly by the Ampere’s Law. On the other hand, when the ocean depth becomes deeper, the self-induction effect gets larger and reduces the amplitude and causes delay in phase of the magnetic field induced by $\mathbf{v}\times\mathbf{F}$. Especially for the ocean depth deeper than 5000 m, the amplitude is attenuated to approximately 70 percent and the phase is delayed by more than 70 degrees compared with the magnetic field due to $\mathbf{v}\times\mathbf{F}$, which can be understood by analogy with ”Frozen Flux”. As for the case of the tsunami dynamo phenomena reported by Toh et al. (2011) as well as Minami and Toh (2013), we can regard the phenomena as the self-induction dominant case because the ocean depth at the observation site, NWP, is approximately 5600m. This is consistent with the fact that sea level changes observed at the two DART sites in the vicinity of NWP are in phase with that of the vertical component of the magnetic field observed at NWP. In addition, our analysis using analytical solutions revealed that magnitudes of the tsunami-induced magnetic field have maximum peaks around the ocean depth of 2000m, when the tsunami height is fixed to 1m. This is because the self-induction and the diffusion effect, which vary differently according to the ocean depth, balances around that specific depth. These results are important because they enable us to predict how EM fields are induced by tsunamis in a variety of ocean depths, even though the number of observed examples of tsunami dynamo phenomena is limited at present. It is possible that our results are applied to tsunami early warning or mitigation of tsunami hazards in the future.

In the presentation, we will report the methodology of our classification of tsunami dynamo phenomena and discuss how tsunami-induced EM fields vary according to the ocean depth. We will also discuss how the ocean depth influences on the recently found initial rise (Minami and Toh, 2013) in the horizontal magnetic component observed prior to tsunami arrivals.

Keywords: tsunami, dynamo, solitary wave, seafloor observation, finite element method

Japan Geoscience Union Meeting 2014
(28 April - 02 May 2014 at Pacifico YOKOHAMA, Kanagawa, Japan)

SEM36-03 Room:413 Time:April 30 15:45-16:00

Electric conductivity of earth's medium derived from earthquake-excited electromagneic siganals

TSUTSUI, Minoru[1*]

[1]Kyoto Sangyo University

We have been observing electromagnetic (EM) pluses excited by earthquakes, using tri-axial electromagnetic sensors installed in a deep borehole of 100 m in depth. We simultaneously captured waveforms of EM pulses in the borehole and of seismic waves installed near the borehole. We have confirmed that the detected EM waves were co-seismic ones readily generated by piezo-electric effect in earth's crusts [1].

We detected an EM pulse in the borehole when an earthquake of M3.0 occurred at 10 km depth and at 5.4 km north of the EM observation site at 03:57 on Dec. 25, 2013. Figure 1 shows waveforms of (a) east-west component (S_{ew}) of the seismic wave, and of (b) east- west component (H_{ew}) of magnetic field of the EM pulse. The waveform of the S_{ew} wave shows an impulsive amplitude at the arrival of its S-wave, which is because the earthquake hypocenter was close to the EM observation site. On the other hand, the waveform of H_{ew} shows that its amplitude was increasing from about 1 sec prior to the S-wave arrival, and after that it was decreasing.

The amplitude change of H_{ew} can be explained as follows: Since the electronic conductivity of the earth's medium is large, the amplitude of an EM wave shows an exponential decrease as a function of the distance, in which the decay rate is so-called Skin depth. Since the source of EM pulse was propagating with the S-wave velocity, the amplitude of the EM wave measured at the EM observation site is exponentially increasing as time goes on, and after the S-wave arrival it is exponentially decreasing. Therefore we obtained the Skin depth ?for the frequency of 20 Hz and the electronic conductivity as 850 m and 0.0175 S/m, respectively.

[1] M. Tsutsui, submitted to IEEE Geoscience, Letters, 2014.

Keywords: seismic wave, electromagnetic wave, observation in the earth, skin depth, electric conductivity

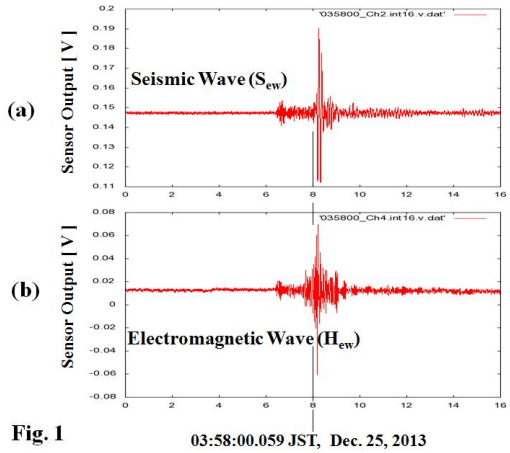

Fig. 1

Japan Geoscience Union Meeting 2014
(28 April - 02 May 2014 at Pacifico YOKOHAMA, Kanagawa, Japan)

SEM36-04 Room:413 Time:April 30 16:15-16:45

Electrical conductivity structures of volcanic areas: a proxy for volcanic gas fluxes

KOMORI, Shogo[1*] ; KAGIYAMA, Tsuneomi[2] ; FAIRELY, Jerry[3]

[1]Institute for Earth Sciences, Academia Sinica (Taiwan), [2]Aso Volcanological Laboratory, Kyoto University, [3]University of Idaho

The efficiency of degassing of volcanic gases in magma is one of the key parameters controlling the explosive potentiality of the eruption and the diversity of the volcanic activity. Therefore, to evaluate the mass flux of volcanic gases is important in considering the constraint conditions of the activity. When volcanic gases are dissolved into the pore water of an aquifer, the aquifer has a high electrical conductivity (E.C.); this is because that the pore water conductivity is increased due to the high-salinity and temperature, and that the surface conductivity of rock matrices is also increased due to hydrothermal alteration. Therefore, the spatial extent of the high E.C. region could be related to the abundance of the mass flux of volcanic gases. We have developed the method to estimate the mass flux of volcanic gases using the E.C. structure of volcanic areas as follows.

[Effect of exposure temperatures on the surface conductivity of rock matrices]

There has already been some quantitative formula about the effect of temperature and salinity on the E.C. of the pore water. On the other hand, it has been known that temperatures are closely related to the generation/stability of smectite, which makes a great contribution to the increase of E.C. However, their effect on the surface conductivity has not been understood quantitatively. We performed the E.C. measurements using drillcore samples obtained from drilling projects, to estimate the surface conductivity. Results showed that the relation between surface conductivities and the temperatures to which the rock matrices have been exposed well corresponds to generation/stable condition of smectite. Thus, the surface conductivity could be represented as relatively simple function of exposure temperatures, and the formula could be incorporated into the modeling of dissipation of volcanic gases (Komori et al., 2010, 2013).

[Simplified model for the dissipation of volcanic gases and its application to Unzen volcanic area]

In Unzen volcanic area, there are various geophysical and geochemical studies to understand the formation process of hot springs associated with magma degassing and the magmatic activity. Ohba et al. (2008) proposed three-stage magma degassing; the first magma degassing occurs at the depths of 4-6 km. Correspondingly, the pressure sources are estimated at the similar depths (Kohno et al., 2008). In addition, the high temperature region greater than 200 ℃ are present above the sources (NEDO, 1988), which corresponds to the high E.C. region inferred from TDEM surveys (Srigutomo et al., 2008).

Based on the above background, we developed the simple model of volcanic gases dissipation into the aquifer at the area, to estimate the mass flux of volcanic gases. The model assumes the isotopic physical properties and the simple geometry of the aquifer. The temperatures and salinity of the pore water are distributed by the simulated flow regime, which is the consequent of the injection of the thermal waters formed by the mixing between volcanic gases and groundwater. Their distributions are converted to the pore water and surface conductivities; which are then converted to the bulk E.C. Results showed that the spatial extent of the high E.C. region is essentially controlled by the volcanic gases flux and rainfall recharge (Komori et al., under review).

[Possibility of effective magma degassing]

The above model was applied to the E.C. structure of the area. The estimated volcanic gas flux was 10^4.8±0.5 t/yr, yielding the CO_2 flux (10^3.1±0.5 t/yr) and the magma input rate (10^0.1±0.5 million t/yr). These values are consistent with other petrology, geochemical and geophysical evidences. Our result suggests that the magma is steadily releasing the volcanic fluids into the aquifer. This effective degassing might lead to the decrease of water content of magma, and be one of the reason of the recent effusive volcanism like dome-forming eruptions (Komori et al., under review).

Keywords: Bulk electrical conductivity, Pore water conductivity, Surface conductivity, Volcanic gas fluxes, Unzen volcanic area

Japan Geoscience Union Meeting 2014
(28 April - 02 May 2014 at Pacifico YOKOHAMA, Kanagawa, Japan)

SEM36-05 Room:413 Time:April 30 16:45-17:00

Audio frequency magnetotelluric imaging and tectonic activity evaluation of the Cimandiri Faullt, West Java, Indonesia

FEBRIANI, Febty[1*] ; YAMAYA, Yusuke[2] ; HATTORI, Katsumi[1] ; WIDARTO, Djedi S.[3] ; HAN, Peng[1] ; YOSHINO, Chie[1] ; NURDIYANTO, Boko[4] ; EFFENDI, Noor[4] ; MAULANA, Iwan[4] ; GAFFAR, Eddy[5]

[1]Chiba University, [2]National Institute of Advanced Industrial Science and Technology, [3]Upstream Technology Center, [4]Indonesian Geophysical, Meteorological, Climatological Agency (BMKG), [5]Research Center for Geotechnology, Indonesian Institute of Sciences (LIPI)

The tectonic activity around the Cimandiri fault zone, Pelabuhan Ratu, West Java, Indonesia, has been analyzed for 30 years (1973-2013). The subsurface electrical resistivity structure close to the Cimandiri fault has been also investigated by twenty five audio-magnetotelluric (AMT) sites. The AMT exploration was carried out during two weeks, from July 27, 2009 to August 8, 2009. The sites were distributed on two lines along about 13 km x 6.5 km profile. There are two profiles of the AMT: (1) the A-A' line of the AMT which is perpendicular to the fault (2) the B-B' line of the AMT which is parallel to the fault. Two-dimensional modelling using the code developed by Ogawa and Uchida 2-D inversion has been applied in the AMT data. The result of tectonic activity analysis shows that the Cimandiri fault is the active fault. The subsurface electrical resistivity structure of the Cimandiri fault zone is characterized by (1) the A-A' and B-B' lines present a conductive zone (1-100 Ωm) from the surface up to the depth of 1 km, which is possibly associated with quarternary volcanics. At the surface, there are also some very conductive spots (1-5 Ωm) which are indicating the existence of the marine sediments in the study area. (2) The gradual conductive-resistive (500-1,000 Ωm) zone at the depth of 1-3.5 km overlays above a low resistivity zone (10-100 Ωm). This low resistivity zone may reflect the combined influences of a fluid network and the presence of the young and less compact sediments with the 500-1,000 Ωm zone as a cap rock that defines the upper boundary of the low resistivity zone (10-100 Ωm). Finally, the result of both methods presents that the Cimandiri fault is the strike-slip fault.

Keywords: audio frequency magnetotelluric, subsurface electrical resistivity structure, 2-D inversion, Cimandiri Fault, Indonesia

Japan Geoscience Union Meeting 2014
(28 April - 02 May 2014 at Pacifico YOKOHAMA, Kanagawa, Japan)

SEM36-06 Room:413 Time:April 30 17:00-17:15

Robust magnetotelluric inversion

MATSUNO, Tetsuo[1*] ; CHAVE, Alan[2] ; JONES, Alan[3] ; MULLER, Mark[3] ; EVANS, Rob[2]

[1]National Institute of Polar Research, [2]Woods Hole Oceanographic Institution, [3]Dublin Institute for Advanced Studies

A robust magnetotelluric (MT) inversion algorithm has been developed on the basis of quantile-quantile (q-q) plotting with confidence band and statistical modelling of inversion residuals for the MT response function (apparent resistivity and phase). Once outliers in the inversion residuals are detected in the q-q plot with the confidence band and the statistical modelling with the Akaike information criterion, they are excluded from the inversion data set and a subsequent inversion is implemented with the culled data set. The exclusion of outliers and the subsequent inversion is repeated until the q-q plot is substantially linear within the confidence band, outliers predicted by the statistical modelling are unchanged from the prior inversion, and the misfit statistic is unchanged at a target level. The robust inversion algorithm was applied to synthetic data generated from a simple 2-D model and observational data from a 2-D transect in southern Africa. Outliers in the synthetic data, which come from extreme values added to the synthetic responses, produced spurious features in inversion models, but were detected by the robust algorithm and excluded to retrieve the true model. An application of the robust inversion algorithm to the field data demonstrates that the method is useful for data clean-up of outliers, which could include model as well as data inconsistency (for example, inability to fit a 2-D model to a 3-D data set), during inversion and for objectively obtaining a robust and optimal model. The present statistical method is available irrespective of the dimensionality of target structures (hence 2-D and 3-D structures) and of isotropy or anisotropy, and can operate as an external process to any inversion algorithm without modifications to the inversion program.

Keywords: Inversion, Probability distribution, Magnetotellurics

Japan Geoscience Union Meeting 2014
(28 April - 02 May 2014 at Pacifico YOKOHAMA, Kanagawa, Japan)

SEM36-07 Room:413 Time:April 30 17:15-17:30

Preliminary report of self-potential observation during a water injection experiment at 1800 m depth in Nojima fault

MURAKAMI, Hideki[1*] ; HIGA, Tetsuya[2] ; SUZUKI, Takeshi[2] ; YOSHIMURA, Ryokei[2] ; GOTO, Tada-nori[3] ; KAWASAKI, Shingo[4] ; OUCHI, Yuhei[5] ; YAMAGUCHI, Satoru[6]

[1]Natural Sciences Cluster-Science Unit,Research and Education Faculty,Kochi University, [2]Graduate School of Science,Kyoto University, [3]Graduate School of Engineering,Kyoto University, [4]Disaster Prevention Research,Kyoto University, [5]Faculty of Science, Osaka City University, [6]Graduate School of Science,Osaka City University

We report self-potential variations during 2013 water injection experiment at 1800 depth in Nojima fault, which is a surface earthquake fault of the 1995 Hyougoken-nanbu earthquake (Mw6.9). The 2013 water injection test started in 15 September and ended in 29 September. Fresh water was injected into the fault system through the open hole part of the borehole (1800m depth). Average injection rate was 20 litter/min and pressure was 5 MPa. Self-potential variations around the 1800m borehole were very smaller than those in the previous water injection experiments (1997, 2000, 2003, 2004, 2006, and 2008) at 540m depth and self-potential variations did not appear clearly to correspond to the operation of the water injection. The previous water injection experiments have been repeated in the same conditions. The observed variations during the experiments have the following features: 1) self-potential variations appeared to correspond to the operation of water injections; 2) the negative voltage appeared around the water injection borehole, and 3) the magnitude of self-potential variations decreased with increasing distance from the borehole. And the self-potential variations in the previous experiments have become larger every experiment. These features suggest that the observed variations were caused by the streaming potential and the permeability around the open hole part of the borehole (540m depth) has decreased. If the line source model to explain the self-potential variations associated with the water injection is correct, the small self-potential variations observed this experiment may suggest that the permeability of the fault fracture zone at 1800m depth is larger than that around the fault at 540m depth.

Keywords: Nojima fault, 1995 Hyogoken-nanbu earthquake, self-potential, water injection experiment, streaming potential

Japan Geoscience Union Meeting 2014
(28 April - 02 May 2014 at Pacifico YOKOHAMA, Kanagawa, Japan)

SEM36-P01 Room:Poster Time:April 30 18:15-19:30

Long-term variation of geomagnetic transfer function in Japan

TAKEDA, Masahiko[1*]

[1]Data Analysis Center for Geomagnetism and Space Magnetism, Kyoto Univ.

Time variation of geomagnetic transfer function in Japan was studied for long period of since 1985. Most of the long-term variation is common at most observatories, and some of then are due to the solar activity. However, different behavior of the variation was found at some observatories, which may be caused by time variation of the local conductivity structure in the earth.

Keywords: geomagnetism, transfer function, long-term variation, induced current, locality

Japan Geoscience Union Meeting 2014
(28 April - 02 May 2014 at Pacifico YOKOHAMA, Kanagawa, Japan)

SEM36-P02 Room:Poster Time:April 30 18:15-19:30

Numerical simulations for the electrical prospecting of the rock samples

SUZUKI, Takeshi[1*] ; YOSHIMURA, Ryokei[2] ; OSHIMAN, Naoto[2]

[1]Graduate School of Science, Kyoto University, [2]Earthquake Hazards Division, Disaster Prevention Research Institute, Kyoto University

For the purposes of oil explorations and surveys of active faults, electrical and electromagnetic methods are powerful tools to reveal the underground properties, since the resistivity images have high sensitivity to the existences of the fluid. Obtained resistivity images are interpreted in relation to the porosity of rock and its connectivity with several mixing lows. In order to verify the applicability of such interpretations, we plan to carry out high-density electrical soundings for hand size rock samples whose other geological characteristics are well known.

As the first step of laboratory experiments, we made numerical simulations to estimate the optimal electrode arrangement and the scale of detectable anomalies. In this presentation, we will report the results of numerical simulations and the future plans of laboratory experiments.

Keywords: rock experiments, electrical conductivity, numerical simulations

Japan Geoscience Union Meeting 2014
(28 April - 02 May 2014 at Pacifico YOKOHAMA, Kanagawa, Japan)

SEM36-P03 Room:Poster Time:April 30 18:15-19:30

Volcano-Loop observation at Kusatsu-Shirane volcano

HINO, Yuta[1] ; OGAWA, Yasuo[2*] ; KANDA, Wataru[2] ; HASE, Hideaki[2] ; SEKI, Kaori[1]

[1]Department of Earth and Planetary Sciences, Tokyo Institute of Technology, [2]Volcanic Fluid Research Center, Tokyo Institute of Technology

We have made successful measurement of time domain electromagnetic signals using transmitting and receiving loops at the same location. This system is being planned to work for monitoring the volcano vent.

The test measurement was conducted in the Kusatsu-Shirane volcano where detailed resistivity structure is known by audio-magnetotelluric method. The stepwise waveform was used and off-time response was measured using a transmitting and receiving loop both with 33m radius. The induced voltage was measured from the 0.1ms to 30ms. The observed voltages as a function of time in logarithm were inverted using Occam's algorithm and the model resistivity and resolution of the model were investigated. We also compared the result with those obtained by magnetotelluric method and found that the upper surface layers which have 1d structure are consistent with volcano loop results. We plant to use the system for repeated measurements or continuous monitoring the volcano in the future.

Keywords: Electromagnetic induction, time domain, loop, volcano, monitoring

Japan Geoscience Union Meeting 2014
(28 April - 02 May 2014 at Pacifico YOKOHAMA, Kanagawa, Japan)

SEM36-P04 Room:Poster Time:April 30 18:15-19:30

Electrical conductivity structure beneath the Gomura Fault (Kyotango, Kyoto)

OUCHI, Yuhei[1*] ; YAMAGUCHI, Satoru[2] ; MISHIMA, Toshiaki[2] ; ODA, Yusuke[2]

[1]Department of Geosciences, Osaka City University, [2]Department of Geosciences, Graduate School of Science, Osaka City University

Fault zone architecture and related permeability structures form primary controls on fluid flow in upper-crustal, brittle fault zone. As the electrical resistivity of rocks is sensitive to distributions of fluids, the magnetotelluric (MT) method can be a powerful tool in investigating the fault zone architecture.

The Yamada Fault is located in Kyoto, Japan. The Yamada Fault zone consists of the main part of the Yamada Fault zone and the Gomura Fault zone. The Gomura Fault zone extends over 34 km and can be grouped into the Gomura Fault, the Chuzenji Fault and so on. The Gomura Fault appeared as a result of 1927 Tango earthquake.

In oreder to delineate subsurface structure of the fault, we made an audio-frequency magnetotelluric survey at 12 stations along the transect (4 km) across the surface trace of the Gomura Fault. The MT response function was obtained at each station, using remote reference processing. After dimensionality analysis by Phase Tensor method (Caldwell et al., 2004; Bibby et al., 2005), two-dimensional inversions for TE and TM modes were carried out, using the code of Ogawa and Uchida (1996).

The model is characterized by two resistive zones and four conductive zones. The most significant conductive zone is recognized beneath the surface trace of Gomura Fault with a width of more than 650 m and located in a depth range of 0.45-1 km. It is noteworthy that the conductive zone beneath the Gomura Fault is comparable in width to the damage zone determined by geological survey.

Keywords: The Gomura Fault, electrical resistivity structure, Magnetotelluric(MT), Damage zone

Japan Geoscience Union Meeting 2014
(28 April - 02 May 2014 at Pacifico YOKOHAMA, Kanagawa, Japan)

SEM36-P05 Room:Poster Time:April 30 18:15-19:30

A Summary report on the investigations of an electrical resitivity structure beneath Chugoku and Shikoku regions, south

SHIOZAKI, Ichiro[1*] ; UTO, Tomofumi[1] ; YOSHIMURA, Ryokei[2] ; OSHIMAN, Naoto[2] ; KUBO, Atsuki[3] ; MURAKAMI, Hideki[4]

[1]Graduate School of Engineering, Tottori University, [2]Disaster Prevention Research Institute, Kyoto University, [3]Kochi Earthquake Observatory, Faculty of Science, Kochi University, [4]Department of Applied Science,Faculty of Science,Kochi University

The purpose of this study is to estimate crossing and longitudinal electrical resistivity structure sections in the southwest Japan arc in order to clarify the relation between the deep crustal low resistivity region and seismic activities. Therefore, based on the investigation research of the electrical resistivity structures in Japan arc and the southwest Japan arc, in Sanin region, it is important to clarify the relation between earthquake occurrences out of the strain concentration zone, volcanoes not having eruption records for a long time and crustal fluid, and to find the structural heterogeneity in the inland earthquake occurrence area, the inland seismic gap (beneath the third class and quaternary volcano) and deep low frequency earthquakes. In Shikoku region, it is also important to find the relation between the occurrence pattern and structural locality of crustal earthquakes and deep low frequency earthquakes and the fluid supposed to be supplied from ocean plate subduction.

Our research group has shown that there is a clear relationship between resistivity and seismicity in the Sanin and Shikoku regions. We investigated deep crustal resistivity structures in the measurement lines that traverse a linear seismic activity area along with the coastal part of Japan Sea. As the result, in the eastern part of San-in region, it was found that a conductive area exists in the deep crust part under the seismic region, which is a resistive area, along with the seismic activity area stretching nearly in the east and west direction

However, Ozaki et al.(2011) showed that the crust has generally a high resistivity in the earthquake occurrence region in the middle-west part of Tottori pref. (2002, Mj5.3). This observation fact conflicts with the model advocated by the group including the author that has studied electrical resistivity in Sanin region. That is, there is a possibility that the deep low resistivity area beneath the Sanin region does not exist in series. Assuming that inland earthquakes occur because of local stress concentration caused by heterogeneity beneath a seismic activity band (Iio, 2009), the heterogeneity should be clarified by a spatial and structure analysis, and a more detailed surfacial structure data should be completed hereafter.

On the other hand, in the Shikoku region, the same investigation was carried out mainly in the outer zone, the south side of MTL and the result suggested that a remarkable conductive area should exist in the upper crust of the outer zone, and that the conductive area in the central and western part should have a clear relation with the non-seismic area.

These studies suggest that high conductivity(low resitivity) is possibly caused by the existence of deep crustal fluids, which probably play an important role in the inland earthquake occurrence mechanism of these regions. As one of the possible interpretations of water supply system, it is thought that the fluids in the deep crust are supplied from the subducting Philippine Sea plate by means of the dehydration processes. However, the existence of the plate is not thoroughly identified in the geological inner zone of the southwestern Japan Arc. Therefore, in order to grasp a whole tectonic setting, from the fore to the back arc side in the southwestern Arc, quantitative discussions based on the wideband MT survey covering whole these regions should be required. Consequently, for making the island arc crossing structure section in the southwest Japan arc, an additional structure investigation in the unmeasured area, the area of Setouchi as the main area is required to clear the northern edge of Philippine Sea plate.

In this presentation, the summary report on joint structure analysis result in Chugoku and Shikoku regions and key features of spatial resistivity distributions in these regions, using the recent data acquired in the Seouchi area incorporated in the existing data, will be shown.

Keywords: electrical resistivity, Chugoku and Shikoku regions, heterogeniety

Japan Geoscience Union Meeting 2014
(28 April - 02 May 2014 at Pacifico YOKOHAMA, Kanagawa, Japan)

SEM36-P06 Room:Poster Time:April 30 18:15-19:30

Electrical resistivity features of the back-arc areas in the NE Japan subduction zone

ICHIHARA, Hiroshi[1*] ; TADA, Noriko[1] ; BABA, Kiyoshi[2] ; KASAYA, Takafumi[1] ; ICHIKI, Masahiro[3] ; KAIDA, Toshiki[3] ; OGAWA, Yasuo[4]

[1]JAMSTEC, [2]ERI, University of Tokyo, [3]Tohoku University, [4]Tokyo Institute of Technology

Electrical resistivity in the crust and upper mantle depends on the pore-fluid distribution, salinity, and connectivity of fluid-filled rock pores. Thus imaging of resistivity distribution based on magnetotelluric surveys gives us fundamental information about fluid distribution of subduction zones. Marine magnetotelluric survey is important to understand dynamics of the NE Japan subduction zone because dehydration of subducting Pacific plate occurs under the Japan Sea. In this study, we discuss resistivity distribution around back-arc areas in the NE Japan subduction zone based on the marine MT data.

We collected natural EM signals with ocean bottom electro-magnetometers (OBEMs) in the eastern Japan sea area between April and August 2013 by MR13-02A and NT13-18 JAMSTEC scientific cruises. In addition, 3 land MT stations were settled in islands in the Japan Sea (Tobishima, Awashima and Sado islands) between April and October 2013. These recorded time-series data were converted to a frequency-domain impedance tensor based on the BIRRP program [1]. The remote reference technique [2] was applied in the data processing using horizontal magnetic field data from Kakioka Station in the period range between 10 and 20000 seconds. As results, high-quality MT responses and geomagnetic tippers in both the trench and back-arc areas.

We calculated phase tensors [3] based on MT impedances by this and previous studies [4] to discuss re-sistivity distribution beneath the back-arc area. The phase tensor ellipse indicates high Φ_{max} ($>$65 degrees) and Φ_{min} ($>$50 degrees) in the long periods ($>$8000 seconds). Large β of phase tensor and large amplitude of geomagnetic transfer function are also shown. These features cannot be explained with bathymetry and sediment effects based on the 3-D forward modeling [5]. Thus strong three-dimensionality and deep conductor possibly distributed beneath the Japan sea. In order to discuss detailed resistivity structure, 3-D inversion approaches are required by using a newly developed 3-D MT inversion code for marine data to treat complicated ocean bottom and land topography [6].

References: [1] Chave, A. D. and D. J. Thomson, Geophys. J. Int. 157, 988-1006 (2004); [2] Gamble, T. D. et al., Geophysics, 44, 53-68 (1979); [3] Caldwell, T. G et al., Geophys. J. Int 158, 457-469 (2004); [4] Toh, H. et al., Ge-ophys Res Lett, 33, L22309 (2006); [5] Baba, N. et al., Geophys. J. Int 158, 392-402 (2002); [6] Tada, N. et al., Earth Planets Space, 64, 10051021 (2012).

Keywords: back arc, NE Japan subduction zone, magnetotelluric, OBEM, phase tensor

Japan Geoscience Union Meeting 2014
(28 April - 02 May 2014 at Pacifico YOKOHAMA, Kanagawa, Japan)

SEM36-P07 Room:Poster Time:April 30 18:15-19:30

Conductivity structure beneath the fault segment gap in the Yamasaki fault zone, southwest Japan (2)

ODA, Yusuke[1*] ; YAMAGUCHI, Satoru[1] ; MURAKAMI, Hideki[2] ; KATOH, Shigehiro[3] ; UYESHIMA, Makoto[4] ; MISHIMA, Toshiaki[1] ; OUCHI, Yuhei[5]

[1]Department of Geosciences, Graduate school of Science, Osaka City Univ., [2]Natural Sciences Cluster-Science Unit, Kochi Univ., [3]Division of Natural History, Hyogo Museum of Nature and Human Activities, [4]Earthquake Research Institute, The University of Tokyo, [5]Faculty of Science,Osaka City Universe

Abstract

The Yamasaki fault zone (YFZ) of southwest Japan is a typical strike-slip fault system consisting of the Nagisen fault, the main strand of YFZ, and the Kusadani fault. The main strand of YFZ extends for over 79km and is divided into northwestern (NW) and southeastern (SE) groups based on their latest seismic activity. The NW group consists of the Ohara, Hijima, Yasutomi and Kuresaka-touge faults, and the SE group consists of the Biwako and Miki faults. The maximum magnitudes of the earthquakes generated by the NW and SE groups are estimated to be 7.7 and 7.3, respectively. Simultaneous activation of both fault groups is also pointed out to be as large as M = ˜8.0 (The Headquarters for Earthquake Research Promotion, 2013).

The subsurface structure beneath the fault segment gap between both groups will be the key information for assessing the possibility of such large earthquake.

To infer the structure, we carried out Audio-frequency Magnetotelluric (AMT) survey at 11 sites along a transect between the NW group and the SE group and showed the two-dimensional resistivity model along the transect based on MT impedances. This model is characterized by three conductive zones. They locate beneath the points where the transect crosses the extension lines of the surface trace of the Yasutomi, Kuresaka-touge, and Biwako fault. We thus concluded that the Yasutomi and Kuresaka-touge faults are extended to southeast and the Biwako fault is extended to northwest further than the recognized terminals of their surface trace.

In this presentation, we show the improved resistivity model which is determined by not only MT impedance but tipper vectors.

Keywords: conductivity structure, active fault, Yamasaki fault system, Magnetotellurics

Japan Geoscience Union Meeting 2014
(28 April - 02 May 2014 at Pacifico YOKOHAMA, Kanagawa, Japan)

SEM36-P08 Room:Poster Time:April 30 18:15-19:30

Electrical Resistivity Imaging at Western Turkey by Wideband Magnetotelluric Method

TUNCER, Mustafa kemal[1*] ; CENGIZ, Ozlem[2] ; TANK, Bulent[3] ; TOLAK-CIFTCI, Elif[4] ; KAYA, Tulay[5] ; OGAWA, Yasuo[6] ; HONKURA, Yoshimori[7] ; MATSUSHIMA, Masaki[8] ; OSHIMAN, Naoto[9] ; CELIK, Cengiz[10]

[1]Istanbul University-Turkey, [2]Bogazici University-Turkey, [3]Bogazici University-Turkey, [4]Bogazici University-Turkey, [5]Tokyo Institute of Technology, Japan, [6]Tokyo Institute of Technology-Japan, [7]Tokyo Institute of Technology-Japan, [8]Tokyo Institute of Technology-Japan, [9]Kyoto University-Japan, [10]Bogazici University-Turkey

The westward migration of large magnitude earthquakes along the North Anatolian Fault Zone indicates that a major event may take place at and around the Marmara region, following the Izmit (Mw7.4) and Duzce (Mw7.2) earthquakes that took place in 1999 in northwest Turkey. For this reason many studies were conducted around Marmara sea, west of these events. These studies focused mostly on the northern part of this area because of the high damage risk near Istanbul, but the similar potential is also present for the southern Marmara. In order to investigate the upper crustal electrical resistivity structure at this location, wide-band magnetotelluric data were collected at sixteen sites forming two parallel profiles. These profiles were constructed to cross the southern branches the North Anatolian Fault. Following the application of Groom and Bailey decomposition that has been applied to remove the surplus features and to deduce the appropriate geo-electric strike direction which is an important requirement for two-dimensional interpretation, an inversion algorithm developed by Ogawa and Uchida (1996) was utilized to develop electrical resistivity models. These models pointed out a relatively complicated shallow (surface-to-5 km) structure which may be associated with the presence of crustal fluids, but below these depths the electrical resistivity is more uniform with only a deep conductor appearing beneath the northern ends of the two profiles. The known faults in the survey area correlate well with the features characterized in the final geo-electric models. A resistive-conductive boundary between Manyas - Karacabey basin and Bandirma-Karadag uplift on the western and Uluabat uplift and Mudanya uplift on the eastern profiles may be associated with the South Marmara Fault.

Keywords: North Anatolian Fault, Fluids, Electrical resistivitiy, Magnetotellurics, geo-electric models

Japan Geoscience Union Meeting 2014
(28 April - 02 May 2014 at Pacifico YOKOHAMA, Kanagawa, Japan)

SEM36-P09 Room:Poster Time:April 30 18:15-19:30

Installation of a Vector Magnetometer for a Ground-based Tsunami Early Warning

KAWASHIMA, Issei[1*] ; TOH, Hiroaki[2] ; YOSHIMURA, Ryokei[3] ; FUJII, Ikuko[4] ; OOGI, Junpei[4] ; ABE, Satoshi[5]

[1]Graduate School of Science, Kyoto University, [2]Data Analysis Center for Geomagnetism and Space Magnetism, Graduate School of Science, Kyoto Univers, [3]Earthquake Hazards Division, Disaster Prevention Research Institute, Kyoto University, [4]Kakioka Magnetic Observatory, Japan Meteorological Agency, [5]GeoSpatial Information Authority of Japan

Conductive sea water moving in the geomagnetic main field generates electromagnetic variations by a physical process called the oceanic dynamo effect. This effect at the time of tsunami passages was recently detected on the seafloor in the northwest Pacific (Toh et al., 2011) and on Easter Island (Manoj et al., 2011). The tsunami-induced electromagnetic field is expected to contribute to existing global tsunami warning systems.

We are carrying out a project that aims to observe geomagnetic variations associated with tsunami passages by ground-based real-time observations. This project requires a pair of geomagnetic observation sites for clear detection of tsunami events. The geomagnetic coast effect and the external field due to ionospheric and/or magnetospheric disturbances can be removed by taking real-time differences between a coastal and an inland geomagnetic sites. We installed a vector magnetometer at Umaji located in the middle of Muroto Peninsula, where artificial electromagnetic noises are very small. This location is selected as a counterpart of the existing observation site at Muroto located at the tip of the peninsula, which is operated by Geospatial Information Authority of Japan (GSI).

In this presentation, we will make a progress report on our ground-based tsunami warning system consisting of a pair of vector magnetometers. This system is intended to detect the geomagnetic field variations induced by tsunamis at the time of Nankai/Tonankai earthquakes.

Keywords: Geomagnetism, Tsunami

Japan Geoscience Union Meeting 2014
(28 April - 02 May 2014 at Pacifico YOKOHAMA, Kanagawa, Japan)

SEM36-P10 Room:Poster Time:April 30 18:15-19:30

The several Records of tsunami induced magnetic field obtained by the JMA Chichijima observation station(CBI).

TATEHATA, Hidee[1*] ; HAMANO, Yozo[2]

[1]JMA, [2]JAMSTEC

Through the geomagnetic field, electrically conducting seawater movement generates electric fields and currents in generally. Furthermore, the current induces secondary magnetic fields. Our Chichijima geomagnetic observation station (CBI) is located on the solitary island in the Pacific Ocean. Addition this, located the tsunami observation station (Futami tide gauge) that is subject to the JMA. We are able to obtain concurrent tsunami and magnetic data because the distance between these observation points is only 1 km. So, this Chichijima Island is suitable in order to research tsunami induced magnetic fields research. We have investigated in CBI data (samples taken every 1 second) and Chichijima Futami tide gauge data (every 15 seconds) from 1995 to 2013, finally obtained 9events tsunami induced phenomena. The many of the signal of these events is small, but three of them has clear record, the 2011 off the Pacific coast of Tohoku Earthquake Tsunami (2001/3/11 M9.0), The 2010 Chile earthquake (2010/2/27 M8.8) and 1996 the Irian Jaya Earthquake Tsunami (1996/2/17 M8.1). The other events are week, but their magnetic signals are detectable enough. it may be worth worldwide renown that so many induced magnetic phenomena have been fund in one observation station Chichijima (CBI). In the low solar activity periods, the induced magnetic signal may be detectable, if the half tsunami amplitude is 20cm or over. Some of these events might have been disturbed and dismissed due to magnetosphere substorm, even though the induced magnetic field was enough to detect. Each of above-mentioned three examples has over 1 m tsunami height, and clear induced magnetic record. Especially, in spite of weak magnetosphere substorm, the record of the 2011 off the Pacific coast of Tohoku Earthquake Tsunami is very clear. So, on 1 m or more-high tsunamis, it is safely said that the induced magnetic fields is detectable definitely. These induced magnetic field records will be one of mediation between the geomagnetic science and the tsunami disaster prevention science.

Keywords: tsunami, Induced magnetic effects, chichijima

Japan Geoscience Union Meeting 2014
(28 April - 02 May 2014 at Pacifico YOKOHAMA, Kanagawa, Japan)

SEM36-P11 Room:Poster Time:April 30 18:15-19:30

Geomagnetic total intensity variations associated with vertical crustal movement in the eastern part of Izu Peninsula

SASAOKA, Masahiro[1*] ; OGAWA, Tsutomu[2]

[1]Kakioka Magnetic Observatory, Japan Meteorological Agency, [2]Earthquake Research Institute, University of Tokyo

In order to detect geomagnetic changes associated with the earthquake swarm and anomalous crustal activities, continuous observations of the geomagnetic total intensity have been conducted in the eastern part of Izu Peninsula. The continuous data of the geomagnetic total intensity were utilized after an analysis of removing the effect of external magnetic field from those data during 2010 - 2012. An association between the geomagnetic field variation and the vertical crustal movement was examined comparing the day-to-day variation of the geomagnetic total intensity with that of the geodetic height measured by GPS (Global Positioning System). It is found that the day-to-day variation in the geomagnetic total intensity shows each seasonal change on the quiet seismic period during 2010 and on the relatively active seismic period during 2011 and shows no significant change on the quiet seismic period during 2012, though the day-to-day variation in the vertical crustal movement shows seasonal changes during 2010 - 2012. It is inferred that the hydrothermal activity related to the Dec. 2009 earthquake swarm caused by magma injection had been lasting up to less than two years and the hydrothermal movement associated with the vertical crustal movement had caused the seasonal changes in the geomagnetic total intensity during 2010 - 2011. This suggests the observed variations of the geomagnetic total intensity were not directly associated with seismic faulting. The continuous observation of the geomagnetic total intensity is expected to have a monitoring advantage in predicting the course of the earthquake swarm activity in the eastern part of Izu Peninsula.

Keywords: eastern part of Izu Peninsula, geomagnetic total intensity, crustal movement, hydrothermal activity

Japan Geoscience Union Meeting 2014
(28 April - 02 May 2014 at Pacifico YOKOHAMA, Kanagawa, Japan)

SEM36-P12 Room:Poster Time:April 30 18:15-19:30

Validity of using space approximation in calculating EM variations generated by the piezomagnetic effect

YAMAZAKI, Ken'ichi[1*]

[1]Kyoto University

Variations in the magnetic field generated by the piezomagnetic effect, which is referred to as the piezomagnetic field, has been discussed in a framework of magneto-statics, in which temporal variations are totally ignored. This treatment is valid for quasi-static processes, but possibly invalid for dynamic processes including fault ruptures. The earlier works by the author has demonstrated that, when the temporal variations in the EM field is considered, finite conductivity of the Earth's crust alters the feature of the piezomagnetic field. However, consideration of the temporal variations in the EM field makes estimation of the piezomagnetic field complicated, even in a simple two-layered model which consists of the Earth's ground with finite conductivity and the air as a perfect resister.

The problem will be largely simplified if the situation is approximated by a finite space model with a uniform electrical conductivity.

In the present work, variations in the EM field generated by the piezomagnetic effect are compared for two situations: finite space and semi-finite space models with finite conductivity, assuming the source of the piezomagnetic field is two-dimensional. It is demonstrated that, for some situations, the simpler model provides a good approximation of the expected piezomagnetic field.

Keywords: piezomagnetic effect, electromagnetic field, electrical conductivity, infinite space, semi-infinite space

Japan Geoscience Union Meeting 2014
(28 April - 02 May 2014 at Pacifico YOKOHAMA, Kanagawa, Japan)

SEM37-01 Room:413 Time:April 30 09:00-09:15

Testing paleointensity determination using Wilson method

FUKUMA, Koji[1*] ; SHCHERBAKOV, V. P.[2] ; SHCHERBAKOVA, V. V.[2]

[1]Dept. Env. Sys. Sci., Doshisha Univ., [2]Borok Geophysical Observatory, Russian Academy of Sciences

The classical Thellier method still remains most reliable for paleointensity determination, but requires a quite demanding and rarely satisfied condition; a natural remanent magnetization (NRM) must be completely replaced by a laboratory thermoremanence (TRM) at every temperature interval. If a significant amount of multidomain grains is present, this condition is not satisfied and resulting in erroneous paleointensities as obtained from curvatures seen on the Arai diagrams.

A single-step heating method, which sounds quite primitive as adopted in early times (e.g., Folgheraiter [1899]) but is essentially still alive as in the Shaw method, escapes from the strict condition posed on the Thellier method. The Wilson method, being a sort of single-step heating methods, was developed a half century ago (Wilson, 1961 & 1962); comparison of high-temperature continuous thermal demagnetization curves, measured for a natural remanent magnetization (NRM) and then a thermal remanent magnetization (TRM) acquired in a known laboratory field, yield a paleointensity. The reason why the Wilson method was rarely used for paleointensity studies is that magnetization needs to be measured at elevated temperature. Yet this method has a great advantage of being extremely quicker than the other paleointensity methods. If using a modern automated high-temperature magnetometer, we can complete a Wilson measurement within one hour for a 1-cc cube.

We performed testing paleointensity measurements based on the Wilson method for 27 1-cc cubes of basalts and scorias of the 1983 eruption in Miyakejima (the expected field of 45.1 microT). A 1-cc cube was heated in air at the rate of ˜40 deg.C per minute along with measuring three-component NRM at elevated temperature using a Orion three-component vibrating sample magnetometer at the Borok Geophysical Observatory. When the magnetization is decreased less than 1 percent of the initial value, heating was stopped and then total TRM was imparted during cooling down in the magnetic field of 45 microT. The total TRM was also continuously demagnetized in the same way as NRM.

We did find nicely straight lines on the NRM-TRM diagrams for 85% of measured samples, indicating that the shapes of unblocking temperature spectrum are essentially unchanged for NRM and TRM. We obtained the expected field intensity of 45.1 microT for the about half of the samples. The Thellier method for the sister samples also gave the expected field, but some of the samples did not. For the another half, the gradients of NRM-TRM lines significantly deviated from unity to higher or lower values. This means that thermal alteration (NOT including domain alteration) increased or decreased TRM capacity but did not appreciably changed unblocking temperature spectrum. Such a kind of alteration is not detected on NRM-TRM diagrams, therefore it is possible to give erroneous paleointensities.

Although the Wilson method is quick and robust even for samples containing multidomain grains, we need to take caution that thermal alteration is not necessarily detected from the linearity on NRM-TRM diagrams. This caution should be exercised for other kinds of single-step heating methods.

Keywords: paleointensity, Wilson method, Thellier method, high-temperature magnetometer

Japan Geoscience Union Meeting 2014
(28 April - 02 May 2014 at Pacifico YOKOHAMA, Kanagawa, Japan)

SEM37-02 Room:413 Time:April 30 09:15-09:30

Microscopic observation of titanomagnetite grains during paleointensity experiments of volcanic rocks

TANAKA, Hidefumi[1] ; YAMAMOTO, Yuhji[2*]

[1]Faculty of Education, Kochi University, [2]Center for Advanced Marine Core Research, Kochi University

Titanomagnetite (Tmt) grains, some partially maghemitized, of various oxidation levels were microscopically observed under reflected light as a function of temperature step in a Kǒnigsberger Thellier Thellier experiment in air. The reflected light microscopy indicated that the brownish colour of homogeneous Tmt turned blue at ∼300 ℃. This false blue colour was caused by submicron scale rugged stripes on the surface, according to scanning electron microscope observations, which was made after the final heating step. The typical grey-to-bluish colour of maghemitized parts of Tmt grains turned to a brownish colour at ∼300 ℃, indicating inversion of titanomaghemite to a mixture of magnetite and ilmenite (Ilm) or haematite (Hem). Although these observations were from Tmt grains on the sample surface, oxidation must have proceeded similarly within samples because the surface changes in the Tmt grains were highly correlated with behaviour of data points on Arai plots. Alterations in Tmt after heating at 610 ℃ in air for increasing times from 10 to 500 min were evaluated by reflected light microscopy and scanning electron microscopy at the end of the experiment. Mottled patches gradually emerged in the Tmt grains during subsequent heatings. However, the formation of new Ilm lamellae was not observed, even after the final 500 min heating. In conclusion, the alteration of Tmt during laboratory heating in air at ∼600 ℃ is likely not due to the typical high-temperature oxidation that forms trellis-type Ilm lamellae. Below ∼400 ℃, the process should be closer to low-temperature oxidation. On the other hand, maghemitized parts of Tmt grains invert instantaneously at 300 ℃, and a trellis-type structure with Hem lamellae soon emerges when heated at 610 ℃.

Japan Geoscience Union Meeting 2014
(28 April - 02 May 2014 at Pacifico YOKOHAMA, Kanagawa, Japan)

SEM37-03 Room:413 Time:April 30 09:30-09:45

Archeointensity trend between 8th and 11th century in Okayama

KITAHARA, Yu[1*] ; YAMAMOTO, Yuhji[2] ; HATAKEYAMA, Tadahiro[3] ; TORII, Masayuki[4] ; KAMEDA, Shuichi[5]

[1]Graduate School of Integrated Arts and Sciences, Kochi University, [2]Center for Advanced Marine Core Research, Kochi University, [3]Information Processing Center, Okayama University of Science, [4]Faculty of Informatics, Okayama University of Science, [5]Faculty of Biosphere-Geosphere Science, Okayama University of Science

This study presents three new archeointensity estimated from Sayama-area (Bizen city, Okayama prefecture), for the period of 8th to 11th century. The baked-earth samples (archaeological artifacts) we used in this study were collected from old kilns (part of floor and wall) of Sue wares. These kilns were found during the course of five excavations which were conducted under an archaeological project (see Archaeological lab, Okayama University of Science, 2012; 2013) aiming to trace development-history of ceramics production activity in Sayama-area between Nara and Heian-era. If we adopt the archeological chronology based on the Sue-mura type (e.g. Nakamura, 2006), the Sayama-Shin-ike kiln and the Sayama-Higashiyama kiln were estimated to be under operation during last half of 8th century (? 775±25 year), and the Sayama-Higashiyama-Oku kiln to be at around 10 century (? 900±50 year) (See Archaeological lab, Okayama University of Science, 2012; 2013).

Various rock magnetic and stepwise thermal demagnetization experiments revealed that (1) the samples are generally resistant to laboratory heating, (2) shape anisotropy is small, and (3) main magnetic carriers are Ti-poor titanomagnetite with high blocking temperature. Archeointensity measurements were done by using the IZZI Thellier method (double heating method; Yu & Tauxe, 2005). We applied this method to 19 specimens from 15 samples of the Shin-ike kiln, 10 specimens from 10 samples of the Higashiyama kiln, and 19 specimens from 9 samples of the Higashiyama-Oku kiln. After applying a set of very strict criteria, averaged archeointensity (with one standard deviation) is obtained as follows: 61.6±4.4 μT for the Shin-ike kiln (N=4), 51.8±6.5 μT for the Higashiyama kiln (N=8), and 49.8±9.8 μT for the Higashiyama-Oku kiln (N=9). These values are not contradicted from the ones obtained by the Tsunakawa-Shaw method (Tsunakawa and Shaw, 1994; Yamamoto et al., 2003) though they are preliminary. Our new data show general agreement with the most recent archeointensity compilation in Japan (Yoshihara et al., 2003) and confirm the rapid intensity decrease at ˜600 AD on average.

Keywords: Archeointensity, IZZI-Thellier method, Tsunakawa-Shaw method, Old kilns of Sue wares

Japan Geoscience Union Meeting 2014
(28 April - 02 May 2014 at Pacifico YOKOHAMA, Kanagawa, Japan)

SEM37-04 Room:413 Time:April 30 09:45-10:00

Absolute paleointensity determinations of welded tuffs: Correlations between relative and absolute paleointensity data

FUJII, Satomu[1] ; MOCHIZUKI, Nobutatsu[2*] ; HASEGAWA, Takeshi[3] ; OKADA, Makoto[3] ; SHIBUYA, Hidetoshi[1]

[1]Department of Earth and Environmental Science, Kumamoto University, [2]Priority Organization for Innovation and Excellence, Kumamoto University, [3]Department of Earth Science, Faculty of Science, Ibaraki University

Absolute geomagnetic paleointensities (APIs) have been estimated from igneous rocks, while relative paleomagnetic intensities (RPIs) have been reported from sediment cores. These two datasets have been treated separately, as correlations between APIs and RPIs are difficult on account of age uncertainties. We present a procedure for directly correlating APIs with RPIs of a RPI stack. Correlations between APIs and RPIs were conducted with virtually no associated age errors using both tephrochronologic correlations and RPI minima. Using the stratigraphic positions of tephra layers in oxygen isotope stratigraphic records, we directly compared the RPIs and APIs reported from welded tuffs contemporaneously extruded with the tephra layers. In addition, RPI minima during geomagnetic reversals and excursions were compared with APIs corresponding to the reversals and excursions. The comparison of APIs and RPIs at these exact points allowed a reliable calibration of the RPI values. In this study, we applied the Tsunakawa-Shaw method to 21 welded tuffs to increase API dataset. We obtained mean paleointensities for 16 of the 21 welded tuffs. Since eight of the 16 welded tuff units were correlated with the oxygen isotope stratigraphy, they can be added to the API data used in the correlation procedure. Combining these API data with the reported data, we correlated API data with RPIs from the PISO-1500 stack and SINT-800 stack. For 13 correlation points, RPIs of the PISO-1500 stack showed a linear relationship with virtual axial dipole moments (VADMs) calculated from the APIs, indicating that the PISO-1500 stack has a linear relation to the axial dipole moment. On the other hand, PRIs from the SINT-800 stack has a tread with VADMs and the correlation coefficient is lower than that of the PISO-1500 stack. The correlation procedure with increased API data can contribute to constraining the relation between RPI of a RPI stack and API and calibrating a RPI stack to absolute values.

Keywords: absolute paleointensity, relative paleointensity, tephra, oxygen isotope stratigraphy, welded tuff

Japan Geoscience Union Meeting 2014
(28 April - 02 May 2014 at Pacifico YOKOHAMA, Kanagawa, Japan)

SEM37-05 Room:413 Time:April 30 10:00-10:15

Rock magnetic study of the North Atlantic sediment during late Pliocene and early Pleistocene

SATO, Masahiko[1*] ; OHNO, Masao[1] ; HAYASHI, Tatsuya[2] ; KUWAHARA, Yoshihiro[1] ; MIYAGAWA, Chizuru[1] ; FUJITA, Shu[1] ; KITA, Itsuro[1]

[1]Kyushu University, [2]Mifune Dinosaur Museum

As the ocean is a major component in the climatic system, it is crucial for palaeoclimatic study to understand the past evolution of the thermohaline circulation. The North Atlantic Ocean is one of the most important sea areas because newly formed deep water mass is redistributed to the global ocean from there (Broecker et al., 1991). In order to recover the past change in deep ocean circulation at the North Atlantic Ocean, a variety of proxies have been studied. However, the change during Pleistocene and Pliocene is still poorly understood.

In this study we conducted rock magnetic measurement of deep-sea sediments recovered from IODP Site U1314 on the Gardar Drift, to investigate the past change in bottom current flows at the North Atlantic Ocean. Since a coercivity of magnetic mineral varies sensitively with its state such as chemical composition, grain size, grain shape, stress, and so on, coercivity spectra can be used as a proxy for the constituent spectra of the sediment.

The samples were collected at 16 - 50 cm resolution from 199.3 to 262.5 mcd of the core, which corresponds to the age between 2.22 and 2.75 Ma according to the age model by Hayashi et al. (2010). Rock magnetic properties were measured for these samples using a MicroMag 2900 Alternating Gradient Magnetometer. The isothermal remanent magnetization (IRM) acquisition curve was obtained by the application of stepwise-increasing uniaxial fields to the sample at 30 steps from 1 mT to 1 T. The ratio of IRM acquired in a back-field of 0.1 T to that in a forward-field of 1 T (S-ratio) was also measured for all samples.

In order to reveal constituents of the sediment, decomposition of coercivity spectra were conducted. The IRM acquisition curve was normalized by the IRM intensity at 1 T and then the first derivative of the curve was calculated with respect to log10 field (hereafter referred to as IRM gradient curve). The least square fit was performed so as to decompose the IRM gradient curve into linear combination of two end-members. Two end-member components were calculated by averaging the IRM gradient curves of selected samples. Samples with low S-ratio ($<$0.57) and younger than 2.4 Ma were chosen for component 1. Samples with high S-ratio ($>$0.88) and during MIS100, which were associated with the ice rafted debris, were chosen for component 2. These components were distinctly different from each other; coercivity distribution of component 1 was magnetically harder than that of component 2.

In consequence of the decomposition, the fitting error was significantly small for all samples, indicating that North Atlantic sediments in the Garder Drift during late Pliocene and early Pleistocene are explained by mixing of two end-member components. The fraction of two components periodically changes with time and agrees well with the LR04 $\delta^{18}O_{benthic}$ stack (Lisiecki and Raymo, 2005): the high-coercivity component dominated during interglacial periods, and the low-coercivity component dominated during glacial periods.

On the basis of the elemental ratio of potassium to titanium (K/Ti), Grutzner and Higgins (2010) reported change in proportion of sources of sediment at Site U1314 during the last 1.1 Ma. They demonstrated that Ti-rich basaltic material transported by the Iceland-Scotland Overflow Water and K-rich particle (continental rock like) derived from the other source dominated during interglacial periods and glacial periods, respectively. Our result is consistent with their result because high-coercivity and low-coercivity components are interpreted as the fine-grain titanomagnetite of Icelandic sources and the coarse-grain magnetic mineral of continental sources, respectively. Therefore the change in fraction of two end-member components represents change in fraction of bottom currents, and the bottom current flow patterns similar to those during the last 1.1 Ma might prevail at the North Atlantic Ocean during late Pliocene and early Pleistocene.

Keywords: North Atlantic Ocean, Deep-sea Sediment, IRM acquisition curve, Bottom current flow

Japan Geoscience Union Meeting 2014
(28 April - 02 May 2014 at Pacifico YOKOHAMA, Kanagawa, Japan)

SEM37-06 Room:413 Time:April 30 10:15-10:30

Magnetic properties of REY rich red clay near Minami-Torishima in the Pacific Ocea

YAMAZAKI, Toshitsugu[1*] ; USUI, Yoichi[2] ; SHIMONO, Takaya[3]

[1]AORI, University of Tokyo, [2]JAMSTEC, [3]University of Tsukuba

Red clay accumulates slowly on the seafloor deeper than CCD in mid-latitudes. Paleoceanographic and paleomagnetic studies were limited so far because red clay does not yield microfossils that can be used for precise age estimation and sedimentation rates were extremely low, less than a few meters per million years. However, red clay has attracted interest since Kato et al. (2011) reported that red clay rich in REY (rare-earth elements and yttrium) distributes widely in the Pacific Ocean. In this paper, we present magnetic properties of red clay cores obtained from the seafloor near Minami-Torishima during the R/V Kairei KR13-02 cruise. From these cores, extremely high REY contents were reported (Fujimoto et al., 2013, JpGU; Suzuki et al., 2013, JpGU). We will discuss a possible relationship between REY content and magnetic properties.

It is known in red clay that magnetostratigraphy can be established back to only ˜3 Ma, and this also holds for the KR13-02 cores. However, noisy but rather coherent inclinations were obtained throughout the cores even where polarity reversal patterns were obscure. Although a possibility that these directions are of magnetic overprint cannot be excluded, the observed inclinations are not much lower than that expected from the GAD model at the present latitude. This may suggest that the sediments including the intervals of high REY content are not very old, possibly Eocene to Oligocene or younger in age, and that they deposited in the northern latitudes not very far from the present sites. This result is not consistent with the idea that the high REY content is influence of hydrothermal activity along the East Pacific Rise. The cores showed a common magnetic susceptibility variation pattern, and a peak of REY content occurs just below an interval of high magnetic susceptibility. The REY peak coincides with a sharp upward decrease in the ratio of ARM to SIRM, which indicates an increase of the mean magnetic grain size and/or an increase in the proportion of detrital to biogenic magnetic mineral component. These results suggest that the increased REY concentration may have occurred in association with a paleoceanographic event.

Keywords: red clay, REY, rock magnetism, environmental magnetism, Pacific, Minami-Torishima

Japan Geoscience Union Meeting 2014
(28 April - 02 May 2014 at Pacifico YOKOHAMA, Kanagawa, Japan)

SEM37-07 Room:413 Time:April 30 11:00-11:15

A method for measuring rapid magnetization change in high field using a pulse magnetizer: A new rock magnetic approach

KODAMA, Kazuto[1*]

[1]Center for Advanced Marine Core Research, Kochi University

Pulse magnetizers have frequently been used in rock magnetic studies for the convenience of the production of high magnetic field without the need for a large electromagnet, enabling the rapid acquisition of isothermal remanent magnetization (IRM) for short (*c*. 10^{-2} sec) period of time. Because the demand for high field is limited as much as 10 T for rock magnetism, the pulse magnetizer can be compact and low-cost, and several commercial systems are available for the purpose of imparting IRM. We propose in this study a new method for measuring the dynamical behavior of magnetization in pulsed high-field, a new cost-effective system comprised of a fast broad-bandwidth digital oscilloscope and a newly designed coil system. We show examples of such dynamical behaviors from a set of natural samples, and discuss these results in comparison with conventional rock magnetic analyses.

Keywords: rock magnetism, pulse magnetic field, magnetic hysteresis

Japan Geoscience Union Meeting 2014
(28 April - 02 May 2014 at Pacifico YOKOHAMA, Kanagawa, Japan)

SEM37-08 Room:413 Time:April 30 11:15-11:30

Paleomagnetic study of the Holocene volcanic rocks and tephras from post-caldera central cones of Aso Volcano

ABIRU, Takuya[1] ; SHIBUYA, Hidetoshi[2*] ; MOCHIZUKI, Nobutatsu[3] ; YATO, Takanori[2] ; MIYABUCHI, Yasuo[4]

[1]Faculty of Science, Kumamoto University, [2]Department of Earth and Environmental Sciences, Kumamoto University, [3]Priority Organization for Innovation and Excellence, Kumamoto University, [4]Faculty of Education, Kumamoto University

We have conducted a paleomagnetic study on Holocene volcanic rocks and tephras from post-caldera central cones of Aso Volcano. Paleomagnetic sampling was made at 25 sites of seven units. Nineteen out of 25 sites gave reliable mean paleomagnetic directions that had a 95% confidence circle of lower than 5 degree. Different sites from a few lavas, which had been treated as a single unit in the geological map of Aso Volcano (Ono and Watanabe, 1985), gave distinct mean directions at 95% confidence level. For Kishimadake lava, Ojodake lava, Nakadake young volcanic edifice, two different mean directions were obtained from multiples sites. These differences in mean directions indicate that multiple flows were extruded with a temporal gap of more than 10 or 100 years. We also found that Kamikomezuka scoria, two sites of Kishimadake lava, two sites of Ojodake lava gave identical mean directions at 95% confidence level. The concordance of the mean directions suggests that the multiple vents erupted simultaneously, in a time interval of the order of 10 years, and these lavas were extruded over a wide area of the post-caldera central cones. In this study, we also made paleomagnetic measurements on tephra layers in a section. Oriented samples were collected from 22 layers of a tephra section, 4km NNE of Nakadake vocano (Miyabuchi and Watanabe, 1997). Seventeen of the 22 layers gave mean paleomagnetic directions that had a 95% confidence circle of lower than 5 degree. Most of the N6 layer, and N5 and N4 layers give an identical direction, which suggests these layers were formed in a short period of several tens of years. A tephra layer record a same direction of a lava flow, which suggests a simultaneous formation of the tephra layer and lava flow.

Keywords: Aso Volcano, paleomagnetic direction, volcanic rock, tephra

Japan Geoscience Union Meeting 2014
(28 April - 02 May 2014 at Pacifico YOKOHAMA, Kanagawa, Japan)

SEM37-09 Room:413 Time:April 30 11:30-11:45

Paleomagnetic secular variation record for the last 7000 years observed in piston cores from the Ichinomegata Maar

ANRAKU, Kazuhiro[1*] ; HAYASHIDA, Akira[2] ; HARAGUCHI, Tsuyoshi[3] ; YAMADA, Kazuyoshi[4] ; SHINOZUKA, Yoshitsugu[5] ; GOTANDA, Katsuya[6] ; YONENOBU, Hitoshi[7]

[1]Graduate School of Science and Engineering, Doshisha University, [2]Department of Environmental Systems Science, Doshisha University, [3]Department of Geosciences,Graduate School of Science,Osaka City University, [4]School of Human Sciences, Waseda University, [5]Faculty of Environmental Earth Science, Hokkaido University, [6]Faculty of Polycy Informatics, Chiba University of Commerce, [7]Graduate School of Education, Naruto University of Education

The Ichinomegata is a maar lake located in Oga peninsula, Akita Prefecture. Thin-wall core samples (IMG06) obtained in 2006 provided a Holocene paleomagnetic secular variation (PSV) record through measurements of natural remanent magnetization (NRM) of u-channel samples. In this study, we collected the piston-core samples (IMG13P-1 and IMG13P-2) from the center of the lake, and measured magnetic susceptibility, anisotropy of magnetic susceptibility (AMS) and natural remanent magnetization (NRM) of 7cc cubic samples. According to correlation between IMG06 and the piston cores based on lithological and magnetic susceptibility data, both IMG13P-1 and IMG13P-2 cover the last 7000 years. Stepwise AF demagnetization of the NRM showed that high intensity NRM decayed toward the origin linearly in most samples, so we determined the directions by applying the principal component analysis. We excluded some by evaluating inclinations of minimum axis and shape parameters q of AMS ellipsoids. Excepting some intervals that probably disturbed in coring, inclination and relative declination are showed consistent variations between IMG13P-1, IMG13P-2 and IMG06 cores. Therefore, we argue that the sediments of the Ichinomegata Maar are suitable for PSV studies. The paleomagnetic record from the Ichinomegata Maar shows a good similarity with the archeomagnetic secular variation from southwest Japan (Shibuya, 1980) and the PSV record from Lake Biwa (Ali et al., 1999), implying a great importance in regional reconstruction of the PSV record in Japan.

Keywords: Paleomagnetic secular variation, remanent magnetization, magnetic susceptibility, Ichinomegata Maar

Japan Geoscience Union Meeting 2014
(28 April - 02 May 2014 at Pacifico YOKOHAMA, Kanagawa, Japan)

SEM37-10 Room:413 Time:April 30 11:45-12:00

Thermomagnetic characteristics in the Hikageyama lava: searching a paleomagnetic record of the Laschamp excursion

NISHIYAMA, Hiroto[1*] ; HAYASHIDA, Akira[2] ; SAWADA, Yoshihiro[3] ; DANHARA, Tohru[4] ; KAWANO, Shigenori[5]

[1]Sci. Environ. Math. Model., Grad. Sci.&Engi., [2]Dept. Environ. Sys. Sci., Doshisha Univ., [3]Shimane University, [4]Kyoto Fission-Track Co., Ltd., [5]Tochigi Prefectural Museum

In the JpGU 2013 Meeting, we reported a paleomagnetic record from the Hikageyama lave. Among the 9 sites, 4 sites in the eastern part of the Hikageyama yielded consistent site mean directions characterized by shallow inclinations and easterly deflection. These site mean directions provide virtual geomagnetic poles (VGP) at around 50 N and 100 W. It can be assumed therefore that the Hikageyama dacite recorded anomalous geomagnetic field at the time of the Laschamp excursion. In addition to the above record, stepwise thermal (TH) demagnetization revealed that the above 4 sites yielded consistent site mean directions.

Thermomagnetic analysis revealed that most samples are composed of a single phase Curie temperature, suggesting magnetite as a remanence carrying mineral. And, the above 4 sites are classified into two groups. One (HKG-9, 10) shows a single phase, similar to the above. The other (HKG-11, 12) shows two phases, suggesting titanohematite and hematite. According to TH demagnetization results, one has two or three NRM components remanence. The other has a single component, which showed highly stable remanence which cannot be demagnetized at peak alternating field of 100 mT as previously reported. We will report these components discussion together with the thermomagnetic results.

Keywords: Rock magnetism, Hikageyama lava, Geomagnetic excursion, Laschamp excursion

Japan Geoscience Union Meeting 2014
(28 April - 02 May 2014 at Pacifico YOKOHAMA, Kanagawa, Japan)

SEM37-11 Room:413 Time:April 30 12:00-12:15

Electromagnetic core-mantle coupling and length-of-day variation in numerical dynamo models

TAKAHASHI, Futoshi[1*]

[1]Tokyo Institute of Technology

Exchange of angular momentum between the core and the mantle is likely to be responsible for the decadal variations in the length-of-day (LOD). If the changes in the angular momentum of the mantle are balanced by the opposite changes of the core, some coupling mechanisms between the core and the mantle should be invoked. Here we examine the electromagnetic (EM) coupling as a possible mechanism of angular momentum exchange. We use numerical dynamo simulations to investigate the mechanism to explain the LOD variations with respect to time including the decadal time scale. In numerical dynamo models, we impose a uniformly electrically conducting layer of about 200 km-thick on the mantle side of the core-mantle boundary corresponding to the D" layer. The electric current associated with the dynamo-generated magnetic field can flow in the conducting layer and the Lorentz force can yield a net EM torque with respect to the rotation axis. The electrical conductivity of the layer is varied from 200 - 500 S/m in dynamo models. The LOD variations can put some feedback effects on flows in the core through the changes in the angular velocity, which emerge as a change in the effective Ekman number and the Poincare force. Influences of such a feedback are also included in numerical models. The Ekman number adopted as a nominal value is 10^{-4}. We have obtained the EM torque resulting in typical angular velocity variation of the order of 10^{-6} relative to the nominal angular velocity in a time scale of the magnetic diffusion time. Much smaller changes in shorter time scale are also observed. Based on the findings in the present study, it is suggested that the EM core-mantle coupling in a likely range of the conductance within the D" layer is a promising mechanism to yield LOD variations in decadal to longer time scale.

Keywords: dynamo, electromagnetic core-mantle coupling, LOD variation, D" layer

Japan Geoscience Union Meeting 2014
(28 April - 02 May 2014 at Pacifico YOKOHAMA, Kanagawa, Japan)

SEM37-12 Room:413 Time:April 30 12:15-12:30

Infulence of surface displacement on fluid motions induced by Joule heating in the inner core of the Earth

TAKEHIRO, Shin-ichi[1*]

[1]Research Institute for Mathematical Sciences, Kyoto University

The elastic anisotropy of the earth's inner core as revealed by recent seismic observations is considered to originate from the alignment of texture formed along the solidification of the core or alignment of the preferred orientation of crystals by plastic deformation of fluid motions. The depth dependency of the anisotropy is difficult to explain by the solidification mechanism, whereas the various factors driving fluid flows in the inner core considered thus far do not appear to yield sufficiently strong stresses for generation of the elastic anisotropy. Takehiro (2011) proposed Joule heating of the magnetic field penetrating diffusively from the inner core boundary (ICB) as a possible source of inner core flows. His specific calculation in the case of toroidal magnetic field with the horizontal structure of spherical harmonics $Y_2{}^0$ showed that downward flow in the equatorial region and upward flows in the polar region are induced by the Joule heating. This flow field has non-zero radial velocity component at the ICB, causing mass exchange between the inner and the outer core. This feature is a result of the constant normal stress boundary condition at the ICB, and it is implicitly assumed that the phase change occurs instantaneously at the ICB. However, the actual speed of the phase change is finite. If the speed of the phase change is slow enough, the ICB would be deformed and the surface displacement is induced by the non-zero radial velocity at the ICB. This surface displacement may prevent inner core flows due to the buoyancy force originated from the density contrast between the inner and the outer cores. Therefore, in this study, we investigate influence of surface displacement on fluid motions induced by horizontally heterogeneous Joule heating in the inner core. We examine the extent of development of the surface displacement and modification of flow field of the inner core.

The difference of the governing equations from those of Takehiro (2011) is the boundary conditions at the ICB. Temperature disturbance at the ICB coincides with the melting temperature which varies depending on the surface displacement. The normal component of stress equates with buoyancy induced by the surface displacement. The toroidal magnetic field and surface displacement with the horizontal structure of $Y_2{}^0$ is given. The flow fields are calculated numerically for various amplitudes of the surface displacement with the expected values of the parameters of the cores.

The results show that, when the surface displacement is the order of 0.01–0.001m or less, the flow and stress fields are similar to those of Takehiro (2011), where the surface displacement vanishes. As the amplitude of the surface displacement is increased, counter flows from the polar to the equatorial regions come to emerge around the ICB, while the flow in the inner regions is directed from the equatorial to the polar regions in the inner region and non-zero radial component of velocity at the ICB still exists. When the surface displacement is about 0.14–14m, radial component of velocity at the ICB vanishes, the surface counter flows becomes stronger than the flow in the inner region, and the amplitude of the stress field near the ICB dominates that of the inner region, which might be inconsistent for the elastic anisotropy in the inner core.

Reference: Takehiro, S., 2011: Phys. Earth Planet. Inter., 184, 134–142.

Keywords: anisotropy of the Earth's inner core, magnetic fields in the Earth's outer core, flows in the Earth's outer core, inner core boundary of the Earth, dynamo action in the Earth's outer core

Japan Geoscience Union Meeting 2014
(28 April - 02 May 2014 at Pacifico YOKOHAMA, Kanagawa, Japan)

SEM37-13 Room:413 Time:April 30 14:15-14:30

Paleomagnetism of the Znp-Ohta tephra in eastern Honshu: relative tectonic rotations at local and regional scales?

HOSHI, Hiroyuki[1*] ; FUTAMURA, Sho[2]

[1]Aichi University of Education, [2]Futagawa Minami Elementary School

We present paleomagnetic data suggesting relative tectonic rotations in eastern Honshu since 3.9 Ma. Samples were collected from a widespread ash bed, called the Znp-Ohta tephra, at three localities. One is the Tomioka locality located to the east of the Abukuma Mountains, where the ash bed (local name = SF4.5 tephra) was samples at three sites. The other two are the Miyobara and Kohsaka localities on the Boso Peninsula, where the ash bed (local name = An85 tephra) was sampled at three sites at each locality. Stepwise demagnetization was performed on all specimens, and the principal component analysis was applied to the demagnetization data to extract characteristic remanent magnetization (ChRM) components. At Tomioka, site-mean ChRM directions were determined at all sites. They are tightly clustered after tilt correction and have a southerly direction of reverse polarity. Interestingly, the direction is deflected significantly counterclockwise with respect to the direction of the correlative tephra at Chita in central Honshu (Hoshi & Deguchi, 2013). At Miyobara and Kohsaka, the locality-mean ChRM directions are significantly different to each other. The paleodeclination of Miyobara is similar to that of Tomioka, and the paleodeclination of Kohsaka is almost identical to that of Chita. The difference in paleodeclination between Miyobara and Kohsaka seems to be related to the difference in the general geological trend of Neogene strata on the Boso Peninsula, suggesting relative rotation on the peninsula. Our results imply that in eastern Honshu, relative rotations have taken place at local and regional scales since the Pliocene.

Keywords: eastern Honshu, paleomagnetism, Pliocene, relative rotation, tectonics, Znp-Ohta tephra

Japan Geoscience Union Meeting 2014
(28 April - 02 May 2014 at Pacifico YOKOHAMA, Kanagawa, Japan)

SEM37-14 Room:413 Time:April 30 14:30-14:45

Past continental shape inferred from GPS data

KAWAI, Keigo[2] ; KATO, Tadayoshi[2] ; HARADA, Yasushi[1*]

[1]Department of Marine and Earth Science, Tokai University, [2]Department of Marine Mineral Resouces, Tokai University

Kono et al.,1985 analyzed paleomagnetic data around Andes and showed past shape of the south American continent about 50Ma and figured the Andes mountain range were more linear shape than at present. We tried to reconstruct the 50Ma shape of the south American continent from the current crustal motion of GPS data. Plate motion vectors observed from space geodesy including GPS, can comparable with plate motions of geological time scale. Gordon, 1993 showed VLBI plate motion (time scale of years) and NUVEL-1 plate motion (3 million years mean motion) are in great harmony with each other.

We applied a method of Harada and Kato(AGU Fall Meeting 2012), and calculated about 50Ma shape of the south American continent (figure below). The shape of the Andes mountain range were linear and in good harmony with the result of Kono et al.,1985. We conclude, thus, decades scale GPS data can compare with plate deformation of ten thousands years.

Keywords: GPS, Past continental shape, Deformation of plates

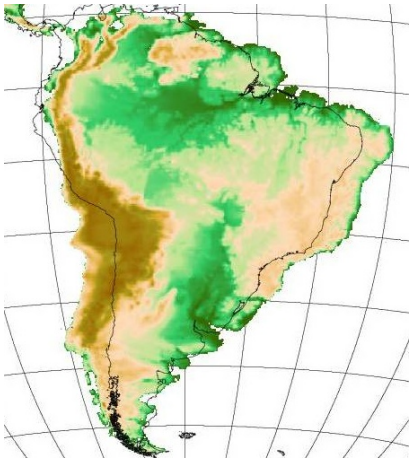

Japan Geoscience Union Meeting 2014
(28 April - 02 May 2014 at Pacifico YOKOHAMA, Kanagawa, Japan)

SEM37-15 Room:413 Time:April 30 14:45-15:00

Problems related to the past motion of the Philippine Sea Plate

TAKAHASHI, Masaki[1*]

[1]Geological Survey of Japan, AIST

Plate motion through geological time is reconstructed based on the correlation of marine magnetic anomaly patterns and/or hot-spot track analysis. But the past motion of the Philippine Sea Plate cannot be clarified because the plate is surrounded by convergent plate boundary (trench) and it has no hot-spot track. Therefore the paleomagnetic approach is the only method to reconstruct the past location and motion of the plate. However this method contains unacceptable problems that the paleomagnetic declination does not indicates the total rotation of the plate around its Euler pole in most cases. The paleomagnetism has been thought as an effective tool to reconstruct the Philippine Sea Plate motion, but actually it is impossible to clarify the past motion of the plate by paleomagnetic method.

Keywords: tectonics, paleomagnetism, Philippine Sea Plate

Japan Geoscience Union Meeting 2014
(28 April - 02 May 2014 at Pacifico YOKOHAMA, Kanagawa, Japan)

SEM37-P01 Room:Poster Time:April 30 18:15-19:30

Environmental rock-magnetism of red clay in the South Pacific Gyre during the Cenozoic: relation with rare-earth content

SHIMONO, Takaya[1*] ; YAMAZAKI, Toshitsugu[2] ; SUZUKI, Katsuhiko[3]

[1]Graduate School of Life and Environmental Sciences, University of Tsukuba, [2]Atmosphere and Ocean Research Institute, The University of Tokyo, [3]Institute for Research on Earth Evolution, Japan Agency for Marine-Earth Science and Technology

Red clay occupies ˜40% of the global ocean floor. Paleoceanographic and paleomagnetic studies of red clay were limited so far because red clay does not yield microfossils that can be used for precise age estimation and sedimentation rates were extremely low, less than a few meters per million years. However, red clay has attracted interest since Kato et al. (2011) reported that red clay rich in REY (rare-earth elements and yttrium) distributes widely in the Pacific Ocean. Among the cores studied by Kato et al. (2011), especially REY-rich mud (2110 ppm at the maximum) of ˜40 m thick occurs below 13.5 m below seafloor (mbsf) at the Deep Sea Drilling Project (DSDP) Site 596 at the western edge of the South Pacific Gyre. However, the core sections have large gaps, and rock- and paleomagnetic studies were not conducted. In 2010, Integrated Ocean Drilling Program (IODP) Expedition 329 Site U1365 occupied at almost the same position as Site 596. Continuous pelagic red clay cores of ˜76 m thick was recovered above the basaltic basement of ˜100 Ma in age.

We conducted an environmental magnetic study using the Site U1365 cores to investigate long-range climatic and paleoceanographic changes during the Cenozoic. We also investigate a relation between magnetic properties and REY of the red clay. On the basis of rock magnetic analyses and transmission electron microscopy, magnetic mineral assemblages are dominated by bacterial magnetites (magnetofossils) throughout the cores (Yamazaki and Shimono, 2013). In the uppermost several meters, terrigenous maghemite probably transported as eolian dust increases. High REY mud (2470 ppm at the maximum) of ˜40 m thick occurs below 8 mbsf. The variation pattern of REY constant is similar to that at Site 596. The ages of the Site U1365 cores were transferred from those of Site 596, which is based mainly on a constant Co-flux model at Site 596 (Zhou et al., 1992), by inter-core correlation using magnetic susceptibility and REY variation patterns. Paleomagnetic stratigraphy is available for the uppermost several meters at Site U1365.

We discuss a possible relationship between REY content and magnetic properties. The REY peak coincides with a sharp upward decrease in the ratio of κ_{ARM} to SIRM, which indicates an increase of the mean magnetic grain size and/or an increase in the proportion of detrital to biogenic magnetic mineral component. A peak of REY content occurs just below an interval of high magnetic susceptibility. These characteristics are similar to those of red clay cores near Minami-Torishima (Yamazaki et al., 2014, JpGU). This suggests that the increased REY concentration may have occurred in association with a common paleoceanographic event. Eolian dust supply may have increased since ˜30 Ma. The Eocene/Oligocene (E/O) transition (˜34 Ma) is known as the time when major ocean gateways (the Drake passage and Tasmanian gateway) opened and the Antarctic Circumpolar Current was formed (Scher and Marting, 2004, 2006; Stickley et al., 2004). The onset and increase of dust supply in the South Pacific may have occurred after this time. Northward movement of Australia continent to an arid region (middle-latitude) may have also contributed an increase of dust supply. Hyeong et al. (2013) suggested that phosphatization on the Mid-Pacific mountains took place between 36 and 12 Ma, and it peaked at the E/O transition. They connected the results to paleo-deepwater circulation. A REY peak occur near the E/O transition at Site U1365, which may be related with the phosphorus budget.

Keywords: Red clay, REY, South Pacific Gyre, Cenozoic, Environmental Magnetism

Japan Geoscience Union Meeting 2014
(28 April - 02 May 2014 at Pacifico YOKOHAMA, Kanagawa, Japan)

SEM37-P02 Room:Poster Time:April 30 18:15-19:30

Regional differences in magnetic properties of topmost sediments of the Northern Lake Biwa

ISHIKAWA, Naoto[1*] ; ISHIKAWA, Kanako[2]

[1]Graduate School of Human and Environmental Studies, Kyoto Univ., [2]Lake Biwa Environmental Research Institute

Rock-magnetic investigations have been performed on topmost sediments above about 30 cm below sediment surface (bss) cored in summer (June to July) and winter (November to December) at eight sites with different water depth, where dissolved oxygen (DO) content in bottom water and its seasonal variation are different, in the first depression at the North Basin of Lake Biwa in order to reveal early diagenetic effect on magnetic properties of the sediments.

Low-temperature magnetometric results indicate that a partially-maghemitized magnetite is a principal magnetic mineral in the sediments. Warning curves from 6 to 300K of isothermal remanence (IRM) imparted at 6K in 1T after zero-field cooling show a remarkable decrease of IRM between 90 and 120K, which is regarded as a suppressed Verway transition of magnetite. The amount of IRM decrease between 90 and 120K increase downcore at all site, implying the dissolution of maghemite skin covering magnetite. The IRM decrease is more slightly remarkable in the sites with shallower water depth. The degree of maghemitization may be lower in the site. Samples from sites with deeper water depth below about 70m show another IRM decrease between 20 and 30K with the inflection point at about 29K. The IRM drop disappears in samples with hydrochloric acid treatments. These low-temperature IRM behaviors may imply the presence of ferro-rhodochrosite. The IRM drop is detected in samples above about 18 cmbss, and the samples in two zones of 0-3 cm-bss and 6-15 cm-bss show the IRM drop more clearly. The IRM drop is more remarkable in samples with deeper water depth. The occurrence of the magnetic mineral with the characteristic low-temperature magnetic behavior seems to be influenced by the DO values and its seasonal change.

As common characteristics in downcore changes of magnetic properties, the downcore decrease of magnetic coercivity is observed in the uppermost sediments above about 10 cm-bss, and the amount and grain size of magnetic minerals subsequently decreases and increases downcore below 10cm-bss, respectively. These changes are considered to be associated with the dissolution of maghemitized magnetite by the early diagenetic effect. The presence of magnetic minerals with finer grain size and higher magnetic coercivity in the sediments above 10 cm-bss is more remarkable in sites with deeper water depth.

Keywords: rock magnetic property, Lake Biwa, topmost sediment, early diagenesis

Japan Geoscience Union Meeting 2014
(28 April - 02 May 2014 at Pacifico YOKOHAMA, Kanagawa, Japan)

SEM37-P03 Room:Poster Time:April 30 18:15-19:30

Magnetic properties of the sediments and suspended solids in the sea surface water at the Hiroshima bay station.

KAWAMURA, Noriko[1*]

[1]Japan Coast Guard Academy

Suspended solids (SS) in sea water are consisted of planktons and insoluble particles, and are an indicator of transparency. SS particles adsorb and incorporate metallic ions. Iron is a metallic ion, and an essential element for phytoplankton. It is supplied from river to sea as bivalent or trivalent ions, and exists as iron compounds as organic complexes in sea water. Aeolian dusts are consisted of SS, and also consists of iron compounds. They will deposit on seafloor, and be sediments as the climatic record. It is important to investigate the distribution and mode of iron compound in SS for the present and past environmental studies. This study aims to diagnose magnetic minerals in SS. Enough amount of SS sample for magnetic measurements are collected by magnetic separation from seawater at the Hiroshima bay station. 4 L of seawater is filtrated, and the particles above 0.45 um in diameter are recovered for XRF analysis. The amount of magnetic particles in sea surface water shows relatively high values from April to July in the bay. The maximum value is found at the station, which is located near an iron works (the supply source). The particle is opaque minerals and looks like needle. The values of IRM imparted at 0.3 T and 2.5 T are not stable. It suggests that SS has strong anisotropy. Results of thermo-magnetometry indicate that magnetic carriers of SS samples are mainly magnetite, and goethite and hematite is also recognized. Magnetic minerals in the sediments at the station are magnetite, hematite, and greigite. It is implied that goethite present in the sea surface water and it may be dissolved on sea floor.

Keywords: Suspended solids, Iron compounds, Goethite

Japan Geoscience Union Meeting 2014
(28 April - 02 May 2014 at Pacifico YOKOHAMA, Kanagawa, Japan)

SEM37-P04 Room:Poster Time:April 30 18:15-19:30

Paleomagnetic study of the turbidite sediments around the Daini Atsumi Knoll

TAMAKI, Machiko[1*] ; SUZUKI, Kiyofumi[2] ; EGAWA, Kousuke[3]

[1]Japan Oil Engineering Co., Ltd., [2]Japan Oil, Gas and Metals National Corporation, [3]National Institute of Advanced Industrial Science and Technolog

This study is a part of the program of the Research Consortium for Methane Hydrate Resource in Japan (MH21 Research Consortium)

Keywords: Paleomagnetic study, Paleomagnetostratigraphy, Anisotropy of magnetic susceptibility, Paleocurrent analysis, turbidite sediments, Dainii Atsumi Knoll

Japan Geoscience Union Meeting 2014
(28 April - 02 May 2014 at Pacifico YOKOHAMA, Kanagawa, Japan)

SEM37-P05 Room:Poster Time:April 30 18:15-19:30

Emplacement mechanism of marine volcaniclastic sediments (IODP Site U1397, 1398) based on rock magnetic properties

SAITO, Takeshi[1*] ; KATAOKA, Kyoko S.[2]

[1]Faculty of Science, Shinshu University, [2]Research Institute for Natural Hazards and Disaster Recovery, Niigata University

Large numbers of marine volcaniclastic sediments with various origins were recovered from the sites U1397 and U1398 during IODP Expedition 340. They were most likely derived from volcanoes on Martinique and possibly from Dominica, Lesser Antilles volcanic arc. Some volcaniclastic units were transported and deposited as turbidites, some were as thin tephra fall deposits and others show both characteristics. They contain various amounts of bioclastic component, pumice and lithic fragments and hemipelagic mud clasts. Therefore, these volcaniclastic sediments are suitable for investigating transport and emplacement mechanisms of volcanic materials and the resultant sedimentary and petro-facies in marine settings. This study focuses on magnetic minerals in the marine volcaniclastic sediments and carried out rock magnetic measurements.

Thermomagnetic measurements showed almost reversible curves and induced magnetization decayed to almost zero below 580 ℃, suggesting little contribution of maghemite or hematite. Two Curie temperatures (Tc) with 350-400 ℃ and 500-550 ℃ indicate that the main magnetic carriers are Ti-rich titanomagnetite and Ti-poor titanomagnetite. The proportion of low-Tc titanomagnetite in central and bottom part of thick turbidite units was larger than that in hemipelagic sediments and in the topmost part of turbidite units, suggesting Ti-rich titanomagnetite is derived from volcanic events. Tephra fall deposits also showed large contributions of Ti-poor titanomagnetite, resulted from large amount of volcanic materials. On the other hand, thin turbidite units showed small contributions of Ti-poor titanomagnetite. This suggests that thin turbidite units are derived from diluted flows which contain few heavy Fe-bearing magnetic minerals.

Magnetic susceptibility and hysteresis measurements showed that heavy and large magnetic minerals in most thick turbidite units were concentrated at the lower part of the unit. Samples from the topmost and bottom part of turbidites showed higher degrees of anisotropy than those from the central part, indicating strong influence of suspension settling at the topmost part and shearing at the bottom part. Bottom parts of fall units contain heavy and large magnetic minerals, whereas upper parts of fall units contain fine magnetic minerals. On the other hand, in thin turbidite units such features cannot be observed and hysteresis parameters and susceptibility values were almost concentrated. Probably thin turbidite units did not experience segregation of specific particles during transportation and settling under the relatively calm condition.

These preliminary results suggest that magnetic minerals are useful indicators of volcanic events and rock magnetic approaches can identify various types of depositional processes about marine volcaniclastic sediments.

Keywords: turbidite, fall deposit, marine sediment, titanomagnetite, magnetic mineral

Japan Geoscience Union Meeting 2014
(28 April - 02 May 2014 at Pacifico YOKOHAMA, Kanagawa, Japan)

SEM37-P06 Room:Poster Time:April 30 18:15-19:30

Paleomagnetic direction of the Tomikusa Group in southern Nagano Prefecture and its tectonic significance

SAKO, Kazuki[1*] ; HOSHI, Hiroyuki[1]

[1]Aichi University of Education

We report here a new paleomagnetic direction from Early Miocene (18-17 Ma) sediments of the Tomikusa Group in southern Nagano Prefecture, and discuss the formation of curvature of the Median Tectonic Line (MTL) in central Honshu. Sedimentary rock samples collected from 24 sites were demagnetized stepwise, and site-mean directions were determined for 23. Rock magnetic experiments suggest that the main magnetic minerals are magnetite and maghemite. The site-mean directions pass a reversal test, indicating primary remanent magnetization. The overall mean direction with a northerly declination is indistinguishable from the Early Miocene reference direction derived from the Asian continent. This comparison suggests no significant rotation in the study area with respect to the continent since 17 Ma. The mean declination is deflected about 15 deg counterclockwise with respect to the strike of the nearby MTL. The same angular relationship is also found in other sedimentary basins in central Honshu (Ichishi in Mie Pref., Chita Peninsula in Aichi Pref., Shitara in Aichi Pref., and Chichibu in Saitama Pref.). Thus we conclude that the MTL was straight in the late Early Miocene (18-17 Ma).

Keywords: paleomagnetism, Tomikusa Group, Median Tectonic Line, Miocene, rock magnetism, tectonics

Japan Geoscience Union Meeting 2014
(28 April - 02 May 2014 at Pacifico YOKOHAMA, Kanagawa, Japan)

SEM37-P07 Room:Poster Time:April 30 18:15-19:30

Rock magnetism and its petrological charactization of fossil Porites coral frameworks in Ishigaki island, Japan

KUMAGAI, Yuho[1*] ; NAKAMURA, Norihiro[1] ; SATO, Tetsuro[1]

[1]Graduate school of Earth Science, Tohoku University.

Radiocarbon (^{14}C) is produced by the cosmic rays in the atmosphere and is utilized for analysis of the past sun activity. But the Earth's geomagnetic field also controls radiocarbon variability, suggesting that a strong field would shield the planet from high energy charged particles. This mimics lower sun activity. Also, the short-term (in decadal or centennial scale) movement of the geomagnetic pole to the low latitude, such as geomagnetic jerk, could lead to an increased cosmic ray flux impinging on the terrestrial atmosphere and thus to a higher ^{14}C production rate. Therefore, in order to study the past sun activity from the ^{14}C production rate, we need to know the movement of geomagnetic pole position, its field strength and the variability of radiocarbon production during decadal to centennial periods. Many researches, which aim to reveal the paleomagnetic secular variation (PSV), have been performed using datasets obtained from volcanic rocks, sediment, and fired kilns. The some reconstruction models of geomagnetic dipole moment are also established from these data sets. But there are few recorders that can be used for the reconstruction of PSV in a decadal or centennial scale. Here we propose an alternative candidate of fossil coral frameworks as a possible paleomagnetic recorder for PSV research. The coral framework has an advantage in reconstructing both the radiocarbon variability and the geomagnetic field, although usual corals show extremely weak intensity of remanence and its low stability. However, it is shown that our recently-ceased coral framework samples from Ishigaki island possess a remanence intensity of 10^{-5} -10^{-4} A/m and a single-domain like stability from Lowrie-Fuller test. We prepared the standard 1-inch core samples cut parallel to the growth direction of coral *Porites*, including coral's growth bands for a ten to several tens of years. Our thermal and AF demagnetization experiments of oriented coral samples show that a characteristic remanence direction is parallel to the present Earth's magnetic field with some fluctuations. On the other hand, some samples exhibit different remanence directions from the present geomagnetic field with a calcite peak of X-ray diffraction analysis. The presence of calcite indicates that the meteoric diagenesis which changes aragonite coral frameworks into calcite affect the direction of initial magnetization. To constrain the remanence carriers, we are conducting a first order reversal curves (FORC) measurement and petrologic observations by a Schottky field-emission scanning electron microscope (FE-SEM) of acid-treated residuals of our corals. Our results suggest that Porites coral framework samples provide a role as a potential use for paleomagnetic recorder for annual to decadal scales with careful examination of calcite content.

Keywords: fossil Porites coral frameworks, paleomagnetism

Japan Geoscience Union Meeting 2014
(28 April - 02 May 2014 at Pacifico YOKOHAMA, Kanagawa, Japan)

SEM37-P08 Room:Poster Time:April 30 18:15-19:30

Effect of thermal expansion on Neel's relaxation nomograph of magnetite and its agreement with the radiocarbon age

SATO, Tetsuro[1*] ; NAKAMURA, Norihiro[1] ; GOTO, Kazuhisa[2]

[1]Earth Science, Tohoku University, [2]International Research Institute of Disaster Science (IRIDeS),Tohoku University

Age gap between the paleomagnetic viscous dating and the radiocarbon age of tsunamigenic boulders in Ishigaki Island is focused. Recent researchers have conducted radiocarbon dating to label tsunami age, being able to calibrate the paleomagnetic viscous dating. These ages should be the same for the initial tsunami event. In the paleomagnetic viscous dating, time-temperature relation assuming Neel's single domain (SD) theory of magnetite is used. This monograph shows the older remagnetized component in nature can be erased by the higher temperature in the laboratory, and younger is its reverse. Thus, we can predict the age acquired the secondary magnetization by calculating demagnetization temperature and heating time. Our viscous dating results sometimes represented that the unblocking temperature of viscous components for tsunamigenic boulders is higher than the temperature predicted from Neel's relaxation theory of single domain magnetite, suggesting the older age than the one determined from the calibrated radiocarbon age. Previous numerous studies confirmed that the departure from Neel's theory is attributed to the presence of multi-domain magnetite. However, Lowrie-Fuller test, FORC (first order reversal curves) experiments and Low-temperature demagnetization of tsunamigenic boulders confirmed the presence of single domain magnetite. To solve this problem, we consider the thermal expansion of magnetite during stepwise thermal demagnetization process and propose a modified time-temperature relation to be able to fill the age gap. Currently, thermal expansion coefficient of magnetite is reported by some researcehrs (e.g. Nikolaev and Shipilin, 2000; Levy et al, 2004). If magnetite volume is bigger than initial volume during thermal demagnetization, unblocking temperature should indicate higher value under the assumption of constant coercive force. To confirm this hypothesis, we conducted stepwise thermal demagnetization to a boulder emplaced by 1771 Meiwa tsunami (242 years ago) and compare them to our new modified time-temperature relation.

Keywords: thermal expansion, Neel's theory, single domain, viscous remanence, blocking temperature

Japan Geoscience Union Meeting 2014
(28 April - 02 May 2014 at Pacifico YOKOHAMA, Kanagawa, Japan)

SEM37-P09 Room:Poster Time:April 30 18:15-19:30

Rock magnetic study of single zircon crystals sampled from river sands

SATO, Masahiko[1*] ; YAMAMOTO, Shinji[2] ; YAMAMOTO, Yuhji[3] ; OKADA, Yoshihiro[4] ; OHNO, Masao[1] ; TSUNAKAWA, Hideo[4]

[1]Kyushu University, [2]The University of Tokyo, [3]Center for Advanced Marine Core Research, Kochi University, [4]Tokyo Institute of Technology

Geomagnetic field paleointensity data provide critical information such as thermal evolution of the Earth (Stevenson et al., 1983). Also a state of geomagnetic field closely relates to a surface environment (Kulikov et al., 2007). It is pivotal to know the variation of geomagnetic field intensity throughout the history of the Earth. Until now we have not yet obtained, however, enough data to resolve billion-year-scale geomagnetic field variation (Tauxe and Yamazaki, 2007) and need to obtain more paleointensity data.

In this study we focus on a paleointensity experiment using single zircon crystal. Since river sand originates in rocks widely distributed in river basin, detrital zircons in the sand have various ages (Rino et al., 2004). Therefore if the geomagnetic paleointensity can be measured using the single zircon crystal, we will probably obtain paleomagnetic data enough to resolve the long-term geomagnetic field variation.

Zircon crystals used in the present study were sampled from sands of the Nakagawa River, Tanzawa Mountain. The Nakagawa River flows along bodies of tonalite, which is a representative rock of the continental crust. Using coarse-grain single zircon crystals with weight of about 0.1 mg, a suite of rock magnetic measurements were conducted: low-temperature demagnetization (LTD) and stepwise alternating field demagnetization (AFD) of saturation isothermal remanent magnetization (SIRM), and low-temperature cycle using an Magnetic Property Measurement System (MPMS).

SIRM intensities of the single zircon crystals vary four orders of magnitude ranging from $1x10^{-12}$ - $2x10^{-9}$ Am^2, and especially a few percent of the grains have strong SIRM larger than $1x10^{-10}$ Am^2. The zircon crystals contain nearly pure magnetite (Fe_3O_4), and they are in both single-domain (SD) and multidomain (MD) states. The SD magnetite contained in the zircon crystals has the potential to record the paleomagnetic information. The existence of MD magnetite suggests that stepwise-demagnetization after LTD treatment is an efficient approach for paleomagnetic measurement. Taking into account the relation between SIRM intensity and thermoremanent magnetization (TRM) intensity for magnetite (e.g., Yu, 2010), TRM of single zircon crystal may be measured with a high-sensitivity magnetometer such as a SQUID magnetometer.

Now we plan to sample river sand at the Mississippi River and to conduct rock magnetic measurements of the zircon crystal collected from the sand. On the basis of the rock magnetic studies for the zircon crystals from the Nakagawa River and the Mississippi River, we will discuss the feasibility of the paleointensity experiment using single zircon crystal.

Keywords: Zircon, Rock magnetic study, Paleointensity

Japan Geoscience Union Meeting 2014
(28 April - 02 May 2014 at Pacifico YOKOHAMA, Kanagawa, Japan)

SEM37-P10 Room:Poster Time:April 30 18:15-19:30

Development of the Japan Archeomagnetism Database

HATAKEYAMA, Tadahiro[1*]

[1]Information Processing Center, Okayama University of Science

Here we will report the online service of Japan Archeomagneitsm Database which is developed since 2012. Now the database includes about 700 site archeodirection dataset, and we are working to add new data from the backyard stocks which has uncertainty about the independent archeological chronology. Therefore we have to confirm that with searching the dating in the original excavation reports.

Moreover we have added new archeomagnetic data from the archeological archives. More than 100 archeomagnetic data have been manually discovered in the reports.

Now we are also providing a paleomagnetic direction at the Far-East region calculated from the Japanese geomagnetic secular variation models.

Keywords: Archeomagnetism, Database, Geomagnetic secular variations

Japan Geoscience Union Meeting 2014
(28 April - 02 May 2014 at Pacifico YOKOHAMA, Kanagawa, Japan)

SEM37-P11 Room:Poster Time:April 30 18:15-19:30

Medium soscale crustal structure based on magnetic and gravity anomalies in the eastern part of Hokkaido, Japan. -part 2

MORIJIRI, Rie[1*] ; NAKAGAWA, Mitsuru[1]

[1]Geological Survey of Japan, AIST

The Pacific coast of the eastern Hokkaido (from Kushiro to Nemuro Peninsula) is characterized by high gravity and high magnetic anomalies. However, it was difficult to get a suitable model due to gravity anomalies on land and aeromagnetic anomalies. We sampled basalts in this area and measured densities, natural remanent magnetization, susceptibilities and other magnetic properties. These results were presented in Japan Geoscience Union Meeting 2007. Moreover, new gravity and magnetic anomaly maps of offshore of cape Ochiishi were published by GSJ, AIST (2012). We picked up profiles and modified previous models. Data including new profiles suggested similar models to previous studies.

Keywords: magnetic property, magnetic anomaly, gravity anomaly, Nemuro, Hokkaido

Japan Geoscience Union Meeting 2014
(28 April - 02 May 2014 at Pacifico YOKOHAMA, Kanagawa, Japan)

SEM37-P12 Room:Poster Time:April 30 18:15-19:30

Seismogenic shear-induced thermal turbulence in Nojima fault gouges: micro-textural and rock magnetic considerations

NAKAMURA, Norihiro[1*] ; FUKUZAWA, Tomohiko[1]

[1]Dep. Earth Science, Tohoku University

Nojima fault gouges exhibit a characteristic flow microtexture of laminated slip zones, billow-like wavy folds and turbulent disordered structures. Power spectral analysis of the wavy folds indicates that the geometry roughly obeys a power-law of -1.9, agreeing well with the previously measured value of Kelvin-Helmholtz (KH) turbulence in natural environments. The well-known example of KH instability is a cloud that the cloud-atmosphere interface becomes an unstable vortex sheet that rolls up into a spiral. The instability occurs at the interface between two fluids of different densities shearing at different velocities (Thorpe 2005). The KH wave in Nojima fault gouges was found along a slip plane in a blackish cohesive gouge (pseudotachylyte-like gouge), resulting in the presence of instability at the slip interface during ancient earthquake or creep. Thin section observations showed the blackish cohesive gouge consisted of granular materials for both sides of the interface and the KH wave occurs in a denser granular material along an earthquake-originated sharp slip plane. Our scanning Magneto-Impedance magnetic microscope observation shows the KH wave dense layer is only magnetized in isothermally-magnetized thin section, revealing the production of magnetic mineral in KH wave. Because the Nojima fault gouge contains iron-carbonate (siderite), the thermal decomposition of siderite produces magnetite more than 400 ℃. Therefore, we suggest that the KH wave is generated through KH instability in a high-temperature (>400 ℃) granular dense layer with different densities and different slip velocities. This result suggests that shear-induced thermal turbulence in the fault gouge plays an important role to weaken a frictional strength during earthquake slip dynamics.

Japan Geoscience Union Meeting 2014
(28 April - 02 May 2014 at Pacifico YOKOHAMA, Kanagawa, Japan)

SEM37-P13 Room:Poster Time:April 30 18:15-19:30

Analyzing the early 19 century's geomagnetic declination in Japan from Tadataka Inoh's Santou-Houi-Ki.

TSUJIMOTO, Motohiro[1*] ; OMOTANI, Akitoshi[2] ; INUI, Takaaki[3] ; MIYAUTI, Satoshi[4]

[1]Japan Cartographers Association, [2]San-in System Consultant, [3]Matsue Municipal comitee of property, [4]Studyies of Inoh's map and writing Assoc

Santou-Houi-Ki national treasure of Japan recorded by cartographer Tadataka Inoh in 1800-1816, is 67 volumes ledger consist of approximately 200,000 magnetic compass land survey azimuth data accuracy of 0 degree 05 min, from eastern coast of Hokkaido to Yakushima Isl in western Japan. We continue the work of analysis that stopped after only analysis in 1917, which done about the survey data at known position of the retirement home of Inoh at Fukagawa in Edo (Tokyo) in 1802-1803.

(1)It is able to change Japan as one of the most concentrated area of accurate geomagnetic declination data in the world, in early 19th century, from insufficient area of data, and supply new data to northeast Asia by analysis of Santou-Houi-Ki.

The total number of analyzed points exceeded 178, and the outline isogonic line in Japan archipelago and the distribution of the declination in every15 minutes in western Japan coast in those days, begun to appear.

(2)Compare the isogonic Atlas by Gauss and Weber (hereinafter Gauss Atlas) consisted of observed data in 1828-1830, with the analysis from Santou-Houi-Ki, the foundational structure of isogonic lines in Japan archipelago is roughly similar. But we recognize the contradiction to reverse with secular variation in Northern Kyushuu area and Tsushima Island. There are no observed data in Japan in the table supplemented with Gauss isogonic Atlas. The recorded observational data in Gauss Atlas in East Asia were inland area from Pekin to Eastern Siberia, Ohotsk, Kamchatka etc. From the analysis of Santou-Houi-Ki, we recognize the magnetic declination supposed as the local geomagnetic anomaly in southern coast of eastern Hokkaido. The isogonic line of declination in surrounding area of Japan in Gauss Weber's Atlas had drawn by calculated estimates, on a matrix of 5 degree in latitude and 10 degree in longitude, one cell of this matrix is 500km long. Therefore the analysis of Santou-Houi-Ki becomes very important. Today it is very important to verify with the isogonic map of Andrew Jackson et al Gufm1 by NOAA (1800-1815).

(3)Procedure and advantage of interdisciplinary and simultaneous analysis of Santou-Houi-Ki across geomagnetism, cartography, and local history. 1.It increase precise evidence to verify the azimuth and the name or short description of the reference point or the target points recorded in Santou-Houi-Ki, with not only the survey diary by Inoh or Inoh map or the survey map of today, add historical local map, historical local source material, the old survey map by former Japan imperial army. 2. Use the recreation software of scenery or digital map of GSI Japan to grasp the outline of particular latitude and longitude of the reference point and target points and real azimuth. 3. Calculate the average of remainder as the declination, to deduct the magnetic azimuth recorded in Santou-houi-Ki from the real azimuth. 4. The important point is to calculate backward the precise position of the reference point should be adjusted to the position, where all of the declination values from the magnetic survey azimuth to different targets at the reference point are approximately equal to each other, to use the consecutive formula of Excel for speed up and keep accuracy. 5. Use GPS transmitter at the reference point to investigate longitude and latitude, and recalculate the position under 0 second in latitude and longitude, minute accuracy declination, more detail and accurate than traditional study. 6.It is able to find areas or points of local geomagnetic anomaly, or to restore the precise position of survey reference point by Tadataka Ino, accuracy of less than second in latitude and longitude, or the objective point of survey in accuracy second where the valuable in local history, including disappeared constructions or big tree etc.

Keywords: declination, Inoh, SantouHouiKI, Reference point, interdisciplinary

Japan Geoscience Union Meeting 2014
(28 April - 02 May 2014 at Pacifico YOKOHAMA, Kanagawa, Japan)

SIT02-01 Room:211 Time:April 29 14:15-14:30

Slab dehydration, intermediate-depth earthquakes, and arc magmatism: A review of seismological observations

NAKAJIMA, Junichi[1*]

[1]RCPEV, Graduate School of Sci., Tohoku Univ.

We review recent seismological observations beneath the Japanese Islands and show important roles of geofluids on seismogenesis at intermediate depths and arc magmatism.

Seismicity in the subducting crust of cold slabs is most active at depths of 70-90 km, where seismic velocity in the crust abruptly increases, suggesting that high pore pressures generated as a result of dehydration reactions in the crust facilitate intermediate-depth seismicity. In contrast, seismicity is almost absent in the subducting crust of warm slabs like Cascadia and Nankai. The aseismic crust may be explained by slow dehydration rates in warm slabs, which cannot increase pore pressures effectively.

Magmatism beneath the arc has been discussed in terms of the heterogeneities in seismic velocities together with geochemical and petrological constraints. We recently developed simple but useful method to estimate seismic attenuation structures and applied it to waveform data in NE Japan. Seismic attenuation provides additional insights into ongoing magmatic processes in subduction zones, because higher-temperature environments or the existence of fluids may have different effects on seismic attenuation from on seismic velocity. The obtained results show that a depth profile of Qp?1 in the back-arc mantle is explained by attenuation expected for a two-dimensional (2-D) thermal model. However, an inclined high-attenuation zone observed in the back-arc mantle wedge, which is interpreted as an upwelling flow, shows higher attenuation than that calculated from the 2-D thermal model. The higher seismic attenuation is probably caused by the concentration of partial melt in the upwelling flow. Our results further imply the breakdown of hydrous minerals in a hydrous layer above the Pacific plate at a depth of ˜120 km.

Keywords: dehydration, pore pressure, eclogitization, seismic attenuation

Japan Geoscience Union Meeting 2014
(28 April - 02 May 2014 at Pacifico YOKOHAMA, Kanagawa, Japan)

SIT02-02 Room:211 Time:April 29 14:30-14:45

Imaging mantle melting processes and the effect of water beneath island arcs and backarc spreading centers

WIENS, Douglas[1*] ; WEI, S. shawn[1]

[1]Washington University, St Louis, MO, USA

We use arrays of land and ocean bottom seismographs to image melting processes in the Mariana and Tonga-Lau mantle wedges. Both regions show arc volcanism, active backarc spreading, and a gradient in mantle water content going from slab to backarc spreading center. The Lau backarc in particular shows a gradient in inferred mantle water content as the spreading centers approach the arc and slab in the south. Water contents range from near-MORB conditions in the Central Lau Spreading Center (CLSC) to high water content for the Eastern Lau Spreading Center (ELSC) and nearly arc-like for the Valu Fa Ridge (VFR).

For both Mariana and Lau we find significant slow velocity and high attenuation anomalies in the upper 100 km of the mantle beneath the volcanic arc and the spreading center. In the Mariana region, the anomalies are separated by a high velocity, low attenuation region at shallow depths (<80 km), implying distinct arc and backarc melting regions, with the anomalies coalescing and possibly allowing material interchange at greater depths. The maximum anomaly in the backarc is shallower (˜30 km) than in the arc (˜65 km), consistent with geochemical indications on the depth of melt production in these regions. The strongest anomaly beneath the backarc spreading center is narrow (˜70 km) and extends from close to the moho to 80 km depth. Data analyses for the Tonga-Lau project are preliminary, but show similarities to the Mariana images. Extremely low seismic velocity and high attenuation are found in a 100 km wide region beneath the spreading center in the upper 80 km. At deeper depths the anomaly is displaced westward in both velocity and attenuation images, suggesting that partial melting occurs along an upwelling limb of mantle flow originating west of the backarc. 3-D images from Rayleigh wave tomography show a much stronger anomaly along the CLSC when compared to the southern ELSC and VFR. The backarc velocity and attenuation anomalies are stronger in the Lau basin than in the Mariana backarc, perhaps due to higher mantle temperatures inferred from petrology.

Both Q and velocity anomalies are larger than expected for temperature effects based on laboratory-derived relationships, and their configuration is inconsistent with the expected temperature field. In addition, the observed anomalies are roughly inversely proportional to inferred mantle water content, suggesting that water content does not cause the observed large seismic anomalies. However, experimental results suggest that seismic attenuation and velocity are highly sensitive to the presence of even very small amounts of partial melt. Therefore we suggest the high attenuation and low velocity anomalies delineate the melt production regions beneath the ridge axis and volcanic arc, but that only small melt fractions (<1 %) are required to explain the seismic data. Smaller amplitude anomalies beneath the VFR, where large amounts of subduction-derived water are incorporated into the melt, may indicate lower mantle melt porosity due to low melt viscosity and more efficient transport of the water-rich melt, or a different topology of melt in the matrix. A lower melt porosity for aqueous melts is also consistent with the smaller seismic anomaly seen for the water-rich volcanic arc melting regions compared to the backarc melt production zone for both regions.

Keywords: seismic tomography, island arcs, backarc spreading centers, seismic attenuation, mantle fluids, melt generation

Japan Geoscience Union Meeting 2014
(28 April - 02 May 2014 at Pacifico YOKOHAMA, Kanagawa, Japan)

SIT02-03 Room:211 Time:April 29 14:45-15:00

Slab Melting in Subduction Zones

SCHMIDT, Max[1*] ; MANN, Ute[1]

[1]ETH Zurich, Switzerland

Depending on temperature, slab-to-mantle element transfer in the subarc region may either occur through fluids or melts. In this contribution we present pelite melting experiments systematically varying H_2O and CO_2 contents and review the presently available information on slab melting. Synthetic pelite model compositions containing variable proportions of H_2O (0.7-4.4 wt%) and CO_2 (0-4 wt%) was melted at 3-4.5 GPa and 750-1200 ^oC. The fluid-saturation concentration at 3-8 GPa (i.e. the H2O stored in phengite as the only hydrous phase) is 0.8-0.9 wt% H_2O. We locate the fluid-absent solidus of the H_2O-pelite system at 3 to 4.5 GPa at 880 ^oC to 1050 ^oC about 150-200 ^oC higher than the wet solidus (3 to 4.5 GPa, 730 to 860 ^oC). CO_2 increases the fluid-saturated solidus temperature by ˜30 ^oC but leaves the fluid-absent solidus temperature unchanged. For all systems considered, the onset of melting is controlled by phengite and only in the fluid-absent experiments K-feldspar becomes a product of melting (at 3 GPa).

Compiling all available information, we parameterize the amount of melt to be formed as a function of temperature for fluid-saturated and fluid-undersaturated conditions. Melt compositions themselves are meta- to peraluminous high Si-granites (71-77 wt% SiO_2 on a volatile free basis) with low Fe,Mg, and Ca contents and are uniform to ˜50% melting when plotted as a function of melt fraction (but not temperature), almost independent of starting compositions. At $>$2 wt% bulk H_2O melts are sodic (K/Na =0.2-0.4), while at $<$1.5 wt% melts are mostly potassic (K/Na=0.9-1.7). Only the fluid-poor H2O-CO2 and the CO2-only experiments of Thomsen and Schmidt (2008, EPSL) and Tsuno and Dasgupta (2011, CMP) produce significantly different melts i.e. rather potassic phonolites (Na being increasingly retained in jadeitic cpx with pressure). Near 5 GPa a fundamental change occurs: the H_2O-silicate solidus comes to an endpoint while in CO_2-rich systems a carbonatite replaces the silicate melt lowering the solidus temperature by more than 100 ^oC to 9 GPa.

Regarding the likelihood of sediment melting in the subarc region, only the wet solidus is within reach of the hottest geotherms of the thermal models that predict the highest slab-surface temperatures, i.e. none of the Arcay et al (2007, EPSL) slab surface P-T paths cross the solidus while for Syracuse et al. (2010, G3) about 7 out of 56 modeled slab segments have P-T-paths that may lead to significant melting for H_2O-saturated pelites at 3-4 GPa. As retention of significant amounts of fluids within a subducting lithology is not an option, flushing with fluids from dehydrating serpentinites would be the only option for achieving significant melting in the hottest subduction zones (at the required P-T conditions, there are no suitable reactions in the mafic crust or the sediments themselves). An alternative option to reach widespread pelite melting would be to dismiss the rigid slab surface concept and allow for sediment diapirs to rise into the hot mantle (Gerya and Yuen, 2003, EPSL; Behn et al, 2011, Nature Geosci.) in which case the pelites could bleed out their incompatible elements completely. Nevertheless, these diapirs are propelled by a density contrast resulting from partial melting and it remains unclear whether they could start rising without melting in the first place.

In conclusion, combining P-T paths, phase diagrams and degrees of melting suggests that significant pelite melting at a rigid slab-mantle interface appears to be a rather rare on present day Earth (and hence much more so for mafic materials), the only option for widespread pelite melting appears to be entrainment of the sediments into the mantle wedge. Removal of CO_2 through melting is utterly inefficient and as subsolidus metamorphic reactions lead to low X_{CO2} fluids, most of the subducted CO_2 will be fed into the deep beyond-arc C-cycle.

Keywords: slab melting, H2O, CO2, pelite

Japan Geoscience Union Meeting 2014
(28 April - 02 May 2014 at Pacifico YOKOHAMA, Kanagawa, Japan)

SIT02-04 Room:211 Time:April 29 15:00-15:15

Diverse magmatic effects of subducting a hot slab in SW Japan: results from forward modeling

KIMURA, Jun-ichi[1*] ; GILL, James[2]

[1]JAMSTEC, [2]University of California Santa Cruz

In response to the subduction of the young Shikoku Basin of the Philippine Sea Plate, arc magmas erupted in SW Japan throughout the late Cenozoic. Many magma types are present including ocean island basalt (OIB), shoshonite (SHO), arc-type alkali basalt (AB), typical sub-alkalic arc basalt (SAB), high-Mg andesite (HMA), and adakite (ADK). OIB erupted since the Japan Sea back-arc basin opened, whereas subsequent arc magmas accompanied subduction of the Shikoku Basin. However, there the origin of the magmas in relation to hot subduction is debated. Using new major and trace element and Sr-Nd-Pb-Hf isotope analyses of 324 lava samples from seven Quaternary volcanoes, we investigated the genetic conditions of the magma suites using a geochemical mass balance model, Arc Basalt Simulator version 4 (ABS4), that uses these data to solve for the parameters such as pressure/temperature of slab dehydration/melting and slab flux fraction, pressure, and temperature of mantle melting. The calculations suggest that those magmas originated from slab melts that induced flux-melting of mantle peridotite. The suites differ mostly in the mass fraction of slab melt flux, increasing from SHO through AB, SAB, HMA, to ADK. The pressure and temperature of mantle melting decreases in the same order. The suites differ secondarily in the ratio of altered oceanic crust to sediment in the source of the slab melt. The atypical suites associated with hot subduction result from unusually large mass fractions of slab melt and unusually cool mantle temperatures.

Keywords: SW Japan, Volcanic rocks, Geochemistry, Forward model

Japan Geoscience Union Meeting 2014
(28 April - 02 May 2014 at Pacifico YOKOHAMA, Kanagawa, Japan)

SIT02-05 Room:211 Time:April 29 15:15-15:30

Fluids and earthquakes in the Japan subduction zone

ZHAO, Dapeng[1*]

[1]Tohoku University, Department of Geophysics

Detailed tomographic images are determined for the source areas of large crustal and megathrust earthquakes that occurred in the Japan subduction zone during 1995-2013, thanks to the availability of the dense Japanese seismic network that could locate accurately the mainshocks and aftershocks of those large earthquakes and provide high-quality arrival-time data for tomographic imaging. Suboceanic events are relocated precisely using sP depth phase. Large crustal earthquakes in the forearc region such as the 1995 Kobe earthquake (M 7.2) and the 2011 Iwaki earthquake (M 7.0) might be triggered by fluids that are released from the dehydration of the subducting slab and directly ascend to the crust and enter an active fault zone. In contrast, along the volcanic front and in back-arc areas, the seismogenic layer in the upper crust is thinned and its mechanical strength is weakened because of ascending hot magmas and fluids which are produced by a combination of slab dehydration and corner flow in the mantle wedge. Large crustal earthquakes are apt to take place at the edge portion of the thinned seismogenic layer which exhibits low velocity, high Poisson's ratio, and high electrical conductivity. To clarify the generating mechanism of the 2011 Tohoku-oki earthquake (Mw 9.0) and the induced tsunami, we determined high-resolution tomographic images of the Northeast Japan forearc. Significant lateral variations of seismic velocity are visible in the megathrust zone, and most large interplate thrust earthquakes are found to occur in high-velocity (high-V) areas. These high-V zones may represent high-strength asperities at the plate interface where the subducting Pacific plate and the overriding Okhotsk plate are coupled strongly. A shallow high-V zone with large coseismic slip near the Japan Trench may account for the mainshock asperity of the 2011 Tohoku-oki earthquake. Because it is an isolated asperity surrounded by low-velocity patches, most stress on it was released in a short time and the plate interface became decoupled after the Mw 9.0 earthquake. Thus the overriding Okhotsk plate there was shot out toward the Japan Trench and caused the huge tsunami. Further details of the role of arc magma and fluids in the nucleation process of a large earthquake can be clarified by high-resolution geophysical imaging and multidisciplinary studies of the earthquake fault zones.

Keywords: fluids, earthquakes, Japan Islands, subduction zones, magma, slab

Japan Geoscience Union Meeting 2014
(28 April - 02 May 2014 at Pacifico YOKOHAMA, Kanagawa, Japan)

SIT02-06 Room:211 Time:April 29 15:45-16:00

Silicate solute in aqueous fluids governs trace element and stable isotope behavior in subduction zones

MYSEN, Bjorn[1*]

[1]Geophysical Laboratory, CIW, USA

Physical and chemical properties of fluids equilibrated with subducting deep crust and overlying upper mantle are saturated in silicate components [1]. These components govern physical and chemical properties of the fluids. For example, the solution behavior of volatile components such as hydrogen, carbon, and nitrogen, which form bonding with silicate components in fluids, will differ from the behavior in pure H_2O fluids [2]. This can also affect isotope fractionation between fluids and condensed silicate materials.

In pure H_2O, hydrogen bonding plays a role to temperatures $<$600 ℃ at pressures in the 1 GPa-range with a $\triangle$H for hydrogen bond formation near 20 kJ/mol. At temperatures less than 600 ℃, physical properties of fluids, including density, compressibility, and viscosity, are non-linear functions of temperature, whereas at higher temperature and in the absence of hydrogen bonding, these properties tend to become linear functions of temperature. Solution of silicate components in aqueous fluids changes these relationship. The silica solubility in equilibrium with quartz/coesite reaches $>$5 mol/kg near 5 GPa and 900 ℃ with polymerized silicate species, SiO_4, Si_2O_7, and SiO_3 in the fluid. In equilibrium with enstatite and forsterite, the silicate solubility is ~50% less and only SiO_4 and Si_2O_7 species exist in the fluids. Those variables affect D/H isotope ratios. For example, the fluid/melt partition coefficients for hydrogen, KH, varies by ~40% as a function of variable silicate speciation in fluids in the 500 ℃-800 ℃/0.5-1 GPa temperature and pressure range. The hydrogen fluid/melt partition coefficient exceeds that of deuterium. Their temperature-dependence also differs so that for the exchange equilibrium of D and H between coexisting water-saturated melt and silicate-saturated aqueous fluid, the $\triangle$H is between -4 and -6 kJ/mol. This difference is because in the more silicate-rich fluids (higher proportion of polymerized silicate species), the abundance ratio, OD/OH, is higher in the more polymerized silicate species in the fluid. As a result, increasing pressure, which leads to increasingly polymerization of silicate, will cause the D/H ratio of the fluid will increase. This also means that D/H fractionation between aqueous fluid and condensed silicate increases with increasing pressure.

Interaction between dissolved silicate components and other elements can also affect their solubility and, therefore, their roles as geochemical tracers. For example, in the system rutile+H_2O, the Ti solubility in the few-GPa-range at ~1000 ℃ is on the order of 1-100 ppm as compared with thousands of ppm in silicate-saturated aqueous solution [3]. This difference between pure H_2O and silicate-saturated fluid is related to interaction with the silicate species dissolved in the fluid, $2M_6Si_2O_7 + 4H_2O + TiO_2 = 4(MH)_2SiO_4 + M_4TiO_4$, where M is a metal cation. Similar situation likely exist for other nominally insoluble, highly charged elements (e.g., Al^{3+}, Zr^{4+}, Hf^{4+}, P^{5+}).

When modeling isotope fractionation and partitioning of nominally insoluble elements between fluid and condensed phases (melts and minerals) in the deep crust and upper mantle of the Earth, the silicate solute concentration and structure in the fluid and the water concentration and structure of silicate melts both can have major effects on the fractionation factors. These factors depend on the element or isotope ratio in question. They also vary with pressure (and likely temperature) because the structure if dissolved silicate in aqueous fluids varies with pressure and temperature.

[1] C. E. Manning, Eart Planet. Sci. Lett. 2004, 223, 1-16.
[2] B. O. Mysen, Lithos 2012, 148, 228-246.
[3] A. Antignano and C. E. Manning, Chemical Geology 2008, 255, 283-293.

Keywords: aqueous fluid, solubility, subduction, stable isotope, structure, fluid property

Japan Geoscience Union Meeting 2014
(28 April - 02 May 2014 at Pacifico YOKOHAMA, Kanagawa, Japan)

SIT02-07 Room:211 Time:April 29 16:00-16:15

D/H intramolecular partitioning in alkali silicate melts: with implications for tracing subduction processes

LE LOSQ, Charles[1*] ; CODY, George[1] ; MYSEN, Bjorn[1]

[1]Geophysical Laboratory, Carnegie Institution of Washington

The D/H ratio is an important probe for studying the cycle of water in the Earth interior in general, and in subduction zones in particular. Indeed, D/H ratios in melt inclusions (MIs) of arc magmas for instance indicate that the δD of subduction fluids is high, near -30 ‰, compared to the δD of the mantle that is near -80 ‰. A possible explanation for these different values is that D/H fractionation during dehydration of the slab in subduction zones enriches the subduction fluids in D, leading to high δD values in subduction magmas. This might be accomplished with hydrogen exchange between the melt and another source enriched in D before entrapment of MIs or a diffusive loss of H from within the inclusion leading to D/H fractionation. However, chemical effects affecting the δD ratio have not been considered because it is usually assumed that D and H have the same chemical and structural properties in silicate melts and glasses.

However, recent results from ^{2}H and ^{1}H MAS NMR of $Na_2Si_4O_9$ glasses quenched from melt (equilibrated with fluid at 1400?C and 1.5 GPa) with various amounts of $(D_xH_{(1-x)})_2O$ (x = D/[D+H]) lead to the conclusion that D and H isotopes occupy different structural positions in the network. From the ^{1}H MAS NMR spectra OH^- groups are distributed in two environments with mean O ⋯ O distances close to 0.26 and 0.29 nm in the $Na_2Si_4O_9$ glass. These environments give rise to two strong NMR lines at 16 and 5 ppm respectively. By contrary, ^{2}H MAS NMR spectra of the same glasses display a strong line at 16 ppm accompanied by a small band near 5 ppm regardless of D/H ratio and total water concentration. This observation leads to the suggestion that OD^- groups are mainly present in an environment with small O ⋯ O distances. In other words, the structural behavior of OH^- and OD^- groups in the quenched silicate melts (glasses) differs.

In $M_2Si_4O_9$ glasses, (M = Li, Na or K) with different concentrations of pure H_2O or D_2O (from 3.3 up to 17.6 mol%), ^{2}H and ^{1}H MAS NMR spectra confirm that by exchanging H with D the intensity of the 16 ppm NMR line increases greatly, whereas the intensity of the 5 ppm line decreases drastically. Interestingly, such a spectral evolution is also observed when increasing the size of the alkali element in the network of hydrous alkali silicate glass. These effects are attributed to steric and electronic effects in the environment of alkali elements, which cause shifts in the equilibrium between H_2O the O^{2-} of the silicate network:

$H_2O_{mol} + O^{2-} \Leftrightarrow 2OH^-$, (1)

The specific preference of OD^- groups for small O ⋯ O sites is in this mind intriguing, but is not in conflict with previous observations. Indeed, increasing the ionic size of alkali elements lead to promote OH^- in the small O ⋯ O environment. Similarly, it appears that increasing the size of the proton (by substituting H by D) promotes their existence in this small O ⋯ O environment. On this basis, we propose that those two observations have a common origin, maybe related to the probability of interaction between H/D and alkali elements depending of their ionic size and/or to molar volume effects related to those ionic sizes.

This large structural-controlled partitioning of D and H in melts, which depends on the melt composition, might be another fractionation process affecting the δD of subduction melts. Consequently, δD values recorded in MIs might be the result of such a structural process and might not reflect the δD of released fluids in the mantle wedge during slab subduction.

Keywords: D/H isotopes, silicate glass, NMR spectroscopy, Raman spectroscopy, Subduction fluids

Japan Geoscience Union Meeting 2014
(28 April - 02 May 2014 at Pacifico YOKOHAMA, Kanagawa, Japan)

SIT02-08 Room:211 Time:April 29 16:15-16:30

Speciation and solubility of F and Cl in coexisting fluids ad silicate melts: implications for F and Cl signature in arc

DALOU, Celia[1*] ; MYSEN, Bjorn[2] ; FOUSTOUKOS, Dionysis[2]

[1]Jackson School of Geosciences, The University of Texas at Austin, [2]Geophysical Laboratory, Carnegie Institution of Washington

The effect of pressure and temperature on the structure of silicate melts coexisting with silica-saturated aqueous electrolyte solutions enriched in fluorine or chlorine in the Na_2O-Al_2O_3-SiO_2-H_2O system has been determined. In-situ measurements were conducted with the samples at desired temperatures and pressures in a hydrothermal diamond anvil cell (HDAC) by using microRaman and FTIR spectroscopy techniques. The data were acquired at high temperature and pressure (up to 800oC and 1264 MPa, respectively), and during cooling/decompression to ambient conditions.

The intensity of the Raman bands assigned to stretch vibration of the OH-groups relative to those of coexisting molecular H_2O in silicate melts is lower in the presence of F and Cl. This difference reflects the interaction of F or Cl with H_2O in the melts. With decreasing pressure and temperature (P-T) conditions, SiF complexes are favored in the melt rather than in the fluid, perhaps because of decreasing silicate concentration in fluids with decreasing temperature and pressure. In melts, the solubility of Cl, likely in the form of $NaCl_{(aq)}$, increases with decreasing P-T conditions, whereas the abundance of such complexes in coexisting fluids decreases.

Our experiments data were employed to help model the ascent of a magma-fluid system from the upper mantle to the shallow crust. The information offers particular insights into F and Cl partitioning between and the speciation of F and Cl in melts and magmatic fluids. We suggest that the formation of stable SiF and NaCl complexes and their increasing solubilities during magma ascent explain the late volcanic degassing of F and Cl, compared to other volatile species.

It explains why F and Cl are often undersaturated in arc basaltic magmas (Carroll and Webster, 1994), indicating that they often do not a significant experience a degassing event. In contrast to H_2O, CO_2 and S, F and Cl signature in primary arc magmas (arc melt inclusions) can be consider as primary and likely retain information on arc magma sources.

Those results also imply that, while Cl is enriched in aqueous fluids from slab dehydration, F preferentially dissolves in slab melts or supercritical fluids, during flows from the subducted slab into the zone of melting in the mantle wedge. It is therefore expected that at given pressure and temperature, the Cl/F ratio is significantly lower in slab melt and supercritical fluids, than in aqueous fluids. This difference in Cl/F signatures decrease when slab components are dragged down to the deep mantle.

Keywords: Fluorine, Chlorine, silicate melt, aqueous fluid, speciation, HDAC

Japan Geoscience Union Meeting 2014
(28 April - 02 May 2014 at Pacifico YOKOHAMA, Kanagawa, Japan)

SIT02-09 Room:211 Time:April 29 16:30-16:45

The Structure of Water-Saturated Carbonate Melts

FOUSTOUKOS, Dionysis[1*] ; MYSEN, Bjorn O.[1]

[1]Geophysical Laboratory, Carnegie Institution of Washington, USA

The structure of water-saturated Ca- and Mg-bearing carbonate melts under reducing and oxidizing conditions was investigated in a series of hydrothermal anvil cell experiments conducted at 400 - 1100 ^{o}C and 442 - 2839 MPa. Equilibria were investigated in the calcite-H_2O, calcite-CaO-H_2O, magnesite-H_2O and magnesite-MgO-H_2O systems, with redox conditions controlled by Re/ReO_2 and Ti/TiO_2assemblages. Melting relationships and the C-O-H speciation of the coexisting aqueous fluid and melt were assessed in-situ by Raman vibrational spectroscopy. Hydrous melting of $MgCO_3$-MgO occurred at ˜850 ^{o}C, 1.5 - 2 GPa. In the $CaCO_3$-CaO-H_2O system, melt was formed at 600 - 900 ^{o}C and pressures of 0.5 - 1.5 GPa because of melting-point depression imposed by the presence of CaO. The C-O-H speciation of the carbonate melts and coexisting supercritical aqueous solutions was mainly H_2O and ${CO_3}^{2-}$, with traces of $CO_{2(aq)}$ and $CH_{4(aq)}$ in the fluid phase. The melt-fluid H_2O partition coefficients attained in the Mg-bearing melt (median 0.5) were higher than in the Ca-bearing melt (median 0.3). Under oxidizing redox conditions, dissolved ReO^{4-} was present in all phases, underscoring the enhanced solubility of trace elements and metals in carbonate-bearing melts and carbonatites. In effect, the enhanced solubility of H_2O along with the ionic nature of the carbonate melts may promote the solvation of ionic species in the melt structure.

From in-situ vibrational spectroscopy, the v_1-${CO_3}^{2-}$ vibration recorded in the melt spectra suggests the presence of intermolecular interactions between the oxygen of the carbonate ion with water dissolved in the melt. The thermodynamic properties of this water appear to be similar to the supercritical aqueous phase. For example, the estimated enthalpy for the breakage of the hydrogen bonding between water molecules attained values of 6.8 $\pm$ 1.5 kcal/mol and 8.4 $\pm$ 1.3 kcal/mol in the melt and fluid phase, respectively. The calculated partial molar volume of H_2O in the melt (˜48 $\pm$ 6 cm^3/mol) is also comparable to the partial molar volume of supercritical water at similar conditions. Interestingly, this value is considerably greater than published partial molar volume values for H_2O in silicate melts (10-12 cm^3/mol).

The pressure-temperature melting relationships of the CaO-CO_2-H_2O and MgO-CO_2-H_2O systems highlight the important role of water and alkali earth oxides on the hydrous melting of the carbonate-bearing subducting oceanic crust. Carbonates present in marine sediments or serpentinized peridotites may melt before complete dehydration at the slap-mantle wedge transition zone, and thus, never reach sub-arc depths. To this end, melting of carbonate minerals at crustal temperatures and pressure can contribute to the volcanic CO_2 flux at the arc through melt/fluid interactions.

Keywords: carbonate melt, aqueous solutions, hydrothermal diamond anvil cell, raman vibrational spectroscopy

Japan Geoscience Union Meeting 2014
(28 April - 02 May 2014 at Pacifico YOKOHAMA, Kanagawa, Japan)

SIT02-P01 Room:Poster Time:April 29 18:15-19:30

Later phase observations and seismic velocity structure in the subducting crust of the Pacific slab beneath Hokkaido

SHIINA, Takahiro[1*] ; NAKAJIMA, Junichi[1] ; TOYOKUNI, Genti[1] ; MATSUZAWA, Toru[1] ; KITA, Saeko[2]

[1]RCPEV, Grad. Sch. of Sci., Tohoku Univ., [2]NIED

The subducting crust at the uppermost part of the oceanic lithosphere is considered to play important roles for generation of intraslab earthquakes (e.g., Kirby et al., 1996) and arc-magmatism in the mantle wedge (e.g., Nakajima et al., 2013), because the crust involves a large amount of water in form of hydrous minerals and these hydrous minerals affect seismic velocities in the crust (e.g., Hacker et al., 2003). Therefore, to understand water circulation in the subduction zones and genesis of intermediate-depth earthquakes, it is important to reveal where dehydration reaction of hydrous minerals occurs in the crust. However, it is generally difficult to obtain the detailed velocity variation in the crust because the thickness of the crust is ˜7 km.

Later phases, such as mode-converted wave and guided wave, are sensitive to heterogeneous structure in the crust because of their longer propagation paths in the crust, and hence they are very useful to resolve small-scale seismic velocity structure in the crust (e.g., Matsuzawa et al., 1986; Abers, 2005).

At the Hidaka mountain range, middle of Hokkaido, northern Japan, some later phases are reported from earthquakes that occurred in the Pacific slab (e.g., Shimizu and Maeda, 1980). A later phase (Xp phase) recorded in this region has some characteristics: 1) amplitudes of Xp phase are similar to or larger than those of the P wave, 2) Xp-P time lies in a range of 2-10 s and increases with epicentral distances. Shiina et al. (2013, SSJ) discussed the origin of the Xp phase with numerical modeling and interpreted the Xp phase as guided P-wave that propagated in the crust. Moreover, we identified a later phase (Xs phase) that arrives several second after the theoretical initial S waves, and such a phase usually appears in seismograms with guided P-wave. We interpreted the Xs phase as guided S-wave by comparison characteristics of guided P-wave and results of numerical modeling.

In this study, based on these interpretations for later phases that observed in the western part of Hidaka mountain range, we estimated P- and S-wave velocity distributions in the subducting crust beneath the eastern part of Hokkaido. The number of arrival times of guided P- and S-waves picked in this study is 117 records and 56 records, respectively. Then, we obtained Vp of 6.8-7.7 km/s and Vs of 3.5-4.0 km/s at depths of 50-100 km in the crust. The obtained Vp in the crust is similar to that observed beneath Tohoku (Shiina et al., 2013) and lower than that expected for fully-hydrated MORB materials (e.g., Hacker et a., 2003). This result suggests that aqueous fluids may co-exist with hydrous minerals in the crust beneath the eastern part of Hokkaido.

Keywords: subducting crust, later phase, guided wave, the Pacific slab

Japan Geoscience Union Meeting 2014
(28 April - 02 May 2014 at Pacifico YOKOHAMA, Kanagawa, Japan)

SIT02-P02 Room:Poster Time:April 29 18:15-19:30

Pore fluid geochemistry and carbonates in cores and cuttings from the Nankai accretionary prism

EVEN, Emilie[1*] ; SAMPLE, James C.[2] ; FUCHIDA, Shigeshi[1] ; IODP EXPEDITION 348, Shipboard scientists[3]

[1]Graduate School of Science, Osaka City University, [2]School of Earth Sciences and Environmental Sustainability, Northern Arizona University, [3]IODP Expedition 348

The recent IODP Exp 348 at Site C0002 has successfully deepened Hole C0002F (Exp 338) down to 3058.5 mbsf, deep into the accretionary prism of the Nankai Trough. During Exp 348, cuttings were collected and analysed from drilled interval of Holes C0002N (875 mbsf- 2325 mbsf) and C0002P (1965 mbsf- 3059 bsf) and limited coring was performed from 2163 to 2218 mbsf in Hole C0002P. The major-element composition of the solid cuttings and the geochemistry of interstitial water in cores was determined. Results provide insights into exchange of elements between minerals and pore water phases, and into geochemical signatures related to lithological changes within the prism. This study reports the main geochemical results from IODP Exp 348.

Interstitial waters were collected using the GRIND method (Wheat et al., 1994), in which core sediments were ground in an agate mill with ultra-pure water. The interstitial water percentage was determined by drying sediments at 60 ℃ and 105 ℃, the former to minimize loss of clay-bound water, and the latter to follow the GRIND procedure used in previous expeditions. Concentrations were interpreted with data corrected for dilution at 60 ℃, 105 ℃ and normalised to chlorinity values. Profiles of carbonates (as $CaCO_3$), organic carbon and total nitrogen were determined from cuttings of 1-4 mm and $>$4 mm sizes and are compared with the observed lithological boundaries. Carbonate veins were observed in a core sample exhibiting a fault zone at ?2205 mbsf, but no increase was observed at the same depth in the carbonates profile.

The GRIND method has limitations in recovering absolute values of dissolved ions in interstitial waters, and yielded very high dissolved-ion concentrations in some samples. But comparison of ions normalized to chlorinity yielded results comparable to what was observed in pore waters at shallower depths of Site C0002. Some of the trend variations in the cuttings profiles of carbonates, organic carbon and nitrogen match the unit boundaries determined by observation of lithological changes in the cuttings. Therefore, it can be suggested to integrate these data when defining geological units.

Wheat, Boulegue and Mottl (1994) Proc. ODP, Sci. Results, 139: College Station, TX (Ocean Drilling Program), 429-437

Keywords: Accretionary prism, GRIND method, IODP Expedition 348, Nankai Trough, Pore water

Japan Geoscience Union Meeting 2014
(28 April - 02 May 2014 at Pacifico YOKOHAMA, Kanagawa, Japan)

SIT02-P03 Room:Poster Time:April 29 18:15-19:30

Solution mechanism of water in depolymerized silicate melts

CHERTKOVA, Nadezda[1*] ; YAMASHITA, Shigeru[1]

[1]Okayama University, ISEI

It is known that the effect of dissolved water on the viscosity of silicate melts is larger for polymerized melts than for depolymerized melts [*e.g.*, 1, 2]. Direct spectroscopic measurements of melt structure and water speciation at high temperature provide information about the mechanism of water dissolution and its influence on the physical properties of the melts. While *in situ* measurements of water speciation were widely conducted for rhyolitic melts and their analogues [*e.g.*, 3, 4, 5], only limited data are available for depolymerized silicate melts.

We performed high-temperature near-infrared and Raman spectroscopic measurements of hydrous $Na_2Si_2O_5$ melts (2.3-8.1wt% H_2O) using externally heated diamond anvil cell (HDAC). $Na_2Si_2O_5$ composition was chosen as a structural analogue of basaltic melt (anhydrous NBO/T = 1). Experimental pressure was monitored with the pressure- and temperature-dependent Raman shift of ^{13}C diamond [6]. Near-infrared spectra of the homogeneous liquid phase, observed above 820 degree C, 1.7GPa in the $Na_2Si_2O_5$+2.3wt%H_2O system and above 700 degree C, 1.6GPa in the $Na_2Si_2O_5$+8.1wt%H_2O system, contain absorption peaks corresponding to molecular H_2O (at ~5200 cm^{-1}) and structurally bound OH groups (at ~4500 cm^{-1}). At 900 degree C and 1.6-1.9GPa the ratio of these peaks height remains approximately constant (2.6-2.2), implying a constant (structurally bound OH)/(molecular H_2O) ratio for this range of water contents. This observation differs from the regularities reported for more polymerized melts (rapid decrease of OH/H_2O with total water content) [*e.g.*, 4, 7]. At the same time no pressure effect on the ratio of 4500 cm^{-1} peak height to 5200 cm^{-1} peak was observed below 2.4 GPa.

References

[1] Whittington A., Richet P., Holtz F. (2000) Geochim Cosmochim Acta 64, 3725-3736.
[2] Giordano D., Russell J.K., Dingwell D.B. (2008) Earth. Planet. Sci. Lett. 271, 123-134.
[3] Sowerby J.R., Keppler H. (1999) Am. Mineral. 84, 1843-1849.
[4] Nowak M., Behrens H. (2001) Earth. Planet. Sci. Lett. 184, 515-522.
[5] Shen A.H., Keppler H. (1995) Am. Mineral. 80, 1335-1338.
[6] Mysen B.O., Yamashita S. (2010) Geochim. Cosmochim. Acta 74, 4577-4588.
[6] Mysen B.O. (2010) Geochim. Cosmochim. Acta 74, 4123-4139.
[7] Botcharnikov R.E., Behrens H., Holtz F. (2006) Chem. Geol. 229, 125-143.

Keywords: water speciation, hydrothermal diamond anvil cell, near-infrared spectroscopy, Raman spectroscopy

Japan Geoscience Union Meeting 2014
(28 April - 02 May 2014 at Pacifico YOKOHAMA, Kanagawa, Japan)

SIT03-01 Room:418 Time:April 29 09:00-09:15

Effect of the upper mantle structure on the Moho geometry

TENZER, Robert[1*] ; CHEN, Wenjin[1]

[1]School of Geodesy and Geomatics, Wuhan University

We investigate the effect of the lateral density structure within the upper (most) mantle on the Moho geometry. The gravimetric forward and inverse modeling methods are applied to determine the Moho depths using the gravity data corrected for major known anomalous density structures within the Earth crust. In our numerical experiment we compute and compare the Moho geometry determined using uniform and laterally varying models of the Moho density contrast. The laterally varying model of the Moho density contrast incorporates the information on the upper mantle lateral density structure taken from the CRUST1.0 global crustal model. For the uniform density contrast model, the constant value of the Moho density contrast is determined based on minimizing the spatial correlation between the gravity data and the Moho geometry. Except for the upper (most) mantle, the deeper heterogeneous mantle density structures including the core-mantle boundary zone are not taken into consideration due to the absence of a reliable 3-D density model of the whole mantle. The numerical results revealed that the consideration of the upper mantle density structure improves the fit of the gravimetric solution with the seismic Moho model.

Keywords: crust, density, gravity, mantle, Moho

Japan Geoscience Union Meeting 2014
(28 April - 02 May 2014 at Pacifico YOKOHAMA, Kanagawa, Japan)

SIT03-02 Room:418 Time:April 29 09:15-09:30

Conductivity anisotropy of partial molten peridotite under shear deformation

ZHANG, Baohua[1] ; YOSHINO, Takashi[1*] ; YAMAZAKI, Daisuke[1]

[1]Institute for Study of the Earth's Interior, Okayama Univ.

Recent ocean bottom magnetotelluric investigations have revealed a high-conductivity layer (HCL) with high anisotropy characterized by higher conductivity values in the direction parallel to the plate motion beneath the southern East Pacific Rise (Evans et al., 2005) and beneath the edge of the Cocos plate at the Middle America trench offshore of Nicaragua (Naif et al., 2013). These geophysical observations have been attributed to either hydration (water) of mantle minerals or the presence of partial melt. Currently, aligned partial melt has been regarded as the most preferable candidate for explaining the conductivity anisotropy because of the implausibility of proton conduction (Yoshino et al., 2006).

In this study, we report development of the conductivity anisotropy of partial molten peridotite in three directions parallel and normal to shear on the shear plane, and perpendicular to the shear plane as a function of time and shear strain. Starting samples were pre-synthesized partial molten peridotite (Fe-free and Fe-bearing systems), showing homogeneous melt distribution. The Fe-free and Fe-bearing partially molten peridotite samples were deformed in simple shear geometry at 1 GPa and 1523 and 1723 K, respectively, in a DIA-type apparatus with uniaxial deformation facility. Conductivity of the partially molten peridotite parallel to the shear direction was initially identical to that normal to shear. However, shear-parallel conductivity increased by more than one order of magnitude after the initiation of shear by piston advancement. Shear-parallel conductivity then stayed constant for the duration of the experimental run. On the other hand, conductivity normal to the shear direction on the shear plane remained constant, whereas conductivity perpendicular to the shear plane decreased gradually after initiation of shear and finally close to that of olivine. Conductivity difference between parallel and normal to shear direction reached one order, which is equivalent to that observed beneath asthenosphere. In contrast, such anisotropic behavior was not found in the melt-free samples, suggesting that development of the conductivity anisotropy was generated under shear stress.

Microstructure of the deformed partial molten peridotite shows partial melt tends to preferentially locate grain boundaries parallel to shear direction, and forms continuously thin melt layer sub-parallel to the shear direction, whereas apparently isolated distribution was observed on the section perpendicular to the shear direction. The resultant melt morphology can be approximated by tube like geometry parallel to the shear direction. This observation suggests that the development of conductivity anisotropy is caused by the realignment of partial melt (forming tube-like melt) parallel to shear direction in the silicate matrix.

In conclusion, the high anisotropy of conductivity in the direction of plate motion can be well explained by anisotropic interconnection of melt in partially molten rocks at the top of asthenosphere, but not hydration of nominally anhydrous minerals. Therefore, our results provide the direct experimental evidence for supporting these geophysically observed high-conductivity anisotropy at the LAB and verify the validity of partial melting hypothesis (Yoshino et al., 2006; Naif et al., 2013).

References

Evans, R. L. et al. Geophysical evidence from the MELT area for compositional controls on oceanic plates. Nature 437, 249?252 (2005).

Naif, S., Key, K., Constable, S. & Evans, R. L. Melt-rich channel observed at the lithosphere?asthenosphere boundary. Nature 495, 356?359 (2013).

Yoshino, T., Matsuzaki, T., Yamashita, S. & Katsura, T. Hydrous olivine unable to account for conductivity anomaly at the top of the asthenosphere. Nature 443, 973?976 (2006).

Keywords: partial melting, asthenosphere, electrical conductivity, upper mantle, anisotropy, shear deformation

Japan Geoscience Union Meeting 2014
(28 April - 02 May 2014 at Pacifico YOKOHAMA, Kanagawa, Japan)

SIT03-03 Room:418 Time:April 29 09:30-09:45

Surface-wave phase velocity maps of North America with inter-station waveform analysis

HAMADA, Kouta[1*] ; YOSHIZAWA, Kazunori[2]

[1]Graduate School of Science, Hokkaido University, [2]Faculty of Science, Hokkaido University

The western United States encompasses a variety of tectonic features, including regions with east-west extension, volcanic areas and relatively stable cratonic regions.

In the last decade, the Transportable Array (USArray) has been installed throughout the U.S, and these waveform data have facilitated a variety of tomographic studies in this region using body and surface waves, and ambient noise analysis making the most of the high-density seismic network.

In this study, we have developed a new method of fully non-linear waveform fitting to measure inter-station phase velocities, using the Neighborhood Algorithm (NA) as a global optimizer. This algorithm searches for model parameters to fit two observed waveforms on a common great-circle path by perturbing the phase term of the fundamental-mode Love and Rayleigh waves. We have employed the reliability parameter, which represents how well the waveforms at two stations can be fitted in a time-frequency domain. This parameter is used as a data selection criterion for the subsequent step of phase velocity mapping.

The method has been applied to observed waveform data of the USArray from 2007 to 2010, and we could collect a large-number of phase speed data (over 45000 for Rayleigh and 15000 for Love) in a period range from 30 and 200 seconds, at short distances less than 1000 km. The phase velocity models for Rayleigh and Love waves indicate good correlation on large scales with the recent tomographic maps derived from different approaches for inter-station phase velocity measurements (Foster et al., 2013); e.g., significant slow velocity anomaly in volcanic regions in western Unites States and extremely fast anomaly in the cratonic region in the longer period range, which implies the robustness of such tectonic features as well as the validity of our new measurement technique. The current method can be expanded for the measurements of inter-station higher-mode phase velocities, which will be of great help in enhancing the vertical resolution of the 3-D shear wave models.

Keywords: surface wave, phase velocity, tomography, North America

Japan Geoscience Union Meeting 2014
(28 April - 02 May 2014 at Pacifico YOKOHAMA, Kanagawa, Japan)

SIT03-04 Room:418 Time:April 29 09:45-10:00

Diffusion to dislocation creep transition in the upper mantle inferred from silicon grain boundary diffusion rates

FEI, Hongzhan[1*] ; KATSURA, Tomoo[2] ; KOIZUMI, Sanae[3] ; SAKAMOTO, Naoya[4] ; HASHIGUCHI, Minako[5] ; YURIMOTO, Hisayoshi[5] ; YAMAZAKI, Daisuke[1]

[1]Institute for Study of the Earth's Interior, Okayama University, Japan, [2]Bayerisches Geoinstitut, University of Bayreuth, Germany, [3]Earthquake Research Institute, The University of Tokyo, Japan, [4]Isotope Imaging Laboratory, CRI, Hokkaido University, Japan, [5]Department of Natural History Sciences, Hokkaido University, Japan

The majority of the dynamical processes in the upper mantle are controlled by creep of minerals. Dislocation creep causes non-Newtonian viscosity and seismic anisotropy whereas diffusion creep causes Newtonian viscosity and no seismic anisotropy. Determination of deformation mechanism in the upper interior is thus essential to understand mantle dynamics. Previous deformation studies on olivine suggested that the shallow regions of the upper mantle should be dominated by dislocation creep and the deeper regions dominated by diffusion creep [Karato, 1992; Karato and Wu, 1993; Hirth and Kohlstedt, 2003]. However, recent study [Fei et al., 2013] demonstrated that those deformation experiments largely misunderstood the creep rate due to the experimental difficulties. Since the creep of olivine is controlled by silicon diffusion, we measured silicon grain-boundary diffusion coefficient in Mg-olivine aggregates as a function of pressure, temperature, and water content. The activation energy, activation volume, and water content exponent are found to be 240-260 kJ/mol, 1.8 ± 0.2 cm^3/mol, and 0.22 ± 0.05, respectively. Together with the silicon lattice diffusion data [Fei et al., 2012; 2013], our results predict the diffusion to dislocation creep transition in the upper mantle, which is in contrast with the previously considered model. In the asthenosphere, dislocation creep should dominate because of the high temperature. In the lithosphere, diffusion creep dominates in shallow regions and dislocation creep dominates in deeper parts. The seismic anisotropy jumps at mid-lithosphere discontinuity beneath continents and at Gutenberg discontinuity beneath oceans are caused by the transition from diffusion to dislocation creep. The weak anisotropy in cold lithospheres could be attributed to the fossil anisotropy formed at the spreading ridges. Dominance of diffusion creep in upper lithosphere accounts for the Newtonian rheology suggested by postglacial rebound.

Fei et al., *EPSL* **345**, 95-103 (2012).
Fei et al., *Nature* **498**, 213-215 (2013).
Hirth and Kohlstedt, *Geophys. Monogr.* **138**, 83-105 (2003).
Karato, *JGR* **19**, 2255-2258 (1992).
Karato and Wu, *Science* **260**, 771-778 (1993).

Keywords: diffusion creep, dislocation creep, upper mantle, silicon, grain boundary diffusion, deformation mechanism

Japan Geoscience Union Meeting 2014
(28 April - 02 May 2014 at Pacifico YOKOHAMA, Kanagawa, Japan)

SIT03-05 Room:418 Time:April 29 10:00-10:15

Aluminum incorporation into phase A - a new hydrous silicate in the deep upper mantle

CAI, Nao[1*] ; INOUE, Toru[1] ; FUJINO, Kiyoshi[1] ; OHFUJI, Hiroaki[1] ; KURIBAYASHI, Takahiro[2] ; YURIMOTO, Hisayoshi[3]

[1]Geodynamics Research Center, Ehime University, [2]Institute of Mineralogy, Petrology and Economic Geology, Graduate School of Science, Tohoku Universi, [3]Division of Earth and Planetary Sciences, Hokaido University

A new aluminum bearing hydrous silicate was found in the experiments under the deep upper mantle conditions, using phase A ($Mg_7Si_2O_8(OH)_6$) and $Al(OH)_3$ as the starting materials. Using electron probe micro analysis (EPMA) and secondary ion mass spectrometry (SIMS), the composition was determined to be very close to $Mg_{5.5}AlSi_2O_8(OH)_6$, which contained about 12 wt % of water. Almost pure phase was obtained in the subsequent experiments. The powder x-ray diffraction pattern and transmission electron diffraction patterns showed a hexagonal structure, with an abnormal large c axis. This new phase has similar stability region with phase A. At lower pressure and higher temperature, it breaks down into Chondrodite + Garnet + Brucite + Fluid, while at higher pressure and higher temperature, it breaks down into Al-superhydrous phase B + Garnet + Brucite + Fluid.

Besides, present study shows that phase A coexists with this aluminum bearing hydrous phase, with a small amount of aluminum ($<$1 wt%) incorporated into phase A structure, which predicts that phase A can preserve only trace of aluminum.

According to Inoue's unpublished data, aluminum can easily incorporate into some dense hydrous magnesium silicates and form aluminum bearing hydrous phases such as phase B, superhydrous phase B, and even perovskite. However, rather than aluminum bearing phase A, the present study shows a small amount of aluminum incorporation into phase A structure, and an appearance of a new aluminum bearing hydrous phase, with the composition very similar to phase A but structure very different from it. Further investigations are needed to clarify these two phases.

Keywords: Phase A, Aluminum incorporation, hydrous phase, upper mantle

Japan Geoscience Union Meeting 2014
(28 April - 02 May 2014 at Pacifico YOKOHAMA, Kanagawa, Japan)

SIT03-06 Room:418 Time:April 29 10:15-10:30

Changbai intraplate volcanism and deep earthquakes in Northeast Asia

ZHAO, Dapeng[1*] ; TIAN, You[1]

[1]Tohoku University, Department of Geophysics

The origin of the intraplate volcanoes in Northeast Asia is considered to be associated with upwelling of hot and wet asthenospheric materials in the big mantle wedge above the stagnant Pacific slab in the mantle transition zone. Among these intraplate volcanoes, Changbai is the largest and most active one, and very deep earthquakes (500-600 km depths) in the Pacific slab under East Asia occur ~300 km to the east of the Changbai volcano. Integrating the findings of geophysical, geochemical and petrologic studies so far, we suggest a link between the Changbai volcanism and the deep earthquakes in the Pacific slab. Many large shallow earthquakes occurred in the Pacific plate in the outer-rise areas close to the oceanic trench, and seawater may enter down to the deep portion of the oceanic lithosphere through the active normal faults which generated the large outer-rise earthquakes. The seawater or fluids may be preserved in the active faults even after the Pacific plate subducts into the mantle. Many large deep earthquakes are observed that took place in the subducting Pacific slab under the Japan Sea and the East Asian margin. At least some of the large deep earthquakes are caused by the reactivation of the faults preserved in the subducting slab, and the fluids preserved in the faults within the slab may cause the observed non-double-couple components in the deep earthquake faulting. The fluids preserved in the slab may be released to the overlying mantle wedge through the large deep earthquakes. Because large deep earthquakes occur frequently in the vicinity of the Changbai volcano, much more fluids could be supplied to this volcano than other areas in Northeast Asia, making Changbai the largest and most active intraplate volcano in the region.

Reference
Zhao, D., Y. Tian (2013) Changbai intraplate volcanism and deep earthquakes in East Asia: A possible link? Geophys. J. Int. 195, 706-724.

Keywords: volcanoes, deep earthquakes, Asia, slab

Japan Geoscience Union Meeting 2014
(28 April - 02 May 2014 at Pacifico YOKOHAMA, Kanagawa, Japan)

SIT03-07 Room:418 Time:April 29 10:30-10:45

Semiconductor diamond heater (SCD): An innovation for ultrahigh temperature experiments in the Kawai cell

XIE, Longjian[1*] ; ITO, Eiji[1] ; YONENDA, Akira[1]

[1]Institute for Study of the Earth Interior , Okayama University

We developed the semi-conductor diamond heater in the Kawai high pressure cell. The starting material of the semi-conductor diamond heater is born(B)-doped burned-graphite. We succeeded to improve the machinability of the B-doped burned-graphite by decreasing porosity. Following is the motivation and the background of the semi-conductor diamond heater project.

It is important to generate extremely high temperature (~3000 ℃) in a large sample volume (~0.1mm^3) in the Kawai apparatus.X-ray transparency is also desirable for in-situ synchrotron analysis. However, any traditional heater used in the Kawai apparatus so far does not satisfy the both requirements simultaneously.

Semiconductor diamond is a candidate material to generate temperatures higher than 3000 ℃ with low x-ray absorption. Anton Shatskiy (2009) have generated a temperature of 3500 ℃ by using the semiconductor diamond heater in a large-volume Kawai-type high-pressure apparatus, although their temperature measurement is questionable from a viewpoint of the power-temperature relation. Furthermore, their semi-conducted diamond heater, made of boron and graphite powders, was not machinable and difficult to control the temperatures. It often became unstable at around 1000~1300 ℃ and impossible to generate higher temperature.

Systematic experiments have done to improve the performance of the semiconductor heater. We used a machinable block of graphite contain 3 wt.% boron as the starting material for the semi-conductor diamond heater. The graphite-diamond transformation started at ~1000-1200 ℃ at 15 GPa in the Kawai apparatus. After the transformation, we stably generated temperature to 2000 ℃. Activation energy of B-doped diamond is about 0.1 eV, which is much lower than that of pure diamond (5.45eV).

References:

Anton Shatskiy, Daisuke Yamazaki, Guillaume Morard, Titus Cooray, Takuya Matsuzaki et al. , Review of Scientific Instruments 80, 023907 (2009).

Keywords: Semiconductor Diamond Heater, Ultrahigh Temperature, Kawai Cell

Japan Geoscience Union Meeting 2014
(28 April - 02 May 2014 at Pacifico YOKOHAMA, Kanagawa, Japan)

SIT03-08 Room:418 Time:April 29 11:00-11:15

Recent Global Tomography Models: Where are We Heading for?

TAKEUCHI, Nozomu[1*]

[1]Earthquake Research Institute, University of Tokyo

Many high-resolution global tomography models have been obtained and we now have consensus about overall features of 3-D heterogeneous structure in the Earth. Majority of models have been obtained by using conventional ray theory which assumes that scale length of lateral heterogeneities is sufficiently large compared with wavelength of seismic waves analyzed.

Primary efforts in recent studies appear to introduce better theories to overcome resolution limits caused by the above-mentioned assumption. The efforts include delay time tomography with finite frequency kernels (e.g., Montelli et al. 2004, Science; Obayashi et al. 2013, GRL) and waveform tomography with 2-D (e.g, Li and Romanowicz 1996, GJI, Panning and Romanowicz 2004, Science) or 3-D (e.g, Takeuchi 2007, GJI; Takeuchi 2012, EPSL) finite frequency kernels. Waveform tomography with further better theories is also becoming feasible (e.g., Lekic and Romanowicz 2011, GJI; French et al. 2013, Science).

In this presentation, I want to propose another direction to improve resolution: use of a new type of dataset. I will propose to use incoherent part of seismic signals (i.e., scattering waves or coda waves). Scattering waves are sensitive to heterogeneities whose scale length is comparable with wavelength of seismic waves analyzed. Use of such waves therefore should provide new information beyond resolution limit of ray theory. At the time of the presentation, I plan to show feasibility and examples of such analyses to reveal distribution of smaller scale heterogeneities in the subduction zone around Japan.

Keywords: tomography, scattering wave, seismology

Japan Geoscience Union Meeting 2014
(28 April - 02 May 2014 at Pacifico YOKOHAMA, Kanagawa, Japan)

SIT03-09 Room:418 Time:April 29 11:15-11:30

Lattice preferred orientation of stishovite in deformation experiment

XU, Fang[1*] ; YAMAZAKI, Daisuke[1] ; TSUJINO, Noriyoshi[1]

[1]ISEI, Okayama University

Seismic observations reveal strong negative anisotropy ($V_{SV}>V_{SH}$) at around 550 km depth in the lower part of mantle transition zone (Visser et al., 2008). The mantle tomography indicates the obvious association of this negative anisotropy with the subduction zones (Panning and Romanowicz., 2006). The observed anisotropy can be caused by lattice preferred orientation (LPO) of constituting material when the material is elastically anisotropic. Majorite and ringwoodite, which are the dominant minerals in this region, are nearly isotropic (Chai et al., 1997; Weidner et al., 1984). On the other hand, stishovite, which may occur in significant amounts in this region derived from the delaminated subducting basaltic layer (Karato et al., 1997) and continental crust (Kawai et al., 2012), shows strong elastic anisotropy (V_{SV}/V_{SH} is as large as 150%) indicated by the acoustic velocities study (Yoneda et al., 2012) on single crystal of stishovite. Therefore, the LPO of stishovite has a high potential to interpret the seismic anisotropy in the lower part of the transition zone and indicate the geometry of mantle flow.

To investigate the LPO of stishovite, deformation experiments on stishovite were conducted in both simple shear and uni-axial geometry. We prepared starting material of polycrystalline stishovite with grain size of ~10 μm at 12 GPa and 1450 ℃ in a Kawai-type high-pressure apparatus. Then deformation experiments were carried out at 12 GPa and 1600 ℃ by Kawai-type apparatus for tri-axial deformation (KATD installed at Tokyo Institute of Technology) and deformation-DIA apparatus (SPEED-Mk. II installed at SPring-8). Sintered diamond piston was used in the uni-axial deformation experiment. Shear strain was ~1.0 estimated from the rotation of platinum strain maker after deformation. From the change of sample length, uni-axial tension and compression strain were 0.4 and 0.1 respectively. The microstructure and crystallographic orientation of the deformed samples were investigated by SEM with EBSD.

The EBSD results reveal that the [001] direction of stishovite tends to be parallel to the shear direction. (100) plane, though not so obvious, tends to parallel to the shear plane. The slip system is consistent with rutile TiO_2 (Blanchin and Faisant., 1979), which has the same structure with stishovite. The calculated seismic anisotropy indicates a fast shear wave along shear direction. Polarization anisotropy reported by Visser et al. (2008) can be attributed by a vertical flow and LPO of stishovite in the transition zone. The negative anisotropy along subduction zones in Panning and Romanowicz. (2006) indicates the type A slabs (slabs which penetrate directly into the lower mantle without much deflection in the transition zone) (Karato et al., 2001).

Keywords: stishovite, deformation, LPO

Japan Geoscience Union Meeting 2014
(28 April - 02 May 2014 at Pacifico YOKOHAMA, Kanagawa, Japan)

SIT03-10 Room:418 Time:April 29 11:30-11:45

Phase transitions and mineral chemistry in pyrolite at 1600-2200C across 660-km seismic discontinuity

ISHII, Takayuki[1*] ; KOJITANI, Hiroshi[1] ; AKAOGI, Masaki[1]

[1]Depertment of chemistry, Gakushuin University

It is widely accepted that pyrolite is a model rock which represents the chemical composition of the Earth's upper mantle. Because the post-spinel transition in pyrolite occurs at about 23 GPa along mantle geotherm (e.g. Litasov et al. 2005), it has been accepted that the transition is responsible for the seismic 660-km discontinuity. Slow velocity anomalies by global seismic tomography which may indicate mantle upwelling have been found in the transition zone and the lower mantle, and these regions are higher in temperature than average mantle. To elucidate the origin and dynamics of the mantle plume, informations on phase relations in pyrolite are essential. However, few investigations on phase relations in pyrolite have been made at hot-plume temperatures (1800-2200C) (Hirose, 2002; Nishiyama and Yagi, 2003). In this study, we demonstrated detailed phase equilibrium experiments in pyrolite composition at hot plume conditions.

The starting material was prepared as the oxide mixture in pyrolite composition after McDonugh and Sun (1995) excluding minor components (MnO, K_2O and P_2O_5). Quench experiments were made at about 20-28 GPa and 1600-2200C for 2-10 hours using a Kawai-type 6-8 multianvil high-pressure apparatus at Gakushuin University. The starting material was packed with pressure calibrants ($MgSiO_3$ and pyrope) in a Re multi-sample capsule. A $LaCrO_3$ heater and a W5%Re-W26%Re thermocouple were inserted in a Cr_2O_3-doped MgO pressure medium. Phases of recovered samples were identified with microfocus-Xray diffractometer and SEM-EDS.

The mineral assemblages of $MgSiO_3$-rich perovskite (Mpv) + magnesiowustite (Mw) + garnet (Gt) + $CaSiO_3$-perovskite (Cpv) and Mpv + Mw + Cpv at 1600-2200C are stable at pressure range of 22-24 GPa and above 24 GPa, respectively. The mineral assemblage of ringwoodite (Rw) + Gt + Cpv at 1600C changes to that of Rw + Mw + Gt + Cpv at 1800-2000C, and Rw disappears perfectly above 2200C. From mass balance calculation of analyzed compositions of the phases, we found that Gt content increases with increasing temperature before and after formation of Mpv. We also calculated the densities in pyrolite at each temperature. The density of average pyrolite mantle (1600C) is higher than pyrolite plume (1800-2200C) across 660-km discontinuity due to increase in Gt content with increasing temperature. Therefore, we conclude that hot-plume ascending nearby 660-km discontinuity has positive buoyancy by the phase transitions.

Keywords: post-spinel transition, 660-km seismic discontinuity, mantle plume, pyrolite, post-garnet transition

Japan Geoscience Union Meeting 2014
(28 April - 02 May 2014 at Pacifico YOKOHAMA, Kanagawa, Japan)

SIT03-11 Room:418 Time:April 29 11:45-12:00

Elastic properties of delta-AlOOH under high-pressure: Implications for high Vs anomaly in the mantle transition zone

MASHINO, Izumi[1*] ; MURAKAMI, Motohiko[1] ; OHTANI, Eiji[1]

[1]Faculty of Science, Tohoku University

delta-AlOOH is a high-pressure polymorph of diaspore (alpha-AlOOH) and boehmite (gamma-AlOOH) (Suzuki *et al*., 2000). Since delta-AlOOH is identified to be stable from 20 to 120 GPa, and temperatures up to 2300 K, this phase is considered to be a possible carrier and reservoir of water in subducting cold slab into the deep mantle (Ohtani *et al*., 2001; Sano *et al*., 2004; 2008). In order to investigate the effect of composition on seismic velocities in subducting slab, it is important to measure the elastic properties of delta-AlOOH at high pressure.

We have conducted high-pressure acoustic-wave velocity measurements of delta-AlOOH using Brillouin spectroscopy and also explored the chemical bonding of delta-AlOOH by Raman spectroscopy at high pressure in a diamond anvil cell. We obtained sharp peaks from transverse acoustic mode (V_S) of delta-AlOOH over the entire pressure range explored up to a pressure of 89 GPa. The peaks from longitudinal acoustic mode (V_P) of delta-AlOOH were masked by the diamond shear acoustic modes from 35 GPa. The pressure dependence of the aggregate velocities for the delta-AlOOH at 300 K suggests that the hydrogen-bonding symmetrization with the space group changes from $P2_1nm$ to $Pnnm$ occurs during compression above 7 GPa. The shear and adiabatic bulk moduli and their pressure derivatives at zero pressure were determined to be K_0 = 192.2(8) (GPa), G_0 = 158.8(3) (GPa), $(dK/dP)_0$ = 3.63(6), and $(dG/dP)_0$ = 1.35(6) for the pressures above 15 GPa. Raman spectroscopic measurements have shown that the B_1 mode frequencies of $P2_1nm$ disappeared around 6 GPa and A_g mode frequencies of $Pnnm$ appeared above 5.6 GPa, which also indicates the hydrogen-bonding symmetrization around 6 GPa. These results indicate that delta-AlOOH becomes harder by the hydrogen-bonding symmetrization and probably exists as a phase ($Pnnm$) with the symmetric hydrogen bonding in the mantle transition zone and lower mantle.

Shear wave velocities for delta-AlOOH are larger than those of hydrous wadsleyite (by 30 %), hydrous ringwoodite (by 29 %), and majorite (by 29 %). Those of delta-AlOOH are approximately 7 % below those of stishovite. The delta-AlOOH phase thus found to be one of the hardest phases compared to the minerals of mantle transition zone. The existence of delta-AlOOH may contribute to the cause of high V_S and V_P anomalies. Shear velocities for sediment containing delta-AlOOH phase are larger than those of pyrolite (by 10 %) and MORB (by 5 %). The subducting slabs often stagnate at the transition zone before reaching the lower mantle. Particularly beneath Korean peninsula, there is a high V_S anomaly (~2 %) in the lower part of the transition zone (Zhang *et al*., 2012). The seismic data under the eastern part of northeast China (NEC) also indicates a slight positive anomaly of V_S (~1 %), but the V_S value observed around 600 km depth under NEC is ~1 % lower than that beneath Korea. We explain the difference in the V_S anomalies beneath the NEC and Korea by the amount of sediment containing the delta-AlOOH phase and the stagnating duration. If sediments stagnate at the transition zone before reaching the lower mantle in this region, we can estimate that the higher V_S anomaly (~1 %) than NEC would correspond to sediments with 13.4 vol% in stagnant slab. The average oceanic crust subduction rate is estimated to be about 8 cm/yr around Japan. Assuming this estimated rate of subduction, the slab stagnetion has lasted for at least 30 million years.

Keywords: delta-AlOOH, Brillouin scattering, Raman spectroscopy, subducting slab, high pressure

Japan Geoscience Union Meeting 2014
(28 April - 02 May 2014 at Pacifico YOKOHAMA, Kanagawa, Japan)

SIT03-12 Room:418 Time:April 29 12:00-12:15

Mechanisms of ultra-deep earthquakes (h>660km) in a slab penetrating the 660-km discontinuity

FUKAO, Yoshio[1*] ; OBAYASHI, Masayuki[1] ; YOSHIMITSU, Junko[1]

[1]IFREE/JAMSTEC

Recent mantle tomography has begun to reveal the characteristic differences between the deep hypocentral distributions associated with stagnant slabs and those associated with penetrating slabs (e.g., Fukao and Obayashi, 2014). We here show that there are differences in focal mechanism as well. Mechanisms of deep shocks within tomographically imaged stagnant slabs (typically in Bonin and Tonga) are characterized by horizontal compression (e.g., Bonnardot et al., 2009). Those within tomographically imaged penetrating slabs (typically in Java and Tonga) are characterized by very steeply dipping compressional axes (e.g., Alpert et al., 2010).

The deepest seismicity is especially active in Tonga, where many shocks occur at depths greater than 660km. Such ultra-deep shocks show in general very unusual mechanisms, typified by nearly vertical tensional axes with a large amount of CLVD component, as demonstrated in Figure 1 (Mechanisms viewed from the side). This figure also shows a remarkble contrast of mechanisms of deepest shocks just above and below the 660km depth. The source region of the ultra-deep shocks (h>660km) is underlain by the greatly deepened post-spinel phase boundary (Niu and Kawakatsu, 1995) so that the source region is at the pre-spinel state while the underlying portion is at the post-spinel state. This situation along with contortion of the slab associated with its interaction with the post-spinel phase boundary (e.g., Cizkova and Bina, 2013) may explain the mechanism change across the 660km depth as observed in Figure 1. We explore the finer velocity structure and hypocentral distribution in the source region by a technique of differential travel time tomography.

Keywords: mantle dynamics, tomography, deep earthquakes

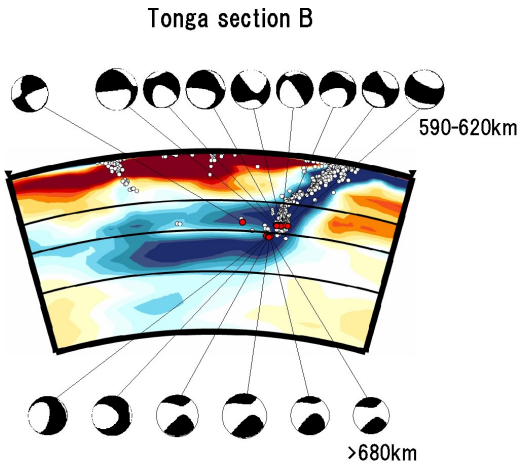

Japan Geoscience Union Meeting 2014
(28 April - 02 May 2014 at Pacifico YOKOHAMA, Kanagawa, Japan)

SIT03-13 Room:418 Time:April 29 12:15-12:30

A pyrolitic lower mantle with $(Mg,Fe^{3+})(Si,Al^{3+})O_3$ perovskite

WANG, Xianlong[1*] ; TSUCHIYA, Taku[1]

[1]GRC, Ehime University and ELSI, Tokyo Institute of Technology

To better understand the Earth's lower mantle (LM), thermodynamic properties (TDPs) of LM minerals with Fe and Al dopant should be illustrated more clearly. We have so far reported the TDPs of Fe-bearing MgO, $MgSiO_3$ perovskite (Pv) and post perovskite. [1-4] We furthermore study the TDPs of Fe- and Al-bearing Pv, where the internally consistent LSDA+*U* method and the lattice dynamics method are applied. Two spin states, high (HS) and low spin state, two substitution sites, Mg and Si site, and several possible distribution configurations are considered. In the LM pressure range, HS Fe^{3+} substituted at the Mg site with Al^{3+} at the adjacent Si site (Fe-Al pair) is the most stable configuration and tends to distribute homogeneously in LM. Furthermore, negative frequency cannot be observed in the Fe-Al pair-bearing Pv, and Al contributes to middle frequency while Fe mainly to low part due to its heavy mass. This indicates that the Fe-Al pair is vibrationally stable. Incorporation of the pair for geophysically relevant concentrations can increase volume of Pv a little and has marginal effects on the TDPs of Pv except for thermal expansivity and Gruneisen parameter. Simulated densities, adiabatic bulk moduli ,and bulk sound velocities show that a composition close to pyrolite is accountable for the reference Earth model.

References:
[1] A. Metsue, and T. Tsuchiya, J. Geophys. Res. 116, B08207 (2011).
[2] A. Metsue, and T. Tsuchiya, Geophys. J. Int. 190, 310 (2012).
[3] H. Fukui, T. Tsuchiya, and A. Q. R. Baron, J. Geophys. Res. 117, B12202 (2012).
[4] T. Tsuchiya, and X. Wang, J. Geophys. 118, 83 (2013).

Keywords: First-principles method, Internally consistent LSDA+*U*, Perovskite, Thermodynamic properties, Pyrolite

Japan Geoscience Union Meeting 2014
(28 April - 02 May 2014 at Pacifico YOKOHAMA, Kanagawa, Japan)

SIT03-14 Room:418 Time:April 29 12:30-12:45

Linear analysis on the onset of thermal convection of highly compressible fluids

KAMEYAMA, Masanori[1*]

[1]GRC, Ehime University

A series of linear stability analysis was performed on the onset of thermal convection in a highly compressible fluid, in order to study the fundamental nature of mantle convection of massive super-Earths in the presence of strong adiabatic compression. We consider the temporal evolution (growth or decay) of an infinitesimal perturbation superimposed to a highly compressible fluid which is in a hydrostatic (motionless) and conductive state in a basally-heated horizontal layer. As a model of pressure-dependence in material properties, we employed an exponential decrease in thermal expansivity and exponential increase in (reference) density with depth. The linearized equations for conservation of mass, momentum and internal (thermal) energy are numerically solved for the critical Rayleigh number as well as the vertical profiles of eigenfunctions for infinitesimal perturbations. The above calculations are repeatedly carried out by systematically varying (i) the dissipation number which measures the effect of adiabatic compression, (ii) the temperature at the top surface and (iii) the magnitude of pressure-dependence in thermal expansivity and reference density.

Our analysis demonstrated that the onset of thermal convection is strongly affected by the adiabatic compression, through modulating the static stability of thermal stratification in the fluid layer. For sufficiently strong adiabatic compression where a sufficiently thick “stratosphere” of stable stratification develops in the layer, for example, the critical Rayleigh number explosively increases with the dissipation number. The explosive changes in the critical Rayleigh number are associated with drastic decreases in the length scales of perturbations both in vertical and horizontal directions. In particular, for very strong adiabatic compression, the vertical motion of fluid is significantly suppressed in a thick “stratosphere”, which narrows the incipient convection in a thin sublayer of unstable thermal stratification. In addition, when the effect of adiabatic compression is extremely strong so that the thermal stratification becomes stable in the entire layer, no perturbation is allowed to grow with time regardless of the Rayleigh number and/or the horizontal wavelength. We also found that the effect of adiabatic compression becomes prominent for higher temperature at the top surface of the fluid layer. These findings may imply the crucial importance of adiabatic compression in understanding the dynamics and evolution of the mantles of massive super-Earths, particularly for those orbiting their parent stars very closely.

Keywords: super-Earths, mantle convection, adiabatic compression, thermal expansivity

Japan Geoscience Union Meeting 2014
(28 April - 02 May 2014 at Pacifico YOKOHAMA, Kanagawa, Japan)

SIT03-15 Room:418 Time:April 29 14:15-14:30

In Situ observation of the Segregation Process of Molten Iron from Partially Molten Silicate using X-ray Radiography

YAGI, Takehiko[1*] ; GOTOU, Hirotada[2] ; IIZUKA, Riko[1] ; SUZUKI, Akio[3]

[1]Geodynamics Research Center, Ehime University, [2]Institute for Solid State Physics, University of Tokyo, [3]Department of Earth Science, Tohoku University

We have made in situ observation of the segregation process of molten iron from partially molten silicate at 5 GPa and 1800 K using X-ray radiography. Earth ' s core is believed to have formed by the similar process in the early stage of Earth formation. Although two measure mechanisms, " rain fall " and " percolation ", have been proposed for this process, experimental results are still quite controversial. Most of the previous works were made either by the texture analysis of the quenched and recovered sample or by the electrical conductivity measurement. In the present study, an uniform mixture of the powders of $Mg(OH)_2$, SiO_2, and Fe was compressed to 5 GPa at room temperature and then X-ray tomography observation was made with increasing temperature up to 1800 K. Addition of H_2O component into silicate-iron system reduces the melting temperature of both silicate and iron considerably. The dynamical process of the formation of iron ball at the bottom of the sample chamber was clearly observed. It was proved that this technique is quite useful to study such process in detail.

Keywords: core formation process, molten iron, x-ray, high pressure and temperature

Japan Geoscience Union Meeting 2014
(28 April - 02 May 2014 at Pacifico YOKOHAMA, Kanagawa, Japan)

SIT03-16 Room:418 Time:April 29 14:30-14:45

Influence of majorite on mantle convection

ICHIKAWA, Hiroki[1*] ; KAMEYAMA, Masanori[2] ; SENSHU, Hiroki[3] ; KAWAI, Kenji[4] ; MARUYAMA, Shigenori[5]

[1]GRC, Ehime University and ELSI, Tokyo Institute of Technology, [2]Geodynamics Research Center, Ehime University, [3]Planetary Exploration Research Center, Chiba Institute of Technology, [4]Department of Earth and Planetary Sciences, Tokyo Institute of Technology, [5]Earth-Life Science Institute, Tokyo Institute of Technology

Influence of $MgSiO_3$ majorite on the mantle convection has been investigated by using numerical simulations. According to a first principles study (Yu et al., 2011), wadsleyite decomposes to an assemblage of majorite plus periclase with a large negative Clapeyron slope. Since stability field of majorite is limited at high temperature, downwellings are considered to be unaffected by this phase boundary. On the contrary, the upwelling plumes may be significantly modified by this phase boundary. The asymmetry on upwelling and downwelling caused by the phase transitions may induce strong effects on the thermal evolution and the thermal structure of the mantle.

In this study, we performed 2-D numerical simulations on thermal convection of the mantle incorporating majorite stability field. According to our numerical results, very hot upwelling plumes are strongly influenced by the phase transitions related to majorite. The dynamics of these upwellings are controlled by the release and the absorption of latent heat induced by the transitions as well as interruption of currents due to the large negative Clapayron slope of the transition between wadsleyite and majorite plus periclase.

Keywords: Mantle convection, Majorite, Phase transition

Japan Geoscience Union Meeting 2014
(28 April - 02 May 2014 at Pacifico YOKOHAMA, Kanagawa, Japan)

SIT03-17 Room:418 Time:April 29 14:45-15:00

Rapid lateral variation of P-wave velocity at the base of the mantle beneath the Western Pacific

TANAKA, Satoru[1*] ; KAWAKATSU, Hotoshi[2] ; OBAYASHI, Masayuki[1] ; NECESSARRAY, Project team[2]

[1]JAMSTEC, [2]ERI, Univ. Tokyo

We examine P-wave velocity structure at the base of the mantle beneath the Western Pacific, where is the western edge of the Pacific Large-Low Velocity Province (LLVP), by using high-quality seismograms that are provided by the NECESSArray project. Forward modeling with the reflectivity method is conducted to explain the variation of P-wave travel times as function of epicentral distance near the core shadow zone after station and ellipticity corrections are applied. Additionally PcP-P travel times are also examined to enlarge the survey area. As a result, a rapid variation of P-wave velocity structure at the base of the mantle is detected. Thin (10 to 60 km thickness) and very low velocity (-2 to -6 %) layers at the base of the mantle are intersected with a 100 km thickness and high velocity (+3%) layer, and a slightly fast layer exists at the north of the region with the thin and low velocity layers. Their spatial separations are typically several hundred kilometers and it would be difficult to explain by only a thermal effect. These observations suggest that very complicated thermo-chemical reactions occur near the edge of Pacific LLVP.

Keywords: P-wave velocity, the base of the mantle, the Western Pacific

Japan Geoscience Union Meeting 2014
(28 April - 02 May 2014 at Pacifico YOKOHAMA, Kanagawa, Japan)

SIT03-18 Room:418 Time:April 29 15:00-15:15

Methods for inversion of body-wave waveforms for localized three-dimensional seismic structure and an application to D”

KAWAI, Kenji[1*] ; KONISHI, Kensuke[2] ; GELLER, Robert J.[3] ; FUJI, Nobuaki[4]

[1]Department of Earth and Planetary Sciences, Tokyo Institute of Technology, [2]School of Earth and Environmental Sciences, Seoul National University, [3]Department of Earth and Planetary Science, Graduate School of Science, University of Tokyo, [4]Institut de Physique du Globe de Paris

We formulate the inverse problem of waveform inversion for localized 3-D seismic structure, computing partial derivatives of waveforms with respect to the elastic moduli at arbitrary points in space for anisotropic and anelastic media. In this study we minimize computational requirements by using the Born approximation with respect to a laterally homogeneous model, but this is not an inherent limitation of our approach. We solve the inverse problem using the conjugate gradient (CG) method, using Akaike’s Information Criterion (AIC) to truncate the CG expansion. We apply our method to invert for three-dimensional shear wave structure in the lowermost mantle beneath Central America using a total of 2154 waveforms at periods from 12.5 to 200 s recorded at stations near the Pacific coast of North America for 29 deep and intermediate-depth events beneath South America. The resulting model shows lateral heterogeneity in the E-W direction which may be associated with a subducted cold slab surrounded by hotter materials with slower velocities. Various tests show that our model is robust.

Keywords: Lowermost mantle, Waveform inversion, Farallon plate

Japan Geoscience Union Meeting 2014
(28 April - 02 May 2014 at Pacifico YOKOHAMA, Kanagawa, Japan)

SIT03-19 Room:418 Time:April 29 15:15-15:30

A magnetic probe into Earth's core and deep-mantle dynamics

SAKURABA, Ataru[1*]

[1]Department of Earth and Planetary Science, University of Tokyo

It is widely recognized that Earth's core dynamics is an important research subject in understanding the past, present and future states of our planet, firstly because the metallic core is a vast domain accounting for one thirds of Earth's mass and plays a significant role in thermal history, and secondly because it dynamically generates the main geomagnetic field that has historically been observed for several hundred years and geologically recorded in rocks since more than a billion years ago. This review attempts to cover this subject with an attention to general questions: how geomagnetic-field data can be used to advance the deep-Earth science, and what theoretical progresses have been made and could be made. I will deal with some of the following particular topics: (1) various driving sources of convection, such as thermal and compositional buoyancy and inertial forcing (e.g., luni-solar precession); (2) a dynamo without a solid inner core; (3) a dynamo that operates in a part (e.g., an inner part) of the outer core; (4) sensitivity of the geomagnetic field structure (e.g., dipolarity), intensity, and time variations (e.g., reversal frequency) to the above mentioned various parameters.

Japan Geoscience Union Meeting 2014
(28 April - 02 May 2014 at Pacifico YOKOHAMA, Kanagawa, Japan)

SIT03-20 Room:418 Time:April 29 15:30-15:45

Relationship between sound velocity and density of liquid alloy under pressure

TERASAKI, Hidenori[1*] ; NISHIDA, Keisuke[2] ; URAKAWA, Satoru[3] ; KUWABARA, Souma[1] ; TAKUBO, Yusaku[1] ; SHIMOYAMA, Yuta[1] ; UESUGI, Kentaro[4] ; TAKEUCHI, Akihisa[4] ; SUZUKI, Yoshio[4] ; KONO, Yoshio[5] ; HIGO, Yuji[4] ; KONDO, Tadashi[1]

[1]Osaka Univ., [2]Univ. Tokyo, [3]Okayama Univ., [4]JASRI, [5]HPCAT

It is important to understand the relationship between sound velocity and density of liquid Fe-alloys under high pressure for obtaining a constraint of the composition of the molten outer core from observed seismic data. We have studied a relationship between sound velocity and density of liquid alloy based on simultaneous measurement of these properties under high pressure and high temperature. Sound velocity was measured using ultrasonic pulse-echo overlapping method and density was measured employing X-ray absorption method combined with X-ray tomography technique. The measured P-wave velocity and density of liquid Ni?S both increase with pressure. From these data, adiabatic bulk modulus (K_{S0}) of the liquid sample can be well constrained to 29 GPa. It is note that the measured P-wave velocity is found to increase linearly with increasing density. This result provides an important issue in terms of Birch's law for liquid material.

Keywords: Sound velocity, density, liquid, high pressure

Japan Geoscience Union Meeting 2014
(28 April - 02 May 2014 at Pacifico YOKOHAMA, Kanagawa, Japan)

SIT03-21 Room:418 Time:April 29 15:45-16:00

Magnetic-Coriolis waves in convection-driven dynamos: Implications for geomagnetic westward drift

HORI, Kumiko[1*] ; JONES, Chris[2] ; WICHT, Johannes[3] ; SHIMIZU, Hisayoshi[1]

[1]Earthquake Research Institute, University of Tokyo, [2]University of Leeds, UK, [3]Max-Planck Institute for Solar System Research, Germany

A prominent feature of the geomagnetic secular variation is the westward motion of the non-dipole part of the field, which is significant in the Atlantic hemisphere with timescales of a few hundred years. Potential mechanisms to account for longitudinal geomagnetic drifts are advection due to large-scale zonal flows in the Earth's core as well as propagation of rotating magnetohydrodynamic (MHD) waves, particularly of slow Magnetic-Coriolis (MC) Rossby waves. More commonly the westward motion is thought to reflect zonal flow advection, an assumption that is used when inverting the secular variation signal for the flow at the top of the core. However, recent geodynamo simulations have successfully reproduced longitudinal magnetic drifts and some authors reported that the drift is at least partly a wave propagation.

To assess to what extent waves could play a role in geomagnetic drift, we explore nonlinear simulations of convection-driven MHD dynamos in rotating spherical shells. By performing a tempo-spatial spectral analysis of simulation data, we identify a slow MC-Rossby mode, that follows the dispersion curve predicted by a quasi-geostrophic linear theory. The result indicates that such waves can be excited in the planetary fluid core and that wave propagation may indeed play a role in the magnetic drifts. This gives a framework for further exploration of different wave types, which can provide valuable information about the physical properties in the deep interior fluid core.

Japan Geoscience Union Meeting 2014
(28 April - 02 May 2014 at Pacifico YOKOHAMA, Kanagawa, Japan)

SIT03-22 Room:418 Time:April 29 16:15-16:30

A generating process of the geomagnetic drifting field

YUKUTAKE, Takesi[1*] ; SHIMIZU, Hisayoshi[2]

[1]None, [2]Earthquake Research Institute, University of Tokyo

The geomagnetic field is comprised of drifting and standing field. The drifting field is the field that drifts westwards nearly steadily over the past several hundred years and the standing field is that stays at the same place. The drifting field has two major characteristic features. When the field is expressed in a spherical harmonic series, the drifting field mainly consists of sectorial harmonics. Secondly the rate of drift is uniform irrespective of the harmonics. This means the drift velocity is non-dispersive.

We here propose a model of the generating process of the drifting field. Because of the non-dispersive nature of the drift velocity, we assume the westward drift is a phenomenon closely tied with material flow rather than a magnetohydrodynamic wave. Furthermore we take it a phenomenon near the surface of the core where the dipole field is dominant.

If the mantle is approximated by an electrical insulator, the electric current in the core normal to the core-mantle boundary must be zero. This provides a strong constraint on the liquid flow near the surface. If we assume infinite conductivity of the core for simplicity, only the sectorial flow is allowed for the toroidal flow, and the meridional flow for the poloidal flow. The sectorial toroidal flow, interacting with the dipole field, induces sectorial poloidal field, whereas the meridional poloidal flow produces the meridional poloidal field. The surface layer, which is rotating westwards as a whole, carries these fields westwards together. Since the rotation of the meridional field is unrecognizable, only the sectorial field is observed as the drifting field.

We present a simplified model that describes the above process.

Keywords: geomagnetic secular variation, westward drift, drifting field, core surface flow

Japan Geoscience Union Meeting 2014
(28 April - 02 May 2014 at Pacifico YOKOHAMA, Kanagawa, Japan)

SIT03-23 Room:418 Time:April 29 16:30-16:45

Electrical resistivitiy of hcp-Fe under Earth's core conditions

OHTA, Kenji[1*] ; KUWAYAMA, Yasuhiro[2] ; HIROSE, Kei[3] ; OHISHI, Yasuo[4]

[1]Department of Earth and Planetary Sciences, Tokyo Institute of Technology, [2]Geodynamics Research Center, Ehime University, [3]Earth-Life Research Institute, Tokyo Institute of Technology, [4]Japan Synchrotron Radiation Insititute

Iron is the primary component of the Earth's core. Convection of the conductive liquid outer core generates the geomagnetic field, and secular cooling of the core induces growth of the solid inner core and dynamics in the Earth's inside. Synchrotron x-ray diffraction study suggests that iron crystallizes in the hexagonal close-packed structure at the inner core conditions (Tateno et al., 2010). Thus, the electrical resistivity of hexagonal close-packed iron (hcp-Fe) is a key piece of information for estimating the transport properties of the core. We report high temperature electrical resistivity for hcp-Fe to 185 GPa measured in a laser-heated diamond anvil cell. We observed resistivity saturation in hcp-Fe under high pressure and high temperature conditions as predicted in a recent laboratory-based model for the conductivity of the Earth's core (Gomi et al., 2013). The saturation effect is significant in estimating electrical and thermal conductivity of the core, which strongly affect the dynamics and thermal evolution of the Earth.

References
Gomi, H. et al. The high conductivity of iron and thermal evolution of the Earth's core. Phys. Earth Planet. Inter. 224, 88-103 (2013).
Tateno, S., Hirose, K., Ohishi, Y., & Tatsumi, Y. The structure of iron in Earth's inner core. Science 330, 359-361 (2010).

Keywords: Electrical resistivity, Earth's core, hcp iron

Japan Geoscience Union Meeting 2014
(28 April - 02 May 2014 at Pacifico YOKOHAMA, Kanagawa, Japan)

SIT03-24 Room:418 Time:April 29 16:45-17:00

Spatial dependence of anisotropic thermal diffusivity and its influence on dynamics in the Earth's core

MATSUSHIMA, Masaki[1*]

[1]Tokyo Institute of Technology

Small-scale fluid motions in the Earth's core are likely to be highly anisotropic because of rapid rotation of the Earth and a strong magnetic field in the core. We have carried out direct numerical simulations of rotating magnetoconvection to investigate the effect of anisotropic diffusivity on dynamics in the Earth's core, as one of pilot studies. When a computational region is expressed in terms of a rectangular box with periodic boundaries in the three-directions, the prescribed anisotropic thermal diffusivities were found not to influence the character of rotating magnetoconvection, such as kinetic and magnetic energies averaged over the computational region. When a computational region is expressed in terms of a rectangular box with rigid boundary surfaces perpendicular to the gravitational direction, the prescribed anisotropic thermal diffusivities have a significant effect on the character of rotating magnetoconvection; that is, kinetic and magnetic energies can be increased even by a small anisotropy. The degree of increase depends on the direction of anisotropy and the direction of gravity corresponding to location of the computational region. These results suggest that anisotropic thermal diffusivity insignificantly influences dynamics in the bulk of the core, but that it should be effective near rigid boundary surfaces. Therefore, it is likely that anisotropic diffusivity has a more significant effect on MHD dynamos in rotating thin spherical shells. Such an implication can be examined through global numerical simulations of MHD dynamo models with anisotropic diffusivity being variable in the core.

Instead of such a study, we perform further direct numerical simulations of rotating magnetoconvection by prescribing anisotropic thermal diffusivities with spatial dependence; for example, in one case, anisotropic thermal diffusivities are presumed to be effective only near rigid boundary surfaces; in another case, anisotropic thermal diffusivities are presumed to be effective only far from rigid boundary surfaces. Hence this is another pilot study. Kinetic and magnetic energies in the former case seem to be larger than those in the latter case. The result is consistent with that obtained in our previous studies.

Keywords: anisotropic thermal diffusivity, core dynamics

Japan Geoscience Union Meeting 2014
(28 April - 02 May 2014 at Pacifico YOKOHAMA, Kanagawa, Japan)

SIT03-25 Room:418 Time:April 29 17:00-17:15

Can a stably stratified layer interrupt the top-down dynamics of Earth's core?

NAKAGAWA, Takashi[1*]

[1]IFREE, JAMSTEC

Takashi Nakagawa

In some of previous studies of numerical dynamo simulation with a stably stratified region below the outer boundary, the long-wavelength feature of radial magnetic field can be only found on the outer boundary because a stratified layer can filter small-scale features of radial magnetic field generated in the convective region below the stratified boundary [Christensen, 2006; Nakagawa, 2011]. The existence of the stably stratified region below the core-mantle boundary (CMB) is recently exposed from high pressure mineral physics [e.g. Pozzo et al., 2012] and seismological data analysis [e.g. Helffrich and Kaneshima, 2013].

Regarding the modeling on geomagnetic secular variation from numerical dynamo simulations, the heterogeneous thermal/chemical anomalies at the core-mantle boundary is important for understanding the time-scale of secular variation such as polarity reversals and excursions suggested from paleomagnetic observations [e.g. Olson et al., 2011; Olson et al., 2013] and current observational magnetic field [Aubert et al., 2013]. However, their investigation was not included in the effects of the stably stratified region below the CMB in their dynamo simulations.

Here we introduce several examples of numerical dynamo simulations with both heterogeneous outer boundary prescribed by the CMB heat flux calculated from numerical mantle convection simulations and a stably stratified layer. Preliminary results are found that the large-scale and ?amplitude of thermal/chemical anomalies induced by the heterogeneous boundary condition, that is, thermal wind type flow, may be trapped at the imposed stratified boundary. This may imply that the geomagnetic secular variations related to the core-mantle coupling may be suggested that the core surface flow would be a key physics.

Keywords: Earth's core, heterogeneity, core-mantle boundary, stably stratified layer, thermal wind

Japan Geoscience Union Meeting 2014
(28 April - 02 May 2014 at Pacifico YOKOHAMA, Kanagawa, Japan)

SIT03-26 Room:418 Time:April 29 17:15-17:30

Sound velocity measurements of liquid Fe-Ni-S alloy at high pressure and temperature via inelastic X-ray scattering

IMADA, Saori[1*] ; NAKAJIMA, Yoichi[2] ; KOMABAYASHI, Tetsuya[3] ; HIROSE, Kei[4] ; TSUTSUI, Satoshi[5] ; UCHIYAMA, Hiroshi[5] ; ISHIKAWA, Daisuke[5] ; ALFRED, Baron[2]

[1]Department of Earth and Planetary Sciences, Tokyo Institute of Technology, [2]Material Dynamics Laboratory, RIKEN SPring-8 Center, RIKEN, [3]School of Geosciences, The University of Edinburgh, [4]Earth-Life Science Institute, Tokyo Institute of Technology, [5]Japan Synchrotron Radiation Research Institute

The liquid Earth's outer core is mainly composed of Fe-Ni alloy with some amounts (5˜10%) of light element(s), such as hydrogen, carbon, oxygen, silicon, and sulfur. Moreover, it has been known that the Mars and Mercury have also liquid (outer) core, although there are less observational data (Dehant, 2003, Margot et al., 2007).

In order to identify the kind and amount of the light elements dissolved in these planetary cores, sound velocity data of iron alloys at high pressure and temperature are important because the seismic wave speeds are the primary observed information in the deep Earth's interior. While sound velocity measurements of solid core materials up to core pressures have been extensively conducted via ultrasonic method, inelastic X-ray scattering (IXS), nuclear resonance IXS, due to its experimental difficulty, there exist few reports on sound velocity measurements of liquid Fe alloys at high pressure (Nishida et al. 2012).

We measured sound velocity of liquid of $(Fe,Ni)_3S$ up to 30 GPa. Sulfur has been considered to be a major candidate for the light element in the Earth's outer core as well as in the Martian and Mercury's cores (e.g. Lodders and Fegley 1997). We conducted high-pressure and -temperature experiments with an externally-heated diamond-anvil cell (EHDAC). The starting materials were a synthesized or a powder mixture of Fe, Ni, and FeS, with compositions of $(Fe_{0.83}Ni_{0.17})_3S$, or $(Fe_{0.64}Ni_{0.36})_3S$. Sound velocity was measured using high resolution IXS at BL35XU, or BL43XU of SPring-8. IXS spectra were collected in the range of the momentum transfer, Q=3.2?6.59 $nm^{?1}$ with a resolution of 0.45 nm^{-1}. EHDAC was put in a vacuum chamber to reduce the background of the spectra.We will present the sound velocity data of liquid and solid of $(Fe,Ni)_3S$ and discuss the composition of the terrestrial, Martian, and Mercury's liquid outer core.

Keywords: sound velocity, inelastic X-ray scattering, planetary outer core, liquid iron alloy, High-PT experiment

Japan Geoscience Union Meeting 2014
(28 April - 02 May 2014 at Pacifico YOKOHAMA, Kanagawa, Japan)

SIT03-27 Room:418 Time:April 29 17:30-17:45

Experimental approach to the core-mantle boundary region of Mercury

OKAMOTO, Miho[1] ; URAKAWA, Satoru[1*]

[1]Dept Earth Sci, Okayama Univ

MESSENGER mission revealed precise moment of inertia parameters of Mercury and its surface chemistry [1, 2]. These data allow to model the internal structure of Mercury, which has a large liquid core with ∼2000 km radius and a solid outer shell with ∼400 km thickness [3, 4]. As density of solid outer portion is apparently higher than that of the expected mantle silicate, the solid outer layer must include dense materials. Recent models [3, 4] showed that the Mercury's core contains sulfur and silicon as light elements due to high S fugacity and low oxygen fugacity of its interior. Those models presented a solid FeS layer at bottom of solid outer shell of Mercury as a dense layer, which separated from liquid outer core as a FeS-rich liquid due to liquid immiscibility of the Fe-S-Si ternary system. To investigate the FeS-rich layer at the top of Mercury's core, we performed the high-pressure experiments on the Fe-S-Si system using a KAWAI-type multi-anvil apparatus.

Pressure is fixed at 5 GPa corresponding to the CMB of Mercury and temperature is 1800 K, which is 200 K above the liquidus of Fe-S-Si system reported by Sanloup and Fei [5]. Fe-S-Si sample was kept for 30 min at this condition, and then it was quenched into room temperature. Oxygen fugacity of run charges was maintained around 3 log unit below IW buffer. Texture and chemistry of recovered samples were examined by electron microprobe.

We found two immiscible liquids in one run charge, which consist of Fe,Si-rich metallic liquid and FeS-rich sulfide liquid. Sulfur content of metallic liquid ranges 6 to 9 at%, which is higher by ∼5 at% than those reported by Morard and Katsura [6]. Differences in texture of recovered samples and run duration between this study and Morard and Katsura [6] suggest that the latter experiments were in disequilibrium state. Our data shows the liquid immiscible region has a narrower extent than the previous estimation and the Mercury immiscible Fe-S-Si core must contain at least 6-9 at% sulfur. The quenched FeS-rich liquid phase consists mainly of crystalline FeS (∼90 vol%) and Fe-Si alloy. In the case that FeS-rich liquid contacted with MgO sample container, $(Mg_{0.8}Fe_{0.2})S$ crystalline phase coexisted with FeS-rich liquid. Mg-sulfide phase could be made by Fe-Mg exchange reaction between MgO and FeS-rich liquid. In the Mercury core, when FeS-rich liquid ascends to add the bottom of the CMB due to its buoyancy, it makes a stable low density layer. Mg-sulfide phase is produced under low oxygen fugacity and high sulfur fugacity at CMB, and then it incorporates into mantle. This is consistent with the results of X-ray fluorescence spectrometry on the Mercury's surface, which indicates the presence of Mg and Ca sulfides [2].

References

[1] Margot JL et al., J. Geophys. Res., 117, E00L09, 2012.
[2] Nittler LR et al., Science, 333, 1847, 2011.
[3] Smith DE et al., Science, 336, 214, 2012.
[4] Hauck II SA et al., J. Geophys. Res.: Planets, 118, 1204, 2013.
[5] Sanloup C and Fei Y, Phys. Earth Planet. Inter., 147, 57, 2004.
[6] Morard G and Katsura T, Geochim. Cosmochim. Acta, 74, 3659, 2010.

Keywords: core, CMB, Mercury

Japan Geoscience Union Meeting 2014
(28 April - 02 May 2014 at Pacifico YOKOHAMA, Kanagawa, Japan)

SIT03-P01 Room:Poster Time:April 29 18:15-19:30

Single crystal elasticity by means of GHz ultrasonics and Brillouin scattering in DAC II

YONEDA, Akira[1*] ; MURAKAMI, Motohiko[2]

[1]ISEI, Okayama Univ., [2]Department of Earth and Planetary Materials Science, Tohoku University

We have been developing simultaneous measurement of GHz ultrasonics and Brillouin scattering in DAC. At JpGU 2013, we presented fundamental feasibility of GHz ultrasonics in DAC. This year, we will present succeeding progress of it.

Keywords: mantle, DAC, single crystal elasticity, GHz ultrasonics

Japan Geoscience Union Meeting 2014
(28 April - 02 May 2014 at Pacifico YOKOHAMA, Kanagawa, Japan)

SIT03-P02 Room:Poster Time:April 29 18:15-19:30

Single-crystal elastic property of silicate perovskites

FUKUI, Hiroshi[1*] ; YONEDA, Akira[3] ; SHATSKIY, Anton[4] ; TSUTSUI, Satoshi[5] ; BARON, Alfred[2]

[1]Graduate School of Material Science, University of Hyogo, [2]Materials Dynamics Laboratory, RIKEN SPring-8 Center, RIKEN, [3]Institute for the Earth's Interior, Okayama University, [4]V.S. Sobolev Institute of Geology and Mineralogy, Russian Academy of Science, Siberian Branch, [5]Research and Utilization Division, SPring-8/JASRI

Information of single-crystal elasticity of silicate perovskite is essential for comprehensive understanding of the lower mantle. We have measured single-crystal elastic property of $Mg_{1-x}Fe_xSiO_3$ perovskite (x = 0 or 0.035) by means of inelastic x-ray scattering at the ambient condition. The present results show relatively low values compared to previous reports for the iron free sample. The effect of iron increases both adiabatic bulk modulus and shear modulus. Combining the present results with pressure and temperature derivatives reported in literature, the chemical composition of the lower mantle will be discussed.

Keywords: silicate perovskite, single-crystal elasticity, the lower mantle, inelastic x-ray scattering

Japan Geoscience Union Meeting 2014
(28 April - 02 May 2014 at Pacifico YOKOHAMA, Kanagawa, Japan)

SIT03-P03 Room:Poster Time:April 29 18:15-19:30

Measurement of thermal conduction of high-pressure minerals at pressures of the transition zone and to the lower mantle

OSAKO, Masahiro[1*] ; YONEDA, Akira[2] ; YOSHINO, Takashi[2]

[1]National Museum of Nature and Science, [2]Institute for study of the Earth's interior

Knowledge of thermal diffusivity or thermal conductivity of the mantle is vital for study of the dynamics of the Earth. So far thermal diffusivity and thermal conductivity of mantle minerals were measured under high pressure using a pulse-heating method of one-dimensional heat flow. This method is a predominant one for study in deep Earth's materials under pressure because it requires comparatively small amount of samples. It is also applicable to materials with anisotropy in thermal conduction. In addition its measurement yields heat capacity data under pressure.

Thermal conductivity or thermal diffusivity of olivine and garnet increases 3-4 % per 1 GPa, and olivine still reveals anisotropy in thermal conduction under the conditions of the upper mantle. Antigorite, a high-temperature form of serpentine, has low thermal diffusivity and low thermal conductivity which are much lower than those of olivine, whereas talc has high thermal diffusivity and thermal conductivity comparable to those of olivine. All those data were obtained from the measurements at pressures up to 10 GPa and temperatures to 1100 K. An advanced cell assembly was needed to expand the pressure range of measurement.

A new pressure-cell assembly similar to our previous one is designed for a sample of 3 mm in diameter and 0.7 mm in thickness. This smaller cell was applied to pyroxene samples of which sizes were necessarily limited. The measurements were conducted using the Kawai-type apparatus at the Institute for study of the Earth's interior, Misasa. This cell enabled to make measurements of thermal properties at pressures exceeding 15 GPa, which will covers the condition in the mantle transition zone.

We made preliminary measurements by this cell for the garnet sample as a test material. The thermal diffusivity showed slightly lower value (5˜10 %) and the thermal conductivity was slightly high (0˜10 %) value compared with the previous results by the large cell. The precision of measurements should be improved by well-controlled machining of the cell assembly and by refining the data acquisition system. After that this cell will be used for measurements of wadsleyite, ringwoodite and majorite. A cell assembly of more reduced in size is planned. This cell will be used for measurements of MgSiO3 perovskite.

Keywords: mantle minerals, thermal diffusivity, thermal conductivity, high-pressure

Japan Geoscience Union Meeting 2014
(28 April - 02 May 2014 at Pacifico YOKOHAMA, Kanagawa, Japan)

SIT03-P04 Room:Poster Time:April 29 18:15-19:30

Elemental partitioning in the Fe-S-Si system at high pressure and temperature: Implications for the Earth's core

SAKAIRI, Takanori[1*] ; OHTANI, Eiji[1] ; SAKAI, Takeshi[2] ; KAMADA, Seiji[1] ; MIYAHARA, Masaaki[3] ; HIRAO, Naohisa[4]

[1]Department of Earth science, Tohku University, [2]Geodynamics Reserch Center, Ehime University, [3]Department of Earth and Planetary Systems Science, Graduate School of Science, Hiroshima University, [4]JASRI

It is widely accepted that the Earth's core is mainly composed of iron and contains light elements to account for the core's density deficit. Alloying with light elements significantly affects the physical properties of iron and the arguments on the chemical structure of the Earth's core. Therefore, the melting relation of the Fe-light elements system is the key to clarifying the chemical structure of the core because the inner core has formed by crystallization of the molten outer core. Although there are many candidates for light elements in the core, based on geochemical modeling and high-pressure partitioning experiments, sulfur and silicon are considered to be the major light elements. Despite the importance of the effect of sulfur and silicon on the physical properties of iron, previous studies, including high-pressure melting experiments in the Fe-S-Si system, did not cover the pressure conditions of the core. To better understand the properties of the core, we investigated the melting relations of the Fe-S-Si system under high-pressure conditions corresponding to the Earth's core.

We report on the melting relations in the Fe-S-Si system up to 135 GPa. Melting experiments were performed in the pressure range of 37-135 GPa and the temperature range of 1800?4100 K using a double-sided laser-heated diamond anvil cell. The composition of the starting material was $Fe_{80.1}S_{12.7}Si_{7.2}$ (Fe-8 wt.% S-4 wt.% Si). Melting relations were examined on the basis of quenched textures of the recovered samples and chemical analysis of observed phases. The chemical composition of the coexisting phases in the samples was obtained with an energy-dispersive X-ray spectroscopy (EDS) system attached to the FEG-SEM. We determined the compositions of the coexisting phases and investigated the partitioning behavior of sulfur and silicon between the metallic melt and the coexisting iron alloy.

We consistently found that a quenched melt with a dendritic texture coexists with a solid Fe alloy in the recovered samples, implying that the samples were partially melted under the experimental pressure and temperature conditions. Based on the present results, the partition coefficients of sulfur and silicon between the liquid and solid Fe alloy were determined in the pressure range from 37 to 135 GPa. The value obtained for D_{sulfur} at 37 GPa was 0.032(28), whereas $D_{silicon}$ was 4.53(73), which is significantly higher than D_{sulfur}. The obtained values of Dsulfur were between 0.032(28) and 0.135(35) and those of $D_{silicon}$ were between 2.63(12) and 5.58(56) in this study. The present results indicate that the solid Fe alloy is silicon rich whereas the metallic melt is enriched in sulfur. We can find that this trend continues up to the core-mantle boundary (CMB) pressure.

The information on partitioning of light elements between the metallic melt and hcp-Fe is the key for clarifying the chemical structure of the Earth's core because the inner core is considered to have crystallized from the liquid outer core during cooling of the Earth. Moreover, previous studies strongly implied that both sulfur and silicon were the plausible candidates for the light elements in the core. Therefore, our experimental results in the Fe-S-Si system offer important clues for understanding the composition of the Earth's core. Based on the present results, if the Earth's core cools down below the melting temperature of the core material, silicon could be preferentially partitioned into hcp-Fe from the Fe-S-Si liquid during crystallization of the inner core. The present data demonstrated that if the Earth's core contains both sulfur and silicon as light elements, the present-day Earth has a sulfur-rich outer core and a silicon-rich inner core.

Keywords: Earth's core, light element, elemental partitioning, crystallization

Japan Geoscience Union Meeting 2014
(28 April - 02 May 2014 at Pacifico YOKOHAMA, Kanagawa, Japan)

SIT03-P05 Room:Poster Time:April 29 18:15-19:30

Influence of the electrical conductivity heterogeneity at the CMB on the flow and magnetic field in the core

SHIMIZU, Hisayoshi[1*]

[1]Earthquake Research Institute, University of Tokyo

The effects of electromagnetic induction in the heterogeneous mantle on the observed electromagnetic fields have been studied numerically to investigate possible causes of short time-scale variation known as the geomagnetic jerk. We found previously that the jerk-like magnetic and electric field variations observed at the surface of Earth can be explained by an input of a sudden variation of the toroidal field at the top of the core and large-scale conductivity heterogeneity of which conductivity is about 100 times higher than the background electrical conductivity. In this study, the effect of the heterogeneity on the flow in the core and magnetic field is evaluated by using a simple plane model of a heterogeneous mantle. Preliminary results suggest that the signature of the magnetic field may be detected as a stationary field at the Earth's surface if the heterogeneity is planetary scale, but the penetration length of its effect in the core is much shorter than the length scale of the heterogeneity.

Keywords: geomagnetic field, CMB

Japan Geoscience Union Meeting 2014
(28 April - 02 May 2014 at Pacifico YOKOHAMA, Kanagawa, Japan)

SIT03-P06 Room:Poster Time:April 29 18:15-19:30

Potassium solubility into the Earth's core at the base of the magma ocean -Implication for the heat source of the core

WATANABE, Kosui[1*] ; OHTANI, Eiji[1] ; KAMADA, Seiji[1] ; SAKAMAKI, Tatsuya[1] ; MIYAHARA, Masaaki[2]

[1]Department of Earth Science, Graduate School of Science, Tohoku University, [2]Department of Earth and Planetary Science, Graduate school of Science, Hiroshima University

Since the densities of the Earth's inner/outer cores are smaller than pure iron at the core conditions, the core has been thought to include light elements, such as H, C, S, O, Si (e.g., Poirier, 1994). Although the light element(s) in the core has not been decided yet, high-pressure experiments and cosmochemical estimations suggested that Si and O are plausible light elements. The energy causing the geodynamo is derived from the accretion energy at the early stage of the Earth, the latent heat of crystallization of the inner core, the gravitation energy associated with the exclusion of light materials from the inner core, and the radioactive decay of radioactive elements which are potentially present in the core. The Earth's core might contain long-lived radioactive elements such as U, Th, and K. In particular, potassium (K) is more depleted in the mantle than other volatile elements. Thus, potassium may be included in the core. In order to verify the amount of potassium in the core, we have performed potassium partitioning experiments under high pressure and temperature.

We studied partitioning of potassium between aluminosilicate (adularia, $KAlSi_3O_8$) and metal containing oxygen and silicon, and partitioning of potassium without light elements (Fe-O, Fe-Si, pure Fe) at pressures up to 50 GPa and 3500 K using a double-sided laser-heated diamond anvil cell. Our results for the pressure, temperature, and compositional effects on the partitioning coefficient of potassium, D_K (i.e., the content of potassium in metal [wt%] divided by the content of potassium in silicate [wt%]), reveal that the temperature effect is slightly positive but weaker than that reported previously, whereas the pressure effect is negative and oxygen in metal increases the potassium content in metal, although silicon in metal has the opposite effect. According to the effects on potassium partitioning, we estimated that the amount of potassium in the core is less than 32 ppm and that it generates less than 0.14 TW heat in the core. This amount of heat is small compared with the heat flux at the core-mantle boundary (5-15 TW).

Keywords: Potassium, magma ocean, high pressure, high temperature, Earth's core

Japan Geoscience Union Meeting 2014
(28 April - 02 May 2014 at Pacifico YOKOHAMA, Kanagawa, Japan)

SIT04-01 Room:414 Time:April 28 09:00-09:25

Thermal structure of the NE Japan-Hokkaido subduction system: The effects of 3-D slab geometry and oblique subduction

WADA, Ikuko[1*] ; JIANGHENG, He[2] ; HASEGAWA, Akira[3] ; TAMURA, Yoshihiko[4] ; NAKAJIMA, Junichi[3]

[1]IRIDeS, Tohoku University, [2]Pacific Geoscience Centre, Canada, [3]Graduate School of Science, Tohoku University, [4]Japan Agency for marine-Earth Science and Technology

In this study, we first examine the effects of along-strike variation in slab geometry and oblique subduction on subduction zone thermal structures by comparing 3-D numerical thermal models with a range of generic subduction geometries and parameters with a 2-D reference model. We found that changes in slab dip along a straight margin have modest effects on the mantle flow pattern and thus the thermal field. However, concave and convex ocean-ward margins result in cooler and warmer mantle wedges, respectively, and oblique subduction results in a warmer mantle wedge, compared to the 2-D reference model. We developed a 3-D thermal model for the NE Japan-Hokkaido margin, using a well-constrained 3-D slab geometry model. In general, there is little 3-D effect on the thermal structure of the shallow part (<70 km depth) of the subduction system, where the mantle does not participate in the slab-driven wedge flow. We also found that the 3-D effect is small in the deeper part of the southern half of the system, where the margin is relatively straight and the slab dip does not vary significantly along the margin. These results indicate that 2-D models provide excellent approximations for the thermal structures of the shallow part and the southern part of the subduction system. However, from the northern part of NE Japan to Hokkaido, the mantle flow pattern is affected by the concave ocean-ward margin and oblique subduction, and the wedge is cooler near the NE Japan-Hokkaido junction and warmer in Hokkaido than the 2-D thermal models for the respective regions. We compare the 3-D thermal modeling results with along-strike variations in surface heat flow, arc magma geochemistry, and earthquake distribution in NE Japan and Hokkaido.

Keywords: Tohoku-Hokkaido subduction system, 3-D thermal model, slab geometry, oblique subduction, mantle wedge flow, earthquakes and volcanism

Japan Geoscience Union Meeting 2014
(28 April - 02 May 2014 at Pacifico YOKOHAMA, Kanagawa, Japan)

SIT04-02 Room:414 Time:April 28 09:25-09:40

Effects of a local deepening of slab-mantle decoupling depth on slab surface temperature

MORISHIGE, Manabu[1*] ; VAN KEKEN, Peter E.[2]

[1]JAMSTEC, [2]University of Michigan

In the subduction zone, we generally observe low seismic attenuation in the forearc mantle. In addition, surface heat flow shows low value in the forearc and a sudden transition to high value in the arc. These observations suggest that the forearc mantle is cold and is not involved in the corner flow in the mantle wedge. We can understand it in terms of slab-mantle decoupling depth (D_{dec}). Above D_{dec}, the mantle does not move with the slab just beneath it. Therefore, it becomes cold quickly due to the cooling from the overriding plate and the slab. Below D_{dec}, on the other hand, the mantle moves with the slab. It keeps this part of mantle warm by advection of hot material due to the corner flow. Thus, D_{dec} is a key parameter which strongly affects thermal structure in the subduction zone. Comparison of the observed surface heat flow and the one predicted with 2D numerical model suggests that D_{dec} does not vary much for each subduction zone and is 70-80km, but in each subduction zone D_{dec} may show some degree of along-arc variation. One such example is the junction between Japan and Kurile arcs, where the down-dip limit of thrust type earthquake is locally deepened by around 15km. In this presentation, we investigate the effects of a local deepening of D_{dec} on slab surface temperature.

Toward the goal, we use time-dependent 3D finite element models to compute mantle flow and temperature. Only mantle wedge is treated as a dynamic entity. We use a simple slab geometry and assume a local deepening of D_{dec} to see its effects. We find that the increase in slab surface temperature at D_{dec} is larger where we assume a deepening of D_{dec}, which produces a warmer region there. It is caused by 3D flow in the mantle wedge due to along-arc variation of D_{dec}. We also calculate surface heat flow from obtained thermal structure, but it does not show significant along-arc variation. These results do not change even when we use a realistic slab geometry which is similar to that of the junction between Japan and Kurile arcs. While the surface heat flow anomaly and deepening of the seismic belt in S. Hokkaido cannot be easily explained by these models, the temperature excursions at the slab surface are significant. These models predict potentially strong variations in the conditions that the fluids leave the slab, which may be visible by various new geothermometers, such as those based on the H_2O/Ce ratio.

Keywords: subduction zone, slab-mantle decoupling depth, slab surface temperature

Japan Geoscience Union Meeting 2014
(28 April - 02 May 2014 at Pacifico YOKOHAMA, Kanagawa, Japan)

SIT04-03 Room:414 Time:April 28 09:40-10:05

Thermal modeling associated with subduction of the Philippine Sea plate in southwest Japan

YOSHIOKA, Shoichi[1*] ; JI, Yingfeng[1] ; MATSUMOTO, Takumi[2]

[1]RCUSS, Kobe University, [2]NIED

By constructing a parallelepiped three-dimensional thermal convection model, we investigated temperature, mantle flow and heat flow distributions associated with subduction of the Philippine Sea (PHS) plate in southwest Japan. We proposed new, realistic, and high-resolution temperature field on the plate interface, and attempted to clarify its relationships with the occurrences of megathrust earthquakes, long-term slow slip events (SSE), and low frequency tremors (LFEs). For this purpose, we newly developed a numerical model to deal with subduction of an oceanic plate with 3D arbitrary geometry. We modeled subduction of the PHS plate by using the up-to-date three-dimensional slab geometry, referring to high resolution P-wave seismic tomography and seismic reflection studies. We also used large number of heat flow data such as BSRs, borehole, heat probe, and Hi-net to constrain calculated temperature field, and took account of complicated subduction history in southwest Japan. The results showed that the interplate temperature was lower by approximately 100^{o}C in western Shikoku where a larger true subduction angle exists than eastern Shikoku. Temperature change due to erosion and sedimentation affected surface heat flow with short wavelength. We also found that the obtained interplate temperature in the Nankai seismogenic zone was wider than that in the Tonankai seismogenic zone. The LFEs occurred near the plate interface with temperatures ranging from 350^{o}C to 450^{o}C at depths of 30 to 40 km. The existence of large temperature gradients from the surface to the inside of the PHS plate was considered to be related to the occurrence of long-term slow slip events beneath the Bungo Channel.

Japan Geoscience Union Meeting 2014
(28 April - 02 May 2014 at Pacifico YOKOHAMA, Kanagawa, Japan)

SIT04-04 Room:414 Time:April 28 10:05-10:20

Slab-wedge mantle boundary preserved in the Sanbagawa belt, SW Japan

WALLIS, Simon[1*] ; MORI, Hiroshi[1] ; NAGAYA, Takayoshi[1] ; KAWAHARA, Hirokazu[1]

[1]Dept. Earth & Planetary Sci., Nagoya Uni.

The Sanbagawa belt of SW Japan is a high-pressure low-temperature subduction type metamorphic belt. The rock types consists of mafic, siliceous and pelitic schists derived from the subducted slab. There are also a series of ultramafic bodies whose origin is disputed: both a slab and wedge mantle origin have been proposed. However, the clear relationship between the distribution of the mantle rocks and metamorphic grade provides strong evidence that they were derived from the wedge mantle. We carried out a detailed study of the Shiragayama body as an example of serpentinized mantle from close to the corner of the wedge. Studies of this region can contribute to our understanding of non-volcanic tremor and fluid flow that occurs in these otherwise inaccessible parts of subduction zones.

Keywords: fore arc mantle, subduction metamorphism, slab mantle boundary

Japan Geoscience Union Meeting 2014
(28 April - 02 May 2014 at Pacifico YOKOHAMA, Kanagawa, Japan)

SIT04-05 Room:414 Time:April 28 11:00-11:25

Phenomenology of Episodic Tremor and Slip

OBARA, Kazushige[1*]

[1]Earthquake Research Institute, UTokyo

Episodic Tremor and Slip (ETS) is a coupling phenomenon composed of continuous weak seismic events and geodetic short-term slow slip event (SSE) in the transition zone between the brittle seismogenic zone and stable sliding regime recognized in southwest Japan and Cascadia. This paper reviews characteristics of ETS and related phenomena to contribute to discussion for subduction process.

ETS is interpreted as a stick slip on the plate interface accompanied by seismic swarm at small patches surrounded by the SSE plane because of coincidence of their sources and linear relationship between the duration of tremor episode and the moment of SSE estimated geodetically for each episode. ETS is distributed in a narrow belt-like zone along the strike of the subducting plate. ETS zone is divided into several segments in which episodes recur at each regular recurrence interval. However ETS is not ”characteristic earthquake” because the rupture area and recurrence interval are fluctuated. Sometimes we observe rupture propagation through a couple of segments. The segment is usually bounded by gap which is considered as not a barrier but an easily sliding portion because of the existence of multi-segment migration.

ETS activity has depth dependent property. At the deeper part of the ETS zone minor episode frequently occurs, on the other hand major episode occurs infrequently at the shallower part. Large ETS usually initiates from the deeper part and migrates upward then activates at the shallower part. This might be caused by gradual change in frictional property with increasing the depth. At the downdip edge of the ETS zone tremor episode easily occur due to weak strength and stress concentration from stable sliding zone. Each small episode transfers the stress to the updip side. Finally a small episode can propagate to the updip edge then develop as a large ETS episode.

The activity style of ETS in southwest Japan and Cascadia is very similar; however there are some differences. One is the existence of deep very low frequency earthquake (VLF). In Japan the VLF earthquake is usually associated with ETS but has not been detected in Cascadia. It might depend on the detection capability or difference in inhomogeneity of the plate interface because the distribution of VLF earthquake in southwest Japan is more localized compared to that of tremor.

The other difference is the existence of long-term SSE. It is detected at the updip side of ETS zone in the Bungo Channel and Tokai in southwest Japan but not detected in Cascadia. The long-term SSE with duration from several months to years activates tremor at the adjacent limited region in the ETS zone. On the other hand, the tremor activity at the downdip part is not affected. Similar long-term SSE has been detected in Alaska and Mexico, where tremor activity was recently detected at the downdip side of the source fault of the long-term SSE. The tremor is seems to be activated during the SSE period like as in southwest Japan. The long-term SSE in Tokai is located above the anomalously high Vp/Vs region in the slab. In Mexico, a ultra slow speed layer was found in the long-term SSE source region. Therefore, the anomalous structure might be a cause of the long-term SSE. ETS and long-term SSE are quite different in the slip velocity. It might reflect the difference in the frictional property. In Tokai, the source region of the long-term SSE and ETS is bounded by the inland Moho discontinuity. Therefore, ETS occurs at the interface between the subducting plate and overlying mantle wedge.

ETS has not been recognized besides in southwest Japan and Cascadia; however ambient tremor has been detected in some regions. We expect that the ambient tremor is triggered by small SSE which is not detected by the current observation. Understanding detail relationship between tremor and SSE based on improvement detection capability is important to reveal the mechanism of ETS.

Keywords: slow earthquake, non-volcanic tremor, slow slip event, subduction zone, plate interface

Japan Geoscience Union Meeting 2014
(28 April - 02 May 2014 at Pacifico YOKOHAMA, Kanagawa, Japan)

SIT04-06 Room:414 Time:April 28 11:25-11:40

Enhancement of slow earthquakes by geometrical irregularity of subducting oceanic crust

KATO, Aitaro[1*] ; OBARA, Kazushige[1] ; TAKEDA, Tetsuya[2]

[1]ERI University of Tokyo, [2]NIED

Along the worldwide subduction zones, slow earthquakes commonly occur on the deep extension of major tectonic boundary which hosts megathrust earthquake rupture. Slow earthquakes silently release stress to the adjacent seismogenic zone, raising the likelihood of promoting unstable fast slip. However, what controls the transitional variations in fault-slip behaviors from fast to slow modes on the deep extension of megathrust fault remains controversial. Here we use a high-resolution receiver function and seismic tomography illustrated by dense seismic arrays to analyze the structural elements in the subduction complex and fore-arc mantle wedge beneath the Shikoku Island, Japan, where episodic tremor and slow-slip events (ETS) have been most intensive for over a decade.

We find out that deformed oceanic crust with irregularity of surface geometry horizontally lies in the ETS zone, where low seismic velocity zone with high Poisson's ratio that we interpret as high pore-fluid pressure. Step-like discontinuous alignments of intra-slab seismicity support the flat-subduction of the oceanic crust with faulting structure. In contrast, at depths shallower than the ETS zone, the low velocity anomaly within the oceanic crust is weak and dipping towards the NW, implying less amount of high-pressured fluid in the tilting oceanic crust. In addition, lithology of the overlying plate changes to partially serpentinized mantle wedge in the ETS zone. Locally flat-geometry of the subducting oceanic crust combined with the contact of serpentine enhances accumulation of high-pressurized fluids along the plate interface, leading to segregation between slow and fast slip modes at the deep transition zone of mega-thrust fault.

Japan Geoscience Union Meeting 2014
(28 April - 02 May 2014 at Pacifico YOKOHAMA, Kanagawa, Japan)

SIT04-07 Room:414 Time:April 28 11:40-12:05

Deformation experiments on serpentinite at high PT conditions with implications for the mechanisms of slow earthquakes

OKAZAKI, Keishi[1*] ; HIRTH, Greg[1] ; PROCTOR, Brooks[1] ; KATAYAMA, Ikuo[2] ; TAKAHASHI, Miki[3]

[1]Department of Geological Sciences, Brown University, [2]Department of Earth and Planetary Systems Science, Hiroshima University, [3]Geological Survey of Japan, AIST

To understand the spatial and temporal distribution of earthquakes and deformation in subduction zones, it is important to constrain the rheological properties of metamorphic rocks (i.e., altered mantle, oceanic crust and sediments), and how they evolve during metamorphic reactions following hydration, carbonation and dehydration of the down-going slab. Especially, antigorite (the high-temperature serpentine polytype) serpentinite, the dominant metamorphic phase in hydrated mantle material at the condition of mantle wedge, is the key metamorphic rock to understand the generation mechanism of slow earthquakes and slab-mantle coupling at the plate interface in subduction zones.

Deformation experiments on antigorite serpentinite were conducted within and above the thermal stability field of antigorite using a gas pressure-medium apparatus and a solid pressure-medium apparatus to understand how dehydration reactions influence the mechanical behavior of antigorite serpentinite. At 400 ℃, within the stability field of antigorite, antigorite serpentinite shows stable sliding and a positive velocity dependence of shear stress (i.e., friction coefficient). Shear stress increased with increasing confining pressure, while the friction coefficient decreases from 0.55 to 0.37 with increasing confining pressure from 200 MPa to 1500 MPa. These results indicate that antigorite serpentinite deforms by brittle and semi-brittle processes in subduction zones.

During the experiments using a gas pressure-medium apparatus at a confining pressure of 200 MPa and temperatures close to the dehydration temperature of antigorite (450-550 ℃), antigorite serpentinite shows a slow stick-slip behaviour, which is characterised by relatively long durations and small stress drops during slip, while this type of behaviour was not observed at higher temperatures when the antigorite becomes completely dehydrated. Stick-slip in this temperature range is consistent with the temperature range where slow earthquakes occur at the corner of the mantle wedge in southwest Japan and Cascadia. The scaling law of slow stick-slip in the antigorite serpentinite gouge is distinct from that of regular earthquakes and a theoretical duration estimated from the apparatus stiffness, but similar to that of slow earthquakes.

We also conducted deformation experiments in which temperature was increased above the thermal stability of antigorite to simulate a prograde metamorphism in subduction zones, similar to the experiments by Chernak and Hirth (2011) but with a general-shear geometry. With increasing temperature from 400 ℃ to 700 ℃ during deformation, differential stress decreased and reached 120 MPa. Recovered sample suggest that the strain localizes within shear fractures and limited dehydration occurred during the experiments.

These results suggest that the dehydration of antigorite can form weak zones within the mantle wedge along the plate interface in subduction zones, even if the extent of the dehydration reaction is limited. In addition, slow instabilities of the slip interface can be caused by the dehydration of antigorite within the weak zone in the antigorite serpentinite layer, which can result slow earthquakes.

Keywords: antigorite, serpentinite, semi-brittle flow, slow earthquakes, dehydration, hydrothermal condition

Japan Geoscience Union Meeting 2014
(28 April - 02 May 2014 at Pacifico YOKOHAMA, Kanagawa, Japan)

SIT04-08 Room:414 Time:April 28 12:05-12:20

Metasomatic fault-zone weakening of subduction plate boundary faults

HIRAUCHI, Ken-ichi[1*] ; SPIERS, Christopher[2]

[1]Shizuoka University, [2]Utrecht University

Fluid influx along faults triggers stress-induced dissolution and precipitation processes, leading to syntectonic growth of weak phyllosilicates. In subduction zones, slab-derived Si-rich fluids may infiltrate into the forearc wedge and transform primary mantle minerals into hydrous phases such as serpentines and talc, changing the mechanical and seismogenic properties of subduction plate boundary faults. However, it remains unclear how frictional strength and sliding stability of the plate boundary faults evolve via Si-metasomatism.

Hirauchi et al. (2013, *Geology*) performed frictional sliding experiments on antigorite (70%) plus quartz (30%) gouges at a pore fluid pressure (P_f) of 200 MPa, an effective normal stress (σ_{eff}) of 200 MPa, temperatures (T) of 20, 300, 400, and 500 ℃, and sliding velocities (V) of 0.1-30 μm/s, using a hydrothermal ring shear machine. At temperatures of 300-500C, the gouges exhibited a peak friction coefficient (μ) of 0.40-0.62, followed by strain weakening towards a quasi-steady-state μ of 0.25-0.47. The weakening was mainly due to the development of through-going, talc-rich boundary shears. The steady-state μ of the gouges decreased systematically as the talc-rich layer widened.

At central California, there are several boundary faults that separate serpentinite bodies from shale-matrix melanges of the Franciscan accretionary complex. The serpentinite body is overprinted by anastomosing development of crack-seal veins of talc, serpentine, and calcite, suggesting that intense water-rock interaction took place in connection with faulting. The serpentinite along the faults represents a cataclastic shear zone that records brittle deformation, consisting of angular fragments that are suspended in fine-grained, randomly-oriented talc matrix. Frictional sliding experiments conducted at P_f = 40, 80, and 120 MPa, σ_{eff} = 60, 120, and 180 MPa, T = 20, 150, and 300 ℃, and V = 0.3-100 μm/s showed that the serpentinite has friction coefficients that agree with Byerlee's law (μ 0.6), while the cataclasite is much weaker with friction coefficients as low as 0.2. Examination of the velocity dependence of friction revealed that the serpentinite exhibits both velocity-weakening and velocity-strengthening behavior, whereas the cataclasite is velocity strengthening under all conditions investigated.

Our results demonstrate that in the lowermost part of the forearc wedge, where silica-saturated fluids infiltrate from the dehydrating slab, metasomatically produced talc will form in the intensely sheared serpentinite, causing a much larger weakening effect than expected for serpentines, even if the total amount of talc formed is minor (<10 vol%). The continued reaction with Si-rich fluid will also result in a transition from seismic to aseismic behavior of the plate boundary faults.

Keywords: subduction zone, serpentinite, metasomatism, fault

Japan Geoscience Union Meeting 2014
(28 April - 02 May 2014 at Pacifico YOKOHAMA, Kanagawa, Japan)

SIT04-09 Room:414 Time:April 28 12:20-12:45

Coupled mass transport and serpentinization at crust/mantle boundary: Insights from hydrothermal experiments

OKAMOTO, Atsushi[1*] ; OYANAGI, Ryosuke[1] ; TSUCHIYA, Noriyoshi[1]

[1]Graduate School of environmental Studies, Tohoku University

Serpentinization commonly proceeds by a supply of water passing through crust, and thus a large mass transport could occur during serpentinization reactions. Especially, silica activity is known as a control of the reaction paths and rate during the hydrothermal alternation of peridotites [1, 2]. However, it is still unclear the role of mass transport on reaction paths, overall hydration rate and volume change during serpentinization. In this study, we conducted two types of hydrothermal experiments on serpentinization. First one is the metasomatic-reaction experiments between olivine (Ol) ? quartz (Qtz) zones as analogue of boundary of mantle and crustal rocks. Second one is the hydrothermal experiments with sintered olivine (analogue of low porosity rock). Both types of experiments were carried out at 250 ?C and vapor-saturated pressure (= 3.98 MPa) in alkaline aqueous solution.

In the Ol-Qtz metasomatic experiments (up to 46 days.), composite powders, which was composed of Qtz zone and Ol zone was set in inner tubes and then loaded into autoclave. After the experiments, the mineralogy and H2O content of the products were evaluated as a function of the distance from Ol/Qtz boundary. The reaction products after olivine are serpentine (Srp), brucite (Brc), magnetite (Mgt) and smectite (Smc) (instead of talc). The products systematically change from the Smc+Srp to Srp+Brc+Mgt with increasing the distance from the Ol/Qtz boundary. The H2O content of the products is low at the Ol/Qtz boundary (i.e., 3.9 wt.% after 46 days), and increases toward the margin of the tube (12 wt.% at ˜30 mm from the Ol/Qtz boundary).

The detailed mass balance calculation between 25 to 46 days reveals the characteristic nature of the metasomatic reactions and porosity change as follows. Near Ol/Qtz boundary (Smc+Srp zone), smectite was formed by supply of silica in two ways; hydration of olivine and dehydration of serpentine. In contrast, at the zone far from the boundary (Srp+Brc zone; $>$20 mm from O/Qtz), the production rate of serpentine and brucite are constant without any silica supply. At the transition zone between Smc+Srp and Srp+Brc zones, a large amount of serpentine is formed by consumption of both brucite and olivine, which results in a largest porosity reduction (˜30 %). In the Smc+Srp zone, dehydration and porosity reduction occurs simultaneously, implying a possible raise of fluid pressure. Silica metasomatic reactions causes a significant variation not only in mineral assemblage but also in porosity and fluid pressure, which will characterize the dynamic change of mechanical properties at crust/mantle boundary.

In the hydrothermal experiments of the sintered olivine, the starting olivine aggregate (initial porosity $<$˜10 %, covered by Pt jacket), which was made by hot press at 1200 degreeC, 1 GPa and 4 days, was emplaced in the alkaline water. After 3 days, we recognized the progress of serpentinization reaction to produce serpentine and brucite. An interesting finding of this experiment is that brucite did not formed in pores of the core sample, but it was formed only at the top of the cylindrcial core of the sample. This result is quite different from with our previous experiments with using olivine powder (initial porosity is ˜50 %) [3], in which brucite and serpentine was formed uniformly. The result of our present study of the sintered olivine suggests that, when the rock porosity is low and volume expansion is difficult, brucite is segregated into open space (c.a. open fracture) during serpentinization; which may also affects on the formation of the local weak zone within the mantle peridotite.

[1] Frost, B. R., & Beard, J. S., 2007. Journal of Petrology, 48, 1351?1368.
[2] Ogasawara, Y., Okamoto, A., Hirano, N., & Tsuchiya, N, 2013. Geochim. Cosmochim. Act, 119, 212?230.
[3] Okamoto, A., Ogasawara, Y., Ogawa, Y. and Tsuchiya, N., 2011. Chemical Geology, 289, 245-255.

Keywords: serpentinization, hydrothermal experiments, silica metasomatism, porosity change, hydration, mass transport

Japan Geoscience Union Meeting 2014
(28 April - 02 May 2014 at Pacifico YOKOHAMA, Kanagawa, Japan)

SIT04-P01 Room:Poster Time:April 28 18:15-19:30

Saline fluids recorded in jadeitites in subduction-zone melanges of southwest Japan

MORI, Yasushi[1*] ; SHIGENO, Miki[1] ; KAWAMOTO, Tatsuhiko[2] ; NISHIYAMA, Tadao[3]

[1]Kitakyushu Mus. Nat. Hist. Hum. Hist., [2]Inst. Geotherm. Sci., Kyoto Univ., [3]Grad. Sch. Sci. Tech., Kumamoto Univ.

Slab-derived fluids play essential roles in mass transfer along subduction-zone channels between the subducting slab and mantle wedge (e.g., Bebout 2013 Metasomatism and the chemical transformation of rocks; Spandler and Pirard 2013 Lithos). Salinity of such slab-fluids probably affects solubility and fluid-rock partitioning of elements; therefore, it remains to be investigated in various rocks. Jadeitite is a rock composed mainly of jadeite (sodium pyroxene, $NaAlSi_2O_6$) and occurs typically in serpentinite mélanges intercalated to high-pressure and low-temperature metamorphic belts. This curious rock is thought to be the product of direct precipitation from aqueous fluids and/or of fluid-induced metasomatism of a protolith (Harlow *et al*. 2007 Geology of gem deposits, Tsujimori and Harlow 2012 Eur J Mineral, and references therein). Fluid inclusions are commonly observed in jadeitites, and they may provide information about the fluid composition in subduction-zone mélanges. We determined major components and salinity of fluid inclusions in the jadeitites collected from eight localities in Japan: Omi-Itoigawa (Omi-Renge belt), Oya and Osa (Suo belt), Kochi (Kurosegawa belt), Mie and Tone (Nishisonogi metamorphic rocks), and Shimonita and Yorii (the origin unclear). In all of the studied rocks, primary fluid inclusions consist of a liquid phase and a gas bubble. Raman spectra show the presence of H_2O liquid and vapor with or without minor CH_4 gas. The freezing point of the liquid phase indicates high-salinity (up to 8 wt% NaCl equivalent) of the primary fluid inclusions. The salinity varies among the localities of the jadeitite. For example, the salinity of the primary fluid inclusions is about 7.1 $\pm$ 0.1 wt% NaCl equivalent in the albite jadeitite from Oya and about 4.6 $\pm$ 1.2 wt% NaCl equivalent in quartz inclusions bearing jadeitite from Tone. Some jadeitite samples contain secondary CH_4-rich fluid inclusions along healed microcracks. The presence of minor CH_4 is also reported in the saline fluids inclusions with 5.1 $\pm$ 1.9 wt% NaCl equivalent from the Myanmar jadeitite (Shi *et al*., 2005 Geochem J). The present findings suggest that saline fluids with or without CH_4 are common in subduction-zone mélanges in Japan as well as in Myanmar. The reduced conditions can be caused by serpentinization processes. This is contrast to the CO_2-bearing saline fluids in the peridotite xenoliths from fore-arc mantle wedge (Kawamoto *et al*., 2013 PNAS). The high-salinity of the slab-fluids probably enhances the mobility of elements such as Pb in subduction-zone channels (Keppler, 1996 Nature, Shigeno *et al*., 2012 Eur J Mineral).

Keywords: saline fluid, jadeitite, fluid inclusion, serpentinite mélange, subduction zone

Japan Geoscience Union Meeting 2014
(28 April - 02 May 2014 at Pacifico YOKOHAMA, Kanagawa, Japan)

SIT04-P02 Room:Poster Time:April 28 18:15-19:30

Serpentinite structure above subduction surface: Analysis of a natural example in Sanbagawa metamorphic belt

MIZUKAMI, Tomoyuki[1*] ; SODA, Yusuke[1] ; YOKOYAMA, Hironori[1] ; HIRAMATSU, Yoshihiro[1]

[1]Kanazawa University

Serpentinization is a key reaction in forearc mantle. Formation of strong schistosities and shear zones under high differential stresses provides anastomosing networks of fluid pathways as well as seismically anisotropic nature in the mantle. Understanding of such structural development is important for both interpretation of seismic analyses and forward modelling of subduction system including thermal structure, material circulation, magma process and slip behaviours of subduction boundaries.

We report results of petrological and structural analyses of layered antigorite (Atg) serpentinite in the marginal part of the Higashi-akaishi ultramafic unit in the Sanbagawa belt. This is a product of hydration of dunite (a rock consisting of almost 100% olivine (Ol)) due to metamorphic fluid from the underlying meta-sediments and meta-basites. Strong shape preferred orientation of Atg and existence of boudinaged layers indicate fluid-rock reaction under extensional deformation.

The layered structure is defined by a centimeter to meter-scale interlayering between Ol-rich and Atg-rich units. The modal amounts of Atg in these units form peaks at 15 vol% and 50 vol%, respectively, showing a bi-modal distribution as a whole. Effects of initial microstructures on the extent of serpentinization are limited: Porphyroclastic and fine-grained dunite, that occupy a large part of the outcrop, are transformed to both Ol-rich and Atg-rich layers although dunite with more than 50 % of coarse Ol grains has been poorly serpentinized. Each Atg layer shows millimeter-scale spaced foliations defined by amounts of Ol and Atg and locally shows a diffusive variation in millimeter to centimeter-scales. Thickness and proportion of Atg-rich layers increase near the contact with crustal rocks.

Reaction for the Atg formation is constrained based on re-distribution of elements among Ol, Atg and opaque minerals. As serpentinization proceeds, Ol is enriched in Fe and Ni owing to their incompatibility in Atg. Taking concomitant formations of minor amounts of magnetite and sulfides into account, the variation of the Ol composition and modal amounts of serpentinization products are quantitatively explained by the following reaction: Ol + $SiO_{2,aq}$ + H_2O $\Rightarrow$ Atg. This indicates that the development of Atg has been controlled by a supply of silica in aqueous fluids.

We measured thickness of 70 layers for each and, taking the layers with the thickness lower than 200 centimeters, we found exponential relationships in cumulative frequency distributions both for Ol-rich and Atg-rich layers. Relative thickness between neighbouring units [d(Ol)/d(Atg)] also shows an exponential distribution. We could not find any regular relationships among width and spacing like Liesegang patterns.

It is known that pattern structures appear in reaction-diffusion systems. The above observations strongly suggest that the development of layered structures in Atg serpentinite is controlled by interaction between reaction and material transfer. In this case, potential causes of heterogeneous serpentinization may be diffusional contrast between H_2O and SiO_2 or permeability contrast between Ol-rich and Atg-rich layers. Scaling analyses of deep low frequency tremors showed that duration-amplitude and size-frequency distributions of tremors in SW Japan can be fit with exponential models rather than power-law models. The seismological observations imply structural heterogeneity with unique scale length. Further examination on the exponential relationships developed in serpentinite may contribute to understand the slip phenomena on plate interfaces.

Keywords: serpentinite, layered structure, reaction-diffusion, expnential frequency distribution, deep low frequency tremor

Japan Geoscience Union Meeting 2014
(28 April - 02 May 2014 at Pacifico YOKOHAMA, Kanagawa, Japan)

SIT04-P03 Room:Poster Time:April 28 18:15-19:30

Awaruite in serpentinites from Oshima Peninsula, Fukui Prefecture, Japan

YAMAGUCHI, Kai[1*] ; UEHARA, Seiichiro[2]

[1]Department of Earth and Planetary Sciences, Faculty of Science, Kyushu University, [2]Department of Earth and Planetary Sciences, Faculty of Science, Kyushu University

Awaruite is one of native Ni-Fe alloys, and the compositional range is Ni_2Fe to Ni_3Fe. The space group is *Fm3m* or *Pm3m* (e.g., Williams, 1960; Ahmed et al., 1981). Typical grain sizes are 10-300 μm, and grain shapes are typically irregular, anhedral or skeletal. It is found only in the serpentinized peridotites and chondritic meteorites (e.g., Ramdohr, 1967; Clarke et al., 1970). In general, awaruite is observed in serpentine vein (Sakai and Kuroda, 1983), and coexist with other metal minerals (Kanehira et al., 1975). This study deals with the characteristic occurrence of awaruite in pseudomorph texture in the Oshima serpentinites from Oshima peninsula, Fukui prefecture, Japan.

All samples were examined with polarizing microscope observation, X-ray diffraction analysis and SEM-EDS analyses. Preparation of TEM specimen and microtexture observation were conducted with an ion milling machine (JEOL EM-09100IS) and TEM (JEOL JEM-2000FX, JEM-3200FSK) in the Research Laboratory for High Voltage Electron Microscopy (HVEM), Kyushu University, Japan. Chemical analyses of microtexture were also examined using JEM-3200FSK equipped with EDS.

Peridotites in this area are partially or perfectly serpentinized. Texture of the serpentinite is mesh texture after forsterite and vein texture. Scarcely serpentinized enstatite is also observed. Each mesh texture is composed of mesh rim shows optical anisotropy and mesh core shows optical isotropy. The serpentinization of mesh texture is strong in close to vein textures. Most mesh rims near vein texture consist of some layers; outer rim, outer-inner rim boundary and inner rim. These rims consist of chrysotile, about 50 nm in width and 2 μm in length, and lizardite, about 300 nm in width and 1 μm in length, and outer-inner rim boundary about 2 μm in width are filled with serpentine fine grains, up to 100 nm in diameter.

A number of awaruite fine grains, 200-300 nm diameter, array along cell boundary, outer-inner rim boundary and rim-core boundary. These awaruite coexist with no other metal minerals; pentlandite, magnetite and etc. In contrast, metal minerals in vein texture are magnetite and minor pentlandite. These results indicate that mesh texture in serpentinite is extremely reductive environment compared with vein texture. The chemical composition of awaruite (average of four analysis) is Ni 73.13% and Fe 26.87%. The cross-section of these awaruite grains is square or rhombic, indicating that these grains are cube or octahedral crystals (fig. 1a). These grains seem to be euhedral from grain shapes, and this is characteristic compared with previous studies (e.g., Rubin, 1991). The SAED pattern recorded along the [001] zone axis shows strong 200, 220 reflections and weak 100, 110 reflections (fig. 1b). This indicates space group of the Oshima awaruite is *Pm3m*, which is ordering phase of *Fm3m* awaruite. Lower symmetry of the Oshima awaruite will be formed lower temperature.

Keywords: Awaruite, Mesh texture, Serpentinite, Microtexture, Serpentine minerals, TEM

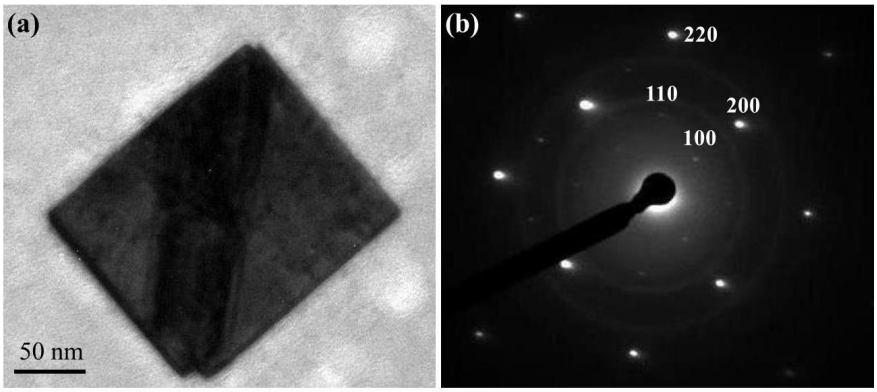

Fig. 1. (a) TEM image of awaruite in mesh texture. (b) The SAED pattern of (a) recorded along the [100] zone axis.

Japan Geoscience Union Meeting 2014
(28 April - 02 May 2014 at Pacifico YOKOHAMA, Kanagawa, Japan)

SIT04-P04 Room:Poster Time:April 28 18:15-19:30

Antigorite CPO measured by U-stage, EBSD and synchrotron X-rays

SODA, Yusuke[1*] ; ANDO, Jun-ichi[2] ; URATA, Yoshito[2] ; WENK, Hans-rudolf[3]

[1]Kanazawa University, [2]Hiroshima University, [3]University of California, Berkeley

Foliated antigorite serpentinite with crystallographic preferred orientation (CPO) probably causes shear wave splitting observed at subduction zones (e.g., Katayama et al., 2009). Therefore, the study of type and intensity of antigorite CPO is an important to understand the detail of this phenomenon.

Soda and Wenk (2014) measured CPOs of antigorite serpentinite from the Sashu Fault at the Saganoseki Peninsula, Oita Prefecture, by three independent methods, U-stage (with optic microscope), EBSD and synchrotron X-rays. The obtained antigorite CPOs by three methods are almost same without the fabric strength, maxima of pole figures in multiples of random distribution. The fabric strength decreases in the following order, U-stage >EBSD >synchrotron X-rays, which is probably caused by the characteristics of three methods. Through U-stage measurement, we can obtain the fabric pattern of antigorite CPO mainly from coarser antigorite grains (>30 μm). In the case of EBSD measurement, we measure antigorite CPO within an area of ca. 0.8 mm $\times$ 0.8 mm. Measurement points of only ca. 30% can be used to make fabric patterns. Residual ca. 70% points are neglect, because the quality of Kikuchi lines from them is too low to identify the orientation. In the synchrotron X-rays method, the result represents the bulk fabric from a volume of ca. 0.5 mm $\times$ 0.5 mm $\times$ 1.0mm.

The serpentinite measured antigorite CPO develops mylonitic structures with a penetrative foliation and lineation (Soda and Takagi, 2010). The antigorite grains show undulose extinction. And their grain boundary is unclear under the microscopy. Mg# (Mg/(Mg+Fe)) of antigorite grains is wide range 0.98-0.88. The BSE images indicate Fe-rich antigorite infilling the grain boundaries and fractures of Mg-rich antigorite.

The same serpentinite has already observed by TEM (Urata et al., 2009). The results indicate that the m-vales of antigorite grains, the number of octahedral along the [100] modulation wave, make two groups, high m-vale (16-18) and low m-vale (13-14). This result suggests that the antigorite are crystallized mainly two stages, which is supported by the variation of Fe contents of antigorite (Fe-rich and Mg-rich). The Mg-rich antigorite grains are main minerals composed of the serpentinite, Fe-rich antigorite grains occupy at the periphery of the others and within the vein. The TEM observation indicates that the Mg-rich antigorite grains are subdivided into sub-grain with 50-100 nm in size, which can be recognized as an undulose extinction under optic microscope.

These microstructures of antigorite grains potentially influence the outcome of CPO measurements. The weaker fabric patterns from the synchrotron X-rays are probably attributed to the fine-grained antigorite crystallized at the deferent stages and to sub-grain. And the U-stage and EBSD measurements focus only the selected grains, which may result in overestimation of elastic wave anisotropy of serpentinite.

References

Katayama et al, 2009, Nature 461, 1114-1117.
Soda and Takagi, 2010, Journal of Structural Geology 32, 792-802.
Soda and Wenk, 2014, Tectonophysics, in press
Urata et al., 2009, AGU2009 abstract. MR41A-1858.

Keywords: antigorite, CPO, synchrotron X-ray, elastic anisotropy

Japan Geoscience Union Meeting 2014
(28 April - 02 May 2014 at Pacifico YOKOHAMA, Kanagawa, Japan)

SIT04-P05 Room:Poster Time:April 28 18:15-19:30

Olivine CPO in non-deformed peridotite due to topotactic replacement of antigorite

NAGAYA, Takayoshi[1] ; WALLIS, Simon[1*] ; KOBAYASHI, Hiroaki[1] ; MICHIBAYASHI, Katsuyoshi[2] ; MIZUKAMI, Tomoyuki[3] ; SETO, Yusuke[4] ; MIYAKE, Akira[5] ; MATSUMOTO, Megumi[6]

[1]Department of Earth and Planetary Sciences, Nagoya Nagoya University, [2]Institute of Geosciences, Shizuoka University, [3]Department of Earth Science, Kanazawa University, [4]Department of Earth and Planetary Science, Kobe University, [5]Department of Earth and Planetary Science, Kyoto University, [6]Center for Supports to Research and Education Activities, Kobe University

Olivine crystallographic preferred orientation (CPO) is thought to be the main cause of seismic anisotropy in the mantle, and its formation is generally considered to be the result of plastic deformation of mantle by dislocation creep. Olivine CPO has been reproduced in laboratory deformation experiments and considerable success has been achieved in understanding the deformation conditions (e.g. stress, temperature and water content) under which different olivine CPO patterns develop. This opens the possibility of mapping conditions in the mantle using seismic anisotropy and has been the subject of considerable study. Here we report an alternative mechanism for olivine CPO without the need for deformation. This process may be important in understanding the seismic properties of mantle in convergent margins.

Metamorphic studies show peridotite in the Happo area, central Japan, formed by the dehydration of antigorite- schist related to contact metamorphism around a granite intrusion. Both field and microstructural observations suggest the olivine has not undergone strong plastic deformation. This was confirmed by TEM work that shows the olivine has very low dislocation densities and lacks low angle tilt boundaries. Such tilt boundaries are general stable even after annealing. These features show that peridotite in the Happo area formed in the absence of solid-state deformation.

The olivine of the Happo peridotite formed dominantly by the dehydration breakdown of antigorite schist. We propose that the olivine CPO formed as a result of topotactic replacement of antigorite by the newly formed olivine. EBSD measurements in samples where both antigorite and new olivine are present and in contact show a very close crystallographic relationship between the two minerals: the *a*-axes are parallel, and the *b*- and *c*-axes are perpendicular. We conclude the strong olivine CPO in the Happo area was inherited from the original CPO of the antigorite. Such a process is likely to also occur in subduction zones where serpentinite is dragged down by plate movement. Topotactic growth of olivine may be an important cause of mantle anisotropy in convergent margins.

Keywords: subduction zones, microstructure, B-type olivine CPO, antigorite, topotaxy

Japan Geoscience Union Meeting 2014
(28 April - 02 May 2014 at Pacifico YOKOHAMA, Kanagawa, Japan)

SIT04-P06 Room:Poster Time:April 28 18:15-19:30

Cr-rich olivine in deserpentinized peridotite and its implication

ENDO, Shunsuke[1*]

[1]Institute of Geology and Geoinformation, AIST

Formation of Cr-rich olivine (Cr_2O_3 >0.1 wt %) in the presence of Cr-spinel ± pyroxene has been thought to require extremely reducing and/or high-temperature conditions. Indeed, terrestrial olivine is Cr-free except for some high-T occurrences from Archaean komatiites, inclusions in diamonds, and ultrabasic pseudotachylytes. Deserpentinization is an important fluid release process in subduction zones. One of the best studied examples of this process occurs in Cerro del Almirez (SE Spain), where the antigorite-out reaction front (Atg = Ol + Opx + Chl + H_2O) at eclogite facies conditions is well preserved. Large elongate olivine crystals (similar to spinifex textures in komatiites) at the reaction front contain abundant exsolution lamellae of Cr-magnetite, and estimated primary compositions of the elongate olivine show high Cr content (0.1-0.4 wt% Cr_2O_3), leading to a proposal of the spinifex-like textured peridotite being pseudotachylyte (>1600 ℃, Evans & Cowan, 2012), in contrast to the generally held view that the elongate olivine crystalized under ambient subduction-zone T (~680 ℃ at 1.9 GPa) but high supersaturation conditions.

To better understand the dehydration process of serpentinite in subduction zones, this study focuses on a deserpentinized peridotite from the Eclogite unit of the Sanbagawa belt (SW Japan). It consists of porphyroblastic olivine (~70 vol %, Mg#=0.952±0.004, NiO=0.37±0.04 wt%), antigorite (Al_2O_3=0.3-0.5 wt%), brucite, zoned Cr-spinel and Ni sulfides. Olivine porphyroblasts contain inclusions of antigorite, brucite, magnetite and Ni sulfides, suggesting that the olivine-forming reaction Atg + Brc = Ol + H_2O took place after serpentinization of a dunitic protolith. Sporadic occurrences of Ni-rich olivine (up to 8.1 wt% NiO) within the olivine porphyroblasts suggest prograde breakdown of Ni-rich sulfides. Zoned Cr-spinel grains are composed of a chromite core, a ferritchromite mantle, and an irregular-shaped overgrowth of Cr-magnetite. The chromite core, being the only primary mineral preserved, shows Cr-rich/Ti-poor compositions [Cr/(Cr+Al)=0.74-0.76, TiO_2 <0.14 wt%] indicative of a forearc wedge mantle origin. The Cr-magnetite rim contains inclusions of Cr-rich olivine (Cr_2O_3 = 0.12-0.70 wt %, Mg#=0.950±0.004, NiO=0.37±0.04 wt%), in addition to Cr-rich antigorite (Al_2O_3=0.5-3.1 wt%, Cr_2O_3=0.3-3.9 wt%), diopside and brucite.

Formation of the Cr-rich olivine inclusions can be explained by dehydration of Cr-rich antigorite that developed around Cr-spinel grains. Slow diffusivity of Cr^{3+} compared to the olivine growth rate may have caused disequilibrium Cr incorporation into olivine under low-T conditions just above the Atg + Brc breakdown equilibrium (~460-500 ℃). Alternatively, a distinct Cr substitution mechanism (Cr^{3+} + Fe^{3+} = Mg + Si) than that proposed for high-T olivine (Cr^{2+} = Mg or 2Cr^{3+} + vacancy = 3Mg) could explain the low-T formation of Cr-rich olivine. In any case, the local uptake of Cr in olivine from the Sanbagawa metaserpentinite does not imply very high-T conditions, and this weakens the main basis of the pseudotachylyte hypothesis for the spinifex-like textured peridotite in Cerro del Almirez. The geological record on the causal link between deserpentinization and deep earthquake nucleation remains elusive.

Keywords: Cr-rich olivine, antigorite, dehydration, subduction zone

Japan Geoscience Union Meeting 2014
(28 April - 02 May 2014 at Pacifico YOKOHAMA, Kanagawa, Japan)

SIT04-P07 Room:Poster Time:April 28 18:15-19:30

Spatial variation in scale length of deep low-frequency tremor inferred from duration-amplitude scaling in western Shiko

HORINO, Kazuki[1*] ; HIRAMATSU, Yoshihiro[2] ; MIZUKAMI, Tomoyuki[2] ; OBARA, Kazushige[3] ; MATSUZAWA, Takanori[4]

[1]Division of Natural System, Graduate School of Natural Science and Technology, Kanazawa University, [2]School of Natural System, College of Science and Engineering, Kanazawa University, [3]Earthquake Research Institute, University of Tokyo, [4]National Research Institute for Earth Sciences and Disaster Prevention

Slip properties on plate interface vary largely along dip direction from seismic to aseismic slip. At the transition zone at depths of 25-35 km, non-volcanic deep low-frequency (DLF) tremor and short-term slow slip event occur in the Nankai subduction zone. Recent detailed studies (e.g. Obara, 2010) reveal along dip and along strike variations in the occurrence and the migration of DLF tremor in the transition zone. We report here an along dip variation in scale length of DLF tremor inferred from duration-amplitude scaling in the western Shikoku.

A physical process of natural phenomena is reflected by scaling law, for example, frequency of occurrence versus size distribution. Watanabe et al. (2007) reported that a duration-amplitude distribution of DLF tremor shows a better fit to the exponential model rather than the power-law model, which is different from regular earthquakes. We investigate the duration-amplitude distribution of DLF tremor using Hi-net data in the western Shikoku. The procedure of analysis is the same as that of Watanabe et al. (2007).

We focus on the slope of the exponential distribution for the duration-amplitude distribution of DLF tremor. The value of the slope is small in the western area and large in the eastern area. Noting along dip direction, we can recognize a weak variation of the value of the slope. Deeper DLF tremor tends to show a larger value of the slope than shallower DLF. A large value of the slope means a small scale length and vice versa.

Beneath the western Shikoku, the configuration and the age distribution of the subducting Philippine Sea plate changes significantly along the strike, generating a large variation in a thermal structure. Such a variation causes various modes of serpentinization in the hanging wall mantle. The resultant structures due to the different modes are the most likely cause of the detected transition of the scale length.

Keywords: deep low-freqency tremor, scaling law, subduction zone, size distribution, serpentinization

Japan Geoscience Union Meeting 2014
(28 April - 02 May 2014 at Pacifico YOKOHAMA, Kanagawa, Japan)

SIT05-01 Room:315 Time:April 28 09:00-09:15

Lithospheric Rheology and Stress and the Dynamics of Plate Tectonics

ZHONG, Shijie[1*]

[1]Department of Physics, University of Colorado

Plate tectonics is a kinematic theory that describes relative motions of Earth ′ s surface tectonic plates. However, with the subduction of cold lithosphere into mantle interiors, plate tectonics has profound implications on the thermal and dynamic evolution of planets. Earth appears to be the only planetary body in the solar system that has active plate tectonics. The cause of plate tectonics remains one of the most important unresolved questions in Earth and planetary sciences. The recent discovery of a large population of exoplanets further raises the question on how common plate tectonics is to planetary bodies and what causes plate tectonics. In this presentation, I will discuss two issues that are important to understanding the origin of plate tectonics: lithospheric rheology and stress. Lithospheric rheology is important for understanding crustal and lithospheric dynamics, and the conditions for plate tectonics. For example, numerical modeling studies suggest that plate tectonics emerge from the dynamics of mantle convection when a small coefficient of friction μ ($<$0.1) or small yield stress for lithosphere is used [Moresi and Solomatov, 1998]. However, both in-situ borehole stress measurement (to ˜10 km depth) and laboratory studies suggest that μ˜0.6 [Kohlstedt et al., 1995; Zoback and Townend, 2001]. A recent study that models the seismically observed elastic flexure and seismicity at Hawaiian islands in response to volcanic loading indicates $\mu>$0.25 [Zhong and Watts, 2013]. The loading study [Zhong and Watts, 2013] also suggests that lithospheric rheology related to low-temperature plasticity is significantly weaker than laboratory studies [Mei et al., 2010] and that lithospheric stress at Hawaiian islands is 100-200 MPa, possibly largest lithospheric stress on the Earth, given that Hawaiian islands represent the largest uncompensated surface loads on the Earth. These studies highlight the importance to understand the evolution of lithospheric stress and rheology from plate interiors to plate boundaries, in order to understand the cause of plate tectonics. I will also discuss the convection-driven stress in the top thermal boundary (lithosphere). Convection-driven stress scales with Rayleigh number and hence mantle viscosity. A larger mantle viscosity or smaller Rayleigh number leads to a larger viscous stress in the lithosphere in mantle convection models. Some recent mantle convection studies for plate tectonics generation reported $>$500 MPa stress in lithosphere. It is important to develop independent observable measures to examine the relevance of modeled lithospheric stress. I will discuss possible measures that may be developed and used in this context.

Keywords: Mantle Convection, Plate Tectonics, Lithospheric Stress, Lithospheric Rheology, Brittle Deformation

Japan Geoscience Union Meeting 2014
(28 April - 02 May 2014 at Pacifico YOKOHAMA, Kanagawa, Japan)

SIT05-02 Room:315 Time:April 28 09:15-09:30

3D numerical modeling of thermal regime and mantle flow associated with subduction of the two oceanic plates

JI, Yingfeng[1*] ; YOSHIOKA, Shoichi[1]

[1]RCUSS, Kobe University, [2]Graduate School of Science, Kobe University

Based on a thermal convection model for an arbitrarily curved oceanic plate, we newly constructed a 3D model for subduction of two oceanic plates, and investigated its thermal regime and mantle flow. The 3D parallelepiped modeled domain for numerical simulations is a length of 840 km, a width of 840 km, and a depth of 300 km, with 72∗72∗72 grids, and the total calculation time up to 15 Myr. Geometry of one continental plate and two oceanic plates are prescribed in the simulation. The two oceanic plates subduct with prescribed velocities beneath the continental plate along neighboring two trenches, adjoining with a right angle. The upper oceanic plate and the lower oceanic plate contact each other at their intersection zone. Both of the oceanic plates are assumed to be 30 km in thickness. Giving boundary conditions of adiabatic and permeable walls, half-space cooling and rigid upper surface, and stratified initial temperature condition, we solved equations of mass conservation, momentum, and energy, using the finite difference method (FDM) and Finite Volume Method (FVM). In this study, the dynamical properties of the thermal regime associated with double subduction are investigated in detail. In our numerical simulation for the subducting two oceanic plates, the convergent rate of the upper oceanic plate should be paralleled to the intersection line of the two plates so as to reach a stable and sustainable subduction. Dip angles of the two oceanic plates, obliquity of the lower oceanic plate, and subduction velocity are assumed to be 10 deg, 0 deg ˜75 deg, and 5 cm/yr, respectively. As a result of numerical simulation, we found that there are remarkable low temperatures in the inter-slab zone due to subduction of the two cold oceanic plates. We also found that obliquity and relative directions of plate subduction velocities contribute to the obliquity of subduction-induced mantle flow convection adjacent to the two oceanic plates, and spiral mantle convection may be produced by the difference of the obliquity of two oceanic plates.

Keywords: thermal regime, plate tetonics, subduction, numerical simulation

Japan Geoscience Union Meeting 2014
(28 April - 02 May 2014 at Pacifico YOKOHAMA, Kanagawa, Japan)

SIT05-03 Room:315 Time:April 28 09:30-09:45

Mantle flow and overriding plate stress state in 3-D models of thermo-mechanical subduction

HOLT, Adam[1] ; BECKER, Thorsten[1*]

[1]University of Southern California

The formation of back-arc basins is a fundamental component of plate tectonics, yet the dominant mechanism for their formation, and whether an individual mechanism is dominant over different tectonic settings, is not entirely clear. On top of the classic mechanism of extension being driven by basal tractions due to poloidal return flow, recent numerical and experimental modeling studies have indicated that, for slabs with finite widths, toroidal return flow around slab edges plays an important role. We investigate the relative contribution of poloidal and toroidal flow field components to back-arc extension by examining the overriding plate stress regime in conjuction with the flow field for various model setups. We characterize the velocity field by decomposing it into toroidal and poloidal components at various stages of subduction, and calculating the ratio of the toroidal to polodial RMS velocities (TPR).

Models are carried out using a thermo-mechanical setup of the finite element code, CitcomCU. We find that the presence of an overriding plate reduces the development of trench curvature, and so 3-D modeling studies that neglect the presence of the overriding plate may be significantly overestimating the rate of development of trench curvature. Within the overriding plate, we observe long wavelength back-arc extensional stresses at a large distance from the trench and more localized forearc compressive stresses. Fixing the position of either the subducting or overriding plate causes the amplitude of back-arc extension to be greater than that for the case when both plates are free. This occurs because, for the fixed overriding plate models, all of the slab rollback is forced to occur at the expense of overriding plate thinning/extension, and for the fixed subducting plate models, increased rollback causes heightened toroidal flow. For all models with significant slab rollback, the poloidal RMS velocity is maximum in the very upper and lower portions of the model whereas toroidal flow is maximum at mid-domain depths due to return flow around slab edges, indicating that slab rollback-induced toroidal flow is focussed at sub-lithospheric depths, where it has the potential to contribute to back-arc extension. Reducing the width of the plate vastly reduces the rate of slab rollback, yet increases the degree of back-arc extension and focuses it closer to the trench. In such models, toroidal flow magnitude is approximately constant throughout the domain resulting in only minor TPR variation with depth, and yet the magnitude of overriding plate extensional stress is large, possibly suggesting an alternate control on back-arc extension.

Finally, we investigate the effect that Byerlee plasticity and a laterally confining side plate has on both overriding plate stress state and the flow field. Including a side plate does not modify the slab dynamics and overriding plate stress state, yet significantly reduces the toroidal RMS velocity component throughout the model, while retaining the systematic variation, which results in uniformly reduced TPR throughout the domain. The inclusion of plasticity, intended to approximate brittle failure, gives rise to elevated forearc compression, due to increased plate convergence, and reduced backarc extension.

Keywords: subduction, mantle flow, slab rollback, overriding plate stress

Japan Geoscience Union Meeting 2014
(28 April - 02 May 2014 at Pacifico YOKOHAMA, Kanagawa, Japan)

SIT05-04 Room:315 Time:April 28 09:45-10:00

Magnetic spectral analysis over the Atlantic Ocean off Portugal

MATSUSHIMA, Jun[1] ; OKUBO, Yasukuni[2] ; ANTONIO, Correia[3] ; UCHIDA, Youhei[2*]

[1]Graduate School of Engineering, [2]Geological Survey of Japan, [3]University of Evora

Magnetic spectral analysis, which has often been applied to estimate Curie point depths, was used to delineate thermal and crustal structure of the Atlantic Ocean off Portugal. The Atlantic oceanic plate covers the study area deepening eastward and volcanic islands rise in the eastern margin. We used EMAG2, the resolution and the altitude of which are 2 arc minute and 4 km above geoid, respectively. Linear magnetic anomalies are dominant over the study area. They are attributed to the seafloor spreading of the oceanic plate. The magnetic lineation forms a strong directional feature not only in the space domain but also in the spectral domain. Taking the directional feature, we developed a pseudo-one dimensional spectral analysis using two dimensional data sets. The gradient of the power spectrum across the lineation depends on the centroid depth of magnetic layer. The bottom depth is easily calculated by the centroid and the seafloor depth, assuming that the top of magnetic layer corresponds to the seafloor. The bottom of magnetic layer over young oceanic plate deepens with time, because the Curie point depth deepens with time. Taking the relationship, we assume that the bottom of magnetic layer over the Atlantic oceanic plate corresponds to the Curie point depth and delineates a thermal structure. The results of spectral analysis show that the bottom depths over the oceanic plate are deepening gradually from the ridge to Europe. The results correlate well with magnetic isochrons and thermal history of the oceanic plate. The bottom depths over the volcanic islands are anomalously shallow indicating a rise of high thermal structure.

Keywords: Magnetic data, spectral analysis, Curie point

Japan Geoscience Union Meeting 2014
(28 April - 02 May 2014 at Pacifico YOKOHAMA, Kanagawa, Japan)

SIT05-05 Room:315 Time:April 28 10:00-10:15

Subduction Processes and a New Hypothesis for "Top-down Hemispherical Dynamics" of the Earth

IWAMORI, Hikaru[1*] ; NAKAMURA, Hitomi[2] ; HANYU, Takeshi[1] ; KIMURA, Jun-ichi[1] ; NAKAKUKI, Tomoeki[3] ; NAKAGAWA, Takashi[1] ; YOSHIDA, Masaki[1] ; TANAKA, Satoru[1] ; SUETSUGU, Daisuke[1] ; OBAYASHI, Masayuki[1]

[1]JAMSTEC, [2]TITEC, [3]Hiroshima University

Water-rock interactions reduce the rock strength, and possibly produce weak plate boundaries, inducing active plate tectonics. Water-rock interactions may also have geochemical impacts, causing the unique differentiation of the Earth (e.g., formation of granitic continental crust and hydrothermal ore deposits). However, how water actually interacts with the rocks and circulates within the solid Earth to contribute to material differentiation and dynamics has been poorly constrained. In this paper, we present numerical models of water and element transport in subduction zones, as well as global geochemical evidences for water and the associated element cycling in the mantle. Then we compare these geochemical evidences with the geophysical observations and modeling to propose "top-down hemispherical dynamics" for the whole Earth's interior.

Water-rock interaction may significantly reduce the viscosity of rocks [1], and affects the subduction zone dynamics. Hydrated subducting slabs release water as the slabs are heated up, which hydrates the bottom of mantle wedge just above the subducting slab, to form a serpentinite layer. In this case, the slab-wedge mechanical coupling is reduced, and weakens the wedge corner flow, decreasing the slab surface temperature. The serpentinite layer is stabilized to extend deeper, enhancing mechanical decoupling between the slab and the wedge. This positive feedback has a large impact on the overall thermal-flow structure and magmatism in subduction zones [2]. We compare the model results and the observations such as position of arc magmatism, heat flow and seismic structures to constrain the actual structure and dynamics.

Water may enhance elemental transport once a fluid phase is formed and
migrates, which potentially causes specific elemental fractionation. We have constructed two-dimensional models of trace element transport in subduction zones, incorporating (i) slab subduction-dehydration, (ii) fluid migration and its reaction with the convecting mantle, (iii) melt generation and (iv) associated elemental partitioning among the solid, aqueous fluid and melt [3]. This model predicts various trace element abundances in solid, fluid and melt, and shows that significant variability in terms of trace element ratios is produced in subduction zones and can be brought down to the deep mantle. The trace element variability must affect long-term radiogenic isotopic evolution of the mantle (e.g., Sr, Nd and Pb isotopic compositions). Recently, a global isotopic structure has been found based on a statistical analysis of a large geochemical data set including MORB, OIB and arc basalts [4]: the eastern mantle hemisphere is enriched in subducted aqueous fluid components compared to the western hemisphere. Magnitude of the radiogenic ingrowth for the hemispherical structure suggests that it has been mostly developed within the last several hundred million years. These observations can be explained by focused subduction towards the supercontinent (Rodinia, Gondwana and Pangea), which has created the large-scale mantle heterogeneity. A strikingly similar pattern is found for the seismic velocity structure of the inner core [5,6]. Such hemispherical structures may be key to understanding the global dynamics of the Earth. We propose that the focused plate subduction governs the flow and thermal structure of the deep interior, in a "top-down" manner.

References: [1] S. Karato, H. Jung, Philos. Mag. 83, 410 (2003). [2] S. Horiuchi, Ph.D. thesis, U. Tokyo (2013). [3] A. Ikemoto, H. Iwamori, Earth Planet. Space, in revision. [4] H. Iwamori, H. Nakamura, Geochem. J. 46, e39 (2012). [5] S. Tanaka, H. Hamaguchi, JGR 102, 2925 (1997). [6] L. Waszek et al., Nature Geo.4, 264 (2011).

Keywords: subduction, water, trace element, isotope, hemisphere, mantle

Japan Geoscience Union Meeting 2014
(28 April - 02 May 2014 at Pacifico YOKOHAMA, Kanagawa, Japan)

SIT05-06 Room:315 Time:April 28 10:15-10:30

Effects of plate-like behavior and material recycling on lateral variation of CMB heat flux

NAKAGAWA, Takashi[1*]

[1]IFREE, JAMSTEC

We studied the relationship between heat flux across the core-mantle boundary (CMB) and seismic anomalies in the CMB region in numerical mantle convection simulations in a 3-D spherical shell with a simple temperature- and depth-dependent viscosity [Nakagawa and Tackley, 2008]. That study suggested that the relationship between CMB heat flux and seismic anomalies was not simple linear function because of the post-perovskite phase transition and/or compositional heterogeneous structure in the deep mantle. However, in that study, we did not include the complicated rheology that occurred to the plate tectonics-like behavior and the segregation of oceanic crust in the deep mantle because they would be important for regulating the heat flux across the CMB [e.g. Nakagawa and Tackley, 2010].

Here we revisit to investigate the relationship between heat flux across the CMB and seismic anomalies in the deep mantle including plate tectonics-like behavior and material recycling. Preliminary result suggests that the heat flux tends to be more linear relationship with seismic anomalies in the deep mantle including plate tectonics-like behavior and material recycling but the uncertainty of this relationship between two quantities is very strong. The peak-to-peak of lateral variation of CMB heat flux is much larger than that obtained from our previous study. This is still problematic for magnetic field generation caused by geodynamo.

Keywords: CMB heat flux, lateral variation, plate tectonics, material recycling

Japan Geoscience Union Meeting 2014
(28 April - 02 May 2014 at Pacifico YOKOHAMA, Kanagawa, Japan)

SIT05-07 Room:315 Time:April 28 10:30-10:45

Petrology and Geochemical Evolution of Lavas from the Ongoing and Voluminous Puu Oo Eruption of Kilauea Volcano, Hawaii

GARCIA, Michael[1*] ; PIETRUSZKA, Aaron[2] ; GREENE, Andrew[3] ; MARSKE, Jared[4] ; RHODES, Michael[5]

[1]Dept. Geology-Geophysics, Univ. of Hawaii, [2]USGS, Denver, [3]Depart. Natural Sciences, Hawaii Pacific University, [4]Dept. Terrestrial Magnetism, Carnegie Institution of Washington, [5]Dept. Geoscience, Univ. Massachusetts

The Puu Oo eruption of Kilauea Volcano is one of the longest-lived (31 years and continuing) Hawaiian eruptions. Volumetrically, it is the most significant historical eruption. It has produced over 4 km3 of lava from several vents along its east rift zone. We have continually monitored the compositional and isotopic signatures of its lavas, which have shown remarkable variations. These variations resulted from diverse crustal and mantle processes including crystal fractionation, magma mixing and storage, assimilation of crust and melting of a heterogeneous plume source. Crystal fractionation is an important process in these lavas based on their wide range of MgO contents (5-10 wt.%) and normally zoned minerals (mostly only olivine). During the first two years, the effects of crystal fractionation were superimposed on hybrid magmas created by mixing two evolved, rift zone-stored magmas with a new, mantle-derived magma. Later lava erupted show no signs of mixing except for one-day, uprift events in 1997 and 2011. Small, systematic variations in Pb and Sr isotopes, incompatible trace element ratios and MgO-normalized (10 wt.%) major element abundances of post-mixing lavas document rapid changes in the parental magma composition unrelated to crustal processes. Lavas erupted between 1985-1998 continued the post-1924 composition trend of Kilauea lavas towards more depleted composition. This trend was initiated by the collapse of summit crater during a period of very low magma supply. Puu Oo lavas showed a systematic temporal evolution towards historical Mauna Loa lava composition from 1998-2003. This trend reversed in 2003 and again in 2008 creating a cyclic pattern of geochemical variations. These reversals in composition are contrary to previous models for geochemical trends during sustained basaltic eruptions. The cyclic variations of Pb isotopic and some trace element ratios during the Puu Oo eruption suggest melt extraction from a mantle source with thin strands of vertically-oriented source heterogeneities. These strands may be 1-3 km in diameter in order to explain the scale of isotopic variations for the Puu Oo eruption. This continuing eruption provides a dynamic laboratory for evaluating models of the generation and evolution of basaltic magmas.

Keywords: volcano, Hawaii, eruption, historical, magma, basalt

Japan Geoscience Union Meeting 2014
(28 April - 02 May 2014 at Pacifico YOKOHAMA, Kanagawa, Japan)

SIT05-08 Room:315 Time:April 28 11:00-11:15

When did the plate tectonics start on the Earth?

MARUYAMA, Shigenori[1*]

[1]ELSI Tokyo Institute of Technology

Initiation of plate tectonics on the Earth is a key to make life-sustaining rocky planet Earth, because primordial ocean was highly toxic and primordial atmosphere had high XCO2. Transportation of huge amounts of CO2 into mantle by plate subduction depends on pH of seawater and composition of oceanic slab.

Plate tectonics has been proposed from the data set of the ocean-floor, firstly by ocean-floor spreading theory followed by rigid lithosphere. Yet, the oldest lithosphere goes back to only 200Ma, hence demonstration of plate tectonics on the Earth is restricted to the Earth after 200Ma.

Hence, we need to make logical framework of pre-200Ma plate tectonics of the Earth. The principle of Accretionary Complex Geology (ACG) is an only key issue which is centered by Ocean Plate Stratigraphy (OPS). ACG is a technology which separates the subducted oceanic slab from trench turbidites, and offers the MORB, OIB, pelagic sediments, and subduction zone magmatic rocks from the mixture of rock units formed at trench.

Application of this technology to 3.8Ga Isua ACs clarified Early Archean plate tectonics which had different aspects of plate tectonics from the modern plate tectonics, e.g., thickness and composition of lithosphere (Komiya et al., 1999). Specifically, thickness of MORB was 20km which seems to be buoyant to prohibit subduction (e.g., Davies, 1992). But if slab-melting is common, the buoyancy turns to be negative to cause more rigorous slab-pull force at subduction zone (Komiya et al., 2002).

For the Hadean Earth, there are no geologic units remained on the modern Earth, except for zircons with back to 4.4 Ga. Mineral inclusions within the Hadean zircons suggest the host melt with granitic magma. Formation of granitic melts could be most probable for the operation of plate tectonics. But this is logically imperfect, because small amounts of granitic melts can be formed and actually present on the Moon. Conversely, the forward modelling of planetary tectonics could be more important than zirconology. Formation of primordial ocean causes the formation of rigid lithosphere, and hydrous minerals on the slab surface would act as liberated lubricants along Benioff plane. This is plate tectonics and plays even in the state of magma pods remains in the asthenospheric mantle (Sleep et al., 2011). If so, initiation of plate tectonics on the Earth could be back to Hadean Earth, presumably back to 4.4Ga.

Japan Geoscience Union Meeting 2014
(28 April - 02 May 2014 at Pacifico YOKOHAMA, Kanagawa, Japan)

SIT05-09 Room:315 Time:April 28 11:15-11:30

Difference of tectonics and rheological structure between Earth and Venus

AZUMA, Shintaro[1*] ; KATAYAMA, Ikuo[1] ; NAKAKUKI, Tomoeki[1]

[1]Department of Earth and Planetary Systems Science, Graduate School of Science, Hiroshima University

Venus has been regarded as a twin planet to the Earth, because of density, mass, size and distance from the Sun. However, the Magellan mission revealed that plate tectonics is unlikely to work on the Venus. The plate tectonics is one of the most important mechanism of heat transport and material circulation of the Earth, consequently, its absence might cause the different tectonic evolution between Earth and Venus. Rheological structure is a key to inferring mantle structure and convection style of planet interiors because the rock rheology controls strength and deformation mechanism. In previous study, the behavior of Venusian lithosphere has been inferred from the power-law type flow law of dry diabase. They indicated that lower crust can be weaker than upper mantle, which might result decoupling at the crust-mantle boundary (Moho depth) and mantle convection without crustal entrainment. However, the power-law creep cannot be applicable to infer the rheological structure at Moho depths, because the dislocation-glide control creep (Peierls mechanism) is known to become dominant at relatively low temperatures in materials with a relatively strong chemical bonding such as silicates. In this study, we conduct two-phase deformation experiments to directly investigate rheological contrast between plagioclase (crust) and olivine (mantle) and discuss the difference between these planets in terms of rheological behaviors. Moreover, one-dimensional and two-dimensional numerical calculation is performed to evaluate the influence of the strength contrast on the Venusian tectonics. Our experiments using solid-medium deformation apparatus directly determine the relative strength between plagioclase (crust) and olivine (mantle) without any extrapolating of flow law. The experimental conditions were ranging 2GPa and 600-1000 degrees under dry conditions. The experimental results show that olivine is expected to always be stronger than plagioclase. This result contradicts to that inferred from power-law creep of olivine and plagioclase, suggesting that Peierls mechanism could be dominant deformation mechanism in both olivine and plagioclase at relatively low temperatures. In the case of the Earth, rheological structure of oceanic lithosphere is constrained well by Byerlee's law and power-law type flow law. The oceanic crust and mantle lithosphere are strongly coupled mechanically because the Moho has no strength contrast, so that they could move and subduct together into the deep. In contrast, our experimental results imply that large strength contrast exists at Moho in Venus, resulting decouple of the motion between the crust and mantle lithospheres because the weak lower crust acts as a lubricant. Also one-dimensional numerical calculations show us that the surface velocity becomes more sluggish in the model with larger strength contrast (from two-digit to four-digit difference in viscosity) at Moho. Therefore the crustal part is less likely to be involved to mantle convection when strength contrast gets larger and larger. In fact, two-dimensional simulations suggest that the crustal portion cannot subduct with the mantle lithosphere if the strength contrast exists at Moho

Keywords: plagioclase, olivine, Venus, rheology, plate tectonics

Japan Geoscience Union Meeting 2014
(28 April - 02 May 2014 at Pacifico YOKOHAMA, Kanagawa, Japan)

SIT05-10 Room:315 Time:April 28 11:30-11:45

On the origin of plate tectonics: Thinking outside of the convective box

SOLOMATOV, Viatcheslav[1*]

[1]Washington University in St. Louis

From the observational point of view, there is no evidence of plate tectonics on other planets in the Solar System. Remote sensing methods for detecting plate tectonics on exoplanets are yet to be developed and are unlikely to be as robust as the surface observations that were conducted for Venus, Mars, and Mercury. The observational constraints on the tectonics of the early Earth are probably the most important clues to the plate tectonics origin and yet, their interpretations remain ambiguous. Some researchers see a very early start of plate tectonics in the data while others do not exclude a relatively late start. From the theoretical point of view, the absence of plate tectonics is easy to explain and can be considered as a normal state of any rocky or icy body. Two decades ago, both the observational data and theoretical studies led to the reversal of the question “why do other planets not have plate tectonics” to “why does the Earth have plate tectonics”. Since then various theories and numerical models focused on the latter question and investigated how plate tectonics began and what conditions are required for plate tectonics to occur on a planet. In most models the starting state of a planet is a non-plate tectonics regime (e.g. stagnant lid convection) which then transitions to plate tectonics. The forces responsible for the transition can be caused by convective motions below the lithosphere and with thermal (e.g. lithospheric relief) and compositional density variations (e.g. continents) near the surface. The role of the factors involved can be complicated. For example, the crust can both hinder and help plate tectonics. The transition to plate tectonics can also be caused by external factors, such as impacts and tidal forces. Similar to the previous, internal factors, these external factors can also either help or hinder plate tectonics initiation. For example, even though impacts are sometimes considered as a possible cause of plate tectonics, they can create conditions that would hinder plate tectonics initiation later on or stop it in case if plate tectonics was previously initiated by other mechanisms. Plate tectonics could also have emerged from a magma ocean, bypassing the stagnant lid regime. In this scenario plate tectonics is a continuation of convection in the magma ocean. As the magma ocean crystallizes, the surface boundary layer, which has little difficulty to recycle in the liquid magma, eventually transforms into tectonic plates as the crystallizing magma ocean undergoes a transition from turbulent convection controlled by melt viscosity to laminar convection predominantly controlled by solid-state creep. Regardless of the origin of the first episode of plate tectonics, the question of how plate tectonics survived and evolved into a relatively stable regime is a challenge for any of these models and may require a combination of many factors such as asthenosphere, surface oceans and volatile cycling.

Keywords: Plate tectonics, Stagnant lid convection, Giant impacts, Magma oceans, Exoplanets

Japan Geoscience Union Meeting 2014
(28 April - 02 May 2014 at Pacifico YOKOHAMA, Kanagawa, Japan)

SIT05-P01 Room:Poster Time:April 28 18:15-19:30

Estimation of the lithosphere-asthenosphere transition from multi-mode surface waves

YOSHIZAWA, Kazunori[1*]

[1]Earth and Planetary Dynamics, Faculty of Science, Hokkaido University

The lithosphere-asthenosphere transition (LAT) is a key to the understanding of the present-day plate motion, but its seismological determination is not straightforward unlike material boundaries such as the Moho and core-mantle boundary. Some recent works on the LAT using body-wave receiver functions have revealed evidences for clear converted signals at the bottom of lithosphere, particularly in oceanic region. To the contrary, receiver functions normally do not show clear converted signals from the expected bottom of cratonic lithosphere at about 200 km depth, where surface wave studies indicate fast wave speed anomalies of the thick continental lithosphere.

In this study, we investigate a quantitative way to estimate the depth and thickness of the LAT from S-wave speed models derived from surface waves. Although surface waves are inherently not very sensitive to the sharpness of boundaries due to their long-wavelength features, the depth of LAT can be roughly estimated from the depth of either the negative peak of velocity gradient or the slowest shear velocity beneath the lithosphere. In this study, we consider that the former represents an upper bound of LAT and the latter a lower bound. The thickness (or sharpness) of LAT can be deduced from the differences between the upper and lower bounds.

We have performed synthetic experiments using several types of S-wave models including different smoothness (or sharpness) of LAT. Synthetic experiments using multi-mode surface waves (including up to fourth higher modes) result in a successful recovery of the smooth LAT (with a depth range over 50 km), which is expected at the base of the cratonic lithosphere. However, if we use the fundamental mode only, the recovery is unsatisfactory even for the smooth boundary, and the effects of the sharpness of boundary are almost indistinguishable in the recovered models. Surface waves have less sensitivity to a sharp boundary (with a transition thickness less than 25 km), but our experiments indicate that the estimated depth from the velocity gradient (upper bound of LAT) are found to be coincide well with the depth of sharp boundary, which may indicate the distribution of oceanic LAT can be well represented by the negative peak of vertical gradient in S-wave speed profiles derived from surface waves.

Keywords: lithosphere, asthenosphere, surface wave, higher mode

Japan Geoscience Union Meeting 2014
(28 April - 02 May 2014 at Pacifico YOKOHAMA, Kanagawa, Japan)

SIT38-01 Room:511 Time:April 30 09:00-09:15

Advances in laboratory acoustic emission study

LEI, Xinglin[1*]

[1]Geological Survey of Japan, AIST, Japan

Acoustic emission (AE) is an elastic wave radiated by rapid cracking in solids. As a technology of nondestructive inspection, AE has a long history of development and has been applied in numerous areas including material sciences, medical sciences and engineering fields. In stressed rocks, macroscopic fracturing is preceded by a very complex pervasive evolution of some pre-failure damage. Thus, studies focusing on both fracture dynamics and pre-failure damage are a subject of interest and can be inferred from AE statistics as the number of AE events is proportional to the number of growing cracks, and the AE amplitudes are proportional to the length of crack growth increments in the rock. In Earth science, since the similarity in size distribution of earthquakes and acoustic emissions (AE) was found in the 1960s, many laboratory studies have been motivated by the need to provide tools for the prediction of mining failures and natural earthquakes. This report aims to draw an outline of laboratory AE studies in the last 50 years, which have addressed seismological problems, with special focuses on some key issues associated with fault nucleation and growth in brittle rocks.

The AE technique, which monitors the spatiotemporal distribution of AE events, is applied to the analysis of the micro-cracking activity inside the sample space, and it can be performed under an artificially controlled pressure, which is very important for the simulation of underground conditions. During the last five decades, a great number of studies were done following developments in experimental technology, AE monitoring technology, and data processing methodology. Fifty years ago, only the hitting time of an AE could be recorded with a single sensor or a small number of sensors. The rock fracture test was performed under simple loading conditions. Later, the number of sensors that could be used in a study increased and thus allowed the determination of the hypocentre of an AE. Developments in transient memory technique in the 1970s through to the 1980s lead to the ability to make a digital multichannel recording of the full waveform of an AE. Hypocentre location was improved greatly by the use of more precise arrival times obtained through waveform analysis. In addition, it became possible to determine the mode of fracture, i.e., the focal mechanism solution of an AE source. In the present day, AE are usually monitored by 16-32 sensors with digital waveform recording at up to a 200 MHz sampling rate and up to a 16 bit A/D resolution. The dead time of a recording is sufficiently short and continuous recording is possible by use of very large amounts of memory. The waveform of most events can be captured with multiple channels, even for the period of dynamic failure in which the AE rate may reach several thousand a second. Rock fracture experiments can be performed under triaxial compression conditions with controlled fluid injection and pore pressure. AE hypocentres are determined with a location error of a few mms. A focal mechanism solution can be determined for individual events or a group of events. As demonstrated by very recent studies progress in laboratory AE study, particularly studies focusing faulting nucleation, is shedding more and more light on earthquake seismology.

By summarising recent results, it can be concluded that the fault nucleation behaviour, including critical size, duration time, and AE productivity, depend on the heterogeneity of the area of weakness of the fault compared with that of the host rock. If the fault is as strong as the host rock then the fracture makes no difference and the rock remains intact. Furthermore, a homogeneous fault or rock mass appears to fracture in unpredictable ways without a consistent trend in precursory statistics, while inhomogeneous faults fracture with clear precursors related to the nature of the heterogeneity.

Keywords: Acoustic emission (AE), Pre-failure damage, Rock fracture, Earthquake, Fault nucleation, Process zone

Japan Geoscience Union Meeting 2014
(28 April - 02 May 2014 at Pacifico YOKOHAMA, Kanagawa, Japan)

SIT38-02 Room:511 Time:April 30 09:15-09:30

Microfracture distributions indicating formation of large-scale cracks in the rock mass ahead of the mining front

NAOI, Makoto[1*] ; MORIYA, Hirokazu[2] ; NAKATANI, Masao[1] ; MURAKAMI, Osamu[3] ; THABANG, Kgarume[4] ; THABANG, Masakale[5] ; LUIZ, Ribeiro[6] ; YABE, Yasuo[2] ; KAWAKATA, Hironori[3] ; ANTHONY, Ward[6] ; RAY, Durrheim[4] ; OGASAWARA, Hiroshi[3]

[1]Univ. of Tokyo, [2]Tohoku Univ., [3]Ritsumeikan Univ., [4]CSIR, [5]OHMS, [6]SeismoGen

We are monitoring Acoustic Emissions (AEs) down to Mw -4 or less at 1km beneath the ground in the Cooke 4 Mine (previously known as the Ezulwini Mine), where many earthquakes up to Mw 2 are induced by stress concentration due to tabular mining. The network consists of 24 AE sensors and 6 three-component accelerometers. Naoi et al. (2013; Pageoph) made a catalog composed of about 360,000 events by using waveform data obtained for three months, and reported that 90% of them aggregated within 10 m ahead of the mining front at the time.

In this study, we extended the analysis term to 9 months and developed a catalog composed of about one million events. We also applied the double difference algorithm (Waldhauser and Ellsworth, 2000) to them so as to examine spatial distributions of the AEs near the mining front in detail. Travel time differences for relative location were calculated from arrival times automatically read by the program of Horiuchi et al. (2011). To efficiently calculate relative hypocenters for a massive amount of events, we adopted the parallelization method of Hauksson and Shearer (2005), where events in subregions overlapping each other are firstly relocated and then the hypocenters relocated redundantly are averaged to make a single catalog. We succeeded in relocating 96% of the one million events.

The relocated AEs near the mining front exhibited two-dimensional, tabular aggregations with a few tens of meters lateral extent (hereinafter referred to as tabular cluster), rather than a three-dimensional distribution spread more or less uniformly (randomly) over the entire zone of the stope-front activity of 10 m breadth. Each tabular cluster was discernible because they were separated by regions of low AE density. That is, AEs ahead of the mining front basically occur selectively in several discrete tabular zones within a highly stressed volume affected by the mining cavity. The tabular clusters strike parallel to the mining face and dip 60-80^o. This resembles similarly large shear fractures along the plane of maximum shear commonly observed by excavation around the stopes (Gay and Ortlepp, 1979; Adams and Jager, 1980; Adams et al. 1981). Ahead of a panel that advanced by 40 m during the analysis period, 10 such tabular zones formed at intervals of 5 m on average.

By the same AE monitoring network, we also have found extremely aggregated (a few tens of centimeter thickness) planar clusters continuous over the cluster's extent, reminiscent of thoroughgoing fracture surfaces. They often coincide with pre-existing geological faults (Naoi et al. 2013; JpGU). In contrast, the AEs of the tabular clusters regularly forming in the mining front were spread over 1-2 m thickness, lacking a dominant aggregation with good continuity. We interpret that the tabular-cluster AEs are microfractures occurring in a formation process of a large-scale shear crack in macroscopically intact rock subjected to high stress ahead of the advancing mining front. Indeed, the activity of tabular clusters gradually increased as the mining front approached and ceased when passed by the front.

Keywords: Acoustic Emission, Induced Earthquake, Rock fracture

Japan Geoscience Union Meeting 2014
(28 April - 02 May 2014 at Pacifico YOKOHAMA, Kanagawa, Japan)

SIT38-03 Room:511 Time:April 30 09:30-09:45

Deformation and acoustic emission of a penetrated granular bed

MATSUYAMA, Kazuhiro[1] ; KATSURAGI, Hiroaki[2*]

[1]Department of Applied Science for Electronics and Materials, Kyushu University, [2]Department of Earth and Environmental Sciences, Nagoya University

In general, the rheological behavior of granular matter can mimic a certain side of the geophysical phenomena. In this experiment, the plunged granular matter is used to model the deformation and/or fracturing of the geophysical materials.

Penetration resistant force and acoustic emission (AE) from a plunged granular bed are experimentally investigated through their power-law distribution forms. The experimental apparatus used in this study is basically similar to that in our previous works [1,2]. In this experiment, AE measurement is used to approach the grain's-level microscopic behavior in a penetrated granular bed. An AE sensor (NF AE-9913) is buried in a glass beads bed. Then, the bed is slowly penetrated by a solid sphere by using a universal testing machine (Shimadzu AG-100NX). The average diameter of glass beads is varied from 0.4 to 2 mm, and the penetrating sphere's diameter ranges from 10 to 40 mm. During the penetration, the resistant force applied to the sphere and the AE signal are simultaneously measured [3]. The penetration speed (in the order of 1 mm/s) is kept slow enough to focus on the quasi-static regime. In this slow-penetration regime, the resistant force is independent of the penetration speed. Moreover, the resistant force shows power-law relation to the penetration depth. The obtained power-law exponent seems to depend on the size of granular column, i.e., the container's size. By comparing the resistant forces obtained by this experiment and other experiments, we confirm the relation between the resistant force and container's size. The smaller the container is, the larger the power-law exponent of resistant force becomes. This might mean that the slow penetration drag is affected by side wall of the container through force chains.

For AE signal, we observe a lot of (more than 1,000) burst-like AE events in each penetration experiment. We define the size of each AE event by its maximum amplitude. Then we find that the size distribution of AE events obeys power-law that is similar to Gutenberg Richter's law of the earthquakes statistics. However, the measured power-law exponent is not universal in this experiment. It rather depends on experimental condition. Particularly, the size of beads composing the penetrated granular bed affects the result significantly. The small glass beads bed shows larger power-law exponent. This tendency of power-law exponent indicates that the deformation of small-grains-bed is rather plastic, and the deformation of large-grains-bed shows brittle-like behavior. Namely, the emitted acoustic signal relates to the mode of deformation or fracturing. Since the grains network constructed in a small grains bed is dissipative, it also influences the statistics of AE events. The large AE events could be dissipated and screened by a lot of contact points in the small grains bed. This effect is also consistent with the current experimental result. In this study, only the AE events are measured and analyzed based on its power-law distribution. Actually, to characterize the mode of fracturing more precisely, electromagnetic emission (EME) should be also measured. Simultaneous measurement of AE and EME would reveal the details of the mechanics of slowly penetrated granular bed. Although this result is still preliminary to directly compare the power-law exponent with actual geophysical phenomena, the systematic behaviors of the power-law exponents are qualitatively informative to understand the deformation of the granular matter which relates to various geophysical phenomena and is quite different from usual continuum.

[1] H. Katsuragi, Material, Chem. Eng. Sci., 76, 165-172 (2012).
[2] H. Katsuragi, Phys. Rev. E, 85, 021301:1-5 (2012).
[3] K. Matsuyama and H. Katsuragi, Nonlin. Processes Geophys., 21, 1-8 (2014).

Keywords: acoustic emission, quasi-static resistant force, granular matter, power law

Japan Geoscience Union Meeting 2014
(28 April - 02 May 2014 at Pacifico YOKOHAMA, Kanagawa, Japan)

SIT38-04 Room:511 Time:April 30 09:45-10:00

Variety of memories of clay paste flows which can be visualized as desiccation crack patterns

NAKAHARA, Akio[1*] ; MATSUO, Yousuke[1] ; OOSHIDA, Takeshi[2] ; OTSUKI, Michio[3] ; KITSUNEZAKI, So[4]

[1]College of Science and Technology, Nihon University, [2]Department of Mechanical and Aerospace Engineering, Tottori University, [3]Department of Materials Science, Shimane University, [4]Graduate School of Human Culture, Nara Women's University

Due to its plasticity, a water-poor clay paste can remember the direction of vibration and flow that it suffered. The memory of flow in clay paste can be visialized as a morphology of crack pattern that appears when the clay paste is dried. When the clay paste remembers the flow direction, desiccation cracks run all parallel to the direction of the flow. Recently, we find that there are some different types of memory of flow, as the direction of crack propagation changes from parallel to perpendicular direction. We would like to discuss on the mechanism of the memory effect of flow.

Keywords: desiccation crack pattern, rheology of clay paste, memory effect of flow

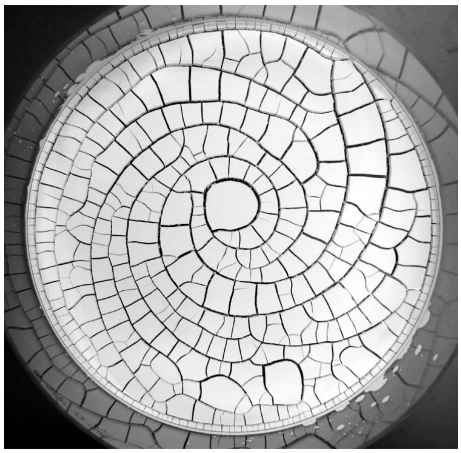

Japan Geoscience Union Meeting 2014
(28 April - 02 May 2014 at Pacifico YOKOHAMA, Kanagawa, Japan)

SIT38-05 Room:511 Time:April 30 10:00-10:15

Precursory Signal of Frontal Thrust Formation: Current status of Large Scale High Precision Sand Box Experiments

HORI, Takane[1*] ; SAKAGUCHI, Hide[1] ; YAMADA, Yasuhiro[2] ; DOTARE, Tatsuya[2] ; FUKUMOTO, Yutaka[3]

[1]JAMSTEC, [2]Depertment of Urban Management Engineering, Kyoto University, [3]Graduate School of Agriculture, Kyoto University

In order to find out the mechanism of the three dimensional complex shape formation in sequential thrust and uplift of a accretion prism, we have developed a large scale high precision sand box experimental apparatus since 2011. After a number of modifications in the experimental apparatus and experimental procedure, we finally performed productive runs in July 2013. In specimen preparation, the thickness of a sand layer is controlled with the precision of less than single particle size. As a result, the shape of a frontal thrust became uniformly straight with high reproducibility and no complex shape has been observed since then. However, with such a well-controlled experimental system, we succeeded to detect the precursory signal prior to frontal thrust formation. In this talk, detailed information of the experimental apparatus and our new findings will be given with the scope of applicability of our finding in the field.

Keywords: precursor, earthquake, sandbox experiment

Japan Geoscience Union Meeting 2014
(28 April - 02 May 2014 at Pacifico YOKOHAMA, Kanagawa, Japan)

SIT38-06 Room:511 Time:April 30 10:15-10:30

New modelling devices to enhance the reproducibility of analogue model experiments

DOTARE, Tatsuya[1*] ; YAMADA, Yasuhiro[1] ; SAKAGUCHI, Hide[2] ; HORI, Takane[2]

[1]Department of Urban Management, Kyoto University, [2]Japan Agency for Marine-Earth Science and Technology (JAMSTEC)

The scaled analogue model experiments have been used for more than 100 years to reproduce the geological development processes in the laboratory scales using the granular material (e.g. dry sand). Recently, we can obtain the small-scale deformation quantitatively by applying digital image analyses. Then, we observed the 'weak shear band' before fault initiation process. However, heterogeneity in the initial model produced by human hand often causes the fluctuation of the experimental results (e.g. fault location, faulting timing and fault geometry).

To solve this problem, we made the experimental device for making the initial model automatically and conducted the experiments to compare the experimental results with the previous method.

We conducted simple convergent experiments. Initial models were made by previous method (human hand) or new method (new device) and experiments were repeated 5 times, respectively.

As a result, while branches of new faults can be seen in the previous method, there are no branches in the new method. In addition, the fluctuation of experimental results was restricted in the new method.

This shows that new experimental device can make the initial model homogeneous and reproduce the same initial model in each experiment.

Keywords: analogue modelling, sandbox, reproducibility, accrationary prism, heterogeniety

Japan Geoscience Union Meeting 2014
(28 April - 02 May 2014 at Pacifico YOKOHAMA, Kanagawa, Japan)

SIT38-07 Room:511 Time:April 30 10:30-10:45

Relaxation processes of granular layer at seismic slip rates and layer thickness.

KUWANO, Osamu[1*] ; NAKATANI, Masao[2] ; HATANO, Takahiro[2] ; SAKAGUCHI, Hide[1]

[1]IFREE, JAMSTEC, [2]ERI, University of Tokyo

A natural fault has the cataclasite core zone, along which shear deformation concentrates. Rheology of these granular matters thus provides us an important insight in considering the nature of friction on faults from a microscopic point of view. In the past two decades, experiments conducted at sub seismic to seismic slip rates (mm/s to m/s) revealed two remarkable phenomena of high-velocity rock friction; very long critical slip distance (Dc) of the order of 1-10m/s and the considerable weakening due to mechanochemical effects by frictional heating [e.g., Di Toro et al., 2011, Nature]. Recently, Chambon et al.[2006, JGR] conducted friction experiment with very large shear displacement experiment on a thick granular layer, and reported significant slip-weakening behavior active over decimetric slip distances. However, the relation between long Dc observed in a thick granular layer and long Dc in the high-velocity friction is still not clear. Here, we report on laboratory experiments designed to explore transient responses of a thick granular layer following a step change in slip velocity at seismic slip rates. We use simple particle and choose relatively low normal stress to exclude the possible mechanochemical effects caused by frictional heat. We find that friction coefficient and layer thickness show similar response that is symmetry with respect to velocity changes, and Dc is of the order of 10m. It appears that these responses are attributed to dynamics of granular matter. We also report how magnitude of the relaxation and Dc are affected by the layer thickness.

Keywords: high-velocity friction, granular matter, rheology

Japan Geoscience Union Meeting 2014
(28 April - 02 May 2014 at Pacifico YOKOHAMA, Kanagawa, Japan)

SIT38-08 Room:511 Time:April 30 11:00-11:15

Porosity and permeability under effective pressure for the Quaternary Kazusa Group siltstones

MARUMO, Haruna[1*] ; UEHARA, Shin-ichi[1] ; TAMURA, Yukie[2] ; MITSUHASHI, Shunsuke[2]

[1]Graduate School of Science, Toho University, [2]Faculty of Science, Toho University

The Kazusa group is a geological formation of the middle Pleistocene - Pliocene marine, and widely distributes in middle and northern part of the Boso Peninsula. Mudstones of the Kazusa Group is in the first stage of consolidation (viscous compaction stage), and porosity is 37.9 - 55.5% [1]. In mudstone formations of the Kazusa Group, high porosity anomaly is observed, of which location is consistent with that of natural gas deposits. This high porosity anomaly is suggested to have been generated by an abnormally excess pore pressure. The development process of the high pore pressure is still unknown. Previous studies have discussed the mechanism in connection with production of natural gas, but sufficiently quantitative analyses have not been performed. H igh pore pressure zone may affect many properties and processes in underground, such as porosity and permeability development in accretionary wedge or sedimentary basins during accretion and depositional process, ground water flows or petroleum migrations in underground, and fault mechanisms. Thus, to elucidate the mechanism of developing the high pore pressure zone is important. We are therefore planning to investigate the mechanism of the high pore pressure zone development by using the 1D model of Tanikawa et al. [2], which include simple deposition and compaction processes. In this study, as the first step of this project, the effective pressure dependences of porosity and permeability were determined for laboratory experiments for siltstone of the Kazusa Group, which are necessary for the modeling.

The measurements were performed using an intra-vessel deformation fluid-flow apparatus at Toho University. The rock samples used in the experiments were collected from outcrops at Umegase Formation, Ota-dai Formation, Kiwada Formation, Ohara Formation and Katsuura Formation of the Kazusa group. The collected samples were shaped into a cylindrical shape about 40 mm in diameter and about 30 mm in height. Distilled water was used for pore fluid and confining pressure was applied by using oil. Permeability and porosity of siltstones were measured at room temperature and under effective pressures from 0 MPa to 35 MPa. To obtain porosity under effective pressure, we measured a volume of water discharged from the specimen when confining pressure was applied. We measured permeability by monitoring flow rate through the specimen under the condition that pore pressure differences at the both side of the specimen is kept constant.

Permeability and porosity ranged from 10^{-17} - 10^{-18} m^2 and to 34 - 42 %, respectively. Permeability and porosity both decreased with increasing effective pressure, and this pressure dependence varies.Based on the results of the experiment, porosity and permeability was expressed in relation to the effective pressure. We have examined the relationship between permeability and porosity.

References
[1] Inami, K., Bull. Geol. Surv. Japan 34, 207-216 (1983)
[2] Tanikawa, W., J. Geophys.Res.,113,B12403 (2008)

Keywords: Kazusa group, porosity, permeability, laboratory experiment

Japan Geoscience Union Meeting 2014
(28 April - 02 May 2014 at Pacifico YOKOHAMA, Kanagawa, Japan)

SIT38-09 Room:511 Time:April 30 11:15-11:30

Rheological properties of mafic schists: Implications for subduction dynamics

OKAZAKI, Keishi[1*] ; HIRTH, Greg[1]

[1]Department of Geological Sciences, Brown University

To understand the spatial and temporal distribution of deformation (e.g., underplating and exhumation of metamorphic rocks) and earthquakes in subduction zones, it is important to constrain the rheological properties of metamorphic rocks (i.e., altered oceanic crust and sediments), and how they evolve during metamorphic reactions following hydration, carbonation and dehydration of the down-going slab. Metamorphism of oceanic crust has stimulated hypotheses on the relationship between intra-slab earthquakes and slab-wedge coupling along plate boundaries in subduction zones. While it is well known that metamorphism has important effects on material fluxes and arc volcanisms at subduction system, it remains unclear how the formation of metamorphic minerals following fluid release influences rheology. Past experimental studies on mafic metamorphic rocks were mostly concentrated on phase equilibrium, thus there are few reports on the mechanical data for these metamorphic rocks.

We conducted triaxial deformation experiments on two mafic schists sampled from the Sambagawa metamorphic belt (Shikoku Island, Japan), using Griggs-type solid pressure- medium apparatus at Brown University. Both mafic schists are mainly composed of amphible, albite, epidote, and chorlite with small amounts of titanite and phengitic mica However, there are differences in the peak metamorphic condition (i.e., the maximun PT condition), amphibole composition and mineral abundance of minerals in the two schists. One, which was metamorphosed at greenschist facies (pressure of ~0.75 GPa and temperature of ~400 ℃), has a relatively high chlorite content (~12 %) and actinolite is the dominant amphibole phase. The other, metamorphosed at the epidote-amphibolite facies (pressure of ~1 GPa and temperature of ~520 ℃), has a lower chlorite content (<2 %) and hornblende is the dominant amphibole phase. Constant strain rate experiments and strain rate stepping experiments were conducted at confining pressures (P_c) from 0.76-2GPa, temperatures (T) from 300-600 ℃ and strain rates from 10^{-5}-10^{-7} 1/s.

At conditions near the peak conditions of the greenschist (P_c = 1 GPa, T = 400 ℃), differential stresses were higher than 1 GPa. The greenschist samples are weaker than the epidote-amphibolite samples under all experimental conditions. Both types of samples exhibit strain rate strengthening; frictional behavior that inhibits earthquake nucleation. Differential stress increased with increasing confining pressure, while friction coefficient decreased with increasing confining pressure and temperature. At T = 400 ℃, the nominal friction coefficient (μ) for the greeschist samples was μ ~0.34 at P_c = 1 GPa and μ ~0.30 at P_c = 1.5 GPa; for the epidote-amphibolite, μ ~0.48 at P_c = 1 GPa and μ ~0.42 at P_c = 1.5 GPa. Stress exponents (n) for the greenschist samples at P_c = 1 GPa were n ~26 at T = 300 ℃, n ~36 at T =400 ℃ and n ~34 at T = 500 ℃; for the epitote-amphibolite, n ~31 at T = 400 ℃ and n ~21 at T = 500 ℃. Microstructures of recovered samples showed modest buckling and several localized shear zones. These features suggest that the deformation of mafic schist is accommodated by semi-brittle deformation resulting in strain localization on faults.

We also conducted deformation experiments in which temperature was increased above the thermal stability of chlorite (~800 ℃) to simulate a prograde metamorphism in subduction zones. With increasing temperature during deformation, differential stress decreased and reached nearly 0 MPa. This suggests that such reaction-enhanced weakening of metamorphic rocks forms weak fault zones in subducting slab, which might promote detachment of oceanic crust from the subducting slab and allow underplating to forearc crust. The strain-rate strengthening behavior of these materials suggests that such faults would be relatively aseismic.

Keywords: mafic schist, subduction zone, deformation experiment, oceanic crust, semi-brittle deformation, intermediate depth earthquake

Japan Geoscience Union Meeting 2014
(28 April - 02 May 2014 at Pacifico YOKOHAMA, Kanagawa, Japan)

SIT38-10 Room:511 Time:April 30 11:30-11:45

Effect of iron content on the creep behavior of olivine under hydrous conditions

TASAKA, Miki[1*] ; ZIMMERMAN, Mark[1] ; KOHLSTEDT, David[1]

[1]University of Minnesota

Since iron and hydrogen play important roles in dynamic processes not only in Earth's mantle but also in Mars's mantle, we conducted triaxial compressive creep experiments on polycrystalline samples of olivine, $(Fe_{1-x},Mg_x)_2SiO_4$, with x = 0, 0.53, 0.77, 0.90, and 1.0 under hydrous condition. A Paterson-type gas-medium apparatus was used for these experiments. The water contents, determined from Fourier transform infrared (FTIR) spectroscopy analyses of larger Fo_{90} crystals embedded in the olivine aggregates, demonstrate that the samples are water-saturated both before and after deformation. The grain sizes of initial and deformed samples were determined using electron backscatter diffraction (EBSD).

Creep tests at 300 MPa confining pressure were conducted at temperatures from 1050 to 1200C at constant stresses in the range 25 to 315 MPa. The values of the pre-exponential term, stress and grain size exponents, and activation energy in the constitutive equation were determined for a wide range of iron concentrations. Samples with high Mg contents are finer grained (1-2 μm) than those with low Mg contents (10-20 μm). Furthermore, samples with high Mg contents ($x \geq 0.90$) exhibit a stress exponent of n = 2, whereas samples with low Mg contents (x <0.90) deform with n = 3. This result is consistent with the dislocation-accommodated grain boundary sliding model of Langdon (1994), which predicts that fine-grained samples that do not contain sub-grains should exhibit n = 2 while coarser-grained samples that do contain sub-grains should exhibit n =3. The flow stress decreases with increasing iron content of the olivine samples at constant temperature, strain rate, and grain size. Following the analysis of previous studies (Mackwell *et al*., 2005; Zhao *et al*., 2009), we fit our creep data to the following flow law: strain rate = $A\sigma^n\ d^{-p}\ (1\text{-}x)^m\ {f_{H2O}}^r\ \exp\{-[Q_0 + \alpha(1\text{-}x)] / RT\}$, where A is a material-dependent parameter, σ is stress, d is grain size, p grain size exponent, m iron content exponent, f_{H2O} water fugacity, r water fugacity exponent, Q_0 activation energy at $(1\text{-}x)$ = 0, and α a constant. The dependence of strain rate on iron concentration is characterized by two parameters - directly, through the iron content exponent m and, indirectly, through the term $\alpha(1\text{-}x)$ in the activation energy. The values of m and α are determined by the rate-controlling mechanism of deformation and the charge neutrality condition for Fe-bearing olivine.

Keywords: olivine, iron content, creep, rheology, experiments, deformation

Japan Geoscience Union Meeting 2014
(28 April - 02 May 2014 at Pacifico YOKOHAMA, Kanagawa, Japan)

SIT38-11 Room:511 Time:April 30 11:45-12:00

High accuracy measurement of activation energy of creep and electrical conductivity of olivine aggregate

NAKAKOJI, Tadashi[1*] ; HIRAGA, Takehiko[1] ; MIBE, Kenji[1]

[1]Earthquake Research Institute, The University of Tokyo

It is believed that creep rate of peridotite being major rock in the Mantle is controlled by diffusion of the slowest ion which is Si^{4+}. However it is suggested that diffusion of the second fastest ion controls the deformation rate in the system of which not only olivine but it including pyroxene also consists (Sundberg and Cooper (2008)). As seen above, the controlling process has not been understood well. Besides the activation energy being indication for deciding the mechanism is often obtained with a large error range. Therefore, in a case of extrapolating the experimental to the Earth's interior value, the large error will produce a large uncertainty. To solving the two problems, we have conducted the compression experiment and electrical conduction test for olivine simultaneously under a continuously changing temperature.

The sample used for the experiment was synthetic olivine composed of forsterite (90vol %) + enstatite (10vol %), which imitates a material in upper Mantle. To inhibit to grain growth during the experiment, the sample was annealed at 1360 ℃ for 24 hours in the furnace before the test conducted. During the experiment, the sample was kept loaded at constant stress, 20MPa, and temperature changed from 1360 ℃ to 1240 ℃ and then increased from 1240 ℃ to 1360 ℃ in order to confirm reproducibility of measurements. Measurement of impedance of the sample was also conducted simultaneously. The sample applied at 20V every ten degree from 1360 ℃ provided us current response, which was used for measurement of impedance of the sample.

The result of the experimental data provided us viscosity and electrical conductivity of the sample. Viscosity was obtained by the relation of stress and strain rate. Arrhenius plot of reciprocal viscosity shows a linear distribution. This indicates that deformation mechanism of the sample did not change at the applied temperature range in the experiment. Electrical conductivity in the sample was obtained by the resistivity derived from the data by impedance measurement. Assuming that the conduction is thermally-activated process, the relation of conductivity times temperature and temperature shows a linear relation in Arrhenius plot. From each these slopes of lines, Activation energy of 627±15 kJ/mol was obtained about creep and that of 297 ±12 kJ/mol was obtained about electrical conduction, respectively. This difference of the activation energies indicates that the creep rate and electrical conduction were controlled by different ion or/and different diffusion in the sample.

Sundberg and Cooper (2008) suggested that deformation mechanism is Mg^{2+} + O^{2-} ion diffusion but not Si^{4+}diffusion in a case of the sample of olivine + pyroxene. Therefore we compare our result with previous works. Activation energy of lattice diffusion of Si^{4+} and O^{2-}in olivine are ≈530 kJ/mol and ≈340 kJ/mol(Dohmen et al. 2002), respectively and that of Mg^{2+}lattice diffusion is about 400±60 kJ/mol (Chakraborty et al. 1994). On other hand, 627±15 kJ/mol was obtained in this study, so that we can infer that lattice diffusion of Si4+ controlled creep rate. ten Grotenhuis et al. (2004) obtained that activation energy of 315±39 kJ/mol by measuring electrical conductivity of olivine aggregate which has the same composition and almost same grain size of ours, and relation of increase electrical conductivity and decrease in grain size. Consequently, from the grain size is the same one of us, we can infer that grain boundary diffusion of Mg^{2+}ion contributed to the conductivity of our sample.

Keywords: olivine, creep, electrical conduction, activation energy, diffusion, polycrystal

Japan Geoscience Union Meeting 2014
(28 April - 02 May 2014 at Pacifico YOKOHAMA, Kanagawa, Japan)

SIT38-12 Room:511 Time:April 30 12:00-12:15

Quantification of grain boundary sliding and grain rotation during diffusion creep of mantle rocks

MARUYAMA, Genta[1*] ; HIRAGA, Takehiko[1]

[1]Department of Earth and Planetary Sciences, Earthquake Research Institute, University of Tokyo

Existence of an anisotropy in the seismic wave velocity in Earth's upper mantle have been known for decades (Tanimoto and Anderson 1984). The seismic anisotropy is often explained by the crystallographic preferred orientation (CPO) of rock-forming minerals, which have anisotropic elasticity. In general, the CPO of olivine produced during dislocation creep is considered to be the primary cause of the anisotropy. Recently, our team showed that the CPO of olivine is produced even during diffusion creep (Miyazaki et al. 2013). However, the mechanism of the CPO development under diffusion creep is still not clear. The purpose of this study is to understand the mechanism in submicron scale by observations of samples surface after the sample deformation where the fine-scale strain markers were imposed.

We used a vacuum sintering technique to synthesize cylindrical samples which were composed of fine-grained forsterite plus 20 vol. % diopside (a combination that we denote Fo80Di20) and forsterite plus 35 vol. % enstatite (En). We polished the lateral side of the sample. Subsequently we imposed grooves on such surface with using a focused ion beam. These marker lines were parallel to the compression axis of sample deformation. We conducted uniaxial compression creep experiments at atmospheric pressure, temperatures of 1300oC and strain rates of 10^{-5} -10^{-4} s^{-1}. After the compression creep experiment, we observed the marker lines under scanning electron microscope (SEM) with field emission gun (JEOL 6500F installed at Nano-Manufacturing Institute, University of Tokyo) to observe how the markers were displaced after the deformation. Such observations allow to quantify the amount of grain boundary sliding and grain rotation due to a plastic deformation of the sample.

We succeeded to observe the marker lines after the deformation. Significant grain boundary sliding was detected from the offsets of the markers at numbers of grain boundaries. No distortion of the markers within the grains was found indicating the absence of intragranular deformation process such as a glide of dislocations. We quantified the grain rotation finding that the rotation angle increases with strain. The average angles in the sample of Fo80Di20 with strain of 3%, 7% and 14% were 1.2^o, 3.9^o, 6.5^o, respectively. We also found larger rotation angle of the grains in Fo80Di20 than in Fo65En35. Fo80Di20 is composed of anisotropic grains of Fo whereas Fo65En35 has isotropic grains, which may explain the difference in the grain rotation between the samples. The shape of anisotropic grains is crystallographically controlled resulting in a development of longer and straight grain boundaries. We assumed that grains were easier to glide at such boundaries resulting in development of CPO during diffusion creep (Miyazaki et al. 2013), which is an modified model of grain rotation during grain boundary sliding creep (Beere 1978). Our present result seems to support our CPO model.

Keywords: grain rotation, grain boundary sliding, CPO, creep

Japan Geoscience Union Meeting 2014
(28 April - 02 May 2014 at Pacifico YOKOHAMA, Kanagawa, Japan)

SIT38-13 Room:511 Time:April 30 12:15-12:30

In-situ observation of crystallographic preferred orientation of olivine deformed in simple shear: Implications for the

OHUCHI, Tomohiro[1*] ; NISHIHARA, Yu[1] ; SETO, Yusuke[2] ; KAWAZOE, Takaaki[3] ; NISHI, Masayuki[1] ; MARUYAMA, Genta[5] ; HIGO, Yuji[6] ; FUNAKOSHI, Ken-ichi[7] ; SUZUKI, Akio[8] ; KIKEGAWA, Takumi[9] ; IRIFUNE, Tetsuo[1]

[1]Geodynamics Research Center, Ehime University, [2]Department of Earth and Planetary Sciences, Kobe University, [3]Bayerisches Geoinstitut, University of Bayreuth, [4]Earth-Life Science Institute, Tokyo Institute of Technology, [5]Graduate School of Science, University of Tokyo, [6]Japan Synchrotron Radiation Institute, [7]Research Center for neutron Science and Technology, [8]Department of Earth and Planetary Materials Science, Tohoku University, [9]Photon Factory, High Energy Accelerator Research Organization

The characteristics of the seismic anisotropy vary depending on the types of crystallographic preferred orientation (CPO) of olivine. Therefore, the pattern of the seismic anisotropy has been interpreted by taking into account the water- and pressure-induced fabric transitions of olivine in recent studies (Jung and Karato, 2001; Ohuchi et al., 2011). The fabric strength of olivine aggregates is also important when we evaluate the magnitude of the seismic anisotropy in the upper mantle. In the upper mantle, the steady-state fabric strength of olivine is expected to be achieved due to long time-scales of flows.

The dependency of the fabric strength of olivine aggregates on strain has been evaluated in only limited numbers of experimental studies (e.g., Bystricky et al., 2000). Bystrikcy et al. (2000) showed that total shear strains higher than 4 are needed to achieve the steady-state fabric strength of olivine (D-type fabric) at 0.3 GPa and 1473 K. However, it has been difficult to evaluate the detailed process of the development of fabrics because fabrics of recovered samples have been evaluated. Recently, we have developed experimental techniques for in-situ simple-shear deformation experiments using a D-DIA apparatus. In this paper, we briefly show that our recent experimental results on in-situ observations of stress, strain, and fabric developments in olivine samples.

Simple-shear deformation experiments on olivine aggregates at pressures P = 2-3 GPa, temperatures T = 1290-1490 K, and shear strain rates of 3E-4 s-1 were performed using a deformation-DIA apparatus installed at SPring-8. Shear strain (up to 5) was measured by the rotation of a platinum strain-marker, which was initially placed perpendicular to the shear direction. Differential stress, generated pressure, and CPO patterns of olivine samples were determined from two-dimensional X-ray diffraction patterns using software (IPAnalyzer, PDIndexer, and ReciPro: Seto et al., 2010; Seto, 2012). The CPO patterns of olivine in the recovered samples were also evaluated by the indexation of the electron backscattered diffraction (EBSD) patterns.

A-type olivine fabric was developed under dry conditions. The fabric strength increased with strain ($<$2), and steady-state fabric strength was achieved at shear strains about 2. The [010] axes strongly concentrated to the shear plane normal and its concentration increased with strain. Preferential alignments of the [100] and [001] axes were developed through increase in strain, though concentrations of the [100] and [001] axes were weaker than those of the [010] axes. Development of B-type olivine fabric was observed under wet conditions (˜700 ppm H/Si). The fabric strength of B-type sample continuously increased with strain (up to 3). As same as the case of A-type samples, concentrations of the [010] axes were stronger than those of other axes in the B-type sample. Because the concentration of the [010] axes efficiently increases at strains larger than 1, seismic anisotropy (e.g., VSH/VSV) at shear strains = 1 is quite similar to that under the steady-state conditions.

Using the CPO data of the steady-state A-type fabrics, V_{SH}/V_{SV} of the asthenospheric upper mantle is estimated to be 1.027 (note that 70 vol.% of preferred-orientated olivine grains and 30 vol.% of random-orientated orthopyroxene grains are assumed in the calculation). This value is consistent with the global one-dimensional model reported by Visser et al. (2008). The V_{SH}/V_{SV} of the asthenospheric upper mantle is expected to have higher values in the case of B-type fabric (e.g., 1.035), which is harmonious with the global one-dimensional model reported by Panning and Romaniwics (2006). Our results show that seismic anisotropy in the upper mantle is mostly explained by the steady-state olivine fabrics (A- and B-types), and other effects (e.g., shape-preferred orientation of melt, CPO of other minerals) would be limited.

Keywords: olivine, crystallographic preferred orientation, in-situ observation, seismic anisotropy

Japan Geoscience Union Meeting 2014
(28 April - 02 May 2014 at Pacifico YOKOHAMA, Kanagawa, Japan)

SIT38-14 Room:511 Time:April 30 12:30-12:45

Simultaneous observations of dehydration and AE activities during the deformation of antigorite at high pressures

IWASATO, Takuya[1*] ; KUBO, Tomoaki[1] ; HIGO, Yuji[2] ; KATO, Takumi[1] ; KANESHIMA, Satoshi[1] ; UEHARA, Seiichiro[1] ; IMAMURA, Masahiro[1]

[1]Kyushu Univ., [2]JASRI

Intermediate-depth earthquakes are seismic activities at depths of 60-300 km, where subducting plates deform plastically rather than brittle failure. Because dehydration embrittlement (Raleigh and Paterson, 1965) may not work for serpentinite at pressures more than ~2 GPa, it is important to understand the mechanisms of shear instability at higher pressure. To conduct simultaneous observation of dehydration reaction, plastic flow and shear instability, we developed an in-situ observation system combined with synchrotron monochromatic X-ray and AE 6-6 system (multiple acoustic emission measurement for multi-anvil 6-6 type system) using Deformation-DIA (D-DIA) apparatus. Using this system, we carried out antigorite deformation experiments up to ~4.5 GPa and ~850 K including the condition of the antigorite dehydration to talc and forsterite.

Deformation experiments were conducted at high pressure and high temperature using a 1500-ton uniaxial press (SPEED Mk. II) with a D-DIA type guide block installed at BL-04B1, SPring-8 (Katsura et al., 2004; Kawazoe et al., 2011). 50 keV monochromatic X-ray were used to measure two-dimensional X-ray diffraction (2D-XRD) patterns and X-ray radiography images, which give reaction kinetics, differential stress, and strain. We developed MA 6-6 type system (Nishiyama et al., 2008) to monitor shear instabilities by AEs from maximum six piezoelectric devices positioned between first and second stage anvils. AE waveforms were recorded in trigger mode using six-channel 8-bit digital oscilloscopes at a sampling rate of 50MHz. Starting material of polycrystalline antigorite cylinder (1.7 mm in diameter and 2.7 mm in length) cored from high-temperature serpetinite (Eigami, Nagasaki, Japan) were first compressed at room temperature, then heated at constant load, and finally deformed with constant strain-rate mode. In some runs, dehydration occurred during heating or deformation. Microstructures of recovered samples were preliminarily observed by optical microscopy.

A total of ten deformation experiments of polycrystalline antigorite were conducted at 1.1~4.5 GPa, 300~850 K, and strain rates of 3.4~6.7 x 10^{-5} s^{-1}. AEs were frequently generated from the sample during the cold compression. Relatively large AEs were also detected when heating the sample to 673 K, while AE activities became zero at higher temperatures. During the constant strain-rate deformation, the flow stress reached steady state at the sample strain of more than 5%, and no stress drops were observed until the final strain of ~30-40%. These flow behaviors and the flow strength are almost consistent with the previous study (Hilairet et al., 2007). We also detected AEs during the deformation stage although the frequency was lower compared to the cold compression and heating stages. The AE activities during the deformation became large at lower temperature and larger stain conditions. Optical microscopic observation revealed that some faults are present in the antigorite samples recovered from each stage. On the other hand, we observed dehydration reaction from antigorite to talc-like phase during the deformation at 800 K. The reaction was very slow and only one AE event was detected at the strain of ~25%. Because the faults were only observed in the relict antigorite region, the AE was possibly originated from antigorite. At higher temperature of 850 K, complete dehydration quickly occurred before the deformation. No AEs were detected during the dehydration and the following deformation of dehydrated materials to more than 30% strain. No faults were observed in the recovered sample. Our simultaneous observations of reaction and AE activities showed that the AE is not generated by dehydration of antigorite at more than ~2 GPa. Instead, the unstable fault slipping that generates AEs occurs during heating and deformation of antigorite without dehydration.

Keywords: Acoustic emission, In situ X-ray observation, deformation-DIA, antigorite, dehydration, stress and strain

Japan Geoscience Union Meeting 2014
(28 April - 02 May 2014 at Pacifico YOKOHAMA, Kanagawa, Japan)

SIT38-15 Room:511 Time:April 30 14:15-14:30

Seismic attenuation measurement by cyclic loading under high pressure and temperature

YOSHINO, Takashi[1*] ; YAMAZAKI, Daisuke[1] ; HIGO, Yuji[2] ; FUNAKOSHI, Ken-ichi[3]

[1]Institute for Study of the Earth's Interior, Okayama Univ., [2]JASRI, [3]CROSS

The estimation of the mantle structure using seismic tomography method has been advanced by understanding of the detailed velocity structure of the Earth interior . On the other hand , Brillouin scattering in the DAC at very high pressure, X-rays inelastic scattering, sound velocity measurement of ultrasonic range in the large press is also improved. These developments can be expected this time as a further declaration of a picture of a more detailed Earth interior. However, as compared to the frequency band of MHz to GHz region, the frequency range of the seismic waves propagating through the earth interior is much lower. We should noted that it is greatly affected by the attenuation of seismic waves. Because the materials are not in a perfectly elastic body, energy loss inside the materials occurs in the wave propagation because of presence of grain boundaries, dislocations, and defects. Thus, seismic attenuation occurs as a function of frequency.

The attenuation of seismic waves (the determination of the Q-1) of mantle material under high pressure has not been reported until recently mostly because it is an experimental quantification is very difficult . Temperature effects and particle size effects were reported for the first time systematically for olivine aggregates at high temperature under low pressure. However, for this system the upper limit of the generated pressure is low because it is a torsion test performed in the gas pressure. So the study of pressure -dependent and high-pressure mineral is difficult . The other group using the D-DIA type press having two differential ram measured $Q^{-}1$ combining an in-situ observation and radiation uniaxial periodic vibration test. This system expands a possibility of experimental determination of Q^{-1} at much higher pressure. In Japan, the DIA type press was installed at SPring8 (D-DIA). Recently we started the measurement of Q^{-1} under high pressure using in situ image acquisition of the high time and spacial resolution at short period of oscillation cycle.

In this paper, some experimental developments for measuring seismic attenuation at high pressure and results of cyclic loading tests are introduced. Time resolved images of the sample and reference material obtained by a synchrotron X-ray radiography provide their strain as a function of time during cyclic loading. Attenuation is determined as the tangent of the angle of phase lag between the strain of the sample and the strain of the reference material. A newly installed short period sinusoidal cyclic loading oil pressure system enable us to determine minimal strain of the sample in a wide frequency range from 2 to 0.01 hertz on olivine aggregates at 1 GPa and up to 1673 K. The detectable minimum strain is around 5×10^{-5}. Several test experiments exhibited resolvable Q^{-1} (10^{-2}) above 1273 K. The results are generally consistent with previously reported data.

Keywords: seismic attenuation, high pressure, oscillation, Q value, shear modulus

Japan Geoscience Union Meeting 2014
(28 April - 02 May 2014 at Pacifico YOKOHAMA, Kanagawa, Japan)

SIT38-16 Room:511 Time:April 30 14:30-14:45

Viscoelastic property of antigorite

YAMAZAKI, Daisuke[1*]

[1]Okayama University

Seismological data reveals the structure and dynamics combined with mineral physics. For example, the velocity structures from observations are interpreted using the elastic properties of constituting minerals obtained from the laboratory measurements. Because the minerals in the earth is not perfect single-crystal but they contain a certain amount of defects (vacancy, dislocation, grain boundary), the viscoelastic relaxation is taken place by the viscous motion of the defects during the propagating the seismic waves with the frequency of 10^{-4}-10 Hz. Serpentinite can be considered to be one of the candidate for the source of the fluid in the wedge mantle. In the present study, therefore, we examine the viscoelastic property of serpentine (antigorite) under uppermost mantle conditions by means of high pressure experiments.

Fine-grained polycrystalline antigorite (a few micrometer of grain size) sintered at 3 GPa and 550 degree C for 4 hours was used as a starting material for the attenuation experiment. We conducted the experiments by using D-DIA press with a short-period cyclic loading system, which was recently installed at BL04B1, SPring-8, Japan. D-DIA, which is a single stage of six-anvil compression device, applied pressure by forcing each of the six anvils to advance on the cubic pressure medium with a main ram. After pressure reaching to the target value of 1 GPa by the pumping the main ram, a sinusoidal stress and strain was applied by advancing and withdrawing the upper and lower anvils operated by the short-period cyclic loading system with the frequency between 0.01-2 Hz at 1 GPa and 500-750 degree C. At high temperature (>˜650 degree C), dehydration is expected. The strain was monitored directly from X-ray radiography of sample located in the pressure medium through the anvil gap during cyclic loading. In the present study, single crystal of forsterite was placed next to the sample along the stress axis of the sample and it can be used as the standard to estimate the stress by recording the X-ray radiography images displaying the lengths of standard and sample simultaneously.

The time lag of strain of sample against that of standard provided us the quality factor, Q, to be 5.4, 4.8 and 4.4 for the periods of 5, 10 and 20 s, respectively, at 600 degree C. Present preliminary results shows the temperature dependence of Q-1. At 500 degree C, Q^{-1}s are ˜0.5 log unit lower than those at 600 degree C. The present values is ˜2 order of magnitude lower than that of olivine aggregates. The shear modulus was estimated to be 15-25 GPa in our experimental condition, which is much smaller than the shear modulus without attenuation (38.5 GPa). The large reduction in shear modulus due to attenuation was previously reported in the case of olivine.

Japan Geoscience Union Meeting 2014
(28 April - 02 May 2014 at Pacifico YOKOHAMA, Kanagawa, Japan)

SIT38-17 Room:511 Time:April 30 14:45-15:00

Experimental study of anelasticity of a polycrystalline material near the melting temperature

YAMAUCHI, Hatsuki[1*] ; TAKEI, Yasuko[1]

[1]Earthquake Research Institute, University of Tokyo

Rock anelasticity is important to interpret seismic wave velocity and attenuation structures in the upper mantle. By using organic polycrystalline borneol ($C_{10}H_{18}O$, melting temperature =204.5 ℃) as an analog to mantle rock, McCarthy et al.(2011) measured Young's modulus and attenuation Q^{-1} as functions of frequency f (=10^{-4} - 2 Hz), temperature T (20-50 ℃) and grain size d (3.3 - 22 micrometer). They also measured viscosity, and calculated the Maxwell frequency fm. When the obtained Q^{-1} spectra were plotted as functions of the frequency normalized by the Maxwell frequency fm, all Q^{-1} spectra obtained for various temperatures and grain sizes collapsed onto a nearly single curve. Moreover, data from olivine aggregates (Gribb and Cooper, 1998; Tan et al. 2001; Jackson et al. 2002) collapsed onto the same master curve as borneol, demonstrating the universality of anelastic behavior. However, experimental frequencies normalized by the Maxwell frequency of the samples were lower than $5*10^4$, which is considerablly lower than those of seismic waves in the upper mantle (f/fm= 10^6-10^9). Therefore, whether the Maxwell frequency scaling is applicable to the seismic waves or not is an open question.

Takei et al. (in preparation) measured anelasticity of organic polycrystalline borneol at lower temperatures (0-20 ℃) and higher frequencies (10^{-4}-50 Hz) than McCarthy et al. (2011). They also investigated the effect of chemical composition on anelasticity, by using the samples made of high-purity borneol and borneol + diphenylamine ($(C_6H_5)_2NH$) (eutectic temperature = 43 ℃). Before obtaining these data, our experimental methodology and data quality were much improved. When the obtained Q^{-1} spectra were plotted as functions of the frequency normalized by the Maxwell frequency, the Q^{-1} spectra collapsed onto a nearly single curve at f/fm $<10^4$, but significantly scattered at f/fm $>10^4$, where the spectra have a broad peak and the scattering is caused by the variation of the peak amplitude and width with temperature, grain size and chemical composition. Therefore, the simple Maxwell frequency scaling is not applicable to the seismic waves in the upper mantle. They found that seismic attenuation predicted from the data of high purity samples and those of the borneol + diphenylamine samples under low temperature conditions is too low to explain the seismic attenuation in the upper mantle (~ 0.01). In other words, enhancement of attenuation near the melting temperature is important to understand high Q^{-1} in the upper mantle.

In this study, we measured anelasticity of borneol + diphenylamine system at various frequencies ($2*10^{-4}$ -50 Hz) and temperatures (20 - 46 ℃), and obtained the detailed behavior of anelasticity near the melting temperature (43 ℃). The result obtained so far show that the change of viscosity and anelasticity near the melting temperature is not discrete but continuous. This result is somewhat different from our previous understanding that physical properties abruptly change when melting starts beyond the solidus. We will further obtain systematic data for various grain sizes and melt fractions.

Keywords: anelasticity, seismic attenuation

Japan Geoscience Union Meeting 2014
(28 April - 02 May 2014 at Pacifico YOKOHAMA, Kanagawa, Japan)

SIT38-18 Room:511 Time:April 30 15:00-15:15

Experimental study of bulk and shear viscosities of partially molten rock analogue

SUZUKI, Ayako[1*] ; TAKEI, Yasuko[1] ; WATANABE, Shun-ichi[2]

[1]Earthquake Research Institute, University of Tokyo, [2]Hydrographic & Oceanographic Dept, Japan Coast Guard

Deformation of partially molten rock is controlled by two independent viscosities: shear viscosity for shear deformation and bulk viscosity for compaction/decompaction. Bulk viscosity and its ratio to shear viscosity, h_b/h_s , play an important role in melt segregation dynamics in the upper mantle (Katz, 2008). However, that value has not been well constrained theoretically nor experimentally especially at small melt fractions. Most numerical studies have used the theoretically predicted value of h_b/h_s = ~f^{-1}, where f is the melt fraction. Takei and Holtzman (2009a) theoretically obtained a constant value of h_b/h_s by taking into account a diffusion creep mechanism. The discrepancy between two models is significant at small melt fractions. There has not been experimentally determined value of h_b/h_s because very few experimental studies have been done about bulk viscosity although shear viscosity has been measured extensively. To discuss the validity of these models based on the experimental data, it is highly important to measure both bulk and shear viscosities by using the equivalent samples. In this study, we measured experimentally these two viscosities as functions of melt fraction using a partially molten rock analogue.

Samples were polycrystalline aggregates of borneol-diphenylamine binary with eutectic temperature of 316K, which has a quite similar equilibrium microstructure to olivine + basalt system (Takei, 2000). Initial melt fraction can be controlled precisely by the concentration of diphenylamine because of its simple eutectic reaction. Before deformation experiments, samples were annealed at 320K for ~100 hours in a sealed capsule to make those grain size large enough (~0.030 mm), resulted in negligible grain growth during the successive deformation tests at the same temperature.

To measure bulk and shear viscosities, we carried out two separate experiments. For bulk viscosity, compaction experiments were performed under the diffusion creep regime. A cylindrical sample was compacted uniaxially in a rigid sleeve (e_{zz} <0, e_{xx} = e_{yy} = 0, where e is the strain). Melt was squeezed out from the partially molten sample into porous metals which contact with the sample at the top and bottom ends until melt fraction becomes nearly zero. Evolution of melt fraction in the sample was calculated from the sample length measured with digital gauge. Apparent viscosities as a function of melt fraction were proportional to exp(-af) with a = ~30 at f >4 %, which is quite consistent with the olivine + melt systems (Renner et al., 2003). At f <3 %, deviation of the viscosity from the exponential curve occurs, suggesting the possible effects of permeability and change of rate limiting process of the volumetric creep (Takei & Holtzman, 2009b). For shear viscosity, uniaxial deformation experiments were performed without a horizontal confining pressure (s_{zz} <0, s_{xx} = s_{yy} = 0, where s is the stress). Melt fraction was nearly constant during the test. Deformation tests were conducted with some constant load steps under the diffusion creep regime. Apparent viscosity is evaluated from the stress and the strain rate at steady state.

From the two apparent viscosities obtained independently, we can calculate each bulk and shear viscosities as functions of melt fraction. We will test the predictions of models and discuss the possible viscosity ratio of the partially molten rocks in the upper mantle.

References:
Katz RF (2008) J.Petrol., 49, 2099-2121.
Renner J, Viskupic K, Hirth G, Evans B (2003) G^3, 4, doi:10.1029/2002GC000369.
Takei Y (2000) JGR, 105, 16665-16682.
Takei Y, Holtzman BK (2009a) JGR, 114, doi:10.1029/2008JB005850.
Takei Y, Holtzman BK (2009b) JGR, 114, doi:10.1029/2008JB005851.

Keywords: viscosity, bulk viscosity, shear viscosity, partial melt

Japan Geoscience Union Meeting 2014
(28 April - 02 May 2014 at Pacifico YOKOHAMA, Kanagawa, Japan)

SIT38-19 Room:511 Time:April 30 15:15-15:30

Role of Mg-O grain-boundary diffusion in rheology and grain-growth in the Earth's mantle

NISHIHARA, Yu[1*] ; NISHI, Masayuki[1] ; MARUYAMA, Genta[2]

[1]Geodynamics Research Center, Ehime University, [2]Earthquake Research Institute, University of Tokyo

Material and heat transports in the Earth highly depends on rheology and grain-growth kinetics of the constituent materials. Although rheology and grain-growth in single phase aggregate have been studied extensively, knowledge of those in multi-phase system is still limited. Sundberg and Cooper (2008) pointed out the importance of a creep mechanism in which strain is produced by Mg-O grain-boundary diffusion accompanied with reaction at olivine-orthopyroxene phase boundary in the Earth's upper mantle. Tasaka and Hiraga (2013) showed that grain-growth in forsterite-enstatite two-phase system is rate-limited by growth of secondary phase through Mg-O grain-boundary diffusion. These reports suggest that Mg-O grain-boundary diffusion plays important role both in rheology and grain-growth. Recently, our group reported Mg-O grain-boundary diffusion coefficients in forsterite and $MgSiO_3$ perovskite (Maruyama et al., 2013; Nishi et al., 2013). In this study, theoretical model using our Mg-O grain-boundary diffusion data are compared with available rheological and grain-growth data, and importance of these mechanisms are discussed.

Flow-law were calculated for Mg-O grain-boundary diffusion creeps accompanied by reaction at forsterite-enstatite phase boundary (upper mantle) or accompanied by grain-growth of periclase (lower mantle) using Coble's (1963) equation and results by Maruyama et al. (2013) and Nishi et al. (2013). The derived flow-law for the upper mantle shows ˜3 orders of magnitude faster strain-rate than that of creep experiments by Tasaka et al. (2013) which suggests this mechanism is not realistic. Although no comparable creep data was reported for the lower mantle, the derived flow-law shows faster strain-rate than that by Si lattice diffusion creep that was assumed in Xu et al. (2011) and the mechanism is a possible candidate deformation mechanism in the most part of lower mantle.

Grain-growth in the forsterite-enstatite two phase system was studied by Tasaka and Hiraga (2013) experimentally and it is already shown that grain-growth in this system is rate-limited by growth of secondary phase through Mg-O grain-boundary diffusion. Based on the same manner as Tasaka and Hiraga (2013), grain-growth law was calculated for the lower mantle assemblage $MgSiO_3$ perovskite-periclase system using Ardell's (1972) theory and Nishi et al.'s (2013) results. Derived grain-growth law was generally consistent with the grain-growth data in $MgSiO_3$ + MgO system reported by Yamazaki et al. (1996). Yamazaki et al.'s results can be explained by initial rapid growth from metastable texture and subsequent normal grain-growth which is rate-limited by Mg-O grain-boundary diffusion. Based on this interpretation, grain-size in the lower mantle is estimated to reach several hundred micro meter by 10^6 years.

Keywords: Upper mantle, Lower mantle, Rheology, Grain-growth, Olivine, Mg-perovskite

Japan Geoscience Union Meeting 2014
(28 April - 02 May 2014 at Pacifico YOKOHAMA, Kanagawa, Japan)

SIT38-P01 Room:Poster Time:April 30 18:15-19:30

Relationship between Skempton's coefficient and diagenesis of the Quaternary Kazusa Group siltstones

MITSUHASHI, Shunsuke[1*] ; UEHARA, Shin-ichi[1] ; MARUMO, Haruna[2] ; TAMURA, Yukie[1]

[1]Faculty of Science, Toho University, [2]Graduate School of Science, Toho University

Skempton's coefficient B is one of fundamental properties of sediments and rocks. B is defined as the change in pore pressure per unit change in total stress applied under undrained conditions. To reveal the evolution of B of sediments and sedimentary rocks during diagenesis is critical for some processes relating to geophysics and geology, such as mechanisms of developing abnormal pore pressure in sedimentary basins (Tanikawa et al., 2008). However, how B depends on diagenesis is still not clear. To understand the dependency, we evaluated B based on porosity measurements under effective stress for siltstones collected from various formations in the Quaternary Kazusa Group. We also tried to measure B directly, and compared the results with B values obtained from measurements of porosity.

We used siltstones of Umegase, Otadai, Kiwada, Ohara and Katsuura Formations of the Kazusa Group as the samples for the experiments. The specimens from the samples were 30 mm in diameter and 40 mm in length. The laboratory experiments were performed using an intra-vessel deformation fluid-flow apparatus at Toho University, at room temperature and under confining pressures from 2 MPa to 35 MPa. Distilled water was used for pore fluid. From the results of the porosity measurements under effective pressure, we estimated the compressibilites of the rock on the assumption that volume change of the rock at effective stress change equals to the pore volume change, and calculated B from the results. In the direct measurements of B, we measured pore pressure changes when confining pressure were applied under undrained conditions.

The results of B estimations from porosity measurements indicated that B tends to decrease with increasing burial depth. But, B of Ohara siltstones was somewhat higher than other samples despite Ohara Formation is relatively lower in the Kazusa Group. This is probably because siltstones at Ohara Formation were not consolidated enough as compared with those at other formations due to some reasons such as developing abnormal pore pressure. Results indicated that the dependency of B on effective pressure is not simple. B was not simply decreased with effective pressure increases, but B was increased at some range of effective pressure, which mostly reflected that the compressibility was increased at the transition from overconsolidation to normal consolidation state. B depends on both compressibility and porosity, and in the case of the Kazusa Group siltstones, the behavior of compressibility has greater effect on B. Thus, B is decreased as a grade of diagenesis increases because compressibility is decreased. The values of B measured directly tended to be higher than B estimated from measurements of porosity. This is probably because a period between step changes of effective stress was not enough for the rocks to reach steady state.

Keywords: Skempton's coefficient, diagenesis, Kazusa Group, porosity, compressibility, laboratory rock experiment

Japan Geoscience Union Meeting 2014
(28 April - 02 May 2014 at Pacifico YOKOHAMA, Kanagawa, Japan)

SIT38-P02 Room:Poster Time:April 30 18:15-19:30

Effects of pore pressure changes on frictional behaviors of talc

UEHARA, Shin-ichi[1*] ; OKAZAKI, Keishi[2] ; SHIMIZU, Ichiko[3]

[1]Faculty of Science, Toho University, [2]Department of Geological Science, Brown University, [3]Faculty of Science, The University of Tokyo

Since the discovery of low frequency earthquake, several classes of physical mechanisms have been proposed to explain this events. Several models and geophysical observations have suggested that the overpressurized fluid along the subducting plate interface have an important role in triggering such events. In addition, the existence of hydrous minerals along the plate boundary at fore-arc wedge may also be important for the seismogenic properties of the slab-mantle interface. Especially, serpentine minerals are generally expected to be the main hydrous mineral present in the fore-arc minerals, and the existence of serpentine in the wedge mantle has suggested by seismological studies. However, talc may also be important in fault mechanism at the plate boundary in the fore-arc wedge mantle, because slab-derived fluids are likely to lead replacement of serpentine by talc at the slab-mantle interface in the fore-arc wedge mantle, and talc is one of the weakest minerals that constitute natural fault zones. However the quantitative influences of pore pressure on the frictional properties of talc are not well constrained. We conducted friction experiments using pre-cut samples of talc with controlling pore pressure P_p and confining pressure P_c adopting several kinds of stress paths during an experiment.

Cylindrical samples of talc (Gvangjsih, China), 20 mm in diameter, were cut at an angle of 30^o to the sample axis. The sliding surfaces were ground with carborundum (#400). A small hole (3 mm in diameter) through the center of each piece ensured adequate communication of the water between the precut surfaces with the rest of the pore pressure system. The specimen was loaded by a triaxial apparatus and sheared under an axial displacement rate of 1 μm/s. We used water as a pore fluid. All measurements were performed at room temperature. Experiments were conducted under several paths of P_c (up to 110 MPa) and P_p (up to 100 MPa). During steady axial loading, either P_c or P_p was changed stepwise.

The stepwise changes of effective normal stress σ (= σ_t - P_p, where σ_t is total normal stress) resulted in a linear elastic response of shear stress followed by a transient evolution of friction. In the case that σ was decreased, friction coefficient μ was temporally increased and then decreased back to steady state, and the normalized transient change of μ to the logarithm of normalized amplitude of σ change ranged from 0.2 to 0.28, which is comparable to that for quartz and Westerly granite reported by previous studies (Linker and Dieterich, *J. Geophys. Res.*, 1992; Hong and Marone, *Geochem. Geophys. Geosyst.*, 2005). While in the case that σ was increased (μ was temporally decreased then increased), the values were smaller (less than 0.12, and negative in some cases), which means that a transient change of μ was less dependent on a change of σ than that for quartz and granite, which may reflect ductile deformation of contacts on fault surfaces during the evolutional transition.

This frictional property might cause slow slip phenomena. After an initiation of a fault slip, possibly triggered by an increase of pore pressure, partially undrained conditions on the slip surface may cause dilatancy hardening, and therefore σ may be increased during the slip. The results of this study suggest that, in the case that a fault plane is covered by talc, the temporal decrease of μ following an increase of σ might be smaller than the case that fault planes are covered by other ordinary minerals. Consequently, a frictional resistance might act more effectively than faults covered by other ordinary minerals and an acceleration of fault slip rate might be mitigated, and therefore a slip rate might be smaller than regular earthquakes.

This research is supported by Grant-in-Aid for Scientific Research on Innovative Areas, KAKENHI.

Keywords: talc, friction experiment, pore pressure, low frequency earthquake

Japan Geoscience Union Meeting 2014
(28 April - 02 May 2014 at Pacifico YOKOHAMA, Kanagawa, Japan)

SIT38-P03 Room:Poster Time:April 30 18:15-19:30

Sintering experiments on fine-grained polycrystalline orthoclase

OHIRA, Akane[1*] ; ISHIKAWA, Masahiro[1]

[1]Graduate school of Environment and Information Sciences, Yokohama National University

K-feldspar is one of the major mineral components of granitic rocks and a wide variety of metamorphic rocks. Its deformational behavior is important for establishing the overall rheology of continental crust. The creep strength is influenced by various factors such as mineral species, grain size and pores. Therefore control of these factors in polycrystalline minerals is essential for rheological experiments. In order to make dense polycrystalline orthoclase, we have carried out sintering experiments.

We prepared submicron mineral powders from a single crystal of orthoclase ($K_{0.83}Na_{0.17}Al_{1.04}Si_{2.96}O_8$). As a result of X-ray fluorescence (XRF) analysis, ZrO2 (<5.65wt.%) which is considered to be contamination from a mill was detected. We formed cylindrical compacts from fine-grained mineral powders by uniaxial dry pressing at room temperature and pressure of 20MPa. Sintering was carried out using a tube furnace at temperature of 970 ℃ for 4 hours, achieving a vacuum condition of $\sim 4.1 \times 10$Pa. We also compared the sintered body with a sample sintered at atmospheric pressure using muffle furnace at the same temperature and the time. Sintered bodies were observed using scanning electron microscope (SEM), and analyzed by XRF and X-ray diffraction (XRD).

As the result of vacuum and atmospheric pressure sintering, we obtained sintered bodies with volume reduction of 52.2% and 44.5%, and porosity of 0.15 and 0.17, respectively. SEM images showed that densification process was advanced by both vacuum and atmospheric pressure sintering. We confirmed that crystal structures (Al/Si order-disorder) were not changed from compacts by XRD patterns.

In this study, we found that dense submicron polycrystalline orthoclase can be made from fine-grained powders by either of vacuum and atmospheric pressure sintering, and confirmed that orthoclase does not cause order-disorder phase transition by a sintering for 4 hours.

Keywords: submicron, orthoclase, sintering

Japan Geoscience Union Meeting 2014
(28 April - 02 May 2014 at Pacifico YOKOHAMA, Kanagawa, Japan)

SIT38-P04 Room:Poster Time:April 30 18:15-19:30

Doping effect on high-temperature creep of polycrystalline anorthite

YABE, Kosuke[1*] ; KOIZUMI, Sanae[1] ; HIRAGA, Takehiko[1]

[1]Earthquake Research Institute, The University of Tokyo

Rheological properties of lower crust are considered to play important roles on the cause of inland earthquakes. Previous studies on creep properties of polycrystalline anorthite indicate that the polycrystalline anorthite will deform under diffusion creep at temperature condition of 400 to 1000C and grain size of <100 um where such conditions are identified in mylonites which are of lower crust origin. Therefore, it is important to know a precise strength of polycrystalline anorthite during diffusion creep.

Previous studies have shown the influence of grain size, temperature, stress, and water content on the strength of polycrystalline anorthite. It is well known that a small amount of impurities segregated at grain boundaries has a significant effect on the strength of polycrystalline oxides. We have shown that our pure anorthite aggregate, which was synthesized using the technique that could minimize the contamination of impurities, had two orders of magnitude larger strength than anorthite aggregates used in previous studies. In this study, we examine the effect of doping a small amount of MgO on high-temperature creep of anorthite aggregates.

MgO-doped anorthite aggregates were fabricated from nano-sized powders of $CaCO_3$, Al_2O_3, SiO_2 ,and $Mg(OH)_2$, all of which have <50 nm in diameter, and vacuum sintering of the powders. We controlled the amount of $Mg(OH)_2$ powders to obtain anorthite doped with 1wt% of MgO. Constant load tests were performed at temperatures ranging from 1150 to 1380C, stresses from 10 to 120 MPa, and confining pressure of 0.1 MPa. We measured Arithmetic mean grain size of specimens by microstructural observations using scanning electron microscopy (SEM) before and after creep tests.

Grain sizes of the specimens were 1˜2um before and after the creep test. Log stress versus log strain rate showed a linear relationship where its slope gave a stress exponent, n of 1, indicating that samples were deformed under diffusion creep. MgO-doped anorhite aggregates exhibited more than one order of magnitude weaker than pure anorthite. We obtained activation energy, Q of 702 kJ/mol which was higher than that of our pure anorthite. The difference in strength between pure and MgO-doped anorthite was attributed to the presence of a small amount of MgO which was probably segregated at grain boundaries.

Keywords: polycrystalline anorthite, diffusion creep, effect of doping

Japan Geoscience Union Meeting 2014
(28 April - 02 May 2014 at Pacifico YOKOHAMA, Kanagawa, Japan)

SIT38-P05 Room:Poster Time:April 30 18:15-19:30

Synthesis of textural polycrystalline forsterite using colloidal processing in a strong magnetic field.

KOIZUMI, Sanae[1*] ; HIRAGA, Takehiko[1] ; SUZUKI S., Tohru[2] ; SAKKA, Yoshio[2]

[1]Earthquake Research Institute, University of Tokyo, [2]National Institute for Material Science

It is well known that the crystallographic preferred orientation (CPO) of minerals is commonly produced in the Earth's interior. Thus, it is important to understand the physical properties of the mineral aggregates that exhibit CPO. However, silicate minerals are often feeble magnetic and have small anisotropic susceptibilities so that it is difficult to apply a magnetic field effectively to rotate the mineral particles. Tendency of finer particles to spontaneously agglomerate due to strong attractive interactions (van der Waals forces) add further difficulty. We used a technique of slip casting in a high magnetic field (12T) to align certain crystallographic axis of mineral particles. For the particles to rotate easily in the solvent under a strong magnetic field, we improve the method of deflocculating. To control the surface potential of the particles, we applied various types of polymer modification. Vacuum sintering of the powders that were composed of the aligned particles was expected to produce a polycrystalline material aggregate that exhibits CPO. The resultant materials were characterized by X-ray powder diffraction (XRD), secondary electron microscope (SEM) and Electron Backscatter Diffraction (EBSD).

The specimen exposed to a strong magnetic field exhibits preferential A-axis alignment to the magnetic direction. Those synthetic specimens allow us to examine the effect of CPO on the physical properties of the earth's materials in future room experiments.

Keywords: forsterite, polycrystalline, magnetic field, orientation, CPO

Japan Geoscience Union Meeting 2014
(28 April - 02 May 2014 at Pacifico YOKOHAMA, Kanagawa, Japan)

SIT38-P06 Room:Poster Time:April 30 18:15-19:30

Grain growth experiment on pyrolite materialunder lower mantle conditions

IMAMURA, Masahiro[1*] ; KUBO, Tomoaki[1] ; KATO, Takumi[1]

[1]Kyushu Univ.

Grain size is a key parameter for understanding viscosity of Earth's mantle. Grain growth rate is one of important factors controlling the grain size. Especially, it is indispensable to examine grain growth kinetics in multiple phases because the grain growth rate of major phase drastically changes with the proportion of secondary phases (e.g., Hiraga et al., 2010). In the lower mantle, Mg-perovskite is major phase, and ferro-periclase, Ca-perovskite, and majoritic garnet are present as secondary phases (e.g., Irifune, 1994; Nishiyama and Yagi, 2003). The previous grain growth experiment (Yamazaki et al., 1996) in the two-phase system of $MgSiO_3$ perovskite and MgO periclase using Mg_2SiO_4 forsterite as a starting material suggests that the grain growth rate is too slow to explain the lower mantle viscosity constrained by geophysical observations. This inconsistency may arise from effects of the eutectoid transformation prior to the grain growth process (e.g., Solomatov et al., 2002). It is also necessary to examine effects of the chemical composition that affects the proportion of secondary phases and diffusivity. Here, we report preliminary results of the grain growth experiment on pyrolite material under lower mantle conditions.

High-pressure and temperature experiments were conducted using a Kawai-type multi-anvil apparatus (QDES) installed at Kyushu University. Starting material is a powder with pyrolite composition that was used in the previous phase equilibrium study (e.g., Irifune, 1994). We conducted annealing experiments at 25-28 GPa and 1600-1800 ℃ for 6-600 min. Chemical compositions, microstructures and grain sizes of recovered samples were examined using a FE-SEM with an energy-dispersive analytical system.

Four phases of Mg-perovskite, Ca-perovskite, ferro-periclase and majoritic garnet were present in recovered samples annealed at 25 GPa and 1600-1800 ℃. The normalized grain size distribution in the recovered samples showed Gaussian-like shape and the largest grain size is smaller than three times of the mean grain size, suggesting that normal grain growth occurred. The grain growth rate is faster than that of the previous study (Yamazaki et al., 1996). Preliminary analysis of the kinetic data of Mg-perovskite obtained showed the smaller grain growth exponent of 4.3 than that reported in the previous study. On the other hand, three phases of Mg-perovskite, Ca-perovskite and ferro-periclase were present at higher pressure of 28 GPa and 1800 ℃, in which the volume fraction of Mg-perovskite increased compared to the four-phases experiment. While the microstructure and the grain size distribution in the three-phase assemblage was similar to those of the four-phase assemblage, the grain size was larger probably due to the smaller proportion of the secondary phases. Our preliminary results provide some insights into the grain-size evolution in the lower mantle and suggest that further quantitative grain growth data with possible lower mantle conditions are needed.

Keywords: lower mantle, multi-anvil, pyrolite, grain growth

Japan Geoscience Union Meeting 2014
(28 April - 02 May 2014 at Pacifico YOKOHAMA, Kanagawa, Japan)

SIT38-P07 Room:Poster Time:April 30 18:15-19:30

Grain boundary diffusion of noble metal elements in mantle composites

MATSUO, Naoya[1*] ; HIRAGA, Takehiko[1]

[1]Eartuquake Research Institute, The University of Tokyo

So far, it is not clear whether Earth's core and mantle have been chemically isolated through geological time. It has been believed that highly incompatible elements such as siderophile elements in the mantle minerals have not been moved from the core to the mantles so that the elemental abundance of highly siderophile elements (HSEs) in the core and mantle were determined when both were separated. Although HSEs are refractory, amounts of HSEs are very little in the mantle (Wood, 2006) so that these elements are expected to be highly concentrated in the core relative to the silicate mantle. However, a recent study has shown that incompatible elements can be concentrated and quickly diffuse at grain boundaries (Hiraga et al., 2004). If HSEs can diffuse from the core to the mantle, the concentration of HSEs in the mantle can change through Earth's history. Therefore, HSEs can be a good tracer to detect the chemical interaction of the core and the mantle.

We conducted grain growth experiments on Au particles in forsterite (Fo) aggregates at 1 atmosphere pressure and temperature of 1360 ℃. We prepared several sintered bodies which were made by dispersing 10vol% Au particles in Fo aggregates and then annealed for several hours. We observed these bodies using a scanning electronic microscope. In the result, Au particles changed their shape from spherical to polygonal. This is due to a balance of interfacial tensions between Au and Fo phases. Further, average grain size of Au particles was found to increase with time. Based on these observations, we conclude that Ostwald ripening of grains, by which Au atoms move from small particles to larger ones to minimize entire interfacial energies of the system, occurred in our experiment. Grain boundaries as diffusion paths should be responsible for Au diffusion. In this case, grain growth of Au particles will follow the relationship of $d^4-d_0^4=kt$, where d is the average grain size of Au particles after annealing, d_0 is the initial average grain size, k is the grain growth coefficient, and t is annealing time. Using the average grain size of each body, we calculated k. In addition, we estimated the interfacial energy of the system from the shape of Au particles and calculated the product of concentration of Au particles at grain boundaries, c, and diffusivity of Au atoms at grain boundaries, D.

Keywords: grain boundary diffusion, grain growth, core-mantle interaction

Japan Geoscience Union Meeting 2014
(28 April - 02 May 2014 at Pacifico YOKOHAMA, Kanagawa, Japan)

SIT38-P08 Room:Poster Time:April 30 18:15-19:30

The effect of partial melting on the mantle viscosity and electrical

SUEYOSHI, Kenta[1*] ; HIRAGA, Takehiko[1]

[1]Earthquake Research Institute, University of Tokyo

In this study, in order to know the change in mantle viscosity and electrical conductivity during partial melting, which corresponds to decompression melting of ascending mantle beneath mid-ocean ridge, mantle analogue sample was synthesized and used to measure its viscosity and electrical conductivity under atmospheric pressure and high temperature conditions. The sample has lherzolite composition of olivine (50%), orthopyroxene(40%) and clinopyroxene(10%) with addition of 0.5 vol% spinel. Constant force was applied to the sample under increasing the temperature where its range includes sample solidus. Sample viscosity and the electrical conductivity by the impedance measurement were calculated for every temperature. We particularly examined how viscosity and conductivity change when the sample transforms from melt-free to melt-bearing system. Temperature ranged from 1100 to 1390 ℃, which resulted in the change of melt fraction (ϕ) from 0 to 0.09, where the melt composition becomes enriched in clinopyroxene component as the temperature increases.

We observed a continuous and gradual reduction of sample viscosity with increasing temperature. The effect of the increasing melt fraction on the sample viscosity should have been added to the viscosity change simply due to thermally activation process. There is a linear relationship between measured 1/T and $\log(1/\eta)$,which goes well with the previous proposed empirical expression of flow law that, which is an function of melt fraction.

Analyzing the observed viscosity change with temperature with this law, the apparent activation energy of 970 kJ/mol is obtained at a temperature range of 1220 ℃ to 1340 ℃ and the effect of increasing melt fraction on sample viscosity roughly corresponds to the activation energy of ˜+35 kJ/mol. The activation energy on the melt ?free system is estimated to be 935 kJ/mol. This value is close to the activation energy of the dislocation creep of orthopyroxene and clinopyroxene indicating that the sample viscosity was essentially controlled by deformation of pyroxenes.

Electrical conductivity did not change dramatically when the experimental temperature reached and exceeded the sample solidus. Grain size dependency on the conductivity was observed at all temperature conditions indicating that the conductivity is simply determined by grain boundary conductivity even at higher melt fraction condition, probably due to fine grain size of the samples. Compared with previously reported grain boundary conductivity in the melt-fee forsterite system, grain boundaries in our sample have 3 to 4 times higher conductivity indicating that the pyroxene grain boundaries have a large effect on the bulk sample conductivity in our experiment.

In this study, it was demonstrated that previously proposed empirical flow law as a function of melt fraction can approximate the viscosity change of the mantle during its transition from melt-free to melt-bearing Taking into account of the incremental rate of melt fraction with temperature and the connectivity of intergranular melt in the mantle highly depend on the volume fraction of the pyroxenes and spinel phases, mineral mode in the mantle should have substantial effects on the mantle rheology and electrical conductivity during mantle melting.

Keywords: rheology, rhelzolite, melt, viscosity, electrical conductivity

Japan Geoscience Union Meeting 2014
(28 April - 02 May 2014 at Pacifico YOKOHAMA, Kanagawa, Japan)

SIT38-P09 Room:Poster Time:April 30 18:15-19:30

Stress calibration of Griggs-type deformation apparatus with solid salt assemblies

KIDO, Masanori[1*] ; MUTO, Jun[1] ; NAGAHAMA, Hiroyuki[1]

[1]Department of Earth Sciences, Tohoku University

Mechanical properties of rocks and minerals can be quantitatively studied by deformation experiments under high-temperature and high-pressure conditions relevant to the Earth's interior. There are several types of deformation apparatus using different confining media such as gases, liquids or weak solids (e.g., Tullis and Tullis, 1986). Liquid medium apparatus have the disadvantage that they cannot be used for temperatures above 500 ℃ because of prevention from alteration of oil at high temperature. Solid medium apparatus can provide us high pressure safely and stably for a long time. However, stress accuracy is not high due to frictional forces between pressure medium and load piston or samples (e.g., Tullis and Tullis, 1986). Gas apparatus has most accurate stress measurement because of the usage of internal load cell; thus measured stresses do not include frictional forces. However, experiments are restricted to confining pressures less than 200 MPa in Japan due to safety issues on the usage of high-pressure gas. Therefore, solid medium apparatus is necessary for generating high temperature and high pressure required to investigate rheological behaviors of rocks and minerals in lower crust or uppermost mantle.

Recently, comparisons of mechanical results obtained for metals at the same confining pressure, temperatures and strain rates deformed in a Griggs apparatus with solid salt assemblies (SSA) and a gas apparatus provide calibration for Griggs apparatus with SSA (Holyoke and Kronenberg, 2010). This calibration law allowed differential stresses to be measured accurately to within $\pm$30 MPa. However, we have not been able to reproduce elastic, yielding and post-yield behaviors because the calibration law was obtained by the comparison of strengths at 5% strain of mechanical results. Calibration law for measured stresses using Griggs apparatus in all deformation behaviors are required for revealing detailed rheological behavior of rocks and minerals.

In this study, we performed axial compression experiments on high-purity nickels to measure differential stresses using a Griggs apparatus with SSA at Tohoku University. Samples were given by Drs. Holyoke and Kronenberg. Experimental conditions were confining pressures of 300 and 1200 MPa, temperatures of 600, 700, and 800 ℃ and strain rates of 2×10^{-4}, 2×10^{-5} and 2×10^{-6} /s. Measured differential stresses agreed with results of the former study within $\pm$30 MPa under the identical confining pressure of 300 MPa. However, differential stresses were larger with confining pressure. We analyzed obtained mechanical data of nickels based on the high temperature viscoelastic constitutive law developed by Shimamoto (1987). We made the master curve which normalized temperature and strain conditions. In the same way, we also made the master curve from mechanical data of nickels using a gas apparatus (mechanical data are from Holyoke and Kronenberg, 2010). Master curves were made of mechanical data of the identical material between Griggs apparatus and gas apparatus under normalized temperature and strain conditions. Therefore, difference in master curves is thought to be derived from apparatus and assembly. We derived calibration law for Griggs apparatus from difference in master curves. Applying this calibration law to differential stresses of nickels obtained using Griggs apparatus with SSA, it became possible to reproduce gas apparatus's differential stresses not only steady state but also elastic, yield and post-yield behaviors within the systematic error of $\pm$30 MPa. However, the error was $\pm$70 MPa when the calibration law was applied to the mechanical data of carbonate rock. Moreover, unlike gas apparatus, measured differential stresses using Griggs apparatus tend to become larger with confining pressures. Therefore, it is necessary to investigate the effect of confining pressures on measured stresses in the calibration law.

Keywords: rheology, deformation experiment, calibration of Griggs-type apparatus

Japan Geoscience Union Meeting 2014
(28 April - 02 May 2014 at Pacifico YOKOHAMA, Kanagawa, Japan)

SIT38-P10 Room:Poster Time:April 30 18:15-19:30

Preliminary experiments on in-situ stress-strain measurements of Ca-Pv and Mg-Pv up to 23 GPa

TSUJINO, Noriyoshi[1*] ; YAMAZAKI, Daisuke[1] ; YOSHINO, Takashi[1] ; SAKURAI, Moe[2] ; NISHIHARA, Yu[3] ; HIGO, Yuji[4]

[1]ISEI, Okayama Univ., [2]Tokyo tech., [3]GRC, Ehime Univ., [4]JASRI

In order to discuss mantle dynamics in the Earth's interior, knowledge of viscosity of the Earth's lower mantle, which is the highest of the whole mantle, is important. Viscosity models of the Earth's lower mantle were reported by geophysical observations. However, observation values of viscosity have large variety (2˜3 order magnitude). Although determination of viscosity of lower mantle minerals by high pressure experiments is needed to understand mantle dynamics, stress-strain relationship for $MgSiO_3$-perovskite (Mg-Pv) and $CaSiO_3$-perovskite (Ca-Pv), which are principal minerals of the Earth's lower mantle, are not reported due to difficulty of high pressure deformation experiments. In this study, we tried in-situ stress-strain measurements of Ca-Pv and Mg-Pv up to 23.0 GPa.

In-situ uniaxial deformation experiments were conducted using a deformation DIA apparatus (SPEED-Mk.II) as Kawai-type apparatus at SPring-8 BL04B1. Experimental conditions of Ca-Pv and Mg-Pv are 13.8 GPa, 1473 K and 23.0 GPa, 1273 K, respectively. cBN anvils, which was transparent material against X-ray, was used along X-ray path. Two-dimensional X-ray diffraction patterns were taken for 120-180 s using CCD detector. To calculate the stress magnitude from the X-ray diffraction data, we used a model of stress-lattice strain relationship (Singh et al. 1998),

$d_{hkl}(\psi) = d_{0hkl}\,[1+(1-3\cos^2\psi)\,\sigma/6\,G_{hkl}]$ (1)

where d_{hkl} is the d-spacing measured as a function of azimuth angle ψ, d_{0hkl} is the d-spacing under the hydrostatic pressure, G_{hkl} is the appropriate shear modulus for a given hkl, and σ is the uniaxial stress. Pressure and stress were estimated using Ca-Pv (110) (200) and Au (111) diffraction in Pressure marker (Au : Fo = 1 : 2 volume ratio) at deformation experiments of Ca-Pv and Mg-Pv, respectively. An X-ray radiograph of the strain markers was taken using an imaging system composed of a YAG crystal and a CCD camera with an exposure time of 60 s.

Uniaxial stress of Ca-Pv at 13.8 GPa, 1473 K and ˜1.2×10^{-5} /s and Mg-Pv at 23.0 GPa, 1273 K and ˜1.5×10^{-5} /s were estimated as ˜2GPa and ˜0.25 GPa , respectively. Stress of Mg-Pv was significantly smaller than that of Ca-Pv though temperature condition of Mg-Pv was lower than that of Ca-Pv. This fact is doubtful. This reason is thought that stress estimated by Au was much smaller than that of Mg-Pv because of framework made by Ringeoodite, which was polymorphic phase of Fo in pressure marker.

Keywords: In-situ measurements, deformation experiments, Stress, Strain, Perovskite, The Earth's lower mantle

Japan Geoscience Union Meeting 2014
(28 April - 02 May 2014 at Pacifico YOKOHAMA, Kanagawa, Japan)

SIT39-01 Room:416 Time:May 2 09:00-09:15

A new form of the dynamics equation of Maxwellian visco-elastic media

MATSUNO, Taroh[1*]

[1]Japan Agency for Marine-Earth Science and Technology

Dynamical property of the earth's interior down to the core-mantle boundary has so far been considered to be a Maxwellian visco-elastic medium. It behaves as an elastic body for short time-scale phenomena, while on a very long time-scale it shows fluid-like behavior. So the Navier-Stokes equation for viscous fluids is considered to be appropriate for describing mantle convection, and numerical simulations have been made based on the equation.

As a phenomenon for which both elastic body property and viscous fluid property are essential post-glacial uplift has been discussed based on the constitutive equation proposed by Maxwell. However, so far most of studies apply Laplace transform to expressing time evolution, so it is not possible to treat this problem by use of finite difference method, just like general circulation models of atmosphere and oceans. Thus it is not possible to extend numerical simulation of mantle convection to include elastic property of the plate near the earth's surface.

With intention to overcome this difficulty to enable us to conduct numerical simulations of mantle-plate general circulation, a new formulation of dynamics equations for Maxwellian visco-elastic media is attempted in this study

Keywords: Maxwellian visco-elsatic media, visco-elastic medium dynamics, mantle convection, plate-mantle coupling simulation

Japan Geoscience Union Meeting 2014
(28 April - 02 May 2014 at Pacifico YOKOHAMA, Kanagawa, Japan)

SIT39-02 Room:416 Time:May 2 09:15-09:30

Effects of Al content on water partitioning between Opx and Ol: Implications for lithosphere-asthenosphere boundary

SAKURAI, Moe[1*] ; TSUJINO, Noriyoshi[2] ; SAKUMA, Hiroshi[3] ; KAWAMURA, Katsuyuki[4] ; TAKAHASHI, Eiichi[1]

[1]Earth and Planet. Sci., Tokyo Inst. Tech., [2]ISEI, Okayama, [3]NIMS, [4]Enviromental Sci., Okayama Univ.

Most minerals in the Earth's upper mantle contain small amounts of hydrogen (i.e. "water"), structurally bound as hydroxyl. Water has an important influence on the behavior of rock system. This small amount of water has an important influence on the behaviours of rock systems. A large viscosity contrast of more than two orders of magnitude was detected at depths of 70 km to 100 km beneath ocean and was defined as the lithosphere-asthenosphere boundary [1]. The origin of the lithosphere-asthenosphere boundary remains an enigma. The water distribution in the Earth is critical to the nature of the boundary. For example, Mierdel et al. (2007)[2] indicated that a high water solubility in aluminous orthopyroxene among mantle geotherm in the Earth's upper mantle would effectively contribute to a stiffening of the lithosphere. Therefore, precise knowledge on the distribution of water among mantle minerals is very important for understanding the Earth's dynamics. The Earth's uppermost mantle is composed mainly of olivine (Ol), orthopyroxene (Opx), clinopyroxene (Cpx), spinel, and garnet. In particular, Ol accounts for a large proportion (60 vol.%) of the Earth's uppermost mantle. In addition, Opx, which contains significantly more water than does Ol in the mantle xenolith, is the second phase of the Earth's uppermost mantle. The FeO content in mantle Ol shows very limited variation in range, whereas the Al content of Opx in the Earth's upper mantle decreases significantly with increasing pressure [3] Therefore, the variation of Al content in mantle minerals can be important for the solubility of water in mantle minerals.

To investigate the partitioning coefficient of water between Opx and Ol ($D_{(Opx/Ol)}$) under low-water concentrations (3 ~ 387 wt. ppm) similar to the Earth's mantle conditions, high-pressure experiments have been conducted at pressures of 1.5-6 GPa and a temperature of 1573 K. The experiments were performed with Kawai-type multi-anvil and piston-cylinder apparatus by using starting materials of natural Ol and synthetic Opx with various Al contents. The water contents were obtained with a vacuum type Fourier transform infrared spectrometer (*Jasco*: FT-IR6100, IRT5000). Water content of minerals was calculated based on Paterson's calibration [4]. IR-spectra of Ol and Al-bearing Opx in this study are similar to those obtained by high-pressure experiments [5] and natural rocks [6], respectively. It is believed that broad bands in IR spectra of natural Opx are due to effect of crystal distortion by large Al substitution. On the contrary, IR-spectra of Al-free Opx are not consistent with those reported by Rauch and Keppler (2002) [7] likely because of the large difference of water fugacity. $D_{(Al-freeOpx/Ol)}$ is ~ 1 at all pressure conditions. However, the water contents of Al-bearing Opx are significantly larger than those of Ol at the same conditions. In addition, the effect of Al concentration in Opx on $D_{(Opx/Ol)}$ becomes larger with increasing pressure. The high Al content in Opx significantly increases $D_{(Opx/Ol)}$ and the trend increases with increasing pressure. $D_{(Opx/Ol)}$ drops sharply at the pressure at which the Al concentration of Opx becomes nearly 0 in the Earth's mantle conditions.

These results imply that viscosity of the upper mantle decreases sharply at depths deeper than those in which orthopyroxene contains no Al. The dramatic change of $D_{(Opx/Ol)}$ may explain the lithosphere-asthenosphere boundary beneath oceans and continents.

[1] D.L. Anderson, (1989) Blackwell Scientific, Boston [2] K. Mierdel et al. (2007) Science, 315, 364-368 [3] M. Obata, (1976) Am. Mineral., 61, 804-816 [4] M. S. Paterson, (1982) Bull. Mineral., 105, 20-19 [5] Q. Bai and D.L. Kohlsted, (1993) Phys. Chem. Minerals, 19, 460-471 [6] K. Grant et al., (2007) Contrib Mineral Petrol, 154, 15-34 [7] M. Rauch, H. Keppler, (2002) Contrib. Mineral. Petrol., 143, 525-536

Keywords: water partitioning coefficient, olivine, orthopyroxene, viscosity, FT-IR, lithosphereasthenosphere

Japan Geoscience Union Meeting 2014
(28 April - 02 May 2014 at Pacifico YOKOHAMA, Kanagawa, Japan)

SIT39-03 Room:416 Time:May 2 09:30-09:45

Acoustic velocities of MgGeO3 gel at high pressure by Brillouin scattering

KAWADAI, Tomofumi[1*] ; MURAKAMI, Motohiko[1] ; OHTANI, Eiji[1]

[1]Tohoku University

Properties of silicate melts are essential for understanding evolution and dynamic behavior of the Earth and terrestrial planets. In the shallow mantle melting processes the density contrast between melts and crystals is well studied, but studies on the deep melting near the core-mantle boundary are still limited due to technical difficulties. The studies of amorphous material, analogs of melt, at high pressure can provide valuable insights about melts in the deep mantle. The Brillouin scattering method is suitable for velocity measurements of amorphous materials. It has been suggested that the change in coordination in the melt or glass structure reflects to the change in acoustic velocity. Thus we conducted sound velocity measurement using the Brillouin scattering method in diamond anvil cell at high pressure. We report in situ high-pressure acoustic velocity measurements of $MgGeO_3$ gel, an analogue of the $MgSiO_3$ melt, revealing the gradual coordination change of Ge from four- to six at least up to 80 GPa. We will conduct experiments at higher pressure in order to confirm the possible Ge coordination change in the gel expected to exist in the terrestrial and extraterrestrial planets.

Keywords: sound velocity measurement, high-pressure experiment, mantle dynamics, silicate melts, super-Earth

Japan Geoscience Union Meeting 2014
(28 April - 02 May 2014 at Pacifico YOKOHAMA, Kanagawa, Japan)

SIT39-04 Room:416 Time:May 2 09:45-10:00

Measurement of differential P-wave travel time between two BBOBSs with Correction for crustal reverberation

OBAYASHI, Masayuki[1*] ; YOSHIMITSU, Junko[1] ; ISHIHARA, Yasushi[1] ; SUETSUGU, Daisuke[1]

[1]JAMSTEC

Seismic observations under the ocean are very important to investigate three-dimensional structure of the whole mantle. However, it is difficult to pick up arrival times of P-waves because noise level of broadband ocean bottom seismometer (BBOBS) is in general high in the period range more than 5 sec. Instead of picking arrival times, differential travel times between two BBOBSs have been measured by cross-correlating the waveforms at a period of around 10 sec or more (e.g. Toomey et al. 1998, Tanaka et al., 2009).

The resolution of P-wave tomography become high effectively by taking dispersion of P-wave travel time into account with the finite frequency theory (e.g. Obayashi et al. 2013 JpGU meeting), and its effect is expected to be significant under the ocean where the observations have been sparse. Obayashi et al. (2004) showed dispersion of PP is generated by interference of crustal reverberations under its bounce point. The reverberation under the station also affects a direct P-wave. Especially the effect of the seawater reverberation is significant.

Obayashi et al. (2013) proposed a method of correction for such reverberations to measure differential travel times between any two stations. In this method a waveform is convolved by the response calculated for the crustal structure under the other station.

We applied this method to the BBOBS array at French Polynesia. In the case of the measurement between a BBOBS and a island station, the waveforms of the two stations become similar each other after the correction, suggesting the correction is effective. We report the characteristics of the observed dispersions and the very first result of P-wave tomography using the new observations.

Keywords: crustal reverberation, broadband ocean bottom seismometer, tomography

Japan Geoscience Union Meeting 2014
(28 April - 02 May 2014 at Pacifico YOKOHAMA, Kanagawa, Japan)

SIT39-05 Room:416 Time:May 2 10:00-10:15

Small shear modulus of cubic CaSiO3 perovskite

KAWAI, Kenji[1*] ; TSUCHIYA, Taku[2]

[1]Department of Earth and Planetary Sciences, Tokyo Institute of Technology, [2]Geodynamics Research Center, Ehime University

Ca-perovskite (CaPv) is considered to be one of the most abundant minerals in the Earth's lower mantle (LM) and was suggested to have distinctly larger shear modulus than MgPv from static calculations and mean-field theory (Karki and Stixrude 1999; Stixrude et al. 2007). In this study the elasticity of cubic CaPv is reinvestigated using density functional constant-temperature first principles molecular dynamics simulations with strict calculation conditions. First, we computed the stable structure of CaPv and found that the cubic phase is more stable than the tetragonal and orthorhombic in the LM P,T condition. The thermal equation of state of CaPv was analyzed using the MD data set, which indicates its thermal properties including Gruneisen parameter quite similar to those of MgPv. Along the adiabatic temperature, CaPv was found to have higher density than the PREM and 12.5% iron-bearing MgPv. Next, we calculated elastic constants of cubic CaPv. Our new results clearly demonstrate that cubic CaPv does not have anomalously large shear modulus suggested by previous calculations with a small computation cell. This is because the cell applied in the previous studies is too small to allow the rotational phonon motion of SiO6 octahedra related to the zone boundary optic phonon instability. Acoustic wave velocities were finally determined from the elastic moduli, indicating no significant differences in velocities between CaPv and iron-bearing MgPv.

Keywords: Ca-perovskite, elasticity, lower mantle, first principles

Japan Geoscience Union Meeting 2014
(28 April - 02 May 2014 at Pacifico YOKOHAMA, Kanagawa, Japan)

SIT39-06 Room:416 Time:May 2 10:15-10:30

Seismic Constraints on an Enstatite Chondrite Earth

HOUSER, Christine[1*] ; GREAUX, Steeve[2] ; DU, Wei[2]

[1]Earth-Life Science Institute, Tokyo Tech, [2]Geodynamics Research Center, Ehime University

Recently, Javoy et al., EPSL, 2010 suggested the possibility that Earth had an initial enstatite chondrite composition due to their similar oxygen isotopes. Currently, the calculations of the bulk silicate Earth (BSE) are based on the assumption that the initial Earth began with a composition very close to that of a carbonaceous chondrite. Thus, it is necessary to evaluate whether the 1D seismic properties of the Earth are more consistent with an initial enstatite or chondritic composition. The BSE of an enstatite chondrite Earth (ECE) is different from that of a carbonaceous chondrite since the magnesium/silicon ratio is much lower for the former, resulting in a lower mantle that is almost devoid of Mg. Hence, the primitive lower mantle of an ECE consists mostly of iron-rich perovskite and pure silica. The seismic velocities of these phases are much slower than Mg-perovskite which, by itself, is faster than PREM (the slower MgO phase is necessary to match PREM velocities). However, the present-day lower mantle would be a mix of the primitive upper mantle (ie. pyrolite) and the Mg-depleted lower mantle. The latest mineral physics results are used to calculate possible 1-D seismic profiles of the Earth associated with these two scenarios and to compare with those observed for the Earth today.

Japan Geoscience Union Meeting 2014
(28 April - 02 May 2014 at Pacifico YOKOHAMA, Kanagawa, Japan)

SIT39-07 Room:416 Time:May 2 10:30-10:45

Thermal property modeling of the core-mantle boundary

TSUCHIYA, Taku[1*] ; DEKURA, Haruhiko[1]

[1]Ehime Univ

Lattice thermal conductivity of minerals under pressure and temperature is a key property to understanding dynamics and evolution of the Earth's interior. We recently established an efficient ab initio technique for calculating the thermal conductivity of silicate minerals with complex structure and chemistry (Dekura, Tsuchiya, Tsuchiya, PRL, 2013). Calculated lattice thermal conductivity of MgSiO3 perovskite agreed satisfactorily with experimental values at room temperature, and post-perovskite was found to have thermal conductivity quite different from perovskite's, indicating that the D" discontinuity is not only the phase transition boundary but also the conductivity boundary. Using the obtained results, we determine the effective conductivity of the lower mantle and estimate the energy flow across the core-mantle boundary (CMB). Our results demonstrate that the CMB heat flux could change significantly from place to place by reflecting temperature heterogeneity located atop the core. A large CMB heat flow recently suggested from the outer core side can be reconciled only by considering polycrystalline assemblages yielding high-thermal conductivity.

Keywords: First principles computation, Thermal conductivity, CMB heat flow

Japan Geoscience Union Meeting 2014
(28 April - 02 May 2014 at Pacifico YOKOHAMA, Kanagawa, Japan)

SIT39-08 Room:416 Time:May 2 11:00-11:15

Waveform inversion for localized 3-D seismic velocity structure in the lowermost mantle beneath the Western Pacific

KONISHI, Kensuke[1] ; KAWAI, Kenji[2] ; GELLER, Robert J.[3*] ; FUJI, Nobuaki[4]

[1]School of Earth and Environmental Sciences, Seoul National University, [2]Department of Earth and Planetary Sciences, Tokyo Institute of Technology, [3]Department of Earth and Planetary Science, Graduate School of Science, University of Tokyo, [4]Institut de Physique du Globe de Paris

We infer 3-D localized shear velocity structure in the lowermost 400 km of the mantle at the western edge of the Pacific large low shear velocity province (LLSVP) by applying waveform inversion to transverse component body-wave waveforms from the F-net seismic array in Japan. Our dataset consists of relatively long period (12.5-200 s) broad-band seismic waveforms of Tonga-Fiji deep focus and intermediate deep earthquakes. We conduct several tests to confirm the robustness of the inversion results. We find two low velocity zones at the bottom of the target region, with a high velocity zone in the middle, and a low velocity zone above the high velocity zone and contiguous with the two deeper low velocity zones at a depth of 200-300 km above the CMB. This supports the idea that the Pacific LLSVP may be an aggregation of small upwelling plumes rather than a single large thermochemical pile.

Keywords: Waveform inversion, Western Pacific, Mantle convection, Lowermost mantle, Plume cluster

Japan Geoscience Union Meeting 2014
(28 April - 02 May 2014 at Pacifico YOKOHAMA, Kanagawa, Japan)

SIT39-09 Room:416 Time:May 2 11:15-11:30

Compressional sound velocity and density measurements of hcp-Fe under core conditions

SAKAMAKI, Tatsuya[1*] ; OHTANI, Eiji[1] ; FUKUI, Hiroshi[2] ; KAMADA, Seiji[1] ; TAKAHASHI, Suguru[1] ; SAKAIRI, Takanori[1] ; TAKAHATA, Akihiro[1] ; SAKAI, Takeshi[4] ; TSUTSUI, Satoshi[5] ; BARON, Alfred[3]

[1]Tohoku University, [2]University of Hyogo, [3]RIKEN, [4]Ehime University, [5]SPring-8/JASRI

Sound velocity measurements of Fe and Fe-alloy at high temperature and high pressure are necessary to understand the Earth's inner core. Despite seismological observations providing density-sound velocity data of Earth's core, there are few experimental reports about sound velocity of hcp-Fe at ultrahigh pressure and temperature conditions. In order to push forward with research, we have developed a portable laser-heating system for diamond anvil cell, which is called COMPAT (Fukui et al., 2013). We have succeeded in measuring the sound velocity of hcp-iron up to 160 GPa and 3000 K by inelastic X-ray scattering measurements combining with a laser-heated diamond anvil cell. The obtained pressure and temperature dependence of the sound velocity suggest that compressional sound velocity of hcp-Fe at inner core boundary (330 GPa and 5500 K) is higher than that of Earth's inner core. Thus, we can conclude that the light elements or combination of the light elements and nickel in the inner core decreases both density and compressional sound velocity of hcp-Fe simultaneously under the inner core conditions.

Reference
Fukui et al., 2013. A compact system for generating extreme pressures and temperatures: An application of laser-heated diamond anvil cell to inelastic X-ray scattering. Review of Scientific Instruments 84, 113902; doi: 10.1063/1.4826497.

Keywords: Earth's core, sound velocity, density, high pressure and high temperature, inelastic X-ray scattering, laser-heated diamond anvil cell

Japan Geoscience Union Meeting 2014
(28 April - 02 May 2014 at Pacifico YOKOHAMA, Kanagawa, Japan)

SIT39-10 Room:416 Time:May 2 11:30-11:45

The P-V-T equation of state of liquid pure Fe and Fe-light elements alloys by ab initio molecular dynamics simulations

ICHIKAWA, Hiroki[1*] ; TSUCHIYA, Taku[1] ; OSUMI, Masanao[2]

[1]GRC, Ehime University and ELSI, Tokyo Institute of Technology, [2]Geodynamics Research Center, Ehime University

The equation of state (EoS) of pure Fe and Fe-light elements alloy liquids were calculated by means of ab initio molecular dynamics simulations at the outer core P-T conditions. In the outer core, many light elements, such as carbon, nitrogen, oxygen, hydrogen, sulfur, and silicon, have been proposed as possible constituents. The concentrations of these elements have been strongly debated for years. In this study, internally consistent thermodynamic and elastic properties of pure Fe and Fe-light elements alloys, in particular density, adiabatic bulk modulus, and P-wave velocity were analyzed in order to clarify the effect of light elements incorporation on seismically observable data. Then the results were compared with the seismological data of the Earth's outer core to confine the plausible compositions of the outer core. The new EoS model of liquid iron alloys as a function of pressure, temperature and fraction of light elements may serve as fundamental data for the composition model of the Earth's core.

Japan Geoscience Union Meeting 2014
(28 April - 02 May 2014 at Pacifico YOKOHAMA, Kanagawa, Japan)

SIT39-11 Room:416 Time:May 2 11:45-12:00

Simultaneous measurement of liquid Fe-C density and sound velocity at high pressure

SHIMOYAMA, Yuta[1*] ; TERASAKI, Hidenori[1] ; TAKUBO, Yusaku[1] ; URAKAWA, Satoru[2] ; KUWABARA, Souma[1] ; KATAYAMA, Yoshinori[3]

[1]Graduate School of Science, Osaka University, [2]Department of Earth Sciences, Okayama University, [3]Japan Atomic Energy Agency

The cores of terrestrial planets, such as Mercury, Mars and Moon are considered to contain some light elements. The effect of light elements on density and bulk modulus of liquid iron is necessary for estimating of these core compositions. Sound velocity of liquid iron alloys is also important for identifying light elements in the core by comparison with observed seismic data.

In this study, we have measured density and sound velocity of liquid Fe-C at SPring-8 beamline BL22XU. Density was measured using X-ray absorption method (Katayama et al., 1993) and sound velocity was measured using pulse-echo overlapping method (Higo et al., 2009). Experimental conditions were 1.2-2.9 GPa and 1650-1850 K. Obtained density values of this study were consistent with our previous results (Shimoyama et al., 2013). In sound velocity measurement, we could observe clear sample wave signal. Measured compressional wave velocity of liquid Fe-C was found to increase with pressure.

Keywords: Density, Sound velocity, liquid Fe-C

Japan Geoscience Union Meeting 2014
(28 April - 02 May 2014 at Pacifico YOKOHAMA, Kanagawa, Japan)

SIT39-12 Room:416 Time:May 2 12:00-12:15

Sound velocity and density measurement of liquid FeSi alloy by laser-shock compression

HOSOGI, Ryota[1*] ; YOKOYAMA, Naoya[1] ; SAKAIYA, Tatsuhiro[1] ; KONDO, Tadashi[1] ; TERASAKI, Hidenori[1] ; SHIGEMORI, Keisuke[2] ; HIRONAKA, Yoichiro[2]

[1]Graduate School of Science, Osaka University, [2]Institute of Laser Engineering, Osaka University

The internal structure of the earth is estimated by observing seismic wave. Comparing seismic wave observations and experimental data of sound velocity of iron(Fe), the composition of the Earth's core is not pure Fe. Several light elements (hydrogen, carbon, oxygen, silicon, sulphur, etc.) have been considered as the candidate of the composition of the Earth's core, but its composition is still unclear. In order to constrain the core composition, it is important to measure the sound velocity of iron alloys because it can be directly compared with the seismic wave. Silicon (Si) has been proposed as a major light element in the inner core [Mao et al., 2012]. So we measured the sound velocity of laser-shocked FeSi alloy in order to investigate the effect of Si for sound velocity of liquid Fe in the outer core condition.

The starting sample was prepared by synthesizing from mixture of Fe (99.98% purity) and Si (99.9% purity) slugs at arc furnace. The compositions of Fe and Si are 66.5 wt.% and 33.5 wt.%, respectively. We measured sound velocities and densities of FeSi at high pressure and high temperature conditions at the large laser facility in Institute of Laser Engineering, Osaka University. The sound velocities were measured by the x-ray radiography [Shigemori et al., 2012].

We obtained the sound velocity and density of FeSi at pressures around 700 GPa. It is seen that Si has the effect of increasing the sound velocity of liquid Fe. Comparing our experimental results and PREM model [Dziewonski and Anderson, 1981], Si may be contained up to 13.1 wt.% at 135 GPa, and up to 5.5 wt.% at 330 GPa in the outer core.

Japan Geoscience Union Meeting 2014
(28 April - 02 May 2014 at Pacifico YOKOHAMA, Kanagawa, Japan)

SIT39-P01 Room:Poster Time:May 2 14:00-15:15

Effects of hydrous rocks on behaviors of subducting slabs

NAKAO, Atsushi[1*] ; IWAMORI, Hikaru[2] ; NAKAKUKI, Tomoeki[3]

[1]Department of Earth and Planetary Sciences, Tokyo Institute of Technology, [2]Institute for Research on Earth Evolution, JAMSTEC, [3]Department of Earth and Planetary Systems Science, Hiroshima University

Introduction: It is widely accepted that Earth's deep mantle contains water in several tens to several hundreds ppm, and that the water causes plate tectonics, volcanoes in subduction zones, deep earthquakes, and large-scale transportation of hydrophilic elements. A number of previous numerical studies on water transportation in the deep mantle are performed. In theses simulations, constant plate velocities and/or fixed plate shapes are synthetically imposed. In this study, we systematically investigated water transportation into the deep mantle and how the water changes the spontaneous behavior of the slab using a numerical model of whole mantle convection without external forces.

Numerical Model: Based on 2-D fluid mechanics simulation (Tagawa *et al*., 2007, *EPS*), the motion of mantle rocks is calculated. Advection of hydrous rocks is calculated using a Marker-And-Cell method, and dehydration/hydration reactions are evaluated by experimentally determined phase diagrams of the hydrous basalt and peridotite (Iwamori, 2007, *Chem. Geol.*). Effects of the hydrous rocks are formularized in constitutive laws (*e.g*. Karato and Wu, 1993, *Science*) and a state equation; therefore, the water transportation and the motion of solid phase are interactive. Only two parameters r (= 0, 0.7, 1.0, 1.93) in constitutive laws (viscosity reduction by hydration) and β (= 0, 1.0, 2.0) in a state equation (density reduction by hydration) are treated as variable, and other settings are equalized.

Results and Discussion: The reaction path (p-T path) of subducting hydrous rocks in each result is the same as that of southwest Japan (Iwamori, 2007), and a hydrous ultramafic layer along the slab surface ($\sim$2000 ppmH_2O in NAMs) is formed beneath $\sim$200-km depth. Large hydration weakening seems essential for back arc spreading because the subducting slab causes tensile stress within the overlying continental plate, and then the expansive deformation is concentrated on the hydrous weak area. Comparing the results with each other, at large r, the subduction rate increases. This is because a hydrous layer reduces viscous resistance above the slab. In contrast, at large β, the subduction rate decreases. This is because the positive buoyancy of the hydrous layer partially canceled to the gravitational instability of the slab. The subduction rate significantly controls the velocity field of the corner flow in the mantle wedge. A rapid corner flow causes strong suction force along the slab surface, which determines the angle of subduction. This also causes effective heat advection from the deep mantle to the back arc, and that contributes rapid, sustainable back arc spreading. The analytical discussion enables us to understand why scenarios differ when r and β are changed. In east Asia, stagnant slabs and back arcs are widely distributed. To realize both, large r and small β are needed. This is because they require strong corner flow, but β declines it. Thus the slab shapes and the period of back arc spreading may constrain scales of hydrous buoyancy and hydrous weakening in the mantle wedge comparing with those in nature.

Keywords: water transportation, free convection, subduction dynamics, plate velocity, big mantle wedge

Japan Geoscience Union Meeting 2014
(28 April - 02 May 2014 at Pacifico YOKOHAMA, Kanagawa, Japan)

SIT39-P02 Room:Poster Time:May 2 14:00-15:15

Regional scale variation of splitting intensity observed in Japanese islands by Hi-net II

OGAWA, Naoto[1*] ; KAWAKATSU, Hitoshi[1] ; TAKEUCHI, Nozomu[1] ; SHIOMI, Katsuhiko[2]

[1]Earthquake Research Institute, the University of Tokyo, [2]National Research Institute for Earth Science and Disaster Prevention

To systematically investigate the spatial variation of seismic anisotropy around the Japanese islands, we measured the splitting intensity (SI) of teleseismic SKS and SKKS phases by Hi-net (Ogawa et al., 2013, SSJ). SI is first introduced by Chevrot (2000) as a method of measuring seismic anisotropy; it is based on cross-correlation of polarized waveforms, and can be modeled like the delay time of seismic tomography considering the effect of finite frequency (e.g., Favier and Chevrot, 2003). In this study, we extend our previous work by measuring SI for a large number of dataset recorded by the dense seismic station network, Hi-net. We use data from tilt-meters of Hi-net from October in 2000 to September in 2013. We have selected the recordings of SKS phases for epicentral distances between 90 and 135 degrees and SKKS beyond 105 degrees, and Mw larger than 6.0, resulting in a total number of events to be 189 that is much larger than the previous case. For the actual analysis, we apply a band-pass filter between 0.05 and 0.125 Hz, and the measurement error of each SI will be carefully estimated using a new formulation, as there appears an error in the Chevrot (2000)'s original treatment. The preliminary analysis indicates regional scale variations of SI patterns that apparently depend on the back azimuth of seismic event, which may be influenced by the subducting slabs.

Keywords: seismic anisotropy, splitting intensity

Japan Geoscience Union Meeting 2014
(28 April - 02 May 2014 at Pacifico YOKOHAMA, Kanagawa, Japan)

SIT39-P03 Room:Poster Time:May 2 14:00-15:15

Comparison of phase relations in pyrolite, MORB and harzburgite across 660-km discontinuity

ISHII, Takayuki[1*] ; KOJITANI, Hiroshi[1] ; AKAOGI, Masaki[1]

[1]Depertment of chemistry, Gakushuin University

Pyrolite is the model rock which composes the average upper mantle. It is accepted that 660-km seismic discontinuity is formed by post-spinel transition of pyrolite. MORB (mid-ocean ridge basalt) and harzburgite in slabs subduct to 660-km seismic discontinuity due to their higher densities than pyrolitic average mantle. It has been considered that the density cross-over between pyrolite and slab materials occurs due to post-spinel transition in pyrolite at the 660-km discontinuity, and MORB and harzburgite are trapped around the depth (e.g. Ringwood and Irifune, 1988). Therefore, the phase transition pressures of these mantle rocks are the important parameters to elucidate the dynamics around 660-km seismic discontinuity. We investigated detailed phase relations of pyrolite, MORB and harzburgite with multi-sample cell technique.

The starting materials were prepared from the oxide mixtures of pyrolite, MORB and harzburgite composition after McDonugh and Sun (1995) (excluding MnO, K_2O and P_2O_5), Melson et al. (1976) (P_2O_5) and Michael and Bonatti (1975), respectively. High-pressure and high-temperature experiments by quench method were performed at about 20-28 GPa and 1600-2200C for 2-10 hours using a Kawai-type 6-8 multianvil high-pressure apparatus at Gakushuin University. These samples were packed with pressure calibrants ($MgSiO_3$ or pyrope) in a Re multi-sample capsule with four holes. Temperature was controlled with a LaCrO3 heater and measured with a W5%Re-W26%Re thermocouple inserted in a Cr_2O_3-doped MgO pressure medium. Phases of recovered samples were identified with microfocus-Xray diffractometer and SEM-EDS.

In pyrolite at 1600-2200C, the mineral assemblage of $MgSiO_3$-rich perovskite (Mpv) + magnesiowustite (Mw) + garnet (Gt) + $CaSiO_3$-perovskite (Cpv) is stable at pressure range of 22-24 GPa, and changes to that of Mpv + Mw + Cpv above 24 GPa. The mineral assemblage of ringwoodite (Rw) + Gt + Cpv at 1600C transforms to that of Rw + Mw + Gt + Cpv due to transition of Rw to Gt + Mw at 1800-2000C, and Rw disappears perfectly above 2200C. In MORB, the mineral assemblage of Gt + stishovite (St) + Cpv changes to that of Mpv + St + Al-rich phase + Cpv with continuous post-garnet transition. In harzburgite at 1600C, the mineral assemblage of akimotoite (Ak) + Rw + Gt changes to that of Mpv + Mw by post-spinel transition after the Ak to Mpv transition. Above 1800C, no Ak was observed.

At 1600C, post-spinel transition in pyrolite occurred by about 0.5 GPa and 2 GPa lower pressure than that of harzburgite and post-garnet transition in MORB, respectively. The Clapeyron slope of post-spinel transition in harzburgite is larger than that of pyrolite, and both boundaries intersect at 2000C. From the comparisons of density profiles at 1600C, MORB and harzburgite have lower densities than pyrolite by post-spinel transition in pyrolite.

Keywords: post-spinel transition, post-garnet transition, 660-km discontinuity, pyrolite, MORB, harzburgite

Japan Geoscience Union Meeting 2014
(28 April - 02 May 2014 at Pacifico YOKOHAMA, Kanagawa, Japan)

SIT39-P04 Room:Poster Time:May 2 14:00-15:15

Melting experiments in the system Fe-Xe and Earth's missing xenon

MORI, Yuko[1*] ; HIROSE, Kei[2] ; TATENO, Shigehiko[1] ; OZAWA, Haruka[3] ; OHISHI, Yasuo[4]

[1]Dept. of Earth & Planetary Sciences, Tokyo Institute of Technology, [2]Earth-Life Science Institute, Tokyo Institute of Technology, [3]Japan Agency for Marine-Earth Science and Technology, [4]Japan Synchrotron Radiation Research Institute,

The abundances of noble gases in the Earth's atmosphere should be consistent with those in CI chondrite. However, xenon in the atmosphere is depleted relative to chondritic abundance, while lighter rare gases, Ne,Ar, and Kr, are less depleted. This is the so-called "missing xenon" problem and its reservoir has been discussed for a long time. Since xenon is too heavy to escape toward outer space, the missing xenon (Xe) might be hidden in the deep Earth.

The potential reservoirs are the mantle and core because xenon has a good reactivity under high pressure. Although extensive studies on the reactions of Xe and various mantle materials have been performed, none of those found a Xe reservoir (e.g., Sanloup et al., 2005; 2011; Brock et al., 2011). On the other hand, the alloying of iron with xenon has been expected based on the fact that Xe becomes metallic above 130 GPa (e.g., Eremets et al., 2000). While first-principle calculations suggested that the solubility of xenon in hcp iron is 0.8 mol% at Earth's core conditions (Lee et al., 2006), experimental study showed that the solid Fe-Xe reaction did not occur at least up to 155 GPa and 3000 K (Nishio-Hamane et al., 2010). Here we performed melting experiments in the Fe-Xe system to 86 GPa and 6450 K.

High pressure and temperature (P-T) conditions were generated in a laser-heated diamond-anvil cell. We used pure iron foil as a starting material. Xe was loaded cryogenically. Angle-dispersive X-ray diffraction (XRD) measurements in-situ at high P-T were conducted at BL10XU, SPring-8. The textural and chemical characterizations of recovered samples were made by using a field-emission-type scannning electron-microprobe (FE-SEM) equipped with energy dispersive x-ray spectrometry (EDS). Both cross section and surface of a sample were carefully examined by combining a focused Ga ion beam (FIB) with FE-SEM.

Any evidence for the reaction was not observed at least up to 83 GPa and 3810 K based on both XRD measurements and chemical analyses. On the other hand, chemical analysis on the sample recovered from 86 GPa and 6450 K, the highest P-T condition achieved in this study, showed Fe alloyed with up to ˜1.6 wt.% Xe as tiny grains. This sample had a difference in the texture between heated and unheated regions. We calculated the concentration of Xe in the entire molten area by assuming the heated region and the small grains of Fe-Xe alloy as a cylinder and spheres, respectively. The xenon content was estimated to be 0.02 wt. % for the heated area which is high enough to account for the missing xenon problem (10^{-10} wt.% Xe in the core). The present results could be a clue to solve the "missing xenon" paradox. Since the temperature of the present Earth's core is most likely lower than 6000 K, xenon might be incorporated into the core during Earth's early history at higher temperature.

Keywords: Missing Xe, melting experiments, High pressure and temperature, core

Japan Geoscience Union Meeting 2014
(28 April - 02 May 2014 at Pacifico YOKOHAMA, Kanagawa, Japan)

SIT39-P05 Room:Poster Time:May 2 14:00-15:15

Whole-mantle P-wave radial anisotropy tomography

KITAGAWA, Hiroki[1*] ; ZHAO, Dapeng[1] ; TOYOKUNI, Genti[1]

[1]RCPEVE, Tohoku Univ.

1. Introduction

When studying seismic anisotropy, it is generally assumed that the medium under study has a hexagonal symmetry (i.e., transverse isotropy). In most cases, the axis of symmetry is assumed in the vertical direction (i.e., azimuthal anisotropy) or in the horizontal plane (i.e., radial anisotropy). Seismic anisotropy is induced mainly by the lattice-preferred orientation (LPO) of anisotropic minerals, especially for the olivine in the mantle (e.g., Zhang & Karato, 1995; Tommasi et al., 2000; Kaminski & Ribe, 2001). Studying seismic anisotropy is very important for understanding the structure and dynamics of the Earth's interior (e.g., Silver, 1996). Many previous studies have investigated P-wave azimuthal anisotropy tomography for several regions including the Japan Islands. Recently, Wang & Zhao (2013) studied P-wave radial anisotropy tomography of the Kyushu and Tohoku subduction zones. In this work, we have attempted to conduct global tomography to understand 3-D P-wave radial anisotropy in the whole mantle.

2. Data and method

In this study we used 12,657 earthquakes recorded by 6765 seismic stations which were selected from the ISC-EHB catalog by Yamamoto & Zhao, 2010. About 1.4 million arrival times of P, pP, PP, PcP and Pdiff waves are used in the tomographic inversion. The method of radial anisotropy tomography by Wang & Zhao (2013) is combined with the flexible-grid global tomography of Zhao et al. (2013) to conduct the whole-mantle tomographic inversion in this work.

3. Result

In comparison with the isotropic tomographic model, our anisotropic tomography model results in a smaller root-mean-square travel-time residual, suggesting that the anisotropic tomography model fits the data better. The isotropic component of this model is very consistent with the previous isotropic tomography. In upper mantle, low-velocity anomalies along the Pacific Rim, and high-velocity anomalies under the stable continents are visible. In addition, low-velocity anomalies exist from the surface down to the core-mantle boundary under South Pacific and East Africa, which represent two superplumes. The anisotropic results show that vertical velocity is greater than horizontal velocity under some regions such as South Pacific, which may reflect the mantle upwelling.

References

Kaminski & Ribe (2001) A kinematic model for recrystallization and texture development in olivine polycrystals. Earth Planet. Sci. Lett. 189, 253?267.

Silver (1996) Seismic anisotropy beneath the continents: Probing the depths of geology. Ann. Rev. Earth Planet. Sci. 24, 385?432.

Tommasi, Mainprice, Canova & Chastel (2000) Viscoplastic selfconsistent and equilibrium-based modeling of olivine lattice preferred orientations: Implications for the upper mantle seismic anisotropy. J. Geophys. Res. 105, 7893?7908.

Wang & Zhao (2013) P-wave tomography for 3-D radial and azimuthal anisotropy of Tohoku and Kyushu subduction zones. Geophys. J. Int. 193, 1161-1181.

Yamamoto & Zhao (2010), Whole-mantle P-wave tomography -Tohoku model-, Chikyu monthly, 32, 312-324.

Zhang & Karato (1995) Lattice preferred orientation of olivine aggregates deformed in simple shear. Nature 375, 774?777.

Zhao, D., Y. Yamamoto, T. Yanada (2013) Global mantle heterogeneity and its influence on teleseismic regional tomography. Gondwana Res. 23, 595-616.

Keywords: tomography, mantle, anisotropy tomography

Japan Geoscience Union Meeting 2014
(28 April - 02 May 2014 at Pacifico YOKOHAMA, Kanagawa, Japan)

SIT39-P06 Room:Poster Time:May 2 14:00-15:15

Melting experiments on the MgO-$MgSiO_3$ system using double CO_2 lasers heated diamond anvil cell

OHNISHI, Satoka[1*] ; KIMURA, Tomoaki[1] ; KUWAYAMA, Yasuhiro[1]

[1]Geodynamics Research Center, Ehime University

Seismological studies suggest the presence of ultralow-velocity zones (ULVZ) near the core mantle boundary (CMB). Partial melting of the lower mantle materials has been proposed to explain these zones, but experimental validation at the appropriate temperature and pressure regimes remains challenging. The melting curve of the lower mantle material is a key to constrain the existence of melt at the base of the mantle. A laser heated diamond anvil cell (LHDAC) provides an enabling tool for determination of melting temperatures of materials under high *P-T* conditions. Although YAG, YLF lasers (the wavelengths are about 1 μm) have been generally used for LHDAC experiments, the use of metal absorber is required to heat silicate materials. However, the thermal absorber may cause a chemical reaction and a temperature gradient in the sample. The accuracy of temperature determination is suffered from the chemical reaction and the temperature gradient. In contrast, the CO_2 laser with the wavelength of about 10 μm can directly heat silicate materials. For the minimization of temperature gradients, double-sided heating system for LHDAC was suggested by Shen *et al*. (1996). This technique using the YAG laser has been widely used to study the behavior of materials under high *P-T* conditions. However, the double CO_2 laser heating system has not been used due to the wavelength of this laser is different from that of visible light.

The requirements for the pressure medium in laser heating experiments are low thermal conductivity and chemical inertness. Ar, which is a noble gas, is one of the suitable pressure mediums. However, loading Ar into the DAC is difficult under room temperature and ambient pressure. Therefore, a simplified method to load Ar into the DAC is required. In this study, I established new experimental technique for the minimization of temperature gradients and chemical reactions and performed melting experiments of the lower mantle materials using LHDAC.

First, a double-sided heating system using CO_2 laser was developed by separating optical elements. This system consists of the heating system using two CO_2 lasers which have the high power (100 W), the observation systems and the temperature measurement system. By using lenses designed for the CO_2 laser wavelength, the laser system is separated from observation and temperature measurement system. Two dimensional images and radiation spectrums are observed by Charge Coupled Device (CCD) camera and spectrometer, respectively.

Second, a simplified method to load Ar into the DAC was developed by the cryogenic technique. In this technique, Ar is cooled using liquefied N_2 until it forms a liquid, and the liquefied Ar is loaded into the sample chamber of the DAC. Cu was used to enhance cooling efficiency.

Finally, I performed melting experiments of the lower mantle materials using the double CO_2 lasers heated diamond anvil cell and Ar as the pressure medium. I used forsterite (Mg_2SiO_4) and mixtures of MgO and $MgSiO_3$ as the starting material. After the complete pressure release, the sample was recovered from the DAC and examined by FE-SEM. From the surface texture of recovered samples, I discussed melting temperatures of the lower mantle materials under high *P-T* conditions.

The double CO_2 laser heating and loading Ar methods developed in this study could powerful tool for determination of melting temperatures of the lower mantle materials.

Japan Geoscience Union Meeting 2014
(28 April - 02 May 2014 at Pacifico YOKOHAMA, Kanagawa, Japan)

SIT39-P07 Room:Poster Time:May 2 14:00-15:15

Ultra high pressure generation using the double-stage diamond anvil cell

SAKAI, Takeshi[1*] ; YAGI, Takehiko[1] ; OHFUJI, Hiroaki[1] ; IRIFUNE, Tetsuo[1] ; OHISHI, Yasuo[3] ; HIRAO, Naohisa[3] ; SUZUKI, Yuya[4] ; KURODA, Yasushi[4] ; ASAKAWA, Takayuki[4] ; KANEMURA, Takashi[4]

[1]Geodynamics Research Center, Ehime University, [2]Earth-Life Scinece Institute, Tokyo Institute of Technology, [3]Japan Synchrotron Radiation Research Institute, [4]HITACHI High-Technologies

1 TPa region is still far frontier for the high pressure physics. The maximum pressure generated by diamond anvil cell is about 400 GPa (Akahama and Kawamura, 2010). On the other hand, recently Dubrovinsky et al. (2012) reported the generation of 640 GPa using double stage diamond anvil cell. This new technique makes 1TPa reagion a realistic goal for static compression experiments. But there are some technical difficulties such as a second-stage anvil's shape controllability, shift under pressure, and the difficulty of a sample filling. These problems depress the reproducibility of experiment.

In this study, second-stage microanvils were made by focused ion beam system from the nano-polycrystalline diamond (NPD) or single crystal (SC) diamond. Micro manufacturing using focused ion beam system enables us to control anvil shape, process any materials (NPD, SC and also sample), and fill the sample between the second-stage anvil gap precisely. Using this method, we generated up to 340 GPa. This method has a high reproducibility of the experiment. Thus, we can optimize the experimental parameters such as an anvil shape, confining pressure and so on.

Keywords: nano-polycrystalline diamond (NPD), microanvil

Japan Geoscience Union Meeting 2014
(28 April - 02 May 2014 at Pacifico YOKOHAMA, Kanagawa, Japan)

SIT39-P08 Room:Poster Time:May 2 14:00-15:15

Ab initio molecular dynamics study on a phase separation in liquid Fe-O

OHSUMI, Masanao[1*] ; TSUCHIYA, Taku[1] ; ICHIKAWA, Hiroki[1]

[1]Geodynamic Research Center, Ehime University

The Earth's outer core is mainly composed of liquid Fe-Ni alloy. The density of the outer core is, however, ˜10% smaller than this alloy. The density deficit indicates that substantial amount of light elements are present in the outer core [Birch, 1964]. Recent seismological observations proposed that seismic wave velocity is ˜3% slower than PREM below a few hundred kilometers of the CMB [Helffrich and Kaneshima, 2010]. The low-velocity anomaly is considered to be cause by stratification. However, mechanisms of the stratification have not been clarified yet. One possible cause is phase separation into Fe-rich and light element-rich liquid. Oxygen is one of the most important light elements, because an iron-oxygen phase separation was observed experimentally at low-pressure condition [Tsuno et al., 2007]. This immiscible behavior is, however, still unclear at the outer core pressure.

In this study, we calculated liquid Fe-O alloy at the outer core condition by means of *ab initio* molecular dynamics simulations. First, we analyzed local structures of liquid Fe-O alloy to detect signs of phase separation. Second, we evaluated its excess enthalpy. Both indicate that the liquid was well-mixed. Finally, we computed P-wave velocity in liquid Fe-O alloy. P-wave velocity was found to increase with increasing the oxygen concentration. All these results suggest that the simple enrichment process is less suitable to explain the low-velocity anomaly.

Keywords: ab initio molecular dynamics simulation, phase separation, liquid Fe-O alloy

Japan Geoscience Union Meeting 2014
(28 April - 02 May 2014 at Pacifico YOKOHAMA, Kanagawa, Japan)

SIT39-P09 Room:Poster Time:May 2 14:00-15:15

In situ X-ray observations of phase transitions in MgCr2O4 to 30 GPa using Kawai-type multianvil apparatus

KUNIMOTO, Takehiro[1*] ; IRIFUNE, Tetsuo[1] ; FUJINO, Kiyoshi[1]

[1]Ehime University

Phase relations in $MgCr_2O_4$ (magnesiochromite) have been studied up to 30 GPa and 1600 ℃, using a large volume Kawai-type multianvil apparatus and in situ X-ray diffraction measurements system installed at SPring-8/BL04B1. $MgCr_2O_4$ spinel dissociates into $Mg_2Cr_2O_5$ (orthorhombic type) + Cr_2O_3 (eskolate) at 9 GPa and 1200 ℃, and then reunion to higher pressure phase ($CaTi_2O_4$ type) at 22 GPa and 1200 ℃. Moreover, another high-pressure phase was observed above $CaTi_2O_4$ type structure phase, and this phase was unquenchable to ambient condition. In addition, pressure-induced phase transition in $MgCr_2O_4$ was confirmed without decomposition under cold compression process. In this cause, Magnesiochromite is directly transformed to high-pressure phase through the mixture of spinel and high-pressure phase. In this study, $CaFe_2O_4$ type and ε-phase, which reported in earlier studies in $MgAl_2O_4$ were not observed. The Birch-Murnaghan equation of state was used for least-squares fitting of the volume data (assuming $K_0{}'$ =4). Thus, determined zero-pressure bulk modulus (K_0) of the $CaTi_2O_4$ type $MgCr_2O_4$ was 195 GPa.

In this presentation, we will discuss further details of high-pressure phase relation and physical properties of high-pressure phases in $MgCr_2O_4$ series.

Keywords: Magnesiochromite, in situ X-ray diffraction measurement, Kawai-type multianvil apparatus, phase transition

Japan Geoscience Union Meeting 2014
(28 April - 02 May 2014 at Pacifico YOKOHAMA, Kanagawa, Japan)

SIT39-P10 Room:Poster Time:May 2 14:00-15:15

Sound velocities of laser-shocked Fe-Ni alloys under Earth core conditions

SAKAIYA, Tatsuhiro[1*] ; YOKOYAMA, Naoya[1] ; HOSOGI, Ryota[1] ; KONDO, Tadashi[1] ; TERASAKI, Hidenori[1] ; SHIGEMORI, Keisuke[2] ; HIRONAKA, Yoichiro[2]

[1]Graduate School of Science, Osaka University, [2]Institute of Laser Engineering, Osaka University

When we consider the structure of Earth's interior, the sound velocity is one of the important physical properties of the interior materials because it can be directly compared with the seismological data (1) which can yield the physical properties of the Earth's interior. Cosmochemical data and the composition of iron meteorites suggest that Earth's core contains mainly Fe-Ni alloy with 5-25 wt.% Ni. Although Lin et al. (2) and Kantor et al. (3) measured compressional sound velocities of Fe-Ni alloys at room temperature by inelastic x-ray scattering (IXS) at diamond anvil cell (DAC), the sound velocity data of liquid Fe-Ni alloys is very few (4).

We performed laser-shock experiments of liquid Fe-Ni alloys at HIPER system of Gekko-XII laser in Institute of Laser Engineering, Osaka University (5). Sound velocities were measured by side-on radiography (6, 7). We obtained sound velocities of Fe-Ni alloys at pressures up to 770 GPa. The sound velocity of Fe-Ni alloy was about 10% lower than that of liquid Fe at inner core boundary (ICB) pressure.

Part of this work was performed under the joint research project of the Institute of Laser Engineering, Osaka University.

References

1. A.M. Dziewonski, D.L. Anderson, Phys. Earth Planet. Inter. 25, 297 (1981).
2. J.F. Lin et al., Geophys. Res. Lett. 30, 2112 (2003).
3. A.P. Kantor et al., Phys. Earth Planet. Inter. 164, 83 (2007).
4. P.M. Nasch, M.H. Manghnani, Geophys. Monograph Ser. 101, 307 (1998).
5. C. Yamanaka et al., Nucl. Fusion 27, 19 (1987).
6. K. Shigemori et al., Rev. Sci. Instrum. 83, 10E529 (2012).
7. T. Sakaiya et al., Earth Planet. Sci. Lett. in press (2014).

Keywords: sound velocity, laser, shock wave, iron alloy, Earth's core, experiment

Japan Geoscience Union Meeting 2014
(28 April - 02 May 2014 at Pacifico YOKOHAMA, Kanagawa, Japan)

SIT40-01 Room:416 Time:May 1 09:15-09:30

3D imaging of geofluid by wideband magnetotellurics

OGAWA, Yasuo[1*] ; ICHIKI, Masahiro[2] ; KANDA, Wataru[1]

[1]Volcanic Fluid Research Center, Tokyo Institute of Technology, [2]Graduate School of Science, Tohoku University

Magnetotelluric measurements have been conducted over the five years in the central part of NE Japan arc surrounding the Naruko Volcano with approximately 3km grid. Over 200 sites were used for modeling the crustal resistivity structure in detail. Full impedance tensors for 8 periods were used for inversion. To alluviate the computational load, first four short periods were used to image upper crustal features and the resultant model was used for a prior model for another set of inversions with longer 4 periods.

The obtained model show the crustal conductor underneath the Mukaimachi caldera and Sanzugawa caldera. Seismic tomography shows low S-wave velocity for both, however, the resistivity image show clear low resistivity for Mukaimachi Caldera, but not for Sanzugawa Caldera. This difference may be due to the salinity of the fluids underlying the volcanic regions.

Keywords: geofluid, magnetotellurics, resistivity, 3d

Japan Geoscience Union Meeting 2014
(28 April - 02 May 2014 at Pacifico YOKOHAMA, Kanagawa, Japan)

SIT40-02 Room:416 Time:May 1 09:30-09:45

Three dimensional electrical conductivity model in the subduction zone beneath northeastern Japan

ICHIKI, Masahiro[1*] ; OGAWA, Yasuo[2] ; KAIDA, Toshiki[1] ; DEMACHI, Tomotsugu[1] ; HIRAHARA, Satoshi[1] ; HONKURA, Yoshimori[2] ; ICHIHARA, Hiroshi[3] ; KANDA, Wataru[2] ; KONO, Toshio[1] ; KOYAMA, Takao[4] ; MATSUSHIMA, Masaki[5] ; NAKAYAMA, Takashi[1] ; SUZUKI, Shu'ichi[1] ; TOH, Hiroaki[6] ; UYESHIMA, Makoto[4]

[1]Grad. School of Sci., Tohoku University, [2]VFRC, Tokyo Institute of Technology, [3]IFREE, JAMSTEC, [4]ERI, The University of Tokyo, [5]Grad. School of Sci. & Eng., Tokyo Tech, [6]Grad. School of Sci., Kyoto University

Our final goal is to infer a geofluid map (GFM) from both of the seismological (seismic velocity, Vp/Vs, Q etc.) and electrical conductivity structures in the wedge mantle of subduction zone beneath northeastern Japan. While plenty of high-resolution three dimensional (3-D) seismic tomographic images has been revealed there, none of 3-D electrical conductivity distribution model, of which the resolution is comparative to those of seismic tomography, has been proposed in terms of wedge mantle in subduction zones. Here, we show a high-resolution 3-D electrical conductivity distribution model in the wedge mantle beneath northeastern Japan used as input of GFM.

We carried out long-period MT observation using the state-of-the-art equipments, LEMI-417 and NIMS. The total 72 site observation has been completed. To remove tilt changes, baseline steps and drifts of fluxgate magnetometers, we first subtracted magnetic field variations to which a median filter was applied, from raw data. The horizontal coordinate of magnetic field data in each site was rotated before the response calculation such that the declination of the averaged horizontal component should be consistent with the 2010 absolute geomagnetic observation map provided by Geospatial Information Authority of Japan. We used the BIRRP processing code (Chave and Thomson, 2004) to estimate MT responses and have successfully retrieved them up to 61440 seconds in period.

The MT impeadance responses were inverted into 3-D electrical conductivity model using WSINV3D (Siripunvaraporn et al, 2005), the data-space Occam inversion method. The all input data error floor was assigned to be 10 percent. We investigated the optimal reference model with trial and errors. The test model was (1) uniform models, (2) layered models and (3) layered models with subducting slab models. The best RMS in each reference model was (1) 2.81, (2) 2.71 and (3) 2.48, respectively. Hence, we adopted the reference model of the layered model with subducting slab.

The conductivity profiles normal to the trench axis in higher latitude than N 39 degrees delineate conductive region on the subducting slab, and the conductive region is raised just beneath the central range of northeastern Japan (Ou-backbone range). This electrical image is well consistent with that obtained by the seismic tomographic model. On the other hand, a profile in lower latitude than N 39 degrees reveals that the conductive region is overturned towards backarc. The top of the overturned conductive body coincides with Gassan Volcano location, one of the outstanding backarc volcanism. However, Chokai Volcano, another distinctive backarc volcanism has no subsurface conductive root originated from deep upper mantle. The overturned mantle convection image is not found in the seismic tomographic image.

Japan Geoscience Union Meeting 2014
(28 April - 02 May 2014 at Pacifico YOKOHAMA, Kanagawa, Japan)

SIT40-03 Room:416 Time:May 1 09:45-10:00

S-wave attenuation on the western side of Nankai subduction zone: implications for geofluid distribution and dynamics

TAKAHASHI, Tsutomu[1*] ; OBANA, Koichiro[1] ; YAMAMOTO, Yojiro[1] ; NAKANISHI, Ayako[1] ; KODAIRA, Shuichi[1] ; KANEDA, Yoshiyuki[1]

[1]JAMSTEC

One major cause of seismic wave attenuation is the presence of fluid in rocks. In this study, we estimated the attenuation structure in southwestern Japan and western Nankai trough by applying the attenuation tomography that takes account of apparent amplitude attenuation due to multiple forward scattering [Takahashi, 2012]. Because the estimated attenuation 1/Q in our tomographic study was much larger than 1/Q due to wide-angle scattering, our estimated 1/Q is composed mainly the intrinsic 1/Q.

High 1/Q (>1/500 at 4-8 Hz) was imaged beneath the Quaternary volcanoes. The highest attenuation (1/Q ˜1/250 at 4-8 Hz) distributes beneath the Beppu-Shimabara rift zone at 40-60km depth. Beneath this rift zone, 1/Q becomes larger as depth increases. Random inhomogeneities in this zone are relatively strong at 0-40 km depth; whereas at 40-60 km depth random inhomogeneities are almost comparable to those in non-volcanic area. Meanwhile, in northeastern Japan, uppermost mantle beneath the volcanoes shows strong inhomogeneities and high attenuation. Apparent attenuation at the uppermost mantle beneath the Quaternary volcanoes is high in both study areas, but relative contributions of scattering and intrinsic attenuation differ between northeastern Japan and the Beppu-Shimabara rift zone. If we consider random inhomogeneities and 1/Q in other areas, the weak random inhomogeneities and high 1/Q beneath this rift zone suggest that random inhomogeneities due to the presence of igneous rocks are not significant, and that any magma inclusions are too small to excite S-wave scattering at 4-32 Hz.

At off Shikoku region, moderate 1/Q (1/800 ˜1/1000 at 4-8 Hz) is imaged at 0-20 km depth. This moderate 1/Q is estimated as 1/Q (f) ˜$10^{-2.5}f^{-0.5}$. Similar moderate attenuation can be found beneath the south of Shikoku at 20-40km, beneath the northern edge of Shikoku at 40-60km depth, and beneath Chugoku area at 40-60km depth. From geometry models of subducting Philippine Sea plate, most of the moderate 1/Q zone is located in and around the oceanic crust of subducting Philippine Sea plate except beneath Chugoku region. In this area, Shelly et al. [2006] pointed out fluid existence in the oceanic crust by estimating Vp/Vs structure. This correspondence implies this moderate 1/Q reflects fluid in the subducting slab. If we suppose that 1/Q of P- and S-wave have the same frequency dependences and that random inhomogeneities of P- and S-wave has the same scale dependences, we can show possible cases of fluid flow induced by the passage of low frequency seismic waves (<1 Hz) by applying a theoretical model of wave attenuation in saturated porous random media [Muller and Gurevich, 2005]. As a phenomenon suggesting such fluid flow by lower frequency seismic wave, triggering of non-volcanic tremors by surface waves passing has been observed [e.g., Miyazawa and Brodsky, 2008]. Even though we further need P-wave studies for detailed examination of this topic, it is likely that random inhomogeneity, intrinsic at 4-32 Hz and triggered tremors can be used to investigate medium properties and fluid dynamics.

Japan Geoscience Union Meeting 2014
(28 April - 02 May 2014 at Pacifico YOKOHAMA, Kanagawa, Japan)

SIT40-04 Room:416 Time:May 1 10:00-10:15

Seismic activity near the Moriyoshi-zan volcano in northeastern Japan: Implications for geofluid migration

KOSUGA, Masahiro[1*]

[1]Graduate School of Science and Technology

The 2011 Off the Pacific coast of Tohoku (Tohoku-oki) Earthquake caused increased seismicity in many inland areas. A seismic cluster that occurred north of the Moriyoshi-zan volcano in the Akita prefecture of the Tohoku District is of interest in light of contribution of geofluids to seismic activity. We observed a seismic cluster characterized by the migration of seismicity, reflected/scattered phases, and deep low-frequency earthquakes. We relocated hypocenters by using the data of temporal observation and by using the Double-Difference location technique, which increased the depth accuracy. We interpreted the spatiotemporal variation of the hypocenters in the most active cluster by estimating the migration of pore fluid pressure. The hydraulic diffusivity of the cluster was in the range of 0.01?1.0 m2/s, and increased with time, implying that the migration of hypocenters accelerated after a pathway for fluids was formed by the fracturing of the wallrock that produced the initial stage of seismic activity. A prominent feature of the seismograms is a reflected/scattered phase observed at stations around the volcano. We have interpreted the phase as S-to-S scattered waves and estimated the location of scatterers using a back-projection method. The scatterers are located about 5 km northwest of the Moriyoshi-zan volcano and at an approximate depth of 13 km. The Moriyoshi-zan area is one of the source areas of deep low-frequency earthquakes that have previously been interpreted as events generated by the migration of geofluids. The depth of scatterers is close to the upper limit of the depth at which low-frequency earthquakes occur. Thus, we regard the observed scatterers to be a reservoir of geofluid that came from the uppermost mantle accompanying contemporaneous low-frequency earthquakes. The geofluid reservoir is the probable source of overpressurized fluid that induces the migration of seismicity in the upper crust. A time delay in seismic activity from the Tohoku-oki Earthquake was considered as the time needed to migrate across a gap between the reservoir and the earthquake cluster with a hydraulic diffusivity comparable to that observed for the initial stage of seismicity, i.e., fracturing of the wallrock.

Keywords: The 2011 Off the Pacific coast of Tohoku Earthquake, triggered seismicity, hypocenter migration, scattering, geofluid

Japan Geoscience Union Meeting 2014
(28 April - 02 May 2014 at Pacifico YOKOHAMA, Kanagawa, Japan)

SIT40-05 Room:416 Time:May 1 10:15-10:30

Is H_2O-NaCl fluid enough to explain high electrical conductivity in the earth's crust?

SAKUMA, Hiroshi[1*] ; ICHIKI, Masahiro[2]

[1]National Institute for Materials Science, [2]Tohoku University

Old continental crust has a high electrical conductivity layer at 20 to 30 km in depth [1]. Presence of aqueous fluids is a plausible hypothesis for explaining the high conductivity zone [2]. Therefore the electrical conductivities of aqueous fluids under high pressure (P), temperature (T) conditions should be investigated in order to evaluate the hypothesis. The phases of water and aqueous NaCl solutions at the P-T conditions of the Earth's crust correspond from liquid to supercritical states.

Experimental approaches to measure the electrical conductivities at high P, T and salt concentration (c) conditions are limited and the data at P <400 MPa, T <1073 K and c <0.6 wt% for aqueous NaCl solutions is only available [3]. Classical molecular dynamics (MD) simulations are useful to obtain the electric conductivities at high P, T and c conditions and for understanding the underlying mechanism controlling the conductivities.

We used the flexible and induced point charge (FIPC) H_2O model [4] for MD simulations of aqueous NaCl solution. The technical details of the model and computational methods are explained in the literature [4]. The unit cell contained 2222 H_2O and 4 NaCl, 2035 H_2O and 22 NaCl, and 2035 H_2O and 66 NaCl for c = 0.6, 3.4, and 9.6 wt% NaCl solutions, respectively.

The isotherms indicate that the conductivity increases with increasing pressures and saturated at high pressures. The conductivity decreased with increasing temperature. This behavior may seem to be strange, since the ionic mobility should be high at high temperatures. This can be explained by the mixed effects of the change of (i) the density, (ii) ionic mobility, and (iii) dielectric constant of water as discussed in Quist and Marshall (1968) [3]. We concluded that the change of the conductivity of H_2O-NaCl fluids along with a geotherm model can explain one order of the increased magnitude at the high conductivity layer in depth, but more change observed by the Magnetotelluric method should be explained by the additional mechanism such as the connectivity of the fluids and the conductivity of H_2O-CO_2 fluids.

References
[1] T. J. Shankland and M. E. Ander (1983) *J. Geophys. Res.* **88** 9475-9484.
[2] B. E. Nesbitt (1993) *J. Geophys. Res.* **98** 4301-4310.
[3] A. S. Quist, and W. L. Marshall, (1968) *J. Phys. Chem.* **72** 684?703.
[4] H. Sakuma, M. Ichiki, K. Kawamura and K. Fuji-ta (2013) *J. Chem. Phys.* **138** 134506.

Keywords: salt water, electrical resistivity, supercritical fluid, molecular dynamics, static dielectric constant

Japan Geoscience Union Meeting 2014
(28 April - 02 May 2014 at Pacifico YOKOHAMA, Kanagawa, Japan)

SIT40-06 Room:416 Time:May 1 10:30-10:45

Connectivity of cracks and pores in a granitic rock

WATANABE, Tohru[1*] ; HIGUCHI, Akiyoshi[1] ; YONEDA, Akira[2]

[1]Graduate school of science and engineering, University of Toyama, [2]Institute for Study of Earth's Interior, Okayama University

Seismic velocity and electrical conductivity are used to map the fluid distribution in the crust. Seismic velocity reflects the contiguity of solid phases, while electrical conductivity the connectivity of fluid phases. The combination of velocity and conductivity could provide us a strong constraint on the fluid distribution. However, mapping of the fluid distribution has not been successful. The connectivity of fluid phases in rocks is poorly understood. In order to understand the connectivity of fluid phases in rocks, we have made conductivity measurements on a fluid-bearing granitic rock under various confining pressures.

Fine grained (100-500μm) biotite granite (Aji, Kagawa pref., Japan) was used as a rock sample. The sample is composed of 52.8% plagioclase, 36.0% Quartz, 3.0% K-feldspar, 8.2% biotite. The density is 2.66(1) g/cm^3, and the porosity 0.8(1) %. The porosity was estimated from the mass of the dry and wet samples. Cylindrical samples have dimensions of 25 mm in diameter and 30 mm in length, and saturated with 0.01 mol/l KCl aqueous solution. Simultaneous measurements of elastic wave velocity and electrical conductivity were made using a 200 MPa hydrostatic pressure vessel. The pore-fluid is electrically insulated from the metal work by using plastic devices (Watanabe and Higuchi, 2013). The confining pressure was progressively increased up to 125 MPa, while the pore-fluid pressure was kept at 0.1 MPa. It took five days or longer for the electrical conductivity to become stationary after increasing the confining pressure.

Elastic wave velocities and electrical conductivity showed reproducibly contrasting changes for a small increase in the confining pressure. Elastic wave velocities increased only by 5% as the confining pressure increased from 0.1 MPa to 25 MPa, while electrical conductivity decreased by an order of magnitude. The increase in velocities is caused by the closure of cracks. Most ($\sim$80%) of the decrease in electrical conductivity occurred below the confining pressure of 5 MPa. The decrease in electrical conductivity must also be caused by the closure of cracks. The decrease in porosity was only 0.07(1) %. Such a small change in porosity caused a large change in electrical conductivity. The connectivity of fluid was maintained at least up to the confining pressure of 125 MPa. A calculation with the effective medium theory (Kirkpatrick, 1973) suggests that the fluid forms a network with small coordination number (average coordination number=2.3), and that the connectivity at higher pressures is maintained by stiff pores. More cracks are open at lower pressures to link pores, drastically increasing electrical conductivity.

Keywords: pore, crack, connectivity, granitic rock, electrical conductivity

Japan Geoscience Union Meeting 2014
(28 April - 02 May 2014 at Pacifico YOKOHAMA, Kanagawa, Japan)

SIT40-07 Room:416 Time:May 1 11:00-11:15

Geometry of intergranular fluids in the mantle xenoliths: Implications for the physical properties of upper mantle

NAKAMURA, Michihiko[1*] ; OKUMURA, Satoshi[1] ; YOSHIDA, Takeyoshi[1] ; SASAKI, Osamu[2] ; TAKAHASHI, Eiichi[3]

[1]Graduate School of Science, Tohoku University, [2]Tohoku University Museum, [3]Graduate School of Science and Engineering, Tokyo Institute of Technology

Recent magnetotelluric (MT) studies have revealed that crust and uppermost mantle are less resistive than dry rocks in various localities in the world. This suggests that interconnected fluid phases present more ubiquitously than previously realized. Intergranular fluids also decrease seismic wave velocities and changes Vp/Vs ratio, thus interpretation of the seismic tomographic images largely depends on the volume faction and geometry of the fluid phase. The conventional view on grain-scale fluid distribution is based on dihedral angle between minerals and fluids in isotropic monomineralic rocks (i.e. ideal equilibrium geometry). Natural rocks are, however, composed of ani-sotropic multiple phases and undergo textural adjustment to minimize interfacial and strain energy such as grain growth and dynamic recrystallization, which results in microstructural complexity. In order to understand real fluid distribution in deep-seated rocks, we conducted an X-ray CT study of xenoliths from the uppermost mantle from various localities.

The mantle xenoliths samples investigated were from Ichinomegata (NE Japan), Eifel (W Gernamy), San Carlos (AZ, USA), Bullen Merri and Shadwell (Victoria, AU), Kilbourne Hole (New Mexico, USA), Longang-hu (NE China), Gi-rona (Spain), Lanzarote (Canary islands), and Moses Rocks (Uta, USA). The micro-focus X-ray CT imaging was performed using Comscantecno ScanXmate-D160TSS105 in Tohoku University Museum with a tube voltage of 100 – 130 kV and current of 90 – 120 mA. The voxel size was typically 43 – 73 μm^3. The 3-D image analysis was carried out with a software package Slice[1].

All the observed spinel lherzolite and Harzburgite xenoliths contained up to a few vol% of intergranular pores, indicating that the rocks were saturated with a free-fluid phase. The imaged pore fluids are typically polyhedral and tens – hundreds of micrometers in scale; this suggests that they were formed via coalescence of smaller pore fluids. The fluids are localized in interphase boundaries (between different mineral phases), while most of the monomineralic triple junctions lack pore fluids. All these characteristics are consistent with the results of grain-growth experiments in a fluid-bearing bimineralic system[2]; in other words, the role of interfacial energy anisotropy and grain growth are crucial in determining fluid distribution in nature. In the ellipsoid approximation, the 3-D shape of the intergranular fluids show deformed rugby-ball shape with aspect rations larger than those of the equilibrium fluid geometry determined by the dihedral angle[3]. The geometry, distribution and thus connectivity of fluids cannot be assessed simply from dihedral angles.

The results of CT imaging suggest that no pervasive grain-scale fluid interconnection is established in the uppermost mantle. To explain the observed low electrical resistivity in the mantle which does not undergo partial melting, concentration (localization) and interconnection of CHO fluids in a larger spacing, such as in meter-scale shear zones should be necessary. Given the observed geometry of the inter-granular fluids, their effects on Vp/Vs ration is limited.

References: [1]Nakano et al. http://www-bl20.spring8.or.jp/slice/ (2006). [2] T. Ohuchi and M. Nakamura J. Ge-ophys. Res. 111, B01201, doi: 10.1029/ 2004JB003340 (2005). [3] Y. Takei JGR 107 (B2) doi:10.1029/2001JB000522 (2002).

Keywords: mantle xenoliths, rock microstructure, elastic wave velocity, electrical resistivity, grain growth

Japan Geoscience Union Meeting 2014
(28 April - 02 May 2014 at Pacifico YOKOHAMA, Kanagawa, Japan)

SIT40-08 Room:416 Time:May 1 11:15-11:30

Ultra-fine textures along grain boundaries in nominally fresh mantle xenoliths

MURATA, Masami[1*] ; UEMATSU, Katsuyuki[2] ; YAMAMOTO, Takafumi[3] ; TANI, Kenichiro[4] ; SHUKUNO, Hiroshi[5] ; MIZUKAMI, Tomoyuki[1] ; MORISHITA, Tomoaki[1]

[1]Kanazawa Univ., [2]Marine Works Japan LTD., [3]Hiroshima Univ., [4]JAMSTEC, [5]non party

It is important for the evolution of the Earth to understand the role of grain boundaries during melts/fluids migrations in mantle peridotites. There are, however, very limited numbers of studies on grain boundaris in natural samples, although many experimental and theoretical approaches have been carried out (e.g., Drury and Fitz Gerald, Geophys. Res. Lett., 1996; Hiraga et al., Nature, 2004).

We focus on nanoscale microstructures of crystal surface (grain boundary) in " nominally fresh " peridotite xenoliths from the San Carlos, USA, which is one of the most famous localities of peridotite xenolith in the world. Thin amorphous films along grain boundaries were already reported in some San Carlos xenoliths (Wirth, Contrib. Mineral. Petrol., 1996).

We recovered mineral grains with a selFrag at the Japan Agency for Marine-Earth Science and Technology (JAMSTEC) in order to minimize mechanical damages during mineral separations. We observed multiple grains of peridotite xenoliths using a high-resolution electron microscope (FE-SEM) at JAMSTEC.

Microstructures of crystal surface of these peridotite xenoliths are classified as follows. (1) over micron scale structures such as moth-eaten structures, vermicular structures, automorphic crystals and etch pits. (2) submicron scale structures. It is interesting to note that (2) submicron scale structures are frequently observed on (1) over micron scale structures. These textures suggest that microstructures were developed by several stages. We analysed on the surface of these textures using a micro-Raman and SEM-EDS techniques. We are also planning to perform transmission electron microscope, combined with chemical analyses in order to identify the surface materials that constrain P-T conditions and fluids for the formation of these textures.

Keywords: peridotite xenolith, Microstructures, TEM, grain boundary, fluids

Japan Geoscience Union Meeting 2014
(28 April - 02 May 2014 at Pacifico YOKOHAMA, Kanagawa, Japan)

SIT40-09 Room:416 Time:May 1 11:30-11:45

Elemental transport under lower-middle crustal condition: example from hydration of basic schist, Sanbagawa belt, Japan

UNO, Masaoki[1*] ; NAKAMURA, Hitomi[2] ; IWAMORI, Hikaru[3]

[1]Graduate School of Environmental Studies, Tohoku University, [2]Department of Earth and Planetary Sciences, Tokyo Institute of Technology, [3]Geochemical Evolution Research Program, Japan Agency for Marine-Earth Science and Technology

To constrain the behavior of geofluids under the lower to middle crustal conditions, hydration reactions and trace element and Sr-Nd-Pb isotopic compositions of basic schists in the Cretaceous Sanbagawa metamorphic belt, a typical regional metamorphic belt in the circum-Pacific orogeny, have been investigated based on the observations of thin-sections and outcrops. The basic schists have undergone significant hydration from 0.8 GPa, 550 ^{o}C to 0.3 GPa, 400 ^{o}C during decompression towards the surface at the final stage of metamorphism. High-field-strength and rare-earth element compositions of the basic schists, as well as the Sr-Nd-Pb isotopic ratios, are different among three mineral zones with different peak P-T metamorphic conditions; the basic schists in the low-grade chlorite zone shows N-MORB-like compositions whereas those in the higher-grades, garnet and oligoclase-biotite zones, show more enriched compositions (E-MORB-like). On the other hand, there is a common feature to all the metamorphic zones; the enrichment degree of some group of elements (e.g., large-ion lithophile elements) relative to high-field-strength and heavy-rare-earth elements is proportional to loss on ignition that approximately measures the bulk rock H_2O content. This correlation suggests that Li, B, K, Cr, Ni, Rb, Sr, Cs and Ba have been added to the basic schists during hydration. The addition of these elements amounts to as much as 60-80% of the bulk abundance, indicating that significant amounts of elements were transported via pervasive fluid flow, which overprinted the variation in the bulk rock compositions of the protolith. The estimated compositions of hydration fluid show high concentrations in large-ion lithophile elements, lead and light-rare-earth elements (10-100 times denser than primitive mantle, Fig. 1) and are similar to those of the slab-derived fluids[1] that induce arc volcanism. These elements (Cs, Rb, Ba, K, La, Ce and Pb) are thought to have been preferentially partitioned into the fluid when it was generated at depth. Such high concentrations indicate a high temperature origin of the hydration fluid, and are consistent with a model of hot slab subduction during exhumation of the Sanbagawa belt.

References:
[1] Nakamura, H., Iwamori, H., and Kimura, J.-I., 2008 *Nat. Geosci.*, **1**, 380-384

Keywords: geofluid, metamorphism, trace elements, Sr-Nd-Pb isotopes, hydration reaction, Sanbagawa metamorphic belt

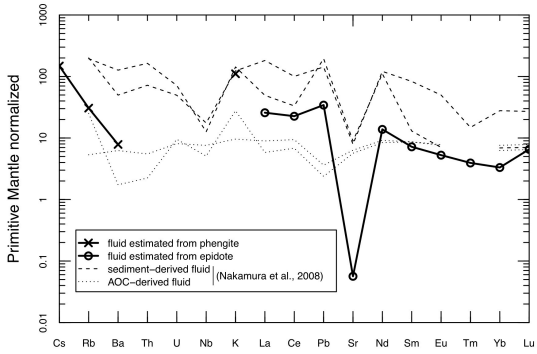

Fig. 1 Estimated compositions of the hydration fluid (solid lines). Compositions of slab-derived fluids estimated for arc volcanism (dotted lines; Nakamura *et al.*, 2008 *Nat. Geosci.*, **1**, 380–384) are shown for comparison. Note that the concentrations of LILE, Pb and LREE in the hydration fluid are in the range of slab-derived fluids.

Japan Geoscience Union Meeting 2014
(28 April - 02 May 2014 at Pacifico YOKOHAMA, Kanagawa, Japan)

SIT40-10 Room:416 Time:May 1 11:45-12:00

Progress of serpentinization in the mantle wedge and its effect on the redox state

KOGISO, Tetsu[1*] ; MIYOSHI, Akane[2]

[1]Human Environ. Stds., Kyoto Univ., [2]JX Nippon Oil & Energy Corporation

Serpentinization of peridotite in the mantle is a key process that significantly changes the physical properties of the mantle. Serpentinization also produces hydrogen, which is essential not only for the activity of microbial systems in hydrothermal fields on the seafloor, but also for controlling the oxidation state of the mantle in subduction zones. Hydrogen is generated along with the formation of magnetite during serpentinization. However, there still remains controversy about what factors promote the mineralogical reactions responsible for magnetite formation during serpentinization in natural ultramafic rocks. Recent petrologic studies have proposed that serpentinization reactions proceed via a two-stage process involving the early formation of serpentine and brucite and subsequent magnetite formation. Many studies proposed that magnetite forms by the break down of ferrous brucite promoted by the addition of aqueous silica, but others proposed that magnetite forms by the breakdown of ferrous serpentine which releases silica component. To solve this controversy, we examined a number of variably serpentinized harzburgite and dunite samples taken from the Iwanaidake ultrama?c body in Kamuikotan belt, Japan (Miyoshi et al. 2014). Petrographic observations of these samples revealed that successive changes in textures, mineral chemistry, whole-rock H_2O contents, and magnetic susceptibility with the progress of serpentinization of harzburgite involved two stages: replacement of olivine by serpentine and brucite, and subsequent formation of magnetite along with more-magnesian serpentine and brucite. The later reactions occurred concurrently with serpentinization of orthopyroxene, which supplied the silica component. In serpentinized dunite, which doesn't contain orthopyroxene, serpentinization involved replacement of olivine by serpentine and brucite, and the fraction of magnetite did not increase with the progress of serpentinization. These observations, and the fact that the Iwanaidake ultramafic body originated from the forearc mantle of the Northeast Japan arc, suggest that the silica supply from serpentinization of orthopyroxene is an essential factor for the formation of magnetite during serpentinization in mantle wedge.

Our observations imply that serpentinization in the mantle wedge of subduction zone produces H_2 along with magnetite if sufficient amounts of silica component are supplied from subducting slab, which will probably occur because dehydration in subducted sediments can supply silica-rich fluids. Since H_2 is expected to exist as immiscible hydrogen-rich gas phases that coexist with H_2O fluids in normal subduction zone conditions, it will be rapidly migrate upwards owing to its very low density. Then the remaining serpentinites will become oxidized. Such oxidation associated with serpentinization would occur in the shallow part of the wedge corner where temperatures are lower than ~600 ℃, but the oxidized (magnetite-bearing) serpentinite will be dragged downwards in the mantle wedge. Thus serpentinization reactions can be one of the main processes to increase the oxygen fugacity of the mantle wedge. On the other hand, the H_2 gas removed from the wedge corner will produce highly reduced fluid phases, which may result in reducing the shallowest part of the forearc mantle and the lower part of the forearc crust. This could be the cause of rare presence of metal phases in subarc peridotite.

Reference:

A. Miyoshi, T. Kogiso, N. Ishikawa, K. Mibe (2014) *American Mineralogist*, in press.

Keywords: serpentinization, hydrogen, magnetite, subduction zone, redox state

Japan Geoscience Union Meeting 2014
(28 April - 02 May 2014 at Pacifico YOKOHAMA, Kanagawa, Japan)

SIT40-11 Room:416 Time:May 1 12:00-12:20

Evolution of porosity structures in a fracture during quartz vein formation

YAMADA, Ryo[1*] ; OKAMOTO, Atsushi[1] ; SAISHU, Hanae[1] ; NAKAMURA, Michihiko[2] ; OKUMURA, Satoshi[2] ; SASAKI, Osamu[3] ; TSUCHIYA, Noriyoshi[1]

[1]Tohoku university, [2]Tohoku university, [3]The Tohoku university museum

Ubiquitous occurrences of quartz veins suggest that dissolution/precipitation of silica provides significant effects on the hydrological and mechanical properties within the crust. For example, a model has been proposed that fracture sealing processes control the change of pore fluid pressure and thus earthquake cycle. Previous studies on natural quartz veins have focused on estimates of P-T conditions, stress and strain fields and fluid compositions; however, details of dynamics of fluid flow and how fractures are sealed during vein formation are still unclear. In this study, we synthesized quartz veins by the hydrothermal experiments, and observed the aperture structures by using X-ray CT to clarify how aperture structures evolve during vein formation.

We conducted the hydrothermal flow-through experiments for quartz precipitation from Si-supersaturated solutions under controlled high temperature and high pressure condition. The experimental apparatus consists of two vessels for preparation of the Si-supersaturated solution and for precipitation, respectively. The precipitation vessel has double-structure : the main flow path was the inner alumina tube (diameter=4mm), and the outer SUS tube was filled with static solutions. The advantage of this system is that we can take out the non-destructive sample for the X-ray CT analyses. We conducted two types experiments: first one is precipitation in porous media with alumina balls, the second one is rock slice as analog of a fracture.

In the alumina-ball experiments, we carried out the precipitation experiment at supercritical (430C, 30MPa) and vapor condition (370C, 20MPa). In both experiments, the significant silica precipitation within few days, but showed contrasting porosity structures. Under supercritical condition, amorphous silica was predominantly formed with covering the surfaces of the alumina balls and alumina tube, and discrete quartz crystal (50 um) within the amorphous silica layers. The porosity (ϕ) gradually decreases with minimal porosity (ϕ = 0.4) at $\sim$ 38mm from the inlet. In contrast, under vapor condition, fine-grained quartz grains (0.1-1 um) were directly nucleated in solutions using surface of vapor, and immediately settled on the bottom. The porosity rapidly decreases from 18 mm (ϕ = 0.8) to 25 mm (ϕ <0.1) from the inlet. These results suggest that a depressurization of crustal fluids related to fault dilation by earthquakes would cause a formation of fine-grained silica particles, and their mineralogy and transport/deposition properties strongly depend on properties water.

In the experiment with rock slits, we evaluated the effect of rock substrate (amount and distribution quartz in the fracture wall). The P-T conditions and solution chemistry are similar to the previous experiments, but we used granite core with a slit ($\sim$ 300 um). The mineralogy and aperture structures changes systematically along the fluid flow path. From the inlet to 35 mm of fracture, nucleation of quartz and other silica polymorphs predominantly occurred, regardless of vein wall minerals. From >35mm low Si concentration, silica precipitates occurred as epitaxial overgrowth from quartz crystal. The wavelength of aperture structures is controlled by distribution and grain size of quartz of the host granite. Accordingly, fractures are not sealed homogeneously, but complex flow pathways are evolved during vein formation. Such a variation in the precipitation mechanism and porosity structures during quartz vein formation may affect the evolutions of permeability and strength of rock fractures in the Earth's crust.

Keywords: Hydrothermal experiments, Quartz, Vein, Fracture, Porosity

Japan Geoscience Union Meeting 2014
(28 April - 02 May 2014 at Pacifico YOKOHAMA, Kanagawa, Japan)

SIT40-12 Room:416 Time:May 1 12:20-12:35

High precision in situ Pb isotope analysis of galena by LAL-ICPMS technique

WAKAKI, Shigeyuki[1*] ; TANIMIZU, Masaharu[1]

[1]Kochi Insititute for Core Sample Research, JAMSTEC

Radiogenic Nd and Pb isotopic compositions of the fluids originated from subdcting Pacific and Philippine Sea plates have been characterized from isotopic trends observed among arctic volcanic rocks (Nakamura et al., 2008). Origin and evolution of the fluids that produced hydrothermal ore deposits may now be investigated by radiogenic isotopic compositions of ore deposits. In this study, we analyzed the micro scale isotopic variation of Pb in a hydrothermal galena to shed light on the macro scale dynamics of the fluids. To investigate the possibly small degree of isotopic changes within a galena sample, both high spatial resolution and high precision are required for the isotopic analysis. We employed the combination of laser ablation in liquid (LAL) micro sampling technique (Okabayashi and Hirata, 2011) and solution-based Pb isotopic analysis by MC-ICPMS technique to meet the analytical requirements. In the LAL micro sampling, laser-ablated sample particles are trapped in the liquid that placed above the sampling area. The trapped samples are then dissolved and introduced to the ICPMS as a solution. The advantage of the combined LAL-ICPMS technique over laser ablation (LA) ICPMS technique is the stable ion signals due to solution form, which allows high-precision isotope ratio measurement.

Sample analyzed in this study was a hydrothermal galena from Hosokura mine (Miyagi, Japan). A microscopic texture of the sample was observed in detail with FE-SEM-EDS system (JEOL JSM-6500F) prior to the isotopic analysis. A fs laser (IFRIT, Cyber Laser, Japan) with a wavelength of 780 nm (˜200 fs pulse width) was used for the LAL micro sampling. Care was taken to avoid sampling of grain boundaries and inclusions. Typical special resolution was 150 micron in diameter and 30 micron in depth. The laser-sampled PbS (300-400ng Pb) trapped in Milli-Q water was dissolved in conc. HNO3, and adjusted to 200 ng/mL Pb solution in 0.15 M HNO3 for Pb isotopic analysis. Pb isotope ratios were determined with a MC-ICPMS, Neptune (Thermo Instruments, Bremen, Germany). An isotopic reference material of Tl (NIST-SRM 997) was added to the final sample solutions for the correction of mass discrimination of Pb in the instrument to have a concentration of 20 ppb Tl.

Galena occurs as discrete layers of ca. 1cm width in between layered CaF_2 as well as sub mm-sized inclusion within thick CaF_2 layer. Galena inclusion and layers were numbered from 1 to 3 according to its precipitation order. Grain size of the galena in each of the layer is several hundred microns to several millimeters. Euhedral quartz with a size of 10-100 micron occurs along the grain boundary of galena and as an inclusion within galena grains.

Small but significant Pb isotopic variation of sub-permil order was observed among and within the 3 galena layers. The analyzed samples clearly form a linear trend in the $^{208}Pb/^{207}Pb$ vs. $^{206}Pb/^{207}Pb$ diagram. The observed Pb isotopic trend indicates that the Pb isotopic composition of the fluid that produced the galena has slightly changed during galena precipitation. The Pb isotopic composition of the galena is consistent with mixing of a sediment component of the Pacific plate (Nakamura et al., 2008) with a deep fluid derived from Pacific Ocean plate (Nakamura et al., 2008) and/or the DMM. With the high-precision isotopic analysis as demonstrated in this study, LAL-ICPMS may have an important contribution to high-spatial-resolution geochemical studies in the future.

Keywords: Geofluids, laser ablation in liquid, Pb isotope ratio, galena, in situ isotope analysis

Japan Geoscience Union Meeting 2014
(28 April - 02 May 2014 at Pacifico YOKOHAMA, Kanagawa, Japan)

SIT40-13 Room:416 Time:May 1 14:35-15:00

Origin of saline waters distributed along the Median Tectonic Line in southwest Japan

AMITA, Kazuhiro[1*] ; OHSAWA, Shinji[2] ; NISHIMURA, Koshi[3] ; YAMADA, Makoto[4] ; MISHIMA, Taketoshi[2] ; KAZAHAYA, Kohei[5] ; MORIKAWA, Noritoshi[5] ; HIRAJIMA, Takao[6]

[1]Department of Earth Science & Technology Faculty of Engineering and Resource Science Akita Universit, [2]Institute for Geothermal Sciences, Graduate School of Science, Kyoto University, [3]Faculty of Economics, Toyo University, [4]Research Institute for Humanity and Nature, [5]Geological Survey of Japan, AIST, [6]Department of Geology and Mineralogy, Graduate School of Science, Kyoto University

To identify of metamorphic dehydrated fluid as source fluid of hot spring water, we conducted chemical and isotopic analyses of water and accompanied gas samples collected from hot-spring wells along the Median Tectonic Line (MTL) in the forearc region of the southwestern part of Japan. As a result, we found hot spring waters having anomalous dD and $d^{18}O$ compositions as compared with modern seawater and shallow groundwater in Wakayama and Shikoku regions. Judging from data in relative B-Li-Cl composition and He isotopic systematics, the source fluid of the hot springs in Shikoku could be identified to be one of diagenetic fluids. On the other hand, the source fluid of the hot springs of Wakayama had different B-Li-Cl composition and higher 3He/4He ratio in comparison with diagenetic dehydrated fluids and then the fluid was thought to be originated from metamorphic dehydrated fluid as well as Oita plain. There was another striking contrast between the source fluid of Wakayama and Oita and that of Shikoku and Miyazaki; accompanied gases by the former were rich in CO_2, whereas those with the latter were rich in CH_4, and CO_2 in the accompanied gases of Wakayama and Oita is mostly derived from marine carbonate like volcanic gases in subduction zones. Moreover, the Li-B-Cl compositions of them showed transitive values between the relative composition of diagenetic fluids and those of volcanic thermal waters. Consequently, the source fluid of hot springs in Wakayama and Oita was likely to be dehydrated metamorphic fluids released from the subducting Philippine-Sea plate.

Keywords: hot spring water, dehydrated fluid from subducting plate, Median Tectonic Line

Japan Geoscience Union Meeting 2014
(28 April - 02 May 2014 at Pacifico YOKOHAMA, Kanagawa, Japan)

SIT40-14 Room:416 Time:May 1 15:00-15:15

Distribution of the helium isotope ratios in northeast Japan in terms of geological setting

HORIGUCHI, Keika[1*] ; KAZAHAYA, Kohei[1] ; TSUKAMOTO, Hitoshi[1] ; MORIKAWA, Noritoshi[1] ; SATO, Tsutomu[1] ; OHWADA, Michiko[1] ; NAKAMA, Atsuko[1]

[1]Geological Survey of Japan, AIST

The distribution of slab fluid defined by high Li/Cl ratios conforms the area of ”hot fingers”(Tamura et al., 2002) in Northeast Japan (Kazahaya et al., submitted). Conversely, the high $^{3}He/^{4}He$ ratios distribute wider and do not match with slab-derived fluids indicating that some of the mantle-derived helium would not be transported with magmas or slab fluids but directly upwells as mantle-derived fluid. The $^{3}He/^{4}He$ ratios vary along the volcanic front showing an areal contrast; such as a low-ratio-area close to volcanoes are observed in the central part of Tohoku. We propose here an extended helium upwell model which can explain the spatial variation of $^{3}He/^{4}He$ ratios with the following concept; 1) The most important constraint for mantle helium upwelling is the crustal structure divided by tectonic lines; Hatagawa Tectonic Line (HTL) divides the Kitakami and Abukuma belts. Ryoke belt and north part of Abukuma belt is torn apart by number of faulting events. The rest of parts, Abukuma granitic province and Kitakami province form very large stable blocks which might prohibit helium to upwell from mantle. 2) A view from U-Th content in the crust is im-portant to understand the flat distribution of mantle helium in back-arc region; Low U-Th crust in the back-arc with less crustal ^{4}He production is favora-ble to explain the flat and high $^{3}He/^{4}He$ signature, such as oceanic crust might have.Tanakura Tectonic Line (TTL) divides the thick crust of con-tinental margin (sedimentary prism and granite) with Ryoke belt.

Keywords: helium isotope ratio, northeast Japan, areal distribution, geological structure

Japan Geoscience Union Meeting 2014
(28 April - 02 May 2014 at Pacifico YOKOHAMA, Kanagawa, Japan)

SIT40-15 Room:416 Time:May 1 15:15-15:30

The Li-Cl-Br systematics of saline groundwater: A new indicator for slab fluid

KAZAHAYA, Kohei[1*] ; TAKAHASHI, Masaaki[1] ; IWAMORI, Hikaru[2]

[1]Geological Survey of Japan, AIST, [2]Geochemical Evolution Research Program, Japan Agency for Marine-Earth Science and Technology

In this study, we propose Br/Cl ratio as a new indicator for slab-derived fluids, which is useful to distinguish their sources between pore water and hydrous minerals in subducting slab. The areal distribution of slab-derived fluids and their sources using Li/Cl and Br/Cl as geochemical evidences will provide a view for water circulation in subduction zones.

Subducting slab contains waters (originally seawater) as pore water and many kinds of hydrous minerals. Hydrous minerals such as opal, clay or mica will decompose to release water during subsiding, and pore water will be released by compaction. Even though such complex process occurs, behavior of halogen ions in the subducting slab may be simple because they are always enriched in aqueous phase (pore water) and the rest are in minerals as a replacement of OH. Some metamorphic fluids in wedge mantle peridotite with Br-enriched signature have been observed and were indicated to be from pore water in the slab. The mineral dehydration process is supposed to be responsible for Br-depletion in slab-derived aqueous fluid. Therefore, halogens are potentially good indicators concerning with the water behavior in subduction processes.

The higher Br/Cl ratios ($>$0.0035 in wt.) have been observed in fossil seawater and oil field brines due to the addition of Br from organic matters. The very low Br/Cl waters ($<$0.0025 in wt.) have feature of ^{18}O-shift to the slab (magmatic) fluid end member, which is quite lower than that in seawater (Br/Cl = 0.0034 in wt.), indicating that these waters originate from dehydration of the slab.

Keywords: Li-Cl-Br, slab-derived fluid, groundwater, subduction process

Japan Geoscience Union Meeting 2014
(28 April - 02 May 2014 at Pacifico YOKOHAMA, Kanagawa, Japan)

SIT40-16 Room:416 Time:May 1 15:30-15:45

Origin of U-Th disequilibrium in subduction zone volcanic rocks

YOKOYAMA, Tetsuya[1*] ; IKEMOTO, Akihiko[1] ; IWAMORI, Hikaru[2] ; UEKI, Kenta[1]

[1]Department of Earth and Planetary Sciences, Tokyo Institute of Technology, [2]JAMSTEC

Subduction zone magmatism is induced by the addition of slab derived fluids to the mantle wedge [1]. Chemical compositions of subduction zone volcanic rocks are largely controlled by the chemical and physical properties of the slab fluid. The nature of slab fluids have been extensively studied by geochemical approach utilizing trace element abundances and isotope compositions in arc basalts [2]. U-series disequilibrim in arc volcanic rocks is a useful tracer to understand the origin of arc magmas as well as the timescales of fluid/melt migration in subduction zones. However, detail of the process that producing ^{238}U-^{230}Th disequilibrium in primary melts in the mantle wedge is still poorly constrained.

In this study, we determined ^{238}U-^{230}Th disequilibrium in volcanic rocks from the Northeast Japan Arc (Iwate, Akitakoma, Yakeyama, Hachimantai, and Kampu). In addition, we performed a numerical simulation that reproduced (^{238}U/^{232}Th) and (^{230}Th/^{232}Th) ratios in primary melts in a subduction zone, by simultaneously calculating mantle dynamics, hydro phase reactions and trace elements transport. To discuss the origin of U-Th disequilibrium in arc volcanic rocks, the new data and previously published U-Th data around Japan were evaluated based on the result of the numerical simulation. The numerical simulation performed in this study

Most of arc volcanic rocks possess ^{238}U-^{230}Th disequilibrium with 238U excesses, suggesting the addition to the mantle wedge of slab fluid enriched in U relative to Th. The feature of ^{238}U enrichment is well reproduced by the numerical simulation. Interestingly, the simulation produced two positive trends in the U-Th diagram; the shallow trend matches data from the Izu-Mariana arc, while the steep slope is consistent with data from the Kamchatka arc. This strongly suggests that the positive trend in the U-Th diagram for a single arc samples simply reflects the variation of (^{238}U/^{232}Th) and (^{230}Th/^{232}Th) ratios in primary melts produced in the mantle wedge, and the slope does not have any age significance. Thus, as discussed in [3], the decoupling of U-Th and Th-Ra ages for arc samples would be explained by assuming that the slab derived fluid have (^{230}Th/^{232}Th) ratios higher than the mantle wedge composition.

Although the NEJ frontal-arc lavas (Iwate) possess ^{238}U-^{230}Th disequilibrium with ^{238}U excesses, the extent of 238U enrichment is moderate ($<$10%) compared to the other frontal-arc samples. In addition, Iwate lavas have relatively low (^{230}Th/^{232}Th) ratios that cannot be explained by the numerical simulation. This implies that the (^{230}Th/^{232}Th) in mantle wedge beneath Iwate volcano is lower than that in the depleted MORB mantle (DMM), due presumably to ancient mantle metasomatism by Th-enriched fluids derived from sediments.

In contrast to the frontal arc samples, the extent of ^{238}U enrichment in the NEJ samples decreases as the slab depth increases, and the rear-arc lavas (Kampu) show 230Th enrichments relative to ^{238}U ($<$10%). This generally reflects gradual decrease of the amount of slab derived fluid mixed into the wedge mantle. The ^{230}Th excesses in rear-arc lavas would be produced by the melting of garnet-bearing upwelling mantle, as reproduced by the simulation. However, our data for Kampu show 230Th excesses with an extremely low (^{230}Th/^{232}Th) ratio (˜0.8) that plots outside the simulation data. This is explained by assuming the existence of metasomatised mantle beneath the NE Japan as discussed above, although the possibility of direct addition of Th-enriched fluid to the DMM-like mantle cannot be ruled out for the generation of rear-arc magmas.

References: [1] Iwamori (1998) *EPSL* 160, 65. [2] Nakamura et al. (2008) *Nature Geosci*. 1 380. [3] Yokoyama et al. (2003) *JGR* doi: 10.1029/2002JB002103.

Keywords: U-Th disequilibrium, Subduction zone, volcanic rocks, slab derived fluid

Japan Geoscience Union Meeting 2014
(28 April - 02 May 2014 at Pacifico YOKOHAMA, Kanagawa, Japan)

SIT40-17 Room:416 Time:May 1 15:45-16:00

Water transport coupled dynamically with a plate-mantle convection system involving a shallow to deep subduction zone

NAKAKUKI, Tomoeki[1*] ; KANEKO, Takeo[1] ; NAKAO, Atsushi[2] ; IWAMORI, Hikaru[3]

[1]Dept. Earth and Planetary Systems Science, Hiroshima Univ., [2]Dept. Earth and Planetary Sciences, Tokyo Inst. Technology, [3]Geochemical Evolution Research Program, JAMSTEC

Numerical study for water transport under a volcanic arc revealed dynamics of the water processes inducing melt generation (Iwamori, 1998; 2007). Back-arc and intra-plate volcanisms also indicate water migration from a deeper section of the subduction zone. Aiming to understand geodynamical processes of water derived and transported from the subducted slab in the deep subduction zone, we developed a numerical model of water transport coupled dynamically with plate-mantle convection system with a whole mantle scale. We here focus on the mechanism of dehydration from stagnating or penetrating slab and water transport from the mantle transition zone (MTZ). We also consider water transport to deeper mantle and the effects on the global distribution of water-compatible elements (Iwamori and Nakamura, 2012).

We assume that a viscous fluid in a 2-D rectangular box with an extended Boussinesq approximation represents the mantle convection system with integrated lithospheric plates (Tagawa et al, 2007). We incorporate water transport and hydrous mineral phase diagram (Iwamori, 1998; 2007) into the numerical plate-mantle model. We assume that the water dehydrated from water-saturated minerals migrates upward with porous flow that is much faster than mantle flow. In our model, the emitted water is instantaneously transported only to the upward direction. We introduce reduction of the density and the viscosity due to the hydration into the density and rheology model according to experimental study (karato and Jung, 2003). We also consider viscous weakening of serpentine or chlorite that is important for water transport in shallow subduction zone [6]. A numerical method developed by Tagawa et al. (2007) is used to solve momentum and energy conservation equations for the mantle convection. To solve an equation for water transport advected by the mantle flow in which the diffusion term is negligible, a Marker-And-Cell (MAC) method is employed to avoid artificial diffusion.

A serpentine layer generated by dehydration of the oceanic crust plays a key role to control water transport by the subducted slab shallower than about 150 km (Iwamori, 1998; 2007; Horiuchi, 2013). To continuously generate this layer, coupling between the serpentine layer and the plate boundary fault is essential. After dehydration of serpentine, nominally anhydrous minerals (NAMs) (Iwamori, 1998; 2007) are a main veneer of the water. In this stage, water capacity of NAMs, which depends on the grain boundary storage as well as that of the hydrous minerals, is the primary factor to control the amount of transported water. This is not so large as about 0.4 wt. % to maintain water-filled region under the arc. The water is carried without dehydration above the 660 km boundary. If the water capacity in the lower mantle is as large as that of NAMs in the mantle shallower than 410 km (˜0.2 wt. %), the water is entirely transported to the lower mantle. When the lower mantle water capacity is lower than that, the water is expelled at the post-spinel phase transition. While the water ascends with the porous flow, the medium rocks descend with asthenospheric flow dragged by the downwelling slab. The repetition of these processes broadens the hydrous layer at the 660 km boundary. A thin water-saturated layer is formed at the 660 km boundary around the penetrating slab. Because of the buoyancy, this becomes unstable so that hydrous plumes are generated. On the contrary to this, the hydrous plume was not formed from the hydrous NAMs layer over the stagnant slab. At the 410 km boundary, the water is ejected from the hydrous plume as the olivine phase minerals can bear the water much less than MTZ minerals. The ejected water rises with porous flow till the emission is completed. The hydrous plumes fill the water within the mantle wedge from the edge to the 500 to 1000 km distant back-arc area, and those erode to thin the overriding lithosphere.

Keywords: subduction zone, water transport, transition zone, slab, hydrous plume, mantle convection

Japan Geoscience Union Meeting 2014
(28 April - 02 May 2014 at Pacifico YOKOHAMA, Kanagawa, Japan)

SIT40-P01 Room:Poster Time:May 1 18:15-19:30

An overview of seismic coupling and crustal deformation on the basis of geofluid and shallow slow earthquakes

ARIYOSHI, Keisuke[1*] ; MATSUZAWA, Toru[2] ; HINO, Ryota[3] ; HASEGAWA, Akira[2] ; HORI, Takane[1] ; NAKATA, Ryoko[1] ; KANEDA, Yoshiyuki[1]

[1]Japan Agency for Marine-Earth Science and Technology (JAMSTEC), [2]Research Center for Prediction of Earthquakes and Volcanic Eruptions, Tohoku University, [3]International Research Institute of Disaster Science, Tohoku University

Due to the use of broadband seafloor seismometers near the trench and dense inland networks of highly sensi-tive seismic stations, very low-frequency events (VLFEs) have been observed in the shallow transition zone near the trench of subduction plate boundaries as well as the deep one. Following the 2004 Sumatra Earthquake, the Japanese government has established the Dense Oceanfloor Network system for Earthquakes and Tsunamis (DONET) along the Nankai Trough. In the Tonankai district, M8-class megathrust earthquakes will probably occur in the near future; DONET-I has now operated since August 2011. In this study, we perform numerical simulations of multiscale earthquake cycles, including a megathrust earthquake and VLFEs, on a 3-D subduction plate boundary, in order to understand the change in VLFE activity after megathrust earthquakes and hydraulic pressure gauge data.

In our simulation, the motion equation for a subduction plate boundary is described by a quasi-dynamic equi-librium between the shear stress (due to reverse dip-slip on the discretized faults) and the frictional stress based on a rate- and state-dependent friction (RSF) law. To perform multiscale earthquake cycle simulations, we as-sumed single large asperity and numerous small asperities arranged along the strike direction, where the large asperity generates megathrust earthquakes and a chain reaction of numerous small asperities generate a migra-tion of slow earthquakes along the strike direction.

From our simulation results, we concluded as follows: (i) For a megathrust earthquake in which the coseismic slip penetrates to the trench, plate coupling in the postseismic stage will be strong in the region from the central part of the source region to the shallower part toward the trench, which will cause the shallow VLF after-events to be quiescent or to occur infrequently in isolation. On the outer rim, shallow VLF after-events will be reac-tivated earlier than they will be in the center because of weak plate coupling. (ii) Since leveling change due to slow earthquakes at DONET is expected to be local and incoherent in the same node because of the short dis-tance between their sources and the (DONET) receiver, it is useful to remove an average from original data in the same node in order to extract a signal.

Keywords: megathrust earthquake, subduction zone, seismic quiescence, high pore pressure, seafloor observation, rate- and state-dependent friction law

Japan Geoscience Union Meeting 2014
(28 April - 02 May 2014 at Pacifico YOKOHAMA, Kanagawa, Japan)

SIT40-P02 Room:Poster Time:May 1 18:15-19:30

Three-dimensional seismic attenuation structure beneath Kyusyu

SAITA, Hiroto[1*] ; NAKAJIMA, Junichi[1]

[1]Tohoku University

The Philippine Sea (PHS) plate is subducting beneath Kyusyu and a clear volcanic front is formed through the middle of the arc. Furthermore, there is a volcanic gap between Aso and Kirishima volcanos. Seismic attenuation provides additional insights into subduction-zone dynamics, because higher-temperature environments or the existence of fluids may have different effects on seismic attenuation from on seismic velocity. Therefore the estimate of seismic attenuation is very important to understand arc magmatism and mantle dynamics in subduction zone. This study estimates seismic attenuation structure beneath Kyushu using a large number of high-quality waveform data. Data and method

We used 5195 earthquakes that occurred from April 2003 to December 2013 by applying the method of Nakajima et al. [2013] to waveform data recorded at a nation-wide seismograph network in Japan. We determined the corner frequency of earthquakes by using the spectral ratio method of S-coda waves. Then, we determined a whole-path attenuation term (t∗), site-amplification factors and spectrum level simultaneously by a joint inversion. Finally, these t∗values (N= 75207) were inverted to obtain three-dimensional attenuation structure.

The obtained results show several interesting feature. First, the subducting PHS slab is imaged as a low attenuation zone. Second, an inclined high-attenuation zone that is interpreted as mantle upwelling flow is served in the back-arc mantle. However, the inclined high-attenuation zone is less developed in the volcanic gap between Aso and Kirishima volcanos. This correspondence suggests the important role of mantle-wedge processes in the genesis of arc magmas.

Keywords: seismic attenuation structure, Philippine Sea Plate, Kyusyu

Japan Geoscience Union Meeting 2014
(28 April - 02 May 2014 at Pacifico YOKOHAMA, Kanagawa, Japan)

SIT40-P03 Room:Poster Time:May 1 18:15-19:30

3D Electrical Resistivity Imaging beneath Kyushu by Geomagnetic transfer function data

HATA, Maki[1*] ; UYESHIMA, Makoto[1] ; HANDA, Shun[2] ; SHIMOIZUMI, Masashi[3] ; TANAKA, Yoshikazu[4] ; HASHIMOTO, Takeshi[5] ; KAGIYAMA, Tsuneomi[4] ; UTADA, Hisashi[1] ; MUNEKANE, Hiroshi[6] ; ICHIKI, Masahiro[7] ; FUJI-TA, Kiyoshi[8]

[1]Earthquake Research Institute, the University of Tokyo, [2]Faculty of Agricultural Science, Saga University, [3]Kyushu Polytechnic College, [4]Graduate School of Science, Kyoto University, [5]Institute of Seismology and Volcanology, Graduate School of Science, Hokkaido University, [6]Geographical Survey Institute, [7]Graduate School of Science, Tohoku University, [8]GSE,Osaka University

The Kyushu island in the Southwest Japan Arc has many Quaternary active volcanoes in relation to the subduction of the Philippine Sea Plate (PSP). The volcanoes exist along the volcanic front of N30^{o}E-S30^{o}W, whereas the volcanoes are densely located in the northern and southern regions of the island. The Kyushu island has a non-volcanic region in the central region of the island between the two volcanic regions. We performed three-dimensional (3D) inversion analyses to obtain a litospheric-scale electrical resistivity model beneath the entire Kyushu island using the Network-Magnetotelluric (MT) data. The electrical resistivity model, however, has a limited resolution in a horizontal direction because of the sparse Network-MT data in several areas of Kyushu. Thus data of geomagnetic variations are used anew to improve the uncertainty of the electrical resistivity structure in a horizontal direction. Data of geomagnetic variations were obtained at the entire Kyushu island and several islands off the western coast of Kyushu from 1980's to 1990's [e.g., Handa et al., 1992; Shimoizumi et al., 1997; Munekane et al., 1997]. In this study, accessible data of geomagnetic variations around Kyushu are compiled. Geomagnetic transfer functions for the data of geomagnetic variations in the northern Kyushu are re-estimated using the BIRRP code [Chave and Thomson, 2004] in order to enhance the quality of the transfer functions and their error estimation. The transfer functions at about 150 sites, which are 12 periods between 20 and 960 s, are obtained with improving quality at the entire Kyushu island. The induction vector representation [Parkinson, 1962] is generally used to delineate the lateral variation of electrical resistivity structure because the vectors point to current concentration in conductive anomalies. Induction vectors determined using the improved transfer functions have the following specific features. First, the vectors on the northern and central Kyushu do not point to the Pacific ocean off the eastern coast of Kyushu but point to the East China Sea of the shallow sea off the western coast of Kyushu. Second, the induction vectors on the southern Kyushu point to the Pacific ocean in the eastern part and point to the East China Sea in the western part at short period, whereas the vectors are arranged along a direction parallel to a direction of the coast line at longer period ($>$300 s). These results are consistent with the previous work [Handa et al., 1992; Shimoizumi et al., 1997; Munekane, 2000]. It is considered that the complex behavior of the induction vectors are influenced by conditions of the Earth's mantle relating to the igneous activities. Then we applied three-dimensional (3D) inversion analyses for geomagnetic transfer functions using the WSINV3DMT inversion code [Siripunvaraporn and Egbert, 2009]. The electrical resistivity of a starting model is based on values of the 3D electrical resistivity model estimated by using the Network-MT data. In this presentation, we will mainly describe features of the 3D electrical resistivity structure using the geomagnetic transfer functions and them of the 3D electrical resistivity structure using only the Network-MT data [Hata et al., 2013].

Japan Geoscience Union Meeting 2014
(28 April - 02 May 2014 at Pacifico YOKOHAMA, Kanagawa, Japan)

SIT40-P04 Room:Poster Time:May 1 18:15-19:30

Influence of confining and pore-fluid pressures on velocity and conductivity of a fluid-saturated rock

SEMA, Fumie[1*] ; MAKIMURA, Miho[1] ; HIGUCHI, Akiyoshi[1] ; WATANABE, Tohru[1]

[1]Department of Earth Sciences, University of Toyama

Pore-fluid pressure in seismogenic zones can play a key role in the occurrence of an earthquake (e.g., Sibson, 2009). Its evaluation via geophysical observation can lead to a good understanding of seismic activities. It is critical to understand how pore-fluid pressure affects seismic velocity and electrical conductivity. We have studied the influence of pore-fluid pressure on elastic wave velocity and electrical conductivity of water-saturated rocks.

Measurements have been made using a 200 MPa hydrostatic pressure vessel, in which confining and pore-fluid pressures can be separately controlled. An aqueous pore-fluid is electrically insulated from the metal work by using a specially designed device (Watanabe and Higuchi, 2013). Elastic wave velocity was measured with the pulse transmission technique (PZT transducers, f=2 MHz), and electrical conductivity the four-electrode method (Ag-AgCl electrodes, f=100 mHz-100 kHz) to minimize the influence of polarization on electrodes.

Berea sandstone (OH, USA) was used for its high porosity (19.1%) and permeability (~10^{-13} m^2). It is mainly composed of subangular quartz grains. Microstructural examinations show clay minerals (e.g., kaolinite) and carbonates (e.g., calcite) fill many gaps between quartz grains. A small amount of feldspar grains are also present. The grain size is 100-200 micrometers. Cylindrical samples have dimensions of 25 mm in diameter and 30 mm in length. Their axes are perpendicular to sedimentation bed. Elastic wave velocity is slightly higher in the direction perpendicular to the axis than in that parallel to the axis.

Confining and pore-fluid pressures work in opposite ways. Increasing confining pressure closes pores, while increasing pore-fluid pressure opens them. For a given pore-fluid pressure, both compressional and shear velocities increase with increasing confining pressure, while electrical conductivity decreases. When confining pressure is fixed, velocity decreases with increasing pore-fluid pressure while conductivity increases. The closure and opening of pores can explain observed changes of velocity and conductivity.

Effective confining pressure is defined by the difference between confining and pore-fluid pressures. Velocity increases with increasing effective confining pressure, while conductivity decreases. However, neither velocity nor conductivity is unique function of the effective confining pressure. For a given effective confining pressure, conductivity significantly increases with increasing confining pressure. Velocity also increases with increasing confining pressure, though it is not so significant. Increasing pore-fluid pressure can compress clay minerals to increase pore space. This might explain observed conductivity change.

Keywords: pore-fluid pressure, seismic velocity, electrical conductivity, geofluid

Japan Geoscience Union Meeting 2014
(28 April - 02 May 2014 at Pacifico YOKOHAMA, Kanagawa, Japan)

SIT40-P05 Room:Poster Time:May 1 18:15-19:30

A study on grain boundary brine in halite rocks using electrical conductivity measurements

WATANABE, Tohru[1*] ; KITANO, Motoki[1]

[1]Graduate school of science and engineering, University of Toyama

Intercrystalline fluid can significantly affect rheological and transport properties of rocks. Its influences are strongly dependent on the style of distribution. When a fluid fills grain boundaries in a rock, it will significantly reduce the strength of the rock. The fluid distribution is mainly controlled by the dihedral angle between solid and fluid phases. The grain boundary wetting is expected only when the dihedral angle is 0o. The dihedral angle of the halite-water system was studied through microstructural analyses of quenched materials (Lewis and Holness, 1996). The dihedral angle is 50˜70o at P<200 MPa and T<300 oC. However, deformation experiments (e.g., Watanabe and Peach, 2002) and cryo-SEM observations (e.g., Schenk et al., 2006) on halite rocks have indicated the coexistence of grain boundary brine with a positive dihedral angle. In order to understand the nature of grain boundary brine, we have conducted electrical impedance measurements on synthetic wet halite rocks over a wide range of pressure and temperature.

Wet halite rock samples (9 mm diameter and 6 mm long) are prepared by cold-pressing (P=140 MPa, 40 min.) of wet NaCl powder and annealing (T=180oC, P=180 MPa, 160 hours). Grains are polygonal and equidimensional with a mean diameter of 50-100 ?m. The porosity is less than 1 %. The volume fraction of brine is estimated to be 11.1% by the thermo gravimetric analysis. Microstructural observation shows that most of brine is enclosed inside halite grains. Electrical impedance is measured in the axial direction of a sample by a lock-in-amplifier (SRS, SR830) with a current amplifier (SRS, SR570). The cylindrical surface of a sample is weakly dried and coated with RTV rubber to suppress the contribution of surface conduction. A conventional externally heated, cold-seal vessel (pressure medium: silicone oil) is used to control pressure and temperature.

Electrical conductivity of wet halite rocks is higher than that of NaCl by orders of magnitude even at the conditions of the dihedral angle larger than 60 degrees. The conduction through brine dominates the bulk conduction. This is also supported by the quick conductivity change in response to the change in pressure. Brine is interconnected over a whole range of pressure and temperature.

No remarkable change in conductivity is observed around the condition of the dihedral angle of 60 degrees. Although the interconnection of triple-junction tubes might drastically change at the dihedral angle of 60 degrees, its influence on the bulk conductivity is masked by more conductive paths. A triple-junction tube is so stiff that it cannot give observed conductivity changes in response to changes in pressure. The dominant conduction paths are not triple-junction tubes. Grain boundary brine must be the dominant conduction paths.

Electrical conductivity decreases with increasing pressure. Larger change is observed for lower temperatures. A simple model of fluid tube with elliptical cross-section shows that the thickness of a fluid tube decreases by less than 10%. The observed large change in conductivity suggests that the conductivity of brine is strongly dependent on the fluid thickness. When the thickness is comparable to the molecular size, the mobility of ions must be sensitive to the thickness. The observed large change in conductivity might be caused by the decrease in ionic mobility.

Keywords: salt, grain boundary, water, electrical conductivity

Japan Geoscience Union Meeting 2014
(28 April - 02 May 2014 at Pacifico YOKOHAMA, Kanagawa, Japan)

SIT40-P06 Room:Poster Time:May 1 18:15-19:30

Estimation of the maximum burial depth of siltstones from the Kazusa Group by laboratory experiments

TAMURA, Yukie[1] ; MARUMO, Haruna[2] ; MITSUHASHI, Shunsuke[1] ; UEHARA, Shin-ichi[1*]

[1]Faculty of Science, Toho University, [2]Graduate School of Science, Toho University

To evaluate maximum burial depth of sedimentary formations is important for many topics in earth science and engineering such as estimating uplift and erosion of sedimentary basins. As a one of effective methods of the evaluation, a laboratory-based method for determining the maximum effective stress have been proposed. This method is based on a conventional method to evaluate preconsolidation stress (maximum effective stress experienced) of soil. However, this method cannot be necessarily applied to sedimentary rocks in simple ways, because sedimentary rocks have experienced not only mechanical compaction but also other processes such as cementation between grains, which should affect the mechanical properties of the rock. Thus applicability of this method to sedimentary rocks should be examined for several sedimentary basins. We performed laboratory experiments to measure porosity of siltstone specimens collected from several formations of the Kazusa Group, Boso peninsula, Japan, and tried to estimate the maximum burial depth based the results. We then compared the results with differences of burial depth ($\Delta Depth$) among locations of collecting samples which were estimated from geological setting, and examined the applicability of this method for estimation of the maximum burial depth in this site.

We collected rock blocks from Umegase (UMG), Otadai (OTD), Kiwada (KWD), Ohara (OHR), and Katsuura (KTR) Formations (in the descending order of stratigraphic horizon), and prepared cylindrical specimens of approximately 40 mm in diameter and 30 mm in length from these blocks. The porosity of these specimens was measured under different confining pressure (up to 35 MPa) and constant pore pressure (1 MPa) by using an intra-vessel deformation fluid-flow apparatus at Toho University. We used water as a pore fluid, and the measurements were performed at room temperature. Porosity under each effective pressure (the difference between confining pressure and pore pressure) was estimated by measuring volume of water drained from a specimen when confining pressure was loaded. The relation between measured porosity and effective pressure could be bilinear in log?log scale. The maximum effective stress experienced ($P_{e,B}$) of the tested rocks was determined from the intersection point of the two straight lines of the compaction curve. The maximum burial depth (D_{max}) was obtained by $D_{max} = P_{e,B} / [(\rho_r - \rho_w)g]$, where ρ_r, ρ_w and g are density of rock, water and gravity acceleration, respectively.

In the case of UMG, OTD and KTR, porosities decrease as the burial depth increases. Porosities of OHR and KWD, however, were relatively high although their burial depth is relatively large. There was a linear correlation between D_{max} and $\Delta Depth$ except for OHR, but the slope of the relationship was less than one (approximately 0.27). Therefore, further investigation is necessary to examine the applicability of this methods to this site. $P_{e,B}$ of OHR was less than that of other specimens, which supports the possibility that pore pressure in this formation was approximately 5 to 12 MPa higher than hydrostatic conditions.

Keywords: porosity, maximum burial depth, maximum effective stress experienced, Kazusa Group, overpressure, laboratory rock experiment

Japan Geoscience Union Meeting 2014
(28 April - 02 May 2014 at Pacifico YOKOHAMA, Kanagawa, Japan)

SIT40-P07 Room:Poster Time:May 1 18:15-19:30

Experimental constraints on the serpentinization rate under the antigorite-stable P-T condition

NAKATANI, Takayuki[1*] ; NAKAMURA, Michihiko[1]

[1]Earth and Planet Materials Sci., Tohoku Univ.

Water transport into the Earth's interior can be limited by the rate of serpentinization reaction proceeding at slow spreading ridges and along bending related faults (Iyer et al., 2012). Moreover, the distribution of H_2O in the mantle wedge may be controlled by the extent of progression of the reaction between the slab-derived fluid and the hanging wall mantle, as suggested by theoretical models (Iwamori, 1998). Previous hydration experiments for kinetic studies have been vigorously conducted at relatively low P-T condition (up to ca. 400 ℃ and 0.3 GPa) where the low T serpentine variety lizardite or chrysotile is stable. In contrast, antigorite is expected to be the dominant serpentine variety under the higher P-T condition corresponding to the deep oceanic lithosphere and the mantle wedge.

In order to constrain the serpentinization rates of peridotite under the antigorite- stbale conditions, we conducted piston-cylinder experiments at 580 ℃ and 1.3 GPa. Four types of starting materials were prepared from the crushed powder of a San Carlos lherzolite xenolith: 1) olivine (Ol), 2) orthopyroxene (Opx) + clinopyroxene (Cpx), 3) Ol + Opx, and 4) Ol+ Opx + Cpx + spinel. These systems were abbreviated as OL, OPX+CPX, OL+OPX, and LHZ, respectively. The starting materials were reacted with 15 wt% distilled water for 4-15 days. The formation of serpentine + talc + magnetite was observed in all the systems except for OL. Based on Raman spectroscopy results and crystal shapes, the synthesized serpentine mineral was identified as lizardite with 6?9 wt% Al_2O_3, rather than antigorite. The high Al_2O_3 content in the system possibly stabilized the aluminous lizardite at the experimental temperatures. Low silica activity precluded olivine reaction in the OL system, whereas olivine reacted with the SiO2 com-ponent in orthopyroxene to form lizardite and talc in the other systems. The reaction progress followed an interface-controlled rate law. The growth rate, G, was estimated to be 2.31 $\pm$ 0.37, 1.23 $\pm$ 0.20, and 2.78 $\pm$ 0.64 μm/day in the OPX+CPX, OL+OPX, and LHZ systems, respectively. As an example, we applied the hydration rates of peridotites, which were obtained experimentally, to a reactive-transport model for the convecting mantle wedge hydartion. In the case of grain-scale pervasive flow, the mass flux ratio of water fixable in the hanging wall peridotites to that supplied from the dehydrating oceanic lithosphere was calculated to be 2.7 $\times$ 105 - 1.5 $\times$ 108. This indicates that the water is completely fixable in the convecting mantle wedge and carried down to the stability limit of serpentine as soon as it is supplied from the slab. Aqueous fluid may penetrate all the way through the serpentine stable layer and reach the hot center of the mantle wedge only when the fluid migrates via crack-like pathways with a spacing $>$270-15000 m, which is not consistent with observations of natural serpentinites.

Keywords: hydration, serpentine, fluid, subduction zone, mantle wedge

Japan Geoscience Union Meeting 2014
(28 April - 02 May 2014 at Pacifico YOKOHAMA, Kanagawa, Japan)

SIT40-P08 Room:Poster Time:May 1 18:15-19:30

Diffusive kinetic isotope fractionaion of water in silicate glasses

KURODA, Minami[1*] ; YAMAMOTO, Daiki[1] ; TACHIBANA, Shogo[1] ; NAKAMURA, Michihiko[2] ; OKUMURA, Satoshi[2] ; ASAKI, Miho[2] ; ISHIBASHI, Atsuko[1] ; SAKAMOTO, Naoya[1] ; YURIMOTO, Hisayoshi[1]

[1]Department of Natural History Science, Hokkaido Unicersity, [2]Deparement of Earth Science, Tohoku University

Oversaturation of dissolved volatiles in an ascending magma leads to bubble nucleation and growth, which depend on volatile solubility and diffusivity, and drives explosive volcanic eruptions in the Earth. It is thus important to clarify the behaviors of volatiles in silicate melts in understanding the mechanism and dynamics of volcanic eruptions.

Hydrogen isotopes record the degassing processes of hydrous magmas due to isotopic fractionation between dissolved and exsolved water. The degree of hydrogen isotopic fractionation is correlated with the water content in natural volcanic rock samples; Deuterium is more deficient in water-poor samples, and the degree of D-deficiency increases as the water content decreases. This trend has been interpreted to reflect the transition of degassing model from that in a closed-system to in an open-system. However, these two extreme degassing schemes do not take the diffusive transport of water in magmas into account, which should be included in a realistic degassing model, because the timescale of diffusion is not necessarily negligibily small compared to that of degassing during magma ascent. Moreover, diffusion of water in silicate melts may cause kinetic isotope fractionation between silicate melt and explosive fluid phases because H_2O is likely to diffuse faster than HDO, of which effect can be overprinted in the D/H ratios of natural samples. The hydrogen isotopic fractionation during water diffusion in silicate melts, however, has not yet been fully determined. In order to determine the isotopic fractionation factor of hydrogen due to water diffusion in silicate melts, we performed diffusion experiments of water in SiO_2 and synthetic rhyolite glasses in a D-enriched systems(H/D=10, 5 and 1).

The experiments were performed for SiO_2 and rhyolite glasses at 850 ℃ and water pressure of 50 bar in sealed silica tubes and at 650 ℃ and water pressure of 500 and 1000 bar in a hydrothermal furnace developed at Tohoku University. Concentration profiles of H and D in run products were measured with the ion microprobe (Cameca ims-6f at Hokkaido University) to evaluate diffusion coefficients of water (including H_2O and HDO) in glasses. The obtained diffusivity (a diffusion coefficient divided by a water content) in SiO_2 glass at 650 and 850 ℃ were consistent with the values reported in previous studies (Davis and Tomozawa, 1995; Berger and Tomozawa, 2003). The D/H ratios along the diffusion profile were also analyzed for SiO_2 glasses with the ion microprobe. The D/H ratio first decreases, but apparently increases along the profile. The decrease of D/H ratio may imply the kinetic isotope fractionation during diffusion. However, the increase of D/H ratio cannot be explained simply by diffusion and may reflect the change of instrumental mass fractionation with water content (Hauri et al., 2006), which should be precisely determined to correct the profile of hydrogen isotopic ratio.

Keywords: eruption dynamics, silicate glass, water, diffusion, hydrogen isotope, isotopic fractionation

Japan Geoscience Union Meeting 2014
(28 April - 02 May 2014 at Pacifico YOKOHAMA, Kanagawa, Japan)

SIT40-P09 Room:Poster Time:May 1 18:15-19:30

Development of high-precision geobarometer

TAKAHATA, Kohei[1*] ; TORIMOTO, Junji[2] ; YAMAMOTO, Junji[2]

[1]Earth and Planetary System Science, Hokkaido University, [2]Hokkaido University Museum

Fluid inclusions in mantle-derived minerals can serve as a messenger from deep Earth. If CO_2 is a dominant phase of the fluid, the relationship between intensity ratio and frequency separation of the Fermi diad bands in the Raman spectra of CO_2 can be used for determination of density of the inclusions.

In this study, we installed new Raman spectrometer that was improved spectral resolution. And we also measured its precision of frequency separation (Δ). As a result of this study, we determined that the error of Δ is $\pm$ 0.003 cm^{-1} (1σ) . Converted into the error of density, this value is $\pm$ 0.0025 g / cm^{-1} .

Keywords: fluid inclusion, carbon dioxide, Raman spectroscopy, mantle xenolith, geobarometer

Japan Geoscience Union Meeting 2014
(28 April - 02 May 2014 at Pacifico YOKOHAMA, Kanagawa, Japan)

SIT40-P10 Room:Poster Time:May 1 18:15-19:30

Applications of rapid and precise 11B/10B isotopic analysis to water and rock samples

TANIMIZU, Masaharu[1*] ; NAGAISHI, Kazuya[2] ; ISHIKAWA, Tsuyoshi[1]

[1]Kochi Institute, JAMSTEC, [2]Marine Works Japan Ltd.

Boron isotope ratio is a powerful tracer in the fields of geochemistry, biochemistry, and environmental chemistry. Boron isotope ratios are determined by TIMS or MC-ICP-MS with precisions of better than 0.1 % RSD, but a large inter-lab discrepancy of 0.6 % is still observed for actual carbonate samples (Foster, 2008). Here, we are trying to determine B isotope ratio by MC-ICP-MS with a simple and common analytical techniques using a quartz sample introduction system with a PFA nebulizer, and compared to recently developed precise B isotope ratio analysis techniques by TIMS in positive ion detection mode determined as Cs2BO2+ ions with sample amount of <100 ng (Ishikawa and Nagaishi, 2011) and by MC-ICP-MS (Foster, 2008, Louvat et al., 2011).

In this year, our developed B analytical method above for carbonate and water samples are applied to rock samples. Resultant analytical reproducibility (twice standard deviation) was +/-0.04 % with a consumption of 50 ng B for several geochemical reference rocks issued from GSJ. Their relative differences from the standard were consistent with those determined by the positive TIMS within analytical uncertainty. Current potential B isotopic analysis by MC-ICP-MS will be discussed.

Japan Geoscience Union Meeting 2014
(28 April - 02 May 2014 at Pacifico YOKOHAMA, Kanagawa, Japan)

SIT40-P11 Room:Poster Time:May 1 18:15-19:30

Water migration with a subducting slab and the dynamic effects on whole mantle convection

KANEKO, Takeo[1*] ; NAKAKUKI, Tomoeki[1] ; IWAMORI, Hikaru[2]

[1]Dept. Earth and Planetary Systems Science, Hiroshima Univ, [2]Geochemical Evolution Research Program, JAMSTEC

Existence of liquid water is a characteristic of the earth. The water of interior of the Earths involved with the subducting plate reduces density and viscosity of the crustal and mantle rocks. These effects are essential to emerge the solid Earth activity such as, plate tectonics and island arc volcanism. Although the most of subducted water circulates through upper mantle, there is a possibility that portion of the water penetrates into lower mantle. Where does the water migrate? How much does the water affect mantle dynamics through the rock rheology and property? We performed numerical mantle convection simulation to investigate the water cycle and dynamic effects on the whole mantle convection.

In this study, we use the numerical model based on the model (Tagawa et al., 2007; Nakakuki et al., 2010) including the subducting oceanic plate driven dynamically. This model includes migration of water with the plate motion. We consider influences of reducing density and viscosity due to the water on the mantle flow (Karato and Jung, 2003). The maximum water content in the upper mantle is determined using phase relations of the basalt and the peridotite (Iwamori, 2004; 2007). We use various values of the maximum water content of rocks in the lower mantle, because it has been not clearly defined. We also treated the following physical properties as varying parameters: friction coefficient at the plate boundary, amount of the water injection at the trench, density-water dependence coefficient, and maximum water content in the lower mantle. Addition to we calculated dislocation creep by non-newtonian fluid or newtonian fluid.

A part of subducted water associate with the subducting oceanic plate is absorbed into peridotitic rocks and transported to about 150 km deep mantle. After that, dehydration with the serpentine decomposition occurs, and transported to deeper mantle by hot nominally anhydrous minerals (NAMs). The amount of dehydration at the 660 km phase boundary depends on the maximum water content of lower mantle, when the slab penetrates into lower mantle. The ejected water forms thin and high-water-content layer over the 660 km phase transition. As a result, the buoyancy of this layer induces instability, so that hydrated plumes are generated. We propose that this mechanism is important for the water cycle in the upper mantle. On the other hand, considerable portion of the water is transported into lower mantle with subducting slab, although notable water capacity of the lower mantle much smaller than that of the upper mantle, and reach core-mantle boundary. We have not yet observed notable water influence on mantle convection at lowermost mantle because of the small water concentration. Also, the hydrated materials do not rise to surface with hot plumes generated at the core-mantle boundary.

Keywords: mantle convection, plume, transition zone, water transport

Japan Geoscience Union Meeting 2014
(28 April - 02 May 2014 at Pacifico YOKOHAMA, Kanagawa, Japan)

SIT41-01 Room:314 Time:April 28 10:00-10:15

Microstructural and fabric characteristics of the uppermost mantle peridotites in the Taitao ophiolite, South America

YOSHIDA, Yoshiaki[1*] ; MICHIBAYASHI, Katsuyoshi[1] ; ANMA, Ryo[2]

[1]Institute of Geosciences, Shizuoka University, [2]Faculty of Life and Environmental Science, University of Tsukuba

The <6Ma young Taitao ophiolite, exposed at the westernmost promontory of the Taitao Peninsula, is located approximately 40 km southeast of the Chile triple junction and consists of a complete sequence of oceanic lithosphere, including ultramafic rocks, gabbros, a dyke complex and volcaniclastic rocks. The ophiolite is surrounded by several contemporaneous granite plutons intruded in between the ophiolite and the Pre-Jurassic metamorphic basement. Several studies have been carried out on the Taitao ophiolite and surrounding granites. Whereas they have focused mostly on petrology and geochemistry, we investigated microstructures and crystal-fabrics of the ultramafic rocks, aiming to understand the origin of the ophiolite. 6 out of 16 ultramafic rocks preserved peridotite textures despite of intense serpentinization and show mostly porphyroclastic textures consisting of pyroxene porphyroclasts with a fine-grained olivine-pyroxene matrix. Their olivine crystal-fabrics shows [100]{0kl} and [100](001) patterns. These indicate that the uppermost mantle section have remarkably been deformed before and/or during the obduction process after their formation beneath the mid-ocean ridge.

Keywords: Taitao ophiolite, mantle section, peridotite, microstructure, olivine fabrics

Japan Geoscience Union Meeting 2014
(28 April - 02 May 2014 at Pacifico YOKOHAMA, Kanagawa, Japan)

SIT41-02 Room:314 Time:April 28 10:15-10:30

Gabbroic petrology of oceanic lithosphere: comparison between Godzilla Megamullion and megamullions in mid-ocean ridges

YAMASHITA, Hiroyuki[1*] ; OHARA, Yasuhiko[2] ; ARIMA, Makoto[3]

[1]Kanagawa Prefectural Museum of Natural History, [2]Hydrog. & Oceanog. Dept. of Japan, [3]Yokohama National University

Godzilla Megamullion is the largest oceanic core complex on the Earth, with the dimension 125 km (along axis) and 55 km (across axis) (Ohara et al., 2001). Our study has revealed systematic petrological characteristics of the gabbroic rocks from the Godzilla Megamullion. In this contribution, we will report these characteristics and compare the results with those of gabbroic rocks from mid-ocean ridges.

Low modal abundance of olivine and high abundances of amphibole and iron oxide minerals are the prominent feature of the majority of the gabbroic rocks recovered from the Godzilla Megamullion. The studied gabbroic rocks are classified into troctolite, olivine gabbro, gabbro, hornblende pyroxene gabbro, pyroxene hornblende gabbro, hornblende gabbro on the basis of the classification by Streckeisen (1976). The chemical compositions of constituent minerals show systematic variations that are indicative of magmatic differentiation. Anorthite content in plagioclase, XMg (Mg/ (Mg + Fe) value in olivine and clinopyroxene decrease from less differentiated to highly siliceous evolved rocks. The mineral compositions indicate that troctolite is the most primitive variety and that trondhjemite is the most differentiated variety in the Godzilla Megamullion.

Troctolite, olivine gabbro and gabbro were recovered only from the distal parts of the Godzilla Megamullion. An age of ˜13 Ma has been reported from this region (Tani *et al*., 2011). On the other hand, trondhjemite was recovered from the medial and proximal parts of the megamullion, with ages of 11 and 8.7 Ma (Tani *et al*., 2011), respectively. Gabbroic rocks with relatively primitive composition were recovered from the Neck Peak region (age of 8.4 Ma; Tani *et al*., 2011). The spatial and temporal distribution of gabbroic rocks in the Godzilla Megamullion suggests the following magmatic model: a robust magmatic activity was predominant in the distal part, a declined magmatic activity in the medial to proximal parts, and a resurgent magmatic activity in the Neck Peak region. This model is consistent to the results obtained independently from petrological analysis on the peridotites from the Godzilla Megamullion (Snow *et al*., in preparation).

The lithological proportions of the gabbroic rocks in the Godzilla Megamullion are characterized by lower primitive gabbro (troctolite and olivine gabbro) ratio than in the Kane Megamullion in the Mid-Atlantic Ridge and in the Atlantis Bank in the Southwest Indian Ridge.

Keywords: Parece Vela Basin, Godzilla Megamullion, gabbro, Oceanic core complex

Japan Geoscience Union Meeting 2014
(28 April - 02 May 2014 at Pacifico YOKOHAMA, Kanagawa, Japan)

SIT41-03 Room:314 Time:April 28 10:30-10:45

The Po/So waves propagating in the Philippine Sea

SHITO, Azusa[1*] ; SUETSUGU, Daisuke[2] ; FURUMURA, Takashi[3]

[1]Institute for Geothermal Science, Kyoto University, [2]JAMSTEC, [3]Earthquake Research Institute, The University of Tokyo

The Po/So waves which have high-frequency content, large amplitude, and long-duration propagate for large distance (up to 3000 km) across the oceanic lithosphere. In our previous study, we analyzed Po/So waves from deep-focus earthquakes occurring in the subducting slab beneath Japan, recorded by broadband ocean bottom seismometers (BBOBSs) at northwestern Pacific [Shito et al., 2013]. We demonstrated that the Po/So waves are developed by multiple forward scattering of P and S waves due to laterally elongated heterogeneities in both the subducting and laterally extending oceanic lithosphere. Following this study, the question when and where do the small-scale heterogeneities form in the oceanic lithosphere comes about. In order to answer this question, the Po/So waves in younger oceanic lithosphere need to be analyzed. Therefore in this study, we investigate the Po/So waves in the Philippine Sea plate (15-60 Ma), which is much younger than the Pacific Plate (130 Ma).

The Philippine Sea is one of the marginal seas of the Pacific Ocean. It is fundamentally divided into two regions bounded by the Kyushu-Palau Ridge. It is thought that these two regions were formed in different episodes of back-arc spreading and that western part (45-60 Ma) is older than eastern part (15-30 Ma) [e.g., Seno and Maruyama, 1984]. The comparison of Po/So waves propagation in the different ages of the oceanic lithosphere is expected to reveal the origin of the small-scale heterogeneities.

Seismological observations using BBOBSs was conducted in the Philippine Sea from 2005 to 2008, and high-quality Po/So waves from earthquakes in subducting Philippine Sea plate were recorded very clearly. The findings from the observed Po/So waves in the Philippine Sea plate are summarized as follows. (1) The Po/So waves propagate much effectively in western part than eastern part of the Philippine Sea. (2) The Po/So waves propagate even in youngest oceanic lithosphere (15 Ma) near the past spreading center of the Shikoku Basin.

In order to reveal the structure of the oceanic lithosphere and propagation efficiency in the Po/So waves, we performed numerical FDM simulations of 2-D seismic wave propagation in a realistic oceanic lithosphere model. The model is developed in the same procedure as the case of the Pacific plate [Shito et al., 2013]. In the oceanic lithosphere, we introduce laterally elongated small-scale heterogeneities, which are described by von Karman type stochastic random distribution function. Because the thickness of the oceanic lithosphere is considered to correlate with the age [e.g., Kawakatsu, et al. 2009], we vary the thickness of the oceanic lithosphere from 80 km to 20 km. To evaluate the fit of the computed waveforms to the data, we use the spatial attenuation of the seismic wave energy along the record section (up to 1500 km). The seismic wave energy is defined as integrated squares of amplitudes in a certain tine window (25 s from the Po/So wave onset). The model with the thickness of the oceanic lithosphere of 60 km and 30 km successfully explain the spatial attenuation of the Po/So waves record section observed at western and eastern parts of the Philippine Sea, respectively. The thicknesses are consistent with those obtained by previous studies [Kawakatsu et al., 2009]

This result suggests that the oceanic lithosphere including small-scale heterogeneities grow as it ages and develop large-amplitude and long-duration of high-frequency Po/So waves. The small-scale heterogeneities may form at the bottom of the lithosphere as it cools. They suggest that small-scale melts in the asthenosphere are frozen and attached at the bottom of the lithosphere, which remain even after the lithosphere is subducted into the mantle.

Keywords: Po/So waves, Philippine Sea plate, oceanic lithosphere

Japan Geoscience Union Meeting 2014
(28 April - 02 May 2014 at Pacifico YOKOHAMA, Kanagawa, Japan)

SIT41-04 Room:314 Time:April 28 11:00-11:15

Multi-scale heterogeneity of abyssal peridotite

TAMURA, Akihiro[1*] ; MORISHITA, Tomoaki[1] ; ARAI, Shoji[1]

[1]Earth Sciences, Kanazawa University

Petrological studies of peridotite have increasingly revealed the origin of magma as well as materials and processes of Earth interior. Although we now only access to the interior indirectly, we can obtain the mantle-derived material brought by magma transporter or by large tectonic reconstruction of the earth surface. At the ocean floor near the mid-ocean ridge spreading center, where the deep seated rock is exposed along spreading axis or fracture zone, abyssal peridotite is collected. The abyssal peridotite studies significantly contribute not only to understanding of the formation of oceanic lithosphere but also to development of analytical way for the mantle material. In mineralogical and geochemical approaches, chromian spinel is a good indicator for the origin; for example, the spinel Cr# reflects a partial melting degree of the upper mantle material (e.g., Dick and Bullen, 1984; Arai, 1987). Trace-element compositions of clinopyroxene allow us to discuss the melting process quantitatively (e.g., Johnson et al., 1990). Recently, further discussions can be available by using ultra-trace elements and PGE isotopes (e.g., Harvey et al., 2006; Ishikawa, 2012).

Several petrological studies of abyssal peridotite samples have demonstrated ”regional-scale” heterogeneity of the upper mantle along Mid-Atlantic Ridge based on their spinel Cr# (e.g., Dick et al, 1984; Michael and Bonatti, 1985). In ”Global-scopic” differences between Atlantic, Indian and Pacific oceans, Niu and Hekinian (1997) proposed that the spinel Cr# of abyssal peridotite is dependent on spreading rate. Contrasting to such a heterogeneity, Ghose et al. (1996) and Dick et al. (2010) showed that the compositional variation of the abyssal peridotite is controlled by local structures at the mid-ocean ridge: for example, spreading axis, fracture zone, abyssal plane and oceanic core complex. Geochemical heterogeneity of each abyssal peridotite sample is recently discussed in aspects of magmatic event during or after partial melting stage (Tamura et al., 2008; Warren and Shimizu, 2010).

In our presentation, to review petrological characteristics of abyssal peridotite, we will demonstrate our compiling data set focused on relationship between their spinel Cr# and sample localities, such as ocean floor structures at the mid-ocean ridge. The example of abyssal peridotite sample heterogeneity are also discussed. Then, we would like to discuss the factor and significance of compositional variation of abyssal peridotite.

Keywords: abyssal peridotite, spinel, ocean floor

Japan Geoscience Union Meeting 2014
(28 April - 02 May 2014 at Pacifico YOKOHAMA, Kanagawa, Japan)

SIT41-05 Room:314 Time:April 28 11:15-11:30

Heterogeneity from mantle to crust at the central Southwest Indian Ridge (1) -Upper mantle-

MATSUNO, Tetsuo[1*] ; SEAMA, Nobukazu[2] ; SATO, Hiroshi[3] ; SATO, Taichi[4] ; SENDA, Ryoko[5] ; MACHIDA, Shiki[6] ; NAKAMURA, Kentaro[5] ; MORISHITA, Tomoaki[7] ; MIZUMA, Keiko[2] ; NOGI, Yoshifumi[1] ; OKINO, Kyoko[8]

[1]National Institute of Polar Research, [2]Kobe University, [3]Senshu University, [4]National Institute of Advanced Industrial Science and Technology, [5]Japan Agency for Marine-Earth Science and Technology, [6]Waseda University, [7]Kanazawa University, [8]University of Tokyo

Mantle is heterogeneous in terms of geophysical (e.g., bathymetry, geomagnetics, and gravity) and geological (e.g., petrology and geochemistry) aspects. Because heterogeneity is enhanced at slow spreading ridge, the ultra-slow spreading Southwest Indian Ridge (SWIR) is suitable for understanding the heterogeneity. We conducted geophysical and geological investigations since 2007 at the segment along the central SWIR between 35^{o}E and 40^{o}E, where the ridge segment is close to the Marion hotspot.

Serpentinised mantle peridotites occurring as clasts in the conglomerate were dredged from a topographic high within the Prince Edward fracture zone at 35^{o}E. A marine electromagnetic experiment was conducted along a 110 km transect across a subsegment at 37^{o}E to reveal an electrical resistivity structure of the upper mantle.

The peditotites are considered to have originally been lherzolite based on petrographic and mineral chemical composition analyses. Chemical compositions of spinel (Cr# and Mg#) in the peridotites suggest that the peridotites have undergone moderate partial melting without enhancement of melting by the hotspot regardless of proximity of the dredge site to the Marion hotspot. Light rare earth elements of clinopyroxene are more depleted than were previously reported for SWIR peridotites, suggesting that the peridotites have undergone little to no metasomatism of a melt-mantle interaction. Osmium isotope ratios are highly depleted, resulting in that a model age of rhenium depletion (T_{RD}) is 1 billion years. These results suggest that the dredged peridotites have not been enriched after the last melt extraction event 1 billion years ago, preserve their initial depleted compositions without hotspot effects, and show the presence of a refractory mantle domain under the central SWIR.

A preliminary 2-D electrical resistivity structure of the upper mantle down to 200 km depth does not show a remarkable conductive melting region beneath the ridge axis and a more conductive asthenospheric mantle than those observed at other mid-ocean ridges. The resistivity model suggests that the presence of the Marion hotspot does not result in enhancement of melt production beneath the ridge and enrichment of conductors like water in the upper mantle at present.

The result of this study suggests that the source mantle contain ancient, refractory, and depleted portion. This mantle may be a part of the depleted mantle prevailed under the Marion Rise, which was proposed by Zhou and Dick (2013) and may be supported by the absence of slow velocity anomalies around the Marion hotspot in upper mantle seismic tomography images (e.g., Zhao, 2007).

Japan Geoscience Union Meeting 2014
(28 April - 02 May 2014 at Pacifico YOKOHAMA, Kanagawa, Japan)

SIT41-06 Room:314 Time:April 28 11:30-11:45

Heterogeneity from mantle to crust at the central Southwest Indian Ridge (2) -Crust-

SATO, Hiroshi[1*] ; SATO, Taichi[2] ; MACHIDA, Shiki[3] ; SENDA, Ryoko[4] ; MATSUNO, Tetsuo[8] ; SEAMA, Nobukazu[5] ; NAKAMURA, Kentaro[6] ; MORISHITA, Tomoaki[7] ; NOGI, Yoshifumi[8] ; OKINO, Kyoko[9]

[1]Senshu Univ., [2]AIST, [3]Waseda Univ., [4]JAMSTEC, [5]Kobe Univ., [6]Dept. System Innovation, Univ. of Tokyo, [7]Kanazawa Univ., [8]NIPR, [9]AORI, Univ. of Tokyo

Mantle is heterogeneous in terms of geophysical (e.g., bathymetry, geomagnetics, and gravity) and geological (e.g., petrology and geochemistry) aspects. Because heterogeneity is enhanced at slow spreading ridge, the ultra-slow spreading Southwest Indian ridge is suitable for understanding the heterogeneity. We conducted geophysical and geological investigations since 2007 at the segment along the central Southwest Indian Ridge (SWIR) between 35E and 40E, where the ridge segment is close to the Marion hotspot.

Recent investigations of topography and geophysics along the central Southwest Indian ridge between 35E and 40E (Sato, T. et al., 2013) classify the segment between the Prince Edward and Eric Simpson fracture zones as four subsegments: PE-1, PE-2, PE-3, and PE-4 from west to east. A long oblique axial valley (NTD-1) is recognized between PE-1 and PE-2. Geochemical and isotopic compositions of MORB samples from these subsegments consist with previously reported MORB and/or SWIR basalts. However, small scale geochemical and isotopic heterogeneity are recognized in these samples. Sato, T. et al. (2013) considered that strong melt-focusing could be principle process to produce volcanic and low volcanic subsegment rather than the effect of proximity to the Marion hotspot. Continuous seafloor morphology and isochrons over off-axis areas of segment PE-1 and NTD-1 suggest that PE-1 shortened after the C2An chron, indicating the magmatic process has changed for several million years.

Among MORB from the subsegments, PE-1 and NTD-1, geochemically enriched sample (e.g. those with La/Sm>1) are enriched in isotope (higher Sr and lower Nd), suggesting that enrichment is due to source enrichment rather than smaller degree of melting of the homogeneous source mantle. Although geochemical and isotopic compositions could be explained by the mixture of depleted MORB source and the Marion components, contribution of the Marion component is limited only in the eastern part of PE-1 and NTD-1 subsegments. Therefore, it is reasonable to consider that source mantle beneath eastern part of PE-1 segment contains the enriched Marion components rather than direct contribution from Marion hotspot. Degree of enrichment (i.e. amount of enriched component) is higher beneath the present eastern part of PE-1 subsegment.

Sato, T. et al. (2013) pointed out that the melt supply center (tip of V-shaped bathymetric structure) between segment PE-1 and NTD-1 has migrated westward. It means that the enriched portion in the source mantle beneath PE-1 and NTD-1 subsegments has migrated westward. Melting of enriched, probably preferentially melting, components induced the strong melt-focusing process to form the V-shape bathymetric structure between PE-1 and NTD-1. This constraints the spatial scale and type of enriched component in depleted mantle.

References

Sato, T., K. Okino, H. Sato, M. Mizuno, T. Hanyu, and N. Seama (2013), Magmatic activities on the Southwest Indian Ridge between 35E and 40E, the closest segment to the Marion hotspot, Geochem. Geophys. Geosyst., 14, 5286?5307, doi:10.1002/2013GC004814.

Keywords: heterogeneity, mantle, crust, MORB, Southwest Indian Ridge

Japan Geoscience Union Meeting 2014
(28 April - 02 May 2014 at Pacifico YOKOHAMA, Kanagawa, Japan)

SIT41-07 Room:314 Time:April 28 11:45-12:00

Origin of Magnetization High at the Yokoniwa Hydrothermal Vent Fields, the Central Indian Ridge

FUJII, Masakazu[1*] ; OKINO, Kyoko[1] ; SATO, Taichi[2] ; SATO, Hiroshi[3] ; NAKAMURA, Kentaro[4]

[1]AORI, University of Tokyo, [2]Geological survey of Japan, AIST, [3]Senshu University, [4]University of Tokyo

Measurement of near bottom magnetic anomalies is an effective method to reveal the spatial extent of hydrothermal alteration zone and to find buried hydrothermal vent fields because hydrothermal alteration processes can change crustal magnetization by destruction and creation of magnetic minerals. In the Yokoniwa vent field (YVF), which is located at the top of the non-transform offset massif, called the Yokoniwa Rise, in the southernmost part of the Central Indian Ridge, a high magnetization zone was discovered by AUV r2D4 in 2009. Basalts and ultramafic rocks were found around the YVF, however the origin of positive magnetization and the relationships between high magnetization and hydrothermal activity are remains to be investigated.

In order to constrain the origin of magnetic source near the YVF, we conducted deep-sea geological observation and magnetic measurements using submersible Shinkai 6500 during the R/V Yokosuka cruises, YK09-13 and YK13-03. Vector geomagnetic field were successfully obtained along the all dive tracks at an altitude of ˜10 m. The distribution of crustal magnetization is estimated by vertical and horizontal components of magnetic anomalies using the 2-dimesional forward modeling technique and frequency analysis.

In the southern slope of the Yokoniwa Rise, serpentinized-peridotites were discovered and absolute magnetization shows entirely low (˜6 A/m). On the other hand, just around the YVF, hydrothermal sulfide deposits, tiny dead chimneys, shimmering and talc were observed and absolute magnetization shows relatively high (9 A/m). This magnetization contrast between the YVF and the surrounding area may be attributed to the difference in amount of magnetite, controlled by the degree and the temperature of serpentinization. One of the serpentinized-peridotite recovered during the cruises showed large amount of magnetite and high natural remanent magnetization. However, the highest absolute magnetization (20 A/m) was discovered at pillow basalt area with thin sediment just ˜700 m away from the YVF, implying recent off-axis volcanic activity. Therefore basaltic intrusion beneath the YVF is also possible for the origin of high magnetization. In addition, magnetic iron sulfide (pyrrhotite) grown during hydrothermal circulation, which is proposed at the Rainbow hydrothermal vent field, is also possible.

Consequently, we proposed three possibilities for the origin of high magnetization at the YVF; serpentinized peridotites with high temperature hydrothermal alteration, basaltic intrusion bodies, and pyrrhotites concentration. All of these hypotheses are related to hydrothermal activity. For the further inspection, recovering subseafloor rocks and inspection of rock magnetic properties are absolutely necessary.

Keywords: Seafloor hydrothermal activity, Mid-ocean ridge, Ultramafic rock, Deepsea magnetic anomaly, Off-axis volcanism, Oceani lithosphere

Japan Geoscience Union Meeting 2014
(28 April - 02 May 2014 at Pacifico YOKOHAMA, Kanagawa, Japan)

SIT41-08 Room:314 Time:April 28 12:00-12:15

Three-dimensional seismic structure of the Rainbow area, Mid-Atlantic Ridge 36 degree N

ARAI, Ryuta[1*] ; DUNN, Robert[1] ; CANALES, Pablo[2] ; SOHN, Robert[2]

[1]University of Hawaii, [2]Woods Hole Oceanographic Institution

Oceanic lithosphere formed along slow-spreading mid-ocean ridges is structurally and compositionally heterogeneous due to spatial and temporal variations in tectonic extension, magmatic accretion, and mantle temperature and composition. While mid-ocean ridges with greater magma supply host a greater abundance of hydrothermal systems, the relative roles of magmatic input, heat advection and faulting in controlling ridge structures are still poorly understood. These are particularly important to understanding formation and evolution of oceanic core complexes where ultramafic-hosted lithologies are exhumed at the seafloor by long-lived detachment faulting. The MARINER (Mid-Atlantic Ridge INtegrated Experiments at Rainbow) seismic and geophysical mapping experiment was designed to examine the relationship between tectonic rifting, heat/melt supply, and oceanic core complex formation at a non-transform offset of the Mid-Atlantic Ridge, 36 ^{o} 14 $'$ N, the site of the ultramafic-hosted Rainbow hydrothermal system. Using the seismic refraction data from this experiment, we constructed three-dimensional tomographic images of the crust and upper mantle around the Rainbow area. The seismic velocity images reveal undulations in crustal thickness across the ultramafic Rainbow massif, indicating temporal variations in melt supply, magmatic processes, and crustal construction. Previous studies suggest that a current heat source for the vents, which probably arises from a magmatic body, is required just beneath the hydrothermal vent, but the tomography does not detect a low-velocity anomaly indicating a significant magmatic system or high-temperature region beneath the Rainbow vent site. The only candidate region for high-temperatures and perhaps melt at shallow levels is much further to the south, and located roughly beneath the central valley of the spreading center. At the Rainbow massif, where mantle rocks have been recovered by direct sampling, mantle velocities near the seafloor are significantly reduced to ~ 5 km/s. This velocity reduction implies that an active hydrothermal circulation system altered the mantle via recharge and discharge of seawater.

Keywords: Slow-spreading ridge, Oceanic core complex, Rainbow hydrothermal field, Mantle alteration, Hydrothermal circulation, Seismic tomography

Japan Geoscience Union Meeting 2014
(28 April - 02 May 2014 at Pacifico YOKOHAMA, Kanagawa, Japan)

SIT41-09 Room:314 Time:April 28 12:15-12:45

Thermal structure of old oceanic upper mantle: Constraints from electrical conductivity imaging in the NW Pacific

BABA, Kiyoshi[1*] ; TADA, Noriko[2] ; LIANG, Pengfei[1] ; ZHANG, Luolei[1] ; SHIMIZU, Hisayoshi[1] ; UTADA, Hisashi[1]

[1]Earthquake Research Institute, The University of Tokyo, [2]Japan Agency for Marine-Earth Science and Technology

Northwestern part of Pacific plate is very old as the crustal age is over 100 Ma. Seafloor subsidence and heat flow change with age for such old ocean have been explained by cooling of a plate with constant thickness (e.g., Parsons & Sclater, 1977; Stein & Stein, 1992). Electrical conductivity of the upper oceanic mantle typically has resistive layer over a conductive zone reflecting the thermal structure. However, our recent results on the electrical conductivity of the upper mantle beneath northwestern Pacific suggest that a simple plate cooling model can not explain the observations.

We have run marine electromagnetic observation in two areas (Areas A and B) of the northwestern Pacific since 2010. Areas A and B locate northwest and southeast of Shatsky Rise, respectively. Although a part of the observation is still going on, we analyzed the data collected by the last year to obtain magnetotelluric responses and one-dimensional (1-D) electrical conductivity structure beneath the observation areas. Here, we compare the results together with a model obtained for the mantle beneath the Pacific ocean off the Bonin Trench (Area C) by a past project. The mean lithospheric ages of Area A, B, and C are about 130, 140, and 147 Ma, respectively. Based on a plate cooling model, the age differences for the thermal structure among the areas are very small. However, the obtained electrical conductivity models show significant difference in the thickness of the resistive layer. The depth the mantle become more conductive than 0.01 S/m are about 80 km for Area A, about 110 km for Area B, and about 200 km for Area C. These differences can not be reconstructed from the age difference of a single plate cooling model.

Our observations revealed that there is large scale lateral heterogeneity in electrical conductivity. We need to consider another factors rather than age difference of the thermal structure to explain such the lateral heterogeneity.

Keywords: oceanic upper mantle, northwestern Pacific, magnetotellurics, electrical conductivity structure, thermal structure

Japan Geoscience Union Meeting 2014
(28 April - 02 May 2014 at Pacifico YOKOHAMA, Kanagawa, Japan)

SIT41-10 Room:314 Time:April 28 14:15-14:30

PGE abundances and Os isotope ratios of troctolites from pacific oceanic lithosphere

SENDA, Ryoko[1*] ; ISHIKAWA, Akira[2] ; MORISHITA, Tomoaki[3] ; SUZUKI, Katsuhiko[1] ; ISHII, Teruaki[4]

[1]JAMSTEC, [2]Department of Earth Science and Astronomy, The University of Tokyo, [3]School of Natural System, Colleage of Science and Technology, Kanazawa University, [4]Fukada Geological Institute

The structure of oceanic lithosphere becomes much clear in these days. Troctolite is a kind of gabbro, mainly consisting of olivine and calcic plagioclase with minor pyroxene, found in oceanic lithosphere. Melt-rock interactions at mantle-crust transition zone are believed to play a main role for troctolite formation. Troctolites are locally found at Atlantis Massif oceanic core complex, Mid Atlantic Ridge 30 iii N (Blackman et al., 2006), at Kane Megamullion, Mid Atlantic Ridge 23N (Dick et al., 2008; 2010), at Uraniwa Hills, Central Indidan Ridge (Nakamura et al., 2009), and at Godzilla Megamullion, Parece Vela Basin of the Philippine Sea (Sanfilippo et al., 2013). They also occurred as sections of the oceanic lithosphere in ophiolites and show similarity to lower crust sections from slow and ultra-slow spreading ridges (e.g., Herbert et al., 1989; Sanfilippo and Tribuzio, 2013). The formation process of the troctolites is in debate. From the ophiolite studies, troctolites were formed as cumulates from primitive basalts in a closed system (Bezzi and Piccardo, 1970; 1971; Borghini and Rampone, 2007). Alternatively, troctolites were the results of a substantial amount of mantle olivine incorporated into the lower oceanic crust (Suhr et al., 2008; Drouin et al., 2009; 2010) based on the studies of oceanic core complex.

Troctolites were also found in the drilled core at site 895 of ODP Leg 147 in Hess Deep, located at a triple junction between EPR and Cocos-Nazca plate boundary. Hess Deep is a small rift with intra-rift ridges, where deep-seated rocks probably formed at EPR are exposed (Francheteau et al., 1990; 1992). Ultramafic and related rocks were expected to be found at the site in fast-spreading ridge system and sequences of dunite, harzburgite, troctolite, and gabbro were actually drilled (Allan and Dick, 1996; Dick and Natland, 1996; Arai and Matsukage, 1996). Troctolite appears to be transitional from dunite to olivine gabbro (Arai and Matsukage, 1998).

Major, trace and platinum group element (PGE) abundances and Os isotope ratios of troctolites from Holes 895C, 895D and 895E were newly measured using XRF, ICP-MS, and TIMS. The samples are clearly divided in two groups by Al_2O_3, MgO and NiO. Prichard et al. (1996) reported the PGE and trace element abundances of the ultramafic rocks from Holes 895. Their PGE concentrations of the troctolites were in a similar range to hartzburgites and dunites from the same sites and Pt and Pd are enriched in some troctolites. They also found platinum-group alloys and base metals in troctolites. New data set with Os isotope ratios possibly make constraints on the forming process of troctolites under the oceanic ridge.

Keywords: troctolite, Os isotope ratio, PGE abundance, oceanic lithosphere

Japan Geoscience Union Meeting 2014
(28 April - 02 May 2014 at Pacifico YOKOHAMA, Kanagawa, Japan)

SIT41-11 Room:314 Time:April 28 14:30-14:45

The origin for the olivine-rich troctolites from the oceanic lithosphere: remnants of a reactive MOHO

SANFILIPPO, Alessio[1*] ; MORISHITA, Tomoaki[2] ; HARA, Kaori[2] ; TAMURA, Akihiro[2] ; ARAI, Shoji[2]

[1]University of Pavia, Kanazawa University, [2]Kanazawa University

Olivine-rich troctolites are documented since the early 1970s in the lower crust and mantle sections of the Jurassic oceanic lithosphere exposed along the Alpine-Apennine belt (Italy). These rocks were first interpreted to be cumulates formed by precipitation of olivine and accessory spinel from primitive basalts (Bezzi A. and Piccardo G.B., 1971. Mem. Soc. Geol. It.). The founding of olivine-rich troctolites bodies within the gabbroic sections of the Hess Deep (East Pacific Rise) and Atlantis Massif and Kane Megamullion (Mid Atlantic Ridge) called into question this idea, suggesting that they may represent portion of the crust-mantle transition entrapped during the growth of the lower crust (Arai and Matsukage, 1996, Lithos; Suhr et al., 2008, G-cubed). Recently, Japanese scientific cruises found olivine-rich troctolites associated with mantle harzburgites at the Godzilla Megamullion (Philippine Sea) [3] and at the Uraniwa Hills (Central Indian Ridge) (Nakamura et al., 2009, EPSL; Sanfilippo et al., 2013, J. Petrol.). We show that the olivine-rich troctolites from all these occurrences show peculiar structural and compositional features: i) highly variable forsterite, Ni and Co contents of olivine; ii) high Mg/(Mg+Fe), high Cr_2O_3 contents, and fractionated incompatible element compositions (i.e. Ti/REE and Zr/REE) of clinopyroxene; iii) the occurrence hydrous silicate mineral inclusions in spinels anomalously enriched in TiO_2. These features agree with the idea that olivine-rich troctolites formed through reactions between a pre-existing olivine-matrix and migrating melts [see also Renna and Tribuzio, 2011, J. Petrol.). In particular, we suggest that these chemical features were acquired at the crust-mantle transition, through interactions between mantle peridotites and melt stagnating at the base of the igneous crust. The occurrence of olivine-rich troctolites both at slow- to intermediate spreading ridges and at back-arc settings suggests that melt-peridotites reaction processes constrain the Moho under the totality of the oceanic plates.

Keywords: Ocean floor, Peridotite, Troctolite, Melt-Mantle reaction, Moho

Japan Geoscience Union Meeting 2014
(28 April - 02 May 2014 at Pacifico YOKOHAMA, Kanagawa, Japan)

SIT41-12 Room:314 Time:April 28 14:45-15:15

Experimental study of anelasticity of a polycrystalline material for seismological application

TAKEI, Yasuko[1*] ; YAMAUCHI, Hatsuki[1] ; KARASAWA, Fumiya[2]

[1]Earthquake Research Institute, Univ. of Tokyo, [2]Yahoo, Japan

Rock anelasticity causes dispersion and attenuation of seismic waves. Therefore, for the quantitative interpretation of seismic low velocity and/or low Q regions in the upper mantle, understanding of rock anelasticity is necessary. However, due to the difficulty of forced-oscillation experiment under high-temperature (>1000^{o}C) and small strain (<10ˆ-6) conditions, systematic data on rock anaelasticity, needed for the understanding of underlying mechanisms, have not been obtained adequately. To address this lack of data, data from rock analogue (polycrystalline organic borneol) will be of merit. Our recent result published in McCarthy et al (2001) has shown that anelasticity of polycrystalline materials is subject to the Maxwell frequency scaling: Q = Q(f/fm). However, the applicability of this scaling to the seismic dispersion and attenuation has not been guaranteed because experimentally testing frequencies normalized to the Maxwell frequency fm of the laboratory samples are usually much lower than the seismic range in the upper mantle (10^6 <f/fm <10^9). In this study, by using borneol as an analogue to mantle rock, we measured anelasticity up to higher normalized frequencies (0.1 <f/fm <10^8), and examined the applicability of the Maxwell frequency scaling to these new data. The obtained data show that the Maxwell frequency scaling is no more applicable to higher normalized frequencies than f/fm = 10^4, where attenuation spectra plotted as functions of f/fm scatter significantly by temperature, grain size, and impurity. Especially, a small amount of impurity (diphenylamine) significantly enhanced the anelastic relaxation. The addition of dyphenylamine to borneol significantly lowers the melting temperature from Tm=477 K to Tm=316 K. From these results, we have speculated that the enhancement of anelasticity with impurity and/or temperature might be scaled by T/Tm. If this speculation is true and can be generalized to the other polycrystalline materials, it will give a crucial insight for the underlying mechanism. Because T/Tm is close to one in the upper mantle and it is important to investigate the detailed behavior of anelasticity near T/Tm=1.

Keywords: anelasticity, polycrystalline material

Japan Geoscience Union Meeting 2014
(28 April - 02 May 2014 at Pacifico YOKOHAMA, Kanagawa, Japan)

SIT41-13 Room:314 Time:April 28 15:15-15:30

Seismic structural changes in the incoming oceanic plate beneath the well-developed horst and grabens

FUJIE, Gou[1*] ; TAKAHASHI, Tsutomu[1] ; KODAIRA, Shuichi[1] ; OBANA, Koichiro[1] ; YAMADA, Tomoaki[2]

[1]JAMSTEC, [2]ERI, Univ. of Tokyo

Recent seismic, electromagnetic, and thermal structure studies in the trench-outer rise region have revealed the structural changes of the incoming plate in the trench-outer rise region. These structural changes are considered to be caused by the plate bending-related faulting and water penetration. However, there are many unresolved questions such as the maximum depth of the structural changes, the mechanisms of the water penetration, and the source of the water.

The northwestern Pacific margin, where extremely old (more than 120Ma) oceanic plate is subducting, is a good place to study structural changes in the incoming plate prior to subduction, because the horst and graben structure, which is caused by the bending-related faulting, is well developed in this region. However, the former seismic survey could not revealed the seismic structure around the trench axis, where seismic structure is expected to be significantly changed, because of the large water depth in the vicinity of the trench axis.

In 2013, we conducted extensive wide-angle seismic reflection and refraction surveys across the Japan trench with use of ultra-deep Ocean Bottom Seismometers (OBSs). Our obtained data enabled us to reveal the seismic structure in the vicinity of the trench axis, and we confirmed that the bending-related structural changes reach to the top of the oceanic crust. In addition, in the record sections obtained at the deep grabens, we observed seismic waves that laterally propagate within the sedimentary layer as well as the phases vertically propagate within the sedimentary layer. These two phases provided us new insights to the sedimentary structure, which implies that the bottom of the sedimentary layer can be the water source to the oceanic crust in the trench-outer rise region.

Keywords: oceanic plate, trench-outer rise region, bending-related faults, seismic structure, water contents, ocean bottom seismometer

Japan Geoscience Union Meeting 2014
(28 April - 02 May 2014 at Pacifico YOKOHAMA, Kanagawa, Japan)

SIT41-14 Room:314 Time:April 28 15:30-15:45

Mafic minerals within a sediment core sampled by ABISMO in Mariana Trench

MICHIBAYASHI, Katsuyoshi[1*] ; TERUMINE, Naonobu[2] ; HARIGANE, Yumiko[3] ; NUNOURA, Takuro[4] ; UEHARA, Shigeki[1] ; OHARA, Yasuhiko[5] ; MIYAZAKI, Junichi[4] ; TAKAI, Ken[4]

[1]Institute of Geosciences, Shizuoka University, [2]Institute of Geosciences, Shizuoka University, [3]AIST/GSJ, [4]JAMSTEC, [5]Hydrographic and Oceanographic Department of Japan

Mariana Trench is one of the deepest oceans in the world more than 10,000 m depth. Although the mantle section outcrops along the land-side slope of the southern Mariana Trench, the studied depth so far is approximately shallower than 7,000 m and therefore few geological information is available for the mantle section deeper than 7,000 m. In 2008, a sediment core has been sampled at 10,350 m in Challenger Deep of Mariana Trench by ABISMO (Automatic Bottom Inspection and Sediment Mobile) during KR08-05 cruise. The sediment core is 161.5 cm in length and contains mafic sandy grains such as olivine and spinel. In this study, we sampled the mafic minerals from the sediment core and analyzed their major element compositions. As a result, the chemical compositions of the mafic sandy grains were compatible with those of mafic minerals within the peridotites along the land-side slope of Mariana Trench shallower than 7,000 m. We will discuss the origin of these sandy grains.

Keywords: ABISMO, Mariana Trench, Challenger Deep, sediment core, spinel, olivine

Japan Geoscience Union Meeting 2014
(28 April - 02 May 2014 at Pacifico YOKOHAMA, Kanagawa, Japan)

SIT41-15 Room:314 Time:April 28 15:45-16:00

High Ni and Mg olivine as a time recorder of chromitite P-T history

MIURA, Makoto[1*] ; ARAI, Shoji[1] ; YAMAMOTO, Shinji[2] ; SHMELEV, Vladimir[3]

[1]Department of Earth Sciences, Kanazawa University, [2]Department of Earth Science and Astronomy, University of Tokyo, [3]Institute of Geology and Geochemistry, Ural Brance Russian Academy of Sciences

High Ni and Mg olivines were found in dunites enveloping podiform chromitites from Oman, Ray-Iz and Luobusa ophiolites. These high Ni and Mg olivines occur only in dunite adjacent to chromitite. This characteristic suggests subsolidus Ni and Mg diffusion from the chromites of the chromitite. In the case of dunite enveloping concordant chromitite from Oman ophiolite, olivines show high NiO (up to 0.5 wt %) and Fo (around 92 mol %) contents. This is not the case, however, for the dunite envelope around the discordant chromitite in the Oman ophiolite. On the other hand, olivines in dunite enveloping UHP chromitites from Ray-Iz and Luobusa ophiolites are extraordinarily high in Fo value (94 - 96) and NiO (around 0.5 wt %). Silicate exsolution lamellae in spinel from UHP chromitites and concordant chromitite suggest that these chromitites have experienced substantial cooling, and probably decompression, for a longer priod than the discordant chromitite from Oman. According to the well-known Ni and Mg diffusion coefficients in olivine, the high-Ni and -Mg olivine in the dunite envelope may constrain the cooling duration of the chromitite and the history of ophiolite. Podiform chromitites are enigmatic in origin, and their origins should be systematically classified to understand concerning mantle processes. Their temporal relationship is a clue to solve this problem.

Keywords: Olivine, Ni and Mg diffusion, Podiform chromitite, Low pressure chromitite, Ultra-high pressure chromitite, P-T history

Japan Geoscience Union Meeting 2014
(28 April - 02 May 2014 at Pacifico YOKOHAMA, Kanagawa, Japan)

SIT41-16 Room:314 Time:April 28 16:15-16:30

Geochemistry and genetic conditions of primary boninites from the Ogasawara Island Group and Oman ophiolite

KITAMURA, Keitaro[1*] ; KANAYAMA, Kyoko[1] ; UMINO, Susumu[1] ; ISHIZUKA, Osamu[2] ; KUSANO, Yuki[1]

[1]Department of Earth Sciences, Kanazawa University, [2]Geological Survey of Japan/AIST

Subduction initiation and arc crust evolution along oceanic plate boundaries are fundamental processes that modify oceanic lithosphere and promotes the material evolution of the Earth. How subduction of oceanic plates initiates and develops largely depend on the thermochemical structure and mechanical strength of the colliding two plates. The resulting conditions of the wedge mantle can be best represented by the varying geochemistry of primary magmas produced through the subduction initiation. For example, the subduction zone in the Izu-Bonin (Ogasawara)-Mariana (IBM) arc started with an intense high-Si to low-Si boninite magmatism during 48-45 Ma (Ishizuka et al., 2006; Kanayama et al., 2012). By contrast, the subduction stage of the Oman Ophiolite lacked typical boninite and is characterized by the low-Si boninite magmatism (Ishikawa et al., 2002; Kusano et al., 2014). Because of its high Mg#s and andesitic chemistry, boninite is generally considered to be a candidate of a primary magma derived from the hydrous upper mantle, and therefore, its compositional variations reflect various thermochemical conditions of the source mantle. The geochemical and petrological studies on boninite magma genesis can provide crucial information on the evolution of arc and the formation of continental crust. Boninites are distinct from ordinary arc magmas in highly depleted U-shaped and depleted spoon-shaped chondrite-normalized rare earth elements (REE) patterns.

We have investigated melt (glass) inclusions enclosed by boninite-derived chrome spinel grains in beach sand, called “uguisu-zuna” from Ogasawara islands, and in wadi sand from the Oman Ophiolite. We analyzed major- and trace-element compositions of the boninitic melt inclusions by EPMA and LA-ICP-MS (Kanazawa Univ.) and H2O by SIMS (Hokkaido Univ. Creative Research Institution). Glass inclusions in spinel have more Mg-rich compositions than aphyric whole rocks, indicating their primitive nature since derivation from the source mantle, which experienced least modification by the processes such as crystal fractionation, and assimilation and contamination by the crust. Volatile measurements of melt inclusions confirmed that they were only slightly degassed and retain primitive contents. Five geochemical types (BIC-1~5) are identified among boninites from the Ogasawara Islands and a single geochemical type from the Oman Ophiolite. Both Ogasawara and Oman low-Si boninites show lower H2O contents than high-Si boninites. Assuming that the most magnesium-rich melts of each geochemical type in Ogasawara and Oman boninites coexisted with olivine and orthopyroxene, the P-T conditions of these primary boninite magmas were estimated by using the geothermobarometers of Putirka et al. (2007) and Putirka (2008). High-Si boninites erupted on the Ogasawara Islands during 48-46 Ma were generated at 1400-1440 ℃ and 0.7-0.9 GPa, whereas the subsequent low-Si boninite at 45 Ma formed at 1380-1400 ℃ and 0.8-0.95 GPa. This suggest that the geothermal gradient descended from 48 Ma to 45 Ma. On the other hand, low-Si boninite from the Oman Ophiolite was generated at 1320 ℃ and 0.5 GPa. Hence, it is apparent that the wedge mantle beneath the proto-IBM arc was significantly hotter than that in the Oman paleoarc.

Keywords: subduction initiation, IBM forearc, Oman Ophiolite, high-Si boninite, low-Si boninite, melt inclusion

Japan Geoscience Union Meeting 2014
(28 April - 02 May 2014 at Pacifico YOKOHAMA, Kanagawa, Japan)

SIT41-17 Room:314 Time:April 28 16:30-16:45

Thermo-chemical evolution of mantle wedge during the incipient stage of the Izu-Ogasawara-Mariana subduction zone

KANAYAMA, Kyoko[1*] ; KITAMURA, Keitaro[2] ; UMINO, Susumu[1] ; ISHIZUKA, Osamu[3]

[1]College of Science and Engeneering, Kanazawa University, [2]Graduate School of Natural Science and Technology, Kanazawa University, [3]Geological Survey of Japan/AIST

It is essential to understand the processes of subduction zone initiation and evolution of oceanic arcs which promote the development of Earth's structure and composition. We present the genetic conditions of the Eocene magmas from the Ogasawara (Bonin) Ridge and discuss the thermo-chemical structure of the mantle wedge beneath the Ogasawara region during the incipient stages of the IBM arc. On the Ogasawara Ridge, MORB-like basalt (forearc basalt: FAB) is generated just after the beginning of subduction of the Pacific Plate at 52 Ma, followed by ultra-depleted high-Si boninite activities began at 48Ma. This high-Si boninite magmatism gradually changed through less-depleted low-Si boninite at 45 Ma to arc tholeiite and calc-alkaline magmatism [1, 2].

Major element compositions of high- and low-Si boninites are similar to those of experimentally produced melts of harzburgite [3] and lherzolite [e.g. 4], respectively. Ultra low concentrations in rare earth elements (Yb$>$0.3 ppm) of high-Si boninite also indicate a depleted harzburgite source. On the other hand, characteristically high Zr/Ti ratio ($<$0.04) of boninites from the Ogasawara Islands reflects high contributions of slab melt [2]. FAB is produced by less than 10 % fractional melting of MORB source mantle, leaving residue of moderately depleted lherzolite. This suggests that the residue of FAB cannot be the highly depleted source of high-Si boninite.

P-T conditions at which the most primitive boninitic melts can coexist with harzburgite are 1430 ℃ and 0.83-0.96 GPa for high-Si boninite (MgO=23, H_2O=3.2 wt%) and 1380 ℃ and 0.86 GPa for low-Si boninite (MgO=19, H_2O=2.6 wt%) [5]. Genetic conditions of magmas other than boninite are dry, ˜1350 ℃ and 1.3-1.7 GPa for FAB and water-undersaturated (0-0.5 wt%), 1300-1350 ℃ and 1-1.2 GPa for arc tholeiitic and calc-alkaline magmas, which were estimated by comparing calculated primitive liquid compositions with experimentally produced liquid compositions of lherzolite melting [e.g.4].

Mantle potential temperatures (T_p) calculated based on MgO content of primary magmas are 1500 ℃ for high-Si boninite and 1450 ℃ for low-Si boninite, which are higher than the ambient mantle (T_p=1300-1400). Especially Tp for high-Si boninite is comparable to T_ps of mantle plumes [6]. This result is consistent with plume-related magmatism (51-45Ma) in the West Philippine Basin simultaneously with the high-Si boninite magmatism in the Ogasawara Ridge [7]. The ultra-depleted source of high-Si boninite is possibly the residue of the plume-related magmatism. T_p of FAB and arc tholeiitic and calc-alkaline magmas is 1400 ℃, equivalent to the ordinary oceanic mantle.

From the above, the thermo-chemical history of the mantle wedge beneath the Ogasawara Ridge during the incipient stage of the IBM subduction zone is advocated as follows; Spontaneous sinking of old, dense Pacific Plate induced upwelling of asthenosphere which melted to produce FAB in eastern margin of the Philippine Sea Plate at 52 Ma. At 48 Ma, depleted residual harzburgite of plume-related magmatism upwelled from deeper (˜3.5 GPa ?) asthenosphere to 1 GPa, suffering flux melting incorporating slab melt to generate the high-Si boninite magma. By 45 Ma, shallow mantle wedge was cooled by the subducted slab and asthenosphere began circulating in the wedge. As a result, magma composition changed from high-Si boninite through low-Si boninite to arc tholeiite and calc-alkaline magmas more fertile than the Quaternary frontal lava. Subsequently the IBM subduction zone changed to a stable arc-trench system.

[1] Ishizuka et al. (2011) EPSL, 306, 229-240. [2] Kanayama et al. (2012) Island Arc, 21, 288-316. [3] Falloon and Danyushevsky (2000) J. Petrol., 41, 257-283. [4] Hirose and Kawamoto (1995) EPSL, 133, 463-473. [5] Kitamura et al. (2014) JPGU. [6] Herzberg and Gazel (2009) Nature, 458, 619-623. [7] Ishizuka et al. (2013) Geology, 41, 1011-1014.

Keywords: Ogasawara (Bonin) Islands, boninite, mantle wedge, IBM arc, mantle potential tempareture, subduction zone

Japan Geoscience Union Meeting 2014
(28 April - 02 May 2014 at Pacifico YOKOHAMA, Kanagawa, Japan)

SIT41-18 Room:314 Time:April 28 16:45-17:00

Hot and ephemeral subduction zone magmatisms in the Oman Ophiolite

KUSANO, Yuki[1*] ; KITAMURA, Keitaro[1] ; ADACHI, Yoshiko[2] ; SHINJO, Ryuichi[3] ; UMINO, Susumu[1] ; MIYASHITA, Sumio[2]

[1]Kanazawa University, [2]Niigata University, [3]University of Ryukyus

Subduction zone is initiated by descending oceanic plate at the plate boundary and a counter flow of the mantle advances growth of the wedge mantle in the Izu-Ogasawara-Mariana arc (e.g. Stern, 2004). But it is questioned that do initial arc always develop a long-survived subduction zone? We present detailed volcanostratigraphy, petrology and geochemistry of short-lived juvenile arc tholeiite and subsequent boninite magmatism from the northern Oman ophiolite.

The Oman ophiolite belonging to the Tethys ophiolite belt is one of the best places to investigate magmatic and volcanic developing processes of an infant arc. The Ophiolite had formed on a spreading axis and followed by subduction stage magmatism at approximately 100 Ma. The V2 sequence was constructed by initial arc magmatism begun $<$2 m.y. after the spreading ridge stage (e.g. Hacker et al., 1996). Based on the radiolarian fossil age, the V2 volcanism ceased 2-3 m.y. after the ridge stage (Kurihara and Hara, 2012), therefore, it seems to record short-spanned island arc magmatism.

An 1110 m thick V2 sequence is divided into the lower 970 m (LV2) and upper 140 m (UV2) thick subsequences by a 1.0 m thick sedimentary layer in Wadi Bidi. Pahoehoe flows dominate in the lower part of the LV2, while the upper part consists mainly of sheet flows with intervened few pelagic sediments, a fissure vent and a cylindrical plug. In addition to the presence of feeder conduits, the flow-dominant lithofacies with a few thin sedimentary interbeds in the LV2 indicates that the study area was the center of a monogenetic volcano grown in a short period. The LV2 consist of arc tholeiite with orthopyroxene phenocrysts increasing in amount upward. The UV2 is composed of sheet flows overlain by a 2.0 m thick subaqueous pyroclastic fall deposit. They are boninite containing olivine and two-pyroxene phenocrysts with plagioclase in the groundmass. Successive orthopyroxene-bearing arc tholeiitic volcanism in the LV2 followed by a relatively small amount of boninite lavas in the UV2 overlain by thick pelagic sediments suggests that the infant arc volcanism was short lived and terminated long before the ophiolite obduction.

Keywords: High-T subduction zone, Initial arc magmatism, Boninite, Oman Ophiolite

Japan Geoscience Union Meeting 2014
(28 April - 02 May 2014 at Pacifico YOKOHAMA, Kanagawa, Japan)

SIT41-19 Room:314 Time:April 28 17:00-17:15

Fate of high-T subduction zone and the obduction of the Oman Ophiolite

UMINO, Susumu[1*] ; KUSANO, Yuki[1] ; KITAMURA, Keitaro[1] ; NAGAISHI, Kazuya[2] ; ISHIKAWA, Tsuyoshi[3] ; KANAYAMA, Kyoko[1]

[1]Department of Earth Sciences, Kanazawa University, [2]Marine Works Japan, [3]JAMSTEC

Obduction of ophiolitic bodies onto continental crust inevitably follows a tectonic event of conversion from divergence to convergence of plates. This is commonly accomplished by the formation of intraoceanic subduction zone near the ridge axis, where lithospheric lid is thinnest and weakest, and accompanies the boninite volcanism [3]. The upper part of the subducted slab is metamorphosed and later thrust over onto a continent with the overlying mantle to become ″ the metamorphic sole ″ . Known examples of metamorphic soles record peak T-P of 600˜840 ℃ and ˜1 GPa, whereas the thickness of overlying ophiolite sheets are only 10-20 km, yielding too small lithospheric load compared to the metamorphic pressure of the sole [4]. This discrepancy has been explained that the ophiolite sheet and the metamorphic sole formed at discrete places were emplaced and superposed at the same place during the obduction process [3].

However, we have demonstrated by examining the trace element geochemistry of the arc magmas and metamorphic sole of the Oman Ophiolite that fluid liberated from the metamorphic sole triggered flux melting of the overlying depleted mantle peridotite and produced arc tholeiitic basalt magma first, and subsequently low-Si boninite magma. Therefore, the ophiolite and the underlying metamorphic sole did not form independently at distant places, but were formed and transported together as an intact body with the present structural relationship. Genetic conditions estimated for a primitive boninite melt with 16 wt% MgO enclosed by Cr spinel indicate the segregation pressure of 0.5 GPa and 1320 ℃ from the mantle with the potential T of 1400 ℃ [1, Kusano et al., this session]. Thus, the boninite magma should have segregated from the mantle at a depth $>$17 km. Nevertheless, the present ophiolite body has the maximum thickness $<$15 km.

The above lines of evidence urged us to propose the following model; Conversion from spreading to closure of the Tethys resulted in the subduction of young and hot oceanic lithosphere beneath the Tethyan ridge axis. The oceanic crust of the subducted slab was metamorphosed to cpx-bearing amphibolite at a depth of ˜35 km and 800 ℃. Trace elements and Nd-isotopic evidence indicate fluids and partial melt of subducted sediments liberated from the dehydrated slab migrated upward and formed a partially melted column in the wedge mantle [6, 7]. Primary boninite magmas segregated from the residual harzburgite on the top of the melting column at a depth of ˜17 km and at 1320 ℃ and ascended to form dunite channels and depleted zones through the uppermost lithospheric mantle [8]. Because serpentine and chlorite are unstable $>$800 ℃, the subducted crustal rocks are metamorphosed to amphibolite and the overlying mantle peridotite becomes amphibolite-bearing lherzolite. The lack of mineral phases which could act as lubricant caused large friction and eventual cohesion of the metamorphic slab and hanging wall of the mantle peridotite. Because of the large mechanical strength of the upper crustal and the lower mantle section of the slab, the lower slab of lithospheric mantle are decoupled from the crustal upper slab and continued to subduct without dehydration because the lower slab was virtually anhydrous. This terminated the Oman arc volcanism in a few million years with the production of boninite magma. The strongly coupled upper slab with the overlying wedge mantle obducted together onto the Arabian Peninsula as the metamorphic sole. During the course of thrusting toward the continent, the hot and partially molten asthenospheric mantle in the wedge was squeezed and flattened by the load of the overlying lithosphere, resulted in the present structure of the thin ($<$15 km) ophiolite sheets underlain by the metamorphic sole formed at a high pressure ˜1 GPa.

Keywords: Oman Ophiolite, boninite, high-T subduction zone, metamorphic sole, subduction initiation, obduction

SIT41-19 Room:314 Time:April 28 17:00-17:15

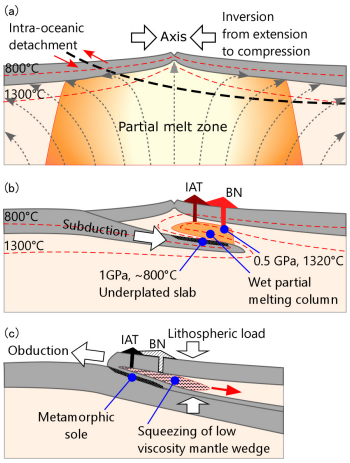

Japan Geoscience Union Meeting 2014
(28 April - 02 May 2014 at Pacifico YOKOHAMA, Kanagawa, Japan)

SIT41-20 Room:314 Time:April 28 17:15-17:30

Magmatic diversity of the ultramafic rock in the oceanic crustal sequence, Oman ophiolite

KANEKO, Ryu[1*] ; ADACHI, Yoshiko[2] ; MIYASHITA, Sumio[2]

[1]Graduate School of Science and Technology, Niigata University, [2]Niigata University

Although all the wehrlitic intrusions in the Oman Ophiolite are regarded as a single group (e.g. Koepke et al. 2009), there are two different types of wehrlitic intrusions. The first are ordinary wehrlitic intrusions that have similar features to the crustal sequence of V1 (MOR basalt). The second are a depleted type characterized by the appearance of true wehrlite and depleted mineral compositions (Adachi & Miyashita 2003; Yamasaki et al. 2006; Goodenough et al. 2010). The former and latter groups are linked to V1 and V2 magmatism, respectively.

We report the discovery of a new occurrence of the ultramafic rock in the oceanic crustal sequence from the Oman ophiolite, which does not intrude into the crustal sequence. This ultramafic rock is referred to as the Lasail-South complex, and the oldest rock in the study area because of being intruded by sheeted dyke complex. TiO2 and Na2O contents of clinopyroxene from the complex range 0.06-0.59 and 0.09-0.42 wt%, respectively, and are similar to the fractional crystallization trend of oceanic gabbro. Co-variation of Mg values of clinopyroxene and An contents of plagioclase show that most of samples plot in the Oman layered gabbro field. Although mineral compositions of the Lasail-South complex show characteristic of mid-ocean ridge magmatism, the complex mainly comprises plagioclase?hornblende lherzolite, olivine clinopyroxenite and clinopyroxenite. Such rock assemblage of is different from the assemblage of the oceanic crust of the Oman ophiolite. The Lasail-South complex shows intermediate characteristic of mid-ocean ridge and island arc magmatisms, and we attempt to discuss the origin of the complex.

References

Adachi and Miyashita, 2003. *Geochemistry Geophysics Geosystems*, **4**(9), doi.org/10.1029/2001GC000272.
Goodenough et al., 2010. *Arabian Journal of Geosciences*, **3**, 439-458, doi.org/10. 1007/s12517-010-0177-3.
Koepke et al., 2009.*Geochemistry Geophysics Geosystems*, **10**, 10002, doi.org/10.1029/ 2009GC002488.
Yamasaki et al., 2006. *Earth and Planetary Science Letters*, **251**, 52-65, doi.org/10.1016/j.epsl.2006.08.027.

Keywords: Oman ophiolite, ultramafic rock, mid-ocean ridge magmatism, island arc magmatism

Japan Geoscience Union Meeting 2014
(28 April - 02 May 2014 at Pacifico YOKOHAMA, Kanagawa, Japan)

SIT41-21 Room:314 Time:April 28 17:30-17:45

Compositionally and genetically distinct domains found in the southernmost Salahi mantle section in the Oman ophiolite

FUJII, Satoru[1*] ; TAKAZAWA, Eiichi[2]

[1]Graduate school Science and Technology, Niigata University, [2]Faculty of Science, Niigata University

We investigate spatial variability in mineral compositions in the southernmost part of the Salahi mantle section and discuss genetic relationship between highly refractory peridotites and less refractory plagioclase-bearing peridotites in this region. The study separates the study area into two domains based on spinel Cr# such as high Cr# domain in the eastern part that is closer to Moho and low Cr# domain in the central part. Concordant dunites commonly occur in the low Cr# domain whereas discordant dunites are common in the high Cr# domain. Plagioclase-bearing peridotites and wehrlite also occur in the low Cr# region.

Highly refractory dunite with spinel Cr# >0.7 frequently occurs in the high Cr# domain. In the low Cr# domain, spinel Cr# is low and ranges from 0.47 to 0.57. We analyzed clinopyroxene (cpx) in dunites and harzburgite from both domains for REE abundances by LA-ICP-MS. The results show that harzburgite cpxs in the high Cr# domain and low Cr# domain are highly depleted in LREE ([Ce]CH =0.01˜0.02) with [Yb]CH=2˜3. Dunite cpxs in the low Cr# domain have REE abundances similar to the harzburgites in the same outcrop whereas those in the high Cr# domain are enriched in LREE relative to the harzburgite cpxs in the same outcrop. This implies that dunite cpxs in the high Cr# domain were reacted with LREE-enriched fluid infiltrated from the base of the ophiolite.

In the low Cr# domain, plagioclase-bearing dunite, plagioclase-bearing lherzolite vein occur and phlogopite-bearing wehrlite discordantly cuts them. The spinel Cr# of these dunites are in a range from 0.46 to 0.56. Abundances of REE in a melt in equilibrium with cpx in plagioclase-bearing peridotites and associated dunites are similar to those of N-MORB. On other hand, a melt in equilibrium with wehrlite cpx resembles to those of boninitic dikes from the Fizh block in the northern Oman ophiolite (Yamazaki, 2013). From the field occurrence, plagioclase-bearing dunite and plagioclase-bearing lherzolite formed by a reaction with MORB melt beneath spreading ridge whereas cumulative wehrlite was crystalized from a boninitic melt.

Japan Geoscience Union Meeting 2014
(28 April - 02 May 2014 at Pacifico YOKOHAMA, Kanagawa, Japan)

SIT41-P01 Room:Poster Time:April 28 18:15-19:30

Mafic and ultramafic rocks along the southern Central Indian Ridge close to the Kairei Hydrothermal Field

NISHIMURA, Takuma[1] ; HARIGANE, Yumiko[2] ; MICHIBAYASHI, Katsuyoshi[3*] ; MORISHITA, Tomoaki[4] ; SATO, Hiroshi[5]

[1]Institute of Geosciences, Shizuoka University, [2]AIST/GSJ, [3]Institute of Geosciences, Shizuoka University, [4]School of Natural System, Colleage of Science and Technology, Kanazawa University, [5]School of Business Administration, Senshu University

The central Indian Ridge (CIR) is situated at the north of the Rodrigues Triple Junction (RTJ) and is a slow- to intermediate-spreading mid-ocean ridge with a spreading rate increasing from 30 mm/year in full rate near the Equator to 49 mm/year in full rate at the RTJ. In the southern CIR near RTJ, the Kairei Hydrothermal Field (KHF) was discovered in August 2000 as the first directly observed hydrothermal vent site in the Indian Ocean. Recently, KH-10-06 cruise aboard R/V Hakuho-maru was organized for understanding the hydrothermal system and geological feature around KHF. In this study, we present the petrography of mafic and ultramafic rocks dredged from the vicinity of the KHF during KH-10-06 cruise. A total of 76 samples have been studied from 9 sites, including 24 ultramafic rocks and 38 mafic rocks and 14 other rocks. Most of them are remarkably altered and hydrated. We classified them into sub-groups based on their textures and mineral assemblies. The ultramafic rocks were classified into 5 sub-groups: 1 peridotite, 2 pyroxenites, 3 serpentinized peridotites, 9 olivine-bearing serpentinites and 9 serpentinites. The mafic rocks were classified into 8 sub-groups: 21 Fe-Ti oxide gabbros, 4 gabbros including 2 mylonites, 3 olivine gabbros, 7 gabbroic rocks with various textures and 8 amphibole-rich gabbros. The other rocks consist of 5 aragonites and 9 hydrothermally altered rocks.

Keywords: mafic rock, ultramafic rock, Central Indian Ridge, Kairei Hydrothermal Field

Japan Geoscience Union Meeting 2014
(28 April - 02 May 2014 at Pacifico YOKOHAMA, Kanagawa, Japan)

SIT41-P02 Room:Poster Time:April 28 18:15-19:30

Upper mantle electrical resistivity structure at the continental margin of East Antarctica

MATSUNO, Tetsuo[1*] ; NOGI, Yoshifumi[1] ; SEAMA, Nobukazu[2]

[1]National Institute of Polar Research, [2]Kobe University

The breakup of the Gondwana supercontinent is one of targets of the study on the plate tectonics and related mantle dynamics. The crust and the upper mantle structure under the western Cosmonauts Sea at the continental margin of East Antarctica, where a rifting of Gondwana and a subsequent seafloor spreading occurred, are anticipated to reflect the breakup process of Gondwana. We carried out a marine electromagnetic experiment to reveal an electrical resistivity structure at depth of the crust and the upper mantle under the western Cosmonauts Sea. Time variations of the electromagnetic field were acquired at two seafloor sites in the experiment. The time variations data were processed on the basis of the magnetotelluric (MT) method. The MT response function was obtained after considering influence of non-plane magnetic field sources at high geomagnetic co-latitude. The obtained MT response functions and polar diagrams imply that the MT responses involve topographic distortion and/or reflect a higher dimensional resistivity structure under the observational sites. Three dimensional forward modeling was conducted to examine influence on the observed MT responses from the topographic variation around the observational sites and a conductive layer just under the sites, which is mostly regarded as sediment. The results of the forward modeling clearly show that the topographic variation and the surface conductive layer have severe influence on the observed MT responses. A series of 3-D forward modeling with the topographic variation and the surface conductive layer was implemented to examine a resistivity structure at depth of the crust and the upper mantle. The results indicate that the resistivity structure is explained by a two-layer resistivity structure, in which the upper layer is resistive and the lower layer is conductive. The upper resistive and the lower conductive layers likely represent dry and water/melt rich oceanic upper mantle, respectively. The thickness of the upper resistive layer is thinner than that expected for a typical oceanic upper mantle of the seafloor age of the study area. The thin upper resistive layer may require high temperature and high water/melt anomalies that were generated through mantle convection, which was related to the breakup process of Gondwana at the continental margin of East Antarctica.

Japan Geoscience Union Meeting 2014
(28 April - 02 May 2014 at Pacifico YOKOHAMA, Kanagawa, Japan)

SIT41-P03 Room:Poster Time:April 28 18:15-19:30

Geochemical characteristics of the peridotites from the southern Mariana forearc

SAKUYAMA, Tetsuya[1*] ; ISHII, Teruaki[4] ; MICHIBAYASHI, Katsuyoshi[2] ; OHARA, Yasuhiko[3] ; CHANG, Qing[1] ; HARAGUCHI, Satoru[5] ; KIMURA, Jun-ichi[1]

[1]JAMSTEC, [2]Shizuoka Univ., [3]Japan Coast Guard, [4]Fukada Geological Institute, [5]Faculty of Engineering, Univ. Tokyo

Dehydration of a subducting oceanic plate and infiltration of the fluid/melt released from the oceanic plate are thought to be the key processes to invoke melting of the wedge mantle. Although a number of studies on volcanic rocks in arcs have been conducted to reveal a material recycling process at subduction zone, understanding of geochemical development process within the wedge mantle is still not as far advanced. The southern Mariana forearc is one of the best locations on the Earth to investigate issues above, since serpentinized peridotites are widely exposed on the inner slope of the Mariana Trench. We have collected peridotite samples obtained by dredging and Shinkai diving from 3000 — 7000 mbsl at the southern Mariana Trench. The dredge and dive points are geographically grouped into three sites: site 1 (KH98-1-D1, KH98-1-D2, and 6K-973), 2 (KH03-3, KH98-1-D3, and 6K-1094), and 3 (6K-1095, 6K-1232, 6K-1233, and 6K-1234) from the east to the west. We conducted EPMA and LA-ICP-MS analyses on minerals in the recovered samples to reveal geochemical development process of the wedge mantle.

Peridotites from the easternmost site 1 consist of olivine (Fo# = 90 — 91), orthopyroxene (Mg# = 90 — 91), spinel (Cr# = 40 — 50), clinopyroxene (Mg# = 89 — 93), tremolite (TiO_2 = 0 — 0.4 wt%), pargasite (TiO_2 = 2.0 — 2.5 wt%), plagioclase, and serpentine. Clinopyroxene and pargasite exhibit LREE-depleted (type C1 and A1, respectively) and orthopyroxene LREE- and MREE-depleted patterns (type O1) in a chondrite-normalized diagram.

Peridotites from the westernmost site 3 consist of olivine (Fo# = 91 — 92.5), orthopyroxene (Mg# = 91 — 93.5), spinel (Cr# = 45 — 75), clinopyroxene (Mg# = 94 — 96), tremolite (TiO_2 = 0 — 0.2 wt%) and serpentine. Some clinopyroxene exhibits LREE-enriched convex upward pattern (type C2), others strong LREE- and MREE-enriched REE pattern (type C3). Tremolite and orthopyroxene exhibit LREE-enriched convex upward (type A3) and weakly LREE-enriched convex upward REE patterns (type O2), respectively. HREE, Ti, and Y abundances of type C3 clinopyroxene are higher and their LREE and Sr abundances lower than those of type C1 clinopyroxene.

Peridotites from the middle site 2 show intermediate characteristics between site 1 and 3. They consist of olivine (Fo# = 90 — 92), orthopyroxene (Mg# = 91 — 92.5), spinel (Cr# = 45 — 52), clinopyroxene (Mg# = ˜95), pargasite (TiO_2 = 0.8 — 1.7 wt%), tremolite (TiO_2 = 0 — 0.2 wt%), plagioclase and serpentine. Some clinopyroxene exhibits C1-type REE pattern and coexists with A1-type pargasite, while other clinopyroxene exhibits LREE- and MREE-depleted patterns (type C2) coexisting with LREE- and MREE-depleted tremolite with weak enrichment in LREE (type A2).

Compared to results of high-pressure melting experiments on peridotite, monotonous increase of Mg# of olivine, clinopyroxene, and orthopyroxene as well as Cr# of spinel from site 1 to 3 suggests increase of melting degree of the mantle peridotite from site 1 to 3. Monotonous decrease of HREEs, Ti, Y, Zr, and Hf abundance from C1- to C3-type clinopyroxene, from A1- to A3-type amphibole, and from O1- to O2-type orthopyroxene, is consistent with major element variations above. However, in contrast to the observation above, LREE and LILE abundance increase from C1- to C3-type clinopyroxene, from A1- to A3-type amphibole, and from O1- to O2-type orthopyroxene, suggesting involvement of melt/fluid enriched in such elements.

LREE-enriched clinopyroxene and amphibole have been found from mantle xenoliths and subaerial peridotite complex. Those clinopyroxene and amphibole have been interpreted as a product of melting and melt separation involving infiltration of LREE-enriched melt/fluid into the melting system. Similarity of geochemical characteristics of type C3 clinopyroxene and A3 amphibole to those in xenoliths or peridotite complexes may suggest involvement of LREE-enriched melt/fluid to the mantle beneath the southern Mariana forearc.

Keywords: Mariana Trench, peridotite, pyroxene, amphibole, trace element

Japan Geoscience Union Meeting 2014
(28 April - 02 May 2014 at Pacifico YOKOHAMA, Kanagawa, Japan)

SIT41-P04 Room:Poster Time:April 28 18:15-19:30

Petrological features of the peridotite xenoliths in the 1991 Pinatubo dacite and mantle metasomatism by subducted ocean

YOSHIKAWA, Masako[1*] ; TAMURA, Akihiro[2] ; ARAI, Shoji[2] ; KOBAYASHI, Tetsuo[3] ; KAWAMOTO, Tatsuhiko[1] ; OKUNO, Mitsuru[4] ; PAYOT, Betchaida[2] ; RIVERA, Danikko[5] ; BARISO, Ericson[5] ; MIRABUENO MA., Hannah T.[6]

[1]Institute for Geothermal Sciences, Kyoto Univ., [2]Department of Earth Sciences, Kanazawa Univ., [3]Department of Earth and Environmental Sciences, Kagoshima Univ., [4]Department of Earth System Science, Fukuoka Univ., [5]PHIVOLCS, [6]Institute of Volcanology and Seismology, University of the Philippines

We observed peridotite xenoliths in the dacite of the 1991 pyroclastic flow deposit of Pinatubo volcano, which is located at the volcanic front of the Luzon (Bataan) arc, Luzon island, the Philippines. The Luzon arc is associated with eastward subduction of the South China Sea plate along the Manila Trench. We also found olivine xenocrysts and xenoliths of amphibolite and granitic rocks in the dacitic deposits. The largest xenolith was up to 14 cm across among about 200 collected samples. Selvage of hornblendite, up to 5 mm width, is common between the peridotite and the dacite host.

Arai et al. (1996) classified peridotite xenoliths from Iraya volcano, Batan Island, the Philippines, into coarse grained (C) and fine grained (F) types depend in terms of olivine grain size. The C-type xenoliths are equivalent to ordinary mantle xenoliths from various localities and the F-type xenoliths are quite different in texture, its individual grains being hardly visible by the naked eye and the fine-grained ($\leq$ 0.1 mm) part occupying $>$10 % by volume (Arai and Kida, 2000). They interpreted that the F-type peridotite was possibly formed from the C-type one by recrystallization assisted by SiO_2-rich fluid or melt originated from subducting slab. Such peculiar F-type xenoliths can be observed in the peridotite xenoliths from Avacha volcano on the volcanic front of the Kamchatka arc, Russia (Ishimaru et al., 2007) and at Tubaf and Edison volcanos, Tabar-Lihir-Tang-Feni island arc, which occur in the fore-arc region of the New Ireland intra-oceanic island arc, Papua New Guinea (McInnes et al., 2001). According to their definition, the F-type peridotites occupy about 50 % of 40 Pinatubo samples. Almost all of the Pinatubo C-type xenoliths are spinel harzburgites (olivine + orthopyroxene + amphibole + spinel $\pm$ clinopyroxene $\pm$ phlogopite) except a wehrlite and a dunite samles. CO_2-bearing saline fluid inclusions were observed in all samples (Kawamoto et al., 2013).

The Sr-Nd isotopic compositions of amphibole from the primary C-type xenolith containing least amounts of fine-grained part are consistent with the most depleted values of the range of andesite and dacite ($^{87}Sr/^{86}Sr$ = 0.70419 - 0.70425, $^{143}Nd/^{144}Nd$ = 0.512863 - 0.512924; Castillo et al, 1991; Bernard et al, 1991). Their compositional variation is within a range of South China Sea oceanic basalt (Tu et al., 1992). Multi-element chondrite-normalized patterns of the amphiboles show depleted signatures with enrichment of Ba, Rb, U, in Pb. These enriching elements are considered as fluid mobile during dehydration of subducting mantle, oceanic crust and sediment (e.g. Tatsumi et al., 1986; McColloch & Gamble, 1991). The present Sr-Nd isotopic and geochemical signatures of the amphibole suggest that the Pinatubo C-type mantle xenoliths have also been metasomatized by aqueous fluids released from subducted oceanic crust beneath the volcanic front.

References; Arai et al., Sci. Rep. Kanazawa Univ., 41, 25-45, 1996; Arai & Kida, Is. Arc, 9, 458-471, 2000; Bernard et al, in Newhall & Punongbayan (eds.) Fire and mud: PHILVOLCS, 767?798, 1991; Castillo & Punongbayan, in Newhall & Punongbayan (eds.) Fire and mud, PHILVOLCS, 799-806, 1991; Ishimaru et al., J. Petrol., 48, 395-433, 2007; Kawamoto et al., PNAS, 110, 9663-9668, 2013; McCulloch & Gamble, EPSL, 102, 358-374, 1991; McInnes et al., EPSL, 188, 169-183, 2001; Tu et al., Chem. Geol., 97, 47-63, 1992.

Keywords: amphibole-bearing peridotite xenolith, Pinatubo, mantle metasomatism, mantle wedge

Japan Geoscience Union Meeting 2014
(28 April - 02 May 2014 at Pacifico YOKOHAMA, Kanagawa, Japan)

SIT41-P05 Room:Poster Time:April 28 18:15-19:30

Petrology of mafic-ultramafic rocks in the East Taiwan Ophiolite, in the Lichi melange, Taiwan

KOMARU, Chihiro[1*] ; MORISHITA, Tomoaki[1] ; TAMURA, Akihiro[1] ; ARAI, Shoji[1]

[1]Graduate School of Natural Science, Kanazawa University

Taiwan is located on the border between the Philippine Sea Plate and the Eurasia Plate. The blocks of cherts, volcanic rocks, plutonic rocks (mafic-ultramafic rocks) are widely distributed as exotic blocks in the Lichi melange, southeastern Taiwan (Liou et al., 1977). These ophiolite-like rocks (cherts, volcanic rocks, plutonic rocks) are defined as the East Taiwan Ophiolite (Liou, 1977). The origin of the East Taiwan Ophiolite is still in debate. Three possible candidates are (1) Philippine Sea Plate (Liou, 1974), (2) the north extension of the Luzon volcanic arc (Ota and Kaneko, 2010), and (3) the South China Sea (Suppe et al., 1981). In this study, we focus on petrological characteristics of gabbros and peridotites in the East Taiwan Ophiolite.

In this research, we collected mafic-ultramafic rocks to cover a wide range of variations in terms of mineral variations at each outcrop. The gabbros are classified into troctolite, olivine gabbro, hornblende gabbro, and gabbronorite. Most of ultramafic rocks are extensively serpentinized, but have equigranular textures based on shape of relic and pseudomorph minerals except for a few serpentine mylonites. The serpentinized peridotites are classified into clinopyroxene-bearing harzburgite and dunite. The Cr# (Cr/(Cr+Al) atomic ratio) and Mg# (Mg/(Mg+Fe) atomic ratio) of spinels in the serpentinized peridotites are 0.3-0.6 and 0.3-0.5, respectively. It is well characterized that the high-Cr# spinel ($>$0.6) coupled with the formation of secondary orthopyroxene are commonly observed in ultramafic xenoliths in Luzon arcs (Arai et al., 2004). We conclude that the East Taiwan Ophiolite is similar with abyssal peridotites and gabbros collected from mid-ocean ridges or back arc basins.

Japan Geoscience Union Meeting 2014
(28 April - 02 May 2014 at Pacifico YOKOHAMA, Kanagawa, Japan)

SIT41-P06 Room:Poster Time:April 28 18:15-19:30

Petrological evidence for arc-metasomatized peridotites beneath mid-ocean ridges

MORISHITA, Tomoaki[1*] ; SENDA, Ryoko[3] ; SUZUKI, Katsuhiko[3] ; NAKAMURA, Kentaro[3] ; SATO, Hiroshi[2] ; OKINO, Kyoko[4]

[1]Kanazawa University, [2]JAMSTEC, [3]Senshu University, [4]University of Tokyo

Here we report for the first time petrological evidence of recycled subduction-modified mantle materials beneath the Mid-Ocean Ridge. We conducted several cruises with submersible SHINKAI 6500 dives and dredges in the south end of the Central Indian Ridges (Phenix knoll). We recovered orthopyroxene-rich lithologies coupled with peridotites and gabbros from a small knoll along the present mid-ocean ridge. The orthopyroxene-rich lithologies can be formed by magmatic processes beneath the present mid-ocean ridges by crystallization from ultra-depleted primary melts (Sobolev and Shimizu, 1993, Nature) in the Mid-Ocean ridge system. Orthopyroxene-rich peridotites are also commonly observed in peridotite bodies of suprasubduction ophiolites (e.g., Morishita et al., 2011 Lithos) as well as in several sub-arc xenoliths (McInnes et al., 2001 EPSL; Arai and Kida, 2000 Island Arc; Arai et al., 2004 J. Petrol; Shimizu et al., 2004 Trans. Royal Soc. London; Ishimaru et al., 2007 J. Petrol). It is also well known that 30% of continental upper mantle samples are enriched in OPX/olivine relative to residual peridotite from partial melting of the primitive mantle (e.g., Boyd, 1989 EPSL; Kelemen et al., 1998 EPSL). Silica-enrichment in the uppermost mantle section under island-arcs is explained by infiltration of silica-rich hydrous fluids/melts derived from subducting slabs. The Re-Os system also supports subduction-metasomatized peridotite origins for orthopyroxene-rich lithologies. The Re-Os isotope system is used for a tracer of recycled crustal materials because oceanic/continental crust possess high Re/Os (parent/daughter) ratios, and develop radiogenic Os isotope compositions over time, which can be readily traced as recycled material if mixed back into the convective mantle. We examined the Os-isotopic compositions of the representative samples: dunite, one harzburgite and one olivine-orthopyroxenite, without signs of petrological and chemical modifications caused by the formation of gabbroic veins. The orthopyroxenite is characterized by a distinctively high in radiogenic Os (187Os/188Os) isotope signatures (0.1475-0.1499) with relatively high in Re contents (382-402 ppt) whereas the Os isotope of the harzburgite is slightly lower than the present-day depleted MORB mantle (0.123-0.126). High 187Os/188Os ratio coupled with high Os and Re contents of the olivine-orthopyroxenite cannot be accounted for by in situ 187Re decay after interaction between MORBs and peridotites for a million years. Radiogenic Os isotope compositions have been reported for MORB glass, and attributed to the presence of recycled oceanic crust in the upper mantle. Mixing of depleted mantle with exotic component that have an isotopic component with high 187Os/188Os ratios, i.e., radiogenic Os components, are required for the sample. We evaluate the effect of metasomatism of mantle by slab-derived fluids or melts on Os systematics observed in the samples. We conclude that ancient subduction-modified mantle domains, probably formed at continental margin of the Gondwanaland, now exists beneath the Central Indian Ridge.

Keywords: Mid-Ocean Ridge, Mantle, Peridotite, arc, recycling

Japan Geoscience Union Meeting 2014
(28 April - 02 May 2014 at Pacifico YOKOHAMA, Kanagawa, Japan)

SGL42-01 Room:419 Time:April 29 09:00-09:30

Why is the IntCal13 special?

NAKAGAWA, Takeshi[1*] ; SUIGETSU 2006, Project members[1]

[1]Department of Geography, Newcastle University (UK)

Please see Japanese abstract (the presentation will be in Japanese).

Keywords: IntCal13, Radiocarbon dating, Radiocarbon calibration, Varved sediment, Lake Suigetsu, Marine reservoir effect

Japan Geoscience Union Meeting 2014
(28 April - 02 May 2014 at Pacifico YOKOHAMA, Kanagawa, Japan)

SGL42-02 Room:419 Time:April 29 09:30-09:45

An evaluation of the effect on 14C dating (AMS) by alkaline treatment of the ABA method on charcoal sample

ATSUMI, Shin[1*]

[1]Tokyo University of Sciences

Charcoal treatment by means of the Acid-Base-Acid (ABA) method (or Acid-Alkali-Acid; AAA method) has been widely used for radiocarbon (^{14}C) dating in the Earth Science and Archaeological field. Although the ABA method is a basic charcoal pretreatment method for ^{14}C dating, the evaluation of processing conditions of the ABA method based on any chemical indicator does exist few until today. This study aims to clarify the error of ^{14}C dating caused by the alkaline pretreatment which is not studied hitherto. The author performed 3 types of experiments for the purpose. The first experiment was performed for confirmation of the reproducibility of ges. The second experiment was performed for confirmation of optimal treatment time of an alkaline solution. The third experiment was performed for confirmation of the optimal concentration of alkaline solution for the ABA pretreatment.

The first experiment: X^2 test of the results shows T=0.45(df=3;5% risk rate T $>$12.59)for the treated samples which means high convergent validity, while T=10.74(df=4;5% risk rate T $>$9.49)for the untreated samples which means large scattering and significant variability.

The second experiment: even after the visual judgment of the completion of alkaline extraction, 3-DF detected humic acid in the retrieved NaOH solution, and Atsumi et. al. (2009) showed that radiocarbon (14C) dating was influenced the existence of humic acid. These results suggest that visual observation is inadequate for the judgment of the completion of alkaline extraction, and that 3-DF is more effective for monitoring the presence of dissolved organic contamination.

The third experiment: three charcoal samples from a single archaeological context were split into 8 aliquots respectively, and treated with 8 different concentrations of NaOH solutions ranging from 0.001 to 2.0 mol/l. Dating results and X^2 tests showed minimum convergence at 1.2 mol/l. This is supported by 3-dimensional fluorescent (3-DF) analysis, which clearly shows different leaching characteristics between 2.0-1.0 and 0.5-0.001 mol/l. 0.5-0.001 mol/l NaOH solutions were too weak in humic leaching capacity at low excitation ranges, which is thought to be the phenomenon that generates the scattering of dates. We recommend using from 1.0 to 1.5 mol/l NaOH for radiocarbon pretreatment.

These results show that the ^{14}C age is affected by difference of the residual of humic acid caused by the difference of chemical conditions of the pretreatment .

Keywords: 14C dating, ABA pretreatment, 3-D fluorescent spectroscopy, Humic acid, Charcoal sample

Japan Geoscience Union Meeting 2014
(28 April - 02 May 2014 at Pacifico YOKOHAMA, Kanagawa, Japan)

SGL42-03 Room:419 Time:April 29 09:45-10:00

Dating of sea-floor hydrothermal barite collected at the Okinawa Trough by ESR and radioactive disequilibrium

FUJIWARA, Taisei[2*] ; TOYODA, Shin[1] ; UCHIDA, Ai[2] ; ISHIBASHI, Jun-ichiro[3] ; NAKAI, Shun'ichi[4] ; TAKAMASA, Asako[5]

[1]Faculty of Science, Okayama University of Science, [2]Graduate School of Science, Okayama University of Science, [3]Faculty of Science, Kyushu University, [4]Earthquake Research Institute, University of Tokyo, [5]National Institute of Radiological Sciences

The temporal change of submarine hydrothermal activities has been an important issue in the aspect of the evolution of hydrothermal systems which is related with ore formation (Urabe, 1995) and biological systems sustained by the chemical species arising from hydrothermal activities (Macdonald et al., 1980). Dating methods using disequilibrium between radioisotopes such as U-Th method (e.g. You and Bickle, 1998), ^{226}Ra-^{210}Pb and ^{228}Ra-^{228}Th method (e.g. Noguchi et al., 2011) have been employed for such studies.

Okumura et al., (2010) made the first practical application of ESR (electron spin resonance) dating technique to a sample of submarine hydrothermal barite to obtain preliminary ages, while Kasuya et al. (1991) first pointed out that barite can be used for ESR dating. Toyoda et al. (2011) determined the optimum ESR condition while Sato et al. (2011) confirmed that the signal is thermally stable enough for an age range of several thousand years. Takamasa et al. (2013) obtained U-Th and ESR ages which are roughly consistent with each other.

The samples were taken by research cruises operated by JAMSTEC. Barite (BaSO4) was extracted from hydrothermal sulfide chimney samples taken from two sites at the Okinawa Trough. Blocks of sulfide deposits were cut into pieces, and about 2.0g was crushed. The samples were soaked in 12M hydrochloric acid, left for approximately 24 hours. Then, 13M nitric acid was added. Finally, after rinsing in distilled water, the sample was filtered and dried. Impurities were removed by handpicking. An X-ray diffraction study was made to confirm that the grains are pure barite. After gamma-ray irradiation at Takasaki Advanced Radiation Research Institute, Japan Atomic Energy Agency, they were measured at room temperature with an ESR spectrometer (JES-PX2300) with a microwave power of 1mW, and the magnetic field modulation amplitude of 0.1mT. The bulk Ra concentration was measured by the low background pure Ge gamma ray spectrometer. Assuming that Ra is populated only in barite, the dose rate was calculated with the alpha effectiveness of 0.043 (Toyoda et al., 2012), where the decay of Ra (a half life of 1600 years) was also taken into account.

The obtained ages range from 4.1 to 16000 years, being consistent with detection of ^{228}Ra in younger samples and radioactive equilibrium/disequilibrium between radium and daughter nuclei. The variation of the ages within each sample is mostly within the statistical error range. The relative order of the ages is consistent with the result of ^{226}Ra-^{210}Pb method, where the difference in absolute ages would be explained by several hydrothermal events that form the chimney. It was found that Yoron Hole field is the youngest, then, Daiyon-Yonaguni Knoll field, Hatoma Knoll field, being nearly equal to Iheya North Knoll field, then Izena Hole field, which is consistent with the direct observation from the submersible.

Keywords: barite, hydrothermal activities, electron spin resonance, dating

Japan Geoscience Union Meeting 2014
(28 April - 02 May 2014 at Pacifico YOKOHAMA, Kanagawa, Japan)

SGL42-04 Room:419 Time:April 29 10:00-10:15

Thermoluminescence property of calcite

OGATA, Manabu[1*] ; HASEBE, Noriko[1] ; FUKUSHI, Keisuke[1] ; FUJII, Naoki[2] ; SATO, Tsutomu[3] ; ITO, Kazumi[4]

[1]Kanazawa University, [2]RWMC, [3]Hokkaido University, [4]AIST

In earth science, the date of past event is very important. To determine accurate age, we have to select suitable dating method for an analyzed sample.

Thermoluminescence dating method calculates a date from equivalent dose estimated by emitted luminescence when mineral is heated. Thermoluminescence dating has been often applied to carbonate minerals because it emits strong luminescence and wider age range applicable than C14 dating method is an advantage of thermoluminescence dating.

However, thermoluminescence dating of calcite is sometimes problematic; e.g., sensitivity change of calcite occurred through repeated heating of samples, possible anomalous fading, difference in characteristics of luminescence response against different kinds of radiation (e.g., gamma-ray, beta-ray, alpha-ray, and x-ray), and so on.

In this study, calcite from Philippine, Mongol, and synthetic calcite are analysed to understand luminescence characteristics of calcite. Mgnesite is also analyzed to see the effect of chemistry. Luminescence was detected by Photon Multiplier (R649, HMA-MATSU) with filter of 600-650nm. Chemical composition, especially impurity concentration was measured by LA-ICP-MS.

First, we evaluate X-ray induced thermoluminescence property of each sample.

Second, we measured luminescence caused by alpha-ray, beta-ray and gamma-ray and compare it to the luminescence induced by the x-ray. .

Finally, the relationship between luminescence characteristics (namely a-x-value, b-x-value and c-x-value) and impurity concentration is examined.

As a result;

1. Most calcites have thermoluminescence peak at 80 and 230 degrees Celsius.
2. In thermoluminescence peak of calcite at 80 degrees Celsius, fading is detected, while at 230 degrees peak is stable.
3. Results show negative or positive relationship between luminescence efficiency factors (a-x-value, b-x-value and c-x-value) and Mg, Mn, Fe and Sr concentrations.
4. The concentration of Fe has a correlation with a luminescence emitting efficiency.

Fe plays an important role for thermoluminescence of calcite. Thermoluminescence property of calcite may be subject to multiple chemical factors (ex; Mg, Mn and Sr), therefore, further analyses on calcites with the variety of impurity is necessary to evaluate a relation between multiple impurity concentration and thermuluminescence properties quantitatively.

Keywords: thermoluminescence, calcite, dating

Japan Geoscience Union Meeting 2014
(28 April - 02 May 2014 at Pacifico YOKOHAMA, Kanagawa, Japan)

SGL42-05 Room:419 Time:April 29 10:15-10:30

Zircon observation by atomic force microscope: Fission track or alpha recoil track?

HASEBE, Noriko[1*] ; ITO, Kentaro[1] ; OHISHI, Shinnosuke[1] ; HONDA, Chiaki[1] ; MATSUKI, Atsushi[1] ; FUKUMA, Takeshi[1]

[1]Kanazawa University

Fission track (FT) method is a dating technique based on the observation of damage (tracks) by spontaneous fission of 238U left in a mineral. The number of tracks is counted under an optical microscope after etching (chemical expansion of a track). However, as FT density per unit area rises, it becomes difficult to count the number of tracks. This is due to the fact that FTs overlap one another and are unable to be readily distinguished. The atomic force microscope has a potential to observe FT with high track density after a short time etching. However, when etching time is too short, the number of counted tracks were increased probably due to difficulties in recognizing the FT among structures other than FT (e.g., alpha recoil tracks). In the observation of young zircons collected from modern volcanic product, the surface structures found in old zircons do not exit, and a hole with the depth of ˜10nm can be found on the smooth surface. These countable holes may lead us to the alpha recoil track dating.

Keywords: zircon, fission track, alpha recoil track, atomic force microscope

Japan Geoscience Union Meeting 2014
(28 April - 02 May 2014 at Pacifico YOKOHAMA, Kanagawa, Japan)

SGL42-06 Room:419 Time:April 29 10:30-10:45

Excess argon in phengite from the Sanbagawa eclogites: Constraints on argon behavior during subduction zone metamorphism

ITAYA, Tetsumaru[1*] ; TSUJIMORI, Tatsuki[2]

[1]Okayama University of Science, [2]Okayama University

K-Ar system dating of phengitic mica is a powerful tool to determine cooling ages of HP?UHP metamorphic rocks. However, discordant ages in a same metamorphic unit have been often reported, particularly from rocks in Alpine-Himalayan type collisional metamorphic belts. For example, UHP-metamorphosed continental crust materials of the Dola Maira massif (western Alps, Italy) show the discrepancy due to the existence of excess argon in metamorphic minerals that has been inherited from the precursor rocks with polyphase metamorphic records. Over the last two decades, we have addressed an excess-argon free hypothesis in oceanic petrogenesis of Pacific-type convergent margins. According to the hypothesis, metamorphosed oceanic materials in Pacific-type HP metamorphic belts with only a monophase metamorphic records do not contain significant amount of excess 40Ar; in other words, the K-Ar system in syn-metamorphic phengitic mica is significantly reset during fluid-induced metamorphic recrystallization at a Pacific-type convergent margin. Well-documented geological examples are of schists from Sanbagawa, Suo and Renge metamorphic belts in SW Japan, and from Otago metamorphic belt in New Zealand. Ar-Ar phengite analyses of HP-UHP metamorphosed oceanic lithologies of the Lago di Cignana (western Alps, Italy) also show negligible excess 40Ar in eclogite-facies syn-metamorphic phengitic mica.

In the year 2000, as a preparation to guide participants for the IEC Conference in Japan, we have determined K-Ar ages of phengite and paragonite from the eclogite-facies Sanbagawa metamorphic rocks in Shikoku; the twenty-two results were obtained from four localities including Seba (84-89 Ma), Gongen (123-136 Ma) and Western Iratsu (78-80 Ma), and Kotsu/Bizan (82-88 Ma). Excepting for the quartz-rich kyanite eclogite from Gongen (GO), phengite and/or paragonite yields similar cooling-age ranges of metasedimentary rocks of the Sanbagawa metamorphic rocks in central Shikoku. Phengite K-Ar ages of GO eclogites are significantly older than syn-metamorphic zircon U-Pb ages at the same unit. These old ages are interpreted as the presence of excess 40Ar in phengitic mica. The bulk-rock compositions of GO eclogites suggest a sedimentary protolith such as greywacke. When, where and how has the excess argon been trapped in phengite crystals? Considering the geological fact that the GO eclogites are closely associated with the Higashi-Akaishi (HA) meta-peridotite body, the false age obtained from phengite were likely attributed to an interaction between the meta-sediment (GO eclogite) and the meta-peridotite (HA peridotite) at eclogite-facies depth. We postulate that the fluids exchange between deep-subducted sediments and mantle material enhanced a hydration of peridotite and mantle-derived noble gas (including extreme 40Ar) was diffused from mantle material to the sediments. During the exhumation of them, the rigid HA peridotite might have prevented a ductile deformation of GO eclogite and consequently mantle-derived argon gained from HA peridotite in GO eclogite might have been inherited by the limited-argon-depletion due to less deformation. This is not only very rare example of false K-Ar age of metamorphosed oceanic materials but also remarkable observation to explain argon behavior during sediments?peridotite interaction at a deep portion of subduction zone environment.

Keywords: Sanbagawa belt, eclogite, phengite, excess argon

Japan Geoscience Union Meeting 2014
(28 April - 02 May 2014 at Pacifico YOKOHAMA, Kanagawa, Japan)

SGL42-07 Room:419 Time:April 29 11:00-11:25

Deciphering early Earth's differentiation using short-lived isotope systematics

IIZUKA, Tsuyoshi[1*]

[1]Tsuyoshi IIZUKA

Knowledge of the timescale and nature of early Earth's differentiation is central to understanding the evolution of the young Earth. Here I discuss short-lived isotope systematics of terrestrial samples that extended our knowledge of early Earth's differentiation. Recent high-precision W isotopic studies revealed positive 182W anomalies of up to 0.15 epsilon unit in ca. 3.8 Ga Itsaq rocks from West Greenland and 2.8 Ga Kostomuksha komatiites from Russia. I explored the geologic significance of the 182W anomalies by combining with trace element and other isotopic data. In this context, the W isotopic data are interpreted to reflect early silicate differentiation events on Earth. Under the assumption that the bulk silicate Earth has a 5% higher Sm/Nd than the chondrite average, the 182W-142Nd-143Nd chronometry constrains the age of the source mantle differentiation for the Itsaq samples to 4.53-4.49 Ga. The age may reflect the timing of silicate differentiation during a sequence of magma ocean solidification.

Keywords: Hadean, early differentiation, extinct radionuclides, non-chondritic Earth

Japan Geoscience Union Meeting 2014
(28 April - 02 May 2014 at Pacifico YOKOHAMA, Kanagawa, Japan)

SGL42-08 Room:419 Time:April 29 11:25-11:40

Formation age of Fengtien Nephrite, Taiwan: Dating low-temperature thin (<20 um) zircon rims by NanoSIMS

YUI, Tzen-fu[1] ; USUKI, Tadashi[1*] ; CHEN, Chun-yen[1] ; ISHIDA, Akizumi[2] ; SANO, Yuji[2]

[1]Institute of Earth Sciences, Academia Sinica, Taiwan, [2]Atmosphere and Ocean Research Institute, The University of Tokyo

Nephrite in the Fengtien area is associated with serpentinites within the subduction-accretionary complex in eastern part of the Central Mountain Range, Taiwan. In addition to nephrite, there are also other metasomatic rocks, such as diopsidefels and epidotite, present between serpentinites and their country rocks (metapelites and metapsammites). Among these metasomatic rocks, diopsidefels is the most common one observed, while nephrite and epidotite are less frequently present in association with diopsidefels. When all these rocks are present at one outcrop, the common lithologic sequence is serpentinite-nephrite-diopsidefels-epidotite- metasedimentary rocks. Nephrite, diopsidefels and epidotite were interpreted resulting from fluid-rock (serpentinite+country rocks) interactions during subduction metamorphism. Field occurrence and petrographic observations clearly showed that while nephrite and diopsidefels are mainly metasomatic products after serpentinite, epidotite is after metapsammite. The formation temperature has been estimated to be 300 - 400 ℃ based on regional geology and thermodynamic calculations by previous studies. Timing of these metasomatic processes, however, has not been constrained, although the hosting subduction-accretionary complex was thought to be of late Cretaceous in age due to paleo-Pacific subduction beneath the Eurasia continent and to be correlated with the Sambagawa belt in Japan. Zircons were separated from one epidotite sample in this study. Most of these detrital zircons were shown to have a thin zircon rim, which is less than 15 - 20 μm in thickness. These zircon rims were considered to be newly formed during metasomatic interactions between serpentinite and country rocks, which also led to nephrite/diopsidefels/epidotite formation. The CAMECA NanoSIMS NS50 at AORI, the University of Tokyo was employed to date these low-temperature thin zircon rims with a ~5 nA O- primary beam confined to a ~15 μm diameter. Sample surface was pre-ablated for 5 minutes to remove the surface Au coating and any possible surface contaminants. Data acquisition time was 500 seconds. The resulting 238U/206Pb-204Pb/206Pb inverse isochron gave a young age of 3.3±1.7 Ma (MSWD = 2.1, n = 5). The date clearly showed that the Fengtien nephrite would have formed during the (initial) exhumation of the subduction-accretionary complex, which should be of late Cenozoic in age related to subduction of the South China Sea plate beneath the Luzon arc. The present study gave a good example that NanoSIMS is able to date zircon rims with a thickness about 15 μm formed under low temperature conditions only a few million years ago. The instrument has a great potential in future studies dating various low-temperature hydrothermal, metasomatic or metamorphic zircon overgrowths.

Keywords: NanoSIMS, zircon, U-Pb dating, Nephrite, Central Mountain Range, Taiwan

Japan Geoscience Union Meeting 2014
(28 April - 02 May 2014 at Pacifico YOKOHAMA, Kanagawa, Japan)

SGL42-09 Room:419 Time:April 29 11:40-11:55

Significance of external morphology and zircon chemistry for precise U-Pb zircon dating

TAKEHARA, Mami[1*] ; HORIE, Kenji[2] ; TANI, Kenichiro[3] ; YOSHIDA, Takeyoshi[4] ; HOKADA, Tomokazu[2] ; KIYOKAWA, Shoichi[5]

[1]Department of Earth and Planetary Sciences, Graduate School of Sciences, Kyushu University, [2]National Institute of Polar Research, [3]Institute for Research on Earth Evolution, Japan Agency for Marine-Earth Science and Technology, [4]Institute of Earth Sciences, Graduate School of Science, Tohoku University, [5]Department of Earth and Planetary Sciences, Faculty of Sciences, Kyushu University

Improvement of U-Pb zircon dating by microbeam analysis has been provided opportunity of discussion about more detailed geological events. Recent analytical precision of less than 2% at Paleogene zircon allows us to investigate shorter period events such as crystallization differentiation in magma chamber. However, the highly precise U-Pb age data yield an importance of confirming their accuracy and assaying disturbance of U-Pb system and incorporation of exotic components. In this study, we introduce data processing method of the highly precise ages based on zircon morphology, trace element abundances as well as statistics.

The precise U-Pb zircon dating by using a sensitive high-resolution ion microprobe (SHRIMP II) at National Institute of Polar Research, Japan, was applied to igneous rocks of the Tertiary Ishizuchi Cauldron in the Setouchi volcanic belt of Miocene age in northwestern Shikoku. A primary ion beam of about 10 nA was used to sputter an analytical spot of about 40 μm diameter. A retardation lens system was utilized as a means to increase signal-to-noise ratio, and a secondary ion optics including slits of source and collector was adjusted to maximum transmission of the secondary ion under suitable mass resolution avoiding isobaric interferences on Pb isotopes. The surfaces of grain mounts were carefully washed with diluted HCl and ultra pure water to remove Pb contamination. A correction for common Pb was made on the basis of the measured ^{204}Pb and the model for common Pb composition.

Weighted mean ages were calculated from ^{206}Pb/^{238}U ratios corrected by ^{207}Pb. In order to ensure the accuracy of U-Pb age, age known zircon, OD-3, was analyzed together with unknown sample. Concentrations of Hf and rare earth element (REE) in zircons were also measured at the same analytical spot of U-Pb dating by SHRIMP.

Zircon grains from the Bansyodani-biotite-rhyolite were divided to two types based on the external morphology: sharply euhedral type and relatively rounded edge of prism and pyramid type. ^{206}Pb/^{238}U data of whole zircon grains were widely scattered beyond analytical uncertainty and show a weighted mean of 14.78 $\pm$ 0.18 Ma (mean square weighted deviation, MSWD: 3.4). On the other hand, the euhedral zircons yielded the weighted mean of 14.21 $\pm$ 0.19 Ma (MSWD: 1.0), whereas the relatively rounded zircons were older than the euhedral zircons, which suggests the incorporation of exotic components.

Zircon chemistry supported the classification by the morphology and the U-Pb dating. An average of Hf contents of the euhedral zircons were 9523 ppm ranging from 8883 to 10496 ppm and those of the relatively rounded zircons were 8475 ppm ranging from 7616 to 8803 ppm. Hf contents of the euhedral zircons were higher than those of relatively rounded zircons. C1 chondrite-normalized REE patterns of the euhedral zircons were characterized by a large fractionation between light REE and heavy REE, large positive Ce anomalies and large negative Eu anomalies. In contrast, those of the relatively rounded zircons were enrichment of light REE, weaker anomalies of Ce and Eu. Difference of the zircon chemistry between the euhedral zircons and the relatively rounded zircons reflects source melt composition. Therefore, the external morphology, Hf content, and REE abundance are useful criteria for the data processing of the highly precise U-Pb age data.

Japan Geoscience Union Meeting 2014
(28 April - 02 May 2014 at Pacifico YOKOHAMA, Kanagawa, Japan)

SGL42-10 Room:419 Time:April 29 11:55-12:10

LA-ICP-MS U-Pb dating of Oki Dozen volcano using non-polished zircons

ITO, Hisatoshi[1*] ; BRENNA, Marco[2] ; MIURA, Daisuke[1] ; TOSHIDA, Kiyoshi[1] ; NAKADA, Setsuya[2]

[1]CRIEPI, [2]Univ. of Tokyo

LA-ICP-MS U-Pb dating using zircon is now widely used with great success. The normal dating process includes polishing zircons. This process is good in terms of avoiding surface contamination of common Pb and/or Pb loss and is essential for SHRIMP, in which only small fraction (drilling depth of 1-2 μm) is used for dating. Compared to SHRIMP, LA-ICP-MS ablates a much larger volume (drilling depth of $>$10 μm) of zircon. This means that it is easy to date zircons from the surface to the inner core of the crystal and examine the existence of inherited cores and potentially investigate the timespan of crystallization. Here we dated non-polished zircons for some reference samples (Fish Canyon Tuff and OD-3) and samples from Oki Dozen volcano. Zircons were ablated for 30 seconds using 213 nm Nd-YAG laser with 10 Hz repetition rate and 4-5 J/cm^2 energy density. Final drilling depth for 5 J/cm^2 was 27 μm and the ^{206}Pb/^{238}U ratio from 9-18μm depth were used to determine ages. It was found that non-polished zircons yield reliable ages because of agreement with reference ages. The Oki Dozen samples yielded 6-7 Ma ages, in agreement with or slightly older than K-Ar ages of 5.4-7.4 Ma.

Keywords: U-Pb dating, zircon, LA-ICP-MS, Oki Dozen volcano

Japan Geoscience Union Meeting 2014
(28 April - 02 May 2014 at Pacifico YOKOHAMA, Kanagawa, Japan)

SGL42-11 Room:419 Time:April 29 12:10-12:25

Crustal noble gases anomaly associated with fault movement and aftershock the 3.11 Northeast Japan Earthquake

SATO, Keiko[1*] ; KUMAGAI, Hidenori[2] ; IWATA, Naoyoshi[3] ; HYODO, Hironobu[4] ; SUZUKI, Katsuhiko[2] ; TAKAOKA, Nobuo[5]

[1]JAMSTEC, SRRP, [2]JAMSTEC, IFREE, [3]Faculty of Science, Yamagata University, [4]Okayama University of Science, [5]Faculty of Science, Kyusyu University

Noble gases have unique characteristics that they are rarely combined with other chemicals as their very stable nature. Because its main reservoir is atmosphere, their isotopic composition is well defined and believed to be uniform all over the world insensitive to disturbance from anthropogenic and/or natural emission of geologically trapped noble gases in the earth interior. Based on our preliminary friction experiment, however, detectable amount of noble gases seem to be emitted accompanied with a fault motion (Sato et al., 2009). After the extreme Northeast Japan Earthquake occurred on March 11, 2011, extraordinary increase of seismic activity as numerous aftershocks e.g. over 4000 felt earthquakes in four months, which may be a source of non-atmospheric component preserved in the earth interior. In terms of anthropogenic component, Nuclear Power Plant) is a potential source, which is frequently monitored by radioactive species of noble gases.

We widely collected atmosphere samples all over Japan from Hokkaido, Honsyu, Chugoku and Kyusyu Is. The atmospheres have been sampled into vacuumed containers, Isotube@, at each sampling site to evaluate time-series changes. The elemental and isotopic compositions of the samples were analyzed mainly by quadrupole residual gas analyzers (RGA-200, SRS Co.) and partly confirmed by sector-type mass spectrometers (GVI-5400, GV instruments). In the duplicated analyses of the selected a few samples, the measured elemental and isotopic compositions were consistent within analytical uncertainties.

The relative elemental abundances were changed at least in heavier noble gases. Argon was enriched to pre-3.11 Earthquake atmospheres associating with a high $^{40}Ar/^{36}Ar$ ratio. It might be contributed by emission of crustal Ar at aftershock earthquakes, deformation and fault movements. In addition, a frictional melting was occurred in a >M5 earthquake as reported by Kanamori et al. (1998). Further, radioactive Ar isotopes (^{42}Ar and ^{39}Ar) were slightly abundant than those in "pre" 3.11 Earthquake atmospheres. These radioactive Ar isotopes were regarded to be detected limitedly in neutron irradiated geological samples especially in Ar - Ar dating. These altered atmospheric Argon isotopic composition in Eastern Japan area were observed until typhoon season.

Keywords: noble gas, 3.11 Northeast Japan Earthquake, aftershock earthquake, nuclear power plant disaster, Ar Isotope

Japan Geoscience Union Meeting 2014
(28 April - 02 May 2014 at Pacifico YOKOHAMA, Kanagawa, Japan)

SGL42-P01 Room:Poster Time:April 29 18:15-19:30

Ultrahigh-sensitive simultaneous determination of halogens and noble gases by an extension of Ar-Ar and I-Xe methods

SUMINO, Hirochika[1*] ; KOBAYASHI, Masahiro[1] ; SAITO, Takehiko[1] ; NAGAO, Keisuke[1] ; TOYAMA, Chiaki[2] ; MURAMATSU, Yasuyuki[2]

[1]Geochemical Research Center, Graduate School of Science, University of Tokyo, [2]Department of Chemistry, Gakushuin University

Noble gas isotope ratios in various geochemical components in the Earth are significantly different, making them useful tracers to constrain origin of volatiles in the mantle. The development of noble gas mass spectrometry during the last two decades has enabled us to detect less than 10000 noble gas atoms (e.g., [1]).

An extension of Ar-Ar and I-Xe dating methods allows us to simultaneously determine trace amounts of noble gases, halogens, K, Ca, Ba, and U by use of ultrahigh-sensitive noble gas mass spectrometry on neutron-irradiated samples. This method has several advantages: (i) detection limits for halogens are three or four orders of magnitude lower than those of other conventional analytical methods, (ii) several components of different origin can be distinguished based on their relations with specific noble gas isotopes such as mantle-derived ^{3}He and by using various noble gas extraction methods such as laser microprobe [2], and (iii) in-situ production of radiogenic noble gas isotopes (such as ^{4}He and ^{40}Ar) after the entrapment of the noble gas component of interest in the sample can be corrected by the simultaneous determined their parent elements, such as U and K, when the age of the entrapment is known or can be assumed.

We have developed a new noble gas mass spectrometric system for this method based on an Ar-Ar and I-Xe dating system [3]. Accuracy and precision of our method were examined by analyzing GSJ and USGS reference materials, their original rocks, and scapolite standards [4] and by comparing the halogen data with those obtained with ion chromatography and ICP-MS followed by pyrohydrolysis extraction [5].

By using this method, we analyzed halogens and noble gases in exhumed mantle wedge peridotites and eclogites from the Sanbagawa-metamorphic belt, southwest Japan and those in mantle-derived xenoliths from Kamchatka and N. Philippines, in all of which relicts of slab-derived water are contained as hydrous mineral/fluid inclusions. The striking similarities of the observed noble gas and halogen compositions with marine pore fluids [6,7] challenge a popular concept, in which the water flux into the mantle wedge is controlled only by hydrous minerals in altered oceanic crust and sediment (e.g., [8]).

On the other hand, halogen ratios of olivines in lavas from the northern Izu-Ogasawara arc [9] indicate insignificant contribution to the mantle wedge of pore fluid-derived halogens. This implies a relatively small amount of the pore water subduction fluids would be released from the Izu slab at a sub-arc depth resulting in further subduction to great depths in the mantle, possibly resulting in the seawater-like heavy noble gas composition of the convecting mantle [10].

Based on the relation with ^{129}Xe produced from decay of short-lived nuclide ^{129}I during stepwise heating noble-gas extraction of the Allende and Shallowater meteorites, intrinsic I and U to the meteorites were distinguished from those of terrestrial contamination origin.

These results demonstrate that simultaneous determinations of noble gases, halogens, K, Ca, Ba, and U in mantle-derived rocks and meteorites provide important information about their origins.

[1] Sumino et al. (2001) J. Mass Spectrom. Soc. Jpn. 49, 61-68. [2] Sumino et al. (2008) J. Volcanol. Geotherm. Res. 175, 189-207. [3] Ebisawa et al. (2004) J. Mass Spectrom. Soc. Jpn. 52, 219-229. [4] Kendrick (2012) Chem. Geol. 292-293, 116-126. [5] Muramatsu & Wedepohl (1998) Chem. Geol. 147, 201-216. [6] Sumino et al. (2010) Earth Planet. Sci. Lett. 294, 163-172. [7] Kobayashi et al. (2013) Mineral. Mag. 77, 1484. [8] Schmidt & Poli (1998) Earth Planet. Sci. Lett. 163, 361-379. [9] Sumino et al. (2013) Mineral. Mag. 77, 2285. [10] Holland & Ballentine (2006) Nature 441, 186-191.

Keywords: noble gas, halogen, mass spectrometry, Ar-Ar dating, I-Xe dating

Japan Geoscience Union Meeting 2014
(28 April - 02 May 2014 at Pacifico YOKOHAMA, Kanagawa, Japan)

SGL42-P02 Room:Poster Time:April 29 18:15-19:30

Unspiked K-Ar dating for lavas from Zao volcano

YAMASAKI, Seiko[1*] ; OIKAWA, Teruki[1] ; BAN, Masao[2]

[1]Geological Survey of Japan, AIST, [2]Faculty of Science, Yamagata Univ.

Zao volcano is located in the central part on the volcanic front of the NE Japan arc. Previous study revealed that the onset of the volcanic activity is ca. 0.8 Ma, the main edifice-building stage is ca. 0.3-0.1 Ma, and the newest stage is from 0.03 Ma to the present. On this volcano, about 50 K-Ar age data are reported, but not all units are covered and some data contradict the stratigraphy probably because of low-K and/or excess Ar contamination. We report new unspiked K-Ar age data for the lavas collected also from unexplored units, in order to construct the detailed history of the volcano.

Keywords: Zao volcano, K-Ar dating

Japan Geoscience Union Meeting 2014
(28 April - 02 May 2014 at Pacifico YOKOHAMA, Kanagawa, Japan)

SGL42-P03 Room:Poster Time:April 29 18:15-19:30

Diffusion experiment by stepwise heating and muscovite

HYODO, Hironobu[1*]

[1]RINS, Okayama Univ. of Sci.

It is generally recognized that diffusion experiment on micas in vacuum during stepwise heating for $^{40}Ar/^{39}Ar$ dating was unsuitable for diffusion studies because of the destruction of crystal structure from dehydration. However, we showed that estimates of closure temperature from single grain biotites during laser heating experiment gives reasonable values. The problem in case of muscovite is that it seems to have structural transition or significant destruction between 600 and 700^{o}C. The recent study using hydrothermal environment reported the activation energy E of 63 kcal/mole and an estimation of closure temperature exceeding 400^{o}C. The high E and closure temperature T_c are derived on the steep slope in Arrhenius plot. Without change in crystal structure, muscovite does not give high E and Tc. This is contradictory for samples with high E and T_c. It is necessary to separate diffusion phenomena from structural change, and even a hydrothermal experiment at high temperatures in a laboratory may not be suitable for such studies. Muscovite is known to have relatively high T_c in field. To make a practical estimate for T_c, it is necessary to consider both laboratory and field setting.

Keywords: diffusion experiment, argon, closure temperature, stepwise heating, muscovite

Japan Geoscience Union Meeting 2014
(28 April - 02 May 2014 at Pacifico YOKOHAMA, Kanagawa, Japan)

SGL42-P04 Room:Poster Time:April 29 18:15-19:30

Luminescence dating and analysis of environmental change of fine grained sediments from Lake Yogo, Japan

ITO, Kazumi[1*]

[1]Geological Survey of Japan, AIST

We applied optically stimulated luminescence (OSL), infrared stimulated luminescence (IRSL), post-IR IRSL (pIRIR) and ^{14}C dating to the sediment core YG11-3 (294cm) from Lake Yogo, Japan. The fine grained quartz and polymineral sample are used for equivalent dose (D_e) estimation. As a result of several basically test, the preheat temperature of 200 ^{o}C for 10 s and a cut heat of 160 ^{o}C were suitable to all OSL measurements. The accepted aliquots are about 90 % per measurement discs and the range of D_e s are 0.3 ˜3.5 (Gy). The bulk ^{14}C ages are ca. 300 years older than these of plant residue. After subtracting this age difference from bulk ^{14}C ages, the corrected ages agree with the OSL ages except the ages of sediments from some depths. Two excepted OSL ages are older than the corrected bulk ^{14}C ages (YG11-3-245, YG11-3-343) and these layers include a lot of plant residue enough to analyze the plant residue ^{14}C ages. It seems that these sediments from two layers have been transported quickly in muddy stream based on a temporary environmental event. Additionally, the result of the $IRSL_{50/225}$ and $pIRIR_{225}$ age confirms the existence of this temporary event. By comparing the OSL ages with ^{14}C, IRSL and pIRIR ages, the quartz from the small catchment area can be applied to reconstruct the age model of sediment core in Japan.

Keywords: OSL dating, pIRIR dating, lake sediments

Japan Geoscience Union Meeting 2014
(28 April - 02 May 2014 at Pacifico YOKOHAMA, Kanagawa, Japan)

SGL42-P05 Room:Poster Time:April 29 18:15-19:30

U-Pb dating of Eoarchaean zircon using a NanoSIMS -implication for the measurement of volatile in the inclusions

ISHIDA, Akizumi[1*] ; TAKAHATA, Naoto[1] ; SANO, Yuji[1] ; DAVID, Jean[2] ; PINTI L., Daniela[2]

[1]AORI the University of Tokyo, [2]University of Montreal

Volatiles, such as hydrogen or sulfur, trapped in the Eoarchaean igneous rocks, are one of the most important tracers of the evolution of the interior of the early Earth. Apatite or glass inclusions found in the zircon crystal, are expected to preserve such volatiles. However, because of their scarceness, high-sensitive, high-resolution analytical methods are required for quantify them and reveal their isotopic compositions. Furthermore, discriminating between pristine compositions and later alteration is problematic. We are trying to approach these issues carrying out analyses by NanoSIMS50.

Euhedral to subhedral zircons were separated from a tonalite which was from the Eoarchaean Nuvvuagittuq supracrustal belt, Surerior Craton, Canada. The reported U-Pb age of this tonalite is 3661±4 Ma by using LA-MC-ICP-MS [1]. The size distribution of zircons was from approximately 50 micrometers to 200 micrometers. Some of them have inclusions of apatite and glass whose size were 10 to 30 micrometers in diameter. Dating measurements were done avoiding such inclusions.

We performed ^{238}U-^{206}Pb and ^{207}Pb-^{206}Pb dating in the same analytical spot of zircon crystals. A 5 nA O^- primary beam, with spot size of approximately 10 micrometers in diameter, was used for ionizing the sample surface, and secondary positive ions were collected in a multicollector. The detector system was modified to measure $^{30}Si^+$, $^{90}Zr_2{}^{16}O^+$, $^{204}Pb^+$, $^{206}Pb^+$, $^{238}U^{16}O^+$, and $^{238}U^{16}O_2{}^+$ ions simultaneously in ^{238}U-^{206}Pb dating session. In ^{207}Pb-^{206}Pb dating session, $^{204}Pb^+$, $^{206}Pb^+$, and $^{207}Pb^+$ ions were collected in the same detector by changing the magnetic field. Detailed analytical procedure and standard calibration is described in Takahata et al.(2008) [2].

Measured ^{206}Pb/^{238}U ratios range from 0.4932 to 0.7993, and the ^{207}Pb/^{206}Pb ratios range from 0.3052 to 0.3443. After the correction of common Pb, those values were plotted on Tera-Wasserburg Concordia diagram, giving a corrected age of 3633±35 Ma, consistent with the previous value obtained by [1]. On the other hand, some samples showed a discordant age. Since such crystals are thought to have suffered metamorphism with subsequent loss of Pb, volatiles in the inclusions might have lost their initial information as well. Now we are proceeding to measure the volatile compositions of inclusions based on the results of U-Pb dating.

[1] David et al., GSA Bulletin,121, 150-163, 2008.
[2] Takahata et al., Gondowana Res., 14, 587-596, 2008.

Keywords: U-Pb dating, NanoSIMS, zircon, inclusion, Archaean

Japan Geoscience Union Meeting 2014
(28 April - 02 May 2014 at Pacifico YOKOHAMA, Kanagawa, Japan)

SGL42-P06 Room:Poster Time:April 29 18:15-19:30

Geochronological-geochemical characterization of Proterozoic age, western part of the Napier Complex, East Antarctic

HORIE, Kenji[1*] ; HOKADA, Tomokazu[1] ; HIROI, Yoshikuni[2] ; MOTOYOSHI, Yoichi[1] ; SHIRAISHI, Kazuyuki[1]

[1]NIPR, [2]Chiba University

The Napier Complex in East Antarctica has attracted considerable interest from a viewpoint of long Archaean crustal history from 3800 Ma to 2500 Ma (e.g., Harley & Black 1997) and >1000 ℃ ultrahigh-temperature (UHT) metamorphism in a regional scale (e.g., Sheraton et al., 1987; Harley & Hensen 1990). The timing of ultrahigh-temperature metamorphism is in argument either >2550 Ma or <2480 Ma (Kelly and Harley, 2005). However, some previous works reported relatively younger ages, such as 2380 Ma, ˜2200 Ma, and ˜1820 Ma (e.g., Grew et al., 2001; Owada et al., 2001; Suzuki et al., 2001, 2006; Carson et al., 2002; Hokada and Motoyoshi, 2006). In addition, Horie et al. (2012) reported similar ages in felsic orthogneiss from Fyfe Hills and quartzite from Mt. Cronus via zircon U-Pb dating. In this study, we try to characterize the ”younger ages” in order to interpret thermal history after the UHT metamorphism in the Napier Complex.

A quartzo-feldspathic gneiss, YH05021606A, collected from Fyfe Hills by Y.H. during the field work at the 2004-2005 Japanese Antarctic Research Expedition was analyzed by using a high-resolution ion microprobe (SHRIMP II) at the National Institute of Polar Research, Japan. The zircon U-Pb ages of the YH05021606A sample are already reported in Horie et al. (2012). The sample shows multiple age peaks centered at ca. 3025, 2943, 2883, 2818, 2759, 2674, 2518, and 2437 Ma, and evidence of the ”younger ages” has never been reported. In this study, primary ion beam was focused up to 10 um in order to observe detailed zircon structure. The U-Pb analysis of zircon yielded similar age population to the previous work and revealed the ”younger ages” of ca. 2273, 2195, 2106, and 1980 Ma. Distribution of the ”younger ages” is consistent with those of a felsic orthogneiss, YH05021603A, in Fyfe Hills and those of a quartzo-feldspathic gneiss, YH05021701A, and a quartzite, YH05021701H, in Mt. Cronus (Horie et al., 2012). The ”younger ages” in this sample could be found in overgrowth rim and single grain, which indicates that both of Fyfe Hills and Mt. Cronus had been affected by any geological events after the UHT metamorphism. Previous workers suggested that the ca. 2200 Ma age that they obtained for beryllium syn-metamorphic pegmatites reflects post-emplacement deformation and metamorphism (Grew et al., 2001), and a ca. 1930-1800 Ma U-Pb upper intercept age for zircons were affected by aqueous fluid from Paleozoic pegmatite (Carson et al., 2002). Horie et al. (2012) only suggests that these 2380-820Ma ages represent local fluid infiltration or a local deformation events. We will discuss about character of the ”younger ages” zircon with trace element signature.

Keywords: East Antarctica, Napier Complex, zircon, U-Pb dating, rare earth element, metamorphism

Japan Geoscience Union Meeting 2014
(28 April - 02 May 2014 at Pacifico YOKOHAMA, Kanagawa, Japan)

SGL42-P07 Room:Poster Time:April 29 18:15-19:30

Sr and Nd isotope systematics of metacarbonate rocks as proxies for reconstructing extinct oceans: Mozambique Ocean

OTSUJI, Naho[1*] ; KAMEI, Atsushi[2] ; TSUCHIYA, Noriyoshi[3] ; G.H., Grantham[4] ; KAWAKAMI, Tetsuo[5] ; ISHIKAWA, Masahiro[6]

[1]Niigata University, [2]Shimane University, [3]Tohoku University, [4]Council for Geoscience, South Africa, [5]Kyoto University, [6]Yokahama National University

Geochemistry of sedimentary rocks is widely used for understanding the depositional environment and tectonic setting, including source rock composition and paleo-ocean signature. In particular, chemically deposited carbonate rocks are directly precipitated from saturated seawater are supposed to hold key information of extinct paleo-oceans. An important geochemical tool that can lead to the identification of contemporaneous seawater is isotopic composition of strontium and neodymium in carbonate rocks, because these elements have distinct residence and mixing time in seawater and also characterized by surrounding continents.

In the Sør Rondane Mountains (SRMs), East Antarctica, metasedimentary rocks including metacarbonate rocks are widely distributed. These rocks were supposed to have formed in the paleo-ocean called as "Mozambique Ocean". SRMs are divided into two terranes, the SW and NE terranes, by the Main Tectonic Boundary (MTB). In the SW terrane, metaigneous rock that were formed at ca. 1000 Ma and metasedimentary rocks occur as main lithological units, which underwent metamorphic evolution along a anticlockwise *P-T* path, whereas the NE terrane is dominated by metasedimentary rocks, with a characteristic clockwise of *P-T* path. Additionally, metapelitic rocks in the SW terrane have similar detrital age population with the nearby metaigneous rocks, in contrast to those in the NE terrane show older detrital ages (˜ca. 3300Ma)(Osanai *et al*., 2013). If it is possible to reveal the relationship between ocean and continents during depositional timing of carbonate rocks in both terranes, we will be able to put forward a model to explain the difference in depositional setting between SW and NE terranes. To achieve this, analyzed detailed study of Sr and Nd isotopic composition of metacarbonate and metamorphosed silicate rocks, such as pelitic, felsic, mafic and ultramafic rocks, from several important outcrops throughout SRMs were carried out. Based on these data, we discuss about the relationship with continent and depositional basin of carbonate sediments before the final amalgamation of Gondwana.

After geochemical screening for post-depositional alteration, using oxygen isotopes, trace elements and REE + Y patterns, strontium isotope chemostratigraphy was applied to the metacarbonate rocks from SRMs and depositional ages of 880-850 Ma and 820-790 Ma (late-Tonian and early-Cryogenian age) were estimated (Otsuji *et al*., 2013). Metacarbonate rocks in the Brattnipene and Tanngarden regions in the SW terrane are showing typical seawater-rock mixing relationship in a εSr vs. εNd cross-plot indicating the deposition of metacarbonate rocks nearby meta-tonalitic and orthogneiss dominated continental arc. By contrast, the Perlebandet region exhibits an extremely different depositional setting of a seamount based on Nd model and depositional age and REE and εNd compositions. Moreover, the Balchen metacarbonate rocks show a signature of depositional setting surrounding a continent, based on the comparison of metacarbonate rocks with continental and oceanic derived rock units. A comparison of isotopic characteristics of Balchen carbonate rocks with the basement rocks from neighboring Gondwana regions suggested the presence of an ancient continent that is different from Kalahari and Dharwar Craton.

Thus, the Sr and Nd isotopic compositions of carbonate rocks deposited in the Mozambique Ocean have preserved important information about depositional setting of sedimentary rocks and relationship with surrounding basement and continents. In summary, geochemical proxies such as Nd and Sr isotopes of metacarbonate rocks can yield key information not only of paleo-oceans but also about the surrounding rocks during depositional timing, which can lead to a better understanding of oceanic closure during the formation of supercontinents.

Reference cited: Osanai et al., 2013. PR, 234, 8-29. Otsuji et al., 2013. PR, 234, 257-278.

Keywords: Sr and Nd isotope ratios, metacarbonate rocks, the Sor Rondane Mountains, Mozambique Ocean, Gondwana

Japan Geoscience Union Meeting 2014
(28 April - 02 May 2014 at Pacifico YOKOHAMA, Kanagawa, Japan)

SGL42-P08 Room:Poster Time:April 29 18:15-19:30

Geochemistry of Archaean Banded Iron Formations in the Chitradurga Schist Belt, Dharwar Craton, Southern India

KOINUMA, Kentaro[1*] ; MADHUSOODHAN, Satish-kumar[1] ; MISHIMA, Kaoru[2] ; UENO, Yuichiro[2] ; HOKADA, Tomokazu[3]

[1]Niigata University, [2]Tokyo Institute of Technology, [3]National Institute of Polar Research

Banded iron formations (BIF) are marine chemical sediment rocks precipitated mostly in Archaean and early Paleoproterozoic between 2.7Ga and 2.3Ga. This time interval record profound changes in the redox state of the oceans and atmosphere, such as the Great Oxidation Event (GOE). We present here the geochemical data obtained from 3.0 Ga banded iron formation (BIF) in the Chitradurga Schist Belt, Dharwar Craton, Southern India. This region exposes the Archaean strata predominated by supracrustal greenstone belts, stratigraphically overlying the Peninsular gneiss. Chitradurga schist belt comprises of three important BIF layers distributed in the Bababudan and Chitradurga groups. We present here the salient geochemical characteristics and strontium and neodymium isotope results of the BIFs and discuss the depositional environment.

BIF contain very low content of Al2O3 ($<$1wt.% except 1 sample) indicating less detrital components. The PAAS-normalized REY patterns shows positive La and Eu anomaly, low concentration of rare earth element, depletion of light rare earth elements (LREEs) relative to heavy rare earth elements (HREEs). These features differ with other Archaean BIFs in terms of lack of positive Y anomaly. The large positive Eu anomalies in Archean BIF of Chitradurga schist belt attribute to high-T hydrothermal fluid fluxes ($>$250 ^{0} C), while the negative Ce anomaly reflects the lack of significant oxidizing agents.

Sr isotopic composition of BIF shows large variations suggesting post depositional alterations, whereas Nd isotope rations gave consistent information. Most of the samples show εNd(3000Ma) in the range of +2 to +4 and T_{DM} model age in accordance with sedimentation age. The εNd(3000Ma) of depleted mantle is about +4, which suggests that most of the Chitradurga BIFs were deposited in an environment strongly affected by input from a depleted mantle. However samples with different REY pattern show higher εNd(3000Ma) between +6 and +14 and their T_{DM} model age are not equal to the sedimentation age. The geochemical results thus suggest that the BIFs in the Chitradurga schist belt were deposited near possible ridges affected by hydrothermal activities.

Keywords: Banded Iron Formations, Dharwar Craton, Archaean, Nd isotope

Japan Geoscience Union Meeting 2014
(28 April - 02 May 2014 at Pacifico YOKOHAMA, Kanagawa, Japan)

SGL43-01 Room:411 Time:May 1 14:15-14:30

Tectonic evolution of Karwar and Coorg blocks, southern India

C, Ishwar-kumar[1*] ; K, Sajeev[1] ; B.F, Windley[2] ; M, Satish-kumar[3] ; T, Hokada[4] ; K, Horie[4] ; T, Itaya[5]

[1]Centre for Earth Sciences, Indian Institute of Science, Bangalore 560 012, India, [2]Department of Geology, University of Leicester, Leicester LE1 7RH, UK, [3]Department of Geology, Niigata University, 2-8050, Ikarashi, Nishi-ku, Niigata 950-2181, Japan, [4]National Institute of Polar Research, 10-3 Midori-cho, Tachikawa, Tokyo190-8518, Japan, [5]Institute of Natural Sciences, Okayama University of Science, 1-1 Ridai-cho, Kita-ku, Okayama 700-0

The Karwar and Coorg blocks in western India are important terranes in the point of paleogeographic study of India and Madagascar. The *c.* 1300 Ma Kumta suture separates the Karwar and Dharwar blocks within the western Dharwar craton of India (Ishwar-Kumar et al., 2013a). The major rock types are quartz phengite schist, chlorite schist, fuchsite schist, garnet biotite schist etc. Isochemical phase diagram estimates of the quartz phengite schist suggest peak metamorphic *P-T* conditions were *c.* 18 kbar and 550^o C. Towards the east of the suture Sirsi shelf contains weakly deformed sedimentary rocks, unconformable on high-grade gneisses of the Dharwar craton. The Karwar block to the west of the Kumta suture is mainly composed of undeformed tonalite-trondhjemite-granodiorite (TTG) with minor enclaves of amphibolite cut by later granites. Whole-rock major and trace element data suggest that the TTGs were derived from a volcanic arc, and that the granites have within-plate signatures. Amphibolites have a chemical composition comparable to basalts to basaltic andesites with MORB signatures. The TTGs from Karwar block shows a U-Pb zircon magmatic ages of *ca.* 3200 Ma (Ishwar-Kumar et al., 2013a). The K-Ar biotite age from the TTGs (1746 Ma and 1796 Ma) and amphibolite (*ca.* 1697 Ma) represents late-stage *c.* 1700 Ma uplift event of both TTGs and amphibolites. The Coorg block, which is about 100 km south of Karwar block, contains mainly granulite grade rocks (Chetty et al., 2012; Ishwar-Kumar et al., 2013b; Santosh et al., 2014). Major rocks types are charnockite, mafic granulites, hornblende-biotite gneiss, garnet-hornblende gabbro, anorthosite and granite. The Coorg (Mercara) suture which separates the Coorg block from the Dharwar craton to the east contains garnet-kyanite-sillimanite gneiss, mylonitic gneiss, calc-silicate granulite, mafic granulite, granite and syenite. Pseudosection calculations indicate that the constituent calc-silicate granulite and mafic granulite were re-equilibrated under high-pressure conditions of 15-20 kbar at a temperature of 800-900^o C (Ishwar-Kumar et al., 2013b). Santosh et al. (2014) recorded a metamorphic age of *c.*1200 Ma from metapelites from the Coorg (Mercara) suture zone. Integration of our structural, geological and geochronological results integrated with published data suggests the presence of a 1300-1200 Ma paleosubduction zone in western India. We propose that the Kumta and Coorg sutures are an eastern extension in western India of the northern and southern parts of the Betsimisaraka suture of north-eastern Madagascar.

Keywords: Karwar block, Coorg block, Kumta suture, Dharwar craton, Southern India, India-Madagascar

Japan Geoscience Union Meeting 2014
(28 April - 02 May 2014 at Pacifico YOKOHAMA, Kanagawa, Japan)

SGL43-02 Room:411 Time:May 1 14:30-14:45

Cambrian tonalite from Horei, Ofunato in southern Kitakami Mauntains, Japan

TSUCHIYA, Nobutaka[1*] ; TAKEDA, Tomoyo[1] ; SASAKI, Jun[1] ; ADACHI, Tatsuro[2] ; NAKANO, Nobuhiko[2] ; OSANAI, Yasuhito[2] ; ADACHI, Yoshiko[3]

[1]Iwate University, [2]Kyushu University, [3]Niigata University

The Lower Cretaceous volcanic rocks of Ofunato Group and plagioclase quartz diorite porphyry dikes are distributed in Ryori district, south Kitakami belt, Japan. The felsic volcaniclastic rocks and tonalite is discovered within the Ofunato Group in Horei, Ofunato, Japan. The felsic volcaniclastic rocks occur as blocks less than 10 m size, and tonalite are found as blocks less than 2 x 1 m in size. The tonalite composed mainly of plagioclase, quartz, biotite, and hornblende and is characterized by poverty of K-feldsper. The tonalite is rich in SiO_2 (73.1–73.4%), and is classified as volcanic arc granite after Pearce et al. (1984). However, it is characterized by low K_2O (0.72–1.27wt%), Rb (16–32ppm), and Ba (91–97ppm) concentrations. This rock is considered to be derived from arc magmatism in immature oceanic arc setting.

U-Pb dating of zircons were carried out using Agilent 7500cx quadrupole inductively coupled plasma mass spectrometer (ICP-MS) with a New Wave Research UP-213 Nd-YAG UV (213 nm) laser ablation system (LA) installed at the Kyushu University (Adachi et al., 2012). Zircon grains from tonalite concentrate around ca. 500 Ma, 8 analyses from 8 grains define a concordia age of 498 +/- 7 Ma. U-Pb zircon age obtained here correspond to latest Cambrian age, and is similar to U-Pb zircon SHRIMP age of the granitic rocks from the Daiouin granite in Hitachi metamorphic rocks (490.8 +/- 6.1 Ma) and the Hikawa granite in Higo metamorphic rocks, Kyushu (502.5 +/- 9.6 Ma) after Sakashima et al. (2003). In addition, Tagiri et al. (2010) described U-Pb zircon SHRIMP age of metamorphic porphyry (505.1 +/- 4.4 Ma) and metamorphic granite clast (499.6 +/- 5.6 Ma), and Tagiri et al. (2011) reported U-Pb zircon SHRIMP age of felsic schist (510.0 +/- 4.0 Ma) from the Hitachi metamorphic rocks. These rocks are considered to be resulted from Cambrian arc-trench system in proto-Japan (Isozaki et al., 2010). In south Kitakami Mountains, Shimojo et al. (2010) described U-Pb zircon SHRIMP age of trondjhemite in Hayachine complex (466 +/- 6 Ma), and Sasaki et al. (2013) reported that the solidification age of the Hikami granites is 450 Ma. In addition, Osanai et al. (in press) described U-Pb zircon LA-ICPMS age of granitic rocks in the Kurosegawa tectonic line in Kyushu (446–472 Ma). These data suggests that the granitic activity in early Paleozoic of proto-Japan arc occurs at ca. 500 Ma and ca. 450 Ma.

Keywords: Kitakami, Cambrian, zircon, U-Pb age, tonalite

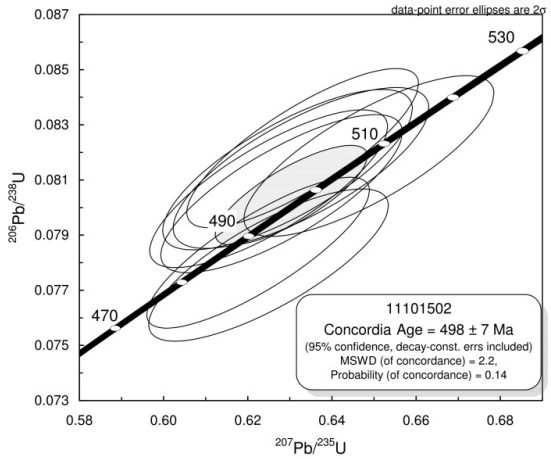

Japan Geoscience Union Meeting 2014
(28 April - 02 May 2014 at Pacifico YOKOHAMA, Kanagawa, Japan)

SGL43-03 Room:411 Time:May 1 14:45-15:00

U-Pb ages of zircon in plutonic rocks within the southern Abukuma Mountains

TAKAHASHI, Yutaka[1*] ; MIKOSHIBA, Masumi[1] ; KUBO, Kazuya[1] ; DANHARA, Toru[2] ; IWANO, Hideki[2] ; HIRATA, Takefumi[3]

[1]Geological Survey of Japan, AIST, [2]Kyoto Fission Track Co., Ltd., [3]Kyoto University

Abukuma Plutonic and Metamorphic Rocks are widely distributed in the southern Abukuma Mountains. These rocks had been studied in detail (e.g. Miyashiro, 1958; Research Group of the Abukuma Plateau, 1969; Kano et al., 1974; Maruyama, 1979). Radiometric age datings of the Abukuma Plutonic Rocks were carried out by Kawano and Ueda (1965), Maruyama (1978), Shibata and Uchiumi (1983), Shibata (1987), Shibata and Tanaka (1987) and others. These studies indicated that radiometric ages of the Abukuma Plutonic Rocks are almost 90 to 120 Ma. Recently, Ar-Ar age dating of hornblende (Takagi and Kamei, 2008) and U-Pb age dating of zircon (Kon and Takagi, 2012) for plutonic rocks in northern Abukuma Mountains were carried out. They showed that the ages of gabbro and granitic rocks are similar. On the other hand, U-Pb age dating of zircon for plutonic rocks in southern Abukuma Mountains is not yet performed. Therefore, U-Pb age dating of zircon for major plutons of southern Abukuma Mountains was carried out, result of which is reported and tectonics of the Abukuma Mountains is discussed based on the cooling history of the plutons.

Plutonic rocks in the southern Abukuma Mountains are classified into gabbro and diorite, fine-grained diorite, hornblende-biotite granodiorite (Irishiken Pluton, Kamikimita Pluton, Tabito Pluton, Ishikawa Pluton, Miyamoto Pluton and Samegawa Pluton), biotite granodiorite (Torisone Pluton), biotite granite and fine-grained leucogranite, based on the geological relations. The U-Pb ages of zircon for gabbro are 102.7+/-0.8 Ma (Tabito Pluton), 109.0+/-1.1 Ma (Hanawa Pluton), 114.2+/-0.8 Ma (Miyamoto Pluton). As for the hornblende-biotite granodiorite, U-Pb ages are 105.3+/-0.8 Ma (IrishikenPluton), 105.2+/-0.8 Ma (Kamikimita Pluton), 113.8+/-0.7 Ma (Tabito Pluton), 104.4+/-0.7 Ma (Ishikawa Pluton) and 106.4+/-0.8 Ma (Miyamoto Pluton). Also for the biotite granodiorite (Hanawa Pluton), the biotite granite and fine-grained leucogranite U-Pb ages are 105.7+/-1.0 Ma, 104.5+/-0.5 Ma and 100.2+/-0.8 Ma, respectively. These data indicate that the intrusion ages of Gabbro and surrounding granitic rocks are similar to each other. Furthermore, K-Ar ages of biotite and or hornblende, and fission track ages of the same rock samples were measured. Accordingly, it is clear that these rocks had been cooled rapidly to 300 degree C (Ar blocking temperature of biotite) after their intrusion. This implies that the Abukuma Mountains were uplifted rapidly after the intrusion of the Abukuma Plutonic Rocks.

References

Kano, H. et al. (1973) Geology of the Takanuki district. Quadrangle series, 1:50,000, Geological Survey of Japan. 115 p.
Kon Y. and Takagi, T. (2012) Jour. Mineral. Petrol. Sci., vol. 107, 183-191.
Maruyama, T. (1978) Jour. Min. Coll. Akita Univ., Ser. A, 5, p. 53-102.
Maruyama, T. (1979) Basement of the Japanese Islands, 523-558.
Miyashiro, A. (1958) Jour. Fac. Sci.,Univ. Tokyo, Sec. C, vol. 8, p. 245-268.
Research Group of the Abukuma Plateau (1969) Mem. Geol. Soc. Japan, no. 4, 83-97.
Shibata, K. (1987) Jour. Min. Petrol. Econ. Geol., vol. 82, p. 36-40.
Shibata, K. and Tanaka, T. (1987) Jour. Min. Petrol. Econ. Geol. vol. 82, p. 433-440.
Shibata, K. and Uchiumi, S. (1985) Jour. Min. Petrol. Econ. Geol. vol. 82, p. 405-410.
Takagi, T. and Kamei, A. (2008) Jour. Mineral. Petrol. Sci., vol. 103, p. 307-317.

Keywords: Abukuma Granites, Gabbro, Abukuma Belt, UU-Pb age, zircon

Japan Geoscience Union Meeting 2014
(28 April - 02 May 2014 at Pacifico YOKOHAMA, Kanagawa, Japan)

SGL43-04 Room:411 Time:May 1 15:00-15:15

Structural trends and tectonic inversion in Miocene sedimentary basins in the Tsugawa-Aizu province, Niigata prefecture

NARISAWA, Sayaka[1*] ; KURITA, Hiroshi[2]

[1]Niigata University, [2]Niigata University

The Tsugawa and Mikawa Sedimentary Basins in the northeastern part of Niigata are composed mainly of Early to Middle Miocene formations that contain so-called ”Green Tuff” volcanic sediments. Previous studies emphasized the NW-SE trend in the basement during the genesis of the Tsugawa basin. This outcrop-based study intends to discuss structural trends in the development of the Miocene sedimentary basin in the Mikawa area, Aga Town, Niigata.

The Miocene in this study area are divided into the Kanose, Tsugawa, and Araya/Igashima Formations in ascending order. Sedimentary facies analysis showed that the Kanose and Tsugawa formations filled half graben or graben. N-S to NNE-SSW trending faults of a map-scale limited the extent of the formations. NW-SE trending faults formed minor steps on the basement as well as minor, syn-sedimentary faults in the Miocene. They also affected the dyke intrusion trend. In short, the genesis of the Tsugawa basin involved 2 structural trends in this study area, while more significant is the N-S to NNE-SSW trend.

At present, the extent of the Miocene in this study area is, in many places, limited by thrust faults. Thrust faults locate at the position where rift-border faults are suggested. This indicates that tectonic inversion occurred with reactivation of N-S to NNE-SSW trending faults of the two. The trend of fault reactivation suggests that development of the basin in this study area is influenced by the Shibata-Koide tectonic line.

Keywords: Niigata sedimentary basin, Miocene, rift, structural trend, inversion

Japan Geoscience Union Meeting 2014
(28 April - 02 May 2014 at Pacifico YOKOHAMA, Kanagawa, Japan)

SGL43-P01 Room:Poster Time:May 1 18:15-19:30

K-Ar whole rock dating of the metamorphic rocks in the Yorii-Ogawa area of the north-eastern part of the Kanto Mountains

ONO, Akira[1*]

[1]none

Atokura Nappe is widely exposed in the Yorii-Ogawa area. It is mainly composed of Permian granitic rocks, Cretaceous Atokura Formation, Cretaceous pyroclastic rocks, Paleogene Yorii Formation and Paleogene Kiroko greenstone melange (Figure 1). Mid-Cretaceous metamorphic and granitic rocks are also distributed as small tectonic blocks. Kiroko greenstone melange mainly consists of high-pressure-type metamorphic rocks (Kiroko metamorphic rocks), meta-gabbro, meta-tonalite, serpentinite, epidote amphibolite and amphibolite. The Atokura Nappe tectonically overlies on the Mikabu greenstones and Chichibu Complex.

K-Ar whole rock ages of the Kiroko metamorphic rocks were determined on three slates and one mafic rock. The results for the slates are 127Ma, 117Ma and 115Ma. Whereas the K-Ar whole rock age of the mafic rock is 57.4Ma. The older ages of the slates are due to the presence of detrital white mica [1]. Based on the results of the K-Ar ages, the Kiroko metamorphic rocks are regarded as members of Sanbagawa metamorphic rocks. This conclusion reveals that nappe tectonics took place even in the region where Sanbagawa metamorphic rocks were exhumed.

The nappe tectonics occurred at many times in Cretaceous and Paleogene forearcs of Southwest Japan. In the northeastern part of the Kanto Mountains weakly metamorphosed Chichibu complex lie on the Mikabu greenstones by thrust faults [2, 3]. The existence of unconsolidated fault gouges suggests the formation of the thrust faults in a surface part of the crust. The thrust faults were formed by Cretaceous nappe tectonics before the formation of the Atokura Nappe.

Radiometric dating of the metamorphic rocks of the Chichibu and Mikabu belts is lack in the surveyed area. Hence, K-Ar whole rock dating was performed on a muscovite-chlorite schist from the Mikabu belt and a slate from the Chichibu belt. The results are presented on the left side of Figure 1. Locations of the samples are described below and are shown by star signs in the geological map.

The sample Yorii-Mikabu is a pelitic schist of the Mikabu belt exposed near the River Arakawa, Yorii town. The sample Sekisonzan is a weakly metamorphosed slate of the Chichibu belt which was exposed near Mt. Sekisonzan, Ogawa town. The sample Suguro-P2 is a black slate rich in carbonaceous materials and fine white mica. The location of the slate is loc. d of Ref. [1]. It is a member of the Kiroko metamorphic rocks.

Particle sizes of white micas vary considerably for each slate specimen studied. This is an evidence for insufficient recrystallization of white mica during regional metamorphism. Therefore, K-Ar whole rock ages of all the studied slates are older than the assumed metamorphic ages.

[1] A.Ono, 2013, Abs. Japan Geosci. Union Meeting, SMP43-P16.
[2] K.Sudo and K.Matsumaru, 1973, Bull. Chichibu Mus. Nat. History, 17, p.13-24.
[3] T. Kimura, 1977, Abs. Geol. Soc. Japan Meeting, p.104.

Keywords: Kanto Mountains, Yorii-Ogawa area, Mikabu greenstones, Chichibu Cmplex, K-Ar dating, Nappe

SGL43-P01 Room:Poster Time:May 1 18:15-19:30

New K-Ar whole rock ages of metamorphic rocks from the Yorii-Ogawa area

Sample	Age (Ma)	^{40}Ar rad (scc/g x10^{-5})	^{40}Ar rad (%)	K (%)
Yorii-Mikabu	89.4 ± 2.2	1.34	95.9	3.76
		1.34	95.1	3.76
Sekisonzan	146 ± 4.0	1.60	95.2	2.75
		1.66	95.4	2.76
Suguro-P2	115 ± 3.0	1.86	97.4	4.01
		1.84	97.9	4.01

λ_β =4.962×10^{-10}/yr , λ_ε=0.581×10^{-10}/yr
^{40}K/K=0.01167 atom%
Geospace Science CO.,LTD.

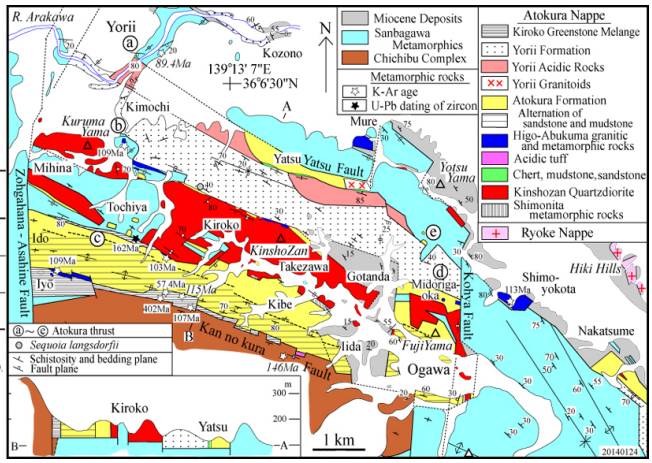

Japan Geoscience Union Meeting 2014
(28 April - 02 May 2014 at Pacifico YOKOHAMA, Kanagawa, Japan)

SGL43-P02 Room:Poster Time:May 1 18:15-19:30

Detrital zircon geochronology of the Tetori Group in the Arimine and Itoshiro areas, central Japan

KAWAGOE, Yuta[1] ; SANO, Shin-ichi[2] ; ORIHASHI, Yuji[3] ; KOUCHI, Yoshikazu[1*] ; UEDA, Tetsuya[1] ; YAMAMOTO, Koshi[4] ; OTOH, Shigeru[1]

[1]Grad. School Sci. Eng., Univ. Toyama, [2]Fukui Prefectural Dinosaur Museum, [3]ERI, Univ. Tokyo, [4]Grad. School Env. Stu., Nagoya Univ.

Introduction Provenance of the Tetori Group in the Arimine (Toyama-Gifu prefs.) and Itoshiro (Fukui Pref.) areas was analyzed using detrital zircon age distribution. In the course of the study, zircon ages of the Hida gneiss and granitoid were also determined.

Geologic Setting The Tetori Group consists of Middle Jurassic to Early Cretaceous shallow marine to terrestrial deposits. The group is divided, in ascending order, into the Kuzuryu, Itoshiro, and Akaiwa subgroups in the Itoshiro area (Maeda, 1961), and into the Higashisakamori, Nagatogawa, and Atotsugawa formations in the Arimine area (Kawai & Nozawa, 1958); the lower, middle, and upper units of the two areas have been correlated with each other. The lower members of the Nagatogawa-Atotsugawa formations consist of gravelly deposits of eastward running braided rivers, whereas the upper members consist of sandstone and mudstone of southward running meandering rivers. The U-Pb age of a tuff bed in the upper member of the Atotsugawa Formation is 120.0 +/- 1.2 Ma.

Zircon ages from surrounding areas The Hida Gneiss to the west of the Arimine area contains abundant 250-220-Ma zircons (Sano et al., 2000). The Korean Peninsula is mainly occupied by Archean-Paleoproterozoic basements of the Nangnim and Yeongnam massifs, covered with Cambrian-Jurassic deposits and cut by 250-160-Ma granitic rocks (e.g. Zhao et al., 2005). On the other hand, Northeast China between the Jiamusi Massif and the Songliao Basin, famous for " Phanerozoic crustal growth " (Wu et al., 2000), is composed primarily of 250-160-Ma granitic rocks and virtually no Precambrian rocks.

Samples and method of study U-Pb ages of zircons from (1) sandstone and sandy siltstone samples from six formations (members) of the Tetori Group from each area, (2) the Shimonomoto, Funatsu and Utsubo bodies of the Hida granite around the Arimine area, and (3) the Hida meta-granite on the north of the Arimine area were determined with laser ablation inductively coupled mass spectrometers (LA-ICP-MS) equipped in the Earthquake Research Institute of the University of Tokyo and Graduate School of Environmental Studies, Nagoya University.

Results There was marked difference in the percentage of Precambrian zircons (%Pc) between the Itoshiro-Akaiwa subgroups and the Nagatogawa-Atotsugawa formations: i.e. the %Pc of the former is 80 or more whereas that of the latter is less than 10. The samples of the Itoshiro-Akaiwa subgroups contained abundant 2500-1500-Ma zircons and a couple of Archean zircons. Age peaks of 190-170-Ma and 250-220-Ma were commonly seen for all samples of the Tetori Group. Among them, the peak of 250-220-Ma was higher in the braided river deposits and that of 190-170-Ma was higher in the meandering river deposits in the Arimine area. The Shimonomoto, Funatsu, Utsubo, and meta-granite bodies mainly contained 200-180-Ma, 250-190-Ma, 205-185-Ma, and 280-220-Ma zircons, respectively, and 180-170-Ma zircons were rare in the Hida Belt.

Discussion The meandering-river deposits in the Arimine area contain abundant 180-170-Ma zircons, which are virtually absent in the Hida Belt, and very few Precambrian zircons (%Pc $<$10). The catchment of the meandering rivers must have been occupied by Triassic-Jurassic igneous rocks with narrow exposures of Precambrian rocks. Considering the geology of eastern margin of Asia, the meandering rivers most likely passed through Northeast China (Jiamusi-Songliao). On the other hand, the braided river deposits of the area contain many 250-220 Ma zircons, suggesting that they were likely supplied at the time of uplifting of the Hida gneiss to the west. On the other hand, the Itoshiro-Akaiwa subgroups have abundant Precambrian zircons (%Pc $>$80). Possible candidates of the Precambrian exposure that could supply the sediments of these subgroups are the Yeongnam-Nangnim massifs. Hence the sediments of the Itoshiro-Akaiwa subgroups were likely carried by rivers that passed through the massifs.

Keywords: U-Pb age, detrital zircon, LA-ICP-MS, Tetori Group, Northeast China, East Asia

Japan Geoscience Union Meeting 2014
(28 April - 02 May 2014 at Pacifico YOKOHAMA, Kanagawa, Japan)

SGL43-P03 Room:Poster Time:May 1 18:15-19:30

Quaternary Tectonic Environments in North-Central Japan

TAKEUCHI, Akira[1*]

[1]Graduate school of Science and Engineering for Research, University of Toyama

The present-day central Japan is located at the convergent junction area among four tectonic plates, Amur, Okhotsk, Philippine Sea and Pacific plates. The Toyama Trough - Fossa Magna region is a major tectonic depression bounding the contrasting, tectonic provinces, i.e. the Northeast Japan (NEJ) arc on the Okhotsk plate and the Southwest Japan (SWJ) arc on the Amur plate. The north-central Japan on the Japan Sea side of Honshu Island is characterized by the latest Cenozoic thrust/fold belts, which are considered as the results of a series of inversion/conversion tectonics in relation to the Quaternary changes in relative motion between Eurasia/Amur and Philippine Sea plates.

This paper aims at describing these changes in crustal movements including active tectonics, and evaluates the existing hypotheses on the plate tectonic framework.

At the end of Pliocene in the NEJ arc, typical basin inversion has been occurred along the NE-SW trending, boundary faults of the Miocene sedimentary basins. While, on the side of SWJ arc, boundary faults of the Miocene basins were not reactivated, but other preexisting fractures have been reused to form the reverse fault and strike-slip fault provinces in response to N-S compression due to the Early Pleistocene northward subduction of the Philippine Sea plate, and to E-W compression due to the eastward motion of Amur plate, although the Present tectonic zone of strain concentration is probably related to the subduction of Pacific plate. In order to account for the Quaternary tectonic environment with a widespread stress field of strike-slip faulting in the basement as inferred from focal mechanism solutions, an accommodation mechanism is likely to have been worked in the asthenospheric mantle of the present arc-arc collision zone.

Considering the above neotectonic circumstances from the existence of the tectonic inversion of north-central Japan and stress field of the seismogenic layer, the hypotheses on eastward motion of Amur plate and on the nascent plate-boundary along the eastern margin of Japan Sea were positively evaluated.

Keywords: Amur Plate, Toyama Trough, Fossa Magna, Quaternary, neotectonics, north-central Japan

Japan Geoscience Union Meeting 2014
(28 April - 02 May 2014 at Pacifico YOKOHAMA, Kanagawa, Japan)

SGL43-P04 Room:Poster Time:May 1 18:15-19:30

Fracture system in the Sawara Granite at the area beside the Hinatatoge-Okasagitoge Fault, northern Kyushu

YUHARA, Masaki[1*] ; MIYAZAKI, Sotaro[1] ; AIZAWA, Jun[1]

[1]Department of Earth System Science, Faculty of Science, Fukuoka University

The Hinatatoge-Okasagitoge Fault has been identified by recent research. This fault continues to the Maebaru and Itoshima-hanto-oki Faults Group, and forms a single fault zone (Shimoyama et al., 2013). Activity rank of this fault is estimated C class. We recorded fractures in the Sawara Granite at the area beside the Hinatatoge-Okasagitoge Fault, and examined formation history of fracture system.

The fractures in the surveyed area are classified by their orientations into three types: NNW-SSE to NW-SE-oriented high-angle fractures, ENE-WSW-oriented high-angle fractures, and low-angle fractures. The fractures are further divided into three groups: minor faults associated with cataclasite, minor faults associated with fault gouge, and joints.

Based on the crosscut relationships of these fractures and the mineralization along joints, the formation process of the fractures related to activity of the Hinatatoge-Okasagitoge Fault involves five stages.

The minor faults associated with cataclasite were formed at the first stage. The laumontite veins were precipitated in spaces formed by the opening of joints at next stage. At the third stage, the minor faults associated with fault gouge were formed. The stilbite veins were precipitated in spaces formed by the opening of joints at next stage. At the last stage, the minor faults associated with fault gouge were formed.

Keywords: Hinatatoge-Okasagitoge Fault, Sawara Granite, fracture system, hydrothermal activity

Japan Geoscience Union Meeting 2014
(28 April - 02 May 2014 at Pacifico YOKOHAMA, Kanagawa, Japan)

SGL43-P05 Room:Poster Time:May 1 18:15-19:30

Bouguer gravity anomaly related to Cretaceous volcanic rocks in the Yanahara area, Okayama prefecture, SW Japan

ISHIKAWA, Nobuyo[1*] ; KOMURO, Hiroaki[1] ; YAMAMOTO, Akihiko[2]

[1]Dept. of Geoscience, Shimane Univ., [2]Dept. of Earth's Evolution Environment, Division of Mathematics, Physics, Earth Science, Ehime Univ.

Cretaceous volcanic rocks (volcanic, pyroclastic and lesser sedimentary rocks) unconformably overlying the basement rocks composed of the Maizuru Group and the Yakuno complex are widely distributed in the region from Okayama to Hyogo Prefectures, central Chugoku, SW Japan. Remarkable low gravity anomalous areas observed in the region of these volcanic rocks suggest some cauldrons. Total 610 observation points including 411 new points and 199 published points (GSJ, 2000; Shichi and Yamamoto, 2001) depict a detailed Bouguer gravity anomaly map of the Yanahara district through the band-pass filter between 1 to 30 km after the terrane and Bouguer corrections with a density of 2670kg/m3.

The Bouguer gravity anomaly map reveals low gravity anomalous areas corresponding with the Cretaceous volcanic rocks and the related granitic intrusive rocks; whereas high gravity anomalous areas corresponding with the Maizuru Group and the Yakuno complex.

The low gravity anomalous areas of the Yanahara district are observed in two parts: western and northeastern areas. The western low gravity anomalous area, measuring 20×7km in size, shows a flat-floor type anomaly surrounded with high gradient margins. The relative anomaly value is 8mgal less than that of the peripheral area. This suggests a flat-floor caldera (cauldron) filled up with thick rhyolitic volcanic rocks. This inferred caldera was possibly produced 80Ma, because quartz diorite intruded into this caldera has been dated as 79.8±1.8Ma by biotite K-Ar method.

Another area northeast of Yanahara shows an elongated funnel floor surrounded with high gradient margin. The anomaly value is 7mgal less than that of the peripheral area. This value is nearly equivalent to the gravity anomaly in the above mentioned western area. Accordingly, another lesser cauldron possibly lies in this area.

Japan Geoscience Union Meeting 2014
(28 April - 02 May 2014 at Pacifico YOKOHAMA, Kanagawa, Japan)

SGL44-01 Room:421 Time:May 2 14:15-14:30

Distribution of stratigraphic units of Middle Pleistocene Izumiyatsu Formation and their arsenic concentrations

YOSHIDA, Takeshi[1*] ; KUSUDA, Takashi[2] ; NIREI, Hisashi[3]

[1]Research Institute of Enviornmental Geology, Chiba, [2]Foremer Research Institute of Enviornmental Geology, Chiba, [3]Institute of medical geology

We identified the strata units of the Pleistocene Izumiyatsu Formation, which extends from the central part of Chiba Prefecture to the northeast, and the distribution of arsenic in these strata. In our summary of the geology, we refer to the Shimofusa Group.

It is possible to divide the facies of the Izumiyatsu Formation, a type locality, into five beds ? a muddy sand layer (facies 1: an estuarine sediment), an interbed of fine sand and mud (facies 2: a tidal flat sediment), a sand layer (facies 3: a tidal channel sediment), a silt layer (facies 4: a freshwater?seawater marsh sediment), and a medium sandy mud layer (facies 5: a inner bay marine sediment). The Izumiyatsu Formation, with changing facies, exhibits the following distribution pattern: facies 1, 2, 3, 4, and 5 in the southwest area, facies 5 only in the central area, and facies 4 and 5 in the northeast area. Only facies 5 is continuously distributed throughout the research areas.

Silt layer(Facies 4), the freshwater?seawater marsh sediment, has lower arsenic concentrations in sediment and in leachate than the other facies. Facies 5, the inner bay sediment, has higher arsenic concentrations in sediment and in than the other facies.

Keywords: Member unit, Groundwater flow, Arsenic

Japan Geoscience Union Meeting 2014
(28 April - 02 May 2014 at Pacifico YOKOHAMA, Kanagawa, Japan)

SGL44-02 Room:421 Time:May 2 14:30-14:45

Chronology of Brunhes-Matuyama geomagnetic polarity transition recoreded in sediments and climate change

ODA, Hirokuni[1*]

[1]National Institute of Advanced Industrial Science and Technology

Channell et al. (2010) suggested that the midpoint of the M-B boundary lies at 773.1 ka, ~7 kyr younger than the previously accepted astrochronological age for this polarity reversal (780-781 ka). Their results are based on the five high-resolution Matuyama-Brunhes polarity transition records from the North Atlantic placed on isotope age models produced by correlation of the d18O record to an ice volume model. They further inferred that the 40Ar/39Ar Fish Canyon sanidine (FCs) standard age that best fits the astrochronological ages is 27.93 Ma, which is younger than the two recently proposed FCs ages of 28.201 +-0.046 Ma (Kuiper et al., 2008) and 28.305 +- 0.036 Ma (Rene et al., 2010). However, recent study by Ganerod et al. (2011) suggested an age of 28.393+-0.194 Ma for FCs based on paired 40Ar/39Ar and 206Pb-238U radiometric dating supporting the calibrations of Kuiper et al. (2008) and Renne et al. (2010). Furthermore, recent study by Rivera et al. (2011) suggested an age of 28.172+-0.028 Ma for FCs based on cross-calibration with an astronomically tuned age of A1 tephra sanidines in the studied sequence of Faneromeni section in Crete. The discrepancy is significant that needs to be investigated carefully especially in terms of climate system involved.

On the other hand, the age model for relative paleointensity stack PISO-1500 (Channell et al., 2009) is based on IODP U1308 from North Atlantic. Channell et al. (2008) developed the age model for U1308 by correlating the benthic oxygen isotope curve with LR04 oxygen isotope stack (Lisiecki&Raymo, 2005). LR04 stack is known as oxygen isotope stack for benthic foraminifarra, whose age model is dependent on ice volume model with a certain time lag. Caballero-Gill et al. (2012) developed an absolute age model based on U-Th dating for stalagmites from China and correlated the oxygen isotope curve with that on planctonic foraminiferra for a deep-sea core from South China Sea. On the basis of the radiometrically calibrated chronology, they estimated that the time constant of the ice sheet is 5.4 kyr at the precession band and 10.4 kyr at the obliquity band. These values are significantly shorter than the single 17 kyr time constant originally estimated by Imbrie et al. (1984), based primarily on the timing of terminations I and II and the 15 kyr time constant used by Lisiecki and Raymo (2005) for LR04 stack.

In the presentation, the chronology of Brunhes-Matuyama geomagnetic polarity transition will be further discussed in relation to the chronology of 10Be records of EPICA Dome C (Dreyfus et al., 2008).

Keywords: Brunhes-Matuyama polarity transition, chronology, sediment, oxygen isotope, ice sheet, astronomical calibration

Japan Geoscience Union Meeting 2014
(28 April - 02 May 2014 at Pacifico YOKOHAMA, Kanagawa, Japan)

SGL44-03 Room:421 Time:May 2 14:45-15:00

SHRIMP U-Pb zircon dating for Byakubi tephra: implication for refined chronology for the Matuyama-Brunhes boundary

SUGANUMA, Yusuke[1*] ; OKADA, Makoto[2] ; HORIE, Kenji[1] ; KAIDEN, Hiroshi[1] ; TAKEHARA, Mami[3] ; SENDA, Ryoko[4] ; KIMURA, Jun-ichi[4] ; KAZAOKA, Osamu[5]

[1]National Institute of Polar Research, [2]Ibaraki University, [3]Kyushu University, [4]JAMSTEC, [5]Research Institute of Environmental Geology, Chiba

Paleomagnetic records from marine sediments have contributed to improved understanding of variations in the Earth's magnetic field and have helped to establish age models for marine sediments. However, lock-in of the paleomagnetic signal at some depth below the sediment-water interface in marine sediments through acquisition of a post-depositional remanent magnetization (PDRM) adds uncertainty to synchronization of marine sedimentary records (e.g., Roberts and 2004; Suganuma et al., 2011; Roberts et al., 2013). Recently, Suganuma et al. (2010) presents clear evidence for a downward offset of the paleointensity minimum relative to the ^{10}Be flux anomaly at the Matuyama-Brunhes (M-B) geomagnetic polarity boundary, which they interpret to result from a 16 cm PDRM lock-in depth. This indicates that a certain age offset probably occurs when a paleomagnetic record is used for dating marine sediments. This phenomenon also suggests that the accepted ages for the geomagnetic polarity boundaries, including the M-B boundary, should be revised (ca. 10 kyr younger in case of the M-B boundary). Contrary, two recently proposed revisions of the age of the ^{40}Ar/^{39}Ar Fish Canyon sanidine (FCs) standard (Kuiper et al., 2008; Renne et al., 2010) would adjust ^{40}Ar/^{39}Ar ages of the M-B boundary from Maui (Singer et al., 2005) to 781 $\pm$ 2 ka and 784 $\pm$ 2 ka, respectively.

Plio-Pleistocene marine sedimentary sequences are widely distributed in the Boso and Miura Peninsula, central Japan. Because these sequences have a significantly high sedimentation rate with well-preserved platonic and benthic foraminifera fossils, it is possible to reconstruct a detailed geomagnetic behavior along the polarity boundaries such as M-B with high resolution oxygen isotope records. In addition, a number of tephra layers are accompanied with these sedimentary sequences, which make it possible to provide absolute age constrains for the boundaries. The Byakubi tephra, located few tens of cm above the M-B boundary, has been investigated based on SHRIMP (Sensitive High Resolution Ion Microprobe) U-Pb dating of single zircon crystals from the tephra. The initial U-Th ratio is also corrected by using ICP-MS (Inductively Coupled Plasma Mass Spectrometer) analysis of volcanic glasses of the tephra. The ^{206}Pb/^{238}U ratio corrected by ^{207}Pb assuming ^{206}Pb/^{238}U-^{207}Pb/^{235}U age concordance from 20 grains are equivalent with a weighted mean of 761.1 $\pm$ 7.6 ka. Although this M?B boundary age is ˜23 kyr younger than previously accepted ^{40}Ar/^{39}Ar ages, this is almost consistent with a younger ice core derived age of 770 $\pm$ 6 ka (Dreyfus et al., 2008), marine sediments age of 770 ka based on ^{10}Be anomaly (Suganuma et al., 2010), and ^{40}Ar/^{39}Ar age of 761 $\pm$ 2 ka adjusted by the K-Ar based FCs standard ages (27.5 Ma: Mochizuki et al., 2010).

Japan Geoscience Union Meeting 2014
(28 April - 02 May 2014 at Pacifico YOKOHAMA, Kanagawa, Japan)

SGL44-04 Room:421 Time:May 2 15:00-15:15

Rockmagnetic and Paleomagnetic examinations for the Matuyama-Brunhes polarity transition recorded in the Kazusa Group

OKADA, Makoto[1*] ; SUGANUMA, Yusuke[2] ; MARUOKA, Toru[1] ; HANEDA, Yuki[1] ; KAZAOKA, Osamu[3]

[1]Ibaraki University, [2]National Institute of Polar Research, [3]Research Institute of Environmental Geology, Chiba Pref.

We report results of rockmagnetic and paleomagnetic examinations for the Matuyama-Brunhes polarity transition recorded a marine sequence of the Kokumoto Formation, Kazusa Group in the Boso Peninsula. We have taken 130 oriented mini-cores from a 13 meters interval of sandy-siltstones spanning across the TNTT bed (Byakubi-ash layer) at the Tabuchi section along to the Yoro River and at the Yanagawa section. Results from thermal magnetic experiments suggested that the samples include iron sulfide, magnetite as a primary remanence carrier and no hematite. Measurements of magnetic hysteresis indicated that a domain state of the samples was PSD. Results of progressive alternating field demagnetization indicated a reversed to normal polarity transition boundary was observed at around 1.5 meter below the TNTT bed as well as previous studies, however the transition boundary was observed at around the TNTT bed in thermal demagnetization results. In the samples showing this discrepancy, a magnetite derived reversed polarity component was observed after a normal polarity component completely demagnetized at around 300-400 ℃. This phenomenon would be due to that the magnetite derived primary component was slightly acquired under a weak magnetic field condition just before the M-B boundary, and then chemically yielded iron sulfide magnetic minerals acquired a much stronger normal polarity component under a strong filed condition after the polarity transition. Those results exhibited that the M-B boundary situated at around the TNTT bed where about 1.5 metes above the position reported in previous studies.

Keywords: Matuyama-Brunhes boundary, rockmagnetism, paleomagnetism, L-M Pleistocene boundary, Boso Peninsula, Kazusa Group

Japan Geoscience Union Meeting 2014
(28 April - 02 May 2014 at Pacifico YOKOHAMA, Kanagawa, Japan)

SGL44-05 Room:421 Time:May 2 15:15-15:30

High-resolution magnetostratigraphy across the Matuyama-Brunhes polarity transition from the Chiba Section

HYODO, Masayuki[1*] ; TAKASAKI, Kenta[2] ; MATSUSHITA, Hayato[2] ; KITABA, Ikuko[1] ; KATOH, Shigehiro[3] ; KITAMURA, Akihisa[4] ; OKADA, Makoto[5]

[1]Research Center for Inland Seas, Kobe University, [2]Department of Earth and Planetary Sciences, Kobe University, [3]Division of Natural History, Hyogo Museum of Nature and Human Activities, [4]Institute of Geosciences, Faculty of Science, Shizuoka University, [5]Department of Earth Sciences, Faculty of Science, Ibaraki University

An oriented 54-m core was collected from the Kokumoto Formation of the Kazusa Group, near the Chiba Section, a candidate for the GSSP of the Early-Middle Pleistocene boundary. The core spans in stratigraphy from a thick sand layer below a mud clast layer up to just below the Ku-2B tuff. A detailed Matuyama-Brunhes (MB) geomagnetic reversal record was obtained, using u-channel samples of 1 m long cut out from 1-m core section. Magnetization components were separated by stepwise alternating field demagnetization (AFD). Low field magnetic susceptibility and anhysteretic remanent magnetization show the core consists of magnetically homogeneous sediments. Magnetizations of discrete samples of 2.2cm x 2.2cm x 2.2cm were also measured, being subjected to progressive thermal demagnetizations (THD) and AFD. The declinations of characteristic remanent magnetization (ChRM) well agree across the boundary of 1m-sections, indicating that orientation of each 1m-core section was successful. Magnetic hysteresis measurements show magnetic grains are of PSD size. THD shows that hematite is included besides magnetite, a main magnetic carrier. Thermomagnetic measurements and THD suggest that the sediments include greigite, ferrimagnetic iron sulfide, which may cause a false reversal due to self-reversal of magnetic minerals. The paleomagnetic results show that the upper boundary of the MB transition lies above the Byakubi volcanic ash layer, which is much higher than the previous result. Our data show normal polarity continues from a depth of about 1m below the Byakubi, but several polarity swings exist above it. From about 70cm above the Byakubi to the top of the core, normal polarity continues. Relative paleointensity data show the lower end of the MB transition lies below the base of the core. The relative paleointensity keeps low values in the lower part below the Byakubi, and gradually increases upward above it, reaching a maximum value at about 39 m above the Byakubi. This linear increase feature is similar to the post-MB reversal intensity pattern observed in the paleointensity stack Sint-2000 (Valet et al., 2005). The low paleointensity kept throughout the basal part suggests the beginning of the MB transition lies much below the base of the core.

Keywords: Matuyama-Brunhes boundary, magnetostratigraphy, Chiba section, oriented core

Japan Geoscience Union Meeting 2014
(28 April - 02 May 2014 at Pacifico YOKOHAMA, Kanagawa, Japan)

SGL44-06 Room:421 Time:May 2 15:30-15:45

Identification of Pleistocene tephra layers in marine sediment core C9001C, offshore Shimokita Peninsula, NE Japan

HASEGAWA, Takeshi[1*] ; SUGAYA, Manami[1] ; OKADA, Makoto[1] ; MOCHIZUKI, Nobutatsu[2] ; FUJII, Satomu[2] ; SHIBUYA, Hidetoshi[2]

[1]Faculty of Science, Ibaraki University, [2]Kumamoto University

Correlations for Pleistocene tephra layers in marine sediment core C9001C was investigated. The core was obtained from near the Shimokita Peninsula, Japan by the CK06-06 D/V CHIKYU Shakedown Cruise in 2006. The stratigraphy of the Hole C9001C (365 m long) has been well established based on the correlation of the benthic d18O curve with the LR04 stack (Domitsu et al., 2011). Tephra layers, a few millimeters to centimeters in thickness, can be often recognized in this sediment core that is mainly composed of dark olive-gray, diatomaceous silty clay. Two tephra layers at 30.3 mbsf and 54.3 mbsf were already correlated with the Spfa-1 and Aso-4, respectively. In this study, we focus on relatively thick and coarse tephra samples from 20 mbsf to 150 mbsf (30 - 240 ka, LR04 age). As the result, seven tephra layers were newly identified on the basis of tephro-stratigraphy and petrology, such as glass chemistry and mineralogy.

We identified the To-Of (BP1) at 19.6 mbsf, To-GP at 24.8 mbsf, Ko-i at 25.5 mbsf, Toya at 61.4 mbsf, Aso-3 at 73.9 mbsf, Mb-1 at 115.6 mbsf and Tn-C at 145.9 mbsf based on tephra databases (e.g. Okumura, 1991; Machida and Arai, 2003; Aoki and Machida, 2005). Descriptions of each tephra layer are as follows: The tephra layer at 19.6 mbsf is 6 cm thick, medium-sand sized, crystal vitric ash, including Cpx and Opx crystals. Chemical composition of glass shards is SiO2=77.5%, K2O=1.2% (100% normalized). The tephra layer at 24.6 mbsf is 3 cm thick, medium-sand sized, vitric crystal (Cpx, Opx) ash, showing Low-K glass composition (SiO2=75.4%, K2O=1.1%). The tephra at 25.5 mbsf is patchy (5 mm in maximum thickness), fine-sand sized, vitric ash, showing the Medium-K composition (SiO2=76.2%, K2O=2.1%). The tephra at 61.4 mbsf is 1.5 m thick, fine-sand sized, vitric ash, containing trace amount of Opx. Glass shards have Medium-K composition (SiO2=79.0%, K2O=2.7%). The tephra layer at 73.9 mbsf is 2 cm thick, medium-sand sized, vitric crystal (Cpx, Opx) ash, characteristically showing High-K glass composition (SiO2=70.3%, K2O=4.6%). The tephra layer at 115.6 mbsf is 4 cm thick, medium-sand sized, vitric crystal ash, characteristically including Bt, Hb crystals in addition to pyroxenes. The glass chemistry is: SiO2=78.1%, K2O=3.9%. The tephra layer at 145.9 mbsf is 20 cm thick, medium to coarse-sand sized, vitric crystal (Cpx, Opx) ash, showing relatively Low-K glass composition (SiO2=78.4%, K2O=1.5%).

We can re-examine the correlations for tephras with marine isotope stages (MIS) based on LR04 age. The To-Of tephra from Towada volcano can be newly correlated with early MIS 2 (<29 ka). The Aso-3 can be correlated with late MIS 6. It is also needed to revise the estimations of eruption volume and distribution of Aso-3. The Tn-C tephra from Osore volcano can be correlated with MIS 7 (<240 ka). Detailed identification of these seven tephras and further correlations for other tephra samples are now in progress, and will be presented elsewhere.

Keywords: Shimokita Peninsula, marine sediment core, Pleistocene, tephra, CHIKYU, glass chemistry

Japan Geoscience Union Meeting 2014
(28 April - 02 May 2014 at Pacifico YOKOHAMA, Kanagawa, Japan)

SGL44-07 Room:421 Time:May 2 15:45-16:00

Overview of tephrochronological study on Kazusa Group, the standard Quaternary marine sediments, central Japan

SUZUKI, Takehiko[1*]

[1]Tokyo Metropolitan University

The author will review tephrochronological study on Kazusa Group, the standard Quaternary marine sediments, central Japan, and will point out issues to study in future. The former will be carried out by referring to previous works by each area such as Boso, Tama Hills, Yokohama, Choshi, and underground of central Kanto Plain. Recent studies have focused on description of characteristic properties of tephras and correlation between areas in Kanto district. Moreover, studies for correlation with proximal tephras around source volcanoes had been carried out.

Keywords: Kazusa Group, Tephrochronology, Quaternary sediments

Japan Geoscience Union Meeting 2014
(28 April - 02 May 2014 at Pacifico YOKOHAMA, Kanagawa, Japan)

SGL44-08 Room:421 Time:May 2 16:15-16:30

The Kazusa Group as a standard tephrostratigraphy of Japanese Lower to Middle Pleistocene formations

SATOGUCHI, Yasufumi[1*]

[1]Lake Biwa Museum

Tephrostratigraphy of the Pliocene to Pleistocene formations at Kyushu and Honshu Island are established (Satoguchi and Nagahashi, 2012). Establishment of stratigraphy and chronological model needs integrative interpretation of biostratigraphy, paleo-magnetostratigraphy and other stratigraphic and chronological studies. In the early stages of the work like this, decision of standard stratigraphy for is valid. Satoguchi and Nagahashi (2012) adopted the Kazusa Group as a standard formation of the Pleistocene stratigraphy of Japan.

The Kazusa Group, which is composed of marine deposits, is investigated about magnetostratigraphy, biostratigraphy, correlated with MIS and other stratigraphical studies. Many tephra beds in this group have been described, and data of characteristic properties of these tephras for correlations are accumulated (e.g. Satoguchi, 1995). Some of these tephras are examined for correlations with widespread tephras, are revealed about their volcanic source area. For example, the Ss-Pnk, the Ss-Az and the Kb-Ks tephras are from Kyushu Island (Hayashida et al., 1996; Kamata et al., 1994; Kikkawa et al., 1991). The Ho-Kd39, Eb-Fukuda, Om-SK110 tephras are from the Chubu Mountains (Nagahashi et al., 2000). The JA-O18L tephra is from north of the Kanto district (Nakamura and Arai, 1998). The As-Kd8 and the Hkd-Ku tephras are from the Tohoku district (Murata and Suzuki, 2011; Suzuki et al., 2005). The Kazusa Group contains tephras from various areas. This thing is important for being standard tephrostratigraphy. Tephras mentioned above are widespread tephras that are distributed over 500km. Some tephras in this group are revealed that they distributed relatively small area. Volcanic source of the Byakubi tephra, which is intercalated around boundary of the Lower-Middle Pleistocene, is the Older Ontake Volcano (Takeshita et al., 2005). The Ks12 tephra above the Byakubi tephra is also from the Older Ontake Volcano. These tephras are important for investigation of volcanic history about the Older Ontake Volcano. Therefore, the Kazusa Group is important formation for Japanese stratigraphic studies and investigation of explosive volcanism in the Pleistocene.

REFERENCES: Hayashida, A. et al. (1996) Quaternary International 34?36, 89?98.; Kamata, H. et al. (1994) Journal of Geological Society of Japan, 100, 848?866.; Kikkawa, K. et al. (1991) Monthly Chikyu, 13, 228?234.; Murata, M. and Suzuki, T. (2011) Daiyonki-Kenkyu, 50, 49?60. Nagahashi, Y. et al. (2005) Journal of Geological Society of Japan, 106, 51-69.; Nakamura, M. and Arai, F. (1998) Chikyu-Kagaku, 52, 153-157.; Satoguchi, Y. (1995) Journal of Geological Society of Japan, 101, 767-782.; Satoguchi,Y. & Nagahashi,Y. (2012) Island Arc, 149-169.; Suzuki, T. et al. (2005) Island Arc, 14, 666?78.; Takeshita, Y. et al. (2005) Journal of Geological Society of Japan, 111, 417-433.

Keywords: Kazusa Group, widespread tephra, Pleistocene, Byakubi tephra

Japan Geoscience Union Meeting 2014
(28 April - 02 May 2014 at Pacifico YOKOHAMA, Kanagawa, Japan)

SGL44-09 Room:421 Time:May 2 16:30-16:45

Reconstruction of paleogeography of Kanto district about 1.6 Ma based on tephrostratigraphy

NAKAJIMA, Eri[1*] ; SUZUKI, Takehiko[2]

[1]Graduate student, Tokyo Metropolitan University, [2]Tokyo Metropolitan University

First Horinouchi Tuff (HU_1) in the Oyamada Formation of the Kazusa Group, erupted about 1.63 Ma, had been found in and around Kanto Plain by previous studies. We examined the correlation of HU_1 and tephras stratigraphically near to HU_1 to reconstruct paleogeography of Kanto district in Early Pleistocene. The tephras collected from the river bed of the Tama River (Tachikawa city), the Sayama Hills, the Yokohama area, the Choshi area, Enoki Trench Core, Tachikawa Core, and Higashiyamato Core were analyzed. The tephras were correlated based on their mineral contents, refractive indices of volcanic glass shards and minerals, chemical compositions of volcanic glass shards and titanomagnetite. As a result, it was newly revealed that three tephra layers (Sayama Gomashio Volcanic Ash in Sayama Formation, pumice fall deposit in the Tachikawa Core Fujimi of Tachikawa, HY-1.1-HY1-6 in the Higashiyamato Core Narabashi of Higashiyamato) are correlated with HU_1. Also, We analyzed Tobiratoge Pyroclastic Rocks and Sanjiro Pyroclastic Rocks occured in the south part of the Utsukushigahara Plateau in order to detect the source volcano of HU_1. As a result, both Tobiratoge Pyroclastic Rocks and Sanjiro Pyroclastic Rocks are not correlated because of difference refractive indices and chemical compositions of volcanic glass shards and refractive indices of hornblende. Thus, it was revealed that HU_1 has not been erupted from the volcano vicinity of Utsukushigahara Plateau. We estimated the accumulation rates of sedimentation based on correlated tephras. The accumulation rates of sediments are 46.3 cm/kyr in the Yokohama area, 59.0 cm/kyr at Tachikawa Core, 2.5-10.3 cm/kyr at Haginaka Core, 3.8-6.7 cm/kyr in the Choshi area. These differences of the accumulation rates of sediments reflect the difference of the sedimental environment. Moreover, in Tachikawa Core and Sayama Hills, HU_1 are accumulated thicker than other areas. It is expected that HU_1had reworked again and again after its primal deposition by the effect of wave action in shallow sea.

Keywords: tephra, Kazusa Group, First Horinouchi Tuff, paleogeography

Japan Geoscience Union Meeting 2014
(28 April - 02 May 2014 at Pacifico YOKOHAMA, Kanagawa, Japan)

SGL44-10 Room:421 Time:May 2 16:45-17:00

Stratigraphy of the L-M Pleistocene boundary section in the Kokumoto Formation with re-definition of the Byk-TNTT tephra

KAZAOKA, Osamu[1*] ; OKADA, Makoto[2] ; KAMEYAMA, Shun[1] ; SUGANUMA, Yusuke[3] ; AIDA, Nobuyuki[4] ; MORISAKI, Masaaki[1] ; KAGAWA, Atsushi[1] ; KUMAI, Hisao[5] ; NIREI, Hisashi[6]

[1]Research Institute of Environmental Geology, Chiba, [2]Ibaraki University, [3]National Institute of Polar Research, [4]Shumei University, [5]Osaka City University, [6]Officer of IUGS-GEM

Detailed stratigraphy of the Kazusa Group was surveyed for development of water-soluble natural gas on many marker tephra in Boso peninsula (Kanehara et al.,1949; Shinada et al.,1951; Mitsunashi et al.,1959; Mitsunashi et al.,1961; Ishiwada et al.,1971; Mitsunashi et al.,1979). Magnetostratigraphy (Nakagawa et al., 1969; Niitsuma, 1976; Okada & Niitsuma, 1989), planktonic foraminifera (Oda,1977), nannofossils (Takayama,1967; Sato et al., 1988) and diatom (Cherepanova et al.,2002) were studied on the detailed stratigraphy for international correlation.

The Early-Middle Pleistocene boundary is in the middle part of the Kokumoto Formation in Kazusa Group (Kumai, 1996). Many marker tephra are interbeded in Kiwada F., Otadai F., Umegase F. and Kakinokidai F. Only 5 marker tephra are intercalated in Kokumoto F. Over twenty thin tephra, pumice bed, scoria bed and vitric fine tuff were fined out in the middle silty part of the Kokumoto F. for detailed stratigraphy around the Early-Middle Pleistocene boundary in Yoro river route, type route of the Kazusa G. (WQSB, 1996). Byakubi(Byk) tephra, 1-3cm thick vitric fine tuff under 27m thick from Ku2 distribute in Byakubi district along Yoro river. Matuyama?Brunhes magnetic reversal was fined out in the middle silty part under Ku2 tephra (Nakagawa et al.,1969). Aida(1997) showed that the magnetic reversal distribute just below the Byk tephra. TNTT tephra and the Matuyama?Brunhes magnetic reversal just below the TNTT tephra were fined under Ku2 on Yanagawa route (Niitsuma,1976). Same tephra and the magnetic reversal were fined on Heizo rute and Chonan route (Okada & Niitsuma, 1989). White vitric tephra are interbeded often in the Kazusa G. So marker tephra is necessary tephra association with over 2 tephra. 4 tephra, 3 scoria bed and 1 vitric fine tuff, were fine out just above Byk tephra on Yoro river route for detailed stratigraphy around the magnetic reversal by this study. And same tephra association were recognized just above the TNTT tephra in Yanagawa route, too.

Byk tephra zone is defined as follows. Byk tephra zone is composed of 5 tephra which in ascending order are Byk-E, Byk-D, Byk-C, Byk-B and Byk-A. Byk-B, Byk-C and Byk-D are medium sand grain scoria lenticular beds. Byk-A is 9 cm thick reddish gray vitric fine tuff. Byk-E is 1-3cm thick white vitric fine tuff. Byk-E tephra is correlated with TNTT tephra.

Keywords: L-M Pleistocene boundary, Kokumoto Formation, Kazusa Group, Byakubi tephra, TNTT tephra, Byk tephra zone

Japan Geoscience Union Meeting 2014
(28 April - 02 May 2014 at Pacifico YOKOHAMA, Kanagawa, Japan)

SGL44-11 Room:421 Time:May 2 17:00-17:15

Lower - Middle Pleistocene Boundary at Chiba Section and istribution situation of Byakubi Ash, central Japan

KIMURA, Hideto[1*] ; KAZAOKA, Osamu[2] ; NIREI, Hisashi[3]

[1]Toho Chisui Co., Ltd. Kanto office, [2]Research Institude of Environmental Geology, Chiba, [3]International Union of Geological Science for Environmental Management(IUGS-GEM)

The Byakubi Ash is distributed over the Ichihara City southern part and is located in the vicinity of a base of the middle-upper member of Kokumoto formation, Kazusa Group. Kokumoto formation is sorted four member by facies, is upper member (sandy alternation), middle-upper member (mussive mud), middle-lower member (sandy alternation) , and lower member (mussive mud). The Matsuyama / Brunhes chron boundary as the Lower - Middle Pleistocene Boundary is attracted by the lower base of the Byakubi Ash, it was confirmed that the Byakubi Ash was distributed from the Yoro River(Tabuchi) , Tabuchi River(Tabuchi), Nishi River(Tsukide), to the Koshikiya River (Koshikiya).

The future follow-up survey comes to need a careful survey, but it is thought that it is to the important clue of the chase because the distribution situation of Ku2(Ku2B' and Ku2B) inserted between the high rank of the Buakubi Ash is considerably confirmed.

Keywords: Byakubi Ash, Kokumoto Formation middle-upper member, Yoro River, Chiba Section

Japan Geoscience Union Meeting 2014
(28 April - 02 May 2014 at Pacifico YOKOHAMA, Kanagawa, Japan)

SGL44-12 Room:421 Time:May 2 17:15-17:30

Tephras of the Kokumoto Formation in the Mobara area

NAKAZATO, Hiroomi[1*] ; NANAYAMA, Futoshi[2]

[1]NARO, [2]AIST

Authors are examining the tephra stratigraphy of the Kazusa Group as part of the geologic map investigation in 1/50,000 Mobara district. The tephras of Ku0.6-Ku6E were confirmed from the Kokumoto Formation. The TNTT tephra (Niitsuma, 1971) which is just above the B/M boundary is pursued to Obota, Chonan town by Okada and Niitsuma (1989). The TNTT is a fine vitric volcanic ash with abundant hornblende (n_2=1.680-1.703) and the pumice type volcanic glass (n=1.505-1.510). This tephra was correlated with the tephras from the Older Ontake Volcano (Takeshita et al., 2005). The distribution of the TNTT was confirmed to Baba, Mutsuzawa town in the authors' investigations. Tephras of Ku0.6, Ku0.9 and Ku2.5 were confirmed in Terasaki, Mobara city where is the northeast limit of distribution of the Kokumoto Formation. The TNTT and the B/M boundary horizon are able to trace to this region.

Keywords: tephra, stratigraphy, TNTT

Japan Geoscience Union Meeting 2014
(28 April - 02 May 2014 at Pacifico YOKOHAMA, Kanagawa, Japan)

SGL44-13 Room:421 Time:May 2 17:30-17:45

The source volcano and age of the Byakubi tephra in the Kazusa Group in Boso Peninsula, central Japan

UCHIYAMA, Takashi[1*] ; TAKESHITA, Yoshihiro[2] ; KUMAI, Hisao[3]

[1]Yamanashi Institute of Environmental Sciences, [2]Shinshu University, [3]Prof. Emeritus, Osaka City University

Introdution

The Kazusa Group in the Boso Peninsula, central Japan is composed of Lower- Middle Pleistocene marine sediments that contain numerous tephra layers (Mitsunashi et al.1959; Machida et al. 1980; Satoguchi 1995; Satoguchi 1996 and so on). One of numerous tephra layers, Byakubi tephra (BYK; Takeshita et al. 2005) is intercalated just above Brunhes/ Matuyama (B/M) boundary in middle part of the Kokumoto Formation (Okada and Niitsuma 1989; Aida et al. 1996). BYK was correlated with YUT4 or 5 from the Older Ontake Volcano, which provide a datum plane of the Lower-Middle Pleistocene boundary in central Japan (Takeshita et al. 2005).

Correlation of the tephra beds in the Kazusa Group with those from the Older Ontake Volcano

Heavy mineral assemblage and chemical compositions of hornblende of nine Lower-Middle Pleistocene tephra beds (Ku6E, Ku5C, BYK, Ka2.4A, Ka2.4B, Ch3, Ch1.5, Ks18, Ks12) from the Kazusa Group, in Boso Peninsula were examined in order to correlate with the tephra from the Older Ontake Volcano in central Japan by Takeshita et al. (2005). Conclusively, hornblende compositions from the nine tephra beds were distinguishable. Two of the nine beds, BYK and Ks12 tephra, were correlated with two tephras from the Older Ontake Volcano, YUT4 or 5 and KZT, respectively . The age of these tephra beds of the Kazusa Group could be inferred from the stratigraphic relationships with 47 dated lava flows on the foot of the Older Ontake Volcano, and from presence of well-known widespread tephras and magnetostratigraphy in the Boso Peninsula. Correlated these two tephra beds became valuable marker tephra for geochronological studies in inland and marine sediments from central Japan. It was also emphasized that the BYK and YUT4 or 5 could provide a datum plane of the Lower-Middle Pleistocene boundary in this region.

Keywords: Lower-Middle Pleistocene Boundary GSSP, Kazusa Group, Byakubi tephra, Ontake Volcano, Bosu Peninsula

Japan Geoscience Union Meeting 2014
(28 April - 02 May 2014 at Pacifico YOKOHAMA, Kanagawa, Japan)

SRD45-01 Room:415 Time:April 28 14:15-14:45

Concentration of Elements Related to Redox Evolution in Oceanic Environments

OTAKE, Tsubasa[1*]

[1]Faculty of Engineering, Hokkaido University

Chemical sedimentary rocks, which are precipitates from ancient seawater, not only concentrate useful elements (e.g., Fe, Mn, Co, Ni, Rare Earth Elements (REEs)), but may also reflect changes in Earth ' s surface environments (e.g., pH, redox conditions, surface temperature). The temporal distribution of Banded Iron Formations (BIFs), the main economic Fe source, has been proposed to indicate changes in atmospheric and ocean chemistry in early Earth related to the evolution of the biosphere. However, to acquire a better understanding of the surface environments, BIFs deposited in various sedimentary setting need to be investigated. In this study, geological and geochemical investigations of BIFs that were deposited in a shallow ocean in the Archean Barberton Greenstone Belt, South Africa, show that the Cr/Ti and U/Th ratios are higher in the BIFs compared with the underlying and overlying clastic sedimentary rocks. Oxygen isotope compositions in each chromite grain, a host mineral of Cr, were determined by SIMS. The results show the chromite has lower δ^{18}O values compared with igneous and metamorphosed chromites, indicating that they were formed under hydrothermal conditions. The results suggest that dissolved Cr and U species in ocean were coprecipitated with ferric (hydr)oxides during the formation of the BIFs, and that chromite was formed by later hydrothermal alteration. Therefore, the results of the study indicate that enrichments of redox-sensitive elements (e.g., Cr, U) in BIFs have already occurred through chemical processes as early as 3.2 billion years ago due to the oxygenation of a shallow part of the ocean.

Volcanogenic Massive Sulfide (VMS) deposits such as Kuroko deposits in the Hokuroku district, Akita Prefecture were formed by ancient submarine hydrothermal activity, and are also associated with Fe-rich chemical sedimentary rocks. Because VMS deposits are primarily composed of sulfide minerals that are unstable in an oxic environment, such as pyrite and chalcopyrite, an anoxic environment in the Hokuroku basin may play an important role in the preservation of sulfide ores. Therefore, REE patterns and Fe isotope compositions of the Fe-rich chemical sedimentary rocks were investigated since geochemical evidence of such an environment being present in the Hokuroku basin is currently lacking. The results of these analyses show that the δ^{56}Fe values of samples occurring directly on and above Kuroko deposits were -1.5 to 0.5 ‰. These values are largely fractionated from the δ^{56}Fe value of the standard (i.e., 0 ‰), which is a similar to that of igneous rocks. The samples that have a large negative value also bears negative Ce anomaly. These signatures indicate that partial oxidation of dissolved ferrous iron occurred by mixing ferrous iron-bearing anoxic water with oxygen-bearing seawater, and therefore that the seafloor of the Hokuroku Basin was anoxic. On the other hand, δ^{56}Fe values of chemical sedimentary rocks formed 2 - 3 Ma after the Kuroko deposits formed ranges from -0.8 to -0.3 ‰. These values are similar to those of dissolved ferrous ion in a modern seafloor hydrothermal fluid. Therefore, the δ^{56}Fe values of the samples indicate near complete oxidation of dissolved ferrous iron in an oxic environment. Therefore, these results suggest that the depositional environment in the Hokuroku basin shifted from anoxic to oxic after the formation of Kuroko deposits.

Keywords: Chemical sedimentary rock, Banded Iron Formation, Barberton Greenstone Belt, Chromium, Volcanogenic Massive Sulfide deposit, Iron isotope

Japan Geoscience Union Meeting 2014
(28 April - 02 May 2014 at Pacifico YOKOHAMA, Kanagawa, Japan)

SRD45-02 Room:415 Time:April 28 14:45-15:00

Os isotope stratigraphy of a ferromanganese crust: Its principles and applications

NOZAKI, Tatsuo[1*] ; GOTO, Kosuke T.[2] ; TOKUMARU, Ayaka[3] ; TAKAYA, Yutaro[4] ; SUZUKI, Katsuhiko[1] ; CHANG, Qing[1] ; KIMURA, Jun-ichi[1] ; KATO, Yasuhiro[4] ; SHIMODA, Gen[2] ; TOYOFUKU, Takashi[5] ; USUI, Akira[6] ; URABE, Tetsuro[3]

[1]JAMSTEC/IFREE, [2]AIST/GSJ, [3]Univ. of Tokyo, [4]Univ. of Tokyo, [5]JAMSTEC/BIOGEOS, [6]Kochi Univ.

Sedimentation age determination by using an Os isotope stratigraphy is one of the effective dating methods for a ferromanganese crust. This dating method is applicable to the almost whole sedimentation age of a ferromanganese crust from the Late Cretaceous to present. So far, we have applied the Os isotope dating method to various ferromanganese crust samples collected from Northwestern Pacific, South Atlantic Oceans and Philippine Sea. In this presentation, we introduce the principles and applications of the Os isotope dating method, and discuss our recent results especially focusing on the growth hiatus of a ferromanganese crust.

Keywords: ferromanganese crust, Os isotope, geochemistry, growth hiatus, paleoceanography

Japan Geoscience Union Meeting 2014
(28 April - 02 May 2014 at Pacifico YOKOHAMA, Kanagawa, Japan)

SRD45-03 Room:415 Time:April 28 15:00-15:15

Occurrence of hydrothermal alteration minerals at the Jade hydrothermal field, in the Izena Hole, mid-Okinawa Trough

MIYOSHI, Youko[1*] ; ISHIBASHI, Jun-ichiro[2] ; YOKOYAMA, Yuka[3] ; TAKAHASHI, Yoshio[3]

[1]National institute of Advanced Industrial Science and Technology (AIST), [2]Department of Earth and Planetary Sciences, Graduate School of Sciences, Kyushu University, [3]Department of Earth and Planetary Systems Science, Graduate School of Science, Hiroshima University

Mineralization at the Jade hydrothermal field, in the Izena Hole, mid-Okinawa Trough, resembles in many aspects the Kuroko type ore mineralization. In the Kuroko type ore deposits, zonal distribution of hydrothermal clay minerals was recognized around the deposit. This study aims to reveal occurrence of hydrothermal clay minerals below the seafloor in the Jade hydrothermal field. We report mineralogy and geochemistry of hydrothermal clay minerals identified in surface sediments in the Jade field and compare with those in the Kuroko type ore deposits.

Surface sediment cores (˜30 cmbsf (centimeters below the seafloor)) were collected by an acrylic push corer (MBARI-type corer) attached to remotely operated vehicle (ROV) Hyper-Dolphin. The core sampling was conducted during the NT10-17 cruise of R/V Natsushima (Japan Agency for Marine-Earth Science and Technology (JAMSTEC)) in September 2010. Minerals in the sediment were identified by X-ray diffraction (XRD), at the Department of Earth and Planetary Sciences, Kyushu University. For some sediment samples, clay fractions ($<2\mu$m) were collected from suspending particles in the distilled water according to the Stokes' law. Clay minerals in the clay fraction samples were identified by the XRD and analyzed chemically using a transmission electron microscope (TEM) equipped with an energy dispersive spectrometer (EDS) in the Research Laboratory for High Voltage Electron Microscopy (HVEM), Kyushu University.

A surface sediment core collected near the sulfide chimney venting high temperature fluid up to 320^{o}C was characterized by occurrence of kaolinite, with sulfide minerals such as sphalerite and galena. The kaolinite would be related to be formed under acidic condition caused by oxidation and dissolution of the sulfide minerals by penetrating seawater. Surface sediment cores collected near clear hydrothermal fluid venting of about 100^{o}C, which is located in 400 m distant from the sulfide chimney, were characterized by assemblage of chlorite and smectite. The chlorite had chemical composition close to Al-rich chlorite (sudoite) which was found around a few Kuroko type ore deposits. In the Kuroko type ore deposits, sudoite was considered to be stable under acidic condition because of the associated clay minerals. This study revealed occurrence of acidic alteration minerals in surface sediment at the Jade hydrothermal field, in the Izena Hole, mid-Okinawa Trough.

Keywords: clay mineral, hydrothermal alteration, Okinawa Trough

Japan Geoscience Union Meeting 2014
(28 April - 02 May 2014 at Pacifico YOKOHAMA, Kanagawa, Japan)

SRD45-04 Room:415 Time:April 28 15:15-15:30

Geochemistry of hydrothermal fluids collected from submarine volcanoes in the Izu-Bonin Arc

ISHIBASHI, Jun-ichiro[1*] ; NAGATOMI, Kentaro[1] ; TAKAHASHI, Minoru[1] ; KODAMATANI, Hitoshi[2] ; TOMIYASU, Takashi[2] ; TAKEUCHI, Akinori[3] ; YAMANAKA, Toshiro[4]

[1]Graduate School of Science, Kyushu University, [2]Graduate School of Science and Engineering, Kagoshima University, [3]National Institute for Environmental Studies, [4]Graduate School of Natural Science and Technology, Okayama University

The Izu-Bonin Arc is an intraoceanic arc related to subduction of the Pacific Plate beneath the Philippine Sea Plate. At some submarine volcanoes on the volcanic front, active hydrothermal fields have been located. Hydrothermal fluids were collected from two active fields, the Suiyo Seamount and Myojin Knoll, and analyzed. Geochemical characteristics of hydrothermal fluids collected from the Izu-Bonin Arc hydrothermal fields will be presented, comparing with those of Okinawa Trough hydrothermal fields.

Hydrothermal fluid samples were collected from the Suiyo Seamount during the NT07-08 cruise in 2007, and from the Myojin Knoll during the NT12-10 cruise in 2012. Fluid samples were collected with ROCS (Rotary Clean Seawater Sampler) installed on ROV Hyper Dolphin (JAMSTEC). Temperature monitored during the fluid sampling showed up to 296 degC at the Suiyo Seamount, and 235 degC at the Myojin Knoll.

Fluid chemistry was characterized as 1) Depletion in Mg and SO_4, 2) Enrichment in K and Ca compared with seawater; especially Ca enrichment is notable, and 3) Low concentration of organic derived species such as NH_4. The fluid chemistry is explained by high-temperature water-rock interactions. Notable enrichment in Ca would be in accordance with low- and Mid-K series chmiecal composition of volcanic rocks. Low NH_4 concentration would be related to depletion in organic-rich terrestrial sediment around the volcanoes.Concentration of minor elements including metal elements will be present, to discuss linkage with mineralogy of hydrothermal deposits in these hydrothermal fields.

Keywords: seafloor massive sulfide deposit, Suiyo Seamount, Myoujin Knoll, fluid-rock interaction

Japan Geoscience Union Meeting 2014
(28 April - 02 May 2014 at Pacifico YOKOHAMA, Kanagawa, Japan)

SRD45-05 Room:415 Time:April 28 15:30-15:45

Relationship between the formation of mercury deposits and the occurrences of organic minerals in subduction zones

ECHIGO, Takuya[1*]

[1]Faculty of Education, Shiga University

Karpatite and idrialite occur in mercury deposits in the West Coast in the USA. In addition, organic matter was also found in mercury deposit in Hokkaido. Both mercury deposits are epithermal type and formed in subducting zone. The relationship between organic minerals and mercury deposits in subducting zone will be discussed.

Keywords: Mercury deposits, Organic minerals, Subducting zone, Polycyclic aromatic hydrocarbons

Japan Geoscience Union Meeting 2014
(28 April - 02 May 2014 at Pacifico YOKOHAMA, Kanagawa, Japan)

SRD45-06 Room:415 Time:April 28 15:45-16:00

A pilot magnetotelluric survey for geothermal exploration in northern Thailand

AMATYAKUL, Puwis[1*] ; RUNG-ARUNWAN, Tawat[1] ; OGAWA, Yasuo[2] ; SIRIPUNVARAPORN, Weerachai[1]

[1]Geophysics Research Group, Department of Physics, Faculty of Science, Mahidol University, [2]Volcanic Fluid Research Center, Tokyo Institute of Technology

One of Thailand's most prominent geothermal field is located in Maechan district, Chiangrai province, along the active Maechan fault which is East-West left-lateral strike-slip fault. Its surface temperature is 99.5 degree Celsius with the flow rate of 3 l/s. Magnetotelluric (MT) survey is proposed to help delineating geothermal fluid and controlling features of the hydrothermal system. In July 2013, 7 magnetotelluric stations were deployed covering the area of Maechan geothermal field. Horizontal magnetic and electric fields (H_x, H_y, E_x and E_y) were collected with the remote reference site located 70 km away in Fang district, Chiangmai province. To obtain 3-D resistivity model, 18 periods of off-diagonal (Z_{xy} and Z_{yx}) elements ranging from 0.003 to 300 second were applied with WSINV3DMT, a 3-D MT inversion widely used among many authors. The obtained resistivity model shows the shallow conductive zones which their locations coincide with the hot springs manifestation. These conductive zone locates from the surface to not more than 500 m and referred as the reservoir of hot geothermal fluid heated by the deeper resistive batholith granite basement. The resistivity contrast in the obtained model up to 2 km northward is corresponding to the lineament of Maechan fault. This also confirms the hypothesis from previous studies that the hot fluid is being stored in fractures of weathered granite which is the damage zone of Maechan fault and reaches the surface where the springs are located through shallow fractures and faults.

Keywords: magnetotellurics, geothermal field, three-dimensional inversion, electrical resistivity, Maechan fault

Japan Geoscience Union Meeting 2014
(28 April - 02 May 2014 at Pacifico YOKOHAMA, Kanagawa, Japan)

SRD45-07 Room:415 Time:April 28 16:15-16:30

Development of in-situ Cu isotope ratio measurement by femtosecond-LA-MC-ICP-MS and its applications to ore minerals

IKEHATA, Kei[1*]

[1]Faculty of Life and Environmental Sciences, University of Tsukuba

A new method for determining copper isotope compositions of copper-rich minerals (native copper, cuprite, chalcocite, chalcopyrite, cubanite and malachite) using a femtosecond LA-MC-ICP-MS has been developed. The standard-sample-standard bracketing technique was applied to correct the instrumental mass fractionation. Matrix effects found in chalcocite, chalcopyrite, cubanite and malachite can be corrected using the matrix-matched calibration standard. The analytical precision ($<$0.14 ‰, 2σ) and accuracy were significantly improved compared with those of previous works using a nanosecond-LA-MC-ICP-MS.

The developed LA-MC-ICP-MS method was applied to the measurements of copper isotope ratios of minute copper ore minerals in igneous rocks (e.g., Horoman peridotite complex) and seafloor hydrothermal deposits (modern: Mariana Trough; ancient: Besshi-type and Kuroko-type volcanogenic massive sulfide deposits) in order to investigate variability of copper isotopic compositions in these samples.

The δ^{65}Cu (where δ^{65}Cu = [(^{65}Cu/^{63}Cu)$_{sample}$/ (^{65}Cu/^{63}Cu)$_{NIST-SRM976}$-1] $\times$ 1000) values of copper-rich sulfide minerals of the active seafloor hydrothermal deposits are significantly large (δ^{65}Cu = -0.7 to 4.0 ‰) compared to those of the ancient submarine hydrothermal deposits (δ^{65}Cu = -0.3 to 0.4 ‰) and the igneous rocks (δ^{65}Cu = -0.3 to 0.3 ‰). These large copper isotope variations in the modern active seafloor hydrothermal deposits are most likely explained in terms of a redox-controlled isotope fractionation during hydrothermal reworking or alteration of precipitated copper-rich minerals. These results also suggest that sub-seafloor and metamorphic recrystallization effects probably have reduced the original range of copper isotopes.

Secondary malachite (δ^{65}Cu = 2.6 to 3.0 ‰) and native copper (δ^{65}Cu = 1.4 to 1.7 ‰) in the Besshi-type deposit have heavier copper isotope values compared to precursor copper-rich minerals. These variations are mainly due to isotope fractionation during redox reactions (weathering) at low temperatures involving the preferential incorporation of heavy copper isotope in secondary Cu(II) solutions. Therefore, copper isotope geochemistry could be a useful tool for understanding geochemical processes of copper transport and deposition in ore-forming systems.

Keywords: copper isotope ratio, femtosecond-LA-MC-ICP-MS, ore minerals

Japan Geoscience Union Meeting 2014
(28 April - 02 May 2014 at Pacifico YOKOHAMA, Kanagawa, Japan)

SRD45-08 Room:415 Time:April 28 16:30-16:45

Origin of Heavy-REE-rich apatite in deep-sea mud from Minami-Torishima area, south-eastern Japan

KON, Yoshiaki[1*] ; SHIN, Ki-cheoul[2] ; HOSHINO, Mihoko[1] ; SANEMATSU, Kenzo[1] ; OKAMOTO, Nobuyuki[3] ; YANO, Nobuhiko[3] ; TANAKA, Mikiya[4] ; TAKAGI, Tetsuichi[1]

[1]Geological Survey of Japan, AIST, [2]Research Institute for Humanity and Nature, [3]JOGMEC, [4]Research Institute for Environmental Management Technology, AIST

We have conducted geochemical and mineralogical investigations of the rare earth and yttrium (REY)-rich mud from Minami-Torishima area in the Pacific in order to clarify the concentration of REY and their host-phase in the mud. X-ray diffraction analysis shows that the mud is mainly composed of phillipsite, fluorapatite, quartz, albite, illite and montmorillonite. Whole-rock CaO, P2O5 and total REY contents of the mud are positively correlated. Relative abundance of apatite is also positively correlated to P2O5 and total REY contents. These correlations suggest that apatite is the main host of the P2O5 and REY in the mud. In order to quantitatively estimate the REY-host phase, we make in-situ compositional analyses of constituent minerals in the REY-mud. The result shows that the apatite is abundant in REY (9300 to 32000 ppm) and characterized by negative Ce-anomaly. In contrast, phillipsite is less abundant in REY (60 to 170 ppm). We conclude that the main REY host phase of the mud is apatite.

Keywords: REE, deep-sea mud, apatite, Minami-Torishima, LA-ICPMS, Nd isotope

Japan Geoscience Union Meeting 2014
(28 April - 02 May 2014 at Pacifico YOKOHAMA, Kanagawa, Japan)

SRD45-P01 Room:Poster Time:April 28 18:15-19:30

Upgradation of silica rich fluvial sands of Bangladesh: Proposals for alternate uses

RAJIB, Mohammad[1*]

[1]Bangladesh Atomic Energy Commission / Graduate Student, Grad. Sch. Sc. Eng., Saitama University

Major rivers of Bangladesh are carrying billions of tons of sediments from the Himalayan mountain range from the north, forming bars almost on every river. These bars inundate in floodwater every year, eroding some sediments as well as depositing more. Thus, almost all the rivers are getting filled with the sediment in course of time. The government of Bangladesh has undertaken a mega plan for Capital Dredging, for raising navigability of the main and important rivers across the country. But there is not enough space to keep those dredged materials. Hence, most of the time, the dredged materials are thrown only in the vicinity of dredging area. In course of very short time, those materials eventually return back to river bed with the precipitation and surface runoff. This makes wastage of time and money.

The river sediments are rich in silicate mineral, mainly quartz and feldspar, along with others, like heavy and micaceous minerals. Quartz (SiO_2) is the raw material for glass production. River sands of Bangladesh also contain some heavy minerals like magnetite, ilmenite, rutile, zircon, garnet, leucoxene, pyroxene etc., and some Mica group minerals like muscovite, biotite, chlorite etc. Industrial use of these minerals are widely accepted. Upgradation of river silica by some physical separation procedures like density, magnetic and electric separators, and chemical composition revealed from X-ray fluorescence analysis shows that 60-70% silica of river sediment can be easily enriched up to 94%. Very low amount of Fe, Al, Ca, Mg and absence of Cr and Ti indicates the probable use of this upgraded silica as glass producing sand.

For industrial use, advance research is necessary for potential use of such silica for silicon extraction or other silicon products e.g. silicon chip, if the upgradation can be reached more than 99%. The heavy and magnetic minerals associated with silica also can be used economically as by-products of the process. Mining of this sediment from the rivers will increase the navigability of the rivers. As dredging is a must in almost every river of Bangladesh, the mining will work as alternative work of dredging, saving huge amount of money to be spent for dredging. This will also lessen the risk of dangerous flood problem of the country.

Moreover, since fluvial sands has been used as earth filling materials for long time and is suitable in many technical aspects, potentiality of using such sediments for artificial islands can be thought. Japan has been implementing several artificial islands where materials like solid waste, soil from mountains are mostly used as filling materials which are not always environment friendly. Feasibility study for using bulk fluvial sand from Bangladesh as earth filling materials for future artificial islands of Japan can a better alternative. This will decrease the risk of potential environmental hazards that can be created from solid waste or hill-cutting. Use of dredged materials from Bangladesh will help decreasing environmental hazards like floods too. Economical sustainability can be achieved through such reduction of hazard risk.

Keywords: Fluvial Sand, Bangladesh, Silica, Heavy Minerals, Capital Dredging, Artificial Islands

Japan Geoscience Union Meeting 2014
(28 April - 02 May 2014 at Pacifico YOKOHAMA, Kanagawa, Japan)

SRD45-P02 Room:Poster Time:April 28 18:15-19:30

Iron isotopic composition of the Palaeoproterozoic Hotazel Formation in the Kalahari Manganese Field, South Africa

ASAKURA, Jun[1*] ; YAMAOKA, Kyoko[2] ; BORROK, David[3] ; WATANABE, Yasushi[2] ; KAWAHATA, Hodaka[1]

[1]Atmosphere and Ocean Research Institute, The University of Tokyo, [2]National Institute of Advanced Industrial Science and Technology, [3]University of Louisiana

Kalahari manganese deposit in the Palaeoproterozoic Hotazel Formation of Transvaal Supergroup of South Africa is the world's largest layered manganese deposit. It has alternating layers structure of three manganese rich layers and banded iron formation. This banded iron formation and manganese deposits of Hotazel Formation were formed at approximately the same time as Global Oxidation Event, which was the period of explosive growth of oxygen in Earth ' s atmosphere. In addition, the relevance of the snowball Earth event of Huronian glaciation has also been suggested from its formation age. Iron isotopes are sensitive indicators of the redox state, and it is suitable for estimating the marine environment when the banded iron formation was formed. Although a prior study on the iron isotope analysis of manganese deposits and banded iron formation of Hotazel Formation has been reported by Tsikos et al. in 2010, it is hard to say enough data is gathered.

In this study, drill core that was collected from the Kalahari manganese deposit in South Africa was subjected to iron isotope analysis with MC-ICP-MS and XRD analysis, and the results were compared with those of Tsikos et al.(2010). In isotopic analysis, δ56Fe values of drill core samples for the standard sample IRMM-14 were measured.

From the results, low δ56Fe values (not higher than -0.70 ‰) throughout the all samples were measured. When limited to manganese-rich layers, δ56Fe values are between -1.66 and -2.86 ‰. Relationship between Fe-Mn ratio and δ56Fe value showed that δ56Fe value have a tendency to drop to a lower value with the increasing abundance ratio of manganese to iron in a formation. This results are consistent with those of Tsikos et al.(2010). In other words, this results support their theory that banded iron formation has a role as a sink of heavy iron isotopes, and manganese are deposited in an environment that was rich in light iron isotopes.

Reference

Harilaos Tsikos, Alan Matthews, Yigal Erel, John M. Moore, 2010. Iron isotopes constrain biogeochemical redox cycling of iron and manganese in a Palaeoproterozoic stratified basin. Earth and Planetary Science Letters 298, 125-134. doi: 10.1016/j.epsl.2010.07.032

Keywords: iron isotope, banded iron formation, Kalahari manganese deposit

Japan Geoscience Union Meeting 2014
(28 April - 02 May 2014 at Pacifico YOKOHAMA, Kanagawa, Japan)

SMP06-01 Room:411 Time:April 28 14:15-14:30

Hydrogen transport into the bottom of the lower mantle by phase H- phase delta solid solution MgSiO2(OH)2-AlOOH

OHTANI, Eiji[1*] ; AMAIKE, Yohei[1] ; OHIRA, Itaru[1] ; KAMADA, Seiji[1] ; SAKAMAKI, Tatsuya[1] ; HIRAO, Naohisa[2]

[1]Tohoku University, [2]SPring-8

Water circulation in a global scale is a key for understanding dynamics and evolution of the Earth. Subducting slabs transport water into the Earth's deep interior. There are many studies on the stability of hydrous phases under the deep mantle conditions, and several hydrous minerals such as phase D and superhydrous phase B have been reported to be stable to the top of the lower mantle. It has been reported that hydrous phase δ-AlOOH is stable up to the bottom of the lower mantle (Ohtani et al., 2005; Sano et al., 2008). Tsuchiya (2013) theoretically predicted that Phase H, $MgSiO_2(OH)_2$, which is the iso-structure with δ-AlOOH, is stable from 45 GPa to 55 GPa. This phase was experimentally confirmed at around 50 GPa (Nishi et al., 2014). Here, we present our recent results on synthesis experiments of hydrous phase H and a solid solution of phase H and phase δ up to the base of the lower mantle along the normal mantle geotherm. The high pressure and high temperature in situ X-ray diffraction experiments were performed by using a double-sided laser heated diamond anvil cell at BL10XU, SPring-8. We observed that the stability field of this new candidate of water reservoir, hydrous phase H, under the lower mantle conditions up to 75 GPa and 2000 K in the MgO-SiO_2-H_2O system, although the previous studies claimed that phase H is broken down at pressures above 55 GPa. Thus, hydrous phase H is a host phase of water in the lower mantle at least up to the depth of 2000 km along both slab and normal mantle geotherms. Our experiments also revealed that the solid solution of phase H and phase δ, AlOOH-$MgSiO_2(OH)_2$, containing 15 mol % of $MgSiO_2(OH)_2$ can coexist with Mg-perovskite and/or Mg-post perovskite up to 135 GPa and 2000 K. If this hydrous phase contacts with the metallic outer core, hydrogen could be dissolved into the core by forming iron hydride, FeH (Terasaki et al., 2012).

Keywords: hydrogen, hydrous phase H, hydrous phase delta, MgSiO2(OH)2, AlOOH, lower mantle

Japan Geoscience Union Meeting 2014
(28 April - 02 May 2014 at Pacifico YOKOHAMA, Kanagawa, Japan)

SMP06-02 Room:411 Time:April 28 14:30-14:45

Influence of H2 fluid on the stability of MgSiO3 enstatite in the upper mantle condition

SHINOZAKI, Ayako[1*] ; KAGI, Hiroyuki[1] ; HIRAI, Hisako[2] ; OHFUJI, Hiroaki[2] ; OKADA, Taku[3] ; NAKANO, Satoshi[4] ; YAGI, Takehiko[2]

[1]GCRC, The university of Tokyo, [2]GRC, Ehime university, [3]ISSP, The university of Tokyo, [4]NIMS

C-O-H fluids affect the phase relation and melting of silicate minerals in the mantle of the Earth. The mantle is expected to become progressively reduced with increasing depth, so that H_2 fluid is considered to exist in the deep mantle with H_2O fluids. In this study, influence of H_2 fluid on stability and phase relation of enstatite, which was the secondary most abundant mineral in the upper mantle, was examined using a laser heated diamond anvil cell.

In this presentation, we will report the results of $MgSiO_3$-H_2 system, which is non-iron-bearing system. After heating at 3.1-13.8 GPa and about 1500-2000 K, decomposition of enstatite and formation of forsterite (Mg_2SiO_4), periclase (MgO) and coesite/stishovite (SiO_2) were observed from XRD measurements. The presence of H_2 fluid were observed from Raman spectra even after the heating. Since the studied P-T range is in the stability field of orthoenstatite and high pressure clinoenstatite under dry condition, the decomposition reaction observed in the present study was presumably induced by H_2 fluid. Formation process of these silicate phases were evaluated by observation of quench texture of the recovered samples using SEM and TEM.

Keywords: enstatite, H2 fluid, upper mantle, laser heated diamond anvil cell

Japan Geoscience Union Meeting 2014
(28 April - 02 May 2014 at Pacifico YOKOHAMA, Kanagawa, Japan)

SMP06-03 Room:411 Time:April 28 14:45-15:00

Dehydration boundary and the EoS of chlorite under high pressure and temperature

SUENAMI, Hideki[1] ; INOUE, Toru[1*] ; KAKIZAWA, Sho[1] ; KIKEGAWA, Takumi[2]

[1]Geodynamics Research Center, Ehime University, [2]High Energy Accelerator Research Organization

Water in hydrous minerals has been transported to deep Earth's interior by subducting slab, which dehydrate at certain pressure and temperature. The existence of deep Earth's water affects the physical properties of Earth's mantle minerals, such as melting point, viscosity, elastic velocity, and so on. Therefore it is important to study the effect of water for the subducting slab materials. Serpentine ($(Mg,Fe)_6Si_4O_{10}(OH)_8$) is major hydrous mineral in subducting slab, and chlorite ($(Mg,Fe,Al)_6(Si,Al)_4O_{10}(OH)_8$) should be also important hydrous mineral in the subducting slab because Al is included in slab materials. In this study, the dehydration reactions of chlorite were determined by time-resolved X-ray diffraction analysis under high pressure and temperature using MAX80, PF-AR, KEK. In addition, P-V-T experiments of chlorite have also been conducted under HPHT. We found that chlorite was quickly dehydrated to forsterite + pyrope + fluid within 1 hour at 3 - 7 GPa when across the phase equilibrium boundary. On the other hand, the kinetic boundary was observed above 7 GPa because of low temperature phase equilibrium boundary, and the dehydration product was Mg-sursassite + unknown + fluid, The result of P-V-T experiments will be also reported.

Keywords: chlorite, hydrous phase, subducting slab, dehydration, equation of state, synchrotron X-ray in-situ experiment

Japan Geoscience Union Meeting 2014
(28 April - 02 May 2014 at Pacifico YOKOHAMA, Kanagawa, Japan)

SMP06-04 Room:411 Time:April 28 15:00-15:15

Composition and nature of melts, supercritical fluids and liquids formed by dehydration of subducted oceanic lithosphere

ULMER, Peter[1*] ; SCHMIDT, Max W.[1] ; PETTKE, Thomas[2] ; LUGINBUEHL, Stefanie[1]

[1]Department of Earth Sciences, ETH Zurich, [2]Inst. Geol. Sciences, University of Bern

At crustal pressures, phase relations in natural rock-H_2O systems involve low density aqueous fluids and/or high density hydrous melts. The wide miscibility gap between these two liquid phases leads to a dichotomy of mobile phases with quite distinct major element solubilities and trace element geochemical signatures. With increasing pressure, the fluid-melt miscibility gap closes until the crest of the miscibility gap intersects the fluid-saturated solidus, leaving a single supercritical liquid that has chemical and physical properties continuously evolving with temperature. The question is if the endpoint of the solidus is relevant for natural rock compositions. We have experimentally determined these endpoints in a variety of systems ranging from MOR basalt, to pelitic systems and to the simplified mantle systems MgO-SiO_2-H_2O (MSH) using different experimental techniques in the P-T range from 2.0 GPa/700 ℃ to 13.5 GPa/1300 ℃. Supercriticality occurs over a wide range of P-T conditions ranging from 1 GPa/1100 ℃ for the SiO_2-H_2O system to 12-13 GPa in the SiO_2-poor part of the MSH system.

In the MORB system, major element compositions of the fluid/melt phase evolve from peralkaline, H_2O-rich, granite-like compositions to metaluminous, andesitic to basaltic compositions with increasing temperature. The endpoint of the fluid-saturated solidus occurs around 5 GPa and 1000 ℃; thus, the dichotomy of fluid versus melt ceases to exist in the oceanic crust. Similar conditions were determined for pelitic to greywacke systems representing deep-sea sediments. In the mantle-like system MSH critical endpoints for fluid/melt solvi along the solidus are located between 12 and 13.5 GPa at 1100 ℃. Melt compositions buffered by olivine and opx remain enstatite - olivine normative below the critical endpoint; in contrast, fluids below the endpoint become progressively enriched in MgO and are silica undersaturated (Mg/Si ratios $>$2) at pressures exceeding 6 GPa. Supercritical liquids coexisting with forsterite and enstatite or dense hydrous silicates are strongly silica undersaturated. The P-T evolution of fluids and liquids in the MSH system allows drawing conclusions regarding the effects of Mg-Si metasomatism in the overlying mantle wedge of a subduction system.

The consequences of the various nature of hydrous mobile phases emanating from hydrated subducted oceanic lithosphere were investigated in the MORB system by determining trace element partitioning between cpx, gar, amphibole, epidote, rutile, titanite, staurolite and phengite and liquid, the latter either being an aqueous fluid, a hydrous melt, or a supercritical liquid. Hydrous melts and supercritical liquids have almost identical trace element pattern. Thus, recycling rates of these elements are not indicative of melting, and in the fast and steep circum-pacific subduction zones, they most likely testify for production of a mobile phase from the subducting crust in the supercritical liquid regime (i.e. at pressure in excess of 4-5 GPa).

Modeling of trace element signatures of fluids, melts and supercritical liquids generated in or passing through eclogitic crustal lithologies during their ascent into the overlying mantle wedge indicate that (1) the mode of fluid advection - porous flow or - focused fluid flow - produces rather contrasting trace element signatures and (2) the presence or absence of accessory phases such as epidote, staurolite, rutile/titanite controls to a large extent the concentrations of high field strength, light REE elements and Th, U. Thus, inversion of geochemical compositions of igneous products in arc settings used to constrain the nature and composition of metasomatizing agents released from the subducted oceanic lithosphere is not straightforward and it is unlikely that an unequivocal solution is obtained.

Keywords: hydrous fluid, supercritical liquid, trace element partitioning, fluid metasomatism, high presssure experiments, subducted oceanic lithosphere

Japan Geoscience Union Meeting 2014
(28 April - 02 May 2014 at Pacifico YOKOHAMA, Kanagawa, Japan)

SMP06-05 Room:411 Time:April 28 15:15-15:30

Trace element mass balance in hydrous adiabatic mantle melting: The HAMMS1 model

KIMURA, Jun-ichi[1*] ; KAWABATA, Hiroshi[2]

[1]JAMSTEC, [2]Kochi University

A numerical mass balance calculation model for the adiabatic melting of a hydrous metasomatized peridotite source was programmed in order to simulate trace element compositions of mid ocean ridge basalt, back arc basin basalt, ocean island basalt, and large igneous province basalt. The Excel spreadsheet-based calculator, Hydrous Adiabatic Mantle Melting Simulator ver.1 (HAMMS1) uses: (1) a thermodynamic adiabatic melting model of mantle peridotite; with (2) experimentally parameterized melting relationships in terms of pressure, temperature, water content, and degree of partial melting. The trace element composition of the model basalt is calculated from the accumulated incremental melts within adiabatic melting, with consideration of source mantle depletion. The mineralogic mode in the mantle in adiabat is calculated using experimental parameterization, and is incorporated into the program. Partition coefficients of the residual mantle minerals are from lattice strain model based parameterization tested by the latest compilations of experimental results. The parameters that control the trace element composition in the model are: (1) mantle potential temperature, (2) water content in the source mantle, (3) depth of termination of adiabatic melting, and (4) source mantle depletion. It is possible to obtain the above controlling parameters by using Monte Carlo fitting calculations and comparing the calculated basalt compositions with primary basalt compositions. Additionally, HAMMS1 compares those melting parameters with its major element model. HAMMS1 provides a unique estimate of the source conditions of basalt genesis using an incompatible trace element mass balance.

Keywords: peridotite, water, adiabatic melting, trace element, forward model

Japan Geoscience Union Meeting 2014
(28 April - 02 May 2014 at Pacifico YOKOHAMA, Kanagawa, Japan)

SMP06-06 Room:411 Time:April 28 15:30-16:00

Very Large Intramolecular D-H Partitioning in Hydrated Silicate Melts Synthesized at Upper Mantle P and T

CODY, George[1*] ; WANG, Ying[1] ; CODY, Samantha[1] ; FOUSTOUKOS, Dionysis[1] ; MYSEN, Bjorn[1] ; LE LOSQ, Charles[1]

[1]Geophysical Laboratory, Carnegie Institution of Washington

Hydrogen isotope fractionation during magnetic processes is key to understanding the deep Earth hydrological cycle and may place constraints on the origin of Earth ' s oceans. It is well established that the D/H content of water in hydrated nominally anhydrous mantle minerals is systematically lower (<-100 ‰) than the standard mean ocean water (SMOW, D/H = 1.5576 x 10^{-4}, defined as 0 ‰). Experiments have revealed significant hydrogen isotope partitioning between melts and fluids or vapors at magmatic temperatures. The origin of such fractionation, given the high temperatures of magmatic processes, is not likely due to classical isotope effects as described by bond energies via statistical mechanics.

It is well known that water has a very high affinity for silicate melts, it both dissolves in the melt as molecular water and hydrolyzes Si-O-Si linkages forming Si-OH. Whereas the molecular forms of water in melts are limited to H_2O and OH, the variety of environments available for water to reside in the melt structure is surprizing large. In order to study water in silicate melts one is restricted to molecular spectroscopy, e.g. Raman spectroscopy in the mid infrared regime, in windowed high pressure devices, e.g. the hydrothermal diamond anvil cell. Alternatively, one can study melts quenched to glass, where the structure of the glass corresponds to the structure of the melt at the glass transition temperature. The advantage of glasses is that one can use Solid State Nuclear Magnetic Resonance (NMR) Spectroscopy. The hydrogen isotopes conveniently provide two stable nuclei with spin, ^{1}H (H) and ^{2}H (D), thus we can use D and H solid state NMR to analyze the nature of water in silicate melts quenched to glass. Given that glass transition temperatures for silicate melts are high (500-600 ∘C), one does not expect H and D to behave differently. D-NMR can, however, be useful in characterizing the molecular dynamics of water in various sites in the glass.

We studied hydrated (with D_2O and H_2O) sodium tetrasilicate glasses, quenched from melts at 1400∘C and 1.5 GPa, using ^{1}H, ^{2}H and ^{29}Si solid state NMR. Whereas D_2O and H_2O depolymerize the silicate melt to similar degrees, as would be expected, we surprisingly find that protium (H) and deuterium (D) intramolecular partitioning between different molecular sites within the glasses is very large and controlled by a strong preferential association of deuterons to sites with short O D O distances. This preference is independent of total water content and D/H ratio. Substantial intramolecular D-H partitioning is also observed in a glass with a model hydrous basalt composition. Such large isotope partitioning cannot result from classic fractionation effects because of the high synthesis temperatures. Potential kinetic isotope effects are excluded via a slow quench experiment. The partitioning is likely governed by density/molar volume isotope effects, where deuterium prefers sites with smaller molar volume. Large intramolecular site partitioning in melts could lead to significant D-H partitioning between water saturated melt and exsolved aqueous fluid (where $D/H_{W,Melt} \neq D/H_{W,Fluid}$) during crystallization of Earth ' s magma ocean, potentially controlling the D/H content of the Earth ' s oceans.

Keywords: Silicate Melt, D-H fractionation, NMR, Magma Ocean

Japan Geoscience Union Meeting 2014
(28 April - 02 May 2014 at Pacifico YOKOHAMA, Kanagawa, Japan)

SMP06-07 Room:411 Time:April 28 16:15-16:30

Chemical dependence of the speciation and structural position of water in silicate melts

LE LOSQ, Charles[1*] ; CODY, George[1] ; MYSEN, Bjorn[1]

[1]Geophysical Laboratory, Carnegie Institution of Washington

Water is the main volatile component affecting the thermodynamic, structural and rheological properties of magmatic liquids in the Earth's interior resulting in major influence on past history and present magmatic activity of the Earth. Previous experiments and modelling have shown that water can be dissolved as H_2O molecules (H_2O_{mol}) and OH^- groups, with the OH^- groups bonded to the silicate network to form Si-OH or Al-OH bonds and perhaps alkali-OH and alkaline earth-OH complexes. However, important questions remain as to how bulk chemistry governs the link between the different OH groups and the silicate network, and the global H_2O_{mol}/OH ratio.

It is now widely accepted that dissolved water reacts with the O^{2-} oxygen composing the silicate network following:

$H_2O_{mol} + O^{2-} \Leftrightarrow 2OH^-$. (1)

As O^{2-} from the silicate network is involved in this reaction, its equilibrium constant must depend on the activities of bridging (BO), non-bridging (NBO), and free oxygen species potentially present in silicate melts, and hence on their global chemistry. Even if Al-OH and Si-OH bonding were the only variables (and, therefore, the Al/Si ratio of a melt), reaction (1) implies that the H_2O_{mol}/OH should depend on silicate melt composition. However, as the activity of NBO species is also affected by the ionic field strength of alkali and alkaline earth cations, we expect the equilibrium of reaction (1) to be affected by those cations.

To test and to quantify the occurrence and the impact of chemical effects on the speciation of water in quenched, hydrous silicate melt (glass), we analysed $M_2Si_4O_9$ glasses (M = Li, Na or K) containing different amounts of water (from 3.3 up to 17.6 mol%) with the help of ^1H and ^{29}Si MAS NRM, Raman and Infrared spectroscopy. Glasses were formed by temperature quenching (∼100 ℃/s) at 1.5 GPa. Raman and infrared spectroscopy show three different bands close to 2300, 2800 and 3600 cm^{-1}. These are assigned to O-H stretching from OH groups bonded to silicate components and from H_2O molecules. Correlation of those frequencies with the O ⋯ O distances in minerals suggest that those three bands arise from OH stretching in two main different environments: one with a mean O ⋯ O distance close to ∼0.26 nm and another one with a ∼0.29 nm O ⋯ O distance. In the ^1H MAS NMR spectra, we retrieved signals near 15 and 5 ppm arising from the ∼0.26 and ∼0.29 nm environments respectively. Increasing the alkali radius tends to increase the intensities of the 15 ppm ^1H MAS NMR peak and of the 2000-2900 cm^{-1} Raman region, indicating an increase of the population of OH groups in the ∼0.26 nm environment. In addition, the higher the alkali radius the higher the effect of water on the polymerization degree is, as testified by changes of the ^{29}Si NMR and Raman signals.

Those NMR and Raman observations suggest that the H_2O_{mol}/OH ratio in quenched hydrous silicate melts decreases in the order Li, Na, K. The greater the radius of alkali, the higher the proportion of OH^- the smaller the mean O ⋯ O distance in their environment, and hence the more extensive hydrogen bonding. We propose that this structural evolution arises from a combination of steric hindrance and electron distribution around alkali elements that affects both equilibrium reaction (1), which will decrease in the order K >Na >Li, and the local environment of the formed OH^- groups. This interplay between the nature of the alkali modifier, the speciation of water and the polymerization of the silicate network must result in non-negligible differences in viscosity of Li, Na and K silicate melts. Therefore, following this study, variation of the concentration of alkali and alkaline-earth elements in natural hydrous magmas, following their origin, will result in changes of their rheological properties, not only because of the different effects of alkali/alkaline earth elements on Si-O bonds, but also because of differences in the water speciation and OH^- environments.

Keywords: water, silicate glass, Raman spectroscopy, NMR spectroscopy

Japan Geoscience Union Meeting 2014
(28 April - 02 May 2014 at Pacifico YOKOHAMA, Kanagawa, Japan)

SMP06-08 Room:411 Time:April 28 16:30-16:45

Large ion lithophile elements delivered by saline fluids to sub-arc mantle

KAWAMOTO, Tatsuhiko[1*] ; MIBE, Kenji[2]

[1]Inst Geotherm Sci, Grad School Sci, Kyoto Univ, [2]Earth Research Institute, Univ of Tokyo

Geochemical signatures of arc basalts are explained by addition of aqueous fluids, melts, and/or supercritical fluids from subducting slab to sub-arc mantle. Partitioning of large ion lithophile elements between aqueous fluids and melts is crucial as these two liquid phases are present in the sub-arc pressure-temperature conditions. Using synchrotron x-ray beams, in-situ x-ray fluorescence (XRF) spectra are obtained from aqueous fluids and silicate melts at high-temperature and high-pressure conditions under varied concentrations of (Na, K)Cl (0-25 wt.%). There is a positive correlation between partition coefficients and pressure, as well as partition coefficients and salinity. In the systems with 13-25 wt.% (Na, K)Cl, partition coefficients of Rb, Cs, and Pb are greater than unity, indicating the capacity of such highly saline fluids to effectively transfer those elements. Enrichment of large ion lithophile elements in arc basalts relative to mid oceanic ridge basalts has been attributed to the mantle source fertilization by aqueous fluids from dehydrating oceanic plate. Such aqueous fluids are likely to contain Cl, although their amount remains to be quantified.

Keywords: subduction zone, magma, high temperature and high pressure, mantle wedge, synchrotron X-ray, chlorine

Japan Geoscience Union Meeting 2014
(28 April - 02 May 2014 at Pacifico YOKOHAMA, Kanagawa, Japan)

SMP06-09 Room:411 Time:April 28 16:45-17:00

In-situ characterization of carbon-speciation in silicate-C-O-H fluid and melt with temperature, pressure, and redox con

MYSEN, Bjorn[1*]

[1]Geophysical Laboratory, CIW, USA

Speciation and partitioning of C-bearing volatiles species in and between silicate-saturated C-O-H fluids and (C-O-H)-saturated melts have been determined in-situ with the samples to pressures and temperatures of ~2GPa and 900^{o}C, respectively. Structural characterization was conducted with vibrational spectroscopy of samples contained in externally-heated, hydrothermal diamond anvil cells. The redox conditions were controlled near that of the Fe+H_2O=FeO+H_2 (reducing, RED) and Ni+H_2O=NiO+H_2 (oxidizing, OX) equilibria, respectively. Melts are, therefore saturated in H_2O, H_2, and C-bearing species (redox dependent) and coexisting fluids saturated in silicate components. Solubility of volatile and silicate components depend on both temperature and pressure.

The melt/fluid partition coefficients of the C-bearing species vary with redox conditions and temperature with the $\triangle H_{RED}{}^{melt/fluid}$ = 44(7) kJ/mol and $\triangle H_{OX}{}^{melt/fluid}$ = -70(32) kJ/mol. Pressure is a dependent variable and increases with increasing temperature. It is assumed no pressure effect of the partition coefficients.

The solution equilibria under reducing and oxidizing conditions, respectively, were; (1) $2CH_3{}^- + H_2O + Q^{n+1} = 2CH_4 + Q^n$ and (2) $2CO_3{}^{2-} + H_2O + 2Q^{n+1} = HCO_3{}^- + 2Q^n$, where the superscript, n, in the Q-species denotes number of bridging oxygen in the silicate species (Q-species). In the absence of H_2O equilibrium (1) changes to $CH_3{}^- + Q^n = CH_4 + Q^{n+1}$. For oxidized carbon, there is an analogous expression expressing equilibrium between molecular CO_2 and structurally bound $CO_3{}^{2-}$-groups. Under both oxidizing and reducing conditions, the abundance ratios, $CH_4/CH_3{}^-$ and $HCO_3{}^-/CO_3{}^{2-}$ increase with temperature. The enthalpy change associated with the species transformation does, however, differ for fluids and melts and also for oxidized and reduced carbon ($\triangle H_{(1)}{}^{fluid}$ = -16(5) kJ/mol, $\triangle H_{(1)}{}^{melt}$ = -49(5) kJ/mol, $\triangle H_{(2)}{}^{fluid}$=81(14) kJ/mol). For the exchange equilibrium of CH_4 and CH_3 species, the temperature-dependent equilibrium constant yields $\triangle$H=34(3) kJ/mol.

Reactions (1) and (2) involve changes in silicate polymerization where increasing abundance ratios, $CH_4/CH_3{}^-$ and $CO_3{}^{2-}/HCO_3{}^-$lead to increased silicate melt polymerization. As a result of the relations between speciation of C-bearing species and melt and fluid structure, stable isotope (C and H) and element partition coefficients between melts and fluids, which depend on and silicate polymerization and silicate speciation, also vary with speciation of C-bearing species in silicate-C-O-H systems. Pressure, temperature, and redox control on the C-speciation also govern those (and other) properties.

Keywords: COH volatiles, fluid structure, melt structure, high pressure, high temperature, redox conditions

Japan Geoscience Union Meeting 2014
(28 April - 02 May 2014 at Pacifico YOKOHAMA, Kanagawa, Japan)

SMP06-10 Room:411 Time:April 28 17:00-17:15

Effect of CO2 content on melting phase relations in kimberlite group I at 6.5 GPa and 1200-1600oC

SHATSKIY, Anton[1] ; LITASOV, Konstantin[1*] ; SHARYGIN, Igor[1] ; OHTANI, Eiji[2]

[1]V.S. Sobolev Institute of Geology and Mineralogy SB RAS, Novosibirsk 630090, Russia, [2]Department of Earth and Planetary Material Science, Graduate School of Science, Tohoku University

Our understanding of kimberlite petrogenesis is significantly hampered by uncertainty about the compositions of kimberlite magma. It is generally accepted that the last equilibration of kimberlite magma with surrounding mantle (garnet lherzolite) occurred beneath cratons at 6-7 GPa prior its rapid ascent (about 70 km/h) to the surface. This conclusion is based on the following facts. The deepest (170-220 km depths) and hottest (1200-1500^{o}C) xenoliths entrapped by kimberlites are sheared garnet lherzolites originating from the lower part of lithospheric mantle. The preservation of deformation features in sheared lherzolites indicates that the rock was undergoing dynamic recrystallization just before it was picked up by the magma and that it reached the surface after less than a few days or even hours in magma rising by crack propagation (Green and Gueguen, 1983; Meyer, 1985; Sparks et al., 2006). Based on our resent study (Sharygin et al., 2013) of melting phase relations in an exceptionally fresh kimberlite group I from Udachnaya-East kimberlite (UEK) pipe at 3.0-6.5 GPa and 900-1500^{o}C, the kimberlite melt had essentially Na-K-Ca carbonatite composition <15 wt.% SiO_2, Na_2O + K_2O = 5-18 wt%, Na/K = 2, Cl >1.5 wt%, and Ca/(Ca+Mg) >0.5. However, the mineral assemblages obtained in these experiments differ from known mantle parageneses. This may be due to unaccounted CO_2 budget missed at shallow depth as a result of decarbonation reactions at 1.5-2.5 GPa. Therefore, in present study we examined the effect of additional CO_2 on melting phase relations in synthetic UEK kimberlite system at 6.5 GPa and 1200-1600^{o}C.

Based on obtained results mineral assemblage equilibrated with kimberlite partial melt gradually changes from peridotite to eclogite paragenesis with increasing its CO_2 content from 13 to 35 mol %. As can be seen at 6.5 GPa kimberlite partial melt (i.e. Na-K-Ca carbonatite melt) becomes equilibrium with garnet lherzolite (i.e. olivine + enstatite + diopside + garnet + FeS + ilmenite assembly) at 1500^{o}C and 23 mol % (20 wt%) CO_2. This value is 10 mol% more than natural abundance of CO_2 in the Udachnaya-East kimberlite rock (group I kimberlite). In other words, the kimberlite magma lost almost half of the CO_2 budget during the eruption.

We greatly thank the Global Center-of-Excellence program at Tohoku University (Sendai, Japan) for the technical and financial support of this study.

Figure. Melting phase relations in Udachnaya-East kimberlite (kimberlite group I) versus temperature and CO_2 content at 6.5 GPa. 13 mol % CO_2 corresponds to the natural abundance of CO_2 in UEK rock.

Keywords: kimberlite, carbonatite, carbon dioxide, high-pressure experiment, Earth's mantle, melting

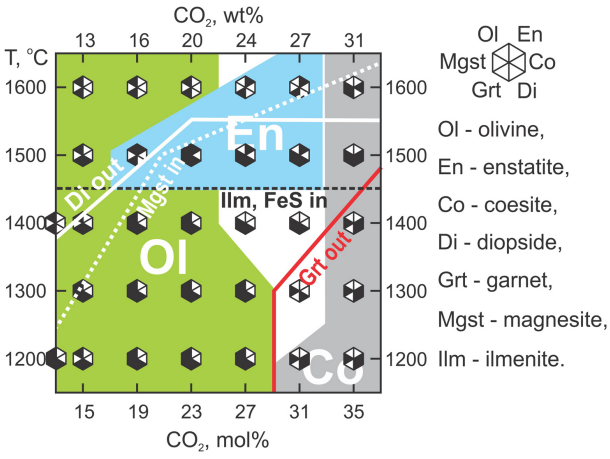

Japan Geoscience Union Meeting 2014
(28 April - 02 May 2014 at Pacifico YOKOHAMA, Kanagawa, Japan)

SMP06-11 Room:411 Time:April 28 17:15-17:30

Carbon dioxide in granitic magma under lower crustal conditions

YOSHIMURA, Shumpei[1*] ; NAKAMURA, Michihiko[2] ; YURIMOTO, Hisayoshi[3]

[1]Department of Earth and Environmental Sciences, Yamagata University, [2]Department of Earth Science, Tohoku University, [3]Department of Natural History Sciences, Hokkaido University

<Introduction>

Carbon dioxide is a major volatile component in the crust and mantle. Its solubility and speciation in silicate melts are important in understanding of mechanisms of magmatism and volcanism. However, they are not well constrained under lower-crustal conditions, especially in granitic magma, which is common in the crustal magmatism. In this study, we carried out equilibrium experiments in the CO_2-H_2O-granitic melt system to investigate the solubility and speciation of CO_2.

<Experimental procedure>

High-PT experiments were performed using a piston cylinder apparatus and a cold-seal pressure vessel. Obsidian flakes of a granitic composition and oxalic acid dehydrate (fluid source) were put in a gold or platinum capsule and run at 1123 and 1473 K and 0.1-1.5 GPa. Oxygen fugacity was estimated to be close to NNO. After quench, volatiles dissolved in the glass were analysed with FTIR spectroscopy. The composition of the coexisting fluid was quantified either by manometric analysis or based on the low-pressure solubility law and volatile contents of the glass.

<Results>

FTIR spectra showed that both CO_2 molecules (CO_{2mol}) and carbonate anions (CO_3^{2-}) were present in all of the glass samples. The concentrations of CO_{2mol}, CO_3^{2-} and total H_2O increased generally with increasing pressure; they were 9200 ppm, 2100 ppm and 6.1 wt%, respectively, at 1.5 GPa and 1473 K. Here, we used new molar absorption coefficients of 2350 cm^{-1} (1192 $\pm$ 130 L cm^{-1} mol^{-1}; CO_{2mol}) and 1410 cm^{-1} (91 $\pm$ 28 L cm^{-1} mol^{-1}; CO_3^{2-}) determined in this study. The fraction of CO_3^2 to total CO2 in the granitic melt increased with increasing total CO2 content, from 0.09 (total CO_2 = 260 ppm) to 0.19 (11300 ppm). The molar fractions of CO_2 in the fluids (X_{CO2}^{fluid}) were 0.25-0.48 for the cold-seal experiments and 0.73-0.79 for the piston cylinder experiments.

<Discussion>

We formulated the solubility law of CO_{2mol} based on a vapour-liquid equilibrium equation. On the basis of the reaction CO_2 (vapour) $\rightleftharpoons$ CO_{2mol} (melt), we calculated the partial molar volume of CO_{2mol} in the granitic melt and the reaction enthalpy to be 24.9 $\pm$ 2.0 cm^3/mol and -22.2 $\pm$ 6.3 kJ/mol, respectively. These values are similar to those in previous experiments carried out at <6.6 kbar (Fogel and Rutherford, 1989; Behrens et al., 2004), indicating that the low-pressure solubility law can be extrapolated to 1.5 GPa. As for the formation of CO_3^{2-}, we assumed a reaction CO_{2mol} + O^{2-} (non-bridging oxygen) $\rightleftharpoons$ CO_3^{2-}. Possible factors shifting the equilibrium to the right-hand side include the total pressure (e.g., Fine and Stolper, 1985; Guillot and Sator, 2011) and water content (King and Holloway, 1992; Behrens et al., 2004). In this study, it was difficult to evaluate these parameters separately, since the water content increased simultaneously with total pressure. If we assume that the effect of water is small enough to be neglected, the change of the partial molar volume of CO_2 in the melt and the reaction enthalpy can be calculated to be -8.6 $\pm$ 6.0 cm^3/mol and -0.4 $\pm$ 3.1 kJ/mol, respectively.

<Application>

Recently, unusually CO_2-rich rhyolitic melt inclusions (up to 1.7 wt% total CO_2) were reported by Blundy et al. (2010). The saturation pressure of this CO_2 content is estimated to be 1.4 GPa when CO_2 dissolved only as CO_{2mol} (X_{CO2}^{fluid} = 1; T=1173 K). If we consider the formation of CO_3^{2-}, the saturation pressure is estimated to 1.2 GPa.

Keywords: CO2, H2O, solubility, granitic melt

Japan Geoscience Union Meeting 2014
(28 April - 02 May 2014 at Pacifico YOKOHAMA, Kanagawa, Japan)

SMP06-P01 Room:Poster Time:April 28 18:15-19:30

Hydrogen positions in hydrous ringwoodite determined by pulsed neutron powder diffraction

PUREVJAV, Narangoo[1*] ; OKUCHI, Takuo[1] ; TOMIOKA, Naotaka[1] ; ABE, Jun[2] ; HARJO, Stefanus[3] ; AIZAWA, Kazuya[3]

[1]Institute for Study of the Earth's Interior, Okayama University, [2]CROSS-Tokai, [3]J-PARC Center, Japan Atomic Energy Agency

The transition zone in the Earth's mantle has been considered potentially large water reservoir. It was experimentally evidenced that its main constituent minerals can uptake significant amount of water as hydroxyl groups in their crystal structures. The ringwoodite [(γ-Mg,Fe)$_2$SiO$_4$] is one of the high pressure polymorph of olivine, which is the most major phase in the lower part of the transition zone, between 525 to 660 km in depth. It was reported that ringwoodite can incorporate up to 2.6 wt.% of water (Kohlstedt et al., 1996). The hydration of ringwoodite strongly affects its physical and chemical properties such as electrical conductivity, compressibility and seismic velocities. However, crystallographic sites of hydrogen and its incorporation mechanism are still unclear mainly due to insensitiveness of X-ray probe for hydrogen. The previous studies of its structure refinement by X-ray diffraction demonstrated that hydrous ringwoodite has cubic spinel structure with Fd-3m space group (Kudoh et al., 2000; Smyth et al., 2003). Here we applied neutron diffraction for hydrous ringwoodite for the first time to analyze its hydrogen positions.

Deuterated ringwoodite powder samples were synthesized at 1300 ^{o}C and 18 GPa for 5 minutes using a scaled-up Kawai-type multi anvil apparatus. The run products were evaluated by micro-focused X-ray, Raman spectroscopy and powder X-ray diffractometer to confirm their purity.

Neutron powder diffraction patterns were taken at BL-19 (TAKUMI) at Materials and Life Science Experimental Facility, J-PARC. The two representative deuterated ringwoodite samples were with identical composition mixed and measured together in a sample holder made of TiZr "null" alloy. The obtained diffraction pattern has been analyzed by Rietveld refinement using the "Z-Rietveld" code in order to determine positions and site occupancies of deuterium atoms in the ringwoodite structure.

We can propose two possible models for the deuterium atomic positions, 96g and 192i. These refined models were given with almost identical R factors. They also gave similar site occupancies and temperature factors for the elements except for the deuterium. However, in terms of deuterium temperature factor, the 192i model is more preferable than the 96g model. The refinement results also showed that the (Mg+Fe)/Si ratio is lower than the ideal ratio of dry ringwoodite [(Mg+Fe)/Si = 2.0] while Si in T sites are fully occupied, which demonstrates that deuterium only substitutes Mg and Fe in M sites and Si in T sites is not affected.

References:
[1] Kohlstedt, et al., Contrib. Mineral. Petrol., 123, 345, 1996.
[2] Kudoh, et al., Phys.Chem.Minerals., 27, 474, 2000.
[3] Smyth, et al., Am Mineral., 88, 1402, 2003.

Keywords: ringwoodite, neutron diffraction, Rietveld refinement

Japan Geoscience Union Meeting 2014
(28 April - 02 May 2014 at Pacifico YOKOHAMA, Kanagawa, Japan)

SMP06-P02 Room:Poster Time:April 28 18:15-19:30

Stability of Hydrous phase H MgSiO2(OH)2 in the lower mantle

AMAIKE, Yohei[1*] ; OHTANI, Eiji[1] ; KAMADA, Seiji[1] ; SAKAMAKI, Tatsuya[1] ; TAKAHASHI, Suguru[1] ; HIRAO, Naohisa[2] ; OHISHI, Yasuo[2]

[1]Department of Earth and Planetary Materials Science, Graduate School of Science, Tohoku University, [2]Japan Synchrotron Radiation Research Institute

Subducting slabs transport water to Earth's deep interior and its circulation on a global scale is the key to understanding the evolution of the planet. However, it is still a matter of debate how deep water can be transported. Therefore, there are many studies on phase relationships in hydrous minerals or MORB-H2O systems. Most dense hydrous magnesium silicates (DHMS) are stable up to 50 GPa (e.g., Komabayashi et al., 2004). Recently, the synthesis of Mg- and Si- bearing δ-AlOOH, which is a solid solution between 2AlOOH-MgSiO2(OH)2, was reported and it might be transported with Mg-perovskite or Mg-post perovskite up to 135 GPa (Ohira et al., 2012, AGU). Tsuchiya (2013) theoretically reported Phase H, the end member of the system, was stable above 45 GPa and up to 55 GPa. And also it was experimentally synthesized at 50 GPa (Nishi et al., 2014). Although the previous studies claimed that Phase H was broken down above 55 GPa, it may be a host phase of water in the deep Earth interior. Here, we report the stability field of a new candidate phase of water reservoir at the lower mantle conditions by investigating the MgO-SiO2-H2O system up to 75 GPa and 2000 K.

A mixture of quartz and brucite (molar ratio 1 : 1) powders were used as starting materials. The high pressure and high temperature experiments were performed by using a double-sided Laser heated diamond anvil cell. A pellet with thickness of about 15 μm was made by a cold compression technique. In situ XRD experiments in the MgO-SiO2-H2O system were performed at BL10XU, SPring-8. In this study we confirmed that hydrous phase H does exist in the MgO-SiO2-H2O system and its stability fields expands at least up to 75 GPa and above 2000 K in contrary with previous reports (Tsuchiya, 2013; Nishi et al., 2014).

If Phase H exists under high pressure conditions corresponding to the pressure of CMB, it may transport water to CMB and thus the core may contains hydrogen as a light element.

Keywords: hydrous phase, hydrous phase, subduction

Japan Geoscience Union Meeting 2014
(28 April - 02 May 2014 at Pacifico YOKOHAMA, Kanagawa, Japan)

SMP06-P03 Room:Poster Time:April 28 18:15-19:30

Partitioning of carbon between metallic- and silicate-liquids in carbonaceous chondrite compositions at high pressure

ASAHARA, Yuki[1*] ; OHTANI, Eiji[1]

[1]Tohoku University

Major volatile elements in the terrestrial planets are oxygen, sulfur, carbon, hydrogen, and nitrogen. They are also candidates for light components in the earth's core which were incorporated into the core at terrestrial magmaocean stage. Partitioning behavior of carbon has not been determined well though it is one of the strong candidates for light elements in the earth's core. We investigated partitioning of carbon with sulfur and oxygen between metallic- and silicate liquids at 6 GPa and 2073 K in carbonaceous chondrite composition (Allende meteorite; CV3). Effect of nitrogen and water as accessory components were also examined. High pressure experiments were conducted with multi-anvil high pressure apparatus. Graphite was used as capsule material. Composition of coexisting metallic- and silicate liquids were measured by electron microprobe with wavelength dispersion type spectrometer except for carbon in silicate liquid. Carbon concentration of bulk recovered sample was measured by elemental analyzer. Then, carbon concentration in silicate liquid was obtained by subtraction of carbon amounts in metallic phase which obtained by electron microprobe and SEM image analyses. Present result suggests that in oxidized carbonaceous chondrite composition, partitioning coefficient of carbon [$D^{Metallicliquid/Silicateliquid} = C^{Metallicliquid}/C^{Silicateliquid}$; C is concentration of carbon in wt.%] is close to 1, and it may increase with increasing the Fe^{metal}/Fe^{oxide} ratio in the carbonaceous chondrite composition.

Japan Geoscience Union Meeting 2014
(28 April - 02 May 2014 at Pacifico YOKOHAMA, Kanagawa, Japan)

SMP06-P04 Room:Poster Time:April 28 18:15-19:30

Microanalysis of H2O and CO2 in silicate melt using laser Raman spectroscopy

YOSHIMURA, Shumpei[1*] ; KAGASHIMA, Shin-ichi[1] ; NAKASHIMA, Kazuo[1]

[1]Department of Earth and Environmental Sciences, Yamagata University

<Introduction>

Water and carbon dioxide are the major volatile components in the crust and mantle. Development of microanalytical techniques of these volatiles has made it possible to investigate mechanisms of igneous and volcanic processes. FTIR has been used as a fundamental tool for this purpose, but its spatial resolution is too large ($\sim$30 μm) to analyse small melt inclusions and micro-scale volatile distribution within a high-pressure experimental sample. In this study, we developed a new technique for volatile analysis in silicate glasses with $\sim$1 μm spatial resolution using laser Raman spectroscopy.

<Experimental and analytical procedure>

Standard glasses were synthesized by using a piston-cylinder apparatus in M. Nakamura's laboratory. Basaltic glass power was loaded into a platinum-sleeved nickel capsule together with oxalic acid and run at 1473 K and 0.5-1.2 GPa. After quench, the H_2O and CO_2 (dissolved as CO_3^{2-}) contents of the glasses were measured by using FTIR. The same glasses were then analysed with a Thermofisher DXR laser-Raman spectrometer. Wave length, power and diameter of the laser beam were 532 nm, 10 mw and 0.7 μm, respectively. We normalized the Raman spectra by the intensity of a peak at 500 cm^{-1} (T-O-T bond) and subtracted the spectrum of the volatile-free glass. The intensities of peaks at 3550 cm^{-1} (H_2O) and 1080 cm^{-1} (CO_3^{2-}) in the resulting spectra were compared with the H_2O and CO_2 contents determined by FTIR spectroscopy.

<Results>

The H_2O and CO_2 contents were determined to be 0.7-2.1 wt% and 0.05-0.82 wt%, respectively. Raman spectroscopy showed that the intensities of peaks at 3550 and 1080 cm^{-1} increased with increasing H_2O and CO_2 contents, respectively. We fitted a linear equation to the data and obtained H_2O (wt%) = $(3.58\pm0.14)\times I_{3550}$ and CO_2(wt%) = $(4.61\pm0.21)\times I_{1080}$.

<Application>

We applied this technique to volatile analysis of an experimentally-produced bubble-bearing basaltic glass. In the experiment, basaltic melt was first equilibrated with H_2O-CO_2 mixture fluid at 1473 K and 1 GPa, and then decompressed to 0.5 GPa and kept for 10 minutes. After quench, the H_2O and CO_2 contents around bubbles were measured along the radial direction at 2-μm intervals for a total of 50 μm. The CO_2 contents decreased on moving towards the bubble, indicating that CO_2 was diffusing into the bubble. Fitting the diffusion equation to this profile, we estimated the diffusivity of CO_2 to be 1.2×10^{-12} m^2/s. This value is consistent with that reported by Zhang et al. (2007). In contrast to CO_2, H_2O showed a flat profile, suggesting that H_2O was already equilibrated with the fluid in the bubble. This is because the diffusivity of H_2O is one order of magnitude greater than that of CO_2. Such a diffusive fractionation was observed also in rhyolitic melt (Yoshimura and Nakamura, 2010).

Keywords: CO2, H2O, glass, Raman

Japan Geoscience Union Meeting 2014
(28 April - 02 May 2014 at Pacifico YOKOHAMA, Kanagawa, Japan)

SMP06-P05 Room:Poster Time:April 28 18:15-19:30

Dynamic and cyclic process of carbon-bearing phases of the terrestrial interior

MIURA, Yasunori[1*]

[1]In & Out Universities

The results of the present study are summarized as follows:

1) Carbon-bearing mineral phases of the terrestrial interior are discussed to elucidate dynamic change of material states (air, liquid and solid) on active Earth planet.

2) Samples used in this study are diamond (Congo,Africa), limestone (Akiyoshi, Japan), carbonatite (Lengai, Tanzania,Africa and Europe-North America), and shungite (Shunga, Russia) together with carbonate grains of Libyan glass (Africa) to observe micro nano-grains of carbon-bearing materials with the FE analytical SEM etc.

3) The present data indicate that micro carbon-bearing grains are easily changed and remained as the three materials states mainly as solidified glasses by high pressure shock waves of earthquake, volcano and impact events to the surface to the interior.

4) Local fluid-bearing depositions irregularly distributed on the surface and interior of active Earth are based on storages on the interior formed by solidified mixtures of multiple carbon-bearing material states originally triggered by impact process on primordial Earth and ocean floors of evolved Earth.

5) The primordial planet Earth with remained heterogeneous surface by original impact-related process is considered to produce dynamic cyclic system of three material states (air, liquid and solid) of carbon-bearing materials with macro-life activity which is formed by huge production from the interior triggered by huge collision process of the giant impact and followed inner movement of active Earth with complicate local reservoir.

Keywords: carbon, interior, cyclic process, shock wave event, irregular distribution, local deposit

Japan Geoscience Union Meeting 2014
(28 April - 02 May 2014 at Pacifico YOKOHAMA, Kanagawa, Japan)

SMP46-01 Room:411 Time:April 28 12:00-12:15

Placing time constraints on a P-T-D evolution: insights from Lu-Hf garnet and U-Th-Pb monazite dating

SKRZYPEK, Etienne[1*] ; SZCZEPANSKI, Jacek[2] ; ANCZKIEWICZ, Robert[3] ; STIPSKA, Pavla[4] ; KRONER, Alfred[5]

[1]Kyoto University, [2]University of Wroclaw, [3]Polish Academy of Sciences, Krakow, [4]Universite de Strasbourg, [5]Universitat Mainz

The best approach for understanding the tectono-thermal evolution of a crustal level is through reconstructing its pressure-temperature-deformation-time (*P-T-D-t*) evolution. Whereas *P-T-D* paths can be inferred from crystallization-deformation relationships, placing absolute time constraints on such paths remains challenging, especially because a link between major element-bearing index minerals and trace element-bearing geochronometers needs to be established.

We present the example of medium-grade metasedimentary rocks (Orlica-Snieznik Dome, EuropeanVariscan Belt) for which results of Lu-Hf garnet and U-Th-Pb monazite dating are linked with prograde and retrograde stages of the *P-T-D* evolution, respectively. On the macroscopic scale, a succession of three metamorphic foliations is recognized: initial subhorizontal S1, intermediate subvertical S2, and late subhorizontal S3. A garnet±staurolite assemblage is ascribed to the S1 foliation, whereas the S2 fabric is associated with staurolite demise producing a garnet-biotite-sillimanite/andalusite assemblage. Post-S2 garnet and cordierite blastesis is followed by chlorite growth during and after the formation of the S3 foliation. Garnet porphyroblasts show a peculiar zoning pattern with a linear Mn-Ca decrease in the allanite-bearing core, an inner rim of alternating Ca-Y- and P-rich annuli, and a Ca-poor outer rim. Monazite is found as subhedral aggregates at garnet rim, and lone matrix grains close to partially resorbed garnet, staurolite or apatite. Textural observations and modelling of the garnet composition suggest that the inner rim with Ca-Y-rich annuli reflects the allanite-to-monazite transition which occurred close to the staurolite isograd. In this inner rim, a Lu oscillatory zoning pattern coincides with the zone of Ca-Y-rich annuli. Since the inner rim dominates the Lu budget of garnet, the associated Lu-Hf garnet-whole-rock isochron age of 344±3 Ma is ascribed to *P-T* conditions of the staurolite isograd, i.e. ∼5 kbar/575 ℃ in the S1 fabric. A subsequent temperature increase to peak conditions of ∼5 kbar/580-625 ℃ in the S2 fabric is indicated by the Ca-poor garnet outer rim that reflects staurolite breakdown. LA-ICP-MS monazite dating yields $^{208}Pb/^{232}Th$ ages defining a dominant group at 313±2 Ma and a secondary peak at 328±2 Ma. Based on monazite textures, these relatively young ages are ascribed to fluid influx during retrograde chloritization.

The short time span between prograde garnet growth (∼344 Ma) and existing Ar-Ar cooling ages on micas (∼335 Ma) points to a tectono-thermal event of about 10 Ma. Assumed high heating and cooling rates during this event are explained by the synchronous intrusion of granitoid sheets. Nevertheless, monazite ages indicate that a low-grade overprint occurred more than 20 Ma after peak conditions.

Keywords: P-T-D-t path, prograde garnet zoning, retrograde monazite

Japan Geoscience Union Meeting 2014
(28 April - 02 May 2014 at Pacifico YOKOHAMA, Kanagawa, Japan)

SMP46-02 Room:411 Time:April 28 12:15-12:30

Microdiamond - bearing UHP chromitite from the Higo Metamorphic Rcoks, Central Kyushu, Japan

NISHIYAMA, Tadao[1*] ; SHIOSAKI, Dai[1] ; EGUCHI, Hibiki[1] ; YOSHIASA, Akira[1]

[1]Graduate School of Science and technology, Kumamoto University

Microdiamond-bearing ultrahigh-pressure (UHP) chomitite was newly found from a spinifex-textured metaperidotite in the Higo Metamorphic Rocks (HMR) , Central Kyushu, Japan. This is the first finding of microdiamond from Japanese metamorphic rocks and the second finding in Japan following the first one from a mantle xenolith in a Cenozoic lamprophyre dyke in Shikoku[1]. The HMR represents a low P/T metamorphism of Cretaceous in age, however, the precursor HP or UHP metamorphism of ca. 250Ma has been inferred[2]. A great deal of debate has been done on whether or how the Dabie-Sulu UHP terrane extends eastward to the Korean Peninsula and also to Japan. The HMR is one of the candidates[3] for the eastern extension in Japan, but no definitive evidence has been given yet.

Metaperidotites occur in two localities in the HMR: one at Yamato Town in the biotite zone and the other in Matsubase Town in the garnet-cordierite I zone[4]. The metaperidotites from Matsubase Town show distinct spinifex-texture with decimeter-sized elongated olivine (mostly serpentinized) and enstatite. Those from Yamato Town shows either spinifex-texture or granular texture of finer grains (several mm to 1 cm across), and is strongly serpentinized. The metaperidotite bodies occur in mostly pelitic gneisses as small lenticular bodies about several ten meters in size, which are concordant to the gneissosity. The mineral assemblage of the metaperidotite is olivine (mostly serpentinized) + enstatite with secondary tremolite and antigorite. Talc occurs locally along the cleavage of enstatite. A podiform chromitite occurs in such a strongly serpentinized metaperidotite at Yamato Town as a nodular form of about 10 cm in diameter, in which we found many inclusions of microdiamond 1 to 10 μm in size. We have made four thin sections, polished with colloidal silica, from one chromitite sample, and found many microdiamond inclusions in all thin sections. Microdiamonds occur both in chromite and in nickeline, and they are all monocrystalline. Many euhedral to subhedral grains (mostly 1 μm in size) of microdiamond occurs in chromite, making several lines of aligned grains. Identification of diamond was carried out with an energy dispersive X-ray spectroscopy (EDS) analysis (carbon peak) and Raman spectroscopy with a He-Ne laser. We observed a Raman peak at 1333.5 cm^{-1}, which is comparable to the peak (1332 cm^{-1}) characteristic of diamond. They show no evidence of partial or total graphitization. The occurrence suggests that the striations represent healed cracks and that microdiamonds precipitated from a reduced C-O-H fluid[5,6]. Our finding presents a convincing evidence for the hypothesis that the Higo Metamorphic Rocks is an eastern extension of the Dabie-Sulu UHP terrane in Japan. The second implication of our finding is on the nature of UHP chromitite. Microdiamonds are found from several UHP metamorphic terranes[5,6,7], however, microdiamond-bearing UHP chromitite has been found from ophiolites in non-UHP metamorphic terrane[8], making the occurrence of UHP chromitite as an enigma[9]. The Higo UHP chromitite represents a deep subduction product as indicated by spinifex-texture in the host metaperidotite due to high pressure breakdown of antigorite (serpentine), instead of a product of mantle migration10. Therefore the origin of the UHP chromitite requires a specific interpretation in each case.

References

1. Mizukami, T., et al., Geology, 36, 219-222, 2008; 2. Osanai, Y., et al.,Gondwana Res.,9, 152-166,2006;3: Omori, S., and Isozaki, Y., J. Geogr., 120, 40-51, 2011; 4: Miyazaki, K., JMG,22, 793-809,2004; 5: Liou J.G., et al., J. Asian Earth Sci.,35, 199-231; 6: Dobrzhinetskaya, L.F.,Gondwana Res., 21, 207-223, 2012; 7. Schertle, H-P., and Sobolev, N.V., J. Asian Earth Sci., 63, 5-38, 2013; 8: Yang, J-S., et al., Geology, 35, 875-878, 2007; 9; Arai,S., JMPS, 105, 280-285, 2010; 10; Yamamoto, S. et al., Lithos, 109, 314-322, 2009

Keywords: microdiamond, UHP chromitite, Higo Metamorphic Rocks, Ultrahigh-pressure metamorphic rocks, Spinifex-texture, Dabie-Sulu UHP terrane

Japan Geoscience Union Meeting 2014
(28 April - 02 May 2014 at Pacifico YOKOHAMA, Kanagawa, Japan)

SMP46-03 Room:411 Time:April 28 12:30-12:45

Grain Size Grading of Garnet in the Liesegang Metamorphism

TORIUMI, Mitsuhiro[1*] ; FUKUYAMA, Mayuko[2]

[1]JAMSTEC, [2]Akita univ.

The very puzzling phenomena is that the grain size of metamorphic garnet shows apparently gradational in both basic and politic schists, for bulk chemistries of large grain and small - grain layers are not different with each other and for chemical zonings of large and small grains of garnet display very similar pattern. These facts suggest that the domain structure by diffusion and growth of garnet should be formed in the layer and the spacing of the domain changes gradually across the grain - size layering in the metamorphism.

The layering shows parallel to subparallel against the schistosity plane, suggesting the parameter changes uniaxialy along the normal direction against the schistosity. The length scales of the grain size layering ranges from several to several ten cm, being likely to those of the compositional banding derived from metasomatism. Judging from these facts, it seems that the size grading process in the plate boundary metamorphism is governed by the diffusion, reaction and grain growth mechanism, that is the precipitation mechanism in the Liesegang bands. The precipitation in the Liesegang band is considered as the Cahn - Hillert - Cook process (1), which is characterized by the relation of average grain size, size distribution, width of the layer, and spacing distribution among grains.

In this paper, we would like to investigate these relations of the size grading of garnet in the subduction zone metamorphism.

References

(1), A. DEWIT, 1999, Advances in Chemical Physics, Volume109, Edited by I. Prigogine and Stuart A. Rice ISBN 0-471-32920-7 0 1999 John Wiley & Sons, Inc

Keywords: grain size, grading, Liesegang, metamorphism

Japan Geoscience Union Meeting 2014
(28 April - 02 May 2014 at Pacifico YOKOHAMA, Kanagawa, Japan)

SMP46-04 Room:414 Time:April 28 14:15-14:30

Metamorphism of sodic pyroxene-bearing quartz schists from the Bizan area, Sambagawa belt, eastern Shikoku, Japan

KABIR, Md fazle[1*] ; TAKASU, Akira[1] ; KAINUMA, Masaaki[1]

[1]Department of Geoscience, Shimane University, Japan

The Bizan area of the Sambagawa metamorphic belt is occurs in easternmost Shikoku, southwest Japan. The Bizan and Kotsu areas are located in the same tectonostratigraphic horizon, i.e. the Kotsu Formation in eastern Shikoku. The Kotsu Formation in the Kotsu-Bizan area is structurally overlying and underlying by the Kawata Formation and the Kawatayama Formation, respectively. The main rock types in the Bizan area include pelitic, basic and siliceous schists, with minor amounts of psammitic and calcareous schists (Iwasaki, 1963). Faure (1983) suggested a melange zone containing tectonic blocks of serpentinite, metagabbro and garnet-amphibolite (garnet-glaucophane schist) occurs along a ductile shear zone between spotted and non-spotted schist zones. Sodic pyroxene-bearing quartz schists consist mainly of quartz and phengite, with minor amounts of amphibole (Fgl, Mrbk, Rbk, Mkt, Wnc, Brs, Fbrs), garnet, Na-Ca pyroxene (hereafter sodic pyroxene) (aegirine, aegirine-augite and omphacite) and albite. Hematite, chlorite, and epidote occur occasionally. A schistosity is defined by preferred orientation of phengite and quartz.

Garnets are spessartine-rich in composition, show a growth zoning with decreasing spessartine (X_{Sps} 0.82-0.35) and increasing almandine (X_{Alm} 0.01-0.41) and pyrope (X_{Prp} 0.03-0.09) from core to the rim and contain inclusions of phengite (6.84 pfu), epidote, hematite and quartz. The garnets are occasionally replaced by chlorite and biotite along cracks and at the rims. Amphiboles occurring as inclusions in porphyroblastic albite are compositionally zoned, with Fbrs and Brs cores and Rbk rims. Matrix amphiboles are Brs and Mkt core, Fgl mantle and Rbk and Mrbk rims, and contain inclusions of phengite (6.50-6.51 pfu), hematite and quartz. Sodic pyroxenes occurring as inclusions in porphyroblastic albite are aegirine, aegirine-augite and omphacite with X_{Jd} 0.08-0.37 contents. Some of them are compositionally zoned, with aegirine-augite and omphacite cores (X_{Jd} 0.34-0.37) to aegirine-augite and aegirine rims (X_{Jd} 0.34-0.21). Matrix sodic pyroxenes are aegirine-augite (X_{Jd} 0.09-0.27), decreasing X_{Jd} from cores (0.22-0.25) to the rims (0.22-0.17). Some other sodic pyroxenes in the matrix display increasing X_{Jd} from core to the mantle (0.13-0.19) and decreasing towards the rim (0.19-0.12). They contain inclusions of amphibole (Brs, Fbrs, Rbk), phengite (6.66-6.82 pfu), hematite and quartz, and are partially replaced by chlorite along their cleavages. Porphyroblastic albite crystals up to 2 mm across contain inclusions of garnet, amphibole (Brs, Fbrs, Rbk), sodic pyroxene (X_{Jd} 0.10-0.37), phengite (6.57-6.76 pfu) and quartz. Matrix phengites show relatively higher in Si (6.33-6.98 pfu) contents than inclusions.

According to the occurrence of mineral assemblage the Kwata, Kotsu and Kawatayama Formation probably correlate with the albite-biotite zone of the Besshi area (Enami *et al*., 1994). Jadeite content in the sodic pyroxenes are significantly higher in sodic pyroxene-bearing quartz schists (X_{Jd} 0.08-0.37) than those of garnet-aegirine augite-alkali amphibole-quartz schist (X_{Jd} 0.30) in the Bizan area (Iwasaki, 1963) and Asemigawa (X_{Jd} 0.15-0.19), Besshi (X_{Jd} 0.14-0.23) and the Sarutagawa area (X_{Jd} 0.17-0.30) in the central Shikoku (Enami *et al*., 1994). This higher jadeite content in sodic pyroxenes suggests metamorphic conditions in the Bizan sodic pyroxene-bearing quartz schists might be higher in pressure than those of the metamorphic zonation in the albite-biotite zone of the Sambagawa belt central Shikoku by Enami *et al*. (1994).

References

Enami *et al*. (1994) *Contrib Mineral Petrol*, 116, 182-198. Faure M. (1983) *J Geol Soci Japan* 89, 319-329. Iwasaki, M. (1963) *J Faculty of Science, Univ Tokyo, Section II*, 15, 1-90.

Keywords: Sambagawa (Sanbagawa) metamorphic belt, Bizan area, quartz schist, omphacite, aegirine-augite

Japan Geoscience Union Meeting 2014
(28 April - 02 May 2014 at Pacifico YOKOHAMA, Kanagawa, Japan)

SMP46-05 Room:414 Time:April 28 14:30-14:45

Application of the Raman carbonaceous material thermometer to the Chichibu-Sanbagawa belt in the Kanto Mountains, Japan

KOUKETSU, Yui[1*] ; SHIMIZU, Ichiko[2]

[1]Geochemical Research Center, Graduate School of Science, The University of Tokyo, [2]Department of Earth and Planetary Science, Graduate School of Science, The University of Tokyo

The structure and tectonic history of the Chichibu-Sanbagawa belt have been investigated by the lithological structure, radiolarian age, radiometric age, deformation microstructural analysis, and X-ray diffraction analysis of carbonaceous material (CM). The structural discontinuities (nappe boundaries) within the Chichibu-Sanbagawa belt are proposed in several studies (e.g., Shimizu 1988, *J.Geol. Soc. Japan*; Isozaki & Maruyama 1991, *J. Geogr.*; Hirajima *et al*. 1992, *J.Geol. Soc. Japan*). However, the boundary between the Chichibu and Sanbagawa belts and their structural relationship are still under debate. In addition, the thermal structure was not well investigated because the geothermometer that can be applied over the temperature range of the Chichibu and Sanbagawa belts was not available. Recently, several studies proposed the geothermometers applying the Raman spectroscopy. Kouketsu *et al*. (2014, *Island Arc*) analyzed the CMs with a wide range of crystallinity, from amorphous carbon to well-crystallized graphite, in sedimentary and metamorphic rocks and proposed a new Raman CM geothermometer. By using this technique, we evaluate the peak temperatures of the rocks in the Chichibu and Sanbagawa belts in the Kanto Mountains, which is the type locality of these belts.

We investigated the mudstone, sandstone, and pelitic schist taken from the Kannagawa, Sanbagawa, and Ayukawa River districts in the Kanto Mountains, Gunma Prefecture. In the studied area, the accretionary complexes of the Northern Chichibu belt are distributed in the south, crystalline schists of the Sanbagawa belt are distributed in the north, and the Mikabu greenstones are exposed between them. The Chichibu belt is divided into three units: Kamiyoshida, Manba, and Kashiwagi units, in descending structural order (Shimizu & Yoshida 2004, *Island Arc*). The Sanbagawa belt is divided into three metamorphic zones: chlorite, garnet, and biotite zones, in order of ascending metamorphic grade (Yano & Tagiri 1998, *J.Geol. Soc. Japan*). The strata gently dip to the north and the metamorphic grade monotonously increases towards the lower structural level.

The Raman spectra of CM in mudstone and sandstone taken from the Chichibu belt include broad peaks that are characteristic of the amorphous carbon structure. The temperatures of most samples estimated by full width and half maximum (FWHM) of the D1-band are around 260-300 ℃. Several CMs in the rocks near the Mt. Nishi-Mikabo show the temperature higher than 300 ℃.

The intensities of Raman spectra of CM in the Sanbagawa schists are one order weaker than those in the rocks taken from the Chichibu belt. The D4-band, which is the characteristic peak in amorphous carbon, is not observed. Instead, G-band, which is the characteristic peak in well-crystallized graphite, becomes the most prominent peak at higher-grade zone. The metamorphic temperatures are estimated by using the FWHM of D1- and D2-bands and area ratio (R2) of CM Raman spectra. The metamorphic temperatures of the samples are estimated around 360-400 ℃, 420-450 ℃, and 460-510 ℃ in the chlorite, garnet, and biotite zones, respectively.

The temperatures estimated from CM show the gap of several tens of degrees or more between the Chichibu and the Sanbagawa belts. Further sampling and analysis will be proceeded.

Keywords: Raman spectroscopy, Carbonaceous material, Geothermometer, Chichibu belt, Sanbagawa belt, Kanto Mountains

Japan Geoscience Union Meeting 2014
(28 April - 02 May 2014 at Pacifico YOKOHAMA, Kanagawa, Japan)

SMP46-06 Room:414 Time:April 28 14:45-15:00

Fission track and U-Pb zircon ages of psammitic rocks from the Harushinai unit of the Kamuikotan belt, Hokkaido

OKAMOTO, Ayumi S.[1*] ; TAKESHITA, Toru[1] ; IWANO, Hideki[2] ; DANHARA, Tohru[2] ; HIRATA, Takafumi[3] ; NISHIDO, Hirotsugu[4]

[1]Hokkaido University, [2]Kyoto Fission-Track Co., Ltd., [3]Kyoto University, [4]Okayama University of Science

In order to discuss exhumation processes and mechanisms for high-*P/T* type metamorphic rocks, it is necessary to obtain correct informations on pressure-temperature-time paths of these rocks from sedimentation to exhumation through maximum burial. We conducted coupled fission-track (FT) and U-Pb dating on detrital zircon grains in two psammitic rock samples collected from the Harushinai unit of the Kamuikotan metamorphic rocks using a Laser Ablation-Inductively Coupled Plasma-Mass Spectrometry (LA-ICP-MS). The results indicate that the concordant zircon U-Pb ages greatly vary between 1980-90 Ma. Among them, the youngest U-Pb age cluster (*c.* 110-90 Ma) is dominant, yielding the weighted mean ages of Albian (100.8±1.1 and 99.3±1.0 Ma with 2σ errors) for both samples. According to an oscillatory zoning of igneous origin without any overgrown rims in the analyzed zircon, the zircon U-Pb ages were not reset by the high-*P/T* type metamorphism, and hence the youngest U-Pb ages indicate the upper bound of sedimentary ages. On the other hand, the zircon FT data show the spectra with a single peak age at 100-90 Ma, which are comparable with the youngest U-Pb age cluster. The fact indicates that these zircon FT ages were once reset at *c.* 100 Ma due to an intense igneous activity at the provenance, but have not been essentially reset since the sedimentation. The scenario is supported by the temperature conditions slightly less than those of brittle-ductile transition of quartz (*c.* 300 ℃, also closure temperature of zircon FT) estimated from the microstructures in deformed quartz detrital grains constituting the psammitic rocks. Combining these results with the previously reported K-Ar ages of white mica, it is inferred that Harushinai unit was deposited after *c.* 100 Ma, dragged down to the maximum depth, and further affected by a localized thermal overprint during exhumation (*c.* 58 Ma).

Keywords: Kamuikotan metamorphic rocks, zircon, U-Pb ages, Fission track ages, deformation microstructure

Japan Geoscience Union Meeting 2014
(28 April - 02 May 2014 at Pacifico YOKOHAMA, Kanagawa, Japan)

SMP46-07 Room:414 Time:April 28 15:00-15:15

Shape evolution of spinel grains in the Horoman Peridotite Complex, Hokkaido

KOIDE, Satoko[1*] ; SHIBATA, Tomoki[2] ; MICHIBAYASHI, Katsuyoshi[1]

[1]Institute of Geosciences, Shizuoka University, [2]Institute of Geosciences, Shizuoka University

We present the evolution of spinel grains in the Horoman Peridotite Complex, Hokkaido. For deformation under differential stresses at high temperature conditions, both diffusion processes including diffusion creep and annealing process and dislocation creep will affect shape change of a crystal inclusion (Okamoto and Michibayashi, 2005 JGR). Grain size and grain shape are related to the shape change of the crystal with respect to given temperature and differential stress conditions. We applied this theory to spinel grains in the Horoman Peridotite Complex, Hokkaido. As a result, grain shapes of coarser spinel grains more than 100 micron are dominantly controlled by dislocation creep, whereas those of smaller spinel grains less than 100 micron are influenced by both diffusion processes and dislocation creep. Moreover, we found that grain shapes of the smaller spinel grains can be only explained by post-tectonic annealing process after their intense deformation. Our result will provide a new insight to understand the deformation processes in mantle.

Keywords: spinel, grain shape, diffusion process, dislocation creep, Horoman

Japan Geoscience Union Meeting 2014
(28 April - 02 May 2014 at Pacifico YOKOHAMA, Kanagawa, Japan)

SMP46-08 Room:414 Time:April 28 15:15-15:30

Verification of ultra-low strain rate effect from microstructural observation on naturally deformed olivine

YAMAMOTO, Takafumi[1*] ; ANDO, Jun-ichi[1] ; OHFUJI, Hiroaki[2] ; MORISHITA, Tomoaki[3] ; TOMIOKA, Naotaka[4]

[1]Department of Earth and Planetary Systems Science, Hiroshima University, [2]Geodynamics Research Center, Ehime University, [3]School of Natural System, Colleage of Science and Technology, Kanazawa University, [4]Institute for Study of the Earth's Interior, Okayama University

Kitamura et al. (1986) and Ando et al. (2001) reported Fe concentration on dislocation core in naturally deformed olivine. They suggested that compositional heterogeneity is formed by Cottrell atmosphere of solute atoms. This phenomenon is well known in the realm of metallurgical science, and only occurs during dislocation creep at very low strain rate condition. The presence of Cottrell atmosphere has a pinning effect on dislocations and prohibits their movements. As a consequence, plastic behavior of materials is drastically changed in the presence of Cottrell atmosphere. On the basis of this compositional heterogeneity, they demonstrate that the study of ultra-low strain rate effect on olivine plasticity is very important to understand the dynamics of the upper mantle.

With this background, the purposes of the present research are: (1) to confirm whether the Fe concentration on dislocation core is a common phenomenon in deformed olivine grains of mantle-derived peridotite, (2) to verify the deformation condition at which Fe concentration was occurred, from the microstructural observation of each studied peridotite samples, (3) to clarify the exact mechanism of Fe concentration, namely Cottrell atmosphere or pipe diffusion. The studied peridotite samples are xenoliths from basalt (Takashima, Megata, Kurose and Salt Lake), and alpine rocks (Uenzaru and Horoman). The techniques employed for the present study include optical microscopy, EPMA, SEM-EBSD, TEM and ATEM.

The main results are as follows:

1) Fe concentration on dislocation core in all olivine samples is detected, which suggests that it is common phenomenon in mantle peridotite.

2) The mechanism of Fe concentration on dislocation core in olivine grains is preferably Cottrell atmosphere than other phenomena such as pipe diffusion. However we need to carry out more careful and detailed observations to confirm it.

3) The microstructural observations indicate that the all peridotites preserve the deformation characteristics developed at the upper mantle. This fact suggests strongly that the Fe concentration on dislocation core in olivine grains occurred in the upper mantle condition.

Ando et al. (2001) Nature, 414, 893; Kitamura et al. (1986) Proc.Japan Acad., 62, 149.

Keywords: Olivine, Cottrell atmosphere, Dislocation creep

Japan Geoscience Union Meeting 2014
(28 April - 02 May 2014 at Pacifico YOKOHAMA, Kanagawa, Japan)

SMP46-09 Room:414 Time:April 28 15:30-15:45

The relationship between microstructures and metasomatism preserved within coarse granular peridotites derived from Kaap

TOMITA, Daiki[1*] ; MICHIBAYASHI, Katsuyoshi[1] ; KATAYAMA, Ikuo[2] ; KOMIYA, Tsuyoshi[3]

[1]Institute of Geosciences, Shizuoka University, [2]Department of Earth and Planetary Systems Science, Hiroshima University, [3]Department of Earth Science & Astronomy Graduate School of Arts and Sciences The University of Tokyo

Kimberlite was generated in deep upper mantle (70-250km) beneath craton and subsequently ascended to surface rapidly. Peridotite xenoliths, which were entrained by kimberlite, record composition and texture formed in upper mantle beneath the craton. We studied coarse granular peridotites obtained from Kimberley pipe, South Africa, as they have a few studies in terms of microstructural development, presumably because of very coarser grains. We performed mineral crystal-fabric analyses of the coarse granular peridotites in order to understand the structure of the cratonic lithosphere. The peridotites consist mostly of olivine and orthopyroxene with clinopyroxene, garnet and a minor amount of spinel and phlogopite. The crystallization of clinopyroxene appears to be associated with melt metasomatism, whereas that of phlogopite could be associated with hydration metasomatism. Garnet grains occur commonly with kelyphite consisting of fine-grained orthopyroxene, clinopyroxene and spinel, indicating that these peridotites could have been uplifted above the phase boundary between garnet peridotite and spinel peridotite stability fields. Although both foliation and lineation are not commonly identified because of coarse granular texture, olivine crystal fabrics are characterized by a single maximum of [010] with single maxima or weak girdles of [100] and [001]. We found that the intensities of olivine and orthopyroxene crystal-fabrics are correlated to the modal composition of clinopyroxene and phlogopite. It suggests that the melt metasomatism weakened crystal-fabrics, whereas the hydration metasomatism intensified crystal-fabrics. As a consequence, the metasomatism could result in the development of different types of microstructures in the peridotites and may weaken the craton lithosphere.

Keywords: kimberlite, peridotite, garnet, olivine, craton, crystal-fabrics

Japan Geoscience Union Meeting 2014
(28 April - 02 May 2014 at Pacifico YOKOHAMA, Kanagawa, Japan)

SMP46-10 Room:414 Time:April 28 15:45-16:00

Corona-forming reaction in the Lutzow-Holm Complex, East Antarctica at Ongul Island

SHIMADA, Asami[1*] ; IKEDA, Takeshi[1]

[1]Kyushu University

[Introduction]

Corona is a microstructure that aggregate of one or several species of mineral surrounds another mineral. This suggests that corona was formed by the reaction between the interior mineral and the matrix minerals (Passchier and Trouw 1996). Estimating this reaction enables us to know which component transferred and how temperature and pressure changed. In this study, we estimated corona-forming reaction by describing the microstructure and chemical composition of a corona in the Lutzow-Holm Complex at Ongul Island.

[Geological Outline]

In the Lutzow-Holm Complex, metamorphic grade increases from amphibolites facies in the northeast to granulite facies in southwest (Hiroi et al., 2006). The granulite facies metamorphic rocks are widely distributed throughout East Ongul Island. The rock types are mainly garnet gneiss and hornblende gneiss (Shiraishi et al., 1994). Ultramafic rocks occur as thin layers in the garnet gneiss. The ultramafic rocks analyzed in this study are composed mainly of hornblende and porphyroblasts of garnet. Corona structure forms around the garnet.

[Microstructure]

In the ultramafic rocks, hornblende-rich domain and plagioclase-rich domain occur. Both domains consist of hornblende, plagioclase, brown biotite and orthopyroxene. The corona consists mainly of green biotite and plagioclase, and occurs around the garnet. Plagioclase in the matrix and the corona has twin and chemical zoning. Garnet porphyroblast (about 15mm diameter) shows concavo-convex shape. In the embayed part of garnet, biotite tends to occur with long axis is at right angles to garnet surface.

[Chemical Composition]

Garnet; Rim shows higher Fe and lower Mg than the interior.

Plagioclase; Ca/(Ca+Na) increases in the order of Pl-rich domain, Hbl-rich domain and corona. Ca/(Ca+Na) in every domain increases from core to rim.

Biotite; Mg/(Fe+Mg) decreases in the order of Hbl-rich domain, Pl-rich domain and corona. Rim in every domain shows lower Al than the core.

Hornblende; Hbl-rich domain shows higher Al and Mg/(Fe+Mg) than Pl-rich domain. The rim of both domains shows higher Al than the core.

Orthopyroxene; Composition is almost homogeneous within the domain.

[Discussion]

The compositional difference between core and rim of each mineral in the matrix can be regarded as growth zoning. We used the rim-composition in each domain to estimate the corona-forming reaction. The average of analyses was used for plagioclase and biotite in the corona and for garnet. The corona-forming reaction employing the compositions of Hbl-rich domain was given as follows.

Grt + 1.10Bt + 3.25Pl + 0.76K + 0.81H2O = 1.91Bt + 3.62Pl

On the other hand, the reaction using the compositions of Pl-rich domain expects garnet as products, which is inconsistent with the observation that garnet was consumed. This suggests that K is supplied from the outside through fluid during corona formation. We also compared volume of left side minerals, that is,

Grt : Bt : Pl = 1 : 1.4 : 2.8

Garnet is minimum in amount. Nevertheless, corona formed around garnet. This suggests that diffusion of component from garnet controlled the rate of the reaction.

Keywords: corona, East Antarctica, Lutzow-Holm Complex

Japan Geoscience Union Meeting 2014
(28 April - 02 May 2014 at Pacifico YOKOHAMA, Kanagawa, Japan)

SMP46-11 Room:414 Time:April 28 16:15-16:30

Possible tectonic models before, during and after mylonitization in the Sor Rondane Mountains, East Antarctica

TOYOSHIMA, Tsuyoshi[1*] ; KANEYA, Akiko[1] ; OSANAI, Yasuhito[2] ; BABA, Sotaro[3] ; HOKADA, Tomokazu[4] ; NAKANO, Nobuhiko[2] ; ADACHI, Tatsuro[2]

[1]Niigata University, [2]Kyusyu University, [3]University of the Ryukyus, [4]National Institute of Polar Research

The deformational history in the Sor Rondane Mountains (SRMs), eastern Dronning Maud Land (DML), East Antarctica, is divided into 13 stages (D1?D13). The tectonic regime varied frequently from extension (D3?D4) to layer-normal compression and layer-parallel extension (D5), to compression (D6), top-to-the S shearing (D7), top-to-the SE shearing and sinistral strike-slip (D8), compression (D9?D11), and ?nally extension related to dextral shearing (D12?D13). In this paper we discuss change in deformation and P-T conditions before, during and after the D7-D8 mylonitization, using mineral textures, assemblage, compositions and microstructures of D7 and D8 mylonites.

Garnet porphyroclasts of the D7-D8 mylonites include high-Ca mantles and crenulation microfolds defined by sillimanite fibrolites. The high-Ca mantles of garnets and their plagioclase inclusions in the mylonites imply an increase in pressure before the D7-D8 mylonitization. S-tectonites having a dominant planar fabric were formed before the D7-D8 mylonites and after the high-Ca mantles of the garnets. The planar fabric (foliation) of the S-tectonites is produced by fan-shaped arrangement of sillimanite and biotite grains. The sillimanite and biotite grains were formed by breakdown of garnet. Most of the sillimanite and biotite grains have been rotated and folded by the D7-D8 mylonitization. The D7-D8 mylonite foliations are parallel to the planar fabric of the S-tectonites. The S-tectonites indicate a flattening type of strain and resulted from the layer-normal shortening after the increase in pressure and before the D7-D8 mylonitization. kyanite-quartz porphyroblasts and randomly oriented crystals of sillimanite/kyanite and biotite were formed after the D7-D8 mulonitization. The randomly oriented crystals of sillimanite/kyanite and biotite resulted from the breakdown of garnet porphyroclasts of the D7-D8 mylonites. The kyanite-quartz porphyroblasts accompany leucogranite veins cutting the D7-D8 mylonite foliations. The randomly oriented crystals and porphyroblasts imply non-deformational conditions after the D7-D8 mylnitization and D9 folding.

Three possible tectonic models for D7 and D8 mylonite-forming events before the D9 deformation can be considered as follows: extensional tectonic model, positive flower structure model and rotated mylonite model. In the former model, D7 and D8 indicate major extensional tectonic activity in the southern part of the East African and Antarctic Orogen (EAAO) before the Pan-African compressional event, and after the 650-600 Ma peak of metamorphism. In the latter two models, D7 and D8 mylonites may have resulted from the compressional events. In the positive flower structure model, the SRMs are the southern half of the E-trending positive flower structure. The flower structure model needs top-to-the N shear zones to the north of the SRMs. In the rotated mylonite model, the present S-dip of the D7 and D8 mylonites results from the rotation and folding of originally N-dipping reverse (top-to-the S-SE, normal-sinistral shear, present day coordinates) mylonites. The Pan-African compressional event resulted in the formation of upright folds with horizontal axes that curve along the coastline in central to eastern DML during the D9 deformation that took place between 600 and 560 Ma. The coastline-parallel fold axes and subvertical axial-planes correspond to the X-axes and the XY-planes, respectively, of strain ellipsoids that were progressively rotated counterclockwise toward the central parts of a sinistral shear zone. Therefore, the curved fold axes and axial-planes suggest the EAAO acted as a zone of sinistral transpression during the collision of parts of East and West Gondwana.

Keywords: S-tectonite, flattening, mylonitization, Sor Rondane Mountains, Gondwana, East Antarctica

Japan Geoscience Union Meeting 2014
(28 April - 02 May 2014 at Pacifico YOKOHAMA, Kanagawa, Japan)

SMP46-12 Room:414 Time:April 28 16:30-16:45

Significance of multi-stage chloride brine activity- An example from Sor Rondane Mountains, East Antarctica

HIGASHINO, Fumiko[1*] ; KAWAKAMI, Tetsuo[1] ; TSUCHIYA, Noriyoshi[2] ; MADHUSOODHAN, Satish-kumar[3] ; ISHIKAWA, Masahiro[4] ; GRANTHAM, Geoffrey H.[5]

[1]Kyoto University, [2]Tohoku University, [3]Niigata University, [4]Yokohama National University, [5]Council for Groscience, South Africa

It has been gradually recognized chloride brine potentially plays an important role in large-scale mass transfer during high-grade metamorphism without partial melting. This is because brine is a powerful solvent, can coexist with CO_2-rich fluid under the granulite facies conditions and has low-H_2O activity (Newton & Manning, 2010; Heinrich et al., 2004). In natural observation, evidence for the presence of brine is often found as fluid inclusions. In metamorphic rocks under granulite facies conditions, however, brine inclusions are only rarely found (Markl & Bucher, 1998). This is partly because brines have a high mobility due to their low viscosity and low wetting angle (Watson & Brenan, 1987; Holness, 1997).

On the other hand, hydrous minerals such as biotite (Bt), hornblende (Hb) and apatite can record the f_{H2O}/f_{HCl} of the last equilibrated Cl-rich fluid as their mineral compositions. In order to understand the metamorphic fluid activity using these minerals, *P-T* condition under which these minerals equilibrated with a fluid as well as the crystallographic requirements for these minerals to record the fluid composition should be known (e.g., Makino, 2000). However, there still are a lot of unsolved issues about brines, for example, cations transported in the fluid, *P-T* condition and areal scale of brine activity, and its origin (Newton et al., 1998).

In order to understand the multiple brine activities and the cation composition in brines, two meta-mafic gneisses are studied in detail in Brattnipene, Sør Rondane Mountains (SRM), East Antarctica.

In a Grt-Bt-Hb gneiss, Cl-rich Bt is exclusively included in garnet (Grt). Bt, Hb, and cummingtonite (Cum) in the matrix are Cl-poor. These compositional differences imply that Bt included in the Grt formed under the presence of chloride brine and Cl-poor fluid infiltrated after Grt formation. Grt is enveloped by the gneissosity defined by the arrangement of Cum overgrown by Hb, and Bt. Therefore, chloride brine activity predated or was simultaneous with the penetrative gneissosity formation in this area. After considering the effect of Mg-Cl avoidance rule and compositional change during retrogression, the geothermobarometry (Holdaway, 2000; Wu et al., 2004) gave 650 $<T<$800 ℃ and 0.96 GPa for the peak *P-T* condition of this sample. The Cl-rich Bt entrapment was probably predated or simultaneous with the attainment of this *P-T* condition.

In a Grt-Opx-Hb gneiss, ca. 1cm-thick Grt-Hb vein cut the penetrative gneissosity in this area. Cl-content of Hb and Bt, and K-content of Hb decrease with the distance from the vein center and become constant at ca. 1.6 cm from the vein center. Plagioclase present next to the vein has a core (An_{55}) and mantle (An_{68}) which is sharply overgrown by Na-richer rim (An_{51}). Plagioclase in the vein is An_{51} without zoning, and development of Na-richer rim gets thinner with a distance from the vein. Therefore, the Grt-Hb vein was probably formed by NaCl-KCl brine infiltration. This is also supported by the isocon analysis of whole-rock chemistry determined for wall rock of the vein. *P-T* condition of the vein formation is estimated as 720 ℃ and 0.70 GPa (Holdaway, 2000; Wu et al., 2004).

P-T conditions of multi-stage chloride brine activity, cation composition of the brine, and outcrop-scale pathways of the brine are constrained in SRM from these two gneisses. From the pelitic gneisses in SRM, Cl-rich fluid or melt activity with a linear distribution over 200 km has been reported (Higashino et al., 2013). Additionally, this study revealed that the brine activity in SRM is not controlled by the lithology or specific deformational stages. It is clear that chloride brine in SRM was not a result of *in situ* fractionation through the selective consumption of H_2O in the fluid (Kullerud, 1995), but substantial amount of brine was actually moving, and was playing an important role in mass transfer.

Keywords: NaCl-KCl brine, fluid infiltration, continental collision zone, Sor Rondane Mountains

Japan Geoscience Union Meeting 2014
(28 April - 02 May 2014 at Pacifico YOKOHAMA, Kanagawa, Japan)

SMP46-13 Room:414 Time:April 28 16:45-17:00

Rate-limiting process and degree of disequilibrium of garnet-forming reaction

MIYAZAKI, Kazuhiro[1*]

[1]GSJ AIST

Water released by dehydration reaction in metamorphic rocks will take a major role in rheology, mass transport, and reactivity of metamorphic rocks. Rate-limiting process of the dehydration reaction can be divided into the following three steps, such as reaction at interface, diffusion, and heat-flow. Garnet is one of the common minerals produced by dehydration reaction in metamorphic rocks. The rate-limiting process of garnet-forming reaction is usually assumed to be diffusion-controlled reaction. However, there are few cases where clear evidences for diffusion-controlled reaction were proposed. In addition, degree of disequilibrium of the diffusion-controlled reaction is not well known. Here, I report evidence of diffusion-controlled reaction and estimation of degree of disequilibrium of garnet-forming reaction in the Tsukuba Metamorphic Rocks.

Garnets in the Tsukuba Metamorphic Rocks are formed by the dehydration reaction of biotite + sillimanite + quartz = garnet + cordierite + K-feldspar + water. Biotite-depleted region surround the irregular shaped garnet. The depleted region of reactant is typically expected for diffusion-controlled reaction, but is rare for natural garnet-forming reaction. Irregular shape of garnet is also expected for diffusional instability of growing interface (Mullins & Sekerka, 1963). These sets of observations strongly suggest that the garnets were formed by diffusion-controlled reaction.

Spherical shape of growing particle under diffusion-controlled reaction becomes unstable due to diffusional instability, but interfacial energy will reduce the instability. Using spherical harmonics function, instability of small perturbation from spherical shape can be evaluated. Assuming interfacial energy of garnet, dominant wavelength in unstable regime is predicted with degree of super-saturation under diffusion-limited reaction. Dominant wavelength of the irregular garnet suggests that degree of super-saturation is less than 0.1. This value can be translated to degree of disequilibrium temperature with entropy change of the garnet-forming reaction. The disequilibrium temperature $\triangle T$ is less than 5 ℃, and is very small. This small value of disequilibrium temperature suggests that spherical or euhedral garnets that are more common than irregular garnets, should be produced near equilibrium condition. Otherwise, such common spherical or euhedral garnets should be produced by interface-controlled reaction associated with influent fluid.

Keywords: garnet, dehydration reaction, disequilibrium, metamorphism, metamorphic rock, metamorphic reaction

Japan Geoscience Union Meeting 2014
(28 April - 02 May 2014 at Pacifico YOKOHAMA, Kanagawa, Japan)

SMP46-14 Room:414 Time:April 28 17:00-17:15

FLUID RELATED ORIGIN OF SILLIMANITE VEINS IN POLYMETAMORPHIC ROCKS FROM THE RYOKE BELT, JAPAN

AMANO, Saori[1*] ; KAWAKAMI, Tetsuo[1]

[1]Graduate School of Science, Kyoto University

In the polymetamorphic area, it is important to distinguish the effect of each metamorphism in order to appreciate the evolution of thermal structure of the area. Some authors have successfully distinguished the regional metamorphism from the postdating contact metamorphism (e.g. Miyake et al., 1992), but studies dealing with a fluid activity during polymetamorphism is not sufficiently available. Veins consisting of fibrous sillimanite (Sil) in a contact metamorphic aureole have been previously interpreted as a result of fluid activity (e.g. Johnson et al., 2003).

In Kasagi area (Kyoto, Japan), Ryoke metamorphic rocks are widely exposed and main lithology is pelitic and psammitic schists and gneisses. Younger Ryoke granites discordantly intrude to the metamorphic rocks and, therefore, the regional metamorphic rocks are overprinted by the heat (Ozaki et al., 2000) and fluid flux from the granites. This area belongs to the Sil zone that is defined by the presence of Sil in the pelitic lithology (Ozaki et al., 2000) whose origin has not been discussed in detail.

However in this area, fibrolite bundles are often observed to cross-cut the gneissosity formed by the regional metamorphism and it seems difficult to explain their formation during the regional metamorphism. In this study, we report the mode of occurrence of Sil veins emanating from the granite into psammitic gneiss and discuss the fluid-related origin of them.

The studied psammitic gneiss containing Sil veins is collected from the Sil zone near the granite intrusion contact. Ryoke granite intrudes discordantly to the gneissosity of this sample, and the Sil vein subparallel to the gneissosity emanate from it. The Sil vein consists of fibrolite and retrograde muscovite (Ms) replacing it. Quartz (Qtz) in the matrix near the vein are coarser-grained and they include fibrolite grains. The amount of fibrolite included in the Qtz decreases as a distance from the Sil vein increases. Fibrolite is present in veins and Qtz grains. Fine, retrograde Ms after fibrolite is present along grain boundaries in the matrix. Although plagioclase (Pl) is a common constituent mineral in the matrix, it is almost completely absent near and in the Sil veins. K-feldspar is absent in the studied sample, but instead, retrograde Ms cutting the schistosity is abundant in the matrix.

Cathodoluminescence (CL) observation of the microstructures around the Sil veins revealed that the brightness of CL signal of Qtz grains increases as the distance from the Sil vein increases. That is, Qtz grains near the vein or including Sil are dark under CL observation. In particular, part of a single Qtz grain including more fibrolite grains appears dark under CL image.

From the observation of microstructural relationships described above, we consider that Sil veins were formed by the fluid released from the Ryoke granite. Formation of fibrous Sil by the action of mobile hydrogen ions on pre-existing minerals has been previously discussed (Vernon, 1979). Moreover, experimental work has shown that Al2SiO5 minerals and Ms can be produced by the action of acidic, aqueous solutions on various common silicate minerals (Burnham, 1967). In this study, fibrolite is present in veins and Qtz grains and the amount of fibrolite crystals included in the Qtz crystals decreases as a distance from the vein increases. Pl is absent in and at the vicinity of the veins. From these pieces of observation, a fluid from the granite would have reacted with the matrix to dissolve Pl and to form coarser-grained Qtz and fibrolite bundles simultaneously. Thermodynamic calculation using SUPCRT92 (Johnson et al. 1992) has revealed that infiltration of the aqueous fluid with low Na+/H+ and K+/H+ ratio can destabilize Pl and stabilize Sil under the presence of Qtz at 3 kbar, 600oC. Therefore, Sil in this study is not regional metamorphic in origin, but is probably a result of fluid infiltration during a contact metamorphism by the Ryoke granite.

Keywords: fibrous sillimanite, Ryoke belt, fluid-related origin, polymetamorphism

Japan Geoscience Union Meeting 2014
(28 April - 02 May 2014 at Pacifico YOKOHAMA, Kanagawa, Japan)

SMP46-P01 Room:Poster Time:April 28 18:15-19:30

Comparison of UHP chromitites from the Higo and Nishisonogi Metamorphic Rocks, Kyushu, Japan.

SHIOSAKI, Dai[1*] ; MORIBE, Yosuke[1] ; EGUCHI, Hibiki[1] ; NISHIYAMA, Tadao[1]

[1]Department of Earth and Environmental Sciences, School of Science and Technology Kumamoto University

We have found microdiamond - bearing ultrahigh-pressure (UHP) chromitites from two metamorphic terranes in Kyushu: the Higo (HMR)[1] and Nishisonogi (NMR)[2] Metamorphic Rocks. This paper describes the similarity and difference between the two UHP chromitites. The HMR are located in west-central Kyushu with an E-W trend. They have undergone low P /T metamorphism, however, precursor HP or UHP metamorphism of ca. 250 Ma has been inferred[3]. The protoliths have affinity to continental shelf deposits[4], consisting mainly of pelitic gneisses and meta-carbonates with minor metabasites and metaperidotites (partly serpentinite). Chromitite occurs very rarely as a nodular form in serpentinized metaperidotites which shows spinifex-texture. The NMR is located in western Kyushu with a N-S trend. They have undergone high P /T metamorphism of epidote-blueschist subfacies. They consists mainly of pelitic and psammitic schists with minor basic schists and serpentinites, some of which show a character of serpentinite melange[5]. Detrital zircon from the pelitic schists show the age of 89-86 Ma[6], whereas zircon from jadeitites in a serpentinite melange does 136 -126 Ma in the core and 84 - 80 Ma in the rim[7,8]. Chromitite occurs as a deformed schlieren-like layer in serpentinite with no reilc minerals. The P-T condition of the HMR has been estimated to be 200 - 600 MPa and 600 - 800 ℃ [3,9,10,11,12,13]. Higher pressure and temperature conditions are reported from the following two samples: a sapphirine-bearing granulite[3,10] as a tectonic block in the spinifex-textured metaperidotite (900 MPa and 950 ℃) and a calc-silicate granulite[13] (900 MPa and 820 ℃) intercalating with garnet - biotite gneiss. We newly estimated the peak P-T condition of Al-spinel and chlorite -bearing metaperidotite as 2.0 GPa and 780 - 990 ℃. In the case of the NMR, the peak metamorphic condition of the crystalline schists is 1.4 GPa and 520 ℃ for a garnet galucophanite[14]. Jadeitites[15] as tectonic blocks in the serpentinite melange shows the peak condition of 1.5 GPa and 500 ℃. Chromite from the HMR has the composition $(Mg_{0.34}Fe^{2+}{}_{0.75}Mn_{0.02})(Cr_{0.81}Al_{0.06}Fe^{3+}{}_{0.04}Si_{0.05)2}O_4$, whereas that from the NMR has similar composition $(Mg_{0.33}Fe^{2+}{}_{0.65}Mn_{0.03})(Cr_{0.84}Al_{0.12}Fe^{3+}{}_{0.04})_2O_4$ in the core and Fe-rich composition $(Mg_{0.06}Fe^{2+}{}_{0.89}Zn_{0.02}Mn_{0.03})(Cr_{0.85}Al_{0.12}Fe^{3+}{}_{0.04})_2O_4$ in the rim. Microdiamonds occur as i*n situ* inclusions in chromite in both chromitites. They are 1 to 10 μm in size in HMR chromite, and those in NMR chromite is much smaller, mostly <1 μm with small number of larger grains. In both chromitites microdiamonds occur in some cases as numerous aligned grains, making diamond - rich zones. Both microdiamonds are identified with Raman spectra. HMR microdiamonds show a broad peak at 1333 cm^{-1}. NMR microdiamond, also shows a broad peak at 1331 cm^{-1} with graphite peak at around 1600 cm^{-1}, suggesting partial graphitization. Both UHP chromitites will be deep subduction origin. HMR can be an eastern extension of the Dabie-Sulu UHP terrane in China, however, NMR is more problematic. No corresponding UHP terrane of ca. 80Ma is found around Kyushu. Our findings of UHP chromitites require reexamination of micro-tectonics in Kyushu, a peculiar location of an arc-arc junction at the continental margin.

References 1:Nishiyama et al., JpGU Meeting, S-MP46, 2014; 2: Nishiyama et al., JpGU Meeting, S-CG08, 2014; 3: Osanai, et al., Gondwana Res.,9, 152-166, 2006; 4: Omori and Isozaki, J.Geogr., 120, 40-51, 2011; 5: Nishiyama, Mem. Geol. Soc. Japan, 33, 237-257, 1989; 6: Kouchi, Y., J. Geogr., 120, 30-39, 2011; 7: Mori, et al., JMG, 29, 673-684, 2011; 8: Yui, et al., EJM., 24, 263-275, 2011; 9: Obata et al., Lithos, 32, 135-147, 1994; 10: Osanai et al., JMG., 16, 53-66, 1998; 11: Maki et al., JMPS, 99, 1-18, 2004; 12: Miyazaki, JMG., 22, 793-809, 2004; 13: Maki et al., JMG., 27, 107-124, 2009; 14: Moribe, Mc thesis, Kumamoto U.; 15: Shigeno et al., EJM, 24, 289-311, 2012

Keywords: microdiamond, chromitite, UHP, Higo metamorphic rocks, Nishisonogi metamorphic rocks, subduction

Japan Geoscience Union Meeting 2014
(28 April - 02 May 2014 at Pacifico YOKOHAMA, Kanagawa, Japan)

SMP46-P02 Room:Poster Time:April 28 18:15-19:30

3D imaging of the Mn-caldera shaped zoning of the garnet found from the Sanbagawa metamorphic belt and its origin.

YOSHIDA, Kenta[1*] ; HIRAJIMA, Takao[1]

[1]Graduate School of Science, Kyoto University

Garnets with a complex compositional zoning were found from the northern proximal area of the Western Iratsu body of the Sanbagawa metamorphic belt of the Besshi district, southwest Japan. The studied garnet shows incipient Mn-reverse (increasing) zoning part (defined as core) and subsequent Mn-bell shape (decreasing) zoning part (defined as mantle), which is almost identical to the " Mn-caldera shaped zoning " described by Banno et al. (2004) in the Asemigawa region of the central Shikoku. In order to describe the chemical characteristic sterically, X-ray chemical mapping were performed by each 0.2-0.3 mm depth step, for one very-coarse-grained garnet with ca. 11 mm in diameter. The result clearly shows that the core/mantle boundary has the highest Mn content with euhedral shape, and that the chemical composition continuously changes through the grain. Internal schistosity defined by sigmoidal inclusion arrays cross-cuts the core/mantle boundary. This fact also suggests the continuous growth of garnet from the central part to the outer part. In the same sample, garnets with Mn-bell shape type zoning are also observed, which are relatively fine-grained up to 5 mm. Raman barometry and thermodynamic modeling suggest the climax *P-T* conditions of the studied sample did not reach the eclogite facies, which are consistent with the conditions of the oligoclase-biotite zone of the Sanbagawa metamorphic belt (610 ℃ and 1.0 GPa, Enami, 1994).

Contrary to the simple Mn-bell shape type zoning which grown up with progressive regional metamorphism, " Mn-caldera shaped zoning " could be generated from the crystal nucleation under oversaturated environment (Matsumoto and Kitamura, 2004). Such oversaturation is expected in a rapid increase of temperature. Recently, Aoya et al. (2013) proposed the eclogite nappe covering the large part of the Besshi district. However, the exact boundary between the eclogite nappe and lower grade surrounding rocks is still under the debate. The conjunction of the eclogite nappe and the lower-grade surrounding rocks are thought to have taken place near the peak metamorphic stage of the surrounding rocks (500-600 ℃ and ca. 1 GPa, Aoya et al., 2013). Mn-caldera shaped zoning garnet found in the Besshi district (this study; Xu et al., 1994) are both found from the northern proximal of the hypothesized eclogite nappe. Those Mn-caldera shaped zonings are possibly originated from the conjunction of the eclogite nappe and surrounding crystalline schist, and corresponding rapid heating. Such features of garnet can help to determine the boundary of the eclogite nappe in the Besshi district.

Keywords: garnet, Sanbagawa metamorphic belt, compositional zoning, disequilibrium crystal growth

Japan Geoscience Union Meeting 2014
(28 April - 02 May 2014 at Pacifico YOKOHAMA, Kanagawa, Japan)

SMP46-P03 Room:Poster Time:April 28 18:15-19:30

Widespread analyses of pressure-temperature trajectory and timing in the Altai Range, Mongolia

NAKANO, Nobuhiko[1*] ; OSANAI, Yasuhito[1] ; OWADA, Masaaki[2] ; SATISH-KUMAR, M.[3] ; ADACHI, Tatsuro[1] ; JARGALAN, Sereenen[4] ; YOSHIMOTO, Aya[1] ; KUNDYZ, Syeryekhan[4] ; BOLDBAATAR, Chimedtseie[5]

[1]Kyushu University, [2]Yamaguchi University, [3]Niigata University, [4]Mongolian University of Science and Technology, [5]Mongolian Exploration Partners, LLC

This study performed large-scale petrographical and geochronological investigation in the Altai Range, Mongolia distributed in the Central Asian Orogenic Belt, which is the typical subduction-accretion-collision orogeny on the Earth. Based on the petrographical observation, clockwise and anti-clockwise pressure-temperature trajectories were identified in whole of the studied area (400 km long). U-Th-Pb monazite dating yields c. 350 Ma and c. 260 Ma. Samples with clockwise pressure-temperature path, containing kyanite in garnet and sillimanite in the matrix, commonly have c. 350 Ma monazite in garnet and c. 260 Ma monazite in the matrix. In contrast, samples with anti-clockwise pressure-temperature path containing sillimanite in garnet and kyanite in the matrix have monazites showing (i) c. 350 Ma both in garnet and the matrix, (ii) c. 260 Ma both in garnet and the matrix, and (iii) c. 350 Ma in garnet and c. 260 Ma in the matrix. Ca zoning pattern in garnet shows either continuous or discontinuous zoning. Samples containing single monazite age cluster (either c. 350 Ma or c. 260 Ma) have continuously zoned garnet, in which samples with anti-clockwise pressure-temperature trajectory at both periods show Ca zoning increasing from core to rim or mantle, whereas some samples with unknown pressure-temperature path at both periods show opposite zoning. These features strongly suggest both clockwise and anti-clockwise evolutions occurred at both periods. Discontinuous Ca zoning in garnet is observed in samples that contain c. 350 Ma monazite inclusions in garnet and c. 260 Ma monazite grains in the matrix, and the zoning patterns show a decrease in Ca at the rim for samples with clockwise paths and an increase in Ca at the rim for those with counterclockwise paths. In some cases, c. 350 Ma monazite grains are included in the large garnet cores but c. 260 Ma monazite grains are found in the garnet rims as well as in the matrix. These rocks might be metamorphosed at c. 350 Ma, whereas they did not exhume to the surface and have remained deep crustal level. Subsequent compression and decompression event formed garnet rim and monazite at c. 260 Ma, which should be caused by same tectonic regime to clockwise and anti-clockwise pressure-temperature path at the period. The presence of the regional-scale clockwise and anti-clockwise trajectories and their repetition during less than 100 My have never reported from any other orogenic belts in the world. Further studies may allow to realize the complex tectonic evolution of the Altai Range.

Keywords: P-T trajectory, U-Th-Pb monazite age, Altai Mountains, Mongolia, Central Asian Orogenic Belt

Japan Geoscience Union Meeting 2014
(28 April - 02 May 2014 at Pacifico YOKOHAMA, Kanagawa, Japan)

SMP46-P04 Room:Poster Time:April 28 18:15-19:30

Temporal change of modal abundance of minerals during formation of arrested charnockite from Sri Lanka

YAMASAKI, Yukiko[1*] ; IKEDA, Takeshi[1] ; MOTOYOSHI, Yoichi[2] ; HIROI, Yoshikuni[3] ; PRAME, Bernard[4]

[1]Kyushu University, [2]National Institute of Polar Research, [3]Chiba University, [4]Geological Survey of Sri Lanka

Charnockite occurs as a number of several-decimeters patches in hornblende-biotite gneiss in central Sri Lanka. This type of charnockite has been called arrested charnockite. Local condition of low-H_2O activity or low-oxygen fugacity could explain the difference of mineral assemblage in local scale. They might be caused by fluid influx and/or partial melting (e.g. Newton et al., 1980; Hiroi et al., 1990; Burton and O'Nions, 1990; Ravindra Kumar, 2004; Endo et al., 2012). The temporal and spatial development of charnockite has been unclear. This study describes variation in modal abundance of hornblende, biotite and orthopyroxene in melanocratic and leucocratic parts from surrounding gneiss to charnockite.

Charnockite and surrounding gneiss have layer structure composed of melanocratic and leucocratic parts. Each part can be traced continuously between the two rock types. Melanocratic parts consist mainly of hornblende and biotite in gneiss, and orthopyroxene added in charnockite. Leucocratic parts are composed of biotite and colorless minerals in gneiss, while biotite is absent in charnockite. Modal abundances of hornblende and biotite have no systematic trend in melanocratic parts of gneiss. Hornblende and biotite decrease drastically and gradually, respectively, while orthopyroxene increases gradually in melanocratic parts of charnockite. Biotite decreases gradually toward charnockite in leucocratic parts in gneiss.

Biotite of leucocratic parts breaks down within gneiss. Orthopyroxene appears in the location of dehydration reaction of biotite and hornblende in melanocratic parts. This suggests that the element released due to break down of biotite in leucocratic layer diffused from leucocratic part to melanocratic part to produce orthopyroxene. It is a possible that hornblende broke down first to produce significant amount of orthopyroxene in melanocratic part. The element released due to break down of biotite in leucocratic part transported to the location of preexisting orthopyroxene in order to grow the crystals. Biotite in leucocratic layers is enriched in Fe as compared with that in melanocratic part. Fe-rich biotite breaks down under lower temperature (or higher activity of H_2O) than Mg-rich biotite. This could explain the decrease of biotite in leucocratic layer in gneiss.

Reference

Burton K. W. and O'Nions R. K., The timescale and mechanism of granulite formation at Kurunegala, Sri Lanka, Contrib. Mineral. Petrol. 106, 66-89 (1990)

Endo et al., Phase equilibrium modeling of incipient charnockite formation in NKCFMASHTO and MnNCKFMASHTO systems: A case study from Rajapalaiyam, Madurai Block, southern India, Geoscience Frontiers 3, 801-811 (2012)

Hiroi Y. et al., Arrested charnockite formation in Sri Lanka: Field and petrographical evidence for low-pressure conditions, Proc. NIPR Symp. Antarct. Geosci. 4, 213-230 (1990)

Newton R. C. et al., Carbonic metamorphism, granulites and crustal growth, Nature 288, 45-50 (1980)

Ravindra Kumar G. R., Mechanism of arrested charnockite formation at Nemmara, Palghat regiom, sourthern India, Lithos 75, 331-358 (2004)

Keywords: Sri Lanka, Charnockite, Hornblende-biotite gneiss, modal abundance

Japan Geoscience Union Meeting 2014
(28 April - 02 May 2014 at Pacifico YOKOHAMA, Kanagawa, Japan)

SMP46-P05 Room:Poster Time:April 28 18:15-19:30

Thermal structure and water transportation in subduction zones: a comparison between NE and SW Japan

ISHII, Kazuhiko[1*] ; OKUNO, Masashi[1]

[1]Graduate School of Sciences, Osaka Prefecture University

Northeastern and southwestern Japan are considered to be typical examples of cold and hot subduction zones, respectively. The old Pacifc plate subducts beneath northeastern Japan at high rate and the young Philippine Sea plate subducts beneath southwestern Japan at low rate. These contrasts in the subduction conditions reveals in several aspects including higher activity of arc volcanism and deeper down dip limit of inter-plate earthquake in northeastern Japan, and deep low-frequency tremors at plate boundary of southwestern Japan. We have investigated thermal structure and geophysical and geochemical processes in these subduction zones using a numerical model. The model includes hydration and dehydration of the slab and mantle wedge, melting and solidification of mantle peridotites, permeable flow of melt and aqueous fluids, and temperature-dependent solid flow of mantle peridotites with water- and melt-induced weakening. We will discuss effects of the subduction conditions on the volcanic and seismic activities through the processes, especially water transportation.

Keywords: subduction zones, NE Japan nad SW Japan

Japan Geoscience Union Meeting 2014
(28 April - 02 May 2014 at Pacifico YOKOHAMA, Kanagawa, Japan)

SMP46-P06 Room:Poster Time:April 28 18:15-19:30

Stress and strain history during the microboudinage for granite intrusion: Mt. Edger granite complex, East Pilbara

MATUMURA, Taroujirou[1*] ; KIMURA, Nozomi[2] ; OKAMOTO, Atsushi[3] ; MASUDA, Toshiaki[2]

[1]Graduate school of science and Technology, Shizuoka University, [2]Institute of Geoscience, Shizuoka University, [3]Graduate school of Environmental studies, Tohoku University

Stress and strain analysis is essential to improving the understanding of deformation process. Microboudinaged columnar minerals can be used as an indicator of stress and strain during the microboudinage for quartzose and calcareous metamorphic tectonites. In this presentation, we discuss the stress and strain history during the microboudinage deduced by the microboudin method with a collaboration of the strain reversal method.

We collected samples of metachert from the Archean Warrawoona greenstone belt around Mt. Edger granite complex, East Pilbara, Western Australia, and identified microboudinaged tourmaline grains embedded within quartz matrix in 10 samples. The result revealed that the samples experienced extensional strain at least -0.56 and differential stress in the range from 3.9 to 11.9 MPa. We obtained stress-strain curves which show increase in differential stress with increasing inverse natural strain (ε_{inv}). The frequency distribution of interboudine gaps between separated grains with respect to ε_{inv} for boudinaged tourmaline grains shows that end of microboudinage occurred immediately after the peak frequency of fracturing. This occurrence commonly appeared in all the 10 samples. These results provided us with keys to discuss a stress-strain history during the microboudinage in relation to evolution of the granite complex. The spectacular implication would be a drop or relaxation in increased differential stress at the end of the microboudinage.

Keywords: microboudin structure, stress, strain, granite complex, Archean

Japan Geoscience Union Meeting 2014
(28 April - 02 May 2014 at Pacifico YOKOHAMA, Kanagawa, Japan)

SMP46-P07 Room:Poster Time:April 28 18:15-19:30

Time scale for formation of diffusion zoning in response to breakdown reaction

IKEDA, Takeshi[1*]

[1]Kyushu University

In high-grade metamorphic rocks, garnet commonly represents an increase in Mn or Fe toward margin. This feature has been interpreted as diffusion zoning owing to garnet-consuming reactions during retrograde metamorphism. In this process, the zoned thickness can be described in terms of distances of internal diffusion and surface retreating. This study preliminaly formulated to express these distances as a function of time and retreating velocity of the surface. Applying the formulation to some high-temperature metamorphic belts yielded that the diffusion zoning with zoned thickness of 0.04 to 0.1 mm was formed by 1 to several million years. This result may be applied to estimate cooling rate provided that the surface equilibrium was mainetained during the formation of diffusion zoning.

Keywords: diffusion zoning, duration time, cooling rate

Japan Geoscience Union Meeting 2014
(28 April - 02 May 2014 at Pacifico YOKOHAMA, Kanagawa, Japan)

SMP46-P08 Room:Poster Time:April 28 18:15-19:30

Integrated radiometric dating of schist clasts from the Eocene and Miocene conglomerates in Shikoku

IIZUKA, Ryota[1*] ; TAKAGI, Hideo[1] ; HONDA, Emi[1] ; IWANO, Hideki[2] ; ISHIDA, Akizumi[3] ; SANO, Yuji[3]

[1]Waseda University, [2]Kyota Fission-Track Co. Ltd., [3]AORI, the University of Tokyo

The age that the high P/T type Sanbagawa metamorphic rocks reached at erosion level gives an important constraints for considering exhumation processes of the Sanbagawa metamorphic rocks. It is shown by the oldest age of the conglomerate containing schist clasts derived from the Sanbagawa Belt. Integrated radiometric dating has been carried out for schist clasts from the Paleogene and Neogene conglomerates in Shikoku. The results of K-Ar and fission-track (FT) ages for the schist clasts from the Eocene Hiwadatoge Formation and the Miocene Furuiwaya Formation (Kuma Group) were already reported (Takagi and Sakisaka, 2012; Takagi et al., 2013). We have been doing U-Pb dating of zircon grains from the same clasts for the FT dating using NanoSIMS 50 ion microprobe of AORI. The youngest U-Pb age of zircon grains approximates the sedimentary age of the protoliths of the schist, because the zircon grains in the low-grade metamorphic rocks are detrital origin. The tentative results shown by the youngest peak yield around 110 Ma in all samples. We will report on details of the U-Pb ages at the meeting. FT dating was also carried out for the schist clasts from Eocene Oyamamisaki Formation in the Shimanto Belt where K-Ar ages (78.2-71.4 Ma) of the clasts have been already reported by Yoshikura et al (1991). The FT ages were 67.3 +/- 9.0 Ma and 68.4 +/- 8.2 Ma. From the results of K-Ar phengite ages and FT zircon ages for schist clasts (Table 1), it is suggested that the exhumation rate of the schist eroded at Eocene time is faster than that eroded at Miocene time.

References :
Takagi and Sakisaka, 2012, 119th Geol. Soc. Japan Congress, Abstracts, p.93.
Takagi et al., 2013, 120th Geol. Soc. Japan Congress, Abstracts, p.49.
Yoshikura et al., 1991, 98th Geol. Soc. Japan Congress, Abstracts, p.434.

Keywords: Sanbagawa belt, schist, radiometric dating

Table1. Phengite K-Ar and zircon fission track ages of schist clasts from the Miocene and Eocene strata in Shikoku.

Series	Formation Name		Sample	Phengite K-Ar age (Ma)	Zircon FT age (Ma)
Miocene	Kuma Group	Furuiwaya Formation	32204-2 psamm.sch.	81.5 ± 1.3	68.7 ± 6.0
			112101-2 pel.sch.	83.5 ± 1.3	64.9 ± 5.8
Eocene	Hiwadatoge Formation		2003-8 psamm.sch.	86.8 ± 1.3	85.2 ± 7.7
	Oyamamisaki Formation		1-B psamm.sch.	78.2 ~ 71.4 (Yoshikura et al., 1991)	67.3 ± 9.0
			1-F psamm.sch.		68.4 ± 8.2

Japan Geoscience Union Meeting 2014
(28 April - 02 May 2014 at Pacifico YOKOHAMA, Kanagawa, Japan)

SMP46-P09 Room:Poster Time:April 28 18:15-19:30

The metamorphic evolution from PrP to LBS facies in a late Paleozoic cold subduction system in Kurosegawa belt

SATO, Eitaro[1*] ; HIRAJIMA, Takao[1]

[1]Graduate School of Science, Kyoto University

Introduction: Recent progress of thermal modeling and thermodynamic calculation can help the general understanding of the thermal structure of subducting plate and the total movement of H2O stored in high-pressure type metamorphic rocks from the trench to the upper mantle depth in various subduction settings (e.g., Peacock & Wang, 1999; Hacker et al., 2003). For example, Peacock (2009) indicated that the oceanic plate in the Philippine Sea plate subducting below the Kii Peninsula would suffer the cold HP/LT type metamorphism represented by zeolite facies, prehnite-pumpellyite facies, pumpellyite-actinolite facies, lawsonite-blueschist facies to jadeite-lawsonite-blueschist to 2GPa. However, the natural example recording abovementioned progressive metamorphic evolution has not been recognized yet.

Recently prehnite-pumpellyite facies and lawsonite-blueschist facies units have been recognized in the Otao unit of Kurosegawa belt in Yatsushiro area, Kyushu, Japan (Kamimura et al., 2012). However, the relationship of two metamorphic units has not been verified yet.

In this paper, we propose the progressive change of metamorphic grade from the prehnite-pumpellyite facies to lawsonite-blueschist facies based on petrography and thermodynamic phase analysis in metabasite system.

Petrography and Mineralogy: We confirmed that the prehnite-pumpellyite facies assemblage is predominant in the Tobiishi subunit of (Kamimura et al., 2012), but we newly found pumpellyite-actinolite facies from the western end of this subunit.

In the lawsonite-blueschist facies unit, Hakoishi-subunit of (Kamimura et al., 2012), located to the west of the Tobiishi-subunit, following mineral assemblage with excess chlorite, quartz, albite and phengite are systematically distributed from the east to the west in the subunit:

lawsonite + pumpellyite + aegirine-augite,pumpellyite + Na-amphibole,lawsonite + pumpellyite + Na-amphibole, lawsonite + Na-amphibole + aegirine-augite.

The compositions of sodic pyroxene, pumpellyite and Na-amphibole also show the following systematic trend westwards in the subunit; jadeite component of sodic pyroxene generally increases from XJd=0.12 to XJd=0.50 with XAeg= up to 0.5. Al content of pumpellyite increases from 3.7 to 4.6 p.f.u. for O=24.5 Fe3+/(Al+Fe3+) in Na-amphibole decreases from 0.8 (riebeckite) to 0.15 (glaucophane).

Thermodynamic phase analysis: To evaluate stability relationship among abovementioned mineral assemblages, the phase diagram was construct-ed in the NCFMASH system with PERPLE_X soft-ware package (Connolly, 2005) for 1-10 kbar and 100-400 C. The considered minerals are stilbite, laumontite, prehnite, pumpellyite, ferro pumpellyite, tremolite, ferro tremolite, diopside, hednbargite, clinochlore, daphnite, lawsonite, glaucophane, ferro graucophane, clinozoisite and albite with excess, quartz and water. As the first order approximation, solid solution in each mineral was ignored. The new-ly constructed phase diagram predicts following representative mineral assemblages appear with the increase of the pressure along the high HP/LT path.

lawsonite + pumpellyite + clinopyroxene,pumpellyite + glaucophane,lawsonite + pumpellyite + glaucophane,lawsonite + glaucophane + clinopyroxene.

This metamorphic evolution in the model system is coincident well with the natural observation in the Hakoishi subunits.

Conclusion: Mineral assemblages observed in metabasites of the Tobiishi and Hakoishi subunits and the newly constructed petrogenetic grid suggest the metamorphic grade increases from prehnite-pumpellyite facies to lawsonite-blueschist facies westward ca. 20km in the Otao unit of Kurosegawa belt. The westward increase of Al content in pumpellyite, Na-amphibole, and Na- clinopyroxene also suggest the metamorphic grade increases westward. Thus, this area would become a type locality of a cold subduction system as proposed by the Peacock (2009)s thermal modeling.

Keywords: lawsonite, blueschist, HP/LT type metamorphic rocks, Kurosegawa belt, petrogenetic grid, cold subduction system

Japan Geoscience Union Meeting 2014
(28 April - 02 May 2014 at Pacifico YOKOHAMA, Kanagawa, Japan)

SMP46-P10 Room:Poster Time:April 28 18:15-19:30

Morphological change of zircon under high temperature metamorphism: Example of the Kiso Ryoke metamorphic rocks

IKAWA, Chiaki[1*] ; MOTOYOSHI, Yoichi[2] ; HOKADA, Tomokazu[2] ; HORIE, Kenji[2]

[1]Department of Polar Science, the Graduate University for Advanced Studies, [2]National Institute of Polar Research

Zircon is an important key mineral to obtain the age of rocks, however zircon newly grew at each metamorphic cycle and its timing of crystallization should have been recorded as U-Pb age. It is not always fully understood how zircon crystal grows at different metamorphic grade. Williams (2001) demonstrated that the behavior of zircon has been changed accompanying with metamorphic grade in Cooma complex, SE Australia. In low grade, there are detrital zircons but in high grade, overgrown or newly formed zircons are observed. Kawakami et al (2013) reported the behavior of zircon in the upper-amphibolite to granulite facies schist/migmatite transition, Aoyama area, Ryoke metamorphic belt. They concluded that the recrystallization of zircon has been controlled by partial melt. Thus, crystal morphology is quite important for understanding the U-Pb age of zircon.

This study reports morphological change of zircon crystal at different metamorphic grades in the Kiso area, Ryoke metamorphic belt in Central Japan, where metamorphic grade continuously increases from non-metamorphic (Mino belt) to migmatite facies, similar with Cooma complex. The district is located in northeastern part of Mt. Kisokomagatake and the study area is about 43km from north to south, and about 22km west to east. In this district, regional metamorphic rocks (metasediments, quartz schist, basic schist, and carbonate rocks, etc.) and non-metamorphic rocks widely occur. Morikiyo (1984) classified the district into nine mineral zones (I to VII) based on the mineral assemblages.

We have studied total 46 samples from all zones. Mineral assembles of the studied samples indicate the following characteristics features: biotite appears in zone II, albite disappears in zone IIIa, chlorite disappears in zone IIIb and sillimanite appears in zone VIa.

On the basis of the optical microscope and SEM observations, morphology of zircon is divided into 3 groups, such as zones I-II, zones IIIa-V and zones VIa-VII.

Zones I-II: Under the optical microscope, each zircon grain shows different color (purple, pale-pink and colourless). Zircon grains are essentially euhedral, and show variable range of grain size (40-220 um). In SEM observation, the abrasion and cracks are notable in zircon crystal surface. The above observations are consistent that the zircons in these zones are detrital origin that were derived from a variety of different source rocks.

Zones IIIa-V: Surface of zircon in these zones are irregular and rough with small holes which are likely to reflect resorption during the metamorphism. In contrast with the zircons from zones I-II, zircon crystal surface is relatively rough and shows no abrasion and cracks. But, even in the same zircon grain, both resorption surface and non-resorption surface can also be observed. Non-resorption surface is considered to preserve detrital surface (same with zone I-II), and resorption surface possibly reflects metamorphic dissolution or recrystallization (similar to zone VIa-VII). According to BSE images, no obvious new growth zone can be observed in many of zircon grains, but a few grains show sign of new overgrowth zone. Grain size of newly growing zircon is relatively small about 30um.

Zones VIa-VII: Surface of zircon in these zones is relatively smooth, which differs from rough crystal surface in zones IIIa-V. It is assumed that the irregular surface of zone IIIa-V zircons are overgrown and filled by smooth surface as temperature increases to zones VIa-VII. In the highest-grade zone VII, the rough surface is disappeared, and smooth zircon grains are dominated.

Thus in the Ryoke metamorphic rocks from Kiso area, crystal morphology of zircons changes from the dominant detrital signature in the lowest-grade zone through irregular and rough resorption and recrystallization features in the middle-grade zone to the more smooth overgrowth recrystallization in the higher-grade. New zircon grain growth can be found in the middle to higher-grade zone.

Keywords: zircon morphology, regional metamorphism, Ryoke belt

Japan Geoscience Union Meeting 2014
(28 April - 02 May 2014 at Pacifico YOKOHAMA, Kanagawa, Japan)

SMP46-P11 Room:Poster Time:April 28 18:15-19:30

P-T estimates of a metapelite containig garnet zoning from Mefjell, Sr Rondane Mountain, East Antarctica

TSUBOKAWA, Yumiko[1*] ; ISHIKAWA, Masahiro[1] ; ICHIKI, Takashi[1] ; KAWAKAMI, Tetsuo[2] ; MADHUSOODHAN, Satishkumar[3] ; TSUCHIYA, Noriyoshi[4] ; GEOFF, Grantham[5]

[1]Yokohama National University, [2]Kyoto University, [3]Niigata University, [4]Tohoku University, [5]Council for geoscience, South Africa

The Sør Rondane Mountains, East Antarctica have been considered to be situated in the Gondwana suture zones. Therefore the mountains have attracted interest as a key area for understanding amalgamation process of the supercontinent. The mountains consist of amphibolite- to granulite-facies metamorphic rocks with granitic intrusions, and the timings of the main metamorphism are interpreted as *c*. 640-600 Ma and *c*. 550-500 Ma. Metamorphic rocks from northern and eastern part of the mountains (Balchenfjella and northern part of Austkampane) record a clockwise *P-T* path, on the other hand, metamorphic rocks from central part of the mountains (Brattnipene and eastern Menipa) record anti-clockwise *P-T* path. This suggests each area records a different *P-T* path. However, pre-peak *P-T* conditions of southwestern part of the mountain such as Mefjell have been still not clear.

In this study, we report a garnet porphyroblast with a prograde zoning in a metapelite from Mefjell. The St-bearing Grt-Sil-Bt gneiss mainly consists of garnet, biotite, sillimanite, quartz and plagioclase, with minor K-feldspar, staurolite, apatite, monazite, ilmenite and magnetite. The garnet grain is 12 mm in diameter, with the change of color from reddish in the core to transparent in the rim. The garnet has core-rim boundary defined by Mn-zoning. The garnet is typically almandine-rich, and shows compositional zoning with decrease in spessartine content from the core ($Alm_{63}Sps_{24}Prp_{14}Grs_{6}$) to the rim ($Alm_{74}Sps_{2}Prp_{20}Grs_{4}$), and spessartine content increase again towards the outer-rim ($Alm_{73}Sps_{11}Prp_{20}Grs_{6}$). The garnet includes staurolite, sillimanite, biotite, chlorite, plagioclase, K-feldspar, quartz, apatite and ilmenite. Garnet-ilmenite and staurolite-garnet geothermometers yield a temperature increase towards rim from 350-400 to 630-700 ℃. Garnet-Al_2SiO_5-quartz-plagioclase geobarometer applied to rim inclusions yields 7.2kbar±0.9kbar for an assumed temperature of 650 ℃.

Keywords: East Antarctica, Sør Rondane Mountain, pressure and temperature conditions

Japan Geoscience Union Meeting 2014
(28 April - 02 May 2014 at Pacifico YOKOHAMA, Kanagawa, Japan)

SMP46-P12 Room:Poster Time:April 28 18:15-19:30

Syn-metamorphic fluid infiltration and petrogenesis of leucogranites in the MCT zone in Eastern Nepal

KAWAKAMI, Tetsuo[1*] ; SAKAI, Harutaka[1] ; SATO, Katsushi[1]

[1]Graduate School of Science, Kyoto University

Syn-metamorphic fluid activity in the continental collision zone is of great importance especially for the petrogenesis of leucogranites and mass transfer through the fluid/melt extraction. Tourmaline (Tur) is a common accessory mineral in the crust having a wide stability field [1]. It is the most important sink of B in metapelites [2, 3, 4]. Although B behaves incompatibly under the absence of its sink minerals and is transported in fluid, once the *P-T-X* condition permits, it can be precipitated as Tur and other borosilicates in the site of fluid/rock interaction. Therefore, Tur can be a good tracer of B-bearing fluid [4]. Since Tur is a polar mineral, different concentrations of cations are incorporated at opposite poles of the crystal as a function of temperature up to 650^{o}C, and this interpolar element partitioning in Tur can be used as a geothermometer [2, 5].

We have investigated the mode of occurrence of Qtz veins and Tur-rich veins in the MCT zone around Dhankuta, Eastern Nepal. In this area, pelitic schists are widely exposed and subordinate amounts of metamorphosed dolostone, quartzite and mafic rocks are intercalated with them. The metamorphic grade decreases from the Ky zone through the St zone to the Grt zone as the distance from the MCT increases toward the south.

Qtz veins are abundant in metapelites of this area. They are mostly deformed by the ductile deformation with top-to-S sense of shear during the activity of the MCT, and are found as lenses. In the Ky zone, Qtz veins contain mm- to cm-sized crystals of Ky and minor Pl. Grt and Ky are coarse-grained only at the vicinity of the Qtz veins, and Ky tends to be formed exclusively around the Qtz veins. This suggests that the fluid activity that formed the Qtz veins took place around the peak metamorphism of the Ky zone, and Si, Al, Na and Ca were mobile in the fluid. Preliminary *P-T* estimate of this fluid activity using Grt-Ky-Pl-Bt-Qtz assemblage gave ca. 8kbar and ca. 600^{o}C. In the St and Grt zones as well, Grt tends to be coarser grained around the Qtz veins. Therefore, these veins are the evidence for the externally derived fluid that infiltrated during the prograde to peak metamorphism of each zone.

Unusually abundant Tur is locally found in metapelites of the MCT zone. It is localized in aluminous, Ms-rich layers and can be formed through the input of external B into the appropriate whole-rock composition for Tur growth. Such a B-bearing fluid infiltration continued from the prograde stage because Grt with prograde chemical zoning includes abundant Tur crystals. B-bearing fluid infiltration continued in the post-peak stage as suggested by the presence of Tur-rich vein cross-cutting the schistosity. Interpolar Ca/Na partitioning of Tur [5] gives 530-590^{o}C for the temperature of the Tur-rich vein formation. A potential source of external fluid could be lower grade metasediments underlying these metamorphic zones, because syn-metamorphic dehydration reactions of hydrous minerals can supply not only H_2O but also B in the fluid.

B-bearing fluid infiltration during the prograde to post-peak metamorphism in the MCT zone is important for the petrogenesis of the Higher Himalayan (HH) and North Himalayan leucogranites whose source region and petrogenesis remain highly controversial [6]. Observation in this study supports the fluid-fluxed melting of the MCT zone or Higher Himalayan Crystallines (HHC) [7]. Tur-bearing leucogranite veins in the HHC just above the MCT could be a potential product of such a fluid fluxed partial melting that took place near the MCT.

References: [1] van Hinsberg et al, 2011, Can Min, 49, 1-16. [2] Henry & Dutrow, 1996, Rev Min, 33, 503-557. [3] Sperlich et al, 1996, Am Min, 81, 1222-1236. [4] Kawakami, 2004, TRSE, 95, 111-123. [5] van Hinsberg & Schumacher, 2007, CMP, 153, 289-301. [6] Guo & Wilson, 2012, GR, 22, 360-376. [7] Le Fort, 1981, JGR, 86, 10545-10568.

Keywords: fluid, tourmaline, boron, inverted metamorphism, partial melting, continental collision zone

Japan Geoscience Union Meeting 2014
(28 April - 02 May 2014 at Pacifico YOKOHAMA, Kanagawa, Japan)

SMP46-P13 Room:Poster Time:April 28 18:15-19:30

Geochronology of the metamorphic rocks from the Masora, Antananarivo and Betsimisaraka domains, east-central Madagascar

ICHIKI, Takashi[1*] ; ISHIKAWA, Masahiro[1] ; OSANAI, Yasuhito[2] ; NAKANO, Nobuhiko[2] ; ADACHI, Tatsuro[2]

[1]Yokohama National University, [2]Kyushu University

In a previous reconstruction of Gondwana supercontinent, Madagascar is located within the interior of the supercontinent (e.g. Jacobs and Thomas, 2004). Therefore, Madagascar is one of the most significant areas to understand the process of Gondwana supercontinent formation. However, it is still controversial whether the central part of Gondwana supercontinent was formed by young arc-arc collision and amalgamation (Stern, 1994), or was reworked of old continent (e.g. Collins and Pisarevsky, 2005; Tucker et al., 2012). In this study we estimated the age of protolith formation by applying LA-ICP-MS zircon dating method to metaigneous rocks and the age of metamorphism by applying EPMA monazite dating method to metasedimentary rocks, to understand the geochronological characteristics of the composed domains in east-central Madagascar.

East-central Madagascar is divided into Masora, Betsimisaraka and Antananarivo domains from east to west based on the geology and geochronology (Tucker et al., 2011). The Masora domain is mainly composed of the felsic metamorphic rocks with subordinate amounts of the metasedimentary rocks. Two metasedimentary rocks gave ages ranging from ca. 520 to 510 Ma. This age range is consistent with the age obtained from the meta-granitoid (ca. 530 to 510 Ma, Smith et al., 2008) and from quartzite (ca. 540 to 520 Ma, De Waele et al., 2011) by U-Pb zircon dating method. The felsic metamorphic rock gave igneous age at ca. 3300 Ma. This age is consistent with the age obtained from the migmatized gneiss (Tucker et al., 2011).

The Antananarivo domain is mainly composed of the felsic metamorphic rocks with subordinate amounts of the metasedimentary rocks. This domain is divided into east and west on the basis of the metamorphic condition and structural geology. The east and west areas are bounded by the low-angle ductile shear zone of top-to-west sense. Monazites from the metasedimentary rock in the east gave ages ranging from ca. 500 to 480 Ma. In the west monazites from the two types of the metasedimentary rocks gave ages ranging from ca. 540 to 500 Ma (Martelat et al., 2000) and ca. 630 to 540 Ma (Jöns and Schenk, 2011) and from the meta-granitoid gave age ranging from ca. 560 to 540 Ma (Grégoire et al., 2009). Therefore, the metamorphic age in the east is relatively younger than in the west. The felsic metamorphic rocks are geochemically classified into two types, which gave individual igneous ages of ca. 2700 Ma in the east and ca. 760 Ma in the west, respectively. The intermediate metamorphic rocks are exposed in the west and gave igneous age at ca. 550 Ma.

The Betsimisaraka domain is mainly composed of the metasedimentary rocks. Monazites from the metasedimentary rocks gave ages of ca. 500 Ma. This age is younger than the ages reported from the quartzite at ca. 550-520 Ma (Tucker et al., 2011) and rim ages from the metasedimentary rock at ca. 550 Ma (Collins et al., 2003) by U-Pb zircon dating method.

As a consequence east-central Madagascar was metamorphosed between ca. 550 and 500 Ma. Both the east of the Antananarivo and Betsimisaraka domains was metamorphosed at the youngest age around ca. 500 Ma. In previously reported geochronological results the oldest igneous activity was at ca. 2500 Ma in the Antananarivo domain (e.g. Kröner et al., 2000) Therefore the ca. 2700 Ma igneous age is new and the oldest igneous age in this domain. The east of the Antananarivo domain was older than the west and the oldest part of this domain. The age transition zone was possibly exposed between the Masora, Betsimisaraka and the west of the Antananarivo domains. The age and geological relationship in Archean domain was recently reported from the Dhawar Craton in southern India (Peucat et al., 2013). The existence of the ca. 2700 Ma igneous activity in the east of the Antananarivo domain could be the significant evidence of the continuity between India and Madagascar since Archean.

Keywords: Gondwana supercontinent, east-central Madagascar, LA-ICP-MS U-Pb zircon dating, EPMA monazite dating

Japan Geoscience Union Meeting 2014
(28 April - 02 May 2014 at Pacifico YOKOHAMA, Kanagawa, Japan)

SMP46-P14 Room:Poster Time:April 28 18:15-19:30

Deformation microstructures of a Kamila amphibolite mylonite and their formative temperatures

ARAI, Tomoyuki[1*] ; KANAGAWA, Kyuichi[1] ; YOSHINO, Takashi[2]

[1]Graduate School of Science, Chiba University, [2]Institute for Study of the Earth's Interior, Okayama University

The Kohistan complex and the Kamila amphibolite belt in the northern Pakistan are considered to represent a Cretaceous island arc crust and a part of its lower crust, respectively. Here we report deformation microstructures of a Kamila amphibolite mylonite sample and their formative temperatures.

The amphibolite mylonite sample studied is composed of 100 μm to 1 mm thick alternating layers of hornblende + pyroxene, plagioclase, and hornblende + plagioclase + quartz, intercalating a 3 mm thick layer of garnet + quartz + plagioclase. Composite planar fabrics of a top-to-south sense of shear are developed in this sample; C plane defined by compositional layering (= foliation), S plane defined by lenticular domains of plagioclase aggregate clockwise oblique to the C plane, and C $'$ plane anticlockwise oblique to the C plane.

Hornblende + pyroxene layers contain pyroxene porphyroclasts of grain sizes $\approx$ 200 μm scattered in matrix mainly composed of hornblende grains with grain sizes $\approx$ 30 μm. Hornblende exhibits a strong crystallographic preferred orientation with (100) and [001] subparallel to foliation and lineation, respectively. Orthopyroxene porphyroclasts are elongated subparallel to foliation, and are accompanied by asymmetric tails mainly composed of hornblende indicating a top-to-south sense of shear. In addition, pyroxene porphyroclasts are surrounded by fine-grained ($\approx$ 10 μm) hornblende and quartz, suggesting a breakdown reaction of pyroxenes (orthopyroxene + clinopyroxene + H2O = hornblende + quartz), which is a retrograde reaction from granulite facies to amphibolite facies.

Plagioclase layers are composed of dynamically recrystallized plagioclase grains of An_{47-54} in composition. Lenticular domains of plagioclase are likely porphyroclasts in origin. Plagioclase grains are polygonal in shape, and weakly aligned clockwise oblique to foliation, which also suggests a top-to-south sense of shear. Plagioclase exhibits a distinct crystallographic preferred orientation with {131} and <1-12>clockwise oblique to foliation and lineation, respectively by $\approx$ 20 degrees. But {131} and <1-12>are aligned subparallel to the S plane, suggesting the dominance of {131}<1-12>during the dynamic recrystallization of plagioclase.

We applied three pyroxene geothermometers to the chemical compositions of orthopyroxene and clinopyroxene porphyroclasts, which yielded temperatures around 850 degrees C. We also applied a hornblende-plagioclase geothermometer to the average chemical compositions of hornblende and plagioclase in hornblende + plagioclase + quartz layers, and obtained a temperature of $\approx$ 610 degrees C. Thus, the amphibolite mylonite studied likely experienced a peak metamorphism of granulite facies at $\approx$ 850 degrees C, and subsequently a retrograde metamorphism of amphibolite facies at $\approx$ 610 degrees C, during which it was sheared by top-to-south thrusting.

Japan Geoscience Union Meeting 2014
(28 April - 02 May 2014 at Pacifico YOKOHAMA, Kanagawa, Japan)

SMP46-P15 Room:Poster Time:April 28 18:15-19:30

The tectonics evolution of metamorphic and igneous rocks embedded in the serpentinite melange from the Kurosegawa Tecton

YOSHIMOTO, Aya[1*] ; OSANAI, Yasuhito[1] ; NAKANO, Nobuhiko[1] ; ADACHI, Tatsuro[1] ; KITANO, Ippei[1] ; YONEMURA, Kazuhiro[2] ; ISHIZUKA, Hideo[3]

[1]Kyushu Univ., [2]JOGMEC, [3]Kochi Univ.

This study focuses petrology of the Kurosegawa Tectonic Zone, which is characterized by serpentinite melange in the Jurassic Chichibu Belt, in SW Japan. The serpentinite melange contains several blocks including high-pressure/low-temperature metamorphic rocks, high-temperature metamorphic rocks and granites. A small amount of age data obtained in previous study suggests that all rock types were formed before the Jurassic. However, detailed petrological and geochronological works on the blocks have been never performed so far. In this study, we carried out regional-scale geological, geochemical and geochronological analyses on the blocks in serpentinite from the western part of Kyushu to the eastern part of Kii peninsula.

Keywords: Kurosegawa Tectonic Zone, U-Pb zre age

Japan Geoscience Union Meeting 2014
(28 April - 02 May 2014 at Pacifico YOKOHAMA, Kanagawa, Japan)

SMP46-P16 Room:Poster Time:April 28 18:15-19:30

Metamorphism of the NE side of the Seba eclogitic basic schist in the Sambagawa metamorphic belt, central Shikoku, Japan

KISHIRA, Naohito[1*] ; TAKASU, Akira[1] ; KABIR, Md fazle[1]

[1]Department of Geoscience, Shimane University, Japan

The Sebadani area belongs to the albite-biotite zone and is located in the central part of the Besshi district. The Sebadani area is composed of the Sebadani metagabbro mass and surrounding Seba basic schists, pelitic and siliceous schists occur as intercalation within the Seba basic schists (Takasu and Makino, 1980; Takasu, 1984). Eclogitic mineral assemblages are sporadically preserved in both the Sebadani metagabbro and the Seba basic schists (Seba eclogitic basic schists) (e.g. Takasu, 1984; Naohara and Aoya, 1997; Aoya, 2001). The Onodani eclogites preserved within the Seba basic schists have a complex metamorphic history, undergoing three different metamorphic episodes (Kabir and Takasu, 2010). The first and second eclogite facies metamorphism is estimated as 530-590 ℃ and 19-21 kbar and 630-680 ℃ and 20-22 kbar, respectively. The second metamorphic event is similar to that of the Seba eclogitic basic schist of Aoya (2001) (610-640 ℃ and 12-24 kbar). The pelitic schists intercalated within the Seba eclogitic basic schists also underwent eclogite facies metamorphism of 520-550 ℃ and *c*. 18 kbar (Zaw Win Ko *et al*., 2005; Kouketsu *et al*., 2010).

The eclogite in the northeastern part of the Seba eclogitic basic schists consist mainly of garnet, epidote, amphibole (glaucophane, barroisite, taramite, Mg-taramite, Mg-katophorite, edinite), omphacite (X_{Jd} 0.27-0.41), phengite (Si 6.5-6.9 pfu). Minor amounts of albite, dolomite, rutile, titanite, biotite, chlorite and quartz. The schistsity is defined by preferred orientation of phengite, amphibole and epidote. Garnets are almandine-rich in composition, increasing almandine (X_{Alm} 0.54-0.60), pyrope (X_{Prp} 0.07-0.13) and decreasing spessartine (X_{Sps} 0.10-0.03) from core to the rim and contain inclusions of epidote, omphacite (X_{Jd} 0.27-0.41), dolomite, quartz and titanite. They also contain inclusions of barroisite/Mg-katophorite and albite symprectite. Amphibole in the matrix are zoned, barroisite/Mg-katophorite cores to edinite rims. Some other amphiboles in the matrix are parallel to the schistosity and occasionally occur as randomly oriented. The cores of these amphiboles are resorbed barroisite, glaucophane in the mantle and barroisite/edenite in the rim.

Based on the mineral paragenesis of the eclogites the metamorphism is divided into three events. The first eclogitic metamorphic event is deduced from symprectites of barroisite/ Mg-katophorite and albite after omphacite inclusions in garnet. The prograde stage of the second eclogitic metamorphic event is represented by the inclusions minerals within the mantle and rim of garnets consisting of epidote, barrosite and dolomite. The peak eclogite facies stage is defined by garnet rim and omphacite inclusins within the garnets with schistosity forming minerals of barroisite, omphacite and phengite. Garnet and omphacite rim-rim pairs yielded 530-570 ℃ and >11-14 kbar, and garnet and omphacite inclusion within garnet yields 520-560 ℃, >11-12 kbar (Ellis & Green, 1979 ; Bannno, 1986). THEMOCALC (Holland & Powell, 1998) average *P-T* calculation for garnet + omphacite + barroisite + phengite assemblage obtained 590-610 ℃ and 19-20 kbar. The retrograde stage is defined by symprectite of barrosite and albite after omphacite. The third metamorphic event is defined by zoned amphibole in the matrix.

The estimated matamorphic temperatures of the eclogites are lower than that of the second high-pressure metamorphic event of the Onodani eclogite and similar to that of the omphacite-bearing metapelites from the NW part of the Seba eclogitic basic schists (Kouketsu *et al*., 2010). This suggests a metamorphic thermal gradient existed within the Seba eclogitic basic schists.

Keywords: Sambagawa (Sanbagawa) metamorphic belt, Seba basic schist, eclogite, glaucophane, P-T path, thermal gradient

Japan Geoscience Union Meeting 2014
(28 April - 02 May 2014 at Pacifico YOKOHAMA, Kanagawa, Japan)

SMP46-P17 Room:Poster Time:April 28 18:15-19:30

Metamorphic history of garnet amphibolite from the Neldy Formation, Makbal district in the Kyrgyz Northern Tien-Shan

KASYMBEKOV, Adil[1*] ; TAKASU, Akira[1] ; KABIR, Md fazle[1] ; BAKIROV, Apas[2] ; SAKIEV, Kadyrbek[2]

[1]Department of Geoscience, Shimane University, Japan, [2]Institute of Geology, Academy of Science, Kyrgyz Republic

The Kyrgyz Tien-Shan Mountains extend from east to west, separating the Kazakhstan plate to the north and the Tarim plate to the south. They are divided into three tectonic units; the Northern Tien-Shan, the Central (or Middle) Tien-Shan and the Southern Tien-Shan. In the Northern Tien-Shan there are two HP and UHP metamorphic complexes, Makbal HP and UHP in the western part, and Aktyuz HP in the eastern part of the complexes. The Makbal complex in the Kyrgyz Northern Tien-Shan is located in the western segment of the CAOB.

The metamorphic rocks exposed in the Makbal district are divided into the Akdzhon and the Scharkyrak Groups based on their metamorphic conditions. The Akdzhon Group contains rocks of the HP and UHP metamorphic conditions, whereas the Scharkyrak Group underwent greenschists facies metamorphism. The Akdzhon Group is divided into two contrasting metamorphic formations, the structurally lower Makbal Formation and the upper Neldy Formation.

The Neldy Formation is mainly composed of garnet-phengite schists and chlorite-carbonate rocks, along with minor metaquartzites and marbles. Amphibolites and garnet amphibolites occur in the garnet-phengite schists as lenses or blocks up to 50 m across. Eclogites preserved in the cores of the garnet amphibolite bodies. Garnet amphibolite consists mainly of amphibole (magnesiohornblende, ferropargasite, ferrotschermakite, tschermakite, barroisite, actinolite), garnet and chlorite, with minor amounts of quartz, epidote and albite. Accessory minerals are paragonite, titanite and calcite. A schistosity is defined by preferred orientation of amphibole.

Garnets in the garnet amphibolite are rich in almandine (X_{Alm} 0.35-0.64), with variable amounts of spessartine (X_{Sps} 0.00-0.20), grossular (X_{Grs} 0.27-0.61) and pyrope (X_{Prp} 0.01-0.07) compositions. Garnet displays a compositional zoning, in which decrease X_{Sps} (0.20-0.04), increases X_{Alm} (0.35-0.60), X_{Grs} (0.31-0.62) and slightly increase X_{Prp} (0.01-0.03) from the core to the rim and contain inclusion of paragonite, titanite, chlorite, epidote and amphibole (actinolite, magnesiohornblende). The garnets are partly replaced by chlorite and aggregates of amphibole (ferrotschermakite, barroisite), chlorite and quartz along the cracks. Amphiboles in the matrix are zoned with magnesiohornblende and barroisite cores to ferrotschermakite and tschermakite rims and contain inclusions of titanite and quartz.

Based on the texture and mineral composition, we consider that the prograde stage probably stable in the epidote-amphibolite facies condition due to the existing of barroisitic amphibole and epidote along with garnet, paragonite, albite and chlorite. The tschermakitic rim of matrix amphibole suggests that the peak stage probably stable in the amphibolite facies conditions. The expecting metamorphic condition of the garnet amphibolite from the Neldy Formation corresponding with peak *P-T* conditions of 610-620 ℃ and 14-16 kbar for the garnet amphibolite from the Makbal complex (Rojas-Agramonte *et al*., 2013).

References:

Rojas-Agramonte Y., Herwartz D., Garcia-Gasco A. *et al*., (2013) Contrib Mineral Petrol, 166, 525-543.

Keywords: Garnet amphibolite, metamorphic history, amphibolite facies, Makbal complex, Neldy Formation, Kyrgyz Tien-Shan

Japan Geoscience Union Meeting 2014
(28 April - 02 May 2014 at Pacifico YOKOHAMA, Kanagawa, Japan)

SMP46-P18 Room:Poster Time:April 28 18:15-19:30

The stress-strain history of metamorphic sole: the case study of Greece, Turkey, Oman and Andaman islands

HOSHINO, Kenta[1*]

[1]Shizuoka University, Graduate School of Science

Metamorphic sole is formed by intra-oceanic thrusting and is found in some locations around the world. Greece, Turkey, Oman and Andaman islands are Tethys type ophiolite exposured area. The microboudin method, which is palaeostress analysis, is based on the proportion of boudinaged mineral grains with respect to applied differential stress. In this study, we used columnar minerals bearing metacherts from four areas and examined the value of palaeodifferential stress. The microboudin method revealed the value of palaeodifferential stress is 3.3˜24.8 MPa and we got stress-strain curve by using strain reversal method. The stress-strain curve indicate the stress history. Palaeodifferencial stress increased until the end of deformation in all samples. This result show that peak P-T condition and peak differencial stress are not simultaneous.

Keywords: microboudin, metamorphic sole, palaeodifferential stress, Tethys, stress-strain history

Japan Geoscience Union Meeting 2014
(28 April - 02 May 2014 at Pacifico YOKOHAMA, Kanagawa, Japan)

SMP46-P19 Room:Poster Time:April 28 18:15-19:30

Late Cretaceous and Paleogene nappe tectonics in the forearc regions of Southwest Japan

ONO, Akira[1*]

[1]none

Nappe tectonics occurred at many times in the Paleogene and late Cretaceous forearcs of Southwest Japan. Upper parts of the crust moved toward trench by the nappe tectonics (Figures A and B). Actually the Atokura and Ryoke Nappes are observed in the northern margin of the Kanto Mountains although most of the nappes were eroded. The Atokura Nappe is mainly composed of Permian granites, mid-Cretaceous granitic and metamorphic rocks, late Cretaceous Atokura Formation, early Paleogene Yorii Formation and late Cretaceous pyroclastic rocks. The Ryoke Nappe mainly consists of late Cretaceous granitic and metamorphic rocks. The Permian granitoids are geological bodies of the Kinshozan-South Kitakami Belt. The mid-Cretaceous granitic and metamorphic rocks were geological members of the Higo-Abukuma Belt. The late Cretaceous granitic and metamorphic rocks were distributed in or near the Ryoke Belt. These various rocks were located in the early Paleogene forearc (Figure B) and were removed by nappe tectonics (Ono, 2011, Abs. Geol. Soc. Japan, Meeting, p. 196).

It is important to reveal the tectonics of the lower crust when the upper crust of about 5km in thickness was moved as a nappe toward trench. The author postulates that the lower crust moved toward mantle. The surface layer of the crust moves as a nappe and the lower crust flows towards the mantle. A thrust is assumed near the base of the lower crust. Figure C shows directions of the movements of crustal materials. Tectonics like this has been repeated in late Cretaceous and Paleogene and almost all the mid-Cretaceous Higo-Abukuma metamorphic rocks were eliminated. The Ryoke Belt was also partly removed after the nappe tectonics.

The tectonics described above is consistent with the geological structure near the Median tectonic Line where the Ryoke Belt is directly in contact with the Shimanto Belt in the central part of the Kii Mountains. In this context, Ryoke granitic and metamorphic rocks are in contact with Sanbagawa metamorphic rocks from surface to lower crust according to the crustal section of Southwest Japan (Ito and Sato, 2010, Journal of Geography, 119, p.235). It is difficult to find a crustal layer which was situated in the deep parts of the Higo-Abukuma and Kinshozan-South Kitakami Belts in the crustal section.

Keywords: Southwest Japan, Forearc, Late Cretaceous and Paleogene, Nappe tectonics, Lower crust

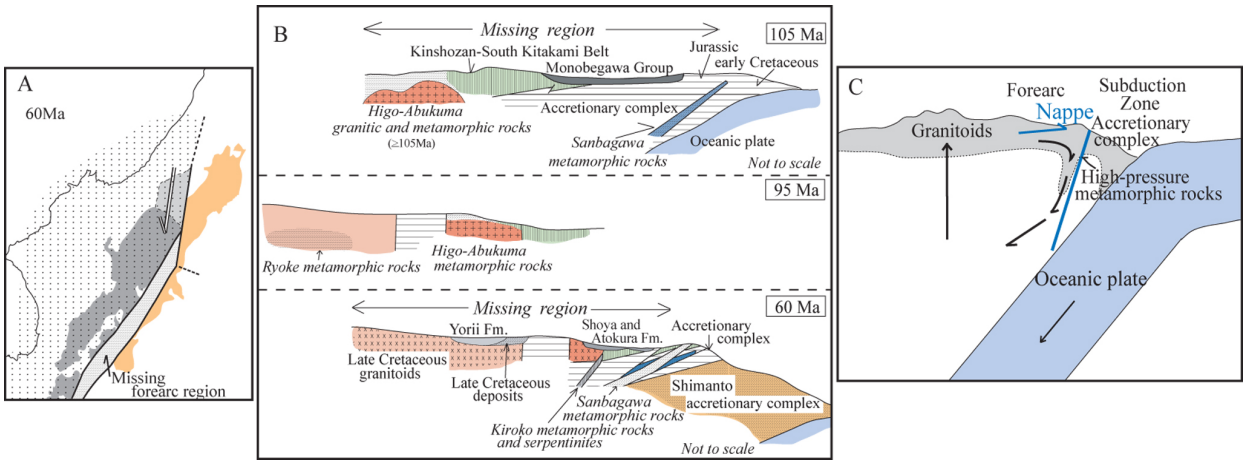

Japan Geoscience Union Meeting 2014
(28 April - 02 May 2014 at Pacifico YOKOHAMA, Kanagawa, Japan)

SMP47-01 Room:422 Time:May 1 09:00-09:15

First-principles calculations of the structure of MgSiO3 melt at high temperature and high pressure

MATSUI, Masanori[1*]

[1]School of Sci., Univ. of Hyogo

Crystals and melts with MgSiO3 composition are important constituents of the Earth's lower crust and mantle. Therefore an accurate knowledge of their structural and elastic properties at high temperatures and high pressures is crucial to investigate the chemical and physical structures, and the conditions of formation and evolution of the Earth. However, reliable experimental data under geophysically relevant conditions are generally lacking for MgSiO3 melt, mainly due to the difficulty in obtaining such data at the combined high temperature and high pressure found in the Earth's interior. Here we use the first-principles molecular dynamics (FPMD) method to study the structures and elastic properties of MgSiO3 melt at high temperatures and high pressures.

All calculations were performed with the Vienna Ab Initio Simulation Package VASP (Kresse and Furthmuller, 1996). The projector-augmented wave (PAW) method was used in the local density approximation (LDA) for the exchange-correlation functional (Blochl, 1994; Kresse and Joubert, 1999). FPMD calculations were carried out in the canonical ensemble (constant temperature T, constant volume V, and constant number of atoms N in the system) using cubic basic cells. N was taken to be 160 (32 MgSiO3) throughout this study. After annealing the system sufficiently at 4000 K, and then 3000 K, we fixed V at 38.54 cm3/mol and T at 2000 K to calculate the interference function S(Q), where Q is the length of scattering vector, and the radial distribution function (RDF) for each atom pair. We found FPMD calculated S(Q) compares reasonably well with the observed data from X-ray analyses at 1973 K by Waseda and Toguri(1990). The FPMD predicted average nearest neighbor bond distances r(ij), and coordination numbers n(ij) between atoms i and j are also compared well with the data by Waseda and Toguri(1990), except the r(MgO) distance, in which the FPMD value of 1.97 A is much shorter than the value [2.12(1) A] by the X-ray analyses. We further apply the FPMD technique to investigate the temperature and pressure dependencies of the structure of MgSiO3 melt.

Keywords: MgSiO3 melt, high temperature, high pressure, first-principles calculation

Japan Geoscience Union Meeting 2014
(28 April - 02 May 2014 at Pacifico YOKOHAMA, Kanagawa, Japan)

SMP47-02 Room:422 Time:May 1 09:15-09:30

Forsterite-$MgSiO_3$ liquid interface : molecular dynamics perspective

NORITAKE, Fumiya[1*] ; KAWAMURA, Katsuyuki[1]

[1]Okayama University

Knowledge about the viscosity and permeability of partial molten rocks is important to understand the thermal history of the Earth and volcanisms. For understanding those obtained by experiments and estimating the physical properties at extreme conditions those are difficult to reproduce in laboratory experiments, the knowledge about structure and properties of silicate crystal-liquid interfaces is necessary. The properties of melt as sandwiched thin films are considered as being different with ones in bulk melts by the effect of crystal surface. For instance, lateral self-diffusivity of water to crystal surfaces shows different from bulk one in the case of water-brucite surface (Sakuma et al. 2003), water-muscovite mica surface (Sakuma and Kawamura, 2009). The dynamic property anomalies on solid - liquid surfaces affect properties of bulk rock such as permeability (Ichikawa et al. 2001).

In this study, structure and properties of the forsterite-$MgSiO_3$ liquid interfaces are investigated by using molecular dynamics simulations. It is essential to know the structure and physical properties of forsterite-$MgSiO_3$ liquid interfaces since forsterite is the liquidus mineral of primordial magmas.

Molecular dynamics simulations were performed with NPT ensemble using MXDORTO code (Sakuma and Kawamura, 2009). The initial structure is a 21440 atom system in which a sheet of MgSiO3 liquid consist of 8000 atoms (˜5 nm) is sandwiched between (010) surfaces of forsterite(Pbnm) and 43440 atom system in which a sheet of MgSiO3 liquid consist of 30000 atoms (˜20 nm) is sandwiched between (010) surfaces of forsterite. Firstly we calculated equilibrated MgSiO3 liquid film in vacuum starting with a randomly generated structure and randomly generated velocities of atoms through 0.5 ns (1,000,000 steps) at 1973 K and quench to 300 K. Secondly we calculated a bulk forsterite crystal with 13440 atoms ($11*5*8$ unit cells of forsterite(Pbnm)) starting with a given experimental crystal structure which was obtained by the experiment [5] and with randomly generated velocities of atoms and then cut along (010) surface. Finally we combined forsterite cut along (010) surface and MgSiO3 liquid film. Under maintaining isobaric and isothermal conditions, we performed the relaxation of 0.5˜1.5 ns. Then the statistical averages of the structure and physical properties were obtained from the velocities and coordinates of each atom in the simulations through 500 ps. The function of inter-atomic potential model was same as used in our previous work (Noritake et al. 2012).

By these simulations, characteristic structures in the forsterite-$MgSiO_3$ liquid interface are observed. The layered structure of alternated crystal surface, Si-rich and Mg-rich layers in the crystal-liquid interface was observed. The layered structure was formed by energy difference between Si-O semi-covalent bonds and Mg-O ionic bonds. Si-O-Si bridging and free oxygen atoms are excessively formed and in the near surface since the energy of Si-O bonding is much lower than that of Mg-O bonding. The difference of layered structure by thickness of MgSiO3 liquid film might be caused by the difference of the degree of freedom of configuration in liquid film. The two-dimensional diffusivity of oxygen atoms is controlled by two factors. The one is the thickness of liquid film that decreases oxygen diffusivity with decreasing the film thickness because of decrease of degree of freedom of configuration in liquid film. The other is composition of sliced layer where oxygen diffusivity increases with increasing the Mg/Si ratio since Si-O bonding is much stronger than Mg-O ones.

Keywords: Interface, High-Temperature, Silicates, Molecular dynamics simulation

Japan Geoscience Union Meeting 2014
(28 April - 02 May 2014 at Pacifico YOKOHAMA, Kanagawa, Japan)

SMP47-03 Room:422 Time:May 1 09:30-09:45

Phase transitions in Zn_2SiO_4: first-principles study

KANZAKI, Masami[1*]

[1]Inst. Study Earth's Interior, Okayama University

Recent experimental study (Liu et al., PCM, 40, 467, 2013) suggested that high-pressure phases of III and IV in Zn_2SiO_4 could be retrograde phases transformed during decompression. In order to check stabilities of these phases under pressure, and to find original high-pressure phases, density functional theory total energy calculations of 12 phases at 0 K have been conducted.

Three pressure-induced "phase transitions" during structural optimization were observed: phase II to spinel structure, phase III to a new high-pressure phase, and phase IV to Na_2SO_4 III-type structure. Phase III, having tetrahedral olivine structure, exhibited extraordinary high compressibility, which is due to large volume reductions in vacant octahedral sites corresponding M1 and M2 sites in olivine structure. Calculated enthalpies of the phases at 0 K confirmed that phase III and IV are not stable at any pressure. It also suggested that Na_2SO_4 III and II phases will be stable phases replacing phase III and IV, respectively.

Keywords: Zn2SiO4, phase transition, high pressure phase, first-principles, transition mechanism

Japan Geoscience Union Meeting 2014
(28 April - 02 May 2014 at Pacifico YOKOHAMA, Kanagawa, Japan)

SMP47-04 Room:422 Time:May 1 09:45-10:00

A new high pressure phase of Fe2SiO4 and the relationship between spin and structural transitions

YAMANAKA, Takamitsu[1*] ; KYONO, Atsushi[2] ; NAKAMOTO, Yuki[3] ; KHARLAMOVA, Svetlana[1] ; STRUZKIN, Viktor[1] ; MAO, Ho-kwang[1] ; HEMLY, Russell[1]

[1]Carnegie Institution of Washington Geophysical Laboratory, [2]Division of Earth Evolution Sciences, Life and Environment Sciences, University of Tsukuba, [3]Center for Quantum Science and Technology Under Extreme Conditions, Osaka University

A structural change in Fe_2SiO_4 spinel (ringwoodite) has been found by synchrotron powder diffraction study and the structure of a new high-pressure phase was determined by Monte-Carlo simulation method and Rietveld profile fitting of x-ray diffraction data up to 64 GPa at ambient temperature. A transition from the cubic spinel structure to a body centered orthorhombic phase (I-Fe_2SiO_4) with space group Imma and Z=4 was observed at approximately 34 GPa. The structure of I-Fe_2SiO_4 has two crystallographically independent FeO_6 octahedra. Iron resides in two different sites of six-fold coordination: Fe1 and Fe2, which are arranged in layers parallel to (101) and (011), and very similar to the layers of FeO_6 octahedra in the spinel structure. Silicon is located in the six-fold coordination in I-Fe_2SiO_4. The transformation to the new high-pressure phase is reversible under decompression at ambient temperature. A martensitic transformation of each slab of the spinel structure with transition vector $<$1/8 1/8 1/8 $>$generates the I-Fe_2SiO_4 structure. Laser heating of I-Fe_2SiO_4 at 1500 K results in a decomposition of the material to rhombohedral FeO and SiO_2 stishovite.

Fe K beta x-ray emission measurements at high pressure up to 65GPa show that the transition from a high spin (HS) to an intermediate spin (IS) state begins at 17 GPa in the spinel phase. The IS electron spin state is gradually enhanced with pressure. The Fe2+ ion at the octahedral site changes the iron radius under compression from 0.78 A at the high-spin state to 0.61 A at the low spin, which results in the changes of the lattice parameter and the deformation of the octahedra of the spinel structure. The compression curve of the lattice parameter of the spinel is discontinuous at approximately 20 GPa. The spin transition induces an isostructural change.

Keywords: Fe2SiO4 spinel, new high-pressure phase, spin transition, X-ray emission, martensitic transition

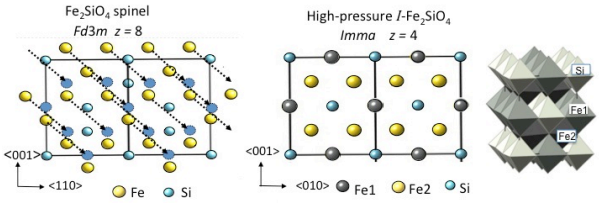

Japan Geoscience Union Meeting 2014
(28 April - 02 May 2014 at Pacifico YOKOHAMA, Kanagawa, Japan)

SMP47-05 Room:422 Time:May 1 10:00-10:15

Synchrotron Mössbauer spectroscopy on Fe_3S, FeO and natural almandine

KAMADA, Seiji[1*] ; HIRAO, Naohisa[2] ; HAMADA, Maki[3] ; SUZUKI, Nanami[1] ; OHTANI, Eiji[1] ; OHISHI, Yasuo[2] ; MASUDA, Ryo[4] ; MITSUI, Takaya[5]

[1]Tohoku Univ., [2]JASRI, [3]School of Nature system, College of Science and Engineering, Kanazawa University, [4]Research Reactor Institute, Kyoto Univ., [5]JAEA

The Earth's core is considered to be composed of an iron alloy with light elements since its density is smaller than that of pure iron under core conditions (e.g., Birch, 1964; Dubrovinsky et al., 2000). Although there are many candidates for these elements, such as H, C, O, Si, and S, sulfur in particular has been considered as one of the most plausible candidates. This is because it is depleted in the mantle, suggesting that it exists in the Earth's core (Murthy and Hall, 1970), and iron sulfides are found universally in iron meteorites, i.e., analogues of the Earth's core. Although the content of sulfur in the Earth's core is not known precisely, the sulfur content in the core is estimated to be at least a few wt% based on cosmic element abundances (McDonough, 2003) and high pressure partitioning experiments (e.g., Hillgren et al., 2000).

Since sulfur is one of the most plausible light elements, a compressibility and phase diagram in the Fe-FeS system has been studied (e.g., Campbell et al., 2007; Chen et al., 2007; Fei et al., 2000; Kamada et al., 2010; Li et al., 2001; Seagle et al., 2006). According to previous studies, Fe_3S is stable from 21 GPa and at least up to 200 GPa. Therefore, Fe_3S can be one of a candidate of the inner core materials. In addition, a synchrotron Mössbauer spectroscopy (SMS) and X-ray emission spectroscopic studies on Fe_3S revealed a spin transition and magnetic transition between 20 and 25 GPa (Lin et al., 2004; Shen et al., 2003). It also showed an abnormal evolution of a and c axes with increasing pressure (Chen et al., 2007).

Synchrotron Mössbauer spectroscopy is a good probe of a small sample under high pressure to investigate magnetic properties and electronic states of Fe of core and mantle minerals. An energy domain Mössbauer spectroscopic system has been recently developed at the BL10XU, SPring-8. We have measured Mössbauer spectra from Fe_3S and FeO under high pressure and a natural almandine at ambient pressure.

A powder mixture was made from ^{57}Fe (96.63%, ISOFLEX) and FeS (99.9%, RAREMETALLIC co., LTD.) with a ratio of Fe:S=75.0:25.0 (in at%). A foil was made from the mixture by a cold compression using a diamond anvil cell (DAC) and loaded into a sample chamber. ^{57}Fe enriched Fe_3S was synthesized from the powder mixture in a DAC at 30 GPa and 1350 K. The synthesis of Fe_3S was confirmed by X-ray diffraction patterns at BL10XU, SPring-8. ^{57}FeO was made by reducing from $^{57}Fe_2O_3$ (ISOFLEX) at ambient pressure and high temperature. A pellet was made from ^{57}FeO powder and loaded into a sample chamber of a DAC. We also measured Mössbauer spectra of a natural almandine ($Py_{15.7}Alm_{78.6}Gros_{4.4}Sp_{1.3}$, Idaho, USA). The energy of used X-ray for Mössbauer spectroscopy was 14.4125 keV.

We have measured Mössbauer spectra of Fe_3S during decompression at 5, 15, 20, 25, and 30 GPa and room temperature at BL10XU and BL11XU. At BL10XU, those of FeO and the almandine were obtained at 200 GPa and ambient pressure, respectively. The magnetic transition in Fe_3S was observed between 20 and 25 GPa, which is consistent with Lin et al. (2004). We observed doublet peaks from FeO. An evidence of Fe^{3+} in the almandine was not detected in this study. We will report the results of the Mössbauer spectra based on the newly developed system at BL10XU, SPring-8.

Keywords: Earth's core, Mantle, Mössbauer, Fe_3S, FeO

Japan Geoscience Union Meeting 2014
(28 April - 02 May 2014 at Pacifico YOKOHAMA, Kanagawa, Japan)

SMP47-06 Room:422 Time:May 1 10:15-10:30

Temperature dependence of Fe^{3+}, Al and Ga distributions and local domain structure in synthetic Ca-clinopyroxene

AKASAKA, Masahide[1*] ; HAMADA, Maki[2] ; NAGASHIMA, Mariko[3] ; EJIMA, Terumi[4]

[1]Dep. Geoscience, Shimane Univ., [2]School of Nature system, Kanazawa Univ., [3]Dept. Earth Sci., Yamaguchi Univ., [4]AIST

Distribution of Fe^{3+}, Al^{3+} and Ga^{3+} among octahedral and tetrahedral sites in synthetic esseneite ($CaFeAlSiO_6$)- and $(CaFe^{3+}GaSiO_6)_{90}(CaGa_2SiO_6)_{10}$-clinopyroxenes at 800 and 1200 ℃ were investigated using ^{57}Fe Mössbauer and X-ray Rietveld methods to find a relation between site occupancies of trivalent cations at the octahedral and tetrahedral sites and ionic sizes of trivalent cations. The esseneite was synthesized from oxide mixture using sintering technique at 1200 ℃ in air. The $FeGaTs_{90}GaTs_{10}$-Cpx was crystallized from glass starting material at 1200 ℃ in air. The Cpxs synthesized and those annealed at 800 ℃ were analyzed using ^{57}Fe Mössbauer spectroscopic and X-ray Rietveld methods. In the synthetic esseneite, $^{VI}Fe^{3+}$:$^{IV}Fe^{3+}$-ratio at 800 ℃ was determined as 82(1):18(1) by Mössbauer method and 78.2(5):21.8(5) by Rietveld method, whereas, at 1200 ℃, 79(1):21(1) by Mössbauer method and 77(1):23(1) by Rietveld analysis. The resulting Fe^{3+} populations at octahedral M1 and tetrahedral T sites in the synthetic esseneite are Fe^{3+}0.782(5)-0.82(1) apfu and 0.218(5)-0.18(1) apfu, respectively. In the synthetic Fe^{3+}-Ga-Cpx, $^{VI}Fe^{3+}$:$^{IV}Fe^{3+}$-ratio at 800 ℃ was 74(3):26(2) (Mössbauer analysis data) and 78(1):22(1) (Rietveld analysis data), while, at 1200 ℃, 71(3):29(1) (Mössbauer analysis data) and 67(1):33(1) (Rietveld analysis), which results in populations at the octahedral M1 and tetrahedral T sites of $[Fe^{3+}_{0.67(1)-0.70(1)}Ga_{0.33-0.30}]^{M1}[Si_{1.0}Fe^{3+}_{0.23-0.20}Ga_{0.77-0.80}]^{T}$ (O = 6) at 800 ℃, and $[Fe^{3+}_{0.64(1)-0.60(1)}Ga_{0.36-0.40}]^{M1}[Si_{1.0}Fe^{3+}_{0.26-0.30}Ga_{0.74-0.70}]^{T}$ at 1200 ℃. This result indicates the temperature dependence of Fe^{3+}, Al^{3+} and Ga^{3+} distributions between M1 and T sites. However, it is evident that, even at different temperatures, distributions of Fe^{3+}, Al^{3+} and Ga^{3+} between M1 and T sites are well correlated with the ratio of ionic radius of larger Fe^{3+}-cation against smaller Al^{3+} and Ga^{3+}, as Akasaka et al. (1997) indicated. Another finding in this study is the splitting of a ^{57}Fe Mössbauer doublet by Fe^{3+} at M1 site into two doublets. This indicates existence of short-range domain structure by two kinds of M1 sites with slightly different distortions, which cannot be detected by X-ray diffraction.

Keywords: clinopyroxene, Mossbauer analysis, X-ray structural refinement, Crystal chemistry, ionic distributions, temperature dependence

Japan Geoscience Union Meeting 2014
(28 April - 02 May 2014 at Pacifico YOKOHAMA, Kanagawa, Japan)

SMP47-07 Room:422 Time:May 1 10:30-10:45

Phase Transformation of Zirconium under High P-T Conditions

ONO, Shigeaki[1*]

[1]JAMSTEC

The behavior of zirconium metal under high pressures is important in the community of the high-pressure study, because changes in resistivity due to the phase transformations of zirconium (Zr) are used as pressure calibration points in the high-pressure experiments. Zirconium metal, which shows the hcp structure at ambient conditions, is known to transform to the bcc structure (beta phase) above 1135 K at ambiant pressure. With increasing pressure, phase transformations to a hexagonal structure (omega phase), at the pressure around 5 GPa and to a bcc structure around 30 GPa have been observed at room temperature. The formation of the high-pressure phases is concerned with changes in the electronic structure. Recent investigations for the phase transformation from the hexagonal to the bcc structures at high temperatures (Zhang et al. 2005 and 2007) were inconsistent with previous study at temperatures around the room-T (Xia et al. 1991). Therefore, we reinvestigated the transformation pressure in zirconium metal.

The starting material used in this study was polycrystalline Zr. High-pressure X-ray diffraction experiments were carried out in an external heated diamond anvil cell. The small sample sandwiched between pellets of NaCl powder was loaded into a hole that had predrilled into a rhenium gasket. The heating temperature was up to 800 K, and was recorded using the R-type of thermocouples. The sample was probed using angle-dispersive X-ray diffraction, located on the synchrotron beam lines, at NE1A of the Photon Factory. Details of the synchrotron X-ray experiments have been described elsewhere (e.g., Ono et al. 2005). The angle-dispersive X-ray diffraction patterns were obtained on the imaging plate of an X-ray data collection system (Rigaku, RAXIS). The pressure was calculated from the NaCl unit cell volume using the equation of state (EOS) for NaCl, as developed by Ono (2010).

The boundary from the omega phase to the bcc phase was determined at high temperatures (300 - 800 K). Our results were in good agreement with those reported in previous room-temperature study. The gradient of dP/dT of the boundary was negative. However, the gradient observed in our experiments was 2-3 times more negative than that reported by previous high-temperature experiments (Zhang et al. 2005 and 2007). Our new data indicated that the difference in the stress conditions of the sample led to the discrepancy of the gradient of dP/dT slope in previous studies.

Keywords: Zirconium, Phase transition, High pressure and high temperature

Japan Geoscience Union Meeting 2014
(28 April - 02 May 2014 at Pacifico YOKOHAMA, Kanagawa, Japan)

SMP47-08 Room:422 Time:May 1 11:00-11:15

Crystal structure analysis of a new high-pressure strontium silicate

SEKINE, Keisuke[1] ; ISHII, Takayuki[1] ; KOJITANI, Hiroshi[1*] ; AKAOGI, Masaki[1]

[1]Dept. of Chemistry, Gakushuin University

$SrSiO_3$ is an analog material to $CaSiO_3$ which is an important component of the Earth's crust- and mantle-constituting minerals. High-pressure phase relation experiments in $SrSiO_3$ showed that δ'-$SrSiO_3$ is stable up to about 10 GPa and decomposes into $BaGe_2O_5$-III -type $SrSi_2O_5$ + larnite-type Sr_2SiO_4 between 14 and 20 GPa (Kojitani et al., 2005). Then, hexagonal perovskite-type $SrSiO_3$ becomes stable above about 20 GPa (Yusa et al., 2005). However, phases except for larnite-type Sr_2SiO_4 appearing in the pressure range between 10 and 14 GPa have been unclear. In this study, crystal structure and composition of one of the unknown phases were determined.

A sample for single-crystal structure analysis was synthesized by heating a mixture of pseudowollastonite-type $CaSiO_3$ and SiO_2 cristobalite (mole ratio of 1:1) with a little amount of water at 12 GPa and 1200 ℃ for 90 min using a Kawai-type multi-anvil high-pressure apparatus. A single-crystal sample with 120x80x60 μm was used for the single-crystal X-ray diffraction measurement. 953 reflection data were analyzed using the SHELX-97 software. Composition analysis of the high-pressure phase was performed using SEM-EDS.

The composition analysis showed that the new high-pressure phase had a composition of $Sr_4Si_9O_{22}$. The single-crystal structure analysis suggests the monoclinic crystal system with the space group of $C2/m$. Lattice parameters were determined to be a = 13.3765(4) $\AA$, b = 5.2321(2) $\AA$, c = 11.6193(6) $\AA$, β = 113.976(4)deg. R factor was 1.25%. The framework of the obtained crystal structure consists of two layers by corner-sharing single chains of edge-shared SiO_6 octahedra or SiO_5 rhombic pyramid polyhedra and by corner-shared SiO_4 tetrahedra and SiO_6 octahedra. It should be mentioned that this structure includes the SiO_5 rhombic pyramids which are very rare in silicates. Strontium ions in the structure are arranged between the two layers and are coordinated by seven oxygens. The structure of δ'-$SrSiO_3$ consists of four-membered rings of SiO_4 tetrahedra and strontium ions coordinated by seven oxygens. On the other hand, $BaGe_2O_5$-III type $SrSi_2O_5$ has a framework by corner-shared SiO_6 octahedra and SiO_4 octahedra and coordination number of Si^{2+} is 12. The crystal structure determined in this study is consistent with the fact that its density would be between those of the lower-pressure and higher-pressure phases.

Keywords: strontium silicate, high-pressure, single-crystal structure analysis, SiO5 polyhedron

Japan Geoscience Union Meeting 2014
(28 April - 02 May 2014 at Pacifico YOKOHAMA, Kanagawa, Japan)

SMP47-09 Room:422 Time:May 1 11:15-11:30

Heat capacity and entropy measurements by PPMS for high-pressure phases in TiO2 and MnSiO3

AKAOGI, Masaki[1*] ; KOJIMA, Meiko[1] ; FUKAI, Aya[1] ; KOJITANI, Hiroshi[1]

[1]Dept. of Chemistry, Gakushuin University

Thermodynamic properties of high-pressure minerals are widely used to calculate phase relations at high pressures and high temperatures and to compare with the properties by the first-principles calculations. Standard entropy, S298.15, is determined by integrating Cp/T in the temperature range between 0 and 298.15 K, where Cp is isobaric heat capacity and T is absolute temperature. To measure Cp at the temperature range, adiabatic calorimetry has been widely used with the highest precision. However, Cp of only a few high-pressure minerals have been measured so far, because a sample of more than several gram is required for the adiabatic calorimetry. Recently, low-temperature Cp measurement with thermal relaxation method using the Physical Properties Measurement System (PPMS) has been developed for samples of about ten milligram quantity. In this method, the sample is cooled with liquid helium and Cp is measured at about 2-310 K. By measuring the sample temperature change associated with applied heat pulse, thermal relaxation process is analyzed to obtain Cp. By this method, we measured Cp and determined S298.15 for Mg2SiO4 wadsleyite and ringwoodite, MgSiO3 akimotoite and perovskite, and SiO2 stishovite, in collaboration with Atake-Kawaji laboratory, Tokyo Institute of Technology. Very recently, we have installed the PPMS apparatus in the laboratory in Gakushuin University, and have investigated Cp and S of rutile-type and α-PbO2-type TiO2 and garnet-type MnSiO3.

Using a multianvil apparatus, rutile- and α-PbO2-type TiO2 phases were synthesized at 3 and 8 GPa, respectively, at 600-700 oC, and MnSiO3 garnet was made at 15 GPa and 1000 oC. All the cylindrical samples were polished and fixed with grease on the stage in the PPMS. The Cp measurements in this study were performed at 2-308 K using the polycrystalline samples of 10-21 mg. The Cp measured for α-Al2O3 (NBS SRM-720) by the PPMS apparatus were consistent within experimental errors with those measured by adiabatic calorimetry by Ditmars et al. (1982).

The measured Cp of rutile-type TiO2 were in good agreement with those by previous studies, and the obtained S298.15 was 50.10 J/molK. Our Cp data of α-PbO2-type TiO2 were almost consistent with those with PPMS measurement by Yong et al. (2014), but substantially smaller than those with DSC measurement by Manon (2008). The S298.15 of α-PbO2-type TiO2 was determined as 46.50 J/molK in this study. The Cp data of MnSiO3 garnet indicated an anomaly at 15 K probably due to magnetic transition, and S298.15 of 90.92 J/molK. High-pressure phase relations calculated using the above data are also reported.

Keywords: heat capacity, entropy, high-pressure phase, PPMS apparatus

Japan Geoscience Union Meeting 2014
(28 April - 02 May 2014 at Pacifico YOKOHAMA, Kanagawa, Japan)

SMP47-10 Room:422 Time:May 1 11:30-11:45

Mechanisms of phase transitions of methane hydrate under high pressure

KADOBAYASHI, Hirokazu[1*] ; HIRAI, Hisako[1] ; HIRAO, Naohisa[2] ; OHISHI, Yasuo[2] ; OHTAKE, Michika[3] ; YAMAMOTO, Yoshitaka[3] ; KOJIMA, Yohei[1]

[1]Geodynamics Research Center, Ehime University, [2]Japan Association of Synchrotron Radiation Institute, [3]National Institute of Advanced Industrial Science and Technology

Methane hydrate (MH), called as " burning ice " , is expected to be a fruitful natural resource, at the same time, methane is rather effective greenhouse gas than carbon dioxide. It is also thought to be a major constituent of icy bodies in and outside the solar system. MH is composed of hydrogen-bonded host water molecules forming cages or frameworks that include guest methane molecules. Three phases of MH have been known so far. The low-pressure phase, sI, is stable below 0.8 GPa and it transforms into a hexagonal structure, sH, at 0.8 GPa and further transforms to a filled ice Ih (FIIhS) at 1.8 GPa at room temperature. At these phase transitions, release of water content is accompanied. As described above, the existence of phase transitions and the structures of transformed high-pressure phases have been clarified by the previous studies. However, transition mechanisms from the lower-pressure phase to individual high-pressure phases have been unresolved issue. In this study, high-pressure experiments were performed to investigate mechanisms of the phase transitions of MH at high pressures.

Clamp type and lever-spring type diamond anvil cells were used in this study. The pressure and temperature conditions were from 0.2 to 3.0 GPa and 300 K, respectively. Pressure measurements were made via a ruby fluorescence method. The initial samples of MH were prepared by ice-gas interface method. The samples were characterized via time-resolved X-ray diffractometry using synchrotron radiation at BL-10XU, SPring-8, and time-resolved Raman spectroscopy at GRC, Ehime University.

As for sI-sH phase transition, Raman spectroscopy revealed that 5^{12} cages of sI survived during the transition and that the 5^{12} cages remained as same 5^{12} cages of sH structure. And, $5^{12}6^2$ cages of sI changed to $4^3 5^6 6^3$ and $5^{12}6^8$ cages of sH. The results suggested that the sI-sH transition may follow a martensitic-like mechanism because of being maintaining 5^{12} cages unchanged in sH structure. On the other hand, at sH-FIIhS transitions, Raman spectroscopy detected abrupt collapse of all constituent cages in sH and release of fluid or solid methane molecules. And then, the framework of FIIhS was gradually reconstructed, absorbing the released methane molecules into the FIIhS structure. The results indicated that the sH-FIIhS transition follows reconstructive mechanism. The explanations may be reasonable, because the former transition is from a cage to another cage structure, and the latter one is from a cage structure to different framework of a filled ice structure.

Keywords: methane hydrate, mechanisms of phase transitions, high-pressure, X-ray diffractometry, Raman spectroscopy

Japan Geoscience Union Meeting 2014
(28 April - 02 May 2014 at Pacifico YOKOHAMA, Kanagawa, Japan)

SMP47-11 Room:422 Time:May 1 11:45-12:00

Incorporation of NaCl into ice VI and ice VII under high pressure.

HIRAI, Hisako[1*] ; YAMASHITA, Fukunori[1] ; KAGAWA, Shingo[1] ; KADOBAYASHI, Hirokazu[1] ; OHISHI, Yasuo[2] ; YAMAMOTO, Yoshitaka[3]

[1]Geodynamics Research Center, Ehime University, [2]JASRI, [3]AIST

Icy satellites have been thought to contain a large amount of salts besides water ices. Ice exhibits a wide variety of forms consisting of hydrogen-bonded water molecules. More than sixteen stable and metastable forms have been reported so far. Liquid water can dissolve various kinds of solutes. Whereas, in the previous idea, when water crystallizes, the dissolved solutes are excluded, which results in formation of pure water ices. Recently, Frank et al. [1] and Komatsu et al. [2] reported that NaCl or other salts was incorporated into ice VI and/or ice VII. In these studies, however, it has been still unclear which ice can incorporate NaCl, and amount of salts incorporated and states of the salt in the ice structure have not yet been clarified. In this study, in order to understand possible incorporation of salts in to ice VI and VII structures, high-pressure experiments were performed with a system of H_2O-NaCl, a typical salt, at room temperature.

Lever-and-spring type diamond anvil cell was used. Pressure range examined was from 0.2 to 10 GPa. NaCl aqueous solutions with three concentrations, 1.5, 2.5, and 5.0 w%, were prepared as starting samples. Characterization was made by optical microscopy, X-ray diffractometry (XRD), and Raman spectroscopy.

Similar phase changes were observed for the samples with three different concentrations. The NaCl aqueous solutions finally crystallized to form iceVI above 1.6 GPa, although in case of pure water ice VI is formed at 1.0 GPa at room temperature. At the pressure range from 2.1 to 3.2 GPa, a new high-pressure phase, of which diffraction pattern was not explained by ice VI, ice VII, and solid NaCl, was observed. Above 3.2 GPa, ice VII and solid NaCl appeared. The high-pressure phase observed may correspond to a phase having a modified structure of NaCl-dihydrate reported by Nakayama et al. [3]. Unit cell volumes of ice VII calculated expanded larger than those of pure ice VII. The result was opposite sense to those by Frank et al, where the volumes decreased smaller than those of pure ice VII. The amounts of the volume expansion for 2.5 and 5.0 w% samples were larger than those of 1.5 w% samples. The volume expansions of the former two samples were almost similar. The results suggested that limitation of incorporation into ice VII is less than 2.5 w%. The O-H vibrational modes shifted to higher frequencies by 10 to 20 cm^{-1} and 5 to 10 cm^{-1} from those of pure ices for ice VI and ice VII, respectively.

All experimental results indicated that NaCl is incorporated both into ice VI and ice VII at room temperature. The amounts of incorporation were estimated to be up to 2.5 w%. Such large amount of incorporation of salt is expected to effect on physical properties of ices, which is important in inferring the interiors of icy bodies.

1. M. R. Frank et al., PEPI 155 (2006) 152; M. R. Frank et al., PEPI 170 (2008) 107; M. R. Frank et al., PEPI 215 (2013) 12.
2. K. Komatsu et al., Abstract od Annual meeting of Jpn. Society High Pressure Tech. (2010).
3. K. Nakayama master thesis (2012).

Keywords: high-pressure ice, NaCl, incorporation, icy satellite

Japan Geoscience Union Meeting 2014
(28 April - 02 May 2014 at Pacifico YOKOHAMA, Kanagawa, Japan)

SMP47-12 Room:422 Time:May 1 12:00-12:15

Structure refinement of legrandite and paradamite : crystal chemistry and hydrogen bonds

JINNOUCHI, Satoshi[1*] ; YOSHIASA, Akira[1] ; SUGIYAMA, Kazumasa[2] ; ARIMA, Hiroshi[2] ; SHIMURA, Reiko[2] ; MIYAWAKI, Riturou[3]

[1]Graduate School of Science and Technology, Kumamoto University., [2]Institute for Materials Research, Tohoku University, [3]National Science Museum

Legrandite, $Zn_2AsO_4(OH)H_2O$ and paradamite, $Zn_2AsO_4(OH)$, are zinc arsenate minerals and have a color between pale yellow and yellowish brown. Related minerals of legrandite and paradamite are adamite, $Zn_2AsO_4(OH)$, and so on with different structures. We performed the structure refinement of legrandite and paradamite Oujela Mine, Mapimi, Durango, Mexico, by (RAPID) RIGAKU single-crystal structure analysis system. We determined the hydrogen position by difference Fourier method. We revealed the detail hydrogen bond using bond valence calculation and hydrogen positions and compared crystal structures of these. The structure of legrandite is constituted by two AsO_4 tetrahedrons, ZnO_6 octahedron and three ZnO_5 trigonal dipyramids that have large unique distortion. AsO_4 tetrahedron, ZnO_5 trigonal dipyramid and ZnO_6 octahedron constitutes the unique framework. The structure of paradamite is constituted by AsO_4 tetrahedron and two ZnO_5 trigonal dipyramid that have large unique distortion. In legrandite, 5 coordination of trigonal dipyrmids have a distance to be expected from ionic radii but interatomic distance of Zn(3)-O(1) has extraordinary distance. Two OH groups bond to Zn1 and Zn2, Zn3 and Zn4 make the $ZnO_3(H_2O)_2$ trigonal dipyramid that is bonded to two H_2O group in legrandite. In paradamite, Zn1 and Zn2 make $ZnO_3(OH)_2$ and $ZnO_4(OH)$ trigonal dipyramid. Hydrogen atoms make a lot of hydrogen bonding in legrandite and paradamite. Crystal structure of legrandite has a tunnel structure continuous that is only parallel to c axis and similar structure is observed in paradamite only parallel to a axis. There are path of proton-conduction in these direction and we conjecture that these proton-conductivity have large anisotropy of one dimension.

Keywords: structure refinement, legrandite, paradamite, crystal chemistry, hydrogen bonds

Japan Geoscience Union Meeting 2014
(28 April - 02 May 2014 at Pacifico YOKOHAMA, Kanagawa, Japan)

SMP47-13 Room:422 Time:May 1 12:15-12:30

Structure analysis of deuterated brucite at pressures to 3 GPa by pulsed neutron powder diffraction

OKUCHI, Takuo[1*] ; TOMIOKA, Naotaka[1] ; PUREVJAV, Narangoo[1] ; HARJO, Stefanus[2] ; ABE, Jun[3] ; WU, Gong[2]

[1]Institute for Study of the Earth's Interior, Okayama University, [2]Japan Atomic Energy Agency, [3]CROSS Tokai

Atomic-scale structures around hydrogen atoms in hydrous minerals may significantly change with increasing pressure, which affect thermodynamic stability, optical properties (Raman, IR, etc.), and transport phenomena of the relevant minerals. To directly observe such structure change around hydrogen atoms, we have conducted neutron diffraction experiments of deuterated brucite at high pressures to 2.8 GPa, using a high-resolution neutron powder diffractometer recently installed at J-PARC Materials and Life Science Experimental Facility. To discriminate subtle structure change of deuterium site positions with increasing pressure, the quality of observed diffraction patterns has been considerably improved from the corresponding previous studies by adopting a new-type experimental apparatus and facility. A newly-designed opposed anvil cell apparatus optimized for the pulsed neutron beam (Okuchi et al., High Pressure Research, 33, 777, 2013) was effectively coupled with the time of flight diffractometer TAKUMI, which was designed to have the resolution of delta-d / d ˜0.3% along with moderately-intense beam and low background (Harjo et al., Materials Science Forum, 524, 199). We used single crystal diamond anvls with culet diameter of 2 mm for sample compression along with deuterated glycerine pressure medium. The combination gives very high neutron transparency as well as high resolution to enable acurate structure refinements of tiny sample volume of the order of less than 1 mm^3. Through Rietveld refinements of the observed patterns, tilting of all OD dipoles in the compressed brucite toward one the three nearest-neighbor oxygen anions in the brucite structure was confirmed to be substantial at the observed pressure regime, suggesting the formation of pressure-induced hydrogen bonding. Therefore, at lower crust and mantle wedge conditions, this pressure-induced bonding may play an important role to constrain hydrogen into the relevant hydrous minerals.

Keywords: hydrogen, brucite, high pressure, neutron diffraction

Japan Geoscience Union Meeting 2014
(28 April - 02 May 2014 at Pacifico YOKOHAMA, Kanagawa, Japan)

SMP47-14 Room:422 Time:May 1 12:30-12:45

Factors controlling barite-water distribution of selenium oxyanion

TOKUNAGA, Kouhei[1*] ; YOKOYAMA, Yuka[1] ; TAKAHASHI, Yoshio[1]

[1]Department of Earth and Planetary Systems Science, Graduated School of Science, Hiroshima University

Geochemical behavior of trace elements is controlled by their interaction with major minerals through ion exchange, sorption/desorption, and coprecipitation/dissolution processes, which govern the concentrations of trace elements in natural water. Especially, the coprecipitation process with mineral is potentially important because trace elements can be incorporated and immobilized in the crystal lattice at least until the minerals are dissolved. Previous studies showed that the partitioning behaviors of trace elements to minerals were controlled by many complex factors, such as crystal constraints of ion substitution, effects of complexation in the aqueous phase, rate of crystallization, and changes in temperature or pressure. For instance, Yokoyama [2011, 2012] demonstrated that, in the case of arsenic (As) and selenium (Se) incorporation into calcite, arsenate rather than arsenite is selectively incorporated into calcite, whereas selenite (Se(IV)) rather than selenate (Se(VI)) into calctite because of the high stabilities of calcium arsenate and calcium selenate complexes compared with those for arsenite and selenite. In this study, we focused on the distribution behavior of Se into barite to determine the factors controlling the partitioning behaviors of the trace elements to minerals at the molecular scale by X-ray absorption fine structure (XAFS). Our previous results suggested that the distribution behavior of Se into barite was controlled by two factors: the stability of the surface complex between barite and Se species (=chemical affinity) at the initial process and the stability of the ion substitution in the crystal structure (=structural affinity) for the subsequent process. In this presentation, the barite-water distributions of Se controlled by the structural affinity are highlighted.

The coprecipitation experiments were conducted to examine the influence of ion substitution structure on the distribution behavior of Se into barite as a function of the reaction time in term of the variation of barite morphology, total concentration, oxidation states, and coordination structure of Se in barite. The results showed that both total Se concentration and the Se(VI)/Se(IV) ratio in barite increased abruptly within first 24 hour and almost reached equilibrium after 24 hours. EXAFS analysis for the initial and aged samples showed that the coordination number of Se-Ba in the aged sample is larger than that in the initial stage. The results indicates that a larger amount of Se(VI) than Se(IV) was incorporated from adsorption site on the surface into the barite crystal by substituting sulfate site because of their high crystallinity that can excludes Se(IV) to a larger degree than Se(VI) due to the similar structure of sulfate ion and sulfate. Based on these results, it is considered that the Se(VI) was preferentially incorporated into barite due to its high structural affinity than Se(IV), thus, the Se(VI)/Se(IV) ratios in barite relatively increased through crystallization. These results suggest that structural affinity is an important factor for controlling the distribution behavior of Se between barite and water.

Keywords: barite, selenite, selenate, XAFS, distribution behavior, structural affinity

Japan Geoscience Union Meeting 2014
(28 April - 02 May 2014 at Pacifico YOKOHAMA, Kanagawa, Japan)

SMP47-15 Room:422 Time:May 1 14:15-14:30

Mid- and far-infrared spectroscopy for Li-Al-Mg micas

MAKIO, Masato[1*] ; ISHIDA, Kiyotaka[1]

[1]Graduate School of Social and Cultural Studies

Mica is a one of the major rock forming minerals and widely spread in the earth crust. The hydrothermal synthetic Li-Al-Mg trioctahedral mica series were measured by mid- and far-infrared spectroscopy and X-ray powder diffraction Rietveld refinement: (a)Trilithionite: $K(Li_{1.5}Al_{1.5})$ $(AlSi_3)O_{10}F_2$- Phlogopite: $KMg_3(AlSi_3)O_{10}F_2$, (b)Polylithionite: $K(Li_2Al)Si_4O_{10}F_2$- Tainiolite: $K(LiMg_2)Si_4O_{10}F_2$, (c)Polylithionite- Eastonite: $K(Mg_2Al)(Al_2Si_2)O_{10}F_2$ and OD- F Mg- Masutomilite: $K(LiAlMg)AlSi_3O_{10}(F, OD)_2$.

The Li-Al-Mg micas synthesized hydrothermally at 600- 650 ^{o}C and 150- 200MPa in cold-seal externally heated Tuttle-type vessels. The starting materials were mixed and then sealed in Pt/Au capsules with 20 wt % D_2O (99.9 % in purity). X-ray Rietveld analysis was done using Rietan- 2000 (Izumi and Ikeda 2000). Mid- and far-infrared spectra were measured with JASCO FTIR- 620 spectrometer. Each sample was scanned 256 times in an evacuated sample-chamber.

All samples could refine monoclinic, C2/m (1M polytype). In the 250- 50cm^{-1} far-infrared region , three kinds of bands are observed: these bands due to an in- plane tetrahedral torsional band between 170- 150cm^{-1}, an interlayer K- O_{inner} stretching band between 120- 140 cm^{-1} and K- O_{outer} stretching band between 90- 100 cm^{-1}. With increasing<K- O_{inner}>, K- O_{inner} stretching band shifts higher frequency, while with increasing <K- O_{outer}>, K- O_{outer} stretching band shifts lower frequency. In the 650- 250cm^{-1} mid- and far-infrared region, two parts of bands are observed. With increasing $^{[4]}$Si→Al, (Si,Al)- O deformational band in the range of 600- 400cm^{-1} became broad and merged.

Keywords: Li-Al-Mg mica, hydrothermal synthesis, mid-infrared, far-infrared, Rietveld analysis

Japan Geoscience Union Meeting 2014
(28 April - 02 May 2014 at Pacifico YOKOHAMA, Kanagawa, Japan)

SMP47-16 Room:422 Time:May 1 14:30-14:45

Cesium (Cs) Sorption Experiments into Weathered Biotite in Fukushima

KIKUCHI, Ryosuke[1*] ; KOGURE, Toshihiro[1]

[1]Earth and Planetary Sci., Univ. Tokyo

After the accident of Fukushima Daiichi nuclear power plant in March 2011, radioactive contamination of the soil around the plant has become an urgent problem in Japan. Previous studies proposed that weathered micaceous minerals present favorable sorption environments for Cs^+. Because the contaminated areas in Fukushima are mainly covered with weathered granite soil, weathered biotite with hydrated (vermiculite) interlayers is abundant. Hence basic understanding of Cs^+ sorption process into the biotite is important to find the recipe for decontamination of radiation. Some of previous studies reported that Cs^+ is adsorbed mainly at the frayed-edge sites of such micaceous crystals. However, other studies indicated that Cs^+ penetrates deeply inside the crystals, along the interlayer regions by ion-exchange. In this study, we performed Cs^+ sorption experiments using single-crystals of Fukushima weathered biotite with well-regulated edge surfaces, and considered the relationship between the weathering state of biotite and Cs^+ sorption property.

Fresh and two kinds of weathered biotite were collected from granodiolite of Abukuma granite body in Fukushima prefecture. For each sample, cross sections of $<$1 mm thick perpendicular to the basal planes were prepared. Surface damage formed by the mechanical grinding/polishing was removed by Ar^+ ion sputtering. These sections were immersed in 30 mL of CsCl aqueous solution of 2000 / 200 / 20 / 0 ppm for 24 hours at room temperature to incorporate Cs^+.

After the reaction, the surfaces of the sections were investigated using scanning electron microscopy (SEM) with energy dispersive X-ray spectroscopy (EDS). SEM-EDS with various acceleration voltage indicated that the concentration of the sorbed Cs^+ does not change in the depth direction of ˜several microns range. Cs^+ was apparently sorbed at 2000 ppm but not at 200 ppm for fresh biotite, whereas Cs^+ was sorbed at both concentrations in the weathered biotite. Back-scattered electron (BSE) images and EDS analysis showed preferred sorption of Cs^+ at the regions probably with dense vermiculite interlayers in the weathered biotite. Moreover, some specimens were processed into this foils using focused ion beam (FIB) and examined using scanning transmission electron microscopy (STEM). High-angle annular dark field (HAADF) imaging in STEM has visualized Cs^+-incorporated interlayer regions individually in the weathered biotite.

Keywords: Biotite, Vermiculite, Cesium, SEM-EDS, FIB, HAADF-STEM

Japan Geoscience Union Meeting 2014
(28 April - 02 May 2014 at Pacifico YOKOHAMA, Kanagawa, Japan)

SMP47-17 Room:422 Time:May 1 14:45-15:00

Pressure-induced phase transitions of vaterite, a metastable phase of calcium carbonate

MARUYAMA, Koji[1*] ; KOMATSU, Kazuki[1] ; KAGI, Hiroyuki[1] ; YOSHINO, Toru[2] ; NAKANO, Satoshi[3]

[1]Geochemical Research Center, Univ. Tokyo, [2]TIRI, [3]National Institute for Materials Science

1. Introduction

Calcium carbonate is one of the most common and ubiquitous minerals on the Earth's surface and plays an important role in global carbon cycle. There are many studies about high-pressure behavior of calcite and aragonite. At ambient temperature, calcite transforms to calcite II at about 1.5 GPa and to calcite III at about 2.0 GPa. The transition from aragonite to post-aragonite phase was observed at about 40 GPa. In contrast, no study has been reported on the high-pressure behavior of vaterite, which is a metastable phase of $CaCO_3$, and is known as a precursor material of more stable $CaCO_3$ polymorphs, calcite and aragonite. In this study, the high-pressure behavior of vaterite was investigated by in situ synchrotron X-ray diffraction (XRD) experiments using a diamond anvil cell.

2. Experimental method

In this study, vaterite was synthesized by mixing two aqueous solutions, 60 mM $CaCl_2$ aq. and 60 mM $NaHCO_3$ aq., kept at 30 degree C. The mixed solution was sealed in a plastic bottle and stirred for 10 min at 30 degree C, and then filtered using an aspirator, washed by pure water, and dried at about 130oC. The obtained white powder was identified as pure vaterite using powder XRD method.

High-pressure experiments were carried out using a diamond anvil cell (DAC). The synthesized vaterite and several tiny ruby crystals were loaded into a gasket hole together with helium as a pressure transmitting medium. The pressure was changed between 0-14 GPa, which was measured by the ruby fluorescence method. XRD patterns were measured at each pressure at room temperature. X-ray diffraction observations were carried out at room temperature using the synchrotron beam line of BL18C in the Photon Factory, Japan.

3. Results and discussion

XRD patterns recorded at pressures lower than 4.7 GPa indicated that the sample consists of vaterite only. At 4.7 GPa, main three peaks of vaterite were split and a peak assignable to calcite III appeared. The discontinuous changes in axial lengths were observed by refinement of lattice constants using a crystal structure model proposed by Le Bail et al. (2011). This change suggests a pressure-induced phase transition from vaterite to a high-pressure form (hereafter vaterite II). Change in the diffraction intensities suggested that vaterite II transformed to calcite III with increasing pressure up to about 9 GPa. At 12.9 GPa, new diffraction spots were observed. These spots were not explainable with the diffraction peaks from any polymorphs of $CaCO_3$. This implies that the new spots are derived from another high-pressure phase of vaterite (vaterite III). After decompression, the recovered sample was identified as a mixture of calcite and vaterite. These results indicate that the transition from vaterite II to calcite III is irreversible. In this study, new high-pressure phases of $CaCO_3$ (vaterite II and III) were discovered by high-pressure experiments of vaterite at ambient temperature.

Keywords: vaterite, phase transition, high-pressure

Japan Geoscience Union Meeting 2014
(28 April - 02 May 2014 at Pacifico YOKOHAMA, Kanagawa, Japan)

SMP47-18 Room:422 Time:May 1 15:00-15:15

Huge plastic deformation of SiO_2 glass at room temperature

WAKABAYASHI, Daisuke[1*] ; FUNAMORI, Nobumasa[1] ; SATO, Tomoko[2]

[1]Department of Earth and Planetary Science, University of Tokyo, [2]Department of Earth and Planetary Systems Science, Hiroshima University

Covalent solids are known to be hard but brittle. Moreover, glasses do not deform plastically by dislocation movement seen in crystals due to the lack of long-range order. However, SiO_2 glass, a highly covalent glass, has long been known to be densified up to about 20% by applying high pressure. This phenomenon is called permanent densification, which is some kind of phase transformation caused by the reconstruction of the network structure consisting of SiO_4 tetrahedra [e.g., Wakabayashi et al., 2011], and could be considered as plastic deformation in a broad sense. Recently, the differential strain of SiO_2 glass in its intermediate-range structure, corresponding to the first sharp diffraction peak, was measured under uniaxial compression by a radial X-ray diffraction method, in which X-rays irradiate the sample from a direction perpendicular to the compression axis (i.e., from a radial direction) [Sato et al., 2013]. In those measurements, very large differential strains were observed under pressure and surprisingly also after decompression. This residual strain may be attributable to the anisotropic reconstruction of the network structure (i.e., anisotropic permanent densification).

In this study, the change in size of bulk samples was measured for uniaxially-compressed SiO_2 glass to clarify whether SiO_2 glass undergoes plastic deformation in a narrow sense, i.e., without density change. X-ray diffraction measurements were also conducted in a wide Q-range with 50 keV monochromatic X-rays by irradiating the recovered sample from the radial direction to clarify whether a differential strain remains only in the intermediate-range network structure or also in the short-range SiO_4 tetrahedral structure. Pressures were generated by using a diamond-anvil cell. The starting material was in the form of a disk, and was adjusted to have an appropriate initial thickness to be compressed under uniaxial conditions, i.e., pinched directly by the two anvils, above a certain pressure. Three independent experiments were conducted with an argon pressure medium up to 20 GPa in run 1, 12 GPa in run 2, and 6 GPa in run 3. The change in size of sample was measured with an optical microscope. X-ray diffraction measurements were carried out at PF AR-NE1. All the experiments were conducted at room temperature.

In runs 1 and 2, the diameter of sample was found to increase significantly with pressure from 6-8 GPa, where uniaxial conditions were achieved, to the maximum pressure of each run without fracturing, and it became about 15% larger at 20 GPa than at 0 GPa. The macroscopic differential strain was about an order of magnitude larger than the microscopic differential strain reported in the previous study [Sato et al., 2013], suggesting that SiO_2 glass deformed plastically at room temperature. The X-ray diffraction measurements clarified that the recovered samples were in the fully densified state (about 20% densified). It was also revealed that a residual differential strain was observed only in the intermediate-range network structure and its magnitude was consistent with the previous study [Sato et al., 2013]. On the other hand, in run 3, the sample did not deform plastically by uniaxial compression from 2-3 GPa to 6 GPa. The X-ray diffraction pattern of the recovered sample was the same as that of the ordinary SiO2 glass. Permanent densification is known to begin at about 9 GPa under hydrostatic conditions [e.g., Wakabayashi et al., 2011], and it is suggested that permanently densified SiO_2 glass easily undergoes plastic deformation even at room temperature.

D. Wakabayashi et al., *Phys. Rev. B* **84**, 144103 (2011).
T. Sato et al., *J. Appl. Phys.* **114**, 103509 (2013).

Keywords: SiO_2 glass, plastic deformation, permanent densification, network structure

Japan Geoscience Union Meeting 2014
(28 April - 02 May 2014 at Pacifico YOKOHAMA, Kanagawa, Japan)

SMP47-19 Room:422 Time:May 1 15:15-15:30

Shock compression of synthetic amino acid - silica gel complex modeling for comet nucreus

MURAI, Takuro[1] ; OKUNO, Masayuki[2*] ; OKUDERA, Hiroki[2] ; ARASUNA, Akane[1] ; MASHIMO, Tsutomu[3] ; CHEN, Liliang[3] ; MIZUKAMI, Tomoyuki[2] ; ARAI, Shoji[2]

[1]Graduate School of Kanazawa University, [2]Kanazawa University, [3]Kumamoto University

Some amino acids were found in comet coma particle and Murchison meteorite [1,2]. These reports may suggest a possibility that basic materials of primitive life on the earth were formed in the space and delivered to the earth.

Greenberg et al. (1997)[3] reported the almost comets are made of organic compounds, silicates and ice. On the other hand, silica gel contains a non crystalline SiO_4-$_n(OH)_n$ framework with water molecules. So, silica gel is a suitable model material for comet. In this study, in order to investigate the stability of amino acid (L-serine) in the comet nucleus during the impact to the earth, synthetic amino L-serine - silica gel complex materials were shock compressed and the structure change of the recovered samples were analyzed by X-ray diffraction measurements, IR and Raman spectroscopies. Shock compression experiments were performed at 8.2, 10.9, 19.7 and 26.9 GPa.

By Raman spectroscopic analyses, it was indicated that synthetic complex materials include two types of L-serine such as crystalline L-serine and hydrated L-serine. Obtained Raman spectra of shocked materials show the L-serine crystal was disappeared and hydrated L-serine molecules survived at 19.7 GPa of shock pressure. Therefore, the sample at 19.7 GPa includes only hydrated L-serine molecules. This may indicate that intermolecular hydrogen bonds of L-serine molecules may be broken by shock compression with water molecule.

The shock pressure of 19.7 GPa is consistent with the estimated impact pressure of about 19% comets to the earth reported by Blank et al. (1999) [4]. This fact may indicate that a possibility for the basic materials of primitive life on the earth were formed in the space and delivered to the earth.

References

[1] Elisila J.E., Glavin D.P., Doworkin J.P. (2009) Commetary glycine in samples returned by stardust. Meteoritics & Planetary Science 44, 1323-1330

[2] Cronin J.R. and Pizzarello S. (1983) Amino acid in meteorites. Advances in space research 3, 5-18

[3] Greenberg J.M., Aigen Li (1997) Silicate core-organic refractory mantle articles as interstellar dust and as aggregates in comets and stellar disks. Advance in space research 19, 981-990

[4] Blank J.G., Millar G.H., Michael J.A., Winas R.E. (1999) Experimental shock chemistry of aqueous amino acid solution and comtary delivery of periodic compounds. Origin of Life and Evolution of the Biosphere 31, 15-51

Keywords: comet, amino acid, silica gel, shock compression

Japan Geoscience Union Meeting 2014
(28 April - 02 May 2014 at Pacifico YOKOHAMA, Kanagawa, Japan)

SMP47-20 Room:422 Time:May 1 15:30-15:45

Microtexture and formation mechanism of impact diamonds from the Popigai crater, Russia

OHFUJI, Hiroaki[1*] ; YAMASHITA, Tomoharu[1] ; LITASOV, Konstantin[2] ; AFANASIEV, Valentin[2] ; POKHILENKO, Nikolai[2]

[1]Geodynamics Research Center, Ehime University, [2]Siberian Branch of the Russian Academy of Sciences

Large meteoritic impact occasionally produces an extensive amount of diamond on the surface of the Earth [1, 2]. Popigai crater located in the north central Siberia is a typical example of such diamond-forming shock events and has recently been brought back into the spotlight due to its vast estimated reserves of the impact diamonds [2-4]. Authigenic impact diamonds occur in shocked graphite-bearing garnet-biotite gneisses that are found as inclusions in impact melt rocks, so-called tagamites and suevites. Popigai diamonds occur as irregular to tabular grains of 0.5-2 mm size (up to 10 mm) and usually show yellow, gray or black colors [3]. Electron microscopic (SEM and TEM) observations in previous studies described that they are polycrystalline aggregates of 0.1-1 μm grains and show a distinct preferred orientation along the [111], which is in a coaxial relation to the [001] of the original graphite source [2-4]. This crystallographic feature as well as the occasional coexistence of lonsdaleite, a metastable carbon polymorph, suggest the Martensitic phase transformation for the potential formation process of the impact diamonds from Popigai crater. However, the textural feature of the impact diamonds and its variation has not fully been examined. Here, we present the result of detailed microtextural observations of impact diamonds from the Popigai crater by transmission electron microscopy (TEM) and discuss the formation mechanism and condition in comparison with those of synthetic diamonds obtained by high pressure and high temperature experiments.

In total 10 diamond grains (7 transparent yellowish and 3 black samples) from the Popigai crater were studied. Each sample was first analyzed by a micro-focus XRD equipped with a Mo target and an IP detector. The results showed that transparent samples consist mostly of diamond and occasionally contain lonsdaleite, while black ones are a mixture of graphite, lonsdaleite and diamond, which are all in a coaxial relation as shown by 2D diffraction patterns collected in transmission geometry. Each sample was then transferred to a focused ion beam (FIB) system to cut out TEM foil sections perpendicular to the surface (of the tabular grains). TEM observation revealed that although all the samples commonly possess layered structures and preferred orientation (mostly along [111] of diamond), there are varieties in crystallite (grain) size (down to 10-20 nm) and degree of preferred orientation. Taking into account the similarity in texture and preferred orientation feature between the Popigai diamonds and synthetic diamond, the variation is likely derived from the small difference in crystallinity of the starting graphite sources and perhaps more significantly from the difference in shock temperature.

According to the shock features recorded in the silicate minerals of the diamond-bearing impactites, the threshold pressure for the onset of the graphite-diamond transformation is estimated to be 34-36 GPa [3]. However, our recent experimental synthesis [5] demonstrated that a similar phase assembly (mostly diamond + traces of lonsdaleite) and microtexture can be produced at much lower pressures of 15-25 GPa at $>$2000 ℃. The shock pressure as well as shock- and post-shock temperature accompanied with the formation of the Popigai crater might be needed to be reevaluated carefully to understand the real nature of the giant impact.

[1] Masaitis V.L. (1998) Meteoritics & Planetary Science. 33. 349-359.
[2] Langenhorst F., Shafranovsky G.I., et al. (1999) Geology. 27. 747-750.
[3] Deutsch A., Masaitis V.L., et al. (2000) Episodes. 23. 3-11.
[4] Koeberl C., Masaitis V.L., et al. (1997) Geology. 25. 967-970.
[5] Isobe F., Ohfuji H., et al. (2013) Journal of Nanomaterials. 2013. 380165.

Japan Geoscience Union Meeting 2014
(28 April - 02 May 2014 at Pacifico YOKOHAMA, Kanagawa, Japan)

SMP47-21 Room:422 Time:May 1 16:15-16:30

Melting and crystal growth textures developed in rapid heating and cooling of olivine fine particles

ISOBE, Hiroshi[1*] ; GONDO, Takaaki[1]

[1]Grad. Sch. Sci. Tech., Kumamoto Univ.

Olivine is one of the most common mineral in the solid Earth and chondritic meteorites. Olivine crystals show characteristic textures in chondrules depending on heating and cooling histories in chondrule formation processes at the early solar system. In this study, quick heating and cooling experiments of mixed olivine particles were carried out with a fine particles free falling apparatus (Isobe and Gondo, 2013). In the run products, characteristic melting and crystal growth textures controlled by phase relations, diffusion, and nucleation and growth behavior of olivine can be seen.

Starting material is mixed powder of natural olivine (Fo90), fayalite and an artificial olivine (Fo55). The typical diameter of the starting material particles is approximately 100 micron meters. Each particle is single crystal of olivine or mixture of two or three kinds of raw materials. Heating and cooling experiments are carried out in a high temperature furnace with mass flow controllers to regulate oxygen fugacity and total gas flow rate. Particles can be heated to 1400 degrees C within two seconds, are kept over 1400 degrees C approximately one second and quenched within a second. Maximum temperature has negative correlation to diameter of the particles, and cooling rate has positive correlation to the diameter depending on the falling velocity of the particles. Run products show spherical shape when the particles mostly melted, and are crystal fragments when the particles did not melt. The outside shape of the retrieved run products are observed with a scanning electron microscope. Inner textures of the particles are observed on polished section of the particles. Chemical compositions are also analyzed on the sections.

Fayalite grains are completely melted and Fo90 olivine grains are not melted by themselves concordantly with the phase relation of olivine. Internal textures of Fo55 olivine crystals show quick partial melting when the temperature reach solidus temperature. In the mixed olivine particles, relict crystals of Fo90 and Fo55 olivines dissolve to iron-rich melt derived from melting of fayalite. The dissolution of relict crystals produce steep chemical gradient at interface between crystals and melt.

Run products like barred olivine chondrules or melted cosmic spherules are produced from completely melted particles. In the particles including relict crystals, overgrowth textures from the relict crystals can be seen. Dendritic olivine crystals with regulated crystallographic orientation are developed in melted particles. Surface texture of melted particles may be affected by the dendritic olivine crystals. Oriented magnetite dendrites may also occur between olivine crystals when oxygen fugacity was in the magnetite stability field. Melting, nucleation and crystal growth processes in a few seconds can be discussed from the textures in the run products.

Keywords: Olivine, chondrule, nucleation, crystal growth, dendrites, quench texture

Japan Geoscience Union Meeting 2014
(28 April - 02 May 2014 at Pacifico YOKOHAMA, Kanagawa, Japan)

SMP47-22 Room:422 Time:May 1 16:30-16:45

Temperature-dependent thermal expansivities of aluminum-free silicate melts and borosilicate melts

SUGAWARA, Toru[1*] ; KATSUKI, Junki[2] ; YOSHIDA, Satoshi[2] ; MATSUOKA, Jun[2] ; MINAMI, Kazuhiro[3] ; OCHI, Eiji[3]

[1]Akita University, [2]The University of Shiga Prefecture, [3]Japan Nuclear Fuel Limited

Thermal expansivities (dV/dT) of silicate melts are essential in a thermodynamic calculation of phase equilibira in magmatic system as a function of pressure and temperature and in a numerical simulation of flow and thermal structures in glass melting furnace. Previous studies have been suggested that the dV/dT of alumino-silicate melts (Lange, 1996; Potuzak et al., 2006) and magmatic silicate melts (Lange, 1997; Ghiorso and Kress, 2004) is a function of composition, but independent of temperature. On the other hand, it has been reported that the dV/dT of SiO_2-TiO_2-Na_2O melt (Liu and Lange, 2001) and 50SiO_2-25CaO-25MgO melt (Gottsmann and Dingwell, 2000) decrease with increasing temperature. Recently, we found that simulated-radioactive waste glass melt which has sodium-borosilicate composition also shows negative temperature-dependent dV/dT (Sugawara et al., 2013). We carried out density measurements for sodium-silicate melts ((100-x)SiO2-xNa2O, x=23 or 32.3 mol%), commercial soda-lime silicate melt (71SiO_2-6MgO-9CaO-14Na_2O, mol%) and borosilicate melts (66.6SiO_2-yB_2O_3-(33.33-y)Na_2O where y=8.3, 16.6, 25; 66.6SiO_2-(12.5+z)B_2O_3-(4.2-z)Al_2O_3-zCaO-(16.7-z)Na_2O where z=0 or 4.2 mol%). The temperature and compositional dependences of the dV/dT are discussed based on the new density data and the literature data.

The high-temperature density (dHT) measurement has been made by double-bob Archimedean method between 1173K and 1665K. The glass samples were annealed around glass transition temperature (Tg) for 6-396 hours and quenched. Then the density of annealed glasses at 298K (d298) and linear thermal expansivity (dL/L) were determined by Archimedean method and TMA. respectively. The densities of supercooled melt around Tg (dTg) were calculated from the d298 and the dL/L of glasses. Then, molar volume as a function of temperature and the dV/dT of melts were obtained by combining the dTg and the dHT.

The dV/dT values of all samples examined in this study show negative temperature dependence. In the sodium silicate melts, the temperature dependence of the dV/dT is remarkable when the SiO2 content increases from 50 to 67 mol%, while the dV/dT becomes close to zero as further increase in the SiO2 content. The negative temperature-dependent dV/dT observed in the 71SiO_2-6MgO-9CaO-14Na_2O melt can be reproduced by an additive sum of the dV/dT of 67.8SiO_2-32.2Na_2O, diopside (Gottsmann and Dingwell, 2000) and wollastonite (Potuzak et al., 2006) melts. High-temperature Raman spectroscopy for the SiO_2-Na_2O and SiO_2-Na_2O-MgO melts has been indicated that amount of Q4 species increases with increasing temperature and SiO_2 and MgO contents (Maehara et al., 2004, 2005). Therefore, the temperature dependent dV/dT for the sodium-silicate, commercial soda-lime silicate and diopside melts can be rationalized by an increase of rigid Q4 species at high temperature. The temperature dependence of the dV/dT is most remarkable in the 66.6SiO_2-8.3B_2O_3-25Na_2O melt among the borosilicate melts. The dV/dT decreases with replacement of Na_2O by B_2O_3 or CaO and of B_2O_3 by Al_2O_3, suggesting that partial molar dV/dT of B_2O_3 depends on temperature-induced coordination change of boron and their composition dependence (Wu and Stebbins, 2010).

Acknowledgements: This work was a part of the research supported by Japan Nuclear Fuel Limited with Grant-in-Aid by the Ministry of Economy, Trade and Industry.

Keywords: silicate melt, thermal expansivity, densitometry

Japan Geoscience Union Meeting 2014
(28 April - 02 May 2014 at Pacifico YOKOHAMA, Kanagawa, Japan)

SMP47-P01 Room:Poster Time:May 1 18:15-19:30

Thermodynamic properties of Mg-postperovskite with Fe^{3+} and Al^{3+} dopant: an internally consistent LSDA+U study

WANG, Xianlong[1*] ; TSUCHIYA, Taku[1]

[1]GRC, Ehime University and ELSI, Tokyo Institute of Technology

Thermodynamic properties of $MgSiO_3$ perovskite (Pv) and postperovskite (PPv) with Fe and Al incorporation at high pressure and high temperature are important to understand the Earth's lower mantle (LM). The thermodynamic properties of Fe^{2+}, Fe^{3+}, and Al^{3+}-bearing Pv[1,2,3] and Fe^{2+}-bearing PPv[4] have been investigated in our previous works uniformally based on first-principles method combined with the internally consistent LSDA+U method and quasi-harmonic approximation (QHA). However, to date, effects of trivalent ions, Fe^{3+} and Al^{3+}, on the thermodynamic properties of PPv are still unclear. In this work, by using the same methods with previous works, the structural, electronic, magnetic, and thermodynamic properties of $(Mg,Fe^{3+})(Si,Fe^{3+})O_3$ and $(Mg,Fe^{3+})(Si,Al^{3+})O_3$ PPv at several pressures, from 0 GPa to 180 GPa, are investigated. Our results show that for $(Mg,Fe^{3+})(Si,Fe^{3+})O_3$ PPv, Fe^{3+} ions substituted at Mg and Si site respectively have the high and low spin state within the deep LM pressure range, while Fe^{3+} in $(Mg,Fe^{3+})(Si,Al^{3+})O_3$ PPv remains in the high spin state. Furthermore, separated phase between Fe_2O_3 and Al_2O_3 in PPv is found unfavorable.

References:
[1] Metsue, A. and Tsuchiya, T. (2012) Geophys. J. Int. **190**, 310.
[2] Tsuchiya, T. and Wang, X. (2013) J. Geophys. **118**, 83.
[3] Wang, X. and Tsuchiya, T. To be submitted.
[4] Metsue, A. and Tsuchiya, T. (2011) J. Geophys. Res. **116**, B08207.

Keywords: First-principles method, Internally consistent LSDA+U, Thermodynamic properties, Postperovskite

Japan Geoscience Union Meeting 2014
(28 April - 02 May 2014 at Pacifico YOKOHAMA, Kanagawa, Japan)

SMP47-P02 Room:Poster Time:May 1 18:15-19:30

Thermal expansion of $Ca(OD)_2$ at high pressure

NAGAI, Takaya[1*] ; SANO, Asami[2] ; IIZUKA, Riko[3] ; KAGI, Hiroyuki[3] ; HATTORI, Takanori[4]

[1]Faculty of Science, Hokkaido Universuty, [2]Japan Atomic Energy Agency, [3]Graduate School of Science, The University of Tokyo, [4]Materials and Life Science Division, J-PARC Center

$Ca(OH)_2$ is one of the important hydrous minerals to understand structural behavior at high pressure and high temperature, because this type of structure is a building unit in more complex hydrous phases such as chondrodite. It is surprising that only a few previous researches can be found on crystallography of $Ca(OH)_2$ in the conditions of simultaneously high pressure and high temperature. We gave an oral presentation about some preliminary results in this conference last year. We have continued to analyze the data carefully and will add some new information.

Deuterated samples were prepared via hydrothermal treatment with CaO fine powders and excess D_2O water in a Teflon lined stainless steel autoclave at 493 K for 4 days. After the hydrothermal treatment was completed, precipitates were filtered out, washed with D_2O water, and then dried at 383 K under vacuum for 3 hours. The products were confirmed to have the CdI2-type structure by conventional powder X-ray diffraction measurements and were checked to be deuterated by IR absorption spectra. Synchrotron X-ray diffraction experiments were performed at the beamline AR-NE5C, KEK, Japan in order to obtain cell parameters of $Ca(OD)_2$ at various P-T conditions from 2-4 GPa and 300-800 K. TOF neutron powder diffraction measurements of $Ca(OD)_2$ were carried out from 300 to 773 K at high pressure at the PLANET beamline in J-PARC, Japan. Pressure was estimated by comparing unit cell parameters with those obtained by synchrotron experiments.

All our TOF data obtained include only $Ca(OD)_2$ peaks and no peaks from sample surrounding materials such as ZrO_2 pressure medium, graphite furnace and WC anvils could be detected owing to radial collimators equipped with the 6-ram pressure apparatus (Atsuhime). The detailed structure parameters such as lattice parameters and atomic coordinates could be reasonably refined by the Rietveld method by using a program GSAS. It is an interesting result that thermal expansion along the *c*-axis seems to be suppressed at high pressure comparing to that at ambient pressure. Mechanism of the thermal expansion of $Ca(OD)_2$ at high pressure will be discussed.

Keywords: portlandite, thermal expansion, high pressure, synchrotron X-ray diffraction, TOF neutron diffraction

Japan Geoscience Union Meeting 2014
(28 April - 02 May 2014 at Pacifico YOKOHAMA, Kanagawa, Japan)

SMP47-P03 Room:Poster Time:May 1 18:15-19:30

High-temperature heat capacity of SiO2-Al2O3-RO (R=Mg, Ca, Sr, Ba) melts

SUGAWARA, Toru[1*]

[1]Akita University

Heat capacity (Cp) of silicate melts is an important property in consideration of phase equilibria in magmatic system and a numerical simulation of flow and thermal structures in glass melting furnace. Heat capacity of aluminum-free melts can be expressed by an additive function of partial molar heat capacities for components (Richet and Bottinga, 1985). On the other hand, it has been reported that the heat capacities of alumino-silicate melts show complicated dependence on both temperature and composition (Richet and Mysen, 2005). However, they are still poorly understood due to the lack of calorimetric data. This study provides new experimental data for the high-temperature heat capacities of Ca, Sr and Ba-bearing alumino-silicate melts.

Drop calorimetry measurements were performed for $50SiO_2$-$25Al_2O_3$-25CaO (An), $36.5SiO_2$-$27Al_2O_3$-36.5CaO (Ca36.5), $8SiO_2$-$30Al_2O_3$-62CaO (Ca62) and $75SiO_2$-$12.5Al_2O_3$-12.5SrO or 12.5BaO (Sr12.5, Ba12.5) melts between 873K and 1889K using a Bunsen ice calorimeter. Heat capacity of melts was determined from the differential of measured relative enthalpy. The heat capacity of anorthite melt is 1.356+0.0001151T(K) (J/K-g), which is consistent with the value reported by Richet and Bottinga (1985). The heat capacities for Ca36.5, Ca62, Sr12.5 and Ba12.5 are 1.532, 1.508, 1.313 and 1.160 (J/K-g), respectively, and they are independent of temperature.

The temperature and compositional dependence of the Cp for SiO_2-Al_2O_3-RO (R=Mg, Ca, Sr, Ba) melts are considered by combining new calorimetric data and literature data by drop calorimetry (n=11, Richet and Bottinga, 1984; Courtial and Richet,1993; Neuville and Richet, 1991; Richet and Neuville, 1992) and by differential scanning calorimetry (n=22, Webb, 2008, 2011). The positive temperature dependence is observed in the SiO_2-Al_2O_3-MgO melts as reported by Courtial and Richet (1993). In the system SiO_2-Al_2O_3-CaO, temperature dependence of the Cp is only observed at anorthite composition. The heat capacity of alkaline-earth aluminosilicate melts can be expressed by a symmetric solution model. The derived heat capacity of mixing is negative value in all of the systems. At constant temperature and oxide ratio, the heat capacity decreases with decreasing field strength of alkaline-earth elements (Ba <Sr <Ca <Mg), suggesting that configurational freedom is restricted in the cations with lower field strength due to the charge compentation effect of aluminum. Further experimental data for Sr and Ba-bearing melts are required to generalize temperature dependence of the heat capacity.

Keywords: Silicate melt, Heat capacity, Calorimetry

Japan Geoscience Union Meeting 2014
(28 April - 02 May 2014 at Pacifico YOKOHAMA, Kanagawa, Japan)

SMP47-P04 Room:Poster Time:May 1 18:15-19:30

Viscosity of titanium-bearing silicate melts at high pressure

SUZUKI, Akio[1*]

[1]Tohoku University

Knowledge about viscosity of silicate melt is valuable for understanding the activity of magma in the planetary interiors. The high-Ti magmas erupted on the lunar surface. These magmas contains TiO2 up to 16 wt%. Because the viscosity change at high pressure is affected by the structural change of TO4-network, it is very interesting to know the influence of Ti on the pressure dependence of viscosity. We performed viscosity measurement of K2TiSi4O11 melt as an analogue of the lunar high-Ti magmas. Viscosity was measured by the falling sphere method using an X-ray radiography system. Experiments were performed at the NE7A station of the PF-AR synchrotron radiation facility in KEK, Tsukuba, Japan. We found that the viscosity of K2TiSi4O11 melt has a viscosity minimum at 3 GPa. Paris et al. (1994) reported that the coordination number of titanium increases with increasing pressure on the basis of the XANES spectra of glasses synthesized under high pressure. Our results suggest that the viscosity minimum of K2TiSi4O11 is strongly related to the coordination change of titanium. The viscosity minimum is also found in the terrestrial MORB magma. Recently, Sakamaki et al. (2013) proposed that the viscosity minimum causes the low velocity zone of seismic wave in the upper mantle. The present study suggests that the high-Ti melt causes an attenuating zone in the deep lunar mantle.

Keywords: magma, viscosity, moon, mantle

Japan Geoscience Union Meeting 2014
(28 April - 02 May 2014 at Pacifico YOKOHAMA, Kanagawa, Japan)

SMP47-P05 Room:Poster Time:May 1 18:15-19:30

Study of physical properties of Fe-Si alloy at high pressureusing using synchrotron radiation Mossbauer spectroscopy

SUZUKI, Nanami[1*] ; OHTANI, Eiji[1] ; HIRAO, Naohisa[2] ; KAMADA, Seiji[1] ; HAMADA, Maki[3] ; SAKAMAKI, Tatsuya[1] ; OHISHI, Yasuo[2] ; MASUDA, Ryo[4] ; MITSUI, Takaya[5]

[1]Department of Earth and planetary materials science, Graduate School of Science, [2]Japan Synchrotron Radiation Research Institute, Hyogo, 679-5198, Japan, [3]School of Natural System, College of Science and Engineering, Kanazawa University, Kanazawa, 920-119, [4]Research Reactor Institute, Kyoto University, Osaka, 590-0494, Japan, [5]Japan Atomic Energy Agency, Hyogo, 679-5148, Japan

The Earth's core is divided into the liquid outer core and solid inner core based on seismological observations. The Earth's core has been geochemically and cosmochemically thought to be mainly composed of Fe. The density of the core is smaller than that of pure iron under the core conditions. Therefore, the core has been considered to contain light elements, such as H, S, Si, C, and O. Si is one of the most important light elements in the core. Although the phase relations and compression behaviors in the Fe-Si alloy have been studied at high pressure and temperature in order to investigate properties of the inner core, magnetic properties of the alloys have not been studied well. In order to clarify the relationship between the magnetic transition and the structural transition of the Fe-Si alloy, we made simultaneous measurements of X-ray diffraction and synchrotron M*ö*ssbauer spectroscopy of the Fe-Si alloy up to 40 GPa at room temperature.

The Fe-Si alloy used for the measurements has a composition of $Fe_{0.95}Si_{0.05}$ enriched with ^{57}Fe. The starting material was synthesized by melting the mixture of ^{57}Fe and Fe-Si alloys under the Ar-H_2 atmosphere by laser heating. M*ö*ssbauer spectra and XRD patterns were obtained at the beamlines, BL10XU and BL11XU of SPring-8 up to 40 GPa at room temperature. Our M*ö*ssbauer data together with X-ray diffraction data revealed that the magnetic transition from magnetic to non-magnetic phase occurs at 18 GPa simultaneously with the bcc to hcp transition. The change in the sound velocity and compression behavior of the Fe-Si alloy has been reported associated with the structural transformation of the alloy from bcc to hcp. The present results imply that the change in these physical properties is caused not only by the structural change but also by the magnetic transition.

Japan Geoscience Union Meeting 2014
(28 April - 02 May 2014 at Pacifico YOKOHAMA, Kanagawa, Japan)

SMP47-P06 Room:Poster Time:May 1 18:15-19:30

Experimental determination of post-spinel transition boundary in Fe_2SiO_4

MATSUZAWA, Taisuke[1*] ; KOJITANI, Hiroshi[1] ; AKAOGI, Masaki[1]

[1]Department of Chemistry, Gakushuin University

It is widely accepted that $(Mg,Fe)_2SiO_4$ ringwoodite is the most abundant mineral in the mantle transition zone. Because spinel-type Fe_2SiO_4 is the endmember of $(Mg,Fe)_2SiO_4$ ringwoodite, many investigators have been studied on phase transitions of Fe_2SiO_4 spinel (Kawada 1977, Ohtani 1979, Morooka 1992, Katsura et al. 1998). Spinel-type Fe_2SiO_4 decomposes into $2Fe_xO+SiO_2$(stishovite)+2(1-x)Fe above about 18GPa. However, the dissociation boundary has not yet been established well due in part to difficulty in oxygen fugacity control. In this study, we determined the post-spinel phase boundary in Fe_2SiO_4 by high-pressure experiments controlling oxygen fugacity with the Fe-FeO buffer.

A starting material of high-pressure experiments was a mixture of Fe_2SiO_4 (fayalite), Fe_xO and Fe with molar ratios of 10:2:1, and it was packed in a Fe capsule. Oxygen fugacity of the sample at high pressure and high temperature was controlled by the Fe-FeO buffer. The high-pressure experiments were performed using a Kawai-type 6-8-type multi-anvil apparatus at 16-20GPa and 1000-1400 ℃. The starting samples were heated at the desired conditions for 3-6 hours, and then quenched and decompressed to ambient conditions. Recovered samples were identified by using powder XRD method and SEM-EDS, and then lattice parameters of FexO were determined by using powder XRD. The x values in Fe_xO were estimated from the composition-lattice parameter relationship of Fe_xO by McCammon (1993).

The post-spinel transition boundary in Fe_2SiO_4 was determined to be P(GPa) = -0.0021T(℃) + 20.0 in the temperature range of 1000-1400 ℃. The phase boundary has a negative slope. Our boundary is almost consistent with those of Ohtani (1979) and Katsura et al. (1998). Katsura et al. (1998) interpreted that the negative slope of the boundary in the previous studies was apparent which was caused by slow kinetics of spinel decomposition. Because our study indicated that the decomposition of Fe_2SiO_4 spinel completed in the runs for 3 hours at 1000 ℃ and that x values of Fe_xO in the run products for 3 and 6 hours at the 1000 ℃ were approximately equal, we conclude that heating at 1000 ℃ for at least 3 hours was enough to reach the equilibrium. Because our transition boundary was determined by the runs for 6 hours at 1000 ℃, 3 hours at 1200 ℃, and 3 hours at 1400 ℃, we suggest that the negative slope of the post-spinel transition boundary in Fe_2SiO_4 is not apparent but the essential feature.

Keywords: Fe_2SiO_4, post-spinel, spinel, high-pressure

Japan Geoscience Union Meeting 2014
(28 April - 02 May 2014 at Pacifico YOKOHAMA, Kanagawa, Japan)

SMP47-P07 Room:Poster Time:May 1 18:15-19:30

Relationship between Raman spectral pattern and crystal orientation of cordierite

ABE, Miyako[1*] ; MADHUSOODHAN, Satish-kumar[1] ; KAGI, Hiroyuki[2]

[1]Niigata University, [2]Tokyo University

In the crystal structure of cordierite, six-membered rings of (Al, Si) O_4 are stacked along the *c*-axis and form a channel structure. This channel structure can trap volatiles such as H_2O and CO_2, and makes cordierite an important mineral for preserving the information of past fluid conditions during metamorphism. Earlier studies have shown that the intensity of CO_2 Raman band represents the contents of CO_2 inside the channel (e.g. Kaindl et al., 2006). Carbon dioxide is aligned linearly along the *a*-axis in the channel (Aines and Rossman, 1984), and therefore the peak intensity of CO_2 at 1383cm^{-1} in the Raman spectra varies considerably depending on the crystal orientation of cordierite (Kolesov and Geiger, 2000). Thus, it is necessary to correct the effect of crystal orientation for the determination of true contents of CO_2 in randomly oriented cordierite grains in metamorphic rocks. As a first step to accurately quantify the CO_2 content in cordierite using Raman spectroscopy, we analyzed euhedral crystals of cordierite for revealing the relationship between Raman spectral patterns and crystal orientation.

In this study, euhedral cordierite crystals collected from the volcanic ash deposit in the Takiga swamp, Gunma Prefecture, Japan were examined in detail using micro-Raman spectroscopy. Raman spectra were observed with different conditions for each analytical point to check the effect of polarization and crystal orientation. Mineral chemical analyses of cordierite crystals indicate homogeneity in its composition (X_{Mg} = 0.735 $\pm$ 0.14). However, different Raman spectral patterns were obtained for (001) plane and (100) plane; the (001) plane show only one pattern, but the (100) plane showed three different patterns. Peak splitting between 554 and 575 cm^{-1}, the peaks of 970 cm^{-1} and 1180 cm^{-1} changed its intensity drastically, whereas the peak at 670 cm^{-1} remained constant. We selected five Raman peaks at 554 cm^{-1}, 575 cm^{-1}, 670 cm^{-1}, 970 cm^{-1}, and 1180 cm^{-1} attributable to the cordierite (Al, Si)O_4 structure and analyzed the intensity ratio of these five peaks in different orientations. A parameter of Δintensity was defined, where the intensity ratios of (001) plane were concentrated around 0, and those of (100) plane deviates from 0. This parameter can be used to identify the crystal orientation of cordierite. The spectral variations observed in cordierite and its relationship with crystal orientation are interpreted based on the stretching and/or bending vibrations of cordierite unit cell structure

Keywords: Cordierite, Raman spectroscopy, Crystal orientation

References

Aines, R. D. and Rossman, G. R. (1984) The high temperature behavior of water and carbon dioxide in cordierite and beryl. American Mineralogist, 69, 319-327

Kaindl, R., Tropper, P. and Deibl, I. (2006) A semi-quantitative technique for determination of CO2 in cordierite by Raman spectroscopy in thin sections. European Journal of Mineralogy, 18, 331-335

Kolesov, B. A. and Geiger, C. A. (2000) Cordierite Ⅱ: The role of CO_2 and H_2O. American Mineralogist, 85, 1265-1274

Keywords: Cordierite, Raman spectroscopy, Crystal orientation

Japan Geoscience Union Meeting 2014
(28 April - 02 May 2014 at Pacifico YOKOHAMA, Kanagawa, Japan)

SMP47-P08 Room:Poster Time:May 1 18:15-19:30

The low-temperature Moessbauer spectroscopy of an M3’ epidote from Osayama, Okayama prefecture, Japan

YAMAKAWA, Junji[1*] ; KAWASE, Masaya[2] ; KUROKUZU, Masayuki[3] ; MORIMOTO, Shotaro[4] ; SAITO, Tadashi[5]

[1]Graduate School of Natural Science and Technology, Okayama University, [2]Nagahama Institute of Bio-Science and Technology, [3]Research Reactor Institute, Kyoto University, [4]Faculty of Pharmacy, Osaka Ohtani University, [5]Radioisotope Center, Osaka University

Epidote, $Ca_2(Al,Fe^{3+},Fe^{2+})Al_2SiO_4Si_2O_7(O,OH)$ is a common rock forming mineral found low-grade metamorphic rocks. The chemical compositions of the epidote vary with the formation conditions and make some complex zoning textures. The distribution of Fe^{2+}-Fe^{3+} ions in the crystal structure will be able to analyze by the Mössbauer spectrometry and the stability/unstability of the sample can be estimated from the distribution.

Moreover, in some sample, the Fe ions are distributed in the characteristic M3′ site that can be detected by the Mössbauer spectroscopy. The distribution ratio of the Fe ions in the M3′ site can not be estimated by the X-ray structure analysis, so the M3′ sites are making a small ordering structures and distribute homogeneously in the crystal. Distribution ratio of Fe in the site of M1/M3/M3′ corresponds to the formation conditions of the sample.

In this study, the low-temperature Mössbauer spectrum and Magnetic susceptibility of the M3′ epidote sample was measured and the characteristics of the M3′ site were analysed.

Keywords: Epidote, Moessbauer spectroscopy, M3’ site, Magnetic susceptibility

Japan Geoscience Union Meeting 2014
(28 April - 02 May 2014 at Pacifico YOKOHAMA, Kanagawa, Japan)

SMP47-P09 Room:Poster Time:May 1 18:15-19:30

Structural change in ikaite ($CaCO_3 \cdot 6H_2O$) near the freezing point temperature of water

TATENO, Natsuki[1] ; KYONO, Atsushi[1*]

[1]Div of Earth Evolution Sciences, Grad Sch of Life & Environmental Sciences, Univ of Tsukuba

Ikaite, one of the calcium carbonate minerals, is thermodynamically stable only at near-freezing temperature and transformed rapidly into calcite and vaterite at ambient temperature. During the phase transformation with dehydration, its crystal shape is preserved as pseudomorphs, termed glendonite, thinolite, and gennoishi. This study aims to clarify the structure change and dehydration mechanisms by using low-temperature single-crystal X-ray diffraction study. At -50 ^{o}C, the crystal structure of ikaite is monoclinic, space group $C2/c$ with the unit cell parameter a = 8.8134 (1), b = 8.3108 (1), c = 11.0183 (1) $\AA$, β = 110.418 (1) ^{o}. It is composed of four $CaCO_3 \cdot 6H_2O$ molecules in the cell. With increasing temperature, the unit cell volume is increased monotonously from 756.3 to 758.0 $\AA^3$ between -50 and -20 ^{o}C, and then jumped to 771.0 $\AA^3$ at -10 ^{o}C. The unit cell lattice anisotropically expands mainly along the c-axis, followed by the a-axis. The intramolecular Ca-O(5) bond distance is drastically elongated at -10 ^{o}C, which is associated with elongations of the intermolecular O(2)-O(3), O(2)-O(5), O(4)-O(5) distances. The a unit cell expansion is directly due to the elongation of the O(2)-O(5) aligned parallel to the a-axis. The drastic elongation of the Ca-O(5) bond distance gives rise to an initial dehydration of the $CaCO_3 \cdot 6H_2O$ molecule. The intermolecular Ca-O(3)-O(2) angle is constantly increased with temperature, leading to rotational motion of the $CaCO_3 \cdot 6H_2O$ molecule along b-axis. This is responsible for the highest expansion coefficient of the c lattice parameter.

Keywords: ikaite, vaterite, calcium carbonate, pseudomorph, low-temperature X-ray diffraction study

Japan Geoscience Union Meeting 2014
(28 April - 02 May 2014 at Pacifico YOKOHAMA, Kanagawa, Japan)

SMP47-P10 Room:Poster Time:May 1 18:15-19:30

Synchrotron powder X-ray diffraction study of the structural thermal properties on hydrogrossular

KATO, Masato[1*] ; KYONO, Atsushi[2]

[1]Graduate School of Life and Environmental Science, [2]Graduate School of Life and Environmental Science

Synchrotron powder X-ray diffraction study on synthetic Si-free hydrogrossular, katoite $Ca_3Al_2(O_4H_4)_3$, were performed at temperature range from 300 to 10 K. The temperature dependence of structure parameters was refined by Rietveld analysis. Since structural contraction with decreasing temperature would directly cause a phase transition on the hydrogrossular structure, three candidates for space group: *Ia*-3*d* (katoite at ambient), *I*-43*d* (katoite at high pressure), and $I4_1/acd$ (majorite), were applied to the X-ray diffraction profile fitting collected at 10 K. The final Rw with the *Ia*-3*d* space group consequently results in the smallest value, which suggests that the katoite structure remains unchanged up to the lowest temperature of 10 K. However, the temperature dependence of the unit cell volume shows two different expansion coefficients at temperatures above and below 100 K. It can be accounted for by the effect of the repulsion between atoms of the same species. Whereas the unit cell of katoite is monotonously contracted with decreasing temperature, the O_4H_4 tetrahedron and AlO_6 octahedron are alternatively expanded and contracted. Compared with the phase transition in katoite under high pressure, moreover, the unit cell volume contraction up to 5 GPa is about eight times larger than that under low temperature. The structural characteristics could therefore explain the reason why no phase transition occurs in katoite at low temperature condition.

Keywords: katoite, synchrotron pwder X-ray diffraction, Rietveld analysis, O4H4 tetrahedron

Japan Geoscience Union Meeting 2014
(28 April - 02 May 2014 at Pacifico YOKOHAMA, Kanagawa, Japan)

SMP47-P11 Room:Poster Time:May 1 18:15-19:30

Structural study on the phase transformation of natural scolecite with increasing temperature

UCHIDA, Takahiro[1*] ; KURIBAYASHI, Takahiro[1] ; NAGASE, Toshiro[2]

[1]Department of Earth Science, graduate school of science, Tohoku University, [2]The Tohoku University Museum, Tohoku University

Scolecite, $CaAl_2Si_3O_{10}\cdot 3H_2O$ is classified to fibrous zeolite group. The sequence of general phase transformation with increasing temperature has been reported for natural scolecite: scolecite→ meta-scolecite → amorphous phase and decomposes to An + Qtz (Rykl *et al.* 1986; Gottardi and Galli 1985).

In this study, the high-T evolution of the structure of natural scolecite from Poona, India were studied up to 573 K to reevaluate the dehydration process of scolecite using TG-DTA and in situ single crystal X-ray diffraction experiments.

As the results from structual refinement at room temperature, the lattice constants of the sample are determined as follows : a= 18.504(3)A, b= 18.971(2) A, c= 6.5262(9) A and β = 90.558(5) ^{0} . The crystal structure of scolecite, $CaAl_2Si_3O_{10}\cdot 3H_2O$, was refined with the space group $F1d1$ from 3567 reflections with Io $>2\sigma(I)$, yielding R= 4.62%, wR= 11.41%. At ∼423 K, the space group was changed to Fdll from $F1d1$, and scolecite underwent a phase transformation to meta-scolecite phase.

As the results from structual refinement at 523 K , the lattice constants of the sample are determined as follows : a= 18.122(3)A, b = 18.847(3) A, c = 6.5408(11) A and α = 88.948(7) ^{0} . The crystal structure of scolecite, $CaAl_2Si_3O_{10}\cdot 2H_2O$, was refined with the space group $Fd11$ from 2782 reflections with Io $>2\sigma(I)$, yielding R= 10.72%, wR= 28.85%. When phase transformation occurs, OW2 in scolecite is expelled and then the half of Ca ions move by ∼1/2c. At 573 K, the number of ovserved reflections was decreased dramatically.

Under high-T experiments from 423 to 523 K, two reciprocal lattices were observed, each lattice is corresponding to twin component with the [00-1] twin law. The [00-1] twinning could be associated with the dehydration mechanism. The X-ray diffraction data suggest the possibility of exist of a new H_2O site in meta-scolecite phase. This may be a key to solve the dehydration process of scolecite.

Keywords: scolecite, dehydration, phase transformation, single crystal X-ray diffraction, twin, high temperature

Japan Geoscience Union Meeting 2014
(28 April - 02 May 2014 at Pacifico YOKOHAMA, Kanagawa, Japan)

SMP47-P12 Room:Poster Time:May 1 18:15-19:30

Near-infrared spectra of ice under high pressure and high temperature

NOGUCHI, Naoki[1*] ; KOMATSU, Kazuki[2] ; SHINOZAKI, Ayako[2] ; SHINODA, Keiji[3] ; KAGI, Hiroyuki[2]

[1]Graduate School of Engineering, Hiroshima University, [2]Geochemical Laboratory, Graduate School of Science, The University of Tokyo, [3]Department of Geosciences, Faculty of Science, Osaka City University

The physical properties of ice VII under high pressure and high temperature (HP-HT) conditions are important to planetary science. Ice VII is considered a primary constituent of the interior of giant icy satellites and planets (e.g., Podolak et al. 1998). Thus, understanding the physical properties of ice VII will contribute to better knowledge about the structure and dynamics of other satellite and planetary interiors. In particular, the ionic conductivity of ice VII, which affects the magnetic fields of these bodies (Stevenson 2003), is controlled by ionic and rotational defects in the ices (Jaccard 1959); moreover, ionic defects have two types: OH^- and H_3O^+. The probability of forming defects in ice VII under the HP - HT conditions that typify the interiors of icy satellites and planets is surely increased by thermal activation.

In the near-infrared (NIR) region, the spectrum of ice VII shows absorption bands of the bending-stretching combination (ν_2 + ν_3) and stretching overtone ($2\nu_3$) modes of the normal vibration of water molecules (Larsen and Williams 1998). These modes correspond to the high vibrational energy level of the potential well, and provide information regarding the potential barrier along the O...O axis. To determine the probability of forming ionic defects in the ice VII structure at elevated temperatures, the NIR spectra of ice VII must be measured. The aim of this study is to investigate the state of protons in ice VII under HP-HT conditions. Thus, we measured the NIR absorption spectra of water at pressures up to 16 GPa and temperatures up to 368 ℃ using an external heating diamond anvil cell and synchrotron NIR radiation of BL43IR at SPring-8.

The absorption band of the first OH stretching overtone mode divided into doublet peaks above 5 GPa at room temperature, suggesting that proton tunneling occurs at the overtone level. As the temperature increased, the doublet peaks gradually reduced to a singlet. This result implies that thermally activated protons hop between the two potential minima along the oxygen-oxygen axis. A P-T diagram for the proton state was constructed from the changing band shape of the overtone mode.

Keywords: ice, proton, icy satellite, near-infrared spectroscopy, high pressure and high temperature

Japan Geoscience Union Meeting 2014
(28 April - 02 May 2014 at Pacifico YOKOHAMA, Kanagawa, Japan)

SMP47-P13 Room:Poster Time:May 1 18:15-19:30

Phase changes of filled ice Ih methane hydrate induced by the orientational ordering of the guest molecules

TANAKA, Takehiko[1*] ; HIRAI, Hisako[1] ; MATSUOKA, Takahiro[2] ; OHISHI, Yasuo[3] ; YAGI, Takehiko[1] ; OHTAKE, Michika[4] ; YAMAMOTO, Yoshitaka[4] ; NAKANO, Satoshi[5]

[1]Geodynamics Research Center, Ehime University, [2]Gifu University, [3]Japan Synchrotron Radiation Research Institute, [4]The National Institute of Advanced Industrial Science and Technology, [5]National Institute for Materials Science

Orientational ordering of guest methane molecules in a filled ice Ih structure of methane hydrate (MH) was observed above 15 to 20 GPa at room temperature in a previous Raman study. However, the change in the fundamental structure was not observed at the pressure region by X-ray diffractometry. In this study, low-temperature and high-pressure experiments were performed with filled ice Ih structure of methane hydrate under pressure and temperature conditions of 2.0 to 77.0 GPa and 30 to 300 K, respectively, using diamond anvil cells and a helium-refrigeration cryostat. Distinct changes in the axial ratios of the host framework were revealed by In-situ X-ray diffractometry. Splitting in the CH vibration modes of the guest methane molecules, which was previously explained by the orientational ordering of the guest molecules, was observed by Raman spectroscopy. The pressure and temperature conditions at the split of the vibration modes agreed well with those of the axial ratio changes. The results indicated that orientational ordering of the guest methane molecules from orientational disordered-state occurred at high pressures and low temperatures, and that this guest ordering led to the axial ratio changes in the host framework. Existing regions of the guest disordered-phase and the guest ordered-phase were roughly estimated by the X-ray data. In addition, above the pressure of the guest-ordered phase, another high pressure phase was developed at a low-temperature region.

Keywords: Methane Hydrate, X ray diffraction, high pressure, Raman spectroscopy

Japan Geoscience Union Meeting 2014
(28 April - 02 May 2014 at Pacifico YOKOHAMA, Kanagawa, Japan)

SMP47-P14 Room:Poster Time:May 1 18:15-19:30

Zirconium local structure in tektite and impact-related natural glasses probed by XAFS

TOBASE, Tsubasa[1*] ; YOSHIASA, Akira[1] ; WANG, Ring[1] ; HIRATOKO, Tatsuya[1]

[1]Graduate School of Science, Kumamoto University, [2]Materials and Structures Laboratory, Tokyo Institute of Technology

The local structures of tektite and natural glasses were studied by Zr K-edge X-ray absorption near edge structure (XANES) and extended X-ray absorption fine structure (EXAFS) in order to provide quantitative data on bonding distances and coordination numbers. The XAFS measurements were performed at the beam line BL-NW10A of the PF-AR in National Laboratory for High Energy Physics (KEK), Tsukuba, Japan. Zr4+ ion in tektite has different kinds of coordination environment. Various natural glasses are formed under different physical conditions. Impact-related glass, fulgurite and volcanic glasses are typical natural glasses. Glass structure is affected by the pressure and temperature conditions during the glass formation and annealing process. This study indicated that different formation process of natural glasses gives different local structure of zirconium ions.

The Zr K-edge XANES spectra of tektite have the double post-edge peaks with different heights. All tektites are classified in same types. Zr-O distances in tektite are 2.198-2.215$\AA$ and XANES spectra of tektite have similar shape. It indicates that tektites have similar Zr local structure with 7-fold coordination Zr ions. Volcanic glasses are classified same type. Impact-related glasses are classified to different types. Impact glasses are formed under different geological process at impact event and are experienced different physical environments.

Keywords: XAFS, Local structure of Zr, Tektite, Natural glass, XANES, EXAFS

Japan Geoscience Union Meeting 2014
(28 April - 02 May 2014 at Pacifico YOKOHAMA, Kanagawa, Japan)

SMP47-P15 Room:Poster Time:May 1 18:15-19:30

Light element quantification using electron microprobe and Os surface coating

OHFUJI, Hiroaki[1*] ; YAMAMOTO, Masashi[1] ; KOJIMA, Yohei[1]

[1]Geodynamics Research Center, Ehime University

Electron microprobe analysis is a non-destructive method widely used for determining the chemical composition of solid materials such as not only minerals and rocks but also industrial and biological materials. Recent advances of solid-state detectors for energy dispersive spectroscopy (EDS) analysis allow us to readily collect precise quantitative data. For SEM and EDS analysis of non-conductive (insulating) materials such as minerals and rocks, surface coating of a thin conductive layer is a prerequisite for sample preparation. For this purpose, carbon and gold are most commonly used; the former with low atomic (Z) number is suitable for microprobe chemical analysis, while the latter is preferable for textural observation of samples with rough, uneven surfaces and/or with high porosity. Recently, osmium coating prepared by chemical vapor deposition (CVD) has been a focus of attention and found to be effective for high-resolution SEM observation of samples with uneven surfaces. In the present study, we applied the sample preparation technique using very thin osmium surface coating for chemical quantification of various mineral samples by EDS.

The SEM-EDS analysis was performed by using FE-SEM (JEOL, JSM-7000F) equipped with a silicon-drift-type EDS detector (Oxford Instruments, X-Max 20). Accelerating voltage and probe current were 15 kV and 1 nA, respectively. Osmium coating of 5 nm thick was carefully made by using a Neoc-ST osmium coater (Meiwafosis). Quantification analyses were conducted on a variety of mineral samples, silicate (including hydrous silicates), carbonate and oxide minerals.

The results showed that the quantification data obtained from samples with osmium coating are as accurate as those from samples with conventional carbon coating for principle elements such as Na, Mg, Al, Si, K, Ca and Fe. With respect to the quantification of light elements such as C, N and O, the results from osmium-coated samples are found to be closer to their stoichiometric values than those from carbon-coated samples. This is likely caused by the absorption correction of the X-rays passing though each coating layer. The thickness of the surface coating layer can be precisely controlled in the case of osmium coating prepared by the CVD technique, but not readily adjusted in carbon coating. As the result, the deviation of the estimated thickness of the coating layer from the actual thickness over/underestimates the effect of X-ray absorption correction, in which low-energy X-rays from light elements are more significantly influenced by the correction. We found that the precise quantification of oxygen as a separate element (not as oxide forms of cations) using osmium surface coating might be helpful and effective in estimation of the valence state of iron in iron-bearing minerals and water (hydrogen) content in hydrous minerals. We also confirmed that the present technique is also useful for precise quantification of carbonate minerals such as $CaCO_3$.

Japan Geoscience Union Meeting 2014
(28 April - 02 May 2014 at Pacifico YOKOHAMA, Kanagawa, Japan)

SMP47-P16 Room:Poster Time:May 1 18:15-19:30

Cathodoluminescence characterization of terrestrial and extraterrestrial alkali-halide minerals

YOSHIDA, Eisuke[1*] ; NISHIDO, Hirotsugu[1] ; NINAGAWA, Kiyotaka[1]

[1]Okayama University of Science

Luminescence of natural alkali halides such as halite and sylvite is characterized by structural defects related to F-center (+p) and V-center (+e). On their CL (cathdoluminescence), however, scarcely has been reported so far. Since asteroidal water was discovered as fluid inclusion in halite from H5 chondrite, Monahans (1998), alkali halides in meteorites have been extensively investigated for understandings of aqueous alteration and thermal metamorphism on the parent body. Therefore, luminescence features of halides can provide valuable information on such issues. In this study we have measured CL spectra of terrestrial and extraterrestrial halite samples to clarify luminescence centers in various types of halite.

Halite crystals of terrestrial origin and small halite particles in ureilite meteorites were selected for CL measurements. All samples were prepared using oil while cutting and polishing without water. Also cleavage fragments of terrestrial samples were used for CL spectral measurements after carbon coating.

All samples exhibit weak blue to greenish blue CL with broad band emissions from 350 to 650 nm. CL spectra corrected for total instrumental response were converted into energy units for spectral deconvolution using a Gaussian curve fitting, because Gaussian curve in energy units can be assigned to one specific type of emission center (Stevens-Kalceff, 2009). The deconvoluted components can be assigned to the emission centers related to V_k (+e), F (+p), V_F (+e), Mn^{2+} (Na^{+}) and Mn^{2+} (interstitial) by referring to Gorobets and Rogojine (2002).

The CL spectra of terrestrial halite at room temperature are consisted of five components at 3.34 eV, 3.05 eV, 2.46 eV, and 2.28 eV and at 2.00 eV. At low temperature the emission of Mn2+ impurity center is enhanced due to an increase in the probability of radiation transition. In the case of high-energy emission, a decrease in sample temperature reduces the intensity of F-center emission, but sensitizes the intensity of V_k-center emission, suggesting the energy transfer from F-center to V_k-center. The CL spectral analysis of terrestrial sylvite at room temperature confirms four emission components at 3.32 eV, 2.97 eV, 2.53 eV and 1.89 eV.

Halite in the meteorite of polymict ureilite (Dar al Gani 319) gives a broad emission band in blue region, which is deconvoluted into two components at 2.70 eV for unknown center and at 3.11 eV for F-center. However, no emission in red region associated with Mn impurity center has not recognized in ureilite halite. It implies that high-energy radiation in cosmic space might break up the crystal fields around Mn ions.

Japan Geoscience Union Meeting 2014
(28 April - 02 May 2014 at Pacifico YOKOHAMA, Kanagawa, Japan)

SMP47-P17 Room:Poster Time:May 1 18:15-19:30

Effects of Mn activator and site occupancy on cathodoluminescence of dolomite

KUSANO, Nobuhiro[1*] ; NISHIDO, Hirotsugu[1] ; NINAGAWA, Kiyotaka[1]

[1]Okayama University of Science

Cathodoluminescence (CL) has been widely applied in mineralogical and petrological investigations, especially for carbonates. Dolomite commonly red CL emission related to an impurity center of divalent Mn in Ca-site and Mg-site (Sommer, 1972; Walker et al, 1989). Furthermore, temperature effect on CL efficiency has not been discussed in spite of potentially important function to control CL emission mechanism. In this study we have clarified luminescent mechanism of dolomite in a wide range of temperature using a SEM-CL, and confirmed a temperature quenching of its emissions. The quenching process has been quantitatively evaluated by CL spectral deconvolution method assuming the Mott-Seitz model.

Five dolomite samples from Hase, Japan (D01), Nakase, Japan (D02), Raura, Peru (D03), Binntal, Switzerland (D04), Arizona, USA (D05) were selected for CL measurements after carbon-coating on their polished surfaces. SEM-CL analysis was conducted using an SEM (JEOL:JSM-5410) combined with a grating monochromator (Oxford: Mono CL2) to measure CL spectra ranging from 300 to 800 nm in 1 nm steps with a temperature controlled stage from -190 to 250 ^{o}C. The dispersed CL was collected by a photon counting method using a photomultiplier tube (R2228) and converted to digital data. All CL spectra were corrected for the total instrumental response.

CL spectra of all samples at room temperature exhibit almost similar pattern with a broad band at 525-800 nm in a red region. The spectral peaks are sharpened and enhanced at lower temperature due to reduction of thermal lattice vibration and an increase in luminescent efficiency, suggesting high spectral resolution of the emission bands at low temperature. Therefore, a Gaussian fitting was conducted to quantitatively deconvolute spectral data obtained at low temperature in an energy unit. The results confirmed that CL of all samples consist of two emission components at around 1.84 eV (Mg-site) and 2.15 eV (Ca-site) in red region, of which variation might be attributable to crystal field (Mn-ligands distance). In general, luminescence efficiency of the material decreases with a rise in temperature due to an increase in non-radiative transitions. This phenomenon has been recognized in several minerals such as quartz, cristobalite and tridymite as temperature quenching. Furthermore, an increasing temperature makes a shift of the emission peak to a higher wavelength side. The emission intensity varies depending on the samples with different concentrations of activator (Mn^{2+}) and quencher (Fe^{2+}), and site occupancy of the Mn^{2+} ion between two cation sites in dolomite structure. The facts suggest that the behavior of the emission intensity with changes in temperature is not explained on the basis of a temperature quenching theory based on an increase in the probability of non-radiative transition with the rise of temperature (Mott-Seitz model). Probably activator (Mn^{2+}) concentration affects temperature quenching effect on CL of dolomite considerably.

Japan Geoscience Union Meeting 2014
(28 April - 02 May 2014 at Pacifico YOKOHAMA, Kanagawa, Japan)

SMP47-P18 Room:Poster Time:May 1 18:15-19:30

Cathodoluminescence of calcite decomposed from dolomite in high-temperature skarn

KUSANO, Nobuhiro[1*] ; NISHIDO, Hirotsugu[1] ; INOUE, Koichi[1]

[1]Okayama University of Science

Purple luminescent calcite associated with periclase has been found from the high-temperature skarn in Kanehira mine located in the eastern part of Hiroshima Prefecture. Calcite usually emits red to orange in cathodoluminescence (CL), but scarcely purple to blue. In this study we have conducted to clarify the emission center related to purple luminescence by using CL spectral analysis and the origin of the calcite during skarn mineralization.

The specimens collected from the skarn zone in the limestone contacted with intrusive granodiorite in the outcrop of the pit-tunnel. The polished thin sections of the selected samples were employed for optical observation and CL measurements. Color CL images were obtained using a cold-cathode type Luminoscope with a cooled-CCD camera. CL spectroscopy was made by a SEM-CL system, which is comprised of SEM (JEOL: JSM-5410LV) combined with a grating monochromator (OXFORD: Mono CL2). The CL emitted from the samples was dispersed by a grating monochromator (1200 grooves/mm), and recorded by a photon counting method using a photomultiplier tube. All CL spectra were corrected for total instrumental response, which was determined using a calibrated standard lamp.

Color CL imaging reveals two types of CL emission, red and purple, in calcite closely associated with spotted periclase. The CL spectra of both calcite show a broad emission band at 620 nm in a red region, which is assigned to an impurity center derived from an activator of divalent Mn ion substituted for Ca, where the intensity of red CL is higher than that of purple CL. Furthermore, the calcite with purple calcite exhibits a broad emission band at 400-500 nm in a blue region, which might be related to a defect center such as ”back-ground blue” found in low-Mn activated calcite.

The calcite with purple CL is accompanied by spotted periclase grains, which is usually found as a component of metamorphosed dolomitic limestone. If the hydrate condition would be presumed during its formation, periclase could easily hydrate and alter to brucite and other magnesium minerals by action of the humidity. According to the results of heating experiments of dolomite, dolomite decomposes to calcite and periclase at around 750 ^{o}C, whereas calcite causes its decarbonation above around 850 ^{o}C. It implies that the calcite with purple CL might be persisting after the decomposition of dolomite under a dry condition at relatively high-temperature near 800 ^{o}C, and leave the defects in the calcite structure during thermal decomposition of dolomite, which can be assigned to the component of an emission band in a blue region.

Japan Geoscience Union Meeting 2014
(28 April - 02 May 2014 at Pacifico YOKOHAMA, Kanagawa, Japan)

SMP47-P19 Room:Poster Time:May 1 18:15-19:30

Cathodoluminescence characterization of terrestrial and extraterrestrial enstatite

OHGO, Syuhei[1*] ; MISHIMA, Maki[1] ; NISHIDO, Hirotsugu[1] ; NINAGAWA, Kiyotaka[1]

[1]Okayama University of Science

Enstatite occurred in meteorite shows various cathodoluminescence (CL) emissions, whereas CL emission in terrestrial enstatite has not been reported so far. We have confirmed several luminescent enstatite in terrestrial samples. In this study, we have conducted to clarify the luminescence centers of terrestrial enstatite and comparatively discuss the CL of terrestrial enstatite and extraterrestrial ones in enstatite chondrite (E-chondrite).

Three enstatite with CL emission from Morogoro, Tanzania and Chandrika, SriLanka were selected for CL measurements. The samples were fixed on a brass disk with low-luminescent epoxy resin, and polished with a diamond paste. The polished thin sections of E-chondrite (Dar al Gani 734 and Y-86004) and Aubrite (Al Haggounia 001) were employed for CL examination. Color CL images were obtained using a cold-cathode type Luminoscope with a cooled-CCD camera. CL spectroscopy was made by a SEM-CL system, which is comprised of SEM (JEOL: JSM-5410LV) combined with a grating monochromator (OXFORD: Mono CL2). The CL emitted from the samples was dispersed by a grating (1200 grooves/mm), and recorded by a photon counting method using a photomultiplier tube. All CL spectra were corrected for total instrumental response, which was determined using a calibrated standard lamp.

Color CL imaging reveals various types of CL emissions, red, blue and purple in the both of terrestrial and extraterrestrial samples. The CL spectra of these enstatite show a broad emission band at 670 nm in a red region, which is assigned to an impurity center derived from activated divalent Mn ion substituted for Mg, and a broad emission band at around 400 nm in a blue region, which might be related to a defect center such as ”intrinsic defect center” possibly raised during crystal growth.

CL spectra corrected for total instrumental response were converted into energy units for spectral deconvolution using a Gaussian curve fitting, because Gaussian curve in energy units can be assigned to one specific type of emission center (Stevens-Kalceff, 2009). The deconvoluted components can be assigned to the emission centers related to impurity centers of trivalent Cr ion (1.71 eV) and divalent Mn ion (1.87 eV) and to defect centers (3.18 eV). Furthermore, enstatite in Y-86004 E-chondrite gives additional emission component (3.87 eV) in a blue to UV region, which might be characteristic of the enstatite formed under the condition of low-oxygen partial pressure.

Japan Geoscience Union Meeting 2014
(28 April - 02 May 2014 at Pacifico YOKOHAMA, Kanagawa, Japan)

SMP47-P20 Room:Poster Time:May 1 18:15-19:30

Cathodoluminescence study of metasomatic feldspar in aegirine syenite from Iwaki Island, Ehime Prefecture

MAKI, Seiya[1*] ; NISHIDO, Hirotsugu[1] ; KAYAMA, Masahiro[2]

[1]Okayama University of Science, [2]Hiroshima University

In Iwaki Island, aegirine syenite was emplaced in the Ryoke granite during late Cretaceous time by alkali-rich hydrothermal metasomatism. The syenite and related rocks show various types of petrographic textures in response to the process of hydrothermal alteration, e.g. feldspar minerals. Feldspar exhibits a variety of cathodoluminescence (CL) colors depending on kinds of impurity elements and their concentrations, and defect densities related to Si-Al ordering and other structural disorder. Recently, the deconvolution method of CL spectra enables to assign the luminescence centers characteristic of the feldspar with satisfactory reliability (Kayama et al., 2010). In this study, we have conducted to clarify the metasomatic process through granite to syenite by CL spectral analyses for various types of feldspar.

Polished thin sections of the rock samples collected from granite, altered granite and syenite were employed for petrographic observations under a polarizing light microscope, CL measurements, and electron microprobe analyses (EPMA). Color CL images were obtained using a cold-cathode type Luminoscope with a cooled-CCD camera. CL spectroscopy was made by a SEM-CL system, which is comprised of SEM (JEOL: JSM-5410LV) combined with a grating (OXFORD: Mono CL2). The CL emitted from the samples was dispersed by a grating monochromator (1200 grooves/mm), and recorded by a photon counting method using a photomultiplier tube. All CL spectra were corrected for total instrumental response, which was determined using a calibrated standard lamp.

The feldspar in the unaltered granite shows apple green and blue CL emissions. The former is identified to plagioclase (Ab80, An20) characterized by divalent Mn activator at 556 nm, and the latter to alkali feldspar (Or90, Ab10) by defect center at 417 nm related to Al-O-Al. Altered granite has albite with red CL emission at around 750 nm, and alkali feldspar with inhomogeneous color of red to violet-blue emissions at around 400 nm and 720 nm. These CL emissions in a red region can be assigned to trivalent Fe activator in tetrahedral sites. The feldspar in syenite are mostly altered to albite with enhanced red emission at 748 nm, but minor alkali feldspar as residual after hydrothermal alteration exhibits dull red emission at 722 nm. The results of the spectral deconvolution reveals oxygen defect centers associated with Al-O-Al and Al-O-Ti bridges and impurity centers of trivalent Fe ions substituted for tetrahedral Al sites according to Kayama et al. (2010). Kayama et al. (2010) investigated the peak changes of a blue emission peak at 420 nm in alkali feldspar and they found that the elimination of Al-O-Al defect center was affected by hydrothermal metasomatism possibly at 250 ^{o}C. Therefore, the disappearance of blue emission in alkali feldspar in syenite implies that alkali-rich (sodium-rich) hydrothermal metasomatism for the formation of syenite could act at relatively high temperature above 250 ^{o}C successively after granitic magmatism.

Japan Geoscience Union Meeting 2014
(28 April - 02 May 2014 at Pacifico YOKOHAMA, Kanagawa, Japan)

SMP47-P21 Room:Poster Time:May 1 18:15-19:30

Provenance study of quartz grains in aeolian desert sediments using cathodoluminescence method

MASUDA, Risa[1*] ; SANEYOSHI, Mototaka[1] ; NISHIDO, Hirotsugu[1] ; TSOGTBAATAR, K.[2] ; CHINZORIG, T.[2] ; MAINBAYAR, B.[2]

[1]Okayama University of Science, [2]Mongolian Academy of Sciences, Mongolia

Cathodoluminescence (CL), the emission of light caused by electron irradiation, has been widely applied in earth science, most extensively used in sedimentology. In such studies CL has the advantage that it can reveal characteristics which are invisible using transmitted light, e.g. growth zones of the crystals such as silica and carbonate minerals. In the case of quartz, its CL spectral feature is so complicated to be simply used for the identification of the provenance due to many emission centers related to various types of structural defects. In this study, we have conducted to clarify the luminescence centers in quartz selected from desert sediments using SEM-CL and evaluate quantitative ratios of the emission components of the CL spectra by the deconvolution method.

The quartz grains (#60-80 mesh size) in the aeolian sediments collected from Djadokhta formation (upper Cretaceous) in the Gobi desert were fixed on the slide glass with low-luminescent epoxy resin, of which surfaces were polished with 1 micron diamond paste. Color CL images were obtained using a cold-cathode type Luminoscope with a cooled-CCD camera. CL spectroscopy was made by a SEM-CL system, which is comprised of SEM (JEOL: JSM-5410LV) combined with a grating monochromator (OXFORD: Mono CL2). The CL emitted from the samples was dispersed by a grating monochromator (1200 grooves/mm), and recorded by a photon counting method using a photomultiplier tube. All CL spectra were corrected for total instrumental response, which was determined using a calibrated standard lamp.

All samples show dark blue CL emission, and exhibit two broad bands at 400 nm in a blue region and at 600-650 nm in a red region. CL spectra corrected for total instrumental response were converted into energy units for spectral deconvolution using a Gaussian curve fitting, because Gaussian curve in energy units can be assigned to one specific type of emission center (Stevens-Kalceff, 2009). The deconvoluted components can be assigned to the emission centers related to trivalent Fe at 1.65 eV, NBOHC at 1.89 eV, tetravalent Ti at 2.75 eV and trivalent Al at 3.19 eV by referring to Stevens-Kalceff (2009). We employed 10 grains randomly selected from collected 80 grains for each sample, and determined quantitative ratios of the emission components for these quartz grains using their integral intensities. We discuss variations of characteristic components among the sediments based on the results by a statistical analysis.

Japan Geoscience Union Meeting 2014
(28 April - 02 May 2014 at Pacifico YOKOHAMA, Kanagawa, Japan)

SMP48-01 Room:313 Time:May 2 14:15-14:30

Science and Technology for Geothermal Frontier

TSUCHIYA, Noriyoshi[1*]

[1]Graduate School of Environmental Studies, Tohoku University

This project should cover multidisciplinary scientific fields such as geology, geochemistry, geophysics, water-rock interactions, rock mechanics, seismology, drilling technology, well logging technologies, reservoir engineering, and environmental science.

(a) Characterization of rock mass in BDT

Preliminary work by the Japanese researchers has revealed some of the behavior of the rock mass in the BDT, such as hydrothermal brecciation and presence of hydrothermally derived fracturing (HDF) (Hirano et al., 2003). However, fundamental understandings of key parameters such as the stress state, lithological structure, mechanical and compositional homogeneity, and thermal characteristics require much additional work. Laboratory tests would be the most effective means to obtain fundamental knowledge on the ductile rock mass in the initial stages of the project combined with analysis of core samples and pore water collected from an experimental borehole. This combination of laboratory and borehole data will generate, new knowledge on the rock mass and provide constraints on, and validation of the laboratory tests.

(b) Creation and control of the reservoirs

The HDF would create a brittle fracture network consisting of very fine fractures at grain boundaries, is created by cooling and depressurization from the borehole in the BDT. If a similar process operates during drilling then cooling of the ductile rock by the drill fluid may be expected to induce a grain-scale fracture network in the near field of the borehole during the drilling phase.

(c) Numerical simulation

To achieve sustainable energy production from EGSs in the BDT, it is essential to design the area of heat exchange between water and rock, and the risk of shortcut flow paths must be carefully evaluated. Simulators with capability to handle T-H-M-C behavior of the rock mass are expected.

Keywords: Geothermal

Japan Geoscience Union Meeting 2014
(28 April - 02 May 2014 at Pacifico YOKOHAMA, Kanagawa, Japan)

SMP48-02 Room:313 Time:May 2 14:30-15:00

Deep seismic reflection profiling in geothermal area: case study of Shirasawa and Shichigashuku calderas

SATO, Hiroshi[1*] ; ABE, Susumu[2] ; UYESHIMA, Makoto[1]

[1]Earthquake Research Institute, The university of Tokyo, [2]Japex Geoscience Institute, Inc.

Along the Ou Backbone Range, northern Honshu, many piston-cylinder type calderas have been developed in Late Miocene to Pliocene. Recently, such calderas formed in late Miocene are focused as a possible resource of geothermal power plants. To obtain the physical data to estimate the sate of deep sited fluids and fractures is significance. Since late 90's, deep seismic reflection profiling was carried out to image the deeper extension of active faults. Some of the seismic lines are crossing such caldera (Sato et al., 2002a Tectonophys,: Sato et al., 2002b EPS). Here, we introduce the seismic sections and results of magnetotelluric investigation and discuss possible strategy for future's site survey.

Shirasawa caldera: The Shirasawa caldera is a piston-cylinder type caldera with 10-km-diameter and welded tuff and lake deposits are cropping out as caldera fill. By seismic reflection profiling using vibroseis trucks, low frequency strong reflectors are imaged 3 to 5 km beneath the caldera and estimated to be a possible evidence showing fluids. The estimation is well accord to the velocity structure obtained seismic tomography (Nakajima et al., 2006 EPS).

Shichigasuku caldera: This caldera is located southern part of Miyagi prefecture and shows piston-cylinder type. Across this caldera, deep seismic reflection profiling was performed in 2013 (Sato et al., 2013: JpGU). Also, magnetotelluric survey is carried out. P-wave velocity structure across the caldera shows low velocity part, which corresponds to the caldera fill, but does not suggest any characteristic feature showing existence of fluids. Magnetotelluric section suggest the distribution of vertical low resistivity zone connected slab to active volcanoes and low resistivity part which located in the md-to upper curst beneath caldera, showing the possibility of existence of fluids.

Significance of integrated geophysical exploration

To understand the physical state and material of deep sited portion beneath caldera, integrated research using several methods, active / passive seismic investigation, MT methods. Seismic reflection survey is not effective for rock unit, which does not have layering. However, it has a potential to evaluate the density of fractures and their pattern.

Keywords: geothermal area, caldera, seismic reflection profiling, magnetotelluric inversion, Shirasawa caldera, Shichigashuku caldera

Japan Geoscience Union Meeting 2014
(28 April - 02 May 2014 at Pacifico YOKOHAMA, Kanagawa, Japan)

SMP48-03 Room:313 Time:May 2 15:00-15:15

Occurrence of rock/mineral fracture under the rapid decompression boiling condition of water

HIRANO, Nobuo[1*] ; AOSHIMA, Satoshi[1] ; KASAHARA, Naoya[1] ; OKAMOTO, Atsushi[1] ; WATANABE, Noriaki[1] ; TSUCHIYA, Noriyoshi[1]

[1]Graduate school of Environmental Studies, Tohoku University

In our previous water-rock interaction experiments under the various hydrothermal conditions using granite or artificial quartz samples, clear cracks or fractures in the samples were observed under the specific hydrothermal condition. We have named this phenomenon as ”Hydrothermally Derived Fracture (HDF)”. Understanding of this fracturing phenomenon may be useful for technological development of geothermal reservoir usage or clarification of vein formation mechanism in the Earth crust. In our previous experimental results, HDF were progressed under the high temperature and low-pressure condition. The result of detailed observation, it was thought that the thermal stress occurred with rapid cooling of rock/mineral sample surface by condensed vapor dew. Similarly, rapid decompression from the high-temperature/pressure state causes, the temperature drop by latent/sensible heat effect. Therefore, when the such rapid decompression was occurred around the rock/mineral samples, HDF may occur under the hydrothermal condition. And so, we attempted rapid decompression experiment from the over 20 MPa / 400?C hydrothermal condition. As a result, the fracturing in the samples was progressed clearly. Therefore, decompression fracturing is possible and the same phenomenon may arise subsurface of near the volcano or hotter and deeper crust with water.

Keywords: Hydrothermally Derived Fracture, Water-Rock Interaction, rapid decompression, granite, fracturing

Japan Geoscience Union Meeting 2014
(28 April - 02 May 2014 at Pacifico YOKOHAMA, Kanagawa, Japan)

SMP48-04 Room:313 Time:May 2 15:15-15:30

Fracturing of granite under pore pressure and evolution of permeability

HAMASAKI, Shohei[1*] ; KATAYAMA, Ikuo[1]

[1]Department of Earth and Planetary Systems Science, Hiroshima University

Hot Dry Rock (HDR) geothermal power generation, which is included in Enhanced Geothermal System (EGS) is characterized by making artificial geothermal reservoir and this is different from conventional geothermal power generation. This system does not require natural hot water and steam. In this system, artificial reservoir is made by hydraulic fracturing in the basement due to high-pressure water injection, and water circulates in the system. Evolution of permeability is important factor in reservoir assessment. To assess this type of geothermal system, we measured effect of pore pressure compared with permeability during triaxial deformation experiment.

Aji granite was used as experimental sample, which is dense and fine, consists of mainly plagioclase, quartz, and biotite. Permeability was measured by intra-vessel deformation and fluid-flow apparatus (IVA) at Hiroshima University. Aji granite was saturated water before triaxial deformation experiments. Confining pressure (Pc) was fixed 20 MPa and pore pressure (Pp) was ranged from 0 MPa (undrain condition during triaxial deformation) to 15 MPa by 5 MPa at room temperature in triaxial deformation. The recovered samples after deformation experiments were fixed by resin and observed by polarizing microscopes and scanning electron microscope (SEM).We discussed relation between permeability and pore pressure - fracture strength from triaxial deformation experiments.

In original sample, permeability is $2.0X10^{-19}$ m^2 at Pc = 20 MPa. Permeability of fractured samples increased against that of original samples. Permeability proportionally increased from $2.5X10^{-18}$ m^2 at Pp = 0 MPa to $7.0X10^{-17}$ m^2 at Pp = 15 MPa. Fracture strength decreased with Pp decreased, from 400 MPa at Pp = 0 MPa to 350 MPa at Pp = 15 MPa. In fractured sample, there are macro fracture surface and microcracks.

The increase of permeability depends on pore pressure suggests that increase of microcrack width and acceleration of crack-connection and propagation in large Pp. And fracture strength relates crack sharps. Therefore, crack sharp and distribution are important parameter in assessment of permeability. We plan to further experiments which try to reproduce hydraulic fracture and high temperature condition.

Keywords: granite, pore pressure, permeability

Japan Geoscience Union Meeting 2014
(28 April - 02 May 2014 at Pacifico YOKOHAMA, Kanagawa, Japan)

SMP48-05 Room:313 Time:May 2 15:30-15:45

The numerical study for behavior of fracture aperture associated with cold fluid flow

KANETA, Kousuke[1*] ; MUKUHIRA, Yusuke[1] ; SWENSON, Daniel[2] ; ITO, Takatoshi[1]

[1]Institute of Fluid Science, Tohoku University, Japan, [2]Mechanical and Nuclear Engineering Department, Kansas State University, USA

Power generation of geothermal power plant sometimes decreases due to reduction of reservoir pressure. Reinjection of used geothermal fluid/cold fluid into the reservoir is conducted in several geothermal power plant to keep/recover the reservoir pressure. It is required for recharge of reservoir pressure that appropriate condition of reinjection in terms of injection pressure, amount of injected fluid, and heat balance. On the other hand, it is empirically observed at some of the geothermal field that amount of injected fluid increases when lower temperature fluid is injected. In this research, we investigated relationship between temperatures of cold fluid and fracture aperture, using numerical simulation.

We conducted numerical simulation for the change in fracture aperture when cold fluid flows into the fracture, using 2D FEM code ″ GEOCRACK2D ″ (Swenson et al., 1995). We set the condition that cold fluid was injected into a single fracture within high temperature rock mass. In this simulation, cold fluid flowed from center of fracture to edge of fracture. Fluid pressure was 1 MPa at center of fracture and 0 MPa at edge of fracture. This given pressure condition made fluid flow from center of fracture to edge of fracture. Initial temperature of rock mass was 300 ℃ and that of cold fluid was 100 ℃. Initial stress condition was 20 MPa in x direction and y direction.

As a result of simulation, the fracture aperture increased with time although 20 MPa of normal stress worked on the rock mass and fluid pressure was at most 1 MPa. It was also simulated that the rock mass around the fracture was cooled down by cold fluid and cooled area extended with time. Normal stress on the fracture decreased. The area where normal stress decreased extended over time.

These results can be interpreted that cooling of rock mass by cold fluid caused thermal shrinkage of rock mass, which decreased normal stress on the fracture surface. Finally, the fracture aperture became large, suggesting increasing in permeability.

We also conducted the simulation for the effect of difference in initial temperature between rock mass and cold fluid. We compared the change in fracture aperture about four temperature difference conditions. Fluid flow, fluid pressure, temperature of rock mass and initial stress condition were same with first simulation. Temperature of cold fluid was 100 ℃, 150 ℃, 200 ℃ and 250 ℃.

As a result of simulation, the fracture aperture increased drastically when the temperature difference between rock mass and cold fluid was bigger than 150 ℃. The fracture aperture slightly increased when the temperature difference is smaller than 100 ℃. The bigger temperature difference was, the earlier fracture aperture opened. The results of simulation suggested that there was the critical value in temperature difference between 100 ℃ and 150 ℃. It was summarized that the fracture aperture increased and that the fracture permeability became large when the temperature difference was bigger than the critical temperature difference.

Keywords: Geothermal reservoir, Fracture, Aperture, Thermal elasticity, Thermal shrinkage, Reinjection

Japan Geoscience Union Meeting 2014
(28 April - 02 May 2014 at Pacifico YOKOHAMA, Kanagawa, Japan)

SMP48-06 Room:313 Time:May 2 15:45-16:00

Slip-able area: New index to evaluate the fault area under critical state based on microseismic data at stimulation

MUKUHIRA, Yusuke[1*] ; ASANUMA, Hiroshi[2] ; HARING, Markus[3] ; ITO, Takatoshi[1]

[1]Institute of Fluid Science, Tohoku University, [2]AIST, [3]Geo Explorer Ltd.

Unexpected occurrence of felt earthquake has been big issue as critical environmental burden associated with geothermal development and other energy extraction. The magnitude of seismic events induced by fluid stimulation is generally small enough to be perceived on the ground. However, at the Basel, Switzerland, some of the events had large magnitude, resulting in the shutdown of engineered geothermal system (EGS) project. Our previous study has revealed the fundamental characteristics and the trigger mechanisms of the large event at Basel. However, we have not reached full understanding of physics of the large events, which enable us to control or manage the magnitude of induced events.

Concept of Slip-able area

Our previous study suggested that the dynamic behavior of pore pressure especially propagation of pressure at the shut-in correlate the event magnitude because many of large events occurred at the shut-in phase in Basel. The pore pressure gradient should exist from the well head to the pressure front during the stimulation. At the shut-in when pumping is stopped, the pressure source despairs and subsequently the pressure gradient may become small with time. Finally, the pore pressure in the reservoir will go back hydrostatic state uniformly. In the relaxation process of the pore pressure gradient, it can be expected that the pore pressure at the far field from the well might slightly increase to average pore pressure increase in whole reservoir. Pore pressure increase at the front of the stimulated zone may put large part of the fault plane into near critical state. In contrast, only some part of the fault plane may become critical state, when the pore pressure increases with the pressure gradient. This is the expected scenario for occurrence of the large event at the shut-in.

So, in this study, we originally defined new concept of Slip-able area, which describes the summation of fault areas in study area, under critical state during/after the stimulation. The informations used in estimating Slip-able are given by the detailed analysis of microseismic events and stress information. Slip-able area can provide the information of the potential fault area which can have shear slip at semi real time. Slip-able area can be directly converted into the event magnitude, suggesting it is also available to the risk assessment of the large event.

Methodology of estimation for Slip-able area

We propose the methodology to estimate Slip-able area as follows.

1.Determine the number of the potential fracture within a given rock volume from microseismic data at the first stage of the stimulation.

2.Characterize the size of the fractures from source parameter of microseismic events and their critical pore pressure for shear slip.

3.Divide the reservoir area into a number of the block with the same size of step1.

4.Determine the stimulated volume in three dimensions by the divided block and information on occurrence of microseismic events.

5.Infer the number of the fracture in a stimulated volume determined in step 4.

6.Estimate maximum increase in pore pressure at given time in each block of stimulated volume.

7.Identify the fault area of the fracture under critical state using the information assummed in step 2.

8.Integrate all fault area of the fractures identified in step 7.

We have to note that the methodology shown above includes some steps with much difficulty or impossible because determination of critical pore pressure is based on the information on orientation of fracture plane and stress information in study area. These informations are not available in many of the geothermal field. Estimation of fault area also required high quality data set of microseismic events. In these cases, it can be valid for simplification to use appropriate constant values like b value as a substitute for characterizing of fault size.

Keywords: Microseismicty, Felt earthquake, Magnitude, Fault area, Risk assessment, Basel

Japan Geoscience Union Meeting 2014
(28 April - 02 May 2014 at Pacifico YOKOHAMA, Kanagawa, Japan)

SMP48-07 Room:313 Time:May 2 16:15-16:30

Hydration of crust through brittle fractures: Example from Sor Rondane Mountains, East Antarctica

UNO, Masaoki[1*] ; OKAMOTO, Atsushi[1] ; TSUCHIYA, Noriyoshi[1]

[1]Graduate School of Environmental Studies, Tohoku University

Arc lower crust is expected to be amphibolite from its seismic velocity, and such lithology contains abundant hydrous minerals. However, the amount and mechanisms for supply of H_2O fluid to arc crust are not well constrained. Pervasive flow and channeling flow are the two mechanisms for the transfer of fluid in the crust. As grain boundaries are closed for crustal P-T condition, channeling flow accompanied by brittle fracture is expected. To investigate the role of brittle fracture to the supply of H_2O fluid for crust, crust-melt hydration reaction was investigated at Sor Rondane Mountains, East Antarctica.

In the survey area, biotite-hornblende-peridotite is intruded by numerous granitic brittle dykes, and reaction zones occurs at the boundaries (Fig. 1). The mineral assemblages indicate that the reaction has occurred under lower crustal P-T condition, thus the area is suitable for investigating both mechanical and physical aspects of fluid-rock interactions under the lower crustal condition. Four reaction zones are identified from the granitic dyke to the host rock as follows:

i) granitic dyke
[quartz + plagioclase + K-feldspar + biotite + rutile + zircon ± muscovite]
ii) hornblende-tremolite zone
[hornblende + tremolite ± quartz ± apatite ± biotite]
iii) tremolite-biotite zone
[tremolite + biotite + spinel ± hornblende ± pyroxene]
iv) biotite-hornblende-peridotite
[olivine + orthopyroxene + biotite + hornblende + Cr-spinel ± magnetite ± apatite]

Those reaction zones are product of hydration reactions of host peridotite with H_2O liberated from granitic melt. From plagioclase in granitic dyke and adjoining hornblende, the temperature of those reactions is estimated[1] to be 700 ^{o}C.

The amount of H_2O liberated from the granitic melt will be quantified by the modes of hydrous minerals formed at the reaction zones. Accordingly, the amount of H_2O supplied thorough hydrous melts, and the mechanisms for transport of H_2O and hydration of the crust will be discussed.

Keywords: geofluid, brittle fractures, melt, hydration reaciton, fluid-rock interaction, Antarctica

Fig. 1 Biotite-hornblende-peridotite (brown) intruded by granitic dykes (white), Sør Rondane Mountains, East Antarctica. Note that reaction zones occur at the boundary: green or black layers are hornblende-tremolite zone and grey to reddish brown layers are tremolite-biotite zone.

Japan Geoscience Union Meeting 2014
(28 April - 02 May 2014 at Pacifico YOKOHAMA, Kanagawa, Japan)

SMP48-08 Room:313 Time:May 2 16:30-16:45

Composite basaltic andesite lava in Iwanuma (Miyagi, Japan): Differentiation along segregation veins and columnar joints

KIMOTO, Kazuki[2] ; ISHIWATARI, Akira[1*]

[1]Center for NE Asian Studies, Tohoku Univ., [2]Dept. Earth Sci., Grad. Sch. Sci., Tohoku Univ.

Occurrence of thin (3-5 m) composite lavas with central phenocryst-rich layers was reported by Kuno (1950; JGSJ, 56, 167-172) and others, but we found very thick (>110 m) composite lava comprising a single cooling unit (with penetrating columnar joints) but consisting of some distinct chemical layers with segregation veins at the layer boundaries.

The basaltic andesite lavas of the middle Miocene age (15˜13 Ma) occur in Iwanuma City, Miyagi Prefecture, Japan. Thickness of the main lava flow measures more than 110 m. Vertical columnar joints of 1 or 2 m intervals are well developed through the outcrop. This lava flow is a composite lava flow with the lower layer (0˜42 m from bottom) having rather felsic composition (SiO_2 55 wt. %) and the upper layer (45˜110 m from bottom) having more mafic compositions (SiO_2 52˜54 wt. %).There are no macroscopic differences between the two layers, but the size of plagioclase in the nearly holocrystalline groundmass of the upper layer is larger (<0.5 mm) than that of the lower layer (<0.3 mm) under the microscope. Red clinker is seen at the bottom of the outcrop, but the top of the flow has been eroded.

Many horizontal segregation veins are observed at the limited portions in the intervals of 6˜14 m (lower vein zone), 45˜64 m (central vein zone) and 80˜95 m (upper vein zone) from bottom. The lower veins are 1 mm in thickness at intervals of 1˜10 cm, have glassy structure and contain plagioclase and augite. The central veins are 5˜15 mm in thickness at intervals of 10˜15 cm at 45 m from bottom and 3˜5 mm at intervals of 5˜15 cm at 52˜64 m from bottom, have crystalline structure and contain plagioclase, pigeonite and subcalcic augite. The upper veins are 3˜5 mm in thickness at intervals of 5˜7 cm and have similar structure and mineral assemblage to the central veins. The segregated melt of the central veins forms after the approximately 70 % crystallization of the host magma. The segregation veins are apparently formed by the migration of the residual melt into the subhorizontal fractures (platy joints) which resulted from the shear deformation and cooling contraction in the crystallizing lava flow, especially near the bottom of the flow and at the bottom part of the flow and relatively mafic layers in the upper part of the composite lava flow. Rare en echelon segregation veins are the evidence for shear deformation.

The columnar joints always perpendicularly cut segregation veins, and the rocks adjacent to the columnar joint plane show low density and increase of vesicles in comparison with the rocks in the middle of the column. This suggests that columnar joints developed far later than the segregation-filled platy joints, but some melt was still present at that time so as to allow its vesiculation promoted by the columnar joint fracturing.

Keywords: composite lava flow, segregation vein, platy joint, colunmar joint, basaltic andesite, crystallization differentiation

Japan Geoscience Union Meeting 2014
(28 April - 02 May 2014 at Pacifico YOKOHAMA, Kanagawa, Japan)

SMP48-09 Room:313 Time:May 2 16:45-17:00

The formation of the permeable-impermeable boundary within the Earth's crust revealed by silica precipitation

SAISHU, Hanae[1*] ; OKAMOTO, Atsushi[1] ; TSUCHIYA, Noriyoshi[1]

[1]AIST, [2]Tohoku University

Silica is one of the dominant constituents of the Earth's crust. The permeable-impermeable boundary corresponds to the brittle plastic transition at 300-450 C [1]. Ubiquitous occurrence of quartz vein is one of the evidences that the spatial and temporal variations in permeability within the Earth's crust are affected by silica precipitation in aqueous fluids. However, the role of silica-water interaction on fracture permeability is still unclear.

The Kakkonda geothermal field, Japan, has the well WD-1a that penetrated the boundary between the hydrothermal convection zone and the heat conduction zone [2]. Calculation of quartz solubility along the well WD-1a revealed that (1) the depth of a local maximum of quartz solubility correlates with that of the strong reflector in seismic data at 350 C isotherm [3], and that of a maximum of fracture numbers revealed by the logs of FMI [4], and (2) the depth of a local minimum of quartz solubility correlates with that of the permeable-impermeable boundary, in either case of hydrostatic or lithostatic conditions [5]. These results indicate that (1) the preservation of open fractures at the margin of the Kakkonda granite is controlled by dissolution of quartz, and (2) the quartz precipitation could occur from both downwards- and upwards-moving fluids, which could divide the hydrothermal convection zone and the heat conduction zone.

The hydrothermal experiments of temperature dependence of silica precipitation were conducted at 24 and 31 MPa and 170-430 C, by using the solution made by dissolution of granite. The large amount of silica precipitation occurred only in the supercritical conditions of water (>390 C). Strong temperature dependence can be explained by the homogeneous nucleation of quartz in the surface energy of quartz of 130 mJ/m^2 [5].

The results of the calculation of silica solubility at the Kakkonda geothermal field and the hydrothermal experiments of silica precipitation suggest that rapid quartz precipitation via nucleation could occur when fluids are brought to the depth in the supercritical conditions of water. The forming and sustaining the permeable-impermeable boundary within the Earth's crust could be controlled by precipitation of silica minerals.

References
[1] Scholz (2002).
[2] Doi et al. (1998) *Geothermics*, **27**, 663-690.
[3] Matsushima et al. (2003) *Geothermics*, **32**, 79-99.
[4] Muraokaet al. (1998) *Geothermics*, **27**, 507-534.
[5] Saishu et al. (in press) *Terra Nova*.

Keywords: Silica precipitation, Quartz solubility, Permeable-impermeable boundary, Hydrothermal experiment

Japan Geoscience Union Meeting 2014
(28 April - 02 May 2014 at Pacifico YOKOHAMA, Kanagawa, Japan)

SMP49-01 Room:314 Time:May 1 16:15-16:30

Introduction of NANO-EPS

SUZUKI, Yohey[1*]

[1]Department of Earth & Planetary Science, The University of Tokyo

Nano, a prefix for 10^-9, represents vast frontiers for both Earth and Planetary Solid Sciences. Conventional tools such as Electron Probe MicroAnalysis (EPMA) for ppm-level quantification at the micrometer scale and Power X-Ray Diffraction analysis (XRD) for the identification of submicron minerals are being transformed into the next generation instruments. In addition, it is possible to reveal the heterogeneity and oscillation of chemical and isotopic compositions at nano-spatial resolutions. It is becoming more aware that nano-sized solids with extremely large surface areas and distorted structures are ubiquitous in planetary materials and intimately relevant to many issues such as soil and groundwater contamination with metals and radionuclides, mineral resources exploitation, carbon sequestration and so on. In my presentation, nano-frontiers from various fields of Earth and Planetary Sciences and key technological advancements will be overviewed as the introduction of this session.

Keywords: nano

Japan Geoscience Union Meeting 2014
(28 April - 02 May 2014 at Pacifico YOKOHAMA, Kanagawa, Japan)

SMP49-02 Room:314 Time:May 1 16:30-16:45

Properties and depositional process of sub-micron scale manganese oxide minerals in the aqueous surface enviromnent

USUI, Akira[1*]

[1]Akira Usui

A large variety of minerals form submicron compounds or minerals in the surface aqueous environments (sea waters, rivers, soils, underground waters, organisms etc.) Especially iron and manganese oxide are most mobile elements among others in such environments. The iron and manganese oxides often scavenge numbers of metallic elements and play significant role in material cycling and geochemical cycles. In this paper, we attempt to introduce several types of occurrences of manganese oxide in the diverse environments. For example a phyllo-manganate minerals, nano-scale aggregate are shown in the paper.

Keywords: manganese oxide mineral, manganese crust, manganese nodule, low-temperature hydrothermal activity, phyllomanganate, redox condition

Japan Geoscience Union Meeting 2014
(28 April - 02 May 2014 at Pacifico YOKOHAMA, Kanagawa, Japan)

SMP49-03 Room:314 Time:May 1 16:45-17:00

Development of PF-STXM and its application to environmental geochemistry

TAKAHASHI, Yoshio[1*] ; TAKEICHI, Yasuo[2] ; SUGA, Hiroki[1] ; INAMI, Nobuhito[2] ; ONO, Kanta[2]

[1]Graduate School of Science, Hiroshima University, [2]Photon Factory, KEK

Scanning transmission X-ray microscopy (STXM) has been applied to various fields in earth and environmental sciences such as aerosol chemistry, geomicrobiology, soil science, and nanomineral sciences. In particular, the technique has been used in the world because of its great importance in imaging distribution of carbon, or in particular carbon functional group, with about 50 nm spatial resolution. However, STXM that can be used to measure NEXAFS at carbon K-edge has not been in use in Japan. We have constructed STXM in Photon Factory (PF-STXM) from 2012 and started to use it for various topics in earth and environmental sciences.

In the PF-STXM, soft X-rays from the undulator are monochromatized by the grating and focused at the four-way aperture slit. The FZP with the outermost zone width of 30 nm is placed at 1 m distant from the aperture slit. First order diffraction selected through an order sorting aperture (OSA) is focused onto the sample with the focal distance of 0.7-5 mm, and then the transmitted X-rays are detected. The PF-STXM at present is mainly operated at BL-13A in Photon Factor, where the energy range available is from 250 eV to 1600 eV, which covers K-edges of carbon, nitrogen, oxygen, potassium, and aluminum. The beamize of the STXM was around 50 nm focused with Fresnel zone plates (FZP). The intensity of focused X-rays at the sample was expected to be up to 10^7 photons/s. Instead of a photomul-tiplier tube (PMT) which is commonly used in STXM, a silicon avalanche photodiode (APD) is utilized to detect the transmitted X-rays in PF-STXM. Compared with other STXM system in the world, our STXM is made so compact and light that it is easily connected to and removed from the multi-purpose beamlines. The experiments reported below are performed at BL-13A and BL-16A of Photon Factory.

The PF-STXM has been used for various applications. Among them, we would like to present recent results on (i) speciation of calcium in mineral dust with 50 nm spatial resolution, (ii) characterization of carbon adsorbed on particulate matter in river water, and (iii) spatial distribution of rare earth elements in bacterial cell.

Keywords: STXM, PF, Aerosol, Particulate matter, Bacteria

Japan Geoscience Union Meeting 2014
(28 April - 02 May 2014 at Pacifico YOKOHAMA, Kanagawa, Japan)

SMP49-04 Room:314 Time:May 1 17:00-17:15

Nano-scale investigation of the microbe-mineral interaction by scanning transmission X-ray microscopy

MITSUNOBU, Satoshi[1*] ; SHU, Mei[1] ; TAKAHASHI, Yoshio[2] ; TAKEICHI, Yasuo[3] ; ONO, Kanta[3]

[1]University of Shizuoka, [2]Hiroshima University, [3]KEK-PF

Microorganisms in the environment critically impact global geochemical cycles and redox reactions of various elements. Many geochemically important redox reactions (e.g., sulfate reduction, Fe(II) oxidation) are largely associated with microbial activity. In addition, microbes can mediate both mineral formation (biomineralization) and mineral dissolution (bioleaching). Recent studies suggest a significant relationship between Fe(II)-oxidizing bacteria and ancient Banded Iron Formation, one of the large geochemical events in Earth's history. The general ecological importance of environmental microbial reaction has been well recognized; however, the specific mechanisms of the reactions in the environments such as the reaction rate and spatial dynamics are poorly understood. In the environment such as sediments, microbial reactions and habitability vary locally and form complicated geochemical networks, which makes it difficult to characterize the specific biogenic reactions in detail.

Scanning transmission X-ray microscopy (STXM), which uses near-edge X-ray absorption spectroscopy (NEXAFS) is a powerful new tool that can be applied to hydrated biological materials with high spatial resolution. The STXM provides spatial resolution of better than 50 nm, which is suitable for imaging bacteria and bacterial biofilms.

In the present study, we applied the STXM into the bioleaching of sulfide mineral (pyrite) to determine carbon, oxygen, and iron species in nano-scale. Both metal and biogenic organic materials in pyrite-microbe interface were investigated in the single cell level. Our study shows that the STXM could be a potential technique to provide direct information on specific biogenic reaction microorganism.

Keywords: STXM, pyrite, bioleaching

Japan Geoscience Union Meeting 2014
(28 April - 02 May 2014 at Pacifico YOKOHAMA, Kanagawa, Japan)

SMP49-05 Room:314 Time:May 1 17:15-17:30

In-situ trace element quantification of geological samples using LA-ICPM

KON, Yoshiaki[1*] ; EJIMA, Terumi[1] ; SUZUKI, Masaya[1] ; HIRATA, Takafumi[2] ; TAKAGI, Tetsuichi[1]

[1]Geological Survey of Japan, AIST, [2]Division of Earth and Planet. Sci., Kyoto Univ.

Laser-Ablation Inductively Coupled Plasma Mass Spectrometry (LA-ICPMS) is a type of mass spectrometry which is capable of in-situ trace element quantification of a solid sample. We introduce an typical application to characterize sub-micron scale particles based on the variation of their geochemical compositions.

Keywords: LA-ICPMS, femtosecond laser, in-situ analyses, trace-element quantification

Japan Geoscience Union Meeting 2014
(28 April - 02 May 2014 at Pacifico YOKOHAMA, Kanagawa, Japan)

SMP49-P01 Room:Poster Time:May 1 18:15-19:30

Formation rate of iron colloids at pH 2-3

NAGASAKI, Sagakuni[1*] ; YOKOYAMA, Tadashi[2] ; HISATOMI, Osamu[2] ; NAKASHIMA, Satoru[2]

[1]Department of physics , Osaka University, [2]Department of Earth and Space Science, Graduate School of Science, Osaka University

Various types of iron colloids are widely distributed in the earth's surface conditions, and their formation process, adsorption characteristic, and the material transport mediated by iron colloids are receiving attention. Iron colloids are often formed through several reactions including the dissolution of Fe^{2+} and Fe^{3+} from minerals, oxidation from Fe^{2+} to Fe^{3+}, hydrolysis, and crystallization. In the present study, the reaction rate was evaluated focusing on the process in which iron colloids are formed from dissolved Fe^{3+}.

A solution of Fe^{3+} 100 ppm was prepared by dissolving $FeCl_3$ into pure water. This solution was reacted at 15, 25, 35, 45, and 55 ℃. At 25 ℃, pH of the solution was ∼2.7 at the start of the reaction and decreased to ∼2.2 as reaction time passed. Such change in pH is known to occur as a result of the following reactions: hydration of Fe^{3+} (release of H^+) → formation of dissolved $Fe(OH)_3$ → formation of solid $Fe(OH)_3$ (Grundl and Delwiche, 1993). Therefore, information of the formation rate of iron colloids can be obtained by monitoring the pH of the solution. After the initial period of the reaction in which the rate of the decrease of dissolved $Fe(OH)_3$ concentration was slow presumably due to nucleation, the concentration of dissolved $Fe(OH)_3$ decreased in a manner like first-order reaction, and the reaction behavior deviated from the first-order reaction at the later stage. By assuming first-order reaction, rate constants of 3.3E-5 - 1.1E-2 s^{-1} were obtained at 15-55 ℃, and good linearity was confirmed in an Arrhenius plot of these rate constants.

In addition to the above experiments in which time variation of the total amount of solid is considered, the time variation of the grain size of iron colloids was evaluated. A solution of Fe^{3+} 100 ppm was prepared and the change of grain size at 25 ℃ was continuously measured using a dynamic light scattering apparatus (Zetasizer μV, Malvern). As a result, enough scattering intensity began to be detected after the mean diameter of iron colloids grew to 10 nm, then the grain size increased. The increase of the grain size almost stopped after 8 hours, and mean diameter at this stage was approximately 30 – 40 nm. By evaluating the number of grains from the total amount of solid and mean grain size, the grain number was estimated to decrease with time.

Japan Geoscience Union Meeting 2014
(28 April - 02 May 2014 at Pacifico YOKOHAMA, Kanagawa, Japan)

SMP49-P02 Room:Poster Time:May 1 18:15-19:30

Surface complexation modeling for lead adsorption on nano-sized aluminum silicate

USHIYAMA, Tomoki[1*] ; FUKUSHI, Keisuke[2]

[1]Graduate School of Natural Science and Technology, Kanazawa University, [2]Institute of Nature and Environmental Technology, Kanazawa University

There are many abandoned lead-produced mines in Japan. The water pollutions by lead due to the weathering of the mine wastes are environmental concern. The concentrations of lead released from the mine wastes is usually low. Therefore, the adsorption process is expected to dominate the mobility of lead in the affected area. It is well recognized that the materials widely occurred in earth surface conditions are comprised with low-crystalline and/or nano-sized minerals. There are some reports for lead adsorption behavior on crystalline phases such as clay minerals and low-crystalline iron oxides. On the other hand, there are very little reports on nano-sized aluminum silicates which must be dominant phases in surface condition. The quantitative understandings of lead adsorption on nano-sized aluminum silicate is essential for the prediction of lead migration in earth surface conditions. The purpose of the study is to clarify the lead adsorption behavior on nano-sized aluminum silicate under wide range of solution conditions and model the adsorption behavior by means of surface complexation modeling.

Keywords: nano-sized aluminum silicate, lead, adsorption, surface complexation modeling

Japan Geoscience Union Meeting 2014
(28 April - 02 May 2014 at Pacifico YOKOHAMA, Kanagawa, Japan)

SMP49-P03 Room:Poster Time:May 1 18:15-19:30

Mineralogical study of serpentinite from Akamatsu, Yatsushiro, Kumamoto prefecture.

IWAKI, Yasuyo[1] ; ENJU, Satomi[1*] ; UEHARA, Seiichiro[1]

[1]Department of Earth and Planetary Sciences, Faculty of Sciences, Kyushu University

Serpentine group minerals are one of the 1:1 layer type sheet silicates and the main component of serpentinite. They are classified into three mineral species chrysotile, lizardite and antigorite. The ideal formula of chrysotile and lizardite is $Mg_3Si_2O_5(OH)_4$and that of antigorite is $Mg_{48}Si_{34}O_{85}(OH)_{62}$.

In our previous study, we researched serpentinite from a large area in Kyushu Kurosegawa belt (Tanaka et al., 2012), but there are only few reports for each area. So, the purpose of this study is to identify the composition minerals of serpentinite in Akamastutaro Pass and Tanoura, located in west of Kyushu Kurosegawa belt, and to conduct a detailed study of serpentine.

Mineral species was identified by XRD pattern and serpentinite was classified into three type: antigorite main serpentine (Type AA, 16 specimens), antigorite rich serpentine (Type A, 10 specimens) and antigorite poor serpentine (Type LC, 8 specimens). Antigorite was most abundant. Magnetite, chromite, clinochlore, brucite and hydrotalcite group minerals were identified in specimens from both areas. Only the specimen from Akamatsutaro Pass had andradite, calcite, heazlewoodite (Ni_3S_2) and millerite (NiS), while forsterite, hydromagnesite, pyroaurite and awaruite (Ni_3Fe) were seen only in Tanoura. The supply of H_2S in Akamatsutaro Pass can be estimated from the presence of heazlewoodite and millerite. Relict forsterite was observed in serpentinites from Tanoura, indicating the smaller degree of serpentization compared to Akamatsutaro Pass.

Sepentine contained in massive serpentinite had variable textures such as vein texture, reed shape texture and mesh texture with core and rim, which was formed after serpentization of olivine. In the specimens of Type LC, mesh texture was often observed, and there were cores with no rim in samples without mesh textures. Also some core texture was replaced by reed shape texture. Chemical compositions obtained by SEM-EDS show some trends for serpentines in each texture. Reed shape texture contains 0.041 (apfu) Al which replaces Mg, while core texture contain 0.07 Al and rim texture contains 0.006 Al, so reed shape texture is rich Al than mesh texture. Reed shape texture contain larger amount of SiO_2 weight percent compared with the ideal formula of chysotile and lizardite, and resemble that of antigorite.

Reference

K.Tanaka, T. Inoo and S. Uehara (2012): Microtexture and chemical composition of serpentine minerals from Kurosegawa belt, Kyushu, Japan. The 2nd Asian Clay Conference, Abstract Book.

Keywords: serpentine, antigorite, reed shape texture, mesh texture, Kyushu Kurosegawa belt, Yatsushiro

Japan Geoscience Union Meeting 2014
(28 April - 02 May 2014 at Pacifico YOKOHAMA, Kanagawa, Japan)

SMP49-P04 Room:Poster Time:May 1 18:15-19:30

The lithium existence form in a lithium ore deposit

SUZUKI, Masaya[1*] ; KON, Yoshiaki[1] ; EJIMA, Terumi[1] ; HIRABAYASHI, Eri[1] ; SATOU, Takumi[1] ; OOWADA, Akira[1] ; TAKAGI, Tetsuichi[1] ; TSUKIMURA, Katsuhiro[1] ; SAWAKI, Takayuki[1] ; MURAKAMI, Takayoshi[2] ; MOTOORI, Masayuki[2]

[1]AIST, [2]JOGMEC

In the ore deposit containing lithium, Spodumene, Petalite, Lepidolite, etc. are known as a lithium mineral, but these minerals are not contained in the lithium ore deposit examined this time. So, in this research, the result analyzed using XRD and SEM+EDS is released.

In the ore deposit containing lithium in this time, it roughly divides of a white portion and a portion of ashes green. From the result of XRD, it mainly becomes a white portion from Searlesite($NaBSiO_5(OH)_2$), Calcite($CaCO_3$), and Orthoclase($KAlSi_3O_8$), and the mineral containing lithium is not shown. On the other hand into the portion of ashes green, Calcite($CaCO_3$), Orthoclase($KAlSi_3O_8$), Illite($K(Al,Mg,Fe)_2(Si,Al)_4O_{10}$), Rozenite($FeSO_4 4H_2O$), and Cryolitionite($Li_3Na_3Al_2F_{12}$) are contained was obtained. Since the peak of various minerals had appeared, it could not declare that Cryolitionite existed clearly, but it was suggested that Cryolitionite may exist as a lithium content mineral.

Next, from the results of SEM+EDS analysis, in the white part, Calcite and Orthoclase were contained at about 10-100 micrometers, and Sealesite existed in it at those circumferences. And in the green gray part, Orthoclase, Calcite, Illite, Rozenite were contained at about 10-30 micrometers, and the particle with a size of 1 micrometer or less existed in those circumferences. Although measurement of Li was not completed in analysis of EDS, it was checked that F is contained in the analysis of these microscopic particles.

From the above result, it was surmised that the lithium content mineral examined this time was Cryolitionite.

Keywords: lithium, ore deposit, mineral

Japan Geoscience Union Meeting 2014
(28 April - 02 May 2014 at Pacifico YOKOHAMA, Kanagawa, Japan)

SVC50-01 Room:315 Time:May 2 09:00-09:15

The mathematical link between stratigraphic grain size variation of fall deposits and its time variation at the source

IRIYAMA, Yu[1*] ; TORAMARU, Atsushi[2] ; YAMAMOTO, Tetsuo[3]

[1]Department of Earth and Planetary Sciences, Graduate School of Sciences, Kyushu University, [2]Department of Earth and Planetary Sciences, Faculty of Sciences, Kyushu University, [3]Center for Planetary Science, Kobe University

Pyroclastic fall deposits which are produced by explosive volcanic eruption have various information on the eruption events. The areal distributions of pyroclastic fall deposits such as maximum grain size, median grain size, thickness, mass per unit area, etc. reflect the intensity in a single eruption and the wind conditions. Stratigraphic grain size variations of pyroclastic fall deposits also reflect the temporal behavior of the eruption intensity. For example, normal or reverse grading structures in the pyroclastic fall deposits have been attributed to temporal variation in the volcanic intensity (column height) and/or in the initial grain size distribution at the vent. However, no quantitative methodology has been developed to relate the temporal variation of source characteristics (column height and initial grain size distribution) to stratigraphic variation of grain size distribution at the deposits. In this study, we consider the mathematical description in 1D fall-sedimentation process, which relates the temporal variation of source grain size distribution to stratigraphic variation of grain size distribution.

The number of grains in a size bin must be conserved during sedimentation process and results in the same value at the arrival time on the deposits. The number of a specific-size grains between at the fallout time and at given times is linked by Lagrangian description. The key point is that the grain size and the departure time at the source are mutually related to the grain size and the arrival time at the deposits. As the arrival time corresponds to the stratigraphic location at the deposit, the stratigraphic variation of grain size in the deposit can be connected to the grain size characteristics and departure time at the source using the condition of grain number conservation. As a result, when the time variations of source grain size distribution and of fallout height are given, we obtain the temporal variation of grain size distribution at the sedimentation surface. It means that different sizes of grains which settle at the same arrival time are traced back to the different source time and height. The arrival time on the deposit can be related to the stratigraphic height in the deposit by the differential equation of increasing rate of the thickness, which equals to the volume flux through the sedimentation surface. By using these mathematical descriptions, we develop the mathematical method to link the temporal variation of eruption intensity to the stratigraphic variation of grain size distribution in the fall deposits.

Keywords: pyroclastic fall deposits, grain size distribution, stratigraphic variation, development of eruption

Japan Geoscience Union Meeting 2014
(28 April - 02 May 2014 at Pacifico YOKOHAMA, Kanagawa, Japan)

SVC50-02 Room:315 Time:May 2 09:15-09:30

Color and grainsize of ash samples collected continuously at Sakurajima volcano, Japan

SHIMANO, Taketo[1*] ; NISHIMURA, Takeshi[2] ; IGUCHI, Masato[3] ; MIKI, Daisuke[3]

[1]Graduate school of Enviroment and Disaster Research, Tokoha University, [2]Department of Geophysics, Graduate School of Science, Tohoku University, [3]Sakurajima Volcano Research Center, Disaster Prevention Research Institute, Kyoto University

Sakurajima volcano, Southwest Japan, is one of the most active volcano, and one of the leading volcano that are characterized by well-established geophysical observation network and enormous amount of data accumulation. Thus, the changes of magma plumbing system and the explosion processes at Sakurajima are now relatively well-understood for the time scale of years and of several hours, respectively (Iguchi et al., 2013). On the other hand, Sakurajima volcano has experienced several giant explosive eruptions every few hundred years, with some plinian eruptions and with erupted volume in the order of $>10^8$ m^3. However, we do not understand the mechanism of phase transition from the recent small eruptions to such bigger ones. Even though we now reached a certain level to recognize that our knowledge of " vulcanian eruption " was too simple relative to real one, the fundamental processes that lead to such eruption variety are not yet constrained well enough. As the variety of eruption styles occurs in a time scale of months to days, we have been focusing on the sample acquisition in this time range and collected daily ash samples for years.

We have been succeeded in collecting daily samples by automatic sampling system for more than five years at the site ca 2 km south of Showa crater, Sakurajima volcano (Shimano et al., 2013). We also analyzed matrix glass composition to track chemical evolution of the magma system, and found a shift of FeO^*/MgO in fall of 2009 before the waxing activity toward 2010. On the other hand, we have been searching for some real-time technique of petrological data for the comparison with geophysical data. The development of useful colorimeter and some results of heating experiments of ash resulted in understanding relationship between color of ash and condition of magma at depths (e.g., Yamanoi et al., 2008; Miyagi et al., 2013). So we have made time-series color measurements of ash samples for years. We found L^* value, degree of brightness, decreased broadly during waxing stage in 2009-2010 whereas a^* and b^* values increased broadly at first several months but decrease gradually. These changes can be explained by increase of black fresh lava block particles, increase at the first stage and gradual fluctuating changes of old red oxidized particles in ash sample. We also measured color change of some grain size group and compared with the color of bulk samples. The preliminary results show that the color differs with particle size as Miyagi et al. (2010) reported, but a correlation was found between the color values of bulk sample and those calculated from the weight fraction and each color values.

Keywords: volcanic ash, continuous observation, color change, Sakurajima volcano

Japan Geoscience Union Meeting 2014
(28 April - 02 May 2014 at Pacifico YOKOHAMA, Kanagawa, Japan)

SVC50-03 Room:315 Time:May 2 09:30-09:45

Numerical Simulation of Volcanic Ash Transport for the Eruptions at Mt. Shinmoe-dake during 26-27 January 2011

HASHIMOTO, Akihiro[1*] ; SUZUKI, Yujiro[2] ; SHIMBORI, Toshiki[1] ; TAKAGI, Akimichi[1]

[1]Meteorological Research Institute, Japan Meteorological Agency, [2]Earthquake Research Institute, The University of Tokyo

The volcanic ash transport associated with the eruptions at Mt. Shinmoe-dake during 26 to 27 January 2011 is simulated using Japan Meteorological Agency Non-Hydrostatic Model (JMA-NHM) to verify the model with satellite observation. In the model, the mixing ratio and number concentration of ash particles are prognosed with the advection, diffusion, sedimentation, and source terms to represent the behavior of ash cloud. Simulation has been performed in the calculation domain covering 2500 km x 2000 km wide area with the horizontal resolution of 5 km.

The model is coupled with one-dimensional eruption column model to define the source term of ash particles, which is simply given as a function of the column height, the level of the release point, and the size of released particle, following Suzuki (1983) and Shimbori et al. (2010). Although the simulated distribution of ash cloud roughly agrees with satellite observation, close examination of the simulation result shows that the model fails to reproduce some of the ash clouds observed by the satellite, which means that much room still remains for improvement in the eruption column model in terms of release point and size spectra of ash particles. Three-dimensional direct numerical simulation has been conducted on a major sub-Plinian eruption during the period at Mt. Shinmoe-dake (Suzuki and Koyaguchi, 2013), in order to make new eruption column model with more realistic function for the source term of ash particles. As a result, it is found that the maximum release rate of the ash particles smaller than 100 μm appears in the height lower than that predicted by the usual eruption column model for same column top height. The authors are developing new eruption column model with realistic profile of release rate, based on this result, so as to improve the reproducibility of the ash transport with JMA-NHM. The sensitivity of the ash transport to altering the new and usual eruption column models will be presented.

Acknowledgement
This study was supported by the Earthquake Research Institute cooperative research program.

References

Shimbori, T., Y. Aikawa, K. Fukui, A. Hashimoto, N. Seino, and H. Yamasato, 2010: Quantitative tephra fall prediction with the JMA mesoscale tracer transport model for volcanic ash: A case study of the eruption at Asama volcano in 2009. *Pap. Met. Geophys.*, **61**, 13-29.

Suzuki, T., 1983: A theoretical model for dispersion of tephra. *Arc Volcanism: Physics and Tectonics. TERRAPUB*, 95-113.

Suzuki, Y. and T. Koyaguchi, 2013: 3D numerical simulation of volcanic eruption clouds during the 2011 Shinmoe-dake eruptions. *Earth Planets Space*, **65**, 581-589.

Keywords: volcanic-ash dispersal, Atmospheric Transport Model,, Shinmoe-dake volcano, 2011

Japan Geoscience Union Meeting 2014
(28 April - 02 May 2014 at Pacifico YOKOHAMA, Kanagawa, Japan)

SVC50-04 Room:315 Time:May 2 09:45-10:00

Weather Radar Investigation of Volcanic Smoke for Disaster-Prevention

MAKI, Masayuki[1*] ; IGUCHI, Masato[2] ; FUJITA, Eisuke[3] ; MAESAKA, Takeshi[3] ; SHUSSE, Yukari[4] ; KOZONO, Tomofumi[4] ; MOMOTANI, Tatsuya[5] ; YAMAJI, Akihiko[5]

[1]Kagoshima University, [2]DPRI, Kyoto Univercity., [3]NIED, [4]Tohoku University, [5]Japan Weather Association

Sakurajima volcano has been active since February 2009. The total number of explosive eruptions was 966 in 2011, which was the highest number in recorded history. Corresponding to volcano activities, the ash accumulation in Kagoshima city increased and total ash amount of 3,500g/ m2 was recorded at Kagoshima local meteorological observatory. Because the volume of volcanic ash in rural area paralyze public ground transportations such as rail road and highway, fast recovery efforts are required to the railroad company and city government. However, no quantitative volcanic ash fall estimation has been established. The present study focuses on utilization of operational weather radar for quantitative ash estimation (QAE), quantitative ash forecasting (QAF), and utilization of crustal movement information for providing ash volume which is necessary for initial conditions of a numerical diffusion model. Although the target volcano of the present study is Sakurajima, the knowledge on volcanic ash and algorithm developed by the present study can be applied to any other volcano which is located in operational weather radar observation area.

Keywords: weather radar, volcanic ash, quantitative ash estimation, Sakurajima, polarimetric radar

Japan Geoscience Union Meeting 2014
(28 April - 02 May 2014 at Pacifico YOKOHAMA, Kanagawa, Japan)

SVC50-05 Room:315 Time:May 2 10:00-10:15

Eruption types determined by the mass flux and volatile component content of ascending magma flow

IDA, Yoshiaki[1*] ; OIKAWA, Jun[2]

[1]Advance Soft Co., [2]Earthquake Res. Inst., Univ. of Tokyo

Volcanic eruptions include the effusive ones that erupt fluid lava and the explosive ones that emit magma fragments in gassy flows or other forms. Traditionally, explosive eruptions are further classified into Plinian eruptions accompanied by high eruption columns, Pelean eruptions involving abundant pyroclastic flows, Vulcanian eruptions with strong instantaneous explosions, Strombolian eruptions involving periodic lava fountains and so on. Effusive and explosive eruptions are clearly controlled by the efficiency of degassing, but what produces various types of explosive eruptions has not yet been explained quite clearly. In this paper I propose a simple idea about how various explosive eruptions arise depending on the natures of ascending deep magma flow based on a stationary conduit flow model.

The state of erupting magma may be represented by exit velocity and the volatile content that determines the vesicularity of volcanic products. The volatile content is specified by its mass ratio to the fluid magma (including solidified part). On the other hand, it is convenient to represent the deep state of magma flow by the mass flux of fluid magma and the volatile contents before degassing takes place. When the magma flow is in a stationary state the mass flux of fluid magma is constant so that it defines the deep state of magma flow with the initial volatile content independently of the specific depth at which magma ascent starts.

The relation between the surface and deep states of ascending magma is calculated using a stationary conduit flow model. In this calculation the volatile component is assumed to move at the same speed as the fluid magma neglecting relative motions. In bubbly magma horizontal permeable flow of volatile gas is assumed to control the rate of degassing. In this treatment, the pressure gradient that drives the permeable flow is considered to arise from the ascent velocity change from center to side and the resulting difference of relaxation of gas expansion due to decompression (Ida, JVGR, 162, 172-184, 2007). The wall friction is assumed to be proportional to ascent velocity in bubbly flow and to the square of ascent velocity in gassy flow with suitable friction coefficients. The relation for water steam in magma is used for solubility of volatiles in magma.

The integration of conduit flow is executed from the surface to a deep conduit. Namely, the deep state of magma flux and volatile content are calculated for various sets of the exit velocity and volatile content at the surface prescribed with the magma pressure equal to the atmospheric pressure. Compiling the calculation results shows that some groups characterize the relation between the surface and deep conditions. Each group can be interpreted in connection with eruption types in the following way.

Firstly, high-speed gassy flow erupts violently when the deep magma contains sufficiently abundant volatile component. This case may produce a Plinian eruption. In this case the exit velocity and gas content are determined by the deep magma flux alone independently of deep gas content because of adjustment by degassing during the ascent process. Secondly, a stationary conduit flow disappears below the critical value of fluid magma flux with high gas content in a deep conduit. In this case magma flow should be non-stationary and may produce Vulcanian or Strombolian eruptions. Thirdly, a relatively slow magma flow with low vesicularity flows out when volatile component is poor. This case likely results in Pelean eruptions because of difficult acceleration of gassy flow in the air.

Our analysis and interpretation suggest that various eruption types arise from different combinations of ascending magma flux and degassing efficiency. It is non-linearity involved in ascending magma flow with vesiculation and degassing that produces separate groups characterizing eruption types.

Keywords: volcanic eruption type, ascending magma flow, conduit flow model, volatile component content, degassing, computer simulation

Japan Geoscience Union Meeting 2014
(28 April - 02 May 2014 at Pacifico YOKOHAMA, Kanagawa, Japan)

SVC50-06 Room:315 Time:May 2 10:15-10:30

Magma eruption rates, eruption styles, and preeruptive magma viscosity

TOMIYA, Akihiko[1*] ; KOYAGUCHI, Takehiro[2] ; KOZONO, Tomofumi[3] ; TAKEUCHI, Shingo[4]

[1]Geological Survey of Japan, AIST, [2]Earthquake Research Institute, University of Tokyo, [3]Department of Geophysics, Graduate School of Science, Tohoku University, [4]Civil Engineering Research Laboratory, Central Research Institute of Electric Power Industry

Magma eruption rate is one of the most fundamental parameters for a volcanic eruption (e.g., Pyle, 2000). It is obtained mainly by geophysical or geological observations. We interpret this important parameter from a petrological point of view and also from a fluid dynamic point of view.

We have collected a hundred of data on magma eruption rates, bulk rock chemical compositions, and phenocryst contents for various styles of eruptions (Plinian, sub-Plinian, basaltic Plinian, lava flow, and lava dome). We are compiling these data on the basis of their 'preeruptive magma viscosities', which are important measures of magma eruptibility (Takeuchi, 2011). Preeruptive magma viscosity is the viscosity of magma (melt + crystals) in the magma chamber at the preeruptive conditions. This value can be obtained by the bulk rock chemical composition and phenocryst content, using an empirical formula (Takeuchi, 2010). We have found that eruption styles are closely correlated to preeruptive magma viscosities but poorly correlated to bulk rock compositions.

We have also examined the difference in magma eruption rates between the explosive phase(s) (e.g., Plinian) and the effusive phase (e.g., dome) in a series of eruptions, in order to understand the transition between these two eruption styles (e.g., Kozono and Koyaguchi, 2009a,b). We have found that the difference is positively correlated to preeruptive magma viscosity.

The above results indicate that preeruptive magma viscosities largely control eruption styles and eruption rates. Our results also show that the eruptive magmas are divided into two types, low-viscosity type (basalt to low-phenocryst-content andesite) and high-viscosity type (high-phenocryst-content andesite to rhyolite). The boundary is at about 10^4 Pa s. These two types may be closely linked to the magma generation processes (e.g., fractional crystallization and melt segregation from crystal mush).

Keywords: magma eruption rates, eruption styles, preeruptive magma viscosity, transition between explosive and effusive eruption, phenocryst content, bulk rock chemical composition

Japan Geoscience Union Meeting 2014
(28 April - 02 May 2014 at Pacifico YOKOHAMA, Kanagawa, Japan)

SVC50-07 Room:315 Time:May 2 10:30-10:45

Conditions for transition from lava dome to explosive eruption

KOZONO, Tomofumi[1*] ; KOYAGUCHI, Takehiro[2]

[1]Department of Geophysics, Graduate School of Science, Tohoku University, [2]Earthquake Research Institute, University of Tokyo

Conduit flow dynamics involving magma vesiculation, gas escape, and crystallization during a lava dome eruption lead to complex processes such as a transition to an explosive eruption. Because the transition from the lava dome to the explosive eruption is accompanied with a drastic increase in eruption intensity, it is important for volcanic hazard mitigation to determine conditions for this transition to occur. In this study, on the basis of a 1-dimensional conduit flow model, we investigated how the conditions for the transition from the lava dome to the explosive eruption depend on magmatic and geological parameters.

In order to systematically investigate the dependence of the transition conditions on the magmatic and geological parameters, we used the relationship between chamber pressure (p_{ch}) and mass flow rate (q) for steady conduit flow (the p_{ch}-q relationship). When the slope of the p_{ch}-q relationship (dp_{ch}/dq) has a positive value (positive differential resistance), the steady flow is stable. When dp_{ch}/dq has a negative value (negative differential resistance), on the other hand, the steady flow is unstable. The negative differential resistance is generated by two positive-feedback mechanisms. First, effective magma viscosity decreases with increasing q because of delay of crystallization, leading to reduced viscous wall friction (feedback 1). Second, magma porosity increases with increasing q because of less efficient gas escape, leading to reduced gravitational load (feedback 2). These two feedback mechanisms induce a sigmoidal p_{ch}-q relationship for some realistic conditions; the positive differential resistance in the low-q and high-q regimes, and the negative differential resistance in the intermediate regime. The analyses of time-dependent conduit flow model indicate that, because of the sigmoidal pch-q relationship, as magma supply at depth gradually increases from the low-q regime to the intermediate regime, magma discharge rate abruptly increases from the low-q to high-q regimes. This abrupt increase in magma discharge rate accounts for the transition from a stable lava-dome eruption to an explosive eruption. We, therefore, define the value of q at the boundary between the low-q and the intermediate regimes as the critical magma supply rate for the transition (q_{cr}).

Our results show that q_{cr} is mainly controlled by the feedback 2 for a wide range of magmatic and geological conditions, whereas it is controlled by the feedback 1 only when phenocryst content is very high. When q_{cr} is controlled by the feedback 2, the value of q_{cr} depends on parameters related to gas escape such as the permeability for vertical gas escape and that for lateral gas escape. We found that for a plausible range of vertical permeability which is constrained from permeability measurements of volcanic rocks, q_{cr} remarkably decreases with decreasing lateral permeability, and it becomes substantially lower than typical magma discharge rates for observed lava-dome eruptions in the limiting case of zero-lateral permeability (i.e. no lateral gas escape). This indicates that the presence of lateral gas escape is a necessary condition for a stable lava-dome eruption to occur. In addition, we found that q_{cr} strongly depends on conduit radius owing to the effects of the change in the conduit radius on the degree of gas escape. As the conduit radius decreases, the ascent of the liquid is suppressed because of the increase in wall friction force, which promotes vertical gas escape. The decrease in the conduit radius also induces an increase in the ratio of the perimeter to the cross-sectional area of the conduit and a decrease in the length scale of pressure gradient that drives lateral permeable gas flow, which promotes lateral gas escape. These promotions of gas escape lead to an increase in q_{cr}. The above results suggest that the variation of conduit radius is a key factor for the transition from a lava-dome to an explosive eruption.

Keywords: conduit flow, numerical model, eruption transition, lava dome, explosive eruption, gas escape

Japan Geoscience Union Meeting 2014
(28 April - 02 May 2014 at Pacifico YOKOHAMA, Kanagawa, Japan)

SVC50-08 Room:315 Time:May 2 11:00-11:15

A phreatic explosion model for Mayon volcano, Philippines, inferred from analyses of an explosion earthquake

MAEDA, Yuta[1*] ; KUMAGAI, Hiroyuki[1] ; LACSON, Rudy[2] ; FIGUEROA, Melquiades[2] ; YAMASHINA, Tadashi[3] ; OHKURA, Takahiro[4] ; BORNAS, Antonia[2]

[1]Nagoya University, [2]PHIVOLCS, [3]Kochi University, [4]Kyoto University

Mayon is one of the most active volcanoes in the Philippines with 49 known historical eruptions from 1616 to 2010. A phreatic explosion took place at Mayon on 7 May 2013 that killed five climbers. In this presentation, we show the results of the waveform inversion for the explosion earthquake and discuss a phreatic explosion model for Mayon.

During the explosion in 2013, a VLP event with a peak frequency of 0.4 Hz was recorded by three broadband seismometers which we had installed in 2011. We performed a frequency-domain waveform inversion in 0.1-0.6 Hz, which pointed to a combination of a subhorizontal tensile crack and a vertical single force at a shallow part beneath the summit crater. Contributions from the crack and force to the waveforms had amplitudes comparable to each other.

The source time functions obtained by the waveform inversion are bandpassed forms (filtered source time functions; FSTFs), which may be different from the source time functions without filters (deconvolved forms of the source time functions; DSTFs). Instead of performing numerically unstable deconvolution operations, we assumed simple step- and impulse-type functions with finite durations as candidates of the DSTFs. We applied the bandpass filter to these functions and compared with the FSTFs. The bandpassed waveforms of the impulse-type functions were similar to the FSTFs for both the crack and force, suggesting that the DSTFs can be approximated by the impulse-type functions. The estimated DSTF for the tensile crack showed an inflation followed by a deflation, whereas that for the single force showed a downward force around the time of the maximum opening of the crack.

The RMS seismic amplitudes, GPS baseline lengths over the volcano, ground surface temperatures around the summit, waveform correlations among the seismic stations, the sulfur dioxide emission, and rainfall did not show clear precursory signals.

Since the analyzed VLP event occurred during the phreatic explosion, the initial inflation in the DSTF for the crack may have been caused by boiling of underground water. This crack is subhorizontal and located at a shallow part, suggesting that the crack may be located on a boundary between permeable and impermeable layers where the water may have accumulated and finally boiled, generating the explosion. The downward force may represent the counter force of the explosion. The deflation of the crack in the latter half of the DSTF may have been caused by outgassing of water vapor during the explosion.

The estimated moment amplitude is explained by a volume change of 400 m $\times$ 400 m $\times$ 0.4 m. A topographic change comparable to this crack size was not observed during the explosion, suggesting that the explosion destroyed only a limited portion of the crack. This crack may repeat the explosion once the fragmented portion of the crack is sealed through the hydrothermal alteration. At Mayon, small ash explosions occurred in 2003, 2004, 2006, and 2009, with intervals of a few days to a few years (mostly longer than one month). These intervals are close to experimentally derived time scales of fracture sealing by the hydrothermal alteration; according to the experiments by Berger et al. (1994, Geochim. Cosmo. Acta), who used basalt samples with chemical compositions similar to magmatic eruption deposits at Mayon, a centimeter-order fracture is sealed in two months for 300 ℃ and 54 months for 150 ℃.

In this model, timings of the explosions are controlled by the sealing of the fracture. Therefore the explosions can occur even with a constant supply of heat and water. This may be the reason why no clear precursory signals were observed before the explosion in 2013. No VLP events other than that associated with the explosion in 2013 have been observed at Mayon since the beginning of the observation in 2011, which may be explained by the sealing of the fracture just prior to the explosion.

Keywords: Phreatic explosion, Waveform inversion, Source time function, Hydrothermal alteration

Japan Geoscience Union Meeting 2014
(28 April - 02 May 2014 at Pacifico YOKOHAMA, Kanagawa, Japan)

SVC50-09 Room:315 Time:May 2 11:15-11:30

Magma accumulation process of Izu-Oshima volcano, as revealed from deep LF earthquakes, deformation and CO2 out-gassing

WATANABE, Hidefumi[1*]

[1]Disaster Prevention Division, Tokyo Metropolitan Government

In order to make successful mid-term eruption predictions, we need to detect particular precursory processes operating in magma-plumbing system. Since 1989, Izu-Oshima volcano has continued its re-inflation, after the last eruption in 1986, and further repeated deflation-inflation cycles, resulting a net inflation of the volcano. The rate of secular inflation decreased exponentially until 2006, while the amplitudes of the deflation-inflation cycles increased. Since 2007, the rate of secular inflation has kept a constant speed and has also increased the activity of deep low-frequency (LF) earthquakes occurring at the depth range of 30-40 km beneath the volcano. Each episodic LF earthquake activity was preceded by the volcano deflation and accompanied by the inflation. Based on these evidences, we may suppose that the volcano inflation is caused by the supply of magma from a source region at the depth range of 30-40 km beneath the volcano, and that an episodic out-gassing from the shallow magma reservoir triggers each deflation-inflation cycle. To demonstrate the proposed mechanism, we need to combine the data on magma accumulation and out-gassing processes. To monitor the out-gassing of basaltic magma accumulating beneath the volcano, CO_2 is most helpful. In September 2005, we started continuous monitoring of soil CO_2 concentration at the summit of Izu-Oshima volcano, and obtained an evidence for the out-gassing process; the correlated increase of soil CO_2 concentration during the periods of not only accelerated inflation but also deflation of the volcano. Integrating the observational data, we suppose that the rate of magma supply from the upper mantle has increased since 2007 and that the increase in amplitude of deflation-inflation cycles might indicate a volume increase of CO_2 over-saturated region at the upper part of the magma reservoir beneath the volcano.

Keywords: Izu Oshima volcano, eruption prediction, precursors to eruption, volcano deformation, CO2 out-gassing

Japan Geoscience Union Meeting 2014
(28 April - 02 May 2014 at Pacifico YOKOHAMA, Kanagawa, Japan)

SVC50-10 Room:315 Time:May 2 11:30-11:45

Spatio-temporal characteristics of volcanic tremor during the 2011 Kirishima eruption by seismic wave analysis

NAKAMOTO, Manami[1*] ; MATSUMOTO, Satoshi[1] ; YAMANAKA, Yoshiko[2] ; SHIMIZU, Hiroshi[1] ; NAKAMICHI, Haruhisa[4] ; ICHIHARA, Mie[3] ; OIKAWA, Jun[3]

[1]SEVO, Kyushu Univ., [2]EVRC, Nagoya Univ., [3]ERI, University of Tokyo, [4]DPRI, Kyoto Univ.

Volcanic tremors are considered as oscillations occurred in magma supply system and provide us important information about condition of the system from magma chamber to crater through a conduit. Therefore, it is important to investigate locations of their source and their characteristics for understanding the condition and process of volcanic activity and modeling the magma supply system. In this study, we reveal features of volcanic tremor using seismic data at Kirishima volcano.

An array observation help us to get information of incident waves on the stations. The two array seismic observations were carried out around Shinmoe-dake during the 2011 Kirishima eruption. One consisted of 25 seismometers located 3 km southwest of the Shinmoe-dake crater (Matsumoto et al., 2013), and the other consisted of 16 seismometers located 5 km northeast of the crater (Nakamichi et al., 2013). The combining data from two arrays enable us to determine the tremor sources. Moreover, we estimated mechanism of the tremor source by using waveforms recorded at temporal seismic station in Kirishima volcanic area and tremor sources obtained by array analysis.

This study focus on the volcanic tremor which occurred on February 2, 2011, and its duration was about 40 minutes. Peak frequencies of the tremor were about 1, 2, 3, and 4 Hz. We investigated temporal variation in the source location of the tremor from the slowness and azimuth of incident wave by MUSIC method. we found that most part of the tremor were radiated around Shinmoe-dake crater. In this part, the tremor that had large slowness and relatively long duration was located in shallow region beneath the crater. In contrast, at some parts of the tremor, source location for waves with short duration were near Ohnami pond, 3.3 km northeast of the crater. Based on amplitude analysis for the seismogram recorded by the seismic network, we also found out difference in radiation patterns of the volcanic tremor among the tremor sources. Assuming single crack model, we found the strike and dip direction of the crack beneath the Shinmoe-dake crater is different from those near Ohnami pond.

Keywords: volcanic tremor, Shinmoedake

Japan Geoscience Union Meeting 2014
(28 April - 02 May 2014 at Pacifico YOKOHAMA, Kanagawa, Japan)

SVC50-11 Room:315 Time:May 2 11:45-12:00

Relationship BH-type earthquake swarms and ground deformations prior to eruptions at Showa crater at Sakurajima volcano

TAMEGURI, Takeshi[1*] ; IGUCHI, Masato[1]

[1]DPRI, Kyoto University

Vulcanian eruptions have occurred at the Minamidake crater at the summit since 1955 at Sakurajima volcano. Principal eruptive activity shifted to the Showa crater at the eastern flank of the summit in 2006. The eruptions at the crater become active and minor vulcanian eruptions occurred about 1,000 times per year in 2010-2013. Ash plume height of the eruptions sometimes reached to 3000m in 2013. The eruptive activities at the Showa crater gradually increase.

Inflationary strain changes are observed by extensometers a few tens of minutes to several hours prior to the eruptions and are caused by pressure sources located at depths of 0-1.5 km (Iguchi et al., 2013). The inflation rates decrease or sometimes suspend about 30 minutes before the eruptions. Small earthquakes dominated by high frequency components (5-6 Hz) swarm when duration of inflation is longer than 1 hour. The hypocenters of the earthquakes are located at a depth of 0.5 km beneath the crater and are close to depth of the pressure source. The earthquakes begin to occur a half hour to 1 hour after the start of the inflation. The amplitudes and number of the earthquakes further increase when the inflation rates decrease or suspend. And, the occurrences of the earthquakes suddenly stop at the start of the eruptions. The occurrences of the earthquake swarms are related to the decrease of inflation rate and the long inflation.

Seismic energy releases of the precursory earthquakes related to every eruption accelerate before eruptions. There are all kinds of large and small seismic energy releases in the eruptions. The accelerations of the seismic energy releases before eruptions with explosive events tend to be larger than those with non-explosive events. And, the accelerations of the seismic energy releases are rapid in the case of large deflations after eruptions. The precursory earthquakes may be generated by release of excess pressure accumulated by inflation of the pressure source. We might be able to predict eruption types and scales from occurrence patterns of the precursory earthquakes.

Keywords: Sakurajima volcano, precursory earthquake, ground deformation

Japan Geoscience Union Meeting 2014
(28 April - 02 May 2014 at Pacifico YOKOHAMA, Kanagawa, Japan)

SVC50-12 Room:315 Time:May 2 12:00-12:15

Volcanic tremor caused by flow-induced oscillation of a magma-filled dike

SAKURABA, Ataru[1*] ; YAMAUCHI, Hatsuki[2]

[1]Department of Earth and Planetary Science, University of Tokyo, [2]Earthquake Research Institute, University of Tokyo

Volcanic tremor (VT) is known to be long-period and long-duration ground motion generally observed during or before eruptions. Majority of VTs show an emergent onset and, when accompanied with eruptions, an exponentially growing phase in amplitude is typically observed (Konstantinou and Schlindwein 2002; McNutt and Nishimura 2008). This characteristic suggests that VT is manifestation of self-oscillation, in which a persistent steady forcing excites an eigen oscillation of a system and the amplitude exponentially grows until a nonlinear process leads to a limit cycle. In volcanic settings, a steady magma flow through an underground conduit may cause flow-induced self-oscillation of bedrocks, and this is the idea first presented by Julian (1994). In the case of the collapse of Tacoma Narrows bridge, which is known to be caused by flow-induced oscillation, the vibrating bridge can be modeled by an elastic plate placed parallel to an infinite flow. Here we consider a reversed setting: a fluid-flowing thin layer in an infinite elastic body. This system is also unstable if the flow speed is high enough, and may be a generation mechanism of some VTs.

We consider a fluid-flowing plane layer sandwiched between two semi-infinite elastic bodies, expanding Julian's idea to a more general elastodynamic model (for details, see Sakuraba and Yamauchi 2014 to appear in *Earth, Planets and Space*). The eigen oscillation that should be excited in this self-oscillation model is an elastic surface wave. Therefore, we solve the Navier-Stokes equation linearized about a laminar flow with the boundary condition that can maintain a surface wave traveling along the layer. We succeeded in obtaining a complex phase speed of the surface wave as a function of wavenumber (and some parameters) using a shooting method, and found that a relatively slow magma flow could lead to instability in which the imaginary part of the phase speed is positive. Remarkably, the most unstable mode exhibits an antisymmetric (flexural) deformation, which has not been discussed in previous similar studies (Balmforth, Craster and Rust 2005; Dunham and Ogden 2012). The unstable mode is identical to two parallel Rayleigh waves traveling against the basic magma flow. The instability can be understood as acceleration of nearly circular particle motion of the Rayleigh wave due to viscous drag of the main laminar flow. As the critical flow speed giving a neutrally stable state decreases in inversely proportional to wavelength, instability will occur with the largest possible wavelength, which could be several kilometers and produce an oscillation period of around 1 second. In that case, the critical flow speed can be reduced to less than 1 m/s when the magma is basaltic. As the magma flow speed in a dike will not exceed several meters per second, there would be a lower bound in the critical wavelength, producing a period of 0.1 second. Thus our model naturally explains typical periods of 0.1-1 seconds observed on volcanoes. Our model also explains typical timescales of the linearly growing phase in some VTs.

Japan Geoscience Union Meeting 2014
(28 April - 02 May 2014 at Pacifico YOKOHAMA, Kanagawa, Japan)

SVC50-13 Room:315 Time:May 2 12:15-12:30

Magnitude-frequency distribution of volcanic eruptions from an open conduit

NISHIMURA, Takeshi[1*] ; IGUCHI, Masato[2] ; MUHAMAD, Hendrasto[3] ; AOYAMA, Hiroshi[4]

[1]Science, Tohoku Univ., [2]DPRI, Kyoto Univ., [3]CVGHM, Indonesia, [4]Science, Hokkaido Univ.

Explosive eruptions such as vulcanian, strombolian, or significant gas burst excite seismic waves. Such seismic signals, which are often called as explosion earthquakes or explosion quake, are used to quantitatively evaluate the magnitude of such volcanic explosions. In the present study, we systematically examine magnitude-frequency distributions of explosion earthquakes observed at Sakurajima and Suwanosejima volcanoes in Japan, and Semeru and Lokon volcanoes in Indonesia. We use the long-term catalog data of Sakurajima explosions for the period from 1963 to 2011, which are routinely summarized by Sakurajima Volcano Research Center (SVRC). Also, we measure the amplitudes of explosion earthquakes from continuous seismic records observed at Suwanosejima and Semeru and Lokon volcanoes in Indonesia. We measure the number of earthquakes that exceed a given amplitude, and then plot the cumulative number of earthquakes versus amplitude, as is often done for examining Ishimoto-Iida's relation, which expresses a power law distribution. However, the observed frequencies of earthquakes at the four volcanoes do not seem to fit the Ishimoto-Iida's relation. The cumulative numbers are well explained by exponential functions. This means that the magnitude of explosion earthquake at each volcano is randomly determined with an average scale.

Keywords: Volcanic Explosion, Vulcano, Gas burst, Magnitude-frequency distribution

Japan Geoscience Union Meeting 2014
(28 April - 02 May 2014 at Pacifico YOKOHAMA, Kanagawa, Japan)

SVC50-14 Room:315 Time:May 2 14:15-14:30

Rheological transition of plagioclase-bearing magma: high-temperature uniaxial deformation experiments of sanukite lava

ISHIBASHI, Hidemi[1*]

[1]Graduate School of Science, Shizuoka University

High-temperature uniaxial compression experiments were done for bubble- and phenocryst-free, plagioclase-bearing lava to investigate the effect of tabular crystals on rheological properties of highly crystalline magma. High-Mg andesite lava from Goshikidai lava plateau, southwest Japan, was used for starting material. The lava is bubble- and phenocryst-free, composed of 60 vol.% rhyolitic glass, 36 vol.% of tabular plagioclase and 4 vol.% of pyroxenes and magnetite and plagioclase crystals are well aligned parallel. High-temperature uniaxial defomation apparatus at Earthquake Research Institute, the University of Tokyo, was used for experiments. The lava was cut to 10 x 10 x 20 mm rectangular solids and deformed under conditions of temperatures of 1238, 1188, and 1138 K and deformation rates from 3.16 to 0.003 mm/min. Run samples were quenched and processed to thin section for textural and compositional analyses by using EPMA.

Phase proportions in all run samples were the same as that of starting material, indicating crystallization did not occur during experiments. The lava behaves as shear thinning fluid under all temperature conditions. Viscosity at strain rate of 10^{-4} s^{-1} increases from $10^{8.7}$ to $10^{9.4}$ Pas with decreasing temperature. Power law exponent [= d(log viscosity)/d(log strain rate)] is ca. 0.64, which is consistent with extrapolation of previous studies for natural plagioclase-bearing magmas. Relative viscosity [= (bulk viscosity)/(melt viscosity)] is ca. $10^{2.4}$ at strain rate of 10^{-4} s^{-1} under all temperatures, indicating that the concept of relative viscosity works well under present experimental condition. The relative viscosity-crystal fraction relation is also consistent with extrapolation of previous studies for natural plagioclase-bearing magmas. Marron-Piece equation well explains the relation with the maximum packing fraction of 0.43. Present results suggest that rheological transition occurs at crystal fraction near 0.43 for plagioclase-bearing natural lava in which plagioclase crystals are well aligned parallel. The value is higher than ca. 0.3 proposed by Picard et al. (2013)'s experiments in which plagioclase orientation is random in starting materials, indicating the first order importance of plagioclase orientation distribution on rheological transition.

Keywords: rheological transition, viscosity, magma, plagioclase, non-Newtonian fluid, sanukite

Japan Geoscience Union Meeting 2014
(28 April - 02 May 2014 at Pacifico YOKOHAMA, Kanagawa, Japan)

SVC50-15 Room:315 Time:May 2 14:30-14:45

Conduit flow of silicic magma: Viscous flow or Frictional sliding?

OKUMURA, Satoshi[1*] ; UESUGI, Kentaro[2]

[1]Department of Earth Science, Graduate School of Science, Tohoku University, [2]Japan Synchrotron Radiation Research Institute

Outgassing rate and bulk magma viscosity that control the style of volcanic eruptions depend on flow type of magma ascending in a volcanic conduit. When magma behaves as a Newtonian fluid, magma in the conduit experiences shear strain large enough to cause effective outgassing. On the other hand, once shear starts to localize, bulk magma viscosity may decrease due to slip deformation and outgassing rate also decreases in parts other than shear-localized region (Okumura et al., 2013 EPSL). Silicic magma experiences shear-induced brittle fracturing and subsequent frictional sliding along the fracturing zone during its ascent (e.g, Gonnermann and Manga, 2003 Nature; Tuffen et al., 2003 Geology). Therefore, outgassing rate and bulk magma viscosity during the ascent are expected to change dramatically. Previous studies (Tuffen et al., 2003 Geology; Gonnermann and Manga, 2005 EPSL) also proposed that fractured magma can heal during magma ascent and that fracturing and healing processes may control the dynamics of magma ascent. In contrast to this model, some experimental studies (e.g. Okumura et al., 2010) indicated that fractured magma cannot heal as long as the deformation continues. In this study, we perform deformation experiments for fractured magma to investigate flow type of magma in the conduit, i.e. viscous flow or frictional sliding, and controlling factors of the transition from viscous flow to frictional sliding.

The deformation experiments were carried out using a custom-made torsional deformation apparatus which was installed in synchrotron radiation X-ray imaging system (BL20B2) of SPring-8. To simulate fractured silicic magma, we crushed rhyolite obsidian and sorted them into fragments of 75-250 μm in size. The powdered sample was sandwiched by two obsidian discs and they were twisted by rotating a piston attached with a rotational motor. The torsional deformation experiments were performed at temperatures of 800 and 900 ℃ under 1-10 MPa pressures. The rotational rate was set to be 0.1 to 10 rpm, corresponding to strain rates of 10^{-2} to 1 s^{-1} if the sample deforms homogeneously. The deformed samples were observed in situ using an X-ray radiography.

At a temperature of 900 ℃ and rotational rates of 0.1-1 rpm, homogeneous deformation through a sample was observed under a pressure of 10 MPa, which indicates viscous deformation. In contrast, the sliding at the interface between powdered obsidian and the disc was observed under 1 and 5 MPa pressures. At a temperature of 800 ℃, the sliding was found under 1-10 MPa pressures. These results indicate that frictional sliding along fractured zone is flow type of magma in shallow parts of the conduit ($<$10 MPa).

We assume that flow type is determined by competition of shear stress necessary for viscous flow and frictional sliding. If magma has high viscosity and shear stress to deform a sample viscously is large, the flow type becomes frictional sliding. At a temperature of 900 ℃, viscous flow and frictional sliding were found at 10 and 1-5 MPa pressures, respectively. At this condition, magma viscosity is approximately 10^7 Pa s (Hess and Dingwell., 1996) and shear stress necessary for viscous deformation is 1 MPa at a strain rate of 0.1 s^{-1}. Because the frictional sliding was observed at pressures of 1-5 MPa, the frictional coefficient is estimated to be ca. 0.1. When we use this value and the criterion for shear-induced brittle fracturing proposed by Okumura et al. (2010), the dynamics of magma ascent is controlled by frictional sliding at shallow parts of the conduit. In addition, silicic magma can ascend quickly due to low frictional coefficient of fractured magma.

Keywords: Silicic magma, Volcanic eruption, Viscous flow, Frictional sliding, Synchrotron radiation X-ray

Japan Geoscience Union Meeting 2014
(28 April - 02 May 2014 at Pacifico YOKOHAMA, Kanagawa, Japan)

SVC50-16 Room:315 Time:May 2 14:45-15:10

Mechanism of delayed brittle-like fragmentation of vesicular magma analogue

KAMEDA, Masaharu[1*] ; SHIDA, Tsukasa[1] ; ICHIHARA, Mie[2] ; TSUGO, Mitsuaki[1] ; OKUMURA, Satoshi[3] ; UESUGI, Kentaro[4]

[1]Mech. Sys. Eng., TUAT, [2]ERI, Univ. of Tokyo, [3]Earth Sci., Tohoku Univ., [4]JASRI

Magma fragmentation is a key phenomenon controlling volcanic eruptions. The fragmentation is classified into two styles: solid-like brittle fragmentation and liquid-like ductile fragmentation. Brittle fragmentation is more hazardous than ductile fragmentation because violent release of pressurized gas in the bubbles contained in the magma may lead to explosive eruptions

The fragmentation of magma, which is a viscoelastic fluid, occurs through a combination of viscoelasticity and rapid deformation. We conducted a rapid decompression experiment over ten years in order to clarify the viscoelastic effect on the fragmentation using a magma analogue, syrup containing gas bubbles (Kameda et al GRL 2008; Kameda et al. JVGR 2013).

Through the experiment we demonstrated the existence of a transitional fragmentation behavior. This transition behavior, which we refer to herein as brittle-like fragmentation, occurred even if the response of material should be in a ductile manner. Comparing the realistic decompression time with the viscoelastic relaxation time for magma, it is more probable that the fragmentation in the real volcanic system occurs in a brittle-like manner.

Observation by high-speed photography using a visible light-source indicated that the onset of brittle-like fragmentation was triggered by the sudden release of a considerable amount of gas from a crack in the specimen. Further observation (Shida et al. IAVCEI 2013) showed that reducing the volume of the specimen suppressed the onset of fragmentation even if their brittleness (Ichihara and Rubin 2010) was close to unity. In our case, the pore distribution of the small samples was more uniform than that of large samples. This observation implies that the crack is initiated from the interior of the specimen due to non-uniform spatial distribution of bubbles.

Then, we observed the interior of the specimen by synchrotron X-ray tomographic microscopy. The X-ray tomographic microscopy was performed at the BL20B2 beamline of the Japan Synchrotron Radiation Research Institute (JASRI, Hyogo, Japan). Initial structure of the specimen was observed by three-dimensional tomographic imaging. High-speed radiography was performed during the decompression. A digital charge-coupled device (CCD) camera was used as the detector whose imaging area is about 16 mm (horizontal) by 5 mm (height) with spatial resolution of 8 μm/pixel. We took 1800 projections over 180 degrees of rotation for tomographic imaging. The framing rate of radiography is 200 frames per second. We successfully captured a series of images during the brittle-like fragmentation. The reconstructed 3D image of the specimen indicated that the brittle-like fracture was initiated at a notch and a chain of small bubbles in the vicinity of a large bubble.

We propose the following scenario for brittle-like fragmentation: It is initiated from ductile growth of internal cracks by connection of bubbles. The stress concentration and the brittleness at crack tip may exceed the critical level at some moment, which leads to brittle failure of the crack. Rapid decompression due to sudden release of a considerable amount of gas from the crack may increase local brittleness to cause partial fragmentation. Such a sequence from ductile crack growth to partial fragmentation may successively occur in brittle-like fragmentation.

Keywords: Magma, Fragmentation, Viscoelasticity, Decompression, X-ray CT

Japan Geoscience Union Meeting 2014
(28 April - 02 May 2014 at Pacifico YOKOHAMA, Kanagawa, Japan)

SVC50-17 Room:315 Time:May 2 15:10-15:35

Approach by volcanic observation for dynamics of volcanic phenomena

IGUCHI, Masato[1*]

[1]DPRI, Kyoto University

Dynamics of volcanic activity has been revealed by various kinds of observation. Inflation of volcanic body prior to eruptions corresponds to intrusion of magma to the underground of volcanoes and deflation is accompanied by eruptive activity.

Prior to vulcanian eruptions, minor deflation is detected. This corresponds to leakage of volcanic gas from a gas pocket formed at the uppermost conduit. The minor deflation reflecting minor pressure decrease induces a sudden degassing in oversatulated magma. The sudden degassing corresponds to a volume increase at a deep part in the conduit, as revealed by outward first motions of explosion earthquakes. The volume increase attained at the top of the conduit and the gas pocket overbursts. As the results of collapse of the gas pocket, infrasound of air-shock type is generated with ejection of incandescent bombs followed by ejection of volcanic ash.

Keywords: vulcanian eruption, Sakurajima

Japan Geoscience Union Meeting 2014
(28 April - 02 May 2014 at Pacifico YOKOHAMA, Kanagawa, Japan)

SVC50-P01 Room:Poster Time:May 2 16:15-17:30

Tephra-Fall Predictions with the JMA Regional Atmospheric Transport Model for the 1914 Eruption at Sakurajima Volcano

SHIMBORI, Toshiki[1*] ; SHIRATO, Shomei[2] ; HASEGAWA, Yoshihiko[3] ; HASHIMOTO, Akihiro[1] ; TAKAGI, Akimichi[1] ; YAMAMOTO, Tetsuya[1] ; YAMAMOTO, Akira[1]

[1]Meteorological Research Institute, [2]Kagoshima Local Meteorological Office, [3]Japan Meteorological Agency

A hundred years ago, the largest eruption in 20th century Japan, *i.e*. the Sakurajima Taisho Eruption occurred on 12 January 1914. With this eruption, tephra-falls were observed large-area in Japan from Kyushu to Tohoku region (Hasegawa, 1914; Omori, 1916). For such large-scale eruptions, the Meteorological Research Institute (MRI) is going to do new research project of the tephra-fall predictions with the JMA Regional Atmospheric Transport Model (JMA-RATM) from this year. The research will lead to the improvement of the Volcanic Ash Fall Forecasts (VAFFs) of the Japan Meteorological Agency (JMA). For the purpose of investigating the predictability of the current JMA-RATM against large-scale eruptions, predictions of volcanic-ash dispersion and tephra-fall for the Sakurajima Taisho Eruption were carried out. The initial values which are the total volume (ash and pumice) of 6×10^8 m^3, the plume height of 3000-18000 m and the eruption duration of 38 hours are assumed based on Yamashina (1999), Yasui *et al*. (2006), Iguchi (2014) and so on. The input GPVs are the JMA Mesoscale Analysis after 28 March 2013. The forecast time by the JMA-RATM is 72 hours from starting time. Results of the calculations indicate that, under the assumption of the ash-density of 1 g/cm^3, the predictions of tephra-fall depths are over 1 m in Sakurajima Island for weak-wind weather condition, several 10 cm at Kagoshima City for easterly wind in summertime, and of the order of 0.1-1 mm at Osaka, Nagoya and Tokyo Metropolitan area for southwesterly wind field. In the atmosphere, dispersions of volcanic-ash up to Tohoku and Hokkaido region are also predicted at the same forecast time.

In the presentation, from the results of volcanic-ash dispersion and tephra-fall prediction, the predictability and problems of the current JMA-RATM for large-scale eruptions will be reported.

References

Hasegawa, K., 1914: Summary report on the Sakurajima eruption. *Geophys. Rev*., **170**, Central Meteorological Observatory, Tokyo, 1-16.

Iguchi, M., 2014: The centennial anniversary of the Taisho Eruption. Lecture note, Ceremony for the Sakurajima Taisho Eruption 100th Anniversary.

Omori, F., 1916: Accumulation and transportation of ashes thrown out during the Sakura-jima eruptions of 1914: The Sakura-jima eruptions and earthquakes II. *Bull. Imperial Earthq. Invest. Comm*., **8**, 113-133.

Yamashina, K., 1999: Volcanic cloud height of the 1914 eruption at Sakurajima volcano - Discussions on documentary records and photographs. *Bull. Volcanol. Soc. Japan*, **44**, 71-82.

Yasui, M., M. Takahashi, K. Ishihara and D. Miki, 2006: Records on the 1914-1915 eruption of Sakurajima volcano, Japan. *Proc. Inst. Nat. Sci*., Nihon Univ., **41**, 75-107.

Keywords: Atmospheric Transport Model, volcanic-ash dispersal, tephra fall, Volcanic Ash Fall Forecast, Sakurajima volcano, 1914

Japan Geoscience Union Meeting 2014
(28 April - 02 May 2014 at Pacifico YOKOHAMA, Kanagawa, Japan)

SVC50-P02 Room:Poster Time:May 2 16:15-17:30

Evaluation of wind data for tephra dispersion simulations

KIYOSUGI, Koji[1*] ; KOYAGUCHI, Takehiro[1] ; SUZUKI, Yujiro[1]

[1]Earthquake Research Institute, University of Tokyo, Tokyo, Japan

Understanding how pyroclasts disperse from volcanic plumes is a fundamental problem of volcanology to reconstruct eruption conditions from tephra fallout deposits. Tephra dispersion is not only a scientifically interesting but also socially and economically important problem. For this reason, advection-diffusion models for tephra transportation have been developed with simplified assumptions (e.g. TEPHA2, PUFF, FALL3D). Simulation results of these advection-diffusion models are affected by the input wind data. For example, in a case study of the Kirishima 2011 eruption with PUFF, simulation results with finer temporal-spatial resolution wind data (Japan Meteorological Agency Mesoscale Model and ERA Interim) reproduced a more wavy shape of observed eastward extending plume (about 900 km from the vent) than that with coarser temporal-spatial resolution wind data (NCEP/NCAR Reanalysis).

Some wind data are available from Japan Meteorological Agency Mesoscale Model, ERA Interim of the European Center for Medium-Range Weather Forecasts and NCEP/NCAR Reanalysis of the National Oceanic and Atmospheric Administration of the United States. Between these wind data, there are differences in data assimilation methods, forecast models and temporal-spatial resolution. In addition, a finer temporal-spatial resolution wind data can be generated with using weather forecast models, such as the Weather Research and Forecasting (WRF) model. The WRF model is a fully compressible, Euler non-hydrostatic mesoscale forecast model developed by a multiagency collaboration. The WRF model is suitable for use in a broad spectrum of applications across scales ranging from meters to thousands of kilometers.

We are developing a system to generate wind data suitable for simulations of the advection-diffusion models. Such wind data should have a spatial resolution of several hundred meters near the vent, that of several kilometers far from the vent and vertically several tens of layers. In addition, it must be required to reproduce the interaction between ambient atmosphere and volcanic plumes. For this purpose, we are carrying out numerical calculations with the WRF model and the available wind data sets; we attempt to generate wind data with higher temporal-spatial resolution using data assimilation based on the observations from the regions of interest (e.g. volcano locations and downwind area) and other observations (e.g. the radar observations).

Keywords: Tephra dispersion simulation, Weather forecast model

Japan Geoscience Union Meeting 2014
(28 April - 02 May 2014 at Pacifico YOKOHAMA, Kanagawa, Japan)

SVC50-P03 Room:Poster Time:May 2 16:15-17:30

Classification of infrasound waveforms and analysis of video images at volcano eruption

SATO, Yusuke[1*] ; YOKOO, Akihiko[1]

[1]Graduate School of Science, Kyoto University

Volcano infrasound is an increasingly useful technique for measuring and analyzing eruptive activity. In order to reveal causes of characteristics of infrasound waveform, we analyzed infrasound records and video images at eruptions that occurred at Yasur Volcano, Vanuatu during an hour at 15:00, 21th September, 2011. Yasur Volcano has three active vents in the summit crater. Infrasound waves are generated every 1-3 minutes at various eruptions with reddish magma, vapor rich gas and ash. Infrasonic waveforms are mostly symmetric with a sharp compressive onset, followed by a small rarefaction phase. In this study, we analyzed infrasound events whose maximum amplitude is more than 50 Pa at one station on the summit crater rim. We conducted cross correlation analysis to 29 wave records and classified them into 3 types; A (13 events), B (12 events) and C (4 events). Time window of the analysis was 5s from a second before the maximum peak time. In contrast to type C, cross correlation coefficient among wave forms of types A and B was very high (>~ 0.75). The compressive ratio and the ratio of positive and negative peak are different between type A and B. On the other hand, we analyzed selected video sequences of these eruptions. We read the RGB and brightness values on horizontal line above each vent until the end of the eruptions from 2s before the ejecta reaches the line. The maximum R and brightness value of type B events was twice as other type eruptions. This result may suggest that type B eruptions release relative much reddish magma and whitish gas compared to those of type A and C.

Keywords: infrasound, volcano eruption

Japan Geoscience Union Meeting 2014
(28 April - 02 May 2014 at Pacifico YOKOHAMA, Kanagawa, Japan)

SVC50-P04 Room:Poster Time:May 2 16:15-17:30

Numerical treatment of dry bed problem in the model of pyroclastic flows based on the 1-D shallow-water equations

SHIMIZU, Hiroyuki[1*] ; KOYAGUCHI, Takehiro[1] ; SUZUKI, Yujiro[1]

[1]Earthquake Research Institute, The University of Tokyo

During explosive volcanic eruptions, a mixture of pyroclasts and volcanic gases is released from the vent. When the mixture loses its upward momentum before the density of the mixture becomes lower than the atmospheric density, the mixture forms a pyroclastic flow. Dynamics of pyroclastic flows can be approximated by that of an inviscid gravity current. The dynamics of inviscid gravity currents are controlled by an inertial-buoyancy balance on the front (e.g., Benjamin, 1968); we refer to this condition as "the front condition". The front condition, and hence, the dynamics of the inviscid gravity currents strongly depends on the density ratio of the current (ρ_c) to the ambient (ρ_a) (e.g., Ungarish, 2009). When $\rho_c/\rho_a \sim 1$, the current is characterized by a high front, whereas a front height does not develop when $\rho_c/\rho_a \gg 1$. In pyroclastic flows, because density ratio ρ_c/ρ_a varies spatially and temporally, the dynamics of pyroclastic flows becomes complicated; the basic features of pyroclastic flows, such as the run-out distance, have not been fully understood. The aim of our study is to develop a unified model of the inviscid gravity currents for various density ratio ρ_c/ρ_a.

In general, the dynamics of shallow inviscid gravity currents can be described by the shallow-water equations. There are two numerical models to solve the shallow-water equations: "shock front condition model" (SFC model) and "artificial bed-wetting model" (ABW model). SFC model is a model, in which the front condition is applied to the boundary condition (e.g., Ungarish, 2009). The boundary condition is given as a function of ρ_c/ρ_a. On the other hand, in ABW model, an artificial wet bed with the height of ϵh_0 is set on the dry bed in order to express the front condition, where h_0 is a characteristic height scale (e.g., Toro, 2001; Larrieu et al., 2006; Doyle et al., 2007). This model has the only parameter ϵ for the front condition. Although the front condition, and hence the appropriate value of ϵ must be a function of ρ_c/ρ_a, the relationship between ϵ and ρ_c/ρ_a has not been studied. In order to resolve these problems, we carried out parameter studies using the two models for solving a simple "one-dimensional (1-D) dam-break problem".

On the basis of systematic comparisons between the results of SFC model and ABW model, we found the relationship between the parameter ϵ and ρ_c/ρ_a : $\epsilon \sim 8.62 \cdot 10^{-2} \cdot (\rho_c/\rho_a)^{-1.87}$. We also found that the application of ABW model should be limited to $15 < \rho_c/\rho_a$. In the case of $1 < \rho_c/\rho_a < 15$, an unphysical shock wave propagates into the artificial bed so that the velocity and height of the current substantially deviate from the solution satisfying the correct front condition.

Keywords: pyroclastic flows, gravity currents, shallow-water equations, numerical simulation, volcanic disaster prevention

Japan Geoscience Union Meeting 2014
(28 April - 02 May 2014 at Pacifico YOKOHAMA, Kanagawa, Japan)

SVC50-P05 Room:Poster Time:May 2 16:15-17:30

Moment tensor representation of elliptical volume sources

MIZUNO, Naoto[1*] ; KUSAKABE, Tetsuya[2] ; ICHIHARA, Mie[2] ; KAME, Nobuki[2]

[1]School of Science, The University of Tokyo, [2]Earthquake Research Institute, The University of Tokyo

A moment tensor inversion is a powerful tool to extract source information from seismic and geodetic observations. However, widely-used moment tensor representation for volumetric sources has been limited to a few basic geometries such as a sphere, a flat crack, and a cylinder. These sources give particular diagonal component ratios: (M_1:M_2:M_3)=(1:1:1) for a sphere, (1:1:3) for a crack, and (2:2:1) for a cylinder. When different component ratios are obtained from the inversion analysis, they are interpreted as combination of these simple geometries without considering internal pressure balance.

Although the moment tensor representation for elliptical sources was obtained 30 years ago (Davis, 1986), the solution has been rarely applied in volcanology. We consider two disadvantages of Davis (1986). The one is that the theories to relate the actual volume change to moment tensor have been proposed but not unified , which has caused some confusion. The accompanying paper (Ichihara et al., 2014, this meeting) presents a unified explanation based on the representation theorem and makes a clear link among volume change, geometry, and moment tensor. In this context, we have confirmed the applicability of Davis (1986) to the observed moment tensor.

The other disadvantage is that researchers have to search in the numerical table to find a geometry fitting to the observed moment tensor. Here we develop a facilitative tool that diagnoses the diagonal part of observed moment tensors to given the aspect ratios and the apparent compressibility. In addition, if the density and the compressibility of the internal material are given, the tool estimates mass change inside the source, which is an important parameter in volcanology.

This tool will provide a reference model satisfying pressure balance and help improving the volumetric source modeling beyond the conventional kinematic summation of simple sources.

Keywords: moment tensor, volumetric source, volcano seismology, magma

Japan Geoscience Union Meeting 2014
(28 April - 02 May 2014 at Pacifico YOKOHAMA, Kanagawa, Japan)

SVC50-P06 Room:Poster Time:May 2 16:15-17:30

Volume source representations: a possible unified explanation based on the representation theorem

ICHIHARA, Mie[1*] ; KUSAKABE, Tetsuya[1] ; KAME, Nobuki[1] ; MIZUNO, Naoto[2] ; KUMAGAI, Hiroyuki[3]

[1]Earthquake Research Institute, The University of Tokyo, [2]School of Science, The University of Tokyo, [3]Graduate School of Environmental Studies, Nagoya University

The moment tensor inversion is a powerful tool to extract source information from seismic and geodetic observations. A moment tensor for earthquake faulting has been determined and its non-diagonal components give the seismic moment (rigidity x slip x fault area), which is one of essential source parameters of an earthquake. The sum of the diagonal components (the trace) of a moment tensor represents volumetric change at the source. A moment tensor determined for a volcanic source frequently has non-zero trace. However, it has been failed to uniquely relate the diagonal components to the actual volume change, which remains a critical issue in volcanic seismology (Kazahaya et al., 2011). For example, two different volume changes DV and dV have been proposed for the seismic moment of a spherical source geometry; DV comes from the moment tensor definition of a seismic fault having opening displacements whereas dV is obtained from the equivalence of resultant displacement fields due to the former moment tensor and an isotropically expanding sphere in an elastostatic equilibrium.

The difference between DV and dV has been discussed in the last decade. Muller (2001) considered an open crack of a spherical shell shape and showed that DV is the volume of the opening and dV is only the part opening outward. Aki and Richards (2002) and Richards and Kim (2005) adopted Eshelby's approach which considers virtual operations consisting of cutting, stress-free transformation, elastic straining, and welding, and concluded that the difference is due to whether the volumetric change occurs in an unconfined condition (DV) or in a confined condition (dV). Kumagai et al. (2013)reconsidered this problem and concluded that the displacement field due to a spherical source does not coincide with that due to a three-perpendicular-crack source though they both are represented by isotropic moment tensors. They also extended the insights into sources in a bimaterial medium. It is worth mentioning that the approaches of AR2002 and RK2005 give a conceptual explanation on how to adjust DV to the actual volume change dV for a sphere, but not for arbitrarily shapes. Here we address how to make such adjustments for general geometries on the basis of the representation theorem. Our imaginary operation below gives a unified explanation for the two different volumetric changes and newly proposes a method of estimating dV of the inversion results for arbitrary source geometries.

We start with the representation theorem that gives the displacement field by two terms (without a body force): a surface integration on the source region with convolution of the surface displacement and the gradient of the Green's function normal to the surface (1), and that with convolution of the surface traction and the Green's function (2). Only (1) has been considered for the seismic fault because (2) vanishes due to the balance of the traction at the contacting surfaces of a fault. On the other hand, (2) does not vanish in the case of a volumetric source, and therefore a quantitative adjustment is required to include the effect of (2) into (1). We here demonstrate that such an adjustment,is always realized by introducing an additional imaginary volumetric change, which works as 'displacement glut' in our representation of moment tensor. Our representation is found to be mathematically equivalent to the rather conceptual 'stress glut' representation proposed by Backus and Mulcahy (1976). We present a unified explanation for the existing various representations and propose a method to practically evaluate the moment tensor components from the boundary conditions of the volumetric source. The proposed representation will be useful in connecting dynamical models of volcanic processes and moment tensors.

Keywords: Moment tensor, Volumetric source, Representation theorem, Green's function, Volcano seismology, Explosion source

Japan Geoscience Union Meeting 2014
(28 April - 02 May 2014 at Pacifico YOKOHAMA, Kanagawa, Japan)

SVC50-P07 Room:Poster Time:May 2 16:15-17:30

X-ray CT observation of delayed fragmentation of vesicular magma analog

SHIDA, Tsukasa[1] ; AOKI, Yamato[1*] ; KAMEDA, Masaharu[1] ; ICHIHARA, Mie[2] ; OKUMURA, Satoshi[3] ; UESUGI, Kentaro[4]

[1]Mech. Systems Eng., TUAT, [2]ERI, Unv. of Tokyo, [3]Earth Sci., Tohoku Unv., [4]JASRI

A laboratory experiment was performed to understand the mechanism of fragmentation of vesicular magma, which is a trigger of explosive volcanic eruption. From the observation of Shinmoe-dake 2011 eruption, the viscosity of magma is not so high as its response is in solid manner. Thus, we aim to reveal the mechanism of brittle-like fragmentation of the magma which behaves in fluid manner.

Rapid decompression test was conducted using syrup containing oxygen bubbles as a magma analogue. The decompression facility consists of a high-pressure chamber in which the specimen can be placed, and an electromagnetic valve. The pore structure of interior of the specimen was observed by X-ray microscopic tomography. The X-ray tomographic microscopy was performed at the BL20B2 beamline of the Japan Synchrotron Radiation Research Institute (JASRI, Hyogo, Japan). Initial structure of the specimen was observed by three-dimensional tomographic imaging. A digital charge-coupled device (CCD) camera was used as the detector whose imaging area is about 2048 pixels (horizontal) by 644 pixels (height) with spatial resolution of 8 μm/pixel. We took 1800 projections over 180 degrees of rotation for tomographic imaging. High-speed radiography was performed during the decompression. The framing rate of radiography is 200 frames per second.

The specimen has a semi-spherical shape whose diameter was 20 mm. The initial pressure (p_0) was 1.5 MPa, the characteristic time of decompression (t_{dec}) was 50 ms, the viscosity of syrup was about 1×10^8 Pa s, the initial averaged void fraction ϕ_0 was about 10%. We tested nine samples whose pore structure was different to each other.

The fragmentation occurred with two samples in which a 10-mm-diameter bubble was contained, while the fragmentation did not occur using the seven samples whose pore structure was relatively uniform. The onset of fragmentation is 960 ms after the decompression was started. The onset was substantially delayed not only from the characteristic decompression time but also from the relaxation time of Maxwellian viscoelastic material (viscosity/rigidity = 150 ms). Referring to the radiographic images, we found that the fracture was initiated from a chain of small gas bubbles and a notch in the vicinity of the 10-mm (large) bubble. The internal crack may grow in ductile manner when the hoop stress around the large bubble increased due to decompression. At a certain instance the stress concentration and the brittleness at crack tip may exceed the critical level, which leads to brittle failure of the crack.

The experimental result indicates that brittle-like fragmentation can occur in the non-uniform vesicular magma even if the response of magma is in fluid manner.

Japan Geoscience Union Meeting 2014
(28 April - 02 May 2014 at Pacifico YOKOHAMA, Kanagawa, Japan)

SVC50-P08 Room:Poster Time:May 2 16:15-17:30

Model experiments on magma migration in a viscoelastic host rock : effect of viscosity

TAKEGUCHI, Izumi[1*] ; SUMITA, Ikuro[1]

[1]Graduate School of Natural Science and Technology, Kanazawa University

Magma generated from partial melting ascends upwards by its buoyancy to the magma chamber, some of which erupt at the Earth's surface. Magma is considered to ascend in the form of diapir in the asthenosphere and transforms to dykes in the lithosphere (Rubin, 1995) . These two end member cases have been studied in detail, but the mechanism of magma ascent in the transitional regime is still poorly known. We have been studying the ascent mechanism in the transitional regime by model experiments using a viscoelastic agar (Sumita and Ota, 2011). Here we report the results of experiments which focus on the effect of fluid viscosity on the magma migration in a viscoelastic medium.

We conducted (1) rheology measurement of agar and (2) fluid injection experiments. We inject magma (CsCl solution to which a thickener is added) using a syringe from the top of a cylindrical acrylic tank (height of 250 and 500 mm). The fluid has a volume of 1ml, density difference with the agar of 0.108 g/ml, and is injected at a constant rate of 0.1 ml/s. We vary the agar concentration in the range of 0.04-0.5 wt% and the fluid viscosity in the range of 10^-3 - 650 Pas. As we increase the agar concentration in this range, we find that the yield stress and the rigidity of the agar increases by 3 orders of magnitude. By shearing the sample under a constant stress (creep test) we find that the agar can be approximated by a Voigt model to which a spring is connected in series. The experiments are recorded using video cameras from two sides and from the bottom of the tank.

From the injection experiments, we find that as the agar rigidity (G) decreases, the crack shape transforms from 2D (blade-like) to 3D (having a bulged head). The critical rigidity (Gc) of the 2D-3D transformation is around Gc=10 Pa, and this value becomes smaller when a high viscosity fluid is injected. The value of Gc is consistent with the rigidity estimated from the balance between the elasticity and buoyancy at which the strain becomes 1. The crack consists of a bulged head and a thin sheet-like tail, and the head becomes thinner and smaller as the crack elongates. When a stiff agar is used as the host, or when a high viscosity fluid is injected, the crack propagation stops within a certain distance from the injection point. We find that this propagation distance becomes shorter as we increase the agar yield stress or the viscosity of the injected fluid, and this result can be associated with the transformation of the crack shape to 2D. We fit the time-distance data to a power-law relation, and find that the exponent varies from 1/3 to 1. An exponent of 1/3 corresponds to the scaling obtained for a 2D crack which thins uniformly as it elongates (Taisne et al, 2011). An exponent larger than 1/3 corresponds to the crack shape becoming more 3D. To conclude, we find that the magma viscosity not only slowers its migration velocity, but also controls the crack shape, its deceleration, and the propagation distance until it stops.

References:

Rubin, A. M., 1995, Ann. Rev. Earth Planet. Sci, 23, 287-336.
Sumita, I. and Y. Ota, 2011. Earth Planet. Sci. Lett., 304, 337-346.
Taisne, B. et al., 2011, Bull. Volcanol., 73, 191-204.

Keywords: viscoelasticity, Magma ascent, rheology, crack

Japan Geoscience Union Meeting 2014
(28 April - 02 May 2014 at Pacifico YOKOHAMA, Kanagawa, Japan)

SVC50-P09 Room:Poster Time:May 2 16:15-17:30

Bubble growth and resorption in magma: insights from dissolved water distributions in volcanic glass

MCINTOSH, Iona[1*] ; LLEWELLIN, Ed[2] ; HUMPHREYS, Madeleine[2] ; NICHOLS, Alex[1] ; BURGISSER, Alain[3] ; SCHIPPER, C ian[4]

[1]IFREE, JAMSTEC, Japan, [2]Department of Earth Sciences, Durham University, United Kingdom, [3]ISTerre, Universite de Savoie - CNRS, France, [4]SGEES, Victoria University, New Zealand

Volcanic eruptions are driven by the growth of gas bubbles in magma, which grow and shrink as volatile species exsolve from and dissolve back into the melt in response to changes in the local environment, particularly in pressure and temperature. This movement of volatiles, particularly water, is recorded in the glass around vesicles and recent studies have used this record to interpret natural samples. Here we investigate the processes that control bubble growth and resorption in magma, by measuring the distribution of dissolved water in experimentally-vesiculated volcanic glasses. Water concentration profiles obtained using SIMS-calibrated BSEM imaging and water speciation data obtained using FTIR spectroscopy, are interpreted in the context of the known pressure and temperature history of the samples.

Samples are found to have undergone partial bubble resorption during the quench to glass at the end of experiments, as a result of increasing water solubility with decreasing temperature. Analysis of the lengthscale and timing of the resulting water concentration profiles demonstrates that the majority of resorption occurs above the glass transition. This quench resorption is associated with a reduction in bubble volumes that creates characteristic textures, such as buckled melt films between adjacent vesicles and reoriented cracks around resorption halos. Highly disequilibrium water speciation ratios within resorption halos are found to be diagnostic of quench resorption and can preserve evidence of pre-quench bubble growth

Quench resorption can increase sample water concentrations and ratios of molecular to hydroxyl water species, and reduce bubble volumes and sample porosities. Studies based on these parameters must therefore consider the potential impact of quench resorption, which is expected to be greatest for samples with high water concentrations, slow quench and low initial sample porosities. Water speciation data offer a way to investigate these impacts in unconstrained natural samples and could provide a tool for forensic interrogation of their eruptive history.

Keywords: Bubble growth, Bubble resorption, Water speciation, FTIR, SIMS, Backscatter SEM

Japan Geoscience Union Meeting 2014
(28 April - 02 May 2014 at Pacifico YOKOHAMA, Kanagawa, Japan)

SVC50-P10 Room:Poster Time:May 2 16:15-17:30

Formulation of the 1-D magmatic flow including vesiculation kinetics

TORAMARU, Atsushi[1*]

[1]Department of Earth and Planetary Sciences, Kyushu University

In most of existing fluid mechanical modeling and numerical calculations, the equilibrium vesiculation has been assumed according to the solubility relation. However, in order to understand the transient behaviors such as triggering of eruptions and shifts of eruption intensity, we need to examine the effect of vesiculation kinetics on the fluid mechanical behaviors in the conduit. In this study, we formulate the governing equations describing the one dimensional fluid mechanics taken into account the vesiculation kinetics, that is, the nucleation and growth of bubbles, assuming the homogeneous flow.

As we adapt the single fluid approximation, we build upon the advantage of the formulation in which the mass conservation equation about density is converted to the pressure equation through the equation of state. We make the similar procedure to obtain pressure equation while in our case the density is a function of not only pressure but also gas phase fraction. The gas phase fraction is calculated by the vesiculation kinetics. As a result we have four equations; 1) pressure equation (mass conservation), 2) equation of motion (momentum conservation), 3) constitutive equations describing vesiculation kinetics. These partial differential equations consisting of pressure, velocity and gas phase fraction, can be solved numerically.

In order to confirm the validity and fundamental characters of the formulation, we numerically solve the shock tube problem, using modified CIP method for advective terms. In the case that the kinetic effect is negligible due to relatively large initial gas fraction in the high pressure region, we obtain the similar solution to that of single fluid, consisting of shock wave in downstream and rarefaction fan in upstream. On the other hand, in the case that kinetics of vesiculation works effectively, we have different behaviors in the high pressure region in which rarefaction front, nucleation pressure front and nucleation event propagate with different velocities, while the behavior in the low pressure region is basically same as the case without the kinetic effect. Each propagation velocity depends on nucleation pressure (liquid/gas interfacial energy), bubble growth rate, initial gas faction in the high pressure region. The essential difference between two cases, the pressure of bubble formation becomes lower in the case with the kinetic effect than in the case without kinetic effect. If the kinetic effect is dominated, it is expected that the time to the vent from the bubble nucleation is relatively short. On the other hand, in the case that the vesiculation proceeds at equilibrium without the kinetic effect, it needs longer time to the vent, suggesting that the relative motion between gas and liquid, the bubble coalescence and degassing become dominate. Thus, this suggests that the kinetics of vesiculation may control the transition of eruption styles such as explosive and non-explosive eruptions.

Keywords: conduit flow, vesiculation kinetics, bubble nucleation, shock tube

Japan Geoscience Union Meeting 2014
(28 April - 02 May 2014 at Pacifico YOKOHAMA, Kanagawa, Japan)

SVC50-P11 Room:Poster Time:May 2 16:15-17:30

Pre-eruptive conditions of rhyolitic magma from Kawagodaira Volcano, Izu Peninsula

TAKASHIMA, Jun[1*] ; ISHIBASHI, Hidemi[1]

[1]Graduate school of science, Shizuoka University

Kawagodaira volcano is a rhyolotic monogenic volcano located in the Higashi-Izu monogenic volcano field at Izu Peninsular. The volcano erupted at ca. 3060˜3190. During the eruption, transition of eruption style was occurred from Plinian explosion to obsidian extrusion. Such transition offen occurred in silicic magma, and depend on pre-eruptive condition and outgassing during magma ascent in the vent. However, detailed mechanism is still under study. In this study, we collect volcanic products of 3 eruption style which are plinian eruption, pyroclastic flow, and lava flow. We conducted petrography and analysis of chemical compositions of glass and phenocryst minerals for these volvanic products, and we estimated the pre-eruptive condition of temperature and pressure and water content to examine mechanism in transition of eruption style.

All samples in this study include ca. 15 vol. % of phenocrysts chiefly composed of hornblende and plagioclase with minor amount of orthopyroxene and magnetite, and include ca. 85 vol. % of grandmas composed of glass. Hornblende phenocrysts show chemical zoning with obvious gap of Al content near rim. Al content is higher in core part (ca. 1.7 atoms per formula unit (apfu)) than rim part (ca. 1.2 apfu).

The estimated pressure using hornblende Al content geobarometer shows bimodal distribution with ca. 100 MPa and 200-300 MPa in each sample. The former and the latter correspond to the crystallization pressure of rim and core part of hornblende, respectively. The estimated temperature using plagioclase-hornblende geothermometer indicate constant in all samples, and average to be 1132K. The water content is estimated to be 5wt. % by using plagioclase-melt geohydrometer, and this value coincident with H2O solubility in rhyolitic melt at 100MPa.

The estimated P-T conditions show that magma decompressed from 200˜300MPa to 100MPa without change of magma temperature. This indicates that transition of eruption style occurred less than 100MPa. The coincidence between water content and the H2O solubility at 100MPa suggest that bubbles were already formed at this pressure. And, we think that magma stopped at 2.5˜3km depth until growth of hornblende and plagioclase phenocrysts finished. During cessation of magma ascent, bubbles rised to upper part of magma chamber, forming bubble zoning in magma chamber. This zoning might relate to transition of eruption style.

Keywords: Higashi-Izu monogenetic volcanic field, rhyolitic magma, eruption style, hornblende

Japan Geoscience Union Meeting 2014
(28 April - 02 May 2014 at Pacifico YOKOHAMA, Kanagawa, Japan)

SVC51-01 Room:312 Time:April 29 14:15-14:30

Hydrothermal system around the Bandaiko hot spring inferred from a 3-D resistivity structure

KANDA, Wataru[1*] ; TAKAKURA, Shinichi[2] ; KOYAMA, Takao[3] ; OGAWA, Yasuo[1] ; SEKI, Kaori[1] ; HINO, Yuta[1] ; HASE, Hideaki[1]

[1]Tokyo Institute of Technology, [2]The National Institute of Advanced Industrial Science and Technology (AIST), [3]Earthquake Research Institute, University of Tokyo

Bandaiko is a hot spring located in the eastern flank of the Kusatsu-Shirane volcano, 3km west from Kusatsu-Onsen. It was discovered in 1967 during excavation of a sulfur mine, and has been utilized as one of the sources of Kusatsu-onsen since 1976. It is presumed that a gush point is located in 505 m west from a tunnel entrance. The ground temperature above the presumed gash point exceeds 80 degrees. About 10 to 20 percent of the hot spring water is always discharged as vapor, so that existence of a two-phase hydrothermal system in a shallow part of tunnel end is considered to be certain. Moreover, since the chemical nature of hot spring is well investigated, Bandaiko is a suitable field which clarifies the resistivity image of a hydrothermal system.

We investigated the shallow resistivity structure around the Bandaiko hot spring using the AMT (audio-frequency magnetotelluric) method. The measurement was done on Oct.19th through Oct.26th, 2013. Five components of EM fields were measured at 19 sites around the presumed gush point: measurements were carried out during the nighttime at 15 of them with sufficient S/N. Because the measuring frequency was 1-10400Hz, information on the resistivity structure from the vicinity of surface to the depths of 1-2km can be obtained. A site for the remote-reference was not installed. Instead, a local-site-reference was applied each other. The 60 Hz noise as well as the 50 Hz noise caused by the local commercial power was extensively seen, because the survey area is located in close proximity to a prefectural border of Nagano where 60 Hz power is used.

Three-dimensional (3-D) analysis was performed in this study. A 3-D resistivity structure model was estimated from the inversion code of Siripunvaraporn and Egbert (2009) using 15 frequencies of all components of impedance data. The inferred model shows low resistivity near the end and the entrance of tunnel. In this presentation, we will report the up-to-date model of the 3-D resistivity structure and discuss the hydrothermal system around Bandaiko in consideration of the measured values of the electrical conductivity of hot spring water, etc.

This study was supported by the Earthquake Research Institute cooperative research program.

Keywords: resistivity structure, Kusatsu-Shirane volcano, hydrothermal system, Kusatsu-onsen, Bandaiko

Japan Geoscience Union Meeting 2014
(28 April - 02 May 2014 at Pacifico YOKOHAMA, Kanagawa, Japan)

SVC51-02 Room:312 Time:April 29 14:30-14:45

Resistivity structure around the Jigokudani valley, Tateyama volcano, Japan, inferred from AMT

SEKI, Kaori[1*] ; KANDA, Wataru[2] ; OGAWA, Yasuo[2] ; HASE, Hideaki[2] ; HINO, Yuta[1] ; KOBAYASHI, Tomokazu[3] ; TANBO, Toshiya[4]

[1]Department of Earth and Planetary Sciences , Tokyo Institute of Technology, [2]Volcanic Fluid Research Center, Tokyo Institute of Technology, [3]Geospatial Information Authority of Japan, [4]Tateyama Caldera and Sabo Museum

Midagahara (Tateyama volcano) is situated in the northern part of the Japan Alps, and fumarolic activity occurs in the Jigokudani valley located in the northeast end of the Midagahara Plateau. Jigokudani valley was formed by the periodically repeated vapor explosions. Increase in volcanic activity is a great concern because of recent events such as a sulfur outflow, a composition change of the fumarolic gases and the emergence of high temperature fumaroles. We investigated the distribution of hydrothermal fluid and gas reservoir beneath Jigokudani using the AMT method to image the 2D resistivity structure and checked the position of fumaroles. In this observation, the AMT sites were installed along the ENE-SWS survey line around the Jigokudani Valley. The final model revealed that there is a conductive body beneath the Jigokudani valley, and that a relatively low resistive body extends through between the high resistivities beneath the conductor. Near-surface conductor is divided into slightly conductive upper part and lower part. The upper part is explained by clay sediments and hydrothermal fluids. The lower part indicates the presence of gases and fluids. Because of clay's impermeability, the upper clay sediments play the role as a cap for gases. The deep resistive layer is estimated to be the basement of granites that are widely exposed around the Jigokudani valley. We inferred that the relativity conductive body separating these granites is a path of the magmatic gases. The most active fumarole in the Jigokudani valley is on extension of this path.

Japan Geoscience Union Meeting 2014
(28 April - 02 May 2014 at Pacifico YOKOHAMA, Kanagawa, Japan)

SVC51-03 Room:312 Time:April 29 14:45-15:00

Hydrothermal system at Tatun Volcano Group, northern Taiwan, inferred from resistivity structure

KOMORI, Shogo[1*] ; UTSUGI, Mitsuru[2] ; KAGIYAMA, Tsuneomi[2] ; INOUE, Hiroyuki[2] ; CHEN, Chang-hwa[1] ; CHIANG, Hsieh-tang[3] ; YOSHIMURA, Ryokei[4] ; KANDA, Wataru[5]

[1]Institute for Earth Sciences, Academia Sinica (Taiwan), [2]Aso Volcanological Laboratory, Kyoto University, [3]National Taiwan University, [4]Disaster Prevention Research Institute, Kyoto University, [5]Tokyo Institute of Technology

Tatun Volcano Group is composed of over twenty volcanoes, which were formed within faults at the northern tip of Taiwan. So far, these volcanoes were regarded as extinct because of no historical record of eruption. However, recent studies have found the relatively young ejecta (Chen and Lin, 2002; Belousov et al., 2010), high 3He/4He ratio (Yang et al., 1999; Ohba et al., 2010), and hypocenter distribution suggesting the fluid flow and the high temperature condition (Konstantinou et al., 2007); that suggest the presence of potentially eruptive magma beneath TVG. Further, active heat discharge from fumaroles and springs also suggests a large amount of the volcanic fluids released from magma beneath Chishinshan volcano. Focusing on this phenomenon, Utsugi et al. (2012, JPGU) conducted AMT surveys at the volcano for a better understanding of this magma degassing, and showed the preliminary resistivity structure suggesting the low resistivity region at the depths of 1-2km.

On the basis of their work, the authors conducted further AMT surveys around Matsao hot spring and Da-you-keng fumarole areas, about 2 km northeast of the volcano. Time series of the electric and magnetic fields were acquired for about 4 hours at each site. Totally 10 observation sites were configured to cover the areas. After data acquisition, the frequency domains were obtained from the time series, using FFT processing. The impedances were estimated for each frequency. The obtained frequency range was between 1 and 10400 Hz. The authors used not only the data of the present study but also those of Utsugi et al. (2012, JPGU).

This study categorized the study area into two areas, mainly from the characteristics of the main axes of the impedance phase tensor ellipse by the method of Caldwell et al. (2004): 1) Mt. Chishinshan area and 2) Matsao and Da-you-keng areas. In this study, two-dimensional resistivity structure was estimated for each area, using the inversion code of Ogawa and Uchida (1996). By incorporating them with the evidences from geochemistry and geophysics (MRSO, 1969, 1970, 1971, 1973; Ohba et al., 2010; Ohsawa et al., 2013; Murase et al., 2013, IAVCEI), the following features of the hydrothermal system was inferred.

Beneath Mt. Chishinshan two-phase fluids are supplied; which is represented by the extremely-low resistivity column (less than 3 Ohm-m) and the deflation pressure source below 1 km depth. As the fluids ascend, their phase is changed into vapor-phase, leading to low to relatively-low resistivities (6-30 Ohm-m) at the depths of 0.3-1 km. The vapor-rich region is covered by the low-permeability cap represented by the extremely-low resistivity layer near the surface (less than 3 Ohm-m). A portion of the vapors is mixed with shallow groundwater, and flows along a topographical relief to form Matsao hot spring; whose area is represented by resistivities less than 10 Ohm-m.

On the other hand, Da-you-keng area has intense fumaroles; whose vapor-dominated fluids are supplied from the region beneath Cing-tian-gang, represented by the low to low-resistivity region (3-30 Ohm-m) and the inflation pressure source below 1 km depth. This vapor-bearing region is covered by the overlying low-permeability cap represented by the extremely-low resistivity region (less than 3 Ohm-m).

This study estimated the horizontally-extending vapor-rich region beneath Mt. Chishinshan, Da-you-keng, and Cing-tian-gang. Actually, this area has experienced a phreatic eruption ca. 6 Ka (Belousov et al., 2010). These suggest that the vapors have been maintained for at least several thousands years, and that there is still a possibility of phreatic explosions.

Keywords: Tatun Volcano Group, Hydrothermal system, Two-phase region, Vapor-dominated region, Pressure sources

Japan Geoscience Union Meeting 2014
(28 April - 02 May 2014 at Pacifico YOKOHAMA, Kanagawa, Japan)

SVC51-04 Room:312 Time:April 29 15:00-15:15

Conductivity distribution of the surface layer in Aso Caldera

KAGIYAMA, Tsuneomi[1*] ; YOSHIKAWA, Shin[1] ; UTSUGI, Mitsuru[1]

[1]Graduate School of Science, Kyoto University

Kagiyama and Morita(2008) proposed that volcanism has a wide range of diversity represented by two typical end members controlled by the easiness of magma storage beneath volcano; Eruption dominant (ED) volcanism in difficult condition and Geothermal activity dominant (GD) volcanism in easier condition. In GD volcanoes, magma stagnates beneath volcanoes and maintains geothermal activity. This seems GD volcanoes continue to give much benefit to human society. However, GD volcanoes sometimes have large eruptions after repeated stagnations of magma. This fact suggests it is very important to understand where and why magma stops ascending. Kagiyama and Morita (2008) indicated magma degassing is one of the important factors to control magma ascending. On this aspect, the authors have carried out VLF-MT survey around some active volcanoes in Japan, because electrical conductivity of ground strongly depends on the conductivity of pore water.

Aso Caldera has an acid crater lake in Nakadake, which is one of the post caldera cones, and has many hot springs such as Uchinomaki, Akamizu. Conductivity distribution shows two typical features; caldera floor has almost homogeneous and high conductivity (>10mS/m), while the post caldera cones show wide range.

Most cones such as Kishima-dake and Ohjo-dake have lower conductivity (<3mS/m), except around Naka-dake Craters and western flank of post caldera cones such as Yoshioka, Yunotani and Jogoku-Tarutama (>30mS/m). Kusasenri Volcano, located between Naka-dake and Yoshioka has also rather high conductivity (3-10mS/m). These areas locate along the E-W trend of the major post caldera cones. Most part of the northern flank of the post caldera cones shows low conductivity (<3mS/m). However, higher conductivity was found around Sensuikyo, just north of Nakadake Craters. This suggests down flow of hydrothermal water from Naka-dake Craters to the caldera floor. Similar features are detected in the southern flank; from Nakadake to Shirakawa Hot Spring, from Jigoku-Tarutama Hot Springs to Tochinoki Hot Springs.

Caldera floor has almost homogeneous conductivity. This feature is explained by the fact that the caldera floor was under the lake until 9 ka and is covered by lake deposit. However, extremely high conductivity was found at three areas (>50mS/m). Two of them correspond hot spring areas; Uchinomaki in the north and Akamizu in the west. The third area is distributed around old post caldera cones, Mietsuka. The age of these cones was estimated around 46 ka, and no hot spring is distributed. High conductive zones, Uchinomaki, Mietsuka and Naka-dake are located along the NNW-SSE line. Hydrothermal water may be supplied along this line.

These results suggest that hydrothermal water is supplied along the E-W trend crack from Naka-dake to Yoshioka, mainly supplied beneath Naka-dake, and expanded to the northern caldera floor. The NNW-SSE trend from Naka-dake to Uchinomaki may suggest a tectonic fault. Aso has wide high conductivity area and degassing in Aso might be large to be GD volcano.

Reference: Kagiyama and Morita, First steps in understanding caldera forming eruptions, J. Disaster Res., 3, 270-275, 2008.

Keywords: Electrical conductivity, Geothermal activity, Failed eruption, Aso Caldera

Japan Geoscience Union Meeting 2014
(28 April - 02 May 2014 at Pacifico YOKOHAMA, Kanagawa, Japan)

SVC51-05 Room:312 Time:April 29 15:15-15:30

The thermal expansion model and the Mogi model for volcanic ground deformation

KITSUNEZAKI, Choro[1*]

[1]none

(1) Basic aspects of the thermal expansion model, which was proposed by the author in this meeting of the last year (Kitsunezaki and Muraoka, 2013), is reorganized in relation to the Mogi model (Mogi,1958). In the Mogi model, the earth's crust is assumed to be a semi-infinite isotropic homogeneous elastic solid with the horizontal free plane (the ground surface). Displacement of the ground surface caused by a spherical pressure source set up in the earth's crust is evaluated. Gravity change associated with the deformation was estimated by Hagiwara(1977). Basically, the inside of the spherical source of this model is void (or material different from the surroundings). As a special case, we assume that the inside is filled with the same material as the surroundings and that temperature in the inside is raised (keeping the outside temperature constant). Thermal expansion of the sphere behaves as a pressure source, and the Mogi model is transformed to the spherical thermal expansion model (ST model). In this case, as the mass of the sphere does not change, the change in gravity on the ground surface is caused by the free-air effect (FE) due to uplift of the ground surface alone.

(2) The above ST model can be extended to the case in which the temperature-rise region (T region) has arbitrary shape. Let the T region be subdivided into a large number of small cubic cells. Every cell effectively behaves as a spherical thermal element. Its outputs (displacement and gravity change on the ground surface) are given by the ST model. The output of the entire T region is given as a sum of the output of each element. Hence in the T region with any shape, the change in gravity is caused by the FE due to the vertical displacement of ground surface alone.∗

∗[Note] The related description in Kitsunezaki and Muraoka(2013) has been corrected here.

(3) Shallow regions of actual volcanoes may be regarded as porous media. Let's assume that the pores are saturated by water and are in open condition. In the thermal expansion model described in (1) and (2), the earth medium is replaced by such a water-saturated porous medium. In this case, pressure of pore water is kept constant. Hence the solid part (skeleton of the medium) behaves in deformation independently from pore water. Thermal expansion of the solid part causes the displacement of the ground surface and the gravity change due to the FE as described in (2). On the other hand in the T region, the pore water expands freely responding to the temperature-rise (below the boiling point), hence its density decreases. (Thermal expansion coefficient of water is more than ten times larger than that of solid part (rock)).This effect causes negative gravity change, which is added to the FE so as to amplify the total gravity reduction to some degree. This example is numerically demonstrated in gravity variation observed in Akita-Komagatake volcano after the 1970-eruption.

[References]

Hagiwara, Y.(1977): The Mogi model as a possible cause of the crustal uplift in the eastern part of Izu Peninsula and the related
gravity change, Bull. Earthq. Res. Inst., Vol.52, 301-309 (in Japanese).

Kitsunezaki, C., and Muraoka, A. (2013): Gravity variation in Akita-Komagatake volcano and thermal expansion model, Japan Geoscience Union Meeting, SVC52-04 .

Mogi, K.(1958): Relations between the eruptions of various volcanoes and the deformations of the ground surfaces around them, Bull. Earthq. Res. Inst., Vol.36.99-134.

Keywords: thermal expansion model, Mogi model, gravity change, ground deformation, Akita-Komagatake, porous media

Japan Geoscience Union Meeting 2014
(28 April - 02 May 2014 at Pacifico YOKOHAMA, Kanagawa, Japan)

SVC51-06 Room:312 Time:April 29 15:30-15:45

El Cobreloa: A geyser with two distinct eruption styles

NAMIKI, Atsuko[1*] ; MUNOZ, Carolina[2] ; MANGA, Michael[2]

[1]DEPS, Univ. of Tokyo, [2]UC Berkeley

We performed field measurements at a geyser nicknamed “El Cobreloa”, located in the El Tatio Geyser Field, Northern Andes, Chile. The El Cobreloa geyser has two distinct eruption styles: minor eruptions, and more energetic and long-lived major eruptions. Minor eruptions splash hot water intermittently over an approximately 4 minute time period. A major eruption begins with an eruption style similar to minor eruptions, but then transitions to a voluminous water-dominated eruption, and finally ends with energetic steam discharge that continues for approximately 1 hour. We calculated eruption intervals by visual observations, acoustic measurements, and ground temperature measurements. All measurements consistently show that each eruption style has a regular interval: 4 hours and 40 minutes for major eruptions, and approximately 14 minutes for minor eruptions. We develop a model, in which the geyser reservoir, connected to the surface by a conduit, is recharged by the deep, hot aquifer. More deeply derived magmatic fluids provide the enthalpy to heat the reservoir. Boiling in the reservoir releases steam and hot water to the overlying conduit causing minor eruptions, and heating the water in the conduit. When the conduit becomes warm enough, the water in the conduit is able to boil, leading to a steam-dominated eruption that empties the conduit. The conduit is then recharged by the shallow, colder aquifer, and the eruption cycle begins anew. El Cobreloa provides insight into how small eruptions prepare the geyser system for large eruptions.

Keywords: geyser, El Tatio, geothermal systems, eruption

Japan Geoscience Union Meeting 2014
(28 April - 02 May 2014 at Pacifico YOKOHAMA, Kanagawa, Japan)

SVC51-07 Room:312 Time:April 29 16:15-16:30

Time variation in the chemical composition of fumarolic gases at Hakone volcano, Japan

OHBA, Takeshi[1*] ; KUNO, Yuki[1] ; SAGOU, Masakazu[1]

[1]Dep. Chem. School Sci. Tokai Univ.

Introduction

Mt Hakone having the caldera structure is an active volcano located on the western end of Kanagawa prefecture. At the central region of caldera, several volcanic cones are located. On the flank of cones, geothermal areas have been developed. The magmatic activity, which formed the cones, started 50 Ka (Kuno, 1972). The activity is estimated to have continued until 3 Ka (Kobayashi et al., 1997). At the last eruption, the western flank collapsed at one of the central cones, resulting in the formation of dammed Lake Ashi (Ooki and Hakamada, 1975).

At Mt Hakone, volcanic earthquakes have been observed frequently, although no historical eruption is known. Especially in 2001, the occurrence of volcanic earthquake was intense. The seismic activity was accompanied with an inflation of body at the central cones. The inflation was interpreted to be brought by a pressure source at 7 km of depth (Daita et al., 2009).

Sampling of fumarolic gas

We sampled fumarolic gas at two sites since May 2013 at Owakudani geothermal area developed on the central cones. One of the sites is located 200m far from the Owakudani car parking in the direction of southeast. At the site we had sampled fumarolic gas in previous study. We call the fumarole as the regular fumarole. Another fumarole is located 500m far from Owakudani car parking in the direction of north. The fumarole has been generated recently. Before the generation, the area was forest. Now many large stout trees were killed by the geothermal effect. We call the fumarole as the new fumarole. Both of the fumarolic gases were sampled in the evacuated Giggenbach bottle containing 20 ml of 5M KOH solution.

Result

The main component of the regular and new fumarole was water vapor (H2O). The molar percentage of H2O was about 98% for the both fumaroles. Both of the gas contain CO2 gas as the major component next to H2O, the percentage was about 1 to 2%. The regular fumarolic gas contained H2S as much as 0.2 to 0.4%. The H2S concentration in the new fumarolic gas was only 0.036 to 0.050%, about 1/10 to the regular fumarolic gas.

The CO2/H2S molar ratio indicated a time variation, a monotonic decrease since May 2013 to Oct 2013. Daita (2013) reported a similar trend based on the observation with detecting tubes. Daita (2013) found an abrupt increase in the CO2/H2S molar ratio on Jan 2013. The increased ratio had been kept until April then decreased gradually toward Oct 2013. According to the seismic observation by Hot Springs Research Institute of Kanagawa Prefecture, volcanic earthquakes occurred frequently in Jan and Feb 2013. We suppose the change in the CO2/H2S ratio has been synchronized with the occurrence of volcanic earthquakes.

Keywords: Fumarolic gas, CO2, Volcanic activity, Hydrothermal system

Japan Geoscience Union Meeting 2014
(28 April - 02 May 2014 at Pacifico YOKOHAMA, Kanagawa, Japan)

SVC51-08 Room:312 Time:April 29 16:30-16:45

Geochemical characteristics and changes of thermal waters around Tokachidake volcano, Japan

TAKAHASHI, Ryo[1*] ; SHIBATA, Tomo[1] ; MURAYAMA, Yasuji[1] ; OGINO, Tagiru[1] ; OKAZAKI, Noritoshi[1]

[1]Geological Survey of Hokkaido, HRO

Tokachidake volcano, located in central Hokkaido, caused three magmatic eruptions (AD 1926, 1962 and 1988-89) in the 20^{th} century. The seismic and thermal activities at the summit crater area have increased since AD 2010. We have continuously investigated thermal waters around the volcano since AD 1986 in order to understand the volcanic activity. Around the AD 1988-89 eruption, the chemical compositions and temperature of the thermal waters had obviously changed (Murayama et al., 1991). Therefore, we need to reveal the origin and changes of the thermal waters in order to forecast the future volcanic activity.

The thermal waters are discharged in the Nukkakushi crater (Ansei crater) and at its lower reaches, which is located at about 2 km southwest from the summit craters. Each thermal water is acidic with pH $<$3.2. At the time of AD 1986, all thermal waters were rich in sulfate ion but were scarce in chloride ion. In addition, anion content of the thermal waters decreases in proportion to the distance from the Nukkakushi crater. Therefore, the thermal waters derived from the Nukkakushi crater area flow, while mixing with groundwater, and are discharged at the lower reaches.

At the Fukiage hot spring area (1,000 m a.s.l.), the concentration of chloride and sodium ions in the thermal waters had abruptly increased since AD 1986. The increase of these chemical concentrations had continued until AD 1992, and the concentration of them had decreased since then. Accompanied with the chemical change, the temperature of the thermal waters had also increased more than 20 ^{o}C around the AD 1988-89 eruption. Such increase of the chemical compositions and temperature of the thermal waters had occurred related to the increase of the volcanic activity. Thus, these increases can be explained by mixing of highly dense NaCl type thermal water into shallow aquifer, and its mixing ratio changed with the volcanic activity. The chemical and thermal changes of the thermal waters have not occurred at the Okina hot spring (1,060 m a.s.l.). This indicates that the input of highly dense NaCl type thermal water has occurred at the lower reaches of the Okina hot spring.

Based on our investigations, the thermal waters in this area are formed by mixing of three end-members, sulfate ion rich thermal water, dense NaCl type thermal water and groundwater. The effect of the dense NaCl type thermal water is recognized only at the Fukiage hot spring area, and the mixing ratio changes according to the volcanic activity. The concentration of chloride and sodium ions in the thermal waters has begun to increase again since AD 2012. However, the increase is obviously small compared with that before the AD 1988-89 eruption, and the oxygen and hydrogen isotopic compositions of these thermal waters have not shown obvious change yet. Observations of the thermal waters will provide useful information to forecast the future volcanic activity in Tokachidake volcano, and hence we will continue the observations.

Keywords: Tokachidake volcano, thermal water, chemical composition, eruption forecasting

Japan Geoscience Union Meeting 2014
(28 April - 02 May 2014 at Pacifico YOKOHAMA, Kanagawa, Japan)

SVC51-09 Room:312 Time:April 29 16:45-17:00

Case study of the behavior of isotope in several hot-spring field

YANAGISAWA, Norio[1*]

[1]AIST

1. Introduction

The behavior of oxygen and hydrogen isotope in geothermal field suggests the origin of fluids and the water rock interaction in fluid path. And there are various origins of high temperature hot springs in Japan, for example, separation from magma, heating meteoric water in the underground.

In this paper, we show the several samples of the isotopic analysis in high temperature hot spring fields including hot spring binary test field and we discuss the diversity of origin of the hot springs.

2. Examples of several hot spring fields

(1) Hachijo Island

There is a geothermal power plant (3.3MW) in Hachijo Island. To clarify hydraulic system, we measured oxygen and the hydrogen isotope ratio of the hot spring fluid, underground water as spring and the fluid at geothermal power plant. The isotope ratio of spring is similar as rain in Hachijo Island and the value of d is about 20 and hydrogen isotope ratio of spring is about -35 ‰. The hot spring fluid in Hachijo Island has two patterns. One is the origin of meteoric water due to similar isotope ratio as spring water. And another is the origin of seawater due to similar isotope ratio as seawater. The isotope ratio of fluid of geothermal plant is higher oxygen ratio than spring and hot spring water and this suggest that the origin of the fluid of geothermal plant is mixture meteoric and magmatic water.

(2) Matsunoyama hot spring field

In Matsunoyama hot spring field, the test of binary power plant is carried out using Takanoyu #3 hot spring fluid with about 100 ℃ and 10,000 mg/l Cl. The hydrogen isotope ratio is about -25 ‰ and oxygen isotope ratio is about 0 ‰ higher than meteoric water. And the isotope ratio of Matsunoyama #4 well with 2,000mg/l shows the mixture of meteoric water and Takanoyu #3. The origin of Takanoyu#3 is fossil salt water with methane gas and geo-pressure structure.

(3) Minami-Izu hotspring field

There is high temperature hot spring with about 100 ℃ and 10,000 mg/l Cl in Minami-Izu hot spring field, too. In this field the temperature and Cl concentration decrease eastern area. The isotope ratios of the several hot springs and underground water exist on the meteoric line. This suggest the origin of hot spring is meteoric water and the reason of temperature and cl concentration decreasing is mixture with low temperature meteoric water.

Keywords: hot spring, geothermal, isotope, meteoric water, fossil salt water

Japan Geoscience Union Meeting 2014
(28 April - 02 May 2014 at Pacifico YOKOHAMA, Kanagawa, Japan)

SVC51-P01 Room:Poster Time:April 29 18:15-19:30

Fluid geochemistry of hot springs at Kotakara-jima,Tokara Islands

TSUTSUMI, Saki[1*] ; ISHIBASHI, Jun-ichiro[1] ; KONNO, Uta[2] ; YOKOSE, Hisayoshi[3]

[1]Department of Earth and Planetary Sciences, Graduate School of Sciences, 33 Kyushu University, [2]JAMSTEC, [3]Graduate School of Science and Technology, Kumamoto University

Yokose et al.(2010) proposed giant calderas related to Quaternary volcanic activity, on the seafloor along the Tokara Islands. Kotakarajima is located on the rim of the Takarajima Caldera, which belongs to this caldera chain. A hot spring called as Yutomari-onsen is located at the coastline of the Kotakarajima island, which water temperature reaches higher than 90 degC. Fluid chemistry of this hot spring was studied with the aim of understanding a hydrothermal sytem associated with the seafloor caldera.

Hot spring water was collected in May, 2013. Temperature, pH, electorical conductivity, and oxidation-reduction potential were measured on site. Fluid samples were filtered with a 0.45 um diskfilter and stored. Major cations and anions were analyzed by ICP-AES and ion chromatography. Alkalinity was determined by HCl titration and Si concentration was determined by colorimetry.

Fluid chemistry of the hot spring water is characterized by high Cl^- concentration, Na/Cl ratio (=0.75) closed to that of seawater, and isotopic composition similar to seawater, which strongly suggests that it is originated from seawater. Depletion in Mg^{2+} and $SO_4{}^{2-}$ and enrichment in K^+ and Ca^{2+} compared with seawter, are in accordance with the idea that the fluid experiences seawater-rock interactions. Fluid temperature in the aquifer where interactions attain to equilibrium is estimated as 250-300 degC based on chemical geothermometers.

From these results, the Yudomari-hotspring at the Kotakarajima Island is considered as fluid discharge of a submarine hydrothermal system that is associated with Takarajima Caldera.

Keywords: Giant caldera, hydrothermal system, seawater-rock interaction

Japan Geoscience Union Meeting 2014
(28 April - 02 May 2014 at Pacifico YOKOHAMA, Kanagawa, Japan)

SVC51-P02 Room:Poster Time:April 29 18:15-19:30

Hydrothermal system beneath Shirahone hot spring, Nagano, Central Japan, revealed by resistivity survey

YAMAYA, Yusuke[1*] ; MOGI, Toru[2]

[1]GSJ, AIST, [2]ISV, Hokkaido Univ.

Shirahone hot spring is one of the most active geothermal area, located in the western part of Nagano prefecture, Japan. A source of hot water has not been clarified, because there are few geophysical exploration and borehole logging. We performed an electrical resistivity exploration employing the magnetotelluric (MT) method in order to identify a hot-water reservoir and whole hydrothermal system providing the Shirahone hot spring. The MT data were measured at six stations along the NNE-SSW line crossing the Shirahone area. The apparent resistivity and impedance phase were inverted to a two-dimensional resistivity section down to 3 km deep with the aid of the code developed by Ogawa and Uchida (1996). The estimated resistivity section generally indicates a range of resistivity 1-3000 Ωm, including two considerable conductors below 3 Ωm. These conductors are found at a depth 400-1000 m and deeper than 2000 m beneath the Shirahone hot spring. The upper conductor is interpreted as a hot-water reservoir which acts as a source of the Shirahone hot spring. The hot water would ascend from this reservoir to the discharge area through a fracture zone. The deeper conductor can be a heat source consisting of high temperature intrusive complex. This source might sustainably supply heat to the upper reservoir, which can keep itself a long time. A high resistivity zone is found beneath the Sakaigawa active fault zone. In general, an active fault is identified as a conductive zone due to saturated water into a fractured zone. Conversely, our resistivity section indicates a relatively resistive zone beneath the fault. This implies a locked part of the fracture zone where groundwater had declined after the last active phase of the fault.

Keywords: hydrothermal reservoir, Shirahone hotspring, resistivity, magnetotellurics, geothermal system

Japan Geoscience Union Meeting 2014
(28 April - 02 May 2014 at Pacifico YOKOHAMA, Kanagawa, Japan)

SVC51-P03 Room:Poster Time:April 29 18:15-19:30

Ground deformation around Ohaaki geothermal field, New Zealand inferred from persistent scatterer SAR interferometry

ISHITSUKA, Kazuya[1*] ; TSUJI, Takeshi[2] ; MATSUOKA, Toshifumi[1] ; FUJIMITSU, Yasuhiro[3] ; NISHIJIMA, Jun[3]

[1]Graduate School of Engineering, Kyoto University, [2]International Institute for Carbon-Neutral Energy Research (I2CNER), Kyushu University, [3]Faculty of Engineering, Kyushu University

There are several producing geothermal fields in Taupo Volcanic Zone (TVZ), northeast-trending zone of mainly andesitic to rhyolitic arc/back arc volcanism, within the central North Island, New Zealand. It has been reported that ground subsidence with the rate of 30-50 mm/year has occurred at the Wairakei geothermal field, one of the biggest geothermal fields in TVZ [Allis et al., 2009]. Such a research on ground deformation around geothermal field is, however, rarely documented. Thus, it would be important to study deformation pattern at the geothermal field.

In this study, we mapped ground deformation around Ohaaki geothermal field located northeast of TVZ using persistent scatterer SAR interferometry (PS-InSAR). Since the analysis makes use of high quality phase information of the coherent target of SAR image, the estimated deformation is more accurate compared with the standard differential SAR interferometry (DInSAR). We processed 21 ALOS/PALSAR images acquired from January 2007 to January 2011 from an ascending orbit. As a result, we estimated ground deformation opposite to line of sight direction, which may correspond to ground subsidence. Moreover, the deformed area showed sharp boundary which we can be attributed to fault location in the area.

Allis, R., C. Bromley, and S. Currie, Update on subsidence at the Wairakei-Tauhara geothermal system, New Zealand, *Geothermics*, vol. 38, pp.169-180, 2009.

Keywords: ground deformation, persistent scatterer SAR interferometry, Ohaaki geothermal area

Japan Geoscience Union Meeting 2014
(28 April - 02 May 2014 at Pacifico YOKOHAMA, Kanagawa, Japan)

SVC51-P04 Room:Poster Time:April 29 18:15-19:30

Gravity Monitoring at Takigami Geothermal Area, Oita Prefecture, Japan

PRATIWI, Maryati[1*] ; FUJIMITSU, Yasuhiro[1] ; NISHIJIMA, Jun[1]

[1]Kyushu University, Fukuoka, Japan

The gravity monitoring at Takigami geothermal area has been applied since November 1996 (Oka et al., 2011). In this area, the nearest geothermal manifestations are about 1-2 km to north and east of Takigami (Furuya et al., 2000). So, there are no geothermal manifestations at the surface. The geothermal power plant was built at Takigami in August 1991. It was reported that its power plant output was changed from 25,000 kW to 27,500 kW in June 2010 (Kyushu Electric Power Co., Inc., 2010)

We analyzed the gravity data from August 2008 until August 2013. We found that the gravity changes at the northern zone, the western zone, and the southwestern zone of this area are quite stable historically. This result indicates that the recovery state for these zones is almost done. However, the data at the eastern zone shows gravity increasing. It was assumed that the subsurface fluid at Takigami area flows from south, which is the direction Kuju Mountain area. Then, we noted that the fluid from south is filling the faults in eastern area in the beginning before going through to northern area (due to its high permeability (Jalilinasrabady et al., 2011)), thus the recovery state in the eastern zone has not been done.

By using theorem of Gauss, we calculated the mass changes based on the gravity changes from August 2009 to August 2012. This calculation is excluding the northern area as it has different water system, and removed the effects of precipitation and evapotranspiration by Gwater-e program (Kazama, 2011). And, we found that the mass increases as much as 10.12 Mt in the Takigami geothermal area. This mass change is associated with the production and reinjection process of geothermal fluids.

REFERENCES

Furuya, S., Aoki, M., Gotoh, H. and Takenaka, T. (2000), " Takigami geothermal system, northeastern Kyushu, Japan, " Geothermics, 29. 191-211.

Jalilinasrabady, S., Itoi, R., Gotoh, H., and Tanaka, T. (2011), " Development of the Optimum Numerical Reservoir Model of the Takigami Geothermal Field, Oita, Japan " Proc. of 36th Workshop on Geothermal Reservoir Engineering Stanford University, Stanford , California, SGP ? TR ? 191.

Kazama, T., K. Yamamoto, and Y. Fukuda (2011), " Hydrological disturbance corrections for relative gravity data observed at Sakurajima Volcano. " 116th Meeting of the Geodetic Society of Japan, 17 (oral presentation at Gifu).

Kyushu Electric Power Co., Inc. (2010). " Introduction to Geothermal Power Station of Kyushu Electric Power Co., Inc. " [Company brochure].

Oka, D., Fujimitsu, Y., Nishijuma, J., Fukuda, Y. and Taniguchi, M. (2011), " Geothermal Fluid Flow Monitoring by the Repeat Gravity Measurement at the Takigami Geothermal Field, Japan — Application of Hybrid Grvaity Measurement by an Absolute Gravimeter (A10) and Relative Gravimeters (CG-3M and CG-5) —" Proc. of 36th Workshop on Geothermal Reservoir Engineering Stanford University, Stanford , California, SGP ? TR ? 191.

Keywords: gravity change, gravity monitoring, mass change, Takigami

Japan Geoscience Union Meeting 2014
(28 April - 02 May 2014 at Pacifico YOKOHAMA, Kanagawa, Japan)

SVC51-P05 Room:Poster Time:April 29 18:15-19:30

Heat balance technique under the condition that the influence of solar radiation can be negligible

FUJIMITSU, Yasuhiro[1*] ; NISHIJIMA, Jun[1]

[1]Faculty of Engineering, Kyushu University

The coefficient of geothermal flux is essential for the heat balance technique (Sekioka and Yuhara, 1974), which is one of the methods for measurement of heat discharge rate from geothermal fields, and is determined by micrometeorological data of a target area. In order to comprehend the temporal change of the micrometeorological conditions and the coefficient of geothermal flux, we have manufactured an automated continuous micrometeorological measurement system and measured micrometeorological data at some geothermal fields. And we have discussed about the coefficient of geothermal flux (Fujimitsu et al., 2009; Fujimitsu et al., 2010; Fujimitsu et al., 2011).

In the heat balance technique, a reference temperature is set on a ground surface where there is no geothermal anomaly, and the area that indicates higher ground surface temperature than the reference temperature is regarded as the geothermally anomalous area. However, the influence of solar radiation on the determination of the reference temperature is one of the main factors in accuracy of the estimated heat discharge rate by the heat balance technique. Therefore, we assumed the condition that the influence of solar radiation can be negligible, and conducted the observation experiments during the nights by using an artificial heating element as a heat source in order to improve the accuracy of the heat balance technique by a new analytical method.

For the new analytical method, we considered the heat balance at the ground surface under the condition of no solar radiation, adopted Richardson number for determination of the transfer velocity, and changed the determination procedure of the reciprocal of the Bowen ratio. As a result, the new analytical method estimated the heat discharge rates that are almost the same as the actual heat generation rates from the artificial heating element.

We are grateful to Mr. Shohei Oshikata who had progressed this study.

Fujimitsu, Y., Nishijima, J. and Ehara, S. (2009) Temporal change of the coefficient of geothermal flux used in the heat balance technique. Abstracts of Japan Geoscience Union Meeting 2009, V161-P012.

Fujimitsu, Y., Nishijima, J. and Ehara, S. (2010) Relationship between the coefficient of geothermal flux and ground surface temperature anomaly. Abstracts of Japan Geoscience Union Meeting 2010, SVC061-P03.

Fujimitsu, Y., Nishijima, J. and Ehara, S. (2011) Relationship between the coefficient of geothermal flux for the heat balance technique and micrometeorological data. Abstracts of Japan Geoscience Union Meeting 2011, SVC049-P10.

Sekioka, M. and Yuhara, K. (1974) Heat flux estimation in geothermal areas based on the heat balance of the ground surface. J. Geophys. Res., Vol. 79, No. 14, 2053-2058.

Keywords: Heat balance technique, coefficient of geothermal flux, micrometeorology, heat discharge rate, solar radiation, reference temperature

Japan Geoscience Union Meeting 2014
(28 April - 02 May 2014 at Pacifico YOKOHAMA, Kanagawa, Japan)

SVC52-01 Room:416 Time:April 28 10:00-10:15

Simulation of the Daisen-Kurayoshi tephra, in the San-in district, SW Japan, using Tephra2

YAMAMOTO, Takahiro[1*] ; SUGIYAMA, Minoru[2] ; TAJIMA, Yasuhisa[2]

[1]Geological Survey of Japan, AIST, [2]Nippon Koei Co Ltd

The Daisen-Kurayoshi tephra, which erupted from Daisen volcano at about 53 ka, is one of the most voluminous Plinian fall deposits in Japan. Its apparent volume was estimated as more than 20 km^3, but quantitative study of this tephra have not be done. So, we try to analyze this tephra using Tephra2 and decide its eruption parameters. In the simulation, we set 5 cases in height of the eruption column from 10 to 18 km, 4 cases in weight of the erupted magma from 1 to 8x10E+18 kg, 4 cases in medium grain size of the ejected materials from 0 to 3 phi, and 5 cases in sorting of the ejected material under the average wind data above Yonago. A total of 400 cases have been calculated. To explain the observed distribution of the tephra, the column height and ejecta weight have to be 18 km and 4 to 8x10E+18 kg (40 to 80 km^3), respectively.

Keywords: Daisen-Kurayoshi tephra, Tephra2

Japan Geoscience Union Meeting 2014
(28 April - 02 May 2014 at Pacifico YOKOHAMA, Kanagawa, Japan)

SVC52-02 Room:416 Time:April 28 10:15-10:30

Insight into setup of typical meteorological conditions for evaluating volcanic ash hazard

HATTORI, Yasuo[1*] ; SUTO, Hitoshi[1] ; GO, Yumiko[2] ; TOSHIDA, Kiyoshi[1] ; HIRAKUCHI, Hiromaru[1] ; ISHIHARA, Shuji[2]

[1]Central Research Institute of Electric Power Industry, [2]Denryoku Computing Center

Estimation of ash concentration and deposition is of practical interest in evaluation of volcanic ash risk on critical infrastructure (e.g. Wardman et al. 2012). For estimating ash concentration and deposition, numerical simulations with an ash transport- and deposition-model have become a powerful tool (e.g. Folch 2012). However, the setup of meteorological conditions, which mainly control the ash transport- and deposition- processes in the atmosphere and on the ground, has not been discussed in details.

In the present study, we examine the estimation of ground deposition for a real test case, a volcanic ash hazard in Kanto-area for an eruption at Mt. Fuji, with various meteorological conditions by using an ash transport- and deposition-model, fall3d. The meteorological conditions are generated with the 53 years reanalysis meteorological dataset, CRIEPI-RCM-Era2, which has a temporal- and spatial resolutions of 1 hr and 5 km; the typical and extreme conditions were sampled by using Gumbel plot and an artificial neural network technique.

The ash deposition is invariably limited to the west area of Mt. Fuji, even with the typical wind conditions on summer, while the isopach of ground deposition depicted various distributions, which strongly depends on meteorological conditions. This implies that the concentric circular distribution must not be realistic. Also, a long-term eruption, such as the Hoei eruption during stage3, yields large deposition area due to the diurnal variations of wind direction, suggesting that the attention to the differences between diurnal variation and fluctuations of wind direction on evaluating of volcanic ash risk is vital.

More details will be presented in the presentation, and we believe that our study must be helpful to develop the numerical simulations for evaluation of volcanic ash risk.

Keywords: Ash transport- and deposition-model, Long-term meteorological reanalysis, Extreme value, Artificial neural network, Advection-diffusion, Numerical simulation

Japan Geoscience Union Meeting 2014
(28 April - 02 May 2014 at Pacifico YOKOHAMA, Kanagawa, Japan)

SVC52-03 Room:416 Time:April 28 10:30-10:45

Numerical model of 3D ballistic trajectory for hazard assessments at Upper Te Maari eruption of Tongariro volcano in New

TSUNEMATSU, Kae[1*] ; FITZGERALD, Rebecca[2] ; KENNEDY, Ben[2]

[1]Graduate School of Environmental Studies, Nagoya University, [2]Department of Geological Sciences, University of Canterbury

Ballistic bombs and blocks are energetic pyroclasts deposited around volcanic craters. Hazard assessments of ballistic projectiles are important for people, buildings, and roads around vent especially in tourist and residential areas. Tongariro volcano, an active volcano in a popular national park in New Zealand, erupted August 6th, 2012 after one hundred years. By combining acoustic signals with eyewitness descriptions, five eruption pulses from fissures around Upper Te Maari crater were characterized and conditions of particle ejection were defined. A distribution of ballistic blocks was mapped from orthophotos and field campaigns. In order to clarify characteristics of ballistics at Tongariro volcano and assess future hazards, a numerical model of ballistics is modified and applied to the 2012 eruption. At first, 3D multiparticle model based on Discrete Event Simulation (DES) method is converted to the model based on semi-Lagrangian method to include an effect of air drag and gas flow around airborne particles. Initial conditions, such as ejection direction and speed, were calibrated to explain both spatial and size distribution of deposit bombs. Finally, an initial particle velocity of 200 m/s and gas flow velocity (constant) of 150 m/s are obtained as conditions of best fit. Furthermore, we applied this model to the assessment of future eruption regarding Tongariro Alpine Crossing, a walking trail in the national park frequented by ˜80,000 people each year. Impacts of two extreme eruption cases are simulated by the numerical model. Negligible probabilities of fatality along the TAC are found from a magnitude smaller eruption, similar in size to the November 2012 eruption. However, a magnitude larger eruption could result in higher probabilities in certain areas of the track which it would be unlikely to survive the eruption. Varying the input parameters from the calibrated model allows for the assessment of future ballistic hazard from larger and smaller eruptions of Upper Te Maari Crater. A possibility of applying this model to the assessment of Japanese volcanoes such as Mt. Fuji will be discussed.

Keywords: Ballistics, Hazard map, Numerical model, Volcanic eruptions, Hazard assessment, Tongariro Volcano

Japan Geoscience Union Meeting 2014
(28 April - 02 May 2014 at Pacifico YOKOHAMA, Kanagawa, Japan)

SVC52-04 Room:416 Time:April 28 11:00-11:15

Estimation of locations and migration of debris flows on Izu-Ohshima Island on 16 Oct., 2013 by seismic amplitudes

OGISO, Masashi[1*] ; YOMOGIDA, Kiyoshi[2]

[1]Matsushiro Seismological Observatory, JMA, [2]Grad. Sch. Sci., Hokkaido Univ.

Typhoon 1326 (Wipha) with heavy rainfall caused severe damage at Izu-Ohshima Island on 16 October 2013 with large-scale debris flow, probably not only a single event but sequence of flows.

Seismic networks on Izu-Ohshima recorded the signals originated from those debris flows. At least five events of large amplitudes are recognized in continuous records of seismographs.

It is hard to estimate the location of such events with conventional methods of epicenter determination because of the difficulty to identify any seismic phase arrivals. We estimate the locations of the five events with spatial distribution of seismic amplitudes (Battaglia and Aki, 2003; Kumagai et al., 2010). In this method, after correcting the site effect of each station, the RMS amplitude of high-frequency seismic waveform is assumed to decay only with geometrical spreading and intrinsic absorption. Although amplitudes depend on radiation pattern of seismic waves, the isotropic distribution of amplitudes could be assumed at high frequencies because of the scattering effect by small scale heterogeneity in the crust (Takemura et al., 2009). The location of each event is derived as the point of the minimum residual between observed and calculated amplitudes of all the seismic stations. Before estimating the locations of the five events, we apply the band pass filter of 5-10Hz to each seismic record. We assume that the filtered waveform is composed of S body waves only, S-wave velocity is 1.44km/s, and Q=100 for intrinsic absorption. We limit the search range of each event only on the surface of the island. Site factors of stations are estimated by amplitudes of coda waves for regional earthquakes.

The estimated locations of all the five events are located in an eastern side of Motomachi district, where huge causalities were suffered, agreeing with the debris flow traces mapped carefully after the disaster occurred. In addition, the location is migrated to the west (i.e., from the volcano flank to the sea coast) within its duration time of 60-80 sec except for one event with small duration time. Such migrations may correspond to the flow of debris, with its speed about few tens km/h. Time series of source amplitudes, that is, the maximum value and duration time of each event show the variability of the debris flows occurred on Izu-Ohshima Island within several hours on that day.

Generally, seismic networks focused on volcanic activities are generally composed of stations of higher density than other seismic networks. The records of such dense seismic networks are useful to analyze not only earthquakes and tremor on volcanoes, but also debris flows or other disastrous events, as shown in this study. The present location method using the spatial distribution of seismic amplitudes is conceptually able to apply in quasi-real time, so it should be useful to early estimation of location and magnitude of various disasters in and around volcanoes.

Acknowledgements

We analyzed the seismic waveforms recorded in the networks on Izu-Ohshima Island which are operated by Earthquake Research Institute of the University of Tokyo, the National Research Institute for Earth Science and Disaster Prevention, and the Japan Meteorological Agency. We used the digital elevation model and topographical map images of Digital Japan Web System provided by the Geospatial Information Authority of Japan.

Keywords: distribution of seismic amplitudes, locations and migration of debris flows, Izu-Ohshima Island

Japan Geoscience Union Meeting 2014
(28 April - 02 May 2014 at Pacifico YOKOHAMA, Kanagawa, Japan)

SVC52-05 Room:416 Time:April 28 11:15-11:30

G-EVER Next-generation Volcanic Hazard Assessment System

TAKARADA, Shinji[1*] ; BANDIBAS, Joel[1]

[1]Geological Survey of Japan, AIST

The Asia-Pacific Region Global Earthquake and Volcanic Eruption Risk Management (G-EVER) is a consortium of geohazard research institutes that was established in Asia-Pacific region in 2012. G-EVER aims to formulate strategies to reduce the risks caused by earthquakes, tsunamis and volcanic eruptions worldwide. The G-EVER next-generation volcano hazard assessment working group is developing a useful system for volcanic eruption prediction, risk assessment, and evacuation strategy at various eruption stages. The assessment system is based on volcanic eruption history datasets, eruption database and numerical simulations. Eruption history datasets including precursor phenomena leading to major eruptions are important for the prediction of future volcanic eruptions. A high quality eruption database which contains compilations of eruption dates, volumes, and styles, is important for the next-generation volcano hazard assessment system. Formulating international standards on how to estimate the volume of volcanic materials is important to establish a high quality volcanic eruption database. GIS-based spatial distribution database of volcanic materials (e.g. Tephra and pyroclastic flow distributions) is important for accurate area and volume estimation and risk assessments. The volcanic eruption database is developed based on past eruption results, which only represent a subset of possible future scenarios. Therefore, numerical simulations with controlled parameters are needed for more precise volcanic eruption predictions. The ”best-fit” parameters of the past major eruptions in the world have to be estimated and the simulation results database should be made.

The use of the next-generation system should enable the visualization of past volcanic eruptions datasets such as distributions, eruption volumes and eruption rates, on maps and diagrams using timeline and GIS software. Similar volcanic eruption types should be easily searchable from the eruption database. Using the volcano hazard assessment system, prediction of the time and area that would be affected by volcanic eruptions at any location near a volcano should be possible using numerical simulations. The system should be able to estimate volcanic hazard risks by overlaying the distributions of volcanic deposits on major roads, houses and evacuation areas using a GIS enabled systems. The next-generation real-time hazard assessment system will be implemented with user-friendly interface, making the risk assessment system easily usable and accessible online.

Preliminary version of the next-generation volcanic hazard assessment system is available since June 2013. This can run energy cone simulations at any volcano in the world using ASTER Global DEM, and the links to major volcanic databases, such as Smithsonian, VOGRIPA and Quaternary volcanoes. Almost all volcanoes in the world can be evaluated using this volcanic hazard assessment system. Currently, the system covers more than 3200 Quaternary volcanoes worldwide. Links to major volcanic databases in the world are useful to examine eruption history in detail. Using Google and Bing maps as base maps provide more information for hazard evaluations. A hazard evaluation system using Titan2D will be available soon. Hazard assessment system using probabilistic analysis is also being planned in collaboration with INGV in Italy. This hazard assessment system is expected to be used for hazard mapping and risk management planning by government authorities and policy makers.

G-EVER Next-generation Hazard Assessment System URL (http://volcano.g-ever1.org/vhazard/HazardAssessment/)

Keywords: volcano, hazard, Asia-Pacific, G-EVER, simulation, database

Japan Geoscience Union Meeting 2014
(28 April - 02 May 2014 at Pacifico YOKOHAMA, Kanagawa, Japan)

SVC52-06 Room:416 Time:April 28 11:30-11:45

An attempt to obtain empirical evidences for petrological assessment of volcanic activity based on magma database

TAKEUCHI, Shingo[1*] ; TOSHIDA, Kiyoshi[1] ; MIURA, Daisuke[1]

[1]Central Research Institute of Electric Power Industry

For Japanese volcanoes, high-quality databases of volcanic eruptions have been developed, for example Japanese active volcanoes (Kudo and Hoshizumi, 2006-) and one-million years chronology of volcanic eruptions (Hayakawa, 1996-). These databases involve eruptive age, eruption style and eruption magnitude, M. In contrast, it is often the case that properties of magma that caused these eruptions remain unrevealed. We have sampled and analyzed eruptive products of ca. 90 eruptions in Japan during the last one hundred thousand years and are constructing a database of magmatic properties (petrological properties), as a magma database. This database involves mainly large scale eruptions with M=4-8 and additionally recent small eruption of M=1-3. In the magma database, we estimate melt compositions, and phenocryst contents, which are important factors controlling physical properties of magmas, and thus eruption dynamics. Based on the magma database, we have attempted to obtain empirical evidences between these magmatic properties and eruption characteristics (eruption magnitude, eruption style and so on).

Examining relationship between eruption magnitude, M, and magmatic properties for ca. 100 eruptions, including 11 eruptions compiled in Takeuchi (2011), some relationships are found.

(1) Rhyolitic melt (>70 wt% SiO2)-bearing magmas (andesitic to rhyolitic magmas) caused M=4-8 eruptions. In contrast, basaltic to dacitic melt (<70 wt% SiO2)-bearing magmas (basaltic to dacitic magmas) caused M=1-5 eruptions.

(2) For rhyolitic melt-bearing magma, the maximum eruption magnitudes are correlated with phenocryst content. Phenocryst-poor magmas with 0-20 vol% caused caldera-forming eruption with M=8 at the maximum, where phenocryst-rich magmas with 20-50 vol% phenocryst have the maximum eruption magnitude with ca.6.

These empirical evidences suggest that petrological properties, such as melt composition and phenocryst content, are some level of constraint on eruption magnitude. Thus, petrological analysis of eruptive materials in early eruptive stage may contribute to constructing eruption scenario.

Keywords: magma, petrological analysis of volcanic rock, assessment of volcanic activity, database

Japan Geoscience Union Meeting 2014
(28 April - 02 May 2014 at Pacifico YOKOHAMA, Kanagawa, Japan)

SVC52-07 Room:416 Time:April 28 11:45-12:00

Temporal variation (2011-2013) of the amount of CO2 dissolved in Lake Monoun, Cameroon

OHBA, Takeshi[1*] ; ISSA, I[1] ; SASAKI, Yuka[1] ; KUSAKABE, Minoru[2] ; YOSHIDA, Yutaka[3] ; UEDA, Akira[2] ; ANAZAWA, Katsuro[4] ; SAIKI, Kazuto[5] ; KANEKO, Katsuya[6] ; MIYABUCHI, Yasuo[7] ; AKA, F t[8] ; TANYILEKE, G[8] ; HELL, J v[8]

[1]Tokai Univ, [2]Univ Toyama, [3]Yoshida Eng Office, [4]Univ Tokyo, [5]Osaka Univ, [6]Kyoto Univ, [7]Kumamoto Univ, [8]IRGM Cameroon

Introduction

On 15th Aug 1984, the people living Lake Monoun, western Cameroon, heard a loud sound and experienced earth tremors. After the event, a deadly phenomenon occurred as 37 people were asphyxiated by gas that was discharged from the lake. Sigurdsson et al (1987) attributed the cause of the outburst of CO2 to landslide that plunged into the Lake's depth, which was CO2-charged. After a scientific consensus that proceeded from a similar phenomenon at Lake Nyos (100 km NW of Lake Monoun) in 1986, the explosive discharge of CO2 gas from lakes was named "limnic eruption". In 2001, the concentration of CO2 dissolved in Lake Monoun approached saturation at the depth of 50 m (Kusakabe et al., 2008), suggesting a possibility of recurrence of the limnic eruption if no preventive measures were taken. To prevent another limnic eruption, a degassing pipe was installed at Lake Monoun in 2003 (Halbwachs et al., 2004), and by 2009, the lake was almost free of dissolved CO2 and lost its natural gas self-lifting capability through the pipes. Recently we observed that concentration of CO2 has increased slightly in the bottom water. To avoid gas re-buildup in the lake, in 2013, we installed a solar energy driven system to artificially pump the CO2-rich water to the surface.

So far we have employed two methods (MK and CTD) to determine a reliable CO2 concentration profile in lakes.

The MK method (Kusakabe et al, 2000)

With this method, we determine CO2 concentration in lake water as follows. A disposable plastic syringe that contains 10 ml of 5M KOH solution is immersed in the lake at a given depth using an MK sampler. After that, we suck 30ml of lake water into the syringe to fix the total dissolved CO2 (CO2 dissolved gas, HCO3- and CO3–) as CO3–. Then a volumetric titration with standard HCl solution allows the determination of the total carbonate in the syringe. The results obtained so far indicate that the MK method is accurate and reliable. However, the method gives discrete data in terms of depth.

The CTD method

The CTD (Conductivity, Temperature, Depth) enables us to estimate the CO2 concentration as a smooth depth profile. The absolute value of CO2 concentration by the CTD method depends strongly on pH and conductivity values, thus the data from the CTD method need to be carefully examined compared to those from the MK method. We introduced an adjustable parameter k as defined by C-corr=k∗C, where C is the measured raw conductivity and C-corr is the corrected conductivity. Assuming an appropriate molar conductivity for HCO3-, the C-corr gives the total CO2 concentration under the assumption of chemical equilibrium among the dissolved carbon species (CO2aq, HCO3- and CO3–). We compared the total CO2 concentration by MK method and CTD method at the every depth where we have the values by MK method. The difference between the two methods was squared and the summation of squared values was calculated. The summation was minimized with changing the parameter k.

Results

As shown in Fig. 1, the thickness of bottom water with CO2 concentration higher than 20 mmol/L increased significantly in 2012 relative to 2011. This tendency continued in 2013, although CO2 concentration of the bottom water decreased slightly. The lake water shallower than 30m is affected by inflowing river water contains low concentration of total CO2. The total CO2 profile was integrated between -98m (near bottom) to -30m and estimate of the total amount of CO2 in the lake were 101, 118 and 119 Mmol in 2011, 2012 and 2013, respectively. Those values are much smaller than 600 Mmol, which was the amount of CO2 gas in lake just before the degassing pipe started functioning (Kusakabe et al., 2008). However, it should be noted the amount of dissolved CO2 is gradually increasing, so a regular monitoring of the lake is imperative.

Keywords: Lake Monoun, CO2, Limnic eruption, Cameroon, Magma

SVC52-07 Room:416 Time:April 28 11:45-12:00

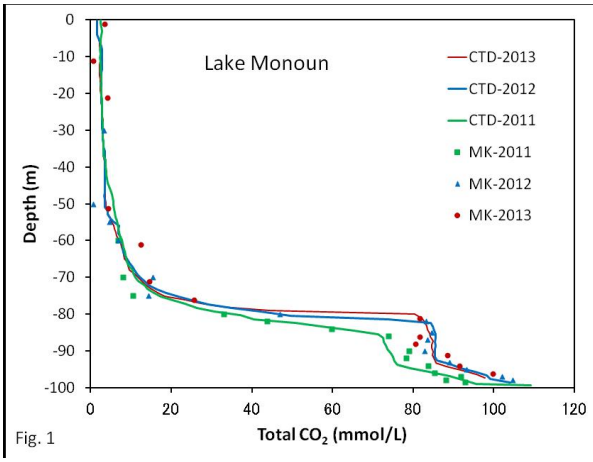

Fig. 1

Japan Geoscience Union Meeting 2014
(28 April - 02 May 2014 at Pacifico YOKOHAMA, Kanagawa, Japan)

SVC52-08 Room:416 Time:April 28 12:00-12:15

Topographical features of Fuji volcano as seen in the polar coordinate system

CHIBA, Tatsuro[1*]

[1]Asia Air Survey Co., Ltd.

Introduction

Fuji volcano is the highest mountain in Japan and the most active volcano in past 12 thousand years, in Japan except for the caldera eruption (Miyaji 1988) . The inclination is loosely about 300,000 people each year climb to the summit.

As a result of repeated eruption of central vent , volcanic body of a huge cone-shaped with a diameter of 10km high specific 2000m is formed around the crater . Fuji volcano had piled up in stages on Komitake , Old-fuji , and New-fuji. The remaining part of the old edifice also so as to project on the slope .Fuji is seen variety profile from the direction by such features .

Study range

In this paper , the technique of polar coordinate conversion. Study subjects ranged circular radius 13.5km centered summit. This point is not the highest point , the approximate center of Dainai-in Institute(The latitude is 35.36295 and longitude is 138.73035) . The terrain data is base map information 0.4 seconds mesh of the Geographical Survey Institute (about 10m) source , was used in resampled to 50m mesh japanese orthogonal coordinate system (VIII, system) .

Angle of repose

Slope gradient of the volcano , is determined by the movement mechanism and state of matter that has been brought to the ground from the crater in general , the angle of repose and stable gradient . Looking at the topography of the polar coordinate transformed , it can be seen that the portions to concentrated lateral cone is higher than ambient , and is raised as acne . In particular , it is found that it is concentrated in a direction 315 degrees and 135 degrees direction . It should be noted that the gap of advanced 250 degrees around , under the influence of Tanzawa is protruding from the east , to the south of Gotemba is lower .

Projected section

Take the elevation direction from the summit , the Y -axis in X -axis , to prepare a projected section shows the projection section color grid point frequency distribution of 50mDEM. If likened to Mount Fuji skirt , bright line of lower limit corresponds to the height of the perimeter of the flared skirt . According to this chart , it can be seen that the low altitude most Fujinomiya direction of southwest . Then , a Fuji-Yoshida direction Gotemba direction , finally . Design such as bubbling southeast and northwest direction direction can be seen , but it is the effect of mountain body side of the volcano . In addition, over the surface of Lake Yamanaka from Oshino of 250 degrees from 200 degrees azimuth , elevation is significantly higher than at the periphery . In this direction there is a mountain slope body of old Fuji.

Literature

Tatsuro Chiba (2010) Landform -50mDEM cylindrical coordinate transform analysis , Fujigaku studies , 7, 1 , 3 -13.

Miyaji Naomichi (1988) Activity history of younger Fuji volcano , Journal of the Geological Society ,94 , 6 , 433 -452.

Keywords: DEM, angle of repose, profile, slush abalanche, lava flow, active fault

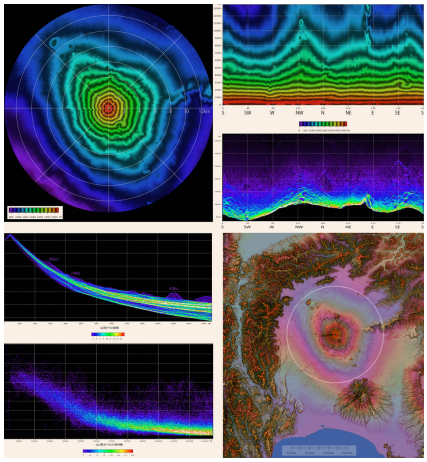

Japan Geoscience Union Meeting 2014
(28 April - 02 May 2014 at Pacifico YOKOHAMA, Kanagawa, Japan)

SVC52-09 Room:416 Time:April 28 12:15-12:30

Tool handing down disaster experiences using Geoparks: examples of Unzen Volcanic Area Global Geopark

OHNO, Marekazu[1*]

[1]Unzen Volcanic Area Geopark Promotion Office

Local inhabitants living in Shimabara peninsula has suffered volcanic disasters of Mt. Unzen repeatedly, which include the worst volcanic disasters occurred in 1792 (Kansei eruption and Shimabara Catastrophe). Nevertheless these conditions, they stay near Mt. Unzen to take good living environments.

Since they continue living in the near active volcano, they are always at risk of the volcanic disasters. If these experiences of disasters pass down to next generations, disaster prevention awareness in local inhabitants and, as the result, risk from disasters should be reduced. However, because of a long eruption interval (a few hundred years) of Mt. Unzen, it is difficult to pass down these experiences to next generations. Furthermore, the information that emphasized a disaster more than required may lead the uneasiness of local inhabitants. The system to overcome these problems is a Geopark.

Education is one of main component of businesses of geoparks. Thus, we have carried out an education program of disaster prevention for local school students as a business of Geopark and promote their awareness of disaster prevention.

Actually, all of 6th grade of elementary school students in Shimabara city visit geosites for a day as a geotour and learn the highlights of the Geopark. Main theme of the geotour is *a Kansei and Heisei eruptions and their disasters*. School students learn what happened at their home town in about 20 years ago through observation of a building of elementary school burned by a fire derived from pyroclastic surge and a memorial park preserved houses buried by lahar. In the tour, I also try to inquire why you stay near the active volcano introducing great landscapes created by big landslides occurred in 1792, spring water sprung out from a head of a lava flow emitted in 1792 and local special foods using local natural environments.

This is not a program to learn disaster prevention directly. However, when local inhabitants (especially children) understand academic value of local resources (e.g. strata, landscapes, human history, culture, and so on) and realize reasons to stay near active volcanoes, their consciousness of disaster prevention must be promoted. I believe the system of Geopark must contribute promotion of volcanic disaster prevention in Japan.

Keywords: Unzen Volcanic Area Global Geopark, Educatiion of disaster prevention, geosites, Heisei eruptopm, Shimabara Catastrophe

Japan Geoscience Union Meeting 2014
(28 April - 02 May 2014 at Pacifico YOKOHAMA, Kanagawa, Japan)

SVC52-P01 Room:Poster Time:April 28 18:15-19:30

Reproduction of the Eruptive sequence of the 2011 Shinmoedake eruption using the kitchen volcano experiments

IMURA, Ryusuke[1*] ; TANIYAMA, Hirokazu[2]

[1]Graduate School of Science and Engineering, Kagoshima University, [2]Takaharu Town Office, Miyazaki Prefecture

For elementary and junior high school students, we conducted a program for the reproduction of the eruptive sequence of the 2011 Shinmoedake eruption using the kitchen volcano experiments. Learning about the Shinmoedake eruption in 2011 will lead to disaster prevention. This program plays an important part of education and disaster prevention activities in the Kirishima Geopark.

Keywords: The 2011 Shinmoedake eruption, kitchen volcano experiment

Japan Geoscience Union Meeting 2014
(28 April - 02 May 2014 at Pacifico YOKOHAMA, Kanagawa, Japan)

SVC52-P02 Room:Poster Time:April 28 18:15-19:30

HOMURA: Development of mobile sensor for volcanic exploration

KANEKO, Katsuya[1*] ; ITO, Koichi[2] ; ANBE, Yuichi[3] ; IWAHORI, Kodai[4]

[1]Human and Environmetal Studies, Kyoto University, [2]Graduate school of Science, Kyoto University, [3]Graduate school of Technology, Kyoto University, [4]Facultiy of Science, Kyoto University

Monitoring of phenomena near craters of active volcanoes is important to learn symptoms of volcanic eruptions and to understand eruption dynamics. At present, some devices such as crater camera, volcanic gas sensors, and seismographs that have been installed in a calm period of volcanic activity are monitoring volcanic phenomena near the craters. On the other hand, we cannot approach the crater and cannot install new devices after beginning of a volcanic eruption, even if we want to observe unexpected volcanic phenomena. Therefore, unmanned robots that observe them on an ad hoc basis are needed. Previously some projects have tried to develop robots for volcanic exploration. However, those projects which required large budgets ended before a practical application.

We hope to destroy the status quo and are trying to develop a practical unmanned-ground-vehicle-type robot for volcanic exploration that carries out monitoring near active craters. We named this system ”Homura”. Homura is controlled by wireless remote control, move in volcanic field, approach an active crater, monitor volcanic phenomena with sensors equipped in the vehicle, and send their data to the base stationin real time. In this presentation, we introduce a prototype of Homura and report a test campaign in Mihara-yama volcano, Izu-Ohshima.

Guidelines of development of Homura are two: (1) the vehicle does not readily become undrivable in volcanic fields, and (2) assemblage and use of Homura require low conts. We produced the prototype of Homura these guidelines. Homura is a six-wheeled vehicle with a vertically symmetric shape. Its size is 750 length x 430 width x height 310 height mm, its weight is about 12 kg. The power source is two-cell lithium polymer battery (7.4 V, about 250 Wh capacity). Some sensors such as camera, GPS, CO2 gas sensors are installed in the vehicle. Homura communicates with the base station by digital radio communication, and receives and send commands from base stations and data in real time. An installed small computer control all telecommunication, movement, and sensors. Production cost of vehicle is about 200,000 JPY, which is much lower than the robots developed in the previous projects.

Means of stable radio communication are needed for practical missions in volcanic field. Homura can use wireless transceiver modules that directly communicate with another module and Docomo FOMA modem using mobile phone network. The former wireless transceiver modules can be used in any volcanic field but distance between Homura and the base must be less than 1 km. The latter FOMA communication needs cell phone network. If the network is available, we can control Homura in any place.

We carried out a test campaign of Homura around Mihara-yama volcano, Izu-Ohshima in November, 2013 to examine remote control with FOMA communication. The base station was placed at Ohshima Spa Hotel which is about 2 km distant from the summit crater. Homura started Ohshima Spa Hotel. We controlled Homura only with information from sensors such as camera, GPS, and gyro. Homura moved on the mountain trail and reached the summit. Then, it climbed down on scoria slope without trail. This campaign result indicate that we can control Homura with remote control in volcanic fields. On the other hand, the radio communication with FOMA was not stable enough in Izu-Ohshima. At four areas where lava walls were barriers between Homura and a relay antenna of FOMA, the communication became unstable or disconnected. This indicates that we cannot move Homura to the summit only by remote control in Mihara-yama. When a UGV robot carries out missions in the volcanic field, we must obtain means of stable telecommunication before the missions. There are some cases where temporal stations of relay antenna are needed to use cell phone network.

Keywords: robot, Remote control, Telecommunication by cell phone, Izu-ohsima

Japan Geoscience Union Meeting 2014
(28 April - 02 May 2014 at Pacifico YOKOHAMA, Kanagawa, Japan)

SVC52-P03 Room:Poster Time:April 28 18:15-19:30

Particle fallout from an eruption column (2) - evaluation of reproducibility

MANNEN, Kazutaka[1*]

[1]Hot Springs Research Institute of Kanagawa Prefecture

One of the major sources of error in tephra fall simulation is considered to be the source term, which depicts amount of particle release as a function of height in eruption column. The source term has been assumed to be linear or modeled using relationship between particle size and plume velocity (Suzuki function); however, no direct observation of the source term has been reported. The author has tried to obtain source term of the 1986 Izu-Oshima B eruption based on inversion technique using a tephra simulation code named Tephra2. Here the reproducibility of the inversion is evaluated.

In this study, two methods are applied to evaluate reproducibility. One is validation using a dummy source term. In this method, a dummy source term is given and tephra loads on each observation point is calculated using Tephra2. Based on the calculated loads, the source term is inversely calculated and compared with the originally given source term.

The other method is jackknifing. In this method, source terms are calculated using dataset in which a single observation is deleted one by one. The calculated source term is called as pseudo-value and the estimated source term is defined as an average of the pseudo-values. The error of the source term is also defined as a standard deviation of the pseudo-values.

In the 1986 Izu-Oshima B eruption, range of reproducible height changes as a function of grain size; 0-7 km for -3 phi particles and 0-4 km for 0 phi particles. The errors of obtained source parameter was limited; less than 10 % in the most cases.

Keywords: Pyroclastic fall, Tephra2, simulation

Japan Geoscience Union Meeting 2014
(28 April - 02 May 2014 at Pacifico YOKOHAMA, Kanagawa, Japan)

SVC52-P04 Room:Poster Time:April 28 18:15-19:30

Detection of thermal anomaly associated with volcanic activity from MODIS data

TSUTSUMI, Rika[1*]

[1]Chiba University

There are a lot of volcanoes in the world.And then, it is difficult to monitor all volcanoes because of costs.But we can monitor efficiently a lot of volcanoes using satellite remote sensing, because a volcanic activity will cause the increase in surface temperature and satellite (whose sensor can observe the surface temperature) remote sensing can cover a large area on surface.Therefore, various approaches have been suggested to monitor volcanic activities using remote-sensing satellite data.

Removing cloud pixel is essential to monitor volcanic activities using remote-sensing satellite data. Therefore, the purpose of this study is to remove cloud accurately and to develop an adequate algorithm continuously to detect thermal anomalies related to volcanic activities (especially lava activity which causes serious damages involve human lives) using MODIS (Moderate Resolution Imaging Spectroradiometer) infrared sensor onboard Aqua satellite.

We investigate spatial-time changes in thermal infrared in the statistical way. In order to detect only hotospots related to lava activities without faints, the developed algorithm investigates the difference temperature behavior between a target point and reference points, and we get spatial difference of brightness temperature (S). The presence of cloud causes large value of S that doesn't related to volcanic activities (Noguchi 2011). Therefore, removing cloud is essential in the proposed algorithm. To remove cloud, we use some BTD(Brightness Temperature Difference) which is sensitive to cloud. And we verified the technique of cloud removal as compared with Lidar data.

Keywords: MODIS, Lidar, Volcanic activity, Shinmoe-dake, lava activity

Japan Geoscience Union Meeting 2014
(28 April - 02 May 2014 at Pacifico YOKOHAMA, Kanagawa, Japan)

SVC53-01 Room:413 Time:April 28 14:15-14:30

Variations of basaltic magmas and their timing of injection into the magma system of Sakurajima volcano since AD 1779

EBIHARA, Kaho[1] ; NAKAGAWA, Mitsuhiro[1*] ; YOSHIMOTO, Mitsuhiro[1] ; KOBAYASHI, Tetsuo[4]

[1]Earth & Planetary System Sci., Hokkaido Univ., [2]Earth & Planetary System Sci., Hokkaido Univ., [3]Earth & Planetary System Sci., Hokkaido Univ., [4]Earth & Enviromental Sci., Kagoshima Univ.

Sakurajima volcano has repeated plinian eruptions three times during the last 600 years and changed the mode of eruptive activity since the AD 1914 plinian eruption. Frequent vulcanian eruptions has continued since AD 1955. Nakagawa et. al(2011) concluded that two-end-member magma mixing of silisic magma(S-magma) and andesite magma(A-magma) occurred in 1471 and 1779, and three-end-member magma mixing of mixed magma(S+A) and basaltic magma(B-magma) since the 20th century. They concluded that the injection of the B magma has frequently occurred since then to change the mode of eruptive activity. Their evidences of the injecting were presence of Olivine and An=90 plagioclase phenocrysts and different mixing trend in SiO2 variation diagrams between the 20th century and previous products. However, petrological features of AD 1779 submarine eruptive products just after the terrestrial plinian eruption have not been revealed in detail. In this study, newly collected 1779 submarine products are investigated to discuss the magma plumbing system.

The AD 1779 submarine products are banded pumice and slightly vesiclated lavas. These contain plagioclase, orthopyroxene, clinopyroxene and magnetite as phenocryst associated with small amounts of olivine microphenocrysts, which were not recognized in the AD 1779 terrestrial products. These olivine phenocrysts do not have reaction rims of orthopyroxene. Average core compositions of these are about Fo=77. Compositional variations of other phenocrysts, except for magnetite, are nearly the same as those in the AD 1779 terrestrial and 20th eruption products. These olivine phenocrysts are diequilibrium with pyroxenes on the basis of Fe-Mg partitioning, suggesting that the basaltic magma injected into the mixed magma between the S and A magmas, which erupted as the AD 1779 terrestrial products. It should be noted that the injection of the basaltic magma had started just before the submarine eruption. On the other hand, olivine phenocrysts in the 20th century products are composed of two types, with or without reaction rims of orthopyroxene. Average core compositions of those without reaction rims are Fo=81, whereas those with reaction rims are less than Fo=74. These suggest that the 20th century products had been repeatedly injected by the basaltic magmas and that the basaltic magma injecting just before each eruption had olivine phenocrsyts with Fo=81. Although the injections of the basaltic magma has occurred just before the AD 1779 submarine eruption, two types of basaltic magma have injected . The basaltic magma in AD 1779 was less magnesian and contained olivine pehnoctysts with Fo=77, whereas those in 20th century were magnesian, having olivine phencorysts with Fo=81. This is consistent with distinct two chemical trends of AD 1779 submarine and 20th century products in SiO2 variation diagrams, such as P2O5 and MgO. Considering the presence and absence of the relict olivine phenocrysts, with reaction rims, the erupted magma during the 20th century were effected by previous injections of basaltic magmas. After the injection of olivine (Fo=77) in AD 1779, these olivine phenocrysts were reacted with more silicic melt not only to form the reaction rim but also to change their chemical compostions with less magnesian. Just before AD 1914 eruption, voluminous another basaltic magma with more magnesian olivine (Fo=81) had injected just before the AD 1914. The injected magma since AD 1955 has been similar to that of AD 1914, whereas volume of the magma has become smaller. However frequent, small scale of injection has continued to cause number of small, but explosive vulcanian eruptions.

Keywords: Sakurajima volcano, magma system, magma mixing, olivine, volcanic eruption

Japan Geoscience Union Meeting 2014
(28 April - 02 May 2014 at Pacifico YOKOHAMA, Kanagawa, Japan)

SVC53-02 Room:413 Time:April 28 14:30-14:45

Bulk density change of juvenile clasts during the climactic phase of the 2011 Shinmoe-dake eruption

SUZUKI, Yuki[1*] ; ICHIHARA, Mie[1] ; MAENO, Fukashi[1] ; NAGAI, Masashi[2] ; NAKADA, Setsuya[1]

[1]ERI, Univ. of Tokyo, [2]NIED

In the 2011 eruption of Shinmoe-dake, three sub-Plinian events occurred intermittently between Jan 26 PM and Jan 27 PM (1/26PM, 1/27AM and 1/27PM). This was followed by lava accumulation in the crater (Nakada et al. 2013, EPS). Based on Suzuki et al. (2013a, JVGR) that clarified characteristics and plumbing system of the erupted magmas, we reveal evolution of conduit magma flow during the climactic phase as above, by using groundmass textures. The questions we would like to address are, 1) mechanisms that led to the intermittent sub-Plinian events, including triggering process of each event, 2) timing and condition of syneruptive magma ascent that were responsible for the shifting eruption intensity and style.

As a preliminary result, we here present bulk density data for samples (gray and brown pumices and lava) of the same chemical and storage conditions just prior to ascent from the reservoir. If lithic fragments in sub-Plinian deposit can be judged juvenile (i.e. from the 2011 magma) based on whole rock composition and appearance under the microscopy, they were included in the sample set for the bulk density analysis. Generally, the bulk density data reflect syneruptive ascent condition and resultant degree of syneruptive outgassing. This time, the data allowed us to select representative samples for further textural analyses. The bulk density data also helped us newly define the horizon corresponding to the start of the second sub-Plinian event.

Following the results in Maeno et al. (revised) and Nakada et al. (2013, EPS), the sub-Plinian deposit was collected at locations on dispersal axes and 2-3km from the crater. The following unit numbers are after Nakada et al. (2013). We had no difficulty in identifying the deposit of the third sub-Plinian event (Layer5), because the field survey was in progress at the time of occurrence. The lower units (Layer2, 3 and 4) exhibit reverse grading from layer2 to layer3 and normal grading from layer3 to layer4, as if it was generated in a single event. This occurrence had prevented us from identifying the boundary between the first and second sub-Plinian events. As far as area of the sampling is considered, we believe no deposition during the resting phase between the first and second sub-Plinian events (Jan 26, 19:00 - Jan 27, 2:00) . The most likely deposit for the resting phase is ash, if plume height of 3.5km and lower (Shimbori and Fukui, 2012; lower than 6-7km during the sub-Plinian events) is considered. We did not find ash layers between the two of the three layers (layer2, 3 and 4).

The bulk densities of the samples change systematically with the subunits; 1.0-1.7 g/cm^3 from Layer2-low to Layer3-low, 1.0-2.0 g/cm^3 in Layer3-up, and 0.8-1.4 g/cm^3 from Layer4-low to Layer4-up. The average densities for the subunits are 1.25 g/cm^3, 1.28 g/cm^3, 1.27 g/cm^3, 1.44 g/cm^3, 1.14 g/cm^3, 1.17 g/cm^3 in order from Layer2-low.

We propose that Layer3-up corresponds to the start of the second sub-Plinian event, based on a judgment that high-density pumices in Layer3-up are from upper-conduit degassed magma that was generated during the resting phase (Jan 26, 19:00 - Jan 27, 2:00). The infrasound and seismic data (Ichihara et al., submitted) recorded no explosion for the resting phase. Therefore, we infer the degassed magma did not block the conduit completely.

We could not know exact time of the Layer4 deposition. However, the lower bulk densities in Layer4, in comparison with those of layer3-up, is consistent with the temporal increase of plume height (e.g. ca. 5km at AM2 of Jan 27 $<$ca. 7km at AM4 of Jan 27) and mass eruption rate (Ueda et al., 2013) during the second sub-Plinian event. In this model, we however must explain smaller pumice sizes in Layer4 in comparison with those of Layer3-up.

Keywords: Shinmoe-dake, Sub-Plinian eruption, Bulk density, Outgassing, Infrasound, Plume height

Japan Geoscience Union Meeting 2014
(28 April - 02 May 2014 at Pacifico YOKOHAMA, Kanagawa, Japan)

SVC53-03 Room:413 Time:April 28 14:45-15:00

Hypocentral migration associated with magma intrusion in the 2000 Miyakejima eruption

MATSUYAMA, Ryotaro[1*] ; MORITA, Yuichi[1] ; SAKAI, Shin'ichi[1] ; UEDA, Hideki[2]

[1]ERI, Univ. of Tokyo, [2]NIED

A dike intrusion is a phenomena that large amount of magma emplaces in the shape of vertical plane. It is much controlled by tectonic stress. A dike intrusion process is one of the important key informations to understand the relation between tectonic stress and volcanoes. In the case of the Miyakejima eruption in 2000, it is confirmed that a large scale dike intruded beneath sea floor from the following observations; Hypocenters migrate from inland area of Miyakejima to the area near by Kozushima and Niijima. Large ground inflation is measured by nation-wide GNSS network. However, the detail process in this event has been unsolved because hypocenter locations cannot be estimated precisely. Therefore, we try to relocate hypocenters and to reveal the dike intrusion process of the 2000 Miyakejima eruption in this study.

Because hypocenters migrated to the offshore of Miyakejima, hypocenters could not be located precisely from the data recorded at inland of islands surrounding hypocenter area. Eight days after the initiation of the activity, ocean bottom seismometers(OBSs) were installed just above hypocenters. The hypocenter locations was improved very much using the OBSs data. However, analysis of OBS's data did not cover a whole period of the activity. We try to relocate hypocenters that has no OBS's data (approximately 30,000 events) relative to the reference hypocenters (approximately 3000 events) that are located precisely using OBSs data. In our analysis, we modify Double Difference method to give constraints not to move the reference hypocenters and apply it to all earthquakes occurring during 26 June and 31 August, 2000. We also use the velocity structure that is smoothly varying in the depth because of prevention of artificial hypocenter concentration.

From the relocated hypocenters, we find out the following features in the seismic activity associated with the 2000 Miyakejima eruption. 1) There are two groups in the seismic activity. One is the hypocenters aligned from the summit of Miyakejima to the point around 8km off the coast line (near coast activity), the other is the seismic activity distributed on a sub-vertical plain located beneath sea floor at the area surrounded by Miyakejima, Kozushima and Niijima (main activity). The alignment of the hypocenters match with the direction of the maximum tectonic stress. 2) The near coast activity began with an initiation of the volcanic activity and concluded on July 1st. The seismicity in this area was active only in the first week of the whole volcanic activity, and earthquakes did not occur after the period at all. 3) The main activity lasted during two months, and it was accompanied with gradual ground deformation measured by nation-wide GNSS network that represents a large scale of dyke intruded at hypocentral area. The vertical section of the hypocenters shows that the vertical alignment changes at the depth of 12 km where the structure discontinues is implied from a seismic survey. 4) In the later periods of the activity, there are many earthquakes at the area next to the main activity. Their focal mechanisms were strike slip types that agree with the direction of tectonic stress.

Considering the features of the hypocentral distribution mentioned above and other observational facts, we can conclude that there are two types of the magma flow during the 2000 Miyakejima eruption. One is horizontal emplacement just after an initiation of the volcanic activity and the other is gradual upward migration from deep zone to the main activity. Because the cost activity was inactive after July 1st, we suppose that the two magma flow is independent during almost whole period except at the beginning of the activity. In other words, the magma that generate the main activity is not supplied horizontally from Miyakejima but from just beneath hypocenter area.

Acknowledgments: We are much grateful to JMA, NIED, Tokyo Pref. for permitting to use their seismic data.

Keywords: dike intrusion, 2000 Miyakejima eruption, hypocenter migration, seismic activity, tectonics

Japan Geoscience Union Meeting 2014
(28 April - 02 May 2014 at Pacifico YOKOHAMA, Kanagawa, Japan)

SVC53-04 Room:413 Time:April 28 15:00-15:15

Temporal variation of mineral composition of Hanafusa Formation distributed in the western area of Aso caldera

SUGIYAMA, Fumiko[1*] ; HASENAKA, Toshiaki[1]

[1]Guraduate school of Science and Technology,Kumamoto university

Aso volcano made four large-scale pyroclastic eruptions, with magma composition changing with time, so that hornblende phenocryst appeared in the latest Aso-4 pyroclastic flow deposits (Watanabe, 1979). Hornblende becomes a key mineral to detect the physicochemical change, as it also appeared as microphenocryst in volcanic products of Omine volcano and associated Takayubaru lava flow, which erupted just before Aso-4 event (Kurokawa et al., 2012). Hanafusa Formation is a lake deposit forming 20 km west of Aso caldera just before Aso-4 pyroclastic eruption, thus it is suitable for finding the appearance time of hornblende from the minerals included in the deposits.

Hanafusa Formation consists of silt and sand with thickness of up to 10 m, and formed between Aso-3 and Aso-4 pyroclastic flow events. We collected samples from pumice deposit and overlying sand in Kajisako, Kikuchi city. We also collected samples from silt layer just below the contact with Aso-4 pyroclastic deposit, and from the type locality of Hanafusa Formation in Kikoji, Kikuchi city. We divided silt layer into upper unit and lower unit with boundary at the tephra layer, which we identified as Ata regional tephra by its mineral assemblage and existence of abundant bubble-shape glass and estimated age of 100 ka.

(1) The lower unit contain plagioclase, clinopyroxene and orthopyroxene. Plagioclase crystals indicate auhedral and have the surface which give a dirty impression.

(2) The upper unit contains euhedral hornblende and euhedral plagioclase crystals which are not observed in the lower unit. The upper unit contains clinopyroxene and orthopyroxene crystals. The mineral assemblage and their ratios are the same as observed among Aso-4 pyroclastic flow deposit.

(3) Chemical compositions of pumice fragments in Pumice layer resembled those of all Aso-4 pyroclastic flow deposits. However, in detail, Oyatsu pumice flow deposit, Benri scoria flow deposit and Omine volcanic products show distinct compositional trends from this pumice layer(Kurokawa et al., 2012; Yamasaki et al., 2013).

(4) Observed crystals in sand just above the pumice layer include plagioclase, clinopyroxene, orthopyroxene, opaque minerals and olivine, which isnot included in the lower pumice layer.

Our findings suggest that the appearance of hornblende was 10,000 years before Aso-4 pyroclastic eruptions, however their source is unknown, because we did not find obvious tephra layers other than Ata regional tephra.

Keywords: Hanahusa formation, hornblende, Aso-4 tephra, Aso-4 pyroclastic flow

Japan Geoscience Union Meeting 2014
(28 April - 02 May 2014 at Pacifico YOKOHAMA, Kanagawa, Japan)

SVC53-05 Room:413 Time:April 28 15:15-15:30

Estimating composition of primitive magma by using opx, and temporal and spatial change of HMA magmatism in NE Shikoku

MORISATO, Fumitoshi[1*] ; OZAWA, Kazuhito[1]

[1]School of science, The University of Tokyo, [2]School of science, The University of Tokyo

In the subduction zone, oceanic plates start sinking into the mantle, and continental crusts are generated and eroded. So it is important for understanding the evolution of plate-tectonics. As for the subduction initiation, temporal change of thermal structure and water content of the mantle wedge is mainly estimated by numerical simulations (Iwamori, 2000 *etc*.), but there are few constraints from material informations. Using magma information is a possible method to estimate thermal structure of the Earth (Green, 1981). Although it is necessary to estimate chemical composition of the primitive magma, the effects of crystal differentiation and, especially in subduction zone, crustal process (magma mixing, crustal assimilation, and degassing) should be evaluated. Moreover, the magmatism in subduction zone is assumed to be affected by mantle flow in mantle wedge (Tatsumi *et al*., 1983; Tamura, 2003). To estimate such upwelling, Sakuyama *et al*. (2009) investigated temporal and spatial change of the magma generation field.

SW Japan is an example of juvenile subduction zone. Shikoku basin initiated to sink 17 Ma ago, and magamatisms migrated from forearc to reararc (Kimura *et al*., 2005). In the Setouchi volcanic zone, the generation of high-Mg andesite (HMA) has been discussed from the view of thermal structure of the mantle wedge and subducting plate (Tatsumi & Hanyu, 2003 *etc*.), but there remains some questions about magma mixing and degassing, and about temporal and spatial change of magma generation field.

In this study, we suggest a method to estimate the primitive magma composition by using oscillationally-zoned opx, and apply to the HMA in the Setouchi volcanic zone. And we try to estimate the magma generation mechanism by evaluating temporal and spatial change of magmatism in the area.

Firstly, we investigated a HMA in Mt. Kiyama, central part of NE Shikoku, Japan (Sato, 1982 *etc*.). It has the most primitive composition (SiO_2: 57.3wt%, MgO: 8.56wt%, Mg#: 69.3), and it contains olivine, opx, and cpx as phenocrysts. The olivine phenocrysts are normally-zoned, and their highest Mg# (87.6) is lower than the equilibrium value calculated from whole rock composition of the HMA (88.7). Therefor the olivine phenocrysts are considered to be crystallized in closed system. On the other hand, opx phenocrysts are reversely-zoned, and their composition boundaries are sharp. Moreover they have higher Mg# (up to 91.5) than calculated equilibrium value (88.8). Accordingly, these opx could record the composition of more primitive melts. And zoning pattern among opx is consistent, so they could reflect compositional change of the same melt.

According to Putirka (2005), the composition of primitive magma can be estimated by adding fractionated olivine or opx until the melt's composition become in equilibrium with the opx which has the highest Mg#. But we must remove the effects of magma mixing before it. Kuritani (1998) used the fact that the An content of plagioclase phenocryst can be changed in a magma chamber reflecting the difference of temperature or water content. He investigated the pattern of zoning and quantity ratio of them, and estimated mixing ratio.

We estimated the change of melt composition. (1) Calculating the melt compositions from opx composition by using distribution coefficients. (2) Comparing the change of the melt composition and modeled composition in Rayleigh fractionation or magma mixing. (3) Estimating mixing ratio by evaluating the pattern of zoning in opx and their quantity ratio, and estimating end member of mixing. (4)According to the true fractionation trend, determining primitive magma composition which is in equilibrium with opx having the highest Mg#.

By applying this method to the HMA in Mt. Shichihousan, western part of NE Shikoku (Kawabata & Suto, 2000), we estimated the spatial change of primitive magma composition and magma generation field.

Keywords: subduction, Southwest Japan, primitive magma, magma mixing, High-Mg andesite

Japan Geoscience Union Meeting 2014
(28 April - 02 May 2014 at Pacifico YOKOHAMA, Kanagawa, Japan)

SVC53-06 Room:413 Time:April 28 15:30-15:45

The relation of volcanic stages for the recent 10000 years of Kirisima and Southern Kyushu volcanoes

TAJIMA, Yasuhisa[1*]

[1]Nippon Koei Co., Ltd.

In this study the eruption ages of tephra and lava generated from Shinmoedake volcano and Ebinokogen volcanic area by 14C dating were determined. Those ages indicate that the Kirishima volcanoes have three eruptive stages among the recent 10,000 years. The eruptive stage C started from 9.0 to 8.0 cal ka BP with RyD-L from Shinmoedake volcano and Fd-TmA tephra and Fudoike lava from Ebinokogen volcanic area. Old-Takachihono volcano and Takachihonomine volcano grew rapidly in this stage. The eruptive stage B continued from 5.6 to 2.3 cal ka BP growing the Shinmodedake and Nakadake volcanic edifices. Three eruptions at the same time, which were the Miike plinian eruption at 4.6 cal ka BP from Miike maar, Sm-Sy eruption at 4.5 cal ka BP from Shinmoedake volcano and Kn-EbD eruption at 4.3 cal ka BP from Ebinokogen volcanic area in this stage. The time interval between eruptive stage B and eruptive stage A was 2.3 to 1.6 cal ka BP. The yougest eruptive stage A started with Fd-EbC tephra from Ebinokogen volcanic area at 1.6 ka. In this stage, the Ohachi volcano grew from 6th century and Shinmoedake volcano erupted from 18th century. This result indicates that the Kirisima volcanoes repeated a few thousand years of eruptive stages and 500 to 1000 years intervals. The current eruptive stage A pasts about 1600 years. The relation of eruption ages of Kirishima volcanoes and Sakurajima volcano is well.

Keywords: Kirishima Volcano, Volcanic stage, Shinmoedake, Ebinokogen, Long term activity

Japan Geoscience Union Meeting 2014
(28 April - 02 May 2014 at Pacifico YOKOHAMA, Kanagawa, Japan)

SVC53-07 Room:413 Time:April 28 15:45-16:00

Investigation report of rootless cone in Iceland -as an analogue of that of on Mars-

NOGUCHI, Rina[1*] ; SARUYA, Tomotaka[1] ; SUZUKI, Yuki[1] ; KURITA, Kei[1]

[1]Earthquake Research Institute, the University of Tokyo

Rootless cone is a pyroclastic cone which has a variety of shape. It's formed by lava-water interaction [e.g. Fagents et al., 2002, Hamilton et al., 2010], but details such as formation conditions are still unknown. Since pervasive existence of various types of rootless cones has been clarified on the martian surface, terrestrial rootless cones are key to understand Martian volcanism and strong interests have been paid in the field of planetary science. We surveyed rootless cones in Iceland by RTKGPS (Real-Time Kinematic GPS) with material-scientific investigations on the constituent materials.

We investigated 3 rootless cone fields; Myvatn (northern Iceland), Landbrot (eastern Iceland), and Thjorsardalur (western of Hekla volcano). In this presentation, we will focus on Myvatn area. In Myvatn, rootless cones were formed by lava-lake water interaction. The lava is basaltic, and emanated from the fissure which locates in east of the lake [Thorarinsson, 1951], and flowed into the lake. We mapped more than 500 rootless cones by aerial photo survey. Most of cones locate around the lake, but some cone locates in in the down-flow region (40 km far from the lava source) area. In Myvatn, here exists unique rootless cone which has an inner cone in the summit crater. We named this as double cone. We focus on this type and conducted detailed morphological survey.

We found that slope angle of rootless cone depends on its size. For double cone, inner cone has gentler slope than that of outer cone. In case of single cone (no inner cone), large cones have steeper slope than that of small cones. Also, large cones have constant slope (repose angle: 32-33 degree), despite the slope angle of small cone varies. In case of the double cone, we found that the constituting material of the inner cone differs from that of the outer cone. The component material of the outer cone is lapilli - coarse ash size pyroclast. On the other hand, that of the inner cone is welded pyroclasts or agglutinate. For small cones, the summit part is covered with agglutinate. These differences should indicate different condition of the formation such as the amount of available water/heat supply by magma.

A We measured bulk chemical composition of the lava and the pyroclasts by XRF confirming no significant change along lava flow traveling. We also measured bulk density and size distribution of the pyroclasts of the rootless cones. We found density of the lava concordantly increases with traveling distance, which means bubbles progressively escaped from the lava during traveling while the formation of rootless cone seems not to be influenced by the vesicularity of lava. The size distribution seems to be correlated with the slope value of the cone, which strongly suggests the control of fragmentation on the formation of rootless cone.

Keywords: rootless cone, Iceland, Mars, Myvatn, double cone

Japan Geoscience Union Meeting 2014
(28 April - 02 May 2014 at Pacifico YOKOHAMA, Kanagawa, Japan)

SVC53-08 Room:413 Time:April 28 16:15-16:30

Volume of magma chamber and eruption ratio for caldera collapse

GESHI, Nobuo[1*]

[1]Geological Survey of Japan, AIST

Mechanism of caldera collapse is modeled with a comparison of a piston-cylinder caldera model and the compiled data of caldera size and eruptive volume in nature.

Collapse caldera is formed by the fracturing and subsidence of the roof of magma chamber with rapid withdrawal of massive magma from a magma chamber. As the fracturing and subsidence of the roof of magma chamber may enhance the additional eruption of magma inside the magma chamber, understanding of the mechanisms of the precursory eruption is crucial to evaluation of the potential eruption from caldera volcanoes.

Collapse calderas are formed only by the largest eruptions of its life, though, in many cases, caldera volcanoes repeat many eruptions with various scales before and after caldera formation. Smaller eruptions have no significant contribution for collapse. Aira caldera in Japan was formed at 29ka eruption during which ~400 km^3 of magma was erupted. Though many smaller eruptions including Fukuyama pumice eruption (10km^3DRE) and Sz-S eruption (4km^3DRE) occurred from the Aira caldera, no significant collapse was occurred. During the 29 ka eruption, Osumi pumice fall was erupted prior to the onset of collapse, and the emission of Ito pyroclastic flow followed the collapse. The erupted volume of Osumi pumice fall (~40 km^3DRE) is larger than those of the eruptions without collapse. This relationship is commonly observed in other caldera volcanoes. The erupted volume during the precursory eruption is in correlation with the size of caldera.

The volume of magma withdrawal to induce collapse is modeled with piston-cylinder model. The driving force of collapse is the decompression in magma chamber by the magma extraction. The friction in the ring fault sustains the roof. Competition between the decompression of magma chamber and the friction controls the onset of collapse. The decompression of magma chamber is in the function of the eruption ratio (volume of magma withdrawal / total volume of magma chamber). This model shows that a larger volume of magma withdrawal is required for the onset of collapse with larger diameter. The critical eruption ratio for collapse is smaller for the larger caldera.

Though this model has potentially large ambiguity from the simplified shape of caldera fault and the assumption of the bulk modulus of magma, this model can give the total volume of magma chamber associating collapse caldera. In the case of Aira caldera, with 15 km in diameter and 6 km to the roof of magma chamber, the total volume of magma chamber before the eruption is estimated as 600 km^3. The caldera collapse occurred when the erupted volume reached to 8% of the total magma chamber, and 60 % of magma was erupted as Ito pyroclastic flow after the onset of collapse.

Keywords: large eruption, caldera volcano, magma chamber

Japan Geoscience Union Meeting 2014
(28 April - 02 May 2014 at Pacifico YOKOHAMA, Kanagawa, Japan)

SVC53-P01 Room:Poster Time:April 28 18:15-19:30

Identification and Geology of Taftan volcano Calderas, Sistan and Baluchestan, Southeast of Iran

BIABANGARD, Habib[1*]

[1]Department of Geology, Sistan and Baluchestan University of Zahedan, Iran

The Taftan volcano, Sistan and Baluchestan province, SE Iran, is above 4050 m sea level and currently dormant, showing fumarolic activity near the summit. This volcano is located in a structural zone along the subduction of Oman oceanic crust below the Eurasia plate. Large volcanic centers including Chah-Shahe, Bazman and Taftan in Iran and Soltan in Pakistan have been developed during the Quaternary. Anjerk and Tamandan are two calderas from of Taftan volcano that identified for the first time. Theses calderas are mostly composed of pyroclastics, lava flows, ignimbrites and tuffs. Various volcanic eruptions had occurred during these calderas formation. The exposed lava flows and pyroclastics of these calderas mainly consist of andesitic and dacitic in compositions. The geochemical evaluation of the major and trace element compositions indicate the magma erupted from this volcano show a calk-alkaline trend.

Keywords: Taftan Volcano, Makran belt, Anjerk caldera, Tamandan caldera, Geochemical evaluation, Iran

Japan Geoscience Union Meeting 2014
(28 April - 02 May 2014 at Pacifico YOKOHAMA, Kanagawa, Japan)

SVC53-P02 Room:Poster Time:April 28 18:15-19:30

K-Ar ages of Kelut-Welirang volcano cluster, East Java, Sunda arc: comparison with clusters that hosts large calderas

TOSHIDA, Kiyoshi[1*] ; TAKADA, Akira[2] ; KITSUKAWA, Takashi[3] ; TAKEUCHI, Shingo[1]

[1]CRIEPI, [2]AIST, GSJ, [3]Ceres, Inc.

Sunda arc, Indonesia, has many active caldera volcanoes and is well suited for studying the evolution of large caldera systems. Volcano groups are distributed in clusters at Sunda arc. Two adjacent volcano clusters in East Java, Semeru-Tengger and Kelut-Welirang, are compared. Semeru-Tengger volcano cluster consist of Semeru and Tengger-Bromo volcano systems. Tengger-Bromo system has formed Ngadisari and Sand Sea calderas. Kelut-Welirang volcano cluster consists of multiple active volcano groups and has comparable footprint and cumulative volume as Tengger-Bromo. However, large-scale eruptions in the order of 10km3 or greater have not taken place at Kelut-Welirang volcano cluster.

Kelut-Welirang volcano cluster consists of five volcano groups. They are Penanggungan, Arjuno-Welirang, Argowayan, Butak-Kawi-Panderman, and Kelut from northeast to southwest. They are classified as active volcanoes except for Argowayan, and Kelut is currently active. However, their formation ages are not understood.

K-Ar dating is performed in order to determine and compare the long-term activity of the two clusters. Mass fractionation correction method is used for argon measurement, for many of the samples are very young. Samples with crystalline groundmass are selected for dating to obtain precise and reliable age. Groundmass is separated from phenocryst and used for dating.

The active periods and the ages of the volcano groups are identified by K-Ar dating as follows. (a) Argowayan, which consists about half of the volume of Kelut-Welirang cluster, has formed between 1.0-0.8Ma. (b) There was long dormancy in the area of this cluster, and the four volcano groups have formed within the past 0.2 m.y. (c) Kelut has started to form by 0.2Ma, and has repeatedly produced lava domes to present. (d) Much of Butak-Kawi-Panderman has formed around 0.2Ma. The group is considered active, but the long-term eruption rate of the group has decreased substantially since the early stage of edifice building activity at 0.2Ma. (e) Arjuno-Welirang is younger and likely started to form by 0.1Ma. (f) Penanggungan is the youngest volcano group and likely to have formed within the past 0.05 m.y.

The obtained ages allow us to compare Kelut-Welirang and Tengger-Semeru volcano clusters. Although Kelut-Welirang cluster has comparable volume to Tengger-Semeru, it consists of separate volcano groups formed at different ages. The long-term eruption rate for the past 0.2Ma is relatively large, but much of the erupted volume is contributed from new volcano group. In contrast, the volcano edifices of Semeru-Tengger have almost entirely formed from 0.5Ma to present. The eruptive centers are concentrated at Tengger and Semeru, and have repeated active periods.

Keywords: age dating, Quaternary, Indonesia, mass fractionation correction method

Japan Geoscience Union Meeting 2014
(28 April - 02 May 2014 at Pacifico YOKOHAMA, Kanagawa, Japan)

SVC53-P03 Room:Poster Time:April 28 18:15-19:30

Correlation between petrology and magneto-stratigrapphy of Holocene volcanic products from Aso central cones

HIRAKAWA, Yuichiro[1*] ; HASENAKA, Toshiaki[1] ; MOCHIZUKI, Nobutatsu[2] ; MORI, Yasushi[3]

[1]Grad School Sci & Tech, Kumamoto Univ., [2]Priority Organization for Innovation and Excellence, Kumamoto University, [3]Kitakyushu Museum of Natural History and Human History

We collected samples from 25 sites where Yato et al. (2013) and Miyabuchi et al. (2012) reported magneto-stratigraphy of six different lava flows distributed in the northwestern region of Aso central cones. We conducted petrographic descriptions and chemical analyses of these samples and correlated them with paleomagnetic directions and stratigraphy of Miyabuchi (2009) based on radiocarbon dating.

Kijimadake lava is divided into two lava flow units with different paleomagnetic directions suggesting interval of at least several hundreds of years. They show the same mineral assemblage, but different groundmass texture, modal composition and whole-rock chemical composition. The upper lava flow unit has the same petrological characteristics as Kishimadake scoria, whose estimation age was 4000 y.b.p. from the radiocarbon dating.

Possibility of multiple eruptions has been suggested for Ojodake lava flows, because they are intercalated by soil, and show different paleomagnetic directions. However, no distinction was made in petrographic descriptions and chemical compositions between these lava flows.

Six different lava flows younger than Akahoya tephra have similar appearance and similar petrographic characteristics, however they are distinguishable by chemical compositions. Lava flow units with possible simultaneous eruptions (e.g. old Kijimadake lava and Nakadake younger stage lava, Kamikomezuka scoria and old Ojodake lava) show about 1% difference in SiO_2 content. A series of Holocene lava flows in Aso central cones are possibly derived from a common magma supply system with different conduits.

Keywords: post-caldera central cones of Aso volcano, volcanic products, Holocene, paleomagnetic directions, petrography, chemical compositions

Japan Geoscience Union Meeting 2014
(28 April - 02 May 2014 at Pacifico YOKOHAMA, Kanagawa, Japan)

SVC53-P04 Room:Poster Time:April 28 18:15-19:30

Magma genesis of Miocene basalts from Ootsu district, Yamaguchi Prefecture, SW Japan arc

HIGASHIYAMA, Yoji[1] ; HASENAKA, Toshiaki[1*] ; SHIBATA, Tomoyuki[2] ; YOSHIKAWA, Masako[2] ; NAGAO, Takashi[3]

[1]Grad School Sci. & Tech., Kumamoto Univ., [2]Beppu Geothermal Res. Lab., Kyoto Univ., [3]Grad School Sci. & Eng., Yamaguchi Univ.

The geological, petrological and geochemical studies of Miocene Ootsu basalts, distributed in Tsunoshima and Yuyashima islands along the coast of the Japan Sea, revealed the temporal and vertical changes in mantle melting processes. Based on their volcanic stratigraphy and petrological data, Ootsu basalts were grouped into; (1) clinopyroxene-olivine basalt (COB), (2) olivine basalt, magnetite-rich type 1 (MRB1), (3) olivine basalt, magnetite-rich type 2 (MRB2), and (4) olivine basalt, magnetite-poor type (MPB). MRB1 and MRB2 are rich in FeO$*$ and TiO_2 contents, and MPB is rich in SiO_2 and Al_2O_3 contents. MRB1, MRB2 and COB are alkalic and MPB is tholeiitic.

Phase diagram and mass balance calculations indicate that these four groups were derived from different primary magmas, and had experienced polybaric crystallization. The compositions of primary magmas for these four groups suggest that MRB1 and MPB were generated at the deepest and shallowest depths, by the lowest and the highest degrees of melting, respectively. Multi trace element plots (normalized by the primitive mantle values) of Ootsu basalts show the strong enrichment of LILE (Rb, Ba, and K), and distinct negative anomaly of Nb and Sm. The compositions of coexisting olivine and spinel (OSMA) suggest that MPB's mantle source is the most fertile among four groups. The different ratios of LREE/HREE among four groups suggest different mantle source and different degree of partial melting. B/Nb ratio of four groups is getting higher with decreasing segregation depth. These systematic differences in B/Nb ratio indicate that the upper mantle beneath Ootsu district is characterized by an increased degree of metasomatism at shallow level.

We concluded that the diversities of chemical composition in Ootsu basalts attribute largely to different segregation depth and heterogeneous mantle source.

Keywords: alkaline rock, tholeiite, boron, rare earth element, mantle

Japan Geoscience Union Meeting 2014
(28 April - 02 May 2014 at Pacifico YOKOHAMA, Kanagawa, Japan)

SVC53-P05 Room:Poster Time:April 28 18:15-19:30

Rifting- and subduction-related volcanism of the northern Fossa Magna related to the formation of the Sea of Japan

OKAMURA, Satoshi[1*] ; INABA, Mitsuru[2] ; YOSHIDA, Takanori[3] ; ADACHI, Yoshiko[4] ; SHINJO, Ryuichi[5] ; IKEDA, Yasuo[6]

[1]Sapporo, Hokkaido Educ. Univ., [2]Japan Petroleum Exploration Co., Ltd., [3]Sapporo, Hokkaido Educ. Univ., [4]Faculty of Science. Niigata Univ., [5]Faculty of Science. Univ. Ryukyus, [6]Kushiro, Hokkaido Educ. Univ.

Specific aims of the research are; 1) to characterize the chemical composition of the magmatic sources for the Cenozoic volcanic suite in the Fossa Magna region, a boundary fault zone between north and south Japan, 2) to relate the magmatic evolution to the simultaneous tectonic process of the opening of the Japan Sea, and 3) to assess the role of rifting and subduction processes in the evolution of the continental margin of the northwestern Pacific rim with inferences for the other tectonic zone.

Keywords: Fossa Magna, Yamato Basin, MORB source, Enrich mantle

Japan Geoscience Union Meeting 2014
(28 April - 02 May 2014 at Pacifico YOKOHAMA, Kanagawa, Japan)

SVC53-P06 Room:Poster Time:April 28 18:15-19:30

The Middle Miocene tectonics and volcanism in the intra-arc and the back-arc region, Northeast Japan

HOSOI, Jun[1*] ; AMANO, Kazuo[2]

[1]Graduate School of Science and Engineering, Ibaraki University, [2]Faculty of Science, Ibaraki University

In northeast Japan, many submarine volcanic rocks related to opening of the Japan Sea in the Early Miocene are widely distributed. They are very important to consider the evolutional process of Japan Arc and to elucidate the submarine volcanism. Despite the importance, there were no detailed sedimentological studies of these volcanic rocks, and the detailed sedimentary processes, sedimentary basin formation, paleo-volcanism and tectonics were poorly understood. In this study, we tried to reconstruct the detail volcanic edifices and volcanism based on the facies analysis of volcanics in typical two area; one is Ou Backbone Ranges in Nishiwaga town, Iwate prefecture and the other is Dewa Mountains in Sakata, Yamagata prefecture, that were located in the intra arc and the back arc in the Miocene respectively.

As results, we could elucidate paleo volcanism in each area. Remarkable tectonic change occurred in 15Ma with active volcanism, counterclockwise rotation and rapid subsidence (Hosoi et al., 2013). Regional paleostress around 15 to 12Ma is NW-SE tensional stress (Otsuki, 1989; Hosoi, 2013). This tectonic change happened in 15Ma with opening of Japan Sea, and active bimodal volcanism, rotation movement and tectonic subsidence occurred.

[References]

Hosoi, J., 2013, Research Report for the Fukada Grant-in-Aid in the H24 fiscal year, 9-23.

Hosoi, J. et al., 2013, Jour. Sediment. Soc. Japan, 72, 141-146.

Sato, H. and Amano, K., 1991, Sedimentary Geology, 74, 323-343.

Keywords: Miocene, tectonics, back-arc, intra-arc, greentuff, Northeast Japan

Japan Geoscience Union Meeting 2014
(28 April - 02 May 2014 at Pacifico YOKOHAMA, Kanagawa, Japan)

SVC53-P07 Room:Poster Time:April 28 18:15-19:30

Paleostress analysis of dilational fractures using genetic algorithm

YAMAJI, Atsushi[1*]

[1]Kyoto University

The attitudes of dilational fractures, including dikes and veins, are clues to the paleostresses under which the structures were formed. A software tool for clustering their 3D orienatations has been developed in this study. The software fits mixed Bingham distributions to them, and detects girdle, elliptical and circular clusters. In addition, it determines the three principal stress axes, stress ratios and maximum fluid pressure for each of the clusters. Fitting a mixed Bingham distribution is not a well posed problem, because the mathematical inversion is highly non-linear and its object function is multimodal. It is demonstrated that genetic algorithm is more effective than the expectation-maximization algorithm which was used by previous researchers (Yamaji and Sato, 2011).

Keywords: real-coded genetic algorithm, magma pressure, mixed Bingham distribution, dike, vein

Japan Geoscience Union Meeting 2014
(28 April - 02 May 2014 at Pacifico YOKOHAMA, Kanagawa, Japan)

SVC54-01 Room:411 Time:May 1 09:00-09:15

Eruption History and Future Scenario of Sinabung volcano, North Sumatra, Indonesia

YOSHIMOTO, Mitsuhiro[1*] ; NAKADA, Setsuya[2] ; ZAENNUDIN, Akhmad[3] ; PRAMBADA, Oktory[3] ; HOKANISHI, Natsumi[2] ; TAKAGI, Natsuko[2] ; HENDRASTO, Muhamad[3] ; IGUCHI, Masato[4]

[1]Faculty of Science, Hokkaido University, [2]Earthquake Research Institute, University of Tokyo, [3]Center for Volcanology and Geological Hazard Mitigation, Indonesia, [4]Sakurajima Volcano Research Center, Disaster Prevention Research Institute, Kyoto University

Sinabung Volcano is an andesitic stratovolcano located 40 km northwest of Lake Toba, North Sumatra. The activity began after the latest caldera-forming eruption of Toba Lake (ca. 74ka). The eruption history can be divided into two stages (old and young stages) based on topographical and geochemical features. The edifice is characterized by multiple thick lava flows/domes, and their collapsed materials of block-and-ash flow and associated surge deposits. The lava spine is located at the southern end of one of the summit craters which trend in N-S. Pumice-fall deposits by relatively large explosive eruptions, such as plinian- to subplinian types, were not recognized. The last magmatic eruption before 2010 occurred during 9 to 10th century, whose products are mainly pyroclastic-flow deposits, distributed in the SE slope.

The present activities began with phreatic events in August and September 2010. It resumed its activity in September 2013 with phreatic events. After the repeated phreatic to phreatomagmatic events, lava appeared in the summit crater in late December and started its partial collapse on 30 December. Several tens collapses occurred everyday in January 2014. Those pyroclastic flows descended on the SE slope of the volcano and traveled 4.5 km in maximum.

Lavas of the volcano are basaltic andesite to andesite in composition, and andesitic lavas contain hornblende phenocrysts. Although old lava have a SiO2 range similar to young lavas, the old lava are more enriched in K2O than the young lava. The lava spine is highly enriched in SiO2 and extremely depleted in Na2O, a result of high alteration by volcanic gases, suggested by the mineralogical features. Bulk composition of 2010 ash seems to be intermediate between the young lava and the altered lava spine. In contrast, pumice of 2013 eruption has a similar composition of juvenile materials of 9-10th eruption.

Before the 2013-2014 events, highly possible scenario for future eruption have been proposed the similar case of lava-dome eruptions at Unzen, Japan, in 1991-95 and at Soufriere Hills, Montserrat, West Indies, in 1995-present, based on the eruption history. The present eruption at Sinabung follows the proposed scenario of the highest probability.

This work was supported by SATREPS research project (Multi-disciplinary Hazard Reduction from Earthquakes and Volcanoes in Indonesia) and the Indonesian Center for Volcanology and Geological Hazard Mitigation (CVGHM).

Keywords: Indonesia, Sinabung, volcanic eruption, eruption history, Scenario, pyroclastic flow

Japan Geoscience Union Meeting 2014
(28 April - 02 May 2014 at Pacifico YOKOHAMA, Kanagawa, Japan)

SVC54-02 Room:411 Time:May 1 09:15-09:30

Petrological study of monogenetic volcanoes in the fore-arc region of the northern Kamchatka Peninsula

NISHIZAWA, Tatsuji[1*] ; CHURIKOVA, Tatiana[2] ; GORDEYCHIK, Boris[3] ; ISHIZUKA, Osamu[4] ; NAKAMURA, Hitomi[1] ; IWAMORI, Hikaru[5]

[1]Department of Earth and Planetary Sciences, Tokyo Institute of Technology, [2]Institute of Volcanology and Seismology Far East Division, Russian Academy, [3]Institute of Experimental Mineralogy, Russian Academy, [4]Research Core for Deep Geological Environments, AIST, [5]Japan Agency for Marine-Earth Science and Technology

The western part of the Pacific Plate is subducting under the Okhotsk Plate along Kuril-Kamchatka Trench, and the northern part of it is subducting under the Bering Sea Plate with high obliquity along the western Aleutians arc. The three plates form the Aleutian-Kamchatka triple junction (Eichelberger *et al*., 2013). The northern edge of the Pacific Plate is separated from Bering Sea Plate by transform fault, and the mantle edge beneath the Kamchatka Peninsula is thought to be open towards the Bering Sea.

There are at least 29 active volcanoes in the Kamchatka Peninsula. From the east to the west, arc volcanism on the Kamchatka Peninsula forms three zones parallel to the Kamchatka trench: the Eastern Volcanic Front (EVF), the Central Kamchatka Depression (CKD) including Klychevskaya Volcano Group (KVG) where the large volcanoes concentrate, and the Sredinny Ridge (SR) in the back arc side.

Along EVF, the straight volcanic chain is terminated around 55^{o}N (near the Kizimen volcano), and in further north the volcanic chain seems to deflect toward KVG corresponding to deeper depth of subducting slab. However, monogenetic volcanoes on the northward extension of the EVF exist and were studied in 1960s, called ‘ Kumuroch range ’ (Fedororenko., 1969). The present-day slab depth beneath the monogenetic volcanoes is about 60km (Gorbatov *et al*., 1997), and the crustal thickness is about 20-30km (Levin *et al*., 2002). These volcanic rocks were reported as basalt to andesite, having relatively high MgO content ($\sim$11.8 wt. %) and low FeO/MgO ratio ($<$1.0) (Uspensky and Shapiro., 1984). In summer 2013, we have identified 15 monogenetic volcanoes in this area (hereafter ‘ East Cone volcanic group ’ , EC) by using stereogram, and had investigated 8 volcanoes by using a helicopter.

In this study, we aim to reveal the origin of the EC lavas. For this purpose, we have first examined mineral assemblages under optical microscope and analyzed the whole rock major element compositions by XRF. All 16 samples are classified as basalt or basaltic andesite, of which the two lavas contain xenoliths, and one sample oxidized to red. The rocks exhibit porphyritic to seriate texture, containing plagioclase, clinopyroxene, olivine, opaque minerals, although, the proportion of minerals varies from sample to sample. The silica contents of all samples are over 50 wt. %, with the FeO/MgO ratio less than 2, indicating relatively undifferentiated characteristics.

In comparison to the typical island arc basalts having a similar silica content, the MgO contents of the EC lavas are higher by $\sim$4 wt. %. Accordingly, the EC lavas are similar to or classified into high-Mg andesite, which is considered to be generated by melting of relatively hydrous mantle (as an example, unsaturated with H_2O, 1.0GPa, 1100-1250 ℃, saturated with H_2O, 1.5GPa, 1030-1150 ℃) (Tatsumi., 1995; 2003).

The EC lavas scarcely include orthopyroxene, on the other hand, volcanic rocks of KG include orthopyroxene (Churikova *et al*., 2013). Mantle xenoliths from the Bezymianny volcano of KG is reported to be spinel harzburgites (Ionov *et al*., 2013). Combining these constraints, we discuss a regional variation in mineral assemblage and H_2O content in source mantle, H_2O content in the primary magma, and the crystallization temperature and pressure of the magmas.

By comparing the petrological characteristics of the EC lavas with those from other regions (e.g., KG), cleare constraints on the relationship between magma genesis and the tectonic setting are expected to be imposed.

Keywords: arc, high-Mg andesite, Kamchatka Peninsula, triple junction

Japan Geoscience Union Meeting 2014
(28 April - 02 May 2014 at Pacifico YOKOHAMA, Kanagawa, Japan)

SVC54-03 Room:411 Time:May 1 09:30-09:45

Geology and petrology of Taisetsu volcano group, Japan; Evolution of magma and long-term time variation of eruption rate

ISHIGE, Kosuke[1*] ; NAKAGAWA, Mitsuhiro[1] ; MATSUMOTO, Akikazu[2]

[1]Department of Natural History Sciences, Graduate School of Science, Hokkaido University, [2]Geological Survey of Japan, National Institute of advanced Industorial Science and Technology

Taisetsu volcano group locates at the northern part of the Taisetsu-Tokachi volcanic chain, which is situated at the southern end of Kuril arc. The volcano group started its activity ca. 1 Ma and is composed of andesitic lava domes and stratovolcanoes. Although previous studies (eg., NEDO, 1990; Katsui, 1979) revealed the outline of structure and eruptive history of the group, detail chronological and petrological studies have not been carried out. We have revealed the volcano stratigraphy and petrological features of the whole area of the volcano group. In addition, K-Ar ages of representative samples are also determined. Based on these data, we focus on the temporal change of eruption rate and magma types during 1 My in the volcano group.

According to the stratigraphy, location of eruption centers, mode of eruptive activity and petrological features, the activity of the volcano group can be divided into four major stages, as follows. Stgae 1(1.0 ˜0.75Ma): Fluidal andesite lava were effused from several eruption centers to form flat-shaped volcanic edifices which are distributed in N-S direction. Their total estimated eruptive volume is 26km^3(DRE). Stage 2: It can be subdivided into sub-stage 2-1 (0.6Ma) and 2-2 (0.35 ˜0.05Ma). Eruptive lavas of the former sub-stage are mostly coverd by younger deposits. Detail structure of the edifice and the distribution of deposits have not been clear. The sub-stage 2-2, is further subdivided into central and western group according to the differences in mode of activity and location of eruption centers. The total estimated eruptive volume of stage 2 is 23km^3. Stage 3(ca. 30 ka): The stage is characterized by most explosive eruptions in the volcano group, resulting to the formation of a plinian column and related pyroclastic flows. These activities formed the Ohachidaira caldera with 2 km in a diameter. The total eruptive volume is estimated to be 13km^3. Stage 4 (ca. 30 ka - present): Main eruption centers moves to the southwestern part of the caldera to form several stratovolcanoes and lava domes. The total eruptive volume of stage 4 is 10km^3.Based on the ages and estimated eruptive volume, the magma discharge stepdiagram of the volcano group is created to discuss a temporal change of magma discharge rate. The eruption rate of each stage is as follows; $>$0.07km^3/ky for stage 1, $>$0.01km^3/ky for stage 2-1, $>$0.06km^3/ky for stage 2-2, $>$0.33km^3/ky for stage 3, $>$0.33km^3/ky for stage 4. According the stepdiagram, the period from 0.7 to 0.4 Ma could be characterized by extremely low eruption rate and/or the presence of dormant stage.

Petrological features of the ejecta of Taisetsu volcano group can be distinguished among stages. All of the rocks are andesite and dacite, often containing mafic inclusions. These rocks contain plagioclase, clinopyroxene, orthopyroxene and Ti-magnetite as phenocrysts, associated with minor amounts of olivine, and quartz phenocrysts in some rocks. Although the rocks of stage 1 do not contain hornblende phenocrysts, those of stage 2 and 3 usually include hornblende phenocrysts. However, there rarely exist hornblende phenocrysts in the rocks of stage 4. The whole-rock SiO_2 contents range from 56.4 to 69.1 wt.% for host rocks and from 52.7 to 57.4 for the inclusions. Almost all the rocks are defined as medium-K in SiO_2 - K_2O and CA types in SiO_2-FeO/MgO diagrams, respectively. The host of the rocks from stage 1 is characterized by high Zr contents, compared with the rocks from other stages, whereas Zr contents in the mafic inclusions in the rocks from stage 1 are the same as those from other stages. Considering Zr contents and occurrence of hornblende phenocryst in andesite, magma type had changed largely during the possible long dormancy from 0.7 to 0.4 Ma. This would be related to the tectonic change at the junction between NE Japan and Kuril arcs.

Keywords: Volcano, Eruption rate, Formation history, Taisetsu, Geology and petrology, Transition of magma

Japan Geoscience Union Meeting 2014
(28 April - 02 May 2014 at Pacifico YOKOHAMA, Kanagawa, Japan)

SVC54-04 Room:411 Time:May 1 09:45-10:00

Reconstruction accuracy of eruptive sequence inferred from the pyroclastic fall deposits of the Asama-Maekake volcano

YASUI, Maya[1*]

[1]Dept. of geosystem sciences, Nihon University

The pyroclastic fall deposits of the Asama-Maekake volcano, such as A (1783AD), B′ and B (12^{th} century), and C (4^{th} century), are mainly composed of pumice layers. On the other hand, ash fall derived from the recent vulcanian eruptions (e.g., 2004 and 2009 eruptions) is too small in scale to be preserved as a geologic unit. Ash particles from such small-scale eruptions are mainly lithic fragments originating from solidified lava in a shallow level of the conduit. After the 1783 eruption, repeated vulcanian eruptions have formed ash and soil mixtures on the flank of the volcano. Similar ash and soil mixtures are also recognized beneath A, B, C, and D pyroclastic fall deposits, respectively. These ash and soil mixtures contain lithic fragments as the ash component, indicating that vulcanian eruptions occurred repeatedly in the period between large-scale eruptions, similarly to the period after the 1783 eruption. Lithic ash layers are also interbedded with pumice fall layers of B′, B, and E pyroclasic fall deposits. There seem to be some cases of intermittent vulcanian and sub-plinian eruptions in the course of the large-scale eruption.

In the case of the 1783 eruption, detailed reconstruction of the eruptive sequence is possible on the basis of correlation between the stratigraphy of the eruptive products and old documents. The large-scale sub-plinian eruption is considered to be associated with the formation of a pyroclastic cone in a proximal area owing to vigorous fountaining. Subsequently, large-scale clastogenic lava flows are generated throughout its climactic eruption. On the other hand, little information is available for eruptions before 1783 because of limited exposure and few old documents. Although the reconstruction accuracy for the eruptions in the 12th century is not as good as that for the 1783 eruption, these eruptions might have occurred with a different sequence from the 1783 eruption. Intermittent events of ash and pumice fall occurred in the initial stage of these eruptions. Phreatomagmatic eruption also occurred in the early stage of the 1128 eruption, resulting in a B′ pyroclastic fall deposit. The existence of many units of pyroclastic flows in the 1108 eruption indicates that pyroclastic flow occurred on multiple occasions. Since the stratigraphic relationship between the B pyroclastic fall and these pyroclastic flows is unclear, the sequence of the eruption is still in question. Furthermore, little information is available for eruptions predating the 12^{th} century.

Comparative study of the distributions of pyroclastic fall deposits using isopach maps reveals that some fall units from B′ and B are larger in scale than that of the climactic pyroclastic fall deposit of the 1783 eruption. In addition, the A′ pyroclastic fall deposit is estimated to be comparable to or smaller than the preclimactic fall unit of the 1783 eruption. Although the isopach maps of A, B′, B, C, and E could be prepared, the accuracy of the isopach maps for the C and E pyroclastic fall deposits is insufficient. The preparation of an accurate map is difficult for deposits of older age. Consequently, at this point, the 1783 eruption is the only example in which the temporal variation in eruptive style and in eruptive volume can be discussed with high accuracy in the history of the Asama-Maekake volcano.

Japan Geoscience Union Meeting 2014
(28 April - 02 May 2014 at Pacifico YOKOHAMA, Kanagawa, Japan)

SVC54-05 Room:411 Time:May 1 10:00-10:15

Polybaric crystallization of H_2O-saturated island arc low-K tholeiite magmas: A case study of the Izu-Oshima volcano

HAMADA, Morihisa[1*] ; OKAYAMA, Yuko[2] ; KANEKO, Takayuki[3] ; YASUDA, Atsushi[3] ; FUJII, Toshitsugu[4]

[1]Japan Agency for Marine-Earth Science and Technology, [2]National Museum of Emerging Science and Innovation, [3]Earthquake Research Institute, University of Tokyo, [4]Crisis and Environment Management Policy Institute

Introduction: The H_2O concentration of pre-eruptive melts, particularly that of primitive melts, provides information on the *P-T* conditions of their generation, their differentiation pathways, and their potential explosivity of eruptions. Consensus with regard to the H_2O concentration of island arc low-K tholeiitic magmas (melts) remains elusive. We investigated conditions of their crystallization differentiation, particularly the H_2O concentration in melts, using geochemical data of volcanic rocks from Izu-Oshima volcano in the Izu arc, along with the results of hydrous melting experiments.

Geochemistry and petrology of volcanic rocks: We selected 68 aphyric volcanic rocks which exhibit multiply saturated liquid compositions of the Izu-Oshima volcano. Among them, two magma groups are distinguished by the K/Zr ratio, a lower-K subgroup (K/Zr$<$60) and a higher-K subgroup (K/Zr$\geq$60). In this study, we focus on the higher-K subgroup liquids. Two endmember trends, referred to here as a higher-Al/Si trend and a lower-Al/Si trend, have been distinguished in the higher-K subgroup liquids. All the liquids are bracketed by these two endmembers, and thus may be mixtures of the two endmembers or may have been derived under intermediate conditions between those responsible for the two endmembers. An experimental study by Hamada and Fujii (2008, *Contrib. Mineral. Petrol.*) suggests that the higher-Al/Si and lower-Al/Si trends can be reproduced by upper crustal crystallization differentiation of primitive basalt under moderately hydrous ($\sim$3 wt % H_2O) and almost dry conditions, respectively.

Hydrous melting experiments on island arc low-K tholeiite magmas: Island arc low-K tholeiite magma is characterized by presence of Ca-rich plagioclase (An$\geq$90), with Ca-poor rim ($\sim$An75). Hydrous melting experiments on two volcanic rocks from the Izu-Oshima volcano, MA43 and MA44 (MgO$\sim$5 wt %), were conducted at 250 MPa to constrain the origin of Ca-rich plagioclase (Hamada and Fujii 2007, *Geochem. J.*). MA43 and M44 represent less differentiated liquid compositions on the higher-Al/Si and lower-Al/Si trends, respectively. In the melting experiments on MA43, plagioclase crystallized as the liquidus phase at all H_2O content (1$\sim$6 wt % H_2O), and anorthite content of the plagioclase increased from $\sim$An80 under nearly dry conditions to An$\geq$90 with $\geq$3 wt % H_2O in melt. In the melting experiments on MA44, plagioclase crystallized as the liquidus phase under low-H_2O ($\leq$2 wt %) conditions, but augite replaced plagioclase as the liquidus phase with more H_2O in melt. Anorthite content of plagioclase increased from about An70 under nearly dry conditions to An80 with $\sim$4 wt% H_2O in melt. Increases in anorthite content of plagioclase crystallized from the MA44 melt were suppressed compared with plagioclase crystallized from the MA43 melt. In short, Ca-rich plagioclase (An$\geq$90) can be crystallized from melts on the higher-Al/Si trend with $\geq$3 wt % H_2O, but cannot be crystallized from melts on the lower-Al/Si trend with any H_2O. Ca-poor rim ($\sim$An75) cannot be crystallized from melts on the higher-Al/Si trend, but can be crystallized from melts on the lower-Al/Si trend.

Summary: Geochemical variations in the liquids from the Izu-Oshima volcano are bracketed by two endmember trends, namely, the higher-Al/Si and the lower-Al/Si trends. Origins of the higher-Al/Si and the lower-Al/Si trends can be explained by crystallization differentiation under moderately hydrous conditions ($\sim$3 wt% H_2O) and almost dry conditions, respectively. We propose that polybaric crystallization of H_2O-saturated melts, at a depth range between the $\sim$4-km-deep magma chamber ($\sim$3 wt% H_2O) and near surface level (nearly dry) beneath the Izu-Oshima volcano, is a ubiquitous feature of island arc low-K tholeiite magmas.

Keywords: Island arc low-K tholeiite, Volcanic front, Ca-rich plagioclase, Izu-Oshima volcano

Japan Geoscience Union Meeting 2014
(28 April - 02 May 2014 at Pacifico YOKOHAMA, Kanagawa, Japan)

SVC54-06 Room:411 Time:May 1 11:00-11:15

The change time from magmatic to phreatomagmatic eruption, in the Hachodaira caldera eruption at Miyakejima Volcano

OIKAWA, Teruki[1*] ; GESHI, Nobuo[1]

[1]GSJ, AIST

The Miyakejima volcano formed the caldera in 2000. This volcano erupted Hachodaira Scoria and Hachodaira Ash at ca.3ka of Hachodaira caldera collapse. Many plant fossils (Miscanthus sp.) are recognized in Hachodaira Scoria and Ash. Based on plant fossils in these tephras occurrence, deposition late of soil in the Miyakejima volcano, and form of the boundary of Hachodaira Scoria and Ash, The change time from magmatic eruption (Hachodaira Scoria eruption) to phreatomagmatic eruption (Hachodaira Ash) is under 1 year, probably it is several days or less. Thus, there was no time gap almost between magma eruption and phreatomagmatic eruption. This eruption style change can be explained such as 2000 eruption (Geshi and Oikawa,2008:JVGR) as follows. The altitude of the summit part approached the sea level by caldera collapse; as a result, phreatomagmatic eruption occurred.

Keywords: volcano, caldera, Miyakejima, eruption, Miscanthus

Japan Geoscience Union Meeting 2014
(28 April - 02 May 2014 at Pacifico YOKOHAMA, Kanagawa, Japan)

SVC54-07 Room:411 Time:May 1 11:15-11:30

Pumice deposits of the pre-Ofunato stage distributed in northwest of the Miyake-jima volcano, northern Izu-Bonin Arc

NANRI, Shohei[1*] ; SUZUKI, Takehiko[2]

[1]Graduate student, Tokyo Metropolitan University, [2]Tokyo Metropolitan University

Miyake-jima Island, a volcanic island of the northern Izu-Bonin Arc, is located in the northwestern Pacific Ocean, approximately 180 km south of Tokyo. A pale-orange-tuff layer had been reported by Issiki (1960) on coastal cliff in the northwestern part of the island. The aim of this study is to clarify (i) distribution, (ii) stratigraphic position, (iii) sedimentary structure, (iv) petrological features, and (v) mineralogical features, for this pyroclastic deposit in more detail. The layer was re-defined as ”Miyake-jima Ofunato Pumice deposit: OFP”. The OFP is distributed from western to northern parts of the island. The OFP exists below the Aira-Tn tephra, erupted at 30 ka. The sedimental facies of OFP deposits suggest it formed as a pyroclastic flow deposit.

The relation between K_2O and FeO concentrations in the OFP is characterized by higher FeO wt.% and lower K_2O wt.%. Tsukui et al. (2006) and Saito & Miyairi (2008) showed that the chemical trends in the volcanic products of forearc of Izu-Bonin Arc such as Izu-Oshima and Hachijo-jima are characterized by high FeO wt.% and low K_2O wt.%, and those of the backarc Izu-Bonin Arc such as Nii-jima and Kozu-shima shows low FeO wt.% and high K_2O wt.%. Consequently, chemistry of the OFP suggests that it was originated from forearc of Izu-Bonin Arc.

This paper concludes that the activities of the Miyake-jima volcano around 30 ka are characterized by a production of pumice by the eruption at the northwestern part of the present island. The current stage of this study, it is not possible to discuss the source vent of the OFP in detail and specify the type of the volcanic eruption produced the OFP. In future, we attempt to find a clue to account for these two problems by the detailed study on the OFP with referring to its faces like a pyroclastic flow deposits.

Keywords: Miyake-jima volcano, Pumice, Miyake-jima Ofunato Pumice deposit, Northern Izu-Bonin Arc

Japan Geoscience Union Meeting 2014
(28 April - 02 May 2014 at Pacifico YOKOHAMA, Kanagawa, Japan)

SVC54-08 Room:411 Time:May 1 11:30-11:45

Formation process of a volcanic island during the 2013-2014 eruption at Nishinoshima, Ogasawara, Japan

MAENO, Fukashi[1*] ; NAKADA, Setsuya[1] ; KANEKO, Takayuki[1]

[1]Earthquake Research Institute, Univ. Tokyo

New volcanic islets created by submarine eruptions are often observed around Japanese Islands. However, in most cases, such new islets are disappeared by wave erosion in short periods. To make a new volcanic island remaining for a long time, an amount of lava flows must occur and reclaim land from the sea. However, such relatively large-scale lava eruptions rarely occur. Therefore, the very initial stage of the formation process of a volcanic island has been poorly understood.

The submarine eruption off Nishinoshima, Ogasawara, has created a new volcanic islet since Nov 2013. The lava flow eruption continues for more than a few months, and the islet keeps growing. This eruption will give an opportunity to understand the birth and growth of a new volcanic islet. We studied variation of eruptive styles and sequences of this 2013-2014 eruption at Nishinoshima based on airborne observations and publicized aerial and satellite images (taken by JCG, GSI, and JAXA).

Nishinoshima forms a part of summit crater rim of a huge submarine volcano. The 2013-2014 eruption occurred inside the summit crater about 400 m off Nishinoshima with a depth of dozens of meters. In the first stage, Surtseyan eruptions repeated due to seawater entering a main crater of an islet. With the growth of the islet, the main crater was dried up and the eruption style changed to Strombolian with a scoria cone formation and lava flows that continuously effuse from the main crater over a few months. Lava flow front is brecciated by rapid cooling, or auto-brecciated, and eventually reclaimed the foreshore from the sea. The lava flows are then branched many times and extended to almost all directions. The continuous activity of Strombolian with lava flows suggests that magma is stably supplied from the deeper part of conduit.

Based on the change of outline of the islet and bathymetry data before the eruption, volume and discharge rate of lava flows are estimated. For the first 2.5 months by early Feb 2014, the volume of lava flow is estimated at about 6 M m^3. The discharge rate is estimated at 0.5-1$*10^5$ m^3/day with some fluctuations. This discharge rate is almost the same as that estimated for lava effusion in the 1934-1935 eruption at Showa Iwojima, southern Kyushu (1$*10^5$ m^3/day; Maeno and Taniguchi, 2006), which is one of the youngest remained volcanic islands in Japan. The volume of the 2013-2014 eruption is so far 1/4 of the total volume (24 M m^3) of the last 1973-1974 eruption, in which the volume of the last eruption was estimated based on bathymetry change before and after the eruption. The eruptive sequence and growth rate of the islet in 2013-2014 is different from the last eruption. This is probably because the eruption began at shallower depth than the last eruption. At the time of early Feb 2014, erosion signatures on lava flows are little, so that the new island is expected to further grow.

Keywords: Nishinoshima, volcanic island, lava flow, Surtseyan eruption, Strombolian eruption

Japan Geoscience Union Meeting 2014
(28 April - 02 May 2014 at Pacifico YOKOHAMA, Kanagawa, Japan)

SVC54-09 Room:411 Time:May 1 11:45-12:00

Petrological characteristics of volcanic materials ejected during 2012-2013 explosive events on Ioto Island

IKEHATA, Kei[1*] ; TAMURA, Tomoya[2]

[1]Faculty of Life and Environmental Science, University of Tsukuba, [2]Graduate School of Life and Environmental Sciences, University of Tsukuba

Ioto is an active volcanic island (8.5km long in NE-SW and 4.5km wide) located about 1250km south of central Tokyo. Since early February 2012, small explosive eruptions have repeatedly occurred at the Old Crater (Million Dollar Hole) in the western part of the island (JMA, 2013). Four (February 2012, March 2012, February 2013 and April 2013) ejected mud materials collected in the vicinity of the crater consist of free crystals (plagioclase, clinopyroxene, olivine, and Fe-Ti oxides), relatively fresh volcanic glass, altered volcanic glass, lithic fragment, altered lithic fragment and pyrite aggregate (Ikehata and Tamura, 2013). Among the mud samples, there is little difference in component of grains except for high abundance of altered lithic fragment in the mud ejected in February 2012.

Detailed SEM/BSE image observation of the relatively fresh volcanic glasses show that even these fresh glasses have pitted alteration and hydration features. The extent of hydration could be different among volcanic glass shards in geothermal field like Ioto because hydration rate depends on chemical compositions of volcanic glasses and groundwater, and soil temperature. To eliminate such hydration effects, heating (400 ℃-12h) is conducted for the relatively fresh volcanic glasses before analyzing. As a result of the chemical analysis, all of these volcanic glasses are trachytic, and their chemical compositions are homogeneous within the analytical error. In conclusion, no juvenile materials existed in the mud samples, suggesting these explosive events were not phreatomagmatic but phreatic eruption.

We would like to thank members of JMSDF Ioto Air Base weather team for sampling around the Old Crater and providing information on the studied area. Ministry of Defense, JMA and NIED are also thanked for their cooperation.

Keywords: Ioto Island, the Old Crater, mud, volcanic glass, phreatic eruption

Japan Geoscience Union Meeting 2014
(28 April - 02 May 2014 at Pacifico YOKOHAMA, Kanagawa, Japan)

SVC54-10 Room:411 Time:May 1 12:00-12:15

Compositions of minerals in volcanic products from pre- and the early stage of Aso-4 large-scale pyroclastic flow

KUROKAWA, Kiyoshi[1] ; YAMASAKI, Hideto[1] ; HASENAKA, Toshiaki[1*] ; MORI, Yasushi[2]

[1]Grad School Sci. & Tech., Kumamoto Univ., [2]Kitakyushu Museum of Natural and Human History

Formation of Omine scoria cone, Takayubaru lava flow, and Oyatsu pumice flow are a series of volcanic events just before and after the large-scale Aso-4 pyroclastic eruption. Compositions of volcanic products change from 62-66 SiO_2 wt.% for Omine scoria, 63-66 SiO_2 wt.% for Takayubaru lava, to 67-69 SiO_2 wt.% for Oyatsu pumice. The difference between Omine-Takayubaru compositional trend and Oyatsu trend is small but evident (Yamasaki et al., 2013). Common phenocrsyt assemblage is plagioclase, orthopyroxene, clinopyroxene, and opaque minerals. In addition, Omine scoria and Takayubaru lava contain hornblende microphenocrysts, whereas Oyatsu pumice contains phenocrysts of hornblende. Most plagioclase characteristically shows sieve texture among Omine-Takayubaru samples. Such texture is not so common among Oyatsu pumice samples. We analyzed these minerals using EPMA in order to characterize the change in magma supply system that lead to large-scale pyroclastic eruption.

In response to different compositional trends observed between Omine-Takayubaru and Oyatsu samples, different mineral compositions are also found. Plagioclase phenocrysts in Omine-Takayubaru samples are An50-An60 with uni-mordal peak, where as those in Oyatsu samples are An37-An56 with three peaks. Slight difference in Mg# are also found between orthopyroxene, clinopyroxene, and hornblende of Omine-Takayubaru and those of Oyatsu samples.

Estimated temperature for Omine scoria using Wells (1977) pyroxene thermometer is 950 ℃, and dry viscosity is 10^5.6 Pa • s. That for Tamaraigawa lava (SiO_2=61 wt.%) extruded before Aso-2 pyroclastic eruption was reported as 1120 ℃ and 10^3.9 Pa • s, respectively, by Kobayashi (2013). The difference in viscosity is reflected by different aspect ratio, i.e. 100 m thick and 7 km long for Takayubaru lava flow, and 10 m thick and 10 km long for Tamaraigawa lava flow.

Sieve texture and microphenocrysts in Omine scoria and Takayubaru lava make an important restriction for making models of magma supply system before and after the large-scale pyroclastic eruption. If sieve texture suggests melting process of plagioclase, it indicates temperature ascent and/or water vapor pressure increase. In contrast, growth of hornblende microphenocryst suggests temperature drop and/or water vapor pressure increase. Omine-Takayubaru samples do not contain mafic inclusions and mafic minerals with reverse zoning, thus possibility of magma mixing and temperature ascent is small. The change in physicochemical condition in Aso-4 magma supply system is yet to be solved.

Keywords: Aso-4 pyroclastic flow, Takayubaru lava, Omine volcano, lava flow

Japan Geoscience Union Meeting 2014
(28 April - 02 May 2014 at Pacifico YOKOHAMA, Kanagawa, Japan)

SVC54-11 Room:411 Time:May 1 12:15-12:30

Forming process of Minamidake stratovolcano, Sakurajima, inferred from paleomagnetic age and volume of lava flows

MIKI, Daisuke[1*]

[1]DPRI, yoto University

A paleomagnetic measurement was carried out on the Arimura lava, which consists uppermost part of the main body of Minamidake stratovolcano, Sakurajima volcano, Kyushu, Japan. A mean paleomagnetic direction, D=4.0 ^{o} E I=40.5 ^{o} down, was obtained from the Arimura lava. By comparison between measured paleomagnetic direction and the paleo-secularvariation of geomagnetic field, the age of the Arimura lava was estimated as about 3.1-2.7 ka, moreover the age of the Kannonzaki lava lying beneath the Arimura lava, was thought as about 3 ka. These two lavas are considerable to be formed by a sequence of intermittent eruption during several hundred years at around 3 ka. The volumes of individual lava that extruded in recent 4,000 years were estimated. The main body of Minamidake stratovolcano had grown rapidly at around 3 ka, since estimated lava volume. The volume of the Nagasakihana lava erupted in 764-766 AD was estimated as about 0.8km^{3}. The scale of 764-766 AD eruption may be greater than previously thought. The long?term magma effusion rate during historic time, particularly recent 240 years, was estimated as larger than earlier.

Japan Geoscience Union Meeting 2014
(28 April - 02 May 2014 at Pacifico YOKOHAMA, Kanagawa, Japan)

SVC54-P01 Room:Poster Time:May 1 18:15-19:30

Morphology of microlite -projections of plagioclase microlite-

SANO, Kyohei[1*] ; TORAMARU, Atsushi[2] ; WADA, Keiji[3]

[1]Department of Earth and Planetary Sciences, Graduate School of Sciences, Kyushu University, [2]Department of Earth and Planetary Sciences, Faculty of Sciences, Kyushu University, [3]Hokkaido University of Education at Asahikawa

At Tokachi-Ishizawa (TI) rhyolite lava, Shirataki, Hokkaido, northern part of Japan, the interior structure transition can be observed, from the outer obsidian layer to the inner rhyolite layer. Thus TI lava is an appropriate target field for correlating textural characteristics with lava interior structure. In order to obtain insights into the magma ascent and outgassing process of viscous magma, we have analyzed oxide microlites of TI rhyolite lava, suggesting that dominant outgassing process is ductile permeable development (Sano et al.,2013 JpGU meeting). However, we have not examined the morphology of microlite. Morphology of crystal is considered to reflect the effective undercooling of the melt and provide the constraint for ascent process and water exsolution processes. In this study, we focused on the morphology of microlites, especially projections of plagioclase microlites. The projections mean localized growth of crystal from plagioclase surface.

In Shirataki, aphyric rhyolite lavas erupted ca. 2.2Ma and composed of 10 flow units. The TI lava is about 50 m in height and stratigraphic sequences from the bottom are a obsidian layer region, a boundary bounded region of obsidian and rhyolite, and rhyolite layer region. The obsidian layer region consists of a single vesicle-free obsidian about 7 m high. The rhyolite layer region consists of rhyolite layers with variable vesicularity, crystallinity and characteristic scales in layer thickness. The boundary banded region, which is located between the obsidian and rhyolite regions, consists of thin obsidian ($<$10mm in width) and rhyolite. In this study, we define the obsidian and rhyolite based on the differences in appearance of hand specimens and rock texture. Rhyolite has perlitic cracks in the glass and contains some amounts of crystalline materials, namely, spherulite and lithophysae. In boundary banded region, the fraction of obsidian decreases toward rhyolite layer region.

From the examination by scanning electron microscope (SEM) for thin sections from obsidian layer region, boundary banded region and rhyolite layer region, we found the projection texture in all samples. We measured projection length and number density (Nv) of plagioclase microlites for obsidian and rhyolite layer regions. The measurement results show that plagioclase microlites in obsidian and rhyolite layer regions indicate the similar number density. Nv for obsidian layer region is 1.8×10^{11} — 3.5×10^{11} [/m^3] and 8.2×10^{10} — 3.0×10^{11} [/m^3] for rhyolite layer region, respectively. However, the length of projection is remarkably different between two regions. The mean values are 2.3 μm in obsidian layer region, and 8.7 μm in rhyolite layer region. The transition of mean length can be observed in boundary layer region.

Since the difference of projection length reflects the growth rate (G [m/s]) and growth time (t [s]) according to the theory of crystal growth (Keith and Padden, 1963; Lofgren, 1971; Rao, 2002), we can estimate the degree of effective undercooling at the formation time of projections. Under the assumption that G is constant for the time, the length of projection can be given by Gdt. Assuming the constant growth rate and growth time, the difference in projection lengths indicate that in growth rate, namely, the undercooling. Using experimental values for growth rate and undercooling, it is found that the rhyolite layer region experiences higher undercooling than obsidian layer region by 30 — 70 K. The projection can be formed after the nucleation of plagioclase microlite, which indicate the similar number density in obsidian and rhyolite layer region. Thus projections reflect the different undercooling after the nucleation of microlites. Based on the quantitative analysis of crystal morphology of microlites, we can obtain the insights into the magma ascent process that rhyolite layer region experienced higher undercooling than obsidian layer region.

Keywords: textural analysis, obsidian, rhyolite, lava, Shirataki

Japan Geoscience Union Meeting 2014
(28 April - 02 May 2014 at Pacifico YOKOHAMA, Kanagawa, Japan)

SVC54-P02 Room:Poster Time:May 1 18:15-19:30

Differentiation process of arc magmas revealed by principal component analysis on trace element composition

UEKI, Kenta[1*]

[1]Volcanic Fluid Research Center, Tokyo Institute of Technology

Chemical composition of magma can be used to address state of the magmatic system and the processes during magma generation, ascendent and eruption. Various processes from the mantle to the crust in various pressure, temperature and chemical composition modify magma composition. Consequently, bulk chemical composition of erupted magma represents a sum of these processes.

Differentiation in terms of major element composition is controlled by non-linear thermodynamic relation. Major element composition of magma is modified by temperature, pressure and H2O content dependent saturation states of mineral phases, and partition between melt phase and mineral phases. In this sense, major element composition can be a proxy of physical state during magma generation and ascendent. However, the non-linarlity of major element processes and a small degree of freedom in compositional space prevent us from decomposition of processes that have derived compositional variation in terms of major element.

On the other hand, partition of trace elements between melt and mineral phase can be modeled with relatively simple equation, and can be considered as a linear process. Consequently, trace element composition of erupted magma represents a simple sum of a melting and differentiation processes. Trace element can be a tracer of the specific phase or reaction, because partition coefficients between various minerals melt show wide range of variation. Therefore, trace element can be used as a proxy of a specific chemical mass reaction process during magma generation and ascendent. In addition, trace element composition shows a large degree of freedom. Therefore, it is expected that nature and the number of processes during magma generation and ascendent can be decomposed by analyzing trace element composition of volcanic rock using multivariate statistics.

In this study, principal component analysis is used to analyze compositional variation of volcanic rocks in Northeastern Japan Arc.

Analysis based on a series of volcanic rocks from single volcanic activity has shown that the differentiation process and/or mantle melting process beneath each volcano (crystal fractionation and magma mixing) can be decomposed by using principal component analysis on trace element compositions. Consistent relationship between the trace element principal components, major element composition, and petrological information such as mineral composition is derived from the analysis.

In order to illustrate the differentiation process in terms of large scale spatial and compositional range, 262 samples from 17 different volcanoes in the Sengan region, northeastern Japan are analyzed with principal component analysis. Result of the analysis clearly demonstrates that differentiation processes in the arc crust, are the primary controlling factor to derive compositional variation of arc magmas. Only three principal components account for the compositional variation of 262 samples. It is estimated the three principal components represent magma mixing, relatively high pressure olivine fractionation, and relatively shallower pressure plagioclase differentiation, respectively. No strong mantle signature is identified by the analysis. This result shows intermediate-felsic magmas (SiO2>60 wt. %) can only be derived through magma mixing, not by crystal fractionation.

Keywords: volcanic rock, arc magma, crystal fractionation, magma mixing, trace element

Japan Geoscience Union Meeting 2014
(28 April - 02 May 2014 at Pacifico YOKOHAMA, Kanagawa, Japan)

SVC54-P03 Room:Poster Time:May 1 18:15-19:30

A preliminary estimation of water content of the mantle beneath Changbaishan Volcano, northeast China

KURITANI, Takeshi[1*] ; OKUMURA, Satoshi[2] ; YOKOYAMA, Tetsuya[3] ; ITO, Yoshinori[2] ; NAKAMURA, Michihiko[2] ; WEI, Haiquan[4]

[1]Osaka City University, [2]Tohoku University, [3]Tokyo Institute of Technology, [4]China Earthquake Administration

In northeast China, Cenozoic intraplate volcanic products are widely distributed. Geophysical studies have suggested that the underlying mantle transition zone is remarkably hydrous (Kelbert et al., 2009) and contains remnants of the subducted Pacific slab (Fukao et al., 1992); therefore, the Pacific slab stagnation and its relation to observed magmatism has received growing attention (e.g., Ohtani and Zhao, 2009; Richard and Iwamori, 2010). Beneath the Changbaishan volcanic field, a prominent low-velocity anomaly with a plume-like shape has been imaged in the upper mantle by P-wave tomography, which is suggestive of an upwelling of a mantle plume from the mantle transition zone (e.g., Zhao et al., 2009). In this study, to characterize the nature of the transition zone-derived mantle plume, the water content of the source mantle is estimated for basaltic products from the Changbaishan volcano.

Basaltic scoria samples were collected from a cinder cone, located about 20 km to the northeast of Tianchi volcano. One scoria sample was used for preliminary analysis of glass inclusions in some plagioclase phenocrysts. Basaltic lavas, which occur with abundant mantle xenoliths, were also collected from the outcrop near the cinder cone to know the primitive magma composition at the volcano. The MgO contents of the scoria and the lava are 5.1 wt.% and 9.1 wt.%, respectively. Major element compositions of quenched glass inclusions in the scoria sample were analyzed using EPMA, and the water contents were estimated by the difference of the analytical total of the major element analysis from 100 wt.%. Through calibration using an in-house standard glass sample of known water content, the water contents of the glass inclusions were obtained to be 0.15-3.4 wt.%. The FT-IR analysis was also performed for one glass inclusion of the estimated water content of 0.15 wt.% by EPMA, which yields the total water content of 0.2 wt.%.

Given that 3.4 wt.% represents the original water content of the melt without leakage, the H_2O/K_2O ratio of the melt of 0.90 is obtained. If we assume that the H_2O/K_2O ratio of the melt was not affected significantly by magmatic processes and the ratio is essentially constant in basaltic magmas at Changbaishan volcano, the water content of the primitive magma (2.4 wt.% in K_2O) is estimated to be 2.2 wt.%. The source mantle for the Changbaishan basalts may contain ˜0.5% sediment component (Kuritani et al., 2011), and the Ce content of the source mantle is estimated to be ˜1.1 ppm using the Ce content of the sediment component of 57.3 ppm (Plank and Langmuir, 1998) and that of the depleted mantle of 0.77 ppm (Salters and Stracke, 2004). If we assume that Ce and H_2O behave similarly during mantle melting (e.g., Michael, 1995), the compositions of the primitive basalt lava (Ce: 70 ppm, H_2O: 2.2 wt.%) yield the water content of the source mantle of ˜350 ppm. This estimated water content is significantly higher than that of the normal depleted mantle (˜120 ppm; Salters and Stracke, 2004), suggesting that the transition zone-derived mantle plume is hydrous compared with the surrounding ambient upper mantle.

In this preliminary study, we have analyzed only seven glass inclusions in a single sample, and therefore, the water content of ˜350 ppm may represent the minimum estimate. It is necessary to increase the number of data by EPMA and FT-IR analyses to more reliably estimate the source water content for the Changbaishan basalts.

Keywords: mantle, water content, China

Japan Geoscience Union Meeting 2014
(28 April - 02 May 2014 at Pacifico YOKOHAMA, Kanagawa, Japan)

SVC54-P04 Room:Poster Time:May 1 18:15-19:30

Petrological and geochemical variations within an off-axial submarine large lava flow from the Oman Ophiolite

OTSUKA, Ryo[1*] ; KUSANO, Yuki[1] ; KANAYAMA, Kyoko[1] ; UMINO, Susumu[1]

[1]Department of Earth Sciences, Kanazawa University

Large submarine lava with thicknesses >100 m and volumes exceeding a few cubic kilometers are not uncommon volcanic constructs of mid-ocean ridges and around Hawaii Islands, yet details of the physical processes of eruption of these large lava flows are poorly understood. The V3 flow of the Oman ophiolite extruded at 90 Ma far off the paleospreading axis as thick lava flows with a minimum areal extent of >11 km by 1.5 km and the maximum thickness >270 m, yielding a minimum estimated volume >1.2 cubic kilometers. The V3 flow was fed by a thick feeder dike in the SW of the flow field and buried off-axial fault-bounded basins with a thick sedimentary cover in ˜40 days. The upper V3 flow field consists of compound lobes that merge upstream into larger and thicker sheet-like lava, which grew endogenously as a vast sheet lobe.

Low-T hydrothermal alteration and weathering slightly modified the bulk compositions as indicated by moderate albitization of plagioclase and partial replacement of titanomagnetite and clinopyroxene by titanite and chlorite, respectively. However, strong positive correlations among incompatible HFSEs and REEs and relatively good correlations with major elements besides LILEs and Pb show that these elements were less mobile and preserve primary characteristics. FeO and TiO2 show moderate increases with a decrease in MgO from 8 to 5 wt%, and then decreases with the decrease in MgO down to 4 wt%. 20-50 times enrichment in Th and depleted HREEs compared to primitive mantle of the V3 flow is similar to differentiated EMORBs.

Whole-rock major and trace element variations through a vertical transect at 8.7 km (T-21) from the feeder dike show fractional crystallization of clinopyroxene and plagioclase, the major phases in the groundmass of the lava, at a pressure of the paleowater depth. The stratigraphic variations show a notable enrichment in MgO and depletion in incompatible elements in the lowermost core, consistent with accumulation of olivine phenocrysts. Enrichment in incompatible elements in the uppermost core of the flow is in accordance with the model that the last solidified, residual melt resided in this horizon.

By contrast, samples collected from the basal crust every 0.5-1 km from the feeder dike, and vertical transects at 6.7 km (T-14) from the dike have whole-rock compositions spread over compositional spaces that could be explained by internal mixing of variably differentiated magmas. Interestingly, incompatible elements like Yb and Ti of the basal crust show increases downflow to ˜5 km from the feeder dike and decreases further downflow. Because the basal crust is the quenched lava that came to rest first at that place, samples farther away from the feeder were extruded and emplaced later in the eruptive event. The downflow variations show extrusion of differentiated lava in the middle stage of the eruption and less differentiated lava in early and late stages. Meanwhile, the transect at T-14 is differentiated in the upper and lower crust and less differentiated in the core.

These intraflow variations in the bulk geochemistry indicate supply of less differentiated magma in an early stage of the eruption, which was progressively replaced by mixed magmas of variably differentiated and less differentiated ones toward the end of the eruption. The eruptive sequence of less differentiated to differentiated magmas with increasing FeO suggests extrusion from a density stratified magma chamber with less dense and Mg-rich magma underlain by more dense Fe-rich magma. The internal mixing among variably differentiated magmas with the progress of the eruption and the extrusion of less differentiated magma toward the end of the eruption suggest a renewal of magma toward the end of the eruption caused mixing of newly supplied less differentiated magma with the differentiated magma within the conduit and the lava tubes.

Keywords: Oman Ophiolite, obduction, V3, Large Lava Flow, chemical variation geochemistry

Japan Geoscience Union Meeting 2014
(28 April - 02 May 2014 at Pacifico YOKOHAMA, Kanagawa, Japan)

SVC54-P05 Room:Poster Time:May 1 18:15-19:30

Factors governing fragmentation of submarine lava - mechanism of hyaloclastite formation

UMEZAWA, Yumi[1*] ; UMINO, Susumu[1] ; KUSANO, Yuki[1] ; KANAYAMA, Kyoko[1] ; KITAMURA, Keitaro[1]

[1]Department of Earth Sciences, Kanazawa University

Hyaloclastite is water-lain volcanic breccia embedded in a matrix of glassy clasts by fragmentation of brittle lava under thermal stress. Fluidal basalt lava tends to form coherent flows like pillow lava and sheet flows. In contrast, viscous lava such as andesite and dacite is more likely to form hyaloclastite. This preference of hyaloclastite on lava composition indicates that mechanical response of solidified lava under stress is strongly dependent on composition. Fracturing of lava occurs when the rate of stress accumulation exceeds the rate of stress relaxation and ultimately reaches the mechanical strength of the lava. The rate of stress relaxation decreases with the increase in lava viscosity. Therefore, hyaloclastite is more common in viscous silicic lava.

However, the occurrences of pillow lava of dacite and rhyolite are known from the Ogasawara Islands, Unalaska Island, Oman Ophiolite, etc. Pillow lava is commonly associated with hyaloclastite of the same compositions. These examples demonstrate that factors other than lava composition determines fragmentation of lava. Then, the problem arises what are the governing factors that control the mechanical response of lava under stress. We will address these issues through comparative study on glass, quenched melt, of pillow lava and hyaloclastite of variable compositions spanning from basaltic andesite to rhyolite from the Eocene submarine volcanic strata in Chichijima, Ogasawara Islands.

Samples of glass from these sites were analyzed by EPMA for major elements and by SIMS for water contents. Eruption temperatures were estimated by clinopyroxene-liquid geothermometer of Putirka (2008). Crystal number densities of groundmass plagioclase and clinopyroxene were determined on COMPO images and modal abundance of constituent minerals were determined on element distribution maps of EPMA. Bulk viscosity of lava was estimated by the methods of Giordano et al. (2008) and Pinkerton and Stevenson (1992).

Dacite has phenocrysts of clinopyroxene, orthopyroxene, plagioclase and magnetite. Groundmass consists of clinopyroxene and plagioclase microlites and magnetite set in glass. In dacite glass, there is little difference in melt composition, eruption temperature, crystal number density between pillow lava and hyaloclastite. However, lower water content in hyaloclastite glass than in pillow margin glass yields higher bulk viscosity.

Andesite has phenocrysts of clinopyroxene, orthopyroxene, plagioclase and magnetite. Groundmass consists of clinopyroxene and plagioclase microlites and magnetite set in glass. Clinoenstatite xenocrysts enclosed by orthopyroxene rim are occasionally present. Hyaloclastite is higher in crystal number density and mode of groundmass plagioclase than associated pillow lava. Hyaloclastite glass is lower in Al2O3 than associated pillow glass, consistent with preferential crystallization of plagioclase. However, the cpx-saturated melt temperatures show little difference between pillow lava and hyaloclastite. Bulk viscosity estimated for the lava to become hyaloclastite is higher than the lava that formed pillows because of the larger crystal number density in hyaloclastite.

The above observations on dacite glass clearly indicate that water played an essential role in formation of hyaloclastite. Degassing either within the conduit or during flowage through lava tubes raised the bulk viscosity of lava and stress relaxation time, resulted in fragmentation of lava to form hyaloclastite. Although water content was not determined for andesite glass, higher crystal number density and modal amount of plagioclase in hyaloclastite with the same temperature as the coexisting pillow lava can be explained by volatile loss which raised the liquidus of plagioclase and its preferential crystallization, resulted in higher bulk viscosity and fragmentation of lava.

Keywords: hyaloclatite, the Bonin Islands Chichijima, viscosity, submarine lava

Japan Geoscience Union Meeting 2014
(28 April - 02 May 2014 at Pacifico YOKOHAMA, Kanagawa, Japan)

SVC54-P06 Room:Poster Time:May 1 18:15-19:30

Eruption history and petrography of Akanfuji in the Me-akan volcano, eastern Hokkaido, Japan

SATO, Eiichi[1*] ; WADA, Keiji[2]

[1]Institute for Promotion of Higher Education, Kobe University, [2]Hokkaido University of Education at Asahikawa

Me-akan volcano is located in the Akan volcanic field, eastern Hokkaido, and ˜250 km inland from the Kuril trench. The volcanic activity of Me-akan volcano began at least a few tens thousand years ago, and eight volcanic bodies with different peaks have been formed.

Akanfuji (1476 m), which is the newest volcanic body in the Me-akan volcano, started its eruptions about 2.5 ka, and the volcanic activity continued for 1,500 years. The eruption products of Akanfuji are composed of scoria fall deposits and lava flows. The scoria fall deposits are distributed from northeast to south from present vent. We described the scoria fall deposits to interpret the complex depositional sequence. As a result, 17 scoria fall layers were recognized for 1,500 years.

Akanfuji had erupted basalts through its history. Two types of basalts (types I and II) are recognized on the basis of phenocrysts assemblage. Type I is orthopyroxene (opx) bearing olivine (ol)-crynopyroxene (cpx) basalt and Type II is cpx bearing ol-opx basalt. They were formed by mixing between different types of basaltic magmas on the basis of the textural and mineralogical evidences.

Keywords: Me-akan volcano, Akanfuji, Eruption history, basalt, magma mixing

Japan Geoscience Union Meeting 2014
(28 April - 02 May 2014 at Pacifico YOKOHAMA, Kanagawa, Japan)

SVC54-P07 Room:Poster Time:May 1 18:15-19:30

Evidence of eruption episodes before AD1741 of Oshima-Oshima Volcano, Hokkaido, Japan

YOSHIMOTO, Mitsuhiro[1*] ; NAKAMURA, Yugo[1] ; FUKUHARA, Genta[2] ; NISHIMURA, Yuichi[1]

[1]Faculty of Science, Hokkaido University, [2]Faculty of Science, Hokkaido University

We newly identified two eruption episodes of Oshima-oshima volcano below eruption products of the AD 1741 eruption at an outcrop on the summit of the volcano. The upper eruption product consists of alternating volcanic lapilli fall and ash fall deposits, and the lower one consists of scoria fall deposits. Tephra from those eruptions have not found in the other area including southern Hokkaido. We also identified two thin tephra layers between three eruption products of Oshima-oshima volcano with intercalating soil layers. They are correlating with well-known wide spread tephras such as Ko-d (AD 1640) from Hokkaido-Komagatake Volcano and B-Tm (ca. AD 940) from Changbaishan Volcano, China-North Korea, based on chemistry of volcanic glass shards. Considering the thickness of soil layers, those eruption episodes would occur at around AD 1450 and BC 600. It suggests that Oshima-Oshima volcano erupted at least 4 times in last 2500 years including 2 historical eruptions in AD 1741-1742 and 1759.

This work was supported by JSPS Grant-in-Aid for Scientific Research C, Grant Number 24540447.

Keywords: Oshima-oshima, eruption history, tephra

Japan Geoscience Union Meeting 2014
(28 April - 02 May 2014 at Pacifico YOKOHAMA, Kanagawa, Japan)

SVC54-P08 Room:Poster Time:May 1 18:15-19:30

Compositional variation and magmatic differentiation at the northern Kita-Hakkoda volcanic group

KOMATSU, Sho[1*] ; OHBA, Tsukasa[1]

[1]Akita Univ.

Since 0.6 Ma, magmatic eruptions have occurred several times at Kita-Hakkoda volcanic group. This study focuses on the activity between 0.4 and 0.2 Ma. Magmatic differentiation process is investigated from whole-rock chemistry and mineralogy along with stratigraphy. This area consists of 12 geologic layers: Hakkoda 2nd Stage Pyroclastic Flow Deposit, Northern Kita-Hakkoda Basaltic Andesite Lavas, Lower Kansuisawa Pumice Flow Deposit, Lower Tamoyachi-dake Andesite Lavas, Upper Kansuisawa Pumice Flow deposit, the Upper Tamoyachi-dake Andesite Lavas, the Tashirotai Lacutrine Deposit, Narusawa Debris Flow Deposit, Maedake Lavas, Narusawa-daichi Andesite Lavas, Okuzuresawa Debris Flow Deposit and Okuzuresawa Pyroclasitic Flow deposit in stratigraphic order. Temporal variation of chemical composition in stratigraphic order is evaluated. The activity initiated with the effusion of differentiated tholeiitic basaltic magma around 0.4 Ma. After a dormancy the activity resumed around 0.2 Ma with effusion of andesitic magma (60wt% SiO_2), followed by a fluctuating activity between tholeiitic basalt and low-silica calc-alkaline andesite magmas. Then, the magma composition jumped to high silica (60wt% SiO_2) calc-alkaline andesite. No evidence for open system process is recorded in phenocrysts in the tholeiitic rocks. Previous studies accounted for the chemical variation of tholeiitic magma by crystallization differentiation, and our new data is consistent with the model. Disequilibrium mineral assemblages in calc-alkaline rocks, e.g., coexistences of magnesian olivine and embayed quartz, and of reversely zoned pyroxenes and normally zoned pyroxenes, implies open system processes. As indicated by linear trends between tholeiitic basalt and the high-silica andesite, magma mixing is a plausible process to produce the series. Stratigraphic chemical variation might be caused by temporal variation in mixing ratios.

Keywords: Magma mixing

Japan Geoscience Union Meeting 2014
(28 April - 02 May 2014 at Pacifico YOKOHAMA, Kanagawa, Japan)

SVC54-P09 Room:Poster Time:May 1 18:15-19:30

The volcanic history and geological structure of Sanzugawa Caldera, Yuzawa, Akita prefecture

OKI, Fumiya[1*] ; OHBA, Tsukasa[1]

[1]Akita Univ.

Sanzugawa caldera, located in the southern part of Akita prefecture, was formed by collapses after eruptions of voluminous ash flows about >ca. 1 Ma. Torageyama Formation, deposited during the caldera formation, thickly infills the caldera depression. The Formation is divided into two members: Torageyama tuff member and Minasegawa tuff member. Torageyama tuff member consists of welded tuff, lapilli tuff, and alternation of tuffaceous sandstone, mudstone, and conglomerate. Thickness of Torageyama tuff member is approximatly 900m. Minasegawa tuff member consists of lapilli tuff, tuff and conglomerate. Thickness of Minasegawa tuff member is about 450m. In this study, on the basis of lithology, Torageyama Formation is divided into 10 layers, including pyroclastic density current deposits (PDC-1 to PDC-8), a debris flow deposit (DF-1) and a lacustrine deposit (LD-1). Stratigraphic order from the bottom is PDC-1, DF-1, LD-1 and PDC-2 to PDC-8. Approximate thicknesses of the layers are 20m, 80m, 140m, 50m, 250m, 200m, 340m, 160m, 90m and 30m, respectively. Pyroclastic density current deposits consist of massive lapilli tuff. The lapilli tuff contains pumice clasts and lithics, and minor amount of wood pieces. Bases of PDC-4 and PDC-6 consist of ground surge deposits. Low-angle cross-laminar and dunes are developed in the ground surge deposits. The ground surge deposit of PDC-6 is further underlied by a ground breccia layer. The ground breccia layer consists of matrix-supported conglomerate, containing lithics with a maximum grain-size of 2.5 m. Lapilli tuff of PDC-1, 3, 4, 8 include welded parts, developing degassing pipes and columnar joints. Welded parts often contain spherulites and exhibit eutaxitic texture. Debris flow deposit (DF-1) consists of clast-supported conglomerate with rounded clasts. The clasts are directed parallel to the bedding plane, showing coarse-tail reverse grading. Lacustrine deposit (LD-1) consists of alternation of tuffaceous sandstone, mudstone, and conglomerate. In mudstone, laminar is well developed. Laminar and bedding are well developed in tuffaceous sandstone. Conglomerate is massive. PDC-2 overlying the lacustrine deposit (LD-1) shows sedimentary structures that imply subaqueous setting. Pyroclastic density current occurred more than eight times, suggested by the number of pyroclastic density current layers. The source of PDC-4 is Takinohara vent, determined from paleocurrent estimated with dunes of a ground surge deposit. Presence of a lacustrine deposit (LD-1) in the middle of the Formation implies that caldera collapsed two times. Half-concentric distribution of strike surrounds Mt. Ishigami and their dips incline outward of the caldera. This structure implies a resurgent dome. This resurgent dome resulted in uplift of Oyasudake area where the center of the caldera. Presence of resurgent dome, thick pyroclastic density current deposits and ring fractures suggests that Sanzugawa caldera is classified as a Valles type caldera.

Keywords: Sanzugawa caldera, Torageyama Formation, Pyroclastic density current deposit, Resurgent dome

Japan Geoscience Union Meeting 2014
(28 April - 02 May 2014 at Pacifico YOKOHAMA, Kanagawa, Japan)

SVC54-P10 Room:Poster Time:May 1 18:15-19:30

Stratigraphy and chemical compositions of eruption products in Umanose agglutinate activity, Zao volcano

KAWANO, Gen[1*] ; BAN, Masao[2] ; OIKAWA, Teruki[3]

[1]Graduate School of Science and Engineering, Yamagata University, [2]Faculty of Science, Yamagata University, [3]Geological Survey of Japan/ AIST

The newest stage of the Zao volcano, central part of NE Japan, began at about 30 ka and the activity has continued to present. The Zao newest stage eruption products are classified into Komakusadaira agglutinate, Umanose agglutinate and Goshikidake pyroclastics. In this study, we examined the stratigraphy of eruption products in the Umanose agglutinate activity (ca. 8-4 ka). Besides, we examined temporal change in chemical compositions of the products.

≪Tephra-stratigraphy≫ We re-examined the tephra-stratigraphy and recognized nine volcanic sand layers (Z-To 5a, 5b, 5c, 5d, 5e, 5, 6, 7, 8) during the Umanose agglutinate activity. The tephra (volcanic sand) layers younger than the Z-To 5e widely distribute around the summit area, while the others are found only in the northern part. Based on ^{14}C ages on paleosols and fossil leaf samples from the tephra-loam succession coupled with the stratigraphy, ages of Z-To 5a to 8, except for Z-To 5, are estimated to be ca. 8.9, 7.3, 6.0, 5.6, 5.3, 4.7, 3.9, 3.6 ka, respectively.

In addition, we found whitish yellow colored wide-spread tephra layer between Z-To 5e and 5d in the northern and bellow 5e in the southern part of the summit area. This tephra is mainly composed of pumice type volcanic glass. This layer can be correlated to To-Cu (Towada-Chuseri) tephra, based on the major element compositions of the volcanic glass and the stratigraphic horizon.

≪Stratigraphy of the proximal layers≫ The proximal layers are well exposed in the central part of the summit area. In this part, the Umanose agglutinate covers the Komakusadaira agglutinate, which include less-vesiculated volcanic bombs with glassy luster as well as scoria. Overlying products of the Umanose agglutinate are composed of alternation of agglutinate, scoria fall deposit, and pyroclastic surge deposit. More than ten layers are recognized by intercalating loam layers.

≪Temporal change in chemical compositions≫ The eruptive products are olivine +- pyroxene andesite (56.0-59.2% SiO_2) and belong to medium-K calc-alkaline series. All samples are plotted on same linear trends in SiO_2 variation diagrams. The silica contents increase gradually from the bottom to the middle part. Afterwards, the content drops to the lowest, and gradually increase upwards again.

Keywords: Zao volcano, Umanose agglutinate, tephra stratigraphy, evolution of magma

Japan Geoscience Union Meeting 2014
(28 April - 02 May 2014 at Pacifico YOKOHAMA, Kanagawa, Japan)

SVC54-P11 Room:Poster Time:May 1 18:15-19:30

Eruptive History of Post-caldera Stage, East-Azuma Volcano -Correlation between ejecta intra-caldera and boring core-

OZAKI, Mamoru[1*] ; FUJINAWA, Akihiko[2]

[1]Ibaraki Univ., [2]Ibaraki Univ.

Introduction

Azuma Volcano is one of the Quaternary stratovolcanoes located at the volcanic front of the Northeast Japan arc. The recent 7ka activities of this volcano are characterized by dominant fall out tephra (Yamamoto, 2005). Eruptive history occurred at the Jododaira explosion caldera (Fujinawa and Kamoshida, 1999) is built by comparing boring core of the Jododaira with the ejecta deposited the intra-caldera area.

Stratigraphy and lithofacies of boring core

Boring site is at about 500m NW from Azuma-Kofuji cone. This core was described most immediately after core-recovery, and stratigraphic sequence was outlined (CCPVE core analysis group, 2011). Layers of andesitic volcanic block and lapilli (11.20m-1.50m in depth) are lithologically correlated to the Azuma-Kofuji volcanic ejecta.

Andesite lava (100.55m-81.07m, sample No.19-17 near the bottom of the core) and welded tuff breccia / lapilli tuff (79.90m-14.20m, No.13-10) are to be the keys to reveal the eruption history. Andesite lava (19-17) is dark-gray in color with dominant plagioclase phenocrysts of 2˜3mm in diameter. Inclusions are rarely recognizable. Welded tuff breccia/lapilli tuff (No. 13-10) are characterized by dark-gray, highly deformed and elongated blocks/lapilli at the densely welded part.

Description of outcrops

3 lava flows and 1 pyroclastic flow deposit were newly found at the outcrops of intra-caldera area.

Lava flow1 (Lf1) does not show distinct lobe topography. This is exposed only at altitudes of 430m along forest road with about 5m thick. Lf1 is massive, dark-gray in color and characterized by dominant plagioclase phenocrysts of 2˜3mm in diameter. Rare cognate inclusion is also recognized.

Pyroclastic flow deposit (Pfl) intermittently cropped out around at altitudes of 470m along the route 126, showing a thickness about 2.5m. The Pfl is overlain by unconsolidated talus deposit. The stratigraphy of these deposits was not confirmed in the field observation. This Pfl includes dark-gray lithic fragments in weakly welded light-gray matrix.

Lava flow2 (Lf2) constitutes thick massive spreading widely on the floor of the Jododaira explosion caldera (Fujinawa and Kamoshida, 1999). Judged from topography, the Lf2 storatigraphically overlies the Pfl. At altitudes of 660m along forest road, the Lf2 of over 10m in thick showing an well-developed columnar joint is cropped out. The Lf2 is directly covered by Ak-Lf at this locality (Kamoshida, 1991MS). Lithology of Lf2 is massive, gray in color and pyroxene phenocrysts are secerned easily.

Lava flow3 (Lf3) is distributed in the southern part of the intra-caldera, well foamed and grey tinged with red in color. The Lf3 topographically overlies the Lf2, furthermore, and covered by Ak-Lf. The Lf3 consists of 3˜5 flow units, lobes and levees at its surface.

Comparison of lithofacies

The lava samples of the core (19˜17) are lithographically similar to those for the Lf1, but distinguishable to those of the Lf2 or Lf3. The core samples of the welded tuff (13˜10) is slightly different from Pfl in the degree of welding, but are similar to each other in terms of including dark-gray lithic fragments in light-gray matrix.

Eruptive history based on comparison of lithofacies

The welded pyroclastic deposits in boring core are as thick as 20m, suggesting that the deposit is the deposit of an enormous pyroclastic eruption. If such eruption occurs, a sort of depression would often be remained in the supply source area. Judging from topography, the Jododaira explosion caldera is the most plausible candidate. Because the Lf1 (=core 19˜17) lie beneath welded Pfl (=core 13˜10), this lava is promisingly erupted during pre-caldera activities. Because the Lf2 and Lf3 are topographically come above the Lf1, it is considered that these lavas erupted in the post-caldera stage.

Keywords: Azuma Volcano, Jododaira, eruptive history, boring core, stratigraphy

Japan Geoscience Union Meeting 2014
(28 April - 02 May 2014 at Pacifico YOKOHAMA, Kanagawa, Japan)

SVC54-P12 Room:Poster Time:May 1 18:15-19:30

Plagioclase phenocrysts and Opx-magnetite symplectite of the Sessho Lava of the Kusatsu-Shirane Volcano

OSHIO, Kazuki[1*] ; UEKI, Kenta[2] ; KAWANO, Munehiro[3] ; INUI, Mutsuko[3] ; NOGAMI, Kenji[2]

[1]Kokushikan University Graduate School of Engineering, [2]Volcanic Fluid Research Center, Tokyo Institute of Technology, [3]Kokushikan University

Chemical composition and crystal size distribution of plagioclase phenocrysts may represent the cooling rate and chemical heterogeneity of the magma chamber. Therefore, chemical and physical conditions in the magma storage before eruption can be constrained by analyzing the morphology and chemical composition of phenocrysts in lava.

For the purpose, we focused on the Sessho lava, a single lava flow erupted from Kusatsu-Shirane volcano. Kusatsu-Shirane volcano is a quaternary active volcano located in the Central Japan arc. According to Uto *et al.*(1983), the Sessho lava is estimated to have erupted from the Moto Shirane cone during an eruption about 3000 years ago. The Sessho lava shows andesitic composition (Takahashi *et al.*, 2010; Ueki and Terada, 2012). In this study, detailed descriptions in morphologies of phenocryst minerals have been carried out. We determined the modal composition of phenocrysts, and measured the aspect ratio and the crystal size distribution of plagioclase phenocryst. We also carried out the detailed description of opx-magnetite symplectite, which have been observed in several samples.

The phenocrysts assemblage of the Sessho lava is plagioclase, clinopyroxene, orthopyroxene, magnetite, and rare olivine. Groundmass shows glassy structure. Modal composition of phenocrysts shows homogeneous value in a single lava flow; 54.0 to 59.0 vol. % for groundmass, 33.4 to 38.1 vol. % for plagioclase, 2.1 to for 4.2 vol. % for magnetite, 3.0 to 6.4 vol. % for pyroxene. On the other hand, the aspect ratios of plagioclase phenocrysts show wide range of variation in a single lava flow. Fine grained plagioclase shows needle-like morphology whereas coarse grained plagioclase shows tabular morphology. Although the modal composition shows the homogeneous value, sizes of plagioclase phenocrysts show wide range of variation; samples rich in fine-grained phenocrysts and samples rich in coarse-grained phenocrysts are both present in the single lava flow.

Observations and quantitative analysis using EPMA and SEM show that the structure of plagioclase phenocrysts can be classified into following five groups; normal zoning, reverse zoning, oscillatory zoning, patchy zoning, dusty zoning. Plagioclase phenocrysts show a wide range of composition in the single lava flow. An# ranges 55-84 %. Olivine phenocryst is observed in some samples, its Mg# is -83, which is a non-equilibrium composition with its host rock.

Opx-magnetite symplectite have been observed in several samples. The symplectite show oval form. Its diameter ranges 2-4 mm. Magnetite shows lamella structure, and is concentrated at the central part of the symplectite. Orthopyroxene is 75-975 μm in diameter and distributes around the magnetite lamella. Orthopyroxene in the symplectite is characterized by its low birefringence than the typical orthopyroxene phenocrysts of the Sessho lava. This structure is estimated to be formed by the rapid oxidation of olivine, indicating that during the formation of andesite magma of Sessho lava, oxygen fugacity in the magma storage may have rapidly increased.

In conclusion, it is estimated that final temperature was homogeneous in the magma strage of the Sessho lava, because modal contents of phenocrysts in the single lava flow show homogeneous value. On the other hand, several types of the chemical composition and size of plagioclase have been observed in the lava flow, indicating rate of crystallization and cooling had variation in the magma storage of the Sessho lava. Existences of orthopyroxene-magnetite symplectite and non-equilibrium olivine indicate magma mixing and oxidization event had occurred during the formation of andesitic magma of the Kusatsu-Shirane volcano.

References

Uto *et al.*, Kusatsu-Shirane volcano geological map, Geological Survey (1983)

Takahashi *et al.*, Nihon University College of Humanities and Sciences, Research bulletins, 45, 205-254 (2010)

Ueki & Terada, Volcano 57, 4, 235-251 (2012)

Keywords: Lava flow, Crystal size distribution, Eruption, Andesite, Active volcano, Symplectite

Japan Geoscience Union Meeting 2014
(28 April - 02 May 2014 at Pacifico YOKOHAMA, Kanagawa, Japan)

SVC54-P13 Room:Poster Time:May 1 18:15-19:30

Boring Core Observation of the Izu Oshima Sembazaki Strain Meter Well.

KAWANABE, Yoshihisa[1*] ; ONIZAWA, Shin'ya[2] ; KOKUBO, Kazuya[3]

[1]Geol. Surv. Japan, AIST, [2]Meteorological Research Institute, [3]Japan Meteorological Agency

We report the boring core observations of strain gauge well that Japan Meteorological Agency has been installed in the Sembasaki, Izu Oshima. The location of the well is at 34 42' 20.5168 "N, and 139 21' 40.7016"E, and well altitude is 51.2m, and drilling depth is 100m. For deeper than about 70m deep, the core was recovered.

Depth from 70m to 86m is composed of volcanic breccia with thin layers of volcanic ash. Volcanic breccia is solidified and including fragments of various basalt, scoria and altered rocks. Some basalt fragments seems to be the essential with a quench rim. From the surrounding geology, this breccia can be compared to the Senzu Formation that is the product of explosive eruption at shallow sea in the first stage of Izu Oshima volcano.

The core, depth of 86m (below sea level 34.8m) or deeper, is made of fresh aphyric basaltic lava flow. At least 2 flow units can be identified. Both lava flows contain very small amount of plagioclase and clinopyroxene phenocrysts. There is no evidence that is water-cooled to the lava flow.

We performed the whole rock chemical composition analysis for basalt fragment of breccia and lava flows. All specimen have SiO_2 = 49.8 ˜52.9wt% and significantly lower K_2O content, about 0.2wt%, than the basalts of Izu Oshima volcano, except for one breccia fragment. The lower K_2O content than that of the rock of Izu Oshima volcano is consistent with the characteristics of the old basement volcanoes such as Fudeshima volcano.

In the sea floor of the west of the Izu Oshima, there are Semba spur accompanied by magnetic anomaly. Oshima et.al.(1987) pointed out that the Semba spur might be the older volcanic body and they named it Semba volcano. The height of the sea cliff is gradually increased from Sembazaki toward the north, and the highest around Tsuwai. The distribution of valleys around Tsuwai also shows the discordant rise in the foot of Izu Oshima volcano, and this discordant may lead to the Semba spur. The basalts from the Semba core indicate that the old basement volcano, Semba volcano, is also present in the Izu-Oshima southwest side.

Keywords: Izu Oshima, boring core, basalt

Japan Geoscience Union Meeting 2014
(28 April - 02 May 2014 at Pacifico YOKOHAMA, Kanagawa, Japan)

SVC54-P14 Room:Poster Time:May 1 18:15-19:30

Origin and deformation of the clastic flow bands in the Takanoobane rhyolite lava

FURUKAWA, Kuniyuki[1*] ; KANAMARU, Tatsuo[2] ; UNO, Koji[3]

[1]Faculty of Business Administration, Aichi University, [2]Department of Geosystem Sciences, College of Humanities and Sciences, Nihon University, [3]Graduate School of Education, Okayama University

In this study, we showed that the clastic flow bands, which are developed in the Takanoobane rhyolite lava, were formed by shear fracturing of the high viscous magma within the shallow conduit. The flow bands broke up into the small particle-rich flow lines, which are ubiquitously observed in obsidian lavas.

The Takanoobane rhyolite lava (TR lava) is located at the Aso caldera in the middle of Kyushu Island in SW Japan. The lava is effused at 51+/-5 ka (Matsumoto et al., 1991). The thickness, estimated volume, and bulk rock chemistry of TR lava are 60-90 m, 0.14 km^3 (Miyabuchi et al., 2004), and 71-72 SiO_2 wt.% (Furukawa, 2006), respectively. In this study, we examined two drill cores (AVL1 and AVL4) provided by the Aso Volcanological Laboratory. Both drill holes penetrated the proximal part of TR lava. TR lava is composed of an inner crystalline part and marginal glassy parts.

The black to dark gray colored flow bands within a few millimeters thick are concentrated around the boundary between crystalline part and basal obsidian. The bands are composed of clastic materials with a diameter below a few mm. The clastic materials are composed of glassy lithics and minerals. Some clasts are rounded and fluidal shapes and show different textural occurrences from the surrounding rhyolite. The chemical compositions of the glassy lithics and those of glassy matrix of the surrounding rhyolite are slightly different. Within the bands, the streak texture, which is defined by difference of clasts and microlite contents, is conspicuous.

The differences in texture and chemical compositions between the clasts in the bands and surrounding rhyolite indicate that the clastic bands were not formed by autobrecciation within the lava. These observations indicate that the clastic bands are likely to be formed by shear fracturing of the high viscous magma within the shallow conduit such as Tuffen et al. (2003). The fractures would become pathway of the volcanic gasses, and the clasts were transported by the gas transport. The streak texture within the bands is interpreted as sedimentary structures, which were formed by gas transportation of clasts through fracture system. The rounded and fluidal shapes of the clasts indicate that the fracturing occurred when the conduit magma was enough hot. The clastic bands consequently break up and disappear. The bands show progressive loosening along the individual streak, where will be the structural weakness. Consequently, the streak develops into the individual thin bands. The small particles, such as glass particles, microlites and lithics, are released from margin of the clastic bands to the surrounding rhyolite. Since the high viscosity of the lava inhibits their homogenization, the particles are likely to be aligned along the flow line. The clastic flow bands, originated from shear fracturing, will thoroughly break up via this process. Our results mean that the clastic flow bands developed within silicic lavas is important for understanding of the shallow conduit system of silicic magma.

Keywords: rhyolite, lava, flow band, conduit, Aso

Japan Geoscience Union Meeting 2014
(28 April - 02 May 2014 at Pacifico YOKOHAMA, Kanagawa, Japan)

SVC54-P15 Room:Poster Time:May 1 18:15-19:30

Magma chamber processes revealed by textures in plagioclase phenocrysts through Taisho eruptions of Sakurajima volcano

YAMASHITA, Shunsuke[1*] ; TORAMARU, Atsushi[2]

[1]Department of Earth and Planetary Sciences, Graduate School of Sciences, [2]Department of Earth and Planetary Sciences, Faculty of Sciences

Textures in volcanic products record important information about the origin of the rock. Especially, plagioclase phenocrysts have been studied in order to understand the magma chamber processes because they are commonly included in various types of volcanic rocks. Two types of plagioclase phenocrysts are found in lavas by the 1914-1915 eruption of Sakurajima volcano, Southern Kyushu, Japan: (1) honeycomb plagioclase(H-Pl) with large melt inclusions in cores; and(2) clear plagioclase(C-Pl) without any melt inclusions. In Sakurajima volcano, magma mixing has been suggested by bimodal compositions of plagioclase phenocrysts. However, relationship between textures and chemical compositions has not been reported. In addition, the crystal size distributions (CSDs) also may provide essential information for the production environment of the crystals. Therefore, in order to obtain insights into magma chamber and magma mixing processes, we conduct chemical composition and crystal size distribution (CSD) analyses.

We carried out chemical compositional analysis by FE-SEM. As a result, it is found that H-Pl phenocrysts have heterogeneous mozaic cores with An75-90 and An55-70 and very low An#(An40-55) around melt inclusions. On the other hand, C-Pl phenocrysts are uniform in compositions while the An contents varies from grain to grain. The histogram of An contents in H-Pl cores shows narrow bimodal distributions around An78 and An86, whereas that of C-Pl cores shows the wide bimodal distribution around An62 and An86. We carried out CSD analysis. It is found that H-Pl and C-Pl phenocrysts showed different trends. CSD of C-Pl is strongly convex-downward showing crossover with two different slopes.

We revealed plagioclase are classified into three types: (1) type-H with an An-rich (An74-89) and heterogeneous core containing large melt inclusions; and (2) type-C-1 with an An62 and homogeneous core not containing melt inclusions; and (3) type-C-2 with an An-rich (An85) and homogeneous core not containing melt inclusions. The results of CSD suggest different formation pocesses between H-Pl and C-Pl, and crossover in the slopes of C-Pl CSDs suggest the mixing of two magmas from which two populations of phenocrysts originate (Higgins, 1996b). In Sakurajima, magma mixing has been suggested, therefore it is important to understand the temperature of magmas. So, we estimated temperature on equilibrium constants by plagioclase- and alkali feldspar-liquid thermobarometers (Putirka, 2008). The results show the temperature on equilibrium constants of the dacitic magma was about 850 ℃, and that of the basaltic magma was about 1050 ℃. Since the honeycomb plagioclases are generated by the skeletal growth under high supercooling condition, the H-Pl phenocrysts is formed in the basaltic magmas during cooling at mixing events. In summary, type-H is formed by skeletal growth due to the thermal interaction during mixing events in basaltic magma, type-C-1 is formed under magma chamber with mixed homogeneous magma, type-C-2 is formed under magma chamber with the basaltic magma before mixing, respectively.

Keywords: plagioclase phenocryst, honeycomb texture, textural analysis, crystal size distribution, magma mixing, Sakurajima volcano

Japan Geoscience Union Meeting 2014
(28 April - 02 May 2014 at Pacifico YOKOHAMA, Kanagawa, Japan)

SVC55-P01 Room:Poster Time:May 1 18:15-19:30

Ground Deformation of Active Volcano in Kunashiri and Etorofu Islands using InSAR time series analysis

ANDO, Shinobu[1*] ; MIURA, Yuji[2] ; MATSUMORI, Toshiyuki[2]

[1]MRI, [2]JMA

ALOS has an L-band SAR (PALSAR), which is not affected by vegetation, and the interference is good even in mountainous areas. So these methods are effective for the crustal deformation observation of volcanic areas.

In previous studies, we have reported the analysis results about all domestic active volcanic areas, using D-InSAR of ALOS since 2007. However, ALOS has suspended the operation in May 2011. Therefore, we did not do D-InSAR analysis for the period thereafter. In recent years, InSAR time series analysis technique called PS-InSAR and SBAS has been developed, a number of cases have been reported.

There are 11 active volcanoes in the Kunashiri and Etorofu island, Southern Kuril Islands. It has still continued an active volcanic activity in the some volcanoes of them. In this report, we have take advantaged of the archive data of ALOS/PALSAR, and tried to analyze the ground deformation of around these 11 active volcanoes using *StaMPS* program was developed by the Stanford Institute of Technology. Note, we analyzed except for the data captured in the winter in order to remove the effect of the snow. Also, besides PS-InSAR and SBAS methods, *StaMPS* program has the analysis methods to merge these results. Therefore, we will also present about the difference of these results.

Some of PALSAR data were prepared by Japan Aerospace Exploration Agency (JAXA) via the Coordinating Committee for the Prediction of Volcanic Eruption (CCPVE) as part of the project ”ALOS Domestic Demonstration on Disaster Management Application” of the Volcano Working Group. Also, we used some of PALSAR data that are shared within PALSAR Interferometry Consortium to Study our Evolving Land surface (PIXEL). PALSAR data belongs to Ministry of Economy, Trade and Industry (METI) and JAXA. In the process of the InSAR analysis, we used ”the ASTER Global Digital Elevation Model” was developed jointly by METI and the United States National Aeronautics and Space Administration (NASA), and Generic Mapping Tools (P.Wessel and W.H.F.Smith, 1999) to prepare illustrations.

Keywords: InSAR time series analysis, Ground deformation, ALOS/PALSAR, Domestic active volcano

Japan Geoscience Union Meeting 2014
(28 April - 02 May 2014 at Pacifico YOKOHAMA, Kanagawa, Japan)

SVC55-P02 Room:Poster Time:May 1 18:15-19:30

Preliminary result of resistivity modeling around Ponmachineshiri crater at Meakandake Volcano, Japan

TAKAHASHI, Kosuke[1*] ; MATSUSHIMA, Nobuo[2] ; TAKAKURA, Shinichi[2] ; YAMAYA, Yusuke[2] ; ARITA, Shin[1] ; NAGAMACHI, Shingo[1] ; OISHI, Masayuki[2] ; KAZAHAYA, Ryunosuke[2] ; FUJII, Ikuko[1]

[1]Kakioka Magnetic Observatory, Japan Meteorological Agency, [2]National Institute of Advanced Industrial Science and Technology

Meakandake Volcano, situated in Eastern Hokkaido, Japan, is an active volcano where a phreatic eruption occurs in every several years. Volcano-tectonic (VT) earthquakes mainly occurred below Ponmachineshiri crater which is one of active craters of the volcano (Japan Meteorological Agency, 2013). A source region of the tremors occurred before the 2008 eruption was estimated beneath the southern slope of the crater (Ogiso and Yomogida, 2012). Significant changes in the geomagnetic field were observed in 2008 and 2009 around the crater. Hashimoto et al. (2009) pointed out that the temporal variations of the geomagnetic field in 2008-2009 were due to the thermal demagnetization of the material beneath the southern slope of the crater.

These VT earthquake, tremor and rock demagnetization events probably associated with the movement of volcanic fluids such as hydrothermal water, gas and melt. Therefore, understanding of a hydrothermal system of the volcano is a key to reveal the mechanism of the tectonic events occurred there.

Resistivity of rock strongly depends on the fluid inclusion. Therefore, an electro-magnetic measurement is an effective method to image the fluid distribution. We conducted audio-frequency magnetotelluric (AMT) surveys in August 2013 on the western slope of the volcano. The objective of the survey is to reveal the resistivity structure around Ponmachineshiri crater and to infer the relationships among the fluid distribution, the seismic focal area, and the demagnetized area around the crater.

Since we have not finished the AMT survey on the eastern slope of the volcano yet, the resistivity structure around the Ponmachineshiri summit crater is not well-constraint. Therefore, we present the two-dimensional resistivity structure beneath the western slope of the volcano as a preliminary result. The characteristics of the resistivity distribution are described as follow.

1) A resistive (more than several hundred Ω m) layer locates at the top of the western slope of the volcano. Its thickness varies from 100 to 300 m on the profile. This layer can be regarded as a permeable lava or pyroclastic fall deposits.
2) Below the resistive surface layer, two conductive (less than 10 Ω m) bodies are found. One is located to the west of Ponmachineshiri crater at depths of 300-1000 m from the surface. This conductor corresponds to a hydrothermal reservoir which relates to the fumarolic activity in the crater. The second conductor is found beneath the western part of the profile at a depth of about 1000 m from the surface. The discharge of hot spring water at the west of our survey region suggests that this conductor can be explained by the presence of the hydrothermal fluid and/or the altered rocks.
3) A resistive area (more than several hundred Ω m) exists below the two conductors. Causes of this high resistivity are unknown yet.

Keywords: resistivity structure, Meakandake Volcano, volcanic fluid

Japan Geoscience Union Meeting 2014
(28 April - 02 May 2014 at Pacifico YOKOHAMA, Kanagawa, Japan)

SVC55-P03 Room:Poster Time:May 1 18:15-19:30

Variation of Geomagnetic Total Intensity at Meakandake Volcano after the Eruptions in 2008

SHIMAMURA, Tetsuya[1*] ; ARITA, Shin[1] ; MASHIKO, Norimichi[1] ; FUJII, Ikuko[1] ; FUKUI, Keiichi[1] ; OGISO, Masashi[2]

[1]Kakioka Magnetic Observatory, JMA, [2]Matsushiro Seismological Observatory, JMA

This study reports on the geomagnetic total intensity change at Meakandake volcano and its relations with volcanic activity after eruptions in 2008.

Meakandake volcano is located in eastern Hokkaido and is a volcanic complex which consists of eight volcanoes, such as Ponmachineshiri, Nakamachineshiri, Akanfuji and so on. Ponmachineshiri has been active in recent years and minor phreatic eruptions repeatedly occurred in 1988, 1996, 1998, 2006 and 2008.

Kakioka Magnetic Observatory, Japan Meteorological Agency has carried out a repeat observation of the geomagnetic total intensity in one or two times a year since 1992 for the purpose of detecting geomagnetic field changes accompanying the volcanic activity of Meakandake volcano. Twelve repeat stations were installed on the east side of summit crators' edge and south slope of Ponmachineshiri in 1992 and since then we have improved the repeat station network step by step. About thirty stations are used recently. A continuous station of the geomagnetic total intensity (MEA) was installed on the south slope of Ponmachineshiri on October 16, 2003 in order to improve the time resolution of the observation. Then, a new continuous station (ME2) was installed between the 96-1 crater of Ponmachineshiri and MEA on September 28, 2013. The geomagnetic intensities are acquired every 5-minutes at MEA and ME2.

A significant decrease of the geomagnetic total intensity was observed at Meakandake volcano in July, 2013 and continues up to now (January, 2014). The total intensity varied with the eruptive activity in 2008, and no remarkable change of the total intensity was seen for thirty months from January 2011 to June, 2013. There has been no significant variations in volcano-tectonic earthquakes, tremors, volcanic smoke and tectonic deformation at Meakandake volcano since July, 2013 (Volcanic Observations and Information Center, Sapporo District Meteorological Observatory, JMA), which differs from the situation at the 2008 eruptions when significant variations of the total intensity and the other tectonic measurements were observed.

It is assumed that the decrease of the geomagnetic total intensity at Meakandake volcano in 2013 is due to the thermal demagnetization accompanying heating of the inside of the volcanic body. A source of the thermal demagnetization was estimated beneath the southern slope of the 96-1 crater at Ponmachineshiri by using geomagnetic total intensity changes at repeat stations for about 3 months from June to September, 2013. This source location is almost the same as that of the demagnetization in 2008. And it is inside the focal area of migrating volcanic tremors which occurred on November 16, 2008 reported by Ogiso and Yomogida (2012). We used MaGCAP-V (Seismology and Volcanology Research Department, Meteorological Research Institute, JMA, 2013) as a support software for the modelling of the demagnetization source.

It is indicated that the position of the thermal demagnetization source has not changed for last four months, because the difference of the geomagnetic total intensities at two continuous stations (MEA and ME2) has been almost constant since the end of September, 2013.

Only the geomagnetic total intensity detects a possible on-going heating process inside the Ponmachineshiri which commenced in July 2013. This case strongly suggests that the observation of the geomagnetic field is important to monitor heating or cooling of the volcanic body. The observation with two or more continuous stations is effective in order to monitor the source position of the thermal demagnetization. In addition, Hashimoto *et al.* (2009) suggested a possibility of the volcanic eruption prediction at Meakandake volcano, because a decrease of the geomagnetic total intensity was observed two days before the eruption on November 18, 2008 when the amplitude of the volcanic tremors had been increased.

Keywords: Meakandake, geomagnetic total intensity, volcano, eruption, thermal demagnetization

Japan Geoscience Union Meeting 2014
(28 April - 02 May 2014 at Pacifico YOKOHAMA, Kanagawa, Japan)

SVC55-P04 Room:Poster Time:May 1 18:15-19:30

Recent volcanic deformations observed by campaign GPS on and around Mt.Tokachi and Mt.Meakan

WADA, Sayaka[1*] ; MORI, Hitoshi, Y.[1] ; OKUYAMA, Satoshi[1]

[1]Hokkaido University, Institute of Seismology and Volcanology

Mt. Tokachi is one of the famous active volcanoes located in the central Hokkaido, Japan. In the recent 100 years, major magmatic eruptions at Mt. Tokachi occurred in 1926, 1962 and 1988-1989. Mt. Meakan sits in the eastern Hokkaido. It is also an active volcano and made phreatic eruptions in 1996, 1998, 2006 and 2008.

In this study, we will discuss the results of the campaign GPS on and around Mt. Tokachi and Mt. Meakan. Each broad area GPS observation had begun at Mt. Tokachi in 2007 and at Mt. Meakan in 2006. The campaign GPS observation for Mt. Tokachi made at 12 sites and that for Mt. Meakan at 8 sites, for several days to weeks in each year.

We used the data of our campaign observations since 2007 for Mt. Tokachi and after the 2008 eruption for Mt. Meakan. For evaluating spatial deformation pattern in more detail, we also used the data of several GPS sites operated by JMA (Japan Meteorological Agency) at the same time. Analyzing these data, annual movements at those stations were estimated. The regional tectonic movement and the coseismic step of Tohoku-oki earthquake on March 11, 2011 are included in those movements. We used the continuous data at GEONET sites by Geospatial Information Authority of Japan (GSI) around the volcanoes to make corrections for non-volcanic deformations. Using the GEONET data from 2007 to 2013, the regional tectonic and the seismic deformations were estimated by linear approximation in space. Seasonal changes should be taken into consideration to study the volcanic deformation. The discussion about deduced volcanic deformations will be made, after the corrections about the regional deformation, the coseismic step and the after slip of 2011 Tohoku-oki earthquake, and the seasonal variations.

Acknowledgements

In this study, JMA, Sapporo District Meteorological Observatory furnish their observation data to us. We would like to express our gratitude to them. Also, we used the data of GEONET sites of GSI with thanks.

Keywords: Mt. Tokachi, Mt. Meakan, volcanic crustal deformation, GPS

Japan Geoscience Union Meeting 2014
(28 April - 02 May 2014 at Pacifico YOKOHAMA, Kanagawa, Japan)

SVC55-P05 Room:Poster Time:May 1 18:15-19:30

The Volcanic activity of Tarumaesan Volcano in 2013 and Trial of Application to the Eruption scenario

NAGAYAMA, Hiroaki[1*] ; MIAYAMOTO, Masashi[1] ; FUJIMATSU, Jun[1] ; USUI, Yuji[1] ; FUSHIYA, Yuji[1] ; MIYAMURA, Jun'ichi[1]

[1]Sapporo Regional Headquarters, JMA

Continuous observation network with tiltmeter and strainmeter in Mt.Tarumae, which is located on the southeastern edge of Shikotsu caldera, operated by Japan Meteorological Agency (JMA) and Hokkaido University Institute of Seismology and Volcanology (ISV) detected volcanic ground deformation during June 19 to July 4, 2013. According to the Mogi model (Mogi, 1958), the ground deformation is interpreted as volume increase of about $10^5 m^3$ at about 3-4km in depth beneath sea level around Mt.Kitayama, is located in about 1.5km northwest from Tarumae summit. It is different from the deformation in shallow region (above the sea level) beneath the summit, reported by MRI (2008), the Meteorological Reaearch Insutitude, and ISV et al.(2011). According to the classification suggested by MRI (2013), it is correspond to slowly accumulation process of magma, as magma chamber or dike intrusion. B-type earthquakes, have been occurred in shallow region (˜sea level) beneath the summit, became active slightly in synchronization with the ground deformation. As a result of the process of volcanic fluid, the actual medium is unknown, rise to the volume increase area (depth 3-4km), it is interpreted as an increase in heat flux to shallow region beneath the summit.

Volcano-tectonic earthquake (VT earthquake) activated at a depth of 3-5km surrounding the deformation area in mid-July, after ground deformation, it is still ongoing. The VT seismicity was very active until August and maximum shock was M3.0 in late September. VT earthquakes have occurred in the relative high resistivity layer (50-500Ωm) of Resistivity imaging by Yamaya et al. (2005, 2012). Whereas, it have not occured in the deformation area and the path to beneath Tarumae summit, that is relative conductive area.

Order to carry out disaster prevention appropriately and promptly in the eruption, JMA has operated the eruption alert level on 31 volcanoes across the country. It is intended to share the consciousness of the local government by flow assuming the transition of volcanic activity, called the eruption scenario. For operating the level effectively, the eruption scenario, flow chart assuming the progress of the volcanic activity of each volcano, has been shared with the local government. As lastest magma eruption is in 1909, major volcanic activity had been occured in the very shallow part around lava dome for a long time. It is unknown what the phenomenon is observed when the magma is supplied to the shallow depth from the deeper. Therefore, the scenario that assumed the magma eruption is supplemented by the general knowledge that was observed at other volcanoes. The mechanism of the deformation and VT-seismicity is not clear. But, it can be considered of the distribution that related to the heat supply system or the geological structure beneath Tarumae. In this study, we tried to apply the interpretation of the ground deformation and VT-seismicity to the eruption scenario. However, our interpretation on the activity is unverifiable evidence so poor at present. In order to improve the eruption scenario certainly, elucidation of the magma supply system in Tarumae is essential, but it is not clear at present. To clarify the magma supply system, it is necessary to more information of geological structures and obseved results such as ground deformation and VT-seismicity in this time. However, we are at present able to investigate detection of the high attenuation region used natural earthquake and to estimate fault plane solutions of VT earthquake (P-axes) using P-waves, and would like to approach. In addition, it is necessary to operate new observation system to capture phenomena such as seismic activity and ground deformation more certainly due to magma rising from the deep.

Acknowledgment:In this study, we use the data of ISV, tiltmeter and strainmeter, and the waveform data. Thank you for permission to use data.

Keywords: tarumae, volcanic activity, eruption scenario, ground deformation, VT seismicity

Japan Geoscience Union Meeting 2014
(28 April - 02 May 2014 at Pacifico YOKOHAMA, Kanagawa, Japan)

SVC55-P06 Room:Poster Time:May 1 18:15-19:30

Volcanic activities of Hakkoda volcano after the 2011 Tohoku-Oki earthquake

YAMAMOTO, Mare[1*]

[1]Geophysics, Science, Tohoku University

The 2011 Tohoku-Oki earthquake of 11 March 2011 is one of the largest earthquakes in recent times, and it generated large displacements and deformation in and around the Japanese islands. Such large crustal deformation, especially the east-west extension exerted on Tohoku area, raises fear of further disasters including triggered volcanic activities as well as triggered seismicity. To assess the potential risks of triggered volcanic activities, understanding of the behavior of volcanic fluids in the crust and volcanic bodies would be a key. In this presentation, as examples of such possibly triggers volcanic activities, we report the recent seismic activities of Hakkoda volcano, and discuss the relation to the movement of volcanic fluids.

Hakkoda volcano is a group of stratovolcanoes at the northern end of Honshu Island, Japan. There are fumaroles and hot springs around the volcano, and phreatic eruptions from Jigoku-numa on the southwestern flank of Odake volcano, which is the highest peak in the main cones of Northern-Hakkoda volcanic group, were documented in its history. Since just after the occurrence of Tohoku-Oki earthquake, the seismicity around the volcano became higher, and the migration of hypocenters of high-frequency volcano-tectonic (VT) earthquake was observed.

In addition to these VT events, long-period (LP) events started occurring beneath Odake at a depth of about 2-3 km from February, 2013, and subtle crustal deformation caused by deep inflation source was also detected by GEONET GNSS network around the same time. The characteristics of LP events are summarized as follows: (1) The spectra of LP events are common between events irrespective of the magnitude of events, and they have spectral peaks at 6-7 sec, 2-3 sec, 1 sec, and so on. (2) The long-period component of LP events appears as a wave packet of a few cycles, and high-frequency ($>$1 Hz) signals sometimes overlaps it. (3) LP events sometimes occur like a swarm with an interval of several minutes. These characteristics of LP events at Hakkoda volcano are similar to those of LP events at other active volcanoes and hydrothermal area in the world, where abundant fluids exist. Our further analysis using far-field Rayleigh radiation pattern observed by NIED Hi-net stations reveals that the source of LP events is most likely to be a nearly vertical tensile crack whose strike is almost parallel to the direction connecting Odake summit crater and Jigoku-numa. The number of VLPs gradually decreased after September, 2013, and high-frequency VT earthquakes became more dominant in the seismicity around Hakkoda volcano. However, there were a burst of earthquakes beneath Southern-Hakkoda volcanic group, that includes a few low-frequency earthquakes, at the end of December, 2013.

These results suggest that the extensional steress field generated by the 2011 Tohoku-Oki earthquake causes the upward movement of volcanic fluids and heat from the deep, and results in an activation of hydrothermal activities at the pre-existent fracture zone at Hakkoda volcanic group.

Acknowledgment: We used Hi-net data provided by the National Research Institute for Earth Science and Disaster Prevention.

Keywords: Volcanic earthquakes, Volcanic fluids, Geofluids, Long-period events

Japan Geoscience Union Meeting 2014
(28 April - 02 May 2014 at Pacifico YOKOHAMA, Kanagawa, Japan)

SVC55-P07 Room:Poster Time:May 1 18:15-19:30

New knowledge of eruptive sequence in Heian eruption of Towada volcano

HIROI, Yoshimi[1*] ; MIYAMOTO, Tsuyoshi[2]

[1]Grad.Sci.Tohoku Univ., [2]CNEAS.,Tohoku Univ.

1. Introduction

Heian eruption is the latest activity at Towada volcano, in Heian period (eruptive episode A : Hayakawa,1985). This eruption has been started from Nakanoumi caldera lake (Kudo,2010) filled with lake water, and repeated magmatic and phreatomagmatic eruption alternately. The details of the eruptive sequence have already been shown by Hiroi and Miyamoto (2010), however, we got and report new knowledge about the activity of first plinian phase and the occurrence mechanism of large pyroclastic flow unit.

2. Ash layers within unit OYU-1

The first plinian pumice fall unit OYU-1 has a SW dispersal axis and it achieves 50km farther. OYU-1 in distal shows very well sorting and uniform grain size distribution , but we found plural outcrops that OYU-1 accompanies with fine ash layers within 12km from source vent. Two kinds of ashes are observed, one is a beige colored ash in the lower part of OYU-1. The thickness is about 1-8 cm, and dispersal area is SW-SSE. Others are gray colored ashes and intercalated in the upper part of OYU-1. Their thicknesses are about 1-3 cm, and each dispersal area is SW-SSW.

All of ashes are intercalated in pumice layer, and the boundary between pumice layer and ash one is almost clear. Because OYU-1 without ash layers in distal shows uniform grain size distribution, the extent of these ashes deposit is limited in narrow area if their ash had been accumulated during the plinian column formation. The clear boundaries between pumice and ash suggest that ash layers are not fall deposit accumulated for a long period, but flow deposit piled in a very short time. Ash layers can be found not only a valley, but the little highland such as a mountain ridge line. This feature of distribution shows that they are regarded as surge deposit.

Because the ashes intercalated with pumice layer in OYU-1indicate the feature of density current, they are intra-plinian flow. As one of their origin these ashes are derived from small-scale density current by the partial column collapse. The dispersal area of the ashes is limited adjacent to source vent and just only the direction of dispersal axis. This tendency of distribution seems that it corresponds with the direction of strong wind of 22[m/s] blew.

On the other hand, the source vent within a caldera lake and the fine grain features of ashes indicate a possibility that ash layers are phreatmagmatic base-surge deposit. In that case the occurrence of magma-water explosion might be caused by satisfying a condition of magma-water ratio partially or temporarily on the surface of eruption collumn. Unit OYU-2, overlying OYU-1 pumice fall directly, is phreatomagmatic base-surge deposit. Thus these ash layers may be a precursor phenomenon of eruptive style transition.

3. Distribution and draining style of KPf

Kemanai Pyroclastic flow is the climax deposit of Heian eruption, the total volume is estimated about 5km3(Hayakawa,1985). KPf distributes only the south area of Towada caldera, except for Oirase River to east direction. The Towada caldera rim is lowest at southwest edge (630m above sea level). The highest outcrop of KPf on caldera rim is located in 760m. In spite of adjacent to the source vent KPf cannot be shown on Mt. Akaiwa(785m) on the south caldera rim. These distribution features suggest that KPf flew out over the lower part of caldera rim. KPf deposit has been regarded that it occurred by plinian column collapse of preceded unit OYU-3 (Matsu-ura et al.,2007,etc.). But the column collapse type pyroclastic flow can be accumulated in high-altitude, KPf seems to be piled on only lower portion. Thus KPf is not occurred by column collapse, but derived by currents over the lower caldera wall. This conclusion agrees with the new eruptive sequence by Hiroi and Miyamoto(2010), that the unit just before KPf is not plinian pumice fall OYU-3, but phreatomagmatic base-surge unit OYU-4 without higher eruption column.

Keywords: Towada volcano, Heian eruption, intra-plinian flow, Soufriere-type pyroclastic flow

Japan Geoscience Union Meeting 2014
(28 April - 02 May 2014 at Pacifico YOKOHAMA, Kanagawa, Japan)

SVC55-P08 Room:Poster Time:May 1 18:15-19:30

Petrological study of northern part of ca. 300-100 ka volcanic edifices in Zao volcano.

TAKANO, Toru[1*] ; INOUE, Tsuyoshi[2] ; BAN, Masao[3] ; OIKAWA, Teruki[4] ; YAMASAKI, Seiko[4]

[1]Graduate School of Department of Earth and Environmental Sciences, Yamagata University, [2]Nippon Koei Co., Ltd., [3] Department of Earth and Environmental Sciences, Faculty of Science, Yamagata University, [4]Institute of Geology and Geoinformation, Geological Survey of Japan, National Institute of Advance

Zao volcano is a Quaternary stratovolcano located in the middle part of the volcanic front of northeast Japan arc. The volcanic activity started at about 800 ka, and has continued to present. During ca. 300 to 100 ka activity of the Zao volcano, several middle sized edifices were formed. These volcanic edifices can be divided into northern and southern parts. We performed petrologic study on eruption products of the northern part to reveal the variation of magma compositions along with the evolutionary history.

Eruption products are divided into 8 units from lower to upper: Yokokurayama lavas, Kanshodaira lavas, Jizosan west lavas, Kumanodake west eruption products, Kumanodake main edifice products, Jizosan east agglutinate and lavas, Kumanodake agglutinate and lavas, Umanose eruption products. Yokokurayama lavas, Kanshodaira lavas, and Jizosan west lavas are composed of andesitic lavas. Kumanodake west eruption products are consisted of andesitic lapilli tuff, tuff breccia, agglomerate, and andesitic lavas. Kumanodake main edifice products are consisted of alternation of andesitic lavas and pyroclastic rocks in the lower part, and andesitic tuff breccia and agglomerate in the upper part. Jizosan east agglutinate and lavas, Kumanodake agglutinate and lavas are consisted of basaltic andesitic agglutinate, agglomerate, and lavas. Umanose eruption products are mainly composed of basaltic andesitic lavas, with subordinate amounts of agglomerate.

The eruption center of the Yokokurayama lavas would be located westward from the main chain of eruption centers. The main eruption centers for the other units were located in between the Kumanodake-Jizosan area. Jizosan east agglutinate and lavas, Kumanodake agglutinate and lavas, Umanose eruption products are characterized by the agglutinate and/or agglomerate distributing near the eruption centers.

All of eruption products belong to medium-K calc-alkaline series. All units other than the Yokokurayama lavas are plotted on same general trends in most of the SiO_2 variation diagrams. The Yokokurayama lavas show a lower trend than the other units in K_2O diagram. Other than the Yokokura lavas, the lower four units are andesitic, whereas upper three units are basaltic andesitic. Looking at in detail, slight differences in compositions can be observed among units. Among the four andesitic units, Kumanodake main edifice products show higher trends in the Cr, Ni, Zr, Nb diagrams and a lower trend in Rb diagram than the others. The Umanose eruption products are plotted in higher part in Cr and Ni diagrams from the trends of the other products.

Keywords: Zao volcano, stratovolcano, eruption history, evolution of magma

Japan Geoscience Union Meeting 2014
(28 April - 02 May 2014 at Pacifico YOKOHAMA, Kanagawa, Japan)

SVC55-P09 Room:Poster Time:May 1 18:15-19:30

Characteristics of data observed by multi-component strainmeter installed at Senba, Izu-Oshima

YAMAMOTO, Tetsuya[1*] ; ANDO, Shinobu[1] ; KOKUBO, Kazuya[2] ; KOBAYASHI, Akio[1] ; KIMURA, Kazuhiro[1]

[1]Meteorological Research Institute, [2]Japan Meteorological Agency

Meteorological Research Institute installed a multi-component borehole strainmeter at Senba Station in Izu-Oshima, one of the most active volcanos in Japan, in February 2013. By the strainmeter, we aim to research on evaluation of volcanic activity by means of crustal deformation and also to monitor the activity of the volcano. In many cases, unavoidable drift were shown in data of strainmeter installed in a borehole from just after the installation for several years. In order to utilize the strainmeter for volcano monitoring effectively, it is important to grasp the drift and noise quantitatively from early stage of observation. We report a result of research about characteristics of the data observed for about a year.

The strainmeter has 4 sensors which measure linear strains in the horizontal plane in every 45 degrees. In data observed by the sensors, tidal variation of about a day or half day period over 500 nano-strains is obvious, as well as a long term variation. Generally only three components are independent in a plane, the strainmeter has redundancy and it makes us possible to evaluate quality of the data. Examining hourly mean values, all strain components look consistent in the period range of a day or half day. It suggests the data of strain are reliable in the period. On the other hand, the long term variation has an inconsistency as much as 4 micro-strains for 6 month. The inconsistency could be caused by only one sensor of the four, it is difficult to conclude what amount of volcanic deformation is observed at the present stage. In the periods shorter than a half day, almost all variation is less than 2-3 nano-strains. It indicates the accuracy of observation for a short interval.

Keywords: Izu-Oshima, Monitoring of active volcano, Strainmeter, Ground deformation

Japan Geoscience Union Meeting 2014
(28 April - 02 May 2014 at Pacifico YOKOHAMA, Kanagawa, Japan)

SVC55-P10 Room:Poster Time:May 1 18:15-19:30

Gravity changes during magma accumulation period in Izu-Oshima volcano

ONIZAWA, Shin'ya[1*] ; TAKAGI, Akimichi[1] ; FUKUI, Keiichi[2] ; ANDO, Shinobu[1]

[1]Meteorological Research Institute, JMA, [2]Kakioka Magnetic Observatory, JMA

Since March, 2004, we have been conducting series of campaign gravity measurements, in order to understand magma accumulation process and to detect eruption precursor of Izu-Oshima volcano. Here, we show calibration results of relative scale factors between gravimeters, and characteristics of temporal gravity changes observed in the volcano.

We have been measuring relative gravity changes in the volcano using three instruments; LaCoste & Romberg Type-D #109, Scintrex CG3M #454, and Scintrex CG5 #033. Gravity differences in our campaign network are about 180 mgal in maximum from the coastal sites to the summit sites. Such large differences easily induce systematic deviations between data obtained by different instruments, when gravimeter scales are not calibrated. Further, temporal changes in the scale factor of Scintrex CG3M have been reported by some previous gravity researches.

Since scale calibrations using absolute gravity networks had not conducted until 2012, we cannot absolutely calibrate for past data. However, we can check relative scales between gravimeters and their temporal changes by comparing campaign data obtained simultaneously. The scale factor for CG3M#454 relative to one for D#109 shows clear temporal decrease. One for CG5#033 also shows change at breakdown occurred in 2010. This can be explained by a parameter change done by the maker during repairing processes. Furthermore, we found a non-linear relationship between D#109 and CG5#033, which implies a non-linear scale factor of either instrument. Probably, the non-linearity occurs in LaCoste & Romberg Type-D, and we should calibrate further.

Although calibrations of each instrument are still not sufficient to discuss smaller gravity changes down to c.a. 10 micro-gal, we can find systematic temporal changes in relative gravity by correcting relative scale factors. Gravity increases at higher altitude sites relative to coastal sites are observed during a two-year period from July, 2008 to June, 2010. Temporal changes in relative gravities reaches up to 100 micro-gal in maximum. A spatial pattern of the changes suggests its center is at the northern caldera, which implies some relationship with ground deformation sources inferred by GPS data. However, both the amplitudes and phases of the relative gravity changes can never be explained by the ground deformation observed during the period. The change seems to be related to temporal changes in precipitation. Increase in water content in vadose zone may be one of possible factor of the changes. Apart from these candidates, we tentatively inferred source location and mass increase by assuming single point mass source. The best fit location after grid searches was at depth of 3 km b.s.l. beneath the northern caldera, where approximately coincides with the ground deformation source. However, the estimated mass increase is as much as 1.8×10^8 ton, which is equivalent to erupted materials of one large scale eruption of the volcano. It is difficult to accept easily such large amount of mass increase without any another significant signs. To detect signs of magmatic activities and to evaluate volcanic activities appropriately by gravity measurments, it is important to calibrate instruments further and to evaluate effects of environmental factors such as precipitations.

Keywords: Izu-Oshima volcano, gravity change, ground deformation

Japan Geoscience Union Meeting 2014
(28 April - 02 May 2014 at Pacifico YOKOHAMA, Kanagawa, Japan)

SVC55-P11 Room:Poster Time:May 1 18:15-19:30

Preparation for the practical use of unmanned observation robots in the next Izu-Oshima eruption

SAIKI, Kazuto[1*] ; ICHIHARA, Mie[2]

[1]Graduate School of Science, Osaka Univ., [2]Earthquake Research Institute, Univ. of Tokyo

In the case of a volcanic eruption, in order to carry out evacuation guidance, it is important to observe the changing situation from just after the eruption to the completion of evacuation. In the 1986 eruption of Izu-Oshima, the explosive eruptions occurred at the unexpected points such as caldera floor and outside of a caldera. Therefore, volcanologists could not approach the vents and the opportunity of observation to gain the precious data for scientific understanding of the eruption phenomenon or disaster mitigation was lost. Moreover, during the evacuation from the island, the situation of the eruption had not been announced correctly to residents, and the mistaken information that the lava flow cut off the traffic between Okada-Motomachi was spread. Today, 20 years or more pass since a previous eruption in Izu-Oshima, and it has become the time to prepare the next eruption. In order to improve the situation at the time of the next eruption, development of the new observation robot which can respond immediately to an eruption and the establishment of an operation framework are required. From such a viewpoint, the author started Izu-Oshima Unmanned Observation Robot Symposium in 2009. This symposium is intended to bring together experts developing unmanned observation robots from different study fields such as volcanology, space engineering, and disaster relief to Izu-Oshima and to provide them the opportunity of field tests and exchange of knowledge to make them accelerate the development of the robots and the establishment of the operation framework. For these four years, many participants gathered to perform field test and to have an active information exchange. 8 UGV and 2 UAV from 9 research groups (2009), 5 UGV and 2 UAV from 5 groups (2010), 13 UGV and 3 UAV from 9 groups (2011), and 13 UGV and 6 UAV from 10 groups (2012) participated in the symposium. In the 2013 fiscal year, Izu-Oshima was hit by the 27th typhoon of the year just before the symposium. While an open lecture meeting was canceled, 5 UGV and 1 UAV from 6 groups performed field tests. In the 2013 fiscal year, we started to obtain an accommodation of the research funds for this activity from the specific joint research B of Earthquake Research Institute of the University of Tokyo. Furthermore, installation of volcano monitor cameras was also begun by inhabitants' cooperation. At the presentation, the results so far and a future view will be shown. For further detail of the symposium in the current fiscal year please refer to the following URL (http://www.volcano-robot.org/index.html). Izu-Oshima monitor camera can be accessed by the following URL (http://www.volcano-robot.org/oshima_camera/monitor_top.php) .

Keywords: Izu-Oshima, unmanned observation robot, robot, Miharayama

Japan Geoscience Union Meeting 2014
(28 April - 02 May 2014 at Pacifico YOKOHAMA, Kanagawa, Japan)

SVC55-P12 Room:Poster Time:May 1 18:15-19:30

Pressure sources of Miyakejima volcano estimated from crustal deformation

FUKUI, Miyo[1*] ; MATSUSHIMA, Takeshi[1] ; OIKAWA, Jun[2] ; WATANABE, Atsushi[2] ; OKUDA, Takashi[3] ; OZAWA, Taku[4] ; MIYAGI, Yosuke[4] ; KOHNO, Yuhki[4]

[1]SEVO, Kyushu University, [2]ERI, University of Tokyo, [3]EVRC, Nagoya University, [4]NIED, Japan

Miyakejima volcano had deflated after the 2000 eruption. The deep region of the volcano has inflated since 2006 (JMA, 2013). It suggests magma accumulation for future eruptions. JMA, GSI, JCG and NIED independently observe crustal deformation using GPS. However, the observation networks are not enough to reveal the magma accumulation model.

A dense GPS campaign observation started in Miyakejima from 2011 associate with Kyushu University, University of Tokyo, Nagoya University and NIED. New GPS observation points have been established every year to improve spatial resolution of crustal deformation and estimation of the magma source parameter. In 2013, our observation network are constructed 21 points in total including new two points near summit crater where no observation after the 2000 eruption.

By assembling all the continuous GPS data that has been observed by each institution, and our observation data, integrated processing was made so as to measure the precise crustal deformation on the island for two years in 2011-2013.

As the result, the obtained deformation in this study indicates inflation in the south region of Miyakejima and deflation around the crater. The estimated magma sources are a shallow deflation sill source under the crater, a southern inflation dyke source and a deep inflation spherical source. Ozawa & Ueda (2011) estimated a flat source under the caldera using InSAR technique. The parameters of this model are consistent with our sill model. Further, only deep spherical inflation source estimated in prior studies cannot be described the observed deformation during this period. We think the supply of magma began to new inflation dyke source from deep spherical inflation source. In order to monitor the inflation source, it is necessary to enhance the southern observation network and obtain more detailed geodetic data.

Keywords: GPS, Miyakejima, Crustal deformation, Volcano, Magma chamber

Japan Geoscience Union Meeting 2014
(28 April - 02 May 2014 at Pacifico YOKOHAMA, Kanagawa, Japan)

SVC55-P13 Room:Poster Time:May 1 18:15-19:30

The products of 2012-2013 mud eruption event at Million Dollar Hole crater, Ioto volcano

NAGAI, Masashi[1*] ; TANADA, Toshikazu[1] ; UEDA, Hideki[1] ; KOBAYASHI, Tetsuo[2]

[1]National Research Institute for Earth Science and Disaster Prevention, [2]Kagoshima University

Explosive eruptions occurred several times in the period from February 2012 to April 2013 at the Million Dollar Hall crater in Ioto (Iwo Jima) Island. The situation of eruptions and properties of the ejecta are summarized as follows.

At the eruption occurred in the duration from 7 to 9 February 2012, muddy volcanic ash were erupted from vents arranged NNW-SSE direction. The main vents were consist of follows. Vent A that occurred within the existing crater (25m in diameter, approximately 10m deep) at south-southeast side, vent C that was occurred in center of the existing shallow crater (30m in diameter) at north-northwest side, and vent B that was probably newly formed between the two. Thickness of ejecta layer was 30 or 40 cm on rim of each vent. Because isopach contours are irregularly shaped, tephra are estimated that were emitted directionally from each vent. Then, small scale muddy volcanic ash release and steam plume activities was followed.

The eruption on 17 to 18 February 2013 was the largest. Muddy volcanic ash were erupted from the location of vent A and B, and fell on the western side. Thickness of ejecta layer are 1 to 3 meter on vent rim. Cinders and minor man-made Objects there were possibility of ballistic ejecta reached distant point approximately 220m at the maximum from the vents. After the eruption, vent A and B were combined into a single crater (35m in diameter, 17m deep). In addition, the formation of collapse crater about 40m in diameter began at the location of vent C.

The eruption on 11 April 2013 was occurred at the collapse crater (vent C). Muddy volcanic ash deposited on the southern side. The maximum thickness of ejecta layer is 45 centimeter on the vent rim. Ballistic cinders were witnessed at the eruption, but the limit of distribution was not estimated. Vent C was combined with vents A. Therefore, the whole shape of the crater became a cocoon (60m in major axis, 17m deep). Thereafter, the crater has remained in calm state.

Volcanic ash that erupted in the series of eruptions were wet at the ejection and deposition. They are composed mainly of hydrothermal alteration clay consisting of smectite and kaolin minerals and also includes large amount of lithic fragments, free crystals and volcanic glass fragments that are altered varying degree. In addition, pieces of glass and iron piece of man-made weaponry, which is said to have been abandoned after World War II. In addition, pieces of glass and iron which were derived from weapons abandoned immediately after World War II are also included. Ballistic cinders consists of such as tuffaceous sandstone, tuff and altered trachyandesite.

Eruptive volume of each eruption are estimated approximately as follows. The eruption in February 2012 is 800 m^3, the eruption on 17-18 February 2013 is 11,000 m^3, and the eruption on April 11, 2013 is 2,000-4,000 m^3. Total volume is 14,000 to 16,000 m^3 approximately. On the other hand, total amount of subsidence in this peroid is 10,000 to 15,000 m^3, it is roughly equal to the eruptive volume.

These eruptions are considered phreatic explosion that blew off strongly altered rocks surrounding the hydrothermal reservoir and shallow non- or weakly altered tuffaceous rocks. It indicates that the hydrothermal activity under Million Dollar Hole crater became active in relation to rapid crustal deformation that occurred in Ioto from early 2011 to May 2012.

Keywords: tephra, depositional structure, surface phenomena, eruption record

Japan Geoscience Union Meeting 2014
(28 April - 02 May 2014 at Pacifico YOKOHAMA, Kanagawa, Japan)

SVC55-P14 Room:Poster Time:May 1 18:15-19:30

2013 eruption of Nishinoshima volcano, Ogasawara islands, Japan

ITO, Koji[1*] ; ONO, Tomozo[1] ; SASAHARA, Noboru[1] ; NOGAMI, Kenji[2]

[1]Japan Coast Guard, [2]Volcanic Fruid Research Center, Tokyo Institute of Technology

Nishinoshima volcano is a basaltic to andesitic maritime volcano on the volcanic front of the Izu-Bonin arc. For the first time ever, the submarine eruption including movement of vents and development and disappearance of new islands happened off the southeastern coast of the Nishinoshima island in 1973. The eruption stopped in May 1974 and the Nishinoshima island and the new volcanic islands were joined by sand drift in June. Then geographic changes was continued by erosion and sand drift till 1990s.

The eruption column and new volcanic island were firstly discovered by the airplane of Japan Defensive Force on 20 Nov. 2014. Then Japan Coast Guard found the new volcanic island with violent phreatomagmatic eruption. The following day, 21 Nov. 2013, phreatomagmatic eruption had occurred and volcanic edifice was developing. The eruption style changed into the Strombolian-type and lava started to flow from the vent on the eastern flank of main edifice on 22 Nov. 2013. In succeeding days, lava emerged from the western vent and pyroclastic cone was built up in the large crater in the center of main edifice. The vent of the pyroclastic cone effused blue-white volcanic gas consistently and spatter occasionally. On 24 Dec. 2013, new vent started to produce eruption colmun at the north of the central vent. These vents are located on the 1973 vents.

The new volcanic island consists of lava flow and water depth around eruption center may be almost constant, so growth rate of the island and magma supply rate should be equal. The growth rate estimated from the air photo is almost constant, hence the magma supply rate may be kept constant.

It is unclear that when did this volcanic activity start. But high temperature anomaly and difference of normalized water-leaving radiance within sea water are shown at the southern sea area in the satellite images published by the Earth Observation Research Center on Nov. 7. The volcanic activity may start on or before Nov. 7.

Future volcanic scenarios are uncertain, but volcanism is still active and shows no sign of end of eruption as of early-February.

Keywords: Nishinoshima volcano, volcanic island, Izu-Ogasawara arc, phreatomagmatic eruption, Strombolian eruption, maritime volcano

Japan Geoscience Union Meeting 2014
(28 April - 02 May 2014 at Pacifico YOKOHAMA, Kanagawa, Japan)

SVC55-P15 Room:Poster Time:May 1 18:15-19:30

The recent volcanic activities of Mt. Asosan

KATO, Koji[1*] ; NAGATO, Shinya[2] ; MATSUSUE, Shinichi[2] ; HIRAMATSU, Hideyuki[2]

[1]Japan Meteorological Agency, [2]Fukuoka District Meteorological Observatory

Mt. Asosan is one of the most active volcanoes in Japan.
In Mt. Asosan, volcanic tremor amplitude and volcanic earthquakes increased on September 2013. On November 2014, water level of crater lake decreased. On December 2014, volcanic tremor amplitude increased again and the emission rate of the SO2 increased. On January 2014, Mt. Asosan erupted. We report about recent volcanic activity of Mt. Asosan

Japan Geoscience Union Meeting 2014
(28 April - 02 May 2014 at Pacifico YOKOHAMA, Kanagawa, Japan)

SVC55-P16 Room:Poster Time:May 1 18:15-19:30

Gravity variation near the crater of Aso volcano and gravity contribution of precipitation

HAYAKAWA, Hideaki[1*] ; KAGIYAMA, Tsuneomi[1] ; OHKURA, Takahiro[1] ; YOSHIKAWA, Shin[1]

[1]Graduate School of Science, Kyoto University

We investigated the gravity variation continuously measured near the active crater of Aso volcano. At the period of low volcanic activity, the gravity variation is dominated by a contribution of water mass movement arisen from percolation of rain water and discharge in a permeable layer under about 100m.

In this study, it is used a time series measured by a superconducting gravity meter, CT-200, which installed in Hondo tunnel under 30m located in about 1000m southwest of Nakadake first crater. An analysis period is for 3 years from February, 1998 to January, 2001. Aso volcano was quiet low active for this period. The hot lake in Nakadake first crater, Yudamari, which its state is an index of the volcanic activity, had been in high water level. There were no events of drying up and eructation of volcanic ash. The gravity variation removed tide and air response shows large seasonality, increasing 20 - 40 μGal at July and August after rainy season and decreasing gradually after that. It also has some minor changes in response to precipitation, for example, an increase of about 10 μGal after autumnal rain.

It is known that precipitation has an affect on gravity. However, the effect near the crater of Aso volcano did not well understand. We computed water flux by percolation into underground and water discharge from a permeable layer using a kind of physical model of storage function method known as tank model. Model input is amount of precipitation measured at Asosan meteorological station by Japan Meteorological Agency. The change of water volume contained in underground is computed from input-output difference of tank model. The gravity contribution is obtained from the corresponding density change in a region of 1400km in north-shouth and in east-west around the gravity meter with thickness from surface to 200m depth. It assumes that there is no gravity change by volcanic activity. Outflow resistance of a tank and permeable layer depth are decided so that the gravity contribution fits in the measured gravity variation as much as possible.

The gravity contribution of water mass movement by model computation is well coincident with the measured gravity variation in the case that rainwater percolates under 100m in vertically and is discharged horizontally from the permeable layer at 100 - 110 m depth. The model value correlates highly with the measured gravity value in the coefficient of 0.9. The root mean squares (RMS) are 10.5 μGal for the measured gravity and 11.4 μGal for the model computation, and 4.8 μGal for difference between the two. The model computation overestimates to a certain degree. It is considered for a reason of the discrepancy that percolation and ground water flow in general are complicate and non-linear phenomena in contrast to our linear model. However, the model computation represents sufficiently figures of the measured variation and explains it in accuracy of 14.4 μGal in 3σ RMS of the difference. The contribution of water mass movement in shallow underground to 110m depth is inferred to be main component of gravity change near the crater.

The water mass movement can be computed at any period of time. In this study, we obtained the gravity contribution under 30m where the gravity meter located in. Converting it to on ground, the model prediction is available for use in correction of values measured near the crater in the repeated gravity survey at Aso volcano area. A part of discharge from the permeable layer in the computing region is considered as a source of ground water flow into Yudamari. A seasonal peak of precipitation is for about a month from June to July, however the ground water flow continues for several months after rainy season. This is coincident with the seasonal water level change of Yudamari. It is expected to estimate a possible quantity of ground water flow into Yudamari as time variation.

Keywords: Aso volcano, Gravity, Water mass movement, Precipitation, Groundwater, Superconducting gravity meter

Japan Geoscience Union Meeting 2014
(28 April - 02 May 2014 at Pacifico YOKOHAMA, Kanagawa, Japan)

SVC55-P17 Room:Poster Time:May 1 18:15-19:30

Thermal activities of the Nakadake first crater at Aso volcano, Japan -Unusual heat discharge events in 2012-2014-

TERADA, Akihiko[1*]

[1]Volcanic Fluid Research Center, Tokyo Institute of Technology

Aso volcano is one of the most active volcanoes in Japan in terms of the persistent release of volatiles and thermal energy from the Nakadake first crater. Throughout most of the calm period, the crater emits significant amounts of volcanic gas, including 200 - 400 tonne/day of SO_2. The first crater contains a hot crater lake, locally referred to as Yudamari with a diameter greater than 200 m. Applying the model of Ryan et al. (1974), which involves the effects of free and forced convection, Terada et al. (2012) estimated that during the calm period, the heat discharge through the lake surface is almost constant, with a value of approximately 220 MW.

The water level falls rapidly preceding an active period. The disappearance of lake water is followed by the emergence of a red-hot crater bottom or wall and a phreatic-to-phreatomagmatic and strombolian eruption sequence that lasts several months. When the volcanic activity subsides to calm period levels, the lake reforms. These dramatic falls/rises in the lake water level are likely caused by increases/decreases in the input of high-temperature steam to the crater bottom (Terada et al., 2012).

In spring of 2012, an unusual event involving the increase in water temperature and rapid decrease in water level occurred at the Yudamari crater lake. The heat discharge rates approached the figure of 600 MW which is three times higher than the representative figure in a calm period. The computational results based on energy and mass conservation indicate that the event is caused by an increase in temperature and flux of fluid inputs from the lake bottom. Preceding the event, silica content in lake water clearly increased, indicating a rise in temperature of hydrothermal system beneath the Yudamari crater lake. The event was accompanied by slight increase in SO_2 emission rate, but seismicity around the crater did not change significantly.

After September 2013, the lake water of Yudamari almost disappeared. Consequently volcanic fluid emitting from the crater bottom ascended as a buoyant plume into the air without transportation of the heat to the lake water. To estimate the rate of heat discharge from the first crater, we applied the plume rise assumption (Briggs, 1969; Kagiyama, 1981). This assumption states that the height h of a given position in a fumarole increases proportionally with time t to the power of 2/3. Video records of surveillance camera operated by Japan Meteorological Agency are used to the analysis.

In September, 2013 and December, 2013 - January, 2014, seismicity including earthquake swarms and volcanic tremors were enhanced, which were accompanied by an increase in SO_2 emission rates up to 2,000 tonne/day. During the periods, heat discharge rates are estimated to be 800-1000 MW which is several times higher than the figure measured in a calm period. The ratio of H_2O/SO_2 has been roughly maintained whereas small amount of volcanic ash including juvenile materials were continuously emitted in January 2014. This may occur as a result of an increase in amount of degassing in the conduit beneath the first crater.

Acknowledgments: I would like to thank Yoshihiro Ushiroshoji, Shinya Nagato and the Fukuoka District Meteorological Observatory, Japan Meteorological Agency for sharing their data and for providing permission for the data to be published.

Keywords: heat discharge rate, Aso volcano, hot crater lake, eruption

Japan Geoscience Union Meeting 2014
(28 April - 02 May 2014 at Pacifico YOKOHAMA, Kanagawa, Japan)

SVC55-P18 Room:Poster Time:May 1 18:15-19:30

The temporal changes of the shallower resistivity structure associated with a small eruptions at Aso Volcano, 2014.

UTSUGI, Mitsuru[1*] ; KAGIYAMA, Tsuneomi[1] ; HAYAKAWA, Hideaki[1] ; INOUE, Hiroyuki[1]

[1]Graduate School of Science, Kyoto Univ.

On Aso volcano, many observations and research have been made to detect the subsurface structure and detailed information about the distribution of the subsurface hydrothermal system have been obtained from previous studies. From the high-density AMT survey, Kanda et al. (2008) found a low resistivity area is localized just beneath the Nakadake first crater. This area is considered as a chamber of the hydrothermal fluid which is formed by a part of the hydrothermal fluid which is supplied from the deeper magma. In recently, the activities of the Nakadake crater were often temporarily increased. Associated with these activities, it is expected that the distribution of the subsurface hydrothermal fluid is changed and subsurface resistivity structure is temporally changed. In order to detect such a temporal change of shallow resistivity structure according to these activities, we carried out the repeated control sourced electromagnetic survey around the Nakadake crater using ACTIVE observation system (Utada et al., 2007). In these observations, we installed electric current transmitter on 1 km NNE from the crater, and magnetic receiver was also installed on the 4 points around crater.

In Aso volcano, a small eruption occurred in January 2014, and this activity has continued after this eruption.

During this activity, we carried out the electromagnetic survey around Nakadake crater of Aso volcano. In our presentation, we will show the observation data and the resistivity structure obtained by the 1-D analysis of our data.

Keywords: registivity structure, Aso volcano

Japan Geoscience Union Meeting 2014
(28 April - 02 May 2014 at Pacifico YOKOHAMA, Kanagawa, Japan)

SVC55-P19 Room:Poster Time:May 1 18:15-19:30

Crustal deformation associated with increase in VLP events activity in Aso Volcano

OHKURA, Takahiro[1*] ; YOSHIKAWA, Shin[1] ; INOUE, Hiroyuki[1]

[1]AVL,Kyoto Univ.

Aso Volcano, one of the most active volcanoes in Japan, is located in the central part of Kyushu and consists of an elliptical caldera with a diameter of 18km in E-W and 25km in N-S, and of central cones with more than 10 volcanoes aligned in E-W direction. Among central cones, Nakadake volcano is the only active cone and its recent activity is characterized by ash and strombolian eruptions and phreatic or phreatomagmatic explosions. The last strombolian eruptions ended in the beginning of the 1990s and after that, surface activities have been restricted to the fumarolic gas and ash emission from the northernmost crater of the volcano accompanying activity of long period tremors(LPT) or very long period (VLP) events.

Since 1990s, observations using broadband seismometers have revealed that the source of LPT is a crack-like conduit located at depths of 1-1.5 km beneath Nakadake, with a length of 1km and width of 2.5km. It is also revealed that at this depth a pressure was located and caused long-period displacements a few minutes before phreatic eruption which occurred in 1993 and 1994.

The Japan Meteorological Agency (JMA) raised the Volcanic Alert Level from 1 (Normal) to 2 (Do not approach the crater) based on rapid increase in numbers volcanic earthquakes and volcanic gas emission in September 2013, and based on increase in amplitude of volcanic tremors in December 2013, respectively.

Remarkable ground deformation was detected by water-tube tilt meters and super invar-rod extensometers which were installed in a 30m observation tunnel, 1km southwest from the active crater, in September 2013 and January 2014 associated with increase in VLP events activity.

By comparing the calculated deformation assuming a Mogi source and a dyke, is found that observed deformation can be attributed to the expansion of the crack-like conduit. At the beginning of the deformation, the radial component of the extensometer showed dilatation and converted to contraction, which indicates initiation of expansion at the deeper portion of the crack and propagation to the shallower part.

Keywords: Aso Volcano, Crustal deformation, VLP events, Volcanic gas, Conduit

Japan Geoscience Union Meeting 2014
(28 April - 02 May 2014 at Pacifico YOKOHAMA, Kanagawa, Japan)

SVC55-P20 Room:Poster Time:May 1 18:15-19:30

Remote temperature sensing on fumaroles in active volcanoes using stable isotopes of trace gases in volcanic plume

KOMATSU, Daisuke[1*] ; TSUNOGAI, Urumu[1] ; NAKAGAWA, Fumiko[2]

[1]Graduate School of Environmental Studies, Nagoya University, [2]Graduate School of Science, Hokkaido University

Molecular hydrogen (H_2) in a high-temperature volcanic fumarole (>400 degreeC) reach to the hydrogen isotope exchange equilibrium with coexisting fumarolic H_2O under the outlet temperature of the fumarole. In this study, we applied this hydrogen isotope exchange equilibrium of fumarolic H_2 as a tracer for the remote temperature sensing on the fumarolic area in the 1^{st} crater of Mt. Naka-dake (Aso volcano) where direct measurement on fumaroles was not practical, by deducing the hydrogen isotopic composition (dD value) of fumarolic H_2 remotely from those in volcanic plume. The reciprocal of H_2 concentration in the plume samples showed a good linear relationship with the dD values. The linear relationships suggested that both the concentrations and the dD values of H_2 in the plume samples can be explained by simple mixing between two end-members, both of which can be classified to a single category at least for the dD values of H_2. By extrapolating the linear relationship between $1/H_2$ and dD to $1/H_2$=0 to exclude the contribution of the tropospheric H_2 from the dD value of each sample, we estimated that the dD value of fumarolic H_2 to be -172+-16 per mil vs. VSMOW and the apparent equilibrium temperature (AET_D) to be 868+-97 degreeC. Although the estimated temperatures using the IR thermometers were much lower than the AET_D, we concluded that the AET_D represented the highest outlet temperature of the fumaroles in Aso volcano and that the dimensions of the fumaroles at surface smaller than the pixel of the IR thermometers was responsible for the temperatures lower than the AET_D. That is to say, temporal variation in the dimensions of fumaroles at surface, probably due to variation in the emission flux of fumarolic gases, was responsible for the temporal variation in the temperature determined by the IR thermometers, while the actual outlet temperature of the Aso fumaroles keeps the high temperature almost equal to the equilibrium temperature of fumarolic gases.

Keywords: fumarolic gases, carbon dioxide, molecular hydrogen, stable isotopes, isotopic exchange equilibrium, remote temperature sensing

Japan Geoscience Union Meeting 2014
(28 April - 02 May 2014 at Pacifico YOKOHAMA, Kanagawa, Japan)

SVC55-P21 Room:Poster Time:May 1 18:15-19:30

Strange seismic, infrasonic, and geodetic phenomena observed 3 days before the 2011 eruption of Shinmoe-dake volcano

ICHIHARA, Mie[1*] ; OIKAWA, Jun[1] ; TAKEO, Minoru[1]

[1]Earthquake Research Institute, University of Tokyo

Shinmoe-dake volcano started its climatic events on January 26 at 14:49. Some precursory phenomena have been found in petrologic studies. The ash from a phreatic eruption on January 19 contained fresh pumice fragments indicating ascent of new magma to a shallow depth (Miyabuchi et al., 2013; Suzuki et al., 2013). Petrologic analyses of the eruption products from the climatic events showed evidences of magma mixing in two stages before the eruptions; Suzuki et al. (2013) estimated the times of the first and second mixing to the eruption as >14 days and 0.7-15 hours, respectively, while Tomiya et al. (2013) conclusively proposed 0.4-3 days and several hours, respectively, and suggested that the first mixing likely triggered the eruption.

On the other hand, no clear precursory signals have been identified in geophysical observations. Considering the above petrologic studies, we reexamined the seismic, infrasonic, and geodetic data in a few weeks to the eruption, and particularly focused on a sequence of strange phenomena on January 23, three days before the eruption. It was the only notable phenomena recognized in several days to the eruption, but has not been reported elsewhere.

Nakada et al. (2013) referred to the JMA report (2012) that volcanic tremor was first recorded at 01:27 on 19 January and continued from the 19 January afternoon to the morning of 23 January. In fact, the tremor started to be recorded at stations around the summit of Shinmoe-dake at 12:45 on 18 January and increased significantly after the phreatic eruption at 01:27 on the 19th. If there was any sign indicating rise of new magma to the shallow depth before the phreatic eruption, the tremor could be the candidate.

On January 23, there was a clear infrasound signal continuing from 4:11 to 4:53 with an amplitude about 1 Pa and a sharp peak frequency at 1.8 Hz. The events was nearly aseismic and the regional seismic stations recorded infrasound shaking of the ground. The bad weather condition prohibited visual observation to see if any surface activity accompanied. At 6:00, the tremor power increased at stations on the north flank while it decreased at a station on the west flank, indicating some change of the source. The tremor power decreased from 8:00 to 8:30, stayed at the low level until 13:15, and then recovered to the previous level by 14:00. It was more distinct at stations close to the summit of Shinmoe-dake; the power decrease was more than an order of magnitude at the nearest station, SMN, 700 m from the summit. After the recovery the tremor stayed nearly same levels until the small eruptive event on the 26th before the main event. During the quiescent period of the tremor, gradual tilt up toward the summit was detected by a broadband seismometer at station SMN. Although, seismic activity except the tremor was low around the days, the quiescent period had more seismic events including relatively low-frequency ones.

Although causal relations among these events or their relation to the magma mixing are totally unclear, the sequence of phenomena on January 23 is potentially important to understand the processes leading to the climatic events of the Shinmoe-dake eruption.

Keywords: Eruption, Tremor, Infrasound, Precursor, Tilt

Japan Geoscience Union Meeting 2014
(28 April - 02 May 2014 at Pacifico YOKOHAMA, Kanagawa, Japan)

SVC55-P22 Room:Poster Time:May 1 18:15-19:30

Relationship between Infrasound Signals and Plume Heights by the JMA's Weather Radar, the Shinmoe-dake 2011 Eruption

TAKAGI, Akimichi[1*] ; SHIMBORI, Toshiki[1] ; YAMAMOTO, Tetsuya[1] ; FUKUI, Keiichi[2]

[1]Meteorological Research Institute, [2]Kakioka Magnetic Observatory

During the continuous sub-plinian eruption of the 2011 Shinmoe-dake eruption, the JMA's weather RADAR detected the sequential echoes from the volcanic plume (Shimbori et al., 2013). We report the brief result of basic analysis for the relationship between the plume heights and infrasound signals.

The eruption cloud echo data observed at the Kagoshima Airport Doppler RADAR (Kagoshima DRAW) were analyzed. While Kagoshima DRAW has the threshold of radar reflectivity factor, its time interval of the volume scan is shorter as 5 minutes. In this study, in order to improve the accuracy of time, the time of the plume top in a volume scan was identified by every scanning time of the antenna.

The relationship between the plume height and discharge rate of magma has the empirical power law, and its power index was estimated to be 0.259 (Sparks, 1997). Assuming that the discharge rate has the proportional relation with the integration of the infrasound signal generated by eruption (Takagi at al., 2013), we estimate the power law between the echo height and infrasound data for this eruption. In the result, the most appropriate power index was estimated to be 0.55, and the delay time and the time window of the infrasound data which make error smaller are 4 minutes and 6 minutes, respectively.

These time delay and window might be subjected to height and velocity of plume top. More advanced analysis for plume heights and infrasound signals would disclose the dynamics of volcanic plume.

Acknowledgements

We would like to thank Drs. Y. Tanaka, O. Suzuki, H. Yamauchi and E. Sato (MRI, JMA) for the use of their "Draft" radar analysis software.

Keywords: lume height, weather radar, infrasound, Shinmoe-dake

Japan Geoscience Union Meeting 2014
(28 April - 02 May 2014 at Pacifico YOKOHAMA, Kanagawa, Japan)

SVC55-P23 Room:Poster Time:May 1 18:15-19:30

Long-period seismic waves propagating over Kyushu as associated with the Sakurajima eruption of August 18, 2013

IKEDA, Ayami[1] ; KUGE, Keiko[1*] ; KAZAMA, Takahito[1] ; MATSUZAWA, Takanori[2]

[1]Dept. Geophysics, Kyoto University, [2]NIED

We found long-period seismic waves propagating over Kyushu after the explosive eruption from Showa crater of Sakurajima volcano at 16:31JST on August 18, 2013. The eruption is one of the most significant ones that Showa crater has experienced since 2006, and the volcanic plume rose approximately 5000 m high. Showa crater is currently very active, causing more than 1000 eruptions a year.

The broadband seismic network F-net recorded the long-period seismic waves traveling in a very wide area covering Amami and the whole Kyushu region. The dominant periods are longer than 5 s. The apparent propagation velocity is approximately 2.75 km/s. In data recorded by Hi-net tilt meters at shorter intervals of around 20 km, the long-period seismic waves arrived earliest at the station AIRH that is the closest to Sakurajima volcano, and propagated with the almost same apparent velocity as observed by F-net. The long-period seismic waves are, therefore, likely to have been radiated from Sakurajima volcano. Assuming that the source is located at Showa crater, we rotated two horizontal components of the F-net and Hi-net data to transverse and radial components. The long-period seismic waves were observed in the radial and transverse components, and the apparent propagation velocity is slightly faster in the transverse component than the radial one. The waves observed in transverse and radial components can be Love and Rayleigh waves, respectively.

For previous eruptions of Sakurajima volcano, we also examined whether or not long-period seismic waves were recorded by F-net. From 5057 eruptions in the period between 2006 and 2013, we selected 43 eruptions that have large amount and height of a volcanic plume as well as large deflation volume. Long-period seismic waves were found for five eruptions including ones from Minami-dake crater. The maximum distances with the observations of long-period seismic waves range from 150 to 331 km, which are much shorter than for the 2013 eruption. Therefore, the 2013 eruption could excite long-period seismic waves more remarkably, compared to the other five eruptions. Observations of long-period seismic waves, on the other hand, did not have clear dependence on the amount and height of a volcanic plume or the deflation volume.

We observed significant transverse components of the long-period seismic waves associated with the 2013 eruption, which are considered Love waves. We also had similar observations for the five eruptions accompanied by long-period seismic waves in F-net data. Eruptions of Sakurajima volcano have been explained by isotropic explosion and contraction of a vertical cylinder (Uhira and Takeo, 1994; Tameguri et al., 2002), and these models cannot excite Love waves. A model for explaining Love waves observed in the present study is to be investigated.

Japan Geoscience Union Meeting 2014
(28 April - 02 May 2014 at Pacifico YOKOHAMA, Kanagawa, Japan)

SVC55-P24 Room:Poster Time:May 1 18:15-19:30

Comparison between areas of VT earthquakes around Sakurajima Volcano and a 3-D velocity model of the upper crust

YAKIWARA, Hiroshi[1*] ; HIRANO, Shuichiro[1] ; MIYAMACHI, Hiroki[1] ; TAKAYAMA, Tetsuro[2] ; ICHIKAWA, Nobuo[2] ; TAMEGURI, Takeshi[2]

[1]GSE, Kagoshima Univ., [2]SVRC, DPRI, Kyoto Univ.

Volcano-tectonic (VT) earthquakes associated with volcanic activities of Sakurajima Volcano also occur beneath Kagoshima Bay around the volcano (Hidayati et al., 2007). Not only seismic observations on land but also ones using Ocean Bottom Seismographs (OBSs) are need to detect micro VT earthquakes beneath the bay, and to improve accuracies of the hypocenter locations of the earthquakes. Authors therefore have performed OBS observations five times since 2009. In the present study, we summarize hypocenter distributions of the VT earthquakes obtained by OBS observations. We also compare the hypocenters and a three-dimensional seismic velocity model derived from regional earthquake data in order to extend knowledge for active area of the VT earthquakes.

The areas where the earthquakes occurred are summarized as follows: 1) Shallow VT earthquakes generated beneath Wakamiko Caldera. Most of the earthquakes were located shallower than or equal to 5 km depth. 2) Small number of VT earthquakes were also located at 5-10 km depth off the northeastern coast of the volcano. This activity may be steadily. 3) No earthquake was detected beneath the western half of Aira Caldera.

On the other hand, we also analyzed a three-dimensional seismic velocity model by use of regional earthquake data (Mera et al., 2013) to compare the hypocenter distribution and the velocity model. As a result of the 3-D inversions, we obtained reliable P- and S-wave velocities at the depth range of 5-12km under the area in and around the volcano. At shallower than 6 km depth, the model delineates an area of Low-Vp (5.3-5.4 km/s) and Low-Vs (3.0-3.1 km/s) beneath the area of south of Wakamiko Caldera. A peak of the low velocity area tends to close the volcano at the portion deeper than 6 km depth. At 10 km depth, a peak of Low-Vp (5.4-5.5 km/s) and Low-Vs (3.1-3.2 km/s) was imaged beneath an area off northeast coast of the volcano (beneath Shin-jima Island). Obviously low velocity areas also spread from the volcano to the area off the south coast of the volcano.

Because several recorder troubles happened among the five OBS observations, we selected the hypocenters of the VT earthquakes which were located using data recorded at common three OBS stations. As a result of the comparison between the hypocenters of the VT earthquakes and the 3-D velocity model, most of the VT earthquakes were located where intermediate velocities were estimated. Furthermore, some of VT earthquakes occurred in close vicinity of the peaks of Low-Vp and Low-Vs areas. The former suggests that the strains by crustal deformation hardly accumulate at areas of high and low velocities. The latter may reflect the increase of pore pressures and stress changes generated by existence of volcanic fluids.

Keywords: Sakurajima Volcano, Volcano-tectonic earthquakes, Three-dimensional seismic velocity model

Japan Geoscience Union Meeting 2014
(28 April - 02 May 2014 at Pacifico YOKOHAMA, Kanagawa, Japan)

SVC55-P25 Room:Poster Time:May 1 18:15-19:30

Repetitive seismic survey 2013 in Sakurajima Volcano.

TSUTSUI, Tomoki[1*] ; MASATO, Iguchi[2] ; NAKAMICHI, Harushisa[2] ; TAMEGURI, Takeshi[2] ; YAKIWARA, Hiroshi[4] ; OHMINATO, Takao[5] ; SUGAI, Akira[3] ; OSHIMA, Hiromitsu[6] ; MIURA, Satoshi[7] ; YAMAMOTO, Mare[7] ; ICHIKI, Masahiro[7] ; NOGAMI, Kenji[8] ; TAKEO, Minoru[5] ; ICHIHARA, Mie[5] ; OIKAWA, Jun[5] ; YAMANAKA, Yoshiko[9] ; OHKURA, Takahiro[2] ; ABE, Yuki[2] ; SHIMIZU, Hiroshi[10] ; YAMASHITA, Yusuke[10] ; MIYAMACHI, Hiroki[4] ; KOBAYASHI, Reiji[4] ; MIKI, Daisuke[2] ; YAMAMOTO, Keigo[2] ; MAEKAWA, Tokumitsu[6] ; HIRAHARA, Satoshi[7] ; ATSUSHI, Watanabe[5] ; OKUDA, Takashi[9] ; HORIKAWA, Shinichiro[9] ; MATSUHIRO, Kenjiro[9] ; SONODA, Tadaomi[2] ; SEKI, Kenjiro[2] ; YOSHIKAWA, Shin[2] ; HIRANO, Shuichiro[4] ; WATANABE, Yukihiro[3] ; USUI, Yuji[3] ; KOBAYASHI, Tsukasa[3] ; IKEDA, Keiji[3] ; NAGATO, Shinya[3] ; KOEDA, Tomoyuki[3]

[1]Akita University, [2]Kyoto University, [3]Japan Meteorological Agency, [4]Kagoshima University, [5]University of Tokyo, [6]Hokkaido University, [7]Tohoku University, [8]Tokyo Institute of Technology, [9]Nagoya University, [10]Kyushu University

The latest report on structural evolution and on effect of the density reduction in the seismic network will be presented through the sixth round of the repetitive seismic experiment in Sakurajima Volcano. Sakurajima Volcano locates in Kagoshima, south Kyushu, which is one of the most active volcanoes in Japan. The repetitive seismic experiment have been carried out since 2008 in order to detect and research structural evolution along volcanic activity, with using 4.5Hz sensors. This round has carried out as a part of the experiment which presented by Nakamichi et al. in this conference.

The detection and researching the structural evolution approach to magma movement under the ground along volcanic activity and will provide essential measure on development of volcanic activity. Extending its result into evaluation on flux and accumulation will bring significant informations on considering scenario about volcanic activity in progress. And the experiments should be sustainable method because of long time scale of the target.

The latest report about structural evolution will be presented. Details and results of the experiment rounds have been reported in these conferences since 2009. The seismic response along the line in the north flank have changed year by year. Two major sweet spots have been found at 4.9km depth in the northeastern Sakurajima and at 8km depth beneath northern flank of Kitadake, the northern edifice, through these experiments. The changes in seismic response are interpreted as a result of mass movement underground with going volcanic activity. Further change is expected associating with development of volcanic activity.

The effect of density reduction will be also discussed. Though the repetitive seismic experiments with two lines have been done with about 250 stations every December until 2012, the latest experiment with the most sensitive line with 74 stations on the northern flank was carried on December 2013. Discussions on the effect of density reduction in the seismic network is necessary in order to have a style of sustainable execution of the research.

Keywords: Sakurajima Volcano, Reflection seismology, Dynamic structure, Controlled source seismology

Japan Geoscience Union Meeting 2014
(28 April - 02 May 2014 at Pacifico YOKOHAMA, Kanagawa, Japan)

SVC55-P26 Room:Poster Time:May 1 18:15-19:30

Active source seismic experiment in and around Sakurajima volcano in 2013 and comparison with the experiment in 2008

NAKAMICHI, Haruhisa[1*] ; TSUTSUI, Tomoki[2] ; TAMEGURI, Takeshi[1] ; IGUCHI, Masato[1] ; YAKIWARA, Hiroshi[3] ; OHMINATO, Takao[4] ; SUGAI, Akira[5] ; OSHIMA, Hiromitsu[6] ; MIURA, Satoshi[7] ; YAMAMOTO, Mare[7] ; ICHIKI, Masahiro[7] ; NOGAMI, Kenji[8] ; TAKEO, Minoru[4] ; ICHIHARA, Mie[4] ; OIKAWA, Jun[4] ; YAMANAKA, Yoshiko[9] ; OHKURA, Takahiro[1] ; ABE, Yuki[1] ; SHIMIZU, Hiroshi[10] ; YAMASHITA, Yusuke[10] ; MIYAMACHI, Hiroki[3] ; KOBAYASHI, Reiji[3] ; MIKI, Daisuke[1] ; YAMAMOTO, Keigo[1] ; MAEKAWA, Tokumitsu[6] ; HIRAHARA, Satoshi[7] ; WATANABE, Atsushi[4] ; OKUDA, Takashi[9] ; HORIKAWA, Shinichiro[9] ; MATSUHIRO, Kenjiro[9] ; SONODA, Tadaomi[1] ; SEKI, Kenjiro[1] ; YOSHIKAWA, Shin[1] ; HIRANO, Shuichiro[3] ; WATANABE, Yukihiro[5] ; USUI, Yuji[5] ; KOBAYASHI, Tsukasa[5] ; IKEDA, Keiji[5] ; NAGATO, Shinya[5] ; KOEDA, Tomoyuki[5]

[1]Kyoto University, [2]Akita University, [3]Kagoshima University, [4]University of Tokyo, [5]Japan Meteorological Agency, [6]Hokkaido University, [7]Tohoku University, [8]Tokyo Institute of Technology, [9]Nagoya University, [10]Kyushu University

We conducted active seismic experiment in and around Sakurajima volcano in December 2013, five years after the similar experiment that was conducted in 2008. We deployed 280 temporary seismic stations, 90% of which were located at the same locations of the experiment in 2008. Six explosive shots with 200 kg or 300 kg charges were detonated in December 5. The 2013 shot locations (S1, S2, S4, S5 and S6) are less than 60 m from the 2008 shot locations except for 1 shot (S3). We successively observed the explosions and volcanic events during nighttime nine hours continuous recording. The continuous records contain not only waveforms excited by the six shots but also by an explosive eruption and volcanic tremor. We evaluate cross-correlations of waveforms at the same station locations that obtained in 2008 and 2013 to detect temporal change of subsurface structure beneath Sakurajima volcano except for S3.

Member organizations of the Research Group of the Seismic Dynamic Structure in Sakurajima Volcano: Graduate School of Science, Hokkaido University, Graduate School of Engineering and Resource Science, Akita University, Graduate School of Science, Tohoku University, Earthquake Research Institute, University of Tokyo, Volcanic Fluid Research Center, Tokyo Institute of Technology, Graduate School of Environmental Studies, Nagoya University, Graduate School of Science, Kyoto University, Disaster Prevention Research Institute, Kyoto University, Graduate School of Science and Engineering, Kagoshima University, and Japan Meteorological Agency

Keywords: active seismic experiment, temporal change, volcanic activity, eruption, Sakurajima volcano, Aira caldera

Japan Geoscience Union Meeting 2014
(28 April - 02 May 2014 at Pacifico YOKOHAMA, Kanagawa, Japan)

SVC55-P27 Room:Poster Time:May 1 18:15-19:30

Active monitoring by using ACROSS in Sakurajima volcano - observation report 3 -

MIYAMACHI, Hiroki[1*] ; ARIKADO, Natsumi[1] ; YAKIWARA, Hiroshi[1] ; YAMAOKA, Koshun[2] ; WATANABE, Toshiki[2] ; KUNITOMO, Takahiro[2] ; IGUCHI, Masato[3] ; TAMEGURI, Takeshi[3] ; MIKADA, Hitoshi[3] ; TAKENAKA, Hiroshi[4] ; SHIMIZU, Hiroshi[5] ; IKUTA, Ryoya[6]

[1]Kagoshima University, [2]Nagoya University, [3]Kyoto University, [4]Okayama University, [5]Kyushu University, [6]Shizuoka University

In 2012, in order to realize quantitative monitoring of magma transport process, we deployed the ACROSS (Accurately Controlled Routinely Operated Signal System) vibrator system composed of two vibrators in the site that is 3.6 km apart from the northwest of the Minamidake crater of Sakurajima.

On September 2012, we have started the full-scale operation under synchronized control of two vibrators with a frequency modulation, in which the modulation period is 50 seconds and the frequency range is 5 to 15 Hz, to produce broad frequency range of signal: one vibrator 'SKR1' with a signal frequency range of 7.510Hz +/- 2.50Hz and the other 'SKR2' with the range of 12.505Hz +/- 2.50Hz. The signal from the ACROSS source is routinely monitored with more than 20 permanent seismic stations in and around Sakurajima volcano. Five temporal seismic stations are also deployed to increase the spatial coverage of monitoring. The signals recorded at the seismic stations are deconvoluted with the source function to obtain the transfer function between the source and the receivers.

In this report, we estimated the daily transfer functions for the SKR2 vibrator at each station by every 5 days stacked data during a whole period (400 days from September 19, 2012 to October 23, 2013) of the operation. It is obviously found that these daily transfer functions vary temporally. To detect quantitatively the temporal variation of the transfer functions, we analyzed the variation of the transverse component (Tt) of the transfer functions at 7 seismic stations located in Sakurajima Island as folllows:

(1) We analyzed the transfer function obtained at temporal seismic station 'GOMI' located at about 50m apart from the ACROSS source to verify the stability of power of the seismic waves generated by the ACROSS source. According to the result, we rejected the transfer function evaluated during a period of the unstable power condition from a whole period of the operation.

(2) We visually inspected arrival times and amplitudes for the specific phases in the transfer functions at each station during the period of the stable power condition of the ACROSS, and obtained the quantitative temporal variation for the specific phases.

(3) On a simple assumption that the specific phases are SH waves (the transverse component of the transfer functions), we presumed the depth range where each specific phase propagated in the 5 horizontally layered model simplified from the results of the exploration seismic experiment (Miyamachi et al., 2013).

(4) We compared the temporal variation of the specific phases with activity of volcanic eruptions by JMA, the temporal change of the N-S and E-W horizontal distances (GPS data) in Sakurajima Island, and the temporal change of strain at the HAR station measured by Kyoto University.

In the presentation, we will show the observation results in detail. This ACROSS research project in Sakurajima volcano is still in a pioneering stage, and we have plans in the future to continue our project.

Keywords: Sakurajima volcano, ACROSS

Japan Geoscience Union Meeting 2014
(28 April - 02 May 2014 at Pacifico YOKOHAMA, Kanagawa, Japan)

SVC55-P28 Room:Poster Time:May 1 18:15-19:30

Vertical ground deformation in Sakurajima volcano and around Aira caldera: results of leveling survey in Oct.-Nov. 2013

YAMAMOTO, Keigo[1*] ; MATSUSHIMA, Takeshi[2] ; YOSHIKAWA, Shin[3] ; OHKURA, Takahiro[3] ; YOKOO, Akihiko[3] ; AIZAWA, Koki[2] ; INOUE, Hiroyuki[3] ; MISHIMA, Taketoshi[3] ; UCHIDA, Kazunari[2] ; SONODA, Tadaomi[1] ; SEKI, Kenjiro[1] ; KOMATSU, Shintaro[1] ; HOTTA, Kohei[3] ; TAKAHASHI, Atsushi[3] ; TOYOFUKU, Takashi[4] ; ASANO, Haruka[4] ; NARITA, Tsugunori[4]

[1]Disaster Prevention Research Institute, Kyoto University, [2]Faculty of Sciences, Kyushu University, [3]Graduate School of Science, Kyoto University, [4]Geospatial Information Authority of Japan

We conducted the precise leveling survey in Sakurajima volcano and around Aira caldera in October and November 2013, following the repeated leveling surveys to evaluate the vertical ground deformation associated with the recent eruptive activity of this volcano. The leveling routes measured in 2013 survey are about 117 km long in total, including Sakurajima coast route, Sakurajima western flank route, Sakurajima northern flank route, Kagoshima Bay western coast route (BM.2469 - BM.2474 - BM.J), Kagoshima Bay eastern coast route (BM.2500 - BM.J.2797) and Soo route (BM.J.2797 - BM.2785). These leveling routes were measured by the joint university team during the period of November 5-22 and by Geospatial Information Authority of Japan (GSI) during the periods from October 25 to November 7 and of November 13-26.

The obtained survey data are compared with those of the previous surveys conducted in October-December 2007 and November-December 2012, resulting in the relative vertical displacements of the bench marks. The resultant displacements show the ground uplift around Aira caldera as well as the ground subsidence near the central part of Sakurajima. From the analysis based on Mogi's model, the inflation and deflation sources are located beneath the center of Aira caldera and beneath the center of Sakurajima, respectively.

These results indicate that the magma storage at the magma reservoir beneath Aira caldera is still progressed. On the other hand, they also suggest the increase of the amount of ejected magma at the magma reservoir beneath the center of Sakurajima volcano, reflecting the recent increase of the eruptive activity at Showa crater.

Keywords: Sakurajima volcano, Aira caldera, precise leveling survey, vertical ground deformation

Japan Geoscience Union Meeting 2014
(28 April - 02 May 2014 at Pacifico YOKOHAMA, Kanagawa, Japan)

SVC55-P29 Room:Poster Time:May 1 18:15-19:30

Movement of pressure source at Sakurajima volcano after 2006 revealed by continuous GPS observation data

HOTTA, Kohei[1*] ; IGUCHI, Masato[2] ; OHKURA, Takahiro[1] ; YAMAMOTO, Keigo[2]

[1]Graduate School of Science, Kyoto University, [2]DPRI, Kyoto University

Ground deformation around Sakurajima has been mainly detected by precise leveling, and has been modeled with 2 spherical pressure sources at the center of the Aira caldera (about 10 km depth) and at beneath the summit crater (about 4 km depth) (Eto, 1989, Annuals of DPRI, Kyoto Univ.). The ground around the Aira caldera turned to uplift since 1993. After continuous GPS observation started at Sakurajima in 1995, explosive activity at summit crater temporally increased at the end of 1999, and Showa crater started eruptive activity at June 2006. Large deformation rate was obtained prior to these eruptive activities, and a pressure source was located at depths 6-8 km near the northern coast of Sakurajima by assuming a spherical source (Hotta et al., 2013, Annual of DPRI, Kyoto Univ.). It is thought that both of pressure sources at the center of the Aira caldera and at beneath the summit crater expanded, and a pressure source apparently moved toward northern coast of Sakurajima. Eruptive activity at Showa crater has increased since 2009. In this study, we analyzed GPS data to make clear process of magma movement accompany with eruptive activity of Showa crater.

GPS data observed by SVO (Sakurajima Volcano Observatory) and GEONET data during 2006-2012 were analyzed by using PPP-AR analysis of GIPSY OASIS II ver. 6.1.2. Although no significant deformations are found during 2006-2009, variable deformation rates are found after around 2009.

Here, we focused on the period of the largest deformation rate after eruptive activity at Showa crater started (from October 2011 to March 2012). At first, we searched average positions of pressure sources whole the period by using GA. Pressure sources located at the center of Aira caldera (8.3 km depth; source A) and beneath Sakurajima (2.9 km depth; source B). Next, fixing the position of source A at the average position (because previous studies also obtained pressure source at the center of Aira caldera around this average position), we set a time window with 4 month period, and shifted it by 10 days. Source B moved from around Kitadake toward the northern part of Sakurajima during 1st time window (October 1, 2011-January 31, 2012) to 6th one (November 21, 2011-March 21, 2012), and then moved toward beneath Minamidake at 7th one (December 1, 2011-March 31, 2012). During the period of November 26, 2011-March 25, 2012, which is middle of 6th and 7th time windows, source B located around Kitadake. Deformation pattern of GPS stations at the northern part of Sakurajima changed around the end of December 2011. Moreover, eruptive activity at Showa crater increased from December 2011. These suggest that magma migrated from Aira caldera toward Sakurajima at around December 2011.

Keywords: Sakurajima volcano, Aira caldera, ground deformation, GPS, Mogi’s model

Japan Geoscience Union Meeting 2014
(28 April - 02 May 2014 at Pacifico YOKOHAMA, Kanagawa, Japan)

SVC55-P30 Room:Poster Time:May 1 18:15-19:30

The importance of hydrological disturbance corrections for relative gravity data: A case study at Sakurajima Volcano

KAZAMA, Takahito[1*] ; YAMAMOTO, Keigo[2] ; FUKUDA, Yoichi[1] ; IGUCHI, Masato[2]

[1]Kyoto Univ., [2]DPRI, Kyoto Univ.

An empirical water balance model was created to correct for hydrological disturbances in relative gravity data repeatedly measured at Sakurajima Volcano, southern Japan. This study aims to quantitatively monitor gravity signals due to magmatic activities of Sakurajima Volcano, and we here present the first applied results of the empirical model. The hydrological disturbances were simply calculated by the product of the instant gravity response to unit precipitation and land water storage, which were estimated using digital topography and observed meteorological data. The calculated hydrological disturbance was consistent with the observed absolute gravity data at Harutayama Station from 2010 to 2011 within 8 micro-gal (1 [micro-gal] = 1 E-8 [m/s2]), which was smaller than the typical accuracy of relative gravity measurements (˜10 micro-gal). In addition, after we subtracted (i.e., corrected) the calculated disturbances from the measured relative gravity data at Sakurajima Volcano, the average amplitude of the corrected gravity changes during 2007-2009 was reduced by 90 % compared with that of the original gravity data. Since gravity changes have been measured using both absolute and relative gravimeters at volcanic areas these days, hydrological disturbance corrections should be applied to the relative gravity data, not only to the absolute one. By sophisticating the effects of spatiotemporal variations in precipitation, evapotranspiration, and infiltration capacity, this model will enable us to robustly monitor long-period and wide-spread gravity variations associated with volcanic activities.

Keywords: Sakurajima Volcano, gravity change, hydrological disturbance, relative gravity measurement, absolute gravity measurement, infiltration capacity

Japan Geoscience Union Meeting 2014
(28 April - 02 May 2014 at Pacifico YOKOHAMA, Kanagawa, Japan)

SVC55-P31 Room:Poster Time:May 1 18:15-19:30

Automated sulfur dioxide flux observation at Suwanosejima volcano, Japan, and comparing to seismic data

MORITA, Masaaki[1*] ; MORI, Toshiya[1] ; IGUCHI, Masato[2] ; NISHIMURA, Takeshi[3]

[1]Geochem. Res. Center, Univ. of Tokyo, [2]DPRI, Kyoto Univ., [3]Dept. Geophys., Tohoku Univ.

Suwanosejima is a remote volcanic island located about 240 km south-southwest of Kagoshima city, Kyushu Island, Japan. This volcano has been erupting very frequently since early-1950s, and is one of the most active volcanoes in Japan. Previous studies on sulfur dioxide (SO_2) flux measurement of Suwanosejima are very limited and reported that daily average SO_2 flux from this volcano ranged about 5–15 kg/s [Mori et al., 2004; Hirabayashi et al., 2005]. Therefore, we conducted automated SO_2 flux measurement at Suwanosejima volcano to understand SO_2 flux variation with long-term observation at Suwanosejima volcano and to evaluate a relation between SO_2 flux and seismic data.

We developed automated SO_2 flux measurement system to conduct automated observation in such a remote island. The power consumption of the scanning instrument was significantly improved compared to that in the previous studies. The observation was conducted for January 21, 2013–May 7, 2013 (Period I) and November 5, 2013–the present (Period II). The observation system has been working without any trouble for more than 200 days in total showing robustness of the developed system.

SO_2 flux was calculated with a corrected differential optical absorption spectroscopy method for radiative dilution effect [Mori at al., 2006; Kern et al., 2009]. In the observation period of over 200 days, SO_2 flux was calculated for 40 days. The average SO_2 flux in the total observation period was 13.4 kg/s, which ranged from 5.9 kg/s to 34.5 kg/s. The average and the standard deviation in Period I were 16.9 kg/s and 6.2 kg/s, and those in Period II were 14.0 kg/s and 5.7 kg/s, respectively.

Since previously reported SO_2 flux in 2000s [Mori et al., 2004; Hirabayashi et al., 2005] were not corrected for the dilution effect, these values might be significantly underestimated. The average and the standard deviation of uncorrected SO_2 flux for the dilution effect in this study were 9.7 kg/s and 4.3 kg/s. This range was comparable to the range of the previous studies in 2000s. Considering above, SO_2 flux range has been stable since at least 2000s.

Surface and seismic activities in Period I (January 21–May 7, 2013) significantly differed from those in Period II (November 5, 2013–the present). Period I was in a continuous volcanic tremor period (September 2012–July 2013), and Period II was in an intermittent explosions and volcanic tremors period. In contrast to the surface and seismic activities, SO_2 flux variations in Period I and II were almost in the same range. This implies that degassing rate of magma for these two periods were similar. Therefore, the difference of surface and seismic activities which was observed in these periods needs to be explained considering the stable degassing magma rate.

Keywords: Volcanic gas, Sulfur dioxide, Flux, Suwanosejima volcano, Automated observation, Seismic data

Japan Geoscience Union Meeting 2014
(28 April - 02 May 2014 at Pacifico YOKOHAMA, Kanagawa, Japan)

SVC55-P32 Room:Poster Time:May 1 18:15-19:30

Shallow active magma body beneath Taal Volcano Island, Philippines

KUMAGAI, Hiroyuki[1*] ; LACSON, Rudy[2] ; MAEDA, Yuta[1] ; FIGUEROA, Melquiades[2] ; YAMASHINA, Tadashi[3] ; BORNAS, Ma. antonia[2]

[1]Nagoya University, [2]PHIVOLCS, [3]Kochi University

Taal volcano, Philippines, is one the world's most dangerous volcanoes in view of its explosive eruption history and close proximity to populations. Electromagnetic, geodetic, and seismic studies have been extensively conducted at this volcano to reveal its magma system. Recent deployment of a realtime broadband seismic network has detected long-period (LP) and volcano-tectonic (VT) events that occurred beneath Taal. Our source location analysis of VT events using both onset arrival times and high-frequency seismic amplitudes points to the existence of a strong attenuation region with a shear-wave quality factor (Q) of around 10 near the surface at the eastern flank of Volcano Island in Taal Lake. This region is located just beneath the active fumarolic area and LP source and above inflation and deflation pressure sources, and is coincident with a low resistivity region. The attenuation region matches with that inferred from an active seismic survey conducted in 1993 at Taal volcano. These features strongly suggest that the attenuation region represents an active degassing magma body near the surface, which persistently existed for more than 20 years. Our study synthesized with previous studies clarifies the magma system beneath Taal, which further addresses volcanic risk at Volcano Island sitting on a shallow active magma body.

Japan Geoscience Union Meeting 2014
(28 April - 02 May 2014 at Pacifico YOKOHAMA, Kanagawa, Japan)

SVC55-P33 Room:Poster Time:May 1 18:15-19:30

Waveform analysis on initial phases of explosion earthquakes at Lokon-Empung volcano, Indonesia

TAISHI, Yamada[1*] ; AOYAMA, Hiroshi[1] ; NISHIMURA, Takeshi[2] ; YAKIWARA, Hiroshi[3] ; NAKAMICHI, Haruhisa[4] ; OIKAWA, Jun[5] ; IGUCHI, Masato[4] ; MUHAMAD, Hendrasto[6] ; YASA, Suparman[6]

[1]Faculty of Sci., Hokkaido Univ., [2]Graduate School of Sci., Tohoku Univ., [3]Faculty of Sci., Kagoshima Univ., [4]DPRI, Kyoto Univ., [5]ERI, Univ. of Tokyo, [6]CVGHM, Indonesia

Excitation mechanism of explosion earthquake that often accompanies explosive Vulcanian eruptions is understood to be macroscopically explained by a downward single force acting in the vent. In the meantime, it is revealed that the excitation of initial phases of explosion earthquake occurs earlier than the explosion at the crater [e.g. Tameguri et al., 2002]. So the excitation of the initial phases of explosion earthquake can be regarded as one of the most important processes to understand the initiation of Vulcanian eruption. However, the researches focusing on the initial phases are not so common in spite of their scientific importance. In this study, we implemented temporary observation of Vulcanian eruption at Lokon-Empung volcano in Indonesia and estimated source parameters of the initial phases of explosion earthquakes to compare them to the previous works at Sakurajima volcano and Suwanosejima volcano.

Lokon-Empung volcano located in the northern part of Sulawesi island is known as one of the very active volcanoes in Indonesia. We deployed seismic and infrasound observation network around Lokon-Empung in September 2012. During about one-year-long observation, 46 events of explosion earthquakes associated with Vulcanian eruptions had been recorded. Seismograms of explosion earthquakes have common features in the initial phases at all stations; the compressional P phase arrives first, and a larger dilatational phase follows it. Comparison between seismic and infrasound record shows that the excitation of the P phase occurs about 1 second earlier than that of infrasound which is thought to be excited by the explosion at the crater. Particle motion analysis reveals that these initial phases consist of P wave and propagate from the direction of the active crater. Since signal to noise ratio of the first compressional wave (P phase) is not good at some distant stations, we focus on the second dilatational phase (D phase). We performed waveform fitting on the D phase using synthetic seismogram to estimate source depth, shape of source time function, contraction mechanism and seismic moment.

For most events, we obtained the best fitting solution with cylindrical contraction source located at 1 km below the crater. We compared the estimated seismic moment of D phase and the amplitude of seismogram and infrasound with those reported in the previous works, and found that the strength of the explosion of Lokon-Empung ranks between those of Sakurajima and Suwanosejima. At Sakurajima volcano, Tameguri et al. (2002) showed that the amplitude of infrasound is independent from the moment of D phase. On the other hand, Hirai (2013) reported a positive correlation between them at Suwanosejima volcano. Estimated focal depths of D phase at these two volcanoes are 2 km and 100 - 400 m, respectively. At Lokon-Empung volcano, we recognized a weak positive correlation between the amplitude of infrasound and the moment of D phase. The comparison suggests that the shallower focal depth of D phase becomes, the stronger the correlation between moment of D phase and strength of infrasound appears. This result we obtained here will provide a new insight into the unrevealed process between the excitation of D phase and the surface explosion.

Keywords: Vulcanian eruption, Explosion earthquake

Japan Geoscience Union Meeting 2014
(28 April - 02 May 2014 at Pacifico YOKOHAMA, Kanagawa, Japan)

SVC55-P34 Room:Poster Time:May 1 18:15-19:30

Recent eruptive activity at Sinabung Volcano, Northern Sumatra, Indonesia

NAKADA, Setsuya[1*] ; YOSHIMOTO, Mitsuhiro[2] ; ZAENUDIN, Ahkmad[3] ; SUZUKI, Yuki[1] ; HOKANISHI, Natsumi[1] ; TAKAGI, Natsuko[1] ; HENDRASTO, Mochammad[3] ; IGUCHI, Masato[4] ; OHKURA, Takahiro[5]

[1]ERI, Univ. of Tokyo, [2]Grad. Sch. Sci., Hokkaido Univ., [3]CVGHM, Indonesia, [4]Disaster Res. Inst., Kyoto Univ., [5]Grad. Sch. Sci., Kyoto Univ.

Sinabung in the Northern Sumatra of Indonesia began its eruptive activity with phreatic events in August and September 2010. It resumed its activity in September 2013 with phreatic events. In November 2013, eruption columns stood about 5 km above the volcano. Volcanic ash issued since the middle November contained juvenile particles, and pumice fragments were ejected on to the NE flank of the volcano by the vulcanian event on 23 November 2013. Small-scale pyroclastic flows descended during the events. Though the eruptive activity had declined since early December, occurrence of low-frequency earthquakes replaced high-frequency events common during explosive events. Following partial collapse of the summit crater outer-slope repeated, lava appearance was confirmed in late December. Lava appeared in the summit crater grew as a dome and started its partial collapse on 30 December, generating pyroclastic flows which descended on the SE slope of the volcano. The lava dome grew into a lava flow moving to the SE, repeating its partial collapse. The horizontal length of the lava flow exceeded 1 km in late January 2014.

Several tens collapses occurred everyday in January 2014. Relatively large collapse (pyroclastic flows) generated on 7, 11 and 21 January and 1 February. Pyroclastic flows on 1 February traveled about 4.5 km, according to newspapers, and 15 local people who invaded into the danger zone, 5 km from the summit, were involved in the flows.

The present eruption at Sinabung is close to the eruption of 9 to 10th Century of this volcano in terms of both eruption site and scale. It is also similar to lava-dome eruptions at Unzen, Japan, in 1991-95 and at Soufriere Hills, Montserrat, West Indies, in 1995-present, where lava dome/flow growth associated with pyroclastic-flow events continued for several years.

Based on the chemical analyses of pumice of the Vulcanian event on 23 November 2013 and pebbles included in pyroclastic flow event on 11 January 2014, magma of this eruption (hornblende andesite) is similar to but a little poorer in SiO_2 (58-59%) than the magma of the 9 to 10th Century (59-60%).

Keywords: Indonesia, Sinabung, volcanic eruption, pyroclastic flow, lava flow, hornblende andesite

Japan Geoscience Union Meeting 2014
(28 April - 02 May 2014 at Pacifico YOKOHAMA, Kanagawa, Japan)

SGC56-01 Room:415 Time:April 30 14:15-14:30

Metal-silicate partitioning of U, Th, Nd, Sm at high P-T: Implications for heat and chemical budget in the core

NOMURA, Ryuichi[1*] ; HIROSE, Kei[1] ; KIMURA, Jun-ichi[2] ; CHANG, Qing[2]

[1]ELSI, Titech, [2]IFREE, JAMSTEC

The excess abundance of siderophile elements in the mantle has been proposed that the core was equilibrated with the mantle at ˜3500 K, ˜30GPa and fO2˜△IW-1 at the Earth ' s formation (e.g. Righter, 2011 EPSL). Much more severe condition (>6500 K) is supposed immediate aftermath the moon-forming giant impact based on the study of numerical simulation (e.g. Canup, 2012 Science). The occurrence of high-temperature equilibrium between the core and the mantle evoked that the early core had once incorporated heat-genic radionuclides (U, Th) and rare earth elements (e.g. Nd, Sm), which are know as highly lithophile elements, suggesting profound implications for the thermal history (Nimmo, 2007 Treatise on Geophysics) and early-formed geochemical reservoirs (e.g. sub-chondritic 142Nd/144Nd, Boyet and Carlson, 2005 Science).

However, partitioning of these elements between liquid metal and silicate melt has been investigated only up to 20 GPa and 2500 K using multi-anvil apparatus (Malavergne et al., 2007 GCA). Here, we extended pressure and temperature conditions up to 138 GPa and 5200 K at △IW-2˜-1 using laser-heated diamond cell (LH-DAC) and field emission-type electron probe microanalyzer (FE-EPMA, JXA-8530F, JEOL) and laser-ablation inductively coupled plasma mass spectrometry (LA-ICP-MS, Kimura and Chang, 2012 JAAS). K (4wt%) and trace elements (U, Th, Nd, Sm, Hf, W, Pb) doped pyrolitic gel, and pure iron were used as starting materials. Iron-free pyrolitic gel was used as a thermal insulator. After high P-T experiments using LH-DAC, recovered samples were analyzed by FE-EPMA and LA-ICP-MS for major and trace elements, respectively. Fe and Mg were used as internal standards for metal and silicate, respectively for LA-ICP-MS. The diameter of ablated area was about 10 um, small enough to measure each (silicate melt/liquid metal) phase.

The results are summarized as follows;

(1) Partition coefficient of U and Th are 10-3-10-2 at 3500-4000 K and △IW-1 to -1.5, resulting in 0.02-0.2 ppb (<0.03 TW) U and 0.08-0.8 ppb (<0.04 TW) Th into the core assuming that the abundance of U and Th are 22 and 83 ppb in the Earth ′ s mantle (McDonough and Sun, 1995). Total <0.1 TW (present-day) heat flow in the core has negligible effect on the thermal history of the Earth with <50 K change in the initial temperature at core-mantle boundary (Nimmo, 2007 ToG).

(2) The ratio of partition coefficients, D_{Nd}(metal/silicate)/D_{Sm}(metal/silicate), was always unity despite of large temperature dependence for each D, suggesting that the core could not be a candidate for an early-formed (with sub-chondritic 142Nd/144Nd) hidden reservoir.

Japan Geoscience Union Meeting 2014
(28 April - 02 May 2014 at Pacifico YOKOHAMA, Kanagawa, Japan)

SGC56-02 Room:415 Time:April 30 14:30-14:45

Element partitioning between mantle minerals and melt under deep lower mantle condition

TATENO, Shigehiko[1*] ; SAKATA, Shuhei[2] ; HIRATA, Takafumi[2] ; HIROSE, Kei[3]

[1]Dept. Earth & Planetary Sciences, Tokyo Institute of Technology, [2]Dept. Earth & Planetary Sciences, Kyoto University, [3]Earth-Life Science Institute, Tokyo Institute of Technology

Melting is a primary mechanism of chemical evolution of our planet. Earth's mantle would have been completely molten due to moon-forming giant impact, leading to a global magma ocean. Resultant fractional crystallization by secular cooling progressively induced the chemical evolution of the Earth. As a consequence, remnant silicate melt left at the present day at the base of the mantle is a possible explanation for the seismically observed ultralow-velocity zones (ULVZs). The knowledge of melting phase relations and element partitioning between mantle minerals and partial melt is crucial to understand the chemical evolution in the early Earth and the nature of ULVZs. However, melting experiments under the middle to deep lower mantle conditions are quite limited.

Here we carried out the melting experiments on KLB-1 peridotite and basalt to deep lower mantle conditions up to 179 GPa by a combination of laser-heated diamond-anvil cell experiments and chemical analyses of recovered samples. Textural characterization and chemical analysis on major and minor elements were made by a field-emission-type electron microprobe (FE-EPMA). Trace element abundances were determined by a laser-ablation inductively coupled plasma mass spectrometry (LA-ICP-MS). Typical crater diameter was 2 or 5 μm by using ArF Excimer laser.

Results shows that the liquids phase was $MgSiO_3$-perovskite at least above 34 GPa and further to post-perovskite in KLB-1 peridotite. The Fe-Mg distribution coefficients (K_D) between perovskite/post-perovskite and melt decreased considerably with increasing pressure, leading to strong Fe-enrichment in partial melts. It supports dense partial melts in a deep lower mantle, which migrate downward to the core mantle boundary (CMB). Furthermore, $CaSiO_3$-perovskite (CaPv) was found to be a liquids phase under whole lower mantle condition in MORB bulk composition. We then investigated the minor/trace element partitioning between CaPv and melt in basaltic composition. Partition coefficient of alkali elements such as Na and K increases with increasing pressure. In particular, potassium, known as highly incompatible element, become compatible with pressure, whose partition coefficient exceeded the unity at 90 GPa. Although pressure effect on D_{Sm} and D_{Nd} was not found even to 80 GPa, D_{Sm}/D_{Nd} decreases with increasing pressure and will reach to the unity at around 100 GPa. Our results shows that Sm and Nd was equally partitioned to partial melt and residual solids upon fractionation of CaPv from primordial deep magma ocean. This has profound implications for the origin of the super-chondritic $^{142}Nd/^{144}Nd$ for all terrestrial rocks.

Japan Geoscience Union Meeting 2014
(28 April - 02 May 2014 at Pacifico YOKOHAMA, Kanagawa, Japan)

SGC56-03 Room:415 Time:April 30 14:45-15:00

Melting relation on FeO-SiO2 system at high pressure and the fate of the subducted banded iron formations

KATO, Chie[1*] ; NOMURA, Ryuichi[1] ; HIROSE, Kei[2] ; MIYAKE, Akira[3] ; OHISHI, Yasuo[4]

[1]Department of Earth and Planetary Sciences, Tokyo Institute of Technology, [2]Earth-Life Science Institute, Tokyo Institute of Technology, [3]Division of Earth and Planetary Sciences, Kyoto University, [4]Japan Synchrotron Radiation Research Institute

Subduction of banded iron formations (BIFs) may have played a significant role on the evolution of the core-mantle boundary (CMB) region and the chemical stratification at the topmost core. Almost all of the BIFs that had been deposited on the seafloor must have been subducted into the mantle and only a small portion was left at the surface today. Because of their high density, BIFs may have fallen down toward the CMB region. The amount of subducted BIFs is estimated to be $2*10^8$ km^3, which roughly matches with the total volume of the ultra-low velocity zones (Dobson and Brodholt, 2005, *Nature*). BIFs would be composed mainly of FeO and SiO_2 in the lower mantle because its oxidation state is close to iron-wustite buffer. We have performed melting experiments on FeO-SiO_2 system by laser-heated diamond-anvil cell technique at 25 - 140 GPa. FE-EPMA and FIB-SEM chemical analysis and observation of the texture of the recovered samples revealed that the liquidus phase was SiO_2 when starting from Fe_2SiO_4 fayalite, and compositions of the quenched melt suggested that the composition of the eutectic point was extremely FeO-rich ($<$0.6 wt% SiO_2). The solidus curve was constrained by observing the existence or no-existence of tiny quenched melt pools in each recovered samples. The solidus temperature at CMB pressure was 3,100 to 3,300 K that were lower than the solidus of pyrolite and the geotherm (Nomura et al., 2014, *Science*). These results imply that when the BIFs reach the CMB, they generate FeO-rich liquid that would be mixed with the basal magma ocean (Labrosse et al., 2007, *Nature*). This liquid would form a thin layer spread along CMB and react with the topmost core. Silicon content in liquid iron varies inversely to the oxygen fugacity when equilibrium with silicate melt (Ricolleau et al., 2011 *EPSL*). Assuming silicon-rich bulk core, exchange of silicon and oxygen would occur between the topmost core and FeO-rich silicate melt. This mechanism may account for the seismic wave speed anomaly observed at the topmost core which is thought to be honor to chemical stratification (Helffrich and Kaneshima, 2010 *Nature*; Buffett and Seagle, 2010 *JGR*).

Japan Geoscience Union Meeting 2014
(28 April - 02 May 2014 at Pacifico YOKOHAMA, Kanagawa, Japan)

SGC56-04 Room:415 Time:April 30 15:00-15:15

Standardless determination of Nd isotope ratios in glasses and minerals using LA-MC-ICP-MS

KIMURA, Jun-ichi[1*] ; QING, Chang[1] ; KAWABATA, Hiroshi[2]

[1]JAMSTEC, [2]Kochi University

We investigated an appropriate instrumental setup for a laser-ablation multiple-collector inductively coupled plasma mass spectrometer (LA-MC-ICP-MS) and found that a reduced oxide setting allowed accurate and precise analysis of Nd isotope ratios in samples with or without concomitant interfering elements. We used an Aridus II solution?excimer laser dual-intake system. The ICP interface used normal sample and skimmer cones with torch shield switched off and an additional large interface rotary pump. The setting accomplished reduced oxide levels NdO+/Nd+ 0.01?0.05%, without significant sacrifice of the instrumental sensitivity (˜70%). Oxide molecular ions for the lighter elements were negligible and accurate internal mass bias corrections were achieved for both Sm and Nd using isotopic ratios derived from thermal ionization mass spectrometry measurements. This report reveals a novel setup that requires no external mass bias corrections (standardless analysis) for Sm and Nd isotope analyses by both solution- and LA-MC-ICP-MS methods. Solution analysis of La Jolla Nd standard gave a 143Nd/144Nd ratio of 0.511860 +/- 0.000026, which is in excellent agreement with the reference value (relative deviation (RD) = +6 ppm). JMC Nd standard solution yielded a 143Nd/144Nd ratio of 0.512216 +/- 0.000044 (RD = -14 ppm) while a Sm-doped JMC solution showed 0.512211 +/- 0.000030 (RD = -23 ppm). For LA analyses, the observed ratios and RDs were 143Nd/144Nd = 0.511921 +/- 0.000013 (RD = -12 ppm) for NIST SRM 610 glass standard (430 ppm Nd/453 ppm Sm); 0.512490 +/- 0.000018 (RD = +14 ppm) for Durango apatite (1121 ppm Nd/147 ppm Sm); 0.512200 +/- 0.000009 (RD = -26 ppm) for Fish Canyon Tuff sphene; 0.512232 +/- 0.000003 (RD = +65 ppm) for EDR monazite; and 0.512890 +/- 0.000147 (RD = +34 ppm) for groundmass of a St. Helena lava (22.7 ppm Nd/˜5.01 ppm Sm). All measurements were in good agreement with the reference values. Examinations on Sm/Nd elemental fractionation have also been made and we confirmed that this was originated from the ICP interface region rather than at laser ablation site.

Keywords: LA-MC-ICP-MS, Nd isotope, glasses, minerals

Japan Geoscience Union Meeting 2014
(28 April - 02 May 2014 at Pacifico YOKOHAMA, Kanagawa, Japan)

SGC56-05 Room:415 Time:April 30 15:15-15:30

Grain boundary diffusion of polycrystalline ice Ih under confining pressure of 100 MPa

NOGUCHI, Naoki[1] ; KUBO, Tomoaki[2*] ; DURHAM, William[5] ; SHIMIZU, Ichiko[4] ; KAGI, Hiroyuki[3]

[1]Graduate School of Engineering, Hiroshima University, [2]Department of Earth and Planetary Sciences, Faculty of Sciences, Kyushu University, [3]Geochemical Laboratory, Graduate School of Science, University of Tokyo, [4]Department of Earth and Planetary Science, Graduate School of Science, University of Tokyo, [5]Department of Earth, Atmospheric and Planetary Sciences, Massachusetts Institute of Technology

Ice I_h is a primary constituent of surfaces of the icy Galilean satellites and ice sheets at the Antarctica. Thus understanding rheological behavior of ice Ih will contribute to better knowledge about the dynamics and tectonics of the surface of the icy satellites and ice sheets. Stress applied by the tidal deformation to the surfaces of the icy satellites was predicted to be very low, ˜1 MPa (Sotin and Tobie 2004), and diffusion and grain-size-sensitive creeps probably control the deformation of the surfaces of the ice satellites. The deformation map under such a low stress condition can be constructed, based on two diffusion constants, grain boundary and volume diffusion coefficients, of polycrystalline ice I_h. The volume diffusion coefficient of ice I_h was determined from experiments using a single crystal of ice I_h (Ramseier 1967; Itagaki 1967), while the grain boundary diffusion coefficient has not been determined yet. Thus we carried out experiments to determine directly the grain boundary diffusion coefficient of polycrystalline ice I_h.

The diffusion couples have been composed of a pair of disks of pore-free polycrystalline H_2O and D_2O ices. The glass beads with a diameter of 2 μm were doped in the diffusion couples to prevent the grain growth during diffusion experiments by Zener pinning effect. The volume fraction of the glass beads was approximately 1 %. The diffusion experiments were carried out under the confining pressure of 100 MPa using a gas apparatus surrounded with a cryostat (Durham et al. 2001). Temperatures were set in the range from 235 K to 256 K. After keeping the diffusion couples in the deformation instrument for 20 ˜94 hours, we shaved off thin sections from the diffusion couples. Two-dimensional diffusion profiles of the thin section were determined with micro- and imaging- Raman spectroscopes and a cryo-stage. The Raman mapping or Raman imaging measurements were carried out with keeping the thin sections at -90 ℃. The concentration of deuteron can be determined from the relative intensity of Raman band of OH stretching mode to that of OD stretching mode using a quantitative curve. The two-dimensional distribution showed enrichment of deuterium at the grain boundaries near the H_2O/D_2O boundary. It indicates that grain boundary diffusion of ice I_h is rapid. The diffusion profiles obtained by the experiments enable to estimate the grain boundary diffusion coefficient of ice I_h which is essential to construct the deformation map.

Keywords: ice, diffusion, grain boundary diffusion, hydrogen isotope, Raman spectroscopy, rheology

Japan Geoscience Union Meeting 2014
(28 April - 02 May 2014 at Pacifico YOKOHAMA, Kanagawa, Japan)

SGC56-06 Room:415 Time:April 30 15:30-15:45

Trace elements and Sr-Nd isotopic compositions of the pre-Komitake volcano

SHIBATA, Tomoyuki[1*] ; YOSHIMOTO, Mitsuhiro[2] ; FUJII, Toshitsugu[3] ; NAKADA, Setsuya[4]

[1]Institute for Geothermal Resarch, Kyoto University, [2]Faculty of Science, Hokkaido University, [3]Crisis & Environment Management Policy Institute, [4]Earthquake Research Institute, University of Tokyo

The chemical charecteristics of magmas from pre-Komitake Volcano, which is a buried and old volcanic body benarth the northeastern ?ank of Mt. Fuji, show the differences to those of Mt. Fuji (Yoshimoto *et al*., 2010). According to Yoshimoto *et al*. (2010), incompatible elements of former magmas increase with increasing SiO2, whereas those of later magmas increase at nearly constant SiO_2. They emphasized that those changes of the magma chemistry at this area from 250 ka to recent may have occurred due to a change in regional tectonics around 150 ka, although this remains unproven. To elucidate this problem, geochemical study for the magmas from pre-Komitake is essential. Therefore, we analyzed trace element and Sr-Nd isotopic compositions of those magmas.The samples are selected from the entire group, which are classified by lithology and chemistry (Group 1-3, Yoshimoto *et al*., 2010), and from 188-412m (core ERI-FJ2) and 426-624m (core ERI-FJ3) in depth. Trace elements are analyzed using by quadrupole inductively coupled plasma mass spectrometer following by the method of Chang *et al*. (2003). Sr-Nd isotopic compositions are measured by thermal ionization mass spectrometer following by the procedure of Shibata *et al*. (2007) and Yoshikawa and Shibata (2003). The enrichments of LILE's, Pb and Sr, which are general characteristics of island arc magma (eg. Wood et al., 1979), are observed from the analyzed samples in the primitive mantle normalized multi-element diagram. High Sr/Y ratios (70 in max.) and the weak positive Eu anomalies ($Eu^* = [Eu]_N/([Sm]_N/2+[Gd]_N/2$; N means condrite normalized value) are also found from several samples. The Sr and Nd isotope ratios show the variations from 0.703320-0.703476, and 0.512885-0.513087, respectively.

The Sr-Nd isotopic compositions of pre-Komitake volcano show a similar range of Mt. Fuji presented by Nagai *et al*. (2004), indicating that those magmas can be generated from the same source materials. Although the variations of Sr isotope compositions are small, significant differences are found. Most of the samples show similar Nd isotope ratios, whereas few samples show lower significant differences. These observations can be explained by 1) difference of slab derived fluid and 2) different degrees of crustal contaminations. It is unlikely that Nd isotope ratio of slab derived fluid is changed, because it is difficult keeping isotopic heterogeneity during the deep processes. Crustal rocks, which have similar Sr-Nd isotope ratios of Tanzawa tonalities (Kawate, 1996), are the candidate producing the whole isotopic variation of pre-Komitake volcano. Therefore, we prefer the contributions of crustal materials to explain the Sr-Ns isotopic variations of pre-Komitake volcano. The Eu∗shows positive correlation with Al2O3. This may indicate the plagioclase accumulation contributed the magma genesis of pre-Komitake volcano, and cause the elevation of Sr/Y ratios.

This study is supported by fund for collaboration from Earthquake Research Institute,The University of Tokyo.

Keywords: pre-Komitake, trace elements, Sr-Nd isotope

Japan Geoscience Union Meeting 2014
(28 April - 02 May 2014 at Pacifico YOKOHAMA, Kanagawa, Japan)

SGC56-07 Room:415 Time:April 30 15:45-16:00

Geochemical connection between HIMU-FOZO-PREMA: link to chemical and water content variation in oceanic crust

SHIMODA, Gen[1*] ; KOGISO, Tetsu[2]

[1]National Institute of Advanced Industrial Science and Technology, [2]Graduate School of Human and Environmental Studies, Kyoto University, Kyoto

One of fundamental concepts of the geochemistry is an existence of mantle reservoirs. Namely, isotopic composition of the ocean island basalts (OIBs) are explained by mixing of distinct and isolated reservoirs in the Earth (White, 1985; Zindler and Hart, 1986; Hofmann, 1997; Stracke, 2012). In early research on the mantle reservoirs, the isotopic composition of OIBs was mainly explained by the mixing of depleted MORB mantle (DMM) and three enriched reservoirs, those are HIMU (high-u: u = 238U/204Pb) EM1 (Enriched Mantle 1) and EM2 (Enriched mantle 2) whose isotopic compositions are enriched extremes. In addition to these reservoirs, importance of reservoirs whose isotopic compositions are common and intermediate has been pointed out, these are, FOZO (Focal Zone, Hart et al., 1992), C (common component; Hanan and Graham, 1996), PREMA (Prevalent Mantle, Zindler and Hart, 1986) and PHEM (Primitive Helium Mantle, Farley et al., 1992). Although the existences of these intermediate reservoirs are still in debated, the isotopic compositions of these reservoirs, in particular FOZO, have been frequently used to describe the isotopic distribution of OIBs. Therefore, elucidating the origin of these reservoirs should be important from the perspective of production of mantle heterogeneity (e.g., Hofmann, 1997; Stracke et al. 2005; Stracke, 2012).

To evaluate the origin of high-u (HIMU), focal zone; (FOZO) and Prevalent Mantle (PREMA), geochemical modeling was conducted from the perspective of chemical fractionation at mid-ocean ridges and subduction zones. For the modeling, MORB compositions from the Mid-Atlantic ridge are compiled for seven trace elements (Rb, Sr, Nd, Sm, Pb, Th and U) and used as representatives of oceanic crust compositions. Effect of chemical fractionation at a mid-ocean ridge is estimated based on magnesium number and frequency distribution. The results suggest that the chemical fractionation at a mid-ocean ridge can produce moderately depleted isotopic compositions those are suitable for PREMA if the age of recycled MORBs is1-2 Ga. It may follow that subduction modification is unnecessary for the production of PREMA, suggesting the importance of recycling of dry MORBs. Dehydration process at a subduction zone can produce FOZO isotopic signatures if degree of dehydration is high (4 %) that may represent maximum amount of dehydrated water. Thus, FOZO-PREMA isotopic array can be explained by mixing between recycled strongly dehydrated and dry MORBs. Consequently, PREMA-FOZO arrays could be produced by mixing between dry and dehydrated MORBs. For the production of HIMU, U and Th enrichment during crystal fractionation at mid-ocean ridge and Pb depletion owing to removal of sulfur during subduction is required in addition to FOZO production condition. As sulfur content in MORBs should be controlled by degassing process at a mid-ocean ridge, key processes that can differentiate HIMU from FOZO may be magma evolution process at mid-ocean ridge.

Keywords: HIMU, FOZO, PREMA, OIBs, recycling, mantle reservoirs

Japan Geoscience Union Meeting 2014
(28 April - 02 May 2014 at Pacifico YOKOHAMA, Kanagawa, Japan)

SGC56-08 Room:415 Time:April 30 16:15-16:30

REY-rich mud deposits around Minamitorishima Island -General overview and future reserach plan-

SUZUKI, Katsuhiko[1*] ; IIJIMA, Koichi[1] ; KATO, Yasuhiro[2] ; FUJINAGA, Koichiro[2] ; KASHIWABARA, Teruhiko[1] ; NAKAMURA, Kentaro[2] ; MACHIDA, Shiki[3] ; NOZAKI, Tatsuo[1] ; TAKAYA, Yutaro[2] ; YASUKAWA, Kazutaka[2] ; OTA, Junichiro[2] ; HARAGUCHI, Satoru[2] ; ARAKI, Shuuhei[2] ; LIU, Hanjie[2] ; NISHIO, Yoshiro[1] ; USUI, Yoichi[1]

[1]JAMSTEC, [2]Gradunate School of Engineering, Univ. of Tokyo, [3]School Creative Sci. Engineering, Waseda Univ.

We report general overview and future reserach planof REY-rich deposits around Minamitorishima Island.

Keywords: REY rich mud, Minamitorishima Island, chemical composition, research cruise, deep-sea mineral resource

Japan Geoscience Union Meeting 2014
(28 April - 02 May 2014 at Pacifico YOKOHAMA, Kanagawa, Japan)

SGC56-09 Room:415 Time:April 30 16:30-16:45

Distribution and characteristics of REY-rich mud in the Minamitorishima EEZ inferred by sub-bottom profiling

NAKAMURA, Kentaro[1*] ; MACHIDA, Shiki[2] ; FUJINAGA, Koichiro[1] ; KATO, Yasuhiro[3] ; SUZUKI, Katsuhiko[4] ; TAKAYA, Yutaro[3] ; YASUKAWA, Kazutaka[1] ; OTA, Junichiro[1] ; HARAGUCHI, Satoru[1] ; ARAKI, Shuuhei[1] ; LIU, Hanjie[1] ; USAMI, Ryo[1] ; MAKI, Ryota[1] ; IIJIMA, Koichi[4] ; NISHIO, Yoshiro[4] ; USUI, Yoichi[4] ; NOZAKI, Tatsuo[4] ; MR13-E02 LEG 2, Cruise members[4] ; KR14-02, Cruise members[4]

[1]Sys. Innovation, Univ. of Tokyo, [2]School Creative Sci. Engineering,Waseda Univ., [3]FRCER, Univ. of Tokyo, [4]JAMSTEC

In recent years, particular attention has been paid to the ”REY-rich mud” (deep-sea sediment enriched highly in rare-earth and yttrium (REY)), because of its high potential as a REY resource. The REY-rich mud was originally reported from the central Pacific Ocean in 2011 (Kato et al., 2011). In January 2013, during KR-13-02 cruise, the mud was also discovered at southern part of the Minamitorisima within the Japanese exclusive economic zone (EEZ) (Kato et al., 2013; Fujinaga et al., 2013; Suzuki et al., 2013). Then, in the late 2013 and early 2014, we further conducted two more research cruises (MR13-E02 Leg2 and KR14-02 cruises) in the northern and eastern part of the Minamitorishima EEZ. During the cruises, we performed an acoustic survey using sub-bottom profiler (SBP), together with mud sampling by piston coring. In this presentation, we report the distribution and characteristics of the REY-rich mud in the northern and eastern part of Minamitorishima EEZ inferred by the SBP survey.

Keywords: rare-earth elements, REY-rich mud, Minamitorishima, EEZ, sub-bottom profiler

Japan Geoscience Union Meeting 2014
(28 April - 02 May 2014 at Pacifico YOKOHAMA, Kanagawa, Japan)

SGC56-10 Room:415 Time:April 30 16:45-17:00

Geochemical features of rare-earth elements and yttrium-rich mud from north region of Minamitorishima EEZ

FUJINAGA, Koichiro[1*] ; KATO, Yasuhiro[1] ; NAKAMURA, Kentaro[2] ; SUZUKI, Katsuhiko[3] ; MACHIDA, Shiki[4] ; TAKAYA, Yutaro[1] ; YASUKAWA, Kazutaka[2] ; OTA, Junichiro[2] ; HARAGUCHI, Satoru[1] ; ARAKI, Shuuhei[2] ; LIU, Hanjie[2] ; USAMI, Ryo[2] ; MAKI, Ryota[2] ; IIJIMA, Koichi[3] ; NISHIO, Yoshiro[3] ; USUI, Yoichi[3] ; NOZAKI, Tatsuo[3] ; MR13-E02 LEG2, Cruise members[3] ; KR14-02, Cruise members[3]

[1]Frontier Research for Energy and Resources, University of Tokyo, [2]Department of Systems Innovation, University of Tokyo, [3]JAMSTEC, [4]Department of Resources and Environmental Engineering, Waseda University

Recently, deep-sea sediment enriched in rare-earth elements and yttrium (REY) (called REY-rich mud) has been reported from a central part of the Pacific Ocean (Kato et al., 2011). Due to its great potential as a completely new REY resource, the REY-rich mud attracts particular attention from a wide field of scientists and non-scientists. In 2013, we have discovered the deep-sea sediments that are extremely enriched in REY (˜6,600 ppm) from the south region of the Minamitorishima within the Japanese exclusive economic zone (EEZ) (Kato et al., 2013; Fujinaga et al., 2013; Suzuki et al., 2013). In 2014, in order to investigate the detailed distribution of REY-rich mud in the EEZ of Minamitorishima, we further conducted research cruises (MR13-E02 Leg. 2 and KR14-02) in the north region of the Minamitorishima. Here, we report the distribution, mineral composition, and geochemical features of the REY-rich mud from the north region of the Minamitorishima EEZ.

Keywords: rare earth elements (REEs), REY-rich mud, Minamitorishima, deep-sea mineral resource

Japan Geoscience Union Meeting 2014
(28 April - 02 May 2014 at Pacifico YOKOHAMA, Kanagawa, Japan)

SGC56-11 Room:415 Time:April 30 17:00-17:15

Independent component analysis to decouple geochemical components of REY-rich mud in the Pacific and Minamitorishima EEZ

YASUKAWA, Kazutaka[1*] ; TAKAYA, Yutaro[2] ; OTA, Junichiro[1] ; FUJINAGA, Koichiro[1] ; NAKAMURA, Kentaro[1] ; KATO, Yasuhiro[2] ; IWAMORI, Hikaru[3]

[1]Sys. Innovation, Univ. of Tokyo, [2]FRCER, Univ. of Tokyo, [3]JAMSTEC

Rare-earth elements and yttrium (REY) are essential for state-of-the-art devices and green technologies including electric vehicles, fiber optics, smart phones, wind power generation etc. Recently, the deep-sea sediments enriched in REY (termed as "REY-rich mud") have been discovered in the Pacific Ocean, which have great potential as a completely new REY resource (Kato et al., 2011). In 2013, the presence of REY-rich mud was also confirmed within the Japanese exclusive economic zone (EEZ) around Minamitorishima (Fujinaga et al., 2013; Suzuki et al., 2013). The maximum total REY content in the REY-rich mud from Minamitorishima EEZ reaches as high as 6,600 ppm, although typical REY-rich mud in other regions of the Pacific Ocean contains less than 2,230 ppm of total REY.

In order to elucidate a component contributing to REY-enrichment in the sediments, Kato et al. (2011) performed independent component analysis (ICA) on the geochemical data set of Pacific deep-sea sediments. ICA is a relatively new multivariate statistical method established in 1980s, which can extract original independent source signals or factors from observed signals based on an assumption that the observed multivariate data are mutually independent but do not form a multivariate normal (Gaussian) distribution (Hyvärinen et al., 2001).

Four independent components (ICs) were found by Kato et al. (2011): two diluting components corresponding to biogenic carbonate and silica, and two components toward high REY contents with Fe and Al values, respectively. Kato et al. (2011) interpreted that the Fe- and Al-rich ICs that are responsible for the REY-enrichment of the mud correspond to end-member minerals of Fe-oxyhydroxide and phillipsite, respectively. Recently, however, X-ray absorption fine structure (XAFS) analysis and μ-XRF elemental mapping using high-energy synchrotron radiation revealed that most of REY are directly bonded to apatite in the REY-rich mud (Toda, 2013; Kashiwabara et al., 2014).

Here, we analyze a new comprehensive geochemical data set of deep-sea sediments from the Pacific Ocean and Minamitorishima EEZ by ICA. In this calculation, we utilize the new chemical composition data of individual crystals of phillipsite and apatite measured by LA-ICP-MS as new end-members for the ICA analysis. We will discuss the results and interpretation of our new analysis.

– References –
Fujinaga, K. et al. (2013) *JpGU Meeting 2013*.
Hyvärinen, A. et al. (2001) *Independent Component Analysis*. John Wiley and Sons.
Kashiwabara, T. et al. (2014) *Chemistry Letters*, **43**, 199-200.
Kato, Y. et al. (2011) *Nature Geoscience*, **4**, 535-539.
Suzuki, K. et al. (2013) *JpGU Meeting 2013*.
Toda, R. (2013) Master's thesis, Univ. Tokyo.

Keywords: deep-sea sediment, REE, independent component analysis

Japan Geoscience Union Meeting 2014
(28 April - 02 May 2014 at Pacifico YOKOHAMA, Kanagawa, Japan)

SGC56-12 Room:415 Time:April 30 17:15-17:30

Mineralogical features of REY-rich mud in EEZ around Minamitorishima and implications for its genesis

OTA, Junichiro[1*] ; TAKAYA, Yutaro[2] ; FUJINAGA, Koichiro[2] ; YASUKAWA, Kazutaka[1] ; NAKAMURA, Kentaro[1] ; MACHIDA, Shiki[3] ; HARAGUCHI, Satoru[1] ; KATO, Yasuhiro[2]

[1]Department of Systems Innovation, University of Tokyo, [2]Frontier Research Center for Energy and Resources, University of Tokyo, [3]Department of Resources and Environmental Engineering, Waseda University

The KR13-02 cruise was conducted in the southern part of the Minamitorishima to explore rare-earth elements and yttrium-rich mud (REY-rich mud) within Japanese Exclusive Economic Zone (EEZ) on January 2013. During the cruise, seven sediment cores were successfully collected. The results of bulk sediment analyses showed that one of the cores (PC05) has an extremely REY-concentrated layer with 6,596 ppm total REY (Kato et al., 2013; Suzuki et al., 2013) which is three times higher than the maximum concentration in the mud previously reported for the eastern South and central North Pacific Ocean (2,230 ppm; Kato et al., 2011). In addition to REY, P concentration in the layer is also noticeably high (Kato et al., 2013; Suzuki et al., 2013), suggesting that Ca phosphate (apatite) is mainly responsible for the REY-enrichment in the layer, as in the case for the mud presented in other areas (Kashiwabara et al., 2014). However, factors contributing the extreme enrichment of REY, which in turn might provide important insights into the genesis of REY-rich mud, are still uncertain. In the present contribution, we report mineralogical features of Minamitorishima REY-rich mud including the extremely REY-concentrated layer and discuss about its genesis.

Keywords: rare-earth elements (REEs), REY-rich mud, deep-sea mineral resource

Japan Geoscience Union Meeting 2014
(28 April - 02 May 2014 at Pacifico YOKOHAMA, Kanagawa, Japan)

SGC56-P01 Room:Poster Time:April 30 18:15-19:30

Helium and halogen compositions in MORB vesicles

KAGOSHIMA, Takanori[1*] ; TAKAHATA, Naoto[1] ; SANO, Yuji[1]

[1]Atmosphere and Ocean Research Institute, University of Tokyo

Degassing behavior of halogens through submarine volcanism is not well understood. We determined helium and halogen compositions of MORB vesicles to constrain halogen flux at ridges. Samples collected at 8 sites (13oN-17oS on EPR; 15oN-37oN on MAR; 24-25oS on CIR) were crushed in dilute NaOH or NH_3 solution at liquid nitrogen temperature and volatiles were extracted from vesicles. Helium isotope compositions were determined with a VG-5400 MS and F and Cl contents were measured with ICS-2100 ion chromatography. For glass matrix, concentration of F and Cl were determined with a NanoSIMS.

For vesicles, the average ^{3}He concentration was (4.5+/-2.1)x10^{-15} mol/g of sample and the average F/^{3}He and Cl/^{3}He ratios were (1.4+/-0.5)x10^6 and (2.9+/-0.6)x10^7. This provides F and Cl flux of (7.1+/-2.8)x10^8 mol/y and (1.5+/-0.4)x10^{10} mol/y at ridges calibrating against the known ^{3}He flux of 530 mol/y. They may be defined as lower limits of MOR flux because F and Cl contents in glass matrix are $>$7000 and $>$100 times higher than those in vesicles and dissolution of only a small part of volatiles staying in oceanic crust into the ocean will increase volatile flux significantly. The large difference between F/Cl ratios in vesicles and glass matrix reflects difference in vesicle/glass partition coefficients of these elements, which suggests that they have significantly different degassing behavior at ridges. From the data of the noble gas method on MORB in literature, Br/Cl and I/Cl ratios in vesicles were calculated to be (1.8+/-0.1)x10^{-3} and (5.4+/-0.1)x10^{-5} which are almost equivalent with those in glass matrix [1], suggesting their vesicle/glass partition coefficients are similar in submarine basaltic magma. Br and I flux at ridges were calculated to be (2.7+/-0.8)x10^7 mol/y and (8.3+/-2.4)x10^5 mol/y based on the Cl flux estimated in this study. They are the first estimate of Br and I flux obtained by indirect calibration against ^{3}He flux and may be lower limits of MOR flux by the same reason as Cl. Combination of the method in this study and the noble gas method on the same sample will give us new insight into degassing behavior and geochemical cycles of halogens.

Reference: [1] Kendrick et al. (2012) GCA 81, 82-93.

Keywords: Mid-ocean ridge basalt, Helium, Halogen, Flux, Geochemical cycle

Japan Geoscience Union Meeting 2014
(28 April - 02 May 2014 at Pacifico YOKOHAMA, Kanagawa, Japan)

SGC56-P02 Room:Poster Time:April 30 18:15-19:30

Magmatic process of Cretacious plutonic complex in Ikoma mountains, SW Japan

KOIZUMI, Naoko[1*] ; OKUDAIRA, Takamoto[1] ; OGAWA, Daisuke[1]

[1]Osaka City University

The Ikoma gabbroic complex is one of the largest Cretaceous mafic pluton in SW Japan are exposed at Ikoma mountains, consisting of mafic rocks (the Ikoma gabbroic rocks) and intermediate to felsic rocks, the Fukihata tonalites and the Kyuanji quartz diorites. These rocks show three modes in whole-rock compositional relation, 1) as Plagioclase (Pl) cumulate, 2) as Hornblende-plagioclase (Hbl-Pl) cumulate and 3) as Hornblende (Hbl) gabbronorite.

The SiO_2 contents of the Ikoma gabbroic complex show 44 to 63 wt.%. Plagioclase cumulate and Hbl-Pl cumulate with SiO_2<50wt.%, their major oxide contents change widely for SiO_2 contents. Hbl gabbronorite are mafic to intermediate with SiO2>50wt.%, major oxide contents show linear trends with respect to SiO_2 contents on compositional variation diagrams.

Plagioclase cumulate shows cumulus structure and consists of mainly Ca-rich plagioclase (An_{85-90}). On the compositional variation diagrams, plagioclase compositions included in Plagioclase cumulate is located to the end-member on the trend of Plagioclase cumulate. Moreover, their plagioclase mode are shown by a positive trend with respect to the variation of CaO contents. It suggests that Plagioclase cumulates were associated with the accumulation of plagioclase. On the other hand, plagioclase compositions in Hbl-Pl cumulate and Hbl gabbronorite are Ca-poor (An_{70-75}). It suggests Hbl-Pl cumulate and Hbl gabbronorite occur after forming Plagioclase cumulate. Whole-rock compositions of the Ikoma gabbroic complex vary linearly with increasing SiO_2 contents, and their $^{87}Sr/^{86}Sr$ initial ratios at 82 Ma show a positive trend with variation of SiO_2 contents. These characteristics suggest a mixing of mafic magma and felsic materials. The mafic end-member is mafic magma of Ikoma gabbroic complex. Granitoids occurred at the same time of the activity of the Ikoma gabbroic complex are plotted on the extrapolation of the compositional trend of Hbl gabbronorite, but their $^{87}Sr/^{86}Sr$ initial ratios at 82 Ma is too low as the felsic end-member in a mixing. It is suggesting that the felsic end-member may not be the granitoids, but other crustal materials.

Keywords: Ryoke belt, Magmatic process, cumulate, accumulation

Japan Geoscience Union Meeting 2014
(28 April - 02 May 2014 at Pacifico YOKOHAMA, Kanagawa, Japan)

SGC56-P03 Room:Poster Time:April 30 18:15-19:30

Volatile compositions of apatite grains from pyroclastic flow deposits of Aso volcano

DOKYU, Marie[1*] ; KOGISO, Tetsu[1]

[1]Graduate School of Human and Environmental Studies, Kyoto University

Water in the Earth is important for life and mantle dynamics. The amount of water in the early Earth is one of the most essential constraints for revealing the origin of the Earth's water.

An important clue to the water budget in the early Earth is apatite inclusions in ˜4.4 Ga zircon from Jack Hills in Australia. Because apatite has volatile components, it is expected to determine the amount of water in the interior of the early Earth from OH composition of the Jack Hills apatite. However, partitioning of OH between apatite and melt is unclear.

We analyzed volatile compositions of apatite grains from pyroclastic flow deposits of Aso volcano in order to reveal the relationship between OH composition of apatite and H_2O composition of melt. The H_2O concentrations in the host magma have been estimated from those of melt inclusions in plagioclase phenocrysts. It shows that mafic melt contains more H_2O than silicic melt does. F concentrations in apatite in each sample show large variations while Cl concentrations are constant, suggesting that F and OH substitute for each other. OH concentration in apatite of mafic sample was larger than that of silicic one, that is, OH concentration in apatite and amount of H_2O in melt show negative correlation.

The negative correlation would have been caused by difference in Ca content between mafic and silicic samples. It is possible that Ca in melt combines F and affect partitioning F between apatite and melt (Mathez and Webster, 2005). Mafic melt contains more Ca than silicic melt and Ca may disturbed partitioning F for apatite and OH concentration can be increase in apatite. Another possibility is that the water compositions of melt inclusions do not represent those in the host melt. The melt inclusions have many bubbles, and the more bubbles they have, the less H_2O they contain. It means that H_2O in melt inclusions was lost to the bubbles, resulting in underestimation of water contents in the host melt. Actually another study calculated the amounts of H_2O in the mafic and silicic melts of the Aso pyroclastic flow and results were 4.1-7.7wt% and 4.1-5.7wt% respectively (Kaneko et al., 2007). If these results are correct, then OH concentration in apatite and the amount of H_2O in melt are positively correlated.

Range of the amount of F and OH in each sample could mean that melt composition gradually changed by degassing or/and crystallization differentiation. For precise determination of OH partitioning between apatite and melt, it is necessary to reveal the effect of Ca or other components to partitioning behavior of volatile components between apatite and melt.

Keywords: apatite, water, volatile component, the early Earth, magma

Japan Geoscience Union Meeting 2014
(28 April - 02 May 2014 at Pacifico YOKOHAMA, Kanagawa, Japan)

SGC56-P04 Room:Poster Time:April 30 18:15-19:30

Measuring osmium isotopic composition of natural polycrystalline diamond (carbonado) and implications for its origin

SHIRAISHI, Noriko[1*] ; SENDA, Ryoko[2] ; KAGI, Hiroyuki[1] ; SUMINO, Hirochika[1] ; SUZUKI, Katsuhiko[2]

[1]Geochemical Research Center, Graduate School of Science, University of Tokyo, [2]Institute for Research on Earth and Evolution, Japan Agency for Marine-Earth Science and Technology

The origin of natural polycrystalline diamond, carbonado, has long been enigmatic. Carbonado is characterized as high porosity, no genetic relations to kimberlites, light carbon isotope ratio, and lack of mantle-derived mineral inclusions. Based on these observations, several hypotheses about the origin of carbonado have been proposed: transformation of subducted organic carbon into diamond in a cold slab (Robinson, 1978); shock metamorphism of organic carbon by meteorite impact (Smith and Dawson, 1985); radiation-induced diamond formation by spontaneous fission of uranium in crustal environment (Ozima *et al*., 1991); formation in an interstellar environment (Garai *et al*., 2006); crystallization from C-O-H fluid in cratonic upper mantle (Ishibashi *et al*., 2012). However, no conclusive evidence has been provided to settle a controversy about the origin of carbonado. In this study, we first tried to measure Os isotopic composition of carbonados collected from placer deposits in the Central African Republic in order to identify its origin.

Natural samples have a wide variety of Os isotopic ratios, $^{187}Os/^{188}Os$, depending on their origin because ^{187}Re, the parent nuclide of radiogenic ^{187}Os, is a mildly incompatible element during mantle melting whereas Os is a strongly compatible element. $^{187}Os/^{188}Os$ ratio of upper continental crust ranges from 1.0 to 1.4 (Peucker-Ehrenbrink and Jahn, 2001), whereas that of primitive upper mantle is about 0.13 (Meisel *et al*., 1996). Os isotopic ratio of the micro diamond crystal itself can reflect the environment where diamond grains crystallized. Carbonado is a porous aggregate of micrometer-size diamond crystals and original chemical characteristics of the grain boundaries could be heavily altered after the diamond growth.

This study was designed to determine Os isotopic ratios within diamond crystals of carbonados and in the grain boundaries separately. Two-step sample chemical leaching was carried out by Carius tube method (Shirey and Walker, 1995). First, carbonado samples were crushed to submillimeter grains and were sealed in a Carius tube with spike solutions and inverse aqua regia (HCl + 3 HNO_3). The solution was heated at 220 ℃ for 24 hours. This procedure was for extract Os in the grain boundaries. Second, the residue of solid samples was heated in a vacuum chamber to convert diamond to graphite. A graphitized sample was decomposed in acid solution in the same way as the first leaching process. The second process was to extract Os within diamond grains. Osmiums in the both solutions were purified with the solvent extraction (Cohen and Waters, 1996) and microdistillation (Roy-Barman, 1993). Osmium isotopic compositions of the samples were determined using thermal ionization mass spectrometry (TIMS). Blank levels of Carius tubes and inverse aqua regia solutions prepared from several chemical regents were checked. As a result, a quartz glass tube was found to have the lowest blank level compared with other glass tubes made from borosilicate glass.

In the presentation, we will report preliminary results of Os isotopic ratios of the carbonado, which have the potential for a decisive evidence to close the debate on the origin of carbonado.

Keywords: carbonado, TIMS, Os isotope, diamond

Japan Geoscience Union Meeting 2014
(28 April - 02 May 2014 at Pacifico YOKOHAMA, Kanagawa, Japan)

SGC56-P05 Room:Poster Time:April 30 18:15-19:30

High-pressure high-temperature phase transitions in $ZnTiO_3$

ABE, Kohei[1*] ; KOJITANI, Hiroshi[1] ; AKAOGI, Masaki[1]

[1]Department of Chemistry, Gakushuin University

It is widely accepted that perovskite-type $MgSiO_3$ is the most abundant mineral in Earth ' s lower mantle. Ilmenite-type $MgSiO_3$ transforms to perovskite at 23 GPa and 1600 ℃. It was reported that ilmenite-type $ZnTiO_3$, an analogue to ilmenite-type $MgSiO_3$, decomposes into ZnO and TiO_2 at about 20-25 GPa (Ito and Matsui, 1979). However, phase relations in $ZnTiO_3$ have not been studied yet in detail. Therefore, we investigated the phase relations in $ZnTiO_3$ by high-pressure high-temperature experiments.

A starting material of ilmenite-type $ZnTiO_3$ was synthesized by heating a mixture of ZnO and TiO_2 with 1:1 mol ratio at 800 ℃ for 32 hours in air. High-pressure phase relation experiments were made by using a Kawai-type 6-8 multi-anvil apparatus in the pressure and temperature ranges of 13-35 GPa and 1000-1400 ℃, respectively. After keeping the starting sample at desired conditions for 1-2 hours, the samples were quenched, and then decompressed to ambient pressure. Recovered samples were identified by using the powder X-ray diffraction method.

We found that the recovered samples which were compressed between 15 and 20 GPa at 1000-1400 ℃ had the $LiNbO_3$-type (LNO) structure. The ilmenite-LNO phase boundary was determined as P(GPa)=19.9-0.0038T(℃). $FeTiO_3$ ilmenite which is an analogue to ilmenite-type $MgSiO_3$ transforms to perovskite above 15 GPa, and the perovskite transforms to the LNO-type structure during decompression (Ming et al., 2006). The ilmenite-perovskite phase boundary in $FeTiO_3$ has a negative slope which is caused by a positive entropy change for the transition due to increase of coordination number of divalent cation from 6 to 8. If the LNO-type $ZnTiO_3$ is a stable phase, the slope of the boundary should be positive because of no change in the coordination number of the divalent cation. Therefore, the negative slope of the boundary implies that the recovered LNO-type $ZnTiO_3$ was originally perovskite-type at 15-20 GPa.

The recovered samples synthesized above 20 GPa were identified to be an assembly of wurtzite-type ZnO and α-PbO_2-type TiO_2. The post-perovskite phase boundary in $ZnTiO_3$ is determined as P(GPa)=9.5-0.010T(℃). Wurtzite-type ZnO transforms to NaCl-type at about 6 GPa (Kusaba et al., 1999). Also, α-PbO_2-type TiO_2 transforms to baddeleyite-type at about 17 GPa (Tang and Endo, 1993). Therefore, we suggest that the phase assembly of NaCl-type ZnO and baddeleyite-type TiO_2 is stable above 20 GPa.

Keywords: $ZnTiO_3$, Perovskite, $LiNbO_3$, High pressure

Japan Geoscience Union Meeting 2014
(28 April - 02 May 2014 at Pacifico YOKOHAMA, Kanagawa, Japan)

SGC56-P06 Room:Poster Time:April 30 18:15-19:30

Quantitative multi-element imaging of geological materials by femto-second LA-ICP-MS

CHANG, Qing[1*] ; KIMURA, Jun-ichi[1]

[1]Japan Agency for Marine-Earth Science and Technology

Elemental mapping analysis of geological materials using X-ray related methods (EPMA, XRF) or SIMS suffers from insufficient sensitivity and poor quantification. LA-ICP-MS has advantages of high sensitivity and less matrix effect, therefore has been developed for elemental and isotopic imaging analyses over the last decade. However, quantification problem by this method remains unsolved because of the lack of a suitable sampling volume correction method and necessity of matrix-matched standard. This work presents multi-element imaging/mapping analysis of orthopyroxene and plagioclase minerals by femto-second LA-ICP-MS using a novel normalization process. Laser sampling volume is corrected for by analyzing ten major elements (SiO2, TiO2, Al2O3, FeO, MnO, MgO, CaO, Na2O, K2O, and P2O5) followed by normalization of the analyzed total sum to 100 wt% to obtain correction factor. This correction method is free from any external analysis (e.g., EPMA) for at least one internal standard element (e.g. Ca), and can be applied for both spot and line scanning LA mode. This allows LA-ICP-MS method standalone and liberates from errors inherited from any local heterogeneity of the samples picked up differently by the different analytical techniques used. Use of USGS basalt glass as a standard eliminates matrix effect in the levels less than 10% RD for these silicate minerals. Two-dimensional elemental distribution images of 43 elements were acquired from 4-6 μm depth of the sample surface with a ˜40 μm lateral resolution. An area of 500$\times$500 μm can be scanned simultaneously for 43 elements in less than 2.3 hours. Trace elements in silicate minerals can be imaged at sub-ppm concentration level, while major elements were mapped at sub-percent concentration.

Key words: femto-second LA-ICP-MS, elemental mapping, minerals

Japan Geoscience Union Meeting 2014
(28 April - 02 May 2014 at Pacifico YOKOHAMA, Kanagawa, Japan)

STT07-01 Room:421 Time:April 29 09:00-09:15

Applicability of fictitious domain method in data processing of marine CSEM exploration

KUSUDA, Kei[1*] ; MIKADA, Hitoshi[1] ; GOTO, Tada-nori[1] ; TAKEKAWA, Junichi[1]

[1]Graduate School of Engineering, Kyoto University

Marine controlled-source electromagnetic (CSEM) survey, one of the electro-magnetic (EM) sounding methods, is considered as a technique in practice for the exploration of hydrocarbon resources including methane hydrate (MH). In the analysis of EM field acquired in CSEM survey, forward modeling is used to model sub-seafloor structure. In the forward modeling, transforming the diffusive Maxwell equation to a fictitious wave domain reduces CPU time (Mittet, 2010). Phase velocities of electromagnetic waves are a function of material properties, i.e., electric conductivity and magnetic permeability. In the fictitious domain, the difference in the phase velocity as a function of materials is exaggerated so that EM field could propagate in the earth with much slower apparent phase velocity compared to the other field propagating through materials above seafloor. However, such character of the fictitious wave domain has not been well exploited for the estimation of subsurface resistivity structure. In the present study, we examine whether the received waveforms in the fictitious wave domain could highlight MH responses better than in the diffusive domain. We conduct numerical simulations using a three-dimensional resistivity model composed of seawater and earth layers, and a thin MH zone of a rectangular shape. Our results show that the sensitivity to the MH response in the received waveform is improved in the fictitious domain. It is mainly due to the separation of EM waves travelling with different phase velocities through the sub-seafloor layers and seawater in the fictitious domain. We then tested to see if the transform from the diffusive domain (e.g., observed EM field) to the fictitious wave domain is possible or not for further utilization of the transform. As a result of the singular value decomposition method to achieve the transform, the transforming EM waves in the fictitious domain indicated that the sensitivity to MH becomes about twice as much than the original EM field in the diffusive domain.

Keywords: CSEM, Fictitious wave domain, methane hydrate

Japan Geoscience Union Meeting 2014
(28 April - 02 May 2014 at Pacifico YOKOHAMA, Kanagawa, Japan)

STT07-02 Room:421 Time:April 29 09:15-09:30

Subsurface imaging with EM migration of magnetic fields from multiple frequencies

HYODO, Daisuke[1*] ; GOTO, Tada-nori[1] ; MIKADA, Hitoshi[1] ; TAKEKAWA, Junichi[1]

[1]Kyoto University

These days, the supply of water is facing a crisis due to the dramatic growth of population, industrialization, etc. As a result, the groundwater demand is becoming more and more stronger than before. Electrical prospecting is a method usually attempted for groundwater exploration, but setting the observation equipment in desert regions, where water shortage is a serious problem, causes us difficulty using this method there, since there is nothing that assures electrical contact between electrode and the earth. In these circumstances, some other methods that do not require any contact of electrode are needed. VLF or ULF is the method that satisfies the condition. However, none of these methods could provide information necessary to locate groundwater and it is strongly necessary to locate water head of survey areas. There is some shortcomings in the present processing of these VLF and ULF data. In this study, the phase-shift method, which is used in seismic migration, is applied to the horizontal magnetic components with multiple frequencies in order to image subsurface resistivity structures to locate groundwater. The survey is conducted more easily and shortly, if only the magnetic sensors above the surface are enough for estimating the structures. As in the seismic migration, both upward/downward imaging and the exploding reflector concepts can be applied to the horizontal magnetic components. The synthetic data examples show that the migration method is effective for imaging the conductive anomaly. However, it is necessary to select appropriate frequency bands in order to estimate correct subsurface structures. We conclude that this technique gives an approximate resistivity structures quickly and that the migration of magnetic components is expected to provide information on the subsurface. This method is also useful for geological interpretations and for an initial model of the more complicated inversion method.

Keywords: electromagnetic exploration, migration, apparent resistivity structure

Japan Geoscience Union Meeting 2014
(28 April - 02 May 2014 at Pacifico YOKOHAMA, Kanagawa, Japan)

STT07-03 Room:421 Time:April 29 09:30-09:50

Application of particle method to forward modeling of marine controlled-source electromagnetic survey

IMAMURA, Naoto[1*] ; GOTO, Tada-nori[1] ; TAKEKAWA, Junichi[1] ; MIKADA, Hitoshi[1]

[1]Kyoto University, Graduate School of Engineering

A new marine controlled-source electromagnetic (MCSEM) forward simulation is presented in this study. The benefit of the method is the better treatment of complicated seafloor topography and/or buried structures than before. Here, we focused on the moving particle semi-implicit (MPS) method. In our method, the Maxwell ' s equations are discretized with particle arrangement without grid structure, which is usually used in finite-difference method (FDM). Each particle denotes the three components of electromagnetic fields at each particle. MPS method has some advantages over the other methods such as finite-element method (FEM), FDM, integral method (IE), etc. An obvious advantage of this approach is a numerical model that can flexibly form arbitrary topography shapes. Although FEM is sometimes employed to treat the topographic structure, especially for MCSEM, pre-process for creating grid or mesh structures require a time-consuming procedure especially in three-dimensional cases. A second advantage is that the three components of electric field and electric current as well as magnetic field and source are defined at the same location of every particle, while not at the same location in the case of Yee ' s grid.

We tested our three dimensional MCSEM forward simulation using the particle method and confirmed that the accuracy of the forward simulation with the simple tilted layered model would be improved. Our forward modeling results show the accuracy sufficient to discuss with the analytical results. The local and arbitrary refinement of particle is conducted to obtain more accurate result using the same model. The local refinement is applied only near the transmitter and receiver dipoles. The accuracy of MPS becomes higher in the local refinement than in the use of isodiametric particles. Our results suggest that the method using MPS with locally refined particles is useful for the forward simulation of electromagnetic field with arbitrary topography in the MCSEM modeling.

Keywords: Marine controlled-source electromagnetic, Forward simulation, Particle method

Japan Geoscience Union Meeting 2014
(28 April - 02 May 2014 at Pacifico YOKOHAMA, Kanagawa, Japan)

STT07-04 Room:421 Time:April 29 09:50-10:10

Simultaneous inversion of self-potential for estimating hydraulic parameters and streaming current coefficient

OZAKI, Yusuke[1*] ; MIKADA, Hitoshi[1] ; GOTO, Tada-nori[1] ; TAKEKAWA, Junichi[1]

[1]Graduate School of Engineering, Kyoto University

In this study, we develop an inversion scheme for the simultaneous estimation of hydraulic conductivity, streaming current coefficient and specific storage, using transient self-potential (SP) data. SP is a natural electrical potential, which is thought to be caused by subsurface fluid flow through the electro-kinetic coupling. Recently, several SP measurements are performed during pumping tests to characterize the parameters of the aquifer. Almost of all SP analysis methods are adaptable to the static SP data, but a huge amount of the transient SP data is not used efficiently. Therefore, we develop an inversion scheme for the analysis of transient SP data. The electrical conductivity, streaming current coefficient, hydraulic conductivity and specific storage are parameters effectively influencing the SP profile on the surface, and can be solved in the inversion. The distribution of electrical conductivity structure can be used if the electrical resistivity tomography (ERT) or other EM measurements are performed with the SP measurement. We employ the relationship between hydraulic conductivity and streaming current coefficient to decreases the number of estimating model parameters, and to enable the simultaneous estimation of hydraulic conductivity and streaming current coefficient. First in this study, we check the sensitivities of the hydraulic conductivity and specific storage obtained at different times. The sensitivities of the hydraulic conductivity and specific storage are different with respect to the phase. The simultaneous inversion of hydraulic conductivity and specific storage from the transient SP profile is turned out possible from the difference in phase. Finally, we apply our inversion scheme to a synthetic SP profile, and reconstruct the subsurface structure of hydraulic conductivity, streaming current coefficient and specific storage simultaneously. As a result, our inversion technique allows us to obtain the hydraulic parameters from SP data on the ground surface, although the conventional hydraulic tomography strongly relies on the borehole data.

Keywords: Self potential, Inversion, Time domain, Hydraulic conductivity, Specific storage, Streaming current coefficient

Japan Geoscience Union Meeting 2014
(28 April - 02 May 2014 at Pacifico YOKOHAMA, Kanagawa, Japan)

STT07-05 Room:421 Time:April 29 10:10-10:25

Numerical study for failure behavior of rock masses including complex free-surfaces using a particle method

TAKEKAWA, Junichi[1*] ; MIKADA, Hitoshi[1] ; GOTO, Tada-nori[1]

[1]Kyoto Univ.

Failure of rock mass including complex free surfaces is of importance in many engineering and scientific fields. This paper applied an advanced discretization approach to simulate quasi-static failure of rock mass within a Hamiltonian particle method (HPM) framework. In HPM, a free surface is introduced in a simple way, just by removing or ignoring outer particles. This potential can be developed to discretize numerical models including complex free surfaces without the increment of time for pre-processing. In the present study, we developed the numerical simulator based on HPM with a staggered particle technique for simulating brittle failure and AE activities in rock mass with incorporating the elasto-plastic damage model. We, first, conducted uni-axial compressive tests for validating the effectiveness of our approach. Next, we adopted rectangular and circular disc specimens with a hole as complex free surface models. Our numerical results had good agreement with those from laboratory experiments. This suggests that HPM would be a method to simulate failure behavior of rock mass without time-consuming pre-processing.

Keywords: particle method, failure behavior, rock mass

Japan Geoscience Union Meeting 2014
(28 April - 02 May 2014 at Pacifico YOKOHAMA, Kanagawa, Japan)

STT07-06 Room:421 Time:April 29 10:25-10:40

Forward calculation of Magnetotelluric responses with MPS method

TANI, Masanori[1*] ; MIKADA, Hitoshi[1] ; GOTO, Tada-nori[1] ; TAKEKAWA, Junichi[1]

[1]Graduate School of Engineering, Kyoto University

In this research, we developed a new 2-D magnetotelluric (MT) forward simulation method based on the MPS (Moving Particle Semi-implicit) method framework. Our final purpose is to calculate MT response with arbitrary three-dimensional topography.

The MPS method is a particle method and was first developed for the simulation of incompressible fluid flow (Koshizuka and Oka, 1996). Recently, the MPS method is used the digital reproduction of failure of materials,for the simulation of elastic wave propagation, etc. We use the MPS method for the simulation of electromagnetic induction.

In our forward calculation, electric and magnetic fields are defined at each particles in a calculation model. MT responses are calculated on the surface of the ground with topography with a horst-graben shape. Our simulation results indicate that MT forward calculation with the MPS method is suitable for free surface like topography, because the MPS method does not require the mesh configuration such as for FDM and FEM, particles in the MPS method could form any shape. The results of MT forward calculation (TE-mode and TM-mode) based on MPS method is reliable enough to calculate MT responses on models with topography. Based on the inherent character of MPS method, the expansion of our code from two-dimension to three-dimension will be easily achieved.

Keywords: Magnetotelluric, MPS, topography

Japan Geoscience Union Meeting 2014
(28 April - 02 May 2014 at Pacifico YOKOHAMA, Kanagawa, Japan)

STT07-07 Room:421 Time:April 29 11:00-11:15

Fluid-physical simulation of silicate scale formation using lattice Boltzmann method

MIZUSHIMA, Akihiro[1*] ; MIKADA, Hitoshi[1] ; GOTO, Tada-nori[1] ; TAKEKAWA, Junichi[1]

[1]Graduate School of Engineering, Kyoto University

Scaling behavior has an important role in various geosciences fields. For example, precipitation of silica can cling to pipes and wells, and prevent the geothermal power generation. Silica precipitation strongly affects the circulation of hydrothermal systems by changing the permeability structure, which is related to the nucleation of seafloor massive sulphide. Self-sealing is of importance in the understanding of long-term radionuclide mobility and the safety of deep geological repositories of radioactive waste.

The deposition of amorphous silica is controlled probably by many processes. There have been a number of experimental studies made on the chemical kinetics of silica deposition as a function of the degree of super-saturation. However scaling estimated by the simple chemical precipitations cannot explain the measured features in laboratory and field experiments. On the other hand, a high rate of deposition could be found where fluid flow stagnates. Although it has been empirically observed that the fluid flow structure can influence silica scaling, relatively little research have been conducted to investigate hydrodynamic effect on silica scaling. The aim of this work is to evaluate the importance of both chemical kinetic and hydrodynamic effects on silica scale growth with a method of numerical simulation.

Here using the lattice Boltzmann method, we calculated velocity, temperature and concentration of dissolved silica in the 2D parallel plate channel and predicted the silica deposition of both chemical kinetic and hydrodynamic deposition processes. The laboratory results by Hosoi and Imai (1982) can be as the reference. We also predicted the silica deposition along the channel with sudden expansion of width. For the latter case, the similar field example in the production pipes of the geothermal well was reported (Mercado et al., 1989).

In our numerical simulations, the silica deposition predicted by the kinetic process has the magnitude extremely lower than the amount of laboratory experiment, but shows the similar magnitude if the hydrodynamic process is considered for scaling. In addition, at the another channel model with the sudden expansion scaling predicted by the hydrodynamic process can explain the observed feature at the geothermal well.

It is found that consideration of the simple kinetics process solely is not sufficient for explanation of the real silica deposition. Therefore, we emphasize the importance of hydrodynamic effect on silica scaling. To predict the silica deposition more quantitatively, an advanced-simulation including behaviors of colloid silica particles in flow.

Keywords: scale prediction, silica scaling, kinetics, hydrodynamics, the lattice Boltzmann method

Japan Geoscience Union Meeting 2014
(28 April - 02 May 2014 at Pacifico YOKOHAMA, Kanagawa, Japan)

STT07-08 Room:421 Time:April 29 11:15-11:30

Distinct element method for solid-fluid coupled interaction in the application of hydraulic fracturing

NAGASO, Masaya[1*] ; MIKADA, Hitoshi[1] ; GOTO, Tada-nori[1] ; TAKEKAWA, Junichi[1]

[1]Graduate School of Engineering, Kyoto University

The hydraulic fracturing is of great interest in many scientific and engineering fields in hydraulic fracturing, such as the hot dry rock geothermal power(HDR). However, the natural fractures have significant influence on the nucleation and growth of fractures created in hydraulic fracturing. In addition, the viscosity of fluid used in hydraulic fracturing also influences the geometry of hydraulically created fractures. Although the influence of both natural fracture and fluid viscosity has been intensively investigated on the distribution of hydraulic fractures, none of the studies has dealt with natural fractures and fluid viscosity at the same time and the interaction between them has not been revealed yet. We, therefore, performed a series of numerical simulations for hydraulic fracturing in naturally fractured rock using a 2D flow-coupled DEM code to examine the influence of the fluid viscosity on the interaction between hydraulic and natural fractures. In this study, a low viscosity fluid of 0.1 m^2/s and a high viscosity fluid of 100.0 m^2/s are used. Our model is a square block with a borehole at the center under a stress field whose maximum and minimum stresses are 10 and 5 MPa, respectively. We apply the hydraulic pressure to the borehole wall, and observe how induced hydraulic fracture would propagate in the presence of a single natural fracture located adjacent to the borehole. The viscosity of fluid and the angle between the maximum stress direction and fracture orientation are the parameters of the numerical simulation. The results show that the lower the oblique intersection angle is, the less linearly the induced fracture crosses the pre-existing fracture. However, when a high viscosity fluid is used, the interruption of natural fractures decreases and the induced fracture tends to go straight along the direction of maximum compression. Our numerical example implies that high viscosity fluid could be used in hydraulic fracturing to reduce the influence of a natural fracture when the hydraulic fracture intersects the pre-existing fracture with certain angles .

Keywords: hydraulic fractureing, viscosity, natural fracture, discrete element method

Japan Geoscience Union Meeting 2014
(28 April - 02 May 2014 at Pacifico YOKOHAMA, Kanagawa, Japan)

STT07-09 Room:421 Time:April 29 11:30-11:45

Numerical simulation for apparent viscosity change under oscillating boundary condition using lattice Boltzmann method

UEDA, Ryuta[1*] ; MIKADA, Hitoshi[1] ; GOTO, Tada-nori[1] ; TAKEKAWA, Junichi[1]

[1]Kyoto University

Unsteady fluid dynamics in Newtonian and non-Newtonian fluid is the main concern of aeronautical engineering, mechanical engineering, chemical engineering, resource engineering and civil engineering. It is also true to the oil industry because the amount of oil production in the world is decreasing recently, it is of importance to seek the technological development for enhanced oil recovery (EOR) in place in the subsurface. Recently, many laboratory experiments and field tests have been performed such as water, gas, chemical, or thermal injections to attempt the enhancement of oil production. Seismic stimulation is known as one of the EOR methods and unsteady flow problem. Numerous observations show that seismic stimulation of oil reservoir may improve oil production. However, for effective usage of seismic EOR, we need to understand the characteristics of changing apparent viscosity under oscillating solid-phase. In this study, we attempt to demonstrate the apparent viscous change in laminar flow under oscillating boundary condition with the models of single pore throats and porous media.

We use Lattice Boltzmann method (LBM) describing Boltzmann equation. We use 2-dimensional 9-velocity (2d9v) model to simulate 2-dimensional incompressible viscous flow. We assume that the background pressure difference between inlet and outlet is constant. The flow is generated by a constant pressure difference.

We discuss the apparent viscosity of a single pore throat and porous media.

First, we discuss four characteristics of an incident elastic wave: amplitude, frequency, angle, and pressure disturbance (P wave). The characteristics of amplitude, frequency and angle are largely related with the amount of changing apparent viscosity. The flux increases under cases with large amplitude, high frequency, and large angle (S wave) of incident to the wall. On the other hand, the pressure disturbance (P wave) is not effective for changing apparent viscosity. We then discuss the possibility of changing apparent viscosity in terms of fluid properties. Wall oscillation can cause improving relative permeability. So, if the rock has water wettability, the oil flux largely increase with wall oscillation. After that, we examine the possibility of changing apparent viscosity in terms of pore scales or shapes under the oscillating boundary condition with LBM. The models of single pore throat consists of two half pore and one pore throat. The models of porous media consist of several pore spaces connected by pore throats from one pore to the others. The shapes of single pore throats are also largely related with changing apparent viscosity. The apparent viscosity decreases with increasing length of the pore throats and radius of the pore throats, and with decreasing width of the pore throats and large pore radius. Comparing single pore throat model and porous media model, we find the apparent viscosity change in porous media models cannot be replaced by linear combination of the apparent viscosity changing in single pore throat models.

Our numerical results imply: i) the flow resistance under oscillating condition increases because the velocity difference between the wall and the center of flow is larger than that in steady flow, ii) the effect of the advection term in oscillating boundary condition is larger than that in steady flow, iii) fluid extrusion is generated by partial pressure gradient near the wall and pore throat, and iv) the oscillating boundary may cause improving pressure loss.

Keywords: Lattice Boltzmann method, Unsteady flow, Seismic EOR, Apparent viscosity, Pore throat scale

Japan Geoscience Union Meeting 2014
(28 April - 02 May 2014 at Pacifico YOKOHAMA, Kanagawa, Japan)

STT07-10 Room:421 Time:April 29 11:45-12:05

Estimation of stress change in ductile part of the crust inferred from seismic scattering

OKAMOTO, Kyosuke[1*] ; MIKADA, Hitoshi[1] ; GOTO, Tada-nori[1] ; TAKEKAWA, Junichi[1]

[1]Graduate School of Engineering, Kyoto University

In the past, stress field in the subsurface has been measured by various techniques. For example, the borehole-breakout, the stress release method, the hydraulic fracturing, the strain gauge buried in the ground are used to measure the stress field after costly drilling the subsurface. Beside the techniques requiring direct access to the subsurface, the stress field is also measured indirectly. The Electro Distance Meter, the Global Positioning System, etc. are used to measure a surface deformation in time, from which the subsurface stress change is estimated. However, the estimated stress change in the subsurface is largely affected by near-surface inhomogeneities. Thus, information on the stress field should be obtained from other indirect techniques.

Here, we focus on seismic scattering wave, particularly the coda-Q value, to measure spatial and temporal variations of subsurface stress field. The coda-Q, derived from the attenuation of coda envelope, is perceived to be an indicator of the inhomogeneity in the subsurface. Meanwhile, it has been proposed that the coda-Q has a proportional relationship with the magnitude of stress using a numerical simulation. In this study, we hypothesize that the coda-Q, obtained from seismic waves traveling over a wide range of the crust, indicates stress change in a deep subsurface. At first we numerically calculate a relationship between the coda-Q and the magnitude of stress using a homogeneous crustal model, and show that the coda-Q systematically increases against the magnitude of the stress. Then we confirm the relationship using a heterogeneous numerical model, which has a low velocity zone near the surface. It is revealed that the coda-Q indicates the magnitude of the stress change in the deep subsurface, beneath the inhomogeneity, while the surface strain distribution is largely affected by the low velocity zone near the surface. For the next step, using real seismic data acquired at the regions of the 2008 Iwate-Miyagi Nairiku earthquake and the 2004 mid-Niigata prefecture earthquake, we examine whether the coda-Q indicates stress change in the deep subsurface. The stress change estimated from the coda-Q corresponds with the theoretical one in the ductile part, calculated by a fault model acquired by a seismic wave analysis, whereas the estimated stress change dose not correspond with the inferred one from GPS measurement. It means that the coda-Q can indicate stress change in the deep subsurface, which could give more accurate investigation than the GPS measurement.

Keywords: seismic scattering, stress change, ductile, heterogeneity

Japan Geoscience Union Meeting 2014
(28 April - 02 May 2014 at Pacifico YOKOHAMA, Kanagawa, Japan)

STT07-11 Room:421 Time:April 29 12:05-12:25

2D simulation of seismic wave propagation for time lapse monitoring of heterogeneous structure and near-surface effects

KAMIMURA, Aya[1*] ; KASAHARA, Junzo[1] ; MURASE, Kei[1] ; TAZAWA, Oshie[1] ; NISHIYAMA, Eiichiro[1] ; KUBOTA, Ryuji[1] ; FUJIMOTO, Osamu[1] ; OHMURA, Takeshi[1] ; NOGUCHI, Shizuo[1] ; OHNUMA, Hiroshi[1]

[1]Kawasaki Geological Engineering Co.,Ltd.

For the time lapse study in CCS and EOR, we have proposed the method using the seismic ACROSS (Accurately Controlled and Routinely Operated Signal System) and geophone array. However, it is considered that the near-surface effects and their temporal changes caused by water content changes, temperature and surface wave generation, might have very large effects for time lapse estimation, and we would like to evaluate and reduce the near-surface effects by the comparison of surface and borehole geophone records. We have carried out simulation studies to evaluate the effects of near-surface and heterogeneities such as the man-made cavities in the green tuff layers (Vp ˜2.5 km/s). We also evaluate the near-surface effects by changing geophone depths. The results of the simulations are as follows.

At the simulation of surface hypocenters, seismic waves passed through the man-made cavities attenuated and seismic waves scattered at the man-made cavities. This shows that there will be a heterogeneous structure like man-made cavities when observed seismic waves were attenuated, and the man-made cavities will become a secondary hypocenter.

As the results of simulation of surface hypocenters, the amplitude of scattered waves observed by borehole geophones were larger than that of surface geophones. This means that the borehole geophones are suitable for time lapse monitoring of heterogeneous structures. The amplitude of scattered waves observed by horizontal components of geophones was larger than that of vertical components of geophones. This means that the horizontal components of geophones are suitable for time lapse monitoring of heterogeneous structures.

At the simulations of deep hypocenters (15Hz, 2Hz) as assumed natural earthquakes, seismic waves scattered by the man-made cavities. Observation of natural earthquakes will be helpful to look at the wide seismic structure.

Japan Geoscience Union Meeting 2014
(28 April - 02 May 2014 at Pacifico YOKOHAMA, Kanagawa, Japan)

STT07-12 Room:421 Time:April 29 12:25-12:45

A time lapse test of seismic waveform changes during several days at the green tuff area in Japan using a seismic vibrat

KASAHARA, Junzo[1*] ; KUBOTA, Ryuji[1] ; YUTAKA, Kanai[1] ; TAZAWA, Oshie[1] ; FUJIMOTO, Osamu[1] ; KAMIMURA, Aya[1] ; NISHIYAMA, Eiichiro[1] ; MURASE, Kei[1] ; NOGUCHI, Shizuo[1] ; OHMURA, Takeshi[1] ; OHUMRA, Hiroshi[1] ; HASADA, Yoko[2]

[1]Kawasaki Geological Enginnering Co. Ltd., [2]Daiwa Exploration and Consulting Co. Ltd., [3]Tokyo Unniversity of Marine Science and Technology

In order to estimate the physical property changes in the subsurface, the time-lapse measurement is quite useful for various cases such as CCS (Carbon Capture and Sequestration) zone, EOR, shale gas exploration, and oil production. The authors have carried out the time lapse experiment at the water pumping area in Kingdom of Saudi Arabia using a very accurate and extremely stable seismic source called ACROSS (Accurately Controlled and Routinely Operated Signal System).

Because this seismic ACROSS has been installed semi-permanently at the Saudi test field, it is not easy to bring to any places. Instead, we alternatively used a much conventional electro-magnetic vibrator for this field test in the green tuff area in Japan.

We used the vibrator for 12 hours a day during five days in 2013. We also used 110 geophones and two borehole geophones placed just above the green tuff miming area with 2km x 3km. We used sweep signal from 10 Hz to 50Hz during 100 second.

We repeated 32 sweep during an hour. 32 stacking of waveforms of 100s second time-windows improved the S/N, and we can identify arrivals up to 3 km distance by this one-hour stacked data. If we look the 12 hours waveforms, it is difficult to find the change of those with time.

Using the subtraction of waveforms every day with 12-hour stack data from the first day, we generated residual waveforms. If we use residuals waveforms from the first day, we can clearly identify the change of waveforms with time. In conclusion we can use the time lapse method during five days by the use of residuals waveforms though the period is short. We can use conventional seismic vibrator(s) for the time lapse for several days.

Keywords: time lapse, ACROSS, seismic method, residual waveforms, vibrator source, green tuff

Japan Geoscience Union Meeting 2014
(28 April - 02 May 2014 at Pacifico YOKOHAMA, Kanagawa, Japan)

STT07-13 Room:421 Time:April 29 14:15-14:30

A Reflectivity Guided Elastic Full Waveform Inversion

JAMALI HONDORI, Ehsan[1*] ; MIKADA, Hitoshi[2] ; GOTO, Tada-nori[2] ; TAKEKAWA, Junichi[2]

[1]JGI, Inc., [2]Kyoto University

Full Waveform Inversion (FWI) of seismic reflection data has become a common technique for producing subsurface images based on local minimization of least squares misfit between observed data and calculated model. Usually, an initial model that is close to the global solution of the problem is needed to obtain satisfactory results without being trapped in a local minimum of the misfit function. Due to the limitations in quantity of the observed data, e.g. using seismic traces from surface receivers to make an image of earth model, the full waveform inversion problem is ill-posed and underdetermined. The problem becomes even worse when dealing with elastic waveforms which require increased number of model parameters, i.e. P wave velocity, S wave velocity, density etc. In order to overcome this problem, inserting a priori model information in to the inversion process helps the algorithm to converge to a solution in the vicinity of the global minimum. This kind of information could be included in the gradient of the misfit function by adding model terms, when using conjugate gradient method to iteratively update the model parameters.

On the other hand, producing reliable velocity model is a key for successful Pre Stack Depth Migration (PSDM) of seismic data. Assuming an available depth section of seismic reflection data, e.g. by time to depth conversion of time migrated section, we estimate the P wave velocity from seismic section by first extracting reflectivity and then using Gardner equation (Gardner 1974) as stated by Hondori et. al 2013. This will produce a P wave velocity model which is used in full waveform inversion as a priori information. Our frequency domain elastic full waveform inversion is developed using finite difference method and perfectly matched layers are used on the boundaries of the computational area. A preconditioned conjugate gradient method is used together with improved pseudo Hessian matrix for updating the model parameters. At each iteration the gradient is calculated using adjoint state method, and then l_2 norm of the model term is added to the gradient to constrain the inversion. We suggest that this method not only improves the full waveform inversion results, but also resulting FWI models provide a good velocity model for pre stack depth migration of seismic data.

References

Gardner, G. H. F., Gardner, L. W., and Gregory, A. R., 1974, Formation velocity and density: the diagnostic basics for stratigraphic traps: Geophysics, **39**, 770?780.

Hondori, E. J., Mikada, H., Goto, T.N, Takekawa, J., 2013, A random layer-stripping method for seismic reflectivity inversion: Exploration Geophysics, **44**, 70?76.

Keywords: Full Waveform Inversion, Frequency Domain, Elastic, Reflectivity

Japan Geoscience Union Meeting 2014
(28 April - 02 May 2014 at Pacifico YOKOHAMA, Kanagawa, Japan)

STT07-14 Room:421 Time:April 29 14:30-14:45

3D-FDFD simulation for high resolution eddy-current testing method

SAITO, Takuya[1*] ; MIKADA, Hitoshi[1] ; GOTO, Tada-nori[1] ; TAKEKAWA, Junichi[1]

[1]Kyoto University

The applicability and the feasibility of eddy-current testing method for the measurement of wall thinning and surface crack of steel structure have been practically confirmed by field and laboratory experiments. Where and how large the cracks would be are roughly understood by this method. However, it is difficult to estimate the exact size and shape of them. For more accurate inspections, there has been a growing demand to quantitatively evaluate the cracks. Therefore, we have developed a numerical simulator for the high accuracy eddy-current method. Eddy-current method measures excitation magnetic and induced magnetic fields, the latter of which is caused by the eddy-current in the inspecting material. In order to calculate induced magnetic field deformed by the cracks, we used three-dimensional finite-difference frequency domain technique to solve Maxwell's equations numerically. As a simulation model, two-layer structure consisting of seawater and steel plate including cracks is used. We simulated a variety of cracks to estimate characteristic of the induced magnetic field, and compared the results in terms of what kind of difference in the induced field would appear. As a result, the effect of surface cracks of steel plate on receiving magnetic field intensity was confirmed as follows: the induced magnetic field intensity increases near the edge of cracks and decays above the cracks with the distance to the edge. The deeper and wider cracks are, the more the magnetic field intensity becomes attenuated. Due to the limitation of our simulation schemes, the response of magnetic field intensity whose detectable scale of cracks was no smaller than mm order. We are introducing a method that could allow us to confirm much finer detectability.

Keywords: NDI, Maxwell's equations, Eddy Current, numerical simulation

Japan Geoscience Union Meeting 2014
(28 April - 02 May 2014 at Pacifico YOKOHAMA, Kanagawa, Japan)

STT07-15 Room:421 Time:April 29 14:45-15:00

Elastic parameter estimation in full waveform well-to-well tomography

TERANISHI, Keisuke[1*] ; MIKADA, Hitoshi[1] ; GOTO, Tada-nori[1] ; TAKEKAWA, Junichi[1]

[1]Graduate school of Engineering, Kyoto university

Seismic full-waveform inversion (FWI) method has been used to estimate velocity and density structures in the subsurface. The waveform analysis is a powerful tool to investigate the properties in the areas of interest, and the importance to use the waveform is widely recognized in the seismic explorations. As the wave propagation is influenced by elastic parameters, Vp, Vs, density, it is necessary to include these parameters in FWI (Virieux and Operto 2009). However, there are few previous studies dealing with density as a parameter in the application of elastic FWI. Density is usually estimated using an empirical formula such as Gardner's relationship (Gardner et al., 1974), or is fixed to a constant value. Almost all elastic FWI studies have neglected the influence of approaches how density parameter is estimated. The objective of this study is to investigate how difficult the estimation of density structure is, and propose a new approach to overcome the problem. We employ 2D numerical simulations in order to investigate the important factor in the inversion of density structure. Our results show that it is difficult to estimate density structure because density structure is less sensitive to waveform than Vp and Vs. Therefore, we hypothesize that the simultaneous inversion of Vp and density structures, using a selected dataset can improve the accuracy of the FWI. For testing this hypothesis, various ways for estimation of Vp, Vs and density using different datasets and approaches. We conclude that Vp and density structures should be estimated simultaneously in the elastic FWI, in which P-wave data separated from the seismic records is used as the input data.

Keywords: full-waveform, tomography, density

Japan Geoscience Union Meeting 2014
(28 April - 02 May 2014 at Pacifico YOKOHAMA, Kanagawa, Japan)

STT07-16 Room:421 Time:April 29 15:00-15:15

Estimation of fluid contact in terms of attenuation

ISHIKURA, Kazuki[1*] ; MIKADA, Hitoshi[1] ; GOTO, Tada-nori[1] ; TAKEKAWA, Junichi[1]

[1]Kyoto University graduate school of engineering

Sonic logging has been widely used for many years to acquire physical properties of formations in the vicinity of hydrocarbon reservoirs. When gaseous phase exists in the formation fluid, the compressional waves traveling through the formation could be strongly attenuated due to low bulk modulus of gas in the fluid, while the shear waves are not. For acquiring physical properties of fluid in the formation, Biot physics or poroelastic analysis would be the best method. Among the available technologies, quality factors based on the Biot's equation could be used. Although the Biot's theory considers the viscous attenuation induced at the interface between pore wall and fluids, the intrinsic attenuation caused by the internal friction in the matrix is ignored.

In the present study, adding the intrinsic attenuation we investigate if we take the effect of the viscous attenuation from the acquired quality factor, and then, on the basis of the result, if we estimate the fluid contact (e.g. gas-oil contact and oil-water contact). We employ a 2D finite-difference scheme to simulate seismic wave propagation in a poroelasic medium. The intrinsic attenuation is included in our model using a filter for frequency-independent quality factor (constant-Q). We then achieve the results of compressional and shear wave in our numerical simulations. Our results show that on compressional and shear waves, obtained the quality factors different from each other. We acquire the effect of the viscous attenuation by subtracting the quality factor of shear wave from the quality factor of compressional wave. We conclude that the effect of viscous attenuation is extracted and the gas-oil contact is estimated.

Keywords: Q, attenuation, poroelastic, Biot, sonic logging

Japan Geoscience Union Meeting 2014
(28 April - 02 May 2014 at Pacifico YOKOHAMA, Kanagawa, Japan)

STT07-17 Room:421 Time:April 29 15:15-15:30

AVO waveform inversion for estimating the fluid contact with fluid transition zone

IWAKI, Yunosuke[1] ; MIKADA, Hitoshi[1*] ; GOTO, Tada-nori[1] ; TAKEKAWA, Junichi[1]

[1]Graduate School of Engineering, Kyoto University

The fluid distribution in the hydrocarbon reservoir affects waveforms acquired in reflection seismic method. A reflected wave changes its waveform at the transition zone of the interface of two different fluids as a function of volume fraction of the two. AVO is in general used to estimate the difference in the P and S wave velocities for the interfacing two media at the interface without any assumptions on the existence of the transition zone. The consideration of the effect of the volume fraction of a fluid to the other in the waveform could be a key for evaluating the fluid mixture around the fluid contact in the reservoir. Therefore, we try to use the waveform directly to estimate fluid distribution in the transition zone that has not been done in the practice of AVO.

In our research, we consider the effects of the transition zone at a gas-water contact (GWC) in a horizontally stratified medium on seismic waveforms. The numerical simulation reveals that the fluid distribution of transition zone distorts the seismic waveform both in amplitude and in phase. Then we use the difference in amplitude and in phase for estimating some necessary parameters expressing the fluid-mixture. We apply a waveform inversion method to the fluid substitution problems to see if the method is applicable to estimate the fluid contact with the transition zone, while the conventional AVO only utilizes the amplitude derived from observed data. Our numerical approach uses full waveform and the results imply the advantages in the estimation of the parameters including the thickness of the transition zone under that assumption of linear trend in the volume fraction in a contrast porosity condition. We suggest that the phase information should be used simultaneously for the inversion process to get the closer contact image.

Japan Geoscience Union Meeting 2014
(28 April - 02 May 2014 at Pacifico YOKOHAMA, Kanagawa, Japan)

STT07-18 Room:421 Time:April 29 15:30-15:45

The insulation effects caused by the scattering of electromagnetic waves by fine spheres against insolation heating

HORIE, Jun[1*] ; MIKADA, Hitoshi[1] ; GOTO, Tada-nori[1] ; TAKEKAWA, Junichi[1] ; TANIGUCHI, Kiyoshi[2] ; ASHIDA, Yuzuru[3]

[1]Kyoto University, [2]West Nippon Expressway, [3]NPO EEFA

The temperature of materials rises when they are exposed to the sunlight (insolation heating). Insolation heating could be suppressed when the materials are coated with paint admixed with fine silica spheres (insulating paint). By coating buildings' walls and roofs with such paint, the temperature in the subjacent rooms could be kept lower thanby coating with regular one. The temperature of the former could be enough low so that no air-conditioning becomes necessary even in the mid summer. These phenomena are well known in a practical manner and have been widely utilized. However,the cause of the phenomena has hardly been analyzed theoretically yet. Moreover, micron-scale ceramic spheres have been known as the best commixture than the other metallic commixture of the same size. Theoretical analysis would greatly enhance the effects of the suppression of insolation heating. We focus on the light scattering by fine spheres under the assumption that the scattering of lights, i.e., electromagnetic waves, attributes to suppression of insolation heating and that the imaginary part of scattering coefficients of the spheres is a key to explain the observed phenomena. In this study, we therefore consider commixture sphere materials to be (i)silica, (ii)aluminum and (iii)copper, distributed in a paint layer coating an iron material, and calculate transmission, reflection and absorption coefficient using the Monte Carlo ray tracing method based on the Mie theory. Using these coefficients, the rise in temperature of surface of the iron layer would be estimated. We finally investigate how the structure of the paint attributes to the insulating effects.

We assume three layers: air, paint, and iron, and commixed fine spheres in the paint layer using Distinct Element method (DEM). A number of photons vertically incident to the paint at random position from the air. We then count the number of photons that reaches the iron to estimate the intensity of the transmitted wave, and count the number of photons that are absorbed by spheres to estimate the intensity of the absorbed wave energy. Fresnel Equations are used to identify photons' behavior stochastically using a random number. Moreover, Mie theory is used to calculate the radiation pattern of scattering at each sphere when a photon incident to the sphere. As a result, it is estimated that the transmission coefficient would be less than 0.1 forthe commixture material of silica whose radius is smaller than ca. 0.7 micrometers. On the other hand, the transmission coefficient could be much less than 0.1 if we use conductive spheres. However, in the latter case, the absorption coefficient would be approximately 0.5, which could cause the rise in temperature of the spheres and the paint.

We estimate the rise in temperature of iron layer using coefficients calculated above. Near-infrared radiation of the sunlight is assumed to be the incident wave. As a result, whereas the temperature would be 63 degrees Celsius if no paint is coated. On the other hand, the temperature would be suppressed to 39, 59 or 56 degrees Celsius, respectively, if we use silica, aluminum or copper spheres of the same radii of 0.5 micrometers. The metallic commixture could lower the temperature rise but the absorption of the energy seems deteriorate the efficiency of the insulation.

In conclusion, silica is one of ideal material for insulating paint in contrast with conductive ones such as aluminum and copper, mainly due to the absorption phenomena of electromagnetic waves by spheres.

Keywords: mie scattering, monte Carlo Ray-tracing, insulating paint, sphere, electromagnetic scattering

Japan Geoscience Union Meeting 2014
(28 April - 02 May 2014 at Pacifico YOKOHAMA, Kanagawa, Japan)

STT07-P01 Room:Poster Time:April 29 18:15-19:30

Three-dimensional joint inversion of gravity and magnetic anomalies using fuzzy c-means clustering

TERANISHI, Yosuke[1*] ; MIKADA, Hitoshi[1] ; GOTO, Tada-nori[1] ; TAKEKAWA, Junichi[1] ; TADA, Ryohei[2]

[1]Kyoto University, [2]INPEX CORPORATION

The gravity and magnetic surveys have been widely carried out over the years, especially for the exploration of metallic mineral deposits and geothermal resources. These intensity data of gravity and magnetic fields could be acquired in much quicker and simpler ways than the other geophysical or geological surveys. The inversion of such potential field data, however, has been known as a non-uniqueness problem expressed in the Green's equivalent layer theory. Because of this problem, gravity and magnetic data have no inherent resolution in depth. We, therefore, would like to develop a way to make use of high exploration efficiency that takes the advantages of the convenience to conduct gravity and magnetic surveys.

We present a 3D joint inversion method to estimate two physical parameters, density and magnetization of subsurface materials. In the method, we introduce the fuzzy c-means (FCM) clustering technique in our joint inversion algorithm to consider the petrophysical relation between density and magnetization of subsurface materials. The fuzzy c-means clustering technique we introduce does not necessitate any empirical equations but deals with a linear combination of the influence from multiple clusters given a piece of data to belong to plural clusters in the parameter space formed by the petrophysical parameters. Adding the simple FCM clustering scheme, we introduced the smoothness constraint to a weight for membership to each clusters, instead of the conventional smoothness constraint to model parameters. Numerical studies using synthetic data indicate the effectiveness of FCM clustering in the joint inversion: the joint inversion results using gravity and magnetic data sets show higher accuracy and resolution than the individual ones.

As the field example, we focus on submarine volcanoes located at Mozambique Channel, because the world-class gas fields were discovered around that area and it is necessitated to estimate structure of submarine volcanoes near gas fields. We apply our inversion method to the real field gravity and magnetic data of the submarine volcanoes at Mozambique Channel. We conclude that our joint inversion method gives the reliable and detailed density/magnetization structures inside the submarine volcanoes in term s of the gravity and magnetic anomalies.

Keywords: joint inversion, gravity, magnetic, submarine volcano

Japan Geoscience Union Meeting 2014
(28 April - 02 May 2014 at Pacifico YOKOHAMA, Kanagawa, Japan)

STT07-P02 Room:Poster Time:April 29 18:15-19:30

Stress field and fracture propagation due to the change of injection pressure

OKUBO, Kurama[1*] ; MIKADA, Hitoshi[1] ; GOTO, Tada-nori[1] ; TAKEKAWA, Junichi[1]

[1]Kyoto University

Hydraulic fracturing is an indispensable scheme to stimulate fluid production in hydrocarbon reservoir development in conjunction with various well testing methods such as drill stem, buildup tests, etc. In recent years, it is also well known that hydraulic fracturing plays a major role in the development of shale oil or gas reservoirs.

The extension length and the orientation of fractures induced by hydraulic fracturing are strongly influenced by the crustal stress field under which any reservoirs are located. Therefore the propagation of fractures is controlled by the regional stress field. It is, in general, necessary to get some understanding of regional stress field before the application of hydraulic fracturing as well as acquiring the rock physical properties of reservoir formations.

However, hydraulically induced fractures may not be created as planned and could cause some environmental issues such as pollution, induced seismicity, etc. It is, we think, very important to estimate how fractures are induced under various crustal conditions to cope with unexpected behavior of fracture propagation.

We focused the effects of the in-situ stress on the stress field around the pre-existing fracture and the fracture propagation with both steady and non-steady hydraulic pressure conditions. To simulate failures in crustal materials under the complicated stress field, we use an extended finite element method (X-FEM) in this study, which can retrieve the stress distribution affected by fractures effectively and estimate the fracture propagation based on linear elastic fracture mechanics (LEFM). Numerical simulations are conducted for a 2D elastic medium having a borehole and a pre-existing fracture. We put the pre-existing fracture around the borehole initially and simulate the propagation of this fracture by applying the hydraulic pressure. The velocity of fracture propagation and the interval of the stress recovery from the stress drop caused by the propagation are set uniformly for the kinetic simulation.

We first simulate the fracture propagation around the borehole under different steady hydraulic pressures with regional stress field. Then we try to see how the fracture could propagate with the non-steady hydraulic pressure during the propagation.

We confirmed that the orientation of the fracture propagation converges to that of the principal stress. Moreover, the convergence speed could be inversely related to the hydraulic pressure. We also found the time delay of the influence of the hydraulic pressure change to the fracture propagation with non-steady hydraulic pressure condition.

From the results of our numerical simulations, we would like to have two conclusions. First, the curvature of the fracture trace depends on hydraulic pressure, but no matter how the fluid pressure is, the orientation of fracture propagation converges to that of principal stress. Second, the transition of the stress field involves the time delay, which leads to the delayed response of the fracture propagation in the non-steady hydraulic pressure condition.

When we develop a hydrocarbon reservoir using hydraulic fracturing, the orientation of maximum in-situ principal stress and the fluid pressure for fracturing should be quantitatively taken into account for the environmental safety and for the stimulation efficiency. It might be also necessary to consider the time delay of the transition of the stress due to the non-steady hydraulic pressure.

Keywords: Hydraulic fracturing, Fracture propagation, X-FEM, Stress field

Japan Geoscience Union Meeting 2014
(28 April - 02 May 2014 at Pacifico YOKOHAMA, Kanagawa, Japan)

STT07-P03 Room:Poster Time:April 29 18:15-19:30

Estimation of the Dispersion Curve for Soil Layers with Lateral Heterogeneity Using Continuous Wavelet Transform

TSAI, Pei-hsun[1*]

[1]Department of Construction Engineering, Chaoyang University of Technology

The MASW method is the normal method regarding surface wave testing, but it requires 12 or more receivers to measure the phase velocity for statistical redundancy. Therefore, the SASW method has potential for use because only two receivers are required. A time-frequency domain analysis is used to extract a dispersion image of Rayleigh waves and select a dispersion curve from the seismic signals of two receivers during surface wave testing. The signals are transformed by continuous wavelet transform, and the products of the transformed signals of the two receivers are summed at the same slowness over the intercept time to construct a dispersion image. This method is unnecessary empirical judgment in the unwrapping of phases and a significant number of receivers. To examine the applicability of the method on evaluating the dispersion curve for soil layers with lateral heterogeneity, three synthetic examples and an experience example of surface wave testing are discussed. The method is applicable for extracting a dispersion image for lateral heterogeneity soil layers. A high-resolution dispersion image is generated in this study by increasing the interval of the receivers. The result of the experience example was in accordance with that of the borehole data.

Keywords: Dispersion curve, Continuous wavelet transform, Lateral heterogeneity

Japan Geoscience Union Meeting 2014
(28 April - 02 May 2014 at Pacifico YOKOHAMA, Kanagawa, Japan)

STT07-P04 Room:Poster Time:April 29 18:15-19:30

Issues and Countermeasures for the Geophysics Investigation of Contaminated with Chlorinated Hydrocarbon

LIU, Hsin-chang[1*] ; LIN, Chih-ping[1] ; WANG, Tzu-pin[2] ; DONG, Tian-xing[3]

[1]Disaster Prevention and Water Environment Research Center, National Chiao Tung Univ., [2]Chien Hsin University of Science and Technology, [3]APOLLO TECHNOLOGY CO., LTD.

Environmental geophysics survey has the advantages of survey rapidly, high resolution result and less affected by the surface topography and objects. It is suitable to either a wide range of general survey or a small-scale precise survey. Recently, non-invaded technologies such as geophysical technology have been introduced to provide the plane and space information of pollution in subsurface by integrating few bore-hole dates. The most common used geophysical technologies are ground-penetrating radar method (GPR) and electrical resistivity tomography (ERT). The electrical resistivity tomography (ERT) is one of the most widely used geophysical methods in geological, hydro-geological, and geo-environmental investigations.This study would first discuss how DNAPL and its soluble-phase components invade into the low permeable layer based on the field observation. Then, the importance of geophysical technology is introduced with comparing to the limitations of bore-hole investigation. Last, the case studies on using geophysical technologies including geophysical well logging are introduced to snapshot the complex profile of DNAPL distribution for improving future application.

Keywords: Geophysical survey, Electrical Resistivity Tomography, Borehole Radar

Japan Geoscience Union Meeting 2014
(28 April - 02 May 2014 at Pacifico YOKOHAMA, Kanagawa, Japan)

STT57-01 Room:423 Time:April 30 16:15-16:30

Development of a laser strain gradiometer and reduction in its thermal noise.

DEGUCHI, Takehiro[1*] ; ARAYA, Akito[1]

[1]Earthquake Research Institute, University of Tokyo

An earthquake is essentially a shear slip on a fault. Because the rupture velocity is roughly constant for most earthquakes, the length, the width, and the slip distance of a fault are respectively proportional to the duration of the rupture, and therefore an earthquake follows the scaling law that its seismic moment is proportional to the cube of its duration. In addition to the ordinary earthquakes, slow earthquakes have been discovered recently. Slow earthquakes include short-term and long-term slow slip events, non-volcanic tremors, low-frequency earthquakes, and very low-frequency earthquakes. They are known to be also shear slips but have slower rupture velocity than the ordinary earthquakes (see the reference [Beroza and Ide, 2011]). Ide et al. (2007) proposed that every slow earthquake has the same mechanism with a new scaling law that its seismic moment is proportional to its duration.

However, no middle-term slow earthquakes with duration of 200 s to 1 day have been reported so far. To understand the reason, we conducted analytical calculations including comparisons of expected signals of slow earthquakes and background seismic noise. It was shown that the middle-term slow earthquakes cannot be observed by a single accelerometer, a strainmeter, or a tiltmeter due to the background seismic motion.

AIST's synthetic analysis using the network of strainmeters, tiltmeters, and groundwater pressure gauges [Itaba et al, 2009] detected smaller slow slips.

Let us take the second spatial derivative of displacement, "the strain gradient". Analytical calculations showed that the signals of slow earthquakes with duration of 200 seconds to 1 day can directly be detected from the strain gradient of the ground. The spatial scale of the background ground motion is larger than the typical distance between a hypocenter and an observatory and the typical size of the fault. Taking spatial derivative emphasizes the small-scale crustal deformation, and makes the detection of local slow earthquakes easier. Thus, measuring the strain gradient will be effective to detect them.

We made a prototype instrument of measuring the strain gradient, "strain gradiometer," with laser interferometry. Before installing it on the ground, we measured its instrumental noise in the atmosphere and found the noise following power spectral density of 10^{-12}[m^{2}s] at 10^{-5}Hz and tendency of 1/f^2 below 0.1Hz. This noise was caused by changes in optical path lengths due to the fluctuation of air pressure. Subsequently, the noise of the interferometer in vacuum was measured; the noise was reduced by 1/10 and had the tendency of 1/f below 0.1Hz. This noise could be reduced by adjusting the optical path difference because it was estimated to be caused by frequency fluctuations of the laser source, which was frequency stabilized by the two-mode method. After the adjustment, there remained noises that had the power spectrum of 1/f^6 in the period between 5000s and 20000s and same power in the period longer than 20000s. This noise had similar waveform to temperature in time-domain. This noise was estimated to be caused by thermal expansion of the optical devices and the optical breadboard. Assuming this noise will be reduced in proportion to the square of the baseline length in terms of the strain gradient, the necessary baseline will be more than 300m. In the presentation, analyses of the noise of the interferometer with thermal insulation by ceramics and the future development will be explained.

References

Ide, S., Beroza, G. C., Shelly, D. R. and Uchide, T., A scaling law for slow earthquakes, Nature, **447**, 76-79, 2007a.

Beroza, G. C. and Ide, S., Slow earthquakes and nonvolcanic tremor, Annu. Rev. Earth Planet. Sci., **39**, 271-296, 2011.

Itaba, S., Koizumi, N., Matsumoto, N. and Ohtani, R., Continuous observation of groundwater and crustal deformation for forecasting tonankai and nankai earthquakes in Japan, Pure Appl. Geophys., **167**, 1105-1114, 2010.

Keywords: laser interferometer, strainmeter, strain gradiometer

Japan Geoscience Union Meeting 2014
(28 April - 02 May 2014 at Pacifico YOKOHAMA, Kanagawa, Japan)

STT57-02 Room:423 Time:April 30 16:30-16:45

Compact Ocean Bottom Cabled Seismic and Tsunami Observation System Using ICT and Installation Plan

SHINOHARA, Masanao[1*] ; YAMADA, Tomoaki[1] ; SAKAI, Shin'ichi[1] ; SHIOBARA, Hajime[1] ; KANAZAWA, Toshihiko[2]

[1]Earthquake Research Institute, University of Tokyo, [2]National Research Institute for Earth Science and Disaster Prevention

The Pacific plate is subducting below the northeastern Japan islands arc. The 2011 Tohoku earthquake occurred at the plate boundary between the Pacific plate and the landward plate below landward slope of the Japan Trench. In 1996, Earthquake Research Institute (ERI), University of Tokyo had installed seismic and tsunami observation system using seafloor optical fiber in the off-Sanriku area. The continuous real-time observation has been carried out since the installation. The system observed seismic waves and tsunamis generated by the 2011 Tohoku earthquake, and the data from the system are indispensable to estimate accurate position of the source faults and the source process of the 2011 event. However, the landing station of the system was damaged by huge tsunami 30 minutes after the mainshock, and the observation is discontinued. Because the data from the real-time system on seafloor are important, we decide to restore the existing system and install newly developed Ocean Bottom Cabled Seismic and Tsunami (OBCST) observation system off Sanriku for additional observation and/or replacement of the existing system. In this paper, we present a system of the new OBCST in detail, and installation plan.

Until 2010, we had already developed and installed the new compact Ocean Bottom Cabled Seismometer (OBCS) system near Awashima-island in the Japan Sea. After the installation, the OBCS system is being operated continuously and we have continuous seismic data for more than 3 years at the present. The new OBCST system for off-Sanriku area is based on this system, and is characterized by system reliability using TCP/IP technology and down-sizing of an observation node using up-to-date electronics. The new OBCST has three accelerometers as seismic sensors. Signals from accelerometers are 24-bit digitized with a sampling rate of 1 kHz and sent to a landing station using standard TCP/IP data transmission. A precise pressure gauge is also equipped as a tsunami sensor. The tsunami data with a sampling rate of 1ms are also transmitted by TCP/IP protocol. In addition, an observation node can equipped with an external port for additional observation sensor instead of a pressure gauge. Additional sensors on seafloor are supplied the power using Power over Ethernet technology. Clock is delivered from the GPS receiver on a landing station using simple dedicated lines. In addition, clocks in observation nodes can be synchronized through TCP/IP protocol with an accuracy of 200 ns (IEEE 1588). The data will be stored on the landing station and sent to ERI in the real-time. A simple canister for tele-communication seafloor cable is adopted for the observation node, and has diameter of 26cm and length of about 1.3m. This small size of the canister has an advantage for burying the system below seafloor.

At the present, we are producing the observation nodes of the new OBCST. The new system has three observation nodes; two have three-component seismometer and a pressure gauge, one has seismometers and an external port by using the PoE technology. We have a plan to connect a pressure gauge and hydrophone via the PoE external port of the third observation node. Total length of the practical system is approximately 100 km and an interval of the observation node is about 30 km. We have a plan to install the practical system in 2015.

Keywords: Cabled ocean bottom seismometer and tsunami gauge, Sanriku, Japan Trench, seafloor observation

Japan Geoscience Union Meeting 2014
(28 April - 02 May 2014 at Pacifico YOKOHAMA, Kanagawa, Japan)

STT57-03 Room:423 Time:April 30 16:45-17:00

Long-period duration of the teleseismic events reported to ISC from Syowa Station since 1967

KANAO, Masaki[1*]

[1]National Institute of Polar Research

Phase identifying procedure for teleseismic events at Syowa Station, East Antarctica have been carried out since 1967 after the International Geophysical Year (1957-1958). From the development of INTELSAT telecommunication link, digital waveform data have been transmitted to the National Institute of Polar Research for utilization of phase identification. Arrival times of teleseismic phases, P, PKP, PP, S, SKS have been reported to the International Seismological Centre (ISC), and published by JARE Data Reports from NIPR. In this paper, hypocentral distribution and time variations for detected earthquakes are demonstrated over the last four decades in 1967-2010. Characteristics of detected events, magnitude dependency, spatial distributions, seasonal variations, together with classification by focal depth are demonstrated. Besides the natural increase in number for occurrence of teleseismic events on the globe, a technical advance in observing system and station infrastructure, as well as the improvement of procedure for reading seismic phases, could be efficiently combined to produce the increase in detection number in last few decades. Variations in teleseismic detectability for longer terms may possibly by associate with meteorological environment and sea-ice spreading area around the Antarctic continent. Recorded teleseismic and local seismic signals have sufficient quality for many analyses on dynamics and structure of the Earth's as viewed from Antarctica. The continuously recorded data are applied not only to lithospheric studies but also to Earths deep interiors, as the significant contribution to the Federation of Digital Seismological Network from high southern latitude.

Keywords: Syowa Station, teleseismic events, detection capability, monitoring observation, global network

Japan Geoscience Union Meeting 2014
(28 April - 02 May 2014 at Pacifico YOKOHAMA, Kanagawa, Japan)

STT57-04 Room:423 Time:April 30 17:00-17:15

Seismic observation on Greenland Ice Sheet by the Japanese GLISN team (2011-2013), and a plan for the 2014 season

TOYOKUNI, Genti[1*] ; KANAO, Masaki[2] ; TONO, Yoko[3] ; HIMENO, Tetsuto[4] ; TSUBOI, Seiji[3]

[1]RCPEVE, Tohoku Univ., [2]NIPR, [3]JAMSTEC, [4]Seikei Univ.

Melting of the Greenland ice sheet is now in progress accompanying the global climate change. Recently, a new type of seismic event called ”glacial earthquakes”, which are generated by the movement of a large mass of ice within the glacial terminus, has been realized as a new way to monitor current ice sheet dynamics. In 2009, the multinational GreenLand Ice Sheet monitoring Network (GLISN), a large broadband seismological network in and around Greenland was initiated to monitor these events.

Japan, a partner country of the GLISN project, has been sending a field team every year since 2011. The joint U.S. and Japanese team first constructed a seismic station (station code: ICESG) on the Greenland ice sheet. In 2012, we serviced two ice sites (ICESG, DY2G) and one rock site (NUUK). In 2013, the same team spent 11 days on ice for maintenance of ICESG and DY2G, and helped rogistics for another ice site (NEEM). This presentation summarizes our field activities on the GLISN project for three years, and show a plan for the 2014 season.

Our activity is supported by JSPS KAKENHI 24403006.

Keywords: Greenland, glacial earthquake, GLISN network

Japan Geoscience Union Meeting 2014
(28 April - 02 May 2014 at Pacifico YOKOHAMA, Kanagawa, Japan)

STT57-05 Room:423 Time:April 30 17:15-17:30

Development and Operation of Wide-area Observation Monitoring (WONM) System

MURATA, Ken T.[1*] ; NAGATSUMA, Tsutomu[1] ; YAMAMOTO, Kazunori[1] ; WATANABE, Hidenobu[1] ; UKAWA, Kentaro[2] ; MURANAGA, Kazuya[2] ; YUTAKA, Suzuki[2]

[1]National Institute of Information and Communications Technology, [2]Systems Engineering Consultants Co., LTD.

This paper is devoted to present an operation system to acquire, to transfer and to storage data for world-wide observation networks, which is named as WONM (Wide-area Observation Network Monitoring) system, developed in NICT (National Institute of Information and Communications Technology). This system provides us with easier management of data collection than legacy systems by means of autonomous system recovery, periodical state monitoring, and dynamic warning procedures. We have equipped world-wide observatories for space weather prediction and research works with this system connected with the NICT Science Cloud. Demonstration and discussion will be presented concerning with this challenging system, especially from the viewpoint that we easily operate world-wide observatories on a web application.

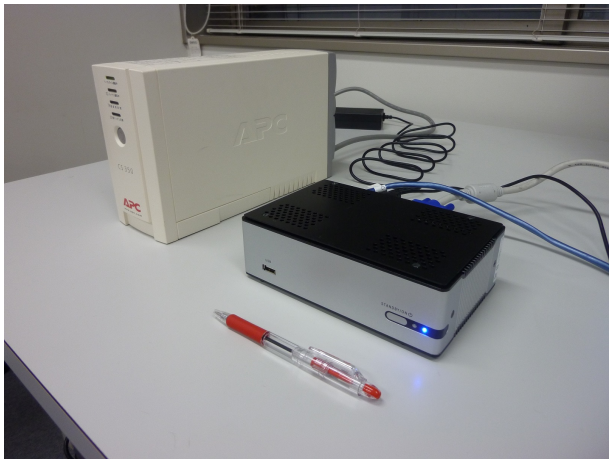

Japan Geoscience Union Meeting 2014
(28 April - 02 May 2014 at Pacifico YOKOHAMA, Kanagawa, Japan)

STT57-06 Room:423 Time:April 30 17:30-17:45

Development of hypocenter location method using envelopes: Application to B-type earthquakes at Miyakejima volcano

UCHIDA, Higashi[1*] ; NISHIMURA, Takeshi[2] ; NAKAHARA, Hisashi[2] ; YAMASATO, Hitoshi[1] ; FUJITA, Eisuke[3]

[1]Japan Meteorological Agency, [2]Geophysics, Science, Tohoku University, [3]NIED

B-type earthquakes are frequently observed in active volcanoes, but it is difficult to locate them by using traditional phase picking methods because most of B-types show emergent onsets of P- and S-waves. We applied the envelope correlation method of Obara (2002) to B-type earthquakes at Miyakejima volcano, but the located hypocenters shifted towards the south-east by 0.5 - 1 km compared to those determined by phase picking method. Such systematic difference is caused by some assumptions such as that the envelope waveforms at each station are all the same. Actually, the envelope waveform broadens as hypocentral distance increases because of the scattering, or the waveform strongly depends on the site condition. In this study, therefore, we develop a new envelope correlation method in which a small number of the B-type earthquakes whose S-wave arrival times are manually picked are used as reference events. The method estimates S-wave arrival times by taking cross-correlations between envelopes of reference events and that of target event at each station. To find appropriate reference events effectively, we use the similarity of concatenated envelopes: the envelopes of all stations are connected in order keeping the amplitude ratios and time differences of envelopes between stations. The similarity of the concatenated envelopes means that the hypocenters and path effects on the envelope waveform at each station are almost the same with those of the reference events. By applying this method to B-type earthquakes at Miyakejima volcano observed from August 2010 to April 2011, we determine 71 % of the observed ones in an automated way. The B-type earthquakes are located within a 1 km diameter centered on the southern part of the summit caldera, where continuous gas emission occurs. On the other hand, A-type earthquakes, which show clear onsets of P- and S-waves, are distributed from southern part to western part of the summit caldera. To check the reliability, we also compare the result to the hypocenters located by picking P- and S-onset times, and there is no systematic difference between them as seen in the comparison to the result of Obara (2002) method. Our new method is applicable to volcanic earthquakes recorded at other seismic networks that consist of at least several stations surrounding hypocenter regions, which will help us to monitor and understand volcanic activity.

Keywords: hypocenter determination, envelope correlation, Miyakejima volcano

Japan Geoscience Union Meeting 2014
(28 April - 02 May 2014 at Pacifico YOKOHAMA, Kanagawa, Japan)

STT57-P01 Room:Poster Time:April 30 18:15-19:30

The annual variation in the teleseismic detection capability at Syowa Station, Antarctica

IWATA, Takaki[1*] ; KANAO, Masaki[2]

[1]The Institute of Statistical Mathematics, [2]National Institute of Polar Research

Kanao et al. [2012a, 2012b] have pointed out the annual variation in the teleseismic detection capability at Syowa Station located in Antarctica. The main cause of the variation is considered to be the increase in area and/or thickness of sea ice in winter, which restrains the generation of sea waves around Antarctica; consequently the noise level in seismic records changes annually [Grob et al., 2011; Kanao et al. 2012c].

This implies that environmental parameters relevant to climate, sea ice, and so forth affect the teleseismic detection capability. To investigate the relationship in detail, a quantitative evaluation of the annual variation in the detection capability is dispensable because the aforementioned studies have revealed the annual variation only qualitatively on the basis of the time history of the minimum magnitude of detected teleseismic events at the station. Therefore, we conducted the following analysis in this study.

The dataset analyzed in this study is the same as the examined one in Kanao [2010] and Kanao et al. [2012]. The data period ranges from 1987 to 2007 and the magnitudes of the events are measured with the body-wave magnitude (Mb) scale. The number of analyzed earthquakes of which magnitudes are determined is 19,044. Because the main interest of this study is to quantify the annual variation, the earthquake sequence is divided into periods of one year and these one-year sequences were stacked.

For the quantification of the detection capability, the model representing a magnitude-frequency distribution of earthquake covering the entire range [Ogata & Katsura, 1993] is used with a small modification. In this model, the distribution is assumed to be the product of the Gutenberg-Richter (GR) law [Gutenberg and Richter, 1946] and the detection probability of earthquakes at magnitude M. As mentioned above, the magnitudes in the examined dataset are given as Mb, which saturates at its large value. Therefore, instead of the original GR law, we introduced a modified type of the GR law, which is suggested by Utsu [1974], that contains the maximum magnitude of earthquake potentials as a parameter. The detection probability was represented by the cumulative distribution of a normal distribution, following the suggestion of Ringdal [1975] and its accompanied studies [e.g., Ogata & Katsura, 1993; Iwata, 2008, 2012, 2013a, 2013b, 2013c]. This formulation results in the introduction of a parameter μ, which corresponds to the magnitude at which 50% of earthquakes are expected to be detected, and this parameter quantifies the quality of the earthquake detection capability.

Then, the annual variation in μ was estimated by adopting a Bayesian approach used in Iwata [2013a, 2013b]. In this approach, the annual variation is represented by a piecewise linear approximation of which breaking points were taken at each of the occurrence times of each events. We determined the variation in μ with a smoothness constraint.

The result of the estimation is summarized as follows. The significance of the existence of the annual variation was evaluated with ABIC [Akaike, 1980]; the value of ABIC in the case with the annual variation is 54.9 smaller than that in the case without the annual variation, suggesting high significance of the variation. The maximum (i.e., the worst detection capability) and minimum (i.e., the best) values of μ appear around the end of December and the middle of August, respectively. The difference between the maximum and minimum values is 0.13. Because the maximum and minimum of the average temperature at Syowa Station also appear in those periods, this result reinforces the relationship between the environmental parameter and teleseismic detection capability.

(The references are listed in the abstract written in Japanese.)

Keywords: earthquake detection capability, annual variation, Antarctica, Syowa Station, Bayesian statistics, statistical seismology

Japan Geoscience Union Meeting 2014
(28 April - 02 May 2014 at Pacifico YOKOHAMA, Kanagawa, Japan)

STT57-P02 Room:Poster Time:April 30 18:15-19:30

Towards Detection of Hydraulic Fracturing Induced Earthquakes Using Neural Network

KIM, Ahyi[1*] ; IIDA, Shuhei[1] ; FUJIHARA, Satoru[2]

[1]Yokohama City University, [2]Itochu Techno-Solutions Corporation

Detection, location and determination of focal mechanism of low frequency and hybrid events such as volcanic and non-volcanic events have been extensively studied. Recently, Das and Zoback (2011) found unusual events which has relatively low frequency in the seismic activity induced during hydraulic fracturing in a gas shale reservoir. Those events were observed in limited frequency band similar to tectonic tremor sequences. It is important to understand the mechanisms of those events for clarifying the fracturing process during the hydraulic stimulation. In this study, we introduce a method to detect the band-limited waveform using neural network. The results of the initial numerical test indicate that the harmonic function waveforms could be identified when they have clear features in shape. As the next step, we will add realistic noise to the synthetic data and perform the synthetic analyses. After we verify the applicability of our method, we will apply the method to real seismic data observed during fluid injection.

Keywords: Neural Network, Waveform detection, Hydraulic fracturing, Low frequency earthquake, Seismic Waveform

Japan Geoscience Union Meeting 2014
(28 April - 02 May 2014 at Pacifico YOKOHAMA, Kanagawa, Japan)

STT57-P03 Room:Poster Time:April 30 18:15-19:30

Background noise characteristics of F-net broadband seismograms

KIMURA, Takeshi[1*] ; MURAKAMI, Hiroshi[2] ; YANO, Tomoko elizabeth[1] ; KIMURA, Hisanori[1] ; KAZAKAMI, Tomoe[1] ; MATSUMOTO, Takumi[1]

[1]NIED, [2]ADEP

National Research Institute for Earth Science and Disaster Prevention (NIED) has operated a broadband seismometer network, F-net. F-net consists of 73 stations in Japan and a broadband seismometer, STS-1/2/2.5 or CMG-1T/3T, has been installed at each station. The seismometers are installed in 30-50 m vault to prevent effects of the temperature and air pressure changes. All the data are openly available on the web, and rapid automated data processing systems, such as AQUA system [Matsumura et al., 2006], have used these data. To evaluate the data quality continually is important for the operation of the observation network, the earthquake monitoring, and the automated analyses. In order to assess the F-net data quality, we investigated the characteristics of their background noise.

To quantify the background noise of F-net waveform data, we used probability density functions (PDFs) of power spectral densities (PSDs) [McNamara & Buland, 2004]. For 1996-2013 continuous waveform data with the interval of 1 sec, PSDs of ground acceleration were computed from overlapping (50 %) 1-day time-windows. Each time-window was divided into 13 time segments (6 hours) overlapping by 75 %, and the 1-day PSD estimate was calculated as the average of the 13 segment PSDs. These 1-day PSDs were gathered by binning periods in 1/8 octave intervals and binning power in one-dB intervals.

We calculated a new noise model for F-net, based on the statistical mode of the obtained PDFs for vertical component of all the F-net stations [McNamara & Buland, 2004]. The noise model was constructed from the minimum PDF mode value among all the stations at each period. The values of the F-net model is ˜5 dB higher than ones of the mode noise model of the continental United States [McNamara & Buland, 2004] around periods of 4 sec and 40 sec. The F-net noise model is mainly defined by the STS-1 mode values. The STS-2 values are ˜5 dB larger than STS-1 ones at the periods of 200-800 sec, and the CMG-1T/3T are ˜15 and ˜10 dB larger than STS-1 at 30-2000 sec and 100-2000 sec, respectively.

Recently, we have equipped a styrofoam cover on the broadband sensor for temperature shielding. This cover has reduced the PDF mode values for vertical component of STS-2 by ˜5 dB at the periods longer than 500 sec, and is useful to obtain such long-period signals with a good signal/noise ratio.

Keywords: background noise, broadband seismometer, F-net

Japan Geoscience Union Meeting 2014
(28 April - 02 May 2014 at Pacifico YOKOHAMA, Kanagawa, Japan)

STT57-P04 Room:Poster Time:April 30 18:15-19:30

Long-term ocean-bottom seismometers in MRI/JMA and some related problems

HIRATA, Kenji[1*] ; TSUSHIMA, Hiroaki[1] ; YAMAZAKI, Akira[1] ; KATSUMATA, Akio[1] ; MAEDA, Kenji[1] ; BABA, Hisatoshi[2] ; MATSUBARA, Tadayasu[3] ; ITOU, Tatsuya[3] ; SUGITA, Tomoya[3] ; HORI, Katsuhiro[4] ; SHIRAKO, Takeshi[4]

[1]Meteorological Research Institute, JMA, [2]School of Marine Science and Technology, Tokai University, [3]Tokyo Sokushin, [4]NiGK Corporation

In 2011 to 2012, seismology and volcanology research department/MRI introduced eight long-term ocean-bottom seismometers (OBSs) by converting existing short-term ones so that we were able to conduct one-year-long, three-component seismographic observation. The conversion was made by changing the control circuit, the AD convert, and the data storage device into low-power consumption ones.

In November 2011, four long-term OBSs were deployed off Boso Peninsula, about 40 km east of Tokyo, to test them and to investigate seismicity in this region that adjoins the southern end of the mainshock rupture area of the March 11, 2011 Tohoku earthquake (Mw9.0). In September 2012, we tried to recover the four long-term OBSs that were deployed in 2011 and re-deploy other four long-term OBSs. However, all transponder units of four long-term OBSs to be newly deployed got out of order soon after the vessel left the port. So we declined to newly deploy other four long-term OBSs. Also, we could not recover two long-term OBSs among four that were deployed. We confirmed that two recovered long-term OBSs recorded ultra-micro earthquake activity successfully.

After the cruise, the OBS transponder units that became out of order were tested in manufacturer's laboratory so that the cause of the trouble was inferred to be (1) possible opening within the housing of transducer unit of OBS transponder due to thermal expansion/contraction thorough high temperature in summer and low temperature in winter, and (2) cavitation in silicon-oil within the housing of transducer unit of OBS transponder due to hull vibration. Countermeasures were devised as follows; (a) overhaul of electric circuits and transducer unit housing filled with silicon oil, (b) use of base-isolation floor-mat on which OBSs should be placed. Both of manufacturer's laboratory tests and actual onboard tests suggest that these countermeasures are effective.

Keywords: long-term, seismographic observation, ocean-bottom seismometer, measure for a glitch

Japan Geoscience Union Meeting 2014
(28 April - 02 May 2014 at Pacifico YOKOHAMA, Kanagawa, Japan)

STT57-P05 Room:Poster Time:April 30 18:15-19:30

Value change of ocean bottom pressure gauge (Paroscientific depth sensor) by inclination of the sensor

OGATA, Naoki[1*] ; SATO, Toshinori[1] ; YAMADA, Tomoaki[2] ; SHINOHARA, Masanao[2]

[1]Graduate School of Science, Chiba Univ., [2]ERI, Univ. Tokyo

Introduction

Ocean bottom pressure gauges (OBP) using depth sensor of Paroscientific Inc. are used for observation of up-down crustal movement at ocean bottom (e.g. Inazu et al., 2012). Observation error of this sensor is about 0.5 hPa (about 5mm in water) (e.g. Kono et al., 2012). So, this sensor is expected to detect coseismic movements and movements with large slow slip events such as the Boso slow slip events. But , it is known that this sensor shows incorrect values when the sensor is inclined. This suggests the possibility that this sensor can not obtain correct value because OBP itself may be inclined by coseismic crustal deformation. This presentation shows measurements of value change by inclination of the sensor, and discusses limits of inclination based on the observation error.

Measurements and results

We used an intelligent depth sensor 8CB2000-I, Paroscientific Inc. We set the sensor upright, then incline it, hold it for some time, then return it upright. We measured differences of the values between upright position and inclined position. We found that if we incline the sensor very fast, it shows very large transient values after inclined. So, we need slow inclination (a few ten seconds par 10 degree inclination) of the sensor. After the measurements, we fit the data using a spherical harmonic function.

The observed data show 2 hPa at 10 degree inclination, 6 hPa at 20 degree, and 12 hPa at 30 degree. The data is not symmetrically with respect to the upright position, but symmetrically at a point which is inclined about 15 degree from the upright position. The reproducibility of the values for inclination is within about 0.3 hPa (STD). From this result, inclination limit of OBP is about 5 degree if OBP sits on the ocean bottom flat. If OBP touches down at steeper inclined bottom, the limit become narrower. If OBP is inclined at 20 degree, the limit is about 2 degree.

Keywords: Pressure gauge, inclination correction, Paroscientific Depth Sensor

Japan Geoscience Union Meeting 2014
(28 April - 02 May 2014 at Pacifico YOKOHAMA, Kanagawa, Japan)

STT57-P06 Room:Poster Time:April 30 18:15-19:30

Evaluating performance of automatic earthquake detection and location system for the nationwide seismic network(2)

NAKAYAMA, Takashi[1*] ; HIRAHARA, Satoshi[1] ; KONO, Toshio[1] ; NAKAJIMA, Junichi[1] ; OKADA, Tomomi[1] ; UMINO, Norihito[1] ; HASEGAWA, Akira[1] ; HORIUCHI, Shigeki[2] ; HORIUCHI, Yuko[2]

[1]Graduate School of Science, Tohoku University, [2]Home Seismometer Corporation

The number of seismic stations has tremendously increased by many temporary seismic networks recently deployed in various areas, in addition to dense routine seismic networks such as the nationwide Kiban seismic network. Effective automatic earthquake detection and location system is anticipated, because the ability of data processing is limited. Manually picking P- and S-wave arrival times etc. from a huge amount of seismic waveform data observed by such many seismic stations is considerably time consuming work.

Horiuchi et al. (2012, 2013) have developed such an automatic seismic waveform processing system. This system was set up at Tohoku University on December 2012, and automatic detection and location processing of the nationwide seismic network data has been operating since then. The system can detect and locate many earthquakes which are difficult to be located by the routine processing based on manual pickings. However, sometimes earthquakes cannot be correctly discriminated by the system: for example, when more than two earthquakes occur almost simultaneously. In order to consider the application of automatic earthquake detection and location system to the actual seismic network, we need to know its performance.

Nakayama et al. (2013) tried to evaluate performance of this earthquake detection and location system for the application to the nationwide seismic network. Results showed that the automatic system could detect and locate earthquakes about 1.5 times more than those in the JMA unified catalogue. The automatic system extended the lower limit of the detection capability to much smaller magnitude range than that by the JMA unified catalogue. The evaluation also showed that S-wave arrival times picked by the automatic system were systematically delayed by ˜0.05-0.1 sec compared with those by the manual pickings of the unified catalogue. Based on this performance evaluation, Horiuchi et al. (2014 this meeting) have tried to improve the system by developing a new algorithm to better pick S-wave arrivals.

We have evaluated performance of this presently improved automatic processing system by using the waveform data for the same period as those in the previous evaluation. Results show that the systematic delay of S-wave arrivals by the automatic pickings is considerably improved and the difference in S-wave arrivals between the new automatic system and the unified catalogue has become nearly the same as that between the manual pickings by Tohoku University and those in the unified catalogue. This indicates that the S-wave arrival times, as well as P-wave arrival times, picked by the automatic system almost stand comparison with those by the manual picking. Moreover, the evaluation shows that the new system also improved the rate of correct discrimination of earthquakes: the percentage of events that were missed to be correctly located decreased from 19% to 14% (most of these events are those located in and around the Izu-Bonin Islands and the Ryukyu Islands), and the percentage of events that were incorrectly defined as earthquakes decreased from 3.1% to 2.5%. This is because of the improvement of algorithm to correctly discriminate more than two earthquakes that occurred nearly simultaneously.

Keywords: automatic arrival time picking, automatic event detection and location system, performance evaluation

Japan Geoscience Union Meeting 2014
(28 April - 02 May 2014 at Pacifico YOKOHAMA, Kanagawa, Japan)

STT57-P07 Room:Poster Time:April 30 18:15-19:30

W-phase analysis with 1Hz GNSS data

UENO, Hiroshi[1*] ; KATSUMATA, Akio[1] ; KAWAMOTO, Satoshi[2] ; YAHAGI, Toshihiro[2] ; MIYAGAWA, Kohei[2]

[1]Meteorological Research Institute, [2]Geospatial Information Authority of Japan

The Japan Meteorological Agency analyze W-phase inversion solution and CMT solution when big earthquakes occur. Now we can analyze W-phase solution with broadband seismograms in Japan after 6 minutes of earthquake occurrence. These W-phase solution are one of information for performing grade changes or cancel of TSUNAMI warning.

Broadband seismic records is used by integrating for W-phase analysis. Because when big earthquake occur, the waveform data recorded at near site from source area may be unstable, it might be difficult for analyzing W-phase solution. On the other hand, the GNSS data to be recorded directly displacement, it can be used as a stable displacement.

In this study, using 1Hz GNSS data of Geospatial Information Authority of Japan(GSI), we analyzed W-phase solutions of Great Tohoku earthquake in 2011, its aftershock, and Tokachi-oki earthquake in 2003.

Keywords: W-phase analysis, 1Hz GNSS data, Great Tohoku earthquake

Japan Geoscience Union Meeting 2014
(28 April - 02 May 2014 at Pacifico YOKOHAMA, Kanagawa, Japan)

STT57-P08 Room:Poster Time:April 30 18:15-19:30

Automated event identification of aftershocks(2)

KATSUMATA, Akio[1*]

[1]Meteorological Research Institute, JMA

We are developing a seismic event identification technique for a quick grasp of aftershock activities of great earthquakes. For the case of the 2011 off the Pacific coast of Tohoku Earthquake, a number of onsets of aftershocks were not clear due to successive occurrence of aftershocks. Envelops of seismic waves are used to make it possible to estimate source locations of events without clear onsets.

The method is based on peak amplitudes and their times as

(1)A band pass filter is applied to the seismic waves.

(2)Envelop of seismic wave is obtained.

(3)Peak amplitudes and times are checked.

(4)Possible events are searched for the data of envelop amplitudes and times.

Formerly we tried to estimate source parameters by searching a solution in five-dimensional space of (origin time, latitude, longitude, depth, magnitude) by the shuffled complex evolution (SCE-UA) method. However, good solutions were seldom obtained because a combination of noise data often show a high score.

We changed the source estimation method. At the first, a group with high S/N data is searched for. We select a key data with highest S/N from the group. Then we estimate the best source parameter which is consistent to the selected data. While searching for the source location, the focal depth is fixed and epicentral distance and azimuth are changed. The origin time is obtained from the time of the envelop peak and epicentral distance, and the magnitude is estimated from the peak amplitude and epicentral distance.

Noise is often selected as the key data. Noises are usually rejected because they do not form a group of consistent data. Data of noise and identified events are removed from dataset to be checked. Data search is continued until no candidate is left.

Events are successfully identified and source locations are properly estimated for the events with a number of data. However source locations are not properly estimated for events with a small number of data.

We used seismic data from the National Research Institute for Earth Science and Disaster Prevention, Hokkaido University, Hirosaki University, Tohoku University, University of Tokyo, Nagoya University, Kyoto University, Kochi University, Kyushu University, Kagoshima University, the National Institute of Advanced Industrial Science and Technology, Aomori prefectural government, Tokyo metropolitan government, Shizuoka prefectural government, Kanagawa prefectural government, the City of Yokohama, the Japan Marine Science and Technology Center, and the Japan Meteorological Agency.

Keywords: automated seismic event identification, envelop of seismic wave

Japan Geoscience Union Meeting 2014
(28 April - 02 May 2014 at Pacifico YOKOHAMA, Kanagawa, Japan)

STT57-P09 Room:Poster Time:April 30 18:15-19:30

Construction of the seismic observation network around Shimokita Peninsula

SEKINE, Shutaro[1*] ; SAWADA, Yoshihiro[1] ; KASAHARA, Keiji[1] ; SASAKI, Shunji[1] ; TAZAWA, Yoshihiro[1] ; YAJIMA, Hiroshi[1]

[1]Association for the Development of Earthquake Prediction

Introduction

Seismic activity in the Shimokita region is not well grasped, because the distribution of the seismic stations is not dense compared with that of Southern Tohoku region. So, it is not enough to estimate the depth of the seismogenic zone. Accordingly, the Association for the Development of Earthquake Prediction (ADEP), determined to newly construct a high-density seismic observation network (AS-net) in the region in question, as a part of its investigation and research into seismic activity in the Shimokita Peninsula. An outline of the observation network is presented below.

Outline of the network

The AS-net consist 36 seismic observation stations. 20 stations were made before the end of 2013. And the other stations will make in 2014.

The sensors of each station are installed in boreholes at a depth of about 20m. We set the short period three dimensional velocity sensors by Lennartz, and accelerometers by Japan Aviation Electronics Industry ltd. And A/D converter is LS-7000XT made by Hakusan Co.

The data of the each station send to ADEP using with Internet, and relay to other facility for research.

Future works

It is anticipated that useful data will be obtained regarding detailed velocity and attenuation structures in the area surrounding the seismic observation network, as well as micro earthquake activity in the regions. The number of the earthquakes we estimate in January, is twice as that of JMA.

Keywords: seismic observation network, Shimokita Peninsula

Japan Geoscience Union Meeting 2014
(28 April - 02 May 2014 at Pacifico YOKOHAMA, Kanagawa, Japan)

STT58-01 Room:313 Time:April 30 16:15-16:30

Regional Airborne Survey for the Evaluation of Geothermal Potential in Japan

SHIMADA, Tadaaki[1*] ; TAKAI, Katsumi[1] ; MIYAKE, Kazuhiro[1] ; HISATANI, Koichi[1] ; TOSHA, Toshiyuki[1]

[1]Japan Oil, Gas and Metals National Corporation

Japan Oil, Gas and Metals National Corporation (JOGMEC) supports smooth development of geothermal resources in Japan by providing assistance to geological, geophysical, and well-drilling surveys, equity capital or liability guarantees, and information and data on geothermal resources.

As part of them, we planned to conduct evaluation of geothermal potential with airborne technique of gravity gradiometer method and time-domain electromagnetic method.

The gravity gradiometer method measures the differential of gravity, and provides information of much detailed geological structures. The time-domain EM method provides deeper penetration data than the frequency-domain EM method.

Since these methods are state-of-the-art techniques, we demonstrated them first in a couple of area with relatively high geothermal potentials and a lot of surveys conducted.

We carried out airborne survey with the technique of the gravity gradiometer method in the Kuju and the Kirishima areas in 2013. We would like to introduce the result of the airborne survey.

The authors thank local municipalities and related organizations for their understanding and cooperation to conduct the airborne survey.

Keywords: airborne survey, geothermal resources, gravity, gravity survey, electromagnetic survey

Japan Geoscience Union Meeting 2014
(28 April - 02 May 2014 at Pacifico YOKOHAMA, Kanagawa, Japan)

STT58-02 Room:313 Time:April 30 16:30-16:45

Study on the prediction of the deep catastrophic landslide using the Airborne Electromagnetic Survey

KAWATO, Katsushi[1*] ; KINOSHITA, Atsuhiko[2] ; TAKAHARA, Teruyoshi[2] ; ISSHIKI, Hiromitsu[2] ; ISHIZUKA, Tadanori[2] ; OKUMURA, Minoru[1] ; UCHIDA, Koichi[1]

[1]Nippon Engineering Consultants Co.,LTD., [2]Public Works Research Institute

Recently, the deep catastrophic landslides were occurred frequently including the disaster of the Kii peninsula by typhoon 12 in 2011. The risk evaluation is demanded to be carried out the measures that we can assume at the both sides of the method constructing sabo dams and evacuation method. Recently, the airborne electromagnetic survey is performed a close-up to evaluate the risk of them. Merits of the airborne electromagnetic survey include that a geological feature border in conjunction with the deep catastrophic landslides having possibilities to become clear, hydrological properties may become clear. On the other hand, there is the uncertain element such as the decision method of the ratio resistance level of the geological feature border and the groundwater not being clear. In this study, we have arranged the results such as in the airborne electromagnetic survey, a geological survey, the hydrological investigations for the points where the deep catastrophic landslides were occurred and where airborne electromagnetic survey was carried out so far. The study areas are Byutano river basin (is about 4.4km2), Fujikawa river basin (about 3.7km2), Himekawa basin (about 15.2km2), and Kumano river basin (about 10.1km2). In these areas, in the past, the deep catastrophic landslides were occurred and the airborne electromagnetic surveys were carried out.

First, we have examined ratio resistance properties every area by the airborne electromagnetic survey. The range of the ratio resistance level to appear in the area for showed 1-2400 Ω-m in 1-1200Ω-m, the Kumano river basin in the Himekawa river basin whereas it was 1-400Ω-m in Byutano river basin and the Fujikawa river basin, and the distribution of the ratio resistance level knew that there was a difference by a geological feature and an area. And we have found that there were three patterns of the distributions of the resistance when we have paid our attention to the ratio resistance pattern of the plumb directions from the surface of the slope at the point with the fear of the deep catastrophic landslides to the deep part. From this, the depth that a ratio resistance level changes in the plumb direction may become the fundus of the deep catastrophic landslide. Boring investigations were carried out in Byutano river basin, Fujikawa river basin, Himekawa river basin, and a weathering department and the geological feature border of the virginity part are authorized by the observation of the boring core. The ratio resistance level corresponding to this geological feature border indicates 100Ω-m in Byutano river basin, 70Ω-m in Fujikawa river basin, and in Himekawa river basin indicates 500Ω-m, 680Ω-m, 1000Ω-m.

From these, it was confirmed that the ratio resistance level to correspond to appearance frequency and the geological feature border of the ratio resistance level varied according to an area and a geological feature. Therefore, it is necessary to carry out the risk evaluation of the deep catastrophic landslide after carrying out a boring investigation in addition at a representative point when we carry out the airborne electromagnetic survey, and having arranged a geological feature and the relations of the ratio resistance level.

In addition, at the deep catastrophic landslide point of Kumano river basin, consecutive low ratio resistance zones and the low ratio resistance zone of the plumb direction are common to the valley part from the ridge and are confirmed and agree with the groundwater situation by the hydrological investigation. We need to accumulate data about the ratio resistance structure in conjunction with the deep catastrophic landslide and want to examine the extracting method of the point with the fear of the deep catastrophic landslide, an estimate method of the collapse depth and collapse volume in future.

Keywords: Airborne Electromagnetic Survey, deep catastrophic landslide

Japan Geoscience Union Meeting 2014
(28 April - 02 May 2014 at Pacifico YOKOHAMA, Kanagawa, Japan)

STT58-03 Room:313 Time:April 30 16:45-17:00

Study on the prediction of the large landslides of the volcanoes using the Airborne Electromagnetic Survey

KINOSHITA, Atsuhiko[1*] ; TAKAHARA, Teruyoshi[1] ; ISSHIKI, Hiromitsu[1] ; ISHIZUKA, Tadanori[1] ; OODAIRA, Tomohide[2] ; OMORI, Tetsuji[3] ; YAMANE, Hiroyuki[3] ; ARAI, Kenichi[4] ; KIYONO, Koji[5] ; TSUJIOKA, Hideki[6]

[1]Public Works Research Institute, [2]Fukushima River and National Highway Office, [3]Fuji Sabo Office, [4]Asia Air Survey Co,. ltd., [5]Nippon Engineering Consultants Co,. ltd., [6]OYO Corporation

In the lower basins of the active volcanoes, there are always the risks that sediment disasters are occurred. Especially, when large landslides are occurred at the time of heavy rains, the landslide sediment become a debris flow and makes a big damage by the sedimentation and the flooding in a lower basin. In late years,the Airborne Electromagnetic Survey is performed a close-up of as means to predict these large-scale landslides. It is necessary to estimate establishing technique to estimate a collapse side, the water sentence process in the slope to predict the slope where there is possibility of the collapse in at the time of heavy rains, but is the situation that is hard to say to be considered about these enough currently.Therefore, in this study, we havetaken Mt. Azuma and Mt. Fuji examples and examined the estimate technique of the collapse side and technique to predict a water sentence process from the result of a geological survey and the quality of the water investigation that we carried out the airborne electromagnetic survey in addition.

First, we performed the documents investigation into the characteristics of the topography, the geological feature, results of the sediment disasters, volcanic activity history there. Next, we performed a field work and confirmed the quality of soil structure in conjunction with the landslides, hydrothermal alteration situation causing the landslides and the hot spring gush situations. We examined areas of the airborne electromagnetic survey in reference to these results.We decided that the top of the mountain body and the representative craters were included and did the investigation object with the area including inclines more than 15 degrees that landslides were possible.The exploration area of Mt. Azuma was about 18km2 and the exploration area of Mt. Fuji was about 120km2.We have arranged themevery depth two-dimensionally so that we could recognizethe result of the helicopter electromagnetic explorationregionally.And, at the area where sediment disasters were easy to be occurred, there were some craters and water level under the ground were high, we have arranged them every depth two-dimensionally so that we grasped ratio resistance levels of the depth direction for running. We have verified the result of the airborne electromagnetic surveyby Comparing with the investigation results of the topographic and geological features.In addition, we investigated hydrology and water quality of the water at 10 neighboring streams in Mt.Azuma for the purpose of confirming the result of the airborne electromagnetic survey in detail.The investigation items werewater discharge, electric conductivity, pH, water temperature and ion silica concentration. In addition, we have carried out the boring investigation for the purpose of checking the ratio resistance levels by the airborne electromagnetic survey and the relations with the geological feature in Mt.Fuji.

We have found that by using the airborne electromagnetic survey in volcano area we could roughly grasp the geological features and underground water levels.From this, wecouldroughly predict the slopes that may collapse at the time of a heavy rain by using the airborne electromagnetic survey. On the other hand, we cannot estimate the collapse depth and the collapse volume in detail when it is only the airborne electromagnetic survey.It is necessary to supplement the results of the in the airborne electromagnetic survey by carrying out other investigations which arethe boring investigations and physics explorations on the ground, the waterquality and hydrological investigation to estimate these.In the near future, we will carry out the investigations including the airborne electromagnetic survey for models in some volcanoes and want to establish the estimate technology of the collapse dangerous points in the volcano areas, estimate technique of the collapse depths and collapse volume by accumulating data.

Keywords: airborne electromagnetic survey, large landslide, volcano

Japan Geoscience Union Meeting 2014
(28 April - 02 May 2014 at Pacifico YOKOHAMA, Kanagawa, Japan)

STT58-04 Room:313 Time:April 30 17:00-17:15

Verification of the tunnel geological structure based on the helicopter-borne magnetometry data analysis

OKAZAKI, Kenji[1*] ; ITO, Yoshihiko[1]

[1]CERI, PWRI

1. Introduction

More detailed geological information of tunnel ground is very important for its construction. Especially, geological complicated area, such as accretionary complex, is needed more accurate information for process control and avoidance of risk during construction of tunnels. The authors carried out helicopter-borne magnetic survey to verify its applicability for geotechnical evaluation of a mountainous planned road tunnel in east Hokkaido, Japan. We describe corresponds with the results of the geological profiles estimated from the outcomes of tunnel construction records and its analysis results of magnetic anomalies which was obtained by helicopter-borne magnetometry data.

2. Outline

The geology of the study area is mainly consists of greenstone, pyroclastic sedimentary rock and hyaloclastite, and is mixed with pillow lava, chert and limestone. Many faults are formed in the area around the survey site due to tectonic movements at the time of formation of the accretionary complex and after that. Surveyed tunnel is planed to 910 m long and maximum overburden is 150 m. The magnetic intensity was measured from a helicopter at low altitude using a cesium magnetometer, and a magnetic intensity map was compiled based on the scalar volume of the magnetic force after reduction to pole magnetism. The probable geological model of the tunnel profile was analyzed using the magnetic anomaly pattern. The forward modeling process for the magnetic data was conducted using Mag2dc software (Cooper, 2003) based on the Talwani algorithm for calculation anomalies. The forward modeling was carried out according to the type of magnetic anomaly over blocks/steps, dependence of anomaly on width, depth, susceptibility contrast and dip angle. The tunnel geological models that estimated using the magnetic anomaly pattern were verified by the geological properties from tunnel construction records.

3. Results of survey

Results of this survey, executed in a mountainous area where accretionary complexes are distributed, are summarized as follows:

1) Helicopter-borne magnetic survey was carried out for a tunnel in northeastern Hokkaido and magnetic intensity map was figured. By the correlation to the other results such as the geological survey or the observation of rock type and fracture shear and conditions in advanced core, high magnetic intensity zone corresponded to the sedimentary rock and the fracture and shear zone of hyaloclastite and massive basalt.

2) Two geological models were made by combining helicopter-borne magnetic survey results with geological survey results and magnetic intensity model. The models were correlated to the detailed data obtained by advanced boring core observation, and these distributions are roughly confirmed by advanced boring core observation.

3) In this case study, helicopter-borne magnetic survey provided useful information for effective interpretation. To analyze geological structure by helicopter-borne magnetic survey is very effective to evaluate potential geotechnical issues when excavating a tunnel.

Keywords: helicopter-borne magnetic survey, magnetic anomalies, accretionary complex, road tunnel

Japan Geoscience Union Meeting 2014
(28 April - 02 May 2014 at Pacifico YOKOHAMA, Kanagawa, Japan)

STT58-05 Room:313 Time:April 30 17:15-17:30

Magnetic structure of the tsunami inundation area of the 2011 off the Pacific coast of Tohoku Earthquake

OKUMA, Shigeo[1*] ; UEDA, Takumi[1] ; NAKATSUKA, Tadashi[1] ; MITSUHATA, Yuji[1] ; JINGUUJI, Motohara[1] ; UCHIDA, Toshihiro[1]

[1]Geological Survey of Japan, AIST

In June 2012, the Geological Survey of Japan (GSJ) conducted an airborne EM and magnetic survey over the inundation area by the tsunami of the 2011 off the Pacific coast of Tohoku Earthquake, northeast Japan. The purpose of the survey was mainly to map the resistivity of the subsurface structure associated with sea water invasion by the tsunami. Airborne EM data were successful for revealing the subsurface resistivity distribution as an aid for groundwater assessment of the study area.

Aeromagnetic data were also observed by the survey and processed (Okuma et al., 2013). However, it turned out that the magnetic data seem to be contaminated by artificial noise with amount of ˜20nT probably caused by the survey helicopter. To mitigate directional errors (Herringbone effect), the generalized mis-tie control method (Nakatsuka and Okuma, 2006) was applied to the observed magnetic data and magnetic anomalies were reduced onto a smoothed observation surface. According to the compiled aeromagnetic anomaly map of the Southern Sendai Plain, magnetic highs lie over the Cretaceous granitic rocks with high magnetic susceptibilities (˜10^{-2} SI; PB-Rock 21) outcropping on the north-trending Wariyama Mountains, which may constrain the groundwater flow system. The magnetic highs also extend NE and reach the Pacific coast, implying the existence of Cretaceous granitic rocks. In a map of the Matsukawaura area, an obvious magnetic high lies over the northern edge of the lagoon without any signatures of magnetic sources on surface. To better understand the subsurface structures of the survey areas, we applied 3D imaging (Nakatsuka and Okuma, 2013) to the observed magnetic anomalies. The preliminary results of the imaging indicate magnetization highs lie below the Wariyama Mountains and coastal regions between the Torinoumi Lagoon and Ushibashi river mouth in the Southern Sendai Plain. An obvious magnetization high is present below the northeastern edge of the Matsukawaura Lagoon, corresponding to granitic rocks with high magnetic susceptibilities (˜10^{-2} SI; PB-Rock 21) at a depth of around 300m below the surface in a hot spring exploration well. The details of the 3D imaging will be shown in the presentation.

Keywords: airborne EM survey, tsunami, groundwater environment, aeromagnetic survey, magnetic structure, basement

Japan Geoscience Union Meeting 2014
(28 April - 02 May 2014 at Pacifico YOKOHAMA, Kanagawa, Japan)

STT58-06 Room:313 Time:April 30 17:30-17:45

Repeated aeromagnetic surveys in Shinmoedake volcano, Japan, by using an unmanned helicopter

KOYAMA, Takao[1*] ; KANEKO, Takayuki[1] ; OHMINATO, Takao[1] ; WATANABE, Atsushi[1] ; TAKEO, Minoru[1] ; YANAGISAWA, Takatoshi[2] ; HONDA, Yoshiaki[3]

[1]Earthquake Research Institute, University of Tokyo, [2]Institute for Research on Earth Evolution, Japan Agency for Marine-Earth Science and Technology, [3]Center for Environmental Remote Sensing, Chiba University

After the 2011 eruptions of Shinmoedake volcano in Japan, we conducted three repeated aeromagnetic surveys around this area, by using an autonomously driven unmanned helicopter. Shinmoedake volcano had sub-Plinian eruptions in the end of January 2011 and its vent was filled by uprising intrusive lavas. After that, some Vulcanian eruptions followed, and then volcanic activities were decreasing gradually up to the beginning of April 2011.

After these events, we conducted aeromagnetic surveys in the end of May 2011, the beginning of November 2011, and the end of October 2013. The Yamaha RMAX-G1 unmanned helicopter was used for our surveys, which was usually used to spray the agricultural chemicals to fields, and can make flights following the programmed tracks within about 1 m precision. Availability of precise flights are a great advantage for repeated surveys in order to detect easily the changes of circumstances, such as, geomagnetic changes due to volcanic activities by measuring at the same positions. Almost 85 km flights in total were made in every survey with a flight speed of about 10 m/s. Flight heights above the ground were almost kept in 100 m.

As the result of some data processing, we clearly detected the change of the magnetic fields around the vent of Shinmoedake, which has a kind of a dipolar pattern with positive changes in South and negative changes in North. This indicates a region around the vent got magnetization due to cooling. The intrusive lava is supposed to be the source of magnetization, and 2.0x10ˆ7 Amˆ2 magnetization of lava is evaluated at the second survey (0.5yr) and 4.8x10ˆ7 Amˆ2 is evaluated at the third survey (2.5yr), compared with the first survey. This means the magnetizing rate is almost related to a square root of the elapsed time and it leads to an implication the lava cooling is dominantly made gradually by thermal diffusion, not by other cooling processes such as thermal convection. The common thermal diffusivity of rocks, however, is too small by one order of magnitude to explain this cooling rate, and intrusion of water in lava, say, rainfall water, may play an important role to raise the effective thermal diffusivity to make the lava cool.

Japan Geoscience Union Meeting 2014
(28 April - 02 May 2014 at Pacifico YOKOHAMA, Kanagawa, Japan)

STT58-P01 Room:Poster Time:April 30 18:15-19:30

The 3D magnetic imaging using the L1 regularization and variable selection procedure.

UTSUGI, Mitsuru[1*]

[1]Graduate School of Science, Kyoto Univ.

Recently some new method to obtain 3D subsurface structure from the gravity or geomagnetic data were proposed. Some of them have a goal to obtain a stable and most simple model which reproduce the observed data in high accuracy. This is because, in generally, most of the traditional way of inversion for the potential data provides distorted or unfocused mages of real gravitational or magnetic structures. In this study, we propose a new method introducing a L-1 penalized least square procedure and tried to obtain a simple, and therefor high- resolution model.

Lasso(Tibshirani,1995) is a linear regression and variable selection procedure based on the L1 penalized least square. L1 penalty has a effect of shrinkage the value of regression coefficients which has only weak contributions to be 0. So, the Lasso does both continuous shrinkage and automatic variable selection simultaneously. On the other hand, Lasso has some limitations and restrictions. One of them is, at most Lasso algorithm can select nonzero variables of same number of observed data. So, in the case of p <<n problem, i.e. in the case of number of unknown regression coefficients (p) is larger than the number of observations(n), this algorithm cannot be adopted or overly shrinkage model will be obtained.To overcome this limitation, Zou and Hastie (2005) proposed a new L-1 penalized method named Elastic Net.This method is a compromise of the L-1 and L-2 regularization method with two control parameters. Using this method, we can treat p <<n problems in the framework of L-1 penalized method.

In our presentation, we will show the results of applying this method to the synthesized and real magnetic data.

Keywords: potential, geomagnetism, magnetic structure, L-1 norm regularization

Japan Geoscience Union Meeting 2014
(28 April - 02 May 2014 at Pacifico YOKOHAMA, Kanagawa, Japan)

STT58-P02 Room:Poster Time:April 30 18:15-19:30

Magnetic structure of the north part of Deception Island based on the aeromagnetic survey by a small unmanned airplane

SAKANAKA, Shin'ya[1*] ; FUNAKI, Minoru[2] ; HIGASHINO, Shin-ichiro[3] ; NAKAMURA, Norihiro[4] ; IWATA, Naoyoshi[5] ; OBARA, Noriaki[6] ; KUWABARA, Mikio[7]

[1]Akita Univ., [2]NIPR, [3]Kyushu Univ., [4]Tohoku Univ., [5]Yamagata Univ., [6]Robotista, [7]RC Service

Aerial magnetic survey was carried out in the part of the flight project of the autonomous unmanned aerial vehicles (UAV). The project was incorporated with National Institute of Polar Research (Japan), Korea Polar Research Institute, Chile Antarctic Institute, Bulgarian Antarctic research and Spanish Antarctic team. Magnetic anomaly data were aquired over the northern part of Deception Island (within South Shetland islands) in Bransfield Strait. It was the first time to succeed to get the geophysical data by a long-flight unmanned aerial vehicle (UAV) in the area of Antarctica as already reported by our team. Due to the severe weather the flight was canceled over the southern half of the Deception Island and its surrounding sae area.

The flight altitude is about 780m averaged. The main survey lines are directed east-west and the intervals of the lines are about 1000m. Longest length of the main survey line is about 18km. Probably due to the unstable atitude of the UAV body by strong wind, some east-west lines are shortcuted regardless of pre-programmed 18km length courses. The flight courses were overlapped on the survey lines along the latitude of 62 degree 53 minute and the longitude of -60 degree 28 minute. On these lines each direction of the flight is opposite. Some unnatural unduration was seen around overlapped lines. These kinds of unduration are occurred due to the difference of the observed magnetic field on each line. These differences have to be corrected, now we have the torerable data for estimate the structure of the Deception Island.

Outstanding high magnetic anomaly is recognized over the eastern peak of the island. Preparing topographic digital data of the Deception Island and bathymetric data on surrounding sea area, we estimated the distribution and the intensity of magnetization.

Keywords: Antarctica, Deception Island, Unmanned Aerial Vehicle, Magnetic Survey, South Shetland Islands

Japan Geoscience Union Meeting 2014
(28 April - 02 May 2014 at Pacifico YOKOHAMA, Kanagawa, Japan)

STT58-P03 Room:Poster Time:April 30 18:15-19:30

Three dimensional inversion for the Grounded Electrical-Source Airborne Transient Electromagnetic (GREATEM) data

ABD ALLAH, Sabry[1*] ; MOGI, Toru[1] ; KIM, Hee[2] ; FOMENKO, Elena[3]

[1]Institute of Seismology and Volcanology, Hokkaido University, [2]Departments of Environmental Exploration Engineering, Pukyong National University, Busan, Korea, [3]Nova Scotia Community College, Halifax, NV, Canada

Previous studies conducted by the Grounded Electrical-Source Airborne Transient Electromagnetic (GREATEM) have shown that, this system is a promising method for modelling 3D resistivity structures in coastal areas, in addition to inaccessible area such as volcano, mountainous area covered by deep forest. To expand the application of the GREATEM system in the future for studying hazardous wastes, sea water incursion,geothermal exploration and hydrocarbon exploration, a 3D-resistivity modelling that considers large lateral resistivity variations is required in case of large resistivity contrasts between land and sea in surveys of coastal areas where 1D resistivity model that assumes a horizontally layered structure might be inaccurate. In this abstract we present the preparation for developing a consistent three dimensional electromagnetic inversion algorithm to calculate the EM response over arbitrary 3D conductivity structure using GREATEM system. In forward modelling the second order partial differential equations for scalar and vector potential are discretized on a staggered-grid finite difference method (Fomenko and Mogi, 2002, Mogi et al., 2011). In the inversion method the 3D model discretized into a large number of rectangular cells of constant conductivity and the final solution is obtained by minimizing a global objective function composed of the model objective function and data misfit. To deal with a huge number of grids and wide range of frequencies in air borne datasets, a method for approximating sensitivities is introduced for the efficient 3-D inversion. Approximate sensitivities are derived by replacing adjoint secondary electric fields with those computed in the previous iteration. These sensitivities can reduce the computation time, without significant loss of accuracy when constructing a full sensitivity matrix for 3-D inversion, based on the Gauss?Newton method (Han, N.et al., 2008).

Firstly, we started testing the algorithm in the frequency domain electromagnetic response of synthetic model considering a 3D conductor embedded in uniform half space. In the second step we tested more complex synthetic model, considering vertical contact between two different high and low resistivity quarter-spaces and a conductor embedded in a high resistive quarter-space. Frequency-domain computation is executed at frequencies of five equal logarithm spacings in one decade in the frequency range of (10^{5}-10^{-2}) Hz. After the computation, we transformed into time domain using FFT and compared forward value with inverted value.The inverted results in case of the simple model, appear to highlight a conductive zone of potential interest within the resistive region. In addition, in case of two quarter spaces model, it was able to the reveal the clear resistivity contrast between the two quarters spaces and highlight a conductive zone within the high resistive quarter space. Both of the forward and inverted models have almost the same EM response which can confirm the accuracy of the inverted method. The next step for preparing this algorithm will be using the field data from previous GREATEM surveys to demonstrate this technique

Keywords: 3D EM inversion, GREATEM, Numerical approximations, Airborne Electromagnetic

Japan Geoscience Union Meeting 2014
(28 April - 02 May 2014 at Pacifico YOKOHAMA, Kanagawa, Japan)

STT58-P04 Room:Poster Time:April 30 18:15-19:30

An Advanced Method of Data Analysis for Gravity Exploration System on a Mobile Vehicle

OGURA, Yumiko[1] ; MATSUDA, Shigeo[2] ; YOKOI, Isamu[3] ; SUDA, Haruo[3] ; KIMA, Sadaharu[3] ; MORIKAWA, Hitoshi[1*] ; SAEKI, Masayuki[4] ; SUZUKI, Takuya[4] ; KOMAZAWA, Masao[5]

[1]Tokyo Institute of Technology, [2]Clover Tech . Inc., [3]Tokyo Sokushin Co.,Ltd.,, [4]Tokyo University of Science, [5]OYO Corporation

A model of ground structure is very important to estimate earthquake ground motions. Gravity survey is one of exploration methods. We can estimate ground structure by using information of gravity anomaly which comes from heterogeneous density structure of the ground. Generally speaking, there are high correlation between density and velocity structure of the ground. Thus, the gravity survey is comparatively easier than other exploration method to estimate the ground structure, so that it is very suitable for the aspect of the seismic hazard projection.

For gravity survey, spring-type relative gravimeter is usually used. This type of gravimeter can provide accurate data, however, it is very expensive and difficult to handle. Furthermore, it takes much time to obtain adequate data. We, thus, began to develop a simple and inexpensive sensor which can measure gravity anomaly on a moving vehicle, such as air, land, and sea vehicles, that is, airplanes, motor vehicles, and ships. In a case where a gravimeter is used with a moving vehicle, we may survey the gravity over larger area in shorter time than using conventional survey techniques.

Generally, the gravity should be measured with resolution of 10 micro Gal at least for survey to estimate ground structure. However, the signal obtained from sensor is contaminated by various noise such as vibration of a moving vehicle etc. This means that a sensor with high resolution and large dynamic range is required. This is difficult to realize because resolution and dynamic range are conflicting requirement. To solve this problem, we have developed a sensor with a new feedback system, which has high resolution and large dynamic range.The performance of this sensor is examined in this study, and we also propose a technique of data processing based on the combination of second order blind identification (SOBI) and Hilbert Huang transform (HHT) technique.For this two different type of observations are carried out.

First, we set the sensor statically in a tunnel to confirm whether the sensor can respond to the gravitational effects caused by earth tides. From this observation, it is found that the sensor is affected by atmosphere. The effect is can be removed by applying second order blind identification (SOBI).

Second, the ship survey is carried out.Through a technique of data processing based,the observed data provide quite good agreement with theoretical gravity in phase and period of the signal.

Keywords: gravity survey, Hilbert-Huang Transform, Second Order Blind Identification

Japan Geoscience Union Meeting 2014
(28 April - 02 May 2014 at Pacifico YOKOHAMA, Kanagawa, Japan)

STT59-01 Room:414 Time:April 29 09:00-09:15

DEM accuracy evaluation in mountain area by utilizing topographic corrected products of high-resolution TerraSAR-X data

NONAKA, Takashi[1*] ; OKAJIMA, Yuki[1] ; TSUKAHARA, Koichi[1]

[1]PASCO CORPORATION

The commercial high-resolution Synthetic Aperture Radar (SAR) sensors have been developed during past few years and became essential source of information in Earth Observation. The production of the maps is examined in the various fields, such as the damaged area caused by disaster, paddy field area, and forest etc. The interpretation of the objects from the images and the positional accuracy of the images are highly important for the map creation and several basic studies for such issues are also conducted by applying high-resolution SAR data.

TerraSAR-X is one of the commercial SAR satellites, and has acquired data worldwide after it was launched in June 2007. Furthermore, TanDEM-X (TerraSAR-X add-on) was launched in 2010. Both satellites are currently acquiring land surface of Earth for creating global and homogeneous Digital Elevation Model (DEM) of very high precision. TerraSAR-X has several processing level products, and the Geocoded Enhanced Ellipsoid Corrected (EEC) is amplitude data projected to the digital elevation model (DEM), which makes possible for users to integrate other optical data and GIS data. Pre-geocoded Single Look Slant Range Complex (SSC) product is complex data with two axes in the azimuth-slant range plane, and used for interferometric and polarimetric analysis.

It was reported that the geometric accuracy of SSC product was better than 1 m in several previous studies, however there are no reports stating details for the validation results of the EEC product using the actual TerraSAR-X data though it is utilized by the most of users. Therefore the authors evaluated the geometric accuracy of the EEC product by performing in-situ experiment using reflectors on the flat area, simultaneously conducted during satellite passed over. The results showed that the accuracy satisfied several meters in case of utilization of SRTM DEM. In the next stage, we developed the model showing the relationships between the geometric accuracy of range direction, DEM accuracy, incidence angle, and it was revealed that the accuracy of the model was about 1 m in the flat area.

The purpose of this study was to evaluate the accuracy of utilized DEM for the topographic correction by applying the model to TerraSAR-X data in the mountain area. The utilized TerraSAR-X data were 2 data sets of high-resolution SpotLight mode (about 2 m resolution) with the different incidence angles, and the DEMs were produced by ASTER with the mesh of 30 m and SRTM with 90 m. We also used the airborne optical data with a geometric accuracy (Digital topographic level of 2,500 scales) for a validation.

Firstly we selected 25 validation points from the intersections and curves of roads easily interpreted both from TerraSAR-X and airborne data. The average, standard deviation, and Root Mean Square Errors (RMSE) value of the difference between TerraSAR-X and reference optical data were evaluated for X-, Y-, and X-Y plane. In the next stage, we examined to apply the model to data in the mountain area. We estimated DEM's errors by assuming that the variation of the differences of the X-direction was corresponded to the errors of the topographic correction since the range direction was almost same for X direction. The results were summarized based on the evaluations of both flat and mountain areas.

Keywords: Geometric accuracy, TerraSAR-X, topographic correction, ASTER, SRTM

Japan Geoscience Union Meeting 2014
(28 April - 02 May 2014 at Pacifico YOKOHAMA, Kanagawa, Japan)

STT59-02 Room:414 Time:April 29 09:15-09:30

Pi-SAR-L2 observation of the landslide caused by Typhoon Wipha on Izu Oshima island

WATANABE, Manabu[1*] ; DAN, Risako[2] ; MOTOHKA, Takeshi[1] ; OHKI, Masato[1] ; SHIMADA, Masanobu[1]

[1]Japan Aerospace Exploration Agency, [2]RESTEC

On October 16, 2013, Typhoon Wipha struck Izu Oshima island, and a large-scale landslide was induced by the heavy rain. Six days after the disaster, Pi-SAR-L2 observation was carried out in four different observation directions (L203201?L203204). One Pi-SAR-L observation (L03801) was carried out before the disaster on August 30, 2000 in same observation direction of L203201. The observation data were used to determine which parameters and directions are preferable to detect landslide areas. Several full polarimetric parameters, including Sigma_0, polarimetric coherence, four-component parameters, and eigenvalue decomposition parameters were obtained using PolSARPro and a self-produced programs. As pointed out by Shimada et al. [1], the change of the land cover from a forest before the disaster to bare soil after the disaster was well detected by the coherence between HH and VV. In addition to this parameter, the eigenvalues and four-component decomposition parameters have the potential to detect landslide areas. The data from observations of the bottom to the top of the landslide detect the landslide well, whereas the observation of the opposite side are not as useful.

Soil from the landslide intruded into the town areas, but none of the full polarimetric parameters show any significant difference between the landslide-affected town areas and the unaffected areas.

[1] Masanobu Shimada, Manabu Watanabe, Noriyuki Kawano, Masato Ohki, Takeshi Motooka, and Yutaka Wada, Detecting Mountainous Landslides by SAR polarimetry: A Comparative Study Using Pi-SAR-L2 and X band SARs, Transactions of the Japan Society for Aeronautical and Space Sciences, Aerospace Technology Japan, 2014, 12, No.ists29, pp. Pn9-Pn15.

Keywords: Full polarimetry, SAR, disaster

Japan Geoscience Union Meeting 2014
(28 April - 02 May 2014 at Pacifico YOKOHAMA, Kanagawa, Japan)

STT59-03 Room:414 Time:April 29 09:30-09:45

Shoreline change analysis using JERS-1/SAR and ALOS/PALSAR amplitude images

ASAKA, Tomohito[1*] ; IWASHITA, Keishi[1] ; KUDOU, Katsuteru[1] ; AOYAMA, Sadayoshi[1] ; SUGIMURA, Toshiro[2]

[1]Nihon University, [2]Remote Sensing Technology Center of Japan

Aerial photo analysis and bathymetric survey are commonly conducted to investigate the actual conditions and temporal variation in beach transformation. In recent years, satellite-based optical imagery has been more widely used to evaluate coastal erosion. However, defining shoreline edges using optical imagery is difficult because the sand under seawater near the shoreline can often be seen through clear water. On the other hand, synthetic aperture radar (SAR) imagery can be used to interpret the boundary between a sandy beach and seawater; this is possible because the incident radio waves are not transmitted through water, and SAR images can be compared to trace the shoreline. In this work, we examine the potential of shoreline change analysis by using Japanese Earth Resources Satellite 1 (JERS-1)/SAR and Advanced Land Observing Satellite/Phased Array type L-band Synthetic Aperture Radar (ALOS/PALSAR) amplitude images. We consider Kujy?kurihama beach in Chiba Prefecture as our test site; along this beach, the shoreline is almost perpendicular to the SAR antenna beam orientation for the descending orbit.

We propose a three-step automated shoreline-tracing method to assess the temporal variation of the shoreline in the study area; the HH-polarized JERS-1/SAR amplitude image captured on February 22, 1993, and the HH-polarized ALOS/PALSAR amplitude image captured on May 20, 2010 were used for this purpose. In our method, a shoreline is traced as vector data. In the first step, edge pixels in SAR images are identified by using the Laplacian of a Gaussian filter. In the second step, unwanted edge pixels are masked on the basis of a discriminant analysis in which candidate shoreline edge pixels are estimated by using statistical information within a moving window. The criteria for identifying shoreline edge pixels is decided on the basis of previously gathered data, the backscattering average, and the standard deviation, in the training area (30 by 10 pixels) encompassing the sea, shoreline, and land. In the third step, shoreline vector data are generated from continuous candidate shoreline edge pixels by an automated shoreline-tracing algorithm.

The results were verified in two ways. We first verified the location of the shoreline edge in the SAR amplitude images by overlaying multispectral images acquired on dates close to the acquisition dates of the earlier mentioned JERS-1/SAR data and ALOS/PALSAR data: the JERS-1/Optical Sensor (OPS) color composite image acquired on May 3, 1993, and the ALOS/Advanced Visible and Near Infrared Radiometer type 2 (AVNIR-2) color composite image acquired on January 8, 2011, were used for this analysis. Next, we calculated the statistical information of the backscattering data in the JERS-1/SAR and the ALOS/PALSAR amplitude images for our selected training area. It is noteworthy that the backscattering average and standard deviation in the shoreline training area is a unique than anything training area.

Our proposed method reproduces the temporal variation of the shoreline by using JERS-1/SAR and ALOS/PALSAR amplitude images. However, a part of the shoreline extracted using the JERS-1/SAR amplitude image was inaccurate. The speckle noise in the JERS-1/SAR amplitude image and the low spatial resolution of the raw data may have caused these errors. In our future work, we intend to improve the algorithm for JERS-1/SAR data and accumulate backscattering information of shoreline edge areas using SAR amplitude images.

Keywords: backscattering, beach erosion

Japan Geoscience Union Meeting 2014
(28 April - 02 May 2014 at Pacifico YOKOHAMA, Kanagawa, Japan)

STT59-04 Room:414 Time:April 29 09:45-10:00

Glacier observations by airbourne synthetic aperture radar, PiSAR2, at Tateyama, Japan

FURUYA, Masato[1*] ; FUKUI, Kotaro[2] ; SUGIYAMA, Shin[3] ; SAWAGAKI, Takanobu[4]

[1]Hokkaido University, Graduate School of Science, [2]Tateyama Caldera Sabo Museum, [3]Institute of Low Temperature Science, [4]Hokkaido University, Graduate School of Environmental Science

Fukui and Iida (2012) reported that three snowy gorges at Tateyama, Japan, were flowing at a rate of 10-30 cm/month and hence could be identified as glaciers. Fukui and Iida's observations are based on ground-based GPS observations. Because glacier flow velocity data sets are one of the fundamental physical quantities to better understand the dynamics, conventional geodetic techniques have been applied, and the measurement accuracy has significantly improved. However, due to the severe environment and logistic problems, SAR-based velocity mapping has been performed with successful results at large glaciers and ice sheets over the past decades. The velocity mapping technique is so called pixel-offset (or feature) tracking. Thus, applying the same technique to the fore-mentioned newly discovered glaciers, we should also be able to detect the spatial distribution of glacier velocities. However, the presently available satellite-based SAR data set does not have enough spatial resolutions to resolve the velocities. In this regard, the 30-cm resolution of Pi-SAR2 seems promising to perform the pixel-offset tracking. Here we report the first observation images of the Japanese glaciers acquired by Pi-SAR2, and will discuss the preliminary report of velocity mapping.

Keywords: SAR, glacier, Tateyama

Japan Geoscience Union Meeting 2014
(28 April - 02 May 2014 at Pacifico YOKOHAMA, Kanagawa, Japan)

STT59-05 Room:414 Time:April 29 10:00-10:15

Monitoring of Ice sheet marginal zone using multi-frequency SAR data

YAMANOKUCHI, Tsutomu[1*] ; DOI, Koichiro[2] ; NAKAMURA, Kazuki[3] ; AOKI, Shigeru[4]

[1]Remote Sensing Technology Center of Japan, [2]National Institute of Polar Research, [3]Nihon University, [4]Institute of Low Temperature Science, Hokkaido University

Environment of Antarctic continent and ice sheet marginal zone is quite important for understanding the mass balance of ice, formation of deep ocean water and other cryospheric phenomena.Previous study showed the usefulness of SAR data to understand what is happen on the bounary area between ice sheet and ice shelf by SAR data analysis, and achieved the mapping of ice sheet surface velocity mapping. In recent, many kinds of satellite equipped SAR sensor plan to launch and these data are available trough the scientific Research Announcement (RA) or Announcement of Oppotunitty (AO).

Based on these facts, this study focuses on the use of multi-frequency SAR data for ice sheet marginal zone monitoring. Especially, we focus on the use of InSAR analysis for grounding line extraction, ice flow velocity mapping by offset tracking, and understanding the image feature difference through the interpretation of X-, C- and L- band SAR data. We use X-band data by TerraSAR-X, C-band data by ENVISAT and ERS-1/2, and L-band data by ALOS/PALSAR data. Then, we will try to describe the applicability and prospectives of ALOS-2 / PALSAR-2 data

TerraSAR-X data were provided by DLRs' AO project (Proposal No. HYD1808), ERS-1/2 and ENVISAT data were provided by ESA Cat-1 AO project, (project C1P.7657) and ALOS/PALSAR data were provided by Research Announcement by JAXA PI project (PI No. P1418002).

Keywords: Ice sheet, multi-frequency, SAR

Japan Geoscience Union Meeting 2014
(28 April - 02 May 2014 at Pacifico YOKOHAMA, Kanagawa, Japan)

STT59-06 Room:414 Time:April 29 10:15-10:30

Evaluation of surface roughness, magnetic permeability and dielectric permittivity using polarimetric SAR data

KOIKE, Katsuaki[1*] ; MASUDA, Takayuki[1] ; SAEPULOH, Asep[2] ; URAI, Minoru[3] ; OMURA, Makoto[4] ; DOI, Koichiro[5]

[1]Graduate School of Eng., Kyoto Univ., [2]Bandung Institute of Technology, [3]Geological Survey of Japan, AIST, [4]Dept. Cultural Studies, Univ. Kochi, [5]National Institute of Polar Research

Synthetic Aperture Radar (SAR) systems have great advantages of observing the Earth surface regardless of meteorological conditions and detecting crustal deformations by Interferometric processing. Another latest technique, polarimetric SAR has also been widely used through its principle that backscattering intensity differs with polarization mode. However, most applications are limited to image classification. In addition, the evaluation method for surface physical properties has not yet been investigated well. To achieve this evaluation from the viewpoints of geological identification and water-content estimation of soils, this study adopts mdPSAR (**m**agnetic permeability and **d**ielectric permittivity from **P**olarimetric **S**ynthetic **A**perture **R**adar) proposed by Saepuloh *et al*. and tries to evaluate roughness, relative magnetic permeability, and relative dielectric permittivity of the surface materials using the HH, VV, and HV mode SAR data.

As the first step of mdPSAR, the surface roughness is calculated from the backscattering coefficient data at the HV mode and an empirical equation based on an assumption of fractal property of the topography (Campbell and Shepard, 1996). Next, using the Small Perturbation Model (Fung and Chen, 2010) of backscattering coefficient and the Nelder-Mead Simplex method (a method of nonlinear optimization), the relative magnetic permeability and the relative dielectric permittivity are calculated by minimizing the difference between the model and the backscattering coefficient data at the HH and VV modes.

The areas around the Tottori sand dunes were selected as a case study of mdPSAR using two scenes of ALOS PALSAR data acquired on 25 October and 27 April 2009. As the result, the average calculation errors were small as about 1% for both the HH and VV modes and the errors were uniform in general over the scenes. The relative dielectric permittivity values of the Tottori sand dunes were evaluated as 13.4 and 10.6. These values correspond with those of wet sands. It is noted that the value is higher in the scene after raining. Higher values of relative magnetic permeability were evaluated in the sand dunes than the surroundings, which is a reasonable trend because the sands are originated from the weathering of granitic rocks containing magnetite. Consequently, the effectiveness of mdPSAR is demonstrated. However, an improvement is necessary for the surface-roughness estimation of the areas occupied by artificial structures such as buildings. This is because the HH mode intensity becomes strong in them.

Application of mdPSAR to the PARSAR data around Syowa Station, Antarctica is in progress. Its purposes are to clarify distribution of outcrops and snow ice areas, melting state of ices, and development of crevasse topography from the spatio-temporal changes of surface roughness and relative dielectric permittivity.

References

Campbell, B.A., Shepard, M.K. (1996) Lava flow surface roughness and depolarized radar scattering, *J. Geophys. Res*., v. 101 (E8), 18941-18951.

Fung, A.K., Chen, K.S. (2010) *Microwave Scattering and Emission Models for Users*, Artech House, Norwood, MA.

Saepuloh, A., Urai, M., Koike, K., Sumantyo, J.T.S.: An advanced technique to identify surface materials on an active volcano by deriving magnetic permeability and dielectric permittivity from polarimetric SAR data, *IEEE Geosci.& Remote Sens. Lett*. (under review)

Keywords: ALOS PALSAR, polarization mode, backscattering coefficient, nonlinear optimization, Tottori sand dunes

Japan Geoscience Union Meeting 2014
(28 April - 02 May 2014 at Pacifico YOKOHAMA, Kanagawa, Japan)

STT59-07 Room:414 Time:April 29 10:30-10:45

New Global Forest/Non-Forest Maps from ALOS PALSAR data (2007-2010)

SHIMADA, Masanobu[1*] ; ITOH, Takuya[2] ; WATANABE, Manabu[1] ; MOTOOKA, Takeshi[1] ; RAJESH, Thapa[1]

[1]Japan Aerospace Exploration Agency, [2]Remote Sensing Technology center of japan

Four global mosaics of Advanced Land Observing Satellite (ALOS) Phased Arrayed L-band Synthetic Aperture Radar (SAR) HH and HV polarization data were generated at 25 m spatial resolution using data acquired annually from 2007 to 2010. Variability in L-band HH and HV gamma-naught for forests was observed between regions, with this attributed to differences in forest structure and vegetation/surface moisture conditions. Region-specific backscatter thresholds were therefore applied to produce from each annual mosaic, a global map of forest and non-forest cover from which maps of forest loss and gain were mapped. Using a combination of Degree Confluence Project (DCP), Forest Resource Assessment (FRA) and Google Earth images as ground data, the overall agreement was 85 %, 91 % and 95 % respectively. Using 2007 as a baseline, decreases of 0.040 and 0.028 dB (with a 0.006 dB confidence level) were observed in the HH and HV gamma-naught respectively suggesting a decrease in forest area and increased smoothing of the global surface at the L-band radar observation. The maps provide a new global resource for documenting the changing extent of forests and contributing to ongoing monitoring through integration with historical (1992-1998) Japanese Earth Resources Satellite (JERS-1) SAR and forthcoming (from 2014) ALOS-2 PALSAR-2 data.

Keywords: SAR, forest/non-forest, SAR mosaic

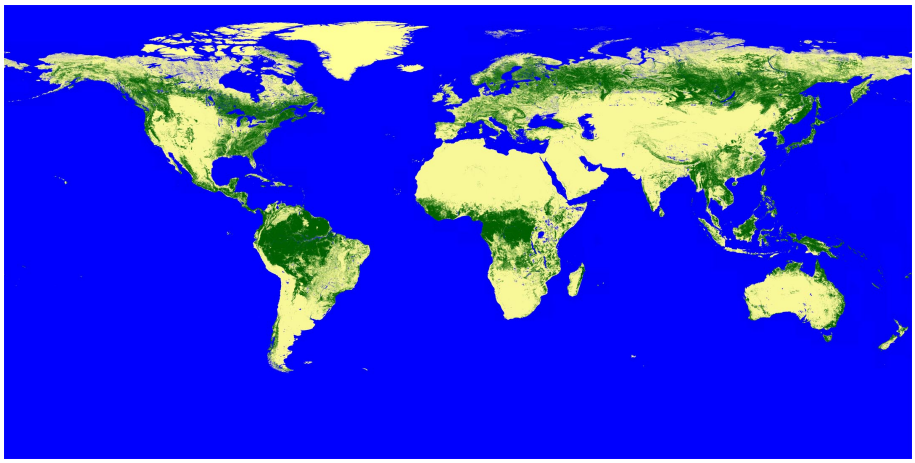

Japan Geoscience Union Meeting 2014
(28 April - 02 May 2014 at Pacifico YOKOHAMA, Kanagawa, Japan)

STT59-08 Room:414 Time:April 29 11:00-11:20

Recent progress in InSAR and PolSAR signal processing

HIROSE, Akira[1*]

[1]The University of Tokyo

This invited talk reviews latest technology in synthetic aperture radar (SAR) signal processing, in particular interferometric SAR (InSAR) and polarimetric SAR (PolSAR), by focusing on the works on adaptive processing made by the author's group. This field attracts more attention because of its usability in solving serious social problems through, e.g., disaster monitoring and mitigation, water resource management, and prevention of global warming. We discuss a radar-physics-based adaptive processing framework, namely complex-valued neural networks, to increase variety of observation functions and/or improve the accuracy. We also introduce a new phase-unwrapping method to discuss its recent progress.

Keywords: synthetic aperture radar, interferometry, polarimetry, complex-valued neural newtork, phase unwrapping, Singularity-spreading phase unwrapping

Japan Geoscience Union Meeting 2014
(28 April - 02 May 2014 at Pacifico YOKOHAMA, Kanagawa, Japan)

STT59-09 Room:414 Time:April 29 11:20-11:35

Uplift and reverse fault rupture of the 2013 Bohol earthquake (Mw 7.2), Philippines, revealed by SAR pixel offset analys

KOBAYASHI, Tomokazu[1] ; TOBITA, Mikio[1*]

[1]GSI of Japan

Applying a pixel offset analysis using RADARSAT-2 SAR data to an inland crustal earthquake that occurred in Bohol Island, Philippines on 15 October, 2013, we succeeded in mapping a ground displacement associated with the earthquake. The most concentrated crustal deformation is located in the northwest of the island with ground displacement exceeding 1 m. The crustal deformation is zonally distributed with the length of approximately 50 km in the ENE-WSW direction. The ground in the mountainous area moves toward the satellite, while in the northern coastal zone the ground moves away from the satellite. A clear displacement discontinuity with the length of about 5 km, probably corresponding to earthquake surface faults, can be identified in the northeastern part. Our fault model that consists of two rectangular planes shows nearly pure reverse fault motions on south-southeast-dipping planes with moderate dip angles. A local rupture located in the northeast occurs at shallow depths, causing appearance of surface ruptures. Applying an additive color process using SAR amplitude images, significant changes in the backscatter intensity are detected along the coast from Maribojoc to Loon, suggesting that the seafloor uplifted and the shoreline shifted seaward resultantly. The area showing the shoreline change is in good spatial agreement with the locally-distributed large ground uplift predicted from our fault model. We can identify a good correlation between the ground upheaval produced by the reverse fault motion and the elevation in the mountainous area, consistent with the idea that the historically-repeated reverse faultings have developed the present-day topography.

Keywords: Bohol earthquake, Crustal Deformation, Pixel offset analysis, uplift, SAR, RADARSAT-2

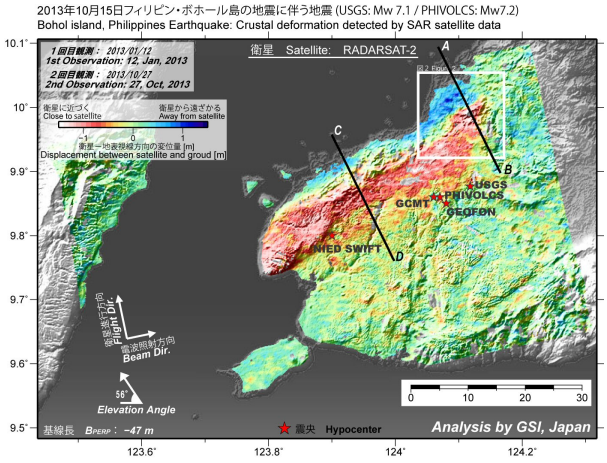

Japan Geoscience Union Meeting 2014
(28 April - 02 May 2014 at Pacifico YOKOHAMA, Kanagawa, Japan)

STT59-10 Room:414 Time:April 29 11:35-11:50

Estimate of error in ALOS/PALSAR interferograms

HASHIMOTO, Manabu[1*]

[1]DPRI, Kyoto University

Large deformation is generated by the subduction of the Philippine Sea plate in Shikoku. GNSS observation reveals a WNW ward horizontal motion and a velocity gradient from south to north. This velocity field is suitable for the observation with SAR, which is sensible to the E-W ward displacement field. Based on these facts, we have conducted to derive average velocity in Shikoku using ALOS/PALSAR. We mainly analyzed ascending images acquired during 4 years, but anomalously large displacements (peak-to-peak displacement ˜50 cm) were often observed possibly due to ionospheric disturbances. We discarded interferograms with such disturbances with visual inspection, and stacked rest of them. However we found E-W velocity gradient in Shikoku that is inconsisntent with GNSS observations, when stacked interferograms are superposed from 4 paths. Furthermore, discontinuities between paths are evident in the Chugoku district. Therefore we made error estimate in order to clarify its magnitude and spatial distribution, comparing line-of-sight displacements derived from InSAR and GNSS.

The procedure is as follows:

(1) Calculate displacements of GNSS stations between the acquisitions of master and slave images for a specific pair from the F3 solution of GEONET and convert them to LOS displacements.

(2) Extract LOS displacements at GNSS sites from the interferogram.

(3) Take differences of LOS displacements between interferogram and GNSS.

(4) Examine dependence of latitude, longitude and height, and interpolate differences of LOS displacements with Surface function of GMT.

(5) Add interpolated differences of LOS displacements to the original interferogram.

One typical example is interferogram for the pair of April 11 and May 27, 2010 for the path 419. Since the time difference is 46 days, little motion is expected. However, we observe LOS changes of ˜40 cm in the E-W direction. We also find a tong-shaped region of LOS decrease in the Chugoku district. Applying the above procedure, we obtain interpolated differences of LOS displacement with the opposite sign to the original interferogram. The standard error of difference of LOS displacements for 36 GNSS sites is 7.8 cm. However, the dependences of longitude and latitude are obviously different at 34 N. Therefore we use the Surface function instead of a simple linear function for the interpolation. Finally, we obtain a fairly flat interferogram consistent with the GNSS result. There still remain displacements with shorter wavelength than 20 km, however.

Applying to other pairs, we evaluate standard errors. The minimum is 1.2 cm (Jan. 6 - Feb. 21, 2009), while the maximum is 18.9 cm (May 27 - Jul. 12, 2010). In total 24 pairs, 4 is less than 2 cm, 7 for 2 ˜4 cm, 6 for 4 ˜6 cm, 3 for 6 ˜8 cm, 2 for 8 ˜10 cm, and 2 is larger than 10 cm. The median is 4.5 cm. For the neighboring path 418 (30 GNSS sites), the minimum is 1.5 cm, while the maximum is 19.8 cm. The median is 4.7 cm. These estimates may give a rough idea of error of PALSAR interferograms including ionospheric disturbances.

We apply this procedure to other paths (417, 418 and 420) and obtain corrected interferograms that cover the entire Shikoku (Attached figure). This map is fairly consistent with the GNSS velocity field, but there is a discontinuity between the paths 417 and 418. We use interferograms with a rather long perpendicular baseline, which causes decorrelation in mountains. We use only GNSS displacements in plain areas for such interferograms, which results in systematic error.

Keywords: SAR interferometry, PALSAR, ALOS, error, crustal deformation

STT59-10 Room:414 Time:April 29 11:35-11:50

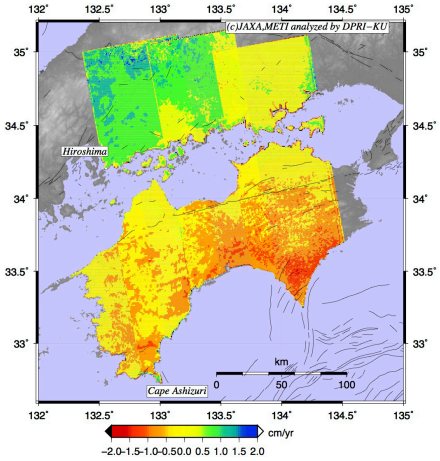

Japan Geoscience Union Meeting 2014
(28 April - 02 May 2014 at Pacifico YOKOHAMA, Kanagawa, Japan)

STT59-11 Room:414 Time:April 29 11:50-12:05

Persistent scatterer SAR interferometry using multi-polarimetric SAR interferograms

ISHITSUKA, Kazuya[1*] ; TAMURA, Masayuki[1] ; MATSUOKA, Toshifumi[1]

[1]Graduate School of Engineering, Kyoto University

Persistent scatterer SAR interferometry (PS-InSAR) is a method to estimate surface deformation using a number of SAR interferograms, and has been applied to aseismic fault slip, volcano and land subsidence as a practical monitoring tool. In recent years, more and more satellites that are equipped with SAR, which can acquire multi-polarimetric data has been operated. In this study, we propose a method to processing PS-InSAR analysis using multi-polarimetric SAR interferograms, and show that the estimation accuracy of surface deformation increases.

In this study, we increase estimation accuracy by processing multi-polarimetric SAR interferograms simultaneously. Since, the amount of noise ratio would differ in different multi-polarimetric SAR interferograms depending on the geometry or electromagnetic characteristics of targets, we determine the weighting coefficient between polarimetric SAR interferograms from observed phase based on maximum likelihood method.

We applied the method to ALOS/PALSAR data acquired in multi-polarimetric mode. First, we processed HH-HH and VV-VV interferograms simultaneously. As a result, weighting of HH-HH and VV-VV interferogram was almost identical, suggesting that decorrelation-induced noise in HH-HH and VV-VV interferograms was almost same. In this case, the accuracy of estimated deformation rate would increase twice. On the other hand, when we processed HH-HH and HV-HV interferograms simultaneously, the weighting of HH-HH interferograms are larger than that of HV-HV interferograms, suggesting that HH-HH interferograms has less amount of noise compared with HV-HV interferograms. Nevertheless, we found that the estimation accuracy increases by using both HH-HH and HV-HV interferograms compared with the standard analysis using HH-HH interferograms.

Keywords: persistent scatterer SAR interferometry, surface deformation, polarimetry

Japan Geoscience Union Meeting 2014
(28 April - 02 May 2014 at Pacifico YOKOHAMA, Kanagawa, Japan)

STT59-12 Room:414 Time:April 29 12:05-12:20

Correction by GNSS data for wide area InSAR analysis

MORISHITA, Yu[1*]

[1]GSI of Japan

InSAR results include not only deformation signals but also noises caused by orbital inaccuracies, tropospheric delay and ionospheric delay. Orbital inaccuracies yield a residual orbital phase ramp. As spatial wavelengths of tropospheric and ionospheric noise are typically long, the effect is trivial for a small area but it can be significant for a large area.

Tropospheric noise can be mitigated by estimating the amount of tropospheric delay from a numerical weather model. However, the mitigation does not always work because of the limitation of spatial and temporal resolution of the numerical weather model. There is no common and effective technique to correct ionospheric noise so far while several techniques have been proposed. The ionospheric noise remains a big problem because, in particular, L-band is greatly affected by ionospheric noise. A residual orbital phase ramp can be reduced by flattening the phase in an area with no deformation. Another effective correction method is estimating model parameters (e.g. bilinear surface) to fit other deformation data such as GNSS continuous observation (Tobita et al., 2005; Fukushima and Hooper, 2011). This method works even if the deformation extends the entire area (Kobayashi, 2011). However, if the area is wide, a bilinear surface model is not sufficient because of noises with long wavelengths. A spline interpolation method has been proposed to overcome this problem (Fukushima, 2013).

In this presentation, I will report a GNSS correction technique using a natural interpolation method for scattered points. This technique can mitigate not only residual orbital phase ramps but also noises with long wavelength. Adjusting correction steps enables realistic extrapolations while conventional steps sometimes result in outliers in extrapolated areas. The results of wide area time series InSAR analysis using ALOS/PALSAR data show less noise and more apparent phase changes with shorter wavelength than the interval of the GNSS stations.

References

Tobita, M., H. Munekane, S. Matsuzaka, M. Kato, H. Yarai, M. Murakami, S. Fujiwara, H. Nakagawa and T. Ozawa (2005): Studies on InSAR data processing techniques, Bull. GSI., 106, 37-49 (in Japanese).

Fukushima, Y. and A. Hooper (2011): Crustal deformation after 2004 Niigataken-Chuetsu earthquake, central Japan, investigated by Persistent Scatterer Interferometry, J. Geod. Soc. Japan, 57, 195-214 (in Japanese with English abstract).

Kobayashi, T., M. Tobita, T. Nishimura, A. Suzuki, Y. Noguchi and M. Yamanaka (2011): Crustal deformation map for the 2011 off the Pacific coast of Tohoku Earthquake, detected by InSAR analysis combined with GEONET data, Earth Planets Space, 63 , 621-625, 2011.

Fukushima, Y. (2013): Correction of DInSAR noise using GNSS measurements, in proceedings of APSAR 2013, 2013.

Keywords: InSAR, GNSS

Japan Geoscience Union Meeting 2014
(28 April - 02 May 2014 at Pacifico YOKOHAMA, Kanagawa, Japan)

STT59-P01 Room:Poster Time:April 29 18:15-19:30

Research on the characteristics of ionospheric disturbance around Japan by GPS-TEC for ionospheric correction to InSAR

NAKAGAWA, Hiroyuki[1*] ; MUNEKANE, Hiroshi[1] ; KUROISHI, Yuki[1] ; KAMIHARA, Masashi[2]

[1]GSI of Japan, [2]Pascalia Co.,Ltd

In the monitoring surface deformation using SAR interferometry (InSAR), it is a serious problem that the long-wavelength noise caused by ionospheric disturbance degrades accuracy of the detection of deformation. Since 2013, Geospatial Information Authority of Japan (GSI) have conducted a research project on the method for ionospheric correction to satellite InSAR based on TEC information obtained from two-wavelength observation data of GEONET.

For the first step, in order to understand the characteristics of ionospheric disturbance around Japan, we identified ionospheric disturbance of the period between 2000 and 2011 by GPS-TEC of GEONET and estimate characteristic values of each event.

In the manner in Munekane (2013), we first estimate zenith TEC and TEC gradient in north-south and east-west component every thirty second during the period from GEONET thirty-second RINEX data. Then, we adopted high pass filter of 3600s to remove low frequency component.

Next, based on this GPS-TEC time series, we identified ionospheric disturbance event in the period. In this step, we focus rather on revealing overall trend of ionospheric disturbance than inspecting accuracy of the characteristic value of each event.

The process of identification is as follows. First hourly RMS of TEC was calculated every hour, and, if the number of sites which hourly TEC-RMS is over threshold is more than a certain criterion, regard the epoch as a part of ionospheric disturbance event. Then, viewing the ”GEONET GPS-TEC maps over Japan” on the web site of NICT, each disturbance event was divided visually into three category according to the pattern of TEC distribution, ”traveling ionospheric disturbance (TID) ”, ”plasma bubble” and ”other”.

After the identification of event category, we decided characteristics such as event start and end time, affected area and its temporal transition based on ten-minute RMS of TEC. Also, we estimate characteristic values associated with event category such as wavelength of a TID or northernmost latitude of a plasma bubble etc. Finally, we derived characteristics of the ionospheric disturbance around Japan statistically.

We identified 8,815 ionospheric disturbance in the period, reaching maximum of 967 events in 2001, decreasing gradually to minimum of 471 in 2007, and having increasing tendency afterwards. This trend is consistent with solar cycle. The occurrence of TID and plasma bubble is found to be consistent with solar cycle, too.

Also, it appears that TID occurs commonly from May to August, in summer season. TID occurrence also concentrates before and after two hours around 22 o’clock in local time. As for plasma bubble, the occurrence is high from the sunset to midnight in local time. These results are consistent with earlier studies.

References

Munekane, H., (2013): On ionospheric correction of ALOS/PALSAR interferograms using GEONET data (preliminary report) , STT57-09, Japan Geoscience Union Meeting 2013

National Institute of Information and Communications Technology: GEONET GPS-TEC maps over Japan, http://seg-web.nict.go.jp/GPS/GEONET/index_e.html

Keywords: InSAR, ionospheric disturbance, TEC, GEONET

Japan Geoscience Union Meeting 2014
(28 April - 02 May 2014 at Pacifico YOKOHAMA, Kanagawa, Japan)

STT59-P02 Room:Poster Time:April 29 18:15-19:30

APPLICATION OF DINSAR TIME SERIES ANALYSIS USING ALOS PALSAR TO EXTERIOR DEFORMATION MONITORING OF DAMS

HONDA, Kenichi[1*] ; MUSHIAKE, Naruo[1] ; SATOH, Wataru[1] ; SATOH, Hiroyuki[2] ; KOBORI, Toshihide[2] ; SASAKI, Takashi[3] ; YAMAGUCHI, Yoshikazu[4] ; SHIMIZU, Norikazu[5]

[1]Kokusai Kogyo Co., Ltd., [2]Public Works Research Institute, [3]National Institute for Land and Infrastructure Management, [4]Japan Dam Engineering Center, [5]Yamaguchi University

The number of aging civil engineering structures is rapidly increasing in Japan. As for dams, it is estimated that 58% of existing dams in the year 2020 will be 50 years old or over after completion. This situation increasingly requires not only efficient deformation monitoring systems for safety management of civil structures but also safe and rapid methods in case of emergencies such as earthquakes.

Remote sensing techniques, especially Synthetic Aperture Radar (SAR), can play an important role to conduct deformation monitoring of civil structures such as dams. Differential Interferometric SAR (DInSAR) analysis using SAR satellite data can be suitable to deformation monitoring in broad areas.

To investigate the applicability of DInSAR analysis for the deformation monitoring, the Taiho Subdam, which is located in the Okinawa Prefecture, Japan, was selected as a study area because the deformation monitoring using GPS have been rigorously conducted since the completion of the dam from December 2006. In this study area, at maximum 114 mm of deformation was measured from December 2006 to December 2010, which corresponds to the observation period by SAR satellite. ALOS PALSAR data, L-band SAR, was used for DInSAR analysis and the results of deformations calculated by DInSAR analysis were compared with the results of the GPS deformation measurements. 28 scenes of ALOS PALSAR data were used: 14 scenes of descending data from December 6, 2006 to December 17, 2010, and 14 scenes of ascending data from January 12, 2007 to January 23, 2011, respectively.

The values of deformations calculated by DInSAR analysis were about 70 or 80% of those measured by GPS during observation period about four years. Although the DInSAR analysis results were expected to have some errors and were different from the GPS measurement results to some extent, DInSAR deformation monitoring is sufficient enough to monitor few-centimeter deformations. Additionally time series changes by DInSAR analysis can well reproduced the tendency of the settlement of the dam. This indicates a possibility that DInSAR analysis is useful for the deformation monitoring for civil structures.

Keywords: Dam, Exterior deformation monitoring, DInSAR, SBAS, GPS

Japan Geoscience Union Meeting 2014
(28 April - 02 May 2014 at Pacifico YOKOHAMA, Kanagawa, Japan)

STT59-P03 Room:Poster Time:April 29 18:15-19:30

Approach for monitoring ground deformation around the active volcanoes in Japan by InSAR time series analysis

MIURA, Yuji[1*] ; ANDO, Shinobu[2] ; NAKAMURA, Masamichi[1]

[1]Volcanological Division, JMA, [2]MRI

In previous studies, we have reported the analysis results about domestic active volcanic areas using D-InSAR of ALOS since 2007. In recent years, InSAR time series analysis technique has been developed. Therefore various studies have been reported for monitoring ground deformation using InSAR time series analysis. In this study, we have applied this procedure to the analysis of the data of ALOS/PALSAR for monitoring ground deformation of the active volcanoes in Japan.

As a result, we can detect ground deformations associated with volcanic activities of Tokachidake, Azumayama, Izu-Oshima, Miyakejima, Satsuma-Iojima and others. These obtained ground deformations by InSAR time series analysis were basically consistent with the results of GPS.

Keywords: InSAR time series analysis, ground deformation, ALOS/PALSAR, active volcano

Japan Geoscience Union Meeting 2014
(28 April - 02 May 2014 at Pacifico YOKOHAMA, Kanagawa, Japan)

STT59-P04 Room:Poster Time:April 29 18:15-19:30

Surface displacement around Hachobaru geothermal field inferred from persistent scatterer SAR interferometry

ISHITSUKA, Kazuya[1*] ; TSUJI, Takeshi[2] ; MATSUOKA, Toshifumi[1] ; FUJIMITSU, Yasuhiro[3] ; NISHIJIMA, Jun[3]

[1]Graduate School of Engineering, Kyoto University, [2]International Institute for Carbon-Neutral Energy Research (I2CNER), Kyushu University, [3]Faculty of Engineering, Kyushu University

Fluid migration around geothermal field can cause surface displacement. Leveling campaign and GPS measurement has been used to estimate surface displacement and shown the usefulness for reservoir monitoring at geothermal field. Recently, persistent scatterer SAR interferometry (PS-InSAR) analysis has been developed as a practical tool for surface displacement monitoring. By making use of the advantage of wide data coverage of satellite image, the analysis enables us to estimate surface displacement at the whole geothermal field with high spatial density. In this study, we applied PS-InSAR analysis on areas around Hachobaru geothermal field, the largest geothermal field in Japan, located Kyushu Island. For the analysis, we used 18 ALOS/PALSAR images acquired from July 2007 to December 2010 from an ascending orbit.

As a result of the analysis, we estimated secular surface displacement with the maximum rate of 15 mm/year opposite to satellite direction, which can be inferred as ground subsidence. We also found temporally irregular displacement along with the secular displacement. This irregular displacement has occurred all of Mt. Kuju, suggesting that displacement at Mt. Kuju has influenced displacement at the geothermal field. Moreover, we found that the secular displacement has decayed over time and has clear boundaries which possibly correspond to fault locations.

Keywords: surface displacement, persistent scatterer SAR interferometry, Hachobaru geothermal area

Japan Geoscience Union Meeting 2014
(28 April - 02 May 2014 at Pacifico YOKOHAMA, Kanagawa, Japan)

STT59-P05 Room:Poster Time:April 29 18:15-19:30

The Steady Crustal Deformation Analysis in Tokai region by InSAR

ANDO, Shinobu[1*] ; IWAKIRI, Kazuhiro[2] ; AOKI, Gen[2]

[1]MRI, [2]JMA

ALOS has an L-band SAR (PALSAR), which is of help to understand of a ground surface state, and its interferometric coherence is highly effective for the crustal deformation observation.

We analyzed the ALOS/PALSAR data around Omaezaki and Kakegawa cities in Shizuoka Prefecture, and tried to detect steady crustal deformation due to the subduction of the Philippine Sea plate. In this study, in order to obtain steady-state deformation (time series), we subjected to interference processing on the image pairs of a number of different imaging date interval. Then, using a variation of the satellite line-of-sight direction in the interference each images and we were calculated the average variation of the 46 days (stacking process). However, to reduce noise, we analysed except for some interferograms with obvious noise. This method can be expected to improve detection accuracy, because of able to reduce the influence of noise caused by the ionosphere.

We used 23 ascending data acquired from January 2007 to October 2010 and 19 descending data acquired from October 2006 to September 2010. Before solving for the displacement time series, we corrected the atmosphere phase delay by Japan Meteorological Agency nonhydrostatic model (JMA-NHM), and calculated the displacement of the satellite line-of-sight direction of the pair of all. The average displacement of the satellite line-of-sight direction of the 46 days was calculated under the assumption that the variation in the period of each pair is constant. The distance between the imaging date is different for each pair, but we did not weight during the averaging process.

As a result, steady-state deformation was hardly observed in the analysis of the ascending orbit data, but in the analysis of the descending orbit data, were observed the steady-state deformation the away from the satellite in the radar line-of-sight direction. This crustal deformation was significant in Omaezaki area, especially. These results are consistent with the displacement vector by GNSS. In this report, we also reported about InSAR time series analysis using *StaMPS* program was developed by the Stanford Institute of Technology.

Some of PALSAR data were prepared by the Japan Aerospace Exploration Agency (JAXA) via the Geospatial Information Authority of Japan (GSI) as part of the project ”ALOS Domestic Demonstration on Disaster Management Application” of the Earth Working Group. Also, we used some of PALSAR data that are shared within PALSAR Interferometry Consortium to Study our Evolving Land surface (PIXEL). PALSAR data belongs to Ministry of Economy Trade and Industry (METI) and JAXA. We would like to thank Dr. Shimada (JAXA) for the use of his *SIGMA-SAR* software. In the process of the InSAR, we used ”the digital elevation map 50m-mesh” provided by GSI, and Generic Mapping Tools (P.Wessel and W.H.F.Smith, 1999) to prepare illustrations.

Keywords: InSAR, Ground deformation, ALOS/PALSAR, Tokai region

Japan Geoscience Union Meeting 2014
(28 April - 02 May 2014 at Pacifico YOKOHAMA, Kanagawa, Japan)

STT59-P06 Room:Poster Time:April 29 18:15-19:30

Monitoring of Sakurajima Volcano using Cosmo-SkyMed

MIYAGI, Yosuke[1*] ; OZAWA, Taku[1] ; SHIMADA, Masanobu[2]

[1]National Research Institute for Earth Science and Disaster Prevention, [2]Japan Aerospace Exploration Agency

Sakurajima volcano is located in southwestern part of Japan, and currently a most active volcano in Japan. Eruptive activities from Showa-crater have activated since 2009, and several explosive eruptions occurred in 2012. On July 24, 2012, another large eruption occurred from Minamidake-crater after a lapse of 18 months. To understand current condition and future unrest of Sakurajima, periodic monitoring is required. Although it is generally difficult to make a field observation in dangerous active volcanoes, a satellite remote sensing can make observations of even ongoing volcanoes periodically. Especially, Synthetic Aperture Radar (SAR) sensor is well-suited for monitoring active volcanoes because it can penetrate ash clouds and can observe targets like an active vent. Moreover, SAR data are applicable to use a Differential Interferometric SAR (DInSAR) technique to detect crustal movement associated with the magmatic activities. In this study, we used COSMO-SkyMed data for monitoring Sakurajima volcano and tried DInSAR processing. Monitoring using high-resolution amplitude images revealed changes of backscattering intensity probably due to some kind of surface change within or around the crater. DInSAR processing suffered from low coherence, therefore we acquired quite limited geodetic information.

Keywords: SAR, Sakurajima, Deformation

Japan Geoscience Union Meeting 2014
(28 April - 02 May 2014 at Pacifico YOKOHAMA, Kanagawa, Japan)

STT59-P07 Room:Poster Time:April 29 18:15-19:30

Volume Increase of Lava within the Kirishima, Shinmoe-dake Crater, Detected by TerraSAR-X/DInSAR

MIYAGI, Yosuke[1*] ; OZAWA, Taku[1] ; KOZONO, Tomofumi[2] ; SHIMADA, Masanobu[3]

[1]National Research Institute for Earth Science and Disaster Prevention, [2]Department of Geophysics, Graduate School of Science, Tohoku University, [3]Japan Aerospace Exploration Agency

Shinmoe-dake in the Kirishima volcano group is located in southwestern part of Japan. In January 2011, eruptive activities started from the Shinmoe-dake crater with a rapid accumulation of lava within the crater. The eruption phase ceased by the beginning of September, and the post-eruptive inflation also ceased by November 2011. After the 2011 eruption, monitoring by TerraSAR-X have continued and revealed a continuous shortening of satellite-ground distance even after the end of the main activity. This LOS shortening means uplifts of the lava surface. We estimated the volume increase of the lava after November 2011, using DInSAR processing of TerraSAR-X data, and concluded that the volume increase still continued in January 2014. The volume change rate has exponentially decreased with a small fluctuation as an overall trend. PSInSAR and long-term DInSAR results show LOS elongation including a subsidence in the northeast flank of the crater. It is interpreted that the subsidence is caused by deflation of a shallow deformation source located just beneath the crater. A total amount of effused lava after November 2011 is comparable to a volume decrease of the shallow source estimated from the deflation deformation. This long-term continuous lava extrusion suggests a possibility of an additional injection from the deeper source.

Keywords: SAR, Kirishima, Shinmoe-dake, Deformation

Japan Geoscience Union Meeting 2014
(28 April - 02 May 2014 at Pacifico YOKOHAMA, Kanagawa, Japan)

STT59-P08 Room:Poster Time:April 29 18:15-19:30

Crustal deformation in Izu-Oshima Island detected by PS-InSAR analysis and estimation of volcanic deformation source

HASEGAWA, Yuichi[1*] ; TABEI, Takao[2] ; OZAWA, Taku[3]

[1]Grad. School Int. Arts Sciences, Kochi Univ., [2]Fac. Science, Kochi Univ., [3]National Research Institute for Earth Science and Disaster Prevention

Mt. Mihara in Izu-Oshima Island have erupted 21 times in the last 800 years. The latest eruption occurred in 1986 inside the caldera. Though spatially and temporally dense observation network is desired to continuously monitor volcanic activities, it is not easy to construct such a network in a mountainous region. In this study, we conduct time-series analysis of ALOS/PALSAR images over Izu-Oshima Island using persistent scatter interferometric SAR (PS-InSAR) method to detect volcanic deformation.

From the analysis of 20 images collected from ascending track during the period from October 2007 to February 2011, we detect distance change of about 15 cm extension in the line-of sight (LOS) direction inside the caldera. Similarly the extension of about 14 cm is detected at the same location from the analysis of 18 images from descending track during the period from January 2007 to March 2010. Next we compare the LOS distance changes with those converted from GPS coordinate time-series at four continuous sites in the island. The RMS between them are as large as 1.3-3.2 cm, implying that SAR results are good enough to monitor volcanic deformation over the island.

Combining the LOS distance changes from the ascending and descending tracks, we derive quasi-vertical and quasi-east-west components of the displacement. The most remarkable is the vertical displacement of the caldera where the subsidence of about 16 cm is detected during 2007-2010 with small occasional uplifts. Moreover uplift of about 11 cm is recognized in the eastern coastal area of the island during the same period. Based on the quasi-vertical component of the displacement, we estimate a spherical pressure source model (Mogi, 1958) below the island. We assume two sources with different depth and estimate the optimum model using a grid search method. Horizontal position of the shallower source is fixed to coincide with the location of the caldera and its depth is varied every 0.5 km in a range of 2.0-4.5 km. Horizontal position of the deeper source is varied every 2 km and its depth is checked every 0.5 km in a range of 5.0-10 km. The optimum model shows that the shallower source is located at a depth of 3.0-4.5 km where inflation and deflation are occurring alternatively while the deeper source is located at a depth of 6.0-9.0 km where nearly constant inflation rate of about 8 million m3 per year is expected. These results can be interpreted that the deeper magma reservoir continues to expand due to magma supply from the mantle while the shallower reservoir is affected by magma supply from the deeper source and gravitational load of lava that spreads within the caldera.

Keywords: PS-InSAR method, time-series analysis, Izu-Oshima Island, crustal deformation, volcanic deformation source

Japan Geoscience Union Meeting 2014
(28 April - 02 May 2014 at Pacifico YOKOHAMA, Kanagawa, Japan)

STT59-P09 Room:Poster Time:April 29 18:15-19:30

Flow velocity measurements of ice streams in the southern part of Soya Coast, Antarctica, by DInSAR

SHIRAMIZU, Kaoru[1*] ; DOI, Koichiro[2] ; AOYAMA, Yuichi[2]

[1]The Graduate University for Advanced Studies, [2]National Institute of Polar Research

Differential Interferometric Synthetic Aperture Radar (DInSAR) is an effective tool to measure flow rate of ice streams on Antarctic continent. In this study, we applied the DInSAR technique to L band (wavelength 23.6cm) SAR data acquired by ALOS/PALSAR, and tried to measure flow velocity around Skallen, in the southern part of Soya Coast, East Antarctica. We used 9 scenes (Path633, Row 571-572), observed during the period from November 23, 2007 through January 13, 2010. In order to remove topographic fringes in the interferograms, we used a digital elevation model ASTER GDEM.

According to the analysis, ice flow rate of up to 3.5cm/day was obtained in the line of sight direction. Although no displacement is expected in areas of outcrops in general, we found displacements up to 37cm in the outcrops of obtained displacement maps. These displacements are considered to be apparent ones and must contain errors induced in the process of analysis. Therefore, it is possible to use apparent changes as a measure of the error contained in ice flow rate estimation.

In this presentation, we will show the results of flow rate estimation of the ice streams, and discuss the errors included in the flow rate estimation.

Keywords: Differential Interferometric SAR, Antarctic ice sheet, ice stream

Japan Geoscience Union Meeting 2014
(28 April - 02 May 2014 at Pacifico YOKOHAMA, Kanagawa, Japan)

STT59-P10 Room:Poster Time:April 29 18:15-19:30

Flow measurements of ice sheets in Arctic region by differential SAR interferometry

DOI, Koichiro[1*] ; YAMANOKUCHI, Tsutomu[3] ; NAKAMURA, Kazuki[4] ; SHIRAMIZU, Kaoru[2]

[1]National Institute of Polar Research, [2]The Graduate University for Advanced Studies (SOKENDAI), [3]RESTEC, [4]Nihon University

Rapid ice sheet mass losses from ice sheets have been found in Greenland and the Canadian Arctic Archipelago on and after 2000 from the observations by the satellite gravity mission GRACE (Svendsen et al. 2012, Gardner et al. 2011). It is considered to be one of the causes that flow rate of ice sheet and ice stream was accelerated and ice mass outflow into the sea increased.

We aim to measure flow rates of ice sheet and ice streams in the Arctic region by applying differential Synthetic Aperture Radar (SAR) interferometry (DInSAR) with a digital elevation model ASTER GDEM to satellite SAR data. In addition, we intend to explore whether changes in the flow rate happen or not.

We obtained displacement maps along line of sight direction for 46 days of three regions in north eastern Greenland and Ellesmere Island of northern Canadian Arctic Archipelago observed by ALOS/PALSAR by applying differential SAR interferometry. We will show the obtained displacement maps in the presentation, and will also intend to discuss changes in the flow rates by applying three or four pass interferometry.

Keywords: Differential SAR interferometry, flow, ice sheet, Arctic region

Japan Geoscience Union Meeting 2014
(28 April - 02 May 2014 at Pacifico YOKOHAMA, Kanagawa, Japan)

STT59-P11 Room:Poster Time:April 29 18:15-19:30

Spatial distribution and classification of rock glaciers in Kyrgyz Ala-Too Range, Central Asia

YAMAMURA, Akiko[1*] ; NARAMA, Chiyuki[1] ; TOMIYAMA, Nobuhiro[2] ; TADONO, Takeo[3]

[1]Niigata University, [2]RESTEC, [3]JAXA

In the arid and semi-arid region of Central Asia, Tien Shan Mountains is known as important water tower in Central Asia. Although the current situation of mountain glaciers and permafrost should be researched for estimate of water resources, mountain permafrost is not clarified in the Tien Shan (Marchenko et al., 2007; Sorg et al., 2012). In recent years, landslides caused by the melting of mountain permafrost in Ak-Shiyrak mountains, show that recent changes of mountain permafrost begin to influence to mountain environment including the disaster. In this study, to clarify mountain permafrost environment, we researched spatial distribution and classification of rock glaciers in Kyrgyz Ala-Too Range, Tien Shan Mountains. In addition, we applied InSAR analysis to the ALOS PALAR data obtained in 2007-2010, to research moving of rock glaciers. We extracted polygon data of rock glaciers based on aerial photo interpretation and ALOS PRISM, using ArcGIS. Rock glaciers were classified an active and inactive-fossil types by NDVI (Normalized Difference Vegetation Index) of ALOS AVNIR-2 and field observation in the summer 2013. The distributions of active rock glaciers show the lower limit of mountain permafrost is 3300m in the northern part and 3500m in the southern part of the Kyrgyz Ala-Too Range. We confirmed moving of some rock glaciers in this mountain area using InSAR analysis. In particularly, the moving of rock glaciers in the southern part of the range is remarkable. The most of these active rock glaciers developed from glacier ice. We report the results in detail in JpGU meeting.

Keywords: mountain permafrost, rock glacier, InSAR, ALOS PALSAR, Tien Shan Mountains

Japan Geoscience Union Meeting 2014
(28 April - 02 May 2014 at Pacifico YOKOHAMA, Kanagawa, Japan)

STT59-P12 Room:Poster Time:April 29 18:15-19:30

Development of InSAR processing tools in NIED ?Part3?

OZAWA, Taku[1*]

[1]National Research Institute for Earth Science and Disaster Prevention

Synthetic aperture radar (SAR) became one of the useful tools for crustal deformation detection. Recently, InSAR processors which can be used freely in scientific research (e.g., ROI_PAC, GMTSAR, and Doris) were released, and enabled anyone to do crustal deformation detection by InSAR. Especially, algorithm of two-pass differential InSAR analysis matured, and it enabled anyone to obtain almost same results. On the other hand, advanced InSAR analysis methods, e.g., time-series analysis, have been recently used to detect precise crustal deformation. However, many issues to improve remains in such analyses. In order to research on improvements for such analysis, we are developing InSAR processor.

In this InSAR processor, general procedure is adopted. (1) Format conversion of SLC and creation of parameter files. (2) Rough co-registration of two SLCs considering parallel shift only. (3) Estimation of affine transformation coefficients. (4) SLC resampling. (5) Generation of the initial interferogram. (6) Simulation of a SAR intensity image and estimation of translation tables between geodetic and radar coordinates based on DEM. (7) Co-registration between simulated and observed SAR intensity images. (8) Correction of translation tables. (9) Simulation of the orbital and the topographic phase components. (10) Generation of differential interferogram. (11) Applying interferogram filter. (12) Geocoding.

In JPGU meeting 2013, we showed comparison between results from our processor and from GAMMA SAR processor. Although their results were roughly the same, it indicated that many improvement points remained. In 120th meeting of the Geodetic Society of Japan, we presented about improvement of coherence by the spectrum shift filter (Gatelli et al., 1994), improvement of calculation speed, and correspondence to skewed images. After that, this processor corresponded to the InSAR processing with FBS-FBD image pair of ALOS/PALSAR using SLC over-sampling and band-pass filter. We added DEM resampling function by over-sampling method and by the bi-cubic spline interpolation. Furthermore, we are attempting to improvement of the image matching now. After this correspondence, the first step of this development will be finished. In next step, we will attempt more improvements and additions of other advanced algorithms.

Keywords: SAR, InSAR, software, tool

Japan Geoscience Union Meeting 2014
(28 April - 02 May 2014 at Pacifico YOKOHAMA, Kanagawa, Japan)

STT60-01 Room:211 Time:April 30 14:15-14:24

Creating future of solid Earth science with high performance computing (HPC): Introduction

HORI, Takane[1*] ; HINO, Ryota[2] ; HONKURA, Yoshimori[3] ; KANEDA, Yoshiyuki[1] ; ARIKAWA, Taro[4] ; ICHIMURA, Tsuyoshi[5] ; TODORIKI, Masaru[5]

[1]JAMSTEC, [2]Tohoku University, [3]Tokyo Institute of Technology, [4]Port and Airport Research Institute, [5]University of Tokyo

In Japan, high performance computing (HPC) had been driven by computer science community (HPC developer). However, recently, computational science community (HPC user) has been expected to contribute to the planning and development of the next generation HPC showing the scientific and/or social issues to be solved for the next 10-20 years using HPC. In various filed of science using HPC, scientists has started to discuss scientific and/or social issues to be solved in each field. Hence, in this session, we aim to examine such issues in solid Earth science, which HPC can contribute to solve. For social issues, we will focus on earthquake and tsunami disaster mitigation. For scientific issues, we would like to discuss construction of the next generation of solid Earth model based on the big data of seismic waves and crustal deformation obtained by high-density observation networks. We will introduce the contents of the ”white paper” of the future plans for computer science in various fields including solid Earth science.

Keywords: HPC, hazard mitigation

Japan Geoscience Union Meeting 2014
(28 April - 02 May 2014 at Pacifico YOKOHAMA, Kanagawa, Japan)

STT60-02 Room:211 Time:April 30 14:24-14:39

The K Computer and Japan Plan for Exascale

HIRAO, Kimihiko[1*]

[1]AICS RIKEN

At the end of September 2012, official operation of the Kcomputer has started. Already in many areas we see many great results. Users of K are actually very much impressed having experienced using K. The K is Japanese supercomputer jointly developed by Fujitsu and Riken and everything is made in Japan. The K computer won the top position on TOP500 in 2011 achieving a LINPACK benchmark performance of 10 petaflops - becoming the first supercomputer ever to reach this milestone. The K fell behind China and US machines on the latest TOP500. We believe that the K is still one of the most powerful and user-friendly machine in the world. K demonstrates an extraordinary level of stability. K is capable of sustained performance of 1 PF on real applications in a wide range of science. K is the strong science machine.

Computer simulation is becoming more and more important for contemporary science and engineering. Nobel Prizes 2013 in chemistry and physics show how computing is changing every field of research. Particularly simulations performed on the supercomputer will drive progress in science and technology and play an important role in solving difficult problems that we face as a society. There are very critical issues that need to be solved - global warming, alternative energy, disaster mitigation, new materials, healthcare, security, etc. The role of simulations will become increasingly larger, and the results that they provide will undoubtedly greatly affect society. The new frontiers opened up by the K computer will be presented.

The post K project will be lauced from April 2014. MEXT selected RIKEN AICS to develop a new exascale supercomputer by 2020. The post K is 100 times faster than the current K computer. Architecture is hybrid of general-purpose plus accelerator components. We will push the state of the art in power efficiency, scalability & reliability. Power consumption is limited in the range of 30-40MW.Total project cost is ca. JPY140 billion with about JPY 110 billion coming from the government’s budget (JPY 1.2 billion for 2014)

Computer simulation will dramatically increase our ability to understand the world around us. With exascale computing, we are reaching a tipping point in predictive science. Its success will have lasting impact on the planet and people all around the world and for generations into the future. With a planned deployment in 2020, the new system is expected to keep Japan at the leading edge of computing science and technology.

Japan Geoscience Union Meeting 2014
(28 April - 02 May 2014 at Pacifico YOKOHAMA, Kanagawa, Japan)

STT60-03 Room:211 Time:April 30 14:39-14:54

The application of simulation studies using HPC to disaster management: current status and future.

YOKOTA, Takashi[1*] ; TAIRA, Yutaro[1]

[1]Cabinet Office

In Central Disaster Management Council, estimations of damage by anticipated earthquakes have been conducted to plan measures for disaster management(preparedness, emergency response and recovery). Also, when a large earthquake occurs early assessments of the damage have been carried out immediately to grasp the situation of the disaster and to support decision-making for emergency response operations in central government. These estimations and assessments require high accuracy to develop more effective measures and to decide more appropriate operations.

It is indisputable that the sophistication of forecasting techniques of natural phenomena is necessary to mitigate human damage by encouraging residents to evacuate.

In this presentation, we will introduce our approaches described above, and would like to talk about what to expect from the application of simulation studies using High Performance Computing to the disaster management of earthquakes and tsunamis in particular.

Keywords: disaster managent, damege estimation, HPC

Japan Geoscience Union Meeting 2014
(28 April - 02 May 2014 at Pacifico YOKOHAMA, Kanagawa, Japan)

STT60-04 Room:211 Time:April 30 14:54-15:09

Development of Integrated Earthquake Simulator on K-computer

ICHIMURA, Tsuyoshi[1*] ; HORI, Muneo[1]

[1]Earthquake Research Institute,The University of Tokyo

Earthquake simulation with high-resolution and high-accuracy could have significant contribution on making rational and effective contour measures against earthquake disaster. Such earthquake simulation must consider whole process from a fault rupture to city responses, since each process has significant effects on the resulting responses. We are now developing such earthquake simulation system on K-computer, which is called Integrated Earthquake Simulator (IES). IES combines spatial data and earthquake simulation with a high-fidelity model to simulate the whole process. The target domain of earthquake simulation is typically very large, making it difficult to prepare sufficient data to construct a high-fidelity model. Even if a high-fidelity model can be constructed, it is difficult to resolve the computational expense due to the discretization of such models. Thus, simplified analyses or analytical methods are typically used in earthquake simulation. However, the construction of high-fidelity models has become popular with recent increases in available spatial data, and a considerable volume of data from high-density observation networks is now available for checking their validity. The realization of analyses using high-fidelity models is desirable. Several examples of analyses using such models can currently be found on the K-class supercomputer, although the resolution is not yet adequate. In this presentation, we discuss the following earthquake simulations (parts of IES) on the K computer, together with problems to be solved: non-linear wave simulation with high resolution, crust deformation analysis with island-scale and the seismic response analysis of soil-structures system.

Keywords: earthquake simulation, high performance computing, high fidelity, high resolution and accuracy

Japan Geoscience Union Meeting 2014
(28 April - 02 May 2014 at Pacifico YOKOHAMA, Kanagawa, Japan)

STT60-05 Room:211 Time:April 30 15:09-15:24

Consideration to the resiliency of protective structures against tsunami by using High Performance Computer

ARIKAWA, Taro[1*] ; OIE, Takayuki[1] ; TOMITA, Takashi[1]

[1]Port and Airport Research Institute

The Committee for Technical Investigation on Countermeasures for Earthquakes and Tsunami Based on the Lessons Learned from the ”Great East Japan Earthquake” (2011) of the Central Disaster Management Council has responded to the Great East Japan Earthquake by proposing that basically, two levels of tsunami must be hypothesized to build future tsunami countermeasures. One is a tsunami hypothesized to build comprehensive disaster prevention countermeasures centered on evacuation of residents. It is set based on a survey of tsunami deposits formed over an ultra-long period and observations of crustal movement, and it is a maximum class tsunami which, although it occurs extremely rarely, causes devastating damage when it does occur. One more is a tsunami which is hypothesized to build coastal protection facilities such as breakwaters and other structures which prevent tsunami from inundating inland regions. It is a tsunami which occurs more often than the maximum class tsunami, and although it is a low type of tsunami, it causes severe damage. At such times, technological development of structures which are capable of resiliently providing effects even under tsunami height which is the object of the design must continue for coastal protection facilities etc. to be improved. So, in this research , the protective effectiveness is considered by using STOC-CADMAS(Arikawa and Tomita, 2005).

Japan Geoscience Union Meeting 2014
(28 April - 02 May 2014 at Pacifico YOKOHAMA, Kanagawa, Japan)

STT60-06 Room:211 Time:April 30 15:24-15:39

Determination of Earth structure using waveform inversion and Spectral-Element Method

TSUBOI, Seiji[1*] ; MIYOSHI, Takayuki[1] ; OBAYASHI, Masayuki[1] ; TONO, Yoko[1]

[1]JAMSTEC

Recent progress in large scale computing by using Spectral-Element Method and the Earth Simulator has demonstrated possibilities to perform full-waveform inversion of three dimensional (3D) seismic velocity structure inside the Earth. Specifically Liu and Tromp (2006) have shown that it becomes feasible to compute finite frequency kernel for seismic velocity structure based on adjoint method. We apply their method to obtain 3D velocity structure beneath East Asia. We take one chunk from global mesh of Spectral-Element Method and compute synthetic seismograms with accuracy of about 10 second. We use GAP-P2 mantle tomography model (Obayashi et al., 2009) as an initial 3D model and try to use as many broadband seismic stations available in this region as possible to perform inversion. We then use the time windows for body waves and surface waves to compute adjoint sources and calculate adjoint kernels for seismic velocity structure. We use the earthquakes, which occurred in East Asia since 2001, with magnitude greater than 5.5 and selected 161 events for this inversion. One iteration of the waveform inversion using 256 cores of massively parallel supercomputer, such as K-computer, requires 0.1 million CPU hours. We have performed several iteration and obtained improved 3D velocity structure beneath East Asia. The result demonstrates that waveform misfits between observed and theoretical seismograms improves with the iteration proceeds and it now becomes feasible to perform waveform inversion within practical computational time. We will use much shorter period in our synthetic waveform computation and will try to obtain seismic velocity structure for basin scale model in our future study.

Acknowledgements: We used F-net seismograms of the National Research Institute for Earth Science and Disaster Prevention. This study was supported by the strategic Programs for Innovative Research ”Field 3” Advanced prediction Researches for Natural Disaster Prevention and Reduction.

Keywords: Earth structure, Seismic tomography, Synthetic seismogram, Spectral Element Method

Japan Geoscience Union Meeting 2014
(28 April - 02 May 2014 at Pacifico YOKOHAMA, Kanagawa, Japan)

STT60-07 Room:211 Time:April 30 15:39-15:54

Mantle convection simulations on HPC: past, present and future

KAMEYAMA, Masanori[1*] ; MIYAGOSHI, Takehiro[2] ; FURUICHI, Mikito[2] ; NAKAGAWA, Takashi[2] ; YANAGISAWA, Takatoshi[2] ; NAKAKUKI, Tomoeki[3] ; OGAWA, Masaki[4]

[1]GRC, Ehime University, [2]JAMSTEC, [3]Hiroshima University, [4]University of Tokyo

In this presentation, we will discuss (a rather personal view of) the possible
directions of the advanced numerical studies of mantle dynamics in concert with the progress of high-performance computing in the next era. We will start with a brief overview of the research targets and outcrops of the numerical modelings of mantle convection to date from a viewpoint of geosciences. Then we will discuss the scientific goals which the mantle dynamics researchers are to tackle with in coming years, together with the technical issues in terms of both software and hardware developments.

Keywords: mantle convection, numerical simulation

Japan Geoscience Union Meeting 2014
(28 April - 02 May 2014 at Pacifico YOKOHAMA, Kanagawa, Japan)

STT60-08 Room:211 Time:April 30 16:15-16:30

Cloud Services to Release Techniques of Data Assimilation

NAGAO, Hiromichi[1*] ; HIGUCHI, Tomoyuki[2]

[1]Earthquake Research Institute, The University of Tokyo, [2]The Institute of Statistical Mathematics

Data assimilation (DA) is a fundamental technique to integrate numerical simulations and observation data in the framework of the Bayesian statistics. The purpose of DA is to provide an assimilation model that enables us to predict the future state and/or to determine parameters in the given simulation model. A sequential Bayesian filter, e.g., Kalman filter and particle filter, alternatively estimates probability density functions of one-step-ahead prediction and filtering, which respectively mean the states conditionally given the past observation data and given both past and present observation data. DA seems to be hard to implement due to complex programing of the procedure and needed numerous computation, which essentially requires High Performance Computing (HPC). Cloud service (CS) can be a solution for this through an implementation of the DA procedure on a parallel computing environment.

We have developed and released several CSs related to DA such as CloCK-TiME (Cloud Computing Kernel for Time-series Modeling Engine) and DA system for seismoacoustic waves. CloCK-TiME enables us to carry out a multivariate time-series analysis using the particle filter through the Internet. Users can, via the user interface, construct observation and system models, and specify optional parameters to control the analysis in detail. DA system for seismoacoustic waves enables us to determine hypocentric parameters through DA based on a numerical simulation related to seismoacoustic wave propagation using the normal model summation and observed infrasound data obtained at Shionomisaki and Sugadaira.

We will discuss the importance and availability of CS for DA researches through introduction of CSs we have developed.

Keywords: cloud computing, data assimilation, time-series analysis, seismoacoustic wave, multivariate analysis

Japan Geoscience Union Meeting 2014
(28 April - 02 May 2014 at Pacifico YOKOHAMA, Kanagawa, Japan)

STT60-09 Room:211 Time:April 30 16:30-16:45

Techniques of Big-Data Processing on the NICT Science Cloud

MURATA, Ken T.[1*] ; WATANABE, Hidenobu[1] ; UKAWA, Kentaro[2] ; MURANAGA, Kazuya[2] ; YUTAKA, Suzuki[2] ; TATEBE, Osamu[3] ; TANAKA, Masahiro[3] ; KIMURA, Eizen[4]

[1]NICT, [2]Systems Engineering Consultants Co., LTD., [3]University of Tsukuba, [4]Ehime University

This paper is to propose a cloud system for science, which has been developed at NICT (National Institute of Information and Communications Technology), Japan. The NICT science cloud is an open cloud system for scientists who are going to carry out their informatics studies for their own science.

The NICT science cloud is not for simple uses. Many functions are expected to the science cloud; such as data standardization, data collection and crawling, large and distributed data storage system, security and reliability, database and meta-database, data stewardship, long-term data preservation, data rescue and preservation, data mining, parallel processing, data publication and provision, semantic web, 3D and 4D visualization, out-reach and in-reach, and capacity buildings.

In the present study, we examine performance of parallelization of I/O on the NICT Science Cloud system. We examine an I/O performance of data file system; distributed file system (Gfarm). The Gfarm file system shows a tremendous fast I/O, as fast as 23 GB/sec using only 30 servers. We should pay attention to this I/O speed (23GB/sec is 184 Gbps) from the viewpoint of network speed. We also discuss that the distributed file system shows high scalability: Parallelization efficiency in the present examination is higher than 90% in case of parallel file system. We finally discuss high-performance data processing on the NICT Science Cloud. We have already archived several examples using our technique for both Earth and Space observation data and simulation data. The speed up of the data processing is more than 60 times for scientific big-data.

Japan Geoscience Union Meeting 2014
(28 April - 02 May 2014 at Pacifico YOKOHAMA, Kanagawa, Japan)

STT60-10 Room:211 Time:April 30 16:45-17:00

Creating future of solid Earth science with high performance computing (HPC): Discussion

HINO, Ryota[1*] ; HORI, Takane[2] ; HONKURA, Yoshimori[3] ; KANEDA, Yoshiyuki[2] ; ARIKAWA, Taro[4] ; ICHIMURA, Tsuyoshi[5] ; TODORIKI, Masaru[5]

[1]Tohoku University, [2]JAMSTEC, [3]Tokyo Institute of Technology, [4]Port and Airport Research Institute, [5]University of Tokyo

How the evolution of High Performance Computing (HPC) contributes to progress in earth sciences? We will develop a perspective in the next 10 to 20 years based on comprehensive discussion provided in the session including invited talks. Especially, we will discuss what is necessary for solving the social issues such as improvement of hazard maps, tsunami warning system, long-term forecast, etc. The aim of the concluding discussion is to integrate the opinions of attendees, both speakers and non-speakers, into a proposal for development of next generation HPC as a solution to important problems in terms of scientific break through and social relevance.

Japan Geoscience Union Meeting 2014
(28 April - 02 May 2014 at Pacifico YOKOHAMA, Kanagawa, Japan)

STT60-P01 Room:Poster Time:April 30 18:15-19:30

Parallel Performance of Particle Method in Many-Core System

FURUICHI, Mikito[1*] ; NISHIURA, Daisuke[1]

[1]Japan Agency for Marine-Earth Science and Technology

We present a computational performance of the smoothed particle hydrodynamics (SPH) simulation on three types of current shared-memory parallel computer devices: many integrated core (MIC: Intel Xeon Phi) processor, graphics processing units (GPU: Nvidia Geforce GTX Titan), and multi-core Central Processing Unit (CPU: Intel Xeon E5-2680 and Fujitsu SPARC64 processors). We are especially interested in the efficient shared-memory allocation methods with proper data access patterns on each chipset. We first introduce several parallel implementation techniques of SPH code for shared-memory system. Then they are examined on our target architectures to find the best algorithms for each processor unit. In addition, the computing and the power efficiency, which are increasingly important to compare multi device computer systems, are also examined for SPH calculation. In our bench mark test, GPU is found to mark the best arithmetic performance as the standalone device and the most efficient power consumption. The multi-core CPU shows the best computing efficiency. On the other hand, the computational speed by the MIC on Xeon Phi approached to that by two Xeon CPUs. This indicates that using MIC is attractive choice for the existing SPH codes parallelized by OpenMP to gain the computational acceleration by the many many-core processors.

Keywords: high-performance computing, many core, SPH, Parallel Computing, Performance analysis, Shared memory

Japan Geoscience Union Meeting 2014
(28 April - 02 May 2014 at Pacifico YOKOHAMA, Kanagawa, Japan)

STT60-P02 Room:Poster Time:April 30 18:15-19:30

Numerical investigation of efficient parallelization of large scale quasi-dynamic earthquake generation cycle simulation

HYODO, Mamoru[1*] ; ANDO, Kazuto[1] ; HIYOSHI, Yoshihisa[1] ; HORI, Takane[1]

[1]Japan Agency for Marine-Earth Science and Technology

Recently, Ohtani et al. (2011) applied an efficient compression method of full matrix to the problem of earthquake cycles. Since an original full matrix is approximated by a set of sub-matrices with the hierarchical structure, a compressed full matrix is called as H-matrices. By multiplying H-matrices to a column vector, they found that the required floating-point operation reduces to O(N)-O(NlogN) where N means the number of discretization of the model fault, though the original multiplication operation using the full matrix is $O(N^2)$. Owing to H-matrices, required memory and computation time are largely reduced for the problems of M8 earthquake cycles with $N=10^5$-10^6, and it enables us to execute capacity computing consisting of many earthquake scenarios using massively parallel computers like the K computer. However, for more realistic simulation with multi-scale earthquakes and their interactions, we must use 100 times larger N at least, and capability computing with massively parallel CPUs will be indispensable.

Following Ohtani et al. (2011), we have implemented MPI parallelization of earthquake cycle simulation with H-matrices. First, we applied a 1D division in the row direction to H-matrices. Then, each MPI process took charge of a divided row band region of H-matrices. Since the original H-matrices have a hierarchical structure consisting of many sub-matrices with large variation in size, it is difficult to divide all sub-matrices into MPI processes without overlapping through the 1D row division. Hence, we arrowed the overlapping sub-matrix to be calculated in both adjacent MPI processes for the simplification of parallelization. Then, through the simulation with $N=3\times10^5$, we confirmed a gradual speed-up with the increase of MPI processes up to about 100. However, further increases of MPI processes caused stagnation of speed-up, because the overlapping operation that is not reduced by the increase of MPI processes became dominant.

Accordingly, for more large-scale simulation with many MPI processes, it is necessary to reconsider the parallelization. At first, based on the current 1D division code, we limit the division number in the row direction so as not to increase the ratio of operations with respect to overlapping sub-matrices to the total operations. Then, each row region is divided into further small sub-regions in the column direction, thus we will apply the 2D division of H-matrices. In dividing a particular row region into further sub-regions, we introduce a reference size for the division, B (Block size). The column directional division of H-matrices requires data transfers between sub-matrices. Moreover, depending on the value of B, we also need data transfer inside the large sub-matrix. Though such 2D division increases the data transfers between neighboring MPI processes, the appropriate choices of B and division number in the column direction will realize the equal load balancing among MPI processes in row bands. Accordingly, parallel implementations with 2D division of H-matrices may overcome the overhead due to the increase of data communications.

As tentative results, for $N=1.3\times10^6$ problem, we implemented parallel calculations with both 1D and 2D divisions. Though the 1D parallelization cannot reduce the computational time with the increase of MPI processes, 2D parallelization successfully achieves speed-up with the increase of the number of parallelization. For the same number of MPI processes (1024 processes), the 2D implementation is more than two times faster than that of 1D.

In the presentation, we will show the more detail of our parallelization algorithm and its dependencies on the values of N, B, and division numbers.

Acknowledgement: Part of the results is obtained by using the K computer at the RIKEN Advanced Institute for Computational Science (Proposal number hp120278). We thank the Fujitsu tuning team for helping us to develop the parallelization of simulation codes.

Keywords: earthquake cycle, capability computing, parallel computing, H-matrices

Japan Geoscience Union Meeting 2014
(28 April - 02 May 2014 at Pacifico YOKOHAMA, Kanagawa, Japan)

SCG08-01 Room:311 Time:April 29 09:15-09:30

The Van, Turkey Earthquake of October 2011: Seismicity, Mechanism and its Aftershocks

KALAFAT, Dogan[1*]

[1]Bogazici University Kandilli Observatory and ERI Cengelkoy, Istanbul Turkey

On 23 October 2011, a strong earthquake (Mw=7.1) occurred east of Van Lake. The earthquake destroyed damage along the Van Fault Zone. Generally, it is caused significant damage in the city of Van with Ercis town, as well as in many villages. The epicenter of the main shock was located in Tabanli Village between Van city and Ercis town. Shortly afterwards the November 9, 2011 earthquake (Mw=5.6) occurred southeastern part of Van Lake, Edremit town area. The main shock and second shocks caused significant damage and deaths of 644 people.

After the main shock 11 important earthquakes ($5.0 \leq M \leq 6.0$) were occurred in the region which has hypo-central distances of 8-38 km. from the main shock location. The main shock triggered mass movement, spreading, and local liquefaction. The important earthquakes and the aftershocks distribution showed that the E-W and NE-SW oriented fault segments caused the earthquake activities. The distribution of the aftershocks supported the presence a rupture of approximately 70 ∓ 10km. Aftershocks occurred within an area of approximately 2300 km^2.

Fault mechanism solution has supported 23 October 2011Van Earthquake was a reverse fault with a northward dipping fault plane. The fault plane solutions of about 225 important earthquakes ($M \geq 4.0$) were calculated using MT inversion solution technique by this study.

In addition, the stress tensor analysis was completed using the focal mechanism solutions. The stress tensor values of the region were calculated using the azimuth and plunge pairs of P and T axes for 225 earthquakes. The maximum principal stress (P-compressional) of the main shock is aligned in an N-S (NNW/SSE) direction and the tensional axis (T-dilatation) is aligned in an E-W (ENE-WSW) direction. The results of the focal mechanism and stress analysis solutions show that earthquakes have occurred on the reverse faulting and the seismic activity has been continuing under the compressional regime in the region. The Van earthquake activity initiated and caused an increase in seismic activity of the region. This may be explained by the triggering of small faults by the Van Earthquake. The Van earthquake is a good example of compressional deformation and the activity of blind reverse faulting.

This study was supported by Bogazici University Research Projects Commission under SRP/BAP project No. 6671.

Keywords: Van Lake, aftershocks distribution, focal mechanism, stress analysis, reverse faulting

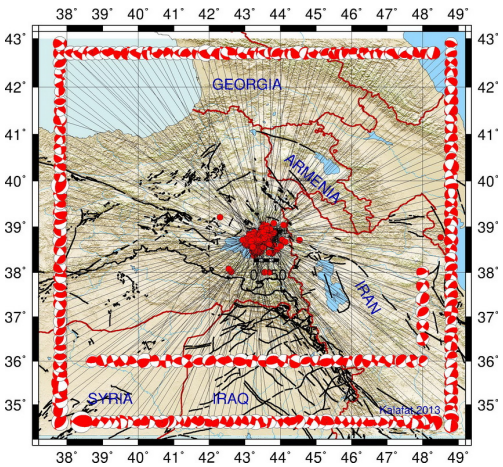

Japan Geoscience Union Meeting 2014
(28 April - 02 May 2014 at Pacifico YOKOHAMA, Kanagawa, Japan)

SCG08-02 Room:311 Time:April 29 09:30-09:45

Microstructural observation of quartz and K-feldspar in quartzo-feldspathic granulite in Sri Lanka

ATHURUPANA, Bhathiya madhura bandara[1*] ; FUKUDA, Jun-ichi[1] ; MUTO, Jun[1] ; NAGAHAMA, Hiroyuki[1]

[1]Department of Earth Science, Tohoku University, Japan

Sri Lankan basement has been considered as high grade terrains which have suffered poly phase deformation and also upper amphibolite to granulite facies metamorphism during Pan-African amalgamation. In order to illuminate the rheological properties of felsic granulite in deep crustal level associated with high grade metamorphism, microstructural and petrographic observations were conducted.

A quartzofeldspathic gneiss sample (Quartz$\sim$40%, K-feldspar$\sim$55% and plagioclase $<$5%) contains highly elongated ribbon quartz which demarcate lineation, in K-feldspar matrix. The sample was collected from the hinge zone of kilometer scale large upright cuspate antiform between two large synforms named Dumbara and Huluganga in Sri Lanka.The lineation as maximum elongation direction is N35^{0}W/horizontal. Thin sections were made parallel and perpendicular to the lineation for petrographic and microstructural observations. Based on energy dispersive X-ray spectroscopic (EDS) measurement, most of K-feldspars in the matrix are sanidine [$(K_{0.59}Na_{0.41})AlSi_3O_8$]composition. Plagioclase is albite (An 0.1) composition and occurs in clusters and exsolution lamellas in K-feldspar. The grain size of sanidine is from $\sim$50 μm to 2 mm. Large sanidine porphyroclasts are partly recrystallized and show core and mantle structures. Grain boundaries of sanidine are sub polygonal to amoeboid shapes with increasing grain size, while plagioclase grains in clusters show perfect polygonal boundaries with grain size ranging from 50 to 200 μm. Around the plagioclase clusters, scapolite reaction corona exists with crosscutting elongated ribbon quartz. Sericite presents in the same region as very low temperature alteration of plagioclase and scapolite. Most importantly ribbon quartz grains are boudinaged in K-feldspar matrix. Any sign of undulatory extinction or dynamic recrystallization is absent in both boudinaged and large ribbon quartz. Measured average axial ratio of ribbon quartz grains is 21:7:1 with respect to X, Y and Z directions.

The crystallographic orientations of both quartz and sanidine were measured by electron backscattered diffraction (EBSD) method, including large ribbon quartz and boudinaged quartz and also matrix sanidine. The lattice preferred orientation (LPO) patterns of sanidine manifest (010)$<$001$>$as a dominant slip system with a minor activation of (010)$<$100$>$slip system. The quartz LPO indicates the activations of prism$<$a$>$and rhomb$<$a$>$slip systems.

According to the presence of K-feldspar as sanidine and their slip systems, we can point out that the sample has prevailed high grade conditions ($\sim$550-800^{0}C and $\sim$0.4-0.8 GPa) during deformation [e.g. Menegon et al. 2008]. Scapolitization which occurs at granulite facies could be indicative of peak metamorphism. Also, reaction coronas of scapolite crosscutting ribbon quartz can be interpreted as strong deformation prior to the peak metamorphism. Exsolution of K-feldspar indicates the post dated cooling relative to the strong deformation and the peak metamorphism.

Reference:
Menegon, L., Pennacchioni G., Spiess R., 2008. Dissolution-precipitation creep of K-feldspar in mid-crustal granite mylonites. Journal of Structural Geology 30(5): 565-579

Keywords: Microstructures, Quartz, K-feldspar, Quartz micro boudins

Japan Geoscience Union Meeting 2014
(28 April - 02 May 2014 at Pacifico YOKOHAMA, Kanagawa, Japan)

SCG08-03 Room:311 Time:April 29 09:45-10:00

Multiple events of metamorphism in lenses of eclogite within marbles of Maykhan Tsakhir Formation, Lake Zone, Mongolia

JAVKHLAN, Otgonkhuu[1*] ; TAKASU, Akira[1] ; BAT-ULZII, Dash[2] ; KABIR, Md fazle[1]

[1]Department of Geoscience, Shimane University, Japan, [2]School of Geology and Petroleum, Mongolian University of Science and Technology, Mongolia

The eclogite-bearing Alag Khadny metamorphic complex in the Lake Zone, SW Mongolia located in the central part of the Central Asian Orogenic Belt, consist mainly of orthogneisses which interleaving with marbles including lenses of garnet-chloritoid schists of Maykhan Tsakhir Formation. Eclogites have two modes of occurrence, i.e. lenses and boudins *eclogite-1* in orthogneisses and *eclogite-2* in marbles. Thermocalc calculations for the peak eclogite facies metamorphism for *eclogite-1* with the assemblage of Grt + Omp + Brs ± Ph ± Ep yielded 570-630 ℃ and 22-25 kbar (Javkhlan et al., 2013a). In contrast, pressure conditions of the garnet-chloritoid schists (10-11 kbar) are distinctly lower than those of the eclogite-1, whereas temperatures (560-590 ℃) are similar (Javkhlan et al., 2013b).

Eclogite-2 in marbles consists of small grains of garnet (<0.1 mm) and omphacite with minor amounts of amphibole, epidote, paragonite, plagioclase, chlorite, calcite, biotite, quartz, titanite and rutile. The matrix of *eclogite-2* shows a pseudomorpous texture, where small grains of garnet crowd cemented by titanite forming isomorphic round shape. Some of cores of garnet grain contain relics of garnet (X_{Ca}=0.32-0.42; X_{Mg}=0.06-0.08) indicating previous mineral were larger porphyroblastic garnet. In addition, small grains of omphacite forming rectangular prismatic nature surrounded by garnet grains.

Garnet grains have compositionally zoning with core (X_{Ca}=0.08-0.20; X_{Mg}=0.10-0.16), mantle (X_{Ca}=0.24-0.39; X_{Mg}=0.08-0.17), rim (X_{Ca}=0.22-0.26; X_{Mg}=0.18-0.23) and outer-rim (X_{Ca}=0.20-0.22; X_{Mg}=0.12-0.18). Few omphacites preserved their core (X_{Jd}=0.27-0.31; Fe_2O_3=1.34-2.22 wt%) whereas most of grains have compositional heterogeneity with X_{Jd} from 0.34 to 0.48 (Fe_2O_3=0.04-2.31) and locally with rims of higher Fe_2O_3 (3.79 wt%)-bearing omphacite (X_{Jd}=0.32). Omphacites partially replaced by symplecites of Pl (An=15-17), amphibole (Ed, Act, Mg-hbl) and Ep. Three types of amphibole are distinguished by their texture, amphibole (Amp1) [zoned with Act (X_{Mg}=0.79-0.81) core, Brs (X_{Mg}=0.54-0.69) mantle and rims with Ts, Mg-Trm and Prg in compositions] coexisting with Grt and Omp, poikiloblastic barroisitic amphibole (Amp2) (X_{Mg}=0.65-0.75) containing eclogitic minerals of Grt and Omp with their symplectitic assemblage and finally actinolitic amphiboles (Amp3) partially replacing Omp and Grt.

Based on the textures we distinguished two metamorphic events, i.e. eclogite facies metamorphism and poikiloblastic barroisitic amphibibole metamorphism. The peak eclogite facies metamorphism characterized by assemblages of Grt (mantle) + Omp + Amp1 (Brs) + Ep + Pg + Rt. Thermocalc calculation yielded 487 ± 46 ℃ and 19.7 ± 2.1 kbar (sigfit=1.80). Thermocalc calculation of Grt (rim) + Omp (rim) + Amp1 (Mg-Trm) + Ep + Pl yielded 666 ± 45 ℃ and 13.7 ± 1.6 kbar (sigfit = 2.11) suggesting a decompression stage after the eclogitic metamorphism. The poikiloblastic barroisitic Amp2 shows decreasing Si (7.01-6.69 pfu) and increasing NaB (0.61-0.70 pfu) from core to rim, suggesting that the Amp2 grew after the peak eclogite facies metamorphism, and probably during the second prograde metamorphic event. Approximate P-T conditions of the poikiloblastic barroisitic Amp2 are estimated as 5-7 kbar at c. 450 ℃.

$^{40}Ar/^{39}Ar$ muscovite ages for eclogites (543 ± 3.9 Ma) in marbles (probably eclogite-2) and the garnet-chloritoid schists (537 ± 2.7 Ma) were determined (Stipska et al. 2010). K-Ar ages for eclogite-1 [603 ± 15 Ma, 602 ± 15 Ma (Amp) and 612 ± 15 Ma (Ph)] within orthogneisses have been obtained (Javkhlan et al., 2014). These ages are interpreted as the exhumation ages for the eclogites (-1 and -2) and the garnet-chloritoid schists.

The peak temperature conditions of eclogite-2 considerably lower than eclogite-1 whereas the pressure conditions are similar. The peak P-T conditions garnet-chloritoid schists are correlated with the poikiloblastic Amp2 metamorphism of the eclogite-2.

Keywords: eclogite-2, pseudomorphous texture, garnet-chloritoid schits, Maykhan Tsakhir Formation, Lake Zone, SW Mongolia

Japan Geoscience Union Meeting 2014
(28 April - 02 May 2014 at Pacifico YOKOHAMA, Kanagawa, Japan)

SCG08-04 Room:311 Time:April 29 10:00-10:20

Multiple exhumation episodes recorded in orogenic garnet peridotites from the Bohemian Massif (Czech Republic)

NAEMURA, Kosuke[1*] ; SVOJTKA, Martin[2] ; ACKERMAN, Lukas[2] ; SHIMIZU, Ichiko[1] ; HIRAJIMA, Takao[3]

[1]Department of Earth and Planetary Science, Graduate School of Science, The University of Tokyo, [2]Geologicky ustav Akademie, Czech Republic, [3]Department of Geology & Mineralogy, Faculty of Science, Kyoto University

Presence of garnet peridotites in *HP/UHP* metamorphic terranes is taken as evidence for interaction between crust and mantle during orogeny. In order to constrain the timing of interaction, *P-T* paths for both peridotites and crustal rocks have been constrained, which demonstrated that there are significant gaps between peak pressure of peridotites and host continental crust. In this contribution, we will show an evidence for multiple exhumations recorded by clinopyroxene (*Cpx*) megacryst discovered in the garnet peridotite from the Bohemian Massif, and will constrain the timing of crust-mantle interaction in the light of the new data.

The Gföhl Unit experienced the highest metamorphic grade in the Moldanubian zone of the Bohemian Massif, and it mainly consists of quartz-feldspathic garnet-kyanite granulite with peak condition at 2.2-2.3 GPa and 1000 ℃ (Vrana et al., 2013, *J. Geosci.* **58**, 347-378), although Kotková et al. (2011, *Geology* **39**, 667-670) recently found diamond and coesite from the Saxony-type granulite. Gföhl granulite occurs as tens km-sized isolated blocks and contains garnet peridotites whose peak conditions were estimated as 2-6 GPa and 850-1350 ℃ (Medaris et al., 2005, *Lithos* **82**, 1-23). We studied *P-T* path for the garnet peridotite at Lom pod Libínem quarry in the Prachatice granulite massif in the south Bohemia. Lom pod Libínem (*LPL*) peridotite generally displays granoblastic texture consisting of mm-sized (0.1-5.0 mm in diameter) garnet, pyroxenes, olivine, and most garnet grains are transformed to kelyphite and are replaced by phlogopite. *LPL* peridotite includes a lot of cm-size Cpx megacrysts. Among them, the largest megacryst (3×5 cm) shows a strong chemical zoning consisting of three zones (Fig. 1), namely, core, mantle and rim: (1) the " pale-green core " is poor in Ca-Tschermak (CaTs.˜6 mol.%) and rich in Enstatite (En.˜9 mol.%) (components after Simakov, 2008, *Lithos* **106**, 125-136) and includes phlogopite and orthopyroxene, (2) the " mantle " is lower in CaTs. (4-5 mol.%) and En. (4 mol.%), and includes hornblende, chlorite, apatite, titanite, andradite, olivine, and celsian, and (3) the " rim ", rich in CaTs. (7-9 mol.%) and En. (9 mol.%), includes olivine, phlgopite, and hornblende, respectively. The mm-size Cpx has identical composition to the megacryst-rim, and (4) the smaller Cpx is richer in CaTs. (12 mol.%) and poorer in En. (7 mol.%). Four mineral stages can be identified: **Stage 1** is defined by megacryst-core coexisting with phlogopite, orthopyroxene. Assuming the co-existence with garnet, the equilibrium condition was estimated at ˜4 GPa and 1000 ℃ by use of the single Cpx geothermobarometer (Nimis & Taylor, 2000, *Contrib. Mineral. Petrol.* **139**, 541-554), **Stage 2** is defined by the " mantle " coexisting with hornblende, chlorite, orthopyroxene, and andradite, which were equilibrated at ˜700 ℃, $P<2.5$ GPa. **Stage 3** is defined by the core of mm-size pyroxenes, garnet and olivine that were equilibrated at ˜3.0 GPa and 1000 ℃ in the garnet lherzolite facies. **Stage 4** is defined by the matrix spinel lherzolite assemblage equilibrated at T˜800 ℃ at 1-2 GPa.

We envisaged the following juxtaposition mechanism: *LPL* peridotite originally came from the upper mantle (4 GPa) that exhumed to the depth of <2.5 GPa and was partially transformed to chlroite peridotite. Assuming that *LPL* peridotite was entrained in the crust at Stage 2, peridotite and host continental crust could have shared the Variscan *UHP* metamorphism at 3 GPa (Stage 3), followed by final exhumation. Although the peak *P-T* condition of Stage 3 is still higher than that of country granulite (<2.3 GPa), this could reflect different degree of retrogression during the final exhumation. Our study suggests some orogenic peridotites were exotically derived from the *UHP* mantle (>4 GPa), where continental crust have not subducted more than 3 GPa. This will give an another solution to the observed pressure gaps between orogenic peridotites and host continental crust.

Keywords: orogenic peridotite, UHP metamorphism, crust-mantle interaction, Bohemian Massif, multiple exhumations

SCG08-04 Room:311 Time:April 29 10:00-10:20

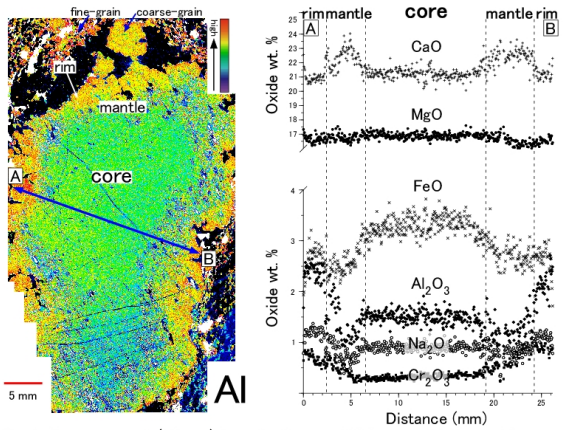

Fig. 1. Cpx megacryst (*Al map*) from the Lom pod Libinem peridotite and its compositions along the line.

Japan Geoscience Union Meeting 2014
(28 April - 02 May 2014 at Pacifico YOKOHAMA, Kanagawa, Japan)

SCG08-05 Room:311 Time:April 29 10:20-10:45

Modelling of the Phase Relations in High- and Ultrahigh-pressure Metabasic Rocks

WEI, Chunjing[1*]

[1]School of Earth and Space Sciences, Peking University

Pseudosections calculated with THERMOCALC predict that for glaucophane- lawsonite eclogite facies conditions (500-600 ℃ and 18-28 kbar), MORB compositions in the NCKMnFMASHO system will contain glaucophane, garnet, omphacite, lawsonite, phengite and quartz, with chlorite at lower temperature and talc at higher temperature. In these assemblages, the pyrope contents (Xpy) in garnet is mostly controlled by variations in temperature, grossular content (Xgr) is strongly controlled by pressure, and the silica content (Si-) in phengite increases linearly with pressure. As the P-T conditions for these given isopleths are only subtly affected by common variations in bulk-rock compositions, the P-T pseudosections potentially present a robust geothermobarometric method for natural glaucophane-bearing eclogites. The maximum Xpy content may define the temperature peak (Tmax) and the minimum Xgr content constrains the pressure peak (Pmax) conditions. An isothermal decompression of these lawsonite-bearing assemblages would result in epidote- bearing assemblages through dehydration reactions such as lawsonite + omphacite = glaucophane + epidote + H2O, releasing a large amount of bound fluid. Thus, most natural HP epidote eclogites may have experienced a metamorphic stage of lawsonite stability.

Under low-T UHP conditions (>28 kb, 550-650 ℃), basic rocks are predicted to contain garnet, omphacite, lawsonite, phengite, coesite and talc. In this assemblage, the Xpy contents steadily increase as temperature rises and the Si-in phengite increases linearly with pressure. However, the Xgr content is very sensitive as pressure changes, showing slowly decrease as pressure rises. The peak P-T conditions for low-T UHP eclogites can be determined using the isopleths of maximum Xpy and Si-in phengite in P-T pseudosections. An isothermal decompression of these low-T UHP eclogites at temperature i.e. 600 ℃ would result in disappearance of lawsonite and talc in the peak stage, but appearance of glaucophane, epidote and kyanite, forming the mineral assemblages involving garnet + omphacite + glaucophane + epidote ? kyanite + quartz/coesite + phengite commonly observed. Moreover, garnet in the low-T UHP eclogites is characteristic of growth zoning with its rims containing lower Xgr and higher Xpy contents.

Under Medium-T UHP conditions (>28 kb and >650 ℃), basic rocks are predicted commonly to contain garnet + omphacite + lawsonite + phengite + coesite. In this assemblage, the Xpy in garnet mostly depends on bulk compositions, whereas the Xgr in garnet and the Si-contents in phengite regularly increase, respectively, as temperature and as pressure rise, and thus, can provide robust thermobarometric constraints. Decompression of the eclogites with lawsonite in the peak stage is inferred to be dominated by lawsonite dehydration, resulting in increase in the mode of anhydrous minerals, or further eclogitization, and formation of epidote porphyroblasts and kyanite-bearing quartz veins in eclogite. As lawsonite dehydration can facilitate evolution of assemblages under fluid-present conditions, the UHP eclogites with lawsonite are hard to memorize their real peak P-T conditions.

Keywords: HP-UHP eclogites, pseudosection, geothermobarometer, basic rock

Japan Geoscience Union Meeting 2014
(28 April - 02 May 2014 at Pacifico YOKOHAMA, Kanagawa, Japan)

SCG08-06 Room:311 Time:April 29 11:00-11:15

DEHYDRATED FLUID AND SEISMIC DEFORMATION IN DEEP SUBDUCTION ZONE ?constraints from lawsonite eclogite and olivine-opx sp

OKAMOTO, Kazuaki[1*]

[1]Saitama University, [2]Joint Graduate school, Tokyo Gakugei University

Introduction: It has been considered that there is a correlation between the double seismic zone and metamorphic dehydration reaction in deep slab. The location of the upper limits of the upper seismic plane correspond to metamorphic facies boundary where H2O contents change in subducting crust; nu-merous earthquakes from 60 to 110 km depths in the lawsonite-blueschist facies, many earthquakes in the lower crust of the slab from 110 to 150 km depths in the lawsonite-amphibole eclogite facies and few earthquakes in the lawsonite eclogite facies. It was considered that the dry eclogite is distributed in the area where there is few earthquake [1] . However, ultrahigh pressure experiments and thermodynamic calculation are both demonstrating that the lawsonite eclogite is stable [2] in the area. In order to unravel relation between dehydration and seismic defor-mation, we have investigated dehydration process of natural metamorphic rocks recording very cold geo-thermal history in the crust and lithosphere in the slab.

Lawsonite eclogite (Alpine Corsica): Alpine Corsica is the best representative field area exhibit-ing lawsonite eclogite and blueschist as a coherent high pressure, low temperature metamorphic belt. Ophiolite sequence (oceanic plate structure) is also well-preserved, and the pillow structure is clearly recognized in the lawsonite eclogite. Recent petro-logical researches have revealed that both blueschist (rims of the pillow) and lawsonite eclogite (core of the pillow) are stable in the same pressure and tem-perature condition [3] because chemical variation including water content creates both law-sonite-amphibole eclogite and lawsonite eclogite in different portion of suducted crust. We carefully observed microtexture of the lawsonite eclogite and blueschist and have found that omphacite vein and lawsonite vein in mylonitized blueschist matrix.

Olivine-opx spinifex in serpentinite (Cerro del Almirez, Nevado complex): Metamorphic olivine after antigorite has been de-scribed in Italian Alps and also from the Mt. Shiraga, Japan. However, the olivine was formed with talc and fluid by antigorite breakdown reaction in pressures lower than 1.5 GPa. Spinifex olivine with opx in the Cerro del Almirez, is the product at pres-sures (P >1.5 GPa) relevant to the lower seismic plane beneath Northeast Japan. In Cerro del Almirez, olivine-opx rocks underlie an-tigorite schist by a contact[4]. In the olivine-opx rocks, the blade-like, elongated olivine and opx were grown, representing spinifex texture. It clearly indi-cates the presence of large amount of water facilitate crystallization of elongated olivine with opx.

Discussion and conclusion: In the lawsonite eclo-gite in the Alpine Corsica, blueschist and lawsonite coexist together reflect-ing chemical difference in pillowed structure or lithology. Omphacite and law-sonite veins are observed along the shear band in mylonitized blueschist. It suggests that decomposi-tion of glaucophene causesd hydro-fracturing and precipitate omphacite and lawsonite vein. Garnet was grown statically close to the vein.

Olivine-opx spinifex in the serpentinite, Cerro del Almirez, were probably recrystallized in the presen-ce of large amount of water. The estimated dehydra-tion reaction has a negative P-T slope at pressures higher than 1.5 GPa. The reaction is volume reduc-ing reaction and the olivine-opx spinifex texture was formed under volume reducing reaction.

References: [1] S. Kita et al., Geophy. Res. Lett., 33, doi:10.1029/2006GL028239. (2006). [2] K. Okamoto et al., Geochem-istry, 46 205-215 (2013). [3] A. Vitale Brova-rone et al., J. Met. Geol., 29, 583-600, (2011). [4] V. Trommsdorff et al., CMP, 132, 139-148 (1998).

Keywords: double-seismic zone, upper seismic plane, Lawsonite eclogite, lower seismic plane, olivine-opx spinifex, dehydrated vein

Japan Geoscience Union Meeting 2014
(28 April - 02 May 2014 at Pacifico YOKOHAMA, Kanagawa, Japan)

SCG08-07 Room:311 Time:April 29 11:15-11:30

Ultrahigh-pressure eclogites: paleo-environment indicators

UR REHMAN, Hafiz[1*]

[1]Department of Earth and Environmental Sciences, Graduate School of Science and Engineering, Kagoshim

Ultrahigh-pressure (UHP) eclogites generally form by the metamorphism of mafic lithologies (gabbros or basalts) at depths greater than 90 km (minimum stability field of coesite) indicating P-T conditions of >2.7 GPa and 600-800 ∘C. At such conditions most minerals reequilibrate their chemical elements (e.g. major and trace and even isotopes) and new minerals crystallize or grow at the expense of other minerals formed during the magmatic crystallization. Some chemical elements, considered as relatively less mobile or immobile (e.g. Sm, Nd, Lu, Hf), are widely used for the extraction of past records the rocks have evolved through. Besides those elements, oxygen, the major component of silicates and oxides, impart important information related to protolith formation of rocks and their metamorphism. In general, most basaltic rocks show a narrow range of δ^{18}O (ca. +5.7 $\pm$ 0.3 ‰ relative VSMOW) and values for altered basalts vary from 0 to +12 ‰.

In this paper, I discuss the origin of low or negative δ^{18}O values; recently we found in the Himalayan UHP eclogites of Kaghan Valley and explain the mechanism how these low values were acquired. These eclogites are formed during Eocene by the India-Asia collision and their protoliths were the Panjal Trap basalts which were emplaced in Permian when Indian Plate was part of Gondwana. The δ^{18}O values are as low as — 2.25 ‰ in the fresh parts of eclogites and increase towards more positive in the retrogressed or amphibolitized parts. The unusually low δ^{18}O values in eclogites are interpreted to have resulted from the hydrothermal alteration of the protoliths by meteoric water interaction when Greater India was still at southern high latitudes (>65 degrees S) during the Permian indicating glacial paleo-environment. These low δ^{18}O values were frozen-in in the protolith rocks and did not change during subduction-related UHP metamorphism. However retrogressive process, due to infiltration of ^{18}O-rich fluids during exhumation, shifted these values towards more positive range.

Keywords: Ultrahigh-pressure eclogites, Himalaya, Oxygen isotope, Paleo-environment

Japan Geoscience Union Meeting 2014
(28 April - 02 May 2014 at Pacifico YOKOHAMA, Kanagawa, Japan)

SCG08-08 Room:311 Time:April 29 11:30-11:45

Role of the second continent

KAWAI, Kenji[1*] ; ICHIKAWA, Hiroki[2] ; YAMAMOTO, Shinji[4] ; TSUCHIYA, Taku[2] ; MARUYAMA, Shigenori[3]

[1]Department of Earth and Planetary Sciences, Tokyo Institute of Technology, [2]Geodynamics Research Center, Ehime University, [3]Earth-Life Science Institute, Tokyo Institute of Technology, [4]Department of Earth and Astronomy, Graduate School of Arts and Sciences, The University of Tokyo

It has been thought that granitic crust, having been formed on the surface, must have survived through the Earth's evolution because of its buoyancy. Recent geological studies have suggested that a significant amount of crustal material has been lost from the surface due to delamination, continental collision, and subduction at oceanic?continental convergent margins (von Huene and Scholl 1991; Yamamoto et al. 2009; Ichikawa et al. 2013a). If so, then the subducted crustal materials are expected to be trapped in the mid-mantle due to the density difference from peridotitic materials induced by the phase transition from coesite to stishovite (Kawai et al. 2013). In order to study the effect of the subducted granitic materials floating around the mantle transition zone, we conducted two-dimensional numerical experiments of mantle convection incorporating a continental drift with a heat source placed around the bottom of the mantle transition zone. We found that the addition of heat source in the mantle transition zone considerably enhances the onset of upwelling plumes in the upper mantle, which further reduces the time scale of continental drift. The heat source also causes massive mechanical mixing, especially in the upper mantle. The results suggest that the heat source floating around the mantle transition zone can be a possible candidate for inducing the supercontinent cycle (Ichikawa et al. 2013b).

Keywords: Second continent, Wilson's cycle, Granite, Tectonic erosion

Japan Geoscience Union Meeting 2014
(28 April - 02 May 2014 at Pacifico YOKOHAMA, Kanagawa, Japan)

SCG08-09 Room:311 Time:April 29 11:45-12:10

Where had the primordial continent gone?

MARUYAMA, Shigenori[1*] ; KAWAI, Kenji[2] ; TSUCHIYA, Taku[3]

[1]ELSI Tokyo Institute of Technology, [2]Tokyo Institute of Technology, [3]Ehime University

There are no Hadean rocks on the Earth ' s surface. This indicates (1) there was no continents on the primordial Earth, or (2) continents were present in the Hadean but lost afterwards. It is well-known that Moon surface was covered by anorthositic continental crust with KREEP basalts with ca. 50-60km thickness. Those rocks are the fractionated final residues of magma ocean after the giant impact at 4.56Ga.

The Earth must have been completely melted if giant impact was correct, but due to 6 times larger gravity, the thickness of anorthositic continents must be 21 km. Moreover, during the consolidation of magma ocean, bulk of anorthositic blobs could be transformed into (1) zoisite+kyanite+quartz, (2) grossular+kyanite+quartz, (3) grossular +kyanite+coesite, (4) grossular +kyanite+stishovite, in 300km depth.

Absence of TTG rocks in the Hadean and nearly absent in early Archean less than 5% among the surface of present continents must be caused by extensive tectonic erosion by subducting slabs which are present even today at trench. Therefore, it is wrong to believe that low-density granite must have accumulated on the surface once formed on the surface of the Earth.

Density calculation of anorthosite, MORB, harzburgite, and pyrolite using first principles calculation showed that anorthosite was heavier if it convected at depth in mantle transition zone. If it turns into lower mantle, it becomes to be heaviest among those as mentioned above, suggesting the stability field at D " layer on the bottom of mantle which is right above CMB.

However, it depends on the geothermal gradient on which phase change of Al2O3 occurs to determine whether or not the heaviest among all rocks at CMB. Depending on cooling the CMB, meta-anorthosite could have been buoyant particularly after the mantle overturn at 2.7-2.6Ga.

Before the overturn, if the basal magma ocean was present in the Archean, the lost primordial continents musty have been melted into basal magma ocean where anorthosite-KREEP basalts mixed with FeO-enriched primordial basal magma ocean. The possible bulk chemistry can be estimated, though qualitatively; it must be super-enriched in anorthositic component. It can be expressed in Ca-Pv, Mg-Pv, Ferro-periclase as major components.

When, mantle overturn occurred at 2.7-2.6Ga, low-temperature materials of upper mantle must have cooled down the basal magma ocean to consolidate to crystalize Ca-Pv rock, bi-mineral Ca-Pv + Mg-Pv rock, and the tri-mineral Ca-Pv + Mg-Pv + FM periclase rock. According to the formation of these rocks, those three rocks would have been behaved differently, although depends on not only density but also mass.

Assuming the enough volume of Ca-Pv rocks, those rocks may be floating in mid-depth of lower mantle.

Japan Geoscience Union Meeting 2014
(28 April - 02 May 2014 at Pacifico YOKOHAMA, Kanagawa, Japan)

SCG08-10 Room:311 Time:April 29 12:10-12:30

Subduction origin for UHP chromitite from the Nishisongi metamorphic rocks, Western Kyushu, Japan

NISHIYAMA, Tadao[1*] ; MORIBE, Yousuke[1] ; ISHIMARU, Satoko[1] ; ARAI, Shoji[2] ; MORI, Yasushi[3] ; SHIGENO, Miki[3]

[1]Graduate School of Science and Technology, Kumamoto University, [2]Department of Earth Sciences, Kanazawa University, [3]Kitakyushu Museum of Natural History and Human History

Ultrahigh-pressure (UHP) chromitite from the Luobsa Ophiolite in non UHP terrane has been an enigima because of its peculiar occurrence. We newly found a UHP chromitite from serpentinite in the Nishisonogi metamorphic rocks (NMR), a member of the Nagasaki Metamorphic Rocks, in Western Kyushu, following our finding[1] of it from the Higo Metamorphic Rocks (HMR), Central Kyushu. The UHP chromitite from NMR documents well a fluid -chromite interaction, showing partial graphitization of microdiamond. Such a fluid - chromite interaction is not observed in HMR chromitite. The NMR are high P/ T (epidote-glaucophane schist subfacies) metamorphic rocks of Cretaceous in age, mainly consisting of pelitic and psammitic schists intercalating with minor basic schists[2]. The peak metamorphic condition of the crystalline schists is estimated as 1.4 GPa and 520 ^{o}C by an assemblage of garnet with inclusions of chloritoid and omphacite, glaucophane, paragonite, and phengite in a garnet galucophanite[3]. Serpentinite and serpentinite melanges occur as elongated bodies or lenses concordant with schistosity trending N-S of the country schists[1]. Jadeitite and omphacitite occur as tectonic blocks in the serpentinite melange, showing the peak condition of 1.5 GPa and 500 ^{o}C by coexistence of jadeite and quartz[4]. Microdiamond - bearing chromitite was found from serpentinite in a melange at Ooseto Town, Saikai City. Chromitite occurs as a thin layer several cm thick and meter-size long in a serpentinite with numerous magnesite (or ankerite) veins. The layer is strongly deformed to show a schlieren - like structure. The serpentinite consists of fine-grained antigorite with no relics of olivine and pyroxenes. The chromitite consists of an aggregate of rounded and fractured chromite crystals with small amounts of talc and magnesite as a matrix and veins. Microdiamond occurs as aligned crystals in narrow zones ranging from a few μm to several tens of μm in chromite. Chromite is zoned, consisting of Mg-rich core $(Mg_{0.33}Fe^{2+}{}_{0.65}Mn_{0.03})(Cr_{0.84}Al_{0.12}Fe^{3+}{}_{0.04})_2O_4$ and Fe-rich rim $(Mg_{0.06}Fe^{2+}{}_{0.89}Zn_{0.02}Mn_{0.03})(Cr_{0.85}Al_{0.12}Fe^{3+}{}_{0.04})_2O_4$. The microdiamond - bearing zones are conspicuously richer in Fe_2O_3 [$(Mg_{0.03}Fe^{2+}{}_{0.94}Mn_{0.04}Zn_{0.01})(Cr_{0.67}Ti_{0.01}Fe^{3+}{}_{0.31}0)_2O_4$], observed as a brighter zone in a BSE image, than other part of chromite in the same grain. The network -like distribution of the zones clearly indicates fluid infiltration associated with the following exchange reaction of trivalent cations between chromite and the fluid: Cr^{3+} + Al^{3+}(in chromite) = Fe^{3+}(in fluid)

Microdiamond occurs either as polyhedral or as platy crystals, 1 to several μm across. Identification of diamond was carried out with an energy dispersive X-ray spectroscopy (EDS) analysis (carbon peak) and Raman spectroscopy with a He-Ne laser. We observed a broad Raman peak at 1331 cm^{-1}, which is comparable to the peak (1332 cm^{-1}) characteristic of diamond. Graphite peak at about 1600 cm^{-1} is also observed, showing partial graphitization of microdiamond. These lines of evidence shows that the fluid infiltration may have occurred after inclusion of microdiamond.

It is quite astonishing that microdiamond is preserved in such a completely serpentinized ultramafic rock. Chromite can be a good container of microdiamond to prevent graphitization during geologically long duration of exhumation and serpentinization. Our finding suggests the subduction origin of UHP chromitite from NMR rather than mantle migration origin[5] in the case of the Luobusa Ophiolite.

References

1. Nishiyama. T., Shiosaki, D., Eguchi, H., and Yoshiasa, A. JpGU Meeting, S-MP46 (2014);2. Nishiyama, T. Mem. Geol. Soc. Japan 33, 237-257 (1989) ;3. Moribe, Y. unpublished Mc thesis, Kumamoto University (2014);4. Shigeno, M., Mori, Y., Shimada, K., and Nishiyama, T. Eur. J. Mineral., 24, 289-311 (2012);5. Arai, S. J. Mineral. Petrol. Sci., 105, 280-285 (2010)

Keywords: microdiamond, UHP chromitite, subduction zone, Nishisonogi metamorphic rocks, ultrahigh-pressure metamorphic rocks

Japan Geoscience Union Meeting 2014
(28 April - 02 May 2014 at Pacifico YOKOHAMA, Kanagawa, Japan)

SCG08-P01 Room:Poster Time:April 29 18:15-19:30

Melt-Peridotite Reactions In The Upper Mantle: Geochemistry Of Peridotite And Pyroxenite From The Beni-Bousera Massif

CHETOUANI, Kamar[1*] ; AMRI, Isma[1] ; TARGUISTI, Kamal[1]

[1]departement de geologie, Faculte des sciences de Tetouan. Maroc

The Beni-Bousera massif contains ubiquitous pyroxenites of various types, organized into conspicuous layers ranging from 0.5 to 100 cm in thickness, hosted by peridotites. Integrated field features, petrographic observations, and geochemical analyses from 92 samples (whole rock major and trace elements data: 55 samples, microprobe data for minerals: 48 samples, and mineral trace elements data: 30 samples) from pyroxenites provide information to classify the rock types into four different groups typified as: (1) garnet pyroxenites, (2) spinel-garnet websterites, (3) spinel websterites, and (4) spinel chromium websterites. Type 1 rocks, occurring at the base of the massif, are considered as the most primitive type, garnet pyroxenites layers represent the vestiges of an old veined subcontinental lithosphere. They generally indicate temperatures <970∘C (based on two-pyroxene thermometry) and a low to very low Mg# (<76%). Trace element contents show enrichment in heavy and middle rare earth elements but strong depletion in light rare earth elements (LREE). Paradoxically, the host peridotites show enrichment in LREE, which give new insights into their genesis history. Based on our field observations and geochemical results, we suggest that garnet-pyroxenite layers metasomatised the host peridotite successively by the partial melting as a consequence of subsequent heating phase(s) of the lithosphere. The magmatic event that led to the diversity and zoning of mafic layers was caused by melting of the base of thinned subcontinental lithosphere by upwelling asthenosphere, followed by infiltration of asthenospheric melts. The different groups of mafic layers record several stages of this event.

Keywords: Geochemistry, Beni Bousera, Pyroxenite, Peridotites

Japan Geoscience Union Meeting 2014
(28 April - 02 May 2014 at Pacifico YOKOHAMA, Kanagawa, Japan)

SCG08-P02 Room:Poster Time:April 29 18:15-19:30

Petrology and geochemistry of the ultramafic metamorphic rocks from the Masora domain, east-central Madagascar

ICHIKI, Takashi[1*] ; ISHIKAWA, Masahiro[1] ; KIMURA, Jun-ichi[2] ; SENDA, Ryoko[2]

[1]Yokohama National University, [2]JAMSTEC IFREE

Madagascar is located within the interior of the Neoproterozoic East African Orogen (Jacobs and Thomas, 2004) that marks the join between East and West Gondwana. In the east Madagascar, the Paleo-Mesoarchean Antongil-Masora domains are exposed (Collins, 2006; Tucker et al., 2011). In this study we report the petrological and whole rock and REE geochemical characteristics of the ultramafic metamorphic rocks exposed within the Masora domain and we discuss their origin and tectonic settings. The Masora domain is mainly composed of the Paleo-Mesoarchean felsic metamorphic rocks with subordinate amounts of metasedimentary rocks (e.g. Randriamananjara, 2008; Tucker et al., 2011). This domain was intruded by Neoproterozoic granitoids and mafic-ultramafic rocks (e.g. Smith et al., 2008).

The ultramafic metamorphic rocks are exposed in the north and south Masora domain. Three types of ultramafic metamorphic rocks are identified in the north: peridotite, pyroxenite and hornblendite. The peridotite is mainly composed of olivine and anthophyllite with subordinate amounts of serpentine, magnesite and magnetite. The pyroxenite is mainly composed of clinopyroxene and hornblende with subordinate amount of magnesite and magnetite. The hornblendite is mainly composed of hornblende with subordinate amount of actinolite and magnetite. Some of the hornblendite has spinel. An ultramafic metamorphic rock body occurs as a lens within metasedimentary rock in the south. This metasedimentary rock is kyanite+biotite+muscovite schist. The mineral assemblage of the ultramafic lens differs between core and rim. It is mainly composed of olivine, tremolite, actinolite and chlorite with subordinate amounts of serpentine, magnetite and altered minerals in the core. The rim is mainly composed of tremolite, actinolite and chlorite with subordinate amount of magnetite and ilmenite.

The ultramafic metamorphic rocks except for the hornblendites have SiO_2 = 42.7-51.7 wt.%, Al_2O_3 = 1.5-7.5 wt.%, MgO = 19.8-35.4 wt.%, and CaO = 3.5-16.5 wt.%. They have high Mg# (molar ratio of $Mg^{2+}/(Mg^{2+} + Fe^{2+})$) of 0.76-0.83. On the basis of bulk rock CIPW normative Ol-Cpx-Opx composition, the ultramafic metamorphic rocks except for the hornblendites plot in the field of the lherzolite, olivine websterite and websterite (Streckeisen, 1976). Compared with the geochemical characteristics of abyssal peridotites (Niu, 2004), the ultramafic metamorphic rocks shows lower MgO, higher TiO_2 and CaO than those in the abyssal peridotites. On the MgO-Ni diagram (Pfeifer, 1990 in Katzir et al., 1999) one of the samples plot in the typical abyssal lherzolite field whereas the others plot in higher-Ni (orogenic) field. Chondrite normalized REE patterns of the ultramafic metamorphic rocks show flat HREE with variable LREE patterns. One of the samples shows enriched LREE pattern and the others show depleted LREE patterns. The depleted LREE samples have flat HREE with about twice amount of chondritic HREE abundances. This is typical characteristic of an orogenic lherzolite such as Ronda massif in the southern Spain and Lanzo lherzolites in the Italian Alps (Bodinier and Godard, 2003). Enriched LREE pattern is also a typical characteristic of pyroxenites occurring in orogenic peridotites (Bodinier and Godard, 2003). On the basis of petrological and geochemical characteristics, their protoliths are orogenic lherzolite, websterite and pyroxenite.

Keywords: Gondwana supercontinent, east-central Madagascar, geochemistry, Masora domain, ultramafic metamorphic rocks

Japan Geoscience Union Meeting 2014
(28 April - 02 May 2014 at Pacifico YOKOHAMA, Kanagawa, Japan)

SCG08-P03 Room:Poster Time:April 29 18:15-19:30

Zircon Nano-SIMS U-Pb dating from the country gneiss beside Horoman peridotite, Hokkaido, Japan

SUZUKI, Ryosuke[1] ; OKAMOTO, Kazuaki[1*]

[1]Saitama university, Japan

Hidaka Metamorphic Belt, Hokkaido, Japan includes the youngest granulites and the Horoman peridotite complex in the highest grade zone. Age of the Hidaka gneiss and amphibolite have been determined by various methods (e.g. K-Ar, U-Pb, Rb-Sr and etc). However, the age of Horoman peridotite complex has not been determined yet. Only Yoshikawa et al (1993) reported the cooling age of the complex as 23 Ma based on whole rock Rb-Sr isochron method. This study performed U-Pb dating of zircons from the paragneiss surrounding the Horoman peridotite complex in order to determine the intrusive age of the Horoman peridotite complex from the upper mantle into the lower crustal conditions. The zircons have detrital cores and thin rims (<20 microns). Therefore we used Nano-SIMS because it is possible to focus the secondary beam diameters down to submicrons for the analysis. As a result of this measurement, rim ages of the zircons show that 238U-206Pb age are 7-11Ma (n=7) and detrital core ages show 25.6 Ma, 34-35 Ma, 78 Ma and 150 Ma (n=8). The rim ages are the youngest in Hidaka metamorphic rocks and there is a discrepancy with zircon rim ages (19Ma) from the granulite (Kemp et al. 2007; Usuki et al. 2006). The present rim ages (7-11 Ma) fit well with the tectonic scenario of the collision process of Hokkaido Island proposed by Yamamoto et al. (2010). It is considered that the Horoman peridotite complex was juxtaposed onto the Hidaka metamorphic belt at 7-11Ma by the subducting Pacific plate after the collision between North American and Eurasian plates.

Keywords: Zircon, U-Pb, Nano-SIMS, Horoman peridotite, country gneiss, juxtaposition age

Japan Geoscience Union Meeting 2014
(28 April - 02 May 2014 at Pacifico YOKOHAMA, Kanagawa, Japan)

SCG08-P04 Room:Poster Time:April 29 18:15-19:30

3 types of Ca-Amp found from Nove Dvory UHP eclogites and their origin, Moldanubian Zone of the Bohemian Massif

YASUMOTO, Atsushi[1*] ; HIRAJIMA, Takao[1]

[1]Department of Geology and Mineralogy, Graduate School of Science, Kyoto University

The upper-stability limit of Ca/Na amphibole (Amp) in meta-mafic rocks are considered to be around 2-3 GPa in pressures (Schmidt & Poli, 1998). Thus, most Ca-Amp in (ultra)-high pressure metamorphic rocks have been considered as retrograde products. The peak metamorphic conditions of Nové Dvory eclogites are estimated to be 4.5-4.9 GPa and 1050-1150^{o}C. However, some Ca-Amp inclusions in Grt are likely to be interpreted as prograde relicts survived the ultra-high pressure metamorphism. This paper reports the mode of occurrence and the chemical compositions of Ca-Amp and the coexisting minerals in Nové Dvory eclogite, and discusses when Ca-Amp crystalized. Investigated two eclogite samples, ND0107 and ND120, collected from the same outcrop, are composed mainly of garnet (Grt) and Omphacite (Omp) with minor amounts of apatite (Apt) and rutile (Rt) at the UHP stage, and suffered hydration reactions, represented by Ca-Amp and plagioclase (Pl) formation, with various degree during the exhumation stage.

Ca-Amp in studied eclogite can be classified into 3 types based on their modes of occurrence; Type 1 Amp occurs in sporadic euhedral shaped polyphase mineral aggregates (PMAs) in Grt along with Omp, Rt, and Apt. Type 1 Amp is identified only from ND0107, and is classified as pargasite (Prg) or kaersutite (Krs). Omp inclusions associated with Type 1 Amp are homogeneous and have high X_{Jd} of 40-45, suggesting that the associated Omp did not suffer retrogressive reactions. On ACF diagram, Type 1 Amp is plotted between the associated Omp and host Grt. It suggests that Type 1 Amp could be a relict of the following reaction, Amp=Omp+Grt+W, during the subduction stage. Type 2 Amp is identified as a member of PMAs in Grt along with spinel (Spl) and diopside (Di). Those PMAs with Type 2 Amp show unidiomorphic shapes and straight alignment in Grt. They are classified as Prg or magnesio-hastingsite (Mg-Hs). Type 3 Amp is a member of the symplectite along with Omp. Di, Spl, and Pl developed at Grt rim. These facts suggest that Type 2/3 Amp were formed during the exhumation stage reacted with infiltrated fluids to the host eclogite.

The different stage origins of Type1/2 Amp mentioned above is supported by F and Cl contents in them. Type 1 Prg contains 0.21-0.30 wt% of F, but is almost free from Cl (<0.01wt%). Type 2 Prg contains 0.43-1.17wt% of Cl. Type 2 Prg in ND0107 with Type 1 Amp contains 0.05-0.29wt% of F. On the other hand, Type 2 Prg in ND120, which is free from Type 1 Amp, is scarce in F (<0.05wt%). Type 3 Amp is free from Cl.

It is generally considered that Ca-Amp enriched in $(Na+K)^{A}$, ^{IV}Al, and $^{VI}Fe^{2+}$ can incorporate more Cl (Makino, 2000). However, Type 1/2 Amp have a similar major element compositions such as $(Na+K)^{A}$=0.79-0.95 pfu (for O+OH+F+Cl=24 basis), ^{IV}Al=2.01-2.45 pfu, and $^{VI}Fe^{2+}$=0.56-0.97 pfu, in spite of a scarce but significant difference in Cl content among them. Cl-free Type 3 Amp contains similar amount of $(Na+K)^{A}$ (0.75-0.96 pfu) and ^{IV}Al (1.95-2.38 pfu), but less in $^{VI}Fe^{2+}$ content (<0.47pfu) compared with those of Type 1/2 Amp.

As a present stage conclusion, Type 1 Amp crystalized under F-bearing and Cl-poor environment during the prograde stage, and Type2/3 Amp crystalized during the retrograde stage along with supply of Cl from outside of the rock. F identified in Type 2 Amp in ND0107 with F-bearing Type 1 Amp could be supplied from the Type 1 Amp through the retrogressive reactions.

Keywords: Eclogite, Amphibole, Ultra-high pressure metamorphism, Bohemian Massif, Fluorine, Chlorine

Japan Geoscience Union Meeting 2014
(28 April - 02 May 2014 at Pacifico YOKOHAMA, Kanagawa, Japan)

SCG09-01 Room:315 Time:April 28 12:00-12:15

carbon and helium in faulted-seismogenic areas

SANO, Yuji[1*]

[1]Atmosphere and Ocean Research Institute, University of Tokyo

Carbon and helium have been discharging for a long time from the Earth's mantle to the atmosphere through volcanic and hydrothermal activity. In addition they are derived from faulted-seismogenic areas. It is obvious that volcanic fluxes are originated in magma source even though they may be partly contaminated by crustal material. In contrast, it is difficult to estimate how deep they are derived in non-volcanic and tectonically active regions. Irwin & Barnes [1] reported that CO_2-rich springs occur worldwide along major zones of seismicity. They further suggested that much of the CO_2 is derived from the mantle and that other important sources are the metamorphism of marine carbonate-bearing sedimentary rocks and the degradation of organic material. Carbon isotopes may provide information of the origin. When the delta13C value of spring gas in faulted-seismogenic area shows -6permil, it is explained by either mantle carbon or a mixing of marine carbonate (0permil) and sedimentary organic matter (-30permil). Thus it is difficult to estimate the origin of carbon. If the data are combined with helium isotopes, however, we can deconvolve the mantle contribution quantitatively [2]. There are several evidences of mantle carbon and helium degassing from active fault. Kennedy et al. [3] suggested the mantle helium flux in the San Andreas fault system located at boundary between the Pacific and North American plate. The bottom may extend the upper mantle. Significant CO_2 discharges were observed at the same time. A part of CO_2, up to 3.3% may be derived from the mantle [4]. Similar discharges have been observed in the North and East Anatolian fault zones [5,6]. These are examples of steady-state degassing from active fault. Non steady-state, catastrophic degassing of carbon and helium were reported in the 1995 Kobe earthquake, even though they are originated in shallow crust [7,8]. On the other hand, increase of helium isotopes in bottom seawater in the trench region after the 2011 Tohoku-oki earthquake suggested substantial input of mantle helium [9]. There may be a fluid flow induced by the earthquake, which would carry helium and methane from the mantle wedge to the trench through the entire plate boundary.

Reference [1] Irwin & Barnes, 1980. *JGR* **85**, 3115-3121. [2] Sano & Marty, 1995. *Chem Geol* **119**, 265-274. [3] Kennedy et al., 1997. *Science* **278**, 1278-1281. [4] Kulongoski et al., 2013. *Chem Geol* **339**, 92-102 [5] de Leeuw et al., 2010. *App Geochem* **25**, 524-539. [6] Italiano et al., 2013. *Chem Geol* **339**, 103-114. [7] Sano et al., 1998. *Chem Geol* **150**, 171-179. [8] Famin et al., 2008. *EPSL* **265**, 487-497. [9] Sano et al., 2014. *Nature Commun* **5**, 3084.

Keywords: Helium, Carbon, Origin, Flux, Fault

Japan Geoscience Union Meeting 2014
(28 April - 02 May 2014 at Pacifico YOKOHAMA, Kanagawa, Japan)

SCG09-02 Room:315 Time:April 28 12:15-12:30

Volatiles in kimberlites:an indicator of possible deep mantle origin

KANEOKA, Ichiro[1*]

[1]Earthquake Research Institute, University of Tokyo

Kimberlites are well known to bear diamonds and their magmas are regarded to have been derived from a depth of at least more than 150km. They are found only in old continental areas and the exposed areas at the surface are quite limited to a diameter of less than 2km in most cases. Although their distributions are quite sparse, they have quite unique characteristics in their chemical and isotope compositions.

In spite of ultrabasic properties, they bear abundant volatiles such as H2O, CO2, halogens, sulfur and they also contain relatively abundant LIL elements. On the other hand, they show more abundant concentrations of Os and Ir compared to those of other kinds of lavas such as MORBs (mid-oceanic ridge basalts) and OIBs (oceanic island basalts). Their magmas are generally regarded to have been produced in relatively less oxidized environments compared to MORBs, OIBs and IABs (island arc basalts). Hence, it is a quite significant issue to clarify the origin of volatiles in kimberlite magmas, which might be related to the chemical circumstances of deep mantle.

Based on Sr-Nd isotope systematics, kimberlites are classified in two groups (Smith, 1983). In the 87Sr/86Sr-143Nd/144Nd diagram, Group I kimberlites are relatively concentrated in an area which is close to the Bulk Earth value. In contrast, Group II kimberlites are located in an area of typical enriched character and widely scattered. Most kimberlies are regarded to belong to Group I. Since Group II kimberlite magmas show the effect of recycled materials with an enriched character, volatiles in Group II kimberlites might have been also affected from them.

On the other hand, distribution of data of Group I kimberlites on the Sr-Nd isotope diagram implies that the magma source of Group I kimberlites is less fractionated from the assumed Bulk Earth material than those of MORBs. Further, Ne isotopes in kimberlites from Russia indicates that its magma source is similar to those of OIBs isotopically and different from those of MORBs (Sumino et al. 2006). Noble gas signatures of OIBs indicate the occurrence primordial components in the OIB source (e.g.Kaneoka, 2008). The magma source of MORBs has been generally assigned to be located in the upper mantle, while those of OIBs are located at a deeper part than those of MORBs. These signatures suggest that volatiles in Group I kimberlites would probably reflect those of the deep mantle. In effect, some diamonds are regarded to have been derived from the upper part of the lower mantle. Thus, at least Group I kimberlites might contain volatiles including carbon of the lower mantle origin which has not always been recycled.

Further, kimberlite magmas are conjectured to have been erupted directly from a magma reservoir located below the thick continental lithosphere within a few hours so that captured diamonds might not be decomposed during the rise of a kimberlite magma. Hence, it is inferred that chemical contamination for a kimberlite magma might be less compred to that for a OIB magma which would take much longer time to be transported to the surface from a magam reservoir. If so, Group I kimberlites might keep more primary information on the chemical state of the lower mantle compared to OIBs.

References

Kaneoka, I. (2008) Geochem. J.42, 3-20.
Smith, C.B. (1983)Nature304,51-54.
Sumino, H. et al.(2006) Geophys. Res. Lett.L16318.

Keywords: volatiles, kimberlite, deep mantle, OIBs, isotopes, diamond

Japan Geoscience Union Meeting 2014
(28 April - 02 May 2014 at Pacifico YOKOHAMA, Kanagawa, Japan)

SCG09-03 Room:315 Time:April 28 12:30-12:45

Carbon isotope systematics during carbonated silicate melting under upper mantle conditions

MADHUSOODHAN, Satish-kumar[1*] ; MIZUTANI, Shogo[2] ; YOSHINO, Takashi[3]

[1]Niigata University, [2]Shizuoka University, [3]Okayama University

Carbon isotope fractionation between graphite and carbonated silicate melt was determined at 5 GPa and in the temperature range between 1400 and 1900 ^{o}C. High pressure experiments were carried out in the carbon-saturated model harzbergite system (Enstatite-Magnesite-Olivine-Graphite), where carbonated silicate melt and graphite were the two stable carbon-bearing phases in the run products. Carbonated silicate melting resulted in an isotopic fractionation between graphite and carbon in the silicate melt, where the carbon in the melt is ^{13}C enriched than co-existing graphite (Mizutani et al., 2014). ^{13}C enrichment in carbonate melt were further confirmed in experiments where redox melting between olivine and graphite produced carbonate melt as well as carbonate reduction experiments to form graphite.

According to the results of carbon isotope fractionation obtained in this study between graphite and carbonated silicate melt, heavier carbon will be selectively partitioned to the melt and graphite will be lighter than the melt in the order of 1 to 2 permil. If locally oxidative or reductive domains are present or melt extraction and a Rayleigh fractionation process dominate in the upper mantle, then carbonate silicate melt-graphite carbon isotope partitioning at upper mantle conditions will have larger effect on carbon isotopic composition. It is possible that carbonate melt will progressively enrich in carbon isotopes, which corresponds to the primary igneous carbonatite values (-5 to -8 permil) and even rare carbonatites having the more enriched ^{13}C (-2 to -5 permil) may be explainable in term of the existence of more reductive environment. Conversely, the graphite coexisting with such melts will have delta13C values corresponding to main mantle carbon reservoir. Recent experiments have shown that carbonate melts can be a medium for the efficient crystallization of diamonds in Earths mantle. Therefore, redox reaction at lower upper mantle is likely to yield the range of carbon isotope variation of mantle derived diamond. Moreover, carbonated mantle melting according to redox melting at upwelling mantle can be an alternative explanation for the formation of ^{12}C enriched diamonds in the deep mantle

Mizutani, S., Satish-Kumar, M. and Yoshino, T., (2014) Experimental determination of carbon isotope fractionation between graphite and carbonated silicate melt under upper mantle conditions, Earth and Planetary Science Letters (in press).

Keywords: carbonated mantle melting, carbon isotopes, graphite, fractionation

Japan Geoscience Union Meeting 2014
(28 April - 02 May 2014 at Pacifico YOKOHAMA, Kanagawa, Japan)

SCG09-04 Room:315 Time:April 28 14:15-14:33

3He/4He distributions near the Tancheng-Lujiang faults zones, at Liaoning, NE China

ZHENG, Guodong[1*] ; XU, Sheng[1] ; NAKAI, Shun'ichi[2] ; WAKITA, Hiroshi[3] ; WANG, Xianbin[1]

[1]Institute of Geology and Geophysics, Chinese Academy of Sciences, [2]Earthquake Research Institute, The University of Tokyo, [3]Faculty of Science, The University of Tokyo

Chemical and isotopic compositions have been measured for natural gases near the NNE trending Tancheng-Lujiang Fault Zones (TLFZ) at Liaoning Province, NE China, including hydrocarbon-rich natural gases from Liaohe basin (121oE-124oE, 40.5oN-42oN) and nitrogen-rich geothermal gases from the eastern Liaoning Mountains. Observed 3He/4He ratios show two orders of magnitude variability from 0.04 RA to 3.5 RA where RA is atmospheric 3He/4He ratio 1.4x10-6. The following geochemical observations are noted: (1) at Liaohe basin and the adjacent geothermal fields, 3He/4He ratios show positive correlations with He contents; (2) in Liaohe basin, the 3He/4He ratios are largely variable (0.04-3.5 RA), generally high in the eastern depress and low in the western depress; (3) in the eastern Liaoning mountains, geothermal 3He/4He ratios are generally low (0.2-0.7 RA) but have closed relationship with distribution of seismic activity and heat flow; and (4) overall there is a spatial distribution pattern that 3He/4He ratios gradually decrease from the TLFZ eastwards and westwards. Such a 3He/4He distribution feature shows strong evidence that the TLFZ played an important role on mantle-derived helium transform from mantle upwards and groundwater circulation along the deep major faults.

Keywords: helium, fault, china, isotopes

Japan Geoscience Union Meeting 2014
(28 April - 02 May 2014 at Pacifico YOKOHAMA, Kanagawa, Japan)

SCG09-05 Room:315 Time:April 28 14:33-14:51

Heterogenous carbon reservoir in sublithospheric mantle: variations of carbon isotopic composition in diamonds from Sao-

ZEDGENIZOV, Dmitriy[1*] ; KAGI, Hiroyuki[2] ; SHATSKY, Vladislav[3] ; RAGOZIN, Alexey[2]

[1]V.S.Sobolev Institute of Geology and Mineralogy, Novosibirsk, Russia, [2]University of Tokyo, Tokyo, Japan,, [3]A.V.Vinogradov Institute of Geochemistry, Irkutsk, Russia

The Juina kimberlite field in Brazil is a well-known source of alluvial sublithospheric diamonds as identified by their properties and mineral inclusions. Taking advantage of the rather common occurrence of superdeep mineral inclusion assemblages in diamonds from Sao-Luis river alluvial deposits (Juina, Brazil), we carried out a study of variations of C isotope in diamonds from this locality.

Diamonds from Sao-Luis are characterized by rough morphologies and have complex growth histories. Episodic growth, plastic deformation and breakages are visible in these crystals and most diamonds have experienced a final episode of resorption before exhumation. Total nitrogen content in studied diamonds reach 1200 ppm and more. Only several studied diamonds are nitrogen-free (type IIa). Some diamonds consist of domains that are also nitrogen-free but other parts may contain nitrogen. Many diamonds have very low (>10 ppm) but still detectable nitrogen impurity. Extremely high nitrogen aggregation state and overall platelet degradation detected in the majority diamonds from Sao-Luis are suggested they have stored at considerably higher temperatures that are typical for continental lithosphere.

Syngenetic inclusions in 59 diamonds from Sao-Luis were represented by phases of superdeep paragenesis as it was described previously. The dominated inclusions are majoritic garnets, ferropericlases, CaSi- and CaSiTi-perovskites, MgSi-perovskites, TAPP, SiO_2 phases, kyanites, AlSi-phases, olivines and Fe-sulfides. Rare inclusions of clinopiroxenes, KFsp (K-hollandite?), CF, NAL, grossular, native iron, magnesite, $CaCO_3$+$CaMgSi_2O_6$ (composite inclusions) have been found in separate diamonds. All majoritic garnets we found are of metabasic affinity and in some cases associated with omphacitic clinopyroxenes.

The studied diamonds from Sao-Luis display wide variations of carbon isotopic compositions (δ^{13}C) ranging from 2.7 to -25.3 ‰. The diamonds with inclusions of ferropericlase have very narrow range of δ^{13}C values from -2.1 to -7.7 ‰, which are closely similar to the normal mantle values [Cartigny, 2005; Stachel et al., 2009]. From this observation, it may be suggested that their formation may proceed from isotopically homogeneous mantle reservoir that do not support the model of large primordial isotopic variability of carbon isotopes in primitive Earth's mantle with a predicted pyrolite composition. Diamonds with inclusions of majoritic garnet and CaSi- and CaSiTi-perovskites in many cases show marked differences from the expected normal mantle values of δ^{13}C values. Low δ^{13}C values (-10 to -25 ‰) have been observed exclusively in a series of superdeep diamonds with calcic-majorite garnets, Ca-silicates, aluminous silicates and SiO_2 from Sao-Luis.

The δ^{13}C measurements in core to rim traverses within some individual crystals varied substantially, indicating multi-stage growth histories. The variations in δ^{13}C within individual diamonds may be attributed to either different source of carbon or fractionation effect during diamond growth. No correlation of carbon isotope composition and nitrogen content has been found in individual diamonds. It therefore appears that the cores and rims of the Sao-Luis diamonds precipitated from different fluids/melts with variable N/C ratios and/or under different growth conditions. The highly negative δ^{13}C values in the core (-20 to -25 ‰) potentially represent organic matter in sediments or altered basalts, and the lower δ^{13}C values may represent mixing trends towards normal mantle compositions [Schulze et al., 2004; Harte, 2011]. In this study, we have also described a series of diamonds which show opposite trend of change carbon source from primordial mantle to subducted/crustal (either biotic or abiotic carbon).

Keywords: carbon, diamond, sublithospheric mantle, subduction

Japan Geoscience Union Meeting 2014
(28 April - 02 May 2014 at Pacifico YOKOHAMA, Kanagawa, Japan)

SCG09-06 Room:315 Time:April 28 14:51-15:06

Chemical composition of nano-inclusions in supe-deep diamonds and implications to the growth condition

KAGI, Hiroyuki[1*] ; ISHIBASHI, Hidemi[2] ; OHFUJI, Hiroaki[3] ; ZEDGENIZOV, Dmitry[4] ; SHATSKY, Vladislav[4] ; RAGOZIN, Alex[4]

[1]Graduate School of Science, University of Tokyo, [2]Graduate School of Science, Shizuoka University, [3]Geodynamic Research Center, Ehime University, [4]Russian Academy of Science

Superdeep diamonds originating from the mantle transition zone and the lower mantle were found from alluvial deposits of Sao-Luis river (Juina, Brazil). We investigated carbon isotopic variations and chemical compositions of nano-inclusions in the superdeep diamonds which can give a clue for the growth condition.

We found syngenetic inclusions of superdeep paragenesis from 59 diamond samples from Sao-Luis. The dominant inclusions in diamonds from studied here are CaSi-perovskite and AlSi-phases. MgSi- and CaTi-perovskites, ferropericlase, native iron, coesite and zircon have also been found. Our SIMS analysis showed the wide variations of carbon isotopic compositions ranging from 2.7 to -25.3 ‰ in δ^{13}C. The details on the carbon isotopic analysis will be reported by Zefgenizov et al. in this session.

Some samples contained microinclusions and FTIR analyses showed that water and carbonates were not major components of these tiny inclusions. To identify the microinclusions, TEM observations were carried out on a foil of carbonado (0.1 micron thick) made from a polished diamond specimen after Au-coating. The foil was fabricated with a Ga ion beam using a focused ion beam (FIB) instrument (JEOL JEM-9310FIB). The foil was observed with a TEM (JEOL JEM-2010) under an accelerating voltage of 200 kV. We found that the microinclusions were euhedral inclusions of several tens nanometers in size. The TEM observations revealed that the nano-inclusions have a negative cystal shape suggesting the syngenetic origin directly related to the diamond growth. In this study, chemical composition of the nano-inclusions were conducted by synchrotron X-ray fluorescence analysis using X-ray micro-beam as an incident light at BL-4A, Photon Factory, KEK. The obtained results clarified that the nano-inclusions contain S, Cr, Mn, Fe, Co, Ni, Cu Zn, and so on. The present study suggests that the growth media of the superdeep diamonds are composed of sufilde melt.

Keywords: diamond, nano inclusion, X-ray fluorescence analysis, super deep diamonds

Japan Geoscience Union Meeting 2014
(28 April - 02 May 2014 at Pacifico YOKOHAMA, Kanagawa, Japan)

SCG09-07 Room:315 Time:April 28 15:06-15:21

High-pressure melting experiments on magma genesis in Hawaiian plume: effect of volatiles

GAO, Shan[1*] ; TAKAHASHI, Eiichi[1] ; IMAI, Takamasa[1] ; SUZUKI, Toshihiro[1]

[1]Earth and Planetary Sciences, Tokyo Institute of Technology

Introduction: Compared with OIB, Hawaiian tholeiitic basalt is thought to be relatively drier (about 0.5 wt.% H2O content; Muenow, 1979). In front of the plume core, overlying mantle is metasomatized by hydrous partial melts derived from the Hawaiian plume. Downstream from the plume core, lavas tap a depleted source region similar to enriched Pacific mid-ocean ridge basalt (Dixon & Clague, 2001). Magma genesis model has been proposed by some authors (Hauri, 1996; Takahashi & Nakajima; 2002; Sobolev et al., 2007) that magma produced near the axis of the plume head may be mixtures of two types of melts 1) basaltic andesite melt formed by melting of eclogite and 2) picritic melts formed by the reactive melting of eclogite and peridotite. A series of high temperature high pressure experiments were conducted to explore the genesis of tholeiite magma from Hawaiian plume and investigate the role of volatiles in magma genesis.

Experiments: A series of experiments were conducted under dry and slightly hydrous conditions at 2.85GPa for 1, 3 to 9 hours and from 1460 to 1520C with a piston cylinder by making basalt peridotite sandwich which using MgO-rich CRB72-180 (Takahashi et al 1998) and a fertile peridotite KLB-1 (Takahashi 1986) as starting materials.

Results: Three factors that might affect melting progress and chemical reaction among minerals – temperature, duration and water content –were examined, respectively.

1) Temperature: (1460˜1520C and every 20C as an interval.)

Basalt went partial molten at 1460C and completely molten when temperature went above 1500C. Orthopyroxene reaction rim formed on the border area due to the reaction between high Si-rich melt and olivine in the peridotite matrix. The opx film becomes more visible and thicker with the increasing of temperature. Partial melting degree of peridotite is also related to the increasing of temperature but the change is not very sensitive when 20C as an interval. The higher temperature, the more peridotite molten. The area of the peridotite near the opx film has a higher degree of partially melting than areas away from the boundary.

2) Duration: (1, 3 and 9 hours.)

Longer time do accelerate the speed of chemical reaction between basalt and peridotite in this study. Basalt molten completely as the running time longer than 3 hours. The orthopyroxene reaction rim on the boundary between peridotite and basalt becomes thicker. Large clinopyroxene crystals formed on the border (the minerals on the border from melt to peridotite are cpx, opx, garnet) momentarily yet faded away as the chemical reaction went on with time.Partial melting of peridotite is also positively related to duration. When the melt of peridotite is too much and unable to support the weight of basalt and it would got rid of the crack and finally went to the basalt side and mixed with the basalt melt.

3) Water content

Basalt layer melted completely, and large orthopyroxene crystallized in the basalt side. Peridotite layer also melted considerably at the same time than its anhydrous counterparts owing to the reason that the join of water could lower the peridotite liquidus line and finally made it more partial melted than in hydrous condition.

Discussion: Under dry conditions below peridotite solidus, melting is limited in eclogite layers and chemical reactions with ambient peridotite is hindered by opx film. On the other hand, under slightly wet conditions, water could accelerate the melting process of both eclogite and peridotite layer. As a result, melts formed under wet conditions are saturated with oliv+opx whereas those formed under dry conditions could be saturated with only opx. Changing nature of Hawaiian magma during the shield building stage will be discussed in the light of present melting experiments.

Keywords: Hawaiian plume, high-pressure, magma, volatiles

SCG09-07 Room:315 Time:April 28 15:06-15:21

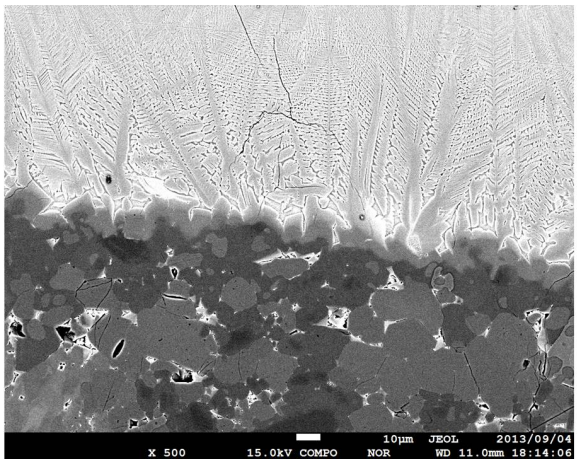

Japan Geoscience Union Meeting 2014
(28 April - 02 May 2014 at Pacifico YOKOHAMA, Kanagawa, Japan)

SCG09-08 Room:315 Time:April 28 15:21-15:36

Partitioning of carbon between metallic- and silicate-liquids in magmaocean of differentiated planetesimals

ASAHARA, Yuki[1*] ; OHTANI, Eiji[1]

[1]Tohoku University

Partitioning behavior of carbon has not been determined well though it is one of the strong candidates for light element in the earth ' s core. We investigated partitioning of carbon with sulfur and oxygen between metallic- and silicate liquids at 6 GPa and 2073 K in carbonaceous chondrite composition (Allende meteorite; CV3). High pressure experiments were conducted with multi-anvil high pressure apparatus. Graphite was used as capsule material. Composition of coexisting metallic- and silicate liquids were measured by electron microprobe with wavelength dispersion type spectrometer except for carbon in silicate liquid. To estimate carbon concentration in silicate liquid, carbon concentration of bulk recovered sample was measured by elemental analyzer. Present result suggests that in oxidized carbonaceous chondrite composition, partitioning coefficient of carbon [$D^{Metallicliquid/Silicateliquid} = C^{Metallicliquid}/C^{Silicateliquid}$; C is concentration of carbon in wt.%] is close to 1, and it increases with increasing the Fe^{metal}/Fe^{oxide} ratio of the bulk carbonaceous chondrite composition.

Japan Geoscience Union Meeting 2014
(28 April - 02 May 2014 at Pacifico YOKOHAMA, Kanagawa, Japan)

SCG09-09 Room:315 Time:April 28 15:36-15:54

Experimental study of Group-I kimberlite: evidences for carbonatite primary melt and implication to mantle plumes

LITASOV, Konstantin[1*] ; SHARYGIN, Igor[2] ; SHATSKIY, Anton[2] ; OHTANI, Eiji[3]

[1]Novosibirsk State University, Novosibirsk, Russia, [2]V.S. Sobolev Institute of Geology and Mineralogy SB RAS, Novosibirsk, Russia, [3]Department of Earth and Planetary Materials Science, Tohoku University, Sendai, Japan

The experiments on the origin of Udachnaya-East kimberlite (UEK) have been performed using a Kawai-type multianvil apparatus at 2-6.5 GPa and 900-1500 ^{o}C. The studied composition represented exceptionally fresh Group-I kimberlite containing (wt.%): SiO_2 = 25.9, TiO_2 = 1.8, Al_2O_3 = 2.8, FeO = 9.0, MgO = 30.1, CaO = 12.7, Na_2O = 3.4, K_2O = 1.3, P_2O_5 = 1.0, Cl = 0.9, CO_2 = 9.9, and H_2O = 0.5. Super-solidus assemblage consists of olivine (Ol), Ca-rich garnet (Gt), Al-spinel (Sp), perovskite (Pv), CaCO3 (calcite or aragonite), and apatite at 4-6.5 GPa with an addition of clinopyroxene at 3-4 GPa and Na-Ca carbonate with molar ratio of (Na+K)/Ca $\sim$ 0.44 at 6.5 GPa and 900 ^{o}C. The apparent solidus was established between 900 and 1000 oC at 6.5 GPa. In the studied P-T range, melt has Ca-carbonatite composition (Ca/(Ca+Mg) = 0.6-0.8) with high alkali and Cl contents (2.8-6.7 wt.% K_2O, 7.3-11.6 wt.% Na_2O, 1.2-3.7 wt.% Cl). The K, Na and Cl contents and Ca/(Ca+Mg) value decrease with temperature. It is argued, that the primary kimberlite melt at depth $>$200 km was essentially carbonatitic ($<$5 wt.% SiO_2), however, evolved toward carbonate-silicate composition (with 15-20 wt.% SiO_2) during ascent. The absence of orthopyroxene among the run products indicates that xenogenic orthopyroxene was preferentially dissolved into kimberlite melt. The obtained subliquidus phase assemblage (Ol + Gt + Sp + Pv) at P-T condition of UEK source region differs from lherzolite lithology of this source. Both petrological observations and experiments indicate that kimberlite magma lost substantial amount of CO_2 at shallow depths.

Our study combined with earlier experiments on carbonate-silicate systems at pressures to 30 GPa implies that liquid phase of thermo-chemical plume generated at the core-mantle boundary is represented by alkali-carbonatite melt. This conclusion has broad geodynamic implication providing insight into fluid regime of mantle melting under hotspots along margins of African large low-shear-wave-velocity province. We conclude that the long term activity of rising hot mantle plume and associated carbonatite melt (i.e. proto-kimberlite melt) causes thermo-mechanical erosion of the subcontinental lithosphere mantle (SCLM) roots and creates hot, oxidized, and deformed metasomatic layer at lower parts of initially depleted SCLM, which corresponds to depths constrained from the sheared Gt-lherzolites. The sheared Gt-lherzolites undoubtedly represent the samples from this layer.

Keywords: mantle, kimberlite, carbonatite, plume, melting

Japan Geoscience Union Meeting 2014
(28 April - 02 May 2014 at Pacifico YOKOHAMA, Kanagawa, Japan)

SCG09-P01 Room:Poster Time:April 28 18:15-19:30

Gas geochemistry and soil CO2 flux in active volcanic areas, China

WEN, Hsinyi[1*] ; YANG, Tsanyao frank[1] ; GUO, Zhengfu[2] ; FU, Chingchou[1] ; CHEN, Aiti[1] ; ZHANG, Maoliang[2]

[1]Department of Geosciences, National Taiwan University, [2]Institute of Geology and Geophysics, Chinese Academy of Sciences

Changbaishan intra-plate volcano and Tengchong hydrothermal area are two of the active volcanic areas in China. In order to better understand current status of magma/hydrothermal activities of the Changbaishan intra-plate volcano and Tengchong hydrothermal area, we have conducted the soil gas survey and bubbling gas sampling from hot springs around the Tianchi crater lake and Rehai geothermal area.

In Changbaishan volcano, the results show that CO_2 is the major component gas for most samples. The maximum value of helium isotopic ratio of 5.8 R_A (where R_A = $^3He/^4He$ in air) implies more than 60% of helium is contributed by mantle component, while carbon isotope values fall in the range of -5.8 to -2.0 ‰ (vs. PDB), indicating magmatic source signatures as well. Nitrogen dominated samples, 18Dawgo, have helium isotopic ratio of 0.7 R_A and carbon isotope value of -11.4 ‰, implying the gas source might be associated with regional crustal components beneath 18Dawgo. The first-time systematic soil CO_2 flux measurements indicate the flux is ca. 22.8 g m^{-2} day^{-1} and 6.8 g m^{-2} day^{-1} at the western and southern flank of Changbaishan, which is at the same level as the background value in the Tatun Volcano Group (24.6 g m^{-2} $day^{-1)}$, implying that Changbaishan may not be as active as TVG.

In Tengchong hydrothermal area, the preliminary results show that CO_2 is the major component gas for most samples. The helium and carbon isotopic ratio fall in the range of 0.5 R_A to 3.5 R_A and -4.7 to -1.6 ‰ (vs. PDB), respectively. We also analyzed the hot springs water. The δD and δ^{18}O values fall in the range from -59.8 to 84.6 ‰ and -6.20 to -12.38 ‰ (vs. SMOW), respectively. Rehai has the highest helium isotopic ratio of 3.5 R_A, which implies ca. 40% of helium is mantle-derived. The δD and δ^{18}O results implied the water in this area was affect by primary magmatic water. Nevertheless, samples from Banglazhang and Shihchiang hydrothermal areas show much lower helium isotopic ratio of 0.8 R_A and 0.5 R_A, respectively. It suggests that the local tectonic setting plays an important role for the gas degassing in this area.

Japan Geoscience Union Meeting 2014
(28 April - 02 May 2014 at Pacifico YOKOHAMA, Kanagawa, Japan)

SCG09-P02 Room:Poster Time:April 28 18:15-19:30

The reaction between $MgCO_3$ and SiO_2 at high pressure and temperature and genesis of ultra-deep diamonds

MAEDA, Fumiya[1*] ; OHTANI, Eiji[1] ; KAMADA, Seiji[1] ; SAKAMAKI, Tatsuya[1] ; TAKAHASHI, Suguru[1] ; TAKAHATA, Akihiro[1] ; OHISHI, Yasuo[2] ; HIRAO, Naohisa[2]

[1]Department of Earth and Planetary Materials Science, Graduate School of Science, Tohoku University, [2]Japan Synchrotron Radiation Research Institute

Carbon, one of the important light elements for the Earth science, is reserved in the deep part of the Earth. The evidence of the deep carbon is found in ultra-deep diamonds or estimations of carbon fluxes between the surface and interior of the Earth. Subducting slabs are considered as an important C-source of the Earth. Following reactions of $MgCO_3$ and SiO2 are potentially important in the slabs descending into the deep mantle:

$MgCO_3$ (magnesite) + SiO_2 → $MgSiO_3$ (perovskite) + CO_2

CO_2 → C (diamond) + O_2

These reactions can play a fundamental role in the deep carbon cycle.

In this work, we investigated the reaction between $MgCO_3$ and SiO_2 up to about 80 GPa and 3000 K using a laser-heated diamond anvil cell combined with in-situ synchrotron X-ray diffraction (XRD) technique and Raman spectroscopy. The starting material is the powered 1:1 (in mole fraction) mixture of natural magnesite (Brazil, Bahia) and reagent α-quartz. 5 wt.% platinum powder was added to the sample mixture in order to absorb laser and estimate the pressure in the sample chamber. NaCl, KCl or SiO_2 glass powder was stuffed into the sample chamber as pressure media. XRD patterns of high P-T samples and recovered samples were acquired at beamline BL10XU of SPring-8. Raman spectroscopy was carried out to high-pressure conditions. Raman spectroscopy was also conducted for the recovered samples.

In the present results made at about 70 GPa, diamond and $MgSiO_3$ perovskite are detected at temperatures greater than 1750 K. The high P-T XRD patterns in the experiments at 50-60 GPa and 2000-3000 K show the appearance of a small amount of $MgSiO_3$ perovskite. Our study demonstrated that formation of diamonds was confirmed in the range of 1300-1500 km depth of the lower mantle in subducting slabs due to the reaction of $MgCO_3$ with SiO_2 and the breakdown of CO_2. This phase relations have a possibility to explain one of the origins of diamonds from the lower mantle.

Japan Geoscience Union Meeting 2014
(28 April - 02 May 2014 at Pacifico YOKOHAMA, Kanagawa, Japan)

SCG10-01 Room:313 Time:May 2 09:00-09:24

Microcracks preceding ruptures: insights gained from laboratory acoustic emission study

LEI, Xinglin[1*]

[1]Geological Survey of Japan, AIST, Japan

Earthquakes in the crust are caused by the rapid shear fracture of a fault. Thus, understanding the source processes of earthquakes relies on the understanding of shear fracturing in rocks. Abundant experimental evidence shows that macroscopic shear fracturing within rocks and other brittle materials does not occur by the growth of a single shear crack in its own plane. Rather, it is preceded by a very complex pervasive evolution of some pre-failure damage. Therefore, studies focusing on both fracture dynamics and pre-failure damage are a subject of interest in seismology. Fracturing dynamics and the pre-failure damage can be inferred from AE statistics as the number of AE events is proportional to the number of growing cracks, and the AE amplitudes are proportional to the length of crack growth increments in the rock. Therefore, the AE technique, which monitors the spatiotemporal distribution of AE events, is applied to the analysis of the micro-cracking activity inside the sample space, and it can be performed under an artificially controlled pressure, which is very important for the simulation of underground conditions.

The fracture of intact rocks as well as rocks containing natural structures (joints, faults, foliations) under constant stress rate loading or creep conditions is generally characterized by typical stages with different underlying physics. Through an integrated analysis of several AE statistics obtained from AE data collected with the high-speed AE waveform recording system, a three-phase pre-failure-damage model has been proposed and further enforced with new data. The primary phase reflects the initial rupture of pre-existing microcrack population in the sample or in the fault zone. Sub-critical growth dominates the secondary phase. The third phases termed nucleation phase corresponds to the initiation and accelerated growth of the ultimate fracture. In earthquake seismology, researchers have a special interest with the nucleation phase since faulting nucleation governs the predictability of earthquakes.

Lithology, density and size distribution of pre-existing cracks, meso-scale and macro-scale heterogeneities all have an overall role in AEs. There are some cases in which some phases are not clear. In general, homogeneous (both fine-grained and coarse-grained) rocks with pre-existing cracks likely show all phases. Heterogeneous or weak rocks such S-C cataclasite normally show a lack of the primary phase. Samples with few pre-existing cracks and samples containing optimally oriented weak structures, likely show an unpredictable fracturing behaviour as well as a lack of primary and secondary phases, in addition the nucleation phase has a small number of AEs.

Rules obtained at the laboratory scale are helpful for understanding natural earthquakes on a significantly larger scale. However, we cannot simply bridge laboratory scale to a scale several orders larger. At every step up from a smaller scale to a larger scale, we encountered something different. The difference could be small for each step but, after many steps, we could see something quite different. Studies on all scales are important. Quantitative investigation of rock fracture using AE techniques is still an interesting field for the future. On one hand, it may shed some light on earthquake seismology. On the other hand, it may provide a fundamental technical background promoting applications including: enhanced geothermal systems (EGS), extraction of shale gas and core bed gas, and CO2 geological storage. The latter of which involves fluids being intensively pumped into the deep Earth under high pressure; injection-induced earthquakes would be a problem that must be well-addressed.

Keywords: Acoustic emission (AE), Microfracture, Pre-failure damage, Fault nucleation

Japan Geoscience Union Meeting 2014
(28 April - 02 May 2014 at Pacifico YOKOHAMA, Kanagawa, Japan)

SCG10-02 Room:313 Time:May 2 09:24-09:39

Radio wave emission in friction or collision of various materials

TAKANO, Tadashi[1*] ; HANAWA, Rikuya[1] ; SAEGUSA, Saegusa[1]

[1]Nihon University

1. Introduction

In fracture of rock, radio wave emission was found experimentally [1]. This phenomenon could be used to detect a rock fracture during an earthquake or a volcanic activity [2] [3]. The cause of the radio wave is expected to be micro-discharges, which are generated by an inhomogeneous potential distribution around micro-cracks [4]. However, the theory of emission is not completely understood yet.

In order to clarify the cause of radio wave emission, we carried out experiments to detect the emission in the cases of friction or collision of various materials. This paper describes the experimental results, and a brief explanation of physical process.

2. Tested systems and experimental results

We tested the following systems using the manufactured measuring system at 1 MHz, 300 MHz, 2.0 GHz, and 18.8 GHz [5].

(1) A lighter using piezoelectricity

This device makes sparkles by knocking a mineral with piezoelectricity. Due to discharges, strong radio wave is emitted, and detected in our measuring system.

(2) A lighter using friction of OL metal

Formerly, this type of a lighter was widely used for igniting cigarettes. The alloy metal of cerium and iron rubs a revolving drum so that sparkles are made changing the friction power to thermal energy. Despite significant sparkles, radio wave could not be detected in this case.

(3) Igniter using a flint stone

A flint stone is struck against iron pyrites so that small flakes of iron are scattered being made hot. The flint stone is mostly chart In Europe, and quartz, sanukite, or obsidian in Japan. Sparkles cannot be made by striking two bulks of flint each other. Radio wave is not emitted in this case.

(4) Striking a steel lump with a steel hammer

Radio wave is emitted in this case. Probably, the kinetic energy is converted not to thermal energy but to the excitation of electrons or atoms so that inhomogeneous potential distribution is realized.

3. Conclusions

In general, sparks are not the origin of radio wave emission. This emission is esteemed a non-thermal phenomenon. An inhomogeneous potential distribution makes micro-discharges that emit radio waves. In some cases, the cause of an inhomogeneous potential distribution makes the sparks.

Further study is needed to clarify the mechanism of the energy transfer to electron excitation.

References

[1] Ken-ichiro Maki, Tadashi Takano, Eriko Soma, Kentaro Ishii, Shingo Yoshida and Masao Nakatani, ”An experimental study of microwave emission from compression failure of rocks” (in Japanese), Jour. of the Seismological Society of Japan, vol.58, no.4, pp.375-384, 2006.

[2] Tadashi Takano, Takashi Maeda and Shingo Yoshida, ”Experiment and Theoretical Study of Earthquake Detection Capability by Means of Microwave Passive Sensors on a Satellite”, IEEE Trans. Geoscience And Remote Sensing, Vol.6, No.1, pp.107-111, 2009.

[3] T. Maeda and T. Takano, ”Discrimination of Local and Faint Changes from Satellite-borne Microwave Radiometer Data”, IEEE Trans. on Geoscience and Remote Sensing, vol 46, issue 9, pp. 2684-2691, 2008.

[4] K. Maki and T. Takano, ”Analysis of the microwave radiation field from the discharge due to an impact destruction”, National Convention of the Institute of Electrical Engineers of Japan (IEEJ), 1-081, p.87, March 2004.

[5] T. Takano, J. Kato, M. Hirashima and K. Saegusa, ”Radio wave emission from 1 MHz to 18 GHz due to rock fracture and the estimation of the emitted energy”, EEIS’12, 978-1-4673-0335-4/12/IEEE, pp.300-303, Cape Town, September 2012.

Keywords: radio wave, friction or collision, various materials, electrical discharge, micro-crack, non-thermal phenomenon

Japan Geoscience Union Meeting 2014
(28 April - 02 May 2014 at Pacifico YOKOHAMA, Kanagawa, Japan)

SCG10-03 Room:313 Time:May 2 09:39-10:03

Seismoelectric phenomena of electrokientic nature associated with the formation of cracks in porous media

REVIL, Andre[1*]

[1]Colorado School of Mines, department of Geophysics

I will describe the physics of the generation of electromagnetic disturbances associated with the formation of cracks in porous media. The mechanism is electrokinetic in nature (i.e., associated with the flow of the pore water with respect to the solid phase of a porous material). I will describe the occurrence of these electromagnetic signals and how they can be inverted jointly with seismic signals to determine the position of the hydromechanical disturbance and its moment tensor. I will also demonstrate that electrical fields of electrokinetic nature are associated with the formation of crack through a set of laboratory experiments (see figure below showing the fluctuation in the electrical potential on the surface of the block and the amount of recorded acoustic emissions). The associated electrical field fluctuations can be remotely monitored and the resulting signals used to localize their causative source. The technique is similar to what is performed in electroencephalography (in the medical world) in which an electrical field (associated with the opening of ionic channels at the synapses between the neurons) can be measured on the scalp of a patient and inverted to localize and monitor brain activity. A laboratory experiment shows how these electrical fields can be recorded at the surface of a cement block during the fracking of the block. The measurements are performed with a research-grade medical electroencephalograph and inverted using the genetic algorithm to localize the causative source of electrical current and therefore localize the evolution of the crack. Two snapshots of electrical signals are used to show how the breakage evolves over time. A second experiment is performed to see if we could localize a pulse water injection from a shallow well in field conditions and in the case of a heterogeneous subsurface.

Keywords: electrokinetic, streaming current, self-potential, moment tensor, source localization, electromagnetic phenomena

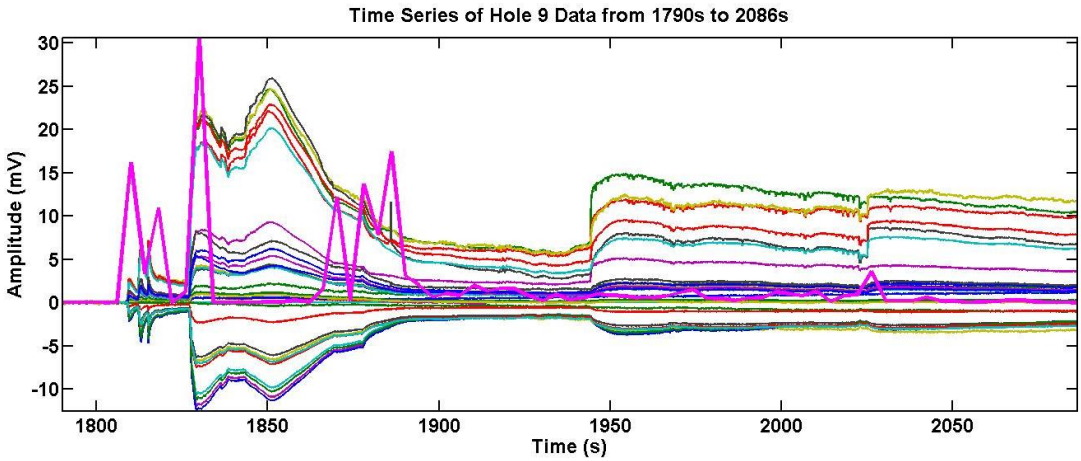

Japan Geoscience Union Meeting 2014
(28 April - 02 May 2014 at Pacifico YOKOHAMA, Kanagawa, Japan)

SCG10-04 Room:313 Time:May 2 10:03-10:18

Waveform analysis of seismo-magnetic signals in Boso, Japan

HAN, Peng[1*] ; HATTORI, Katsumi[1] ; FEBTY, Febriani[1] ; HIROKI, Yamaguchi[1] ; CHIE, Yoshino[1]

[1]Graduate School of Science, Chiba University

To clarify the seismo-magnetic phenomena, it is essential to establish theoretical models to explain how the phenomena come out. A reliable model should coincide with field observations. Thus, the fundamental part is to find out what are the signals associated with earthquakes. Therefore, in this study we have checked detailed waveform of seismo-magnetic signals observed in Boso, Japan. Our preliminary results indicate that there are mainly two kinds of seismo-magnetic signals: one is noise-like signals; the other is transient/quasi-rectangular signals. The former are mainly detected before the 2005 M6.1 Boso earthquake; the latter is observed mainly during slow slip events.

Keywords: ULF seismo-magnetic phenomena, waveform analysis, slow slip events

Japan Geoscience Union Meeting 2014
(28 April - 02 May 2014 at Pacifico YOKOHAMA, Kanagawa, Japan)

SCG10-05 Room:313 Time:May 2 10:18-10:42

Quantitative evidence of the coupling between seismic and electromagnetic signals

HUANG, Qinghua[1*]

[1]Peking University

There are some reports of the coupling between seismic and electromagnetic signals from both the natural earthquakes and the active field experiments. Such coupling effect may provide some useful information of earthquake process and/or oil exploration. Although the coupling mechanisms are not well understood at the current stage, there are some candidate mechanisms, such as the electrokinetic effect and piezoelectric effect. We focused this study on seismic and electromagnetic coupling for the data observed during earthquakes or synthesized from our numerical simulation method based on electrokinetic effect and earthquake models. We presented a quantitative analysis method of the correlation between seismic and electromagnetic signals. As an example of the field data, we investigated the data recorded during the Ms5.7 Ningqiang earthquake, China. The results indicated that there is a clear coupling between seismic and electromagnetic signals. As a further example of the synthetic data of seismic and electromagnetic signals, we obtained the synthetic seismic and electromagnetic signals using our numerical simulation method and confirmed the existence of coupling between the seismic and electromagnetic signals in the synthetic data.

This study is supported by the National Natural Science Foundation of China (41025014, 41274075).

Keywords: Co-seismic electromagnetic signals, Rupture model, Source time function, Electrokinetic effect

Japan Geoscience Union Meeting 2014
(28 April - 02 May 2014 at Pacifico YOKOHAMA, Kanagawa, Japan)

SCG10-06 Room:313 Time:May 2 11:00-11:15

The Development of self-potential tomography to estimate the ground water condition

OTSUBO, Hiroshi[1] ; HATTORI, Katsumi[1] ; YMAZAKI, Tomohiro[1*]

[1]Graduate school of science, Chiba University

Landslides are one of the most severe natural disasters in the world and there are two types; rainfall induced landslides and landslides triggered by an earthquake. In this research, basic study on early warning system for landslides will be performed to understand rainfall-induced landslide process by hydrological and electromagnetic changes. The final goal of this research is to develop a simple technology for landslide monitoring/forecasting using self potential method. The advantages of this method are lower cost and easier to set up than the hydrological approaches using pore pressure sensors. The laboratory experiments show that the self-potential variation has relationship with the water and soil displacements. But, we can not estimate the ground water condition by self-potential yet. So, in this study, we developed self-potential tomography to estimate the ground water condition.

Measured self-potential value under the ground and charge distribution to estimate is given by the Coulomb's law. Therefore, this is inverse problem. To solve the inverse problem, we adapt Phillips-Tikhonov regularization with Generalized Cross Validation (GCV). To evaluate the reconstructed charge distribution and investigate the relationship with the ground water condition, computational simulations and applications to practical data by using the sandbox experiment has been examined.

It is found that the developed algorithm is effective through numerical simulations. Results of application to sandbox experiments show good performance but there are some problems to solve.

The details will be given in our presentation.

Keywords: landslide, self-potential

Japan Geoscience Union Meeting 2014
(28 April - 02 May 2014 at Pacifico YOKOHAMA, Kanagawa, Japan)

SCG10-07 Room:313 Time:May 2 11:15-11:30

Induced seismicity due to fluid injection at a deep well in Youngstown, Ohio, USA

KIM, Won-young[1*]

[1]Lamont-Doherty Earth Observatory, Columbia University, [2]Earthquake Research Institute, University of Tokyo

Over 100 small earthquakes (Mw 0.4-3.9) were detected during January 2011- February 2012 in the Youngstown, Ohio, USA area, where there were no known earthquakes in the past. These shocks were apparently close to a deep fluid injection well, and hence, were immediately suspected as induced by the fluid injection. This 14-months seismicity included a half-dozen felt earthquakes and culminated with a Mw 3.9 shock on 31 December 2011, about 24 hours after the fluid injection ceased in the deep well in Youngstown. Among the 109 shocks, 12 events greater than Mw 1.8 were detected by regional network, whereas 97 small earthquakes (0.4 <Mw <1.8) were only detected by using the waveform correlation detector.

Among these shocks, 21 earthquakes were accurately located by using the local portable station data. All of the accurately located earthquakes were distributed along a set of subsurface faults striking N265 (due East-west) and dipping steeply to the north – consistent with the focal mechanism of Mw 3.9 mainshock on 31 December 2011. All of the well-located earthquakes have occurred at depths ranging from 3.5 to 4.0 km in the Precambrian crystalline basement.

We conclude that the recent earthquakes which occurred during 2011 - 2012 in Youngstown, Ohio were indeed induced by the waste fluid injection at a deep injection well due to increased pore pressure along the preexisting East-west trending faults located close to the wellbore in the Precambrian basement. We found that the earthquakes are located along a 1.2 km-long, East-west trending subsurface en echelon fault, and that the seismicity initiated at the eastern end of the subsurface fault – close to the injection point, and migrated toward the west – away from the wellbore, indicating that the expanding high fluid pressure front increased the pore pressure along its East-west trending path and progressively triggered the earthquakes. Further, we observe that the occurrence of these earthquakes is generally correlated to the total daily injection volume and that several sharp peaks in the daily injection volume correlate with the occurrence of earthquakes. We observed that several periods of quiescence of seismicity follow gaps in surface injection volumes and pressure (sudden drops in injection pressure followed by prolonged low pressure), which may indicate that the earthquakes were directly caused by the pressure buildup in the fractured Precambrian basement and stopped when pressure dropped. Geohydrologic properties of the Youngstown, Ohio area behaved as a fractured Precambrian rock similar to the Rocky Mountain Arsenal, Colorado, USA site of induced earthquakes during 1960s.

Keywords: Induced seismicity, Fluid pore pressure, Shale gas extraction, Space and tme migration of earthquakes

Japan Geoscience Union Meeting 2014
(28 April - 02 May 2014 at Pacifico YOKOHAMA, Kanagawa, Japan)

SCG10-08 Room:313 Time:May 2 11:30-11:45

Characteristics of Microcracks in the Nucleation Stage of Natural Earthquake

FUJINAWA, Yukio[1*] ; NODA, Yoichi[2] ; TAKAHASHI, Kozo[3]

[1]MierukaBosai Inc., [2]Tierra Tecnica Ltd., [3](former) Communication Research Laboratory

At the last JpGU meeting we reported that a deep underground electric field measurement using special antenna could detect micro-cracks appearing in the nucleation stage of the Tohoku Earthquake (Fujinawa et al., 2013). Here we report several results of further analysis on the characteristic pulse-like phenomena.

1) Detection Distance:

Some events of B-type variation have clear first and second phases (Figure 1). The S-P time is 25ms corresponding to about 180m of the epicentral distance. Majority of events have no apparent P phases due to the small strength of the P phase and/or large dissipation. The detection distance of P phase is about 200m. On the other hand the S phase of the frequency of some 100Hz and amplitude of 2mV suggests detection distance of some 10km, much larger than that of the acoustic emission signal of order several hundred meters by elastic observation.

The characteristic electric field variation induced by crack through electro-kinetic mechanism have been discussed by systematic formulations (Pride, 1994; Revil and Leroy, 2004). As to the wave mode, there are four kinds of wave, slow P and fast P wave (ordinary p wave), S-wave (ordinary S wave) and electromagnetic wave (EM). Events containing P phase have occasionally small forerunners at about the origin time possibly corresponding to (see Fig.1).

2) Correspondence to main shock:

The seismological approaches (e.g., Kato et al., 2012) showed that there were two slow seismic slip events from mid-February to the Tohoku Earthquake and microearthquake activities around the foreshocks and mainshocks. Those activities were whole around the epicentral zone, about 300 km northeast from the observation site. The detection distance of the electric field change by the borehole antenna is at most 100 kilometer. Our observational evidence including temporal evolution of the microcrack activity and b value of 0.7 suggest that the micro-cracks of B-type are related to the nucleation process of the main shock, though they occurred at the edge of the giant rupture area. We propose that the nucleation process is not limited at around the asperity, but extends to whole rupture zone. More extensive monitoring of the microcrack of magnitude less than -5 can provide clue to this question.

3) Intermittent Criticality

There appeared undulation of microcrack activity after the most active period around 9th March , 2011. The undulation has been suggested to reflect the intermittent criticality indicating another phase of nucleation (Sornette and Sammis, 1995; Kapiris et al., 2005). As approaching to the main shock there appeared two kinds of events. One kind is a superposition of several smaller events. It is interpreted that small events substantially increased with the result of picking up more smaller events in the time interval of data length of 100ms. The second kind is like a long chain of small events. These feature suggest that microcrack activity has changed at the last stage of nucleation stage.

4) It is well known that the crust of the earth is elastic-porous medium filled with fluid as water. The research on the rupture of such kind of medium had a remarkable development in early 1990 contributing to interpret the mysterious seismo-electric phenomena associated earthquakes enabling systematic treatment and suggesting new method of geophysical prospecting. The formulation of Pride and Revil have been used to interpret the phase of faster propagation of EM signal with velocity much larger than the p-wave speed (Fujinawa et al., 2011), the ULF band anomalies associated the slow-slip (Han, 2013) . And, our electromagnetic method has been suggested to detect micro-cracks preceding natural earthquakes to identify the nucleation stage providing a break-through for the short term prediction method. The converted electromagnetic mode at the material contrast from elastic seismic wave has been proved to be profitable means to survey for oil and gas.

Keywords: Microcrack, Earthquake Prediction, Nucleation Stage, Seismo-electric- signal, Electrokinetic effect, Tohoku Earthquake

SCG10-08 Room:313 Time:May 2 11:30-11:45

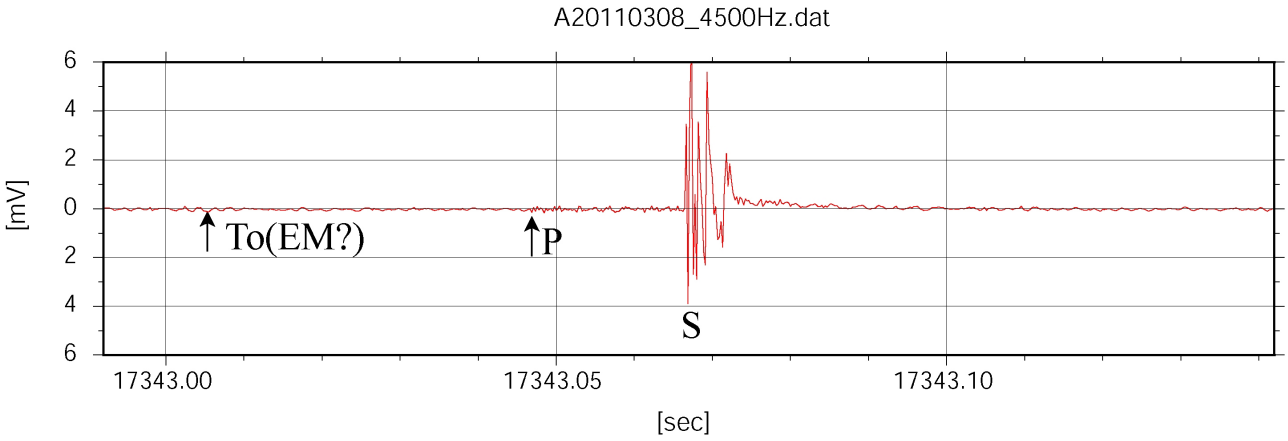

Japan Geoscience Union Meeting 2014
(28 April - 02 May 2014 at Pacifico YOKOHAMA, Kanagawa, Japan)

SCG10-P01 Room:Poster Time:May 2 16:15-17:30

Electromagnetic emissions from fracture of semiconductor pyrite

OZAWA, Mitsuyuki[1*] ; MUTO, Jun[1] ; NAGAHAMA, Hiroyuki[1] ; NAGASE, Toshiro[2]

[1]Department of Geoenviromental Sceinces, Graduate School of Science, Tohoku University, [2]The Tohoku University Museum

Introduction

When elastic waves propagate in orebodies composed of semiconductor minerals, electromagnetic (EM) radiation with radio frequency occurs. Its frequencies were 10-100 times higher than those of the elastic waves. They were observed by geophysical exploration surveys and laboratory experiments. These previous studies suggested that generation of radio waves is closely related to the rectifying property of orebodies which is attributed to semiconductor minerals. Semiconductor minerals are divided into p- or n-type conductivity by its charge carrier. When p- and n-type are joined, the resulting junction (p-n junction) has the rectifying property. Because many p-n junctions of semiconductor minerals exist as which connect in parallel and in series in the orebody, they also show rectifying property. Previous research measured only large scale rectifying property of orebody to understand the generation mechanism of radio wave. However, due to the lack of the measurement of rectifying properties of each micro p-n junction in semiconductor minerals, quantities evaluation was difficult.

Composition of semiconductor minerals is heterogeneous due to the presence of impurities and lattice defects. Because rectifying property depends crucially on the composition, clarifying the composition at each micro region is needed. In this research, we measured the composition and rectifying property of semiconductor pyrite to discuss the possibility of EM emission from the ore bodies.

Methods

Semiconductor pyrite sample was obtained from Waga-Sennin mine, Akita prefecture, Japan. It was cut into slabs with a thickness of about 0.38 cm and an area of 1.4 cm^2.

We obtained composition of the sample surface by electroetching method and SEM-EDS. Thermal probing method allowed us to discriminate between p- and n-type conductivity. By electrical probing, we quantified the rectifying properties.

Results

After the electrolytic etching, heterogeneity of composition in the sample surface was emerged as the difference in solubility. The difference of soulubility caused etching figure and zonal structures. Thermal probe method revealed that the differences of p-n type regions corresponded to the difference in solubility of each region. P-types regions showed a higher solubility than n-type regions. According to the SEM-EDS analysis, about 1.0 wt.% of Pb inclusions were precipitated parallel to crystallographic planes in the p-type regions.

In the electrical probing method, rectifying effects were observed at p-n junctions. We obtained the current and voltage characteristic of p-n junction. The reverse and forward breakdown voltages were estimated to be 1.5 V and 0.3 V, respectively.

Discussion and conclusion

When two types of rocks make contact, electrons move between the surfaces of rocks, producing the potential difference between them. This electrification becomes a possible source of EM radiations during separating rocks. If we regard p- and n-type semiconductor minerals as the two types of rocks, the contact potential is given by the forward breakdown voltage of p-n junction. When the junction is split into two pieces, separated surface can be regarded as capacitance plates. If the surface charge density of plates reaches the Paschen's minimum charge density of breakdown (e.g. air 5.0×10^{-5} C/m^2), corona discharge occurs. We estimated the charge density of separated plates at p-n junction to be 2.7×10^{-4} C/m^2. Given the effect of charge relaxation, we must take into account separation velocity of plates. In this case the critical separation velocity to cause corona discharge is estimated to be 2.0 km/s. Therefore, it is expected that the pyrite fractured by propagation speed higher than 2.0 km/s can cause corona discharge.

In conclusion, the fracturing of pyrite becomes a possible source of EM radiations. Further investigation is needed to clarify the properties (e.g. frequency) of EM radiations from the orebodies.

Keywords: Seismic electromagnetic signals, Semiconductor minerals, Radio wave, P-n junction

Japan Geoscience Union Meeting 2014
(28 April - 02 May 2014 at Pacifico YOKOHAMA, Kanagawa, Japan)

SCG61-01 Room:311 Time:May 2 09:00-09:15

Pulsed granitic crust formation revealed by comprehensive SHRIMP zircon dating of the SW Japan granitoids

TANI, Kenichiro[1*] ; HORIE, Kenji[2] ; DUNKLEY, Daniel[3] ; ISHIHARA, Shunso[4]

[1]Japan Agency for Marine-Earth Science and Technology, [2]National Institute of Polar Research, [3]Curtin University, [4]Geological Survey of Japan/AIST

The origin of continental crust is a fundamental question in Earth's evolution. Granitoids, its volcanic equivalents, and metamorphic and sedimentary rocks with granitic compositions, are the main components of the upper continental crust. It is therefore important to understand the geodynamic settings in which juvenile granitic magma is generated from mantle-derived sources. Convergent plate margins, such as the Mesozoic circum-Pacific orogenic belts, are regarded as one of the plausible candidates for the post-Archean continental crust formation, as they are associated with abundant calc-alkaline I-type batholiths. However, the fundamental tectonic processes that triggered these voluminous granitic crust formations in the Mesozoic have remained largely unresolved due to the lack of precise temporal constraints on the granitic magmatism. We are currently undertaking a comprehensive geochronological study of the granitic batholith exposed in the Southwest Japan Arc, which is typical of the Mesozoic circum-Pacific orogenic belts utilizing high-precision zircon U/Pb geochronology.

In order to precisely determine the space-time distribution of the granitic magmatism that occurred in the SW Japan Arc during the Mesozoic, we have used the zircon U/Pb method to date a comprehensive suite of granitic rocks from the Chugoku Region in the SW Japan. Contrary to the results previously obtained using conventional geochronological methods, which suggested that the magmatism occurred gradually from ~100 to ~50 Ma, with the plutons forming over long time intervals, the newly obtained zircon ages reveal three clear pulses of granitic crust formation at 85, 60 and 35 Ma separated by 25 million year intervals. The 85 Ma magmatism was the most voluminous and was distributed in a broad zone that extends ~120 km across-strike, whereas the magmatism at 60 and 35 Ma were focused on the northern margin of the SW Japan Arc. Furthermore, the granitic magmatism at 85 Ma involved sediment-incorporated, ilmenite series granitic rocks, while the magmatism at 60 and 35 Ma involved more juvenile, mantle-derived, magnetite series rocks. Thus, not only did the granitic magmatism in SW Japan occur in pulses, there was also a spatial and compositional transition in the magmatism through time. This can be best explained by enhanced subduction zone magmatism during the Mesozoic, rather than the previously proposed model in which it was suggested that the granitic crust was formed by the subduction of a mid-ocean ridge on the Pacific Plate during the Middle Cretaceous.

Japan Geoscience Union Meeting 2014
(28 April - 02 May 2014 at Pacifico YOKOHAMA, Kanagawa, Japan)

SCG61-02 Room:311 Time:May 2 09:15-09:30

Petrology and zircon geochronology of the Hikami Granitic Rocks in south Kitakami Mountains,Japan

SASAKI, Jun[1*] ; TSUCHIYA, Nobutaka[1] ; ADACHI, Tatsuro[2] ; NAKANO, Nobuhiko[2] ; OSANAI, Yasuhito[2] ; ADACHI, Yoshiko[3]

[1]IwateUniversity, [2]KyushuUniversity, [3]NiigataUniversity

The Hikami Granites,pre-Cretaceous older granitic complex of the South Kitakami Terrane,has long been controversial on their age of intrusion. Since unconformable relationship between the granites and the Silurian formation was shown by Murata et al.(1974). However CHIME age determinatin for the grainites (Adachi et al.,1994),indicates Silrian to Permian age.We examined the zircon U-Pb ages of 13 samples from the Hikami Granitic Rocks, and solidification age of around 450Ma were obtained.

Bulk rock chemical compositions of the Hikami granites were compared with Paleozoic granitic rocks in Japan. Petrochemical similarity between Hikami Granitic Rocks and the granitic rocks in the Kurosegawa Belt is consistent with the correlation between the South Kitakmi and Kurosegawa Belts.

Keywords: HikamiGranites, zircon, U-Pb age, Petrochemistry

Japan Geoscience Union Meeting 2014
(28 April - 02 May 2014 at Pacifico YOKOHAMA, Kanagawa, Japan)

SCG61-03 Room:311 Time:May 2 09:30-09:45

Sr-Nd-Pb-Hf isotopic variations of Cretaceous to Paleogene granitic rocks from northeast Japan

TSUCHIYA, Nobutaka[1*] ; KAGASHIMA, Shin-ichi[2] ; HIRAHARA, Yuka[3] ; TAKAHASHI, Toshiro[3] ; SENDA, Ryoko[3] ; CHANG, Qing[3] ; KIMURA, Jun-ichi[3]

[1]Iwate University, [2]Yamagata University, [3]JAMSTEC

The Japanese Islands represent a segment of a 500 Ma old subduction related orogen developed along the western Pacific convergent margin, and most tectonic units are composed of late Paleozoic to Cenozoic accretionary complexes and their high P/T metamorphic equivalents (e.g., Maruyama, 1997; Isozaki et al., 2010). Maruyama (1997) described the formation of the Japanese Islands has been taken as the standard model for an accretionary orogeny. He also stated that the most important cause of the orogeny is the subduction of an oceanic ridge, by which the continental mass increases through the transfer of granitic melt from the subducting oceanic crust to the orogenic belt. On the other hand, Jahn (2010) described that the subduction-accretion complexes consisting of granitic and sedimentary rocks in southwest Japan are composed mainly of recycled old continental crust. Kagami et al. (1999) described that the Honshu Arc can be divided into three groups based on their Sr-Nd isotope characteristics: the Kitakami, North (Abukuma belt), and South (Ashio/Mino belts) Zones, in order of increasing Sr isotopic enrichment, with Nd isotopic depletion from NE to SW. We present Sr-Nd-Pb-Hf isotopic ratios for granitic rocks in northeast Japan.

Sr-Nd-Pb-Hf isotopic study are made for granitic rocks from the Kitakami belts (Kitakami Mountains), the Abukuma belts (Shirakami Mountains, Obonai area, Taihei Mountain, Sekiryo Mountains, and Abukuma Mountains), and the Ashio/Mino belts (Okutone area, Tadami area, Okutadami area, Taisyaku Mountains, and Ashio Mountains). Newly isotopic data from these granitic rocks show increasing enrichment of crustal component in order of the Kitakami, Abukuma, and Ashio/Mino belts. Multi-isotope plots of these rocks indicate that the trend in variation could result from the mixing of depleted and enriched components. The depleted component is likely to originate from the magmatic flux related to the Lower Cretaceous ridge subduction. On the other hand, the mixing model of subducted sediments and depleted mantle cannot explain the variation of Nd-Hf isotopic compositions of granitic rocks. The enriched component requires existence of a reservoir with low Hf initial isotope ratio, which is considered to be zircon-rich sediment derived from old continental protolith (Chauvel et al., 2008). In addition, the granitic rocks in Kitakami zone shows rather different trend from the granitic rocks in other districts. It can be explained by the hypothesis that the granitic rocks in the Kitakami zone were derived from the mixing of mantle component with enriched end menber of lower Hf initial isotope ratio. This model is consistent with the fact that the Kitakami zone is characterized by the occurrence of adakitic rocks related to Lower Cretaceous ridge subduction.

Keywords: Northeast Japan, granite, Sr-Nd-Pb-Hf isotope, petrochemistry

Japan Geoscience Union Meeting 2014
(28 April - 02 May 2014 at Pacifico YOKOHAMA, Kanagawa, Japan)

SCG61-04 Room:311 Time:May 2 09:45-10:00

Garnet-bearing acidic igneous bodies in Mt. Kenashi-yama area, Fujikawaguchiko-machi, Yamanashi, Japan

NAGAHATA, Hiromi[1*] ; ISHII, Teruaki[2]

[1]Graduate school, Open University of Japan, [2]Fukada Geological Institute

Introduction The gernet-bearing quartz porphyrite body in Mt. Kenashi-yama area Fujikawaguchiko-machi, Yamanashi, Prefecture was described by Katada (1956). On the other hand, there are many reports on garnet-bearing boulders in this area (Togawa et al., 1996; Togawa et al., 1997; Matsubara et al., 2008; Tamura et al., 2010).

On the detailed field works, we recognized three groups of garnet-bearing acidic igneous bodies in this area.

Geology The studied area is in the northern end of Izu-Bonin Arc, and is located east side of Misaka group, middle to late Miocene.

Lithology Three garnet-bearing acidic igneous bodies are recognized, which are named A, B and C groups.

[A group (lava flow(?))] This group exists in 1,100m to 1,200m above sea level, and is located from WSW to ENE over 2km long. The rock consists of quartz (10%-20%, md : maximum diameter = 5mm), feldspar (10%-25%, md = 4mm), garnet (1%, md = 3mm) and groundmass(60%-65%). The rock of A group shows high dense appearance.

[B group (volcanic ash(?))] This group exists at 1,200m, and this group may be exist along above the A group. This group can be assumed as garnet-bearing volcanic ash, because this group contains volcanic glasses (at under microscope) and rock fragments (If B group is not volcanic ash, this group may be the weathered zoon of A group). The B group consists of quartz (10%, md = 5mm), garnet (1%, md = 3mm) and clay matter 80%.

[C group (dike)] This group exists in 1,300m to 1,400m, and is located from WSW to ENE, over 3km long. The rock is little fragile, and consist of quartz (3%-20%, md = 4mm), feldspar (3%-20%, md = 3mm), garnet (0.1%, md = 3mm), hornblende (1%, maximum length = 9mm) and groundmass (65%-85%).

Chemical analysis Representative samples of each groups are analyzed by X-lay fluorescent analysis on 10 major elements. The SiO_2 contents of three groups are 72wt%-76wt%. It mean that these rocks are classified into rhyolite according to alkali-SiO_2 diagram (Le Bas, et al., 1986). There are slightly high in Na_2O, and slightly low P_2O_5 than Tanzawa Hosokawadani rhyolite (Yamashita, 1997).

Discussion and Consideration It can be assumed that three groups of garnet bearing acidic igneous bodies are recognized in Mt. Kenashi-yama area. They are located along WSW-ENE direction 2-3km long. A, B and C groups are possibly lava flow, volcanic ash and intrusive rock, respectively. All of them may be classified into garnet-bearing rhyolite.

Keywords: garnet, quartz, feldspar, rhyolite, Mt. Kenashi-yama, Fujikawaguchiko-machi

Japan Geoscience Union Meeting 2014
(28 April - 02 May 2014 at Pacifico YOKOHAMA, Kanagawa, Japan)

SCG61-05 Room:311 Time:May 2 10:00-10:15

Two types of websterite from the Ust'-Belaya ophiolite, Far East Russia: Origins and implications

MACHI, Sumiaki[1*] ; ISHIWATARI, Akira[2] ; MORISHITA, Tomoaki[1] ; HAYASAKA, Yasutaka[3] ; ARAI, Shoji[1] ; TAMURA, Akihiro[1]

[1]Natural Sci & Tec., Kanazawa Univ., [2]NE Asia Center, Tohoku Univ., [3]Earth & Planet. Sys. Sci., Hiroshima Univ.

The Ust'-Belaya ophiolite is located in the Koryak Mountains, Far East Russia. We report two types of websterite in the mantle section of the ophiolite.

The lithology of the mantle peridotites from the ophiolite is variable from very fertile lherzolite to moderately depleted harzburgite. The mineral chemistry of the very fertile lherzolite shows similar signature to those of the subcontinental peridotite. The two types of websterite (type1 and type2) occur in them as dikes/veins. Type1 is composed of brownish colored cpx, opx and Al-spinel. On the other hand, type2 is composed of green colored cpx, opx and Cr-spinel.

Type2 websterite is similar to those reported from many other ophiolites. Websterites, which are characterized by extremely aluminous spinel similar to the type1 websterite, are never found in ophiolitic peridotites but are described in passive margin peridotites (e.g. Zabargad Island in Red Sea and Iberia Abyssal plain peridotites). These websterites are generally interpreted as high-pressure cumulates and the host peridotites are considered as fragments of subcontinental mantle.

The mantle section of the Ust'-Belaya ophiolite represents, at least partly, fragments of subcontinental mantle. The two types of websterite might be related to two different magmatisms in two different tectonic settings; type1 is formed former subcontinental to oceanic environment and then type2 is formed later oceanic to arc environment.

Keywords: Ust'-Belaya ophiolite, websterite, subcontinental mantle

Japan Geoscience Union Meeting 2014
(28 April - 02 May 2014 at Pacifico YOKOHAMA, Kanagawa, Japan)

SCG61-06 Room:311 Time:May 2 10:15-10:30

Field geological considerations on the formation mechanism of platy joints in lava flows

SATO, Kei[1*] ; ISHIWATARI, Akira[2]

[1]Grad. School Sci., Tohoku Univ., [2]CNEAS, Tohoku Univ.

Columnar jointing and platy jointing are characteristic types of jointing in volcanic rocks. The origin of columnar joints has been discussed for centuries, and at the present day it is considered that they are the result of cooling and contraction of lava (Aydin and DeGraff, 1988). However, platy joints have far less attracted researchers than columnar joints and their formation mechanism is still controversial. Platy joints can develop in thick (>100 m) and voluminous lava flows which have glassy margins such as ”flood andesite” in Kyushu, Japan (Nagao et al., 1995) and ridge-forming lava flows at Mount Rainier (Lescinsky and Sisson, 1998), probably reflecting stress distribution or physical property within solidifying lava. Previous studies attributed formation of platy joints (sheeting joints) to late stage shear of lava flow and/or microlite orientation (Lescinsky and Fink, 2000), deflation of flow (Spörli and Rowland, 2006) or both flowage and shrinkage of lava (Bonnichsen and Kauffman, 1987). Although absolute evidence for the origin of platy jointing has not been found, restraining of internal lava by solidified flow margin would be an important factor in any case and density (volume ratio of crystals to glass) difference between flow margin and interior would be also important when we consider thermal contraction. It is also a problem when platy joints form, especially in the case that columnar and platy joints intersect without terminating each other. Occasionally platy joints are filled with tridymite and/or mica mineral with or without andesitic to dacitic melt, which might be segregated from the crystallizing lava body, suggesting that platy joints start to form at early stage of cooling of lava.

References:
Aydin and DeGraff, 1988, Science, 239, 471-476.
Bonnichsen and Kauffman, 1987, GSA Special Papers, 212, 119-145.
Lescinsky and Fink, 2000, J. Geophys. Res., 105, 23711-23726.
Lescinsky and Sisson, 1998, Geology, 26, 351-354.
Nagao et al., 1995, Mem. Geol. Soc. Japan, 44, 155-164 (in Japanese with English abstract).
Spörli and Rowland, 2006, J. Volcanol. Geotherm. Res., 157, 294-310.

Keywords: platy joints, flood andesite, internal flowage, thermal contraction, segregation vein

Japan Geoscience Union Meeting 2014
(28 April - 02 May 2014 at Pacifico YOKOHAMA, Kanagawa, Japan)

SCG61-07 Room:311 Time:May 2 10:30-10:45

Oxidation stats of Fe within constituent minerals in spinel-lherzolite xenolith from Tariat Depression, Mongolia: Signif

EJIMA, Terumi[1*] ; OSANAI, Yasuhito[2] ; OHFUJI, Hiroaki[3]

[1]National Institute of Advanced Industrial Science and Technology, [2]Kyushu Univ., [3]Ehime Univ.

The Tariat depression is one of the most famous areas of deep-seated megacrystic xenoliths and mantle-derived xenoliths in the Baikal-Mongolia rift. Spinel-garnet-bearing websterite, garnet lherzolite and spinel lherzolite have been found in this area (Osanai et al. 2010). In this study, oxidation state of Fe in olivine (Ol), orthopyroxene, clinopyroxene and spinel in fresh spinel-lherzolite xenolith, and olivine in host basalt in Tariat depression were investigated using Mossbauer spectroscopy, X-ray FeL?/FeL?-intensity ratio analysis (EPMA method) and transmission electron microscopy (TEM).

Olivine, clinopyroxene, orthopyroxene and spinel have homogeneous chemical compositions. Olivine is forsterite with average composition of Fo90Fa10, Clinopyroxene is Na-bearing diopside [(Na0.17Ca0.71Mg0.81Fe0.09Al0.20)?2.00(Si1.89Al0.11)?2.00O6], and have symplektite consisting of diopside and glass on the rim with the width of ˜50 micro m. The chemical composition of the glass is similar to that of feldspar with compositions of An. Orthopyroxene is [(Mg0.85Fe0.09Al0.04Ca0.02)(Si0.94Al0.06)O3]. Spinel is [(Mg0.81Fe2+0.22)?1.03(Al1.80Cr0.17)?1.97O4].

The Fe2+: Fe3+ ratios of forsterite, orthopyroxene, clinopyroxene and spinel determined by Mossbauer analysis are 97(1):3(1); 85(8):15(1); 74(4):26(3); 66(8):34(5), respectively. Fe3+ in olivine is not attributed to any precipitates nor minute inclusions, which was confirmed by TEM observation, and, thus, exists in olivine structure. Fe of olivine phenocrysts from host basalt lava is only Fe2+ which was proved by EPMA method.

Fe3+-bearing forsterite in spinel-lherzolite xenolith is considered to have been stable under mantle condition.

Keywords: olivine, oxidation state of Fe, spinel-lherzolite xenolith, Mossbauer methods, Mongolia

Japan Geoscience Union Meeting 2014
(28 April - 02 May 2014 at Pacifico YOKOHAMA, Kanagawa, Japan)

SCG61-08 Room:311 Time:May 2 11:00-11:15

Al/Si disordered anorthite in anorthite megacryst from Miyake-jima: effect of non-stoichiometry on Al/Si distribution

ECHIGO, Takuya[1*] ; HOSHINO, Mihoko[2] ; KIMATA, Mitsuyoshi[3] ; SHIMIZU, Masahiro[3] ; MATSUI, Tomoaki[4] ; NISHIDA, Norimasa[5]

[1]Faculty of Education, Shiga University, [2]Mineral Resources Research Group, AIST, [3]Earth Evolution Sciences, University of Tsukuba, [4]Faculty of Education, Kagoshiama University, [5]Research Facility Center for Science and Technology, University of Tsukuba

The crystal chemistry of anorthite with the low content of albite (An92.0Ab3.4), part of a rapid cooled, anorthite megacryst occurring in 1940 ejecta from Miyake-jima volcano, Japan, has been investigated using single-crystal X-ray diffractometer and electron microprobe analyzer with wavelength dispersive X-ray spectroscopy (EMPA-WDS). The structure was refined in space group P-1 and cell parameters, a = 8.182(6) Å, b = 12.883(4) Å, c = 7.092(4) Å, α = 93.19(4) ^{o} , β = 115.91 (4) ^{o} , γ = 91.18 (4) ^{o} . The final weighted R-factor is 3.77 % for 1549 reflections. Averaged T-O distances are 1.681 Å for T1(0), 1.674 Å for T1(m), 1.677 Å for T2(0) and 1.680 Å for T2(m), indicating each Al occupancy of 0.501, 0.453, 0.472, and 0.496, respectively. These results suggest that the Al/Si-distribution in the tetrahedral framework is highly disordered (QOD = 0.06), which results in having the c-axis in half along that determined in Al/Si ordered anorthites (c ˜14 Å).

Keywords: Anorthite, Al/Si order-disorder, Anorthite megacryst, Structual heterogeneity

Japan Geoscience Union Meeting 2014
(28 April - 02 May 2014 at Pacifico YOKOHAMA, Kanagawa, Japan)

SCG61-09 Room:311 Time:May 2 11:15-11:30

Formation temperature of perlite and its texture by heating experiments of obsidians from Hokkaido

IKEYAUCHI, Ryo[1] ; WADA, Keiji[1*] ; SAITO, Takeaki[1]

[1]Hokkaido University of Education at Asahikawa

The obsidians from Hokkaido were heated in electric furnaces to transform the perlite in a form like pumice in vitreosity, because remained water in obsidians becomes the gas and makes air bubbles by heating.

We examined foaming temperature of the obsidians from 13 samples in 7 Hokkaido sources, and the relations with its foaming temperature and the water content of the obsidians. In addition, we changed a heating temperature and a condition of the heating time and examined the difference in foaming form of the perlite.

Finally, we considered a relations with foaming process of the obsidians and the internal structure of the perlite through the microscopy of the perlite.

Keywords: obsidian, heating experiment, perlite, vesiculation, glass

Japan Geoscience Union Meeting 2014
(28 April - 02 May 2014 at Pacifico YOKOHAMA, Kanagawa, Japan)

SCG61-10 Room:311 Time:May 2 11:30-11:45

Estimation of intracrystalline distribution coefficient of Mg-Fe ions in olivine using Cs-corrected STEM

MIYAKE, Akira[1*] ; TOH, Shoichi[2] ; FUKUNAGA, Keiichi[3] ; KURIBAYASHI, Takahiro[4]

[1]Kyoto Univ., Sci., [2]Fukuoka Univ., Sci., [3]JFCC, [4]Tohoku Univ., Sci.

Intracrystalline distribution coefficient of Mg-Fe ions between the two types of the octahedral sites (M1, M2-site) of olivine, $(Mg,Fe)_2SiO_4$, have been estimated using X-ray or neutron diffraction studies. Recently, the high angle annular dark field (HAADF) method using scanning transmission electron microscopy with the correction of spherical aberration (Cs-corrected STEM) visualizes the element column sites in crystalline samples. In the present study, the intracrystalline distribution coefficient of Mg-Fe ions in olivine were tried to estimate using HAADF-STEM. And furthermore, Crystal Structure Analysis of same sample was carried out using e four-circle X-ray diffractometer. We used the synthetic forsterite and the natural olivine from San Carlos, Sri Lanka and Miyake-jima. HAADF-STEM images parallel to a-axis show the Mg / Fe atom columns and the columns which alternately formed of Si and O atoms. Intracrystalline distribution coefficients estimated from the brightness in M1/M2-sites for synthetic forsterite, the olivines from San Carlos and SriLanka are good agreement with those estimated from X-ray method. On the other hand, that obtained from Miyake-jima is different with that obtained from X-ray method.

Keywords: STEM, olivine, intracrystalline distribution coefficient

Japan Geoscience Union Meeting 2014
(28 April - 02 May 2014 at Pacifico YOKOHAMA, Kanagawa, Japan)

SCG61-11 Room:311 Time:May 2 11:45-12:00

A Novel Approach for the Classification of Mineral Ore Particles by A Statistical Raman Spectroscopic Method

SASAKURA, Daisuke[1*] ; HAYAUCHI, Aiko[1]

[1]Malvern Instruments Division of Spectris Japan

[Introduction]

Mineral ores extracted by mining go through a milling process before ore dressing. An important factor in both milling and ore dressing operations is the determination of the particle size distribution of the materials being processed, commonly referred to as particle size analysis. An elemental analysis technique such as X-Ray fluorescence and destructive wet chemical analysis can determine the quantity of mineral species present in the ore, however, these chemical analysis methods do not allow the study of the composition of individual particles of different size and shape. The statistical Raman spectroscopic method is a novel approach which can resolve this problem. Using this method the Raman spectra of several hundred particles is determined after size and shape classification of each individual particle by automated particle image analysis. Raman spectroscopy can be used to acquire the spectra of any inorganic compounds such as metal oxides and nitrides which are Raman active. Many mineral resources are mined as inorganic compounds. Therefore, Raman spectroscopy can be used for the identification of the chemical composition of mineral ores. Using the statistical Raman spectroscopic method described herein, it is possible to calculate the particle size distribution and proportion by mass or volume of each chemical component or mineral species based on Raman spectroscopic information. This study will report and discuss the capability of the statistical Raman spectroscopic method using iron ore as a model material.

[Material and Method]

Iron ore samples were purchased from a vendor. These samples had been through the ore dressing process. Statistical Raman analysis was carried out using a Morphologi G3SE-ID instrument (Malvern Instruments, UK) equipped with a dry powder sample dispersion unit (SDU) and Raman module. The laser wavelength of Raman excitation was 785nm the laser power was less than 5mW and the irradiation time was 5 sec. The particle image measurements were made in diascopic mode with a total magnification 250x. Iron ore dry powder samples were dispersed using the SDU using a short duration pulse of compressed air. Measurements were made automatically using Standard Operating Procedures (SOPs) which define the software and hardware settings used. Measurement sample was dispersed on to glass plate as sample carrier which was minimized environmental exposure by the enclosed sample chamber unit. Particle identification by Raman analysis used the spectrum correlation coefficient approach.

[Results and Discussion]

A Total of 66,436 particles of iron ore were measured by image analysis. The circle equivalent diameter particle size distribution by volume (VCED) exhibited a monomodal distribution with size distribution percentiles as follows: 8.62μm (d10), 21.83μm (d50), 51.29μm (d90). A subset of 700 particles were selected and the Raman spectra were measured. Particles over 20 micron in size were selected randomly from the image analysis data and Raman spectra were acquired. The spectra enabled identification of 4 components (Fig.1). The relative proportion of each component by volume or number of particles is shown in Table 1. Component (A) comprised approximately 90% of the sample. This component exhibited a Raman spectrum typical of α-Fe_2O_3 [1]. It is assumed that components (B) and (C) are polymorphs based on the ratio of the intensities at 221cm^{-1} and 245cm^{-1}. Component (D) exhibited a spectrum typical of α-FeOOH and composed less than 3% of the sample. This result does show that the statistical Raman analysis approach can detect components present at quite low concentrations.

[Summary]

This report illustrated the application and capability of statistical Raman analysis for the characterization of mineral ores using a new approach based on combining chemical and particle size / shape information.

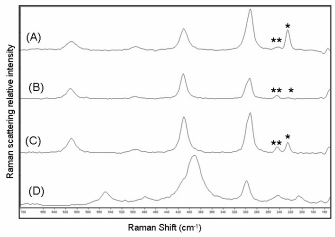

Fig 1. Raman Spectrums of iron ore.
(* : 221cm^{-1},** : 245cm^{-1})

Table 1.
Ratio of each component based on Raman spectrum

Component	Number (%)	Volume(%)
A	87.6	90.2
B	2.5	2.1
C	7.2	6.3
D	2.7	1.4

Japan Geoscience Union Meeting 2014
(28 April - 02 May 2014 at Pacifico YOKOHAMA, Kanagawa, Japan)

SCG61-12 Room:311 Time:May 2 12:00-12:15

Assessment of Nakhile porphyry Cu mineralization potential using geological, geochemical and statistical studies: a case

BOOMERI, Mohammad[1*] ; NAKASHIMA, Kazuo[2] ; F, Yavari[1]

[1]Univ. of Sistan and Baluchestan, [2]Yamagata Univ.

The Nakhile Cu mineralization is located in 145 km northwest of Zahedan in Sistan and Baluchestan province of Iran. This area is geologically located in boundary part of Lut block and flysch zone of east Iran. Geology of the study area consists of Cretaceous to Eocene andesitic lavas and tuffs that were intruded by a dioritic to quartz-dioritic stock. The intrusive rocks are mainly altered and mineralized. Based on the petrography and XRD studies, main mineral in all types of the igneous rocks is plagioclase and the main texture is porphyry. Other minerals are clinopyroxene, amphibole, biotite, quartz, and secondary minerals that vary in the igneous rocks. A large part of the intrusive rocks is rich in pyrite. The pyrite occurs as veins, veinlets and disseminated in the stock. Cu mineralization occurs as vein and can be divided into hypogene and supergene mineralization. Hypogene mineralization is characterized by chalcopyrite and pyrite while supergene mineralization is characterized by malachite, azurite, jarusite, ghothite, hematite and limonite. The propylitic alteration is dominant feature of the intrusive rocks as a wide outer zone. Potassic, phyllic and argillic alterations are also important in the area. The potassic alteration is probably important in the center part of the stock in depth. phyllic and argillic alterations are mainly formed by supergene processes.

The samples that were collected from the least altered and altered rocks in the study area were analyzed by ICP were processed by convenient software such as EXEL and SPSS to obtain statistic parameters of: skewness, maximum, minimum and standard deviation. Then, the histograms for the amount of Cu, Au and related elements were drawn and their correlation coefficients were calculated. There are remarkable positive correlations between Cu, Au and Ag indicating their similar origin. The highest content of Cu is 7000 ppm in the study samples. The Cu anomalies are mainly observed in central and eastern parts of the area. The highest content of Au is 6000 ppb. The Au anomalies are mainly observed in western parts of the area. The higher contents of Pb, Zn and Ag are observed more away from the intrusive rocks.

The outcrops in the area are mainly similar as propylitic alteration zone of porphyry Cu deposits that is characterized by secondary hydrothermal epidote and chlorite and pyrite. The Cu porphyry mineralization and other alteration zones specially potassic probably occur in depth in the area.

Japan Geoscience Union Meeting 2014
(28 April - 02 May 2014 at Pacifico YOKOHAMA, Kanagawa, Japan)

SCG61-P01 Room:Poster Time:May 2 16:15-17:30

A leucogranite stock rich in high field strength elements, Kanamaru-Oguni area on the Niigata-Yamagata border, NE Japan

KAMEI, Atsushi[1*] ; NAITO, Kazuki[2] ; TAKAMURA, Sayaka[3] ; KAGASHIMA, Shin-ichi[4] ; OKUZAWA, Koichi[5] ; SEKI, Yoji[6] ; WATANABE, Yoshio[2]

[1]Department of Geoscience, Shimane University, [2]Geological Survey of Japan/ AIST, [3]Ricoh Japan Corporation, [4]Department of Earth and Environmental Sciences, Yamagata University, [5]Technical Research Institute, Obayashi Corporation, [6]Faculty of Science and Technology, Tokyo University of Science

A small stock of leucocratic Grt-two mica granite enriched in high field strength elements (HFSEs) has recently been found in the Kanamaru?Oguni district of the Asahi?Iide mountains in the Ashio Belt of the NE Japan arc. The granite has a high-K peraluminous composition, and is categorized as an A-type within-plate granitoid, according to several geochemical discriminants based on HFSEs. However, total Zr+Nb+Ce+Y contents are lower (166-192 ppm) and Rb/Ba ratios are higher (19-48) than those typical of A-type granitoids (Zr+Nb+Ce+Y $>$350, Rb/Ba $<$10). This suggests that this stock is in fact a highly fractionated granite, rather than an A-type intrusive. The stock solidified at shallow depth (about 3 - 6 km) from a silisic granitic magma, under moderately water-rich conditions. Geochemical modeling shows that the petrogenesis of the granite can be explained by partial melting of crustal rocks, leaving abundant plagioclase as a residual phase, with subsequent active fractional crystallization of plagioclase + alkali-feldspar. Many other small stocks composed of Grt-two mica granite occur in the Asahi and Iide mountains. The granitic activity ranges from Late Cretaceous (ca 90 Ma) to Paleogene in age. Although most of these stocks were derived from melting of various crustal rocks, some are highly differentiated, and have HFSE concentrations similar to the Kanamaru-Oguni stock studied here.

HFSE-rich granitoids also occur sporadically within the other Japanese geological units, but they are restricted in the southwestern Japan. The granitoids in the Inner and Outer Zones of SW Japan differ in composition. The HFSE-rich granitoids in the Inner Zone originated from middle to lower crustal materials, and were then strongly differentiated before emplacement. This is similar genesis to the granite in the Kanamaru?Oguni district. In contrast, the solitary HFSE-rich granitoid in the Outer Zone crops out at Cape Ashizuri. This occurrence is the only classic A-type intrusion in Japan, and is considered to have formed by a low degree of partial melting of the upper mantle or mafic lower crust. Although the HFSE-rich granitoids within the SW Japan arc may be similar geochemically to within-plate or ocean-ridge granites, they are in fact volcanic arc granites produced within the subduction zone by specific activities.

Keywords: Granite, HFS elements, Niigata-Yamagata, NE Japan

Japan Geoscience Union Meeting 2014
(28 April - 02 May 2014 at Pacifico YOKOHAMA, Kanagawa, Japan)

SCG61-P02 Room:Poster Time:May 2 16:15-17:30

Rare earth element compositions of the Kitahata body in the Fukae granite, northern part of Kyushu

KAWANO, Yoshinobu[1*]

[1]Department of Environment Systems, Faculty of Geo-environmental Science, Rissho University

Cretaceous granitic rocks are widely distributed in northern part of Kyushu (Karakida, 1985), and Fukae granite is located in Kitahata district, Karatsu city, Saga Prefecture. The Fukae granite in this area (hereinafter, Kitahata body) consists of granite, aplite and felsic inclusion. The felsic inclusion is an oval figure about 50 cm in diameter, and is gradually changing from the surrounding granite. Main constituent minerals of the Kitahata body are quartz, k-feldspar, plagioclase and biotite, with apatite, zircon, opaque minerals as accessories. K-Ar biotite age of the body is 95.8+/-2.4 Ma (Kitahata village history compilation committee, 2008). Rare earth element compositions are analyzed about ten samples, for comparison with estimated result of Kawano (2013).

In chondrite normalized REE patterns, values of LREE of the Kitahata body are the highest, and, aplite and felsic inclusion are lower than them. Normalized La/Lu ratios of the Kitahata body are also higher than those of the aplite and the felsic inclusion. Although the negative abnormalities of Eu are not observed in the Kitahata body and the felsic inclusion, it is clearly observed in the aplite. That is, Eu/Eu∗ratio of the aplite is low and the Kitahata body and the felsic inclusion show a similar value. SiO_2 contents increase from the Kitahata body to the felsic inclusion and the aplite. The values of LREE and La/Lu ratio of the felsic inclusion and the aplite which are rich in SiO_2 are lower than those of the Kitahata body, and it is suggested that they have the different origin from the Kitahata body. Although aluminum saturation index of the Kitahata body is larger than 1.0, it of the felsic inclusion is less than 0.9 and shows the character of meta-aluminous. The origin of the felsic inclusion not be considered to be a sedimentary rock, but it may originate in different felsic magma.

Keywords: Kyushu, Fukae granite, Kitahata, rare earth element

Japan Geoscience Union Meeting 2014
(28 April - 02 May 2014 at Pacifico YOKOHAMA, Kanagawa, Japan)

SCG61-P03 Room:Poster Time:May 2 16:15-17:30

Petrographic and geochemical studies of granitoids from the Inbi intrusives, Inner Zone of Southwest Japan

SATO, Kei[1*] ; KAMEI, Atsushi[2] ; MINAMI, Masayo[1] ; ASAHARA, Yoshihiro[3] ; KATO, Takenori[1]

[1]Center for Chronological Research, Nagoya University, [2]Department of Geoscience, Shimane University, [3]Department of Earth and Planetary Scicences, Nagoya University

We report a data set of whole rock compositions of seven granitoids from the early Paleogene Inbi intrusives and a granitoid from the mid Paleogene Namariyama intrusives, Inner Zone of Southwest Japan. The Inner Zone where voluminous granitic plutons occur is subdivided from the north to the south into three areas in terms of mineralogical and petrological characteristics of granitoids: the San-in Belt, the San-yo Belt, and the Ryoke Belt. The examined Paleogene intrusives, which belong to the San-in Belt, show volcano-plutonic association on the eastern side of younger Daisen volcano at the southern part of Tottori Prefecture and the northern part of Okayama Prefecture [e.g. 1-5].

Seven early Paleogene granitoids were collected from three plutons of the Inbi intrusives: Tottori granite, Ningyo Toge granite, and Sangenya granite [4]. Minerals in polished thin sections were first described under microscope. All of the granitoids from the Inbi intrusives contain quartz, feldspars, biotite and iron oxide. Most of them except for Tottori granite contain amphibole. Sphene is found as accessory mineral in some thin sections.

Each mixture of lithium tetraborate and powdered rock was put into a platinum crucible, and then ignited in a furnace at 1000 degree-C and cooled for preparing a glass bead. And then, major and trace elements were measured using XRF analyzer. To prepare sample solutions for measuring trace elements including REEs, the powdered rocks were first digested in a PTFE beaker with HF/HClO4 mixture on a hotplate at 120-140 degree-C, and then residue probably including heavy minerals such as zircon was dissolved in sealed high-pressure container with HF/HCl mixture at 180 degree-C. The first step decomposed fraction and residual one were well-mixed, and then this mixture was split into two aliquots: one was separated from other elements using a quartz column filled with cation exchange resin for measuring REEs, and the other aliquot was for analysis of trace elements except for REEs. These solutions were analyzed using ICP-MS.

Chemical analyses for whole rock compositions of seven Inbi granitoids yielded the following results. Molecular Al2O3/(CaO+Na2O+K2O) values are given as I-type with a range from 0.96 to 1.10. Relationship of Na2O+K2O vs. total FeO vs. MgO shows calc-alkaline series on AFM diagram. SiO2 content ranges from 65.7 wt% to 73.4 wt%, and relationship between Si and other major elements gives clear differentiation trend on Harker variation diagrams. Five samples of the granitoids are categorized as high-K series. Many granitoids in this area suffer weathering. The resulting in weathering yields a decrease of CaO (from 2.5 wt% to 1.7 wt%) and Na2O (from 4.1 wt% to 3.6 wt%) for Ningyo Toge granites. Whereas Sangenya and Ningyo Toge granites contain about 200 to 360 ppm Sr, Tottori granite contains only 90 ppm Sr. The values of Ti normalized by the mean MORB composition [6] against seven granitoids yield a trend of depletion in Ti. Those of REEs normalized by the MORB composition are given as enriched LREE pattern, negative Eu anomaly, and relatively flat MREE and HREE patterns. All of these normalized patterns have characteristics as volcanic arc granites [e.g. 7].

References:

[1] Shibata, H. and Saruyama (1959) Paper. ITSR, Okayama Univ., 25, 1-12 (in Japanese with English abstract); [2] Shibata, K. and Yamada (1965) Bull. Geol. Surv. Japan, 16, 437-442; [3] Kawano and Ueda (1966) Jour. Mineral. Petrol. Econom. Geol., 56, 191-211 (in Japanese with English abstract); [4] Sasada et al. (1979) Memoir. Geol. Soc. Japan, 17, 19-34 (in Japanese with English abstract); [5] Shibata, K. (1979) Memoir. Geol. Soc. Japan, 17, 69-72 (in Japanese with English abstract); [6] Albarede (2005) Geophys. Monogr. R.D. van der Hilst, J. Bass, J. Matas and J. Trampert. Washington D.C., Amer. Geophys. Union, 160, 27-46; [7] Imaoka et al. (2011) Jour. Asian Earth Sci., 40, 509-533.

Keywords: granitoid, San-in Belt, XRF, ICP-MS, trace element, REE

Japan Geoscience Union Meeting 2014
(28 April - 02 May 2014 at Pacifico YOKOHAMA, Kanagawa, Japan)

SCG61-P04 Room:Poster Time:May 2 16:15-17:30

Petrology of ultramafic rocks in the Gosaisho series, northeastern Japan: Is the Gosaisho series the SSZ ophiolite?

SATO, Yuki[1*] ; ISHIWATARI, Akira[2]

[1]Dept. Earth Sci., Grad. Sch. Sci., Tohoku Univ., [2]Center for NE Asian Studies, Tohoku Univ.

The Abukuma plateau, which extends ˜180km in N-S and ˜50km in E-W directions, is located along the Pacific coast of northeastern Japan. This plateau is composed mainly of Cretaceous granitic rocks and regional metamorphic rocks. In the Gosaisho-Takanuki district that is located in the central part of the plateau, the Gosaisho metamorphic rock series in the east overthrust onto the Takanuki metamorphic rock series in the west (e.g. Umemura, 1979). The Gosaisho series is mostly composed of mafic and siliceous rocks, and the Takanuki series is mainly composed of pelitic-psammitic rocks. In the Gosaisho series, many small ultramafic bodies are present in the areas adjacent to the Takanuki series. Metamorphic rocks in the Abukuma Plateau have been well studied since the late 19th century, excepting these ultramafic rocks.

The ultramafic rocks in the Gosaisho-Takanuki distinct are affected by contact metamorphism of the Cretaceous granitic rocks in various degrees, but their protoliths are judged as mantle peridotites and ultramafic cumulates based on their bulk rock chemistry. The ultramafic cumulates are sometimes accompanied by metagabbros. In an ultramafic body called Mount Ohtsube, mantle peridotites are distributed at the foot of the mountain and cumulates occupy its top part. It is likely that the ultramafic bodies in this area are the fragments of the lower part of an ophiolite. We also note that cortlandites and associated gabbroic rocks are present in this area. They are always contained in granitic bodies, and it is likely that intrusion of cortlandites coincided with the Cretaceous felsic magmatism.

The bulk rock chemistry of the peridotite is poor in Ca and Al contents (CaO $<$0.6 wt. %, Al_2O_3 $<$1.6 wt. %). This suggests that they are highly depleted mantle peridotite. On the one hand, Cr# of spinel in the peridotite, which supposedly correspond to the degree of mantle depletion, show a wide range (14 - 87) from place to place. The spinel is poor in Ti content (TiO_2 $<$0.2 wt. %). These characteristic features of spinel suggest that the mantle section was of arc origin (Arai et al., 2011). This is consistent with the bulk rock chemistry of the associated metagabbro which is rich in Ca and Al, and poor in Ti contents (CaO = 11.6 - 17.0 wt. %, Al_2O_3 = 13.8 - 18.5 wt. %, TiO_2 = 0.06 - 1.06 wt. %). It is also noteworthy that some ultramafic cumulates are very rich in Fe (up to Fo = 73).

In the Gosaisho series, siliceous rock contain early Jurassic radiolarian fossils (Hiroi et al., 1987). In addition, some low-grade metamorphic rocks show original pillow structure (Nohara and Hiroi, 1989). Hiroi et al. (1998) argued that the Gosaisho Series represents the mid-ocean ridge origin oceanic crust which overthrust onto the terrigenous Takanuki Series. However, in some places, there are calc-alkaline intrusions which have experienced regional metamorphism with the country rocks (Umemura, 1970). This is consistent with our idea that the ultramafic rocks are of arc origin. Therefore, it is suggested that the Gosaisho Series is the arc-related, supra-subduction zone ophiolite which thrust onto the Takanuki Series in the Jurassic period. However, it is also possible that the early Paleozoic Hayachine-Miyamori ophiolite (e.g. Machida and Ishiwatari, 2013). Comprehensive study of mafic and ultramafic rocks in the Gosaisho series is needed to solve this problem.

Keywords: supra-subduction zone ophiolite, ultramafic rock, Abukuma metamorphic rocks

Japan Geoscience Union Meeting 2014
(28 April - 02 May 2014 at Pacifico YOKOHAMA, Kanagawa, Japan)

SCG61-P05 Room:Poster Time:May 2 16:15-17:30

Experimental petrology of Goseong volcanoes,Korea

FUJINAGA, Nozomi[1*] ; SANO, Takashi[2]

[1]Graduate School of Geo-environmental Science, Rissho University, [2]Department of Geology and Paleontology, National Museum of Nature and Science

Genozoic volcanoes with composition of alkali basalts are widely distributed in Southwest Japan, Korea, and East China.On the basis of geochemical studies, several models to explain magma origin of the alkali basalts were proposed (e.g., upwelling of hot asthenosphere, melting of stagnant slab, and so on).However, little is known about differentiation processes for the alkali basalts based on petrological studies.We therefore performed a series of experimental determinations of melting relation in alkali basalts on Goseong volcanic field, Goseong-do, Korea.Goseong volcanic field consists of seven volcanic plugs, and some of them are accompanied by lava flows.We have carried out petrological studies on alkali basalts from all the seven plugs.The alkali basalts have phenocrysts of olivine and augite and microphenocryst of spinel.Whole rock compositions show that the alkali basalts are relatively primitive (FeO/MgO $<$0 and MgO $>$11 wt %), and mineral chemistry supports this (Forsterite content in olivine $>$87).The most primitive rock was selected for melting experiments at 1110-1220 ℃ and 1 bar under the oxygen fugacity along the fayalite-magnetite-quartz buffer.The experimental results show that mineral assemblage (olivine, spinel, and plagioclase) is different from natural one (olivine, spinel, and augite), indicating that crystallization pressures were probably higher than the melting pressure (1 bar).Thus, we will conduct melting experiments at high pressures in future work.

Japan Geoscience Union Meeting 2014
(28 April - 02 May 2014 at Pacifico YOKOHAMA, Kanagawa, Japan)

SCG61-P06 Room:Poster Time:May 2 16:15-17:30

Metamorphic evolution of garnet-sillimanite gneiss from Ambatofotsy region, Antananarivo domain, east-central Madagascar

ICHIKI, Takashi[1*] ; ISHIKAWA, Masahiro[1]

[1]Yokohama National University

Madagascar is situated within the central part of the Neoproterozoic East African Orogen (EAAO: Jacobs and Thomas, 2004) that marks the join between East and West Gondwana. Therefore, Madagascar is one of the most significant areas to understand the process of Orogen formation. In this study we report the newly found inclusion of kyanite + staurolite + muscovite + rutile in garnet and the mode of occurrence and discuss the metamorphic evolution of the garnet-sillimanite on the basis of estimated results by using various geothermobarometers and phase equilibrium by constructing psuedosection.

The Antananarivo domain is mainly composed of the felsic metamorphic rocks with subordinate amounts of the metasedimentary rocks (Tucker et al., 2012). There exposed magnetite-orthopyroxene-quartz gneiss (metamorphosed banded iron formation), garnet-orthopyroxene rock and garnet-hornblende-biotite gneiss around the garnet-sillimanite gneiss in the eastern part of the domain. The garnet-sillimanite gneiss is mainly composed of garnet, sillimanite, k-feldspar, plagioclase, and quartz with subordinate amounts of biotite, muscovite, monazite, zircon, rutile and graphite. Sillimanite is present in the matrix and as inclusion in garnet. Kyanite is only present as inclusion in garnet. Garnet (X_{Mg}=0.17-0.18) also contains spinel and abundant quartz and monazite inclusions. Spinel shows Mg poor (X_{Mg}=0.21-0.22) and Zn rich (ZnO = 18.4-19.0 wt.%) compositions. We newly found kyanite + staurolite + muscovite + rutile in the garnet. This staurolite shows Mg poor (X_{Mg}=0.12) and Zn rich (ZnO=3.1 wt.%) composition. Garnet is replaced rim of grain by radial aggregate of biotite (X_{Mg}=0.58) + sillimanite.

As a result of the petrographic observation, the metamorphic condition of the garnet-sillimanite gneiss was increased from the stability field from staurolite + quartz to garnet + kyanite (Spear and Cheney, 1989). Garnet + sillimanite + spinel + quartz was stable during the peak metamorphic condition. The estimated peak pressure and temperature condition is ca. 800 ℃ at 0.9 GPa by using garnet-sillimanite-plagioclase-quartz geobarometer (Spear, 1993) and garnet-sillimanite-spinel-quartz geothermobarometer (Nichols et al., 1982) with garnet activities calculated after Berman (1990). Garnet is replaced rim of grain by radial aggregate of biotite (X_{Mg} = 0.58) with sillimanite. This reaction is hydrous reaction from garnet + k-feldspar + H_2O to biotite + sillimanite + quartz with decreasing temperature (Le Breton and Thompson, 1988). This retrograde metamorphic condition is almost consistent with the estimated P-T condition from the garnet-hornblende-biotite gneiss. The estimated pressure and temperature condition is ca. 700 ℃ at 0.6 GPa by using garnet-hornblende geothermometer (Graham and Powell, 1984), hornblende-plagioclase geothermometer (Holland and Blundy, 1994) and garnet-hornblende-plagioclase-quartz geobarometer (Kohn and Spear, 1990). In summary we newly identified the clockwise P-T path from the garnet-sillimanite gneiss exposed in Ambatofoty region, eastern part of the Antananarivo domain.

Keywords: Gondwana supercontinent, east-central Madagascar, Antananarivo domain, Garnet-sillimanite gneiss, Clockwise P-T path

Japan Geoscience Union Meeting 2014
(28 April - 02 May 2014 at Pacifico YOKOHAMA, Kanagawa, Japan)

SCG61-P07 Room:Poster Time:May 2 16:15-17:30

Petrogenesis of garnet-clinopyroxene rocks from the Gondwana collisional orogeny

TAKAMURA, Yusuke[1*] ; TSUNOGAE, Toshiaki[1] ; IINUMA, Minako[1] ; KOIZUMI, Tatsuya[1] ; SANTOSH, M.[2] ; MALAVIARACHCHI, Sanjeewa[3]

[1]Univ. Tsukuba, [2]China University of Geosciences Beijing, [3]Univ. Peradeniya

Madagascar - Southern India - Sri Lanka - East Antarctica region, which is regarded as a part of the East African - Antarctic Orogenic Belt formed by complex subduction-accretion-continent tectonic events related to the amalgamation of Gondwana Supercontinent during Neoproterozoic, is characterized by the presence of major suture zones (e.g. Palghat-Cauvery Suture Zone in southern India) which correspond to paleo-plate boundaries formed by the closure of Mozambique Ocean at ca. 530-550 Ma. The dominant lithologies of the suture zones are felsic to intermediate orthogneiss, metasediments, and mafic-ultramafic suites. Particularly, the occurrence of mafic-ultramafic suites (ophiolite or layered intrusion) is a unique character of the suture zones compared to surrounding granulite blocks and cratons. Here, we report new petrological and geochemical data of metagabbroic garnet-clinopyroxene rocks from Sri Lanka and discuss its petrological implications. Mineral assemblages of the rocks are garnet + clinopyroxene + orthopyroxene + ilmenite + hornblende + plagioclase (type 1), and garnet + plagioclase + clinopyroxene + orthopyroxene + quartz + ilmenite (type 2). Type 2 rock shows a decompression texture of orthopyroxene + plagioclase symplectite formed by a reaction: garnet + quartz=>orthopyroxene + plagioclase. Similar rocks and textures have been reported from the Palghat-Cauvery Suture Zone in South India (Nishimiya et al., 2008; Sajeev et al., 2009; Saitoh et al., 2011), Highland Complex in Sri Lanka (Osanai et al., 2006), and Lutzow-Holm Complex in East Antarctica (Saitoh et al., 2012). Temperature and pressure conditions inferred for the type-1 Sri Lankan metagabbro based on pseudosection analysis in NCFMASHTO system is 970-1040C and 8-10.5 kbar, which is significantly lower in pressure than the results of Osanai et al. (2006) (>18 kbar, >1000C). Recent petrological and geochemical studies of the Palghat-Cauvery suture zone in southern India suggest that similar metagabbros and related mafic-ultramafic suites occur as various blocks within ortho- and paragneisses as melange. Similar occurrences and P-T evolution of metagabbro bodies in several Gondwana fragments suggest that the Palghat-Cauvery Suture Zone might continue to the Lutzow-Holm Complex (East Antarctica) through Highland Complex (Sri Lanka).

Keywords: granulite, Gondwana, suture zone, pseudosection

Japan Geoscience Union Meeting 2014
(28 April - 02 May 2014 at Pacifico YOKOHAMA, Kanagawa, Japan)

SCG61-P08 Room:Poster Time:May 2 16:15-17:30

Neoarchean and Middle Neoproterozoic bimodal magmatism in the Gondwana orogeny, South India

KOBAYASHI, Airi[1*] ; TSUNOGAE, Toshiaki[1] ; KOIZUMI, Tatsuya[1]

[1]Univ. Tsukuba

Detailed petrological investigations for bimodal association of basaltic and rhyolitic magmas, which is regarded to have formed at subduction or rift zones, provides important information to investigate magma petrogenesis and tectonic evolution in a convergent or divergent margin settings. Here, we report first preliminary petrological and geochemical data of the Neoarchean charnockite-mafic granulite association in the Madras Block and Middle Neoproterozoic granite-amphibolite association in the Mesoarchean Coorg Block, southern India. Irregular-shaped mafic granulite (basaltic andesite) occurs as blocks of about tens of centimeter within charnockite (dacitic) in the Madras Block, while amphibolite (basaltic trachy-andesite) blocks in the Coorg Block are surrounded by sub-alkaline granite. Although there is no obvious texture of magma mixing in the Madras samples probably due to post-magmatic high-grade metamorphism and complete recrystallization, plagioclase in the contact zone between mafic enclave and host granite from the Coorg Block shows oscillatory and dusty zonings, which might suggest bimodal magmatism in Middle Neoproterozoic divergent margin in southern India.

Japan Geoscience Union Meeting 2014
(28 April - 02 May 2014 at Pacifico YOKOHAMA, Kanagawa, Japan)

SCG61-P09 Room:Poster Time:May 2 16:15-17:30

Infiltration of CO_2-H_2O binary fluid and formation of patchy charnockite from Southern India

ENDO, Takahiro[1*] ; TSUNOGAE, Toshiaki[1] ; M., Santosh[2]

[1]Univ. Tsukuba, [2]China University of Geosciences Beijing

Since the first discovery of patches, veins and ladders of coarse-grained orthopyroxene-bearing felsic granulite (incipient charnockite) within foliated amphibolite-facies gneiss from Kabbal in Karnataka, southern India, by Pichamuthu (1960), the origin and petrogenesis of charnockite and its implications for granulite processes in lower crust have been the focus of many petrologists. According to previous studies, charnockite formation in the SGT is considered to have resulted by the infiltration of CO_2-rich anhydrous fluids along structural pathways within upper amphibolite-facies gneisses, resulting in the lowering of water activity and stabilization of orthopyroxene through breakdown of biotite (e.g. Janardhan et al., 1979; Newton et al., 1980; Hansen et al., 1987; Santosh et al., 1990; Newton, 1992; among others).

This study presents new petrological data of ‘ incipient ’ charnockite developed within garnet-biotite (Grt-Bt) gneiss from Kakkod with the western Trivandrum Granulite Block (TGB), India. In this locality, bulk rock compositions of charnockite and the host Grt-Bt gneiss are almost equivalent. The result of conventional geothermobarometry using Grt-Opx-Pl-Qtz assemblage shows the peak metamorphic condition of 860-960 ℃ and 6.9-8.4 kbar, which is consistent with the results of mineral equilibrium modeling. The metamorphic condition certainly corresponds to granulite-facies event, and it is higher than those reported from other incipient charnockite localities in the TGB and adjacent Nagercoil Block. Furthermore, the estimated metamorphic condition is too high for the stability of the host Grt-Bt gneiss that contains a mineral assemblage formed at amphibolite-facies condition. In addition, althought pseudosecondary fluid inclusions are composed of pure CO_2, secondary fluid inclusions contain CO_2-H_2O binary fluid. Therefore, patchy chanorckite in Kakkod from the TGB is considered to have formed by infiltration of CO_2-H_2O binary fluid during a retrograde stage. The petrogenetic model of incipient charnockite formation proposed in this study is therefore different from reported petrogenesis from other localities.

Keywords: incipient charnockite, metamorphic fluid, pseudosection, geothermobarometry, Trivandrum Granulite Block, southern India

Japan Geoscience Union Meeting 2014
(28 April - 02 May 2014 at Pacifico YOKOHAMA, Kanagawa, Japan)

SCG61-P10 Room:Poster Time:May 2 16:15-17:30

Relationship of zeolites and host rocks

SHIMIZU, Kouhei[1*] ; YASUI, Mana[2]

[1]Department of Natural Sciences, Faculty of Knowledge Engineering, Tokyo City University, [2]Department of Resources and Environmental Engineering, Waseda University

Natural zeolites occur in various rocks, such as igneous rocks, sedimentary rocks, and metamorphic rocks, at surface and shallow zone of upper crust.

In this research, the relationship between chemical composition of the host rocks and zeolite species are discussed in terms of the basis of chemical analysis of samples from Izu Peninsula and the Chichijima of Ogasawara (Bonin) Islands.

Although origin relations between the microscopic zeolite species and host rock compositions are seen under the conditions of low water/rock ratio, like a burial diagenesis, low degree regional metamorphism, and contact metamorphism, it has reported that macroscopic crystals occur in veins and geodes, not controlled by host rock composition, as they produced under the conditions of high water/rock ratio of hydrothermal alteration, in a previous work. (Utada 1995)

Result and discussion

The identification of the zeolites species are characterized by X-ray diffractometry and bulk rock chemical composition of host rocks are analized by X-ray fluorescence.

To research 10 pointss of Chichijima (Ogasawara islands) and 2 points of Izu Peninsula, eight kinds of zeolite (Heulandite, Analcime, Chabazite, Mordenite, Erionite, Phillipsite, Stilbite and Yugawalite) were able to be identified.

Samples from Chichijima, Stilbite was detected on Miyanohama, Hatsuneura north side, Hatsuneura south side, Suzaki, Buta seashore, and Kin-shi beach.. Stilbite did not occur on the samples from other 4 points

As a resalts Si/Al ratio of the host rocks are clearly different between the points of Stilbite occured and not occured, Si/Al ratio of former rocks were 5.248˜7.672, the latter rocks were 4.230˜4.768. The boundary of Stilbite occurrence S1/Al ratio of host rock seems to be around 5. . In the Chichijima (Ogasawara islands), correlation was found between host rocks and formed zeolites.

Keywords: zeolites, host rocks, Chichijima,Ogasawara islands

Japan Geoscience Union Meeting 2014
(28 April - 02 May 2014 at Pacifico YOKOHAMA, Kanagawa, Japan)

SCG61-P11 Room:Poster Time:May 2 16:15-17:30

Three pyroxene andesite (pigeonite-augite-hypersthen andesite) from Hakone volcano

ISHII, Teruaki[1*]

[1]Fukada Geological Institute

Pigeonite phenocryst bearing volcanic rock is very rare in the world. Pigeonite-augite-hypersthen andesite (= three pyroxene andesite or pigeonite andesite) from Hakone volcano is very famous according to the detailed studies on the pyroxenes using microscope by the late professor Kuno (Kuno 1935, Kuno 1936).On the bases of the detailed EPMA analyses of the pyroxene crystallization sequences as well as estimated magmatic temperatures using pyroxene geothermometer, for the pigeonite andesite, the author suggests the following working hypothesis, i.e. the pigeonite andesit was induced by magma mixing between three pyroxenes andesite magma (about 1070 degree C) originated from the primitive high temperature hydras tholeiite magma within secondary magma reservoir opened for water, and the high temperature magma (about 1110 degree C) in the secondary magma reservoir. The key concept is that cocrystallization of three pyroxene phenocrysts under open system for water in the secondary magma reservoir.

Keywords: Hakone volcano, pyroxene geothermometer, pigeonite, magma mixing, three pyroxene andesite, magmatic temperature

Japan Geoscience Union Meeting 2014
(28 April - 02 May 2014 at Pacifico YOKOHAMA, Kanagawa, Japan)

SCG61-P12 Room:Poster Time:May 2 16:15-17:30

The structural water in hydrothermally synthesized monazite

ABE, Takeyasu[1*] ; NAKAMURA, Michihiko[1]

[1]Department of Earth Sciences, Tohoku University

Introduction: The U-Th-Pb dating of accessary minerals such as zircon and monazite is widely applied for various types of rocks [1,2,3]. There has been proposed another method to obtain geochronological information from these minerals: quantifying the degree of metamictization (destruction of crystal structure by radioactive components). It is reported for zircon that the water content (up to 10 wt%) is in proportion to the degree of metamictization, thus to the concentration of radioactive nuclei and geological age[4]. Monazite on the other hand usually undergoes much less metamictization than zircon due to the higher bond strength of P and O compared to that of Si and O; this results in the lower water content in the metamictized monazite. Determination of the structural water content in monazite without radioactive damage is thus necessary to constrain the ”initial” water content prior to hydration. The water content bears significance also for better understanding the crystal chemistry of monazite. In this study, we synthesized monazite single crystals at hydrothermal condition and determined the content of structural water as a function of pressure.

Experimental method: The hydrothermal synthesis of monazite was conducted at a temperature of 800 degC and pressures of 1.5, 10 and 15 kbar using a cold-seal pressure vessel and a piston cylinder apparatus. The $CePO_4$ reagent was encapsulated with H_2O or H_2O-NaCl solution and run for ca. 100 hours. The FT-IR analyses of the obtained monazite single crystals were conducted to determine the concentration of structural OH on the basis of Lambert-Beer’s Law. The molar absorption coefficient was estimated by linear calibration curve against the OH stretching vibration wavenumber [5].

Results and Discussion:The broad absorption band was observed at 3100-3600 cm^{-1} in the crystals synthesized in all the experimental conditions. The water content of synthesized monazite was estimated approximately to be 20-70 ppm, showing no large pressure dependence. FT-IR analyses of pleochroic absorption are on-going to determine the OH dipole orientation within the crystal structure.

References: [1]J. M. Langille, M. J. Jessup, J. M. Cottle, G. Lederer, T. Ahmad, Journal of Metamorphic Geology, 30, 769-791 (2012)
[2]E. Janots, A. Berger, E. Gnos, M. Whitehouse, E. Lewin, T. Pettke, Chemical Geology, 326-327, 61-71 (2012)
[3]T. Imayama, K. Suzuki, American Mineralogist, 98, 1393-1406 (2013)
[4]M. Zhang, E. K. H. Salje, R. C. Ewing, Journal of Physics: Condensed Matter, 14, 3333-3352 (2002)
[5]M. S. Paterson, Bulletin de Mineralogie, 105, 20-29 (1982)

Keywords: hydrothermal synthesis, accessory mineral, monazite dating, metamictization, nominally anhydrous minerals, FT-IR

Japan Geoscience Union Meeting 2014
(28 April - 02 May 2014 at Pacifico YOKOHAMA, Kanagawa, Japan)

SCG61-P13 Room:Poster Time:May 2 16:15-17:30

Phase relation in ternary feldspar system at high temperature

KODAMA, Yu[1*] ; MIYAKE, Akira[1] ; HOKADA, Tomokazu[2] ; KAWASAKI, Toshisuke[3]

[1]Kyoto Univ., Sci., [2]National Institute of Polar Research, [3]Ehime Univ., Sci.

During cooling of rocks or by change of chemical composition of feldspar, feldspar transforms to other polymorphs and forms various micro-textures. Observing micro-textures of feldspar is a useful approach to give a constraint to the thermal history of the rock. It has been known that the feldspars in ultrahigh-temperature (UHT) metamorphic rocks have ternary feldspar (Tfs) composition and those have the various and complex microtextures. However, the occurrence and the formation process of micro-textures in Tfs had not been studied in detail and they could not be interpreted by the widely used phase diagram with 2nd-order C2/m-C-1 phase transition at high temperature. And furthermore, although many experimental studies were performed, with respected to the phase relation on the plagioclase feldspar and alkali feldspar systems, the detailed experiments for the phase relations in the An-Ab-Or ternary feldspar system were restricted and its phase relations still remain ambiguous. Due to the high crystallization temperature of ternary feldspar (Tfs), Tfs would preserve the information about thermal history in more detail than those recorded on alkali feldspars and plagioclase feldspars. Previous thermodynamic studies on the C2/m - C-1 phase transition (Kroll et al., 1980; Salje et al.1985, Carpenter, 1988) were carried out using the in situ powder X-ray experiments on pure Ab compositions. Due to the spatial resolution of analytical instruments, they missed the formation of the micro-texture on C2/m - C-1 phase transition. In this study, high temperature and high pressure experiments were carried out to decide the phase relation at high temperature including the phase relation between the C2/m and the C-1 in the An-Ab-Or ternary feldspar system at 1100 - 1300C and 10 kbar. We reveal the formation process of complex micro-textures of Tfs in UHT metamorphic rock by the present phase diagram.

We employed mixture of powdered lamellae-free oligoclase and sanidine crystal as starting materials. Bulk composition of starting materials was prepared by varying ratio of oligoclase and sanidine. We focused whether micro-textures derived from the C2/m - C-1 phase transition were formed or not. Experimental products were observed using field emission scanning electron microscopy (FE-SEM, JEOL JSM-7001F) and annular dark-field scanning transmission electron microscopy (ADF-STEM, JEOL JEM-2100F) to observe micro-textures.

Exsolution lamellae by a compositional gap between the C2/m and the C-1 which has near (010) interface, were observed in the run products synthesized at 1100 - 1200C. This result strongly suggests that the C2/m - C-1 transition is the first order phase transition. Moreover, the glass phase was observed in run products synthesized at 1250 - 1300C. From these experimental results, we propose the phase diagram on the Olg (An25Ab75) -Or pseudo-binary.

Napier Complex in northern Enderby Land, East Antarctica is one of the most famous regional ultrahigh-temperature (UHT) metamorphic terranes in the world. Although Tfs in Napier Complex has the complex microtextures (e.g., Harley 1985; Sheraton et al. 1987; Hokada, 2001), the occurrence and the formation process of micro-textures in Tfs have not been understood in detail. By the phase diagram obtained in the study, the formation process of Tfs in the felsic gneiss and the micro-texture in Tfs were revealed as following process. At first heterogeneous distribution of Olg, Tfs, and myrmekite-like textures were result of melting of the felsic gneiss and following crystallization. And then, the peak metamorphic temperature is estimated to be at least 1200 - 1250C. At the cooling process, the complex exsolution textures of Tfs are composed of (010) coarse lamellae derived from C2/m - C-1 first order phase transition and (-901) fine lamellae derived from spinodal decomposition.

Keywords: ternary feldspar, phase relation, high temperature experiment

Japan Geoscience Union Meeting 2014
(28 April - 02 May 2014 at Pacifico YOKOHAMA, Kanagawa, Japan)

SCG61-P14 Room:Poster Time:May 2 16:15-17:30

Quantitative Analysis of Rock Samples by ICP-Quadrupole Mass Spectrometer (QMS)

AJIRO, Takuya[1*] ; OOKI, Seigo[2] ; CHAKO TCHAMABE, Boris[3] ; OHBA, Takeshi[2]

[1]Cource of Chemistry, Graduate School of Science, Tokai University, [2]Department of chemistry, School of Science, Tokia University, [3]School of Science and Technology, Tokai University

ICP-Quadrupole Mass Spectrometers (QMS) can analyze multi-element quickly with high sensitivity. One problem is the interference by polyatomic molecules. For example, polyatomic molecules, such as ArO and ArCl, obstruct the analysis of Fe and As, respectively. In order to remove polyatomic molecules, ICP-QMSs using the collision gas was developed. For collision gas, generally inert gas such as He gas has been used. In this study, we try to analyze major and trace elements of standard rocks and volcanic rocks of Cameroon Volcanic Line by a ICP-QMS with He collision cell.

The iCAP-Q (ThermoScientific Inc) was selected for study. The plasma was operated at 1.7 kW and 27 MHz. The flux of Ar was about 16 L/min. The sampling cone can be removed easily without any tools and cleaning procedure is simple. The plasma gas, which is injected to vacuum system, is bended to 90 degree by an ion lens and reach to He Collision Cell. Neutral molecules are removed efficiently by the ion lens. Helium collision cell has a function as small QMS, removing interfering ions lighter than target element. The polyatomic molecules are also removed due to the reduction of their kinetic energy with He collision. The ions passing He collision cell go to the main QMS and their signals are detected by analog or pulse detections.

We used three standard rocks (JA-2, JB-2, and JB-3) and volcanic rocks at Borombi Mbo Volcano, Cameroon. The 50 mg of rock powder was put into 100 mL Teflon digestion vessel with 2.0 mL of 35 wt% HCl, 1.0 mL of 60 wt% $HClO_4$, and 0.5mL of 50 wt% HF. The vessel was set in microwave heating system (Multiwave 3000, Parkin Elmer Inc.). The microwave power was increased to 500 W by 50 W/min and kept over 60 min. After heating, the digestion vessel was cooled down to 50 ℃. In the cooled vessel, 2.5 mL of saturated H3BO3 water and 2.5 mL of pure water were added, and the vessel was heated by microwave heating system again. The micro wave power was increased to 1400W by 280 W/min and kept for 20 min. After cooling, pure water was added to the sample solution and total volume was adjusted to 50 mL.

Yields of major elements in standard rocks, except for Si, were almost more than 70 %. In case most of trace elements, those were also more than 70%. Furthermore, there was no significant difference in the yield of most elements when we analyzed several times for a common sample. It is found that major elements, except Si, and most of trace elements of volcanic rocks can be analyzed by using a single ICP-QMS. In case of volcanic rock samples of Cameroon, type of these samples were identified to be an alkali basalt based on Nb/Y versus Zr/TiO_2 diagram. This result is consistent to the previous study on Cameroon Volcanic Line (A. Marizoli et al., 2000).

Keywords: ICP-QMS, microwave digestion, volcanic rock, quantitative analysis, Cameroon

Japan Geoscience Union Meeting 2014
(28 April - 02 May 2014 at Pacifico YOKOHAMA, Kanagawa, Japan)

SCG61-P15 Room:Poster Time:May 2 16:15-17:30

Validation of mass attenuation coefficients in quantitative electron probe microanalysis (EPMA)

KATO, Takenori[1*] ; JEEN, Mi-jung[2] ; CHO, Deung-lyong[3] ; SATO, Kei[1]

[1]Center for Chronological Research, Nagoya University, [2]Center for Research Facilities, Pusan National University, [3]Geological Mapping Department, Korea Institute of Geoscience and Mineral Resources

Mass attenuation coefficients (m.a.c.s) are important factors of accuracy in quantitative electron probe microanalysis (EPMA). New m.a.c.s are calculated from the latest version of two datasets[1][2] for Z = 1 - 92. The combination of two datasets solves the problems within them, such as spurious discontinuity and unnatural increase at high-energy sides of absorption edges. New m.a.c.s improve accuracy including geological applications.

[1] Henke B.L., Gullikson, E.M. and Davis, J.C. (1993) At. Data Nucl. Data Tables, 54, 181 - 342.
[2] Hubbel J.H. and Seltzer S.M. (1995) NISTIR, 5632, pp. 116.

Keywords: electron probe microanalysis (EPMA), quantitative analysis, mass attenuation coefficients, matrix correction

Japan Geoscience Union Meeting 2014
(28 April - 02 May 2014 at Pacifico YOKOHAMA, Kanagawa, Japan)

SCG61-P16 Room:Poster Time:May 2 16:15-17:30

SEM-EDS Automated Particle Analysis of Mineral Compositions of Rocks

MUTOU, Hitomi[1*] ; SHIMADA, Aiko[2] ; ONODERA, Hiroshi[3]

[1]JEOL Ltd.SM APPLICATION DEPARTMENT SM BUSINESS UNIT, [2]JEOL RESONANCE Inc. SM APPLICATION DEPARTMENT, [3]JEOL Ltd.SA APPLICATION DEPARTMENT SA BUSINESS UNIT

Rocks consist of various kinds of minerals depending on their localities and formation processes. Mineral compositions of rocks are very important to study their sources and formation processes. X-ray fluorescence analysis (XRF) is commonly needed for mineral composition analysis. The XRF analysis provides the average composition of elements in a rock. Analysis of mineral particles in a rock is sometimes more important to find features of a rock. However, the analysis of a large number of mineral particles in a rock one by one requires a great deal of time. In recent years, the automated particle analysis combined with a scanning electron microscope (SEM) on energy dispersive X-ray spectrometer (EDS), which is called SEM-EDS automated particle analysis has rapidly been advancing. This method enables fast analysis of a large number of particles one by one directly.

In this report, analysis of the mineral compositions of two rocks -the Koujaku granite and the Hakkoda second-stage pyroclastic flow deposition (Ht2) - was carried out with SEM (JSM-IT300LA, JEOL)-EDS (JED2300, JEOL) automated particle analysis. The samples for this analysis were prepared as follows: rocks were crushed separately and each crushed rock embedded in resin was polished. More than a few thousand particles of the rocks were analyzed. In the Koujaku granite, quartz was a dominant constituent. K-feldspar and alkali feldspar were contained in a higher concentration than plagioclase. In addition, some colored minerals were contained. In the Ht2, pumice was a dominant constituent. In addition, quartz, feldspar and some colored minerals were contained. Additionally, many particles in the Ht2 consisted of multiple minerals unlike in the Koujaku granite. In the presentation, we will give more detailed descriptions of minerals and their components of the rocks.

Keywords: Mineral, Particles Analysis, SEM-EDS

Japan Geoscience Union Meeting 2014
(28 April - 02 May 2014 at Pacifico YOKOHAMA, Kanagawa, Japan)

SCG61-P17 Room:Poster Time:May 2 16:15-17:30

Dependence of water concentration distribution of columnar joints formation in analogue experiments

HAMADA, Ai[1*] ; TORAMARU, Atsushi[2]

[1]Earth and Planet. Sci., Kyushu Univ., [2]Earth and Planet. Sci., Kyushu Univ.

Columnar joints of igneous rocks and ignimbrites have various morphological patterns. As their unit structure, column structure can be classified in terms of straight or curved. Columnar joint is formed by volume contraction due to cooling and tensile stress accumulated inner the volume is released as sequentially cracks according to the temperature gradient during cooling. Basic research to explain how curved columns are formed has not been conducted. In this study, we report the results of reproducing curved structure in analogue experiments by drying starch and water mixture. We put the mixture into a cylindrical container and light a lamp (60W) 1.5cm above the surface of mixture. We take images with X-ray CT of the specimen before drying perfectly and observe the spatial distribution of water concentration of the mixture on the way to form columnar joints. As a result, we recognize that water concentration distribution at a depth in mixture increases with the horizontal distance from just below the lamp. The direction of crack developing from the surface of the mixture to inner is almost perpendicular to the contour of water concentration. We confirm that the effect of heat from the lamp on the surface of the mixture differs with the distance from the lamp and it suggests inhomogeneous water concentration in mixture is caused by the difference of drying rate depending on the distance from the lamp. We also report the relationship between the direction of crack advance and the change of water concentration distribution with time.

Keywords: columnar joint, analogue experiment, crack formation, Micro-focus X-ray CT, concentration distribution

Japan Geoscience Union Meeting 2014
(28 April - 02 May 2014 at Pacifico YOKOHAMA, Kanagawa, Japan)

SCG62-01 Room:502 Time:May 2 09:00-09:15

Slab-fluids contain chlorine

KAWAMOTO, Tatsuhiko[1*]

[1]Institute for Geothermal Sciences, Kyoto University

We found that the fluid inclusions of sub-arc mantle peridotites have 5.1 wt. % NaCl beneath the Pinatubo, a frontal volcano (Kawamoto et al., 2013 PNAS) and 3.7 wt. % NaCl beneath the Ichino-megata, a rear-arc volcano (Kumagai et al., under review). Based on these observations, we suggest that the slab-derived fluids are saline fluids.

In order to understand the effects of salinity on the arc-magma chemsitry, two series of elemental partitioning experiments between silicate melts and aqueous fluids have been carrying out with and without Cl in synchrotron facilities. The experiments show that highly saline fluids can transfer Pb, Rb, and Cs more effectively than Sr and Ba from subducting oceanic lithosphere to the mantle wedge. As suggested by Keppler (1996, Nature), saline fluids can be an important agent to transfer large ion lithophile elements. Geochemical studies have suggested that three chemical components are involved in the formation of arc-basalts: the depleted mantle, aqueous fluid, and melt components (Pearce et al., 2005 G-cube). If supercritical fluids contain Cl and then subsequently separate into aqueous fluids and melts (Kawamoto et al., 2012, PNAS), then it follows that such aqueous fluids will inherit much of the Cl and also some of the large ion lithophile elements to explain qualitatively the geochemical features of Mariana arc basalts. In contrast, Cl-free aqueous fluids may not be able to transfer Pb to the magma source. Our partitioning experiments were conducted using highly saline fluids (12-25 wt % (Na, K)Cl). Based on the geochemical features, slab-fluids are likely to contain Cl, although their amount remains to be quantified.

References

Kawamoto T., Kanzaki M., Mibe K., Matsukage K.N., Ono S. (2012) Separation of supercritical slab-fluids to form aqueous fluid and melt components in subduction zone magmatism. Proc. Nat. Acad. Sci. USA 109, 18695?18700.

Kawamoto T., Yoshikawa M., Kumagai Y., Mirabueno M.H.T., Okuno M., Kobayashi T. (2013) Mantle wedge infiltrated with saline fluids from dehydration and decarbonation of subducting slab. Proc. Nat. Acad. Sci. USA 110, 9663-9668.

Keppler H. (1996) Constraints from partitioning experiments on the composition of subduction-zone fluids. Nature 380, 237 - 240.

Pearce J.A., Stern R.J., Bloomer S.H., Fryer P. (2005) Geochemical mapping of the Mariana arc-basin system: Implications for the nature and distribution of subduction components. Geochem. Geophys. Geosys. 6, Q07006.

Keywords: subduction zone, H2O, fluid inclusion, mantle wedge, synchrotron X-ray, magma

Japan Geoscience Union Meeting 2014
(28 April - 02 May 2014 at Pacifico YOKOHAMA, Kanagawa, Japan)

SCG62-02 Room:502 Time:May 2 09:15-09:30

Numerical modeling of water-rock reaction with a focus on the earth's surface environment

YOKOYAMA, Tadashi[1*]

[1]Osaka University, Graduate School of Science, Department of Earth and Space Science

Water-rock interaction proceeds by the interplay between dissolution/precipitation, diffusion of ions, and water flow in rock pores. The reaction-transport process in rock is quantitatively described by:

$\phi(\partial c/\partial t) = D_e(\partial^2 c/\partial x^2) - v\phi(\partial c/\partial x) + Ar_0 f(c)$

This equation is an example of the one-dimensional reaction-transport equation, and c is the solute concentration (mol/cm^3), t is the time (s), x is the distance (cm), ϕ is the porosity (dimensionless), D_e is the effective diffusion coefficient (cm^2/s), v is the flow rate in pores (cm/s), A is the surface area per unit volume of rock (cm^2/cm^3), r_0 is the rate constant (mol/cm^2/s). $f(c)$ is the function that expresses the concentration dependence of the dissolution rate (mol/cm^2/s), and for quartz, $f(c)=(1-c/c_{eq})$ (c/c_{eq} is the equilibrium Si concentration) (Scott et al., 2009). By solving the reaction-transport equation, we can know how the distributions of the solute concentration and dissolution rate and the amounts of primary and secondary minerals change with time. Such analysis is called the reactive transport modeling and has been applied to the studies of various processes including soil formation (Maher et al., 2009) and the reactions associated with geologic storage of CO_2 (Xu et al., 2010).

The parameters used in the reaction-transport equation can be estimated by direct measurement in the field, laboratory experiment, and fitting in the modeling. To reproduce natural process accurately, we need to estimate each parameter as precisely as possible. However, it is difficult to evaluate what value is most proper. For example, the reactive surface area A is often determined by measuring the volume of gas adsorbed on the mineral or by approximating the geometry of the mineral. However, the proportion at which the reactive surface area determined by these processes contributes to actual reaction is often unclear. In addition, there are cases where various $f(c)$ have been proposed for a specific mineral and the dissolution rate varies with time (White and Brantely, 2003). In such case it is unclear what equation should be used. Therefore, the way of setting appropriate parameter is one of the main subjects of research.

In water-rock reaction on the earth's surface environment, evaluation of the effect of water saturation is important because water saturation changes dynamically as a result of the occurrence of intermittent drying and infiltration. It has been reported that both the hydraulic conductivity and effective diffusion coefficient in rock decrease with decreasing water saturation and this significantly affects the result of the reactive transport modeling (Yokoyama, 2013). In addition, how water saturation affects the reactive surface area has been revealed recently (Nishiyama and Yokoyama, 2013).

Keywords: Reactive transport modeling, Water-rock reaction

Japan Geoscience Union Meeting 2014
(28 April - 02 May 2014 at Pacifico YOKOHAMA, Kanagawa, Japan)

SCG62-03 Room:502 Time:May 2 09:30-09:45

Kinetics of overall silica precipitation within the Earth's crust

SAISHU, Hanae[1*] ; OKAMOTO, Atsushi[2] ; TSUCHIYA, Noriyoshi[2]

[1]AIST, [2]Tohoku University

The kinetics of dissolution and precipitation of silica minerals is important to reveal the geochemical reaction and to estimate how long silica deposits forms in the Earth's crust. The present kinetic equation for silica-water reactions was determined at 0-300 C and in the low Si saturated solution, where quartz growth on quartz surfaces occurs than that of nucleation of silica polymorphs [1]. However, the precipitation experiments of the high Si supersaturated solution showed that the co-precipitation of silica polymorphs via nucleation could occur [2], and the euhedral quartz crystals precipitates without precursor of silica polymorphs from the solution with minor components (Al and Na) [3].

In this study, the overall precipitation rate of silica minerals, which includes surface reaction of quartz (first term) and nucleation of silica polymorphs (second term), is derived empirically to estimate the total amount of silica precipitation within the Earth's crust. The previous kinetic equation of surface reaction [1] is applied as the first term. Based on the precipitation experiments of flow rate, the nucleation-controlled precipitation of silica minerals is expressed in a first order rate equation in the second term. The applicability of the nucleation term determined as the nucleation parameter is only in the conditions that precipitation occurs: in the solution supersaturated with respect to quartz, and in the supercritical conditions of water. The rate constant of nucleation is derived as a function of Al concentration in the solution based on the experiments of silica precipitation [3].

By using the new kinetic equation, silica-water interaction was simulated at the wel WD-1a of the Kakkonda geothermal field, Japan, which penetrated the boundary of the hydrothermal convection and heat conduction zones [4]. Amount of dissolution and precipitation of silica minerals increases with decreasing of the fracture permeability. The largest amount of silica precipitation occurs in the downflow fluid at the permeable-impermeable boundary regardless of the fracture permeability.

The equilibrium consideration [5] and the kinetic results indicate that, if open fractures forms at the depth of the permeable-impermeable boundary, the impermeable zone could be reproduced by precipitation of silica minerals, which cause the sustainable division between the permeable zone and the impermeable zone in the Earth's crust.

References

[1] Rimstidt and Barnes (1980) *Geochim. Cosmochim. Acta*, **44**, 1683-1699.
[2] Okamoto et al. (2010) *Geochim. Cosmochim. Acta*, **74**, 3692-3706.
[3] Saishu et al. (2012) *Am. Min.*, **97**, 2060-2063.
[4] Doi et al. (1998) *Geothermics*, **27**, 663-690.
[5] Saishu et al. (in press) *Terra Nova*.

Keywords: Silica precipitation, Hydrothermal experiment, Kinetic equation, Nucleation, Permeable-impermeable boundary

Japan Geoscience Union Meeting 2014
(28 April - 02 May 2014 at Pacifico YOKOHAMA, Kanagawa, Japan)

SCG62-04 Room:502 Time:May 2 09:45-10:00

Sedimentary pore-fluid origin of H_2O-rich fluid in mantle wedge revealed by halogens and noble gases

KOBAYASHI, Masahiro[1*] ; SUMINO, Hirochika[1] ; NAGAO, Keisuke[1] ; ISHIMARU, Satoko[2] ; ARAI, Shoji[3] ; YOSHIKAWA, Masako[4] ; KAWAMOTO, Tatsuhiko[4] ; KUMAGAI, Yoshitaka[4] ; KOBAYASHI, Tetsuo[5]

[1]GCRC, Univ. Tokyo, [2]Dept. Earth Environ. Sci., Kumamoto Univ., [3]Dept. Earth Sci., Kanazawa Univ., [4]Inst. Geothermal Sci., Kyoto Univ., [5]Dept. Earth Environ. Sci., Kagoshima Univ.

H_2O plays an important role in mantle processes in subduction zones. Yet its subducting processes to the mantle remain unknown because of scarcity of direct observations of H_2O in mantle-derived materials. Since halogen and noble gas are strongly partitioned into ?uids and they show distinct elemental and/or isotopic ratios depending on their origins, their compositions in mantle rocks can provide complementary constraints on the behavior and origin of H_2O in the mantle. Although only few researches have been conducted, the subduction of halogens and noble gases derived from sedimentary pore fluids (seawater trapped in pores of deep-sea sediments) has been suggested. Pore fluid?like halogens and noble gases were found in mantle wedge peridotites which captured H_2O-rich fluids just above a subducting slab [1]. H_2O-rich fluid inclusions whose salinity is similar to that of pore fluids (salinity of pore fluids is the same level as that of seawater [2]) are found in a mantle xenolith from a subduction zone [3]. We investigated halogen and noble gas compositions of mantle wedge peridotites from subduction zones to better constrain how far the in?uence of subducted sedimentary pore fluids extends into the mantle.

The samples studied are harzburgitic xenoliths from the Avacha volcano in Kamchatka and the Pinatubo volcano in the Philippines, and alpine-type peridotite from the Horoman massif in Japan. H_2O-rich ?uid inclusions have been found in olivine of those mantle peridotites [3,4,5].

We applied the noble gas method, in which halogens (Cl, Br, and I) are converted to corresponding isotopes of Ar, Kr, and Xe by neutron irradiation in a nuclear reactor and then the concentrations of noble gas isotopes are determined by noble gas mass spectrometry. Halogen detection limits of this method are from two to ?ve orders of magnitude lower than conventional method, which enable to determine the low halogen abundances in mantle-derived materials. By crushing samples under ultra-high vacuum, noble gases are selectively extracted from H_2O-rich fluid inclusions. Unirradiated peridotites were also analyzed to obtain precise noble gas isotope compositions.

The halogens of all peridotites are heavily enriched in I, although the halogen ratios are distinctive in each locality. These high I/Cl ratios show a strong contribution of sedimentary pore fluids [2]. The noble gases except for He have the elemental and isotopic ratios similar to elementally fractionated atmospheric noble gases dissolved in seawater, which is probably equivalent to those dissolved in sedimentary pore fluids. The $^3He/^4He$ ratios are similar to that of the mantle and distinctly higher than the atmospheric ratio. This indicates that the fluids derived from subducting slabs acquired He from the ambient mantle, where He is much more enriched than in seawater.

These pore fluid?like halogen and noble gas signatures are strong evidence that the H_2O-rich fluids in the studied peridotites are derived from sedimentary pore fluids and transported to the mantle.

References: [1] Sumino *et al.* (2010) *EPSL* **294**, 163. [2] *e.g.* Muramatsu *et al.* (2007) *Appl. Geochem.* **22**, 534. [3] Kawamoto *et al.* (2013) *PNAS* **110**, 9663. [4] Ishimaru *et al.* (2007) *J. Petrol.* **48**, 395. [5] Arai & Hirai (1985) *Nature* **318**, 276.

Keywords: water, halogen, noble gas, subduction zone, mantle, peridotite

Japan Geoscience Union Meeting 2014
(28 April - 02 May 2014 at Pacifico YOKOHAMA, Kanagawa, Japan)

SCG62-05 Room:502 Time:May 2 10:00-10:15

Relations among temperature, dehydration of the PHS plate, and a large earthquake, a SSE, and LFEs in the Tokai district

SUENAGA, Nobuaki[1*] ; YOSHIOKA, Shoichi[2] ; MATSUMOTO, Takumi[3]

[1]Graduate School of Science, Kobe Univ., [2]RCUSS, Graduate School of Science, Kobe Univ., [3]NIED

In this study, we performed numerical simulations of temperature distribution at the plate boundary and estimated the dehydration process of hydrous mid ocean ridge basalt (MORB) in the oceanic crust in the Tokai district, central Japan. We discuss the relationships among temperature, dehydration, and a future megathrust earthquake, deep low-frequency earthquakes (LFEs), and a slow slip event (SSE). Our results identified a strongly coupled region for an expected megathrust Tokai earthquake based on temperature conditions at the plate boundary. The depth range of the plate boundary where the megathrust earthquake may occur is 9∼21 km, narrowing toward the east. An SSE is estimated to have occurred in the transition zone between unstable and stable sliding. Hypocentral depths of LFEs deviating from the isodepth contours of the Philippine Sea plate toward the east may be explained by differences in the dehydration process associated with phase transformations in hydrous MORB.

Keywords: 2-D thermal modeling, megathrust earthquake, low-frequency earthquake (LFE), slow slip event (SSE), temperature, dehydration from hydrous MORB

Japan Geoscience Union Meeting 2014
(28 April - 02 May 2014 at Pacifico YOKOHAMA, Kanagawa, Japan)

SCG62-06 Room:502 Time:May 2 10:15-10:30

The regional and single-vein scale distribution of the CO2 fluids in the Shimanto accretionary complex, Muroto area, SW

MUSHA, Michimasa[1*] ; TSUCHIYA, Noriyoshi[1] ; OKAMOTO, Atsushi[1]

[1]Enviromnetal Studies of Tohoku University

Carbon dioxide and methane are major carbonic components of the fluids in the crust. The crustal fluids generally have composition of C-H-O system, mainly composed of H_2O, CO_2, and CH_4, and they may be carried down into Earth's interior at subduction zones. Many studies have examined fluid components in various accretionary prisms under low-grade metamorphic conditions, and CH_4 is showed as the only carbonic species. Therefore, there is little information on the variation of the components of C-H-O fluids in subduction zones.

The Tertiary (Paleogene and Neogene system) Shimanto belt, southwest in Japan, is one of the best-studied ancient accretionary complexes. The Muroto Peninsula belongs to the Tertiary Shimanto belt, and it is mainly composed of sandstones, mudstones and conglomerates with small amount of basalt. Mineral veins were mainly composed of quartz, with small amount of calcite near the vein walls, while many studies have showed CH4 is the only carbonic component in the Shimanto belt, therefore it is unclear why calcite precipitated in the veins in absence of CO_2. Lewis (2000) reported the fluid inclusions of CH_4 and CO_2 mixture at one area in the Muroto Peninsula, but the extensive distribution of CO_2 fluids in the whole peninsula is not clear. In this study, we examined the distribution of C-H-O fluids from the Murotohanto Peninsula, as fluid inclusions in the mineral veins, using microthemometry and Laser Raman spectroscopy, in regional scale and single vein scale.

Fluid inclusions from quartz in the veins are composed of one-phase carbonic inclusions (only CH_4) and two-phase aqueous inclusions (carbonic vapor and H_2O liquid). Carbonic components of the vapor phase in the two-phase inclusions are gradually transited from CH4-dominant in the north area of the belt to a CO_2?CH_4 mixture in the south; the $CO_2/(CO_2 + CH_4)$ ratio in mole fraction (X_{CO2}) vary from 0 ˜0.3 in the north area to 0 ˜0.9 in the south.

In single vein scale, we examined single CO_2-bearing vein from the south area of the Peninsula, where X_{CO2} is 0 ˜0.8. The CO_2 ratio in the carbonic species is decreased from the vein wall (X_{CO2} = 0.5?0.8) to the vein center, in which carbonic species in the fluids is only CH_4 (X_{CO2} = 0). The existence of CO_2 only near the vein walls is in good agreement of the precipitation of calcite near the vein walls. The homogenization temperature increases from ˜180 ℃ to 240?250 ℃, indicating the transition of the carbonic species from CO_2?CH_4 to CH_4 during vein formation.

The dominant species of carbonic species in most accretionary prisms is CH_4 under low-grade metamorphic conditions, and thermodynamic calculation about equilibrium in the C-H-O fluids also shows that CH4 is dominant carbonic species in the equilibrium with graphite under the P?T conditions of formation of the CO_2-bearing veins (235?245 ℃, 165?200 MPa). The CO_2-fluids are preferentially distributed close to an out-of-sequence thrust that brings the Murotohanto sub-belt into contact with the late Oligocene?early Miocene Nabae sub-belt with its many volcanic lavas and intrusive rocks. Therefore, the CO_2-fluids were considered to be magmatic-origin, and that the fluids were injected and mixed with the CH_4pore-fluids of the sediments in the accretionary prism in the timing of formation of CO_2-bearing veins.

Keywords: fluid inclusions, accretionary complexes, calcite, mineral veins, C-H-O fluid, Shimanto belt

Japan Geoscience Union Meeting 2014
(28 April - 02 May 2014 at Pacifico YOKOHAMA, Kanagawa, Japan)

SCG62-07 Room:502 Time:May 2 10:30-10:45

Visualization of deep-seated fluid flow in Tokusa Basin, Yamaguchi Prefecture

NISHIYAMA, Nariaki[1*] ; TANAKA, Kazuhiro[2] ; SUZUKI, Koichi[3]

[1]Yamaguchi University, [2]Yamaguchi University, [3]Central Research Institute of Electric Power Industry

It is known that highly saline fluids spout out in spite of inland area in Japan (Sakai et al. 1978). These fluids spout out not only at the surface of the ground surface but also at the flowing borehole. However, the erupted region of ascending fluid from flowing borehole and its relationship to the geological structure is not identified. Electromagnetic surveys applying Controlled Source Audio-frequency Magneto-Telluric Method was carried out in the Tokusa basin, Yamaguchi Prefecture to obtain the two dimensional distribution of resistivity to clarify the geological structure and the distribution of deep-seated fluid.

The study area is consisted of the Late Cretaceous welded tuff, rhyolitic lava, and the Holocene sediments. Low resistivity zone continuously is distributed along the Tokusa-Jifuku fault (Sagawa et al, 2008) in bedrock more than 2.5km long and is distributed in north side of the fault in sediments like a tongue shape. Resistivity of erupted highly saline water corresponds to that obtained by CSAMT. Groundwater of the shallow wells drilled in the sediments shows the NaCl type. Therefore, low resistivity zone in the sediments corresponds to the highly saline water diluted by surface groundwater. As a result, deep-seated fluid in the Tokusa basin rises along the Tokusa-Jifuku fault in the basement rock and then flows to river subjected to the dilution by surface groundwater.

Keywords: Deep-seated fluid, CSAMT method, Tokusa-Jifuku fault, Groundwater flow

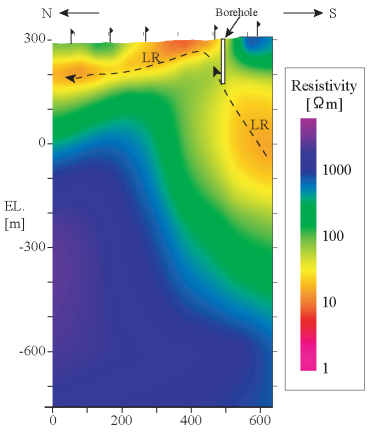

Fig.1 The resistivity profile by the CSAMT survey.

Japan Geoscience Union Meeting 2014
(28 April - 02 May 2014 at Pacifico YOKOHAMA, Kanagawa, Japan)

SCG62-08 Room:502 Time:May 2 11:00-11:15

Can clay minerals account for the non-asperity on the subducting plate interface?

KATAYAMA, Ikuo[1*] ; KUBO, Tatsuro[1] ; SAKUMA, Hiroshi[2] ; KAWAI, Kenji[3]

[1]Department of Earth and Planetary Systems Science, Hiroshima University, [2]National Institute for Materials Science, [3]Department of Earth and Planetary Sciences, Tokyo Institute of Technology

Seismicity along the subducting plate interface shows a regional variation, in which large earthquakes occur repeatedly at the strongly coupled patches that are surrounded by weakly coupled regions. This model suggests that the subduction plate interface is heterogeneous in terms of frictional properties; however, mechanism making the difference in strong and weak coupling is still not well understood. We consider this difference to relate to the alternation of plate interface due to aqueous fluids that result in the spatial distribution of clay minerals. In this study, we measured the frictional healing of clay minerals and discuss whether the frictional properties of clays can account for the weakly coupled non-asperity regions in the subducting plate interface.

We carried out a series of slide-hold-slide frictional experiments to examine the time-dependent frictional restrengthening of the simulated fault gouge. In the experiments, the axial loading was interrupted for periods ranging 10 to 3000 s after steady-state friction, and we measured the difference between the steady-state friction and the peak friction after each holding period. Mechanical data were recorded continuously with a sampling rate of 10 Hz and the frictional coefficient was calculated from the shear force divided by the normal force assuming zero cohesion.

The preliminary results show that the frictional strength of clay minerals (smectite and chlorite) slightly increases with holding time; however, the healing rate is significantly smaller than that of dry silicates such as quartz. Similar weak healing rate has been reported in the serpentinized simulated faults (Katayama et al., 2013). These experimental results suggest that the recovery of fault strength is different in materials, in which clay minerals show weak and slow recovery whereas dry materials show relatively quick and thereby strong coupling on the fault surface. Aqueous fluids that are released from the descending plate may change the mineralogy on the plate interface where clay minerals become dominant at the channel of fluid flow surrounding the unaltered dry patches that potentially act as a seismic asperity. Thus, the heterogeneous fluid pathway and spatial distribution of clay minerals may play a key role for the formation of asperity and non-asperity on the subducting plate interface.

Keywords: Interplate earthquake, Asperity, Clay minerals, Frictional experiment, Frictional healing

Japan Geoscience Union Meeting 2014
(28 April - 02 May 2014 at Pacifico YOKOHAMA, Kanagawa, Japan)

SCG62-09 Room:502 Time:May 2 11:15-11:30

Oxidation state of arc primary magma-inferred from sulfur speciation of melt inclusions

SHIMIZU, Kenji[1*] ; KASHIWABARA, Teruhiko[1] ; TAMENORI, Yusuke[2]

[1]JAMSTEC, [2]JASRI, SPring-8

Oxidation state of arc magmas highly influences the chemical behaviors of redox sensitive elements such as chalcophile and some siderophile elements in subduction zone. Therefore, Oxidation state of arc magmas is essential to understand arc magma geneses and evolutions of ore deposits. It has been suggested that sub-arc mantle is oxidized by subducted materials such as fluid, sediments and oceanic crust. However, recent studies contradicted that the oxidation state of primary arc magma (sub-arc mantle) is similar to the average upper mantle and oxidation is caused by differentiation associated with crystallization and interaction within preexisting crust (e.g. Lee et al., 2012, Science, v336, p64).

In order to constrain oxidation state of primary arc magmas at an immature subduction zone, we have analyzed S6+/ΣS of boninitic and tholeiitic melt inclusions within Cr-spinel from Bonin Islands and Guam by soft X-ray microbeam at SPring-8/BL27SU. Boninite in Bonin Islands uniquely formed at the early stage of subduction formation (~50 Ma) by melting of highly depleted hydrous mantle and 0-7 myrs later, related arc tholetiites erupted in southern Bonin Islands and Guam by melting of depleted mantle (Ishizuka et al., 2011, EPSL, v306, p229). Compositions of melt inclusions fully cover compositional ranges of whole-rocks and some boninitic melt inclusions have MgO higher than 20 wt%, showing that they are very primitive magmas. S6+/ΣS of boninitic and tholeiitic melt inclusions are 0.57 to 0.78 and 0.47 to 1, respectively; S6+/ΣS of all high-MgO (7 to 12 wt%) tholeiitic melt inclusions are >0.9. Oxygen fugacities of primary boninite and tholeiite are estimated to be ΔFMQ >+1 and >+1.5, respectively by experimental results of Jugo et al. (2010, GCA, v74 p5926), indicating that sub-arc mantle is oxidized even at an early stage of subduction zone. Between the period of eruption of boninite and tholeiite, not only mantle sources but also the subducting component in term of oxidation state of sub-arc mantle may have changed.

Keywords: melt inclusion, boninite, arc, sulfur

Japan Geoscience Union Meeting 2014
(28 April - 02 May 2014 at Pacifico YOKOHAMA, Kanagawa, Japan)

SCG62-10 Room:502 Time:May 2 11:30-11:45

Evaluating slab-fluid contribution into inhomogeneous mantle source: geochemical variation of Central and East Java arc

HANDINI, Esti[1*] ; HASENAKA, Toshiaki[1] ; WIBOWO, Haryo edi[2] ; SHIBATA, Tomoyuki[3] ; MORI, Yasushi[4] ; HARIJOKO, Agung[2]

[1]Graduate School of Science and Technology, Kumamoto University, [2]Geological Engineering, Gadjah Mada University, [3]Institute for Geothermal Sciences, Kyoto University, [4]Kitakyushu Museum of Natural History and Human History

The spatial distribution of the volcanoes in Central and East sections of Java arc denotes the widest and the narrowest of Java Island. Central Java section corresponds to the largest range and depth of Wadati-Benioff Zone along the island (180-360 km), whereas East Java section shows the narrowest range (190-220 km). However, both sections equally show wide geochemical variation with the function of slab-depth. Both also mark the appearance of the rear-arc alkaline suites in a different slab depth (360 km for Central Java, and 220 km for East Java). Geochemical datasets of basalt to basaltic andesite (further screened on Zr/Nb basis) from these sections were compiled to evaluate the contributions of slab-derived fluid to the mantle sources, and to assess the possible mantle sources of these magmas.

We group the lavas of the Central and East Java into two series: (1) the volcanic front series (VF), calc-alkaline suites of frontal- and middle-arc region volcanoes of Central and East Java, and (2) the rear-arc series (RA) consists of alkaline suites from Central and East Java (Muria, and Ringgit-Beser and Lurus, respectively). The VF series consistently shows typical island arc geochemistry, with strong LILE enrichment (Sr, Ba, Pb, and Rb) relative to HFSE. The RA series, mainly Muria, indicate stronger enrichment of LILE than other volcanoes closer to the trench. Ringgit-Beser and Lurus, the rear-arc lavas of East Java, behave differently in LILE enrichment. Ringgit-Beser lavas shows stronger LILE enrichment than that of lavas from Lurus, within the same enrichment range of Muria lavas. In the other hand, Lurus lavas are showing obvious HFSE depletion compared to OIB. The decreasing trend of LILE/HFSE and LILE/LREE (e.g. Ba/Nb, Ba/La, Pb/Ce, Pb/Nb) is observed across both Central and East Java sections. These ratios become lower toward the rear-arc of both sections, and the lowest in the rear-arc of Central Java. In various normalized plots (such as Nb vs. Ba/Nb), the VF series are plotted within the range of typical island arc basalts (IAB). Muria lavas, the rear-arc alkaline suite of the Central Java, resemble OIB and other non-arc type alkaline rock characteristics, but with positive indications of being island arc, such as negative Nb and Ti anomalies. Ringgit-Beser and Lurus alkaline lavas of East Java, however, are associated with other arc-type alkaline rock characteristics, with stronger signature of island arc than Muria.

Our analyzed samples show that lavas from East Java are closer in compositions to primitive magmas compared to Central Java's. The thicker overriding crust beneath Central Java than East Java possibly acts as the magma retainer that allows extensive fractionation. Across-arc variation of slab-derived fluid in both sections are observed as shown by decreasing LILE/HFSE and LILE/LREE toward rear-arc, suggesting the decreasing amount of slab-fluid added to the great slab-depth. The slab-fluid added to the volcanic front of East Java is slightly higher than that of Central Java, which may be controlled by the narrow range of slab dehydration area in the former that allows more fluid to concentrate. The low ratio of these trace elements in the rear-arc of both sections suggests that these parts have also been affected by dehydration of subducted slab. The stronger slab-fluid contributions in the rear-arc alkaline lavas of East Java than that of Central Java may reflect the role of shallower slab depth. Different mantle characteristics between the rear-arc of Central and East Java may reflect several possibilities: (1) the inhomogeneous mantle plume (E-type/EMI) beneath both sections, or (2) stronger EMI-type mantle contribution to Central Java than to East Java, or (3) the combination of both.

Keywords: Sunda arc, slab-derived fluid, across- and along-arc variations, trace elements

Japan Geoscience Union Meeting 2014
(28 April - 02 May 2014 at Pacifico YOKOHAMA, Kanagawa, Japan)

SCG62-11 Room:502 Time:May 2 11:45-12:00

Reaction progress and porosity change in hydrothermal alternation at Olivine/Quartz boundary

OYANAGI, Ryosuke[1*] ; OKAMOTO, Atsushi[1] ; TSUCHIYA, Noriyoshi[1]

[1]Graduate School of Environmental Studies, Tohoku University

Serpentinization in oceanic lithosphere is a fundamental process to bring water into deep earth ' s interior. It is known that silica activity controls the reaction paths during the hydrothermal alternation of peridotites [e.g. 1,2], however the detailed reaction mechanism induced by silica transport is poorly understood. In this study, we conducted hydrothermal experiments in olivine (Ol)-quartz (Qtz)-H2O system for investigating the mechanism of silica metasomatism at crust/mantle boundary.

Composite powders, which was composed of Qtz zone and Ol zone was set in inner tubes, with diameters of 1.7 mm and heights of 50 mm, and then loaded into autoclave with alkaline solution (NaOH,aq, pH = 13.8 at 25 ℃). Temperature and pressure are 250 ℃ and vapor-saturated pressure (= 3.98 MPa), respectively. After the experiments, the inner tube was cut into ten segments to evaluate the reaction progress as a function of the distance from Ol/Qtz boundary (hereafter denoted X), by Thermogravimetry and XRD. In order to evaluate the spatial variation of the reactions, the area of each minerals (olivine and reaction products) and pore was measured from the back-scattered electron (BSE) images of the thin section.

After 46 days, the H2O content near the Ol/Qtz boundary is lower (3.9 wt.% H2O) than that in (12 wt.%) at the margin of the reaction tube. The reaction products after olivine changed systematically as away from Ol/Qtz boundary from smectite+serpentine zone to the serpentine+brucite zones. In the smectite+ serpentine zone, the (Mg+Fe)/Si ratio of the products increases from 0.5 to 1.5, indicating that proportion of serpentine with respect to smectite increased away from the boundary. With increasing time, the smectite+ serpentine zone was enlarged, where as the serpentine+brucite zones was retreated.

Based on the combined analyzes of BSE images, TG and SEM-EDS, we obtained the reaction progresses of individual elementary reactions between 25 and 46 days as follows:

(1) In the smectite+ serpentine zone, smectite was formed via hydration of olivine and dehydration of serpentine by supply of silica. As the result, overall reaction has a variation in the smectite+ serpentine zone; △mH2O is negative (hydration) at X=0-4 mm, it is positive (dehydration) at X=4-10 mm. Volume expansion factor (V/V0) is much higher (=1.4) at Ol/Qtz boundary than other zones (=˜1.1), mainly due to Si-metasomatic reaction.

(2) Far from the Ol/Qtz boundary(X = 20-40 mm), there is no influence of silica supply, indicating that silica was completely consumed in the smectite+ serpentine zone. In these area, serpentinization proceeds as the typical olivine hydration reaction to produce brucite and serpentine with constant Srp/Brc ratio.

(3) In the transient zone, serpentine was formed by two ways: hydration of olivine and dehydration of brucite by supply of silica. These two serpentine forming reaction resulted in a large amount of serpentine in this area, and high volume expansion factor (=˜1.4).

Due to these two volume expansion reactions, low porosity (˜5%) area developed locally, never-theless porosity of other area is 30%. The amount of silica (△mSiO2,aq), which consumed from 25 to 46days, is largest at Ol/Qtz boundary, and monotonically decreases with increasing distance. If excess silica are available, the zones affected by silica will increase gradually with increasing time during hydrothermal alteration around mantle/crust boundary. In contrast, the porosity has a minimum around X = 15 mm in the transition zone, because Ol-hydration and Brc-dehydration reaction proceed with large volume expansion. Such volume expansion reaction and mineral changes causes the mechanical strength of boundary.

References:

[1] Frost, B. R., & Beard, J. S. (2007). Journal of Petrology, 48(7), 1351?1368.
[2] Ogasawara, Y., Okamoto, A., Hirano, N., & Tsuchiya, N. (2013). Geochimica et Cosmochimica Acta, 119, 212?230.

Keywords: serpentinization, ultramafic rock, Si-metasomatism, Hydrothermal alternation

Japan Geoscience Union Meeting 2014
(28 April - 02 May 2014 at Pacifico YOKOHAMA, Kanagawa, Japan)

SCG62-12 Room:502 Time:May 2 12:00-12:15

Distribution and transportation of melt in subduction zones

ISHII, Kazuhiko[1*]

[1]Graduate School of Sciences, Osaka Prefecture University

Volcanic and seismic activities in subduction zones are the result of complex interaction of geophysical and geochemical processes. I have investigated the hydration and dehydration and the generation and transportation of melt in subducting slab and adjacent mantle wedge using a numerical model. The model includes hydration and dehydration of the slab and mantle wedge, melting and solidification of mantle peridotites, permeable flow of melt and aqueous fluids, and solid flow of mantle peridotites with water- and melt-induced weakening. The model shows the melt distribution in the mantle wedge beneath the volcanic front and extending sub-parallel with the subducting slab. The detailed geometry of the melt distribution is strongly dependent on the parameters including water solubility of peridtites and permeable flow velocities of melt and aqueous fluids. I will discuss the effect of these parameters on the melt distribution and the interdependence among the geodynamic processes in the subduction system.

Keywords: subduction zones, melt, distribution and transportation

Japan Geoscience Union Meeting 2014
(28 April - 02 May 2014 at Pacifico YOKOHAMA, Kanagawa, Japan)

SCG62-13 Room:502 Time:May 2 12:15-12:30

Effects of mineral grain size variation on fluid migration in the mantle wedge

WADA, Ikuko[1*] ; BEHN, Mark D.[2]

[1]IRIDeS, Tohoku University, [2]Woods Hole Oceanographic Institution, USA

In this study, we investigate the effect of mineral grain size on the migration paths of aqueous fluids in the mantle wedge. Grain size is an important parameter that controls the grain-scale permeability of the mantle; in general, the smaller the grain size, the less permeable the mantle is, provided that the pores between grains are connected. The migration paths of aqueous fluids are therefore dependent on the grain size distribution, influencing the location and the degree of hydrous melting in the mantle wedge and the location of arc volcanism. We develop a 2-D fluid migration model with generic subduction zone geometry. In the model, we adopt grain size distributions calculated by coupling a subduction zone thermal model with a laboratory-derived grain size evolution model for a range of subduction parameters (Wada et al., 2011). The fluid migration model also includes the effects of mantle flow velocities and mantle-flow-induced pressure gradients, both of which are also calculated from the thermal model. The calculated grain size immediately above the slab is on the order of 10?100 micrometers beneath the forearc region, depending on the slab thermal structure, and it increases down-dip to a few cm beneath the arc region. Our preliminary modeling results with a simplified fluid influx pattern indicate that the aqueous fluids tend to become trapped in the down-going mantle due to low permeability and dragged down-dip until permeability becomes high enough for the fluids to migrate upward. Grain size above a colder slab tends to be smaller than that above a warmer slab, and therefore fluids become dragged down-dip further in a cold-slab subduction zone than in a warm slab subduction zone. A colder slab also tends to release fluids at deeper depths than a warmer slab, influencing the pattern of fluid influx into the mantle wedge. In this study, we calculate the fluid influx along the base of the mantle wedge, using the thermal modeling results and thermodynamic calculations based on Perple_X, and quantify fluid migration in the mantle wedge with the grain size and fluid influx distributions that are consistent with a given slab thermal structure.

Keywords: subduction zone, mantle wedge, aqueous fluid migration, grain size, slab dehydration, arc volcanism

Japan Geoscience Union Meeting 2014
(28 April - 02 May 2014 at Pacifico YOKOHAMA, Kanagawa, Japan)

SCG62-P01 Room:Poster Time:May 2 16:15-17:30

Temperature dependence of seismic velocities in a antigorite serpentinite at 1 GPa

SHIRAI, Ryo[1*] ; WATANABE, Tohru[1] ; YONEDA, Akira[2] ; MICHIBAYASHI, Katsuyoshi[3]

[1]Deaprtment of Earth Sciences, Faculty of Science, University of Toyama, [2]Institute for Study of Earth's Interior, Okayama University, [3]Institute of Geosciences, Shizuoka University

Serpentines play key roles in subduction zone processes including water transport, seismogenesis, exhumation of high-pressure rocks, etc. Geophysical mapping of serpentinized regions in the mantle wedge leads to further understanding of these processes. Seismic properties of serpentinized peridotites are critical to interpretation of seismological observations. Antigorite is a major form of serpentine, which is stable to higher temperatures. The single-crystal elastic properties were recently revealed via Brillouin scattering technique (Bezacier et al., 2010; 2013). However, the temperature dependence of elastic properties is still poorly understood. We have measured elastic wave velocities in a antigorite serpentinite at high temperature and pressure conditions.

A black massive antigorite serpentinite was collected from the Nagasaki metamorphic rocks, western Japan. It is composed of antigorite (98.0 vol.%), diopside (1.5 vol.%) and magnetite (0.5 vol.%). Microstructural observation reveals an interpenetrating texture characterized by randomly oriented antigorite blades. Antigorite CPO data shows weak concentration of antigorite axes. Elastic wave velocities measured at 180 MPa shows very weak anisotropy in elasticity. Cylindrical samples (D=L=6mm) were made with ultrasonic machining.

Measurements were made at the pressure of 1 GPa and the temperature of up to 550 C, by using a piston-cylinder type high pressure apparatus at ISEI, Okayama University. The pulse reflection technique was employed for velocity measurement. One LiNbO3 transducer with the resonant frequency of 5 MHz was used to transmit and receive ultrasonic signals. The length of the sample at high pressure and temperature conditions was estimated from the length of the recovered sample.

Both compressional and shear wave velocities linearly decrease with increasing temperature. The temperature derivatives are -3.6$\times 10^{-4}$ (km/s/K) and -2.7$\times 10^{-4}$ (km/s/K) for compressional and shear wave velocities, respectively. The temperature derivative of compressional wave velocity is close to that observed in the direction subparallel to antigorite *c*-axis (Yano et al., in prep.). The temperature dependence of c33 might dominate that of the effective elastic constants of a randomly oriented polycrystalline aggregate. Applications to seismological observations will also be discussed in this presentation.

Keywords: seismic velocity, serpentinites, antigorite, subduction zone, fluid

Japan Geoscience Union Meeting 2014
(28 April - 02 May 2014 at Pacifico YOKOHAMA, Kanagawa, Japan)

SCG62-P02 Room:Poster Time:May 2 16:15-17:30

Detection of structured water on quartz interface by Raman-FTIR spectroscopy and its evaluation by molecular dynamics

ISHIKAWA, Satoru[1*] ; SAKUMA, Hiroshi[2] ; TSUCHIYA, Noriyoshi[1]

[1]Graduate School of Environmental Studies, Tohoku University, [2]National Institute for Materials Science

Molecular structure of water in thin film shows different characteristics compared with that of free water. Thin film water was observed at mineral grain boundaries, and its structure might be influence by mineral surface.

High temperature-pressure cell for micro-Raman and Fourier-transform infrared (FT-IR) spectroscopy have been developed to investigate molecular structure of thin film water at high temperature and pressure conditions. As a result of micro-Raman and FT-IR spectroscopic measurements of water, the broad peak around 3400 cm^{-1}, attributed to OH stretching vibration mode of water molecular, was observed at ambient temperature and pressure. The broad peak shifted to higher wavenumber with increasing temperature on metal reflector. Compared with the result of IR properties of water on metal reflector, IR properties of water on artificial quartz surface exhibit different trend: the broad peak contained the peak component of the lower wavenumber (around 3200 cm^{-1}), even at high temperature.

In addition, molecular dynamics simulations were performed under the conditions of the experiment using MXDORTO. In the simulation, the water of a few nanometers of quartz near the surface was structured. The distribution of water density was different from the free water. These properties are discussed in the hydrogen bond between water molecular and silanol (Si-OH) of quartz.

Keywords: Raman spectroscopy, IR spectroscopy, interfacial water, subcritical, quartz, molecular dynamics

Japan Geoscience Union Meeting 2014
(28 April - 02 May 2014 at Pacifico YOKOHAMA, Kanagawa, Japan)

SCG62-P03 Room:Poster Time:May 2 16:15-17:30

Generation process of brecciated marble at Hiraodai karst, Kyushu, Japan

ISHIYAMA, Saya[1*] ; ANDO, Jun-ichi[1] ; NAKAI, Shun'ichi[2] ; OTA, Yasuhiro[3] ; DAS, Kaushik[1]

[1]Department of Earth and Planetary Systems Science, Hiroshima University, [2]Earthquake Research Institute, the University of Tokyo, [3]Kitakyushu Museum of Natural history & Human history

Geofluid is believed to be closely related to the seismic and volcanic activities. However, the detail relationship of geofluids with seismicity and volcanic activity is not studied properly through geological observations. We have found recently the brecciated marble widely distributed at Hiraodai karst plateau, Fukuoka Pref. This brecciated marble offers unique opportunity to study the relationship between geofluid and seismicity. Here, we shall explore the generation process of this brecciated marble through geological, microstructural and geochemical methods using polarization microscope, SEM, TEM, EPMA, microthermometric and MC-ICP-MS techniques.

The marble in Hiraodai karst plateau was thermally metamorphosed due to Cretaceous Hirao granodiorite intrusion. The brecciated marble occupies about 0.7 km x 1km of area in the central part of the karst. The main results of the present study are as follows.

1) The brecciated marble is composed of the rock fragments with variety of sizes ranging from millimeter to meter scale, and having angular to rounded shapes.
2) Numerous fluid inclusions are observed in the thin section of the brecciated marble.
3) TEM observation shows that the dense tangled dislocations are formed in calcite grains of the brecciated marble.
4) The homogenization and freezing temperatures of the fluid inclusions are about 240 deg C and 0 deg C, respectively.
5) The whole-rock and mineral separates (biotite and plagioclase) of Hirao granodiorite yields Rb-Sr isochron age of 129.4 +/- 2.4 Ma. Interestingly, Rb-Sr data of the fluid inclusions also lie on the Rb-Sr isochron of Hirao granodiorite.

The above-mentioned results of 1) and 2) suggest that the brecciation occurred by fluid infiltration and that the fragments were moved and rotated at very high speed. The result 3) demonstrates that the calcite grains of the brecciated marble experienced high stress. These three results together indicate that the brecciation process might generate seismic wave. On the other hand, the results of 4) and 5) suggest that the possible origin of the fluid inclusion is the released fluid from the Hirao granodiorite magma. Therefore, the brecciation of marble distributed at Hiraodai karst plateau was probably generated by magmatic fluid from Hirao granodiorite under high stress condition at 129.4 +/- 2.4 Ma ago.

Keywords: Brecciated rock, Hiraodai karst, Hirao granodiolite, Fluid inclusion, Rb-Sr isotope

Japan Geoscience Union Meeting 2014
(28 April - 02 May 2014 at Pacifico YOKOHAMA, Kanagawa, Japan)

SCG62-P04 Room:Poster Time:May 2 16:15-17:30

Equation of state of topaz-OH in the subducted sediment under high pressure and high temperature

NIIZATO, Mizuki[1*] ; INOUE, Toru[2] ; CAI, Nao[2] ; SUENAMI, Hideki[2] ; KAKIZAWA, Sho[2]

[1]Department of Earth Sciences, Ehime University, [2]Geodynamics Research Center, Ehime Univercity

Dehydration reactions of hydrous minerals in the subducted sediment produce a H_2O-rich fluid which causes generations of magma, decreases of melting temperature of sediment, and variations of magma compositions. Topaz-OH [$Al_2SiO_4(OH)_2$], which is one of hydrous minerals, is considered to be existed in the sediment of the subducting slab. Topaz-OH is the end-member of natural topaz [$Al_2SiO_4(OH,F)_2$]. The stability field of topaz-OH extends to 1500 degree C at 5-10 GPa (Wunder *et al*., 1993; Ono. 1998; Schmidt *et al*., 1998). The equation of state (EoS) for the natural topaz has been also estimated (Komatsu *et al*., 2003; Gatta *et al*., 2003). However, the EoS of the end-member topaz-OH has not been performed yet. In this study, we performed *in situ* X-ray diffraction (XRD) experiments under high pressure and high temperature for determining the thermal elastic properties of topaz-OH.

The starting material of topaz-OH was synthesized at 10 GPa and ˜1000 degree C from the quench experiment using multi-anvil apparatus. The high pressure (3-8 GPa) and high temperature (up to 800 degree C) *in situ* XRD experiments were carried out using MAX80 installed at beam-line NE5C at PF-AR, KEK, Japan. These XRD patterns were collected by the energy dispersive method. Thermal elastic properties were calculated from EoS fit v5.2 software (Angel, 2000) using 3rd order Birch-Murnaghan EoS.

From *in situ* XRD experiments, we successfully determined thermal elastic properties using all-data for fixed K'=4 as below: V_0=354.7(1) Å ^{3}, K_0=169.8(22)GPa, $(dK_T/dT)_P$=-0.013(7) GPaK^{-1}, a_0=1.61(23)$\times10^{-5}K^{-1}$, b_0=1.36(41)$\times10^{-8}K^{-2}$. From the detailed analysis of compression data, we found the change of the compression properties near 7 GPa. This change was also seen in a- and b-axis. Therefore we re-calculated the thermal elastic properties using two data sets: (I) below 7 GPa (II) above 7 GPa at room temperature. These calculation results from low pressure data show V_0=355.2(1) Å ^{3}, K_0=160.1(2)GPa, however those from the high pressure data show V_0=356.5(9) Å ^{3}, K_0=153.1(89) GPa (K'=4 fixed). Compared to the natural topaz, topaz-OH shows relatively large volume and bulk modulus. This shows that the volume and bulk modulus increase with increasing OH content. Compared bulk modulus with density, topaz-OH locates near the line for Birch's law and indicates large bulk modulus and density as same as Phase D [$Mg_2SiO_4(OH)_2$]. We suggest that high density topaz-OH enhances the slab subduction and transports water to deeper earth's interior.

Keywords: topaz-OH, high pressure hydrous phase, subducting slab, equation of state, synchrotron X-ray in-situ experiment

Japan Geoscience Union Meeting 2014
(28 April - 02 May 2014 at Pacifico YOKOHAMA, Kanagawa, Japan)

SCG62-P05 Room:Poster Time:May 2 16:15-17:30

Water content in arc basaltic magma in northeast Japan and Izu-Mariana arc estimated from melt inclusions in olivine and

USHIODA, Masashi[1*] ; IKEGUCHI, Naoki[1] ; TAKAHASHI, Eiichi[1]

[1]Dept. Earth and Planetary Sciences, Tokyo Institute of Technology

Primitive arc basalt magma is generated by partial melting of sub-arc mantle with adding aqueous fluid which was derived from dehydration of subducting slab. Aqueous fluid has profound effects on melting temperature of the mantle, crystallization pathways of generated magmas, and explosivity of magmas. Precise estimation of H_2O content in arc basalt magma is important to evaluate the effect of water on generation, differentiation, and eruption of magmas in subduction zones. We estimated variation of water content of arc basaltic magmas in the northeast Japan arc and the Izu-Mariana arc using a simple plagaioclase phenocryst hygrometer and melt inclusion analysis of olivine phenocrysts.

A simple plagaioclase phenocryst hygrometer was constructed by high-pressure and high temperature experiments using internally heated pressure vessels: SMC-2000 and SMC-5000 installed at the Magma Factory, Tokyo Tech (Ushioda et al., 2013, VSJ fall meeting). High-pressure and high-temperature experiments were conducted for relatively primitive basalt from Miyakejima volcano under hydrous conditions. OFS (Ofunato scoria: Tsukui et al., 2001; Niihori et al., 2003) is one of the most primitive basalt in the last 10,000 years. All experiments were conducted near the liquidus of plagioclase ($\pm$magnetite) and therefore the composition of melt is essentially the same as the starting material. H_2O content of melt was calculated by weight ratio of melt using mass balance calculation of all phases assuming that water was concentrated only in melt. Partition coefficient ${K_D}^{pl-melt}{}_{Ca-Na}$ is proportional to H_2O content in melt. In the experimental conditions, both pressure and temperature effects are negligible.

We then chose geochemical data sets of relatively primitive basaltic rocks (with no evidence of magma mixing) and most frequent Ca-rich plagioclase phenocrysts from 15 arc basaltic volcanoes, which includes both frontal arc volcanoes and rear-arc volcanoes from literature. In 15 volcanoes, plagioclase phenocrysts of high anorthite content (An$>$90) are commonly observed, whereas plagioclase phenocrysts in rear arc volcanoes usually have lower anorthite content (90$>$An$>$80). Estimated H_2O content of basaltic magma is 3 wt.% H_2O or higher.

We also analyzed H_2O content of melt inclusions in olivine phenocrysts using FTIR micro reflectance measurement (Yasuda, 2011) and FTIR micro transmission measurement (absorption coefficient: Yamashita et al., 1996) in order to compare H_2O content between melt inclusion analysis and this simple plagioclase phenocryst hygrometer. For example, melt inclusions of olivine phenocrysts in scoria from Ko-Fuji volcano had up to 3.7 wt.% H_2O which was consistent with estimate from our simple plagioclase phenocrysts hygrometer. In Miyakejima volcano, melt inclusions of olivine phenocrysts from OFS contained up to 3.3wt.% H_2O although H_2O content was 5.2 wt.% estimated from this hygrometer. In either case, basaltic magmas in volcanic front have 3 wt.% H_2O or higher.

Keywords: water in magma, melt inclusion, equilibrium between plagioclase and melt

Japan Geoscience Union Meeting 2014
(28 April - 02 May 2014 at Pacifico YOKOHAMA, Kanagawa, Japan)

SCG62-P06 Room:Poster Time:May 2 16:15-17:30

DEM simulation on fracturing induced by hydration and dehydration reactions

OKAMOTO, Atsushi[1*] ; SHIMIZU, Hiroyuki[2]

[1]Graduate School of environmental Studies, Tohoku University, [2]Institute of Fluid Science, Tohoku University

Dehydration and hydration reactions play significant roles on the global water circulation in the solid Earth, and cause drastic change in the mechanical properties of the subduction zone interface. Progress of both reactions requires an effective transport of water (release or supply) between the reaction sites and outer system, and are commonly characterized by large changes in solid volume, porosity, and fluid pressure. Reaction textures with fracturing are commonly observed both in hydration and dehydration hydration reactions. However, the dynamic relationship among reactions, fluid transport and deformation (fracturing, plastic deformation) is too complicated to be understood solely by observations of natural occurrences.

In the present study, we carried out numerical simulations on fracturing induced by hydration or dehydration reactions by using distinct element method (DEM). At first, we consider a dehydration reaction like a dehydration of serpentine. In the model, the following factors are introduced: (1) pressure dependence of reaction rate, (2) grain boundary as weak and water-saturated region, and that (3) mineral grains become permeable after fracturing or reacted. In this model, reaction rate drastically decreases with progress of dehydration reaction, when fluid cannot escape from the system.

We examined two rock systems; one is composed of reactive minerals (uniform-reactive system) and the other one is composed of reactive minerals embedded in unreative matrix minerals (reactive minerals in matrix system). In both systems, one is drain-boundary, whereas all the others are undrain-boundary. The spatial variation in fractures and progress of reactions are contrasting between the two systems. In the uniform-reactive system, fracturing does not occur and reactions uniformly occur from the drain-boundary, because fluid effectively escapes through newly-produced pore-network. In contrast, the reactive-mineral-in-matrix-system, the fracture network is produced among the reactive grains, and heterogeneous distributions of reaction progress was produced in the rocks. We will further discuss the key parameters to controls the fracture patterns and difference between hydration and dehydration reactions.

Keywords: hydration, dehydration, fracturing, distinct element method

Japan Geoscience Union Meeting 2014
(28 April - 02 May 2014 at Pacifico YOKOHAMA, Kanagawa, Japan)

SCG63-01 Room:418 Time:May 2 14:15-14:35

Investigation on the temporal change in attenuation within ruptured fault zone of the 1999 Chi-Chi, Taiwan earthquake

MA, Kuo-fong[1*] ; WANG, Yu-ju[1]

[1]Department of Earth Sciences, National Central University

Attenuation, noted as 1/Q, had been considered as a geophysical parameter related to the fluid content, temperature and fracture of the medium. The attenuation parameter related to S-wave named as Qs has more significant indication to the factors indicated above. The damage zone of a large earthquake was often considered as a fracture zone, especially the hanging wall of a thrust faulting earthquake, which suggests a zone with possible high attenuation (decrease in Q). Earlier Qp and Qs tomography studies revealed the feature with high attenuation on the hanging wall of the ruptured Chelungpu fault of the 1999 Chi-Chi earthquake. To examine the attenuation character in the rupture fault, we further investigate the temporal variation of the attenuation, specifically in Qs, within the hanging wall before, following and after the earthquake. We observed a decreasing in Qs within the fault rupture zone two years following the 1999 Chi-Chi earthquake by Qs tomography images and an analysis of single-path Qs near the Chelungpu fault. The synthetic and sensitivity tests of the Qs determination were carried out accordingly to justify the temporal variation. A Qs value within the hanging wall above the hypocenter was determined to be 157 two years following the Chi-Chi earthquake, which is significantly lower than the values of 238 and 289 prior to and two years after the main shock, respectively, from the Qs tomography. Similar values using a signal-path Qs analysis, from events within the ruptured fault zone to stations along the fault were obtained. The corresponding Qs values were 247 prior to the Chi-Chi earthquake. After the earthquake, we obtained the Qs values of 158 and 318 for the time, two years following and two years after the earthquake, respectively. Considering the two independent methods in determination of Qs, the reduction in Qs of 89 two years following the Chi-Chi earthquake in both method is significant. Along with 1% Vs reduction revealed by the analysis of repeating earthquakes, our studies suggested possible reduction both in Vs and Qs within the fault zone after the Chi-Chi earthquake. The observation of temporal changes in Qs after the Chi-Chi earthquake implies variations of pore fluid saturation in the ruptured fault zone. The reduction in Qs two years following the Chi-Chi earthquake might indicates high pore-fluid saturation within fractured fault zone rocks due to post-seismic redistribution of the fluid.

Keywords: attenuation, fault zone, temporal variation, earthquake rupture

Japan Geoscience Union Meeting 2014
(28 April - 02 May 2014 at Pacifico YOKOHAMA, Kanagawa, Japan)

SCG63-02 Room:418 Time:May 2 14:35-14:50

Chemical characteristics of hot springs in Southwestern part of Taiwan

SUGAI, Shuto[1*] ; TANAKA, Hidemi[1] ; TERUSAWA, Shuji[1] ; TSUNOMORI, Fumiaki[2] ; MURAKAMI, Masaki[3] ; KAWABATA, Kuniyo[2]

[1]School of Science, The University of Tokyo, [2]Geochemical Research Center, Graduate School of Science, The University of Tokyo, [3]OYO Corporation

Taiwan is located at the junction of the Ryukyu Trough and the Manila Trench which are the boundaries of the Philippine Sea Plate and the Eurasian plate. While the Philippine Sea plate is subducting beneath the Eurasian plate at the offshore of eastern Taiwan, the Eurasian plate is subducting beneath the Philippine Sea plate at Manila Trench at the south offshore of western Taiwan. The plate boundary is riding on the Taiwan Island in the vicinity of Kaohsiung, southern Taiwan, and the plate boundary appears as active faults to the north. Many faults striking NE - SW have been developed, and there are some hot springs and mud volcanoes (Hamada et al., 2009) along those faults.

We focused on the hot springs around Chiayi and Tainan, southwestern Taiwan in this study. These hot springs show temperature around 34 - 70 ℃ which are distributed about 20 km apart from the active faults to the east, arranging from north to south. We have conducted chemical analyses for the hot spring water taken from these springs and report the results of these analyses in this presentation.

Keywords: Taiwan, hot springs

Japan Geoscience Union Meeting 2014
(28 April - 02 May 2014 at Pacifico YOKOHAMA, Kanagawa, Japan)

SCG63-03 Room:418 Time:May 2 14:50-15:05

Estimate of isotopic composition and flux of Arima type fluid

TANAKA, Hidemi[1*] ; TERUSAWA, Shuji[1] ; SUGAI, Shuto[1] ; TSUNOMORI, Fumiaki[2] ; MURAKAMI, Masaki[3] ; KAWABATA, Kuniyo[2]

[1]School of Science, University of Tokyo, [2]Geochemical Research Center, Graduate School of Science, University of Tokyo, [3]OYO Corpoartion

It has been well known that change in chemical compositions of ground water is associated with crustal activities including large earthquakes. Research for change in chemical compositions of fluids associated with earthquakes is still continuing all over the world. However, reasons to choose the location of wells to measure the chemical and isotopic compositions of the fluids, and to choose particular chemical and isotopic compositions for measurements have not been unambiguous so far.

Because no deterministic theory has been established to predict large earthquake from anomalous chemical precursor signals so far, and fluid-monitoring research to explore earthquake precursor is significantly declined in the community, it would be less meaning to collect more chemical precursors of the earthquakes by repeating procedure in future.

Instead, there are some meaning if observed chemical change can be explained by physical and chemical process in the crust associated with crustal activities. At present, following three subjects are especially important. First, establishing the reliable basis to choose proper fluids and wells, second, designing and constructing the mass-spectrometer which has sufficient performance for fluid continuous monitoring at on-site close to the fault zone, and finally, establishing and improvement of diagnostic theory of fault zone fluid.

Based on the idea mentioned above, the results of examination of fluid of hot springs at Arima area are presented. There are several hot spring sources which are flown out continuously to the surface. After hot spring drillings at the 1940 to 1950's constant amounts and quality of these hot springs are maintained by branch of coal government office of Kobe City. Many researches have been done for the hot springs so far, including surface geology, shallow underground structure, source of fluids and fluids paths. Fluid paths are inferred to be fracture zones of particular fault zones by results of geological survey and resistivity analysis. It is important to recognize these kinds of fluids as "fault zone fluids", since identification whether monitored fluids flow through fault zone or not is important issue to examine the crustal activities from the chemical and isotopic compositions of the fluids. It is also well known that fluids from Arima hot springs show specific isotopic compositions which is inferred to be very deep origin. In this presentation, we discuss about quantity of flux of deep source fluids of Arima hot spring which is important issue to answer the question why we need to observe the fluids for crustal activities and where? and compare the results between this and previous studies.

Keywords: crustal fluids, Arima type Hot spring, fluid flux, saline water, isotopic composition

Japan Geoscience Union Meeting 2014
(28 April - 02 May 2014 at Pacifico YOKOHAMA, Kanagawa, Japan)

SCG63-04 Room:418 Time:May 2 15:05-15:20

Basic experiments for continuous monitoring of CH3 in the field by Mass spectrometer

KAWABATA, Kuniyo[1*] ; TSUNOMORI, Fumiaki[1] ; MURAKAMI, Masaki[3] ; TANAKA, Hidemi[2]

[1]Geochemical Research Center, Graduate School of Science, The University of Tokyo, [2]Department of Earth and Planetary Science, Graduate School of Science, The University of Tokyo, [3]OYO Corporation

Continuous gas monitoring in the field is important issue for various purposes such as for heat trapping gas monitoring, poisonous gas monitoring and scientific objective. In order to analyze the gas in the field, small-sized gas analyzer using mass spectrometer have been developed in our group. In the field, identifying the location of the emitted gas is needed. To detect gas-emission in distant places from the analyzer, we made basic laboratory experiments using methane gas. In this presentation, we introduce the results of the experiment.

Keywords: Mass spectrometer, methane, monitoring, in the field

Japan Geoscience Union Meeting 2014
(28 April - 02 May 2014 at Pacifico YOKOHAMA, Kanagawa, Japan)

SCG63-05 Room:418 Time:May 2 15:20-15:35

Geophysical Research of Tachikwa Fault Zone by Rn-222 and Cl- Concentration in Groundwater

SHIMODATE, Tomoya[1*] ; TSUNOMORI, Fumiaki[2] ; YASUHARA, Masaya[3] ; HAYASHI, Takeshi[4]

[1]International Christian University, [2]The University of Tokyo, [3]AIST, [4]Akita University

The 2011 off the Pacific coast of Tohoku Earthquake enhanced the probability of earthquake in Tachikawa Fault Zone. To evaluate the physical condition of Tachikawa fault zone, we researched Rn-222 concentration in groundwater, which is known as a precursory anomaly of earthquake. Additionally, we focused on the connection between the concentration of chloride ion in groundwater and fault damage zone and measured chloride ion in groundwater as well. Our purpose in this paper is to detect suitable groundwater for continuous measurement: (1) The depth of aquifer is deep enough to reach the bedrock. (2) Water contains much enough radon to monitor. (3)Water contains chloride ion whose concentration is controlled by the condition of fault damage zone.

Radon concentration in confined aquifer is supplied by alpha decay of radium in the surface of the grain. If the specific surface area of the grain changes according to physical condition of fault, radon concentration in the groundwater would change. The upper edge of bedrocks, main source of radon, has a depth of under 2,000 m around Tachikawa Fault Zone and it deepen in the west.

We focus on the distribution of chloride ion around Ayasegawa Fault is similar to one around Tachikawa Fault Zone. Low concentration of chloride ion in groundwater around Ayasegawa Fault is affected by fault damage zone, and we expect that groundwater around Tachikawa Fault Zone also shows low concentration of chloride ion due to fault damage zone. We use RTM1688(SARAD) for radon measurement, and ion chromatography for chloride ion measurement.

As a result, samples around the fault show high concentration of radon and low chloride ion. This suggests that the well around fault reach the bedrock and contain low concentration of chloride ion due to fault damage zone. These samples would show concentration change according to earthquake.

Keywords: radon, chloride ion, Tachikawa Falut Zone, spring water

Japan Geoscience Union Meeting 2014
(28 April - 02 May 2014 at Pacifico YOKOHAMA, Kanagawa, Japan)

SCG63-06 Room:418 Time:May 2 15:35-15:50

Precursory Change of Radon Concentration in Groundwater before 2011 Tohoku Earthquake

TSUNOMORI, Fumiaki[1*]

[1]Graduate School of Science, University of Tokyo

We will report characteristics of radon concentration changes in groundwater at the Nakaizu observatory around the Tohoku earthqauke, 2011.

Radon concentration in groundwater sometimes responds to crustal deformation before the earthquakes. The phenomenon was well known in 1980, and many scientists tried to detect such anomalous signals in order to find a chemical indicator of earthquakes. However few researches have studied a mechanism of the phenomenon. Nonetheless a lot of anomalies of the radon concentration relating to earthquakes are reported every year, thus it is important to clarify the fundamental process of radon concentration change in an aquifer. We would like to report the characteristics of radon concentration change around the 2011 Tohoku earthquake, and to discuss a fundamental model of the radon concentration change in an aquifer.

An anomalous increase in radon concentration was measured at the Nakaizu observatory on the Izu Peninsula prior to the 2011 Tohoku earthquake using a custom-made radon counter. Since the increase was more than three times the standard deviation of radon concentration variations over 35 years of recorded data, it is considered likely that it is a precursor to the earthquake. Following the earthquake, the radon concentration decreased exponentially to the background level. The anomalous increase is explained using a modified volatilization model containing three important aquifer parameters: the groundwater saturation ratio, the fracture surface area per unit volume, and the porosity. The modified model can also explain the radon concentration behavior prior to the 1978 Izu-Oshima-Kinkai earthquake.

Keywords: Radon, Groundwater

Japan Geoscience Union Meeting 2014
(28 April - 02 May 2014 at Pacifico YOKOHAMA, Kanagawa, Japan)

SCG63-P01 Room:Poster Time:May 2 16:15-17:30

Cooling history of a fracture zone in the Kojyaku granite, Tsuruga area: Constraints from multi-system thermochronology

SUEOKA, Shigeru[1*] ; YASUE, Ken-ichi[1] ; NIWA, Masakazu[1] ; SHIMADA, Koji[1] ; ISHIMARU, Tsuneari[1] ; UMEDA, Koji[1] ; YAMADA, Ryuji[2] ; DANHARA, Tohru[3] ; IWANO, Hideki[3] ; GOUZU, Chitaro[4]

[1]Japan Atomic Energy Agency, [2]National Research Institute for Earth Science and Disaster Prevention, [3]Kyoto Fission-Track Co., Ltd., [4]Hiruzen Institute for Geology and Chronology Co., Ltd.

Ages of faulting are generally estimated from ages of displaced geomorphic markers, e.g., terrace surfaces, alluvial deposits, or artificial structures. However, these markers are not always available, such as for faults in basement rocks. Such faults have been attempted to date by detecting chronological anomalies (e.g., Ikeya et al., 1982; Murakami and Tagami, 2004; Yamada et al., 2013; Gansawa et al., 2013) or dating hydrothermal veins or clay minerals formed after faulting (e.g., Zwingmann et al., 2004; Watanabe et al., 2008; Siebel et al., 2009; Yamasaki et al., 2013). However, definitive procedures to determine faulting ages based on such geochronological methods have not been established because thermogenesis and mass transport along fault zones are not simple. More basic and case studies are desirable to improve these methods.

We introduce an attempt to date a fracture zone observed in the northwestern part of the Tsuruga peninsula, southwest Japan, by constraining its cooling history from fission-track (FT), K-Ar, and U-Pb thermochronometries. In the northern part of the Kinki Triange, including the Kohoku and Tsuruga bay areas, NE-SW or NW-SE strike-slip faults such as the Kohokusanchi and Nosaka-Shufukuji fault zones, are dominant (e.g., The Headquarters for Earthquake Research Promotion, 2003a, b). Strike-slip faults in mountainous areas are generally difficult to date by using geomorphic markers. The fault we study is a strike-slip fault formed in the Tsuruga body of the Kojyaku granite (Kurimoto et al., 1999), along which no gromorphic marker is available. We dated 1) the fault gauge, 2) uncrushed host granitic rock, and 3) dolerite intruding within a few meters from the fault. The dispersions between zircon U-Pb ages and zircon fission-track ages of 1) and 2) are not significant at 2 sigma level and both of the zircon fission-track lengths are not shortened, implying 1) and 2) shared the cooling histories between closure temperatures of zircon U-Pb (>900 deg. C) and zircon fission-track methods (210-350 deg. C). On the other hand, apatite fission-track ages of 50.8 +/- 18.5 Ma for 2) and 28.4 +/- 13.6 Ma for 1) may be interpreted to be reflections of different cooling histories below 90-120 deg. C, closure temperature of apatite fission track method. Although the younger age of a) is attributable to the faulting during the Neogene/Quaternary or intrusion of the dolerite at 19.1-18.8 Ma inferred from plagioclase and whole-rock K-Ar ages, definitive conclusions are difficult to be drawn because of the wide error bars of the apatite FT ages and luck of apatite fission-track length data. In this presentation, we are going to give more precise discussions based on apatite fission-track length analyses.

Keywords: dating of a fault, fission-track thermochronology, K-Ar dating method, U-Pb dating method, Kojyaku granite

Japan Geoscience Union Meeting 2014
(28 April - 02 May 2014 at Pacifico YOKOHAMA, Kanagawa, Japan)

SCG63-P02 Room:Poster Time:May 2 16:15-17:30

Chemical and isotopic examinations of Arima-type high saline hotspring water in south-west Japan

TANAKA, Hidemi[1*] ; TERUSAWA, Shuji[1] ; SUGAI, Shuto[1] ; TSUNOMORI, Fumiaki[2] ; MURAKAMI, Masaki[3] ; KAWABATA, Kuniyo[2]

[1]School of Science, University of Tokyo, [2]Geochemical Research Center, Graduate School of Science, University of Tokyo, [3]OYO Corpoartion

Many researches have been conducted to explore component source, heat source and water source of hot spring in Japan. Matshubaya et al.,(1974) classified hot springs into four types by isotopic ratio of hydrogen and oxygen in water and geology (1) volcanic type, (2) Arima type, (3) coastal type, (4)Green tough type. Of these, Arima type is said to have deep origin source because hydrogen and oxygen isotope ratios suggests that the origin is mixture of meteoric water and magmatic water, and dissolving gas have abnormally high He isotopic ratio.

Sugimoto (2012) selected 180 hot springs that seem to be classified as Arima type from 6058 hot springs in Japan, using Li/Cl and Br/Cl values. Li/Cl is used as index of temperature of water was experienced (You et al., 1996). Br/Cl expresses influence from sea water and biological effect (Hurwitz et al., 2005: Uemura et al., 1988). He selected hot springs which have more Li/Cl and less Br/Cl as Arima type. But, his discussion was only about dissolving ion and not discussed hydrogen and oxygen isotope ratios used in the definition of Arima type.

So, we reselected 185 hot springs that seems to Arima type by Sugimoto (2012) method from 9887 hot springs in Japan and sampled 67 hot springs for isotopic analysis and ion analysis. As a result, the hot spring with the isotope shift in the same way as Arima hot spring is found along Median Tectonic Line (MTL) at Kinki, Western Shikoku and Central Japan (Kashio) districts. All mixing lines are converged to one point. Thus, we refer the fluid with this isotopic composition as origin water of Arima type. Since they converge to one point in the relationship of the hydrogen isotope ratio of the chloride ion concentration, the composition of the original water is as δD = -35 ‰, δ18O = 5 ‰, Cl- = 42g/l. The method to determine the isotopic composition and the resultant value of δD and δ18O is more convincing than those from previous results. Because shift lines from several regions are coincided at one point.

Keywords: Arima hot spring, Oxygen Isotope, Hydrogen Isotope, Brine fluids, original composition

Japan Geoscience Union Meeting 2014
(28 April - 02 May 2014 at Pacifico YOKOHAMA, Kanagawa, Japan)

SCG64-01 Room:501 Time:April 30 11:00-11:15

Spatial and temporal evolution of slip and seismicity during the 2013-2014 Boso slow slip event

FUKUDA, Jun'ichi[1*] ; KATO, Aitaro[1] ; OBARA, Kazushige[1] ; MIURA, Satoshi[2]

[1]Earthquake Research Institute, University of Tokyo, [2]Graduate School of Science, Tohoku University

GPS time series data show that transient crustal deformation has been occurring in the Boso peninsula, central Japan, since December 2013. Observed spatial and temporal patterns of surface displacements suggest the occurrence of transient aseismic slip on the subducting Philippine Sea plate. In addition, an increased rate of seismicity was observed from 31 December 2013 to 9 January 2014 off the east coast of the Boso peninsula. The location of the increased seismicity partly overlaps with the areas of seismic activity during the past Boso slow slip events.

To estimate spatial and temporal evolution of aseismic slip, we use GPS data from 71 stations of the GEONET in the Kanto region and data from 6 stations located along the east coast of the Boso peninsula, which are operated by Earthquake Research Institute of University of Tokyo and Tohoku University. The data are analyzed with GIPSY-OASIS II software to obtain daily coordinate time series at the 77 stations. Secular velocities, seasonal variations, and postseismic deformation following the 2011 Tohoku-oki earthquake are removed from the time series. We use a modified version of the Network Inversion Filter to estimate spatial and temporal evolution of daily cumulative slip and slip rate on the Philippine Sea plate. Slip slowly started around 20 December 2013 off the east coast of the Boso peninsula and then slip rapidly accelerated around 28 December and propagated to the west. Slip continued to accelerate until 3 January and then rapidly decelerated until 9 January.

To investigate spatial and temporal correlation of slip and seismicity, we use a matched-filter technique to detect earthquakes in the area of increased seismic activity. The detected earthquakes are located along the northern edge of the large aseismic slip and migrated from east to west during the period of rapid aseismic slip (31 December to 9 January). This migration pattern is consistent with the propagation of rapid aseismic slip, suggesting that the earthquakes are triggered by stress loading due to the propagation of aseismic slip. We do not identify significant seismic activity before 28 December, indicating that the slow slip event started well before the initiation of the seismic activity.

Keywords: slow slip event, seismic activity, GPS

Japan Geoscience Union Meeting 2014
(28 April - 02 May 2014 at Pacifico YOKOHAMA, Kanagawa, Japan)

SCG64-02 Room:501 Time:April 30 11:15-11:30

A slow slip event near the Boso Peninsula immediately triggered by the 2011 Tohoku-Oki earthquake

KATO, Aitaro[1*] ; IGARASHI, Toshihiro[1] ; OBARA, Kazushige[1]

[1]ERI University of Tokyo

It has been recognized that a series of slow slip events, accompanying with ordinary earthquakes, take place with recurrence intervals from 5 to 7 years near the Boso Peninsula along the plate interface of the subducting Philippine Sea plate [e.g., Hirose et al., 2012]. Immediately after the 2011 Tohoku-oki earthquake, intensive afterslip have been detected to start along the plate interface of the Pacific plate from off Tohoku region to southward Kanto region [e.g., Munekane et al., 2012; Fukuda et al., 2013]. It is well known that both the Pacific and the Philippine Sea plates are subducting beneath the Kanto region, and interacting with each other. Therefore, it is expected that the Philippine Sea plate might be dragged by the speeding Pacific plate during the intensive afterslip. We hypothesize that the dragging of the Philippine Sea plate by the Pacific plate leads to triggering of a slow slip event near the Boso Peninsula immediately after the Tohoku-Oki earthquake.

In order to verify the above hypothesis, we analyzed the seismicity including small repeating earthquakes, applying the matched filter technique to continuous waveforms. We used all available earthquakes associated with three sequences of slow slip events in 2007, 2011, and 2014 as template events. Then, we searched for events those have similar waveforms to ones of each template event from continuous waveforms. Based on the new earthquake catalog, we found out an abrupt increase in the swarm-like seismicity at the slow slip source area from March 12 to 14, 2011. In addition, some repeating earthquakes were extracted in the swarm, indicating aseismic slip transient. We, thus, interpret that the seismic swarm were linked to a newly detected slow slip event, which has not been previously recognized. However, based on the amount of aseismic slip deduced from the repeating earthquakes, moment released by the slow slip event is estimated to be smaller that by previously recognized slow slip events. We thus conclude that a small slow slip event might be triggered through the dragging of the Philippine Sea plate by the Pacific plate immediately after the Tohoku-Oki earthquake.

Japan Geoscience Union Meeting 2014
(28 April - 02 May 2014 at Pacifico YOKOHAMA, Kanagawa, Japan)

SCG64-03 Room:501 Time:April 30 11:30-11:45

Tidal correlations of earthquake swarms associated with slow slip events off Boso Peninsula

TANAKA, Sachiko[1*]

[1]NIED

We investigated statistical correlations between Earth tides and earthquakes in the four swarms associated with slow slip events (SSEs) off Boso Peninsula in 2002, 2007, 2011, and 2014. Following Hirose et al. (2012), we selected the SSE-related events from the Hi-net earthquake catalog. For each event, we assigned the tidal phase angle at the origin time by theoretically calculating tidal Coulomb failure stresses with a frictional coefficient of 0.2. For the fault plane, we assumed a landward-dipping reverse fault from the F-net moment tensor solution of the largest earthquake (Mw 4.9) in the 2014 swarm. Based on the distribution of tidal phase angles, we statistically tested whether they concentrate near some particular angle or not by using the Schuster test. In this test, the result is evaluated by p-value, which represents the significance level to reject the null hypothesis that the earthquakes occur randomly irrespective of the tidal phase angle. The result of analysis shows the 2014 swarm was strongly correlated with tidally-induced stresses (p = 0.01%). The distribution of tidal phase angles exhibited a peak near the angle 0, which corresponds to the time of the maximum tidal stress promoting fault slip. We suggest that tidal stress fluctuations can trigger earthquakes when superimposed on stress buildup caused by nearby slow slip. On the other hand, the other three swarms show insignificant correlations with tides. The resultant p-values are 87%, 16%, and 14% for the 2002, 2007, and 2011 activities, respectively. Geodetic observations indicate larger slow slip in these three episodes than in 2014 (Hirose et al., 2013; Kimura, 2014). It is highly likely that the swarm earthquakes in those activities were fully triggered by stress perturbations imparted by large slow slip. Tides appear to have exerted little or no influence on triggering in that case.

Keywords: Boso Peninsula slow slip events, Earth tides, earthquake triggering

Japan Geoscience Union Meeting 2014
(28 April - 02 May 2014 at Pacifico YOKOHAMA, Kanagawa, Japan)

SCG64-04 Room:501 Time:April 30 11:45-12:00

Interplate coupling and SSE in the Tokai region after 1981 using leveling data

OCHI, Tadafumi[1*]

[1]AIST

The long-term SSE in the Tokai region, central Japan, from mid-2000 to mid-2005 [Suito and Ozawa (2009)], had continued five years, which was much longer than other SSEs around the world [e.g. Schwartz and Rokosky (2007)]. After the termination of the SSE in 2005, no obvious long-term SSE has been detected and that makes difficult to discuss a recurrence interval of the events. In order to reveal whether the event repeats or not, and if it repeats, in order to clarify the interval and a temporal and spatial change of the interplate coupling and the slow slip, I analyzed a leveling data before the era of GEONET.

Various types of geodetic observations have been conducted in the Tokai region and there are some previous works about the temporal change of the crustal deformation using the data of these observations. For example, Kimata and Yamauchi (1998) analyzed EDM data and Kobayashi and Yoshida (2004) analyzed tidal data to detect irregular feature in the crustal deformation. In this study, I analyzed leveling data in the Tokai region from 1981 to 1999 and reveal spatially the temporal change of the vertical deformation velocity. Leveling observations have been conducted four times a year along the route from Kakegawa City to the Omaezaki Cape and once a year along the others around the Omaezaki Cape. I used all the data from these observations and inferred two-year-averaged vertical deformation rate using the time-dependent network adjustment [Fujii (1991)]. The estimated error of the rate is about 2 mm/yr, which is twice as much as the error of GNSS vertical data in this region [Ochi and Kato (2013)]. Comparing with the other geodetic data, the biggest advantage of the leveling data is that it can produce a spatial view of the crustal deformation with small error.

From the results of the analysis, two patterns of the crustal deformation that may correspond to existence and non-existence of the SSE appear alternately. The pattern that resembles that of in the 2000-05 was detected around 1982-83, 1988-90 and 1997. The duration of the event in 1982-83 is shorter than that of 1988-90, which is again shorter than that of 2000. Summing up these results, it is clear that there are various durations in the SSEs. In addition, if the small event in 1997 is taken into account, small and large events occur alternately and the intervals after the large event may tend to get longer. However, as the 1997 event is temporally close to the large long-term SSE after 2000, the SSE would affect the analysis of 1997 data and it should be considered further.

I also inferred the temporal change of the interplate coupling and slow slip using the results. In order to overcome the lack of temporal resolution, I fixed the distribution center of the slow slip to the same place by the results by Ochi and Kato (2013), the northwestern part of the Lake Hamana with the depth around 30-40 km. According to the forward modeling, the pattern of the crustal deformation in the 1982-83 and 1988-90 require somewhat smaller amount of SSE. On the other hand, the interplate coupling beneath the Omaezaki Cape constantly continues whether the SSE occurs or not.

Keywords: leveling data, interplate coupling, slow slip event, the Tokai region

Japan Geoscience Union Meeting 2014
(28 April - 02 May 2014 at Pacifico YOKOHAMA, Kanagawa, Japan)

SCG64-05 Room:501 Time:April 30 12:00-12:15

A shallow slow-slip-event in northern Hokkaido in 2012-2013: An event triggered by seismic waves.

IKEDA, Shohei[1*] ; HEKI, Kosuke[2]

[1]Graduate School of Science, Hokkaido University, [2]Department of Natural History Sciences, Faculty of Science, Hokkaido University

GNSS (Global Navigation Satellite System), as represented by GPS (Global Positioning System), enabled us to study SSE (Slow Slip Event), slow displacement of fault without exciting seismic waves. In this study, we report that baseline length between the Horonobe and the Nakatombetsu GNSS stations (part of the GEONET, GNSS Earth Observation Network) in Northern Hokkaido, shortened by ˜2 cm over 4-5 months period from 2012 summer to the early 2013. We assumed that an SSE is responsible for this change, and inferred fault parameters of this unique SSE. There have been lots of reports on repeating SSE at plate boundaries, e.g. off the Boso Peninsula, the Nankai Trough, and the Ryukyu Trench. In the Northern Hokkaido, a block boundary is considered to run north-south (Loveless and Meade, 2010) with the convergence rate of about 1 cm/year. This shallow SSE we report here is considered to have occurred at this boundary.

At first, we analyzed time series of the distance change between Horonobe and Nakatombetsu, together with a few additional GNSS stations nearby and estimated the fault parameters of this SSE by grid searches. The estimated slip was about 10 cm (Mw was ˜5.9), which suggests that a similar SSE recurs every decade. However, these GNSS stations started in 2002, and we do not have information on the previous SSE. We modeled the time series using lines with two breaks, and we constrained the onset time and the ending time of the SSE by minimizing the root-mean-square of the post-fit residuals. The optimal onset and termination was 2012.64 and 2013.08, respectively. Around the onset time, there was a deep earthquake beneath Sakhalin (M7.7) on August 14, 2012, and there were four M4 class earthquakes close to the Horonobe station in July, 2012. Seismic waves generated by these earthquakes may have triggered this SSE. At the termination time, there was an M4.8 earthquake on 3 Jan. 2013 at the depth of 24 km on the westward extension of the SSE fault. From mechanical point of view, it is difficult to consider that this earthquake encouraged the termination of SSE.

Keywords: GPS, Slow Slip Event, Northern Hokkaido, seismic waves

Japan Geoscience Union Meeting 2014
(28 April - 02 May 2014 at Pacifico YOKOHAMA, Kanagawa, Japan)

SCG64-06 Room:501 Time:April 30 12:15-12:30

Seismicity and pressure changes observed around DONET at the same time

SUZUKI, Kensuke[1*] ; TAKAHASHI, Narumi[1] ; HORI, Takane[1] ; KAMIYA, Shin'ichiro[1] ; NAKANO, Masaru[1] ; KANEDA, Yoshiyuki[1]

[1]JAMSTEC

The Philippine Sea plate is subducting to northwest below the Eurasian plate along the Nankai trough in southwestern Japan at a convergence rate of about 65 mm/year. In this region mega-thrust earthquakes have repeatedly occurred along the Nankai trough and caused serious and widespread damages in central and western Japan. The Japan Agency for Marine-Earth Science and Technology (JAMSTEC) installed permanent ocean bottom observation stations named as Dense Oceanfloor Network System for Earthquakes and Tsunamis (DONET) off the Kii Peninsula to monitor earthquakes and tsunamis and to decrease damage due to those. Because several kinds of continuous data have sent to JAMSTEC in real time, we can discuss continuous seismicity and other seismic/geodetic information. It is important for considering occurrence of large earthquakes to judge seismicity of small earthquake and to monitor crustal deformation.

Suzuki et al. (2013) has reported that quiescence of seismicity and ocean bottom pressure changes around DONET have occurred almost at same time from Feb. 2013 to Sep. 2013. In this study we extended observational period until Jan. 2014. As a result of investigation by using similar method with Suzuki et al. (2013), these changes seem to have continued after Sep. 2013. Quiescence of seismicity has not finished yet; seismicity is lower than one predicted from ETAS model (Ogata, 1989) represented by five parameters fitted by using data between 2012. Although pressure changes have been observed at only three stations (KMB05, KMB06 and KMB07) on Sep. 2013, pressure change at KMB08 was also observed on extended time series in addition to the three stations. We will try to estimate fault slip model that can cause these pressure changes and investigate how that fault slip influence to seismicity.

Keywords: seismicity, ocean bottom pressure gauge, DONET, ETAS model

Japan Geoscience Union Meeting 2014
(28 April - 02 May 2014 at Pacifico YOKOHAMA, Kanagawa, Japan)

SCG64-07 Room:501 Time:April 30 12:30-12:45

Detection of short-term slow slip events along the Nankai Trough by observations of groundwater level or pressure

KITAGAWA, Yuichi[1] ; KOIZUMI, Naoji[1*]

[1]Geological Survey of Japan, AIST

Non-volcanic deep low-frequency (DLF) tremors are detected on plate boundaries along many subduction zones around the world [Obara,2002; Ide, 2012]. Short-term slow slip events (S-SSEs), which cause small crustal deformation with no usual seismic waves, are also detected in subduction zones [Rogers and Dragert, 2003; Schwartz and Rokosky, 2007; Sekine et al., 2010]. There is a close spatial and temporal correlation between DLF tremors and S-SSEs. However, S-SSEs do not always occur in areas where DLF tremors occur and vice versa. Therefore, it is important to clarify the detailed spatial and temporal correlations in order to know what occurs on the plate boundaries along subduction zones. In general, detecting S-SSEs via crustal deformation is more difficult than with DLF tremors when using a seismograph. One major reason for this is that the decay of crustal deformation by distance is much larger than that of seismic waves. Therefore, it is necessary to develop new tools or techniques to detect S-SSEs. For this purpose, we attempted to detect S-SSEs in the Nankai Trough, Japan by conducting groundwater pressure observations at ANO station in Mie Prefecture, Japan. The ANO is a groundwater observation station operated by the Geological Survey of Japan, AIST, for earthquake prediction research. The groundwater pressures changed due to six S-SSEs that occurred near ANO from June 2011 to April in 2013. The fault models of these S-SSEs, which were estimated mainly by observing the crustal strains and tilts, explained the changes in the groundwater pressures. We also considered the conditions for detecting S-SSEs via groundwater observations. The volumetric strain changes caused by the S-SSEs along the Nankai Trough were 10-20 nstrain/day at most [Kobayashi et al., 2006], where nstrain means 10^{-9} strain. Therefore, the strain-converted noise level should be 5 nstrain/day or smaller to detect the S-SSEs. Taking the actual conditions of groundwater observation into consideration, it is necessary that the noise level should be smaller than 50 mm/day and that the strain sensitivity of the groundwater pressure or level should be larger than 1 mm/nstrain for the required strain-converted noise level.

Keywords: Slow slip event, Deep low-frequency tremor, Groundwater, Poroelastic theory, Strain, Earthquake forecast

Japan Geoscience Union Meeting 2014
(28 April - 02 May 2014 at Pacifico YOKOHAMA, Kanagawa, Japan)

SCG64-08 Room:501 Time:April 30 14:15-14:30

Time evolution of non-volcanic tremor episode

OBARA, Kazushige[1*] ; MATSUZAWA, Takanori[2] ; TANAKA, Sachiko[2] ; MAEDA, Takuto[1]

[1]Earthquake Research Institute, Univ. of Tokyo, [2]NIED

Non-volcanic tremor in subduction zones like as Nankai is one of slow earthquake phenomena in the transition zone between the seismogenic zone and the stable sliding zone on the subducting plate interface (Obara, 2002). Major tremor episodes with duration longer than several days are always accompanied by short-term slow slip events (SSEs). The space-time correlation of tremor and SSE suggests that the time evolution of tremor episode reflects the rupture process of SSE. Based on the similarity, studying the mechanism of slow earthquakes is important to understand the activity style of megathrust earthquake. Therefore, we investigate the time evolution of tremor episode based on the clustering catalog (Maeda and Obara, 2009, Obara et al., 2010) because the tremor is well-detected compared to other slow earthquakes.

Tremor belt-like zone is divided into some segments based on their spatial extent and recurrence interval (Obara, 2010). Each segment includes some sub-segment as units of tremor activity (Obara et al., 2013). Tremor episode usually initiates from the deeper part of the tremor belt-like zone. If the episode reaches to the updip part of the tremor zone, it becomes a major episode associated with detectable SSE (Obara et al., 2011). We sometimes observe major episodes initiated from the shallower part. The time evolution of tremor energy at the beginning stage of the tremor episode depends on the location of initiation point. If the episode starts from the deeper part, the evolution velocity is small for a while then increases rapidly after the tremor migration front reaches to the updip edge. On the other hand, the evolution velocity is high if the episode starts from the shallower part. This suggests that the tremor patches radiating high energy concentrate at the updip side. The time evolution of tremor energy at the beginning stage of each episode is not related to the final size of the episode. The size of episode may be controlled by the strain energy accumulation at each portion on the way of migration. This is the same for along-strike evolution of tremor episode. The propagation of tremor episode depends on the slip deficit in each sub-segment ahead of the rupturing sub-segment. We observed temporal deceleration of migration speed in front of the small gap as the sub-segment boundary. On the other hand, we detect acceleration of the migration speed at a common spot during passage of the major tremor episode several times. This spot is considered as a sweet spot where tiny tremor activity continuously occurs in the shallower part of the tremor zone. This spot frequently generates tremor episodes and is considered to be strongly inhomogeneous. Such variation on the plate interface may control the rupture process of SSE.

Keywords: non-volcanic tremor, slow earthquake, source migration, segmentation

Japan Geoscience Union Meeting 2014
(28 April - 02 May 2014 at Pacifico YOKOHAMA, Kanagawa, Japan)

SCG64-09 Room:501 Time:April 30 14:30-14:45

Fundamental properties of non-volcanic low frequency tremor catalogues

TAKEDA, Naoto[1*] ; KOIZUMI, Naoji[1] ; MATSUZAWA, Takanori[2] ; TANAKA, Sachiko[2] ; OBARA, Kazushige[3] ; MAEDA, Takuto[3]

[1]GSJ, AIST, [2]NIED, [3]ERI, Univ. of Tokyo

Since a discovery of non-volcanic low frequency tremor (NVT) in the subduction zone of southwest Japan (Obara, Science, 2002), the NVT has been found in various subduction zones or bottom of faults all over the world, and has been studied by many researchers. In these studies, an envelope cross-correlation technique for NVT detection and making a catalogue of NVT is important to discuss spatial and temporal activity of NVTs (e.g.; Maeda & Obara, JGR, 2009; Ide, Nature, 2010; Nakata et al., Nature Geoscience, 2008; Imanishi et al., GRL, 2011). There are some differences in NVT catalogues in the same region, since each study developed an original program for NVT catalogue. Furthermore, in some cases, even if they use a same program, parameters to detect NVT in the program were changed depending on a scope of the study. Consequently, there are some different features of NVT activity between the catalogues. In this report, we compare three catalogues, made by Japan Meteorological Agency (JMA), National Research Institute for Earth Science and Disaster Prevention (NIED) and Geological Survey of Japan, National Institute of Advanced Industrial Science and Technology (AIST), regarding a resolution of location and a NVT scale-sensitivity property as fundamental properties of the NVT catalogue.

Based on the method to estimate the resolution of location from a standard deviation of relative location (Ide, Nature, 2010), we calculated the resolution of location in each catalogue using several standard deviations of relative location. The estimated epicentral resolutions in three catalogues are almost 2-3km.

The NVT scale-sensitivity was estimated by a ratio of NVT counts in catalogues. For example, the sensitivity of the NIED catalogue for magnitude (M) based on the JMA catalogue was defined as $N_{nied-jma}(M)/N_{jma}(M)$. Here, $N_{jma}(M)$ is total counts of low frequency earthquakes (LFEs) with M listed in the JMA catalogue, and $N_{nied-jma}(M)$ is total counts of NVT in the NIED catalogue which is also listed in the JMA catalogue. To examine the relationship between the scale and the sensitivity in the catalogues, we used magnitude and NVT energy as the scale in the JMA and the other catalogues, respectively. By comparison of the NVT scale-sensitivity properties, it is found that these catalogues have characteristic scales in the sensitivity. Furthermore, the sensitivities of all catalogues decrease for large scale NVT. This is attributed to the increase of lost counts due to complex waveforms of highly active NVT. In our presentation, we show some examples of different features of NVT activities arising from different scale-sensitivity properties.

We conclude that these fundamental properties are useful not only for a comparison of catalogues, but also for an optimization of parameters in the programs of NVT detection.

Acknowledgments: We use the earthquake catalogue reported by JMA, and seismic waveform data provided by NIED (Hi-net), AIST, JMA, University of Tokyo, Kyoto University, Kyushu University, Kochi University, and Nagoya University.

Keywords: non-volcanic low frequency tremor, catalogue, position resolution, NVT scale-sensitivity property

Japan Geoscience Union Meeting 2014
(28 April - 02 May 2014 at Pacifico YOKOHAMA, Kanagawa, Japan)

SCG64-10 Room:501 Time:April 30 14:45-15:00

Determination of focal mechanisms of non-volcanic tremors using S-wave polarization: Correction for shear wave splitting

IMANISHI, Kazutoshi[1*] ; UCHIDE, Takahiko[1] ; TAKEDA, Naoto[1]

[1]Geological Survey of Japan, AIST

Non-volcanic tremors (NVTs) have been found at various plate boundaries during the last decade. Focal mechanisms of NVTs are important for better understanding physical mechanisms of tremor generation. Stacking of many similar event waveforms greatly enhances the signal to noise ratio of tremor signals, which enables us to use conventional focal mechanism determination methods based on P-wave first motion polarities and/or waveforms (Ide et al., 2007; Bostok et al., 2013). However, the stacking approach cannot resolve spatio-temporal variations of focal mechanisms, so a new method is needed.

Imanishi and Takeda (2010) conducted a polarization analysis to continuous seismic data and showed that the scatter in the particle motion directions becomes small in accordance with a period of NVT activity. The same conclusion was reported for Cascadia tremors by Bostock and Christensen (2012). Because NVTs are primarily composed of shear waves (e.g., Obara, 2002), our observed particle motions contain information regarding focal mechanisms. However, the shear wave particle motion should be treated in caution, since shear-wave splitting may distort the particle motion excited by a seismic source (e.g., Zhang and Schwartz, 1994).

In this study, we first explored the existence of seismic anisotropy using tremor signals. A standard shear-wave splitting analysis (Silver and Chan, 1991) was used to determine the fast polarization direction (LSPD) and the lag time between fast and slow shear waves (DT). The analysis detected clear split arrivals separated by about 0.1 s, indicating the need of the correction for splitting effects to recover radiation pattern of S-wave. The LSPD shows two major directions which are normal or subparallel to the strike of the plate margin. These results are consistent with previous studies using regular earthquakes (e.g., Saiga et al., 2011), demonstrating that tremor signals are also available to investigate seismic anisotropy.

We then determined focal mechanisms of NVTs by correcting for splitting effects on particle motions. The actual procedure is as follows:

(1) We rotate two horizontal seismograms to the fast and slow directions, advance the slow wave by the lag time, and rotate back to NS and EW directions.

(2) A polarization analysis is subject to 1 minute windows to determine S-wave polarization angles.

(3) Average and standard deviation of polarization angles are calculated at each hour.

(4) A grid search approach is performed at each hour to determine the best double-couple solution using polarization angles of multiple stations. Here the epicenter is determined by an average of locations using our ECM catalogue. The depth is assumed to be 35 km.

(5)Uncertainty is estimated based on a bootstrap approach.

We applied the above method to a tremor sequence at northern Mie prefecture that occurred at the beginning of April 2013. Most solutions show NW-dipping low-angle planes or SE-dipping high-angle planes. Because of 180 degrees ambiguity in polarization angles, the present study alone cannot distinguish compressional quadrant from dilatational one. Together with the observation of very long frequency earthquakes near the present study area (Ito et al., 2007), however, it is reasonable to consider that they represent shear slip on low-angle thrust faults. It is also noted that some of focal mechanism solutions contain large strike-slip component. We will present the spatial and temporal characteristics of focal mechanism solutions based on the analysis of more tremor sequences.

Acknowledgements: Seismograph stations used in this study include permanent stations operated by NIED (Hi-net), JMA, and Earthquake Research Institute. This work was supported by JSPS KAKENHI Grant Number 24540463.

Keywords: Non-volcanic tremors, Focal mechanism, Polarization analysis, Shear wave splitting

Japan Geoscience Union Meeting 2014
(28 April - 02 May 2014 at Pacifico YOKOHAMA, Kanagawa, Japan)

SCG64-11 Room:501 Time:April 30 15:00-15:15

Improved estimation of seismic energy radiation from deep low-frequency tremor

ANNOURA, Satoshi[1*] ; OBARA, Kazushige[1] ; MAEDA, Takuto[1]

[1]Earthquake Research Institute, the University of Tokyo

Deep low-frequency tremor occurs associated with slow slip event on the subducting plate interface at the downdip part of the megathrust seismogenic zone. Studying these phenomena is considered to play an important role to understand the mechanism of the megathrust earthquake. Until now, spatio-temporal distribution of tremor has been well investigated to get a whole picture of tremor activity. In this paper, we proposed a method for assessing energy radiation of tremor more quantitatively.

The Hybrid Method (HM) [Maeda and Obara, 2009] is a technique which determines epicenter and seismic energy of tremor simultaneously by using relative arrival time and amplitude distribution of the tremor envelope. To avoid false event detection, the " HM selected catalog " constructed with a threshold of a high Variance Reduction (VR>90) has been used for tremor study. However, when tremor activity is very high, envelope correlation between stations is relatively poor because of complicated waveforms. Then the VR generally becomes low and some parts of tremor during the active stage are not included in the HM selected catalog [Takeda et al., 2014]. Therefore, in order to investigate the energy release of tremor activity precisely, we have to re-evaluate it by using the waveform data.

Here, we developed a method for estimation of tremor energy by using measurement of tremor duration time from envelope waveform and the HM catalog. We started to search the duration around an origin time of tremor in the HM selected catalog. Then we determined the tremor duration when the amplitude is higher than noise level at each station simultaneously. At each tremor duration, we determined epicenter using centroid location of hypocenters of HM selected catalog within corresponding time and determined energy radiation by summing up of energy of tremor epicenters with VR of larger than 60.

As a result, we found characteristic spatial distribution of energy. It has been already known that there are two peaks of the number of tremors in the dip direction [Obara et al., 2010]. In this study, we found that high-energy region is distributed in the shallower part of the source area of tremor along the strike of the subducting Philippine Sea plate. This biased distribution of high-energy radiation suggests that the shallower part is more brittle in the brittle-ductile transition zone where tremor occurs. This brittle part may radiate higher seismic energy when shear slip occurs. This research will lead to quantitative assessment of the role of tremor in the stress relaxation process in the subduction zone.

Keywords: tremor, Nankai trough, slow earthquake

Japan Geoscience Union Meeting 2014
(28 April - 02 May 2014 at Pacifico YOKOHAMA, Kanagawa, Japan)

SCG64-12 Room:501 Time:April 30 15:15-15:30

The role of tectonic tremor in slow earthquake

YABE, Suguru[1*] ; IDE, Satoshi[1]

[1]Dept. EPS, The University of Tokyo

Since the discovery of the slow earthquake, tectonic tremors, very low frequency earthquakes (VLFs), and slow slip events (SSEs) are thought to have close relation. Although the tremor activity is often regarded as a proxy of SSEs, the degree of proximity is yet unclear due to the lack of detailed quantitative comparison between them, especially for tectonic tremors. Here, we develop a method to estimate the seismic energy of tremors and apply it to tremors in four subduction zones (Nankai, Japan; Cascadia, USA-Canada; Jalisco, Mexico; South Chile). This method estimates the seismic energy of tremors, after evaluating the regionally averaged seismic attenuation and the site amplification factors, which has not been considered enough in previous studies estimating the seismic energy of tectonic tremors. Then the catalog of the energy rate, which is the seismic energy divided by the tremor duration, is compared with some characteristics of tremors, VLFs, and SSEs.

We have observed three types of spatial distributions in terms of energy rate; heterogeneous, homogeneous, and isolated. In regions where the energy rate is heterogeneously distributed on the plate interface, such as Nankai and northern Cascadia, tremor activities almost always initiate from where the energy rate is low. Sometimes the initial tremors trigger more energetic tremors nearby, which are further followed by a long-distance tremor migration along the strike of the subducting plate. These energetic tremors tend to have longer recurrence intervals, and seem to control the onset of a large-scale tremor migration, which probably corresponds to a SSE. In Nankai, the energy rate of tremors estimated between 2-8 Hz is large where VLFs have been detected in the frequency range of 0.02-0.05 Hz. These observations suggest that the characteristics of tremors are regionally various, but similar in different frequency ranges. In the region where tremor activities are isolated, such as East Shikoku, Jalisco and South Chile, each tremor activity has occurred independently, and the relations between the energy rate and the recurrence intervals cannot be seen. In the region where the energy rate is homogeneously distributed on the plate interface, such as a part of southern Cascadia, tremor activities have occurred spontaneously in the entire tremor zone.

Our observation suggests a possibility that the spatial distribution of the energy rate of tectonic tremors might control the behavior of slow earthquakes in the region. When the energy rate is distributed heterogeneously, some energetic tremors seem to control the activity of SSEs, as a switch that ignites a large-scale migration. When tremor patches are isolated, they are passively controlled by the tectonic loading. When it is homogeneously distributed, minor tremor activities, which rupture the only part of the tremor zone, cannot occur.

Keywords: Slow Earthquake, Tectonic Tremors, Seismic wave energy

Japan Geoscience Union Meeting 2014
(28 April - 02 May 2014 at Pacifico YOKOHAMA, Kanagawa, Japan)

SCG64-13 Room:501 Time:April 30 15:30-15:45

Effect of long-term SSE and megathrust earthquake on tremor activity

IDO, Miki[1*] ; SUDA, Naoki[1]

[1]Graduate school of Science, Hiroshima University

Tremor activity migrates with a velocity of ∼10 km/day along the strike of subducting plate boundary. Recently it has been shown that migration front draws a parabolic pattern in spatio-temporal distribution of tremors, indicating that tremor migration is diffusional process [Ide 2010]. We analyzed activities from 2001 to 2013 in western Shikoku, and obtained diffusion coefficients on the order of 10^4 m^2/s for all the activities. Relatively large values ($>1.5\times10^4$ m^2/s) were obtained for the activities during long-term slow slip events (SSEs) in the Bungo Channel region or just after the 2011 Tohoku earthquake (SSJ2013). In this study we investigate the relation between these activiteis and external stress perturbations.

To evaluate perturbations due to these events, we calculated Coulomb stress changes (ΔCFF) using Coulomb 3.3 [Toda et al. 2011]. The long-term SSEs in 2003 and 2010 produced ΔCFF of 28.7 and 5.4 kPa, respectively. These values are large enough to affect tremor occurrences because they are on the same order of magnitude as the tidal effect, which modulates tremor occurrences. The Tohoku earthquake produced ΔCFF of 0.4 kPa. Although it is smaller than the tidal effect by an order, a long-time stress change due to possible viscoelastic response would give some effect on tremor occurrences. Since such a stress perturbation is widespread on the plate interface, it could accelerate tremor migration observed as high diffusion coefficient. We also compare tremor activities with the seismicity calculated with a rate- and state-dependent friction law.

Keywords: deep non-volcanic tremor, tremor migration, Coulomb stress change, long-term slow slip event, megathrust earthquake, subduction zone

Japan Geoscience Union Meeting 2014
(28 April - 02 May 2014 at Pacifico YOKOHAMA, Kanagawa, Japan)

SCG64-14 Room:501 Time:April 30 15:45-16:00

Improvement of tectonic tremor detecting and locating methods: Case study in Shikoku and Kanto

CHAO, Kevin[1*] ; OBARA, Kazushige[1]

[1]ERI, the University of Tokyo

Obtaining accurate tremor sources in time and space is important because it provides essential information that reveals the mechanism of tremor activity. Recent findings of triggered tectonic tremor in recently discovered regions in Hokkaido (Obara, GRL, 2012), Kyushu, and Kanto (Chao and Obara, AGU Meeting, 2012) provide an ideal dataset with which we can test the clock-advanced model, which predicts the occurrence of triggered tremor in regions where ambient tremor occurs. In this study, we improve upon two existing tremor detecting and locating methods: 1) the WECC (Waveform Envelope Correlation and Clustering) auto-detecting algorithm (Wech and Creager, GRL, 2008), which auto-detects tremor episodes, and 2) the improved conventional envelope cross-correlation technique (Obara, Science, 2002; Chao et al., BSSA, 2013), which accurately pinpoints the locations of short duration tremor sources in space. Using WECC, we detected tremor episodes in western Shikoku and compared the results with existing NIED tremor catalogs (Maeda and Obara, JGR 2009; Obara et al., GRL, 2010). Our preliminary results indicate that during testing period (i.e., tremor episodes between 2012/05/25 and 2012/06/02), the WECC was able to successfully auto-detect the same ambient tremor episodes listed in the NIED tremor catalogs. The tremor detections by WECC show similar tremor migrations pattern as the features from the NIED tremor catalog. In addition, the WECC is able to capture more small tremor episodes that are not included in the NIED catalog. Our next step will be to apply the WECC to the entire dataset to determine whether it can successfully detect all tremor episodes while minimizing noise. Using the modified envelope cross-correlation technique, we plan to conduct a 3D grid search to locate accurate triggered tremor sources in Kanto following several teleseismic earthquakes. This modified technique has been used to locate micro-earthquakes (M<=0.5) in western Shikoku, and a comparison of the hypocenter of these micro-earthquakes with those from the JMA earthquake catalog showed that they were located within 5km of one another.

Keywords: ambient tremor, Shikoku, Kanto, tremor auto-detection technique

Japan Geoscience Union Meeting 2014
(28 April - 02 May 2014 at Pacifico YOKOHAMA, Kanagawa, Japan)

SCG64-15 Room:501 Time:April 30 16:15-16:30

Volcanic Deep Low-Frequency Earthquakes and Cooling Magma

ASO, Naofumi[1*] ; TSAI, Victor[2] ; IDE, Satoshi[1]

[1]Graduate School of Science, The University of Tokyo, [2]Seismological Laboratory, California Institute of Technology

Deep low-frequency earthquakes (LFEs) are deep earthquakes that radiate low-frequency seismic waves. While tectonic LFEs on plate boundaries are thought to be slip events, the physical mechanism of volcanic LFEs around the Moho beneath volcanoes is not well understood. For initial brittle failure to be produced at these temperature-pressure conditions, high strain rates should exist there.

Since an ascending magma diapir tends to stagnate near the Moho, where there is a density discontinuity, we suspect its thermal contraction acts as a driving force of volcanic LFEs. In the present study, we estimated thermal strain rates caused by a cooling magma near the Moho beneath volcanoes.

We calculated thermal evolution after an initial perturbation of 400K uniformly within planar and cylindrical magma intrusions. Then, we estimated thermal strain rates within the region of δT $<$200K, where the medium can be treated as a Poissonian elastic body. We assume a thermal diffusivity of 6×10^{-7}m^2/s and a thermal expansion coefficient of 2×10^{-5}/K, taking into account latent heat release and the density change caused by a phase change of partially molten material.

As a result, strain rates larger than the effect of tectonic loading ($>5\times10^{-14}$/s) is observed for planar magmas of width of $<$200m and cylindrical magmas of radius of $<$160m. Even if the initial crack were not observed because of small amplitude and high attenuation, an exited larger-scale deformation such as a resonance would be observed as an LFE.

The orientation of produced strain rates differs between planar intrusions and cylindrical intrusions. Assuming that magma shape and strain rate correspond to source distribution and source mechanism, respectively, we expect a correlation between source distribution and source mechanism for volcanic LFEs. Although a part of this relationship has been recognized for the LFEs in eastern Shimane in western Japan [Aso and Ide, 2014], more mechanism analyses are needed to verify our model.

Keywords: volcanic low-frequency earthquakes, cooling magma, CLVD

Japan Geoscience Union Meeting 2014
(28 April - 02 May 2014 at Pacifico YOKOHAMA, Kanagawa, Japan)

SCG64-16 Room:501 Time:April 30 16:30-16:45

Spatiotemporal Distribution of Shallow Very Low Frequency Earthquakes along the Nankai Trough and the Ryukyu Trench

ASANO, Youichi[1*] ; MATSUZAWA, Takanori[1] ; OBARA, Kazushige[2]

[1]National Research Institute for Earth Science and Disaster Prevention, [2]Earthquake Research Institute, The University of Tokyo

We have investigated spatiotemporal distribution of shallow very low frequency earthquakes (sVLFEs) along the Nankai trough and the Ryukyu trench. Three component seismograms recorded at 40 broadband stations of the NIED F-net were analyzed by using waveform-correlation and back-projection techniques after processing a band-pass filter (0.02 to 0.05 Hz). Here we used known 6 sVLFEs and 17 regular interplate earthquakes near the trench axis as template events. Time series of cross-correlation function (CC) at each station was calculated from continuous waveform data and triggered seismograms of template events. Assuming surface wave propagation, CCs are back-propagated onto possible origin times and horizontal locations. We obtained sVLFE epicenters by performing a grid search in time and space domains to maximize the averaged CCs from all stations under the condition of high signal to noise ratios that was defined as amplitude ratios between two time windows before and after the surface wave arrivals from the epicenters. As the result of this analysis for the last decade, we detected infrequent activity of sVLFE episodes at a few clusters adjacent to the locked zone related to the megathrust earthquakes along Nankai trough: in 2004 and 2009 of Kii peninsula, in 2003 and 2009 off cape Muroto, and in 2003 and 2010 off cape Ashizuri. On the other hand, sVLFE episodes in Hyuga-nada and areas along the Ryukyu trench are frequent. Such a variation of seismicity of sVLFEs revealed from this study based on the same detection capability may suggest the difference of the plate coupling in the seismogenic zone.

Keywords: Very Low Frequency Earthquakes, Nankai Trough, Ryukyu Trench

Japan Geoscience Union Meeting 2014
(28 April - 02 May 2014 at Pacifico YOKOHAMA, Kanagawa, Japan)

SCG64-17 Room:501 Time:April 30 16:45-17:00

Relationship between very low frequency earthquakes and repeating slow slip events in the south Ryukyu Trench

NAKAMURA, Mamoru[1*] ; SUNAGAWA, Naoya[1]

[1]Faculty of Science, Univ. Ryukyus

The repeating slow slip events (SSEs) occur on the upper interface of subducted Philippine Sea plate at the depth from 30 to 50 km in the south Ryukyu Trench region (Heki & Kataoka, 2008). The afterslip of the March 2002 earthquake (Mw=7.2) is distributed at the west of the fault of the repeating SSEs. This afterslip continued from March 2002 to 2005 (Nakamura, 2009).

Recently, very low frequency earthquakes, which occurred continuously along the Ryukyu Trench, were detected (Ando et al., 2012). The occurrences of SSEs, afterslip, and very low frequency earthquakes reflect the state of slip in the plate interface.

Then we investigated the relation between the SSEs with very low frequency earthquakes.

We employed the broad-band seismometer network of NIED (F-NET) and IRIS. We used the station of Ryukyu Islands, Kyusyu, SSE (Shanghai), and TATO (Taipei). The used the waveforms of vertical component for the analysis. The period we used are from January 1, 2002 to September 30, 2013. We filtered the band-pass range of 0.02-0.05 Hz to the waveforms, and detected the low-frequency events and picked the arrival times of surface waves manually. The local and teleseismic earthquakes were eliminated using the earthquake catalogue. The local events were also eliminated with checking the high-pass filtered record. Then we determined the location of low frequency events assuming that the observed waves were Raleigh waves.

We determined the 6299 low frequency events for 12 years. Almost events are distributed along the Ryukyu Trench axis. The low frequency events are clustering at the south Iriomote Island, south of Okinawa Island, and near Amami Island. The events are also distributed near the Okinawa Trough. However, the events in the Okinawa Trough would be the apparent distribution by miss-location of hypocenter determination which is caused by the linear distribution of seismic stations along the Ryukyu Arc.

Next we investigated the cumulative number of low frequency earthquakes in the clusters. The activity of the low frequency events at the cluster of the south of Iriomote Island decreased from 2005 to 2010, and increased since late of 2011. The activation of very low frequency events occurred after the occurrence of repeating SSEs. The 24 SSEs had occurred since 2002, and the 14 activation of the low frequency events occurred after the SSEs. The occurrence rates of the VLFEs during the SSEs increased about 2-3 times than the averaged ones. However, the activation of usual earthquakes during the SSEs occurred only two times. These suggest that the SSEs would trigger the VLFEs.

Keywords: very low frequency earthquake, slow slip event, Ryukyu Trench

Japan Geoscience Union Meeting 2014
(28 April - 02 May 2014 at Pacifico YOKOHAMA, Kanagawa, Japan)

SCG64-18 Room:501 Time:April 30 17:00-17:15

Activity characteristics of deep very low frequency earthquake and asperity structure

NIZATO, Taro[1] ; SUDA, Naoki[1*] ; MATSUZAWA, Takanori[2]

[1]Hiroshima Univ., [2]NIED

Deep very low frequency earthquake (VLF) and deep nonvolcanic tremor (NVT) concurrently occur with short-time slow slip event (SSE) in the Nankai subduction zone. Among them VLF is least known since seismic records are usually noisy at dominant periods of VLF signals (20-50 sec). We have developed a new grid-based method for monitoring VLF activity in the Nankai subduction zone. In this method we assume that VLF occurs at equally-spaced grids on model plate boundary, and that VLF at each grid has a fixed source mechanism predetermined from plate boundary model and observed plate convergence direction. Previous studies have used the grid moment-tensor method in which depth and source mechanism are freely determined. These parameters are predetermined in the present method, so that it is expected that small VLFs can be detected even from low S/N records.

As a preliminary study we analyzed Hi-net accelerometer records for two activities in western Shikoku in September 2006 and March 2007. We detected a large number of VLFs compared with previous studies, and observed the following characteristics: (1) Some VLF occurrences were rapidly activated than NVT occurrences, and VLF activity highs were sometimes delayed relative to NVT activity high, (2) There was an NVT cluster with or without VLF depending on activity, (3) Rapid tremor reversals are associated with VLFs, (4) Clusters with maximum moment release were different between VLF and NVT, (5) The cluster of maximum VLF moment release was located in the updip portion next to the region of maximum SSE moment release. Some of these characteristics can be explained by a nested or fractal asperity model, in which small NVT asperities are contained in a VLF asperity.

Keywords: Nankai subduction zone, slow earthquake, very low frequency earthquake, nonvolcanic tremor, automatic detection, asperity

Japan Geoscience Union Meeting 2014
(28 April - 02 May 2014 at Pacifico YOKOHAMA, Kanagawa, Japan)

SCG64-19 Room:501 Time:April 30 17:15-17:30

Preseismic behaviors involving slow slip in rate-state earthquake sequence models with a hierarchical asperity concept

NODA, Hiroyuki[1*] ; NAKATANI, Masao[2] ; HORI, Takane[1]

[1]JAMSTEC, IFREE, [2]The University of Tokyo, ERI

Understanding preseismic phenomena before large earthquakes is of critical importance in assessing possibility of disaster mitigation by detecting and recognizing them. The 2011 Tohoku-Oki earthquake has long recorded geophysical data for tens of years prior to it. Since the earthquake, multiple studies have reported potentially important phenomena involving slow slip which may be particular to ripe asperities. It is our mission for modelers to see if they are consistent with, or appear naturally without fine tuning of numerical models of earthquake sequences accounting for interseismic processes, as well as earthquake ruptures.

The off-Miyagi to off-Fukushima region was locked at least from Apr. 1995 to Mar. 2002 [Nishimura et al. 2004], with the shallower region not being able to be constrained by on-land GPS stations [Loveless and Mead, 2011]. The region started creeping from 2005 [Ozawa et al., 2012]. Recently, Katsumata [2013, JpGU] pointed out that seismic quiescence [Katsumata, 2011] correlates with the locked period, and inferred that this region may have been creeping at least from 1980 to 1988. In the shallower region near the hypocenter of the Tohoku-Oki earthquake, a couple of slow slip events were reported by Ito et al. [2013], one in Nov. 2008 and the other in Feb. 2011. This interval is much shorter than that for the larger scale events inferred by Katsumata [2013].

Suito et al. [2011] reported that M7-class earthquakes along the Japan Trench after 2005, including the Mw 7.3 preshock 2 days before the Tohoku-Oki earthquake, had unusually large amount of afterslips. The postseismic moment releases are comparable to or even larger than the coseismic ones, with the centroid being located close to the epicenters, not deeper than them.

In the present talk, we present that qualitatively similar behaviors to those observations are recognized in numerical models reported by Noda et al. [2013, JGR]. They presented rate-state earthquake sequence simulations accounting for a hierarchical asperity concept [Ide and Aochi, 2005]; a large tough patch has a small fragile patch in it. Importantly, those simulations were not meant to mimic the Tohoku-Oki earthquake through fine tuning of the model, and are representing general behaviors characteristic to the rate-state (aging law) earthquake sequence with a certain kind of heterogeneity in the parameter distribution.

In those simulations, interseismic penetration of a creep front into a locked velocity-weakening patch often becomes non-steady and accompanied by aseismic transients before nucleation. This is because the critical length scale for impossibility of coherent steady-state slip [Rice et al., 2001] can be smaller than the nucleation size [Rubin and Ampuero, 2005]. In the simulation, the transients take place both in the large tough patch and in the small fragile patch when a creep front penetrates inwards to a certain extent. A transient does not necessarily, but may lead to nucleation. In addition, such an elevated aseismic slip rate in the large patch seems to be a necessary condition for cascade-up rupture growth from the small patch if it is smaller than the nucleation size of the large patch.

A small event which only ruptures the small patch is sometimes followed by a large event before the afterslip smearing out. Such small events are classified as precursory events, since clear causality is recognized between them and the following large ones; the large ones are initiated either by delayed cascade-up or by large nucleation hosted by the afterslip. The precursory small events tend to have larger afterslip than non-precursory ones.

In the rate- and state-dependent friction law, logarithmic slip rate is, by definition, proportional to stress minus strength which correlates with fracture energy. Therefore temporal changes in the aseismic slip rate in a so-called asperity, if detectable, could be used to infer the ripeness of it.

Keywords: Earthquake sequence, Preseismic phenomena, Hierarchical asperity, Numerical simulation

Japan Geoscience Union Meeting 2014
(28 April - 02 May 2014 at Pacifico YOKOHAMA, Kanagawa, Japan)

SCG64-20 Room:501 Time:April 30 17:30-17:45

Numerical simulation of slow slip events before the 2011 Tohoku-Oki Earthquake

NAKATA, Ryoko[1*] ; ARIYOSHI, Keisuke[1] ; HYODO, Mamoru[1] ; HORI, Takane[1]

[1]JAMSTEC

In the Japan Trench, the M9.0 great interplate earthquake occurred on 11 March 2011, off the coast of Tohoku, Japan. Before this earthquake, two slow slip events (SSEs) were observed on 2008 and 2011. The second SSE occurred on February 2011 at the downdip end of the huge-coseismic-slip region, and it continued at least until the occurrence of the M7.3 largest foreshock on March 9 [Ito et al., 2013]. In addition, following the largest foreshock, postseismic slip propagated to the location of the mainshock hypocenter and triggered the dynamic rupture there [Ando & Imanishi, 2011].

In this study, we numerically simulated cycles for occurrences of seismic and aseismic events along the Japan Trench with the 3D geometry of the Pacific plate. We model the M9 2011 Tohoku-Oki Earthquake, the largest foreshock of the M9 earthquake, and the SSE before the foreshock using the slowness law, which is a type of rate- and state-dependent friction law. We set frictional properties at source area of earthquakes and SSEs to satisfy a condition of unstable slip and slow slip, respectively. We evaluated simulation results achieved using different values of frictional parameters with respect to characteristics such as the slip history leading to the 2011 Tohoku-Oki earthquake and crustal deformation before and after the Tohoku-Oki earthquake.

As a result, we quantitatively reproduced the observed scenario. Temporal characteristics of the resultant scenario were sensitive to both sizes and locations of the circular fault patches. Now, we are improving our model to reproduce various characteristics qualitatively. Based on some of the reasonable results achieved, we will discuss frictional conditions for the pre-seismic process of the 2011 Tohoku-Oki earthquake.

Japan Geoscience Union Meeting 2014
(28 April - 02 May 2014 at Pacifico YOKOHAMA, Kanagawa, Japan)

SCG64-P01 Room:Poster Time:April 30 18:15-19:30

Deep Triggered Non-Volcanic Tremor in the Slow Earthquake Active Regions in South Chile and Ecuador

CHAO, Kevin[1*] ; OBARA, Kazushige[1]

[1]ERI, the University of Tokyo

Deep non-volcanic tremor has been observed at many major plate-boundary faults and intraplate faulting systems. Recent studies have shown that the tremor triggered by surface waves of teleseismic earthquake occurs on the same fault patches as the spontaneously occurring ambient tremor. The observations suggest that the triggered tremor can be used as a proxy to estimate the background tremor activity. Here we search for tremor triggered by teleseismic earthquakes in south Chile and Ecuador where the ambient tremor and slow slip event have been observed respectively. In south Chile, we analyzed a temporal array data between 2004 and 2006 and observed clear triggered tremor following the 2004 Mw9.0 Sumatra, 2005 Mw8.6 Nias, and 2006 Tonga earthquakes. Triggered tremor sources are located at the central of the ambient tremor zone. The results indicate both Love and Rayleigh waves promote the tremor triggering potential. The tremor triggering threshold is around 2 kPa, similar to which in Parkfield. In Ecuador, we can only use single station to infer the existence of triggered tremor due to lack of seismic stations in this region. During the period between 2004 and 2012, we observed triggered tremor following the 2010 Mw8.8 Chile and 2007 Mw8.0 Peru earthquakes. Since there is no other station within 500 km near that station, we roughly estimate that the triggered tremor sources are located within 50 km from the station based on the attenuation of tremor from previous studies and the estimation of the time difference between P- and S-waves of triggered tremor. We infer that the triggered tremor source might be located at the region where the slow slip event has been observed. The apparent tremor triggering threshold in Ecuador is about 40 kPa. The high threshold infer a low background tremor rate or simply due to the network capability.

Keywords: non-volcanic tremor, triggered tremor, south America

Japan Geoscience Union Meeting 2014
(28 April - 02 May 2014 at Pacifico YOKOHAMA, Kanagawa, Japan)

SCG64-P02 Room:Poster Time:April 30 18:15-19:30

Shallow low-frequency tremor activity in the Hyuga-nada, revealed by ocean bottom seismographic observation

YAMASHITA, Yusuke[1*] ; YAKIWARA, Hiroshi[2] ; UCHIDA, Kazunari[1] ; SHIMIZU, Hiroshi[1] ; HIRANO, Shuichiro[2] ; MIYAMACHI, Hiroki[2] ; UMAKOSHI, Kodo[3] ; YAMADA, Tomoaki[4] ; NAKAMOTO, Manami[1] ; FUKUI, Miyo[1] ; KAMIZONO, Megumi[1]

[1]Institute of Seismology and Volcanology, Kyushu Univ., [2]Nansei-Toko Observatory for Earthquakes and Volcanoes, Kagoshima Univ., [3]Graduate School of Fisheries Science and Environmental Studies, Nagasaki Univ., [4]Earthquake Research Institute, Univ. of Tokyo

In order to reveal the detail of microseismicity from the shallower part of the plate boundary to seismogenic zone in the Hyuga-nada region, we have conducted Ocean Bottom Seismographic observation from May 19 until July 6, 2013. We used 12 Ocean Bottom Seismometers (OBSs) with a three-component short-period seismometer. During this observation, we observed many low-frequency tremors (SLFT) which mainly occurred from end of May to end of July 2013 [*Yamashita et al*., 2013 AGU fall meeting]. We report the detail of SLFT activity in the Hyuga-nada region based on the semi-automatically analysis using envelope correlation method (ECM)[*Obara*, 2002].

The differential arrival times between OBS stations using ECM were obtained from the lag times with maximum cross-correlation coefficient between the pair of the root mean square (RMS) envelopes which were converted from composite horizontal components waveform with applying a 2-8 Hz bandpass filter. RMS envelopes were smoothed by using 5 s window and performed down-sampling with a 20Hz. The length of RMS envelops for calculating of cross-correlation coefficients was set for 150 s. If the maximum cross-correlation coefficient for a pair was larger than 0.85, and more than or equal to 6 pairs, we searched minimum RMS residual position by a grid search algorism. These processing were performed automatically for the continuous RMS envelope records every 75 s (i.e., overlapping two moving window for 75 s). After the calculation, we carefully examined the candidate tremor events to distinguish ”regular” earthquakes, T-phase signals, or background noise.

Based on the result of SLFT location by ECM, we identify two migration episode of the SLFT: 1st episode started in east off Tanegashima Island from end of May, 2013, migrated northward along strike of subducting plate, veered away to the north-west in the around S08 station, then reached under the S06 station on July 12 - 14. 2nd episode started in the south of S08 station on July 17, migrated northward and veered away to the north-west in the around S08 station, reached around the S07 station, veered away to the east, reached around the S09 station.

These migration episodes suggest that undetected short-term slow-slip event may have occurred at the same time in the shallow part of the Hyuga-nada region. Around the focal area of SLFT, the Kyushu-Palau ridge is subcudting: the SLFT activity was only found on the south side (i.e., Ryukyu arc side). In particular, the depth of plate boundary around the S08 station is southwestward deepening down to 10 km depth [*Park et al*., 2009]. Therefore, the episodic slow-slip extended to northward with SLFT activity, and shifted to northwest-ward caused by the Kyushu-Palau ridge which act a segment boundary to controle the interplate slip phenomena.

Acknowledgements: We thank the crews of T/S Nagasakimaru (Faculty of Fishers, Nagasaki University) for OBS observation.

Keywords: Shallow low-frequency tremor, Ocean Bottom Seismographic observation, Hyuga-nada

Japan Geoscience Union Meeting 2014
(28 April - 02 May 2014 at Pacifico YOKOHAMA, Kanagawa, Japan)

SCG64-P03 Room:Poster Time:April 30 18:15-19:30

The Slow Slip Event off the Boso Peninsula on January 2014 and the associated earthquake swarm

KIMURA, Hisanori[1*]

[1]National Research Institute for Earth Science and Disaster Prevention (NIED)

Introduction

Off the Boso Peninsula, at the southeastern Kanto, central Japan, slow slip events (SSE) accompanied with earthquake swarms recurs with time interval of 4-7 years. SSEs have occurred in 1983, 1990, 1996, 2002, 2007, and 2011 and the latest SSE recurred from Dec. 2013 to Jan. 2014 with interval of 2 years and 2 months. In this study, detailed activity of the earthquake swarm and a fault model of the Boso SSE were determined.

Data and Methods

High precision hypocenter distribution was determined for earthquakes shallower than 30 km off the Boso Peninsula, from Jan. 1, 2005 by Double Difference method incorporating waveform correlation analysis. Hypocentral parameters determined by NIED Hi-net (automated hypocenters were partly included) were used as initial hypocenters.

A rectangular fault model with uniform slip was determined using genetic algorithm inversion for fault location and geometry and the weighted least squares method for slip amounts, following a method of Obara *et al*. (2004) based on tilt data recorded by high sensitivity accelerometer co-installed in NIED Hi-net station. In this analysis, slip direction was fixed to the direction of relative plate motion.

Results

Most earthquakes occurred around the northern edge of the seismic region where seismic swarms associated with the previous Boso SSEs occurred. Seismic swarms first occurred at the eastern offshore area and then migrated to the western onshore area. Migration from offshore to onshore regions is common feature among the previous Boso SSEs. Distribution of earthquake swarms is similar to that of the 2007 SSE, although spatial distribution and number of events are slightly smaller than the 2007 SSE.

The maximum crustal tilting of about 0.4 μ radian with northwestward direction was observed at KT2H station and the fault model was determined to be located off the Boso Peninsula with size of M_W6.1. Location of SSE slip overlaps with locations of the 2007 (Sekine *et al*., 2007) and initial stage of the 2011 (Hirose *et al*., 2012) SSEs. Tilting direction is similar to tilting direction of the 2007 SSE, however, its amount is about a half of the 2007 SSE (M_W6.4) and the SSE size is also smaller. Smaller number of earthquakes is likely to reflect smaller size of the SSE. In the 2011 SSE, west-northwestward tilting of about 0.3 μ radian was observed for the first two and a half days and size for this period was estimated as M_W6.2. Its direction and amount are similar to those of the 2014 SSE and the SSE size is also close.

Discussion

Recurrence interval of the 2014 SSE was shortest for the last about 30 years. The size of the 2011 SSE was estimated to be comparable to previous SSEs and a possibility that the 2011 SSE was hastened by the stress increase caused by the 2011 Off Tohoku Earthquake and its afterslip has been proposed (Hirose *et al*., 2012). On the contrary, size of the 2014 SSE is likely to be smaller than previous SSEs. This result infers that the SSE slip is smaller supposing the same source area and the SSE recurred with shorter interval with smaller stress accumulation. Further analysis is necessary to reveal the detailed source process of the Boso SSE for monitoring of the stress accumulation.

Acknowledgements:

In this study, seismic data obtained by Earthquake Research Institute (ERI) and Japan Meteorological Agency (JMA) were used.

Keywords: Slow Slip Event, plate boundary, earthquake swarm, Kanto region

Japan Geoscience Union Meeting 2014
(28 April - 02 May 2014 at Pacifico YOKOHAMA, Kanagawa, Japan)

SCG64-P04 Room:Poster Time:April 30 18:15-19:30

A long-term slow slip event in central Shikoku in 2013

KOBAYASHI, Akio[1*]

[1]Meteorological Research Institute

A long-term slow slip event in central Shikoku is investigated using the GEONET GNSS data. We estimated the steady deformation rate at each GNSS station from the daily coordinates for the period from January to December 2012. Then the steady deformation rates were subtracted from all the coordinate data. The artificial offsets of the coordinate were corrected using data set shown on the web site of the Geospatial Information Authority of Japan. We can see south-eastern displacements less than 1 cm at GNSS stations in central Shikoku for one year from October 2012. These unsteady displacements are also seen in the time series of the baseline lengths between central Shikoku and Chugoku district.

We estimated slip distribution on the plate boundary, assuming the unsteady displacements were caused by a slip on the plate boundary. The estimated slip is distributed in central Shikoku. Center of the slip is located slightly southeast of the belt of deep low-frequency earthquakes. The size of the slip is equivalent to Mw 6.2, which is smaller than other long-term SSEs along the Nankai Trough.

Keywords: long-term slow slip, GNSS, crustal deformation, central Shikoku

Japan Geoscience Union Meeting 2014
(28 April - 02 May 2014 at Pacifico YOKOHAMA, Kanagawa, Japan)

SCG64-P05 Room:Poster Time:April 30 18:15-19:30

Rate and state simulation of Yaeyama slow slip events in the southwestern part of the Ryukyu Arc, Japan

OKUDA, Ryosuke[1*] ; HIRAHARA, Kazuro[1] ; MIYAZAKI, Shinichi[1] ; KANO, Masayuki[1] ; OHTANI, Makiko[1]

[1]Graduate School of Science, Kyoto Univercity

Slow slip events (SSEs) are recurring on the plate interface beneath the source regions of the interplate large earthquakes. It has been proposed that the activity of SSE possibly changes before the occurrence of large interplate earthquakes. Hence, it is essential to know the frictional properties for producing SSEs to predict the occurrence of large earthquakes. Our final goal is to optimize frictional parameters on the fault related to SSE through a data assimilation method which combines the observational data and the forecast ones derived from a simulation model, and then to give information on the occurrence of large interplate earthquakes. In this paper, as a first step of such a data assimilation, we construct a simulation model reproducing the observed spatio-temporal slip evolution of SSE.

In this paper, we consider the Yaeyama SSEs. Around the Yaeyama islands in the southwestern part of the Ryukyu Arc, Japan, GPS observations have caught the frequent recurrence of SSE activity. Around there have occurred almost no large earthquakes that affect the SSE activities during the observational period, which leads to a relatively simple simulation model of SSE. Those are the reasons that we select SSE on this area.

Heki and Kataoka(2008) reported the following features of Yaeyama SSEs; 1) SSEs recur on a plate interface at depths of 20-40km, 2) the average recurrence interval is 6.3 months, 3) its standard deviation is 1.2 months, 4) the slip rate released by SSEs is 11.0 cm/yr, in spite of the estimated convergence rate of 12.5 cm/yr.

We construct a simulation model which reproduces the above mentioned features of SSE. We set a dipping fault embedded in a homogeneous elastic half space. The friction on the fault is assumed to obey a rate-and state-dependent friction law, and the slowness law of state evolution (Dietrich, 1979). To simulate SSE, following Kato(2003), we set an asperity at depths of 20-40 km on a stable sliding plate interface, whose frictional properties are characterized by frictional parameters A, B and L. The asperity has the rate weakening frictional property of $A-B<0$ and its radius is nearly equal to or less than the nucleation radius determined by frictional parameters. We also consider the possible presence of a locked zone, namely an asperity, at the shallow portion of the plate boundary close to the Ryukyu Trench, which might cause the 1771 Meiwa tsunami (Nakamura, 2009). Dating of tsunami stones suggests a possible recurrence of 150-400 years of large tsunami (Araoka et al., 2013), and the large tsunami events close to the Ryukyu Trench might have recurred in several hundred years.

It is found that the interval of SSE can be adjustable by changing the friction parameters. For example, if a single asperity with the size of 80 km has frictional parameters of A=50 kPa, B=56kPa, and L=2.2 mm, the interval is about 6 months. Further, if we add another asperity with 40 % slip deficit rate of the convergent rate of 12.5 cm/yr just above the SSE asperity zone, the slip rate released by SSEs reduces to the observed rate of 11.0 cm/yr. The released slip rate depends on the location, size and assigned slip deficit rate of the shallow asperity. The locking state at the shallow portion is important to give information on the occurrence of possible tsunami earthquake, and we need the further investigation. For reproducing the observed fluctuation of recurrence intervals of SSE, we need to consider the interaction among multiple asperities or the hierarchical asperity model where a large asperity has small asperities with different properties inside itself.

Keywords: slow slip events, Yaeyama, a rate- and state-dependent friction law

Japan Geoscience Union Meeting 2014
(28 April - 02 May 2014 at Pacifico YOKOHAMA, Kanagawa, Japan)

SCG64-P06 Room:Poster Time:April 30 18:15-19:30

Array observation of short span strainmeter in the Kii peninsula

KANO, Yasuyuki[1*] ; HOSO, Yoshinobu[1] ; ONOUE, Kensuke[1]

[1]DPRI, Kyoto Univ.

Crustal deformations have been observed associated with deep low-frequency tremors occurring below the Kii peninsula and Shikoku. Strain measurements by an extensometer at Kishu operated by DPRI, for example, show that the sources with epicentral distance of 30 - 40 km causes strain changes of $10^{?9}$ to $10^{?8}$ occurring within several days. Although the traditional extensometer observations can detect these strain changes, it is difficult to make detailed analyses because of the limited number of stations. We designed a short-span extensometer with 1.5 m-long standard measure. Strong coupling of the instrument to the ground is important for stable observations, so three anchor bolts fixed to the base of the instrument are cemented into a 50-cm-deep hole. We observed crustal deformation associated with deep low-frequency tremors by the short-span extensometer installed at Nakaheji. We detected strain change associated with low frequency events occurred on March 2013. We are preparing another sites for installation of the strainmeter around the western Kii Peninsla to constract array of strainemters. The array observation contributes to improve the detection capability of crustal deformation by eliminating noise caused by weather disturbance and to have better understanding of slow slip events such as slip distribution.

Keywords: strainmeter, slow earthquakes, array observation

Japan Geoscience Union Meeting 2014
(28 April - 02 May 2014 at Pacifico YOKOHAMA, Kanagawa, Japan)

SCG65-01 Room:423 Time:May 2 09:00-09:15

Reconstraction of paleostress states in the Walanae fault zone in South Sulawesi using the multiple inverse method with

NISHIKAWA, Osamu[1*]

[1]Akita University

Paleostress analysis using the multiple inverse method with calcite twin data was performed in the East Walanae fault (EWF) zone in South Sulawesi, Indonesia. The geomorphic trace of the EWF can be recognised as a distinct line between the Bone Mountains and the Walanae Depression, around which an intensive deformation zone characterised by various scales of faults and folds are developed. Carbonate rocks with numerous calcite twins and mesoscale faults are ubiquitous around the EWF trace. Therefore EWF zone is a useful location for testing the inclusion of calcite twin data in the multiple inverse technique to determine paleostress states. One to three poles of differently oriented twin lamellae and c-axis orientation were measured for each grain from three mutually perpendicular thin sections for 11 samples using a U-Stage optical microscope. The data set for multiple inverse method consists of the attitude of the e-plane, gliding direction and sense of shear of e-twinning. We prepared data files not only for twinned e-planes but also for the remaining untwinned e-planes in a grain with one or two twin sets. We incorporated the untwinned e-plane data for determining stress states with the multiple inverse method using calcite twins. In the analysis, the identified stress states by twinned e-plane data were tested calculating misfit angle β, the angle on the untwinned e-plane between the calculated maximum shear stress direction for every identified stress state and the observed potential gliding direction. It is possible to say that the sampled rocks had never experienced stress states to activate any of the untwinned e-planes. Therefore, if most untwinned e-plane data (95% or more in this study) are incompatible(β >30 degree) with the stress state identified from twinned plane data, then the stress state is viable for both the twinned and untwinned e-planes.

The analysis using calcite twin yielded reliable paleostress states similar and consistent with those from fault-slip data throughout the study area. Dominant and common stress states are characterized by NE-SW-to-E-W-trending σ1 and vertically to moderately-south-plunging σ3 with generally small values of stress ratio ϕ. These stress states were most likely caused by collision of eastern Sulawesi with the Australian fragments since the Pliocene, and they could have activated the EWF as a reverse fault with a dextral shear component, accounting for the contraction deformation structures and landforms along the trace of the fault. Calcite twin and mesoscale faults were activated predominantly during the fold tightening stage and subordinately before folding.

Keywords: multiple inverse method, calcite twin, Walanae fault zone

Japan Geoscience Union Meeting 2014
(28 April - 02 May 2014 at Pacifico YOKOHAMA, Kanagawa, Japan)

SCG65-02 Room:423 Time:May 2 09:15-09:30

Capability of calcite twin for estimating stress magnitudes and orientations

YAMAJI, Atsushi[1*]

[1]Kyoto University

Calcite has three e-twin planes, each of which has a critical resolved shear stress at ˜10 MPa along the twin gliding direction; and the planes and direction have certain crystallographic orientations (e.g., Lacombe, 2010). We quantified the tightness of the constraints from twin and untwin data on stress conditions. It is shown that twin and untwin data place tight constraints if differential stress is low and large, respectively. Their tightness converges to the same value with increasing differential stress. The constraint from a calcite grain becomes tighter with increasing number of twin sets in the grain. It is also shown to be important to cope with sampling bias to utilize untwin data: The number of twin data compared to the total of twin and untwin ones tend to be underestimated by ˜25%. It is found that calcite e-twin loses resolution in determining stress magnitudes and orientations if differential stress is greater than ˜200 MPa.

Keywords: twin, calcite aggregate, stress

Japan Geoscience Union Meeting 2014
(28 April - 02 May 2014 at Pacifico YOKOHAMA, Kanagawa, Japan)

SCG65-03 Room:423 Time:May 2 09:30-09:45

Enhanced detectability of stress tensor inversion from heterogeneous fault-slip data with preferred orientations

SATO, Katsushi[1*]

[1]Div. Earth Planet. Sci., Kyoto Univ.

Fault planes occasionally have preferred orientations according to the slip tendency (e.g., Lisle and Srivastava, 2004), which is defined as the ratio between normal and shear stresses (Morris et al., 1996). In contrast, most stress tensor inversion methods calculate crustal stress states from fault-slip data on the assumption that faults slip along the resolved shear stress vectors on their surfaces. This assumption called Wallace-Bott (W-B) hypothesis allows low values of slip tendency on ”misoriented” faults so as to consider faulting along pre-existing weak surfaces in rock masses. However, the weak assumption causes the loose constraint on stress. For example, when a set of conjugate faults is observed, one usually determines principal stress axes as bisectors of fault planes. On the contrary, W-B hypothesis permits only to constrain the axes within the angle between fault planes. Such a disadvantage severely lowers the detectability of multiple stress conditions from heterogeneous fault-slip data. To avoid this problem, this study proposes a new method of stress tensor inversion by combining the W-B hypothesis and the slip tendency.

This study employed a stress tensor inversion method called HIM (Yamaji et al., 2006; Sato 2006) which maximize the fitness between observed slip directions and shear stress vectors. The fitness value is modified to be the product of the conventional fitness and the slip tendency. Artificial fault-slip data are analyzed to examine the performance of the new method. The data set includes 200 faults compatible with N-S compressional stress and 50 faults compatible with E-W tensional stress. The former has random orientations of fault planes and the latter has a preferred orientation so that they have large values of slip tendency. As the result, the conventional HIM could not detect the latter stress, while the new method could detect both stresses.

The new method is applied to fault-slip data from Late Miocene Awa Group in eastern Boso Peninsula. Mesoscale faults in this area have at least two different origins; reverse-faulting stress and normal-faulting one (e.g., Angelier and Huchon, 1987). The new method successfully detected both stresses without a priori classification of faults into subsets.

References

Angelier, J. and Huchon, P. 1987, Earth Planet. Sci. Lett., 81, 397-408.
Morris, A., Ferrill, D.A. and Henderson, D.B., 1996, Geology, 24, 275-278.
Lisle, R.J. and Srivastava, D.C., 2004, Geology, 32, 569-572.
Sato, K., 2006, Tectonophys., 421, 319-330.
Yamaji, A., Otsubo, M. and Sato, K., 2006, Journal of Structural Geology, 28, 980-990.

Keywords: stress tensor inversion, heterogeneous fault-slip data, slip tendency, orientation distribution

Japan Geoscience Union Meeting 2014
(28 April - 02 May 2014 at Pacifico YOKOHAMA, Kanagawa, Japan)

SCG65-04 Room:423 Time:May 2 09:45-10:00

Reconstruction of absolute stress based on a condition of aftershock occurrence

IMANISHI, Kazutoshi[1*] ; UCHIDE, Takahiko[1]

[1]Geological Survey of Japan, AIST

Absolute crustal stress is essential to understand the earthquake generation process. If focal mechanisms both before and after an earthquake together with the fault slip model of the earthquake are available, the magnitude of absolute stress can be constrained (e.g., Hardebeck and Hauksson, 2001; Wesson and Boyd, 2007; Yang et al., 2013). However the application of those methods is inherently limited, because background seismicity is generally low. In this study, we propose a method to reconstruct an absolute stress field incorporating a condition of aftershock occurrence, which is applicable to areas without enough pre-mainshock focal mechanisms.

We suppose that there are pre-existing weak planes represented by aftershock focal mechanisms. Because these planes were locked before the mainshock but afterwards activated, it is reasonable to expect that the slip-tendency, defined by the ratio of shear to normal stress acting on a given plane (Morris et al., 1996), increases after the occurrence of the mainshock. On the basis of this consideration, we search the best absolute stress field as follows.

(1) We assume a pre-mainshock homogeneous absolute stress field (**B**) in the study area. We then compute a post-mainshock stress field (**A**) at each aftershock location by combining the stress change due to the mainshock and the aforementioned pre-shock stress field.

(2) For the fault plane of each aftershock, we compute a pre- and a post-mainshock slip-tendency ($T_s{}^b$ and $T_s{}^a$, respectively) based on the pre- and post-mainshock stress fields, **B** and **A**, respectively. Regarding the computation of $T_s{}^a$, we adopt the component of stress acting in the slip direction on a fault instead of the shear stress itself. Therefore, $T_s{}^a$can have a negative value.

(3) We compute the summation of $T_s{}^a$ of aftershocks that satisfy the condition of $T_s{}^a > T_s{}^b$. If both nodal planes satisfy the condition, the larger $T_s{}^a$ is used for the summation.

(4) We repeat the procedure (1) to (3) by changing the initial stress field **B**, and search a stress field that has the largest sum of $T_s{}^a$.

Numerical tests of this method work well. It is noted that multiple candidates of stress fields were inferred, if we did not incorporate the condition of $T_s{}^a > T_s{}^b$, suggesting that the condition is important in the situation without pre-mainshock focal mechanisms. We then applied the method to the 2013 M6.3 Awaji Island earthquake. Focal mechanisms of 115 aftershocks were determined from P-wave polarity data as well as body wave amplitude. A finite fault slip model of the mainshock was derived from slip inversion analysis (see Uchide and Ide, 2007) of KiK-net strong-motion data. A preliminary analysis shows that the pre-mainshock stress field is characterized by a reverse-faulting regime with a WSW-ENE oriented maximum compression and the differential stress of 200-300 MPa.

Acknowledgements: Seismograph stations used in this study include permanent stations operated by NIED (Hi-net, KiK-net), JMA, ERI, and DPRI. We modified a program coded by Satoshi Ide to estimate the focal mechanism solutions. We thank Yoshimitsu Okada for the use of his code in our stress change computation.

Keywords: absolute stress field, aftershock, focal mechanism, 2013 Awaji Island earthquake, slip-tendency

Japan Geoscience Union Meeting 2014
(28 April - 02 May 2014 at Pacifico YOKOHAMA, Kanagawa, Japan)

SCG65-05 Room:423 Time:May 2 10:00-10:15

Motions after rainfall in borehole tiltmeters and the azimuth of crustal stress before and after 2011 Tohoku Earthquake

SHIMADA, Seiichi[1*] ; KIMURA, Takeshi[1]

[1]NIED

Shimada (1987) has revealed that in borehole telemeter generally the tilt motions after rainfall are tilting to a certain azimuth which is named 'rainfall component', and the perpendicular azimuth is named 'rainfall-free (RFF) component'. In the time series of the RFF component, very little motions are seen after rainfall. From the observations of tiltmeters in NIED Kanto-Tokai network, Shimada (1987, 1989) has found that the azimuths of the RFF component are generally coincided with the azimuth of the crustal maximum compressive stress obtained from the experiments of hydrofracturing and the mechanisms of middle or large scale earthquakes. This is interpreted that the azimuth of the strike of the nearby open crack of the borehole is generally coincided with the azimuth of the crustal maximum compressive stress.

In this study, we examine the azimuth of tilt motions after rainfall for Hi-net borehole high-sensitivity accelerometer (tiltmeter) in the periods from April to December in 2010, 2011, and 2012 before and after the 2011 Great Tohoku Earthquake in the region of the border of Ibaraki and Fukushima prefectures, and the time variations of the azimuth of the maximum principal crustal stress.

The left figure shows the azimuth of the RFF component of the seven borehole tiltmeters in this area obtained from the time series from April to December 2010. In IWEH site, the azimuth of the RFF component is almost N-S direction, suggesting in the nearby area of this site the maximum compressive stress was not E-W direction even before the 2011 Great Tohoku Earthquake. Among the sites south of IWEH site, in the sites near IWEH site and coastal sites the RFF components are generally almost NE-SW direction, suggesting in the area the maximum compressive stress does not coincide with E-W direction which is seen widely in NE Japan before the 2011 Great Tohoku Earthquake.

The right figure shows the azimuth of the RFF component of the same seven borehole tiltmeters obtained from the time series from April to December 2011 or 2012. In this period, there occurs many offsets and large drifts after those offsets arose by the induced earthquakes and aftershocks of the 2011 Great Tohoku Earthquake, and it is not so easy to detect the detections of the motions after rainfall and the azimuth of the RFF components comparing with the period in 2010. In HTAH and YBKH sites, there seems very little time variations in the azimuth of the RFF component. Also in IWEH site, the time variation of the azimuth of the RFF component is only 10 degree. In IWWH site, the azimuth of the RFF component changes significantly, and almost N-S direction. In DGOH site also the azimuth of the RFF component changes from the NE-SW direction before the earthquake to the NNE-SSW direction. In THGH sites, there are very large noises in N-S component in 2012, which is probably mechanical faults, and there seems very little time variations in the azimuth in 2011 compared with that in 2010. In JUOH site, very little tile motions are seen after rainfall, suggesting the closing of the crack opened in 2010 because of the time variations of the azimuth of crustal stress.

Estimating from the tilt motions after rainfall before and after the 2011 Great Tohoku Earthquake in the Hi-net sites in the area of the border of Ibaraki and Fukushima prefectures, it is suggesting that the area with the N-S direction maximum compressive stress is exist near the IWEH site even before the earthquake, and that mainly in the area west of IWEH site the maximum compress stress shifts near N-S direction after the earthquake.

Keywords: borehole tiltmeter, tilt motions after rainfall, azimuth of crustal stress, 2011 Great Tohoku Earthquake

SCG65-05 Room:423 Time:May 2 10:00-10:15

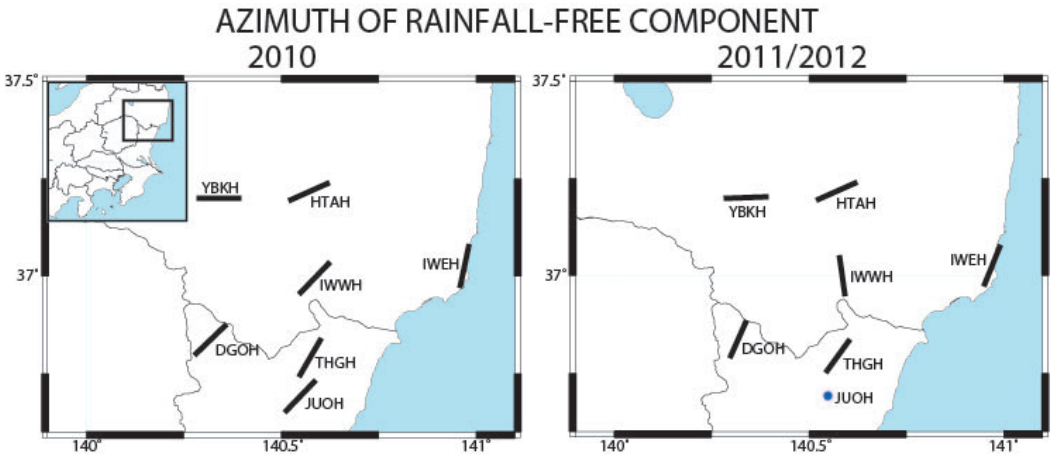

Japan Geoscience Union Meeting 2014
(28 April - 02 May 2014 at Pacifico YOKOHAMA, Kanagawa, Japan)

SCG65-06 Room:423 Time:May 2 10:15-10:30

Evaluation of faults in the site of power plants and stress analyses

SHIGEMATSU, Norio[1*]

[1]Active Fault and Earthquake Research Center, AIST

The expert meeting on the investigation of fracture zones in the site of the Ohi power station of NRA (Nuclear Regulation Autority) concluded that the F-6 fault in the site is not an active fault. Stress tensor inversion was a key technique to make the conclusion during the discussion. In this talk, I will explain how stress tensor inversion was used to evaluate the faults.

It is difficult to evaluate faults based on paleoseismological techniques in the site of many of the power plants, due to the lack of young sediments and tectonic landforms. For the evaluation of the safty of the power plants, it is important to evaluate if the faults in the site are active. Degree of the activity of the faults is not always important. Stress tensor inversion based on the fault slip data is useful because the phenomenon is relatively clear.

There are two concepts to evaluate if the faults are active or not using stress analyses. One is to compare the structures in the fault with the present stress such as slip tendency. The other is that stress tensor inversion is used as a tool to construct the tectonic histories. The former concept may have a problem concerning the stability of stress, especially after large earthquakes. The later concept used stress tensor inversion to determine the sequence of tectonic stages. Tectonic stage is the period during which faults had repeated to move due to the control of similar stress condition. Once the structures in faults at different places were identified to be controlled by the same stress condition, those structures were formed during the same tectonic stage. The comparison of the result of this analysis with the result of fault trenching enables us to evaluate if the faults are active or not.

Keywords: power plant, fracture zones in the site, stress tensor inversion, tectonic stage

Japan Geoscience Union Meeting 2014
(28 April - 02 May 2014 at Pacifico YOKOHAMA, Kanagawa, Japan)

SCG65-07 Room:423 Time:May 2 10:30-10:45

Stress rate dependency and effect of volatile element on seismicity of volcano-tectonic earthquakes

MORITA, Yuichi[1*]

[1]ERI, Univ. of Tokyo

Even in a quiescent period, magma is charged and discharged intermittently beneath volcanoes, and volcano-tectonic earthquakes often occur with ground inflation that is caused by upward migration of magma. Moreover, an increasing volatile element sometimes leads an increasing seismicity. Therefore, it is well known that the seismicity around a volcano is one of the well-established indicators of volcanic activities. Many evidences show that increasing seismicity is followed by volcanic eruptions or magma intrusions because magma migration makes large stress change. On the other hand, the increasing seismicity does not always result in volcanic eruptions. We need to evaluate seismicity quantitatively and discriminate some kinds of effects that generate earthquakes. At present, research in this field has not been established well. It is partly because we cannot propose the model that express temporal variation of seismicity quantitatively, and we do not have enough observation data except some volcanoes where dense observation networks are installed multi-disciplinary.

We proposed to apply the Rate and State Friction (RSF) law to the seismicity occurring at Izu Oshima volcano where dense GPS network as well as seismic one are installed. At the volcano, stress rate changes are observed every 1 to 2 years because of the intermittent magma charging and discharging processes. We presented in last fall meeting of volcanological and seismological society that a simple RSF law model cannot reproduce the observed seismicity fully. We try to revise the model and get remarkable improvement. Aim of this presentation is to reveal the effect of stress rate as well as the other effect, such as volatile element emitted from magma that affect the seismicity around volcanoes, and demonstrate that the seismicity has large potential to monitor the condition not only in the stress rate but also in the volatile density beneath volcanoes.

In Izu-Oshima volcano, seismicity is well correlated with stress rate caused by magma accumulation except the period after the long-term inflation is weaken in 2011. In several volcanoes, increasing volatile component causes decreasing normal stress at fault plane in seismogenic zone and earthquakes are generated intensely (e.g. Northern Volcanic Rift zone in Iceland, La Fossa volcano in Italy). The weakened inflation means that fresh magma is less supplied and emission of volatile decreases in Izu-Oshima volcano. Therefore, we added the effect of the increasing and decreasing volatile element in the previously proposed RSF law, and revised the model. Finally, we can complete successfully the revised model that realize the observed seismicity for all analyzed period.

In conclusion, temporal variation in seismic activity around volcano is mainly due to changes in stress field generated by the magma accumulation and partly caused by effect of volatile element that affects the confining pressure of the fault surface at seismogenic zone. The effect of the stress field is well modeled by ordinary RSF law, and its parameters can be estimated from the data in quiescent period. If observed seismicity exceeds the level that estimated from the model, the volatile element much emitted from magma and it may be precursor to the volcanic eruptions. Therefore, the difference between observed seismicity and the calculated one based on the RSF law is one of the powerful indicator to forecast volcanic eruptions. We propose that there are two kinds of earthquake generating mechanisms around the volcano. Further study at other volcanoes will be helpful to understand the volcano-tectonic earthquake systematically. In future, we should examine the model from direct observation of volcanic gas at volcanoes.

Acknowledgements: We are much grateful to GSI for providing GNSS data.

Keywords: volcano-tectonic earthquakes, seismicity, stress rate change, ground deformation, volatile element

Japan Geoscience Union Meeting 2014
(28 April - 02 May 2014 at Pacifico YOKOHAMA, Kanagawa, Japan)

SCG65-08 Room:423 Time:May 2 11:00-11:15

Investigation into stress field and strength at hypocenters at South African gold mines

OGASAWARA, Hiroshi[1*] ; KATO, Harumi[2] ; HOFMANN, Gerhard[3] ; ROBERTS, Dave[3] ; CLEMENTS, Trevor[4] ; PIPER, Phil[4] ; YABE, Yasuo[5] ; NAKATANI, Masao[6] ; NAOI, Makoto[6]

[1]Ritsumeikan University, [2]3DGeoscience Inc., [3]Anglogold Ashanti ltd., [4]Groundwork ltd., [5]Tohoku University, [6]The university of Tokyo

We report on in-situ stress measurements at seven sites at South African gold mines. The depth ranged from 1.0 to 3.4 km (deepest level in the world where mining is in progress). The measured maximum stress ranged from to 146MPa. In the ranges of stress above 100 MPa have not been able to be measured before we introduced a downsized Compact Conical-ended Borehole Overcoring technique (CCBO; ISRM suggested) in South African gold mines, which has several advantages over the methods widely used in South Africa.

The in situ measurements were carried out at the sites with minimal disturbance by mining or geological features at depths of 3.3 and 3.4 km at Tau Tona and Mponeng mines, respectively, both allowing confirmation that the virgin stress assumptions in the mine were acceptable with slight modification. With the modified virgin stress assumptions, the loading conditions for seven seismic events (ML >2.9) over a 9-year period at Tau Tona mine were back-analyzed with an elastic boundary element method that allows non-linear ride and closure on displacement discontinuity elements (Map3D Fault-SlipR), successfully constraining the stress or the strength on the source faults. At the Pink and Green dykes at 116L at Mponeng mine, the rupture plane of a ML2.1 event was finely delineated by the Japanese-German acoustic emission (AE) network with eight AE sensors deployed within several tens of meters from the rupture plane. It was confirmed that, with the virgin stress assumption and the strength, Map3D was able to reproduce an area of ride consistent with the rupture plane delineated by the AE network. A hole of about 90m length was drilled to intersect the ML2.1 rupture plane to constrain stress by analyzing borehole breakout and core discing. The stress thus constrained was consistent with those estimated with Map3D although the former is a little bit larger than the latter. In situ stress measurements were carried out near seismic damage caused by a ML1.5 event, which took place in the area that a Map3D model with simplest geology structure could not predict high stress. The measured stress state was comparable to that evaluated at the above-mentioned seismic sources.

Seismicity is high at a shaft pillar at 1.0 km depth at Ezulwini mine, where BX CCBO stress measurement was carried out. The measured maximum principal stress was significantly higher than the stress at sites at 3.4km depth with no mining activities.

Keywords: SA gold mines, Seismogenic areas, Stress, Strength, In-situ observation

Japan Geoscience Union Meeting 2014
(28 April - 02 May 2014 at Pacifico YOKOHAMA, Kanagawa, Japan)

SCG65-P01 Room:Poster Time:May 2 16:15-17:30

Comparison of stress modeling with in-situ strain monitoring at seismogenic area in South African gold mines

OGASAWARA, Hiroshi[1*] ; KATSURA, Taishi[2] ; HOFMANN, Gerhard[3] ; NAKATANI, Masao[4] ; YABE, Yasuo[5] ; ISHII, Hiroshi[6] ; NAKAO, Shigeru[7] ; OKUBO, Makoto[6] ; ANTHONY, Ward[8] ; JERRY, Wienand[9] ; PATRICK, Lenegan[9] ; KAWAKATA, Hironori[1] ; MURAKAMI, Osamu[1] ; UCHIURA, Taka[1]

[1]Ritsumeikan University, [2]Hitachi Solutions, ltd., [3]Anglogold Ashanti ltd., [4]The university of Tokyo, [5]Tohoku University, [6]Tono Research Institute of Earthquake, [7]Kagoshima University, [8]Seismogen CC, [9]Sibanye Gold ltd.

Compared with continuous in-situ strain monitoring in other mines, we discussed the time evolution of stress in rock mass at a depth of 3.3km for a ˜1.5-year period 90m beneath a dip pillar at Mponeng mine. The pillar contained a 30m-thick dyke which a ML2.1 seismic event obliquely bisected. We analyzed the recordings of two multi-component Ishii borehole strainmeters which had been already installed nine months prior to the ML2.1 event. One of the strainmeters was installed in the dyke (gabbros) and the other in the host rock (quartzite) near the dyke contact, both being within a few tens of meters from the ML2.1 rupture plane.

The magnitudes and directions of the principal strain changes were similar for both strainmeters in the period prior to the ML2.1 event. This suggested that the increase in stress in the dyke was significantly larger because the dyke was significantly stiffer than the host rock.

After the ML2.1 event, associated with the start of mining on the eastern side of the strainmeters, the pattern of deformation changed between the two strainmeters.

The above-mentioned characteristics of deformation were compared with numerically modelled deformation by an elastic boundary element method using Map3D Fault-Slip. The magnitude of the Map3D strain changes were, however, several times smaller than the observed strain changes both prior to and after the ML2.1 event. The rock mass just around a stope in deep tabular mining is fractured and behaves time-dependently and non-linearly. Whatever the inelastic deformation, the stress field in an elastic area can be reproduced within reason provided that the boundary condition (deformation, force or stress) is appropriately specified on the elastic-inelastic boundary. Because it is well known that time-dependent inelastic stope closure is much larger than instantaneous elastic stope closure, as a trial, we analyzed a response to an additional forced stope closure using Map3Di (Seismic Integrator version). It was then found that the forced additional stope closure better accounted for both the magnitude and the deformation pattern observed by in situ strain monitoring. We concluded that the effect of inelastic deformation around the stope was significantly larger than the elastic effect induced by the advance of mining faces, and the direct effect of the very close ML2.1 event was not so significant.

A great amount of better maintained data sets of strain are now being accumulated in four gold mines, which will allow us to discuss in further depth.

Keywords: SA gold mines, Seismogenic areas, In-situ strain continuous monitoring, Stress time evolution

Japan Geoscience Union Meeting 2014
(28 April - 02 May 2014 at Pacifico YOKOHAMA, Kanagawa, Japan)

SCG65-P02 Room:Poster Time:May 2 16:15-17:30

Distribution of fault plane solutions of smaller events associated with the motion of Kuril forearc sliver

HIRATSUKA, Shinya[1*] ; SATO, Tamao[2] ; SUGAWARA, Sou[3] ; IMANISHI, Kazutoshi[4]

[1]ISV, Faculty of Science, Hokkaido Univ., [2]Sci. and Tech., Hirosaki Univ., [3]JGI, Inc., [4]AIST

In order to find the direct evidence of motion of fore-arc sliver along the Kuril trench, we investigated the distribution of fault plane solutions along the estimated boundary of Kuril fore-arc sliver in Hokkaido. Using the P-wave polarity data as well as P- and SH-wave amplitudes, we determined the fault plane solutions of smaller events ($2.0<M<3.5$) with the number of P-wave polarity data are 10 or greater. The result is summarized as follows. Along the volcanic front in eastern Hokkaido, strike-slip fault type of events with WNW-ESE trending P-axes are distributed, which is consistent with the motion of Kuril fore-arc sliver along the volcanic front. In the western side of Hidaka Mountains, reverse fault type of events with P-axes sub-parallel to the trench are widely distributed, which is consistent with ongoing process of collision of Kuril fore-arc sliver with northeastern Japan arc. In more detail, we found that reverse fault type of events with NE-SW trending P-axes, which rotates counterclockwise from trench parallel direction are concentrated near the epicenter of 1982 Urakawa-oki earthquake (M7.1). The P-wave velocity perturbation derived from tomography study for the lower portion of the overriding plate show a good correlation with the distribution of events with NE-SW trending P-axes. The seismic tomography study suggests that the lower half of the delaminated lower crust extends to the source region of the 1982 Urakawa-oki earthquake, which may cause counterclockwise rotation of P-axes near the epicenter of 1982 Urakawa-oki earthquake (M7.1).

Japan Geoscience Union Meeting 2014
(28 April - 02 May 2014 at Pacifico YOKOHAMA, Kanagawa, Japan)

SCG65-P03 Room:Poster Time:May 2 16:15-17:30

Permeable fractures detected by geophysical loggings and their relation to in-situ stress

KIGUCHI, Tsutomu[1*] ; KUWAHARA, Yasuto[1] ; SATOH, Takashi[1] ; KOIZUMI, Naoji[1]

[1]GSJ, AIST

We examine a relation between the orientation of permeable fractures and the state of in-situ stress by using several logging data measured in 16 boreholes at hard rock sites. Geological Survey of Japan, AIST has constructed 16 integrated borehole observation stations in and around the Kii Peninsula and the Shikoku Island since 2006. Three boreholes with different depths of about 600, 200, 30 m were drilled at each site and various kinds of geophysical loggings were conducted. We obtained the values of strike and dip angle of all fractures including the permeable ones from the borehole wall images of borehole televiewer/camera. Permeable fractures intersecting the borehole were detected by analyzing the logging data of fluid electric conductivity, sonic and temperature. The magnitude and orientation of horizontal principal stress were estimated from hydraulic fracturing stress measurements at 6 sites and the orientation of maximum horizontal stress (SHmax) were evaluated at 11 sites from the images of borehole breakout and/or induced tensile fracture.

The preliminary results from the 6 hydraulic fracturing sites are as follows: The total numbers of all fractures and the permeable ones at each site are in ranges from about 2,000 to 5,000 and from about 20 to 30, respectively. The distribution of the orientation of all fractures at each site shows various values of strike and dip angle. We classify the fractures in three types: tensile fracture (Mode I fracture), shear one and others among the distribution by considering the in-situ state of stress at each site. The tensile type has orientations parallel to SHmax and relatively high dip angles. The shear fracture is optimally oriented for shear failure in the current stress field. It is difficult at any sites to say that characteristics of the distribution of the orientation of all fractures are described only with tensile or shear failure types. Next, an examination of the permeable fracture orientation shows that large number of the permeable ones at the Niihama site have strike orientations almost parallel to SHmax and high dip angles. This feature is different from that for all types of fractures at this site. This suggests that the current stress field controls the existence of the permeable fractures at Niihama site. On the other hand, the distributions of the orientations of permeable fractures at other 5 sites have different characters from the Niihama case: The orientations of permeable fractures have the same tendency with all fractures including non-permeable fractures.

Keywords: permeable fracture, geophysical logging, in-situ state of stress, tensile fracture, shear fracture

Japan Geoscience Union Meeting 2014
(28 April - 02 May 2014 at Pacifico YOKOHAMA, Kanagawa, Japan)

SCG65-P04 Room:Poster Time:May 2 16:15-17:30

Change in paleostress in offscraped accretionary complex, Kayo formation, the Shimanto Belt, Okinawa island

HASHIMOTO, Yoshitaka[1*] ; MOTOMIYA, Yuhei[1] ; UJIIE, Kohtaro[2]

[1]Kochi University, [2]Tsukuba University

It is important to understand a stress state of subduction zone because it is strongly related to development of accretionary complex, strength of fault, geometry of subduction zone and earthquake process. The purpose of this study is to examine paleo-stress in a off-scraped accretionary complex in Shimanto Belt, Okinawa island.

The study area is Kayo formation in the northeastern coast of Okinawa island. The Kayo formation consists mainly of coherent turbidites, and it was highly deformed by folds and thrusts. Those geological structures of the formation represent characteristics of fold-thrust belt in forearc area[Ujiie,1998].

Flexural slip associated with folding is commonly observed. In addition, many micro-faults cutting bedding are also observed. On the slip surfaces both of flexural slip surfaces and micro-faults, slicken lines and slicken steps are identified. From the structures, slip data (strike and dip of fault plane, slip direction and slip sense) was obtained.

The number of slip data for micro-fault is 153 in ˜2 km wide of study area. Using the slip data, we conducted micro-fault inversion analysis to examine the stress orientation and stress ratio. The stress ratio is defined as ϕ=(σ2-σ3)/(σ1-σ3). We used software MIM (Yamaji,2000) for stress analysis and K-means clustering (Ostubo et al, 2007) for automated picking of center of cluster. After the stress analysis, we combined the stress data with stress polygon to examine stress magnitude semi-quantitatively. The stress polygon is based on Anderson ' s theory. We assumed the vertical stress is always gravity force, which is converted from assumed depth.

As a result of analysis, 4 stress solution (KY1-KY4) were obtained. KY1) NE-SW horizontal compression with high stress ratio, (ϕ=0.88), KY2) KY3) NW-SE high angle compression with low to intermediate stress ratio (ϕ=0.22,0.45), and KY4) NW-SE horizontal compression with intermediate stress ratio (ϕ=0.65).

We picked up the micro-fault with misfit angle less than 40? for each stress. Misfit angle is the angle between calculated slip direction and observed slip direction on the micro-fault surface. Reverse faults are dominant in KY1 and KY4 and normal faults are dominant in KY2 and KY3.

The stresses are projected to horizontal surface and to Shmax (perpendicular to fold axis), Shmin (parallel to fold axis), and Sv. Using stress ratio and stress projection above, linear functions in Shmax and Shmin space are obtained. We can examine the semi-quantitative Shmax and Shmin value for the stresses in overwrapping area between the linear functions and stress polygon.

Magnitudes of shear stresses for KY2, KY3, KY1 and KY4 on the horizontal decollement were also estimated as τ2=39.2˜54.7[MPa], τ3=52.1˜64.2[MPa] and τ1=79.0˜212.3[MPa], τ4=48.0˜137.7[MPa]. The shear stress for reverse fault (KY1, KY4) is bigger than the shear stress for normal fault (KY2, KY3). If the differences in stress represent the stress change in seismic cycle, the differences in shear stress indicate stress drop as -16.2˜173.1[MPa]. Stress drop in general earthquake ranges 0.03˜30[MPa]. The obtained stress drop in this study includes the range of general stress drop.

Keywords: Stress, micro-fault inversion, Shimanto Belt, Okinawa

Japan Geoscience Union Meeting 2014
(28 April - 02 May 2014 at Pacifico YOKOHAMA, Kanagawa, Japan)

SCG66-01 Room:414 Time:April 30 09:00-09:15

Development of heterogeneous rheological model of the Tohoku Island arc-trench system

MUTO, Jun[1*] ; SHIBAZAKI, Bunichiro[2]

[1]Dept. Earth Sci., Tohoku Univ., [2]Building Res. Inst.

Subduction zone earthquake cycles can be characterized by various deformation processes taking place around the plate boundary and surrounding area. For example, after slip, viscoelastic relaxation and locking of the plate boundary are three primary processes among them. In order to illuminate the recovery of plate coupling after the Mw 9.0 Tohoku-Oki earthquake and strain budgets of island arc during cycles, the detailed viscoelastic structure of the Tohoku region is developed using seismologically determined subsurface structures and densely measured geothermal gradient data. The model is oriented perpendicular to the Japan Trench and also transects an area of large coseismic slip of the 2011 Tohoku Oki earthquake. Petrological model proposed by the laboratory measurement of seismic velocity of various rocks [Nishimoto et al., 2005] was utilized to infer rheologically major minerals from seismic velocity structures. We used geothermal gradient data from the inland Hi-net borehole [Matsumoto, 2007], as well as geothermal gradient data compiled from around Japan [Tanaka et al., 2004]. The strain-rate-dependent, steady state effective viscosity was calculated using constitutive laws of various rocks under the assumption of homogeneous geologic shortening rate [Sato, 1989]. The calculated viscosity structures show lateral viscosity gradients both parallel and normal to the trench axis. Moreover, the minimum viscosities are predicted to be 10^{19} Pa s in the mantle wedge and 10^{20} Pa s in the oceanic mantle. The values are consistent with previous estimates obtained by postseismic deformation analysis of subduction zone earthquakes with similar magnitudes (Mw ˜9). However those minimum values only appear in depths of 30-100 km in the upper mantle and the viscosity increases further with depths because of the pressure hardening effect. Taking the high values of viscosities in shallower part of the lithosphere, the thickness of high viscous layers found to have lateral variations implying the heterogeneous elastic layer thickness. Model viscosity structures of the Tohoku region utilizing realistic temperature and rheological properties of rocks can be used to evaluate the effect of rheological heterogeneity in the postseismic deformation field of the Tohoku-Oki earthquake observed by dense network of geodetic observations. In the presentation, we will mention the detailed information on the choice of the flaw law parameters, and physical and ambient conditions for NE Japan to calculate the viscosity structures. We also show how these heterogeneities affect the crustal deformation of the NE Japan during subduction zone earthquake cycles.

Keywords: rhology, Tohoku, viscoelastic relaxation, earthquake cycle, Tohoku oki earthquake

Japan Geoscience Union Meeting 2014
(28 April - 02 May 2014 at Pacifico YOKOHAMA, Kanagawa, Japan)

SCG66-02 Room:414 Time:April 30 09:15-09:30

Detailed seismic attenuation structures beneath the Hokkaido corner, northern Japan (3)

KITA, Saeko[1*] ; NAKAJIMA, Junichi[2] ; HASEGAWA, Akira[2] ; UCHIDA, Naoki[2] ; OKADA, Tomomi[2] ; KATSUMATA, Kei[3] ; ASANO, Youichi[1] ; KIMURA, Takeshi[1]

[1]NIED, [2]RCPEV, Graduate School of Science, Tohoku University, [3]ISV, Hokkaido University

1. Introduction

In the Hokkaido corner, the Kuril fore-arc sliver collides with the northeastern Japan arc. Using travel-time data compiled from the nationwide Kiban seismic network and a dense temporary seismic network [Katsumata et al, 2002], Kita et al. [2012] determined high-resolution 3D seismic velocity structure beneath this area for deeper understanding of the collision process of the two fore-arcs. In this study, we merged waveform data from the Kiban-network and from the temporary network, and estimated the seismic attenuation structure to understand seismotectonics and collision process beneath Hokkaido.

2. Data and method

We estimated corner frequency for each earthquake by the spectral ratio method of coda waves [e.g. Mayeda et al., 2007]. Then, we simultaneously determined values of t∗and the amplitude level at low frequencies from the observed spectra after correcting for the source spectrum. Seismic attenuation (Q-1 value) structure was obtained, inverting t∗values and employing the 3-D ray-tracing technique of Zhao et al. [1992]. The study region covers an area of 41-45N, 140.5-146E, and a depth range of 0-300 km. We obtained 154,293 t∗at 316 stations from 6,196 events (Mj>2.0) that occurred during the period from Aug. 1999 to Dec. 2012. Horizontal and vertical grid nodes were set with spacing of 0.1-0.3 degrees and 10-30 km, respectively.

3. Results

The calculated stress drops are distributed from 0.1 to 100 MPa. Stress drops of intraslab earthquakes increase with focal depth. The values of stress drops of events in the slab mantle tend to be larger than those in the slab crust at depths of 80 to 170 km, which might contribute to understanding of the physical nature of intraslab earthquakes.

Seismic attenuation structure is imaged for the region above the subducting Pacific slab at depths down to ˜80 km. For the forearc side of the eastern and western parts of Hokkaido, high-Qp zones are generally imaged at depths of 10 to 80 km in both the crust and mantle wedge above the Pacific slab. In contrast, low-Qp zones are clearly imaged in the mantle wedge of the backarcside.They are distributed in deeper parts and reach the Moho beneath the volcanic front. Locations of these low-Qp zones correspond to the low-Vp and low-Vs zones imaged by Zhao et al. [2012]. These suggest that the upper head of the mantle-wedge upwelling flow is detected beneath Hokkaido also by our seismic attenuation imaging.

In the Hokkaido corner, to the west of the Hidaka main thrust a broad low-Qp zone is imaged at depths of 0?60 km. Location of this broad low-Qp zone almost corresponds to that of the low-V zone in the collision zone found by Kita et al. [2012]. Fault planes of the 1970 M6.7 and 1982 M7.1 earthquakes are located at the edges of a broad low-Qp zone, being in contact with a high-Qp zone at 10 to 35 km. These results suggest that the occurrence of these anomalously deep and large inland earthquakes is related to the presence of hydrous minerals or fluids.

The subducting oceanic crust beneath the Hidaka region is imaged as a low-Q zone whose location corresponds to the low-Vp and low-Vs zone of Kita et al. [2012], suggesting the existence of hydrated materials at the top of the slab. Just above the slab surface, moderately low-Q zones are imaged at depths of 90 to 100 km beneath eastern and southern Hokkaido and at depths of 110 to 130 km beneath the corner, which are located at depths deeper than the upper plane seismic belt. These observations suggest the existence of the hydrated mantle wedge by the aqueous fluids supplied from the oceanic crust right below.

Keywords: Seismic attenuation structure, Seismotectonics, arc-arc collision process, Stress drops of intraslab earthquakes

Japan Geoscience Union Meeting 2014
(28 April - 02 May 2014 at Pacifico YOKOHAMA, Kanagawa, Japan)

SCG66-03 Room:414 Time:April 30 09:30-09:45

Crustal deformation in the Mid-Niigata area and its implication for strain concentration

SAGIYA, Takeshi[1*] ; MENESES, Angela[1]

[1]Nagoya University

The Mid-Niigata area is located within the concentrated strain belt along the eastern margin of the Japan Sea. This area suffered from two large earthquakes, the 2004 Chuetsu and the 2007 Chuetsu-oki earthquakes. Based on GPS velocity data calculated from daily coordinate time series of GEONET, we identified significant time dependence of the interseismic crustal deformation patterns before, between, and after these two earthquakes. Modeling results of the deformation pattern changes are summarized as follows. 1) Contraction before 2004 occurred between the source regions of the two earthquakes and it was attributed to aseismic faulting across almost the whole elastic layer, implying that the observed strain was largely inelastic. This interpretation is also supported from a fact that the historical seismic energy release in this area is much smaller than that expected from geodetic strain accumulation. 2) After two earthquakes, aseismic faulting seems to have continued without explicit time decay. The aseismic faulting is estimated close the source fault of the main shocks, implying that postseismic strength recovery did not occur on the main shock fault or a nearby parallel fault was activated to accommodate regional contraction. This is consistent with an idea that the upper crust in this area is segmented to smaller blocks and the mechanical behavior is very sensitive to external stress changes.

Keywords: Strain concentration, Niigata-Kobe Tectonic Zone, 2004 Chuetsu earthquake, 2007 Chuetsu-oki earthquake, aseismic faulting, inelastic deformation

Japan Geoscience Union Meeting 2014
(28 April - 02 May 2014 at Pacifico YOKOHAMA, Kanagawa, Japan)

SCG66-04 Room:414 Time:April 30 09:45-10:00

Tectonic stress fields in subduction zones governed by frictional strength of plate interfaces

MATSU'URA, Mitsuhiro[1*] ; NODA, Akemi[2] ; TERAKAWA, Toshiko[3] ; FUKAHATA, Yukitoshi[4]

[1]Institute of Statistical Mathematics, [2]Kozo Keikaku Engineering Inc., [3]Nagoya University, [4]Kyoto University

Tectonic crustal motion in plate convergence zones varies from mountain building (e.g., Himalaya) to back-arc spreading (e.g., Mariana) [1, 2, 3]. Such difference in tectonic crustal motion reflects the diversity of tectonic stress fields. So our question is what causes the diversity of tectonic stress fields in plate convergence zones. Recently, from a theoretical study [4], we revealed that the tectonic stress field consists of basically two different sorts of stress fields; one of which is a horizontally compressional stress field due to frictional resistance at plate interfaces, and another is a horizontally tensile stress field due to steady plate subduction. On a geological timescale, the former can be regarded as constant in time, but the latter increases with time. So, if the earth's crust were infinitely strong, tectonic stress fields in plate convergence zones would become tensile in time everywhere. Actually, the earth's crust includes a number of defects with low strength, over which inelastic deformation (brittle fracture and/or plastic flow) occurs so as to release the tectonic stress caused by mechanical interaction at plate interfaces. From these considerations, we may conclude as follows. When the plate interface is very weak in comparison with the earth's crust, a horizontally tensile stress field becomes dominant, which causes back-arc spreading as in the case of Mariana. When the plate interface is very strong, a horizontal compressional stress field becomes dominant, which causes mountain building as in the case of Himalaya. Tectonic stress fields in most subduction zones, where the strength of plate interfaces are comparable to that of the earth's crust, are between these two extreme cases.

References

[1] Takada, Y. and M. Matsu'ura, 2004. A unified interpretation of vertical movement in Himalaya and horizontal deformation in Tibet on the basis of elastic and viscoelastic dislocation theory, Tectonophysics, 383, 105-131.

[2] Hashimoto, C. and M. Matsu'ura, 2006. 3-D simulation of tectonic loading at convergent plate boundary zones: Internal stress fields in northeast Japan, Pure Appl. Geophys., 163, 1803-1817.

[3] Hashima, A., Y. Fukahata, and M. Matsu'ura, 2008. 3-D simulation of tectonic evolution of the Mariana arc-back-arc system with a coupled model of plate subduction and back-arc spreading, Tectonophysics, 458, 127-136.

[4] Matsu'ura, M., A. Noda, and T. Terakawa, 2013. Strength of plate interfaces and tectonic stress fields in subduction zones, Seismological Society of Japan 2013 Annual Meeting, D22-08, Yokohama.

Keywords: subduction zone, tectonic stress field, plate interface, frictional strength, mountain building, back-arc spreading

Japan Geoscience Union Meeting 2014
(28 April - 02 May 2014 at Pacifico YOKOHAMA, Kanagawa, Japan)

SCG66-05 Room:414 Time:April 30 10:00-10:15

Sequential inversion of GPS time series data to estimate spatiotemporal change in interplate coupling

NODA, Akemi[1*] ; MATSU'URA, Mitsuhiro[2]

[1]Kozo Keikaku Engineering Inc., [2]Institute of Statistical Mathematics

To estimate steady increase rates of slip deficits at plate interfaces, first, we obtain linear trends of the time series of GPS daily coordinate data by removing seasonal variations and coseismic and postseismic changes due to episodic events. Then, we invert the linear trends (surface displacement rates at GPS stations) into steady slip-deficit rate distribution on a plate interface with completely relaxed slip-response functions for an elastic-viscoelastic layered half-space model under gravity (Noda et al., 2013, GJI). Noda et al. (SSJ 2012 Annual Meeting) demonstrated that this method is applicable to GPS time series data in northeast Japan for the interseismic period (March 1997-February 2008) before the 2008 Ibaraki-oki (Mw6.8) and Fukushima-oki (Mw6.9) earthquakes. After these events, the trends of GPS time series data gradually change with time (Suito et al., 2011, EPS), indicating spatiotemporal change in interplate coupling preceding the 2011 Tohoku-oki mega-thrust earthquake.

The change in slip-deficit rate distribution disturbs a steady stress state in the asthenosphere, and so we need to use the viscoelastic transient slip-response functions for the analysis of GPS time series data after the 2008 events (Noda et al., 2013, GJI). An exact treatment of the viscoelastic inverse problem to estimate cyclic slip processes at a plate interface has been given by Fukahata et al. (2004, GJI), but it is not applicable to the present problem because the change in slip-deficit rate distribution is not a cyclic but transient process. So, we propose a simple inversion technique, called sequential inversion of GPS time series data, to estimate spatiotemporal changes in slip-deficit rates at plate interfaces. A similar sequential inversion technique has been used by Lubis et al. (2013, GJI) for the analysis of afterslip distribution following the 2007 southern Sumatra earthquake (Mw8.5) on the assumption that the asthenosphere has been in a steady stress state until the 2007 event.

In the present study, we estimate the spatiotemporal change in interplate coupling by applying the sequential inversion technique to GPS time series data for March 2008-February 2011, and reveal the slip history at the North American-Pacific plate interface off Tohoku during the 14 years before the 2011 Tohoku-oki mega-thrust earthquake.

Keywords: GPS time series data, sequential inversion, viscoelastic transient response, change in interplate coupling, the 2011 Tohoku-oki earthquake

Japan Geoscience Union Meeting 2014
(28 April - 02 May 2014 at Pacifico YOKOHAMA, Kanagawa, Japan)

SCG66-06 Room:414 Time:April 30 10:15-10:30

Middle Miocene swift migration of the TTT triple junction and rapid crustal growth in SW Japan

KIMURA, Gaku[1*] ; HASHIMOTO, Yoshitaka[2] ; KITAMURA, Yujin[3] ; YAMAGUCHI, Asuka[4] ; KOGE, Hiroaki[1]

[1]Dept. Earth and Planetary Science, The University of Tokyo, [2]Kochi University, [3]Kagoshima University, [4]Atmosphere and Ocean Research Institute, The University of Tokyo

We review recent progress in geological and geophysical investigation in SW Japan, the Nankai Trough and the Philippine Sea Plate (PSP), and propose a comprehensive hypothesis for the Miocene tectonics of the Nankai Trough. New interpretations are as follows: Near-trench magmatism in the outer zone of SW Japan might have various reasons. The possibility of an arc-arc collision in particular should be examined, in addition to the previous model of an oceanic ridge and hot PSP subduction. The indentation structure at Capes Ashizuri, Muroto in Shikoku, and Shiono on the Kii Peninsula may be explained by the collision of the active arc or topographic peaks such as seamounts, contrary to the previous ”kink-folding” model due to recent E-W compression. This inference is drawn from comparison between the many modern examples of seamount collision and sandbox analogue experiments. Crustal components of SW Japan might consist mainly of igneous plutonic rocks, in contrast to the previous inference of Cretaceous to Tertiary accretionary complexes. This is especially the case in the outer zone to the north of Capes Ashizuri, Muroto and Shiono. This is inferred from geophysical observation of gravity anomalies, velocity and resistivity, together with geological estimations of caldera age and the size of its root pluton. Episodic crustal growth due to intrusion of igneous rock and subduction of the PSP may have stopped after ˜11 Ma and restarted at ˜7-8 Ma. New accretionary prism was again developed after ˜6 Ma. This inference is suggested by recently conducted ocean drilling program.

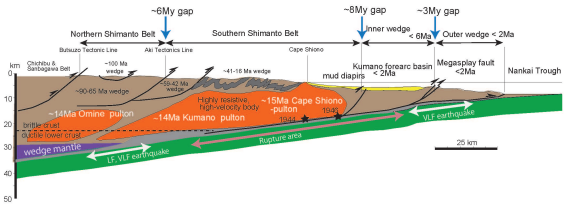

Japan Geoscience Union Meeting 2014
(28 April - 02 May 2014 at Pacifico YOKOHAMA, Kanagawa, Japan)

SCG66-P01 Room:Poster Time:April 30 18:15-19:30

Spatial relationship between the volcanic chain and high gravity anomalies in subduction zones

FUKAHATA, Yukitoshi[1*]

[1]DPRI, Kyoto University

The most conspicuous features of arc-trench systems are active seismicity, characteristic topography and gravity anomalies, and volcanism. The topography and gravity anomalies are low in the trench and high in the arc, which can be theoretically explained by mechanical interaction between the subducting oceanic plate and the overriding plate (Sato & Matsu'ura, 1993, GJI; Hashimoto et al, 2004, PAGEOPH). Because the topography is more complicated to be understood, free-air gravity anomaly is more suitable to be compared to the theoretical model. Free-air gravity anomalies with long wave length basically represent the effect of tectonic force, which disturbs gravity equilibrium.

Volcanoes align along the volcanic front in most arcs. Since both of the high free-air gravity anomalies and volcanic front have a subparellel strike to the trench, it should be possible to classify arc-trench systems according to the spatial relationship between them. Based on such an idea, Fukahata (2008, JPGU meeing) classified arc-trench systems, but there was a problem that the recognition of the location of high gravity anomalies was quite subjective. So, in this study, I improved this process.; the location of high gravity anomalies were more quantitatively recognized. As a result, the location of high gravity anomalies relative to the volcanic front did not change for most arcs, but I found that it was difficult to define its location in some arcs (mostly tensile). Using the result, I discuss the spatial relationship between the volcanic chain and high gravity anomalies in subduction zones and consider causes of topographic evolution of island arcs.

Keywords: island arc, subduction zone, gravity anomaly, volcanic front

Japan Geoscience Union Meeting 2014
(28 April - 02 May 2014 at Pacifico YOKOHAMA, Kanagawa, Japan)

SCG66-P02 Room:Poster Time:April 30 18:15-19:30

Uplift and denudation history of the Yoro-Suzuka-Nunobiki Mountains: Constraints from apatite FT thermochronology

SUEOKA, Shigeru[1*] ; TSUTSUMI, Hiroyuki[2] ; TAGAMI, Takahiro[2] ; HASEBE, Noriko[3] ; TAMURA, Akihiro[3] ; ARAI, Shoji[3] ; SHIBATA, Kenji[1]

[1]Japan Atomic Energy Agency, [2]Kyoto University, [3]Kanazawa University

The Yoro-Suzuka-Nunobiki Mountains are fault block mountains distributed along the Isewan-Tsurugawan Tectonic Line, a tectonic boundary between the Kinki and Chubu districts. The Kinki district on the west of the mountains is characterized by predominance of reverse faults and alternation of N-S trending mountain ranges and basins (Kinki Triangle; Huzita, 1962), whereas the Chubu district on the east of the mountains has predominance of strike-slip faults and westerly tilting landforms (Chubu tilting block; Kuwahara, 1968). Miyoshi & Ishibashi (2008) mentioned that the Philippine Sea Plate slab beneath the region around the Yoro-Suzuka-Nunobiki Mountains has shallow subduction angle and form a convex shape (Isewan-Kohoku slab) and proposed this shallow slab resulted in the tectonic boundary between the Kinki and Chubu districts in the region. On the eastern and western sides of the Yoro-Suzuka-Nunobiki Mountains, two major subsidence areas have formed and moved northward since the end of the Miocene as recorded by deposition of the Tokai group and Kobiwako group (e.g., Yokoyama, 1995; Yoshida, 1990). On the other hand, there is some debate over the formation process and mechanism of the Yoro-Suzuka-Nunobiki Mountains; Okada (2004) speculated the mountains have uplifted from south to north generally corresponding to the northward moving of the subsidence areas, whereas Ohta and Takemura (2004) proposed the formation of the mountains were still later and independent from the formation of the subsidence areas.

We are attempting revealing uplift and denudation history of the Yoro-Suzuka-Nunobiki Mountains in the past few million years by using apatite fission-track (AFT) thermochronology. We have obtained AFT ages and length distribution data in one site for the Yoro Mountains, eight sites for the Suzuka Range, and one site for the Nunobiki Mountains. Highlights of the results are as below: 1) the AFT ages range 47-30 Ma, 2) the ages were youngest in the middle to south parts of the Suzuka Range and get older to the north and south, 3) thermal histories calculated from the AFT ages and length distributions indicate rapid cooling events in the past few million years in the middle to south parts of Suzuka Range, but not in the Yoro and Nunobiki Mountains and the north part of the Suzuka Range, 4) the rapid cooling events in the past few million years are attributable to the the uplift of the Suzuka Range since ~1.3 Ma (Yokoyama, 1995). We are conducting additional AFT analyses in seven sites of the Nunobiki Mountains to expand our results to the south. In this presentation, we are planning to provide progressed discussions containing the results of the additional data.

Keywords: Yoro-Suzuka-Nunobiki Mountains, apatite fission-track thermochronology, denudation, eastern margin of the Kinki Triangle

Japan Geoscience Union Meeting 2014
(28 April - 02 May 2014 at Pacifico YOKOHAMA, Kanagawa, Japan)

SCG66-P03 Room:Poster Time:April 30 18:15-19:30

Self-affinities for Amplitude and Wavelength of Folds

KIKUCHI, Kazuhei[1*] ; NAGAHAMA, Hiroyuki[1]

[1]Department of Earth Science, Graduate School of Science, Tohoku University

In general, many folds are apparently curved or jagged on a wide range of scales, so that their geometries appear to be similar when viewed at different magnifications. By Matsushita and Ouchi (1989a, b)'s method, we also analyzed the self-affinities of folds in the North Honshu Arc, Japan (Kikuchi et al., 2013). Based on this analysis, geometries were found to be self-affine and can be differently scaled in different directions. We recognize the self-affinities for the amplitude and the wavelength of folds and a crossover from local to global altitude (vertical) variation of the geometries of folds in the Northeast Honshu Arc.

Buckingham's Pi-theorem is sufficient to the first problems of fold systems (Shimamoto, 1974). However, the complete similarity cannot give us the self-affinities of folds. A general renormalization-group argument is proposed to the applicability of the incomplete self-similarity theory (Barenblatt, 1979). Based on the general renormalization-group argument, we derive the self-affinities for the wavelength (L) and the amplitude (a) of folds:

$$L^{(1-d)} \propto a.$$

The relationship between Hurst exponents H of fold (Kikuchi et al., 2013) and d are equation:

$$1\text{-}d=H,$$

where H is index of the continuity of a given fold curve and obtained by the ratio between horizontal scaling exponent and vertical scaling exponent. d is an exponent of a given incomplete self-similarity theorem.

In $d \neq 0$ case, the Hurst exponent $H \neq 1$ indicates self-affinities for the given fold curve. In this case, scale invariance of the fold might be affected by a variety of tectonic processes under the anisotropic stress field. In $d = 0$ particular case, the Hurst exponent $H = 1$ indicates self-similarity for the given fold curve. In this case, scale invariance of the fold might not be affected by a variety of tectonic processes under the anisotropic stress field. These results imply that anisotropic stress fields by gravitation and tectonic stresses might cause self-affinities of folds. Self-similarity and self-affinities of the fold might be affected and by a variety of tectonic processes under the isotropy or anisotropic stress field.

Reference

Barenblatt, G.I. (1979)*Consultants Bureau*, New York.
Kikuchi, K., K. Abiko, H. Nagahama, H. Kitazato, and J. Muto (2013) *Acta Geophysica*, **61**, 6, pp. 1642-1658.
Matsushita, M. and S. Ouchi (1989a) *Physica D*, **38**, 1, pp. 246-251.
Matsushita, M. and S. Ouchi (1989b) *Journal of the Physical Society of Japan*, **58**, 5, pp. 1489-1492.

Keywords: Fold, Self-affinity, Buckingham's Pi-theorem, Incomplete self-similarity theory

Japan Geoscience Union Meeting 2014
(28 April - 02 May 2014 at Pacifico YOKOHAMA, Kanagawa, Japan)

SCG66-P04 Room:Poster Time:April 30 18:15-19:30

Reason for strange appearance of Mt. Hakone, and Reason why the Boso Triple Junction has moved to the west most

MASE, Hirofumi[1]*

[1]none

(Refer to the chart)

Mt. Fuji penetrates through the north end of the Philippine Sea Plate(PHSP), and is the front of land side plate incision, and is the starting point of Suruga and Sagami Trough(1). Mt. Hakone and Mt. Mihara have decided the position of Sagami Trough.

”Tokai Slab” seems to stop beneath the north side of Mt. Fuji. On the other hand, ”Sagami Slab” seems to sink and reach the interior of Kanto.(3) It is unnatural as one board. Though the crustal deformation that GPS caught shows that the Izu Peninsula moves to the west, tendencies of Izu islands and Southern part of Kanto to move to the north are strong(4). In 135-140∗east, it has been understood that the section of especially 140∗meets the requirement of the temperature structure that the power to make the Pacific Ocean’s side go north is generated. In a word, I think that only the side of ”Sagami Slab” sank greatly in PHSP in the past and the current situation was caused.

Then, where is the crack (lateral fault) that becomes a boundary? There is the earthquake-prone zone that symbolizes subducting of Slab on the north side of the Mt. Hakone(5). If the edge of west side within the range of that distribution is traced, the Mt. Hakone and Mt. Mihara can be connected in a smooth line(red broken line). The line of blank for south-north, that divides the earthquake-prone zone to the east and the west, passes the Mt. Hakone(blue broken line). Because there was no fault in the south from Mt. Mihara, I think the slipping fault shifted to the fault shown in blue broken line though there was an age that the fault shown in red broken line slipped. The Mt. Hakone has the meaning of the west edge of PHSP in the Izu-islands-east and of the starting point of subducting.

On the other hand, why has the trench axis around the Boso Triple Junction moved to the west most? Pacific Plate that goes west compresses land side Plate and PHSP that get on on it into the direction of east-west. And, pulls them for south-north. The Part where land side Plate and PHSP overlap shifts mutually and the overlap becomes shallow. The upper plates expand for south-north to Pacific Plate. As a result, the trench axis becomes easy to go west by the east-west compression. Land side Plate and PHSP and Pacific Plate become tight in the direction of east-west. And, fold and collapse occur in them. As a result, the trench axis becomes easy to go west further. Because usual stresses are absorbed to the fold and collapsing, the trench axis is not easy to returns east even if a massive earthquake occurs. This is the cause that the trench axis moves to the west.

Reference literature

(1)Hirofumi MASE(2009)/SSJ2009/P3-64/http://jglobal.jst.go.jp/detail.php?JGLOBAL_ID=200902239527416838

(3)Shinji TODA(2005)/A new image of plate configuration and seismotectonics of the triple junction beneath the Kanto region/Fig.1(Noguchi1999)/AFRC.AIST/release06/10/2005/http://www.aist.go.jp/aist_j/new_research/nr20050610/nr20050610.html

(4)GSI/Animation of Crustal Deformation in Japan/http://mekira.gsi.go.jp/ENGLISH/crstanime.html

(5)JMA/Monthly Report on Earthquakes and Volcanoes in Japan December 2001/Tokai and South-Kanto/Fig.5/http://www.seisvol.kishou

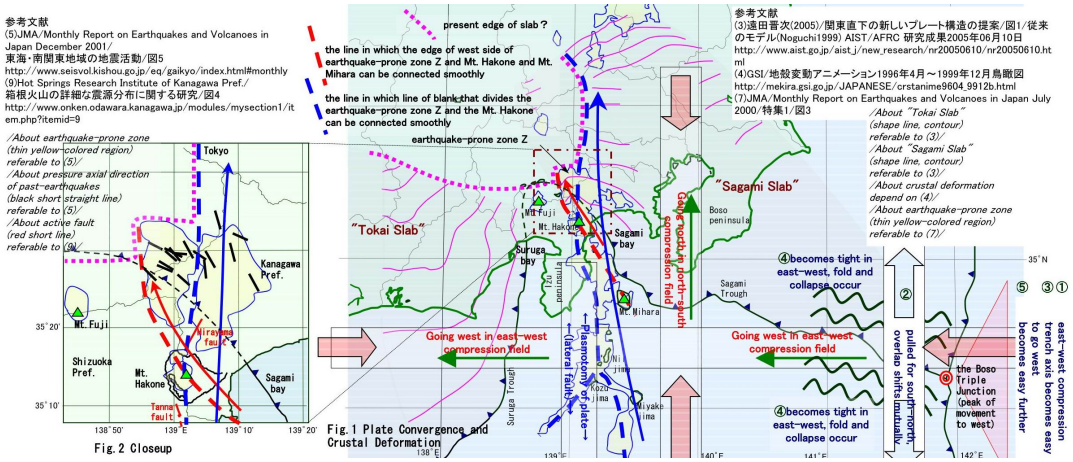

Japan Geoscience Union Meeting 2014
(28 April - 02 May 2014 at Pacifico YOKOHAMA, Kanagawa, Japan)

SCG67-01 Room:414 Time:May 1 14:15-14:30

The Ocean Floor was Expanded by Increasing Seawater

MADO, Shinichiro[1*]

[1]MAROSA

Introduction

I wrote this paper in order to present the negation of a hypothesis which supports the plate tectonics. The hypothesis is 'Spreading Oceanic Floor Hypothesis'. This negation is based upon a new fact that has been revealed recently. I concluded the negation by such facts and my original reasoning. I already presented another fact negating the hypothesis of 'Spreading Oceanic Floor'. The abstract titled 'it was not switching global geo-magnetic fields that created the alternating anomalies over oceanic ridges' was presented at the Japan Geoscience Union Meeting 2013. Therefore, one of reasons that support the hypothesis of spreading oceanic floor was already denied. In this paper I will deny another reason of the hypothesis, which says that the plates of the oceanic floors are spreading.

What is the question

The Hypothesis of Plate tectonics was evolved from Wegener's 'Continental Drift Hypothesis' and based upon 'The Hypothesis of Spreading Oceanic Floor'. However, the hypothesis of spreading oceanic floor is denied as far as it means the spreading plate of oceanic floor. It is denied by the fact that the oceanic floors spread not because the oceanic plates themselves spread but merely because the seawater increased. Therefore, the hypothesis of plate tectonics lost one of its evidences.

The Expanding Oceanic Floor

The hypothesis of plate tectonics is supported by the hypothesis of spreading oceanic floor. The rapidity of the movement of the plate was estimated by the switching pattern of geo-magnetic anomaly near the ridges. The farer and farer it comes from the ridges, the older and older the dates of the basalts and fossils become. The estimated dates fit well the dates estimated from the pattern of geo-magnetic anomalies. It was proved that the rapidity was estimated 2cm par one year for the Pacific Ocean[1],[2].

Rising Sea Level Caused by Increasing Seawater

However, the hypothesis of spreading oceanic floor neglected the fact that the sea level increased greatly. The sea level increased more than 6000m after the creation of oceanic plates. That fact was revealed by the remaining river valleys on the oceanic floors. For instance the Kushiro River reaches more than 6000m in depth$^{[Fig1-B]}$. The Itoi River reaches about 3500m in depth$^{[Fig1-A]}$.

These facts revealed that the seawater increased greatly after the creation of the oceanic plates. It takes very long time to raise sea level to recent level. Gradually the amount of seawater is increasing even now.

Provably the increase of seawater is caused by crustal movements squeezing water from the rocks of the crust. The squeezed water becomes hot springs.

The date of the fossils near the ridges are newer because those places are higher and newly became under the sea level.

Conclusion

The oceanic floors spread not because the oceanic plates spread but because the seawater increased largely after the creation of the oceanic floor plates.

Therefore, it has no relation between the dates of the oceanic plates and the date of fossils contained in upper layers. Therefore, one of evidences of plate tectonics was lost.

References

[1] Maxwell, A. & Von Herzen, R. et al. 'Deep Sea Drilling in the South Atlantic', SCIENCE, Volume 168, pp.1047-1059, 29 May 1970.

[2] Dietz, R. 'Continent and Ocean Basin Evolution by Spreading of of the Sea Floor', NATURE, Volume 190, pp.854-857, June 3, 1861.

[3] Shinichiro Mado, 'It was not switching global geo-magnetic fields that created the alternating anomalies over oceanic ridges', ABSTRACT of Japan Geoscience Union Meeting, SEM36-P01, 2013.

SCG67-01 Room:414 Time:May 1 14:15-14:30

Keywords: Dating the Ocean Floor, Rise in the Sea Lebel, Increase of Seawater, Expansion of the Ocean Floor

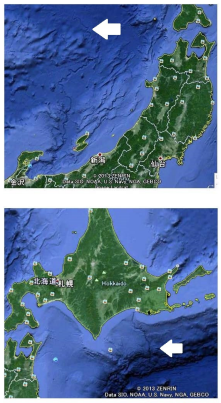

Fig 1

Japan Geoscience Union Meeting 2014
(28 April - 02 May 2014 at Pacifico YOKOHAMA, Kanagawa, Japan)

SCG67-02 Room:414 Time:May 1 14:30-14:45

Noble gas evidence of deep plume origin of the Louisville hotspot

HANYU, Takeshi[1*]

[1]Japan Agency for Marine-Earth Science and Technology

Louisville seamount chain has been considered to be one of the long-lived hotspot tracks on the Pacific plate, but its magmatic source has not been well understood. I report noble gas compositions of the drill cores from four of the five seamounts drilled during IODP Expedition 330. Because the samples are aged (50-74 Ma), a stepwise crushing test for noble gas extraction from olivine phenocrysts and submarine glasses was made to assess contamination of post-eruption radiogenic nuclides. This test confirmed extraction of magmatic noble gases with minimal release of post-eruption radiogenic nuclides from the olivine samples; however, this was not always the case for the glass samples. The 3He/4He ratios in the olivine phenocrysts range from a value similar to those of mid-ocean ridge basalts (MORB) to slightly elevated ratios up to 10.6 Ra. Although these ratios are not as high as those observed in other ocean island basalts, two Louisville seamount basalts exhibit a primordial Ne isotopic signature that can be clearly discriminated from MORB Ne. The He and Ne isotopic compositions of the Louisville seamount basalts can be explained by the mixing of less degassed mantle and depleted upper mantle with different He/Ne ratios. The presence of the less degassed mantle component in the source of the Louisville seamounts documents the deep origin of the mantle plume.

One of the major objectives of the IODP Expedition 330 was to test the geodynamic model that predicts lateral advection of mantle plumes in the convecting mantle [Koppers et al., G-cubed, 2004; Steinberger and Antretter, G-cubed, 2006]. This model assumes a primary mantle plume that is rooted deep in the mantle, and the trajectory of a plume conduit is influenced by the overall mantle flow, which can be monitored by the hotspot drift on the Earth's surface [Tarduno et al., Science, 2009]. The paleomagnetic and dating results from IODP Expedition 330 verified the geodynamic modeling predictions for the Louisville seamount chain together with the Hawaiian-Emperor seamount chain [Koppers et al., Nat. Geosci., 2012]. The present noble gas data gives a guarantee for the deep-rooted Louisville plume assumed in the geodynamic model.

Keywords: Louisville seamount, mantle plume, deep mantle, noble gases, IODP

Japan Geoscience Union Meeting 2014
(28 April - 02 May 2014 at Pacifico YOKOHAMA, Kanagawa, Japan)

SCG67-03 Room:414 Time:May 1 14:45-15:00

Preliminary result of the oceanic mantle structure revealed by ”Normal Oceanic Mantle Project”

ISSE, Takehi[1*] ; SHIOBARA, Hajime[1] ; SUGIOKA, Hiroko[2] ; ITO, Aki[2] ; TAKEO, Akiko[1] ; UTADA, Hisashi[1] ; KAWAKATSU, Hitoshi[1] ; TONEGAWA, Takashi[2] ; TANAKA, Satoru[2]

[1]ERI, Univ. of Tokyo, [2]Institute for Research on Earth Evolution, Japan Agency for Marine-Earth Science and Technology

The oceanic mantle is an important region to understand the Earth system, because more than 2/3 of the surface is covered by oceanic area. Since 1990s, we have operated several seafloor observations by using newly developed long-term broadband ocean bottom seismometers (BBOBSs) in the northwest and central part of the Pacific Ocean. These observations have revealed the structures in and around the subduction zone in the Pacific Ocean and in the Pacific superswells, respectively. However, we have no observation and result in the normal oceanic regions. To reveal the normal oceanic mantle structure from observational approach, we conduct a long-term observation called “ Normal Oceanic Mantle Project ” (NOMan project) from 2010, deploying ocean bottom geophysical (seismic and electromagnetic) instruments in the northwestern Pacific Ocean. We conduct two arrays in that region. One is northwest side of the Shatsky Rise (Area A) and the other is southeast side of the Shatsky Rise (Area B). Sea floor age of Area A is 125 - 135 Ma, that of Area B is 135 - 145 Ma, so that the shear wave structures of those area should be similar.

By using seismograms of the NOMan project, other BBOBS observations, and permanent broadband seismic stations on land, we have determined the three-dimensional shear wave velocity structure of the upper mantle in the northwestern Pacific Ocean to reveal this area to be really normal. We used a surface wave tomography technique in which multimode phase speed of the surface wave are measured and inverted for a 3-D shear wave velocity structure by incorporating the effects of finite frequency and ray bending.

Our obtained model shows that lateral heterogeneity of each area is not strong and that average structures are different in two areas. Area A is consistent with previous models, whereas Area B is faster than previous models. We think for the present that Area A seems to be normal oceanic mantle, though Area B is not. We will recover all BBOBSs in this year. These BBOBS’s data enable us to obtain more reliable mantle structures.

Keywords: upper mantle, BBOBS, surface wave, tomography

Japan Geoscience Union Meeting 2014
(28 April - 02 May 2014 at Pacifico YOKOHAMA, Kanagawa, Japan)

SCG67-04 Room:414 Time:May 1 15:00-15:15

Seismic anisotropy in the oceanic lithosphere/asthenosphere system estimated by the broadband ocean bottom seismology

TAKEO, Akiko[1*] ; ISSE, Takehi[1] ; NISHIDA, Kiwamu[1] ; KAWAKATSU, Hitoshi[1] ; SHIOBARA, Hajime[1] ; SUGIOKA, Hiroko[2] ; ITO, Aki[2] ; UTADA, Hisashi[1]

[1]Earthquake Research Institute, University of Tokyo, [2]IFREE, JAMSTEC

The uppermost mantle structure beneath the oceanic basins is essential to discuss the oceanic lithosphere/asthenosphere system, the most simple and representative system of the theory of plate tectonics. Seismic anisotropy within the oceanic lithosphere and asthenosphere is especially important, as it reflects the flow and deformation in the uppermost mantle. Previous structural studies have been, however, limited in terms of the depth range: the top of lithosphere at depths of ˜10-20 km by refraction surveys, and the structure deeper than ˜30 km by surface-wave tomography studies. There has been no discussion from the top of the lithosphere continuously to the asthenosphere, which needs the broadband analysis of surface waves at periods of 3-100 s. In addition, there has been limited discussion about the intensity of seismic anisotropy because of the difficulty of estimating the absolute value of seismic anisotropy by surface-wave tomography studies.

We have developed a new multi-band method to analyze surface waves in broadband array records of ocean bottom seismometers for determining seismic anisotropy structure at depths of ˜10-100 km quantitatively (Takeo et al 2013 JGR, submitted to GJI). The method uses the ambient noise cross-correlation method for analyzing surface waves at periods of 3-30 s and to determine structure at depths shallower than ˜50 km, as well as the array analysis method of teleseismic waveforms at longer periods for determining deeper structures.

In previous studies, we have applied the multi-band method to records obtained in three oceanic regions: the Shikoku Basin region (Takeo et al. 2013 JGR), the southwestern region of the Shatsky Rise (Takeo et al. submitted to GJI) and the French Polynesia region (Takeo et al. 2012 SSJ Fall Meeting). In this study, we applied the same method to the records of broadband ocean bottom seismometers obtained by the normal oceanic mantle (NOMan) project at two oceanic regions (northwestern and southeastern regions of the Shatsky Rise) from 2010 to 2013. By combining the results for five oceanic regions with different seafloor ages between 20 and 155 Ma, we can discuss the seismic structure and its anisotropy in the oceanic lithosphere and asthenosphere, and the deformation of mantle related to plate motions.

The results for five oceanic regions can be summarized into five points: (i) the high-velocity lid and the low velocity zone corresponds to the oceanic lithosphere and asthenosphere, (ii) the transition from the lithosphere to the asthenosphere occurs at depths of 40-90 km, (iii) the average intensity of S-wave radial anisotropy is 3-6 % at depths of 10-150 km with the velocity of horizontally propagating and vertically polarized S-wave slower than the horizontally polarized S-wave, (iv) the intensity of S-wave azimuthal anisotropy at depths of 10-100 km is weaker than that of S-wave radial anisotropy and weakens with depths, and (v) the azimuth of maximum S-wave velocity is not perpendicular to ancient spreading axis in general. These results indicate complex deformation system in the present and ancient oceanic asthenosphere related to the presence of partial melting, the unusual fabric of olivine and so on. We will summarize these results and discussions, and will also present the potential of the broadband ocean bottom seismology to elucidate structure and deformation in the oceanic lithosphere/asthenosphere system and in other oceanic systems such as hotspots, mid-ocean ridges and subduction zones.

Keywords: surface wave, ambient noise, anisotropy, plate tectonics

Japan Geoscience Union Meeting 2014
(28 April - 02 May 2014 at Pacifico YOKOHAMA, Kanagawa, Japan)

SCG67-05 Room:414 Time:May 1 15:15-15:30

Locality and cause of the characteristics of high-frequency Po/So wave propagating in heterogeneous oceanic lithosphere

FURUMURA, Takashi[1*] ; KENNETT, Brian[2]

[1]Earthquake Research Institute, The University of Tokyo, [2]Research Schoole of Earth Sciences, The Australian National University

In our previous study (Kennett & Furumura 2013; Geophys. J. Int.) we described the characteristics of the propagation of the high-frequency mantle phases Po and So. These oceanic Pn and Sn phases can be observed after propagation over many thousands of kilometres from the source, retaining high frequencies but acquiring a long and complex coda. This study concentrated on the way in which these characteristics can be sustained by fine-scale heterogeneity in the oceanic lithosphere that reinforces the influence of multiple P reverberations in the ocean and sediments as recognized by Sereno & Orcutt (1985; 1987). A form of quasi-laminar heterogeneity with horizontal correlation lengths around 10 km and vertical correlation lengths of about 0.5 km provides a good representation of the Po and So wavefield as also noted by Shito et al. (2013). This class of heterogeneity creates a strong scattering environment within the lithosphere that helps to sustain the Po and So phases over long distances. Propagation of So is most effective in thick old lithosphere, e.g., in the northwest Pacific Plate. Amplitudes of So are reduced significantly by propagation through thinner lithosphere in the Philippine Plate.

In this study we look at the entire Pacific basin and map out the propagation patterns for Po and So, which have the general characteristic of much more efficient propagation in the western sector than in the east that is much less well sampled. There are stronger changes in the nature of So than Po. For the same frequency S waves have a shorter wavelength than P waves, and so the So phase is more sensitive to the effects of both lateral variations in lithospheric structure and seismic attenuation.

We explore the relation of the nature of the observations of Po and So and the age of the lithosphere, based on 2-D FDM simulation seismic wave propagation for examining the influence of changes in lithospheric structure across fracture zones and similar features. The strong diffuse scattering field created in the oceanic lithosphere is hard to destroy and it is quite difficult to explain situations where So is very much weaker than Po, except by introducing enhanced seismic attenuation for younger lithosphere and the warmer asthenosphere in the neighborhood of spreading centers.

Japan Geoscience Union Meeting 2014
(28 April - 02 May 2014 at Pacifico YOKOHAMA, Kanagawa, Japan)

SCG67-06 Room:414 Time:May 1 15:30-15:45

Distribution of petit-spot volcanoes in relation to deformation and structures on a subducting plate

HIRANO, Naoto[1*] ; NAKANISHI, Masao[2]

[1]Center for Northeast Asian Studies, Tohoku University, [2]Graduate School of Science and Technology, Chiba University

Tiny submarine volcanoes, known as petit-spots, occur in regions of plate flexure prior to subduction and seamount-loading (Hirano *et al.*, 2006, 2013). The surface morphology and distribution of petit-spot monogenetic volcanoes are influenced by the stress field in the lithosphere. The magmas produced by the accumulation of melt originating from asthenosphere just below the site of plate-flexure, are able to rapidly ascend to the surface from the base of the lithosphere (Hirano *et al.*, 2006; 2011; Valentine & Hirano, 2011). As monogenetic petit-spot volcanoes are too small to be detected by satellite altimetry, their study requires a research vessel equipped for shipboard acoustic multibeam surveys. Although previously surveyed areas are limited to the regions off the Japan Trench, the eruption ages of petit-spot volcanoes in this region represent monogenetic eruptions over a period of >9 Myr over a large area, and the eruptions are related to the outer rise bathymetry. Such tiny volcanoes are ubiquitous in regions of plate flexure worldwide, and have been recently reported from the Tonga Trench (Hirano *et al.*, 2008), the Basin and Range province (Valentine & Hirano, 2010), south of Greenland (Uenzelmann-Neben *et al.*, 2012), the Chile Trench (Hirano *et al.*, 2013), an accretionary complex in Costa Rica (Buchs *et al.*, 2013), and submarine French Polynesia (Hirano *et al.*, submitted).

The spatial distribution of submarine petit-spot volcanoes remains poorly constrained because shipboard bathymetry has not covered the entire northwestern Pacific Plate. If petit-spot volcanoes occur only in regions of plate flexure, then tiny submarine volcanoes should appear homogeneously on the submarine surface of outer rises. However, areas devoid of volcanoes and lava have been found surrounding areas of petit-spot volcanoes (i.e., sites A?C in Hirano *et al.*, 2006), indicating that the local characteristics of the lithosphere, in addition to plate flexure, control the occurrence of petit-spot volcanoes. Here we report that the distribution of petit-spot volcanoes is controlled by the tectonic structure of the seafloor. We conducted submersible dives along the linearly distributed petit-spot knolls by JAMSTEC *Shinkai6500* in April 2014. Areas with tectonic fabrics appear on the subducting Pacific Plate off the Japan Trench, including a ridge-perpendicular fabric zone (RPPFZ), ridge-parallel abyssal hills (RPRAH), and subducting 'horst and graven' structures (HAGS) (Nakanishi *et al.*, 2011). At Site C, which is a trench-oceanward slope offshore from Soma City, Fukushima Prefecture, the trend of the Japan Trench changes from N?S in the north to NE?SW in the south, where two areas of trench-parallel HAGSs are intersecting in a complex manner (Nakanishi *et al.*, 2011). The distribution of young volcanic cones of more than 80 petit-spots, reported from Site C by Hirano *et al.* (2008), seems to be controlled by the fabrics of RPPFZ and RPRAH, the trends of which are continuous with the HAGS to the north and south along the trench-oceanward slope, respectively. Although the RPPFZ is not recognized as a fracture zone, its trend is sub-parallel to that of the neighboring Nosappu and Kashima fracture zones (Nakanishi, 1993). As the RPPFZ and RPRAH that control the petit-spot distribution are clearly original structures of the lithosphere (in contrast to HAGS), the occurrence of petit-spot eruptions is possibly related to lithospheric structures.

Keywords: petit-spot, alkali-basalt, Pacific plate, outer rise, lithosphere

Japan Geoscience Union Meeting 2014
(28 April - 02 May 2014 at Pacifico YOKOHAMA, Kanagawa, Japan)

SCG67-07 Room:414 Time:May 1 15:45-16:00

Magnetic Anomalies in the Southern Indian Ocean Revisited

NOGI, Yoshifumi[1*] ; SATO, Taichi[2] ; HANYU, Tomoko[3]

[1]National Institute of Polar Research, [2]National Institute of Advanced Industrial Science and Technology, [3]Graduate University for Advanced Studies

Magnetic anomalies in the Southern Indian Ocean are vital to understanding initial breakup process of Gondwana. However, seafloor age estimated from magnetic anomalies still remain less well-defined because of the sparse observations in this area. To understand the seafloor spreading history related to the initial breakup process of Gondwana, vector magnetic anomaly data as well as total intensity magnetic anomaly data obtained in the Enderby Basin, Southern Indian Ocean, are used. The strikes of magnetic structures are deduced from the vector magnetic anomalies.

Magnetic anomaly signals, most likely indicating Mesozoic magnetic anomaly sequence, are obtained almost parallel to WNW-ESE trending lineaments just to the south of Conrad Rise inferred from satellite gravity anomalies. Most of the strikes of magnetic structures indicate NNE-SSW trends, and are almost perpendicular to the WNW-ESE trending lineaments. Mesozoic sequence magnetic anomalies with mostly WNW-ESE strikes are also observed along the NNE-SSW trending lineaments between the south of the Conrad Rise and Gunnerus Ridge. Magnetic anomalies originated from Cretaceous normal polarity superchron are found in these profiles, although magnetic anomaly C34 has been identified just to the north of the Conrad Rise. However, Mesozoic sequence magnetic anomalies are only observed in the west side of theWNW-ESE trending lineaments just to the south of Conrad Rise and not detected to the east of Cretaceous normal superchron signals. These results show that counter part of Mesozoic sequence magnetic anomalies in the south of Conrad Rise would be found in the East Enderby Basin, off East Antarctica. NNE-SSW trending magnetic structures, which are similar to those obtained just to the south of Conrad Rise, are found off East Antarctica in the East Enderby Basin. However, some of the strikes show almost E-W orientations.

Moreover, the thickness of the crust increase just to the north of the Conrad Rise and clear magnetic anomaly signals considered to be magnetic anomaly C34 in this region may indicate continental-ocean boundaries while taking dredged continental origin rock samples at the Ob seamount into account. Therefore, magnetic anomaly C34 identified in the Indian Ocean must be reconsidered. These suggest complicated ridge reorganization occurred during initial breakup of Gondwana in the Indian Ocean.

Keywords: magnetic anomaly, Indian Ocean, Gondwana, continental crust

Japan Geoscience Union Meeting 2014
(28 April - 02 May 2014 at Pacifico YOKOHAMA, Kanagawa, Japan)

SCG67-08 Room:414 Time:May 1 16:15-16:30

Origin of the Palau Basin and a revised spreading model of the West Philippine Basin deduced from three-component magnet

SASAKI, Tomohiro[1] ; YAMAZAKI, Toshitsugu[2*] ; ISHIZUKA, Osamu[3]

[1]University of Tsukuba, [2]AORI, University of Tokyo, [3]GSJ, AIST

The western part of the Philippine Sea (PHS) plate was occupied by the West Philippine Basin (WPB) in the north and the Palau Basin (PB) in the south. The WPB is generally considered to have opened from about 50 to 30 Ma, but the details are still unclear; in particular the origin and age of the PB was unknown. Studying the history of the WPB is important for understanding better the initiation and evolution of the IBM Arc. Here we discuss the spreading history of the WPB using new data on three-component magnetic anomaly and swath bathymetry acquired in the PB as well as those obtained previously by JAMSTEC fleets in the southern WPB. NS-trending magnetic boundaries and seafloor fabrics occur in the PB, indicating the formation by EW seafloor spreading. With a constraint from a 40Ar/39Ar age of 40.4 Ma obtained from the northernmost part of the PB, we interpret that the observed magnetic anomalies correspond to polarity reversals from C16n1r to C18n/C18r (35.6 to 38/39 Ma). Previous models of WPB spreading incorporated a spreading-rate decrease around 40 Ma from about 4.4 to 1.8 cm/year. Our study in the southern WPB, however, suggests that the decrease is unnecessary for correlating observed three-component anomalies to the GPTS. A typical profile along 130E corresponds to C16r to C21 (36.3 to 45.3 Ma). The cessation age of the spreading in our interpretation, about 35 to 37 Ma, is older than the previous estimation (about 30 to 33 Ma). It was difficult to constrain rotation of the PHS plate from the magnetic anomaly skewness.

Keywords: Philippine Sea plate, West Philippine Basin, Palau Basin, magnetic anomaly, seafloor spreading

Japan Geoscience Union Meeting 2014
(28 April - 02 May 2014 at Pacifico YOKOHAMA, Kanagawa, Japan)

SCG67-09 Room:414 Time:May 1 16:30-16:45

The composition of back-arc basin basalts in the West Philippine Basin and association with mantle dynamics

HARAGUCHI, Satoru[1] ; ISHII, Teruaki[2*]

[1](Faculty of Engineering, University of Tokyo, [2]Fukada Geological Institute

The Philippine Sea Plate was expanded by multiple extensions of backarc basins. Ishizuka et al. (2011) and Haraguchi et al. (2012) pointed out that the enriched mantle was flowed from backarc side during the spreading of the Shikoku Basin from 25 to 15 Ma (Okino et al., 1994, 1999). Haraguchi et al. (Meeting of the Volcanological Society of Japan, 2013) considered that the process of flowing of the enriched mantle estimated by the composition of the backarc basin basalts (BABB) recovered by the drilling of the Deep Sea Drilling Project (DSDP), Ocean Drilling Program (ODP) and Integrated Ocean Drilling Program (IODP). In this study, we attend the BABB of the West Philippine Basin, precede backarc spreading of the Shikoku Basin, and consider mantle dynamics by geochemical characteristics of BABB.

The first drillings in the West Philippine Basin by the Deep Sea Drilling Project are the Leg 31 same as the Shikoku Basin, and following operations are Leg 59 and the Ocean Drilling Program (ODP) Leg 195. And the diving of the R/V *Shinkai 6500* during the Y9611 cruise by R/V *Yokosuka* and dredges during the KR9801 cruise by R/V *Kairei* at the spreading axis (e.g. Fujioka et al., 1999). In this study, we discuss the new analyzed data of the basements of DSDP Leg 58 Site 446 and ODP Leg 195 Site 1201, and compare the data of the former studies.

Site 1201 is located in the west of the West Philippine basin, about 500km north from the Central Basin fault, axis of the spreading center. The main purpose of this site is the set up of the borehole site WP-1. Thickness of covered sediments at this site is more than 500m. The chemical characteristics of basements at this site are the typical BABB, not find the island arc characteristics. SiO_2 and MgO contents of these basalts are 49-53 and 5-8 wt%, respectively, and are similar to the basalts from the DSDP Leg 58 Site 442˜444 in the Shikoku Basin. The TiO_2 contents of these basalts are 0.9˜1.0 wt%, lower than those of the Shikoku Basin. The alkali elements are 1.5-2.8 wt% of Na_2O and 0.1-1.6 wt% of K_2O, similar K_2O and lower Na_2O contents to Shikoku Basin BABB. The trace elements are 320-420 ppm of Cr, higher than Shikoku Basin BABB, and lower Sr, Y and Zr. The Zr/Y and Nb/Zr ratio are also lower than Shikoku Basin BABB. We consider that these characteristics are the existence of the depleted parent mantle before the spreading of the Shikoku Basin pointed by Ishizuka et al. (2011) and Haraguchi et al. (2012).

Site 446 ate located in the Minami Daito Basin between the Daito and the Oki Daito Ridges. Thickness of covered sediments is about 350m. These volcanic rocks are considered to the intrusion in the sediment layer, different from the basement. The chemical characteristics of this volcanics are classified into alkali basalts, and prominent enrichment of TiO_2, more than 4 to 5 wt%. This extremely enrichment of TiO_2 is not found from other inner plate volcanism in the Philippine Sea Plate. Therefore, we assume that the different inner plate volcanism from the mantle plume in the West Philippine Basin about 40 Ma (Deschamps and Lallemand 2002) were more active in the other Philippine Sea region.

We discuss these analyzed data and former data of the basements in the Philippine Sea Region, and consider parental material composition and magma dynamics before 30 Ma.

Keywords: Backarc basin basalts, Incompatible element ratio, Parent material of magma, Mantle dynamics

Japan Geoscience Union Meeting 2014
(28 April - 02 May 2014 at Pacifico YOKOHAMA, Kanagawa, Japan)

SCG67-10 Room:414 Time:May 1 16:45-17:00

Long-distance magma transport from oceanic island arc volcanoes

ISHIZUKA, Osamu[1*] ; GESHI, Nobuo[1] ; KAWANABE, Yoshihisa[1] ; OGITSU, Itaru[1] ; TUZINO, Taqumi[1] ; SAKAMOTO, Izumi[2] ; TAYLOR, Rex[3] ; ARAI, Kohsaku[1] ; NAKANO, Shun[1]

[1]Geological Survey of Japan/AIST, [2]Tokai University, [3]University of Southampton

Long-distance lateral magma transport away from volcanic centers is emerging as a common phenomenon where the regional stress regime is favorable. It should also be recognized as an important factor in the construction and growth of island arcs, and a potential trigger for devastating eruptions. In this contribution, we report on recent investigations into the magma dynamics of Izu-Oshima volcano: an active basaltic volcano with an extensive fissure system.

Geophysical observations in the Izu-Bonin intra-oceanic island arc indicate that magma periodically is moved away from the main basaltic composite volcanoes. When Miyakejima erupted in 2000, seismic activity migrated about 30km northwestward from the volcanic centre (Geshi et al., 2002). This event is interpreted to reflect magma injection and dike propagation at a depth range between 12 and 20km (Kodaira et al., 2002). Long-distance lateral magma transport has also been identified at the Nishiyama volcano on Hachijojima Island using petrological, geochemical and structural studies of satellite vents (Ishizuka et al., 2008). Nishiyama has provided evidence for two types of magma transport: Primitive magma moving laterally for $>$20km in the middle to lower crust (10-20km deep) and short distance transport ($<$5km) from shallow, differentiated magma reservoirs. Of these the long-distance transport seems to be controlled by a regional extensional stress regime, while short distance transport may be controlled by the local stress regime resulting from the load of the main volcanic edifice.

Izu-Oshima is flanked by numerous, subparallel NW-SE trending submarine ridges extending up to 22 km to the NW and SE from the center of the volcano. During a recent diving survey we have identified that these ridges are fissures which erupted basaltic spatter and lava flows. Furthermore, lavas are petrographically similar along each ridge, while there are noticeable differences between ridges. The subparallel ridges are observed to transect a series of knolls, the Izu-Tobu monogenetic volcanoes (ITMV), which are dispersed across this area of the rear-arc. However, there is a consistent petrographic difference between these seamounts and the ridges.

We have found similar, and in some cases a matching, geochemistry between the submarine ridges and subaerial ridges of eruptions found ascending the flanks of Izu-Oshima. This implies that the subaerial ridges and submarine ridges together represent the track of a magma transport episode away from the storage system beneath the central volcano.

ITMV and the transecting ridges are found to have quite distinct geochemical characteristics, indicative of different magma sources. Yet, they are essentially found interspersed in outcrop. The most appropriate scenario for their development is one where ITMV are fed by an ”in-situ” underlying source, while the NW-SE ridges are fed by lateral magma transport from Izu-Oshima. Unlike Nishiyama volcano, Izu-Oshima does not show a compositional variation along the length of the ridges, and has no evidence of primitive magmas. Hence, the magma transport is likely to be derived from a crustal chamber where crystal fractionation and plagioclase accumulation has taken place.

Japan Geoscience Union Meeting 2014
(28 April - 02 May 2014 at Pacifico YOKOHAMA, Kanagawa, Japan)

SCG67-11 Room:418 Time:May 2 09:00-09:15

Seafloor geodetic observation along the Nankai Trough - Progress report after the 2011 Tohoku-oki earthquake -

SATO, Mariko[1*] ; WATANABE, Shun-ichi[1] ; YOKOTA, Yusuke[1] ; UJIHARA, Naoto[1] ; ISHIKAWA, Tadashi[2] ; MOCHIZUKI, Masashi[3] ; ASADA, Akira[3]

[1]Hydrogr. and Oceanogr. Dept. of Japan, [2]Japan Coast Guard Academy, [3]IIS, Univ. of Tokyo

We have been carrying out GPS/acoustic seafloor geodetic observation on the landward slope of the major trenches around Japan, such as the Japan Trench and the Nankai Trough. From the past observations, we detected intraplate deformation caused by the subduction of oceanic plates and coseismic displacements associated with large earthquakes.

Along the Nankai Trough, we deployed six seafloor reference points in the sea area from off-Omae-zaki through off-Muroto in 2002-2004 and had been carrying out campaign observations. From the observations conducted before the 2011 Tohoku-oki earthquake, we obtained the intraplate velocities of 2-5 cm/year toward WNW, which were generally consistent with those detected by on-land GPS measurements. A closer look gives us the differences of the velocities by sea areas.

Furthermore, to monitor seafloor movement spatially in the whole expected focal regions along the Nankai Trough, we deployed nine new seafloor reference points mainly off Shikoku in January 2012. If we obtain crustal velocities at all the site, it is expected that a spatial variation of interplate coupling will be revealed in the sea area along the Nankai Trough. It has been two years after the expansion of seafloor reference points and seafloor movements westward and northward are being observed at most of the sites.

In this report, we present a progress report on seafloor geodetic observation along the Nankai Trough after the 2011 Tohoku-oki earthquake.

Keywords: Seafloor geodetic observation, Seafloor geodesy, Nankai Trough

Japan Geoscience Union Meeting 2014
(28 April - 02 May 2014 at Pacifico YOKOHAMA, Kanagawa, Japan)

SCG67-12 Room:418 Time:May 2 09:15-09:30

Postseismic seafloor movements following the 2011 Tohoku-oki earthquake detected by GPS/acoustic positioning

WATANABE, Shun-ichi[1*] ; SATO, Mariko[1] ; YOKOTA, Yusuke[1] ; UJIHARA, Naoto[1] ; ISHIKAWA, Tadashi[2] ; MOCHIZUKI, Masashi[3] ; ASADA, Akira[3]

[1]Hydrographic and Oceanographic Department, Japan Coast Guard, [2]Japan Coast Guard Academy, [3]Institute of Industrial Science, University of Tokyo

The Hydrographic and Oceanographic Department, Japan Coast Guard, have been developing precise seafloor positioning systems using the GPS/acoustic combination technique and carrying out campaign observations along the major trenches in the Pacific Ocean, such as the Japan Trench and the Nankai Trough. For example, after the 2011 Tohoku-oki earthquake (Mw = 9.0), we detected a huge coseismic displacement of 24 m toward ESE at MYGI which is located above the epicenter. We have been continued the geodetic observations along the Japan Trench in order to detect postseismic deformation.

The results of the observations show that the displacements vary with the sites even in the directions. MYGI and KAMS had moved toward west-northwest at constant rate. MYGW had moved toward south-southeast. KAMN had moved toward northwest. FUKU and CHOS had moved toward east-southeast. In addition, the displacements at FUKU and CHOS decay with time. For vertical component, significant subsidence was detected at all sites except CHOS where no vertical displacement was detected within the accuracy range.

In this presentation, we will report and discuss the latest results of the seafloor geodetic observation along the Japan Trench.

Keywords: seafloor geodetic observation, the 2011 Tohoku Earthquake

Japan Geoscience Union Meeting 2014
(28 April - 02 May 2014 at Pacifico YOKOHAMA, Kanagawa, Japan)

SCG67-13 Room:418 Time:May 2 09:30-09:45

A summary of the achievement in the project for advanced GPS/acoustic survey

KIDO, Motoyuki[1*] ; FUJIMOTO, Hiromi[1] ; HINO, Ryota[1] ; OHTA, Yusaku[2] ; OSADA, Yukihito[1] ; IINUMA, Takeshi[1] ; AZUMA, Ryosuke[1] ; WADA, Ikuko[1] ; SUZUKI, Syuichi[2] ; TOMITA, Fumiaki[3] ; IMANO, Misae[3]

[1]IRIDeS, Tohoku Univ., [2]RCPEV, Tohoku Univ., [3]Sci., Tohoku Univ.

GPS/acoustic survey is known as a most probable way to measure the crustal deformation of seafloor far from the coasts, where dense GPS network is not available. We, Tohoku University, together with Nagoya University and Japan Coast Guard dedicated in GPS/acoustic survey for more than decade. MEXT has been strongly promotes our activities though financially support as governmental project. We summarize individual topics in the project.

For the moored buoy, collaborating with JAMSTEC and JAXA, we have started long-term continuous and realtime seafloor geodetic survey at Kumano-nada. At the early stage of the project, we employed a small buoy, which can be also used as towing survey, at off-Miyagi site. Because the size of battery is limited, sea-trials was lasting only for two days. However, using this platform, we developed an automatic ranging system and simple on-demand operation technique via UHF communication. In 2012, we have started developing a automatic ranging system in a realistic working condition using a time-proven platform, m-TRITON buoy, operated by JAMSTEC. Together with JAMSTEC and JAXA, satellite communication part and GPS positioning part have been shared for multi-purpose. Tohoku University group concentrate acoustic ranging part and onsite data processing to compute precise traveltimes. Using a limited onsite resource in the buoy, we have eliminated unnecessary and redundant procedure and data as possible. The first sea-trial took place in 2013 for four months and the ongoing second trial has started in 2014 for six months. In the second trial, acoustic ranging data has been successfully transmitted to onshore station every week and we can monitor it from our laboratory.

For the Autonomous Surface Vehicle (ASV) system, we aimed to develop an automatic survey system, which can also be used simultaneous measurements from other platform, such as a research vessel, for improve the ranging accuracy with multi-acoustic-paths. In our system, vehicle is like an unmanned boat (2.4m long and 400kg in weight), whose propulsion system is driven by electric power from onboard diesel generator lasting for a week. As the ASV system demonstrates sufficient performance for our use in GPS/acoustic survey, it can be a candidate of multi surface platform for simultaneous ranging to achieve high accuracy GPS/acoustic measurement taking the spatial sound speed variation into account.

After the Tohoku-Oki earthquake in 2011, the project has an extra mission that significantly enhance the survey framework, especially in deep seafloor ($>$5000m) near the trench axis. In this extra mission, we have developed a new type of seafloor transponder that works at over 5000m depth and its acoustic communication range is greater than 15km. We made 86 transponders in total and constructed 20 new GPS/acoustic station along the Japan Trench in 2012. In addition, we chartered a research ship for about 50 days per year to construct and observe the new stations. At present we have carried out four times of campaign surveys during 2012-2013. At these new stations, we conducted both moving and stationary surveys, the former generally took several hours and the latter 12 hours for each station. We found a problem in acoustic property in the new transponders, which can be corrected with post-processing shown in Azuma et al. (2014, JpGU). Campaign surveys ranges only about one year, but we have observed post-seismic movement at selected stations. These results are reported in Tomita et al. (2014, JpGU). The new transponders are hybrid type so that Japan Coast Guard has started to make measurements with their own system at several stations above.

This work has been supported by MEXT project for advanced GPS/acoustic survey. Stuffs in RCPEV and IRIDeS, Tohoku University gave dedicated support and collaborative operation in the onboard and GPS surveys. The construction and surveys in the new stations were collaboration with Nagoya University.

Keywords: GPS/acoustic, moored buoy, autonomous surface vehicle, Japan trench

Japan Geoscience Union Meeting 2014
(28 April - 02 May 2014 at Pacifico YOKOHAMA, Kanagawa, Japan)

SCG67-14 Room:418 Time:May 2 09:45-10:00

Detection of post-seismic movement after Tohoku-oki Earthquake using GPS/Acoustic technique

TOMITA, Fumiaki[1*] ; KIDO, Motoyuki[2] ; OSADA, Yukihito[2] ; AZUMA, Ryosuke[2] ; FUJIMOTO, Hiromi[2] ; HINO, Ryota[2] ; IINUMA, Takeshi[2] ; OHTA, Yusaku[1] ; WADA, Ikuko[2]

[1]Graduate School of Science, Tohoku University, [2]International Research Institute of Disaster Science, Tohoku University

Using GPS/Acoustic seafloor geodetic observation (GPS/A observation), we can directly measure seafloor movements, which cannot be obtained from on-land geodetic observation. For example, Kido et al. (2011) and Sato et al. (2011) detected huge co-seismic displacements associated with 2011 off Pacific coast of Tohoku Earthquake near the Japan Trench, 150km distant from the coast.

After the occurrence of the Tohoku-oki Earthquake, we deployed new seafloor benchmarks at 20 sites along the Japan Trench from Ibaraki-oki to Sanriku-oki. Including three sites installed before 2011, we totally have 23 sites to monitor the post-seismic movement for the Tohoku-oki Earthquake. We have conducted four GPS/Acoustic surveys at present (09/2012, 11/2012, 07/2013, 10/2013) at these sites.

The surveys consists of two types of observations; they are moving survey to locate the position of individual seafloor transponders that make up each geodetic site and point survey to determine the precise location of the center of the transponder array. The displacement at each site is estimated from the temporal change of the array center position. However, we identified two dominant factors that influence the precision of the array center positioning in our observation.

The first factor is the instability in the waveforms of acoustic signals. In GPS/A analysis, we calculate cross-correlation waveform between received and transmitted signals, and determine the timing of maximum peak as round trip travel time. However, multiple peaks separated by 0.3-0.5ms each other are found in a cross correlation waveform, whose relative amplitudes are influenced by the relative position between the hydrophone on the research ship and the seafloor transponder. We have developed an algorithm that can automatically picks up the first peak from the multiples and reduces the error in determining round trip travel time. The detail of this problem and the algorithm will be reported by Azuma et al. (2014, JpGU).

The second factor is uncertainty in the position of the hydrophone equipped on the research ship with respect to three GPS antennas at the top of the ship for attitude determination. In our observations, it is difficult to directly measure the relative position of the three GPS antennas and the hydrophone attached at the end of the pole mounted on the ship's side; the provisional position based on the drawing has about 1m offset. The horizontal component of the offset causes systematic deviation in the apparent position of the transponders depend on ship's heading. Taking this behavior into account, we can correct for the horizontal offset with about 5cm in accuracy. The vertical offset is thought to have less influence on the estimation of the array center position because the sound speed correction intrinsically includes the vertical offset. However, accuracy of offset estimation is still insufficient, hence the estimation technique must be refined further.

After these correction, we have succeeded to obtain preliminary movements at 10 sites using the data in two of the four surveys (09/2012 and 07/2013) at present. These preliminary results generally indicate eastward seafloor movements at the northern Sanriku-oki sites and westward movements at off-Miyagi sites. In this talk, we introduce outline of the analysis and up-to-date results of evaluation of the post-seismic movement incorporating the data in 11/2012 and 10/2013.

Keywords: seafloor geodesy, Tohoku-oki Earthquake, Japan Trench, post-seismic movement

Japan Geoscience Union Meeting 2014
(28 April - 02 May 2014 at Pacifico YOKOHAMA, Kanagawa, Japan)

SCG67-15 Room:418 Time:May 2 10:00-10:15

Understanding recoupling process using a seafloor geodesy in megathrust earthquake zone

OSADA, Yukihito[1*] ; ITO, Yoshihiro[2] ; KIDO, Motoyuki[1] ; HINO, Ryota[1] ; IINUMA, Takeshi[1]

[1]IRiDes, Tohoku University, [2]DPRI, Kyoto Uniersity

The 11 March 2011 Tohoku-Oki earthquake ruptured the interplate boundary off the eastern shore Honshu, generated a devastating tsunami that swept the coastal area along the northeastern Japan. The seafloor geodesy brought important results that showthat the large slip was near the Japan Trench and suggested the heterogeneity of the coseismic slip distribution in the plate interface. The maximum displacement region for interplate earthquake is mainly located offshore region. Therefore it is important to monitor the postseismic displacement and the stress accumulation process using seafloor geodesy. And if we can observe the postseismic displacement near the Japan Trench, we contribute to understand the coupling condition of plate boundary. There is a seafloor acoustic ranging system for direct observation of horizontal displacement on seafloor. We improve this system that adapted for the axis of Japan Trench. The system is designed to measure distances of up to 3 km and to adapt the pressure vesselof 9000m water-depth. We deployed the seafloor acoustic ranging system between 2013 May and 2013 Sep. We observed across the Tranch baseline (about 7km), baseline between the bottom of Tranch to the seaward side of Japan Trench (about 3.6km). We get data both baseline results for 4 month. We report this results on this presentation.

Keywords: seafloor crustal movement, Japan Trench

Japan Geoscience Union Meeting 2014
(28 April - 02 May 2014 at Pacifico YOKOHAMA, Kanagawa, Japan)

SCG67-16 Room:418 Time:May 2 10:15-10:30

Sea trial of tsunami and crustal movement observation buoy system in real-time under environment with high speed sea cur

TAKAHASHI, Narumi[1*] ; ISHIHARA, Yasuhisa[1] ; FUKUDA, Tatsuya[1] ; OCHI, Hiroshi[1] ; TAHARA, Jun'ichiro[1] ; MORI, Takahito[1] ; KIDO, Motoyuki[2] ; OHTA, Yusaku[2] ; HINO, Ryota[2] ; MUTOH, Katsuhiko[2] ; HASHIMOTO, Gosei[3] ; MOTOHASHI, Osamu[3] ; KANEDA, Yoshiyuki[1]

[1]Japan Agency for for Marine-Earth Science and Technology, [2]Tohoku University, [3]Japan Aerospace Exploration Agency

Japan Agency for Marine-Earth Science and Technology (JAMSTEC), Tohoku University and Japan Aerospace Exploration Agency (JAXA) have developed real-time observation system for tsunami and crustal movement using a buoy since 2011. Although observation interval of crustal movement is generally sparse, because the timing depends on availability of observation ship, we aim to construct to observe tsunami in real-time and crustal movement when it is necessary. Because Japan is surrounded by seismogenic zones with large earthquakes and such large event brought huge damages on coastal region people, early detection is needed to reduce the severe damage. Although online cable system is best for it, the cost for the construction and implementation is huge. Therefore, we point use of the buoy as the removable temporal early detection system. The system is composed of a pressure seafloor unit with pressure sensor and acoustic transmission unit, six seafloor transponders and buoy station incorporating some loggers, transducers to communicate with seafloor systems and data transmission system to land. The seismogenic zones, however, are under the environment of high speed sea current like the Kuroshio. Therefore, we use the slack mooring on our system, but the some technical development is needed for adoption of the mooring. For example, low consumption electricity due to high power acoustic signals for the data transmission and We tried sea trial for three months in last year, and confirmed to fully resistance for high speed sea current over 5.3 knots. On the other hand, the issued to be resolved are clarified, which are on acoustic transmission between the pressure seafloor unit and the buoy, the resistance for the fishery activities and so on. We took measures for above issues and deploy the revised system at off the Kumano Basin. The observation period of the second sea trial is six months. In addition to the measures, we implement tsunami mode. In normal case, we obtain tsunami data with an interval of 15 minutes, but, it is switched to be 15 seconds in tsunami mode. The tsunami mode is triggered when a ratio of average for short period of time (STA) and that of long one (LTA) exceed the threshold level. And, we move the timing of the STA and LTA and try to detect the first arrivals of tsunami. Now, we obtain real-time tsunami and crustal movement data via iridium transmission and introduce it in this presentation.

Japan Geoscience Union Meeting 2014
(28 April - 02 May 2014 at Pacifico YOKOHAMA, Kanagawa, Japan)

SCG67-17 Room:418 Time:May 2 10:30-10:45

Study for improving efficiency in seafloor geodetic observation by means of multi acoustic ranging

YOKOTA, Yusuke[1*] ; SATO, Mariko[1] ; WATANABE, Shun-ichi[1] ; ISHIKAWA, Tadashi[2]

[1]Hydrographic and Oceanographic Department, Japan Coast Guard, [2]Japan Coast Guard Academy

Japan Hydrographic and Oceanographic Department (JHOD) and the Institute of Industrial Science, University of Tokyo, have been developing a system for precise seafloor geodetic observation with the GPS/Acoustic combination technique. In this observation, the movements of the seafloor reference points are measured with 2 - 3 centimeters precision. JHOD has been carrying out seafloor geodetic observations 2 - 4 times a year for each station and reported the inter-seismic deformation before and after the 2005 Miyagi-oki earthquake and the co- and post-seismic deformations of the 2005 Miyagi-oki earthquake and the 2011 Tohoku-oki earthquake and so on.

After the 2011 Tohoku-oki earthquake, this observation is expected to be broadened and densely-arranged with the objective of large-scale earthquake disaster prevention. In order to expand further seafloor geodetic observation, shortening of observation time, which is about one day for one campaign, is required. Therefore, we are considering a new acoustic ranging method. In this new method, we conduct the acoustic ranging for multi seafloor transponders not individually but sequentially. We report the details of this new multi acoustic ranging method and discuss how much efficiency will be improved by the introduction of the new method.

Keywords: seafloor geodetic observation, acoustic ranging

Japan Geoscience Union Meeting 2014
(28 April - 02 May 2014 at Pacifico YOKOHAMA, Kanagawa, Japan)

SCG67-18 Room:418 Time:May 2 11:00-11:15

Hydrothermal heat mining due to the aquifer thickening toward the trench axis: A model for the Japan Trench

KAWADA, Yoshifumi[1*] ; YAMANO, Makoto[1] ; SEAMA, Nobukazu[2]

[1]ERI, Univ of Tokyo, [2]Kobe University

Observation: At the Japan Trench, a 135-Myr-old Pacific plate is subducting beneath the Japan Island. Heat flow on such an old oceanic plate is expected to be 50m W/m^2 by a thermal model of the oceanic plate. However, observed heat flow values range from 50 to 120 mW/m^2 and the averaged value is 70 mW/m^2 (Yamano et al., 2008, Int. J. Earth Sci.). In the area of high heat-flow anomalies, a high V_p/V_s layer (highly porous, and probably highly permeable) is observed within the uppermost part of the oceanic plate (Fujie et al., 2013, JpGU Meeting). The layer thickness is observed to increase toward the trench axis.

Hypothesis: Permeability within the uppermost several hundred meters of oceanic plate is measured to be high for fluid to convect; this layer is called an aquifer. We assume that thickening of the observed high V_p/V_s layer is a consequence of thickening of this highly permeable layer. Accordingly, we construct a numerical model including hydrothermal circulation within an aquifer being thickened with time, and calculate the resulted heat flow anomalies.

Results: Calculations show that heat flow is increased as the aquifer thickness begins to increase. With typical parameter values for the Japan Trench, the result accounts for the observed high heat-flow anomaly of 20 mW/m^2. This high heat-flow arises due to the mining of heat from the base of the thickening aquifer. Downward thickening of the aquifer invades the high-temperature region, and incorporates the heat into convection. As a result, this heat is transported upwards through sediments above the aquifer, and heat flow is increased.

Keywords: hydrothermal circulation, heat flow, the Japan Trench, seismogenic zone

Japan Geoscience Union Meeting 2014
(28 April - 02 May 2014 at Pacifico YOKOHAMA, Kanagawa, Japan)

SCG67-19 Room:418 Time:May 2 11:15-11:30

Seismic structure and seismicity surevey at the Kairei hydrothermal vent field in the Indian Ocean

SATO, Toshinori[1*] ; TAKATA, Hiroyoshi[1] ; IMAI, Yuki[2] ; NOGUCHI, Yui[1] ; KOUNO, Akihiro[1] ; YAMADA, Tomoaki[3] ; SHINOHARA, Masanao[3]

[1]Graduate School of Science, Chiba Univ., [2]Dep. Science, Chiba Univ., [3]ERI, Univ. Tokyo

1. Introduction

In the first segment of the central Indian Ridge from the Rodriguez triple junction, the Kairei hydrothermal vent field exists and extrudes hydrothermal fluid with richer hydrogen content compared to other hydrothermal vents in the world. Around the Kairei hydrothermal field, serpentinized peridotite and troctolites, and gabbroic rocks were discovered. These deep-seated rocks exposed around the Kairei field may cause the enrichment of H2 in the Kairei fluids. At the Kairei field, a hydrogen-based subsurface microbial ecosystem and various hydrothermal vent macrofauna were found. In the TAIGA Project (Trans-crustal Advection and In situ reaction of Global sub-seafloor Aquifer), this area is a representative field of TAIGA of hydrogen. To investigate how the deep-seated rocks (originally situated at several kilometers below seafloor) are uplifted and exposed onto seafloor, and the hydrothermal fluids circurate in subsureface, we conducted a seismic refraction/reflection survay and seismicity observation with ocean bottom seismometers (OBSs).

2. Observation

We conducted a seismic survey around the Kairei hydrothermal field from January 27 to March 19 in 2013 using S/V Yokosuka of Jamstec. We used 21 OBSs, an air gun (GI gun) and a single channel streamer cable. Deployed intervals of OBSs are about 7.5 km, and 2 km near the Kairei field. Survey lines are 5 lines NNW-SSE direction parallel to the ridge axis, 5 lines E-W direction, and 5 lines NNE-SSW direction. Line lengths are from 7 km to 30 km. In addition, we conducted other 5 lines pass around the point just above the Kairei hydrothermal field and the Yokoniwa Rise. The air gun was a GI gun with 355 cu. in. (5.5 l), and the shot interval was 40 s (about 100 m).

3. Results

From seismicity observation, we found many micro earthquakes in this area. A swarm of micro earthquakes exists at a location about 1 km northwest of the Kairei field. The swarm has a NNW-SSE strike, parallel to the ridge axis. The depth of the swarm is very shallow (˜4 km from seafloor). This swarm may be relateted to the hydrothermal activities of the Kairei field. At the first segment of the central Indian Ridge, many micro earthquakes occurred. The depth of these events is deeper than that of the swarm near the Kairei field.

Acknowledgements

We thank the captain and the crew of S/V Yokosuka of Jamstec for their support. This work was supported by Grant-in-Aid for Scientific Research on Innovative Areas of the Ministry of Education, Culture, Sports, Science and Technology (Grant Number 20109002, TAIGA project).

Keywords: TAIGA, hydrothermal area, seismicity, Triple junction in the Indian Ocean

Japan Geoscience Union Meeting 2014
(28 April - 02 May 2014 at Pacifico YOKOHAMA, Kanagawa, Japan)

SCG67-20 Room:418 Time:May 2 11:30-11:45

Origin of boron in Okinawa Trough hydrothermal fluids using B isotope as a tracer

TOKI, Tomohiro[1*] ; EBINA, Naoya[1] ; SHINJO, Ryuichi[1] ; ISHIBASHI, Jun-ichiro[2]

[1]University of the Ryukyus, [2]Kyushu University

The Okinawa Trough is a back-arc basin located around the Ryukyu Arc, where several hydrothermal systems have been discovered. The Okinawa Trough has a very thick sedimentary cover, and the chemistry of the hydrothermal fluids appeared to be influenced by interaction with the sediment. However, the temperature environments below the seafloor have not been clarified yet in detail. In this study, we investigated B isotope ratios (δ^{11}B) in hydrothermal fluids from Okinawa Trough, and discussed the origin of the boron and the reaction temperature.

The hydrothermal fluid samples were collected by WHATS with Hyper Dolphin and *Shinkai 6500* from Iheya North Knoll, Izena Caldron, Hatoma Knoll, and Yonaguni Knoll IV. The sample was filtered and acidified by HNO_3. B was isolated by microsublimation, and δ^{11}B measurement was carried out using a MC-ICP-MS (Neptune plus). The precision was within 0.3%. All values reported in this study are presented in delta notation relative to NBS SRM 951.

The concentrations of B in the hydrothermal fluids from Okinawa Trough were higher than those from sediment-starved MOR, and the δ^{11}B showed ^{10}B enrichments. A difference of δ^{11}B among Okinawa Trough hydrothermal fields was found; Yonaguni IV ‹ Izena Caldron ‹ Iheya North ‹ Hatoma Knoll. The δ^{11}B in the hydrothermal fluids showed the strong correlation with the carbon isotopic ratios of methane (δ^{13}C-CH_4) in the hydrothermal fluids, suggesting the factor controlling the variation of δ^{11}B in the hydrothermal fluids is identical with the one controlling the variation of δ^{13}C-CH_4 in the hydrothermal fluids. The controlling factor for the variation of δ^{13}C-CH_4 in the hydrothermal fluids is a mixing ratio between thermogenic methane and microbial methane, implying the controlling factor for the variation of δ^{11}B would be a mixing ratio between B derived from sediment at higher temperature and lower temperature.

We calculated the reaction temperature based on the correlated equation of reaction temperature with δ^{11}B fractionation between solid phase and aqueous phase. For δ^{11}B of the solid phase, reported δ^{11}B of surface sediment from Okinawa Trough (– 5.4 and – 2.2 ‰) was used. However, all observed δ^{11}B in the hydrothermal fluids could not be explained. Instead, δ^{11}B of solid phase was estimated between 50 and 400 ℃; the lowest temperature of leaching B from sediment is 50 ℃ and the highest temperature of sub-critical water is 400 ℃. δ^{11}B of sediment involved in B leaching was estimated to be from – 20 to – 10 ‰, which are lower than the δ^{11}B in surface sediment from Okinawa Trough. Hydrothermal alteration lowered δ^{11}B in sediment, suggesting the origin of the B in Okinawa Trough hydrothermal fluids would be altered sediment. For the reaction temperature, the lowest value among Okinawa Trough hydrothermal fluids was obtained in Hatoma hydrothermal fluids, following Iheya North, Izena, and Yonaguni IV, suggesting a large amount of sediment is distributed in recharge zone in Hatoma Knoll, and the B would be derived from the sediment at relatively low temperature. On the other hand, sediment is distributed in reaction zone beneath Yonaguni IV, and the B would be derived from the sediment at relatively high temperature.

Keywords: hydrothermal fluid, Okinawa Trough, boron isotope

Japan Geoscience Union Meeting 2014
(28 April - 02 May 2014 at Pacifico YOKOHAMA, Kanagawa, Japan)

SCG67-21 Room:418 Time:May 2 11:45-12:00

The structure of iron- and silica-rich mounds at hydrothermal environment in shallow marine, Satsuma Iwo-Jima

KURATOMI, Takashi[1*] ; KIYOKAWA, Shoichi[1] ; IKEHARA, Minoru[2] ; GOTO, Shusaku[3] ; HOSHINO, Tatsuhiko[4] ; IKEGAMI, Fumihiko[1] ; MINOWA, Yuto[1]

[1]Kyushu University, [2]Center for Advanced Marine Core Research, Kochi University, [3]Geological Survey of Japan, AIST, [4]Japan Agency for Marine-Earth Science and Technology

Satsuma Iwo-Jima Island, located 38km south of Kyusyu, Japan, is a volcanic island in the northwestern rim of Kikai caldera. Iron- and silica-rich mounds develop with hydrothermal activity (pH=5.5, 50-60 degree Celsius) in Nagahama bay located southwestern part of the island. The brownish seawater at the bay is due to mixing of the hot spring water with seawater (Shikaura and Tazaki, 2001). Very high deposition rate (33 cm per year) of iron-rich sediments was observed in the bay (Kiyokawa et al., 2012). In this study, we analyzed samples (20-30 cm long) recovered from mounds at the seafloor of Nagahama bay by the observation with X-ray CT scan, FE-SEM, and the thin-sectioned sample, and the chemical analysis with EDS, XRF, XRD and DNA, and found that the structure of mounds has unique information.

Visual observation indicated that the samples were made from two layer: black high-density hard layer and brownish low-density soft layer. X-ray CT scan observation shows that the inside of samples is constructed from the aggregation of convex structure (3-4 cm). Soft layer is covered by a hard layer as a rim. The soft layer has many pipe-like structures (typical radius: 1 mm). Petrographic observations indicate that soft and hard layers have filament-like forms, and the form in soft layer is perpendicular to that in the hard layer. The number of small particles (about 20 μm) observed on filament-like forms in soft layer increases toward hard layer. FE-SEM observation shows that filament-like form in hard layer consists of aggregation of bacillus-like form as the chain of particle (about 2 μm). At soft layer, on the other hand, bacteria-like form with smaller particles ($<$0.5 μm) is observed. Bacteria-like form could be classified into 3 types (helix, ribbon-like, twisted). Furthermore, the result of XRD and XRF show that hard layer consists of ferrihydrite and opal-A (Si: 26.8%, Fe: 56.0%) and soft one is composed by ferrihydrite, opal-A, quartz, cristobalite and tridimite (Si: 36.5%, Fe: 43.5%). DNA analysis indicated predominance of *Mariprofundus ferrooxydans* that is known as iron-oxidizing bacteria belonging to Zeta-proteobacteria.

The forming process of the mounds at Nagahama bay is that firstly chemical and biological reaction made soft layer. During occurrence of the reaction, volcanic ash originating from Iwo-dake was contained as silica in the soft layer. Bacteria-like form in soft layer is considered to be the stalk made by iron-oxidizing bacteria according to the result of DNA analysis. Such neutrophilic iron-oxidizing bacteria prefers an environment of redox interface between hydrothermal water and seawater (Chan et al., 2011), and their activity made hard rim at outer soft layer. Inside of hard rim, the keeping of both reaction resulted in relative iron-rich layer and layering at hard rim. Because such process occurred repeatedly, the mounds at Nagahama bay had the aggregation of convex structure with many pipes as the hydrothermal vent. The high depositional rate of iron hydroxides is likely to be influenced by the activity of bacteria.

Keywords: hydrothermal activity, iron-hydroxide, iron-oxidizing bacteria, shallow marine

Japan Geoscience Union Meeting 2014
(28 April - 02 May 2014 at Pacifico YOKOHAMA, Kanagawa, Japan)

SCG67-P01 Room:Poster Time:May 2 16:15-17:30

GPS/acoustic measurement using a multi-purpose moored buoy system

IMANO, Misae[1*] ; KIDO, Motoyuki[2] ; OHTA, Yusaku[1] ; FUKUDA, Tatsuya[3] ; OCHI, Hiroshi[3] ; TAKAHASHI, Narumi[3]

[1]Graduate School of Science, Tohoku University, [2]IRIDeS, Tohoku University, [3]Japan Agency for Marine-Earth Science and Technology

For monitoring crustal deformation and tsunami occurrence in the source region of the upcoming Nankai and Tonankai earthquake, JAMSTEC, JAXA, and Tohoku University have jointly developed a realtime continuous observation system using a moored buoy, called m-TRITON, and have started its sea-trial. The system consists of a seafloor pressure sensor for monitoring tsunamis and vertical crustal deformation, a GPS system for monitoring sea-level and position/attitude of the buoy, and a GPS/acoustic system for monitoring horizontal crustal deformation. Measuresd data are transmited to onshore station via satellite communication so that they can be monitored in realtime. The first sea-trial was carried out in Kumano-nada in 2013, and the second trial has been started in 2014 after improvement of the system. In this presentation, we focus on the issues particular to acoustic ranging of GPS/acoustic measurement for the purpose to remedy the system based on the data acquired in 2013, and report new data being acquired in the ongoing second trial in 2014.

The GPS/acoustic system measures horizontal movement of a seafloor banchmark, which consists of six transponders by combining GPS analysis of the buoy and acoustic ranging between the buoy and seafloor transponders. Considering bit-rate of the satellite communication, it is not realistic to send full acoustic waveform. So, it is required to send only the result processed on the buoy. In order to proceed acoustic wave with a low-powered device on the buoy, it is necessary (1) to cut out recorded waveform to the minimum requirement and (2) to send the processed data containing minimum but sufficient information. As for (1), in the current system recorded acoustic waveform is cut out by a window of $\pm$ 20 ms centered at synthetic traveltime calculated from provisional position of the buoy and each seafloor transponder. After that, cross-correlation waveform between the transmitted signal and the received signal is calculated to obtain an accurate observed traveltime. Then (2) send the correlogram only a 1 ms window centered at the maximum correlation peak, which is sufficient to include the sidelobe. Since correlation wave is represented in 8 bit and the sampling rate is in 100 kHz, the size-per-signle wave to be transmitted can be reduced only to 101 byte.

As a result of considering the fluctuating range for the uncertainty of provisional position obtained by the NMEA output of the GPS (˜10 m at most) and the average sound speed variation (˜2 m/s) that affect the synthetic traveltime, the window width of $\pm$ 20ms employed in (1) is a minimum requirement. In order to certainly cut out maximum correlation peak for all acoustic ranging, it is desirable to set the width to $\pm$ 30 ms. As for correlogram to be sent to onshore station, since the envelope of the correlation peak is within the 1 ms, current width is reasonable. However, apparent maximum correlation peak often known to appears due to multiples at sea surface. In that case, it is not possible to achieve proper adjustment only by the width. Therefore the development of an algorithm to detect the true correlation peak is required. We verified based on actual data about the condition that the multiple occurs, and found that it is explained by the incident angle of the sound wave and the directivity of transducer. We are developping an algorithm that automatically detects the true correlation peak based on this hypothesis.

Keywords: crustal deformation, moored buoy

Japan Geoscience Union Meeting 2014
(28 April - 02 May 2014 at Pacifico YOKOHAMA, Kanagawa, Japan)

SCG67-P02 Room:Poster Time:May 2 16:15-17:30

Inversion analysis for slip deficit rate along the Nankai Trough using on- and offshore crustal velocities

WATANABE, Tsuyoshi[1*] ; TADOKORO, Keiichi[1] ; YASUDA, Kenji[1] ; FUJII, Cosumo[1] ; IKUTA, Ryoya[2] ; OKUDA, Takashi[1] ; KUNO, Masahiro[3]

[1]Graduate School of Environmental Studies, Nagoya University, [2]Department of Geosciences, Shizuoka University, [3]Mie Prefecture Fisheries Research Institute

Along the Nankai Trough, megathrust earthquakes occur every 100-150 years. A nationwide continuous GPS observation network in Japan has measured precise crustal deformation in this area for the past decade. However, the sources of these earthquakes are located offshore where slip resolution is generally poor. Since the early 2000s, seafloor geodetic observations using GPS/Acoustic techniques have been conducted against such a background in Japan. Today, seafloor geodetic observations are recognized as an effective and essential procedure for understanding the source process of earthquakes that occur in offshore areas. In this study, we show the result of seafloor geodetic observations using GPS/Acoustic techniques from 2004 to 2012 and estimate slip deficit rates along the Nankai Trough using both onshore GPS velocities and offshore crustal velocities derived from seafloor geodetic observations. We conducted inversion analysis with a priori information, and then, a high slip deficit rate of more than 50 mm/yr was detected off the Shikoku district. This decreases to approximately 30-50 mm/yr off the Kii Peninsula, and then it falls to approximately 10-30 mm/yr around the Suruga Trough relative to the Amurian plate, except for slip deficit rate of nearly 40 mm/yr which was detected at a fault segment beside the seafloor benchmark at the Suruga Bay. In addition, we investigated slip resolution by adding new established seafloor benchmarks off Shikoku district. As a result, we found that slip resolution was still poorer in offshore areas such as off the Ashizuri Cape, the Muroto Cape, and the Kii Peninsula near the trench axis than in onshore areas. Thus, it is important to conduct seafloor geodetic observations in areas with poor slip resolution.

Keywords: GPS/Acoustic, Nankai Trough, crustal deformation, slip deficit rate, slip resolution

Japan Geoscience Union Meeting 2014
(28 April - 02 May 2014 at Pacifico YOKOHAMA, Kanagawa, Japan)

SCG67-P03 Room:Poster Time:May 2 16:15-17:30

Development and examination of new methods for traveltime detection in GPS/A geodetic data to high-precise and automatic

AZUMA, Ryosuke[1*] ; TOMITA, Fumiaki[2] ; IINUMA, Takeshi[1] ; HINO, Ryota[1] ; KIDO, Motoyuki[1] ; FUJIMOTO, Hiromi[1] ; OSADA, Yukihito[1] ; OHTA, Yusaku[3] ; WADA, Ikuko[1]

[1]IRIDeS, Tohoku Univ., [2]Graduate School of Science, Tohoku Univ., [3]RCPEVE, Tohoku Univ.

The development of a technique for GPS-acoustic (GPS/A) geodetic observations has enabled us to understand the slip distribution of the 2011 Tohoku-oki earthquake. However, there remains an issue with the precision of GPS/A measurement is still lower by two orders of magnitude than that of on-land GPS measurement due to problems in observations and data processing methods. In this study, we focus on the problem for determination of traveltimes of acoustic signals obtained from GPS/A measurement.

The conventional approach for determining the two-way traveltime of observed acoustic signals is to determine the maximum peak of the cross-correlation waveforms between the transmitted and returned signals. However, the maximum peak often differs from the true peak due to the distortion in the correlation waveform which depends on the relative spatial geometry of the ship and station. These misread traveltimes have been re-read manually so far. Such procedure is no longer applicable for processing vast array of data obtained at newly installed over 20 GPS/A stations after the 2011 Tohoku-oki earthquake. The aim of this study is to develop fully automated algorithms for analyzing GPS/A data with high precision. We introduce here two algorithms.

1) We read the maximum peak in the observed correlogram and then deconvolve it by the synthetic correlogram. Then, we apply the same operation to the deconvolved waveform. This procedure is iterated until the correlation coefficient decreases lower than a pre-defined threshold. A true traveltime is defined as the fastest traveltime during the iterations.

2) We classify the observed correlograms into several groups based on their similarity through cluster analyses and choose a master waveform in each group. Then evaluate the traveltime residual between the maximum peak and the true peak in the observed correlogram. Thus obtained residual is applied as the correction value of each clustered group.

We also use a seismic data analysis tool to visually inspect whether above algorithms work properly. We confirmed that the both new methods properly correct for misreadings in the current method, which sometimes amount to several hundred micro seconds. This corresponds roughly to a 0.3-m difference in the slant range. Therefore, with the new algorithms, significant improvement in the estimation of the station location is expected. However, both methods have to be assigned an arbitrary value as a threshold. Further analyses are needed to determine arbitrary threshold values and to construct fully automated algorithms.

Keywords: ocean bottom geodetic observation

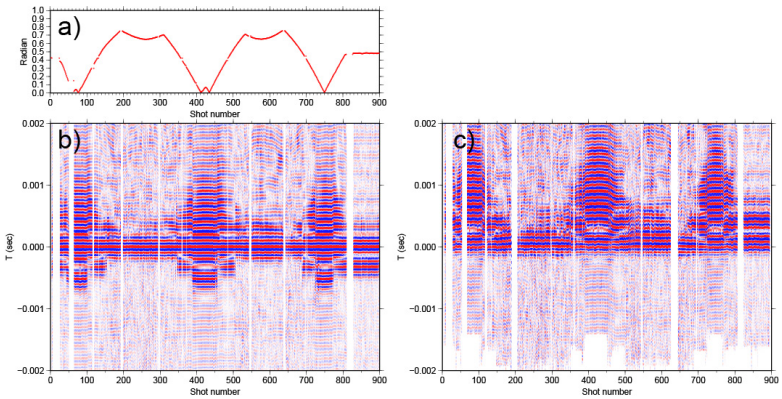

Fig. Incident angle of transmitted signals (a). Pasted corelation waveforms analyzed by reading maximum peak (b) and reading iteratively-deconvolved peak (c). Each trace was moved out by the observed traveltime.

Japan Geoscience Union Meeting 2014
(28 April - 02 May 2014 at Pacifico YOKOHAMA, Kanagawa, Japan)

SCG67-P04 Room:Poster Time:May 2 16:15-17:30

A NaI spectrometer for long-term radon measurement at the sea floor

NINAGAWA, Kiyotaka[1*] ; TOYODA, Shin[1] ; FUJIWARA, Taisei[1] ; NAKAGAWA, Masuo[1] ; YAMAMOTO, Isao[1] ; KUMAGAI, Hidenori[2] ; KINOSHITA, Masataka[2] ; KUBO, Shin[3]

[1]Okayama University of Science, [2]Japan Agency for Marine-Earth Science and Technology, [3]CLEAR-PULSE

In the Japanese Islands, the Tokai, Tonankai and Nankai earthquakes are expected within a few decades. It is a very important scientific issue to understand the physicochemical process occurring in the earthquake occurrence belt and the mechanism of earthquakes near the oceanic trench for damage mitigation of human lives and social basis. Increases of the radon concentration in atmosphere and in groundwater before earthquake are reported in the Southern Hyogo Prefecture Earthquake in 1995. In this research, gamma rays from radon daughter radionuclides at the sea floor will be continuously measured on the Kumanonada offing, where is the epicentral area of the expected Tonankai earthquake. The correlation between micro earthquakes and radon concentrations is also investigated to contribute the fundamental research on the response of the fluid in the crust corresponding to change of the crust.

Investigation on the gamma ray at the sea floor has been made only in a certain limited duration up to several hours while the submersible stays at the site for measurement. This time, a time variation of the gamma ray for several months is planned in order to investigate correlation between earthquakes and radon concentration. A battery drive type NaI spectrometer, which will be set on sea floor and can automatically record gamma ray, was designed. In this January it is almost constructed. A preliminary measurement is scheduled in February. After improvements of software and hardware, it will be set on spring water area of the Kumanonada offing from April to September, and will measure for more than about 4.6 months.

Specification of the NaI spectrometer for long-term radon measurement at the sea floor is as follows;
Name: Low consumed power type gamma-ray spectrometer for deep sea
PMT High-voltage : programmable (+1000V max)
Amplifier: Charge sensitive Memory Capacity: 1Gbit (NOR Flash)
Connection: RS-232C 921,600 bps Current: 110mA (on), 10mA (off)
Operation:
1. After initial setting with PC, measurement starts automatically, and records gamma-ray spectra.
2. It has the intermittent mode for electric power saving.
3. Battery Power Supply 30 AA alkaline batteries, 6 series, 9V
4. When the battery power supply voltage falls to 6V or spectral data is over memory capacity, measurement is suspended automatically and the battery power supply is disconnected.
5. It can connect with PC after measurement, and transfer the recorded spectra to PC.

Keywords: Radon, sea floor, long-term measurement, NaI

Japan Geoscience Union Meeting 2014
(28 April - 02 May 2014 at Pacifico YOKOHAMA, Kanagawa, Japan)

SCG67-P05 Room:Poster Time:May 2 16:15-17:30

Time stamp experiment of MEMS-gyro for the observation of seafloor crustal deformation using multi-buoy system

MUKAIYAMA, Haruka[1*] ; IKUTA, Ryoya[1] ; TADOKORO, Keiichi[2] ; NAGAI, Satoru[2] ; WATANABE, Tsuyoshi[2]

[1]Graduate school of science , Shizuoka University, [2]Earthquake research center, Graduate school of environmental study, Nagoya University

We are developing a new method for the observation of seafloor crustal deformation using multi-buoy system. The system measures seafloor crustal deformation by determining position of benchmarks on the seafloor using multi-buoy which link-up GPS and acoustic signals. Acoustic ranging is used to measure distance between the buoys and seafloor benchmarks. And kinematic GPS is used to locate the multi-buoy every 0.2 seconds. Now we have deployed 4 seafloor benchmark units at Suruga Bay and 4 units at Kumano Basin. At each survey site, three seafloor transponders are settled to define a benchmark unit. In November 2012, first observation of seafloor crustal deformation using the buoys was held in Suruga Bay. Analyzing observed data, errors of traveltime ' s residual were about 0.2ms(Mukaiyama et al 2012JPGU). These errors were too large. From approximate calculation, it is predicted that these errors of 0.16ms at maximum can be removed by introduction of a gyro compass. So, we introduced MEMS-gyro to multi-buoy observation to monitor the attitude of the buoys at Suruga Bay at November 2013. The MEMS-gyro was NAV440CA by Crossbow Co.. For the attitude monitoring of the observation of seafloor crustal deformation, time stamp is important. Although the gyro introduces time stamp provided by its GPS processor, its accuracy was not evaluated. In this study, we conducted rotation experiments to evaluate the accuracy of its time stamp. In the experiment, we used another GPS antenna system as a time reference. The GPS antenna and the gyro were deployed on a rotation table to synchronize their motions and the time stamp of the rotated gyro was checked with reference to the GPS time. Timing between their motions was evaluated by cross correlation between GPS circular trajectory and the rotation angle of the gyro. Specifically, we rotated the table for 3 min every 1 hour. This subset was repeated 3 times. As a result, delay times in first two sets were about -38ms. But third set was -58ms. The delay became lager. Offset of the average angle between GPS and gyro was also deferent from first two sets to third set. This deference might be caused by that of rotation speed between three subsets. We tried additional experiment with different parameter settings of MEMS-gyro under controlled rotation speed. We will also report the result of this additional experiment.

Keywords: Seafloor crustal deformation, buoy, GPS, MEMS-gyro, Time stamp, Rotation experiment

Japan Geoscience Union Meeting 2014
(28 April - 02 May 2014 at Pacifico YOKOHAMA, Kanagawa, Japan)

SCG67-P06 Room:Poster Time:May 2 16:15-17:30

Three year observations of ocean infragravity waves by broadband seismometers and pressure gauges of Japanese seafloor n

TONO, Yoko[1*] ; NISHIDA, Kiwamu[2] ; FUKAO, Yoshio[1] ; TO, Akiko[1] ; TAKAHASHI, Narumi[1]

[1]JAMSTEC, [2]ERI

Ocean infragravity (IG) waves are sea-surface gravity waves with periods of several minutes and wavelengths up to tens of kilometers. We used a slant-stack technique to detect IG waves from the three-year period records (2011-2013) of the vertical component broadband seismograms and pressure gauges of the seafloor network deployed in the Nankai Trough region (DONET). IG signals show good match in waveform between the seafloor displacement and pressure with propagation speeds consistent with the seafloor depths of 2000 m. The signal intensities are strongly azimuth-dependent. Except for the days with extreme weather, waves incoming from the SE direction (from the deep ocean to the coast across the Nankai Trough) are by far dominant. The incoming direction sharply splits into two, SSE and ESE. Waves from the deeper ocean in the SSE direction are more dominated in longer-period components than those from the shallower ocean in the ESE direction. Amplitudes of these waves clearly show a seasonal variation, high in winter and low in summer. The effect of typhoon is to generate IG waves incoming from the source direction and those incoming from the NE-ENE direction through the corridor between the coast and the Nankai trough. The latter is often stronger than the former.

Keywords: Infragravity wave, Nankai Trough, DONET

Japan Geoscience Union Meeting 2014
(28 April - 02 May 2014 at Pacifico YOKOHAMA, Kanagawa, Japan)

SCG67-P07 Room:Poster Time:May 2 16:15-17:30

Evaluation of resolution and estimation error of vessel-based seafloor displacement observation using AUV bathymetry

FUJIWARA, Toshiya[1*] ; MASAKI, Yuka[1] ; YAMAMOTO, Fujio[1]

[1]JAMSTEC

Bathymetry is basic information for any kind of seafloor observation, and therefore vessel-based multi-narrow beam bathymetric surveys are conducted quite often. In recent years, previous bathymetric data exist in most scientifically-important areas. A repeated bathymetric survey reveals seafloor displacement related to geodynamics [e.g. Fujiwara et al., Science 2011]. However, the spatial resolution and estimation error of the seafloor displacement observation from the vessel-based bathymetric survey are not exactly known. Because the observation compares a pair of limited-resolution bathymetric data. Water depth (distance from the vessel's echo sounder to the seafloor) degrades the spatial resolution and precision of depth measurement from the vessel-based survey. While on the other hand, a near-seafloor Autonomous Underwater Vehicle (AUV)-based survey enables us to obtain high-resolution bathymetric data. In this paper, we evaluated the spatial resolution and estimation error of the seafloor displacement observation from vessel-based bathymetric survey. In this evaluation, bathymetric data from vessel-based and AUV-based surveys in the Iheya-North knoll of the Okinawa Trough were used.

AUV Urashima bathymetric survey was conducted in YK07-07 cruise aboard the R/V Yokosuka in May 2007 [Yamamoto et al., 21st Mtg, Japan Society for Marine Surveys and Technology 2009]. The applied multi-narrow beam echo sounder was a SEABAT 7125. R/V Yokosuka bathymetric survey was performed using a SeaBeam 2112 echo sounder in YK06-09 cruise from 18 to 24 July 2006 [Masaki et al., JAMSTEC R&D 2011]. The vessel passed over the survey area six times with each constant speeds and obtained bathymetric data. One survey track was treated as one's independent survey in this evaluation. The beam angle (angle formed by the vertical line and a narrow sounding beam) was within 40^o in the survey area.

AUV bathymetry shows hills (the shallowest depth ∼870 m) in the western side and basins (the deepest ∼1070 m) in the eastern side. The average/median depth is 1010 m. Hydrothermal chimney mounds ∼30 m in diameter and ∼10-20 m in height were found on the hillside in the high-resolution bathymetry. Vessel-based bathymetry is spatially-smoothed as a function of the footprint (area of the narrow sounding beam projected onto the seafloor) size. The footprint size of the Yokosuka survey at a depth of 1000 m is ∼35×35 m-43×55 m (∼5% of water depth). In the vessel bathymetry, geographical features smaller than the footprint size, such as the hydrothermal chimney mounds, cannot be recognized. And seafloor morphology is slightly different from each other track surveys due to distribution of sounding points and measuring error. Standard deviations of depth differences between the AUV- and the vessel-based data were 2.67-3.08 m. The AUV bathymetry are assumed to be the "true" bathymetry, and therefore the precision of the vessel-based depth measurement (standard deviation of measuring error) is considered to be ∼0.2-0.3 % of water depth.

Simulated vessel-based bathymetric data "before and after" the seafloor displacement were made using AUV-based bathymetric data. The displacement was verified by comparing these simulated data using the analysis conditions that neither depth accuracy variation within the area nor locational errors of beam sounding points are allowed. We used the method of Fujiwara et al. [2011] to estimate horizontal displacement. As a result, we found that estimation error of the seafloor horizontal displacement depends on the precision of the depth measurement and is ∼0.2-0.3 % of water depth. As for the seafloor vertical displacement, the smallest displacement that can be detected occurs when the horizontal extent of the deformation is larger than several times the size of the footprint, and in the situation that the amplitude of the depth difference is greater than the precision of depth measurement.

Keywords: Multi-narrow beam bathymetry, seafloor displacement, Iheya-North knoll, AUV Urashima, R/V Yokosuka

Japan Geoscience Union Meeting 2014
(28 April - 02 May 2014 at Pacifico YOKOHAMA, Kanagawa, Japan)

SCG67-P08 Room:Poster Time:May 2 16:15-17:30

Bathymetric survey and discovery of hydrothermal plume in the Daiichi-Amami Knoll using autonomous underwater vehicle

MINAMI, Hiroki[1*] ; OHARA, Yasuhiko[2]

[1]Hydrographic Surveys Division, Hydrographic and Oceanographic Department, Japan Coast Guard, [2]Ocean Research Office, Hydrographic and Oceanographic Department, Japan Coast Guard

Many submarine volcanoes exist along the volcanic front in the Ryuku Arc. The Daiichi-Amami Knoll, which is located about 70 km off Amami Oshima Island, is one of those submarine volcanoes. Detailed bathymetric survey of this knoll has not been done before, therefore its shape and size have not been known. Japan Coast Guard conducted a high resolution bathymetric mapping of the knoll using survey vessel and autonomous underwater vehicle (AUV) and discovered hydrothermal plumes which are rising from the seafloor, indicating that the presence of hydrothermal activities in the Daiichi-Amami Knoll.

1. Method

The survey was conducted in August and September, 2013 using survey vessel Takuyo and AUV Gondo. The knoll was surveyed with multibeam echo sounder (MBES) installed on S/V Takuyo. Then the detailed survey was done with MBES on AUV Gondo.

2. Bathymetry

The bathymetry of the Daiichi-Amami Knoll indicates that the knoll is a volcanic high. The knoll has flat areas, a caldera with a diameter of 1.6 km and some volcanic cones at its summit. The knoll also has two small depressions near to the volcanic cones and they are deeper about 40 m than the surrounding areas. The relative high of the knoll is about 500 to 700 m and the shallowest depth of the knoll is 245 m.

3. Hydrothermal plume

Water column data acquired by MBES on S/V Takuyo detected the clear hydrothermal plumes in the two depressions. The plumes were especially clear at the rim of the depression. Some plumes were observed to rise from the seafloor of 350 m depth to near sea surface (although no discolored water was visually observed on the sea surface). Plumes were also detected at the slope areas of the volcanic cones. AUV Gondo dived to the depressions at the altitude 40-50 m above seafloor and conducted a detailed survey. The high resolution bathymetric map shows a presence of a numerous small depressions near the plume points. The side scan image by AUV Gondo also shows the plumes acoustically at its nadir.

4. Water temperature

AUV Gondo observed the water temperature at the altitude 40-50 m in the depresions, but distinguished temperature increases were not observed. Temperature profile observation, which was conducted using expendable bathythermograph launched from S/V Takuyo, showed over 2 degrees temperature increase near the seafloor in the depression. This observation along with the presence of plumes indicate the presence of hydrothermal activity in the Daiichi-Amami Knoll.

5. Importance of this survey result

The detailed bathymetry and the presence of plumes in the Daiichi-Amami Knoll were revealed by the survey using survey vessel and AUV. The discovery of plumes suggests the presence of hydrothermal deposits and chemosyhthetic community, therefore being important in terms of seafloor resources. The high resolution bathymetric map acquired by AUV is fundamental information which is useful for scientific research and mineral exploration. This result is a first step for further survey to understand the geological history of the knoll and to secure new seafloor resources.

Keywords: Daiichi-Amami Knoll, submarine volcano, plume, AUV, bathymetry

Japan Geoscience Union Meeting 2014
(28 April - 02 May 2014 at Pacifico YOKOHAMA, Kanagawa, Japan)

SCG67-P09 Room:Poster Time:May 2 16:15-17:30

Topography, geology, tectonics and ore deposit of the Bayonnaise knoll caldera, Izu-Ogasawara arc

HONSHO, Chie[1*] ; URA, Tamaki[1] ; ASADA, Akira[3] ; KIM, Kangsoo[3] ; NAGAHASHI, Kenji[3]

[1]Atmosphere and Ocean Research Institute, The University of Tokyo, [2]Center for Socio-Robotic Synthesis, Kyushu Institute of Technology, [3]Underwater Technology Research Center, Institute of Industrial Science, The University of Tokyo

Several hydrothermal sites have been discovered in the volcanic front of the Izu-Ogasawara arc: Myojin knoll caldera, Myojinsho caldera, Smith caldera, Suiyo seamount, and Kaikata seamount. The Hakurei hydrothermal site in the Bayonnaise knoll caldera is the only hydrothermal site discovered in the rift zone of the arc. We analyzed deep-sea multibeam and side scan sonar data obtained using autonomous underwater vehicle Urashima in the caldera and discussed the topography, geology, tectonics, and ore deposit of the caldera.

The survey area ∼3 km x ∼2 km wide covers the southern half circle of the caldera. Major geomorphic elements are, from the outside to the inside, the knoll slope, the steep caldera wall, the flat caldera floor, the central cone with three peaks, and the central depression surrounded by the peaks. The high-resolution bathymetric map shows that large slope failures occurred in the southeastern caldera wall and that the Hakurei deposit is distributed over the failure area. Slope failure is also going on in the southwestern wall and a large collapse may shortly occur. The eastern hill, the main part of the central cone, seems to be a lava dome: it has a small flat surface on the top, convex slopes in the upper part, and rectilinear to concave slopes near the base. The northeastern slope of the dome is relatively flat from top to bottom, indicating that a slope failure occurred there. A series of depressions lying in a NW-SE direction in the western caldera floor would be a crater row, seeing that the terrain gently slopes down from the rim of the depressions. The direction of the crater row suggests that the caldera is under the extension stress in a NE-SW direction.

Morphological and textural characteristics of the Hakurei site were determined by three kinds of analyses. The gray-level co-occurrence matrix was used to describe the texture of the side scan sonar image and to classify the seafloor using cluster analysis. The Hakurei area was distinctly classified to a group that was characterized by high entropy and low homogeneity, and a broad area from the top to the northeast slope of the eastern lava dome was also classified to the group. Some areas belonging to the group were distributed around the top of the southern central cone, in the eastern caldera wall northeast of the Hakurei site, in the southwestern caldera wall, and around the crater row. A band-pass filtered topography was used to determine areas where short-wavelength topographic features like chimneys and mounds observed in the Hakurei site dominate. The band-pass filtering was also performed on the multibeam backscattering intensity data to detect similar patterns to numerous spots of strong backscattering from chimneys observed in the Hakurei area. These results commonly show that areas of similar characteristics to the Hakurei site are distributed in a zone crossing the caldera in a NW-SE direction, from the Hakurei site to the crater row through the central cone.

The Izu-Ogasawara rift zone is separated to many segments ranging in a N-S direction. The Bayonnaise knoll caldera is located on the northeastern margin of an oval depression called the North Myojin rift, which has a longer N-S axis of ∼20 km. It appears that the direction of the crater row, the distributions of hydrothermal or volcanic features, and the distribution of slope failures are along the rim of the North Myojin rift going through the caldera. The North Myojin rift is surrounded by seven knolls including the Bayonnaise knoll. Although hydrothermal activity has been discovered only in the Bayonnaise knoll so far, the geological settings that volcanoes of acidic rocks lying along a circular fault of a depression host ore deposits closely resembles that of the Hokuroku Kuroko region in northern Akita. It is suggested that the Hakurei site is the present field of the Kuroko ore formation.

Keywords: hydrothermal deposit, Izu-Ogasawara rift, multibeam sonar, side scan sonar, GLCM, Kuroko deposit

Japan Geoscience Union Meeting 2014
(28 April - 02 May 2014 at Pacifico YOKOHAMA, Kanagawa, Japan)

SCG67-P10 Room:Poster Time:May 2 16:15-17:30

Electrical resistivity structure of the Snail site at the Southern Mariana Trough spreading center

MATSUNO, Tetsuo[1*] ; KIMURA, Maho[2] ; SEAMA, Nobukazu[2]

[1]National Institute of Polar Research, [2]Kobe University

The electrical resistivity of the oceanic crust is sensitive to the porosity of the crust and the fluid temperature within crustal fractures and pores. The spatial variation of the crustal porosity and the fluid temperature that is related to a hydrothermal circulation can be deduced by revealing an electrical resistivity structure of the oceanic crust involving a hydrothermal site. We carried out a magnetometric resistivity experiment using an active source to reveal an electrical resistivity structure of the oceanic crust at the Snail site on the ridge crest of the Southern Mariana Trough. Active source electric currents were transmitted along and across the ridge axis in a 4000 m^2 area including the Snail site. Five ocean bottom magnetometers were deployed around the Snail site as receivers to measure the magnetic field induced by the transmission of the active source electric currents. The amplitude of the induced magnetic field was calculated by maximizing data density and the signal to error ratio in the data, and locations of the transmissions were determined using several types of calibration data. An optimal 1-D resistivity structure of the oceanic crust, averaged over the experimental area, was deduced by least squares from the data of the amplitude of the magnetic field and the location of the transmission. After calculating magnetic field anomalies, which are deviations of the observed amplitude from the prediction of the optimal 1-D resistivity model, an optimal 3-D resistivity structure was deduced from the magnetic field anomalies through trial and error 3-D forward modeling. The optimal 1-D resistivity structure is a two-layer model, which consists of a 5.6 Ω-m upper layer having a 1500 m thickness and a 0.1 Ω-m underlying half-space. Using Archie's law and porosity profiles of the oceanic crust, the resistivity of 5.6 Ω-m at depths ranging from 800 to 1500 m suggests the presence of high-temperature fluid related to the hydrothermal circulation. The resistivity of 0.1 Ω-m below 1500 m depth may represent a magma mush that is a heat source for the hydrothermal circulation. The optimal 3-D resistivity structure includes a conductive anomaly (0.56 Ω-m in approximately 300 m^2 area down to 400 m depth) just below the Snail site, two resistive anomalies (56 Ω-m with slightly larger volumes than the conductive anomaly) adjacent to the conductive anomaly on the across-ridge side, and three conductive anomalies away from the Snail site. The conductive anomaly just below the Snail site suggests hydrothermal fluid, and the adjacent resistive anomalies suggest areas of low porosity. The size and distribution of the conductive and resistive anomalies near the Snail site constrains the size and style of the hydrothermal circulation.

Keywords: electrical resistivity structure, temperature and porosity, oceanic crust, hydrothermal circulation, magnetometric resistivity method

Japan Geoscience Union Meeting 2014
(28 April - 02 May 2014 at Pacifico YOKOHAMA, Kanagawa, Japan)

SCG67-P11 Room:Poster Time:May 2 16:15-17:30

Crustal Imaging of initial structure in Izu-Ogasawara forearc region obtained by seismic reflection survey

YAMASHITA, Mikiya[1*] ; NO, Tetsuo[1] ; SATO, Takeshi[1] ; KODAIRA, Shuichi[1] ; TAKAHASHI, Narumi[1] ; MIURA, Seiichi[1] ; ISHIZUKA, Osamu[1]

[1]JAMSTEC

The Izu-Bonin (Ogasawara)-Mariana (IBM) arc is known to the typical oceanic island arc, and it is the most suitable area to understand the growth process of island arc. The existence of two paleo arc which consists of Oligocene and Eocene paleo age is known in IBM forearc region by geological and geophysical studies. The Ogasawara ridge is also known to locate the initial structure of arc evolution from geologic sampling of research submersible. In this region, IODP drilling site: IBM-2 is proposed in order to understand the temporal and spatial change in arc crust composition from 50 to 40Ma magmatism. Site IBM-2 consists of two offset drilling holes (BON-1, BON-2). BON-1 designed to first encounter forearc basalt and will reach the sheeted dykes. BON-2 will start in boninites and finish in fore arc basalts. The purpose of these drilling is sampling the full volcanic stratigraphy from gabbro to boninite. This drilling project is already scheduled in 2014. The survey lines along the proposed sites, however, there are no crossing seismic data around BON-1 and BON-2. Therefore, it is need to conduct the MCS survey until 2013 for the evaluation of proposed site.

Japan Agency for Marine-Earth Science and Technology (JAMSTEC) newly carried out multi-channel seismic reflection (MCS) survey using 7,800 cu.in. air gun, 5 km streamer with 444 ch hydrophones in April, 2013. We obtained two seismic reflection profiles of lines IBr11n and IBr11 across from Shikoku Basin and current volcanic front to the paleo arc. The preliminary results show the distribution of volcanic sediments and basement.We also identified the block type structure associated with the uplift in northern side of Kinyo seamout. We will discuss about the characteristics between backarc and forearc from north to south.

Keywords: MCS survey, IBM forearc, initial arc structure

Japan Geoscience Union Meeting 2014
(28 April - 02 May 2014 at Pacifico YOKOHAMA, Kanagawa, Japan)

SCG67-P12 Room:Poster Time:May 2 16:15-17:30

Across-arc geochemical variation of Quaternary Basalts dredged from central part of Izu-arc

YOSHIDA, Takanori[1*] ; OKAMURA, Satoshi[1] ; SAKAMOTO, Izumi[2] ; ADACHI, Yoshiko[3] ; IKEDA, Yasuo[4] ; SHINJO, Ryuichi[5] ; SUGAWARA, Makoto[6]

[1]Hokkaido University of Education Sapporo, [2]Tokai University, [3]Niigata University, [4]Hokkaido University of Education Kushiro, [5]Ryukyu University, [6]Mitsubishi Materials Techno Corporation

The Izu-Bonin arc located western margin of the Philippine sea plate extend to ca. 1200 km south from central Honshu of Japan with ca. 400 km width. The Izu-Bonin arc is a match for NE Honshu arc (Nishimura and Yuasa, 1991). Although volcano lying on the volcanic front (VF) of northern part of this arc expose above the sea level (e.g. Izu Oshima, Miyakejima), almost this arc sink down to sea surface. Active rifts (AR) exist just behind VF with 20-30 km width. These are parallel to the VF and Izu-Bonin Trench and enclosed with escarpment. Ishizuka et al. (2003b) reported Ar-Ar age of igneous rocks dredged from central part of Izu-Bonin arc. According to these age data, recent volcanism (<1Ma) occurred only VF and AR. In this study, we report geochemical data of basalt dredged from Myojin volcano, Myojin rift and Aogashima rift. Basalts exhibit evident across-arc variations. Ba/La ratio, Sr, Nd and Hf isotopic ratios decrease correspondingly distance from Izu-Bonin trench toward rear-arc. Whereas (La/Sm)N increase correspondingly distance from Izu-Bonin trench. Based on ratios of trace elements and each isotopic feature, we conclude that VF basalts generated from flux melting of mantle due to adding aqueous fluid to wedge mantle from subducting slab. On the other hand, genesis of AR basalt is to supply supercritical melt (e.g. Kessel et al. 2005) of slab to wedge mantle. Chromian spinel composition, Cr# of inferred chromian spine equilibrated with mantle is 0.75, held in olivine of VF basalt suggest that residual mantle equilibrated with VF primary magma is dunite. Degree of partial melt of AR basalt decrease correspondingly distance from Izu-Bonin trench toward rear-arc. Tollstrup et al. (2010) interpreted magma genesis of basalt after cessation of Shikoku back-arc basin. They proposed that basalts of western seamount chain (WS) and back-arc knolls (BAK) derived from partial melting of mantle due to adding supercritical melt to mantle wedge from subducting slab, whereas aqueous fluid contributed to partial melting of mantle beneath AR and VF. In their discussion, activity age and activity region are not considered. According to their conclusions, supercritical melt related to genesis of basalts from WS and BAK is not contribute to partial melting of mantle wedge recent volcanism (<1Ma). Bryant et al. (2003) revealed that VF basalt volcanism has continued since 15Ma. Moreover, Ishizuka et al. (2003b) reported volcanism has traveled eastward with time in the central Izu-Bonin arc. It means Izu-Bonin arc volcanism has become narrow range with time. Distinct slab flux between VF and AR in this study suggest that occurrence of supercritical melt is traveling with time toward VF side due to change subducting angle of slab into more steep angle since 15Ma to 3Ma (Honda et al., 2007). Therefore supercritical melt related to genesis of basalt from WS and BAK at predate volcanism contribute to AR recent volcanism.

Keywords: basalt, Izu-Bonin arc, geochemical across-arc variation, Myojin seamount, Aogasima rift, Myojin rift

Japan Geoscience Union Meeting 2014
(28 April - 02 May 2014 at Pacifico YOKOHAMA, Kanagawa, Japan)

SCG67-P13 Room:Poster Time:May 2 16:15-17:30

The variety of silisic rocks around the Myojin volcano, central Izu-Bonin arc

YOSHIDA, Takanori[1*] ; OKAMURA, Satoshi[1] ; SAKAMOTO, Izumi[2] ; ADACHI, Yoshiko[3] ; IKEDA, Yasuo[4] ; SHINJO, Ryuichi[5] ; SUGAWARA, Makoto[6]

[1]Hokkaido University of Education Sapporo, [2]Toukai University, [3]Niigata University, [4]Hokkaido University of Education Kushiro, [5]Ryukyu University, [6]Mitsubishi Materials Techno Corporation

The Izu-Bonin arc located western margin of the Philippine sea plate (PSP) extend to ca. 1200 km south from central Honshu of Japan with ca. 400 km width. The Izu-Bonin arc is a match for NE Honshu arc (Nishimura and Yuasa, 1991). Active rifts (AR) exist just behind volcanic front (VF) with 20-30 km width. These are parallel to the VF and Izu-Bonin Trench and enclosed with escarpment. Generally primitive basalts possibly erupted at oceanic arc volcano without any process in the oceanic crust due to be thinner than continental crust. Although it is well known that Izu-Oshima and Miyakejima, located on VF, erupted basalts, Kouzushima, Niijima and Myojin reef are represented volcanoes which provide mostly felsic products exist on the Izu-Bonin arc VF (Tamura et al., 2009). Nowadays extensive seismic experiments in the Izu-Bonin arc have documented the occurrence of middle crust with P-wave velocity of 6.0-7.0km/s (e.g. Suyehiro et al., 1996). Because of the rock, with P-wave velocity of 6.0-7.0km/s, correspond to tonalite exposed Tanzawa complex Izu collision zone and tonalitic xenoliths in the volcanic rocks sampled VF, inferred middle crust of Izu-Bonin arc composed of tonalitic igneous rocks (Suyehiro et al., 1996). In this study, our aim is to understand mechanism of felsic volcanism contribute to making continental crust. Therefore we consider about felsic rocks dredged from Myojin volcano, Myojin rift and Aogashima rift.

Felsic rocks in this study are divided into three suites (type 1, type 2, type 3) on the basis of Zr/Y versus Zr diagram. Type 1 is lowest Zr/Y ratio trend, type 3 exhibit highest Zr/Y ratio and type 2 have intermediate Zr/Y ratio. Type 1 occur mainly VF, and small amount of type 1 appear AR. Type 2 collected overall from VF to AR. Type 3 occurs only AR.

Although Sr and Nd isotopic compositions of type 1 is similer to the basalt from the VF, Hf isotopic compositions of type 1 differ from VF basalt, and Hf isotopic compositions of type 1 is same as mafic xenoliths in VF lava rather than VF basalt. Isotopic features of type 2 are distinguished from lavas erupted normal-arc magmatism after cessation of Shikoku basin. And Isotopic features of type 2 dredged from more AR-side have higher Nd, Hf isotope ratios. Although Sr and Nd isotopic compositions of type 3 is similer to the basalt from the AR, Hf isotopic compositions of type 3 differ from AR basalt, and isotopic compositions of type 3 is different from lavas erupted normal-arc magmatism after cessation of Shikoku basin and tephra data from ODP boring (Straub et al., 2010).

On the basis of Na2O vs ASI diagram, three type felsic rocks in this study agree with compositions of experimental liquids which derived from basaltic source materials (e.g. Sission et al., 2005). There is possibility that felsic rocks derived from associated basalt. But because of Hf isotope ratio, all felsic rocks are not derived from associated basalt. Therefore all felsic rocks, provided by recent volcanism, are rejuvenated products of old arc crust.

Because of isotopic compositions of type 1 are similer to mafic xenoliths in VF lava, type 1 derived from remelting of arc crust which have postdate VF basalt composition (Bryant et al., 2003). Altough There is possibility that type 2 derived from remelting of Oligocene mafic arc crust, type 2 dredged from more AR-side have higher Nd, Hf isotope ratios. It suggests that AR-side type 2 is possibly affected by PSP. Geochemical data which is similer to type 3 have been found out in previous ODP boring data, and it is possible exist crustal material which is peculiar to AR. We long for IODP projects which start at this year to accumulate new AR crustal material data to consider source of type 3. We propose heterogeneous crust model. It have made by underplating or intrusion of mafic magma derived from mantle into PSP for 50Ma.

Keywords: acidic rock, Izu-Bonin arc, Myojin volcano, Myojin rift, Aogashima rift

Japan Geoscience Union Meeting 2014
(28 April - 02 May 2014 at Pacifico YOKOHAMA, Kanagawa, Japan)

SCG67-P14 Room:Poster Time:May 2 16:15-17:30

General remarks of velocity structures of the Ogasawara Plateau, revealed by the Contineltal Shelf Survey of Japan

KANEDA, Kentaro[1] ; NISHIZAWA, Azusa[1*] ; OIKAWA, Mitsuhiro[1] ; MORISHITA, Taisei[1]

[1]JHOD

Japan Coast Guard conducted seismic refraction surveys with OBSs and multi-channel seismic surveys over more than 10 survey lines on the Ogasawara Plateau which is located on the Pacific Plate, close to a plate boundary to the Philippine Sea Plate. Analysis of these seismic data in 2006-2007 revealed that 1)the Ogasawara Plateau collide and partly accreted with the Philippine Sea Plate, 2)crustal thickness of the Ogasawara Plateau is approximately 25 km, close to that of the Izu-Ogasawara Arc, and 3)low velocity structure in lower crust extends below flat seafloor to the south-east to the plateau.

Recently, re-analyzing of the data by utilizing various later phases and MCS profiles revealed more detailed velocity structure of 1')plate boundary between the Pacific Plate and the Philippine Sea Plate, 2')under plating below the Ogasawara Plateau and 3')low velocity structure distributing around the plateau.

Keywords: velocity structure, Ogasawara Plateau, seismic experiment

Japan Geoscience Union Meeting 2014
(28 April - 02 May 2014 at Pacifico YOKOHAMA, Kanagawa, Japan)

SCG67-P15 Room:Poster Time:May 2 16:15-17:30

Acoustic characterization of abyssal plain, northwestern Pacific region

OKINO, Kyoko[1*] ; HONSHO, Chie[1] ; MACHIDA, Shiki[2] ; OIKAWA, Mitsuhiro[3] ; NAKAMURA, Kentaro[4]

[1]AORI, The University of Tokyo, [2]School of Creative Science and Engineering, Waseda University, [3]Hydrographic and Oceanographic Department, Japan Coast Guard, [4]School of Engineering, The University of Tokyo

The old seafloor covered by pelagic sediment has not attracted large scientific attention and remained untouched for many years, however, the recent studies on intra-plate volcanism as well as the increasing interest in deep-sea natural resources focus spotlight on the abyssal plains. We analyzed the multi-beam bathymetry, beam intensity, and side-scan images of abyssal plain in the northwestern Pacific, around the Minami-Torishima (Marcus) Island. The data were collected by Japan Coast Guard as part of Japanese EEZ survey and by R/V Yokosuka for decades. The beam intensity data from multi-beam echo sounder were processed to create a backscatter mosaic without geometric distortion. The mosaic shows a large variation of acoustic characteristics in whole study area. The high backscattering areas at the foot of large seamounts likely reflect the distribution of volcaniclastic sediments and debris. We can also recognize another type of high backscattering areas in flat seafloor, where neither remarkable seamounts nor knolls exist. The latter type partly corresponds to the area where the high concentration of rare-earth elements were reported and may suggest a thin cover of uppermost soft sediment layer. We try to integrate the backscattering mosaics and the statistic analysis of bathymetry and to establish a new method of acoustic characterization of abyssal plain. We also plan to compare our results with piston core samples as ground references and to discuss the sedimentation process and the relationship with intra-plate volcanism on old seafloor.

Keywords: marine acoustics, muti-beam echo sounder, backscattering intensity, abyssal plain

Japan Geoscience Union Meeting 2014
(28 April - 02 May 2014 at Pacifico YOKOHAMA, Kanagawa, Japan)

SCG67-P16 Room:Poster Time:May 2 16:15-17:30

Spreading stability at the mid-ocean ridges derived from 3D magnetic survey

MATSUMOTO, Takeshi[1*] ; SATOH, Yukitaka[1] ; NOGI, Yoshifumi[2]

[1]University of the Ryukyus, [2]National Institute of Polar Research

The Shipboard Three Component Magnetometer (STCM) has provided vector data of the geomagnetic filed provided detailed information more than total magnetic force measurement. Previous study shows the results about relationship with ocean floor topography and standard deviation of magnetic boundary strike (MBS) calculated from Intensity of the Differential Vectors (ISDV) in Southeast Indian Ridge (SEIR) classified intermediate spreading rate. In this study, the standard deviation of MBS and half spreading rate were analyzed from STCM data in East Pacific Rise (EPR) of fast spreading ridge, Explorer Ridge (ER) and Southeast Indian Ridge (SEIR) classified intermediate spreading ridge and Mid Atlantic Ridge (MAR) categorized as slow spreading ridge. In EPR existing axial high, the results shows that standard deviation and half spreading rate are stable in west of EPR whereas standard deviation and half spreading rate are variability in east of EPR. However standard deviation is low and spreading rate is stable on both sides in MAR developed axial valley. Thus there is no relationship with topographic features and spreading of stability. Additionally, standard deviation of MBS is the low although half spreading rate has variability in ER. The results show differential MBS at the same position in SEIR. As a result, dispersion of MBS is caused by inaccurate measurements of magnetic anomaly. In addition, there is no clear relationship though the simulation was run about plate reconstruction. Therefore spreading stability is controlled by the balance among plate reconstruction, slab pull and magma provided from mantle.

Keywords: mid-ocean ridge, spreading rate, 3D magnetometry

Japan Geoscience Union Meeting 2014
(28 April - 02 May 2014 at Pacifico YOKOHAMA, Kanagawa, Japan)

SCG67-P17 Room:Poster Time:May 2 16:15-17:30

Detailed bathymetry and magnetic anomaly in Central Ryukyu: Implications on westward shift of volcanic front after 2.1Ma

SATO, Taichi[1*] ; ODA, Hirokuni[1] ; ISHIZUKA, Osamu[1] ; ARAI, Kohsaku[1]

[1]Institute of Geology and Geoinformation, Geological Survey of Japan, AIST

Detailed bathymetry and magnetic anomaly were obtained by GH12 cruise in 2012 using R/V Hakurei, in the southern part of Central Ryukyu. Volcanic structures such as caldera were observed on the southwestward extension of the present-day volcanic front, implying recent volcanic front of the Ryukyu arc. Furthermore, bathymetric highs which are sub-parallel to the recent volcanic front were observed and is located ~20 km east. These are accompanied by spotted magnetic anomalies, which continue to Kume-jima via Aguni-jima Islands to the south, suggesting an existence of an ancient volcanic front. The ages of volcanic rocks from these Islands suggest that the magmatic activity along the ancient volcanic front had been active at least until ~2.1 Ma. The magmatic anomalies connecting two volcanic fronts suggest that a volcanic front have moved gradually westward. This shift would be explained by the termination of asthenospheric upwelling and/or rapid retreat of Ryukyu Trench.

Keywords: Ryukyu arc, Volcanic front, Okinawa Trough, magnetic anomaly, seafloor bathymetry

Japan Geoscience Union Meeting 2014
(28 April - 02 May 2014 at Pacifico YOKOHAMA, Kanagawa, Japan)

SCG67-P18 Room:Poster Time:May 2 16:15-17:30

Evolution of depositional basin accompanied by recurring caldera collapses in Kikai caldera, southern-off Kyushu, Japan

IKEGAMI, Fumihiko[1*] ; MINOWA, Yuto[1] ; KURATOMI, Takashi[1] ; KIYOKAWA, Shoichi[2] ; OIWANE, Hisashi[3] ; NAKAMURA, Yasuyuki[4] ; KAMEO, Katsura[5]

[1]Department of Earth and Planetary Sciences, Kyushu University, [2]Faculty of Sciences, Kyushu University, [3]Mishima-mura, [4]JAMSTEC, [5]Atmosphere and Ocean Research Institute, Tokyo University

Kikai caldera (Matsumoto, 1943) is a mostly submerged highly active caldera volcano located in 40 km off Kyushu Island. The caldera is recognized as the product of 7300 cal. BP super-colossal eruption with Akahoya tephra (Machida and Arai, 1978; Fukuzawa, 1995) which is widely distributed along the western part of Japan. Previous studies for near-vent onshore geology strongly suggests such a large eruption was not occurred only once, but multiple times in the Kikai caldera (Ono et al., 1982).

In Kikai caldera, 24 lines of multi-channeled seismic reflection surveys were held in two survey cruises (KT-10-18 and KT-11-11) in 2010 and 2011 using R/V Tansei-maru of JAMSTEC (Japan Agency for Marine-Earth Science and Technology). The acquired seismic data for subseafloor structures spotted thick sedimentary basin at the eastern margin of the caldera. The basin covers 70 square km of the 20 km-wide caldera and is next to caldera rim fault. The infill of the basin is characterized by the group of onlapping stratified deposits named B which maximum thickness is more than 600 m. The B-sequence has two major depositional discontinuities in the middle and the top. The lower one is paraconformity and the upper one is disconformity though, the both of them are associated with similar deformation of the basin itself. The deformation is characterized by 1. Dragged-up reflectors along the caldera rim fault, and 2. Slight outward rotation of the deposits. Both characteristics intensify along the depth, which means lower deposits were experienced much more deformation.

The both two types of the deformation suggest the basin was experienced at least two major subsidence event. The former dragged-up structure is interpreted as the incomplete slip of the caldera rim fault for the relief of the subsidence, while the latter rotation shows the slippages were slightly listric. The displacements of the subsidence events could be estimated from the top and bottom of the dragged-up structures, as more than 100 m in the lower-older event and more than 50 m in the upper-newer event. The subsidence would be an abrupt event, as the paraconformity was formed in the lower-older event. The most likely candidate for such a significant subsidence is caldera collapse. As therefore, the basin might be the one of the pre-caldera structure, and it has been experienced multiple caldera collapse events in the past.

Keywords: caldera, seismic reflection survey, Kikai caldera, Akahoya

Japan Geoscience Union Meeting 2014
(28 April - 02 May 2014 at Pacifico YOKOHAMA, Kanagawa, Japan)

SCG67-P19 Room:Poster Time:May 2 16:15-17:30

Estimates on fluid migration and material recycling via offshore mud volcanoes

KIOKA, Arata[1*] ; ASHI, Juichiro[1]

[1]Atmos. Ocean Res. Inst., U. Tokyo

About 300-400 offshore mud volcanoes are currently confirmed and the double is inferred. Mud volcanism can be viewed as a tectonic window to understand geological frameworks at much greater depth, since mud volcanoes bring up deep substances and fluids to seafloor and are consequently good tools to explore their migration mechanism. Herein we present a global catalog of offshore mud volcanoes and estimate their contributions to subsurface fluid migration and material recycling.

Keywords: Submarine mud volcanoes, fluid migration, material recycling, overpressure

Japan Geoscience Union Meeting 2014
(28 April - 02 May 2014 at Pacifico YOKOHAMA, Kanagawa, Japan)

SCG67-P20 Room:Poster Time:May 2 16:15-17:30

New Marine Sediment Core Database ”COEDO”

NAKANO, Yukihiko[1*] ; ICHIYAMA, Yuji[1] ; HORIKAWA, Hiroki[1] ; TOMIYAMA, Takayuki[1] ; SATO, Yusuke[2] ; KANESHI, Toko[2] ; OGIDO, Eriko[2] ; TAKAESU, Yuki[2] ; NAGAYAMA, Anri[2] ; OSHIRO, Satoshi[2]

[1]Japan Agency for Marine-Earth Science and Technology, [2]Marine Works Japan Ltd.

Japan Agency for Marine-Earth Science and Technology (JAMSTEC) established basic policies on the handling of data and samples (http://www.jamstec.go.jp/e/database/data_policy.html). On the basis of the policies, JAMSTEC provides data and samples in an easily accessible manner. Data and sample information of geological sediment core has been published at ”JAMSTEC Core Data Site” since 2008. In order to improve quality and usability, we reconstructed and released new database in January 2014.

Details of the new database are shown below:

<Name>

COre Electronic Database of Ocean floor (COEDO)

<URL>

http://www.godac.jamstec.go.jp/coedo/e/

<Search Method>

Multiple-filter search using interactive map and basic information filters (Cruise ID, date, location etc.)

In the previous version of the database, users have to take longer steps to reach sample information, because only one of two methods (map search for general users and Cruise ID list menu for science parties) were available. In COEDO, all users can search samples by multiple filters in a single step on a single window.

<On-line accessible data>

Basic information of sediment core (Cruise ID, date of collect, chief scientist, ship name, position, depth), core photo, scanned image, visual core description, X-ray photo, X-ray scanned image, physical property data, literature, link for geochemical data.

We are planning further updates to improve the usability, as follows:

1. Acquiring information of sedimentary ages of core, and making them easily accessible on the database as numerically searchable information.
2. Integration with sample inventory information of JAMSTEC core sample collection, which is currently available at the Kochi Institute for Core Sample Research.
3. Publishing other data, which have not been incorporated into the database yet.

We aim not only improving services to current users, but also making effort to propagate the user community. JpGU and Yokohama city government have a special geological training course for junior/senior high school students at Keio University High School in Yokohama city on April 13. JAMSTEC cooperates with the training course, and provides lecture and practices using actual database and real core samples. In the training course, trainers give lectures on how to obtain marine sediment core onboard and how to study core sample data in COEDO, then trainees observe the actual core samples for which they have just pick up the associated data on the database. The course stimulates trainees’ interest and curiosity on the geological study, and we can nurture the new generation. As a result of this cooperation, we can hopefully increase educational users of JAMSTEC core samples.

Keywords: JAMSTEC, marine sediment core, database, ocean floor, piston corer, geology

Japan Geoscience Union Meeting 2014
(28 April - 02 May 2014 at Pacifico YOKOHAMA, Kanagawa, Japan)

SCG67-P21 Room:Poster Time:May 2 16:15-17:30

Geological Annotation for the Deep-Sea Images

IREI, Kazuhiro[1*] ; OGIDO, Moritaka[1] ; KAYO, Makino[1] ; NAKAMURA, Makoto[1] ; TANAKA, Katsuhiko[2] ; KITAYAMA, Tomoaki[2] ; SAITO, Hideaki[2] ; HANAFUSA, Yasunori[2]

[1]Marine Works Japan LTD., [2]JAMSTEC

The Global Oceanographic Data Center (GODAC) of the Japan Agency for Marine-Earth Science and Technology (JAMSTEC) has been collecting, archiving and disseminating videos and photos acquired by deep-sea research programs using submersibles and remotely operated vehicles owned by JAMSTEC. We register those videos and photos to our database with annotations (keywords), which are names of geological features or organisms, and enable users to search for images of their interest. Those videos and photos with annotations are distributed from the data site called, ″ JAMSTEC E-library of Deep-sea Images (J-EDI)∗1 ″ on the Internet.

Researchers of deep-sea can use the videos and photos distributed by J-EDI as materials for their research or lecture, and also for planning of research cruises or dives, etc. Through the database for marine biodiversity, ″ Biological Information System for Marine Life (BISMaL)∗2 ″ , biological annotations are used to visualize the distribution of organisms or to accumulate the observation record of them, since those videos and photos of deep-sea organisms are not only valuable data, but also indicate the proof of existence of organisms at those points.

We put annotations which can be recognized from the images itself by clicking icons from the prefixed palette or selecting classification name from hierarchical tree. The videos and photos with annotations concerning to the ocean floor geoscience are 41,000 with 95 different kinds of terms out of approximately total 120,000 videos.

To promote the use of deep-sea videos and photos especially in the solid earth science we tried to register more detailed annotations by using scientific papers, reports or documents about research dives and we found that registration of precise annotations takes considerable time. In order to progress the annotating work efficiently we think it necessary to select contents of annotations that lead to an efficient expansion of its use.

In this presentation, we introduce the current status of annotating work for the geological features of the deep-sea and we also show our approach to expand its use.

∗1 http://www.godac.jamstec.go.jp/jedi/
∗2 http://www.godac.jamstec.go.jp/bismal/

Keywords: deep-sea video and photo, geological environments, annotation

Japan Geoscience Union Meeting 2014
(28 April - 02 May 2014 at Pacifico YOKOHAMA, Kanagawa, Japan)

SCG68-01 Room:502 Time:April 30 09:00-09:15

Vp/Vs ratio in the southernmost Japan Basin and its transition area, Japan Sea deduced from the seismic survey

SATO, Takeshi[1*] ; NO, Tetsuo[1] ; KODAIRA, Shuichi[1] ; TAKAHASHI, Narumi[1] ; KANEDA, Yoshiyuki[1]

[1]JAMSTEC

The Japan Sea is one of very well studied back-arc basins in the northwestern Pacific. To clarify the formation process of the back-arc basin in the Japan Sea, many seismic surveys using ocean bottom seismographs (OBSs) and control sources have been conducted in the sea. The Japan Basin, which located in the northern to eastern Japan Sea, has an oceanic crust formed by seafloor spreading (Hirata et al., 1992; No et al., submitted). On the other hand, the ocean-continent transition area between the Japan Basin and the continental shelf in the eastern margin of this sea may have a thick oceanic crust (No et al., submitted). However, it is unknown the origin and the nature of this thick oceanic crust, due to the lack of the information about lithology in the transition area. To understand the origin and the nature of this thick oceanic crust, it is necessary to obtain the information lithology in the crust of the transition and the basin areas. For this study, we will present the Vp/Vs ratio of the crust from the southernmost Japan Basin to its transition area.

From the southernmost Japan Basin to the continental shelf off the west of Aomori and the northern Oga Peninsula, seismic surveys using OBSs and an air-gun array were undertaken. In vertical record sections of several OBSs, not only the first arrived phases but also later phases reflected from interfaces in the crust and uppermost mantle are visible. Moreover, in horizontal record sections of several OBSs, converted phases from P- to S-waves are apparent. In this study, we have obtained the S-wave velocity structure using travel times of these converted phases. Then, we have obtained the Vp/Vs ratio in the crust from the southernmost Japan Basin to its transition area using the obtained P- and S-wave velocity structures.

In the southernmost Japan Basin off west of Aomori, the Vp/Vs ratio in the sedimentary layer of shows 4 to 8 and has a lateral variation. The Vp/Vs ratios in the crustal upper and lower parts show around 1.85 and 1.8, respectively. On the other hand, in the transition area, the Vp/Vs ratio in the crustal upper part is similar to that in the southernmost Japan basin. This Vp/Vs ratio may show that the nature of the whole crust in the basin area and of the crustal upper part in the marginal area has an oceanic origin. Therefore, the crusts in southernmost Japan Basin and in its transition area are suggested as an oceanic crust and a thick oceanic crust, respectively. The oceanic crust formed by the opening of the Japan Sea may extend to the transition area of the southernmost Japan Basin.

Japan Geoscience Union Meeting 2014
(28 April - 02 May 2014 at Pacifico YOKOHAMA, Kanagawa, Japan)

SCG68-02 Room:502 Time:April 30 09:15-09:30

Crustal structure study of the Sea of Japan: Recent results and future perspectives

NO, Tetsuo[1*] ; SATO, Takeshi[1] ; KODAIRA, Shuichi[1] ; ISHIYAMA, Tatsuya[2] ; SATO, Hiroshi[2] ; TAKAHASHI, Narumi[1] ; OIKAWA, Nobutaka[1] ; KANEDA, Yoshiyuki[1]

[1]JAMSTEC, [2]ERI, Univ. of Tokyo

In recent years, crustal structure study of the Sea of Japan has advanced. Various new seismic data have been obtained in the Sea of Japan; for example, the two ship seismic surveys study (Sato et al. 2007) and onshore-offshore seismic survey (Earthquake Research Institute, 2013) conducted by the University of Tokyo, and 2D/3D seismic reflection survey conducted by R/V SHIGEN (JOGMEC, 2013).

From 2007 to 2012, we conducted marine seismic surveys using the multichannel seismic reflection system and ocean bottom seismometers; the surveys covered the area between the Japanese coast of the Sea of Japan and the Yamato and Japan Basins. Based on the results, the crustal structure of the eastern margin of the Sea of Japan was classified into three types: island arc crust, thick oceanic crust, and oceanic crust (Sato et al. 2014; No et al. submitted). In addition, our studies found that the contractive deformation zones of the eastern margin of the Sea of Japan are associated with the crustal structure distribution. Further, seismic data suggests that the crustal structure in the south (off Yamagata to Niigata) differs from that of the north (off Akita to Nishi-tsugaru). These differences are critical in understanding the relation between the spatial distributions of the seismogenic and contractive deformation zones (JAMSTEC, 2013). These results can contribute to the review of long-term evaluations of earthquake occurrence potentials and the discussion of the seismogenic study in the eastern margin of the Sea of Japan.

In 2013, new projects have been observing and studying earthquakes and tsunamis in the Sea of Japan. *Integrated Research Project on Sei* scheduled in 2014 in order to conduct a seismic survey in the blind areas of the existing observations, which are in the southwest region of the Sea of Japan and off western Hokkaido. The addition of new observation data will advance the study of crustal structure in the Sea of Japan. In this study, we aim to improve the accuracy of the position and size of the source faults in the Sea of Japan. In addition, we investigate the relation among tectonic history, crustal structure, and factors that form source faults in the Sea of Japan. In the future, we aim to clarify the seismogenic zone of the Sea of Japan using new seismic data.

Keywords: the Sea of Japan, crustal structure, MCS, OBS

Japan Geoscience Union Meeting 2014
(28 April - 02 May 2014 at Pacifico YOKOHAMA, Kanagawa, Japan)

SCG68-03 Room:502 Time:April 30 09:30-09:45

Results of 2013 Off-Joetsu and Hokuriku survey for the integrated research project on seismic and tsunami hazards around

SATO, Hiroshi[1*] ; ISHIYAMA, Tatsuya[1] ; SHIRAISHI, Kazuya[2] ; ABE, Susumu[2] ; KATO, Naoko[1] ; KURASHIMO, Eiji[1] ; TAKEDA, Tetsuya[3]

[1]Earthquake Research Institute, Univ. Tokyo, [2]JGI. Inc., [3]NIED

An obvious convergent plate boundary cannot be recognized in the Sea of Japan, and convergence accommodates in defused wide area of the back arc. To estimates Tsunami and seismic hazards along the coastal area of Sea of Japan, more detailed survey to identify source faults are needed. A new research project funded by MEXT named ”the integrated research project on seismic and tsunami hazards around the Sea of Japan” began in FY 2013. To obtain the information of source faults, we performed deep seismic reflection profiling off-Joetsu and Hokuriku area in the central part of Honshu, Japan. We used two vessels; a gun-ship with 3020 cu. inch air-gun and a cable-ship with a 2-km-long, streamer cable with 156 channels and 480 cu. inch air-gun. Common-mid point reflection data were acquired along 9 seismic lines with total 715 km in length. The seismic profiles portray the structure of failed rift basins, such as Toyama trough and Sado strait, bounded by rift axis reverse faults with rift axis vergence, which represents reactivation of boundary faults between mafic intrusion and pre-rift basement. Noto Peninsula is marked by syn-rift normal faults and their reactivation by shortening deformation. The back arc side of the SW-Japan arc experienced NS trending shortening deformation in the latest Miocene. From the Noto peninsula, undeformed Pliocene sediments covers folded Miocene. Some normal faults reactivated as active strike-slip and reverse faults. The survey results contributed to construct source faults models of Tsunami and seismic hazards estimation.

Keywords: Sea of Japan, source fault, crustal structure, seismic reflection profiling, Off-Joetsu, off-Hokuriku

Japan Geoscience Union Meeting 2014
(28 April - 02 May 2014 at Pacifico YOKOHAMA, Kanagawa, Japan)

SCG68-04 Room:502 Time:April 30 09:45-10:00

Lithospheric Structure of the Hidaka Collision Zone, Hokkaido, from Reanalysis of 1998-2000 Hokkaido Transect Data IV

IWASAKI, Takaya[1*] ; TSUMURA, Noriko[2] ; ITO, Tanio[3] ; SATO, Hiroshi[1] ; KURASHIMO, Eiji[1] ; HIRATA, Naoshi[1] ; ARITA, Kazunori[4] ; NODA, Katsuya[5] ; FUJIWARA, Akira[5] ; ABE, Susumu[5] ; KIKUCHI, Shinsuke[6] ; SUZUKI, Kazuko[7]

[1]Earthquake Research Institute, the Univsesity of Tokyo, [2]Chiba University, [3]Teikyo Heisei University, [4]Hokkaido University, [5]JGI. Inc., [6]JAPEX, [7]Schlumberger Ltd.

The Hidaka region in the central part of Hokkaido Island, Japan, is known as an arc-arc collision zone ongoing from the middle Miocene. In 2012, we started reinterpretation for a series of seismic reflection/refraction surveys from 1994 to 2000 in this collision zone. In this analysis, we used integrated and sophisticated processing and analysis techniques. including CRS/MDRS method for seismic reflection data and refraction tomography both very dense arrival time data from both the reflection and refraction/wide-angle reflection data. The most important finding so far obtained is a clear image of the NE Japan Arc subducting eastward under the northern part of the collision zone. However, the following problems are remained unsolved.

(1) Shallow structure beneath the Hidaka Collision zone is still unsolved. Particularly, the structure just east of the Hidaka Main Thrust is not sufficiently evaluated from our seismic data.
(2) Delamination of the Hidaka crust as in the southern part of this collision zone is not unclear. Our CRS/MDRS processing for the reflection data provided no positive evidence for the delamination.
(3) Deeper collision structure of the NE Japan Arc and the Kuril Arc is still not constrained. It is necessary to elucidate the subducting structure of the NE Japan Arc from amplitude data as well as travel time data.

In this paper, we focus the items (1) and (3) from seismic refraction/wide-angle reflection approach. Previous refraction tomography elucidated a thick (4-5 km) undulated sediments in the hinterland, the outcrop of crystalline crust beneath the Hidaka Metamorphic Belt with higher Vp and Vp/Vs and an enormously thick (>8-10 km) sedimentary package beneath the foreland. In order to obtain the more reliable structure model, we intensively revised the travel time data obtained both from seismic reflection/wide-angle reflection line and reflection lines. The seismic tomography using these revised data sets indicate a clearer high velocity (>6.1 km/s) anomaly just east of the HMT. We also recognized some wide-angle reflections around 5-10 km deprth beneath the HMT, from which we expect to determine the finer structure at the collision front. Our present analysis indicates the wide-angle reflection data sample a part of the lower crust of the subducting NE Japan Arc beneath the fold-and-thrust belt. According to the preliminary result, its velocity is ranging from 6.5-7.0 km/s. By combining the amplitude analysis, we expect to estimate the more reliable Moho depth of the NE Japan Arc than in the previous analyses.

Keywords: active source seismic experiment, collision, arc, crustal structure, lithosphere

Japan Geoscience Union Meeting 2014
(28 April - 02 May 2014 at Pacifico YOKOHAMA, Kanagawa, Japan)

SCG68-05 Room:502 Time:April 30 10:00-10:15

Seismic crustal structure beneath the southeastern part of northeast Japan by dense seismic array observation

KURASHIMO, Eiji[1*] ; SATO, Hiroshi[1] ; ISHIYAMA, Tatsuya[1] ; HIGASHINAKA, Motonori[2] ; ABE, Susumu[2] ; IWASAKI, Takaya[1]

[1]ERI, Univ. Tokyo, [2]JGI, Inc.

The 2011 Tohoku-Oki Earthquake (Mw9.0), that occurred on the Japan Trench off the eastern shore of northern Honshu, Japan, generated enormous crustal deformations. Seismic activity in northeastern Japan increased significantly after the 2011 Tohoku-Oki Earthquake. Detailed crustal structure and deep geometry of the active fault is important to constrain the process of earthquake occurrence. Active and passive seismic experiments were conducted to obtain a structural image beneath the southeastern part of NE Japan (Sato et al., 2013). The geometry of the active faults have been revealed by seismic reflection profiling (Sato et al., 2013). Natural earthquake data set is useful to obtain a deep structural image. Forty portable seismographs were deployed along a 70-km-long line between Souma and Takahata during the period from August 16, 2012 to December 24, 2012. Each seismograph consisted of a 1-Hz 3-component seismometer and off-line data recorder (Shinohara et al., 1997). Waveforms were continuously recorded at a sampling rate of 200 Hz. In the area of the present study, deep seismic reflection profiling was conducted using vibrators (Sato et al., 2013). The off-line recorders observed the controlled seismic signals as well as natural earthquakes. During the seismic array observation, the JMA located 2956 earthquakes in a latitude range of 37.2-38.5 N and a longitude range of 139.6-141.3 E. We selected 200 earthquakes, all of which occurred near the survey line. In order to obtain a high-resolution velocity model, a well-controlled hypocenter is essential. Due to this, we combined the seismic array data with permanent seismic station data. The arrival times for the first P- and S waves obtained from local earthquakes and Vibrator shots were used in a joint inversion for earthquake locations and three-dimensional Vp and Vp/Vs structures, using the iterative damped least-squares algorithm, simul2000 (Thurber and Eberhart-Phillips, 1999). Permanent seismic stations observed the controlled seismic signals as well as natural earthquakes. We added the arrival time data of these controlled sources into the dataset to improve the shallow velocity structure. The depth section of Vp structure along the survey line shows that lateral variation of the Vp value at a shallow depth. This lateral variation correlates with the surface geology along the profile.

Keywords: dense seismic array observation, seismic tomography, the 2011 Tohoku-Oki Earthquake

Japan Geoscience Union Meeting 2014
(28 April - 02 May 2014 at Pacifico YOKOHAMA, Kanagawa, Japan)

SCG68-06 Room:502 Time:April 30 10:15-10:30

Shallow geologic structure around the northern part of the Futaba Fault, northeast Japan, based on gravity survey

KOSHIYA, Shin[1*] ; TERUI, Kyoko[2] ; YONEZAWA, Kenta[1] ; SATO, Hiroshi[3] ; KATO, Naoko[3] ; ABE, Susumu[4] ; HIGASHINAKA, Motonori[4]

[1]Faculty of Engineering, Iwate Univ., [2]Graduate School of Engineering, Iwate Univ., [3]ERI, Univ. of Tokyo, [4]JGI, Inc.

The Futaba Fault, bounding the eastern margin of the Abukuma Mountains, is known as a left lateral fault in the Cretaceous and Paleogene period with a remarkable fracture zone of a few hundreds meter win width. It trends NNW-SSE and divides into two branches between which the Wareyama horst develops. During early to middle Miocene, E-W extensional stress field caused large normal displacement along the western fault to form a half graben filled with sediments including breccia. In late Miocene, it had been a right lateral fault. In present, the eastern fault is active, along which left lateral offsets with western upheaval ingredient are geo-morphologically observed. Thus the Futaba Fault has experienced the complicated history of development. In this study, we modeled two dimensional shallow geological structure across the faults mainly based on gravity survey. The gravity survey was conducted across the faults with a G-type gravity meter (G827; LaCoste and Romberg Inc.) along two E-W survey lines, one of which is ca. 12 km long, (line 1), and the other of which is ca. 13km long (line 2). Each interval of observation sites is about 200 m. The elevation of observation sites was surveyed with a electric level and a RTK-GPS. Acquired gravity data was processed to obtain Bouguer anomaly mostly according to the methodology of Geological Survey of Japan, AIST (2004). We assumed that the density for Bouguer and terrain corrections were 2.2 g/cm^3. In each survey line, Bouguer anomalies after trend correction show the highest value around the Wareyama horst consisting of pre-Paleogene basement rocks and a few maxima in the western side of the horst. We assume four layers in our model, which have densities of 2.00 g/cm^3 (layer 1), 2.2 g/cm^3 (layer 2), 2.55 g/cm^3 (layer 3), and 2.67 g/cm^3 (layer 4) , respectively. The interpretation of the model is as follows. Layer 1 is correlated to the surface covers and Pliocene sedimentary rocks, layer 2 lower to middle Miocene sedimentary rocks, layer 3 Miocene breccia and layer 4 basement rocks. We will discuss the shallow structure across the faults in detail.

Keywords: Futaba fault, gravity anomaly, active fault

Japan Geoscience Union Meeting 2014
(28 April - 02 May 2014 at Pacifico YOKOHAMA, Kanagawa, Japan)

SCG68-07 Room:502 Time:April 30 10:30-10:45

Structural characters of active faults, crustal architecture, and permanent deformation of the Hokuriku region

ISHIYAMA, Tatsuya[1*] ; SATO, Hiroshi[1] ; KATO, Naoko[1] ; TAKEDA, Tetsuya[2] ; KURASHIMO, Eiji[1]

[1]Eathquake Research Institute, University of Tokyo, [2]NIED

We discuss in this study about characters of crustal architectures around the Toyama trough revealed by new seismic reflection and refraction profiles and seismic tomography, and active structures based on Neogene geology and tectonic geomorphology. As revealed by onshore offshore deep seismic reflection profiling across the Toyama trough funded by MEXT named as The Integrated Research Project on Seismic and Tsunami Hazards around the Sea of Japan since 2013, crustal architectures across the Toyama trough is characterized by three domains: (1) crustal thrust wedge comprising the northwestern flanks of the Hida Mountains, (2) Neogene sedimentary basin near the axis of the Toyama trough, and (3) reactivated normal faults as thrust (or obliquely slipping) faults beneath the Noto peninsula, comprising structural higher domain west of the Toyama trough. These structural patterns and permanent, late Quaternary crustal deformation recorded by tectonic geomorphology are quite similar to adjacent Neogene sedimentary basins in the backarc failed rifts in the Sea of Japan, including northern Fossa Magna, Niigata, and Akita.

Japan Geoscience Union Meeting 2014
(28 April - 02 May 2014 at Pacifico YOKOHAMA, Kanagawa, Japan)

SCG68-08 Room:502 Time:April 30 11:00-11:15

Phase changes and temperature of the subducted crust of Philippine Sea slab beneath Kanto, Japan

ISHIKAWA, Masahiro[1*] ; NAKAGAWA, Shigeki[2] ; SAKAI, Shin'ichi[2] ; HIRATA, Naoshi[2] ; SATO, Hiroshi[2] ; KASAHARA, Keiji[3]

[1]Graduate School of Environment Information Sciences, Yokohama National University, [2]Earthquake Research Institute, The University of Tokyo, [3]Association for the Development of Earthquake Prediction

The Philippine Sea plate subducts beneath the Greater Tokyo Area of Japan. Devastating M8-class earthquakes occurred on the upper surface of the Philippine Sea plate, examples of which are the Genroku earthquake of 1703 (magnitude M8.0) and the Kanto earthquake of 1923 (M7.9). A M7 or greater (M7) earthquake in this region may occur either on the upper surface or intra slab of Philippine Sea plate. To evaluate seismic hazard in the Greater Tokyo Area of Japan we need to clarify the lithological properties of Philippine Sea slab. This study presents an interpretation of the crustal and mantle structure of the Philippine Sea slab beneath Kanto based on recent MeSO-net seismic tomography data. The seismic tomography reveals that P wave velocity of the subducted crust of the Philippine Sea slab increases stepwise at 30 km and 40 km depths beneath the Kanto area. The cause of these two stepwise increases in P wave velocity of subducted crust is expected to correspond to metamorphic phase changes. Mineralogical assemblages of forearc basalt composition of the Izu arc was calculated by Theriak-Domino software, and the phase diagram shows that phase changes to garnet amphibolite and eclogite can account for these two stepwise increase in P wave velocity of the subducted crust of the Philippine Sea slab.

Keywords: slab, phase change, slab temperature, Kanto, Philippine Sea Plate, crust

Japan Geoscience Union Meeting 2014
(28 April - 02 May 2014 at Pacifico YOKOHAMA, Kanagawa, Japan)

SCG68-09 Room:502 Time:April 30 11:15-11:30

Geologic structure in and around the Beppu Bay estimated by gravity analysis

YAMAKITA, Satoshi[1*] ; KUDO, Takeshi[2] ; ITO, Tanio[3]

[1]University of Miyazaki, [2]Chubu University, [3]Teikyo-Heisei University

Seismic profiling in the Beppu Bay and the Bungo Straight performed by Kyoto University and JGI inc. from 1988 to 1990 (Yusa et al., 1992) raised new progresses of studies on the geologic structure of the Median Tectonic Line (MTL) in Kyushu and the development of the Beppu Bay Sedimentary Basin (BSB) accompanying it (Yamakita et al., 1995; Ito et al., 1996). The P-wave velocity assumed by Yusa et al. (1992) for the rocks in Ryoke Belt, however, was too low for granitic and metamorphic rocks constituting this Belt, and it is likely that the dip of the MTL beneath it was underestimated. Besides, the structure of the basin in the innermost part of the Beppu Bay has remained uncertain because this part is located in the terminal part of the seismic lines. On the other hand, there are plenty of gravity data in and around the Beppu Bay (Yusa et al., 1992; GSJ, 2000; Gravity Research Group in Southwest Japan, 2001). It can be expected that these gravity data clarify the structure of BSB, combined with correct seismic profiles. Fortunately, a profile reprocessed with re-estimated P-wave velocity along the Bungo straight (J-line) was presented last year (Abe et al., 2013). Using this reprocessed profile and gravity data, we tried to determine the subsurface structure along the G-line of Yusa et al. (1992), trending N70E, 35 km long, from on-land area, across the Asamigawa fault (AF) and the Beppu Bay Central Fault (BCF), to the mouth of the Beppu Bay (Fig. A), occupied by Sanbagawa metamorphic rocks (Sm, ρ=3.0g/cm^3), Ryoke granitic and metamorphic rocks (Rk, ρ=2.8g/cm^3), lower (Bl, ρ=2.6g/cm^3) and upper (Bu, ρ=2.4g/cm^3) sediments of BSB. Assuming only the depth and form of the MTL estimated from the reprocessed profile of J-line and geologic constraints, and the position of the AF on the surface, we determine other subsurface structures to fit with the gravity data through traial and error (Fig. B). In this profile, the upper surface of the Ryoke basement almost coincides with that in the Yusa et al. (1992)'s profile. This fact suggests high reliability of this profile. We concluded the structure of BSB from this and Yusa et al.(1992)' s profiles as follows.

1. The innermost part of the BSB was formed by two listric normal fault systems, NE-dipping Asamigawa Fault System (AFS) and SW-dipping Beppu Bay Central Fault System (BCFS). Both systems formed roll-over structure in the sediments of BSB.
2. The AFS consists of three faults (I, II, III), which converge to the MTL. It is uncertain whether the fault AFS-II reaches the uppermost part of the sediments. The total amount of the vertical displacement of ASF may be up to 3000m, although it depends on the thickness of sediment in the SW-side on AF and the amount of erosion of Ryoke basement
3. Two faults BCFS-I and BCFS-II vertically displaced the bottom of the Bu in 250m and 150m respectively and reach the uppermost part of it, although it is difficult to recognize in this figure because of its highly reduced scale. Both, however, did not displace the bottom of the Bl (= the upper surface of the Ryoke basement).
4. BSB is inferred to be formed and developed by eastward movements of the hanging wall (Ryoke basement), strike-slip on the MTL and downward on the AF. The BCFS was secondarily formed in eastward moving sediments.

These results are almost concordant with the model of a strike-slip basin proposed by Yamakita and Ito (1999), which assume a not vertical but moderately dipping strike-slip fault with a releasing bend. This model ignored the effects of secondary listric normal faults in sediments, dipping toward the main oblique normal fault forming the oblique ramp, but they contributed to the development of BSB to some extent. Their effects, however, are rather small as indicated by the fact that they did not displace the basement.

Keywords: Gravity analysis, Beppu Bay, MTL, Asamigawa Fault, Beppu Bay Central Fault

SCG68-09 Room:502 Time:April 30 11:15-11:30

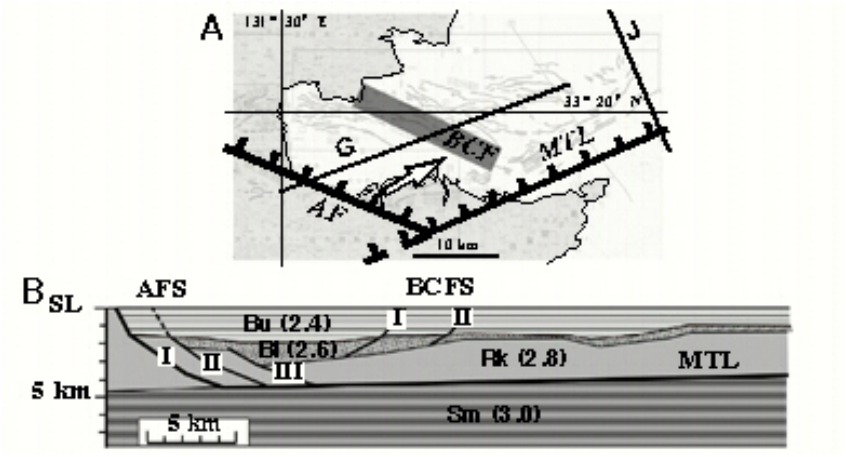

Japan Geoscience Union Meeting 2014
(28 April - 02 May 2014 at Pacifico YOKOHAMA, Kanagawa, Japan)

SCG68-10 Room:502 Time:April 30 11:30-11:45

Structure and evolution of the lower crust constrained from alkaline basalts and xenoliths in southwest Japan

IGATA, Eri[1*] ; OMORI, Soichi[2] ; IWAMORI, Hikaru[3]

[1]Department of Earth and Planetary Sciences, Tokyo institute of technology, [2]The open university of Japan, [3]Japan Agency for Marine-Earth and Technology

The continental crust is unique to the Earth and, in spite of its small mass, is geochemically an important reservoir, concentrating about half of the radiogenic heat producing elements. In order to understand the differentiation history of the Earth, it is essential to decipher how and when the continental crust has been formed.

In contrast to the upper continental crust, which has been well surveyed with direct means, the lower continental crust is largely unknown in terms of composition, mineralogy and age distribution of formation. In this study, we investigate the xenoliths that have been derived possibly from the lower crust, in terms of petrology (mineral assemblages and their composition, modal abundances and bulk composition) and geochronology (zircon U-Pb age dating of both the xenoliths and the host basalt). Study area is located on the Kibi Plateau in southwest Japan. The xenoliths are classified into 4 types by petrography and EPMA analysis; Type 1, pyroxenite; Type 2, eclogitic gabbro; Type 3, anorthosite: Type 4, kyanite/garnet-bearing felsic granulite. Pseudosection and mineral stability analyses were performed by a thermodynamic program "Perplex". These analyses have revealed that pyroxenite is stable beneath the Moho and its seismic velocity estimated from pseudosection ranges from 7.23 to 7.65 km/s. Therefore pyroxenite corresponds to the olivine-pyroxenite layer under the Moho. Gabbro was formed at 8-10 kbar and 873-940 K and its velocity is higher than pyroxenite. Granulite is stable at 7.5- kbar and about 1000 K and its velocity is very low. In spite of the density gap between the eclogitic gabbro and granulite (3900 and 2740 kg/m^3), the analysis suggests that the felsic granulite exhibits a higher equilibration pressure and may even underlay the eclogitic gabbro. Moreover, composition of the lower crust becomes more felsic than previously thought.

Ages of the eclogitic gabbro xenolith and the host basalt coincide, showing 70 Ma. It is argued that the subducted sediments (now appear as felsic granulites) were subdcuted and underplated to the bottom of the lower crust during the last 30 million years or so. If such a mechanism operates worldwide, then the continental crust may have an intermediate to felsic composition even without a hypothetical process of lower crustal delimitation.

The authors thank T. Hirata, K. Tani, Jl. Kimura and Q. Chang for U-Pb zircon age dating.

Japan Geoscience Union Meeting 2014
(28 April - 02 May 2014 at Pacifico YOKOHAMA, Kanagawa, Japan)

SCG68-11 Room:502 Time:April 30 11:45-12:00

Three-dimensional seismic velocity structure beneath East Asia using adjoint tomography

MIYOSHI, Takayuki[1*] ; OBAYASHI, Masayuki[1] ; TONO, Yoko[1] ; TSUBOI, Seiji[1]

[1]JAMSTEC

East Asia is the complicated region where tectonic plates meet. In many studies, travel-time tomography based on ray theory has clarified three-dimensional (3D) velocity structure of the Earth. On the other hand, the recent studies show waveform inversion based on wave theory can construct realistic 3D structure (e.g. Obayashi et al., 2010 SSJ; Miyoshi et al., 2013 SSJ). In the present study, we have inferred 3D heterogeneous structure precisely beneath the eastern Asia region by using adjoint tomography method. We selected 161 earthquakes (M >5.5, half duration <5 second) occurred in the region based on Global CMT catalog. Displacement seismograms used in this study were recorded at broadband seismic stations in the region. The average number of stations used in inversion is about 180. Theoretical waveforms were calculated using the spectral-element method (Komatitsch and Tromp, 2001). We used GAP-P2 mantle tomography model (Obayashi et al., 2009) as an initial 3D model of inversion. Both observed and theoretical waveforms were filtered between 12.5 and 100 second to extract time windows of P- and S-waves, and between 30 and 150 second to extract time windows of surface waves. We applied adjoint method (Liu and Tromp, 2006) for calculating the misfit kernel, which is related to velocities, and performed inversion by using the steepest descent method. The parallel computing of theoretical waveforms and misfit kernels were used 256 CPU cores of supercomputers, such as K computer at Riken. The computing time was required 0.1 million CPU hours in each iteration. We have iterated four times on inversion. The VR value was improved about 10% by using the revised model. The Vp and Vs of improved model showed a few percent slower than the initial model. The ratios of the velocity perturbation show slightly large value than the initial model at a depth of 100 km in a wide area of the eastern Asia region. Acknowledgements: We used F-net seismograms of the National Research Institute for Earth Science and Disaster Prevention. This study was supported by the strategic Programs for Innovative Research ”Field 3” Advanced prediction Researches for Natural Disaster Prevention and Reduction.

Keywords: adjoint method, tomography, velocity structure, East Asia

Japan Geoscience Union Meeting 2014
(28 April - 02 May 2014 at Pacifico YOKOHAMA, Kanagawa, Japan)

SCG68-12 Room:502 Time:April 30 12:00-12:15

Seismological evidence for a transition from ”hydrous” oceanic crust to typical oceanic crust in the Lau back-arc basin

ARAI, Ryuta[1*] ; DUNN, Robert[1]

[1]University of Hawaii

The Lau back-arc basin, associated with subduction of the Pacific plate beneath the Indo-Australian plate at the Tonga Trench, provides a superb study area to understand the interaction between plate subduction and back-arc spreading: Subducting oceanic lithosphere induces mantle corner flow within the mantle wedge above the subducting plate and releases a large amount of water and other elements into this wedge, producing heterogeneous chemical compositions and fluid gradients beneath the back-arc basin. While petrological studies suggest that the heterogeneity in the mantle source composition, mainly caused by slab-derived fluids, plays an important role for melt supply to the back-arc ridges, variations in thickness and internal structure of crust formed along back-arc ridges are poorly documented. On the basis of seismic tomography analyses, we present a structural model of crust formed along the Eastern Lau Spreading Center within the Lau back-arc basin as evidence for a transition from a “ hydrous ” type of oceanic crust to a more typical oceanic crust. The seismic data indicate that as the back-arc spreading center moved away from the active arc, the crust thinned from 8-9 km to ˜7 km, the lower crust changed from high P wave velocity values (7.2-7.4 km/s) to typical values for oceanic crust (7.0-7.2 km/s), and the upper-crustal volcanic layer changed from a thick low-velocity layer to a thinner layer with more typical wave speeds. The seismic results, in combination with other geophysical and geochemical data, suggest that crustal formation along the ELSC is strongly controlled by the influence of slab water: When a spreading center is near the active arc, water from the downgoing slab is entrained in the melting zone beneath the back-arc ridges where it enhances melting. Thereafter, the water enhances crustal differentiation within sub-ridge magma chambers. This creates an anomalous “ hydrous ” form of oceanic crust with a thick felsic volcanic layer and a mafic/ultramafic lower crust - features that are not typically observed in crust formed at mid-ocean ridges. The Lau basin has a zoned structure with an abrupt transition from this type of oceanic crust to more typical oceanic crust, which resulted from a rapid change in the influence of slab water as the ridge moved away from the arc. The unique geodynamic setting of the Lau basin, such as proximity of the back-arc ridges to the volcanic arc (<100 km), the relatively low subduction angle of the slab (˜45 degrees), and the fast subduction rate at the Tonga trench (>20 cm/yr), probably operate to effectively deliver slab-derived water far beyond the volcanic arc to the back-arc ridges and produce this “ hydrous ” oceanic crust in the back-arc basin. The abundance and high rate of production of the “ hydrous ” crust suggests that such crust may make up a significant proportion of the arc-like crust that forms continents.

Keywords: Back-arc basin, Crustal differentiation, Oceanic crust, Slab water, Seismic tomography, Eastern Lau Spreading Center

Japan Geoscience Union Meeting 2014
(28 April - 02 May 2014 at Pacifico YOKOHAMA, Kanagawa, Japan)

SCG68-P01 Room:Poster Time:April 30 18:15-19:30

Tectonic province of the northern Fossa Magna region based on the crustal movement and seismic activity

IMAI, Yuki[1*] ; TAKEUCHI, Akira[2]

[1]Graduate school of Science and Engineering for Education, University of Toyama, [2]Graduate school of Science and Engineering for Research, University of Toyama

The northern Fossa Magna region is located in an area where the Niigata-Kobe tectonic zone (Sagiya *et al.*, 2000) and geological strain concentration zone along the eastern margin of the Japan Sea (Okamura, 2002) is duplicated. In the past, inland crustal earthquakes, such as the Zenkoji earthquake in 1847 (M7.4) and the Niigata-ken Chuetsu earthquake in 2004 (M6.8), have occurred in this region. In order to discuss the current tectonics of the northern Fossa Magna region that has active crustal movement and seismic activity, it is necessary to clarify the characteristics of ”tectonic province”. The purpose of this paper is to reveal a detailed three-dimensional tectonic province model from the crustal movement and seismic activity of this region in the recent years. In order to clarify the characteristics of crustal movement and seismic activity, we have analyzed the GEONET observation data (from October 2007 to March 2011) using the GAMIT 10.4 software, and made the E-W cross-sectional view of the JMA hypocenter data.

The horizontal strain distribution for three and a half years just before the 2011 Tohoku-Oki earthquake shows that strain concentration zone with NW-SE directional contraction extends from the Niigata plain to the Matsumoto basin continuously. Moreover, the eastern margin of this zone corresponds roughly to the position of the Shibata-Koide tectonic line (Yamashita, 1970) running NNE-SSW direction in the eastern margin of the Niigata plain. The strain rate in the Echigo mountain range is smaller than in the Niigata plain. Takeuchi (1999) showed tectonic province based on the activity and characteristics of active faults. The strain distribution revealed from GPS data corresponds approximately to active faults provinces. The large and small strain region corresponds approximately to the reverse fault province (Shin’etsu ˜Niigata sedimentary basin) and strike-slip faults province (Central upheaval zone and Echigo mountain range) respectively. Focusing on the depth distribution of the seismogenic layer in the E-W cross-section, the depth of the lower limit of seismogenic layer is shallow (D = 10-15 km) in the strike-slip province but is deeper (D = 20-30 km) in the reverse fault province. The seismogenic layer is located beneath the low P-wave velocity zone corresponding to the thick sediments layer in the sedimentary basin.

According to the above results, there is obvious spatial variation of the depth of seismogenic layer and strain distribution at the boundary of the sedimentary basin and Central upheaval zone. It is conceivable that two different tectonic provinces are adjacent along the tectonic boundary where characteristics of the crustal activity are changing greatly. The moderate-large crustal earthquakes around the northern Fossa Magna, such as the Zenkoji earthquake in 1847, the Niigata-ken Chuetsu earthquake in 2004 and the Nagano-ken Hokubu earthquake in 2011, have occurred on or near the tectonic boundary. Stress concentration is likely to occur due to large changing of the physical properties in the tectonic province boundary, and a large crustal earthquake tend to occur at the tectonic province boundary than at the inside province.

Keywords: tectonic province, northern Fossa Magna, crustal movement, seismic activity, seismogenic layer

Japan Geoscience Union Meeting 2014
(28 April - 02 May 2014 at Pacifico YOKOHAMA, Kanagawa, Japan)

SCG68-P02 Room:Poster Time:April 30 18:15-19:30

Results of 2013 Off-Kanazawa and Noto peninsula survey for the integrated research project on seismic and tsunami hazard

SATO, Hiroshi[1*] ; ISHIYAMA, Tatsuya[1] ; SHIRAISHI, Kazuya[2] ; ABE, Susumu[1] ; KATO, Naoko[1] ; IWASAKI, Takaya[1]

[1]Earthquake Research Institute, Univ. Tokyo, [2]JGI. Inc.

To estimates Tsunami and seismic hazards along the coastal area of Sea of Japan, more detailed survey to identify source faults are needed. A new research project funded by MEXT named ”the integrated research project on seismic and tsunami hazards around the Sea of Japan” began in FY 2013. To obtain the information of source faults, we performed deep seismic reflection profiling off-Kanazawa and Noto area in the central part of Honshu, Japan. The source faults were estimated together with the results of seismic sections in the epicentral area of the 2007 Noto peninsula earthquake (Sato et al., 2007, BERI). We used two vessels; a gun-ship with 3020 cu. inch air-gun and a cable-ship with a 2-km-long, streamer cable with 156 channels and 480 cu. inch air-gun. Common-mid point reflection data were acquired along 4 seismic lines with total 245 km in length. The seismic profiles portray the reactivation of normal faults, which formed during syn-rift periods, associated with the opening of the Sea of Japan. 2007 Noto peninsula earthquake occurred by the oblique motion on source fault dipping 60 degrees, which is favorable normal faulting. The back arc side of the SW-Japan arc experienced NS trending shortening deformation in the latest Miocene. From the Noto peninsula to the west, undeformed Pliocene sediments covers folded Miocene. Some normal faults reactivated as active strike-slip and reverse faults in Quaternary. The survey results contributed to construct source faults models of Tsunami and seismic hazards estimation.

Keywords: Sea of Japan, source fault, crustal structure, seismic reflection profiling, Off-Kanazawa, Off-Noto Penisula

Japan Geoscience Union Meeting 2014
(28 April - 02 May 2014 at Pacifico YOKOHAMA, Kanagawa, Japan)

SCG68-P03 Room:Poster Time:April 30 18:15-19:30

Results of 2013 Off-Joetsu survey for the research project on seismic and tsunami hazards around the Sea of Japan

KATO, Naoko[1*] ; SATO, Hiroshi[1] ; ISHIYAMA, Tatsuya[1] ; SHIRAISHI, Kazuya[2] ; ABE, Susumu[2] ; KURASHIMO, Eiji[1]

[1]Earthquake Research Institute, Univ. of Tokyo, [2]JGI. Inc.

To estimates Tsunami and seismic hazards along the coastal area of Sea of Japan, more detailed survey to identify source faults are needed. A new research project funded by MEXT named ”the integrated research project on seismic and tsunami hazards around the Sea of Japan” began in FY 2013. To obtain the information of source faults, we performed deep seismic reflection profiling off-Joetsu area in the central part of Honshu, Japan. The seismic lines were located in the offshore extension previous onshore seismic lines forming onshore-offshore integrated seismic lines. We used two vessels; a gun-ship with 3020 cu. inch air-gun and a cable-ship with a 2-km-long, streamer cable with 156 channels and 480 cu. inch air-gun. Common-mid point reflection data were acquired along 3 seismic lines. Two offshore seismic lines are connected to the onshore seismic sections. The survey area consists of stretched continental crust, such as Noto peninsula and Sado island, and failed rift area with large amount of large mafic intrusive rocks, such as Sado strait and Toyama trough. Stretched continental area is marked by densely distributed syn-rift normal faults. On the other hand, in the Sado strait and Toyama trough, fault-related folds were developed, which show small amount of vertical displacement. Along the boundary between continental crust area and oceanic crust, thrusts with rift axis vergent well imaged by seismic reflection profiles. The survey results contributed to construct source faults models of Tsunami and seismic hazards estimation.

Japan Geoscience Union Meeting 2014
(28 April - 02 May 2014 at Pacifico YOKOHAMA, Kanagawa, Japan)

SCG68-P04 Room:Poster Time:April 30 18:15-19:30

Onshore offshore, deep seismic survey across the Toyama trough

ISHIYAMA, Tatsuya[1*] ; KATO, Naoko[1] ; SATO, Hiroshi[1] ; SHIRAISHI, Kazuya[2] ; ABE, Susumu[2] ; TAKEDA, Tetsuya[3] ; KURASHIMO, Eiji[1]

[1]Earthquake Research Institute, University of Tokyo, [2]R&D Department, JGI, Inc, [3]NIED

To estimates Tsunami and seismic hazards along the coastal area of Sea of Japan, more detailed survey to identify source faults are needed. A new research project funded by MEXT named " the integrated research project on seismic and tsunami hazards around the Sea of Japan " began in FY 2013. To obtain the information of source faults, we performed onshore offshore deep seismic reflection profiling across the Toyama trough. The seismic line extends from Unazuki at the foot hill of the Hida mountains to the shoreline for 15 km and connected with bay cable of 3 km in length. Seismic signals produced by four vibroseis trucks were recorded by onshore receivers and bay cable. For offshore, we used two vessels; a gun-ship with 3020 cu. inch air-gun and a cable-ship with a 2-km-long, streamer cable with 156 channels and 480 cu. inch air-gun. The P-wave velocity profile by refraction tomography, suggests that the upper surface of Vp 5 km/sec is located 5 km below the mean sea level at the Toyama trough. Vertical offset of Vp 5 km/sec layer is about 8 km. Trough fill sediments beneath the Kurobe alluvial fan show northward dipping. Beneath the apex of this fan, velocity profile and reflection profile suggest the existence of south dipping thrust at 4 km in depth. This fault extends northward as a blind thrust. The seismic section suggests the reverse fault at the northern edge of Toyama trough. Based on the distribution of 5e coastal terraces along the southern part of Noto peninsula, the reverse fault prayed a significant roll for the uplift of Noto peninsula. Such basin structure is analogues to the Niigata sedimentary basin, and northern Fossa magna basin. The survey results contributed to construct source faults models of Tsunami and seismic hazards estimation.

Japan Geoscience Union Meeting 2014
(28 April - 02 May 2014 at Pacifico YOKOHAMA, Kanagawa, Japan)

SCG68-P05 Room:Poster Time:April 30 18:15-19:30

Structure analysis of the Ryukyu arc by the receiver function

ARASHIRO, Yasuhisa[1*] ; NAKAMURA, Mamoru[1]

[1]Graduate School of Science,Ryukyu University

The Ryukyu arc have converted plate boundary and back arc basin. The volcanic front in Tokara Islands is the main volcanism. Moreover, The activity of shaped Trough is supposed (Kimura, 1985). In addition, by the survey of igneous activity, the Okinawa Trough have upper flow mantle. Analyzed by receiver function in the Ryukyu arc, McCormack et al., (2013) ware anisotropy structure of slab beneath F-net station.

The Ryukyu arc have converted plate boundary and back arc basin. The volcanic front in Tokara Islands is the main volcanism. Moreover, The activity of shaped Trough is supposed (Kimura, 1985). In addition, by the survey of igneous activity, the Okinawa Trough have upper flow mantle. Analyzed by receiver function in the Ryukyu arc, McCormack *et al.,* (2013) ware anisotropy structure of slab beneath F-net station.

However, it was unknown how changed the structure in the slab and wedge mantle structure changed in the subducting direction. Therefore we clarified I sank by making a receiver functional analysis section at right angles to an errand, the trench including a seismometer record in addition to F-net broadband seismometer record in a short period of the Japan Meteorological Agency,(JMA) and how a Slavic angle changed into the direction.

In the receiver function analysis, we use 8 of short-period seismograph by JMA and 3 of broadband seismometers by NIED F-NET established in central Ryukyu . An analysis period is 2002 to 2013. and used 113 remote earthquake events more than M6.0 for analysis.

In receiver functional analysis, the discontinuity imaging depth is as same as JMA , in Okinawa-honto beneath 40km.

Keywords: receiver function, Ryukyu arc, mantle wedge

Japan Geoscience Union Meeting 2014
(28 April - 02 May 2014 at Pacifico YOKOHAMA, Kanagawa, Japan)

BAO01-01 Room:502 Time:April 28 09:00-09:15

Superflares on Solar-Type Stars

SHIBAYAMA, Takuya[1*] ; MAEHARA, Hiroyuki[2] ; NOTSU, Yuta[3] ; NOTSU, Shota[3] ; HONDA, Satoshi[4] ; NOGAMI, Daisaku[3] ; SHIBATA, Kazunari[3]

[1]Nagoya University, [2]University of Tokyo, [3]Kyoto University, [4]University of Hyogo

Stellar flares emit harmful UV and high-energy particles such as protons. Although the atmosphere protects the surface of the planets, certain amount of UV penetrates the atmosphere and high-energy particles reach the ground as secondary radiation. These radiations are thought to affect habitability and evolution of life.

High precision photometry of Kepler spacecraft enables us to detect superflares on G-type dwarfs. By extending Maehara et al. (2012, Nature), we found 1547 superflares on 279 G-type dwarfs detected from light curves of 500 days (Shibayama et al., 2013, ApJS). In the case of the Sun-like stars (with surface temperature 5600 - 6000 K and slowly rotating with a period longer than 10 days), the frequency of superflares with energy of 10^{34} - 10^{35} erg (100 - 1,000 times larger than the largest solar flare) is once in 800 - 5000 years. No hot Jupiters were found in these superflare stars. These superflare stars often show quasi-periodic brightness variation, which might be evidence of the large star spot. Rotational period can be estimated from the brightness variation period. It is interesting that superflares are detected on slowly rotating stars (P $>$10 days) like the Sun. Using these data, we studied the statistical properties of superflares. We compare the flare frequency distribution of the superflare and solar flare, and study the similarity of them. We also found that some G-type dwarfs show very high activity and exhibit superflares once in ~ 10 days. In the case of Sun-like stars, the most active stars show one superflare in ~ 100 days.

Keywords: Stellar flare, Solar flare, Habitability, Evolution

Japan Geoscience Union Meeting 2014
(28 April - 02 May 2014 at Pacifico YOKOHAMA, Kanagawa, Japan)

BAO01-02 Room:502 Time:April 28 09:15-09:30

Survey Observations of A Glycine Precursor, Methylenimine (CH2NH)

SUZUKI, Taiki[1*] ; OHISHI, Masatoshi[2] ; HIROTA, Tomoya[2] ; SAITO, Masao[2]

[1]Department of Astronomy, the Graduate University for Advanced Studies (SOKENDAI), [2]National Astronomical Observatory of Japan

It is widely thought that prebiotic chemical evolution from small to large and complex molecules would have resulted in the Origin of Life. The interstellar medium (ISM), where more than 170 molecules ranging from simple linear molecules to COMs were detected, show chemically rich environment. Ehrenfreund et al. (2002) argued that exogenous delivery of COMs to the early Earth by comets and/or asteroids could be more than their terrestrial formation by two orders of magnitude; molecules delivered from the Universe might have played an important role in early Earth chemistry. From this point of view, many observations were conducted to search for prebiotic molecules in the ISM, which might turn into the " Seeds of Life " when delivered to planetary surface. Especially, great attention was paid to amino acids, essential building blocks of terrestrial life; many surveys were made unsuccessfully to search for the simplest amino acid, glycine (NH_2CH_2COOH), towards Sagittarius B2 and other high-mass star forming regions (e.g., Brown et al. 1979; Snyder et al. 1983; Combes et al. 1996, ...).

In these days, the Atacama Large Millimeter/submillimeter Array (ALMA) is expected to break through such difficulties associated with glycine survey. Garrod (2013) used her chemical reaction network simulation and argued the possibility in detecting glycine with very high spatial resolution (~0.1 ″) and the collecting power of ALMA. It would be important to know which are potential glycine-rich sources for future surveys. However, the chemical evolution of N-bearing molecules, including glycine, is poorly known. We would need to better understand formation mechanisms of N-bearing COMs including amino acids and to have carefully selected good candidate sources for amino acids before conducting searches for amino acids by ALMA.

Although the chemical evolution of interstellar N-bearing COMs is poorly known, methylamine (CH_3NH_2) has been proposed as a precursor to glycine. Theoretical and laboratory studies have demonstrated that glycine is formed on icy grain surface from CH_3NH_2 and CO_2 under UV irradiation (Holtom et al. 2005). It is suggested that CH_3NH_2 can be formed from abundant species, CH_4 and NH_3, on icy dust surface (Kim & Kaiser 2011). Further methyleneimine (CH_2NH) would be related to CH_3NH_2. Another possible route to form these species is hydrogenation to HCN on the dust surface (Dickens et al. 1997; Theule et al. 2011).

However, a source number of such precursor molecules is very limited. In order to increase the number of CH_2NH sources and to better understand formation paths to CH_2NH, we conducted survey observations of CH_2NH, with the NRO 45 m telescope and the SMT telescope towards 11 high-mass and three low-mass star-forming regions. As a result, CH_2NH was detected in eight sources, including four new sources. The estimated column densities were roughly 10^{14}-10^{15}, 10^{15}-10^{16}, and 10^{16}-10^{17} cm^{-2}, respectively, for extended, 10 ″ , and 2 ″ sources. G10.47+0.03 and Orion KL are found to be especially CH_2NH-rich sources. We used chemical reaction network simulations to investigate formation process of CH_2NH in the ISM. Under the dark cloud condition, the simulated CH_2NH abundance in the gas phase is more than 10 times lower than our observations even if we conservatively estimate the CH_2NH abundance with an extended source. On the other hand, if we include hydrogenation reaction to HCN in our model, the CH_2NH abundance increased about by two orders of magnitude, enabling us to reconcile the observed abundance of CH_2NH. We also showed that this reaction is dominant in the early, low temperature phase of cloud evolution.

Keywords: Origin of Life, Chemical Evolution, Interstellar Medium, Glycine

Japan Geoscience Union Meeting 2014
(28 April - 02 May 2014 at Pacifico YOKOHAMA, Kanagawa, Japan)

BAO01-03 Room:502 Time:April 28 09:30-09:45

Formation, alteration and delivery of interstellar organics: Verification with experiments on ground and in space

KOBAYASHI, Kensei[1*] ; SHIBATA, Hiromi[2] ; TAMURA, Motohide[3] ; TAKAYAMA, Ken[4] ; KANEKO, Takeo[5] ; FUKUDA, Hitoshi[6] ; OGURI, Yoshiyuki[6] ; YOSHIDA, Satoshi[7] ; KANDA, Kazuhiro[8] ; YAMAGISHI, Akihiko[9] ; TANPOPO, Working group[10]

[1]Yokohama National University, NINS, [2]Osaka University, [3]University of Tokyo, NAOJ, NINS, [4]High Energy Accelerator Research Organization, [5]Faculty of Engineering, Yokohama National University, [6]Graduate School of Science and Engineering, Tokyo Institute of Technology, [7]National Institute of Radiological Sciences, [8]University of Hyogo, [9]Tokyo University of Pharmacy and Life Science, NINS, [10]JAXA/ISAS

As a wide variety of organic compounds have been found in meteorites and comets, their relevance to the origin of life is discussed. Many kinds of amino acids have been identified in extracts of carbonaceous chondrites, their origin is controversial. Possible carriers of organic compounds to the Earth were meteorites, comets and interplanetary dust particles (IDPs). It is said that IDPs could deliver organics more safely than meteorites and comets, the nature of organics in IDPs are little known since they have been collected usually in terrestrial biosphere. In addition, IDPs are directly exposed to cosmic and solar radiation, which might destroy organics in IDPs.

When possible interstellar media (a mixture of carbon monoxide or methanol, ammonia and water) was irradiated with high-energy particles, amino acid precursors were formed in high energy yields. We are planning to irradiate possible interstellar media with high energy heavy ions from a newly developed Digital Accelerator in KEK to confirm it. It suggested that amino acid precursors could be formed in interstellar space in prior to the formation of the solar system. Before the incorporation of interstellar organic compounds into comets or parent bodies of meteorites, they could be altered with high energy photons from the yound Sun. Soft X-rays irradiation of simulated interstellar organics resulted in the formation of hydrophobic compounds as seen in comets.

We are planning a novel astrobiology mission named Tanpopo by utilizing the Exposed Facility of Japan Experimental Module (JEM/EF) of the International Space Station (ISS). Two types of experiments will be done: Capture experiments and exposure experiments. In the exposure experiments, organics and microbes will be exposed to the space environments to examine possible alteration of organic compounds and survivability of microbes. Selected targets for the exposure experiments of organic compounds are as follows: Amino acids (glycine and isovaline), their possible precursors (hydantoin and 5-ethyl-5-methyl hydantoin) and complex precursors (CAW) synthesized from a mixture of carbon monoxide, ammonia and water by proton irradiation. In capture experiments, we will collect space dusts by using ultra-low density silica gel (aerogel), and will analyze them after returning them to the Earth. Amino acid enanthiomers will be analyzed after HF digestion and acid hydrolysis, as well as characterization of complex organic compounds in space dusts. The mission is planned to be started in 2015.

Keywords: origins of life, interstellar organic compounds, cosmic rays, interplanetary dust particles, Tanpopo Mission, particles irradiation

Japan Geoscience Union Meeting 2014
(28 April - 02 May 2014 at Pacifico YOKOHAMA, Kanagawa, Japan)

BAO01-04 Room:502 Time:April 28 09:45-10:00

Polymerization of methionine: Ignition of sulfur metabolism?

KAKEGAWA, Takeshi[1*]

[1]Graduate School of Science, Tohoku University

Methionine, sulfur-bearing amino acid, is one of protein-forming 20 amino acids. On the other hand, peptide formation using methionine is known to be difficult, because of large thermal stability of methionine. Incorporation of methionine into peptide has importance to form metal-sulfur-cluster in protein or other biologically important molecules, such as taurine. In order to overcome difficulties to make methionine-bearing peptide, new series of experiments were performed in the present study. Experiments were performed at 175 C and 150 MPa, using various mixtures. Methionine-trimers, which were not formed by previous investigators, were produced in the present study. Surprisingly a part of methionine was converted into glycine and then glycine-methionine peptide was newly formed. Those results demonstrated that high T and P conditions were suitable for not only methionine-peptide formation but also making multi-component peptide. Sulfur isotope compositions were determined on run products of the present study. Run products were enriched or depleted in 32S compared to starting materials. Hydrogen sulfides were preferentially released from methionine for the 32S-depleted samples. The 32S-enriched samples are explained by loss of sulfate from methionine, although oxidants of methionine-sulfur are still unclear. Modern living organisms metabolically produce sulfide and sulfate from methionine and cysteine. Such metabolic path is similar to the abiological production of sulfide and sulfate in the present study. This may imply that course of sulfur metabolism was most likely established early in the prebiotic age when methionine was incorporated in prebiotic protein.

Keywords: prebiotic, methionine, peptide, sulfur

Japan Geoscience Union Meeting 2014
(28 April - 02 May 2014 at Pacifico YOKOHAMA, Kanagawa, Japan)

BAO01-05 Room:502 Time:April 28 10:00-10:25

Formation of extraterrestrial oceans: Cradles of life

SASAKI, Sho[1*] ; KIMURA, Jun[2] ; KONDO, Tadashi[2] ; MATSUMOTO, Koji[3] ; SENSHU, Hiroki[4] ; SEKINE, Yasuhito[5] ; SHIBUYA, Takazo[6] ; KUBO, Tomoaki[7] ; NAMIKI, Noriyuki[4] ; HORI, Yasunori[3] ; KAMATA, Shunichi[8]

[1]Department of Earth and Space Sciences, Osaka University, [2]ELSI, Tokyo Institute of Technology, [3]National Astronomical Observatory, [4]PERC, Chiba Institute of Technology, [5]The University of Tokyo, [6]Japan Agency for Marine-Earth Science and Technology, [7]Department of Earth and Planetary Sciences, Kyushu University, [8]Hokkaido University

As one of research groups on ”Astrobiology in the Solar System” (a proposal submitted to MEXT), our group will study the origin of icy satellites around giant planets, and the origin and evolution of the interior ocean(s) of those icy bodies and their universality. Outside the so-called snowline of H_2O, the mass of protoplanets could be large enough to collect surrounding gas rapidly to form massive gaseous giant planets. Icy satellites would have been formed or trapped by the circumplanetary gas disks around giant planets. In multisatellite cases, orbital resonances may stabilize satellite migration and tidal dissipation would provide heat for sustaining interior oceans. Even when surface temperature is lower at a further distance from the sun, additional ice component (NH_3, CH_4, CO, etc.) would decrease the melting temperature. As a result, the more extended condition for presence of liquid water can be considered in comparison with the conventional habitable zone (with surface water).

Keywords: icy satellites, habitability, interior ocean, habitable zone, gas giant planets, origin of planetary systems

Japan Geoscience Union Meeting 2014
(28 April - 02 May 2014 at Pacifico YOKOHAMA, Kanagawa, Japan)

BAO01-06 Room:502 Time:April 28 10:25-10:40

Tanpopo: Astrobiology Exposure and Micrometeoroid Capture Experiments - Experiments at the Exposure Facility of ISS-JEM

YAMAGISHI, Akihiko[1*] ; YOKOBORI, Shin-ichi[1] ; YANO, Hajime[2] ; HASHIMOTO, Hirofumi[2] ; IMAI, Eiichi[3] ; TABATA, Makoto[2] ; KAWAI, Hideyuki[4] ; YABUTA, Hikaru[5] ; HIGASHIDE, Masumi[6] ; KOBAYASHI, Kensei[7] ; MITA, Hajime[8]

[1]Tokyo University of Pharmacy and Life Sciences, [2]ISAS/JAXA, [3]Nagaoka University of Technology, [4]Chiba University, [5]Osaka University, [6]Innovative Technology Research Center, Japan Aerospace Exploration Agency, [7]Yokohama National University, [8]ukuoka Institute of Technoology

Tanpopo, a dandelion in Japanese, is a plant species whose seeds with floss are spread by wind. We propose this mission to examine possible interplanetary migration of microbes, and organic compounds at the Exposure Facility of Japan Experimental Module (JEM: KIBO) of the International Space Station (ISS). The Tanpopo mission consists of six subthemes: Capture of microbes in space (Subtheme 1), exposure of microbes in space (Subtheme 2), analysis of organic compounds in interplanetary dust (Subtheme 3), exposure of organic compounds in space (Subtheme 4), measurement of space debris at the ISS orbit (Subtheme 5), and evaluation of ultra low-density aerogel developed for the Tanpopo mission (Subtheme 6). 'Exposure Panel' for exposure of microbes and organic materials and 'Capture Panels' for capturing micro particles with aerogel will be launched. The panels will be placed on the Exposed Experiment Handrail Attachment Mechanism (ExHAM) in the ISS. The ExHAM with the panels will be placed on the Exposure Facility of KIBO (JEM) with the Japanese robotic arms through the airlock of KIBO. The panels will be exposed for more than one year and will be retrieved and returned to the ground for the analyses.

Keywords: Panspermia hypothsis, Microbes, Organic compounds, Aerogel, Space exposure experiments

Japan Geoscience Union Meeting 2014
(28 April - 02 May 2014 at Pacifico YOKOHAMA, Kanagawa, Japan)

BAO01-07 Room:502 Time:April 28 11:00-11:25

Rock Magnetic Constraints on the origin of putative biological magnetite in the Martian ALH84001 Carbonates

KIRSCHVINK, Joseph[1*] ; KOBAYASHI, Atsuko[2] ; BUZ, Jennifer[1] ; THOMAS-KEPRTA, Kathie[3] ; CLEMETT, Simon[3]

[1]California Institute of Technology, Pasadena USA, [2]Earth/Life Science Institute, Tokyo Tech., [3]ESCG at NASA/Johnson Space Center, Houston TX

McKay et al. (1996) discussed 4 lines of evidence that were consistent with the possible presence of ancient life on Mars. Although none of these have been falsified, the one that has triggered the most intense debate concerns the claim that some of the fine-grained magnetite crystals embedded in small carbonate deposits might have been formed by the magnetotactic bacteria. These magnetite particles, when examined by high-resolution transmission electron microscopy, are indistinguishable from particles only produced by magnetotactic bacteria on Earth (Thomas-Keprta et al., 2001). Unfortunately, the magnetic and microscopic analyses done to date do not allow us to provide a direct statistical test of the probability that these particles are of biological origin, vs. the hypothesis they form from high-temperature decomposition of siderite (FeCO3).

In the past decade, developments in superconducting magnetometry and electron microscopy now provide new experimental approaches that can be applied to this problem. First, the new Ultra-High Resolution Scanning Magnetic Microscopes (UHRSMMs) can detect magnetic moments 3 to 4 orders of magnitude below the sensitivity of the best superconducting rock magnetometers, and robust dipole-fitting routines allow the 3-D vector magnetic moment of tiny particles to be resolved quantitatively. We have shown recently that individual fragments of the famous ALH84001 carbonate blebs can be imaged clearly using this technique, opening the possibility of experimental tests that should distinguish low-temperature (biological) from high-temperature (thermal decomposition) magnetite. Magnetite produced by thermal decomposition of carbonate during shock heating should carry a relatively strong Thermo-Remanent Magnetization (TRM), whereas biological magnetite trapped during carbonate growth should have a much weaker detrital magnetization (DRM). Fuller et al. (1988) reported a simple technique that compares the relative intensities of the Natural Remanent Magnetizations (NRMs) to Isothermal and Anhysteretic magnetizations (IRMs and ARMs) that can easily distinguish TRMs from DRMs; this new sensitivity now be applied to these particles. Second, because the magnetotactic bacteria use genetic control to manufacture their magnetite crystals, particles within the same cell are of very similar size and shape. When these cells die and leave their magnetite crystals in the sedimentary record as magnetofossils, they produce clumps of similarly-sized crystals because they stick together magnetically with very strong force (Kobayashi et al., 2006). Sediment transport and removal processes cannot disaggregate them, but they do get scrambled together during extraction and high-resolution TEM studies. We therefore need to do very high-resolution studies that can demonstrate the position of these crystals within the carbonate matrix of the ALH 84001 carbonate precipitates. We propose to use the new focused ion-beam (FIB) milling techniques available at the Earth-Life Science Institute of TiTech to make 3-dimensional reconstructions, at a 5 to 10 nanometer scale, of rectangular chunks of the ALH84001 carbonate. At this resolution, the putative magnetosomes will be represented by up to 500 voxel elements, each with definitive elemental composition. We should be able to determine whether clusters of particles within these carbonates are of similar size and shape, as expected from collapsed magnetosome chains. It will then be very simple to do statistical tests to determine whether these clumps are non-random assemblages sampled from the background crystal size distribution. The debate about life on Mars may rise again!

Fuller et al.,1988, Geophys. Res. Lett., v. 15, p. 518-521.
Kobayashi, et al.,2006,: Earth and Planetary Science Letters, v. 245, no. 3-4, p. 538-550.
McKay et al.,1996, Science, v. 273, no. 5277, p. 924-930.
Thomas-Keprta, et al.,2001, Proc. Natl. Acad. Sci. USA, v. 98, no. 5, p. 2164-2169.

Keywords: Martian Magnetofossils, Rock Magnetism, Panspermia, Carbonate

Japan Geoscience Union Meeting 2014
(28 April - 02 May 2014 at Pacifico YOKOHAMA, Kanagawa, Japan)

BAO01-08 Room:502 Time:April 28 11:25-11:40

Cu-Zn ores in 2.7 Ga komatiite-basalt assemblages in Abitibi Greenstone Belt, Canada, and their associations to microbs

KAKEGAWA, Takeshi[1*]

[1]Graduate School of Science, Tohoku University

Archean greenstone belts are hosting many massive sulfide ores. In particular, komatiite-basalt sequences are hosting Ni-Cu ores, which are mostly considered as a magmatic in origin. Some Ni-Cu ores are associated with serpentinization near seafloor. Such serpentinization may have been important for early life as hydrogen donors with alkaline fluids. Cu-Zn-Pb ores are also reported from the same komatiite-basalt sequences, although the origin of these ores are still uncertain. One representative 2.7 Ga komatiite-basalt sequence appears in the Munro area of the Abitibi Greenstone Belt. In order to understand the origin of Cu-Zn-Pb ores, mineralogical and geochemical studies are performed on ores at Munro area. Sulfide ores are essentially developed in black shale zones, and some ores are disseminated in altered volcanic rocks. Chalcopyrite, sphalerite, pyrrhotite are major minerals associated with minor galena, electrum, pentlandite, etc. Sulfur isotope compositions of those sulfides are ranging are not magmatic values. Some ores are rich in Se and As. Host volcanic rocks are extensively hydrated (followed by metamorphism) forming tremolite, chlorite and talc. Those features are similar to the modern submarine hydrothermal deposits, rather than magmatic ore deposits. Therefore, Cu-Zn-Pb ores in komatiite-basalt sequences were formed by black smoker type submarine hydrothermal activities. Carbon isotope analyses of organic matter in ore-associated sediments suggest that methanogens were active when komatiite became serpentinite, followed by submarine hydrothermal activities.

Keywords: Komatiite, ore, submarine, Abitibi, microbe

Japan Geoscience Union Meeting 2014
(28 April - 02 May 2014 at Pacifico YOKOHAMA, Kanagawa, Japan)

BAO01-09 Room:502 Time:April 28 11:40-12:05

Microbial community development in deep-sea hydrothermal vents in the Earth, and the Enceladus

TAKAI, Ken[1*] ; SHIBUYA, Takazo[1] ; SEKINE, Yasuhito[2] ; RUSSELL, M. J.[3]

[1]Japan Agency for Marine-Earth Science & Technology, [2]Department of Complexity Science & Engineering, University of Tokyo, [3]Jet Propulsion Laboratory, California Institute of Technology

Over the past 35 years, researchers have explored seafloor deep-sea hydrothermal vent environments around the globe and studied a number of microbial ecosystems. Bioinformatics and interdisciplinary geochemistry-microbiology approaches have provided new ideas on the diversity and community composition of microbial life living in deep-sea vents. In particular, recent investigations have revealed that the community structure and productivity of chemolithotrophic microbial communities in the deep-sea hydrothermal environments are controlled primarily by variations in the geochemical composition of hydrothermal fluids. This was originally predicted by a thermodynamic calculation of energy yield potential of various chemolithotrophic metabolisms in a simulated hydrothermal mixing zone. The prediction has been finally justified by the relatively quantitative geomicrobiological characterizations in various deep-sea hydrothermal vent environments all over the world. Thus, there should be a possible principle that the thermodynamic estimation of chemolithotrophic energy yield potentials could predict the realistic chemolithotrophic living community in any of the deep-sea hydrothermal vent environments in this planet. In 2005, a spacecraft Cassini discovered a water vapour jet plume from the sole pole area of the Saturnian moon Enceladus. The chemical composition analyses of Cassini's mass spectrometer strongly suggested that the Enceladus could host certain extent of extraterrestrial ocean beneath the surface ice sheet and possible ocean-rock hydrothermal systems. An experimental study simulating the reaction between chondritic material and alkaline seawater reveals that the formation of silica nanoparticles requires hydrothermal reaction at high temperatures. Based on these findings, we attempt to built a model of possible hydrothermal fluid-rock reactions and bioavailable energy composition in the mixing zones between the hydrothermal fluid and the seawater in the Enceladus subsurface ocean. The physical and chemical condition of the extraterrestrial ocean environments points that the abundant bioavailable energy is obtained maximally from redox reactions based on CO_2 and H_2 but not from with other electron accepters such as sulfate and nitrate. In the low-temperature zones, the available energy of the Enceladus methanogenesis and acetogenesis is higher than those in any Earth's environment where the methanogens sustain the whole microbial ecosystem. Our model strongly suggests that the abundant living ecosystem sustained by hydrogenotrophic methanogensis and acetogenesis using planetary inorganic energy sources should be present in the Enceladus hydrothermal vent systems and the ocean.

Japan Geoscience Union Meeting 2014
(28 April - 02 May 2014 at Pacifico YOKOHAMA, Kanagawa, Japan)

BAO01-10 Room:502 Time:April 28 12:05-12:20

Light absorption and energy transfer in photosynthesis: Toward extending our current biosignatures

KOMATSU, Yu[1*] ; UMEMURA, Masayuki[1] ; SHOJI, Mitsuo[1] ; KAYANUMA, Megumi[1] ; YABANA, Kazuhiro[1] ; SHIRAISHI, Kenji[2]

[1]University of Tsukuba, [2]Nagoya University

In the recent success in detecting for extrasolar planets, several habitable planets, which can sustain liquid water, have already been discovered. From reflection spectra on exoplanets, what and how to detect signs of life, biosignatures, have been controversial (Kiang et al. 2007). One of proposed biosignatures is vegetation red edge (VRE), which is observed from reflectance spectra on the Earth. VRE is identified as a sharp contrast in about 700 - 750 nm due to the absorption in visible region by photosynthetic pigments like chlorophylls and the reflection in NIR region. However, VRE is an effective as biosignature only if exovegetation shows the same spectral feature to that on the Earth (Seager et al. 2005). Therefore, the criterion as biosignature needs to be extended when the primary stars are totally different. Because in future missions searching for a second earth, the M type stars (cooler than Sun) will be the main targets, as the first step, we focused on the fundamental properties of purple bacteria which absorbs longer wavelength radiation (1025 nm).

We investigated light absorptions and excitation energy transfers (EETs) based on quantum dynamics simulations for light harvesting complexes (LHCs), which contain array of photosynthetic pigments. After light reaches in LHCs, effective EET is accomplished by corporative electronic excitation of the pigments. We used theoretical models for LHCs in purple bacteria (LH2s). LH2 is made of 2 rings: inner ring (B850) and the outer (B800), as shown in Figure. In our model, a dipole-dipole approximation was used for the electronic excitations. The low-lying electronic excited states of a LH2 were computed by using transition dipole moment of first excited state of each pigment calculated at time-dependent density functional theory. Corresponding to the light absorption process, the oscillator strength in the system could be computed. The oscillator strength of one LH2 was in a good agreement with the experimental value. Subsequently, quantum dynamics simulations were performed by Liouville equation to examine the EET process. In this model, the densities relaxed according to energy gradient. This treatment corresponded with the EET process. The relaxation parameters were determined based on the energy transfer time from B800 to B850 (0.8 ps). The calculated transfer time between two LH2s was determined to 2.72 - 3.67 ps in good agreement with the experiment values (2.0 - 10.0 ps). In order to deal with more realistic system, we calculated at a macro structural model. The calculated systems were composed of 7 LH2s and 19 LH2s, where LH2s were aligned in triangle lattice. As the system size increases, the oscillator strength shifted longer and the transfer velocity became faster. In photosynthesis, collected energies are efficiently transferred to lower energy sites where redox reactions take place, very efficiently by EET. When two pigments in central LH2 in the system were exchanged to pigments absorbed longer wavelength radiation (850 nm to 890 nm), the transfer velocities became faster. Moreover, in order to examine for what environments the absorption spectra of purple bacteria were optimized, the absorption efficiency was calculated from blackbody spectra expected in typical extrasolar planets. As a result, the absorption efficiency was maximum at the emission spectrum of a black body at around 200 K. Furthermore, the Light absorptions and EETs in purple bacteria, cyanobacteria and plants will be examined by using our methodology.

Keywords: biosignatures, extrasolar planets, photosynthesis, quantum chemical calculation, light harvesting, purple bacteria

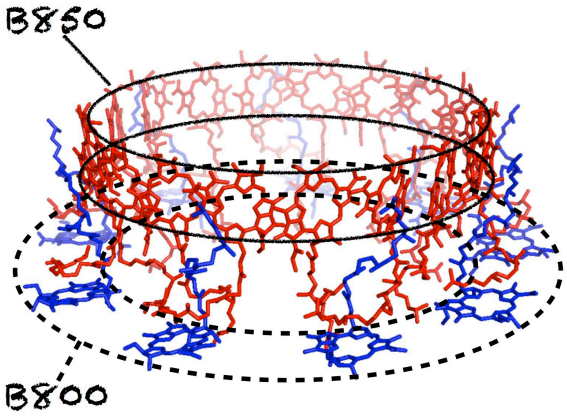

Japan Geoscience Union Meeting 2014
(28 April - 02 May 2014 at Pacifico YOKOHAMA, Kanagawa, Japan)

BAO01-11 Room:502 Time:April 28 14:15-14:30

Ancient Habitable-Trinity Mars and Future Targeting of potential Signs of Life

DOHM, James[1*] ; MARUYAMA, Shigenori[1]

[1]Earth-Life Science Institute, Tokyo Institute of Technology

Mars, the most Earth-like planet in our solar system, once had Habitable-Trinity conditions: an interfacing ocean, atmosphere, and nutrient-enriched primordial crustal materials with energy circulation driven by the Sun. Mars is thus considered the best target to search for life beyond Earth, as there are no other planetary bodies in our solar system that record Habitable-Trinity conditions. Following the termination of Habitable Trinity conditions nearly 4.0 Ga, when a strong dynamo shut down prior to the post-heavy-bombardment Hellas and Argyre impact events, the atmosphere was thinning, and plate tectonism was ongoing though waning, life would have found it increasingly difficult to survive at or near the surface, and thus would have migrated to the subterranean to persist. Vent structures, such as those located in the western part of Elysium Planitia where oceans once occupied the Martian surface and long-term magma-water interactions (billions of years) may be still ongoing, as evidenced through pristine lavas, faults that cut youthful surfaces, and geologically-recent flood events, are thus considered to be optimal targets to search for signs of life on Mars. The vent structures were formed by the transferal of subterranean materials to the surface likely due to magma-water interactions. The geologically youthful vent structures could be readily investigated in situ through current mission design.

Keywords: Habitable Trinity, potential signs of life

Japan Geoscience Union Meeting 2014
(28 April - 02 May 2014 at Pacifico YOKOHAMA, Kanagawa, Japan)

BAO01-12 Room:502 Time:April 28 14:30-14:55

Origin of life component of the Earth

MARUYAMA, Shigenori[1*] ; KOUCHI, Akira[2]

[1]ELSI Tokyo Institute of Technology, [2]Hokkaido University

The Earth is highly depleted in volatile in general. Water is one of them and only 0.023wt% among mass of the solid Earth. If the parental chondrite is carbonaceous with 2.3wt% water, the Earth must have been covered by 380km thick ocean, where too much amount of water was present, hence no life was born because of no supply of nutrients (Maruyama et al., 2013). Origin of water is critical to control the birth of life on rocky planet. Snowline is a concept of the boundary whether solid ice or vapor (gas) is stable at 2.7AU. If the Earth was formed at 1.0AU, the Earth must have been dry, no atmosphere and no ocean.

By this reason, there are several ideas to make the Earth with thinly covering ocean. One of such ideas is that Earth was born as a dry planet with Moon at 4.5-4.6Ga, followed by late bombardments to transport water components to the Earth at 4.4Ga (Maruyama et al., 2013).

Here we propose that late bombardment delivered not only water component but also carbon and nitrogen together at 4.4Ga. The organic lines are present within a narrow region around 2.1AU which is much closer to the Earth than the snowline. Asteroids derived from chondritic materials were transported to the Earth at 4.4Ga, and their organic matters turned to be primordial atmosphere from which primordial ocean was born. C and N with respect to O and H are enriched to make reduced atmospheric composition which could be favorable to synthesize complex organic compounds at the interface between atmosphere and ocean.

Japan Geoscience Union Meeting 2014
(28 April - 02 May 2014 at Pacifico YOKOHAMA, Kanagawa, Japan)

BAO01-P01 Room:Poster Time:April 28 18:15-19:30

Theoretical investigation of amino acid formations on interstellar dusts

KIDACHI, Kaori[1*] ; UMEMURA, Masayuki[1] ; KOMATSU, Yu[1] ; KYANUMA, Megumi[1] ; SHOJI, Mitsuo[1] ; YABANA, Kazuhiro[1] ; SHIRAISHI, Kenji[2]

[1]University of Tsukuba, [2]Nagoya University

Molecular evolution in the interstellar space remains unsolved. Formations of molecules in space have been extensively studied by experiments and space observations. Formations of complex organic molecules are expected in the interstellar space. In fact, some amino acids were found in meteorites and amino acids were detected after UV irradiation of interstellar ice analogs.

In the amino acid formation in space, many precursors and molecular evolution pathways are expected. Among these possible pathways, it is very important to know the energy profiles and molecular structures in the major formation pathways. In this study, possible amino acid formation pathways are investigated by using accurate quantum chemistry methods at the density functional theory levels.

Two formation pathways of glycine and alanine were examined: (1) hydrolysis of aminoacetonitrile and (2) hydrolysis of hydantoin derivatives. In the aqueous solution model, Polarizable Continuum Model was used.

Calculated formation energy of glycine is the most stable in the formation pathway in vacuum and no excessively stable intermediates existed. In aqueous solution, hydantoin pathway was slightly unstabilized. In conclusion, glycine production is considered to be occured easily if the components exist. Similar trend is expected for the alanine production.

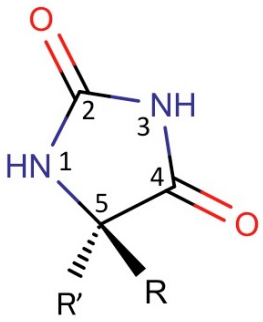

Japan Geoscience Union Meeting 2014
(28 April - 02 May 2014 at Pacifico YOKOHAMA, Kanagawa, Japan)

BAO01-P02 Room:Poster Time:April 28 18:15-19:30

Cosmic dusts capture on the International Space Station: Progress of the ground-based experiment

YABUTA, Hikaru[1] ; OGATA, Yuichiro[1*] ; OKUDAIRA, Kyoko[2] ; KOBAYASHI, Kensei[7] ; MITA, Hajime[6] ; NAKASHIMA, Satoru[1] ; MORIWAKI, Taro[3] ; IKEMOTO, Yuka[3] ; HASEGAWA, Sunao[4] ; TABATA, Makoto[4] ; YOKOBORI, Shin-ichi[5] ; IMAI, Eiichi[8] ; KAWAGUCHI, Yuko[5] ; SUGINO, Tomohiro[5] ; HAMASE, Kenji[15] ; FUKUSHIMA, Kazuhiko[9] ; AOKI, Dan[9] ; NOGUCHI, Takaaki[10] ; TSUCHIYAMA, Akira[11] ; NAKAMURA, Tomoki[12] ; ITO, Motoo[13] ; MIKOUCHI, Takashi[14] ; YANO, Hajime[4] ; YAMAGISHI, Akihiko[5] ; TANPOPO, Wg[4]

[1]Osaka University, Department of Earth and Space Science, [2]University of Aizu, [3]SPring-8, [4]JAXA, [5]Tokyo University of Pharmacy and Life Science, [6]Fukuoka Institute of Technology, [7]Yokohama National University, [8]Nagaoka University of Technology, [9]Nagoya University, [10]Ibaraki University, [11]Kyoto University, [12]Tohoku University, [13]JAMSTEC, [14]Tokyo University, [15]Kyusyu University

Introduction: Organic matter in interplanetary dust particles (IDPs) records the primitive chemical history in the early Solar System as well as it is thought to have delivered the building blocks of life to the early Earth (Chyba and Sagan, 1992). The Japanese Astrobiology working group, Tanpopo, is planning to collect the IDPs using a low-density silica aerogel (0.01 g/cm^3) (Tabata et al. 2011) on the International Space Station (Yamagishi et al. 2009). The mission has a great advantage that collection of the pristine IDPs without atmospheric entry heating and terrestrial contamination will be expected. One thing that has to be considered is a possible modification of the chemical composition of organic matter in IDPs upon their high velocity impact to the aerogel. This issue has been also concerned in the Stardust cometary dust sample return mission. Although the laboratory simulations have been conducted to study the alteration of minerals (Okudaira et al. 2004; Noguchi et al. 2007), the alteration of organics under a realistic condition has not been well understood. As a ground-based experiment, we have conducted a laboratory experiment of aerogel capture of Murchison meteorite powder at 4 km/s using a two-stage light gas gun, in order to evaluate the extent of modification of organic matter in the meteorite.

Experimental: The Murchison meteorite powder (˜500 ug) of a particle diameter of 30-100 um in a polycarbonate sabot was shot at ˜4 km/s using a two-stage light gas gun at JAXA/ISAS. The penetrations of the meteorite powder formed ˜70 tracks of ˜10 mm length in aerogel. Six terminal particles were extracted from the aerogel tracks using a tungsten needle and were pressed between two Al foils. The particles on the Al foils were analyzed by micro-Fourier transmission infrared (FTIR) spectroscopy at the beamline 43IR, Spring-8 and Osaka Univ., and micro-Raman spectroscopy at Osaka Univ. For a comparison, pre-shot Murchison meteorite powder was analyzed by these micro-spectrometers.

Results and discussion: The IR imaging detected the regions of absorptions of aliphatic carbons, CH3 at 2960cm^{-1} and CH2 at 2920cm^{-1} within the two Murchison terminal particles captured by aerogel. Thus, organic matter is survived through the high velocity impact at 4 km/s. The spectral intensities of aliphatic carbons in the terminal particles are slightly lower than those in the pre-shot Murchison meteorite. CH2/CH3 ratios obtained from the IR spectra of the terminal particles were 0.3 ? 3, while those of the pre-shot sample were 1.3 ? 2. The difference in the ratios may be reflected by modification of aliphatic chains of organic macromolecules in the meteorite, e.g., demethylation, methylation, or cracking, due to the high velocity impact heating. From the two terminal particles, D- and G- bands, which are derived from carbonaceous matter, were detected by micro-Raman analyses. Peak widths and positions of the two bands showed similar values to those for pre-shot Murchison meteorite. Thus, modification of aromatic structures after the aerogel capture is unlikely. Although relative amounts of organics were low in the four other terminal particles, this may be reflected by original heterogeneity of the meteorite.

Keywords: International Space Station, Cosmic dusts, Organic matter, Astrobiology, Origin of life, Aerogel

Japan Geoscience Union Meeting 2014
(28 April - 02 May 2014 at Pacifico YOKOHAMA, Kanagawa, Japan)

BAO01-P03 Room:Poster Time:April 28 18:15-19:30

Possibility of production of amino acids by impact reaction using a light-gas gun as a simulation of asteroid impacts

OKOCHI, Kazuki[1*] ; MIENO, Tetsu[2] ; KONDO, Kazuhiko[1] ; HASEGAWA, Sunao[3] ; KUROSAWA, Kosuke[4]

[1]Dept.Physics, Shizuoka Univ., [2]Grad.School of Sci. and Technol, Shizuoka Univ., [3]ISAS/JAXA, [4]Planetary Exploration Research Center, Chiba Institute of Technology

We are interested in the production process of amino acids in space. Especially, asteroids coming to Titan satellite have made impact reaction on the surface including nitrogen gas, water ice and methane. On the Titan surface, various material, produced by the impact reactions, have been stored under low temperature and dark condition. To do the simulation experiment, a JAXA 2-stage light-gas gun has been used. A projectile with 6.5km/s of speed hits a water + iron target in 1 atm of nitrogen gas, causing an impact reaction. Figure 1 shows a crater on the target. Figure 2 shows produced black soot which deposited onto the aluminum sheet. The samples produced are carefully collected and analyzed by HPLC, FTIR, TOF-MS. As a result of HPLC, peaks suggesting the existence of glycine and alanine in the samples produced were confirmed.

Keywords: impact reaction, gas gun, Titan, asteroid, amino acid, HPLC

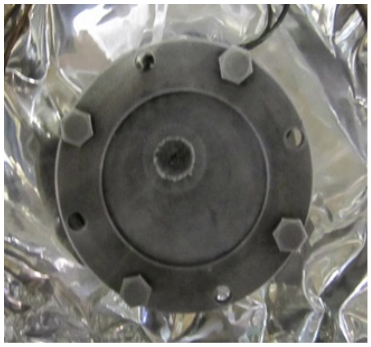

Fig.1 A crater on the target.

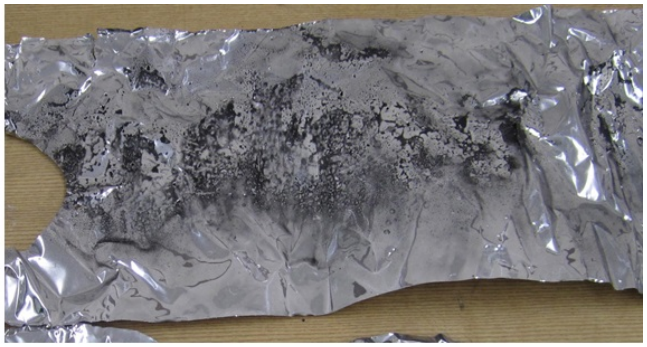

Fig.2 Produced black soot deposited onto the aluminum sheet.

Japan Geoscience Union Meeting 2014
(28 April - 02 May 2014 at Pacifico YOKOHAMA, Kanagawa, Japan)

BAO01-P04 Room:Poster Time:April 28 18:15-19:30

Amino acid formation from simulaed mildly-reducing primitive atmospheres by spark discharges and proton irradiation

ISE, Jun-ichi[1*] ; KANEKO, Takeo[2] ; OBAYASHI, Yumiko[2] ; FUKUDA, Hitoshi[3] ; OGURI, Yoshiyuki[3] ; KOBAYASHI, Kensei[4]

[1]Grad. School of Eng., Yokohama Natl. Univ., [2]Faculty of Eng., Yokohama Natl. Univ., [3]Grad. School of Sci. & Eng., Tokyo Inst. Tech., [4]Yokohama National University, NINS

Miller (1953) reported that amino acids were abiotically formed in a gas mixture of methane, ammonia, hydrogen and water. However, It is suggested that the primitive Earth atmosphere was less reducing, and its major components were carbon dioxide and nitrogen. It is quite difficult to form amino acids from such non-reducing gas mixtures. If it is mildly reducing, i.e. it contained some carbon monoxide or methane, amino acid production could be expected.

We examined possible formation of amino acids from mildly reducing gas mixtures by spark discharges or by proton irradiation. A mixture of carbon dioxide and methane (total 50 %) and nitrogen (50 %) was introduced into a glass tube with liquid water. Spark discharges in the gas mixtures were performed with a Tesla coil for 12 hours. Proton beams (2.5 MeV, 2 mC) were irradiated to the gas mixtures from a Tandem accelerator (TIT). The resulting products were acid-hydrolyzed, and amino acids were determined by ion-exchange HPLC with post-derivatization with o-phthalaldehyde and N-acetyl-L-cystein.

A mixture of methane and nitrogen gave amino acids in high yields by either spark discharges or proton irradiation. When carbon dioxide was added to the gas mixture, amino acid yields decreased. In the case of spark discharges, amino acids could not be detected when methane ratio in total carbon sources (carbon dioxide + methane) was less than 30 %. In the case of proton irradiation, the mixture with the methane ratio was 5 % still gave amino acids. Thus, it was suggested that, in the case that the primitive Earth atmosphere was only slightly reducing, a major energy source for the production of amino acids was not thundering but cosmic rays.

Keywords: mildly-reducing primitive atmospheres, spark discharge, proton irradiation, origins of life, amino acids

Japan Geoscience Union Meeting 2014
(28 April - 02 May 2014 at Pacifico YOKOHAMA, Kanagawa, Japan)

BAO01-P05 Room:Poster Time:April 28 18:15-19:30

Stability and reactions of amino acids in simulated submarine hydrothermal systems

AKAMATSU, Ryota[1*] ; BALASANTHIRAN, Kuhan C.[1] ; OBAYASHI, Yumiko[2] ; KANEKO, Takeo[2] ; KOBAYASHI, Kensei[2]

[1]Grad. School or Eng., Yokohama Natl. Univ., [2]Faculty of Eng., Yokohama Natl. Univ., [3]National Institutes of Natural Sciences

The discovery of hydrothermal systems in the late 70s brought a new hypothesis to the origin of life. Previously, the Urey-Miller experiment had made waves in this new field, indicating that a reducing atmosphere could form amino acids from basic chemicals. The further discovery of hydrothermal systems with earth prebiotic conditions added another notion to the field. Since then, different kinds of simulation were conducted to test the hypothesis. Initially and autoclave was extensively used due to its robustness and durability, however this system was not an ideal system, hence a flow-type simulator was proposed instead. We tested the stability and reaction of several amino acids using a flow reactor simulating submarine hydrothermal systems at 200 — 250 ℃. This study generally showed that there is a variation in the individual amino acids survivability in the simulators. This is mainly attributed to the following factors; heat time, cold quenching exposure, metal ions and also silica.We observed that, in a rapid heating flow reactor, high aggregation and/or condensation of amino acids could occur even during a heat exposure of 2 min. We also monitored their stability in a reflow-type of simulator for 120 min at 20 min intervals. The non-hydrolyzed and hydrolyzed samples for this system showed a similar degradation only in the absence of metal ions. We also tested the possible condensation that could be forming peptide bonds among the amino acids in one of the flow rectors. We utilized the Lowry protocol to determine the concentration of the peptide bonds in several hydrothermal temperatures. Concentration of peptide bonds was significantly higher when the temperature was at 300 ℃. This is despite the decomposition of amino acids by more than half. However, the contribution of peptide bonds in the combined amino acids was less than 10%, even in the 300 ℃ sample, which showed the highest contribution of peptides. The major heat products were non-peptide amino acid condensates (NPACs) that only possess partial peptide bonds. The role of NAPCs should be examined though they were often ignored in the classical chemical evolution scenario so far.

We experimented with Gly, Ala, Asp and Val in the SCWFR at 200 ℃, 250 ℃ and 300 ℃. We recorded the recovery of the samples and performed the Lowry method to quantify the peptide bond concentration. Peptide bonds ' concentrations are significantly higher when the temperature is at 300 ℃. This is despite the decomposition of amino acids by more than half. The highest peptide bond concentration among the samples constitute only about 10% of the total product yield of the amino acid mixture.

We also examined possible formation of amino acid condensates by using single amino acid (Gly, Ala, Asp or Val) and compared the results with those with all of four amino acids.

Keywords: submarine hydrothermal systems, amino acids, origins of life, flow reactor

Japan Geoscience Union Meeting 2014
(28 April - 02 May 2014 at Pacifico YOKOHAMA, Kanagawa, Japan)

BAO01-P06 Room:Poster Time:April 28 18:15-19:30

Scanning electron microscopic observation of organic microspherules formed by Maillard-type reaction

TAKAHASHI, Ayako[1*] ; YABUTA, Hikaru[1]

[1]Osaka University, Department of Earth and Space Science

It has been suggested that organic microspherules played a role as a physical container to maintain catalytic molecules and their reaction intermediates at concentrations high enough to sustain catalysis in prebiotic chemistry on the early Earth (Weber, 2005). Experimental studies on the formation of organic microspherules from a variety of organic compounds, such as amino acids (Fox and Harada, 1958), gelatin and gum arabic (Oparin, 1976), organic extracts from meteorite (Deamer, 1985; Deamer and Pashley, 1989), interstellar organic analogue (Dworkin et al. 2001), fatty acids and polycyclic aromatic hydrocarbons (Groen et al. 2012), formaldehyde and ammonia (Cody et al. 2009; Kebukawa et al. 2013) have been reported. However, the formation process and stability of these organic microspherules have been unexplored. In this study, sizes, shapes, and distributions of organic microspherules formed during the progress of Maillard-type reaction of formaldehyde and ammonia were investigated.

Experimental:
Paraformaldehyde (120mg), glycolaldehyde (120mg), ammonium hydroxide (54ul), calcium hydroxide (30mg) in 2ml of water in a glass tube was heated at 50-90 degrees C for 71-720 hours. For comparison, the samples without ammonium hydroxide were heated under the same conditions. After heating, the sample solutions were centrifuged. The precipitated material were rinsed with 2N HCl to dissolve calcium, and dried at 50 degrees C to obtain organic solids. The organic solid samples were pressed on a indium plate, gold-coated, and observed by a scanning electron microscopy (SEM).

Results and discussion:
After several minutes in heating, all the sample solutions turned yellow and eventually turned brown to black. Organic solids were produced at 90 degrees C but 50 degrees C. The yields of organic solids from sample solutions with ammonia were 10 times higher than those without ammonia. The yields gradually increased during heating. While distorted-shaped aggregates are produced from the samples heated for 71-120 hours, micron-sized organic microspherules (0.4-4.0 um) were observed from those heated for 240-720 hours. The samples with ammonia show perfectly round shapes of microspherules. Some microspherules are large and oval in the sample heated for 480 hours. The sizes of the microspherules increased with heating time. Organic solids produced by the same reaction as this study's at 90 degrees C for 72 hours consist of approximately equal abundances of aromatic and aliphatic carbons (Kebukawa et al. 2013). This molecular composition could result in amphiphilicity that is related to formation of the stable microspherules observed in this study. Formaldehyde and ammonia are thought to have been commonly present on the early Earth, and thus the organic microspherules formed by these molecules which proceed polymerization efficiently under mild conditions, could have played a role as a precursor of prebiotic cell membrane.

Keywords: organic microspherules, Maillard reaction, prebiotic cell membrane

Japan Geoscience Union Meeting 2014
(28 April - 02 May 2014 at Pacifico YOKOHAMA, Kanagawa, Japan)

BAO01-P07 Room:Poster Time:April 28 18:15-19:30

Fluorescence imaging of microbe-containing micro-particles that had been shot from a two-stage light-gas gun into an ult

KAWAGUCHI, Yuko[1*] ; SUGINO, Tomohiro[2] ; TABATA, Makoto[1] ; OKUDAIRA, Kyoko[3] ; IMAI, Eiichi[4] ; YANO, Hajime[1] ; HASEGAWA, Sunao[1] ; YABUTA, Hikaru[5] ; KOBAYASHI, Kensei[6] ; KAWAI, Hideyuki[7] ; MITA, Hajime[8] ; HASHIMOTO, Hirofumi[1] ; YOKOBORI, Shin-ichi[2] ; YAMAGISHI, Akihiko[2]

[1]ISAS/JAXA, [2]Tokyo University of Pharmacy and Life Sciences, [3]University of Aizu, [4]Nagaoka University of Technology, [5]Osaka University, [6]Yokohama National University, [7]Chiba University, [8]Fukuoka Institute of Technology

We previously proposed an experiment (the Tanpopo mission) to capture microbes and organic compounds on the Japan Experimental Module of the International Space Station. An ultra low-density silica aerogel will be exposed to space for one year. After retrieving the aerogel, particle tracks and particles found in it will be visualized by fluorescence microscopy after staining it with a DNA-specific fluorescence dye. In preparation for this study, we simulated particle trapping in the aerogel so that methods could be developed to visualize the particles and their tracks. During the Tanpopo mission, particles that have an orbital velocity of about 8 km/s are expected to collide with the aerogel. To simulate these collisions, we shot *Deinococcus radiodurans*-containing Lucentite particles into an aerogel from a two-stage light-gas gun (acceleration 4.2 km/s). The shapes of the captured particles and their tracks and entrance holes were recorded with a microscope/camera system for further analysis. The size distribution of the captured particles was smaller than the original distribution, suggesting that the particles had fragmented. We were able to distinguish between microbial DNA and inorganic compounds after staining the aerogel with the DNA-specific fluorescence dye SYBR green I as the fluorescence of the stained DNA and the autofluorescence of the inorganic particles decay at different rates. The developed methods are suitable to determine if microbes exist at the International Space Station altitude.
Keywords: Aerogel, Space experiment, Hypervelocity impact experiment, DNA-specific fluorescence dye.

Keywords: Aerogel, Space experiment, Hypervelocity impact experiment, DNA-specific fluorescence dye

Japan Geoscience Union Meeting 2014
(28 April - 02 May 2014 at Pacifico YOKOHAMA, Kanagawa, Japan)

BAO01-P08 Room:Poster Time:April 28 18:15-19:30

Studies on life detection methods by using enzymatic activities: Phosphatase and Catalase

AOKI, Kohei[1*] ; KURIZUKA, Taihei[1] ; OBAYASHI, Yumiko[1] ; OGAWA, Mari[2] ; YOSHIMURA, Yoshitaka[4] ; MITA, Hajime[3] ; NAVARRO-GONZALEZ, Rafael[5] ; KANEKO, Takeo[1] ; KOBAYASHI, Kensei[6]

[1]Graduate School of Engineering, Yokohama National University, [2]Faculty of Education, Yasuda Women's University, [3]College of Agriculture, Tamagawa University, [4]Faculty of Engineering, Fukuoka Institute of Technology, [5]National Autonomous University of Mexico, [6]Yokohama National University and Natural Institutes of Natural Sciences

We have recognized that microorganisms can survive in such extreme environments as polar environments, deserts, hot springs and stratosphere. It is quite difficult to evaluate microbial activities in extreme environments, since most microorganisms in extreme environments are hard to cultivate. We are discussing how to detect microorganisms in extreme environments including Mars. In MELOS mission, a proposed Japanese Mars exploration, fluorescence microscope will be applied to life detection. In addition to the technique, we examined amino acid analysis and enzyme assay as possible chemical strategies for life detection in terrestrial and extraterrestrial extreme environment.

One of the most well studied enzymes in environments is phosphatase. Phosphatases hydrolyze phosphate esters to produce phosphate that is essential for terrestrial life, and they are known to be stable in environments. We assayed rocks and soils in extreme environments such as submarine hydrothermal core samples and Antarctic soil samples, and found that it can be a good indicator for microbial activity. Here we analyzed phosphatese activity in Atacama Desert soil samples. Atacama desert is know to be one of the driest and harshest environments on the Earth, and regarded as Mars simulant. Samples were collected in 2002 by USA-Mexico team. Phosphatase activity was correlated to precipitation rate.

Such extreme environments as Mars, Antarctica and deserts have commonalities. Strong UV causes formation of peroxides that will damage bioorganics. Thus, we supposed that catalase and peroxidase are quite important for the survival of organisms living there, and it would be a good biomarker. We are now studying the assay methods for catalase in soil samples.

Keywords: extreme environments, Mars, life detection, enzymatic activities, phosphatase, catalase

Japan Geoscience Union Meeting 2014
(28 April - 02 May 2014 at Pacifico YOKOHAMA, Kanagawa, Japan)

BAO01-P09 Room:Poster Time:April 28 18:15-19:30

Molecular approach to the characterisation of Sri Lanka red rain cells

MIYAKE, Norimune[1*] ; MATSUI, Takafumi[1] ; WICKRAMASINGHE, Chandra[2] ; WALLIS, Jamie[3] ; WALLIS, Daryl[2] ; WICKRAMARATHNE, Keerthi[4] ; SAMARANAYAKE, Anil[4]

[1]Planetary Exploration Research Center, Chiba Institute of Technology, Chiba, Japan, [2]Buckingham Centre for Astrobiology, University of Buckingham, Buckingham, UK, [3]School of Mathematics, Cardiff University, Cardiff, UK, [4]Medical Research Institute, Colombo, Sri Lanka

The recent mysterious phenomenon that has attracted much attention is that of the red rain which fell in Polonnaruwa, Sri Lanka, on 13 November 2012. The microbial content in red rain shows generic similarities to that of the Indian red rain which fell in 2001. The morphological property of those microbes has been well documented [1,2]. Various microscopic analyses of our Sri Lankan red rain sample indicate that the defining red rain cells (RRC) exist in the presence of other microorganisms including diatoms. In our past paper, the ultrastructure of RRC shows that it is possibly a spore-form and so allowing them to thrive in the extreme upper biosphere conditions [3]. We also show the presence of uranium in the abnormally thick cell wall of RRCs.

In this report, we present the molecular approach to the characterisation of microbial communities in red rain and reveal the genus of RRCs. A beads-beating protocol is carried out for the efficient extraction of DNA and denaturing gradient gel electrophoresis (DGGE) for the analysis of microbial communities.

References

[1] Louis and Kumar (2006) New red rain phenomenon of Kerala and its possible extraterretrial origin, *Astrophys. Space Sci*, **302**, 175-187.
[2] Samaranayake et al. (2013) Microorganisms in the coloured rain of Sri Lanka, *J. Cosmol*, **21**, 9805-9810.
[3] Miyake et al. (2013) Discovery of Uranium in Outer Coat of Sri Lankan Red Rain Cells, *J. Cosmol*, **22**, 1-8

Keywords: Red rain, Extremophile, Polonnaruwa

Japan Geoscience Union Meeting 2014
(28 April - 02 May 2014 at Pacifico YOKOHAMA, Kanagawa, Japan)

BAO01-P10 Room:Poster Time:April 28 18:15-19:30

The mechanism that had formed the oldest organic carbon with the banded ironstone formations

KARASAWA, Shinji[1*]

[1]Miyagi National College of Technology (Professor emeritus)

The band iron layers were formed about 3.8 billion years ago. M. T. Rosing reported that the oldest organic carbon was found in the sedimentary rock from west Greenland that formed at the same period [1]. That is, the value of carbon isotope ratio ($^{12}C/^{13}C$) on 2- to 5-micrometers graphite globules in the rock is larger than that of inorganic carbon. Since photosynthesis is realized by a system of molecules with chain of reactions, the production of that carbon by the photosythesis is difficult. The author proposes the mechanism that a slightly large amount of ^{12}C was incorporated in the floating substances which were produced with the banded ironstone formations (BIF).

We can observe the phenomena by adding fine iron particles in carbonated water as shown in the [photograph 1]. Bubbles were produced at the surface of iron in the bottom of water. The bubbles transfer the fine particles of iron from the bottom to the surface. Since the electronegativity of carbon is larger than that of hydrogen, the carbon atom released from carbonated water by oxidation of iron was adhered to iron particle. The intermolecular bonding of iron with carbon beomes floating substance. The iron atom will be released from the floating substance as the form of iron oxide. So, the carbon atom that was released from the iron will constitute the floating substances [2].

At about 3.8 billions years ago, earth's surface was covered with compounds such as oxides, sulfides and carbonates. Although there were carbon dioxide gasses in the atmosphere, the seawater at mild temperature became dissolve the carbon dioxide. There occurred volcanic eruptions frequently. Iron particles were emitted by the volcanic eruption and the iron oxides were deposited at the bottom on the sea. that is the process of BIF. On the other hand, the carbn dioxide molecules in the syk smashed into surface of the sea water frequently. It is possible to produce an organization of molecules from the floating substance of intermolecular bonds by the energy that comes from outer world such as ultraviolet ray. The floating substances will accuulate at surface of water. At last, the substances deposited at bottom of the sea. That is, the carbon atoms those were included in sedmentary rocks fromk west Greenland had come from the sky.

[**References**]

[1] Rosing M. T. (1999). ^{13}C-Dpleted Carbon Microparticles in >3700-Ma Sea -Floor Sedimentary Rocks from West Greenland, *Science* Vol.283 No.5402 pp.674-676.

[2] karasawa S. (2010). Inorganic production of membranes together with iron carbide via oxidization of iron in the water that includes carbon dioxide plentifully, *AbSciCon* 2010, #5168

[**Photograph 1**]

Accumulation of the floating substances those are produced by adding fine iron particles in carbonated water (Left: old #300 meshed fine particles, Center: new #300meshed fine particles, right: #200 meshed particles)

Keywords: 3.8 billion years ago, Banded iron formation, Organic carbon, Carbon dioxide, Carbon isotope ratio

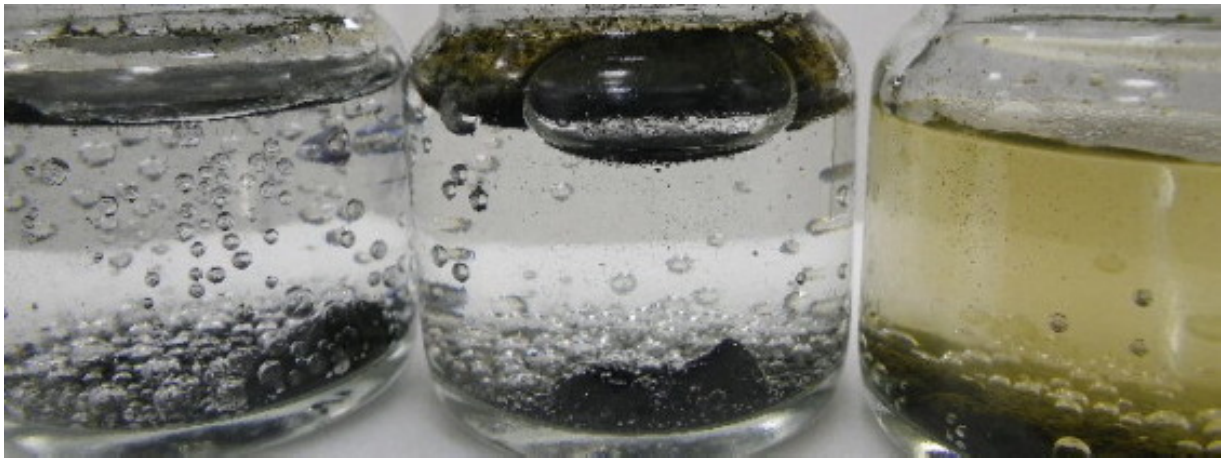

Japan Geoscience Union Meeting 2014
(28 April - 02 May 2014 at Pacifico YOKOHAMA, Kanagawa, Japan)

BBG21-01 Room:213 Time:May 1 09:00-09:15

Ocean Acidification and its effect on calcification since the late 19th century revealed by d11B of Ogasawara coral

KUBOTA, Kaoru[1*] ; YOKOYAMA, Yusuke[1] ; ISHIKAWA, Tsuyoshi[2] ; SUZUKI, Atsushi[3]

[1]Atmosphere and Ocean Research Institute, University of Tokyo, [2]Japan Agency for Marine-Earth Science and Technology, [3]National Institute of Advanced Industrial Science and Technology

Boron isotopes ($d^{11}B$) of coral skeleton are known as a pH meter in the seawater. As pH of seawater is closely related to partial pressure of CO_2 (pCO_2) in the atmosphere, it is expected that $d^{11}B$ becomes pCO_2 indicator in the geological past too. However, $d^{11}B$-pH is under scrutinized since coral calcification itself probably affects the relationship. Although many studies have focused on $d^{11}B$ measurements for cultured corals under pH-controlled aquarium, those for living corals outdoors have rarely measured, which are limited to, for example, Great Barrier Reef and Guam. Here we show 125 years-records (AD1873-1998) of $d^{11}B$ and boron concentration (B/Ca ratio) for long-lived massive coral (Porites sp.) that was sampled at Chichi-jima, Ogasawara Islands, North West Pacific. They clearly reveal Ocean Acidification after the industrial revolution. We will discuss a relationship between ocean acidification and coral calcification from a slope of pH decline that is obtained from observational data. We will also discuss how B/Ca of calcium carbonate skeleton that is produced by marine calcifiers is reliable proxy for seawater pH, which is being paid a great attention mainly due to relative easiness to measure compared to isotopes.

Keywords: boron, Ogasawara, coral, calcification, Ocean Acidification

Japan Geoscience Union Meeting 2014
(28 April - 02 May 2014 at Pacifico YOKOHAMA, Kanagawa, Japan)

BBG21-02 Room:213 Time:May 1 09:15-09:30

Ocean acidification influences on coral growth of temperate species

KIM, So[1*] ; SUZUKI, Atsushi[2] ; HAYASHI, Masahiro[3] ; YAMAMOTO, Yuzo[3] ; HOTTA, Kimiaki[3] ; ISONO, Ryosuke[3] ; WATANABE, Yusuke[3] ; YAMANO, Hiroya[4] ; NOMURA, Keiichi[5] ; NISHIDA, Kozue[2] ; INOUE, Mayuri[6] ; ZHANG, Jing[1] ; NOJIRI, Yukihiro[4]

[1]Toyama University, [2]Geological Survey of Japan, AIST, [3]Marine Ecology Research Institute (MERI), [4]National Institute for Environmental Studies, [5]Kushioto Marine Park, [6]Atmosphere and Ocean Research Institute, The University of Tokyo

Carbon dioxide concentration in the atmosphere has steadily increased since the industrial revolution due to burning of fossil fuel and will cause the global warming and ocean acidification. It will raise the ocean temperature around Japan and reduce the seawater pH and then it may bring serious threat to corals dwelling around Honsyu Island, Japan. Last year, our research group did temperature-controlled culture experiments of temperate coral species from the Pacific side of Honsyu Island of Japan under the present level of the partial pressure of CO_2 (pCO_2). But, synergetic effect of the global warming and ocean acidification on these corals has not been tested yet in detail. In this study, we focus on the how the different pCO_2 levels (past, present, and future) can influence skeletal growth of temperate *Acropora* coral species under the different temperature setting using a precise control system. This system was used to generate six different pCO_2 levels: (i) pre-industrial, ˜300 μatm, (ii) present-day pCO_2, ˜400 μatm, and at four near-future conditions, (iii) ˜550 μatm, (iv) ˜750 μatm, (v) ˜1000 μatm and (vi) ˜1200 μatm at three temperature conditions (17, 25, and 27 deg C). Our early results suggested a negative influence of higher pCO_2 levels on skeletal growth of temperate *Acropora* corals, but not so sensitive compared to tropical and subtropical *Acropora* corals.

Keywords: Ocean acidification, temperate coral, calcification, global warming

Japan Geoscience Union Meeting 2014
(28 April - 02 May 2014 at Pacifico YOKOHAMA, Kanagawa, Japan)

BBG21-03 Room:213 Time:May 1 09:30-09:45

Projecting impacts of rising water temperature on the distribution of seaweeds around Japan

TAKAO, Shintaro[1] ; FUJII, Masahiko[1*] ; KUMAGAI, Naoki[2] ; YAMANO, Hiroya[2] ; YAMANAKA, Yasuhiro[1]

[1]Faculty of Environmental Earth Science, Hokkaido University, [2]National Institute for Environmental Studies

Using monthly mean sea surface temperature (SST) from 1950 to 2035 obtained by a high-resolution climate projection model (MIROC4h) and SST-based indices of the distribution of tropical-subtropical and temperate seaweeds (*Sargassum duplicatum* and *Ecklonia cava*, respectively), we evaluated the effects of SST rises on the potential distribution of the species in seas close to Japan. Estimated distributions from the 1950s to 2000s showed that the potential southern limit of the temperate seaweed shifted to higher latitudes due to rising water temperature-induced barren ground, while there was little change in the potential northern limit of them. In contrast, the tropical-subtropical seaweed *S. duplicatum* expanded their distribution polewards during the same period. Under the global warming scenario (RCP4.5), the potential distribution of *S. duplicatum* can replace the one of *E. cava* in coastal area of Kochi Prefecture by the 2010s. This replacement of the temperate seaweed species with the tropical-subtropical one could consequently change coastal productivity and food web structure, and therefore may affect ecosystem services around Japan.

Keywords: seaweed bed, global warming, climate model, Ecklonia cava, Sargassum duplicatum

Japan Geoscience Union Meeting 2014
(28 April - 02 May 2014 at Pacifico YOKOHAMA, Kanagawa, Japan)

BBG21-04 Room:213 Time:May 1 09:45-10:00

Standing genetic variation of coral populations under changing environments

IGUCHI, Akira[1*]

[1]Department of Bioresources Engineering, Okinawa National College of Technology

How genetic diversities affect ecosystem functions is one of key questions to understand the maintenance of genetic diversities and their roles in ecosystem. To evaluate the functional genetic diversities of corals which are main composers of coral reefs, I genotyped 20 colonies (collected in front of Sesoko Station) of *Acropora digitifera* which is one of dominant coral species around the Ryukyu Archipelago where is the northern peripheral area of coral reefs, and performed common garden experiment using five clonal fragments from each colony (to reduce accidental response in each genotype) to estimate variations of growth and photosynthetic efficiencies among colonies, namely, genotypes. Genotyping was performed with microsatellite markers for coral host and ITS2 direct sequencing for symbiotic algae, indicating that all host colonies were genetically distinct and belonging to major populations around the Ryukyu Archipelago and mainly maintaining clade C symbionts which are dominant around this region. In common garden experiment, all colonies showed different growth patterns whilst the photosynthetic efficiencies showed similar optimal peaks among colonies. The experimental approach above suggests that there are standing genetic variations in host itself of *A. digitifera*, which might guarantee the adaptive potential of coral population for future global warming in northern peripheral reef area. These genetic variations might also contribute to the change of material cycles in future coral reefs.

Japan Geoscience Union Meeting 2014
(28 April - 02 May 2014 at Pacifico YOKOHAMA, Kanagawa, Japan)

BBG21-05 Room:213 Time:May 1 10:00-10:15

Carbon flows in estuarine and shallow waters: blue carbon study

KUWAE, Tomohiro[1*] ; TOKORO, Tatsuki[1] ; WATANABE, Kenta[1] ; MIYOSHI, Eiichi[1] ; MOKI, Hirotada[1] ; TADA, Kazufumi[2]

[1]Port and Airport Research Institute, [2]Chuden Engineering Consultants Co., Ltd.

Blue Carbon, which is carbon captured by marine living organisms, has recently been highlighted as a new option for climate change mitigation initiatives. In particular, coastal ecosystems have been recognized as significant carbon stocks because of their high burial rates and long-term sequestration of carbon. However, unlike sequestration in terrestrial ecosystems, coastal carbon burial does not lead directly to an uptake of atmospheric CO_2. This is because the water column separates the atmosphere from benthic systems, and buried sedimentary carbon is composed of allochthonous sources in addition to autochthonous sources. Our research project is aiming to in situ measurements of carbon flows, including air-sea CO_2 fluxes, dissolved inorganic carbon changes, net ecosystem production, and carbon burial rates in estuarine and shallow waters.

Keywords: climate change, carbon sequestration, carbon storage, blue carbon, seagrass meadows, estuarine waters

Japan Geoscience Union Meeting 2014
(28 April - 02 May 2014 at Pacifico YOKOHAMA, Kanagawa, Japan)

BBG21-P01 Room:Poster Time:May 1 18:15-19:30

Field investigation and the path analysis of air-sea CO2 flux in shallow waters of Ishigaki Island

TADA, Kazufumi[1*] ; TOKORO, Tatsuki[2] ; WATANABE, Kenta[2] ; MOKI, Hirotada[2] ; KUWAE, Tomohiro[2]

[1]Chuden Engineering Consultants Co., Ltd., [2]Port and Airport Research Institute

The Blue Carbon, which is carbon captured by marine living organism, is recently focused as an important option for climate change mitigation initiatives. The Blue Carbon is equivalent to approximately 55% of carbon fixed by photosynthesis activity of the earth. In particular, vegetated shallow waters have been recognized as significant carbon stocks due to the high burial rates and long term sequestration. However, the contribution of Blue Carbon sequestration to atmospheric CO_2 in subtropical shallow waters is unclear, because the investigation and analysis technologies are unmatured.

In this study, using an approach combining field investigations and path analysis, we examined the mechanisms by which environmental factors directly and indirectly affecting air-sea CO_2 flux. Field investigations were performed to examine air-sea CO_2 flux and environmental factors (e.g., wind speed, water temperature, salinity, total alkalinity (TA), dissolved inorganic carbon (DIC)) in shallow waters (Fukido, Shiraho, Nagura, and Kabira) of Ishigaki Island, July 2013. In addition, we implemented the path analysis to infer important environmental factors and interactions affecting the air-sea CO_2 flux.

Keywords: blue carbon, coastal vegetation, air-sea CO2 flux, path analysis

Japan Geoscience Union Meeting 2014
(28 April - 02 May 2014 at Pacifico YOKOHAMA, Kanagawa, Japan)

BBG21-P02 Room:Poster Time:May 1 18:15-19:30

Spatial distribution and its characteristics of stable nitrogen isotopic composition of macroalgae in Nagura Bay

TOMITA, Mami[1*] ; KAWACHI, Atsushi[2] ; MARUOKA, Teruyuki[2] ; TSUJIMURA, Maki[2]

[1]Graduate School of Frontier Sciences, The University of Tokyo, [2]Faculty of Life and Environmental Sciences, University of Tsukuba

This study, focusing on Nagura Bay in the west of the Ishigaki Island, conducted a field sampling and measurement of δ^{15}N values of macroalgae, *Padina* spp. and sea grass, *Thalassia hemprichii* in order to evaluate effects of land-derived nitrogen load on the coral reef ecosystem, and to discuss the reasons for the nitrogen load distribution in the bay.

In June 2013, 55 samples for each species were collected at about 50 m intervals on 7 transect lines, and their δ^{15}N and δ^{13}C values were measured in the laboratory. At the same time, water samples at stream, spring and sea were collected and their water qualities were measured. Moreover, areas for each land use in related watershed were calculated using GIS to examine the relationship between the nitrate concentration in river water samples and land use, and to identify the source of land-derived nitrogen.

As a result, most of the δ^{15}N values of macroalgae and sea grass linearly decreased from +6 to +2 ‰ with increasing distance from the shoreline. However, the transect lines around the river mouth of Nagura River relatively showed high δ^{15}N values by about 1 km away from the shoreline comparing with the other transect lines. One of the reasons is probably water flow condition around the river mouth. Some previous studies had showed that the water flow stagnates around there due to the south monsoon wind in spring and summer. Before this field sampling, the mode of wind direction for 3 months was surely south wind. This is why the land-derived nitrogen loads through Nagura River remained around river mouth due to water stagnation and lower dilution in seawater, and the plants could have higher δ^{15}N values.

On the other hand, NO_3-N concentrations have high correlations with ratios of farm land and cultivated areas. Thus, they were perhaps the main nitrogen sources in this study area. Additionally, NO_3-N flux [mg/s], which calculated by flow rate [m3/s] and NO_3-N concentration [mg/l], estimated 81.9 mg/s at the river mouth of Nagura River, and 59.4 mg/s at the upstream. Mangrove swamps and tidal flat exist between the two locations. Thus, the nitrogen source increasing the flux 22.5 mg/s could come from the swamps or their upstream.

Keywords: Padina spp., Thalassia hemprichii, Stable nitrogen isotopic composition, land-derived nitrogen, Nagura Bay, mangrove swamps and tidal flat

Japan Geoscience Union Meeting 2014
(28 April - 02 May 2014 at Pacifico YOKOHAMA, Kanagawa, Japan)

BBG21-P03 Room:Poster Time:May 1 18:15-19:30

Propagation of suspended matter from aquacultures as traced by stable C and N isotope ratios of bivalves

MORIMOTO, Naoko[1*] ; UMEZAWA, Yu[2] ; TANAKA, Yoshiyuki[3] ; REGINO, Genevieve L.[4] ; WATANABE, Atsushi[5] ; MCGLONE, Maria lourdes s.d.[4] ; MIYAJIMA, Toshihiro[1]

[1]Atmosphere and Ocean Research Institute, The University of Tokyo, [2]Faculty of Fisheries, Nagasaki University, [3]Mutsu Institute for Oceanography, Japan Agency for Marine-Earth Science and Technology, [4]Marine Science Institute, Unversity of the Philippines, [5]Graduate School of Information Science and Engineering, Tokyo Institute of Technology

Recently there is growing concern about the impact of densely-deployed aquacultures on coastal marine ecosystems in the Philippines. As suspension-feeding bivalves are expected to reflect local food sources, their effectiveness as an environmental indicator were examined by analyzing stable carbon and nitrogen isotope ratios of bivalves living in aquaculture and neighboring seagrass areas. As a whole, the δ^{13}C and δ^{15}N of bivalves collected in the seagrass areas ranged from -13.1 to -11.0 and from +4.0 to +6.6, respectively, but in seagrass area where water mass from aquaculture area passed through typically lower values (-18.9 ˜-16.1 and +2.7 ˜+5.2, respectively) were observed, and they were the lowest in the aquaculture area (-24.4 ˜-19.8 and +3.4 ˜+4.3, respectively). It suggests that bivalves mainly fed on sinking particles, and presumably also seagrass-derived particles in seagrass areas. Higher C/N ratio was observed at sites where impact of aquaculture was larger. Although the interspecies differences and food selectivity etc. may affect the variability of the bivalve δ^{13}C and δ^{15}N to some extent, these results demonstrated that stable isotope ratios of bivalves could be used as an effective indicator to evaluate propagation areas and actual effects of suspended matter resulting from anthropogenic source on ecosystems.

Keywords: suspension-feeding bivalve, seagrass, aquaculture, stable carbon and nitrogen isotope ratios

Japan Geoscience Union Meeting 2014
(28 April - 02 May 2014 at Pacifico YOKOHAMA, Kanagawa, Japan)

BBG21-P04 Room:Poster Time:May 1 18:15-19:30

Organic carbon preservation in tropical seagrass-bed sediments: importance of sorptive vs. non-sorptive mechanisms

MIYAJIMA, Toshihiro[1*] ; HORI, Masakazu[2] ; SHIMABUKURO, Hiromori[2] ; ADACHI, Hiroshi[3] ; HAMAGUCHI, Masami[2] ; NAKAOKA, Masahiro[4] ; NADAOKA, Kazuo[5]

[1]The University of Tokyo, [2]Fisheries Research Agency, [3]Geoact Co.,Ltd., [4]Hokkaido University, [5]Tokyo Institute of Technology

Large benthic primary producers such as seagrasses and seaweeds often exhibit extremely high CO_2-fixing ability and are expected to have a potential to mitigate the deteriorative influence of ocean acidification on local communities. In particular, the seagrass community has also a capacity of accumulating and sequestering organic carbon (OC) in the sediment underlying it, which implies that it functions as a self-complete, long-term CO_2 sink in the biogeochemical carbon cycle. This feature has been recognized as one of the major ecosystem services of the coastal marine ecosystem. In this study, we investigated the distribution, the physical state, and the potential origins of OC stored in the sediments from tropical, subtropical, and temperate seagrass communities.

The concentration of OC per salt-corrected dry weight of sediment normally ranged between 500 and 1300 μmol C g^{-1} in both temperate and subtropical seagrass beds, although extremely high values up to 4000 μmol C g^{-1} have been found in some tropical seagrass sediments that were affected by OC inputs from adjacent mangrove forest. The carbon isotopic composition (δ^{13}C) of OC varied broadly from -28 ‰ to -12 ‰ (vs. VPDB), although the majority of seagrass bed sediments exhibited -20 $\pm$ 3 ‰. The variability in δ^{13}C could be interpreted by varying contribution of multiple OC sources to the sediment, including seagrasses (c. -10 ‰), sinking particles derived from phytoplankton (c. -22 ‰), and allochthonous OC including terrestrial plant and mangrove detritus (c. -28 ‰).

The specific surface area (SSA) of sediment grains ranged between 1 - 20 m^2 g^{-1} for seagrass bed sediments. In the case of temperate seagrass sediments, the concentration of OC was closely correlated to SSA (r = 0.9405), with the average OC/SSA ratio being 0.72 mg C m^{-2}. This trend, as well as the OC/SSA ratio, is consistent with the well-known sorptive preservation model of sediment OC originally proposed for shelf sediments (OC/SSA = 0.6 - 0.9 mg C m^{-2}; Keil et al. 1994, Mayer 1994). In contrast, no clear relationship between OC and SSA was detected for subtropical and tropical seagrass sediments. The OC/SSA ratio was generally higher for subtropical (up to 4.2) and tropical (up to 8.5) samples than temperate ones. Two clearly different trends of the δ^{13}C of OC vs. the OC/SSA ratio could be distinguished for tropical and subtropical samples. In one trend, the δ^{13}C converged to between -28 ‰ and -26 ‰ with increasing OC/SSA ratio. This trend was typically observed in mangrove-affected tropical seagrass beds and therefore could be ascribed to accumulation of mangrove-derived OC particles within seagrass sediments. The other trend, in which the δ^{13}C gradually increased up to -12 ‰ with increasing OC/SSA, was found mainly in subtropical seagrass beds. This trend indicates an accumulation of OC particles of relatively high δ^{13}C, putatively derived from the underground parts of seagrasses.

Overall, the above results demonstrated that the seagrass community actually has a large capacity to accumulate and store organic carbon of both autochthonous and allochthonous origins. However, the physical state of OC stored in the sediment seemed contrasting between temperate and tropical/subtropical seagrass communities. In the former, OC seemed to be stabilized by adsorption onto mineral particles as suggested by the consistent OC/SSA ratio. In the latter, accumulation of refractory detrital OC particles apparently played the major role in the OC storage in the sediment. The source of refractory OC particles could have been autochthonous (e.g. seagrass roots) or allochthonous (e.g. mangrove debris) depending on the environment. We are now investigating what causes such a difference in the accumulation state of OC depending on climatic and/or biological factors.

Keywords: carbon cycle, organic matter, coastal ocean, seagrass beds, sediment, specific surface area

Japan Geoscience Union Meeting 2014
(28 April - 02 May 2014 at Pacifico YOKOHAMA, Kanagawa, Japan)

BBG21-P05 Room:Poster Time:May 1 18:15-19:30

Inorganic carbon cycle at the Fukido estuary in Ishigaki Island

TOKORO, Tatsuki[1*] ; WATANABE, Kenta[1] ; MIYOSHI, Eiichi[1] ; MOKI, Hirotada[1] ; TADA, Kazufumi[2] ; HOSOKAWA, Shinya[1] ; KUWAE, Tomohiro[1]

[1]Port and Airport Research Institute, [2]Chuden Engineering Cosulatants

″ Blue Carbon ″ , which is carbon captured by marine living organisms and about 55 % of biological captured carbon in the world, is an important carbon budget in the global carbon cycle. The Blue Carbon in coastal regions is recently focused as an effective option for the climate change initiatives because the part of the Blue Carbon is separated from the atmosphere for long periods as the sediment in the soil. The potential of the carbon sequestration in tropical-subtropical coastal regions is expected to be high due to the abundant vegetations such as seagrass meadows and mangroves. Meanwhile, there is the potential that the coastal regions release CO_2 to the atmosphere due to the high decomposition rate of organic matters in vegetations and from land.

The precise measurement of the carbon cycle including the air-sea CO_2 flux is necessary for the evaluation of tropical-subtropical coastal regions related to atmospheric CO_2. Because the temporal variation in tropical-subtropical regions is generally larger than that in other climate regions, the measurement should have a certain level of continuity for long periods. In this study, we analyzed the subtropical inorganic carbon flow base on the measurement of air-sea CO_2 flux by the eddy covariance method and the biomass of seagrass at an estuary in Ishigaki Island.

The measured air-sea CO_2 flux by the eddy covariance method (-1.00 $\pm$ 0.11 μmol/m^2/s; 95 % confidential limit) indicates that the estuary was atmospheric CO_2 sink during the measurement period; the value is almost the same as the flux measured by other method such as the bulk formula method or the floating chamber method. In addition, the measured flux shows different tendency before and after a typhoon approach at the site. Because the seagrass was autotrophic during the measurement period, the linkage between the Blue Carbon production and the absorption of atmospheric CO_2 was confirmed at the measurement site. The presentation will discuss about the potential of the Blue Carbon fixation at subtropical coastal regions based on the comparison of the carbon flow measurement in other climate zone.

Keywords: Carbon cycle, Blue Carbon, Air-sea CO2 flux, Seagrass, Eddy covariance method

Japan Geoscience Union Meeting 2014
(28 April - 02 May 2014 at Pacifico YOKOHAMA, Kanagawa, Japan)

BBG21-P06 Room:Poster Time:May 1 18:15-19:30

Skeletal records in sclerosponges from Miyako-jima, Ryukyu Islands

MATSUMORI, Taketo[1*] ; ASAMI, Ryuji[1] ; SAKAMAKI, Takashi[2]

[1]University of the Ryukyus, Japan, [2]Tohoku University, Japan

Sclerosponges, living in dark environments of tropical to subtropical shallow oceans, precipitate calcium carbonate skeleton with growth bands. They grow slowly at an approximate rate of $<$1 mm/year unlike corals (about 1 cm/year) but can be so long-lived for several decades to hundred years like corals (e.g., Benavides and Druffel, 1986). Skeletal oxygen isotopic ratios (δ^{18}O) reflect variations in sea surface temperature and seawater δ^{18}O with the latter being closely related to salinity reflecting the precipitation-evaporation balance at the sea surface and changes in water mass transport (e.g., Wu and Grottoli, 2009). In contrast to zooxanthellate corals, which commonly show positive correlations between skeletal δ^{18}O and carbon isotopic ratios (δ^{13}C), there do not exist vital effects in the secretion of sclerosponge skeleton (Druffel and Benavides, 1986). Previous studies showed significant decrease trends in the δ^{13}C records toward the present, which is probably a result of $^{12}CO_2$ added into the atmosphere/ocean from fossil fuel burning (e.g., Bohm et al. 1996). Therefore, sclerosponges are shown to provide annually resolved time series of proxy records of ocean environments since the Industrial Revolution. However, longer ($>$100 year) proxy records from sclerosponges were derived only from the Atlantic Ocean.

Here we present δ^{18}O and δ^{13}C records from high-Mg calcite skeleton of two sclerosponges (*Acanthochaetetes wellsi*) collected at a water depth of about 10 m from Miyako-jima, Ryukyu Islands in the North Pacific. The samples were slabbed to a thickness of 5 mm parallel to the skeletal growth and subsamples for stable isotope measurements were taken every 1 mm. External precision of replicate measurements of interlaboratory calcite material throughout the stable isotope analysis using a continuous flow isotope ratio mass spectrometer system (Delta V Advantage and Gasbench II: Thermofisher Scientific Inc.) of Ryukyu University was $\pm$0.05 per mil for δ^{18}O and δ^{13}C. Soft X-ray images showed highly developed skeletal growth bands with $>$100 high/low density layers. The secular changes in δ^{13}C of the two sclerosponges were quite similar to previously reported δ^{13}C records from Atlantic and Pacific corals and sclerosponges. The long-term δ^{18}O trends of the two samples are characterized by slight depletions throughout their living periods, indicative of an overall trend toward warmer ocean environment around Miyako-jima. Our sclerosponge-based estimates of sea surface temperature and salinity may document thermal and hydrologic variations in the Ryukyu Islands, furthering a good understanding of northwestern tropical-subtropical Pacific climate change for the last several centuries in conjunction with coral-based long proxy records.

Keywords: sclerosponge, skeleton, oxygen isotope composition, carbon isotope composition, paleoenvironment, Ryukyu Islands

Japan Geoscience Union Meeting 2014
(28 April - 02 May 2014 at Pacifico YOKOHAMA, Kanagawa, Japan)

BBG21-P07 Room:Poster Time:May 1 18:15-19:30

Paleoenvironmental analysis using Tridacnidae shells from archaeological sites in Okinawa-jima, subtropical southwestern

ASAMI, Ryuji[1*] ; KONISHI, Mika[1] ; TANAKA, Kentaro[1] ; UEMURA, Ryu[1] ; FURUKAWA, Masahide[1] ; SHINJO, Ryuichi[1]

[1]University of the Ryukyus, Japan

Symbiont-bearing Tridacnidae giant clams living in shallow waters of the Indo-Pacific tropical and subtropical regions can be a used as an archive for documenting high-resolution record of thermal and hydrologic variations in coral reef environments for the past. Their shells, composed of dense aragonitic increments, are less sensitive to diagenetic alteration than porous skeleton of corals. They have annually and daily banded shells structure, providing chronological controls (e.g., Bonham 1965). The oxygen isotope composition (δ^{18}O) of shells, which are precipitated isotopically equilibrium with seawater, can reflect the temperature and seawater δ^{18}O (e.g., Aharon & Chappell 1986). Several studies on paleoenvironmental reconstructions around the Ryukyu Islands were performed using geochemistry in fossil corals from Okinawa-jima (Mitsuguchi et al. 1998), Yonaguni-jima (Suzuki et al. 2001), Kikai-jima (Morimoto et al. 2007), and Kume-jima (Seki et al. 2012). However, only a δ^{18}O record has been published from 6.2 ka giant clams from Kume-jima (Watanabe et al. 2004).

Here we present seasonally resolved δ^{18}O time series of fossil Tridacnidae shells recovered from two archaeological sites (the Kogachibaru Shell Mound and the Second Aragusuku-Shichabaru Ruin) in Okinawa-jima, southwestern Japan to reconstruct subtropical coral reef environments of the past. The samples, mainly composed of aragonite shells with limited amounts of calcite cements, were selected for geochemical analyses. The radiocarbon dating results indicated that they lived during the early and middle Shell Mound periods in Okinawa-jima, corresponding to the middle-to-late Holocene, which is in good agreement with ages inferred from excavation (Okinawa Prefectural Board of Education 1987; Okinawa Prefectural Archaeological Center 2006). The shell δ^{18}O values roughly showed seasonal variations, coincident with the occurrence of annual growth bands. The averages of annual, summer, and winter δ^{18}O values of fossil shells were significantly lower than aragonite theoretically precipitated in present-day coral reef water of Okinawa-jima. These results demonstrate that the seawater temperature was higher and/or salinity was lower at the sites than today. It is likely that the giant clams lived in relatively small and/or closed coral-reef lagoons with less water circulation where seawater is highly susceptible to insolation-induced temperature increase and input of fresh water; the effect could be enhanced by the fisheries lifestyle that stonewalling would be constructed at shallow waters through the use of tidal variation during the Shell Mound period in Okinawa-jima.

Although it is extremely difficult to find well-preserved fossil Tridacnidae shells from carbonate sediments that are not fragmented, archaeological ruins and shell mounds can yield many fossils. Results of our study suggest that the use of fossil shells from archaeological sites can enable the reconstruction of temporal and spatial variations in coral reef environments and of the history of lifestyles and culture during prehistoric and protohistoric ages.

Keywords: coral reef, Tridacnidae, shells, fossil, oxygen isotopic composition, archaeological site

Japan Geoscience Union Meeting 2014
(28 April - 02 May 2014 at Pacifico YOKOHAMA, Kanagawa, Japan)

BBG21-P08 Room:Poster Time:May 1 18:15-19:30

Evaluation of natural break water of coral reefs affected by typhoons in the near future

HONGO, Chuki[1*] ; KIGUCHI, Masashi[2]

[1]Dept. Physics & Earth Sciences, University of the Ryukyus, [2]Institute of Industrial Science, the University of Tokyo

Tropical cyclones are one of the most extreme natural catastrophic events over the world and devastate coastal areas affected by floods and coastal erosions. Ryukyu Islands in the northwest Pacific is especially prone to many typhoons every year (Emanuel et al. 2008 Bull Amer Meteor Soc). However, the region is moderately protected from storm surge and wave during typhoons because coral reefs play a role in natural break water. For the last several decades, coral cover and species diversity on coral reef have shown dramatic declines in the region, influenced by global and local stresses (e.g., Hongo and Yamano 2013 PLoS ONE). According to the numerical modeling of global warming at the end of 21 st century, moreover, the mean intensity of tropical cyclones will probably increase significantly in the near future (Meehl et al. 2007 IPCC 4th Report). It is thus of some interest to understand the impact of tropical cyclones on the coastal areas in the region and the evaluation of coral reefs as natural break water.

To calculate a hydraulic force on a natural break water, we measured 9 transects using the echo sounder system (HFD-1000; Hongo et al. 2013 The Quat Res) on from the coast to the reef crest at Ishigaki Island in Ryukyu Islands during November 2013. To evaluate a contribution to reef formation by corals, moreover, we observed species abundance (cover) of tabular corals at the island. We shows that a change of role in natural break water of coral reefs in the island from present to end of 21 st century. Furthermore, we suggest necessary information of corals (e.g., cover and species) for maintenance of natural break water in the near future. The information are like to be one of basic criterion for determination of species in terms of direct transplantation of juvenile or adult corals, if the coral reefs will decline in the near future.

This research was supported by Nippon Life Insurance Foundation and JSPS Research Fellowships for Young Scientists (24-4044).

Keywords: typhoon, coral reef, Ishigaki Island, Ryukyu Islands, natural break water

Japan Geoscience Union Meeting 2014
(28 April - 02 May 2014 at Pacifico YOKOHAMA, Kanagawa, Japan)

BGM22-01 Room:415 Time:April 30 09:00-09:15

Plant rhizopsphere is a hotspot for greenhouse gas emissions

MINAMISAWA, Kiwamu[1*]

[1]Consortium for Rhizosphere Biogeochemistry, Graduate School of Life Sciences, Tohoku University

Nitrous oxide (N_2O) is a greenhouse gas that also degrades stratosphere ozone. Marked N_2O emission were detected from soybean root systems with degraded nodules during late growth stage in field-grown soybeans. A model system developed to produce N_2O emissions from soybean fields. Soybean plants inoculated with *nosZ* mutant of *Bradyrhizobium japonicum* USDA110 (lacking N_2O reductase) were grown in aseptic jars. After 30 days, shoot decapitation (D, to promote nodule degradation), soil addition (S, to supply soil microbes), or both (DS) were applied. N_2O was emitted only in the DS treatment. Thus, both soil microbes and nodule degradation are required for the emission of N_2O from the soybean rhizosphere. The N_2O flux peaked at 15 days after DS treatment. A ^{15}N tracer experiment indicated that the N_2O was derived from N fixed in the nodules. As for nitrification, the addition of nitrification inhibitors significantly reduced N_2O flux. Both AOA and AOB were detected by PCR analysis with N_2O emission profile in soybean rhizosphere. The N_2O flux from the *nirKnosZ* mutant rhizosphere was significantly lower than that from *nosZ* mutant, but was still 30% to 60% of that of *nosZ* mutant, suggesting that N_2O emission is due to both *B. japonicum* and other soil microorganisms. Only *B. japonicum nosZ+* strains could take up N_2O. In particular, *Fusarium* spp., a soil fungus may contributed to N_2O emission in soybean rhizoshere. From these results, the organic-N inside of the nodules was mineralized to NH_4^+, and N_2O producing processes (nitrification and denitrification) simultaneously occur in the soybean rhizopsphere. We continue to examine which microbes really mediated N_2O methabolism using isotopic techniques including ^{15}N site preference of N_2O molecules. N_2O emissions from soybeans ecosystems can be mitigated by inoculting *B. japonicum* mutants with increased N_2O reductase activity (Nos++ strains). The mutation of *nasS* gene is responsible for the Nos++ phenotype. We propose that *nasS* mutation might be an effective strategy to induce higher Nos activities in N_2O-reducing rhizobia, such as indigenous isolates from local soybean fields or even from other important leguminous crops such as alfalfa, and thus to mitigate N_2O emission.

Plants have mutualistic symbiotic relationships with rhizobia and fungi by the common symbiosis pathway, in which Ca_2^+/calmodulin-dependent protein kinase (encoded by *CCaMK*) is a central component. Although *OsCCaMK* is required for fungal accommodation in rice roots, little is known about the role of *OsCCaMK* in rice symbiosis with bacteria. Here, we report the effect of a *tos17*-induced *OsCCaMK* mutant (NE1115) on CH_4 flux in low-nitrogen (LN) and standard-nitrogen (SN) paddy fields as compared with wild-type (WT) Nipponbare. Growth of NE1115 was significantly decreased compared with that of WT, especially in the LN field. The CH_4 flux of NE1115 in the LN field was significantly higher (156?407% in 2011 and 170?816% in 2012) than that of WT, although no difference was observed in the SN field. The copy number of pmoA was significantly higher in the roots and rhizosphere soil of WT than those of NE1115. However, mcrA copy number did not differ between WT and NE1115. These results were supported by a ^{13}C-labeled CH_4-feeding experiment. In addition, the natural abundance of ^{15}N in WT shoots (3.05 permile) was significantly lower than in NE1115 shoots (3.45 permile), suggesting higher N_2 fixation in WT due to dilution with atmospheric N_2 (0.00 permile). Thus, CH_4 oxidation and N_2 fixation were simultaneously activated in the root zone of WT rice in the LN field, and both processes are likely controlled by *OsCCaMK*.

Keywords: methane, nitrous oxide, rhizosphere, Bradyrhiozbia, bacteria, stable isotope

Japan Geoscience Union Meeting 2014
(28 April - 02 May 2014 at Pacifico YOKOHAMA, Kanagawa, Japan)

BGM22-02 Room:415 Time:April 30 09:15-09:30

Does microbial ecology expand our understandings of nitrogen cycle in forests?

ISOBE, Kazuo[1*] ; OHTE, Nobuhito[1]

[1]The University of Tokyo

Forests cover approximately 70% of Japan's total land area, representing a largest reservoir of diversity of organisms including plants, animals, fungi protists and prokaryotes on land. These organisms are closely associated each other in material cycles if not directly. Thus, we need to know how materials are cycling between the organisms in order to address a fundamental question in ecosystem ecology: why do forests have the richest biodiversity on land? However, it is not easy to understand the material cycles in a forest because the forest has the various environmental heterogeneity which greatly affect the cycle. For example, nitrogen dynamics can be different in soils around hills and valleys in forests. Such spatial heterogeneity of the dynamics in the soils has been explained mainly from phenomenological perspectives using abiotic information such as soil moisture, soil temperature or litter quality. However, these perspectives have not fully explained the dynamics. Here, we suggest that such heterogeneity need to be explained in the context of ecology of microbial communities which mediate the nitrogen dynamics. More specifically, we suggest that understanding the nitrogen dynamics based on the physiology, population dynamics and diversity of the microbial communities can provide the mechanistic insights into the nitrogen cycle in forests.

We analyzed the spatial heterogeneity of nitrogen dynamics and associated microbial communities in natural and planted forest soils in Asia. Specifically, we focused on nitrification in which ammonium are oxidized to nitrate and found the close association between gross nitrification rates and population size of nitrifiers in the soils. Additionally, nitrification rates cannot be fully explained by using environmental properties including substrate supply, soil moisture and litter quality, but can be explained by using the population size of nitrifiers. This shows that the better understandings of the microbial ecology allows us to more accurately explain and even predict the spatial heterogeneity of material cycles. In this presentation, we will discuss how information on microbial ecology expands our understandings of nitrogen cycle in forests.

Keywords: microbial ecology, nitrogen cycle, forest

Japan Geoscience Union Meeting 2014
(28 April - 02 May 2014 at Pacifico YOKOHAMA, Kanagawa, Japan)

BGM22-03 Room:415 Time:April 30 09:45-10:00

Diversity of microbial arsenic transformation pathways associated with arsenic cycling in the environment

HAMAMURA, Natsuko[1*] ; KATAOKA, Takafumi[1] ; FUKUSHIMA, Koh[1]

[1]CMES, Ehime University

Arsenic (As) is a naturally occurring toxic element that is widely distributed in nature. Although the concentrations of As in natural systems are generally low (~15 μg g^{-1} in soil and ~10 μg L^{-1} in surface waters), the elevated levels of As have been released via natural sources (i.e. volcanic activity) and anthropogenic activities due to its increasing industrial use. As can exist in four oxidation states (-III, 0, III and V), while they are mainly found as trivalent [arsenite; As(III)] and pentavalent [arsenate; As(V)] in natural systems. Depending on its oxidation state, As exhibit different mechanisms of toxicity to microorganisms and other biota. As(III) is highly reactive with thiol containing proteins and is considered more toxic than As(V). Despite its toxicity, microorganisms have developed mechanisms to tolerate As and/or utilize the element for respiratory metabolism. Although various microorganisms have been identified to catalyze As transformation including both oxidation and reduction, we have just began to unveil the full diversity of different microbial processes associated with the redox cycling of As in the environment.

To gain insight into microbial roles in the geochemical dynamics of As, the combined geochemical, physiological and molecular biological analyses were applied to examine As-impacted environments and microcosms. Microbial populations were analyzed using 16S rDNA-based molecular approach combined with metagenomic sequencing. The presence of indigenous microbial populations capable of As transformation was examined by using both molecular approach targeting As functional genes and cultivation approach. The genes coding for arsenite oxidase (*aioA*), which catalyzes the oxidation of As(III) coupled to O_2 reduction, have been recovered from geochemically distinct geothermal habitats (pH 2.6-8) as well as the soils from mine tailing. Successful cultivation of various As(III)-oxidizing bacteria confirmed the microbial attribute in As oxidation *in situ*. In contrast, from the As impacted lake sediments and soils, diverse sequences of anaerobic arsenite oxidase (*arx*) and arsenate respiratory reductase (*arr*) genes were detected, while no *aio* genes were recovered. The anaerobic arsenite oxidase, Arx, is known to catalyze arsenite-oxidation coupled to nitrate reduction or photosynthesis. Consistent with the molecular approach, the anaerobic arsenite-oxidizing nitrate reducer and arsenate-reducing bacteria were isolated from the lake sediments.

Our results showed that As redox metabolisms are widespread within phylogenetically and physiologically diverse bacteria, including both chemolithotrophic and organotrophic aerobes and anaerobes. This study revealed the diversity of As transformation pathways associated with geographically and geochemically distinct environments and presented the mechanisms behind microbial processes controlling the redox cycling of As.

Keywords: arsenite oxidase, arsenate reductase, microbial arsenic transformation, soil microbiology

Japan Geoscience Union Meeting 2014
(28 April - 02 May 2014 at Pacifico YOKOHAMA, Kanagawa, Japan)

BGM22-04 Room:415 Time:April 30 10:00-10:15

Biosignature found in iron oxide mineralogy of iron-oxidizing microbe origin?

MAKITA, Hiroko[1*] ; KIKUCHI, Sakiko[2] ; NUNOURA, Takuro[1] ; MITSUNOBU, Satoshi[3] ; HIRAI, Miho[1] ; TAKAKI, Yoshihiro[1] ; YAMANAKA, Toshiro[4] ; TOKI, Tomohiro[5] ; NAKAMURA, Kentaro[6] ; ABE, Mariko[1] ; MIYAZAKI, Junichi[1] ; NOGUCHI, Takuroh[1] ; WATANABE, Hiromi[1] ; TAKAHASHI, Yoshio[2] ; TAKAI, Ken[1]

[1]JAMSTEC, [2]Hiroshima University, [3]University of Shizuoka, [4]Okayama University, [5]University of the Ryukyus, [6]The University of Tokyo

Recently, many iron mats have been discovered at deep-sea hydrothermal fields in all over the world. It has been thought that microbes, especially iron-oxidizing microbes, are the key players for forming the iron mats. However, there was no direct evidence to this, due to cultivation difficulty of iron oxidizers. Recently, '*Mariprofundus ferrooxidans*' that belong to the Zetaproteobacteria was successfully isolated. From this isolation, it has been proved that this microbe can oxidize ferrous iron as the electron donor, and can widely be observed in various deep-sea low-temperature hydrothermal fields. Therefore we have investigated how these microbes contributed to the formation of the iron mat using mineralogical and culture independent approaches.

We tried to clarify mineralogical properties of natural or lab-prepared iron oxides of iron-oxidizing microbes by using XAFS, SEM and EDX. Natural samples were collected at 3 sampling sites: iron mats from deep-sea hydrothermal fields in the Mariana Volcanic Arc, Mariana Trough and the Okinawa Trough. Lab-prepared iron-oxide synthesis was carried out using chemoautotrophic bacterium Mariprofundus ferrooxydans PV-1 (ATCC BA-1020) and was cultured by diffusion cell's method (Kikuchi et al., 2011, 2014). SEM observation showed similar morphology to all samples, which have distinctive plait-like structure, and at where iron oxides precipitate around distinctive materials. Although each natural iron-oxide sample was precipitated at different environments and with different dominant microbial species within the natural samples, XAFS showed identical spectrum. Regardless of medium employed in the cultivation, lab-prepared iron oxides also showed similar spectrum to natural samples. XANES fitting suggested that iron mats consist of ferrihydrite and iron-organic complex being the same as the lab-prepared iron oxides. These results strongly supported the iron-oxidizing chemolithoautotrophs had significant ecological roles in producing the iron mat. These mineralogical analyses may help to find biosignature in the deep-sea environments.

Keywords: iron-oxidizing bacteria, Biosignature, Mineralogical property, deep-sea, hydrothermal fields

Japan Geoscience Union Meeting 2014
(28 April - 02 May 2014 at Pacifico YOKOHAMA, Kanagawa, Japan)

BGM22-05 Room:415 Time:April 30 10:15-10:30

The trench biosphere observed from the transect water sampling for the Japan Trench

NUNOURA, Takuro[1*] ; HIRAI, Miho[1] ; YOSHIDA, Yukari[1] ; NISHIZAWA, Manabu[1] ; KAWAGUCCI, Shinsuke[1] ; MAKITA, Hiroko[1] ; MIYAZAKI, Junichi[1] ; SUNAMURA, Michinari[2] ; TAKAI, Ken[1]

[1]JAMSTEC, [2]The Univ. Tokyo

We have discovered the presence of the trench biosphere that harbored distinct microbial populations comparing to those in the upper water masses in the Challenger Deep, Mariana Trench (Nunoura et al. in preparetion). The deep locates under the oligotrophic ocean and is isolated from the other trenches while the Japan Trench locates under eutrophic ocean and in a series of long trenches in north Pacific. Therefore, the Japan Trench has one of the best environments to test the universality of the occurrence of trench biosphere. In this study, we conducted CTD casts in 8 stations across the Japan Trench in 2011 after the big earthquake and analyzed microbial structures for each sample in order to examine the occurrence of the trench biosphere.

Keywords: Japan Trench, nitirification

Japan Geoscience Union Meeting 2014
(28 April - 02 May 2014 at Pacifico YOKOHAMA, Kanagawa, Japan)

BGM22-06 Room:415 Time:April 30 10:30-10:45

SUP05 contribution for Carbon and Nitrogen cycles in semi-closed water mass

SUNAMURA, Michinari[1*] ; TAKAKI, Yoshihiro[2] ; NUNOURA, Takuro[2] ; TAKAI, Ken[2]

[1]Earth & Planet. Science, The University of Tokyo, [2]JAMSTEC

In the deep sea hydrothermal plume, significantly elevated microbial biomass has been reported depending on chemolithoautotrophic activities by hydrothermal reduced chemicals. The potential energetic is sulfur, methane and hydrogen oxidation, and microbial production is up to date. The most important microbes in the plume is SUP05 phylotype (genus Thioglobes), which is known to have sulfur and H2 oxidation pathway, RubisCO carbon assimilation pathway, and denitrification pathways. In this study, we compared the bicarbonate and inorganic nitrogen species with SUP05 cell densities in the hydrothermal plume of the TOTO caldera hydrothermal field with half-closed water mass system in the Southern Mariana Trough. The cell densities of SUP05 is strong negative correlation with bicarbonate and nitrate, however, the correlation slope indicated the nitrogen assimilation but not the nitrogen respiration (denitrification). Only the nitrogen assimilation occurred in the plume is also supported by the lack of denitrification genes in the plume sample with the metagenomic analysis.

Keywords: Chemolithoautotroph, SUP05, TOTO, metagenomics

Japan Geoscience Union Meeting 2014
(28 April - 02 May 2014 at Pacifico YOKOHAMA, Kanagawa, Japan)

BGM22-07 Room:415 Time:April 30 11:00-11:15

From who, where, how many and what to ’Earth science’

KENJI, Kato[1*]

[1]Department of Geosciences, Graduate School of Science, Shziuoka University

Glancing at 50 years’ history of aquatic microbial ecology since Wright and Hobbie proposed an uptake kinetics using radio-labeled glucose, I may pose issue(s) of consideration for microbial ecology as an earth science.

Keywords: 14C-glucose uptake vs. 3H-Thymidine uptake, Production vs. Respiration, sec vs. year

Japan Geoscience Union Meeting 2014
(28 April - 02 May 2014 at Pacifico YOKOHAMA, Kanagawa, Japan)

BGM22-08 Room:415 Time:April 30 11:15-11:30

Microbial potential and carbon cycle in deep aquifer of the accretionary prism of Southwest Japan

MATSUSHITA, Makoto[1*] ; KIMURA, Hiroyuki[1]

[1]Department of Geosciences, Graduate School of Science, Shizuoka University

The accretionary prism situated along the Pacific side of Southwest Japan forms thick sediments. The sediment contains deep aquifers that anaerobic groundwater is accumulated. In addition to the anaerobic groundwater, it has been reported that dissolved natural gases composed mainly of methane are present in the deep aquifers. The groundwater and natural gases are collected from deep wells (150-1500 m depth) which are drilled at the accretionary prism. In the past study conducted in a deep well situated Shimada, Shizuoka Prefecture, Japan, it has been shown that methane has been produced by subterranean microbial community in deep aquifer associated with accretionary prism. However, microbial and geochemical studies have not yet been performed at other areas of accretionary prism. In this study, we collected groundwater and natural gases from 14 deep wells of Shizuoka Prefecture, and we performed measurements of physical and chemical parameters, anaerobic cultivations of microbial communities and 16S rRNA gene analysis to understand microbial potential and carbon cycle in subterranean environments of the accretionary prism.

The temperature of groundwater samples ranged from 24.2 to 49.3 ℃, and pH was weakly alkaline. Oxidation-reduction potential suggested -325 to -114 mV at all deep wells. Electric conductivity ranged widely from 92 to 2,110 mS m^{-1} at each groundwater sample. NO_3^-, SO_4^{2-} and S^{2-} in groundwater was below the detection limit. Dissolved organic carbon (DOC) ranged from <0.3 to 50 mg l^{-1}. From componential analysis of the natural gases, methane was predominant gas component at many sites (>90%). On the other hand, we detected several natural gas samples contained a large amount of N_2 (20-50%). Stable carbon isotopic analysis of methane in the natural gases and dissolved inorganic carbon (DIC) in groundwater suggested that methane of biogenic origin are contained in the natural gases at a lot of sites.

Anaerobic incubations using groundwater amended with organic substrates revealed the high potential of H_2 and CO_2 generation by H_2-producing fermentative bacteria. Furthermore, methane generation by syntrophic consortium of H_2-producing fermentative bacteria and H_2-using methanogen was also observed in 3-5 days after the start of incubation.

Bacterial 16S rRNA gene analysis indicated the dominance of H_2-producing fermentative bacteria. The presence of denitrifying bacteria was also observed at the sites where N_2 is contained in the natural gas samples. In archaeal 16S rRNA gene analysis, H_2-using methanogens dominant in the groundwater.

From these date, it was shown that carbon cycle that methane has been produced from organic matters which are contained in the sediments by syntrophic consortium of H_2-producing fermentative bacteria and H_2-using methanogens exist in wide area of the subterranean environments of the accretionary prism. In addition to methane production, the presence of denitrification using NO_3^- or NO_2^- and organic matter or methane was also suggested at a few site.

Keywords: accretionary prism, deep aquifer, methanogenesis, fermentation, syntrophic biodegradation, subsurface environment

Japan Geoscience Union Meeting 2014
(28 April - 02 May 2014 at Pacifico YOKOHAMA, Kanagawa, Japan)

BGM22-09 Room:415 Time:April 30 11:30-11:45

The global methane cycle revealed through geomicrobiological analysis

YANAGAWA, Katsunori[1*]

[1]JAMSTEC

Methane is one of the major end products of anaerobic microbial metabolism. Based on stable carbon and hydrogen isotopic compositions of methane, geochemical studies have systematically classified the origin of methane; 1) biological pathways consisting of carbon dioxide reduction coupled to molecular hydrogen oxidation and methyl-type fermentation, and 2) abiological pathways such as thermal degradation of organic matter and Fischer-Tropsch type reaction. In contrast, regarding methane consumption, recent advances in subseafloor biosphere research have unveiled the complexity of processes involved in the transformation, migration and fate of methane. Particularly, it has been recognized that marine sediments with high methane flux harbor novel lineages of microorganisms, the physiological traits of which are largely unknown due to their resistance to cultivation. Recent advances in subseafloor biosphere research indicate that microbes play much more important roles in methane production and consumption than previously assumed. Though these biogeochemical processes are not fully understood, future combined approach of geochemistry and geomicrobiology will shed light on the global methane cycle on Earth.

Keywords: subseafloor biosphere, methane, methanogen, methanotroph

Japan Geoscience Union Meeting 2014
(28 April - 02 May 2014 at Pacifico YOKOHAMA, Kanagawa, Japan)

BGM22-10 Room:415 Time:April 30 11:45-12:00

Isotope systematics among H_2, CH_4 and H_2O in fluid associated with serpentinization

KONNO, Uta[1*]

[1]JAMSTEC

Serpentinite-hosted hydrothermal systems have attracted considerable attention as sites of abiotic organic synthesis and as habitats for the earliest microbial communities, because hydrothermal fluids derived from ultramafic rocks are characterized by high concentrations of H_2 and CH_4. During water-rock reactions, Fe (II) in olivine of ultramafic rock is oxidized to Fe (III), which accompanies the reduction of water to yield H_2. Methane and hydrocarbons are often observed in serpentinite-hosted hydrothermal systems and are thought to be produced from H_2 and CO_2 via Fischer-Tropsch-type (FTT) reactions. On the other hand, H_2 and CH_4 can be consumed and produced by microorganisms such as methanogens and methanotrophs around the hydrothermal systems. When we collect and analyze samples, those chemical compositions could have been altered due to microbial activities. Therefore, it is very difficult to clarify processes related to H_2 and CH_4 around the serpentinite-hosted hydrothermal systems.

Isotopic compositions are useful tool to discriminate origins and reaction pathways of chemical components. As representative controlling factors of isotopic compositions are temperature equilibrium, isotopic compositions of substrate, and isotopic fractionation, the dynamics of isotopic compositions are complicated in natural environments. Therefore, polyphasic aspects, such as hydrological, geological and microbiological interpretations, are needed. However, even complete hydrogen isotopic analysis of H_2, CH_4 and H_2O from serpentinite-hosted systems and basic laboratory experiments has been reported in only a few studies. As the isotope systematics among H_2, CH_4 and H_2O in fluid associated with serpentinization remain unexplored, I will present the review of some previous studies and results of explorations of hydrothermal systems at Mid Cayman Ridge during YK13-05 cruise.

Keywords: serpentinization, stable isotope, hydrogen, methane

Japan Geoscience Union Meeting 2014
(28 April - 02 May 2014 at Pacifico YOKOHAMA, Kanagawa, Japan)

BGM22-11 Room:415 Time:April 30 12:00-12:15

Acetate-oxidation activities in the deep subseafloor biosphere associated with coalbeds off the Shimokita Peninsula

IJIRI, Akira[1*] ; INAGAKI, Fumio[1]

[1]JAMSTEC

The IODP Expedition 337 was the first riser-drilling expedition dedicated to subseafloor microbiology using the drilling vessel Chikyu. During Expedition 337, we penetrated a 2466 m deep sedimentary sequence at Site C0020A with a series of coal layers at 2000 m bellow the seafloor (mbsf) off the Shimokita Peninsula, Japan. One of the primary scientific objectives of Expedition 337 was to understand ecological roles of subseafloor microbial activity in biogeochemical carbon cycles associated with the deeply buried coalbeds in the ocean. It has been hypothesized that immature coalbeds (i.e., lignite) release substantial dissolved organic compounds such as volatile fatty acids or hydrocarbons during the burial alternation process, which compounds may play important roles for supporting microbial population and activity in the deep sedimentary habitat. Alternatively, it is also conceivable that deep subseafloor microbial activities may contribute to the hydrocarbon reservoir system.

To examine those hypotheses, we measured methanogenic and acetate-oxidation activities by radiotracer incubation experiments using 2 cm^3 of the innermost sediment core samples that were supplemented with ^{14}C-labelled substrate ([2-^{14}C]-acetate) immediately after core recovery. Activities of aceticlastic methanogenesis were observed in the sediment above the coalbed layers (>1990 mbsf), ranging from 0.2 to 4 pmol cm^{-3} d^{-1}. The highest activity was observed in a coalbed horizon at 1990 mbsf; however, no aceticlastic methanogenesis activities were observed below the 2 km-deep coalbeds. Activities of acetate oxidation to CO_2 were measured by $^{14}CO_2$ production rate from [2-^{14}C]-acetate. Interestingly, the acetate-oxidation activities were observed in sediments above the coalbeds, which values were generally higher than those of methanogenesis with the maximum value of 150 pmol cm^{-3} d^{-1} at 1800 mbsf. The rates gradually decreased with increasing depth from 1800 mbsf and reached bellow the detection limit in 2 km-deep coalbeds. The occurrence of relatively high acetate oxidation at around 1800 mbsf above the coalbeds indicates the presence of available electron acceptors (e.g., glauconitic iron oxides) in the deep sedimentary habitat.

Japan Geoscience Union Meeting 2014
(28 April - 02 May 2014 at Pacifico YOKOHAMA, Kanagawa, Japan)

BGM22-12 Room:415 Time:April 30 12:15-12:30

Temperature effect of sulfur isotope fractionation by sulfate reducers when used glucose as electron donor

MATSUURA, Fumihiro[1*] ; UENO, Yuichiro[1] ; MAKITA, Hiroko[2] ; TAKAI, Ken[2]

[1]Tokyo Institute of Technology, [2]Japan Agency for Marine-Earth Science and Technology

Sulfate reducing microbe (SRM) is responsible for over 50 % of organic carbon remineralization in marine sediments and thus plays a prominent role in sulfur cycle. Based on a large number of culture experiments of SRM, sulfur isotope fractionation by SRM changes depending on environmental factors including temperature, sulfate concentration and availability of electron donor. The isotope fractionation is recorded in sedimentary sulfates and sulfides. Hence, the sulfur isotopic fractionation is useful to reconstruct ancient environmental condition. However, the mechanism controlling the degree of the sulfur isotopic fractionation is still unclear. Particularly, we have to consider the physiology. Previous culture experiments of SRM indicated that the temperature effect varies with species of SRM. However, there is little temperature control experiments using various electron donor with same strain. We carried out temperature control experiments at 25 ℃, 30 ℃ and 37 ℃, by sulfate reducing bacteria DSM 642 using glucose as electron donor. Our results revealed growth rate of DSM 642 is fastest at 30 ℃, when using glucose as electron donor. Growth rate is the fastest at 37 ℃ when using lactate as an electron donor. Sulfate reduction rate is thought to primary factor controlling isotope fractionation. In addition, growth rate and sulfate reduction rate have basically positive correlation. Accordingly, the shift of sulfur isotope fractionation by temperature must be changed when used glucose as electron donor. This result indicates that we should pay attention not only sulfate reduction pathway but also oxidation pathway of electron donor. We report temperature dependency of sulfur isotope fractionation by DSM 642 using glucose as electron donor at the first time, to elucidate the mechanism controlling the degree of the sulfur isotopic fractionation during microbial sulfate reduction.

Keywords: sulfur isotope, sulfate reducing bacteria

Japan Geoscience Union Meeting 2014
(28 April - 02 May 2014 at Pacifico YOKOHAMA, Kanagawa, Japan)

BGM22-13 Room:415 Time:April 30 12:30-12:45

A hot-alkaline DNA extraction method for deep subseafloor communities

MORONO, Yuki[1*] ; TERADA, Takeshi[3] ; HOSHINO, Tatsuhiko[1] ; INAGAKI, Fumio[1]

[1]Kochi Institute for Core Sample Research, JAMSTEC, [2]Submarine Resources Research Project, JAMSTEC, [3]Marine Works Japan Ltd.

Many of the DNA-based researches have greatly enhanced our understanding on stratified nature in subseafloor microbial communities. An important prerequisite for DNA-based microbial community analysis is even and effective cell disruption for DNA extraction. With a commonly used DNA extraction kit, in average, roughly two-third of subseafloor sediment microbial cells remain intact (i.e., the cells are not disrupted), indicating that microbial community analyses may be biased at the DNA extraction step, prior to subsequent molecular analyses. To address this issue, standardized a new DNA extraction method using alkaline treatment and heating by precisely monitoring microbial cell numbers in the treated samples. Upon treatment with 1 M NaOH at 98oC for 20 min, over 98% of microbial cells in subseafloor sediment samples collected at different depths were disrupted. However, DNA integrity tests showed that such strong alkaline and heat treatment also cleaved DNA molecules into short fragments that could not be amplified by PCR. Subsequently, we optimized the alkaline and temperature conditions to minimize DNA fragmentation and retain high cell-disruption efficiency. The best conditions produced a cell disruption rate of 50-80% in subseafloor sediment samples from various depths, and retained sufficient DNA integrity for amplification of the complete 16S rRNA gene (i.e., ˜1,500 bp). The optimized method also yielded higher DNA concentrations in all tested samples compared with extractions using a conventional kit-based approach. Comparative molecular analysis using real-time PCR and pyrosequencing of bacterial and archaeal 16S rRNA genes showed that the new method produced an increase in archaeal DNA and its diversity, suggesting it provides better analytical coverage of subseafloor microbial communities than conventional methods.

Keywords: Subseafloor microbial community, DNA extraction, bias, archaea

Japan Geoscience Union Meeting 2014
(28 April - 02 May 2014 at Pacifico YOKOHAMA, Kanagawa, Japan)

BGM22-P01 Room:Poster Time:April 30 18:15-19:30

Effect of antimony on arsenite oxidation by soil microbial community

KATAOKA, Takafumi[1*] ; HAMAMURA, Natsuko[1]

[1]Center for Marine Environmental Studies

Antimony (Sb) and arsenic (As) are naturally occurring toxic elements in the earth’ s crust, and both elements exist commonly in sympatric environment. The chemical properties and the mode of toxicity of those elements depend on their oxidation states. Although both oxidation states are toxic, trivalent is more toxic than pentavalent chemical form. The microbiological oxidation of As(III) can impact on the geochemical cycling of arsenic in the contaminated environment, and more than 30 phylogenetically diverse As(III)-oxidizing bacterial strains have been isolated. Although natural microbes are exposed to multiple contaminants in situ, the effect of co-contamination on microbial As(III)-oxidation activity is not well understood. To gain insight into the microbial roles in the biogeochemical cycles of As, we evaluated the effect of co-contamination of Sb and As on the microbial community and their As-oxidizing activity by using solid-phase culturing which was inoculated with antimony mine tailing soil (Ichinokawa, Ehime, Japan). As(III) oxidation rates increased exponentially and reached steady state at day-8 in which 0.15 mM As(III) was oxidized to As(V) in 22.9 hrs. The addition of antimonite tartrate (Sb[III]-tar, 0.15 mM) at day-9 inhibited arsenite oxidation, which was then reduced to 40% by day-15. Successional changes in bacterial community compositions were observed after Sb(III)-tar addition by 16S rDNA- and arsenite oxidase gene (aioA)-targeted analyses. Total of 69 As(III)-oxidizing strains were isolated from the solid samples obtained before and after the Sb(III)-tar addition, and the Sb(III)-tar tolerance of representative isolates were determined. Various As(III)-oxidizing strains exhibited different levels of Sb(III)-tar tolerance in growth response and As(III)-oxidation rates. These results indicated that the co-contamination of As and Sb affect the community composition and activity of As(III)-oxidizing microbial population reflecting the differences in cellular responses among strains to Sb toxicity.

Keywords: Heavy metal pollution, Arsenic, Antimony, Solid phase advective culturing, Soil bacterial community

Japan Geoscience Union Meeting 2014
(28 April - 02 May 2014 at Pacifico YOKOHAMA, Kanagawa, Japan)

BGM22-P02 Room:Poster Time:April 30 18:15-19:30

Bacterial community structure in different subsurface sediments of the southern Kanto Plain

OHKUBO, Satoshi[1*] ; OHNISHI, Jun-ichi[1] ; A.K. AZAD, Muhammad[1] ; SUDA, Wataru[2] ; SAITO, Takeshi[1] ; SAITO, Hirotaka[3] ; TAKEMURA, Takato[4] ; HAMAMOTO, Shoichiro[5] ; KOMATSU, Toshiko[1]

[1]Graduate School of Science and Engneering, Saitama University, [2]Graduate School of Frontier Science, University of Tokyo, [3]Department of Ecoregion Science, Tokyo University of Agriculture and Technology, [4]College of Humanity and Science, Nihon University, [5]Graduate School of Agriculture, University of Tokyo, [6]CREST, JST

Ground source heat pump (GSHP) systems have become popular because of their efficiency in energy conservation and reduction of CO2 emission. GSHP utilizes the groundwater or subsurface sediment, with an almost constant temperature during the year, as the heat source or sink. Although the temperature changes in subsurface would affect geological structure, groundwater quality, and subsurface microorganisms, very few studies have addressed temperature effects on subsurface biophysical processes. For evaluation of subsurface environmental effects and ensuring overall sustainability of GSHP use, it is essential to investigate how the temperature change may affect the subsurface microbial community structure . Before that, however,, it is necessary to know the subsurface microbial community structure that has not yet been affected by temperature change. The purpose of this study was therefore to investigate initial (non-thermal-change-affected) bacterial community structure in deep boring core samples from three different sites in southern Kanto plain. The three sites were the university campuses of College of Humanity and Science, Nihon University (NU; Setagaya-ku, Tokyo), Saitama University (SU; Saitama-city) and Fuchu campus of Tokyo University of Agriculture and Technology (TAT; Fuchu-city, Tokyo). At all three sites, tests of GSHP systems and their environmental response are planned in the near future.

At each site, 10 to 12 sediment core samples were collected from different depths, and whole DNA was extracted from those core samples. PCR-amplified V2-V3 region of bacterial 16S rRNA gene was analyzed by pyrosequencing. The results showed that bacterial community structures of 0-30 m depth were distinctly different among the three boring sites. At the NU site, bacteria belonging to Actinobacteria and Firmicutes accounted for more than half of the whole bacteria population. On the other hand, Chloroflexi, γ-, and δ-proteobacteria were predominant at the SU site, and α-, β-, and γ-proteobacteria were mainly detected at the TAT site. Especially, OTUs assigned to the classes Dehalococcoidetes and Anaerolineae (both belonging to phylum Chloroflexi) were predominant in a wide range of depths at the SU site, and they were particularly detected in former marine sediment. Below 30-m depth, β-, and γ-proteobacteria were predominant at all sites. The relative amounts of some taxonomic groups of bacteria were correlated with depth, pH, electric conductivity of pore water, and particle size distribution. Thus, the variety of bacterial community structure could be attributed to the differences of the depositional ages and environments and/or present subsurface environment at each site. The fundamental data on subsurface bacterial community structures in the southern Kanto Plain from this study will be a useful platform for evaluating the future GSHP-induced temperature change effects on the subsurface environments.

Keywords: subsurface microorganisms, ground source heat pump, next generation DNA sequencing, bacterial community structures

Japan Geoscience Union Meeting 2014
(28 April - 02 May 2014 at Pacifico YOKOHAMA, Kanagawa, Japan)

BPT02-01 Room:421 Time:May 1 09:00-09:15

TOWARDS THE NEXT GENERATION OF CARBONATE-BASED PROXIES

DE NOOIJER, Lennart jan[1*] ; TOYOFUKU, Takashi[2] ; BIJMA, Jelle[3] ; REICHART, Gert-jan[4]

[1]NIOZ - Royal Netherlands Institute for Sea Research, [2]JAMSTEC, [3]Alfred Wegner Institute for Polar- and Marine Science, [4]NIOZ/Utrecht university

Reconstructions of past climate and environments are largely based on stable isotopes and trace element concentrations measured on fossil foraminiferal calcite. Element and isotope composition of foraminiferal calcite roughly reflects seawater composition and physical conditions, which in turn, is related to paleoceanographic parameters. Additional biological controls on test composition biases such correlations and needs to be corrected for when aiming at precise and accurate reconstructions. The various physiological processes involved in foraminiferal biomineralization have, however, different impacts on different elements and isotopes. For instance transmembrane transport of Ca-ions has a large impact on Mg fractionation (and hence the Mg-temperature proxy), whereas is has very little effect on Na/Ca ratios (a novel proxy for salinity). Many foraminifera-based proxies are thus impacted by more than one physiological process, which can only be corrected for by 1) quantification of the impacts of these processes (ion pumping, photosynthesis, pH regulation, etc) on calcitic element and isotope composition and 2) combine high-resolution multi-element and isotope analysis to simultaneously correct for these impacts. Since trace metals and isotopes are affected by multiple parameters, combining analyses not only makes reconstructions more robust, but also fundamentally more accurate.

Japan Geoscience Union Meeting 2014
(28 April - 02 May 2014 at Pacifico YOKOHAMA, Kanagawa, Japan)

BPT02-02 Room:421 Time:May 1 09:15-09:30

The evolution of shell microstructure of protobranch bivalves

SATO, Kei[1*] ; SASAKI, Takenori[2]

[1]Graduate School of Science, The University of Tokyo, [2]The University Museum, The University of Tokyo

Molluscs are the second largest taxa and most of them have the shell of calcium carbonate. Molluscan shells are composed of the complex structural units that are called shell microstructures. Molluscs demonstrate a great variety of microstructures which are similar in phylogenetically close taxa. Thus, investigations of shell microstructures can provide clues for systematic and phylogenetic analyses of molluscs, including fossil taxa. Additionally, these trends suggest the possibility that the shell microstructure had a crucial role in the evolution of Mollusca.

The Protobranchia is an ancestral group of the Bivalvia and comprise four superfamilies (Nuculoidea, Nuculanoidea, Manzanelloidea, and Solemyoidea). However, the systematics of protobranch bivalves has been also problematic, because their simple external shell morphology can provide an insufficient number of informative characters. Therefore, Comprehensive investigation of the shell microstructure and molecular phylogenetic study of protobranch bivalves are required for understanding molluscan evolutionary history. The purpose of this study is to reveal the relationship between the shell micro- structure of protobranch bivalves and molecular phylogeny, and to discuss the evolution of the shell microstructures and their significance as novel morphological characters.

As the result of molecular phylogenetic analysis, it is revealed that the species of protobranch bivalves formed a distinct clade with long branches expect for one exception. One species of Sareptidae were included in Nuculanoidean clade while Sareptidae is placed within Nuculoidea in earlier systematics. SEM observation revealed that each of four superfamilies has a distinct trend in the composition of shell microstructures. And the results of the molecular phylogenetic analysis and the observation of the shell microstructure were consistent with each other. This condition indicates the shell microstructures of the Resent protobranch bivalves show a phylogenetic constraint. Nevertheless, previous study shows this trend is imperfect in fossil taxa. Some fossil nuculoids have nacreous structures and some fossil nuculids possess homogeneous structures. The foliated aragonite that resembles nacreous structure is known as the most primitive shell microstructure. Ancestral nacreous structure was first originated in the Paleozoic protobranch bivalves prior to any other structures that are found in protobranchs of younger ages. Thus, the absence of the nacreous structure may represent the secondary condition in protobranchs. However, the loss of nacreous might be unreasonable, because nacreous structure is considered to be the strongest shell microstructure. In further studies, the evolution of the shell microstructure of protobranchs should be discussed in terms of the habitats and the production costs of the shells as well as protective functions of shells.

Keywords: shell microstructure, mollusca, bivalve, protobranch

Japan Geoscience Union Meeting 2014
(28 April - 02 May 2014 at Pacifico YOKOHAMA, Kanagawa, Japan)

BPT02-03 Room:421 Time:May 1 09:30-09:45

Tube mechanical properties and structural design of Hydroides elegans under multiple stressors

LI, Chaoyi[1*] ; CHAN, Vbs[1] ; MENG, Yuan[1] ; HE, C[2] ; YAO, H[2] ; YEUNG, Kwk[3] ; THIYAGARAJAN, V[1]

[1]Swire Institute of Marine Sciences and School of Biological Sciences, The University of Hong Kong, [2]Department of Mechanical Engineering, The Hong Kong Polytechnic University, [3]Department of Orthopaedics and Traumatology, The University of Hong Kong

Most marine calcifiers construct robust calcareous skeletons or shells through biomineralization to protect themselves from predatory attacks. Due to increased anthropogenic emission of CO_2 in recent years, reduced global ocean pH and decreased carbonate concentration in seawater are expected to impede the CaCO3 accretion in shell formation and produce a mechanically brittle shell structure. In addition, the effect of elevated pCO2 level can act synergistically with temperature and salinity changes in seawater, further affecting the calcification process adversely. To investigate the combined effects of multiple environmental stressors on calcifying marine organisms, we studied the effects of pH (8.1 and 7.8), salinity (34 and 27 ‰), and temperature (23 ℃ and 29 ℃) on the mechanical properties of the tubes built by the tubeworm, *Hydroides elegans*. By employing Micro-CT scanning and micro-force testing, information on tube topography and mechanical properties were analyzed using finite element analysis (FEA). Markedly, despite the structural deterioration observed in reducing pH and salinity, the level of elevated temperature counteracts these effects and even strengthen the overall mechanical properties. This may suggest that warming conditions in the early subtropical summer seawater may rescue the tapeworms from decreasing pH and salinity in the near future.

Keywords: calcifiers, biomineralization, stressors, Hydroides, tubeworm

Japan Geoscience Union Meeting 2014
(28 April - 02 May 2014 at Pacifico YOKOHAMA, Kanagawa, Japan)

BPT02-04 Room:421 Time:May 1 09:45-10:00

The mechanical consequence of ocean acidification - the application of finite element analysis

LI, Chaoyi[1] ; CHAN, Vbs[1] ; MENG, Yuan[1*] ; HE, C[2] ; YAO, H[2] ; SHIH, H[3] ; THIYAGARAJAN, V[1]

[1]Swire Institute of Marine Sciences and School of Biological Sciences, The University of Hong Kong, [2]Department of Mechanical Engineering, The Hong Kong Polytechnic University, [3]Department of Civil Engineering, The University of Hong Kong

We studied the effects of low pH (near-future average pH 7.8) seawater on the structure and mechanical properties of the calcifying serpulid tubeworm, *Hydroides elegans*, compared to normal pH (current average pH 8.1).

We found that tubes produced at pH 7.8 altered tube ultrastructure, volume and density, and decreased the mean tube hardness and elasticity to a large extent by ˜80% and ˜70%, respectively. Specifically, mechanical properties of the outer and inner surfaces of the tube were curbed by pH 7.8, and the tube breaking force required to damage the tube was reduced by 64%.

Nano-indentation to spatially map the micromechanical properties of tubes built by the biofouling serpulid tubeworm, *Hydroides elegans*. The mechanical information was analyzed by computational model, finite element analysis (FEA). In order to study the details of strength properties of the shell, finite element analysis (FEA) was used to simulate the consequence of predatory attack in nature for both shells produced in the control and treatment seawater. The finite element analysis provided a reasonable answer to this phenomenon: altered mechanical properties shifted the stress development and distribution within the tubes and therefore resulting in mechanical weaker part of that were suffering from higher stress concentration.

Keywords: Hydroides, ultrastructure, tubeworm, calcifyer, mechanical properties

Japan Geoscience Union Meeting 2014
(28 April - 02 May 2014 at Pacifico YOKOHAMA, Kanagawa, Japan)

BPT02-05 Room:421 Time:May 1 10:00-10:15

Visualization approach on foraminiferal calcification under various pH

TOYOFUKU, Takashi[1*]

[1]JAMSTEC

Foraminifera, marine unicellular organism, have been thought as one of the major carbonate producer in ocean. Their calcareous tests are commonly utilized as paleo-environmental indicators in various studies of earth science because their tests have been archived as numerous fossil in sediment for long time and various environmental information are brought by population, morphology and geochemical fingerprints. The calcareous test itself is interested by many foraminifer scientists. The knowledge about the cytological process on carbonate precipitation has been described for couples of decade using by multi approaches. Foraminiferal regulations of calcium and carbonate ion uptake into calcareous tests from ambient seawater udner different pH conditions are of great interest. Our previous studies showed the potential to understanding the biomineralization of foraminifera by the application of fluorescent indicators. Recently, we apply the method to show the spatial distributions of cytological calcium and pH in living cell at several pH conditions (7.5-8.1). Observed results show that foraminifera controls pH variation and concentration of calcium at even different environmental pH. These observations results will help to consider how the geochemical compositions arranging on the foraminiferal test, sensitivity of pH proxy of boron and others.

Japan Geoscience Union Meeting 2014
(28 April - 02 May 2014 at Pacifico YOKOHAMA, Kanagawa, Japan)

BPT02-06 Room:421 Time:May 1 10:15-10:30

Live confocal imaging of cytoplasmic structure and calcification processes in Amphisorus kudakajimensis

OHNO, Yoshikazu[1*] ; FUJITA, Kazuhiko[2] ; TOYOFUKU, Takashi[3]

[1]Graduate school of Engineering and science, University of Ryukyus, [2]Department of Physics and Earth Sciences, University of Ryukyus, [3]Institute of Biogeosciences (BioGeos), Japan Agency for Marine-Earth Science and Technology

Although complex processes of calcification processes have been reported in Foraminifera, details of the cellular events generating organic templates and causing calcification are still unknown. To better understand cellular mechanisms in foraminiferal calcification, it is important to observe the molecular dynamics in vivo (e.g., calcium ion, matrix proteins). Here we report confocal microscopic observations of cytoplasmic structures in a live cell of a *porcelaneous symbiotic foraminifer Amphisorus kudakajimensis* and discuss the application of calcium imaging combined with pharmacological manipulations to study intracellular calcium dynamics. In addition, we succeeded in observing the elevated pH (pH 9.0) in organic templates, and lowered pH (pH 6.0) around thread-like cells using a cell-impermeable fluorescent pH indicator (HPTS).

Keywords: calcification, calcium imaging, Live-cell imaging, confocal microscopy

Japan Geoscience Union Meeting 2014
(28 April - 02 May 2014 at Pacifico YOKOHAMA, Kanagawa, Japan)

BPT02-07 Room:421 Time:May 1 11:00-11:15

Internal pH distribution and post-metamorphic biomineralization in the tubeworm, Hydroides elegans

CHAN, Vbs[2] ; TOYOFUKU, Takashi[1*] ; WETZEL, G.[4] ; SARAF, L.[4] ; THIYAGARAJAN, V.[2] ; MOUNT, A.s.[3]

[1]JAMSTEC, [2]Hong Kong University, [3]Department of Biological Sciences, Clemson University, [4]Advanced Material Research Laboratory (AMRL), Clemson University

The serpulid tubeworms produce a diverse tube structure through controlled calcification. Cellular environment associated with actively calcifying serpulid tubeworms at metamorphosis were studied using pH and calcium sensitive indicators. With a notable degree of compartmentation, the thoracic region between the collars showed a high pH value above 8.5 and elevated calcium ion levels. As suggested by SEM-EDX results, such region also demonstrated a higher Ca signal. To analyze the presence of crystalline CaCO3, the unpolished sample was characterized using SEM-EBSD at 20kV, this low voltage and non-destructive approach showed the direct formation of aragonite. Applying in situ lift-out technique at the calcified region, TEM specimen was prepared for structural analysis using selected area diffraction pattern. This study documents the cellular environment during the first calcification event in the serpulid tubeworm at the transition of metamorphosis and the subsequent aragonite formation.

Keywords: imaging, serpulid tubeworms, visualization, calcifyer, biomineralization

Japan Geoscience Union Meeting 2014
(28 April - 02 May 2014 at Pacifico YOKOHAMA, Kanagawa, Japan)

BPT02-08 Room:421 Time:May 1 11:15-11:30

Genomic Exploration of the Nautilus' Shell Matrix Hydrophilic Proteins: An Insight To Their Evolution in Mollusks

SETIAMARGA, Davin[1*] ; ENDO, Kazuyoshi[2]

[1]Japan Society for The Promotion of Science, [2]Graduate School of Science, The University of Tokyo

The presence of a calcium-carbonate-based shell is a defining feature of most members of Mollusca. Thus, research on the genomic aspects of biomineralization of this group is interesting, since the resulting knowledge can be useful for understanding their evolutionary success. Interestingly, most members of cephalopods have secondarily lost their external mineralized shells. The nautiloids, however, is one of the two extant cephalopod groups still maintaining their true shells. Phylogenetically, the nautiloids had diverged from the ancestors of non-shelled, extant cephalopods (Neocoleoidea) in the mid-Paleozoic (Silurian/Devonian boundary, ±416MYA), older than the split between ammonoids and neocoleoids. This makes studies on nautiloid shell biomineral-proteins important and interesting, since insights from the nautiloids might shed light on how shell internalization and de-mineralization events evolved in cephalopods, while at the same time, might help to elucidate the evolution and identification of core components of mollusk shell biomineralization proteins, through comparisons with other molluscan biomineral-related protein data. In this talk, we are reporting our result of the genomic explorations to identify biomineralization-related proteins in the nautiloid *Nautilus pompilius*. To do so in our research, we first determined the total transcriptome sequences from the mantle tissue using pyrosequencing, while simultaneously did a total proteome analysis of the shell's hydrophilic proteins by orbital-trap mass-spectrometry. We then conducted a transcriptome-proteome comparative analysis in order to identify the hydrophilic components of shell biomineral-related proteins in the Nautilus, where we identified 51 distinct shell specific EST/proteins sequences. In the talk, we are also going to discuss how the findings provide an insight to the study of the evolution of mollusk shell biomineralization.

Keywords: Shell matrix protein, Nautilus, Transcriptome, Proteome, Biomineralization

Japan Geoscience Union Meeting 2014
(28 April - 02 May 2014 at Pacifico YOKOHAMA, Kanagawa, Japan)

BPT02-09 Room:421 Time:May 1 11:30-11:45

Using Acropora digitifera to bridge the gap between genome biology and geochemistry

BELL, Tomoko[1*] ; YOKOYAMA, Yusuke[1] ; IGUCHI, Akira[2] ; SUZUKI, Atsushi[3]

[1]Atmosphere and Ocean Research Institute, the University of Tokyo, [2]Department of Bioresources Engineering, Okinawa National College of Technology, [3]The National Institute of Advanced Industrial Science and Technology

Coral's calcification mechanism has been receiving great attention in the fields of both geochemistry and biology. In geochemistry, high-resolution proxies using coral skeletal elements have been developed to reconstruct climate history (Gagan et al, 2012). In parallel, coral genomes have been sequenced progressively. However, trials that connect these two different fields of studies focusing on coral calcification have not been conducted yet. In this study, we focused on *Acropora digitifera* as the target species because enough genomic information is available (Shinzato, 2011) and its potential as geochemical proxies (Inoue, 2011). First, using ZoophyteBase, which has been recently developed as coral's proteome database (Dunlap et al, 2013), we investigated the genes that are potentially related to metabolism using inorganic minerals in seawater and analyzed their gene components and the correlations with seawater chemistry. Second, using next-generation sequencing, we are currently comparing *Acropora digitefera*'s gene expression between fast and slow calcification lineages of this species. In addition, coral skeletal elements of these materials have been analyzed by ICP-AES. In this presentation, we report the progress of these analyses focusing on calcification related genes and skeletal elements.

References: [1] Dunlap et al, 2013.BMC Genomics. DOI: 10.1029/2011PA002215 [2] Gagan, et al, 2012. Paleoceanography. DOI: 10.1029/2011PA002215 [3] Inoue et al, 2011. Geophysical Research Letters. DOI: 10.1029/2011GL047786 [4] Shinzato et al, 2011. Nature. DOI:10.1038/nature10249

Keywords: Acropora digitifera, Calcification, Gene, Skeletal elements

Japan Geoscience Union Meeting 2014
(28 April - 02 May 2014 at Pacifico YOKOHAMA, Kanagawa, Japan)

BPT02-10 Room:421 Time:May 1 11:45-12:00

Comprehensive identification of shell matrix proteins in brachiopods

ISOWA, Yukinobu[1*] ; SARASHINA, Isao[2] ; OSHIMA, Kenshiro[3] ; KITO, Keiji[4] ; HATTORI, Masahira[3] ; ENDO, Kazuyoshi[1]

[1]Graduate School of Science, Univ. Tokyo, [2]University Museum, Univ. Tokyo, [3]Graduate School of Frontier Sciences, Univ. Tokyo, [4]School of Agriculture, Meiji Univ.

Brachiopods are marine invertebrates that appeared in the Cambrian, and they have two shells like bivalves composed of calcium carbonate or calcium phosphate. Shells contain organic matrix, which have important roles in the biomineralization processes. Recently, many shell matrix proteins in molluscs have been identified, and their roles in shell formation have been discussed. On the other hand, shell matrix proteins in brachiopods have not been identified, except for partial amino acid sequences of a chromoprotein, named ICP-1. In this study, we performed comprehensive identification of shell matrix proteins of the brachiopod *Laqueus rubellus* using proteomics combined with transcriptomics. As a result, we identified a total of 18 shell matrix proteins. BlastP search showed that these proteins have no homologues in skeletal proteins identified from other phylum, suggesting that brachiopod and mollusc shells are different in origin.

Japan Geoscience Union Meeting 2014
(28 April - 02 May 2014 at Pacifico YOKOHAMA, Kanagawa, Japan)

BPT02-11 Room:421 Time:May 1 12:00-12:15

Utility of nitrogen isotopic composition of amino acids in shell protein

CHIKARAISHI, Yoshito[1*] ; NOMAKI, Hidetaka[1] ; TSUCHIYA, Masashi[1] ; TOYOFUKU, Takashi[1] ; OHKOUCHI, Naohiko[1] ; KITAZATO, Hiroshi[1]

[1]Japan Agency for Marine-Earth Science and Technology

Stable isotopic composition of sedimentary organic nitrogen has been employed as a proxy to understand biogeochemical nitrogen cycles in marine and lacustrine environments. However, modification of the isotopic signals during early diagenesis (including heterotrophic assimilation/disassimilation, recycling, and reproduction) in water column and sediments always leads to much uncertainty on the interpretation of bulk isotope data. Recently, we found that a proteinogenic amino acid, phenylalanine, shows little change in the nitrogen isotopic composition during heterotrophic degradation even in long-length grazing food webs, whereas the other proteinogenic amino acid, glutamic acid, shows significant 15N-enrichment at each step of food webs. Moreover, the isotopic signals of these amino acids in shell protein are always identical to those of biomass protein (e.g., muscle tissue) when the shell was produced. These results imply that the nitrogen isotopic composition of phenylalanine and glutamic acids from shell protein (e.g., in microfossils of foraminifera) captures (1) primary isotopic signals of organic nitrogen in the environment where the shell was produced and (2) trophic position of the shell-owner in ecosystems when the shell was produced.

In the presentation, we will show comparative data sets on the isotopic composition of amino acids between muscle and shell protein from various organisms, and discuss its applicability as a proxy to estimate the primary isotopic signals in environments and the trophic position of organisms of interest.

Keywords: amino acid, nitrogen isotope, food web

Japan Geoscience Union Meeting 2014
(28 April - 02 May 2014 at Pacifico YOKOHAMA, Kanagawa, Japan)

BPT02-12 Room:421 Time:May 1 12:15-12:30

Variation of North Atlantic nitrogen fixation in Caribbean coral skeletons

YAMAZAKI, Atsuko[1*] ; HETZINGER, Steffen[2] ; REUMONT, Jonas V.[2] ; MANFRINO, Carrie[3] ; TSUNOGAI, Urumu[4] ; WATANABE, Tsuyoshi[5]

[1]AORI, The University of Tokyo, [2]GEOMAR Helmholtz-Zentrum fur Ozeanforschung Kiel, [3]Central Caribbean Marine Institute, [4]Graduate School of Environmental Studies, Nagoya University, [5]Faculty of Science, Hokkaido University

Oceanic nitrogen fixation is important as new nitrogen in oligotrophic oceans and balances with denitrification in global nitrogen cycle controlling primary production. North Atlantic ocean is known to have higher nitrogen fixation rates, although the controlling factors have been debated by modern observations and sediment cores in geological time scales. Reef corals have been widely used as paleo-environmental proxy in oligotrophic oceans. Recent studies suggested that nitrogen isotopes of organic matter preserved in coral skeletons $\delta^{15}N_{coral}$ have the potential to record coral nitrogen sources on decadal to millennia scale. In this study, we report recent 90-year records of nitrogen isotopes in Diploria sp. coral cores from Cayman Islands. $\delta^{15}N_{coral}$ values were +1.9±2.6 (σ) ‰ (n=139), which suggested that the variation of $\delta^{15}N_{coral}$ was controlled by nitrogen fixation (˜0 ‰) in ambient seawater. The trend line of $\delta^{15}N_{coral}$ increased ˜4 ‰ from 1920s to 2010s. This result suggests that nitrogen fixation rate in Caribbean Sea decreased during the past 90 years. Detrended $\delta^{15}N_{coral}$ showed a negative correlation between Atlantic Multi-decadal Oscillation (AMO) index (R=-0.71, P ‹‹ 0.001), which suggested that nitrogen fixation rate increased in higher SST condition leading an index for hurricane activity on multi-decadal scales. In this presentation, we discuss the relationship between nitrogen fixation and hurricane activity in global warming state.

Keywords: Coral skeletons, nitrogen isotopes, nitrogen fixation, Caribbean Sea, North Atlantic Ocean

Japan Geoscience Union Meeting 2014
(28 April - 02 May 2014 at Pacifico YOKOHAMA, Kanagawa, Japan)

BPT02-13 Room:421 Time:May 1 12:30-12:45

Fluorometric analysis of photosymbiosis: Toward quantitative validation of ecological proxy of planktic foraminifers

TAKAGI, Haruka[1*] ; KIMOTO, Katsunori[2] ; FUJIKI, Tetsuichi[2] ; KURASAWA, Atsushi[2] ; HIRANO, Hiromichi[3]

[1]CSE Grad. School, Waseda University, [2]Japan Agency for Marine-Earth Science and Technology, [3]Dep. Earth Sci., Sch. Edu., Waseda University

Endosymbiosis of planktic foraminifers with photosynthetic algae (photosymbiosis) is established especially among species which dominate in warm, low-nutrient surface water. Here, photosymbiosis probably plays an important role for host foraminifers, and can be considered as an adaptive ecology to live in such oligotrophic oceans. Therefore, back in geologic time, photosymbiosis could have been involved with species adaptive radiation as well. In such viewpoint, stable isotopic change of foraminiferal test through ontogeny, attributed to change of symbiont photosynthetic effect, has been used as an indicator to detect fossil photosymbiosis. However, how host-symbiont association change through ontogeny, if any, is practically unknown and has never been quantified. Here, we offer new insights for photosymbiosis based on photosynthetic characteristics of symbionts, obtained by in vivo fluorometric analysis (Fast Repetition Rate Fluorometry, FRRF).

We cultured two symbiont-bearing species, *Globigerinoides sacculifer* and *Globigerinella siphonifera*, and conducted FRRF measurement on individual host-algal consortium during the culture period. FRRF can identify photosymbiosis of individual foraminifer instantly in a non-destructive manner, and gives us various photosynthetic characteristics of symbionts, i.e., maximum fluorescence yield (Fm, index of chlorophyll content), photochemical efficiency (Fv/Fm, index of potential photosynthetic activity), and effective absorption cross-section of photosystem II (σ_{PSII}, capability of the absorbed energy to promote a photochemical reaction).

Sequential FRRF analyses on single individuals revealed that Fm increases with growth, and then decrease drastically at the end of their life, which means that the algal biomass per individual foraminifer increases through ontogeny, but the symbionts are rapidly digested at the end. Fv/Fm and σ_{PSII} values were constant through ontogeny, though Fv/Fm drops in correspondence with the decrease of Fm. Compared between the two species, average values of both Fv/Fm and σ_{PSII} showed statistically significant differences. Fv/Fm was significantly higher in *Gs. sacculifer*, which means that symbionts are more actively photosynthesizing in *Gs. sacculifer*. Because Fv/Fm is mainly depends on nutrient availability, it is a direct evidence of nutrient (metabolite) flow from host to symbionts. On the other hand, σ_{PSII} was higher in *Gn. siphonifera*, indicating that this species can utilize low light energy more efficiently, i.e., more " low-light-adapted " than *Gs. sacculifer*. Actually, it is consistent with inferred habitat preference of *Gn. siphonifera*, which is relatively deeper than *Gs. sacculifer*.

These FRRF results provide us information of foraminiferal photosymbiosis both quantitatively and qualitatively. When the information is combined with test geochemistry mentioned above, it will presumably enable us to quantify the photosynthetic activity from foraminiferal tests. Then, it can be applied to fossil specimens as a validated ecological proxy of photosymbiosis.

Keywords: planktic foraminifers, photosymbiosis, Fast Repetition Rate Fluorometry

Japan Geoscience Union Meeting 2014
(28 April - 02 May 2014 at Pacifico YOKOHAMA, Kanagawa, Japan)

BPT02-14 Room:421 Time:May 1 14:15-14:30

Skeletal isotope compositions of Acropora coral primary polyps experimentally cultured at different temperatures

NISHIDA, Kozue[1*] ; ISHIKAWA, Kei[2] ; IGUCHI, Akira[3] ; TANAKA, Yasuaki[4] ; SATO, Mizuho[1] ; INOUE, Mayuri[5] ; NAKAMURA, Takashi[2] ; SAKAI, Kazuhiko[4] ; SUZUKI, Atsushi[1]

[1]Geological Survey of Japan, National Institute of Advanced Industrial Science and Technology (AIST), [2]Faculty of Science, University of Ryukyus, [3]Department of Bioresources Engineering, Okinawa National College of Technology, [4]Sesoko Station, Tropical Biosphere Research Center, University of the Ryukyus, [5]Atmosphere and Ocean Research Institute, The University of Tokyo

We investigated temperature and growth-rate dependency of skeletal oxygen and carbon isotopes in primary polyps of *Acropora digitifera* (Scleractinia: Acroporidae) by culturing them at 20, 23, 27, or 31 ℃. We cultured primary polyps of *A. digitifera* at Sesoko Station, University of the Ryukyus, Motobu, Okinawa Prefecture, Japan for 10 days. From the results of the polyp weight and polyp area, calcification was most rapid at 27 and 31 ℃. The δ^{18}O — temperature relationship (– 0.18 ‰/℃) is consistent with reported ranges for *Porites*, indicating that juvenile *Acropora polyps* can be used for paleotemperature reconstruction. We found a gap between curves for the experimental polyps and the equilibrium curves for inorganic aragonite of about 3.0 ‰ for δ^{18}O and 8.0 ‰ for δ^{13}C, with the primary polyp values being lower than the equilibrium values of inorganic aragonite. The kinetic isotope effect was evident in the polyps cultured at low temperature but disappeared at high temperatures, despite relatively low light levels. The estimated upper calcification flux limit for a kinetic isotope effect (~0.4 – 0.7 g $CaCO_3$ /cm^2·y) was similar to that of *Porites* colonies with a linear extension rate of <5 mm/ y, suggesting that the calcification flux may be used as a measure of kinetic isotope effect dominance in different genera at different growth stages.

Keywords: coral, temperature, stable isotopes, polyp, kinetic effect

Japan Geoscience Union Meeting 2014
(28 April - 02 May 2014 at Pacifico YOKOHAMA, Kanagawa, Japan)

BPT02-15 Room:421 Time:May 1 14:30-14:45

Corals at marine volcano of Satsuma iwo-jima: Implication for a new proxy of hydrothermal events and biological adaptati

WATANABE, Tsuyoshi[1*] ; KAMIMURA, Kanae[1] ; YAMAZAKI, Atsuko[2] ; OHMORI, Kazuto[1] ; LE GUERN, Francois[3] ; KIYOKAWA, Shoichi[4]

[1]Grad. Sch. of Science, Hokkaido University, [2]AORI, University of Tokyo, [3]CNRS, LSCE (Deceased), [4]Grad. Sch. of Science, Kyushu University

Coral cores from massive corals could record marine environmental and ecological changes in their annual bands with monthly temporal resolution in the present and/or the past. We discovered large massive Porites corals living at active volcanic island of Satsuma Io-Jima, located 50 km south from Kyushu area, southern part of Japan. Satsuma Io-Jima provides a unique opportunity to observe marine organism living under extreme environments of volcanic gases emission and different types of hydrothermal activities from sea flower. We collected eleven coral cores from four different conditions around the island to test if corals could record volcanic and hydrothermal activities and how corals could survive in extreme environments such as very low pH condition with CO2 emission. Coral annual bands recorded in x-ray images revealed that these corals have been survived at least during last a few hundreds years. Coral extension rate for the site near hydrothermal vent was significantly small (1-2mm/year) relative to that for general condition of Porites corals (ca. 10-20 mm/year), suggesting that coral growth was influenced by hydrothermal activity. We will demonstrate our preliminary results of geochemical approaches of δ^{18}O, δ^{13}C, Sr/Ca, Mg/Ca, Ba/Ca, and F/Ca in coral skeletons and in surrounding seawater and discuss the possibility for reconstructing the past hydrothermal events and relationship between marine ecosystem and extreme environments at volcanic activity as the analogues for coral adaptation to future ocean acidification.

Keywords: Coral geochemistry, hydrothermal activity, coral adaptation, ocean acidification

Japan Geoscience Union Meeting 2014
(28 April - 02 May 2014 at Pacifico YOKOHAMA, Kanagawa, Japan)

BPT02-16 Room:421 Time:May 1 14:45-15:00

Sediment ecosystems dynamics on proxies development of foraminifera

KITAZATO, Hiroshi[1*]

[1]Japan Agency for Marine-Earth Science and Technology

I would like to discuss how sediment ecosystems dynamics give affection to forminiferal environmental proxies developments.

Keywords: Sediment ecosystems, dynamics, deep-sea foraminifera, environmental proxies

Japan Geoscience Union Meeting 2014
(28 April - 02 May 2014 at Pacifico YOKOHAMA, Kanagawa, Japan)

BPT02-17 Room:421 Time:May 1 15:00-15:15

Benthic Foraminifera from the deep-water Niger delta (Gulf of Guinea): Assessing acitivity of hydrate pockmark

FONTANIER, Christophe[1*] ; KOHO, Karolina[3] ; GONI-URRIZA, M.[4] ; DEFLANDRE, B.[5] ; GALAUP, S.[6] ; IVANOVSKY, A.[5] ; GAYET, N.[7] ; DENNIELOU, B.[2] ; GREMARE, A.[5] ; BICHON, S.[4] ; ANSCHUTZ, P.[5] ; DURAN, R.[4] ; REICHART, G.-j.[8] ; SULTAN, N.[2]

[1]IFREMER/Universite de Nantes/Angers/Le Mans, [2]IFREMER, Laboratoire Environnements sedimentaires, [3]Faculty of Geosciences, Utrecht University, [4]Universite de Pau et des Pays de l'Adour, [5]Universite de Bordeaux, [6]Ecole d'ingenieurs en Environnement, Georessources et Ingenierie du Developpement durable,, [7]IFREMER, Laboratoire Environnements Profonds, [8]Royal Netherlands Institute for Sea Research

We present an ecological study of foraminifera from 4 deep-sea stations sampled in a pockmark field from the deep-water Niger delta (Gulf of Guinea, Equatorial Atlantic Ocean). All stations are located very close to each other (less than 1.2 km distance). Both sites GMMC-01 and GMMC-02 settle in an active pockmark where methane seepages were recorded by ROV observations. A third station (GMMC-03) is located in a topographic depression which is interpreted as a collapsed pockmark where no gas seepage takes place. The site GMMC-04 is a reference station, without past or present seepages. The main objective of this study is to define whether fossilizing benthic foraminifera are reliable and relevant proxies to detect gas emission in relation to hydrocarbon resources. We focus on living (stained) and dead individuals from present environments, and combine our observations with an outstanding analysis of stable isotopes (δ^{13}C, δ^{18}O) in tests of living and dead foraminifera. Our observations show that degraded organic matter with low bio-availability is present at all stations with a preferential burial of organic compounds in topographic depression (GMMC-03 station). Mudclast breccias cemented by authigenic carbonates (mainly aragonite) are recorded at both station of active pockmark (GMMC-01 and -02). There, prokaryotic consortia involved in both sulphur and methane cycles underline that both sulphide production and methane oxidation take place in the sediment close to sediment-water interface. Compared to the reference site GMMC-04, living foraminifera recorded at active and inactive pockmark show only minor changes in terms of diversity, standing stocks and faunal composition. However, the δ13C signal of some living and dead (but well-preserved) foraminiferal species (*Ceratobulimina contraria, Melonis barleeanus, Uvigerina peregrina*) is moderately depleted in active pockmark compared to both other stations. This depletion may be related to (1) a discrete geochemical imprint of anaerobic methane oxidation in upper sediments and (2) a potential effect of prokaryotic ^{13}C-depleted biomass as a potential food source for benthic foraminifera. Overgrowth of authigenic carbonate on badly preserved foraminifera generates an important shift to lower δ^{13}C values. Whereas living faunas reflect "snapshot" environmental conditions at the sampling period (November 2011) when seepages were likely discrete, dead faunas (modern thanatoceonosis) carry a reliable message integrating temporal variability of gas emission. They reveal major faunal differences that are quite reliable to detect gas hydrate seepages in different pockmark stages with some key-species (i.e., *Bulimina marginata*, *Bolivina albatrossi*) underlining periods of enhanced methane emission and pockmark collapsing.

Japan Geoscience Union Meeting 2014
(28 April - 02 May 2014 at Pacifico YOKOHAMA, Kanagawa, Japan)

BPT02-18 Room:421 Time:May 1 15:15-15:30

Potentials and challenges on the use of environmental DNA to reconstruct deep-sea ecosphere and environmental changes.

SINNIGER, Frederic[1*] ; YAMAMOTO, Hiroyuki[1] ; HARII, Saki[2] ; TAKAMI, Hideto[1] ; OSHIMA, Kenshiro[3] ; CREER, Simon[4] ; CARVALHO, Gary[4] ; PAWLOWSKI, Jan[5]

[1]Japan Agency for Marine Science and Technology, [2]University of the Ryukyus, [3]University of Tokyo, [4]Bangor University, [5]University of Geneva

Deep sea is one of the most difficult to access environment, and consequently one of the most poorly known. However, deep-sea sediments and the organisms inhabiting this environment play a crucial role in the oceans geochemical cycles. Benthic communities are often well adapted to their local environment and therefore can reflect accurately the present conditions but also can provide insights into the past history of environmental changes. Unfortunately, except for a few specific taxa, most knowledge on deep-sea biodiversity is still missing. Deep-sea fauna is very patchy and rarity of most taxa adds to the sampling difficulty using traditional methods. Environmental DNA (eDNA) presents the advantage not to rely only on living organisms present in the sample. The presence of a species in an environment can also be detected using trace DNA left by the organism in the sediments (fragment of dead organisms, fecal pellets, etc). Recent development of DNA sequencing technologies led to promising results in the large-scale exploration of biodiversity from deep-sea environments based on eDNA using environmental DNA.

Here we will examine the use of environmental DNA as a proxy to reconstruct deep-sea communities and estimate environmental conditions in the deep-sea ecosphere. We will present data obtained from deep-sea (500-9000 m) around Japan as well as from worldwide deep-sea oceans to explore the potential use of eDNA as a proxy at various geographical and historical scales and levels of resolution. The data obtained from Iheya North vent field in the Okinawa Trough allowed us to compare the signal of eDNA along extreme environmental gradients at a very restricted geographical scale, while worldwide deep-sea eDNA survey provided us with information of on the global deep-sea environment history and colonisation. Potential of eDNA obtained from sediments to obtain information on water column processes such as plankton blooms will also be discussed.

Keywords: Deep Sea, Environmental DNA, Biodiversity, Sediment, Hydrothermal vent

Japan Geoscience Union Meeting 2014
(28 April - 02 May 2014 at Pacifico YOKOHAMA, Kanagawa, Japan)

BPT02-19 Room:421 Time:May 1 15:30-15:45

Long term monitoring of oxygen distributions at sea floor, Sagami bay, Japan.

OGURI, Kazumasa[1] ; KITAZATO, Hiroshi[1*] ; NOMAKI, Hidetaka[1] ; SAKAI, Saburo[1] ; TOYOFUKU, Takashi[1] ; IWASE, Ryoichi[1]

[1]JAMSTEC

Oxygen (O_2) distributions at the sediment water interface (SWI) are fluctuated by physical, chemical and biological interactions. Especially, bioturbation and bioirrigation at SWI enhance O_2 supply into the sediment, and such benthic activities play significant role on maintaining oxic environment at sediment surface. However, studies of these interactions in deep sea SWI have been limited due to technical limitations for the instrument developments and the operations. In order to investigate the SWI, we constructed a planar O_2 optode system to visualize O_2 distributions across SWI. This system was optimized for low O_2 concentrations, which value was equivalent to the typical O_2 minimum zone, ˜50μM. Using with a platform (so-called lander) to mount the planar O_2 optode, the system was set on the sea floor. On 21/Jan/2008, the deployment for the measurement was stated at Sagami bay, 1170m in water depth by extension of the power cable from Hatsushima deep-sea observatory. Until 31/Jan/2008, the two dimensional O_2 profiles were obtained at 1 hour interval. Throughout the deployment, 245 O_2 profile images and the corresponding grayscale images were obtained. Throughout the analysis of the images, we found the following aspects and phenomena: (1) O_2 penetration depth ranged 5˜8mm. (2) O_2 irrigations sporadically enhanced the O_2 penetration depth to ˜10mm. (3) O_2 concentrations in the sediment were fluctuated by time. (4) Microtopography and hydrodynamics affected to the O_2 concentrations on the sediment surface. (5) Meiobenthic activities suggesting anoxic metabolism were found below O_2 penetration depth. In the presentation, we present these characteristics with the O_2 images obtained from the *in situ* measurement.

Keywords: sediment-water interface, oxygen, optode, meiobenthos

Japan Geoscience Union Meeting 2014
(28 April - 02 May 2014 at Pacifico YOKOHAMA, Kanagawa, Japan)

BPT02-P01 Room:Poster Time:May 1 18:15-19:30

New evidence for halite co-precipitation during coral calcification

MOTAI, Satoko[1*] ; NAGAI, Takaya[1] ; KAWANO, Jun[2] ; WATANABE, Tsuyoshi[1]

[1]Hokkaido University Faculty of Science, [2]Creative Reseach Institution, Hokkaido University

In the last JpGU Meeting, we reported halite grains in coral skeleton through the observation of massive coral skeleton of *Porites lobata* by Analysis Transmission Electron Microscope (ATEM). Each halite grain typically shows a square shape and its grain size is around 80 nm. The spatial distribution of halite grains is inhomogeneous and seems to be independent on the arrangement of growth lines.

We observed new evidence that the halite grains in coral skeleton could precipitate during coral calcification. The electron diffraction patterns from some selected areas including both an aragonite and a halite grain show that there are special crystallographic orientation relationships between them. In consideration of misfit ratios between some selective bond lengths of halite and those of aragonite, crystallographic orientations of halite and aragonite seem to be a kind of hetero-epitaxial relationship.

This is the first observation for a primary precipitated mineral phase other than aragonite in coral skeletons. The halite phase in coral skeleton will provide a new perception for understanding the process of coral calcification.

Keywords: reef-building coral, calcification, biomineral, aragonite

Japan Geoscience Union Meeting 2014
(28 April - 02 May 2014 at Pacifico YOKOHAMA, Kanagawa, Japan)

BPT02-P02 Room:Poster Time:May 1 18:15-19:30

Ocean acidification in the tropical Northwest Pacific since the mid-20th century reconstructed from coral boron isotope

SHINJO, Ryuichi[1] ; ASAMI, Ryuji[1*] ; HUANG, Kuo-fang[2] ; YOU, Chen-feng[2] ; IRYU, Yasufumi[3]

[1]University of the Ryukyus, Japan, [2]National Cheng Kung University, Taiwan, [3]Tohoku University, Japan

Ocean acidification has been accelerating as a result of absorption of increasing anthropogenic CO_2 in the atmosphere emitted by fossil-fuel combustion and land-use practices since the Industrial Revolution, which can be resulting in decreased surface ocean pH and posing a critical threat to marine ecosystems (e.g., Sabine et al., 2004; Orr et al., 2005). By the end of the 21st century, predictions based on different scenarios indicate that ocean pH will decrease by 0.3-0.4 pH units. Only a few long-term continuous observations of sea surface pH have been derived from Station ALOHA off the Hawaiian Islands in the North Pacific, near the Bermuda Islands, and near the Canary Islands in the North Atlantic. A decreasing pH trend in the western North Pacific surface waters for 1983-2007 was estimated from the observational data of oceanic CO_2 partial pressure and related properties (Midorikawa et al., 2010). To elucidate the natural variability of ocean pH and assess the actual trend in ocean acidification more accurately, we must go further back in time. For these reasons, we rely on paleo-pH archives or other related parameters.

Massive corals, an informative archive of past ocean environments, precipitate annually banded calcium carbonate skeletons at a relatively rapid rate (about 1 cm per year), allowing for accurate chronological control and high-resolution sampling. Because of pH-dependent isotopic fractionation between the two dominant boron species in seawater, boron-isotopic systematics in marine carbonates provide a potential proxy for ocean pH in the past (e.g., Hemming and Hanson, 1992). Nevertheless, only two previous investigations provided boron-isotope time series from long-lived corals from the Great Barrier Reef in the South Pacific for the last 300 years. Unlike seawater temperature and salinity records (Asami et al., 2005; Felis et al., 2009), no coral-based reconstruction of long-term pH variation in the North Pacific has been reported.

Here, we generated an annually resolved 60-year-long (1940-1999 A.D.) record of seawater pH from boron isotope composition in a *Porites* coral collected in Guam Island, located in the Western Pacific Warm Pool which contains the highest annual sea surface waters and serves as a heat engine for the earth climate. The first long-term continuous boron isotope-pH proxy record in the North Pacific from the coral provides evidence of a slight ocean acidification trend (equivalent to 0.05-0.08 pH units for surface water) since the mid-20th century, although the critical factors that affect interannual variability remain unknown (Shinjo et al., 2013). From this perspective, the results of this study will provide improved constraints on global atmosphere-ocean interaction models and understanding of the future coral reef ecosystems.

Keywords: coral skeleton, boron isotope composition, pH, ocean acidification, North Pacific

Japan Geoscience Union Meeting 2014
(28 April - 02 May 2014 at Pacifico YOKOHAMA, Kanagawa, Japan)

BPT02-P03 Room:Poster Time:May 1 18:15-19:30

15N/14N mapping of the isotope labeling cultured foraminifera using ultra thin section

NOMAKI, Hidetaka[1*] ; ISHIDA, Akizumi[2] ; SHIRAI, Kotaro[2] ; CHIKARAISHI, Yoshito[1] ; UEMATSU, Katsuyuki[3] ; TAME, Akihiro[3] ; TSUCHIYA, Masashi[1] ; TOYOFUKU, Takashi[1] ; TAKAHATA, Naoto[2] ; SANO, Yuji[2] ; OHKOUCHI, Naohiko[1]

[1]JAMSTEC, [2]AORI, University of Tokyo, [3]Marine Works Japan

Shallow water benthic foraminifera, *Ammonia beccarii*, survive under anoxic conditions in conjunction with possible endobionts. Based on the amino acid analysis, those endobionts are expected to utilize nitrate pool in the foraminifera. However, nitrogen cycles in the foraminiferal cell and endobionts are still unclear. Here, we obtained two dimensional-nitrogen isotopic compositions of *A. beccarii* which had been incubated under oxic and anoxic conditions with ^{15}N-labeled nitrate. After observing with transmission electron microscope to confirm cellular ultrastructure and endobiont distribution, same ultra thin section was examined for nitrogen isotopic composition analysis using secondary ion mass spectrometer. Nitrogen isotopic compositions were measured with spatial resolution better than 400 nm. ^{15}N-enriched parts were found in certain structures in the cell, but not in the endobionts in this experiment.

Keywords: Benthic foraminifera, nitrate respiration, symbiotic microbe, NanoSIMS

Japan Geoscience Union Meeting 2014
(28 April - 02 May 2014 at Pacifico YOKOHAMA, Kanagawa, Japan)

BPT23-01 Room:411 Time:April 30 09:00-09:15

Snowball Earth and GCM simulation

MARUYAMA, Shigenori[1*] ; SUZUKI, Ryohei[2] ; OHFUCHI, Wataru[3]

[1]ELSI Tokyo Institute of Technology, [2]Tokyo Institute of Technology, [3]JAMSTEC

Numerical simulation of snowball Earth, using out-of-date supercomputer program has been performed recently in USA, France and Germany. It seems to be difficult to reconstruct Snowball state by their simulation, while freezing more than 55% of ocean. If continents are gathered along the equatorial region such as Rodinia in the case of Sturtian and Marinoan Snowball Earth in Neoproterozoic, total surface irradiance (TSI) seems plausible to be 95% of present day and CO2 level as same as today.However, if the atmospheric CO2 is 2-6 times more than today, Snowball state cannot appear (Voigt et al., 2011). More realistic CO2 concentration of Neoproterozoic Earth was 20-50 times more than today. In addition, the temperature fluctuation of Snowball Earth period, from Sturtian to Marinoan, was -40 ℃ to +40 ℃ and vice versa within a short period $<$10 m.y. which seem to be impossible because input and output of CO2 by plate tectonics usually takes time more than several hundreds of millions years.

GCM simulation exaggerates positive feedback of CO2 too much. It is time to remodel GCM, considering the amount of clouds and its effect.

Japan Geoscience Union Meeting 2014
(28 April - 02 May 2014 at Pacifico YOKOHAMA, Kanagawa, Japan)

BPT23-02 Room:411 Time:April 30 09:15-09:30

Glaciation carbon cycle in Neopaleozoic and Phanerozoic by numerical carbon cycle box model to fix carbon isotope ratio

TAHATA, Miyuki[1*] ; EBISUZAKI, Toshikazu[2] ; SAWAKI, Yusuke[1] ; NISHIZAWA, Manabu[4] ; YOSHIDA, Naohiro[1] ; UENO, Yuichiro[1] ; KOMIYA, Tsuyoshi[3] ; MARUYAMA, Shigenori[1]

[1]Tokyo institute of Technology, [2]RIKEN, [3]The University of Tokyo, [4]Japan Agency for Marine-Earth Science and Technology

In Ediacaran period, some environmental changes are proposed (e.g. Oxidation, nutrient and carbon cycle) before the Cambrian explosion and macroscopic multicellular metazoan first appeared and their sizes became drastically large. It suggests that carbon cycle in ocean changes in Ediacaran period. Therefore, we assumed box model that there were two carbon reservoirs in Ocean and fluxes are taken as the first order reaction of each reservoir (Rothman et al., 2003; Ishikawa et al., 2012). Thus, we could estimate both d1 and d2 by changes of parameters to trace analyzed d13Ccarb and d13Corg curves from drilling core samples in Three Gorges through the Ediacaran to the early Cambrian (Tahata et al., 2012; Kikumoto et al., 2013; Ishikawa et al., 2012). The d13Ccarb in Three Gorges shows negative excursions in Gaskiers glaciation (ca. 580 Ma), Shuram excursion (ca. 570-550 Ma) and Precambrian/Cambrian boundary (ca. 542 Ma). On the other hand, the d13Corg in Three Gorges show constant ca. -30 per mill in early Ediacaran and correlation to d13Ccarb after Shuram excursion.

The parameter sets suggested carbon cycle changes in Ediacaran period. This Reconstructed Three Gorges carbon cycle quantitatively estimated carbon cycle changes in these periods. The results indicate the rate of remineralization need to increase before the Shuram excursion and the rate of organic carbon burial increase to ca. 100 times in the late stage of Shuram excursion. The increase of remineralization might indicate step-by-step changes of dominant metabolism from anaerobic respiration to aerobic respiration. In addition, the change of organic carbon burial is possibly consistent with the first appearance of mobile metazoan and zooplankton.

The parameters in early Ediacaran apply to carbon cycle in Marinoan glaciation before Ediacaran period. On the other hand, parameters in modern Ocean apply to carbon cycle in P-T boundary. It has possibility that there is glaciation in P-T boundary. The DOC reservoir size differed in Marinoan and P-T boundary. The different DOC reservoir size cause different carbon isotope changes in Marinoan glaciation and P-T boundary.

Keywords: Glaciation, Carbon cycle, Ediacaran, Marinoan, Phanerozoic

Japan Geoscience Union Meeting 2014
(28 April - 02 May 2014 at Pacifico YOKOHAMA, Kanagawa, Japan)

BPT23-03 Room:411 Time:April 30 09:30-09:45

Evidence for meteoric diagenesis during Gaskiers glaciation recorded in the Ediacaran carbonate in South China

FURUYAMA, Seishiro[1*] ; KUNIMITSU, Yoko[1] ; KANO, Akihiro[1]

[1]Kyushu University

Carbon isotope ratios fluctuate globally in association with environmental changes in atmosphere and ocean system. The major carbon isotopic excursions happened in Earth history would be linked to biological evolutions and extinctions and these causes have been investigated actively (e.g. Grotzinger et al., 2011). The Ediacaran period when multicellular animals dramatically evolved also have two major excursions reflected from the Gaskiers glaciation (Sawaki et al., 2010) and the Shuram event (Fike et al., 2006). The Ediacaran Yangtze block in South China is unmetamorphosed sedimentary rocks, and high-resolution carbonate carbon isotopic data have been extensively reported from this block (e.g. Jiang et al., 2011). Although these data could have reflected characteristic oceanic structure and influenced by oceanic oxidation in Ediacaran, those causes have been not fully understood. This study investigated the Yangjiaping section that records large fluctuation of bulk carbonate carbon isotope (e.g. Kunimitsu et al., 2011) and analyzed the cause of fluctuation by measuring the bulk strontium isotope ratios and the carbon-oxygen isotopes of cement components.

Yangjiaping section is about 470 m thick and divided into the Nantuo Formation, the Doushantuo Formation and the Dengying Formation in ascending order. The Nantuo Formation is extensively distributed as post-Marinoan diamictite in the Ediacaran Yangtze platform. The Doushantuo Formation consists of carbonate, black shale, chert and phosphate and the Dengying Formation consists of carbonate and chert. Kunimitsu et al. (2011) subdivided the Doushantuo Formation into Unit 1, Unit 2 and Unit 3 in ascending order, based on the trends of carbonate carbon isotope. The large fluctuation of carbon isotope occurs in Unit 3. Coarse-grained carbonate in upper Unit 2, Unit 3, and the Dengying Formation are available for analyzing isotopic composition of the cement components. Unit 2, lower part of Unit 3 and the Dengying Formation exhibit only minor difference between the bulk and the cement parts in carbon and oxygen isotopes. While, middle to upper parts of Unit 3 record significantly lower isotopic composition of the cements, which are lower than the bulk values by ˜25 permil for carbon and by ˜7 permil for oxygen. Additionally, the strontium isotopic ratios in Yangjiaping section ranging from 0.7079 to 0.7105 indicate an increasing trend from Unit 3 to upward.

Extremely low carbon isotope of the cement parts is responsible for the large fluctuation of the bulk values in Unit 3. It was formed by secondary addition of cement in meteoric diagenetic environments. Upper part of Unit 2 and Unit 3 consist of very shallow water lithofacies implying that the platform was easily exposed during sea level fall. Oxygen-rich meteoric diagenetic water induced remineralization of organic matter that occurred in pore spaces, and formed low carbon isotope of the diagenetic water. Additionally, increase of strontium isotope in Unit 3 reflected an enhanced continental fluxes that could be attributed to the promotion of continental weathering at the Gaskiers glaciation (ca. 580 Ma). The line of evidence suggests that very shallow part of the Yangtze platform was exposed above sea level during the Gaskiers glaciation.

Keywords: South China, Ediacaran, meteoric diagenesis, the Gaskiers glaciation, carbon isotope

Japan Geoscience Union Meeting 2014
(28 April - 02 May 2014 at Pacifico YOKOHAMA, Kanagawa, Japan)

BPT23-04 Room:411 Time:April 30 09:45-10:00

Nitrogen isotope chemostratigraphy of the Early Cambrian platform sequence at Three Gorges, South China

TSUCHIYA, Yuki[1*] ; TAHATA, Miyuki[2] ; NISHIZAWA, Manabu[3] ; SAWAKI, Yusuke[2] ; SATO, Tomohiko[2] ; KOMIYA, Tsuyoshi[1]

[1]Department of Earth and Planetary Science, The University of Tokyo, [2]Department of Earth and Planetary Science, Tokyo institute of technology, [3]Japan Agency for Marine-Earth Science and Technology (JAMSTEC)

The earth is only the planet where higher forms of life exist. The appearance and evolution of metazoans are the most important issue of the evolution of the earth and life, but the causes are still obscure. We made multi-isotope and elemental chemostratigraphies of drill core samples from the Ediacaran to Cambrian in South China. The results show that secular changes of nutrients influenced the evolution of the metazoan. We focused nitrogen that is one of the most important nutrients in bioessential elements, and reconstructed the temporal variation of the oceanic nitrate contents in the early Cambrian.Preservation of continuous and fossiliferous strata from the Ediacaran to the Cambrian, South China provides reconstruction of secular change of compositions of seawater through the time.

Kikumoto et al.(2014) analyzed the nitrogen isotope ratios of the organic nitrogen. The results show that the nitrogen isotope ratios were high from early to middle Ediacaran, and decreased from middle Ediacaran to earliest Cambrian and then became high. They interpreted the change in the nitrogen isotope as secular change of nitrate contents of seawater through the time. And Shimura et al.(2014) showed phosphorus contents in carbonate rocks and minerals from the Ediacaran to the Cambrian, and estimated secular change of phosphorus contents of seawater through the time. As a result, they interpreted that the seawater was depleted in nitrate contents from the early to the middle Ediacaran due to high phosphorus contents. From the middle Ediacaran to the earliest Cambrian, the seawater had higher nitrate contents because of decrease of phosphorus contents possibly due to oxidation of seawater and then lower nitrate contents after the early Middle Cambrian.

The hypothesis is very attractive, but many problems remain, especially in the Cambrian samples. One is whether the change in the nitrogen isotope values is controlled by lithological change. The second is which the change was transient or abrupt because the previous work showed no nitrogen isotope variation between them. Correlation of the nitrogen isotope values with other proxies was unclear, too. This work presents the nitrogen isotope ratios of organic nitrogen in black shales and carbonate rocks of drill core samples from the Shuijintuo and Shipai formations.The nitrogen isotope ratios gradually increase from +2 to -2 ‰ in the Shuijingtuo Formation, whereas they are fluctuated from ca. +1 to +3 ‰ in the Shipai Formation. In addition, the variation of the nitrogen isotope ratios is not related with difference of lithology: carbonate rocks and black shales, respectively. Although low nitrogen isotope anomalies are found in samples with low organic nitrogen contents, no clear correlation between the total organic nitrogen contents and nitrogen isotope ratios is observed. The results indicate that the variation in the nitrogen isotope values is not artificial due to lithological change and secondary alteration but it was caused by environmental change through the Early Cambrian. The increase of the nitrogen isotope ratios was gradual, and was found in the black shales at the upper part of the Shuijingtuo Formation, indicating that the change was transient. There is no correlation between the nitrogen and carbon isotope values of organic matter through the time.

The increase of the nitrogen isotope ratios indicates that the nitrate content of the surface seawater decreased. In other words, it shows that the nitrate-rich environment was completed in the early Cambrian and that nitrate started to be limited with increasing primary production and denitrification activity became significant. It shows that the modern-style marine nitrogen cycle was established in the early Cambrian. Higher primary productivity led to increase of the oxygen content of the atmosphere and ocean, promoting the Cambrian explosion.

Japan Geoscience Union Meeting 2014
(28 April - 02 May 2014 at Pacifico YOKOHAMA, Kanagawa, Japan)

BPT23-05 Room:411 Time:April 30 10:00-10:15

Dendroid multicellular thallophytes preserved in a Neoproterozoic black phosphorite in southern China

DU, Wei[1*] ; WANG, Xunlian[1] ; KOMIYA, Tsuyoshi[2]

[1]China University of Geosciences, [2]Tokyo University

Both metaphytes and metazoans are reported from the well-preserved multicellular assemblage in the Neoproterozoic Doushantuo phosphorite in Weng'an of the Guizhou province, southern China. Here, a new form of dendroid multicellular thallophytes is documented. The new thallus is slightly heteromorphic. Several lateral branches extend from upper portion of the main axis, bearing terminal vegetative vesicles, carpognial vesicles, monosporangium-like discoidal vesicles and urn-shaped pseudoparenchymatous structures. The vegetative vesicle gives rise to a club-shaped pseudoparenchymatous structure, characterised by the medulla?cortex thallus differentiation, which may represent the early stage of the thallus. An oogamous conceptacle arising from one carpognial vesicle is a highly specialised goblet-shaped conceptacle. The discovery and identification of these new dendroid multicellular thallophytes not only document the first fossil-histological evidence for the heteromorphism of Precambrian organisms but also provide a potential insight for our enhanced understanding of the life cycle of the Precambrian red algae.

Keywords: Neoproterozoic, Doushantuo, multicellular thallophytes, dendroid, heteromorphic

Japan Geoscience Union Meeting 2014
(28 April - 02 May 2014 at Pacifico YOKOHAMA, Kanagawa, Japan)

BPT23-06 Room:411 Time:April 30 10:15-10:30

Marine biomass changes after the Neoproterozoic Marinoan Glaciation in Australia

SHIZUYA, Atena[1*] ; KAIHO, Kunio[1] ; CHEN, Zhong-qiang[2] ; GORJAN, Paul[3] ; OBA, Masahiro[1] ; TAKAHASHI, Satoshi[4]

[1]Grad. Sch. of Sci., Tohoku Univ., [2]China University of Geosciences, [3]Washington University in St. Louis, [4]School of Science, The Univ. of Tokyo

The late Neoproterozoic Marinoan glaciation (ca. 635 Ma) was one of the most severe ice ages in the Earth history. It is thought that the glaciation affected the biosphere and caused some succeeding evolutionary events, such as the occurrence of the Lantian biota, the first known macroscopic multicellular eukaryotes (Yuan et al., 2011, 2013). We analyzed sedimentary organic molecules from post-Marinoan deposits in three Australian cores and a section: the Wallara-1 drillhole in the Amadeus Basin, the GILES-1 drillhole in the Officer Basin, the SCYW79-1A drillhole in the Adelaide Geosyncline, and the Moonlight Valley type section in the Kimberley region.

The analysis identified more than 10 types of sedimentary organic molecule, and some of these were used as indicators of biomass for this time. The trends and correlations among the indicators through the researched formations revealed that sum of pristane and phytane (biomass of photosynthetic organisms), 2-alpha-methylhopane (biomarker of cyanobacteria), aryl isoprenoids (photosynthetic organisms and/or green sulfur bacteria), and Cholestane (biomarker of eukaryotes) relative to total organic carbon (TOC) had a positive peak(s) in the lowermost Ediacaran System, which represents an increase in biomass of photosynthetic organisms and eukaryotes immediately after the retreat of the Marinoan glacier, probably caused by an increased nutrient flux to the sea. Except for aryl isoprenoids, those indicators relative to TOC increased through the upper part of the lowermost Ediacaran formations, which may correspond to a recovery and/or evolution of eukaryotes after the Marinoan glaciation.

Yuan, X., Chen Z., Xiao, S., Wan, B., Guan, C., Wang, W., Zhou, C. & Hua, H. (2013) The Lantian biota: A new window onto the origin and early evolution of multicellular organisms. Chinese Science Bulletin 58, 701-707.

Yuan, X., Chen, Z., Xiao, S., Zhou, C. & Hua, H. (2011) An early Ediacaran assemblage of macroscopic and morphologically differentiated eukaryotes. Nature Letter 470, 390-393.

Keywords: Organic Geochemistry, Neoproterozoic, Ediacara, Marinoan Glaciation

Japan Geoscience Union Meeting 2014
(28 April - 02 May 2014 at Pacifico YOKOHAMA, Kanagawa, Japan)

BPT23-07 Room:411 Time:April 30 10:30-10:45

Oceanic oxidation mechanisms spanning the Snowball Earth and early animal diversification

KAIHO, Kunio[1*] ; SHIZUYA, Atena[1] ; OBA, Masahiro[1] ; YAMADA, Kenji[1] ; KIKUCHI, Minori[1] ; SENBA, Naoto[1] ; CHEN, Zhong-qiang[2] ; TONG, Jinnan[2] ; TAKAHASHI, Satoshi[3] ; TIAN, Li[2] ; KOMIYA, Tsuyoshi[3]

[1]Tohoku University, [2]China University of Geosciences, [3]University of Tokyo

The late Neoproterozoic (780 million years ago (Ma)) to early Cambrian (520 Ma) interval witnessed the rise and evolution of early animals. Oceanic oxidation is believed to be crucial in driving the early animal evolution. However, the oxygenation mechanism in seas during this critical period remains unknown. Here we found (i) oceanic anoxia before and during the Marinoan global glaciation (MGG) (660-635 Ma), (ii) surface-water reoxidation immediately after the MGG (635 Ma), (iii) intermediate-water oxidation in the mid-Ediacaran (600 Ma), (iv) deep-water oxidation in late Ediacaran (580 Ma), (v) oceanic anoxia at the end of the Ediacaran (541 Ma), and (vi) reoxidation in the early Cambrian (535 Ma). Thus, a stepwise marine oxygenation took place from shallow to deep water through the Ediacaran epoch, and every major changes in oxygen levels coincided with an important revolutions of marine life, suggesting a coevolution of ocean chemistry and early animals occurred during this period.

Keywords: Ediacaran, Cryogenian, Neoproterozoic, oxygen, biomarkers

Japan Geoscience Union Meeting 2014
(28 April - 02 May 2014 at Pacifico YOKOHAMA, Kanagawa, Japan)

BPT23-08 Room:411 Time:April 30 11:00-11:15

Geochemical identification of projectile from the Upper Triassic ejecta deposits in Japan

SATO, Honami[1*] ; YAMASHITA, Katsuyuki[2] ; YONEDA, Shigekazu[3] ; SHIRAI, Naoki[4] ; EBIHARA, Mitsuru[4] ; NOZAKI, Tatsuo[5] ; EBIHARA, Mitsuru[5] ; ONOUE, Tetsuji[6]

[1]Kyushu University, [2]Okayama University, [3]National Museum of Nature and Science, [4]Tokyo Metropolitan University, [5]Japan Agency for Marine-Earth Science and Technology, [6]Kumamoto University

Our previous studies have revealed that the Sakahogi section in central Japan contains an impact ejecta layer in the Late Triassic, which was derived from an extraterrestrial impact event. This ejecta layer is characterized by platinum group element (PGE) positive anomalies and Os isotope negative excursion together with enrichments in Ni and Cr, and abundant occurrences of Ni-rich magnetite grains and microspherules. PGE anomalies in the Late Triassic sediments were also discovered from deep-sea claystone layers at three bedded chert sections in southwest Japan as follows: (i) Unuma section in the Inuyama area, Mino Belt, (ii) Hisuikyo section in the Kamiaso area, Mino Belt, and (iii) Enoura section in the Tsukumi area, Chichibu Belt. Combined PGE and various isotope data from these ejecta layers are insightful so as to identify the meteoritic material which has caused the Late Triassic impact event. Here we report the PGE element ratios, and Cr and Os isotope compositions of these ejecta layers to understand the projectile component.

The Ru/Ir and Pt/Ir ratios of all the claystone samples from the study sites are plotted along the mixing line between chondrites and upper continental crust. Although a chondrite cannot be distinguished from iron meteorites by using PGE/Ir ratios, the claystone layers show Cr/Ir ratios between 10^4 to 10^5, indicating that the claystone layers are clearly contaminated by chondritic material. The Os isotope compositions ($^{187}Os/^{188}Os$ ratios) in the claystone have a narrow range from 0.126 to 0.128 and these values are well similar to those of chondrites. The Cr isotope data are useful to identify the extraterrestrial components in the ejecta deposits because meteorites of different classes have a distinct ^{54}Cr isotope anomaly. The presence of positive $\varepsilon^{54}Cr$ anomaly in all claystone samples strongly suggests that a carbonaceous chondrite-like material was involved in the studied ejecta layers. Consequently, these geochemical lines of evidence indicate that the Upper Triassic ejecta layers in the Japanese accretionary complexes have been most likely derived from a carbonaceous chondrite.

Keywords: impact event, platinum group element, osmium isotope, chromium isotope

Japan Geoscience Union Meeting 2014
(28 April - 02 May 2014 at Pacifico YOKOHAMA, Kanagawa, Japan)

BPT23-09 Room:411 Time:April 30 11:15-11:30

Stratigraphic Sequence in the Axim-Princess Town section of the coastal Paleoproterozoic Greenstone Belt in the Birimian

KIYOKAWA, Shoichi[1*] ; ITO, Takashi[2] ; TETTEH, George M.[3] ; NYAME, Frank K.[4]

[1]Kyushu Univ. Earth and Planetary Sci., [2]ibaraki Univ. Dep. Education, [3]University of Mines and Technology, Tarkwa, [4]University of Ghana

The coastal Axim-Princess Town sequence of the Paleoproterozoic Birimian Greenstone Belt contains very thick volcaniclastic and organic rich sedimentary rocks. Recent work in this area has revealed more than 5 km wide excellently preserved and continuously outcropping rocks which generally exhibit isoclinal fold with west vergence and east-ward younging lithologies of over 1000m total thickness.. Stratigraphically, the lower portion contains thick vesicular volcaniclastic rocks probably of sub-aerial origin. The middle portion is made up of well laminated alternation of volcaniclastics and black shale but the upper portion is dominated by well laminated black shale sequence. This fining upward sequence is likely indicative of shallow to deep sea depositional conditions of the rocks. Though preliminary evidence gathered suggests an oceanic island arc in shallow to deep ocean setting for the rocks, highly negative deltat13 C values ranging from -43 ? -37 per mil obtained from the black shale further suggests deep ocean anoxic conditions prevailed during deposition of the rocks, presumably with carbon derived from organic matter via cyanobacteria.

Keywords: Paleoproterozoic, Berimian Greenstone belt, island arc ocean floor environment

Japan Geoscience Union Meeting 2014
(28 April - 02 May 2014 at Pacifico YOKOHAMA, Kanagawa, Japan)

BPT23-10 Room:411 Time:April 30 11:30-11:45

Geochemistry of the Nsuta Mn deposit in Ghana: Implications for the Paleoproterozoic ocean redox state

GOTO, Kosuke T.[1*] ; ITO, Takashi[2] ; SUZUKI, Katsuhiko[3] ; KASHIWABARA, Teruhiko[3] ; TAKAYA, Yutaro[4] ; SHIMODA, Gen[1] ; NOZAKI, Tatsuo[3] ; KIYOKAWA, Shoichi[5] ; TETTEH, George M.[6] ; NYAME, Frank K.[6]

[1]GSJ, AIST, [2]Ibaraki University, [3]JAMSTEC, [4]University of Tokyo, [5]Kyushu University, [6]University of Ghana

Oxygenation of the atmosphere and oceans may have influenced the ocean chemistry and diversified contemporaneous life. A number of large manganese (Mn) deposits are distributed in the Paleoproterozoic sedimentary successions that were formed during the great oxidation event (GOE) around 2.4-2.2 Ga (Maynard, 2010 Econ. Geol.). Due to the high redox potential of Mn, occurrences of Mn deposits have been regarded as important evidence for a highly oxidized environment during the Paleoproterozoic (Kirschvink et al., 2000 PNAS). Furthermore, because Mn oxides are efficient scavengers of various elements, including bio-essential elements such as Mo, formation of large Mn deposits may have affected the seawater chemical composition and ecology during the Paleoproterozoic. However, due to lack of detailed geochemical records constraining the genesis of each Mn deposit, the relationships among the formation of Mn deposits, the evolution of atmospheric and ocean chemistry, and the diversification of early life are still ambiguous.

In this study, we report the Re-Os isotope compositions, rare earth element (REE) compositions, and abundance of manganophile elements in the Mn carbonate ore and host clastic sedimentary rock samples collected from the Nsuta Mn deposit of the Birimian Supergroup, Ghana. The Nsuta deposit is one of the largest Paleoproterozoic Mn deposits, although its genesis remains controversial (Melcher et al., 1995 Mineral. Mag.; Mucke et al., 1999 Miner. Deposita). The composite Re-Os isochron age (2149 +/- 130 Ma) of the Mn carbonate and sedimentary rock samples is consistent with the depositional age of the sedimentary rocks (?2.19 Ga) obtained from U-Pb zircon age of the volcanic rocks (Hirdes and Davis, 1998 J. Afr. Earth Sci.), suggesting that the timing of Mn ore deposition was almost equivalent to the host rock sedimentation. The PAAS-normalized REE patterns show positive Eu anomaly in all samples and a positive Ce anomaly only in the Mn carbonate ore. These REE patterns suggest possible contribution of Eu-enriched fluids derived from hydrothermal activity and Ce enrichment due to the oxidation of Ce(III) by Mn(IV) during ore formation. Among the manganophile elements, only Mo is enriched in the Mn carbonate ore compared to the host sedimentary rocks. The profile of manganophile elements is similar to that of modern hydrothermal Mn oxide (Kuhn et al., 2003 Chem. Geol.), although the Mo/Mn ratio is much lower. These geochemical lines of evidence provide the following plausible genetic model for the Nsuta deposit: (1) Mn(II) was derived from hydrothermal fluids, (2) Mn(II) was oxidized to Mn(IV) oxide by the oxygenated seawater, (3) the precipitation of Mn oxide is almost concurrent with the deposition of the host sedimentary rocks, (4) Mn oxide was diagenetically transformed to Mn carbonate ore by the reaction with organic matter.

The geochemical features of the Nsuta deposits suggest that, as in the present oxic oceans, Mn oxide was a potential sink for several trace elements in the Paleoproterozoic oceans. The low Mo/Mn ratio in the Mn carbonate ore may reflect the large difference between the chemical compositions of Paleoproterozoic and present seawater. As the Paleoproterozoic black shales also tend to show low Mo abundance (Scott et al., 2008 Nature), the observed low Mo/Mn in the Mn carbonate ore suggests low Mo inventory in the Paleoproterozoic seawater. In the presentation, we will also discuss the oceanic redox condition responsible for the low Mo inventory during the Paleoproterozoic.

Keywords: Paleoproterozoic, Great Oxidation Event, Mn ore, Re-Os isotope, manganophile elements, Birimian Supergroup

Japan Geoscience Union Meeting 2014
(28 April - 02 May 2014 at Pacifico YOKOHAMA, Kanagawa, Japan)

BPT23-11 Room:411 Time:April 30 11:45-12:00

Geochemical study on the variation and stability of atmospheric oxygen in Paleoproterozoic

NAKAMURA, Umi[1*] ; SEKINE, Yasuhito[1] ; TAJIKA, Eiichi[1] ; GOTO, Kosuke T.[2] ; SENDA, Ryoko[3] ; SUZUKI, Katsuhiko[3] ; TADA, Ryuji[1] ; MARUOKA, Teruyuki[4] ; OGAWA, Nanako O.[3] ; OHKOUCHI, Naohiko[3]

[1]The University of Tokyo, [2]AIST, [3]JAMSTEC, [4]University of Tsukuba

Atmospheric oxygen level is considered to have dramatically increased during the early Paleoproterozoic (i.e., 2.4-2.2 Ga). Severe glaciations occurred at least three times in this same interval. The rises of atmospheric oxygen have been indicated just after the second (Bruce) and third (Gowganda) glaciations (Sekine et al., 2011 EPSL, 2011 nature comm.). However, the atmospheric oxygen level between the two glaciations remains unclear.

In this study, we investigated the evolution of redox conditions of the atmosphere and oceans between the second and third Paleoproterozoic glaciations, by analysing redox sensitive elements, such as osmium (Os), rhenium (Re), and molybdenum (Mo), and stable isotope analyses of organic carbon and sulfur for the sedimentary rocks from the Huronian Supergroup, Ontario, Canada. We found no enrichment of redox sensitive elements in these rocks. The Re-Os data yields an isochron age of 3089 +/- 98 Ma, which is significantly older than the depositional age of the Huronian Supergroup (˜2.45-2.2 Ga; Young et al., 2001 Sediment. Geol.). The obtained Re-Os isochron age indicates that Os and Re in the sediments were mainly supplied as detrital components originally formed at ˜3.1 Ga without any significant disturbance of Re-Os system during chemical weathering and sediment transport. This, in turn, implies that Os and Re were highly depleted in the seawater at the time of deposition, suggesting that oxidative weathering did not occur in the time interval between the second and third Paleoproterozoic glaciations. This conclusion is supported by the little varition of $d^{34}S$ and low abundance of other redox sensitive elements in the sediments.

Together with the geochemical data from the previous studies, we suggest that atmospheric oxygen level increased shortly after the second Paleoproterozoic glaciation, but then, returned to low levels. In the aftermath of the third glaciation, a shift to an oxidizing atmosphere would have occurred.

Japan Geoscience Union Meeting 2014
(28 April - 02 May 2014 at Pacifico YOKOHAMA, Kanagawa, Japan)

BPT23-12 Room:411 Time:April 30 12:00-12:15

Reconstruction of 3.2Ga sea floor environment: Carbon and sulfur isotopic ratios of DXCL drill cores.

MIKI, Tsubasa[1*] ; KIYOKAWA, Shoichi[2] ; NARAOKA, Hiroshi[2] ; TAKAHATA, Naoto[3] ; ISHIDA, Akizumi[3] ; ITO, Takashi[4] ; IKEHARA, Minoru[5] ; YAMAGUCHI, Kosei E.[6] ; SAKAMOTO, Ryo[7] ; SANO, Yuji[3]

[1]Department of Earth and Planetary Sciences, Graduate School of Sciences, 33 Kyushu University, [2]Department of Earth and Planetary Sciences, Faculty of Sciences, 33 Kyushu University, [3]Department of Chemical Oceanography,Atmosphere and Ocean Research Institute, The University of Tokyo, [4]Teacher Training Course (Science Education), College of Education, Ibaraki University, [5]Graduate School of Integrated Arts and Sciences, Kochi University, [6]Department of Chemistry, Faculty of Science, Toho University / NASA Astrobiology Institute, [7]Mitsui Oil Exploration CO., LTD

In the Pilbara Coastal Greenstone Terrane in Western Australia, the Dixon Island and Cleaverville formations of 3.2-3.1 Ga is exposed. DXCL Drilling Project was performed in 2007 and 2011 for the purpose of the high-resolution reconstruction of the change of past sedimentary environment in this area, and four core samples (DX, CL1, CL2, and CL3) were acquired. Through these cores except for CL3, previous study revealed carbon isotopic ratio (=δ^{13}C) with about -30 ‰ and sulfur isotopic ratio (=δ^{34}S) of black shale from DX core obtained by combustion method with wide range of fluctuation and had very high values (δ^{34}S=-10.1∼+26.8 ‰, n=93: Sakamoto, MS2010; Kobayashi, MS2013). This is dissimilar to the previously reported sulfur isotopic ratio of sedimentary sulfides of the early Archean (δ^{34}S=-16.8∼+8.7 ‰, n=351: Strauss, 2003).

In this study, we evaluated the change of carbon and sulfur isotopic ratio through whole DXCL cores. Moreover, in order to clarify the cause of positive shift and dispersion, we performed in situ analysis with NanoSIMS focusing minute spherical pyrites observed in the DX core.

Three cores (CL2: 44.4m, CL1: 66.1m, CL3: 200m to the top) were collected from the Cleaverville Formation which consists of lower Black Shale Member and upper Banded Iron Formation Member. DX core (100.40m) of the upper part of Dixon Island Formation is composed of black shale, gray chert, and alternated pyrite layers. Especially, the DX core contains the layer of tens-hundreds micrometer euhedral pyrites and the layer of the minute spherical pyrites (about 10 μm in diameter) which are fulfilled with silica. We considered that the minute spherical pyrites formed at early stage of sedimentation from their morphology and occurence.

We did whole-rock analysis of sulfur isotope by NA 1500NCS (EA) manufactured by FISONS and DELTA plus XL (IRMS) manufactured by Thermo Finnigan. The instruments are equipped in Organic Geochem. & Cosmochem. Lab., Kyushu University. In situ analysis of sulfur isotope was performed using NanoSIMS50 manufactured by CAMECA at Atmosphere and Ocean Research Institute, Tokyo University. Carbon isotope analysis was performed using Delta Plus Advantage (EA/IRMS) manufactured by Thermo Finnigan at the Center for Advanced Marine Core Research, Kochi University.

As a result, minute spherical pyrites were revealed to have 5∼10 ‰ isotopic fractionation on the inside, showing distribution that area of high value is in ring-shape on the inside and area of low value is in the outer side and the central part of the crystal. Besides, CL3 core (n=27) showed δ^{34}S=+1.33∼+21.52 ‰, $\delta^{13}C_{org}$=-30.79∼-28.57 ‰, C_{org}=0.09∼1.65wt%.

In this analysis, most of carbon isotopic data had value between -30 to -28 ‰ in about 400m forming the Dixon island to Cleaverville formations. The carbon isotope result indicates that the same kind of carbonaceous material was deposited on the seafloor and the value corresponds with photosynthetic bacteria like cyanobacteria origin. Besides, pyrites formed in the anoxic marine sediment rich in organic matter. Particularly, closed system to sulfate was formed and Rayleigh fractionation was promoted by sulfate reducing bacteria. As a result, the feedback occurred and pyrites isotopically heavier than contemporary seawater sulfate (+2 ‰: Ohmoto, 1992) formed on the inside of pyrite shell. Although generally, in case sulfate reducing bacteria is concerned, sulfur isotopic ratio of sulfides has negative value, but +20 ‰ or more is observed in these sequence. It is possible that sedimentary sulfides in that time were in a condition that they had high sulfur isotopic ratio.

Keywords: Archean, carbon isotopic ratio, sulfur isotopic ratio, pyrite, SIMS, sulfate reducing bacteria

Japan Geoscience Union Meeting 2014
(28 April - 02 May 2014 at Pacifico YOKOHAMA, Kanagawa, Japan)

BPT23-13 Room:411 Time:April 30 12:15-12:30

S-MIF geochemistry of the Early Archean in the Onverwacht Suite, South Africa

MISHIMA, Kaoru[1*] ; UENO, Yuichiro[1] ; DE WIT, Maarten[2] ; FURNES, Harald[3] ; SAITOU, Takuya[1]

[1]Department of Earth and Planetary Sciences, Tokyo Institute of Technology, [2]EON-Africa Earth Observatory Network, and Faculty of Science, Nelson Mandela Metropolitan University, [3]Department of Earth Science and Centre for Geobiology, University of Bergen

The recent study of sulfur mass independent fractionation (S-MIF) in the Archean sedimentary rocks represented that multiple sulfur isotope ratios (32S/33S/34S/36S) could be useful new tracer for Archean sulfur cycles. Farquhar et al. (2000) first discovered that Archean sedimentary rocks before 2.4 Ga have Δ^{33}S anomaly, whereas no such anomaly was found in younger samples. This contrast implies the rise of atmospheric oxygen content that fundamentaly changed atmospheric sulfur cycle. The hypothesis are based on the studies from Western Australia and South Africa (Kaufman et al., 2007; Ono et al., 2009; Zerckle et al., 2013). High-resolution stratigraphic studies provide a detailed view into the late Archean marine sulfur cycle, which can help our understanding of both atmospheric and biological processes. In the early Archean, S-MIF data are almost from hydrothermal sulfate and sulfide. For comparing early nad late Archean data precisely, it is necessary to investigate stratigraphical and petrological distributions and variations of the multiple sulfur isotopes. We have studied Early Archean sedimentary sulfides which are well preserved in the Barberton Greenstone Belt, South Africa. Sulfur isotope analysis of extracted sulfide of sedimentary rocks from Barberton Greenstone Belt, show a clear MIF (>1 ‰) and δ^{34}S-Δ^{33}S, Δ^{33}S-Δ^{36}S correlation. The Noisy Complex whchi is consist of fluvial sediments and diamictite show negative δ^{34}S-Δ^{33}Scorrelation, and Δ^{36}S/Δ^{33}S slope of -0.72. On the other hand, the Kromberg Formation which compose of deep marine sediments show positive δ^{34}S-Δ^{33}S, and scattered Δ^{36}S/Δ^{33}Sslope. δ^{34}S-Δ^{33}S, Δ^{33}S-Δ^{36}S relation from each stratigraphic level shows somewhat different trend, possibly reflecting local environment and/or bacterial sulfate reduction activity.

Keywords: South Africa, Sulfur, MIF

Japan Geoscience Union Meeting 2014
(28 April - 02 May 2014 at Pacifico YOKOHAMA, Kanagawa, Japan)

BPT23-14 Room:411 Time:April 30 12:30-12:45

Atmospheric oxygen in the Earth's 4.6-billion-year history

SATO, Tomohiko[1*] ; MARUYAMA, Shigenori[2]

[1]Department of Earth and Planetary Sciences, Tokyo Institute of Technology, [2]Earth-Life Science Institute, Tokyo Institute of Technology

The oxygen content of the Earth's surface environment is regarded to have increased in two steps; the Great Oxidation Event (ca. 2.4 Ga) around the Archean-Proterozoic boundary and the Neoproterozoic Oxygenation Event (ca. 800-550 Ma). These two events are supported by geochemical or paleobiological evidences; however, the estimation of the oxygenation level of the surface environment through time still have many problems to solve. We will review and discuss the previous researches for the better quantitative estimation of the atmospheric oxygen content in the Earth's 4.6-billion-year history.

Japan Geoscience Union Meeting 2014
(28 April - 02 May 2014 at Pacifico YOKOHAMA, Kanagawa, Japan)

BPT23-15 Room:411 Time:April 30 14:15-14:30

Convective stirring versus compositional stratification in the early mantle of terrestrial planets of various sizes

OGAWA, Masaki[1*]

[1]University of Tokyo at Komaba

Systematic numerical studies of magmatism in the convecting mantle of terrestrial planets suggest that how the compositional differentiation by magmatism in the earliest mantle affects its subsequent history depends on the size of the planets. In large planets like the Earth and Venus, the global scale magmatism induced by the high initial temperature of the mantle does not differentiate the mantle so much because of a strong positive feedback that arises between magmatism and mantle convection: Ascending flow of mantle convection induces decompression melting, but the buoyancy of the melts further enhances the ascending flow itself. This ascending flow enhanced by melt buoyancy strongly stirs the mantle and suppresses prominent compositionally stratified structure to develop in the early mantle. In Mars, the positive feedback still works, but the convection does not stir the mantle so strongly and the initial global scale magmatism makes the mantle compositionally stratified; the subsequent mantle evolution occurs as a convective relaxation of the compositionally stratified structure. In the moon and Mercury, the positive feedback itself does not work, and the convective current is mild even in the earliest stage of the history of the mantle. In the moon where the heat flux from the core is negligible and the gravity is small in deep mantle, in particular, a compositionally stratified structure formed in early mantle survives the subsequent stirring by such a mild convective flow.

Keywords: planetary size, magmatism, mantle convection, compositional stratification

Japan Geoscience Union Meeting 2014
(28 April - 02 May 2014 at Pacifico YOKOHAMA, Kanagawa, Japan)

BPT23-16 Room:411 Time:April 30 14:30-14:45

Lunar and Planetary Cratering Records: Evidences for and against the Cataclysmic Late Heavy Bombardment

MOROTA, Tomokatsu[1*]

[1]Nagoya Univ.

In this talk, I will discuss about the cataclysmic late heavy bombardment hypothesis based on the findings from studies of lunar and planetary cratering records.

Keywords: Late Heavy Bombardment, Crater, Moon

Japan Geoscience Union Meeting 2014
(28 April - 02 May 2014 at Pacifico YOKOHAMA, Kanagawa, Japan)

BPT23-17 Room:411 Time:April 30 14:45-15:00

Timing of late veneer on Earth: a siderophile element perspective

ISHIKAWA, Akira[1*] ; KOSHIDA, Keiko[1] ; SUZUKI, Katsuhiko[2] ; KOMIYA, Tsuyoshi[1]

[1]The University of Tokyo, [2]JAMSTEC

The short-lived ^{182}Hf-^{182}W decay system (half life is ca. 9 Myr) has long been recognised as a powerful tracer for accretionary and differentiation processes on the early Earth. Recent advances in analytical technique made it possible to conduct high-precision ($\pm$ 5 ppm or better) W isotope ratio measurements and have allowed exploitation of ^{182}W/^{184}W variations (expressed in the conventional ϵ^{182}W notation) in a wide variety of geological samples. To date, the presence of ϵ^{182}W anomalies have been documented for the 3.8 Ga Isua supracrustal belt in West Greenland, the 2.8 Ga Kostomuksha komatiites, the $\geq$ 3.8 Ga Nuvvuagittuq greenstone belt in Northeastern Canada and the 4.03 Ga Acasta gneiss complex in Northwestern Canada, all of which exhibit similar positive ϵ^{182}W anomalies up to 15 ppm relative to modern terrestrial samples (ϵ^{182}W $\simeq$ 0). These ^{182}W enrichments have been interpreted to represent the composition of anciently isolated domains in Earth's mantle that escaped addition of the chondritic late veneer (ϵ^{182}W $\simeq$ -2). This hypothesis is apparently consistent with the idea that $\sim$0.5% of the Earth's mantle was added after the cessation of core formation, required to account for the overabundance of highly siderophile elements (HSEs) in modern mantle. In order to test this hypothesis, we produced the HSE concentration data for basaltic amphibolites in the 4.03 Ga Acasta gneiss complex, meta-komatiites and meta-dunites in the $\geq$ 3.8 Ga Saglek-Hebron segment in Northern Labrador, Canada with the motivation in the search for the pre-late veneer mantle almost devoid of HSEs. The results demonstrated that the relative and absolute HSE abundances in all these rocks are akin to their late Archean to modern equivalents, indicating the delivery of late-accreted materials prior to 3.8-4.0 Ga at the period of late heavy bombardment on the Earth-Moon system. Considering the results of other studies demonstrating high-HSE contents of the mantle sources for the 3.8 Ga Isua rocks and the 2.8 Ga Kostomuksha komatiites, we can now conclude that ^{182}W enrichments are largely decoupled from HSE depletions, inconsistent with the pre-late veneer hypothesis. Further studies are necessary focusing on the siderophile element behaviors in Eoarchean rocks to advance in the knowledge of late accretion on Hadean mantle and the source of ^{182}W enrichments.

Keywords: siderophile element, late veneer, Archean, mantle

Japan Geoscience Union Meeting 2014
(28 April - 02 May 2014 at Pacifico YOKOHAMA, Kanagawa, Japan)

BPT23-18 Room:411 Time:April 30 15:00-15:15

Destruction and melting of Hadean continent by Late Heavy Bombardment

SHIBAIKE, Yuhito[1*] ; SASAKI, Takanori[2] ; IDA, Shigeru[3]

[1]Department of Earth and Planetary Sciences, Tokyo Institute of Technology, [2]Department of Astronomy, Kyoto University, [3]Earth-Life Science Institute, Tokyo Institute of Technology

There are no rocks, which were made in Hadean Earth. In recent years, however, sedimentary rocks including zircons made in Hadean indicated the existence of some continental crusts in Hadean. So, how were the continental crusts to disappear? One hypothesis to solve this problem is destruction and/or melting of the crusts by the Late Heavy Bombardment (LHB), a concentration of impacts in last phase of Hadean. However, there are few quantitative studies so far.

We developed the expressions to deduce the effects of LHB to the Hadean crusts, and showed that the concentration of impacts could not destruct/melt the whole Hadean crust. We assumed the impact flux of based on the following three models: ”Cataclysm” model, ”Soft-Cataclysm” model, and ”Standard” model.

First, we estimated the scale of LHB through the main asteroid belt’s size-frequency distribution by the basins on the moon (Cataclysm model), results of numerical simulations (Soft-Cataclysm model), and cratering rates of the moon (Standard model). We approximated the main asteroid belt’s size?frequency distribution estimated by observations as a power-law scaling, and gave some power indexes as a parameter. This parameter can change the effects of LHB widely. Then we estimated the sum of volume and area of craters made by LHB using the scaling low of cratering.

The result is that the LHB in any models had a chance to melt roughly same volume of the Hadean crusts, but could not cover the whole surface of the Earth by the craters. As the Hadean crusts are considered to be dotted on the surface, it would be impossible to melt the all dotted crusts by impacts. In conclusion, the Late Heavy Bombardment could not destruct/melt the whole Hadean crusts.

Keywords: Late Heavy Bombardment, Hadean, continental crust, asteroid, crater, impact

Japan Geoscience Union Meeting 2014
(28 April - 02 May 2014 at Pacifico YOKOHAMA, Kanagawa, Japan)

BPT23-19 Room:411 Time:April 30 15:15-15:30

The first recovory of impact-shocked zircons from the Jack Hills metasedimentary rocks, Western Australia

YAMAMOTO, Shinji[1*] ; KOMIYA, Tsuyoshi[1]

[1]Department of Earth and Astronomy, Graduate School of Arts and Sciences, The University of Tokyo

The first 500 million years of the Earth history remain poorly understood because terrestrial rock records during Hadean era (>4.0Ga) are scarcely preserved, probably due to surface and/or tectonic erosion and intense meteorite bombardment. The Late Heavy Bombardmend (LHB) is the period from ca. 3.85-3.95, an intense flux of asteroidal bodies into inner solar system originally proposed to have impacted the Moon. To date, the oldest impact structure on the Earth is the 2.02 Ga Vredefort Dome, South Africa, and another oldest evidence of bolide impact is 3.47-3.24 Ga spherule layers in the Barberton Greenstone Belt, South Africa (e.g. Lowe et al., 2003). The impact chronology from these spherule layers suggest that the impactor flux was significantly higher 3.5 Ga than today (Jhonson & Melosh, 2012).

Geological conditions during Hadean era can be deduced from detrital zircon grains as old as 4.4 Ga preserved in metasedimentary rocks at Jack Hills in the Narryer Gneiss Complex, Western Australia (e.g. Compston & Pidgeon, 1986; Wild et al., 2001). Jack Hills metaconglomerates deposited in ca. 3 Ga contain detrital zircons with ages continuously spanning from 3.0 to 4.4 Ga. Previous investigations of these grains have suggested the existence of a thermal excursion during LHB era (Abbott et al., 2012; Bell and Harrison, 2013), but temperature approach of detrital zircons do not restrict impact-related heating.

Here, we first report zircons with shock-induced textures, such as granular (polycrystalline) texture, from the Jack Hills metaconglomerate. Granular-textured zircons have been frequently reported from impact ejecta layers and craters, such as K-Pg boundary, the Chicxulub crater (e.g. Bohor et al., 1993; Krogh et al., 1993) and also from shock experiments (Wittmann et al., 2006). Polycrystalline zircon grains recovered from the Jack Hills metaconglomerates represents several micro-meter sized crystallites of zircon in a glassy ZrSiO4 matrix that may resulted from shock-induced amorphization and subsequent recrystallization (Witmann et al., 2006). Several grains show the granular texture with abundant micro-vesicles and tiny ThSiO4, suggesting incipient melting and vaporization. The first recovery of shock-induced zircons from the Jack Hills metaconglomerate would provide significant clues on the early Earth environment and on constructions/destructions of Earth early crust.

Keywords: early Archean, Hadean, Jack Hills, zircon, shock metamorphism

Japan Geoscience Union Meeting 2014
(28 April - 02 May 2014 at Pacifico YOKOHAMA, Kanagawa, Japan)

BPT23-20 Room:411 Time:April 30 15:30-15:45

Trace element variety of mafic rocks in the Acasta Gneiss Complex

KOSHIDA, Keiko[1*] ; ISHIKAWA, Akira[2] ; IWAMORI, Hikaru[3] ; KOMIYA, Tsuyoshi[2]

[1]Department of Earth and Planetary Science, The University of Tokyo, [2]Department of Earth Science and Astronomy, Graduate School of Arts and Sciences, University of Tokyo, [3]Geochemical Evolution Research Program, Japan Agency for Marine-Earth Science and Technology

The Hadean from birth of the Earth to 4.03 Ga is the earliest period of the history of the earth, and defined by no preservation of rock records in the earth. Eoarchean crustal records are also rare, so that the details of early Earth are not revealed yet.

Acasta Gneiss Complex (AGC), located in the western part of the Slave Province, Canada, is one of the Early Archean terranes, and mainly consists of 3.6-4.0 Ga felsic and layered gneiss suites and mafic rocks. Minor mafic rocks are distributed all over the AGC and occur as rounded to elliptical enclaves and inclusions in the felsic and layered gneisses. These field occurrence of the mafic rocks suggest that they were formed before the formation of granitoid precursor of felsic gneisses and have potential to demonstrate the Early Archean mantle evolution. However, the AGC is subjected to numerous metamorphic and alteration events. The Acasta mafic rocks mainly consist of amphibolites with hornblende, plagioclase and quartz, suggesting that they underwent at least amphibolite facies metamorphism. No relict igneous minerals are preserved. At some localities, hornblendites with over 90 % modal abundance of hornblende occur as restites of anatexis. This study constrain the Early Archean mantle characteristics from the least altered samples, which selected based on the effects of alteration process by methods of whole rock major and trace element compositions.

The compositions of the amphibolites range from basalt to basaltic andesite (SiO2=48-57 wt. %, MgO=2.1?9.8 wt. %) and negative correlations can be seen between Al_2O_3 and MgO contents and Na_2O and MgO contents respectively. The hornblendites have higher MgO and lower Al_2O_3 and Na_2O contents than amphibolites, supporting the geological evidence that the hornblendites were derived from residue of anatexis. Amphibolites are divided into three groups based on their major elements and primitive mantle (PM)-normalized trace element patterns: Low-Al, Intermediate-Al and High-Al amphibolite respectively.

The Low-Al amphibolites are plotted between the Intermediate-Al amphibolites and hornblendites on the $Al2O_3$ vs MgO diagram. They have relatively higher LREE contents than the Intermediate-Al amphibolites. They display negative Zr and Ti anomalies on the PM-normalized trace element patterns. Those characteristics are similar to those of hornblendites. On the other hand, PM-normalized trace element patterns of the High-Al amphiblites are highly scattered. The geochemical characteristics of the amphibolites suggest that the Low-Al amphibolites were formed as a residue with incomplete melt loss due to the partial melting of the Intermediate-Al amphibolites, whereas the High-Al amphiblites as the melts addition. The geological and geochemical evidence indicates that the compositions of almost mafic rocks at the AGC were affected by secondary partial melting, but some mafic rocks, the Intermediate-Al amphibolites, possibly preserve their primary characteristics.

Except for Nb, the Intermediate-Al amphibolites have flat PM-normalized trace element patterns. Their negative Nb anomalies suggest that they were generated at the subduction setting, implying slab-dehydration process already occur in the Early Archean. Mantle evolution through geologic time is an alternative candidate for the Nb negative anomaly.

Keywords: Archean, mafic, mantle

Japan Geoscience Union Meeting 2014
(28 April - 02 May 2014 at Pacifico YOKOHAMA, Kanagawa, Japan)

BPT23-21 Room:411 Time:April 30 15:45-16:00

Growth curve of continental crust on the surface of the Earth

SAWADA, Hikaru[1*] ; MARUYAMA, Shigenori[2] ; HIRATA, Takafumi[3]

[1]Department of Earth and Planetary Sciences, Tokyo Instite of Technology, [2]Earth and Life Institute, Tokyo Instite of Technology, [3]Division of Earth and Planetary Sciences, Kyoto University

The growth curve of continental crust through the Earth's history has been estimated by many methods, which include geologic-geophysical-, and geochemistry-based. Many studies through geophysical and geochemical modeling indicate that there was rapid formation of continental crust during the early part of the history of the Earth. The geological record shows, however, that less than 20% of continental crust before 2.6 Ga remains and an absense Hadean geological body. The difference between the formation of continental crust, indicated by modeling to be more extensive than what is observed in the geological record has been thought to be effect of crustal recycling or subduction of crustal material into the mantle. Recently, the importance of arc subduction (Yamamoto et al., 2009) and large scale subduction erosion around circum-Pacific active subduction zones has been revealed through geologic investigation of the Japanese islands (Isozaki et al.,2010; Suzuki et al., 2010). The crustal material subducts into the mantle transition zone and forms a second continent (Kawai et al.,2009;2013). It is the aim of this study to delineate the growth history of continental crust which takes into account the subduction of continental crustal material into the mantle global scale.

River sand zircon method is one of the most powerful methods to determine the age frequency distribution of the continental crust (Rino et al.,2004;2008). In this study, the global unconformities are regarded to be past continental margins, with river sand in clastic rocks occuring above them. The age frequency distributions of detrital zircons at given global unconformities with ages of 2.6, 1.0 and 0.6 Ga were determined in this study. This included analyzing detrital zircons separated from sedimentary rocks which occur above global uncconformities with surfaces covering the Pilbara, Kaapvaal, Zimbabwe and Wyoming cratons, with U-Pb ages determined through the LA-ICP-MS at Hirata Laboratory in Kyoto University. In addition, in oreder to make this more of a global study, published data was also were used to determine the age frequency distribution of continental crust at 2.6, 1.0 and 0.6 Ga.

The growth history of continental crust is discussed by showing the compilations of age frequency distribution of detrital zircons at 2.6, 1.0, 0.6 Ga (this study) and at present (Rino et al., 2008). The shape of these curves indicates that there was rapid formation of continental crust with large scale subduction of crustal materials into the mantle during a time range of 4.5 to 2.6 Ga, and that during 1.0 Ga to present, continental crust on the Earth's surface has been declining due to subduction erosion being more dominant than crustal formation. In addition, the growth history of continental crust was estimated in this study by using the evolution of oceanic Sr isotope ratio recorded in carbonate rocks (Shields and Veizer, 2002). In this study, the Sr flux estimated from the carbonates is assumed to be proportional to the volume of the continents.

Based on these works, a model of growth history of the continental crust is proposed here. From the Hadean through the Archean to the early part of the Proterozoic, there was rapid formation of granitic crust as most oceanic island arcs were subducted into the mantle with only a limited number of them colliding and contributing to the growth of continental crust of the surface of the Earth. At 2.6 Ga, the amount of continental crust was 75% of that at present. Subsequently, magmatism at subduction zones was superior to subduction erosion with about 150% continental crust at 1.0 Ga compared to that at present. Since about 1.0 Ga, the continental crust has been reducing in volume due to subduction erosion being superior to growth at subductions zones.

Keywords: U-Pb age, detrital zircon, global unconformity, growth of continental crust

Japan Geoscience Union Meeting 2014
(28 April - 02 May 2014 at Pacifico YOKOHAMA, Kanagawa, Japan)

BPT23-22 Room:411 Time:April 30 16:15-16:30

Geological and geochemical studies about the Eoarchaean-aged Banded Iron Formations in Nain Province, Northern Labrador.

AOKI, Shogo[1*] ; SHIMOJO, Masanori[1] ; YAMAMOTO, Shinji[1] ; HIRATA, Takafumi[2] ; KOMIYA, Tsuyoshi[1]

[1]Department of Earth Science and Astronomy, Graduate School of Arts and Sciences, University of Tokyo, [2]Division of Earth and Planetary Sciences, Graduate School of Science, Kyoto University

Banded iron formations (BIFs) are chemical sediments, deposited in seawater before the Paleoproterozoic, and are often utilized as proxies for chemical compositions of seawater. However, the scarcity of >3.6 Ga supracrustal rocks including BIFs hampers the use of BIFs for estimate of the seawater composition, especially bioessential elements, in the early earth. Recently, Konhauser et al. (2009) showed secular change of Ni/Fe ratios of BIFs through geologic time, and suggested that the Archean seawater was enriched in dissolved Ni, suitable for methanogenic bacteria. But, their data show quite large variations in Ni/Fe ratios at the same ages from the modern value to about ten times value. Therefore, more comprehensive investigation of the BIFs through geological time is necessary to estimate secular change of chemical composition of seawater. For the purpose, we performed comprehensive investigations of geology, geochronology, stratigraphy and geochemistry of the oldest supracrustal rocks, in >3.96 Ga Nulliak Supracrustal rocks in the Nain Province, Northern Labrador, Canada (Shimojo et al., 2013).

Based on the lithostratigraphy and accompanied rocks, we classified into two types of BIFs: BIFs interlayered with metabasite in the Nulliak Island and BIFs accompanied with carbonate and/or chert layers, respectively. The former are Algoma-type BIFs, which was deposited in deep-sea near basaltic volcanism. The latter are uncommon in the Early Archaean, which are possibly formed in shallow-water environment.

Their PAAS-normalized REE+Y patterns display positive La, Eu and Y anomalies, suggesting that they were deposited in a mixing zone of seawater and hydrothermal water. In addition, transitional element contents such as Ni and Zn (>50 ppm) are high, similar to other Archean BIFs (Konhauser et al., 2009, Mloszewska et al., 2012). But, HFSE (e.g. 1˜20 ppm in Zr contents) and Al2O3 (0.5˜2 wt%) contents are variable, and positively correlated with REE+Y and the transitional element contents, suggesting that the variation in the REE+Y contents is due to detrital inputs so that samples with low Zr and Al2O3 contents preserve the detritus-free compositions. The samples with low detritus inputs show a negative correlation between Eu/Eu∗and REE and Y/Fe ratios, and between Eu/Eu∗and LREE/REE and Y ratios, respectively. The similar correlations are reported for iron-rich suspended particulates collected from the TAG hydrothermal field (German et al., 1990). Therefore, the REE+Y variations can be explained by continuous scavenging processes by iron-oxyhydroxide particles. Moreover, no Ce/Ce∗anomaly is consistent with anoxic seawater in the Early Archaean.

In addition, transition metals (Ni, Zn, Co)/Fe ratios correlate negatively with Eu/Eu∗. The correlations were also shown in BIFs in the Isua Supracrustal Belts and the Nuvvuagittuq Supracrustal Belts (Bolhar et al., 2004; Mloszewska et al., 2012), suggesting that their variations are due to same scavenging processes by iron-oxyhydroxide particles as REE+Y. Namely, the transition metals/Fe ratios of BIFs don't provide direct estimate of those concentrations of seawater. We normalize their transitional metals by rare earth elements (e.g. Sm), which are adsorbed on iron-oxyhydroxide similar to the transition metals. Sm-normalised transitional metals contents of the Archaean BIFs are higher than those of Proterozoic BIFs, suggesting that the Archaean seawater was enriched in transitional metals such as Ni and Zn, which are essential for protein synthesis of the early life.

Reference : Konhauser et al., 2009. Nature 458, 750-754. ; Shimojo et al., 2013. Goldschmidt 2013, Florence, Italy.; German et al., 1990. Nature 345, 516-518. ; Bolhar et al., 2004. EPSL 222, 43-60. ; Mloszewska et al., 2012. EPSL 317-318, 331-342.

Keywords: Eoarchaean, bioessential elements, Banded Iron Formations

Japan Geoscience Union Meeting 2014
(28 April - 02 May 2014 at Pacifico YOKOHAMA, Kanagawa, Japan)

BPT23-23 Room:411 Time:April 30 16:30-16:45

In-situ iron isotope analysis of pyrite in ca. 3.8 Ga metasediments from Isua supracrustal belt, Greenland

YOSHIYA, Kazumi[1*] ; SAWAKI, Yusuke[2] ; KOMIYA, Tsuyoshi[3] ; HIRATA, Takafumi[4] ; MARUYAMA, Shigenori[1]

[1]Earth life Institute, Tokyo Insititute of Technology, [2]Dept. of Earth & Planetary Sciences, Tokyo Insititute of Technology, [3]Dept. of Earth Sci. and Astro., The University of Tokyo, [4]Dept. of Geology and Mineralogy, Kyoto University

The timing of emergence of life still remains one of the unresolved questions in the early Earth. Early life could be identified and characterized by its metabolic processes, which must be deposited and preserved in the old rocks. The oldest (ca. 3.8Ga) sedimentary rocks on Earth occur in the Isua supracrustal belt (ISB), southern West Greenland. These rocks have been subjected to until amphibolite facies metamorphism (Nutman, 1986; Hayashi et al., 2000). Despite the contribution of the intense thermal metamorphism, carbon isotope compositions from the Isua metasediments suggested the evidence for biological carbon fixation. Microbial dissimilatory iron reduction (DIR) is also considered to be one of the earliest metabolisms on Earth. σ^{56}Fe value of $Fe^{2+}{}_{aq}$ generated by DIR is expected to have lower value, whereas negative σ^{56}Fe values lower than -1 ‰ are not found in the sedimentary record prior to 2.9Ga. Here, we report the *in-situ* iron isotope analysis of pyrite in sedimentary rocks from the ISB, using femtosecond laser ablation multi-collector ICP-MS technique (fs-LA-MC-ICP-MS). We obtained a large variation of iron isotope data from -2.41 to +2.35 ‰ in σ^{56}Fe values, from 212 points of pyrite grains in 15 rock specimens, including metachert, muddy metachert, BIF, carbonate rock and conglomerate. The distribution of σ^{56}Fe values varies depending on the lithologies and depth gradient, whereas no correlation could be found between σ^{56}Fe values and the metamorphic zone.

Low σ^{13}C values of graphite in ISB muddy metachert suggested the existence of biological carbon fixation(e.g., Schidlowski et al.,1979). σ^{56}Fe values of pyrite grains from the shallow water samples show lower σ^{56}Fe values, which suggested the occurrence of microbial DIR in the Early Archean.

Keywords: Early archean, Isua supracrustal belt (ISB), iron isotope ratio, pyrite, microbial dissimilatory iron reduction (DIR)

Japan Geoscience Union Meeting 2014
(28 April - 02 May 2014 at Pacifico YOKOHAMA, Kanagawa, Japan)

BPT23-24 Room:411 Time:April 30 16:45-17:00

The origin of carbonaceous material in the Early Archean Nain Complex, northern Labrador, Canada

TASHIRO, Takayuki[1*] ; HORI, Masako[3] ; ISHIDA, Akizumi[3] ; IGISU, Motoko[4] ; SANO, Yuji[3] ; KOMIYA, Tsuyoshi[2]

[1]Department of Earth and Planetary Science Graduate School of Science The University of Tokyo, [2]Department of Earth Science & Astronomy Graduate School of Arts and Sciences The University of Tokyo, [3]Atmosphere and Ocean Research Institute The University of Tokyo, [4]Japan Agency for Marine-Earth Science and Technology

Presence of early life in the Early Archean is still controversial, and it is a key issue to find evidence for early life from the Early Archean rocks. Carbon isotope ratio ($\delta^{13}C_{org}$) of carbonaceous matter (CM) is widely used as an indicator of existence of life (Schidlowski, 2001). CM in the 3.80 Ga metasediments of the Isua Supracrustal Belt (ISB), southern West Greenland has low $\delta^{13}C$ values, interpreted as evidence for organism in the Early Archean (Rosing, 1999). Recently, Ohtomo et al (2013) showed the nano-scale microstructure of the CM, evident for originating from organisms. In contrast, it is presumed that CM in the Nuvvuagittuq Supracrustal Belt (˜3.75Ga) has a secondary metamorphic origin because the crystallization temperature (˜380 ℃) of the CM estimated from LA-Raman spectrums is much lower than than metamorphic temperature (˜640 ℃) (Papineau et al., 2011). Moreover, a putative banded iron formation in the Akilia Island (˜3.83 Ga) including apatites with carbonaceous inclusions with the low $\delta^{13}C$ provides another evidence for the life, but the precursor is still controversial (Fedo and Whitehouse, 2002). Thus, there is no obvious evidence for presence of life in the Early Archean except for that from ISB.

Shimojo et al. (2013) showed that >3.96Ga metasediments exist in the Nain Complex, northern Labrador, Canada. The Nain Complex is *ca*. 100 million years older than the Akilia association, which has the oldest supracrustal rocks in the world. The purpose of this research is to reveal the origin of the CM in the sedimentary rocks in the Nain Complex.

We selected pelitic gneisses (n=70), conglomerates (n=14), carbonate rocks (n=39), cherts (n=30), chert nodules in carbonate rocks (n=3) and amphibolites (n=5) from over 2000 samples over the Nain Complex based on the metamorphic grade, geography, their field occurrence and degree of alteration. Among the metasedimentary rocks (n=156), 54 specimens including pelitic gneisses (n=21), conglomerates (n=4), carbonate rocks (n=26) and chert nodules in carbonate rocks (n=3) contain CM. Seven CM-bearing rock samples were selected for $\delta^{13}C_{org}$ analysis: pelitic gneisses (n=4), conglomerates (n=1), carbonate rocks (n=1) and chert nodules (n=1), and 3 carbonate rock samples for $\delta^{13}C_{carb}$ analysis, respectively.

Metamorphic grade was estimated for mineral paragenesis and garnet-biotite thermometry. Among the seven CM-bearing rock samples, the six samples were metamorphosed under up to the amphibolite facies condition, and a sample under the lower granulite facies condition, respectively. The metamorphic temperatures are consistent with the estimated crystallization temperature of the CM calculated by Raman spectral parameters.

$\delta^{13}C_{carb}$ values range from -3.75 to -2.63 ‰. Because it is well known that secondary alteration and metamorphism decrease a $\delta^{13}C_{carb}$ value (Schidlowski et al., 1979), a primary $\delta^{13}C_{carb}$ value was estimated to be higher than -2.63 ‰. As a result, the $\delta^{13}C_{carb}$ value of marine bicarbonate was at least -2.63 ‰ in the Early Archean.

$\delta^{13}C_{org}$ values of pelitic gneisses range from -28.86 to -14.07 ‰. The $\delta^{13}C_{org}$ values of conglomerate, carbonate rock and chert nodule are -17.52, -5.72 and -10.60 ‰, respectively. Metamorphism, generally speaking, increases a $\delta^{13}C_{org}$ value of CM due to partial thermal decomposition, especially methane degassing, suggesting that the variation in the $\delta^{13}C_{org}$ values is due to secondary thermal decomposition. The correlation of the $\delta^{13}C_{org}$ values with distribution of organic matter under microscopic observation also supports the partial decomposition and consequent increase of the $\delta^{13}C_{carb}$ values. As a result, the lowest δ13Corg value is a maximum estimate of the $\delta^{13}C_{org}$ value.

The minimum fractionation between the $\delta^{13}C_{org}$ and $\delta^{13}C_{carb}$ reaches 25 ‰, indicating biologic origin for the CM. This work presents the organism has already existed *ca.* 3.96 Ga.

Keywords: CM, Labrador, early life, carbon isotopic ratio

Japan Geoscience Union Meeting 2014
(28 April - 02 May 2014 at Pacifico YOKOHAMA, Kanagawa, Japan)

BPT23-25 Room:411 Time:April 30 17:00-17:15

Sr-Nd-Pb isotopic compositions of hot spring water in the Toyoha Mine, Hokkaido Japan: Implications for the origin of hy

NAKAMURA, Hitomi[1*] ; IWAMORI, Hikaru[2] ; ARAKI, Shuuhei[3] ; HIEDA, Yuki[3] ; FUJINAGA, Koichiro[3] ; KATO, Yasuhiro[3] ; NAKAI, Shun'ichi[4] ; KIMURA, Jun-ichi[2] ; CHANG, Qing[2]

[1]Titech, [2]JAMSTEC, [3]Univ. of Tokyo, [4]ERI, Univ. of Tokyo

Chemistry and dynamics of slab-derived fluids in subduction zones have been rigorously studied by high pressure experiments, geochemical and hydrological modellings, and geophysical observations [1-5]. Surface manifestation of deep slab-derived fluids are now suggested by geochemistry, such as slab fluid-like chemical affinities found in volcanic rocks [6,7] and in hot spring waters [8] . In this study, we aim to examine the presence (or absence) of slab derived fluid signatures in hot spring water related with the Toyoha Mine ore deposits in Hokkaido, one of the largest hydrothermal vein-type deposits in Japan. We applied Sr-Nd-Pb isotope analyses of the hot spring water and compared the results to those from the volcanic rocks and the ore minerals from the Toyoha Mine.

For this purpose, we have examined a ferric co-precipitation pre-concentration method for the hot spring water from the Toyoha Mine. This was necessary because the abundances of Nd and Pb were very low, less than several ppb for Nd, in particular. The method has previously been applied to brines with high chlorine concentration at Arima hot spring [9], and the method worked well with the Toyoha hot spring water. The concentrated sample has been analyzed by Q-ICP-MS and MS-ICP-MS for both element abundances and Sr-Nd-Pb isotopic compositions. We examined origin of the hot spring water by using Sr-Nd-Pb isotope systematics in comparison with the data from the ore deposit, volcanic rocks related with the ore deposition, and the basement rocks of the Toyoha Mine. A recent study has shown that Sr-Nd-Pb isotopic ratios of sulfide ores in the Toyoha Mine exhibit a high contribution of slab-derived fluid from the Pacific Plate slab [10]. Our preliminary results on the hot spring water suggest that the water may also preserve the slab-fluid signatures and/or may also be affected by the chemical components in the basement rocks.

[1] Schmidt and Poli, 1998, EPSL [2] Hacker et al., 2003, JGR [3] Iwamori, 1998, EPSL [4] Arcay et al., 2005, PEPI [5] Cagnioncle et al., 2007, JGR [6] Pearce et al., 2005, G3 [7] Nakamura et al., 2008, NGeo [8] Kusuda et al., in revision [9] Nakamura et al., submitted [10] Hieda, 2013, Master Thesis, Univ. of Tokyo

Keywords: hot spring, isotope, Toyoha, mine, ore

Japan Geoscience Union Meeting 2014
(28 April - 02 May 2014 at Pacifico YOKOHAMA, Kanagawa, Japan)

BPT23-26 Room:411 Time:April 30 17:15-17:30

The contribution of slab-fluids to the formation of hydrothermal vein-type deposits

FUJINAGA, Koichiro[1*] ; KATO, Yasuhiro[1] ; HIEDA, Yuki[1] ; ARAKI, Shuhei[1] ; TANIMIZU, Masaharu[2] ; SUMINO, Hirochika[3] ; SHIMIZU, Toru[4] ; NAKAMURA, Hitomi[5] ; IWAMORI, Hikaru[2]

[1]Department of Systems Innovation, School of Engineering, University of Tokyo, [2]JAMSTEC, [3]Geochemical Research Center, Graduate School of Science, University of Tokyo, [4]AIST, [5]Dep. of Earth and Planetary Sciences, Tokyo Institute of Technology

It has been recently pointed out that ”geofluids” released from the subducting plates are involved in various products in subduction zones, such as arc magmas, deep-seated hot springs and hydrothermal vein-type deposits. Systematic investigations of these various materials are needed for identifying the geochemical characteristics of the geofluids. Nakamura et al. (2008) revealed the heavy isotopic compositions of slab-fluids derived from two subducted plates (the Pacific plate and the Philippine Sea plate) which contribute largely to the genesis of arc magmas in Central Japan.

In this study, we focus on the hydrothermal vein-type deposits in Japan. It has been previously considered that hydrothermal fluids that form sul-phide mineral (pyrite, chalcopyrite, sphalerite, galena etc.) deposits were originated from magmatic and/or meteoric waters [2]. However, we reported that Pb isotopic compositions of the sulphide ore samples were plotted between Philippine Sea plate (PHS)-fluid and Pacific plate (PAC)-fluid, suggesting that ore fluids responsible for the hydrothermal deposits are directly derived from deep slab-fluids. Here we report multi-isotopic compositions (Pb-Nd-He) of sulphide ores, associated volcanic rocks, and the surrounding country rocks from the Toyoha polymetallic (Zn-Pb-Ag-Cu-Sn-In) vein-type deposit (one of the largest hydrothermal vein-type deposits in Japan) in order to understand the rela-tionship between slab-fluid and formation of vein-type deposit in more detail.

Results and Discussion: We collected twenty-six sulphide ore samples, and fifteen associated volcanic and country rocks from the Toyoha Mine. The 206Pb/204Pb values of sulfide ore samples are significantly larger than those of the Muine volcanic rocks which have been long thought to be genetically related to the formation of Toyoha deposit. In addi-tion, the 3He/4He values of Toyoha galena samples range between 5 and 6 times the atmospheric ratio, implying the significant contribution of the mantle component, and strongly suggest that there is a contribution from deep-derived fluid to the Toyoha ore fluid. The correlation between 207Pb/204Pb and 143Nd/144Nd shows that the relative contribution of PAC fluid component in the Toyoha ores is significantly higher than that involved in the Muine volcanic rocks. It can be estimated that more than ˜80% of Pb of the Toyoha ore deposit is derived from slab-fluids. Based on the present measurements and mass balance calculations, it is very likely that the slab-fluids supplied the major part of Pb and other metals concentrated in the Toyoha district.

Keywords: Pb isotopic composition, hydrothermal deposit, slab-fluid

Japan Geoscience Union Meeting 2014
(28 April - 02 May 2014 at Pacifico YOKOHAMA, Kanagawa, Japan)

BPT23-27 Room:411 Time:April 30 17:30-17:45

The Archean hydrothermal alteration: Significance of silicification for seawater composition and biological evolution

KOMIYA, Tsuyoshi[1*]

[1]Komaba, University of Tokyo

The earth is the active planet, where higher forms of life live. Presence of liquid water on surface of planet is necessary to organisms: thus a planet with the liquid water is called a habitable planet. But, enrichment in bioessential elements is also important because they are demanded for their activity. In addition, it is required that they are continuously supplied to biosphere through the elemental cycle. Especially, phosphate is one of the most important nutrients because the DNA and RNA contain large amounts of phosphate contents. Nickel is a bioessential element for methanogen, which was more active in early Earth. However, phosphorus, iron, and nickel are highly depleted in modern seawater because oxic modern seawater causes precipitation of iron oxyhydroxide, which effectively remove the phosphorus and nickel through their adsorption on iron precipitates. The evolution of seawater composition through geologic time accounts for the apparent paradox, namely ancient seawater was enriched in the phosphorus and nickel contents (Planavsky et al., 2010; Konhauser et al., 2009). But, the mechanism of high phosphorus and nickel contents in seawater is still ambiguous. This works presents silicification plays important roles not only on the supply of the phosphorus and nickel into seawater but also on preventing adsorption of the elements on iron hydroxide.

Comparison between major element compositions of modern altered and non-altered MORB (Alt & Honnorez, 1984) indicates present-day hydrothermal alteration increased phosphorus contents relative to titanium contents in the altered basalts because altered MORBs commonly contain over four times higher phosphorus contents than the fresh equivalents (e.g. Alt & Honnorez, 1984, CMP). Therefore, the hydrothermal fluid has relatively low phosphorus content. On the other hand, comparison between Archean altered and non-altered MORB indicates the Archean altered basalts contain relatively lower phosphorus contents than the fresh equivalents (Komiya et al., 2002, IGR, Nakamura & Kato, 2004, GCA). The different behavior of phosphate during the hydrothermal alteration of basalts suggests higher phosphate contents in the Archean hydrothermal fluids. In addition, silicified basalts in the Archean greenstone belts are completely depleted in phosphorus, indicating much amounts of phosphorus were supplied into seawater. Comparison between nickel contents of altered and non-altered basalts and peridotitic komatiites indicates the altered rocks are more enriched in nickel under the moderate hydrothermal alteration condition, contrast to previous hypothesis (Konhauser et al., 2009). However, silicified basalt and peridotitic komatiite are completely depleted in sodium, phosphorus and nickel except for potassium, indicating silicification effectively supplied nickel and others to ocean. It is considered that formation of banded iron formation caused effective removal of nickel and phosphorus from seawater. Especially, recent study of their rare earth element patterns, namely Y/Ho and Sm/Yb ratios, indicate iron oxyhydroxide were precipitated much more from seawater in the Early Archean, suggesting phosphorus and nickel were more efficiently removed from seawater. Higher silica content of seawater in the early Earth accounts for the apparent paradox. The high silica content of ancient seawater had a significant role of the preventing adsorption of phosphorous and nickel on iron oxyhydroxide as well as supplying more phosphorus and nickel to seawater at the hydrothermal alteration.

We propose that high silica contents of ancient seawater resulted in high phosphorus and nickel contents of seawater in the early Earth.

Keywords: Silicification, Early Earth, Paleo-seawater, Nutrient and biological evolution, Basalt and komatiite

Japan Geoscience Union Meeting 2014
(28 April - 02 May 2014 at Pacifico YOKOHAMA, Kanagawa, Japan)

BPT23-28 Room:411 Time:April 30 17:45-18:00

Potential nitrogen fixation by hyperthermophilic methanogens on the early Earth

NISHIZAWA, Manabu[1*] ; MIYAZAKI, Junichi[1] ; TAKAI, Ken[1]

[1]JAMSTEC

Hyperthermophilic hydrogenotrophic methanogens are considered to represent one of the most important classes of primary producers in hydrogen (H_2)-abundant hydrothermal environments throughout the history of Earth. Despite extensive studies of methanogenesis, comprehensive research on nutrient anabolism in hyperthermophilic methanogens is limited. We first investigated the physiological properties and isotopic characteristics of experimental cultures of hyperthermophilic methanogens during the fixation of dinitrogen (N_2), an abundant but less-bioavailable compound in hydrothermal fluids. We found that these hyperthermophilic methanogens actively assimilated N_2 via molybdenum (Mo)-iron (Fe) nitrogenase under broad ranges of Mo and Fe concentrations relevant to present and past oceanic and hydrothermal environments. Furthermore, the methanogens produced more ^{15}N-depleted biomass than that previously reported for diazotrophic photosynthetic prokaryotes. These results indicate that diazotrophic methanogens can be broadly distributed in seafloor and subseafloor hydrothermal environments, where the availability of the transition metals is variable and organic carbon and nitrogen compounds and ammonium are extremely scarce. The possible emergence and function of diazotrophy coupled with methanogenesis 3.5 billion years before the present may be inferred from the nitrogen and carbon isotopic records of kerogen and fluid inclusions from hydrothermal deposits.

Japan Geoscience Union Meeting 2014
(28 April - 02 May 2014 at Pacifico YOKOHAMA, Kanagawa, Japan)

BPT23-P01 Room:Poster Time:April 30 18:15-19:30

Reconstruction of tectonic history of the Cleaverville area in Coastal Pilbara Terrane ,western Australia

AIHARA, Yuhei[1*] ; KIYOKAWA, Shoichi[1] ; TANAKA, Ryoji[2] ; NAKAMURA, Eizo[2] ; SAKAGUCHI, Chie[2]

[1]Earth and Planetary Science, Kyushu Universiy, [2]Pheasant Memorial Laboratory, Institute for the Study of the Earth's Interior at Misasa

The Dixon Island - Cleaverville formations of the Coastal Pilbara Terrane, Western Australia, is one of the most complete sections of a volcano-hydrothermal sequence of the immature island arc (Kiyokawa &Taira, 1998). These formations composed of the Dixon Island (DX) Formation, Dixon pillow basalt and the Cleaverville (CL) Formation. The CL Formation is uncomformably overlain by the Lizard Hills Formation. The Lizard Hills Formation was formed in syncline basin (66 Hill Member) during collisional D1 deformation and pull-apart basin (44 Hill Member) during sinistral slip D2 deformation (Kiyokawa et al., 2002).

In this study, depositional ages of the CL Formation and the Lizard Hills Formation (44 Hill Member and 66 Hill Member) were examined by the analysis of U-Pb zircon dating. Zircons were measured using SHRIMP2 at National Institute of Polar Research. Metamorphic age of the DX Formation was obtained by the whole-rock 87Rb-86Sr isochronusing TIMS (Thermo TRITON and MAT253) at the Pheasant Memorial Laboratory, Institute for the Study of the Earth's Interior at Misasa.

As a result, U-Pb zircon age of felsic tuff in the CL Formation is 3108(+14/-7) Ma. Detrital zircon ages of the 44 Hill Member showed main peaks at 3280-3200Ma and 3030-3020Ma. Detrital zircon ages of the 66 Hill Member also showed peaks at 3300-3200Ma, 3100-3050Ma, and miner group of 3700Ma. The Rb-Sr data define clear correlation line in the 87Rb-87Sr evolution diagram which corresponds to an age of 2210+/-60 Ma.

In conclusion, sedimentation age of the DX formation is 3195+/-12Ma (Kiyokawa et al.,2002) and the CL Formation is 3108(+14/-7) Ma. The average of sedimentation rate in DX-CL formations is 2˜3mm/ky as total thickness between these ages is 250m. After the sedimentation of the CL Formation, syncline basin (the Sity-Six Hill Member) was formed by D1 during 3088˜3020 Ma. D2 faulting with pull-apart basin (44 Hill Member) was formed after the quartz porphyry (3020Ma) and the massive tonalite became to expose on land surface. The Rb-Sr age in the DX Formation as 2210+/-60 Ma corresponds to the timing of Ophthalmian orogeny (2145˜2215Ma) in the southern margin of the Pilbara Craton (Rasmussen & Sheppard, 2005). The DX-CL formations probably had been affected by wide scale metamorphism at this timing.

Japan Geoscience Union Meeting 2014
(28 April - 02 May 2014 at Pacifico YOKOHAMA, Kanagawa, Japan)

BPT23-P02 Room:Poster Time:April 30 18:15-19:30

Lu-Hf isotope systematics of 3.45Ga Barberton basalts : implications for early mantle evolution

YAMAGUCHI, Takao[1*] ; IIZUKA, Tsuyoshi[1] ; HOKANISHI, Natsumi[2] ; NAKAI, Shun'ichi[2] ; DEWIT, Martin[3]

[1]University of Tokyo, Graduate school of Science Department of Earth and Planetary Science, [2]Earthquake Research Institute, University of Tokyo, [3]Neison Mandela Metropolitan University

Lu-Hf isotope systematics of Archean rocks can provide valuable insights into early crust-mantle evolution. In particular, those of Archean mafic rocks allow us to constrain the degree of early mantle depletion. Furthermore, a combination of Lu-Hf and Sm-Nd isotope systematics provides constraints on the physical condition of the mantle differentiation. Recent studies have indicated that 3.8 Ga mafic rocks from Isua have highly positive ϵHf with nearly chondritic ϵNd, suggesting that the source mantle had differentiated under a lower mantle condition. This may reflect that the differentiation of the Earth ' s deep mantle occurred much earlier than 3.8 Ga, possibly during the solidification of a magma ocean. In this study, we report new ^{176}Lu-^{176}Hf data for 3.45 Ga basalts in the Kromberg Complex of the Barberton Greenstone Belt, South Africa. The data for all analyzed samples define an isochron age of 2801±690 Ma(MSWD=49, 2σ, N=8), whereas those for relatively pristine samples yield an age of 3890±1100 Ma (MSWD=9.6, 2σ, N=4). The latter age is consistent with the formation age. We obtained the average ϵHf value at 3.45 Ga of 2.63 ± 0.33 (2σ) for the pristine samples. This indicates that the source mantle of the basalts had been depleted in incompatible elements by 3.5 Ga, but the extent of the depletion was not as strong as that of the source mantle of 3.8 Ga Isua mafic rocks. Furthermore, we found that there is no resolvable Hf isotopic difference between Barberton basalts and komatiites. This observation suggests that Barberton komatiites and basalts share the source mantle, and their formation mechanisms resulted in their petrologic difference. By combining our results with previously reported Sm-Nd isotopic data, we propose that the source mantle of the Barberton experienced early differentiation under high pressure conditions possibly during magma ocean solidification, and subsequently the differentiated mantle had been re-homogenized by mantle mixing.

Keywords: Mantle Evolution, Basalts, Barberton, Lu-Hf, Archean, Isotopic Analysis

Japan Geoscience Union Meeting 2014
(28 April - 02 May 2014 at Pacifico YOKOHAMA, Kanagawa, Japan)

BPT23-P03 Room:Poster Time:April 30 18:15-19:30

Major element composition and forming condotion of the hidden reservoir

KONDO, Nozomi[1*] ; KOGISO, Tetsu[1]

[1]Graduate School of Human and Environmental Studies, kyoto University

Solidification of the magma-ocean and subsequent mantle-crust differentiation could have significant influence on the evolution of the solid Earth and hydrosphere, but its detail is still unclear. Previous studies have suggested that the difference in $^{142}Nd/^{144}Nd$ between chondrites and bulk silicate Earth (BSE) resulted from the formation of an incompatible element-rich reservoir that had formed in the early Earth and then got hidden into the Earth ' s interior or lost outside the Earth. Although various models for the composition and the origin of such a " hidden reservoir " have been proposed, they have not focused on the major element composition of the hidden reservoir. However, the major element composition is crucial to know the density of the hidden reservoir and to examine whether the hidden reservoir rose to form the proto-crust or sunk in the early mantle. In order to determine the major element composition of the hidden reservoir, we estimated the melting condition for the formation of the hidden reservoir with constraints of $^{142}Nd/^{144}Nd$ and $^{143}Nd/^{144}Nd$ systematics in the ancient and modern mantle.

This study assumed that the hidden reservoir had formed at pressures less than 10 GPa, on the basis of previous studies that estimated the initial depth of melt segregation to be at this pressure range in the solidifying magma ocean. Then we calculated the Sm/Nd ratio that is conformable to the difference in $^{142}Nd/^{144}Nd$ between chondrites and BSE, and estimated the melt fraction that satisfies this Sm/Nd ratio. From this calculation, the melt fraction was estimated to be $<5.2\%$ at 1 GPa, $<3.2\%$ at 3 GPa and $<1.4\%$ at 7 GPa. From these calculated melt fractions and previous experimental data, we estimated that the major element compositions of the hidden reservoir were incompatible element-rich tholeiite, picrite, and komatiite, respectively.

Ancient hotter mantle should have melted at higher pressure, but on the other hand, the melt fraction was estimated to be small. In order to satisfy the small melt fraction at deep melting, the lithosphere must be thick, as suggested by Korenaga (2009) who showed the possibility of thick lithosphere in the hotter mantle. From these results, a likely composition of the hidden reservoir is incompatible element-rich picrite-komatiite.

Solomatov and Stevenson(1993),*Journal of Geophysical Research*, **98**, 5407-5418
Korenaga(2009), *Geophysical Journal International*, **179**, 154-170

Keywords: hidden reservoir, proto-crust, $^{142}Nd/^{144}Nd$

Japan Geoscience Union Meeting 2014
(28 April - 02 May 2014 at Pacifico YOKOHAMA, Kanagawa, Japan)

BPT23-P04 Room:Poster Time:April 30 18:15-19:30

Differentiation and material recycling of Archaean mantle estimated from North pole basalt, Western Australia

SANO, Ayane[1*] ; NAKAMURA, Hitomi[1] ; KOMIYA, Tsuyoshi[2] ; YOKOYAMA, Tetsuya[1] ; UNO, Masaoki[3] ; KIMURA, Junichi[4] ; CHANG, Qing[4] ; IWAMORI, Hikaru[1]

[1]Tokyo Institute of Technology, [2]The University of Tokyo, [3]Tohoku University, [4]JAMSTEC

Mid-ocean ridges and hotspots are the prominent surface manifestations of mantle upwelling with different mechanisms. In these domains, two types of basalts:, i.e., mid-oceanic basalt (MORB) and oceanic island basalt (OIB) occurare occurred, in the respective settingsly. Recent statistical analysis on the global data set of the Sr-Nd-Pb isotopic compositions demonstrates that modern MORB and OIB are clearly separated: MORB is derived from a mantle source that has undergone long-term depletion in a " melt component ", while OIB is derived from a mantle source with long-term enrichment in the melt component through the recycling of subducted plate material (Iwamori and Albarede, 2008; Iwamori et al., 2010). Therefore, when plate recycling started to develop the geochemical domains is of great importance to understand the material differentiation and evolution of the Earth.

In this study, we present new trace element and Sr,-Nd isotope composition of Archaean MORB and OIB, in order to discuss the differentiation of the mantle at that period and compositional evolution of the mantle for a longer period of the Earth's history. The basaltic rocks of ca. 3.5 Ga from North Pole in northwestern Australia have been analyzed, which include have been classified as MORB and OIB by their geological occurrence and stratigraphy in by Komiya et al. (2002). The rocks have undergone greenschist to /amphibolite facies transition metamorphism (Komiya et al., 2002). The original rock compositions may have been modified by metamorphism. In order to examine potential metamorphic modification of the bulk rock composition, so we have measured composition of igneous clinopyroxene which shows original igneous texture, in addition to bulk composition, with special reference to equilibrium/disequilibrium partitioning of trace elements between clinopyroxene and the bulk rocksestimate the effect of metamorphism using partition coefficient.

The composition of North Pole MORB (NP MORB) and OIB (NP OIB) show slightly different trace element patterns. Some spikes in alkaline elements and alkaline earth metal elements and variabilityety of the initial Sr isotopic compositions may result from metamorphic modificationeffect. The initial Nd isotopic compositions of NP MORB and NP OIB are similar to each other. However, most of the samples have εNd$<$0, which is not typically expected for a mantle-derived basalt. characteristic is typical for felsic rocks. The apparent elemental partitioning between partition coefficient of clinopyroxene and the estimated ' melt ' , as well as a relatively clear correlation between Sm/Nd and Nd isotopic ratio, suggests that metamorphism has also disturbeds Nd isotopic compositions even for clinopyroxene which preserves igneous texture, resulting in εNd$<$0 of the bulk rocks. The isochron may show the metamorphic age of ca. 3.1 Ga. These approaches, therefore, may provide a quantitative measure for metamorphic geochemical modification of us, we need to gain the original composition from Archaean rocks, and will be useful, or even compulsory to discuss the true mantle signatures. to discuss the differentiation of mantle.

Keywords: Archaean, North Pole, basalt, mantle, isotope, differentiation

Japan Geoscience Union Meeting 2014
(28 April - 02 May 2014 at Pacifico YOKOHAMA, Kanagawa, Japan)

BPT23-P05 Room:Poster Time:April 30 18:15-19:30

Development of the African continent constrained from U-Pb chronology of detrital monazite

ITANO, Keita[1*] ; CHANG, Qing[2] ; IIZUKA, Tsuyoshi[1] ; KIMURA, Jun-ichi[2]

[1]Department of Earth and Planetary Science, The University of Tokyo, [2]Institute For Research on Earth Evolution,Japan Agency for Marine-Earth Science and Technology

Monazite, a light rare earth element phosphate, occurs as an accessory mineral in peraluminous felsic rocks and metamorphic rocks from subgreenschist- to granulite-facies. Because monazite has high U and Th and low common Pb contents, it is suitable for precise U-Pb chronology. In addition, monazite is moderately resistant to chemical and mechanical weathering, detrital monazites are well preserved and potentially record the timing and nature of peraluminous igneous activities and a wide range of metamorphic events in their provenance area. Consequently, detrital monazites from large rivers can provide valuable insights into orogenic events in the drainage basins on a continental scale (Hietpas et al., 2013). In this study, we have determined U-Pb ages of ca. 100 detrital monazite grains from the Nile and Niger Rivers, which give chronological information on orogenic events in the African continent with a high time resolution.

The African continent comprises several Archean-Paleoproterozoic cratons, which are rimmed by orogenic belts. A significant part of igneous and metamorphic basement rocks are covered by sediments and therefore inaccessible to in situ sampling at present. Considering that detrital monazites sampled from river sands would partly be derived from the currently inaccessible basement rocks over an extensive area, U-Pb dating of detrital monazite from large rivers can provide chronological information of the basement rocks complementary to studies of the exposed geology. The samples used in this study were collected at the river mouths of the Nile and Niger Rivers. The sand samples used in this study were previously used for zircon U-Pb dating and Hf isotopic studies by Iizuka et al. (2013). Monazite grains were newly concentrated from the river sand samples using the conventional magnetic and heavy liquid separation techniques. Monazites were randomly hand-picked from the aliquots of monazite concentrates and mounted in an epoxy mount. Before analysis, each grain was imaged by BSE using FE-SEM to check elemental zonation and the presence of inclusions. Monazite U-Pb isotopic dates were measured using 200nm-FsLA-ICP-MS. Reference monazite 44069 (U-Pb age 425 Ma) is used to correct for instrumental Pb/U fractionation.

The monazite grains from the Nile River gave U-Pb ages between 560 and 2100 Ma with a dominant population at 580-800 Ma. Furthermore, the U-Pb age population indicates a sharp peak at 600 Ma. The age peak at 600 Ma of Nile River suggests metamorphic and/or felsic igneous events occurred at that time in the drainage basin, probably related to the collision of the East and West Gondwana continents.

The monazite age population of Niger River is dominated by Neoproterozoic ages with the most prominent peak at 580 Ma and peaks at 625 and 645 Ma. The peaks shown in the Niger River monazite (580 Ma and 620-630 Ma) correspond with the timing of previously known orogonic events in Northwest Africa. A peak at 620-630Ma is consistent with a metamorphic event at ca. 625 $\pm$ 29 Ma, likely related to the collision of the West Africa Craton and West Gondwana continent (Agbossoumonde et al., 2007). The other peak at 590-600Ma is consistent with a ca. 576 $\pm$ 4 Ma post-collisional igneous event at the Pan-African Belt in Cameroon (Kuekam et al., 2013).

The age difference in the most prominent peaks of Nile and Niger monazites suggests that the timing of orogonenic event in Northwest Africa was prior to that of in East Africa by ca. 10 Ma.

The accumulated monazite age distribution shows populations at 580-590 Ma, 630-640 Ma and 710-720 Ma, corresponding with the timing of Snowball Earth glaciation events. The chronological correspondence can be interpreted that the multiple Pan-African orogenic events during the Gondwana supercontinent assembly enhanced the rates of erosion and weathering via supermountain building that in turn decrease atmospheric carbon dioxide concentration resulted in glaciation.

Keywords: monazite, U-Pb age, LA-ICP-MS, Pan-African

Japan Geoscience Union Meeting 2014
(28 April - 02 May 2014 at Pacifico YOKOHAMA, Kanagawa, Japan)

BPT23-P06 Room:Poster Time:April 30 18:15-19:30

Significance of serpentinization of lower crust in deep-sea hydrothermal biosphere

ANDO, Yumi[1*]

[1]Department of Education,Saitama University

Hydrothermal activity in the Archean-Ridge system has been considered to play a major role to maintain the oldest biosphere in early Earth. In the present ridge-system, hydrogen production in the serpentinized peridotite layer, is considered as major energy source. However, low temperature hydrothermal zone in the lower crust layer in the ridge has been recognized as hydrogen producing zone. Thickness of oceanic crust is less then 10 km in the present Earth. However, the thickness of Archean oceanic crust has been estimated as 50 km. That is, hydration process of oceanic crust in the Archean-ridge is significantly important. Hydration rate of the peridotite layer in the Archean ridge is less extensive than Phanerozoic because thicker oceanic crust prevents hydration in the peridotite layer. Lower crustal rocks of accreted oceanic plateau is one of the best sample to describe hydration process due to deep-sea-hydrothermal alteration because it is easy to observe huge outcrops and collect samples systematically in whole section. We have collected gabbroic rocks from Mikabu high P/T rocks in Toba area and from Ootoyo area, Japan because there are large scale trench cliffs in the mine. Serpentinization of olivine gabbro and troctolite and hydrogen production rate will be shown in the present poster.

Keywords: the oldest biosphere in early Earth, serpentinization, gabbroic rocks

Japan Geoscience Union Meeting 2014
(28 April - 02 May 2014 at Pacifico YOKOHAMA, Kanagawa, Japan)

BPT23-P07 Room:Poster Time:April 30 18:15-19:30

Production mechanism for hydrocarbons in serpentinite-hosted hydrothermal systems: Hakuba Happo hot spring

SUDA, Konomi[1*] ; UENO, Yuichiro[1] ; MARUYAMA, Shigenori[2]

[1]Department of Earth & Planetary Sciences, Tokyo Institute of Technology, [2]Earth-Life Science Institute, Tokyo Institute of Technology

Serpentinite-hosted hydrothermal systems have been considered to be important environment for birth or evolution of earlier life. Serpentinite is a rock that results from the geological processes of hydration and metamorphic transformation of ultramafic rock from the Earth's mantle. Although ultramafic rocks are rarely exposed at the surface of the Earth today, they were likely to be an abundant component of the early crust owing to the higher potential temperatures compared to the present-day mantle [Komiya et al., 2004]. The presence of hydrocarbons has been reported in serpentinite-hosted systems at not only seafloor but also continental settings [e.g., Charlou et al., 2002; Proskurowski et al., 2008; Etiope et al., 2011; Szponar et al., 2013]. However, production mechanisms of the hydrocarbons in serpentinite-hosted hydrothermal systems so far has not been satisfactorily understood. In this study, we conducted chemical and isotopic analyses of hydrocarbons from a continental serpentinite-hosted hydrothermal system; Hakuba Happo hot spring in central Japan. Hakuba Happo hot spring is situated in the ultramafic rock body and is a site where serpentinization processes are likely to be ongoing at low-temperature of 50-60 [Suda et al., 2014]. The water at Hakuba Happo is strong alkaline (pH $>$10.5) and rich in H_2 and CH_4. Gas and water samples were obtained directly from two drilling wells in November 2013. Water temperature, pH, dissolved oxygen level (DO), oxidation-reduction potential (ORP) and salinity were measured at the sampling points using portable sensors. The water temperatures and chemistries were almost exactly the same as that at previous investigations conducted in 2010 and 2011. The hydrocarbon constituents of CH_4, C_2H_6, C_3H_8, iso-C_4H_{10} and normal-C_4H_{10} were detected from gas samples of Hakuba Happo hot spring. We report the isotopic analyses of hydrocarbons and discuss the process of hydrocarbons generation in serpentinite-hosted hydrothermal systems.

Keywords: serpentinite-hosted hydrothermal system, hydrocarbon, isotopic analyses, abiotic synthesis

Japan Geoscience Union Meeting 2014
(28 April - 02 May 2014 at Pacifico YOKOHAMA, Kanagawa, Japan)

BPT24-01 Room:213 Time:April 29 09:15-09:30

Geology and biology of the Shinkai Seep Field in the Southern Mariana Forearc

OHARA, Yasuhiko[1*] ; TAKAI, Ken[2] ; WATANABE, Hiromi[2] ; KONNO, Uta[2] ; ISHII, Teruaki[3] ; BLOOMER, Sherman[4] ; OZAWA, Genki[5] ; ONISHI, Yuji[6] ; FUJII, Masakazu[7]

[1]Hydrographic and Oceanographic Department of Japan, [2]Japan Agency for Marine-Earth Science and Technology, [3]Fukada Geological Institute, [4]Oregon State University, [5]Kitasato University, [6]Okayama University, [7]Atmosphere and Ocean Research Institute, University of Tokyo

The Shinkai Seep Field (SSF), located in the inner trench slope of the southern Mariana Trench, ˜80 km northeast of the Challenger Deep, is a serpentinite-hosted ecosystem mainly consisted of vesicomyid clams. Although vesicomyid clams are among the dominant invertebrates of chemosynthesis-based communities found principally at methane cold seeps derived from sediment diagenesis (such as at the Japan Trench, Nakai Trough, and Sagami Trough) and high-temperature hydrothermal vents (such as at the Galapagos Rift and Okinawa Trough), there have been no live examples from a serpentinite-hosted hydrothermal system including serpentinite mud volcanoes.

The SSF was serendipitously discovered by a Shinkai 6500 dive to map the mantle peridotite in the southern Mariana forearc, during YK10-12 cruise of R/V Yokosuka in September 2010. Although the dive was successful in collecting mantle peridotites and vesicomyid clams, no water and sediments were collected. TN273 cruise of R/V Thomas G. Thompson in January 2012 performed Deep-towed IMI-30 sonar backscatter imaging. The result indicates that the SSF is associated with a small, low backscatter feature that may be a small mound. Such low backscatter features can be widespread in the mapped area.

In order to understand the SSF, YK13-08 cruise had the following objectives:
(1) Finding and locating active fluid venting in the SSF. If successful, sampling the vent fluid and associated sediment for chemical and microbiological study.
(2) Finding seep fields other than the SSF in the southern Mariana forearc, using the low backscatter feature on IMI-30 image as a guide.
(3) Comprehensive understanding of the geology of the SSF. It is important to understand the geological background of the SSF including tectonic development of the southern Mariana forearc.

During YK13-08 cruise, Shinkai dives 1362, 1365 and 1366 successfully revisited the SSF, obtaining core samples for investigation of faunal composition, microbial and geochemical analyses in sediments, Niskin and pressure-tight water samples for geochemical analyses, and discovering chimneys. Shinkai dives 1363 and 1364 investigated the landward slope of the southern Mariana Trench ˜7 km west of the SSF, revealing that the mapped slope is entirely consisted of serpentinized harzburgites. New seep fields were not discovered during the cruise, indicating that not all low backscatter features on IMI-30 image correspond to seep fields. In this talk, we will show the preliminary results of YK13-08 cruise and discuss the geology and biology of the SSF.

Keywords: chemosynthetic community, serpentinite, Shinkai Seep Field

Japan Geoscience Union Meeting 2014
(28 April - 02 May 2014 at Pacifico YOKOHAMA, Kanagawa, Japan)

BPT24-02 Room:213 Time:April 29 09:30-09:45

Deep-sea hydrothermal vent fauna on the Central Indian Ridge

WATANABE, Hiromi[1*] ; BEEDESSEE, Girish[2]

[1]Japan Agency for Marine-Earth Science and Technology, [2]Mauritius Oceanography Institute

In deep-sea hydrothermal vent fields, faunal distribution is associated with the geochemical environments generated by hydrothermal vent activity. Hydrothermal vent fields on the Central Indian Ridge (CIR) are associated with vent fauna which is a mixture of Atlantic and Pacific and are discretely distributed along the ridge axis of more than 1000 km apart. In this presentation, faunal distribution in hydrothermal vent fields on the CIR is summarized at the intra- and inter-field levels. The species composition of the vent fauna in the four vent fields hitherto known is reviewed and updated, and faunal resemblance among the four vent fields of the CIR appears to reflect the number of species recorded, indicating that faunal surveys are not sufficient in describing the total vent fauna on the CIR. All the genetic studies of the CIR vent fauna have indicated a high genetic connectivity among the local populations, despite the many potential dispersal barriers existing between the vent fields. On the basis of the spatial distribution of vent species in a vent field, typical vent fields on the CIR were classified into six zones, of which the central two zones are often covered by *Rimicaris* swarms in the Kairei and Edmond fields. The close relationship between vent fauna from the CIR and the western Pacific, compared to those from other regions, is highlighted. Knowledge of the Indian Ocean vent fauna is limited, and further quantitative information on the biodiversity of vent fauna will provide clues to the formation of biogeographical regions and the dispersal of vent fauna among deep-sea hydrothermal vent fields.

Keywords: chemosynthetic biological community, biogeography, faunal similarity

Japan Geoscience Union Meeting 2014
(28 April - 02 May 2014 at Pacifico YOKOHAMA, Kanagawa, Japan)

BPT24-03 Room:213 Time:April 29 09:45-10:00

A trial on evaluating hydrothermal system evolution using geochronological dating and biological diversity analyses

KUMAGAI, Hidenori[1*] ; WATANABE, Hiromi[2] ; YAHAGI, Takuya[3] ; KOJIMA, Shigeaki[4] ; NAKAI, Shun'ichi[5] ; TOYODA, Shin[6] ; ISHIBASHI, Jun-ichiro[7]

[1]Submarine Resources Research Project, JAMSTEC, [2]Japan Agency for Marine-Earth Science and Technology, [3]Graduate School of Frontier Sciences, The University of Tokyo, [4]Atmosphere and Ocean Research Institute, The University of Tokyo, [5]Earthquake Research Institute, University of Tokyo, [6]Department of Applied Physics, Faculty of Science, Okayama University of Science, [7]Department of Earth and Planetary Sciences, Faculty of Science, Kyushu University

To elucidate the evolution of hydrothermal activities, we conducted an interdisciplinary study including geochemistry and biology to develop a method of obtaining reliable age information. Because there was a small amount of constraint on the lifetime of activity at hydrothermal sites, this study is one of the principal goals of the TAIGA-project,"Trans-crustal Advection and In-situ biogeochemical processes of Global sub-seafloor Aquifer" funded by a Grant-in-Aid for Scientific Research on Innovative Areas. As geochemical dating techniques, two methods applicable for hydrothermal ore minerals were developed and improved to fill the gap of the time-ranges in the conventional dating methods: electron spin resonance method and uranium-thorium disequilibrium method. Cross checks between the two methods generally showed good agreement for the range of hundreds to thousands of years. Except for the extreme values for each hydrothermal site, geochemical ages exceed 9ka for the southern Mariana Trough and for 16ka for the Okinawa Trough, respectively. As biological analysis, the biodiversity among faunal communities in the targeted areas was analyzed at the species and DNA levels. In the southern Mariana Trough, *Alviniconcha* gastropods and *Neoverruca* barnacles clearly show the greater genetic diversity with greater distances from the ridge axis, which fairly corresponds to the geochemical ages for ore minerals. In the Okinawa Trough, *Bathyacmaea* limpet showed greater genetic diversity at the Hakurei site in the Izena Hole where the ore minerals show oldest ages among the studied sites (Fig.).

Species and genetic diversity of the local fauna were not always correlated to geochemical dating, either in the southern Mariana Trough region or in the Okinawa Trough region. Although the results are not simple, comparison of age information obtained from analyses of these two disciplines potentially provides important constraints for discussion of the history and evolution of hydrothermal activities.

Figure caption (upper): Genetic divergence of COI gene indicated as mismatches in base sequences of *Bathyacmaea secunda* limpet of the Okinawa Trough. Scale bars are shown as five mismatches of partial COI sequences. (lower) Geochemical age range determined from the sulfide and sulfate deposits in Okinawa Trough. Active sites are shown from approximately SW to NE. The left-hand side is the southwestern end. Colored bars represent reliable age ranges for respective sites. The localities are denoted as follows: Yg, Daiyon-Yonaguni Knoll; Ht, Hatoma Knoll; Ir, Irabu Knoll; Izh, Hakurei-site in Izena Hole; Izj, JADE-site in Izena Hole; Ik, Iheya North Knoll; Yr, Yoron Hole; Me, Minami-Ensei Knoll.

Keywords: geochronology, biodiversity, TAIGA-project, ESR, U-Th disequilibrium, mitochondrial mismatch analysis

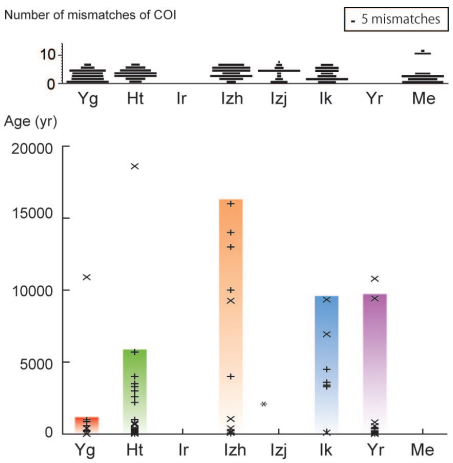

Japan Geoscience Union Meeting 2014
(28 April - 02 May 2014 at Pacifico YOKOHAMA, Kanagawa, Japan)

BPT24-04 Room:213 Time:April 29 10:00-10:15

Chemosynthesis-based ecosystem discovered on a Cretaceous sea turtles from Japan

JENKINS, Robert[1*] ; KAIM, Andrzej[2] ; MORIYA, Kazuhiro[4] ; HIRAYAMA, Ren[3] ; HIKIDA, Yoshinori[5]

[1]School of Natural System, College of Science and Engineering, Kanazawa University, [2]American Museum of Natural History; Instytut Paleobiologii PAN, [3]Faculty of International Research and Education, Waseda University, [4]Graduate School of Natural Science and Technology, Kanazawa University, [5]Nakagawa Museum of Natural History

One of the basic types of chemosynthetic ecosystems is known to develop on vertebrate carcasses. Within the framework of efforts to trace the evolution of chemosynthetic animals thriving in the modern vents and seeps, it has been hypothesized that these chemosynthetic animals adapted to the vent and seep environments via the transient environment formed by the decomposition of bones of vertebrate animals (e.g. Distel et al., 2000). Thus a study of the geological record of chemosynthetic ecosystems on vertebrate carcasses became of increasing importance in understanding the evolution of chemosynthetic animals. However, such studies were not fully assessed so far. Kaim et al. (2008) reported the existence of chemosynthetic ecosystems on plesiosaurid carcasses, marine reptiles which flourished in the Cretaceous oceans. However, we still were uncertain whether any other marine reptile carcasses could support chemosynthetic ecosystems. Here we document the first chemosynthetic community found on carcasses of the Cretaceous sea turtles.

The fossil sea turtle (*Mesodermochelys* sp.) has been collected from the Upper Cretaceous Campanian deposits cropping out along the Nio River, Nakagawa Town, Hokkaido. Sediments surrounding the turtle yielded provannid gastropods and thyasirid bivalves, both known to be members of chemosynthetic communities. Those chemosynthetic molluscan fossils have also been found in Cretaceous hydrocarbon seeps and on plesiosaurid carcasses (Kaim et al., 2008; 2009; Kiel et al., 2008).

This finding indicates that the chemosynthetic communities were supported not only by plesiosaurid carcasses but also by decomposing sea turtles. The sea turtles are a rare example of Cretaceous marine reptiles surviving the Cretaceous/Paleocene extinction event. Thus, it is reasonable to assume that sea turtle carcasses could continuously support chemosynthetic ecosystems linking the Mesozoic reptile fall communities with Cenozoic and modern whale fall communities, the latter occurring in the fossil record not earlier than Eocene.

Japan Geoscience Union Meeting 2014
(28 April - 02 May 2014 at Pacifico YOKOHAMA, Kanagawa, Japan)

BPT24-05 Room:213 Time:April 29 10:15-10:30

A chemosynthetic community on plesiosaurid carcass: with focus on distributions of microbes and invertebrate fossils

MORIYA, Kazuhiro[1*] ; JENKINS, Robert[2] ; KAIM, Andrzej[3] ; KOBAYASHI, Yoshitsugu[4] ; ECHIZENYA, Hiroki[4]

[1]Graduate School of Natural Science and Technology, Kanazawa University, [2]School of Natural System, College of Science and Engineering, Kanazawa University, [3]American Museum of Natural History; Instytut Paleobiologii PAN, [4]Hokkaido University Museum

Chemosynthesis - based communities are known to have been established not only in hydrocarbon seeps and/or hydrothermal vents but also on Cretaceous plesiosaurid carcasses (Kaim et al., 2008a). However, no detailed reconstruction of chemosynthetic ecosystems on plesiosaurid carcasses has yet been undertaken. To reconstruct the detailed development of ecosystems, we examined distribution patterns of chemosynthetic molluscs and micro- and macroborings around/on a plesiosaurid carcass. The examined carcass derived from a Cretaceous marine deposit distributed in Haboro Town, Hokkaido, and thought to have perhaps supported chemosynthetic ecosystems (Kaim et al. 2008a).

We observed the surface and a cross section of the plesiosaurid specimen. Chemosynthetic gastropods (Abyssochrysoidae) were densely distributed around the plesiosaurid bones (especially on the upper side). Several types of borings (e.g. micron-sized filamentous miroborings and rounded boring holes with apertures) could be found on the plesiosaurid bones. On the basis of their genera shapes and juxtaposition to pyrites, we hypothesize that the filamentous borings might have been formed by sulfur-oxidizing bacteria. The rounded boring holes with apertures within the bones are similar to modern borings made by *Osedax*.

The borings were distributed on the upper side of the bones relative to the lower side, resembling the distribution pattern of chemosynthetic gastropods. Most Recent abyssochrysoid gastropods are known to graze bacterial mats. The coherent distribution patterns of abyssochrysoid gastropods and microborings on the plesiosaurid bones indicate that the gastropods grazed bacterial mats even in the Cretaceous age. In addition, bone-eating animals also accumulated on the upper side of the bones. These distribution patterns might be influenced by the difference in exposure duration times of the upper and lower bone surfaces (upper side exposed on sea floor for a longer time than the lower side due to continuous sedimentation).

Keywords: Reptile fall, Plesiosauridae, distribution patterns, borings, chemosynthetic molluscs

Japan Geoscience Union Meeting 2014
(28 April - 02 May 2014 at Pacifico YOKOHAMA, Kanagawa, Japan)

BPT24-06 Room:213 Time:April 29 10:30-10:45

Paleoecology of the Upper Cretaceous echinoderms from cold seep carbonates in South Dakota, USA

KATO, Moe[1*] ; OJI, Tatsuo[2]

[1]Graduate School of Environmental Studies, Nagoya University, [2]Nagoya University Museum

Echinoderms were thought to be rare in a cold seep environment and had not been considered as a member of the chemosynthetic community until recent years, whereas the chemosynthesis community consists of a variety of other taxa. In the last 10 years, some species of echinoderms have been reported as a member of the modern chemosynthetic community, and some fossil echinoderms have also been found from or near carbonate mounds associated with cold seep. However the taxonomic and paleoecologic studies about these echinoderms have not been sufficiently done, and the ecologic relationship between these echinoderms and cold seeps has been also unsolved. The purposes of this study is to discuss paleoecology and process of adaptive evolution of echinoderms associated with a cold seep environment found from the Upper Campanian Pierre Shale in South Dakota, by field surveys, taxonomic of and morphological observation of fossil echinoderms. Chemical analyses of fossil echinoderm skeletons were also conducted, including element analysis for estimating the degree of diagenesis, and stable carbon isotopes analysis for clarifying the degree of relation between the echinoderms and the seep hydrocarbon.

As a result of field surveys, it is proved that the diversity of fossil species from carbonate mounds associated with cold seeps is different among mounds, even between adjacent mounds. Such a difference of species diversity is considered to reflect the difference of environments during the time when the carbonates were formed. It is presumed that the carbonate mounds with high diversity were exposed on the sea floor for a long time and provided a suitable environment for epifauna such as many echinoderms. Fossil crinoid from seep carbonates has low values of δ^{13}C (-20 ‰ or less). These values are considerably lower than modern crinoids which inhabit non-seep environments, and are also lower than the values of other fossil echinoderms from seep carbonates of the Pierre Shale. The crinoid from seep carbonates also has very strange, characteristic morphology, not seen in other stalked crinoids. Considering these chemical and morphological data, the crinoid from seep carbonates had probably adapted to the environments of cold seeps. On the other hand, echinoids from cold seeps do not have low values of δ^{13}C, and morphologically they are not significantly different from those found from non-seep environments. Therefore, it is considered that the echinoids from seep carbonates are not regarded as a true member of chemosynthetic community, but they came into cold seeps to benefit irregular, hard substrate to live on, or to obtain ample food sources from this cold seep environment.

The degrees of adaptation to cold seeps are therefore different among echinoderm species.

Keywords: cold seep, echinoderms, paleoecology, chemosynthetic community

Japan Geoscience Union Meeting 2014
(28 April - 02 May 2014 at Pacifico YOKOHAMA, Kanagawa, Japan)

BPT24-07 Room:213 Time:April 29 11:00-11:15

Molecular phylogenetic evidence for host switching in chemoautotrophic symbionts of deep-sea *Calyptogena* clams

OZAWA, Genki[1*] ; KANEKO, Takashi[3] ; SHIMAMURA, Shigeru[2] ; TAKAKI, Yoshihiro[2] ; KOSHIISHI, Takeshi[2] ; KATO, Chiaki[2] ; MARUYAMA, Tadashi[2] ; YOSHIDA, Takao[2]

[1]Department of Marine Biosciences, School of Marine Biosciences, Kitasato university, [2]Tokyo College of Biotechnology, [3]Japan Agency for Marine-Earth Science and Technology (JAMSTEC)

Calyptogena clams are living in deep-sea chemosynthetic habitats and globally distributed in seeps and hydrothermal vents. They are nutritionally dependent on chemoautotrophic sulfur oxidizing bacteria, which are harbored within their gill epithelial cells. The *Calyptogena* symbionts are thought to be vertically transmitted via clam ′ s egg to the next generation. Both host and symbiont are though to coevolve, because topologies of the phylogenetic trees of them form a mirror image. However, their phylogenetic trees have not been robust enough for analyzing their coevolutional relationship, because of using partial gene sequences of host (mitochondrial *cox1* and rrnL genes) and symbiont (16S rRNA gene). The possibility of lateral acquisition of the symbiont has been reported in some *Calyptogena* lineages. To improve the phylogenetic trees of *Calyptogena* clams and of symbiont, we sequenced the mitochondrial genomes of *Calyptogena* clams, and several their symbiont genes, and analyzed the phylogenetic trees by using the concatenated sequences.

Mitochondrial genomes of *C. phaseoliformis*, *C. okutanii* and *C. fossajaponica* were sequenced. Based on these mitochondrial genome sequences, primer sets for PCR of mitochondrial genes of other *Calyptogena* clams were designed. Using them, 11 mitochondrial genes (*cox1*, *cox2*, *cox3*, *nad1*, *nad3*, *nad4*, *nad5*, *cytb*, *atp6*, *atp8* and rrnL) of other 8 *Calyptogena* species (*C. fausta*, *C. kawamurai*, *C. kilmeri*, *C. laubieri*, *C. nautilei*, *C. pacifica*, *C. soyoae*, *C. stearnsii*) were amplified by PCR and sequenced. Eight genes (16S rRNA, 23S rRNA, *uvrA*, *uvrD*, *mfd*, *groEL*, *groES* and *gyrb*) of symbionts of these *Calyptogena* clams were also sequenced. Phylogenetic trees of clams and symbionts were constructed by maximum likelihood and bayesian analysis based on concatenated 11 mitochondrial and 8 symbionts genes, respectively.

The reliabilities of phylogenetic trees of the hosts and their symbionts were significantly improved by using the concatenated genes sequences (Fig.1). Bootstrap values and posterior probabilities of inernal nodes were better supported than those of the previous phylogenetic trees using partial gene sequences. Topological congruence of host and symbiont that was supported by bootstrap value (100%) and posterior probabilities (1.0), was shown in *C. okutanii*, *C. soyoae*, *C. kilmeri*, *C. pacifica* and *C. fausta*. These results suggested that these symbionts were cospeciated with their host clams (green boxes in Fig.1). Although the topologies of host and symbiont were congruent with *C. fossajaponica* and *C. phaseoliformis*, there were the low bootstrap values and low posterior probabilities in the host clade.

Topological incongruence between host and symbiont trees was shown in *C. kawamurai* - *C. laubieri* clade and *C. nautilei* - *C. stearnsii* clades (Fig.1) Congruence of topologies was rejected by approximately unbiased test using sitewise log-likelihoods (red branches in Fig.1). This result suggested that these symbionts have not cospeciated with their host clams. Host switching of the symbionts in the clades of *C. kawamurai* - *C. laubieri* and *C. nautilei* - *C. stearnsii* were examined by coevolution software, which compared the topologies of host and symbiont. Host switching is the event that symbiont is transferred from a host to a new host in a different lineage during speciation. The host switching of symbiont between *C. kawamurai* and *C. laubieri* was suggested by this software. Moreover, both clams are living in different depths of the same area (blue box on Fig.1). However, this software did not suggest the host switching of symbionts between *C. nautilei* and *C. stearnsii*. They are living in different areas. In this study, we show the phylogenetic relationships of cospeciation and non-cospeciation species with the symbionts among examined 11 *Calyptogena* species. It was suggested that topological incongruence of host and symbiont trees in clade of *C. kawamurai* - *C. laubieri* may be due to the host switching

Keywords: symbiosis, deep-sea *Calyptogena* clams, coevolution, host switching

BPT24-07 Room:213 Time:April 29 11:00-11:15

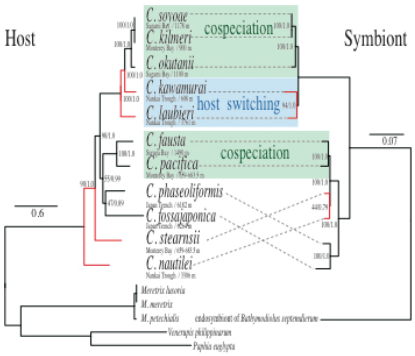

Fig1. cospeciation and host swithing on *Calyptogena* clam and symbiont trees.
Numbers in the nodes correspond to maximum likelihood bootstrap values and posterior probabilities.
Reg branches correspond to topological congruence rejected by approximately unbiased test using
sitewise log-likelihoods.

Japan Geoscience Union Meeting 2014
(28 April - 02 May 2014 at Pacifico YOKOHAMA, Kanagawa, Japan)

BPT24-08 Room:213 Time:April 29 11:15-11:30

Two forms of Calyptogena (Ectenagena) nautilei recognized in shell morphologies

MOROKUMA, Akitoshi[1*] ; NAKASHIMA, Rei[2] ; FUJIKURA, Katsunori[3] ; ANMA, Ryo[4] ; MAJIMA, Ryuichi[1]

[1]Yokohama National University, [2]Geological Survey of Japan, [3]JAMSTEC, [4]University of Tsukuba

Calyptogena (*Ectenagena*) *nautilei* was originally described by Okutani and Métivier (1986) from the cold seep sites in the Tenryu Canyon at the Nankai Trough based on six living specimens. After that, this species has been reported from the continental slope off Kumano, the Daiichi-Minami-Muroto Knoll, Zenisu Ridge, and Shionomisaki Canyon in the Nankai Trough (Fujikura et al., 2000; Okutani et al., 2002; Kojima et al., 2004; Anma et al., 2010). Okutani et al. (2002) examined the species from the Tenryu Canyon, the continental slope off Kumano, and the Daiichi-Minami-Muroto Knoll, and described that the species had a great variety in the shell outline. We observed the shell morphologies and structures of *C*. (*E*.) *nautilei* from some localities above including the type materials, and concluded that this species can be divided into two forms (form 1 and 2) by the shell morphologies and the shell structure.

We examined three type specimens from the Tenryu Canyon (Nautile Dive KD-3 and KD-5: Holotype, MNHN 26983, Paratype, MNHN 26984, Paratype, MNHN 26985), four specimens from the continental slope off Kumano (Shinkai 6500 Dive 615), five specimens from the Shionomisaki Canyon (Shinkai 6500 Dive 889, 890, and 891), and eight specimens from the Daiichi-Minami-Muroto Knoll (KAIKO Dive 189, 192, and 193). All specimens were observed with an optical microscope and bare eyes, and two specimens from the Shionomisaki Canyon were observed with a scanning electron microscope in the shell surfaces and cross sections.

The specimens from the Tenryu Canyon are assigned to form 1, and the other specimens are assigned to form 2. Two forms are most easily distinguished in the shell inner surface characters. That is, form 1 has smooth inner surface whereas from 2 is ornamented nearly overall the surface in hole-like structures that consist of about 61-548 μm in diameter. In addition to the inner surface ornamentation, form 1 is distinguished from the form 2 in having a subumbonal pit in the hinge plate of both valves, anterior ramus of right subumbonal cardinal tooth, and pallial sinus.

Keywords: Vesicomyidae, Calyptogena (Ectenagena) nautilei, Shell morphology, Hole-like structure

Japan Geoscience Union Meeting 2014
(28 April - 02 May 2014 at Pacifico YOKOHAMA, Kanagawa, Japan)

BPT24-09 Room:213 Time:April 29 11:30-11:45

Archives of long-term deep seafloor videos at chemo-synthetic biological community off Hatsushima Island in Sagami Bay

IWASE, Ryoichi[1*] ; TAKAHASHI, Ichiro[2]

[1]JAMSTEC, [2]Marine Works Japan, Ltd.

More than 20 years of multidisciplinary long-term observation, including visual observation, has been carried out with a cabled observatory on deep seafloor at a depth of 1175 m off Hatsushima Island in Sagami Bay since the first deployment in 1993, experiencing entire replacement for upgrade in 2000. The observatory was installed at a cold seepage site where large chemo-synthetic biological communities mainly consisted of vesicomyid clams exist. The observatory is composed of several kinds of sensors, including video cameras, a hydrophone, CTD sensor and seismometer in order to observe biological phenomena visually and also to investigate environmental fluctuation on deep seafloor.

All those data obtained with the underwater unit are transmitted through a submarine cable to the shore station in Hatsushima Island. The video signal was recorded on S-VHS videotape before the replacement of the observatory in 2000 and mainly on DVCAM videotape after the replacement, both with acoustic signal obtained with a hydrophone on soundtrack as audible sound. The shore station is usually uninhabited, and daily visual monitoring of seafloor, 30 minutes a day before the replacement and 26 minutes a day after the replacement, has been performed automatically. The videotape has been replaced once a week on the day when manual observation is performed usually for 6 hours. As for lighting, six halogen lights were attached at first and two of them were turned on simultaneously by turn for usual observation considering lifetimes. However, most of those lights were broken by 2008 and since then an LED light is used which is darker but has longer lifetime than the halogen lights, resulting narrow view.

Although visual observation has been performed about ten hours a week, more than 20 year observation produced thousands of videotapes. Archiving those videotapes becomes important because they degrade over time and the devices to replay them are going out of production and the opportunities to utilize them are being lost.

Meanwhile, vocalizations of sperm whales were found in the acoustic signal recorded on the soundtrack of the videotapes and, in order to utilize them as one of the *in situ* data for the remote species identification, archiving the videotapes started under one of the research project in Core Researches for Evolutional Science and Technology (CREST) founded by Japan Science and Technology Agency (JST) since December 2011. At the end of the fiscal year 2013, more than half of those videotapes will be archived. Although the main target of the CREST project is acoustic data, video signals on the videotapes are converted to MPEG-2 files for S-VHS tapes and both AVI and MPEG-2 files for DVCAM tapes before extracting acoustic data.

In those video images, not only the long term change of the clam colony but also some episodic events, such as spawning of the clams, sudden increase of snails and other unidentified events have been recognized, which would be invaluable data for the investigation of chemo-synthetic ecosystems. Those archived video images will be able to supply researchers outside the project in near future. However, there still exists a problem that the number of hard disks in which the video images are stored is very large even though it is less than a thousand.

Keywords: off Hatsushima Island in Sagami Bay, long-term visual observation, archives of videos

Japan Geoscience Union Meeting 2014
(28 April - 02 May 2014 at Pacifico YOKOHAMA, Kanagawa, Japan)

BPT24-10 Room:213 Time:April 29 11:45-12:00

Paleoecology of Neogene vesicomyids from Niigata, Japan and their adaptations to geochemical environments of cold seeps

MIYAJIMA, Yusuke[1*] ; WATANABE, Yumiko[1] ; KOIKE, Hakuichi[2] ; MATSUOKA, Hiroshige[1]

[1]Graduate school of Science, Kyoto University, [2]Shinshushinmachi Fossil Museum

Living vesicomyid bivalves are known to adapt to different hydrogen sulfide concentration and various habitats such as methane seeps, hydrothermal vents, whale falls, and petroleum seeps depending on species. Fossil vesicomyids are reported especially from Neogene seeps worldwide, but their adaptations to the geochemical environments of ancient seeps, which can help to understand the diversity and evolution of them, remain unrevealed. This study examined the paleoecology of fossil vesicomyids and geochemical environments of seeps to which they adapted by investigating their modes of fossil occurrence and geochemistry and petrography of seep carbonates from the two Neogene seep localities in Niigata Prefecture.

The lower Pliocene part of the Kurokura Formation mainly consists of gray to dark gray siltstones which deposited in upper bathyal depth. At the riverside cliff of Echido River at Matsunoyama-Matsuguchi, Tokamachi City, pebble-sized carbonate concretions are contained in 60 cm-thick massive gray siltstone. Fossil vesicomyids, *Archivesica kannoi*, are contained in the concretions some of which are gradually bounded by surrounding siltstone. A large individual (ca. 90 mm length) and surrounding small individuals (ca. 20 mm in the mean length) of *A. kannoi* are contained in the same concretions with various other bivalves, gastropods, and scaphopods which are not unusual to the modern cold-seep communities. Lucinid bivalves are contained in surrounding siltstone and burrows filled with carbonates are also observed in the siltstone. Concretions are mainly composed of micritic Mg-calcite, containing abundant pyrite crystals, and stable carbon isotopic compositions of them are very low values (-43.3 to -27.1 ‰ vs. PDB), showing their derivation from methane, whether they contain fossils or not. Only fossil-bearing concretions contain clast-like carbonates (ca. 5 mm in diameter) which are triangular or oval-shaped in cross section and composed of many fine dolomite crystals surrounded by Mg-calcite matrices in thin section. Dolomite formation is related to the removal of dissolved sulfate by sulfate reduction, thus it may suggest active produce of hydrogen sulfide. It can be concluded that *A. kannoi* was adapted to the habitat where hydrogen sulfide concentration was relatively higher due to more active sulfate reduction than surroundings, or pumping activity of *A. kannoi* supplying sulfate was active enough to promote active sulfate reduction.

The upper Miocene Nodani Formation consists of alternation of gray sandstone and dark gray siltstone which deposited in upper bathyal depth as submarine fan turbidites. At the river cliff of Nakanomata River at Nakanomata, Joetsu City, pebble-sized carbonate concretions are contained in dark gray siltstone just below gray, oily sandstone. Fossil vesicomyids, *Calyptogena pacifica*, are contained in these concretions or surrounding siltstone. Some of them are preserved in life position. Fossils and concretions are contained in a narrow range of 30 cm wide and 5 cm thick, and pipe-shaped carbonate concretions are contained parallel to bedding in siltstone 50 cm below. These concretions are mainly composed of micritic calcite and carbon isotopic values of them are moderately low (-21.7 to -13.2 ‰), suggesting their derivation from crude oil. In thin section, the fossil-bearing concretion contains many micritic peloids. Central void space of pipe-shaped concretion is fringed with bladed calcite which also shows low carbon isotopic value (-22.6 ‰), suggesting that these pipes acted as conduits of seepage. *C. pacifica* lives in the Recent methane seeps, but it is suggested that this species was also adapted to narrow-ranged, local petroleum seep in the Miocene.

Keywords: vesicomyids, Neogene, sulfide concentration, petroleum seep

Japan Geoscience Union Meeting 2014
(28 April - 02 May 2014 at Pacifico YOKOHAMA, Kanagawa, Japan)

BPT24-11 Room:213 Time:April 29 12:00-12:15

Recent trials of laboratory culture with chemosynthetic organisms

NAGAI, Yukiko[1*] ; TOYOFUKU, Takashi[1] ; NOMAKI, Hidetaka[1] ; WATSUJI, Tomoo[1] ; IKUTA, Tetsuro[1] ; TAKAKI, Yoshihiro[1] ; YOSHIDA, Takao[1] ; SHIGENO, Shuichi[1] ; INOUE, Kouji[3] ; KONISHI, Masaaki[2]

[1]JAMSTEC, [2]Kitami Institute of Technology, [3]The University of Tokyo

Chemosynthetic ecosystem is dominated by the organisms what has symbiotic bacteria in their body. Deep-sea bivalve *Bathymodiolus septemdierum* have been hosting some sulfur oxidizing bacteria in their gills. The bacteria have ability to synthesize such organic compounds as sugars from inorganic carbon source with hydrogen sulfied (H_2S). Many questions have been still remaining about the emergence and maintenance mechanisms of such symbiotic relationship between host animal and bacteria. Even though the development of laboratory culture techniques of such chemosynthetic bivalves are very useful approach to understand the detailed ecology and for further experiments, the technique is not developed very well. Our research group try to set chemostat water bath up with hydrogen sulfide to keep *B. septemdierum* as healthy condition. We try to use the culture system to evaluate the bivalves can keep their symbiotic bacteria to make much longer life time in laboratory. The activity of symbiotic bacteria has been tested by the uptake ability of ^{13}C labeled inorganic carbon into their body.

Individuals of *B. septemdierums* are captured during dive series of ROV Hyper-dolphin system of two cruises of R/V Natsushima operated by Japan Agency for Marine-Earth Science and Technology (JAMSTEC) in April of 2012 and in March of 2013. The samples are collected around Myojin-Sho submarine volcano on the Izu-Ogasawara Ridge. Collected samples were kept under 4 ℃ water tank in an on-board low-temperature room till the end of cruise. Then, the individuals are immediately transfer to on-land laboratory water tank after cruise to avoid the unfavorable environment. The water tank has been designed as chemostat system with H_2S supply to maintain symbiotic bacteria of deep-sea chemosynthetic animals. The individuals are cultured in this system for three months and fourteen months respectively. Here, previous study shows the symbiotic bacteria disappeared within three months without H_2S source. Therefore, we prefer to confirm the bacteria have been hopefully maintained more than three months in our chemostat system or not. For this purpose, carbon isotope labeling experiments were carried out to clarify the existence of symbiotic bacterial activity. The carbon isotope will be taken into organic matter of *B. septemdierums* if the symbionts are active after laboratory culture. We have compared the carbon isotopic uptake between under H_2S positive and under H_2S negative (control) conditions, respectively. Meantime, dissolved oxygen (DO) of each cultivation was monitored to check health and activity of individual bivalves. The results show the labeled ^{13}C signals were detected on the organic matters of both gills and foot especially under H_2S positive condition. Surprisingly, the activity was much positive even the individuals were kept for fourteen months in the chemostat system.

Keywords: laboratory culture, chemosynthetic organisms, Bathymodiolus septemdierum

Japan Geoscience Union Meeting 2014
(28 April - 02 May 2014 at Pacifico YOKOHAMA, Kanagawa, Japan)

BPT24-P01 Room:Poster Time:April 29 18:15-19:30

Distribution and internal structure of the nodules occuring in the Shimanto sedimentary rocks,Muroto Peninsula,Shikoku

YAMAMOTO, Ryouta[1*] ; FURUKAWA, Nadaska[1] ; SHIBATA, Tadahiro[2] ; HAGA, Takuma[1] ; INUI, Mutsuko[1]

[1]School of Science and Engineering,Kokushikan University, [2]Muroto Geopark,

Nodules has often been discovered on the deep-sea floor. The mechanism of their formation however is not yet clear. Nodules found in the outcrops of the Tertiary Shimanto belt in Muroto Peninsula are found as concretions that can easily be separated from the host rock. Those nodules very likely record the formation process at the deep-sea floor, and also the accretional process thereafter. This study aims to show the origin of the nodules through the spatial distribution, the occurrence, the shape, and the internal structure of the nodules sampled in Muroto Peninsula.

Spatial distribution of carbonate nodules were investigated along the coastline of Muroto Peninsula. Nodules were found in almost every outcrop, the abundance, however, varied from one locality to another. Outcrops with abundant nodules had more than 50 nodules within the area of 100 m2. Six localities were discovered with abundant nodules. Four of them were mudstone outcrops, and two the alternation of sandstone and mudstone. Most nodules occurred in the mudstone layers within the alternation of sandstone and mudstone. It is indicated that the distribution of nodules as are mainly controlled by lithology. The localities were scattered along the coastline of Muroto Peninsula. Comparing the distribution with the temperature estimated using vitrinite reflectance by Laughland and Underwood (1993), the distribution of nodules was not correlated with the thermal structure of the Shimanto Belt.

The length of the long axis of the nodules were 12-250 mm and the length of the minor axis were 10-180 mm, most of them with aspect ratios of 1.3 to 1.4. The aspect ratio is the ratio of the long axis diameter to the short axis diameter of an ellipse. At one outcrop, all nodules withthe short axis diameter of 40mm or less were long in shape, with the aspect ratios 3 or larger. This can be explained if the nodules were originally equivalent in size and weredeformed during the accretinal process. The locality is where high vitrinite reflectance has been reported(Laughland and Underwood, 1993).

Surface of section of 18 nodules were examined. Dark colored matrix, which was similar to the country mudstone, composed most of the interior of the nodules. One of the nodules had small whitish core near the center. The size of the core was approximately 4 mm in length with irregular shape. Triangular or quadrangular pyrite grains, with the length of the sides approximately 50-450 μm um, are often found scattered within the nodules. The shape of the pyrite grains indicated chemical origin. Heterogeneity was observed in the matrix: darker and lighter colored bands with 1 to 2 mm width were observed. The chemical mapping image of the matrix obtained using EDS showed that different colored bands contained different mineral assemblage. One band was mainly composed by quartz and calcite, the other was presumably rich in clay minerals.

In conclusion, nodules were formed mainly in the mudstone layer in Shimanto Belt of Muroto peninsula, indicating that the nodules were originally formed near the surface of the mud of the quiet deep-see floor. One of the nodules had small whitish core near the center, indicating the origin of the nodules being trace fossils produced by probable annelid worm. Observation of the internal structure indicated that the activity of the habitant of the trace likely accelerated the concretion of the mud in the vicinity.

References

Laughland and Underwood (1993) Geological Society of America Special Paper 273, 1-24, 25-43

Keywords: noduie, Shimannto belt, mudstone layer, pyrite, trace fossil

Japan Geoscience Union Meeting 2014
(28 April - 02 May 2014 at Pacifico YOKOHAMA, Kanagawa, Japan)

BPT24-P02 Room:Poster Time:April 29 18:15-19:30

New localities of fossil cold-seep assemblages from the Pleistocene Otsuka Formation of the Nakatsu Group, central Japan

SETO, Hiroki[1*] ; MAJIMA, Ryuichi[1]

[1]Yokohama National University

We report two new localities of fossil cold-seep assemblages from the Pleistocene Otsuka Formation, Nakatsu Group, exposed along the northeastern bank of the Sagami River, Sagamihara City, centaral Japan. The Otsuka Formation is composed mostly of massive mudstones in which pumice-rich lapilli tuff beds (several cm to several dozen cm in thickness) and thin sandstone beds are intercalated.

Our new localities (Locs. 1 and 2) occur lucinid fossils in the massive mudstones associated sporadically with the authigenic carbonate concretions (several cm to several dozen cm in size). In Loc.1, scoria and pumice grains (0.5 to 2 mm in size) are scattered and lenticular fine grained sandstone, 7 cm in maximum thickness, is intercalated. The 17 large bivalve fossils, mostly articulated lucinids, occur sporadically in 0.4 m in height and 1 m in width of the outcrop. Most of the fossils are entirely dissolved in this locality. The commissure planes of articulated bivalves are arranged perpendicular to the bedding plane, with their umbos oriented upward. In Loc.2, scoria and pumice grains (0.5 to 2 mm in size), and granule-size pumice grains are scattered. The 42 articulated and disarticulated bivalve fossils, mostly lucinids, occur sporadically in 2 m in height and 1.2 m in width of the outcrop. Most of the fossils are entirely dissolved as well as in Loc.1. The articulated and disarticulated bivalve fossils are counted, respectively, 27 and 15 in numbers. The commissure planes of many articulated bivalve fossils are arranged perpendicular to the bedding plane, with their umbos oriented upward, whereas the commissure planes of disarticulated shells are arranged parallel to the bedding plane with convex-down (8 in number) and convex-up (4 in number) in positions.

Lucinids are known to live in their umbos oriented upward to the sediment (Stanlay, 1970 ; Kondo, 1990 and Kanno, 1993). So that, the many articulated lucinid fossils reported herein are interpreted to be preserved in their life positions.

Keywords: Nakatsu Grooup, fossil cold-seep assemblage, Pleistocene

Japan Geoscience Union Meeting 2014
(28 April - 02 May 2014 at Pacifico YOKOHAMA, Kanagawa, Japan)

BPT24-P03 Room:Poster Time:April 29 18:15-19:30

Cretaceous chemosynthetic communities in Japan

JENKINS, Robert[1*]

[1]School of Natural System, College of Science and Engineering, Kanazawa University

The earliest occurrences of many molluscan genera, which are living in modern chemosynthetic ecosystem, were in the late Mesozoic. In addition, the oldest occurrences of chemosynthetic communities on decomposed vertebrate bones and sunken-drifted wood were in Cretaceous. Japanese Islands are located at junction of several continental and oceanic plates since hundreds of millions of years ago and provide many important material to establish evolutionary history of modern-type chemosynthetic ecosystems. Here I review Cretaceous chemosynthetic ecosystems with special focus on Japanese material.

Keywords: chemosynthetic community, whale bone, sunken wood, hydrocarbon seep, hydrothermal vent, cold seep

Japan Geoscience Union Meeting 2014
(28 April - 02 May 2014 at Pacifico YOKOHAMA, Kanagawa, Japan)

BPT25-01 Room:416 Time:May 2 14:15-14:30

Rapid change of atmosphere in the Hadean Earth: Beyond Habitable Trinity on a tightrope

OMORI, Soichi[3] ; ARAI, Tatsuyuki[2] ; MARUYAMA, Shigenori[1*]

[1]ELSI Tokyo Institute of Technology, [2]Tokyo Institute of Technology, [3]Open University

Surface environment of Hadean Earth is a key to bear life on the Earth or not. All of previous works assumed that high PCO2 has been decreased to a few bars in the first a few hundreds millions of years (e.g., Zhanle et al., 2011). However, this process is not easy because of material and process barriers as shown below. Four barriers are present.

First, the ultra-acidic pH (<0.1) of 4.4Ga ocean prevented the precipitation of carbonates at mid-oceanic ridge or its pseudo-system through water-rock interaction after the birth of primordial ocean. To overcome this barrier, primordial (anorthosite + KREEP) continents must have been above sea-level to increase pH rapidly through hydrological process.

Second, major cap rocks on the Hadean oceanic crust must have been komatiite with minor basaltic rocks to precipitate carbonates through water-rock interaction and transport them into mantle through subduction at higher than the intermediate P/T geotherm on the Benioff plane. If not, carbonate minerals are all decarbonated at shallower depths than the Moho plane. Komatiite production depends on mantle potential temperature which must have been rapidly decreased to yield only Fe-enriched MORB by 3.8Ga.

Third, the primordial continents composed of anorthosite with subordinate amounts of KREEP basalts must have been annihilated until 4.0Ga to alter pH to be possible to precipitate carbonates by hydrothermal process. The value of PCO2 must have been decreased down to a few bars from 35 bars at TSI (total surface irradiance) = 75% under the restricted time limit. If failed, the Earth must have been Venus state which is impossible to bear life on the planet.

Fourth is the role of tectonic erosion to destroy and transport the primordial continent of anorthosite into deep mantle by subduction. Anorthosite + KREEP was the mother ' s milk grow life on the Earth, but disappeared by 4.0Ga or even earlier, but alternatively granites were formed and accumulated on the Earth to supply nutrients for life. This is time-dependent process to increase new continents.

Fifth is the water content 3-5km thick, if the value was over, no way to bear life nor evolution afterwards.

After all, the Hadean Earth has passed the really naive tightrope processes to bear life. If any of above five conditions was lost, life has not been appeared.

Japan Geoscience Union Meeting 2014
(28 April - 02 May 2014 at Pacifico YOKOHAMA, Kanagawa, Japan)

BPT25-02 Room:416 Time:May 2 14:30-14:45

Global paleogeography and life evolution: 3. Paleozoic

ISOZAKI, Yukio[1*] ; MARUYAMA, Shigenori[2]

[1]Univ. Tokyo/Dept. Earth Sci. & Astronomy, [2]Tokyo Inst. Technology/ELSI

In modern oceans, there is no remaining information about past oceans older than 200Ma. For reconstructing paleo-plate motions with respect to collision-amalgamation of continents, on-land geology, in particular, orogenic belts that cemented older continents provide a sole source of information.

The onset of the Paleozoic is marked by the Gondwana semi-superocntinent formation at 540Ma around the South Pole. During the Paleozoic, Gondwana broken up, whereas Laurentia aggregated to form a real supercontinent by 430 Ma. Immediately after that, Gondwana began to be rifted, and its fragments and other blocks such as Baltica, Kazakhstan, Siberia, N China, South China, Indochina, and smaller pieces of Cimmeria, were dispersed; most of these were eventually amalgamated to from the northern half of Pangea, i.e., Laurasia.

The mode of mantle dynamics was represented by the high MORB production rate during 540-350Ma, almost the same as that in the Cretaceous, but it dropped after 350 Ma, probably by the activation of Pacific superplume. According to such continental assembly/ disassembly, sea-level changed remarkably as represented by the glaciation/deglaciation; the major Gondwana glaciations during the Carboniferous-Permian with 3 more minor episodes; the Paleozoic-Mesozoic transition interval might be close to the snowball Earth condition with extremely cold climate. The continent dispersion/amalgamation likely drove the development of remarkable floristic provincialism, e.g., Gondwana, North America, and Angara, that particularly reflected the formation of Laurentia. Not only the post-Ordovician land trees, this also controlled the diversification pattern of soil bacteria, moss, and land animals. Biodiveristy changes including mass extinctions occurred in accordance with the secular change in seawater Sr isotope ratio; extremely high in the Cambrian with high bio-divesrification, and the minimum at the G-L boundary (Permian) with onset of the greatest mass extinction.

Keywords: paleogeography, Paleozoic, supercontinent, Gondwana, Pangea, evolution

Japan Geoscience Union Meeting 2014
(28 April - 02 May 2014 at Pacifico YOKOHAMA, Kanagawa, Japan)

BPT25-03 Room:416 Time:May 2 14:45-15:00

Neodymium isotopic signature for deep/intermediate water formation in the late Cretaceous northwestern Pacific

MORIYA, Kazuyoshi[1*] ; MOIROUD, Mathieu[2] ; PUCEAT, Emmanuelle[2] ; DONNADIEU, Yannick[3] ; BAYON, Germain[4] ; DECONINCK, Jean-francois[2] ; BOYET, Maud[5]

[1]Dep. Earth Sci., Kanazawa Univ., [2]UMR CNRS Lab. Biogeosciences, Univ. Bourgogne, [3]UMR CEA/CNRS Lab. Sci. Climat Environ., CE Saclay, [4]IFREMER,Unite Recherche Geosciences Marines, [5]UMR CNRS Labo. Magmas Volcans, Univ. Blaise Pascal

The Cretaceous is known to be one of the archetypal greenhouse periods, and intensively studied for evaluating the climate sensitively in the high pCO2 region. The meridional sea surface temperature distribution, secular changes in sea surface and deep water temperatures have also been discussed globally. In addition to the thermal structure, analyses of ocean circulations on the basis of neodymium isotope signatures become more popular especially in the Atlantic Ocean. On the other hand, the ocean circulation in the Pacific Ocean is still uncertain, because of fundamental lack of deep sea sediments in the Pacific. In this study, instead of deep sea sediments, fore arc basin sediments have been utilized for discussing the ocean circulation in the late Cretaceous (late Turonian through early Campanian) northwestern Pacific.

Neodymium isotopic signatures in fish remains obtained from clayey sediments in the Yezo Group show highly radiogenic values of -1 to -2 ϵ-unit. These values are significantly higher than those in the Atlantic and the equatorial Pacific. This result indicates the presence of highly radiogenic intermediate/deep water formation in the northwestern Pacific, because it is expected that the radiogenic neodymium has been delivered from volcanic arcs in the northwestern Pacific. This results is also supported by climate models showing the potential deep water formation in the late Cretaceous northwestern Pacific.

Keywords: Cretaceous, Ocean circulation, Neodymium isotopes, North Pacific, Deep water, Intermediate Water

Japan Geoscience Union Meeting 2014
(28 April - 02 May 2014 at Pacifico YOKOHAMA, Kanagawa, Japan)

BPT25-04 Room:416 Time:May 2 15:00-15:15

Campanian-Maastrichtian clay-rich sequences along North Pacific Margin: Early Cooling History of Cretaceous Greenhouse

HASEGAWA, Takashi[1*] ; MORIYA, Kazuyoshi[2] ; HAGGART, James[3]

[1]Kanazawa Univ., Univ. BC, Geol Serv. Canada, [2]Kanazawa Univ., Univ. British Columbia, [3]Geol. Serv. Canada, Univ. British Columbia

Cretaceous shelf and fore-arc basin sandstone and mudstone are preserved in the coastal regions of Japan, Far East Russia, and the Pacific coast of Canada and USA. Several of these sequences have been variously assessed in terms of their biostratigraphy and chemostratigraphy, and correlated to the Aptian through Maastrichtian. In addition to macro- and microfossil biostratigraphy, carbon isotope (δ^{13}C) stratigraphy has also identified some important event horizons within these successions, such as OAE2. Owing to the clay-rich nature of the strata, parts of the sequences yield excellently preserved calcareous fossils available for oxygen isotope thermometry (Moriya et al., 2003).

This study examines the Campanian-Maastrichtian interval. Its chronostratigraphy, including detailed δ^{13}C stratigraphy, has been summarized recently (Voigt et al., 2012) and it records the initial phase of global cooling of the Cretaceous greenhouse Earth (Moriya, 2011; Friedrich et al., 2012). As the northern paleo-Pacific Ocean had a large heat capacity, its paleoceanography should provide insights for understanding the subsequent environmental transition from greenhouse to ice house Earth.

The Yezo Group and its equivalent in Hokkaido (Japan) and Sakhalin (Russian Far East), as well as the Nanaimo Group of the Canadian Pacific coast (British Columbia), are examined in this study. From the Yezo Group, a clear negative δ^{13}C excursion as large as 1.4?2 ‰ has been identified. On Sakhalin, its Campanian-Maastrichtian boundary age is constrained by local bio- and magnetostratigraphy, and the excursion is thus identified as the Campanian Maastrichtian Boundary Event (CMBE), associated with some subevents.

Carbon isotopic event, CMBE, suggested from magneto- and biostratigraphy (Haggart et al., 2011; Ward et al., 2012) of the Nanaimo Group near the top of the Northumberland Formation is well observed at the expected mudstone-dominated interval of the formation with negative 1.5 ‰ excursion. These progresses of stratigraphic correlational potential enable us to correlate CMBE interval between NW and NE Pacific with higher resolution.

Friedrich, et al., 2012, Geology, 40, 107-110; Haggart et al., 2011, Can. Paleont. Conf., Field Trip Guidebook No. 16, 31-62; Hasegawa et al., 2003, Palaeo-3, 189, 97-115; Moriya, 2011, Paleont. Res, 15, 77-88; Moriya et al., 2003, Geology, 31,167?170; Voigt et al., 2012, Newsl. Str., 45, 25-53; Ward et al., 2012, GSA Bull., 124, 957-974.

Keywords: Cretaceous, Greenhouse, Cooling, Campanian, Maastrichtian

Japan Geoscience Union Meeting 2014
(28 April - 02 May 2014 at Pacifico YOKOHAMA, Kanagawa, Japan)

BPT25-05 Room:416 Time:May 2 15:15-15:30

Composite trace fossils: Phymatoderma reburrowed by Chondrites/Phycosiphon and its paleoecological implications

IZUMI, Kentaro[1*]

[1]Department of Earth and Planetary Science, University of Tokyo

Composite *Phymatoderma* specimens from the Pliocene deep-sea Shiramazu Formation in Japan, particularly those reburrowed by *Chondrites* and *Phycosiphon*, were analyzed to reveal the differences caused by the activities of these trace-makers. *Phymatoderma* reburrowed by *Phycosiphon* is significantly larger than non-reburrowed *Phymatoderma*, whereas *Phymatoderma* reburrowed by *Chondrites* shows no significant difference in burrow diameter compared with non-reburrowed *Phymatoderma*. The recognized size selectivity (i.e., preference for larger burrows) by the *Phycosiphon* trace-makers can be explained by considering the different feeding strategies of these two ichnogenera; namely deposit-feeding *Phycosiphon*-makers, which must have processed a significant mass of sediment to obtain sufficient organic matter, whereas chemosymbiotic *Chondrites*-producers, which did not require a lot of sediment to obtain nutrients. In order to test these interpretations, records of the Phanerozoic trace fossils reburrowed by *Chondrites*/*Phycosiphon* were compiled. Consequently, the *Phycosiphon* -preference toward relatively larger burrows was recognized, which supports the results of this study. The compilation also indicates that the burrow size has become a limiting factor for the *Phycosiphon*-producers that tried to rework the sediments within previous subsurface burrows, at least for 80 million years.

Japan Geoscience Union Meeting 2014
(28 April - 02 May 2014 at Pacifico YOKOHAMA, Kanagawa, Japan)

BPT25-06 Room:416 Time:May 2 15:30-15:45

The influences of durations of geologic time units on diversity assessments

UBUKATA, Takao[1*]

[1]Shizuoka University

The study on global diversity change has been at the center of paleontological studies during the past quarter-century. It is well known that the diversity estimates are readily biased by unevenness of sampling density and there have been many debates on how to remove sampling overprints. In addition, taxonomic richness in a given chronological interval can be also biased by variation in time interval duration because the piled up diversity becomes much greater as the interval gets longer. However, there is no simple solution for this problem because the rate of taxonomic turnover is not uniform through time; that's why we can define discrete chronostratigraphic units with various durations. In addition, actual data registered in the Paleobiology Database indicate less correlation between sampled-in-bin taxonomic richness and time interval duration.

In the present study, the following simple computer simulations were performed to understand biases on diversity estimates derived from variation in time interval duration of chronologic units. A total of one million hypothetical taxa originated and went extinct at each time step (= 0.1 Ma) during the Phanerozoic at a given rate. In the present simulations, most (80%) of the turnovers were set to be concentrated at the boundary between intervals. The following different conditions were adopted for the turnover rates and sampling probability per time step within the interval; 1) fixed independent of the interval duration or 2) inversely proportional to the interval duration. The sampled-in-bin richness was counted for each age in each simulation.

As a result of the above simulation, a positive correlation between piled up diversity and time interval duration was generated when sampling probability was fixed through time. This result seems a natural consequence because the number of sampling for each bin depends on the duration of the time interval and the sample-size effect was not removed in the present analysis. The correlation was particularly remarkable when the mean turnover rate was high and/or probability of sampling was low. However, such a correlation was found also in some cases even when the sampling probability per time step was inversely proportional to the interval duration. In the latter case, the correlation was significant when the sampling probability was moderate.

Keywords: paleobiodiversity, time interval duration

Japan Geoscience Union Meeting 2014
(28 April - 02 May 2014 at Pacifico YOKOHAMA, Kanagawa, Japan)

BPT25-07 Room:416 Time:May 2 16:15-16:30

Upper Oligocene to Lower Miocene radiolarian biostratigraphy in the Northwest Pacific

MOTOYAMA, Isao[1*] ; SAWADA, Taiki[2]

[1]Yamagata University, [2]Japan Petroleum Exploration Co.,Ltd.

Ocean Drilling Program Leg 145 Hole 884B core provides the most continuous Neogene sequence of pelagic sediments in the northwest Pacific. We examined radiolarians from the Upper Miocene to Lower Miocene sediment of the core to establish subdivided radiolarian biozones.

The Upper Oligocene sequence can be divided into three zones, *Actinomma* sp. A, *Hexacontium* sp. B and *Cyrtolagena laguncula* Zones, in ascending order. The Lower Miocene sequence can be divided into four zones, *Botryopyle* sp. B, *Pentactinosphaera hokurikuensis* *Stichocorys subligata* and *Dendrospyris sakaii* Zones, in ascending order. Each of *Botryopyle* sp. B Zone and *P. hokurikuensis* Zone has been subdivided into subzones a, b and c.

Some episodes of significant faunal changes of radiolarians are identified within the studied interval. They seem not to reflect global cooling events but to reflect some regional events.

Keywords: Radiolaria, biozone, Site 884, North Pacific

Japan Geoscience Union Meeting 2014
(28 April - 02 May 2014 at Pacifico YOKOHAMA, Kanagawa, Japan)

BPT25-P01 Room:Poster Time:May 2 16:15-17:30

Available or unavailable? : nomenclatural examination of the Cretaceous ammonite genus Polyptychoceras

IKUNO, Kenji[1*] ; HIRANO, Hiromichi[1]

[1]Waseda University

It goes without saying that scientific names are useful for representing kinds of organisms. However, using names properly in accordance with the rules of nomenclature is not necessarily easy and a confusion of names could damage the objectivity of researches.

Polyptychoceras Yabe, 1927 from the Upper Cretaceous is a genus of heteromorph ammonites, which is characterized by paper clip-like shell morphology. It has been pointed out that this genus needs re-examination of species-level classification whereas occurrences of 12 species have been reported from Japan since *P. pseudogaultinum* (Yokoyama, 1890) was described. However, there are still many unclear points in the species names of this genus proposed until today. For example, *P. yubarense* has been attributed to Yabe, 1927 in many literatures probably because Yabe (1927) first proposed this name. In fact, Yabe (1927) is not the original description of this species by reason that the literature only listed the name of this species and gave no biological description (the *Code's* Article 12.1).

In the present study, we examined the nomenclature of these 12 species on the basis of the currently used *International Code of Zoological Nomenclature Fourth Edition* (International Commission on Zoological Nomenclature, 1999). As a result, nomenclatural availability, authors, dates of publication, and original descriptions were revealed. These results will ensure the objectivity of relevant studies and will contribute to future taxonomic works.

For your information, this abstract is not issued for the purposes of zoological nomenclature (Disclaimer based on Art. 8.2).

References

International Commission on Zoological Nomenclature, 1999, *International Code of Zoological Nomenclature, Fourth Edition*, International Trust for Zoological Nomenclature, London, xxix + 306 p.

Yabe, H., 1927, *The science reports of the Tôhoku Imperial University, 2nd series (geology)*, **11**, 27-100.

Keywords: Polyptychoceras, heteromorph ammonite, scientific names, International Code of Zoological Nomenclature, Cretaceous

Japan Geoscience Union Meeting 2014
(28 April - 02 May 2014 at Pacifico YOKOHAMA, Kanagawa, Japan)

BPT25-P02 Room:Poster Time:May 2 16:15-17:30

Assessment of local diversity in Cretaceous ammonoids from the Yezo Group using individual taxonomic abundance

YAMASHITA, Shuhei[1] ; UBUKATA, Takao[1*]

[1]Shizuoka University

Exploring global diversity change across the Phanerozoic has been an important part of paleontology in the past quarter-century. It is widely known that the diversity estimates are seriously biased by variation in the volume of paleontological data and there have been many debates on how to remove the sampling intensity biases. The taxonomic richness has been standardized by sampling proxies such as collection-based occurrences and the amount of rock records. On the other hand, use of the number of individuals observed in each taxon is limited to the studies on sample level diversity at the outcrops because those data are not available at the global level. An intermediate approach between at the global and sample levels is commonly found in the tabulation of number of species for a particular taxonomic group through a restricted geologic time interval at the local level. However, such a local database compiled in a traditional manner does not record any information on abundance of each species in most cases.

Here, we studied chronological change in species diversity of Cretaceous ammonoids from the Yezo Group exposed in central Hokkaido, Japan, using the diversity indices that take into account the abundance of each species. This study was based on the fossil collections collected from Soya, Nakagawa, Haboro, Kotambetsu, Obira, Mikasa, Oyubari or Hobetsu areas and stored at Shizuoka University, National Museum of Nature and Science, Tokyo, Nakagawa Museum of Natural History, Mikasa City Museum and Hobetsu Museum. The number of individuals was counted for each species for each stratigraphic unit from the Cenomanian to Maastrichtian. A total of 9,834 individuals of 266 species was identified and counted.

The patterns of diversity change estimated in the present analysis were considerably different among collections even when the same diversity index was adopted. A plausible reason of this discrepancy is the difference in relative species abundance observed among collections. The only exception is the Shannon-Weiner function which exhibited a consistent pattern of diversity change independent of which collection was utilized. This result suggests that the Shannon-Weiner function is the most robust against variation in relative species abundance. The diversity estimates based on species richness tended to be correlated with the proportion of the rare species to the total number of species. This result suggests that these diversity estimates are readily distorted by the impact of rare species.

Keywords: paleobiodiversity, Cretaceous, ammonoids, Yezo Group, individual taxonomic abundance

Japan Geoscience Union Meeting 2014
(28 April - 02 May 2014 at Pacifico YOKOHAMA, Kanagawa, Japan)

BPT26-01 Room:421 Time:May 2 09:00-09:15

Estimation of the environmental temperatures at the early evolutionary periods by resurrection of ancient proteins

YOKOBORI, Shin-ichi[1*] ; AKANUMA, Satoshi[1] ; NAKAJIMA, Yoshiki[1] ; YAMAGISHI, Akihiko[1]

[1]Sch. Life Sci., Tokyo Univ. Pharm. Life Sci.

To understand the origin and history of terrestrial life, it is important to clarify the environment where early life evolved. Geological records on the early evolution of terrestrial life are quite limited. Therefore, it is not easy to assume the ancient environment where our extinct ancestors had lived.

The 16S/18S rRNA based-tree of life by Woese et al. (1990, PNAS, 87: 4576-4579) has been treated as the "standard" tree of terrestrial life, although there are many objections. In this tree, all extant terrestrial organisms have common ancestor (the last common universal ancestor: LUCA or Commonote), and are classified into three domains, Bacteria, Archaea, and Eukarya. If all extant terrestrial life has the Commonote, its nature is the next question. In particular, the growing temperature of Commonote (or LUCA) has been interested and discussed. Pace (1991, Cell, 65: 531-533) proposed that the LUCA (or Commonote) was thermophilic. However, there are many objections. However, the discussion on this issue has been done mostly based on the predicted growth temperature estimated from the GC contents and amino acid frequencies of LUCA's genes and proteins inferred with molecular phylogenetic analyses, so that they are not proven by the experimental data (e.g. Galtier et al. (1999, Science, 283:220-221)). Recently, as one of powerful tools to evaluate the characteristics of extinct organisms, it has become to be used that experimental resurrection of ancient proteins based on the estimation of ancient amino acid sequences being possessed by ancient organisms estimated from the molecular phylogenetic analysis (e,g, Gaucher et al. (2003, Nature, 425: 285-288)).

To evaluate the growth temperature of ancient organisms, we resurrected amino acid sequences of nucleoside diphosphate kinases (NDKs) of the last archaeal common ancestor (LACA) and the last bacterial common ancestor (LBCA) with the maximum likelihood method for tree reconstruction by using NDK amino acid sequences of extant archaea and bacteria. The ancestor NDKs with resurrected amino acid sequences were expressed in *Escherichia coli* cells, purified, and then temperature-dependence of their denaturation was measured. The T_m of denaturation of resurrected NDKs of LACA and LBCA were higher than 100 ^{o}C. Since there is strong correlation between the T_m of NDKs and optimal growth temperature of their host organisms, both LACA and LBCA are suggested to be hyperthermophiles. Errors of estimation of ancestral sequences and different tree topologies used for resurrection of sequences did not affect seriously on the thermal stabilities of resurrected NDKs of LACA and LBCA. We also estimated the possible NDK sequences carried by the Commonote based on the sequences of resurrected NDKs of LACA and LBCA. The T_m of the most thermally unstable Commonote's NDK we resurrected was 90 ^{o}C (Akanuma et al. 2013, PNAS, 110: 11067-11072). This suggests that the Commonote was thermophilic organism.

Keywords: Commonote, resurrection of proteins, nucleotide diphisphate kinase, thermophiles

Japan Geoscience Union Meeting 2014
(28 April - 02 May 2014 at Pacifico YOKOHAMA, Kanagawa, Japan)

BPT26-02 Room:421 Time:May 2 09:15-09:30

Evolution of the Earth's environment: A view from sedimentary alkyl porphyrins

OHKOUCHI, Naohiko[1*] ; CHIKARAISHI, Yoshito[1] ; SUGA, Hisami[1] ; OGAWA, Nanako[1]

[1]JAMSTEC

Alkyl porphyrins are derivatives of chlorophylls that are formed in the surface of the Earth by photosynthesizers. Structural changes associated with the diagenetic processes have been intensively studied during the last half a century. Now we know that some alkyl porphyrins are derived only from specific chlorophylls that are originated from a specific type of photosynthesizers. Together with carbon and nitrogen isotopic compositions, such structural information provides a profound insight on the critical evaluation of the surface water environment in the geological past. In this presentation, I will review the diagenetic alteration of chlorophyll structures and review the current evidence.

Keywords: Porphyrins, Sediment, Earth's surface environment

Japan Geoscience Union Meeting 2014
(28 April - 02 May 2014 at Pacifico YOKOHAMA, Kanagawa, Japan)

BPT26-03 Room:421 Time:May 2 09:30-09:45

The close correlation between environmental change and evolution of metazoans: Genome duplication and rapid adaptation

KOMIYA, Tsuyoshi[1*]

[1]Komaba, University of Tokyo

The Neoproterozoic to Cambrian is one of the most exciting periods when Metazoa first appeared and quickly evolved. The origin and early evolution of Metazoa are very attractive firstly because the events suddenly happened after very long calmness, over 2000 m.y. since the emergence of eukaryotes, and proceeded very quickly, and secondly because appearance of new phylum was limited to this period (Cambrian explosion). Recent paleontology, biomarker study and molecular biology suggested early origin, especially of sponges and cnidarians, and cryptic evolution of the metazoans (e.g. Maloof et al., 2010; Love et al., 2010; Peterson et al., 2008: Sperling et al., 2010, Erwin et al., 2011). On the other hand, recent comprehensive study of multi-elemental and multi-isotopic chemostratigraphies of drill core samples in Three Gorges, Tianping and Beidoushan areas revealed that redox condition and bioessential element contents of seawater such as P, Ca, NO_3^-, Fe, Mn, Mo, and Sr drastically changed from the Neoproterozoic to the Early Cambrian. Sr isotope values display positive excursions at ca. 580, 570-550 and 540 Ma, indicating repeated high continental influxes at those times. P contents of carbonate minerals were very high until ca. 550 Ma, and then decreased, suggesting the seawater was enriched in phosphorus before 550 Ma and then depleted due to oxidation of seawater and deposition of phosphorite. High nitrogen isotope values of organic matter and high Ca isotope values of carbonate rocks indicate that seawater was depleted in NO_3^- and Ca contents until ca. 550 Ma, and then increased. Mo isotopes of black shale, and Fe and Mn contents and REE patterns of carbonate rocks indicate that seawater became more oxic since ca. 550 Ma. In addition, the Mo contents of black shale increased in the Late Ediacaran and Early Cambrian, indicating Mo content of seawater increased due to the oxidation of seawater. On the other hand, iron and manganese contents of carbonate rocks decreased, suggesting that iron and manganese contents of seawater decreased because of the oxidation of seawater.

Comparison of the geochemical evidence with biostratigraphy suggests that the emergence of Metazoan in the Early Ediacaran was caused under the relatively less oxic and P-rich condition, whereas their diversification occurred under oxic, NO_3^- and Ca-rich condition. Especially, the transition from phosphorus-rich to NO_3^--rich seawater possibly increased Redfield ratio, and contributed to diversification of more actively mobile multicellular animals. In addition, the comparison of geochemical and paleontological evidence indicates that the biological evolution occurred just after the environmental changes, especially the timing of increase in nutrients, allowing a new insight of biological evolution of multicellular animals. The quick response of biological evolution to the environments suggests that the fundamental innovation for biological functions was already established long before the environmental changes. The quick adaptation implies that early metazoans or a common ancestor have genomes for the functions before they acquired the functions, indicating genome duplication plays important role on the early evolution of metazoans.

Keywords: Biological evolution, paleoenvironmental change, Ediacaran, Nutrients of seawater, Evolution of Metazoa and Cambrian explosion, Genome duplication

Japan Geoscience Union Meeting 2014
(28 April - 02 May 2014 at Pacifico YOKOHAMA, Kanagawa, Japan)

BPT26-04 Room:421 Time:May 2 09:45-10:00

Reconstruction of the gene sets for the developmental signaling ligands in ancestral protostome animals

ENDO, Kazuyoshi[1*] ; SETIAMARGA, Davin[1] ; SHIMIZU, Keisuke[1]

[1]Dept. Earth and Planetary Sci., Tokyo Univ.

Recently, a draft genome sequence of the pearl oyster Pinctada fucata was reported, enabling to infer a possible evolutionary scenario of the gene sets that are important for body plan formation in protostomes including both lophotrochozoans and ecdysozoans. We report the results of phylogenetic character mapping carried out for the gene families that encode developmental signaling ligands (Fgf, Hedgehog, PDGF/VEGF, TGF-b, and Wnt families) to reconstruct possible copy numbers of signaling molecule-coding genes for hypothetical ancestral protostomes. Our reconstruction suggests that P. fucata retains the ancestral protostome gene complement, providing further justifications for the use of this taxon as a model organism for developmental genomics research.

Keywords: paleogenomics, metazoan evolution, evo-devo, signaling ligand genes, Cambrian explosion, lophotrochozoans

Japan Geoscience Union Meeting 2014
(28 April - 02 May 2014 at Pacifico YOKOHAMA, Kanagawa, Japan)

BPT26-05 Room:421 Time:May 2 10:00-10:15

Reconstruction of paleo genomic information of metazoan based on a microsyteny analysis

KAWASHIMA, Takeshi[1*]

[1]Okinawa Institute of Science and Technology, [2]National Institute of Basic Biology

Since a variety of metazoan genome decoding, the conservation of gene order on the DNA (synteny) is recognized as a common event in the metazoan. For example, Putnam reported the some amounts of signatures of macrosynteny between human and sea anemone (Nematostella vectensys) (Putnam et al 2007). Subsequently, Irimia reported their hypothesis that two adjacent genes that shared their 5'cis region (head to head) may restraint their translocation. Because of this situation, I'm trying to use these syntenic constraint for reconstructing the ancient genome. To the start of such reconstruction analyses, I'm compared among the genome of Hemichordate, Sea urchin and Amphioxus. These analyses revealed their possible common developmental mechanisms kept since their common ancester.

Keywords: metazoan, genome, microsyntey, reconstruction

Japan Geoscience Union Meeting 2014
(28 April - 02 May 2014 at Pacifico YOKOHAMA, Kanagawa, Japan)

BPT26-06 Room:421 Time:May 2 10:15-10:30

A close relationship between global oceanic environmental changes and seafloor mineral deposition during the Phanerozoic

KATO, Yasuhiro[1*]

[1]Department of Systems Innovation, Graduate School of Engineering, University of Tokyo

Metal deposition on seafloor is strongly controlled by marine redox conditions. Fe-Mn and Mn oxide deposits are formed under oxygenated oceans. In striking contrast, Cu and Zn-bearing sulfide deposits are stable under anoxic oceans. Seafloor mineral deposits in turn are good indicators to redox conditions or redox changes of modern and ancient oceans.

There are numerous strata-bound ore deposits in the Japanese accretionary complexes. These deposits are mainly divided into three types; umber (Fe-Mn), Mn-rich, and volcanogenic massive sulfide (VMS; Besshi-type). The Mn-rich deposits are further divided into two subtypes that are associated with greenstone and NOT associated. Ages of these deposits provide us important constraints for a secular change of marine redox conditions over the past ˜360 Myr. Depositional ages of umber and Mn deposits were previously determined by microfossils including radiolarians and conodonts. On the other hand, ages of the Besshi-type deposits are determined by Re-Os method (Nozaki et al., 2013). Oxide ore deposits such as umbers and Mn deposits were very likely precipitated in the modern-style oxygenated deep-sea. In contrast, Mn carbonate and VMS deposits were precipitated in the stagnant, O2-deficient deep-sea during the Triassic and Jurassic periods. Seafloor mineral deposition closely related to global oceanic environmental changes may give us a hint for exploring the causes of mass extinction, and further for elucidating the evolution of life.

Nozaki, T., Y. Kato, K. Suzuki (2013) Late Jurassic ocean anoxic event: evidence from voluminous sulphide deposition and preservation in the Panthalassa. Scientific Reports, 3: 1889; doi:10.1038/srep01889.

Keywords: oceanic environmental change, seafloor mineral deposit, Japanese accretionary complexes, marine redox condition, Phanerozoic

Japan Geoscience Union Meeting 2014
(28 April - 02 May 2014 at Pacifico YOKOHAMA, Kanagawa, Japan)

BPT26-07 Room:421 Time:May 2 10:30-10:45

Global paleogeography and life evolution: 2. Mesozoic

ISOZAKI, Yukio[1*] ; MARUYAMA, Shigenori[2]

[1]Univ. Tokyo/Dept. Earth Sci. & Astronomy, [2]Tokyo Inst. Technology/ELSI

The Mesozoic witnessed the Pangean breakup. Since the Triassic, the southern half of Gondwana successively rifted/separated, kicking out numbers of continents northward to form Laurasia, i.e., the northern half of Pangea, ca. 200 Ma. Multiple collisions among the Russian platform, Kazakhstan, Siberia, N. China, S. China, Indochina, Tarim, and other minor continental blocks were completed mostly in the Triassic or in the Early Jurassic at the latest. Gondwana has started to be fragmented immediately after its birth at 540Ma, except the collision of Laurentia at 430 Ma. The apparent supercontinent Pangea formed when Laurasia came in shape by 200 Ma. Its disassembly began first by the opening of the central Atlantic domain induced by the eastward moving of Africa for ca. a few thousands of km. The birth of South Atlantic Ocean was delayed until ca. 120Ma, whereas the opening of Northern Atlantic already started. The separation of S. America from Africa occurred ca. 120Ma. There was a pulse period of Pacific superplume ca. 120-85Ma when the production rate of MORB was 150-300 % higher than the rest of the Mesozoic. Numbers of huge oceanic plateaus were formed in the Pacific domain, including the Caribbean plateau. The birth of Indian Ocean occurred at ca. 100-120Ma by the separation of India from Gondwana. It is composed of 4 distinct oceanic lithospheres (separated by NS-trending major transform faults) behaved uniquely. The sea-level was kept relatively high according to such Mesozoic global tectonics; warm period without global glaciation but with oceanic anoxia and remarkable production of oil, gas, and coal. The climate was generally dryer than the Cenozoic, with higher production of evaporites. The mammalian diversification was triggered by the ca. 120Ma separation of the final bridge among Africa, S. America, and Laurasia. The appearance of the fox monkey in Madagascar, and of new-world monkeies in S. America, was likely connected to Indian migration and narrow arc bridge to S. America.

Keywords: paleogeography, Mesozoic, supercontinent, Pangea, Atlantic Ocean, evolution

Japan Geoscience Union Meeting 2014
(28 April - 02 May 2014 at Pacifico YOKOHAMA, Kanagawa, Japan)

BPT26-08 Room:421 Time:May 2 11:00-11:15

Recent results of foraminiferal calcification

TOYOFUKU, Takashi[1*]

[1]JAMSTEC

Foraminifera, marine unicellular organism, have been thought as one of the major carbonate producer in ocean. Their calcareous tests are commonly utilized as paleo-environmental indicators in various studies of earth science because their tests have been archived as numerous fossil in sediment for long time and various environmental information are brought by population, morphology and geochemical fingerprints. The calcareous test itself is interested by many foraminifer scientists. The knowledge about the cytological process on carbonate precipitation has been described for couples of decade using by many legacy technology. Cellular regulations of ions uptake into calcareous tests from seawater are of great interest for broad fields of earth sciene. Our recent studies showed the potential to understanding the biomineralization of foraminifera by the application of fluorescent indicators. Recently, we visualize the spatial distributions of cytological calcium and pH in living cell at same time under several pH conditions (7.5-8.1). Observed results show that foraminifera controls very detailed timing of pH variation and concentration of calcium at any stage of chamber formation dynamically even ambient pH are varied. These observations results will help to consider how the geochemical compositions arranging on the foraminiferal test, sensitivity of pH proxy of boron and others.

Japan Geoscience Union Meeting 2014
(28 April - 02 May 2014 at Pacifico YOKOHAMA, Kanagawa, Japan)

BPT26-09 Room:421 Time:May 2 11:15-11:30

Left-right reversal in unicellular eukaryotes, planktonic foraminifera

UJIIE, Yurika[1*] ; ASAMI, Takahiro[1]

[1]Department of Biology, Shinshu University

Aquatic unicellular organisms are little motile and passively disperse in general. Holoplankton, which spend their entire life-cycle floating in the water column, are likely carried by water flow and exposed to diverse conditions of environment. Their morphology may vary over wide distribution ranges by phenotypic plasticity or allelic variation. Among these organisms, planktonic foraminifera are an excellent system to examine diversity and evolution in cellular responses to the environment because of two reasons: (1) occurrence in every ocean and (2) visible asymmetry in coiled shell. Both left- and right-coiled forms are often found within single morphospecies. Their coiling direction has traditionally been thought to change phenotypically depending on environmental factors, especially water temperature, based on coil-morph distributions but without statistical evidence. Molecular phylogenetic studies have revealed that morphospecies often contain multiple cryptic species. The arguments on the role of temperature for coil reversal most probably confused cryptic species into single taxa. In the present study, we examined the dependence of morph frequency on temperature by focusing on populations that are dimorphic for coiling direction and occur across wide ranges of temperature. *Globorotalia truncatulinoides* includes five genetically isolated species, and each of them is dimorphic for coiling direction. The statistically meaningful regression analysis was possible in three species that are distributed in global ranges. The results showed that morph frequency does not depend on water temperature in warm or cold seasons or on the annual mean temperature. Moreover, the geographic patterns of frequency variation among water masses in these species suggest that gene flow affects morph frequency. The majority exhibits the same coiling direction among populations that inhabit water masses connected by ocean circulation system. In contrast, morph frequency greatly varies between unconnected water masses regardless of climatic conditions. The present results, therefore, reject temperature-dependence of coiling direction and suggest the presence of genetic basis for coiling direction in planktonic foraminifera. Our study provides a base to explore the evolution on left-right asymmetry in unicellular eukaryotes.

Keywords: left-right asymmetry, coiling direction, cryptic species, unicellular eukaryote

Japan Geoscience Union Meeting 2014
(28 April - 02 May 2014 at Pacifico YOKOHAMA, Kanagawa, Japan)

BPT26-10 Room:421 Time:May 2 11:30-11:45

Were marine microplankton in the Japan Sea geographically isolated during the Last Glacial Maximum?

ISHITANI, Yoshiyuki[1*] ; TAKISHITA, Kiyotaka[2]

[1]School of Geophysical and Earth Science, Glasgow University, [2]Japan Agency for Marine-Earth Science and Technology

The Japan Sea is connected by three straights (the Soya, Tsugaru, and Tsushima Straights) to the Sea of Okhotsk and Pacific Ocean with the shallow sill depth (140 m). During the last glacial maximum (LGM: 23-19 kilo years before present), the sea-level was decreased at least 120 m lower than today and the Japan Sea was almost isolated from surrounding seas. It is possible that such geographic isolation reduced and/or impeded gene flow of marine organisms between the Japan Sea and surrounding seas. Previous phylogeographic studies of coastal vertebrates (only whose larval stage is planktonic) have actually suggested that the Japan Sea was closed during the LGM. However, there is no phylogeographic study with marine microplankton, which inhabit the water column throughout their entire life cycle.

Radiolaria, the major marine planktonic protists, are passively transported in the pelagic ocean. Their geographic distribution would be easily affected by geographic changes through geological time. Moreover, their siliceous shells have been preserved in marine sediments and form a good fossil record. The sensitivity to geographic changes and well-preserved fossil record of Radiolaria could allow us to elucidate a past geographic isolation of marine microplankton. *Larcopyle buetschlii*, a morphospecies of radiolarians analyzed in the present study, is found in the surface waters in the Pacific Ocean, whereas it has a characteristic distribution vertically ranged from the surface to deep layers in the Japan Sea. In addition, its fossil specimens are continuously observed in the Japan Sea before the LGM. Therefore, *L. buetschlii* could be a good model to study a link between geographic isolation during the LGM and reproductive isolation of marine microplankton.

Heterogeneity of internal transcribed spacer regions of ribosomal DNA (ITS1 and ITS2) is observed in many eukaryotes (e.g., vertebrates, dinoflagellates, and diatoms). The ITS1 and ITS2 regions are spliced out during the maturing process of ribosome, causing a nucleotide substitution rate higher than ribosomal DNA coding regions. Nevertheless, the ITS1 and ITS2 sequences are functionally important for their splicing, because the premature transcript composed of 18S, 28S, 5.8S rRNA, ITS1, and ITS 2 is folded into a secondary structure followed by the self-splicing of ITS1 and ITS2. Based on the secondary structures of ITS1 and ITS2 sequences, compensatory base changes (CBCs: base changes occurring on both sides of a double-stranded portion) and hemi-CBCs (HCBCs: base changes occurring on one side of a double-stranded portion) are often observed among closely related species. The correlation between CBCs and HCBCs in the ITS2 sequences likely reflects sexual compatibility among individuals of a closely related species. Thus, the CBCs/HCBCs correlation is a useful marker to infer whether geographically isolated populations are reproducible.

We demonstrated that there is heterogeneity of the ITS2 sequences within an individual of *L. buetschlii* and that all individuals of *L. buetschlii* collected from the surface to deep layers in the Japan Sea do not have a significant difference in the CBCs/HCBCs of the ITS-2 sequences. Furthermore, the CBCs/HCBCs of the ITS-2 sequences do not show a significant difference between individuals of the Japan Sea and Pacific Ocean. These findings suggest that *L. buetschlii* in the Japan Sea and Pacific Ocean likely forms a reproducible single population. Thus, the geological isolation during the LGM is unlikely effective for the reproductive isolation of this radiolarian species.

Keywords: Japan Sea, Larcopyle buetschlii, Radiolaria, secondary deep-sea plankton

Japan Geoscience Union Meeting 2014
(28 April - 02 May 2014 at Pacifico YOKOHAMA, Kanagawa, Japan)

BPT26-11 Room:421 Time:May 2 11:45-12:00

Non-coding sequences conserved independently in four different mammalian orders

SAITOU, Naruya[1*] ; BABARINDE, Isaac[2]

[1]National Institute of Genetics, Division of Population Genetics, [2]SOKENDAI, Department of Genetics

Conserved noncoding sequences (CNSs) of vertebrates are considered to be closely linked with protein-coding gene regulatory functions.We examined the abundance and genomic distribution of CNSs in four mammalian orders: primates, rodents, carnivores, and cetartiodactyls. We defined the two thresholds for CNS using conservation level of coding genes; using all the three coding positions and using only first and second codon positions. The abundance of CNSs varied among lineages, with primates and rodents having highest and lowest number of CNSs, respectively,whereas carnivores and cetartiodactyls had intermediate values. These CNSs cover 1.3?5.5% of the mammalian genomes and have signatures of selective constraints that are stronger in more ancestral than the recent ones. Evolution of new CNSs as well as retention of ancestral CNSs contribute to the differences in abundance. The genomic distribution of CNSs is dynamic with higher proportions of rodent and primate CNSs located in the introns compared with carnivores and cetartiodactyls. In fact, 19% of orthologous single-copyCNSs between human and dog are located in different genomic regions.

If CNSs can be considered as candidates of gene expression regulatory sequences, heterogeneity of CNSs among the four mammalian orders may have played an important role in creating the order-specific phenotypes. Fewer CNSs in rodents suggest that rodent diversity is related to lower regulatory conservation. With CNSs shown to cluster around genes involved in nervous systems and the higher number of primate CNSs, our result suggests that CNSs may be involved in the higher complexity of the primate nervous system. This study was published in Genome Biology and Evolution (Babarinde and Saitou, 2013; vol. 5:2330?2343).

Keywords: genome, mammals, Primates, Rodents, Artiodactyla, Carnivores

Japan Geoscience Union Meeting 2014
(28 April - 02 May 2014 at Pacifico YOKOHAMA, Kanagawa, Japan)

BPT26-12 Room:421 Time:May 2 12:00-12:15

Development for new hyphenated analytical technologies for paleogenomics research

HIRATA, Takafumi[1*]

[1]School of Science, Kyoto University

Cytometry is the analytical technique, basically applied for quantitative analysis of cells and cell systems. In general, cytometry measures optical properties of cells, and most often uses fluorescence to measure specific antigen molecules, intracellular ions and DNA/RNA. Cells may be live or fixed, depending on the application, and individual cells can often be physically sorted. ? Other optical signals can be measured, including light scatter. The cytometry has blossomed to become the key technique to evaluate the nutritional status or to understand the elemental metabolism for animals. Several advantages can be derived by the cytometry, such as analysis speed, detection sensitivity, the ability to measure many parameters simultaneously, and the ability to sort individual cells (i.e., single cell spectroscopy). Recently, new generation cytometry utilizing the sensitive mass spectrometers (i.e., mass cytometry) was described. With the mass cytometry, further sensitive detection of ions or proteins and higher capability for the multiparameter analysis of individual adherent cells (e.g.,; Benfall et al., Science, 2011; Bodenmiller et al., Nature Biotechnology, 2012). With the extensive number of information collected from cells or samples through the cytometry, reliable and objective evaluation for the changes in biochemical functions could be achieved. This approach can also be applied to understand the solar system evolution based on the numerous number of age data. In recent ten years, we have demonstrated the unique study approach using the distribution pattern of sample ages based on the series of precise age data collected from large number of samples (i.e., age-cytometry) (e.g., Rino et al., PEPI, 2008; Iizuka et al., Geology, 2008; Iizuka et al., Iizuka et al., Chem. Geol., 2009; Iizuka et al., GCA, 2010). The mass cytometry will become a powerful tool to promote the big-data science for various research fields such as metallomics, medical sciences or the geochemistry. For elemental or isotopic analysis of trace- or ultratrace-elements, plasma ion source mass spectrometry (ICP-MS) has been widely employed because of its high analytical capabilities such as high-elemental sensitivities, minimal sample preparation procedures, high-analysis throughput or user-friendly operations (Bandura et al., Anal. Chem., 2009). With the laser ablation sample introduction technique, distribution of both the elemental and isotopic data for trace- or ultratrace-elements can be successfully derived directly from large-sized solid samples (>10cm). Despite the obvious success in obtaining elemental and isotopic data (age data), it should be noted that stable isotope ratio data for light elements (e.g., C and O) could not be derived by the present LA-ICPMS technique because of serious contribution mass spectrometric interferences on C and O isotopes, which provides key information concerning the physico-chemical conditions for the sample formation. To overcome this, we would like to develop a new analytical technique to measured the C isotopes, at a same time with elemental analysis using the LA-ICPMS technique. Newly developed spectroscopy technique combined to the LA-ICPMS technique can become a major analytical tool to expand the analytical capability for mass cytomery for biochemical samples and geochemical samples through precise, reliable and uniform quality data. The analytical technique develop here will promote the big-data science for various research fields including geochemistry and biochemistry.

Keywords: mass spectrometry, laser ablation, paleogenomics, hyphenated technology, analytical chemistry, geochemistry

Japan Geoscience Union Meeting 2014
(28 April - 02 May 2014 at Pacifico YOKOHAMA, Kanagawa, Japan)

BPT26-P01 Room:Poster Time:May 2 16:15-17:30

Conditions for photic zone euxinia deduced from ocean biogeochemical cycle model

OIDE, Kana[1*] ; OZAKI, Kazumi[2] ; TAJIKA, Eiichi[1]

[1]University of Tokyo, [2]Atmosphere and Ocean Research Institute, University of Tokyo

It is widely thought that atmospheric oxygen concentration has been kept in a level of the same order of magnitude as that of today over the Phanerozoic, based on both charcoal records and geochemical cycle modeling.

On the other hand, several lines of geological/geochemical evidence indicate that the oceans below photic zone were strongly de-oxygenated on a global scale at some geological intervals. Such oxygen deficient events are known as ”Oceanic Anoxic Events (OAEs).”

In the anoxic water column, hydrogen sulfide is produced via bacterial sulfate reduction. Therefore, if sulfate and metabolizable organic matter are sufficient, hydrogen sulfide builds up in some cases, which is called ”ocean euxinia.”

Biomarkers derived from photosynthetic green sulfur bacteria have been discovered in the sedimentary rocks deposited during the Mesozoic OAEs(e.g., early-Triassic superanoxia and Cretaceous OAE2) indicating that hydrogen sulfide existed in the photic zone ($\sim$100m) at those intervals. However, the conditions required to generate the photic zone euxinia remains unrevealed.

Here we investigate the conditions required for occurrence of photic zone euxinia, using an ocean biogeochemical cycle model developed by Ozaki and Tajika (2013). We further improve the model to have the surface ocean with higher resolution to evaluate the vertical profiles of H_2S, NO_3, HPO_4, and O_2, We try to understand the changes of marine primary producer during photic zone euxinia quantitatively.

Keywords: oceanic anoxic events, biogeochemical cycles, phosphorus cycle, anoxia/euxinia, photic zone euxinia

Japan Geoscience Union Meeting 2014
(28 April - 02 May 2014 at Pacifico YOKOHAMA, Kanagawa, Japan)

BPT26-P02 Room:Poster Time:May 2 16:15-17:30

Partial pressure of atmospheric CO2 during the Paleoproterozoic global glaciation

SHIBUYA, Takazo[1*] ; UENO, Yuichiro[2] ; KOMIYA, Tsuyoshi[3] ; NISHIZAWA, Manabu[1] ; KITAJIMA, Kouki[4] ; YAMAMOTO, Shinji[3] ; SAITOU, Takuya[2] ; TAKAI, Ken[1] ; YOSHIDA, Naohiro[2] ; MARUYAMA, Shigenori[2] ; RUSSELL, Michael[5]

[1]JAMSTEC, [2]Tokyo Institute of Technology, [3]University of Tokyo, [4]University of Wisconsin, [5]Jet Propulsion Laboratory

The Paleoproterozoic Makganyene Glaciation is a particular enigmatic geologic event in that ice covered the oceans even at low latitude (Snowball Earth). This event might have drastically curtailed biological productivity but melting of the oceanic ice presumably induced a cyanobacterial bloom, leading to an acceleration of global oxygenation. It has been predicted that this event occurred as a result of the drawdown of greenhouse gases in the atmosphere. However, atmospheric CO2 levels at that time are still under debate. Here, we constrained the CO2 concentration in seawater based on fluid inclusions in subseafloor hydrothermal quartz deposits from the 2.2 billion years (Gyr) old Ongeluk volcanics, South Africa, in which the ancient water and carbon dioxide are preserved. The quantitative analysis of the concentration and stable carbon isotopes of CO2 in the fluid inclusions revealed that the CO2 concentration in the seawater was limited to be less than 7 mmol/kg. Because the Ongeluk seawater was locally open to the atmosphere, atmospheric CO2 level was also estimated to be lower than 33 times the present atmospheric level (PAL) ($<1.3\times10$?2 bar) assuming equilibrium between the Ongeluk seawater and atmosphere. This CO2 level was not enough to compensate the faint young sun and keep the ocean temperature sufficiently above freezing point by itself. Although the behavior of other greenhouse gases is still unknown, our results demonstrate that the deficient atmospheric CO2 level was a significant contributing factor to the 2.2 Gyr global glaciation.

Japan Geoscience Union Meeting 2014
(28 April - 02 May 2014 at Pacifico YOKOHAMA, Kanagawa, Japan)

BPT27-01 Room:213 Time:April 28 12:00-12:15

Impact-driven ocean acidification as a mechanism of Cretaceous?Palaeogene mass extinctions

OHNO, Sohsuke[1*] ; KADONO, Toshihiko[2] ; KUROSAWA, Kosuke[1] ; HAMURA, Taiga[3] ; SAKAIYA, Tatsuhiro[4] ; SHIGEMORI, Keisuke[4] ; HIRONAKA, Yoichiro[4] ; SANO, Takayoshi[4] ; WATARI, Takeshi[4] ; OHTANI, Kazuto[5] ; MATSUI, Takafumi[1] ; SUGITA, Seiji[3]

[1]Planetary Exploration Research Center, Chiba Institute of Technology, [2]University of Occupational and Environmental Health, [3]University of Tokyo, [4]Osaka University, [5]Institut national de la recherche scientifique

The Cretaceous?Paleogene (K?Pg) mass extinction event at 65.5 Ma triggered by a meteorite impact is one of the most drastic events in the history of life on the Earth. Many hypotheses have been proposed as killing mechanisms induced by the impact, including global darkness due to high concentrations of atmospheric silicate dust particles, global wildfires, greenhouse warming due to CO2 release, and global acid rain. However, the actual mechanism of extinction remains highly controversial. One of the most important clues for understanding the extinction mechanism is the marine plankton record, which indicates that plankton foraminifera, living in the near-surface ocean, suffered very severe extinction in contrast to the high survival ratio of benthic foraminifera. No proposed extinction mechanism can account for this globally observed marine extinction pattern. Here, we show that SO3-rich impact vapor was released in the K-Pg impact and resulted in the occurrence of global acid rain and sudden severe ocean acidification at the end of the Cretaceous, based on the new results of impact experiments at velocities much higher than previous works ($>$10 km/s) and theoretical calculations on aerosol coagulation processes. Sudden severe ocean acidification can account for many of the features of various geologic records at the K?Pg boundary, including severe extinction of plankton foraminifera. This extinction mechanism requires impact degassing of SO3-rich vapor, which is not necessarily found at impact sites other than Chicxulub, suggesting that the degree of mass extinction was controlled greatly by target lithology.

Keywords: K/Pg mass extinction, impact, laboratory experiment, acid rain, ocean acidification, mass spectroscopy

Japan Geoscience Union Meeting 2014
(28 April - 02 May 2014 at Pacifico YOKOHAMA, Kanagawa, Japan)

BPT27-02 Room:213 Time:April 28 12:15-12:30

Platinum group element anomalies in the Triassic-Jurassic deep-sea sediments

FUJISAKI, Wataru[1*] ; SAWAKI, Yusuke[1] ; YAMAMOTO, Shinji[2] ; YOKOYAMA, Tetsuya[1] ; MARUYAMA, Shigenori[3]

[1]Department of Earth and Planetary Sciences, Tokyo Institute of Technology, [2]The University of Tokyo, [3]Earth-Life Science Institute, Tokyo Institute of Technology

One of the biggest mass extinctions in the Phanerozoic occurred at the Triassic-Jurassic (T-J) boundary. The large magmatic activity associated with the breakup of Pangaea (CAMP event) or a bolide impact attract interests as causes of the mass extinction at the T-J boundary. However, the cause of the mass extinction is still controversial because of insufficient geological evidences. PGE abundances and radiogenic Os isotope ratios are powerful tracers that potentially distinguish ancient basaltic magmatism from the effect from extraterrestrial.

We conducted detailed geological survey at the Inuyama area, where Triassic to Jurassic deep-sea sediments well crop out. We developed detailed a geological map of the study area and reconstructed ocean plate stratigraphy. We collected ca. 70 siliceous shale samples bed-by-bed were also collected to measure PGEs concentration and Os isotopes with a high spatial resolution. The rock powder was spiked with ^{190}Os, ^{185}Re, ^{191}Ir, ^{99}Ru, ^{194}Rt, and ^{105}Pd and digested by 2:1 mixture of HNO_3 and HCl in a sealed Carious tube at 240oC for 48 hours. After chemical separation using an anion exchange resin, the isotope ratios of PGE were measured by a quadrupole type ICP-MS at Tokyo Tech. The Os isotope ratios were determined by N-TIMS (Triton plus) at Tokyo Tech.

PGEs concentrations and Os isotope composition are determined from 28 siliceous shale samples across the T-J boundary. Re and Os contents varies from 14.7 to 128.6 pg/g and from 4.9 to 99.2 pg/g, respectively. ^{187}Os/^{188}Os decreases from 0.77 to 0.34 before the T-J boundary. The ^{187}Os/^{188}Os values in the Jurassic siliceous shales fluctuated around ca. 0.5. The highest Os concentration and negative Os isotope anomaly corresponds to the first occurrence of Jurassic type radiolarian. Also, Ir/Pt vs Pd/Pt cross plot and C1 chondrite-normalized PGE patterns of siliceous shales across the T-J boundary show similar trend to CAMP and upper continental crust (UCC). This indicates that the origin of PGEs detected from siliceous shales are the mixture of CAMP and UCC, and that extraterrestrial influence at the T-J boundary was minor.

Keywords: T-J boundary mass extinction, deep-sea sediments, platinum group element

Japan Geoscience Union Meeting 2014
(28 April - 02 May 2014 at Pacifico YOKOHAMA, Kanagawa, Japan)

BPT27-03 Room:213 Time:April 28 12:30-12:45

Impact event and radiolarian faunal turnover across the middle-upper Norian transition at Sakahogi section in Japan

ONOUE, Tetsuji[1*] ; YAMASHITA, Daisuke[1] ; TOMINAGA, Takashi[1] ; SATO, Honami[2]

[1]Kumamoto University, [2]Kyushu University

Anomalously high platinum group element (PGE) concentrations have been reported for Upper Triassic (middle Norian) deep-sea claystone layer in the Sakahogi section, central Japan, which have been interpreted to be derived from an extraterrestrial impact event that formed the 90 km Manicouagan crater in Canada. Here we report middle to upper Norian radilarian biostratigraphy from the Sakahogi section across the impact ejecta layer. Based on the radiolarian biostratigraphy from the Sakahogi section, three radiolarian zones are recognized in ascending order as follows: Capnodoce?Trialatus zone, Trialatus robustus?Lysemelas olbia zone, and Lysemelas olbia zone. Detailed high-resolution sampling and biostratigraphical data allowed us to data precisely the ejecta layer, which occur in the base of the radiolarian Trialatus robustus?Lysemelas olbia zone. Our biostratigraphc analysis suggests that there was no mass extinction of radiolarians across the impact event horizon. Only one species became extinct at the ejecta horizon and the extinction rate of radiolarians (extinct species divided by total species at the same level) is estimated to be about 5% at the horizon. Major turnovers of radiolarians occur above the ejecta horizon within the Trialatus robustus?Lysemelas olbia zone. Biostratigraphic analysis shows that 20 radiolarian species became extinct in this zone and the extinction rate is estimated to be 83%. This turnover is associated with a deposition of spicular chert, suggesting temporal changes in marine ecosystems after the impact event. Given that the average sedimentation rate of the middle to upper Norian chert succession is 2.7 mm per thousand years, this turnover occurred 400 kyr after the impact event. Thus the meteorite impact did not direct cause of radiolarian extinction event.

Keywords: Triassic, Meteorite Impact, Radiolaria

Japan Geoscience Union Meeting 2014
(28 April - 02 May 2014 at Pacifico YOKOHAMA, Kanagawa, Japan)

BPT27-04 Room:213 Time:April 28 14:15-14:30

A global ocean oxidation event immediately after the Early Triassic thermal maximum

KAIHO, Kunio[1*] ; TAKAHASHI, Satoshi[2] ; GORJAN, Paul[3] ; CHEN, Zhong-qiang[4] ; TONG, Jinnan[4]

[1]Tohoku University, [2]University of Tokyo, [3]Washington University, [4]China University of Geosciences

Biotic recovery after the largest mass extinction at the end of the Permian (252.3 million years ago, Ma) became evident in early Spathian (250.1 Ma), Early Triassic, and was eventually completed in middle-late Anisian (ca. 244 Ma), early Middle Triassic. Recent studies showed that this much delayed recovery was impacted by several biocrises and associated environmental and climatic stresses during the Early Triassic. For instance, the end-Smithian extinction and associated thermal maximum and Smithian oceanic anoxia may have prevented biotic recovery initiated in early Smithian (251 Ma). Our new study not only confirmed the oceanic anoxia in late Smithian but also found an oxygenation event just after the Smithian thermal maxima (STM) using sulfur isotope fractionation between sulfate and sulfide. Newly obtained sulfur isotope ratios of carbonate-associated sulfate (d34SCAS) in the surface water and sulfide (d34Ssulfide) in the Panthalassic deep water during the late Permian to the Early Triassic compiled with published data show a significant increase in fractionation between the d34SCAS and d34Ssulfide during the early Spathian (41-51 permil to 62 permil). The latter indicates an increase in global oceanic dissolved oxygen levels, which also coincided with a climatic cooling and may have facilitated biotic recovery in late Early Triassic.

Keywords: Early Triassic, ocean dissolved oxygen, sulfur isotope

Japan Geoscience Union Meeting 2014
(28 April - 02 May 2014 at Pacifico YOKOHAMA, Kanagawa, Japan)

BPT27-05 Room:213 Time:April 28 14:30-14:45

Cyanobacterial proliferation during the Early Triassic

SAITO, Ryosuke[1*] ; KAIHO, Kunio[1] ; OBA, Masahiro[1] ; TONG, Jinnan[2] ; CHEN, Zhong-qiang[2] ; TAKAHASHI, Satoshi[3] ; CHEN, Jing[2]

[1]Institute of Geology and Paleontology, [2]Institute of Geology and Paleontology, [3]Institute of Geology and Paleontology, [4]China University of Geosciences, [5]China University of Geosciences, [6]Department of Earth and Planetary Science, University of Tokyo, [7]China University of Geosciences

Recent studies have shown that microbes bloomed in the aftermath of several major Phanerozoic biocrises. Microbial proliferation, as indicated by widespread microbialites, characterized marine ecosystems after the end-Permian mass extinction, which constituted the most severe biocrisis for life on Earth. The microbialite builders, including cyanobacteria and other unknown microalgae or bacteria, acted as primary producers in the trophic structure of the earliest Triassic marine ecosystem. However, the stratigraphic distributions of cyanobacteria and eukaryotic algae during the Permian?Triassic transition remain unknown. Thus, we conducted studies for the interval from the latest Permian to the Middle Triassic using the monomethyl heptadecane ratio (MHR) and 2-methyl hopane index (2-MHI) as cyanobacterial proxies, and the n-alkyl-cyclobenzene ratio (ACBR) as a biomarker for eukaryotic algae. We detected a proliferation of eukaryotic algae during the latest Permian and early Middle Triassic, whereas cyanobacteria flourished during most of the Early Triassic. The new findings are consistent with previously determined stratigraphic distributions of microbialites and the species richness of eukaryotic algae. The erosion intensity and temperature fluctuated in conjunction with changes in the populations of cyanobacteria and eukaryotic algae. Therefore, we postulate that these population changes were primarily the result of enhanced water turbidity from elevated bedrock erosion and lethally hot temperatures.

Keywords: biomarker, Early Triassic, extinction, cyanobacteria

Japan Geoscience Union Meeting 2014
(28 April - 02 May 2014 at Pacifico YOKOHAMA, Kanagawa, Japan)

BPT27-06 Room:213 Time:April 28 14:45-15:00

Mo depleted ocean after the end Permian mass extinction referred from Mo and U behaviors in pelagic deep-sea sedimentary

TAKAHASHI, Satoshi[1*] ; YAMASAKI, Shin-ichi[2] ; OGAWA, Yasumasa[3] ; KIMURA, Kazuhiko[4] ; KAIHO, Kunio[5] ; YOSHIDA, Takeyoshi[5] ; TSUCHIYA, Noriyoshi[2]

[1]Department of Earth and Planetary Science, the University of Tokyo, [2]Graduate School of Environmental Studies, Tohoku University, [3]Graduate School of Engineering and Resource Science, Akita University, [4]School of food, Agricultual and Environmental Science, Miyagi University, [5]Department of Earth Science, Graduate School of Science, Tohoku University

The end-Permian mass extinction was the largest biotic catastrophe of the Phanerozoic, and evidence of global oceanic anoxia during this event has been reported (e.g. Wignall and Twitchett, 1996). Such anoxic?euxinic conditions have also been revealed by enrichments of redox-sensitive elements (Fio et al., 2010; Grasby et al., 2009, 2011; Algeo et al., 2012). Among redox-sensitive elements, uranium increased in sediments and finally result uranium drawdown, suggested by a decrease in sedimentary uranium isotope ratio (238/235U) and a increase in Th/U ratio from the shallow marine carbonates (Brennecka et al., 2011). In this presentation, we will show the possible evidence of Mo drawdown after the mass extinction event from the continuous deep-sea Permian-Triassic boundary section which located in the low latitude pelagic Panthalassa (Akkamori section-2; Takahashi et al., 2009).

High resolution ICP-MS analysis using sedimentary rock samples from the study section (Takahashi et al., in review) indicates vertical distribution of UEF and MoEF (Enrichment factor of U and Mo), the Mo/U ratio. MoEF and UEF show a synchronous increase from the Upper Permian bedded chert to the overlying siliceous claystone, while the Mo/U ratio increases from 3.9 to 47.3 showing continuous elevation from the 1.0 $\times$ modern seawater Mo/U ratio to 9.0 $\times$ the modern ratio. Accepting the previous study's criteria (Algeo and Tribovillard, 2009), increased Mo/U ratios that clearly exceed 9 (3 times the value of modern seawater) suggest the presence sulphidic bottom water at that time. Considering possibility of U drawdown suggested by Brenecka et al. (2011), decrease in seawater U concentration (possibly up to 1/7) would also help the rise of Mo/U ratio. Further elevations of MoEF and the Mo/U ratio reach values of more than 1000, and MoEF reaches values of several thousands from Upper Permian siliceous claystone to the basal 20cm end-Permian black claystone, indicating that sulphidic bottom water was increasingly developed and that Mo transportation by the particulate shuttle was activated. The particulate shuttle, proposed by Algeo and Tribovillard (2009), is a process by which Mn oxyhydroxides absorb molybdate oxyanions above the oxic?anoxic chemocline in the water column and then sink and finally dissolve on at or just below the sediment-water interface, releasing Mo to the sediments. Additionally, in such a developed sulphidic water column, syngenetic pyrite formation in the euxinic water column could possibly have contributed to Mo transportation to the sediment (Algeo and Maynard, 2004). Above the 20 cm horizon of the black claystone, MoEF decreases to values lower than 100 and the Mo/U ratio takes values of more than 3 but less than 20. These values could be interpreted to indicate that sulphidic bottom water was still present but that the particle shuttle had subsided to some extent after the time of the mass extinction. Low Mo/U values occur in earliest Triassic siliceous claystone bed, despite high MoEF and UEF values. Because MoEF and UEF are high, reducing bottom water conditions still existed. Thus, the decrease in Mo/U does not indicate a return to oxic conditions, but rather a Mo drawdown in the earliest Triassic seawater. The study examples of such trace-metal drawdown in geologic past have been reported by Algeo (2004) and Hetzel et al. (2009). In fact, the trend of low Mo/U values with high MoEF and UEF is consistent with that of the Mo-depleted seawater condition identified in the modern Black Sea (Algeo and Tribovillard, 2009), suggesting a drawdown of seawater Mo in the pelagic ocean.

Keywords: molybdenum, mass extinction, Permian, Triassic, deep-sea, Panthalassa

Japan Geoscience Union Meeting 2014
(28 April - 02 May 2014 at Pacifico YOKOHAMA, Kanagawa, Japan)

BPT27-07 Room:213 Time:April 28 15:00-15:15

Nitrogen isotope chemostratigraphy across the Permian-Triassic boundary at Chaotian, Sichuan, South China.

SAITOH, Masafumi[1*] ; UENO, Yuichiro[1] ; NISHIZAWA, Manabu[2] ; ISOZAKI, Yukio[3] ; TAKAI, Ken[2]

[1]Tokyo Institute of Technology, [2]JAMSTEC, [3]The University of Tokyo

Nitrogen isotopic compositions of upper Permian to lowermost Triassic rocks were analyzed at Chaotian in northern Sichuan, South China, in order to clarify changes in the oceanic nitrogen cycle during the Changhsingian (Late Late Permian) prior to the end-Permian extinction. The analyzed interval across the Permian-Triassic boundary (P-TB) at Chaotian consists of three stratigraphic units: the upper Wujiaping Formation, the Dalong Formation, and the lowermost Feixianguan Formation, in ascending order. The upper Wujiaping Formation is mainly composed of dark gray limestone with diverse shallow-marine fossils deposited on the shallow shelf. In contrast, the overlying Dalong Formation is mainly composed of thinly bedded laminated black mudstone and black siliceous mudstone containing abundant radiolarians, deposited on the relatively deep slope/basin under anoxic condition. The lowermost Feixianguan Formation is composed of thinly bedded gray marl and micritic limestone with minor fossils deposited on the shallow shelf. d15N values are in positive values in the upper Wujiaping Formation implying denitrification and/or anammox in the ocean. d15N values gradually decrease in the lower Dalong Formation and are consistently low in the middle Dalong to lowermost Feixianguan Formation. In particular, no clear d15N shift is recognized across the extinction horizon. The consistently low d15N values at Chaotian suggest the enhanced nitrogen fixation in the ocean during the entire Changhsingian to early Induan (Early Early Triassic), accompanied with the emergence of anoxic condition. The d15N trend at Chaotian was possibly a regional isotopic signature in northwestern South China and not a global one, because the composite d15N profiles document that no d15N trend similar to that at Chaotian is observed in other P-TB sections around the world. Nonetheless, the protracted oceanic nitrogen depletion during the Changhsingian suggested by the present results at Chaotian may have acted as a stress to shallow-marine biota.

Japan Geoscience Union Meeting 2014
(28 April - 02 May 2014 at Pacifico YOKOHAMA, Kanagawa, Japan)

BPT27-08 Room:213 Time:April 28 15:15-15:30

A remarkable sea-level drop and global cooling in the late Middle Permian: record from the mid-superoceanic limestone

KOFUKUDA, Daisuke[1*] ; ISOZAKI, Yukio[1] ; IGO, Hisayoshi[2] ; KANI, Tomomi[3] ; ISHIMURA, Toyoho[4]

[1]The University of Tokyo, Komaba, [2]Insititute of Natural History, [3]Kumamoto University, [4]AIST

For clarifying the global environmental changes relevant to the Guadalupian-Lopingian boundary (G-LB) extinction, i.e. the first major biodiversity drop during the Permian, litho-, bio-, and chemo- stratigraphy of $\delta^{13}C_{carb}$ and $^{87}Sr/^{86}Sr$ were analyzed in the Middle-Upper Permian paleo-atoll limestone at Akasaka in central Japan, which was derived from a paleo-atoll complex deposited primarily in the low latitude in the mid-Panthalassa. Between the Capitanian (upper Middle Permian) black limestone (the *Yabeina* fusuline Zone) and the Wuchiapingian (lower Upper Permian) light gray limestone (the *Codonofusiella-Reichelina* Zone), a unique black-white striped limestone is intercalated, of which top marks the G-LB horizon.

The major extinction occurred in the uppermost black limestone, large-tested fusuline and large bivalve that were adapted to low-latitude extremely warm conditions sharply became extinct. Most parts of the Akasaka Limestone consist of shallow marine wackestone/packstone deposited in low-energy settings of the subtidal zone likely within a lagoon on the top of a seamount.

We newly identified 1) a remarkable hiatus with erosional features at the top of the striped limestone, 2) large-scale cross-beddings in the striped limestone immediately below the hiatus, and 3) the dominance of grainstone in the basal light gray limestone immediately above the hiatus. These lines of evidence altogether suggest that a remarkable sea-level drop has occurred around the G-LB in the mid-oceanic paleo-atoll complex, and that a cool climate has appeared in the Capitanian. The isotope stratigraphy for the Capitanian interval with extremely high $\delta^{13}C_{carb}$ values over +5 ‰ and the extremely low $^{87}Sr/^{86}Sr$ ratios below 0.7070 indicate the high productivity in the superocean and the suppressed continental weathering on Pangea, respectively. Both isotope signatures can be concordantly explained by the appearance of a putative global cooling in the Capitanian. After all, the litho-, bio-, and chemostratigraphical records from the Permian mid-superocean positively suggest a possible link between the Capitanian global cooling and the end-Capitanian extinction.

Keywords: G-L boundary, mid-superoceanic limestone, sea-level drop, cooling, carbon isotope, strontium isotope

Japan Geoscience Union Meeting 2014
(28 April - 02 May 2014 at Pacifico YOKOHAMA, Kanagawa, Japan)

BPT27-09 Room:213 Time:April 28 15:30-15:45

Middle to Late Permian seawater Sr isotope variation linked to the glaciation/deglaciation

KANI, Tomomi[1*] ; KOFUKUDA, Daisuke[2] ; ISOZAKI, Yukio[2]

[1]Department of Earth and Environmental Sciences, Kumamoto University, [2]Department of Earth Science and Astronomy, The University of Tokyo

We report the detailed secular change of the Middle to Late Permian seawater $^{87}Sr/^{86}Sr$ ratio for the Akasaka and Iwato limestone in SW Japan. The studied two sections were originally deposited as paleo-atoll complexes on the low-latitude, mid-Panthalassa seamounts. We also analyzed coeval sections at Sizipo and Liangshan deposited on the shallow marine shelf of South China. Commonly in the four studied sections, extremely low values ($<$0.7069; the lowest values of the Phanerozoic) continued from upper Wordian (middle Middle Permian) to the topmost Capitanian (upper Middle Permian) immediately below the Middle-Late Permian boundary. The $^{87}Sr/^{86}Sr$ ratios increased to 0.7072 in the early Late Permian. This increase recorded the most rapid in the entire Phanerozoic. The ca. 5 m.y.-long minimum interval and the following rapid increase in Sr isotope ratio can be explained by the remarkable changes in continental erosion/weathering rate; in particular, by the onset of glaciation and the following deglaciation, that is supported by global sea level change, in addition to the initial doming/rifting of Pangea. After the Capitanian cooling, the long-term climatic regime shifted to a warmer one during which covering ice was removed from continents to expose crustal silicates for to erosion/weathering. The continental rifting with new drainage systems likely increased decisively the highly radiogenic continental flux to the superocean.

Keywords: Permian, Sr isotope, seawater, limestone

Japan Geoscience Union Meeting 2014
(28 April - 02 May 2014 at Pacifico YOKOHAMA, Kanagawa, Japan)

BPT27-10 Room:213 Time:April 28 15:45-16:00

A unique low-latitude-type molluskan assemblage from the Permian Iwaizaki limestone in the S. Kitakami belt, NE Japan

ISOZAKI, Yukio[1*] ; KASE, Tomoki[2]

[1]Dept. Earth Science & Astronomy, University of Tokyo, [2]National Science Museum

Permian large gastropod *"Pleurotomaria" yokoyamai* was found for the first time from the Capitanian (Upper Guadalupian) Iwaizaki limestone in the South Kitakami belt, NE Japan. A smaller planispiral gatropode *Porcellia* sp. was also associated. These taxa have been scarcely reported, except from the coeval Akasaka limestone in SW Japan. The Akasaka Limestone was deposited as a low-latitude atoll on a mid-Panthalassan seamount, whereas the Iwaizaki limestone as a patch reef within terrigenous clastics-dominant facies on a shallow marine continental shelf. The occurrence of this unique gastropod assemblage, together with large bivalves and large-tested fusulines, suggests that the Iwaizaki Limstone was originated also in a Permian low-latitude domain, and that the South Kitakami belt likely formed a part of the continental margin of South China representing its eastern extension to NE Japan.

Keywords: Permian, bivalve, gastropod, South Kitakami belt, South China

Japan Geoscience Union Meeting 2014
(28 April - 02 May 2014 at Pacifico YOKOHAMA, Kanagawa, Japan)

BPT27-11 Room:213 Time:April 28 16:15-16:30

Mechanisms regulating the redox state of an atmosphere-ocean system during the Paleozoic

OZAKI, Kazumi[1*]

[1]AORI, University of Tokyo

There is now a great interest in understanding paleoredox conditions of an atmosphere-ocean system because it is essential for investigating links between oxygenation of biosphere and major biological innovation/extinction. Therefore, understanding the regulating mechanism(s) of secular (over millions of years) changes of redox state of Earth's surface environments is one of the fundamental topics. Early Paleozoic is marked by the prominent biological evolution/diversification events (i.e., Cambrian explosion, Great Ordovician Biodiversification Event, and advent of land plants). On the other hand, multiple lines of geological and geochemical evidence (such as black shale deposition, low C/S ratio of buried sediments, low molybdenum isotopic value, and iron speciation data) suggest that oxygen-depleted waters were generally more common and widespread in the ocean interior than they are today until the Devonian. Among these, recent finding of an increase in molybdenum isotopic value from ~1.4 ‰ to ~2.0 ‰ between ~440 Ma and ~390 Ma (Dahl et al., 2010 PNAS) attracts the attention because it implies the oceanic redox transition to a well-oxygenated condition. However, the ultimate cause of this transition remains uncertain.

Considering the fact that the ocean oxygenation event correlates with the diversification of land plants since the Late Ordovician, causal linkage between them are intriguing; an enhanced chemical weathering on the continent by land plants could lead to an increase in the burial rate of terrigenous organic matter, giving rise to an oxygenation of an ocean-atmosphere system. However, it remains unclear whether the radiation of land plants is necessary to cause such redox transition.

The evolution of atmospheric oxygen concentration has been studied intensively, but reconstructed atmospheric oxygen evolution varies widely between models, demonstrating that further understanding on the mechanisms controlling atmospheric oxygen level is still required. Because oxygen is most likely regulated by a combination of several feedbacks in the Earth system, it is essential to evaluate the impact of plant diversification on the oxygenation state of an ocean-atmosphere system with the aid of a biogeochemical cycle model. In this study, a model is designed to explore the roles of several feedback mechanisms regulating the redox state of the atmosphere and oceans during the early Paleozoic, and to reconstruct the paleoredox history of an ocean-atmosphere system during the early Paleozoic. The results of systematic sensitivity experiment demonstrate that (1) oceans before the advent of land plant had been kept in suboxic-anoxic condition, that (2) the diversification of land plant since Late Ordovician could cause an increase in atmospheric oxygen level to >16% by the Devonian and ocean could be oxygenated by the Middle Devonian, and that (3) a redox dependent burial efficiency of phosphorus at sediment-water interface and degradability of particulate organic matter (POM) play substantial roles in atmospheric oxygen level before the advent of land plant. The modeling results confirm the causal linkage between plant diversification and the oxidation of Earth's surface environments. Our result also highlights the need for more quantitative and process-based knowledge of the decomposition process of POM in order to reveal the redox evolution of atmosphere-ocean system during the Paleozoic.

Keywords: Paleozoic, atmospheric oxygen level, biogeochemistry, land plant evolution, biogeochemical cycle model

Japan Geoscience Union Meeting 2014
(28 April - 02 May 2014 at Pacifico YOKOHAMA, Kanagawa, Japan)

BPT27-12 Room:213 Time:April 28 16:30-16:45

Compound-specific carbon isotope ratios from the Ediacaran-lower Cambrian in the Three Gorges area, South China

YAMADA, Kentaro[1*] ; SASAKI, Kazunori[2] ; UENO, Yuichiro[3] ; YAMADA, Keita[4] ; YOSHIDA, Naohiro[4] ; MARUYAMA, Shigenori[5]

[1]Earth Sci. and Astro., the Univ. of Tokyo, [2]Human Metabolome Technologies Inc., [3]Earth and Planetary Sci., TITech, [4]Environmental Sci. and Tech., TITech, [5]Earth-Life Science Institute

In order to reveal the organic carbon cycle in the early Cambrian ocean, compound-specific carbon isotope ratios of aliphatic hydrocarbons which records the change of the composition of organic matters derived from phototrophs were first measured for the drill cores from the Three Gorges area. The differences between the carbon isotope ratios of short chain n-alkanes and pristane (Δap) show relatively high ($\sim$-3-4 ‰) in the Ediacaran, decreased down to $\sim$-6 ‰, and subsequently increased up to $\sim$6 ‰ in the early Terreneuvian (the earliest Cambrian; 541-521 Ma), and again decreased down to $\sim$-4 ‰ in the Epoch 2 (the early Cambrian; 521-509 Ma). The differences between the carbon isotope ratios of pristane and phytane (Δpp) were $\sim$0 ‰, decreased down to $\sim$-5 ‰ in the Terreneuvian, and increased up to $\sim$6 ‰ in the Epoch 2. ^{13}C-depleted β-carotane was found only from the black shale at the Series 2.

Δpp indicate that a single phototroph community has existed in the Ediacran, whereas multiple phototroph communities existed in the early Cambrian. The decrease in Δap indicates enhanced burial of lipids derived from eukaryotic phototrophs, probably in response to the emergence of faecal pellets, which has consumed the large dissolved organic carbon reservoir. ^{13}C-depleted β-carotane and negative Δpp values indicate that the anaerobic phototrophs utilized CO_2 derived form degraded organic matters.

Thus, the aerobic phototrophs and the anaerobic phototrophs coexisted on the continental shelf in the early Cambrian. An anoxic water reached on to the photic zone on the continental shelf, and that lasted until Epoch 2. The increase of the burial of lipids derived from aerobic phototrophs is consistent with the intensified biological pump by the radiation of SSFs in the early Terreneuvian.

Keywords: Ediacaran, Cambrian, oxygen level, molecular fossil, South China

Japan Geoscience Union Meeting 2014
(28 April - 02 May 2014 at Pacifico YOKOHAMA, Kanagawa, Japan)

BPT27-13 Room:213 Time:April 28 16:45-17:00

Ancient ocean environment in the Ediacaran to Cambrian.

SAWAKI, Yusuke[1*] ; MARUYAMA, Shigenori[1]

[1]Tokyo Tech

The Ediacaran to Cambrian period is one of the most important intervals for the evolution of life. However, the scarcity of well-preserved outcrops of Ediacaran and Cambrian rocks still leaves ambiguity in deciphering ambient surface environmental changes and biological evolution.

Recent paleontologists, mainly Chinese scientists, revealed that life on the Earth have evolved through multiple stages. Some of the metazoan fossils were discovered from Ediacaran sedimentary rocks. This suggests that so-called Cambrian Explosion already started from the Ediacaran, not from the Cambrian. Therefore, unraveling surface environmental changes during the Ediacaran attract interests.

The Ediacaran to Cambrian strata in South China are almost continuously exposed and contain many fossils, which is suitable for study of environmental and biological changes in the Ediacaran and Cambrian. We (Tokyo Institute of Technology and The University of Tokyo) conducted on-land drilling through the Nantuo, Doushantuo, Dengying, Yanjiahe, Shuijintuo, Shipai and Tianheban Fms at six sites in the Three Gorges area to obtain continuous samples. We systematically analyzed some kinds of isotope ratios (carbon isotope ratios of carbonate and organic carbon, oxygen isotope ratios, nitrogen isotope ratios of organic matter, radiogenic strontium isotope ratios, calcium isotope ratios, molybdenum isotope ratios and iron isotope ratios of pyrite) and elemental concentrations (cerium, phosphorus, manganese and iron concentration in carbonate), using these core samples. The combination of these detailed chemostratigraphies enables us to decipher the surface environmental changes in the Ediacaran and Cambrian. The most important discovery is that surface environment also had evolved through multiple stages during the Ediacaran and the Cambrian.

I will talk about summary of our complehensive work in the speech.

Japan Geoscience Union Meeting 2014
(28 April - 02 May 2014 at Pacifico YOKOHAMA, Kanagawa, Japan)

BPT27-14 Room:213 Time:April 28 17:00-17:15

Neoproterozoic accretionary complex exposed in the Anglesey island and Lleyn peninsula, northwestern Wales

ASANUMA, Hisashi[1*] ; OKADA, Yoshihiro[1] ; SAWAKI, Yusuke[1] ; YAMAMOTO, Shinji[2] ; HIRATA, Takafumi[3] ; MARUYAMA, Shigenori[4]

[1]Department of Earth and Planetary Sciences, Tokyo Institute of Technology, [2]Department of Earth and Astronomy Graduate School of Arts and Sciences The University of Tokyo, [3]Graduate School of Science,Kyoto University, [4]Earth-Life Science Institute, Tokyo Institute of Technology

Accretionary complex is formed by subduction of oceanic plate, and records a history of the subduction. Subduction-related Precambrian rocks crop out in central England to Wales. The subduction with eastward polarity is considered to have continued from the Neoproterozoic to the Ordovician. Those are supported by three evidences: existences of (1) 680-480 Ma calc-alkaline volcano-plutonic complexes, (2) a high-P/T metamorphic belt formed by regional metamorphism, which has barroisite 40Ar/39Ar ages of 560-550 Ma (peak ages), (3) pelagic to hemipelagic-sedimentary rocks and mafic to ultramafic rock in Monian Supergroup. Based on these evidences, previous studies suggested that the region from the central England to the Wales had been formed by subduction-related orogeny. However, there have been a few constraints on a depositional age in the Monian Supergroup. The age constraint is necessary to reveal tectonic history of the central England to the Wales.

The Monian Supergroup is exposed in the Anglesey island and Lleyn peninsula, northwestern Wales. This complex is divided into three groups; South Stack Group (Gp), New Harbour Gp and Gwna Gp. This study focuses on Gwna Gp beacause sedimentary rocks consist of lower to middle Cambrian acritarchs. The Gwna Gp has been described as melange since 1919 and is located at structural top than the other two groups. The Gwna melanges include pillow basalts, bedded or jaspery cherts, carbonates, mudstones, sandstones and quartzites, and these rocks are typical rocks of an ocean plate stratigraphy (OPS). At eight areas in the Lleyn peninsula, we conducted geological survey to reconstruct OPSs. In addition, we determined U-Pb ages of zircons from tuffs, mudstones, claystones or sandstones with LA-ICP-MS at the University of Kyoto.

Twenty-six OPSs are reconstructed, and then repetitions of the OPSs by layer-parallel thrusts are confirmed. We separated zircons from three tuffs, two mudstones, four claystones and three sandstones of each OPS. The U-Pb ages of the zircons range from 637 $\pm$ 13 Ma (the oldest) to 541 $\pm$ 16 Ma (the youngest). We constrained arrival time of each OPS to a trench by the youngest age of detrital zircons.

Although the Gwna Gp has been treated as a single unit, this group can be divided into three types based on the arrival times. The arrival times of Type1, Type2 and Type3 are 630-610 Ma, 610-570 Ma and younger than 560 Ma, respectively. This result indicates the structural upper sequence is older than the lower. This structurally downward growth is the characteristic of typical accretionary complex, and was formed by the eastward subduction. This trend is also supported by the spatial and temporal relation of both volcano-plutonic complexes and regional metamorphic belt. From these evidences, we concluded that the Gwna Gp is the accretionary complex formed by a series of the subduction-related orogeny.

Keywords: Wales, Neoproterozoic, U-Pb age of detrital zircon, Accretionary complex, Subduction-related orogeny

Japan Geoscience Union Meeting 2014
(28 April - 02 May 2014 at Pacifico YOKOHAMA, Kanagawa, Japan)

BPT27-15 Room:213 Time:April 28 17:15-17:30

Deep-sea anoxia during the Marinoan Snowball Earth

SATO, Tomohiko[1*] ; OKADA, Yoshihiro[1] ; ASANUMA, Hisashi[1] ; MARUYAMA, Shigenori[2] ; SHOZUGAWA, Katsumi[3] ; MATSUO, Motoyuki[3]

[1]Department of Earth and Planetary Science, Tokyo Institute of Technology, [2]Earth-Life Science Institute, Tokyo Institute of Technology, [3]Graduate School of Arts and Sciences, The University of Tokyo

The oxidation of the deep ocean in the Earth's history is regarded to have occurred in the Neoproterozoic, coincident with the metazoan diversification; however, the geological record of the Neoproterozoic environment has been restricted only to shallow-sea sediments. Here we present the discovery of the Neoproterozoic deep-sea sediments in the accretionary complex in Llyen Peninsula, Wales, UK. In the studied section, the oceanic plate stratigraphy consists of mid-ocean ridge basalts, bedded dolostones, ca. 10 m-thick black mudstones, hemipelagic siliceous mudstones and turbidite sandstone, in ascending order. The detrital zircons separated from sandstone give the youngest age of 637+-13 Ma. Within ca. 10 m-thick black mudstones, lithological changes are observed; (1) alternating black mudstone and dolomitic carbonate layers, (2) black mudstone with less developed lamination, (3) pyrite-enriched black mudstone, and (4) rhythmically bedded black mudstone, and gradually turns into bedded greenish gray chert sequence. The overlying greenish gray cherts show red color in some place. We analyzed these mudstones and cherts by 57Fe Mossbauer spectroscopy, and identified six iron species, i.e., hematite, pyrite, two paramagnetic Fe3+, and two paramagnetic Fe2+ with different quadrupole splittings. About a quarter of iron content in the black mudstones consist of pyrite, and other component belong to paramagnetic Fe2+ or occasionally paramagnetic Fe3+. The overlying red cherts contain hematite as the main iron mineral. In the analyzed samples, hematite and pyrite never co-existed. The occurrence of hematite in deep-sea chert essentially indicates a primary oxidizing depositional condition, and that of pyrite a reducing one, respectively. The present results confirmed that a reducing condition persisted in the Neoproterozoic deep-sea through the interval of the black mudstone deposition. The overlying partly-red hematite-bearing cherts give evidence of recover from reducing to oxidizing condition before the arrival to the trench. Here we propose that the black mudstone in Llyen Peninsula shows the global-scale oceanic anoxic event during the Marinoan Snowball Earth, and name this event the 'Marinoan Superanoxia'. During the black mudstone deposition, the whole ocean may have turned into anoxic like the Permo-Triassic boundary Superanoxia; although further discussions for the depositional model based on other geochemical proxies are needed.

Japan Geoscience Union Meeting 2014
(28 April - 02 May 2014 at Pacifico YOKOHAMA, Kanagawa, Japan)

BPT27-16 Room:213 Time:April 28 17:30-17:45

Paleogeography of the Earth; Neoproterozoic

MARUYAMA, Shigenori[1*] ; ISOZAKI, Yukio[2]

[1]ELSI Tokyo Institute of Technology, [2]University of Tokyo

Neoproterozoic Earth was a transient state to bridge Precambrian mono-cellular world to Phanerozoic Earth of metazoans and plants. The snowball Earth from 770Ma to the onset of Cambrian time, was another environmental pressure to force the life evolution.

(1) Continent configuration

Supercontinent Rodinia was consolidated ca. 1.0Ga around the equatorial region, and began to be rifted in Neoproteorozoic. After ca.600Ma, it became fragmented by rising superplume in the center to give a birth of Pacific Ocean. Immediately after the fragmentation, continents were removed to the South Pole to assemble again to make a semi-supercontinent Gondwana by 540Ma.

(2) Environmental change

Owing to the leaking Earth (Maruyama and Liou, 2005; Maruyama et al., 2014), the rapid emergence of huge landmass caused the raid diversification of surface environment and birth of metazoans, as wells as algae evolution. Preceding to the Cambrian explosive evolution of life, the snowball Earth event which was a warm-cold fluctuation, GCR-triggered cloud cover, rapid sea-level change, nutrients supply, and probably wet and dry climate change, forced the rapid evolution of life. The first appearance of sponge was between Sturtian and Marinoan snowball Earth event, but the most explosive diversification of metazoans occurred between 540 and 520Ma.

Chemostratigraphy more than 10 were completed for the drilled cores in S. China and the detailed environmental changes were analyzed (Special issue in GR, 2014). Weakened paleomagnetic intensity caused severe radiation for the evolving life on the surface of the Earth.

(3) Life-evolution and mass extinction

By this reason, and presumably the rift volcanism related to atomic bomb magma caused local mass extinction to promote mutation-induced quick evolution to diversify life.

(4) Biomass, Ecosystem, mass extinction

Sr isotopic change recorded in platform carbonate clearly indicate the huge amount of nutrients supply for continents and sea-level drop caused the birth of paradise of metazoans on the continental visible platform with enough nutrients supply. A new diversified ecosystem was appeared.

The most extensive mass extinction occurred during the Ediacaran to Cambrian time, more than 10 times in this restricted period, from 635Ma to 488Ma.

(5) Role of Universe

This could be due to the starburst in our Milky Way Galaxy, and promoted volcanic eruption of atomic bomb magama along the continental rifts on the Rodinia and Gondwana.

Japan Geoscience Union Meeting 2014
(28 April - 02 May 2014 at Pacifico YOKOHAMA, Kanagawa, Japan)

BPT27-P01 Room:Poster Time:April 28 18:15-19:30

Spherules layer of the uppermost Triassic (Rhaetian) limestone sequence in the Kardolina section, Slovakia

SHIROZU, Hideko[1*] ; JOZEF, Michalik[2] ; KUSAKA, Soichiro[3] ; YAMASHITA, Katsuyuki[4] ; YAMASHITA, Misa[4] ; ONOUE, Tetsuji[1]

[1]Graduate School of Science and Technology, Kumamoto University, [2]Slovak Academy of Sciences, [3]Research Institute for Humanity and Nature, [4]Graduate School of Science and Technology, Okayama University

Triassic/jurassic (T/J) boundary of approximately 201 million years ago is known as a stratigraphic boundary recorded one of the big five Phanerozoic mass extinctions. Catastrophic processes such as widespread eruption of the Central Atlantic Magmatic Province (CAMP) flood basalts and extraterrestrial impacts have been proposed to account for the mass extinction event. Here we show the results of our analysis of enigmatic spherules in the Upper Rhaetian of the Kardolina section, Slovakia. The Kardolina section is situated on a steep western slope of the Mt Palenica in the Belianske Tatry Mts as the most continuous section of the uppermost Triassic (Rhaetian) Fatra Formation. The Fatra Formation is shallow marine carbonate sequence and is overlain with a sharp contact by marine shale of the lowermost Jurassic (Hettangian) Kopieniec Formation. The Kopieniec Formation consists of a sequence of brown claystone with sandtone and limestone intercalations. The position of the T/J boundary is constrained by foraminiferal assemblages.

The limestone sequence containing the spherules exists in the upper part of Fatra Formation. A negative δ^{13}C excursion and a positive δ^{18}O peak have been known from spherules layers. Analysis of the foraminiferal assemblages shoed the diversity of foraminifera have decreased in spherules layers. Spherules are found in at least six sedimentary layers in the Fatra limestone. The size of spherules is approximately 200-300 μm. Spherules are contained ˜10 % in the layers and the other component grains consist of lithoclasts, bivalves, and crinoids. These grains were relatively rounded and have reworked fabrics. The results of SEM-EDS analysis indicated that spherules were composed mainly of Si, Al and Mg, and contain small sulfide particles with Fe, Zn, and Cu. Such a geochemical composition was clearly different from ooids and peloids in Fatra Formation, though the origin of spherules in Kardolina section remains uncertain.

Keywords: Triassic/Jurassic boundary, Rhaetian, limestone, spherule, extinction

Japan Geoscience Union Meeting 2014
(28 April - 02 May 2014 at Pacifico YOKOHAMA, Kanagawa, Japan)

BPT27-P02 Room:Poster Time:April 28 18:15-19:30

Global paleogeography and life evolution: 1. Cenozoic

ISOZAKI, Yukio[1*] ; MARUYAMA, Shigenori[2]

[1]Univ. Tokyo/Dept. Earth Sci. & Astronomy, [2]Tokyo Inst. Technology/ELSI

Continental configuration in the Phanerozoic were synthesized, by the integration of not only continents and oceans, but also, plates, ridge-transform system, ocean current, desert, glacier, major rivers, plume-driven bulge, rifts, mountain belts, lakes, vegetation, and the location of first fossils appeared on the Earth. Methods employed here are as follows; plate reconstruction after Scotese (1996, 2002, 2008), for the oceans by Engebretson et al. (1985; 1992), Cogne and Humler (2006), and Seton et al. (2012), and OIB by Utsunomiya et al. (2008).

The Earth system has been changed drastically at 20 Ma under the strong influence by the internal phenomena of solid-Earth, in particular, by the generation of 410 km-depth swarm of hydrous plumes immediately above the ”2nd continents”. The Cenozoic is clearly divided into the two periods at ca. 20 Ma on the basis of the secular change in seawater Sr isotopic composition (Veizer et al., 1999). This sharp change reflects the increased material flux from continental crusts to ocean by the plume-driven topographic elevations and collision orogeny along the Himalayan-Tethyan domain all the way from Europe to Papua New Guinese. It should be emphasized that the former is nearly 10 times greater in magnitude than the latter. The uplifted regions include Tibet-East Asia, Rocky Mtn./Colorado plateau/Basin-and-Range/Rio Grande Rift in North America, and Middle America. The A-subdcution of the main S. America block caused the uplift of the Andean Mtn. The separation

of S. America from Antarctica was critical to have isolated Antarctica around the South Pole to have triggered the glaciation by virtue of cold-water circulation around the Antarctica.

The rapid glaciation both in Arctic and Antarctica started the Quaternary Period at 1.8 Ma, although the Cenozoic glaciation had already started on Antarctica back to 20 Ma. The ultimate cause of the Quaternary glaciation can be blamed to the encounter of our galaxy with a small ”dark cloud” since 20 Ma, and to that with nearby supernovae since 1.8 Ma. The low-temperature on the planet surface and the resultant glaciation was triggered likely by the increased galactic cosmic radiation (GCR) through the extensive development of cloud.

The appearance of the cold weather initiated two independent but critical driving forces for nutrient supply in ocean; i.e., cold-water formation in high-latitudes coupled with accelerated upwelling, and intensified the Hadley atmospheric circulation induced by the plume-driven development of topographic highs on-land closer to the altitude of basal stratosphere, as monitored by the secular curve of seawater Sr isotope ratio. As to the changes in ecosystem after the end-Cretaceous extinction, the promoted nutrients supply caused the increased volume of biomass and various biological innovations; e.g., replacemnt of radiolarians by diatom, the appearance of C4 plants etc. The collision of India against Asia, caused the species mixing between two continents. On the other hand, the resultant Tibetan uplift and birth of Asian Monsoon brought contrasting climate within Eurasia. The birth of human being along the Rift Valley in E. Africa ca. occurred 5-7Ma was caused likely by the episodic eruption of ”atomic bomb” magma along the prominent rift zone. In addition to the local mass extinction by radiations, this led the episodic human escapes from Africa into Eurasia in multiple times after 1.2 Ma.

Keywords: paleogeography, Cenozoic, Pacific Ocean, land bridge, evolution

Japan Geoscience Union Meeting 2014
(28 April - 02 May 2014 at Pacifico YOKOHAMA, Kanagawa, Japan)

G01-P01 Room:Poster Time:April 29 18:15-19:30

An experiment of tsunami-like flow through coastal vegetation designed for classrooms

LIU, Tzu-yu[1*] ; LIU, Chi-min[2] ; LIU, Ting-hsuan[1]

[1]Taipei Municipal Dunhua Elementary School, [2]Chienkuo Technology University

This paper present an experiment for simulating tsunami-like bores passing over coastal vegetations designed for being performed in classrooms. Easy experimental facilities are used to display and study which layout of coastal vegetations can greatly reduce the bore speed. An acrylic tank which is divided into two regions by a movable gate is used to generate a tsunami-like bore. At the downstream region, different layouts of acrylic cylinders are placed to simulate the planting of coastal vegetations. When the gate is suddenly removed, the water in the upstream regions will flow through cylinders and go outside of the open end of the tank. The longest distance of the flow out of the tank is measured by a video camera. Finally the longest distances of all layouts are compared to find out the best design of layout for reducing the flow speed. The experiment not only can be performed in classrooms, but also provides an insight to the role of coastal vegetations in disaster reduction.

Keywords: experiment for classrooms, tsunami-like flow, coastal vegetation, disaster mitigation

Japan Geoscience Union Meeting 2014
(28 April - 02 May 2014 at Pacifico YOKOHAMA, Kanagawa, Japan)

G01-P02 Room:Poster Time:April 29 18:15-19:30

Western classical music about ocean

LIU, Chi-min[1*] ; CHEN, I-chun[2]

[1]Chienkuo Technology University, [2]Taipei Municipal Xinyi Junior High School

The influence of ocean phenomenon on western classical music is preliminarily studied. Main purposes of this interdisciplinary study are to explore the corelation between natural ocean phenomenon and music elements and how they affect each other. Ocean phenomenon considered include the climate, wave conditions, coastal landform, and other natural events around or on the sea. For some specific music pieces, it is clear that all these phenomenon greatly influence the composers' moods and the music pieces they composed. Some music compositions specially in the 19th and the early 20th centuries will be introduced herein to elucidate the whisper between ocean and music. Finally, present idea may give a way for music teachers to include the ocean elements in their classes.

Keywords: western classical music, ocean phenomenon, interaction with ocean

Japan Geoscience Union Meeting 2014
(28 April - 02 May 2014 at Pacifico YOKOHAMA, Kanagawa, Japan)

G01-P03 Room:Poster Time:April 29 18:15-19:30

Mathematical tools for studying internal wave equations

LIU, Chi-min[1*]

[1]Chienkuo Technology University

For undergraduate students who are interested in physical oceanography, fluid mechanics, or wave dynamics, mathematical tools are basic and important to analyze and derive model equations and wave theories. In this paper, the derivation of internal wave equations is introduced as an example of using some mathematical tools. Two important techniques used are the perturbation analysis and the Pade approximation. Based on these techniques the long-wave equations for a two-fluid system are derived and analyzed. Some wave properties predicted by the model equations are also investigated. As mathematical tools play an important role in ocean studies, the teaching of these techniques is of great importance in classrooms.

Keywords: mathematical techniques, internal wave equations, perturbation analysis, Pade approximation

Japan Geoscience Union Meeting 2014
(28 April - 02 May 2014 at Pacifico YOKOHAMA, Kanagawa, Japan)

G02-01 Room:423 Time:April 29 14:15-14:30

Field Lectures at the Classroom sessions of The Open University of Japan

HAGIYA, Hiroshi[1*]

[1]Tokyo City University

Classroom Sessions (Schooling) of The Open University of Japan, is a good opportunity to outreach Earth Science in the context of Lifelong Learning Program. 4 field program planed and held at 3 Study Center, each program limited about 20 students to join, but there were 80 applicant in average. The student had a wide range in age and background, half of them were over 60, which belong hiking and climbing mountain lover generation, and often had knowledge about biology and other field of science. These multi dicipline field works set by biologist and geologist, is a suitable way to recognize how Earth Science is important for our life.

Keywords: Fieldworks, Open University of Japan, Lifelong Learning, Natural History

Japan Geoscience Union Meeting 2014
(28 April - 02 May 2014 at Pacifico YOKOHAMA, Kanagawa, Japan)

G02-02 Room:423 Time:April 29 14:30-14:45

Geological structure of the Kanto sedimentary basin ?An analog model-

TAKAHASHI, Masaki[1*]

[1]Geological Survey of Japan, AIST

The geologic history of the Kanto Plain, central Japan, is briefly introduced for the purpose of educational promotion of the geology and earthquake disaster prevention. Thick sediments were accumulated between Northeast and Southwest Japan during the Japan Sea opening (20-15 m.y. ago). The grabens and half-grabens were developed under extensional stress field during this stage. The topographic up-and-down structure in basement rocks was then covered by marine sediments widely from 15 m.y. until ca. 10 m.y. ago in the Kanto district. The tectonic deformation had been slight between 15 and 3 m.y. ago. However E-W contractive deformation has suddenly begun at 3 m.y. ago, and reverse-faulting and folding were started in the Japanese islands. The thick sediments below the Kanto Plain were then deformed and active faults, such as the Tachikawa Fault, were finally cut the surface. The scenario of this history is useful for interpretation of subsurface structure deduced from geophysical exploration.

Keywords: outreach, earth science, geology, educational promotion

Japan Geoscience Union Meeting 2014
(28 April - 02 May 2014 at Pacifico YOKOHAMA, Kanagawa, Japan)

G02-03 Room:423 Time:April 29 14:45-15:00

Gelatin experiments on magma ascent and eruption for outreach program

TAKADA, Akira[1*]

[1]AIST, Geological Survey of Japan

Analog experiments are useful for outreach program. We cannot see the inside of a volcano directly, though an eruption is caused by underground magma. I develop the see-through experiments to understand a process from magma system to eruption. Liquid-filled cracks are injected in gelatin under the stress field. We can examine the factors controlling magma ascent to eruption, such as density, viscosity, the physical properties of the earth, the stress field etc. I introduce several examples of the experiments: magma ascent to eruption, crack behaviors under the stress field, magma movement with bubbles, the crack interactions, two phase flows, crustal behavior in the liquid filled crack. These experiments were carried out at elementary schools, junior high schools, science museums, the open house in AIST, training course for school teachers in YIES, and lectures of university, the international training course of JICA, APEC, COV.

Keywords: outreach, volcanology, magma, eruption, analog experiment, dike

Japan Geoscience Union Meeting 2014
(28 April - 02 May 2014 at Pacifico YOKOHAMA, Kanagawa, Japan)

G02-04 Room:423 Time:April 29 15:00-15:15

GANSEKI as an educational material: Application of JAMSTEC deep seafloor rock sample database

TOMIYAMA, Takayuki[1*] ; SOMA, Shinsuke[2] ; HORIKAWA, Hiroki[1] ; FUKUDA, Kazuyo[1] ; ICHIYAMA, Yuji[1]

[1]Japan Agency for Marine-Earth Science and Technology, [2]Marine Works Japan, Ltd.

On the basis of Data-Sample Handling Policies of the Japan Agency for Marine-Earth Science and Technology (JAMSTEC)[1], data and samples obtained during research cruises of JAMSTEC vessels are treated as common properties of the human community; data and samples are stored and publicized to the public for second-hand uses with research/educational purposes. After two-years of moratorium period during which on-board researchers and colleagues have a priority to use data and samples, information on data and samples are disclosed through JAMSTEC data sites, and are utilized for foreign/domestic activities of research, education, press report and public relation.

JAMSTEC vessels collect several hundreds of rocks from the deep seafloor each year. These rock samples and associated data are also subject to be publicized. Sampling information and associated data of rock samples are accessible from the website "Deep Seafloor Rock Sample Database (GANSEKI)[2]". Currently, GANSEKI exhibits information of more than 19,800 entries of JAMSTEC rock samples including inventory information of ~9,000 actually available samples, and geochemical data and literature information of JAMSTEC/non-JAMSTEC rock samples.

After the major update in 2013, minor system tuning and data maintenances have been applied to GANSEKI. Now GANSEKI is attracting general educators and students, as well as limited number of research specialists. New GANSEKI search system allows complex filters for screening samples to support various users with different purposes. Improvements on sample/thin-section photo view allow users to effective data handling using visual information.

JAMSTEC maintains several data sites other than GANSEKI. Some of these data sites are linked together so that users can utilize data more effectively. Users can come-and-go between GANSEKI and "Data Research System for Whole Cruise Information of JAMSTEC (DARWIN)[3]" to pick up rock sample information in GANSEKI and associated information in DARWIN, such as cruise/dive information, geophysical observation data, cruise reports and literature information. Rock sample information in GANSEKI is also linked to dive movies/photos in "JAMSTEC E-library of Deep-sea Images (J-EDI)[4]", and users can comfortably look into sampling scenes of interested rock samples and surrounding geology.

GANSEKI users can now access to massive online data, which are almost comparable to those provided to onboard researchers. Disadvantages for second-hand users are getting smaller and these users can perform more practical research/educational activities. GANSEKI can be utilized not only for mineralogical/petrological purposes, but also for other various purposes, such as surveys of contemporary activities in ocean geology, case studies for observation data handling or online database system, and so on.

References: [1] "JAMSTEC Basic Policies on the Handling of Data and Samples" http://www.jamstec.go.jp/e/database/data_policy.html. [2] "Geochemistry and Archives of Ocean Floor Rocks on Networks for Solid Earth Knowledge Information (GANSEKI)" http://www.godac.jamstec.go.jp/ganseki/e. [3] "Data Research System for Whole Cruise Information in JAMSTEC (DARWIN)" http://www.godac.jamstec.go.jp/darwin/e. [4] "JAMSTEC E-library of Deep-sea Images (J-EDI)" http://www.godac.jamstec.go.jp/jedi/e.

Keywords: rock sample, curation, on-line database, outreach, marine geology

Japan Geoscience Union Meeting 2014
(28 April - 02 May 2014 at Pacifico YOKOHAMA, Kanagawa, Japan)

G02-05 Room:423 Time:April 29 15:15-15:30

Quaternary Scientific Programs for School and Lifelong Education of Kikai Island located in the Amami Islands, Japan

OGATA, Takayuki[1*]

[1]Faculty of Education, University of the Ryukyus

The Amami and Okinawa Islands show active tectonics indicated by uplifted marine terraces consisting mainly of raised coral reefs. Especially, Kikai Island shows a rapid rate in uplift (reaches 1.8 m/ka) due to subduction along the Ryukyu Trench. This study arranges geoscientific contents and produces a geostory for school and lifelong educational programs of Kikai Island. The geostory focuses groundwater springs, limestone caves, uplifted terraces (uppermost surface is 214 m) and coral stones, and highlights geomorphic processes characterized by the most rapid uplift in Japan and a hydrologic cycle in the Quaternary limestone region. This geostory was repeated and practiced in half-day geotour targeting undergraduate students and residents of Kikai including high school students. Their comments suggest the significance and the interest on field observation of local landscape related with a global geoenvironmental system.

Keywords: Quaternary, limestone, geostory, geotour, Kikai Island, Amami Islands

Japan Geoscience Union Meeting 2014
(28 April - 02 May 2014 at Pacifico YOKOHAMA, Kanagawa, Japan)

G02-06 Room:423 Time:April 29 15:30-15:45

Educational Approach for Risk Reduction in Himalayan Seismic Zone I -Bridging the Gap Between Knowledge and Practice-

KIMURA, Motoko[1*] ; ADACHI, Tomoyuki[2] ; HANAOKA, Naoya[2] ; TAKAMINE, Ryo[2] ; KATO, Airi[2] ; BETSUYAKU, Shoichi[2] ; ITO, Takamori[3] ; KOKETSU, Kazuki[1] ; OKI, Satoko[2]

[1]Earthquake Research Institute, University of Tokyo, [2]Faculty of Environment and Information Studies, Keio University, [3]Graduate School of Media and Governance, Keio University

How can we encourage people to take preventive measures against damage risks and empower them to take the right actions in emergencies to save their lives?

The conventional approach taken by scientists had been disseminating intelligible information on up-to-date seismological knowledge. However, it has been proven that knowledge alone does not have enough impact to modify people's behaviors in emergencies (Oki and Nakayachi, 2012). On the other hand, the conventional approach taken by practitioners had been to conduct emergency drills at schools or workplaces. The loss of many lives from the Great East Japan Earthquake and Tsunami has proven that these emergency drills were not enough to save people's lives, unless they were empowered to assess the given situation on their own and react flexibly.

Our challenge is to bridge the gap between knowledge and practice. With reference to best practices observed in Tohoku, one of which is known as "*The Miracles of Kamaishi*," our endeavor is to design an effective Disaster Preparedness Education Program that is applicable to other regions in the world, even with different geological, socio-economical and cultural backgrounds.

The two key concepts for this new approach are "community-based understanding of disaster risks" and "personal empowerment to take preventive actions." This approach requires collaboration and participation from people from diverse fields of expertise, cultures, and generations, touching on interdisciplinary areas of study including seismology, geology, community development, education and psychology.

In this presentation, we will introduce how we designed the programs and activities for disaster preparedness workshop held at a high school in the Lesser Himalayan Region in North India,under an Indo-Japan collaborative project[i], and share good practices and lessons learned from this experience.

[i]Project on Information Network for Natural Disaster Mitigation and Recovery (DISANET) http://disanet.interliteracy.info/about/?lang=e

Keywords: Disaster Preparedness Education, International Cooperation, Hazard Map Making, Workshop

Japan Geoscience Union Meeting 2014
(28 April - 02 May 2014 at Pacifico YOKOHAMA, Kanagawa, Japan)

G02-07 Room:423 Time:April 29 15:45-16:00

Educational approach for risk reduction in Himalayan seismic zone II -Hazard map making workshop at a high school

KATO, Airi[1] ; BETSUYAKU, Shoichi[1] ; HANAOKA, Naoya[1] ; TAKAMINE, Ryo[1] ; ADACHI, Tomoyuki[1] ; KIMURA, Motoko[2] ; KOKETSU, Kazuki[2] ; ITO, Takamori[1] ; OKI, Satoko[1*]

[1]SFC, Keio University, [2]Earthquake Research Institute, Univ. of Tokyo

The 2011 Great East Japan Earthquake confronted us with the fact that the knowledge of science alone would not motivate someone take preventive action. This indicates that risk reduction cannot be completed only by hazard assessments but also by motivating people to take preventive action.

With the concept of ”community-based understanding of disaster risks” and ”personal empowerment to take preventive action”, we held a workshop at a high school in the Lesser Himalayan Region. The workshop consists of 2 sessions; 1) understanding the scientific backgrounds of earthquakes and disasters, and 2) hazard map making. Prior to the workshop, we carried out a questionnaire survey to high-school students about how they perceive the risk of the local hazard. After the first session, we provided about an hour of question time, and carefully analyzed what they said. Together with the answers of the questionnaire, it is strongly implied that they understood scientific backgrounds but do not have awareness of disaster and are not motivated to take preventive action.

Session-2 consists of several parts such as giving clear images of earthquake consequences, leading them to imagine each victim’s life that was broken up all of the sudden on March 11th 2011 as well as showing hot to find out and manage risks by making hazard map. The workshop was closed with their presentation that clearly shows the internal change of the participants. Many of them referred to the importance of lives such as ”Life is a precious gift to us from God. Don’t take it as a fun. And if you take it as a fun, then remember your family.”

In the presentation, we share the good practice that can be applied to other disaster-prone countries if we pay regard to the community-based understanding of disaster risks.

Keywords: disaster prevention, earthquake, hazard map

Japan Geoscience Union Meeting 2014
(28 April - 02 May 2014 at Pacifico YOKOHAMA, Kanagawa, Japan)

G02-08 Room:423 Time:April 29 16:15-16:30

Educational Materials for the Community-based Understanding of Disaster Risks -Taking Advantage of four-frame Cartoon

SAITO, Aya[1*] ; OKI, Satoko[1]

[1]SFC, Keio University

One of the lessons from the 2011 Great East Japan Earthquake is that educational approach to prevent natural disasters can compensate the limitations of earthquake science and technologies. Hereinafter we call it as ”BOSAI education”. BOSAI can be translated as disaster prevention based on individual awareness of disaster risks and leading to personal empowerment to take preventive action. After the earthquake, more schools started to conduct BOSAI education, while the government had not provided schools with certain time, textbooks, and curriculum guidelines.

As well as learning how to react to protect lives at the moment, one of the goals of BOSAI education for mid-school students is to deal with a dilemma situation that may take place afterwards. We provided a BOSAI educational material to take up the situation of evacuation site to ask students how to distribute aid supply if the total number is less than that of evacuees. The educational material is made as a four-frame cartoon as follows: 1) 12 hours after the earthquake at an evacuation site... 2) Person1: ”There arrived 100 of aid supply!”, 3) Person2: ”What? We have 500 people here.” 4) Person1: ”Mmm... ”. Students have to give an appropriate line that follows ”Mmm...” Some of the answers were ”We should put a priority to elderly persons and small kids” or ”Why don’t we ask for cooperation to those who brought their own emergency supplies in their backpacks?”

Another point of great importance of this material is to let the local school teachers join and share. We asked for advice to improve the material, and collected comments and suggestions. Some said they will have another class with the improved material. They can arrange the contents to bring community-based understanding of disaster risks. In the presentation, we share the material and report good practices.

Keywords: disaster prevention, education, earthquake, tsunami, evacuation site, mid-school

Japan Geoscience Union Meeting 2014
(28 April - 02 May 2014 at Pacifico YOKOHAMA, Kanagawa, Japan)

G02-P01 Room:Poster Time:April 29 18:15-19:30

Analog model of basement structure below the Kanto Plain

TAKAHASHI, Masaki[1*]

[1]Geological Survey of Japan, AIST

It is commonly discussed the difficulties on promoting the geologic results for the students as well as citizens. To solve this problem, I made three-dimensional analog model of basement structure below the Kanto Plain. The horizontal scale of model is 1/200,000 but vertical scale is emphasized as 400%. Because the model was painted by gradations in color from yellow (Shallow) to dark blue (deep), it can be easily recognized the contrast between subsurface steep precipice and gentle slope of basement structure. Among them, the Tachikawa Active Fault is characterized by sharp drop of basement depth below the Kanto Plain. Thus the analog model of basement structure below sedimentary basin would be helpful to understand why long-period ground motion is amplified in the sedimentary plain.

Keywords: outreach, earth science, geology, educational promotion

Japan Geoscience Union Meeting 2014
(28 April - 02 May 2014 at Pacifico YOKOHAMA, Kanagawa, Japan)

G02-P02 Room:Poster Time:April 29 18:15-19:30

How does the understanding of volcano advance? ; An example from the experiment on forming stratovolcano

KASAMA, Tomohiro[1*]

[1]Kanagawa prefectural museum of natural history

Experiment on Polygenetic stratovolcano using waste food oils and colored sands (Kasama et al. , 2010) was demonstrated at grade schools to high schools in Kanagawa prefecture and Shizuoka prefecture. Two cross section pictures of stratovolcano were drawn by many students. One is a imagination sections before experiment and another is a sketches after experiment. These pictures were divided into several types by inner stratigraphy (Kasama, 2012a) and had a tendency corresponding to age (Kasama, 2012b). Furthermore, many educational practices have done from 2012 to 2014. Many data from 1409 people have obtained. According to the result, it becomes clear that the tendency corresponding to age, residential area and scientific interest of volcano, especially Mt. Fuji. The experiment type (ET) was drawn by lines changed from lower horizontal lines to upper tilted lines. ET was found in the experimental stratovolcanoes and was considered to be exact depiction. Textbook type (TT) was drawn by piling similar triangles. Horizontal type (HT) was drawn by horizontal lines like stratum (Kasama, 2012a).

Fig.1 shows a relation between horizontal type drawn before experiment (HTB) and experimental type drawn after experiment (ETA). They had negative correlation. ETA indicates observation capability. ETA increases with age. HTB indicates misunderstood prior knowledge. Misunderstanding was thought to be caused by the education of the stratum of the 6th grader. Because HTB was not so high at the 3th to 4th grader, but the 6th grader was highest of all. There was found no HTB in a science club which consisted high school and junior high school students, Kanagawa. But, teachers of elementary school of Kanagawa drew same HTB, and ETA did not beyond the high school students. It is an important problem that we must think about.

TTB and ETA had correlation. TTB indicate right back ground but it is not so exact. ETB and ETA also had correlation. ETB is thought to be the best expectation, but its proportion was low.

How to write outside slope lines of stratovolcano is divided into three types. Simple straight lines (SL) which like the side slopes of a scoria cone, convex curves (CV) which like the side slopes of a lava dome and concave curves (CC) which are suitable for the slopes of a stratovolcano. Ratios of three types were not so much depended on age, but heavily depended on arias in which students live. Many students living in Shizuoka prefecture wrote concave curves before experiment (CCB). A high school at Shimizu, Shizuoka indicated the highest CCB ratio. It was thought that students can see Mt. Fuji and its frank easily.

References

Tomohiro Kasama, Daiji HIRATA, Shuichi NIIDA, Hiroyuki YAMASITA and Saeko ISHIHAMA (2010) Development of Experiment on Polygeneteic Volcanoes Using Waste Food Oils. Earth Science Education, 63, 5.6, 163-179.

Tomohiro KASAMA (2012a) Cross sections of stratovolcanoes drawn by sixth grader. Japan Geoscience Union Meeting 2012, G02-P-9, Chiba.

Tomohiro KASAMA (2012b) Cross sections of experimental stratovolcanoes drawn by students of various age. The Geological Society of Japan Meeting 2012 Osaka, R19-O-8.

Keywords: experiment, stratovolcano, cross section, Mt. Fuji, children and students, teachers

G02-P02 Room:Poster Time:April 29 18:15-19:30

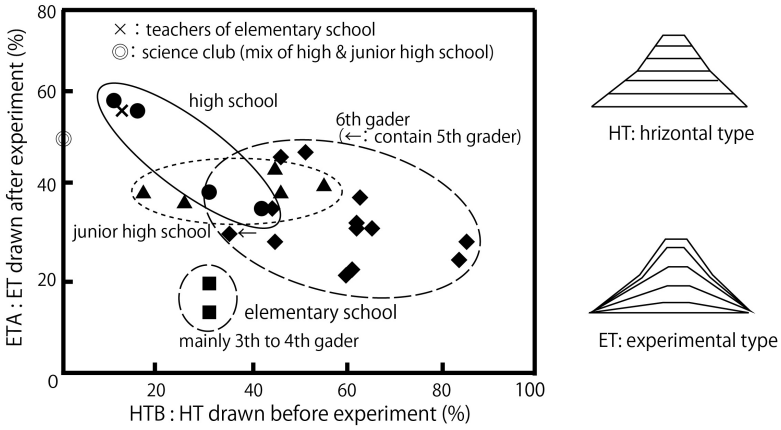

Fig.1 An analysis of pictures, showing a correlation between HTB and ETA.

Japan Geoscience Union Meeting 2014
(28 April - 02 May 2014 at Pacifico YOKOHAMA, Kanagawa, Japan)

G02-P03 Room:Poster Time:April 29 18:15-19:30

3D visualization and outreach of subsurface geological information using multi-layered miniature produced by 3D plotter

SHIBAHARA, Akihiko[1*]

[1]Geological Museum, National Institute of Advanced Industrial Science and Technology

In recent years, people can access to geological information quickly and easily with the help of information technologies. However, it is difficult to recognize three dimensional distribution of geological structure without professional training of map reading. To solve this problem, several techniques were established to build up finely-detailed miniature with rapid prototyping and projection mapping. There are extremely small contours on the surface of the miniature. These contours are used for marker to calibrate projection. This miniature, called Highly realistic Projection system (HiRP system) is used for outreach and research activities in museums, schools, geoparks etc.

I, the present writer, will report about 3D visualization about subsurface geological information using multi-layered miniature. A number of geological datasets, such as borehole datasets, 3D subsurface structure model published by Geological Survey of Japan (GSJ) are also used to modeling interior structure of the model. I will also report about interactive miniature coupled with GIS, and global trends in rapid prototyping.

Keywords: Geological information, 3D model, Rapid prototyping, Projection mapping, 3D plotter, Geopark

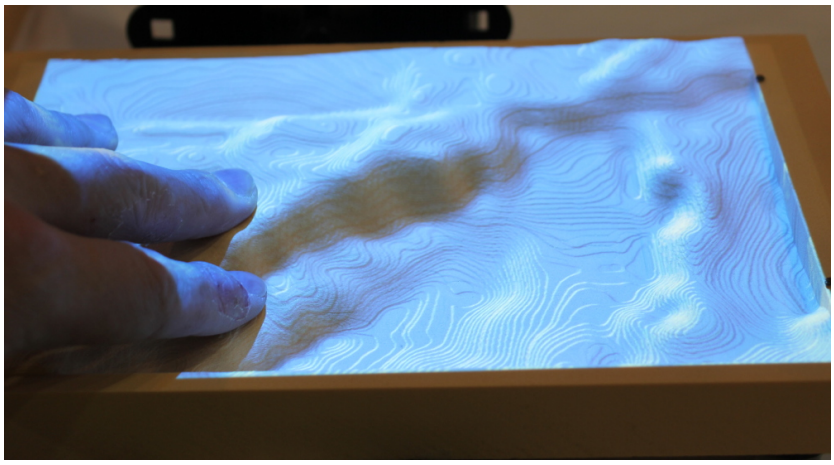

Japan Geoscience Union Meeting 2014
(28 April - 02 May 2014 at Pacifico YOKOHAMA, Kanagawa, Japan)

G02-P04 Room:Poster Time:April 29 18:15-19:30

Benefit of intergenerational course training as a ”Science Seminar” in earth science

KUSANO, Yuki[1*] ; NISHIYAMA, Maki[2] ; NAKANO, Michika[2] ; DOI, Kohei[3] ; IGARASHI, Yuriko[4]

[1]Kanazawa University, [2]Niigata University, [3]Tohoku Gakuin University, [4]Niigata Seiryo University

A science outreach program ”Science Seminar” has been given to junior and senior high school students by graduate students in Niigata University since 2009. We will present an effective age to educate earth science exhibited by statistics of questionnaire and how the intergenerational course training is arranged in the science seminar.

Keywords: Delivery lesson, Graduate student, Earth science for junior high school students, Career education for young scientist

Japan Geoscience Union Meeting 2014
(28 April - 02 May 2014 at Pacifico YOKOHAMA, Kanagawa, Japan)

G02-P05 Room:Poster Time:April 29 18:15-19:30

How should the outreach activity for the earth and planetary sciences be promoted?

CHIBA, Takashi[1*] ; YAMADA, Kentaro[2] ; SATO, Kenji[3] ; YUKI, Asuka[4] ; OSHIMA-YAMADA, Yui[5]

[1]Faculty of Life and Environmental Sciences, Univ. of Tsukuba, [2]Grad. Sch. Of Arts and Sciences, the Univ. of Tokyo, [3]KRI International Corp, [4]ex-Musashino Art Univ, [5]Grad. Sch. of Biosciences and Biotechnology, Tokyo Institute of Technology

The earth and planetary sciences cover various scientific and technological fields so that it is clear that the earth and planetary sciences are one of the most important fields of academic study for the society, and meanwhile the public is responsible for them. Many outreach activities have been held, and interactive ways have been especially remarkable in this decade. The communication which is mediated with scientific knowledge and perspectives is called as ”Science Communication”. Science Communication is not only the enlightenment of science by academic groups for the public but also the role for picking up the voice of the public. The context for Science Communication has been changed over time, therefore, it is more important how the Science Communication should be promoted as needed than why it should be. However, the schematic concepts for Science Communication less have been established.

We ”Universal Earth” have hypothetically proposed the concept of Science Communication and verified it through the science events. Science Cafe is one of useful ways to promote Science Communication with the available facilities and also it is one of the largest number of events are held in Japan. However, Science Cafe is just one way of Science Communication so that we had another symposium to discuss how Science Communication should be promoted and what we can do with other Science Communication tools.

In this presentation, we report the conclusions of the Science Cafe and the symposium about Science Communication held in 2013. We hope our presentation generate the discussions.

Keywords: Outreach, Science Communication, Science Cafe

Japan Geoscience Union Meeting 2014
(28 April - 02 May 2014 at Pacifico YOKOHAMA, Kanagawa, Japan)

G02-P06 Room:Poster Time:April 29 18:15-19:30

Delivery lecture for elementary school students with hand auger boring

KOMORI, Jiro[1*] ; MORIBE, Tatsuhiko[2] ; TAKAHASHI, Akira[3] ; TOYODA, Jyunko[4]

[1]Teikyo Heisei University, [2]Myoeizan Honoji, [3]Japan Geotechnical Consultants Association, [4]Road and highway bureau, Yokohama city

In order to awareness building of earth and environment science for elementary school students, we conducted outdoor practices as a delivery lecture at a Buddhist temple on the Toshima upland (the Musashino I surface), Tokyo. The first lecture in the summer of 2012 was unsuccessful due to miss allocation of time and excessive schedule of study topic with indoor lecture. Even an auger boring using handy soil corer(hand auger LS-3 series, Sanyo testing machines Co. ltd.) took 3 hours, despite that the work was carried out by four adults. In the aftermath, the students could not advance sample treatment and description works, and finding ground water.

In the summer of 2013, the schedule focused on the boring, sample treatment and measurement. As a result, students experienced the following subject; boring work in 4 meters in depth, sample description, measurement of soil color and temperature, verification of ground water. The answers of the questionnaire after the lecture shows the students amazed a variety of characteristics of geology and environmental study and long history of the earth which were recorded at under their foot. We are planning further lecture and boring at the temple in next year.

Keywords: earth science education, summer homework, core description, the Kanto loam, soil temperature, ground water

Japan Geoscience Union Meeting 2014
(28 April - 02 May 2014 at Pacifico YOKOHAMA, Kanagawa, Japan)

G02-P07 Room:Poster Time:April 29 18:15-19:30

Approach to the improvement of the field work

KITAYAMA, Tomoaki[1*] ; KOMORI, Jiro[3] ; IIDA, Kazuya[2] ; GEO EDUCATION, Member[4]

[1]JAMSTEC, [2]Tokyo Institute of Technology, [3]Teikyo Heisei Univ, [4]Geo Education

We started up a new project " Geo Education " in 2012. This project purpose is increase awareness for geo-scientific education in elementary and secondary level through field excursions. In other words, it is the knowing the earth by touching and seeing the real. The members consist of scientist, engineer, teacher and university students specialize in earth science. It is probably new activity which prepares the operation methods and the instructor cooperation with the school.

In 2012, we held the field excursions with two junior high schools in Tokyo. Through the two field excursion, we will clarify figuring out of field materials and future problems involved. In 2013, we did activities about the development of field materials to the improvement of the field excursions.

In this presentation, we will introduce our project " Geo Education " and report the results and problems on this year's activities.

Keywords: Geoscience education, field materials, field excursion, awareness activity, elementary and secondary level

Japan Geoscience Union Meeting 2014
(28 April - 02 May 2014 at Pacifico YOKOHAMA, Kanagawa, Japan)

G02-P08 Room:Poster Time:April 29 18:15-19:30

Outreach activities of AIST for geothermal energy, 2013: simple paper materials

MIZUGAKI, Keiko[1*] ; YOSHIOKA, Mayumi[1] ; YANAGISAWA, Norio[1] ; SAWAKI, Takayuki[1] ; UCHIDA, Youhei[1] ; SAKAGUCHI, Keiichi[1] ; YASUKAWA, Kasumi[1]

[1]AIST

We developed a pen-and-paper game to study verious uses of geothermal enengy in 2012, and reported it in last JpGU meeding (Mizugaki et al., 2013). In 2013, we developed an additional material, a simple paper model illustrating cascade use of geothermal energy.

These materials are used in following outreach events:
AIST Tsukuba open house 2013
Geoscience Exhibition in Miyagi 2013

Keywords: outreach, geothermal energy, paper model, pen-and-paper game

Japan Geoscience Union Meeting 2014
(28 April - 02 May 2014 at Pacifico YOKOHAMA, Kanagawa, Japan)

G02-P09 Room:Poster Time:April 29 18:15-19:30

An Evaluation of Sieving Effect of Volcanic Ash Fine Particles by A Statistical Particles Image Analysis

HAYAUCHI, Aiko[1*] ; SASAKURA, Daisuke[1]

[1]Malvern instruments A division of Spectris Co., Ltd.

1. Introduction

The analysis of particle size and shape characterization is an important evaluation of volcanic ash. It is well known that particles size and shape is one of dominant parameter of volcanic ash for flowability, flying property and abrasively. A sieving is used for particle size analysis of volcanic ash as common method. However, particle has possibility to have shape effect when it goes on through mesh of a sieve. In conventionally, a manual microscope approach has been used for few number of particles shape observation. It is not able to described particle shape as significant number. On the other hand, a fine particle characterization of volcanic ash (less than 50μm) has also importance to hazard protection issue which is a fine particle has possibility to long duration time in air. Our group has reported particle characterization and classification of a volcanic ash fine particle using by images for the purpose of determining particle size distribution which is based on described in ISO13322. The particles are appropriately dispersed and fixed on an optical microscope implemented a fully automated sample stage and an automated real time particle image analysis function on software. This report will be discussed for effect of sieving and precise classification against volcanic ash fine particle by a statistical particle image analysis.

2. Material and method

In this study, the volcanic ash was sampling from Ito flow in Kagoshima. This sample was already filtered coarse particles before, and sieved by a analytical sieve (TOKYO SCREEN CO.,LTD), these mesh size were 75μm, 50μm, 32μm. It was passed to 75μm, 50μm and only trapped on 32μm. As a statistical particle image analysis, Morphologi G3-SE (Malvern Instruments) was used for evaluation of particle size and shape. The observation mode was diascopic mode (Transmittance mode) and magnification was 100x in total magnification. The sample was dispersed with SDU (Sample Dispersion Unit) which attached Morphologi G3-SE. Number of measured particles was 120,000 and a parameter filter function on software was used based on shape and pixel number of particle image.

3. Result

A classification based on sieving were under 32μm sample (sample 1), over 32μm sample (sample 2) and no pretreated sample (sample 3). Those samples were analyzed on over 60,000 particles by statistical particle image analysis. As a result, Number Based Circle Equivalent Mean (NCED Mean) was 8.7μm (sample1), 13.9μm (sample 2) and 9.6μm (sample 3) on each. However, 510 particles of over 32μm particles were detected in sample 1. It was assuming from this result that shape effect happened. Therefore the result of focus on over 32μm particle to consideration of more precise classifications was shown in Table 1. This result showed sample 1 was the most elongate in the same size particles. Intensity Mean (IM) is reflected to sample thickness and transparency. High IM particles are tin particles or glass like particles in normally. Therefore, it can possible to classification glass liked particle or non glass like particle in volcanic ash based on IM parameter. According to results, sample 1 was most of including a glass like particle in amount of particles (Table 2, Fig 1).

4. Conclusions

In summarize of this study, it was clarified particle shape effect against sieving.This report will be more discuss about application and capability of numerical definition of volcanic ash by the statistical particle image analysis as new approach for this research area.

Keywords: Volcanic ash, Particle size, Particle shape, Particle image analysis, Sievng

G02-P09 Room:Poster Time:April 29 18:15-19:30

Table 1: Each Class Data

Class	sample	Number of particles	CE Diameter Mean (μm)	Aspect Ratio Mean
Class 1 (32~37um)	sample 1	357	34.8	0.62
	sample 2	3,540	34.6	0.65
	sample 3	991	34.4	0.64
Class 2 (37~42um)	sample 1	115	39.8	0.55
	sample 2	4,046	39.5	0.66
	sample 3	633	39.3	0.63
Class 3 (over 42um)	sample 1	38	45.2	0.52
	sample 2	4,910	47.0	0.62
	sample 3	578	46.6	0.59

Table 2: Intensity Mean by Class

class	sample	Mean Intensity	Intensity mean > 80	
			Number	%
class 1 (32~37um)	sample 1	59	138	39%
	sample 2	61	882	25%
	sample 3	54	306	31%
class 2 (37~42um)	sample 1	63	54	47%
	sample 2	57	1,558	39%
	sample 3	56	239	37%
class 3 (over 42um)	sample 1	70	24	63%
	sample 2	68	2,857	58%
	sample 3	68	352	61%


High intensity (glass like) particle

Low intensity (no glass like) particles

Figt: Picture with intensity mean

Japan Geoscience Union Meeting 2014
(28 April - 02 May 2014 at Pacifico YOKOHAMA, Kanagawa, Japan)

G02-P10 Room:Poster Time:April 29 18:15-19:30

Primary environmental radioactivity education

ENDO, Misaki[1*] ; YAMANAKA, Masanori[2]

[1]College of Science and Technology, Nihon University, [2]College of Science and Technology, Nihon University

The physics of radioactivity or the radiation has very close relation to developments of physics from the beginning of the 20th century. The human being does not have an organ taking in radioactivity directly, which is different from visible light, hearing, temperature, and the taste. The radioactivity is an extremely mysterious phenomenon historically in this way, and this is why the elucidation was pushed forward. In addition, the radiation is statistical phenomenon because radiation is a phenomenon caused by an atomic nucleus change and an electronic state change of the atom. However, this historically important and mysterious phenomenon is not almost taught in a beginning class or the secondary education. It is only handled for a last unit in physics II of the high school. A public, who did not learn physics about the radioactivity and who experienced the nuclear power plant accident that it follows East Japan great earthquake disaster of 2011, face the radioactivity. As a result, confusion occurred about intuitive and sensible understanding about the radioactivity. On the basis of the above-mentioned background, we make a teaching plan about the beginning class in the radioactivity education and report the result that we practiced in high school and university cooperation educations.

Keywords: Radioactivity education

Japan Geoscience Union Meeting 2014
(28 April - 02 May 2014 at Pacifico YOKOHAMA, Kanagawa, Japan)

G02-P11 Room:Poster Time:April 29 18:15-19:30

Investigation of disaster memorials of the 2005 Fukuoka Earthquake and the 1982 Nagasaki Flood

YAMADA, Nobuyuki[1*] ; SONODA, Hana[1]

[1]Fukuoka Univ. of Education

After the huge tsunami disaster of 2011, the existence such as the monuments which ticked away the teaching of the ancestor who conveyed a disaster was performed a close-up of in each place. The history of the past valuable teaching and disasters such as monuments might be forgotten with time. Therefore, it is an opportunity to raise disaster prevention awareness to convey history of disaster and a disaster sign.

We investigated the disaster memorials of the 2005 Fukuoka Earthquake and the 1982 Nagasaki Flood. We surveyed in 24 sites around Fukuoka and 23 sites around Nagasaki, we was able to confirm some disaster memorials. And we made the map which could take a walk through these damage traces.

Keywords: 2005 Fukuoka Earthquake, 1982 Nagasaki Flood, Disaster memorials

Japan Geoscience Union Meeting 2014
(28 April - 02 May 2014 at Pacifico YOKOHAMA, Kanagawa, Japan)

G02-P12 Room:Poster Time:April 29 18:15-19:30

The Earthquake-making Event of Meteorological Research Institute

KIMURA, Kazuhiro[1*] ; KOBAYASHI, Akio[1]

[1]Meteorological Research Institute

The Otenki-Fair at Tsukuba has been conducted in every August by Meteorological Research Institute, Aerological Observatory, and Meteorological Instrument Center. The Earthquake-making Event is one of the exhibitions in the Otenki-Fair. Participants jump on the floor 1 m away from a seismometer, then calculated magnitude will be displayed on the screen of a PC. The magnitudes usually range from -4 to -6. This event is popular with children.

The software for the Earthquake-making Event worked on a PC9801 computer by a program written in N88BASIC. Because a long time has passed since the cessation of production of PC9801, this event faced possible discontinuance due to hardware trouble. Therefore we transplanted the program into VisualBasic to continue the event with current Windows machines. At the poster meeting place, we will demonstrate the event.

Keywords: event, earthquake, magnitude

Japan Geoscience Union Meeting 2014
(28 April - 02 May 2014 at Pacifico YOKOHAMA, Kanagawa, Japan)

G02-P13 Room:Poster Time:April 29 18:15-19:30

”Listen to the sound of earthquake!” - Experiment of sonificated seismic wave in public relations events

HAYASHI, Yutaka[1*]

[1]Meteorological Research Institute

Meteorological Research Institute (MRI) located in Tsukuba city carries out an annual public relations event titled ”Otenki Fare Tsukuba” on a weekday during the summer school holiday. Every event has two to three thousands visitors mostly from Tsukuba city or neighbor cities. Typical visitors are a group of school child(ren) and their mother. This event is a good opportunity for MRI not only to appeal its research activities but also to diffuse basic knowledges widely on weather, earthquakes and so on.

Edutainment titled ”Listen to the sound of earthquake!” has developped (Hayashi and Takayama, 2009; *QJS*), by which we can hear a sound of any earthquake selected from a menu. The substance of the edutainment is just a presentation file created by Microsoft PowerPoint(R); and interactive operating environment with a menu is realized by using PowerPoint’s functions of slide-show and animation. Therefore, the file can easily be modified by other technicians than the author.

The contents, or various sounds of earthquakes, are WAVE-formatted sound data produced by 10 - 1000 times fast-forwarding using actually observed seismograms. The process, which assume that seismograms are time-series of compression wave transmitted in the air, sacrifices the physical accuracy, but the process without accompanying frequency modulation conserves the scaling law of the sound source; and then, we can feel a material of the source of ”sounds of earthquakes” by listening differences of pitches, intensities and tones. The edutainment intends to make listeners understood on the existence of the diversity of earthquake based on various type of earthquake. By the way, ”sounds of deep low frequency earthquake”, which were processed by the same method as above, were used in the TV program of NHK titled ”Megaquake III” in 2013 so that the difference of source mechanism between slow earthquakes and ordinary ones were explained.

”Listen to the sound of earthquake!” has been displayed for one of the attractions in ”Otenki Fare Tsukuba” every year since 2007. Its display and contents have been improved; the line out from each personal computer (PC) is now divided into three headphones, in order to match the requirements of number of visitors increasing year by year, and the typical guests consisting of a mother and two children; in addition, contents has replaced after the occurrence of major earthquakes.

However, there are still several problems remained. The first one is that 45-seconds experience is too short for most primary school children to feel the diversity of earthquake, which the edutainment want to teach them, from listening their sounds. They just simply enjoy and end. The second one is that the interface using mouse and selecting contents from the displayed menu is becoming user-unfriendly for children in the age of smart phones and tablet PC. The last one is essentialness of multi-language interface.

In the JpGU2014 meeting, PCs installed ”Listen to the sound of earthquake!” will be displayed, after experiment, discussions on possible improvements and application to other public relations event will be welcomed.

Keywords: diversity of earthquake, edutainment, elementary school children, PowerPoint, sonification of seismic wave

Japan Geoscience Union Meeting 2014
(28 April - 02 May 2014 at Pacifico YOKOHAMA, Kanagawa, Japan)

G02-P14 Room:Poster Time:April 29 18:15-19:30

Survey of educational study on disaster prevention

YAMADA, Nobuyuki[1*] ; HAYASHI, Shinsaku[1]

[1]Fukuoka University of Education

The consciousness of importance and need of the disaster prevention education for the natural disaster is increasing more. In this study, we tried that we grasped the actual situation of the study on previous disaster prevention education through compiling of research paper title by the some keywords. We set that the keywords are the causing phenomenon of the disasters, e.g. earthquake, tsunami, volcano, typhoon, and directly expression word of disaster prevention education, safety education. Our result shows these selected words are not so many used in the title of previous research papers. Although this procedure has an inadequacy, we can understand a tendency and the actual situation about the methods and contents of the disaster mitigation education.

Keywords: Disaster mitigation education, Title of reserch paper

Japan Geoscience Union Meeting 2014
(28 April - 02 May 2014 at Pacifico YOKOHAMA, Kanagawa, Japan)

G03-01 Room:423 Time:April 29 09:00-09:15

Student science continuation study on rocks and minerals weathering experiment 2

KOMORI, Nobuo[1*]

[1]Kamata ota ward junior high school

I have been instructing the continuation study to check rocks and minerals change experimentally as a student study of junior high school science club for 23 years. In this continuation study, I l have valued the study of the change basalt and fayalite with ultraviolet rays and the water most. This study is for a purpose to clarify one of the causes with much iron oxide on Mars. Therefore, students irradiate ultraviolet rays to the basalts and fayalites soaked into purified water and check their change. There is much basalt and fayalites on Mars probably. In addition, it is estimated that water existed on past Mars. Therefore, in past Mars, it is thought that ultraviolet rays and water were one of the factors to change rocks .

At first I am interested in the study and I decide directionality and the plan of the study of science club and prepares for tools. And the student who was interested in the study joins the scientific club and studies it. In other words it is a teacher-led science continuation study, but values the idea and opinion of the students. In a junior high school and the elementary school science, I think that such a teacher-led science study should be carried out more lively in Japan. And I think that it is easy to practice such a teacher-led science continuation study in the field of earth planet science and the field of biological science in particular.

Keywords: student syudy, ultraviolet rays, water, fayalite, basalt, change

Japan Geoscience Union Meeting 2014
(28 April - 02 May 2014 at Pacifico YOKOHAMA, Kanagawa, Japan)

G03-02 Room:423 Time:April 29 09:15-09:30

Planning and practice of our delivery lecture at Betsukai elementary school

NANAYAMA, Futoshi[1*] ; SHIGENO, Kiyoyuki[2] ; NAKAYAMA, Riku[3] ; TSUJI, Takafumi[3] ; SATO, Shin[3] ; IKEDA, Yasuo[3]

[1]Geological Survey of Japan, AIST, [2]Meiji Consultants Ltd., [3]Kushiro Branch, Hokkaido University of Education

Triggered by the Tohoku Earthquake on March 11, 2011, science education for disaster prevention and mitigation, are reviewed the importance of earth science education, especially in the field of education. However, we hear often from teachers in elementary school, junior high, and high school. ”There are no instructional materials about local geology and geomorphology on the science textbook around here.

Kazuto Ishiwata in Betsukai museum was consulted me about ”In the study period, which is expected to occur in November, I want you to plan visiting lectures about local geology for target 13 people in grade 5 and 6 of Betsukai elementary school ”. At that time, it was to be three students from Hokkaido University of Education, Kushiro branch aimed at teachers in future come in field training associated with Prof. Yasuo Ikeda. Therefore, we plan to conduct a special science class with them in Betsukai elementary school in last November. We will report our planning delivery lecture at Betsukai elementary school about ”Let’s examine the origin of land using by geological and geomorphological information!” and responses from students.

Keywords: Betsukai elementary school, delivery lecture, geomorphology and geology, origin of land, eastern Hokkaido, marsh

Japan Geoscience Union Meeting 2014
(28 April - 02 May 2014 at Pacifico YOKOHAMA, Kanagawa, Japan)

G03-P01 Room:Poster Time:April 29 18:15-19:30

Computer Based Educational Seismology System for Regional Elementary School Students

IWAMOTO, Sui[1*] ; KIYOMI, Masashi[1] ; KIM, Ahyi[1]

[1]Yokohama City University

Japan is one of the most seismically active countries in the world. Catastrophic earthquake can happen anywhere in the country and large offshore earthquake sometimes cause destructive Tsunami. Since no one can predict the exact date and location of the earthquakes, it is important to get prepared in advance to protect their homes and families. For this purpose, education of disaster preparedness is crucial for everyone. After the 2011 great Tohoku Oki earthquake occurs, importance of the education of disaster preparedness was rediscovered and various educational activities were held in schools and other public facilities. However the mechanism of earthquake itself (Why and how it happens, why the strong ground motion can be generated, what controls the ground motion intensity, etc.) is rarely taught in the classroom. Both comprehensive knowledge of the earth science and disaster drill should go together for the effective disaster prevention. In addition, the education of the earth science including seismology for younger generation is very important to encourage them to be a future scientist or/and leader of disaster prevention. In this study, we develop a computer based educational seismology system targeted for elementary school students. The system will be aimed at being used in the classroom to support their better understanding of earthquake and earth system. Prior to this project, we performed a series of survey in the local elementary school to figure out what teachers want for this type of learning system and how to adopt it in their class. Based on the survey, we developed a prototype of the system. Since it is targeted for little children, we made efforts so that it to be not only practical but also enjoyable. For example, as the prototype, we developed the computer game to determine the hypocenter of earthquakes, which is practical and visually enjoyable. In the game, students will pick P- and S-wave by themselves and compete the score. Furthermore, since we are trying to distribute the system to the local elementary school, we included the learning contents of the local geology, tectonics and historical earthquakes in the system so that they can learn them effectively and prepare for the future earthquake that affects their home town.

Keywords: Disaster prevention education, Educational seismology, Outreach, Computer game, Elementary school

Japan Geoscience Union Meeting 2014
(28 April - 02 May 2014 at Pacifico YOKOHAMA, Kanagawa, Japan)

G03-P02 Room:Poster Time:April 29 18:15-19:30

A direction of geographic education for disaster prevention after Great East Japan Earthquake

ENDO, Yu[1*] ; YAMAMOTO, Ryuta[2]

[1]Aichi Univ of Education, [2]Waseda Univ

One perspective from environmental education after the Great East Japan Earthquake (GEJE) gives us an opportunity to rethink the following attitude: learning about nature and physical environment makes you a person solving problems among them. This can be described as the gap between recognize and action. This concept is lack also in geographic education, where recently problem solving learning often carried out on the context of Education for Sustainable Development.

The aim of disaster prevention education in school is to foster children's competence for recognition and action about disaster and its prevention. However in geographic education so far, the learning approaches were categorized in 2 patterns as point out the correlation between disaster and topographic condition through evaluating map and aerial photographs (1), and find out place of danger with comparing old-new topographical map (2). They were just recognize approach for disaster and would lead to scientific rational recognition like hazard map. The action was not to be in considered. Moreover GEJE shows us the needs of mental- and ethical behavior should be foster in education. Against these challenging ethics education offer a new approach from the theoretical background of Kohlberg's stages of moral development. Life is getting to be an issue also in geographic education.

This presentation shows the cross-linking approach of scientific rational- and ethical aspects of disaster prevention education with concrete example.

Keywords: Great East Japan Earthquake, Geographic Education, Education for Disaster Prevention, Education for Sustainable Development, cross-linking approach

Japan Geoscience Union Meeting 2014
(28 April - 02 May 2014 at Pacifico YOKOHAMA, Kanagawa, Japan)

G04-01 Room:423 Time:April 29 09:30-09:45

Learning Tsunami Physics by Numerical Simulation: A Curriculum of Physical Oceanography Education in High School

NIWA, Yoshihiro[1*] ; SATO, Shunichi[2] ; SUZUKI, Yuta[1]

[1]Center for Marine Education, Ocean Alliance, The University of Tokyo, [2]Tokyo Metropolitan Hibiya High School

In this study, we have developed the curriculum for high school students to learn the physics of tsunami waves. A special feature of this curriculum is that students try to perform numerical simulations to understand the basic behavior and dynamics of tsunami waves. This curriculum is composed of two successive classes of physics for second grade high school students (each class is 45 minutes in length). In the first class, we explain the physical characteristics of tsunami waves, the physical laws governing tsunami waves, and the basics of numerical simulation approach. In the second class, every student plays the numerical simulations of tsunami waves by using PC.

Keywords: Tsunami Wave, Numerical Simulation, Physical Oceanography Education, Marine Education

Japan Geoscience Union Meeting 2014
(28 April - 02 May 2014 at Pacifico YOKOHAMA, Kanagawa, Japan)

G04-02 Room:423 Time:April 29 09:45-10:00

Geoscience curricurum on High School research program

KURI, Miwa[1*] ; MURAKAMI, Yuko[2]

[1]International Research Institute of Disaster Science, Tohoku University, [2]Graduate School/Faculty of Arts and Letters, Tohoku University

Background: A new system for researchprogram on high school had started at 2013. And some school has started the research program as SSH, SPP and so on. Many universities and research instituts suports research by high school students. In many case scientist suport sturents on specific skill not basic skill. As increeasing the number of SSH, theme for research had diversed lile as the interraction of science and society.

Basic skill Lesson: Authors had suported for the resson of basic skill to cross the filds, referenc skill, cretical thinking and so on.

Activities: Lessons from the Great East Japan Earthquake are summarized in White Paper on Science and Technology 2012. The public trust in scientist declined from the gap between expectation and real. Promotion of integrated research of different fields such as seismology, geology, archaeology and history to enough understand earthquake and tsunami is a pressing need. Risks and uncertainty involved in science and technology have not been seriously considered with regard to the provision of information by the government and experts for the public. Therefore most of the people did not have an adequate understanding of the situation. Social Engineering, Social Sciences, and Humanities have to be considered in implementing countermeasures.Anticipating massive earthquakes and tsunamis by taking every possibility into account.

Propose: The uncertainty of geocience has been the reason to avoid geosience in school curricurum.

Keywords: geoscience, statistics, refference

Japan Geoscience Union Meeting 2014
(28 April - 02 May 2014 at Pacifico YOKOHAMA, Kanagawa, Japan)

G04-03 Room:423 Time:April 29 10:00-10:15

Multi-site observation program of sprites in collaboration with high schools and universities: from 10-year activities

YAMAMOTO, Masa-yuki[1*]

[1]Kochi University of Technology

As one of the educational projects in geoscience, TLE (Transient Luminous Events: sprites, elves, etc.) triangulation has been carried out since 2004 with collaborating many high schools in Japan and Kochi University of Technology (KUT). Since 2006, some high schools has been funded by Japan Science and Technology Agency (JST). In this decade, collaboration has been improved educationally and scientifically, resulting almost full-coverage of Northern sky over Japan by high-sensitivity CCD video cameras (Wat-100N) and motion-detective software (UFOCapture V2) operated by high school students. The activity generated the largest TLE observation network in the world by participating 30 or more high schools. After ended the funding from the JST as the SSH consortium or Core SSH, high school teachers and students continued their relationship to study the science of TLEs with having internal meetings twice per year until now.

The first sprite detection was made in Dec. 2004. More than 3000 TLE events were detected by high school students, creating many scientifically interesting results, i.e., the world first triangulation of elves in 2008, a few examples of gigantic jets with VLF signals. Existence of an elf with apparent stripe wave pattern was clearly confirmed by simultaneous observation of the elf, suggesting modulation by gravity waves. Such results were and will be presented by high school students with their impression at the domestic scientific meetings like JpGU high school student session as well as some international conferences (see Shirahata et al., 2014; a scientific paper submitted by Iwata Minami high school team).

Thus, the campaign was very successful to obtain new results of TLE as well as the special educational project for high school students. Their research activities were widely introduced to people in Japan by NHK special TV program ”The cosmic shore” in 2012. In this talk, 10 years collaboration between high schools and universitiy activities will be presented.

Reference: Shirahata et al., Striped structure observed in the elves: Relation to turbulences in the upper atmosphere, AS28 session, AOGS 2014, Sapporo, 2014.

Keywords: high school student, collaboration with high school and university, Astro-HS, Super Science High school (SSH), multi-site observation, sprite

Japan Geoscience Union Meeting 2014
(28 April - 02 May 2014 at Pacifico YOKOHAMA, Kanagawa, Japan)

G04-04 Room:423 Time:April 29 10:15-10:30

Deployment of a teaching material for observing electric field by sprite parent storm at high school

SUZUKI, Tomoyuki[1*] ; SUZUKI, Yuko[1] ; KAMOGAWA, Masashi[1] ; MIYASHITA, Atsushi[2]

[1]Dpt. of Phys., Tokyo Gakugei Univ., [2]Seikei senior high school

Sprites are observed by many high school students by means of high sensitivity CCD cameras. They have revealed the optical characteristics of sprites (e.g. morphology and 3-dimintional location). However, they do not have materials to observe electrical phenomena originating from sprites. So, we developed a low cost field mill data acquisition system observing surface electric field change produced by sprite parent storms. Then, we deployed some field mills at high school in Tokyo. We will present some sample of the data observed and problems on the observations revealed.

Keywords: sprite, electric field observation, teaching material

Japan Geoscience Union Meeting 2014
(28 April - 02 May 2014 at Pacifico YOKOHAMA, Kanagawa, Japan)

G04-05 Room:423 Time:April 29 10:30-10:45

Let's Observe the Sun with Hinode! - Coordinated Observation Campaign with High School Students -

YAJI, Kentaro[1*]

[1]National Astronomical Observatory of Japan

Hinode is the solar observation satellite that launched in 2006. Since its launch, Hinode has given us great new observation results. In addition, it is encouraged to use of the observation data for education. So, as one of education and public outreach(EPO) activities of Hinode, we have proposed to perform coordinated observations with high school students, public observatories and science museums, every year since 2010. The proposal is adopted as "EPO campaign observation mainly for high school students(HOP173)". The goals are that they have interests in Hinode data and compare their own data with Hinode data. They compare Hinode data with their data and obtain new solar knowledge, which make their motivation higher on their activities. The students have a presentation on the observation results at a science contests. Foreign researchers have high interests in the coordinated observations, which contribute to extension of Hinode mission.

In this presentation, we repot the results of the coordinated observations, and the effects.

Keywords: Hinode, sun, astronomical education, outreach, coordinated obsevation, high school

Japan Geoscience Union Meeting 2014
(28 April - 02 May 2014 at Pacifico YOKOHAMA, Kanagawa, Japan)

G04-06 Room:423 Time:April 29 11:00-11:15

Making ”high schools list of the whole country which can study Earth Science”

OBI, Yasushi[1*] ; MIYAJIMA, Satoshi[2] ; MAKINO, Yasuhiko[3]

[1]Kanagawa Prefectual Sagamihara Seiryo High School, [2]Saitama Prefectural Fukaya dai-ichi High School, [3]Ibaraki University

In Japan Society of Earth Science Education, it is tackling making ”high schools of the whole country which can study Earth Science” list beginning in the 2013 fiscal year, and has posted on the society homepage.

From the result of this list, the present condition of today’s high school earth science education is considered.

Keywords: high schools, Earth Science

Japan Geoscience Union Meeting 2014
(28 April - 02 May 2014 at Pacifico YOKOHAMA, Kanagawa, Japan)

G04-07 Room:423 Time:April 29 11:15-11:30

Finding Instructional Difficulties on Basic Earth Science for High School Students

KAWAMURA, Norihito[1*]

[1]Faculty of Education and Human Studies, Akita University

In February 2011, the author carried out a questionnaire research to science teachers about the awareness of any difficulties on new subject Basic Earth Science lesson for senior high school students under the new Course of Study in Japan. One of aim of the research was to get some responses from science teachers in Akita and Kagawa prefectures. In this year, the author conducts the second research to teachers so that to discuss any perception gap of difficulties between the 2011 and 2014 researches.

Keywords: science teacher, senior high school, Basic Earth Science, questionnaire research

Japan Geoscience Union Meeting 2014
(28 April - 02 May 2014 at Pacifico YOKOHAMA, Kanagawa, Japan)

G04-08 Room:423 Time:April 29 11:30-11:51

Is the Earth Science Education of High School at the Stable Standing ?

NAKAJIMA, Takeshi[1*]

[1]Shiga Pref. Ohtsu-seiryo High School

As a result of the revision of the government guidelines for teaching, the number of students who learn the *Basic Earth Science* increased sharply from *Earth Science I* of the previous guidelines. However, it cannot necessarily mean that the educational world had a new appreciation of the importance of earth science education in high school. This problem is considered from a viewpoint of the number of textbooks demand and the number of teachers' adoption. Also, it to be discussed how the contents of this subject have changed in comparison to the previous ones.

Keywords: high school earth science education, textbook demand, teacher adoption, Basic Earth Science

Japan Geoscience Union Meeting 2014
(28 April - 02 May 2014 at Pacifico YOKOHAMA, Kanagawa, Japan)

G04-09 Room:423 Time:April 29 11:51-12:06

Development of laboratory seismic exploration experiment for education and demonstration

KUWANO, Osamu[1*] ; NAKANISHI, Ayako[1]

[1]IFREE, JAMSTEC

We developed laboratory seismic exploration experiment apparatus for education and demonstration. As an elastic medium, we use agarose-gel. Because agarose-gel is transparent and its s-wave velocity is 3 orders of magnitude smaller than the seismic waves that propagate earth's crust, we can easily observe wave-propagation by the photo-elastic technique. We report the detail of the experimental apparatus and practice of seismic exploration using the apparatus for high school students.

Japan Geoscience Union Meeting 2014
(28 April - 02 May 2014 at Pacifico YOKOHAMA, Kanagawa, Japan)

G04-10 Room:423 Time:April 29 12:06-12:21

A simplified focal model constructed with prastic spheres and slinky springs

OKAMOTO, Yoshio[1*]

[1]Osaka Kyoiku University

In the high-school earth-science text books, it is written that the P-wave first motions of an earthquake show a four quadrant distribution, which is related to the focal mechanism. However the detail of mechanism about this phenomenon is never shown. Among the seismology text book, although there are many introduction about this quadrant polarity using mathematical formula, which is too difficult to understand for non-professionals. Therefor, we developed a simplified focal model with cheap cost and easy construction.

By this model we can demonstrate the relation between the focal mechanism and the P-wave first arrivals for educational and outreach purposes. The model consists of 1) Two transparent plastic half spheres purchased at home centers eg. Tokyu Hands. 2) Two acrylic plates 3) Four Slinky Springs(plastic springs can be used as alternatives) attached to spheres with tapes. Two alternate plates mimic a buried fault and a sudden dislocation of this fault causes an earthquake. If the fault moves, the four slinky springs attached to two plastic spheres might show compressional or dilatational first P-wave motions consistent with the fault geometry. We can observe the detail of this phenomenon with high speed video movies. In our tests of this model, we can barely recognize the polarity of the first motions. We also try to improve our model to carry out more comprehensive demonstration.

Keywords: focal sphere, P-wave first motion, earthquake mechanism, fault, slinky spring

Japan Geoscience Union Meeting 2014
(28 April - 02 May 2014 at Pacifico YOKOHAMA, Kanagawa, Japan)

G04-P01 Room:Poster Time:April 29 18:15-19:30

Problems and Possibility of ”Science and Human Life”

NAKAJIMA, Takeshi[1*]

[1]Shiga Pref. Ohtsu-seiryo High School

Science and Human Life was established in the revision of the government guidelines for teaching, the number of students who learn *Science and Human Life* is about 400000, and is much larger than the number of students who learn *Basic Earth Science*. Contents of earth science field that are covered by the *Science and Human Life* is about one fifth of the whole, but they should not be ignored for earth science education, because one in three high school students takes this subject. In addition, this subject deals with the relationship between humans and nature, the benefits received from nature, and natural disasters in particular. However, the contents of this subject can not be said to be enough. In order for the students to master the skill necessary to make our society sustainable, it is necessary to further review the contents of this subject.

Keywords: high school earth science education, textbook demand, Science and Human Life, general subject of science

Japan Geoscience Union Meeting 2014
(28 April - 02 May 2014 at Pacifico YOKOHAMA, Kanagawa, Japan)

G04-P02 Room:Poster Time:April 29 18:15-19:30

A reconstruction of ”Film Case Seismometer” employing ”Arduino” and ”Processing”

OKAMOTO, Yoshio[1*]

[1]Osaka Kyoiku University

We reconstruct so called ”Film Case Seismometer (Okamoto,1999)” for class room use. The legacy system had developed about two decades ago and was a full seismograph involving a moving magnet sensor and a PC recording system as a simplified mimic of a modern digitalized seismograph and a logger system. While the sensor was simplified and easy constructed enough, however the recording system was somewhat complicated and employ a specific program language on the limited PC. Therefore, the system was not so far contributed and/or demonstrated at mid-school’s class rooms. In this regard, now we try to fully model-change the old system to an innovative style using ”Arduino” (one chip micro-computer including both I/O and A/D converter devices) and ”Processing” (Java based language for easy programing). The main aspects are as follows,

1) The sensor consists a rounded coil on a acrylic pipe and a strong Neodymium bar magnet hanging with a series rubber band from a main pillar hook. The Neodymium magnet can supply a sufficient signal and an appropriate damping by induced current with a surrounded metal pipe.

2) The recording system and software are improved more simplified and can applicable on any PC or even tablet.

3) The micro-tip used for I/O and A/D converting is ”Arduino Uno” (Italian made and a cheap cost, 30 USD), which is easily controlled by a simple software written in Processing language and exchanges signals via USB port.

4) Processing language is used for A/D driving and logging, which is running on any operation system such as Windows, Mac, Linux and even Android.

5) The additional hardware for natural earthquake observation is a circuit employing OP amps for signal boost, which is divert from our legacy system.

6) All system is constructed in a transparent acrylic box for recognizing mechanism at a glance.

7) The wave signal is displayed on PC or tablet at real time with second time-marks and also save to PC as a graphic mode or digital mode at each moment.

8) The logging and displaying capacity can be extended to three channels easily.

Keywords: seismograph, Arduino, Processing, education, USB

Japan Geoscience Union Meeting 2014
(28 April - 02 May 2014 at Pacifico YOKOHAMA, Kanagawa, Japan)

G05-01 Room:423 Time:April 29 12:30-12:45

Development of an educational tool for seismic exploration study using piezoelectric buzzer and general-purpose laptop

GOTO, Akio[1*]

[1]CNEAS, Tohoku University

I have developed an inexpensive ground motion detecting system as an educational tool for seismic exploration study, consisting of geophone which uses a piezoelectric buzzer as a sensor and general-purpose laptop.

Piezoelectric buzzer, which is used to transmit electric signal to sound in general, excites electric pressure when an external force is applied. To catch the ground motion it is fixed on the bottom of a cylindrical plastic bin, and a nail is put into the open mouth of the buzzer through a hole opened on the bin lid. When the vertical motion hits the bin from beneath, the nail behaves as a fixed point by its inertia, push the buzzer, and then the electric pressure is excited. We install these sensors near the shot point and the observation site, and record the signal from them synchronously. From the distance and the signal arrival time delay we can determine the elastic wave velocity of the ground.

We need high rate sampling multi-channel data logger for recording, which is not necessarily inexpensive. Instead of it we use a laptop whose audio stereo inlet is available for synchronous recording. A sound recording software may be preinstalled in PC, but it depends on the OS. Because the laptop differs from student to student, and to unify the instruction, we adopt a freeware *Audacity* for recording. A wav format signal file recorded by *Audacity* will be transformed into text format using a freeware *WaveGraph*. Another compatible software may be available for recording and transforming. You should notice there is another *WaveGraph*, which does not have a function for wav to text transform and is not available for our purpose. The transformed text file can be opened by some graphic software to read the time delay between the two sites.

In the classes students firstly constructed the sensor, and then confirmed the utility of their laptop for signal recording. At the field we hit the ground by large wooden hammer to excite the ground motion for one minute with five seconds interval. In case the sensor was far from the shot we heightened the gain by putting some amount of clay on the nail to enhance the inertia. Twelve signals by one-minute recording were stacked to confirm the noise reduction. We confirmed the arrival time to the sensors delayed linearly with distance between 3 and 24 m from the shot point with 3 m interval, and obtained direct wave velocity as 560 m/s. We did not detect refractive wave, it may be because the test field in the university campus was not appropriate for this purpose.

The present system, consisting of inexpensive hand-built sensors and general-purpose laptop, is an educational tool not only for seismic exploration study but to show students the possibility of overcoming the difficulty from the lack of expensive sophisticated equipment for experiments by their ingenuity. On another front this system obviously has some weak points. For examples, it is unclear our sensor is really suitable for ground motion detection, because we have no data on its frequency response, which may depend not only on the property of piezoelectric buzzer and the inertia of the nail but on the manufacturing precision such as the position of the hole on the lid to insert the nail. Due to the insufficient electrical insulation between right and left channels of most laptop stereo inlet we have to attenuate the intense signal from the shot using a resistance to prevent it from interfering. We have found the signal through the laptop stereo inlet is low-cut filtered and is not suitable for precise recording, although it does not seem to affect our present use seriously. If we count the performance evaluations of the present system in a part of the experiment, it may improve the education effect more.

Japan Geoscience Union Meeting 2014
(28 April - 02 May 2014 at Pacifico YOKOHAMA, Kanagawa, Japan)

MIS01-01 Room:314 Time:April 29 14:15-14:30

Evolution and variability of East Asian monsoon and the potential relationship with Himalaya-Tibet uplift

TADA, Ryuji[1*]

[1]Graduate School of Science, the University of Tokyo

Monsoon is climatic phenomenon driven by heat capacity contrast between the continent and ocean, so every continent has its own monsoon system. Asian Monsoon is by far the largest monsoon system on the globe. Although it is regional phenomenon, it exerts significant influence on the global climate. The extremely large size of Asian Monsoon system is considered as having been caused by the presence of Himalaya and Tibetan Plateau (HTP). The large size and high altitude of HTP resulted in higher temperature at ca. 5000 m altitude compared to the surrounding area during summer that resulted in ascending air and development of low pressure cell over the plateau. Topographic effect could be also important to enhance summer monsoon. Large size of Asian continent enhanced cooling over continent during winter, resulted in development of high pressure cell known as Siberian High. HTP plays a role of topographic barrier that keeps Siberian High stronger and stable. Consequently, presence of HTP could have been playing a crucial role to strengthen Asian Monsoon. If correct, uplift of HTP could have resulted in intensification of Asian Monsoon.

Climatic simulations can be used to test the hypothesis that uplift of HTP has intensified Asian Monsoon if uplift history of HTP is known well. However, timings, modes, and magnitudes of HTP uplift have been poorly understood until recently. Situation is rapidly improved recently due to accumulation of thermo-chronological data from the various parts of HTP. Namely, collision of Indian Subcontinent against Eurasian Continent approximately at 40 Ma caused the 1st phase of Tibetan uplift that raised southern Tibet close to the present height by 35 Ma. From 25 Ma to 15 Ma, Main Central Thrust (MCT) and South Detachment System (STDS) in frontal Himalaya were activated and lower crust was extruded and eroded extensively. Approximately at 15 Ma, these fault system ceased their movements and east-west extension started in Tibet. From 15 Ma to 10Ma is the 2nd phase when Tibetan Plateau grew southeastward and possibly also northward. The 3rd phase of uplift started from approximately 5 Ma when northwestern Tibet, TienShan and Altai Mountains uplifted. Using this uplifting history of HTP as a boundary condition, it is possible to estimate what kind of paleoclimatic changes are expected in response to these 3 uplift phases based on climate simulation results.

In this presentation, I will review a recent progress in researches on tectonics-climate linkage as HTP uplift and Asian Monsoon evolution as an example.

Keywords: Monsoon, Himalaya-Tibet, Tectonics-Climate Linkage, East Asia, Japan Sea, Westerly Jet

Japan Geoscience Union Meeting 2014
(28 April - 02 May 2014 at Pacifico YOKOHAMA, Kanagawa, Japan)

MIS01-02 Room:314 Time:April 29 14:30-14:50

Pre-Miocene Birth of the Yangtze River

ZHENG, Hongbo[1*] ; CLIFT, Peter[1] ; WANG, Ping[1] ; TADA, Ryuji[1] ; JIA, Juntao[1] ; HE, Mengying[1] ; JOURDAN, Fred[1]

[1]Nanjing Normal University

The development of fluvial systems in East Asia is closely linked to the evolving topography following India-Eurasia collision. Despite this, the age of the Yangtze River system has been strongly debated, with estimates ranging from 40?45 Ma, to a more recent initiation around 2 Ma. Here, we present new $^{40}Ar/^{39}Ar$ ages from basalts interbedded with fluvial sediments from the lower reaches of the Yangtze together with detrital zircon U/Pb ages from sand grains within these sediments. We show that a river containing sediments indistinguishable from the modern river was established before ˜23 Ma. We argue that the connection through the Three Gorges must post-date 36.5 Ma because of evaporite and lacustrine sedimentation in the Jianghan Basin before that time. We propose that the present Yangtze River system formed in response to regional extension throughout eastern China, synchronous with the start of strike-slip tectonism and surface uplift in eastern Tibet and fed by strengthened rains caused by the newly intensified summer monsoon. Birth of the eastward flowing Yangtze River around the Oligocene/Miocene boundary changed largely the 'source to sink' regime in the East Asia-West Pacific region

Keywords: Yangtze River, birth, Tibetan Plateau, drainage capture, Asian monsoon

Japan Geoscience Union Meeting 2014
(28 April - 02 May 2014 at Pacifico YOKOHAMA, Kanagawa, Japan)

MIS01-03 Room:314 Time:April 29 14:50-15:10

The missing volcanic record captured by dispersed ash in sediment of the Japan Sea/East Sea and NW Pacific Ocean

MURRAY, Richard[1*] ; SCUDDER, Rachel P.[1] ; DUNLEA, Ann G.[1] ; IKEHARA, Ken[2] ; IRINO, Tomohisa[3] ; TADA, Ryuji[4] ; ALVAREZ-ZARIKIAN, Carlos A.[5] ; KUTTEROLF, Steffen[6] ; SCHINDLBECK, Julie[6] ; SCIENTIFIC PARTY, Expedition 346[5]

[1]Boston University, [2]Geological Survey of Japan, [3]Hokkaido University, [4]University of Tokyo, [5]IODP-TAMU, [6]GEOMAR, Kiel

Volcanic ash in marine sediment provides a wealth of information not only about volcanism and arc evolution, but also potentially regarding climate change, geochemical mass balances, hydration of marine sediment during alteration, the geodynamics of subduction zones, and other key components of the earth-ocean-atmosphere system. Ash occurs both as discrete *layers* as well as isolated grains and shards *dispersed* throughout the bulk sediment, and with highly variable grain sizes.

The study of this dispersed component has lagged behind the sedimentologic and chemical assessment of the ash layer record. For example, while decades of smear-slide studies of bulk sediment in volcanic-rich regimes have presented visual estimations of the abundance of volcanic glass, shards, and other components, the quantitative importance of the dispersed ash or cryptotephra remains largely unconstrained on local, regional, and global scales. Also, compared to the often visually stunning ash layer records, which in certain settings can leave single layers with thicknesses of 10s of cm, the dispersed ash component and cryptotephra are unable to be visually differentiated from detrital clay.

We summarize here preliminary results regarding the distribution, composition, and accumulation of dispersed ash in sediment from the Japan Sea/East Sea (gathered during IODP Expedition 346, Asian Monsoon, and ODP Legs 127/128), and compare it to the record provided by discrete ash layers. We will interpret our work in the context of our ongoing studies of dispersed ash throughout the northwest Pacific, Nankai, and Izu-Bonin regions, which is based on sediment from DSDP/ODP/IODP Sites 52, 444, 579/581, and 1149, as well as from Sites C0011 and C0012.

Multivariate statistical treatments are an integral part of our approach, as the bulk determination of the major, trace, and REEs provides the chemical context for our determination of provenance, and the statistical models allow distinctive resolution of the different aluminosilicate components based on their individual geochemical signature(s). A corollary benefit of our approach is an improved determination of the eolian component, as we are able to discern how contributions of dispersed ash have been inadvertently attributed to the eolian aluminosilicate inventory. Q-mode Factor Analysis can help determine the number, and composition of, potential end member contributions. Applying these results in conjunction with Total Inversion, a linear regression technique, allows determination of the compositional variation of these end members.

Consistent with the qualitative smear-slide estimates, in these ash rich regions we find that the dispersed component can account for up to 40% of the total sediment. We are able to document abundances to a relatively high degree of precision (+/- 3-5%) on a sample-by-sample basis, and are further able to distinguish between different chemistries of the dispersed component, and document sources that change through time and space. In addition to providing an overview of " the missing volcanic record ", we will discuss some ongoing challenges, including how to best examine the relationship between the composition of the discrete ash layers compared to the discrete component, and what information can be gained from examining similarities and differences between their respective sources.

Keywords: volcanic ash, sediment chemistry, Japan Sea, East Sea, volcanism

Japan Geoscience Union Meeting 2014
(28 April - 02 May 2014 at Pacifico YOKOHAMA, Kanagawa, Japan)

MIS01-04 Room:314 Time:April 29 15:10-15:25

Tephrochronology and evolution of volcanic activities in Japanese islands during late Cenozoic

IKEHARA, Ken[1*]

[1]Geological Survey of Japan, AIST

The Japanese islands are located along an active plate margin, and are home to many active volcanoes along an island arc. Large, explosive volcanic eruptions have yielded numerous volcanic ash layers (tephras) over geological time. Because tephras are deposited in both onland and seafloor areas, they represent a unique and important link between the geological records of the two settings. There are several source volcanoes to provide tephras to the Japan Sea floor. These are, for example, Kikai, Aira and Aso volcanoes in Kyushu, Sanbe and Daisen volcanoes in Chugoku, Asama volcano in north Kanto, Towada volcano in Tohoku, Toya volcano in Hokkaido, Ulleung volcano on Ulleung Island in the western Japan Sea, and Baegdusan volcano on Korean Peninsula. Most of the previous marine tephra studies in the Japan Sea have been concentrated for the late Quaternary in age. Because of shallow CCD and shallow gateways of the Japan Sea, oxygen isotope stratigraphy is not a perfect tool for age determination, especially in the deep-sea basins. Under the condition, wide-spread tephra works as a key bed connecting among marine cores, and give us a good time-marker. Quaternary Japan Sea sediments are characterized by alternating light- and dark-colored layers. The late Quaternary dark layers were deposited basin-wide in relation to enhanced summer monsoon during the interstadials of the Dansgaard-Oeschger cycles. Recent study on marine tephras among several marine cores in the central Japan Sea suggested the synchronicity of the dark layer deposition. This is clear evidence on significance of marine tephra study for inter-core correlation. Furthermore, tephra may connect the events in marine environments and those in terrestrial and lacustrine environments. Thus, tephras in the Japan Sea sediments are important for the paleoceanographic and paleoclimatic study in and around the Japan Sea. Information on longer time-scale occurrence of tephra layers and their source volcanoes will give us spatio-temporal variation of volcanic activities and their relations to the regional tectonic movements around the Japan Sea, because the continuous and muddy Japan Sea has been a good recorder of tephra layers after its opening.

Keywords: tephra, Japan Sea, stratigraphy

Japan Geoscience Union Meeting 2014
(28 April - 02 May 2014 at Pacifico YOKOHAMA, Kanagawa, Japan)

MIS01-05 Room:314 Time:April 29 15:25-15:40

Identification of Asian dust in hemipelagic sediments of East Asian marginal seas

IRINO, Tomohisa[1*]

[1]Hokkaido University

Detrital fraction contained in marine sediments can be generally used as climate proxies because variations in provenance and mineralogy could be affected by the precipitation distribution and weathering intensity. Element composition of marine sediment is essentially controlled by the mineral composition that is also affected by sorting effect during their transport process. The inland deserts such as Taklimakan and Gobi are large detrital sources for the East Asian marginal seas, and the detrital fraction in the sediments collected from the abyssal part of the Japan Sea / East Sea has been regarded as the mixture of eolian dust and the detritus derived from the Japan Arc. This feature can be used to reconstruct the variability of provenance and transport pathway of detrital fraction in the sediments. Relative contribution of dust from Taklimakan / Gobi could be strongly affected by dust availability in source area and wind system transporting the dust. Major changes in such detrital provenance are more easily reconstructed from the proximal soil record at loess plateau, where many provenance studies have been conducted. Loess can be classified into two types based on their element composition. One is typical loess distributed close to desert area. The other is peripheral soil (weathered loess) distributed surrounding typical loess and desert area. Weathered loess is distributed in the northeastern and southern China in modern times. Spatial distribution of these two types of soils have been also changed from time to time. In order to detect the change in provenances and interpret the terrestrial environment using detrital proxies in the marginal sea sediments, it is necessary to know the variability or range of the element and mineral composition of a particular provenance during the targeted time periods as well as the sorting biases during the transportation.

Keywords: hemipelagic sediment, aeolian dust, provenance, mineral composition, element composition, isotope composition

Japan Geoscience Union Meeting 2014
(28 April - 02 May 2014 at Pacifico YOKOHAMA, Kanagawa, Japan)

MIS01-06 Room:314 Time:April 29 15:40-16:00

Carbon and Sulfur Cycling in Shallowly Buried Sediment of the Japan Sea/East Sea

DICKENS, Gerald[1*] ; KINSLEY, Christopher W.[2] ; DUNLEA, Ann G.[3] ; ANDERSON, William A.[4] ; DA COSTA GURGEL, Marcio H.[5] ; LEE, Kyung eun[6] ; MURRAY, Richard W.[3] ; TADA, Ryuji[7] ; ALVAREZ ZAREKIAN, Carlos[8] ; EXPEDITION 346, Scientific party[8]

[1]Rice University, [2]Massachusetts Institue of Technology, [3]Boston University, [4]Florida International University, [5]Universidade de Sao Paulo, [6]Korea Maritime University, [7]University of Tokyo, [8]Texas A&M University

Continental slopes cover about 10% of Earths surface and represent the primary repository for sediment and organic carbon accumulation on long-time scales. For decades, the geochemical community has introduced and discussed various models for how ocean carbon and sulfur chemistry changes over time. Remarkably, in most of these models, the seafloor on continental slopes is either absent or passive. In the latter case, the prevailing view is as follows. During burial, organic carbon passes through a gauntlet of microbially mediated reaction in shallow sediment, especially including organoclastic sulfate reduction and methanogenesis. Although these reactions generate dissolved species (HCO3-, HS-, CH4), burial fluxes exceed those of upward advection or diffusion. The end process, therefore, is accumulation of remnant solid organic carbon, authigenic carbonate, and authigenic Fe-sulfides. As suggested in several recent papers, this view may be incorrect. Instead, on the slope, a good fraction of solid organic carbon bypasses organoclastic sulfate reduction to produce dissolved inorganic carbon, dissolved organic carbon, and methane at depth. Large portions of these species return toward the seafloor because upward dissolved fluxes exceed burial. However, upward migrating methane reacts with dissolved SO42- to produce HCO3- and HS- via AOM in shallow sediment. The end process is still accumulation of remnant solid organic carbon, authigenic carbonate, and authigenic Fe-sulfides, but the fluxes are linked through the formation, storage and consumption of methane.

It is entirely possible that variations in methane cycling within slope sediments drive significant long-term and short-term changes in ocean carbon and sulfur concentrations. To entertain this idea, however, the broad Earth Science community needs quantified fluxes of solid and dissolved components from appropriate settings. One current problem is that very few locations on continental slopes that have detailed pore water profiles extending 200 m below the seafloor with companion sedimentary records.

IODP Expedition 346 drilled multiple holes at seven sites across the Japan Sea/East Sea. The primary objective behind this cruise was late Neogene and Quaternary paleoceanography: more specifically, to reconstruct changes in surface and deep ocean water properties, riverine outflow, and dust input over the last 5-10 million years, which might be linked to the evolution and temporal differences in the Asian monsoon system. One interesting outcome of this goal was that the sites span a wide range of slope environments with considerable variation in organic carbon accumulation. Another was exquisite sediment recovery, with spliced cores between holes giving complete records from the seafloor to several hundred meters.

Expedition 346 provided a golden opportunity to chase the dynamic geochemical cycling of carbon and sulfur on continental margins. Using a combination of rhizon sampling and whole round squeezing, about 680 pore water samples were collected at the seven sites and analyzed for a broad array of dissolved species. The shipboard pore water geochemistry profiles generated on Expedition 346 are truly remarkable in terms of species examined, their detail across zones of chemical reaction, and the ability to directly couple them to the sedimentary record. Here, on behalf of the Expedition 346 scientists, we discuss the generation of the pore water profiles and their significance to carbon and sulfur cycling on continental slopes. For example, at Site U1427, there is no question as to the dominant process and where species are being produced and consumed in shallow sediment. Upward migrating CH4 is reacting with SO42- via AOM to produce HCO3- and HS-, the first product leaking to the seafloor, the latter product being consumed into sulfide minerals.

Keywords: Methane, AOM, carbon cycle, sulfur cycle

Japan Geoscience Union Meeting 2014
(28 April - 02 May 2014 at Pacifico YOKOHAMA, Kanagawa, Japan)

MIS01-07 Room:314 Time:April 29 16:15-16:30

N.incompta Mg/Ca-paleothermometry in the Japan Sea and its application to Holocene climate reconstruction

HORIKAWA, Keiji[1*] ; KODAIRA, Tomohiro[1] ; IKEHARA, Ken[2] ; MURAYAMA, Masafumi[3] ; ZHANG, Jing[1]

[1]University of Toyama, [2]AIST, [3]The Center for Advance Marine Core Research, Kochi University

We present new core-top calibration for *Neogloboquadorina incompta* Mg/Ca-paleothermometry in the Japan Sea using 15 core-top surface sediments taken from the southern Japan Sea. Using this new Mg/Ca-paleothermometry, we generate the first high-resolution Mg/Ca-derived SST record for the past 7000 years from the sediment core (YK10-7-PC09) taken from 738 m water depth off Niigata. The age model for core YK10-7-PC09 was based on 8 AMS ^{14}C data of mixed planktic foraminifera, and the conventional ^{14}C ages were converted to the calendar ages using Marin13 and delta R of 0±100 yr. Trace metal/Ca ratio of *N.incompta* was measured by a SF-ICP-MS (Thermo Fisher Element II) and the precision (1sigma) of Mg/Ca ratios of the international $CaCO_3$ standard (BAM-RS3) was 0.786±0.008 (n=100).

We have performed paired analyses of δ^{18}Oc and Mg/Ca ratios of *N. incompta* at 15 sites. First, to calculate the mean temperatures of waters in which the foraminiferal shells were formed (i.e., calcification temperature), we have used modern local salinity and temperature data (http://www.jodc.go.jp/) in the following paleotemperature equation; T (℃) = 21.4-4.19×(δ^{18}Oc-δ^{18}Osw) + 0.05×(δ^{18}Oc-δ^{18}Osw)^2 (Oba, 1980). The δ^{18}Osw was calculated from the following salinity-δ^{18}Osw equation in the Japan Sea (δ^{18}Osw (‰ VSMOW) = 0.27×Salinity-8.98; this study). The comparison of the predicted δ^{18}Oc values with the measured δ^{18}Oc shows that *N. incompta* shells were formed at 0-125 m water depths from June to December in the Japan Sea. Given that previous studies show that *N.incompta* dwells in the shallow waters (<100 m) in November to December (Kuroyanagi and Kawahata., 2004; Sagawa et al., 2013), we calculated the calcification temperatures at each site assuming shells were formed in November to December. The cross plot of the calcification temperatures and the Mg/Ca ratios for our core-top samples gives the following equation; Mg/Ca (mmol/mol) = 0.361×exp (0.043×Temp).

Using this new Mg/Ca-paleothermometry, the 7000-years *N.incompta* Mg/Ca records (0.6 to 0.9 mmol/mol, n=127) from core YK10-7-PC09 were converted to the temperature record. Compared to the present winter SST of ca.15 ℃, the 7000-year SSTs varied from 13.5 ℃ to 20.8 ℃. We identified four periods (ca.6000 yr BP, 4000-3500 yr BP, 3000-2300 yr BP, and 800 yr BP) that were warmer than the present and distinct colder periods at ca.4500 yr BP and ca.1500 yr BP than the present. This SST variability for the past 7000 years was almost consistent with the record of relative abundance of F.doliolus, which is the dominant species in the Tsushima Current (Koizumi et al., 2006). This finding indicates that the Tsushima Current influx might have changed with time and altered the heat transport into the Japan Sea, and probably induced significant changes in terrestrial precipitation and vegetation over the northern part of Japan facing the Japan Sea.

Keywords: Japan Sea, Holocene climate change, Mg/Ca-paleothermometry, Tsushima Current, Neogloboquadorina incompta

Japan Geoscience Union Meeting 2014
(28 April - 02 May 2014 at Pacifico YOKOHAMA, Kanagawa, Japan)

MIS01-08 Room:314 Time:April 29 16:30-16:45

Shallow water environmental change in the Sea of Japan during the last 30 kyr deduced from foraminiferal isotopes

SAGAWA, Takuya[1*] ; UCHIDA, Masao[2] ; MURAYAMA, Masafumi[3] ; TADA, Ryuji[4]

[1]Department of Earth and Planetary Sciences, Faculty of Sciences, Kyushu University, [2]National Institute for Environmental Studies, [3]Center for Advanced Marine Core Research,, Kochi University, [4]Department of Earth and Planetary Science, Graduate School of Science, The Univeristy of Tokyo

The Sea of Japan is a marginal sea that connects with North Pacific and adjacent marginal seas by four shallow straits. Because water depth of the deepest straits today is ˜130 m (Tsushima Strait and Tsugaru Strait), environments of Sea of Japan have been strongly affected by sea level fluctuations related to the glacial-interglacial cycles. Previous studies report that foraminiferal oxygen isotope variation from Sea of Japan is distinct from that commonly seen in seas of the world. Since Sea of Japan is nearly isolated from adjacent seas during the glacial maxima, salinity of surface water significantly decreases, and therefore foraminiferal isotopes show the lowest values due to the unique fresh water balance. The peak value of oxygen isotope is ˜0.5 per mil at the last glacial maximum, which is ˜2.5 per mil lighter than at 30 ka. We review literature data and present new results of two sediment cores from northeastern and southern part of Sea of Japan. The new data from southern core has ˜70-yr resolution and shows abrupt shift that may correspond to abrupt climate change reported from the Greenland ice core and Asian monsoon proxy data of Chinese Cave and Loess. The new results suggest that the surface environment of Sea of Japan is sensitive to eustatic sea level change as well as abrupt climate changes.

Keywords: Sea of Japan, oxygen isotope, planktonic foraminifer

Japan Geoscience Union Meeting 2014
(28 April - 02 May 2014 at Pacifico YOKOHAMA, Kanagawa, Japan)

MIS01-09 Room:314 Time:April 29 16:45-17:00

Micropaleontological evidence of oceanic circulation changes in the Japan Sea during Pliocene to Pleistocene transition

ITAKI, Takuya[1*]

[1]Geological Survey of Japan, AIST

Oceanic circulation in the Japan Sea is characterized by flowing of the Tsushima Warm Current and deep-water formation during the interglacial periods, while deep circulation was stagnant due to weakened deep convection with development of the low salinity surface water during the glacial periods. Such cycles of oxic and anoxic deep-water conditions recorded in sediments as alternations of light and dark hemi-pelagic mud layers occurred since ca. 2.5 Ma near Pliocene to Pleistocene transition. The results of micropaleontological studies from previous ocean drilling sites and many onshore sequences have provided various insights into oceanic changes related to global climatic and regional tectonic events during Pliocene to Pleistocene.

Fossil records of shallow dwelling plankton and shelf related benthos are composed of the assemblage associated with upper water environments. Warm-water ostracods and molluscs are rarely recognized from onshore sequences in Japan along the Japan Sea side during the Pliocene climatic optimum (3.2 to 2.7 Ma), and they were most likely associated with subtropical water mass entered from the southern strait. However, planktonic foraminiferal and radiolarian assemblages in hemipelagic sediments suggest that the warm-temperate water was originated from the northern strait during this period. Such conflict interpretation could be explained by a characteristic surface circulation, which was composed of two different water sources from the northern and southern straits. The warm water mass from the southern strait was restricted flowing along the Japanese coastal area, while another water mass from the northern strait was present offshore areas of the sea. Abundance of cold-water calcareous nannofossil species increased significantly at 2.75 Ma corresponding to the global cooling. In this period, ostracode assemblage also indicates cooling in the intermediate water. According to planktonic foraminifers and radiolarians, significant inflow of the subtropical water from the southern strait started at 1.7 Ma, which might be related to the deepened Tsushima Strait and the Okinawa Trough (ca. 2 Ma).

Deep-water environments in the Japan Sea are little known compared with that of shallow environments. Benthic foraminifers in deep-sea sediments changed their faunal composition from agglutinated fauna to calcareous fauna through 3 to 2 Ma. Similarly, deep-water radiolarians show faunal replacement from the Pacific-type deep dwellers to the Japan Sea-type deep dwellers at ca. 2.6 Ma. Such faunal changes recognized from benthic foraminifers and radiolarians imply that the unique deep-water circulation in the Japan Sea was formed with geographical isolation from the Pacific deep water. In actual, this timing is almost coincident with beginning of oxic and anoxic cycles in the Japan Sea. It is likely resulted from either the global cooling or local tectonic motion during the Pliocene to Pleistocene transition.

Keywords: Microfossils, Paleoceanography, Grobal cooling event, Tectonic event, Tsushima Warm Current, Deep water

Japan Geoscience Union Meeting 2014
(28 April - 02 May 2014 at Pacifico YOKOHAMA, Kanagawa, Japan)

MIS01-10 Room:314 Time:April 29 17:00-17:20

Evolution of the Kuroshio Current and its impact on East Asian marginal seas

LEE, Kyung eun[1*]

[1]Korea Maritime and Ocean University

Quaternary is characterized by the onset of the Quaternary ice ages as well as the progressive cooling of the high latitude. Many proxy records from high latitude evidence this. On the other hand, records from low latitudes indicate that the sea surface temperature of the tropical warm pool regions remained relatively stable during the last 4 Ma. Hence these suggest a dramatic increase in the zonal (west?east) and meridional (north?south) gradients in sea surface temperature, which was accompanied by a progressive cooling of the water upwelled along the eastern margins of the Pacific. It is most likely believed that the evolution of the west-east and north-south temperature gradients in the North Pacific is closely related to the evolution of the western boundary current and North Pacific subtropical gyre during the Plio-Pleistocene. It, in turn, caused changes in weather and climate patterns of East Asian margins. In this presentation, previously published data and hypothesis will be reviewed to clarify future researches related to these.

Keywords: Kuroshio, North Pacific Subtropical Gyre, sea surface temperature

Japan Geoscience Union Meeting 2014
(28 April - 02 May 2014 at Pacifico YOKOHAMA, Kanagawa, Japan)

MIS01-11 Room:314 Time:April 29 17:20-17:35

Variations in intermediate water and ocean circulation during the last 26 ka based on a new benthic Mg/Ca calibration

KUBOTA, Yoshimi[1*] ; KIMOTO, Katsunori[2] ; ITAKI, Takuya[3] ; YOKOYAMA, Yusuke[4] ; MATSUZAKI, Hiroyuki[5]

[1]National Museum of Nature and Science, [2]Japan Agency for Marine-Earth Science and Technology, [3]Geological Survey of Japan, AIST, [4]Atmosphere and Ocean Research Institute, University of Tokyo, [5]School of engineering, University of Tokyo

In order to understand variations in ocean circulation at intermediate depth in the North Pacific in subtropical area, bottom water temperatures (BWT), carbon isotope of benthic foraminifera, and oxygen isotope of seawater were reconstructed since 26 ka off east main Okinawa Island, northwestern Pacific. A new regional Mg/Ca calibration for benthic foraminifera *Cibicidiodes wuellerstorfi* was established in order to convert benthic Mg/Ca value to temperature, based on twenty-nine surface sediment samples, including core top samples, retrieved around main Okinawa Island. On the other hand, in order to reconstruct changes in water properties since 26 ka,core GH08-2004 that was retrieved from water depth of 1166 m off east main Okinawa Island was used in this study. As a result, during the LGM from 24 ka to 18 ka, BWT showed relatively constant as approximately 2 ℃, which was ~1.5-2 ℃ lower than today. One of the prominent features of our BWT records was a millennial scale variation in BWT during the last deglaciation. During the last deglaciation, BWT was higher in Heinrich Stadial 1 (H1) (~17 ka) and Younger Dryas (YD) (~12 ka), while lower in Bølling/Allerød (BA) interval (~14 ka). During the interval from 17 to 15 ka, BWT tended to decrease in association with a decrease in carbon isotope of *C. wuellerstorfi,* likely interpreted as increased upwelling of the older water mass that was stored in the abyssal Pacific during the glacial time. The timing of the signal of the upwelling coincided with deglacial atmospheric CO_2 rise initiated at ~17 ka, suggesting the increased upwelling in the subtropical northwestern Pacific from 17 to 15 ka contributes the carbon release to the atmosphere from the Pacific.

Japan Geoscience Union Meeting 2014
(28 April - 02 May 2014 at Pacifico YOKOHAMA, Kanagawa, Japan)

MIS01-12 Room:314 Time:April 29 17:35-17:50

Long-term evolution of the North Pacific subtropical gyre: Implication from the late Quaternary record

UJIIE, Yurika[1*]

[1]Faculty of Science, Shinshu University

The North Pacific subtropical gyre drives a transportation of huge amount of heat from low to high latitude area to maintain warm climate in the northwestern Pacific area. This gyre system largely controls the zonal temperature gradient and west-east asymmetric climate, currently observed in the Pacific Ocean. The stepwise enhancement of these temperature gradients has partly been observed in the equatorial and east Pacific area since the late Pliocene. However, a lack of long-term observation in the west Pacific Ocean impedes a better understanding of the development of the Pacific climate.

The Kuroshio Current, flowing from the Okinawa Trough to eastward off the Japan, act as a heat-transfer along the North Pacific subtropical gyre margin. The variation in this surface current would reflect to the changes of the West Pacific climate. Especially, the Okinawa region is an ideal place for paleocenographic reconstruction, as (1) the Kuroshio Current shows an oscillation with surrounding water masses and (2) the sediments are buried in high rate. Through the short-term paleoceanographic records in the Okinawa region, the planktonic foraminiferal assemblage showed the decrease of the Kuroshio indicator and increase of the coastal- and cold-water masses indicators under the modern Kuroshio path (the East Chia Sea) during MIS 2. Interestingly, the long-term record, which was the first to cover the past 200 kyrs in this region, represented different oceanic condition during MIS 6. The indicator of the upper intermediate water in the subtropical gyre increased over whole of the Okinawa region at this time. Moreover, the Mg/Ca paleo-temperatures in the surface and upper intermediate layers showed that warming in the upper intermediate layer was continuing from MIS 6 to MIS 5e, while warming in this layer was rapidly stopped at MIS 2. Both records of the paleo-temperature and planktonic foraminiferal assemblage congruently suggest the development of the intermediate water in the North Pacific subtropical gyre during MIS 6, instead of the dominance of cold water mass observed during MIS 2. The intermediate water has likely been undergone an independent process from the changes of the surface water masses at least by MIS 5. Even the 200 kyrs record successfully inferred two different glacial mechanisms of MIS 2 and 6, associating with the changes of surface water masses and deeper waters. Future study with longer record will lead a comprehensive understanding how the modern water column structure has been developed in the Pacific Ocean.

Keywords: North Pacific subtropical gyre, Kuroshio, water column structure, Pleistocene

Japan Geoscience Union Meeting 2014
(28 April - 02 May 2014 at Pacifico YOKOHAMA, Kanagawa, Japan)

MIS01-P01 Room:Poster Time:April 29 18:15-19:30

Changes of water structures in the Sea of Japan during the Late Pliocene

YAMADA, Katsura[1*] ; IRIZUKI, Toshiaki[2]

[1]Shinshu University, [2]Shimane University

An analysis of fossil ostracode assemblages in the Kuwae Formation, central Japan, clarify the paleoenvironmental changes related to glacial and interglacial cycles during MIS G19 and G10 (Irizuki et al., 2007). Added to this, temperate intermediate waters which were warmer than those of today, were existed in interglacial periods during 3.5 to 2.8 Ma. Radiolarian faunas inferred that enhancement of ventilation due to global cooling started at approximately 2.5 Ma (Kamikuri and Motoyama, 2007). However, temperatures of the temperate intermediate waters and the timing are uncertain. So, our aims are to clarify quantitative temperatures of shallow and intermediate waters during the late Pliocene based on Mg/Ca, and to discuss change of water structures in the Sea of Japan.

Siltstones collected from the Kuwae Formation along the Tainai River were soaked in H_2O_2 for 24 hours before they were washed. Ostracode shells of genus *Krithe* (intermediate water species) and *Cytheropteron miurense* and *Cytheropteron sawanense* (shallow water species) were taken from the residues, and their Mg/Ca were measured by ICP-AES at Kochi University. Two intervals were identified in the study section based on quantitative temperature of intermediate and shallow waters and their vertical changes. Intermediate water temperatures ranged between 0 and 10 ℃ and fluctuated in short-time intervals during MIS G19-G16, although they were stable and showed a small amplitude between 3 and 7 ℃ during MIS G15-G13. Moreover, difference in temperature between shallow and intermediate waters was large in MIS G19 and G16, but was small in MIS G15-G13. These temperature difference and shifts suggest that strong stratification of shallow and intermediate waters during MIS G19-G16 changed to a condition in which temperature gradients were small due to enhance of ventilation in the Sea of Japan. MIS G15 and G13 were characterized by a large oxygen isotope values compared with those in other inter-glacial periods of the study intervals. The relative cooling in inter-glacial periods might be caused a beginning of ventilation in the Sea of Japan.

Keywords: Sea of Japan, Late Pliocene, ostracode, Mg/Ca, water structure

Japan Geoscience Union Meeting 2014
(28 April - 02 May 2014 at Pacifico YOKOHAMA, Kanagawa, Japan)

MIS01-P02 Room:Poster Time:April 29 18:15-19:30

Sedimentary Rhythms in the Middle Miocene Onnagawa Formation in Northern Japan

KUROKAWA, Shunsuke[1*] ; TADA, Ryuji[1] ; TAKAHASHI, Satoshi[1] ; MIZUTANI, Akane[1] ; KUBOKI, Yui[1]

[1]Department of Earth and Planetary Science, Graduate School of Science, The University of Tokyo

The Middle to Late Miocene bedded siliceous rocks, are widely distributed in the Pacific rim. Typical examples are the Monterey Formation, distributed along the coast of California, and the Onnagawa Formation in northern Japan. The Onnagawa Formation is mainly composed by alterations of porcellanite and siliceous mudstone, called ” hard-soft alternation ” , and finer alternations of light and dark porcellanites, in which parallel lamination is relatively well preserved. These alternations show centimeter- to meter-scale rhythms, where meter-scale rhythm is interpreted as reflecting variations in the water mass structure within the Japan Sea induced by sea-level oscillations paced by Milankovitch cycles (Tada, 1991). On the other hand, centimeter-scale rhythm reflects millennial-scale changes whose origin and cyclicity are still poorly understood.

In this study, we aim to reveal origin and cyclicity of light-dark alternation in the Onnagawa Formation, their relationship with variation of water mass structure in the Japan Sea, and implication to global climatic change.

We will create the perfectly continuous column of the Onnagawa Formation and construct detailed age model based on micro-fossil biostratigraphy and cyclo-stratigraphy. Then we will calculate the silica and detritus fluxes, respectively, from chemical composition of the siliceous rocks. We will discuss temporal variation of the water mass structure in the Japan Sea and its relation with global climatic changes.

In this presentation, we will introduce the results of our field study in Yashima area in northern Japan.

Keywords: Miocene, Onnagawa formation, Sedimentary rhythm

Japan Geoscience Union Meeting 2014
(28 April - 02 May 2014 at Pacifico YOKOHAMA, Kanagawa, Japan)

MIS01-P03 Room:Poster Time:April 29 18:15-19:30

Reconstruction of detrital flux to Lake Suigetsu during the past 20kyrs based on Color and XRF data

SUZUKI, Yoshiaki[1*] ; TADA, Ryuji[1] ; NAKAGAWA, Takeshi[2] ; NAGASHIMA, Kana[3] ; HARAGUCHI, Tsuyoshi[4] ; GOTANDA, Katsuya[5] ; IRINO, Tomohisa[6] ; SUGISAKI, Saiko[1] ; SG12/06, Project members[7]

[1]Univ. Tokyo, [2]Univ. Newcastle, [3]JAMSTEC, [4]Osaka City University, [5]Chiba University of Commerce, [6]Hokkaido University, [7]SG12/06 Project

Lake Suigetsu is known for its highly precise age-depth model based on numerous ^{14}C dating combined with varve counting and wiggle matching with Chinese stalagmite record. For this reason, the sediments are capable of providing extremely precise and high resolution records of past climatic changes. Several paleo-climate reconstruction studies have been conducted based on pollen and diatom analyses of the Lake Suigetsu sediments. However, studies focusing on its detrital material were rare because its detrital component is expected to be a mixture of eolian dust, detrital material derived from surrounding slope of the lake, and suspended material derived from Hasu River that flew into Lake Mikata and came into Lake Suigetsu through a narrow and shallow channel, and it is difficult to separately evaluate materials from these different sources. However, our recent study revealed that it is possible to evaluate the contribution of the detrital material derived from Hasu River through Lake Mikata (See our presentation #01575 in Paleoclimatology and paleoceanography session).

In this study, we tried to reconstruct temporal changes in the flux of detrital material derived from Hasu River during the past 20kyrs based on Color data and XRF data of the major element composition of the sediments analyzed by XRF. We estimated the end-members to explain variations in major element chemical composition using Q-mode factor analysis and oblique rotation of reference vectors. We extracted 4 end members and found that characteristics of factor 2 resemble those of Hasu River suspension. Because number of major element composition data are limited, we estimate contribution of factor 2 to the sediment based on color data. We estimated contents of factor 2 using Multi-regression analysis between color data and factor 2 loading (composition). Factor 2 flux was calculated from factor 2 contents, dry bulk density, and linear sedimentation rates, and the result shows long-term and short-term trends. The short-term trend is characterized by sudden increases and subsequent gradual decreases of factor 2 flux where the sudden increases coincides with sedimentation of ”event layers” that could represent earthquake. The long-term trend, which seems to reflect intensity of river discharge from Hasu-River , seems to reflects rainfall intensity, shows mirroring image against stalagmite record in China suggesting that precipitation decreased in Suigetsu area when precipitation increased in South China.

Keywords: Lake Suigetsu, Deglaciation, Holocene, Factor analysis, Multi-regression analysis

Japan Geoscience Union Meeting 2014
(28 April - 02 May 2014 at Pacifico YOKOHAMA, Kanagawa, Japan)

MIS01-P04 Room:Poster Time:April 29 18:15-19:30

The East Asian winter monsoon variability during the past 150,000 years

YAMAMOTO, Masanobu[1*] ; SAI, Hirotaka[1] ; CHEN, Min-te[2] ; ZHAO, Meixun[3]

[1]Faculty of Environmental Earth Science, Hokkaido University, [2]National Taiwan Ocean University, [3]Ocean University of China

The response of the East Asian winter monsoon variability to orbital forcing is still unclear, and hypotheses are controversial. We present a 150,000 yr record of sea surface temperature difference (delta SST) between the South China Sea and other Western Pacific Warm Pool regions as a proxy for the intensity of the Asian winter monsoon, because the winter cooling of the South China Sea is caused by the cooling of surface water at the northern margin and the southward advection of cooled water due to winter monsoon winds. The delta SST showed dominant precession cycles during the past 150,000 yr. The delta SST varies at precessional band and supports the hypothesis that monsoon is regulated by insolation changes at low-latitudes (Kutzbach, 1981), but contradicts previous suggestions based on marine and loess records that eccentricity controls variability on glacial-interglacial timescales. Maximum winter monsoon intensity corresponds to the May perihelion at precessional band, which is not fully consistent with the Kutzbach model of maximum winter monsoon at the June perihelion. Variation in the East Asian winter monsoon was anti-phased with the Indian summer monsoon, suggesting a linkage of dynamics between these two monsoon systems on orbital timescale.

Keywords: The East Asian winter monsoon, The South China Sea, The Western Pacific Warm Pool, Precession, Sea surface temperature

Japan Geoscience Union Meeting 2014
(28 April - 02 May 2014 at Pacifico YOKOHAMA, Kanagawa, Japan)

MIS21-01 Room:511 Time:April 28 09:00-09:15

Geochemical and molecular biological characterization of nitrogen dynamics in (hado)pelagic sediments

NISHIZAWA, Manabu[1*] ; HIRAI, Miho[1] ; NOMAKI, Hidetaka[1] ; YANAGAWA, Katsunori[1] ; MAKABE, Akiko[2] ; KOBA, Keisuke[2] ; NUNOURA, Takuro[1]

[1]JAMSTEC, [2]TUAT

Great progress has been made in understanding the nitrogen cycle in oceanic waters by the recent identification of ammonia-oxidizing archaea and anaerobic ammonia oxidizer (anammox), and by the following comprehensive approaches to clarify the abundance and activity of each component in the nitrogen cycle. However, nitrogen dynamics in marine sedimentary habitats is still uncertain. To further characterize nitrogen dynamics in the deep-sea sediments, we have quantified i) gene abundance of putative nitrifers, denitrifers and anammox, and ii) potential rate of denitrification in the hadopelagic sediment cores taken from the Ogasawara Trench (water depth of 9760m). We have also determined nitrogen and oxygen stable isotopic compositions of nitrate in the interstitial water in the hadopelagic sediments. Abundance of potential proteobacterial denitrifers correlated with that of nitrifers through the depth, and anammox also likely co-occurred with nitrifers. Further, nitrate isotope compositions suggest the enrichment of 18O by nitrification process and co-occurrence of nitrification and denitrification in nitrate reduction zone. The data suggest that aerobic and anaerobic processes of the nitrogen cycle coupled in the nitrate reduction zone in the hadopelagic sediments.

Japan Geoscience Union Meeting 2014
(28 April - 02 May 2014 at Pacifico YOKOHAMA, Kanagawa, Japan)

MIS21-02 Room:511 Time:April 28 09:15-09:30

Niche separation of nitrifiers and anammox in deep-sea sediments.

NUNOURA, Takuro[1*] ; HIRAI, Miho[1] ; NISHIZAWA, Manabu[1] ; -, Juliarni[1] ; NOMAKI, Hidetaka[1] ; SUGA, Hisami[1] ; TASUMI, Eiji[1] ; MIYAZAKI, Junichi[1] ; MAKABE, Akiko[2] ; KOBA, Keisuke[2] ; TAKAI, Ken[1]

[1]JAMSTEC, [2]TUAT

We revealed the distribution patterns of nitrifiers and anammox along with geochemical gradients in a hadopelagic sediment core from the Ogasawara Trench (Nunoura et al. 2013). The results presented novel insights into the inorganic nitrogen cycle in deep-sea sediments as shown below. 1) Thaumarchaeotes and *Nitrospina* predominates in the ammonia and nitrite-oxidizing communites, respectively. 2) The pore-water nitrate recorded isotopic signatures of nitrification. 3) Abundance of anammox was likely regulated by not only by redox potential but also by nitrite supply from ammonia oxidation. 4) Maximum abundance of denitrifier occurred at sediment surface.

The purpose of this study is to know the roles of benthic microbial inorganic nitrogen cycle in diverse deep-sea environments. In this study, we compared pore water chemistry, and abundance and composition of nitrifier and anammox populations in 6 distinct regions, and will discuss about the roles of dynamic nitrogen cycle in deep-sea benthic environments.

Keywords: nitrification, anammox

Japan Geoscience Union Meeting 2014
(28 April - 02 May 2014 at Pacifico YOKOHAMA, Kanagawa, Japan)

MIS21-03 Room:511 Time:April 28 09:30-09:45

Ecology of viruses in deep-sea hydrothermal vents

YOSHIDA, Yukari[1*]

[1]JAMSTEC

Since the discovery of ubiquitous and highly abundant viruses in aquatic ecosystems, many studies have been conducted to discern the role of viruses within aquatic microbial communities. As a result, viruses are now recognized to be significant components of all aquatic ecosystems. It has been suggested that they affect global nutrient and biogeochemical cycles in the world's oceans, and play a role in regulating abundance and composition of microbial communities. Viruses can also mediate lateral gene transfers and drive the diversification of microbial communities and the co-evolution between viruses and hosts.

Deep-sea hydrothermal vents are sites having great microbial biomass, high productivity, and physiologically and genetically high diversity, contrasting sharply with the surrounding sparsely populated deep-sea environments. The primary production in the deep-sea vent ecosystem is sustained by chemolithoautotrophic microorganisms that utilize reduced chemical compounds from the earth interior as energy sources. To date, the biogeochemical processes, ecophysiological functions, and evolutionary significance of deep-sea vent microbial communities have been extensively studied, but the ecological and evolutionary impacts of viruses on the deep-sea vent microbial communities remain to be fully elucidated.

Here, I provide an overview of current hot research topics related to viruses in aquatic ecosystems, and then introduce our studies on the viral functions and ecology in deep-sea hydrothermal vents in addition to several previous studies on virus-host interactions.

Keywords: virus, hydrothermal vent, chemolithoautotrophs

Japan Geoscience Union Meeting 2014
(28 April - 02 May 2014 at Pacifico YOKOHAMA, Kanagawa, Japan)

MIS21-04 Room:511 Time:April 28 09:45-10:00

Iron redox cycling and subsurface offshore transport in the eastern tropical South Pacific oxygen minimum zone

KONDO, Yoshiko[1*] ; MOFFETT, James W.[2]

[1]National Institute of Polar Research, [2]University of Southern California

Iron (Fe) is well known as an essential element involved in a number of biochemical processes in the ocean such as nitrogen metabolism. The distribution of dissolved Fe in seawater depends on the nature and magnitude of the sources and sinks, and the transport mechanisms. The thermodynamically favored oxidation state of Fe, Fe(III), is strongly hydrolyzed and its removal is mainly constrained by the formation of strong complexes with natural organic ligands such as humic substances and siderophores. These organic ligands control not only the solubility of dissolved Fe in seawater, but also the bioavailability of Fe(III) for phytoplankton. Fe(III) in seawater can be reduced to Fe(II), which is more soluble and kinetically labile, although is rapidly oxidized in the oxygenated seawater. Recent studies have suggested that dissolved Fe(II) substantially exists in surface seawater (e.g., Hansard et al., 2009), suboxic layers in oxygen minimum zones (OMZs) (e.g., Kondo and Moffett, 2013), hypoxic shelf waters and sediments (Lohan and Bruland, 2007), hydrothermal vents and shallow submarine eruption (Santana-Casiano et al., 2013). Since Fe(II) is more bioavailable than Fe(III), the existence of Fe(II) could provide a big advantage for the organisms in these environments even though it is ephemeral. These results suggest the importance to investigate chemical and redox speciations of Fe to elucidate carbon and nitrogen cycles in the ocean.

The distribution of dissolved Fe, Fe(II) and Fe(III)-binding organic ligands were investigated in the upper 1000 meters of the eastern tropical South Pacific from January to March 2010, during El Nino event. Dissolved Fe concentrations were exceedingly low in surface waters, showed minima near chlorophyll maximum, and increased below that depth. While high rates of nitrogen fixation have been inferred for this region from models, our data suggest that surface Fe is much too low to support diazotrophs. Dissolved Fe and organic Fe(III) ligands concentrations at mid-depth were elevated in the nearshore stations, where virtually all dissolved Fe(III) was bound to these ligands. Maxima in the concentration of Fe(II) were seen in the oxygen-deficient and high-nitrite layers of the OMZ. Fully 8 to 68% of dissolved Fe existed as Fe(II) in the samples collected at these depths. Dissolved Fe concentration was higher in the OMZ where Fe(II) and nitrite were present. We propose that this region, the most reducing part of the OMZ, plays an important role in subsurface, offshore Fe transport.

Keywords: iron, Fe(II), oxygen minimum zone, eastern tropical South Pacific, organic ligand

Japan Geoscience Union Meeting 2014
(28 April - 02 May 2014 at Pacifico YOKOHAMA, Kanagawa, Japan)

MIS21-05 Room:511 Time:April 28 10:00-10:15

Biogeochemical cycles on the deep-sea floor revealed by isotope labeling experiments

NOMAKI, Hidetaka[1*]

[1]JAMSTEC

Deep-sea benthic food webs are mainly sustained by sinking aggregates of phytodetritus derived from the water column. Although the majority of organic matter is consumed before reaching the deep-sea floor, phytodetritus still transports a significant amount of fresh material from the surface ocean to the seafloor. A portion of the phytodetritus is converted to benthic biomass, and the remaining refractory organic matter not utilized by the benthic community is preserved in the sedimentary record. The activity of the benthic community is thus expected to be an important factor in controlling the quality of organic matter, and biogeochemical cycles on the deep-sea floor. We carried out some different types of *in situ* isotope labeling experiments to reveal these benthic processes. Results quantitatively demonstrated the fate of phytoplankton, bacteria, dissolved organic carbon, and dissolved inorganic carbon on the deep-sea floor.

Keywords: Sediment-water interface, Benthos, isotope tracer, Biogeochemical cycle

Japan Geoscience Union Meeting 2014
(28 April - 02 May 2014 at Pacifico YOKOHAMA, Kanagawa, Japan)

MIS21-06 Room:511 Time:April 28 10:15-10:30

Nitrogen isotopic record of chlorophylls as a tool for understanding of nitrogen dynamics in the oceanic photic zone

OGAWA, Nanako O.[1*] ; YOSHIKAWA, Chisato[1] ; SUGA, Hisami[1] ; OHKOUCHI, Naohiko[1]

[1]JAMSTEC

Nitrogen isotope record of chlorophylls has a large potential as a tool for reconstructing the nitrogen cycle and its dynamics in the photic zone. In this study, we determined the nitrogen isotopic compositions of chlorophyll *a* ($\delta^{15}N_{chl}$) and pheophytin *a* ($\delta^{15}N_{Phe}$) as well as nitrate ($\delta^{15}N_{NO3}$) collected from two sites (S1 and K2) in the northwest Pacific as a case study. Both chlorophyll a and pheophytin a were extracted from the particulate organic matter (POM) and purified by the fraction collector of high-performance liquid chromatography. The nitrogen isotopic composition of the isolated chlorophylls was determined by our ultra-sensitive elemental analyzer / isotope ratio mass spectrometry. The estimated isotopic fractionation associated with the chlorophyll synthesis is -7.9 ‰ to -13.1 ‰, confirming the previous studies. However, the $\delta^{15}N$ of POM is not consistent with those of chlorophylls, suggesting that the POM from both sites is a mixture of phytoplankton and other materials like detritus of zooplankton. The $\delta^{15}N_{chl}$ value provides pure $\delta^{15}N$ signature of phytoplankton, which is crucial for better understanding of nitrogen dynamics in the surface ocean. Chlorophylls are also buried and preserved in the sediments for long, and thus useful for the reconstruction of nitrogen cycle in the surface ocean in the geological past. In this presentation, we will summarize the evidence and discuss advantages and pitfalls of this tool for the future use in the oceanography and paleoceanography.

Keywords: nitrogen isotope, oceanic photic zone, nitrogen dynamics, photosynthetic pigments, nitrate

Japan Geoscience Union Meeting 2014
(28 April - 02 May 2014 at Pacifico YOKOHAMA, Kanagawa, Japan)

MIS21-07 Room:511 Time:April 28 10:30-10:45

Heterotrophic bacterial production and extracellular enzymatic activity in sinking particulate matter

YAMADA, Namiha[1*] ; FUKUDA, Hideki[2] ; OGAWA, Hiroshi[2] ; SAITO, Hiroaki[3] ; SUZUMURA, Masahiro[1]

[1]AIST, [2]AORI, The University of Tokyo, [3]Fisheries Research Agency

Heterotrophic activities on sinking particulate matter (SPM) have important role for flux of SPM. To demonstrate regional differences in heterotrophic activities on SPM, we measured heterotrophic bacterial production (HBP) in seawater and SPM as well as potential extracellular enzyme activity (EEA) in SPM on a transect along 155E in the western North Pacific Ocean in the subarctic (44N), the Kuroshio Extension area (35N), and the subtropical gyre (20N).

Samples were collected from the western North Pacific Ocean during cruise KH08-2 (Leg 2) on R/V Hakuho-maru from 23 August to 16 September 2008.

Hydrographic data were provided by a shipboard CTD profiler equipped with a carousel multi-sampling system. We obtained water-column depth profiles of dissolved nutrients including nitrate, phosphate, and silicate, Chl a, bacterial cell abundance (BA), and HBP.

We deployed standard cylindrical multi-traps, with eight acrylic trap tubes mounted at each depth. The traps were set vertically on the array line at three targeted depths of 50 m, 200 m, and 500 m at 44N, and 100 m, 200 m, and 500 m at 35 and 20N. The upper deployment depths were chosen to be just under or near the bottom of the euphotic zone. The euphotic zone was defined as the depth at which photosynthetically active radiation was 1% of the value just below the surface.

Before deployment, all trap tubes except tube for HBP and EEA in SPM on each array were filled with seawater that had been collected from 4 m below the surface at each station using the ship ' s pump, pre-filtered through a 0.2-μm capsule cartridge filter to minimize biological contamination, and mixed with sodium chloride to a final concentration of 4% (w/v) to create a density gradient. Trap tube at each depth was used for collecting samples for measuring HBP and EEM in SPM, and was filled with seawater filtered as described above that was collected just before deployment from the depth corresponding to the target layer of trap deployment with a 12-L Niskin bottle. The arrays were attached to a buoy and allowed to drift freely for 24 h at 44N, and 48 h at 35 and 20N.

Upon recovery, the traps were stored upright in the dark and left to settle for 1 h. After the contents had settled, the upper portion of the trap volume above the collection cup was gently drained by siphoning. During the siphoning, only about trap tube for HBP and EEA, an aliquot of the supernatant was subsampled approximately 30 cm from the top of the tube. After siphoning was complete, the upper cylinder of the trap tube was separated from the collection cup. The particle-rich water in each collection cup was pre-screened through a 500-μm-mesh sieve to remove swimmers and then mixed to disrupt large amorphous particles. The pre-screened filtrates were used for measurements of total mass flux of SPM, particulate organic carbon (POC) and nitrogen (PON) content, and HBP and EEA (leucine aminopeptidase (LAPase), s-glucosidase (BGase), lipase, and alkaline phosphatase (APase)).

Depth-integrated HBP in seawater from the surface to 500 m was comparable between the locations, whereas HBP in SPM at 44N was substantially lower than at the other sites. We found the highest POC export flux and export efficiency to bathypelagic depths, and the lowest water temperatures, at 44N. We found significant correlations between LAPase activity, BGase activity, POC flux and particulate organic nitrogen flux. LAPase activity was two orders of magnitude higher than BGase activity, with a BGase:LAPase activity ratio of 0.027. There were no significant correlations between HBP and EEA in SPM except for lipase, and lipase activity was significantly correlated with temperature. We propose that hydrographic conditions are an important factor controlling heterotrophic bacterial activity and export efficiency of organic carbon to the deep ocean, as are the sources and abundance of SPM produced in the euphotic zone via primary production.

Keywords: Sinking particulate matter, Sediment trap, Heterotrophic bacterial activity, Extracellular enzyme activity, western North Pacific

Japan Geoscience Union Meeting 2014
(28 April - 02 May 2014 at Pacifico YOKOHAMA, Kanagawa, Japan)

MIS21-08 Room:511 Time:April 28 11:00-11:15

Enigmas concerning sterols and their surrogates in eukaryotic cell membranes

TAKISHITA, Kiyotaka[1*] ; YABUKI, Akinori[1] ; CHIKARAISHI, Yoshito[1] ; TAKAKI, Yoshihiro[1] ; YOSHIDA, Takao[1] ; OHKOUCHI, Naohiko[1]

[1]Japan Agency for Marine-Earth Science and Technology

A large fraction of eukaryotes and bacteria respectively possess sterols and hopanoids, which function as potent stabilizers of cell membranes. Sterols are also associated with fluidity and permeability of eukaryotic cell membranes, and are key to fundamental eukaryotic-specific cellular processes such as phagocytosis. Several steps of *de novo* sterol biosynthesis require molecular oxygen. For example, the epoxidation of squalene is the first oxygen-dependent step in the sterol pathway; the epoxidized squalene is then cyclized to either lanosterol or cycloartenol by the enzyme oxidosqualene cyclase. In contrast, prokaryotic hopanoid biosynthesis does not require molecular oxygen as a substrate, and the squalene is directly cyclized by the enzyme squalene-hopene cyclase.

Until now, it was unclear how bacterivorous unicellular eukaryotes that are abundant in anoxic or low oxygen environments could carry out phagocytosis. These eukaryotes cannot obtain sterols from food bacteria as the latter generally lack them and sterols cannot be synthesized *de novo* in the absence of molecular oxygen. We have previously provided evidence that the molecule tetrahymanol is synthesized by some anaerobic/microaerophilic eukaryotes and possibly functions as an analogue of sterols in these organisms. Nevertheless, neither sterol, nor tetrahymanol, nor their related molecule has been found in the other anaerobic/microaerophilic eukaryotes, and so it is still enigmatic how these organisms maintain their fluid and permeable membrane system specific to eukaryotes.

One more area of confusion is regarding sterols in bivalves with chemosynthetic bacteria inhabiting areas of deep-sea hydrothermal vents and methane seeps, such as *Calyptogena* spp. and *Bathymodiolus* spp. In general, bivalves cannot synthesize sterols *de novo* and it is necessary for them to obtain these molecules from small eukaryotic prey. On the other hand, *Calyptogena* spp. and *Bathymodiolus* spp. mainly or exclusively acquire nutrients produced by their bacterial symbionts, rather than from eukaryotes rich in sterols. Nevertheless, these ”chemosynthetic bivalves” contain sterols. More curiously, *Calyptogena* spp. have intermediate metabolites of phytosterols (24-methylenecycloartanal, cycloeucalenol, and obutusifoliol), while *Bathymodiolus* spp. have high amounts of cholesterol typical of animals. Little attention has been given to how chemosynthetic bivalves produce or acquire these kinds of sterols.

In my talk, I will discuss potentially controversial topics regarding sterols and their surrogates in eukaryotic cell membranes, which do not appear in biochemical and geochemical textbooks.

Keywords: eukaryotes, sterols, tetrahymanol, cell membrane

Japan Geoscience Union Meeting 2014
(28 April - 02 May 2014 at Pacifico YOKOHAMA, Kanagawa, Japan)

MIS21-09 Room:511 Time:April 28 11:15-11:30

Structural differences of humic acid isolated from estuarine sediments at several fields around Ariake Sea

IWAMOTO, Yuya[1] ; YAMAUCHI, Noriaki[2*] ; NARAOKA, Hiroshi[2]

[1]Dept. of Earth and Planetary Sci., Grad. School of Sci., Kyushu Univ., [2]Dept. of Earth and Planetary Sci., Fac. of Sci., Kyushu Univ.

Material transfer and circulation of coastal areas, and the form and state of the organic matter in the estuary tidal flat area, is attracting attention at various angles from the biological importance of the river estuaries. Analysis and evaluation of the sediment material and coastal water has been carried out around the river basin. So far, we have analyzed the chemical structure of humic substance in the Chikugo River basin near or vary by region. The Ariake Sea, from the fact that environmental issues such as hypoxic water and red tide has occurred, environmental analysis have been made from various points of view in recent years. However, research of organic matter deposition simultaneous in a wide range of areas of the Ariake Sea coast is a few instances.

In this study, humic acid fraction were extracted from the surface sediment of the tidal flat areas, including rivers and estuaries tidal flats, tidal flats as well as less affected by other rivers a broad area of the northern half of the Ariake Sea. Then, the extracted humic acids were analyzed such as stable isotopic analysis and elemental composition, and regional differences were compared. And the use of humic acid as environmental indicator was evaluated from the point of some differences to the several conventional analyses of the environmental indicators at the coastal area.

Sediment samples were collected at a total of seven locations of tidal flat (estuaries at Hayatsue-gawa, Rokkaku-gawa, Hama-gawa, Kikuchi-gawa, Shira-kawa, and tidal flat at Arao and Tara) and two places of the downstream of Chikugo River from May 2011 to August 2013. Humic acid fraction were prepared according to the IHSS soil humic acid extraction method. Multiple analysis, such as the elemental analysis, stable isotope ratios, ultraviolet-visible absorption analysis (application of (A2/A4) ratio of 270nm/407nm that has been proposed by Fooken and Liebezeit (2000)) were applied to the humic acid of coastal areas.

Correlation derived from the source materials was observed between stable isotope ratio, and the atomic ratio calculated from elemental analysis, ultraviolet-visible absorption ratio and the regional differences of humic acid. Contribution of terrigenous organic matter is poor at Hama-gawa estuary Tara and Arao tidal flat. Further, trend in nitrogen isotope ratio is different from the other regions and the 2 points (Hama-gawa mouth and Tara tidal flat). Conditions such as denitrification and nitrogen sources is somewhat different in the Ariake Sea northwest side was suggsted.

Keywords: Ariake Sea, estuarine, stable isotope ratio, UV, humic substance

Japan Geoscience Union Meeting 2014
(28 April - 02 May 2014 at Pacifico YOKOHAMA, Kanagawa, Japan)

MIS21-10 Room:511 Time:April 28 11:30-11:45

Origin of fluorescent dissolved organic matter in forested headwater stream during base-flow period

OBARA, Akihiro[1*] ; OHTE, Nobuhito[1] ; EGUSA, Tomohiro[1] ; TOKUCHI, Naoko[2] ; KOBA, Keisuke[3] ; YAMASHITA, Youhei[4] ; SUZUKI, Masakazu[1]

[1]Graduate School of Agricultural and Life Sciences, The University of Tokyo, [2]Field Science Education and Research Center, Kyoto University, [3]Graduate School of Agriculture, Tokyo University of Agriculture and Technology, [4]Graduate School of Environmental Science, Hokkaido University

In this study, we focus on fluorescent dissolved organic matter (FDOM) such as humic substances (HSs) and aromatic amino acids, which constitutes the main portion of streamwater DOM. Our objective is to estimate the origin of streamwater FDOM during baseflow period, by comparing its composition with soil infiltration water, saturated groundwater and bedrock spring water.

Our study site is Inokawa watershed (watershed area 503 ha) in The University of Tokyo Chiba Forest. We collected stream water samples and bedrock spring water at 142 points in the watershed in 2009, 2010 and 2012, and also soil waters and groundwater in Fukuroyamasawa Experimental Watershed (2ha) which is one of most headwater hollows. Rainwater was collected at the weather station in the watershed. The water samples were filtered with 0.45mm membrane filters and analyzed for DOC concentration by wet-oxidation method, and Excitation-Emission Matrix (EEM) using 3D-spectrofluorometry. EEMs were compiled and further analyzed by Parallel Factor Analysis based on Murphy et al., (2013), and decomposed into five components with distinctive fluorescence spectra. Chemical characteristics of components were identified by comparing their spectral shapes with previous studies as follows: C1 as humic acid type HS-like, C2 as fulvic acid type HS-like, C3 as microbial-derived HS-like, C4 as tryptophane-like and C5 as tyrosine-like.

Groundwaters and bedrock spring waters were classified into three groups based on the ratio of three HS-like components, as C1-dominant group, C2-dominant group and C3-rdominant group. Although groundwater in Fukuroyamasawa watershed belonged to C1-dominant group, and showed seasonal change in DOC concentration, the composition of HS-like components of groundwaters and bedrock spring waters in three groups were temporally relatively stable. This suggests that these groups can be used as end-members in identification of the origin of streamwater FDOM.

Ratios of three HS-like components in streamwaters fell in between groundwater groups and soil waters in about half of the samples. In other samples, however, ratios could not be explained by mixing of such hillslope end-members. FDOM of those streamwaters had higher abundance of C1 and C2, and also relatively higher DOC concentrations, suggesting that it was originated not only from soil and/or groundwater in the hillslope, but also from organic materials in the stream such as deposited litters, woody debris and/or other organic-containing sediments. As to aromatic amino acid-like components, streamwater FDOM tended to have lower C5/C4 ratio relative to hillslope waters, and often had C5 undetectable, suggesting that C5 was more labile than C4 in stream envirnment.

This study showed that HS in streamwater is produced not only in hillslope but also in stream itself, and in-stream produced HS can show different fluorescence spectral characteristics from hillslope-produced HS.

Keywords: fluorescent dissolved organic matter (FDOM), forested watershed, streamwater chemistry, excitation-emission matrix (EEM), parallel factor analysis (PARAFAC)

Japan Geoscience Union Meeting 2014
(28 April - 02 May 2014 at Pacifico YOKOHAMA, Kanagawa, Japan)

MIS21-11 Room:511 Time:April 28 11:45-12:00

Pseudopolarographic estimation of copper complexing ligands in freshwater of Lake Biwa, Japan

MARUO, Masahiro[1*] ; OBATA, Hajime[2]

[1]School of Environmantal Science, The University of Shiga Prefecture, [2]Atmosphere and Ocean Research Institute, The University of Tokyo

Pseudopolarography (Croot P. L. et al., Mar. Chem., 67, 219-232 (1999), Wiramanaden C. I. E., et al., Mar Chem., 110, 28-41 (2008)) is useful method to detect metal (copper) complexation that is very stable compared with that detected by other methods: AdCSV: adsorptive cathodic stripping voltammetry, ion selective electrode etc. in water. It was applied in seawater analysis especially for coastal area where large amount of organic material with high complexing capacity was detected. Also in freshwater lake, there is high potential of existence of very stable copper complexes in water, as it sometimes includes high concentration of sulfur containing compounds and concentration of competing metals such as calcium and magnesium are very low compared with those in seawater. Existence of very stable ligands was investigated using freshwater sampled in Lake Biwa, Japan.

As reference ligands, EDTA, DPTA and CDTA were used at pH 8.8 using borate buffer solution. Copper was deposited on HDME (hanging mercury drop electrode) by varying potential from -0.2 to -1.5 V, and deposition time was 420 s. After deposition, deposited copper was stripped by scanning from the deposition potential to 0 V. Peak height was plotted against deposition potential, and half wave potential was determined. By comparing the half wave potential with that of reference ligands, stability of copper complexing ligands in the sample was estimated.

Half wave potentials measured by references were -0.4 V for EDTA, -0.58V for CDTA, and -0.65 V for DTPA, respectively. By measuring water sampled at north basin of Lake Biwa, half wave potentials at -0.5 V and -1.1 V was obtained for surface water. Only single half wave potential at -0.5 V was obtained for waters at 2m and 10m depth. Existence of strong ligands that has stability close to EDTA was detected all samples tested. These ligands were also detected by AdCSV using salicylaldoxime as competing ligands. But ligand detected at half wave potential at -1.1 V is not detected or undetectable. It might suggest significance of very stable complexes in water of Lake Biwa.

Keywords: freshwater, Lake Biwa, copper, ligand, electroanalysis

Japan Geoscience Union Meeting 2014
(28 April - 02 May 2014 at Pacifico YOKOHAMA, Kanagawa, Japan)

MIS21-12 Room:511 Time:April 28 14:15-14:30

Isotopic composition of chlorophylls as a new indicator of energy flow in stream ecosystems

ISHIKAWA, Naoto F.[1*] ; SUGA, Hisami[1] ; OGAWA, Nanako O.[1] ; OHKOUCHI, Naohiko[1]

[1]JAMSTEC

In most freshwater (e.g., stream) ecosystems, periphytic algae attached to a substrate (periphyton) play an important role as benthic primary producer. However, the energy flow, which is transferred from periphyton to animal consumers through trophic pathways, has not yet been adequately assessed because few studies have traced algal signatures from periphyton matrix to food webs. Here we present a new application of the isotopic composition of chlorophylls in periphyton to the tracer of *in situ* primary production. Chlorophylls can be used as a biomarker of photosynthetic autotrophs, including periphytic algae. We purified chlorophylls from periphyton matrix using a high performance liquid chromatograph (HPLC), and measured carbon and nitrogen stable isotope ratios of chlorophylls, pheophytins, the bulk of periphyton, and algal grazing specialists (e.g., *Epeorus latifolium*: mayfly larva) using an elemental analyzer coupled with an isotope ratio mass spectrometer (EA/IRMS). We will compare the results with traditional isotope maps, and discuss the potential of the isotopic composition of chlorophylls in aquatic food web studies.

Keywords: periphyton, photosynthetic pigments, biomarker, HPLC, stable isotopes

Japan Geoscience Union Meeting 2014
(28 April - 02 May 2014 at Pacifico YOKOHAMA, Kanagawa, Japan)

MIS21-13 Room:511 Time:April 28 14:30-14:45

Biodiversity indicators of trophic structure measured by stable isotope ratios

TAYASU, Ichiro[1*] ; KATO, Yoshikazu[1] ; ISHIKAWA, Naoto F.[2] ; YOSHIMIZU, Chikage[1] ; HARAGUCHI, Takashi, F.[1] ; OKUDA, Noboru[1] ; TOKUCHI, Naoko[3] ; KOHMATSU, Yukihiro[3] ; TOGASHI, Hiroyuki[4] ; YOSHIMURA, Mayumi[5] ; OHTE, Nobuhito[6] ; KONDOH, Michio[7]

[1]Center for Ecological Research, Kyoto University, [2]Japan Agency for Marine-Earth Science and Technology, [3]Field Science Education and Research Center, Kyoto University, [4]Tohoku National Fisheries Research Institute, Fisheries Research Agency, [5]Kansai Research Center, Forestry and Forest Products Research Institute, [6]Graduate School of Agricultural and Life Sciences, The University of Tokyo, [7]Faculty of Science and Technology, Ryukoku University

The term ”biodiversity” is considered as multi-level diversity, ranging from genetic, species, to ecosystem level. However, it is difficult to measure arbitrary level of biodiversity, therefore, biodiversity assessment at species level is often applied to an ecosystem. Biodiversity assessment at species cannot directly be related to ecosystem function, thus, a grouping method, such as functional feeding group (FFG), is often used in stream ecology.

Our project, funded by the Environment Research and Technology Development Fund (4D-1102), aimed at developing a method to evaluate functions of biodiversity in watershed ecology, especially streams. Stable isotope tools have been used to study watershed ecology, which covers researches on nutrient cycling and food web structure among forest, river, lake and coastal ecosystems. Recently, nitrogen isotope ratios of individual amino acids have been measured to estimate trophic positions of animals. However, this technique has not been applied to complex food web analysis, such as freshwater systems, which are based on both autochthonous and allochthonous productions. We have proved that this method is applicable to various freshwater food webs, including the system to which the bulk-isotope method could not be applied. Application of the method to archived biological specimen allows us to study long-term trophic changes in the ecosystem. Natural abundance of radiocarbon is another signature that separates carbon sources in freshwater ecosystems.

We suggest that a trophic structure estimated by various isotope signatures, together with estimated biomass of each taxonomic group, is an alternative index of describing biodiversity in watershed ecosystems.

Keywords: Stable isotope ratios, Food web, Trophic position

Japan Geoscience Union Meeting 2014
(28 April - 02 May 2014 at Pacifico YOKOHAMA, Kanagawa, Japan)

MIS21-14 Room:511 Time:April 28 14:45-15:00

Vertical distribution of the triple oxygen isotopic compositions of DO in oligotrophic/mesotrophic environments

TSUNOGAI, Urumu[1*] ; MINAMI, Sho[1] ; SAKUMA, Hiroki[1] ; KOMATSU, Daisuke[1] ; NAKAGAWA, Fumiko[2]

[1]Graduate School of Environmental Studies, Nagoya University, [2]Faculty of Science, Hokkaido University

In order to quantify the gross production rate of dissolved oxygen molecules (DO) in hydrosphere beneath thermocline, vertical distributions of the triple oxygen isotopic compositions of DO in oligotrophic/mesotrophic lakes were determined, together with their temporal variations.

Keywords: oligotrophic lake, mesotrophic lake, dissolved oxygen, triple oxygen isotopes, vertical profile, seasonal variation

Japan Geoscience Union Meeting 2014
(28 April - 02 May 2014 at Pacifico YOKOHAMA, Kanagawa, Japan)

MIS21-15 Room:511 Time:April 28 15:00-15:15

Biogeochemistry on glaciers and icesheets ? Microbial process of glacier darkening and material cycles

TAKEUCHI, Nozomu[1*]

[1]Chiba University

Glaciers and icesheets have been reported to shrink worldwide, probably caused by recent global warming. They are inhabited by diverse organisms, which adapted to the cold environment. Snow and ice algae grow photosynthetically on their surface and sustain heterotrophic microbes. Organic matter including their bodies and products can reduce surface albedo and accelerate melting of glaciers. Thus, shrinkage of glaciers and icesheets is not only due to climate change, but also possibly due to change of glacier ecosystems. Therefore, it is important to assess quantitatively biogeochemical process of carbon and nitrogen cycles on glaciers. In this talk, I would like to review our present knowledge on glacial ecosystems including Asian and polar glaciers and discuss possible reasons of recent darkening of the Greenland icesheet.

Keywords: glacier, Greenland, albedo, algae, microbe, carbon cycle

Japan Geoscience Union Meeting 2014
(28 April - 02 May 2014 at Pacifico YOKOHAMA, Kanagawa, Japan)

MIS21-16 Room:511 Time:April 28 15:15-15:30

How does anthropogenic nitrogen input affect the nutrient dynamics and food web structures?

OHTE, Nobuhito[1*] ; TOGASHI, Hiroyuki[3] ; TOKUCHI, Naoko[2] ; YOSHIMURA, Mayumi[6] ; KATO, Yoshikazu[7] ; ISHIKAWA, Naoto F.[5] ; KONDO, Michio[4] ; TAYASU, Ichiro[7]

[1]Graduate School of Agricultural and Life Sciences, University of Tokyo, [2]Tohoku National Fisheries Research Institute, Fisheries Research, [3]Field Science Education and Research Center, Kyoto University, [4]Kansai Research Center, Forestry and Forest Products Research, [5]Center for Ecological Research, Kyoto University, [6]Japan Agency for Marine-Earth Science and Technology, [7]Faculty of Science and Technology, Ryukoku University

In last five decades, impacts of anthropogenic nutrient inputs on river ecosystems have continuously been a major concern for the governments and residents of the catchments in Japan. Major sources of anthropogenic nitrogen (N) include leachate from forest ecosystem, surplus fertilizers and sewage. Impacts of anthropogenic N inputs on nutrient dynamics and food web structures were investigated using stable N isotope techniques in the Arida river catchment, Japan. Riverine survey utilizing 5 regular sampling points showed that δ^{15}N of nitrate (NO_3^-) increased from forested upstream (˜2 ‰) to the downstream (˜7 ‰) due to the sewage loads and fertilizer effluents from agricultural area. Correspondingly the δ^{15}N of benthic algae and aquatic insects increased toward the downstream. This indicates that primary producers of each reach strongly relied on the local N sources and it was utilized effectively in their food web. Simulation using a GIS based mixing model considering the spatial distributions of human population density and fertilizer effluents revealed that strongest impacts of N inputs was originated from organic fertilizers applied to orchards in the middle to lower parts of catchment. Differences in δ^{15}N between primary producers and predators were ˜6-7 ‰ similarly at all sampling points. Food web structural analysis using food network unfolding technique based on observed δ^{15}N suggested that the structure of nutrient pyramid did not differ significantly along the riverine positions, while the members of species in each trophic revel changed and the impact of anthropogenic N input was visible along the river.

Keywords: river ecosystem, nitrogen input, stable isotope, food web

Japan Geoscience Union Meeting 2014
(28 April - 02 May 2014 at Pacifico YOKOHAMA, Kanagawa, Japan)

MIS21-17 Room:511 Time:April 28 15:30-15:45

Aerobic methane production in oxygenated water column of a lake ecosystem

IWATA, Tomoya[1*] ; KOBAYASHI, Ai[1] ; NAITO, Azusa[1] ; KOJIMA, Hisaya[2]

[1]University of Yamanashi, [2]Hokkaido Univerisity

Methane is a potent GHG with about twenty times the global warming potential of carbon dioxide. Globally, half of CH_4 emissions are linked to industry and the extraction of fossil fuels, while the remainder of emissions is related to natural sources such as wetlands, freshwaters, oceans, forests, and termites. Among such various natural sources, lake ecosystems are now recognized as the important source of atmospheric CH_4, evading the 8-48 Tg CH_4 yr^{-1} (6-16% of total natural CH_4 emissions and greater than oceanic emission)(Bastviken et al. 2004). Therefore, identifying the pathways and mechanisms of CH_4 production in lake ecosystems is prerequisite to predict the GHG concentrations in the atmosphere and the resultant global warming in the future of the earth.

In lake ecosystems, the majority of methane production has long been believed to occur in anoxic sediments via methanogenesis. However, we have recently found the novel pathway of methane production in aerobic environments with well-oxygenated water in oligotrophic lakes. In particular, in lakes with phosphorus-deficient conditions, dissolved CH_4 concentrations often exhibit a large subsurface maximum during the stratified period. Moreover, seasonal occurrence of the CH_4 maximum was closely related to the abundance of planktonic microbes (such as *Synechococcus*) in the oxygenated water, suggesting active methane production by microbes even in the presence of O_2. Furthermore, the microcosm experiments confirmed the aerobic methane production when methylphosphonic acid (MPn) was added to the P-deficient lake water, suggesting the expression of *phn* genes encoding a carbon-phosphorus (C-P) lyase pathways for P utilization and producing methane from MPn. These findings are contradict to the conventional theory of methane production (methanogenesis in the absence of oxygen) but correspond to the recent findings on the aerobic CH_4 production in the North Pacific gyre (Karl et al. 2008); this study showed that marine microorganisms use MPn as a source of phosphorus when inorganic phosphate is scarce and generate CH_4 as a byproduct of MPn metabolism.

In this session, we will present such novel methane production pathway observed in an oligotrophic lake, central Japan. Spatial and temporal dynamics of dissolved methane and planktonic microbes, as well as the laboratory microcosm experiments show the causal relationships between aerobic microorganisms, their phosphonate metabolism, and aerobic methane production in lake ecosystems.

Keywords: Aerobic methane production, cyanobacteria, Synechococcus, methylphosphonic acid, P-deficient lake

Japan Geoscience Union Meeting 2014
(28 April - 02 May 2014 at Pacifico YOKOHAMA, Kanagawa, Japan)

MIS21-18 Room:511 Time:April 28 15:45-16:00

Effect of fertilizer use and N deposition on global terrestrial nitrogen cycling in 1960-2010

NISHINA, Kazuya[1*] ; ITO, Akihiko[1] ; HANASAKI, Naota[1] ; MASAKI, Yoshimitsu[1]

[1]National Institute for Environmental Studies

Human activities have considerably disturbed terrestrial nitrogen cycling especially after the industrial revolution. Because Harbor-Bosch techniques and fossil fuel combustions have been large sources of reactive nitrogen to the terrestrial ecosystems. The recent N loading derived from these sources on terrestrial ecosystems was estimated 2 times higher than biogenic N fixation in terrestrial ecosystems (Gruber et al., 2009). In this study, we evaluated N fertilizer and N deposition on global terrestrial N cycling using ecosystem model 'VISIT' and global datasets. For the cropland, we made spatial temporal explicit N fertilizer input data (as NH4+ and NO3- respectively) made by FAO statistics, historical land-use dataset and global crop calendar in SAGE dataset. For N deposition, we used global grid data from Galloway et al. (2004) with simple interpolation in time-series. From the simulation results, we evaluated historical N cycling changes by land-use changes and N depositions in N cycling (e.g., N leaching, N2O, NO) at global scale.

Keywords: N fertilizer, N deposition, N2O, Land use change, N leaching

Japan Geoscience Union Meeting 2014
(28 April - 02 May 2014 at Pacifico YOKOHAMA, Kanagawa, Japan)

MIS21-19 Room:511 Time:April 28 16:15-16:30

The diversity-stability relationship in soil microbial community investigated by a diversity-manipulation experiment

USHIO, Masayuki[1*]

[1]Center for Ecological Research, Kyoto University

How biodiversity influences the stability of ecosystem processes is the central question in environmental science, but empirical investigations on the biodiversity-stability relationship in soil microbial community is still limited. To investigate the diversity-stability relationship in soil microbial community, microbial community composition was manipulated using taxon-specific biocides, and changes of community functions (i.e., soil decomposition activities) against changes in external environmental factors (i.e., plant materials to be decomposed) imposed to the soil microbial communities were investigated in a microcosm experiment.

Distilled water, bactericide (oxytetracycline) and fungicide (cycloheximide) were added to forest soils to create communities that are intact (i.e. fungi and bacteria are coexisting), fungi dominated and bacteria dominated, respectively. For decomposition substrates, fresh leaves of eastern hemlock and sugar maple were collected from the same location as the soil collection. The leaves, whose chemical qualities differ from each other, were dried, powdered, then mixed to fixed proportions to produce the substrate quality variations. The substrates were then added to each microbial community, and soil decomposition activity (soil respiration rate and activities of acid phosphatase, N-acetyl-glucosamidase, β-D-glucosidase and cellbiohydrase) was measured after the substrate addition.

Soil respiration rates of the bacterial and fungal communities showed highly significant change along the substrate quality variation, but those of the coexisting community changed less significantly. Dependence of the enzyme activity on the substrate quality in the coexisting community was the weakest in general. These results indicated that the decomposition activity of the coexisting community was generally more stable than those of the less-diverse communities. In addition, microbial community compositions, which were estimated by soil lipid profile, changed more flexibly along the substrate quality variation for the coexisting community. These results can be interpreted as that, for the coexisting community, substrate quality influenced the microbial composition, and in turn, the shift in the microbial composition buffered the influences of the changes of substrate quality. The results could indicate that belowground microbial diversity as well as aboveground plant biodiversity is essential for the stability of terrestrial ecosystem processes, which are driven by the interaction of production and decomposition.

Great cautions should be taken because the specificity of the taxon-specific biocides used in this study was not perfect. For example, there must be many bacteria species that could not be inactivated by the addition of the bactericide. In order to understand the diversity-stability, or diversity-function, relationship in microbial community, more sophisticated methodology to manipulate microbial community composition is required. Limitations of current methodologies as well as possible techniques for the better manipulation of microbial community composition will be discussed in this presentation.

Keywords: biocides, enzyme activity, diversity, soil microbial community, soil respiration rate, stability

Japan Geoscience Union Meeting 2014
(28 April - 02 May 2014 at Pacifico YOKOHAMA, Kanagawa, Japan)

MIS21-20 Room:511 Time:April 28 16:30-16:45

Determination of phosphorus species and bioavailavility in allophanic and non-allophanic Andisols

TAKAMOTO, Akira[1*] ; HASHIMOTO, Yohey[1] ; WAGAI, Rota[2]

[1]Tokyo University of Agriculture and Technology, [2]National Institute for Agro-Environmental Sciences

Andisols have high phosphorus (P) retention capacity due to abundant active aluminums (Al) and irons (Fe). Such characteristics result in a significant inhibition of plant growth in Andisols, if not properly managed. Andisols are categorized into two groups on the basis of the difference in the clay mineral compositions. One group is called as allophanic Andisols, including allophane and imogolite in the clay fraction. The other is called as non-allophanic Andisols, including Al- and Fe- humus complexes and 2:1 phyllosillicates. These soil colloids are considered a major cause of high P retention capacity of allophanic and non-allophanic Andisols. Soil P forms have been investigated using chemical extraction methods. Chemically extracted P fractions of H_2O-P and $NaHCO_3$-P are considered readily soluble P, while NaOH-P is modelately labile P associated with Al and Fe, and HCl-P is apatite-like P. However, there are no studies determining chemical species and hosting phases of P in allophanic and non-allophanic Andisols at the molecular levels. This study was conducted to characterize the species and sorption hosts of P in allophanic and non-allophanic Andisols using Hedley's sequential P extraction method, solution ^{31}P-NMR and X-ray absorption near-edge structure (XANES) spectroscopy. For revealing the behavior of P in soils precisely, it is required to separate the different soil colloids along with their density and then identify P speciation and hosting mineral phases. This study used a density separation method that can classify soil colloids including humus and Al/Fe (oxy)hydroxides by their density.

The total concentration of P in the allophanic and non-allophanic Andisols was 6.2 g P kg^{-1}. The sequential fractionation of bulk soil showed that the largest P pool of both allophanic and non-allophanic Andisols was NaOH-P. The density fractions of 2.0-2.25, 2.25-2.5, and $>$2.5 g cm^{-3}accounted for 88% of allophanic Andisols, and among five fractions, the 2.0-2.25 g cm^{-3} fraction was largest (44%). On the other hand, the density fractions of 1.8-2.0, 2.0-2.25, 2.25-2.5, and $>$2.5 g cm^{-3} accounted for 88% of non-allophanic Andisols. The sequential fractionation of allophanic Andisols showed that the NaOH fraction had a large proportion of inorganic P (Pi, 76-92%) and organic P (Po, 72-99%). The sequential fractionation of non-allophanic Andisols also showed NaOH-Pi (46-83%) and Po (54-97%) were consisted largely of phosphorus pool, with exceptions in $>$2.25 g cm^{-3} fractions. The results combined with the density separations and sequential extraction indicated that i) P in allophanic and non-allophanic soils is primarily associated with Fe and Al minerals, ii) Pi and Po in the 2.0-2.25 g cm^{-3} fraction accounted largely for the total P of allophanic Andisols (Pi: 61%, Po: 68%), iii) Pi and Po in 1.8-2.0 g cm^{-3} fraction accounted largely for allophanic Andisols (Pi: 48%, Po: 64%). According to the solution ^{31}P-NMR results, orthophosphate monoester accounted largely for Po in allophanic and non-allophanic Andisols. Further investigations on XANES and NMR spectroscopy will be presented for more detailed P speciation in the soils.

Keywords: phosphorus, ecosystem, Andisols

Japan Geoscience Union Meeting 2014
(28 April - 02 May 2014 at Pacifico YOKOHAMA, Kanagawa, Japan)

MIS21-21 Room:511 Time:April 28 16:45-17:00

Developement of a carbonized wood passive sampker for atmospheric mercury

OKUMA, Akihiro[1*] ; SATAKE, Kenichi[1]

[1]Geo-environmental Sci, Rissho Univ

[Intro]

UNEP and WHO require reduce the amount used and mercury emission because it is a toxic metal. As a result, reduce and discharge in the world but Southeast Asia and China increase coal production and used by gold mining, And so increase emission to atmosphere. Emitted mercury to atmosphere is Hg^0 (elemental mercury) with over 95%. It can be transported and deposited to remote place from the sources because calculated atmospheric residence time of Hg^0 was estimated about 1 to 2 year. Furthermore deposited Hg can be converted to organic mercury and accumulated in the food chain, posing a potential threat to human′ s health. As a result, it is important to monitoring atmospheric mercury pollution. The present, atmospheric mercury sampler is active sampler with gold amalgam collection glass tube, but it is difficult to sampling cover wide area for high costs and need electrical power. So we made simple passive sampler for mercury monitoring with carbonized wood and experimented.

[Method]

Sticked a wood (*c.japonica*) to acrylic laboratory dish with double-stick tape after it had been cut to 2.5cm×4.5cm×1.5cm and carbonized at 300 ℃ 2h in a electric muffle furnace. We conducted Uryu Exoerimental Forest of Hokkaido University, Sapporo campus of Hokkaido University, Kumagaya campus of Rissho University, Kuniiriyama in Gunma , Kanazawa University, Tottori University, Hiroshima University and Chiang Mai University (Thailand). Moreover, we compared the active sampler at Center for Environmental Science in Saitama.

[Result]

Mercury concentration in propose passive sampler increased as day passed at All conducted sites. Mercury concentration in part of carbonized woods were 0.39 (for 33 days), 0.44 (for 66 days), 0.63 (for 95days), 0.86 (for 127 days), 0.91 ng Hg cm^{-2} (for 158 days), and correlation coefficient was 0.95 at Center for Environmental Science in Saitama.

Atmospheric mercury concentration range were 2.0 to 2.6 ng Hg m^{-3} during experiment. Absorption mercury speed into carbonized wood was uniform in steady atmospheric mercury. Propose passive sampler and active sampler were correlated, slope was y=14.7x, correlation coefficient was 0.95. Propose passive sampler was agreement with the data obtained by an active sampler by these results.

Keywords: mercury, carbonized wood, passivesamplerq, monitoring of air pollution

Japan Geoscience Union Meeting 2014
(28 April - 02 May 2014 at Pacifico YOKOHAMA, Kanagawa, Japan)

MIS21-22 Room:511 Time:April 28 17:00-17:15

Mechanisms and regulating factors of dissolved organic matter production in beech forest soils in northern Kyoto

FUJII, Kazumichi[1*] ; NAKADA, Yuji[2] ; YOSHIDA, Makoto[2] ; HAYAKAWA, Chie[3] ; SUGIHARA, Soh[3] ; FUNAKAWA, Shinya[3]

[1]Forestry and Forest products Research Institute, [2]Tokyo University of Agriculture and Technology, [3]Kyoto University

In forest ecosystems, most of the organic matter supplied to the organic layer mineralizes to CO_2, but a proportion (˜30%) is leached as dissolved organic matter (DOM), as soil water percolates. DOM plays important roles in carbon and nutrient cycling in forest soils, however, the controlling factors and mechanisms of DOM production remain to be clarified. Since DOM contains high concentrations of aromatic compounds derived mainly from lignin, the roles of microorganisms in lignin solubilization and DOM production were investigated under field condition.

The concentrations and fluxes of dissolved organic carbon (DOC) in soil solution were quantified under beech forest in northern Kyoto. The activities of lignin-degrading enzymes, lignin peroxidase (LiP) and manganese peroxidase (MnP), and fungal community composition were analyzed.

The DOC fluxes increased in the organic layer (344 kg C ha^{-1} yr^{-1}), followed by a decrease with depth in the mineral soil layers (20 kg C ha^{-1} yr^{-1}). The seasonal fluctuation of DOC concentrations showed that DOC production increased in summer with increasing temperature, highlighting the importance of microbial activity to DOM production. The activities of both lignin-degrading enzymes, MnP and LiP, were detected in the organic layers, and several potential producers of enzymes, namely basidiomycete fungi, were also identified. These findings could support the central roles of fungi in lignin solubilization and DOC production in organic layers under beech forest in northern Kyoto, where the large fluxes of DOM leaching was observed.

Japan Geoscience Union Meeting 2014
(28 April - 02 May 2014 at Pacifico YOKOHAMA, Kanagawa, Japan)

MIS21-23 Room:511 Time:April 28 17:15-17:30

Soil nitrite transformation along a forest slope and controlling factors

KUROIWA, Megumi[1*] ; ISOBE, Kazuo[1] ; KATO, Hiroyu[1] ; MURABAYASHI, Sho[1] ; KANEKO, Yuka[1] ; ODA, Tomoki[1] ; OHTE, Nobuhito[1] ; OTSUKA, Shigeto[1] ; SENOO, Keishi[1]

[1]Graduate School of Agricultural and Life Sciences, The University of Tokyo

We conducted a tracer study to clarify the spatial heterogeneity of nitrite (NO_2^-) dynamics in forest soils. Because of its reactive nature, NO_2^- does not usually accumulate in forest soils. This low concentration and experimental difficulties of accurate quantification have hampered quantitative detailed analyses of gross NO_2^- production and consumption in terrestrial environments. However, NO_2^- is an intermediate in many N transformation processes including nitrification and denitrification. Furthermore NO_2^- can also be reduced to gaseous N and react with organic matter not only biologically but also chemically. Thus NO_2^- dynamics may control whole N retention/emission characteristics in forest soils.

We added $^{15}NO_2^-$ to mineral top soils derived from a slope of a Japanese cedar forest. Primary properties of soils such as concentration of inorganic N, pH and water content differed geographically; N concentration, pH and water content are lower in the upper soils. NO_2^- production and consumption rates gradually increased from upper slope to lower slope. Quite short mean residence time of NO_2^- implies that NO_2^- consumed very rapidly anywhere in slope. The dominant pathway of NO_2^- consumption change geographically. It is suggested that the conversion to DON and gaseous N is more important in upper soils. On the other hand, conversion to NO_3^- (nitrification) is dominant in lower soils.

At this presentation, we focus on geographical difference of NO_2^- dynamics and their regulation by environmental factors.

Keywords: Forest soil, Nitrite, 15N tracer, Dissolved organic nitrogen, Nitrification

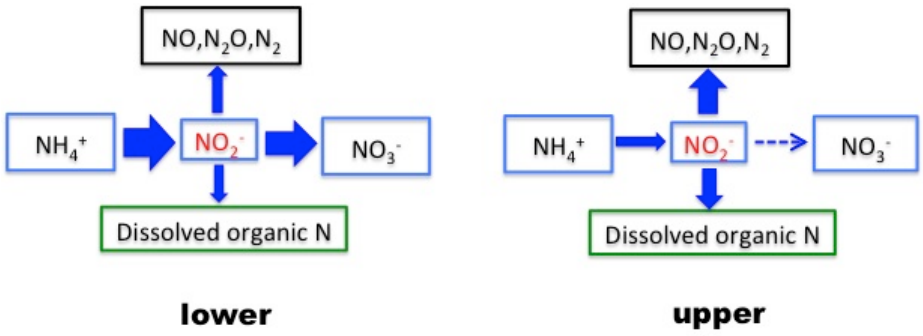

Fig.1 Schematic picture of nitrite dynamics along a forest slope.
Difference between upper and lower soils.

Japan Geoscience Union Meeting 2014
(28 April - 02 May 2014 at Pacifico YOKOHAMA, Kanagawa, Japan)

MIS21-24 Room:511 Time:April 28 17:30-17:45

The availability of atmospheric nitrate in a forested ecosystem

OSAKA, Ken'ichi[1*] ; KOMAKI, Naoto[1] ; KAWAMURA, Yuya[1] ; MURATA, Tetsuya[1] ; KUGO, Tatsuro[1] ; NAKAMURA, Takashi[2] ; NISHIDA, Kei[2] ; NAGAFUCHI, Osamu[1]

[1]University of Siga prefecture, school of environmental science, [2]University of Yamanashi, ICRE

Nitrogen is an important element for forest ecosystems; shortage of nitrogen limits plant growth [Vitousek andHowarth, 1991], however, nitrogen discharged from forested ecosystems link to various environmental problems, such as eutrophication of aquatic ecosystems and deterioration of drinking water quality. Recently, atmospheric nitrogen deposition into terrestrial ecosystems is increasing [Galloway et al., 2008]. However, influence of the increase of atmospheric nitrogen deposition on forested ecosystem is not clear because the interaction between nitrogen input/output and inner nitrogen cycle is not sufficiently understood. In this study, to clarify the interaction between nitrogen input/output and inner nitrogen cycle, we investigate the atmospheric nitrate discharge rate from forested watershed and discuss the availability of atmospheric nitrate deposited into forested watersheds.

Keywords: forested watershed, stable isotope, nitrate, atmospheric deposition

Japan Geoscience Union Meeting 2014
(28 April - 02 May 2014 at Pacifico YOKOHAMA, Kanagawa, Japan)

MIS21-25 Room:511 Time:April 28 17:45-18:00

Estimation of leaf biomass and nitrogen uptake in a hinoki cypress forest

INAGAKI, Yoshiyuki[1*] ; SAKAI, Atsushi[1] ; MIYAMOTO, Kazuki[1]

[1]Forestry and Forest Products Research Institute

Nitrogen uptake by aboveground vegetation in forest ecosystems is determined from nitrogen loss by litterfall plus nitrogen allocated to aboveground biomass increment. Nitrogen in littefall is accurately estimated by littertrap while that in stem increment is by measurement of tree growth. In contrast, estimation of leaf biomass increment is difficult. Although there is close correlation between leaf biomass and cross-sectional area at lowest live branch in the crown, it is difficult to measure diameter at the lowest live branch. Recently, the simple method to estimate leaf biomass is developed by using tree height, height at lowest live branch and diameter at breast height. The applicability of this method depends on tree species and information about hinoki cypress is not known. In this study, we determined the equation for estimating leaf biomass by this method to hinoki cypress trees in Kochi prefecture, southern Japan. In addition the obtained equation is applied for a hinoki cypress forest where tree biomass and litterfall is measured for 20 years.

In two areas at different altitude in Kochi prefecture, 14 hinoki trees were felled and leaf biomass was measured. The relationship between leaf biomass (Wleaf), and tree height (H), height at lowest live branch (HB), and cross-sectional area at breast height (A1.3) was determined by following equation.

Wleaf=1.02[0.0364ABˆ1.10] (r2=0.926, p<0.0001)

AB = A1.3 [(H - Hb) / (H - 1.3)].

This equation is applied for a hinoki cypress forest in Kochi prefecture. Leaf biomass is determined at seven periods between 21 to 41 years old. Leaf production is calculated as leaf-litterfall plus increase of leaf biomass. Nitrogen uptake was calculated as sum of nitrogen in litterfall, increase of nitrogen in leaf and stem biomass. Nitrogen use efficiency of aboveground biomass was calculated as sum of leaf and stem production divided by nitrogen uptake. There was no significant correlation between forest age and leaf biomass, leaf production, stem production, nitrogen uptake and nitrogen use efficiency. However, nitrogen uptake was positively correlated with leaf biomass and leaf production. Nitrogen uptake was not correlated with stem production. These results suggest that nitrogen use of hinoki cypress does not show clear trend in relation to stand age but hinoki cypress utilize nitrogen efficiently to sustain stem production when nitrogen uptake is lower.

Keywords: hinoki cypress, leaf biomass, Stem, nitrogen, forest age

Japan Geoscience Union Meeting 2014
(28 April - 02 May 2014 at Pacifico YOKOHAMA, Kanagawa, Japan)

MIS21-P01 Room:Poster Time:April 28 18:15-19:30

A metabolic model of stable isotope dynamics

ISHII, Reiichiro[1*] ; NOGUCHI, Maki[1] ; WADA, Eitaro[1]

[1]JAMSTEC

Carbon and nitrogen stable isotope analysis have been a powerful tool used for identifying food-web structures. Our recent study suggested that the ratios of trophic fractionation of carbon and nitrogen isotopes ($\triangle\delta$15N/$\triangle\delta$13C) throughout food chain are similar in various ecosystems (Wada et al. 2013), although the general mechanisms determining isotopic incorporation rates and discrimination factors are poorly understood.

Here, we developed a mechanistic model of the isotopic fractionation in metabolic processes that are common to animals composing most grazing food chains. Particularly, we calculate fluxes of carbon and nitrogen stable isotopes within an organism by following fluxes of molecules involved in some of physiological reactions: the synthesis of amino acids and their carbon skeletons, the rates of which are governed by energy-producing systems such as glycolysis, the TCA cycle, and oxidative phosphorylation, that is, the ratio of the rate of amino-acid syntheses to that of energy-yielding processes. The active metabolic pathways above are assumed to be changed by the conditions of supply (diet quantity and quality) and demand (growth rate).

The model result suggests that the instant isotopic composition of animals are sensitive to the change of their diet composition and growth rate, but on the other hand, the isotopic composition converges as the integrating period becomes long. With further temporal scaling-up, in turn, the isotopic compositions of animal body reflect the spatio?temporal variability due to their life history, migration and foraging patterns. This gives mechanistic insight to what information we can acquire from the observation.

Japan Geoscience Union Meeting 2014
(28 April - 02 May 2014 at Pacifico YOKOHAMA, Kanagawa, Japan)

MIS21-P02 Room:Poster Time:April 28 18:15-19:30

Tracing environmental history of macroalgae by the use of radiocarbon and stable isotope ratio analyses

SATO, Naomi[1*] ; FUKUDA, Hideki[1] ; MIYAIRI, Yosuke[1] ; YOKOYAMA, Yusuke[1] ; NAGATA, Toshi[1]

[1]Atmosphere and Ocean Research Institute, the University of Tokyo

In the bays located along the Sanriku coastal area (northeast Japan), where the Kuroshio and Oyashio mix in a complex manner, environmental conditions (e.g. water temperature, irradiation and nutrients) may largely change depending on which current predominantly enters into the bays. Changes in environmental conditions, in turn, may exert a large influence on growth of and interactions between organisms residing there. However, knowledge is limited regarding relationships between shifts in hydrographic conditions and physiological responses of organisms to environmental variability. The purpose of this presentation is to report our attempt to trace environmental history of individual macroalgae (wakame, *Undaria pinnatifida*), a widespread benthic primary producer and an important aquaculture product in the Sanriku area, by a combined use of radiocarbon and stable isotope ratio analyses. The key concept was to use distinct ^{14}C abundance between the two water currents, i.e., ^{14}C abundance of dissolved inorganic carbon in the Oyashio water is lower than that in Kuroshio water due to upwelling of old deep water. We assumed that ^{14}C abundance profile of pinnate blades of macroalgae (blades near the top are older than those near the bottom) reflects a temporal change in dissolved inorganic carbon ^{14}C (hence, shift in water current) via photosynthetic fixation. We also analyzed carbon and nitrogen stable isotope ratios (δ^{13}C and δ^{15}N) of the blades to gain insights into changes in physiological state of the macroalgae during their growth.

We collected sporophytes of *U. pinnatifida* cultured between October 2012 and March 2013 at two stations (one located near the bay center and the other located near the river mouth) in Otsuchi Bay. One individual (length, ca. 190 cm) was collected at each station. For each individual, a tip of each pinnate blade was cut, treated with HCl, reduced to graphite, and served for determination of radiocarbon composition ($\triangle^{14}$C) profile using an accelerator mass spectrometer. δ^{13}C and δ^{15}N of the corresponding samples were also measured using a stable isotope ratio mass spectrometer.

$\triangle^{14}$C of pinnate blades of the saprophyte collected near the bay center varied between 0 and 40 permil. $\triangle^{14}$C values were high for the blades located at the upper and lower parts of the macroalgae, whereas they were low for the blades situated at the middle part. These results indicate that the sporophyte experienced the intrusion of the Oyashio water during the period of the development of the middle blade. Similar to the pattern in $\triangle^{14}$C, δ^{13}C and δ^{15}N values were also lowest at the middle part, although the position of the minimum was skewed toward bottom relative to the position of the $\triangle^{14}$C minimum. There was a significant positive correlation between δ^{13}C and δ^{15}N, suggesting that the variation in stable isotope ratios reflected macroalgal physiological responses and associated shifts in isotope fractionation. Collectively, these results were interpreted as an indication that the physiological state of the saprophyte was altered with a time lag after the intrusion of the Oyashio water into the bay. In contrast, $\triangle^{14}$C profile of pinnate blade was complex for a saprophyte collected near the river mouth. For this individual, there was no clear pattern in distribution of δ^{13}C and δ^{15}N among blades. Complex variations in isotopic compositions for this individual might be ascribed to the influence of inflow river water.

Keywords: macroalgae, Sanriku coast, water current, radiocarbon, stable isotope

Japan Geoscience Union Meeting 2014
(28 April - 02 May 2014 at Pacifico YOKOHAMA, Kanagawa, Japan)

MIS21-P03 Room:Poster Time:April 28 18:15-19:30

Accumulation of humic-like fluorescent dissolved organic matter in the Japan Sea interior

TANAKA, Kazuki[1] ; KUMA, Kenshi[2] ; HAMASAKI, Koji[3] ; YAMASHITA, Youhei[4*]

[1]Graduate School of Environmental Science, Hokkaido University, [2]Faculty of Fisheries Science, Hokkaido University, [3]Atomospher and Ocean Research Institute, The University of Tokyo, [4]Faculty of Environmental Earth Science, Hokkaido University

Marine dissolved organic matter (DOM) is the largest reduced carbon reservoir in ocean. Most marine DOM is produced by marine biota and is resistant to rapid microbial degradation. Thus, it is crucial to know the dynamics of recalcitrant DOM for determining whether the marine DOM reservoir is stable or not. Even though there have been several hypotheses regarding with the recalcitrant mechanism of marine DOM, the microbial production of recalcitrant DOM (defined as microbial carbon pump) has been considered as the main process. Humic-like fluorescent DOM ($FDOM_H$) has found to produce during microbial incubation. Even though $FDOM_H$ has known to easily degrade by sunlight, linear relationships between fluorescence intensity of $FDOM_H$ and indicators of microbial remineralization, e.g., apparent oxygen utilization (AOU), have been observed throughout the ocean. These experimental and observational results imply that $FDOM_H$ is a product of microbial carbon pump. Another important source of $FDOM_H$, especially in coastal environments and marginal seas, is riverine supply. Even though the major fractions of $FDOM_H$ have been considered to be photo-degraded in coastal environments, substantial contribution of terrestrial $FDOM_H$ into ocean interior has been suggested. Thus, in addition to accumulation of in situ produced $FDOM_H$, recalcitrant terrestrial $FDOM_H$ might occur in deep ocean, especially in marginal seas. However, it is not clear whether recalcitrant autochthonous and/or terrestrial $FDOM_H$ is accumulated in deep ocean of marginal seas or not.

We determined vertical profiles of $FDOM_H$ at 5 stations in the Japan Sea and 5 stations in the western North Pacific using excitation emission matrix fluorescence with parallel factor analysis (EEM-PARAFAC). Seawater samples from surface to bottom waters of the Japan Sea and the western North Pacific were collected during T/S Oshoro-maru (C184) and R/V Tansei-Maru (KT-11-17) cruises, respectively. Two $FDOM_H$ were obtained after EEM-PARAFAC and assigned as traditional terrestrial and marine (microbial) $FDOM_H$, respectively. In the Japan Sea, levels of both $FDOM_H$ were lowest in surface waters, gradually increased with depth below surface waters, and were highest in waters distributed depths greater than 2000 m that were corresponding to the lower part of Japan Sea Proper Water (JSPW), i.e., lower part of the Japan Sea Deep Water (JSDW) and the Japan Sea Bottom Water (JSBW). Levels of both $FDOM_H$ were linearly correlated with AOU in the JSPW, suggesting that both $FDOM_H$ were produced in situ in the JSPW. Interestingly, levels of both $FDOM_H$ in the JSPW were similar or slightly higher compared with those in deep waters of the western North Pacific, even though AOU in the JSPW were significantly lower than those in deep waters of the western North Pacific. Such distributional characteristics of $FDOM_H$ in the JSPW imply that $FDOM_H$ is accumulated in the interior of the Japan Sea. We will discuss possible origin and accumulation mechanism of $FDOM_H$ in the Japan Sea interior.

Keywords: Japan Sea, Dissolved Organic Matter, Humic-like fluorescence

Japan Geoscience Union Meeting 2014
(28 April - 02 May 2014 at Pacifico YOKOHAMA, Kanagawa, Japan)

MIS21-P04 Room:Poster Time:April 28 18:15-19:30

Sources of hydroxyl radical photochemically produced in headwater streams from nitrogen-saturated forest

CHIWA, Masaaki[1*] ; HIGASHI, Naoko[1] ; OTSUKI, Kyoichi[1] ; KODAMA, Hiroki[2] ; MIYAJIMA, Tohru[2] ; TAKEDA, Kazuhiko[3] ; SAKUGAWA, Hiroshi[3]

[1]Kyushu University Forest, [2]Graduate School of Science and Engineering, Saga University, [3]Graduate School of Biosphere Science, Hiroshima University

Hydroxyl radical (·OH) is the most oxidative reactant among the active oxygen species and oxidation reactions with ·OH are involved in important biogeochemical processes. In this study ·OH photoformation rate (R_{OH}) was determined in headwater stream samples from nitrogen (N)-saturated forests, 1) to quantify the sources of ·OH in headwater streams and 2) to evaluate the nitrate (NO_3^-)-induced enhancement of ·OH formation in stream water caused by N saturation in forested watersheds. Stream water fulvic acid extracted from the forested watersheds was used to quantify the contribution of dissolved organic matter (DOM) to R_{OH}. The results showed that almost all (97%; 81-109%) R_{OH} sources in our headwater stream samples were quantitatively elucidated; the photolysis of NO3- (55%; 34-75%), nitrite [N(III)] (2%; 0.5-5.2%), and DOM-derived ·OH formation, from which photo-Fenton reactions (18%; 12-26%) and the direct photolysis of fluorescent dissolved organic matter (FDOM) (22%; 10-40%), was successfully separated. FDOM, which accounted for 53% (24-96%) of DOM in total organic carbon bases, was responsible for ·OH formation in our headwater streams. High NO_3^- leaching caused by N saturation in forested watersheds increased R_{OH} in the headwaters, indicating that N-saturated forest could significantly change photoinduced and biogeochemical processes via enhanced ·OH formation in downstream water.

Keywords: hydroxyl radical, dissolved organic matter, nitrate, photo-Fenton reaction, stream, photoinduced processes

Japan Geoscience Union Meeting 2014
(28 April - 02 May 2014 at Pacifico YOKOHAMA, Kanagawa, Japan)

MIS21-P05 Room:Poster Time:April 28 18:15-19:30

Effects of clear-cutting on the loss of ion and DOC from cool-temperate forested watershed in northern Japan

FUKUZAWA, Karibu[1*] ; SHIBATA, Hideaki[1] ; TAKAGI, Kentaro[1] ; NOMURA, Mutsumi[1]

[1]FSC, Hokkaido University

Nitrate and dissolved organic carbon (DOC) concentrations in stream water before and after clear-cutting of trees and subsequent strip-cutting of understory vegetation, dwarf bamboo (Sasa spp.) were investigated to understand the effect of these disturbances on biogeochemical processes in forested watershed in Teshio Experimental Forest in northern Japan. Trees of 8 ha watershed except riparian zone were clear-cut in January-March of 2003. Sasa was strip-cut in October of 2003 and larch seedlings were planted on the cut line immediately after the Sasa cutting. Stream water was sampled every two or three weeks from 2002 to 2013. Tree-cutting did not cause a significant increase of nitrate concentration in stream water during the growing season after the cutting. Subsequent Sasa-cutting caused significant increase of stream nitrate concentration to ca. 15 micro mol L-1. At the cut site, it has been reported that Sasa compensated the decrease in tree fine root biomass. Thus, we suggest that nitrogen uptake by Sasa was very important in mitigating nitrogen leaching after tree-cutting, and the decline of this nitrogen uptake after Sasa-cutting lead to marked nitrate leaching to the stream. However, after that stream nitrate concentration fluctuated in the range of $<$0.1 to $>$20 micro mol L-1 depending on date and year, and was especially high in 2007 throughout the year. It did not get back to pre-cutting level. Cation (K+, Na+, Ca2+, Mg2+) concentration and pH fluctuated much depending on the flow rate and changes by both cutting were not observed. On the other hand, ammonium was detected in 2007 and synchronized with increase in nitrate concentration. DOC concentration in stream water was not changed after both cuttings of tree and Sasa and had clear seasonal pattern that peaked in late summer. Stream DOC concentration increased in growing period with low runoff from late May to August and then decreased after runoff increased in fall, indicating that dilution by the runoff reduce stream DOC concentration after late summer. However, DOC concentration remained low during winter when runoff was stably low, suggesting that high temperature also promote DOC production in soil during the early summer. DOC loss from ecosystem was not influenced by the cutting of trees and Sasa in this watershed owing to the adsorption to the soil at the cut area. These results indicate the response to cutting is different between NO3- and DOC due to the different source area of these solutes in the watershed with cool climate and the gentle basin topography.

Keywords: nitrate, DOC, cation, Sasa, stream discharge

Japan Geoscience Union Meeting 2014
(28 April - 02 May 2014 at Pacifico YOKOHAMA, Kanagawa, Japan)

MIS21-P06 Room:Poster Time:April 28 18:15-19:30

Microbial contributions to biochemical commonalities of decaying organic matter

HOBARA, Satoru[1*] ; AE, Noriharu[1] ; HASEGAWA, Yuki[1] ; OGAWA, Hiroshi[2] ; SATOU, Takayuki[3] ; IMAI, Akio[3] ; BENNER, Ronald[4]

[1]Rakuno Gakuen University, [2]The University of Tokyo, [3]National Institute for Environmental Studies, [4]The University of South Carolina

Natural organic matters including dead organisms are decayed (decomposed) under various environmental conditions, but some parts of them, residues, remain for long time. Organic matter residues are major components of organic matter in soil and marine ecosystems, and play important functions and roles. The residues are originated from various organisms, organs, and cellular components, and in various stages of organic matter decay. Recently, it has been suggested that organic matter produced by microorganisms increase its percentage in residues during decay process. However, researches are limited especially on the quality of the produced organic matter and its producing processes. In this research, we investigate biochemical differences between original organic matters and organic residues and biochemical changes of organic matter during decaying process to clarify microbial contributions to the organic matter residues. Biochemical molecular compositions of original organic matters was more variable than those of organic residues in soil and water: for example, glycine:lysine (Gly/Lys) ratio and glucosamine:galactosamine (GlcN/GalN) ratio of original organic matters varies widely with origins, while those of decayed residues indicates considerably narrower ranges for both ratios. An incubation test, litterbag experiment, in a terrestrial ecosystem showed a clear trend that Gly/Lys ratio increased and GlcN/GalN ratio decreased during decay for all three species litter. These changes were also observed for litterbag experiments conducted in water, suggesting that it might be uniformly-observed biochemical directivity for decaying organic matter. In addition, amino acids and amino sugars are biomoleculars, which increase during decaying processes, suggesting that this directivity results from microbial products. Another biochemical directivity was observed for molecular weight distribution of decaying organic matters, suggesting that organic residues derived from microbial products contribute to biochemical directivities and commonalities of decaying organic matter in various environmental conditions.

Keywords: Organic matter decay, Soil, Ocean, Amino acids, Amino sugars, Molecular weight distribution

Japan Geoscience Union Meeting 2014
(28 April - 02 May 2014 at Pacifico YOKOHAMA, Kanagawa, Japan)

MIS21-P07 Room:Poster Time:April 28 18:15-19:30

Spatial modelling of water, nitrogen and sediment for systematic conservation of multiple ecosystem services

FAN, Min[1*] ; SHIBATA, Hideaki[2]

[1]Graduate School of Environmental Science, Hokkaido University, [2]Field Science Center for Northern Biosphere, Hokkaido University

Spatial modelling and analysis of multiple ecosystem service (ES) under land use and climate changes provides useful support for decision making in sustainable planning, management and policies of large landscapes. This study aimed to integrate the GIS modelling approach of spatial explicit ESs (water yield, and retention of nitrogen (N) and sediment) into system conservation model under various land use and climate changes in Teshio river watershed located in northern Hokkaido, Japan. In this study, we applied hydrology and material flow model (Soil and Water Assessment Tools, SWAT model), land use change model (CLUE) and system conservation model (Marxan). The multiple scenario includes three different land use maps in past (1976), current (2006) and future (2036), and three climate change scenarios (short-term (2010-2039), mid-term (2040-2069), and long-term (2070-2099)).

Our results indicated that various land use and climate change scenarios showed different impact on ES and system conservation in the watershed. The forest land use change significantly affected on magnitudes and spatial patterns in water yield, sediment and N retention. It was suggested that south western and northern part of the studied watershed should be conserved to match the given conservation targets of multiple ESs (0.3 and 0.5 of maximum ES values). The protection area to satisfy each ES conservation target increased with increase of differences between each ES and maximum ES values under land use and climate changes. Our results indicated that the land distribution and area of optimal ES protection for multiple ESs were totally different from those for single ES. The conservation area for multiple ESs was more compact than those for single ES. The proposed approach in this study provided useful information to assess the responses of ESs and system conservation under the land use and climate changes. The system conservation area of ES protection for multiple ESs provided an effective trade-off tool between environmental protection and agriculture expansion.

Keywords: Ecosystem services, SWAT, Marxan, Land use and climate change

Japan Geoscience Union Meeting 2014
(28 April - 02 May 2014 at Pacifico YOKOHAMA, Kanagawa, Japan)

MIS21-P08 Room:Poster Time:April 28 18:15-19:30

Spatial variability of mineralization and nitrification in soil nitrogen along the hillslope in Japanese cedar forest

KATO, Hiroyu[1*] ; OHTE, Nobuhito[1] ; ISOBE, Kazuo[1] ; ODA, Tomoki[1] ; MURABAYASHI, Sho[2] ; URAKAWA, Rieko[1] ; SENOO, Keishi[1]

[1]University of tokyo, graduate school of agricultural and life sciences, [2]University of tokyo,faculty of agriculture

introduction Precise understandings of mechanism of nitrogen (N) cycle is one of the most important subjects for ecosystem conservation in forests and rivers. Especially, the responses of N mineralization and nitrification to environmental changes are especially important due to their role in entire N cycling. Previous studies suggest that nitrification and mineralization have spatial variation in forest, which are controlled by the geophysical condition such as topography and water condition. The aim of this study is to clarify the mechanisms behind the spatial variety of nitrification and mineralization rate in soil along the hillslope.

Methods The field observations and soil samplings were conducted at Fukuroyamasawa Experimental Watershed (Catchment Area 0.8ha) which belongs to the University of Tokyo, Chiba forest. Dominant vegetation on the slope consisted of Cryptomeria japonica plantation. Along the hillslope (entire length: 110m), soil samples were collected at organic layer (O-layer) and mineral layer (0-10cm) at 10m intervals. After measuring water content and pH, the NO_3^- and NH_4^+ concentration of soil extract (by 2M KCl solution) were measured. The net mineralization and nitrification. Rate were measured by laboratory incubations (28 days). Then, the gross mineralization and nitrification rate were determined using the ^{15}N pool-dilution method.

Results Soil moisture content was higher at the down slope part. Similarly, the pH value was higher at down slope part. The pool size of NO_3^- was significantly low at the up slope part, and gradually increased along the slope toward the lower portion. On the other hand, the pool size of NH_4^+ did not have visible pattern along the slope. Moreover, there was not significant spatial variations in net and gross mineralization rate over the hillslope while net and gross nitrification had significant spatial pattern with higher rate at the down slope part.

Discussion Difference in the spatial patterns of mineralization and nitrification suggested that nitrification is more sensitive to the geophysical conditions such as the soil moisture content. We are attempting to explain the mechanisms of these spatial patterns from the spatial distributions of related microbial communities in the next step of this study

Japan Geoscience Union Meeting 2014
(28 April - 02 May 2014 at Pacifico YOKOHAMA, Kanagawa, Japan)

MIS21-P09 Room:Poster Time:April 28 18:15-19:30

Nitrogen mineralization rates in forest soils in the Japanese archipelago measured by field incubation

URAKAWA, Rieko[1*] ; OHTE, Nobuhito[1] ; SHIBATA, Hideaki[2] ; ODA, Tomoki[1] ; WATANABE, Tsunehiro[2] ; FUKUZAWA, Karibu[2] ; INAGAKI, Yoshiyuki[3] ; TATENO, Ryunosuke[4] ; OYANAGI, Nobuhiro[5] ; HATTORI, Daichi[6] ; NAKATA, Makoto[6] ; HISHI, Takuo[7] ; FUKUSHIMA, Keitaro[4] ; NAKANISHI, Asami[4] ; TODA, Hiroto[8]

[1]Graduate School of Agricultural and Life Sciences, University of Tokyo, [2]Field Science Center for Northern Biosphere, Hokkaido University, [3]Forestry and Forest Products Research Institute, [4]Filed Science Education and Research Center, Kyoto University, [5]Environmental Science Research Niigata, [6]Graduate School of Science and Technology, Niigata University, [7]Graduate School of Agriculture, Kyushu University, [8]Graduate School of Agriculture, Tokyo University of Agriculture and Technology

1. Introduction

To predict the effect of climate change on nitrogen dynamics in the forest ecosystem, it is necessary to investigate nitrogen mineralization and nitrification at various locations allowing for modeling of nitrogen dynamics in soils. In this study, we selected 20 sites from the Japanese archipelago and conducted field incubation for measuring net nitrogen mineralization and nitrification. We also considered whether parameters obtained from laboratory incubation were applicable in the field by comparing the ratios between field and laboratory incubations (Urakawa et al., 2013).

2. Method

We conducted buried bag method to investigate field net nitrogen mineralization and nitrification rate. In autumn 2012, we established an experimental plot (20 $*$20 m) at each site, and at each plot, five soil sampling locations were established. At each sampling location, mineral soil samples were collected from 0-10, 10-30, 30-50 cm depths. Soil samples were sieved (4 mm mesh) to remove roots and gravel, and composited soils from five plots into one sample at each depth. After collecting soils for the initial extraction, buried bags were made and buried in the plots again. We collected them in spring, summer, and autumn 2013, and measured net nitrogen mineralization and nitrification for three seasons (autumn 2012 - spring 2013, spring - summer, summer - autumn). Soil samples were extracted with 2M-KCl solution (1:10) and concentrations of ammonium nitrogen and nitrate nitrogen were measured by colorimetric method. Net nitrogen mineralization and nitrification amount of each season were summed to evaluate the annual amount.

Simultaneously with the field incubation, inorganic nitrogen leaching was investigated by resin column method. Resin columns containing ion exchange resin was installed at depths of 0 and 50 cm. Inorganic nitrogen absorbed by ion exchange resin was extracted with 1M-KCl and concentration of inorganic nitrogen was analyzed by colorimetric method.

3. Results and Discussion

Annual net nitrification in 0-50 cm layer ranged widely from 40 to 140 kgN ha^{-1} y^{-1}. Nitrification amount in 10-50 cm layer was comparable to that in surface soil layer (0-10 cm) due to large bulk density and thickness, while nitrification in 0-10 cm layer accounted for about a half of that of all soil layers.

There was a significant positive correlation between nitrification measured by field and laboratory incubation. This suggests that estimation of field nitrification using parameters obtained from laboratory incubation is possible.

4. Reference

Urakawa et al. (2013) Characteristics of nitrogen mineralization rates and controlling factors in forest soils in Japanese archipelago, 2013 AGU Fall Meeting, San Francisco, 9-13 December 2013

Keywords: forest soil, nitrogen mineralization, nitrification, field incubation, nitrogen leaching, ion exchange resin

Japan Geoscience Union Meeting 2014
(28 April - 02 May 2014 at Pacifico YOKOHAMA, Kanagawa, Japan)

MIS21-P10 Room:Poster Time:April 28 18:15-19:30

Analysis of transportation and consumption processes of atmospheric nitrate in forested watershed by using oxygen isotop

KUGO, Tatsuro[1*] ; OSAKA, Ken'ichi[1] ; NAKAMURA, Takashi[2] ; II, Yumi[1] ; IWAI, Misako[1] ; NISHIDA, Kei[2] ; NAGAFUCHI, Osamu[1]

[1]University of Shiga Prefecture, [2]ICRE University of Yamanashi

Some studies reported that atmospheric nitrogen deposition into terrestrial ecosystem has recently increased due to increase of anthropogenic emission of nitrogen compound into atmosphere. However, dynamics of atmospheric nitrogen deposition in forested watersheds is not clearly understood. Moreover, that leads our poor understanding of influence of increasing atmospheric nitrogen deposition on nitrogen cycle in forested ecosystem and nitrogen discharge from forested ecosystem. The purpose of this study is to clarify the mechanisms of transportation and consumption of atmospheric nitrate deposition in forested ecosystems. We collected rainfall, throughfall, surface water, soilwater (10cm, 30cm), groundwater, spring water and streamwater at a forested watershed planted with Japanese cypress in central Japan at biweekly. Samples were analyzed for total nitrogen, dissolved nitrogen, nitrate, ammonium, nitrite, and oxygen isotope of nitrate. Isotope analysis was conducted at ICRE in University of Yamanashi. We also collected soil at several month intervals, and measured nitrate, ammonium in soil and net mineralization rate, and net nitrification rate. We are planning to present transportation rate of nitrogen compounds and atmospheric nitrate through the forested watersheds and discuss the interaction between nitrogen cycle and atmospheric nitrate deposition in forested ecosystem.

Keywords: oxygen isotope of nitrate, transportation and consumption processes of nitrogen, forested watershed

Japan Geoscience Union Meeting 2014
(28 April - 02 May 2014 at Pacifico YOKOHAMA, Kanagawa, Japan)

MIS21-P11 Room:Poster Time:April 28 18:15-19:30

The effect of soil freeze-thaw on nitrogen transformation though the root litter changes

HOSOKAWA, Nanae[1*] ; WATANABE, Tsunehiro[2] ; FUKUZAWA, Karibu[2] ; TATENO, Ryunosuke[3] ; SHIBATA, Hideaki[2]

[1]Graduate School of Environmental Science, Hokkaido University, [2]Field Science Center for Northern Biosphere, Hokkaido University, [3]Field Science Education and Research Center, Kyoto University

Soil freeze-thaw cycles are considered to alter soil nitrogen (N) cycle through physical disturbances of soil, changes in root litter quality, inhibition of microbial N immobilization and others. However, these mechanisms have not been well elucidated yet. Plant litter is important substrate for N mineralization by soil microbes. It has been reported that root litter mass is quantitatively comparable to those of leaf litter in various forest ecosystems. Previous studies suggested that physical disruption of root litter by freeze-thaw cycle in winter affect soil N dynamics through the change in substrate availability. In this study we aimed to clarify that effect of root litter on the rates of soil N mineralization and nitrification under various conditions of soil freeze-thaw.

This study was conducted at Shibecha experimental forest, Kyoto University located in Eastern Hokkaido, Japan. The study site is dominated by Natural oak (*Quercus crispula*) with dense dwarf bamboo (*Sasa niponica*) as understory vegetation. Soil is Humic Andosol. In July 2013, we collected 0-10cm mineral soil and fine root (<2mm) of oak in the 2500 cm^2 square plot. The collected soil was sieved to 2mm to remove coarse gravel and coarse organic matter. Fine roots for incubations were separated manually from the organic matter. The fine roots were added to 25g soil as 0, 5 and 15 mg g $soil^{-1}$, respectively. The soil were exposed to three different freeze-thaw treatments: +5 ℃ ∼-5 ℃, -5 ℃ ∼0 ℃, -5 ℃ constant and +5 ℃ constant for 7days in low temperature incubator. After these freeze-thaw treatments, the soil were incubated at +5 ℃ for 2 days. For the samples exposed at +5 ℃ ∼-5 ℃ and -5 ℃ constant were also incubated at +5 ℃ for 7 days and at +10 ℃ for 2 and 7 days. Each treatment had four replications. Soils were extracted using potassium chloride (KCl) before and after incubations, and were measured for ammonium (NH_4) and nitrate (NO_3) concentrations in the extracts. Net production rates of NH_4 and NO_3 were calculated as differences of NH_4 and NO_3 contents in soil between before and after the incubations. After the freeze-thaw treatment, roots were extracted using distilled water, and were measured for dissolved organic nitrogen (DON) in the extracts.

Root litter addition significantly increased the net NH_4production incubated at 5 ℃ for 2 days after all freeze-thaw treatments (15 mg added >0mg added) with maximum at -5 ℃ ∼0 ℃ treatment followed by -5 ℃ constant treatment. However, these effect were not observed in higher incubation temperature (10 ℃) and longer incubation period (7days), rather dominated by N immobilization in those treatments. Similarly, the root litter additions significantly increased the net NO_3 production rate (nitrification rate) incubated at 5 ℃ for 2 days after all freeze-thaw treatments (15 mg added >0mg added) with maximum at +5 ℃ ∼-5 ℃ treatment. However, these effect were not observed in higher incubation temperature (10 ℃) and longer incubation period (7days) as same as the effects to the NH_4 production. The DON supply by water extraction from root litter tended to be large at -5 ℃ ∼0 ℃ treatment.

These results indicated that increases of soil freeze-thaw cycles with root litter addition increased the net NH_4 production and nitrification. It was suggested that DON supply from root litter by soil freeze-thaw cycle related to these impacts. These effect seems to be remarkable in shorter period (2 days) and lower temperature (5 ℃ incubation). Furthermore, net NH_4 production, the sum of net NH_4+NO_3 productions and DON supply from root rate were higher at -5 ℃ ∼0 ℃ treatment than those at +5 ℃ ∼-5 ℃ treatments, implying that magnitude (temperature ranges) of freeze-thaw cycle was not simple explain variables to impact of freeze-thaw on the microbial NH_4 production and nitrification activities.

Japan Geoscience Union Meeting 2014
(28 April - 02 May 2014 at Pacifico YOKOHAMA, Kanagawa, Japan)

MIS21-P12 Room:Poster Time:April 28 18:15-19:30

Estimation of trace gas fluxes in the forest of Mount Fuji using the multi layer model

NIIJIMA, Kohei[1*] ; HIDA, Yuki[1] ; WADA, Ryuichi[1] ; MOCHIZUKI, Tomoki[2] ; TANI, Akira[2] ; NAKAI, Yuichiro[3] ; TAKANASHI, Satoru[3] ; NAKANO, Takashi[4] ; TAKAHASHI, Yoshiyuki[5] ; MIYAZAKI, Yuzo[6] ; UEYAMA, Masahito[7]

[1]Teikyo University of Science, [2]University of Shizuoka, [3]FFPRI, [4]Yamanashi Institute of Environmental Science, [5]National Institute for Environmental Studies, [6]Hokkaido University, [7]Osaka Prefecture University

We measured vertical profiles of nitrogen oxide, NO, nitrogen dioxides, NO_2, ozone, O_3, and VOC in the atmosphere in Fujiyoshida and Hokuroku forest observation sites at the foot of Mt. Fuji in summer 2012. The concentration of ozone increased gradually with the height, but the concentrations of NO and NO_2 did not changed obviously. VOCs showed characteristic vertical profiles. We calculated O_3 fluxes at parts of in and under the canopy, and around the surface layer as -2.6 $\pm$ 3.2 nmol m^{-2} s^{-1}, 0.2 $\pm$ 2.9 nmol m^{-2} s^{-1}, -8.7 $\pm$ 5.2 nmol m^{-2} s^{-1}, respectively.

Keywords: forest, atmosphere, nitrogen oxides, ozone, VOC, vertical profile

Japan Geoscience Union Meeting 2014
(28 April - 02 May 2014 at Pacifico YOKOHAMA, Kanagawa, Japan)

MIS21-P13 Room:Poster Time:April 28 18:15-19:30

Locaization of delta-34S value distribution in tree ring of Japanese cedar and evaluation on the S deposition history

ISHIDA, Takuya[1*] ; TAKENAKA, Chisato[1] ; TAYASU, Ichiro[2]

[1]Nagoya univ., [2]Kyoto univ.

Anthropogenic sulfur emissions have been changed with human activities and affected sulfur dynamics in terrestrial ecosystems. Therefore, the information on sulfur deposition change should be important for understanding of the effects of anthropogenic sulfur on its dynamics. The stable sulfur isotope ratios (δ^{34}S) in tree rings are a useful archive for the history of sulfur deposition (Kawamura et al. 2006), since the δ^{34}S of various origins have specific values and there is few isotopic fractionation through absorption of sulfur by plant. However, only few studies have been conducted about the δ^{34}S in tree ring, and factors affecting the δ^{34}S in tree ring have not been understood.

The aim of this study is to clarify the localization of δ^{34}S distribution in tree ring. We also perform the evaluation of sulfur deposition history at locations received heavy anthropogenic sulfur deposition using tree ring.

The investigation was carried out at two study sites, Yokkaichi (YOK) and Inabu (INA) in central Japan. Both study sites have different histories of sulfur deposition. YOK had been affected by quite high anthropogenic sulfur deposition during 1960s. INA is located about 60 km NE of main urban area (Nagoya City). Three disk samples were obtained from Japanese cedar (*Cryptomeria japonica*) stump in 2013 at YOK and in 2012 at INA. The stumps at YOK were 63-year-old cut down in 2012 and those at INA were170-year-old cut down in 2007. In addition, at INA, three 40-year-old living stems were cut down in 2013 at INA and the disk samples were obtained. After washing and dried, the tree ring samples were divided into 5 year increments from bark toward the pith, and ground using power mill. The ground samples were digested with HNO_3 and H_2O_2 on a hot plate and after filtration $BaCl_2$ was added to obtain the $BaSO_4$. The δ^{34}S values (VCDT) were measured using EA-IRMS.

To evaluation the localization of δ^{34}S in sapwood, heartwood and pith, the data from the stump and the living wood samples at INA were compared. These samples showed the different localization of δ^{34}S against the age. There were no difference of δ^{34}S between the sapwood (living wood) and the heartwood (stump) at the same age. However, the δ^{34}S values of the pith (living wood) were higher than those of heartwood (stump). This result indicated that the specific composition of sulfur compound might be consisted in pith and the δ^{34}S of the pith should be unsuitable for evaluation of sulfur deposition history.

The δ^{34}S values in ring at YOK declined from the late 1950s to early 1970s and then increased again. This trend was almost homologized in ring at INA and air SO_2 concentration at near the YOK. In contrast, the minimum value of at YOK (-7.3 ‰) was lower than that at INA (-1.6 ‰). These results should be reflected by the deposition history of anthropogenic sulfur with low δ^{34}S value at each site.

Keywords: Tree ring, Sulfur isotope, Morphology, Sulfur deposition

Japan Geoscience Union Meeting 2014
(28 April - 02 May 2014 at Pacifico YOKOHAMA, Kanagawa, Japan)

MIS21-P14 Room:Poster Time:April 28 18:15-19:30

Distribution of radiocesium in a small forest at Namie town in Fukushima Prefecture

OGATA, Hiroko[1*] ; KUROSHIMA, Hiroto[1] ; OKOCHI, Hiroshi[1] ; TOKONAMI, Shinji[2] ; SORIMACHI, Atsuyuki[3] ; HOSODA, Masahiro[4] ; IGARASHI, Yasuhito[5] ; KATAOKA, Jun[1] ; OHSUKA, Shinji[6]

[1]Waseda University, [2]Hirosaki University, [3]Fukushima Medical University, [4]Hirosaki University Graduate School, [5]Meteorological Research Institute, [6]Hamamatsu Photonics K.K.

Fresh leaf/needle, litter, surface soil, stream water and bottom sand were monthly collected in a deciduous broadleaf forest and an evergreen needleleaf forest in Fukushima Prefecture during non-snowfall period. The concentration of radiocesium (^{134}Cs and ^{137}Cs) was measured by commercially available NaI(Tl) scintillation detector.

The air dose rate at a broadleaf forest (5.64 μSv/h) was higher than that at a needleleaf forest (4.11 μSv/h) in November 2012. The average concentration of radiocesium in each sample was also higher at broadleaf forests than at needleleaf forests. The order of the concentration of radiocesium was litter $>$surface soil $>$fresh leaf/needle $>$bottom sand at both sites, indicating that radiocesium was accumulated in litter. Radiocesium was not detected in precipitation, throughfall, and stream water.

Surface soil samples at each sampling point were taken using a scraper plate in April and December 2013. Samples were taken with 0.5 cm increments for the depth of 0-5 cm and 1.0 cm increments for the depth of 5-10 cm. The maximum concentration was found at the surface at the broadleaf forest in April and December 2013. The maximum concentration was also found at the surface at the needleleaf forest in April 2013 but at 1-1.5 cm in December 2013, indicating that the radiocesium in surface soil penetrated deeply at the needleleaf forest. These differences were likely caused by the soil type and the composition of tree species at the sampling points.

A photostimulable phosphor (PSP) image plate was used to record a two-dimensional image of radioactivity distribution on the leaf/needle and root of the broadleaf tree samples. We used the CR^{x}25P (General Electric Company). The image of the needleleaf sample of Japanese cedar showed some high intensity spots on the needles, indicating the presence of radioactive dusts attached onto the plant's surface. On the other hand, the image of the broadleaf showed uniform distribution, suggesting that contamination with radiocesium occurred internally.

In the presentation, we will also report about the runoff processes of the radiocesium with the stream bottom sand.

Japan Geoscience Union Meeting 2014
(28 April - 02 May 2014 at Pacifico YOKOHAMA, Kanagawa, Japan)

MIS21-P15 Room:Poster Time:April 28 18:15-19:30

Monitaring of atmospheric mercury pollution using a leaf camphor tree (cinnamomum campora (L.) Sieb.)

CHIKAMASA, Takaya[1*] ; KAMIYAMA, Naoko[1] ; SATAKE, Kenichi[1]

[1]Faculty of Geo-environmental Science, Rissho University

Source of mercury is divided into two anthropogenic sources such as incineration and sludge of fossil fuel and natural sources, such as by volcanic activity. Mercury discharged from these sources is present in the gaseous atmosphere mainly. On the other hand, trees are accumulated by adsorption or absorption in the leaves and bark of contaminants in the atmosphere. I am thought to absorb atmospheric pollution from the pores in the case of accumulation by the leaves. I was aimed at performing mercury pollution monitoring of air by measuring the mercury content in the leaves in this study. The absorption in the two years up fallen leaves from the deployment of new buds and evergreen broad-leaved tree, using the camphor tree(*Cinnamomum camphora* (L.) Sieb.) accumulation is expected to indicators of mercury pollution in the atmosphere. I was monitoring for the full year, including the winter an increase in use of fossil fuels is expected by this. It was possible sampling points you ′ ve covered as being human influenced due to its proximity to urban areas, in Rissho University campus is located in Kumagaya, Saitama Prefecture. In addition, a point of performing region comparison was a sampling Kirryu City in Gunma, Ogose town in Saitama, Ueno Park in Tokyo, Sarue Park in Tokyo and Katsuura City in Chiba.

1. Changes in mercury concentration due to dry and weight change due to drying temperature of leaf

After drying for five hours, respectively 70 ℃ leaves, at 130 ℃, it was found that 60 minute in 70 ℃ , it is 10 minute at 130 ℃ to constant weight.Mercury concentration at each temperature was 33.4ngg^{-1} at 70 ℃, 33.0ngg^{-1} at 130 ℃.

2. Mercury concentration in the leaves within the site-specific mercury concentration in leaves

I was measuring the mercury concentration of each site by dividing the top, middle, at the bottom toward the petiole from the tip of the leaf camphor tree. As a result, mercury concentration was 62.0ngg^{-}1 at the top, 67.0ngg-1 at middle, 66.5ngg^{-1} at the bottom. In addition, I compared the mercury concentration in leaves in removing the mercury deposited in the leaf and total mercury concentration in the leaves. It is a leaf inside was revealed that much of the mercury contained in the leaves.

3. Changes in mercury concentration in the leaves by the time series variation

I investigated the time series changes in mercury concentration accumulated in the leaves by the use of leaves of different leaf age.

Keywords: mercury, camphor tree, environment

Japan Geoscience Union Meeting 2014
(28 April - 02 May 2014 at Pacifico YOKOHAMA, Kanagawa, Japan)

MIS21-P16 Room:Poster Time:April 28 18:15-19:30

Restoration of Soil Physical Properties by No-tilled Management in Tropical Sugarcane.

MORI, Yasushi[1*] ; ARAI, Miwa[2] ; KANEKO, Nobuhiro[2] ; SWIBAWA, Gede[3] ; NISWATI, Ainin[3]

[1]Okayama Univesity, [2]Yokohama National University, [3]Univresity of Lampung

...

Keywords: Non-till, Sugarcane, Infiltration

Japan Geoscience Union Meeting 2014
(28 April - 02 May 2014 at Pacifico YOKOHAMA, Kanagawa, Japan)

MIS21-P17 Room:Poster Time:April 28 18:15-19:30

A study of soil organic matter stabilization using physical fractionation, isotopic, and spectroscopic approaches

WAGAI, Rota[1*] ; ASANO, Maki[1] ; HAYAKAWA, Chie[1] ; INOUE, Yudzuru[2] ; KAJIURA, Masako[1] ; HIRADATE, Shyuntaro[1] ; YAMAGUCHI, Noriko[1] ; INAGAKI, Yoshiyuki[7] ; UCHIDA, Masao[3] ; TAKEICHI, Yasuo[4] ; SUGA, Hiroki[5] ; JINNOU, Muneaki[4] ; ONO, Kanta[4] ; TAKAHASHI, Yoshio[5]

[1]National Institute for Agro-Environmental Sciences (NIAES), [2]Kyushu University, [3]National Institute of Environmental Studies (NIES), [4]High Energy Accelerator Research Organization (KEK), [5]Hiroshima University, [6]TOYAMA Co. Ltd., [7]Forestry and Forest Products Research Institute

Volcanic-ash soil (Andisol) is unique among the world soil types due to the strong physical stability of organo-mineral aggregate structure at micro and submicron scales (Asano and Wagai, 2013, Geoderma) and its high capacity to store organic matter (OM) even in upland surface horizons under warm, moist climate regime where microbial heterotrophic activity is high. Several hypotheses have been proposed to account for these features of Andisol including (i) strong interaction of OM with dissolved metals (Al, Fe) and/or short-range-order (SRO) minerals that are quite abundant in this soil type, and (ii) preservation of recalcitrant compounds such as char.

Here we present some highlights from the 3-year project (GR091, NEXT Program, JSPS) examining the mechanisms of soil OM stabilization with a focus on organo-mineral interactions at various spatial and temporal scales using multiple analytical methods and experimental approaches. After careful consideration of the degree of soil aggregate disruption levels, we physically fractionated Andisol surface horizon sample based on particle size and density. Chemical composition of each physical fraction was assessed by elemental analysis, selective dissolution of inorganic phases, and solid-state ^{13}C-NMR. The origin and degree of microbial alteration of OM was estimated from C and N stable isotope ratios while the turnover time of C was assessed by radiocarbon measurements. Physical features of soil mineral and organo-mineral aggregate surfaces were characterized by specific surface area (N_2-BET), XPS, and microscopic methods. We also conducted tracer experiments to further assess the residence time of the OM in each density fractions. Based on these results, we will discuss the progression of organo-mineral associations from fresh plant detritus to the aggregates of varying structure and stability for the studied Andisol.

Japan Geoscience Union Meeting 2014
(28 April - 02 May 2014 at Pacifico YOKOHAMA, Kanagawa, Japan)

MIS22-01 Room:213 Time:April 29 14:15-14:30

Formation evaluation and production interval determination at the 1st offshore methane hydrate production test site

FUJII, Tetsuya[1*] ; TAKAYAMA, Tokujiro[1] ; SUZUKI, Kiyofumi[1] ; YAMAMOTO, Koji[1]

[1]Japan Oil, Gas and Metals National Corporation

In order to evaluate productivity of gas from marine methane hydrate (MH) by the depressurization method, on March 2013, the first offshore production test form MH concentrated zone (MHCZ) was conducted by the Research Consortium for Methane Hydrate Resource Development in Japan (MH21) at the AT1 site located in the north-western slope of Daini-Atsumi Knoll in the eastern Nankai Trough, Japan.

Before the production test, during the pre-drilling campaign conduced in 2012, extensive geophysical logging and pressure coring using Hybrid Pressure Coring System were conducted at monitoring well (AT1-MC) and coring well (AT1-C), in order to obtain fundamental information about reservoir properties of MH bearing formation for reservoir characterization, and also to decide on the production interval.

The MHCZ confirmed by the geophysical logging at AT1-MC has a thin-turbidite assemblage (from several tens of centimeters to a few meters) with 60 m of gross thickness; it is composed of lobe/sheet type sequences in the upper part, and relatively thick channel sand sequences in the lower part. The MHCZ at AT1-MC is thicker than those found in wells drilled in 2004 (β1, 45 m), which were located about 150 m northeast of MT1-MC. This fact indicates that the predictions provided by a seismic interpretation and an inversion analysis were reasonable. Moreover, we confirmed that the silt-dominant formation just above the MHCZ was more than 20 m thick ; this was expected to be a seal formation. The well-to-well correlation between two monitoring wells (AT1-MC and MT1) in a 40 m distance shows fairly good lateral continuity of these sand layers (upper part of MHCZ), indicating an ideal reservoir for the production test.

In the upper part of the MHCZ, hydrate pore saturation (Sh) estimated from resistivity log showed distinct difference in value between sand and mud layers, compared to Sh from Nuclear Magnetic Resonance (NMR) log. Resistivity log has higher vertical resolution than NMR log, so it is favorable for these kinds of thin bed evaluation. In this part, 50 to 80% of Sh was observed in sandy layer. On the other hand, lower part of the MHCZ, Sh estimated from both resistivity and NMR log showed higher background value and relatively smoother curve than upper part. In this part, 50 to 80% of Sh was observed in sandy layer as well.

On the basis of the above observations, a production interval was planed. When we consider an effective depressurization, the existence of sealing layers is critical both above and below the interval. We expect that thin silty layers within the lower part of MHCZ will serve as a sealing layer that will prevent water coning from water-bearing layers. Therefore, we stopped drilling the production well at about 20 m above BSR, and decided to produce from approximately 40 m from the top of the MHCZ.

Our future (ongoing) work is to integrate reservoir characterizations based on well logs and pressure core data for the history matching of production test results.

This study is a part of the program of the Research Consortium for Methane Hydrate Resources in Japan (MH21 Research Consortium).

Keywords: methane hydrate, offshore production test, formation evaluation, production interval, eastern Nankai Trough, Daini-Atsumi Knoll

Japan Geoscience Union Meeting 2014
(28 April - 02 May 2014 at Pacifico YOKOHAMA, Kanagawa, Japan)

MIS22-02 Room:213 Time:April 29 14:30-14:45

P-wave velocity features of Methane Hydrate-Bearing turbidity sediments sampled by Pressure Core Tool

SUZUKI, Kiyofumi[1*] ; SANTAMARINA, Carlos J.[2] ; WAITE, William[3] ; WINTERS, William J.[3] ; ITO, Takuma[4] ; NAKATSUKA, Yoshihiro[1] ; KONNO, Yoshihiro[4] ; YONEDA, Jun[4] ; KIDA, Masato[4] ; JIN, Yusuke[4] ; EGAWA, Kosuke[4] ; FUJII, Tetsuya[1] ; NAGAO, Jiro[4] ; YAMAMOTO, Koji[1]

[1]JOGMEC/TRC, [2]Georgia Institute of Technology, United State, [3]USGS, [4]AIST/MHRC

Turbidity sediments around the production test site at Daini-Atsumi knoll were deposited under channels and lobes of a submarine fan environment. It implies that sediments contain property difference caused by depositional environment, fundamentally. In addition, MH crystals among sediment grains overprint their original physical properties. Thus, difficulties in MH reservoir arise in clarifying the properties of MH-bearing sediments and normal sediments from logging data. To analyze their physical properties, core samples of MH-bearing sediments were taken at the first offshore production test site using a wireline tool called the hybrid pressure coring system (Hybrid PCS), which prevents dissociation of MH in the sampled cores.

Nondestructive, high-pressure analyses were conducted in both the 2012 summer drilling campaign and the 2013 winter collaboration study. To handle Hybrid PCS cores during the pressure coring campaign in the summer of 2012, a pressure core analysis and transfer system (PCATS) was installed on the research vessel Chikyu (Yamamoto et al., 2012). The measurements can be taken at the in situ water pressure at depth without causing any core destruction or MH dissociation. In January 2013, GT, USGS, AIST, and JOGMEC researchers conducted a collaborative study. In this study, the pressure core characterization tools (PCCTs) developed by GT also measured P-wave velocity of MH-bearing sediments.

In the PCATS analysis, the results showed a difference of more than 1,200 m/s in P-wave velocities between the MH-bearing sandy and muddy layers. This difference in P-wave velocities was confirmed by PCCTs measurements. Also, P-wave velocity of a turbidite interval tend to decrease upward as same as grading of a turbidite. The result implies that MH concentration is related with pore size of sediments.

Acknowledgement

Authors would like to express thanks to Geotek at 2012 pressure core operation/analysis. Authors are grateful to USGS and Georgia Tech members who struggled with PCCTs operation/experiments in AIST Hokkaido. This research is conducted as a part of MH21 research and the authors would like to express their sincere appreciation to MH21 and the Ministry of Economy, Trade and Industry for disclosure permission for this research.

Keywords: Gas hydrate, P-wave velosity, Turbidite, Pore-filling type, Grain size distribution

Japan Geoscience Union Meeting 2014
(28 April - 02 May 2014 at Pacifico YOKOHAMA, Kanagawa, Japan)

MIS22-03 Room:213 Time:April 29 14:45-15:00

Reservoir Characterization and geological modeling for methane hydrate-bearing sediments around the 1st Offshore Product

TAMAKI, Machiko[1*] ; SUZUKI, Kiyofumi[2] ; FUJII, Tetsuya[2] ; SATO, Akihiko[1]

[1]Japan Oil Engineering Co., Ltd., [2]Japan Oil, Gas and Metals National Corporation

The eastern Nankai trough is considered as an attractive potential resource of methane hydrates (MHs) and the first offshore production test was performed around the Atsumi-oki in 2013. The objective of this study is to conduct MHs reservoir characterization of methane hydrate (MH)-bearing turbidite sediments around the test site.

The depositional environment of MH-bearing sediments around the production test site is a deep submarine-fan turbidite system (e.g., Takano et al., 2009). To evaluate MH dissociation and gas production performance, we require precise geological models that describe facies variations of turbidite sediments and their corresponding petrophysical properties. In this study, we performed MHs reservoir characterization integrated from well log, core and 3D seismic data, and the 3D geological models were constructed based on geostatistical approach.

In accordance with the geological modeling workflow, (1) layering and gridding along the geological horizon and facies variations (framework modeling) and (2) defining internal properties (property modeling) were performed for the reservoir. Property modeling includes calculation of the distribution of facies and petrophysical properties such as hydrate saturation, porosity, and permeability, which are required as input to the reservoir flow simulation for predicting gas production performance.

This study is a part of the program of the Research Consortium for Methane Hydrate Resource in Japan (MH21 Research Consortium).

Japan Geoscience Union Meeting 2014
(28 April - 02 May 2014 at Pacifico YOKOHAMA, Kanagawa, Japan)

MIS22-04 Room:213 Time:April 29 15:00-15:15

Source of iodine and methane in gas hydrate layers in the Kumano Basin, Nankai Trough

YAMAMOTO, Itsuki[1] ; TOMARU, Hitoshi[1*] ; MATSUZAKI, Hiroyuki[2]

[1]Department of Earth Sciences, Chiba University, [2]MALT, University of Tokyo

Because iodine has a strong biophilc behavior in marine system, pore waters in methane hydrate layers are often enriched in iodine as well as methane. The presence of long-lived radioisotope of iodine in nature therefore provides the potential age of source formations for methane. We have determined iodine isotopic ratios of pore waters collected frequently form sandy methane hydrate zone between 200 and 400 m below the seafloor in the Kumano Basin, Nankai Trough to examine the loci of source formations and processes to deliver and accumulate methane in the present methane hydrate stability.

Concentrations of iodine dissolved in pore waters peak at the top of sandy gas hydrate layers at 200 mbsf, where the iodine isotopic ratios also show the lowest/oldest values. Methane and iodine could have been derived from the landward old sediments through the sandy aquifers to the present methane hydrate zone. Transport of methane from old organic-rich sediments to the hydrate stability preferentially accumulates methane hydrates in thick sandy layers in the Kumano Basin.

Keywords: Methane hydrate, Iodine isotope, Pore water

Japan Geoscience Union Meeting 2014
(28 April - 02 May 2014 at Pacifico YOKOHAMA, Kanagawa, Japan)

MIS22-05 Room:213 Time:April 29 15:15-15:30

Trials of the methane hydrate observations in the local governments

AOYAMA, Chiharu[1*]

[1]Japans Independent Institute

Nine prefectures of 1 local government prefecture of the Sea of Japan side established ”Association of Ocean Energy Exploitation of Resources Promotion Sea of Japan” (the following, Association of Sea of Japan) in September, 2012. They support methane hydrate exploitation of resources of the government and aim at the local activation and job creation. Niigata and Hyogo that were members of the association of Sea of Japan carried out a prefecture original methane hydrate investigation. They appeal to the government for development promotion of the government by showing the result. On the other hand, Wakayama located on the Pacific side wants to appeal to the government for the reexamination of the development sea area by showing that outer layer type methane hydrate exists to the sea area that is nearer the landside than the sea area that the government develops. The Independent Institute carried out collaborative investigation each with Niigata, Hyogo and Wakayama in 2013. I show the results of research.

In the joint investigation with Niigata, plural plumes were observed in Mogami trough east slope (from depth of the water 200m 600m) .

In the joint investigation with Hyogo, I carried out observation of a methane plume and the structure and the seafloor topography under the sea bottom in Oki east sea area. Furthermore, I performed a piston core ring and gathered five samples and confirmed plural traces of the methane hydrate.

In the joint investigation with Wakayama, plural plumes were observed in Shionomisaki canyon (from depth of the water 1,700m 2,200m). There is hardly the report of the plume on the Pacific side so far. Therefore I want to continue observing it in future.

Keywords: methane hydrate, methane plume, quantitative echo shounder, piston core

Japan Geoscience Union Meeting 2014
(28 April - 02 May 2014 at Pacifico YOKOHAMA, Kanagawa, Japan)

MIS22-06 Room:213 Time:April 29 15:30-15:45

Quantify methane seeping flux from Ashizuri knoll, Nankai Trough

HARA, Shuichi[1*] ; TSUNOGAI, Urumu[1] ; KOMATSU, Daisuke[1] ; ASHI, Juichiro[2] ; NAKAMURA, Ko-ichi[3] ; SUNAMURA, Michinari[4] ; NAKAGAWA, Fumiko[5] ; TOKI, Tomohiro[6]

[1]Graduate School of Environmental Studies, Nagoya Univ., [2]ORI.,Tokyo Univ., [3]National Institute of Advanced Industrial Science and Technology, [4]Division of Earth and Planetary Sciences, Grad. School Sci., Tokyo Univ., [5]Division of Earth and Planetary Sciences, Grad. School Sci.Hokkaido Univ,., [6]Department of chemistry, Bioligy and Marine Science,Ryukyu Univ,.

The Ashizuri Knoll is located on the southern margin of Tosa Basin (ca. 1000 m depth) in the western Pacific Ocean. The top of the knoll is 534 m depth.The BSR have been detected around the knoll. Beside, seepage methane bubbles were found at top of the knoll. Extensive geochemical surveys on the water column around Ashizuri Knoll were done in September, 2013.The primary purpose of the study was to quantify the seeping flux of methane from the knoll by measuring the spatial distribution of methane around the knoll. Besides, we akso tried to clarify the origin of methane by determining both δ13C and δD values.

Enrichment of thermogenic methane up to 145 nmol/L was detected just above the top of knoll. Besides, the methane enriched plume spread northeastward of the knoll at the water depth of 450- 660 m. The calculated methane flux was almost the same with that of off Joetsu hydrate area.

Japan Geoscience Union Meeting 2014
(28 April - 02 May 2014 at Pacifico YOKOHAMA, Kanagawa, Japan)

MIS22-07 Room:213 Time:April 29 15:45-16:00

Characteristics of natural gas hydrates retrieved off the southeastern and southwestern Sakhalin Island

HACHIKUBO, Akihiro[1*] ; SAKAGAMI, Hirotoshi[1] ; MINAMI, Hirotsugu[1] ; YAMASHITA, Satoshi[1] ; TAKAHASHI, Nobuo[1] ; SHOJI, Hitoshi[1] ; VERESHCHAGINA, Olga[2] ; JIN, Young K.[3] ; OBZHIROV, Anatoly[2]

[1]Kitami Institute of Technology, [2]Pacific Oceanological Institute, FEB RAS, [3]Korea Polar Research Institute

Gas hydrate samples were retrieved at the southeastern and southwestern Sakhalin Island in the cruises of LV59 and LV62 (R/V Akademik M. A. Lavrentyev). Sakhalin Slope Gas Hydrate (SSGH) project started in 2007, and we retrieved sediment cores including gas hydrates off northeastern Sakhalin Island in 2009-2011. In the recent cruises (2012-2013), we sampled sediment cores at the Terpeniya Ridge and the Tatarsky Trough (SE and SW Sakhalin Island, respectively). We found a lot of gas plumes ascend from the sea bottom and the dissolved methane in sediment pore water was rich. Gas hydrate crystals were recovered from both areas and stored into liquid nitrogen tank. Their dissociation heat and hydration number were measured by a calorimeter and Raman spectrometer, respectively. Dissociation heat of gas hydrates was almost the same as that of pure methane hydrate. Raman spectra showed that the hydrate crystals of both Terpeniya Ridge and Tatar Trough belonged to the structure I, and the hydration number was estimated about 6.0. Molecules of hydrogen sulfide were detected in both large and small cages of the structure I. Therefore, the hydrate crystal is similar to that obtained from NE Sakhalin Island in our previous cruises.

We obtained hydrate-bound gas and dissolved gas in pore water on board and measured their molecular and stable isotope compositions. Empirical classification of the methane stable isotopes; δ^{13}C and δD indicated that the gases obtained at the Terpeniya Ridge are microbial origin via carbonate reduction, whereas some cores at the Tatarsky Trough showed typical thermogenic origin. We retrieved three sediment cores with gas hydrate at the Tatarsky Trough, and their δ^{13}C of hydrate-bound methane were -47.5 ‰, -44.2 ‰, and -68.8 ‰, respectively. Therefore, gas hydrates encaged both microbial and thermogenic gases yield at the Tatarsky Trough. Ethane-rich (up to 1% of the total guest gas) hydrates were found at the Terpeniya Ridge and the Tatarsky Trough, and encaged ethane was also detected in their Raman spectra. Ethane δ^{13}C of the all gas samples suggested their thermogenic origin.

Keywords: gas hydrate, stable isotope, Sea of Okhotsk, Raman spectroscopic analysis, Calorimetry

Japan Geoscience Union Meeting 2014
(28 April - 02 May 2014 at Pacifico YOKOHAMA, Kanagawa, Japan)

MIS22-08 Room:213 Time:April 29 16:15-16:30

First attempt to drill down hydrate mound and gas chimney by BGS Rockdrill 2

MATSUMOTO, Ryo[1*] ; WILSON, Michael[2]

[1]Meiji University-Gas Hydrate Laboratory, [2]British Geological Survey

A series of shallow piston coring (PC) has identified dense accumulation of massive gas hydrates in the upper part of hydrate mounds and gas chimneys in Japan Sea since 2004, however, because of limited penetration of PC, distribution and resource potential of gas hydrate below ˜10 mbsf have not been clearly answered as yet. On the other hand, 3D seismic profiles have revealed significant pull-up structure, a characteristic velocity pseudo-structure, in gas chimneys, suggesting an accumulation of significant amount, probably 20 to 30 vol.%, of gas hydrates in gas chimneys. In the summer 2013, Meiji University and British Geological Survey deployed BGS benthic drilling machine, Rockdrill 2, on hydrate mounds in Joetsu basin, Japan Sea, and successfully drilled through inhomogeneous, gas hydrate- and carbonate-bearing hard sediments and occasional soft and gassy sediments down to 32 mbsf. Core recovery was unfortunately low throughout the coring due to extensive dissociation of gas hydrate and gas expansion during and after coring. However, we could recover massive gas hydrate samples, 5 to 12 cm long, from a number of horizons down to 32 mbsf. Several 2 to 7 m thick zones of gas hydrate accumulation have been inferred from integrated profiles of drill logs, video-monitor observation, and discontinuous sediment core record. Shallow drilling of Rockdrill 2 is likely to have proved a dense distribution of gas hydrates in deeper part of hydrate mounds and gas chimneys.

Keywords: gas hydrate, Japan Sea, hydrate mound, gas chimney, Rockdrill 2

Japan Geoscience Union Meeting 2014
(28 April - 02 May 2014 at Pacifico YOKOHAMA, Kanagawa, Japan)

MIS22-09 Room:213 Time:April 29 16:30-16:45

Formation of shallow gas hydrates and geochemistry of gas and pore water from UT13 cruise in the Japan Sea

OWARI, Satoko[1*] ; SUZUKI, Yoshiharu[1] ; TOMARU, Hitoshi[1] ; UCHIDA, Takashi[2] ; KOBAYASHI, Takeshi[3] ; TANI, Atsushi[5] ; NUMANAMI, Hideki[4] ; MATSUMOTO, Ryo[6]

[1]Graduate school of Science , Chiba university, [2]Akita Univesity Faculty of Engineering and Resource Science, [3]Tokyo University of Marine Science and Technology, [4]Department of Home Economics, Faculty of Home Economics, Tokyo Kasei-Gakuin University, [5]Dept. Earth and Space Science, Graduate School of Science, Osaka University, [6]Gas Hydrate Laboratory

Active gas venting and distribution of massive gas hydrates are largely observed on the summits of the Umitaka Spur and Joetsu Knoll in the eastern margin of the Japan Sea, where the fault system associated with strong anticline structure constrains the accumulation of gas and following gas hydrate formation. The UT13 cruise has conducted to collect shallow sediments from the Oki Trough, north eastern of Noto Peninsula, and offshore Akita-Yamagata areas, where gas chimney structure and strong backscatter indicate migration of gas-charged fluid and potential formation of gas hydrates near the seafloor. Geochemistry of pore water, dissolved gas, and hydrate-dissociated gas reflect the geochemical environments associated with the delivery of gas and fluid and formation/dissociation of gas hydrates in the shallow sediments.

Flake-like and nodular gas hydrates were observed at 1-6 mbsf in the Oki Trough and offshore Akita-Yamagata, respectively. Concentrations of methane dissolved in pore water are high, comparable to those in the Umitaka Spur and Joetsu Knoll area, and the SMI depths are accordingly shallow at ~2.7 mbsf in the entire research area, indicating high potential of gas hydrate accumulation in the shallow sediments. Concentrations of chloride are sporadically low in all areas due to gas hydrate dissociation during core recovery, accumulations of small gas hydrates with saturations up to 20% were observed, reflecting ubiquitous formation of gas hydrates in the research area. Concentrations of calcium and magnesium show fine increase and decrease in response to sulfate changes at deeper than SMI, reflecting the change of the methane flux mainly, the formation/dissociation of gas hydrates may have changed seafloor topography and geochemical properties of pore water and gas in the shallow sediments.

Contrary to the Umitaka Spur and Joetsu Knoll area where thermogenic gas dominates in the shallow gas hydrates, chemical and isotopic compositions of gas indicate that the majority of gas is of biogenic origin with minor contribution from thermogenic ethane and hydrogen sulfide, the latter may result in expanding gas hydrate stability and forming gas hydrates near the seafloor.

This research is supported by the MEXT Grand-in-Aid for Scientific Research (KAKENHI) to R. Matsumoto (Meiji University).

Keywords: Shallow gas hydrates, pore water, dissolved gas, SMI

Japan Geoscience Union Meeting 2014
(28 April - 02 May 2014 at Pacifico YOKOHAMA, Kanagawa, Japan)

MIS22-10 Room:213 Time:April 29 16:45-17:00

Distribution of methanogenic and methanotrophic archaea in subseafloor sediment collected during UT12

IMAJO, Takumi[1*] ; KOBAYASHI, Takeshi[1] ; IMADA, Chiaki[1] ; TERAHARA, Takeshi[1] ; MATSUMOTO, Ryo[2]

[1]The graduate school of marine science and technology, TUMSAT, [2]Meiji University

Methane hydrate is now one of the most popular energy sources in the world, and various amounts are presumed to be buried around Japan's continental margins. Methane contained in methane hydrate in the deep sea sediment is produced by microbial or thermogenic system. In the microbial system, methanogenic and methanotrophic archaea play an important role in this environment. However, the studies on characteristics and abilities of these microorganisms are still underway in the Sea of Okhotsk. Therefore, this study focuses on isolation of the methanogenic archaea and analysis of community construction and diversity of these microorganisms.

Sediment samples were collected from the subseafloor by the piston coring, during UT12 (Umitaka-maru Gas Hydrate Research Cruise 2012). Samples were collected from each core sample at appropriate intervals. The samples were stored at 4 ℃ for the microbiological cultivation experiment use, and at -80 ℃ for the microbiological diversity analysis use, respectively.

For the isolation, cultivation was carried out by enrichment culture using H_2/CO_2 medium. The cultivation temperatures were 15 ℃ and 30 ℃, respectively. We successfully isolated several methanogenic archaea from the samples of the surface of the subseafloor. The result of the 16S rRNA gene sequence analysis showed that some of the strains were identified as closely related strains of *Methanogenium marinum*. In a previous literature, *M. marinum* was isolated from the cold marine sediment from the Scan Bay, Alaska. We also conducted the experiment to measure the methane productivity of our isolates by the range of the cultivation temperature.

For the analysis of community structure and diversity of methanogens, DNA was extracted from each sediment sample, using the ISOIL kit following the manufacturer's protocol. The 16S rRNA gene of methanogenic archaea and the mcrA gene of methanogenic and methanotrophic archaea were amplified by PCR. The PCR product was purified by FastGene Gel/PCR Extraction Kit following the manufacturer's protocol. The purified products were analyzed by T-RFLP method and clone library method. The results of the T-RFLP analysis showed that the various fragments were observed. Clone library sequencing analysis of mcrA genes indicated that some of them were identified as related sequences to *Methanogenium*. Also, results from T-RFLP method were used for MDS (Multi-Dimensional Scaling) analysis.

This experiment was supported by grants-in-aid for scientific research <KAKENHI>(Ryo Matsumoto, Meiji University).

Keywords: shallow gas hydrate, methanogenic archaea, methanotrophic archaea

Japan Geoscience Union Meeting 2014
(28 April - 02 May 2014 at Pacifico YOKOHAMA, Kanagawa, Japan)

MIS22-11 Room:213 Time:April 29 17:00-17:15

Environmental variability of the Japan Sea clarified by

OGIHARA, Shigenori[1*]

[1]Earth and Planetary Science, The University of Tokyo

Environmental variability of the Japan Sea was presumed using MD179 Cruse 3312 sediment core by inorganic and organic geochemical analysis. Analysis of this study went focusing on mainly thin-laminated dark layer (TL-1 to 3). TOC was about 0.8% in TL-2 and 3, on the other hand, the TL-1 layer showed nearly 2%. In the central part of TL-2 to the upper part, all the samples of a C/S ratio are 1 or less. This has suggested strong reduction environment at the upper part of TL-2 layer.

The Pristane/Phytane ratio (Pr/Ph ratio) traditionally used as an oxidation-reduction index is shown that most analysis data are <3.0 and it was the reductive environment. Pentamethylicosane (PMI) which is the membrane lipid origin of the anaerobic methanotrophic archaea (ANME), C18-isoprenoid ketone characteristically detected to a cold-seep carbonate and hop-22 (29) ene (diploptene) also the origin were not clear, characteristically found out at a methane seeping point, those depth distribution was plotted and considered. Distribution of the AMNE marker in the inside of TL layers is heterogeneous, and the possibility of the sudden methane eruptions during the TL-2 deposition was suggested.

This study was supported by MH21, Research Consortium for Methane Hydrate Resources in Japan.

Keywords: Japan Sea, biomarker, TL layer, sulfur isotope compositon, anoxic environment, C/S ratio

Japan Geoscience Union Meeting 2014
(28 April - 02 May 2014 at Pacifico YOKOHAMA, Kanagawa, Japan)

MIS22-P01 Room:Poster Time:April 29 18:15-19:30

Overview of well logging operations at the 1st offshore methane hydrate production test in the eastern Nankai Trough

TAKAYAMA, Tokujiro[1*]

[1]Japan Oil, Gas and Metals National Corporation

Overview of well logging operations at the 1st offshore methane hydrate production test in the eastern Nankai Trough

T.Takayama*, T.Fujii, K.Suzuki, K.Yamamoto (JOGMEC)

Objective

The objective of well logging operations at the 1st offshore methane hydrate production test is to evaluate the formation lithology and reservoir properties. We will construct an integrate reservoir model based on the well logging data for assessing an accurate prediction of production performances for the methane hydrate (MH) production test.

Well logging results

Our focused area around the offshore production test site comprised unconsolidated turbidite formations with a thickness of thin turbidite sand and mud layers according to the previous well logging data. These formations typically show significant washed out after the drilling and its effect of the quality of data is serious issues for the formation evaluation by well logging data.

The well logging results in the monitoring wells indicate that the significant washed out was found particularly in the intervals of thin bed turbidite formations above the reservoir interval and below the BSR(Bottom Simulating Reflectors). However, other intervals exhibit stable caliper logging data, which indicating there are no significant washed out effect even in the WL(Wireline Logging) data. This is probably due to the tight formation of the mud-rich and MH-rich intervals.

Conclusions and Future works

a) Operation of both LWD(Logging While Drilling) and WL was successfully completed without any significant trouble.

b) Borehole condition was bad due to the borehole washed out above the reservoir interval and below the BSR. This was mainly due to the unconsolidated turbidite formation with the thin thickness of sand and mud layers. In spite of the washed out effect, reservoir and seal intervals showed good quality of well logging results which correspond to significant tight formations of mud-rich and MH-rich sediments.

c) In LWD operation, we used pulse neutron generator without radioactive sources. This operation was quite rare in the world and we could successfully obtain fairly good well logging data in the seal and reservoir intervals.

d) In the drilling of the MH reservoirs in the offshore exploration, the borehole washed out is inevitable because it exists in the shallow marine unconsolidated sediments. Hence, several challenging and technical issues are significantly important for our future study.

Acknowledgment

This work was supported by Methane Hydrate 21 Research Consortium. We would like to thank the Ministry of Economy, Trade and Industry for providing permission to publish this paper.

Keywords: methane hydrate, offshore methan hydrate production test, Nankai Trough, Well logging

Japan Geoscience Union Meeting 2014
(28 April - 02 May 2014 at Pacifico YOKOHAMA, Kanagawa, Japan)

MIS22-P02 Room:Poster Time:April 29 18:15-19:30

Depicting Thermal History of the Forearc Basin Pleistocene Turbiditic Sedimentary Sequences around Daini Atsumi Knoll

AUNG, Than tin[1*] ; FUJII, Tetsuya[1] ; UKITA, Toshiyasu[1] ; KOMATSU, Yuhei[1] ; SUZUKI, Kiyofumi[1]

[1]Methane Hydrate R&D Division, Technology & Research Center, JOGMEC

Thermal history of sedimentary basin is a key to understand hydrocarbon maturation and generation of the source rock within the basin. In terms of gas hydrate accumulation, high pressure and low temperature boundaries, the gas hydrate stability zone, is mandatory to simulate in order to understand accumulation mechanisms of gas hydrate in the studied basin. We have determined heat flow history of Pleistocene sedimentary sequences in the forearc basin round the Daini Atsumi knoll, along the eastern Nankai Trough, Japan, by simulating gas hydrate stability zone. World first offshore production test of gas hydrate was successfully done in the vicinity area of Daini Atsumi knoll during March 2013.

Simulation in 3D gas hydrate petroleum systems of the forearc basin filling with Pleistocene turbiditic sedimentary sequences around the Daini Atsumi knoll was firstly performed by applying assumed heat flow of 45 mW/m2. Temperature at seabed is applied as 3.5 C throughout the model area and depositional period. Simulated sedimentary sequences consist of Pleistocene Ogasa Group of sand and shale alternative turbiditic sedimentary layers. Older upper Kakegawa Group is also included between the model basement and Ogasa group. Lithologies are interpreted from grain size analysis of cores data. Lateral facies distribution are based on seismic facies analysis. Global sea level changes are considered in applying paleo-water depths of the geologic horizons.

Simulated hydrostatic pressure matches hydrostatic pressure calculated from XPT data at well A1-L. Simulated temperature was calibrated by DTS (distributed temperature sensor) Temperature of gas hydrate reservoir zone at well AT1-MC. Calibration result reveals that heat flow has to low down to 32 mW/m2 in order to fit pressure and temperature at well. Result of simulated temperature using calibrated heat flow matches with a resolution of ˜1C of the well data. This heat flow value is lower than the reported value (˜50 mW/m2, Harris et al., 2014) around the vicinity of the studied area. Validation of this heat flow value requires 1) to reanalyze model layer thickness and total thickness of model, and 2) to reanalyze thermal conductivity of applied lithology.

In addition to above works, model is planned to update with paleo-water depth based on paleo-bathymetry from structural restoration, and reported depth from foraminiferal measurement of core samples at A1-L well. Because mass and lateral distribution of gas hydrate accumulation are considerably affected by tectonic uplift at Daini Atsumi Knoll.

This study is a part of the program of the Research Consortium for Methane Hydrate Resources in Japan (MH21 Research Consortium).

Keywords: Gas Hydrate Petroleum Systems, Daini Atsumi Knoll, Heat Flow, Pleistocene Ogasa Group, 3D, Simulation

Japan Geoscience Union Meeting 2014
(28 April - 02 May 2014 at Pacifico YOKOHAMA, Kanagawa, Japan)

MIS22-P03 Room:Poster Time:April 29 18:15-19:30

Methane Hydrate trapping system of the turbidite channel complex in Daini-Atsumi Knoll, eastern Nankai Trough, Japan

KOMATSU, Yuhei[1*] ; FUJII, Tetsuya[1] ; SUZUKI, Kiyofumi[1]

[1]Japan Oil, Gas and Metals National Corporation

The 1^{st} offshore gas hydrate production test was conducted at gas hydrate concentrated zone (reservoir) of the Eastern Nankai Trough, which is considered stratigraphic accumulation. However, the accumulation mechanism for this concentrated zone is not yet well understood.

In this study, in order to examine gas hydrate trapping system in the accumulation mechanism, we identify the depositional process and controlling factors based on facies analysis and sequence stratigraphy using the core and geophysical log data.

Seven depositional sequences are identified based on grain size, bed thickness, sedimentary structure, and stacking pattern in this study. The sequence boundaries are also identified by terminations of seismic reflection. These sequences are attributed to a fourth to fifth-order eustatic sea-level changes, because the stacking pattern cycle is in phase with global oxygen isotope curves, the cycle is also identified in the onshore formation during the same period. The reservoir was interpreted as Falling-Stage Systems Tract (FSST) and Lowstand Systems Tract (LST).

In the reservoir, it was observed the channel complex set characterized by relatively strong reflections and paleocurrent flowing from northeast to southwest on 3-D seismic data. The channel complex set changes into muddy facies in the south direction. The channel complex set is characterized by hemipelagic setting or slope (F1), abandonment mud drape (F2), nonamalgamated channel element (F3), and semiamalgamated channel element (F4). The channel elements (F3, 4) are the fundamental unit and record a single phase of downcutting and filling. The muddy deposits (several 10 m; F1) above reservoir are interpreted as condensed section because they are consistent with a peak of foraminifer abundance. The condensed section divide different sediments of gas hydrate saturation.

These features suggest that condensed section deposits become top seal and channel deposits interpreted as FSST and LST become reservoir in gas hydrate trapping formation. The trapping system has the ability to seal lateral gas leakage because the channel reservoir is located around structural wing, the direction of sand pinch-out to structural highs becomes oblique to the direction of sediment supply. Consequentially, gas hydrate trapping system is constrained by sedimentary facies, systems tracts, and geographic and tectonic setting. Concepts and data generated in this study can be used for gas hydrate petroleum system analysis such as basin simulation.

Keywords: gas hydrate system, sequence stratigraphy, sea level change, submarine channel, sedimentary facies

Japan Geoscience Union Meeting 2014
(28 April - 02 May 2014 at Pacifico YOKOHAMA, Kanagawa, Japan)

MIS22-P04 Room:Poster Time:April 29 18:15-19:30

Relationship of permeability and particle breakage of experimental fault -Evaluation for the methane-hydrate reservoir-

KIMURA, Sho[1*] ; KANEKO, Hiroaki[1] ; ITO, Takuma[1] ; MINAGAWA, Hideki[1]

[1]Reservoir Modeling Team, Methane Hydrate Research Center, AIST

Methane hydrate is expected to be an energy resource in the future. As results of coring and logging, the existence of a large amount of methane-hydrate is estimated in the east Nankai Trough, offshore central Japan, where many folds and faults have been observed. Permeability in methane hydrate-bearing sediment is important factors for estimating the efficiency of methane gas production. In this study, we use a ring-shear apparatus to examine the relationship between the permeability and grain size reduction of silica sand sample after large displacement shearing under tested effective normal stresses ranging from 0.5 MPa to 8.0 MPa. The grain size distribution in the shear zone of sand specimen after ring-shearing at each normal stress level is analyzed by laser particle analyzer. The permeability and grain size reduce with the increasing the effective normal stress due to particle breakage. The relationship between permeability and grain size distribution after ring-shearing is expressed well by a curve in each sand, silt and clay size content. In the first group, the sand size content is up to about 80 %, permeability drastically decreases by two orders of magnitude. In the second group, the sand size content is less than about 80 %, the permeability is almost constant. In the silt and clay size, the both contents are up to about 10 %, the permeability abruptly decreases, while, the permeability gradually decreases over about 10 %. The results are indicated that the grain size reduction and the effective normal stress during shearing are one of the controlling factors of the permeability in fault of sand. This study is financially supported by METI and Research Consortium for Methane Hydrate Resources in Japan (the MH21 Research Consortium).

Keywords: Fault, Particle breakage, Permeability, Grain size distribution, Ring-shear test

Japan Geoscience Union Meeting 2014
(28 April - 02 May 2014 at Pacifico YOKOHAMA, Kanagawa, Japan)

MIS22-P05 Room:Poster Time:April 29 18:15-19:30

Methane seepage and possibility of hydrate-bearing layers around Kuroshima Knoll, SW Ryukyu

MATSUMOTO, Takeshi[1*] ; AOKI, Tae[2]

[1]University of the Ryukyus, [2]Weathernews Inc.

A reconnaissance survey expedition of Kuroshima Knoll, located south of Ishigaki Island, southwest Ryukyu Islands, was carried out for the first time in 1996. During the expedition dead Calyptogena shells were identified on the summit plane of the knoll. Several advanced reconnaissance survey expeditions afterwards for the geological study in this area by 2001 revealed an active eruption of methane, which suggested a methane hydrate layer beneath the knoll. In this study, we carried out a mapping of the bottom sediment on the top flat plane of Kuroshima Knoll from the video images obtained by JAMSTEC submersibles and ROVs since 2002 in order to create a complete geological route map. The result shows that the whole area of the summit plane of the knoll with the water depth of around 640m was covered by dead Calyptogena community and calcareous rocks. Live Bathymodiolus community was located densely around 24deg. 07min. 48sec.N, 124deg. 11min. 33sec.E. Bubble eruption was located at 35 sites. The area of the suggested methane seepage was estimated to be 40,000 square meters.

Next, the vertical profile of the sea water temperature with its seasonal variability around the knoll was examined in order to verify if methane hydrate exists stably beneath the seafloor of the knoll by use of the JODC data catalogue. It is, however, hard to expect a methane hydrate layer underneath the knoll considering the water temperature at the seafloor in this area. Examination of the vertical profiles of the sea water temperature along the whole Ryukyu Arc also shows that a possible methane hydrate layer is confined to the area with more than 700m in water depth in the fore-arc area.

Keywords: methane hydrate, Kuroshima Knoll

Japan Geoscience Union Meeting 2014
(28 April - 02 May 2014 at Pacifico YOKOHAMA, Kanagawa, Japan)

MIS22-P06 Room:Poster Time:April 29 18:15-19:30

Hydrogen isotope of hydrate-bound hydrocarbons at Lake Baikal

HACHIKUBO, Akihiro[1*] ; SAKAGAMI, Hirotoshi[1] ; MINAMI, Hirotsugu[1] ; YAMASHITA, Satoshi[1] ; TAKAHASHI, Nobuo[1] ; SHOJI, Hitoshi[1] ; KHLYSTOV, Oleg[2] ; KALMYCHKOV, Gennadiy[3] ; DE BATIST, Marc[4]

[1]Kitami Institute of Technology, [2]Limnological Institute, SB RAS, [3]Vinogradov Institute of Geochemistry, SB RAS, [4]Ghent University

Natural gas hydrates exist in sublacustrine sediments of Lake Baikal. Gas hydrates were first obtained from sub-bottom depths of 121 and 161 m in the Baikal Drilling Project well located at the southern Baikal basin. Recently, MHP (Multi-phase Gas Hydrate Project, 2009-2013) revealed distribution of gas hydrate in sub-bottom sediment at the southern and central Baikal basins. We obtained gas hydrate crystals from more than 25 places, and retrieved hydrate-bound gas onboard. We measured molecular and isotopic compositions of hydrate-bound gas.

According to the δ^{13}C-δD diagram for methane (Whiticar, 1999), high and low methane δ^{13}C values indicate thermogenic and microbial origins, respectively, and methane δD provides information on methyl-type fermentation or CO_2 reduction in the microbial field. Kida *et al.* (2006) and Hachikubo *et al.* (2010) reported that hydrate-bound methane of Lake Baikal was microbial origin via methyl-type fermentation, because methane δD was about -300 ‰. We found heavier methane (δ^{13}C ranged from -50 ‰ to -40 ‰) in the Kukuy Canyon area (central Baikal basin), indicating thermogenic origin. Methane δD was distributed from -330 ‰ to -270 ‰. Generally, δD of thermogenic methane of marine gas hydrates is much more heavier (more than -200 ‰). Methane δD of Lake Baikal gas hydrate seems to be about 100 ‰ smaller than that of marine gas hydrate. Matveeva *et al.* (2003) reported that δD of the lake bottom water was about -133 ‰. Possiblely, methane δD of hydrate-bound methane derives from δD of water.

Hachikubo A, Khlystov O, Krylov A, Sakagami H, Minami H, Nunokawa Y, Yamashita S, Takahashi N, Shoji H, Nishio S, Kida M, Ebinuma T, Kalmychkov G, Poort J (2010) Molecular and isotopic characteristics of gas hydrate-bound hydrocarbons in southern and central Lake Baikal. *Geo-Mar Lett* **30**: 321-329. doi:10.1007/s00367-010-0203-1

Kida M, Khlystov O, Zemskaya T, Takahashi N, Minami H, Sakagami H, Krylov A, Hachikubo A, Yamashita S, Shoji H, Poort J, Naudts L (2006) Coexistence of structure I and II gas hydrates in Lake Baikal suggesting gas sources from microbial and thermogenic origin. *Geophys Res Lett* **33**: L24603. doi:10.1029/2006GL028296

Matveeva TV, Mazurenko LL, Soloviev VA, Klerkx J, Kaulio VV, Prasolov EM (2003) Gas hydrate accumulation in the subsurface sediments of Lake Baikal (Eastern Siberia). In: Woodside JM, Garrison RE, Moore JC, Kvenvolden KA (eds) Proc 7th Int Conf Gas in Marine Sediments, 7-11 October 2002, Baku, Azerbaijan. *Geo-Mar Mett* **23(3/4)**: 289-299. doi:10.1007/s00367-003-0144-7.

Whiticar MJ (1999) Carbon and hydrogen isotope systematics of bacterial formation and oxidation of methane. *Chem Geol* **161**: 291-314. doi:10.1016/S0009-2541(99)00092-3

Keywords: gas hydrate, crystallographic structure, Lake Baikal, methane, stable isotope

Japan Geoscience Union Meeting 2014
(28 April - 02 May 2014 at Pacifico YOKOHAMA, Kanagawa, Japan)

MIS22-P07 Room:Poster Time:April 29 18:15-19:30

Sedimentary environments and pore properties of subseafloor sediments in the eastern margin of Japan Sea

UCHIDA, Takashi[1*] ; HORIUCHI, Sena[1] ; KATO, Yuki[2] ; MATSUMOTO, Ryo[3]

[1]Faculty of Engineering and Resource Science, Akita University, [2]Graduate School of Frontier Sciences, the University of Tokyo, [3]Organization for the Strategic Laboratory of Research and Intellectual Properties, Meiji University

Sediment samples below the seafloor were retrieved as long as 40 meters at the Umitaka Spur, Joetsu Channel, Toyama Trough, Japan Basin, Nishi Tsugaru and Okushiri Ridge areas in the east margin on Japan Sea. Small amounts of sandy sediment have been retrieved as thin intercalations in Pleistocene and Holocene muddy layers, where trace fossils and strong bioturbations are commonly observed. Those sandy sediments consist of very fine- to fine-grained sands, and are sometimes tuffaceous. These sandy sediments might have been transported approximately around 3 to 30 ka according to the tephra ages, where supplying sediments might have not been abundant due to sea level fluctuation during the Pleistocene ice age.

It is important to clarify the relationship between burial depths and absolute porosities of the argillaceous sediments. Therefore, macroscopic observations and descriptions, measurements of porosities and the pore size distributions, thin-section observations, SEM (scanning electron microscope) observations, and the X-ray diffraction analyses have been performed. They consist of silt- to clay-grained particles, and they sometimes contain very fine- to medium-grained thin sandy layers. Average porosities are 50 % in all study areas, but mean pore sizes in the Nishi Tsugaru are around 1000 nm while 100 nm in the other areas, which tend to decrease as increasing of depths. It is suggested that repacking of the muddy particles dominantly advances by physical compaction in early diagenesis.

They generally contain much opal-A, quartz, feldspar, illite and smectite that do not change definitely with depth, because they are tuffaceous and are suffered only from early diagenesis. By optical and microscopic observations, diatom tests, foraminifers and framboidal pyrites are commonly observed, and, in particular, the shapes of diatom are usually various, dominantly fragmental and infrequently preserved.

The sedimentological properties of subseabottom argillaceous sediments in early diagenesis can be discussed in terms of physical and geochemical aspects such as porosity, permeability, pore size distribution, diagenetic mineral composition as well as microscopic observation. It is remarked that the physical diagenesis proceeds first as repacking of clastic grains due to mechanical compaction, whereas the chemical diagenesis advances very slowly in early diagenesis.

This study was performed as a part of the MH21 Research Consortium on methane hydrate in Japan.

Keywords: hydrate, Japan Sea, pore

Japan Geoscience Union Meeting 2014
(28 April - 02 May 2014 at Pacifico YOKOHAMA, Kanagawa, Japan)

MIS22-P08 Room:Poster Time:April 29 18:15-19:30

Isotopic and microbial compositions of carbonate nodules from sea bottom sediments in the Japan Sea

MORI, Taiki[1*] ; KANO, Akihiro[1] ; OKUMURA, Tomoyo[2] ; MATSUMOTO, Ryo[3]

[1]SCS Kyushu University, [2]JAMSTEC, [3]Meiji University

Carbonate precipitates on sea bottom sediments and shallow core in methane seep areas are often associated with methanogens. Anoxic methane oxidization is a particularly important metabolism for carbonate precipitation in terms of raising local alkalinity and supersaturation. We recovered carbonate nodules from sea bottom sediments from Umitaka Spur, Joetsu Knoll and Akita offshore during an expedition fro gas hydrate in the Japan Sea in August-October 2013. We investigate microbial metabolisms for carbonate precipitation based on textural observation, isotopic measurement, and gene analysis.

Many specimens appear grapestone textures consisting of aggregated small nodules, which indicate multiple generation of carbonate precipitation. Aragonite needles are commonly observed on outer margin and in pore spaces in the grapestone. Core part of the nodules are often black color due to concentration of organic substance. Isotopic compositions were measured for sub-samples that were micro-drilled from the section of the nodules. Some of the Umitaka specimens exhibit large variation in carbon isotope, which generally decrease from core to margin. Methanogenesis is only accountable microbial processes for the highest values up to +12 permil. This metabolism can separate organic carbon into 13C-depleted methane and 13C-enriched carbon dioxide species. On the other hand, nodules from Joetsu and Akita are relatively homogenous and very low (-45 to -60 permil) in carbon isotope. This indicate that carbonate carbon in the nodules was largely originated from methane. Gene analysis for an Umitaka specimen extracts many sulfate resucers, but no methanogens. This specimen was calcified by sulfate reduction of organic matter.

We would like to thank onboard scientists and crews for their kind support during the expedition. We appreciate British Geological Survey for drilling.

Keywords: gas hydrate, carbonate nodule, stable isotope, microbes

Japan Geoscience Union Meeting 2014
(28 April - 02 May 2014 at Pacifico YOKOHAMA, Kanagawa, Japan)

MIS22-P09 Room:Poster Time:April 29 18:15-19:30

Microstratigraphic studies using UT13 piston cores around methane seep areas, eastern margin of the Japan Sea

OI, Takeshi[1*] ; ISHIHAMA, Saeko[2] ; AKIBA, Fumio[3] ; NUMANAMI, Hideki[4] ; MATSUMOTO, Ryo[1] ; HASEGAWA, Shiro[5]

[1]Meiji University, OSRI, [2]Kanagawa Prefectual Museum of Natural History, [3]Diatom Minilab Akiba, Co. Ltd., [4]Tokyo Kasei University, [5]Kumamoto University

1. Introduction

Microbiostratigraphy is important for the submarine resoueces survey to research the chronology and paleoceanography. Furthermore, benthic foraminiferal studies are also useful to clear the environmental impacts caused by the dissociation of subsurface methane hydrate in shallow sediments of the Umitaka Spur and Joetsu Knoll of the Joetsu basin 30 km off Joetsu city, Niigata Prefecture (Matsumoto et al., 2009). It is possible to estimate the age and environments of core sediments in detail, because the Microbiostratigraphy during the past 130 ka could be evident in the giant piston cores recovered by MD179 cruise in June 2010.

In this poster, we introduce the late Quaternary microbiostratigraphy of diatom and foraminifera off Joetsu in the eastern part of the Japan Sea, and applied these results and foraminiferal ^{14}C dates to the core sediments in the other hydrate areas of the Japan Sea.

2. Microbiostratigraphy of diatom and foraminifera off Joetsu

12 foraminiferal biozones (Biozone I to XII in descending order) in the last 32 ka and 8 diatom zones (A-H diatom zones) in the last 130 ka were recognized based on some piston cores off Joetsu and indicate the paleoenvironmental changes of the surface and bottom sea water, respectively (Nakagawa et al., 2009; Akiba et al., 2014).

3. UT13 studies

In July 2013, Umitaka-maru sailed to two new areas to delineate the entire sequence of gas hydrate mound in the Oki-Trough and the Mogami-Trough. Piston corer penetrated down to 6-8 mbsf on hydrate mounds and recovered some massive methane hydrate and 13 core sediments. We analyzed microfossil assemblages and ^{14}C dating of these sediments and estimated each sedimentation rate by comparing with the previous studies.

3-1. Result 1 - Sedimentation rates of Oki Trough

Main core sediments in the Oki Trough have similar sedimentation rates (about 15 cm/kyr) from 3-4 ka to present, but PC1302 reduced top sediments has a higher rate and PC1305 included methane hydrates a relative lower rate. The sediment age upon massive hydrates from the bottom of PC1305 was calculated ca. 40 ka.

3-2. Result 2 - Microbiostratigraphic features in Mogami Trough

Three cores in the Mogami Trough indicate the lack of sediments around LGM because of older ^{14}C dates and occurrences of the extinct benthic foraminifera, *Epistominella pulchella*. In particular, whole foraminiferal assemblages of PC1311 sediments are characterized by the distributions of *E. pulchella* and poor preserved specimens, whereas mixed the well-preserved subtropical planktonic species. These features might indicate the gas hydrate activities from the deep seafloor.

Keywords: the eastern margin of the Japan Sea, methane hydrate, microbiostratigraphy, stable isotope, sedimentation rate, extinct species

Japan Geoscience Union Meeting 2014
(28 April - 02 May 2014 at Pacifico YOKOHAMA, Kanagawa, Japan)

MIS22-P10 Room:Poster Time:April 29 18:15-19:30

Deposition process based on foraminiferal stratigraphy

UMEZAKI, Yosuke[1*]

[1]Graduate School of Science and Tecnology Kumamoto University

There are mound called Joetsu Knoll and Umitaka Spur which was associated with the formation of methane hydrate off the coast of Joetsu city, Niigata Prefecture. There are valley in east side of Joetsu Knoll, there have a very special geographical features. In this area, previous researches recognized 12 foraminiferal biozones and 8 diatom biozones. These are the good stratigraphic indicators in contrast of sediment core. Sediment core I use to study (MD179-3308) collected from the valley. The length of this core is 30.9m and water depth is 1224m. This core recognized 4 diatom biozones and at 5 layers of this core, radiometric age was measured. From these researches, it was estimated that there was a large age gap around 1620cmbsf in the sediment core.In the valley, it is considered that landslides and flows from the shallow occurred. For clarify depositional process and relationship of valley and mound, in this study, foraminifera in this sediment core was analysed.

Around 1620cmbsf in the sediment core, benthic foraminifera association and planktonic foraminifera numbers are changed. It is considered that the layer of 0 ˜1620cm have a sedimentary record of about 30,000 years. In this layer, benthic foraminifera associations are similar to previous researches. It is considered that layer of 1620cm˜2820cm have a sedimentary record of about 70,000 years ˜110,000 years. Benthic foraminifera is alternated crowd in which Brizarina pacifica is priority species, and crowd in which Eilohedra rotunda, Islandiella sp are priority species. In particular, foraminifera in 1700cmbsf is characterized by Brizarina pacifica and maximum number of foraminifera.

Rutherfordoides rotundata output from 1000 ˜1800cmbsf and 2280cmbsf. It is the related species of Rutherfordoides corunata which is methane-related species. Therefore, it is considered that sediment of these layers are derived from the methane seep.

Keywords: benthic foraminifera, planktonic foraminifera, foraminiferal number, methane hydrate, Deposition process

Japan Geoscience Union Meeting 2014
(28 April - 02 May 2014 at Pacifico YOKOHAMA, Kanagawa, Japan)

MIS23-01 Room:415 Time:May 2 09:00-09:15

Marine biomarkers deposited on land by the 2011 Tohoku-oki tsunami

SHINOZAKI, Tetsuya[1*] ; FUJINO, Shigehiro[2] ; IKEHARA, Minoru[3] ; SAWAI, Yuki[4] ; TAMURA, Toru[4] ; GOTO, Kazuhisa[5] ; SUGAWARA, Daisuke[5] ; ABE, Tomoya[6]

[1]University of Tsukuba, [2]University of Tsukuba, [3]Kochi University, [4]GSJ, AIST, [5]Tohoku University, [6]Nagoya University

Tsunami deposits, especially sand deposits is generally used for estimating paleotsunami event. Sand deposit is mainly identified as tsunamigenic on the basis of geological, chemical, biological, archaeological, anthropological, geomorphological, and contextual feathers, especially geological and biological features such as lateral changes in thickness and grain size of deposit, presence of marine-origin microfossils and others have been frequently utilized as identifying proxies. However, these characteristics do not always get preserved, in which case it is difficult to identify paleotsunami deposit. If evidence of seawater inundation can be detected, it became a good criterion for marine source of sand deposits. As a proxy of seawater evidence, in this study, we focused on biomarker which is molecular fossils originated from formerly living organisms. Biomarker has two advantages. One is their high preservation potential. It is confirmed to be stable in geological time scale. Another is the obvious difference between terrigenous and marine biomarkers; To take the *n*-alkane, lower *n*-alkane homologs, notably C_{15}, C_{17}, and C_{19} *n*-alkanes, tend to be predominant in many algae whereas higher *n*-alkane homologs, such as C_{27}, C_{29}, and C_{31}, tend to be predominant in leaf waxes of higher plants. To verify whether marine biomarkers are deposit on land by tsunami inundation, samples of the 2011 Tohoku-oki tsunami deposit and underlying soil were collected at Sendai and Odaka, Northeast Japan.

In Sendai, a 3 cm-thick fine sand deposits was formed by the 2011 tsunami at the top of core, and there was paddy soil beneath the sand deposits. Biomarkers were measured at 1 layer in sand deposits and 7 layers in soil deposits. Short-chain *n*-alkanes (C_{16}, C_{17}, C_{18}, and C_{19}) mainly elaborated from algae and fish were occurred only at 5-6 cm depth. It seems that theses short-chain *n*-alkanes were penetrated sandy tsunami deposit and concentrated at 5-6 cm depth. In Odaka, sand deposits were found at 8-15 cm and 18-20 cm depth, and there was paddy soil beneath sand deposits. Organic-rich mud deposits (15-18 cm depth) was intercalated between two sand layers. This mud drape was seems to be formed by first wave together with thin sand layer (18-20 cm depth), and then following waves formed thick sand layer (8-15 cm depth). Biomarkers were measured at 1 layer in surface soil deposits, 8 layers in the 2011 tsunami deposits, and 3 layers in underlying soil deposits. Short-chain *n*-alkanes (C_{16}, C_{17}, C_{18}, and C_{19}), pristane, and phytane were detected only from 20-21 cm deep. Pristane is predominately elaborated from zooplankton, benthos, and fish, while phytane is predominately elaborated from zooplankton or sediment itself by biological activity. Presence of these hydrocarbons suggests a contribution from marine/aquatic, and this characteristic is similar to the results of Sendai.

Marine origin hydrocarbons, such as short-chain *n*-alkanes, pristane, and phytane, were detected at soil layers below sandy tsunami deposits in both sites. Since no marine biomarkers were presented further deep soil layer in both sites and surface soil layer overlying tsunami deposit in Odaka, it is highly possible that these biomarkers were transported by the tsunami. Each sediment samples were collected more than two years after the tsunami, it means marine biomarkers have been preserved at least two years. Our study present the first evidence for the marine biomarkers detected from the modern tsunami event, and we propose possibility of biomarkers as a proxy of paleotsunami identification.

Keywords: biomarker, hydrocarbon, tsunami deposit, 2011 Tohoku-oki tsunami

Japan Geoscience Union Meeting 2014
(28 April - 02 May 2014 at Pacifico YOKOHAMA, Kanagawa, Japan)

MIS23-02 Room:415 Time:May 2 09:15-09:30

Geochemical identification of the tsunami deposit using machine learning machine learning techniques

KUWATANI, Tatsu[1*] ; NAGATA, Kenji[2] ; OKADA, Masato[2] ; WATANABE, Takahiro[1] ; OGAWA, Yasumasa[1] ; KOMAI, Takeshi[1] ; TSUCHIYA, Noriyoshi[1]

[1]Graduate school of environmental studies, [2]Graduate school of frontier science

Tsunami deposit is a direct evidence of inundation area of past tsunamis. A large number of publications have been written about the diagnostic signatures and identification criteria for past tsunamis, including sedimentological, micropalaeontological evidences. However their identification is still difficult because all criteria is neither necessary condition nor sufficient condition due to various origin, mechanism and temporal variation of tsunami deposits. Geochemical discrimination is now recognized as other useful proxy which dose not depend on the researcher's subjectivity, especially in the case that other proxies can not be used. Especially, geochemical indicator is suggested to be useful in identification beyond the limit of recognizable sand deposition. In this study, we established the criteria for geochemical discrimination of 2011 Tohoku-oki tsunami deposits and their background marine sediments using machine learning techniques. For 18 analyzed elements, several tens of elemental combinations show the discrimination rates higher than 99%. By applying the criteria to past tsunami deposits in the Sendai Plain, we discuss the validity and effectiveness of the method.

Keywords: tsunami deposit, machine learning, Geochemistry

Japan Geoscience Union Meeting 2014
(28 April - 02 May 2014 at Pacifico YOKOHAMA, Kanagawa, Japan)

MIS23-03 Room:415 Time:May 2 09:30-09:45

Chemical composition of historical tsunami deposits in the Sendai plain and proposal of geochemical discrimination

HOSODA, Norihiro[1*] ; WATANABE, Takahiro[1] ; TSUCHIYA, Noriyoshi[1] ; YAMASAKI, Shin-ichi[1] ; NAKAMURA, Toshio[2] ; NARA, Fumiko[1] ; OKAMOTO, Atsushi[1] ; HIRANO, Nobuo[1]

[1]Graduate School of Environmental Science, Tohoku University, [2] Center for Chronological Research, Nagoya University

A magnitude 9.0 earthquake and huge tsunami occurred off the Pacific coast of Tohoku area in Northeast Japan. After the 2011 Tohoku earthquake and tsunami, disaster science is much focused to reduce the damage around costal area, and it plays an important role as making the set of guidelines in an emergency. Because Japanese islands are located on the plate boundaries among the Pacific, Eurasian, Philippine Sea and North American plates, large earthquakes and tsunamis have repeatedly occurred during historic and prehistoric times. A huge tsunami more than 10m-height is often accompanied with submarine earthquakes around the Pacific Rim. The 2011 Tohoku tsunami was the one of the most destructive natural disasters. By the effect of that, study on earthquakes and tsunami become more and more significant, and it a major issue of social concern in Tohoku and other areas. After the 2011 Tohoku tsunami, these invasion areas were covered by a huge amount of tsunami deposits more than 10 million tons. In addition, we are able to obtain past tsunami deposits with the age of ˜1000-2000 years before present (BP) in the same area using boring corer. In order to make an expecting tsunami invasion map in other areas as soon as possible, we must provide the information about the distribution of past tsunami deposits. However, it is difficult to discriminate the one of tsunami and other events, such as storm and flood. Additionally, we must establish a new technique to detect invisible muddy and thin tsunami deposits. We need historical archives and geological proxy of past tsunami invasion, but it is rare to have both evidences in many cases. Geochemistry is useful techniques to know the source of terrestrial deposits and these weathering processes. Therefore, we tried to apply geochemical techniques in this study.

Keywords: Jogan tsunami sediments, The 2011 Tohoku tsunami, geochemistry

Japan Geoscience Union Meeting 2014
(28 April - 02 May 2014 at Pacifico YOKOHAMA, Kanagawa, Japan)

MIS23-04 Room:415 Time:May 2 09:45-10:00

Scour and deposition by the 2011 Tohoku-oki tsunami at Takata-matsubara in Rikuzentakata City, Japan

TAKASHIMIZU, Yasuhiro[1*] ; SHIBUYA, Takahiro[2]

[1]Faclty of Education, Niigata University, [2]Graduate school of Education, Niigata University

The behavior of the 2011 Tohoku-oki tsunami at the Takata-matsubara in Rikuzentakata city was reconstructed using sedimentary facies analysis, grain size properties and magnetic fabric were summarized as follows;

1) Vertical variations in grain size of the tsunami deposits show ten and several tsunami inflows and outflows of the tsunamis.

2) The deposits were mainly formed by backwash of the tsunami based on the paleocurrent analysis using magnetic fabric measurements.

3) The tsunami flow over the artificial sea wall and destroyed the sea wall with large scours on ground surface. Following ten and several tsunamis with minor wave height can ran-up in order to destroying the sea wall.

Keywords: tsunami deposits, Rikuzentakata City, shooting flow, hydraulic jump, Takata-matsubara, Seawall

Japan Geoscience Union Meeting 2014
(28 April - 02 May 2014 at Pacifico YOKOHAMA, Kanagawa, Japan)

MIS23-05 Room:415 Time:May 2 10:00-10:15

Traces of the 2011 Tohoku-oki tsunami as seen from the topography and geology in rias coast, Iwate Pref.

SAKAMOTO, Izumi[1*] ; YOKOYAMA, Yuka[1] ; YAGI, Masatoshi[1] ; IIJIMA, Satsuki[1] ; IMURA, Riichiro[1] ; NEMOTO, Kenji[1] ; KITO, Takeshi[2] ; FUJIMAKI, Mikio[3] ; FUJIWARA, Yoshihiro[4] ; KASAYA, Takafumi[4]

[1]TOKAI Univ., [2]FODECO, [3]COR, [4]JAMSTEC

The recent 2011 Tohoku tsunami strongly affected the coastal area of the Pacific coast of Tohoku. Tokai University with JAMSTEC investigated the Tohoku coastal area as a part of Tohoku Ecosystem-Associated Marine Sciences (TEAMS). We have succeeded in capturing traces of tsunami in various sea-bottom.

The trace in the bottom topography:Many uneven terrain has distributed around 15 ˜20m water depth. Many of its terrain is denudation mark, mark denudation of these exhibits an axial direction southeast of Toni-bay case. In the Okirai-bay a distance of approximately 20km from Toni-bay, denudation phenomenon that traces to develop in 15-25m water depth around has been confirmed. This denudation mark is presumed to have been formed by mud flowing toward the sea floor off the coast on the tsunami wave at the time of argument.

The trace in the high-resolution geo-stratigraphic survey: We have defined the A layer between the reflective surface and 1 seafloor. The A layer is located below a few tens of cm seafloor, and is widely distributed. The A layer is equivalent to the unit 1 of core samples described below. Reflecting surface enriched unevenness is also confirmed A layer below, which are estimated to be the traces of past tsunami activity.

The trace in the sea-bottom columnar core section:We estimate that the surface U-1 layer with grading structure (fine sand at the surface and coarse sand with gravel from lower part) of columnar core was the sediment gravity flow caused by the tsunami activity. The U-2 layer with bioturbation structure estimated by the normal bay sediment. There is some sandy layer with 10cm thick in the U-2 layer and also under the U-2 layer. It is estimated that these sandy layer have been formed by the historical tsunami activity.

Keywords: Tsunami deposit, Sanriku coast

Japan Geoscience Union Meeting 2014
(28 April - 02 May 2014 at Pacifico YOKOHAMA, Kanagawa, Japan)

MIS23-06 Room:415 Time:May 2 10:15-10:30

Shallow-marine sedimentary processes of the 2011 Tohoku earthquake tsunami, inferred from sediment c

TAMURA, Toru[1*] ; SAWAI, Yuki[1] ; SAWAI, Yuki[1] ; NAKASHIMA, Rei[1] ; HARA, Junko[1]

[1]Geological Survey of Japan, AIST

While subaerial tsunami deposits have been much explored in recent years, our knowledge of shallow-marine tsunami sedimentation and its resultant deposits is limited. In August and September 2012, we practiced vibrocore drilling at 44 sites in Sendai Bay off the Pacific coast of northeastern Japan to investigate features of the open-sea shallow-marine deposits of the 2011 Tohoku earthquake tsunami and their variations. The tsunami deposit was inferred in the uppermost part of the cores based on the extent of bioturbation and concentrations of short-lived radionuclides. The preserved tsunami deposit, where identifiable, is typically 10-50 cm thick. Its grain size is basically similar to that of the original sediment at each site, which differs from medium to fine sand in the lower shoreface, through very fine sand to clay in the inner shelf, to poorly-sorted gravel, sand and mud offshore. This suggests the limited extent of cross-shelf sediment transport. Several lower shoreface sites show a yellowish coarse sand layer at the top. This yellowish layer is differentiated from the underlying greenish gray sand, and is possibly composed of beach sand transported by the tsunami backwash. In the inner shelf, the tsunami layer tends to show multiple inverse and normal grading of grain size as known in some of subaerial tsunami deposits. These features may help identify older shallow-marine tsunami deposits although more research in different settings is needed for establishing comprehensive criteria.

Japan Geoscience Union Meeting 2014
(28 April - 02 May 2014 at Pacifico YOKOHAMA, Kanagawa, Japan)

MIS23-07 Room:415 Time:May 2 10:30-10:45

Sediment transport induced by the 2011 Tohoku-oki tsunami: A shallow seafloor survey at southern part of the Sendai Bay

YOSHIKAWA, Shuro[1*] ; KANAMATSU, Toshiya[1] ; SAKAMOTO, Izumi[2] ; FUJIMAKI, Mikio[3] ; IMURA, Riichirou[2] ; YAGI, Masatoshi[2] ; NEMOTO, Kenji[2] ; GOTO, Kazuhisa[4] ; SAKAGUCHI, Hide[1]

[1]JAMSTEC, [2]Tokai University, [3]Coastal Ocean Research CO., LTD., [4]Tohoku University

After the 2011 Tohoku-Oki earthquake (Mw 9.0), to examine the tsunami-generated sediment transport and topographic change, and inundation area, a large number of investigations have been conducted on land, particularly at the coastal area of Sendai plain (e.g., Goto et al., 2012, 2014). Understanding the linkage of the transport between land and seafloor is also important. In the present study, to examine the influence of the tsunami and offshore sediment transport, high-resolution shallow seismic survey, sampling of surface sediments, vibracoring, and seafloor observation by underwater video camera were conducted on the shallow seafloor at the southern part of the Sendai Bay, northeastern Japan. The present study will help to understand not only modern sedimentary process induced by tsunami but also identification of paleo-tsunami records, because our knowledge of shallow marine tsunami deposits is limited in contrast to the subaerial tsunami deposits.

One of the principal results is as follows. One or two sharp and continuous reflectors are recognized on the sub-bottom profiles in water depths approx. 6-15 m, excluding the area of outcrops in the southern part of the survey area. With decreasing water depth, depth of the reflectors from the seafloor generally increases (up to approx. 1.5 m). A comparison between the seismic profiles and vibracores infers that the sharp reflectors are erosional surface formed during the 2011 tsunami.

Keywords: shallow marine tsunami deposit, 2011 Tohoku-oki tsunami

Japan Geoscience Union Meeting 2014
(28 April - 02 May 2014 at Pacifico YOKOHAMA, Kanagawa, Japan)

MIS23-08 Room:415 Time:May 2 11:00-11:15

Paleo tsunami events determination using radiogenic nuclides

YOKOYAMA, Yusuke[1*]

[1]Atmosphere and Ocean Research Institute, University of Tokyo

Recent advancement of mass spectrometry enables us to determine timing of past events using trace amounts of geological samples. Accelerator Mass Spectrometry (AMS) and Inductively Coupled Plasma Mass Spectrometry (ICP-MS) are amongst them and long-lived nuclides can be measured precisely. We have been conducted paleo Tsunami studies applying 14C and U-series dating employing these techniques. Together with geophysical modeling as well as paleo climate proxy data, paleo Tsunami events are clearly reconstructed from these measurements. Also newly developed AMS, single stage AMS, that is dedicated for 14C measurements can produce large number of data to constrain the timing in different manner. In this presentation, several examples of these studies will be introduced along with perspectives of age determinations of paleo Tsunami events.

Keywords: Radiocarbon, Accelerator Mass Spectrometry, Uranium series, Quaternary, Dating

Japan Geoscience Union Meeting 2014
(28 April - 02 May 2014 at Pacifico YOKOHAMA, Kanagawa, Japan)

MIS23-09 Room:415 Time:May 2 11:15-11:30

Marker-tephras for the chronological study of tsunami deposits along the Pacific coast of Eastern Japan

SODA, Tsutomu[1*]

[1]Institute of Tephrochronology for Nature and History Co., Ltd.

Tephras are effective markers for chronological studies of tsunami deposits along the Pacific coast of Eastern Japan. Because the information on marker-tephras in the tephra catalog of Japan and its surrounding area (Machida and Arai, 2003) is only basic, this author describes the detailed characteristics of some important tephras for their identifications.

The Kikai-Akahoya ash (K-Ah), one of representative widespread marker-tephras on the Japanese Islands, erupted 7.3 ka from the Kikai Caldera, covering most of the Pacific coastal area of Eastern Japan. Towada-Chuseri tephra (To-Cu, ca.6.0 ka), Towada-a tephra (To-a, 915 A.D.) and Baegdusan-Tomakomai ash (B-Tm, the 10^{th} century A.D.) are markers in the northern Tohoku area. To-Cu and To-a cover the southern Tohoku area, as well. Tephras erupted from Numazawa, Asama and Haruna volcanoes are useful in the southern Tohoku area. They are Numazawa Lake tephra (Nm-N, ca.5.0 k.y.BP), Haruna-Futatsudake-Shibukawa tephra (Hr-FA, the early 6^{th} century A.D.), Haruna-Futatsudake-Ikaho tephra (Hr-FP, the middle of the 6^{th} century A.D.) and Asama-Kasukawa tephra (As-Kk, 1128 A.D.).

Likewise, tephras from Asama and Haruna volcanoes are useful for chronological studies of tsunami deposits in the Kanto area. They are Asama-C tephra (As-C, the latter half of the 3^{rd} century A.D.), Hr-FA, Asama-B tephra (As-B, 1108 A.D.) and Asama-A tephra (As-A, 1783 A.D.). Tephras from Fuji, Amagi, Izu-Oshima, Niijima and Kozushima volcanoes are distributed in the southern Kanto area. As a scoriaceous tephra has difficulty in identification, it is also necessary to check its stratigraphic relationships with silisic marker-tephras, archeological and historical data and radiocarbon ages.

Machida, H. and Arai, F. (2003) Atlas of tephra in and around Japan. Unie. Tokyo Press, 336p.

Keywords: tephra, chronology, tsunami deposit, Eastern Japan, Towada-a tephra, Towada-Chuseri tephra

Japan Geoscience Union Meeting 2014
(28 April - 02 May 2014 at Pacifico YOKOHAMA, Kanagawa, Japan)

MIS23-10 Room:415 Time:May 2 11:30-11:45

Modern and possible paleotsunami deposits in Samenoura, Sanriku Coast, and their relation to tsunami source mechanisms

SUGAWARA, Daisuke[1*] ; NISHIMURA, Yuichi[2] ; GOTO, Kazuhisa[1] ; GOFF, James[3] ; JAFFE, Bruce[5] ; RICHMOND, Bruce[5] ; CHAGUE-GOFF, Catherine[4] ; SZCZUCINSKI, Witold[6] ; YOKOYAMA, Yusuke[7] ; MIYAIRI, Yosuke[7] ; SAWADA, Chikako[7]

[1]Tohoku University, [2]Hokkaido University, [3]University of New South Wales, [4]Australian Nuclear Science and Technology Organisation, [5]U.S. Geological Survey, Pacific Coastal and Marine Science Center, [6]Adam Mickiewicz University in Poznan, [7]Tokyo University

Samenoura is situated in the bay head of a small inlet on the Pacific coast of Oshika Peninsula, one of the nearest places to the epicenter of the 2011 Tohoku-oki Earthquake. According to the Joint Survey Group, wave heights were measured at more than 20 m near the coastline. This area was severely damaged as a result of both co-seismic subsidence and tsunami inundation.

We carried out field surveys of the Tohoku-oki and paleotsunami deposits at Samenoura in March, May and October 2013. Sandy deposits laid down by the Tohoku-oki tsunami were up to 20 cm thick at locations with an elevation greater than 10 m, and were several cm thick within the forest higher up. The tsunami deposit also contained numerous shell fragments and foraminifera. Although some possible sources of the tsunami deposits can be attributed to narrow sandy beaches near the study area, the deposition of such a thick sandy deposit is more or less enigmatic, considering the steep Ria-type coastal topography.

Using a gouge auger and geoslicer, we found at least two sand layers intercalated within muddy sediments. A volcanic ash layer, which corresponds to the AD 915 Towada-a tephra, was also identified from a horizon between these sand layers. The underlying sand layer was most probably laid down by the 869 Jogan earthquake tsunami, one of the large-scale events known to have affected the region. Previous studies of the Jogan tsunami have proposed several possible source models that involve an interplate thrust earthquake. Given that the local bathymetry and topography of Samenoura Bay may be sensitive to the waveform of a large-scale tsunami, paleotsunami deposits found from this area may be the key to determining the source mechanisms of events on the Sanriku Coast.

In this presentation, the possible correlation of the sandy deposits with known paleotsunami events based on detailed radiocarbon dating is discussed. The hydrodynamic character and processes of tsunami sediment erosion and deposition in Samenoura Bay are analyzed using numerical modeling of both interplate and outer-rise earthquake scenarios.

Keywords: tsunami deposit, 2011 Tohoku-oki and 869 Jogan earthquake tsunamis

Japan Geoscience Union Meeting 2014
(28 April - 02 May 2014 at Pacifico YOKOHAMA, Kanagawa, Japan)

MIS23-11 Room:415 Time:May 2 11:45-12:00

Identification and ages of paleotsunami deposits in Sanriku Coast: Trench survey in Koyadori, Iwate Prefecture

ISHIMURA, Daisuke[1*] ; MIYAUCHI, Takahiro[1] ; ABE, Kohei[2] ; HAYASE, Ryosuke[3] ; OHARA, Keiichi[3]

[1]Chiba Univ. Sci., [2]OYO Co., [3]Institute of Accelerator Analysis Ltd.

We show new geological evidence of some historical tsunami deposits based on many radiocarbon dating and tephra analysis. Firstly, we sought study area matching for paleotsunami research based on geomorphological analysis and field survey, and excavated trench in coastal lowlands in Koyadori, Iwate Prefecture, northeast Japan. In trench, eleven event deposits (E1-E11: E1 is the 2011 Tohoku-oki tsunami deposits) interbedded within peat/peaty sediments were discovered. Thus, we revealed roundness of each event deposits and modern beach and river deposits to deduce the origin of event deposits. Consequently, we correlated tsunami deposits to historical tsunami events; E1: the 2011 Tohoku-oki tsunami, E2: 1896 Meiji Sanriku tsunami, E3: 1611 Keicho Sanriku tsunami, E4: 869 Jogan tsunami, and identified total eleven tsunami deposits during the last 3000-4000 years.

Keywords: tsunami deposits, Sanriku Coast, 2011 Tohoku-oki earthquake, historical tsunami, AD869 Jogan tsunami

Japan Geoscience Union Meeting 2014
(28 April - 02 May 2014 at Pacifico YOKOHAMA, Kanagawa, Japan)

MIS23-12 Room:415 Time:May 2 12:00-12:15

Geological survey of paleotsunamis at Noda Village, Iwate Prefecture, Japan

GOTO, Kazuhisa[1*] ; IIJIMA, Yasutaka[1] ; NISHIMURA, Yuichi[2] ; SUGAWARA, Daisuke[1] ; YOKOYAMA, Yusuke[3] ; MIYAIRI, Yosuke[3] ; SAWADA, Chicako[3] ; NAKAMURA, Yugo[2]

[1]Tohoku University, [2]Hokkaido University, [3]The University of Tokyo

Along the Sanriku coast, pre-historic tsunami record is still poorly understood in contrast to the well-documented historical tsunamis of past 400 years. AD869 Jogan tsunami is one of these cases. The tsunami affected the Sendai Bay area, as tsunami deposits were reported on Sendai and Ishinomaki Plains, but evidence is unsure if the tsunami was also reached along the Sanriku coast. To explore the paleotsunami histories along the Sanriku coast with emphasis on the possible inundation of AD869 event, we conducted field survey along the coast of Noda Village, Iwate Prefecture. Our survey site is now occupied by paddy and the 2011 Tohoku-oki, 1869 Meiji Sanriku and the 1933 Showa Sanriku tsunamis inundated to this site. We took ˜3 m long cores and found several gravel and sand deposits in peat buried by surface paddy soil. Considering the continuous distribution of deposits over 0.7 km from the present shoreline and analytical results of grain size and mineral composition, the deposits are likely formed by the tsunami although further investigation is required. Among these tsunami-like layers, a ˜10 cm thick gravel layer is deposited below tephra layers. One of the tephra layers is identified as Baitoushan-Tomakomai tephra (B-Tm) that was deposited in early to middle 10th Century. Volcanic glasses that can be identified as Towada-a tephra (To-a) of AD915 also is observed in patches at the similar horizon as B-Tm tephra. Radiocarbon dating results above the gravel layer is consistent with the tephra chronology. These analytical results as well as tsunami numerical modeling result suggest the inundation of potentially large tsunami before early to middle 10th Century along the northern Sanriku coast.

Keywords: tsunami, tsunami deposit, Noda village, Jogan tsunami

Japan Geoscience Union Meeting 2014
(28 April - 02 May 2014 at Pacifico YOKOHAMA, Kanagawa, Japan)

MIS23-13 Room:415 Time:May 2 12:15-12:30

Origin of a tsunami-drifted rock in Raga, Tanohata, Iwate Prefecture, transported by the Meiji Sanriku Tsunami in 1896.

OJI, Tatsuo[1*] ; OISHI, Masayuki[2]

[1]Nagoya University Museum, [2]Iwate Prefectural Museum

There are two large boulders on the hill of Raga, Tanohata, Iwate Prefecture. They are located at 24 m above sea level, and approximately 350 m from the coastline. Local villagers have told that these two boulders were derived as tsunami-drifted rocks at the time of Meiji Sanriku Tsunami in 1896. The eastside boulder is approximately 2-3 m in length, 2 m in width and at least 1.5 m in height, and it is estimated to weigh approximately 20 t. This boulder consists of calcarenite, containing numerous individuals of *Orbitolina* sp. that is a common large benthic foraminifera of the Lower Cretaceous. *Orbitolina* is found in '*Orbitolina* Facies' of the Miyako Group, and it is particularly abundant in the upper and uppermost part of the Hiraiga Formation. This *Orbitolina*-abundant horizon is exposed near the mouth of Raga inlet, just southwest of Hiraname coast. Therefore, this boulder is estimated to be located originally near the mouth of Raga inlet, and it should be transported as long as approximately 500 m by (a) tsunami(s). It is not certain whether this boulder was moved by one tsunami, or stepwisely by multiple tunamis. On the other hand, another boulder on the west side of the calcarenite boulder consists of conglomerate with rounded and subrounded pebbles of siliceous shale and chert, and this is considered as derived from the lower part of the Tanohata Formation, which is also exposed just on the southeastern slope of the boulder. This boulder is possibly derived from the southeastern hill, and thus it is not considered as a tsunami-derived rock. In Haipe inlet located about 1.2 km south of Raga, many new tsunami-drifted rocks have arrived onshore particularly on the northwestern side of the bay. The concentrated distribution of these rocks are in concordant with the direction of Tsunami current that came from the southeastern direction toward the erthquake epicenter located off Miyagi Prefecture. On the other hand, the tsunami-drifted rock in Raga is located in the west southwest of Raga inlet. Considering that the epicenter of Meiji Sanriku Earthquake was located off Kamaishi, this location reflects that the Tsunami current came from the east.

Keywords: Miyako Group, Orbitolina, tsunami-drifted rock

Japan Geoscience Union Meeting 2014
(28 April - 02 May 2014 at Pacifico YOKOHAMA, Kanagawa, Japan)

MIS23-14 Room:415 Time:May 2 12:30-12:45

Estimation of the magnitude of tsunami earthquakes along Japan Trench -Re-evaluation of the 1677 Enpo Boso-oki tsunami-

YANAGISAWA, Hideaki[1*] ; GOTO, Kazuhisa[2] ; SUZUKI, Keita[1] ; KANEMARU, Kinuyo[3] ; SUGAWARA, Daisuke[2] ; YANAGISAWA, Hinako[2] ; HASHIMOTO, Kohei[2] ; IWAMOTO, Naoya[4] ; TAKAMORI, Yoshibumi[5]

[1]Tohoku Gakuin University, [2]Tohoku University, [3]Kansai University, [4]Choshi Geopark, [5]Choshi City Board Education

Along the Japan Trench, unusual earthquakes sometimes trigger much larger tsunamis than expected from their seismic waves, which were called ”Tsunami earthquake”. The Enpo Boso-oki earthquake tsunami on November 4th of 1677 killed more than 500 persons was a so-called ”Tsunami earthquake”. The magnitude of this earthquake and tsunami has been estimated based on the historical documents which were recorded more than three hundred years ago. However, it is difficult to conduct accurate estimation for the magnitude of the 1677 earthquake and tsunami because the documents include ambiguous and insufficient descriptions. The aim of this study is to determine the magnitude of the 1677 earthquake and tsunami integrating the analysis of historical documents, field survey of tsunami deposit and numerical simulation. From field survey in Choshi city, Chiba prefecture, we found the candidate tsunami deposit in the Kobatke pond. Radiocarbon dating and tephra analysis indicated that the sand deposit was formed between AD1100 and AD1700. Based on these results as well as the interpretation of historical documents, we concluded the sand deposits were formed by the 1677 Enpo boso-oki earthquake tsunami. We further conducted numerical simulation to estimate the magnitude of the earthquake and tsunami and the magnitude of the 1677 earthquake was estimated as Mw=8.34. This magnitude is equivalent to that of the 1896 Meiji Sanriku earthquake tsunami which is well known as ”Tsunami earthquake”. Our results would be very important information to understand the magnitude and nature of ”Tsunami earthquake” along Japan Trench.

Japan Geoscience Union Meeting 2014
(28 April - 02 May 2014 at Pacifico YOKOHAMA, Kanagawa, Japan)

MIS23-15 Room:415 Time:May 2 14:15-14:30

The assemblages of foraminifera in paleo-tsunami sediments on Ishigaki island

TU, Yoko[1*] ; ANDO, Masataka[2] ; CHIEN, Chih-wei[4] ; KITAMURA, Akihisa[5] ; SHISHIKURA, Masanobu[6] ; NAKAMURA, Mamoru[7] ; ARASHIRO, Yasuhisa[7]

[1]Department of Natural History Sciences, Hokkaido University, Japan., [2]Center for Integrated Research and Education of Natural Hazards, Shizuoka University, Japan, [3]Institute of Earth Sciences, Academia Sinica, Taiwan., [4]Department of Earth Sciences, National Chen Kung University, Taiwan, [5]Department of Geosciences, Shizuoka University, Japan, [6]Activity Fault and Earthquake Research Center, The National Institute of Advanced Industrial Scie, [7]Department of Physics and Earth Sciences, Ryukyu University, Japan

The Ryukyu subduction zone is generally believed to be aseismic because no large thrust earthquake (M>8) has recently occurred; GPS velocity vectors on the islands are parallel but opposite to the relative motion of the oceanic plate. These observations support the idea that the Ryukyu trench is aseismic or unlocked. However, in 1771 a tsunami struck Ishigaki and Miyako islands with the maximum run-up height of 30 m and caused destructive disaster, which implies that a significant earthquake occurred along the Ryukyu subduction zone. According to Nakamura (2009), the source of this event is a tsunami (slow) earthquake near the Ryukyu trench. Moreover, slow-slip events at depths of 30km (Heki and Kataoka, 2009) and very-low frequency earthquakes at shallow depths near the trench axis (Ando et al., 2012) have been identified in the western Ryukyu trench. These findings suggest that the western Ryukyu subduction zone has a potential to generate large thrust earthquakes.

To estimate recurrence intervals and sizes of paleo-tsunamis near the Ryukyu trench, we excavated Holocene deposits at 5 sites on Ishigaki Island during the years of 2011 to 2013. We analyzed the assemblages of foraminifera in the sediments that were transported by tsunamis from the deep seafloor. Most of foraminifera detected from the deposits are benthonic and planktonic foraminifera are rare in all samples at the excavation sites. Species of benthonic foraminifer such as *Calcarina defrancii* (living at 15 to 50 m depths) are dominant in the tsunami deposits compared to the current beach sand. In addition, some mesopelagic species that commonly live at continental shelf depths are also identified from the tsunami sediments. We found that the percentage of mid epipelagic and mesopelagic species in the deposits can provide a significant key to identify paleo-tsunamis. On the western Ishigaki Island, if the population density of these species in a deposit exceeds 10 %, it can be concluded as a tsunami origin, while on the eastern coast if the population density exceeds 20 %, it can be a tsunami deposit because of the bathymetric reasons.

Together with the results of stratigaraphic facies and C14 dating data of the above tsunami sediments, we identified three large tsunamis (similar to the 1771 tsunami) in the past 2000-3000 years: in 1771, between 10-11th C and between 2000 and 2900 cal. B.P. The average recurrence interval of large earthquake was found to be very long, 500 to 1000-2000 years along the western Ryukyu trench.

Keywords: tsunami sediments, foraminifera, Ryukyu dubduction zone, paleo-tsunami, 1771 tsunami

Japan Geoscience Union Meeting 2014
(28 April - 02 May 2014 at Pacifico YOKOHAMA, Kanagawa, Japan)

MIS23-16 Room:415 Time:May 2 14:30-14:45

Tsunami sediment in the Okinawa Island

SHIGA, Shota[1*] ; NAKAMURA, Mamoru[1] ; FUJITA, Kazuhiko[1] ; ARASHIRO, Yasuhisa[1] ; YAMASHIRO, Sakaki[1] ; SUNAGAWA, Naoya[1] ; SANA, Tomoko[1] ; TAMAKI, Naoyuki[1]

[1]Faculty of Science, University of Ryukyus

The occurrence interval of mega-tsunamis in the south Ryukyu arc was estimated to 200-500 years from the ages of tsunami boulders (Nakata, Kawana 1994, Araoka et al., 2013). The source of 1771 Yaeyama tsunami (Meiwa tsunami), which was the latest mega-tsunami, is interpreted as the M8 class thrust-type earthquake in the Ryukyu trench from the numerical simulation of tsunami. However, past tsunamis have not been found in the central Ryukyu arc because the tsunami boulders were not detected in this area. No tsunami records were documented in the old literatures of central Ryukyu arc. We conducted a tsunami sediment survey in the Okinawa Island to investigate the history of large tsunami on the central Ryukyu Trench. We performed drilling survey from 4 to 15 March 2013 in the Okinawa Island in a collaboration with the coastal disaster prevention section of civil engineering and construction division, the Okinawa Prefectural Office. Survey sites were is Kijoka (Ogimi Village), Teima (Nago), Yaka (Kin Town), Yagi (Nakagusuku Village), Oyama (Ginowan). The sand layers, which have the possibility of tsunami sediments, were found at the cores samples of Teima and Yagi from visual observation. Then, we analyzed the sand layers and their overlying and underlying layers, and compared them with the sand layers. Teima-1 (elevation 4.5m, 0.4km from the coast) is located at the back marshes of the inner part of Oura Bay. We collected five samples at the depth between 1.85m to 1.25m from the surface ground. Yagi1-3 (elevation 2.8-3.1m, 0.1-0.2km from the coast) are located at the coastal lowlands along Nakagusuku. We collected 7 samples at the depths between 0.8m to 4.15m at Yagi-1, 4 samples at the depths between 1.35m to 2.05m at Yagi-2, and 1 sample at the depth of 1.95m at Yagi-3. Furthermore, we sampled modern coastal sands near the survey sites. First, the samples were charged with 10-fold diluted hydrogen peroxide solution after drying completely at the temperature of about 60 degrees. Then samples were washed by the water flow during sieving 63um. After that, the samples were divided to a particle size of five types for using sieve. Foraminifera analysis method was conducted the particle size of 1.00mm ˜0.5mm from sample collection. We picked the samples so as to contain over 150 individuals of foraminifera. Next we classified them to dominant species foraminifera and other species. In addition, we compared their foraminifera composition with those of modern coastal sand, and estimated the origin of the sediment. From the core samples of Teima-1, we detected 3 individuals of *Anomalinella* at the depths of 1.55 m and 1.65 m, and 2 individuals of *Calcarina Mayori* at the depth of 1.65 m. This suggests that the sediments at the depths of 1.55 m and 1.65 m were moved from out of the reef because these species live out of the reef. From the core samples of Yagi-1, we detected 2 individuals of *Anomalinella* at the depths of 3.75 m and 3.85 m, and 4 individuals of *Dendritina* and 3 individuals of *Operculina* at the depth of 3.75 m. Since these species live out of the reef, the sediments at the depths of 3.75 m and 3.85 m were moved from out of the reef. Next we detected 4 individuals of *Dendritina* and 4 individuals of *Operculina* at the depth of 1.85 m in the core sample of Yagi-2. As well, we detected 2 individuals of *Dendritina* at the depth of 2.05 m in the core sample of Yagi-2. These suggest that the sediments at the depth of 1.85 m and 2.05 m were moved from the out of the reef. Thus, we found that the species, which live in the out of reef, were included in the core samples of Teima and Yagi. A possible mechanisms to move the sediment from seafloor to land are ocean waves, storm surges, and tsunamis. However, since ocean waves and storm surge are attenuated by the reef, these could not move the sediments from out of the reef. The sediments which contain the species living out of the reef would have been moved by tsunamis.

Keywords: tsunami, tsunami sediment, foraminifera

Japan Geoscience Union Meeting 2014
(28 April - 02 May 2014 at Pacifico YOKOHAMA, Kanagawa, Japan)

MIS23-17 Room:415 Time:May 2 14:45-15:00

Recognition of washover deposits in the Shizuoka Plain, based on analysis of shape of sand grains

KITAMURA, Akihisa[1*] ; OGURA, Kazuki[1] ; UBUKATA, Takao[1]

[1]Shizuoka Univ

Three-dimensional morphometric analyses were performed to compare the shape of the sand grains as mentioned below. The surface of the upper part of the sand grain was first scanned to collect the x-, y- and z-coordinates of each point on the grain surface using a Shimadzu OLS4000 confocal laser scanning microscope. The obtained upper surface was connected with its vertically reflected shape to obtain a symmetric closed surface model. The surface model was then converted into a solid model by filling the inside of the surface model with equally spaced points. The axes of sand grains were defined as the principal component axes for the 3D coordinate data of the points consisting of the solid model. The aspect ratios of the sand grain was computed as the square roots of the ratios between eigenvalues of the covariance matrix between the coordinates. The collected coordinate data for the upper surface were normalized for location, orientation, and size so that the centroid of the solid model is placed at the origin, the major axis is placed along the x-axis, and the volume of the solid model is fixed at a constant value. A series of the normalized z-coordinates of individual points was defined as the shape function of the corresponding x- and y-coordinate data and was then decomposed into a 2D domain using a two dimensional Fourier transform. The shape of the sand grain was represented by a set of Fourier amplitudes of each frequency. The angularity was assessed for each grain by the sum of the Fourier amplitudes of the first and higher harmonics divided by the magnitude of the 0th harmonic.

The results of the morphometric analyses clearly indicated that the ratio of the minor axis length to the major axis length well defines the difference in grain shape between beach sands and inferred flood sediments. Most of the flood sediments have smaller aspect ratio (i.e., elongate form) than do most of the beach sands. Scatter plots of the angularity against the aspect ratio for the two sedimentary environments were fairly separated with only slight overlap along the axis of the aspect ratio. Variation in angularity was greater among flood sediments than among beach sands and there was no beach-sand grain with the angularity larger than 7.89. The composition of inferred tsunami deposits seems a mixture of the flood and beach sediments in terms of their grain shape.

Keywords: washover deposits, sedimentary grains, analysis of shape

Japan Geoscience Union Meeting 2014
(28 April - 02 May 2014 at Pacifico YOKOHAMA, Kanagawa, Japan)

MIS23-18 Room:415 Time:May 2 15:00-15:15

Two paleotsunami layers in Kushiro Wetlands and their wide correlation in eastern Hokkaido

NAKAMURA, Yugo[1*] ; NISHIMURA, Yuichi[1]

[1]Institute of Seismology and Volcanology, Hokkaido University

Two paleotsunami sand layers, Ks-TS1 and Ks-TS2, were identified in peatland in Kushiro, eastern Hokkaido. Ks-TS1 occurs several cm beneath Ko-c2 (AD 1694) and Ta-b (AD 1667) tephras, and Ks-TS2 occurs 10 cm above B-Tm tephra (ca. 1000 yBP). Thicknesses of these layers are less than 1-3 mm. Particle size of Ks-TS1 is around 2 phi and Ks-TS2 is around 4 phi. They can be identified by their particle size distribution in the precision of 1/16 phi using Morphologi G3. Ks-TS1 is found at the site located about 2120 m from the modern coastline, 5.9 m above the mean sea level, and Ks-TS2 about 1810 m from the modern coastline, 5.7 m above the mean sea level. The actual run-up limit of paleotsunami may exceed these deposition areas.

At present analytical method is not available to correlate paleotsunami layers across distant regions. However, the tsunami layers in Kushiro are likely correlated with paleotsunami layers in other regions in eastern Hokkaido (Urahoro, Kinashibetsu, Onbetsu, Akkeshi, and Nemuro) on the basis of the stratigraphic relationships between the paleotsunami layers, marker tephras, and peat layers. In Kushiro region, thickness of the peat layer between Ta-b and Ks-TS1 is 16 % of the total peat thickness between Ta-b and B-Tm, and thickness between Ta-b and Ks-TS2 is 81 %. These ratios are similar between Kushiro and other regions, although 10-20 % difference can be seen. According to previous researches, up to eight paleo-tsunami layers in the last 3000 years were identified in eastern Hokkaido. The paleo-tsunami layers in Kushiro are correlated with the last two events and presumed to be the greatest events in the last 3000 years.

Keywords: Paleotsunami deposit, correlation, Precise grain size analysis, Morphologi G3, Hokkaido

Japan Geoscience Union Meeting 2014
(28 April - 02 May 2014 at Pacifico YOKOHAMA, Kanagawa, Japan)

MIS23-19 Room:415 Time:May 2 15:15-15:30

Insight of large tsunami recurrence around the Sea of Japan revealed by surveys of historical and pre-historical tsunami

NISHIMURA, Yuichi[1*] ; RAZJIGAEVA, Nadya[2] ; GANZEY, Larisa[2] ; GREBENNIKVA, Tatiana[2] ; KAISTRENKO, Viktor[2] ; GORBUNOV, Alexsey[2] ; NAKAMURA, Yugo[1]

[1]Hokkaido University, [2]Far East Branch of Russian Academy of Sciences, Russia

Tsunami deposits provides essential information for assessing tsunami and earthquake hazards in areas where recurrence of tsunamis are not known or poorly recorded. Northern coast of the Sea of Japan is one of these areas. Recent earthquakes such as the 1940 Shakotan-oki, the 1983 Nihonkai-chubu and the 1993 Hokkaido Nansei-oki earthquakes caursed severe damage along the coastal communities in SW Hokkaido, Japan, however, the past tsunami in this region are not known. The historical tsunamis inundated not only in the Japanese coast but also along the Primorye coast, Russia, located at the other side of the Sea of Japan. We repeated reconnaissance along the Primorye coast to find the historical and pre-historical tsunami evidences. In the region, there are natural lowlands facing sandy beach that are suitable for tsunami deposit formation and preservation. The surveys were done from 2010 to 2013 as a joint research project with Hokkaido University and the Russian Academy of Science. We could trace sandy or muddy tsunami deposits buried in the peat associated with the modern tsunamis, and also found candidate of tsunami deposits at multiple sites along the coast. The sandy layers include significant amount of marine diatoms. Based on the C14 dating results of peat sandwiching the sandy layers, age of the events are estimated to be ca. 350 BP, 600 BP, 800 BP and 2100 BP. In Kit Bay, the southernmost site in our survey area, B-Tm tephra (ca. 1000 AD) were deposited patchy between the 800 BP and 2100 BP. Most of the paleo-event deposits are traced inland up to a few hundred meters from the present coast and they are distributed at 4-5 m above the sea level. These might be the first evidence for the recurrence of large tsunamis around the Sea of Japan in the past.

Keywords: tsunami deposit, Primorye, Sea of Japan, paleo-tsunami, historical tsunami

Japan Geoscience Union Meeting 2014
(28 April - 02 May 2014 at Pacifico YOKOHAMA, Kanagawa, Japan)

MIS23-20 Room:415 Time:May 2 15:30-15:45

Preliminary study for evidence of tsunami deposits from Holocene sediments along the coastal area of the Wakasa Bay.

YAMAMOTO, Hirofumi[1*] ; URABE, Atsushi[2] ; SASAKI, Naohiro[1] ; TAKASHIMIZU, Yasuhiro[3] ; KATAOKA, Kyoko S.[2]

[1]Fukui University, [2]NHDR, Niigata University, [3]Niigata University

This study reconstructed the Holocene sedimentary environment and researched the distribution of possible tsunami deposits in the coastal plain along the Wakasa Bay area in Fukui Prefecture.

Around the Wakasa Bay Area, some historical documents suggested the tsunami event of AD 1586 (Tensho Tsunami), but no sedimentary evidence of this event was reported from this area. So, we carried out reconnaissance along the coastal area of the Wakasa Bay to find the natural lowlands facing sandy beach that are suitable for tsunami deposit reservation. For example, at the Sonobe area in Takahama-cho, a low land behind the beach ridges was said to have been a marshes area, and our preliminary study show that this area had shifted from inner bay environments to marshes area about 3000 years ago. At these places, we study the Holocene sediment using the Geoslicer of 5 meters long.

Keywords: Wakasa Bay area, coastal plain, tsunami deposits, Holocene

Japan Geoscience Union Meeting 2014
(28 April - 02 May 2014 at Pacifico YOKOHAMA, Kanagawa, Japan)

MIS23-P01 Room:Poster Time:May 2 16:15-17:30

Bleaching of K-feldspar grains contained in the tsunami deposits of the 2011 off the Pacific coast of Tohoku Tsunami

HAYASHIZAKI, Ryo[1*] ; SHIRAI, Masaaki[1]

[1]Tokyo Metropolitan University

Optically stimulated luminescence (OSL) dating is feasible method to obtain depositional age from sediments and then, it is expected to be useful for tsunami deposits dating. However, it is not clear that the degree of sun bleaching during tsunami transport processes. Firstly, bleaching of K-feldspar grains during tsunami transport processes was investigated with post-IR IRSL (pIRIR) dating using the 2011 off the Pasific coast of Tohoku Tsunami deposits. Then, single-grain OSL dating was attempted to obtain accurate equivalent doses of tsunami deposits. Equivalent doses of K-feldspar grains obtained from various sampling locations and positions.

Comparing IRSL and pIRIR equivalent doses which showed different decreasing rates of OSL intensities with the sunlight exposure time, sandy tsunami deposits were hardly exposed sunlight during tsunami transport processes. However, nearly zero equivalent dose of single-grain OSL measurement was often acquired. Probably, these " zero-dose " K-feldspar grains had been exposed enough to sunlight before the tsunami. Upper position of one run-up tsunami deposits seemed to be rich in K-feldspar grains suggesting the accurate depositional age.

Keywords: tsunami deposits, Optically Stimulated Luminescence, post-IR IRSL, K-feldspar, sedimentary structure, Fukushima

Japan Geoscience Union Meeting 2014
(28 April - 02 May 2014 at Pacifico YOKOHAMA, Kanagawa, Japan)

MIS23-P02 Room:Poster Time:May 2 16:15-17:30

Sedimentological features of tsunami deposit caused by the 2011 Tohoku-oki earthquake tsunami

YOSHII, Takumi[1*] ; HAMADA, Takaomi[1] ; SASAKI, Toshinori[1] ; MATSUYAMA, Masafumi[1] ; TANAKA, Shiro[1] ; ITO, Yuki[1] ; WATANABE, Masakazu[2] ; OKUZAWA, Koichi[3]

[1]Central Research Institute of Electric Power Industry, [2]Ceres, Inc., [3]Obayashi Corporation

In some areas, the inundation distances of the 2011 Tohoku-oki earthquake tsunami was comparable to that of the 869 Jogan tsunami estimated by geological investigations of tsunami deposits. This fact revealed the potential of research of tsunami deposits to speculate the scales of future tsunamis, resulting in strong social demand to detect ancient tsunamis, especially giant tsunamis, using geological studies. Investigation of present tsunami deposits is crucial to understanding sedimentological features of tsunami deposits because the present tsunami deposits can be identified with high reliability and the investigation of the surrounding circumstances is also feasible. In this study, we collected tsunami deposits caused by the 2011 Tohoku-oki earthquake tsunami from 19 areas with different topography. The obtained cores were observed by the unaided eye and by using CT images. In this presentation, we will discuss sedimentological features of these tsunami deposits and relationship with the surrounding circumstances.

Keywords: Tsunami deposit, The 2011 Tohoku-oki earthquake, Tsunami

Japan Geoscience Union Meeting 2014
(28 April - 02 May 2014 at Pacifico YOKOHAMA, Kanagawa, Japan)

MIS23-P03 Room:Poster Time:May 2 16:15-17:30

Characteristic of tsunami deposit left by 2011 Tohoku earthquake, case study of Toni bay

IIJIMA, Satsuki[1*] ; SAKAMOTO, Izumi[1] ; YOKOYAMA, Yuka[1] ; YAGI, Masatoshi[1] ; IMURA, Riichiro[1] ; NEMOTO, Kenji[1] ; FUJIMAKI, Mikio[2] ; FUJIWARA, Yoshihiro[3] ; KASAYA, Takafumi[3]

[1]Tokai University, [2]COR, [3]JAMSTEC

The recent 2011 Tohoku tsunami strongly affected the coastal area of the Pacific coast of Tohoku. The result of onshore features for tsunami impact is well researched, but offshore is only a few researches.

In this presentation, we will show about characteristic of tsunami deposit left by 2011 Tohoku earthquake, case study of Toni bay. We researched about tsunami deposit using acoustic equipments (Multi beam echo sounder ; MBES, Sub bottom profiler ; SBP) and Vibration core sampler (VCS).

The first of all, as the characteristic of submarine topography was sectionalized to 4 areas from topography profile of the valley axis direction.

Second, SBP data was seen signature reflecting surface (40-100cm down from seabed), and it was able to track at the wide area. Thickness of this reflecting surface and seabed were estimate 25-110cm in this bay. This thickness corresponded with the characteristic of the submarine topography.

Moreover, columnar sample of 13T_V_2 (water depth 14 m) could be divided into U1 (sand), U2 (mud), and the U3 (gravel bed). Sand to silt sediments layer with grading (fine sand to gravel) structure observed at the U1.We assume this U1 is 2011 tsunami deposit. The boundary of between U1 and 2 has continuity reflecting surface by SBP data and confirm distribution of this reflecting surface and thickness.

Finally, we were able to estimate tsunami deposit distributed with thickness approximately 25-110cm, and high thickness was distributed to the valley axis.

Keywords: Tsunami deposit, Sanriku Coast

Japan Geoscience Union Meeting 2014
(28 April - 02 May 2014 at Pacifico YOKOHAMA, Kanagawa, Japan)

MIS23-P04 Room:Poster Time:May 2 16:15-17:30

Characteristic of tsunami deposit left by 2011 Tohoku earthquake, case study of Hirota bay

YOKOYAMA, Yuka[1*] ; SAKAMOTO, Izumi[1] ; YAGI, Masatoshi[1] ; IMURA, Riichiro[1] ; IIJIMA, Satsuki[1] ; KANEI, Tatsuki[1] ; NEMOTO, Kenji[1] ; KITO, Takeshi[2] ; FUJIMAKI, Mikio[3] ; FUJIWARA, Yoshihiro[4] ; KASAYA, Takafumi[4]

[1]Tokai University, [2]FODECO, [3]COR, [4]JAMSTEC

The recent 2011Tohoku tsunami strongly affected the coastal area of the Pacific coast of Tohoku. The study of onshore features for tsunami impact is well researched, but offshore is only a few researches. In this presentation, we will show about characteristic of tsunami deposit left by 2011Tohoku earthquake at Hirota bay using by Sub bottom profiler (SBP) and Vibration core sampler (VCS).

We took the total 17sites columnar core (2012:5sites, 2013:12sites) at water depth 8-25 m. The columnar cores were able to sectionalize to 2 units from lithofacies. Unit-1 consists of sand layer and Unit-2 consists of muddy sediment.

Unit-1 was sand to silt sediments layer with grading (fine to very coarse consists gravel and shell fragments) and lamination, and has forms the erosion surface with the lower layer. We assume that denudation is boundary of previous or after tsunami sediment and upper layer (Unit-1) is 2011tsunami deposit. And, Unit-1 was able to sectionalize to some subunits (Unit1a-1e) by grain size analysis and soft X-ray photo.

Unit-2 was massive sediments with fine sand to silt layer characterized by bioturbation. We assume this unit is normal sediment in this bay. And, some columnar cores have Unit-3(underlying layer of Unit-2) that has similar characteristics of Unit-1.

We estimate the 2011tsunami deposit distribution with thickness approximately 20-50 cm, and high thickness area was valley axis and estuarine region, and those area have sedimentation axis each other (NNW-SSE and NW-SE), and join together at offshore area (around 20m). So, tsunami deposits become thicker by overlap with a few tsunami deposits at offshore area.

Keywords: Tsunami deposit, Sanriku coast

Japan Geoscience Union Meeting 2014
(28 April - 02 May 2014 at Pacifico YOKOHAMA, Kanagawa, Japan)

MIS23-P05 Room:Poster Time:May 2 16:15-17:30

Characteristic of tsunami origin submarine topography -Case study of Toni Bay and Okirai Bay

YAGI, Masatoshi[1*] ; SAKAMOTO, Izumi[1] ; YOKOYAMA, Yuka[1] ; MIZUNO, Ren[1] ; IIJIMA, Satsuki[1] ; NEMOTO, Kenji[1] ; FUJIMAKI, Mikio[2] ; FUJIWARA, Yoshihiro[3] ; KASAYA, Takafumi[3]

[1]School of Marine Science and Technology, Tokai University, [2]COR, [3]JAMSTEC

The recent 2011 Tohoku tsunami strongly affected the coastal area of the Pacfic coast of Tohoku. Toni Bay located south of Kamaishi city and open toward east. Also Okirai bay open toward east. Tokai University started survey there to confirm effect of Tsunami in 2012

Survey of first year, we make extensively submarine topography. As a result, anomaly topography was observed at Toni Bay (depth of 20-25m) and Okirai (depth of 15-20m). Transparent layer with poor internal reflection was observed as the surface layer within the anomaly topography by Sub Bottom Profiler (SBP). Characteristic of columnar core have grading structure (fine to coarse) of sand sediment and erosion structure between sand sediment and clay sediment. It was guessed that erosion structure was made by turbidity current by tsunami activity. For the above reason, estimated anomaly topography is Tsunami origin topography. So we survey around anomaly topography area more closely in 2013. Describe below the character of Toni Bay and Okirai Bay.

[Toni Bay]

In this research area, submarine topography can be divided into three: 1)gentle slope (0.9 degrees) at depth of 15-22m, 2)planation surface at depth of 22-24m, 3)gentle slope at depth of 24m or more. On the 1)-3), these are a lot of protuberance has distributed. Around the protuberance, current marks like a fan or delta shape extend to toward offshore. And groove mark also observed. And we assume this tsunami origin submarine topography have control by protuberance in this way.

[Okirai Bay]

In this research area, topography can be divided into three: 1)gentle slope (1 degrees) at depth of 8.5-17.5m, 2)planation surface at depth of 17.5-19m, 3)gentle slope at depth of 19.5m or more. On the 1), these are a lot of protuberance has distributed. Some tool mark that is cause of protuberance distribute similar to Toni bay, but most of current mark show scour mark.

Tsunami origin submarine topography has almost same character (ex. Water depth) at both bays. But formation factor is different from Toni and OKirai bay.

Keywords: Tsunami orijin submarine topography, Toni Bay, Okirai Bay, Current mark

Japan Geoscience Union Meeting 2014
(28 April - 02 May 2014 at Pacifico YOKOHAMA, Kanagawa, Japan)

MIS23-P06 Room:Poster Time:May 2 16:15-17:30

Relationship between the inundation limit and the maximum extent of the sandy tsunami deposit in Sendai Bay coasts

ABE, Tomoya[1*] ; GOTO, Kazuhisa[2] ; SUGAWARA, Daisuke[2]

[1]Department of Geography, Nagoya University, [2]IRIDeS, Tohoku University

Maximum landward extent of the sandy tsunami deposits can be regarded as the minimum inundation limit. Before the 2011 Tohoku-oki tsunami, recent post-tsunami field surveys along low-lying coastlines showed that sandy tsunami deposits commonly extend to approximately over 90% of the actual inundation limit (MacInnes et al., 2009). On the other hand, after the 2011 Tohoku-oki tsunami, some researches of the 2011 tsunami pointed out that the significant gap (0.6-2.0 km) between the inundation limit and the maximum landward extent of the sandy tsunami deposit where the inundation distance was more than 2.5-3.0 km (Goto et al., 2011; Abe et al., 2012; Shishikura et al., 2012). However, it is uncertain why the gap appeared. This study focuses on the relationship between the maximum extent of sandy tsunami deposits and inundation limit of the 2011 Tohoku-oki tsunami.

Inundation limits of the Tohoku-oki tsunami were assessed over 15 shore-normal transects in the Sendai Bay coast. Inundation distances of the 15 transects were found to range from 0.60 to 5.07 km. The maximum limit of the sand layer extended to 2.3-3.0 km (55-74% of the inundation distance) along 6 transects in the wide coastal plain in the northern-middle part of the Sendai Plain. Absence of the sandy tsunami deposits over 3.0 km inland may explained by the limitation of the sand supply from sand beach and sand dune.

Keywords: 2011 Tohoku-oki tsunami, Sendai Bay coast, Inundation limit, Maximum extent of sandy tsunami deposit

Japan Geoscience Union Meeting 2014
(28 April - 02 May 2014 at Pacifico YOKOHAMA, Kanagawa, Japan)

MIS23-P07 Room:Poster Time:May 2 16:15-17:30

Historical tsunami deposits in Numanohama on the Sanriku coast, Japan

GOTO, Tomoko[1*] ; SATAKE, Kenji[2] ; SUGAI, Toshihiko[1] ; ISHIBE, Takeo[2] ; HARADA, Tomoya[3] ; MUROTANI, Satoko[2]

[1]GSFS, the University of Tokyo, [2]ERI, the University of Tokyo, [3]CIDIR/ERI, the University of Tokyo

We conducted tsunami deposit survey in a small valley along the Sanriku coast, Japan, just north of Taro (Miyako city, Iwate prefecture), where the 2011 tsunami heights from the Tohoku earthquake ranged from 17 to 34 m. We identified six tsunami deposits during the recent 500 yrs from the 3-m long Geo-slicer sample. The uppermost one is located on or just below the ground surface and probably from the 2011 Tohoku earthquake. The ^{210}Pb and ^{137}Cs dating analyses indicated that the 2^{nd} to 4^{th} uppermost tsunami deposits can be correlated with historical tsunamis: the 1960 Chilean tsunami, the 1933 and 1896 Sanriku tsunamis. According to Japanese historical documents, other candidate tsunamis since the 15^{th} century are from the 1793 Miyagi-oki earthquake, the 1763 and 1677 Aomori-oki earthquakes, the 1677 Boso-oki earthquake, and the 1611 Sanriku earthquake. Other trans-Pacific tsunamis includes the 1700 Cascadia tsunamis severe damage along the Sanriku coast and these tsunami deposits may be also preserved.

After the 2011 Tohoku earthquake, many surveys for tsunami deposits have been conducted in Sendai plain (Goto *et al*., 2011, Marine Geology; Shishikura *et al*., 2012, Annual Report on Active Fault and Paleoearthquake Researches). There are few reports of tsunami deposit studies along the Sanriku coast. Furthermore, depositional ages of many identified tsunami traces along the Sanriku coast were estimated to be several thousand years before present. The reasons for absence of recent tsunami deposits include that the Sanriku coast is a ria coast characterized by sawtooth-shaped coastline. Because of the steep-sloped valleys, alluvial deposits are very limited and tsunami traces are difficult to be preserved. Around the survey site, however, a marsh is separated from open sea by a beach ridge of $\sim$ 4m high. In this marsh, well-decomposed peat has been developed. The sand deposits were brought by large tsunamis over the beach ridge and preserved in the marsh peat. Our study is the rare case that the geological evidence of recent historical tsunamis was continuously identified.

To identify tsunami deposits, we sketched the sedimentary structure, measured the distribution of grain sizes, and analyzed the microfossils. Depositional ages of tsunami deposits were estimated on the basis of radiocarbon (AMS) dating and ^{210}Pb, ^{137}Cs analysis. The ^{210}Pb dating is useful to determine the depositional rate during the recent 100 years because of its short decay time (the half life time is 22.3 year). The ^{137}Cs dating is useful to judge whether the depositional ages are before or after the start of atmospheric nuclear experiments in AD 1954.

Peat and sand layers are alternated with their thickness of several centimeters to several tens centimeters. Each sand layer consists of beach pebble and sand or rock pieces from host rock in this area. The sand layers have structure characteristic to tsunami deposit: erosional contact, alternation of normal- and inverse-grading, lamination and thin mud layer sandwiched between two sand layers. The sand layer can be traced continuously along the landward transect. Abundant marine microfossils in the sand layers indicate that the sea water flow into the marsh with the tsunami sand.

The ^{14}C result shows that peat at around 3 m depth deposited after the 15^{th} century. The ^{210}Pb decay curve indicates that the deposition ages of the upper four tsunami deposit layers are during recent 100 yrs. The 2^{nd} uppermost tsunami deposit can be correlated with the 1960 Chilean tsunami because ^{137}Cs was detected down to this layer.

Acknowledgment

We thank Kazuomi Hirakawa and Javed N. Malik for giving useful comments and suggestions in the field. We also thank Jun Muragishi, Ryutaro Naruhashi, Satoshi Kusumoto, Akira Takigawa, Tsuyoshi Yamaichi and Ravi K. Parabhat for helping the field survey.

Keywords: Tsunami deposit, Sanriku coast

Japan Geoscience Union Meeting 2014
(28 April - 02 May 2014 at Pacifico YOKOHAMA, Kanagawa, Japan)

MIS23-P08 Room:Poster Time:May 2 16:15-17:30

A Study of Paleo-Tsunami along the Coastal Area of Akita Prefecture, the eastern margin of Japan Sea

KAMATAKI, Takanobu[1*] ; HOSOYA, Takashi[2] ; KUROSAWA, Hideki[3]

[1]Akita University, [2]Chuo Kaihatsu Corporation, [3]OYO Corporation

Tsunami is the most destructive natural disaster on the coastal area. North-eastern Japan along the Japan Sea has been suffered by tsunamis, such as the 1833, 1983, and 1993 tsunamis. Recently, tsunami deposits have been reported from various areas and environments in Japan. However, paleo-seismological study based on the tsunami deposits has not been reported from along the coastal area of Akita Prefecture. We report a study of paleo-tsunami along the coastal area of Akita Prefecture. These results will be presented in this session.

Keywords: tsunami deposit, paleo-tsunami, eastern margin of Japan Sea, Akita Prefecture

Japan Geoscience Union Meeting 2014
(28 April - 02 May 2014 at Pacifico YOKOHAMA, Kanagawa, Japan)

MIS23-P09 Room:Poster Time:May 2 16:15-17:30

Paleoenvironmental changes and tectonic movements reconstructed from diatoms in Tokushima, during the last 4000 years

CHIBA, Takashi[1*] ; FUJINO, Shigehiro[1] ; KOBORI, Emmy[2]

[1]Faculty of Life and Environmental Sciences University of Tsukuba, [2]College of Geoscience, School of Life and Environmental Sciences, University of Tsukuba

The average recurrence interval of the interplate earthquakes along the Nankai Trough is estimated from many histrical records and archaeological data (Sangawa 2008). However, the studeis of tectonic movement related to Nankai earthquakes is still limited (Maemoku 1989, Shishikura et al. 2008).

Yuki city, Tokushima prefecture, which located in north part of the Nankai Trough, has been subsided and many tsunamis attacked along the coast of the Shikoku islands accompanied by the previous Nankai earthquakes. Therefore, some historical documents and memorial monuments written about the past Nankai earthquakes and tsunamis remain in this city.

In order to obtain the geological evidences of tectonic movements and tsunami depsosits, we conducted a 7m long core drilling at a small marsh behind a barrier spit in Tainohama of Minami city nearly Yuki city. The core includes more than 12 sand layers in organic-rich muddy sedimentary succession up to 5 m depth in this core. And we analyzed fossil diatoms from the core.

The diatom assemblages included in the peat and peaty mud deposits were predominated by fresh and brackish water species, especially *Pseudostaurosira brevistriata*, *Pseudostaurosira subsalina*, *Staurosirella pinnata*, *Tabellaria fenestrate*. *Pinnularia* spp. and *Eunotia* spp. are also dominated. In contrast to the above mentioned sand layers, brackish water and marine species, especially *Diploneis smithii*, *Mastogloia recta* were increased. The diatom assemblages from the organic rich muddy sediments and radiocarbon ages indicates that freshwater marsh or saltmarsh formed in this region during at least the past 4000 years. On the other hand, the diatoms from the sandy layers indicates that salinity of environments when the layers were formed was higher than freshwater or salt marsh. The diatom assemblage suggest that the sand layers were transported from seaside by past tsunamis. On the other hand, changes of diatom assemblages in the muddy sediments show increase or a decrease of freshwater species, suggesting a paleo coastal environment changes due to past earthquakes along the Nankai Trough.

Keywords: Nankai trough, Tsunami deposit, Tectonic movement, Pleo coastal environment, Diatom

Japan Geoscience Union Meeting 2014
(28 April - 02 May 2014 at Pacifico YOKOHAMA, Kanagawa, Japan)

MIS23-P10 Room:Poster Time:May 2 16:15-17:30

Study of tsunami deposits along west coastal area of Kagoshima Prefecture, Japan

OSHIMA, Akihiro[1*] ; HARAGUCHI, Tsuyoshi[2] ; TAJIRI, Yuuta[3]

[1]West Japan Engineering Consultants, Inc., [2]Osaka City University, [3]Kyushu Electric Power Co., Inc.

In the west coast of the Kyushu district, there is no plate boundary in the front, and there is few record of an earthquake and tsunami. There are little investigations and researches of tsunami deposits in this area compared with East Coast facing the Pacific Ocean. However, reexamination of the disaster prevention planning in a coastal area is advanced by the occurrence of the 2011 off the Pacific coast of Tohoku Earthquake, and it is necessary to expand the data about the past tsunami history.

We have investigated the literature about records of the disasters of tsunami, and observed drilling core. We read aerial photos and topographical maps, and classified topography such as beach ridge, sand dune, backswamp. Based on the geographical classifications, we confirmed geographical features and existence of reclaimed land, and determined the survey sites. Drilling cores were taken in ten sites along the west coastal areas of Kagoshima Prefecture. In order to clarify lateral continuity of sediments, several cores were taken at each site. In consideration of sea level change, we collected sediments after about 6,000-7,000 years ago.

We acquired X-rays CT images to visualize internal structure of sediment three-dimensionally without destroying core. After having photographed X-rays CT image, we divided the core into half in lengthwise direction and observed the surface. Sediments are dated using radiocarbon dating and tephrochronology.

Some event deposits are identified in the drilling core taken from Gumizaki site, Nakayama site and Hashima site. Ages of these event deposits are around 7,000 cal BP and 9,500 cal BP (Gumizaki site), 3,500-2,500 cal BP (Nakayama site). However, these event deposits are not defined in other sites. These event deposits were possibly made by local event.

We found the layer including volcanic glass derived from the Kikai-Akahoya tephra in drilling core which were taken from Gumizaki site. The layer was possibly carried by the event accompanied with explosion of Kikai caldera.

In this presentation, we discuss the depositional environmental changes and the origin of event deposits by analysis of microfossil and detail observation of cores.

Keywords: tsunami deposits, event deposits, Kagoshima Prefecture

Japan Geoscience Union Meeting 2014
(28 April - 02 May 2014 at Pacifico YOKOHAMA, Kanagawa, Japan)

MIS23-P11 Room:Poster Time:May 2 16:15-17:30

Tsunami deposits in eastern coast area of Ishigaki Island, Japan.

KITAMURA, Akihisa[1*] ; ANDO, Masataka[1] ; TU, Yoko[4] ; OHASHI, Yoko[1] ; NAKAMURA, Mamoru[2] ; MIYAIRI, Yosuke[3] ; YOKOYAMA, Yusuke[3] ; SHIGA, Shota[2] ; IKUTA, Ryoya[1]

[1]Shizuoka University, [2]Ryukyu University, [3]The University of Tokyo, [4]Institute of Earth Sciences, Academia Sinica

We found two tsunami deposits in eastern coast area of Ishigaki Island, Japan. The tsunami deposits contain many pebble-sized bioclasts such as coral fragments and mollusks, and clay rip-up clasts comprising material from the underlying soil. These deposits have erosive basement and fine upward. These layers thin abruptly at the landward margins, and fine inland. The altitude of the landward end of the lower and upper tsunami deposits attain up to 6 and 8 m, respectively. We referred to as deposits T-II and T-I in order of ascending stratigraphic position. Radiocarbon ages of excellent preserved and articulated marine bivalves mean that T-I and T-II were caused by the AD 1771 Meiwa tsunami and by tsunami at 740-500 cal. yrs BP (AD 1210-1450), respectively. It is noteworthy that abundant fragments of coral and molluscs remains are found from the debris flow deposit below T-II. Radiocarbon ages suggest these fragments were transported up to 8 m elevation by tsunami between 2490-2240 and 930-620 cal. yrs BP.

Keywords: tsunami deposits, Ishigaki Island

Japan Geoscience Union Meeting 2014
(28 April - 02 May 2014 at Pacifico YOKOHAMA, Kanagawa, Japan)

MIS23-P12 Room:Poster Time:May 2 16:15-17:30

The use of benthic foraminifera within tsunami sediments

MAMO, Briony[1*] ; TOYOFUKU, Takashi[1]

[1]Japan Agency for Marine and Earth Science and Technology

Tsunami hazard assessment begins with a compilation of past events that have affected a specific location. Given the inherent limitations of historical archives, the geological record has the potential to provide an independent dataset useful for establishing a richer, chronologically deeper time series of past events. Recent geological studies of tsunami are helping to improve our understanding of the nature and character of tsunami sediments. Wherever possible, researchers should be increasingly working to improve the research ' tool kit ' available to identify past and analyse modern tsunami events. Marine, benthic foraminifera (single celled heterotrophic protists) have often been reported as present within tsunami-deposited sediments but in reality, little information about environmental conditions, and by analogy, the tsunami that deposited them, has been reported even though foraminifera have an enormous capacity to provide meaningful palaeo-environmental data. In light of more recent tsunami events, the use of foraminifera has increased yet their full potential in this capacity is still often not frequently utilised. We discuss the potential use of foraminifera within tsunami research using results from specific case studies from Japan, south Asia, North America, Europe, the UK and New Zealand. We present an updated review in the gaps in our understanding on this topic area and reassert models for ' better ' practice where possible, to assist researchers who examine foraminiferal assemblages within tsunami geology.

Keywords: Tsunami, Foraminifera, Benthic, Tsunami deposit

Japan Geoscience Union Meeting 2014
(28 April - 02 May 2014 at Pacifico YOKOHAMA, Kanagawa, Japan)

MIS24-01 Room:313 Time:April 28 12:00-12:15

Measuring the relative humidity within an error of 0.1% by Arduino

MATSUO, Ryo[1*] ; SAKAI, Satoshi[1]

[1]Graduate School of Human and Environmental Studies, Kyoto University

It is said that the forest is cooler than the city. We measure the temperature and relative humidity at Kyoto University and Mt.Yoshida to find what causes the diffarence.

We used humidity and temperature sensor IC within an error of 0.1 percent.

We found that always forest is cooler and wetter than city. However the latent heat of vaporization of water did not cool the air on a day change.

Keywords: relative humidity, tempature, measure, Arduino, Forest and City

Japan Geoscience Union Meeting 2014
(28 April - 02 May 2014 at Pacifico YOKOHAMA, Kanagawa, Japan)

MIS24-02 Room:313 Time:April 28 12:15-12:30

Spontaneous rotation of a block of ice on a flat surface of a warm metal column

TANAKA, Masashi[1*] ; HOHOKABE, Hirotaka[1] ; YOSHIDA, Shigeo[2] ; NAKAJIMA, Kensuke[2]

[1]Graduate School of Science, Kyushu University, [2]Faculty of Science, Kyushu University

Summary

We have discovered that a block of ice placed on a flat surface of a warm brass column rotates slowly without any external mechanical driving force.

Description of the Phenomenon

A column of brass, whose radius and height are 8cm and 16cm, respectively, is placed with its flat surface set horizontally. After it is warmed at least to the room temperature, a flat bottomed block of home-made ice, whose radius and height are 10cm and 4cm, respectively, is placed on the flat surface of the brass column. As the block of ice melts, it begins to rotate about the vertical axis spontaneously. The direction of the rotation does not change by itself. However, it reverses instantaneously if we gently tap the ice block to the opposite direction. The rotation period is typically about 20 seconds. The rotation stops when the brass column cools or when the ice block melts and the brass surface becomes exposed.

The Importance of Bubbles between the Ice and the Brass Surface

If we use a block of factory-made ice which contains no bubbles, the ice does not rotate. However, if we drill non-through holes on the bottom surface of the ice block so that air bubbles shall be supplied between the ice and brass surface as the ice block melts, the ice rotates. The behavior of the air bubbles observed when the ice rotates and that observed when the ice rotation is blocked are quite different. When the ice rotates, the air bubbles tend to elongate radially and are nearly stationary relative to the brass surface. When the ice is anchored and does not rotate, the air bubbles flow outward, deforming and moving randomly. The observed behaviors above imply a crucial role played by the bubbles in the physics of this phenomenon.

The Importance of Heat Supply

We measured temperature distribution within the brass column, and found a strong positive correlation between the vertical temperature difference in the column and the angular velocity of the ice rotation. We also conducted a similar experiment using a column of stainless steel, whose thermal conductivity is considerably smaller than brass, the rotation period tends to be quite longer. These observations imply that the flux of heat supplied by the heat conduction in the column of metal is crucial to the emergence of the phenomenon.

Future Directions

Presently, we have no concrete idea on the dynamics of the phenomenon, even though the strong relationship between the heat supply and the angular velocity suggests that the phenomenon may be interpreted as a kind of heat engine. In the near future, we will conduct more experiments with parameters being better controlled, and with the results of such additional experiments, we will investigate physics of the phenomenon from various aspects.

Keywords: bubble, ice, rotation, heat engine, phase change, spontaneous motion

Japan Geoscience Union Meeting 2014
(28 April - 02 May 2014 at Pacifico YOKOHAMA, Kanagawa, Japan)

MIS24-03 Room:313 Time:April 28 12:30-12:45

Regimes of solutions of an axisymmetric flow in a cylindrical tank with a rotating bottom

IGA, Keita[1*]

[1]AORI, The University of Tokyo

Non-axisymmetric flows are often observed even in axisymmetric environments in the terrestrial and planetary atmospheres. Such a non-axisymmetry is realized in a simple laboratory experiment using a cylindrical container which is filled with water driven by a rapidly-rotating disk at the bottom. We have been reported on the results of the experiments. When we investigate the mechanism of these phenomena, the solution of the axisymmetric flow realized under this condition is necessary, and we reported last year the expression of the analytical solution obtained using boundary layer theories.

We investigated the features of this analytical solution precisely and extracted some features related to its stability. Applying the solution to the situation with water free surface, we can classify the realized axisymmetric flow into three regimes: (i) Cases where all part of the bottom disk is covered with water and it is divided into inner rigid-body rotation region and outer region with constant angular momentum (ii) Cases where the water exposes the center part of the bottom disk air and the water is divided into inner rigid-body rotation region and outer region with constant angular momentum, and (iii) Cases where the water exposes the center part of the bottom disk air and all the water keeps constant angular momentum. Applying the analytical solution, we elucidated the parameter dependence of the transition between these regimes. Each regime has different characteristic waves, which affects crucially the stability of the flow.

Moreover, in the boundary layer along the side wall, transverse velocity distribution has a jet like structure, which forms negative vorticity gradient region. It is also an important factor which may cause critical layer instability.

Keywords: rotating flow, symmetry breaking, boundary layer, axisymmetric flow, stability

Japan Geoscience Union Meeting 2014
(28 April - 02 May 2014 at Pacifico YOKOHAMA, Kanagawa, Japan)

MIS24-04 Room:313 Time:April 28 14:15-14:30

Benchmark experiments for Venus AGCM: sensitivities to model and astronomical parameters

YAMAMOTO, Masaru[1*] ; TAKAHASHI, Masaaki[2]

[1]Kyushu University, [2]University of Tokyo

Benchmark experiments and inter-comparisons of atmospheric general circulation models (AGCMs) have been conducted in the climate and Geophysical Fluid Dynamics (GFD) communities. Recently, the AGCM inter-comparisons are extended to Venus and hot extrasolar planets. The ISSI inter-comparison project of Venus AGCM (Lebonnois et al. 2013) shows that there are large differences among the models under the same Venus-like condition, and some model parameters influence the general circulation structures. At the present stage, in the inter-comparisons project, the wave analyses have yet to be fully conducted. For Venus' atmospheric modeling, we need to investigate sensitivity to model parameter (such as resolution), in order to understand the numerical properties of the AGCM and to confirm the model results. In terms of GFD, sensitivity to astronomical parameter (such as planetary rotation) is interesting in profoundly understanding the dynamics of superrotation in a mimic slowly rotating planet, which is represented by the base simulation in the inter-comparison. By using the widely-used benchmark, we can easily compare with previous models. In the present study, the base simulation of the ISSI project is applied to a MIROC AGCM for checking the validity of the Venus model, and is extend to the sensitivity experiments for model resolution (T21, T42, T63, and T106) and planetary rotation (Venus, Titan, and Earth), in which the general circulations and waves are analyzed. In the Venus case, as the model resolution is increased, the total angular momentum of the whole atmosphere becomes larger, although the cloud-top superrotation weakens. This indicates that the high-resolution contributes to the accumulation of the angular momentum in the lower atmosphere. The eddy momentum and heat fluxes in the lower atmosphere are also sensitive to the horizontal resolution. Associated with the eddy heat flux, the indirect circulation is also influenced by the resolution. In T42 and higher resolution experiments, the high-latitude jet and polar indirect circulation are extended to the lower atmosphere. The lower-atmospheric high-latitude jet induces large equatorward eddy angular momentum fluxes. In this presentation, we discuss the sensitivities to model resolution and planetary rotation, based on the transformed Euler mean and Eliassen-Palm flux analyses, which are useful even for slowly rotating planet with very small Coriolis force (although they are not widely used in atmospheric researches of Venus).

Japan Geoscience Union Meeting 2014
(28 April - 02 May 2014 at Pacifico YOKOHAMA, Kanagawa, Japan)

MIS24-05 Room:313 Time:April 28 14:30-14:45

Relationship between structure and replacememt of concentric eyewalls in idealized tropical cyclones

TSUJINO, Satoki[1*] ; TSUBOKI, Kazuhisa[1]

[1]HyARC, Nagoya University

Eyewall is a ring of convective clouds that encircles the eye of a tropical cyclone (TC) such as typhoon and hurricane. TC occasionally has some eyewalls which are called as concentric eyewalls. Once concentric eyewalls are formed, eyewall replacement often occurs. The eyewall replacement is a process that the inner eyewall gradually decays and the outer eyewall moves into the position of the inner (old) eyewall. The wind speed of TC rapidly varies during the replacement (Willoughby, 1987). However, the eyewall replacement does not always occur even if concentric eyewalls are formed and the process of eyewall replacement is not fully known. Tsujino and Tsuboki (2013; the Fall Meeting of the Meteorological Society of Japan) indicated that, on the basis of some analyses of Typhoon Bolaven (2012), the vertical flow of the outer eyewall is weaker than that of the inner eyewall and the outer eyewall tilts relative to the inner eyewall in the long-lived concentric eyewalls. Therefore, we suspect that the eyewall replacement is related to the structure of the concentric eyewalls of TC.

In this study, we investigate the relationship between structure and replacement of concentric eyewalls in some idealized TCs. We conduct some parameter experiments for structure of concentric eyewalls in TC, using the Cloud Resolving Storm Simulator (CReSS; Cloud Resolving Storm Simulator, Tsuboki and Sakakibara, 2007) which is a three-dimensional, nonhydrostatic model. And we investigate the structure of concentric eyewalls in these experiments. In our experiments, the initial wind field was axisymmetric and cyclonic vortex, which is hydrostatic and gradient wind. This wind field was based on the eq. (2) and (3) of Terwey and Montgomery (2008, hereafter TM08). The initial thermodynamic field was given by Jordan (1958; hereafter J58). The horizontal grid spacing was 2 km. The number of vertical grids was 45 and the vertical grid interval on the lowest layer was 100 m. The calculating domain had 2000 km x 2000 km x 22.5 km. The simulation time for each experiment was 500 hour. For each experiment, SST value was constant, horizontally uniformed and did not change during the simulation. We considered that structure of concentric eyewalls varies with the radial profile of the tangential wind of TC, on the basis of TM08. Therefore we conducted some parameter experiments for SST and vertical instability in the atmosphere. Because these parameters are sensitive for the maximum tangential wind of TC (Rotunno and Emanuel, 1987). We had four experiments: (1) SST = 301 K, thermodynamic field was J58, (2) SST = 302 K, thermodynamic field was J58, (3) SST = 302 K, thermodynamic field was J58 + 3 K, (4) SST = 300 K, thermodynamic field was J58 + 1 K. Here “ J58 + 3 K ” means that 3 K was uniformly added to the potential temperature profile of J58, and “ J58 + 1 K ” was the same of “ J58 + 3 K ” but except for the added value of 1 K. We named experiments of (1) - (4) as “ CTL ”, “ S302 ”, “ ST302 ”, “ ST300 ”, respectively.

In CTL and S302, eyewall replacements occurred on several occasions during the last 100 hours. On the other hand, in ST302, clear concentric eyewalls were formed. However, eyewall replacement did not occur over 500 hours. In ST300, concentric eyewall was not formed. In CTL and S302, the outward slope associated with height of the outer eyewall was similar to that of the inner eyewall. Moreover, the vertical wind speed in the outer eyewall was comparable with that in the inner eyewall. The other hand, in ST302, the outward slope of the outer eyewall was more gradual than that of the inner eyewall. For the vertical wind speed, it was weaker than that of the inner eyewall.These characters is also indicated in the simulated Typhoon Bolaven (2012) of Tsujino and Tsuboki (2013). Thus, we think that the occurrence of eyewall replacement is related to the similar extent of the slope between the inner and outer eyewall associated with height.

Keywords: tropical cyclone, concentric eyewall, eyewall replacement, vortex dynamics

Japan Geoscience Union Meeting 2014
(28 April - 02 May 2014 at Pacifico YOKOHAMA, Kanagawa, Japan)

MIS24-06 Room:313 Time:April 28 14:45-15:00

Mechanism of vortex movement in environmental vorticity gradient and its estimation

YAMADA, Kao[1*] ; IGA, Keita[1]

[1]AORI, The University of Tokyo

Yamazaki and Itoh(2013) proposed SAM(selective absorption mechanism) as the maintenance mechanism of the blocking which is known as quasi-steady state of the atmosphere. The essence of SAM is vortex-vortex interaction and the blocking can subsist for a prolonged period by absorbing eddies of the same polarity. The movement of tropical cyclones and mid-latitude cyclones have also been investigated by vortex-vortex interaction (e.g. Fiorino and Elsberry, 1989; Oruba et al., 2012). Also, it has been indicated that the key parameters of vortex movement are the absolute vorticity gradient of the environment, the radius of vortex and its strength (e.g. DeMaria, 1985; Chan and Williams, 1987), but these researches remain at a posteriori argument of the results of the numerical simulations. In this study, we conducted numerical simulations using variety of combinations of these parameters by means of two-dimensional nondivergent barotropic model. Besides, we investigated the mechanism of the vortex movement by vortex-vortex interaction and evaluated it quantitatively.

It was found that the time-development of the vortex movement is divided into two periods with different features: the acceleration regime at the initial stage and the vortex pair translation regime with quasi-steady movement. In each regime, the vortex excites characteristic vorticity field around it and the vortex movement showed different dependence on the parameters. While the vortex slightly rotates and deforms the background field in the acceleration regime, another prolonged vortex with opposite sign appears in the eastside of the original vortex in the vortex pair translation regime.

In the acceleration regime, we evaluated the acceleration by applying directly the concept of SAM and obtained the results that the movement velocity is proportional to the product of the absolute vorticity gradient, the circulation of the vortex and the elapsed time. In the vortex pair translation regime, the velocity of the vortex movement can be evaluated by a few number of the parameters which characterize the counterrotating vortex beside, considering the mechanism of the vortex pair propagation. As a result, it is shown that the velocity is proportional to the product of the two-thirds power of the circulation of the vortex and the one third power of the planetary vorticity gradient. These estimations represent the dependence of the each-period velocity on the parameters well, and we succeeded in clarification of the physical effect on the vortex movement by the parameters and estimation of the vortex displacement.

We evaluated these parameters of the experiments for the effective beta and revealed that the difference of the influence of the planetary vorticity gradient and the relative vorticity gradient on the vortex movements results in the shear of the background flow, which has not clearly shown by previous researches.

Keywords: vortex

Japan Geoscience Union Meeting 2014
(28 April - 02 May 2014 at Pacifico YOKOHAMA, Kanagawa, Japan)

MIS24-07 Room:313 Time:April 28 15:00-15:15

A phase-independent expression for the energy flux associated with inertia-gravity waves

AIKI, Hidenori[1*]

[1]Japan Agency for Marine-Earth Science and Technology

For diagnosing the effect of stationary Rossby waves on atmospheric circulation, a phase-independent expression for the wave activity flux has been developed by Takaya and Nakamura (2001) using quasigeostrophic equations. On the other hand, concerning inertia-gravity waves, a phase-expression has not been derived in previous studies. Recently we have developed a phase-independent expression for both the energy flux and the pseudo momentum flux associated with inertial-gravity waves. We have investigated the performance of the new expression using high-resolution simulations for internal waves in the ocean, such as internal gravity waves generated by a moving storm (figure) as well as tidal internal waves in JCOPE-T. The new expression for the energy flux may be used to reduce a noise associated with sampling errors in a model output, while the new expression for the pseudomomentum flux may be used for the diagnosis of mountain waves.

Keywords: inertia-gravity waves, energy flux, phase dependency

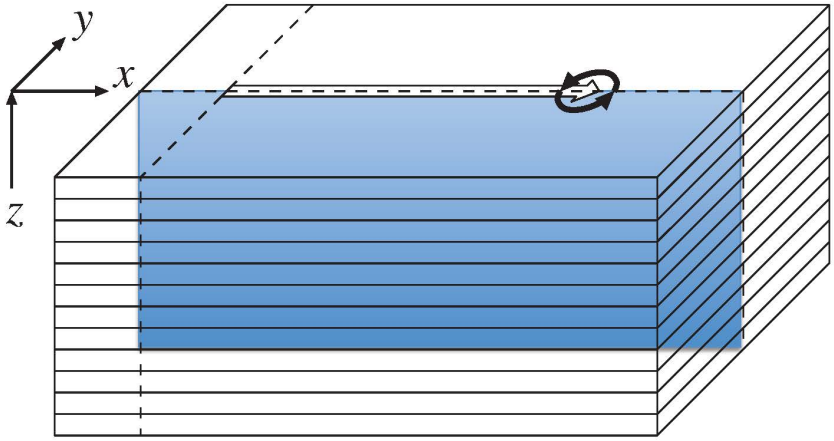

Japan Geoscience Union Meeting 2014
(28 April - 02 May 2014 at Pacifico YOKOHAMA, Kanagawa, Japan)

MIS24-08 Room:313 Time:April 28 15:15-15:30

A mechanistic model of double-diffusive intrusions

NOGUCHI, Takashi[1*]

[1]Graduate School of Engineering, Kyoto University

Dynamical structure of double-diffusive interleaving at a density-compensating thermohaline front is investigated. Numerical simulations successfully reproduced a series of sloped intrusive motions (fig. a). It is revealed that the finger convection and its collective vertical buoyancy transport drastically changes the inner structure of the layers as well as the slope of the intrusion layers. To understand the dynamical balance of the motions in layers, a mechanistic model of intrusive layers was devised for an idealised configuration in which a unit layer repeats in vertical direction (fig. b). Transports of heat and salt by small-scale convective motions are parameterised in terms of large-scale quantities. Balances between parameterised transports yielded results qualitatively consistent with that of the numerical simulations.

Acknowledgements: This work was supported by JSPS Grant-in-Aid for Young Scientists B 23740354.

Keywords: double-diffusive convection, lateral mixing

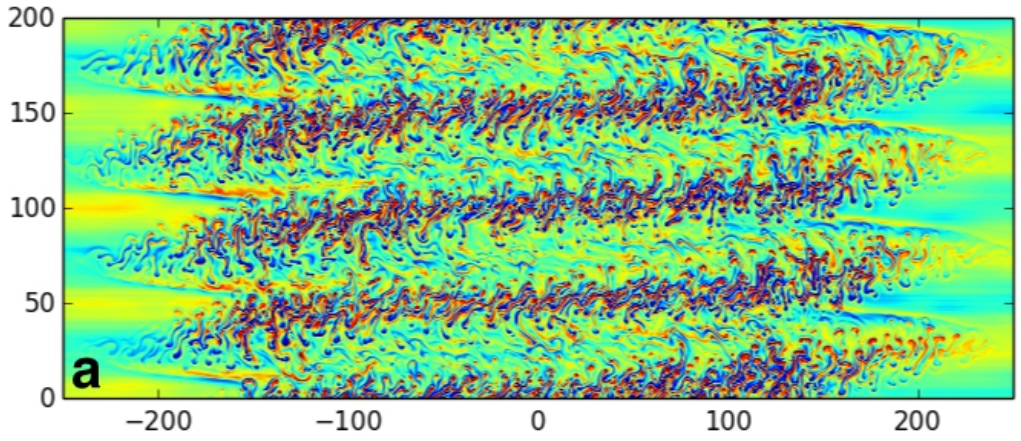

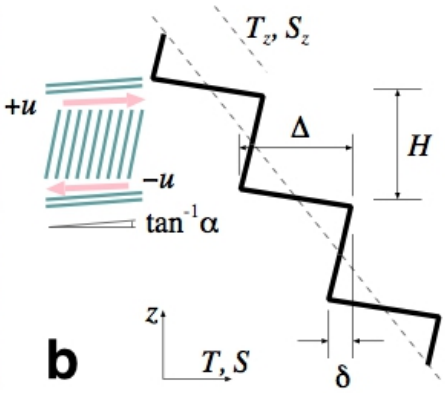

Japan Geoscience Union Meeting 2014
(28 April - 02 May 2014 at Pacifico YOKOHAMA, Kanagawa, Japan)

MIS24-09 Room:313 Time:April 28 15:30-15:45

Low-frequency internal waves in Shiozu Bay, Lake Biwa: A numerical approach

AUGER, Guillaume[1*] ; NAGAI, Takeyoshi[2] ; YAMAZAKI, Hidekatsu[2]

[1]Department of Civil Engineering, Ritsumeikan, [2]Department of Ocean Science, TUMSAT

In this study, we present results from the three-dimensional unstructured numerical simulator SUNTANS, used to understand the dynamics of the low-frequency internal wave field inside Shiozu Bay, a bay in the Northern part of Lake Biwa. Initial conditions for a fine-scale grid were generated in using a coarse grid with measured heat fluxes and wind stress. After being compared against observational data, the simulation reproduced consistently the low-frequency internal wave field, (similar frequencies and waves features). Based on the analysis of integrated potential energy and integrated dissipated energy time series, this study shows that the low-frequency internal wave field that enters Shiozu Bay does not either completely dissipate or break. Moreover isotherm elevation associated to the internal the first horizontal mode and first vertical mode Kelvin wave highlights the cyclonic rotation pattern, which is characteristic of the Kelvin wave, within the bay. This result shows that the part of the Kelvin wave entering the bay goes in and out. Moreover the dynamic of the internal wave field within the bay displays an peculiar process at the narrowing of the bay. At the contraction of the bay, the flow speeds up and deep isotherms deepen further. These two processes generated turbulence by shear and strain; according to the turbulence model (Mellor and Yamada, 1982) turbulent kinetic dissipation rate reached 10^{-6} W kg^{-1}, occurring during the trough phase of the internal wave field. Additionally the occurrence of these enhanced turbulent events appears to depend on the amount of energy detained by the low frequency internal wave. When the internal wave field was energized by the wind the turbulent events were enhanced. Such events could modify the long-term distribution of material in the lake.

Keywords: wind forcing, internal waves, contraction, strain

Japan Geoscience Union Meeting 2014
(28 April - 02 May 2014 at Pacifico YOKOHAMA, Kanagawa, Japan)

MIS24-10 Room:313 Time:April 28 15:45-16:00

Anomalous wave dispersion of distant tsunamis in a coupled system between the self-gravitating elastic Earth and ocean

WATADA, Shingo[1*]

[1]Earthquake Research Institute, University of Tokyo

Traveltime delay and waveform dispersion of distant tsunamis that propagated over the Pacific after the 2010 Chilean and 2011 Tohoku-Oki earthquake can be understood as a propagating wave in a unified gravitationally and elastically coupled system between the solid Earth and ocean.

Keywords: Tsunami propagation delay, Tsunami phase velocity measurements, Tsunami waveform dispersion, Tsunami initial phase with reversed polarity, Tsunami precursor, DART tsunami records from the 2010 Tohoku?Oki earthquake and

Japan Geoscience Union Meeting 2014
(28 April - 02 May 2014 at Pacifico YOKOHAMA, Kanagawa, Japan)

MIS24-11 Room:313 Time:April 28 16:15-16:30

On the vigor of mantle convection and stagnant lid formation in super-Earths

MIYAGOSHI, Takehiro[1*] ; KAMEYAMA, Masanori[2] ; OGAWA, Masaki[3]

[1]JAMSTEC, [2]Ehime University, [3]University of Tokyo

Super-Earths are extra-solar terrestrial planets which have large sizes and masses (up to about ten times the Earth's mass). Understanding mantle convection in super-Earths is a key to clarifying their evolution, surface environment, and habitability. In large super-Earths, the mantle depth far exceeds the thermal scale height, and adiabatic compression strongly influences super-Earths' mantle convection in contrast to the Earth's one. In this paper, we present numerical models of mantle convection in super-Earths with high compressibility, high Rayleigh number, temperature-dependent viscosity and depth-dependent thermal expansivity.

Thermal convection of compressible infinite Prandtl number fluid is solved in a rectangular box under anelastic approximation by the ACuTEMAN (Kameyama et al. 2005). The model of the super-Earths includes depth-dependent thermal expansivity and density, as well as a strong temperature-dependence of viscosity. We assume the mass of the planet is ten times the Earth's. The Rayleigh number defined with the viscosity at the core-mantle boundary (CMB) Ra is 1E10. A viscosity contrast r up to 1E7 arises between the CMB and the surface owing to the temperature-dependence of viscosity. The employed grid number is 1024 (horizontal) and 256 (vertical).

We identified the stagnant lid regime in the model of super-Earths. When the viscosity contrast r is larger than about 1E6, a stagnant lid of highly viscous fluid is formed along the surface. The lid hardly moves and is not involved in the convection, as has been observed earlier for the Boussinesq model of the Earth's mantle convection (Kameyama and Ogawa, 2000). The lithosphere is as thick as about thirty percent of the depth of the whole mantle, and the Nusselt number is about three at r=1E7 and Ra = 1E10. This value is comparable to that of the Earth's model at the same r but at much lower Ra of 6E6 (Kameyama and Ogawa, 2000). The lithosphere is much thicker than has been expected earlier for super-Earths (e.g., Valencia et al. 2007), and the thick lithosphere is likely to affect the possibility of plate tectonics at the surface of super-Earths. The strong effect of adiabatic compression also affects the dynamics of hot plumes that ascend from the CMB when the temperature-dependence of the viscosity is strong: At r $>\sim$1E3, hot plumes from the CMB are strongly suppressed. They do not ascend to the surface of the planet. The overall pattern of convective circulation in the mantle is, therefore, dominated by the cold plumes that descend from the lithosphere to the CMB. The low efficiency of heat transport by the mild convection would strongly affect the evolution history of super-Earths, and is likely to weaken the core convection, and thus, the magnetic field of super-Earths.

Keywords: super-Earths, mantle convection

Japan Geoscience Union Meeting 2014
(28 April - 02 May 2014 at Pacifico YOKOHAMA, Kanagawa, Japan)

MIS24-12 Room:313 Time:April 28 16:30-16:45

Heater size effect on generation of thermal plumes

KUMAGAI, Ichiro[1*] ; YAMAGISHI, Yasuko[2]

[1]Meisei University, [2]IFREE, JAMSTEC

Mantle plumes from the CMB experience a filtering effect by the endothermic phase change at the 660-km phase transition. Fluid dynamics predicts that the hot mantle plumes stagnate at and locally heat the upper-lower mantle boundary, which causes generation of the secondary plumes in the upper mantle, and hence hotspots volcanic activities on the surface. To understand the effects of heater size on the plumes generation, we have experimentally investigated the behaviors of thermally buoyant plumes generated from a localized heat source (circular plate heater) using quantitative visualization techniques of temperature (TLC) and velocity (PIV) fields. Scaling laws for their ascent velocity and spacing of the plumes are experimentally determined. We also estimate the onset time of the secondary plumes in the upper mantle which depends on local characteristics of the thermal boundary layer developing at the upper-lower mantle boundary.

Keywords: plume, mantle, fluid dynamics, experiment

Japan Geoscience Union Meeting 2014
(28 April - 02 May 2014 at Pacifico YOKOHAMA, Kanagawa, Japan)

MIS24-13 Room:313 Time:April 28 16:45-17:00

Waves and linear stability of magnetoconvection in a rotating cylindrical annulus

HORI, Kumiko[1*] ; TAKEHIRO, Shin-ichi[2] ; SHIMIZU, Hisayoshi[1]

[1]Earthquake Research Institute, University of Tokyo, [2]Research Institute for Mathematical Sciences, Kyoto University

Magnetohydrodynamic waves in a rapidly rotating planetary core can cause the magnetic secular variation. To strengthen our understanding of the physical basis of such waves, we revisit the linear stability analyses of thermal convection in a quasi-geostrophic rotating cylindrical annulus with an applied toroidal magnetic field, and we extend the investigation of the oscillatory modes to a broader range of the parameters. Particular attention is paid to influence of thermal boundary conditions, either fixed temperature or heat-flux conditions.

While the non-dissipative approximation yields a slow wave propagating retrograde (westward), termed as a Magnetic-Coriolis/Magnetic-Coriolis-Archimedes (MC/MAC) Rossby wave, dissipative effects produce a variety of waves. When magnetic diffusion is much stronger than thermal diffusion, this can cause a very slow wave propagating prograde (eastward). Retrograde-travelling slow waves appear when magnetic diffusion is weaker. Emergence of the slow modes allows convection to occur at lower critical Rayleigh numbers than in the nonmagnetic case. When the magnetic diffusion is strong, the onset of the convection occurs with the prograde-propagating slow wave, whereas when it is weak, a slow MC mode conducts the critical convection.

Fixed heat-flux boundary conditions have profound effects on the marginal curves, which monotonically increase with the horizontal wavenumber, and lead to larger length scales at the onset of the convection, provided there is sufficient field strength that the Lorentz force is balanced with the Coriolis force. The effect, however, becomes less clear as the magnetic diffusion is weakened and various magnetohydrodynamic waves emerge.

Japan Geoscience Union Meeting 2014
(28 April - 02 May 2014 at Pacifico YOKOHAMA, Kanagawa, Japan)

MIS24-14 Room:313 Time:April 28 17:00-17:15

Investigation of cell patterns on a rotating convection by ultrasonic velocity profile measurements

FUJITA, Kodai[1*] ; TASAKA, Yuji[1] ; MURAI, Yuichi[1] ; OISHI, Yoshihiko[1] ; YANAGISAWA, Takatoshi[2]

[1]Hokkaido University, [2]IFREE JAMSTEC

Rayleigh-Benard convection is the well-known topic as fundamental system in fluid dynamics. In particular, the effect of rotating field on the convection is one of essential piece for geophysics. The influence of centrifugal force and Coriolis force on convection pattern formation was experimentally showed by Rossby (1969). The flow structure of Rayleigh-Benard convection in a rotating field is described by Rayleigh number (Ra), Taylor number (Ta) and Prandtl number (Pr). Especially, it is important to study the behavior of low Pr fluid like liquid metals, because this knowledge helps to understand the dynamics of metallic cores in planets. In low Pr fluids, the flow regimes dramatically changes in comparison with ordinal fluid with Pr $>$1. For example, Rayleigh-Benard convections in a liquid metal layer easily take transition to turbulent state. Generally, adding rotating field stabilizes the flow. On the other hand, flows of low Pr fluids with background rotation are expected to become oscillatory and irregular motion near the marginal stability conditions. These characteristics of low Pr fluids, however, have not been studied experimentally so much, because it is impossible to capture the convection patterns of liquid metal flows optically. To solve this problem, the authors adopt Ultrasonic Velocity Profile (UVP) method to visualize convective flow of liquid metal in a rotating field. As the data set of UVP measurement is one-dimensional velocity distribution, it is difficult to guess flow fields of convection from only a result of UVP without any criterion of translation. In this study, as preparations for liquid metal experiments, we performed two different visualizations using optics and ultrasound on ordinal transparent fluid, water (Pr = 7), to understand flow field from spatio-temporal velocity distribution obtained by UVP. Optical visualization provides path line images for the comparison. In addition, we purpose to take the knowledge about spatio-temporal velocity distribution of high Pr contrasted with low Pr.

Experiments were performed on a rotating table. The vessel of fluid layer has a square geometry, which aspect ratio is seven. The bottom of fluid layer was heated by electrical heating and the upper surface was cooled by circulating water through flow channel made of glass plate. Optical visualization images were obtained from a horizontal section of the fluid layer. An ultrasonic transducer for UVP measurement was mounted horizontally on the side wall of fluid layer.

The path line showed many small round convective cells in the fluid layer, and it represented that the size of cells become smaller as Ta takes larger. In addition, the size of cell and cell motions were also detected by spatio-temporal velocity distributions acquired by UVP. For example, cells moved in certain direction and passed over measurement line of transducer. Staying time of cell on the line was observed and means speed of cells moving. As Ta gets larger, it was found that the speed of each cell motion became slower. The cell diameter was calculated from velocity data. When cells stay next to each other, there is 0 mm/s on cells boundaries in spatial velocity distribution at the time. We defined distances between neighboring cells on the spatial line respectively as scales of cell size. Then we extracted all distances from spatio-temporal distribution and calculated the expected value of these. The expected value represents dominant cell diameter. We confirmed that the cell size on the distribution roughly corresponds to that on the path line. Thereby we obtained information of convective cell from only UVP data.

Keywords: Rayleigh Benard convection, Rotating field, Flow pattern

Japan Geoscience Union Meeting 2014
(28 April - 02 May 2014 at Pacifico YOKOHAMA, Kanagawa, Japan)

MIS24-15 Room:313 Time:April 28 17:15-17:30

Roll convection in a liquid metal layer subject to a horizontal magnetic field

TASAKA, Yuji[1*] ; IGAKI, Kazuto[1] ; YANAGISAWA, Takatoshi[2] ; ECKERT, Sven[3] ; MURAI, Yuichi[1]

[1]Facukty of Enginnering, Hokkaido University, [2]JAMSTEC, [3]Helmholtz center at Dresden-Rossendorf

Recent investigations using ultrasonic velocity profiling (UVP) on Rayleigh-Benard convection in a liquid metal layer under horizontal magnetic field gave good understanding for typical temperature fluctuations shown in previous studies (Yanagisawa, et al., 2013). For example, regime transition against variations of Rayleigh number (Ra) and Chandrasekhar number (Q), variation of the roll number and spontaneous, random flow reversal that consists of spontaneous transition between two modes having different number of rolls, mainly N = 4 and 5. This flow reversal may be due to non-integer number of stable wave number in corresponding conditions of Ra and Q. The rolls can take only integer number even though the stable wave number determined by flow instability is, for example, N = 4.3. In this case the dominant condition is N = 4, and it is sometime modified into N = 5 due to external noise. However, N = 5 is not stable, and thus Skewed varicose instability occurs to restore N into 4. Time average of instantaneous N may correspond to stable wave number for the corresponding conditions.

This study aims to widen the flow regimes into larger Ra and larger Q by one order to clarify the influence of strong magnetic field: Past studies predict that the strong magnetic field greatly modifies the critical Rayleigh number at the onset of the convection. Experiments were done in Helmholtz center at Dresden-Rossendorf (HZDR) to utilize strong magnetic field generator that can provide quasi uniform magnetic field with 30 mT in the intensity. The test fluid layer is almost same with our previous study (Yanagisawa, et al., 2013) and its main aspects are, 5 in aspect ratio, 40 mm in height and sandwiched between copper plates for cooling at top and heating at bottom. The obtained regime diagram shows that the fraction rule on Ra/Q determining the regimes is still almost valid in the widen region of Ra and Q. But the number of rolls is slightly modified from expectations by the rule. Also we observed ”regular” flow reversals instead of random one. This may be due to stable number of rolls larger than N = 4.5 and aspect ratio of the vessel, 5. The dominant roll number also depends on the side boundary of the vessel. Velocity profiles parallel to the roll axes clarified three dimensional motion during the regular flow reversals.

Keywords: Rayleigh-Benard convection, Liquid metal, Magnetic field, Convection pattern

Japan Geoscience Union Meeting 2014
(28 April - 02 May 2014 at Pacifico YOKOHAMA, Kanagawa, Japan)

MIS24-16 Room:313 Time:April 28 17:30-17:45

Flow reversals in liquid metal convection by the skewed-varicose instability

YANAGISAWA, Takatoshi[1*] ; SAKURABA, Ataru[2] ; HAMANO, Yozo[1]

[1]IFREE, JAMSTEC, [2]School of Science, Univ. Tokyo

The natures of turbulence and large-scale flow pattern in the outer core are controlled by the magnetic field. It is important to know the basic behavior of flow in relation to the magnetic field, for understanding the flow patterns observed in real Earth and core dynamo simulations. By recent laboratory experiments of Rayleigh-Benard convection with liquid gallium, a regime diagram of convection patterns was established under various intensities of a uniform horizontal magnetic field for a wide square geometry (Yanagisawa et al. 2013, PRE). Five flow regimes are recognized; (I) fluctuating large-scale pattern without roll, (II) weakly constrained roll with fluctuations, (III) continuous oscillation of roll, (IV) repetition of roll number transitions with random reversals of the flow direction, and (V) steady 2-D rolls. In these, regime (IV) with flow reversals is the most interesting behavior. Flow reversals have been observed so far in narrow vessels with small aspect ratio, and the proposed processes for reversals are reorientation and cessation. Experiments with liquid metal under horizontal magnetic field suggest the existence of new type of reversal, via the skewed-varicose instability.

We performed numerical simulations of magnetoconvection in a same setting as the experiment with no-slip velocity boundary conditions. Both the Prandlt number and magnetic Prandtl number of the working fluid are set small to simulate liquid metals. Our numerical result successfully reproduced all regimes that observed in the experiments. The process of flow reversal is illuminated by the simulation. Axis of roll is skewed with a roll shrinking, and the number of rolls is reduced. In case the reduced roll number structure is not fit the vessel, new small circulation grows to a roll again, and then reversed flow state is established. The process repeats with irregular time interval. It works in 3-dimensional geometry, and should play important role in various flow systems.

Keywords: thermal convection, liquid metal, flow reversal

Japan Geoscience Union Meeting 2014
(28 April - 02 May 2014 at Pacifico YOKOHAMA, Kanagawa, Japan)

MIS24-P01 Room:Poster Time:April 28 18:15-19:30

Spectrum of internal waves in bounded domains of the Atmosphere and the Ocean

GINIATOULLINE, Andrei[1*]

[1]Department of Mathematics, Los Andes University, Bogota, Colombia, South America

We consider the spectral properties of internal waves for three-dimensional compressible rotating exponentially stratified fluid. This model describes the flows in the Atmosphere and the Ocean which include simultaneously the rotation of the Earth over the vertical axis, and the non-homogeneous initial stratification of density caused by the gravitational force. We obtain theoretical results for the spectrum of the resulting internal waves in terms of its structure, localization, and its possible usage in computational algorithms. The applications of the spectral properties of such internal waves can be found, in particular, in the models of the resonance effect. We consider both the general case of bounded domains, and the explicit results of some particular domains, such as cubes and cylinders.

Keywords: computational fluid dynamics, compressible fluid, rotating stratified fluid, essential spectrum, internal waves, fluid dynamics of the Atmosphere and the Ocean

Japan Geoscience Union Meeting 2014
(28 April - 02 May 2014 at Pacifico YOKOHAMA, Kanagawa, Japan)

MIS25-01 Room:411 Time:April 28 09:15-09:30

Relationship between the Kamiaso unit and the Nabi unit in the Mino terrane of the Mino-Seki area, Gifu Prefecture

KITAGAWA, Yusuke[1*] ; MATSUOKA, Atsushi[2]

[1]Graduate School of Science and Technology, Enviromental Science and Technology, Earth Science, Niiga, [2]Department of Geology, Faculty of Science, Niigata University

The Mino terrane, one of the disrupted terranes in central Japan, is divided into several tectonostratigraphic units on the basis of composition, fabric and age. However, there is a problem that these data are biased, because detailed studies have been conducted only in limited areas. The Mino-Seki area of the central part in Gifu Prefecture is one of such area. According to Wakita (1988b), this area is occupied by the Kamiaso unit characterized by repeating coherent chert-clastic sequences and the Nabi unit characterized by broken formation composed of sandstone / mudstone and melange. The Wadano Coglomerate (Kanuma, 1956), characterized by breccias of chert, siliceous claystone, limestone and basaltic rocks, is also distributed in the study area. Here, I will discuss relationship between the Kamiaso unit and the Nabi unit in the Mino terrane.

As a result of a detailed field work, accretionary complexes in the Mino-Seki area are divided into a coherent unit (Kamiaso unit), melange unit (Nabi unit) and the Wadano Coglomerate. The Kamiaso unit is characterized by a tectonic pile composed of chert-clastic sequences that retain the oceanic plate stratigraphy. Chert samples yield Middle Triassic to Early Jurassic radiolarians, while mudstone samples yield Early Bathonian radiolarians. The Nabi unit includes melange and alternating beds of chert and siliceous micrite. There are also differences in the lithology of chert. Black chert with weathered red surface is commonly found in the Nabi unit especially along the Nagara River. These lithofacies generally are not recognized in the Kamiaso unit. Chert samples yield Middle Triassic to Early Jurassic radiolarians, while siliceous mudstone samples yield Middle Jurassic radiolarians. A chert sample in alternating beds of chert and siliceous micrite yields of Late Triassic radiolarians. Igo and Koike (1975) reported Late Norian conodonts from a limestone sample in alternating beds of chert and limestone. The Wadano Coglomerate consists mainly of conglomerate and massive sandstone. It is characterized by blocks of basaltic rock chert, siliceous claystone, and limestone. The Upper Triassic siliceous micrite-chert facies of the Nabi unit differs in containing siliceous micrite from the coeval chert of the Kamiaso unit. This relationship has already been pointed out by Sano et al. (2010).

Keywords: Mino terrane, Kamiaso unit, accretionary complex, chert-clastic sequence, radiolaria

Japan Geoscience Union Meeting 2014
(28 April - 02 May 2014 at Pacifico YOKOHAMA, Kanagawa, Japan)

MIS25-02 Room:411 Time:April 28 09:30-09:45

Recognition of the Olenekian-Anisian Boundary Sequence from Ogama, Ashio Belt

MUTO, Shun[1*] ; TAKAHASHI, Satoshi[1] ; YAMAKITA, Satoshi[2] ; SUZUKI, Noritoshi[3] ; AITA, Yoshiaki[4]

[1]Department of Earth and Planetary Science, Graduate School of Science, The University of Tokyo, [2]Department of Earth Sciences, Faculty of Education and Culture, University of Miyazaki, [3]Institute of Geology and Paleontology, Graduate school of Science, Tohoku University, [4]Geology Lab, Faculty of Agriculture, Utsunomiya University

Pre-Jurassic pelagic sedimentary sequences are known to have accumulated in the pelagic Panthalassa over millions of years (Matsuda and Isozaki, 1991; Ando et al., 2001). These pelagic sequences are considered to preserve environmental record of the pelagic Panthalassa. However, spatial variations of pelagic sequences are not fully understood, due to the scarcity of well-preserved sequences. In order to face this problem, this study reconstructed the stratigraphic sequence ranging from Lower to Middle Triassic with high resolution at the Ogama section of the Ashio Belt, which is located in Tochigi, Japan (Kamata, 1996; Kamata 1997).

The section consists of three parts, which occur in separate outcrops; Og-A section, Og-B section and Og-C section. The boundaries of these outcrops were not directly observed, but the major difference in lithology suggests that these outcrops are in contact with faults. The Og-A section consists of approximately 2.5 m thick black claystone overlain by bedded chert. The Og-B section consists of alternating claystone and chert. Claystone in the Og-B section has two types: black claystone and grey siliceous claystone. The Og-C section consists entirely of bedded chert. Components of bedded chert are 1 to 10 cm thick chert beds and 2 to 25 mm thick intercalated claystone beds.

Age diagnostic conodonts were recovered from the Og-B section. Spathian conodonts indicating the *Triassospathodus homeri* zone (*Neospathodus homeri* zone; Koike, 1981), early Anisian conodonts indicating the *Chiosella timorensis* zone (*Neogondolella timorens* zone; Koike, 1981), Middle Anisian conodonts indicating the *Neogondolella bulgarica* zone (Koike, 1981) were recovered. Radiolarian fossils were recovered from the Og-C section. Early-middle Anisian radiolarian *Triassocampe eruca* (Sugiyama, 1997) and late Anisian radiolarian *Triassocampe coronata* (Bragin) group were recovered.

The reconstructed stratigraphic sequence spans from upper Spathian of Lower Triassic to upper Anisian of Middle Triassic. The Spathian-Anisian boundary determined by the first occurrence of conodont Ch. timorensis is placed at the lower part of the Og-B section. The Lower to Middle Triassic pelagic sequence of the Ogama section has two important characteristics. One is the lithofacies change from claystone dominant facies of upper Spathian to bedded chert facies of middle Anisian. The other is the 4 m thick interval of black claystone and black chert, which spans from uppermost Spathian to lower Anisian.

Lower to Middle Triassic pelagic sequences are also exposed in other Jurassic accretionary complexes. A particularly well-studied sequence belongs to the Mino Belt, and is situated in the Inuyama area, Gifu, Japan. This area has been the target of intensive biostratigraphical examinations (Sugiyama, 1997; Yao and Kuwahara, 1997) and cyclostratigraphical researches (Ikeda et al., 2010). The comparison of the two pelagic sequences from the Ashio Belt and the Mino Belt revealed the common general trend of increasing chert content within the lower to middle Anisian interval. However, it is also noteworthy that the interval consisting of black claystone and black chert is remarkably thicker in the Ogama section than in the Inuyama area. Takahashi et al. (2009) indicated the uppermost Spathian interval consisting of black claystone and black chert in the Inuyama area is the result of an oceanic anoxia. The thicker interval at Ogama section may represent longer duration of this event, or a greater sedimentation rate during the event, at the depositional setting than that of Inuyama area. Further correlations by biostratigraphy and carbon isotope stratigraphy are required to compare the onset and offset timing of this event in both depositional settings. The comparison of timing between the two sections may reveal the cause of this regional difference in pelagic sequences.

Keywords: Ogama section, Ashio Belt, Olenekian-Anisian Boundary, Conodont, Radiolarian, Equatorial Panthalassa

Japan Geoscience Union Meeting 2014
(28 April - 02 May 2014 at Pacifico YOKOHAMA, Kanagawa, Japan)

MIS25-03 Room:411 Time:April 28 09:45-10:00

Upper Triassic conodont, ammonoid, and radiolarian biostratigraphy in a pelagic sequence of Japan

YAMASHITA, Daisuke[1*] ; YASUDA, Chika[2] ; SATO, Honami[3] ; ONOUE, Tetsuji[4]

[1]Earth and Environmental Sciences, Graduate School of Science and Engineering, Kagoshima University, [2]INPEX Corporation, [3]Graduate School of Earth and Planetary Sciences, Kyushu University, [4]Earth and Environmental Sciences, Graduate School of Science and Technology, Kumamoto University

The chronology for the Triassic pelagic deposits in the Panthalassa Ocean is based on the radiolarian zonation, which is well studied in the Middle and Upper Triassic bedded chert successions in the Japanese accretionary complex. Although accurate calibration for the chronostratigraphic stages and substages are established basically by means of ammonites and conodonts, most of the Japanese radiolarian zones were calibrated through correlation with zonal schemes in other regions, and have not been calibrated with ammonoid and conodont biostratigraphy. Here we present the results of Late Triassic (Carnian-early Norian) conodont biostratigraphy from the two pelagic sections in the Jurassic accretionary complex of southwest Japan. Samples for this study were collected from the Sakahogi section of a bedded chert sequence in central Japan and the Nakijin Formation of a pelagic limestone sequence in the northern tip of the Okinawa Island. We found 56 platform conodonts from 36 samples in the Sakahogi section, where the radiolarian biostratigraphy have previously been investigated. The biostratigraphy of the Carnian-Norian sequence of the Nakijin Formation is based primarily on ammonites, since the rare occurrence of conodonts minimizes the stratigraphic potential of these groups. However, our study revealed that the clastic limestones intercalated within the Nakijin Formation contain rich conodonts assemblages. Based on detailed study of the conodont biostratigraphy from the interval of the Carnian and the early Norian in the Sakahogi section and the Nakijin Formation, three conodont zones are recognized in ascending order as follows: lower Carnian *Paragondolella praelindae* - *Metapolygnathus polygnathiformis* zone, upper Carnian *Metapolygnathus lindae* - *Metapolygnathus primitius* zone, and lower Norian *Epigondolella quadrata* zone. This result is consistent with the presence of the lower to upper Carnian ammonites assemblages in the Nakijin Formation.

Keywords: Late Triassic, Carnian to early Norian, conodont, ammonoid, and radiolarian biostratigraphy, Sambosan Terrane, Mino Terrane, Panthalassa Ocean

Japan Geoscience Union Meeting 2014
(28 April - 02 May 2014 at Pacifico YOKOHAMA, Kanagawa, Japan)

MIS25-04 Room:411 Time:April 28 10:00-10:15

Toward reconstruction of oceanic plate paleogeography in the NW Pacific: a subject from the NE Japan arc.

UEDA, Hayato[1*] ; KIMURA, Sho[1] ; ORIHASHI, Yuji[2]

[1]Hirosaki Univ., [2]ERI, Univ. Tokyo

Spatial distribution of oceanic plates in the Mesozoic NW Pacific has been indirectly assumed extrapolating from magnetic anomalies tracked back to the mid-Pacific. However, common occurrences of suprasubduction ophiolites and arc terranes, existence of the Philippine Sea plate originated in the Jurassic, and lower mantle tomography suggesting remnants of subducted slab in the mid-Pacific all imply that plates occupied NW Pacific were distinct from those in the middle to east Pacific in the Mesozoic. To test this possibility, it is important to reconstruct oceanic plates from geology and chronology of accretionary complexes and ophiolites independently from the traditional methods based on magnetic anomaly. Here we present a subject for the oceanic plate reconstruction raised from NE Japan.

In this study, we datermined U-Pb ages of zircons extracted from a tuff bed in a coherent clastic sequence of the Cape Shiriya accretionary complex (Shimokita Peninsula) at the northeastern tip of the North Kitakami belt. These zircons yielded a mean age of ca. 130 Ma (about Hauterivian / Barremian boundary). Almost identical ages were also obtained from the youngest zircon grains in sandstone. The 130 Ma age is concurrent with (a) Trench sedimentation in the Idonnappu accretionary zone, (b) high-P/T metamorphism in the Kamuikotan zone, and (c) island arc volcanism in the upper Sorachi Group, all in the central Hokkaido far in the east. A shift of the NE Japan trench from the North Kitakami belt to central Hokkaido has been assumed, with contemporaneous onset of arc volcanism in central Hokkaido. However, our result implies dual subduction in the both areas at 130 Ma. If this hypothesis stands, arc-trench system in central Hokkaido could have formed not along the Eurasian continental margin but belonging to another plate.

We also dated a diorite dike as a member of microdiorites, which commonly occur associated with serpentinites in central Hokkaido. These rocks have been attributed to Cretaceous arc magmatism based on chemistry and K-Ar ages. The diorite sample yielded a 160 Ma zircon U-Pb age of Late Jurassic, within the period of trench accretion in the North Kitakami belt. This age thus also suggest the hypothesis of dual subduction, where arc activity occurred outside the trench of Eurasian continental margin.

NE Japan has been held other problems difficult to be explained by simple, single subduction schemes. For example, adakite magmatism (suggesting slab melting) in the Kitakami mountains occurred contemporaneously with lawsonite-blueschist metamorphism (suggesting very cold subduction) in the Kamuikotan zone. Our new age data encourages to test possibilities that another subduction zone existed in the NW Pacific distinct from Eurasian active continental margin at least during Late Jurassic to middle Early Cretaceous.

Keywords: Pacific, oceanic plate paleogeography, zircon, U-Pb age, accretionary complex, ophiolite

Japan Geoscience Union Meeting 2014
(28 April - 02 May 2014 at Pacifico YOKOHAMA, Kanagawa, Japan)

MIS25-05 Room:411 Time:April 28 10:15-10:30

Philippine sea plate motion since the Pleistocene viewed from deformed conglomerates of the Ashigara group

KOBAYASHI, Kenta[1*]

[1]Dep. Geol., Fac. Sci., Niigata Univ.

On the northern convergence border of the Philippine Sea plate, Pleistocene Ashigara group (1.6-0.5Ma) filled a trough. Miocene Tanzawa group is distributed on the north side, and both are bounded with the Kannawa fault system. The Kannawa fault system is divided into the Kannawa fault (E-W direction, dextral sense) of the narrow sense, Hisari fault system (NE-SW, sinistral-normal), Nakatsugawa fault system (NW-SE, dextral-reverse), Shiozawa fault system (NE-SW, sinistral-reverse), etc. The Shiozawa formation (conglomerates) which is the high-end strata of the Ashigara group is distributed over the southeastern side of the Shiozawa fault. Parts of the conglomerates are deformed remarkably. These deformation zones are divided into six types (P-R1 cataclasite: A, B, C; fault gouge: Dr, Dg, Db) based on the fault rock property, shear sense, cutting relations. The cataclasites are distributed over the range of 600m from the Shiozawa fault. The shear sense is reverse fault mainly, but shows sinistral in a part of the B and Db type. Quartz grain becomes fine fragment by crush, and biotite does basal slip, it is thought that this cataclasite was formed under environment of 150-300 oC, and 5-10km in depth. The influence of the subducting Philippine Sea plate might have increased. In addition, the moving direction was not constant, northwest and north might be mixed in the Pleistocene age.

Keywords: Kanagawa Prefecture, Ashigara group, Shiozawa formation, cataclasite, fault gouge, Philippine sea plate

Japan Geoscience Union Meeting 2014
(28 April - 02 May 2014 at Pacifico YOKOHAMA, Kanagawa, Japan)

MIS25-06 Room:411 Time:April 28 10:30-10:45

Radiolarian morphology as a proxy for reconstructing pelagic environments: problem and perspective

MATSUOKA, Atsushi[1*]

[1]Niigata University

Late Paleozoic and Mesozoic radiolarian cherts are widely distributed within accretionary complexes in the Circum-Pacific and Alps-Himalaya orogenic belts. These cherts are materials for reconstructing the paleoenvironment of the Panthalassa and the Tethys. Many proxies have been developed to elucidate the environment of the past pelagic realm. Species diversity in radiolarian assemblages is expected to be one of proxies for monitoring paleoenvironmental change. However, the species concept of radiolarians is not always consistent throughout the Phanerozoic time. This makes a serious problem to use radiolarian diversity for elucidating environmental fluctuations. This paper documents the present status of taxonomy for Mesozoic and recent radiolarians. Detailed morphological analysis of radiolarian tests and the understanding of the morphogenesis through culture work are clues toward reconstructing pelagic environments in the past oceans.

Keywords: radiolarians, taxonomy, species concept, morphological diversity, pelagic realm

Japan Geoscience Union Meeting 2014
(28 April - 02 May 2014 at Pacifico YOKOHAMA, Kanagawa, Japan)

MIS25-07 Room:411 Time:April 28 11:00-11:15

Lifestyle of adherent benthic foraminifers in the open ocean based on stable of isotope records

KIMOTO, Katsunori[2] ; HASEGAWA, Shiro[1*] ; NAMIKAWA, Hiroshi[3] ; KITAMURA, Minoru[1] ; KAWAKAMI, Hajime[1] ; HONDA, Makio[1]

[1]Japan Agency for Marine-Earth Science and Technology, [2]Kumamoto University, [3]National Museum of Nature and Science, Tokyo

Colonization of new habitat of benthic foraminifers is related to their diversion, survival strategies and evolutions. However their dispersal mechanisms are not well documented and still poorly understood. Last year, we reported a new lifestyle of neritic benthic foraminifera: They had lived on the stems of hydrozoan attaching to observational moorings in the Pacific Ocean. This is a new insight of dispersal strategy of benthic foraminifera to the open ocean. However there are no evidences whether benthic foraminifera developed their calcareous shells in the water column or not. Here we report the new evidences of benthic foraminiferal lifestyles based on micropaleontological and geochemical methods.

Physical and biogeochemical observational mooring systems (POPPS & Sediment trap) were deployed on July, 2012 at the Station S1 (30N, 145E, water depth: 5,900m). Moored periods were from July 2012 to July 2013 (1 year). Hydrozoan attaching on the both mooring systems were observed at the surface of the winch, sensor buoy, sediment trap and float at shallower depths (˜200 m) and we could not observed hydrozoan at the 500 m water sediment trap. More than 300 individuals of benthic foraminifers attached of the surface of hydrozoan body. At least, fourteen living benthic foraminifers were identified under the microscope and faunal assemblages were basically same (calcareous, agglutinated, and sessile) with that of previous year. We performed the stable isotope analysis for these calcareous specimens including some porcellanic benthic and planktic foraminifera. As the results, oxygen and carbon isotopes of calcareous benthic foraminifera showed remarkably lighter and heavier values than planktic foraminifera, respectively. It suggested that calcareous benthic foraminifera in this study built their calcareous shells at shallower water depth than planktic species.

Keywords: adherent benthic foraminifera, Stable isotopes, Lifestyle, Hydrozoan

Japan Geoscience Union Meeting 2014
(28 April - 02 May 2014 at Pacifico YOKOHAMA, Kanagawa, Japan)

MIS25-08 Room:411 Time:April 28 11:15-11:30

Comparison between morphological dissimilarity and morphological richness

UBUKATA, Takao[1*]

[1]Shizuoka University

Morphological disparity, another look at biodiversity, has recently attracted attention of paleontologists in the context of mass extinction and recovery. The measure of disparity has commonly been based on morphological dissimilarity between objects, e.g., sum of variance, mean pairwise distance, range of variation etc. It is widely known that this sort of disparity is robust against sample size and is not seriously affected by a nonselective extinction, whereas selective extinctions should readily reduce the disparity. On the other hand, another aspect of disparity is morphological richness, which is assessed through compilations of the number of character states; e.g., number of pairwise character-state combinations and number of morphospace divisions occupied by observation. Unlike the morphological dissimilarity, the morphological richness appears to be fairly sensitive to nonselective extinctions as well as to selective ones.

The comparison among the diversity measures based on the morphometric data obtained from the ammonoids revealed that the patterns of disparity change were totally different between dissimilarity and richness, while comparison within the same categories tended to indicate a consistent result. This result suggests that comparison between morphological dissimilarity and morphological richness provides a powerful tool to assess the selectivity of an extinction event.

Keywords: disparity, biodiversity, morphological dissimilarity, morphological richness

Japan Geoscience Union Meeting 2014
(28 April - 02 May 2014 at Pacifico YOKOHAMA, Kanagawa, Japan)

MIS25-P01 Room:Poster Time:April 28 18:15-19:30

Is the growth hiatus of ferromanganese crusts a local or global event?

NOZAKI, Tatsuo[1*] ; GOTO, Kosuke T.[2] ; TOKUMARU, Ayaka[3] ; TAKAYA, Yutaro[4] ; SUZUKI, Katsuhiko[1] ; CHANG, Qing[1] ; KIMURA, Jun-ichi[1] ; KATO, Yasuhiro[4] ; SHIMODA, Gen[2] ; TOYOFUKU, Takashi[5] ; USUI, Akira[6] ; URABE, Tetsuro[3]

[1]JAMSTEC/IFREE, [2]AIST/GSJ, [3]Univ. of Tokyo, [4]Univ. of Tokyo, [5]JAMSTEC/BIOGEOS, [6]Kochi Univ.

Recent applications of an Os isotope dating method revealed that some ferromanganese crusts collected from the Pacific Ocean might have experienced the growth hiatus. However, it is still controversial whether this growth hiatus was a local or global event. In the present study, we discuss the geological trigger of this growth hiatus based on our results of the Os isotope dating on various ferromanganese crust samples collected from Northwestern Pacific, South Atlantic Oceans and Philippine Sea.

Keywords: ferromanganese crust, Os isotope, geochemistry, growth hiatus, paleoceanography

Japan Geoscience Union Meeting 2014
(28 April - 02 May 2014 at Pacifico YOKOHAMA, Kanagawa, Japan)

MIS25-P02 Room:Poster Time:April 28 18:15-19:30

Sedimentation rate of the end-Permian to earliest Triassic black claystone strata in the Panthalassic deep-sea

TAKAHASHI, Satoshi[1*] ; YAMAGUCHI, Asuka[2] ; YAMAKITA, Satoshi[3] ; MIZUTANI, Akane[1] ; ISHIDA, Jun[1] ; YAMAMOTO, Shinji[1] ; IKEDA, Masayuki[4] ; OZAKI, Kazumi[2] ; TADA, Ryuji[1]

[1]Department of Earth and Planetary Science, the University of Tokyo, [2]Atmosphere and Ocean Research Institute, the University of Tokyo, [3]Department of Earth Science, Faculty of Culture, Miyazaki University, [4]Department of Earth Sciences, Graduate School of Science and Engineering, Ehime University

The greatest mass extinction occurred at the end-Permian, its aftermath continued during following Early Triassic. This period, especially interval between the end-Permian and Induan is characterized by occurrences of the black claystone in the pelagic deep-sea depositional area where now locate in Japan and western North America etc. This black claystone generally contains high organic matter and few silicic fossils, in contrast that bedded chert before the mass extinction event has few organic matter and abundant radiolarian tests. Detailed background of this black claystone has not been fully understood due to the scarcity of well-preserved lithologic sequences. Herein, we show preliminary achievement on continuous black claystone strata based on the one of most continuous Permian-Triassic Boundary section (Akkamori-2 section; Takahashi et al., 2009).

We polished the outcrops of the study section using hand grinders with diamond-blades and diamond-polishing pad for observation of sedimentary facies and structures. Observing the outcrop, structural geology examination was conducted (See Yamaguchi et al. in this session). Using their results, we divided the outcrop into 20 subsections that preserve continuous lithologic stratigraphy. Then, high-resolution lithologic column was reconstructed from these subsections.

After careful observation on the polished surface of the outcrop, we found many key bed layers. For instances, dolomitic layers, light and dark grey colored siliceous claystone interbeded within black claystone, and alternations of black and grey colored claystones. Using these key beds, we correlated the lithologic columns from each subsection. In the case of that useful key beds were not found, we simply built the columns up, because no duplication of strata was recognized. After these processes, totally ca. 10 m thick lithologic column of black claystone was reconstructed. Its lower most horizon accords to carbon isotopic negative excursion (Takahashi et al., 2010) coinciding with the main mass extinction event, ca. 252.2 Ma (U-Pb dating by Shen et al., 2011). Meanwhile, in the thick grey-color siliceous claystone horizon from uppermost part of the strata, conodont fossils of Neospathodus waageni and Eurygnathodus costatus were recovered. This combination indicates lowest Smithian. After interpolation by Geologic Time Scale 2012 (Gradstein et al., 2012), beginning of Smithian (end of Induan) is ca. 250.0 Ma. Using these absolute ages, sedimentation rate of black claystone is calculated 4.34mm/kyr (= 10000 mm /2300 kyr). This calculation is still comprehensive. Also, we can calculate the sedimentation rate in another way using the earliest Triassic conodont occurrence of Hindeodus parvus in the 7.5 m above the base of black claystone. The first occurrence horizon is estimated to be 252.3Ma in the type section of Permian-Triassic Boundary (Shen et al., 2011). The calculated sedimentation rate of black claystone in this way is 7.5 mm/kyr (750 mm/100 kyr). As the fossil age is uncertain between the basal 7.5 m interval, this is a maximum estimation. These two results of sedimentation rate indicate that the black claystone beds were accumulated in several millimetres per a thousand year. This rate is in similar class of sedimentation rate of radiolarian chert deposited before and after the black claystone deposition. In fact, recent study of Ikeda et al. (2010) concluded several centimetres thick one chert-clay couplet accords about 20 kyr. The sedimentation rate of the black claystone as similar as silicic fossil rich bedded chert before mass extinction event implies that some materials increased into the pelagic deep-sea at and after the extinction event instead of significantly decreased radiolarian tests (Takahashi et al., 2009). Possible materials are terrigenous clastic material (Algeo and Twitchett, 2009; Sakuma et al., 2012) and very fine silicic biotic crust (such as silicic sponges).

Keywords: Permian, Triassic, pelagic deepsea, black claystone, mass extinction

Japan Geoscience Union Meeting 2014
(28 April - 02 May 2014 at Pacifico YOKOHAMA, Kanagawa, Japan)

MIS25-P03 Room:Poster Time:April 28 18:15-19:30

Stratigraphy and formation process of Late Cretaceous pelagic sediments in the Wadi Hilti area of the Oman Ophiolite

AGUI, Yumi[1*] ; HARA, Kousuke[1] ; KURIHARA, Toshiyuki[1]

[1]Graduate School of Science and Technology, Niigata University

The Oman Ophiolite consists of mantle peridotites, gabbros, a sheeted dyke complex, and basaltic lavas. The extrusive rocks have been subdivided into three volcanic units: the V1 lava with the N-MORB signature, the V2 lava formed by intra-oceanic volcanism, and the V3 lava generated by intra-plate seamount magmatism (Ernewein et al., 1988). Pelagic sediments commonly occur at the boundaries between these volcanic units. Thick sediments upon the V1 lava in the Wadi Jizzi area are subdivided into the Suhaylah and Zabyat formations; the former is composed of metalliferous and fine-grained pelagic sediments of Cenomanian-Santonian? age, and the latter consists of conglomerate derived mainly from a collapsed oceanic crust during the thrusting stage (Fleet and Robertson, 1980; Tippit et al., 1981; Woodcock and Robertson, 1982; Robertson and Woodcock, 1983).

The V2 and V3 lavas are widely distributed in the Wadi Hilti area, about 25 km west of Sohar, northern Oman Mountains. Recently, the eruption and emplacement mechanism of the V3 lava has been studied by Umino (2012). Pelagic sediments, about 50 m thick at a maximum, overlie the V2 lava and are covered by the V3 lava. The sediments also occur on and within the V3 lava. Based on our field examination for several sections in the Wadi Hilti area, the stratigraphy of the pelagic sediments on the V2 lava consists of metalliferous sediments, micritic limestone, red mudstone, conglomerate, V3 lava, and siliceous mudstone, in ascending order. We first found conglomerate containing gravels of lavas and pelagic cherts from this area. From fine-grained pelagic sediments on the V2 and V3 lavas, we obtained *Rhopalosyringium scissum* O'Dogherty and *Hemicryptocapsa polyhedra* Dumitrica that can be assigned to a Turonian age (O'Dogtherty, 1994). In addition, *Rhopalosyringium petilum* (Foreman) and *Guttacapsa biacta* (Squinabol) were recovered from a block of siliceous mudstone probably within the conglomerate. According to O'Dogtherty (1994), the co-occurrence of these species is restricted to be middle to late Cenomanian.

Based on these age assignments, the fine-grained pelagic sediments on the V2 lava (metalliferous sediments, micritic limestone, and red mudstone) in the Wadi Hilti area can be correlated with the Turonian part of the Suhaylah Formation in the Wadi Jizzi area. This reveals that the activity of the V2 lava was terminated in Turonian. The conglomerate and the siliceous mudstone on the V3 lava are correlated with the Zabyat Formation, indicating that the eruption of the V3 lava occurred in Turonian. These age constraints for basaltic extrusive rocks imply that the tectonic setting from subduction to oceanic-thrusting changed rapidly in a short period of Turonian time.

Keywords: Oman Ophiolite, pelagic sediments

Japan Geoscience Union Meeting 2014
(28 April - 02 May 2014 at Pacifico YOKOHAMA, Kanagawa, Japan)

MIS25-P04 Room:Poster Time:April 28 18:15-19:30

Stratigraphy and radiolarian age of the Zabyat Formation at Lasail section in the Wadi Jizzi area, Oman Ophiolite

HAYASHI, Rina[1] ; HARA, Kousuke[2] ; KURIHARA, Toshiyuki[2*]

[1]Department of Geology, Faculty of Science, Niigata University, [2]Graduate School of Science and Technology, Niigata University

The Oman Ophiolite consists of mantle peridotites, gabbros, a sheeted dyke complex, and extrusive lavas overlain by pelagic sediments. The basaltic extrusive rocks have been subdivided into three volcanic units (the V1, V2, and V3 lavas) (Ernewein et al., 1988). The overlying pelagic sediments, named the Suhaylah Formation, consist of metalliferous and fine-grained calcareous sediments of Cenomanian-Santonian? age (Fleet and Robertson, 1980; Tippit et al., 1981). The Zabyat Formation, which covers conformably the Suhaylah Formation, is composed of conglomerate derived mainly from a collapsed oceanic crust during the thrusting stage (Woodcock and Robertson, 1982; Robertson and Woodcock, 1983). Although Robertson and Woodcock (1983) investigated the sedimentation process of this formation, they did not study the biostratigraphic age of fine-grained sediments intercalated with conglomerate at Lasail section in the Wadi Jizzi area.

At Lasail section, the stratigraphy of the Zabyat Formation consists of the lower conglomerate interbedded with micritic limestone and red mudstone and the upper red mudstone and siliceous mudstone. The micritic limestone of the lower part contains *Alievium superbum* and *Rhopalosyringium scissum*, indicating Turonian in age (O'Dogtherty, 1994). From the red mudstone of the upper part, we obtained *Pseudoaulophacus lenticulartus*, *Pseudoaulophacus praefloresensis*, and *Theocampe salillum*. The occurrence of these species assigns the upper part of the Zabyat Formation to Coniacian (Pessagno, 1976; Bandini et al., 2008). Our biostratigraphic result of the Zabyat Formation, taken together with that of the Suhaylah Formation, shows that the change of the tectonic setting from mid-ocean ridge through subduction zone to oceanic thrusting occurred in a short period (c.a. 4 m.y.) of latest Cenomanian to Coniacian time.

Keywords: Oman Ophiolite, pelagic sediments

Japan Geoscience Union Meeting 2014
(28 April - 02 May 2014 at Pacifico YOKOHAMA, Kanagawa, Japan)

MIS25-P05 Room:Poster Time:April 28 18:15-19:30

Deformational features of Permian-Triassic boundary preserved within an on-land accretionary complex

YAMAGUCHI, Asuka[1*] ; TAKAHASHI, Satoshi[2] ; YAMAKITA, Satoshi[3]

[1]Atmosphere and Ocean Research Institute, the University of Tokyo, [2]Department of Earth and Planetary Science, the University of Tokyo, [3]Faculty of Education and Culture, University of Miyazaki

Pelagic siliceous sediment covering on oceanic crust is one of the components in subduction plate boundaries where old oceanic plate subduct. Its mechanical, frictional and fluid transport properties are key to understand faulting and earthquake mechanics in such settings (Kimura et al., 2012; Yamaguchi et al., this meeting). Plate boundary deformations are strongly affected by inhomogeneity of incoming sediments: in the case of Jurassic accretionary complex in Japan (Mino-Tanba belt), siliceous/black claystone at Permian-Triassic boundary horizon within bedded chert functioned as plate boundary decollement, and only Triassic-Jurassic chert is preserved in the complex, whereas Carboniferous-Permian chert is lacking (Nakae, 1993). However, few outcrops in the Jurassic accretionary complex comprise continuous sections across Permian-Triassic boundary. To understand the limitation of lithology-controlled deformations, we investigated structural analysis of the Permian-Triassic boundary section in the North Kitakami Belt (Akkamori-2 section; Takahashi et al., 2009), where the most continuous Permian-Triassic boundary is observed.

Permian gray-color siliceous claystone to Triassic gray-color siliceous claystone through black claystone is successively observed in this outcrop (lithology detail: see Takahashi et al., this session). Orientations of 36 bedding dips, 90 low-angle cleavages, 17 high-angle cleavages, and 22 faults are measured from the outcrop. Strikes of bedding and low-angle cleavage vary NW-SE to NE-SW, gently dip eastward. Faults have two populations: one is subparallel to bedding and low-angle cleavage; the other is dipping gently to the north. Shear sense of the faults is unclear because of the lack of shear sense indicators due to intense development of overprinting high-angle cleavage.

In contrast to the scattered orientations of low-angle cleavage, strike of high-angle cleavage is limited to N40-70E with subvertical dip. The high-angle cleavages are recognized as axial plane cleavage of map-scale Hiraniwa-dake Syncline (Sugimoto, 1974) striking NW-SE and plunging southeastward, since the studied section is located nearby the axis of the syncline. Orientations of bedding, low-angle cleavage, and fault would be also rotated by secondary-order outcrop-scale open folds.

Hiraniwa-dake syncline involves several chert-clastics sequences in this region (Ehiro, 2008). Substracting fold-related deformations, bedding-parallel cleavages and low-angle faults (likely to be thrust) are only initial deformations observed in the studied outcrop. Those deformational features are also typical in off-scraped and underthrusted accretionary complex (Kimura and Hori, 1993, Raimbourg et al., 2009). Lack of intense deformation in the black claystone suggests that not only lithology-controlled physical properties but other factors (e.g. topographic and thermal effects) would be also important to constrain the position where decollement develops.

Keywords: Permian-Triassic Boundary, subduction zone, accretionary complex, Deformation structure

Japan Geoscience Union Meeting 2014
(28 April - 02 May 2014 at Pacifico YOKOHAMA, Kanagawa, Japan)

MIS26-01 Room:422 Time:April 29 09:00-09:15

Magnetosphere-Ionosphere coupling events and Atmospheric electricity at Syowa station, Antarctica

MINAMOTO, Yasuhiro[1*] ; KADOKURA, Akira[2] ; KAMOGAWA, Masashi[3]

[1]Kakioka Magnetic Observatory, Japan Meteorological Agency, [2]National Institute of Polar Research, [3]Department of Physics, Tokyo Gakugei University

At Syowa Station(69.0S, 39.6E), located on East Ongul Island near the continent of Antarctica, atmospheric electric field observation has been carried out with an electric field mill. We extracted 'fair-weather' electric field data over six years, from 2006 to 2012. We considered the 'fair-weather' electric field data and Geomagnetic field by comparison, and found an event which suggests variations of electricity in ionosphere caused by magnetosphere-ionosphere coupling. In this presentation, we will show atmospheric electric field, aurora activity, HF radar, etc. during the event, and discuss the influence of Solar-Terrestrial environment on atmospheric electricity.

Keywords: fair-weather, Antarctica, atmospheric electricity, Magnetosphere-Ionosphere coupling, global circuit

Japan Geoscience Union Meeting 2014
(28 April - 02 May 2014 at Pacifico YOKOHAMA, Kanagawa, Japan)

MIS26-02 Room:422 Time:April 29 09:15-09:30

Changes in atmospheric electricity over about eighty years

HIRAHARA, Hideyuki[1*] ; MINAMOTO, Yasuhiro[1]

[1]Kakioka Magnetic Observatory

The Japan Meteorological Agency has observed atmospheric electric field at Kakioka magnetic observatory (KMO) since 1929. This observation has been carried out by a water-dropper instrument without replacing. Meteorological observations at KMO stopped in 1997, and fair-weather days of atmospheric electricity have been extracted from data of atmospheric electricity itself and precipitations. We extracted clear weather days with weather satellite images and all-sky photos at KMO, and derived diurnal variation of the atmospheric electric field in calm days. In this presentation, we will show the diurnal curve at present and past, from 1931 to 1935, and discuss changes in atmospheric electricity over about eighty years.

Keywords: atmospheric electricity, diurnal variation, fair weather, water dropper, cloud grid information

Japan Geoscience Union Meeting 2014
(28 April - 02 May 2014 at Pacifico YOKOHAMA, Kanagawa, Japan)

MIS26-03 Room:422 Time:April 29 09:30-09:45

Snow electrification observed at Memanbetsu

KAMOGAWA, Masashi[1*] ; KADOKURA, Akira[2] ; MINAMOTO, Yasuhiro[3] ; SATO, Mitsuteru[4] ; SAITO, Shogen[1]

[1]Dpt. of Phys., Tokyo Gakugei Univ., [2]National Institute of Polar Research, [3]Kakioka Magnetic Observatory, Japan Meteorological Agency, [4]Department of Cosmoscience, Hokkaido University

We investigate the snow electrification observed at Memanbetsu. In this presentation, we report a preliminary analysis of atmospheric data observed in Memanbetsu.

Keywords: Atmospheric electric field, Snow electrification

Japan Geoscience Union Meeting 2014
(28 April - 02 May 2014 at Pacifico YOKOHAMA, Kanagawa, Japan)

MIS26-04 Room:422 Time:April 29 09:45-10:00

Spatio-temporal characteristics of subionospheric perturbations associated with annular solar eclipse

INUI, Daiki[1*] ; HOBARA, Yasuhide[1]

[1]Graduate School of Informatics and Communication Eng., The University of Electro-Communications

In this paper, we analyse UEC's VLF/LF transmitter observation network data associated with annular solar eclipse in 2012. Clear temporal dependences of the VLF amplitude are observed by various transmitter-receiver paths. Numerical computations of VLF/LF signals with the ionospheric perturbations due to the solar eclipse are carried out by using 2D-FDTD method. As a result, temporal variations of the VLF/LF amplitude are in rather good agreement with those from the numerical modeling.

Keywords: Annular solar eclipse, Ionospheric perturbations, VLF radio waves, FDTD method

Japan Geoscience Union Meeting 2014
(28 April - 02 May 2014 at Pacifico YOKOHAMA, Kanagawa, Japan)

MIS26-05 Room:422 Time:April 29 10:00-10:15

Electrical characteristics of the lightning discharges generating long-recovery VLF events

YAMASHITA, Junpei[1*] ; HOBARA, Yasuhide[1]

[1]Graduate School of Informatics and Communication Eng., The University of Electro-Communications

In this paper, we focus on the special type of early/fast VLF event so-called long-recovery VLF event to study its generation mechanism. We identify many long-recovery VLF events by using UEC's VLF/LF transmitter signal receiving network. Electrical properties of causative lightning discharges of the long-recovery events are presented based on both the peak current and electrical charge moment changes by the ELF waveform observations.

Keywords: long-recovery event, ionospheric perturbations, charge moment, early/fast event, lightning discharge

Japan Geoscience Union Meeting 2014
(28 April - 02 May 2014 at Pacifico YOKOHAMA, Kanagawa, Japan)

MIS26-06 Room:422 Time:April 29 10:15-10:30

Signature of subionospheric LF wave perturbations associated by Hokuriku winter lightning observed at the Zao station

MORINAGA, Yosuke[1*] ; TSUCHIYA, Fuminori[1] ; OBARA, Takahiro[1] ; MISAWA, Hiroaki[1]

[1]Planetary Plasma and Atmospheric Research Center,Tohoku University

Intense electromagnetic pulses (EMP) radiated from lightning discharge could cause heating and ionization and alter the conductivity in the ionospheric D-region. Quasi-electrostatic fields (QE Fields) which are generated due to the removal of electric charge could also affect it. The purpose of this study is to reveal influence of the lightning on the lower ionosphere and its dependence on properties of lighting discharges. The VLF/LF signature of subionospheric perturbations associated with winter lightning in the Sea of Japan (around Hokuriku) has been observed during December 16-31, 2009. LF (60kHz) radio observation was made at Zao (Miyagi) for Haganeyama JJY transmitter (border between Saga and Fukuoka) whose great circle path (GCP) passes over the coast area of Hokuriku. The amplitude and phase of the JJY signal are recorded every 0.1 seconds. In addition to the subionospheric LF observation, lightning locations are determined by a lightning location network (WWLLN). The number of total lightning event identified in the area of 35-37 degrees N and 134-137 degrees E is 1002. Based on the LF observation, subionospheric perturbations which occur immediately after the causative lightning (early event) were detected. The number of the total detection of the early event in the selected area is 72. Early events identified will be compared with peak current and charge moment of the causative lighting which are derived from LF and ELF waveform observations, respectively, to investigate the relation between early event properties and magnitude of EMP and QE fields.

Keywords: lightning, subionospheric perturbations, electromagnetic pulses, quasi-electrostatic fields

Japan Geoscience Union Meeting 2014
(28 April - 02 May 2014 at Pacifico YOKOHAMA, Kanagawa, Japan)

MIS26-07 Room:422 Time:April 29 10:30-10:45

Generating position identification of high-energy radiation associated with the summer thundercloud

SHOJI, Tomomi[1*] ; SAITO, Shogen[1] ; KAMOGAWA, Masashi[1] ; TORII, Tatsuo[2]

[1]Dpt. of Phys., Tokyo Gakugei Univ., [2]Japan Atomic Energy Agency

We perform the observation on the Fuji mountaintop in the summer from 2008 to elucidate mechanism of the high energy radiation of the thundercloud origin. This presentation is the result of observation in 2013.

Keywords: thundercloud, high-energy radiation, Mt. Fuji

Japan Geoscience Union Meeting 2014
(28 April - 02 May 2014 at Pacifico YOKOHAMA, Kanagawa, Japan)

MIS26-08 Room:422 Time:April 29 11:00-11:15

Development of broadband lightning monitoring system and its application

YOSHIDA, Satoru[1*] ; WU, Ting[2] ; USHIO, Tomoo[2] ; KENICHI, Kusunoki[1]

[1]Meteorological Research Institute, [2]Graduate school of Engineering, Osaka University

We have been designing and developing Broadband Observation network for Lightning and Thunderstorm (BOLT) in Kinki area to study lightning discharges and thunderstorms. The BOLT consists of 11 sensors which detect LF radiation form lightning discharge and locate emission sources in 3D. We have been developing both hard ware and algorithm to locate lightning so that the BOLT produces detail progression of lightning discharges, including stepped leader and negative recoil leader in negative charge region. In this presentation, we show clear 3D BOLT images of lightning discharges and compare the results with VHF source locations.

Keywords: lightning discharge, thundercloud monitoring, remote sensing

Japan Geoscience Union Meeting 2014
(28 April - 02 May 2014 at Pacifico YOKOHAMA, Kanagawa, Japan)

MIS26-09 Room:422 Time:April 29 11:15-11:30

Simultaneous observations of VHF waves and optical emissions for lightning from the International Space Station

KIKUCHI, Hiroshi[1*] ; MORIMOTO, Takeshi[2] ; USHIO, Tomoo[1] ; SATO, Mitsuteru[3] ; YAMAZAKI, Atsushi[4] ; SUZUKI, Makoto[4]

[1]Osaka University, [2]Kinki University, [3]Hokkaido University, [4]Japan Aerospace eXploration Agency

Since Novenber 2012, Global Lightning and sprIte MeaSurements (GLIMS) mission has been conducted on Exposed Facility of Japanese Experiment Module (JEM-EF) of the international space station (ISS) which is orbiting the earth at an altitude 400 km. The VHF broadband digital interferometer (VITF) attached on JEM-EF is designed to estimate the direction of arrival of electromagnetic waves. The VITF has th bandwidth from 70 MHz to 100 MHz. The VITF consists of two antennas, band-pass filters, amplifiers, and 2-channel-AD-converter. The electromagnetic radiations from lighting discharges received by the antennas are digitized by the AD converter synchronizing with another channel through the filters and the amplifiers. The band-pass filter and the amplifier of the VITF are exactly the same as the ones of the VHF sensor on Maido-1 satellite. The basic specification and most of devices in the AD converter of VITF.

In previous study, the Array of Low Energy X-ray Imaging Sensors (ALEXIS) satellite (1993) had a high-speed VHF receiver/digitizer (Blackbeard) for studying the effect of lightning and electromagnetic impulse from lightning and other man-made noise, which means TV and FM carrier interference. Furthermore, the Blackbeard reported the unique characteristics of VHF waves radiated from lightning known as transionospheric pulse pairs (TIPP). In 1997, the Fast On-orbit Rapid Recording of Transient Events (FORTE) satellite recorded many VHF pulses associated with lightning discharges.

The observation results of the VITF of the JEM-GLIMS mission were described. As a case study, the lightning event captured by the two optical sensors (photometers and CMOS sensor) was analyzed. In these events, the waveform data of VITF were used to estimate the arrival direction of EM waves. There are two methodologies which are the interferometry technic and the group delay characteristic of EM waves. We compared the results of direction of arrival estimation with CMOS sensor data. The results agreed with the position of the lightning emission captured by the CMOS sensor. We also compared the results of VITF with that of the photometers in order to find the temporal relationship. The results indicated that the frequency of the VHF radiations recorded with the VITF had a positive relationship with optical waveform captured with the photometers.

Keywords: lightning, radio wave propagation, VHF waves

Japan Geoscience Union Meeting 2014
(28 April - 02 May 2014 at Pacifico YOKOHAMA, Kanagawa, Japan)

MIS26-10 Room:422 Time:April 29 11:30-11:45

Magnetotelluric measurements of volcanic lightning at Sakurajima, Japan

AIZAWA, Koki[1*] ; YOKOO, Akihiko[2]

[1]Institute of Seismology and Volcanology, Kyushu University, [2]Aso Volcanological Labotatory , Kyoto University

Magnetotelluric (MT) method uses the natural electromagnetic (EM) field variation to image subsurface resistivity structure, and usually involves measuring two horizontal electric field components (Ex and Ey) and three magnetic field components (Bx, By, and Bz) at the Earth's surface, where the subscripts x and y indicate the N?S and E?W directions, respectively. In the MT data recorded 3 km away from the active crater of Sakurajima volcano, pulse-like signals that synchronize with the volcanic lighting are frequently observed within 3 minutes from the eruption onset (Aizawa et al. 2010). However the sampling rate on that paper was so low as 15 Hz that the physical properties of volcanic lightning, such as waveform of EM radiation, amplitude of electric current, and its duration, were not investigated.

In the presentation, we show the result from the temporal MT observation with the sampling rate of 65 kHz. The MT data were recorded at two sites approximately 3km away from the active crater between October 27 and November 6, 2013. The preliminary analysis shows the following features of volcanic lightning;

(1) There are two types of discharges. One is the assemblage of several pulses. Another is the EM burst that continues several ms.

(2) The duration of each pulse in the assemblage type is short as a few tens of micro seconds, but its amplitude is far strong than that of EM burst.

(3) Regarding the discharges of the pulse type, there are examples that the first discharge is weaker than the second and third discharges.

The points of (1) and (2) are similar to the lightning in the thundercloud. However, its duration is approximately 1/10˜1/100 of that of thundercloud. In addition, we will show the data of physical unit (mv/Km and nT) which was recovered by incorporating the frequency response of the logger and induction coil, and will closely investigate the relationship between MT signals and the corresponding lighting movie. In addition, the 32 Hz MT data since December 2011 will be presented.

References

Aizawa, K., A. Yokoo, W. Kanda, Y. Ogawa, and M. Iguchi (2010), Magnetotelluric pulses generated by volcanic lightning at Sakurajima volcano, Japan, Geophysical Research Letters, 37, L17301, doi:10.1029/2010GL044208.

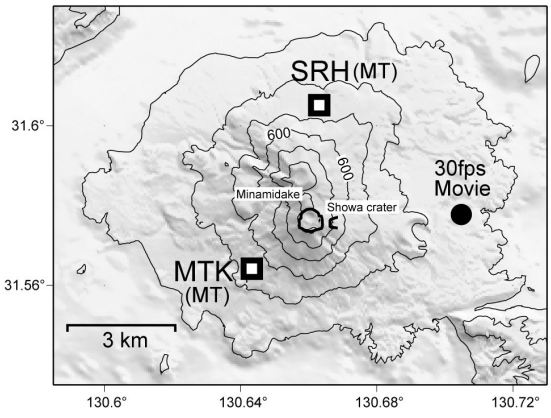

Fig.1

Japan Geoscience Union Meeting 2014
(28 April - 02 May 2014 at Pacifico YOKOHAMA, Kanagawa, Japan)

MIS26-11 Room:422 Time:April 29 11:45-12:00

Pressure field of a tornado observed by POTEKA project

KOBAYASHI, Fumiaki[1*] ; NOROSE, Keiko[1] ; KURE, Hirotaka[2] ; MORITA, Toshiaki[2]

[1]Dep. Geoscience National Defense Academy, [2]Meisei Electric co.,ltd

A tornado event, which occurred in Midori city Gunma prefecture on 16 September 2013, was observed by the fine-mesh surface weather station network named as POTEKA. The pressure field around the tornado revealed the pressure dip pattern at the time of the wind damage and useful for the judgement of the cause of wind damage.

Keywords: surface weather station, tornado, downburst, gust front

Japan Geoscience Union Meeting 2014
(28 April - 02 May 2014 at Pacifico YOKOHAMA, Kanagawa, Japan)

MIS26-12 Room:422 Time:April 29 12:00-12:15

Discrimination between downburst and gust-front by the surface dense observation network POTEKA

NOROSE, Keiko[1*] ; KOBAYASHI, Fumiaki[1] ; KURE, Hirotaka[2] ; MORITA, Toshiaki[2]

[1]National Defense Academy, [2]Meisei Electric

On the evening of 11 August 2013, a severe thunderstorm passed over the Takasaki and Maebashi city, Gunma prefecture, and produced gusty wind damages. The change of surface weather elements was recorded by dense observation POTEKA when gust occurred. In this study, we follow the development and propagation of gust-front and downburst through the analysis of features of pressure field observed by POTEKA. The result of this analysis reveals that the reason of gust caused damages in Maebashi city is downburst.

Japan Geoscience Union Meeting 2014
(28 April - 02 May 2014 at Pacifico YOKOHAMA, Kanagawa, Japan)

MIS26-13 Room:422 Time:April 29 12:15-12:30

Doppler Observation of Cumulonimbus Turret Generation by 95GHz Cloud Radar in Boso Peninsula on 30 August 2012

KASHIWAYANAGI, Taro[1*] ; KOBAYASHI, Fumiaki[2] ; OKUBO, Takumi[2] ; YAMAJI, Mika[2] ; TAKANO, Toshiaki[3] ; TAKAMURA, Tamio[4]

[1]Center for Environmental Remote Sensing, Chiba University/Japan Radio Co., Ltd., [2]National Defense Academy, [3]Graduate School of Engineering, Chiba University, [4]Center for Environmental Remote Sensing, Chiba University

Simultaneous observations of cumulonimbus turrets using a 95GHz W-band cloud radar, an X-Band radar, the MTSAT-1R rapid scan and photogrammetry were held during the summer in 2012 in Kanto Region, Japan to understand the convection initiation and the structure of cumulonimbus turrets. During these observations, the cloud radar was installed in the middle of Boso Peninsula, where cumuli and cumulonimbi frequently generate in mid-summer season.

Cumulonimbus turrets were developed above the W-band cloud radar after 12:30 on 30 August 2012. The turrets continued development and degeneration for two hours above the radar. In a previous study, we have shown the Doppler analysis by X-band radar which indicated convergence of horizontal winds below 1.5 km around the cloud radar site at the initiation of the first cumulonimbus turret generation.

In this presentation, we show the vertical Doppler analysis result of the cloud radar at the initiation of the cumulonimbus turret generation. The result indicates the existence of a strong updraft of over 6 m/s at the initiation of the first cumulonimbus turret generation.

Keywords: cumulonimbus, turret, cloud radar, Doppler

Japan Geoscience Union Meeting 2014
(28 April - 02 May 2014 at Pacifico YOKOHAMA, Kanagawa, Japan)

MIS26-P01 Room:Poster Time:April 29 18:15-19:30

Surface Temperature and Pressure Distributions of Downburst captured by High Dense Ground Observation Network ”POTEKA”

KOJIMA, Shinya[1*] ; SATO, Kae[1] ; MAEDA, Ryota[1] ; KURE, Hirotaka[1] ; YADA, Takuya[1] ; MORITA, Toshiaki[1] ; IWASAKI, Hiroyuki[2]

[1]Meisei Electric co., ltd, [2]Faculty of Education, Gunma University

Meisei developed low-cost compact weather sensor (POTEKA Sta., hereinafter referred to as the POTEKA), which can measure temperature, relative humidity, pressure, sunlight, and rain detection per one minute and achieve higher density weather observation system economically. We installed economical and high dense ground observation network (total 55 stations, 1.5˜4 km-mesh) in Gunma, Japan. This paper presents observation of wind gust phenomena around Takasaki city and Maebashi city on 11 August 2013.

The wind gust occurred from Takasaki thru Maebashi city around 18:00 JST and caused damages to private houses. Temperature changes obtained from POTEKA network show that surface temperature dropped by up to 13.9 deg. C in 12 minutes.

The following figure exhibits the change of sea surface pressure calculated from POTEKA around the gust pathway reported by JMA (Maebashi). Although pressure at Maebashi station increased gradually with 10 minutes resolution, pressure jumps of 1-2 hPa were recorded at POTEKA with one minute resolution, indicating that the temporal high pressure was caused by downburst downflow. Beside, two pressure jump can be found at some stations. The first and second jumps are coincided with gust fronts and down flow of downburst, respectively (Discrimination between downburst and gust-front by the surface dense observation network POTEKA).

Local weather observation network consisting of POTEKA succeeded in capturing the change of surface pressure caused by gust wind phenomena with unprecedented spatio-temporal resolution, which enables us not only to distinguish between gust fronts and downbursts but also to detect such wind phenomena earlier.

Acknowledgments: The authors would like to thank SANDEN Corporation, SAVE ON, and Board of Education of Isesaki city for support POTEKA project.

Keywords: high dense ground observation network, Downburst, Gust fronts

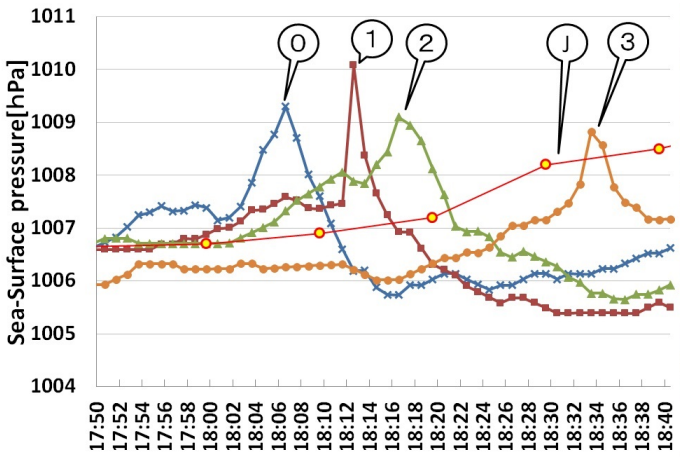

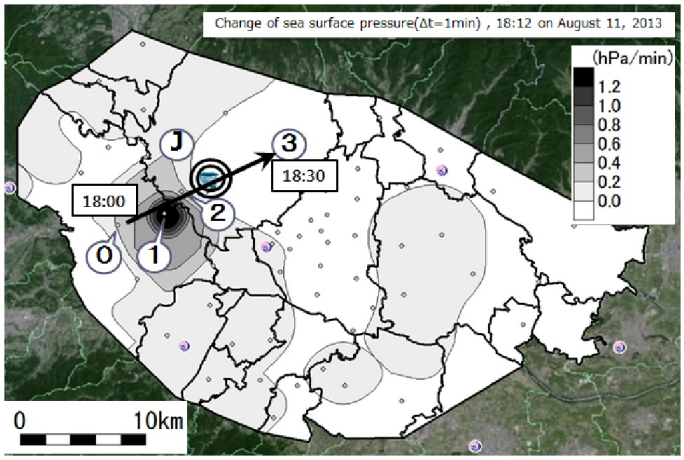

Japan Geoscience Union Meeting 2014
(28 April - 02 May 2014 at Pacifico YOKOHAMA, Kanagawa, Japan)

MIS26-P02 Room:Poster Time:April 29 18:15-19:30

Preliminary Reports of Summer Sprite Observation Campaign at Summit of Mt. Fuji, Japan

SUZUKI, Yuko[1*] ; SUZUKI, Tomoyuki[1] ; KAMOGAWA, Masashi[1]

[1]Dpt. of Phys., Tokyo Gakugei Univ

Many investigations of transient luminous events (TLEs) such as sprites and elves have been carried out since the 1990s. However, there are still unsolved issues like the morphologies of sprites. One of approach to investigate this issue is statistical study with collecting many events. In this study, we report a preliminary result of a mountain observation which enables us to observe the TLEs for a long term at the fixed point. The mountain observation was conducted at the summit of Mt. Fuji (3776 meter altitude), Japan, which enables us to detect the TLEs above off the coast of Boso peninsula, Chiba, Japan and the coast of Japan Sea which a large number of summer TLEs and the winter TLEs due to energetic positive cloud-to-lighting occurs. In particular, the altitude of the summit is located over the summer cloud covering the wide regions, so that the distant TLEs can be observed and low pressure and clean air yield better color images of TLEs. Moreover, the lower cost operation is possible, comparing with than the aerial and balloon measurement.

In the summer of 2013, we detected several events of TLEs with sensitive black-and-while CCD cameras at the fixed point for one month and with the color single-lens reflex camera. We will show the detailed analysis in the presentation. Such a mountain observation gives us a high chance to detect low-altitude blue-jets and starters and a 360-degree view from the isolated mountain, Mt. Fuji, also gives us a high change to detect a number of TLEs. In this presentation, we show the results of sprite images taken at the summit of Mt. Fuji on Aug. 2, 2014.

Keywords: Sprite, Lightning, TLEs

Japan Geoscience Union Meeting 2014
(28 April - 02 May 2014 at Pacifico YOKOHAMA, Kanagawa, Japan)

MIS26-P03 Room:Poster Time:April 29 18:15-19:30

Development of polarimetric 2-D phased array weather radar using minimum mean square error method

KIKUCHI, Hiroshi[1*] ; WU, Ting[1] ; USHIO, Tomoo[1] ; SHANG, Jin[1] ; KIM, Gwan[1] ; GOTO, Hideto[2] ; MIZUTANI, Humihiko[2]

[1]Osaka University, [2]Toshiba

We have been developing a polarimetric 2-D phased array weather radar which detects small scale phenomena such as tornadoes and downbursts. In this paper, we compare Beam Former method (BF), which is a conventional method in Digital Beam Forming signal processing of array antenna, with Minimum Mean Square Error method (MMSE), which is our proposed method, and discuss simulation results estimated by each method. In BF, antenna pattern is uniform and unique in the radar system, and its sidelobe level is high. As a result, if there are obstacles, for example high building, or very heavy rain area, the observation results of array antenna is imprecision in the region near them. In contrast, we can turn the null-point to interference wave direction at the same time we turn the mainlobe to the desired signal direction in MMSE.

Keywords: phased array radar, MMSE

Japan Geoscience Union Meeting 2014
(28 April - 02 May 2014 at Pacifico YOKOHAMA, Kanagawa, Japan)

MIS27-01 Room:423 Time:May 2 14:15-14:30

Metal Flux of Ferromanganese from Northwest and Equatorial Pacifc

HISAAKI, Sato[1*] ; USUI, Akira[1] ; NAKASATO, Yoshio[1] ; NISHI, Keisuke[1] ; IAN, Graham[2]

[1]Department of Integrated Arts and Sciences, Kochi university, [2]GNS science

The hydrogenetic ferromanganese crust is a slowly-growing chemical sedimentary rock composed iron and manganese oxides, with minor heavy metal elements, for example, Co, Ni, Pt, and REEs. We selected some seamounts on the Pacific plate and equatorial seamount for two typical model areas. We carried out occurrence observation of the crusts in a slope of the seamounts at water depths of 1000m to 3000m continually with high-vision camera equipped with ROV, and took intact and unbroken samples with the manipulator at Takuyo-5th seamount. We described substrate rocks, mineralogy and chemistry, and microstructures on fine-microscopic scales with radiometric dating (I. Graham, GNS).

The chemical analysis and calculation of metal flux indicated that, the Mn, the major component has concentrated continuously and fairly constantly in all areas and the depths, while the accumulation of Co depends mainly on water depth. On the other hand, elements which are of clastic origin including Fe and Al greatly reflect the distance from the continental source. Thus the hydrogenetic ferromanganese crusts are probably regarded as useful paleoceanographic archive.

Keywords: ferromanganese crusts, metal flux, northwest pacifc, equatorial pacific

Japan Geoscience Union Meeting 2014
(28 April - 02 May 2014 at Pacifico YOKOHAMA, Kanagawa, Japan)

MIS27-02 Room:423 Time:May 2 14:30-14:45

Comparing rare earth elements in the surface layers of ferromanganese crusts and ambient seawater from the Takuyo Daigo

TOKUMARU, Ayaka[1*] ; ZHU, Yanbei[2] ; NOZAKI, Tatsuo[3] ; TAKAYA, Yutaro[4] ; GOTO, Kosuke T.[5] ; SUZUKI, Katsuhiko[3] ; CHANG, Qing[3] ; KIMURA, Jun-ichi[3] ; KATO, Yasuhiro[4] ; USUI, Akira[6] ; URABE, Tetsuro[7] ; SUZUKI, Yohey[1]

[1]Dept. Earth Planet., Univ., Tokyo, [2]NIST/AIST, [3]IFREE/JAMSTEC, [4]Dept. System Innovation, Univ. of Tokyo, [5]GSJ/AIST, [6]Natural Sciences Cluster, Kochi Univ., [7]JMEC

Hydrogenetic ferromanganese (Fe-Mn) crusts are strongly enriched relative to the Earth's lithosphere in many rare and precious metals, including Co, Te, Mo, Bi, Pt, W, Zr, Nb, Y, and rare earth elements (REEs) (e.g. Hein et al., 2013). Accumulation of these trace metals from seawater is generally controlled by sorption (Koschinsky and Halbach, 1995; Koschinsky and Hein, 2003). REEs, except for Ce, behave as a dissolved trivalent cation in seawater and concentrated in the solid phase by adsorption (Nakada et al., 2013). Although a set of REE concentrations in Fe-Mn crusts is frequently used as a proxy to distinguish formation processes (e.g. Usui and Someya, 1997; Hein et al., 2000), it is not certain if REE concentrations in Fe-Mn crusts are correlated to those in surrounding seawater. In order to verify the correlation, REE concentrations in the outermost surface of Fe-Mn crusts and the surrounding seawater were directly compared at various depths (957-2987 m) on the Takuyo Daigo Seamount. We normalized the REE concentrations in the outermost surface of Fe-Mn crusts with its formation age, as the relative age of Fe-Mn crusts can be determined using osmium isotopic ratio (e.g. Klemm et al., 2005; 2008). For measurement of REE concentrations in seawater, inductively coupled plasma mass spectrometry (ICP-MS) was applied and solid phase extraction (SPE) techniques using chelating resins were conducted as pretreatment (Zhu et al., 2013). In this study, we compare depth profiles of the normalized REE concentrations in the outermost surface of Fe-Mn crusts and the REE concentrations in surrounding seawater.

Keywords: ferromanganese crust, seawater, Os isotope, rare earth elements, geochemistry

Japan Geoscience Union Meeting 2014
(28 April - 02 May 2014 at Pacifico YOKOHAMA, Kanagawa, Japan)

MIS27-03 Room:423 Time:May 2 14:45-15:00

Iron isotopic composition of seawater recorded in ferromanganese deposits

YAMAOKA, Kyoko[1*] ; BORROK, David[2] ; USUI, Akira[3]

[1]Geological Survey of Japan, AIST, [2]Univ. of Louisiana, [3]Kochi Univ.

Iron isotopic composition of marine ferromanganese deposits could be a useful tool to understand the biogeochemical cycle of iron in the ocean. In this study, we measured the iron isotopic compositions (δ^{56}Fe relative to IRMM-14) of hydrogenetic and diagenetic ferromanganese deposits from the Pacific Ocean (1400-6000 m water depth). The hydrogenetic ferromanganese crusts and nodules had a consistent average Fe isotopic composition of -0.32±0.12 ‰ (2SD). The consistent δ^{56}Fe values imply homogenous Fe isotopic composition of modern deep seawater in the central to northwestern Pacific. Despite differences in mineralogy and chemistry, the δ^{56}Fe values of diagenetic nodules (-0.34 to -0.20 ‰) were indistinguishable from those of hydrogenetic origin. These observations suggest that dissolution and re-precipitation of Fe in sediments resulted in no significant Fe isotope fractionation. These values are apparently lower than the δ^{56}Fe values of seawater from <900 m in the central Pacific ranging from +0.01 to +0.58 ‰ (Radic et al., 2011), implying that deep water is enriched in isotopically light iron. We also reconstructed the temporal variations of iron isotopic compositions in three hydrogenetic ferromanganese crusts from different water depths (1440, 2239, 2987 m) in the northwest Pacific. Regardless of water depth, the δ^{56}Fe values of these crusts showed essentially constant (-0.31±0.13 ‰, 2SD) throughout the past ~ 20 Ma. This is remarkably consistent with the constant iron isotopic compositions of ferromanganese crust (-0.31±0.10 ‰, 2SD) in the central Pacific over the last 10 Ma (Chu et al., 2006). Thus, it is suggested that the Pacific deep water has remained constant in iron isotopic composition for long time scale.

Keywords: iron isotope, ferromanganese crust

Japan Geoscience Union Meeting 2014
(28 April - 02 May 2014 at Pacifico YOKOHAMA, Kanagawa, Japan)

MIS27-04 Room:423 Time:May 2 15:00-15:15

Fractionation of Hafnium-Zirconium in ferromanganese crusts

INOUE, Minami[1] ; SAKAGUCHI, Aya[1*] ; KASHIWABARA, Teruhiko[2] ; USUI, Akira[3] ; TAKAHASHI, Yoshio[1]

[1]Hiroshima Univ., [2]JAMSTEC, [3]Kochi Univ.

The couples of High Field Strength elements (HFS elements), e.g. Zirconium (Zr)-Hafnium (Hf) and Niobium (Nb)-Tantalum (Ta), are called Twin-element due to the consistency of their valences and ionic-radii in the environment. As a consequence, these couples must show uniform ratio, which is theoretically same as that of chondrite meteorite. However, the significant fractionations among HFS elements in natural samples have been found, and it was proposed as enigma of Zr-Hf and Nb-Ta fractionation (Niu et al. 2012). The large fractionation of these elemental couples has also been found in the ferromanganese crust (FMC) (Bau 1996). In this study, we attempted to clarify the accumulation mechanism of HFS elements in FMCs with some methods including X-ray absorption fine structure (XAFS) technique for synthesised and natural samples to serve as an aid to approach to this enigma.

Six FMC samples were collected from the Takuyo-Daigo and Ryusei seamounts, from 950 m (summit) to 3000 m water depth, with hyper-dolphin (remotely operated vehicle) equipped with live video camera and manipulators. Near urface layer (less than 1 mm) of all FMC was analysed with XRD and XAFS to confirm the mineral composition and speciation of Zr together with chemical reagents, Zr minerals and rock samples as standard materials. The concentrations of Zr and Hf in these samples were also measured by ICP-MS after appropriate treatments. Furthermore, to serve as an aid to clarify the fractionation mechanism between Zr and Hf in FMCs, distribution coefficients (Kd) and chemical states were determined through the co-precipitation experiments of Hf and Zr with ferrihydrite and δ-MnO_2. To analyse the chemical states on the solid phase, XAFS was employed.

The major mineral composition of Fe and Mn had no significant variation with the water depth of these seamounts. The concentrations of Zr and Hf were increased with depth, and their ratios were varied without showing any trends. However, these ratios were totally fractionated from that in the seawater (Firdaus et al., 2011). For all samples, Hf was enriched in FMC compared to Zr. The chemical state of Zr in FMCs through the depth showed, 1) coprecipitation with ferrihydrite, 2) coprecipitation with δ-MnO_2, and 3) basalt-like composition, and the rate of basalt-like composition of Zr was increased with water depth. The concentrations of Zr in the fraction between ferrihydrite and δ-MnO_2 were uniform through with the depth. Furthermore, the concentration of Zr in these fraction was also uniform, that is, the increased-concentration of Zr in the samples from deeper seamounts could be explained by the increase in basalt-like fraction. From the results of co-precipitation experiments of Zr and Hf with ferrihydrite and δ-MnO_2, it was found that the Hf-DFO was more precipitated compared with Zr-DFO. In this case, the bond length of Hf-O was significantly shorter than that of Zr-O.

Keywords: Zirconium, Hafnium, Ferromanganese crust

Japan Geoscience Union Meeting 2014
(28 April - 02 May 2014 at Pacifico YOKOHAMA, Kanagawa, Japan)

MIS27-05 Room:423 Time:May 2 15:15-15:30

Paleoceanographic Record on the Dual Structure of Hydrogenetic Ferromanganese Crusts

NISHI, Keisuke[1*] ; USUI, Akira[1] ; NAKASATO, Yoshio[1] ; HISAAKI, Sato[1] ; IAN, Graham[2] ; YAMAOKA, Kyoko[3] ; GOTO, Kosuke T.[3]

[1]Kochi University, [2]The Institute of Geological and Nuclear Science, [3]National Institute of Advanced Industrial Science and Technology

Most Hydrogenetic ferromanganese crusts in the Pacific consist of two growth generations: a phosphatized older grows generation and a non-phosphatized growth generation. This study attempts some detail analyses such as macroscopy, microscopy, chemistry, mineralogy, age and growth rate determination to consider how the dual structures are formed. As a result of age growth rate determinations supported by GNS, the boundary of two growth generations concentrates approximately 15-10 Ma regardless of water depth and region. In the middle to late Miocene, the climate was prominently cold by Antarctic glaciation. As a result, a phosphogenesis of ferromanganese crusts may have occurred because the dissolves phosphate rich and oxygen rich deep water were redistributed to the intermediate water depths by upwelling at the seamounts.

Keywords: ferromanganese crust, marine environment, pacific, seamount

Japan Geoscience Union Meeting 2014
(28 April - 02 May 2014 at Pacifico YOKOHAMA, Kanagawa, Japan)

MIS27-06 Room:423 Time:May 2 15:30-15:45

Proposed valid description of ferromanganese crusts and the significance of this method

NAKASATO, Yoshio[1*] ; USUI, Akira[1] ; HISAAKI, Sato[1] ; NISHI, Keisuke[1] ; GOTO, Kosuke T.[2]

[1]Department of Integrated Arts and Sciences, Kochi University, [2]Geological Survey of Japan

This study shows valid description of ferromanganese crusts for acid solution method. Before this, we used some detail analyses such as chemistry, mineralogy and microscopy. This method can extract the dissolution fragments from ferromanganese crusts and is more useful than the method used up, until now. The fragments consists of several kinds of minerals, for example, quartz, magnetite and clay mineral. These fragments, possibly, can be classified into detrital, biogenetic, volcanic and hydrogenetic origins.

Keywords: Ferromanganese crusts, Microstratigraphy, Paleoceanography

Japan Geoscience Union Meeting 2014
(28 April - 02 May 2014 at Pacifico YOKOHAMA, Kanagawa, Japan)

MIS27-07 Room:423 Time:May 2 15:45-16:00

Comparative analysis of microbial community on hydrogenetic ferro-manganese crusts from North-West Pacific Ocean

NITAHARA, Shota[1*] ; KATO, Shingo[2] ; YAMAGISHI, Akihiko[1]

[1]Tokyo University of Pharmacy and Life Sciences, [2]RIKEN

Ferro-manganese crust (Mn crusts) is rock covered with iron and manganese oxides, and present on the boundary layer between hydrosphere and lithosphere. Mn crusts grow with sedimentation of these oxides from seawater. Growth rate is 1-10 mm/Myr, estimated by radiometric dating and magnetic stratigraphy (Usui and Someya, 1997). Mn crust is widely distributed on outcrop of seamount and sea plateau with slow sedimentation rate.

Mn crust contains several metals (ex. Cu, Co, Ni, Pt and Rare Earth Element etc. Hein, 2000). Considering content of rare metals and rare earth element, and abundance of Mn crust on seafloor, it is expected to use of Mn crust as a resource.

Our knowledge about microbes on surface and inside of Mn crust is limited. We analyzed the microbial community on the surface of Mn crust from Takuyo-Daigo Seamount at the depth of 2991 m. We show that high abundance of microbes and highly diversed microbial community on the surface of Mn crust and microbial community on Mn crust is different from that of sediment or seawater (Nitahara et al., 2011). However, it is not clear that these characteristics are general between Mn crust on different area or different depth. So we collected and analyzed Mn crust from several seamounts including Takuyo-Daigo seamount using 16S rRNA gene phylogeny.

We compared microbial communities of Mn crust from Takuyo-Daigo seamount and Ryusei seamount, there is a little difference. Comparative analysis between Mn crust, sediment and seawater from Takuyo-Daigo seamount and Ryusei seamount shows that microbial community composition of Mn crust and sediment are similar, while that of seawater is different from that of Mn crust and seawater.

In this presentation, in addition to Takuyo-Daigo seamount and Ryusei seamount, we will discuss about comparative analysis including Mn crust from Daito Ridge and Ogasawara sea plateau.

Hein, J.R.K., A.; Bau, M.; Manheim, F.T.; Kang, J.-K.; Roberts, L. (2000) Cobalt-rich ferromanganese crusts in the Pacific. In Handbook of marine mineral deposits. Cronan, D. (ed): Boca Raton: CRC Press, pp. 2-279.

Nitahara, S., Kato, S., Urabe, T., Usui, A., and Yamagishi, A. (2011) Molecular characterization of the microbial community in hydrogenetic ferromanganese crusts of the Takuyo-Daigo Seamount, northwest Pacific. FEMS Microbiol Lett 321: 121-129.

Usui, A., and Someya, M. (1997) Distribution and composition of marine hydrogenetic and hydrothermal manganese deposits in the northwest Pacific. Geological Society, London, Special Publications 119: 177-198.

Japan Geoscience Union Meeting 2014
(28 April - 02 May 2014 at Pacifico YOKOHAMA, Kanagawa, Japan)

MIS27-P01 Room:Poster Time:May 2 16:15-17:30

On-site deposition and exposure experiments at a low-temperature hydrothermal area

USUI, Akira[1*] ; HINO, Hikari[1] ; SUZUKI, Yohey[2] ; YAMAOKA, Kyoko[3] ; OKAMURA, Kei[4]

[1]Kochi University, [2]Earth & Planetary Sciences, Univ. Tokyo, [3]Geological Survey of Japan, AIST, Tsukuba, [4]Kochi Core Center, Kochi University

An on-site deposition and on-site adsorption experiments were carried out at a possible hydrothermal area in the Izu-Bonin arc, NW Pacific. The mineralogical and chemical analyses on the exposed glass, ceramics and on the artificial buserite samples suggested a new precipitation during 12 years and positive accumulation of some transitional metals. This finding was the first evidence of modern active precipitation of manganese oxide from normal sea water/ hydrothermal waters in the ocean floors.

Keywords: low-temperature hydrothermal activity, bayonaise hill, manganese minral, buserite, todorokite, adsorption

Japan Geoscience Union Meeting 2014
(28 April - 02 May 2014 at Pacifico YOKOHAMA, Kanagawa, Japan)

MIS27-P02 Room:Poster Time:May 2 16:15-17:30

Uranium isotope composition in ferromanganese crusts: Implications for the paleoredox proxy

GOTO, Kosuke T.[1*] ; ANBAR, Ariel D.[2] ; GORDON, Gwyneth W.[2] ; ROMANIELLO, Stephen J.[2] ; SHIMODA, Gen[1] ; TAKAYA, Yutaro[3] ; TOKUMARU, Ayaka[3] ; NOZAKI, Tatsuo[4] ; SUZUKI, Katsuhiko[4] ; MACHIDA, Shiki[5] ; HANYU, Takeshi[4] ; USUI, Akira[6]

[1]GSJ, AIST, [2]Arizona state University, [3]The University of Tokyo, [4]JAMSTEC, [5]Waseda University, [6]Kochi University

Variations of the 238U/235U ratio (d238U) in sedimentary rocks have been proposed as a possible proxy for decoding the paleo-oceanic redox conditions, although the marine U isotope system is not fully understood (Stirling et al., 2007 GCA; Weyer et al., 2008 EPSL).

Here we investigate the spatial variation of d238U in modern ferromanganese crusts by analyzing U isotopes in the surface layer (0-3 mm depth) of 19 samples collected from 6 seamounts in the Pacific Ocean. The d238U values in the surface layers show little variation and range from -0.59 to -0.69 permil. The uniformity of d238U values is consistent with the long residence time of U in modern seawater (Dunk et al., 2002 Chem. Geol.), although the d238U values are lighter than that of present-day seawater by ˜0.24 permil (Stirling et al., 2007 GCA; Weyer et al., 2008 EPSL). The light d238U is consistent with the isotope offset found during the adsorption experiment of U to birnessite (Brennecka et al., 2011 ES&T). Our results suggest that removal of lighter U from seawater to ferromanganese crusts is responsible for the second largest uranium isotopic fractionation in the modern marine system and could provide a source of heavy U to seawater.

Depth profiles of U isotopes (d234U and d238U) in two ferromanganese crusts were investigated to reconstruct the evolution of oceanic redox state during the Cenozoic. The depth profiles of d238U show very limited ranges, and have similar values with those of the surface layer samples. The absence of any resolvable variations in the d238U depth profiles suggests that the relative proportions of oxic and reducing uranium sinks have not varied significantly over the past 40 Myr. However, the d234U depth profiles in the same samples suggest the possible U redistribution after deposition. Therefore, the d238U values may have been overprinted by secondary mobilization with pore-water or seawater. These results suggest that careful evaluation of secondary disturbance is required before applying chemical and isotope depth profiles of ferromanganese crusts to understand paleocean environmental changes.

To assess the potential effect of U removal by Mn oxides on seawater d238U, we calculated the seawater d238U under different fractions of U removal by Mn oxides using a simple isotope balance model. This calculation suggests that seawater d238U could have varied significantly throughout the Earth's history along with the changes of the Mn oxides accumulation rate.

Keywords: Uranium, 238U/235U, 234U/238U, paleoredox, ferromanganese crust, isotope geochemistry

Japan Geoscience Union Meeting 2014
(28 April - 02 May 2014 at Pacifico YOKOHAMA, Kanagawa, Japan)

MIS28-01 Room:313 Time:May 1 09:00-09:15

Amplification of induced current due to complicated resistivity structure in the earth

GOTO, Tada-nori[1*]

[1]Graduate School of Engineering, Kyoto University

Abrupt changes of geomagnetic field can make large induced electric current on the earth, and yield damages to pipelines, cables and other architectures. For understanding the phenomena and future risks, explorations of sub-surface resistivity structure are necessary because the heterogeneous resistivity structure in the crust and mantle amplifies the induced electrical current locally. The hazard prediction based on the homogeneous earth may result in the under-estimation. Here, I introduce possible cases of induced current near the coastal areas, based on two-dimensional (2D) and three-dimensional (3D) earth structure including the sea layer. My study is based on the numerical forward calculation of induced electric field in the earth. The former case comes from 2D forward simulation. In this case, the straightly elongated coastal line is assumed, and various sub-surface and sub-seafloor resistivity structures are imposed. The numerical results suggest that the amplitude of induced current becomes about 6 times larger than the homogeneous earth without the sea layer. The width of affected land zone is about 20 km from the coast line. In the second case, the 3D forward modeling is employed to express the complicated coastal line and bathymetry. As a result, the amplitude goes double at the cape zones. These phenomena come from the boundary charge along the coastal area. I conclude that electrical structure around the coast line (not only below the land, but also below the seafloor) should be focused for the huge induce current.

Keywords: Geomagnetic field, Induced current, Land-Ocean interaction, resistiivty

Japan Geoscience Union Meeting 2014
(28 April - 02 May 2014 at Pacifico YOKOHAMA, Kanagawa, Japan)

MIS28-02 Room:313 Time:May 1 09:15-09:30

A Numerical Simulation of the Geomagnetically Induced Electric Field with the Three-Dimensional Resistivity Model

ENDO, Arata[1*] ; FUJITA, Shigeru[2] ; FUJII, Ikuko[3]

[1]Japan Meteorological Agency, [2]Meteorological College, [3]Magnetic Observatory

The Geomagnetically induced current (GIC) sometimes causes power-line failure in the geomagnetically high-latitude regions like Canada and Sweden. On the other hand, it has been regarded that Japan is free from this danger because it is located in the lower-latitude region. However, this assumption may not be valid when an extremely severe space weather event happens. In addition, as the GIC and the induced electric field are strongly controlled by non-uniform distribution of the Earth's electric resistivity, we need to evaluate these values taking the non-uniform distribution into account. It is noted that there has been no works about it. In this talk, we will present the geomagnetically induced electric field based on the modeled electric resistivity distribution by using a numerical code applicable to the three-dimensional induction problems. As the results, there are large anomalies in the intensity of the electric field in Japan.

Keywords: Geomagnetically Induced Current, SC, resistivity, conductivity, magnetic storm

Japan Geoscience Union Meeting 2014
(28 April - 02 May 2014 at Pacifico YOKOHAMA, Kanagawa, Japan)

MIS28-03 Room:313 Time:May 1 09:30-09:45

Simultaneous inversion of temporal magnetotelluric signal change and conductivity structure using the time domain simula

IMAMURA, Naoto[1*] ; SCHULTZ, Adam[2] ; GOTO, Tada-nori[1] ; TAKEKAWA, Junichi[1] ; MIKADA, Hitoshi[1]

[1]Graduate School of Engineering, Kyoto University, [2]Oregon State University

Magnetotelluric method is mainly used for estimation of subsurface resistivity structure. However, the time-domain analysis of source field is normally omitted, although its estimation should be included at the cases such as in the high-latitude zones or on the global scale. In previous research, simultaneous inversion is proposed to estimate both magnetotelluric signal and resistivity structure in the earth. Koch and Kuvshinov (2013) proposed inversion algorithm that iteratively estimates magnetotelluric signal and resistivity structure, although this inversion method cannot determine both unknowns in a seamless manner. In this study, we developed simultaneous inversion that can determine both unknowns at the same time. Because magnetotelluric signal is considered non-stationary time series, we try a direct inversion of time-domain electromagnetic field, not in the frequency -domain. It has a chance to give higher accuracy than the frequency domain inversion.

Our new inversion results applied to the synthetic model suggested that we could estimate both magnetotelluric signal and resistivity structure properly even under the condition of noise contamination in the observed data. Moreover, when the time domain and frequency domain inversions are applied to same synthetic time series, the result using time domain inversion has higher resolving capability than result using the frequency domain inversion.

Keywords: Magnetotelluric method, Time domain modelling, Simultaneous inversion

Japan Geoscience Union Meeting 2014
(28 April - 02 May 2014 at Pacifico YOKOHAMA, Kanagawa, Japan)

MIS28-04 Room:313 Time:May 1 09:45-10:00

Geoelectric Field at Kakioka, Kanoya, and Memambetsu

FUJII, Ikuko[1*]

[1]Kakioka Magnetic Observatory, JMA

Kakioka Magnetic Observatory, Japan Meteorological Agency (JMA) has continuously observed the geoelectric field at Kakioka, Kanoya, and Memambetsu for decades. I checked the JMA collection of the geoelectric field from a view point of applicability to studies on the geomagnetically induced current (GIC).

Two horizontal components (northward and eastward components) of the geoelectric field are obtained on the geographical coordinates at the three sites by measuring voltage differences between two pairs of electrodes. Details of the measurements such as locations and materials of the electrodes, baseline lengths, sampling intervals, and filtering responses of the systems differ time to time giving fluctuations on data quality.

I picked up a 11-year data segment ranging from Jan 1, 2000 to investigate the characteristics of the geoelectric field obtained by JMA.

It turned out that the geoelectric fields at three sites ware unstable on the long-term basis because the baseline lengths are as short as a few hundred meters and the instability of the electrodes are relatively noticeable. However, the electric field highly correlates with the geomagnetic field at periods from 100 sec to 1 day at any of three sites, suggesting the geoelectric field induced by a change of the geomagnetic field is successfully obtained at least on the short-term basis. Amplitudes of the geoelectric field are different among the sites. For instance, the eastward component of the field is about 10 times larger than the other at Kakioka, while the northward component is larger than the other at Memambetsu.

The MT response was computed at the three sites to evaluate the signal and infer effects of electrical conductivity structures. A robust procedure BIRRP (Chave and Thomson, 2004) was applied to 0.1 sec, 1 sec and 1min values of the geoelectric and geomagnetic fields at large-scale geomagnetic storms in 2003 and 2004 to estimate the MT response at periods shorter than 10000 sec. Since the 0.1 and 1 sec values of the geoelectric and geomagnetic fields are affected by system filters, shortest periods were not able to be included into the response estimation even after corrections of the filters were made. As for that at periods longer than 10000 sec, I verified a procedure to decompose a time series by Fujii and Kanda (2008) so that a noisy data set can be treated. Then, a trend with step-like anomalies and outliers were estimated from a 11-year segment of 1 hour values of the geoelectric field. Then, the MT response was estimated from the geoelectric field with the trend and outliers removed. In the end, the MT response was obtained at periods from several sec to 12 days. If this response is converted into the time domain by convolution, filter coefficients to estimate the geoelectric field from the geomagnetic field will be obtained.

Effects of local small-scale structures on the MT response were checked as a next step. The Zyx at Kakioka shows an unusually high value (˜1000 ohm m) even at a period of 10days and the comparison with the C value by Fujii and Schultz (2002) suggests it is about 100 times amplified by the local small-scale structures.

Yanagihara and Yokouchi (1965) explained a biased distribution of the electric field at a short frequency range at Kakioka by heterogeneities of a near surface structure. If these affects even at very long periods, use of the geoelectric field at Kakioka for GIC or induction studies should be done with a certain caution.

The electric field at three sites basically reflects the induction as it is supposed to be, although the measurement system and procedure can be verified so that data of higher quality are obtained.

Keywords: geoelectiric field, induction, geomagnetically induced current, MT response

Japan Geoscience Union Meeting 2014
(28 April - 02 May 2014 at Pacifico YOKOHAMA, Kanagawa, Japan)

MIS28-05 Room:313 Time:May 1 10:00-10:15

Magnetotelluric method and the source field with finite wave number

OGAWA, Yasuo[1*]

[1]Volcanic Fluid Research Center, Tokyo Institute of Technology

Magnetotelluric method is now widely used for mapping the crustal and upper mantle structure in three-dimensions. In magnetotelluric method, we normally assume the source field as a plane wave. However, if the source field has a finite wave length, the impedances (apparent resistivity, and impedance phase) and the geomagnetic transfer functions will be affected. In a simple case with uniform earth where the source field has a wave number is considered. The apparent resistivity inferred from the impedance (ratio of horizontal electric field to the orthogonal horizontal magnetic field), by assuming a plane wave source will be biased downward and impedance phase will be biased upward. Also the geomagnetic transfer function will have phase of pi/4, even without any lateral heterogeneity.

Some magnetotelluric studies at the high latitude and under the magnetic equator will be reviewed.

Keywords: magnetotelluric method, source field

Japan Geoscience Union Meeting 2014
(28 April - 02 May 2014 at Pacifico YOKOHAMA, Kanagawa, Japan)

MIS28-06 Room:313 Time:May 1 10:15-10:30

Electromagnetically coupled system between non-uniformly and anisotropically conducting inner earth and upper atmosphere

YOSHIKAWA, Akimasa[1*]

[1]International Center for Space Science and Education, Kyushu University

lectromagnetically coupled system between upper atmosphere and inner earth, is discussed. It is well known that upper atmosphere and inner earth system is electromagnetically coupled across very small conducting atmospheric region, which means 'primary' induced electric field produced by the mutual coupling is almost inductive (divergence free). However if the conductivity distribution is inhomogeneous, 'secondary' polarization (curl-free) electric field can be produced at the region of conductivity gradient. In the ionosphere, non-uniform Hall conductivity distribution induces the Hall polarization field, which becomes cause of current concentration and potential deformation by the Cowling effect. Formation of Cowling channel is one of the most important and peculiar nature of weakly ionized system under strongly background magnetic field distribution.

In this presentation, we will introduce basic feature of electrodynamics at the non-uniform and anisotropically conducting ionosphere, and will discuss a possible electromagnetic coupling mechanism when the telluric conductivity distribution is non-uniform and anisotropic.

Keywords: ionospheric current, telluric current, electromagnetically coupled system

Japan Geoscience Union Meeting 2014
(28 April - 02 May 2014 at Pacifico YOKOHAMA, Kanagawa, Japan)

MIS28-07 Room:313 Time:May 1 10:30-10:45

The distribution of the internal geomagnetic field during a magnetic storm

IWASHITA, Kodai[1*] ; TOH, Hiroaki[2]

[1]Graduate School of Science, Kyoto University, [2]Data Analysis Center for Geomagnetism and Space Magnetism,

We calculated the Gauss coefficients of magnetic potential and estimated the current in the earth during a magnetic storm.

There are two kinds of magnetic storms. One is sudden. The other is synchronized to the sun's rotation period. How does the earth react to such a strong disturbance of external magnetic field?

We quantitatively estimated the induced current in the earth which had reacted to the large change of magnetic field like a strong magnetic storm, using a spherical harmonic expansion and a three dimensional forward calculation code. With a spherical harmonic expansion, we used geomagnetic data of the surface of the earth and calculated the internal and external geomagnetic field. With a three dimensional forward calculation code, we used the time variation of the external Gauss coefficients calculated by the spherical harmonic expansion and visualized and quantified the induced current in the earth during a magnetic storm.

We expect that we estimate the electric conductivity of the earth with the internal Gauss coefficient to the external Gauss coefficients ratio as a development of this study.

Keywords: induced current, magnetic storm

Japan Geoscience Union Meeting 2014
(28 April - 02 May 2014 at Pacifico YOKOHAMA, Kanagawa, Japan)

MIS28-08 Room:313 Time:May 1 11:00-11:15

Why did the Carrington storm recover very rapidly?

KEIKA, Kunihiro[1*] ; EBIHARA, Yusuke[2] ; KATAOKA, Ryuho[3]

[1]Solar-Terrestrial Environment Laboratory, Nagoya University, [2]Research Institute for Sustainable Humanosphere, Kyoto University, [3]National Institute of Polar Research

Intense geomagnetic storms are accompanied by rapid recovery, as represented by a quick increase of the Dst index after its minimum. As far as the geomagnetic storms that we have observed since the early 20th century, the more intense storms experienced the more rapid recovery. The Carrington event on 2 September 1859 also experienced an extremely rapid recovery (>1000 nT/h at Bombay, India; >300 nT/h with 1-hour average data). At least three major processes that occur in the Earth's inner magnetosphere are proposed to explain such rapid recovery: (1) the neutralization of energetic O^+ ions through charge exchange, (2) flow-out of energetic ions to the interplanetary field, and (3) loss of energetic ions into the atmosphere through pitch-angle scattering due to interactions with electromagnetic ion cyclotron (EMIC) waves. In addition, a sudden increase in the solar wind dynamic pressure around the storm maximum could cause a quicker recovery.

In this talk, we focus on intense magnetic storms with the Dst minimum smaller than -200 nT for which solar wind data are available. We first examine whether the rapid recovery can be explained by an ion flow-out effect associated with sudden changes of solar wind density, by modifying the empirical Burton's equation. We also estimate the amount of energetic O^+ ions, the spatial extent of EMIC wave active regions, and the increase rate of the solar wind dynamic pressure that could be required to reproduce the storm rapid recovery. In addition, we discuss how quickly the geomagnetic field could change during the recovery of an extremely intense storm such as the Carrington event.

Keywords: The Carrington event, Geomagnetically induced currents (GICs), Ring current, Magnetopause current, Interplanetary shocks, Coronal mass ejections (CMEs)

Japan Geoscience Union Meeting 2014
(28 April - 02 May 2014 at Pacifico YOKOHAMA, Kanagawa, Japan)

MIS28-09 Room:313 Time:May 1 11:15-11:30

Consideration of geomagnetically induced currents — a case of geomagnetic sudden commencement(SC)

ARAKI, Tohru[1*] ; SHINBORI, Atsuki[2]

[1]Polar Research Institute of China, [2]RISH, Kyoto University

Siscoe et al.(1968) assumed a relationship between the SC amplitude, dH, and solar wind dynamic pressure, Pd, as dH = fgk d(Pd)∗∗0.5 and experimentally determined the proportional constant, k. Here f is a constant associated with the solar wind-magnetosphere interaction and g shows effects of currents induced in the Earth. This constant g has been traditionally taken as 1.5 without detailed check of its meaning for a long time. Here we make a physical consideration on it based upon the present SC model.

The disturbance field of SC, Dsc, is expressed as Dsc = DL + DPpi + DPmi.

Here, DL is caused by the magnetopause current (MC) enhanced during sudden compression of the magnetosphere and dominant in low latitudes on the ground. DP is produced by field-aligned currents (FAC) and FAC- produced ionospheric currents (IC) and larger in the higher latitude region.

The DP shows a two pulse structure where the first pulse is called pi (preliminary impulse) and the following pulse is denoted as mi (main impulse). Thus we have to assume 3 current sources in the consideration of induction effects of SC.

The magnetopause current, MC induces currents both in the ionosphere and Earth. As the induced ionospheric current reduces the amplitude of SC on the ground while the earth currents enhance it, induction current effects will be small for the DL field. Ionospheric currents causing the DP field induces currents only in the Earth which enhances the DP field on the ground.

The LT variation of SC amplitude shows the maximum in the D-component and minimum in the H-component around 8h LT in low and middle latitudes. On the other hand, calculation of a global distribution of ionospheric currents produced by a pair of FACs shows that the current direction is in north-south near 8h LT. This means that the H-component amplitude of SC observed near 8h LT consists of only the DL field which is less affected by induction effects..

Keywords: sudden commencement, induced current, ionospheric current,, magnetopause current, DL/DP-field

Japan Geoscience Union Meeting 2014
(28 April - 02 May 2014 at Pacifico YOKOHAMA, Kanagawa, Japan)

MIS28-10 Room:313 Time:May 1 11:30-11:45

Quasi-periodic DP2 fluctuations in the geomagnetically induced currents

KIKUCHI, Takashi[1*] ; WATARI, Shinichi[2] ; HASHIMOTO, Kumiko[3] ; EBIHARA, Yusuke[4]

[1]Solar-Terrestrial Environment Laboratory, [2]National Institute of Information and Communications Technology, [3]Kibi International University, [4]Research Institute for Sustainable Humanosphere

The geomagnetically induced current (GIC) has been attributed to the time change in the Bx component of the ground magnetic field. However, the GIC was found to be well correlated with By component at mid latitudes [e.g., Watari et al., Space Weather 2009]. Braendlein et al., JGR 2012] reported that the GIC has diurnal and seasonal variations, and suggested that the GIC could be a return current of the ionospheric currents via the wave front of the TM0 mode waves in the Earth-ionosphere waveguide [Kikuchi and Araki, JATP 1979]. We analyzed the quasi-periodic fluctuations in the GIC recorded in Hokkaido on December 14 2006, which accompany the DP2 fluctuations in the equatorial electrojet (EEJ) and D-component magnetic field at midlatitudes. We found that the GIC is well correlated with the EEJ as well as the madlatitude D-components. We suggest that the midlatitude GIC is a part of the magnetosphere-ionosphere-ground (MIG) circuit currents [Kikuchi, JGR 2014], and therefore, the GIC is the return current of the ionospheric currents via the wave front of the TM0 mode waves.

Keywords: midlatitude geomagnetically induced current, midlatitude D-component magnetic field, equatorial electrojet, TM0 Earth-ionosphere waveguide mode

Japan Geoscience Union Meeting 2014
(28 April - 02 May 2014 at Pacifico YOKOHAMA, Kanagawa, Japan)

MIS28-11 Room:313 Time:May 1 11:45-12:00

Statistical properties of superflares on solar-type stars

MAEHARA, Hiroyuki[1*] ; SHIBAYAMA, Takuya[2] ; NOTSU, Yuta[2] ; NOTSU, Shota[2] ; HONDA, Satoshi[3] ; NOGAMI, Daisaku[2] ; SHIBATA, Kazunari[2]

[1]University of Tokyo, [2]Kyoto University, [3]University of Hyogo

Solar-flares are energetic explosions in the solar atmosphere. The energy released by a solar flare is typically of the order of 10^{29} - 10^{32} erg. Recent high-precision photometry from space shows that ”superflares”, which are 10-10000 times more energetic

than the largest solar-flares, occur on Sun-like stars (slowly rotating G-type main sequence stars).

We present recent results on superflares on solar-type stars using the high time-resolution data. We search for superflares from the short-cadence data (time resolution: 1 min) of about 1300 solar-type stars observed with the Kepler space telescope and found about 150 superflares on 20 stars. The energy of detected flares ranges from 10^{33} to 10^{35} erg, which is equivalent to that of X100 - X10000 class solar flares. These superflare data, combined with the previous results from the low time-resolution data (1547 superflares on 279 solar-type stars), indicate that the occurrence frequency distribution of superflares can be fitted in the energy range $>10^{33}$ erg by a simple power-law function with the index of about -2. Moreover, the frequency distribution of superflares on Sun-like stars and that of solar flares are roughly on the same power-law line. The average occurrence frequency of superflares with energy of 10^{33} erg (X100 class) is about once in 100 years and that of superflares with energy of 10^{34} erg (X1000 class) is about once in 1000 years. The duration of superflares depends on the total energy released by superflares. Larger flares tend to have longer duration time. The duration of superflares is proportional to the 1/3 power of the flare energy. This correlation between energy and duration of superflares on solar-type stars is similar to that of solar flares. These results suggest that statistical properties of superflares on solar-type stars is basically the same as thoes of solar flares.

Keywords: superflare, solar flare

Japan Geoscience Union Meeting 2014
(28 April - 02 May 2014 at Pacifico YOKOHAMA, Kanagawa, Japan)

MIS28-12 Room:313 Time:May 1 12:00-12:15

Extreme value statistics analysis of the auroral electrojet indices

NAKAMURA, Masao[1*] ; YONEDA, Asato[1] ; TSUBOUCHI, Ken[2]

[1]Osaka Prefecture University, [2]Tokyo Institute of Technology

The worst space environment phenomena have a possibility of damaging electric transmission grids due to large induced currents on the earth and causing satellite anomalies due to increased high energy plasma on satellite orbits. Therefore a statistical study of the worst substorm events is important. For the study, we utilize extreme value statistics, which focus on the statistical behavior in the tail of a distribution. We analyze the one-minute values of the auroral indices (AE, AU, AL) in 1996-2012. These indices are derived from geomagnetic variations in the horizontal component observed at twelve observatories along the auroral zone in the northern hemisphere. The AU and AL indices are the uppermost and lowermost envelopes of the superposed horizontal component perturbations, and are thought to represent the maximum eastward and westward electrojet currents over the auroral zone, respectively. The AE index is defined by the separation between the upper and lower envelopes (AE=AU-AL) and commonly used as an index of the aurora activity. As a result of the analysis, we can estimate the upper limit of AU and the lower limit of AL, which suggests the maximum strengths of the eastward and westward electrojet currents. However, it is found that the AE index is not suitable for the extreme value statistics analysis, because it is a combined index. The largest values of AE are not generated by a single process and do not show a simple extreme value distribution.

Keywords: Auroral electrojet index, Extreme value statistics

Japan Geoscience Union Meeting 2014
(28 April - 02 May 2014 at Pacifico YOKOHAMA, Kanagawa, Japan)

MIS28-13 Room:313 Time:May 1 12:15-12:30

Statistical estimations of geomagnetic disturbances at Kakioka, Memambetsu and Kanoya

MINAMOTO, Yasuhiro[1*] ; FUJITA, Shigeru[2] ; OOGI, Junpei[1] ; HARA, Masahiro[1]

[1]Kakioka Magnetic Observatory, Japan Meteorological Agency, [2]Meteorological College, Japan Meteorological Agency

We investigated scale of geomagnetic disturbances which can cause extremely large geomagnetically induced current with record of geomagnetic phenomena by The Japan Meteorological Agency with statistical analyses. In this presentation, we will show the following items,

1. an estimation of the scale of millennium magnetic storm calculated from 1932 cases of observations at Kakioka magnetic observatory.
2. estimations of the scale of millennium storm sudden commencements and sudden impulses calculated from 2848, 2408 and 2257 cases of observations at Kakioka, Memambetsu and Kanoya respectively.
3. probable geomagnetic disturbances suggested from one-minutes data of geomagnetic field at Kakioka, Memambetsu and Kanoya over about thirty years.

Keywords: magnetic storm, sudden impulse, storm sudden commencement, statistics, magnetic observatory

Japan Geoscience Union Meeting 2014
(28 April - 02 May 2014 at Pacifico YOKOHAMA, Kanagawa, Japan)

MIS28-P01 Room:Poster Time:May 1 18:15-19:30

Analysis of geomagnetically induced current measured in Japan

WATARI, Shinichi[1*]

[1]National Institute of Informaton and Communications Technology

It is known that there is a possibility of failure of power grids caused by geomagnetically induced currents associated with intense geomagnetic storms. It is believed that effect of GIC is small in Japan because Japan locates low geomagnetic latitude comparing with its geographical latitude. Damage of transformer is reported from the Republic of South Africa associated with the October, 2003 storm. The Republic of South Africa locates in similar geomagnetic latitude with that of Japan. We made GIC measurements of a transformer of the Memanbetsu substation between 2005 and 2007. Those data are compared with geoelectric data observed by the Memanbetsu geomagnetic observatory of Japan Meteorological Agency. We estimated GICs associated with past intense geomagnetic storms using the geoelectric field data based on the result of the comparison. The result of our analysis will be reported.

Keywords: Geomagnetically Induced Current, geomagnetic storm, earth current, power grids, space weather

Japan Geoscience Union Meeting 2014
(28 April - 02 May 2014 at Pacifico YOKOHAMA, Kanagawa, Japan)

MIS28-P02 Room:Poster Time:May 1 18:15-19:30

Global MHD simulation of the magnetospheric response to large and sudden enhancement of the solar wind dynamic pressure

KUBOTA, Yasubumi[1*] ; KATAOKA, Ryuho[2] ; DEN, Mitsue[1] ; TANAKA, Takashi[3] ; NAGATSUMA, Tsutomu[1] ; FUJITA, Shigeru[4]

[1]NICT, [2]NIPR, [3]Kyushu University, [4]Meteorological College

A large and sudden enhancement of the dynamic pressure in the solar wind generates a geomagnetic sudden commencement (SC). The magnetic field variation of SC at auroral latitudes shows a bipolar change which consists of preliminary impulse (PI) and main impulse (MI). Fujita et al. [2003a, 2003b] reproduced the PI/MI magnetic field variation using a magnetosphere-ionosphere coupling simulation and clarified the fundamental mechanisms. Interestingly, Araki et al. [1997] reported an anomalously large-amplitude SC of more than 200 nT with an unusually spiky waveform at low latitude, which occurred when the magnetopause was pushed inside geostationary orbit. Such a super SC is the target of this study. We investigate the large-amplitude SC at auroral latitudes when a large solar wind dynamic pressure impinges on the magnetosphere using a newly developed magnetosphere-ionosphere coupling simulation which has advanced robustness. We simulate two SC events of dynamic pressure enhancement of 16 times larger than the standard value, caused by the density enhancement and velocity enhancement, respectively. As an initial result of the comparison with the SC events, it is found that magnetic field variation of PI/MI is larger and sharper in the case of velocity rise than the case of density rise. It is therefore suggested that high-speed solar wind may be needed to create large and sharp SC. It is also found that a magnetic field variation similar to so-called Psc appears after PI/MI only in the case of velocity rise. When the high-speed solar wind impinges on magnetosphere, vortices are repeatedly formed at the equatorial magnetopause, probably due to the K-H instability. It seems that the high pressure of the vortices play an essential role as a current generator to drive the field-aligned currents and the magnetic field oscillation. In this presentation, we discuss the mechanisms of super SC in more detail, combining the other interesting simulation results.

Japan Geoscience Union Meeting 2014
(28 April - 02 May 2014 at Pacifico YOKOHAMA, Kanagawa, Japan)

MIS29-01 Room:313 Time:April 29 14:15-14:30

Radiations of earthquake-excited electromagnetic waves from the ground

TSUTSUI, Minoru[1*]

[1]Kyoto Sangyo University

We have been observing electromagnetic (EM) pluses excited by earthquakes, using tri-axial electromagnetic sensor system installed in a borehole of 100 m in depth in the campus of Kyoto Sangyo University. During the period of 13 months from December 20, 2011 to March 26, 2013, we had nineteen earthquakes with magnitude of M>2 occurred around our EM observation site. They were within a circle of radius of 40 km centered at the EM observation site. We have confirmed detections of clear EM pulses for thirteen earthquakes among them. Seismic intensities at the EM observation site by these earthquakes were mostly 1 or less. From March, 2013, we added EM measurement above the ground. Furthermore, we began to capture waveforms of EM pulses in the borehole and above the ground and of seismic waves installed near the borehole simultaneously. Then we have confirmed that the detected EM waves were co-seismic ones readily generated by piezo-electric effect in earth's crusts [1].

Figure 1(a) shows a waveform of seismic wave detected at the EM observation site when an earthquake of M3.0 occurred at 10 km depth and at 5.4 km north of the EM observation site at 03:57 Dec. 2013, and (b) shows a waveform of magnetic H_{ew} components of the EM pulse detected in the borehole. Figure 1(c) also shows a waveform of H_{ew} component of the EM pulses detected above the ground where is on a hill of 60 m at about 600 m south-east of the EM observation site, in which the waveform have delayed 0.257 sec from that measured in the borehole. Therefore, this result shows clear evidence that earthquake-excited EM pulse has been radiated from the ground. We had another evidence of EM pulse radiation out of the ground surface when a large earthquake (M6.3) occurred at 14.8 km depth and at 130 km south-west of the EM observation site, in which earthquake-excited EM pulse was detected above the ground of the EM observation site in the campus. In that case, EM pulse was detected above the ground at 13.063 sec prior the detection in the borehole.

Next step is to detect and confirm EM pulses radiated at the occurrence of earthquakes. The final destination is to detect EM pulses radiated before earthquakes. For these purposes, we need to accomplish measurements of EM pulses in deeper earth (at about 1 km depth) after improving the sensitivity of the EM sensors.

[1] M. Tsutsui, submitted to IEEE Geoscience, Letters, 2014.

Keywords: seismic wave, electromagnetic wave, observations above and under ground, EM wave radiation from the ground

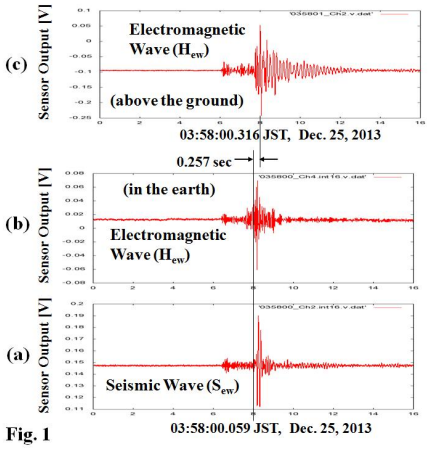

Fig. 1

Japan Geoscience Union Meeting 2014
(28 April - 02 May 2014 at Pacifico YOKOHAMA, Kanagawa, Japan)

MIS29-02 Room:313 Time:April 29 14:30-14:45

A statistical study for relationship between anomalous transmission of VHF band radio waves and earthquakes at Hidaka

MORITA, Shou[1*] ; MOGI, Toru[1]

[1]Institute of Seismology and Volcanology, Hokkaido University

Electromagnetic phenomena precursors to earthquakes, such as variations of geo-electric current, total electron contents in the ionosphere and anomalous transmission of radio waves, have been observed (ex. Hayakawa, 1996). The statistical relationship between such anomalies and an earthquake has investigated statistically (Liu et al., 2011; Orihara et al., 2012).

Anomalous transmission of VHF-band radio wave beyond the line-of-sight has been investigated by many researchers (Kushida and Kushida, 2002), and anomalous FM broadcasting wave (VHF range) has observed close to the epicenter of impending (Moriya et al., 2010). Radio waves transmitted from a given FM radio station are considered to be scattered, such that they could be received by an observation station beyond the line of sight. A quantitative correlation between total duration of scattered wave transmission and the magnitude, or maximum seismic intensity has been proposed (Moriya et al., 2010).

Nevertheless, a statistical relation between the anomalies transmission in VHF-band and impending earthquakes has not been investigated yet. We carried out statistical consideration by using the anomalous transmission data documented by Hokkaido University, and discuss the significance of this relation in this study.

The anomalous VHF-band radio wave data used in this research was observed at the Erimo observatory in Hidakra area from June 1st 2012 to December 31th, 2013. To judge anomalous data, we refer to the statistical method proposed by Liu et al. (2011) that they had used to detect abnormal signals of GPS TEC (total electron content) variations. We adopt a certain standard from median of observed data, and we identified anomalies if data beyond the standard value over 10 minutes.

As a result, some earthquakes were observed precursory anomalous radio propagation, but others are not observed a precursory anomaly. If we set the standard values strictly, the numbers of misdetections are decreased.

Big noises are found because of the appearance of a sporadic E layer in the ionosphere and so on especially in summer. We have to overcome the problem that how to remove such noises.

The earthquakes that we have cheese as targets were magnitude is more than 4.0 and the distance from Erimo observatory is less than 50km as the first trial.

We will investigate the statistical method in many conditions such as duration time, threshold of anomaly, magnitude, hypocenter distance etc and also discuss reasonable method to remove big noise. After that, we need to discuss probability of prediction using the relation between the occurrence of earthquake and anomalous transmission of radio wave propagation.

Keywords: ionosphere, anomalous transmission, relation with earthquakes

Japan Geoscience Union Meeting 2014
(28 April - 02 May 2014 at Pacifico YOKOHAMA, Kanagawa, Japan)

MIS29-03 Room:313 Time:April 29 14:45-15:00

Preseismic geomagnetic deflection synchronized with GPS-TEC enhancement 2011 Tohoku-Oki earthquake

HEKI, Kosuke[1*]

[1]Toyama Industrial Technology Center

The GPS-TEC enhancement stating ?40 minutes before the 2011 Tohoku-Oki earthquake has been observed (Heki, GRL, 2011). The geomagnetic declination change was confirmed nearby the fracture zone, at Easashi (ESA), Mizusawa (MIZ) by GSI and at Kakioka (KAK), Kanozan (KNZ) by JMA in respect to Kanoya (KNY) in synchronization with the GPS-TEC anomaly(Heki & Enomoto, JGR, 2013).These anomalies satisfy the criteria of earthquake precursor candidate (Wyss, AGU, 1991).

The magnetic declination; the difference between the direction of the horizontal components H of the Earth's magnetic field and the magnetic north is normally ?6.9 degree westward (=-415.7 arc min) from true north at the ESA site, but, as seen in the Figure, Δ D ([ESA]-[KNY]) gradually changes to the positive direction (eastward) starting from 40 minutes to the maximum Δ D value of Δ D? +0.32 arc min (= 9.31×10^{-5} rad) just before the main shock. This change should be affected by generation of preseismic magnetic field ?Δ B?. As Δ D is small, we can approximate the relationship between Δ H, Δ D and ?Δ B? as shown in an insert of the Figure; i.e.

?Δ B?[nT] ? ?**H**? [nT]?Δ D[rad]

The amount of H is normally 29037nT at ESA. The ?Δ **B**? is then 29037 nTx9.31×10^{-5} rad = 2.70 nT, which is in agreement with the observed preseismic variation of Δ H (?2.38 nT) as seen in the Figure.

The preseismic geomagnetic field | Δ **B**|, resulting from the time-varying current at the earthquake nucleus zone by Biot-Savalt's law, is expressed, by assuming the time-varying source current element of the length w_c t∗, as:

?Δ **B**?=μ0 ?**I**? sinθ w_ct∗/4πR^2,

where μ_0 is the permittivity of free space, ?**I**? is the pressure-impressed current, which is 170kA in the Tohoku-Oki earthquake (Enomoto & Heki, GJI, submitted), is an angle shown in the Figure, w_c is the earthquake nucleation size, t∗is the normalized preseismic time duration, R is the distance between observation site from the epicenter. The present model of the above equation at t∗=1 gives ?Δ B?=1.78 nT with R=181km: distance between the ESA and the epicenter of which the agreement with the observed value of 2.38nT is rather well.

Keywords: Tohoku-Oki earthquake, Precursor phenomena, Geomgnetic, Declination, GPS-TEC, Modelling

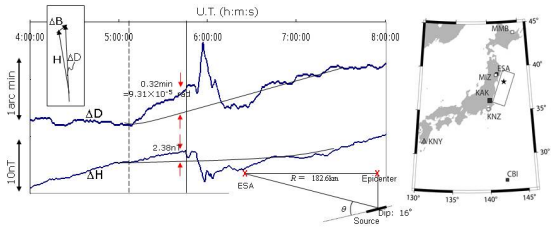

1

Japan Geoscience Union Meeting 2014
(28 April - 02 May 2014 at Pacifico YOKOHAMA, Kanagawa, Japan)

MIS29-04 Room:313 Time:April 29 15:00-15:15

Preseismic ionospheric electron enhancements, revisited : Discrimination from TID and interfrequency receiver bias estim

HEKI, Kosuke[1*]

[1]Dept. Natural History Sci., Hokkaido University

Possible enhancement of ionospheric Total Electron Content (TEC) immediately before the 2011 Tohoku-oki earthquake (Mw9.0) has been reported by Heki [2011]. Later, Kamogawa and Kakinami [2013] attributed the enhancement to an artifact falsely detected by the combined effect of the highly variable TEC under active geomagnetic condition and the occurrence of a tsunamigenic ionospheric hole [Kakinami et al., 2012]. Recently, Heki and Enomoto [2013] showed that preseismic TEC increase did occur by studying vertical TEC (VTEC) rather than slant TEC (STEC) before and after the 2011 Tohoku-oki earthquake and by comparing them with other geophysical data including the electron density profile from radio occultation, foEs at the Kokubunji ionosonde, and geomagnetic declination changes. In this paper, I focus on a few remaining problems in preseismic TEC enhancement, i.e. (1) possibility to discriminate preseismic TEC anomalies from space-weather origin TEC changes represented by the large-scale traveling ionospheric disturbances (LSTID), (2) estimation of site-specific inter-frequency biases for stations outside Japan, (3) possible difference of amplitudes of preseismic TEC anomalies between mid-latitude and equatorial regions, and (4) comparison between the TEC drops occurring ~10 minutes after earthquakes with preseismic enhancements.

References

Cahyadi, M. N. and K. Heki, Ionospheric disturbances of the 2007 Bengkulu and the 2005 Nias earthquakes, Sumatra, observed with a regional GPS network, J. Geophys. Res., 118, 1-11, doi:10.1002/jgra50208, 2013.

Heki, K., Ionospheric electron enhancement preceding the 2011 Tohoku-Oki earthquake, Geophys. Res. Lett., 38, L17312, doi:10.1029/2011GL047908, 2011.

Heki, K. and Y. Enomoto, Preseismic ionospheric electron enhancements revisited, J. Geophys. Res., 118, 6618-6626, doi:10.1002/jgra.50578, 2013.

Kakinami, Y., M. Kamogawa, Y. Tanioka, S. Watanabe, A. R. Gusman, J.-Y. Liu, Y. Watanabe, and T. Mogi, Tsunamigenic ionospheric hole, Geophys. Res. Lett. 39, L00G27, doi:10.1029/2011GL050159, 2012.

Kamogawa, M. and Y. Kakinami, Is an ionospheric electron enhancement preceding the 2011 Tohoku-oki earthquake a precursor?, J. Geophys. Res., 118, 1-4, doi:10.1002/jgra.50118, 2013.

Maeda, J. and K. Heki, Two-dimensional observations of mid-latitude sporadic-E irregularities with a dense GPS array in Japan, Radio Sci., 49, 1-8, doi:10.1002/2013RS005295, 2014.

(Figure caption) Residual vertical TEC time series for seven large earthquakes for which precursory TEC enhancements have been observed. Below the two examples of the 2011 Tohoku-oki earthquake, the rest (six) of the events are arranged by their moment magnitudes. Distinct trend changes seem to occur about 40 minutes before the earthquake. In some cases, they are cancelled by sudden drops 10 minutes after the earthquakes (e.g. 2007 Bengkulu, 2004 Sumatra-Andaman). In other cases, they decay gradually with a timescale of 20 minutes or so (e.g. 2012 North Sumatra earthquakes). Site names and satellite PRN numbers are given at the right end of the time series.

Keywords: GNSS, GPS, ionosphere, earthquake, precursor, TEC

MIS29-04 Room:313 Time:April 29 15:00-15:15

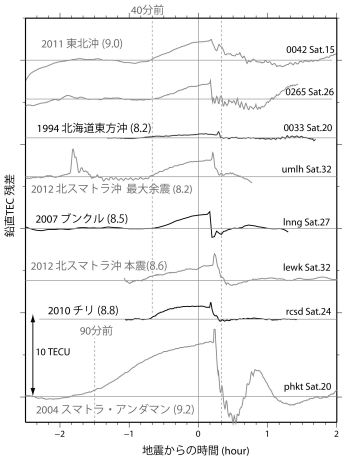

Japan Geoscience Union Meeting 2014
(28 April - 02 May 2014 at Pacifico YOKOHAMA, Kanagawa, Japan)

MIS29-05 Room:313 Time:April 29 15:15-15:30

A Decision Process of the Observation and Research Program of Earthquakes and Volcanoes

KODAMA, Tetsuya[1*]

[1]Tetsuya KODAMA

A Decision Process of the Observation and Research Program of Earthquakes and Volcanoes for Contribution to the Reduction of Disaster will be presented.

Keywords: Subdivision on Geodesy and Geophysics, Earthquake and Volcanoes Subcommittee, Next Research Program Review Committee

Japan Geoscience Union Meeting 2014
(28 April - 02 May 2014 at Pacifico YOKOHAMA, Kanagawa, Japan)

MIS29-06 Room:313 Time:April 29 15:30-15:45

New coordination program of next ”earthquake prediction research” based on the electromagnetic methods

NAGAO, Toshiyasu[1*] ; KODAMA, Tetsuya[2]

[1]Earthquake Prediction Research Center, Tokai University, [2]JAXA

FY 2013 is the final year of the currentfive years program called the University’s earthquake prediction research study. During the current program, devastating Tohoku earthquake occurred in 2011. Therefore extensive revision is requested by the evaluation committee. Unfortunately, the short-term prediction research is not on the map among the current program. We believe that the most important issue in the prediction is the short-term prediction. Therefore, for the next five years’ program we proposed and adopted the unified project based on the electromagnetic methods, which includes Tokai University, Hokkaido University, Earthquake Research Institute, Kyushu University and so on. This really needs close coordination of the SEMS community. In the presentation, we would like to present the outline of impending research plan and tactics.

Keywords: Earthquake Prediction, Electromagnetics, VLF, VHF

Japan Geoscience Union Meeting 2014
(28 April - 02 May 2014 at Pacifico YOKOHAMA, Kanagawa, Japan)

MIS29-07 Room:313 Time:April 29 15:45-16:00

Review of seismo-electromagnetics and earthquake predictology

HAYAKAWA, Masashi[1*]

[1]University of Electro-Communications

This paper consists of a few parts. The 1st part deals with the review of electromagnetic precursors to the 2011 Japan earthquake (EQ). The 2nd part is based on the general review of seismo-electromagnetics, and the 3rd, the proposal of a new science field of EQ predictology. In the 1st paper we present our own results on electromagnetic precursors to the 2011 EQ, including (1) subionospheric VLF/LF propagation anomaly, (2) ULF (ultra-low-frequency) magnetic field depression, and (3) atmospheric VLF/ELF radiation. The 2nd part deals with the present situation of seismo-electromagnetics (DC geoelectric measurement, ULF emissions, atmospheric effect and ionospheric effects), in which the ionospheric precursor has already been found to be statistically correlated with EQs based on long-term data. Finally, by using such EQ precursors we are ready to perform the short-term EQ prediction and to propose a new science field of EQ predictology.

Keywords: Earthquake precursors, Earthquake predictology

Japan Geoscience Union Meeting 2014
(28 April - 02 May 2014 at Pacifico YOKOHAMA, Kanagawa, Japan)

MIS29-08 Room:313 Time:April 29 16:15-16:30

Let’s make use of foretelling an earthquake information.

KUNIHIRO, Hidemitsu[1*]

[1]JYAN meeting for the study

The observation information of 1 JYAN meeting for the study (a foretelling an earthquake amateur net = volunteer group)
(1) Our society for the study performs the NET observation of the FM broadcasting electric-wave, but recorded a decisive harbinger by Awajishima earthquake in last April, and elsewhere much observation records are accumulated, and act for high-reliability as a law learned by experience of the earthquakes.When I could go ahead through the high-reliability in three kinds of observation networks such as the low inside, all frequency to the short wave zone, FM broadcast 100, observation of the ground electromagnetism, and the (2)JYAN meeting for the study collated each observation result, I understood a correlative thing.(3) A great variety of seismometry is carried out, and we demand the collection and feedback of the information there, and can go ahead through the preparations for an exhibition of the observation information nationwide.**I announce the electromagnetism observation to contribute to the mechanism elucidation of 2 earthquakes**.(1) The electric wave propagation change (3) others which appear for several months of the electromagnetism change (2) earthquake that appeared before an earthquakeThe cause that **3 ”foretelling an earthquake information” is not valid**?(1) When ”the foretelling an earthquake is very difficult”, the Japanese Seismological Society of Japan announced it, but do not progress before can announce the foresight information of the earthquake, and therefore cannot start the yet most recent ”foretelling an earthquake information”.(2) If earthquake information is accompanied with a panic and information responsibility, and the information of the major earthquake is announced, a panic is worried about ahead of an earthquake, and if earthquake information is wrong again, is asked the responsibility, and, therefore, cannot be involved in administration and the media either.**4 problems and good solution**?(1) It is necessary let the advancement of the observation technology is necessary, and the promising field of the foretelling an earthquake observe it with enough studies with the earthquake study that the accuracy of the earthquake forecast is necessary for foretelling an earthquake to becoming it there, and to plan the advancement of the foresight technology, and knowledge and the cooperation of the field of extensive arts and sciences let all integrates scientific study or observation information because necessary, and visualize it, and the earthquake study plans the development of the new technology again.(2) Is a panic and information responsibility, but if wake up a large panic in little information, and the warning information of the earthquake cooperates with the media there, and the commuter rush of the city just announces the observation information of the earthquake in the same way as typhoon information because daily life is an abnormal situation, and change it to use earthquake information by a self-judgment anytime, the panic is controlled, and do not have the responsibility problem besides now. **To convey the earthquake forecast that 5 is ideal for** If it is with more right seismometry information if it establishes a seismometry center (a tentative name) to make environment let unify all observation information, and to be able to give synthetic judgment to to do earthquake information precisely because necessary, and let unify a study and observation information, and feed back information again necessary for each observation spot., and may start the earthquake forecast that the nation can rely on, and there are administration and cooperation of the media, may change in the country more reliable safely.

Japan Geoscience Union Meeting 2014
(28 April - 02 May 2014 at Pacifico YOKOHAMA, Kanagawa, Japan)

MIS29-09 Room:313 Time:April 29 16:30-16:45

3-D visualization of the preseismic ionospheric anomalies

HIROOKA, Shinji[1*] ; HATTORI, Katsumi[1] ; ICHIKAWA, Takashi[1]

[1]Graduate School of Sci., Chiba Univ.

The ionospheric anomalies possibly associated with large earthquakes have been reported by many researchers. However, a physical mechanism of pre-seismic ionospheric anomalies has not been clarified. To understand the mechanism, monitoring of three-dimensional distributions of ionospheric electron density is considered to be effective. In this study, to investigate the three-dimensional structure of ionospheric electron density prior to large earthquake, the Neural Network based tomographic approach is adapted to GEONET and ionosonde data. In the case of the 2011 Off the Pacific Coast of Tohoku Earthquake (Mw9.0), the significant enhancements are found in Total Electron Content (TEC) investigation, 1, 3-4 days prior to the earthquake. Especially, TEC increase of 3 days prior to the earthquake was remarkable. As a result of tomographic analysis, the reconstructed distribution of electron density was decreased above the epicenter around 250 km altitude (below the hmF2 altitude) in comparison with 15 days backward median distribution. Meanwhile, we found the electron density enhancement above hmF2 altitude. Moreover, the similar structures were found in many other earthquake occurred in Japan. Especially, in the case of long-term GIM-TEC anomalies (10 hours per day and over) were found, the similar structure was detected at a high rate (85%). Details will be shown in the presentation.

Keywords: Ionospheric tomography, GPS-TEC, Preseismic ionospheric anomaly

Japan Geoscience Union Meeting 2014
(28 April - 02 May 2014 at Pacifico YOKOHAMA, Kanagawa, Japan)

MIS29-10 Room:313 Time:April 29 16:45-17:00

Study on lithosphere-atmosphere-ionosphere coupling inferred from the data of GPS surface displacement and ionopheric pe

HOBARA, Yasuhide[1*] ; MIYAKE, Risa[1] ; CHEN, Chieh-hung[2]

[1]Graduate School of Information and Engineering Department of Communication Engineering and Informati, [2]Institute of Earth Sciences, Academia Sinica, Taiwan

Various scenarios of coupling mechanisms between the major seismic activities on the ground and overlaying ionosphere have been proposed, experimental evidence has not been observed clearly. In this paper we analyze long-term data from ground movement and ionospheric anomalies in relation with major earthquakes occurred around Japan. In association with major earthquakes, anomalous surface displacements are observed by dens GPS network whilst lower ionospheric perturbations are identified by continuous measurement of VLF/LF transmitter signals. As a result, we found that the ionospheric anomalies are observed preferably associated with the thrust type earthquakes. GPS surface displacements tend to occur in association with any types of earthquakes.

Keywords: ionopheric perturbations, GPS surface displacement, lithosphere-atmosphere-ionosphere coupling, earthquake

Japan Geoscience Union Meeting 2014
(28 April - 02 May 2014 at Pacifico YOKOHAMA, Kanagawa, Japan)

MIS29-11 Room:313 Time:April 29 17:00-17:15

Precursor Ionization Anomaly (PIA) caused by earthquake electric field- with and without natural eastward electric field

OYAMA, Koichiro[1*] ; KAKINAMI, Yoshihiro[2]

[1]Plasma and Space Science Center, National Cheng Kung Universoty,Taiwan, [2]School of Systems Engineering, Kochi University of Technology

In the low/midlatitude ionosphere, feature which is similar to Equator Ionization anomaly (EIA) is produced about 5 days before large earthquake (Oyama et al., 2010). The phenomenon was found by using the data obtained by US satellite DE-2, which was in orbit during 1981-1982. We named this phenomenon Precursor Ionization Anomaly (PIA). To find the PIA, satellite altitude should be below 400 Km. PIA seems to show different feature depending on the magnitude of electric field associated with earthquake, distance from the magnetic equator, and the height of the ionosphere to be studied. Depending on the magnitude of the earthquake electric field, and the height to be measured, the electron density shows the minimum or the peak. PIA is also influenced by natural electric field. When EIA exists, two minima of the electron density appear; one is caused by natural eastward E filed, another by earthquake electric field. sometimes three minima appear. Here we present two cases: 1.PIA under the existence of natural eastward electric field. 2. PIA without/or weak natural eastward electric field. We stress here that constellation of small satellites will provide a breakthrough for precursor study of large earthquake.

Keywords: Earthquake, electric field, plasma density, fountain effect

Japan Geoscience Union Meeting 2014
(28 April - 02 May 2014 at Pacifico YOKOHAMA, Kanagawa, Japan)

MIS29-12 Room:313 Time:April 29 17:15-17:30

Mission Analysis of Micro-Satellite for Earthquake Precursor Study

SUTO, Yushi[1*] ; NAKAMURA, Maho[1] ; KAMOGAWA, Masashi[1]

[1]Dpt. of Phys., Tokyo Gakugei Univ.

A mitigation of the disasters attributed to mega-earthquake should be prioritized for saving human lives. In order to promote earthquake prediction, we take particular notice of one of plausible ionospheric precursors, the decrease of VLF electromagnetic wave intensity. Then we statistically verify such a precursor associated with world-wide large earthquakes, and finally conclude whether earthquakes are predicable or not. For this purpose, a dedicated satellite with 2.5- year operation is proposed.

Keywords: Earthquake, Ionospheric Precursors, Micro-Satellite

Japan Geoscience Union Meeting 2014
(28 April - 02 May 2014 at Pacifico YOKOHAMA, Kanagawa, Japan)

MIS29-13 Room:313 Time:April 29 17:30-17:45

Satelite orbit of detecting Ionospheric Earthquake Precursor

TOGO, Shoho[1*] ; SUTO, Yushi[1] ; KAMOGAWA, Masashi[1]

[1]Dpt. of Phys., Tokyo Gakugei Univ.

In general, it is difficult to show a statistical correlation between the precursor and the large earthquake, because of infrequent occurrences of the large earthquake. In particular, to prove the causation required by the identification criteria 5 needs a number of much larger earthquakes, which are further less number according to Gutenberg- Richter relation. In addition, the events of earthquakes in the ocean and far from the ground observation site might be undetectable. Supposing that a number of precursors are detectable on the ground-based station, it might take the long term of thousand years. Theses plausible atmospheric-ionospheric precursors last for a few hours to a few days before the mainshock. Therefore, some of precursors are detectable by satellites because the orbit sampling of satellite is less than the duration of the precursors. Moreover, the satellite observation can cover the whole of a region of active seismicity, when the inclination of satellite is more than 60 degrees. In this presentation, we propose ideal orbits of dedicated satellite for this study.

Keywords: Earthquake, Ionosphere, Satellite

Japan Geoscience Union Meeting 2014
(28 April - 02 May 2014 at Pacifico YOKOHAMA, Kanagawa, Japan)

MIS29-P01 Room:Poster Time:April 29 18:15-19:30

Investigation of ”positive hole excitation” for stressed igneous rocks with a control of water content

OSADA, Akira[1*] ; YAMANAKA, Chihiro[1]

[1]Graduate School of Science, Osaka University

Piezo electric effects, positive hole excitation for stressed igneous rocks and streaming potential have been considered possible mechanisms that explain pre-seismic electric signals. Especially, positive hole excitation, (Freund et al. 2006), explains long-term anomalous electromagnetic signals and telluric current signals observed for a long distance, therefore attracts a lot of attention.

To clarify the mechanism of pre-seismic electric signals, we performed following experiments for stressed igneous rocks with saturated by water. Samples of granite and gabbro sized 3×3×10cm. Then, the samples were loaded from 1.08MPa to 5.45MPa, with recording of water content. Current-flows from -40pA to -20pA and around -1.5nA were observed for granite and gabbro samples respectively, while any current changes were not observed from bone-dry rocks. These results indicate that pore water is closely tied to current changes. Samples with different size were also tested. The values of current-flow agree well with results of observation of pre-seismic anomalous telluric current signals in Kozu-shima Island (Orihara et al. 2012), assuming the resistivity 10-1000Ωm.

Reference

1) F.T.Freund, A.Takeuchi, B.W.S.Lau, ’Electric currents streaming out of stressed igneous rock - A step towards understanding pre-earthquake low frequency EM emissions’, Physics and Chemistry of the Earth 31. pp.389-396. (2006)

2) Y.Orihara, M.Kamogawa, T.Nagao, S.Uyeda, ’Preseismic anomalous telluric current signals observed in Kozu-shima Island, Japan’, Proceedings of the National Academy of Sciences Vol.109 No.47 pp.19125-19128. (2012)

Keywords: Seismic electric signals, Streaming potential, Positive hole excitation, Igneous rocks

Japan Geoscience Union Meeting 2014
(28 April - 02 May 2014 at Pacifico YOKOHAMA, Kanagawa, Japan)

MIS29-P02 Room:Poster Time:April 29 18:15-19:30

Analysis of geomagnetic diurnal variations at Esashi station from 1997˜2012

ASHIDA, Ryo[1*] ; HATTORI, Katsumi[1] ; HAN, Peng[1] ; FEBRIANI, Febty[1] ; YOSHINO, Chie[1]

[1]Graduate School of Science, Chiba University

There have been many reports on ultra-low-frequency (ULF) electromagnetic phenomena associated with earthquakes in a very wide frequency range. In this study, unusual behaviors of geomagnetic diurnal variations prior to the 2011 off the Pacific coast of Tohoku earthquake (Mw9.0) have been reported. Ratios of diurnal variation range between the target station Esashi (ESA) which is about 135 km from the epicenter and the remote reference station Kakioka (KAK) have been computed. The results showed that there had been clear anomalies exceeding the statistical threshold in the vertical component about 2 months before the mega event. These anomalies are unique over a 16 years background. The original records of geomagnetic fields of the ESA station also exhibited continuous anomalous behaviors for about 10 days in the vertical component from Jan.3, 2011-Jan.13, 2011, about two months prior to the Mw 9.0 earthquake. During the same period, other independent geophysical parameters such as seismicity and crustal deformation also show clear unusual changes, which suggests these anomalies might be related with the mega event.

Keywords: ULF seismo-magnetic phenomena, earthquake, geomagnetic diurnal variations

Japan Geoscience Union Meeting 2014
(28 April - 02 May 2014 at Pacifico YOKOHAMA, Kanagawa, Japan)

MIS29-P03 Room:Poster Time:April 29 18:15-19:30

Identification of seismo - ionospheric signatures by using amplitude and phase information of VLF/LF transmitter waves

TATSUTA, Kenshin[1*] ; HOBARA, Yasuhide[1]

[1]Graduate School of Informatics and Communication Eng. , The University of Electro-Communications

In this paper, we analyse the VLF/LF transmitter signals in association with major seismic activities over Japan. Particular attention is paid to phase in addition to amplitude information of the VLF/LF signals. As a result, significant change both in the phase and amplitude are identified as an anomaly of seismo - ionospheric signatures. Moreover, the results of numerical analysis of VLF/LF transmitter waves in the earth - ionosphere waveguide by using FDTD method are in good agreement with the experimental results. We conclude that simultaneous use of amplitude and phase information of VLF/LF signal will be useful to identify the special scale of seismo - ionospheric anomalies.

Keywords: seismo - ionospheric perturbation, FDTD method, VLF/LF transmitter, earthquake

Japan Geoscience Union Meeting 2014
(28 April - 02 May 2014 at Pacifico YOKOHAMA, Kanagawa, Japan)

MIS29-P04 Room:Poster Time:April 29 18:15-19:30

Ionospheric Anomaly as an Earthquake Precursor : Statistical Study during 1998-2012 around Japan

KUNIMITSU, Mayuka[2*] ; HATTORI, Katsumi[3] ; HAN, Peng[3] ; LIU, Jann-yenq[1]

[1]Faculty of science, Chiba University, [2]Graduate School of Science, Chiba University, [3]Institute of Space Science, National Central University, Taiwan

Many anomalous electromagnetic phenomena possibly associated with large earthquakes have been reported. TEC (Total Electron Contents) anomaly is one of the most promising phenomena preceding large earthquakes. We investigated statistically TEC anomalies before large earthquakes around Japan region during 1998-2012. In this study, superposed epoch analysis (SEA) and Molchan's error diagram (MED) analysis have been taken to investigate correlation and predictability in the statistical manner. The results of SEA show that positive anomaly 1-5 days before the large earthquake (M>=6.0 and depth <= 40 km) is significant. The results of MED analysis indicate the some gain against the random estimation (Poisson model). That is, the prediction using TEC anomaly around Japan is not random and has an information. The details will be given in the presentation.

Japan Geoscience Union Meeting 2014
(28 April - 02 May 2014 at Pacifico YOKOHAMA, Kanagawa, Japan)

MIS29-P05 Room:Poster Time:April 29 18:15-19:30

Detection of thermal anomaly associated with Earthquake from MODIS data

TSUTSUMI, Rika[1*]

[1]Chiba University

It is a critical issue to mitigate of disasters including earthquake. And it is required to develop of technique to monitor and predict major earthquakes. Therefore, the purpose of this study is to develop an adequate algorithm to detect LST (Land Surface Temperature) anomalies related to earthquakes using MODIS (Moderate Resolution Imaging Spectroradiometer) infrared sensor onboard Terra/Arqua satellite.

We investigate spatial-time changes in LST in the statistical way. In order to detect only hotspots related to earthquakes without faints, the developed algorithm investigates the difference temperature behavior between a target point and spatial average, and we get spatial difference of brightness temperature(delta-T). In order to evaluate the temporal singularity of delta-T, we calculate the following equation.

R=(delta-T(x,y,t)-ave(x,y))/sigma(x,y)

where ave(x,y) is multi year plus minus 15 days moving average. And sigma(x,y) is multi year plus minus 15 days moving standard deviation.

We detect LST anomaly 8 days before L'Aquila earthquake. And it continued for several hours. This result represents that it has potential for monitoring/predicting major earthquakes to develop algorithms to detect thermal anomalies using MODIS data.

Keywords: MODIS, Earthquake, L'Aquila, thermal anomaly

Japan Geoscience Union Meeting 2014
(28 April - 02 May 2014 at Pacifico YOKOHAMA, Kanagawa, Japan)

MIS30-01 Room:501 Time:April 28 09:00-09:15

diatom assemblages in INW2012 drilling cores from Lake Inawashiro , Tohoku, Japan

HIROSE, Kotaro[1*] ; NAGAHASHI, Yoshitaka[1]

[1]1Fukushima University

Inawashiro-ko Formation is named by a 28.13m sediment core taken from Lake Inawasiro- ko, Fukushima Prefecture, Japan. Stratigraphy and facies analysis combined with tephra and AMS radiocarbon dating were carried out on INW-2012. The Inawashiro-ko Formation are divided into three stratigraphic units: the Lower part (37.17-26.60m) consisted by medium sand-sandy silt (vertically varied in grain size) with granule and wood fragments, the Middle part (26.60-24.89m) consisted by very fine sand-silt with upper level grain refinement, and the Upper part (24.89-0.00m) consisted by dense alternation of brighter and darker clay layers including fallout tephra and Lahars by sediment gravity flow. Each unit are formed by fluvial basin before the form of the lake, early stage of the lake, lake with deep water as present, respectively. ^{14}C dating indicate that Lake Inawashiro-ko is formed 42 cal k BP, and characteristic dense alternation of brighter and darker clay layers deposit continuously except for the most early stage of the Lake. The sedimentation late in the upper part is 0.3-1.0(mm/yr). Additionally, We report the temporal variation of diatom assemblage and its relation to water environment in the past 2000 years from upper 2.00m of IN2012.

Keywords: Lake Inawashiro-ko, lacustrine sediment core, stratigraphy, diatom assemblage, late Pleistocene, 14C dating

Japan Geoscience Union Meeting 2014
(28 April - 02 May 2014 at Pacifico YOKOHAMA, Kanagawa, Japan)

MIS30-02 Room:501 Time:April 28 09:15-09:30

Two different types of regime shift appeared in a 2900-yr record of Japanese sardine abundance

KUWAE, Michinobu[2*] ; YAMAMOTO, Masanobu[2] ; SUGIMOTO, Takashige[3] ; TAKEOKA, Hidetaka[1]

[1]CMES, Ehime Univ., [2]Faculty of Environmental Earth Science, Hokkaido Univ., [3]Institute of Civilization, Tokai University,

Regime shift, revealed in climates and marine ecosystem, is one of key dynamics to predict rapid changes in marine ecosystems and fisheries resources for decades. The regime shift is defined as a relatively rapid change (occurring within a year or two) from one decadal-scale period of a persistent state (regime) to another decadal-scale period of a persistent state (Minobe 1997; King 2005). In the Pacific it has been detected in Pacific Decadal Oscillation (PDO) (Mantua et al., 1997) and species replacement between anchovy and sardine (Lluch-Belda et al., 1989). There is so far no sufficient evidence of how regime shift changes in its feature on longer timescales because of paucity of long-term high-resolution marine records in the Pacific. Here we present a 2900-year record of ecosystem regime shift in the western North Pacific using Japanese sardine abundance which can be reconstructed from fossil scales in the coastal marine sediments; timing of decreases and increases in the abundance can be used as an index of regime shift. Sardine abundance showed two different types of regime shift in the time series. One is a regime shift similar to that previously detected in the 20th century, which repeatedly occurs on interdecadal timescales. The other is a regime shift in relation to centennial-scale variability in sardine abundance, which could be followed by a centennial-scale low or high abundance period characterized by respective small or large amplitudes of decadal variations in abundance. Our estimation suggests that the maximum abundance is depleted one-quarter to one-tenth of that in the sardine regime in 1980s. Similar patterns of the latter regime shift are revealed in the time series of sardine abundance off California (Baumgartner et al., 1992) and Chile (Valdes et al. 2008), PDO index reconstructed from North America (Macdonald and Case 2005), and abnormal snow index in East Asia (Chu et al., 2008). This indicates that the latter regime shifts that we found are associated with those of marine ecosystems and climate over the Pacific. The recent high sardine abundance period lasted 200 years in the Pacific, suggesting transition to next centennial low abundance period in the near future. Careful examinations on whether the latest regime shift in 1990s is the case of the latter regime shift are important for the long-term prediction of climate and fisheries resources.

Keywords: regime shift, marine ecosystem, sardine fossil scale record, Pacific, Beppu Bay

Japan Geoscience Union Meeting 2014
(28 April - 02 May 2014 at Pacifico YOKOHAMA, Kanagawa, Japan)

MIS30-03 Room:501 Time:April 28 09:30-09:45

Modern changes of sedimentary environments in the brackish Lake Shinji, the east part of Shimane prefecture,Japan

SETO, Koji[1*] ; IKEDA, Hiroko[2] ; YAMAGUCHI, Keiko[3] ; KURATA, Kengo[3]

[1]ReCCLE, Shimane Univ., [2]Geoscience, Shimane Univ., [3]Life and Environmental Science, Shimane Univ.

Lake Shinji is oligohaline brackish lake in the east part of Shimane prefecture. Area of Lake Shinji is 79.1km^2, water depth shows less than 6m. The water column of Lake Shinji is divided into oligohaline surface water, mesohaline pycnocline, and mesohaline bottom water.

In recent years, Lake Shinji is observed environmental events such as Cyanobacterial water?bloom, anomaly overgrowth of aquatic plants, decrease in the catch of Corbicula and so on. The purpose of this study is to reveal the changes in the sedimentary environment by using the comparison with the spatial investigation of surface sediments in 2006 and 2013 and the result of monitoring since 2010 in Lake Shinji.

The surface sediments in Lake Shinji in 2006 are sandy deposits shallower than 3.5m in water depth, but are muddy deposits deeper than its depth. Mean grain size of surface sediments deeper than 3.5m tend to be fine-grained with water depth, and shows 7.5 phi in deepest site. In shallower than 3.5m, many surface sediments shows fine to medium sand around 2 phi. Total organic carbon (TOC) contents of surface sediments was less than 4%.TOC contents shows high positive correlation coefficient 0.85 with mean grain size. This is suggested that the spatial distribution of TOC contents depend on grain size. Total Sulfur (TS) contents of surface sediments were less than 1 %, and tend to be decreased with water depth. However, TS contents were less than 0.2 % shallower than 4.5m. In deeper than its depth,TS contents decreases dramatically.

The surface sediments in Lake Shinji in 2013 are sandy deposits shallower than 3.5m in water depth, but are muddy deposits deeper than its depth. Mean grain size in 2013 was similar to the 2006. TOC contents of surface sediments were 6 to 8 %. TS contents were less than 2 %. TS contents were less than 0.2 % shallower than 3.0m. This depth is shallow clearly than in 2006.

TOC contents in monitoring site from 2010 to 2013 fluctuated greatly in the range of 4% to 10%. TOC contents shows low values in summer season, and high values in winter season.It is considered that the fluctuation of TOC contents is caused by the dilution effect of inorganic sediment due to rainfall in the summer. In addition, TOC contents tend to increase from 2010 to 2013. TS contents fluctuated greatly in the range of 0.5 % to 2.0 %. TOC contents shows high values in summer season, and low values in winter season, and tend to increase from 2010 to 2013 as with the TOC contents.This is suggested that the increase of TS contents is caused by the inflow of mesohaline water and the decrease of dissolved oxygen in bottom water.

From the results of these, surface sediments and bottom water environments in Lake Shinji are a distinct change during term from 2006 to 2013. We are thinking that some of this cause.

Keywords: Lake Shinji, Surface sediments, Total organic carbon contents, Total Sulfur contents, Grain size analysis

Japan Geoscience Union Meeting 2014
(28 April - 02 May 2014 at Pacifico YOKOHAMA, Kanagawa, Japan)

MIS30-04 Room:501 Time:April 28 09:45-10:00

Provenances of detrital materials in the Lake Suigetsu sediment and quantitative evaluation of their mixing ratio

SUZUKI, Yoshiaki[1*] ; TADA, Ryuji[1] ; NAKAGAWA, Takeshi[2] ; NAGASHIMA, Kana[3] ; HARAGUCHI, Tsuyoshi[4] ; GOTANDA, Katsuya[5] ; IRINO, Tomohisa[6] ; SUGISAKI, Saiko[1] ; SG12/06, Project members[7]

[1]Univ. Tokyo, [2]Univ. Newcastle, [3]JAMSTEC, [4]Osaka City University, [5]Chiba University of Commerce, [6]Hokkaido University, [7]SG12/06 Project

Lake Suigetsu, central Japan, is characterized by annually laminated sediment, and extremely high resolution and precise age-depth model was established using drilled cores retrieved on 1993 and 2006. For this reason, Lake Suigetsu sediment is ideal subject of high resolution and precise paleo-climate reconstruction. Detrital material accumulated in Lake Suigetsu is thought to have 3 provenances with 3 different transport paths. One is eolian dust transported by wind from Asian continent. Second is detrital material transported by small rivers from surrounding slopes. Third is suspended sediment supplied from Hasu River and transported through Lake Mikata, which is connected to Lake Suigetsu with shallow channel. Mechanism and flux of detrital materkals from these 3 sources could be controlled by the behavior of westerly jet, slope failure due to flood and/or earthquake, and rainfall and erosional process within the drainage area. Therefore, if we could reconstruct the flux of detrital materials from each provenance, we could gain detailed information on histories of paleo-climate and disasters.

In this study, we did factor analysis of chemical composition of detrital fraction extracted from the sediment by chemical treatment. Each end-member extracted by factor analysis was characterized with respect to mineral composition, color, and grain-size distribution. We compared these characteristics with samples taken from probable sources and from event layers in the sediment, and tried to re-construct the flux change of each detrital component.

Keywords: Lake Suigetsu, Deglaciation, Holocene, Factor analysis, Multi-regression analysis

Japan Geoscience Union Meeting 2014
(28 April - 02 May 2014 at Pacifico YOKOHAMA, Kanagawa, Japan)

MIS30-05 Room:501 Time:April 28 10:00-10:15

Wetter condition during the Heinrich Event 1? deduced from detrital flux and provenance records from Lake Suigetsu

NAGASHIMA, Kana[1*] ; NAKAGAWA, Takeshi[2] ; SUZUKI, Yoshiaki[3] ; TADA, Ryuji[3] ; HORIUCHI, Daishi[4] ; SUGISAKI, Saiko[3] ; GOTANDA, Katsuya[5] ; HARAGUCHI, Tsuyoshi[6] ; SG06/12, Project member[7]

[1]JAMSTEC RIGC, [2]University of Newcastle, [3]The University of Tokyo, [4]Japan Coast Guard, [5]Chiba University of Commerce, [6]Osaka City University, [7]http://www.suigetsu.org

Stalagmites in Chinese caves, loess/paleosol sequence of the Chinese Loess Plateau, and lacustrine sediments in Asian countries are favorable to monitor the past changes in East Asian summer monsoon (EASM). However, not much is known about EASM spatial changes during the last deglaciation mostly due to the large uncertainty in the chronologies of the lacustrine and loess/paleosol sediments.

Lake Suigetsu in Central Japan is known for the varved sediments which cover at least last 70 kyr. Recently, accurate age model is established for SG06 core based on varve counting and more than 800 radiocarbon dates (e.g., Ramsey et al., 2012; Staff et al., 2013). Here we examine the precipitation changes in Central Japan during the last deglaciation from the flux and provenance changes of the detrital materials found in the SG06 core sediment.

We analysed flux of detrital materials for the last glacial part of the SG06 core (1402-1810 cm interval of the SG06 composite depth) with 1 cm resolution (corresponding to 7-13 yrs) and estimated provenance of the detrital materials using chemical and mineral compositions, grain sizes, and electron spin resonance intensity and crystallinity of the quartz. The reconstructed flux of detrital materials are characterized by the millennial-scale increases exceeding 12 mg/cm^2/yr at 16,600-14,800 and 13,700-12,800 $SG06_{2012}$ yr BP and short-lived (decadal to centennial) episodes of higher flux repeated more than thirty times throughout the deglaciation interval.

The grain size, color, chemical composition, and crystallinity of quartz records suggest that the increase of the detrital materials during 16,600-14,800 $SG06_{2012}$ yr BP was mainly due to increase of suspended particles supplied from Hasu river through Lake Mikata, that is located immediately upstream of Lake Suigetsu and trapping most of coarse detrital grains. In contrast, the increase of detrital materials during 13,700-12,800 $SG06_{2012}$ yr BP likely reflects local slope erosion around the lake and partly the long-distance aeolian transport from the Asian deserts. Our result suggests the wetter condition in Central Japan during the Heinrich Event 1 in contrast to the dry condition in Yangtze River Basin, China, according to the δ18O stalagmite record (Wang et al., 2001).

Keywords: Lake Suigetsu, Heinrich Event, East Asian Summer Monsoon, detrital material, quartz

Japan Geoscience Union Meeting 2014
(28 April - 02 May 2014 at Pacifico YOKOHAMA, Kanagawa, Japan)

MIS30-06 Room:501 Time:April 28 10:15-10:30

Variation of very fine grained elemental carbon deposition to the Rebun Island, Hokkaido, during the last 5 ky

NAKAI, Yoshie[1*] ; IRINO, Tomohisa[1] ; YAMAMOTO, Masanobu[1] ; MIYAZAKI, Yuzo[1] ; KAWAMURA, Kimitaka[1] ; YAMADA, Kazuyoshi[2] ; YONENOBU, Hitoshi[3]

[1]Hokkaido University, [2]Waseda University, [3]Naruto University of Education

Elemental carbon (EC) is a combustion product which is composed of rich C and depleted O, H, S, N. Biomass burning is major source of Pre-industrial EC, while fossil fuel burning has been the most important source since the 18th century. Black carbon (BC) transfered in the atmosphere as aelosols, including EC have a great impact on the climate. EC is also the second strongest contributor to global warming, and has effect to darken snow and ice surface. On the other hand, aerosols including EC have also negative effect on radiative forcing, which lead cooling. Although it is difficult to evaluate the net EC effect on climate, it is necessary to discriminate EC produced by fossil fuel burning from those from biomass burning. EC is not a single chemical compound, but it can be classified into two types , char and soot. Char is produced by pyrolysis, while soot is formed via gas-to-particle conversion. The char particles which are countable under microscope are called charcoal. There are many researches to reconstruct paleo-fire by counting charcoal, and in the late Holocene, the fire sometimes synchronized with human activity. Therefore, it is very important to understand the past EC variation to examine the relationship between climate change and history of human.

There are some methods for analysis of EC, and in this study, we use the method called thermal optical reflectance (TOR) -method. This method is principally used to analyze EC/OC in aelosols, where we can evaluate an interference of pyrolyzed OC produced during the temperature rise under He atmosphere by measuring the transmittance of near-infrared laser. In order to apply TOR-method to analysis of sediment, we examined thermograms for sucrose, fulvic acid, humic acid, and fullerene in advance. As a result, we confirmed that carbon fraction decomposed at 700-850 ℃ under O2 atmosphere can be regarded as an EC.

The sediment sample we used was collected from the Kusyu Lake in the Rebun Island. We established the stratigraphy of the sediment core of 20 m long as well as the sedimentation rate of the surface sediment. From variation of the ratio of coarse/fine particles down to12 m depth , the sedimentary environment would be changed from marine to fresh water at 600 cm. We analyzed EC/OC both for coarse and fine particles for 0-600 cm interval. The result shows that the variation of EC in coarse particle reflects local variation, while the EC in the fine fraction reflects local and/or distal variation. The local biomass burning increased at 521 cm. The influence of distal EC variability was larger in the interval of >217 cm, with the maximum at 217 cm and the minimum at 263 cm. The long-distance transportation of EC could be influenced not only by increase and decrease of supply from biomass burning but also by the variation of wind pathway which transports distant EC.

Keywords: elemental carbon, biomass burning, Holocene, Rebun Island

Japan Geoscience Union Meeting 2014
(28 April - 02 May 2014 at Pacifico YOKOHAMA, Kanagawa, Japan)

MIS30-07 Room:501 Time:April 28 10:30-10:45

Chronological study on widespread tephras for the past 50,000 years in and around Japanese Islands

OKUNO, Mitsuru[1*] ; TORII, Masayuki[2] ; NAKAMURA, Toshio[3]

[1]Fac. Sci., Fukuoka Univ., [2]Grad. Sch., Sci. Tech., Kumamoto Univ., [3]CCR, Nagoya Univ.

After discovery of Aira Tn (AT) tephra, many widespread tephras have been recognized. The tephra for the past 50,000 years can be dated by the radiocarbon (^{14}C) age determination. All ^{14}C dates for tephras after Spfa-1 can be calibrated to a calendar year using calibration dataset "IntCal13". On the other hand, the stratigraphy and the age of tephras intercalated with core sample from marine and lake have been made highly precise. In this presentation, we review the chronological research on widespread tephras for the past 50,000 years, and then present its perspective

Keywords: widespread tephra, radiocarbon dating

Japan Geoscience Union Meeting 2014
(28 April - 02 May 2014 at Pacifico YOKOHAMA, Kanagawa, Japan)

MIS30-08 Room:501 Time:April 28 11:00-11:30

The door that the IntCal13 and Suigetsu dataset opened for us all

NAKAGAWA, Takeshi[1*] ; SUIGETSU 2006, Project members[1]

[1]Department of Geography, Newcastle University (UK)

See the Japanese abstract (the presentation will be in Japanese)

Keywords: IntCal13, Radiocarbon dating, Radiocarbon calibration, varved sediment, climate change, age-based correlation

Japan Geoscience Union Meeting 2014
(28 April - 02 May 2014 at Pacifico YOKOHAMA, Kanagawa, Japan)

MIS30-09 Room:501 Time:April 28 11:30-12:00

A new high resolution dating method using tree-ring cellulose oxygen isotope ratio

NAKATSUKA, Takeshi[1*] ; SANO, Masaki[1] ; XU, Chenxi[1] ; KIMURA, Katsuhiko[2]

[1]Research Institute for Humanity and Nature, [2]Fukushima University

Introduction

Dendrochoronology is the most accurate dating method by comparing of inter-annual variations in tree-ring width of wood samples from sedimentary layers, archaeological remains or old architectures against the predated standard ring width variations. Master chronologies of tree-ring width, necessary to be built for each region and species, have been established all over world. Some of them based on many living and buried trees cover the whole Holocene in Northern Europe and New Zealand. Tree rings contain other parameters than ring width, applicable for dendrochronological dating. Oxygen isotope ratio (d18O) of cellulose is one of them. Here, we demonstrate merits, methods and problems of the tree-ring d18O chronology in details.

Merits of tree-ring cellulose d18O chronology

Because tree-ring cellulose d18O is controlled solely by two meteorological factors, precipitation d18O and relative humidity, its inter-annual variation is usually independent from ecophysiological conditions of each tree. As the result, highly correlated tree-ring cellulose d18O variations between different trees ensure high success rate of dating. Moreover, the master chronology of tree-ring cellulose d18O built on cedar and cypress trees can be applied to date wood samples from all other tree species living in the same region and period. Therefore, many tree-ring d18O chronologies are now being created very rapidly all over Japan during the late Holocene, and the established tree-ring cellulose d18O chronologies have been applied for dating of various natural and artificial wood samples to promote new inter-disciplinary studies in both natural and human sciences.

Methods in tree-ring cellulose d18O chronology

There are two important progresses in analytical method behind the emergence of tree-ring d18O chronology. One is the combined instrument of a pyrolysis-type elemental analyzer and an isotope ratio mass spectrometer. The other is ”plate method for cellulose extraction” from tree ring samples. Before 2000AD, it was extremely difficult to measure d18O of organic matter because combustion of samples to gases inevitably causes terrible oxygen contamination. The development of an instrument, which converts organic oxygen to CO without any oxidant at 1400 degree C and transfer the CO to mass spectrometer directly, solved the question how to measure d18O in huge numbers of tree ring cellulose. So far, cellulose extraction from many tree ring samples has been too time-consuming and labor-intensive to meet the huge number of samples in dendrochronological purposes. In 2010, we have developed a new method to extract cellulose directly from thin wood plates with hundreds of rings, which enabled us to start the tree-ring cellulose d18O chronology at last.

Perspectives of tree-ring cellulose d18O chronology

Although it is much more time-consuming to analyze tree-ring cellulose d18O than to measure tree ring width, we have accumulated many tree-ring d18O data from various kinds of samples and obtained many essential knowledge. While some data have successfully dated important archaeological remains, new problems have also emerged. Here, we show those problems and discuss future perspective of the tree-ring d18O chronology. <Tree Species>There are usually high correlations in tree-ring d18O time series between conifer and deciduous hardwood. But, evergreen hardwood may be somewhat different due to the longer photosynthetic season. <Spatial Correlation>Tree-ring d18O chronology in central Japan is coincident with those in western Japan, reflecting inter-annual changes of stationary rain band (Baiu front) activity in early summer. However, tree-ring d18O time series on Japan Sea side sometimes becomes complicated due to effect of heavy snow cover. <Analytical Method>”Plate method” sometimes destroys ring boundary of buried wood, so that it is necessary to further improve cellulose extraction procedure.

Keywords: tree ring, cellulose, oxygen isotope ratio, dendrochronology

Japan Geoscience Union Meeting 2014
(28 April - 02 May 2014 at Pacifico YOKOHAMA, Kanagawa, Japan)

MIS30-10 Room:501 Time:April 28 14:15-14:30

Calcareous nodules for sea floor paleothermometry

HASEGAWA, Takashi[1*] ; KOBIYAMA, Yosuke[2] ; YONEZAWA, Shunsuke[2] ; SUZUKI, Takaaki[4] ; JENKINS, Robert[1] ; MORI, Takami[3]

[1]College of Natural Science and Engineering, Kanazawa University, [2]Graduate School of Natural Science and Technology, Kanazawa University, [3]Kanazawa University (currently Marine Work Japan), [4]Kanazawa University (currently Itochu Oil Exp. Co. Ltd.)

Paleothermometry is one of the most important proxies for paleoceanographers. Benthic foraminifers have been used for reconstructing paleotemperature on the bottom of the sea. They are excellent materials for calcareous ooze, while mudstone sequences shows lots of difficulty to apply this technique for terrigenous sediments distributed around Pacific. Calcareous nodules are commonly observed in mudstone sequences, however, no study discussed potential paleothermometry based on calcareous nodules. It might supplements the role of benthic foraminifers. We described occurrences at outcrops, general configurations including their cut sections, analyzed carbon content, total organic carbon, and carbon and oxygen isotopes of nodules collected from Cretaceous starata of several regions in Hokkaido including the Haboro area.

Structure suggesting consolidation just below the sea floor includes burrows that eject calcareous material from nodule. Nodules consolidated associated with anaerobic oxidation of methane with sulfate reduction appear to be just-below-the-sea-bottom origin. Such nodules show the exactly same oxygen isotope values with that of benthic foraminifers. A bivalve fossil found on one of the methane seep nodules preserved aragonite of the shell and yielded close oxygen isotope temperature with that of host nodule.

Carbonate content and oxygen isotope values had positive relation suggesting carbonate content was controlled by the depth of nodule production. Nodules with lower carbonate content ($<$50%) exclusively show low oxygen isotope values and inappropriate for the sea bottom paleothermometry.

Study on nodules from the Haboro area showed that selections in front of outcrops and at laboratory enable us to select ”high quality nodules” for oxygen isotope paleothermometry. As it is simple procedure, large numbers of analyses are available. The cross-plot of these data can emerge ”upper limit line” of oxygen isotope values. The paleotemperature based on that value could provide reliable temperature for the sea bottom. On the other hand, nodules with similar condition from the Oyubari area appeared to be recrystalized and inappropriate for paleothermometry. It might be derived from the difference of burial depth between sediments of the Haboro and Oyubari areas. Even if it was originally consolidated near the bottom of the sea, strong compaction during burial would have caused permeation of pore water into the nodule. Carbon dioxide or bicarbonate ions derived from decomposed organic matter would have caused recrystallization of calcite with oxygen isotopes as low as -10 permil in the nodule.

Keywords: nodules, paleothermometry, oxygen isotope

Japan Geoscience Union Meeting 2014
(28 April - 02 May 2014 at Pacifico YOKOHAMA, Kanagawa, Japan)

MIS30-11 Room:501 Time:April 28 14:30-14:45

Identification of single pollen grains found in a glacier using a whole genome amplification method

NAKAZAWA, Fumio[1*] ; SUYAMA, Yoshihisa[2] ; IMURA, Satoshi[1] ; MOTOYAMA, Hideaki[1]

[1]National Institute of Polar Research, [2]Tohoku University

Pollen taxon in sediment samples can be identified by analyzing pollen morphology. Identification of related species based on pollen morphology is difficult and is limited primarily to genus or family. Because many pollen grains in glaciers contain protoplasm, genetic information of pollen grains should enable identification of plant taxa below the genus level. The present study attempted to analyze the DNA of *Pinus* pollen grains collected from subsurface snow layers on the Belukha Glacier in the Altai Mountains of Russia in the summer of 2003 in order to identify them. *Pinus* is a taxon with approximately 111 recognized species in two subgenera, four sections and 11 subsections. Each *Pinus* pollen grain was amplified using a whole genome amplification method, and some regions of chloroplast genome were sequenced. As a result, each pollen grain was identified at subsection level and was narrowed down to around 10 species.

Keywords: glacier, ice core, pollen analysis, *Pinus*, DNA, WGA

Japan Geoscience Union Meeting 2014
(28 April - 02 May 2014 at Pacifico YOKOHAMA, Kanagawa, Japan)

MIS30-12 Room:501 Time:April 28 14:45-15:00

Dissolution process of G. bulloides shell observed by X-ray CT based on dissolution experiment

IWASAKI, Shinya[1*] ; KIMOTO, Katsunori[2] ; SASAKI, Osamu[3] ; KANO, Harumasa[3] ; HONDA, Makio[2] ; OKAZAKI, Yusuke[1]

[1]Graduate School of Sciences, Kyushu University, [2]Japan Agency for Marine-Earth Science and Technology, [3]Tohoku University Museum

We performed nine-day dissolution experiments with shells of the planktic foraminifera *Globigerina bulloides* at a pH of 6.7 ± 0.1 in water undersaturated with respect to calcite. *Globigerina bulloides* shells were collected from sediment trap samples in the western subarctic Pacific. The process of dissolution of the shells was quantitatively evaluated with observations made with X-ray micro-computed tomography (CT). On the basis of these observations, we divided the shell structures of *G. bulloides* shells into three categories: early-developed calcite formed during the juvenile stage, inner calcite, and outer calcite. The early-developed and inner calcites had low CT numbers (low density) and were sensitive to dissolution. In contrast, the outer calcite had high CT numbers (high density) and resisted dissolution. Both the mode and frequencies of the CT numbers of *G. bulloides* shells decreased as dissolution progressed. Temporal changes of the histogram of CT numbers as the shells dissolved were quantified in terms of the percentage of calcite volume accounted for by low-density calcite (%low-CT-number calcite volume). There was a linear relationship (R^2 = 0.62) between the volume ratio of low-density calcite and shell weight loss. This relationship indicates that shell weight loss can be estimated from the CT number distribution, regardless of the initial condition of the shell, such as size or thickness. We suggest that the X-ray micro-CT method may be used to estimate the extent of foraminiferal shell dissolution with respect to effects on internal structure and shell density.

Keywords: carbonate, planktic foraminifera, X-ray CT, shell weight, shell density, dissolution index

Japan Geoscience Union Meeting 2014
(28 April - 02 May 2014 at Pacifico YOKOHAMA, Kanagawa, Japan)

MIS30-13 Room:501 Time:April 28 15:00-15:15

Relationship between modern speleothem formation and surface weather in an Asian tropical cave

HASEGAWA, Wataru[1*] ; WATANABE, Yumiko[1] ; MATSUOKA, Hiroshige[1] ; OHSAWA, Shinji[2] ; TAGAMI, Takahiro[1]

[1]Earth and Planetary Sciences, Graduate school of Science, Kyoto Univ., [2]Geophysics, Graduate school of Science, Kyoto Univ.

Introduction

For precise climate prediction, it is necessary to reconstruct high time and space resolution paleo-climate (especially past 2000 years) from paleo-climate proxies and assimilate the result to climate model. Tropical Asia, including Indonesia, is well affected by El Nino Southern Oscillation (ENSO). The ENSO does not only directly affect on precipitation in tropical Asia, but also indirectly on middle and high latitude climate through teleconnection [1]. In Indonesia, Watanabe et al. [2] suggested inverse-correlation between δ^{18}O and δ^{13}C in speleothems and instrumental precipitation. However, relationship between modern speleothem formation and surface weather is not revealed clearly.

Therefore, the cave monitoring program, which included cave air temperature, relative humidity, airflow current, air CO_2 concentration monitoring and δ^{18}O and δ^{13}C analysis of dripwater and farmed speleothems, was initiated from 2011 in Petruk Cave (Central Java, Indonesia) in order to study the recording mechanism of precipitation variation into the δ^{18}O and δ^{13}C fluctuation in speleothems.

Result and Discussion

Air CO_2 concentration in Petruk Cave is fluctuated daily and seasonally until over 100 m deep site from the entrance.

It is revealed that cave air CO_2 concentration may be a significant factor that controls stable isotope value in speleothems, because temperature, humidity and drip rate in Petruk cave are nearly stable.

A scenario of precipitation recording is as follows: (1) surface rainfall cools outside air temperature; (2) cave airflow direction is inversed; (3) outside fresh air flows into the cave and air CO_2 concentration is dropped; (4) pCO_2 difference between cave air and dripwater becomes higher and calcite precipitation is promoted; (5) δ^{18}O and δ^{13}C in dripwaters and speleothems are decreased.

In addition to above discussion, we will show you δ^{18}O and δ^{13}C values in dripwaters and farmed speleotems and confirm the scenario by these data.

[1] Hastenrath (1991) Climate dynamics of the tropics. [2] Watanabe et al. (2010) Palaeogeography, Palaeoclimatology, Palaeoecology 293, 90?97.

Keywords: cave monitoring, speleothem, isotope, peleo-climate

Japan Geoscience Union Meeting 2014
(28 April - 02 May 2014 at Pacifico YOKOHAMA, Kanagawa, Japan)

MIS30-14 Room:501 Time:April 28 15:15-15:30

Millennial changes recorded in a stalagmite from central Gifu, Japan

SONE, Tomomi[1] ; KANO, Akihiro[1*] ; MORI, Taiki[1] ; OKUMURA, Tomoyo[2]

[1]SCS Kyushu University, [2]JAMSTEC

A 13-cm-long stalagmite collected from Gujyo City (central Gifu Prefecture) was formed from Marine isotopic stage 3 (MIS-3) to mid-Holocene. The stalagmite is divided into the lower and upper parts by a long-time hiatus during the Last Glacial time. Textural difference appears between the homogenous and transparent upper part and the dark-colored lower part. Oxygen isotopic values are also different; the values of the lower part are 0.5-1.0 permil higher than the values of the upper part. This difference is comparable to one that has been reported from stalagmites in south China, revealing that the Gifu stalagmite was formed under the influence from East Asian summer monsoon.

The most prominent feature of this stalagmite is cyclic changes of ~1 cm intervals in the lower stalagmite. Assuming that the lower part had grown continuous with a uniform rate, it includes a period from 56-35 ka. Eight cyclic changes could coincide to the dark layers in deep-sea sediments from the Japan Sea, which are likely associated with Dansgaard-Oschger (D-O) events. In each cycle, the stalagmite increases transparency to the upward, and suddenly becomes darker at the base of the upper cycle. Similarly, oxygen isotopic values gradually increase in each cycle and rapidly decrease at the base of the upper cycle.

Millennial changes in the Gifu stalagmite indicate D-O cycles, and further records regular intervals that cannot be seen in the Greenland ice sheet. Records of the lower stalagmite support the global extension of D-O events, and suggest that D-O cycles were not necessary originated from the phenomena in North Atlantic. Assuming that the oxygen isotopic values reflect precipitation intensity, it became dry during a gradual cooling period and shifted wet with an abrupt warming.

U-Th dating was performed in National Taiwan University under the guidance of Prof. C.C. Shen.

Keywords: stalagmite, oxygen isotope, late Pleistocene

Japan Geoscience Union Meeting 2014
(28 April - 02 May 2014 at Pacifico YOKOHAMA, Kanagawa, Japan)

MIS30-15 Room:501 Time:April 28 15:30-15:45

Changes in precipitation over the last 2000 yrs recorded in a stalagmite and famine and disaster records in Iwate Pref.

KATO, Hirokazu[1*] ; YAMADA, Tsutomu[1]

[1]Graduate School of Science, Tohoku University

Stalagmites are excellent archives of terrestrial paleoclimate information. Some of them are formed in caves near the noosphere and may have recorded past climatic chaneges influenced human activity. Stable oxygen isotopic compositions of stalagmites especially have been utilized in many paleoclimate studies. However, many factors controlling stalagmite oxygen isotopic composition are known and the degrees of their influence varied from region to region. It is not easy to specify the main controlling factor in Northeast Japan, because the climate is influenced by the East Asian Monsoon and surrounding continental and oceanic air masses struggling with each other. Therefore stalagmite climatic studies is not advanced in this region.

We collected growing stalagmite UT-A from Uchimagi-do Cave, Iwate Prefecture, Northeast Japan. UT-A is 25 cm in height and obvious annual growth layers are found entirely under UV light. The age model of UT-A was based on these growth bands and it revealed that the mean growth rate is 0.12 mm/year and the stalagmite has continuously grown over the last 2000 years. In order to specify the major factor controlling isotopic composition of UT-A, we analyzed changes in annual layer thickness and oxygen isotopic composition of the uppermost part of UT-A and examined the correlations between these changes and weather around the cave over the last 30 years. As the changes in $d^{18}O$ correlates well with the growth rates and amount of precipitation, the oxygen isotopic profiles of UT-A could be interpreted as a proxy of precipitation change over the last 2000 years. The past precipitation deduced from oxygen isotopic composition of UT-A has a 100-200-year cycle and synchronized with famine and disaster caused by excess and lack of precipitation in regional historical records (e.g. Nihon'yanagi, 1968MS). Thus oxygen isotopic composition of stalagmites in Northeast Japan could be a good proxy of past precipitation and we can reconstruct past precipitation and possible famine and disaster events in prehistoric times. Moreover, we may be able to forecast the near future precipitation change in this region by the cyclic fluctuation.

Reference

Nihon'yanagi, S., 1968MS. *Small history of famines in Nanbu-Hachinohe Han in the Thousand Years* (in Japanese). Aomori.

Keywords: stalagmite, d18O, precipitation, famine and disaster records, Uchimagi-do Cave, Iwate Prefecture

Japan Geoscience Union Meeting 2014
(28 April - 02 May 2014 at Pacifico YOKOHAMA, Kanagawa, Japan)

MIS30-16 Room:501 Time:April 28 15:45-16:00

Skeletal records in a long-lived Porites coral from Okinoerabu-jima, Ryukyu Islands

ASAMI, Ryuji[1*] ; TAMASHIRO, Shota[1] ; TSUCHIYA, Maika[1] ; KAWAKAMI, Saya[1] ; MURAYAMA, Masafumi[2] ; IRYU, Yasufumi[3]

[1]University of the Ryukyus, [2]Kochi University, [3]Tohoku University

Tropical and subtropical ocean-atmosphere interactions play a significant role in global climate changes on seasonal, interannual and decadal timescales. Knowledge of past ocean variability is crucial for understanding and modeling current and future climate. However, spatial and temporal instrumental time series from tropical and subtropical oceans before 1950 are quite limited. There is, therefore, a strong need for high-resolution paleoclimate proxies such as corals and sclerosponges from the oceans that extend beyond the instrumental data.

Massive *Porites* corals, living in shallow waters of the tropical to subtropical oceans, precipitate annually banded aragonite skeletons. These colonies provide robust chronological control and allow sub-sampling at monthly-to-seasonal resolution. Oxygen isotope composition of coral skeleton reflects variations in sea surface temperature and seawater oxygen isotope composition (salinity) with the latter being closely related to the precipitation-evaporation balance at sea surface and changes in water mass transport (e.g., Gagan et al., 1998). Long-lived corals are an excellent archive for documenting high temporal resolved time series of thermal and hydrologic changes at sea surface for the last several centuries (e.g., Quinn et al., 1998). Nevertheless, there are a few published long coral records of more than 100 years in the tropical northwestern Pacific (Guam: Asami et al., 2005; Ogasawara: Felis et al., 2009; Ishigaki: Mishima et al., 2010).

We collected a 4.5-m-long skeleton core from a modern *Porites* coral colony in Okinoerabu-jima, Ryukyu Islands on October 2011. Our continuous observational data at the coral living site for the years 2009-2011 are consistent with gridded sea surface temperature and salinity products, suggesting that the site is exposed directly to open sea surface conditions. X-ray images of the coral skeleton showed well-developed annual density bands for the last several centuries. Here we present monthly-to-bimonthly resolved oxygen and carbon isotope composition time series from the coral skeleton to reconstruct secular trend of oceanographic changes before and after the Industrial Revolution. Along with previously published long coral records, our coral-based climate reconstruction will document spatial changes in thermal and hydrologic conditions in the northwestern Pacific for the last several centuries.

Keywords: coral skeleton, oxygen isotope composition, carbon isotope composition, paleo-temperature, paleo-salinity, Ryukyu Islands

Japan Geoscience Union Meeting 2014
(28 April - 02 May 2014 at Pacifico YOKOHAMA, Kanagawa, Japan)

MIS30-17 Room:501 Time:April 28 16:15-16:30

Particle flux and paleoceanographic studies in the subarctic Pacific and the Arctic Ocean

TAKAHASHI, Kozo[1*]

[1]Hokusei Gakuen University

Particle flux studies employing time-series sediment traps have been very useful in obtaining novel knowledge concerning the environmental conditions in ever changing upper water columns of the subarctic Pacific since there had essentially been no such information available prior to our attempt. We employed T/S Oshoro-maru of the Hokkaido University in deploying the sediment traps in two remote areas of the subarctic Pacific during 1989-2010, for >20 years: one in the pelagic central subarctic Pacific (49.5 degree N, 174 degree E) and the other at a hemipelagic site of the Aleutian Basin of the Bering Sea (53.5 degree N,177 degree E). Major biogenic particles in the flues include siliceous shells such as diatoms, radiolarians, and silicoflagellates as well as carbonate shells such as coccolithophores, foraminifers.

These shell-bearing plankton particles are useful in identifying detailed environmental conditions concerning seasonal and inter-annual changes. In particular, the effectiveness of biological pumps has been clarified, showing uptake of atmospheric CO_2 into the upper water columns at a different extent depending of the sites for the first time. Another important aspect of the biogenic particles is initial fossilization process during the settling phase in the water column, which also will be discussed.

Furthermore, application of what had been learnt from the particle flux studies to the sediment records of the past climate changes has been quite a challenge, but rewarding. Integrated Ocean Drilling Program (IODP) Expedition 302 (Arctic Coring Expedition: ACEX) in the vicinity of the North Pole at 88 degree N on the Lomonosov Ridge provided an opportunity of studying the middle Eocene environmental conditions of the paleo-Arctic. The conditions revealed for the first time mainly by siliceous microfossils such as diatoms, silicoflagellates, ebridians and chrysophytes are: fresh water at the top, brackish water next within the euphotic layer, and salty marine water supplied from the outside palegic realm. Another important aspect of the paleoceanographic exploration had been focused on the Bering Sea as IODP Expedition 323, for which the author proposed during the ODP era and materialized during the IODP era after 14 years of drilling preparation effort. The successful drilling down to ca. 5 Ma led to novel knowledge of many aspects such as evolution of sea-ice, the linkages both to the Pacific Ocean and the Arctic Ocean through the Beringian gateway. The Bering Sea drilling data linking to the intensification of the Northern Hemisphere Glaciation (NHG) ca. 2.7 Ma as well as the Mid-Pleistocene Transition (MPT) during 1.2-0.8 Ma are of extremely of interest and will be discussed in details.

Keywords: particle flux, Bering Sea, Arctic Ocean, Northern Hemisphere glaciation, Oceanic gateway

Japan Geoscience Union Meeting 2014
(28 April - 02 May 2014 at Pacifico YOKOHAMA, Kanagawa, Japan)

MIS30-18 Room:501 Time:April 28 16:30-16:45

Calcareous nannoplanktons and nannofossils as useful tools for paleoceanography

OKADA, Hisatake[1*]

[1]Hokkaido University

Microfossils are useful tools for paleoceanographic studies in two ways: age identification by detailed biostratigraphy, and reconstruction of sea state such as water temperature, productivity and dynamic properties of water mass. Needless to say, calcareous nannofoiils are powerful age-diagnostic tool for oceanic sediments, but because of their minute size, its usefulness for oxygen and carbon isotopic analysis are limited. On the other hand, the unique existence of *Florisphaera profund*, a deep photic-zone dweller, provide an useful method for paleoproductivity and dynamic analysis of water column. By the way, new discoveries or break through in any disciplines are often resulted from unexpected encounters or conversations between researchers. Personal relationships are also very important factor to progress career and to accomplish scientific achievement for young scientists. Utilizing this opportunity, I will summarize major points for paleoceanographic applications of calcareous nannofossils, and also, I will explain my own experiences of various encounters that resulted fruitful scientific achievements.

Keywords: paleoceanography, calcareous nannofossils, biostratigraphy, water dynamics, lower photic-zone

Japan Geoscience Union Meeting 2014
(28 April - 02 May 2014 at Pacifico YOKOHAMA, Kanagawa, Japan)

MIS30-19 Room:501 Time:April 28 16:45-17:00

Mechanism of ice age cycle and paleoclimate modeling

ABE-OUCHI, Ayako[1*]

[1]University of Tokyo (AORI) and JAMSTEC

The 100-kyr cycle of the waxing and waning of the large Northern Hemisphere ice sheets and fast termination of the glacial cycles are the prominent pattern known from paleoceanographic records which can not be explained by the summer insolation proposed by the Milankovitch theory alone. Conceptual models imposing a threshold for the terminations by a large size of the ice sheet and/or large insolation can reproduce the patterns of glacial cycles, however, a physical explanation was not given. Here we simulated the past seven glacial cycles successfully with an ice sheet model in combination with a general circulation model imposing the time series of insolation and atmospheric CO2. The response of climate to ice sheet, greenhouse gases and orbital forcings is examined with high resolution. The stationary wave feedback of ice sheet is also taken into account. Our model reproduces 100-kyr periodicity of the glacial cycles even with the astronomical forcing alone under a certain range of CO2 level for the case of North America ice sheet. We show that the threshold which leads to the termination of the glacial cycle is governed by how the ice sheet responds to a given insolation. The characteristics of how the ice sheet responds to external forcing strongly depends on the climatic condition, such as the north-south temperature gradient and the topographic condition for each continent.

Keywords: climate, paleoclimate

Japan Geoscience Union Meeting 2014
(28 April - 02 May 2014 at Pacifico YOKOHAMA, Kanagawa, Japan)

MIS30-20 Room:501 Time:April 28 17:00-17:15

Cretaceous-Paleogene stratigraphy in Northwest Pacific and its significance for paleoenvironmental study

NISHI, Hiroshi[1*] ; TAKASHIMA, Reishi[1] ; YAMANAKA, Toshiro[2] ; ORIHASHI, Yuji[3] ; HAYASHI, Kei-ichi[4] ; KANETSUNA, Masaya[1]

[1]Tohoku University, [2]Okayama University, [3]The University of Tokyo, [4]Geological Survey of Hokkaido

The Cretaceous – Paleogene period is known as the latest Greenhouse climate in the history of earth. In order to understand ocean – climate system during past Greenhouse climate, numerous attempt has long been made for the marine sequences in the Atlantic and Southern oceans and the Tethyas Sea. The Pacific Ocean was the outstandingly largest ocean during Cretaceous – Paleogene, and it may have played important roles in Earth's ocean – climate system. Despite its importance, very little work has been done to establish detailed paleo-oceanographic changes during Cretaceous – Paleogene. This is largely because most of the Cretaceous – Paleogene Pacific oceanic crusts have subducted under continents, and bad recoveries of Cretaceous – Paleogene sediments of the ODP and DSDP cores from the Pacific sites have prevented researchers from studying paleoenvironmental changes of the Pacific Ocean.

First, we establish the detailed integrated stratigraphy (planktic foraminiferal and dinoflagellate cyst biostratirgraphy, carbon isotope stratigraphy and U-Pb dating of tuff beds) of the Cretaceous – Paleogene marine sequences exposed in Hokkaido Japan because the resolution of international stratigraphic correlation of these strata is not enough to identify important climatic and/or extinction events such as the OAEs, K/Pg, PETM and others. The strata used in this study is as follows; the Yezo Group (early Aptian – early Campanian: 125 – 75 Ma), the Nemuro Group (Campanian?– early Eocene: 75?– 53 Ma), the Poronai Formation (late Eocene: 42 – 35 Ma) and the Onbetsu Formation (late Eocene – early Oligocene: 34 – 32 Ma). Our integrated stratigraphy enables to identify the exact horizons of following climatic and extinction events. The Cretaceous Oceanic Anoxic Events (OAEs) of the OAE1a (125.5 – 124 Ma), Leenhadlt Level of OAE1b (110 Ma), OAE1c (107 Ma), OAE1d (101 Ma), OAE 2(94 – 93.5 Ma) are identified in the Yezo Group exposed in Oyubari and Tomamae areas. Although no so-called black shales were found in these horizons, evidences of oxygen depletion were identified from the most of these horizon based on the analyses of benthic foraminifera, degree of pyritilization and sedimentary structure such as degree of bioturbation. The horizons of the K/Pg (66 Ma) and PETM (Paleocene Eocene Thermal Maximum; 56 Ma) in the Nemuro Group and Late Eocene Warming (37 Ma) in the Poronai Formation exhibit no obvious differences in lithology. Especially, the strata across the K/Pg boundary in the Shiranuka Hill consists of massive mudstone and a few intercalations of thin felsic tuff and turbidite sandstone. The middle – late Eocene cooling (40 – 39 Ma) is characterized by abundant occurrences of glendonites and buliminids (benthic foraminifera) in the middle part of the Poronai Formation, which indicates that cooling and eutrophication of surface water occurred in the northwest Pacific. The prominent positive excursion of oxygen isotope around Eocene/Oligocene boudanry (34 – 33.6 Ma) is placed at the top of the Urahoro Group. The overlying Onbetsu Formation includes Oi-1a and Oi-1b of early Oligoene. Flood occurrence of buliminids in the lower part of the Onbetsu Formation suggest that surface water eutrophication occurred in response to global cooling after the Oi-1 glaciation.

The horizons of climatic and extinction in Hokkaido have continuous outcrop without significant hiatus and faults. High resolution analyses of these horizons will improve our understanding of climatic and environmental changes in northwest Pacific during the latest greenhouse period.

Keywords: Cretaceous, Paleogene

Japan Geoscience Union Meeting 2014
(28 April - 02 May 2014 at Pacifico YOKOHAMA, Kanagawa, Japan)

MIS30-21 Room:501 Time:April 28 17:15-17:30

Milankovitch forcing and carbon cycle during the Toarcian Oceanic Anoxic event

IKEDA, Masayuki[1] ; HORI, S., Rie[1*] ; IKEHARA, Minoru[2]

[1]Department of Earth Science, Faculty of Science, Ehime University, [2]Center for Advanced Marine Core Research, Kochi University

One of the most profound environmental changes in the Mesozoic took place during Toarcian (Early Jurassic), including oceanic anoxia (Toarcian Oceanic Anoxic Event; T-OAE). The T-OAE is characterized by negative carbon isotope excursion (CIE) of up to ˜8 ‰. The T-OAE is considered to have resulted from the release of CO2 by Karoo-Ferrar volcanism and possible methane hydrate dissociation. However, the origin of these perturbations remains strongly debated, primarily due to lack of radiometric age constraints across the T-OAE (e.g. Palfy and Smith, 2000; Kemp et al., 2005, 2011; Suan et al., 2008).

Here we present the orbitally-tuned bio-, and $\delta^{13}C_{org}$ stratigraphy of the Lower Jurassic deep-sea bedded chert sequence at the Katsuyama-Sakahogi section, in the Inuyama area, central Japan, which covers the T-OAE (Ikeda and Tada, 2013; Ikeda and Hori, in review). The sedimentary rhythms of the bedded chert display a full range of climatic precession related cycles; ˜20 kyr cycle as a chert-shale couplet and ˜100 kyr, 405 kyr, ˜2000 to 4000 kyr cycles as chert bed thickness variations (Ikeda et al., 2010; Ikeda and Tada, 2013). Chert-shale cycles and variations in chert bed thickness are interpreted as resulted from changes in the burial rate of biogenic silica (Hori et al., 1993).

By using 405-kyr eccentricity cycle of constant and stable periodicity (Laskar et al., 2004) observed in the Inuyama bedded chert, we established the astronomical time scale (ATS) by counting 405 kyr cycle (˜20 bed cycle; Ikeda and Tada, 2013). Then, this ATS is anchored at the end-Triassic radiolarian extinction level of which age is estimated as 201.4 $\pm$ 0.2 Ma based on projection of the U-Pb date measured at the Pucara section, Peru, using the conodont and radiolarian biostratigraphy (e.g. Carter and Hori, 2005; Schoene et al., 2010; Ikeda and Tada, 2013).

This astronomical time scale suggests the absolute ages of the T-OAEs. The timing of two black bedded chert intervals (T-OAEs 1 and 2) and the negative CIE of ˜5 ‰ are within the time interval of radiometric ages from thKaroo-Ferror Lips (Svencen et al., 2007; Jourdan et al., 2008). This result supports the volcanic degassing origin of these carbon cycle perturbations (Palfy and Smith, 2000; Suan et al., 2008).

The termination of black shale deposition occurred at the minimum of 40 kyr obliquity amd 100 kyr and 405 kyr eccentricity cycles. These temporal relations imply the possible impacts of these orbital forcing on the stabilization of carbon cycle perturbation through Earth system dynamics, such as weathering and nutrient cycles.

Keywords: Milankovitch cycle, carbon cycle, volcanism, silica cycle, hydrological cycle

Japan Geoscience Union Meeting 2014
(28 April - 02 May 2014 at Pacifico YOKOHAMA, Kanagawa, Japan)

MIS30-22 Room:501 Time:April 28 17:30-17:45

Paleoceanographic evolution of Miocene to Pliocene mud sea in the Ryukyus based on calcareous nannofossil assemblages

IMAI, Ryo[1*] ; SATO, Tokiyuki[2] ; IRYU, Yasufumi[1]

[1]Institute of Geology and Paleontology, Graduate School of Science, Tohoku University, [2]Institute of Applied Earth Sciences, Faculty of Engineering and Resource Science, Akita University

The Cenozoic sedimentary succession in Okinawa-jima, including the upper Miocene to Pleistocene siliciclastic deposits (Shimajiri Group) and the Pleistocene reef to shelf deposits (Ryukyu Group), suggests a drastic paleoceanographic change from a mud sea to a coral sea. To delineate the paleoceanographic evolution of the mud sea, we quantified the stratigraphic distribution of the calcareous nannofossil assemblages from the Shimajiri Group in a 2119.49 m-deep well (Nanjo R1 Exploratory Well) drilled in southern Okinawa-jima (Ryukyu Islands, southwestern Japan). Four late Miocene and Pliocene datum planes were found in the studied interval. The calcareous nannofossil assemblages suggest the existence of oligotrophic conditions between 5.3 and >8.3 Ma followed by eutrophic conditions and a return to oligotrophic conditions at 3.5 Ma. Micropaleontological evidence suggests that these oceanographic changes were likely caused by local tectonic movement (shallowing of the sedimentary basin in which the Shimajiri Group was deposited). We will report calcareous nannofossil records from two exploratory wells drilled in southern Okinawa-jima in 2013 – 2014 as well.

Keywords: calcareous nannofossil, Miocene, Pliocene, Ryukyu Islands

Japan Geoscience Union Meeting 2014
(28 April - 02 May 2014 at Pacifico YOKOHAMA, Kanagawa, Japan)

MIS30-23 Room:501 Time:April 28 17:45-18:00

East Antarctic deglaciation and the link to global cooling since the Pliocene

SUGANUMA, Yusuke[1*] ; MIURA, Hideki[1] ; ZONDERVAN, Albert[3] ; OKUNO, Jun'ichi[2]

[1]National Institute of Polar Research, [2]JAMSTEC, [3]GNS, Science

Reconstructing past variability of the Antarctic ice sheets is essential to understand their stability and to anticipate their contribution to sea level change as a result of future climate change in a high-CO2 world. Recent studies have reported a significant decrease in thickness of the East Antarctic Ice Sheet (EAIS) during the last several million years. However, the geographical extent of this decrease and subsequent isostatic rebound remain uncertain and a topic of debate. In this study, we reconstruct magnitude and timing of ice sheet retreat at the Sor Rondane Mountains in Dronning Maud Land, East Antarctica, based on detailed geomorphological survey, cosmogenic exposure dating, and glacial isostatic adjustment modeling. Three distinct deglaciation phases since Pliocene for this sector of the EAIS are identified, based on rock weathering and 10Be surface exposure data. We estimate that during the Plio-Pleistocene the ice sheet thinned by at least 500 m. This thinning is attributed to the reorganization of Southern Ocean circulation associated with the global cooling into the Pleistocene, which reduced the transport of moisture from the Southern Ocean to the interior of EAIS. The data also show since the Last Glacial Maximum the ice surface has lowered less than ca.50 m and probably started after ca. 14 ka. This suggests that the EAIS in Dronning Maud Land is unlikely to have been a major contributor to postglacial sea-level rise and Meltwater pulse 1A.

Japan Geoscience Union Meeting 2014
(28 April - 02 May 2014 at Pacifico YOKOHAMA, Kanagawa, Japan)

MIS30-24 Room:501 Time:April 29 09:00-09:15

Past 2 Myr Radiolarian Assemblages and Paleoceanographic Changes off the Southwestern Japan (IODP Site C0001)

MATSUZAKI, Kenji M.[1*] ; NISHI, Hiroshi[1] ; SUZUKI, Noritoshi[2] ; HAYASHI, Hiroki[3] ; IKEHARA, Minoru[4] ; GYAWALI, Babu R.[2] ; TAKASHIMA, Reishi[1]

[1]The Center for Academic Resources and Archives, Tohoku University Museum, Tohoku University (Japan), [2]Institute of Geology and Paleontology, Graduate School of Science, Tohoku University (Japan), [3]Interdisciplinary Faculty of Science and Engineering, Shimane University (Japan), [4]Center for Advanced Marine Core Research, Kochi University (Japan)

The effects of Quaternary paleoceanographic events on the Kuroshio Current off the southwestern Japan, including the mid-Pleistocene Transition (MPT) (1,200?700 ka) and the mid-Brunhes event (MBE) (400?300 ka), are poorly documented at this time because of a lack of long core recovering the MBE and the MPT. In this context, this study aims to establish paleoceanography of this region since the Early Pleistocene, using radiolarian assemblages as paleoceanographical proxy. The Holes C0001E and F, drilled by the R/V Chikyu during IODP Expedition 315 at a depth of 2198 m in the Shikoku Basin off the Kii Peninsula on the slope of the Nankai accretionary prism (southern Japan) are used in this study. The upper 190 m LSF sediments cover the Quaternary based on the shipboard results, the dominant lithology consisted of greenish-gray to grayish-green mud. The age model of Site C0001 is based on calcareous nannofossils datums, planktic foraminifers datums, radiolarians datums and Globorotalia inflata oxygen isotope stratigraphy. In this study, 240 samples of 20 cc, covering the Early to Middle Pleistocene, were used for radiolarian faunal analysis. The examination of the polycystine radiolarians was performed using an optical microscope at a magnification of 100?400x. In each sample, 400 to 1000 polycystine radiolarians were identified. The radiolarian-based sea surface temperature (rSST) was estimated using a Modern Analogue Technique (MAT). Several warming event is recorded during the Early Pleistocene. However, the strongest warming event is recorded during the MPT, where the subtropical fauna abundances increased consequently.

Keywords: Pleistocene, Paleoceanography, Mid Pleistocene Transition, Radiolarian

Japan Geoscience Union Meeting 2014
(28 April - 02 May 2014 at Pacifico YOKOHAMA, Kanagawa, Japan)

MIS30-25 Room:501 Time:April 29 09:15-09:30

Sea-ice conditions in the Okhotsk Sea during the last 550 kyr deduced from environmental magnetism

YAMAZAKI, Toshitsugu[1*] ; INOUE, Seiko[2] ; SHIMONO, Takaya[2] ; SAKAMOTO, Tatsuhiko[3] ; SAKAI, Saburo[4]

[1]AORI, University of Tokyo, [2]Tsukuba University, [3]Mie University, [4]JAMSTEC

Reconstructing past sea-ice conditions in the Okhotsk Sea is important because sea-ice conditions vary in response to global climate changes, which in turn may affect global ocean circulation through intermediate water mass formation. We conducted an environmental magnetic study of six cores from three stations in the central Okhotsk Sea to better understand temporal and spatial sea-ice variations. Inter-core correlations and age estimations are based mainly on geomagnetic paleointensity; an oxygen-isotope stratigraphy is available for one station. Magnetic susceptibility (MS) minima are accompanied by maxima in color b*, the ratio of the anhysteretic remanent magnetization susceptibility to saturation isothermal remanent magnetization (k_{ARM}/SIRM), and the S-ratio, which indicates a higher proportion of biogenic to terrigenous magnetic components. This reflects enhanced ocean productivity. First-order reversal curve diagrams and IRM component analyses support the dominance of biogenic magnetite at MS minima. In contrast, color b*, k_{ARM}/SIRM, and S-ratio values are low when MS is high, which indicates an increased proportion of the terrigenous component that was probably transported as ice-rafted debris (IRD). For the southern two stations, IRD accumulation increased in glacial and deglacial periods, which implies mobile sea-ice conditions even in full glacials. This was succeeded by extremely enhanced ocean productivity in early interglacials, which suggests nearly ice-free conditions. For the northernmost station, on the other hand, IRD accumulation was low in glacials and increased in early interglacials, which indicates perennial sea-ice coverage with little mobility in glacials. Succeeding ocean-productivity enhancement was delayed compared to the southern stations.

Keywords: Okhotsk Sea, paleoceanography, environmental magnetism, sea ice, IRD

Japan Geoscience Union Meeting 2014
(28 April - 02 May 2014 at Pacifico YOKOHAMA, Kanagawa, Japan)

MIS30-26 Room:501 Time:April 29 09:30-09:45

Pliocene and Pleistocene paleoceanography in the northwestern Pacific and the Bering Sea based on diatom analyses

KATO, Yuji[1*] ; ONODERA, Jonaotaro[2] ; SUTO, Itsuki[1] ; TERAISHI, Akihito[3] ; TAKAHASHI, Kozo[4]

[1]Graduate School of Environmental Studies, Nagoya University, [2]Research Institute for Global Change, JAMSTEC, [3]NTT COMWARE Co, Ltd., [4]School of Social Welfare, Hokusei Gakuen University

Late Pliocene-Pleistocene fossil diatom assemblages from Ocean Drilling Program (ODP) Leg 145 Hole 884B in the western Subarctic North Pacific were investigated and the paleoceanographic records were compared with those at Integrated Ocean Drilling Program (IODP) Expedition 323 Holes U1341B and U1343E in the Bering Sea for an interval of 2.5-0 Ma.

As the results, in Hole 884B, five diatom zones, from the *Neodenticula koizumii-N. kamtschatica* Zone to the *N. seminae* Zone, were identified. The cold-water indicators from Hole 884B, which represented high abundances throughout the interval, suggest the cold environmental conditions analogous to the modern sea-surface conditions in the western subarctic Pacific. The drastic decrease of the temperate-water species at ca. 2.2 Ma is related to a rapid cooling event at ˜2 Ma. Sporadic appearances of sea-ice related species from ca. 2.3 Ma and a slight increase of neritic species observed at ca. 2.0 Ma may be reflection of a series of the Northern Hemisphere Glaciation (NHG) events. Slightly higher abundances of the sea-ice related species at 1.0-0.8 and 0.4 Ma and those of the neritic species at 2.0, 1.8, 1.2, and 0.9 Ma are likely to correspond to the southward advance of the subarctic front and drop in sea-surface temperature mentioned by Sancetta and Silvestri (1986).

The age differences of the distinct decreases of temperate-water species recognized at ca. 1.9 Ma for Hole U1343E, ca. 2.1 Ma for Hole U1341B and ca. 2.2 Ma for Hole 884B indicate that the East Kamchatka Current in the Western Subarctic Gyre was strengthened and the westward advection of the Alaskan Stream was weakened at ca. 2.2 Ma. In the Bering Sea, the limited input of temperate waters via the Near Strait resulted as a decrease of warm water supply to the region around Site U1341 at ca. 2.1 Ma, while the eastern Bering slope region had been still affected by the warm water masses advected from the Amchtka and Amukta Passes. Further global cooling might have restricted the continuous warm water supply to the Bering slope region around Site U1343 at ca. 1.9 Ma.

Keywords: diatom, paleoceanography, subarctic Pacific, Bering Sea, IODP Expedition 323, ODP Leg 145

Japan Geoscience Union Meeting 2014
(28 April - 02 May 2014 at Pacifico YOKOHAMA, Kanagawa, Japan)

MIS30-27 Room:501 Time:April 29 09:45-10:00

Millennial-scale rock-magnetic variation indicating instability of North Atlantic environments during MIS 100

OHNO, Masao[1*] ; SATO, Masahiko[1] ; HAYASHI, Tatsuya[2] ; KUWAHARA, Yoshihiro[1] ; KITA, Itsuro[1]

[1]Graduate School of Integrated Sciences for Global Society, [2]Mifune Dinosaur Museum

Ocean thermohaline circulation (THC) plays an important role in global climate change linked with continental ice sheets. To clarify the variation of ocean THC in the early stage of glaciations in the northern hemisphere, we studied a deep-sea sediment core with high sedimentation rate recovered at IODP Site U1314 in the North Atlantic. Rock magnetic study of the sediments during marine oxygen isotope stage (MIS) 100 indicated links between the millennial-scale variability in deep water circulation and iceberg discharge. The observed abrupt decreases of magnetic coercivity associated with ice-rafted debris (IRD) are interpreted to be reduced transport of high-coercivity material from Icelandic source indicating reduced formation of North Atlantic Deep Water (NADW). In these periods, a current from the south, Lower Deep Water, transports sediments with low magnetic coercivity contributed by coarse grained magnetite of continental sources. Repetition of vigorous and weaken NADW production linked to IRD was observed during MIS 100 in a similar manner to that in the last glacial suggests that the regime of climate change in the millennial-scale was already established in the early stage of glaciations in the northern hemisphere.

Keywords: rock magnetism, thermohaline circulation, North Atlantic Deep Water, Ice rafted debris

Japan Geoscience Union Meeting 2014
(28 April - 02 May 2014 at Pacifico YOKOHAMA, Kanagawa, Japan)

MIS30-28 Room:501 Time:April 29 10:00-10:15

Paleoceanographic reconstruction of the Holocene Arctic Chukchi Sea using fossil diatoms

KONNO, Susumu[1*] ; JORDAN, R. W.[2]

[1]Graduate School of Sciences, Kyushu University, [2]Faculty of Science, Yamagata University

The Chukchi Sea, in the Arctic Ocean, receives the warm outflowing waters of the Bering Sea. These waters are one of the causes of Arctic sea ice decline, and change their flow according to the sea ice distribution in the Chukchi Sea. Sea ice in the global climate system has a significant impact on the global environment (e.g., atmospheric circulation, biological production and ocean circulation), due to the albedo effect, maintenance of low temperatures, and high salinity bottom waters. Therefore, the reconstruction of the past sea ice history of the Chukchi Sea is important in understanding the climate system of the Arctic Ocean as well as the global climate system. However, piston cores previously obtained from the Chukchi Sea were too short and/or contained few or no microfossils, making detailed paleoenvironmental analyses and age determinations difficult.

I started working on the diatom analysis of sediment cores taken during the HLY0501 cruise of the United States Coast Guard icebreaker cutter ”Healy” in 2005. They took 8 sediment cores, although diatoms were not obtained at six of the sites. So here I show the diatom analysis results from the remaining two cores (cores 5 and 8).

Keywords: Chukchi Sea, Diatom, Holocene

Japan Geoscience Union Meeting 2014
(28 April - 02 May 2014 at Pacifico YOKOHAMA, Kanagawa, Japan)

MIS30-29 Room:501 Time:April 29 10:15-10:30

Thermal threshold of the Atlantic meridional overturning circulation as a trigger for glacial abrupt climate changes

OKA, Akira[1*] ; ABE-OUCHI, Ayako[1] ; YOKOYAMA, Yusuke[1] ; KAWAMURA, Kenji[2] ; HASUMI, Hiroyasu[1]

[1]Atmosphere and Ocean Research Institute, University of Tokyo, [2]National Institute of Polar Research

Abrupt climate changes known as Dansgaard-Oeschger events (DO events) took place frequently during glacial climate. Geological evidences support the idea that changes of the Atlantic meridional overturning circulation (AMOC) are related to these events, but question on what triggers the AMOC changes remains unsolved. Although most studies have regarded freshwater flux from melting ice sheet as a cause of the AMOC changes, we recently identified the existence of the thermal threshold of the AMOC during glacial climate. Here, from the results of numerical simulations about the glacial AMOC, we report that the thermal threshold of the AMOC serves as a triggering mechanism of DO events. We investigated the structure of the thermal threshold in glacial climate by conducting ocean general circulation model simulations under various thermal conditions in which degrees of sea surface cooling are systematically changed separately or simultaneously in northern and southern hemispheres. The results suggest that the threshold is located near the condition under which the climate is slightly warmer than the coldest glacial conditions. We also found that the amplitude of AMOC changes in crossing the threshold depends on thermal conditions in northern and southern hemispheres. The most prominent threshold is identified where the southern hemisphere is somewhat warmer than the coldest glacial conditions. It is also demonstrated that gradual warming in the southern hemisphere from the colder glacial climate leads to crossing this threshold and can cause significant strengthening of AMOC. Our results indicate that the thermal threshold could be a triggering mechanism of DO events, especially for those accompanying the gradual warming of southern hemisphere before their abrupt warming in northern hemisphere.

Japan Geoscience Union Meeting 2014
(28 April - 02 May 2014 at Pacifico YOKOHAMA, Kanagawa, Japan)

MIS30-30 Room:501 Time:April 29 10:30-10:45

Role of Southern Ocean stratification in glacial atmospheric CO2 reduction

KOBAYASHI, Hidetaka[1*] ; OKA, Akira[1]

[1]Atmosphere and Ocean Research Institute, The University of Tokyo

The global temperatures and atmospheric carbon dioxide (pCO_2) concentrations varied during the last 800 thousand years. During the glacial times, such as Last Glacial Maximum (LGM), the atmospheric partial pressure of carbon dioxide (pCO_2) was about 80-100ppmv lower than interglacial times, such as Holocene. Compared to interglacial conditions, terrestrial carbon stocks were reduced during glacial conditions. Marine carbon cycles must have been the main driver for lowering atmospheric pCO_2 during ice ages. A number of candidate mechanisms to explain the reduction in glacial atmospheric pCO_2 have been proposed. However, they failed to explain full amplitude of 80-100ppmv reduction. Based on paleo-proxy reconstructions, $\delta^{13}C$ gradient between surface and deep ocean was larger than today, suggesting that the glacial ocean circulation state was different from today. In the deep glacial Southern Ocean, very saline water was identified from paleo proxy data. Moreover, radiocarbon record showed the existence of radiocarbon-depleted old waters in glacial ages. One hypothesis that has been proposed to explain the glacial atmospheric pCO_2 is the isolated reservoir hypothesis: a carbon-rich, radiocarbon-depleted water mass was isolated from the atmosphere during the glacial periods. The stratification of the Southern Ocean water column may have contributed to a reduction of atmospheric pCO_2.

In this study preindustrial and LGM marine carbon cycle sensitivity experiments are conducted to estimate a role of stratification in glacial Southern Ocean quantitatively, by using an ocean general circulation model (OGCM). In the control case, atmospheric pCO_2 between Modern case and LGM case is about 44ppmv, which was comparable to previous AOGCM study. However, LGM case cannot explain the saline glacial Southern Ocean.

Previous study using intermediate complexity models suggested that glacial atmospheric pCO_2 and $\delta^{13}C$ distribution can be reproduced by considering brine induced stratification.

Therefore, we also consider the effect of brine induced stratification. We partly succeeded in reproducing the saline glacial South Atlantic Ocean by imposing body forcing near the bottom in the Weddell Sea, Ross Sea and Eastern Antarctica, whereas saline glacial Southern Ocean resulted in increased northward flow of AABW and increased atmospheric pCO_2. Additionally, we used stratification-dependent vertical eddy diffusivity parameterization suggested by Gargett (1984) to discuss changes in vertical eddy diffusivity in Southern Ocean. Contrary to our expectation, vertical eddy diffusivity in high latitude becomes very higher under glacial conditions, and sequestered carbon in deep ocean was released into the atmosphere and resulted in higher atmospheric pCO_2.

Finally, very stratified Southern Ocean achieved by extremely small vertical eddy diffusivity also cannot reduce glacial atmospheric pCO_2. Other processes, which are not taken into account in our study may be important to reproduce the glacial condition.

Keywords: ocean carbon cycle, Last Glacial Maximum, Southern Ocean, Ocean general circulation model

Japan Geoscience Union Meeting 2014
(28 April - 02 May 2014 at Pacifico YOKOHAMA, Kanagawa, Japan)

MIS30-P01 Room:Poster Time:April 28 18:15-19:30

A tree-ring oxygen isotope chronology from Yakushima Island and its dendroclimatic potential

SANO, Masaki[1*] ; YASUE, Koh[2] ; KIMURA, Katsuhiko[3] ; NAKATSUKA, Takeshi[1]

[1]Research Institute for Humanity and Nature, [2]Shinshu University, [3]Fukushima University

Recent progress in isotope dendroclimatology showed that tree-ring oxygen isotopes are a promising proxy to reconstruct past precipitation and/or relative humidity. In the present study, we developed a 300-year tree-ring oxygen isotope chronology using Japanese cedar (Cryptomeria japonica) growing in Yakushima Island, southern Japan, and explored its dendroclimatic potential. Two tree samples that were crossdated by visually matching ring-width variations were used for oxygen isotopic analysis. The resulting oxygen isotope series for the period 1700-2009 C.E. were highly correlated with each other (r = 0.68), indicating that common signals related to local climate are preserved in these data. Both the delta-18O series were individually normalized to have zero mean and unit variance, and the resulting series were averaged to build the final chronology. Response analysis with monthly climatic records (temperature, precipitation and relative humidity) from the Kagoshima station revealed that tree-ring delta-18O was primarily controlled by relative humidity and precipitation in the summer season (May-September). Perhaps the most striking feature of the delta-18O chronology is a significant increasing trend over the 20th century, indicating a decrease in summer relative humidity in the study region. We will present an extended version of the tree-ring delta-18O chronology over the past 1000 years or so.

Keywords: tree ring, oxygen isotope ratios, Yakushima Island, monsoon

Japan Geoscience Union Meeting 2014
(28 April - 02 May 2014 at Pacifico YOKOHAMA, Kanagawa, Japan)

MIS30-P02 Room:Poster Time:April 28 18:15-19:30

Assessment of Sungkai tree-ring δ18O proxy for paleoclimate reconstruction

HARADA, Mao[1*] ; WATANABE, Yumiko[1] ; NAKATSUKA, Takeshi[2] ; TAZURU, Suyako[3] ; HORIKAWA, Yoshiki[3] ; BAMBANG, Subiyanto[4] ; SUGIYAMA, Junji[3] ; TSUDA, Toshitaka[3] ; TAGAMI, Takahiro[1]

[1]Graduate School of Science, Kyoto University, [2]Graduate School of Environmental Studies, [3]Research Institute for Sustainable Humanosphere, Kyoto University, [4]Indonesian Institute of Sciences

We measured annual δ18O variations of two sungkai trees that were collected in the same area as previous study, in order to assess the reproducibility of sungkai δ18O as paleoclimate proxies. Two sungkai δ18O variations has a significant correlation (r = 0.80; P $<$0.001) with each other and also with the previous analysis, suggesting that δ18O values of sungkai are affected by external climatic factors. The annual δ18O of SungkaiNAN7 has significant, positive correlations with temperature, sunlight hours and air pressure whereas it has significant, negative correlations with relative humidity and SOI. Moreover, the seasonal δ18O variation acquired during severe drought of 1997-98 El Nino event shows that the maximum δ18O value around 1997 latewood corresponds to rainfall/relative humidity minimum and temperature/sunlight hours/air pressure maximum with a significant time lag.

Keywords: tree ring, cellulose, stable isotope geochemistry, tropics, paleoclimate

Japan Geoscience Union Meeting 2014
(28 April - 02 May 2014 at Pacifico YOKOHAMA, Kanagawa, Japan)

MIS30-P03 Room:Poster Time:April 28 18:15-19:30

Characteristics of ESR and TL of natural quartz from river bed sediments

SHIMADA, Aiko[1*] ; TOYODA, Shin[2] ; TAKADA, Masashi[1]

[1]Application Support Team, JEOL RESONANCE Inc., [2]Department of Applied Physics, Okayama University of Science, [3]Department of History, Sociology and Geography, Faculty of Letters, Nara Women's University

The sediment provenance would give important information on the erosion processes, uplift of the mountains and so on, suggesting the environments at the time of sediment transportation. The sediment is made of fine grains such as sand and silt. When a new procedure for clarifying provenance of such sediments is established, it will be useful to elucidate the provenance of sediments in the geohistorical environments, which may occasionally be related to stream piracy, regional tectonic setting and/or the environment changes of the hinterland.

There have been already some Electron Spin Resonance (ESR) and luminescence studies on sediment provenance. The intensity of the E_1' center in quartz is shown to be a useful parameter to investigate the provenance of aeolian dust as well as of sediments [1][2]. The crystallinity index (CI) in combination with ESR is employed to discriminate two different sources of eolian dust in the sediment core taken from the Japan Sea [3]. Quartz of four distinct origins can be distinguished using impurity (Al, Ti-Li, Ti-H, Ge) centers observed after beta irradiation [4]. Shimada and Takada (2008) and Shimada et al. (2013) also show that the Al, Ti-Li and E_1' center signal intensities from the natural quartz are useful to distinguish the sediment provenance [5][6]. Volcanic quartz is reported to emit stronger red thermoluminescence (TL) than blue one whereas plutonic quartz does vice versa [7]. Quartz of eolian origin transported from China can be distinguished from volcanic quartz originated in Japanese tephra by looking at TL color of quartz grains [8].

In this study, we report the characteristics of ESR and TL of quartz taken from present river bed sediments, to discuss the possibilities of identifying sediment provenance.

[1] Naruse T, Ono Y, Hirakawa K, Okashita M, and Ikeya M, 1997. Source areas of eolian dust quartz in East Asia: a tentative reconstruction of prevailing winds in isotope stage 2 using electron spin resonance. Geographical review of Japan 70A-1, 15?27.

[2] Toyoda S and Naruse T, 2002. Eolian Dust from Asia Deserts to Japanese Island since the last Glacial Maximum: the Basis for the ESR Method, Japan Geomorphological union 23-5, 811-820.

[3] Nagashima K,Tada R, Tani A, Toyoda S, Sun Y, and Isozaki Y, 2007. Contribution of aeolian dust in Japan Sea sediments estimated from ESR signal intensity and crystallinity of quartz. Geochemistry, Geophysics, Geosystems, doi:10. 1029/2006GC001364.

[4] Duttinea M, Villeneuvea G, Bechtela F, Demazeaub G, 2002. Caracterisation par resonance paramagnetique electronique (RPE) de quartz naturels issus de differentes sources. C.R.Geoscience 334, 949?955.

[5] Shimada A and Takada M, 2008. Characteristics of Electron Spin Resonance (ESR) signals in quartz from igneous rock samples: a clue to sediment provenance. Annual Reports of Graduate School of Humanities and Sciences, 23, 187-195.

[6] Shimada A, Takada M and Toyoda S, 2013. Characteristics of ESR signals and TLCLs of quartz included in various source rocks and sediments in Japan: A clue to sediment provenance. Geochronometria, 40, Issue 4, 334-340.

[7] Hashimoto T, Koyanagi A, Yokosaka K, Hayashi Y and Sotobayashi T, 1986. Themoluminecence color images from quartz of beach sands. Geochemical journal 20,111-118.

[8] Ganzawa Y, Watanabe Y, Osanai F and Hashimoto T, 1997. TL color images from quartzes of loess and tephra in China and Japan, Radiation Measurements 27, 383-388.

Keywords: Electron Spin Resonance, Sediments provenance, Quartz, Sediments, Thermoluminescence, River bed sediments

Japan Geoscience Union Meeting 2014
(28 April - 02 May 2014 at Pacifico YOKOHAMA, Kanagawa, Japan)

MIS30-P04 Room:Poster Time:April 28 18:15-19:30

A chronostratigraphic study of the upper Anno formation, in the Awa group

HANEDA, Yuuki[1*]

[1]Ibaraki Unioversity

We took oriented mini-core samples for paleomagnetic and rockmagentic measurements at 79 sites and rock samples to extract fossil folaminifera from at sites from the upper Anno formation distributed along the Shikoma river. We carried out rock magnetic, paleomagnetic, oxygen isotopic and carbon isotopic measurements.

Magnetic carrier was interpreted as pused-single domain magnetites based on the results of hysteresis and thermal demagnetization, thermomagnetic analyses.

We carried out analysis of principal component to results from the thermal demagnetization and extracted Characteristic Remanent Magentizations (ChRMs). In the result, a relatively short reversed polarity zone found in the previous study is defined as the Mammoth subchronozone.

We obtained an oxygen isotopic curve from the result of isotopic measurements which is correlatable with the LR04 oxygen isotopic standard curve (Lisiecki & Raymo, 2005). Then we detected 6 tie points to establish an age model for this sequence

Keywords: paleomagnetic stratigraphy, oxygen isotopic stratigraphy, chronostratigraphy

Japan Geoscience Union Meeting 2014
(28 April - 02 May 2014 at Pacifico YOKOHAMA, Kanagawa, Japan)

MIS30-P05 Room:Poster Time:April 28 18:15-19:30

Palaeoclimatic analysis for 600 ka based on the TOC contents of MD01-2407 core from the Oki Ridge, Japan Sea

TAKIZAWA, Yuko[1*] ; YAMAMOTO, Hiroki[3] ; HAYASHIDA, Akira[4] ; KUMON, Fujio[2]

[1]Graduate school of Science and Technology, Shinshu University, [2]Faculity of Science, Shinshu University, [3]a former student of Faculty of Scinece, Shinshu Univ ersity, [4]Faculty of Science and Engineering, Doshisha University

We have measured total organic carbon (TOC) and total nitrogen (TN) contents of a sediment core, MD01-2407 (932 m depth, 55.28 m length), at 2 cm interval, This core was taken from the Oki ridge at the southern part of the Japan Sea in AD 2001. We used the age model which shows age-depth relation for MD01-2407 core proposed by Kido et al. (2007). This age model used 6 marker tephra layers, 7 ^{14}C dates, 3 TL layers and 14 delta ^{18}O events. This core covers the past 670 kyr.

TOC content is generally high in MIS 15, 13, 11, 9, 7, 5, 3 and 1 (about 1.5 - 5.0 %), and low in MIS 16, 14, 12, 10, 8, 6, 4 and 2 (about 0.8 - 1.2 %). This fluctuation pattern is very similar to the marine oxygen isotope curve LR04. TN content shows similar fluctuation with TOC. C/N ratio is constantly 9 - 10, suggesting that TOC is originated mainly from marine planktons. Temporal change of TOC of the sediment can reflect the change of biological productivity in the Japan Sea (Oba and Akasaka, 1990), which may be controlled climate change. This is an excellent record of paleoclimate over Middle and Late Pleistocene in the middle latitude region.

Keywords: TOC, TN, Japan Sea, MD01-2407

Japan Geoscience Union Meeting 2014
(28 April - 02 May 2014 at Pacifico YOKOHAMA, Kanagawa, Japan)

MIS30-P06 Room:Poster Time:April 28 18:15-19:30

A standard local chronology of late Quaternary based on the TOC profiles of the sediment cores from the Japan Sea

URABE, Tasuku[1*] ; KUMON, Fujio[2]

[1]Faculty of Science, Shinshu University, [2]Department of Environmental Sciences, Faculty of Science, Shinshu University

The TOC content was measured for the late Quaternary sediments of the Japan Sea with high time resolution (ca. 100 yrs interval), and show the good similarity to the delta 18O curve of NGRIP not only in the orbital scale but also the D-O cycle scale (Urabe et al., 2013). In this study, we use TOC profile of the MD179-3312 core from the Japan Sea, and we align the TOC profile to the delta ^{18}O in NGRIP using signal matching, the Match protocol (Lisiecki and Lisiecki, 2002). Before this matching process, there were ca. 4000 years gaps in maxima between both signals, and the gaps are variable. Based on the matched TOC profile, we calculated the ages of TOC peaks, and we proposed a new age of TL layers recognized in MD179-3312 (Kakuwa et al., 2013) on the basis of the matched chronology.

Recently, detailed TOC profiles of the sediment cores were reported from several sites in the Japan Sea, and they show very similar profiles. Therefore, we tried to compile the TOC profiles, using the same match protocol. The matched MD179-3312 profile mentioned above is used as a tentative standard, and TOC profiles of three sediment cores, namely MD179-3304 off Joetsu, MD01-2407 at Oki bank and MD01-2408 off Akita were matched to the tentative standard. This compiled TOC curve (TOC_{JSCOM}; Japan Sea TOC compile) has a reliability due to averaging the four cores data. This TOC_{JSCOM} have a good similarity with the TOC profiles from lake sediments in Japan. When we compared the TOC_{JSCOM} with the delta ^{18}O of stalagmites from the Hulu/Sanbao caves in the south of China (Wang et al., 2001, 2008), we found the improved chronological correspondence between both proxies in MIS 1/2 boundary, lower MIS 3, 4, 5.1, and 5.2. The difference of the trends is recognized in MIS 5.5, and a part of this discordance is due to the local environmental condition of the Japan Sea.

Keywords: Late Quaternary, Japan Sea, TOC, Chronology

Japan Geoscience Union Meeting 2014
(28 April - 02 May 2014 at Pacifico YOKOHAMA, Kanagawa, Japan)

MIS30-P07 Room:Poster Time:April 28 18:15-19:30

A Long-term pollen record of the C9001C core from the deep-sea bottom, off Shimokita peninsula, northeastern Japan

SUGAYA, Manami[1*] ; OKUDA, Masaaki[2] ; OKADA, Makoto[1]

[1]Ibaraki University, [2]Natural History Museum and Institute of Chiba

We used a pollen analysis method for a deep-sea core to reconstruct paleoclimatic changes with the Milankovitch time scale.

In this study, we obtained a continuous pollen record and reconstructed paleovegetation and paleoclimate changes for the past several kyrs from the C9001C core, drilled from off Shimokita Peninsula.

We have applied the Modern Analogue Method to obtain a quantitative paleochimate reconstruction. In the results, a positive correlation has shown on between the paleotemperature parameter and the glacial - interglacial cycle. On the other hands, the summer precipitation parameter matches with the precession cycles but not with the glacial - interglacial cycles. The annual temperature parameter variability show strong negative correlation. These results are support hypothesis of the East Asia monsoon fluctuation mechanism

Keywords: pollen, monsoon, marine core

Japan Geoscience Union Meeting 2014
(28 April - 02 May 2014 at Pacifico YOKOHAMA, Kanagawa, Japan)

MIS30-P08 Room:Poster Time:April 28 18:15-19:30

Carbon and oxygen stable isotope records of benthic foraminiferal shells at DSDP Site 296

OKAZAKI, Yusuke[1*] ; YAMAMOTO, Madoka[1] ; KAWAGATA, Shungo[2] ; IKEHARA, Minoru[3]

[1]Kyushu University, [2]Yokohama National University, [3]Kochi University

Carbon and oxygen stable isotope records of benthic foraminifera at DSDP Site 296 (2920 m water depth) from the Kyushu-Palau Ridge were measured. Sediment samples for upper 300 m of DSDP Site 296 were taken at every ˜2 m and freeze-dried and washed on a 63 micro m mesh sieve and dried in an oven at 40 degree C. The dry samples were sieved through a mesh with 250 micro m opening. Two epifauna species, Cibicides wuellerstorfi and Cibicidoides mundulus were picked for isotope measurements. The foraminiferal shells were cleaned by soaking them in 99.5% methyl alcohol, followed by ultrasonication until all chambers were open. After confirming that all dirt had been removed, we washed the shells in Milli-Q water and dried them in an oven at 40 degree C. The dried samples were analyzed using IsoPrime mass spectrometry (Center for Advanced Marine Core Research, Kochi University). Analyses were calibrated to the CO-1, and the average analytical errors for delta 13C and delta 18O were less than 0.03 permil and 0.10 permil, respectively.

Age model of DSDP Site 296 is established by planktic foraminiferal and calcareous nannoplankton stratigraphy (Elias, 1975; Ujiie, 1975). Continuous stable isotope records except for a stratigraphic gap at ˜250 mbsf are obtained for the past 20 Myrs. These records are basically consistent with those by Zachos et al. (2001).

Keywords: North Pacific, Benthic foraminifera, Stable isotope, Miocene, Pliocene

Japan Geoscience Union Meeting 2014
(28 April - 02 May 2014 at Pacifico YOKOHAMA, Kanagawa, Japan)

MIS30-P09 Room:Poster Time:April 28 18:15-19:30

A Southern Ocean trigger for Northwest Pacific ventilation during the Holocene?

RELLA, Stephan[1] ; UCHIDA, Masao[1*]

[1]National Institute for Environmental Studies

Holocene ocean circulation is poorly understood due to sparsity of dateable marine archives with submillennial-scale resolution. Here we present a record of mid-depth water radiocarbon contents in the Northwest (NW) Pacific Ocean over the last 12.000 years, which shows remarkable millennial-scale variations relative to changes in atmospheric radiocarbon inventory. Apparent decoupling of these variations from regional ventilation and mixing processes leads us to the suggestion that the mid-depth NW Pacific may have responded to changes in Southern Ocean overturning forced by latitudinal displacements of the southern westerly winds. By inference, a tendency of in-phase related North Atlantic and Southern Ocean overturning would argue against the development of a steady bipolar seesaw regime during the Holocene.This study was also published in Scietific Reports.

Keywords: Holocene, Northwest Pacific, Radiocarbon, Southern Ocean overtuning, Southern westerly winds

Japan Geoscience Union Meeting 2014
(28 April - 02 May 2014 at Pacifico YOKOHAMA, Kanagawa, Japan)

MIS30-P10 Room:Poster Time:April 28 18:15-19:30

Multiple early Eocene hyperthermals reconstructed from the Indian Ocean deep-sea sediments

YASUKAWA, Kazutaka[1*] ; NAKAMURA, Kentaro[1] ; KATO, Yasuhiro[2] ; IKEHARA, Minoru[3]

[1]Sys. Innovation, Univ. of Tokyo, [2]FRCER, Univ. of Tokyo, [3]Center for Advanced Marine Core Research, Kochi Univ.

From the late Paleocene to the early Eocene (ca. 56 Ma), an extreme global warming by 5-8 ℃ occurred within several thousand years, which is termed as the Paleocene-Eocene Thermal Maximum (PETM). The PETM is known to accompany severe ocean acidification and a prominent negative carbon isotope excursion in both marine and terrestrial environments, which indicate a massive and rapid injection of isotopically light (^{12}C-enriched) greenhouse gas into the ocean-atmosphere system. Recently, additional PETM-like global warming events (called as "hyperthermals") have also been identified during the early Eocene period of ca. 56-52 Ma [2]. As is the case with the PETM, the early Eocene hyperthermals also accompanied rapid and pronounced negative carbon isotope excursions. Besides, the hyperthermals appear to be in phase with the oscillations in the eccentricity of Earth's orbit [2, 3], which suggests that the orbital forcing affected to earth's climate and global carbon cycle even in the warmer Earth without large continental ice sheet during this period.

Geologic records of the hyperthermals have so far been reported from all over the world (e.g., the Pacific, the Atlantic, the Arctic, Europe and North America). The Indian Ocean, however, is the exception where only few published data are available for reconstruction of the hyperthermals and thus, the global extent of the hyperthermals remains uncertain. Here, we analyzed δ^{13}C, δ^{18}O and $CaCO_3$ contents of 376 bulk sediment samples taken from four DSDP/ODP cores (DSDP Site 213, DSDP Site 259, ODP Site 738C, ODP Site 752). The analytical results show that sediments from Site 738C and Site 752 contain multiple negative carbon and oxygen isotope excursions and reductions of carbonate contents, which appear to corresponding to the PETM and the early Eocene hyperthermals. Observed hyperthermals from the both sites are inferred to be H1 (Eocene Thermal maximum 2; ETM2)/H2 and I1/I2 events [3]. The observed carbon isotope excursions of ETM2 event (~ -1 ‰ at Site 752 and ~ -0.5 ‰ at Site 738C) and I1 event (~ -0.6 ‰ at both sites) are comparable with those reported from the other regions, such as the Pacific and the Atlantic Oceans. Our results strongly suggest that the hyperthermals in the early Eocene period were a global event including the Indian Ocean.

– References –
[1] McInerney and Wing (2011) Annu. Rev. Earth Planet. Sci., 39, 489-516.
[2] Zachos et al. (2010) Earth Planet. Sci. Lett., 299, 242-249.
[3] Cramer et al. (2003) Paleoceanography, 18, 1097. doi: 10.1029/2003PA000909.

Keywords: deep-sea sediment, Indian Ocean, climate change, hyperthermals

Japan Geoscience Union Meeting 2014
(28 April - 02 May 2014 at Pacifico YOKOHAMA, Kanagawa, Japan)

MIS30-P11 Room:Poster Time:April 28 18:15-19:30

Preliminary analyses on a LGM simulation using MIROC-ESM :climate and dust aerosol representation

OHGAITO, Rumi[1*] ; ABE-OUCHI, Ayako[2] ; TAKEMURA, Toshihiko[3] ; SUEYOSHI, Tetsuo[1] ; WATANABE, Shingo[1] ; HAJIMA, Tomohiro[1] ; O'ISHI, Ryouta[4] ; OKAJIMA, Hideki[1] ; SAITO, Fuyuki[1] ; CHIKAMOTO, Megumi[5] ; KAWAMIYA, Michio[1]

[1]JAMSTEC, [2]AORI, U. Tokyo, [3]Kyusyu U., [4]NIPR, [5]IPRC, U. Hawaii

Future Projection using Earth System Model (ESM) is an important contribution for Intergovernmental Panel on Climate Change Assessment Report 5 (IPCC AR5) from the modelling studies. Therefore, it is important to investigate ability of models and improve them. Especially, Last Glacial Maximum (LGM, 21,000 years before present) is recognized as a benchmarking period because it is the coldest time during relatively recent past. We report the preliminary analyses on climate and dust aerosol representation of the LGM experiment using an ESM, MIROC-ESM (Watanabe et al. 2011).

MIROC-ESM which contributed to IPCC AR5 was used for the study. The resolution of the Atmosphere General Circulation Model is T42 with 80 layers for the vertical levels and the resolution of the Ocean General Circulation Model part is about 1 o with 44 vertical levels. An aerosol module SPRINTARS (Takemura et al. 2000, 2002, 2005) is calculated online.

Following the protocol of Coupled Model Intercomparison Project phase 5, we performed two experiments. One experiment is called PI, which corresponds to pre-industrial time, i.e., 1850 A.D. The other is called LGM, which is supposed to represent climate at LGM (Sueyoshi et al. 2013). The differences of the boundary condition from PI are lower greenhouse gases, the orbit of the Earth and the topography (ice sheets and sea level drop).

The climate of PI is reasonably well represented as a state-of-the-art model (Watanabe et al. 2011). The sea surface temperature drop at LGM is reasonably comparable with MARGO dataset (MARGO project members 2009). However the 7 to 10 oC temperature drop suggested by the Antarctic ice cores (Stenni et al. 2010, Uemura et al. 2012) is reasonably represented, the 21 to 25 oC cooling suggested by the Greenland ice cores (Cuffey et al. 1995, Jonsen et al. 1995, Dahl-Jensen et al. 1998) is not enough simulated in the model. The modelled net cooling over the Greenland summit is about 15 oC. Tackling this defect is important to improve future projection. One of the conceivable reasons is the problem on representing enhancement of mineral dust aerosol in the model, which has been pointed out in IPCC AR5. We have compared the modeled dust amount with a dataset called DIRTMAP (Kohfeld and Harrison 2001). As a result, there are problems on the representation of dust over the Greenland both for PI and LGM. In the LGM experiment, the plant functional types (PFT) are basically unchanged from PI. Taking into account the change of PFT may lead more dust generation at LGM and enhance the cooling. The Antarctic dust is significantly lower than the dataset at LGM. The dust emission from Patagonia, the major dust source of the Antarctic ice core, is too low in the LGM experiment. This seems to be caused by too high soil moisture. The precipitation over Patagonia is already too high in the PI. Improving the PI precipitation amount may also affect the LGM precipitation amount and improve the soil moisture conditions.

We present the preliminary analyses on the dust at LGM using MIROC-ESM. As a result, there is a difficulty on representation of the dust enhancement over the ice sheets. Further improvements of the model, for example, taking into account the PFT change or better representation of the precipitation at PI may work to better representation of dust amount/distribution at LGM. Over the Antarctica, the cooling at LGM is expressed in the model but the dust amount is far from the estimation of the ice core data, i.e., the current simulated cooling may be a result of wrong reasons. We are going to improve the processes of the dust emission and investigate deposition procedures and estimation of radiative forcing.

Keywords: LGM, dust, climate sensitivity, Earth System Model

Japan Geoscience Union Meeting 2014
(28 April - 02 May 2014 at Pacifico YOKOHAMA, Kanagawa, Japan)

MIS30-P12 Room:Poster Time:April 28 18:15-19:30

A 3.3-kyr record of environmental changes in Asian continental interior by Lake Baikal core analysis

IKEDA, Hisashi[1*] ; MURAKAMI, Takuma[2] ; KATSUTA, Nagayoshi[3]

[1]Graduate School of Education, Gifu University, [2]Japan Atomic Energy Agency, [3]Faculty of Education, Gifu University

We report chemical analysis (TOC, TN, TS, BioSi, and etc) of Lake Baikal sediment.

Japan Geoscience Union Meeting 2014
(28 April - 02 May 2014 at Pacifico YOKOHAMA, Kanagawa, Japan)

MIS30-P13 Room:Poster Time:April 28 18:15-19:30

Observation of stalagmite laminae for paleoclimate reconstruction at Taga Mine Cave, Shiga Prefecture, Japan

HISAMOCHI, Ryo[1*] ; WATANABE, Yumiko[1] ; ABE, Yuji[2] ; TAGAMI, Takahiro[1]

[1]Graduate School of Science, Kyoto University, [2]Taga Town Museum

A lot of studies on paleoclimate reconstruction using stalagmites have been done all over the world. However, there are only a few stalagmite paleoclimate researches in Japan. In this study, we observe laminae of stalagmites collected at Taga Mine Cave, Shiga Prefecture, Japan (TAGA3,TAGA5,TAGA7,TAGA11,TAGA12) for paleoclimate reconstruction.

Stalagmite paleoclimate reconstruction has a potential to get high-resolution (anuual˜decadal) age proxy data, if stalagmite samples have anuual laminae. However, some stalagmites have a few types of laminae within a sample (Baker et.al,2008). In this case, it is important to elucidate which types of laminae is anuual.

When we observe the thin section of our samples by microscope, all samples show laminae. These laminae consist of natural organic matters because of fluorescent by UV excitation (Baker et.al,2008). Laminae interval is variable from several μm to a few hundred μm. Laminae of our samples are similar to the one from China and Turkey (Tan et.al,2006 , Baker et.al,2008).

Especially, sample TAGA3 has more obvious laminae than the other samples, but has the laminae which looks like sub-annual or supra-annual laminae reported in China (Tan et.al,2006). In addition, laminae are wavy in some parts of TAGA3. If we can distinguish annual laminae by U-Th age and find the feature of annual laminae, we will get high-resolution paleoclimate proxy data.

Keywords: stalagmite, laminae, paleoclimate

Japan Geoscience Union Meeting 2014
(28 April - 02 May 2014 at Pacifico YOKOHAMA, Kanagawa, Japan)

MIS30-P14 Room:Poster Time:April 28 18:15-19:30

New age model of off Takashima drilling sediment

INOUCHI, Yoshio[1*] ; YAMADA, Kazuyoshi[1] ; OKAMURA, Makoto[2] ; MATSUOKA, Hiromi[2] ; SATOGUCHI, Yasuhumi[3] ; HAYASHI, Ryouma[3] ; KUMON, Fujio[4] ; MATSUHISA, Koki[5] ; OKADA, Ryousuke[5] ; KAWASHIMA, Shouhei[5]

[1]Faculty of Human Sciences, Waseda University, [2]Faculty of Science, Kochi University, [3]Lake Biwa Museum, [4]Faculty of Science, Shinshu University, [5]School of Human Sciences, Waseda University

Several kinds of studies have been carried out regarding Off Takashima drilling core in Lake Biwa, Japan and a lot of achievements have been reported. In recent years, we have been carrying out chemical analysis on biogenic silica content of cored sediment with high time resolution. However, there have been some age problems regarding uppermost part of the core, namely the last 45 k years. In order to solve the age model problem, we carried out piston core sampling near the Off Takashima drilling site in 2012. About 30 carbon-14 data have been obtained. In addition to well-known wide spread tephra dates, these C-14 dates are converted into new age model. Correlation between Off Takashima drilling core and newly obtained piston core sediment enabled to establish new Off Takashima age model. Last year we reported tentative correlation based on water content profile of both cores. This time, we analyzed grain size, total organic carbon content and total nitrogen content of piston core sediment and compared with those of Off Takashima drilling core. Based on total organic carbon content, correlation between two cores and age model of Off Takashima drilling core are improved greatly.

Keywords: Lake Biwa, sediment, paleoenvironment, age model

Japan Geoscience Union Meeting 2014
(28 April - 02 May 2014 at Pacifico YOKOHAMA, Kanagawa, Japan)

MIS30-P15 Room:Poster Time:April 28 18:15-19:30

Climate change history of the last 45ka of Lake Biwa based on grain size and TOC,TN of BWK12-2 piston core

MATSUHISA, Koki[2*] ; MATSUNOSHITA, Kouji[2] ; OKADA, Ryosuke[2] ; KAWASHIMA, Shyohei[2] ; YAMADA, Kazuyoshi[1] ; INOUCHI, Yoshio[1] ; KUMON, Fujio[3] ; OKAMURA, Makoto[4] ; MATSUOKA, Hiromi[4] ; SATOGUCHI, Yasufumi[5] ; HAYASHI, Ryoma[5]

[1]Faculty of Human Sciences, Waseda University, [2]School of Human Sciences, Waseda University, [3]Department of Environmental Sciences,Faculty of Science,Shinshu University, [4]Faculty of Science, Kochi University, [5]Lake Biwa Museum

Based on newly established age model of BWK12-2 piston core sediment, obtained near the Off Takashima drilling station in Lake Biwa, Japan and with about 30 C-14 dates and well dated wide spread tephra, we analyzed grain size and total organic carbon (TOC) and total nitrogen (TN) contents of the sediment. Analyzing interval of those sediments were, 4cm to grain size and 2cm to TOC and TN whose time resolutions were 30 to 120 years and 15 to 60years respectively. Comparison with Marine Isotope Stage profile shows distinct resemblance to MIS1, however, difference between MIS2 and MIS3 is not clear. On the other hand, abrupt cooling events, such as Heinrich events and Younger Dryas, are clearly recognized. Abrupt warming , such as Dansgaard Oeschger events are not clearly recognized.

Keywords: Lake Biwa, sediment, paleo climate, grain size, TOC, TN

Japan Geoscience Union Meeting 2014
(28 April - 02 May 2014 at Pacifico YOKOHAMA, Kanagawa, Japan)

MIS30-P16 Room:Poster Time:April 28 18:15-19:30

Late Holocene change in lacustrine environment inferred from diatom fossil analysis of lake bed core

SATO, Yoshiki[1*] ; MATSUOKA, Hiromi[2] ; OKAMURA, Makoto[3] ; KASHIMA, Kaoru[4]

[1]Faculty of Science, Kyushu University, [2]Faculty of Science, Kochi University, [3]Science Research Center, Kochi University, [4]Faculty of Science, Kyushu University

Detail diatom fossils analysis of a lake bed core provided successive reconstruction of lacustrine environmental change after ca. 4700 cal BP in the Lake Hamana, central Japan, with high temporal resolution. In addition, two suspected thin layers as some kind of event deposits were recognized based on allochthonous sediments and/or diatom fossils.

Lake Hamana is a coastal brackish lake located along the Enshu-nada coast. Ikeya *et al*. (1990) performed numerous geological and paleontological analyses on lake bed sediments and reconstructed roughly the Holocene lacustrine environment and geomorphological development of the lake. According to them, after sea area had expanded landward associated with the Jomon Transgression, an inner bay and a fresh water lake occurred at a relatively stable sea-level condition. Furthermore, Morita *et al*. (1998) suggested that fresh water and brackish water conditions had been formed alternately during the Late Holocene, which indicating geomorphological changes presumably caused by some mega thrust earthquakes occurred in the Nankai trough. However, lower temporal resolution made impossible them to clarify detail lacustrine environmental changes.

In order to reconstruct detail lacustrine environmental change of the Lake Hamana during the Late Holocene, diatom fossil assemblages of the 350 cm-long lake bed core were investigated. The core sediments consisted of muddy deposits mainly including a thin sandy layer and two obvious tephra layers. The refractive index of volcanic ashes and core stratigraphy indicated that the lower tephra layer was the Amagi-Kawagodaira pumice (Kg, 3126-3145 cal BP, Machida and Arai, 2003) and the upper one was the Fuji-Osawa scoria (Os, 2.5-2.8 ka, Machida and Arai, 2003). The age model of the core was reconstructed based on the tephra layers and seven radiocarbon ages.

Six diatom zones were identified based on major species composition changes in the diatom assemblages. Stepwise development of the lacustrine environment in the Lake Hamana was suggested as below: Vigorous seawater inflow inferred by marine diatoms (Stage I, 4600-4700 cal BP); A closed inner bay environment with laminated sediments due to formation of sand barriers (Stage II, 4500-4600 cal BP); A circulative brackish lacustrine environment by active mixture of riverine fresh water with enhanced inflow of seawater since 3500 cal BP (Stage III, 2650-4500 cal BP); Gradual salinity decrease of the lake water by reduced seawater inflow (Stage IV, 2250-2650 cal BP); Lake water from brackish to fresh since 2250 cal BP with intermittent salinity increase in the middle of this period, water depth of the lake getting deeper (Stage V, 1498 AD-2250 cal BP); Re-development of an inner bay environment after the Meio earthquake in 1498 AD with temporal salinity increase during 1600 AD to 1750 AD (Stage VI, after 1498 AD).

Additionally, two possible event layers (A and B layer in ascending order) were found. The A layer, during 321-322 cm depth, was characterized by exceptionally high percentage of *Plagiogramma* sp. This temporal abundance accompanying increases of *Thalassiosira* sp. and *Thalassionema nitzschioides* indicates an abrupt environmental change and/or an allochthonous sediments supply. Nevertheless, it is difficult to specify the cause of this layer because the habitat of *Plagiogramma* sp. is still unknown. On the other hand, the B layer was corresponding to the thin sand layer in the range of 285-288 cm depth showed short-term abundance of fresh water diatom species. This indicates that relative coarse sediments supplied abruptly from fresh water environment, ponds and/or marshes, around the lake to the central part of the lake.

Reference
Ikeya, N. *et al*. 1990. Mem. Geol. Soc. Japan 36, 129-150.
Morita, H. *et al*. 1998. Laguna 5, 47-53.
Machida, H. and Arai, F. 2003. Atlas of Tephra in and around Japan. University of Tokyo Press. 337p.

Keywords: LakeHamana, lacustrine environment, coastal lagoon, diatom fossil, 1498 Meio earthquake, Holocene

Japan Geoscience Union Meeting 2014
(28 April - 02 May 2014 at Pacifico YOKOHAMA, Kanagawa, Japan)

MIS30-P17 Room:Poster Time:April 28 18:15-19:30

Reconstruction of the Last glacial to Holocene climate changes in Shaamar loess-paleosol succession, northern Mongolia

ORKHONSELENGE, Aleksandr[1] ; HASEGAWA, Hitoshi[2*]

[1]School of Geography and Geology, National University of Mongolia, [2]Nagoya University Museum

Two atmospheric circulation systems, the mid-latitude Westerlies and the Asian monsoon, play key roles in northern-hemisphere climatic changes. However, the variability of the Westerlies in mid-latitude Asia and their relationship to the Asian summer and winter monsoon remain unclear. We examined the variations in the grain size and elemental composition from the 30 m long loess-paleosol succession in Shaamar area, northern Mongolia, which could be recorded the interplay of the Westerlies and Asian winter monsoon for the last 30 k.y. We then compared our results with the multi-proxy paleoclimate records (e.g., eolian grain sizes, lake levels, pollen assemblages) of the Asian summer and winter monsoon regions and the Westerlies affected region.

According to the compiled data of the Wang and Feng (2013), the Holocene climatic variation patterns (mainly from lake levels and pollen records) in Asia are categorized into 4 characteristic regions, such as the Summer monsoon region (southern and northeastern China), Westerlies affected region (northwestern China), Winter monsoon region (southern Siberia), and Mixture of westerlies and winter monsoon affected region (Mongolia). Specifically, summer monsoon region is characterized by dry earliest Holocene (12-11 ka), humid early to middle Holocene (11-6 ka), and the moderate-humid late Holocene (last 6 ka), corresponding to the Northern hemisphere summer insolation changes. Westerlies affected region is characterized by dry early Holocene (12-8 ka) and humid middle to late Holocene (last 8 ka). Winter monsoon region is characterized by the humid early Holocene (12-8 ka) and dry middle to late Holocene (last 8 ka). On the other hand, Mongolian records (e.g., Lake Khuvsgul, Lake Gun Nuur) demonstrate humid early Holocene (12-9 ka), dry middle Holocene (9-5 ka), and humid late Holocene (last 5 ka), which seems mixture of westerlies and winter monsoon affected region.

Shaamar loess-paleosol succession record is characterized by the humid early Holocene (12-8 ka) and dry middle to late Holocene (last 8 ka), similar to the winter monsoon region in southern Siberia. Thus, it is suggested that the eolian sediment record in Shaamar could be affected more strongly by winter monsoon influence, although Shaamar section is located closely to the mixture of westerlies and winter monsoon affected region (e.g., Lake Khuvsgul and Lake Gun Nuur). Except for the Chinese Loess Plateau, Shaamar loess-paleosol succession is only the continuous eolian sediment record in mid-latitude Asia. Thus, Shaamar loess-paleosol succession should provide us rare glimpse for understanding the interplay of westerlies and winter monsoon in Asian mid-latitude. We will further examine the Last glacial records of the Shaamar loess-plaeosol succession and compare with other records of the Asian summer and winter monsoon regions and the Westerlies affected region.

Keywords: Mongolia, Loess-paleosol succession, Westerlies, Winter monsoon, Holocene, LGM

Japan Geoscience Union Meeting 2014
(28 April - 02 May 2014 at Pacifico YOKOHAMA, Kanagawa, Japan)

MIS30-P18 Room:Poster Time:April 28 18:15-19:30

Reconstruction paleoenvironment by using diatom fossil assemblage analysis in Imuta-ike wetland, Satsumesendai, Kagoshim

GOTO, Daichi[1*] ; KASHIMA, Kaoru[1] ; YAMADA, Kazuyoshi[2] ; HARAGUCHI, Tsuyoshi[3] ; IMURA, Ryusuke[5] ; YONENOBU, Hitoshi[4]

[1]Department of Earth and Planetary Sciences, Faculty of Sciences, Kyushu University, [2]School of Human Sciences, Waseda University, [3]Department of Geosciences,Graduate School of Science,Osaka City University, [4]Graduate School of Education, Naruto University of Education, [5]Graduate School of Science and Engineering, Kagoshima University

Paleoenvironmental reconstruction, using diatom assemblage analysis have been carried out in Imuta-ike, Satsumasendai, Kagoshima, Japan. In this site, there are deposit peat layer which is rare in west Japan, 6 visible tephra layer and 2.5m depth laminated layer. Boring survey conducted center of Imuta-ike at Feb. 2011, we was able to got 25m depth core. It can be traced back to 30,000 years past, can be reconstructed until modern environment from ice age. Following environment changes are reconstructed. Since about 30,000 years ago, peat and silt continuously has deposited, but accumulate speed has changed.

About 30,000 yr BP to 23,400 yr BP, we can't reconstruct detail environment change, because of the small number of diatom. About 23,400 yr BP to 13,600 yr BP, inflow river has been existed. And edge of the lake, moor has been formed. About 13,600 yr BP to 10,800 yr BP, moor became land, then pH rose. About 10,800 yr BP to 4,600 yr BP, it starts the postglacial age, increase precipitation and water level was rose. After K-Ah, tephra deposited the lake and water depth was shallow. About 4,600 yr BP to 1,500 yr BP, those days was dystrophic lake and it started to form wet land in west side of the lake. About 1,500 yr BP to present, it continues aggradation, water depth has been shallow. It progresses wet land formation so that water pH was dropped.

Keywords: diatom, Holocene, climatic change, pH change, volcanic stratigraphy, annually laminated lake deposit

Japan Geoscience Union Meeting 2014
(28 April - 02 May 2014 at Pacifico YOKOHAMA, Kanagawa, Japan)

MIS30-P19 Room:Poster Time:April 28 18:15-19:30

Reconstruction of Paleo-environment at coastal lakes along the Soya Coast, Antarctica, using fossil diatom assemblages

KANG, Ijin[1*] ; KASHIMA, Kaoru[2] ; SETO, Koji[3] ; TANI, Yukinori[4] ; MATSUMOTO, Genki I.[5]

[1]Department of Earth and Planetary Sciences, Graduate School of Sciences, Kyushu University, [2]Department of Earth and Planetary Sciences, Graduate School of Sciences, Kyushu University, [3]Research Center for Coastal Lagoon Environments, Shimane University, [4]Institute of Environmental Sciences, University of Shizuoka, [5]School of Social Information Studies, Otsuma Women's University

Soya Coast, located at East Antarctica distribute wide ice-free areas such as Langhovde, Skarvsnes, Skallen and Rundvagshetta. The research areas of this study are five lakes in the ice-free coast as follows; Lake Nurume-ike and Lake Yukidori-ike at Langhovde, Lake Oyako-ike at Skarvsnes and Lake Maruwan-minami-ike and Lake Maruwan-oike at Rundvagshetta.

Matsumoto et al.2014 described the Holocene paleo-limnological changes at Lake Oyako-ike. They described soft-x-ray analysis, carbon 14 dating, elemental analyses, Chlorphyll compounds and carotenoids, and algae and cyanobacteria analyses. The paleo-environment of the lake shifted from the open coastal environment, through stratified saline lake, and then to high productive fresh water lake during these two thousand years. They presume that these environmental changes have been affected by isostatic uplift by retreating continental glaciers.

Diatom fossil assemblages at the lake deposit (Ok4C-1) divided into five assemblages zones, from Zone 1 to Zone 5 to upward. The dominated species of each zone is as follows. Zone 1:*Paralia sulcata*, marine species, Zone 2:*Staurosira construens*, Zone3:*Tryblionella littoralis*, marine species, Zone4:*Chamaepinnularia cymatopleura*, brackish species and Zone 5:*Amphora oligotraphent* *Navicula gregaria*, *Diadesmis* spp., freshwater species. The shifts of diatom assemblages presumed the lake water environment shifted from coastal marine environment through freshwater lake environment. This result was fitted to the results of the previous study. Now, we are analyzing other four lake sediment cores.

Keywords: Antarctic coastal lakes, paleolimnology, diatom, the Holocene, Sediment core

Japan Geoscience Union Meeting 2014
(28 April - 02 May 2014 at Pacifico YOKOHAMA, Kanagawa, Japan)

MIS30-P20 Room:Poster Time:April 28 18:15-19:30

Holocene climate changes detected in the bottom sediments of the glacier lake, southern Peru

YAMADA, Kazuyoshi[1*] ; SHINOZUKA, Yoshitsugu[2] ; SETO, Koji[3] ; HARAGUCHI, Tsuyoshi[4] ; YONENOBU, Hitoshi[5]

[1]Waseda University, [2]Hokkaido University, [3]Shimane University, [4]Osaka City University, [5]Naruto University of Education

We attempt to reconstruct climate changes during the Holocene by using a glacier lake on the southern Peru. For this, we had undertaken field investigation as echo sounding and piston coring at Lake Yauriuiri, which is 130 km apart from Nazca city. The lake is one of typical glacier lake at height of 4,384 m. By the seismic record of the lake bottom from echo sounding, it is identified that 10-m thick mud layer with the intercalated fine sand layers on the bedrooks. And, two sediment cores were taken from the southwestern point at 50 m in water depth. The length of the cores is 50, and 170 cm, respectively. Lithology of the sediment shows that almost homogenous dark grey slit with two thin brownish flood-origin layers. We have analyzed physical properties, magnetic susceptibility, color reflectance, chemical compounds by XRF, CNS and ICP-AES with multiple radiocarbon dating for the whole core section. Our results indicated abrupt changes of S and Ti contents at 4,000 and 7,000 cal BP, suggesting that past lake level fluctuation and precipitation over the last 11,000 years caused by climate changes. These past environmental variations in Lake Yauriuiri may have the similar pattern with other records in inland area of Peru as well as off shore Peruvian marine records.

Keywords: Peru, Laguna YauriUiri, climate change, Nazca Culture

Japan Geoscience Union Meeting 2014
(28 April - 02 May 2014 at Pacifico YOKOHAMA, Kanagawa, Japan)

MIS31-01 Room:511 Time:May 2 09:00-09:15

Extensions of RCP2.6/4.5 with zero emission after 2100: as 2K/3K stabilization scenarios for MIROC-ESM

TACHIIRI, Kaoru[1*] ; HAJIMA, Tomohiro[1] ; KAWAMIYA, Michio[1]

[1]Japan Agency for Marine-Earth Science and Technology

Focusing that MIROC-ESM (an earth system model, no atmospheric chemistry version) output around 2K/3K rise in global mean surface air temperature in 2100 with the Representative Concentration Pathways (RCP) 2.6 and 4.5, we extend the experiments with zero-emission after 2100, as 2K/3K stabilization scenarios for the model. As MROC-ESM is a ”pessimistic” (with high climate sensitivity and small ecosystem carbon uptake) model, stabilization for this model means large chance of stabilization for many other models. The experiment, with fixed land use and other non-CO_2 forcing after 2100, is designed to 2300,and we are now just after 2200.

In the 2K stabilization scenario, RCP2.6 followed with zero emission, temperature rise from the pre-industrial state (PI) is slightly over 2K in 2100, and slowly decreased after the zero-emission period starts, and is just below 2K at 2200. Atmospheric CO_2 concentration (pCO_2) is 421ppm at 2100 and around 400ppm at 2200. On the other hand, in the 3K stabilization scenario, RCP4.5 followed with zero emission, temperature rise from PI is just over 3K, and then decreased after that slightly more rapidly than 2K stabilization scenario and is around 2.8K at 2200. pCO_2 is 540ppm at 2100 and just below 500ppm at 2200.

Looking at air temperature after stabilization (i.e., 2100), the 2K stabilization scenario have temperature rise in and around Antarctica, in Siberia and in Greenland, and decrease in Amazon and in northern lands. The 3K stabilization scenario has similar pattern, but with relatively small rise in and around Antarctica, and no significant increase in Greenland. Some increase in Siberia, and with significant decrease in Arctic Sea. Precipitation decreases in Western Pacific and increases in a part of Eastern Pacific and around Indian Ocean for 2K stabilization scenario. For 3K stabilization scenario, precipitation is decreased in some areas in southern Pacific.

Keywords: Representative Concentration Pathways, zero emission, stabilization, Earth system model

Japan Geoscience Union Meeting 2014
(28 April - 02 May 2014 at Pacifico YOKOHAMA, Kanagawa, Japan)

MIS31-02 Room:511 Time:May 2 09:15-09:30

Parallel and integrated processes of climate-impact-socioeconomics for climate research

EMORI, Seita[1*]

[1]National Institute for Environmental Studies

The need to take mitigation measures in order to hold the increase in global average temperature below 2 degree C above pre-industrial levels are recognized in international negotiations of the United Nations Framework Convention on Climate Change (UNFCCC). According to the fifth assessment report (AR5) by the Working Group (WG) I of Intergovernmental Panel on Climate Change (IPCC) which was published last September, attaining the temperature goal with a probability of 50% will require cumulative CO2 emissions from all anthropogenic sources to stay approximately 300 GtC from the present. If the current level of anthropogenic CO2 emission, 10 GtC yr-1, continues, the cumulative emissions will reach this upper limit in only 30 years. If we will seriously pursue the goal of temperature increase below 2 degree C, global CO2 emission should be turned to decline as soon as possible, and to be reduced at nearly zero by around the end of this century.

A great deal of research on climate change impacts and mitigation measures exist; however, large uncertainties remain in their overall pictures. So far, nobody can grasp clearly risks for human society and ecosystem associated with global warming exceeding ”2 degree C”, and risks for socioeconomics due to severe emission reductions of greenhouse gases. Furthermore, the risks will be realized in different ways by country, region, generation, and social attribution, and therefore, either if no specific response measures are conducted or if strong measures are conducted, a part of people in the world will have benefits and another part of people will make a loss. Climate change impact is not just an issue on benefits and losses of each person; but it relates to issues how we feel distress on risks for ecosystem, developing countries, and future generations. It relates to different value judgment among people.

Climate research plays a role to provide scientific information to help the societal decision making process of such an uncertain, complex and ambiguous risk problem. To pursue it, there has been a serious international activity to promote interaction across the three research communities, that is, climate, impact and socioeconomics (corresponding to the WG I, II and III of IPCC, respectively). I will look back the idea of parallel and integrated processes of the three research communities, that was attempted during the discussion of Representative Concentration Pathways (RCP) around 2010, from the present where IPCC AR5 was released, and discuss its progress and future prospects.

Japan Geoscience Union Meeting 2014
(28 April - 02 May 2014 at Pacifico YOKOHAMA, Kanagawa, Japan)

MIS31-03 Room:511 Time:May 2 09:30-09:45

Development of the climate model MIROC and initialization system using LETKF for the next IPCC report

TATEBE, Hiroaki[1*] ; OGURA, Tomoo[2] ; WATANABE, Shingo[1] ; WATANABE, Masahiro[3] ; SUZUKI, Tatsuo[1] ; KOMURO, Yoshiki[1] ; NITTA, Tomoko[3] ; O'ISHI, Ryouta[3] ; TAKATA, Kumiko[5] ; KOYAMA, Hiroshi[1] ; ISHII, Masayoshi[4] ; KIMOTO, Masahide[3]

[1]RIGC, JAMSTEC, [2]NIES, [3]AORI, Univ. of Tokyo, [4]MRI, JMA, [5]NIPR

We have been updating the climate model MIROC and developing a data assimilation and initialization system based on the local ensemble transform Kalman filter (LETKF) for reconstructing global centennial climate, understanding of mechanisms of climatic periodic changes, regime shifts, and extreme events, and improving skills in seasonal-to-decadal climate predictions. For the previous fifth assessment report of IPCC-AR5, decadal climate forecasts and retrospective predictions taking into account both of the global warming due to increase of anthropogenic green house gases and intrinsic variability of the climate system were performed using a series of MIROC with various resolutions and physics. As a result, for example, the mid-latitude SST signals in the North Pacific associated with the Pacific decadal oscillations, the abrupt stepwise climate shift occurred in the late 1990s, and the tropical cyclone activity over the western North Pacific are suggested to be predictable for a few to several years. After the experiments for IPCC-AR5, we additionally performed retrospective climate predictions on seasonal-to-interannual timescales focusing ENSO. Prediction skill of the equatorial SST in MIROC is as high as those in climate models of operational centers over the world. However, because MIROC has remarkable systematic climate biases of stronger equatorial trade winds and resultant deeper thermocline, more subtropical clouds in the lower troposphere and relating colder SST, weaker mid-latitude westerly jets, warmer SST and larger precipitations around Antarctica than observations, so-called anomaly assimilation technique is used in initializing the climate model, and thus the seamless climate predictions cannot be performed by the present system. Therefore, our modeling group is devoting effort to reduce the model biases and to realize the seamless predictions by MIROC based on full field assimilation. In my talk, recent update of MIROC will be introduced along with preliminary results from a newly developing initialization system.

Keywords: climate model, initialization, seamless climate prediction

Japan Geoscience Union Meeting 2014
(28 April - 02 May 2014 at Pacifico YOKOHAMA, Kanagawa, Japan)

MIS31-04 Room:511 Time:May 2 09:45-10:00

Climate projections using high-resolution MRI-AGCM

MIZUTA, Ryo[1*] ; OSE, Tomoaki[1] ; MURAKAMI, Hiroyuki[2] ; ARAKAWA, Osamu[3] ; YOSHIDA, Kohei[1] ; NAKAEGAWA, Toshiyuki[1]

[1]Meteorological Research Institute, [2]International Pacific Research Center, [3]University of Tsukuba

A high-resolution atmospheric general circulation model of the Meteorological Research Institute (MRI-AGCM), with a horizontal grid size of about 20 km, have been developed, and applied to climate projections for extreme weather events such as tropical cyclones and heavy precipitation. Given the observational sea-surface temperature (SST) as the lower boundary condition, the model can simulate not only global-scale climate of temperature and precipitation, but also climatic characteristics of small-scale phenomena such as geographical distribution and intensity of tropical cyclones, and seasonal march of the East Asian monsoon.

Under the KAKUSHIN program (2007-2012; sponsored by MEXT), giving SST changes from atmosphere-ocean coupled models, time-slice experiments with this model have been performed to investigate detailed and localized changes as a consequence of global warming. The uncertainty of the change has been also evaluated, using many ensemble experiments with 60 km version of the model. The simulation results has been used for many purposes, including impact accessments of disasters, water resources, and agriculture, as well as analyses from meteorological point of view. The results has been also provided to the researchers worldwide, for the researches of regional climate changes of their own countries. Over Japan area, dynamical downscaling experiments have been performed using a regional climate model with horizontal grid sizes of 5km and 2km.

Under the SOUSEI program (2012-2017; sponsored by MEXT), in order to evaluate and reduce the uncertainty of the climate projections, ensemble experiments with the 20-km model with different geographical patterns of SST changes are being performed, using results of CMIP5 coupled models.

Keywords: global warming, atmospheric general circulation model

Japan Geoscience Union Meeting 2014
(28 April - 02 May 2014 at Pacifico YOKOHAMA, Kanagawa, Japan)

MIS31-05 Room:511 Time:May 2 10:00-10:15

Earth system modeling - a brief history and future direction

WATANABE, Shingo[1*]

[1]JAMSTEC

A brief history of Earth system modeling will be outlined, and its future direction will be discussed.

Keywords: Earth system model

Japan Geoscience Union Meeting 2014
(28 April - 02 May 2014 at Pacifico YOKOHAMA, Kanagawa, Japan)

MIS31-06 Room:511 Time:May 2 10:15-10:30

Findings in climate change and global carbon cycle from model inter-comparison analyses

HAJIMA, Tomohiro[1*]

[1]Japan Agency for Marine-Earth Science and Technology

Interactions between climate and carbon cycle are essential for making long-term climate projection, since some part of carbon cycle processes in land and ocean display slow responses to environmental change in a longer timescale, with giving feedbacks on climate. Climate-carbon cycle models, sometimes referred as ”Earth system models (ESMs)”, have been developed and utilized for the long-term climate projection. Recent model inter-comparison analyses have revealed some problems in the models, and provided new findings on climate-carbon cycle relationships. For example, a new index ”TCRE” is introduced in the latest IPCC report. This index can capture the entire response of global climate-carbon cycle system to anthropogenic CO2 emission, with suggesting some useful political messages. In this presentation, new findings on climate-carbon cycle system such as TCRE will be reviewed, based on the results from model inter-comparison analyses.

Japan Geoscience Union Meeting 2014
(28 April - 02 May 2014 at Pacifico YOKOHAMA, Kanagawa, Japan)

MIS31-07 Room:511 Time:May 2 10:30-10:45

Cyber Earth: A new technical approach for global studies of Earth

MURATA, Ken T.[1*]

[1]NICT

In the present paper, the author proposed a concept of the Cyber Earth as a basic approach for the global understanding of the Earth system. In order for our global understandings from a variety of observation and simulation data of Earth sciences, we need a methodology to analyze huge size of big science data. The Cyber Earth is a concept to declare that, for our global understandings, mash-up of information and communication technologies for big data plays an important role. This concept is based on several technological ideas, such as data centric/intensive science, the fourth paradigm, science cloud, big-data science. All of the data, observation data and simulation data, are once transferred and stored on a science cloud system. Data preservation and data stewardship is important since most of the data is so precious that they are never observed again at the observed time and location. Big data processing, including visualization, is also important. The data processing must be applicable for any types of digital data from either Earth observation or simulation. Integrated data processing technology for such variety of data type is preferable.

The Cyber Earth is composed of three methodologies; the Network Earth, the Digital Earth and the Virtual Earth. The Network Earth is a concept that role of network is important for data transfer and collection to the cloud. For global monitoring we often build up global observatories on the Earth. Integrated operations and easy management of the remote sites are significant for labor-saving. The Digital Earth is a concept that long-term data preservation is one of the most expected functions to a science cloud. Data files must be saved and managed under DR (disaster recovery) environment. Easy data publication should be functionally synchronized with data preservation. The Virtual Earth is a concept that every digital data must be processed or visualized to be shown on the same framework with other data. Inter-disciplinary data preview, in space and/or in time, makes our global and functional understanding of the Earth system. Immersive visualization may work effectively to understand or discover any interactions between data.

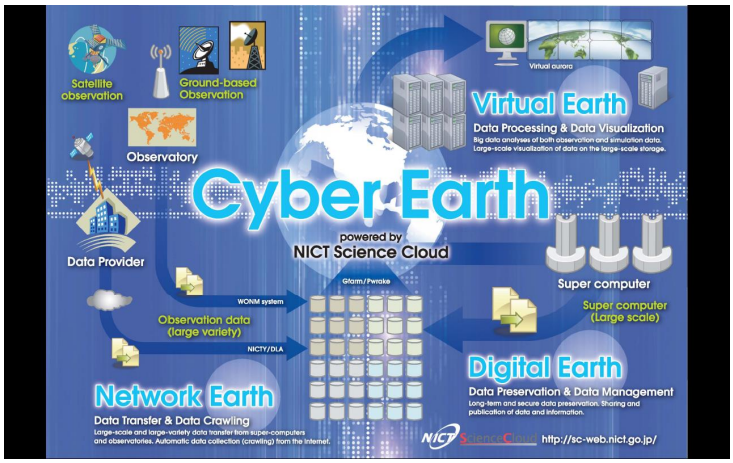

Japan Geoscience Union Meeting 2014
(28 April - 02 May 2014 at Pacifico YOKOHAMA, Kanagawa, Japan)

MIS31-08 Room:511 Time:May 2 11:00-11:15

Current trends of international assessments of greenhouse gas emission mitigation scenarios

AKIMOTO, Keigo[1*]

[1]Research Institute of Innovatitve Technology for the Earth

The IPCC 5th Assessment Report (AR5) are scheduled to be completed in 2014. The Working Group III assesses mitigation options and the report ”Climate Change 2014: Mitigation of Climate Change”, will be released in April 2014 after the approval in the 39th Session of IPCC. Scenario analysis and modeling exercise by the integrated assessment model (IAM) provide a key element in the AR5 report. A number of international inter-model comparison projects are formulated mainly in the United States and EU countries in an effort to make contribution to the IPCC AR5 report.

This paper introduces that the current trends of international assessments of greenhouse gas (GHG) emission mitigation scenarios with the key points which have been described in the AR5 and the key outcomes of the international IAM comparison projects. In addition, international research cooperation activities for harmonizing socioeconomic scenarios for the future IAM assessments, which is named SSPs (Shared Socioeconomic Pathways), will be introduced.

The Fourth Assessment Report (AR4) of IPCC WGIII which was published in 2007 provided six categories for broad ranges of several emission pathways provided by IAM estimations. The lowest level of GHG concentration stabilization is 445-490 ppm CO2eq and the emission pathways correspond to 85-50% reductions of global emission by 2050 relative to the 2000 level. The report summarized that the emission pathways will be expected to the equilibrium global mean surface temperature of 2.0-2.4C increase relative to pre-industrial level. The assessment had a strong impact on the international climate change negotiations and domestic measures of climate change response. Long-term target of 2C and halving global emissions by 2050 have been widely discussed in international negotiations such as UNCCC/COP and G8 after the release of AR4, while IPCC never recommends a specific target and policy.

A lot of assessments for emission reduction scenarios by IAMs particularly for deep emission reduction scenarios such as 450 ppm CO2eq, have been conducted after the AR4. The assessments also include many overshoot scenarios which are temporally over 450 ppm CO2eq and then achieve 450 ppm CO2eq in 2100 as well as 450 ppm stabilization scenarios, because current global emission increases are large due to the increases in developing countries, and it is difficult to develop emission reduction pathways with reality in near-term emissions for 450 ppm CO2eq stabilization without overshoot.

One of the inter-model comparison projects, AMPERE (Assessment of Climate Change Mitigation Pathways and Evaluation of the Robustness of Mitigation Cost Estimates) project which was funded by the European Commission provided the feasibility of significant emissions reduction for a variety of mitigation technology portfolios. The project assessed that the feasibility for deep emission reductions such as 450 ppm CO2eq and the emission reduction costs under several conditions of technology unavailability and the near-term emissions locked into by the Cancun pledges. With significant emission reduction until 2030, the required annual emission reduction to meet 450 CO2eq target diverges from the historical rates of change. If the emissions pathways are locked into the low ambitious Cancun pledges to 2030, further improvement is required after 2030. There are many infeasible results to meet the stringent target in model calculation, if there are technological constraints in the availability of CCS, nuclear and renewable energy particularly under the near-term emissions locked in. The emission reduction costs are also very high and almost double or more compared with the idealistic conditions. These assessments which consider realistic conditions in IAMs are one of the progresses after the AR4.

The AR5 of IPCC will includes such new assessments will make impacts on international climate policies after the release.

Keywords: climate change, global warming mitigation, emissions scenarios, IPCC, integrated assessment model

Japan Geoscience Union Meeting 2014
(28 April - 02 May 2014 at Pacifico YOKOHAMA, Kanagawa, Japan)

MIS31-09 Room:511 Time:May 2 11:15-11:30

Integrated assessment model structure and linkage with climate model

KUROSAWA, Atsushi[1*]

[1]The Institute of Applied Energy

1. History and basic structure of integrated assessment model

Integrated assessment model (IAM) has been developed as a tool to analyze climate change countermeasures. Edmonds-Reilly model in 1980s was the one of initial trials to indicate the importance of the relationship between climate change and energy issues, through explicit analysis of energy CO_2 and global warming. Since 1990s, model development has been active to evaluate comprehensive measures from interdisciplinary knowledge in climate change, energy system, land use, etc. The new keywords of the models developed are 'interdisciplinary', 'large scale', 'very long-term dynamics', 'scale integration'. These models are called IAMs because their scope is very wide in time, space and disciplines. For example, GRAPE model, developed by the GRAPE development team, consists of modules dealing with energy, climate, land use, macroeconomics and environmental impacts. Intergovernmental Panel on Climate Change (IPCC) working group III reviewed IAM intercomparison results such as economic impacts of Kyoto Protocol, multiple GHGs mitigation including non-CO_2 gases mitigation potential and its effects in the past assessment reports.

2. Linkage with climate model

There are various types of linkage of climate model in IAMs. Major categories are 'hard-link' and 'soft-link'. The former includes all equations and variables of climate module in the entire model structure, while the latter exchanges the information (e.g. GHG emissions) between climate module and other parts of the model.

DICE model, one region global model, is the one of initial famous IAMs. It uses hard-link optimization methodology and simple one-dimension climate model with two ocean layers and one atmospheric layer. Radiative forcing of CO_2 is calculated endogenously but other aggregated forcing values are exogenously provided. After obtaining the global mean temperature, macroeconomic damage feedback is assessed as the function of temperature rise.

It is great challenge to include large scale climate model in the hard-link type IAMs. Because of climate system nonlinearity and many constraints including inequalities, it is quite difficult to get solutions especially under dynamic climate constraints such as long-term forcing stabilization. Climate module of GRAPE includes carbon cycle representation of one-dimensional version of the ISAM, one of the reference model in IPCC WG I third assessment report. Global carbon stock is distributed to the atmosphere, ocean, and terrestrial biospheres. The ocean part has 40 deep layers and terrestrial biosphere has six boxes. Energy exchange among atmosphere and ocean layers are also modeled.

Recently, coupled analyses combining earth system model and IAMs are in progress in the area of climate impact assessment with fine mesh-scale, or climate feedback of energy consumption level, etc. Climate information is quite useful and essential in these assessments.

3.Future issues and summary

GHG reduction would not be on the track to avoid potential dangerous impacts to global climate change because it is difficult to get consensus in global climate policy. Adjustment to climate condition (i.e. 'adaptation') could be the realistic solution in the short to medium term. Vulnerability to climate change varies by region and economic condition, and climate information in the future is important to design regional adaptation policies.

'Geoengineering', such as solar radiation management (SRM) and carbon dioxide removal (CDR), is included in the IPCC working group I fifth assessment report sentences. Negative emission feasibility through implementation of CDR needs further considerations with low GHG emissions scenarios with assistance of climate models.

IAM has close and essential linkage with climate model from initial development stage, and more interaction are crucial to resolve global and regional agenda in the future.

Keywords: Integrated Assessment Model, Climate Model

Japan Geoscience Union Meeting 2014
(28 April - 02 May 2014 at Pacifico YOKOHAMA, Kanagawa, Japan)

MIS31-10 Room:511 Time:May 2 11:30-11:45

Integration of climate and economic modeling studies

MATSUMOTO, Ken'ichi[1*] ; TACHIIRI, Kaoru[2]

[1]The University of Shiga Prefecture, [2]Japan Agency for Marine-Earth Science and Technology

So far, there have not been many studies which integrate climate modeling and economic modeling research. The purpose of this presentation is to show one way to integrate climate and economic studies with regard to climate change issues. Here, we present an example of the integration of these two areas, which analyzes socioeconomic impact of achieving a specific radiative forcing level considering the uncertainties of Earth system models using a computable general equilibrium (CGE) model.

Although much uncertainty exists in climate system and simulations of future climate profiles with Earth system models (ESMs), it has not been evaluated in relation to socioeconomic aspects. In this study, we analyze the socioeconomic impact (including that on energy) of three emission pathways, all of which possibly achieve 4.5 W/m^2 of radiative forcing in the year 2100 within uncertainties estimated by an ESM of intermediate complexity (EMIC) tuned for full ESMs using a CGE model, a type of economic models. The model used here is a multi-regional and multi-sectoral recursive dynamic CGE model on a global scale, with energy and environmental components. Thus, the model is also called an integrated assessment model or IAM.

The emission pathways considered in this study are allowable emission pathways obtained by using an EMIC with the Representative Concentration Pathway 4.5 scenario. Here, we analyze the emission pathways of the 5th (lower bound), 50th (mean), and 95th (upper bound) percentiles of the weighted ensemble members in the parameter perturbation experiment. Different pathways are derived from different physical and biogeochemical properties. The global CO_2 emissions in 2100 and the cumulative CO_2 emissions in this century in the upper bound case are 5.1 GtC/yr and 917.6 GtC, while those in the mean case are 3.0 GtC/yr and 764.9 GtC respectively, and those in the lower bound case are 0.91 GtC/yr and 619.7 GtC respectively.

The results indicate that the socioeconomic impacts are larger in the lower bound emission pathway to achieve 4.5 W/m^2 as expected, although the economy and energy demand (both primary and final energy demand) increase continuously in this century. For example, the global gross domestic product (GDP) in each emission pathway is $212 trillion in the lower bound case, $217 trillion in the mean case, and $221 trillion in the upper bound case in 2100 ($30 trillion in 2001), which are 4.2 – 8.1% smaller than that of the reference scenario ($230 trillion in 2100). On the other hand, the global primary energy demand in 2100 in the lower bound case is slightly larger than in the mean case; this can be interpreted because biomass energy with carbon capture and storage technology is enhanced to achieve very low carbon dioxide emissions in the lower bound case. In a comparison between the upper bound and lower bound emission pathways, the carbon price of the latter is approximately three times higher in 2100. The GDP in the latter is 4.1% smaller than that in the former in 2100, which is equivalent to only a 0.042% decrease in the annual GDP growth rate. Thus, the socioeconomic impacts caused by ESM uncertainties, here evaluated by GDP and energy demand, are not insignificant but are smaller than the differences in the emission pathways to achieve 4.5 W/m^2.

Keywords: earth system model, computable general equilibrium model, climate change

Japan Geoscience Union Meeting 2014
(28 April - 02 May 2014 at Pacifico YOKOHAMA, Kanagawa, Japan)

MIS31-11 Room:511 Time:May 2 11:45-12:00

Model Inter-comparison projects of Integrated Assessment Models and the Collaboration with Impact Assessmemts

FUJIMORI, Shinichiro[1*] ; HANASAKI, Naota[1] ; TAKAHASHI, Kiyoshi[1] ; MASUI, Toshihiko[1] ; KAINUMA, Mikiko[1] ; HIJIOKA, Yasuaki[1] ; HASEGAWA, Tomoko[1]

[1]National Institute for Environmental Studies

This presentation talks about two topics; namely model inter-comparison projects (MIP) of integrated assessment models (IAM) and the collaboration with impact assessments.

MIP of IAM is carried out by sharing main themes, assuming model conditions and parameter settings, and comparing results. The themes dealt with the last couple of years were, for example the influence of the technological availability (e.g. nuclear) and mitigation starting year on the mitigation cost. The outcomes are eventually summarized as special issues of international journals. The harmonization of the scenario assumptions is generally quite limited to narrative story. The numerical future socioeconomic conditions are dependent on individual models. This intends to encourage as many as IAMs participating MIPs since IAMs have several types and some variables which are exogenous parameters for some IAMs can be endogenous variables for others. The activities relevant to model validation have become much more important than before and some MIPs treat such themes. The activities are ongoing now and model documentations, development of model diagnostics protocol and comparison hind-casting with historical observation are discussed. In regard to the collaboration with Impact, Adaptation and Vulnerability (IAV) assessment, we can classify two types according to the way how the IAM is used. First is the case where IAMs are used as a provider of socioeconomic conditions to IAV. RCP (Representative Concentration Pathways) and SSP (Shared Socioeconomic Pathways) are well known such information. Hanasaki, et al. is an example and AIM/CGE provided information to the water assessment model H08. They assessed the water scarcity. Second is the case where IAMs assess climate change impacts by themselves. Hasegawa, et al. is an example and crop productivity model GAEZ calculated a potential crop productivity change and it is fed into AIM/CGE. They assessed a risk of hunger. The fields of water and agriculture overlap with the IAM coverage through land use and energy supply. We expect one of the possibilities for the further studies would incorporate transactions between them. All studies are made by the combination of emissions scenarios and the outcome of the Earth System Models (ESM). The release of SSP would encourage much more IAV studies.

Meanwhile, several issues might remain even after SSP processes are completed. Here we show two issues. First, SSPs exclude information relevant to climate mitigation and the case with climate mitigation would be different from the case without climate mitigation. The combination of the RCP and CMIP5 (Coupled Model Intercomparison Project Phase 5) is not consistent for such case. Second, we would face the case where the stabilization targets other than existing four RCPs needed to be assessed. The accuracy of the pattern scaling would be the key point. If the pattern scaling had an accuracy which is acceptable for IAV, the existing RCP and CMIP5 are available with the pattern scaling. Otherwise, a set of new climate scenarios is required. However, multi-model ensemble examination similar to CMIP5 takes extra a few years and it would be unrealistic for IAV. Hence, a specific combination of IAM and ESM in Japan (e.g. AIM/CGE and MIROC) associated with the new set of emissions scenarios might be one of the solutions. Although it would take many efforts in order to achieve it, we might be able to identify the usefulness for society and scientific novelty. We hope that this presentation would be one of the indications for such discussions.

Hanasaki, N. et al. A global water scarcity assessment under Shared Socio-economic Pathways ? Part 1: Water use. Hydrol. Earth Syst. Sci. 17, 2375-2391, doi:10.5194/hess-17-2375-2013 (2013).

Hasegawa, T. et al. Climate Change Impact and Adaptation Assessment on Food Consumption Utilizing a New Scenario Framework. Environmental science & technology 48, 438-445, doi:10.1021/es4034149 (2014).

Keywords: Integrated Assessment Models, Impact, Adaptation and Vulnerability, Model inter-compasion projects, Scenarios

Japan Geoscience Union Meeting 2014
(28 April - 02 May 2014 at Pacifico YOKOHAMA, Kanagawa, Japan)

MIS31-12 Room:511 Time:May 2 12:00-12:15

Climate and socioeconomic scenarios for climate change impact and adaptation assessments in Japan

TAKAHASHI, Kiyoshi[1*] ; HANASAKI, Naota[1] ; HIJIOKA, Yasuaki[1]

[1]National Institute for Environmental Studies

In order to assess the overall impacts of climate change on a nation and investigate effective adaptation measures, it is important to collect scientific understanding beyond academic disciplines, because impacts of climate change emerge every aspect of the society. Modeling is a widely accepted method to assess future climate change impacts: develop climate and socioeconomic environment assumptions in the future (scenarios), run statistical or process based models using the scenarios, and simulate the future situation for each subject and discipline. If a large number of modelers conduct simulations using a set of common scenarios, one can obtain a multidisciplinary national perspective of climate change impacts and potential adaptation strategy.

We have been conducting a strategic research project funded by the Ministry of Environment, which is named 'Comprehensive research on climate change impact assessment and adaptation policies' (Abbr.: S-8 project; Period: FY2010-2014; Project leader: Prof. Nobuo Mimura, Ibaraki University). In S-8 project, we are working on quantitative analyses of climate change impact on various sectors and adaptation in Japan for the purpose of supporting adaptation policy makings as well as of evaluating possibility of the society that can adapt to the anticipated climate change. The sectors covered in the project include water resource, coastal, disaster prevention, natural vegetation, agriculture, and human health. In S-8 project, climate and socioeconomic scenarios for Japan were discussed for climate change impact assessment and adaptation measures investigation by reviewing earlier literature and latest research activities. Based on the discussion, with keeping in step with the research schedule of the project, sets of scenarios were developed twice covering the whole Japan (the 1st version: March 2011, the 2nd version: November 2013), utilizing information available at the respective timings.

For the 2nd version of the S-8 scenario set, we used the climate projection of four climate models and three radiative forcing scenarios of the Coupled Model Intercomparison Project Phase 5 (CMIP5). We utilized the results of dynamical downscaling using a regional climate model which is consistent with the global scenarios after applying bias-correction techniques. Regarding the population projection scenarios, we developed nine scenarios taking into account not only uncertainty range of the total numbers but also uncertainty in its spatial distribution. We also proposed land use scenarios compatible with the population projections.

In the JPGU session, as a case of multidisciplinary collaboration, we will introduce the background and procedure of the S-8 scenarios development. We will also mention future challenges, which have been found in the scenario development process.

Keywords: climate change, climate change impact, adaptation, scenario

Japan Geoscience Union Meeting 2014
(28 April - 02 May 2014 at Pacifico YOKOHAMA, Kanagawa, Japan)

MIS31-13 Room:511 Time:May 2 12:15-12:30

Introduction to global climate change impact assessment

HANASAKI, Naota[1*]

[1]National Institute for Environmental Studies

In this presentation, a typical methodology used in modern climate change impact assessments is introduced. Some latest research activities to tackle key problems are discussed as well. This presentation mainly focuses on water resources sector at global scale, but the contents can be broadly applicable to other sectors and scales.

Climate change impact assessment requires scenarios on future climatic and socio-economic conditions and a model which quantitatively describes how the system of interest responses to those changes. In this presentation the latest scenarios namely CMIP5, RCP, and SSP are introduced. Then, a global water resources model H08 is explained which delineates the water cycle and water use of the globe.

Climate change impact assessment typically takes three steps. First, a model of interest is prepared and a simulation is conducted using the present climatic and socio-economic conditions. Second, some simulations are conducted using various future scenarios. Third, the differences in outputs between the future and present are examined since these are considered the impact due to climatic and socio-economic change. In this presentation, the geographical spread of water stressed regions and the number of affected population are discussed under 10 different future scenarios.

A number of challenges remain unsolved on climate change impact assessments. Two international research activities are highlighted to address some of the challenges. The first item is quantification of uncertainties in assessments caused by models. Although the models used in climate change impact assessment basically reproduce the present conditions well, none of them is perfect and outputs include errors. An ongoing international research project termed ISI-MIP is introduced which conducts climate change impact assessment by using a set of common scenarios and multiple models. ISI-MIP analyzes the variations in results and reasons. The second item is implementation of adaptation options. Although humans are expected to take adaptation measures when the impacts of climate become intolerable, adaption is seldom implemented in earlier simulations. Some pioneering works including adaptation are reviewed and future research directions are discussed.

Keywords: climate change, impact, global, water resources

Japan Geoscience Union Meeting 2014
(28 April - 02 May 2014 at Pacifico YOKOHAMA, Kanagawa, Japan)

MIS31-14 Room:511 Time:May 2 12:30-12:45

Impact assessment of natural disaster due to global warming

MORI, Nobuhito[1*]

[1]Disaster Prevention Research Institute, Kyoto University

Climate changes in give significant impacts on natural disasters such as typhoon, river flooding, storm surge, landside and etc. The different natural disasters require different forcing from GCMS. The spatial and temporal resolutions of forcing also give significant impact on the impact assessment of natural disasters. This study summarize current activity of impact assessment of natural disasters by SOUSEI program in Japan and discuss importance of cooperative research between GCM modelers and IAM group.

Japan Geoscience Union Meeting 2014
(28 April - 02 May 2014 at Pacifico YOKOHAMA, Kanagawa, Japan)

MIS31-15 Room:511 Time:May 2 14:15-14:30

Downscaling in Climate Information and applications

DAIRAKU, Koji[1*]

[1]National Research Institute for Earth Science and Disaster Prevention

Climate effects caused by human activities will continue for centuries and natural climate influences have always been a risk. Mitigation is a complex, uncertain approach and will need at least several decades. It is necessary, therefore, to put adaptation together immediately. The impacts and potential applications of interest to the stakeholders are mostly at regional and local scales as the essential resources of water, food, energy, human health, and ecosystem function respond to regional and local climate. Climate information and services for Impacts, Adaptation and Vulnerability (IAV) Assessments are of great concern.

Users of climate scenarios produced by global climate models with coarse grid-spacing involve an inadequate mismatch of spatial scale. Downscaling technique is used to obtain the regional climate scenarios, especially in regions of complex topography, coastlines, and in regions with highly heterogeneous land surface covers where those results are highly sensitive to fine spatial scale climate processes. Dynamical and statistical downscaling techniques available for generating regional climate information have the respective strengths and weaknesses. To produce useful climate assessments for dicision-making, interaction between the downscaling community and the IAV community are necessary.

To facilitate its interaction, author will present,

- Overview of downscaling techniques in particular for regional climate modelling.
- current International activities (WCRP-CORDEX, etc.)
- Applications of downscaling in Japan from the ”REsearch program on Climate Change Adaptation (RECCA)” and the ”Program for Risk Information on Climate Change (SOUSEI)” sponsored by the Ministry of Education, Culture, Sports, Science and Technology(MEXT)

Keywords: Downscaling, Regional Climate Model, Climate Change, CORDEX, RECCA, SOUSEI

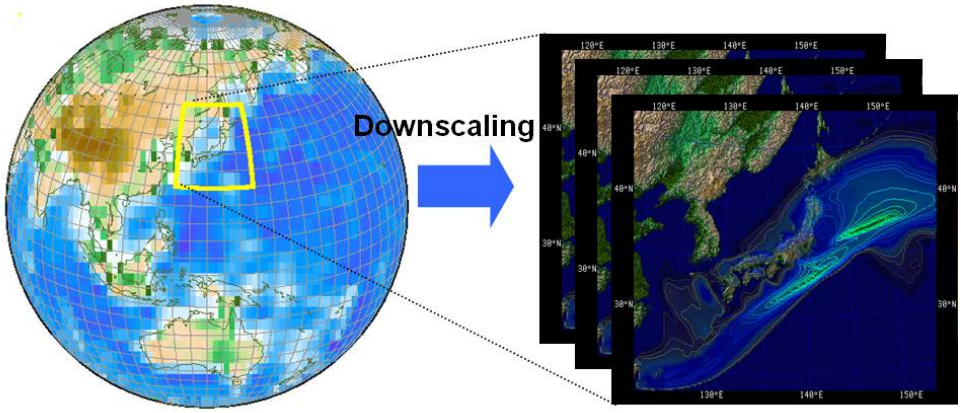

Japan Geoscience Union Meeting 2014
(28 April - 02 May 2014 at Pacifico YOKOHAMA, Kanagawa, Japan)

MIS31-16 Room:511 Time:May 2 14:30-14:45

Pattern scaling approach for generating regional projections of future extreme events associated with tropical cyclones

TSUTSUI, Junichi[1*]

[1]Central Research Institute of Electric Power Industry

The assessment of a wide range of greenhouse-gas-emission scenarios in climate change studies employs a simple climate model and pattern scaling based on ensemble projections with complex climate models for a few representative scenarios. The simple climate model deals with the global mean surface temperature as a prediction variable, and the pattern scaling specifies the spatial distributions of different climate variables with prescribed spatial patterns that do not depend on specific scenarios and time points. Although mean temperature and precipitation are typical variables specified by pattern scaling, the present study applies the concept of pattern scaling to extreme events, which are essential for assessing the impact of climate change. An example shown here is a scheme to assess changes in the minimum sea-level pressure and precipitation extreme of the most intense class of tropical cyclones that make landfall in Japan.

This scheme is based on the theory of potential intensity of tropical cyclones and general precipitation extremes. Although real tropical cyclones do not necessarily attain their potential intensities because of various environmental restrictions, the annual cycle of the lower limit of observed minimum sea-level pressures is well represented by climatological potential intensity. An extremely strong tropical cyclone with high societal impact forms only occasionally, within large fluctuations of natural climate variability, regardless of background warming. It is generally difficult to assess relatively small background changes in the intensity of such a rare event by observation statistics or numerical climate projections. The scheme overcomes this difficulty by focusing on large-scale thermodynamic conditions alone, with no consideration of the dynamic conditions that dominantly control the frequency of tropical cyclones. The thermodynamic conditions are scaled with global mean surface temperature anomalies by referring to results (patterns) of ensemble climate model experiments, and reflected in changes in the potential intensity of a target tropical cyclone. Then, the formulation of precipitation extreme incorporates the dynamic effect associated with the intensification of the target tropical cyclone by scaling the vertical structure of the base updraft with that potential intensity change, in addition to thermodynamic change in the amount of water vapor.

Figure 1 shows the assessment results for three different scenarios. The scheme formulates changes in the pressure drop and precipitation extreme of a target tropical cyclone as a function of global mean surface temperature anomaly. The temperature anomaly is calculated using a simple climate model, which has been developed separately, for 3000 cases for each scenario, taking the uncertainty of climate sensitivity into consideration. The computation load of the scheme is negligible, which enables the assessment of many scenarios with different conditions. The scheme also incorporates another uncertainty, not shown here, associated with the amplification of the upper-air temperature anomaly in the troposphere, which greatly affects the minimum sea-level pressure. Thus, the combination of a simple climate model and pattern scaling handles different types of uncertainties in a distinctive way, which is one of the advantages of this approach.

Figure 1: Probabilistic analysis of a target tropical cyclone for three different scenarios labeled RCP2.6, RCP4.5, and Z650. (a), (b): Secular change in the atmospheric multigas concentration and reference global-mean surface temperature anomaly, (c)-(e): Probability density function of the temperature anomaly, increase in pressure drop, and increase in precipitation extreme in 2081-2100 relative to 1981-2000.

Keywords: tropical cyclone, potential intensity, precipitation extreme, pattern scaling, simple climate model, emission scenario

MIS31-16 Room:511 Time:May 2 14:30-14:45

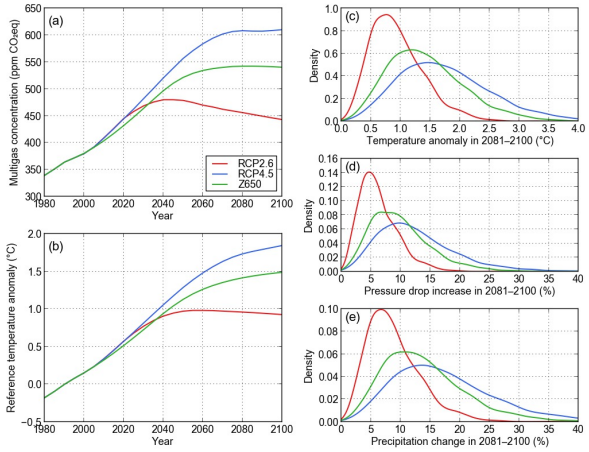

Japan Geoscience Union Meeting 2014
(28 April - 02 May 2014 at Pacifico YOKOHAMA, Kanagawa, Japan)

MIS31-17 Room:511 Time:May 2 14:45-15:00

Emission scenario dependency of pattern scaling and linear additivity of climate forcing-response relationship

SHIOGAMA, Hideo[1*]

[1]Center for Global Environmental Research, National Institute for Environmental Studies

Human activities are changing the climate, and the consequent impacts on humans and ecosystems are becoming increasingly serious. It has been recognised that adapting to and mitigating anthropogenic climate change is a matter of immediate concern for the world. To inform adaptation and mitigation policies, it is essential to assess the impact of climatic changes under a wide range of scenarios for the stabilization of emissions of greenhouse gases (GHGs) and anthropogenic aerosols (sulfate, black carbon, and organic carbon aerosols). Impact assessments are based on climate change projections from coupled atmosphere-ocean general circulation models (GCMs). Therefore, uncertainties in climate projection propagate to impact assessments and affect subsequent policy decisions for adaptation and mitigation.

Due to the large computational costs of GCMs, only a limited number of emissions scenarios can be made for GCM simulations. To overcome this difficulty and obtain climate scenarios under a wide range of emissions scenarios, the so-called pattern scaling method is often used. By multiplying climate change patterns per 1K of global warming from an AOGCM (called a scaling pattern) by the global mean warming projections from a simple climate model, this method provides projections of precipitation, as well as other variables, at global and regional scales under many emission scenarios. Although the pattern scaling method is widely used, applicability of pattern scaling has been evaluated by only a few studies, and further investigations are clearly warranted.

The basic assumption of pattern scaling method is that scaling patterns are independent on the emission scenarios. Here I show a robust emission-scenario dependency (ESD) in scaling patterns of annual mean precipitation; smaller global precipitation sensitivities occur in higher GHG and aerosol emission scenarios in all the CMIP3 GCM. Different aerosol emissions lead to this ESD. The ESD of precipitation pattern potentially propagates into considerable biases in water resource assessments via pattern scaling.

It is possible to scale climate response patterns to individual forcing agents to obtain climate scenarios. This 'separated pattern' approach is useful to overcome the influences of the ESD. However, this approach requires care in its use. An important assumption of the separated pattern is that individual climate responses to individual forcing agents can be linearly added to obtain the total climate response to the sum of the forcing agents. We explored whether linear additivity holds in 5-year mean temperature/precipitation responses to various combinations of forcing agents in the 20th century and in a future-emissions scenario at global and continental scales. We used MIROC3 GCM, which includes the first and second indirect effects of aerosols. The forcing factors considered were well-mixed greenhouse gases, the direct and indirect effects of sulphate and carbon aerosols, ozone, land-use changes, solar irradiance and volcanic aerosols (the latter three factors were specified only in the 20th-century runs). By performing and analysing an enormous matrix of forcing runs, we concluded that linear additivity holds in temperature responses for all of the combinations of forcing agents at the global and continental scales, but it breaks down for precipitation responses in certain cases of future projections.

Keywords: Climate scenario, pattern scaling, impact assessment

Japan Geoscience Union Meeting 2014
(28 April - 02 May 2014 at Pacifico YOKOHAMA, Kanagawa, Japan)

MIS31-18 Room:511 Time:May 2 15:00-15:15

Evaluation of the nexus of risks under global climate change

YOKOHATA, Tokuta[1*] ; NISHINA, Kazuya[1] ; KIGUCHI, Masashi[2] ; ISERI, Yoshihiko[3] ; SUEYOSHI, Tetsuo[4] ; YOSHIMORI, Masakazu[2] ; YAMAMOTO, Akitomo[2] ; HONDA, Yasushi[5] ; HANASAKI, Naota[1] ; ITO, Akihiko[1] ; MASAKI, Yoshimitsu[1] ; SHIGEMITSU, Masahito[6] ; IIZUMI, Toshichika[7] ; SAKURAI, Gen[7] ; IWASE, Kenta[8] ; TAKAHASHI, Kiyoshi[1] ; EMORI, Seita[1] ; OKI, Taikan[2]

[1]National Institute for Environmental Studies, [2]University of Tokyo, [3]Tokyo Institute of Technology, [4]Japan Agency for Marine-Earth Science and Technology, [5]University of Tsukuba, [6]Hokkaido University, [7]National Institute for Agro-Environmental Sciences, [8]Nomura Research Institute

Climate change caused by the increase in atmospheric greenhouse gas has various impacts on human society and ecosystem. Features of the impacts have a large variety, and most part them is adverse impact (damage), although some part is positive impact (benefit) in some locations. It is very important to have reliable predictions of possible damage and benefit (= risks) under the climate change, in order for us to have effective adaptation and mitigation measures.

Future risks caused by the climate change can happen in various sectors. In addition, the various risks are connected across sectors. Especially, a “ nexus ” between the water, food and energy sectors is considered to be very important (Hoff 2011, Understanding the Nexus. Stockholm Environment Institute).

In this study, we are going to present our two activities related to the nexus of risks under the climate change. One is the investigation of qualitative feature of the various links of risks caused by the future climate change. We made a comprehensive list of the possible damage and benefit in the human society and ecosystem possibly caused by the future climate change (“ item of risk ”). This list is generated by the experts of climate, water resources, energy, food, health, security, industry, society, and ecosystem sectors. The experts of these fields in our group members choose all of the possible impacts related to the climate change based on their “ expert judgment ”. The number of items of risks is about 200 currently, such as “ decrease in river runoff ”, “ decrease in crop productivity ”, and “ increase in forest fire ”. Then, we also made a comprehensive list of the possible causal link between the items of risks as described above (“ item of causal link ”). This list is also generated by the experts of the various fields as described above. The number of items of causal link is about 400 currently, such as “ decrease in river runoff ” causes “ decrease in crop productivity ”. Finally, we visualize all of the causal links based on the network diagram using the Fruchtman & Reingold force-directed layout algorithm. Using the data of item of risks and causal links as well as the network diagram, we are going to discuss the nexus of the risks under the climate change.

The other topic is on the development of a “ terrestrial integrated model ” of our group. We coupled a global climate model called “ MIROC5 ” (Watanabe et al. 2010, J. Climate), global water resources model called “ H08 ” (Hanasaki et al. 2008, HESS), global terrestrial ecosystem model called “ VISIT ” (Ito and Inatomi 2012, Biogeosciences, and global crop model called “ PRYSBI2 ” (Iizumi et al. 2013, J. Agricultural Meteorology). The status of our model development and analysis on the nexus of the risks under the climate change as described above are discussed.

Keywords: climate change, risk, water resources, ecosystem, health, society

Japan Geoscience Union Meeting 2014
(28 April - 02 May 2014 at Pacifico YOKOHAMA, Kanagawa, Japan)

MIS31-19 Room:511 Time:May 2 15:30-15:45

Discussion on the challenges for comprehensive global warming studies

TACHIIRI, Kaoru[1*]

[1]Japan Agency for Marine-Earth Science and Technology

Discussion on the challenges raised.

Keywords: Comprehensive Global Warming Studies

Japan Geoscience Union Meeting 2014
(28 April - 02 May 2014 at Pacifico YOKOHAMA, Kanagawa, Japan)

MIS31-P01 Room:Poster Time:May 2 16:15-17:30

Atmospheric Chemistry Transport Modeling of Organic Nitrogen Input to the Ocean

ITO, Akinori[1*] ; LIN, Guangxing[2] ; PENNER, Joyce[2]

[1]JAMSTEC, [2]University of Michigan

Human activities for energy and food production have substantially perturbed the biogeochemical cycle of nitrogen (N) since the industrial revolution. The atmospheric emissions of N-containing compounds from fossil-fuel combustion, intensive agricultural activities, and other anthropogenic processes have substantially increased the supply of reactive N over the oceans downwind of major industrialized regions since 1860. The dominant reactive N species are emitted in the form of nitrogen oxide (NO) and ammonia (NH3) from fossil fuel combustion and agricultural practices, are transformed to a number of other nitrogen oxides (NOy) and ammonium (NHx) during the long-range transport, and then deposited to the oceans. Little is known about the chemical composition of organic N (ON) in the atmosphere or its spatial distribution, due to the limitations of available analytical methods. Over the North Atlantic, a significant fraction of the wet deposition of total soluble N has been measured in the form of soluble ON at coastal and marine locations. The effect of atmospheric ON input on marine ecosystems can either be helpful or harmful depending on the deposition rate and chemical form of ON. Dissolved ON such as urea, amino acids and humic substances can provide an important nutrient source to marine environments These studies suggest that atmospheric models need to predict the chemical speciation of reactive N species to accurately predict the effects of changes in N inputs on marine ecosystems and climate. Here we use a process-based chemical transport model to investigate global supply of soluble organic nitrogen (ON) from continental sources to the ocean.

Keywords: atmospheric deposition, soluble organic nitrogen, environmental changes

Japan Geoscience Union Meeting 2014
(28 April - 02 May 2014 at Pacifico YOKOHAMA, Kanagawa, Japan)

MIS31-P02 Room:Poster Time:May 2 16:15-17:30

Ecosystem sustainability of 2 degrees celsius scenario using BECCS

KATO, Etsushi[1*] ; YAMAGATA, Yoshiki[1]

[1]National Institute for Environmental Studies

Bioenergy with Carbon Capture and Storage (BECCS) is a key component of mitigation strategies in the future socio-economic scenarios to keep mean global temperature rise below 2 ℃ above pre-industrial, which would require net negative fossil fuel emissions in the end of the 21st century. Large scale BECCS requires additional production of biofuels, which could potentially cause substantial carbon emissions from the land-use change. Developing sustainable low carbon scenarios requires careful consideration of the land-use implications involving large scale BECCS.

We use a global terrestrial biogeochemical cycle model to evaluate effects of land-use change in RCP2.6, which is a scenario with net negative fossil fuel emissions aiming to keep the 2 ℃ temperature target used in CMIP5. We also use a global crop model to examine BECCS attainability in the land-use scenario of RCP2.6. In the evaluation, we consider deployment of bioenergy with both first-generation second-generation biofuels.

Our analysis reveals that first generation bioenergy crop production would not be sufficient to achieve the required BECCS of RCP2.6 scenario even if we consider the higher fertilizer and irrigation use cases. It would require more than doubling the area for bioenergy crops around 2050 assumed in RCP2.6, however, such scenarios implicitly induce large scale land-use changes that emit significant amount of carbon from deforestation.

Keywords: BECCS, land-use, crop yield, bioenergy

Japan Geoscience Union Meeting 2014
(28 April - 02 May 2014 at Pacifico YOKOHAMA, Kanagawa, Japan)

MIS31-P03 Room:Poster Time:May 2 16:15-17:30

Climate Restoration via Zero Emissions Stabilization: Examination using Earth System Models

NOHARA, Daisuke[1*] ; WATANABE, Shingo[2] ; TACHIIRI, Kaoru[2] ; HAJIMA, Tomohiro[2] ; OKAJIMA, Hideki[2] ; TSUTSUI, Junichi[1] ; MATSUNO, Taroh[2]

[1]Central Research Institute of Electric Power Industry, [2]Japan Agency for Marine-Earth Science and Technology

Zero-emissions stabilization is a newly proposed concept that targets reduction of CO_2 emissions to zero in a distant future, after which the atmospheric CO_2 concentration is reduced by a natural atmospharic CO_2 removal process, eventually allowing the atmosphere to reach an equilibrated stable state. The zero-emissions pathway, Z650, has been designed based on this concept as a flexible alternative toward a climate stabilization target. It allows cumulative emissions of 650 GtC during the 21st century and aims to attain zero emissions in the middle of the 22nd century. To confirm the decreases in CO_2 concentrations and temperature that would be achieved with the Z650 pathway, long-term climate and carbon cycle projections have been conducted up to the year 2300 by emission-driven experiment using the Earth system models, CESM1 and MIROC-ESM. Both the models show gradual decreases in the atmospheric CO2 concentration subsequent to the occurrence of temporal peaks of the concentration due to oceanic and terrestrial CO_2 uptakes. The models also project decreases in the globally averaged surface air temperature after the peak temperature increase. These results imply that the climate is eventually stabilized from a temporal warming state to less warmed under the zero emissions with the Z650 pathway. However, the experiments show considerably different increases in the peak concentration and temperature values, which are attributable to the different carbon and climate sensitivities.

Japan Geoscience Union Meeting 2014
(28 April - 02 May 2014 at Pacifico YOKOHAMA, Kanagawa, Japan)

MIS31-P04 Room:Poster Time:May 2 16:15-17:30

On the 6th phase of Coupled Model Intercomparison Project

KAWAMIYA, Michio[1*]

[1]JAMSTEC

From 2013, when the 5th Assessment Report of IPCC WG1 was approved, scientists started discussion on framework of the next (6th) phase of Coupled Model Intercomparison Project (CMIP6). A couple of meetings were held in Aspen, USA in August and in Victoria, Canada in October to arrange a system for implementing CMIP6 protocol for global warming projection experiments. It has been suggested that CMIP6 will be jointly managed by multiple communities in a distributed manner. That is, the ”traditional” CMIP community only manages fundamental experiments common to most modeling groups regardless of their specific interest, while other model intercomparison projects (MIPs) cover those specific to their interest: MIPs possibly include, among others, C4MIP for carbon cycle, PMIP for paleoclimate, and GeoMIP for Geoengineering. These activities as a whole will construct CMIP6. The above-mentioned fundamental experiments might include idealized experiments such as CO2 1%/y increase, and experiments based on scenarios with and without mitigation policy. According to the schedule currently proposed, the socio-economic scenarios will be developed by the end of 2015, experimental design will be mostly fixed in early 2016, and scenario experiments will be conducted by modeling groups from 2017, whereas those fundamental experiments can be started earlier.

Keywords: CMP6, IPCC, Global Warming Projection, Model Intercomparison Project, Socio-economic Scenario, Climate Model

Japan Geoscience Union Meeting 2014
(28 April - 02 May 2014 at Pacifico YOKOHAMA, Kanagawa, Japan)

MIS32-01 Room:416 Time:April 30 09:00-09:15

7 years of NanTroSEIZE: Achievements and Lessons Learned

KINOSHITA, Masataka[1*] ; TOBIN, Harold[2]

[1]JAMSTEC, [2]Univ. Wisconsin-Madison

The objectives of Integrated Ocean Drilling Program (IODP) Nankai Trough Seismogenic Zone Experiment (NanTroSEIZE) include characterizing the nature of fault slip and strain accumulation, fault and wall rock composition, fault architecture, and state variables throughout an active plate boundary system. A deep riser drilling into the locked portion of the Tonankai asperity at IODP Hole C0002F began during IODP Expedition 326 in 2010. After one-year delay due to 3.11 Tohoku event (which gave severe damage to D/V Chikyu), the hole was deepened to 2005 m below seafloor during Expedition 338 in 2012, then deepened to ˜3000 m during Expedition 348 in 2013. In addition to the intermittent coring, continuous information was acquired through logging-while-drilling, mud-gas monitoring and cutting analyses. NanTrosEIZE also targets understanding shallow characteristics of subducting Shikoku Basin, forearc slope and Kumano forearc basin.

Through LWD and core analyses, shallow stress state along NanTroSEIZE transect has been revealed. Fault regime changes from normal/strike-slip at <˜500m to strike-slip in the deeper part (>˜500 m). Maximum compressional stress is vertical throughout the transect, indicating that the gravitational effect is dominant. Maximum horizontal stress is parallel to the subduction direction, with secondary contribution by the plate convergence. It is consistent with the result from circular air-gun shooting around the vertical seismic array in the central Kumano Basin, which revealed a Vp anisotropy (˜5%) in the Kumano Basin that suggests subduction-parallel compression.

Through drilling at two subduction input sites in the Shikoku Basin, we identified a significant Source of fluid in seismogenic zone; ˜30 vol% saponite in the basalt sample. This suggests that in the deeper portion of plate boundary, fluid production from basaltic rock (saponite-chlorite) can be greater than from smectite-illite conversion and sediment compaction.

Lab. friction studies in the shallow megasplay fault zone confirmed that shallow faults are velocity-strengthening at slow slip rates. On the other hand, the frictional coefficient during high-velocity (˜1 m/s) slips is very low under the undrained condition, suggesting that earthquake rupture propagates easily through clay-rich fault gouge by high-velocity weakening.

Lines of evidence strongly support the activity of shallow portion of megasplay and decollement. Mud breccia in the surface of splay footwall side indicates the earthquake-induced collapse and reworking. Vitrinite reflectance anomaly localized at the fault reveals past thermal anomaly >380degC, indicative of coseismic slip near the deafloor that should have generated a huge tsunami. XRF scanner analysis of microbreccia fault zone in the shallow megasplay indicates an increased illitization relative to surrounding host rock, representing an additional evidence of possible frictional heating and mechano-chemical clay mineral alteration.

Borehole observatories are essential in order to detect and monitor a small and low-frequency deformation that is continuing around the plate boundary. First complex borehole observatory, including geodetic, seismic and hydrological sensors, was successfully installed in the southern Kumano Basin and connected to cable network for realtime monitoring.

So far we drilled at 13 sites, participated by >170 scientists from 15 countries, and published more than 60 scientific papers. Such achievements were made possible by tremendous efforts by CDEX, who tackled with numerous technical challenges such as mechanical setbacks of riser and vessel, concern about the expedition time available (cost and budget), typhoon/low pressure evacuation, and riser drilling in the 5-knot Kuroshio current.

Keywords: IODP, Chikyu, seismogenic zone, Nankai Trough

Japan Geoscience Union Meeting 2014
(28 April - 02 May 2014 at Pacifico YOKOHAMA, Kanagawa, Japan)

MIS32-02 Room:416 Time:April 30 09:15-09:30

Ultra-deep riser drilling into the Nankai accretionary prism: Preliminary results of IODP Expedition 348

HIROSE, Takehiro[1*] ; TOBIN, Harold[2] ; SAFFER, Demian[3] ; TOCZKO, Sean[1] ; MAEDA, Lena[1] ; KUBO, Yusuke[1] ; KANAGAWA, Kyuichi[4] ; KIMURA, Gaku[4] ; EXPEDITION 348, Scientists[6]

[1]JAMSTEC, [2]University of Wisconsin-Madison, [3]Pennsylvania State University, [4]Chiba University, [5]The University of Tokyo, [6]IODP Expedition 348

The Nankai Trough Seismogenic Zone Experiment (NanTroSEIZE) is a multi-disciplinary scientific project designed to investigate fault mechanics and seismogenesis along subduction megathrusts through seismic imaging, direct sampling, in situ measurements, and long-term monitoring in conjunction with laboratory and numerical modeling studies. As part of the NanTroSEIZE program, International Ocean Discovery Program (IODP) Expedition 348 started on 13 September 2013 and was completed on 29 January 2014. During Expedition 348, the drilling vessel *Chikyu* advanced the ultra-deep riser hole at Site C0002, located 80 km offshore from the Kii Peninsula, from a depth of 860 meters below sea floor (mbsf) to 3058.5 mbsf, the world record for the deepest scientific ocean drilling, and cased it for future access. The drilling operation successfully obtained data on formation physical properties from logging while drilling (LWD) tools, as well as from lithological analyses of cuttings and core from the interior of the active accretionary prism at the Nankai Trough. IODP Site C0002 is the currently only borehole to access the deep interior of an active convergent margin. We will present preliminary scientific results as well as key aspects of riser-drilling operations, including two sidetrack borehole drilling operations conducted in this never-before accessed tectonic environment.

Keywords: IODP, NanTroSEIZE, Nankai Trough, accretionary prism

Japan Geoscience Union Meeting 2014
(28 April - 02 May 2014 at Pacifico YOKOHAMA, Kanagawa, Japan)

MIS32-03 Room:416 Time:April 30 09:30-09:45

Costa-Rica Seismogenesis Program (CRISP) to understand characteristic magnitude of subduction earthquake

SAKAGUCHI, Arito[1*] ; HARRIS, Robert[2]

[1]Yamaguchi Univ./JAMSTEC, [2]Oregon State University

Variations in earthquake magnitude and recurrence intervals of fault behavior are best understood in the context of regional tectonics. Convergent margins may be divided into two end-member types termed erosive and accretionary plate boundaries (e.g. von Huene and Scholl, 1991; Clift and Vannucchi, 2004). These margins may differ greatly in lithology, physical properties and hydrology. The Nankai accretionary margin has a 1300-year historical earthquake record with a recurrence interval of 100-150 years (Ando, 1975). Great earthquakes at Nankai are typically tsunamigenic and include the 1944 Tonankai (Mw=8.1) and 1946 Nankaido (Mw=8.1) earthquakes (Kanamori, 1977). In contrast, the Middle America trench offshore Costa Rica events of M=7.6 reoccur on average of every 40 years. The CRISP drilling area is offshore Costa Rica just northwest of the Osa Peninsula. Comparisons between these margins may produce insights into mechanisms that influence characteristic magnitudes and recurrence intervals of subduction earthquakes.

The IODP Costa-Rica Seismogenesis Program (CRISP) has carried out the first step toward the deep riser drilling by characterizing the shallow lithologic, hydrologic, stress, and thermal state at offshore Osa Peninsula (Vannucchi et al., 2011; Harris et al., 2013). CRISP drilling reveals that the shallow basement of upper plate crust is forearc basin material consisting of lithic sedimentary units with terrigenous sediment accumulated at a high rate. A large sediment flux to the forearc may have originated from the uplifted back-arc Talamanca Cordillera due to Cocos-Ridge subduction (Lonsdale and Klitgord, 1978; van Andel et al., 1971). Both the Nankai and the CRISP drilling areas are characterized by the subduction of young oceanic crust with high heat flow and active fluid flow (Spinelli and Wang, 2008; Spinelli and Harris, 2011; Harris et al., 2010). The Nankai and Costa Rica margins are ideal ares to better understand the relation between the earthquake magnitudes and other subduction zone factors.

Keywords: Large subduction earthquake, seismogenic fault, accretion and erosive margin

Japan Geoscience Union Meeting 2014
(28 April - 02 May 2014 at Pacifico YOKOHAMA, Kanagawa, Japan)

MIS32-04 Room:416 Time:April 30 09:45-10:00

Estimation of the past bottom-ocean environment of 2Ma based on the benthic foraminifera stratigraphy: IODP Exp. 344

UCHIMURA, Hitomi[1*]

[1]Graduate School of Science and Technology, Kumamoto University

IODP Exp.344 (Costa Rica Seismogenesis Project: CRISP 2) is designed to understand the processes that control nucleation and seismic rupture of large earthquakes at erosional subduction zones and drilled five sites off the western coast of Costa Rica around the southern end of the Middle America Trench, where the oceanic Cocos Plate is subsiding beneath the Carrbbean Plate.

Site U1414 is the reference site and its 2Ma is characterized by lower slope assemblages and also there is not any big change of assemblages. However, a lot of Chilostomella oolina are in the upper samples. This means sea bottom environment is a little change from at least 0.12Ma to recent.

The assemblages of Site U1412 are very similar to U1414. The differences are two biozones; one has a lot of Cibicidoides mackkannai, and the other has Brizalina bicostata. These species are originally on upper shelf, and that means these zones are allocated layers.

Main objective of this study in the Site U1413 is to understand the tectonic-induced submergence/ uplifting history or paleoslope instabilities in the upper slope area. Benthic foraminifera (BF) are a useful tool to estimate the past bottom-ocean environment. Based on benthic foraminiferal biostratigraphy of U1413, we have recognized the following four biozones for the sequence of past 2 million years and identified plausible slump mass came from the shallower-water environment

The BF divided into Group A (Zone I) is distributed on the lower continental slope in the modern equatorial Pacific. (Smith, 1963, 1964). Group B in Zone II is reported mainly from the lower to middle slope environment of the Pacific. Group C in Zone III is estimated to be distributed in the upper slope. Group D in Zone IV lives in the upper to middle slope as well as the drill site.

On the other hand, some shelf species such as Brizalina bicostata, Cibicorbis inflatus and Uvigerina incilis (Group E) occur throughout the sequence of the hole. Those species are, however, considered to be reworked specimens from shallower environment, because they co-occurred with deeper water species as Groups A to D, and because a similar occurrence has been reported in the Peru-Chile Trench area by Ingle and Kolpack (1980).

In Zone III, another species group composed of Brizalina spp., (Group C), which is distributed mainly in the upper slope areas in the modern oceans. Because Group C is not accompanied by Group D or other deeper-water species, the interval of Cores 17H-11H in Hole A apparently correspond to the upper continental slope, at least shallower than the depth of Group D. Also, the tests of Brizalina spp. are well-preserved in contrast to the co-occurred Group E. These results imply that Zone III is allocated Mass transported sediments, like a slump. This interpretation has been also supported by geochemical and logging data. The slump mass has been inferred at the interval between 45-150 mbsf based on the irregular profiles for organic matters and a fold structure plausibly formed by slumping. The slump mass might reflects the active subsidence due to tectonic erosion or passage of subducting seamount at the plate interface.

Keywords: benthic foraminifera, paleobathymetry, Subduction zone

Japan Geoscience Union Meeting 2014
(28 April - 02 May 2014 at Pacifico YOKOHAMA, Kanagawa, Japan)

MIS32-05 Room:416 Time:April 30 10:00-10:15

Limits and Habitability of the Deep Subseafloor Biosphere: New Insights from IODP Expeditions 329 and 337

INAGAKI, Fumio[1*] ; IODP, Expedition 329 and 337 scientists[2]

[1]Geomicrobiology Group, Kochi Institute for Core Sample Research, JAMSTEC, [2]IODP Expedition 329 and 337 Scientists

In the past decade, the Integrated Ocean Drilling Program (IODP) has offered unique opportunities to explore how life persists and evolves in ecosystems of the Earth interior. There are very few natural environments on surface of the Earth where life is absent; however, the limits to life are expected in the subsurface world. Processes that mediate genetic and functional evolutions of the deep subseafloor life may be very different to those in the Earth surface ecosystems. Previous studies of subseafloor sedimentary habitats demonstrated that activity of microbial communities is generally extremely low, mainly because of the limit of nutrient and energy supply. Nevertheless, microbial activity plays important ecological roles in biogeochemical element cycles over geological timescale.

In 2010, during Expedition 329, we explored limits and habitability of life in deep-sea sediments and basalts in the South Pacific Gyre, the largest oceanic province where surface chlorophyll concentrations and primary productivity in the gyre are lower than any other regions of the world ocean. In 2012, during Expedition 337, we also explored the deep subseafloor coalbed biosphere off the Shimokita Peninsula of Japan. Using riser system of the *Chikyu*, we successfully drilled, cored and logged down to the depth of 2,466 meters below the seafloor.

The IODP Expeditions 329 and 337 represent aerobic and anaerobic subseafloor microbial ecosystems on our planet, respectively, both of which realms have never been explored by previous scientific drilling; therefore, these provide unprecedented opportunities to address the issue of limits and habitability in the deep subseafloor biosphere. A variety of geophysical and geochemical properties, such as temperature, pH, pressure, salinity, porosity, and availability of nutrient and energy are conceivable to constrain biomass and activity of deep life and extent of the subseafloor biosphere. These are systematically investigated by international and multidisciplinary teams of the Expedition 329 and 337 scientists.

Japan Geoscience Union Meeting 2014
(28 April - 02 May 2014 at Pacifico YOKOHAMA, Kanagawa, Japan)

MIS32-06 Room:416 Time:April 30 10:15-10:30

Geophysical logging at the Shimokita IODP Expedition 337

YAMADA, Yasuhiro[1*] ; SANADA, Yoshinori[2] ; KUBO, Yusuke[2] ; INAGAKI, Fumio[2] ; NAKAMURA, Yasuyuki[2] ; MOE, Kyaw[2]

[1]Kyoto Univ, [2]JAMSTEC

Research achievements using the geophysical logging data obtained at the Shimokita IODP expedition 337 would be presented.

Japan Geoscience Union Meeting 2014
(28 April - 02 May 2014 at Pacifico YOKOHAMA, Kanagawa, Japan)

MIS32-07 Room:416 Time:April 30 10:30-10:45

History of the Mediterranean Sea based on drilled core samples

KURODA, Junichiro[1*]

[1]Japan Agency for Marine-Earth Science and Technology

Mediterranean Sea has experienced an extreme event called Messinian Salinity Crisis (MSC) that represents a formation of gigantic evaporite deposits in deep basins. Although theis event has long been studied, a fundamental question whether the Mediterranean Sea was desiccated or not, still remains unsolved. In this presentation we review the recent achievements of the MSC. To understand hydrological conditions of the Mediterranean Sea during the Miocene-Pliocene, we report a series of Os isotopic record of marine sediment cores from four deep-sea drilling sites in the Balearic Basin, the Tyrrhenian Sea, the Ionian Basin and the Florence Rise, in comparison with the coeval sediments in North Atlantic. Osmium isotopic ratios of the pre-Messinian sediments in the western Mediterranean basin are almost identical to that of the coeval ocean water. In contrast, the pre-Messinian sediments in the eastern Mediterranean basin have significantly low $^{187}Os/^{188}Os$ values. This suggests that Os in the eastern Mediterranean was not fully mixed with western Mediterranean and North Atlantic, and that the basin isolation has already started much earlier than the MSC. The less radiogenic Os would have been supplied to the eastern Mediterranean by selective weathering of ultramafic rocks cropping out in the drainage areas, which contains high amount of non-radiogenic Os. The isotopic compositions of Os in gypsum and halite samples are significantly lower in eastern Mediterranean basins, compared with those of gypsum samples from the western Mediterranean basin, supporting the idea that limited exchange of seawater between eastern and western basins sustained also during the MSC. In all sites Pliocene sediments show more radiogenic Os isotopic ratios, which are close to the coeval oceanic values, indicating that Os started mixing with global seawater again.

Keywords: Mediterranean Sea, Messinian Salinity Crisis, osmium isotope

Japan Geoscience Union Meeting 2014
(28 April - 02 May 2014 at Pacifico YOKOHAMA, Kanagawa, Japan)

MIS32-08 Room:416 Time:April 30 11:00-11:15

Exp. 325 Great Barrier Reef Environmental Changes

YOKOYAMA, Yusuke[1*]

[1]Yusuke YOKOYAMA

The Great Barrier Reef is the largest coral reef in the world and a world heritage site. Integrated Ocean Drilling Program (IODP) Expedition 325 drilled fossil corals and obtained 225m of core materials from 42 to 167 m below sea-level. The site is suited for reconstructing paleo climate data because: 1) reconstructed sea-level data is relatively immune from isostatic effect since it is located at site far from former ice covered regions (far-field), 2) it locates in or near the Indo Pacific Warm Pool (IPWP) where paleo sea surface temperature (SST) data will constrain climate model strongly, and 3) the growth history of the reef since the LGM is to unlock a key factors for reef system response against environmental changes. Both sea level and climate data have been reconstructed by the science party and they provides new insights of the climate system. In this presentation, I will overview and introduce some key findings of IODP 325 GBR environmental changes (Yokoyama et al., 2011)

Reference: Yokoyama, Y. et al. (2011) ”IODP Expedition 325: Great Barrier Reefs Reveals Past Sea-Level, Climate and Environmental Changes Since the Last Ice Age” Scientific Drilling, 12, 32-45.

Keywords: Sea level change, Glacier, Last Glacial Maximum, Sea Surface Temperature, Coral, The Great Barrier Reef

Japan Geoscience Union Meeting 2014
(28 April - 02 May 2014 at Pacifico YOKOHAMA, Kanagawa, Japan)

MIS32-09 Room:416 Time:April 30 11:15-11:30

Determination of hydrocarbon gas in drilling mud and cores during Expedition 348 at the Nankai Trough, Japan

FUCHIDA, Shigeshi[1*] ; HAMMERSCHMIDT, Sebastian[2] ; EXPIDITION 348, Shipboard scientists[3]

[1]Osaka City University, [2]University of Bremen, [3]University of Wisconsin and others

The recent International Ocean Discovery Program (IODP) Nankai Trough Seismogenic Zone Experiment (NanTroSEIZE) Expedition 348 at Site C0002 drilled and cored successfully up to 3058.5 mbsf. During drilling and coring, hydrocarbon and other inorganic gas concentrations were monitored on board. Here, we will report the distribution and origin of the hydrocarbon gas in Holes C0002N (838 to 2330 mbsf) and C0002P (1954 to 3058 mbsf).

Methane, ethane, and propane concentrations in the headspace gas were measured by Geoservices and by using the scientific drilling mud gas monitoring system onboard D/V Chikyu. Total gas concentrations were dominated by methane, with the highest concentrations of up to 8% at around 1305 mbsf. Downhole gas concentrations steadily decreased to values <0.2 %. Ethane and propane were only present in minor concentrations, and higher homologues (i.e. n-butane, i-butane, n-pentane, i-pentane) stayed typically below 0.01 %. Below 2200 mbsf, ethane and propane increase steadily with depth. Bernard diagram (i.e. Bernard parameter vs. $d^{13}C_{CH4}$, Bernard et al., 1978) indicates that the gas in Hole C0002NP was gradually changed from biogenic to thermogenic with increasing depth.

Headspace gas samples from cores in Hole C0002P (2160-2220 mbsf) were all dominated by methane, with up to 23455 ppm. Methane concentration in the headspace gas samples was higher than the drilling mud gas samples at the same interval. This underestimation of methane in the drilling mud is due to the influence of drilling parameter (e.g. rate of penetration), mud properties (e.g. mud weight) and degassing efficiency.

Keywords: IODP, Expedition 348, Nantrosize, hydrocarbon

Japan Geoscience Union Meeting 2014
(28 April - 02 May 2014 at Pacifico YOKOHAMA, Kanagawa, Japan)

MIS32-10 Room:416 Time:April 30 11:30-11:45

New approach for subsurface methanogenesis

KANEKO, Masanori[1*] ; TAKANO, Yoshinori[1] ; OHKOUCHI, Naohiko[1]

[1]JAMSTEC

Quantitative understanding of microbially mediated methanogenesis is important in biogeochemistry for many reasons; Firstly, methanogenesis plays an important role in the carbon cycle on the Earth mediating a terminal process of organic matter degradation and a major metabolic process in anoxic sediments. Secondly, methane produced by methanogens results in methane hydrate formation which is a potential energy resource, while methane released to the atmosphere acts as a greenhouse gas. Thirdly, since methanogens are primitive organisms, clarification of their distribution and environmental factors controlling their activity provides better understanding of subsurface biosphere and environmental constraints for early life.

Although quantitative understanding of distribution and activity of methanogens is requisite for better understanding of methane biogeochemistry, available techniques are restricted to address this issue. Particularly, it is difficult to quantitatively detect a signal of modern methanogenesis from deep marine sediment cores where methanogenic activity is low and complex mixture of organic matter is accumulated during a geologic time scale. However, if function-specific compound directly involved in the methanogenic reaction can be quantified, we would be able to extract information about distribution and activities of methanogens in the marine sediments.

Recently we developed analysis of coenzyme F430. Since F430 catalyzes a terminal step of methanogenesis and possessed by all methanogens, it should be a good biomarker for methanogenesis. High sensitive detection of F430 by LC-MS/MS (sub-femto mol level) allows to detect F430 in marine sediment. We will present the developed methodology and application to sediment core samples.

Keywords: coenzyme F430, methanogenesis, LC-MS/MS, marine sediment

Japan Geoscience Union Meeting 2014
(28 April - 02 May 2014 at Pacifico YOKOHAMA, Kanagawa, Japan)

MIS32-11 Room:416 Time:April 30 11:45-12:00

Lake drilling in Japan: Biwa and Suigetsu

HAYASHIDA, Akira[1*] ; TAKEMURA, Keiji[2] ; NAKAGAWA, Takeshi[3]

[1]Doshisha University, [2]Kyoto University, [3]University of Newcastle

Lake drilling is an important subject of the International Continental Scientific Drilling Program (ICDP), where several projects were implemented in ancient-type lakes utilizing the GRAD200 and GRA800 systems. However, proposals for attempting lake drilling in Japan have not been submitted to ICDP so far. In 2002, an ICDP workshop, entitled ”Lake Biwa and Lake Suigetsu: Recorders of Global Paleoenvironments and Island Arc Tectonics” was held in order to assemble an international team and prepare a full proposal. Subsequently, piston coring and deep drillings were made in Lake Biwa supported by the grant-in-aid from Monbusho. Studies of these core samples are now ongoing in various disciplines including sedimentlogy, paleomagnetism, organic and inorganic chemistry, and radiocarbon dating. In Lake Suigetsu, an international collaborative research has been carried out aiming to provide a high-resolution paleoenvironmental record of the East Asian monsoon. It also contributed toward establishing a purely terrestrial radiocarbon calibration model, based on analysis of the annually laminated sediment. As the next step of the current researches in Lake Biwa and Lake Suigetsu, we expect a new drilling project targeting a 250-m thick continuous clay member of the Lake Biwa sediments.

Keywords: ICDP, Lake drilling, Lake Biwa, Lake Suigetsu

Japan Geoscience Union Meeting 2014
(28 April - 02 May 2014 at Pacifico YOKOHAMA, Kanagawa, Japan)

MIS32-12 Room:416 Time:April 30 12:00-12:15

How the stress state changes with time in and aroud faults

OMURA, Kentaro[1*]

[1]NIED

It is an important factor for forecast a future earthquake how the strength of a fault plane is recovered and how the stress in and around the fault plane accumulate during an earthquake cycle. However, it is difficult to inspect the time variation of stress state in and around a faults in the field because the period of an earthquake cycle is very long. I introduce examples to be concerned with time variations of stress states by downhole in-situ stress measurement (Ikeda et al., 1996a; Ikeda et al., 1996b; Ikeda et al., 2001; Tsukahara et. al., 2001; Omura et al., 2004; Yamashita et al., 2004; Hickman and Zoback, 2004; Lin et al., 2007; Yabe et al., 2010; Yamashita et al., 2010; Yabe and Omura, 2011; Kuwahara et al., 2012; Ito et al., 2013; Lin et al., 2013). Those examples indicade that stress increases since after an earthquake toward the next earthquake. However, it is not clear whether the stress increase linearly with time, or change largely just after an earthquake, or increase rapidly just before the next earthquake. We need repeated measurements of in-situ stress to detect directly a time variation of stress state in and around a fault after an earthquake.

Hickman, S., and M. Zoback, 2004, Geophys. Res. Lett., 31, L15S12, doi:10.1029 2004GL020043

Ikeda, R, K.Omura and Y.Iio,.H. Tsukahara, 1996a, Proc. VIIIth Int'l. Symp. on the Observation of the Continental Crust through Drilling, 30-35.

Ikeda,R., Y.Iio and K.Omura, Y.Tanaka, 1996b, Proc. VIIIth Int'l. Symp. on the Observation of the Continental Crust through Drilling, 393-398.

Ikeda, R., Y. Iio and K. Omura, 2001, The Island arc Special Issue. 10, Issue 3/4, 252-260.

Kuwahara, Yasuto, Tsutomu Kiguchi, Xinglin Lei, Shengli Ma, Xueze Wen, and Shunyun Chen, 2012, Earth, Planets and Space, 64, 13-25.

Lin, W., E.-C. Yeh, H. Ito, J.-H. Hung, T. Hirono, W. Soh, K.-F. Ma, M. Kinoshita, C.-Y. Wang, and S.-R. Song, 2007, Geophys. Res. Lett., 34, L16307, doi:10.1029 2007GL030515.

Lin, Weiren, Marianne Conin, J. Casey Moore, Frederick M. Chester, Yasuyuki Nakamura, James J. Mori, Louise Anderson, Emily E. Brodsky, Nobuhisa Eguchi, and Expedition 343 Scientists, 2013, Science, 339, 687-690.

Omura, K., R. Ikeda, T. Matsuda, A. Chiba, and Y. Mizuochi, 2004, Earth Monthly, extra edition No.46, 127-134.

Tsukahara, H., Ikeda, R. and Yamamoto, K. , 2001, Island Arc, 10, 261-265.

Yabe, Yasuo, Kiyohiko Yamamoto, Namiko Sato, and Kentaro Omura, 2010, Earth Planets Space, 62, 257-268.

Yabe, Yasuo and Kentaro Omura, 2011, Island Arc, 20, 160-173.

Yamashita, Furoshi, Eiichi Fukuyama and Kentaro Omura, 2004, Science, 306, 261-263.

Yamashita, F., Mizoguchi, K., Fukuyama, E. and Omura, K., 2010, J. Geophys. Res., 115, B04409, doi:10.1029 2009JB006287.

Keywords: stress, fault, in-situ measurement, hydraulic fracture, borehole breakout, downhole measurement

Japan Geoscience Union Meeting 2014
(28 April - 02 May 2014 at Pacifico YOKOHAMA, Kanagawa, Japan)

MIS32-13 Room:416 Time:April 30 12:15-12:30

Physicochemical process during earthquake slip: An example from the TCDP

HIRONO, Tetsuro[1*]

[1]Department of Earth and Space Science, Graduate School of Science, Osaka University

Several fault-drilling projects have been conducted with the common aim of seeking direct access to zones of active faulting and understanding the fundamental processes governing earthquakes and fault behavior, as well as the factors that control their natural variability. Here, we review recent scientific drilling project on the the Chelungpu Fault which slipped during the 1999 Taiwan Chi-Chi earthquake. One of the main findings of fault-drilling research is a better understanding of the physicochemical processes of the primary slip zone during an earthquake, which is closely related to the mechanism of dynamic fault weakening. In the case of the Chelungpu fault, integrated research with borehole experiments, core sample analyses, and numerical simulations were performed, and the results indicate that thermal pressurization occurred during the 1999 earthquake, explain ing the peculiar seismic behavior during the earthquake. Such fault-drilling project related to active fault certainly improve our knowledge and understanding of earthquakes.

Keywords: Onland fault drilling, Active fault

Japan Geoscience Union Meeting 2014
(28 April - 02 May 2014 at Pacifico YOKOHAMA, Kanagawa, Japan)

MIS32-14 Room:416 Time:April 30 12:30-12:45

Deep Fault Drilling Project, Alpine Fault, New Zealand

SHIGEMATSU, Norio[1*] ; SUTHERLAND, Rupert[2] ; TONWEND, John[3] ; TOY, Virginia[4]

[1]Active Fault and Earthquake Research Center, AIST, [2]GNS Science New Zealand, [3]Victoria University of Wellington, [4]University of Otago

The Alpine Fault is mature (>460 km offset), active (25 mm/yr), and late in its seismic cycle. It ruptured in AD 1717, has a 330 yr return time, and M8 earthquake probability is c. 30% in the next 50 yrs (Berryman et al. 2013). The objective of the Deep Fault Drilling Project (DFDP) is to collect materials, measure ambient conditions, and monitor at depth on the Alpine Fault, to understand earthquake processes and the formation of a continental orogen.

Pilot drilling (DFDP-1) was completed in 2011. Two boreholes were drilled, wireline geophysical loggings collected, and observatory installed. The followings were revealed as Initial results. A low-permeability alteration zone overprints the boundary between fault core and damage zone. The alteration zone significantly affects physical properties and likely evolves during the seismic cycle. There is a fluid pressure step of 0.53 MPa across the fault at 128 m depth, and probable greater difference at greater depth. Geothermal gradient is 63 +/- 2 C/km. Physical properties are highly asymmetric, suggesting a possible (northeastward) preferred rupture direction.

Planning is now underway for the next phase of drilling (”DFDP-2”), which is scheduled to start in 2014. The target total depth (TD) is 1.3 km, with contingency to reach 1.5 km. We drill, sample, and monitor the Alpine Fault to address fault zone evolution via brittle and ductile processes operating in the upper and mid-crust in this novel experiment.

Keywords: Fault zone drilling, the Alpine Fault, Earthquake processes, Brittle and ductile processes

Japan Geoscience Union Meeting 2014
(28 April - 02 May 2014 at Pacifico YOKOHAMA, Kanagawa, Japan)

MIS32-15 Room:416 Time:April 30 14:15-14:30

An Overview of IODP Expedition 346: Asian Monsoon

TADA, Ryuji[1*] ; MURRAY, Richard W.[2] ; ZARIKIAN, Carlos alvarez[3] ; EXPEDITION 346, Scientists[4]

[1]Graduate School of Science, the Univerity of Tokyo, [2]Earth and Environment, Boston University, [3]Texas A&M University, [4]IODP

In IODP Expedition 346, Joides Resolution (JR) started her cruise from Valdez,Alaska on August 2nd, sailed all the way to the Japan Sea/East Sea (JS/ES), drilled 7 sites in the JS/ES and 2 sites in the northern East China Sea (ECS), and ended her cruise at Pusan, Korea on September 28th. During six weeks of drilling, we recovered 6135.3 m of core, with an average recovery of 101%, which is a record of IODP. The expedition was originally aimed to test the hypothesis that Plio-Pleistocene uplift of Himalaya and Tibetan Plateau (HTP) and/or emergence and growth of the northern hemisphere ice sheets and consequent establishment of the two discrete modes of westerly jet (WJ) circulation is the cause of the millennial-scale variability of the East Asian summer monsoon (EASM) and amplification of the Dansgaard-Oeschger cycles (DOC). The expedition is also aimed to test the hypothesis that surface and deep water conditions of the JS/ES has been controlled by the nature and strength of the water influx through the Tsushima Strait which are strongly influenced by EASM precipitation, eustatic sea level changes, and EAWM cooling.

In order to explore the linkage between WJ circulation and EASM precipitation, it is critical to obtain high-resolution, continuous sedimentary records that preserve proxies of both WJ and EASM. In this respect, the JS/ES is ideal because its hemipelagic sediments contain significant amount of the eolian dust transported from East Asia by the WJ, and alternations of dark and light layers that characterize Quaternary sediments of the sea record variations of EASM precipitation over South China (Tada et al., 1999). Sites are also arranged along the north-south transect to monitor the behavior of the WJ. The sites are arranged to make the depth transect to monitor the behavior of deep water through changes in calcium carbonate compensation depth and bottom water oxygenation level. Northern East China Sea is ideal to monitor changes in EASM precipitation because its surface water salinity and temperature during summer is significantly influenced by the discharge of the Yangtze River whose drainage area covers the majority of the South China where EASM precipitation is most intense (Kubota et al., 2010).

Because of recent advances in drilling technology and newly developed analytical tools, we were able to collect and examine sediment records that were impossible to acquire even a few years ago. The newly engineered half piston core system (called the half APC) enabled us to recover the deepest piston core in DSDP/ODP/IODP history (490.4 m in Hole U1427A). That achievement was also the deepest continuously recovered piston cored sequence, initiated at the mudline and penetrating to the ˜500 m depth solely by piston coring. These technological advances delivered a series of new surprises. Examples are pristine dark?light laminae from ˜12 Ma sediment recovered by piston core from 410 m core depth below seafloor, Method A [CSF-A] at Site U1425 and from 210 m CSF-A at Site U1430.

Through this expedition, we collected the geological evidence necessary to test the hypotheses described above through drilling in the JS/ES and northern part of the ECS, and are trying to 1) specify the onset timing of orbital and millennial-scale variability of EASM, EAWM and WJ and reconstruct their evolution process and spatial variation patterns, and 2) reconstruct orbital and millennial-scale paleoceanographic changes in the JS/ES to clarify the linkage between the paleoceanography of the JS/ES and EASM, EAWM and/or sea level. Comparison of the obtained results with the uplift history of HTP and/or ice volume changes will enable us to test the hypotheses.

Keywords: IODP, Expedition 346, Japan Sea/East Sea, East China Sea, Dansgaard-Oeschger Cycle, East Asian Monsoon

Japan Geoscience Union Meeting 2014
(28 April - 02 May 2014 at Pacifico YOKOHAMA, Kanagawa, Japan)

MIS32-16 Room:416 Time:April 30 14:30-14:45

Sediment cores recovered from the Sea of Japan/East Sea during IODP Expedition 346 and preliminary result of foraminifer

SAGAWA, Takuya[1*] ; TADA, Ryuji[2] ; MURRAY, Richard W.[3] ; ALVAREZ-ZARIKIAN, Carlos A.[4] ; EXPEDITION 346, Scientists[5]

[1]Department of Earth and Planetary Sciences, Faculty of Sciences, Kyushu University, [2]Department of Earth and Planetary Science, Graduate School of Science, The Univeristy of Tokyo, [3]Earth & Environment, Boston University, USA, [4]Integrated Ocean Discovery Program, Texas A&M University, [5]IODP Expedition 346

Integrated Ocean Drilling Program (IODP) Expedition 346 (29 July?27 September 2013) recovered 6135.3 m of core from seven sites in the Sea of Japan/East Sea and two adjacent sites in the East China Sea. One of the objectives of this expedition is to explore the orbital- and millennial-scale variation and evolution of the East Asian monsoon and its impact on the paleoceanography in the Sea of Japan/East Sea. We recovered centimeter- to meter-scale alternation of dark and light layers in the Pleistocene sediments that could be correlated across the six sites in latitudinal and depth transects of the Sea of Japan/East Sea (U1422?U1426 and U1430), suggesting that the Sea of Japan/East Sea responded as a single system to climatic and/or oceanographic perturbations. Sediments of shallower sites (U1426: 903 mbsl and U1427: 330 mbsl) contain well preserved calcareous fossils and are expected to provide high-quality oxygen isotope stratigraphy that will be a key age controls for the entire region. In particular, high sedimentation rate (˜36 cm/kyr) and a complete splice down to ˜400 m at Site U1427 make it possible to produce centennial-scale continuous records in shallow water environments for the last ˜1.2 Ma. We conducted preliminary oxygen and carbon isotope analyses of benthic and planktonic foraminifera for core catchers from Site U1427A (87 samples). The oxygen isotope variations correspond to lithological change alternating low isotope values in darker clay-rich and high values in light biogenic component-rich sediment and therefore show similar variation to physical properties of the sediment, such as bulk density, magnetic susceptibility, natural gamma ray, and color reflectance. These results confirm high potential of this site for paleoceanographic investigation in orbital, millennial, and centennial timescales.

Expedition 346 Scientists:
Anderson, W., Bassetti, M-A., Brace, B., Clemens, S., Dickens, G., Dunlea, A., Gallagher, S., Giosan, L., Gurgel, M., Henderson, A., Holbourn A., Ikehara, K., Irino, T., Itaki, T., Karasuda, A., Kinsley, C., Kubota, Y., Lee, G-S., Lee, K-E., Lofi, J., Lopes, C., Peterson, L., Saavedra-Pellitero, M., Singh, R., Sugisaki, S., Toucanne, S., Wan, S., Xuan, C., Zheng, H., and Ziegler, M.

Keywords: IODP, Expedition 346, Asian Monsoon, Sea of Japan/East Sea

Japan Geoscience Union Meeting 2014
(28 April - 02 May 2014 at Pacifico YOKOHAMA, Kanagawa, Japan)

MIS32-17 Room:416 Time:April 30 14:45-15:00

Preliminary results from shipboard research during IODP Expedition 341 (Alaska Tectonics, Climate and Sedimentation)

SUTO, Itsuki[1*] ; ASAHI, Hirofumi[2] ; FUKUMURA, Akemi[3] ; KIOKA, Arata[4] ; KONNO, Susumu[5] ; MATSUZAKI, Kenji[6] ; NAKAMURA, Atsunori[4] ; OJIMA, Takanori[7] ; EXPEDITION, 341 scientists[8]

[1]Nagoya Univ., [2]Pusan National Univ., [3]Hokkaido Univ., [4]Univ. of Tokyo, [5]Kyushu Univ., [6]Tohoku Univ., [7]Univ. of Tokyo, [8](none)

The North American Cordillera is an active orogen, which in the Pleistocene is, at times, covered by the Cordilleran Ice Sheet. Ice sheet dynamics are likely impacted by global climate and likely enhanced the erosion in the Cordillera. The melt water discharge to the ocean may play an important role in the rich ecosystem in the Gulf of Alaska by delivering nutrients. In the modern Gulf of Alaska, a rich diversity of marine microorganisms is associated with the seasonal nutrient supply derived from glacial melt water. Continuous paleoceanographic reconstruction by marine microfossils (radiolarians, diatoms, foraminifers etc.) can provide the history of the nutrient supply that may be associated with ice sheet dynamics and glacial runoff into the Gulf of Alaska.

Since the late Miocene, ice sheets formed on the North American continent and intensified around 2.5 Ma during Northern Hemisphere glaciation, which had a strong impact on global and regional environments. On the other hand, the large ice sheet may also have enhanced the erosion process in the higher latitudes and supplied terrigenous inputs such as glacial sediments to the coastal zone. Therefore, it is expected that the sediments in the Gulf of Alaska have recorded directly the history of the Cordillera ice sheet formation and erosion process since the Neogene. In this background, the Integrated Ocean Drilling Program (IODP) Expedition 341 held between May to July 2013, targeted this high-resolution sediment record from late Cenozoic in order to investigate the relevance of climate change in the North Pacific Ocean and the erosion process of Cordilleran glaciers. The drilling was conducted from deep-sea fan to continental shelf occupied by glaciers during glacial expanses.

According to preliminary ship-board results, the sediments recovered during this expedition record paleoceanographic changes in the Gulf of Alaska since the late Miocene and extremely high sedimentation rates which could be one of the greatest achievements in this expedition. In addition, microscopic observation, organic and inorganic chemical analysis and measurement of the physical properties suggest that a large amount of the terrestrial sediments have been transported. A large amount of glacial sediments (ice-rafted debris) have been also recorded. Although it was expected that calcareous microfossils are poorly preserved in this area, the sediment samples obtained in this cruise contained a continuous and rich foraminifera record which will allow the establishment of a long continuous oxygen isotopic curve. Siliceous microfossil and p-mag analyses enable the building of firm chronostratigraphy when combined with the oxygen isotopic curve. Under this well-constrained age determination, other chemical/physical/biological investigations will be done and then we will clarify the paleoenvironmental fluctuation that is unprecedented in the North Pacific.

Keywords: IODP Exp. 341, Gulf of Alaska, land/ocean paleoenvironment, Glacier

Japan Geoscience Union Meeting 2014
(28 April - 02 May 2014 at Pacifico YOKOHAMA, Kanagawa, Japan)

MIS32-18 Room:416 Time:April 30 15:00-15:15

IODP Exp. 345: The first sample of primitive layered gabbros from fast-spreading lower oceanic crust

ABE, Natsue[1*] ; AKIZAWA, Norikatsu[2] ; HARIGANE, Yumiko[5] ; HOSHIDE, Takashi[4] ; MAEDA, Jinichiro[3] ; MACHI, Sumiaki[2] ; NOZAKA, Toshio[6] ; PYTHON, Marie[5] ; GILLIS, Kathryn[7] ; SNOW, Jonathan[8] ; SHIPBOARD SCIENTIFIC PARTY, Iodp expedition 345[9]

[1]IFREE, JAMSTEC, [2]Department of Earth Sciences, Kanazawa University, [3]AIST, [4]Akita University, [5]Hokkaido University, [6]Okayama Univesity, [7]University of Victoria, B.C., [8]University of Houston, [9]IODP, Texas A&M University

Three-quarters of the ocean crust formed at fast-spreading ridges is composed of plutonic rocks whose mineral assemblages, textures and compositions record the history of melt transport and crystallization between the mantle and the seafloor. However, owing to the nearly continuous overlying extrusive upper crust, sampling in situ the lower crust is challenging. Hence, models for understanding the formation of the lower crust are based essentially on geophysical studies and ophiolites. Integrated Ocean Drilling Program (IODP) Expedition 345 recovered the first significant sections of primitive, modally layered gabbroic rocks from the lowermost plutonic crust formed at a fast-spreading ridge, and exposed at the Hess Deep Rift (Gillis et al., Nature, 2014, doi:10.1038/nature12778).

Keywords: layered gabbro, oceanic lower crust, Hess Deep, fast-spreading ridge, East Pacific Rise, primitive gabbro

Japan Geoscience Union Meeting 2014
(28 April - 02 May 2014 at Pacifico YOKOHAMA, Kanagawa, Japan)

MIS32-19 Room:416 Time:April 30 15:15-15:30

Results of Previous Drilling on Cretaceous Oceanic Plateaus and Future Outlook

SANO, Takashi[1*] ; NAKANISHI, Masao[2]

[1]National Museum of Nature and Science, [2]Chiba University

Oceanic plateaus, reach volumes of several 10^6 to several 10^7 km^3, are characterized by anomalously high rates of mantle melting that represent the largest volcanic events in the Earth's history. There is currently a lively debate about the oceanic plateau volcanism: whether they are built by plume heads from the lower mantle, changes in plate stress, or even meteor impacts. One difficulty with their research is that several of oceanic plateaus (e.g., Kerguelen Plateau) were erupted on remnants of continents where assimilation of continental lithosphere can obscure the primary mantle signature of the lavas. In contrast, Cretaceous oceanic plateaus in the western Pacific (Ontong Java Plateau, Shatsky Rise, and so on) have no effect of the crustal assimilation, permitting its primary origin in mantle to be resolved. The time of productions of the western Pacific plateaus coincides with increases in climate warming, resulting oceanic anoxic event, and eustatic sea level change; and therefore, its origin receives attention from paleo-environment aspects, too. It is proposed that the western Pacific plateaus were formed by the upwelling of very large plume head of mantle material, superplume, that erupted beneath the Pacific basin (Larson, 1991, *Geology*, 19, 547-550). The present-day South Pacific superswell is probably the nearly exhausted remnant of the original upwelling. Moreover, the remnant of the superplume is likely detected by seismic data (e.g., Suetsugu *et al*., 2009, *Geochem Geophys Geosyst* 10, Q11014).

The plume head phenomenon occurs naturally in numerical and laboratory experiments, but there is currently no unequivocal geological evidence proving that a starting plume head in convecting mantle has operated with Earth. Thus several alternative explanations (described above) or more complex plume head models are proposed to explain origin of the oceanic plateaus.

To test the plume head model, petrological and geochemical data from igneous rocks are important. Although a small number of dredges have recovered basalts from the western Pacific plateaus, almost of all such samples were highly altered. The best way to obtain fresh samples is by drilling of holes. Thus, operations during Ocean Drilling Program (ODP) Leg 192 and Integrated Ocean Drilling Program (IODP) Expedition 324 drilled Ontong Java Plateau and Shatsky Rise, respectively, seeking evidence that would test the plume head hypothesis (Mahoney *et al*., 2001, *Init Rep ODP*, 192; Sager *et al*., 2010, *Proc IODP*, 324). Based on drilling of several holes in the oceanic plateaus, both expeditions have extended our knowledge of the compositions and origin of the plateaus magmas considerably. However, both expeditions uncovered complications that do not fit the simple model, so debate over plume head hypothesis continued.

One of the main reasons for the previous failure to test the plume head model is that the previous drilling holes in the oceanic plateaus were too thin; only $<$300 m basement lavas were recovered among the thick oceanic plateaus ($>$30 km). The information of such thin drilling holes is difficult to evaluate the plume head model that is proposed by numerical and laboratory experiments. The laboratory experiments of "thermo-chemical" plumes containing both thermal and chemical density anomalies are characterized by a strong time-dependence and could develop for mantle density anomalies lower than 2% (e.g., Kumagai *et al*., 2008, *Geophys Res Lett*, 35, L16301). Such thermal or chemical density anomalies would be detected by geological researches of long drilling cores (e.g., ˜3000 m basement lavas which construct ˜10% of total thickness of the oceanic plateaus). To date, such long cores were difficult to recover, but a riser drilling vessel Chikyu has made drilling $>$3000 m basement lavas technically feasible.

Keywords: oceanic plateau, large igneous province, plume, magma genesis

Japan Geoscience Union Meeting 2014
(28 April - 02 May 2014 at Pacifico YOKOHAMA, Kanagawa, Japan)

MIS32-20 Room:416 Time:April 30 15:30-15:45

Recent progress in paleo- and rock magnetism and its applications produced by IODP

YAMAZAKI, Toshitsugu[1*]

[1]AORI, University of Tokyo

Paleomagnetists have sailed most of the IODP expeditions, and greatly contributed to the achievement of the aims of individual expeditions. At the beggining of the new phase of IODP, I will review progress in paleomagnetism and rock magnetism and their applications produced by IODP for the last about 10 years.

Results of the two IODP coring programs, one in the North Atlantic (Exp. 303/306) and the other in the east equatorial Pacific (Exp. 320/321), greatly improved our understanding of the past geomagnetic field variations. High-resolution paleointensity records during the Pleistocene with precise age control were obtained from North Atlantic drift sediments. These records led the establishment of the PISO-1500 paleointensity stack, which is now used as the standard curve for paleointensity-assisted chronostratigraphy. Detailed records of polarity reversals and excursions were also obtained. From the equatorial Pacific sediment cores, continuous Miocene to Eocene relative paleointensity records were obtained for the first time, although resolution is not high. Previously, continuous paleointensity records were available only for the last ca. 3 m.y. No discernible relation between paleointensity and polarity length was recognized, despite that a weak positive correlation was suggested previously. On the other hand, volcanic rocks from seamounts (Exp. 330) and oceanic plateau (Exp. 324) were utilized for obtaining absolute paleointensity in the Mesozoic.

Rock- and paleomagnetism was applied to resolve various geological and geophysical problems in IODP. First of all, paleomagnetism contributed progress in the mantle dynamics; paleomagnetic inclinations revealed that the Louisville hotspot did not move in concert with the Hawaiian hotspot (Exp. 330), which is known to have shifted southward about 15 degrees between about 80 and 50 Ma. Magnetic techniques such as the anisotropy of magnetic susceptibility were successfully utilized for studying subduction zone dynamics (NanTroSEIZE, CRIPS). Rock magnetic techniques become widely used in paleoceanographic and paleoenvironmental applications. It was recently revealed using IODP cores that biogenic magnetite prevails in marine sediments (e.g., Exp. 320/321 and 329). Its role to remanent magnetization acquisition processes and potential applications to paleoceanography are attracted attention.

Keywords: paleomagnetism, rock magnetism, IODP, paleointensity

Japan Geoscience Union Meeting 2014
(28 April - 02 May 2014 at Pacifico YOKOHAMA, Kanagawa, Japan)

MIS32-21 Room:416 Time:April 30 16:15-16:30

Chikyu logging review in IODP and future of well logging in scientific drilling

SANADA, Yoshinori[1*] ; KIDO, Yukari[1] ; KYAW, Moe[1]

[1]JAMSTEC

It has passed seven years since Chikyu joined the IODP expeditions. There were many expeditions where well logging were conducted: NanTroSEIZE exp314 in 2007, expeditions 319 and322 in 2009, exp332 in 2010, exp338 in 2012-2013, exp348 in 2013-2014; Japan trench fast drilling project (J-FAST) exp343 in 2012; Deep coalbed biosphere off Shimokita exp337 in 2012. The total logged length on Chikyu during IODP Expeditions are 26.2 km in the seven years period. Well logging has increased its importance in science and operations. The reasons are 1) sensor and technological innovation brings more geological and geophysical information, 2) spot or partial interval coring in combination of logging-while-drilling and mudlogging is best option in deepwater expeditions, and 3) need of LWD real time data in decision making for precise location of observatory installation and spot coring. Riser drilling by Chikyu improves hole condition by means of drilling fluid control, which improves logging data quality, and its large hole diameter bring us more selections of tools, measurements, and downhole experiments.

The logging companies have been developing new measurement, higher accuracy and resolution tools. For example, resisitivity image tools have wider azimuthal coverage and higher resolution, which helpto deeper geological interpretations and breakout analysis. The new sonic tool improves accuracy of velocity in soft sediment and more availability of measurement in shear velocity.

With accessing deeper, more challenging management of time (coring is a time consuming operation),combination of spot coring in the most interesting interval and continuous logging may be one of solutions under limited cruise schedule.

Realtime LWD data acquisition and interpretation were required to install observatory at proper depth. Current LWD technology sends more data to surface, which helps to understand the lithology in real time.

To use large diameter of riser pipes brings us a lot of advantages against lowering logging tools through small drill pipes. Proper tool size and sensor position in the borehole improve data quality. Increasing of tool selection brings more variety of measurement and experiment. FMI resistivity borehole imager covers more image area of borehole wall. Pressure test by dual packer and fluid sampling were available with large diameter tools.

Logging activities and results by Chikyu as part of IODP (2003-2013) will be reviewed and discuss its potential, role, and challengs in the future scientific drilling.

Keywords: logging, Chikyu, IODP

Japan Geoscience Union Meeting 2014
(28 April - 02 May 2014 at Pacifico YOKOHAMA, Kanagawa, Japan)

MIS32-22 Room:416 Time:April 30 16:30-16:45

Mud logging for scientific drilling on D/V Chikyu: results of the past riser operations in the 1st phase IODP

SUGIHARA, Takamitsu[1*] ; AOIKE, Kan[1] ; MOE, Kyaw thu[1]

[1]CDEX/JAMSTEC

Mud logging has been a key technology for scientific drilling operation by D/V Chikyu. In order to penetrate into deeper formation by riser drilling, full-coring operation to targeted total depth is difficult due to taking much operation time. Therefore mud logging obviously contributes to acquiring continuous geological and geochemical data from formation and circulating fluid in formation to targeted total depth. In the IODP 1st phase, riser drilling operations with mud logging were conducted 4 times by the Chikyu (Expeditions 319, 337, 338, and 348). In this paper, we highlight some results of mud logging operated in the past operation and discuss on technical challenging for future riser operations by the Chikyu.

Mud logging is roughly composed of three components, lithological logging on cuttings, mud gas monitoring, and mud circulation/drilling parameters monitoring. As well known, cuttings lithology logging and mud gas monitoring are important tool to understand geological characteristics beneath drilling site based on results of not only the IODP riser operations by the Chikyu but also ICDP onshore drilling projects (e.g., Unzen and SAFOD). However, potential of mud circulation and drilling parameters monitoring associated with cuttings and mud gas analyses has not been discussed in detail in scientific drilling community. d-exponent is an indicator to detect zone of high pore pressure during drilling and it is well developed in the petroleum industry. d-exponent is defined as normalized rate of penetration (ROP) with rotation speed (RPM) and weight on bit (WOB), and in general case, d-exponent gradually decreases as entering into high pore pressure zone increasing ROP. During Expedition 348, we often faced formation with difficulty of drilling, and supposed there was relatively higher pore pressure zone based on the d-exponent analysis. In this presentation, we will discuss on comprehensive mud logging data analysis including data of d-exponent acquired in the past riser drilling operation and assess its potential for future expeditions.

Keywords: D/V Chikyu, IODP, Mud logging, Cuttings, Mud gas monitoring, Scientific drilling

Japan Geoscience Union Meeting 2014
(28 April - 02 May 2014 at Pacifico YOKOHAMA, Kanagawa, Japan)

MIS32-23 Room:416 Time:April 30 16:45-17:00

Downhole Logging Data Acquisition and Integration: Changing Tactics in the IODP and Its Future Direction

MOE, Kyaw[1] ; KIDO, Yukari[1*] ; SANADA, Yoshinori[1]

[1]CDEX-JAMSTEC

Since the initiation of IODP in 2003, three drilling platforms, Chikyu, JOIDES Resolution (JR) and Mission Specific Platform (MSP), operated at various environments of global locations using varieties of new techniques. Overcoming many difficulties, longest serving ship JR reached the maximum time in operations with 32 expeditions even ship was modified in dock for 38 months, new riser ship Chikyu with 13 expeditions, and MSP with 5 expeditions. Varying in their capabilities, JR expeditions covered most global areas and research themes where MSP and Chikyu expeditions were targeted to the most challenging and extreme environments. Further addition of riser technology and very shallow locations for MSP brought wider choice of new logging and coring tools, rigfloor parameter, and very high-resolution slim-hole logging tools.

In the downhole logging data acquisition, JR continued her standard set of basic wireline logging with best cost and performance factor but MSP and Chikyu were used expedition/project specific measurements with higher cost and better technology. For the new challenges in the various IODP expeditions, things changed from the previous program were new tools and better measurements, data integration applications and facilities, increased staffing for science support.

Those new techniques covering laboratory and downhole measurements, extended widely in measurement types and improved their capability and efficiency in data integration and onsite decision making. All these large volume of data with wider choice of software further enhanced the integrated studies like cuttings/core-log-seismic integration for the very deep-riser holes.

In this talk, dowhhole measurements data acquisition and wider data integration in the IODP will be summarized, operational-technical-scientific highlights and lessons will be reviewed, and future direction will be discussed.

Keywords: IODP, Logging, Data Integration, Chikyu, JOIDES Resolution, MSP

Japan Geoscience Union Meeting 2014
(28 April - 02 May 2014 at Pacifico YOKOHAMA, Kanagawa, Japan)

MIS32-24 Room:416 Time:April 30 17:00-17:15

Overview of IODP drilling in Izu-Bonin-Mariana arc

ISHIZUKA, Osamu[1*] ; TAMURA, Yoshihiko[2]

[1]GSJ/AIST, [2]IFREE, JAMSTEC

What is raw and juvenile continental crust? Furthermore, how does it form and evolve into mature continental crust? The continental crust we observe on the surface of the earth has been deformed, metamorphosed, and otherwise processed perhaps several times from its creation in subduction zones to the present.

Although there are many examples of accreted arc crust on the margins of continents, during- and/or post-collision geochemical changes are widespread, and we do not have the ability to observe active crust-forming processes in modern arcs except by what we can infer from eruptions at the surface, and by remote sensing of arc interiors. ULTRA-DEEP DRILLING INTO ARC CRUST is the best way to sample unprocessed juvenile continental-type crust, to observe these active processes that produce the nuclei of new continental crust, and to examine the nature of juvenile continental crust as first generated at intra-oceanic arcs.

Key questions for comprehending arc crust formation are: (1) What is the nature of the crust and mantle in the region prior to the beginning of subduction? (2) How does subduction initiate and initial arc crust form? (3) What are the spatial changes of arc magma and crust composition of the entire arc? (4) How do the middle arc crust evolve? Possible strategies for answering these questions include drilling by IODP at the Izu-Bonin-Mariana (IBM) arc system. IODP has proposals to drill at the IBM, including three non-riser holes (IBM-1, IBM-2 and IBM-3) and one riser, ultra-deep hole (IBM-4), which answer these questions, respectively, and the four drillings result in comprehensive understanding of the arc evolution and continental crust formation. Drillings by Joides Resolution at three sites (IBM-1, IBM-2 and IBM-3) are scheduled in 2014. This presentation will give an overview of these 3 cruises and their perspectives.

Japan Geoscience Union Meeting 2014
(28 April - 02 May 2014 at Pacifico YOKOHAMA, Kanagawa, Japan)

MIS32-25 Room:416 Time:April 30 17:15-17:30

Tsunami deposits sciences as geohazard research program of ICDP

FUJIWARA, Osamu[1*]

[1]Active Fault and Earthquake Research Center, AIST

Tsunamis initiated by the 2004 Indian Ocean earthquake (Mw 9.1?9.3) and the 2011 Tohoku-oki earthquake (Mw 9.0) have provided recent demonstrations of the widespread catastrophic damage and loss of life that can be caused by mega tsunamis. Mega tsunamis have dramatic impacts on geological processes as well as on human societies. Large-scale erosion and the mass transport of sediments by tsunamis cause rapid environmental change and biological turnover in coastal areas. Mega tsunamis leave evidence of their passage in the geological record on a time scale far beyond human memory.

Over geological time, mega tsunamis have been caused by events such as subduction-zone earthquakes, volcanic eruptions, landslides (on land and submarine), and meteorite impacts. Large submarine collapses of gas-hydrate-bearing sediments may also have caused mega tsunamis. These facts demonstrate that the risk of catastrophic tsunamis is not limited to active tectonic margins. Although the frequency of these catastrophic events is low compared to a human lifetime, there is no telling when and where the next events will occur.

The 2004 and 2011 events, and the recognition that mega tsunamis have occurred many times on both historical and geological time scales, have prompted international efforts to better understand the hazards associated with tsunamis and to design disaster control strategies at regional and global levels. The foundation on which mega-tsunami risk management is built is hazard assessment, including knowledge of the location, frequency, and magnitude of past events. This basic research leads to a better understanding of the dynamics of geological and biological evolution in coastal regions. Historical documents provide important information for regional analysis of past tsunamis, but their value is limited by the short length of the historical record. Studies of tsunami deposits provide a useful means of extending the length of those records onto a geological time scale.

To solve the above mentioned problems and aim at further development in these study field, following research programs are prospected.

Understanding past mega tsunamis from geological records.

+ Mega tsunami events during earth history.

+ Mega tsunami impacts through human history.

Global coordination of research to develop an inventory of tsunami deposits

+ Catalogue of mega tsunamis (size, source, age) at plate subduction zones.

+Catalogue of mega tsunamis (size, source, age) for island countries that have suffered far-field effects of mega tsunamis.

Outreach to and nurturing of young scientists in the field of tsunami geology

Keywords: Tsunami deposit, Geohazard, Continental drillig

Japan Geoscience Union Meeting 2014
(28 April - 02 May 2014 at Pacifico YOKOHAMA, Kanagawa, Japan)

MIS32-26 Room:416 Time:April 30 17:30-17:45

Japan Beyond-Brittle Project

ASANUMA, Hiroshi[1*] ; TSUCHIYA, Noriyoshi[2] ; ITO, Hisao[3] ; MURAOKA, Hirofumi[4]

[1]AIST, [2]Tohoku University, [3]Independent Scientist, [4]Hirosaki University

New conventional geothermal energy projects have not been actively promoted in Japan for the last decade because of perceptions of high relative cost, limited electricity generating potential and the high degrees of uncertainties and associated risks of subsurface development. More recently however, EGS (Enhanced Geothermal System) geothermal has been identified as a most promising method of geothermal development because of its potential applicability to a much wider range of sites, many of which have previously been considered to be unsuitable for geothermal development. Meanwhile, some critical problems with EGS technologies have been experimentally identified, such as low recovery of injected water, difficulties in establishing universal design/development methodologies, and the occurrence of induced seismicity, suggesting that there may be limitations in realizing EGS in earthquake-prone compression tectonic zones.

We propose a new concept of engineered geothermal development where reservoirs are created in ductile basement. This potentially has a number of advantages including: (a) simpler design and control of the reservoir, (b) nearly full recovery of injected water, (c) sustainable production, (d) lower cost when developed in relatively shallower ductile zones in compression tectonic settings, (e) large potential quantities of energy extraction from widely distributed ductile zones, (f) the establishment of a universal design/development methodology, and (g) suppression of felt earthquakes from/around the reservoirs.

To further assess the potential of EGS reservoir development in ductile zones we have initiated the ”Japan Beyond-Brittle Project (JBBP)”. It is intended that the first few years of the JBBP will be spent in basic scientific investigation and necessary technology development, including studies on rock mechanics in the brittle/ductile regime, characterization of ductile rock masses, development of modeling methodologies/technologies, and investigations of induced/triggered earthquakes. We expect to drill a deep experimental borehole that will penetrate the ductile zone in northeast Japan after basic studies are completed. The feasibility of EGS reservoir development in the ductile zone will then be assessed through observations and experimental results in the borehole. An ICDP supported workshop on JBBP has been held March 12-16 in Sendai, Japan, where feasibility, necessary breakthroughs, and roadmap has been discussed from scientific and technological points of view.

Keywords: Geothermal, Brittle-ductile transition, EGS

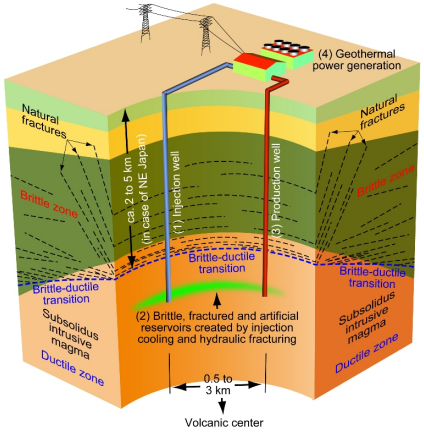

Japan Geoscience Union Meeting 2014
(28 April - 02 May 2014 at Pacifico YOKOHAMA, Kanagawa, Japan)

MIS32-27 Room:416 Time:April 30 17:45-18:00

Expectations for the new decade of drilling science

YAMADA, Yasuhiro[1*]

[1]Kyoto Univ

What kind of roles the 'drilling science' should undertake? This presentation proposes directions of 'drilling science' in the coming decades, to bridge the three methods to explore subsurface; exploration geophysics, drilling technology and usage of boreholes, and geology as material science.

Japan Geoscience Union Meeting 2014
(28 April - 02 May 2014 at Pacifico YOKOHAMA, Kanagawa, Japan)

MIS32-P01 Room:Poster Time:April 30 18:15-19:30

Hydraulic properties and pore structure of the sedimentary rocks at Site C0020, IODP Expedition 337 in Sanriku-oki basin

TANIKAWA, Wataru[1*] ; TADAI, Osamu[2] ; INAGAKI, Fumio[1] ; KAI-UWE, Hinrichs[3] ; KUBO, Yusuke[4] ; OHTOMO, Yoko[1]

[1]JAMSTEC/Kochi Kore Center, [2]Marine Works Japan Ltd., [3]University of Bremen, [4]JAMSTEC

Microbial biomass in the ocean sediments is controlled by physical, chemical and biological factor and conditions. The biomass in sediments reduces with increasing depth, and the limit of life and the reduction rate of biomass is partly controlled by physical conditions because lithification and diagenesis of oceanic sediments induce reduction of porosity, permeability and pore size. However the relationship between biomass and physical property for deep oceanic sediments is not well known. Therefore, in this study, a series of physical property measurements (Water potential, permeability and porosity) were conducted on the sediment cores at site C0020 from IODP expedition 337 and at site 902 from the Chikyu shakedown cruise (CY06-06) in Sanriku-oki basin. We measured water potential under atmospheric condition and permeability under confining pressure up to 40 MPa. Then we estimated the correlation between water potential and microbial biomass in the sediments.

Keywords: permeability, water potential, water activity, off-Sanriku basin, IODP expedition 337, biomass

Japan Geoscience Union Meeting 2014
(28 April - 02 May 2014 at Pacifico YOKOHAMA, Kanagawa, Japan)

MIS32-P02 Room:Poster Time:April 30 18:15-19:30

Coring disturbances with the riser drilling system of the D/V Chikyu during IODP Exp. 337 off Shimokita, Japan

MURAYAMA, Masafumi[1*] ; MORITA, Sumito[2] ; YAMADA, Yasuhiro[3] ; KUBO, Yusuke[4] ; HINRICHS, K-u[5] ; INAGAKI, Fumio[6]

[1]Center for Advanced Marine Core Research, Kochi University, Japan, [2]Institute for Geo-Resources and Environment, National Institute of Advanced Industrial Science and T, [3]Depertment of Urban Management Engineering, Kyoto University, [4]CDEX, Japan Agency for Marine-Earth Science and Technology, [5]University of Bremen, Germany, [6]Kochi Institute for Core Sample Research, Japan Agency for Marine-Earth Science and Technology

Coring disturbances were observed using the riser drilling system of the D/V Chikyu during IODP Exp. 337 off Shimokita, Japan. Injections of drilling mud and fluid with high density and pressure used in riser drilling during Expedition 337 caused complications to visual core observations. Semiconsolidated materials were commonly observed in this Hole, and drilling mud often easily penetrated the semiconsolidated sandstones and siltstones, causing possible false lamination structure in the cores, which might be misinterpreted as natural sedimentary structure preserved in the cores. Here, we report various kind of coring disturbances which were observed on board with riser drilling system.

Keywords: Coring disturbance, riser drilling, IODP, Exp. 337

Japan Geoscience Union Meeting 2014
(28 April - 02 May 2014 at Pacifico YOKOHAMA, Kanagawa, Japan)

MIS32-P03 Room:Poster Time:April 30 18:15-19:30

Lithology and XRF analysis data at drilled Site C0020 off the Shimokita Peninsula, IODP Exp. 337

MURAYAMA, Masafumi[1*] ; HIGASHIMARU, Naotsugu[1] ; IJIRI, Akira[2] ; INAGAKI, Fumio[2]

[1]Center for Advanced Marine Core Research, Kochi University, Japan, [2]KCC/JAMSTEC

Marine subsurface hydrocarbon reservoirs and the associated microbial life in continental margin sediments are among the least characterized Earth systems that can be accessed by scientific ocean drilling. We penetrated a 2,466 m-deep sediment sequence with a series of coal layers around 2 km below the seafloor. Here, we present the 160 XRF data and lithology of sediments and paleoenvironments from drilling Site C0020, IODP Expedition 337. We defined four different lithologic units present in Site C0020. The succession of lithofacies at Hole C0020A also provides insight into the evolution of depositional environments in this region.

Keywords: Lithology, XRF, IODP, Exp.337

Japan Geoscience Union Meeting 2014
(28 April - 02 May 2014 at Pacifico YOKOHAMA, Kanagawa, Japan)

MIS32-P04 Room:Poster Time:April 30 18:15-19:30

Structural characteristics of Nankai accretionary prism at C0002: Preliminary results from IODP Expedition 348

YAMAMOTO, Yuzuru[1*] ; OHTSUBO, Makoto[2] ; BROWN, Kevin[3] ; CRESPO-BLANC, Ana[4] ; EXPEDITION 348, Scientist[5]

[1]JAMSTEC, [2]AIST, [3]SCRIPS, [4]University of Granada, [5]IODP Expedition 348

Integrated Ocean Discovery Program (IODP) Expedition 348 has deepened hole down to 3058.5 mbsf at Site C0002, and collected cutting and core samples of Upper Miocene Nankai accretionary prism. The structural key observation made on cuttings in Holes C0002N and C0002P, and cores retrieved in Hole C0002P are:

a) The structures observed in intact cuttings include slickenlined surfaces, scaly fabric, deformation bands, minor faults and mineral veins. Slickenlines are observed throughout the whole interval, but scaly fabric is increasingly observed below ˜2200 mbsf. The other types of structures are scattered throughout the whole section.

b) The cored interval is characterized by steep bedding planes (more than 75?). A fault zone, 90 cm in thickness, with a few mm-size angular clasts is present in one of the cores (2204.9?2205.8 mbsf). In its present position, the brittle fault zone is associated with a normal faulting sense. It is unclear if this represents an early thrust rotated after its development or late normal fault.

c) SEM images in the upper part of Hole C0002N show little evidence for opal diagenesis, implying T<60?80 ℃ at 1225.5 mbsf. In Hole C0002N, the fabric lacks a strongly preferred orientation in clay-rich materials, except along striated micro-faults formed by clays. These zones are extremely localized with a thickness of a few microns or less. In Hole C0002P, below 2200 msbf, SEM images show the development of a regularly spaced fabric in sandstones, constituted by thin (<0.1?1 um), clay-dominated shear planes. Towards the base of the hole, below 2625 mbsf, compaction fabrics in clay?rich materials can be observed. Very thin shear zones with almost no wall damage zone have cut this fabric.

The overall character of the deformation (independent particulate flow with limited evidence for cataclastic deformation) is suggestive of that deformations occurred in a relatively shallow environment (approximately 0?4 km in burial depth).

Keywords: Expedition 348, C0002, Fault zone, Core, Cuttings

Japan Geoscience Union Meeting 2014
(28 April - 02 May 2014 at Pacifico YOKOHAMA, Kanagawa, Japan)

MIS32-P05 Room:Poster Time:April 30 18:15-19:30

Seismic reflection survey investigating subduction inputs at the Sagami Trough

MIURA, Seiichi[1] ; NO, Tetsuo[1*] ; SATO, Takeshi[1] ; YAMASHITA, Mikiya[1] ; SAITO, Saneatsu[1] ; TAKAHASHI, Narumi[1] ; KODAIRA, Shuichi[1]

[1]Japan Agency for Marine-Earth Science and Technology

The Sagami Trough is a plate convergent zone of the Philippine Sea Plate underneath the NE Japan including the Kanto area. Varied seismic events occurred associated with the plate convergence. Maginitude (M) 8-class earthquakes, for example 1703 Genroku and 1923 Taisho-Kanto events, damaged the Kanto area seriously. On the other hand, slow-slip events have been observed in the Boso area with 5-7 year interval, whose released energies were comparable to Mw 6. Source depths of the M8-class earthquakes and slow-slip events are almost same. One possible reason of the varied seismogenesis is different subduction inputs at the Sagami Trough. To understand the varied seismogenesis, structural and material information are important. A drilling proposal for subduction input at the Sagami Trough is planned to be submitted. Japan Agency for Marine-Earth Science and Technology was conducted a seismic reflection survey in April, 2013 at the southward of the Sagami Trough on the Philippine Sea Plate. Although a planned seismic line had been 270-km length at the 50-km southward of the trough in WNW-ESE direction, acquired data is limited in half of the planned line for rough weather from volcanic front to landward slope of the trench axis, showing sediment distribution and basement morphology. Sediments can be divided in three units. Basement morphology is rugged as basement highs reaching seafloor at the volcanic front and rising at the Frontal Arc and Outer Arc High of the former arc in the Izu-Ogasawara area, and as depressions as 4-km from seafloor filled by thick sediments. The sediments and basement are comparable to those in the vicinity of the Sagami Trough using conducted seismic profiles at the cross points. In this presentation, we will show the seismic profiles around the Sagami Trough, deduce the ages and materials of sediments and basements comparing previous results, infer the subduction inputs of the Sagami Trough, and discuss the seismogenesis around the Sagami Trough.

Keywords: MCS survey, Sagami Trough, subduction input

Japan Geoscience Union Meeting 2014
(28 April - 02 May 2014 at Pacifico YOKOHAMA, Kanagawa, Japan)

MIS32-P06 Room:Poster Time:April 30 18:15-19:30

Core quality evaluation with X-CT data

KUBO, Yusuke[1*] ; AOIKE, Kan[1]

[1]CDEX, JAMSTEC

Xray Computed Tomography (X-CT) is a powerful tool for an observation of internal structures and conditions of core samples. In the laboratory of D/V Chikyu, X-CT data has been used in initial evaluations of sample lithology, structure and physical properties such as density, before splitting the sample. In addition, the non-destructive measurement is particularly useful to evaluate the sample quality, based on which we can optimize the sampling and sample distribution plan. For example, intact pieces are passed to high-priority and contamination-sensitive analyses after observation of X-CT image. However, the evaluation of core quality has been mostly based on visual observation. While visual observation is good for quick evaluation, it sometimes lacked consistency and detailed survey.

In this study we propose a quantitative way to evaluate the core quality from X-CT data. The core quality index (CQI) is calculated as the ratio of area with CT value higher than a threshold value in a sliced image of core sample. The threshold value is determined from the representative CT value in the core section and varies depending on lithology. The data in the region of interest, which is 15 cm^2 of central part of core sample, is binarized with the threshold value to provide normalized index through all sections. The plot of CQI reveals the position and degree of damages inside a core sample.

The method is applied to X-CT data of a total of 176 sections from IODP Exp 337. The results show that CQI profile clearly differentiates intact part and disturbed part of core section. Comparison with other core quality indicators in pore water chemistry and chemical tracer experiments suggests that CQI can be used to identify intervals suitable for contamination-free sampling.

The figure shows an example of binarized X-CT slice of a core sample. Red in the central part (purple) shows porous part in the core sample.

Keywords: Chikyu, IODP, X-CT, core sample

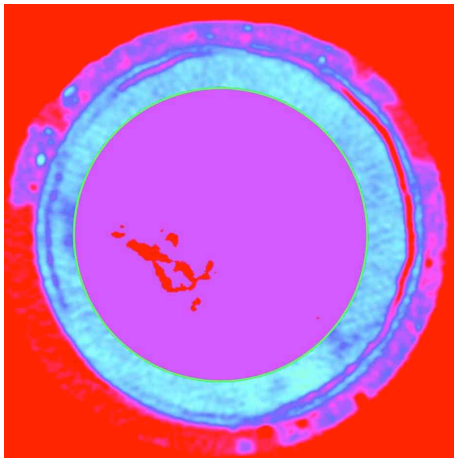

Japan Geoscience Union Meeting 2014
(28 April - 02 May 2014 at Pacifico YOKOHAMA, Kanagawa, Japan)

MIS33-01 Room:501 Time:April 30 09:00-09:15

Comparison of seabeds at <2000 m in water depth off Miyagi before and after the 2011 Tohoku-Oki earthquake

WADA, Ayaka[1] ; KAWAMURA, Kiichiro[1*] ; ROMER, Miriam[2] ; STRASSER, Michael[3] ; FINK, Hiske[2] ; ARAI, Kazuno[4] ; HINO, Ryota[5] ; ITO, Yoshihiro[6] ; FUJIKURA, Katsunori[7]

[1]Yamaguchi University, [2]University of Bremen, [3]ETH Zurich, [4]Chiba University, [5]Tohoku University, [6]Kyoto University, [7]JAMSTEC

The 2011 Tohoku-Oki earthquake of Mw 9.0 occurred on 11 March 2011. This earthquake excited large tsunamis, which were generated turbidity current as a tsunamigenic turbidity current (Arai et al., 2013). We do not know well how such turbidity currents will record in sediments in the future.

We investigated the impact of the tsunamigenic turbidity currents by seabed observations. Additionally, we discussed how the tsunami event will be preserved in deep-sea sediments.

We observed the video data of six dive surveys. The two dive surveys of 3K#483 and 2K#1220 have done on 5 September 2000 and on 19 September 2000 during the cruise NT00-09 by R/V NATSUSHIMA. A deep-sea camera survey of YKDT#100 has done on 21 June 2011 during the cruise YK11E-04 Leg 2 using R/V YOKOSUKA. The site P08 was dived on 25 September 2011 during the cruise by HAKUYO3000. OFOS-1 and -2 were dived on 18 March 2012 during the cruise SO219A by R/V SONNE. In addition, seabed sectional view ware made by PARASOUND in the cruise SO219A.

We observed the change of seabed before and after the Tohoku-Oki earthquake. We could see various alive benthic animals (e.g. sea anemones, sea pens and star fishes) on the muddy mounded seabed. There are no strong flow signals being a strong bottom current from the video observations. We found many dead bodies of benthic animals which were covered with bacterial mats by YKDT#100 and P08 videos. The size of bacterial mats was about 1 m in diameter. After one year from the earthquake, the size of bacterial mats had become small about 10 cm in the OFOS video data. Therefore, the bacterial mats ware made after earthquake by seabed disturbance, but bacterial mats would not record in sediment.

On the other hand, we found lines of evidence on the turbidity current which have the potential of preservation in sediments. We observed the bio-fragments scattered on seabed by YKDT#100 and OFOS videos. We measured these direction and we found majority of these faced the SW-NE. Thus, these indicate the direction of the strong flow (e.g. turbidity current) in recent. Our results support the direction of the turbidity current indicated by Arai et al.,(2013). The benthic animals as bio-fragments would record in sediments and would become evidence of tsunami/earthquake events.

Keywords: R/V SONNE, Tsunami deposit, biofragment, paleocurrent

Japan Geoscience Union Meeting 2014
(28 April - 02 May 2014 at Pacifico YOKOHAMA, Kanagawa, Japan)

MIS33-02 Room:501 Time:April 30 09:15-09:30

Evidence of Tohoku-oki earthquake in the deep sea sediment

KANAMATSU, Toshiya[1*] ; IKEHARA, Ken[2] ; USAMI, Kazuko[2]

[1]Japan Agency for Marine-Earth Science and Technology, [2]Institute of Geology and Geoinformation, National Institute of Advanced Industrial Science and Techn

A study on differences in bathymetric data between before and after 2011 Tohoku-Oki earthquake revealed a large coseismic displacement of the overriding plate, and a seafloor elevation in the Japan Trench axis (e.g. Fujiwara et al. 2012). Detail sub-seafloor structures around the axis obtained after the earthquake image offscraped trench and incoming sediments due to compression during coseismic slip in the plate interface close to the trench (Kodaira et al. 2012, Nakamura et al. 2013). Strasser et al. 2013 suggests that a large scale slump of the wedge toe significantly impacted the geometry and evolution of the plate boundary in the axis of Japan Trench based on data from sediment samples. Kawamura et al., 2012 and Tsuji et al., 2013 also point out that the coseismic displacement of the wedge. These recent researches indicat that remarkable co-seismic deformation and displacement occurred in the toe of slope near to the trench in the case of 2011 Tohoku earthquake. Thus geological evidences for the phenomenon should be recorded in the sediment around the trench axis. We have conducted research cruises to collect surface sediments in order to seek such features as evidences for 2011 and past Tohoku earthquakes. Piston cores were collected from the trench axis and the landward slope in Japan Trench by R/V ”Mirai” and R/V ”Sonne” in 2012. Intervals in the upper several ten-cm consisting of turbidite units which have been formed just after the earthquake were recovered from the trench axis. This discovery demonstrated that the trench axis is one of the feasible areas to reconstruct Tohoku earthquake history. As ensuring, the older turbidites were also recovered in the area. Contrarily debrite and inclined strata were recovered from the surface of landward slope near to the trench. Those lithologies could be evidences for the wedge displacement or slope failure induced by 2011 or past earthquakes. In the landward slope of Japan Trench, the elongated terrace developed in water depth of 4,000-6,000m is another interesting area to seek evidence related to Tohoku earthquakes. We collected sediment samples from the depth widely using R/V ”Natsushima”. Frequent thin turbidite occurrences were identified in the several cores. Ductile deformations, probably induced by slope failures, recognized in three cores. Those features could be regarded as evidences of past-other Tohoku earthquakes.Thus it is worth researching farther in these deep-sea areas of Japan trench to document the Tohoku earthquake record. Documentation spatiotemporal distribution of such geological evidences will improve our understanding of Tohoku earthquakes.

Keywords: 2011 Tohoku-oki earthquake, Japan Trench, deep sea sediment

Japan Geoscience Union Meeting 2014
(28 April - 02 May 2014 at Pacifico YOKOHAMA, Kanagawa, Japan)

MIS33-03 Room:501 Time:April 30 09:30-09:45

Turbidites collected from the Japan Trench inner slope, during the NT13-19 cruise

USAMI, Kazuko[1*] ; IKEHARA, Ken[1] ; MCHUGH, Cecilia[2] ; KANAMATSU, Toshiya[3]

[1]Geological Survey of Japan, AIST, [2]JAMSTEC / Queens College, C.U.N.Y., [3]JAMSTEC

To understand the recurrence of large earthquakes along the Japan Trench, we collected 24 sediment cores from the Japan Trench inner slope, 37.5-40 N, 143.5-144.16 E, water depth 4000-6000 m, during the NT13-19 cruise. Many deep-sea turbidites were intercalated in the sediment cores. We examined the interval and structures of the turbidites using soft-X radiographs. In general, number of the turbidites in a core is high in the southern part off Sendai, but is low in the northern part off Miyako. Meanwhile, intercalated tephras such as Haruna-Ikaho (Hr-FP), Towada-Chuseri (To-Cu) and Towada-a (To-a) were identified in the 13 cores. Based on the eruption ages of the tephras, we estimated the averaged recurrence intervals of 100-500 years in average in almost cores. But there are cores that display different intervals over 1500-2000 years.

Keywords: earthquake, Japan Trench, turbidite, tephra

Japan Geoscience Union Meeting 2014
(28 April - 02 May 2014 at Pacifico YOKOHAMA, Kanagawa, Japan)

MIS33-04 Room:501 Time:April 30 09:45-10:00

Tsunami-generated turbidite as a proxy for large-scale earthquakes

NARUSE, Hajime[1] ; ARAI, Kazuno[2*]

[1]Graduate School of Science, Kyoto University, [2]Graduate School of Science, Chiba University

We summarize the researches of tsunami-generated turbidites, and examine their possibility to be a proxy for ancient earthquakes. A tsunami-generated turbidity current is a kind of seismically triggered turbidites. Arai et al. (2013) reported the first real-time record of a turbidity current associated with a great tsunami. It was recognized after the Mw 9.0, 2011 Tohoku-Oki event offshore Japan. After the 2011 Tohoku-Oki earthquake and tsunami. An anomalous event on the seafloor consistent with a turbidity current was recorded by ocean-bottom pressure recorders and seismometers deployed off Sendai, Japan. Freshly emplaced turbidites were collected from a wide area of seafloor off the Tohoku coastal region. These measurements and sedimentary records to determine conditions of the modern tsunamigenic turbidity current. It can be anticipated that this discovery is a starting point for more detailed characterization of modern tsunamigenic turbidites, and for the identification of tsunamigenic turbidites in geologic records.

Keywords: Earthquake, turbidite, sediment gravity flow, tsunami

Japan Geoscience Union Meeting 2014
(28 April - 02 May 2014 at Pacifico YOKOHAMA, Kanagawa, Japan)

MIS33-05 Room:501 Time:April 30 10:00-10:15

An abrupt seafloor water-temperature increase in the epicentral region of the 2011 Tohoku earthquake

INAZU, Daisuke[1*] ; ITO, Yoshihiro[2] ; SAFFER, Demian[3] ; HINO, Ryota[4]

[1]NIED, [2]Kyoto University, [3]The Pennsylvania State University, [4]Tohoku University

We report an abrupt seafloor water-temperature increase observed just after the 2011 Mw9 Tohoku earthquake. Ocean bottom pressure variations during the Tohoku earthquake were observed by a deployment of pressure gauges at eight stations in the epicentral region (Ito et al. 2013 Tectonophys.). The temperature sensors for pressure sensor compensation built into the pressure gauges recorded seawater temperature variations that are presented here.

The temperature data documented the following. Abrupt temperature increases were evident at two stations (TJT1 and GJT3: ocean depth of 3000-6000 m) where maximum slip occurred during the Tohoku earthquake. The temperature increases started less than 10 hours after the earthquake occurrence, reaching up to 0.1 ℃ above background temperature, and last for a few weeks. Comparable temperature increases were not evident at other stations farther landward, where the ocean depth is less than 2000 m. Prior to the Tohoku earthquake, there were no temperature changes related to other earthquakes at any of the stations. Thus the observed temperature increases are probably associated with the Tohoku earthquake, particularly in the region of maximum coseismic slip.

Geochemical analyses of the seawater sampled near the seafloor suggest that formation pore water was released in the region of maximum coseismic slip following the earthquake. The pore water was thought to originate at about 1 km below seafloor, based on analysis of methane (Kawagucci et al. 2012 Sci. Rep.), with a contribution from the mantle at deeper than 15 km below seafloor as suggested by helium isotope analysis (Sano et al. 2014 Nat. Comm.).

Here we suppose that the observed temperature anomaly is related to pore water release from greater than 1-km depth. In order to explain the timing of the temperature anomalies, required flow velocity of the released water is $>10^{-1}$ m/s. This is several orders of magnitude more than typical velocities of background fluid flow driven by dewatering of subduction zone sediments (10^{-9} m/s) (e.g., Screaton and Saffer 2005 EPSL). The high velocities ($>10^{-1}$ m/s) most likely reflect fluid flow due to enhanced permeability along fractures and fissures (Tsuji et al. 2013 EPSL) extending to depths of kilometers or more below seafloor, generated by the greatest slip of the Tohoku earthquake.

Keywords: Seafloor water temperature, 2011 Tohoku earthquake

Japan Geoscience Union Meeting 2014
(28 April - 02 May 2014 at Pacifico YOKOHAMA, Kanagawa, Japan)

MIS33-06 Room:501 Time:April 30 10:15-10:30

A sedimentological and paleomagnetic study of deep-sea sediments collected from the Sagami trough

NAKAJIMA, Arata[1*] ; KAWAMURA, Kiichiro[1] ; KANAMATSU, Toshiya[2] ; SAITO, Saneatsu[2] ; MURAYAMA, Masafumi[3]

[1]Yamaguchi University, [2]JAMSTEC, [3]Kochi University

Introduction

M7-8 class earthquakes occur repeatedly in the Kanto region, central Japan. We have studied earthquake history around the Kanto region using mainly distribution and geologic age of marine terraces so far (Shishikura, 2012). In contrast to the terrestrial study, we have discussed to identify any seismogenic events from deep-sea sediments (Ikehara, 2001). Recently, Noda et al. (2008) suggested that we could exclude mostly flood deposits by choosing the sampling site carefully. Thus, paleoseismology was developing by these previous studies.

In this study, we collected deep-sea sediments from west Sagami Bay. We described the sediments sedimentologically and paleomagnetically in detail. We discussed a sedimentary process and challenged to extract the earthquake history in the region from these data.

Studied specimens

We collected two cores from a gentle submarine slope (KT-12-35 PC01; 35:04.00N, 139:12.99E, water depth 991 m and KT-12-35 PC03; 34:58.30N,139:13.40E, water depth 1,235 m) using a piston corer during the cruise KT-12-35 of Tansei-maru in December 2012. Ikehara et al (2012) reported probable seismogenic turbidites nearby these coring sites.

Results and discussion

We described and measured the two cores PC01 and PC03 as follows.

1.Sample description using microscope: PC01 and PC03 were mainly olive black hemipelagic sediments including foraminifers and diatoms. Both core were observed several volcanic ash layers and sand layers.

2.X-ray CT analysis: Many sandy clay layers in the hemipelagic sediment layers were confirmed by the difference of CT value. These sandy layers would be event layers (e.g. seismogenic and/or flood events).

3.Physical properties: The porosities in PC01 and PC03 decrease from 72% to 58% and from 76% to 65% with increasing burial depth, respectively. The pososity decreases should result from burial consolidation.

4.Magnetic properties: We analyzed simply a paleocurrent direction using anisotropy of magnetic susceptibility and paleomagnetism. The paleocurrents were roughly judged from E to W in PC01 and PC03 throughout the cores.

5.Volcanic glass: Index properties of volcanic glasses was measured at two horizons at 11 cm and 95 cm below seafloor (hereafter cm-bsf) in PC03. We could identify the 1707 Fuji Houei eruption at 11 cm-bsf and the 838 Tentsujima Tenjyouzan eruption at 95 cm-bsf.

6.C14 dating: We measured C14 for age determination at two horizons at 136 cm-bsf in PC01 and 172 cm-bsf in PC03. We collected 30820±210BP and 2850±30BP, respectively. We could calculate the average sedimentation rates as 64 cm/kyr in PC03 and 4 cm/kyr in PC01, even though we could identify the geologic age only at one horizon in PC01.

Based on these results, we discuss the recurrence intervals of the event layers and its depositional processes.

Keywords: Sagami trough, Seismic deposit, XrayCT, Volcanic glass, C14 dating, Magnetic properties

Japan Geoscience Union Meeting 2014
(28 April - 02 May 2014 at Pacifico YOKOHAMA, Kanagawa, Japan)

MIS33-07 Room:501 Time:April 30 10:30-10:45

DEVELOPMENT OF MULTI-PARAMETER BOREHOLE SYSTEM TO EVALUATE THE EXPECTED LARGE EARTHQUAKE ?N THE MARMARA SEA, TURKEY

OZEL, Oguz[1*] ; GURALP, Cansun[2] ; PAROLAI, Stefano[3] ; BOUCHON, Michel[4] ; KARABULUT, Hayrullah[5] ; AKTAR, Mustafa[5] ; MERAL OZEL, Nurcan[5]

[1]Istanbul University-Turkey, [2]Guralp Systems-UK, [3]Geoforsungszentrum-Germany, [4]CNRS-France, [5]Kandilli Observ. & Earthq. Res. Inst.-Turkey

The Istanbul-Marmara region of northwestern Turkey with a population of more than 15 million faces a high probability of being exposed to an hazardous earthquake. The 1999 Izmit earthquake in Turkey is one of the best recorded in the world. For the first time, researchers from CNRS and Kandilli Observatory (Istanbul) observed that the earthquake was preceded by a preparatory phase that lasted 44 minutes before the rupture of the fault. This phase, which was characterized by a distinctive seismic signal, corresponds to slow slip at depth along the fault. Detecting it in other earthquakes might make it possible to predict some types of earthquakes several tens of minutes before fault rupture.

In an attempt to understand where and when large earthquakes will occur, and the physics of the source process prior to large earthquakes, we proposed to install multi-parameter borehole instruments in the western part of Marmara Sea in the frame of an EU project called MARSITE. This system and surrounding small-aperture surface array is planned to capable of recording small deformations and tiny seismic signals near the active seismic zone of the North Anatolian Fault passing through the Marmara Sea, which should enable us to address these issues.

The objective is to design and build a multi-parameter borehole system for observing slow deformation, low-frequency noise or tremors, and high frequency signals near the epicentral area of the expected Marmara earthquake. Furthermore, it is also aimed to identify the presence of repeating earthquakes and rupture nucleation, to measure continuously the evolution of the state of stress and stress transfer from east to west with high resolution data, and to estimate the near-surface geology effects masking the source related information. The proposed location of the borehole system is right on the Ganos Fault and in a low ambient noise environment in Gazikoy in the western end of the North Anatolian Fault in the Marmara Sea, where the Ganos Fault goes into the Marmara Sea. The proposed instrumentation will be consisted of broadband seismometer with very wide dynamic range, strainmeter, tiltmeter, hydrostatic pressuremeter and thermometer. These instruments will be installed in 150m deep borehole. Additionally, a surface microearthquake observation array, consisting of 8-10 seismometers around the borehole will be established to obtain continuous high resolution locations of micro-seismicity and to better understand the existing seismically active structures and their roles in local tectonic settings.

Keywords: Borehole system, repeating earthquakes, slow motion, microearthquake activity, rupture mucleation, MARSITE

Japan Geoscience Union Meeting 2014
(28 April - 02 May 2014 at Pacifico YOKOHAMA, Kanagawa, Japan)

MIS33-P01 Room:Poster Time:April 30 18:15-19:30

Seabed topography and geologic structure of 2000˜3500 m in water depth, off Miyagi prefecture

HAMADA, Mari[1] ; KAWAMURA, Kiichiro[1*] ; NAKAMURA, Yasuyuki[2] ; KODAIRA, Shuichi[2]

[1]Yamaguchi University, [2]JAMSTEC

Introduction

After three days from the 2011 Tohoku-oki earthquake, an emergency seismic survey was carried out in the Japan trench area, off Iwate and Miyagi. By this surveys, we collected seismic reflection images along 16 survey lines from fore-arc basin area at 2500 - 3500 m in water depth to trench floor area at ˜7000 m in water depth. We analyzed in detal geologic architecture of the fore-arc basin mainly in the 14 seismic reflection images across the Japan trench.

Research Overview

The fore-arc basin of the Japan trench consists of two sedimentary units; Paleogene and Neogene. At the base of the Paleogene unit, an Oligocene unconformity overlies Cretaceous rocks. Because of the complexity of the geologic architecture in the Japan trench, it could not easily decipher the spatial distribution of the sedimentary units.

Results and discussion

Based on the observations of 14 seismic reflection images, we noticed same structural features in the fore-arc basin region (e.g. thickness of seismic units, active faults, deformation structures, topography and so on), so that we divided the region into 5 areas as follows.

Area 1:

It is characterized by a thick seismic unit (probably Paleogene unit) above the Oligocene unconformity. The sides of this area are bounded by faults or folds. These features can see about 100 km from north to south. This unit thickening might be related to wedge extensional processes as shown in Tsuji et al. (2013).

Area 2:

The feature of the Area 2 is similar to that of Area 1. But we found two different points from the Area 1; 1) the continuity of the Area 2 is about 50 km from north to south. This is a half continuity of the Area 1. 2) the Area 2 is located further east (sea) side from the Area 1.

Area 3:

It is characterized by erosive features. This area is located in north of Area 2, but there is not features associated with Area 2. This erosive feature might be related to long-term erosion by subduction erosion processes as shown in von Huene et al. (1989).

Area 4:

This area is characterized by landward dipping Neogene sedimentary units. The depositional centers were shifted from sea (east) side to land (west) side. This shift might be related to tectonic erosion as shown in Arai et al. (2007).

Area 5:

This area is characterized by several active faults that extend and dislocate the seabed. This area is located relatively near the hypocenter of 2011 Tohoku-Oki earthquake, so that here might be active in recent.

Concluding remarks

In this analysis, we found five unique areas in the fore-arc basin region. These features would be a key to understanding for a further study associated with global and long-term tectonics in this region.

Keywords: Japan Trench, Seismic survey, Forearc Basin, Unconformity, 2011 Tohoku-Oki earthquake

Japan Geoscience Union Meeting 2014
(28 April - 02 May 2014 at Pacifico YOKOHAMA, Kanagawa, Japan)

MIS33-P02 Room:Poster Time:April 30 18:15-19:30

The development of the self pop-up ocean bottom pressure gauge (OBP) with precision thermometers attached

SUZUKI, Syuichi[1*] ; ITO, Yoshihiro[2] ; HINO, Ryota[3] ; INAZU, Daisuke[4] ; OSADA, Yukihito[3]

[1]Graduate School of Science, Tohoku University, [2]Disaster Prevention Research Institute, Kyoto University, [3]International Research Institute of Disaster Science, Tohoku University, [4]National Research Institute for Earth Science and Disaster Prevention

We have installed autonomous ocean bottom pressure recoreders (OBPRs) off Miyagi and off Nemuro to observe seafloor vertical displacements in response to large earthquakes and aseismic slip. Most notably, an uplift of 5 m due to the 2011 Tohoku-Oki earthquake (Ito et al., 2011) and transient crustal deformations accompanied by slow slip events that occurred before the earthquake (Ito et al., 2013) were measured by the OBPRs which had been installed off Miyagi since 2008. Recent our observations on seafloor show a seawater-temperature anomaly after the 2011 Tohoku-Oki earthquake (Arai et al., 2013.) Here we show our new OBPRs with precise thermometers to observe both of vertical displacement and temperature anomaly on seafloor.

We design the new OBPR with two precise thermometers. The two thermometers are exterior to our ordinal OBPR. A quartz crystal pressure sensor within the ordinal OBPR is firstly equipped with a thermometer, which is used for temperature compensation of output frequency of quartz oscillator. This means the thermometer with the ordinal OBPR measures a temperature within the vessel of the pressure sensor. By the new attached two thermometers, a actual seawater-temperature are measured accurately.

The development of OBPs with precise thermometers attached enables us to record temperatures of seafloor and seawater along with OBP observations. We are planning to deploy these newly developed OBPs around Japan trench and east off North Island of New Zealand. Especially at the landward Japan Trench slope, increase in the amount of water discharge has been reported by the submarine observation after the 2011 Tohoku-Oki earthquake. Therefore, the installation of the new OBPs with thermometers around this area is expected to allow us to observe not only the seafloor vertical displacements accompanying the postseismic deformation but also the time variation of seafloor water temperature associated with the time variation of the amount of water discharge.

Keywords: Two precise thermometers, Sea-bottom water temperature, Ocean bottom pressure gauge

Japan Geoscience Union Meeting 2014
(28 April - 02 May 2014 at Pacifico YOKOHAMA, Kanagawa, Japan)

MIS34-01 Room:414 Time:May 2 14:15-14:30

Sources of freshwater to the Antarctic continental shelf -distributions and multi-decadal changes-

AOKI, Shigeru[1*]

[1]ILTS, Hokkaido University

The Antarctic continental shelf is the gateway to the global ocean from the Antarctic Ice Sheet, the largest freshwater reservoir on Earth surface. Discharge of the freshwater occurs as the processes such as basal melting of ice shelves and calving of icebergs. On the other hand, sea ice formation and melting on the shelf redistribute the freshwater, affecting the overturning circulations of oceans. These two processes of freshwater transport are closely related to the surrounding oceanic and atmospheric conditions, and therefore estimating their contributions and clarifying their relationships with underlying environments are necessary to quantify the overall impacts to the ocean and its temporal change.

From observed salinity and stable oxygen isotope ratio of sea water with a few assumptions applied, meteoric and sea ice fractions in sea water are estimated on the shelf and their geographical distributions are studied. Meteoric ice fraction is largest in the surface layer of West Antarctica, but the water column inventory is largest in the Ross Sea and surprisingly uniform around Antarctica. The column inventory of meteoric ice retains the broadly consistent signature of ice shelf basal melting, which is proposed by the recent studies, but its oceanic stock is rather homogenized due to the effects such as oceanic advection and basin-scale circulation. Sea ice fraction contributes large production in the areas of strong katabatic wind and shows negligible production/net melting in the West and central East Antarctica. The vigorous vertical mixing due to high production also distributes the meteoric fraction to a wider depth range.

Observed salinity trend suggests a possibility of temporal change in these freshwater transports. The salinity trend at the bottom of the shelf for the recent four decades reveals the salinification in the West Antarctica and freshening in the Ross Sea. Repeated observations on the shelf region off the Adélie Land Coast indicate freshening for the recent two decades. These signatures might be consistent with the accelerating discharge of the west Antarctic ice sheet. The signatures are consistent with the structure of the recent salinity change of Antarctic Bottom Water, suggesting the on-going impact of the Antarctic shelf on the global scale.

Japan Geoscience Union Meeting 2014
(28 April - 02 May 2014 at Pacifico YOKOHAMA, Kanagawa, Japan)

MIS34-02 Room:414 Time:May 2 14:30-14:45

The fourth Antarctic Bottom Water: Cape Darnley Bottom Water

OHSHIMA, Kay I.[1*] ; FUKAMACHI, Yasushi[1] ; WILLIAMS, Guy D.[2] ; NIHASHI, Sohey[3] ; TAMURA, Takeshi[4] ; KITADE, Yujiro[5] ; HIRANO, Daisuke[5] ; AOKI, Shigeru[1] ; WAKATSUCHI, Masaaki[1]

[1]Institute of Low Temperature Science, Hokkaido University, [2]Antarctic Climate and Ecosystem Cooperative Research Centre, University of Tasmania, Australia, [3]Tomakomai National College of Technology, [4]National Institute of Polar Research, [5]Tokyo University of Marine Science and Technology

Antarctic Bottom Water (AABW) is the cold, dense water that occupies the abyssal layer of the global ocean, accounting for 30-40 % of its mass (Johnson, 2008). The production of AABW is a key process in the global overturning circulation, representing a significant sink for heat and CO_2. It is currently recognized that AABW is formed in the Weddell Sea, the Ross Sea and off the Adelie Coast (Orsi et al., 1999). A fourth variety of AABW has been identified in the eastern sector of the Weddell-Enderby Basin (Meredith et al., 2000). However, its production has never been observed, nor its exact dense shelf water (DSW) source located. Recently, satellite-derived estimates of sea ice production suggest that the Cape Darnley Polynya (65-69E), located northwest of the Amery Ice Shelf, has the second highest ice production after the Ross Sea Polynya (Tamura et al., 2008). As such, this polynya is promoted as a strong candidate for DSW source of the AABW identified in the Weddell-Enderby Basin.

As part of the Japanese International Polar Year program, we conducted mooring observations in 2008-2009 offshore from the Cape Darnley Polynya, and revealed that the enhanced sea-ice production in this polynya is the missing source of the AABW (Ohshima et al., 2013). Moored instruments observed overflows of newly formed AABW, about 300 m thick and bottom-intensified, cascading down the canyons north of Cape Darnley. We propose to name this AABW Cape Darnley Bottom Water (CDBW). This result is novel because this AABW is produced purely from sea-ice production without the assistance of an ice shelf and/or large storage volume on the continental shelf, in contrast to the traditional paradigm. We therefore speculate that there could be further AABW-formation discoveries in similar polynyas, particularly those in East Antarctica.

We estimate that 0.3-0.7 Sv of DSW is transformed into CDBW, accounting for 6-13 % of the circumpolar total. The CDBW migrate westward, and increase its volume by gradual mixing with Circumpolar Deep Water, to ultimately constitute part of the AABW in the Weddell Sea (Atlantic sector) referred to as Weddell Sea Deep Water (WSDW). Production of WSDW originating from CDBW is estimated to be 0.65-1.5 Sv, which is about 13-30 % of the Atlantic AABW production. The WSDW is a major component of the AABW driving the lower limb of the meridional overturning circulation (MOC) of the Atlantic Sector. It has been reported that WSDW has been warming since the 1980s, with its volume possibly contracting (Purkey and Johnson, 2012), and that this could result in a weakening of the MOC. Additionally, sediment-core records taken around the CDP indirectly suggest that there has been millennium-scale variability in the local AABW production. It is vital that CDBW be incorporated into the global assessment of the MOC, a key element of the climate system. This will improve numerical simulations predicting its response to long-term climate change.

Keywords: Antarctic Bottom Water, coastal polynya, sea-ice production, dense shelf water, mooring, Cape Darnley

Japan Geoscience Union Meeting 2014
(28 April - 02 May 2014 at Pacifico YOKOHAMA, Kanagawa, Japan)

MIS34-03 Room:414 Time:May 2 14:45-15:00

Southern Ocean: the key factor of climate change

TAMURA, Takeshi[1*] ; SHIMADA, Keishi[2] ; MATSUMURA, Yoshimasa[3] ; KUSAHARA, Kazuya[3] ; SATO, Tatsuru[3] ; NOMURA, Daiki[3]

[1]National Institute of Polar Research, [2]Tokyo University of Marine Science and Technology, [3]Institute of Low Temperature Science

Ocean keeps a lot of heat, oxygen, CO2, and nutrients, and transports these to the world ocean by the global ocean circulation. Polar oceans having sea ice is ”Canary of Climate”, and are very sensitive to the climate change, e.g., the global warming. Antarctic Bottom Water (AABW) formed in the Southern Ocean is the main actor for these two mechanisms, however, it is still difficult to clarify the whole image of AABW only by the in-situ observation. Our purpose is the estimation of AABW formation, sinking process, and its spread in the bottom layer by the numerical modeling, by using the following three different methods; monitoring of sea ice production by the satellite remote sensing, high-resolution mapping of water temperature and salinity by in-situ observation, and numerical modeling by high-resolution model. This study is challenging to the final and most difficult blank area for the global climate system, and could contribute to the prediction of future climate change.

By our recent results, we got the following two progresses; (1) hemispheric-scale and long-term monitoring of sea ice production which directly links to the AABW formation becomes possible by the accumulation of satellite data and the development and improvement of the algorithms (Tamura et al., 2008) and (2) the result from the numerical modeling could compare to the in-situ results directly by the improvement of the numerical model (Matsumura and Hasumi, 2011). Under these our past works, it is possible to detect the actual dynamics of AABW by the following three independent methods; (a) monitoring of sea ice production by the satellite remote sensing, (b) high-resolution mapping of water temperature and salinity based on the in-situ observation data, and (c) high-resolution ocean modeling.

This study try to clarify the process of AABW formation quantitatively by using our dataset, algorithm, and numerical model. Specifically, our purpose is to estimate the AABW formation, its sinking process, and its expansion in the bottom layer. By using the latest in-situ and satellite data and numerical modeling, we try to clarify the following three questions; Where and how much does the dense water (the origin of the AABW) generate?, How much does the dense water mix with the surrounding water during the process of sinking around the shelf break?, and Where and how much does the AABW exist in the bottom of the world ocean and how does AABW spread?

In our talk, we will introduce updated results for our three ongoing projects; (I) mapping of sea ice production by the satellite remote sensing, (II) improvement of in-situ ocean observation data set, (III) ice shelf-sea ice-ocean coupled modeling, and (IV) micro-scale modeling.

Keywords: Southern Ocean, Antarctic Bottom Water, Sea Ice Production, In-situ Ocean Observation Data Set, Ice shelf - Sea ice - Ocean Interaction, Micro-scale Modeling

Japan Geoscience Union Meeting 2014
(28 April - 02 May 2014 at Pacifico YOKOHAMA, Kanagawa, Japan)

MIS34-04 Room:414 Time:May 2 15:00-15:15

High resolution Modeling on the Antarctic Bottom Water Formation

MATSUMURA, Yoshimasa[1*] ; OHSHIMA, Kay I.[1] ; HASUMI, Hiroyasu[2]

[1]Institute of Low Temperature Science, Hokkaido University, [2]Atmosphere and Ocean Research Institute, University of Tokyo

At the Antarctic continental margin, a great amount of dense water is created due to intense cooling and active sea ice formation. A part of this dense water descends down to the depth on the continental slope and provides a source of Antarctic Bottom Water (AABW), the densest water mass of the world ocean. This deep water formation drives and controls the global thermohaline circulation. Thus, quantitative understanding of where and how much such dense water descends to which depth with what water mass property is necessary for discussing the structure and intensity of the global thermohaline circulation and hence the earth's climate.

The AABW formation involves various processes with wider range of spatial and temporal scales, such as turbulent mixing induced by vertical velocity shear of descending dense water, influences of small scale submarine ridges and canyons of O(1) km, the surface buoyancy flux highly controlled by openings and closings of coastal polynyas. It is very difficult to perform a numerical simulation which resolves all of these processes because such simulation requires a huge amount of computational resource. Therefore, modeling studies on the AABW formation have been restricted to very idealized experimental settings. In particular, small scale processes such as turbulent mixing and vertical convection cannot represented by widely used general ocean circulation models with hydrostatic approximation, and a non-hydrostatic model is required. The numerical cost of non-hydrostatic models has been much greater than the hydrostatic models due to the cost of three-dimensional Poisson solver required to diagnose pressure field. To overcome this problem, we developed a non-hydrostatic ocean model with a very numerically-efficient and scalable Poisson solver using the multigirid method. The totla cost of our non-hydrostatic model stays less than twice of that of hydrostatic one even with huge amount of grid cells on massively parallel super computers. With using this newly developed model code and present days computational resources, multi-scale and multi-process modeling on the AABW formation, whose results are competent to be quantitatively compered with direct observations, is becoming a reality.

In our talk, we will introduce the outline of the newly developed numerical model and discuss the results of high-resolution AABW formation simulation with focusing on the effects of small scale topographic features and the turbulent entrainment processes induced by Kelvin-Helmholtz instability.

Keywords: Antarctic Bottom Water, non-hydrostatic model

Japan Geoscience Union Meeting 2014
(28 April - 02 May 2014 at Pacifico YOKOHAMA, Kanagawa, Japan)

MIS34-05 Room:414 Time:May 2 15:15-15:30

Modeling basal melting of Antarctic ice shelves

KUSAHARA, Kazuya[1*] ; HASUMMI, Hiroyasu[2]

[1]Institute of Low Temperature Science, Hokkaido University, [2]Atmosphere and Ocean Research Institute, the University of Tokyo

We have incorporated an ice shelf component into a sea ice-ocean coupled model. Basal melting of all Antarctic ice shelves are investigated with the circumpolar ice shelf-sea ice-ocean coupled model and we have estimated the total basal melting of 770-944 Gt/yr under present-day climate conditions. We present a comparison of the basal melting with previous observational and modeling estimates for each ice shelf in detail. It is found that heat sources for basal melting are largely different among the ice shelves. From a series of numerical experiments, sensitivities of the basal melting to surface air warming and to enhanced westerly winds over the Antarctic Circumpolar Current are investigated. In this model the total basal melting strongly depends on the surface air warming but is hardly affected by the change of westerly winds. The magnitude of the basal melting response to the warming varies widely from one ice shelf to another. The largest response is found at ice shelves in the Bellingshausen Sea, followed by those in the Eastern Weddell Sea and the Indian sector. These increases of basal melting are caused by increases of Circumpolar Deep Water and/or Antarctic Surface Water into ice shelf cavities. By contrast, basal melting of ice shelves in the Ross and Weddell Seas is insensitive to the surface air warming, because even in the warming experiments there is high sea ice production at the front of the ice shelves that keeps the water temperature to the surface freezing point. Weakening of the thermohaline circulation driven by Antarctic dense water formation under warming climate conditions is enhanced by basal melting of ice shelves.

Keywords: Antarctic ice shelves, Ice shelf-sea ice-ocean coupled model, Climate change

Japan Geoscience Union Meeting 2014
(28 April - 02 May 2014 at Pacifico YOKOHAMA, Kanagawa, Japan)

MIS34-06 Room:414 Time:May 2 15:30-15:45

A possible scenario of a drastic change in Antarctic coastal polynyas associated with ice sheet loss

NIHASHI, Sohey[1*] ; OHSHIMA, Kay I.[2] ; FRASER, Alexander D.[2]

[1]Department of Mechanical Engineering, Tomakomai National College of Technolog, [2]Institute of Low Temperature Science, Hokkaido University

Coastal polynyas, which are newly-forming sea-ice areas surrounded by pack ice, are formed by divergent ice motion driven by winds and/or ocean currents. Antarctic coastal polynyas are very high sea-ice production areas, because the heat insulation effect of sea ice is reduced significantly in the case of thin ice and accordingly huge heat loss to the atmosphere occurs. The resultant large amount of brine rejection leads to dense water formation. The dense water is a major source of Antarctic Bottom Water (AABW), which is a key player in the global climate system as a significant sink for heat and possibly carbon dioxide. Coastal polynyas are also sites of biological ”hot spots”, because of much-enhanced primary productivity.

Very recent studies have suggested that landfast sea ice, which is stationary sea ice attached to coastal features such as grounded icebergs and glacier tongues play an important role in the formation of some coastal polynyas by blocking ice advection to cause divergence. Key examples are the Cape Darnley Polynya and Mertz Polynya, both of which are major source areas of AABW.

In this study, we present the first combined circumpolar mapping of Antarctic coastal polynyas and fast ice, based on satellite observation to examine and quantify the linkage between coastal polynyas and fast ice. The map reveals that most coastal polynyas are formed on the western side of fast ice, suggesting that fast ice is an essential element for the formation of most coastal polynyas. Furthermore, we demonstrate that a drastic change in fast ice extent, which is particularly vulnerable to climate change, causes dramatic changes in associated polynyas and possibly AABW formation that can potentially contribute to further climate change.

The map presented in this study reveals that many of the coastal polynyas are formed along the East Antarctic coast where fast ice dominates. In the West Antarctic sector, it was suggested that intrusion of relatively warm Circumpolar Deep Water (CDW) onto the continental shelf causes the basal melting of ice shelves, possibly leading to acceleration of iceberg calving. Future climate change might precipitate a similar situation also in the East Antarctic sector where the location of CDW is relatively close to the continent. This possibly causes drastic changes of fast ice extent directly by melting, or indirectly by acceleration of iceberg calving. The drastic change in fast ice extent is expected to cause a dramatic change in the polynya area and sea-ice production. Further, a huge tabular iceberg can directly affect the polynya area by covering over as shown in the Ross Sea Polynyas area in 2000 and 2002; giant icebergs B-15 and C-19, calved from the Ross Ice Shelf, causing a significant reduction of the polynya area and sea-ice production. The results of this study suggest that fast ice and precise polynya processes should be addressed by next-generation models to reproduce the formation and variability of sea-ice production, dense water, and AABW properly. The mapping presented in this study would give the boundary/validation data of fast ice and sea-ice production for such models.

Keywords: Coastal polynya, Landfast sea ice, Antarctic Bottom Water, Iceberg, Ice sheet

Japan Geoscience Union Meeting 2014
(28 April - 02 May 2014 at Pacifico YOKOHAMA, Kanagawa, Japan)

MIS34-07 Room:414 Time:May 2 15:45-16:00

Wind-buoyancy dichotomy of the Southern Ocean carbon storage

ITO, Takamitsu[1*] ; TAKANO, Yohei[1] ; DEUTSCH, Curtis[2]

[1]School of Earth and Atmospheric Sciences, Georgia Institute of Technology, [2]School of Oceanography, University of Washington

We use a hierarchy of ocean climate-carbon models to investigate the future scenarios of the Southern Ocean carbon storage. Intensified and poleward-shifted westerly wind is hypothesized to enhance the upwelling of deep water and thermocline ventilation, which may be counteracted by the warming and freshening of the surface waters. We analyze the solubility and biological carbon pumps in the Southern Ocean as simulated by the Climate Model Inter-comparison Project phase 5 (CMIP-5) models. Model-model differences in the regional carbon storage are significant, O(100PgC), reflecting the organized changes in the two carbon pumps. To investigate the underlying mechanisms, we perform a suite of numerical sensitivity experiments using an ocean biogeochemistry model, where we purposefully impose (1) a global warming of sea surface temperature, (2) an intensification of freshwater forcing and (3) an increase in the Southern Ocean wind. Comparing the simulated patterns of carbon and oxygen changes, we find that the future increase in the biological carbon storage is likely due to the warming and freshening of the surface water dominating over the increasing wind.

Japan Geoscience Union Meeting 2014
(28 April - 02 May 2014 at Pacifico YOKOHAMA, Kanagawa, Japan)

MIS34-08 Room:414 Time:May 2 16:15-16:30

Incorporation of trace elements by diatom frustules: Significance of sediment-trap observation in the Southern Ocean

AKAGI, Tasuku[1*]

[1]Department of Earth and Planetary Sciences, Kyushu University

Diatoms contribute to more than half of the primary production of the oceans and it is well established that the formation and dissolution of diatom opal governs the distribution of dissolved silica in ocean columns (Nelson et al., 1995). Owing to the physical and chemical difficulty in isolating diatom opal from clays (Shemesh et al., 1988; Beck et al., 2002), however, it is difficult to clarify the trace composition of opal and thus to understand how diatoms contribute to the ocean circulation of trace elements. To date, no direct determination of rare earth elements (REEs) in diatoms has been made, and the role of diatoms has not been considered in the circulation of REEs (Sholkovitz et al., 1994; Oka et al., 2009; Siddall et al., 2008; Arsouze et al., 2009; Tachikawa et al., 2003).

The recent study, based on the dissolution kinetics of diatom silica frustules and the incorporation theory of silicic acid complexes, unveiled the composition of diatom frustules and identified the role of diatoms in the oceans (Akagi et al., 2011: Akagi, 2013). Diatoms incorporate metal-silicate complexes, silicate minerals as well as dissolved silica, to form their silica frustules. They recycle rare earth elements in the water column and disintegrate silicate minerals to change rare earth elements in refractory silicates to readily dissolvable forms. Diatom frustules are no longer regarded as pure hydrated silica, but impure matter able to transport some elements to the deep water. In the Bering Sea diatoms are found to incorporate island-arc matter with a high εNd value (Akagi et al., in press). Diatoms are important in distributing this high εNd signature to the ocean. This new insight may affect the interpretation of the Nd isotope variation recorded in ferromanganese crusts and foraminifera, which synchronizes with the glacial-interglacial periodical variations.

The new insight on diatom frustules has been established based mainly on sediment trap samples from the Bering Sea, a rather special sea, and ocean chemists tend to treat the insight a rather exceptional case. To generalize the insight, the same line of study should be extended to the sediment trap samples from more normal oceans such as the Southern Ocean.

To date, the possibility of silicic acid complex formation with metal ions has not been explored in the research on marine chemistry. Some elements classified as high field strength elements, HFSEs, are considered to be in the form of OH complex in seawater (Byrne, 2002). Most of elements classified to high field strength elements (HFSEs) have a valency of 3+ or 4+, and considering their thermodynamic properties, it was found that they are likely to have fairly high complex formation constants with silicic acid (Wang et al., 2009; Wang and Xu, 2001). Although silica has been long studied, this study is the first to discover the possibility that it is an important carrier of many elements in marine chemistry. To establish this view, again, studies using trap samples from the Southern Ocean would be highly requested.

Keywords: diatom frustules, trace elements, sediment trap, Southern Ocean

Japan Geoscience Union Meeting 2014
(28 April - 02 May 2014 at Pacifico YOKOHAMA, Kanagawa, Japan)

MIS34-09 Room:414 Time:May 2 16:30-16:45

Millennial-scale sea ice expansion in the glacial Southern Ocean

IKEHARA, Minoru[1*] ; KATSUKI, Kota[2] ; YAMANE, Masako[3] ; YOKOYAMA, Yusuke[4]

[1]Center for Advanced Marine Core Research, Kochi University, [2]Korea Institute of Geoscience and Mineral Resources (KIGAM), [3]JAMSTEC, [4]Atmosphere and Ocean Research Institute, University of Tokyo

The Southern Ocean has played an important role in the evolution of the global climate system. Area of sea ice shows a large seasonal variation in the Southern Ocean. Sea ice coverage on sea surface strongly affects the climate of the Southern Hemisphere through its impacts on the energy and gas budget, on the atmospheric circulation, on the hydrological cycle, and on the biological productivity. In this study, we have conducted fundamental analyses of ice-rafted debris (IRD) and diatom assemblage to reveal a rapid change of sea ice distribution in the glacial Southern Ocean. A piston core COR-1bPC was collected from the Conrad Rise, Indian sector of the Southern Ocean. Core site is located in the Polar Frontal Zone. Sediments are composed of diatom ooze. Age model of COR-1bPC was established by 14C dating and oxygen isotope stratigraphy of planktic foraminifera. Records of IRD concentration suggest millennial-scale pulses of IRD delivery during the last glacial period. The depositions of rock-fragment IRD excluding volcanic glass and pumice were associated with increasing of sea-ice diatoms, suggesting that the millennial-scale events of cooling and sea-ice expansion were occurred in the glacial South Indian Ocean. Similar episodic IRD depositions were identified in the South Atlantic during the last glacial period (Kanfoush et al., 2000). However, Nielsen et al. (2007) proposed that the tephra-rich grains in the South Atlantic IRD events (SA-IRD events) were mainly derived from South Sandwich Island volcanic arc, and concluded that sea-ice was the dominant ice rafting transport of such IRD grains. Preliminary provenance study of IRD grains suggest that the source of IRD in the South Indian Ocean was also volcanic arc in the South Atlantic, based on chemical compositions of rock-fragment IRD grains. Thus prominent IRD layers in the glacial South Indian Ocean correlate the SA-IRD event, suggesting episodes of sea ice expansion and cooling in the Atlantic and Indian sectors of the Southern Ocean.

Keywords: Southern Ocean, sea ice, millennial-scale, dust

Japan Geoscience Union Meeting 2014
(28 April - 02 May 2014 at Pacifico YOKOHAMA, Kanagawa, Japan)

MIS34-10 Room:414 Time:May 2 16:45-17:00

The ANDRILL Coulman High Project: Japanese contribution to the next phase of the Antarctic Geological Drilling

SUGANUMA, Yusuke[1*] ; IKEHARA, Minoru[2] ; SUTO, Itsuki[3] ; NOGI, Yoshifumi[1]

[1]National Institute of Polar Research, [2]Kochi Core Center, [3]Nagoya University

The Coulman High Project (CHP) proposes to recover two, high-quality, continuous drill-cores by drilling into Paleogene to lowest Miocene strata beneath the Ross Ice Shelf on the Coulman High in the Ross Embayment, Antarctica. The overarching objective is to establish a history of Cenozoic climate, tectonic and glacial changes in an ice-proximal setting to determine the sensitivity of Antarctica's ice sheets to a range of climatic and tectonic forcings. The sedimentary archives to be recovered in these two ˜800-m drill holes will offer a window into the range of environments, ecosystems and tectonic events in the Ross Sea region as it stepped from the warm, high-CO_2 Greenhouse world of the Eocene into the lower-CO_2 and highly variable Icehouse climate of the Oligocene and early Miocene. Antarctica was the keystone in this global climate transition and hosted the growth of ice sheets that started major cryosphere influence on global systems. The sensitivity of the climate system to elevated levels of greenhouse gases, the strength of polar amplification, and the behavior of the AIS in a world warmer than today remain fundamental questions to be addressed by CHP's integrated data-climate modeling studies. These seek to reduce the large uncertainties in predictions of future ice-sheet dynamics and sea level, in part by testing models with ancient scenarios under conditions warmer than today. To improve predictions of long-term future climate and sea level, it is imperative to obtain geological records of past polar climates and ice sheets from time intervals when atmospheric CO2 was two to four times higher than present levels. Modern observations and instrumental records provide details regarding current and short-term change, but high-fidelity climate records that span previous periods characterized by higher-than-present CO2 are only available from the Earth's geological records.

The Japanese ANDRILL consortium has decided to join the CHP. In this talk, we will introduce the scientific backgrounds, logistics, and schedule of this drilling project.

Japan Geoscience Union Meeting 2014
(28 April - 02 May 2014 at Pacifico YOKOHAMA, Kanagawa, Japan)

MIS35-01 Room:211 Time:May 2 11:00-11:15

Global circumstance on Geopark

WATANABE, Mahito[1*]

[1]Geological Survey of Japan,

The concrpt of Geopark is getting tto be known to wide range of people in many countries including Japan, such as reserchers, citizens and officials in both municipal and central governments. Every people has every point of view on Geoparks. This situation will contribute to improve the concept of Geopark through the discussion of wide range of people.

Global Geoparks Network (GGN) and UNESCO are discussing about the formal link between them in the worrking group composed of member country and GGN hosted by Ecololgy and Earth Science division of UNESCO. When the formalization of Geopark in UNESCO is achieved the present style of evaluating Geopark by GGN may change. As a UNESCO program, support to the least developing countries that try to establish Geopark is important and necessary. The discussion between member countries and GGN is good opportunity to review the activity of Geopark until present with the point of view from outside.

In Japan, on-site evaluation by scientists and manager within Geoparks as well as members of Japan Geopark Committee (JGC) has started in 2012. It was a start of the peer review process between geoparks. Discussion on the policy to evaluate geoparks and candidate areas is getting more active since last May when first meeting on the evaluation policy between evaluators from JGC and geoparks. In those discussion they actively discuss on where Japanese geoparks go and how to promote geopark activity.

The author will present the situation around Geopark as mentioned above and propose issues that should be discussed in the Japanese geopark community.

Keywords: Geopark, UNESCO, Global Geoparks Netork, Japanese Geoparks Network, Japan Geopark Committee

Japan Geoscience Union Meeting 2014
(28 April - 02 May 2014 at Pacifico YOKOHAMA, Kanagawa, Japan)

MIS35-02 Room:211 Time:May 2 11:15-11:30

Geoscience in Japanese Geoparks: Significance of Multidisciplinary and Interdisciplinary Geostories

OGATA, Takayuki[1*]

[1]Faculty of Education, University of the Ryukyus

Geoparks target all geoscientific disciplines consisting of space and planetary sciences, atmospheric and hydrospheric sciences, human geosciences, solid earth sciences, and biogeosciences, presented as the science sections in Japan Geoscience Union (JpGU). In JpGU, academic meetings of geoparks have been held in the public session since 2010 and the multidisciplinary and interdisciplinary session since 2012. However, geostories of Japanese Geoparks Network (JGN) are likely to incline toward specific themes based on URL information uploaded on the JGN official website. Especially, physical geography, such as climatology, hydrology and geomorphology, seems to be slighted in many Japanese geoparks. Physical geography, studying interaction among atmosphere, hydrosphere and geosphere in multidisciplinary and interdisciplinary scopes, should be given more consideration in all Japanese geoparks.

Keywords: geoparks, geostory, geoscience, physical geography, Japanese Geoparks Network, Japan Geoscience Union

Japan Geoscience Union Meeting 2014
(28 April - 02 May 2014 at Pacifico YOKOHAMA, Kanagawa, Japan)

MIS35-03 Room:211 Time:May 2 11:30-11:45

Provision of the Risk Information for Geopark guests in Japan

KOMORI, Jiro[1*]

[1]Teikyo Heisei University

The exact provision of risk information are important to geopark guests. The possible of the risk on the guests are consulted with the statistical police white paper of the mountain accident in Japan. The consideration shows that the major risk factors on geoparks are fall and slip drop, encounters with dangerous animal and rock fall. However, it is impossible to find an alart, description and discussion regarding their risks in published articles and books which specialized in the geopark activity. Furthermore, more than two thirds of the official geopark websites are devoid of the provision of the risk information. Even the remaining one-third place some simple or little paragraph of hazardous issue. For the safety administration with the advertising of attractiveness of geopark, effective provision through the official websites and printed materials are required in the future.

Keywords: geo-site, geo-tour, alpine accident, alert, accountability, official website

Japan Geoscience Union Meeting 2014
(28 April - 02 May 2014 at Pacifico YOKOHAMA, Kanagawa, Japan)

MIS35-04 Room:211 Time:May 2 11:45-12:00

Democratic governance of the Japanese geopark movement

MOKUDAI, Kuniyasu[1*]

[1]Pro Natura Foundation Japan

Japanese geopark movements needs separation of powers. I would like to propose a model for the governance of a Japanese geopark movement.

Keywords: Japanese Geoparks Network, Japan Geopark Committee, academic society, science communication, bottom-up

Japan Geoscience Union Meeting 2014
(28 April - 02 May 2014 at Pacifico YOKOHAMA, Kanagawa, Japan)

MIS35-05 Room:211 Time:May 2 12:00-12:15

Program of Treasure Stones : Making an original rock specimen using a virtual geotour -

OHNO, Marekazu[1*]

[1]Unzen Volcanic Area Geopark Promotion Office

We developed a making a rock specimen combined technique of a virtual geotour. To practice this program, a presentation file explaining highlights of geosites, rock samples and an original sheet which put on rock samples. To finish the program within 30 minutes, we limited 5 geosites in explanation and number of rock samples was 10. We carried out this program at Science Agora, which is a big scientific festival holding at Nihon Kagaku Mirai Hall in recent 2 years.

Participants of the program was mainly school students. They selected their favorite stone samples put them on the original sheet with a bond. In the virtual geotour, we explain not only rocks and landscapes but also relationship rock and people, histories of geosites and local foods using local special products. In 2012, we carried the program out with Shimonita Geopark and 151 participated (Sekiya, 2013). In 2013, 129 persons participated the program nevertheless a number of participates was limited. This program was almost popular with participants and received the Science Agora Award in 2012. Furthermore, this program became the fifth place in all programs by a guest popularity vote in 2013.

This program can be carried out regardless of a place, if machine parts and a place are set. And because people participating in this program have many families, various age groups can publicize the highlight of the Geopark. If participates get interests for the geopark, it is expected the increase of tourists of geopark area. In 2014, we hope some of geoparks join the program in Science Agora.

Keywords: Unzen Volcanic Area Global Geopark, virtual geotour, rock specimen, Science Agora

Japan Geoscience Union Meeting 2014
(28 April - 02 May 2014 at Pacifico YOKOHAMA, Kanagawa, Japan)

MIS35-06 Room:211 Time:May 2 12:15-12:30

Development of the textile with a geological map motif-To carry back geo-stories from geopark or natural history museum

SAITO, Makoto[1*]

[1]Geological Survey of Japan, AIST

The textiles with the Seamless Digital Geological Map of Japan (1:200,000) motif were launched September in 2013. These textiles were developed under the two basic concepts such as making a superior textile by using the geological map as a design of the earth, and the other is making the product which the visitors can carry back a geological story home from natural history museum or geopark. To achieve these concepts, it was important that a designer cooperated with a geologist.

The textiles were developed with Nikko area of the Seamless Digital Geological Map of Japan (1:200,000) motif. The designer changed the color of each legend of the geological map on Geographic Information System (GIS) software and printed it on cloth. The products contained a handkerchief, a porch, and a mini-tote bag with purplish, greenish and pinkish colors each. Because the cloth for product is clipped out from the large cloth which a geological map was printed on, there are 10 areas of porch or 3 areas of mini-tote bag from one printed cloth. As a result, we made the many kinds of textiles such as 3 kinds of handkerchiefs, 30 kinds of porches and 9 kinds of mini-tote bags.

Since the Seamless Digital Geological Map of Japan (1:200,000) is a digital geological map made with a uniform legend throughout Japan, anyone can cut out any local geological map from it. Therefore, it is possible to make the product of the different design every area. If these textiles are made in each geopark, the visitors can carry back the textile with special stories of the geopark.

It is easy to make the T-shirts which a geological map was printed on now. However, it is difficult to make an attractive commercial product, and only an attractive product in cooperation with a designer increases the number of customers. As a result, the product with the geologic map increases the number of people who are interested in geology.

As we push forward a plan to make a product with the geological map of another area motif now, the new products are released soon.

Keywords: textile, geological map, geopark, natural history museum, GIS, geographical Information system

Japan Geoscience Union Meeting 2014
(28 April - 02 May 2014 at Pacifico YOKOHAMA, Kanagawa, Japan)

MIS35-07 Room:211 Time:May 2 12:30-12:45

The accretionary prism experiment for geoparks using powdered sugar, cocoa, and a cooking paper

HAYASHI, Shintaro[1*]

[1]Fac. of Edu.and Human Studies, Akita Univ.

The analog experiment for understanding an accretionary prism was developed. The experiment is developed for children, students, and the tourists of geoparks. The experiment is simple and is using only familiar materials, such as powdered sugar, cocoa, and a kitchen paper.

Accretionary prism is usual in the Japanese geoparks. But, it is difficult to explain the mechanism of accretion to a child and a student, and the tourist of a geopark.

The accretionary prism experiment proposed until now had a thing adapting a sand box experiment (2004 besides Yamada, 2006, and Kaneda), and flour fault experiment (Okamoto, 1999, 2000).

<The method of an experiment>

Ingredients: powdered sugar, raw cocoa, creep, a cooking paper, a tea strainer, a spoon, a paper cup, the lap for kitchens, papier-mache.

Directions:

1. Papier-mache is wrapped in a lap to make continents.
2. Cut cooking paper into about 40 cm.
3. Build the layer of cocoa (the thickness is around 2mm) on an cooking paper using a tea strainer.
4. Sprinkle powdered sugar with a tea strainer on the layer of cocoa. The thickness is around 2 mm.
5. Wrapped papier-mache ”continent” is set at the end of a cooking paper.
6. Sprinkle milk over the continent and continent side of the layer of cocoa and powdered sugar.
7. A cooking paper is pulled.
8. Cocoa and powdered sugar are added to a continent and duplex structure is formed.
9. Put cocoa, powdered sugar, and milk into a paper cup collectively, and pour out and process hot water to make cocoa drink.

Keywords: geopark, accretionary prism, analog experiment, kitchen experiment

Japan Geoscience Union Meeting 2014
(28 April - 02 May 2014 at Pacifico YOKOHAMA, Kanagawa, Japan)

MIS35-08 Room:211 Time:May 2 14:15-14:30

Approach of Educational Activities in Hakusan Tedorigawa Geopark

MOCHIDA, Shuichi[1*] ; HIROSE, Osamu[1] ; HIBINO, Tsuyoshi[1]

[1]Hakusan Tedorigawa Geopark Promotion Council

The Hakusan Tedorigawa Geopark which was certified as a Japanese geopark in 2011 sets the theme ”the journey of water” (water circulation seeing the Tedorigawa River) which is generally easy to understand. The geopark highlights the sites related to earth sciences, nature, people’s lives and culture such as fossils, debris flow, an alluvial fan, brewing industry and ”haiku” (Japanese poetry).

We have been utilizing these sites for children’s education since the beginning, and promoting the activities in school education to popularize the geopark to children. Our aim is also on sustainable local activities.

Although it is said that teachers which don’t have the know-how to teach children in the fields have been increasing, the new educational government guidelines given notice in March 2008, show that teachers need to teach children in the nature and daily lives. The activities of the geopark correspond with the guidelines, and it seems that we need to assist the teachers who have less time to study the new course. Study Supporters, who are retired science teachers, have been supporting teachers in the geopark. We aim to teach children in the fields only by in-service teachers.

Keywords: Hakusan Tedorigawa Geopark, educational activity, school education

Japan Geoscience Union Meeting 2014
(28 April - 02 May 2014 at Pacifico YOKOHAMA, Kanagawa, Japan)

MIS35-09 Room:211 Time:May 2 14:30-14:45

Introduction of teaching and materials the theme of Geo, and Disaster awareness of high school students in Shizuoka

KAZUHIDE, Tsuda[1*] ; MURAKOSHI, Shin[2]

[1]NPO Whole Earth Institute, [2]Faculty of Education, Shizuoka University

[Introduction]

Science and Environmental Education Project (SEEP) , such as researchers, nature guide school teachers work together , we have developed educational content on the theme of natural science (Tsuda, et al. , 2013) . Developing Model class and geoscience materials 12 types aim it at the Izu Peninsula Geopark human resources development projects , and performed on the geo- guide with more than 150 people and described in three years , that capture the characteristics of the earth in Shizuoka Prefecture getting high marks from geo- guides of almost all .

We researched as ” Fuji Disaster prevention Fellow training course ” , a statistical study of disaster prevention survey of model class.

[Method]

The subjects were about 320 students in high schools in Shizuoka Prefecture.

As a method we used, hands-on educational materials, interpreter, communication, sub- materials, learning worksheet.

Specifically, you have used the materials of three main lessons. Experimental observation and for each group a stone of four areas of Shizuoka Prefecture, select the age quiz that is specified in the introduction. It captures the age order in the puzzle by geologic province of Shizuoka Prefecture, including the area of each rock is in the deployment. Conclusion, I confirmed the origin of the earth in Shizuoka picture-story show the history of the land in Shizuoka (wood panel) or not there was any such events to the geological era.

[Results]

In order to know the understanding of the individual, the question, ”earthquake”, ”plate”, ”Nankai Trough earthquake in the past”, ”Mount Fuji eruption”, ”active volcano in the prefecture”, ”rock in the prefecture”, ”Geopark”. We found that that is not known for most of the Geopark in high school outside of Geopark area.

It resulted in materials (60%) interest in the interpreter (22%) accounted for many, teaching increases the interest geology, geo-on (earth) as the reason

It is expected that by the SPSS statistical analysis, to present a detailed analysis of the data in the announcement.

Keywords: Geoscience materials, Geopark guides training programs, Visiting lectures in high schools, Disaster awareness

Japan Geoscience Union Meeting 2014
(28 April - 02 May 2014 at Pacifico YOKOHAMA, Kanagawa, Japan)

MIS35-10 Room:211 Time:May 2 14:45-15:00

Progress of school education through Geopark Studies in the Itoigawa Global Geopark

TAKENOUCHI, Ko[1*] ; MIYAJIMA, Hiroshi[1] ; IBARAKI, Yousuke[1] ; TORIGOE, Hiroko[2] ; BROWN, Theodore[2] ; WATANABE, Seigou[2] ; MATSUNAWA, Takayuki[1] ; CHIKAATO, Hisaki[1] ; FUJITA, Eishi[3] ; ICHIKAWA, Satoshi[3]

[1]Itoigawa City Board of Education, [2]Itoigawa Geopark Promotion Office, [3]Itoigawa Science Education Center

Geoparks are parks where visitors can learn about the relationship between mankind and the earth, but they are also part of a movement to develop sustainable regional societies. Education is regarded as one of the most important elements of the Geopark Movement which includes a system to foster the human resources that will manage our sustainable society in future. Itoigawa has begun to construct a sustainable regional society since Global Geopark certification in 2009. The Itoigawa City Board of Education recognized the important role of the Geopark in school education and has included a Geopark Studies program within the compulsory education (elementary and junior high school) curriculum. The first action was to establish a new education plan called the Unified Education Policy for Children Aged 0 through 18 in 2009 in which Geopark Studies was first introduced. Since then, the City Board of Education's continuing support of Geopark Studies has provided the following results: (1) Number of staff member of the Science Education Center has been increased and a Geopark Department has been established in the Itoigawa Teachers Organization's Society of Education Research. (2) Training programs (outdoor and indoor) have been held by these organizations and the Itoigawa Geopark Council, showing educators how geoparks can be used for classroom education. (3) City-wide Geopark Studies Conferences have been held to give students a chance to share what they have learned. (4) Supplementary textbooks for grades 3 through 9 have been published and distributed by various editorial boards, providing invaluable resources for the study of earth science and history as well as regional culture. (5) Geosites have been equipped with information panels and leaflets which cater to school education. (6) The Geopark has become a valuable tool in the teaching of disaster prevention, with a local elementary school receiving national and prefectural awards for its efforts. (7) Every first Wednesday of each month has been set as the geo school lunch date which features regional cuisine made with local ingredients to allow students to learn the relation of Itoigawa's land, cuisine and local produce. (8) And finally, an exchange program has begun for elementary and junior high school students with Itoigawa's Sister Geopark in Hong Kong.

Keywords: geopark, school education, Itoigawa

Japan Geoscience Union Meeting 2014
(28 April - 02 May 2014 at Pacifico YOKOHAMA, Kanagawa, Japan)

MIS35-11 Room:211 Time:May 2 15:00-15:15

CPD program for improvement of guide skill in the San-in Kaigan Geopark

SAKIYAMA, Tohru[1*] ; MATSUBARA, Noritaka[1]

[1]Graduate School of Management of Regional Resources, University of Hyogo

San-in Kaigan Geopark is the largest global geopark in Japan and there are thirty guide groups in the geopark. Some group members which receive following training programs are registered as official guides of the geopark. (1) Principles of geopark and outline of the San-in Kaigan Geopark, (2) Geology, geography, biology, history and others in the individual area, (3) Manner and technique of guide, (4) Conservation and related ordinances, and (5) Emergency resuscitation methods and system of insurances. License of the official guide is renewed every three years. They must participate at least fifteen seminars and events and improve the skill to guide the geopark during valid period of the license.

It is not easy to prepare enough programs for all official guides because of the wide area of the geopark. On the other hand, there are many educational facilities represented in the San-in Kaigan Geopark. They have many lifelong educational programs independent to the guide training of geopark. But some of them are available to upgrade the guide skill. Accordingly, CPD (continuous professional development) system has been adopted as the improvement program of the official guides in the San-in Kaigan Geopark. Official guides of geopark take the programs provided as CPD program by the educational facilities and they get a CPD-point. Not only such seminars but promotion to out-reach events (symposium, caravan, festival and others) and participation to national and international geopark conferences (GGN, APGN, EGN, JPN and others) is available to CPD-point. In order to renew the license of official guide, they must have fifteen CPD-points in three years.

CPD-program have following effects: (1) Securing of improvement programs for guide, (2) Exchange between people and geopark guides, (3) Deepening of interesting to guide activities, and (4) Development of lifelong education in the geopark.

Keywords: geopark, San’in Kaigan, continuous professional development, lifelong education

Japan Geoscience Union Meeting 2014
(28 April - 02 May 2014 at Pacifico YOKOHAMA, Kanagawa, Japan)

MIS35-12 Room:211 Time:May 2 15:15-15:30

Restoration of the coastal geo-environment along Tottori Sand Dunes

KODAMA, Yoshinori[1*]

[1]Fac. Regional Sciences, Tottori-Univ.

Along the coast of Tottori Sand Dunes, south-west Japan, dimensions of offshore bars were illustrated from air photos taken in 1968-2008 at 5 year intervals and grain size distributions at berm crests on the beach have been investigated over a half century since 1955. The results show that beach environments have been restoring naturally after damages induced by human activities, such as sand and gravel harvesting in the Sendai River during 1960-1975, which had caused diminishing of offshore bars, coastal erosions and beach sediment coarsening (>1.0 mm) at1980's and finally vegetation covering of the Tottori Sand Dunes . After stopping sand and gravel harvesting, large floods occurred in 1998 and 2004. These floods transported lots of sediment from upper parts of the drainage area to the main Sendai River. Around 2000, offshore bars along the coast became larger and grain sizes on the beach changes finer (<0.4mm) after 2011. These grain size values are similar to those in 1955. We are expecting that weeds on the Tottori Sand Dunes will relief naturally by activating blown sand. These phenomena are a good story to get visitors notice well-coordinated natural systems as a geo-park site in the San'in-kaigan Global Geo Park.

Keywords: Tottori sand Dunes, weeding of sand dunes, offshore bar, grain size distribution of beach deposit, sand and gravel harvesting, changes over a last half century

Japan Geoscience Union Meeting 2014
(28 April - 02 May 2014 at Pacifico YOKOHAMA, Kanagawa, Japan)

MIS35-13 Room:211 Time:May 2 15:30-15:45

Various effects that the shape of volcano has brought to the local area: an example of the Takachihonomine volcano

ISHIKAWA, Toru[1*]

[1]The Council for the Promotion of the Kirishima Geopark

When it comes to a volcanic blessing, it will be reminded of hot springs, spring water, and geothermal energy in many cases. However, these are only partial views of the blessing of a volcano directly useful to a life of people. In order to know deeply what kind of benefit the volcano itself has brought human society, it is necessary to see a volcanic blessing from many sides. As the beginning, this study focuses the shape of volcano.

The Takachihonomine volcano located at the eastern part of the Kirishima Volcano Group, SW Japan is the stratovolcano formed about 7,000 years ago, and has an acute summit and twin volcanoes on its both sides. Such a magnificent shape of the volcano is often dealt with as an icon of Kirishima, and is expected to have brought great influence to people's culture, a sense of values, and a religion view. In this research, I investigate where and how the influence of the topographical features of the Takachihonomine volcano has worked.

Keywords: Kirishima Volcano Group, Takachihonomine, Volcanic blessing

Japan Geoscience Union Meeting 2014
(28 April - 02 May 2014 at Pacifico YOKOHAMA, Kanagawa, Japan)

MIS35-14 Room:211 Time:May 2 15:45-16:00

The Activities of MLIT on the Hakusan Tedorigawa Geopark

KANATANI, Takao[1*] ; YAMAGUCHI, Takashi[2]

[1]Kanazawa Office of River & National Highway, Ministry of Land, Infrastructure, Transport & Tourism, [2]Hakusan Tedorigawa Geopark Promotion Council

The national flood control project in the Tedorigawa River by MLIT (Ministry of Land, Infrastructure, Transport & Tourism) is deeply related to the Hakusan Tedorigawa Geopark themes 'the journey of water and rocks'.

Some sabo structures in the geopark, constructed in the early Showa era, are designated as a Civil Engineering Heritage and as Registered Tangible Cultural Properties. MLIT, as a member of the Hakusan Tedorigawa Geopark Promotion Council, offers learning opportunities that allow people to look closely at these structures.

A massive flood, the most disastrous in history to that point, occurred in the Tedorigawa River in 1934. A huge rock known as the Shiramine Hyakumangan-no-iwa Rock (literally 4,800 ton rock) that cascaded along with it now sits neatly in the middle of the river. It is a reminder of the sheer scale of the event and is visited on elementary school field trips or on the geo-tours.

Opened in 2001, the Hakusan Sabo Science Museum introduces scientific information on landslide control measures based on the nature, geology, history, and lifestyle of Mt. Hakusan through video and exhibits in cooperation with the Hakusan Tedorigawa Geopark Promotion Council and is visited annually by more than 10,000 people.

The Ishikawa Coast Field Museum, managed in collaboration with the geopark, is an outdoor museum located on a coastal area that offers information on local history and the formation of the coast.

Keywords: Hakusan Tedorigawa Geopark, "Journey of Water", "Journey of Rocks", Sabo at Mt.Hakusan, Ministry of Land, Infrastructure, Transport & Tourism

Japan Geoscience Union Meeting 2014
(28 April - 02 May 2014 at Pacifico YOKOHAMA, Kanagawa, Japan)

MIS35-15 Room:211 Time:May 2 16:15-16:30

The link among Geopark, Biosphere Reserve, and National Park in Hakusan, Japan

NAKAMURA, Shinsuke[1*] ; SAKAI, Akiko[2] ; MATSUKI, Takashi[3]

[1]Hakusan Tedorigawa Geopark Promotion Council / Mt. Hakusan Biosphere Reserve Council, [2]Graduate School of Environment and Information Sciences, Yokohama National University / JCC for MAB, [3]Hakusan Ranger Office, Ministry of the Environment

Mt. Hakusan (2,702m) is an independent mountain on the Japan Sea side of Central Japan. An area extending over 4 prefectures (Toyama, Ishikawa, Fukui, Gifu) was designated as a national park in 1962, and as a biosphere reserve in 1980 by UNESCO. In 2011, the whole area of Hakusan City (in Ishikawa Prefecture) including the peak of Mt. Hakusan was designated as a Japanese geopark. Therefore, 3 systems on conserving and utilizing nature became to coexist in Mt. Hakusan, and since then, the link among these three is not only a complicated issue but a big chance.

National Parks are locations where human activities are restricted to protect the superb natural landscapes that are representative of Japan and where facilities have been installed to provide essential information and other functions to help visitors come in closer contact with nature (31 national parks in Japan). Biosphere reserves are sites seeking to reconcile conservation of biological and cultural diversity and economic and social development, recognized under UNESCO's Man and the Biosphere (MAB) Programme. To make the 3 functions (conservation, development and logistic support) effective, they have 3 zonations; core area(s), buffer zone(s), and transition area (5 biosphere reserves in Japan). Geoparks are sites enjoying earth and geotourism, supported by UNESCO (6 global geoparks and 27 Japanese geoparks in Japan).

Biosphere reserves and geoparks are both aiming at sustainable development. They attach importance to not only conservation but also utilization of nature, in contrast with the World Heritages. In addition, both form global networks each, which support each site together and diffuse their ideas. However, you can find some differences between these two. For instance, biosphere reserve is an official program of UNESCO, while geopark is a program supported by UNESCO. And the largest difference is that biosphere reserves pay most attention on ecosystems when geoparks pay most attention on earth.

However, they are not only focusing on ecosystems or earth, but they are also focusing on their connections formed with culture or lives. For example, there is a settlement called Shiramine around Mt. Hakusan, located on the river terrace which is a limited flatland in this mountainous area. In Shiramine, fire burned fields were established and forestry was conducted, which could say as a utilization of both topography and biological resources. In the summit of Mt. Hakusan, we could see various alpine vegetations affected by some topographical factors such as the quantity of snow or the formation of the earth. The earth, ecosystems and culture are connected tightly, which connection will be more clarified by both biosphere reserves and geoparks. From this context, you can say that geotours and ecotours might be held as same tours such called geo-ecotours, as it were which Koizumi (2011) said.

National parks are underlying biosphere reserves and geoparks. Both remain under national sovereign jurisdiction, but on the other hand are requested to take effective measures of nature conservation by each state's laws. National parks are representative institution of conservation in Japan, which have some zonations to restrict human activities in phases. Besides, national parks carry out some activities that could be more attractive by cooperating with biosphere reserves and geoparks which have more precise themes.

However, this cooperation depends on the link among the 3 organizations. So in Mt. Hakusan, the secretariats of Hakusan Tedorigawa Geopark Promotion Council and Mt. Hakusan Biosphere Reserve Council are both carried out by Hakusan City, assigning the same staffs, to strengthen the link between these two. Moreover, Ministry of the Environment which manages national parks, takes part in both councils.

The link among the three has just started. We are aiming to create new values and attractions transmitting from Mt. Hakusan, using this beneficial opportunity.

Keywords: Geoparks, Biosphere Reserves, National Parks, Mt. Hakusan, Geodiversity, Biodiversity

Japan Geoscience Union Meeting 2014
(28 April - 02 May 2014 at Pacifico YOKOHAMA, Kanagawa, Japan)

MIS35-16 Room:211 Time:May 2 16:30-16:45

What we learned from the verification of the Dinosaur Valley Katsuyama Geopark reexamiation results

YOSHIKAWA, Hirosuke[1*]

[1]Hirosuke Yoshikawa

We truly feel that reviewing the reexamination results of our geopark verification with local residents and geopark staff members provide us with the opportunity to fundamentally improve its construction. Furthermore, we can use these results to plan future initiatives and development strategies.

We will explain how we can fully utilize these results, such as raising the standards of the overall community and policies and efforts that Katsuyama should undertake as a whole.

Keywords: the reexamination resuits, our geoparku’s verification, development strategies, plan future initiatives

Japan Geoscience Union Meeting 2014
(28 April - 02 May 2014 at Pacifico YOKOHAMA, Kanagawa, Japan)

MIS35-17 Room:211 Time:May 2 16:45-17:00

Present state and Future outlook of Mishimamura Geopark Project

OIWANE, Hisashi[1*]

[1]Mishimamura Village

Mishimamura Village intends to become a member of Japanese Geopark Network desterilizing its natural, historical, and cultural background. The village consists of three islands. The central island, Satsuma Iwo-Jima is located at the edge of Kikai Caldera, which erupted about 7300 years ago. Its volcanic, fumarolic, and hydrothermal activities are very good resources of tourism. In relation with these activities, historical sulfur mining, sulfur trading, and appearance on palaeographies are also good resources of tourism. In addition, a famous Kabuki actor comes to play because of historical background of the island, and famous djembe player comes to play djembe with children in the island. In spite of these interesting resources, the village has not constructed sightseeing tours that organize these resources. Here, the village started to desterilize these resources in order to vitalize the village. In this presentation, I will present our original approach and future plan to be a member of Japanese Geopark Network.

Keywords: geopark, caldera

Japan Geoscience Union Meeting 2014
(28 April - 02 May 2014 at Pacifico YOKOHAMA, Kanagawa, Japan)

MIS35-18 Room:211 Time:May 2 17:00-17:15

Introduction of the Nankikumano Geopark activity research project

MORINO, Yoshihiro[1*] ; TANIWAKI, Tomokazu[2]

[1]Pacific Consultants Co.,Ltd., [2]Natural Environment office of Wakayama Prefectural Goverment

Various business (spread activity, utilization as education, tourist attractions, the Geopark guide training) is developed mainly on ”Nankikumano Geopark promotion meeting” from 2012. ”Nankikumano Geopark activity research project” was carried out to plan accumulation and the regional activation of the academic document of the Nankikumano Geopark design in 2013. As for this project, an individual, a local group, a private enterprise work on an academic investigation and the spread together in a Geopark design area.

Keywords: Geo-resources, Local promotion, Geo-tourism

Japan Geoscience Union Meeting 2014
(28 April - 02 May 2014 at Pacifico YOKOHAMA, Kanagawa, Japan)

MIS35-19 Room:211 Time:May 2 17:15-17:30

Plan to aim at the revival and activation of disaster region by disaster heritage of the Great East Japan Earthquake

TANIGUCHI, Hiromitsu[1*] ; TASHIRO, Kan[2] ; MIYAHARA, Ikuko[3] ; AIHARA, Junichi[4] ; TANAKA, Michi-hisa[5] ; MSC GP, Prep. com.[1]

[1]Tohoku Univ, [2]Tohoku Inst Tech, [3]Miyagi Univ, [4]Tohoku History Museum, [5]Asia Air Survey

The coastal area of Miyagi Prefecture was destroyed almost completely on 11 March 2011 by the Great East Japan Earthquake. Now, many people are working hard and trying to recover from the destruction. As a member of the victims and as a researcher living in the affected areas, we are planning to create a Minami Sanriku Coast Geopark to the affected coastal areas, and to contribute to the reconstruction also.

Simultaneously with general subject such as a stratum, fossil, geographical feature and a cultural heritage, we use the affected heritage which was born in the Great East Japan Earthquake.

At the same time as the scientific understanding of an earthquake or tsunami, the reason to focus on these because we want to help local disaster management in the future. To date, we have finished the investigation of tour point of about 50 places. In the present talk we will focus on an example of Yamamoto town geosite located on the border with Fukushima Prefecture and Miyagi Prefecture.

Keywords: geopark, Minami Sanriku Coast, disaster heritage, revival, Yamamoto Town

Japan Geoscience Union Meeting 2014
(28 April - 02 May 2014 at Pacifico YOKOHAMA, Kanagawa, Japan)

MIS35-P01 Room:Poster Time:May 2 16:15-17:30

”100 Earth Heritages” and its Geographical Concept

ARIMA, Takayuki[1*]

[1]AJG Geopark Committee, Commitee for ”100 Earth Heritages” Selection

1. The Association of Japanese Geographers and ”100 Earth Heritages”

Geopark Committee in the AJG aims to choose ”100 Earth Heritages”. They organized three symposiums and four questionnaire surveys. Furthermore, Committee of 100 Earth Heritages Selection has launched in 2012 and started the selection. This committee has members of the AJG who are both researchers of physical and human geographies. This article introduces a manner of the selection work for understanding a priority of value in Japanese geography.

2. Manner of 100 Earth Heritages Selection

The committee proposed questionnaire survey to members of the AJG several times in order to reflect their opinions in the selection. As a result, 264 places of proposed sites were shown (including some overlap); 155 from speakers and 40 from the audiences in March of 2012, 7 from speakers and 38 from the audiences in March of 2013, 20 from questionnaire respondents and 4 from questionnaire on the web. Based on the list of a total 264 places of proposed sites, the vote by the member of the committee and an argument were performed in July, 2013, and an 65 Earth Heritages were picked up. Enumeration and the vote of the new proposed site by the committee have been held again, and 33 Heritages were added afterwards. It has remaining two places at January 31th, 2014.

3. Contents of 100 Earth Heritages

In January 2014, 98 places of Earth Heritages are chosen. As for the Earth Heritages, 47 prefectures have one heritage at least. It depends on consideration in that the heritages should be used for geographical education in schools in Japan. However, on the other hand, the difficulty of the evaluation of the geographical value hides in the back of this consideration. In other words, geographical valuableness can insist on in area wherever of Japan.

4. Geographical Values from the perspectives of 100 Earth Heritages

For each heritage, the commentary sentence for choice reason is written. This article clarifies geographical value by considering the contents of the commentary sentence. The contents of sentences mostly consist of the plural sites. This is because a certain reciprocal viewpoint (story) was made between the sites. A nature and human reciprocal relations are seen in the contents. For example, in one of Yoshino River District, this district has mountains of steady sedimentary rocks and rivers cutting sharply between the mountains, this becomes the precondition of the creations of small and unique bridges for movements between the villages for settlements. Such nature and human relations are frequent in the commentary sentences of other heritages. In other words, it is thought that the geographical value from ”100 Earth Heritages” is these reciprocal relationships.

On the other hand, the contents of the commentary sentence can point out the problem, too. This article points out two dimensions. First one is seen in the contents. A writer of the commentary sentence is only physical geographer or humanities geographer. Therefore the contents are slightly deflected to physical or human geographical contents so that they should start to learn about each other’s fields. The second problem can point out that there is a giving an environmental determinism like impression for a reader, because a natural condition is described as a precondition in the sentence. So, it may be said that it is necessary for geography to discuss the environmental determinism. If the general relationship of a natural phenomenon and the humanities phenomenon is proved scientifically, it is one of the geographical directionality for Geoparks.

Keywords: Earth heritages, Physical geography, Human geography, Regional geography, Environmental determinism

Japan Geoscience Union Meeting 2014
(28 April - 02 May 2014 at Pacifico YOKOHAMA, Kanagawa, Japan)

MIS35-P02 Room:Poster Time:May 2 16:15-17:30

Activity support for the educational continuity from primary through early secondary levels in the Mikasa Geopark

KURIHARA, Ken'ichi[1*] ; NII, Tadahiro[2]

[1]Mikasa City Museum, [2]Promotion Policy Division, Mikasa City Office

In the Mikasa Geopark, the educational continuity from primary through early secondary levels has been carried out since 2005. In this educational project, there is a subject "Regional Studies", which learns about attributes of Mikasa (eg., history, nature, and industry).

On the other hand, the Mikasa City Museum was established in 1979 to preserve materials of human, natural, and industrial histories of Mikasa. The curators of the museum have supported the subject "Regional Studies" as a museum activity since the first year (2005) of the educational project. Recently, the cooperation program between the educational and geopark activities is exploring.

In the presentation, we introduce the cooperation among the educatioal, museum, and geopark acitivities, and discuss the results and subjects.

Keywords: educational continuity, regional study, museum activity, geopark activity, Mikasa Geopark

Japan Geoscience Union Meeting 2014
(28 April - 02 May 2014 at Pacifico YOKOHAMA, Kanagawa, Japan)

MIS35-P03 Room:Poster Time:May 2 16:15-17:30

The effects of experience-based science and environmental education on Byobugaura geosite in Choshi Geopark

ANDO, Takao[1*]

[1]Chiba Institute of Science

Choshi geopark is certified by Japan Geopark Committee (JGC) at September 24, 2012. In this study, we will introduce the contents and the effects of geoscience education program for junior high school students using Byoubugaura geosite in Choshi Geopaek.

Choshi, located at the east end of the Boso peninsula, 100km east of Tokyo, Chiba prefecture, Japan, has many geological heritages that should be preserved and passed on to future generations. Representative geological features in Choshi are as follows. First, the Bioubugaura geosite, comprising Pliocene and Pleistocene sedimentary rocks, is approximately 9 km in length and 30˜50 m in height and faces the Pacific Ocean. This topography, which is also called ”Dover in the East”, consists of sharp cliffs formed by land erosion resulting from sea waves. According to a previous report, the speed of erosion is 5˜6 m per year. To prevent erosion, seawall was constructed in 1966. The seawall was a necessity for the residents’ safety even though it negatively affected the geo-heritage. Second, Inubouzaki geosite, the Cretaceous shallow sea sediments, designated as a government national monument, are exposed in the Inubouzaki coastal area at the east end of the Choshi peninsula. Third, the ”Inuiwa” geosite, carried on the tradition of the ”Yoshitune legend” which is a legend concerning a samurai warrior in the medieval period of Japan, are composed of Jurassic greywacke, mud stones, and conglomerates that includes calcareous coarse fragments with fusulina fossils.

Our education program using Byoubugaura geosite designed it to be usable by a curricular science class of the junior high school, and it conclude for one day. The contents of this program compose two parts, the morning part contain geotour and tephra sampling in the Byoubugaura geosite, and the afternoon part consisted of geological lecture and stereomicroscope observation of tephra constituents, e.g. volcanic grass and minerals etc.

The results of questionnaire analysis for participants show (1) this program is understandable for major part of attended students, (2) this program have good effects for induction of affection for local environment, and (3) this program increase desiring to learn for earth science.

Keywords: Geopark, Choshi, Science education, tephra, Byoubugaura, Life cycle thinking

Japan Geoscience Union Meeting 2014
(28 April - 02 May 2014 at Pacifico YOKOHAMA, Kanagawa, Japan)

MIS35-P04 Room:Poster Time:May 2 16:15-17:30

Analuzing the Efficcy of Natulal Disaster Awareness Programs based on the Understanding of Geophysical Mechanisms

SUZUKI, Yusuke[1*] ; KOYAMA, Masato[2] ; UENISHI, Tomoki[3]

[1]Izu Peninsula Geopark Promotion Council, [2]CIREN, Shizuoka University, [3]Izu-sogo High-school

Izu Peninsula was once a submarine volcano situated in the south sea. This area collided with Honshu with the Northward movement of the Philippine sea plate and formed a peninsula from about 10 Million years back.

After this land volcanism took place that formed multiple large volcanoes. In this geopark we made attempts to popularize earth science and disaster management by conquicting questionnaires with local schools. As a result we understood the efficacy of natural hazards education by using familiar examples. From the participants there were even demands for more information and more comprehensive training programs.

Keywords: Geopark, Disaster Mitigation Education

Japan Geoscience Union Meeting 2014
(28 April - 02 May 2014 at Pacifico YOKOHAMA, Kanagawa, Japan)

MIS35-P05 Room:Poster Time:May 2 16:15-17:30

Detection, Observation, Preservation, and Utilization of Sand Boiling Traces along an Active Fault : Effort of Hakusan T

KOZAKA, Yutaka[1*] ; HIRAMATSU, Yoshihiro[2]

[1]Hakusan Tedorigawa Geopark Promotion Council, [2]Kanazawa University

The Morimoto-Togashi Fault Zone which goes through Kanazawa City to Tsurugi District, Hakusan City, is one of geosites where people can learn about the formation of earth in the Hakusan Tedorigawa Geopark. On the eastside of the fault mountains (elevation of 650 meters) were formed by the upheaval. On the other hand, on the westside of the fault the Tedorigawa River transported much sediment, and an alluvial fan was formed by them.

In recent years two excavation surveys of the buried cultural properties were carried out in the western margin of the active Togashi Fault. One at the Bunyudo ruins (Hiramatsu and Kozaka, 2013) and the other at the Netsuno ruin which was excavated in 2013. Sand boiling traces were found in the both ruins, which showed a huge earthquake occurred between the late Yayoi Era and the Heian Era. It is difficult to identify the active fault which the earthquake happened, causing the sand boiling traces. However, from a survey in Umeda District along the Morimoto Fault, it was reported that the latest activity occurred after approximately 2000 years ago, prior to the fourth century (Headquarters for Earthquake Research Promotion, 2013). Therefore, the sand boiling traces are likely to be caused by the activity of the Togashi Fault, considering that the sedimentary layer which the sand boiling traces were found is correlated to the era the fault movement occurred.

We report people's activities related to these ruins where they are located on slight elevations of the alluvial fan, together with an introduction of the sand boiling traces. Additionally, we report about a study tour held in 2013 for the citizens to walk around and observe the both ruins and the Togashi Fault.

The Hakusan Tedorigawa Promotion Council is planning to peel off the sand boiling traces, panel it, and then utilize it as learning materials of the geopark to learn about the formation of earth and disaster prevention.

Keywords: Hakusan Tedorigawa Geopark, Active Fault, Morimoto-Togashi Fault Zone, Sand boiling traces, ruins

Japan Geoscience Union Meeting 2014
(28 April - 02 May 2014 at Pacifico YOKOHAMA, Kanagawa, Japan)

MIS35-P06 Room:Poster Time:May 2 16:15-17:30

A practical use of geoparks as university educational materials

NIINA, Atsuko[1*]

[1]Regional Innovation Research Center, Tottori University of Environmental Studies

The purpose of this presentation is to show the practical use of geoparks as university education and to discuss the relationship between local universities and local communities. Tottori University of Environmental Studies opens four classes of *Project Research* for freshmen and sophomore. The classes of Geoparks started in 2012. The aim of the geopark classes is to learn the method of a field survey. There were various topics on geoparks; for freshmen, the development of virtual geotour, the land use survey of Yoshioka hot springs town and the development of geo product, and for sophomore, the development of geo guided tour at Aoshima of Koyamaike Lake and the regional survey of Yoshioka. These output share with local communities and geoparks. It becomes clear that a geopark makes a good use of social learning.

Keywords: university education, regional survey, social learning, San'in Kaigan Geopark, Tottori University of Environmental Studies

Japan Geoscience Union Meeting 2014
(28 April - 02 May 2014 at Pacifico YOKOHAMA, Kanagawa, Japan)

MIS35-P07 Room:Poster Time:May 2 16:15-17:30

Geopark guide training program in Amakusa area

UGAI, Hiroaki[1] ; HASE, Yoshitaka[1*]

[1]Amakusa Geopark planning promotion committee

Amakusa Geopark planning promotion committee trained 149 geopark guides in Amakusa area in 2013. We introduce a state of the Geopark guide training at the geosites.

”Amakusa Geopark plan” is an action for ”Amakusa Geopark” aiming at authorization of the Japanese Geoparks Network. The five elements, geology, geography, viewing point, culture and industry, comprise the main core of the Amakusa area which is shown at the geosites throughout the islands.

The purpose of Geopark guide training program, through a lecture in room and the local training in field, is aimed for the interpreter of the local geology, creature, culture and industry. The committee confers the qualification of the guide to the person who passed an authorized examination. Geopark guides perform their activity after the enrollment to each local tourism guide association.

Through this program we expect an effect guide authorization, common knowledge of the activity for local inhabitants and the interpreter for geopark which can convey resources in this area to anyone clearly. Geopark guide is important as a diffuser explaining ”What is geopark” precisely and is necessary for an action united with local inhabitants or the education spread.

Residents and officials alike collaborate to preserve the geologic inheritance of Amakusa with an educational perspective. Exposing the unique beauty of this inheritance as a tourist attraction in conjunction with the history and culture of the area, an attractive geo-tourism will be found aim at the promotion of the Amakusa area.

Point of the local promotion by the tourism is comment on an earth science-like element for constitution of the earth and a story about the local history and culture.

Keywords: geopark, guide, inhabitants

Japan Geoscience Union Meeting 2014
(28 April - 02 May 2014 at Pacifico YOKOHAMA, Kanagawa, Japan)

MIS35-P08 Room:Poster Time:May 2 16:15-17:30

Program for broadening the knowledge base and awareness of geopark guides -An example of Amakusa Goshoura Geopark-

HASE, Yoshitaka[1*] ; UGAI, Hiroaki[1] ; HIROSE, Koji[1] ; TSURUOKA, Seiya[2]

[1]Goshoura Cretaceous Museum, [2]Association of Goshoura Geo-Tourism Guide

It is very important for any geopark that its guides are actively involved in geo-tourism. Guides must strive to continually increase their awareness and broaden their knowledge base of not only their geopark, but also of neighboring areas. We will use the Amakusa Goshoura Geopark as an example to demonstrate a guide awareness-raising program in action with regard to the geology, geography, history and culture of its neighboring areas.

The Amakusa Goshoura Geopark contains strata and fossils in deposits spanning 100 million years. The strata were deposited in the Cretaceous and Paleogene periods of earth's history, and contain abundant fossils including dinosaurs from the Cretaceous period and large mammals common to the Paleogene.

From the peak of Karasu-toge, a geosite in the geopark, we can see a 360-degree panoramic view of the Yatsushiro Sea and landscape of Kyushu Island including Fugen-dake, Yatsushiro Plane, Aso Mountain, Hitoyoshi Basin, Mt. Shiraga, Ontake and Yahazudake on the Hisatsu Volcanic Plateau, Izumi Plane, Mt. Shibi, Nagashima, Shishijima and Koshikijima.

Members of the Association of Goshoura Tourism Guide group are trained to explain not only about the panorama from Karasu-toge including geologic composition and topographical features of Kyushu Island, but the wealth of information stored in its strata. As an example, the association had a tour to study the geology, geography, history and culture on the coastal area from Ashikita to Nagashima along the Yatsushiro Sea in 2014. Similarly, it will take part in the study of the Shimabara peninsula at the Shimabara Global Geopark in the near future. Training programs like these have been instituted as a means of support for the Amakusa Goshoura Geopark guide's continuing education.

Keywords: Geopark guide, neighboring areas, broadening knowledge

Japan Geoscience Union Meeting 2014
(28 April - 02 May 2014 at Pacifico YOKOHAMA, Kanagawa, Japan)

MIS35-P09 Room:Poster Time:May 2 16:15-17:30

Mt. Apoi Geopark telling a global dynamic movement of the earth

NIIDA, Kiyoaki[1*] ; MT. APOI GEOPARK, Promoting council[2]

[1]Hokkaido Univ. Museum, [2]Samani

Mt. Apoi geopark is located at the southwestern end of the Hidaka mountains, facing to the Pacific southward. Recently, a tectonic map showing a distribution of major plates in the northern hemisphere and suggesting a global sense of plate motion between the North American plate and the Eurasian plate was published. This map gives an easy understanding on a background of the Hidaka mountain building and a simultaneous interpretation on a global dynamic movement of the earth.

We have an excellent example of global mobile belt of the earth, which is the Tethys ophiolite belt from the European Alps ˜Greek ˜Turkey ˜Iran ˜Oman ˜Pakistan ˜Indus Suture ˜Andaman ˜Great Sunda toward the east, including the continent-continent collisions between Africa and Europe, and India and Asia. Also, we have an above example of active tectonic event such as the Hidaka mountain building, here in Mt. Apoi geopark, Hokkaido, Japan.

Keywords: Mt. Apoi geopark, peridotite, upper mantle, basaltic magma, plate boundary, global dynamic movement

Japan Geoscience Union Meeting 2014
(28 April - 02 May 2014 at Pacifico YOKOHAMA, Kanagawa, Japan)

MIS35-P10 Room:Poster Time:May 2 16:15-17:30

Communication of Information on the Internet By Geopark: Case Study of Sanriku Geopark

ITO, Taku[1*] ; HASHIMOTO, Tomoo[1] ; UENO, Ayumi[2]

[1]Chuo Kaihatsu Co., [2]Sanriku Geopark Promotion Conference

The Sanriku geopark certified the Japanese geopark in 2013. It is the largest geopark in Japan that consists of 16 cities in Aomori, Iwate, and Miyagi prefecture. The Sanriku geopark promotion conference is disseminating information at the Internet.

In February 2011, we created the general-oriented website which summarized geological history and the highlight of Sanriku regions. Then, in response to the Great East Japan Earthquake, we have created a new web site for education travel and academic investigation in September 2011, and then, the variety of information was added to the general-oriented website towards the authorization to a Japanese geopark.

Furthermore, through the information by SNS, such as a blog, Facebook and Twitter, we increase the update frequency of information, promotion meeting was to update the content and functionality depending on the purpose or object. We increased the updating frequency of informaton, and updated contents and function according to the purpose.

Now, the degree of name recognition or comprehension of the “ geopark ” are not increasing. However, exposure to mass media and concern of local and a surrounding area are increasing in response to Japanese geopark authorization of Sanriku regions.In order to correspond to this, we decided to newly renew a website in 2014.

In this presentation, we introduce our renewal case and information transmission method and the results of a survey of website on other geoparks.

Keywords: geopark, communication of information, internet, Sanriku

Japan Geoscience Union Meeting 2014
(28 April - 02 May 2014 at Pacifico YOKOHAMA, Kanagawa, Japan)

MIS35-P11 Room:Poster Time:May 2 16:15-17:30

Utilization of Earth sciences for regional development

ONUMA, Saori[1*] ; KORIYAMA, Suzuka[1] ; MAEDA, Tomoyuki[1] ; KIKUTA, Ryota[1] ; ISHIKAWA, Natsumi[1] ; IKETO, Hirokuni[1] ; MATSUHISA, Yuko[1] ; FUKUNAGA, Chie[1] ; SAWAHATA, Yurie[2] ; FURUKAWA, Yohei[2] ; HOSOI, Jun[2] ; AMANO, Kazuo[1]

[1]Faculty of Science, Ibaraki University, [2]Graduate School of Science and Engineering, Ibaraki University

The information on earth sciences is useful for disaster prevention of a natural hazard like earthquake and volcanic eruption etc. The new trend utilizing the information of earth sciences to lifelong learning and tourism occurred in recent years. The geopark can be the best place providing this information.

Ibaraki University Geological Information Utilizing Project team is providing geological informations for the management of North Ibaraki Geopark. Main act is creation of 15 sightseeing guidance maps. Now, we are improving the contents of previous maps. Furthermore, we are having strong cooperation with local residents and companies for the regional development.

Keywords: Geopark, North Ibaraki Geopark, regional development

Japan Geoscience Union Meeting 2014
(28 April - 02 May 2014 at Pacifico YOKOHAMA, Kanagawa, Japan)

MIS35-P12 Room:Poster Time:May 2 16:15-17:30

Activity of Misato-Kai in Sado Island Geopark

ICHIHASHI, Yayoi[1*]

[1]Sado city board of education Geopark promotion office

We introduce the activity of Misato-Kai, which played an important role for Sado Island Geopark to be a member of Japanese Geoparks Network.

Misato-Kai is the association that was established in 2006 by hostesses of local Japanese inns and hotels to keep close relationship with each other and revitalize tourism in Sado Island. Until now, they've made eco-friendly chopsticks and OMOTENASHI pocket notebooks.

Also, they make place mats as their activities. These mats are made of paper and have some pictures and captions on them to introduce some tourist attractions and promotional programs to guests. This time, they made the place mat under the theme of Sado Island Geopark and many groups and associations such as, Misato-Kai, Sado City and welfare facilities give much support to make it. The cooperation is the significant feature for this activity.

Now, these place mats are attracting favorable comments from hotel guests. Some guests bring it home and others leave some messages on it for people of welfare facilities in Sado Island. It is a useful tool for communication between the hotel guests and the hostesses in local Japanese inns.

In Sado Island, many associations are extremely active. They are very important for Sado Island Geopark activities. We hope that we can work together for our geopark in the future.

Keywords: Sado Island Geopark, Misato-Kai, tourisum

Japan Geoscience Union Meeting 2014
(28 April - 02 May 2014 at Pacifico YOKOHAMA, Kanagawa, Japan)

MIS35-P13 Room:Poster Time:May 2 16:15-17:30

Let us Enjoy Geo-Tetsu - the Sixth Geo-tour through Train Windows, Nakamura and Sukumo Line of the TOSA KUROSHIO RAILWAY

FUJITA, Masayo[1*] ; YOKOYAMA, Shunji[1] ; KATO, Hironori[1] ; UENO, Shoji[1] ; YASUDA, Tadashi[1] ; IMAO, Keisuke[1] ; SUGA, Yasumasa[1]

[1]Geo-Tetsu Project Committee of the Fukada Geological Institute

1. Aims of Geo-Tetsu activities

Geo-Tetsu is the name of the activity that shows everyone ways to enjoy and learn about geology and related sciences, using railways (Kato et al., 2009). Following five year's Geo-Tetsu promote activities are continued by geological engineers who love railways, organized with the corporation of the Fukada geological institute since 2009 (Fujita et al.,2013) and established Geo-Tetsu Project Committee since 2013.

Geo-Tetsu offers the chance to get acquainted with geological features, not only through train windows but also along paths accessible from the stopovers alongside the railway routes. We selected enjoyable Geo-Tetsu courses and Geo-points. As much information is obtainable and can be gathered from various perspectives; the railway itself, geology, geography, cultural heritage and sight-seeing as well. We hope that the general public will enjoy a new style of railway traveling provided by the Geo-Tetsu. The Nakamura and Sukumo Line of TOSA KUROSHIO RAILWAY is presented in this as sixth route of Geo-tetsu.

2. The Nakamura and Sukumo Line, the sixth Geo-Tetsu project

(1) Abstract of the Nakamura and Sukumo Line

The Nakamura and Sukumo Line run from Kubokawa at Shimanto Town to Sukumo City in the western region of Kochi Prefecture. The railway connects from Kubokawa to Nakamura at 43.0km, and from Nakamura to Sukumo at 23.6km. Both are single track, and the route not electrified. In the line, there are characters designed by Takashi YANASE. Additionally, they have seven wrapped vehicles of municipalities. John Mung (Manjiro Nakahama), Whales, Whale Sharks, Kashiwa-jima Island, Kyoto cultures of the Shimanto City, and the event character of the Sukumo City etc. are painted there. The vehicles not only transport passengers but also inform the charms of the western region of Kochi Prefecture.

The Nakamura Line and the Sukumo Line have a different history of construction. At first, the construction of the Sukumo Line had been promised. However, the Nakamura Line was given to priority by the political motivation. The Nakamura Line was started constructing in 1956, and opened in 1970. On the other hand, the Sukumo Line was started constructing in 1974, but it was interrupted by the Japanese National Railways reconstructing promote measure law in 1981. Afterwards, both routes were succeeded by TOSA KUROSHIO RAILWAY Ltd. as the third sector railway. At last, when the Sukumo Station opened, it became a present route in October, 1997.

(2) The rich geological and sight-seeing resources of the Nakamura and Sukumo Line

The Nakamura and Sukumo Line runs on the Shimanto terrane that consists of sandstone and the mudstone from Cretaceous to Paleogene. The train leaves Kubokawa Station (asl 210m) and goes to Kaina Station (asl 47m),descending the inclination of 23 permil or less. Especially, "the First Kawaoku Tunnel (2031m) " is well worth as loop of 350m in radius, descending 20 permil, and the exit appears below by 40m. If you have the compass, you can confirm its needle will be made one rotation in the tunnel. When we goes out there, train runs along Iyoki River. Soon we arrive at the Tosa-Saga Station in famous of bonito's single-hook fishing. The train passes under a lot of short tunnels with the outcrops of turbidite of Shimanto terrane around Tosa-Shirahama. Between Ukibuchi and Tosa-Irino Station, you can visit the river-mouth deviation of the Fukiage River. There are almost stone monuments of the Nankai Earthquake at the Kamo shrine in woods of pine at Irino.

Through the Kotsuka Station,the train changes front to the west. It crosses the Shimanto River in parallel to a red bridge as old national road. In the downstream, there is a long dam for the flood disaster evasion. The train advances straight in the Nakasuji lowland (Kano et al., 2003), which understood the slope-basin deposit (Domeki Formation). Lastly, the train comes out of Hijirigaoka Tunnel (5084m), we arrive at the Sukumo Station.

Keywords: Geo-Tetsu, Geo Point, Nakamura and Sukumo Line of the TOSA KUROSHIO RAILWAY, loop tunnel, Shimanto terrane, Nakasuji lowland

Japan Geoscience Union Meeting 2014
(28 April - 02 May 2014 at Pacifico YOKOHAMA, Kanagawa, Japan)

MIS36-01 Room:314 Time:May 1 10:00-10:30

Collectivity and individuality of particle dispersion under gravity

HARADA, Shusaku[1*]

[1]Faculty of Engineering, Hokkaido University

Collective motion of fine particles in liquid can be widely seen not only in engineering processes but also in natural phenomena such as water treatment [1], sediment transport [2], bio-convection [3] and lava convection [4]. It is well-known that the spatial variance of particle concentration brings about large-scale convection flow under gravity and sometimes it affects macroscopic motion of particles. In this study, of particular interest is whether collective or individual motion of particles reveals in liquid under the gravity field. The existence of concentration interface, which is an ambiguous interface between suspended particles and pure fluid, plays a significant role in these extreme behaviors.

Figure indicates the settling behaviors of stratified-suspended particles in a vertical Hele-Shaw cell filled with liquid [5]. In cases of small particle size with high concentration, the interfacial instability occurs at the lower concentration interface and the suspended particles behave as an immiscible fluid even though there is no distinct border with pure fluid [6]. Consequently the settling velocity is much faster than that of an isolated particle. On the other hand, in case of large particles with low concentration, the concentration interface is less distinct and the suspended particles settle individually. The transition from these collective to individual motions of suspended particles is controlled by the border resolution of concentration interface. We define the dimensionless parameter which describes the border resolution of concentration interface by the ratio of average particle distance $d_P/\phi^{1/3}$ (d_P: particle diameter, ϕ: concentration) to the dominant wavelength of the instability λ. As can be seen in Figure, the dimensionless parameter well describes the transition from fluid-like to particle-like behaviors. The suspended particles (and the interstitial fluid) perfectly behaves as continuum for $d_P/\phi^{1/3}\lambda$ <0.03 and behaves individually relative to fluid for $d_P/\phi^{1/3}\lambda$ >0.2 [5].

The similar collective motion of suspended particles has been studied on the settling of particle clouds in viscous fluid. Some researchers have suggested that the collective motion of particles in clouds can be explained by the swarm of Stokeslet [7]. They have found that the particle cloud behaves collectively when the flow generated by each particle (Stokeslet) enough screens the surrounding flow. If the above parameter is rewritten by number density of particles N, it is expressed as $(6/\pi)^{1/3}/N^{1/3}\lambda$. Therefore the border resolution of concentration interface express the discretization of space by Stokeslet $1/N^{1/3}$ for a given lengthscale λ.

One more interesting similarity to previous study is the wavelength of instability. From the linear stability analysis of Rayleigh-Taylor instability on both miscible and immiscible interfaces of pure fluids [8], it is found that the dominant wavelength of miscible interface with no diffusion and immiscible interfaces with no interfacial tension are asymptotically close to constant value. The wavelength at concentration interface is also close to the asymptotic value [9]. From this point of view, the concentration interface can be interpreted both as the the immiscible interface with no interfacial tension and the miscible interface with no diffusion.

References

[1] E. Guyon et al., Physical Hydrodynamics, Oxford University Press (2001).
[2] J. D. Persons et al., Sedimentology, 48, 465-478, (2001).
[3] T. J. Pedley and J.O. Kessler, Annu. Rev. Fluid Mech., 24, 313-358, (1992).
[4] H. Michioka and I. Sumita. Geophys. Res. Lett., 32, L03309, (2005).
[5] S. Harada et al., Eur. Phys. J. E, 35, 1-6, (2012).
[6] C. Voltz et al., Phys. Rev. E, 65, 011404, (2001).
[7] B. Metzger et al., J. Fluid Mech., 580, 283-301, (2007).
[8] J. Fernandez et al., Phys. Fluids, 13, 3120-3125, (2001).
[9] S. Harada et al., Chem. Eng. Sci., 93, 307-312, (2013).

MIS36-01 Room:314 Time:May 1 10:00-10:30

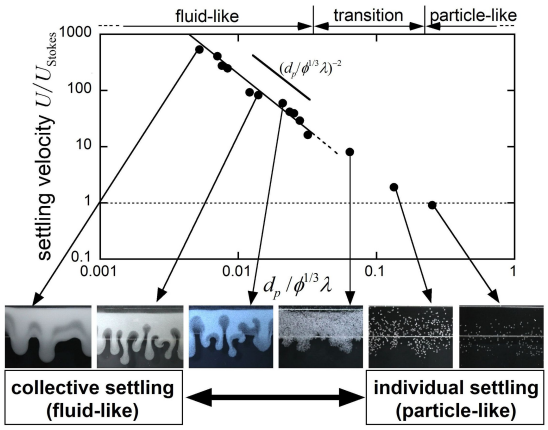

Figure 1: Collective and individual settlings of suspended particles in Hele-Shaw cell.

Japan Geoscience Union Meeting 2014
(28 April - 02 May 2014 at Pacifico YOKOHAMA, Kanagawa, Japan)

MIS36-02 Room:314 Time:May 1 10:30-10:45

Reverse chemical garden reaction of cementitious materials

SATOH, Hisao[1*] ; FURUKAWA, Erika[2] ; KIMURA, Yuki[2]

[1]Mitsubishi Materials Corporation, [2]Tohoku University

Recent advances in the nano-scale mineralogy extend from the extraterrestrial materials known as in cosmic dusts and asteroids to ordinary industrial materials like the cementitious materials. The distinct property of nano materials can be characterized from the points of view of (1) nucleation, (2) self-assembly behavior and (3) flexibility in the form.

A very common industrial material, cement is a typical one consisted of nano particles of calcium silicate hydrartes (C-S-H).

Crystal growth experiment of cementitous materials can be recently performed using interferometric and nanoscopic techniques. Although the cement reaction producing C-S-H from silicates with $Ca(OH)_2$ (portlandite: CH) or more alkaline solution is extensively occurring at buildings under and after construction, similar reaction is expected at the interface of natural rock and concrete-building such like tunnel, dam and underground repository for radioactive wastes.

Hyper alkaline alteration experiment using vertical scanning interferometer revealed the precipitation behavior of C-S-H by reverse chemical garden reaction on natural rock (Satoh et al., in press). Very slow growth rate of the C-S-H on rock was observed to be ˜2.4E-3 nm/s. The ionic selection of the solutes through the C-S-H wall having nanopores like membrane was also confirmed.

Most recently, we applied newly developed ultramicroscopic technique with fluid reaction TEM (FR-TEM: Poseidon) for study of reverse chemical garden reaction between silica fume (Elkem Microsilica 940-U, ˜150 nm) and CH-saturated solution. It revealed that the reaction caused silica hydration (volume expands) and subsequently form string and veil of C-S-H. The growth rate of string C-S-H was calculated to be ˜4.5E-2 nm/s, which is fast enough to form frame network preparing veil-formation. It was chemically confirmed by FESEM-EDS that this C-S-H veil evolved toward Ca-rich over time. Our observed result could be a fundamental process of reverse chemical garden reaction, i.e., cement-solidification.

Ultramicroscopic investigation of C-S-H growths may improve the simulation of groundwater conditions in the future.

Keywords: reverse chemical garden reaction, cementitious material, C-S-H, fluid reaction TEM

Japan Geoscience Union Meeting 2014
(28 April - 02 May 2014 at Pacifico YOKOHAMA, Kanagawa, Japan)

MIS36-03 Room:314 Time:May 1 11:00-11:30

General nature of liquid-liquid transition in aqueous organic solutions

MURATA, Ken-ichiro[1*] ; TANAKA, Hajime[1]

[1]Institute of Industrial Science, University of Tokyo

Contrary to the conventional wisdom that there exists only one unique liquid state for any material, there are growing experimental and numerical pieces of evidence for the existence of more than two liquid states in a single component substance. The transition between them is called liquid-liquid transition (LLT). LLT has attracted considerable attention because of its importance in the fundamental understanding of the liquid state. However, the physical nature of the transition has remained elusive. Particularly for water, the possible existence of LLT has special implications not only on its fundamental understanding, but also on a link of various thermodynamic and transport anomalies with critical anomaly associated with LLT. Here we reveal that 14 aqueous solutions of sugar and polyol molecules, which have an ability to form hydrogen bonding with water molecules, exhibit liquid-liquid transitions. We find evidence that both melting of ices and liquid-liquid transitions in all these aqueous solutions are controlled solely by water activity, which is related to the difference in the chemical potential between an aqueous solution and pure water at the same temperature and pressure. Our theory shows that water activity is determined by the degree of local tetrahedral ordering, indicating that both phenomena are driven by structural ordering towards ice-like local structures. This has a significant implication on our understanding of the low-temperature behaviour of water.

Keywords: liquid-liquid transition, water and aqueous solution, supercooled liquids and glasses

Japan Geoscience Union Meeting 2014
(28 April - 02 May 2014 at Pacifico YOKOHAMA, Kanagawa, Japan)

MIS36-04 Room:314 Time:May 1 11:30-11:45

Direct Observation of Crystallization Process in a Solution using Transmission Electron Microscopy

KIMURA, Yuki[1*] ; YAMAZAKI, Tomoya[1] ; FURUKAWA, Erika[1] ; NIINOMI, Hiromasa[2] ; TSUKAMOTO, Katsuo[1] ; GARCIA-RUIZ, Juan M.[3]

[1]Tohoku University, [2]Nagoya University, [3]Universidad de Granada

Nucleation is a fundamental event that determines the size, number and morphology of produced crystals. Therefore, the nucleation process must be clarified to form products efficiently and to predict mineralization in various environments. The direct approach to understanding nucleation would be atomic-scale in-situ observation, for which a transmission electron microscope (TEM) would be a most powerful tool. However, the experimental conditions for TEM are limited, and there have been only a few reports on the in-situ observation of nucleation processes to date. In particular, since TEM needs a high vacuum, crystallization experiments in a solution are generally impossible. Recently, the processes of formation of nanoparticles and coalescence in a solution were finally observed using specially designed cells in a TEM [1-3]. However, live observation of the dynamics of the earliest stages of nucleation - those taking place before the formation of a stable crystal - had never been achieved before our recent work [4]. We overcame the difficulty by using an ionic liquid, which has negligible vapor pressure and is not charged up by the electron beam due to its relatively high electron conductivity, and by aiming to visualize the dynamics of nucleation under conditions very close to equilibrium, where the nucleation rate must be small but the conditions for TEM observation are more stable. We used two TEMs at an acceleration voltage of 200 kV (Hitachi H-8100, installed at Tohoku University, Japan) for the nucleation experiment and 300 kV (Hitachi H-9500, installed at Hitachi High-Technologies Corporation, Ibaraki, Japan) for the in-situ heating experiment.

An ionic solution could be observed stably under normal electron irradiation conditions as expected. Nucleation of sodium chlorate crystals was directly observed in the TEM at room temperature. Then, the sample was heated up in the TEM. The main results of the heating experiment were as follows:

1. Nanocrystals were not only dissolved but also newly formed even in the totally dissolving system, i.e., probably an undersaturated condition.
2. Both stable and metastable crystals nucleated independently of their respective solubility. However, metastable crystals were dissolved in a shorter residence time.
3. The total number of smaller particles decreased with the formation of new particles by the Ostwald ripening at or near equilibrium conditions.
4. High-density fluctuations may lead to nucleation even under equilibrium conditions.

We describe the ongoing results to elucidate the dynamics of nucleation at the nanoscale, as well as the growth, coalescence and dissolution of nanocrystals in a solution.

[1] Yuk, J. M., Park, J., Ercius, P., Kim, K., Hellebusch, D. J., Crommie, M. F., Lee, J. Y., Zettl, A. & Alivisatos, A. P. High-resolution EM of colloidal nanocrystal growth using graphene liquid cells. *Science* **336**, 61-64 (2012).

[2] Li, D., Nielsen, M. H., Lee, J. R. I., Frandsen, C. Banfield, J. F. & De Yoreo, J. J. Direction-specific interactions control crystal growth by oriented attachment. *Science* **336**, 1014-1018 (2012).

[3] Liao, H.-G., Cui, L., Whitelam, S. & Zheng, H. Real-time imaging of Pt_3Fe nanorod growth in solution. *Science* **336**, 1011-1014 (2012).

[4] Kimura, Y., Niinomi, H., Tsukamoto, K. & Garcia-Ruiz, J. M. In-situ live observation of nucleation and dissolution of sodium chlorate nanoparticles by Transmission Electron Microscopy. *J. Am. Chem. Soc.*, DOI: 10.1021/ja412111f. (2014).

Keywords: Nucleation, In-situ observation, TEM, Ionic liquid

Japan Geoscience Union Meeting 2014
(28 April - 02 May 2014 at Pacifico YOKOHAMA, Kanagawa, Japan)

MIS36-05 Room:314 Time:May 1 11:45-12:00

Emergence and Amplification of Chirality via Achiral-Chiral Polymorphic Transition in Sodium Chlorate Solution Growth

NIINOMI, Hiromasa[1*] ; HARADA, Shunta[1] ; UJIHARA, Toru[1] ; MIURA, Hitoshi[2] ; KIMURA, Yuki[3] ; UWAHA, Makio[4] ; TSUKAMOTO, Katsuo[3]

[1]Graduate School of Engineering, Naogya University, [2]Graduate School of Natural Sciences, Nagoya City University, [3]Graduate School of Scienece, Tohoku University, [4]Graduate School of Science, Nagoya University

Chirality is the concept that widely spreads in nature at various levels from elementary particles to morphology of plants. Although both the enantiomers have equal stability, lives on the earth preferentially selects one-type of the two enantiomers. This phenomenon is called homochirality, and its origin (the emergence of chirality) and the amplification of chirality are great puzzles in the evolution of life on the primitive earth. One candidate of the origin includes chiral crystallization of achiral compounds. Sodium chlorate($NaClO_3$) undertakes chiral crystallization from achiral solution. $NaClO_3$ has chirality in its crystal structure due to the enaniomorphic space group of $P2_13$ (cubic). A *static* solution of the compound yields statistically equal numbers of the two enantiomorphs. However, Kondepudi *et al.* have strikingly revealed that a *stirred* solution yields only one-type of the enantiomorphs[1]. The mechanism of the significant chiral bias has not been elucidated. Diverse crystallization experiments have implied that the emergence and the amplification proceed during the early stage of crystallization. However, a direct investigation of the early stage is still missing. We therefore have carried out in-situ observations focusing on the early stage. The observations have revealed that achiral metastable crystals having $P2_1/a$ symmetry (monoclinic) appear prior to the formation of chiral crystals. The authors have reported this result in JpGU 2011[2]. Here, we present more detailed observations, and demonstrate that polymorphic transformation from the achiral phase to the chiral phase can be responsible for the emergence and the amplification.

A droplet (6 μl) of $NaClO_3$ aqueous solution saturated at 22 ℃ was put on a glass slide whose temperature is controlled at 22 ℃ by a Peltier device, allowing the droplet to evaporate isothermally. We observed crystallization process induced by the evaporation using a polarized light microscope. The microscope enables us to distinguish cubic crystals from non-cubic crystal by detecting birefringence, allowing us to distinguish chiral crystals from achiral crystals, and it can identify handedness of the chiral crystals by detecting optical rotation.

Polymorphic transformation from an achiral crystal to a chiral crystal was observed. The transformation could be classified into two kinds according to their transition rate. The slower one proceeds at 35 μm/sec (Fig.**A**), and the faster did at 2000 μm/sec (Fig.**B**). The slower transformation was induced by a contact with a chiral crystal. It is noteworthy that the resulting enantiomorph generated through the contact-induced transformation was certainly the same as the enantiomorph that contacted with the achiral crystal. The double digit difference in a rate of the two transformations is probably ascribed to difference in the mechanism, indicating the slower transformation and the fast one are solvent-mediated phase transformation (SMPT) and structural phase transition (SPT), respectively. The SPT probably generates both the enantiomorphs in equal probability since the activation energy required to transform should be equal. In contrast, the contact-induced SMPT preferentially generates the same enantiomorph as the contacted crystal. This inheritance of chirality through the contact-induced SMPT is possibly responsible for the amplification of chirality.

So far, the emergence and the amplification have been explained by primary nucleation of a chiral crystal and secondary nucleation from the crystal. In contrast, our observation provided a new sight based on the achiral-chiral polymorphic transformation: the emergence of chirality through the SPT and its amplification through the contact-induced SMPT.

References

[1] D.K. Kondepudi, R. J. Kaufman & N. Singh, (1990). *Science*, Vol. 250, pp.975-976.

[2] H. Niinomi, T Kuribayashi, H. Miura & K. Tsukamoto, Japan Geoscience Union Meeting 2011, MIS020-06.

Keywords: sodium chlorate, chiral symmetry breaking, chiral crystallization, metastable phase, polymorphic transformation, in-situ observation

MIS36-05 Room:314 Time:May 1 11:45-12:00

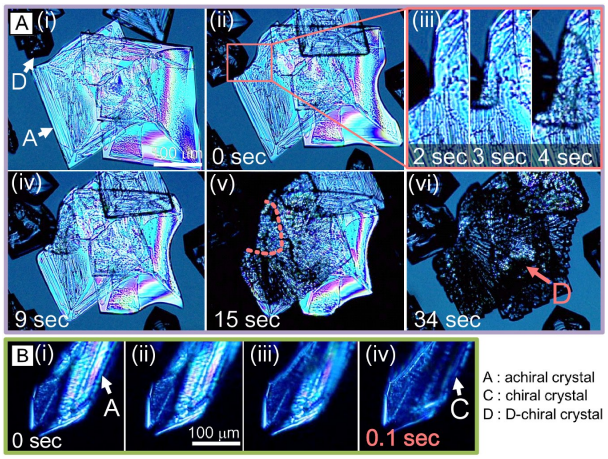

Japan Geoscience Union Meeting 2014
(28 April - 02 May 2014 at Pacifico YOKOHAMA, Kanagawa, Japan)

MIS36-06 Room:314 Time:May 1 12:00-12:15

Theoretical analysis on the stability of divalent cations in the surface sites and clusters of calcium carbonate

KAWANO, Jun[1*] ; SAKUMA, Hiroshi[2] ; NAGAI, Takaya[3]

[1]CRIS, Hokkaido Univ., [2]NIMS, [3]Grad. School of Science, Hokkaido Univ.

Formation process of calcium carbonate polymorphs, calcite, aragonite and vaterite has been extensively investigated, and impurity effect has been proposed as controlling phenomena in order to account for the formation of a particular polymorph. For example, it has been reported that an addition of Mg^{2+} in a solution inhibits calcite formation and promotes aragonite formation, however incorporation mechanism of this kind of impurities is poorly understood.

In general, smaller divalent cations than Ca^{2+}, like Mg^{2+}, cannot form solid solution with aragonite. However, the structure of a crystal surface or small cluster forming at an initial stage of crystal growth can be different from the bulk crystal because of its flexibility, and it can act as the site for incorporation of ions which is unstable in the bulk structure. In the present study, the stability of divalent cations, especially Mg^{2+}, (1) on hydrated aragonite surface and (2) in the cluster forming in an early stage of nucleation was investigated by quantum-chemical calculations, and the impurity effects on the formation of polymorphs were discussed.

The calculation results show that Mg^{2+} is easier to be incorporated into a small cluster, while the hydration energy of Mg^{2+} is higher than that of other divalent cations. This indicates that Mg^{2+} is difficult to be released from hydration shell, however, once released, it is easy to incorporate into the cluster. Atomic arrangement of these clusters including Mg^{2+} is different from that of additive-free $CaCO_3$ clusters. Furthermore, Mg^{2+} on the aragonite surface considerably affects the surface structure and has an influence on the stability of aragonite. Thus, incorporation of Mg^{2+} into the clusters and surfaces sites should play an important role on the formation of the crystalline nuclei and the consequent crystal growth.

Keywords: calcium carbonate, impurity, crystal growh

Japan Geoscience Union Meeting 2014
(28 April - 02 May 2014 at Pacifico YOKOHAMA, Kanagawa, Japan)

MIS36-07 Room:314 Time:May 1 12:15-12:30

Atomic scale in situ observation of solid-liquid interface of calcite

ARAKI, Yuki[1*] ; TSUKAMOTO, Katsuo[2] ; KIMURA, Yuki[3] ; MIYASHITA, Tomoyuki[4] ; OYABU, Noriaki[5] ; KEI, Kobayashi[6] ; YAMADA, Hirofumi[5]

[1]Graduate school of Science, Kobe University, [2]Graduate school of Science, Tohoku University, [3]Institute of Low Temperature Science, Hokkaido University, [4]Faculty of Biology-Oriented Science and Technology, Kinki University, [5]Department of Electronic Science and Engineering, Kyoto University, [6]The Hakubi Center for Advanced Research, Kyoto University

Calcium carbonate is one of common minerals on the earth. Calcium carbonate crystals are utilized industrially in various fields, so that the control of crystal growth is required. It has been known that organisms control the morphology and polymorph of calcium carbonate crystals by utilizing inorganic and organic additives in biomineralization. Understanding the additive effects on growth of calcium carbonate crystal is necessary to control the crystal growth.

The effect of additives on growth of calcite which is a stable polymorph of calcium carbonate has been investigated. The additive effect on calcite surface, such as incorporation of magnesium ions into calcite and pinning of step propagation by organic molecules has been confirmed. On the other hand, the additive effect on hydration of calcite has remained unclear even if that effect has been suggested by the measurement of growth rate of calcite in the presence of additives. Hydration affects adsorption and surface diffusion of ions on calcite surface. Also, the dehydration has been considered as rate-determining process in solution growth by the estimation of energy barriers of solution growth processes. Therefore, hydration is a key to control the kinetics of calcite growth.

Hydration at the vicinity of calcite surface has been measured by surface X-ray diffraction. Although this technique made the description of hydration structure clear, it does not show the local difference of hydration structure between on the terrace and the step front which is capture site of ions. Hence, we employed the newly frequency modulation atomic force microscopy (FM-AFM) for in situ observation of local hydration structure in atomic scale. This technique is expected to provide insight into the atomic scale distribution of hydrated water molecules in growth solution even at step front. This study describes the first in situ examination of the additive effect of organic molecules and magnesium ions on local hydration structure of calcite surface in atomic scale utilizing FM-AFM. The hydration images were compared with the growth rate of calcite measured using phase shift interferometry so as to validate the influence of hydration on the growth rate of calcite.

The findings are summarized as follows:

(1) The synthetic polypeptide, even that with high hydrophilicity, does not affect hydration at the surface of calcite.

(2) Combination of magnesium ions and the synthetic polypeptides provides a rigid hydration on calcite surface.

(3) Magnesium ions and the synthetic polypeptides influence hydration and the surface pattern of calcite, respectively.

(4) Structured water distribution eases the energy gap between the calcite surface and solution. As a result, the interfacial tension between the calcite surface and the solution is decreased.

(5) Magnesium ions and the synthetic polypeptide act in unison to accelerate nucleation via changes in hydration structure.

(6) Hydration contributes to interfacial energy between the calcite and the solution, but not for the adsorption of ions on the calcite steps.

This study demonstrated that additives affect the interfacial tension via altering hydration structure by application of FM-AFM for crystal growth experiment for the first time. Our results also showed that there is hardly any change in the adsorption of ions on calcite surface due to the hydration structure. That suggests that dehydration is not a rate-determining process, an observation that is contrary to the currently prevailing theory. The further observation of hydration of step front will be carried out by FM-AFM to demonstrate the effect of hydration on adsorption of ions. These findings indicate that the control of interfacial tension is possible utilizing the additive effect on hydration. That provides a new knowledge to regulate the polymorphism of calcium carbonate.

Keywords: Calcite, Hydration, FM-AFM

MIS36-07 Room:314 Time:May 1 12:15-12:30

FM-AFM images of Hydration structure on calcite

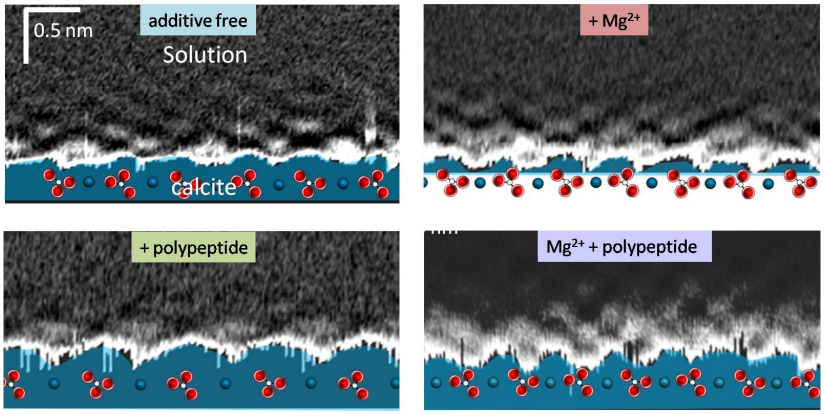

Japan Geoscience Union Meeting 2014
(28 April - 02 May 2014 at Pacifico YOKOHAMA, Kanagawa, Japan)

MIS36-08 Room:314 Time:May 1 12:30-12:45

Impurity partitioning in colloidal crystallization

NOZAWA, Jun[1*] ; HU, Sumeng[1] ; KOIZUMI, Haruhiko[1] ; FUJIWARA, Kozo[1] ; UDA, Satoshi[1]

[1]Institute for Materials Research, Tohoku University

Colloidal crystals are regarded as a promising tool to investigate diverse basic physical phenomena. We have applied this colloidal crystal to impurity partitioning in the melt growth. Since no research has been focused to detail partitioning behavior of colloidal crystals, the objective of the present work is to reveal a partitioning behavior during colloidal crystallization.

A few amount of impurities (2 percent) were doped to the colloidal dispersion, from which colloidal crystals were grown with convective assembly method. Polystyrene particles (PS) were used for fabricating colloidal crystals, and different sizes of PS and fluorescent bearing PS (w/fluor.) were doped as impurity particles.

In each particle size for two kinds of impurity, effective partition coefficient (k_{eff}) were measured at various growth rates. Obtained keff gives k_0 by using BPS plot. The k_0 is decreased as the difference between the size of the impurity and the 500 nm host particle increased. The k_0 of each w/fluor. was larger than that of the corresponding pure PS. Moreover, the value of k0 for the 520 nm w/fluor. surpassed unity, whereas the PS is always less than unity.

We have employed a Thurmond and Struthers (T&S) model (J. Phys. Chem. 57, 831 (1953)) to discuss the difference of k_0 for PS and w/fluor. particles. T&S model shows k_0 as; k_0 = exp((Δ G_{Tr} –Δ H)/RT). Here, Δ G_{Tr} is free energy difference between the solid and liquid phases of an impurity at the transition temperature, T, Δ H is the excess enthalpy which is caused by incorporation of the impurity into the host material, and R is a gas constant. We have determined the phase transition volume fraction for PS and w/fluor. to evaluate the Δ G_{Tr}. It was shown that Δ G_{Tr} of w/fluor. is positive whereas PS is zero. This leads to larger Δ G_{Tr} –Δ H of w/fluor. than that of PS, which corresponds to larger k_0 of w/fluor., and in a small –Δ H range, k_0 of w/fluor. surpasses unity. We have found the difference of k_0 for different kinds of impurity particles, and succeeded in applying concept of T&S model to partitioning of colloidal crystals.

Keywords: Colloidal crystal, Impurity partitioning

Japan Geoscience Union Meeting 2014
(28 April - 02 May 2014 at Pacifico YOKOHAMA, Kanagawa, Japan)

MIS36-09 Room:314 Time:May 1 14:15-14:30

Mechanism of ice nucleation on (100) plane of calcium oxalate monohydrate: a molecular dynamics simulation study

NADA, Hiroki[1*] ; ISHIKAWA, Masaya[2] ; ECHIGO, Takuya[3]

[1]EMTECH, National Institute of Advanced Industrial Science and Technology (AIST), [2]National Institute of Agrobiological Sciences, [3]Shiga University

Calcium oxalate monohydrate (COM) is the most thermodynamically stable polymorph of calcium oxalate. COM is known as an organic mineral formed on the surface of the Earth, under the bottom of sea, in atmosphere, in meteorites, in plants and in kidney stones. So far, COM has been studied in fields of mineralogy, biology and medical science.

Recently, Ishikawa et al. suggested that COM plays as an ice nucleation promoter, like silver iodide and ice nucleation-active bacteria. They speculated that the structure of COM (100) plane induces ice nucleation. Studies on the mechanism of ice nucleation promotion by COM are important, because the studies may help provide development of new materials to make artificial snow. Molecular dynamics (MD) simulation is a helpful method to investigate the mechanism of ice nucleation at the molecular scale. Thus, we performed a MD simulation to elucidate the mechanism of ice nucleation on the (100) plane of COM.

In the simulation, the intermolecular interaction between a pair of water molecules was estimated using a six-site model. The water-COM interaction was estimated using a COM potential model proposed by Tommaso et al. In the <100>direction of COM, two different molecular layers are piled up by turns; one is positively-charged Ox-1 layer consisting of calcium ions and oxalate ions, and the other is negatively-charged Ox-2 layer consisting of oxalate ions and water molecules. In this study, the simulation was performed for a rectangular parallelepiped system in which supercooled water consisting of 4000 water molecules was sandwiched by Ox-1 and Ox-2 layers. Temperature was set to 268 K. Total run was 4 ns or longer. The simulation indicated the formation of a polar cubic ice structure near the Ox-2 layer. However, the formation of a hexagonal ice structure was not observed. Details of the simulation results will be shown at the presentation.

This work was supported by a Grant-in-Aid for Scientific Research (No. 22107004) on Innovative Areas of ”Fusion Materials (Area No. 2206)” from the Ministry of Education, Culture, Sports, Science and Technology (MEXT).

Keywords: crystal growth, nucleation, ice, organic mineral, computer simulation, calcium oxalate

Japan Geoscience Union Meeting 2014
(28 April - 02 May 2014 at Pacifico YOKOHAMA, Kanagawa, Japan)

MIS36-10 Room:314 Time:May 1 14:30-14:45

Observation of admolecule on the crystal surface in liquid by non-contact atomic force microscopy

NAGASHIMA, Ken[1*]

[1]Institute of Low Temperature Science, Hokkaido University, Japan

The highest resolution AFM images are obtained by non-contact atomic force microscopy (NC-AFM). Fukuma et al. (2005) succeeded in obtaining true atomic resolution images by NC-AFM in spite of the liquid environment [1]. We are interested in the crystal growth process. However, previous NC-AFM studies were only about insoluble crystals in liquid. NC-AFM is not good at investigating the moving surface because NC-AFM is a very sensitive method for detecting weak interaction force. Therefore, we tried to observe several soluble crystals in liquid by NC-AFM at first.

At first, we observed tetragonal lysozyme (110) face in saturated solution by using homebuilt Non-Contact AFM (NC-AFM). We could observe individual molecules on the lysozyme (110) face in liquid for the first time and determine the crystallographic position of each molecule [2]. In addition, we also observed admolecule and point defect on the lysozyme surface in liquid.

Acknowledgments
We thank Prof. S. Morita of Osaka University, M. Abe of Nagoya University, and Shimadzu Corporation for observation of AFM.

[1] T. Fukuma et al., Appl. Phys. Lett. 87, 034101 (2005).
[2] K. Nagashima et al., J. Vac. Sci. Technol. B 28, C4C11 (2010).

Keywords: AFM, Crystal growth, Atomic resolution image, Admolecule, Protein crystal

Japan Geoscience Union Meeting 2014
(28 April - 02 May 2014 at Pacifico YOKOHAMA, Kanagawa, Japan)

MIS36-11 Room:314 Time:May 1 14:45-15:00

In-Situ Observation of Protein Crystal Growth in The International Space Station

MURAYAMA, Kenta[1*] ; YOSHIZAKI, Izumi[2]

[1]Katsuo Tsukamoto, [2]JAXA

In-situ observation of protein crystal growth was conduced at the international space station in 2012. Both growth rate and surface topography of lysotyme crystals vs supersaturation and purity of the solution were measured for the first time by interferometry in space. The differences from groud-base experiments became clear to answer the question ”Why better crystal could be grown in space?”.

Keywords: crystal growth, space experiment, microgravity

Japan Geoscience Union Meeting 2014
(28 April - 02 May 2014 at Pacifico YOKOHAMA, Kanagawa, Japan)

MIS36-12 Room:314 Time:May 1 15:00-15:15

In situ simultaneous SEM/STEM observation of Pt/C catalysts in a gaseous atmosphere

SATO, Takeshi[1*] ; MATSUMOTO, Hiroaki[1] ; NAGAOKI, Isao[1] ; NAGAKUBO, Yasuhira[1] ; YAGUCHI, Toshie[1]

[1]Hitachi High-Technologies Corporation

In order to gain fundamental understanding of the degradation mechanisms of Pt/C catalyst, there is an increasing demand on the nanostructural characterization using TEM. We have developed the humid-air supply system in TEM, H-9500 300 kV TEM and we have success the deterioration mechanism of fuel cell electrocatalyst[1]. Recently, we developed in situ simultaneous SEM/STEM observation technique for surface analysis of catalyst materials using a HF-3300 Cold-FE TEM with SEM/STEM function. We succeeded in visualizing of three-dimensional movement of the Pt particles on the carbon support in the gas atmosphere by this observation technique.

In situ simultaneous SEM/STEM observation of the platinum catalysts on carbon support (Pt/C; Pt: 29 wt.%) in the air conditions were carried out using HF-3300 equipped with the Cold-FE gun and the SEM/STEM function. A gas injection-heating specimen holder[2] was used for the Pt/C powder heating and gas injection. Pt/C powder mounted on the tungsten wire was heated to 200 deg C in a TEM, and then, while air was spraying (up to 1.2 x 10^{-2} Pa) from the injection nozzle to the Pt/C, the behavior of the Pt/C was recorded as the movie file. After the air injection at about 1.0 x 10^{-3} Pa, the coalescence growth between Pt particles on the carbon support was observed, and the Pt particles gradually started inserting into the carbon support. After that, most all of the Pt particles on the carbon support disappeared from the surface of the carbon support. And the carbon support structure was changing into a porous morphology.

We can observe that the behavior of the Pt particles on the carbon support was penetrated into the carbon support by in situ simultaneous SEM/STEM observation. These results demonstrate that the penetration of Pt particles to carbon support affects the degradation mechanism of a Pt/C electrocatalyst.

1. T. Yaguchi et. al., Journal of Electron Microscopy 60(3), 217?225, (2011)
2. T. Kamino et. al., Journal of Electron Microscopy 54(6), 497?503, (2005)

Keywords: electron microscope, in situ observation

Japan Geoscience Union Meeting 2014
(28 April - 02 May 2014 at Pacifico YOKOHAMA, Kanagawa, Japan)

MIS36-13 Room:314 Time:May 1 15:15-15:30

Low temperature crystallization of free-flying silicate nanoparticles investigated by in-situ IR measurement experiment

ISHIZUKA, Shinnosuke[1*] ; KIMURA, Yuki[1] ; SAKON, Itsuki[2]

[1]Depatment of Earth and Planetary Science, Tohoku University, [2]Depatment of Astronomy, University of Tokyo

Dust is typically 100 nm sized nanoparticles which can be observed ubiquitously in the universe. Dust forms from the high temperature gas in the out flow of evolved stars and dispersed into interstellar space. Silicate dust is one of the most abundant minerals in the universe including, shells around evolved stars [1], disks around young stars [2], comets [3] and so on. So its formation mechanism is the key process to understand the lifecycle of dust. Especially, 10 μm IR band structure from 8 μm to 12.5 μm in wavelength arising from Si-O stretching provides us mineralogical character of silicate. The Infrared Space Observatory mission revealed the existence of crystalline silicates around evolved stars based on the 10 μm band feature mainly attributed to amorphous silicate [4]. Numerous laboratory experiments to reproduce the observed spectra such as direct condensation [e.g. 5] and annealing of amorphous silicates [e.g. 6] showed variation in the IR spectra due to structure, chemical composition, temperature, size and shape, and proposed formation mechanisms of crystalline silicates. Nevertheless the scenario is not fully understood. One of the most important discrepancies concerning the dust formation process is a detection of an IR feature attributed to crystalline silicates at low temperature region, typically $<$300 K [1] in contrast to amorphous silicates at high temperature region [4]. Low temperature crystalline silicates cannot be explained by direct condensation or annealing involving high temperature process.

Recently, we have investigated new IR measurement technique for free-flying nanoparticles which enabled direct comparison with astronomical observation without KBr medium effects which pervert its band structure such as peak wavelength, FWHM and relative intensity [7]. Applying the new IR technique, we investigated condensation of Mg-bearing silicate from thermally evaporated magnesium and silicon oxide under the atmosphere of O_2 and Ar based on 10 μm band.

In-situ IR measurement revealed initial condensates were amorphous or droplet of Mg-bearing silicate and its crystallization took place at $<$500 K. Furthermore, crystallization kept proceeding through lower temperature region. Produced particles showed core-mantle like structure, amorphous silica covered with polycrystalline forsterite observed by Transmission Electron Microscope.

Prevailing annealing experiments reported that 1000 K is required for crystallization of forsterite [8]. This critical discrepancy may be explained by nano size effects. When immoderately small particle nucleates, a particle takes metastable amorphous or droplet phase because of lower melting point of a nanoparticle [9] and larger diffusion coefficient of molecules in a nanoparticle distinct from in bulk [10]. In case the condensates were droplet due to the size effects, activation energy of crystallization is significantly low compared to amorphous [11]. We concluded such characteristic phenomena in nanometer scale enabled low temperature crystallization in the same way as the circumstellar environments.

References: [1] Waters, L. B. F. M., et al. 1996, A&A, 315, L361, [2] Bouwman, J., et al. 2001, A&A, 375, 950, [3] Hanner, M., et al. 1994, ApJ, 425, 274, [4] Molster, F., & Kemper, C. 2005, Space Sci. Rev., 119, 3,[5] Tsuchiyama, A. 1998, Mineralogy journal, 20, 59, [6] Hallenbeck, S. L., et al. 2000, ApJ, 535, 247, [7] Bohren, C. F., & Huffman, D. R. 1983, Absorption and Scattering of Light by Small Particles (New York: Wiley), [8] Koike, C., et al. 2010, ApJ, 709, 983, [9] Qi., 2005, Physica B, 368, 46, [10] Yasuda, H., et al. 1992, JEM, 41, 267, [11] Tanaka, K., K. et al. 2008, JCG, 310, 1281

Keywords: astromineralogy, nanoparticle, experiment, IR

Japan Geoscience Union Meeting 2014
(28 April - 02 May 2014 at Pacifico YOKOHAMA, Kanagawa, Japan)

MIS36-14 Room:314 Time:May 1 15:30-15:45

Free energy of cluster formation and a new scaling relation for the nucleation rate

TANAKA, Kyoko[1*] ; DIEMAND, Juerg[2] ; ANGELIL, Raymond[2] ; TANAKA, Hidekazu[1]

[1]Institute of Low Temperature Science, Hokkaido University, [2]University of Zurich

Recently we performed molecular dynamics (MD) simulations of homogeneous nucleation from vapor for systems of (1-8) $\times$ 10^9 Lennard-Jones atoms [Diemand etal. J. Chem. Phys. 139, 074309 (2013)]. The very large MD simulations allow us to determine the formation free energy of clusters accurately over a wide range of cluster sizes, for the first time. This is now possible because such large simulations allow for very precise measurements of the cluster size distribution in the steady state nucleation regime. The peaks of the free energy curves give critical cluster sizes, which agree well with independent estimates based on the nucleation theorem. Using these results, we derive an analytical formula and a new scaling relation for nucleation rates: ln J' / η is scaled by ln S / η, where the supersaturation ratio is S, η is the dimensionless surface energy, and J' is a dimensionless nucleation rate. This relation can be derived using the free energy of cluster formation at equilibrium which corresponds to the surface energy required to form the vapor-liquid interface. At low temperatures (below the triple point), we find that the surface energy divided by that of the classical nucleation theory does not depend on temperature, which leads to the scaling relation and implies a constant, positive Tolman length equal to half of the mean inter-particle separation in the liquid phase.

Keywords: nucleation, molecular dynamics simulation, nucleation rate, scaling, free energy of cluster formation

Japan Geoscience Union Meeting 2014
(28 April - 02 May 2014 at Pacifico YOKOHAMA, Kanagawa, Japan)

MIS36-P01 Room:Poster Time:May 1 18:15-19:30

High-speed polarized in-situ observation in a nucleation process of nanoparticles produced by the gas evaporation method

KIMURA, Yuki[1*] ; MIHARA, Arata[2] ; ONUMA, Takashi[2] ; ISHIZUKA, Shinnosuke[1] ; MURAYAMA, Kenta[1] ; TSUKAMOTO, Katsuo[1]

[1]Tohoku University, [2]Photron

The gas evaporation method has been investigated for more than half a century since the Kubo effect was reported (1962). There have been many studies on the produced nanoparticles mainly using a transmission electron microscope, which have elucidated the different physical properties of nanoparticles from those in bulk. On the other hand, there have been almost no reports on nucleation in smoke related to crystal growth. Recently, we achieved in-situ observation of the nucleation process in smoke using a double-wavelength Mach-Zehnder-type interferometer, which can determine the temperature and pressure at the nucleation simultaneously. A series of experiments clearly showed that smoke particles condense homogeneously only in a very high supersaturated environment [1-3]. In a preliminary experiment using tungsten trioxide, the smoke particles condensed with a degree of supersaturation as high as $\sim 10^6$. In this process, since evaporant is continuously supplied into the surrounding of the evaporation source, the flow of smoke after the nucleation and growth of nanoparticles has been simply considered as a consecutive process. The nucleation and growth of smoke particles should be a rapid process (ms order) due to high supersaturation, so the concentration of the evaporated vapor drastically decreases. However, the details of the formation process remain unknown.

In this study, we attempted to visualize the nucleation of nanoparticles and motion of smoke using a high-speed polarization image sensor (Photron Inc.) to clarify the details of the nucleation process of smoke particles. Since the sensor itself has pixels with micro-polarizers, a phase shift interferogram can be obtained in less than a millisecond because of the lack of mechanical movement free, and can therefore be applied to rapid phenomena such as nucleation in vapor phase. Here, we show the preliminary results of homogeneous nucleation of tungsten oxide from vapor phase.

[1] Y. Kimura, H. Miura, K. Tsukamoto, C. Li, T. Maki, Interferometric in-situ observation during nucleation and growth of WO_3 nanocrystals in vapor phase, *Journal of Crystal Growth*, 316 (2011) 196-200.

[2] Y. Kimura, K. Tsukamoto, Interferometric observation of temperature distributions in the smoke experiment, *J. Jpn. Soc. Microgravity* 28 (2011) S9-S12.

[3] Y. Kimura, K. K. Tanaka, H. Miura, K. Tsukamoto, Direct observation of the homogeneous nucleation of manganese in the vapor phase and determination of surface free energy and sticking coefficient, *Crystal Growth & Design*, 12 (2012) 3278?3284.

Keywords: Nucleation, High-speed polarized camera, in-situ observation

Japan Geoscience Union Meeting 2014
(28 April - 02 May 2014 at Pacifico YOKOHAMA, Kanagawa, Japan)

MIS36-P02 Room:Poster Time:May 1 18:15-19:30

In-situ observation of nucleation process of calcium carbonate by the fluid-reaction TEM

YAMAZAKI, Tomoya[1*] ; FURUKAWA, Erika[1] ; KIMURA, Yuki[1]

[1]Tohoku University

Recent studies have reported achievements of in-situ observation of the nucleation and crystallization studies using transmission electron microscope (TEM), and several new perspectives for non-classical pathway of crystallization [1-4]. Calcium carbonate generates a lot of attention because of complex nucleation due to appearance of various polymorphs in addition to availability for industrial materials such as paper and paint, and reservoir of carbon dioxide, and biomineralization. We also focus on the calcium carbonate in view of selection of polymorph in nucleation process. In case of nucleation from relatively higher supersaturated solution, nucleation of amorphous phase prior to crystalline phase has been known [5,6]. Kawano et al. have been reported an in-situ observation of solution-mediated phase transition from amorphous phase into crystalline phase under optical microscope [6]. The Ostwald law of stages has been believed to occur in many cases. Contribution of prenucleation cluster, which was confirmed by using the cryo-TEM [8], to the nucleation has also been reported [7]. However the generality or solution condition to take these processes is still not obvious.

Now, we have performed energetically a project to observe crystallization and dissolution processes in an aqueous solution using ionic liquid instead of water or the ”Poseidon” (Protochips Inc.), which is a sample holder having a liquid cell for TEM observation. We call our TEM fluid-reaction TEM (FR-TEM), which is able to perform crystallization experiments in a solution including both methods. Here, we have been tried to observe whole the process of crystallization of calcium carbonate via amorphous phase using fluid-reaction TEM and actually observed a solid-state phase transition from amorphous phase into a crystalline phase by in-situ observation.

[1] Yuk, J. M., Park, J., Ercius, P., Kim, K., Hellebusch, D. J., Crommie, M. F., Lee, J. Y., Zettl, A. & Alivisatos, A. P. *Science* **336**, 61-64 (2012).
[2] Li, D., Nielsen, M. H., Lee, J. R. I., Frandsen, C., Banfield, J. F. & De Yoreo, J. J. *Science* **336**, 1014-1018 (2012).
[3] Liao, H.-G., Cui, L., Whitelam, S. & Zheng, H. *Science* **336**, 1011-1014 (2012).
[4] Kimura, Y., Niinomi, H., Tsukamoto, K. & Garcia-Ruiz, *J. M. J. Am. Chem. Soc.*, DOI: 10.1021/ja412111f. (2014).
[5] Ogino, T., Suzuki, T. & Sawada, K. *Geochim. et Cosmochim. Acta*, **51** (1987) 2757.
[6] Kawano, J., Shimobayashi, N., Kitamura, M., Shinoda, K., & Aikawa, N. *J. Cryst. Growth*, **237** (2002) 419.
[7] Gebauer, D., & Colfen H. *Nano Today*, **6** (2011) 564.
[8] Pouget, E.M., Bomans, P. H., Goos, J.A.C.M., Frederik, P.M., de With, G. & Sommerdijk, N. A. *Science*, **323** (2009) 1455.

Keywords: Fluid-reaction TEM, In-situ observation, Calcium carbonate, Nucleation

Japan Geoscience Union Meeting 2014
(28 April - 02 May 2014 at Pacifico YOKOHAMA, Kanagawa, Japan)

MIS36-P03 Room:Poster Time:May 1 18:15-19:30

In-situ TEM observation of dissolution processes in aqueous solutions using ”Poseidon”

FURUKAWA, Erika[1*] ; YAMAZAKI, Tomoya[1] ; KIMURA, Yuki[1]

[1]Tohoku University

Recently, we started a new project to observe crystallization and dissolution processes of crystals in a solution using two different methods under transmission electron microscope (TEM). To overcome the difficulties to introduce a solution into a TEM, Kimura et al. used ionic liquid to avoid evaporation of a solvent in the high-vacuum of a TEM [1]. As the result, several new insights were found: solubility-independent formation of polymorph; crystals do not dissolve smoothly but in a fluctuating manner; and new crystals form even in a totally dissolving system. Another advantage of this method is that the growing crystal does not have a hydrated layer on their surface. It has been believed that dehydration process has a largest potential barrier to incorporate a unit cell into the crystal. However, no one ever visualized the process and it has been totally veiled. The water free experiment using an ionic liquid may give us a new perspective on the dehydration process by comparison with experiments in general aqueous solutions. Now, we are forwarding a project to observe crystallization and dissolution processes in an aqueous solution in atomic-scale using the ”Poseidon”, which is a sample holder having a liquid cell for TEM observation. We call our TEM fluid-reaction TEM (FR-TEM) including both solution growth experiments using an ionic liquid and the Poseidon.

Poseidon (Protochips Inc.) give us the opportunity to visualize the three-dimensional process with several advantages compared with previous works using an atomic force microscope, which is able to observe only two-dimensional, and an optical microscope, which has much less lateral resolution. Growth and dissolution processes at the first top layer (surface) of a crystal have been energetically studied long time using these tools. However, the detail process in atomic scale has been observed very limited. Therefore, the aims of our project is understanding of three dimensional nucleation including Ostwald law of stages based on phase determination by electron diffraction, determination of very slow dissolution rates, and dissolution process in terms of an influence of defects. Here, we will show the first pictures about the movements of nanoparticles and dissolution of amorphous silica and crystalline silicate samples.

[1] Kimura, Y., Niinomi, H., Tsukamoto, K. & Garcia-Ruiz, J. M. In-situ live observation of nucleation and dissolution of sodium chlorate nanoparticles by Transmission Electron Microscopy. *J. Am. Chem. Soc.*, DOI: 10.1021/ja412111f. (2014).

Keywords: Fluid-reaction TEM, Dissolution, In-situ observation

Japan Geoscience Union Meeting 2014
(28 April - 02 May 2014 at Pacifico YOKOHAMA, Kanagawa, Japan)

MIS36-P04 Room:Poster Time:May 1 18:15-19:30

Mineral size distribution modeling during dissolution of montmorillonite

YAMAGUCHI, Kohei[1*] ; MIURA, Hitoshi[2] ; SATOH, Hisao[1]

[1]Mitsubishi Materials Co., [2]Nagoya City University

In the geological disposal of radioactive waste, the waste is sealed by cement-based materials and bentonite-based material to prevent leakage into environment. The bentonite-based material protect the radioactive waste from the groundwater flow around the geological disposal area, so its low permeability should be maintained for a long term. The low permeability could be achieved by the swelling of montmorillonite in the bentonite-based material. However, montmorillonite will dissolve by a reaction with high-alkaline pore water, spoiling the low permeability of the bentonite-based material. In addition, precipitation of secondary minerals such as zeolite will promote the dissolution of montmorillonite through changes in composition of the pore water. In order to assess the long-term permeability of the bentonite-based material, it is necessary that the dissolution of montmorillonite and crystallization of secondary minerals are comprehended over a long time of several tens of thousands years.

In the pore water, there are numerous montmorillonite particles of various sizes. When montmorillonite of various sizes co-exists in the same solution, the smaller particle dissolves faster than the larger one because of the Thomson-Gibbs effect. The mean size of montmorillonite will increase gradually, leading to a delay of further dissolution. In addition, an evolution of size distribution is also important for the crystallization process of the secondary minerals, e.g., zeolite. Since zeolite is not present in the initial solution, the crystallization process is described in the nucleation and subsequent growth. Evolution of the size distribution of zeolite affects the dissolution of montmorillonite through changes in solution composition. This implies that the evolution of the size distribution of montmorillonite and zeolite should be considered to assess the long-term behavior of the permeability of the bentonite-based materials. However, in the previous chemical equilibrium calculations, the evolution of the size distribution has not been considered.

In this report, we numerically modeled the time evolution of the size distribution of montmorillonite due to dissolution according to a theoretical model described in Yao et al. (1993). The crystallization of zeolite was neglected as a first step. We consider the dissolution of montmorillonite in a closed system. The evolutions of the size distribution, bulk concentration of solution, and mean radius of montmorillonite were successfully calculated.

The model given in this report is a model in a closed system. On the other hand, the geological disposal environment is not a closed system because there is an actual mass transfer due to the flow of groundwater and diffusion. To couple the local mineral dissolution/crystallization and the global mass transfer, some chemical reaction-mass transfer calculation codes have been developed. However, these codes assumed chemical equilibrium, so the evolution of the size distribution of minerals did not considered. The evolution of the size distribution of minerals would significantly affect the long-term behavior of the permeability of the bentonite-based materials. Therefore, it is important to compare the calculation results of the model with the evolution of the size distribution and chemical equilibrium calculation result.

Keywords: montmorillonite, dissolution, Mineral size distribution

Japan Geoscience Union Meeting 2014
(28 April - 02 May 2014 at Pacifico YOKOHAMA, Kanagawa, Japan)

MIS36-P05 Room:Poster Time:May 1 18:15-19:30

Advanced techniques in the latest quantitative image analysis for crystal growth experiments

YOKOMINE, Makoto[1*] ; SATOH, Hisao[2] ; TSUKAMOTO, Katsuo[3] ; SAZAKI, Gen[4]

[1]TOYO Corporation, [2]Mitsubishi Materials Corporation, [3]Tohoku University, [4]Hokkaido University

In the research field of crystal growth science, the targeted scales are varied from nano-scaled small space to visible large space. Recently the spatial scale expands toward underground or orbital space. In the metrology field, there is the scaling-law for xyz-t space-time space, beyond which we extend the measurable limits.

The contactless microscopes like interferometers or laser microscopes are very valuable tools for analyzing crystal growth in long time and surface-features in wide area because they have advantages to obtain data in high speed without spoiling the sample surface. Their time-scale is variable in the off-line processing, if the data were sequentially obtained by auto-measurements, so that we can trace the real growth phenomena. By this method, we succeeded to observed lysozyme growths in the International Space Station laboratory, ice-water interface and dissolving clay.

Moreover, the spatial scale can be changed by shifting the field of view with observing and the off-line process of these obtained images as stitching. In general, huge data fragments measured by certain time interval or position shifting contain offsets or distortions and the data amount is much bigger than the speed of manual corrections. Hence, there are many cases that whole data cannot be utilized for final analysis. We attempted to eliminate artifacts generated by microscopes using a system consist of commercially supplied software and dedicated plug-in programs for consistent normalizations and corrections between planes to be stitched.

In this session, we will introduce some examples tried quantitative analysis of huge multiple data including the time-line display expressing time-based changes at certain line on a plane of growing and dissolving crystal surfaces.

Keywords: image analysis, time-space scale, topography, huge stitching

Japan Geoscience Union Meeting 2014
(28 April - 02 May 2014 at Pacifico YOKOHAMA, Kanagawa, Japan)

MIS36-P06 Room:Poster Time:May 1 18:15-19:30

IP6 as a silver carrier agent and formation of Ag nanostructures

TATSUOKA, Hirokazu[1*] ; MENG, Erchao[2] ; KOBAYASHI, Tsuyoshi[3] ; SHIMOMURA, Masaru[1] ; TOMODA, Waichi[1] ; MIYABAYASHI, Keiko[1]

[1]Graduate School of Engineering, Shizuoka University, [2]Graduate School of Science and Technology, Shizuoka University, [3]Koba Technology

In recent years, people have become aware of the importance of natural organic materials in geological systems. It would be important to clarify the interaction between natural organic materials and metallic ions.

Phytic acid, known as inositol hexakisphosphate (IP6), or phytate, $C_6H_{18}O_{24}P_6$, is found within the hulls of nuts, seeds, and grains, and it is the principal storage form of phosphorus in many plant tissues, especially bran and seeds. IP6 is not digestible to humans and animals, and phytic acid chelates make unabsorbable certain important minerals such as zinc, iron, calcium and magnesium.

On the other hand, for many years, it has been known that silver works for its catalytic activities, anti-microbial activities, and used to avoid infections and prevent spoilage. Many researchers have focused on the anti-bacterial, ability to kill microorganisms and multi-functional properties of silver nano-particles.

In this study, it is demonstrated that IP6 plays a role as a metal carrier agent for the formation of metallic nanostructures. For the preparation of the IP6 with Ag elements (Ag-IP6), The commercial IP6 solution (50 %) was diluted with distilled H_2O at the H_2O:IP6 solution ratio of 9:1, then 1g of $AgNO_3$ was added to the diluted IP6 solution of 100 ml, and long-term stabilized small Ag clusters were formed in the solution. A drop of the solution was dripped onto metallic substrates, then kept for the treatment time of 10 s to several min at room temperature. The solution was immediately dried using a gas burner or hot plate. Then, the reaction of the Ag-IP6 with several kinds of metals was examined. The structural and morphological properties of the Ag nanostructures were characterized by scanning electron microscopy (SEM) along with energy dispersive X-ray spectroscopy (EDS), transmission electron microscopy (TEM) and scanning transmission electron microscopy (STEM) with EDS. In addition, the surface condition of the Ag nanostructures reacted with Cu or Al and dried IP6 complexes was characterized by X-ray photoelectron spectroscopy (XPS) using a VG, ESCA-LAB Mk II with a non-monochromatized Al K$\alpha source (h\nu$ = 1486.6 eV). The energy calibration for a charge correction in the spectra was made using the C1s peak. The FTIR spectra of the dried IP6 complexes were measured using KBr disks. Each disc was composed of powders consisting of IP6:KBr˜1:100. The spectra were recorded in the range of 400 to 1400 cm^{-1}. Raman spectra were obtained using an NR-1800 triple Raman system with backscattering geometry using the SHG(532 nm) of a Nd:YAG laser as the excitation source. All measurements were carried out at room temperature. It was found that various kinds of Ag nanostructures were formed with additional metallic sources using the Ag-IP6. Ag nanostructures with the three-dimensional dendritic structures replaced by Cu and Mn, the two-dimensional dendritic structures replaced by $CaSi_2$ and Mg, the two-dimensional fractal structures replaced by Fe, Ti, Al and Ni, the particles replaced by $SrSi_2$ and the nanowires replaced by Mo and W were formed. It is noted that the IP6 plays an important role as a silver carrier agent to control the structure and morphology of the Ag nanostructures. In addition, the experimental results suggest that the structural evolution of the Ag-IP6 reacted with Cu takes place to form the Cu-IP6 complex. However, the reaction of Ag-IP6 with Al is not active.

The structural properties of the Ag nanostructures were examined, and the growth evolution of the nanostructures was discussed. The results would help us to understand the nanostructure formation by the reaction between natural organic materials and metals in nature.

Keywords: IP6, nanostructure, dendrite growth, silver

Japan Geoscience Union Meeting 2014
(28 April - 02 May 2014 at Pacifico YOKOHAMA, Kanagawa, Japan)

MIS36-P07 Room:Poster Time:May 1 18:15-19:30

Development and application of 3-D interferometer for analysis of the concentration field in protein crystal growth

MURAYAMA, Kenta[1*] ; TSUKAMOTO, Katsuo[1]

[1]Graduate School of Science, Tohoku University

When the crystal is growing in a supersaturating solution, the solute concentration is decreasing towards the crystal/ solution interface because the crystal consumes solute in the solution as it grows. Due to this large vertical concentration gradient, buoyancy driven solutal convection develops. As a result, the distribution of concentration around the crystal become complicated compared to the case when there is no convection.

Thus, not only concentration gradient but also the flow and convection of the solution influences the state of the crystal surface. So that visualizing the whole concentration field of a crystal interface including convection is required.

There have been many reports concerning the measurement of the concentration field, but many of them were two-dimensional (2-D) observations, namely, the objects were observed only from one direction. The information obtained by the 2-D observations is integrated in average along the direction of the observation, so the local information, e.g., concentration distribution around the crystal-liquid interface, was not obtained.

To improve the disadvantage on the 2-D observation, a method of computer tomography (CT) has been adopted in this study. By using the CT method, we can reconstruct the information of the three-dimensional (3-D) concentration field around the growing crystal based on 2-D observations obtained from several directions (3-D observation).

In this study, 3-D measurement of the concentration field with convection and without convection around inorganic and protein crystals was carried out to reveal the concentration distribution over the crystal surfaces. Normal growth rate of the face from points to points are also measured to discuss the effect of concentration distribution on the surface.

Keywords: interferometer, lysozyme, convection

Japan Geoscience Union Meeting 2014
(28 April - 02 May 2014 at Pacifico YOKOHAMA, Kanagawa, Japan)

MIS36-P08 Room:Poster Time:May 1 18:15-19:30

Dependence of impurity adsorption on the step morphologies and growth rate of tetragonal lysozyme crystal

OSHI, Kentaro[1*] ; YOSHIZAKI, Izumi[2] ; KIMURA, Yuki[1] ; YAMAZAKI, Tomoya[1] ; TSUKAMOTO, Katsuo[1]

[1]Graduate School of Science, Tohoku University, [2]Japan Aerospace Exploration Agency (JAXA)

High quality protein crystals are required to get the information of the 3-dimensional structure of protein molecules. Impurities, mainly dimer molecules, affect the quality of protein crystal strongly (Yoshizaki et al., 2006). In addition, it is known that the step morphology on {110} faces of the tetragonal lysozyme crystal is changed by impurities. Until now, a lot of space experiments were carried out to get high quality protein crystals under microgravity conditions (McPherson, 1993, etc.). However, the relevance between impurity effects and microgravity condition is not clear. In addition, the step morphology corresponding to the crystal external form is not observed in preceding studies.

We performed ”in situ” observations under terrestrial environment and space environment using a tetragonal lysozyme crystal as the model protein. The purpose of this paper is to reveal ”the influence of microgravity condition to the impurities adsorption on the {110} faces” and ”the reason why the step morphology corresponding to crystal external form does not appear”. We made it possible to observe the step morphology and to measure the face growth rate at the same time by using a Michelson type interferometer.

As a result of growth rate measurement, the face growth rate under microgravity condition was higher than that under terrestrial condition. An impurity works to suppress the growth rate of a crystal. Because the buoyancy-driven convection was suppressed under the microgravity condition, we assumed that the larger impurity-depletion-zone was formed around a crystal.

As a result of the observation of the step morphology, we succeeded in observing the lozenge shape step which was corresponding to an external form by a space experiment for the first time. In addition, the step morphologies were classified in four types. It is considered that the impurity adsorption on the crystal surface is different depending on the crystal orientation of the step.

Japan Geoscience Union Meeting 2014
(28 April - 02 May 2014 at Pacifico YOKOHAMA, Kanagawa, Japan)

MGI37-01 Room:413 Time:April 29 09:00-09:15

A Report of Big-Data Processing and Operation of the NICT Science Cloud

MURANAGA, Kazuya[1*] ; UKAWA, Kentaro[1] ; YUTAKA, Suzuki[1] ; MURATA, Ken T.[2] ; WATANABE, Hidenobu[2] ; MIZUHARA, Takamichi[3] ; TATEBE, Osamu[4] ; TANAKA, Masahiro[4] ; KIMURA, Eizen[5]

[1]Systems Engineering Consultants Co., LTD., [2]National Institute of Information and Communications Technology, [3]CLEALINKTECHNO Co.,Ltd., [4]University of Tsukuba, [5]Ehime University

This paper is to propose a cloud system for science, which has been developed at NICT (National Institute of Information and Communications Technology), Japan. The NICT science cloud is an open cloud system for scientists who are going to carry out their informatics studies for their own science.

The NICT science cloud is not for simple uses. Many functions are expected to the science cloud; such as data standardization, data collection and crawling, large and distributed data storage system, security and reliability, database and meta-database, data stewardship, long-term data preservation, data rescue and preservation, data mining, parallel processing, data publication and provision, semantic web, 3D and 4D visualization, out-reach and in-reach, and capacity buildings.

In the present talk we discuss the basic concept of the NICT Science Cloud: (1) data transfer and crawling, (2) data preservation and stewardship and (3) data processing and visualization. After brief introductions of several functions and tools for them, we discuss systems via mash-up of these technologies, which are for practical research works.

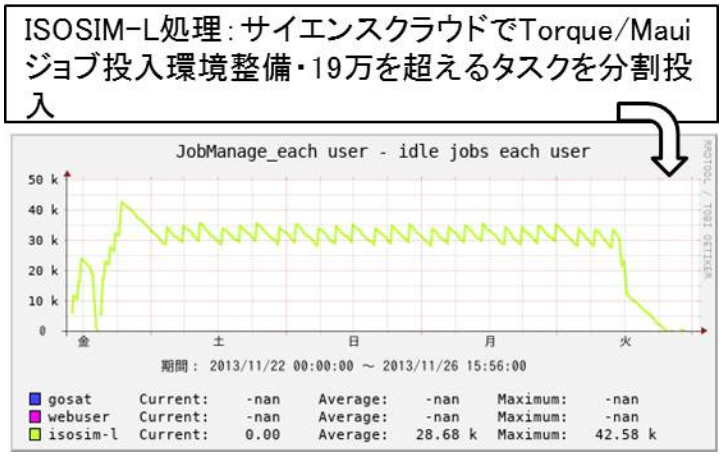

Japan Geoscience Union Meeting 2014
(28 April - 02 May 2014 at Pacifico YOKOHAMA, Kanagawa, Japan)

MGI37-02 Room:413 Time:April 29 09:15-09:30

High-speed File Transfer Tool with the Gfarm File System

WATANABE, Hidenobu[1*] ; KUROSAWA, Takashi[2] ; MURATA, Ken T.[1]

[1]National Institute of Information and Communications Technology, [2]Hitachi Solutions East Japan, Ltd.

A distributed storage system of scale-out type is gradually being used in the High Performance Computing (HPC) to store large scale data. NICT is also running an about 3 petabyte-scale (PB) distributed storage system with the Gfarm file system and a 10Gbps Layer 2 network (JGN-X) in Japan. Gfarm is open source software of a distributed file system for a petabyte-scale grid computing, and has been adopted as a shared storage of the High Performance Computing Infrastructure (HPCI).

When Gfarm copies data between storage servers in long-distance network, it uses a multiple TCP streaming technique to transfer data faster because TCP single streaming is known to produce a low network throughput in a long distance network. However, efficiency of high-speed by the technique becomes low as more distant.

We developed a high-speed file transfer tool worked with Gfarm. The tool adopts the UDT protocol as a data transfer protocol and has a control function for a parallel data transfer. UDT is a reliable UDP based application level data transport protocol over wide area high-speed networks, and uses UDP protocol to transfer bulk data with its own reliability control and congestion control mechanisms. In fact, UDT can provide a high network throughput than TCP in a long distance network.

We explain our tool and report the performance results of the tool in basic evaluation.

Japan Geoscience Union Meeting 2014
(28 April - 02 May 2014 at Pacifico YOKOHAMA, Kanagawa, Japan)

MGI37-03 Room:413 Time:April 29 09:30-09:45

An Examination of Data I/O Speed on a Parallel Data Storage System

MURATA, Ken T.[1*] ; WATANABE, Hidenobu[1] ; UKAWA, Kentaro[2] ; MURANAGA, Kazuya[2] ; YUTAKA, Suzuki[2] ; TATEBE, Osamu[3] ; TANAKA, Masahiro[3] ; KIMURA, Eizen[4]

[1]National Institute of Information and Communications Technology, [2]Systems Engineering Consultants Co., LTD., [3]University of Tsukuba, [4]Ehime University

This paper is to propose a cloud system for science, which has been developed at NICT (National Institute of Information and Communications Technology), Japan. The NICT science cloud is an open cloud system for scientists who are going to carry out their informatics studies for their own science.

The NICT science cloud is not for simple uses. Many functions are expected to the science cloud; such as data standardization, data collection and crawling, large and distributed data storage system, security and reliability, database and meta-database, data stewardship, long-term data preservation, data rescue and preservation, data mining, parallel processing, data publication and provision, semantic web, 3D and 4D visualization, out-reach and in-reach, and capacity buildings.

In the present study, we examine performance of parallelization of I/O on the NICT Science Cloud system. We examine two types of data file system; parallel file system (GPFS) and distributed file system (Gfarm). The later file system shows a tremendous fast I/O, as fast as 23 GB/sec using only 30 servers. We should pay attention to this I/O speed (23GB/sec is 184 Gbps) from the viewpoint of network speed. Since general network speed so far is 10 Gpbs or 40 Gbps in a cloud system, this 184 Gpbs is fast enough that the I/O cannot be a bottle-neck for big data processing.

We also discuss that the distributed file system shows better scalability compared with the GPSF system. Parallelization efficiency in the present examination is higher than 90% in case of parallel file system. This suggests that, in the near future, we can expect higher I/O speed using more file servers. For instance, if the I/O speed is as fast as 100 GB/sec, it takes only 1,000 sec. (17 min.) to read 100 TB data files.

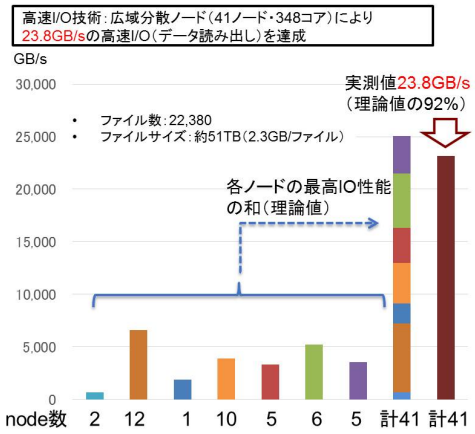

Japan Geoscience Union Meeting 2014
(28 April - 02 May 2014 at Pacifico YOKOHAMA, Kanagawa, Japan)

MGI37-04 Room:413 Time:April 29 09:45-10:00

STARS touch: A web-application for time-dependent observation data

UKAWA, Kentaro[1*] ; MURANAGA, Kazuya[1] ; YUTAKA, Suzuki[1] ; MURATA, Ken T.[2] ; SHINOHARA, Iku[3] ; KOJIMA, Hirotsugu[4] ; NOSE, Masahito[4] ; WATANABE, Hidenobu[2] ; TATEBE, Osamu[5] ; TANAKA, Masahiro[5] ; KIMURA, Eizen[6]

[1]Systems Engineering Consultants Co., LTD., [2]National Institute of Information and Communications Technology, [3]Japan Aerospace Exploration Agency, [4]Kyoto University, [5]University of Tsukuba, [6]Ehime University

This paper is to propose a cloud system for science, which has been developed at NICT (National Institute of Information and Communications Technology), Japan. The NICT science cloud is an open cloud system for scientists who are going to carry out their informatics studies for their own science.

The NICT science cloud is not for simple uses. Many functions are expected to the science cloud; such as data standardization, data collection and crawling, large and distributed data storage system, security and reliability, database and meta-database, data stewardship, long-term data preservation, data rescue and preservation, data mining, parallel processing, data publication and provision, semantic web, 3D and 4D visualization, out-reach and in-reach, and capacity buildings.

In the present study, we discuss a Web application for time-dependent science data, which is named ”STARS touch”. This Web application is based on a technique of asynchronous data transfer of graphic files for several types of data plots. The cloud system create a huge number of data plots with various time scale (e.g., from few minutes to few years) for each data-set. Parallel processing techniques to create such huge number of graphic data files are also discussed. We also make a live demonstration of the STARS touch to show several types of applications not only for research works but also for social data previews.

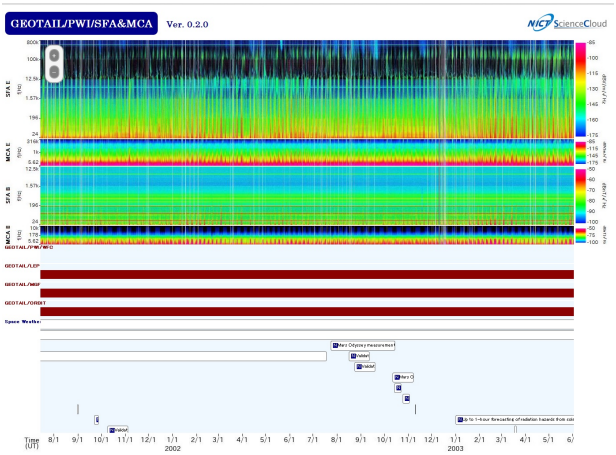

Japan Geoscience Union Meeting 2014
(28 April - 02 May 2014 at Pacifico YOKOHAMA, Kanagawa, Japan)

MGI37-05 Room:413 Time:April 29 10:00-10:15

High performance data processing for detection of bipolar waveforms from KAGUYA/WFC-L using the NICT Science Cloud

DAISUKE, Yagi[1*] ; MURATA, Ken T.[2] ; KASAHARA, Yoshiya[1] ; GOTO, Yoshitaka[1]

[1]Kanazawa Univ, [2]National Institute of Information and Communications Technology

Lunar orbiter named KAGUYA was launched in September, 2007, and was operated until June, 2009. The WFC (waveform capture) onboard KAGUYA measures plasma waves below 1MHz around the moon. The WFC-L, one of subsystems of WFC, is a waveform receiver measuring waveform from 100 Hz to 100 kHz with its sampling frequency at 250 kHz. Characteristic bipolar waveforms which can be classified into some patterns were observed by the WFC-L. We developed an automatic detection algorithm to pick up these bipolar waveforms , but it takes huge computation time because the total amount of the WFC-L data is about 190 GB.

In the present study, we introduced the Science Cloud system served by National Institute of Information and Communications (NICT) in order to improve the performance of trial and error process for the development of detection algorithm. The NICT Science Cloud is a cloud system built for scientific research and data service especially for big data science. We utilized parallel data processing under the work flow control implemented in the NICT Science Cloud. We report the performance of the NICT Science Cloud in the present paper.

In order to define an appropriate workflow to the data processing servers, Pwrake (Parallel Workflow extension for Rake) was introduced as a task scheduler. Pwrake is extended for file sharing systems from Rake which is a build tool described by Ruby language. It is possible to assign tasks to each node and to perform parallel data processing by describing the contents of processing, the node to be used, and the number of cores.

We confirmed that total processing time reduced down to 1/140 times compared with a case of 1 node and 1 core, when we used 10 nodes and 24 cores. Because of the effect of hyper-thread technology, processing speed is not proportional to the number of the resources. By utilizing the system, it is expected that a higher-precision detection algorithm can be developed efficiently. As further works, development of more intelligent detection algorithm as well as evaluation of the performance using much larger resources of the NICT Science Cloud will be necessary.

Keywords: Lunar Orbiter KAGUYA, Waveform Capture, NICT Science Cloud, parallel processing

Japan Geoscience Union Meeting 2014
(28 April - 02 May 2014 at Pacifico YOKOHAMA, Kanagawa, Japan)

MGI37-06 Room:413 Time:April 29 10:15-10:30

Comparison of grid data formats in meteorology: the reason for indexed sequential access method (ISAM) used in JMA

TOYODA, Eizi[1*]

[1]NPD, Japan Meteorological Agency

Many format standards are used for grid data of simulation such as numerical weather prediction (NWP). Wright and Gao (2008) argued there are direct-access and sequential formats, and a choice is needed between fastness of partial read and compactness of data files. However, a JMA's local standard NuSDaS (Toyoda, 2001) uses the third category, ISAM (indexed sequential access method) which achieves both fastness and compactness. These three types of file formats are comared (Table 1).

In the operational NWP (1) data structure is often sparse, (2) each file is written by a single process, and (3) many subsequent processes read a part of data tile. In this situation the weakness (cost of indexing) is not outstanding and the strength (fastness and compactness) are enjoyed.

It is also noted that the weakness of sequential access (full scan for partial data) will be aggravated in the future computing with larger data size.

References

Bruce WRIGHT and Feng GAO, 2008: GRIB vs NetCDF: Evaluation of the Technical Aspects. WMO ET-ADRS Doc.2.3(1) http://goo.gl/AFrsls

TOYODA Eizi, 2001: NuSDaS: Numerical Prediction Standard Data-set System. JpGU presentation A2-011 http://goo.gl/JE0a3M

Keywords: GRIB, netCDF, NuSDaS, grid data, indexed sequential access method

Types of File Structure

	Sequential Access	Direct Access	Indexed Sequential Access Method (ISAM)
Partial Write	Simple: *append to EOF (end of file)*	Simple: *seek and write*	Complex: *append to EOF, then index location*
File Size	Most Compact	Sparse array Bloated	Compact
Partial Read	Slow: *all records must be scanned*	Fastest: *only seek and read*	Fast: *look up index, seek and read*
Other Strength	No definition needed when creating file	Parallel write to single file	
Meteorological Examples	GRIB GTOOL3	GrADS Binary netCDF	NuSDaS

Japan Geoscience Union Meeting 2014
(28 April - 02 May 2014 at Pacifico YOKOHAMA, Kanagawa, Japan)

MGI37-P01 Room:Poster Time:April 29 18:15-19:30

Construction of the Large-Scale Statistical Analysis Environment of the STP field data based on the NICT Science Cloud

YAMAMOTO, Kazunori[1*] ; NAGATSUMA, Tsutomu[1] ; KUBOTA, Yasubumi[1] ; MURATA, Ken T.[1] ; WATARI, Shinichi[1] ; TATEBE, Osamu[2] ; TANAKA, Masahiro[2] ; KIMURA, Eizen[3]

[1]National Institute of Information and Communications Technology, [2]University of Tsukuba, [3]Ehime University

There are two major research methods for geo-space science; one is computer simulation, and the other is satellite and/or ground-based observation. Both methods have their advantages and disadvantages: Computer simulations can provide data in whole time and space in the simulation domain, whereas satellite observation data are expected to provide more accurate information. Therefore it is effective for the improved reliability of data and the increased possibilities of explaining phenomena to utilize multi-satellite observation data in combination with sophisticated simulation data with high time resolution. It has a potential to lead to data assimilations in the future.

However, the amount of both multi-satellite observation data and simulation data with high time resolution is very large. We need computational techniques to analyze both data simultaneously. For statistical analysis and visualization, the typical data processing of both multi-satellite observation data and simulation data with high time resolution is called data intensive processing. In the data intensive processing, the same processing is applied to plenty of data files.

We have built a large-scale environment for the statistical analysis where the data obtained through satellites observations and computer simulation are used to construct a uniform, integrated dataset. In this environment, plenty of data are integrated in the following manner: (1)Archiving large quantities of data files, (2)Resampling time series and convert coordinates, (3)Extracting parameters from simulation data, and (4)Merging both data into one file.

(1)Archiving large quantities of data files: Using the STARS (Solar-Terrestrial data Analysis and Reference System) meta-database that provides meta-information of observation data files managed at distributed observation data sites over the internet, users download data files without knowing where the data files are managed. On the other hand, simulation data is saved from supercomputer to petabyte-scale distributed storage that is connected to 10GbE (JGN-X).

(2)Resampling time series and convert coordinates: We developed an original data class (SEDOC class) to support our reading of data files and converting them into a common data format. The data class defines schemata for several types of data. Since this class encapsulates data files, users easily read any data files without paying attention to their data formats. The SEDOC class supports a function of resampling time series through linear interpolations and converting them into major coordinates systems.

(3)Extracting parameter from simulation data: We have developed a 3-D visualization system that visualizes both of these data simultaneously and extract parameters from simulation data in the arbitrary coordinate value.

(4)Merging both data into a single file: Time scale and coordinate are regularized over data files.

We found a practical problem of the system, especially in case of long durational data analyses. It is the problem of the computational load on the processes two to four. It is necessary to solve this problem in order to achieve data-intensive processing for plenty of data files with non-negligible file I/O and CPU utilization.

To overcome this problem, we developed a parallel and distributed data analysis system using the Gfarm and Pwrake based on the NICT Science Cloud. The Gfarm shares both computational resources and perform parallel distributed processing. In addition, the Gfarm provides the Gfarm file system which behaves as a virtual directory tree among nodes. The Pwrake throws a job for each Gfarm node that has a target data file in the local disk. It utilizes local disk I/O to achieve effective load balance.

In today's presentation, we show latest results using archived long durational data and discuss the present Gfarm+Pwrake system extended to wide area.

Keywords: computer simulation data, satellite observation data, parallel distributed processing, Gfarm, Pwrake, NICT Science Cloud

MGI37-P01 Room:Poster Time:April 29 18:15-19:30

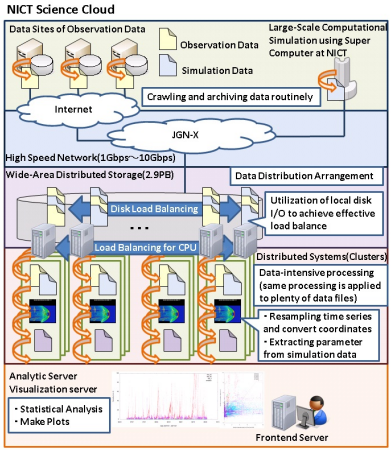

Japan Geoscience Union Meeting 2014
(28 April - 02 May 2014 at Pacifico YOKOHAMA, Kanagawa, Japan)

MGI37-P02 Room:Poster Time:April 29 18:15-19:30

Radio observation network of Tohoku University

YAGI, Manabu[1*] ; OBARA, Takahiro[1] ; KAGITANI, Masato[1] ; YONEDA, Mizuki[1] ; KUMAMOTO, Atsushi[1] ; MISAWA, Hiroaki[1] ; TSUCHIYA, Fuminori[1] ; IWAI, Kazumasa[2] ; TERADA, Naoki[1] ; OHYA, Hiroyo[3]

[1]Tohoku Univ., [2]NAOJ, [3]Chiba Univ.

Planetary Plasma and Atmospheric Research Center (PPARC) of the Tohoku University is now in progress to build a upper atmosphere, planetary, and space physics database under collaboration with the Inter-university Upper atmosphere Global Observation NETwork (IUGONET). The core data of the database are planetary and solar radio observation by Iitate Planetary Radio Telescope (IPRT) and Jupiter/galaxy decameter radio receiver working in Iitate observatory, that is one of the observatory of Tohoku University. Development of database of LF/VLF wave observation at Athabasca, Ny-Alesund, and Asia VLF Observation Network (AVON) are undergoing collaborated with Chiba University. In the presentation, we will introduce the observations of solar radio burst with high time resolution using the AMATERAS spectrometer of IPRT, as well as lightning and precipitation of high energy electrons into the atmosphere observed by LF/VLF wave.

Keywords: radio observation, database, upper atmosphere

Japan Geoscience Union Meeting 2014
(28 April - 02 May 2014 at Pacifico YOKOHAMA, Kanagawa, Japan)

MAG38-01 Room:501 Time:May 2 09:00-09:15

Cs-bearing spherical particles emitted from an early stage of the FDNPP accident

ADACHI, Kouji[1*] ; KAJINO, Mizuo[1] ; ZAIZEN, Yuji[1] ; IGARASHI, Yasuhito[1]

[1]Meteorological Research Institute

We found radioactive Cs-bearing, spherical particles from the filters collected in March 14 and 15, 2011, just after the Fukushima Daiichi Nuclear Power Plant (FDNPP) accident, in Tsukuba. These particles mainly consist of Fe and Zn but contain detectable amounts of Cs using a scanning electron microscope (SEM) and energy-dispersive X-ray spectrometer (EDS). They are several micro meter and are hardly water soluble. They are mostly spherical, suggesting they formed through rapid cooling of radioactive materials. These particles were only found in the filters collected on March 14 and 15, 2011, and these filters had many spots of radioactive materials when measured using an imaging plate (IP). To date, we have identified six such Cs-bearing particles in the filter.

The finding of such Cs-bearing spherical particles suggests the following implications; understandings of the accident and health effects for the radioactive materials emitted at the early stage of the accident and estimations of the current and future environmental radioactivity contaminated by the particles.

Reference: Adachi K., Kajino M., Zaizen Y., and Igarashi Y., Emission of spherical cesium-bearing particles from an early stage of the Fukushima nuclear accident, Scientific Reports, 2013, 3, Article number: 2554.

Keywords: Cesium, electron microscope, aerosol, radioactive material

Japan Geoscience Union Meeting 2014
(28 April - 02 May 2014 at Pacifico YOKOHAMA, Kanagawa, Japan)

MAG38-02 Room:501 Time:May 2 09:15-09:30

Measurement of Cs-137 in atmopshieric aerosols in Fukushima prefecture and the surrounding area

NINOMIYA, Kazuhiko[1*] ; ZHANG, Zijang[1] ; OSUMI, Yuji[1] ; MATSUNAGA, Shizuka[1] ; KAKITANI, Shunsuke[1] ; YAMAGUHI, Yoshiaki[2] ; TSURUTA, Haruo[3] ; WATANABE, Akira[4] ; KITA, Kazuyuki[5] ; SHINOHARA, Atsushi[1]

[1]Graduate School of Science, Osaka University, [2]Osaka University Radioisotope Research Center, [3]Atomosphere and Ocean Research Institute, University of Tokyo, [4]Fukushima University, [5]Ibaraki University

A large amount of radioactive materials were released in the environment by the accident at the Fukushima Daiichi Nuclear Power Station. We have been collecting air-dust using high volume air sampler at Fukushima city (Fukushima Pref.), Marumori town (Miyagi Pref.) and Hitachi city (Ibaraki Pref.) since the accident. We identified the radioactivities of 134Cs and 137Cs in filters using HPGe detector. We will discuss time variations of radioactive cesium concentration.

Keywords: Atmospheric observation, Air dust, Radioactivity Measurement, Cs-137 concentration

Japan Geoscience Union Meeting 2014
(28 April - 02 May 2014 at Pacifico YOKOHAMA, Kanagawa, Japan)

MAG38-03 Room:501 Time:May 2 09:30-09:45

Estimate of possible sources of high Cs-137 in atmospheric aerosols measured in south Miyagi during 2 years (2012-2013)

TSURUTA, Haruo[1*] ; SHIBA, Kaoru[1] ; YAMADA, Hiroko[1] ; KUSAMA, Yuko[1] ; ARAI, Toshiaki[1] ; WATANABE, Akira[2] ; NAGABAYASHI, Hisao[3] ; KITA, Kazuyuki[4] ; SHINOHARA, Atsushi[5] ; NINOMIYA, Kazuhiko[5] ; ZHANG, Zijian[5] ; YOKOYAMA, Akihiko[6] ; KAJINO, Mizuo[7] ; NAKAJIMA, Teruyuki[1]

[1]AORI, The University of Tokyo, [2]Fukushima University, [3]Nihon University, [4]Ibaraki University, [5]Osaka University, [6]Kanazawa University, [7]Meteorological Research Institute

A volunteer team organized by the Japan Geoscience Union has started an intensive field study to monitor radioactive materials in the atmosphere, which were released by the Fukushima Daiichi Nuclear Power Plant (FD1NPP) accident, and by re-suspension of radioactive materials from soils and forests in a regional scale in and surrounding Fukushima area since April 2011. At present, the continuous measurement has been made at Marumori town in Miyagi prefecture, Fukushima city and Koriyama city in Fukushima prefecture, and Hitachi city in Ibaraki prefecture. In this paper, a case study on high concentrations of atmospheric radiocesium frequently measured at Marumori will be reported. At the Marumori town office in south Miyagi, atmospheric aerosols have been collected since December 2011, on a quartz fiber filter every several days by using a high volume air sampler, and radioactive materials in the aerosols were measured with a Ge detector. Forward trajectory analysis by a Lagrangian model was made to trace air masses started from the FD1NPP for 48 hours. The atmospheric concentration of Cs-137 at Marumori was in a level of 10^{-4} Bq m^{-3} until April 2012, and then gradually decreased to the level of 10^{-5} Bq m^{-3} in the latter half of 2013. High concentrations of Cs-137 more than 10^{-4} Bq m^{-3} were measured in the winter and early spring of 2012 and 2013 when the wind speed was high and relative humidity was low. It strongly suggests that the possible source of high Cs-137 could be re-suspension of radioactive materials from soils. In September and November 2012 and from May to August 2013, however, high concentrations more than 10^{-4} Bq m^{-3} were also frequently measured, and the highest concentration of $4.6x10^{-3}$ Bq m^{-3} was measured in a sampling period of 16-20 August 2013. On 19 August, unusual high Cs-137 concentration of $7.1x10^{-1}$-$8.7x10^{-1}$ Bq m^{-3} and $5.8x10^{2}$ Bq m^{-3} was measured at a monitoring post of Koriyama in Futabamachi 2.8 km north of the FD1NPP, and in front of a building inside the FD1NPP, respectively. According to the forward trajectory analysis, the air masses started from the FD1NPP at 09:00 and 12:00 on August 19 2013 arrived at Marumori on the afternoon of 15:00 and 18:00, respectively. It indicates that radioactive materials released from the FD1NPP were directly transported to Marumori about six hours later. The transport pathways similar to those on August 19 were also shown by the forward trajectory analysis in the other periods when the high Cs-137 concentrations were measured except for winter and early spring. These results clearly demonstrate that radioactive materials were still released into the atmosphere from the FD1NPP. We acknowledge the staff members of the Marumori town office for continuous sampling of atmospheric aerosols for these two years.

Keywords: atmospheric aerosols, radiocesium, source estimate, forward trajectory analysis

Japan Geoscience Union Meeting 2014
(28 April - 02 May 2014 at Pacifico YOKOHAMA, Kanagawa, Japan)

MAG38-04 Room:501 Time:May 2 09:45-10:00

Study on the carrier of airborne radiocesium collected for six month in Tsukuba after the Fukushima nuclear accident

KANEYASU, Naoki[1*] ; KOGURE, Toshihiro[2] ; MUKAI, Hiroki[2] ; OHASHI, Hideo[3] ; SUZUKI, Fumie[3] ; AKATA, Naofumi[4] ; OKUDA, Tomoaki[5] ; IKEMORI, Fumikazu[6]

[1]National Institute of Advanced Industiral Science and Technology, [2]Graduate School of Science, The University of Tokyo, [3]Tokyo University of Marine Science and Technology, [4]National Institute for Fusion Science, [5]Faculty of Science and Technology, Keio University, [6]Nagoya City Institute for Environmental Sciences

To obtain the knowledge on the physico-chemical properties of airborne radionuclides, we had been collected size-resolved aerosol in Tsukuba, Japan, since April 28, 2011, although the data obtained do not include the first radioactive plumes that reached to Tsukuba on March 15, 2011. From the initial result, we proposed a hypothesis that the sulfate aerosol was the potential carrier of the ^{134}Cs and ^{137}Cs that had undergone the middle- to long-range transport from the damaged reactor. We further inferred that re-suspended soil particles that attached radionuclides were not the major airborne radioactive substances from late April to May, 2011 (Kaneyasu et al., 2012).

Nevertheless, there are some issues to be addressed on the nature of airborne radionuclides. Those are, a) until when the sulfate aerosol acted as a carrier of the radiocesium released from the reactor, or the other substances acted as carriers instead, and b) what is the carrier substance when the re-suspension or re-emission of became the dominant source in the airborne radiocesium.

In this study, we address these subjects by analyzing the long-term aerosol samples collected later than those presented in the previous study. The temporal change in the activity size distribution of radiocesium for six month will be discussed. In addition, the carrier substance of radiocesium in the coarse mode size range aerosol is investigated by use of the autoradiograph and scanning electron microscope to the aerosol sample collected in 2011 summer.

Keywords: radiocesium, size distribution, re-suspension, electron microscope, autoradiograph

Japan Geoscience Union Meeting 2014
(28 April - 02 May 2014 at Pacifico YOKOHAMA, Kanagawa, Japan)

MAG38-05 Room:501 Time:May 2 10:00-10:15

Resuspension of radioactive cesium from soil and forest

KITA, Kazuyuki[1*] ; TANAKA, Misako[1] ; KINASE, Takeshi[1] ; FUJISAWA, Haruka[1] ; YAMAGUCHI, Ryusuke[1] ; KINO, Himiko[1] ; DEMIZU, Hiroyuki[1] ; IGARASHI, Yasuhito[2] ; MIKAMI, Masao[2] ; ADACHI, Kouji[2] ; YOSHIDA, Naohiro[3] ; TOYODA, Sakae[3] ; YAMADA, Keita[3] ; SHINOHARA, Atsushi[4] ; NINOMIYA, Kazuhiko[4] ; OKOUCHI, Hiroshi[5] ; ISHIZUKA, Masahide[6] ; KAWASHIMA, Hiroto[7] ; NAKAI, Izumi[8] ; ABE, Zenya[8] ; ONDA, Yuichi[9]

[1]Ibaraki University, [2]MRI, [3]TiTech, [4]Osaka Univ., [5]Waseda Univ., [6]Kagawa Univ., [7]Akita Pref. Univ., [8]Tokyo univ. of Science, [9]Tsukuba Uinv

Radionuclides emitted from the Fukushima dai-ichi nuclear power plant (FNDPP) accident have been deposited on the soil, ocean and vegetation. Re-suspension of radioactive cesium from the soil and vegetation to the atmosphere may be one of signi?cant path in the diffusion of radionuclides after the accident. Therefore, the quantitative understanding of these re-suspensions is important to understand future transition of radionuclides. Identification of aerosol species which bring Cs-134/137 is necessary to understand the mechanism of re-suspension, and its efficiency.

We have measured atmospheric concentration of radiation by Cs-134/137 in Namie high school Tsushima-branch where is away 30km from FNDPP. Relationship between Cesium radioactivity and aerosol size destribution show that multiple re-suspension mechanisms contribute and their contribution varies with the season. The mechanisms of re-suspension will be shown and discussed.

Japan Geoscience Union Meeting 2014
(28 April - 02 May 2014 at Pacifico YOKOHAMA, Kanagawa, Japan)

MAG38-06 Room:501 Time:May 2 10:15-10:30

Evaluation of radioactivity resuspension by dust emission using a size-resolved 1-D vertical model in Namie, Fukushima

ISHIZUKA, Masahide[1] ; MIKAMI, Masao[2*] ; TANAKA, Yasuhito[2] ; IGARASHI, Yasuhito[2] ; KITA, Kazuyuki[3] ; YAMADA, Yutaka[4] ; YOSHIDA, Naohiro[5] ; TOYOTA, Sakae[5] ; SATO, Yukihiko[6] ; TAKAHASHI, Yoshio[7] ; NINOMIYA, Kazuhiko[8] ; SHINOHARA, Atsushi[8]

[1]Kagawa University, [2]Meteorological Research Insitute, [3]Ibaraki University, [4]RIKEN, [5]Tokyo Institute of Technology, [6]Tsukuba University, [7]Hiroshima University, [8]Osaka University

Radioactive materials released into the atmosphere by the Fukushima Daiichi Nuclear Power Plant Accident in March 2011 were deposited over a wider area. Those materials adhered to the soil particles (dust particles) and its resuspension by strong winds is apprehensive about as secondary emissions. We have proposed a size-resolved, one-dimensional resuspension scheme to calculate the concentration of radioactivity in the atmosphere, in the last annual meeting. The results underscore the importance of taking into account soil texture when calculating the concentrations of resuspended, size-resolved atmospheric radioactivity. However, various assumptions were incorporated into both the scheme and evaluation conditions. In this study, we made analyses of soil particle size distribution and soil radioactivity at a school ground in Tsushima District, Namie Town, Fukushima, which was heavily polluted by the accident. The model results were compared with in situ observational data of the size spectrum of atmospheric radioactivity. We validated the applicability of the scheme and the behavior of resuspended radioactive aerosols.

Keywords: Secondary emission, Radioactive aerosol, Dust, Fukusihma accident

Japan Geoscience Union Meeting 2014
(28 April - 02 May 2014 at Pacifico YOKOHAMA, Kanagawa, Japan)

MAG38-07 Room:501 Time:May 2 10:30-10:45

Simulation of I-131 in the atmosphere emitted from the Fukushima Daiichi Nuclear Power Plant

TAKIGAWA, Masayuki[1*] ; TSURUTA, Haruo[2]

[1]JAMSTEC, [2]AORI, Univ. of Tokyo

A large amount of radioactive materials was released into the atmosphere after the accident of the Fukushima Daiichi Nuclear Power Plant (FD1NPP). Inhalation of iodine 131 is important for internal exposure, but the observation of iodine is quite limited especialy in the early phase of the accident. We have conducted the simulation of radionuclides using a regional chemical transport model for March 2011. Calculated accumulated deposition of iodine 131 and caesium 137 was compared with the estimation using aircraft monitoring by MEXT and DOE (Torii et al., 2013). The model well captured the meridional gradient in the ratio of iodine 131 to caesium 137 around FD1NPP. The ratio of iodine 131 to caesium 137 is larger than 15 in the south of FD1NPP, and relatively small (around 0.7) in the northwest. This result implies that the regional model and the source term estimated by JAEA can generally reproduce eventual releases which cause large depositon ofer the land in March 2011.

Keywords: numerical simulation, atmospheric environment

Japan Geoscience Union Meeting 2014
(28 April - 02 May 2014 at Pacifico YOKOHAMA, Kanagawa, Japan)

MAG38-08 Room:501 Time:May 2 11:00-11:15

The applicability of lichens as indicator of radiocaesium fall-out following the Fukushima Daiichi nuclear accident

DOHI, Terumi[1*] ; OHMURA, Yoshihito[2] ; KASHIWADANI, Hiroyuki[1] ; FUJIWARA, Kenso[1] ; IIJIMA, Kazuki[1]

[1]Japan Atomic Energy Agency, [2]National Museum of Nature and Science

Lichens are symbiotic organisms consisted of fungi and algae. A number of studies was carried out after the nuclear weapons tests and Chernobyl accident, and demonstrated that lichens were useful for indicator of radioactive fallout because (i) they spread in almost all terrestrial habitats e.g. on rocks, tree barks, and soils, (ii) they could take up large amount of radionuclides directly from their thallus due to lack of root system and retain them, and (iii) they were long-lived. It is necessary to understand the behavior of radiocaesium released into the environment from the Fukushima Daiichi nuclear power plant (FNPP) on March 2011, because it is considered to migrate in the ecosystem over a long period. For this purpose, some indicators of initial amount of deposited radiocaesium are required to be compared. Though, the amount of deposited radiocaesium on the topsoil gradually decreases by weathering, while lichens are expected to retain radiocaesium for long time. However, very little work is currently available on the concentration of radiocaesium in lichens and there is no experience of applying lichens to indicator of fall-out in Japan.

In this study, an applicability of lichens as an indicator for amount of deposited radiocaesium was discussed based on the following investigations related to the Fukushima Daiichi nuclear accident. The lichens were widely collected from the area in Fukushima prefecture (mainly west side) and Kanto region affected by the accident since December 2012. Lichen species were focused on parmelioid lichens which were widely distributed around FNPP. (1) After the lichens were removed from barks and dried, the concentrations of ^{134}Cs and ^{137}Cs in the lichens were measured with a CsI scintillation detector or a Ge semiconductor detector and compared to amount of ^{137}Cs deposited on the topsoil on June 2011 and air dose rate. (2) The retention capability of radiocaesium was evaluated by comparing radiocaesium concentrations in lichens to those of barks of lichen habitat.

The radiocaesium concentrations in lichens tended to be higher than those of barks, indicating that parmelioid lichens had retention capability of radiocaesium than tree barks. It was observed that the radiocaesium concentrations in lichens increased with increasing the amount of ^{137}Cs deposited on the topsoil and air dose rate. These results suggested the applicability of parmelioid lichens as an indicator of radiocaesium fall-out in Fukushima.

Keywords: Fukushima daiichi nuclear accident, Parmelioid lichens, radiocaesium

Japan Geoscience Union Meeting 2014
(28 April - 02 May 2014 at Pacifico YOKOHAMA, Kanagawa, Japan)

MAG38-09 Room:501 Time:May 2 11:15-11:30

Estimation of radioactive cesium translocation by litterfall, stemflow and throughfall in the forest of Fukushima

ENDO, Izuki[1*] ; OHTE, Nobuhito[1] ; ISEDA, Kohei[1] ; HIROSE, Atsushi[1] ; KOBAYASHI, Natsuko[1] ; TANOI, Keitaro[1]

[1]The University of Tokyo

The accident of Fukushima Daiichi nuclear power plant after the earthquake and Tsunami in March 11th 2011 caused large amount of radioactive cesium (Cs) deposition onto the forest in surrounding areas. Deposited radioactive Cs that were caught by the tree canopy, reaches to the forest floor via various several pathways. To estimate the annual flux of radioactive Cs translocate to forest floor, we investigated the component and amount of those which move from tree canopy based on the measurements of litterfall, stemflow and throughfall.

Field study was conducted in a forest at the upstream part of the Kami-Oguni River catchment, northern part of Fukushima Prefecture. Three plots (2 deciduous-pine (*Pinus densiflora*) mixed stands and 1 Japanese cedar (*Cryptomeria japonica*) plantation) were set in the forest. Five litter traps were set in each plot and collected every month from October 2012 to September 2013. Litter samples were sorted among tree species and also branches, seeds and barks. Throughfall and stemflow were collected every 1 or 2 months. Water samples were filtered and particulate matters were collected for radioactive Cs measurement. Radioactive Cs concentration of all samples were measured by germanium semiconductor detector and NaI(Tl) scintillation counter. Both concentrations of ^{137}Cs and ^{134}Cs were measured but only data for ^{137}Cs were discussed in this report.

The concentration of ^{137}Cs in leaf litter samples varied from non-detected level to above 30 kBq/kg. The ^{137}Cs concentration was highest in pine needles and followed by cedar. Leaf litters of deciduous tree species showed significantly lower concentration compared to those of evergreen trees. This was because deciduous trees were before leafing stage at the time of the accident. However, significant levels of ^{137}Cs in the leaves even of deciduous trees suggest that ^{137}Cs have been translocated from some part of tree body. On the other hand, deposited ^{137}Cs at the time of the accident still remains on the leaves of evergreen tree. Amount of ^{137}Cs translocated from canopy to forest floor in cedar plantation was about 3 times higher than that of deciduous-pine mixed forest. This was due to higher ^{137}Cs concentration and larger litter biomass of cedar.

^{137}Cs concentration of throughfall and stemflow were comparable. Since the amount of throughfall was larger than that of stemflow, significant amount of ^{137}Cs moved to the forest floor by throughfall. Higher ^{137}Cs translocation occurred according to the high precipitation. ^{137}Cs concentration fluctuated depending on the season, but there was no apparent tendency to decrease between 2013 and 2012. Since the concentration of ^{137}Cs in open rainwater was below the detection limit, it is suggested that ^{137}Cs is still supplied constantly from the tree canopy and source limitation is not occurring from leaves and trunks, despite the fact that it has past more than one and half year from the fallout.

Japan Geoscience Union Meeting 2014
(28 April - 02 May 2014 at Pacifico YOKOHAMA, Kanagawa, Japan)

MAG38-10 Room:501 Time:May 2 11:30-11:45

Effect of Radiocesium Transfer on Ambient Dose Rate in Forest Environment

KATO, Hiroaki[1*] ; ONDA, Yuichi[1] ; LOFFREDO, Nicolas[1] ; HISADOME, Keigo[2] ; KAWAMORI, Ayumi[3]

[1]Center for Research in Isotopes and Environmental Dynamics, University of Tsukuba, [2]Asia Air Survey Co., LTD., [3]Masters Program of Environmental Sciences, University of Tsukuba

We investigated the transfer of canopy-intercepted radiocesium to the forest floor following the Fukushima Daiichi nuclear power plant accident. The cesium-137 (Cs-137) contents of throughfall, stemflow, and litterfall were monitored in two coniferous stands (plantation of Japanese cedar) and a deciduous broad-leaved forest stand (beech with red pine). We also measured an ambient dose rate at different height in the forest by using a survey meter (TCS-172B, Hitachi-Aloka Medical, LTD.) and a portable Ge gamma-ray detector (Detective-DX-100T, Ortec, Ametek, Inc.).

In decreasing order of total Cs-137 deposition from the canopy to forest floor were the mature cedar stand, the young cedar stand, and the broad-leaved forest. The ambient dose rate in forest exhibited height dependency and its vertical distribution varied by forest type and stand age. The ambient dose rate showed an exponential decrease with time for all the forest sites, however the decreasing trend differed depending on the height of dose measurement and forest type. The ambient dose rates at the canopy (approx. 10 m-) decreased earlier than physical attenuation of radiocesium, whereas those at the forest floor varied among three forest stands. These data suggested that an ambient dose rate in forest environment can be variable in spatially and temporally reflecting the transfer of radiocesium from canopy to forest floor.

Keywords: Fukushima Daiichi NPP accident, Cesium-137, Forest environment, Canopy interception, Transfer, Ambient dose rate

Japan Geoscience Union Meeting 2014
(28 April - 02 May 2014 at Pacifico YOKOHAMA, Kanagawa, Japan)

MAG38-11 Room:501 Time:May 2 11:45-12:00

Three different structures of radionuclide ratios on the surface soil in the northwestern area from the FDNPP

SATOU, Yukihiko[1*] ; SUEKI, Keisuke[1] ; SASA, Kimikazu[1] ; MATSUNAKA, Tetsuya[1] ; SHIBAYAMA, Nao[1] ; TAKAHASHI, Tsutomu[1] ; KINOSHITA, Norikazu[2]

[1]AMS Group, University of Tsukuba, [2]Institute of Technology, Shimizu Corporation

The Fukushima Dai-ichi Nuclear power plant (FDNPP) accident caused radioactive contamination on the surface soil at Fukushima and its adjacent prefectures. Substantial contamination has been found in the northwestern area from the FDNPP, according to the airborne monitoring survey and the ground base survey by MEXT, Japan. Radionuclide ratios would have characteristic information on emission source because each nuclearreactor at the FDNPP had different amount of radionuclide and different activity ratio. The activity ratios can be used to make emission source and transport process in the contamination more obvious . We address the issue of radioactive contaminated process, we have measured radionuclides on the surface soil at the town of Namie in the northwestern region from the FDNPP, in the viewpoint of activity ratio.

This study focused on the gamma-ray emitting radionuclides of ^{134}Cs, ^{137}Cs, and ^{110m}Ag. The activities were decay-corrected as of 11 March 2011 when all nuclear reactors scrammed. Data of activity ratios by our results and the Japanese official report classified the investigated northwestern region into 3 groups. Ratios of 0.02 for ^{110m}Ag/^{137}Cs and 0.90 for ^{134}Cs/^{137}Cs were observed northern area of inside 15 km from the FDNPP. On the other hand, two kinds of ^{110m}Ag/^{137}Cs ratios of 0.005 and 0.002 were distributed broadly in the area 60 km away from the plant. The ^{134}Cs/^{137}Cs ratio was 0.98 there.

The activity ratio in the northern area from the FDNPP corresponds to those of nuclear fuel in Unit 1 according to estimation using the ORIGEN code. The ^{134}Cs/^{137}Cs in the northwestern area from the FDNPP agrees with that of Unit 2 and 3. The ^{110m}Ag/^{137}Cs ratios of 0.005 and0.002 are 1/5 ? 1/10 of the Unit 2 and 3. Official report has announced that discharges of radionuclides from Unit 2 and 3 occurred on 14th March. It is known that contamination in the northwestern area from the FDNPP took place on 15th March. Ag has higher boiling point than Cs. Reactor core would be cooled down to lower temperature below the boiling point of Ag at the timing when contamination occurred. Thus, Ag with higher boiling point was not much released than Cs with lower boiling point. The ^{110m}Ag/^{137}Cs ratio has served to identify the specific sources of contamination in the northwestern area from the FDNPP.

Keywords: Fukushima Nuclear Power plant Accident, 110mAg/137Cs ratio, Surface soil

Japan Geoscience Union Meeting 2014
(28 April - 02 May 2014 at Pacifico YOKOHAMA, Kanagawa, Japan)

MAG38-12 Room:501 Time:May 2 12:00-12:15

Depth profiles of ^{129}I and ^{137}Cs in soil before and after the FDNPP accident

MATSUNAKA, Tetsuya[1*] ; SASA, Kimikazu[1] ; SUEKI, Keisuke[1] ; TAKAHASHI, Tsutomu[1] ; MATSUMURA, Masumi[1] ; SATOU, Yukihiko[1] ; SHIBAYAMA, Nao[1] ; KITAGAWA, Jun-ichi[2] ; KINOSHITA, Norikazu[3] ; MATSUZAKI, Hiroyuki[4]

[1]University of Tsukuba, [2]High Energy Accelerator Research Organization, [3]Shimizu Corporation, [4]The University of Tokyo

Massive nuclear fission products such as radioiodine and radiocesium were deposited on the land surface of Fukushima via radioactive pollution plumes derived from the Fukushima Dai-ichi Nuclear Power Plant (FDNPP) accident. In order to evaluate inventory and penetration of accident-derived ^{129}I and ^{137}Cs in the land surface, depth profiles of ^{129}I, ^{129}I / ^{127}I atomic ratio and ^{137}Cs in 30-cm-long soil cores before (May 2008) and after (November 2012) the accident were compared at two sites (Iw-2 and Iw-8) on the western area within 10 km from the FDNPP.

Total ^{129}I inventories in soil core at two sites after the accident were estimated to be 0.74 - 1.96 Bq m^{-2}, 14 - 34 times higher than those before the accident (53.6 - 57.0 mBq m^{-2}). Average ^{129}I / ^{127}I ratios ((1.4 - 6.2) $\times$ 10^{-7}) in soil core after the accident were consistent with the ^{129}I / ^{127}I ratio of the radioactively-contaminated surface soils in Fukushima (1.5 $\times$ 10^{-8} - 7.2 $\times$ 10^{-6}, Miyake et al., 2012). We also estimated that total ^{137}Cs inventories after the accident were 0.60 - 3.15 MBq m^{-2}, 280 - 470 times higher than those before the accident (2.1 - 6.7 kBq m^{-2}). Average ^{134}Cs / ^{137}Cs activity ratios (1.07 - 1.08) in soil core fell within the activity ratio in Unit 1 - 3 (0.94 - 1.08) of the FDNPP calculated by ORIGEN2 code (Nishihara et al., 2012). These results suggested that accurate total inventories of accident-derived ^{129}I and ^{137}Cs in soil could be determined by deduction of those backgrounds at almost same site, thus, the FDNPP accident caused ^{129}I deposition of 0.69 - 1.90 Bq m^{-2} and ^{137}Cs deposition of 0.59 - 3.14 MBq m^{-2} on the western area within 10 km from the FDNPP. Moreover, deposited ^{129}I and ^{137}Cs at Iw-2 (4.2 km west from the FDNPP) were respectively, 2.9 and 5.3 times higher than those at Iw-8 (8.4 km west from the FDNPP).

Depth profiles of ^{129}I concentration, ^{129}I / ^{127}I atomic ratio and ^{137}Cs concentration before the accident were essentially declined from upper layer with depth at two sites. On the basis of the highest values in these profiles, background levels were determined to be 420 $\pm$ 11 Bq kg^{-1} for ^{129}I, 1.6 $\pm$ 0.1 $\times$ 10^{-8} for ^{129}I / ^{127}I and 48 $\pm$ 2.5 Bq kg^{-1} for ^{137}Cs. After the accident, significant elevated values of ^{129}I (40.2 - 130 mBq kg^{-1}), ^{129}I / ^{127}I ((0.9 - 9.3) $\times$ 10^{-6}) and ^{137}Cs (44.6 - 255 kBq kg^{-1}) were found in the uppermost layer at the two sites, then these profiles exponentially declined with depth. Approximately 90% of deposited ^{129}I and ^{137}Cs at two sites were absorbed upper 37.4 - 50.5 kg m^{-2} (4.1 - 4.3 cm) and upper 13.3 - 21.3 kg m^{-2} (1.0 - 3.1 cm) in depth, respectively. In addition, since the relaxation mass depths (h_0) of ^{129}I were 9.2 - 12.8 kg m^{-2} greater than those of ^{137}Cs (6.8 - 11.7 kg m^{-2}) at two site, radioiodine was considered to penetrate slightly deeper than radiocesium in upper layer of both sites as Kato et al. (2012) found at 40 km northwestern site from the FDNPP. This is not contradicting to increasing tendency of ^{129}I / ^{137}Cs activity ratio with depth at both sites. Based on the fact that both ^{129}I and ^{129}I / ^{127}I in soil after the accident declined to a background level under 84.8 kg m^{-2} in depth at Iw-2 and under 133 kg m^{-2} in depth at Iw-8, about 8 - 9% of accident-derived ^{129}I were likely to penetrated 37.4 - 84.8 kg m^{-2} (4.3 - 8.6 cm) in depth at Iw-2 and 50.5 - 133 kg m^{-2} (4.1 - 10.2 cm) in depth at Iw-8.

Keywords: FDNPP accident, Radioiodine, Radiocesium, AMS, Gamma-ray analysis, Soil profile

Japan Geoscience Union Meeting 2014
(28 April - 02 May 2014 at Pacifico YOKOHAMA, Kanagawa, Japan)

MAG38-13 Room:501 Time:May 2 12:15-12:30

Distribution of ^{129}I in the environment released from the FDNPP accident and estimation of ^{131}I/^{129}I ratio

SASA, Kimikazu[1*] ; MATSUMURA, Masumi[1] ; SUEKI, Keisuke[1] ; TAKAHASHI, Tsutomu[1] ; MATSUNAKA, Tetsuya[1] ; SATOU, Yukihiko[1] ; SHIBAYAMA, Nao[1] ; KINOSHITA, Norikazu[2] ; NISHIHARA, Kenji[3] ; MATSUZAKI, Hiroyuki[4]

[1]University of Tsukuba, [2]Shimizu Corp., [3]Japan Atomic Energy Agency, [4]The University of Tokyo

Radioiodine is one of the most important radionuclides released from the Fukushima-Daiichi Nuclear Power Plant (FDNPP) accident. ^{131}I (half-life: 8 d) has a short half life time. Because of the difficulty of measuring ^{131}I at this time, it is expected to estimate ^{131}I precipitation from ^{129}I (half-life: 1.57×10^7 y) with the long half-life in the surface soil. We have measured ^{129}I concentrations in the surface soil at Fukushima. ^{129}I/^{127}I ratios were measured by accelerator mass spectrometry (AMS) at the MALT, the University of Tokyo (Matsuzaki et al., 2007). Stable iodine of ^{127}I was determined by inductively coupled plasma mass spectrometry (ICP-MS). We already got a result that the average ^{129}I concentration was $(2.74 \pm 1.35) \times 10^8$ atoms/g prior to the FDNPP accident as ^{129}I background at Fukushima. After the accident, average isotopic ratio of ^{131}I/^{129}I at Fukushima is estimated to $(4.02 \pm 0.81) \times 10^{-2}$ as at March 11, 2011. The results of calculation about ^{131}I/^{129}I ratio made by the ORIGEN2 code are 3.18×10^{-2} for the Unit 1, 4.57×10^{-2} for the Unit 2 and 4.81×10^{-2} for the Unit 3 (Nishihara et al., 2012). In this presentation, we report the distribution of ^{129}I in terrestrial environment at Fukushima and ^{131}I/^{129}I ratios by region.

Keywords: FDNPP accident, Radioiodine, ^{131}I/^{129}I, AMS

Japan Geoscience Union Meeting 2014
(28 April - 02 May 2014 at Pacifico YOKOHAMA, Kanagawa, Japan)

MAG38-14 Room:501 Time:May 2 12:30-12:45

Desorption behavior of intrinsic cesium in smectite: Effect of aggregation on the cesium fixation in clay particles

FUKUSHI, Keisuke[1*] ; SAKAI, Haruka[2] ; ITONO, Taeko[3] ; TAMURA, Akihiro[3] ; ARAI, Shoji[3]

[1]Institute of Nature and Environmental Technology, Kanazawa University, [2]College of Science and Engineering, Kanazawa University, [3]Graduate School of Natural Science and Technology, Kanazawa University

The radiocesium from the Fukushima Daiichi nuclear power plant accident is retained at the surface soils around the power plant. The expandable fine grained clay minerals such as smectite and vermiculate are the candidates for the host phases of radiocesium. The sorption mechanism of cesium in the clay minerals is expected to be cation exchange reaction in the interlayer of the clay minerals. Therefore, the retained Cs must be desorbed to the solutions in the presence of high concentrations of major cations. On the other hand, some natural observations after the Fukushima accident have shown that the radiocesium in the contaminated soils or sediments is merely desorbed to the water even in saline solutions (e.g. Aoi et al 2013 JPGU meeting). The purpose of the study is to reproduce the unexpected fixation of cesium in clay minerals from the laboratory experiment by using standard well characterized smectite (Kunipia-F). The desorption behavior of intrinsic trace Cs (10 nmol/g from LA-ICP-MS) in smectite by major cations were systematically examined. The results of the present study showed that the aggregation of smectite by the presence of the divalent cations or high concentration of monovalent cations lead to the fixation of cesium in the clay aggregates.

Keywords: cesium, smectite, desorption, fixation, aggregation

Japan Geoscience Union Meeting 2014
(28 April - 02 May 2014 at Pacifico YOKOHAMA, Kanagawa, Japan)

MAG38-15 Room:501 Time:May 2 14:15-14:30

Evaluation of the migration of radiocesium based on chemical speciation

TANAKA, Kazuya[1*] ; FAN, Qiaohui[2] ; KONDO, Hiroaki[2] ; SAKAGUCHI, Aya[2] ; TAKAHASHI, Yoshio[2]

[1]ISSD, Hiroshima University, [2]Graduate School of Science, Hiroshima University

Chemical form of radiocesium is fundamental information for evaluation of its migration in the environment. After the Fukushima Daiichi Nuclear Power Plant (FDNPP) accident, we analyzed ^{137}Cs in aerosols, rock, soil, leaves, river suspended sediment and river water collected in Fukushima. Here, we review the migration of radiocesium in the environment based on our up-to-date data.

Many particles with high radioactivity were found in aerosols collected in March, 2011, where 50% to 90% of radiocesium was water-soluble. This means that radiocesium was still present mostly in a water-soluble fraction of aerosols before deposition and just after deposition on the ground. However, it was found that little amount of radiocesium was contained in a soluble fraction in soil and weathered rock samples by leaching experiments with water at various pH conditions. Possibly, such a soluble fraction of radiocesium was strongly fixed on rock and soil particles after dissolution in water (e.g. rainfall) on the ground. At the moment, chemical species of radiocesium would have changed from soluble to insoluble form. This strong fixation of radiocesium in soils can be explained by formation of inner-sphere complex in phyllosilicate minerals of clay minerals, which was confirmed by extended X-ray absorption fine structure (EXAFS) analysis. Field-scale observation reflected well the strong adsorption of radiocesium because most of the radiocesium stayed within 5 cm from the surface in soil layers.

In particular, in river and ocean systems, whether radiocesium is particulate or dissolved form is closely related to uptake by organisms and incorporation into food chain in ecosystems. We have monitored radiocesium concentrations in the Abukuma River system since summer in 2011. Total ^{137}Cs concentration in river water including both dissolved and particulate fractions decreased drastically from summer to winter in 2011, and then gradually decreased with time except at heavy rainfall events. From the strong fixation of radiocesium on soil particles, it was expected that radiocesium was predominant in particulate matter in river systems. More than 70% of radiocesium was particulate form, where the contribution of silt size (3 ? 63 μm) fraction was the largest. However, radiocesium in dissolved fraction suggested an increase at estuary. This implies desorption of radiocesium from particulate matter because of an increase in salinity.

We made adsorption experiments to determine distribution coefficient, K_d, between fluvial sediment and river water, and further desorption experiments to examine the reversibility of adsorption-desorption process. Kd values determined by adsorption and desorption experiments were consistent, indicating that radiocesium adsorption was a reversible process. In addition, when artificial seawater was used for desorption experiment, the resulting K_d value was lower than that obtained using river water. This clearly demonstrated the influence of ionic strength on adsorption-desorption process through competition of cesium ions with other ions (e.g., K^+, Na^+ and Ca^{2+}), which is consistent with the field observation as noted above. Furthermore, we applied generalized adsorption model (GAM) to predict the distribution of radiocesium between particulate matter and water in the Abukuma River system. As a result, it was demonstrated that GAM can predict the apparent K_d values calculated from ^{137}Cs concentrations in fluvial sediment and river water as well as lower K_d values at estuary.

Keywords: Fukushima, Radiocesium

Japan Geoscience Union Meeting 2014
(28 April - 02 May 2014 at Pacifico YOKOHAMA, Kanagawa, Japan)

MAG38-16 Room:501 Time:May 2 14:30-14:45

Radiocesium wash-off associated with soil erosion from various land uses after the Fukushima Dai-ichi NPP accident

WAKIYAMA, Yoshifumi[1*] ; ONDA, Yuichi[1] ; YOSHIMURA, Kazuya[2] ; KATO, Hiroaki[1]

[1]Center for Research in Isotopes and Environmental Dynamics, University of Tsukuba, [2]Headquaters of Fukushima Partnership Operations, IAEA

Soil erosion is the initial process which drives radiocesium into the aquatic systems and therefore the quantification of radiocesium wash-off associated with soil erosion is indispensable for mitigating the risks. This study presents two year ' s observation of soil erosion and radiocesium wash-off to quantify differences in radiocesium behavior in various land uses. Seven runoff plots were established in four landscapes; uncultivated farmland (Farmland A1, Farmland B1), cultivated farmland (Farmland A2, Farmland B2), grassland (Grassland A, Grassland B) and Japanese cedar forest (Forest) in Kawamata town, an area affected by the Fukushima Dai-ichi Nuclear Power Plant accident. The discharged sediments were collected approximately every two weeks. In laboratories, collected sediments were dried and weighed for calculating soil erosion rates (kg m^{-2}) and served for measurements of radiocesium concentration (Bq kg^{-1}) with HPGe detectors. The erosivity factor of the Universal Soil Loss Equation (R-factor: MJ mm ha^{-1} hr^{-1} yr^{-1}) was calculated based on the data of precipitation. Standardized soil erosion rates (kg m^{-2} MJ^{-1} mm^{-1} ha hr yr), observed soil erosion rates divided by R-factor, was 1.8×10^{-4} in Farmland A1, 6.0×10^{-4} in Farmland A2, 1.5×10^{-3} in Farmland B1, 8.3×10^{-4} in Farmland B2, 9.6×10^{-6} in Grassland A, 5.9 × 10-6 in Grassland B and 2.3×10^{-6} in Forest. These erosion rates were basically proportional to their vegetation cover of soil surfaces except for cultivated farmlands. Concentrations of Cs-137 in eroded sediments basically depended on the local deposition of Cs-137 and varied enormously with ranging several orders of magnitude in all the landscapes. For the observation period of time decreasing trends in concentrations of Cs-137 in eroded sediments were not obvious. To compare these results with those of Chernobyl, we calculated normalized solid wash-off coefficient (m^2 g^{-1}) with dividing the mean total concentration of Cs-137 in sediments by local deposition of Cs-137 (Konoplev et al., 1992). The coefficient was 4.4 × 10-5 in Farmland A1, 1.3×10^{-5} in Farmland A2, 6.4×10^{-5} in Farmland B1, 1.0×10^{-5} in Farmland B2, 2.2×10^{-5} in Grassland A, 1.0×10^{-5} in Grassland B and 8.2 × 10^{-5} in Forest. High erodibilities and relatively low values of normalized wash-off coefficients in cultivated farmlands can be attributed to the mixing of surface soil by ploughing. These values almost corresponded to those of Chernobyl. It was found that the total solid wash-off coefficient of radiocesium from farmlands is high and for 2 years period of time after the accident reaches 10%. Generally high precipitation in the region and steep slopes promote higher wash-off of radiocesium as compared to the Chernobyl case. Also, normalized wash-off coefficients exhibited relatively less volatility than erodibilities in the landscapes. These results suggest that soil erosion management is crucial for mitigating risks of radiocesium.

Keywords: soil erosion, erosion plot, Cs-137

Japan Geoscience Union Meeting 2014
(28 April - 02 May 2014 at Pacifico YOKOHAMA, Kanagawa, Japan)

MAG38-17 Room:501 Time:May 2 14:45-15:00

The distributed models to predict interannual changes in inventory and discharge of rCs from river basin

KONDOH, Akihiko[1*] ; ONDA, Yuichi[2]

[1]CEReS, Chiba University, [2]CRiED, University of Tsukuba

Radioactive materials emitted from Fukushima Dai-ichi Nuclear Power Plant (FDNPP) in March 11, 2011, are spreading to wide area and deposited on the ground. Abukuma mountains where vast amount of radioactive nuclides are deposited, is mostly covered by forest. Transition of radioactive nuclides arises with hydrologic and material cycles in forested mountain watershed, and the redistribution will proceed for a long time. Monitoring of the distribution and time changes in radioactive materials are necessary. At the same time, the prediction of long term behavior of radioactive materials is necessary to make use of restoration of contaminated area. The purpose of the study is to calculate erosion rate in wide area, and predict long term change in the inventory of radioactive cesium, especially cesium 137, by distributed parameter model.

Spatial resolution of the distributed model is 25m, same as aerial monitoring of dose rate and inventory maps published by MEXT. The area of calculation is the extent of 36 river catchment within the 80 km zone from FDNPP including Abukuma River Basin.

Members of USLE (Universal Soil Loss Equation) to calculate erosion rate are derived from observation in USLE plots established in different land cover in Yamakiya District, Kawamata Town, Fukushima Prefecture, by team Tsukuba University.

Land use type for each grid cels is derived from present vegetation map prepared by Ministry of Environment. Gridded land use map with 25m resolution is created from shape file of the vegetation map. Topographic parameters are extracted from 25m resolution DEM re-constructed from 10m DEM by GSJ (Geospatial Information Authority of Japan). Vegetation cover ratio map is created from MODIS NDVI datasets with 250m resolution processed by Tokyo University of Information Sciences.

Erosion rates on each grid cell are calculated and make distribution map. Erosion rate is high in crop land, and low in forested area. Average erosion rate in crop land is about 1.4 ton/ha/year, and the one in forested area is about 0.1 ton/ha/year.

The model that calculate the transition of cesium-137 is developed and the changes in the inventory from 2011 to 2041 are calculated. The erosion rate is annual value, so time step is set to one year. The eroded sediment is transported to down slope. Sediment Delivery Ratio (SDR), the ratio of transported sediment over total sediment, should be determined, however, the proper SDR is knot known, so SDR=1 is adopted in the calculation and maximum transportation rate is assumed.

The amount of cesium-137 is calculated by introducing Sc. Sc is the ratio of effluent cesium-137 (Bq/kg) over inventory (Bq/m2). Sc is determined by observations at the USLE plots of different land use. Out flowing cesium-137 is calculated by erosion rate multiplying by Sc.

The movement of debris along the slope is generally very slow, however, after the debris reach to the valley bottom, where saturation usually occur at the precipitation events, sediment is removed by flowing water. DEM is used to calculate Topographic Index (TPI) to designate the area of stream flow generation. When sediments reach to the area, cesium-137 flushes to the outlet of the watershed. In this calculation, all the cesium-137 is considered to be removed to the cell, and flushes to the outlet.

The calculation shows the average inventory of cesium-137 is about 10% lower than the one that only radioactive decay is considered. Total amount of discharge of cesium-137 at Iwanuma point, Abukuma River, is the order of 10ˆ13 Bq in both case in the first year after the deposition of radioactive materials. Discharge of cesium-137 sharply decrease in the first years, after the sharp drop, discharge decreased in exponential form.

The result of the study is based on the empirical model, however, it considers the established knowledge in the field of stream flow generation. The results reflect the actual condition of cesium-137 transition.

Keywords: Universal Soil Loss Equation, erosion rate, radioactive cesium, inventory change, distributed model, FUKUSHIMA

Japan Geoscience Union Meeting 2014
(28 April - 02 May 2014 at Pacifico YOKOHAMA, Kanagawa, Japan)

MAG38-18 Room:501 Time:May 2 15:00-15:15

Cs-134 and Cs-137 radioactivity of riverine suspended solids in the Abukuma River after the heavy rain in June 2012

NAGAO, Seiya[1*] ; KANAMORI, Masaki[2] ; OCHIAI, Shinya[1] ; TOMIHARA, Seiichi[3] ; YAMAMOTO, Masayoshi[1]

[1]LLRL, INET, Kanazawa University, [2]Grad. School of NST, Kanazawa University, [3]Environmental Aquarium Aquamarine Fukushima

About 15 PBq of both Cs-134 and Cs-137 was released from the Fukushima Daiichi Nuclear Power Plant (NPP) after the 2011 Tohoku earthquake and tsunami. Surface deposition pattern of Cs-134 and Cs-137 occurred at Fukushima, Tochigi and Gunma Prefecture by a combination with wind direction and precipitation. It is important to elucidate the short-term to long-term impacts of the Fukushima Daiichi NPP accident on ecosystems of river watershed environments. This study was conducted to investigate transport of Cs-134 and Cs-137 in the Abukuma River running through Fukushima and Miyagi Prefecture in Japan, 15 months after the Fukushima Dai-ichi NPP accident. Field experiments were carried out at Shirakawa (upper), Motomiya, Data (middle) and Iwanuma (lower) during June 19-21, 2012. We also carried out the research at the Uta, Niida, Natsui and Same Rivers. Typhoon Guchol struck Japan on June 20. Fukushima Prefecture had rainfall of 77-136 mm during June 19-21. The suspended particles were separated using continuous centrifugation. The radioactivity of Cs-134 and Cs-137 was measured with gamma-ray spectrometry after drying them by freeze-dry method.

Total radioactivity of Cs-134 and Cs-137 in river waters was 0.091-3.83 Bq/l in high flow conditions by heavy rain. The particulate fractions of Cs-134 and Cs-137 were 77-89% at the normal flow condition, but were close to 100% after the typhoon. The radioactivity of Cs-134 and Cs-137 increased from 500 Bq/kg-ss in the upper site (Shirakawa) to 3470 Bq/kg-ss in the lower site (Iwanuma). The Cs-137 radioactivity was 3200 Bq/ kg-ss in the Uta River, 42440 Bq/ kg-ss in the Niida, 850 Bq/ kg-ss in the Natsui River and 550 Bq/ kg-ss in the Same River. These results indicate that the input of radiocesium associated with suspended particles from the watershed to the river water is controlled by the accumulation of radiocesium on the ground surface in the river watershed and transport processes of suspended solids in the river systems.

Keywords: river water, radioesium, particulate forms, migration, heavy rain event

Japan Geoscience Union Meeting 2014
(28 April - 02 May 2014 at Pacifico YOKOHAMA, Kanagawa, Japan)

MAG38-19 Room:501 Time:May 2 15:15-15:30

Transportation of radiocesium through rivers in Fukushima

TANIGUCHI, Keisuke[1*] ; YOSHIMURA, Kazuya[2] ; SMITH, Hugh[3] ; BLAKE, Will[4] ; TAKAHASHI, Yoshio[5] ; SAKAGUCHI, Aya[5] ; YAMAMOTO, Masayoshi[6] ; ONDA, Yuichi[1]

[1]Center for Research in Isotopes and Environmental Dynamics, University of Tsukuba, [2]JAEA, [3]University of Liverpool, [4]School of Geography, Earth and Environmental Sciences, Plymouth University, [5]Department of Earth and Planetary Systems Science, Graduate School of Science, Hiroshima University, [6]Low Level Radioactivity Laboratory, Kanazawa University

Due to Fukushima Daiichi Nuclear Power Plant accident, radioactive materials including Cs-134 and Cs-137 were widely distributed in surrounded area. The radiocesiums have been transported in river networks. This study showed the monitoring results of radiocesium concentration in river waters and suspended sediments in Abukuma river basin and smaller coastal river catchments.

The monitoring started at 6 sites from June 2011. Subsequently, additional 24 monitoring sites were installed between October 2012 and January 2013. Flow and turbidity (for calculation of suspended sediment concentration) were measured at each site, while suspended sediments and river water were collected every one or half month to measure Cs-134 and Cs-137 activity concentrations by gamma spectrometry.

Activity concentrations of Cs-134 and Cs- 137 on suspended sediments were generally decreasing at all sites. The decreasing rate changed lower at about one year later from the accident. Activity concentration in river waters also showed the same tendency although there are only few data within 1 year from the accident.

Activity concentrations measured at the same day are proportional to the mean catchment inventory. Therefore, the activity concentration can be normalized by the mean catchment inventory. The normalized activity can be fitted to following double exponential function:

[At] = 1.551 exp (-5.265 t) + 0.069 exp (-0.266 t), where t is the time from the accident [year].

Radioceasium flux at a monitoring site was measured from the flow and turbidity data and the radioceasium concentration. Suspended sediment concentration (SSC) could be estimated from the turbidity data. Suspended sediment flux was calculated by multiplying the SSC by flow rate. Then, multiplying the suspended sediment flux by radioceasium concentration gave the radioceasium flux. The highest radioceasium flux occurred in Sep. 2011 due to the typhoon roke. Then, the radioceasium flux declined, however the flux increased in the summer and autumn of 2013 due to typhoon events.

There is no time evolution of Kd between suspended sediments and river water. Instead, Kd was varied spatially. Although the reason of the spatial variation is not clear for now, geology of the catchment (i.e. mineral composition of suspended particles) seems to relate the variation.

Keywords: Radioceasium concentration, suspended sediment

Japan Geoscience Union Meeting 2014
(28 April - 02 May 2014 at Pacifico YOKOHAMA, Kanagawa, Japan)

MAG38-20 Room:501 Time:May 2 15:30-15:45

A sediment transport model for analyzing the environmental dynamics of radionuclides in estuarine and coastal oceans

UCHIYAMA, Yusuke[1*] ; YAMANISHI, Takafumi[1] ; TSUMUNE, Daisuke[2] ; MIYAZAWA, Yasumasa[3]

[1]Kobe University, [2]Central Research Institute of Electric Power Industry (CRIEPI), [3]Japan Agency for Marine-Earth Science and Technology (JAMSTEC)

Several oceanic dispersal modeling have been conducted by multiple institutions on dissolved radionuclides leaked at the Fukushima Dai-ichi Nuclear Power Plant (FNPP). Among others, we developed a multi-nesting oceanic model at the lateral grid resolution down to 1 km and performed the comprehensive dispersal reanalysis of the direct release of ^{137}Cs from FNPP occurred in March and April 2011 (Uchiyama *et al*., 2013, *J. JSCE*). The model reveals that the current field on the continental shelf off Fukushima varied with surface wind stress and largely confined in the narrow coastal strip by about 30 km offshore. The spectral coherence analysis suggests that predominant alongshore transport of nuclides is caused by coastal jets on the shelf, presumably as forced shelf waves associated with the alongshore component of the wind stress. The coastal dispersal of the radionuclides is affected not only by direct release but also by atmospheric fallout (deposition) and discharge from the rivers. The last process introduces a time lag behind the direct release with hydrological process because the nuclides mostly attach to suspended particles (sediments) that are transported quite differently to the dissolved matter in the ocean.

In the present study, an Eulerian sediment transport model as an active tracer conservation equation with a prescribed settling velocity added to the vertical advection term, a wave-enhanced bed boundary layer model and a simple stratigraphy model proposed by Blaas *et al*. (2007) are implemented into ROMS (Shchepetkin and McWilliams, 2005, 2008). Three classes of sediments, viz., fine sand, silt and clay fractions, are considered here. The modeling procedure is approximately the same as Uchiyama *et al*. (2013), whereas the third embedding is done at the horizontal resolution dx of 250 m within the existing 1-km domain to develop the triple nested configuration forced by the assimilative JCOPE2 reanalysis (Miyazawa et al., 2009) as the outer-most boundary conditions. Thus the grid refinement occurs from JCOPE2 (dx ~ 10 km) to ROMS-L1 (dx = 3 km), to ROMS-L2 (dx = 1 km), and finally to ROMS-L3 (dx = 250 m). Sediments are taken into account in ROMS-L3 model carried out for March through August 2011. The bed skin stress is evaluated by a combined wave-current stress model of Soulsby (1995) with the wave field computed by a SWAN spectral wave modeling at dx = 1 km embedded in the JMA GVP-CWM spectral wave reanalysis. The bathymetry is provided by the 50-m resolution dataset compiled by Japan's Cabinet Office. The initial distributions of fractions of the marine bed sediment classes are estimated with an optimally interpolated field of the observations reported by Miyagi and Fukushima Prefectures (1991, 2013). Daily discharges of 6 major rivers and 14 minor rivers in the L3 domain are provided from the hydrological surface water model HYDREEMS conducted in CRIEPI. An empirical, mean relation between river discharge and sediment flux based on Takekawa *et al*. (2013) is employed for estimating the section-averaged sediment flux at each river mouth. Fraction of sediment classes in the river water is estimated from a USLE based river model conducted by JAEA (2013). The passive tracer is additionally considered to track dissolved ^{137}Cs released from FNPP as the direct release, whereas its absorption and desorption to the sediments (i.e., suspended ^{137}Cs) are not considered yet.

We intend to talk at the conference on initial dispersal of dissolved ^{137}Cs at dx = 250 m, extent of the land-derived sediments from each river mouth, resuspension and recirculation of the deposited bed sediments during storm conditions, in conjunction with corresponding oceanic states. We will further touch on potential distribution of suspended and dissolved ^{137}Cs if absorption and desorption occur.

Keywords: multi-class sediment transport model, radioactive cesium 137, multiple nesting approach, ROMS (Regional Oceanic Modeling System)

Japan Geoscience Union Meeting 2014
(28 April - 02 May 2014 at Pacifico YOKOHAMA, Kanagawa, Japan)

MAG38-21 Room:501 Time:May 2 15:45-16:00

Distribution of radionuclides in the surface seawater developed by aerial radiological survey

INOMATA, Yayoi[1*] ; AOYAMA, Michio[2] ; HIROSE, Katsumi[3] ; SANADA, Yukihisa[4] ; TORII, Tatsuo[4] ; TSUBONO, Takaki[5] ; TSUMUNE, Daisuke[5] ; YAMADA, Masatoshi[6]

[1]Asia Center for Air Pollution Research, [2]Fukushima University, [3]Sophia University, [4]Japan Atomic Energy Agency, [5]Central Research Institute of Electric Power Industry, [6]Hirosaki University

This study investigated the distribution of anthropogenic radionuclide in the surface seawater derived from the Fukushima Daiichi Nuclear Power Plant (FNPP1) observed by aerial radiological survey as an initial attempt. The aerial radiological survey over the coastal region was performed by the U.S. Department of Energy National Nuclear Security Administration (DOE/NNSA) within a 30 km radius of the FNPP1 on 18 April 2011. We found good correlations between the in-situ activities of radionuclide (131I, 134Cs, 137Cs) in the surface seawater and gamma-ray peak count rates by aerial radiological surveys (correlation coefficients for 131I, 0.89; 134Cs, 0.96; 137Cs, 0.92). Based on these relations, we find that the area with high concentrations extend south-southeast from the FNPP1. The maximum concentrations of 131I, 134Cs, and 137Cs reached 329, 650, and 599 Bq L-1, respectively. The131I/134Cs ratios in surface waters of the high activities area on 18 April were about 0.6-0.7. Considering the radioactive decay of 131I (half-life: 8.02 d), we determine that the radionuclides in this area are due to direct release from FNPP1 to the ocean. These also confirm that the aerial radiological survey might be very effective to investigate the surface distribution of anthropogenic radionuclides in the surface seawater. Furthermore, the model reproduced the distribution pattern of the FNPP1 derived radionuclides, although simulated results by regional ocean model are underestimated.

Keywords: Airborne surveys, Ocean, Anthropogenic radionuclide, Gamma-ray peak count, Regional Ocean Modeling System, Fukushima Daiichi Nuclear Power Plant

Japan Geoscience Union Meeting 2014
(28 April - 02 May 2014 at Pacifico YOKOHAMA, Kanagawa, Japan)

MAG38-22 Room:501 Time:May 2 16:15-16:30

Approach taken by oceanography specialists toward building emergency system and analyzing radiocesium in bottom sediment

IKEDA, Motoyoshi[1*]

[1]Hokkaido University

Eastern Japan along the Pacific coast has been damaged seriously and is still trying to recover after the nuclear power plant accident in Fukushima due to the magnitude-9 earthquake on March 11, 2011. In addition, we should prepare ourselves for another accident in future. The necessary system is to predict and monitor radionuclide distributions immediately following a possible accident, even if it is a rare case. We have started a plan of testing an emergency system based on ocean simulation models. The other actions include monitoring and modeling of radiocesium concentration, which still keeps a high level in the bottom sediments. The dedicated members of the Oceanographic Society of Japan have been making estimations and discussion to find which processes are responsible for the high concentration, while symposia have been held from time to time. We have so far reached the tentative conclusion that any process could be a possible one for the present condition among absorption/adsorption by plankton, detritus and disturbed sediments, direct adsorption of seawater cesium and inflow of suspended solids from rivers, with a particular attention to re-suspending sediments.

Keywords: radionuclide, emergency system, sediments

Japan Geoscience Union Meeting 2014
(28 April - 02 May 2014 at Pacifico YOKOHAMA, Kanagawa, Japan)

MAG38-23 Room:501 Time:May 2 16:30-16:45

Long-term behavior of Cs-137 activity in the ocean following the Fukushima Daiichi Nuclear Power Plant Accident

TSUMUNE, Daisuke[1*] ; AOYAMA, Michio[2] ; TSUBONO, Takaki[1] ; TATEDA, Yutaka[1] ; MISUMI, Kazuhiro[1] ; HAYAMI, Hiroshi[1] ; TOYODA, Yasushi[1] ; YOSHIDA, Yoshikatsu[1] ; UEMATSU, Mitsuo[3]

[1]Central Research Institute of Electric Power Industry, [2]Fukushima University, [3]Tokyo University

A series of accidents at the Fukushima Dai-ichi Nuclear Power Plant following the earthquake and tsunami of 11 March 2011 resulted in the release of radioactive materials to the ocean by two major pathways, direct release from the accident site and atmospheric deposition.

We reconstructed spatiotemporal variability of Cs-137 activity in the ocean by the comparison model simulations and observed data. We employed a regional scale and the North Pacific scale oceanic dispersion models, an atmospheric transport model, a sediment transport model, a dynamic biological compartment model for marine biota and river runoff model to investigate the oceanic contamination.

Direct releases of Cs-137 were estimated for two years and six months after the accident by comparing simulated results and observed activities very close to the site. The estimated total amounts of directly released was 3.6±0.7 PBq. Directly release rate of Cs-137 decreased exponentially with time by the end of December 2012 and then, was almost constant. The daily release rate of Cs-137 was estimated to be 3.0 x 10^10 Bq/day by the end of September 2013. The activity of directly released Cs-137 was detectable only in the coastal zone after December 2012. Simulated Cs-137 activities attributable to direct release were in good agreement with observed activities, a result that implies the estimated direct release rate was reasonable, while there is no observed data of Cs-137 activity in the ocean from 11 to 21 March 2011. Observed data of marine biota should reflect the history of Cs-137 activity in this early period. We reconstructed the history of Cs-137 activity in this early period by considering atmospheric deposition, river input, rain water runoff from the 1F NPP site and absorption in sediment. The comparisons between simulated Cs-137 activity of marine biota by a dynamic biological compartment and observed data also suggest that simulated Cs-137 activity attributable to atmospheric deposition was underestimated in this early period. In addition, river runoff model simulations suggest that the river flux of Cs-137 to the ocean was effective to the Cs-137 activity in the ocean in this early period. The sediment transport model simulations suggests that the inventory of Cs-137 in sediment was less than 10% of total released Cs-137. Sediment is not dominant sink of Cs-137 in the ocean.

Keywords: Fukushima Daiichi NPP accident, Regional Ocean Model System, Cesium 137

Japan Geoscience Union Meeting 2014
(28 April - 02 May 2014 at Pacifico YOKOHAMA, Kanagawa, Japan)

MAG38-P01 Room:Poster Time:May 2 16:15-17:30

Characteristics of radioactive Cs in reservoir sediment in Iwaki, Fukushima prefecture

AOI, Yusuke[1*] ; FUKUSHI, Keisuke[2] ; TOMIHARA, Seiichi[3] ; NAGAO, Seiya[2] ; ITONO, Taeko[1]

[1]Graduate School of Natural Science and Technology, Kanazawa University, [2]Institute of Nature and Environmental Technology, Kanazawa University, [3]Aquamarine Fukushima

Large amount of radioactive elements, mainly Cs, were emitted from Fukushima Daiichi Nuclear Power Plant (FDNPP) because of Tohoku Earthquake occurred in March, 2011 and Fukushima prefecture and prefectures of the neighborhood were contaminated. Nuclear Regulation Authority, Japan (2013) reported that air dose rates evaluated based on the airborne monitoring results clearly show larger declines than those calculated based on the physical half-life of radioactive Cs. The reasons for such larger declines may include the effects of natural environmental erosion, such as rainfall. We have applied the sediment trap to sample the reservoir sediment. Sediment trap can observed the erosion continuously. Our purpose is to examine the characteristics of Cs contaminated soil continuously from summer to winter in 2013 in detail in Iwaki city, Fukushima prefecture.

Keywords: Radioactive Cs, Sediment, Erosion, Soil, Clay mineral

Japan Geoscience Union Meeting 2014
(28 April - 02 May 2014 at Pacifico YOKOHAMA, Kanagawa, Japan)

MAG38-P02 Room:Poster Time:May 2 16:15-17:30

Deposition and Migration of Radioactive Cs in the Matsukawa Ura and Feeder Rivers, Fukushima, Japan (Preliminary report)

KAMBAYASHI, Shota[1*] ; ZHANG, Jing[2] ; NARITA, Hisashi[3] ; SHIBANUMA, Seiichiro[4] ; SOMA-FUTABA FISHERIES COOPERATION, Members[5]

[1]Graduate School of Science and Engineering for Education, University of Toyama, [2]Graduate School of Science and Engineering for Research, University of Toyama, [3]School of Marine Science and Technology, Tokai University, [4]Cbec, [5]Soma-Futaba Fisheries Cooperation Matsukawa Ura Branch

Radionuclides were released into the environment by the associated accident at the Fukushima Daiichi Nuclear Power Plant (FDNPP). Radioactive Cs that are released from FDNPP and is deposited on the land will migrate to the ocean finally through the surface flow. In this study, we were intended to determine the actual transport of radioactive material in the system of river - estuary - ocean as a model area the feeder rivers and Matsukawa Ura located in Soma City, Fukushima Prefecture. Sediment sampling were continuously obtained from Matsukawa Ura and feeder rivers (Uda River, Koizumi River, Ume River and Nikkeshi River) from September 2013. The radioactivity of the Gamma ray nuclide was measured using a Ge semiconductor detector. Radioactive Cs activity in the Ume River and Nikkeshi River, which are located on the south side were higher than that in the Koizumi River and Uda River, located on the north side, because that reduced rainfall led to the increases in radioactive Cs concentration, except for the Nikkeshi River effected by heavy rain. Thus, it is thought there is a strong correlation between precipitation and radioactive Cs inventory of Matsukawa Ura, and the river flow in brackish area is dominant by the increasing precipitation which led to the increasing of flow rate, result in the river bed sediment inflowing to Matsukawa Ura. So it suggests that radioactive Cs activity has decreased because of increasing precipitation. In the Nikkeshi River, radioactive Cs activity was increased and sediment was changed to fine grain size at the same time after heavy rain as compared with before. This is considered that fine particles have been transported due to salt water intrusion during returning from overflow to the calm water after the heavy rain event. Transport situation of radioactive material in the river - estuary - ocean system revealed that physical and chemical process contributes significantly influence on it such as water flow and dynamics of fine sediment.

Keywords: Radioactive Cs, Matsukawa Ura, Brackish water area

Japan Geoscience Union Meeting 2014
(28 April - 02 May 2014 at Pacifico YOKOHAMA, Kanagawa, Japan)

MAG38-P03 Room:Poster Time:May 2 16:15-17:30

Rapid determination of Radiostrontium in seawater sample using DGA Resin

TAZOE, Hirofumi[1*] ; YAMAGATA, Takeyasu[2] ; OBATA, Hajime[3] ; YAMADA, Masatoshi[1]

[1]Institute of Radiation Emergency Medicine, Hirosaki University, [2]College of Humanities and Sciences, Nihon University, [3]Atmosphere and Ocean Research Institute, the Tokyo University

A large amount of radionuclides were dispersed to the environment as a result of the accident at the Fukushima Daiichi Nuclear Power Plant in March 2011. Assessment of Sr-90, one of the major fission products, is crucial from the perspective of its bioavailability depending on behaviour similar to that of Ca, although few reports exist, so far. Traditional analytical procedures applies harmful huming nitric acid or large scale ion chromatography in order to separate between Sr and Ca prior to beta counting. In this study, rapid and robust purification technique for the daughter radionuclides yttrium-90 of Sr-90 using DGA chelating resin (Eichrom) without separation of Sr from Ca. DGA resin shows high distribution coefficient in high hydrochloric and nitric acid concentrations. Furthermore, we optimize the preconcentration method of Sr in seawater.

Keywords: Sr-90, Yttrium, Fuskuhima, Nuclear power plant, seawater

Japan Geoscience Union Meeting 2014
(28 April - 02 May 2014 at Pacifico YOKOHAMA, Kanagawa, Japan)

MAG38-P04 Room:Poster Time:May 2 16:15-17:30

Synchrotron radiation X-ray analyses of the radioactive single airborne particle emitted by the Fukushima nuclear accide

IIZAWA, Yushin[1*] ; ABE, Yoshinari[1] ; NAKAI, Izumi[1] ; TERADA, Yasuko[2] ; ADACHI, Kouji[3] ; IGARASHI, Yasuhito[3]

[1]Tokyo University of Science, [2]JASRI/SPring-8, [3]Meteorological Research Institute

The Fukushima Daiichi nuclear power plant (FDNPP) accident released radioactive materials into the air environment over the entire Northern Hemisphere in March 2011. In order to elucidate environmental transfer of the radioactive materials from the FDNPP accident, a large number of studies have been carried out until today. However, we still do not know the exact physical and chemical properties of the radioactive materials. Such knowledge is necessary to construct the numerical models to estimate the geographical distributions and to evaluate the human exposures during and after the FDNPP accident. Therefore, we studied the radioactive materials which were released in the air environment by a FDNPP accident based on the multiple SR (synchrotron radiation) X-ray analyses of the single airborne particles with strong radioactivity trapped in Tsukuba, Ibaraki Prefecture at the time of the FDNPP accident. The samples were the radioactive single particles collected on quartz fiber filter at the Meteorological Research Institute, Tsukuba using a high-volume aerosol sampler on March 14-15. We selected the radioactive single particles out of this filter using micromanipulator and transferred to the KaptonR tape on an acrylic plate for SR X-ray analyses.

SR experiments were performed at the beam line BL37XU of SPring-8. The monochromatic SR X-ray beams were focused to about 1 μm (horizontal) x 1 μm (vertical) by K-B mirror. Two excitation X-ray energies were selected depending on the target elements for analysis: i.e., 15.0 keV (low-energy mode) and 37.5 keV (high-energy mode). SR X-ray fluorescence (XRF) imaging was applied to obtain elemental distribution, and X-ray absorption near edge structure (XANES) analysis was used for chemical state analysis, and X-ray powder diffraction (XRD) analysis was carried out to obtain crystal structural information of the particles.

We have successfully analyzed three radioactive single airborne particles. XRF analysis has revealed the existence of Cs in all of them. We were able to detect various elements shown below depending on the excitation energy. In addition, XRF imaging shows that each element exhibited uniform distribution in the particles.

High-energy mode: Cs, Ba, Te, Sn, Mo, Zr, Rb, Zn, Fe

Low-energy mode: Fe, Mn, Cr, Zn, Ti

Each particle showed different chemical compositions. XANES analysis of Sn,Mo,Zn,Fe in the particles showed that these metallic elements existed in high oxidation states in glass matrix. Furthermore, XRD analysis shows that the particle was amorphous because no diffraction line was observed. These results suggest that the detected elements are components of materials constituting the reactor and fission products. It is presumed that the reactor materials including the nuclear fuel melted at a high temperature and quenched by releasing to the air environment as a glassy materials.

Keywords: Fukushima Daiichi nuclear power plant, Synchrotron radiation X-ray analysis, airborne particle, strong radioactive particle

Japan Geoscience Union Meeting 2014
(28 April - 02 May 2014 at Pacifico YOKOHAMA, Kanagawa, Japan)

MAG38-P05 Room:Poster Time:May 2 16:15-17:30

An approach to chemical reactions in the atmosphere

AOYAMA, Tomoo[1*] ; WAKAZUKI, Yasutaka[1]

[1]Center for Research in Isotopes and Environment Dynamics, University of Tsukuba

1. Introduction

We discuss an approximate approach to simulate time series reactions in the atmosphere. At first, we write a reaction at definition time-t, as A+B=C. Next, we suppose that densities of the compounds are written by Gaussians. The Gaussian is a solution for general small particles diffusion processes. The time-t is discrete about the interval is dt. If 2 particles of compound A and B are interacted within the interval, the reaction reaches equilibrium, and a compound C is generated.

2. Descriptions

Considering properties of the atmosphere, we adopt Gaussian having different parameters for the horizontal and vertical directions.

$GA\{A\}(r,z)=QA\{A\}\exp\{-\alpha A\ (r-rA)^2-\beta A(z-zA)^2\}$, (1)

The suffix A corresponds to compound A. The Q is density and the unit is [M/volume] of compounds. In case of uncertain compounds chemically, it is replaced by [kg/volume]. A vector r is for x- and y-coordinates, and z is for z-coordinate. The function exp(whose arguments is 3-dimensional distance) is a kind of the volume. Eq. (1) is a relation of [M]; that is, a reaction equation, which is defined at any time.

The α and β (which are positive) are diffusion parameters and they depend with elapsed time from the generation. The dependency is very complex and the evaluation is difficult. In the puff-model approach, it is calculated by many turbulence parameters. However; we wonder that model is significant in case of very diffused case. We wish to adopt Lagrangian particles (L-particles), where alpha-beta-parameters are not, and effects of the turbulence are expressed by random numbers.

L-particles are a finite volume of the air, and have no shape. Therefore; we redefine it to be Gaussian. The multiply of Gaussians is a Gaussian; it is an appropriate function to express reactions.

Under the representation, alpha-beta-parameters are fixed coefficients to define a unit volume. They are a kind of mesh intervals. The re-defined Gaussians are moved by meteorological fields, as if they were L-particles. The Gaussian is like as a mesh-unit in Euler approach, which has a finite volume. They are in a space, and are moved by wind fields; however, they are not arranged orderly in Euler approach. Here, if the arrangement is introduced as following;

A transformation between L-particle and Euler-mesh:

Q(mesh coordinates)=Integral{GA(r,z)G(on mesh)dv},

{GA(r,z)}–>{Q(on mesh)}.

The transformation seems to be usable to evaluate diffused mist.

3. Reactions

In an interval time, chemical equilibrium is,

Keq=[C]/([A][B]). (2)

For every times,

QA(t+dt)=QA(t)-QC(t), QB(t+dt)=QB(t)-QC(t), (3)

rA (t+dt)=rA (t)+{u,v}Adt+Rand(), (4)

ZA (t+dt)=ZA (t)+{w}Adt+Rand(), (5)

Where, a vector {u,v,w} is wind speeds. Rand() is normal distributed random numbers.

In another reaction, A+B=C+D, we get,

Keq=([C][D])/([A][B]), (6)

Since the distributions of C and D are same at the first step,

$GC=GD=(KeqGAGB)^{0.5}$. (7)

4. Progress of the research

We try to simulate some reactions in the atmosphere now.

Keywords: atmospheric reaction, SPM, L-particle

Japan Geoscience Union Meeting 2014
(28 April - 02 May 2014 at Pacifico YOKOHAMA, Kanagawa, Japan)

MAG38-P06 Room:Poster Time:May 2 16:15-17:30

Secular distribution of radioactive strontium concentration in the atmosphere after after the accident of FD-NPP

ZHANG, Zi jian[1*] ; NINOMIYA, Kazuhiko[1] ; TAKAHASHI, Naruhito[1] ; YAMAGUCHI, Yoshiaki[2] ; YOSHIMURA, Takashi[2] ; SAITO, Takashi[3] ; KITA, Kazuyuki[4] ; TSURUTA, Haruo[5] ; WATANABE, Akira[6] ; SHINOHARA, Atsushi[1]

[1]Graduate School of Science, Osaka University, [2]Radioisotope Research Center, Osaka University, [3]Faculty of Comprehensive Human Sciences, Shokei Gakuin University, [4]College of Science, Ibaraki University, [5]Atmosphere and Ocean Research Institute, the University of Tokyo, [6]Fukushima University

1.Introduction

On March 12, 2011, a large amount of radioactive nuclides have been released into the environment by the nuclear accident at the Fukushima Daiichi Nuclear Power Station. Measurement about radioactive nuclides will give us much information about the accident circumstance. Furthermore, radioactivities in the air dust are critical for estimation of internal exposure. There are many measurements results of I-131, Cs-134, Cs-137 in environment samples. However, in other nuclides, such as the pure beta emitter nuclide Sr-90 has not been measured sufficiently. Sr-90 is considered one of the harmful radioactive nuclides. Therefore, measurement of Sr-90 in the air dust is important for calculating exposure. We developed a new simple and quick strontium isolation technique using solid-phase extraction for determination Sr-90 in the air dust by liquid scintillation counter (LSC).

2. Method

In this study, we used 3M EmporeTM Strontium Rad Disk to extract strontium ion from air dust samples. This filter can collect Sr2+ ion efficiently. However, it is known that this filer also catches Pb2+. Natural radioactive nuclide Pb-210 seriously will be interferences in Sr identification in beta ray counting. In this study, cation exchange with EDTA adopted for Sr isolation. We made test experiments with radioactive Sr tracer and obtained that the chemical yield was about 90 %. The time for chemical operation was about 3-4 hours. To determine Sr-90, Cherenkov radiation of Y-90 has been measured by LSC, 1220 QUANTULUSTM Ultra Low Level Liquid Scintillation Spectrometer. With Sr-90 standard solution, we obtained that the Y-90 Cherenkov light detection efficiency was 68.7% and the Sr-90 detection limit was 0.004 Bq. With sequential measurement, the growth curve of Y-90 was described to determinate activity of Sr-90.

3.Results

We measured Sr-90 in the air dust samples of Fukushima, Hitachi, Kawasaki and Osaka. We chose some air dust samples that have high Cs-137 activity for Sr-90 measurement. Strontium isolation with solid phase extraction was performed. In Hitachi, the Sr-90 activity concentration in air is decreased with time and the ratio of Sr-90/Cs-137 is about 10-3. It is possible that after April, Sr-90 has been the same behavior of Cs-137. We observed a long time variation of Sr-90 air concentration in Hitachi and Fukushima and found that the Sr-90/Cs-137 activity ratio increased over time. We are going to discuss about behaviors of the Sr-90 and Cs-137 in the atmosphere.

Japan Geoscience Union Meeting 2014
(28 April - 02 May 2014 at Pacifico YOKOHAMA, Kanagawa, Japan)

MAG38-P07 Room:Poster Time:May 2 16:15-17:30

Correlation between Atmospheric Re-entrainment of Radioactive Cs and Meteorological Phenomena Conditions.

KINO, Himiko[1*] ; KITA, Kazuyuki[1] ; TANAKA, Misako[1] ; KINASE, Takeshi[1] ; DEMIZU, Hiroyuki[1] ; IGARASHI, Yasuhito[2] ; MIKAMI, Masao[2] ; KAJINO, Mizuo[2] ; ADACHI, Kouji[2] ; KIMURA, Toru[2] ; ISHIZUKA, Masahide[3] ; KAWASHIMA, Hiroto[4] ; YOSHIDA, Naohiro[5] ; TOYODA, Sakae[5] ; YAMADA, Keita[5] ; OKOCHI, Hiroshi[6] ; SHINOHARA, Atsushi[7] ; NINOMIYA, Kazuhiko[7] ; ONDA, Yuichi[8]

[1]Ibaraki University, [2]Meteorological Research Institute, [3]Kagawa University, [4]Akita Prefectural University, [5]Tokyo Institute of Technology, [6]Waseda University, [7]Osaka University, [8]Tsukuba University

1.Introduction

Massive earthquake attacked the eastern Japan on March 11 2011. It triggered the Fukushima Daiichi Nuclear Power Point accident, where large amount of radioactive substances were released. Released radioactive substances are diffused with atmospheric diffusion process, and eventually deposit on the ground surface and vegetation. Deposited radioactive Cs are released again from the ground surface and vegetation.

Today's main factor of atmospheric radiation concentration fluctuation is atmospheric Re-entrainment of radioactive Cs. Re-entrainment mechanism of radioactive Cs is a complex and unprecedented problem. We must consider an interdisciplinary study on deposited radioactive Cs for long-term estimation.

We infer that so Cs has a property that is taken in by clay minerals in soil that one of carriers of radioactive Cs is soil particles. The purpose of this study is to make clear how long does atmospheric radiation concentration increase by its re-entrainment, under what meteorological phenomena conditions.

2.About sampling

Since December 2012, we have been observing atmospheric radiation concentration of radioactive Cs by High-Volume Air Sampler on ground at Namie high school. It collects aerosols by passing through quartz filter. Wind velocity is measured at three altitudes by Three Cup Anemometer..Soil moisture is measured by Moisture Meter of Time Domain reflectometry system.

3.Correlation between seasonal re-entrainment of radioactive Cs and meteorological phenomena conditions

4.Investigation of direct transport by back-trajectory analysis

Keywords: Radioactive Cs, Atmospheric Re-entrainment, Fukushima Daiichi Nuclear Plant accident, Environmental Radioactivity

Japan Geoscience Union Meeting 2014
(28 April - 02 May 2014 at Pacifico YOKOHAMA, Kanagawa, Japan)

MAG38-P08 Room:Poster Time:May 2 16:15-17:30

Estimate of relationship between composition of aerosol and radioactive cesium observed in Namie Town, Fukushima Pref.

TANAKA, Misako[1*] ; KITA, Kazuyuki[1] ; KINASE, Takeshi[1] ; KINO, Himiko[1] ; DEMIZU, Hiroyuki[2] ; IGARASHI, Yasuhito[3] ; MIKAMI, Masao[3] ; ADACHI, Kouji[3] ; KIMURA, Toru[11] ; KAWASHIMA, Hiroto[4] ; YOSHIDA, Naohiro[5] ; TOYODA, Sakae[5] ; YAMADA, Keita[5] ; OKOCHI, Hirosi[6] ; YAMANOKOSHI, Eri[6] ; SHINOHARA, Atsushi[7] ; NINOMIYA, Kazuhiko[7] ; NAKAI, Izumi[8] ; ABE, Yoshinari[8] ; ISHIZUKA, Masahide[9] ; ONDA, Yuichi[10]

[1]Faculty of Science, Ibaraki University, [2]Faculty of Engineering, Ibaraki University, [3]Meteorology Research Institute, [4]Akita Prefectural University, [5]Interdisciplinary Graduate School of Science and Engineering, Tokyo Institute of Technology, [6]Faculty of Science and Engineering, Waseda University, [7]Graduate school of Science, Osaka University, [8]Faculty of Science, Tokyo University of Science, [9]Faculty of Engineering, Kagawa University, [10]Center for Research in Isotopes and Environmental Dynamics, Tsukuba University, [11]ATOX Co., Ltd.

Radionuclides emitted from the Fukushima dai-ichi nuclear power plant (FNDPP) have been deposited on the soil, ocean and vegetation. Re-suspension of radioactive cesium from the soil and vegetation to the atmosphere may be one of signi?cant path in the diffusion of radionuclides after the accident. Therefore, the quantitative understanding of these re-suspensions is important to understand future transition of radionuclides. Identification of aerosol species which bring Cs-134/137 is necessary to understand the mechanism of re-suspension, and its efficiency.

We have measured atmospheric concentration of radiation by Cs-134/137 in Namie high school where is away 30km from FNDPP. We have set seven high-volume air samplers (HV) at the site and one operated for 24 hours day by day.

Then gamma-ray emission from HVsamples was measured with Ge detector.

In this way we have gotten atmospheric concentration of radiation which interval is one day.

While sampling, we measure atmospheric concentration of aerosol: black carbon, sulfate, and the number of particle which have size dependence using Electrical Low Pressure Impactor (ELPI).

We have analyzed the aerosols which had collected on HV filter with chemical analysis such as chromatograph.

We examined for correlation between the results of analysis and atmospheric concentration of radiation. And we examined what factor affects atmospheric concentration of radiation, and where the factor comes from using Positive Matrix Factorization (PMF). The PMF is multivariate analysis which estimates factor profile and factor contribution from observed value. The analysis needs only the observed value and number of factor (i.e. need not source profile), so there is possibility of finding the unexpected source.

This study used the date of March and August , 2013 .

Keywords: Fukushima daiichi nuclear plant accident, environmental radioactivity

Japan Geoscience Union Meeting 2014
(28 April - 02 May 2014 at Pacifico YOKOHAMA, Kanagawa, Japan)

MAG39-01 Room:502 Time:May 1 09:00-09:15

The trial which presupposes the surface ground motion using an underground seismograph; MeSO-net

SAKAI, Shin'ichi[1*] ; NAKAGAWA, Shigeki[1] ; HIRATA, Naoshi[1]

[1]Earthquake Research Institute, University of Tokyo

We have been constructing an ultra dense seismic observation network; Metropolitan Seismometer Observation Network; MeSO-net. MeSO-net consists of 296 seismic stations. The signals from seismometers are sampled 200 Hz by a 24-bit analog to digital converter at the bottom of 20m-borehole. The surface ground motion differs from the waveform observed at the underground. Then, we tried presumption of the surface ground motion using an underground seismograph.

The present study is supported by two Special Projects for Earthquake Disaster Mitigation in Tokyo Metropolitan Area and reducing vulnerability for urban mega earthquake disasters from the Ministry of Education, Culture, Sports, Science, and Technology of Japan.

Keywords: groud motion, MeSO-net

Japan Geoscience Union Meeting 2014
(28 April - 02 May 2014 at Pacifico YOKOHAMA, Kanagawa, Japan)

MAG39-02 Room:502 Time:May 1 09:15-09:30

Attenuation Structure beneath Kanto Region using Maximum Amplitude

SEKINE, Shutaro[1*] ; TAKEDA, Tetsuya[2] ; KASAHARA, Keiji[1]

[1]Association for the Development of Earthquake Prediction, [2]National Research Institute for Earth Science and Disaster Prevention

Introduction

The seismic attenuation structure beneath the Japanese islands should be three-dimensionally complex to a similar degree as the velocity structure. Especially, in the Kanto region, the similarity with the velocity structure is unlikely to be seen in other parts of the Japanese islands because seismic attenuation implies inelasticity or scattering, whereas seismic velocity represents elastic properties. A precise estimate of the seismic attenuation leads to a better estimate of the strength of an earthquake source, in turn allowing for proper scaling. Information on seismic attenuation is also important in the simulation of strong ground motions. In this study, tomographic inversions are performed for the three-dimensional (3D) attenuation structure beneath the Kanto Region.

Data and Grid setting

In this study, tomographic inversions are performed for the three-dimensional (3D) attenuation structure beneath the Japanese islands from NIED Hi-net catalog. Vertical amplitudes of ground velocities reported between January 2004 and February 2009 are used in this study. Amplitudes from 11766 earthquakes are selected for P- and S-wave tomography. The number of the ray is 552,935 for P and 393052 for S, respectively. A grid with interval of 0.1 in Kanto region and 0.5 in other region is applied to this region at depths of every 5 km.

Results

We estimate regional detail attenuation structure in Kanto region using tomography method with NIED Hi-net maximum amplitude data. In Kanto region, a High-Q zone is clearly found along the upper boundary of the Philippine Sea slab, and below the slab, we found a distinct wedge mantle low-Q zone.

Keywords: Q, Attenuation Structure, Kanto Region

Japan Geoscience Union Meeting 2014
(28 April - 02 May 2014 at Pacifico YOKOHAMA, Kanagawa, Japan)

MAG39-03 Room:502 Time:May 1 09:30-09:45

A highly attennuative zone beneath the Tokyo Metropolitan area.

PANAYOTOPOULOS, Yannis[1*] ; HIRATA, Naoshi[1] ; SAKAI, Shin'ichi[1] ; NAKAGAWA, Shigeki[1] ; KASAHARA, Keiji[2]

[1]Univ. Tokyo, ERI, [2]Assoc. Develop. Earthquake Prediction

The material properties of the complex subduction zone beneath the Tokyo Metropolitan area can be estimated by the seismic attenuation Q of seismic waves observed at local seismic stations. Previous studies have provided us only with the large scale attenuation structure for all Japan (Jin & Aki, 2005; Nakamura et al., 2006; Edwards & Rietbrock, 2009) or only for the shallow part inside the Kanto basin (Kinoshita, 1994; Yoshimoto & Okada, 2009). In this study we aim to derive a detailed picture of the attenuation structure in the crust and upper mantle beneath the Kanto basin. The waveform data used in this study are recorded at the dense seismic array of the Metropolitan Seismic Observation network (MeSO-net). The station network is distributed on five lines with an average spacing of 3 km and in an area with a spacing of 5 km in the central part of Kanto plane. The 296 MeSO-net stations are equipped with a three-component accelerometer at a bottom of a 20-m-deep borehole, signals from which are digitized at a sampling rate of 200 Hz with a dynamic range of 135 dB. The attenuation of seismic waves along their path is represented by the $t*$ attenuation operator that can be obtained by fitting the observed seismic wave amplitude spectrum to a theoretical spectrum using an omega square source model. In order to accurately fit the spectral decay of the signal, only earthquakes that are recorded with intensity greater than 1 in the Japan Meteorological Agency (JMA) intensity scale are selected. The waveforms of 154 earthquakes were selected from the JMA unified earthquake list from January 1st 2010 to May 31st 2011. A grid search method is applied to determine the $t*$ values by matching the observed and theoretical spectra. The $t*$ data where then inverted to estimate a 3D Qp structure under the Tokyo Metropolitan area, using a layered initial Q model. Grid points were set at 15 km spacing in the horizontal direction and with 10 km spacing at depth. We implemented the 3D velocity model estimated by Nakagawa et al., 2012 and in addition we set the initial Q values at 116 for the 0 km grids and to 400 for all the grids below them. The obtained model suggests average Q values of 50$\sim$100 inside the Kanto basin. Furthermore, a low Q zone is observed in the area where the Philippine Sea plate meets the upper part of the Pacific sea plate. This area is located at approximately 40 km depth, beneath the north-east Tokyo and west Chiba prefecture areas and is represented by Q values of 100$\sim$200. Earthquakes occurring on the Pacific plate pass through this low Q area inside the Philippine sea plate and are attenuated significantly. Combined with the detailed velocity structure beneath the Kanto basin, our results help us to understand the material properties of the subducting plates. The implementation of our findings in strong motion simulation studies could help towards a better understanding of the damage area of future earthquakes and mitigate the disaster of the affected areas.

Keywords: attenuation, tomography, MeSO-net

Japan Geoscience Union Meeting 2014
(28 April - 02 May 2014 at Pacifico YOKOHAMA, Kanagawa, Japan)

MAG39-04 Room:502 Time:May 1 09:45-10:00

Viscoelastic effects on stress on the active faults around the Tokyo metropolitan area after the 2011 Tohoku earthquake

HASHIMA, Akinori[1*] ; FREED, Andrew[2] ; BECKER, Thorsten[3] ; SATO, Hiroshi[1] ; OKAYA, David[3] ; SUITO, Hisashi[4] ; HATANAKA, Yuki[4] ; MATSUBARA, Makoto[5] ; TAKEDA, Tetsuya[5] ; ISHIYAMA, Tatsuya[1] ; IWASAKI, Takaya[1]

[1]Earthquake Research Institute, the University of Tokyo, [2]Purdue University, [3]University of Southern California, [4]Geospatial Information Authority of Japan, [5]National Research Institute for Earth Science and Disaster Prevention

Beneath the Japan islands, the Pacific plate descends from the east and the Philippine sea plate descends from the south, causing interaction of two slabs at depth. The 2011 M9 Tohoku earthquake in northern Japan had a source region with a length of ˜500 km and a width of ˜200 km and forced broad lithospheric and mantle regions to deform. In addition, seismicity rates in the surrounding regions drastically increased. As the effect of the Tohoku earthquake on crustal deformation and seismicity in the Japan region is so large, it is required to quantitatively evaluate the temporal change of stress due to this earthquake. On the other hand, the mechanism of postseismic deformation is considered to be afterslip around the source region, viscoelastic stress relaxation in the asthenosphere and so on. Here, we investigate the effects of slab geometry and 3D heterogeneity on the inversion of inferred coseismic slip, the resulting broad coseismic deformation and the propagation of stress throughout the region.

We construct a 3-D finite element model (FEM) to generate Green functions for use in a coseismic inversion study that allows the influence of complex slab geometry as well as heterogeneities in elastic structure on inferred slip. We utilize the large, land-based Japan GPS array as well as seafloor geodetic constraints in the inversion. We are particularly interested in how coseismic seafloor constraints influence inversion results. Our FEM considers a region of 4500 km x 4900 km x 670 km, incorporating the Pacific and the Philippine sea slabs by interpolating models for the Tohoku region and the Nankai trough, as well as the Kuril, Ryukyu and Izu-Bonin arcs. As the geometry of the plate boundaries, we used the model interpolating the existing local plate boundary models. As the crustal thickness, we simply take the uniform value of 30 km for the continental plate and 6 km for oceanic plates. For the underlying mantle, we give the elastic constants according to the PREM model. The slabs are assumed to have 5 % higher P- and S-wave velocity than the surrounding mantle. The model region is divided into about 500,000 tetrahedral elements with average dimension ranging from 5-100 km. We also test the role of gravity on coseismic results, with initial results suggesting that gravitational loading is not an important factor because of the shallow dip of the upper Pacific slab. Based on the coseismic slip obtained by the inversion, we computed the temporal change of the Coulomb failure stress change on the active faults in the Tokyo metropolitan area considering viscoelastic relaxation in the asthenosphere. Our long-term objective is to study the influence of the Tohoku earthquake on evolution of stresses throughout Japan due to both coseismic and postseismic processes, the latter including afterslip and viscoelastic relaxation. An accurate accounting of coseismic slip is very important to such an endeavor.

Keywords: 2011 Tohoku earthquake, Coulomb failure stress change, Crustal structure, Active fault, Finite element modeling, Viscoelasticity

Japan Geoscience Union Meeting 2014
(28 April - 02 May 2014 at Pacifico YOKOHAMA, Kanagawa, Japan)

MAG39-05 Room:502 Time:May 1 10:00-10:15

Distribution and structures of blind thrust faults beneath the Tokyo metropolitan area

ISHIYAMA, Tatsuya[1*] ; SATO, Hiroshi[1] ; KATO, Naoko[1] ; ABE, Susumu[2] ; WATANABE, Hidehisa[3] ; SHIGA, Nobuhiko[3]

[1]Earthquake Research Institute, University of Tokyo, [2]R&D Department, JGI, Inc, [3]Mitsui Mineral Development Engineering Co., Ltd.

We show subsurface geometries of several active blind thrusts beneath this highly urbanized area, based on tectonic landforms, high-resolution seismic reflection data, gravity anomaly data, and Quaternary stratigraphy. Deep seismic reflection profiles corroborate the notion that steeply dipping blind thrusts are reactivated normal faults originally formed by middle Miocene extensional tectonics. Despite very slow (less than 0.1 mm/yr) late Quaternary slip rates, our work suggests the presence of previously unrecognized faults that pose more seismic hazards to Tokyo and outlying communities, and urges more intense efforts to shed more light on the recent slip rates, magnitude and recurrence of the past earthquakes on them.

Japan Geoscience Union Meeting 2014
(28 April - 02 May 2014 at Pacifico YOKOHAMA, Kanagawa, Japan)

MAG39-06 Room:502 Time:May 1 10:15-10:30

Tsunami damage in Tokyo Bay from the 1703 Genroku Kanto Earthquake

MURAGISHI, Jun[1*] ; SATAKE, Kenji[1]

[1]Earthquake Research Institute, the University of Tokyo

The 1703 Genroku Kanto earthquake was a great inter-plate earthquake along the Sagami Trough on December 31st, 1703 and caused severe damage in southern Kanto region (Usami et al., 2013). For the tsunamis in Boso Peninsula, Hatori (1975, 1976) and Koyama (1982, 1983, 1987) investigated historical documents and stone monuments recording casualties, and Tsuji (2003) revealed the number of washed-away houses at each village.

For the tsunami in Tokyo Bay, Hatori (1976, 2006) estimated the tsunami heights as 2 m in his compilation of tsunami heights in the Kanto region. While this height has been often used for tsunami countermeasure in Tokyo Bay, the ground for this estimation is not clear.

On the other hand, the Cabinet Office (2013) concluded that no tsunami damage occurred in the eastern coast of Tokyo Bay, although some tsunami description is recorded in Edo, the capital in those days. It is necessary to conduct an investigation of tsunami damage along the coast of Tokyo Bay through historical documents.

The notice from Edo-Machi-Bugyo (Edo City Commissioners)to residences in Edo recorded that there were four major arrivals of tsunami along the Uchikawa River (Sumida River), and tsunami came up to the upper limit of the river. According to the “ Omurochuki ”, tsunami inundated up to the Eitai-bashi Bridge. There were seven ebbs and flows of tide. Tides were filled twelve times on the next day after the earthquake. “ Saihen-onkoroku ” recorded that the person(s) were thrown off their ship during their evacuation.

There is a document which recorded tsunami damage in Funabashi City, Chiba Prefecture. Petition from fishermen to public office, which was written 41 years after the 1703 Genroku earthquake, recorded that fishing boats and tools for fishermen such as fishing nets were washed away, and that fishermen requested the public assist for the poor catch of fish due to the lack of sea weeds.

“ Shiohama-Yuraigaki ” reported the origin of salt farm and its damage at Ichikawa City due to the subsidence accompanied by the 1703 earthquake. These historical records are materialized in 1756 and afterwards. The embankments were collapsed and the salt farm has been ruined. However, no tsunami damage is described. This document described storm surge damage on September 28, 1680. It says that 55 persons were killed in Kakemama-mura by the storm surge, 100 persons died and millets and household goods were completely washed away in Hanzaemon Ina ’ s territory. It seems that there was wide range and large-scale storm surge damage according to the historical record. Although the 1680 storm surge damage is recorded in detail, there is no record of the 1703 tsunami, indicating that the 1703 tsunami damage, if any, must be smaller than the storm surge of 1680.

We found the historical records which had not been used in previous tsunami studies, and revealed that the 1703 Genroku tsunami caused some damage in inner Tokyo Bay area. We would like to continuously collect historical-records and examine the tsunami damage and heights.

Acknowledgements

This study was supported by the Special project for reducing vulnerability for urban mega earthquake disasters from the Ministry of Education, Culture, Sports, Science and Technology of Japan.

Keywords: the 1703 Genroku Earthquake, Historical earthquakes, Tsunami

Japan Geoscience Union Meeting 2014
(28 April - 02 May 2014 at Pacifico YOKOHAMA, Kanagawa, Japan)

MAG39-07 Room:502 Time:May 1 11:00-11:15

A new direction of the MeSO-net

HIRATA, Naoshi[1*] ; SAKAI, Shin'ichi[1] ; NAKAGAWA, Shigeki[1] ; KASAHARA, Keiji[2] ; KIMURA, Hisanori[3] ; HONDA, Ryou[4]

[1]Earthquake Research Institute, the University of Tokyo, [2]ADEP, [3]NIED, [4]Hot Springs Research Institute of Kanagawa Prefecture

We have developed the Metropolitan Seismic Observation network (MeSO-net) under the Special Project for Earthquake Disaster Mitigation in Tokyo Metropolitan Area (FY2007-FY2011) and maintain it by the Special Project for Reducing Vulnerability for Urban Mega Earthquake Disasters (FY2012-FY2016), which are supported by MEXT. The network consists of 296 seismic observation stations, from which data are continuously transmitted and recorded at a data management center in ERI. We developed an intelligent data transmission protocol for MeSO-net System, which is referred to as Autonomous Cooperative data Transfer (ACT)(Morita et al., 2010) . As culture noise in urban areas is very high, we use a 20-m-deep shallow borehole to install wide-band accelerometers but a signal-to-noise ratio is still low. A large number with short interval of station configuration helps us to obtain better resolution and high quality seismic data. We are now developing a new automatic data processing function in the MeSO-net: automatic event detection and P- and S-phase picking. We also develop a method to predict ground and building motions from the MeSO-met data.

Keywords: MeSO-net, accelerometer, continuous recording, Autonomous Cooperative data Transfer, automatic event detection, seismic tomography

Japan Geoscience Union Meeting 2014
(28 April - 02 May 2014 at Pacifico YOKOHAMA, Kanagawa, Japan)

MAG39-08 Room:502 Time:May 1 11:15-11:30

Overview of 'Maintenance and Recovery of Functionality in Urban Infrastructures'

NAKASHIMA, Masayoshi[1*] ; KOSHIKA, Norihide[2] ; KAJIWARA, Koichi[3] ; NOZAWA, Takashi[1]

[1]Disaster Prevention Research Institute Kyoto University, [2]Kobori Research Complex, [3]Hyogo EERC, NIED

The 2011 Tohoku earthquake caused unprecedented damage to the island of Japan. The damage was spread to the Tokyo Metropolitan Area, hundreds kilometers away from the epicentral region, which sustained serious disruption, most notably to businesses. Measures have to be taken to reduce such disruption before the island of Japan receives another mega earthquake, which is expected by the middle of this century. Issues to be addressed:

1. Quantification of collapse margin of high-rise buildings.
2. Monitoring and prompt condition assessment of buildings.

The project deals with high-rise buildings which are prevalent in urban areas and focuses on the following three themes.

(1) Quantification of collapse margin of high-rise building structures.
(2) Monitoring and condition assessment for the health of buildings.
(3) Evaluation and monitoring of soil-foundation-structure interaction systems.

To achieve these goals, state-of-the-art theory and high-fidelity simulation are utilized, together with a series of large-scale tests as well as continuous observation of vibrations to actual structures. The project will offer technical guidelines and associated materials useful for the design, construction, and maintenance of buildings and urban infrastructure systems. A research team consisting of members from industry, academia, and government authorities has been formed to run the project most effectively.

鉄骨造試験体
の最終崩壊形

Japan Geoscience Union Meeting 2014
(28 April - 02 May 2014 at Pacifico YOKOHAMA, Kanagawa, Japan)

MAG39-09 Room:502 Time:May 1 11:30-11:45

Urban Resilience

HAYASHI, Haruo[1*]

[1]Disaster Prevention Research Institute, Kyoto University

With a high probability in the first half of 21st century, Nankai Trough earthquakes will cause a tremendous amount of damage and losses which might exceeds Japanese national annual budget. In addition, we might take into account the possible occurrence of Tokyo Metropolitan earthquake which may cause a serious threat to our national security. It is virtually impossible to complete all the works needed to prevent those possible damage and losses due to these mega earthquakes before they will happen. It means that we need to develop a science and technology to minimize the resulting damage and losses due to these mega scale earthquake disasters and to realize high disaster resilience for quick and steady recovery based on the lessons taken from past earthquake disasters including 3.11 Tohoku Earthquake and Tsunami Disaster in 2011.

Recent progress in information and communication technology such as internet and mobile device with GPS should be adapted for effective disaster response and recovery. In this project, we will develop two ICT based system for creating common operational pictures among stakeholders. First system will be web-GIS system to provide an informational platform in which various kinds of information provided from seismology to social psychology will be mashed up for creating a new value. Second system will be Micro Media Service which will provide the information selected for each uses to meet their needs.

It is our ultimate goal to improve disaster preparedness of each individual who might be function as disaster response personnel or disaster victims. We will develop a Web portal site named as Disaster Literacy Hub to provide educational materials prepared for all disciplines related for earthquake disaster reduction based on the theory of instructional design.

All the academic achievements will be presented through the website shown below:

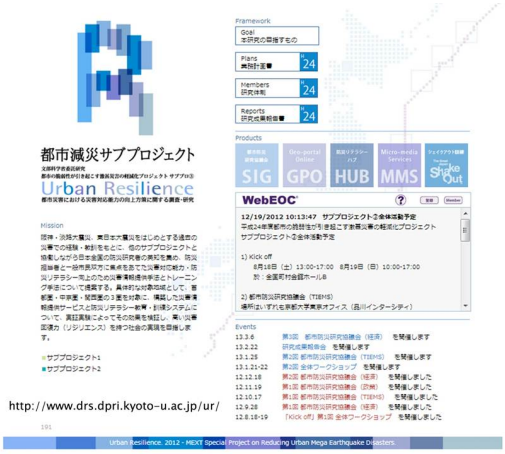

Japan Geoscience Union Meeting 2014
(28 April - 02 May 2014 at Pacifico YOKOHAMA, Kanagawa, Japan)

MAG39-10 Room:502 Time:May 1 11:45-12:00

Past large earthquakes beneath metropolitan Tokyo: Issues for estimation of occurrence probability and disaster

SATAKE, Kenji[1*] ; ISHIBE, Takeo[1] ; MURAGISHI, Jun[1]

[1]Earthquake Research Institute, the University of Tokyo

Two types of large earthquakes, great interplate (M~8) earthquakes along Sagami Trough and M~7 earthquakes beneath southern Kanto region, have caused damage in metropolitan Tokyo and are expected to occur in the future. The 1923 Taisho Kanto earthquake (September 1, M 7.9) and the 1703 Genroku Kanto earthquake (December 31, M~8.2) are the first type, and the typical example of the second type is the 1855 Ansei Edo earthquake (November 11, M~7.0).

The Cabinet office and the Earthquake Research Committee of the Japanese government recently re-examined the source area of the interplate earthquake along Sagami Trough, estimated that the maximum possible size would be M 8.6, and that the 1703 earthquake may be closer to the maximum size. Previous Kanto earthquakes have not been well studied; recent studies of tsunami deposits (Shimazaki *et al*., 2011, JGR) concluded that the 1293 earthquake (May 20) was the Kanto earthquake along Sagami Trough. The 1495 earthquake (September 3) has been considered as a fake earthquake, possibly confused with the 1498 Meio earthquake along Nankai Trough, but Kaneko (2012, Ito-shi Kenkyu) proposed that the 1495 earthquake was another interplate earthquake along Sagami trough. Studies of historical documents and tsunami deposits have revealed the recurrence of Kanto earthquakes. Details of each event, such as the source area or possibility of simultaneous rupture on Kozu-Matsuda fault, need to be studied to clarify the diversity of recurrent interplate earthquakes.

A hypothetical earthquake beneath Tokyo at the deeper plate interface, the northern Tokyo Bay earthquake, had been considered for disaster estimation of metropolitan Tokyo. Recent damage estimation by the Cabinet Office (2013), however, assumed an earthquake in the Philippine Sea Plate, which would cause similar seismic intensity with the 1855 Ansei Edo earthquake. The hypocenter of the 1855 earthquake has been studied on the basis of seismic intensity and damage distribution from historical literature, and various estimates ranging from a shallow crustal source to 100 km deep source within the Pacific Plate have been proposed. The seismic intensity distribution in Kanto region is strongly influenced on both deep and shallow subsurface seismic velocity structures, hence quantitative comparison with recent earthquakes or simulation on three-dimensional velocity structure would be necessary to accurately estimate the 1855 hypocenter.

The Earthquake Research Committee (2004) estimated the 30-year probability of M~7 earthquake in southern Kanto region as 70 %, on the basis of five earthquakes since 1885 and the Poisson process. The five events are: 1894 Meiji Tokyo earthquake, 1895 and 1921 Ibraki earthquakes, 1922 Uraga channel earthquake, and 1987 eastern Chiba earthquake. Among them, at least three (1921, 1922 and 1987) occurred in the Philippine Sea Plate, and one (1895) occurred in the Pacific Plate (Ishibe *et al*., 2012, Coord. Comm. Earthquake Prediction). For more accurate estimation of future probability, studies of older earthquakes from historical records and estimation of their epicenter, depth and earthquake types are required.

Keywords: Tokyo Metropolis, historical earthquake, Kanto earthquake, long-term forecast

Japan Geoscience Union Meeting 2014
(28 April - 02 May 2014 at Pacifico YOKOHAMA, Kanagawa, Japan)

MAG39-11 Room:502 Time:May 1 12:00-12:15

Activity change of aftershocks of the Ansei Edo earthquake of November 11th, 1855

TSUJI, Yoshinobu[1*] ; MATSUOKA, Yuya[2]

[1]Fukada Geolog. Inst., [2]Editorial Room of Chronicle, Sendai City Museum

Ansei Edo earthquake occurred at 11 PM, November 11th, 1855 at a point just below the city zone of Edo (Tokyo at present). Due to this earthquake, it is suggested that more than 10,000 people were killed in Edo. The location of the epicenter, its magnitude, and its fault mechanism is still not clarified. In the present study, we studied on the activity change of aftershocks by using descriptions of felt earthquakes written in diaries. We made a data base of felt earthquakes occurred in the period between the beginning of the first year of Kaei (1848) and the end of the first year of Man-en (1860) in Kanto district including the Edo city zone. In general, more than ten kinds of diaries were kept in the Tokyo city zone. Most reliable one is ”Reiken Kobo” which is the diary kept at the Edo Astronomical Observatory in Kudan-Ue street. Diaries with descriptions of felt earthquakes were kept at more than ten cities on the Kanto Plain. We compiled a database of those records of felt earthquakes. We gathered electronic 3,192 cards of records of felt earthquakes in total. It is clarified that earthquakes were felt at Tokyo 543 times in total. The left figure shows the diagrams of felt earthquakes at Edo in two two years from the beginning of 1855 to the end of 1856. We can recognize that the aftershock period is finished generally at May 1856. An eminent earthquake occurred at Tokorozawa, about 40 kilometers WNW of Tokyo, which is considered as an earthquake induced by the Ansei Edo Earthquakes (an aftershock in wider sense). The right figure shown diagram of felt earthquakes in the period of 13 years between 1848 to 1860. The activity of earthquakes induced by the Ansei Edo earthquakes continued up to the end of the year of Ansei 5 (1858).

Keywords: historical earthquake, earthquake in metropolitan zone, aftershocks, the 1855 Ansei Edo Earthquake

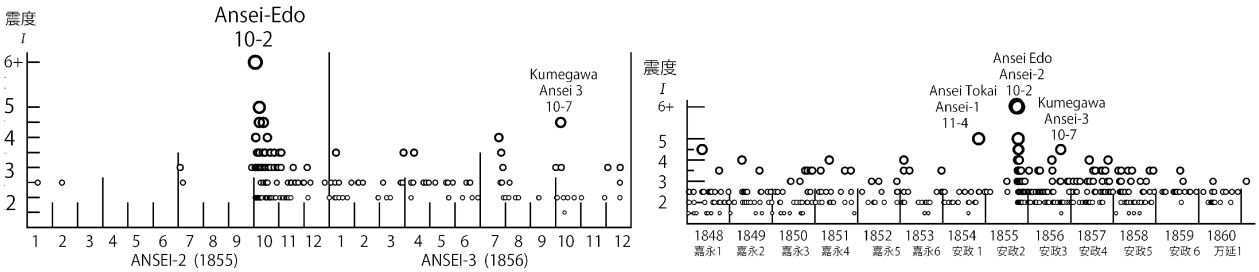

Japan Geoscience Union Meeting 2014
(28 April - 02 May 2014 at Pacifico YOKOHAMA, Kanagawa, Japan)

MAG39-12 Room:502 Time:May 1 12:15-12:30

Compiling S-P times and first motion polarities for recent eqks and classification of the 1921 and 1922 eqks

ISHIBE, Takeo[1*] ; SATAKE, Kenji[1] ; MURAGISHI, Jun[1] ; TSURUOKA, Hiroshi[1] ; NAKAGAWA, Shigeki[1] ; SAKAI, Shin'ichi[1] ; HIRATA, Naoshi[1]

[1]Earthquake Research Institute, the University of Tokyo

We compiled S-P times and first-motion polarities for earthquakes in Kanto region, central Japan on the basis of seismic phase data from 1923 to 2011 provided by the Japan Meteorological Agency (JMA), and that for 3,086 earthquakes which occurred from April 1st, 2008 to June 5th, 2012, from the Metropolitan Seismic Observation Network (MeSO-net). The number of target stations, where these data can be comparable with 26 stations which had operated in early stage of instrumental observations is 69 by JMA, and 19 by MeSO-net and other networks.

These data would be helpful for determining hypocenters and focal mechanism solutions of old earthquakes with limited instrumental data by comparing with S-P times and first-motion polarities for old earthquakes. As an example of application, we then compiled the characteristics of S-P times and first-motion polarities in southwestern Ibaraki and northwestern Chiba regions where the inter-mediate depth earthquakes frequently occur, and inferred the hypocenters and focal mechanism solutions of the 1921 Ibaraki-Ken-Nambu (M7.0) and 1922 Uraga-Channel (M6.8) earthquakes. Eleven first-motion polarities for the 1921 event are inconsistent for inter-plate earthquakes between the Okhotsk and Philippine Sea plates, and between the Philippine Sea and Pacific plates. Fourteen first-motion polarities and six S-P times for the 1922 event are similar for intra-slab earthquakes within PHS in and around southwestern Chiba with strike-slip fault mechanisms. These results strongly suggest that both the 1921 and 1922 events were not inter-plate earthquakes but intra-slab earthquakes.

In Japan, instrumental observation started in 1870's and seismographs and phase data (e.g., arrival times of typical phases, maximum amplitudes, first-motion polarities) have been persisted while some data were lost due to the fire. On the basis of these data, source parameters (hypocenters, focal mechanism solutions, and magnitude) for old earthquakes with limited instrumental data were estimated and cataloged. Determining hypocenters and focal mechanisms as back as possible prior to the start of JMA catalog is important to discuss long-term changes in seismicity. In Kanto, this period is especially important because it corresponds several tens of years before the 1923 Kanto earthquake and damaging earthquakes frequently occurred. However, the determinations of source parameters for old earthquakes have some difficulties. By using S-P times and first-motion polarities for recent earthquakes as "template", the accuracies in hypocenter locations and focal mechanism solutions for old earthquake would improve.

Acknowledgements

We used phase data for earthquakes provided by JMA and that by the MeSO-net. We also used focal mechanism solutions for earthquakes provided by National Research Institute for Earth Science and Disaster Prevention and JMA, and a program modified from HASHv2 (Hardebeck and Shearer, 2002) to calculate the azimuths and take-off angles for first-motion polarities at each observation station. This study was supported by the Special project for reducing vulnerability for urban mega earthquake disasters from the Ministry of Education, Culture, Sports, Science and Technology of Japan.

Keywords: S-P time, first motion polarity, 1921 Ibaraki-Ken-Nambu earthquake, 1922 Uraga-Channel earthquake

Japan Geoscience Union Meeting 2014
(28 April - 02 May 2014 at Pacifico YOKOHAMA, Kanagawa, Japan)

MAG39-13 Room:502 Time:May 1 12:30-12:45

Field Survey for the Memorial Matters from the 1923 Great Kanto Earthquake in Central Kanagawa Prefecture

TAKEMURA, Masayuki[1*]

[1]Disaster Mitigation Research Center, Nogoya-Univ.

Many memorial towers and monuments have been contracted for the heavy toll of life and for the restoration of villages or cities in Southern Kanto district. Death claimed a toll of about 105000 totally from the 1923 Great Kanto earthquake. These towers and monuments must be forever witnesses to the tragedy of the earthquake damage and spokesmen for the victim's dying wish "don't repeat such damages". However, most of them have been already forgotten by the citizens. We thought its sacrilege and must use them for the public education of earthquake disaster prevention. This manuscript is a report on the field survey for the memorial matters from the Great Kanto earthquake in Central Kanagawa Prefecture. The number of the matters is 126. This survey will be continued next two years in Western and Eastern Kanagawa Prefecture.

Keywords: memorial tower, Great Kanto Earthquake, Kanagawa Prefecture

Japan Geoscience Union Meeting 2014
(28 April - 02 May 2014 at Pacifico YOKOHAMA, Kanagawa, Japan)

MAG39-P01 Room:Poster Time:May 1 18:15-19:30

Composition of the subducted slab beneath Izu collision zone, Japan

ISHIKAWA, Masahiro[1*]

[1]Graduate School of Environment Information Sciences, Yokohama National University

The Philippine Sea plate subducts northwesteward under the Honshu arc, Japan. The presence of the Izu-Bonin arc within the Philippine Sea plate causes a complex tectonic environment. In eastern Kanto area, an accretionary wedge composed of late Cenozoic sediments overlies the downgoing Philippine Sea plate. In western Kanto area, the Izu-Bonin arc has collided with the Honshu crust; remnant pieces of the Izu-Bonin arc such as the Tanzawa block were accreted to the Honshu crust. A megathrust separates the Philippine Sea slab from the Honshu crust. According to seismic servey (Sato et al., 2005), the megathrust fault separates the upper/middle crust from the Izu-Bonin arc beneath the Izu collision zone. Devastating M8-class earthquakes occur on the megathrust fault, and the epicenter of the Kanto earthquake of 1923 (M7.9) is located in the Izu collision zone. To evaluate seismic hazard in the Greater Tokyo Area of Japan we need to clarify the lithological properties of Izu collision zone.

This study presents an interpretation of the crustal structure of the Izu collision zone. This study infers that amphibole is a main constituent mineral of the subducted lower crust of the Izu-Bonin arc. Dehydration embrittlement process resulting from the dehydration of hydrous minerals (e.g. amphibole) in the subducting lower crust is expected, and it may have induced the microearthquakes by enhancing pore pressures along the pre-existing faults/fractures in the subducting lower crust beneath the Izu collision zone. Stability filed of amphibole within the gabbroic composition from the Tanzawa plutonic complex was calculated by Theriak-Domino software, and the phase diagram shows hot subduction can account for seismicity of the microearthquakes beneath the Tanzawa Mountains and the resulting dehydrated dry slab may therefore account for the observed absence of seismicity below the northern part of Tanzawa Mountains and Kanto Mountains.

Keywords: collision zone, slab

Japan Geoscience Union Meeting 2014
(28 April - 02 May 2014 at Pacifico YOKOHAMA, Kanagawa, Japan)

MAG39-P02 Room:Poster Time:May 1 18:15-19:30

Tsunami Heights of the 1854 Ansei-Tokai Earthquake Tsunami in Gokasho Bay Region, Mie Prefecture

NARUHASHI, Ryutaro[1*] ; SATAKE, Kenji[1]

[1]Earthquake Research Institute, Univ. Tokyo

The Kumano-nada Sea coastal area has been repeatedly attacked by tsunamis from the Nankai Trough subduction-zone earthquake. For historical tsunamis, since this area is close to Kinki region, many historical records exist. For the recent 1944 Showa-Tonankai earthquake tsunami and the 1854 Ansei-Tokai earthquake tsunami, not only historical records and monuments but also many folklores still remain. However, the 1944 Showa Tonankai earthquake tsunami has a comparatively small scale, and is unsuitable for examining the average scale about the tsunami from the Nankai Trough. Based on above-mentioned reason, we studied for the 1854 Ansei-Tokai earthquake tsunami.

Gokasho Bay is a blockade inner bay which has typical ria coasts and drowned valleys. It is located in central Kii Peninsula and faced with the Nankai Trough. In this bay area, measurement points of the tsunami height for the 1854 Ansei-Tokai earthquake tsunami and the data on height were mainly based on historical records and oral traditions. In particular, in Konsa district, it is based on the words of the Bon festival dance currently kept in there called ”Shongai kudoki” or ”Tsunami kudoki”. Tsunami heights were measured by level measurement using laser range finder TruPulse360 and a hand level on the basis of the spot elevation given by 1/2500 topographical maps.

As a result, a total of 40 points of tsunami height were obtained in Gokasho Bay region. The average inundation height of whole bay area was approximately 4 - 5 m.

In Konsa, located in the most closed-off section of the bay, dendritic valley plains which have small-sized rivers spread. According to distribution of both inundation and run-up points by this research, it is supposed that tsunami ran-up to every valleys of those. Tsunami heights in Konsa ranged 4 - 11 m, and were higher than those in other districts. The maximum run-up height was 11.5 m in the valley of Ushirogochi.

Keywords: Gokasho Bay, 1854 Ansei-Tokai Earthquake Tsunami, tsunami height, run-up height, inundation height

Japan Geoscience Union Meeting 2014
(28 April - 02 May 2014 at Pacifico YOKOHAMA, Kanagawa, Japan)

MAG39-P03 Room:Poster Time:May 1 18:15-19:30

Publication of the Japan University Network Earthquake Catalog of First-Motion Focal Mechanisms (JUNEC FM^2)

ISHIBE, Takeo[1*] ; TSURUOKA, Hiroshi[1] ; SATAKE, Kenji[1] ; NAKATANI, Masao[1]

[1]Earthquake Research Institute, the University of Tokyo

We determined focal mechanism solutions for 14,544 earthquakes that occurred in and around the Japanese Islands from July 1985 to December 1998 by using first-motion polarities reported by the Japan University Seismic Network, and compiled the Japan University Seismic Network Earthquake Catalog of First-Motion Focal Mechanisms (JUNEC FM^2). JUNEC can be obtained from ftp site provided by ERI: ftp://ftp.eri.u-tokyo.ac.jp/pub/data/junec/hypo/. JUNEC FM^2 also can be obtained via ftp site: ftp://ftp.eri.u-tokyo.ac.jp/pub/data/junec/mech/. The Earthquake Research Institute, the University of Tokyo has compiled observed data with the cooperation of universities and determined hypocenters amounting to about 190,000.

This catalog covers small-magnitude earthquakes (M$\geq$2.0) prior to the recent development of seismic observation networks and automated waveform data processing systems, and it will prove helpful in understanding the spatial and temporal heterogeneities of stress fields by combing recent focal mechanism solutions. Abundant focal mechanism solutions will be useful for statistical analyses. Their distribution is spatially and temporally heterogeneous, and it clearly reflects both the development of observation station network and spatial variations of first motion polarity report rate (i.e., first motion polarity report number / the number of picked onsets). Determined focal mechanisms are basically consistent with previously reported ones such as Full-range Seismograph Network of Japan (F-net; Okada et al., 2004) moment tensor solutions provided by National Research Institute for Earth Science and Disaster Prevention (NIED), or P-wave first motion focal mechanisms provided by the Japan Meteorological Agency (JMA) though some focal mechanisms are significantly different from them.

In Japan, an abundance of first-motion focal mechanism solutions for earthquakes have been determined after the 1995 Kobe earthquake (magnitude according to JMA-, M_{JMA} 7.3) through the development of the High Sensitivity Seismograph Network Japan (Hi-net). In addition, moment tensor solutions for moderate- to large-magnitude earthquakes have been routinely determined since 1997 using the F-net and improved data processing systems. These focal mechanism solutions have provided a good understanding of the fault structures and the local/regional stress fields in which earthquakes occur. However, focal mechanism solutions for earthquakes covering the Japanese Islands prior to the development of recent seismic observation networks have been very limited, barring a few studies (e.g., Ichikawa, 1961, 1971). Following the 2011 off the Pacific coast of Tohoku earthquake (moment magnitude according to the JMA, Mw9.0), the distribution of focal mechanism solutions has drastically changed especially in and around the source region. This indicates that stress fields or focal mechanism solutions are temporally variable. In light of this, data on the focal mechanisms of earthquakes extending as far back as possible are desirable in order to investigate intermediate- to long-term spatial and temporal heterogeneities of focal mechanism solutions and local/regional stress fields.

Acknowledgements

We used a program modified from HASH (Hardebeck and Shearer, 2002) to estimate the focal mechanism solutions and the pick files observed by Hokkaido University, Hirosaki University, Tohoku University, the Earthquake Research Institute of the University of Tokyo, Nagoya University, the Disaster Prevention Research Institute of the Kyoto University, Kochi University, Kyushu University, and Kagoshima University. We also used focal mechanism solutions for earthquakes provided by NIED and JMA. This study was supported by the Special project for reducing vulnerability for urban mega earthquake disasters from the Ministry of Education, Culture, Sports, Science and Technology of Japan.

Keywords: first-motion focal mechanism solution, Japan University Network Earthquake Catalog (JUNEC)

Japan Geoscience Union Meeting 2014
(28 April - 02 May 2014 at Pacifico YOKOHAMA, Kanagawa, Japan)

MAG39-P04 Room:Poster Time:May 1 18:15-19:30

Three-dimensional earthquake forecasting model for the Kanto district: Completeness magnitude of earthquake catalogs

YOKOI, Sayoko[1] ; TSURUOKA, Hiroshi[1*] ; HIRATA, Naoshi[1]

[1]Earthquake Research Institute, The University of Tokyo

We started to construct a 3-dimensional (3D) earthquake forecasting model for the Kanto district in Japan under the Special Project for Reducing Vulnerability for Urban Mega Earthquake Disasters based on the Collaboratory for the Study of Earthquake Predictability (CSEP) experiments. Because seismicity in this area ranges from shallower part to a depth of 80 km due to subducting Philippine-Sea and Pacific plates, we need to study the effect of earthquake depth distribution.

We tried to construct a prototype of 3D earthquake forecasting model for the area based on the Relative Intensity model (Nanjo, 2011) which forecasts earthquake probabilities using historical data. For a large earthquake forecasting, we need a longer period of earthquake data than current studies. Therefore, we analyzed completeness magnitude (Mc) every 10 km in a depth from 0 to 100 km of earthquake catalogs of Utsu (1979, 1982), Japan Meteorological Agency (JMA) and National Research Institute for Earth Science and Disaster Prevention (NIED) which are partially covered from 1885 to 2013 by the Maximum curvature method (Wiemer and Wyss, 2000) to assess a quality of their catalogs considering a depth of hypocenters. In the case of JMA catalog, an average and its standard deviation of Mc for a year from 1923 to 1970's showed 3.7 and 0.4, respectively. Then, they decreased from 1970's to 2000, which means that quality of the catalog improved with time. After the 1980's, Mc showed heterogeneous distribution with depth. Mc in shallower depth are smaller than that in deeper one. For example, averaged Mc and its standard deviation from 2000 to 2010 is 0.25 and 0.14 with 0 to 30 km in depth against 0.67 and 0.10 with 60 to 100 km in depth. In this presentation, we discuss how use the heterogeneous catalog to develop a 3-dimensional forecasting model in Japan.

The authors thank JMA and NIED for their earthquake catalogs. This work is sponsored by the Special Project for Reducing Vulnerability for Urban Mega Earthquake Disasters from Ministry of Education, Culture, Sports and Technology of Japan.

Keywords: Three-dimensional forecasting model, Kanto district, Collaboratory for the Study of Earthquake Predictability, earthquake catalogs

Japan Geoscience Union Meeting 2014
(28 April - 02 May 2014 at Pacifico YOKOHAMA, Kanagawa, Japan)

MAG39-P05 Room:Poster Time:May 1 18:15-19:30

Sparse Modeling to Estimate Spatial Distribution of Ground Motion Required for Rapid Prediction of Structural Damages

MIZUSAKO, Sadanobu[1*] ; NAGAO, Hiromichi[1] ; HIROSE, Kei[2] ; KANO, Masayuki[3] ; HORI, Muneo[1]

[1]Earthquake Research Institute, The University of Tokyo, [2]Graduate School of Engineering Science, Osaka University, [3]Graduate School of Science, Kyoto University

A rapid prediction of structural damages due to a large earthquake is important to prevent secondary disasters. The first step of the prediction is to estimate ground motion at a targeted construction from observed seismic data, and the second step is to predict structural damage using the estimated ground motion. An accurate damage prediction requires ground motions with spatially-high resolution although the spatial density of constructions is much higher than that of seismometers in urban area. We have been developing a statistical method to model such ground motions using seismograms obtained by a seismometer array. Our target is Tokyo metropolitan area in which seismogram of MeSO-net (Metropolitan Seismic Observation network) is available.

Mizusako[2013, graduation thesis] proposed a method based on the Taylor expansion, and applied it to MeSO-net data when the Great East Japan Earthquake occurred. This method was found never to account for ground motions higher than 0.15 Hz, which was insufficient when considering that the eigenfrequency of constructions is usually between 1-10 Hz. Mizusako[2013] determined the partial differential coefficients, which appear in the Taylor expansion, from five nearest observatories with a truncation of the first order, but a better selection of a truncation of order and a group of observatories, which is hereinafter called “ cluster ”, could more accurately explain ground motions higher than 0.15 Hz.

We propose an algorithm based on sparse modeling that automatically and objectively determine the truncation of order and the size of the cluster. Our algorithm adopts the lasso, which is able to select dominant partial differential coefficients owing to the L1-norm regularization term. Moreover, the group lasso is implemented on our algorithm in order to select the coefficients of the same order associated with different components. We will report initial results obtained by the proposed method, comparing with the results of Mizusako[2013].

Keywords: Sparse modeling, lasso, urban disaater, MeSO-net

Japan Geoscience Union Meeting 2014
(28 April - 02 May 2014 at Pacifico YOKOHAMA, Kanagawa, Japan)

MSD40-01 Room:312 Time:April 29 17:15-17:30

Let’s make a space food by using Peucedanum Japonicum which is medicinal harbs

WAKITA, Mari[1*] ; TAKASE, Yoshimi[1] ; KAWAI, Mika[1] ; HAYASHI, Yoshino[1] ; KOBAYASHI, Mizuki[1] ; KAJIWARA, Satomi[1] ; KATAYAMA, Naomi[1]

[1]Nagoya Women’s University

Purpose

In a long-term stay in the space, the meal is very important. It is necessary to have the balanced meal every time not to get sick. Therefore it is necessary for space foods to prepared dishies with medicinal herbs. The reinforcement or cancer prevention of immunity were intended that superior efficacy made space foods using prospective Peucedanum japonicum. The Peucedanum japonicum has bitter taste, but considered the method that we could use Peucedanum japonicum as snacks, deliciously.

Method

At first we made a liquid of Peucedanum japonicum by using a mixer. I made three kinds of snacks which are pound cake, dumpling and shortbread with the liquid of the Peucedanum japonicum. We did a sensuality test for subjects and we get the result of taste and the result of smell. The perfect scores of sensuality test is 10 points. To make a pound cake, we mixed 200 g of pancake mixture with 180g of Peucedanum japonicum. And we baked it by using 180 degree oven during 30 minutes. Furthermore, I made the poundcake which I added 10 g of powdered green tea in this basic recipe. In addition, the dumpling mixed 150 g of powder with 130g of nonglutinous rice powde.And we mixed Peucedanum japonicum in that dumpling. We steamed it with 100 degrees for 30 minutes. The shortbread mixed 250 g of weak flour, powder from nonglutinous rice 50 g, sugar 80 g, butter 175 g, Peucedanum japonicum 25 g and leaf 6 g of the mint. And we baked it at 170 degrees for 45 minutes.

Result

We were able to eat deliciously without feeling bitterness of the Peucedanum japonicum by eating snacks. I judged even a sensuality examination to be delicious from a primary schoolchild to an elderly person. By butter, by wheat flour and by the cooking process, Peucedanum japonicum taste is better than before. It is easy to eat after cooking.

Consideration

The Peucedanum japonicum taste was not bitter after cooking. And it was able to eat. Peucedanum japonicum have cancer protective efficacy. It is necessary to take as medicinal herb to keep our body health in the space. The space radiation including danger of the carcinogenesis may be accompanied in the space. Next, we would like to make the side dish by using peucedanum japonicum. And we would like to say utilization of medicinal herbs widely generally in future.

Keywords: Space foods, medicinal harbs, medicinal meal, Peucedanum Japonicum, snacks

Japan Geoscience Union Meeting 2014
(28 April - 02 May 2014 at Pacifico YOKOHAMA, Kanagawa, Japan)

MSD40-02 Room:312 Time:April 29 17:30-17:45

Low GL menu by using Low GI food is good as Space food

KOBAYASHI, Mizuki[1*] ; KAJIWARA, Satomi[1] ; WAKITA, Mari[1] ; TAKASE, Yoshimi[1] ; KAWAI, Mika[1] ; HAYASHI, Yoshino[1] ; KATAYAMA, Naomi[1]

[1]Nagoya Wone's University

Purpose

We became able to stay in the space for a long term. The offer of the meal appropriate to the active mass in the space is necessary. Therefore a menu offer to become the meal contents which are hard to go up of the blood sugar level is necessary. Metabolic syndrome becomes the problem on the earth. It is necessary to inform how it is important that we prevent hyperglycosemia after a meal widely. Similarly, in the space, you should consume the meal which is hard to go up of the blood sugar level. It is important that we do disease prevention. Therefore in this study, we made a menu (low GL food menu) which was hard to go up it of the blood sugar level using food (low GI food) which was hard to go up of the blood sugar level.

Method

We collected low GI foods. We put low GI food together and made the low GL food menu which was hard to go up of the blood sugar level.This menu is Unpolished rice, Wheat, Miso soup, Meuniere of the salmon, Boiled vegetables, Black sugar syrup agar. We use this menu and we measured blood sugar level by using peripheral blood. We checked our menu which is really became the low GL by using peripheral blood . We check our blood sugar level by using Kit (product made in Terumo Corporation) , before eating this food and after 15 minutes, 30 minutes, 45 minutes, 60 minutes, 90 minutes and 120 minutes.

Result

Cooking method was very important to make low GL menu. When we make soft food and eat it, our blood sugar level become high easily. Because when we make rice and boiled vegetables softly, the GL level of the actual survey became higher.

Discussion

We think that it is desirable to perform by using low GI food to make low GL menu. And we think that the cooking method is very important to low GL menu. The space food must be good balance diet. By feeling of satisfaction and slow digestion and slow absorption, it is possible to prevent a sudden rise of the blood sugar level.

Keywords: Low GI, Low GL, Blood sugar level, Diabetes, Spece food

Japan Geoscience Union Meeting 2014
(28 April - 02 May 2014 at Pacifico YOKOHAMA, Kanagawa, Japan)

MSD40-03 Room:312 Time:April 29 17:45-18:00

Two weeks stay in Mars Desert Research Station(MDRS)

KATAYAMA, Naomi[1*]

[1]Nagoya Women's University

I obtained an opportunity to participate in MDRS137. I cooked food for crew in MDRS137.

I made a menu using the commercial article that long-term preservation was possible as space foods. The basic meal was that, rice of the freeze dry, vegetables of the freeze dry, soup of the freeze dry, a retort pouch, canned food, dried fruit, a cookie and a candy. I can keep that food during long time.

Three women and five men participated in this study. The nutrient and the energy of the meal calculated it in consideration of the age, sex and active mass of the subject.I provided a meal of 1600kcal to woman 53 years old. I provided a meal of 1750kcal to woman 21 years old. I provided a meal of 1800kcal to male 50 years old. I provided a meal of 2000kcal to male 41 years old.

The significance of this study is the point that not only the use of the commercial preservation food as space foods but also the food problem at the time of the disaster can solve. It is necessary to make 42 kinds of menus to spend 14 days in MDRS. I thought about a combination of the commercial freeze dry rice and canned food of the fish. In addition, I thought about the combination of freeze dry soup and freeze dry vegetables.

Because 42 menus were gathered up as a booklet, I want to distribute this result widely in future. I hope that people will have interest in the space after to read that booklet. And I can enlighten people about combination of commercial food for the disaster.

Keywords: Closedown space, Life-support system, Space foods

Japan Geoscience Union Meeting 2014
(28 April - 02 May 2014 at Pacifico YOKOHAMA, Kanagawa, Japan)

MSD40-P01 Room:Poster Time:April 29 18:15-19:30

The recommendation of using the commercial disaster food as Breakfast -To consider it as space foods-

KAJIWARA, Satomi[1*] ; WAKITA, Mari[1] ; TAKASE, Yoshimi[1] ; KAWAI, Mika[1] ; HAYASHI, Yoshino[1] ; KOBAYASHI, Mizuki[1] ; KATAYAMA, Naomi[1]

[1]Nagoya Women's University

Purpose

At the present, the people who do not eat breakfast increase in Japan.

The Japanese Government recommends that we have breakfast well. As same as, the importance of the meal in the space rise more. Development of the space food which can store for a long term is urgent business. Because, we think about an exploration and emigration to Mars. Delicious space food is very important for the astronaut to keep their appetite. We perform questionary survey about the breakfast. I clarify the frequency of the breakfast intake. In addition, I clarify what kind of breakfast was eaten. Therefore in this study, we examined sensuality of the commercially food which can keep for a long term. And based on the result, we thought about the taste and smell in future space foods.

Methods

Fifty female college students(20-21 years old) answered the questionnaire about breakfast intake frequency and about contents of breakfast. Fifty female college students (20-21 years old), they eat some commercially available rice things (eight kinds) which can store for ?ve years. And we performed to do sensuality examination for them. Students carried out the sensory examination and scoring (Perfect score is 10) of food. The marketing products are cooked with hot water in 15 minutes and cold water in 60 minutes. Vegetable rice, shrimp pilaff, perilla and seaweed rice, chirashi-sushi, white rice, fried rice, beef rice, dry curry of the magic rice (product made in Satake Corporation) .

Results

The contents of breakfast were one or two kind of food. People have no time to make breakfast because of busy. An evaluation was high in the taste in order of vegetable rice, dry curry, beef rice, chirashi- sushi, fried rice, perill and seaweed rice, and white rice.

Conclusion

Because people were busy in the morning, a balanced meal to be able to make in a short time was required. This disaster food is just fit as breakfast very much. As for both the taste and the incense, five vegetable rice, fried rice with meat, vegetables and curry rice, stewed beef rice occupied the high rank. Space foods passing globally are necessary. This commercially available disaster food is suitable for both space foods and breakfast very much. We want to examine not only the rice but also the side dish in future.

Keywords: Breakfast, th ecommercial disaster food, Space food

Japan Geoscience Union Meeting 2014
(28 April - 02 May 2014 at Pacifico YOKOHAMA, Kanagawa, Japan)

MSD40-P02 Room:Poster Time:April 29 18:15-19:30

The need of the lactic acid veverage in space foods

HAYASHI, Yoshino[1] ; KOBAYASHI, Mizuki[1*] ; KAJIWARA, Satomi[1] ; WAKITA, Mari[1] ; TAKASE, Yoshimi[1] ; KAWAI, Mika[1] ; KATAYAMA, Naomi[1]

[1]Nagoya Women's University

Purpose

The long-term space stay makes it possible to perform many studies. We think that the development of space foods will develop more in future. The meal management to maintain the health of an astronaut working busily is important. With lactic acid bacterium beverage, we thought that we want to perform the health care of the astronaut. Therefore we decided to check the effect on bowel movement of the lactic acid bacterium beverage.

Method

We assumed towenty adult women (average age 20.5 years old) as subjects. Before experiment start, during two weeks , we took the bowel movement record.Townty students participated in an experiment. We divided it into two groups of ten students of the constipation and ten students of the non-constipation. We boiled Y Company lactic acid bacterium beverage (40% of calorie off) at 100 degrees during three minutes. During two weeks, we let the ten constipaton consume the lactic acid bacterium beverage which we boiled and recorded the state of the bowel movement. Another two weeks, we let them consume the lactic acid bacterium beverage which we did not boil and recorded the situation of the bowel movement afterwards. Ten students of the non-constipation tested it in order to reverse-turn with ten students of the constipation. After the experiment end, we recorded the situation of the bowel movement during two weeks. The record contents were the stool frequency, smell, shape and number of times of the gas.

Result

Stool frequency was improved in the constipation group by the lactic acid bacterium intake. In the case of the non-constipation group, the big change was not seen in stool frequency. However, in both groups, the degree of smell was improved clearly.

Discussion

In constipation group, stool frequency was increased after drinking of the lactic acid beverage.A bowel movement state might be improved by an oligosaccharide and the lactic acid included in the lactic acid bacterium drink.However, when constipation group stopped the intake of the lactic acid beverage, their stool frequency was not good as before. It is necessary to consume the lactic acid bacterium drink continuously

Keywords: Lactic acid, Beverage, Space foods

Japan Geoscience Union Meeting 2014
(28 April - 02 May 2014 at Pacifico YOKOHAMA, Kanagawa, Japan)

MTT41-P01 Room:Poster Time:April 28 18:15-19:30

Publication of redesigned multicolor 1:25,000 topographic maps

UNE, Hiroshi[1*] ; NEMOTO, Masami[1]

[1]Geospatial Information Authority of Japan

With rapid development of the information and communication technology, the national basic map accomplishes a big change. As for the 1:25,000 topographic map produced by the Geospatial Information Authority of Japan (”GSI”), which underpins the geo-science studies, publication of newly designed multicolored 1:25,000 topographic map was started from November 2013, with different production process and more detailed contents which the topography was easy to understand.

New 1:25,000 topographic map is based on ”digital Japan basic map (DJBM)”, and the production process was greatly changed. A Plotting work using aerial photo, which was the biggest characteristic of the past topographical map making, is not included in the process, and a part of the vector data in the digital Japan basic map is directly clipped and printed.

It is enactment of ”the Basic Act on the Advancement of Utilizing Geospatial Information (NSDI act of Japan)” of 2007 that became the starting point of such a change. By this law, it was prescribed in particular that the government shall prepare and use ”the fundamental geospatial data (FGD)” as a standard of the positions on the digital map. The GSI executed the production of FGD utilizing 1:2,500 city planning base map and 1:25,000 topographic map to mostly complete for the whole country by the end of 2011, and produced DJBM using FGD as a frame.

New 1:25,000 topographic map is based on DJBM, which means that the contents became more detailed than the conventional one. Furthermore, introduction of process printing enabled multicolor production, and some expression methods were realized for the first time.

Contents becoming more detailed means that the information becomes the precision of 1:2,500 level in city planning area. This comes from that DJBM is maintained at 1:2,500 level in the city planning area, where in the area except it at 1:25,000 level. All the buildings are displayed without being generalized even in the crowded city areas. In addition, the indication density of the road rises because all the roads are displayed without thinning.

Introduction of process printing allowed to add green shadows to grasp the topography intuitively. Orange colored buildings can avoid the congestion with roads or the place names. In addition, expressions using various colors improved the readability of the topographic map, e.g., expressways, national highways and public roads are colored in green, red and yellow respectively, and national highway numbers are displayed in inverse triangle type of the blue.

Besides, GSI started to present ”digital topographic map 25,000” to provide image data clipped from DJBM online using internet from 2012. Users can choose the central position, size and the direction of the map image depending on the purpose of use, and can choose colored/monochromatic map and with/without the shadows. It makes it easier to use it as the background map of geo-science study.

As for 1:25,000 multicolored topographical map, around ten sheets a month are published newly for the time being, and conventional topographic maps are going to be replaced several years later.

Keywords: 1:25,000 topographic map, NSDI Act of Japan, Digital Japan Basic Map, process printing

Japan Geoscience Union Meeting 2014
(28 April - 02 May 2014 at Pacifico YOKOHAMA, Kanagawa, Japan)

MTT41-P02 Room:Poster Time:April 28 18:15-19:30

Design of the PNG Elevation Tile and Rapid Response of Disaster Prevention-related Web Site

NISHIOKA, Yoshiharu[1*] ; NAGATSU, Juri[1]

[1]Institute of Geology and Geoinformation, AIST

In order to achieve the advancement of elevation data use, we designed the PNG Elevation Tile. We create PNG elevation tiles based on the elevation tile of CSV currently published from the Geospatial Information Authority of Japan, and tested using test applications. In such applications, the redraw which took several minutes until now can be performed in several seconds, and a high-speed response can be realized using the PNG Elevation tile.

Keywords: PNG Elevation Tile, tile, disaster prevention, energy cone, Seamless Geological Map, 3D

Japan Geoscience Union Meeting 2014
(28 April - 02 May 2014 at Pacifico YOKOHAMA, Kanagawa, Japan)

MTT41-P03 Room:Poster Time:April 28 18:15-19:30

The monitoring of the NIED Hi-net by using the mobile application

EMOTO, Kentaro[1*] ; SAITO, Tatsuhiko[1] ; UENO, Tomotake[1] ; HARYU, Yoshikatsu[2] ; NASU, Kenichi[2] ; SHIOMI, Katsuhiko[1] ; AOI, Shin[1]

[1]NIED, [2]NIED/ADEP

For the geophysical research and the disaster prevention, monitoring the seismic activity is important. By monitoring of the seismicity, for example, we can detect the unusual event and know the fault plane. Monitoring of the real time wave filed is also important for the early warning. In order to correctly monitor the seismic activity, we have to monitor the seismic stations. The trouble of the station causes the decrease of the accuracy and the wrong interpretation. NIED runs the Hi-net seismic network which has more than 80 seismic stations with the average separation of 20 km all over Japan. NIED provides the waveform data and automatically detected earthquake information through the internet. All stations are always watched and the trouble information is reported. Usually, this watching is done by checking the individual waveform. The map information, however, is easier to understand the station condition than the waveform. In this study, we propose a method to monitor the seismic network by using the mobile device and develop the mobile application. Also we develop the applications to check the automatic hypocenter determination system.

First, we develop the application which shows the seismicity on the map. We plot earthquakes listed on the catalog determined by the Hi-net automatic system on the embedded map application. We also plot the cross section of the seismicity. We can enlarge, reduce and rotate the map. Corresponding to these gestures, the cross section is also changed. Therefore, we can see the subducting slab and the fault plane from arbitrary directions. By plotting the past seismicity on the background, we can check that the recent earthquake is usual or unusual.

Second, we develop the application which shows the wave traces of selected stations and the earthquake information on the same image in order to know whether the automatic hypocenter determination system works properly. On the Hi-net web site, we can see the 100-trace image of selected Hi-net stations. By looking this image, we can roughly know the location, the origin time and the magnitude of the earthquake. We can see some earthquakes are correctly determined but some earthquake is not determined by the automatic system by plotting the earthquake information on the trace image.

Finally, we develop the application for the manager of the Hi-net network, which shows the real time Hi-net records on the map. We get the real time data from the data server of the Hi-net and make the map image of the RMS (1s) velocity amplitude. We stock this image every second and download it from the mobile device. On the device, we can see the real time record of all stations of Hi-net every second. Hence, we can visually find abnormal behaviors of stations. By changing to the map application and showing the detail station information, we can check which station has some troubles. We also plot the information of the rapid source parameter determination system, named AQUA, on the real time map. We can see the wavefield and the source location at the same time. By comparing this information, we can check both AQUA system and station condition.

By using first two and third applications, we check the Hi-net automatically hypocenter determination system and stations, respectively. We can watch the Hi-net in terms of the wavefield, the waveform and the hypocenter by integrating three applications.

Keywords: Hi-net, mobile, real time

Japan Geoscience Union Meeting 2014
(28 April - 02 May 2014 at Pacifico YOKOHAMA, Kanagawa, Japan)

MTT41-P04 Room:Poster Time:April 28 18:15-19:30

Red Relief Image Map of the terrain representation method of the moon

CHIBA, Tatsuro[1*] ; KAMIYA, Izumi[2] ; TAKAKUWA, Noriyuki[2] ; SATO, Takenori[2]

[1]Asia Air Survey Co., Ltd., [2]Geospatial Information Authority of Japan

Summary

Although detailed terrain data of the lunar surface is obtained, terrain representation technique has become an issue. So called Red Relief Image Map (RRIM), which has been developed specifically for volcanic terrain analysis by LiDAR was applied to the topographic representation of the moon that seems to be similar to the volcanic terrain on the earth. The resulted RRIM of the moon showed effectiveness for visual interpretation of the lunar terrain.

Terrain of the Moon

The moon terrain may be characterized by high land and mariner of basaltic plane. There are several commonly used terrain representation methods. Contouring is very effective method for representing high relief topography, but not quite suitable for enhancing low relief terrain such as lunar surface. Many small scale maps and map atlas employ shaded-relief and/or gradation representation method. Even for the small scale topographic representation of the lunar surface, the shaded-relief and gradient method was used to be employed most of the cases. However, these traditional methods have issues to be solved since there are many craters lie one upon another on the lunar surface. These dipped terrains sometimes erroneously expressed by shaded-relief method depending on the direction of illumination light. Development of more effective terrain representation method is expected to solve these issues.

The RRIM

The RRIM is a method for enhancing terrain relief and is based on concept of slope map. In the RRIM, the slope is expressed by red graduation, and ridge-valley is expressed by intensity of light. Namely, the steeper the slope, the more ridge area, the lighter, and the valley and more dipped terrain, the darker on the RRIM. This image, although it is single ortho-image, provides 3D perspective.

The RRIM of the Moon

The RRIM was applied for making map of the moon. Digital terrain data (DEM) used for making the RRIM was acquired by ”Kaguya” lunar mission by JAXA. The DEM has 1/20 degree mesh interval. Presently, The RRIM of the moon can publicly be viewed at home page of Geospatial Information Authority of Japan , MILIT. It is also possible to 3D high speed viewing using Secium and Three.js.

Acknowledgement

Authors acknowledge JAXA and NAOJ for providing the lunar terrain data from ”KAGUYA” mission. .

Keywords: moon, DEM, terrain representation, red relief image map, crater, selene

MTT41-P04 Room:Poster Time:April 28 18:15-19:30

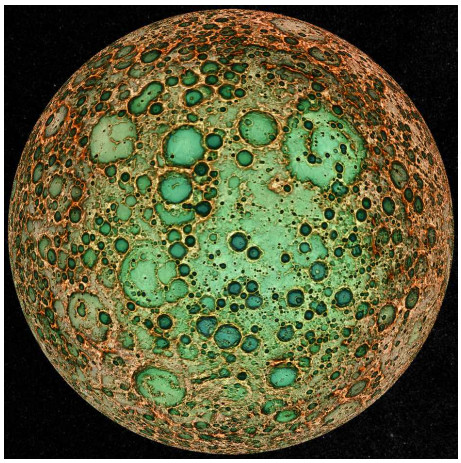

Japan Geoscience Union Meeting 2014
(28 April - 02 May 2014 at Pacifico YOKOHAMA, Kanagawa, Japan)

MTT41-P05 Room:Poster Time:April 28 18:15-19:30

Development of the CS (Curvature and Slope) topographical map

TODA, Kenichiro[1*] ; DAIMARU, Hiromu[2] ; KOARAI, Mamoru[3] ; NAKANO, Takayuki[3] ; IWAHASHI, Junko[3]

[1]Nagano Prefecture Forestry Recerch Center, [2]Forestry and Forest Products Reserch Institute, [3]Geospatial Information Authority of Japan

For the topographical interpretation, we developed CS (Curvature and Slope) topographical map to visualize micro-relief that affect landslide susceptibility in mountain area. The CS topographical map represents valleys by blue color and ridges by red color, simultaneously steep slopes are assigned to dark color. We produced CS topographical map for the entire area of Nagano Prefecture from airborne LiDAR DEM and conducted many micro landslide such as linear depressions in landslide blocks, valley head hollows were recognized, and they were confirmed by subsequent field survey. The CS topographical map provides us with many information about distribution of micro-relief in mountain area, and it may be a prominent tool for evaluating landslide susceptibility.

Keywords: CS topographical map, topographical interpretation, curvature, slope

Japan Geoscience Union Meeting 2014
(28 April - 02 May 2014 at Pacifico YOKOHAMA, Kanagawa, Japan)

MTT41-P06 Room:Poster Time:April 28 18:15-19:30

The map of a geopark

KOARAI, Mamoru[1*] ; MOKUDAI, Kuniyasu[2]

[1]GSI of Japan, [2]Pro Natura Foundation Japan

The authors reviewed about the deployment of geopark activity and the practical use of maps of geopark in Japan, and reported the actual condition of the map in the geoparks of all Japan. In this work, the authors collected many pamphlets of geopark with map information, reviewed all pamphlets in the points of view for expression of geographical feature.

There are many maps like tourist resort maps. But, some maps for Geopark had tried geographical feature expression in base map. For example, some maps express the landform using color for each elevation simply, and some maps were carried out 3D expression of the shade figure using DEM. These type maps were considered to be easy to understand the outline of geographical feature, compared with a contour drawing map.

Keywords: geopark, map, expression of geographical feature

Japan Geoscience Union Meeting 2014
(28 April - 02 May 2014 at Pacifico YOKOHAMA, Kanagawa, Japan)

MTT41-P07 Room:Poster Time:April 28 18:15-19:30

Landslide Geomorphological Map of the Northern Hida Mountains, Japan

SATO, Go[1*] ; KARIYA, Yoshihiko[2]

[1]Teikyo Heisei University, [2]Senshu University

The northern Hida Mountains located in central Japan consist of high-relief mountain ranges. A previous study has reported the distribution of the glacial topography and explained the landform development caused by glaciers in this region. In 2008, we published the *Landslide Geomorphological Map of the Northern Hida Mountains*. This map revealed the landslide distributions and glaciated topographies. Our poster shows this map and explains the methods and criteria for geomorphological mapping, as well as the development and characteristics of landslide distribution.

Keywords: Geomorphological map, Landslide topography, Glacial topography, Geomorphological development, The Northern Hida Mountains

Japan Geoscience Union Meeting 2014
(28 April - 02 May 2014 at Pacifico YOKOHAMA, Kanagawa, Japan)

MTT41-P08 Room:Poster Time:April 28 18:15-19:30

Geographic Environment Reconstruction and Geo-visualization using High Resolution DEM and Old Printed Map

SUZUKI, Atsushi[1*]

[1]Rissho University

This study combines high resolution DEM (5m or 10m) with topographical maps published in the early 20th century and make 2D and 3D maps. By such a work, I try the then geographical environmental reconstruction and geo-visualization.

The main study area is Sakishima Islands of the early 20th century.In Sakishima islands in the first half of the 20th century, 1000 to 2000 malarial patients were reported in every year. According to the old research findings, there was much endemic malaria in Sakishima islands in the island of continentality or volcanic island, and it was distributed over the area where there is a vertical interval of land and the basin system network progressed.

Keywords: High Resolution DEM, Printed Map, Geographical Environment, Geo-visualization

Japan Geoscience Union Meeting 2014
(28 April - 02 May 2014 at Pacifico YOKOHAMA, Kanagawa, Japan)

MTT41-P09 Room:Poster Time:April 28 18:15-19:30

Visualization of tsunami and circumstances during initial evacuation and its effectiveness for disaster education

KIMURA, Hiroyuki[1*] ; SUGAWARA, Daisuke[2] ; IMAMURA, Fumihiko[2]

[1]FUKKEN CO.,LTD., [2]International Research Institute of Disaster Science, Tohoku University

Public interests in forthcoming large-scale tsunami have been increasing since the notification of the large-scale projected tsunami scenario along Nankai Trough. It is important for people to keep their high consciousness of tsunami hazards by means of continuous and effective tsunami-disaster prevention education. With regard to safe evacuation from tsunamis, people must evacuate as early as possible, and they should prepare an appropriate plan and method for evacuation, which is corroborated by understandings on tsunami behavior and situations of the initial stage of tsunami evacuation. In this study, we will present visualizations of tsunami behavior and circumstances during initial evacuation activity. We will further investigate effectiveness of the visualization for disaster prevention education.

Coastal areas of the Pacific coast of Tohoku have been photographed before and after the Great East Japan Earthquake. These photographs have been taken as both orthographical and diagonal (oblique) aerial imageries. The diagonal photographs are useful for people to figure out the elevations of features, such as buildings and topography three-dimensional and clearly. The oblique photographs and inundation map computed from the numerical simulation of 2011 Tohoku-oki tsunami are synthesized, to derive a realistic visualization of the tsunami flooding. This visualization will be useful for people to understand tsunami behavior, which is influenced by land use and local topography.

Visualization of circumstances during initial evacuation activity will be useful information for people to understand imminency and available time for tsunami evacuation. Airborne orthographical photographs and satellite imageries are superimposed by concentric circles centered by selected representative points that is familiar with local people, as well as main roads and evacuation facilities, because they are crucial for evacuation plan. It is unlikely that people may stay in their own houses and offices at the time of the earthquake and tsunami. The visualization proposed by this study will lead people to understand plausible circumstances and will provide useful information for various alternative measures for initial evacuation activity, as well as existences of insusceptible areas for evacuation.

Keywords: tsunami behavior, tsunami evacuation, visualization, disaster prevention education

Japan Geoscience Union Meeting 2014
(28 April - 02 May 2014 at Pacifico YOKOHAMA, Kanagawa, Japan)

MTT41-P10 Room:Poster Time:April 28 18:15-19:30

A Web-based Volcano Hazard Map with Information on Evacuation Shelters, Hospitals and Facilities for Vulnerable People

ISHIMINE, Yasuhiro[1*]

[1]National Institute of Public Health

National Institute of Public Health is a governmental agency that belongs to Ministry of Health, Labour and Welfare. It provides with training courses related to public health, environmental hygiene and social welfare as well as conducts research on the fields. It revises the countermeasures to protect lives and health of citizens during large-scale disasters on the lessons learned from the experience during the Tohoku Earthquake and Tsunami Disaster. As a part of the revision, I am now developing an information-sharing system to facilitate support teams to effectively and efficiently distribute a limited number of staff and resources during large-scale disasters. The mapping of relevant facilities, such as evacuation shelters and hospitals, is the key function of the information-sharing system because the understanding of geographical relationships is the first step to visit and work in an unfamiliar area during disasters. I adapted the information-sharing system to volcanic eruptions to display potentially hazardous areas. I will show an example of the application by using the hazard map of Mt. Fuji, which has been published by Mt. Fuji Volcanic Disaster Prevention Conference in 2002.

Keywords: Hazard Map, GIS, Volcanic Eruption, Mt. Fuji, Disaster Medicine, Public Health

Japan Geoscience Union Meeting 2014
(28 April - 02 May 2014 at Pacifico YOKOHAMA, Kanagawa, Japan)

MTT41-P11 Room:Poster Time:April 28 18:15-19:30

Mapping the supply-demand gap in childcare services with GIS: A case study in Tokyo

WAKABAYASHI, Yoshiki[1*] ; KOIZUMI, Ryo[1] ; KUKIMOTO, Mikoto[2] ; YUI, Yoshimichi[3]

[1]Tokyo Metropolitan University, [2]Oita University, [3]Hiroshima University

The aim of this study is to visualize the spatial pattern of the gap between childcare supply and demand on a map. Study area is Tokyo where the number of children awaiting enrollment in licensed childcare centers is extremely large. To map the supply-demand gap with geographic information systems, we calculated difference between supply and demand densities after converting the vector data concerning childcare supply from the public sector and pre-school children into raster data using kernel density estimation. The result of the analysis showed a spatial imbalance between childcare supply and demand. The map that added the distribution of unlicensed childcare centers proved that the shortage of the childcare supply by the public sector is spatially complemented by the services by the private sector.

Keywords: childcare services, supply-demand gap, kernel density estimation, raster calculation, Tokyo

Japan Geoscience Union Meeting 2014
(28 April - 02 May 2014 at Pacifico YOKOHAMA, Kanagawa, Japan)

MTT41-P12 Room:Poster Time:April 28 18:15-19:30

Geo-interactive Guidebook Services: Design and Development of LBS Applications Featuring Geo-enabled Illustrations

LU, Min[1*] ; ARIKAWA, Masatoshi[1]

[1]Center for Spatial Information Science, The University of Tokyo

The current location-based mobile applications for tourists usually use Web maps as base maps with attached objects like POIs (points of interest) to provide relevant guide information. Their services rely on accuracy of positioning functions on the handsets and accessibility of the Web maps. However, their diversity of maps and geo-information representation methods are insufficient, and are regardless of the differences in cultures as well as target users. Meanwhile, such services provide information mainly based on points, but storytelling and plots are less concerned. On the other hand, conventional paper-based guidebooks and magazines are still popular because they are good at dealing with subdivided topics, content arrangement, illustrations and stories to provide tentative travel plans with attractiveness and readability. However, they lack the capability of interactions with readers' actions and locations.

In considering of combining the advantages of positioning-enabled devices and well-designed guidebooks, we researched on a framework to create geo-enabled pages for designing applications and services providing better user experience when traveling in the real world. By analyzing the graphic components of the pages of a guidebook from the viewpoint of geo-information representation, a structured description of both graphic and geographic information of the components is established. Different geo-reference methods for geocoding the components are discussed. Especially, the methods of positioning using illustrated-maps and lines on pages are focused. Possible location-based events in the procedures of interactions with users and their locations are summarized. The design principles of user interfaces for both content creators and final users are discussed.

Finally, prototypes named "Manpo" including a content editor and a content browser are developed based on Apple Inc.'s iOS platform. Contents created by the prototype editor from existing guidebooks were used with Manpo by experimenters, to show the usability of the framework and the potential to be a commercial product.

Keywords: guidebooks, illustrated maps, geo-reference, mobile applications

Japan Geoscience Union Meeting 2014
(28 April - 02 May 2014 at Pacifico YOKOHAMA, Kanagawa, Japan)

MTT41-P13 Room:Poster Time:April 28 18:15-19:30

Development of a Learning Environment based on Spatio-temporal Historical Story Mapping Animation

INOUE, Yasushi[1*] ; TSURUOKA, Ken'ichi[1] ; ARIKAWA, Masatoshi[1]

[1]Center for Spatial Information Science, The University of Tokyo

The purpose of leaning history is to have the capability of imaging the future by using the knowledge in historical facts. In history learning, it is important for users to understand effectively causal relationships of events. However, paper textbooks have a limitation of dynamically representing historical stories, because articles of paper textbooks consist of pieces of texts and pictures such as photos, maps, diagrams, and chorological tables. These kinds of articles are fragmental and static descriptions from the viewpoint of visual presentations. A learning environment that the user can easily understand causal relationships of events for a historical story is desired.

For resolving the limitation of paper textbooks, we propose a new framework for visualization of historical stories with relationships of events. A historical story can be defined what to combine causal relationships of events along the axis of time. We classified and defined simple data models for visualization according as time series and locations of events. We have implemented an application software system that has an interactive user interface by displaying sequences of graphics with our data models. Visual representation of our user interface is realized by three basic methods for depicting historical stories as follows:

(1)Visualization of causal relationships with arrow icons on chorological tables and maps
(2)Visualization of hierarchies of events with chorological tables and maps
(3)Visualization of the focal position in storytelling

We are creating animation content telling the story about the government's actions for the aftermath of the 2011 Tohoku earthquake and tsunami by using our prototype system as a model case. The purpose of our study is to realize a learning environment for users to easily understand causal relationships of events, in brief, and to prove effectiveness of historical learning through the model case.

Keywords: History Learning, Visualization, Ubiquitous Mapping

Japan Geoscience Union Meeting 2014
(28 April - 02 May 2014 at Pacifico YOKOHAMA, Kanagawa, Japan)

MTT41-P14 Room:Poster Time:April 28 18:15-19:30

Integrating Maps in Photos with Relative Spatial References

SI, Ruochen[1*] ; ARIKAWA, Masatoshi[1] ; LU, Min[1]

[1]Center for Spatial Information Science, The University of Tokyo

1. Introduction

Signboard maps are widely distributed in public places, such as parks, subway stations, universities, and so on. Signboard maps are usually designed specially for the local area. POIs are usually highlighted in the maps. Many signboard maps are also drawn in an artistic way, and the mapping styles are various in different signboard maps. Except for the content, the locations of the signboard maps also provide rich information. The locations of the signboard maps are usually important places, such as the entrance of the facility and the place people easily miss the way. However, one of the disadvantage of the signboard maps is that they are not accessible anytime anywhere if users are far from them. To solve the problem, we propose a method to integrate the signboard maps in photos with digital maps to provide location based services with the signboard maps on smart phones.

2. Mapping Signboard Maps onto Digital Topographical Maps

An example of a signboard map we are going to integrate is a map of Kashiwa Campus at the University of Tokyo. We took the high resolution photos of the signboard maps in the campus. And we use a digital topographical map provided by The Geospatial Information Authority of Japan as the base maps.

We use the road intersection points as the control points of the photos. All the road intersection points are picked and are given the same coordinates as the corresponding points on the base maps. With the control points, we can map a user's location coordinates onto the photos including the signboard maps. However, factors such as the generalization, exaggeration, and the different of map projection used in the signboard maps make errors of the mapped user's location on the photo. And the errors of relative spatial relations, like locating the user on the wrong side of roads intersection, will easily mislead the users.

To ensure the relative spatial relationship of user's location with roads, we depict the roads on the photos, record their coordinates, and find the corresponding roads on the base maps. Instead of mapping the user's location directly onto the photos, we first map it onto the base map. Then we find the nearest road in the base map from the user's location. Then we map the location from the base map to the photo, so that the relative distance from user's location to the road keeps same and the foot point cuts the road with same proportion. As shown in the figure, AB and A'B' are corresponding roads in base map and in the photo, U and U' are the user's locations, V and V' are the nearest point on the road from user's location. Then, AV/VB=A'V'/V'B', UV/AB=U'V'/A'B'.

3. Integrating Multiple Various Signboard Maps

As we have mentioned, the locations of signboard maps themselves are usually important places. We annotate in each signboard map the locations of other signboard maps. By doing so, we do not only tell the users the locations of other signboards, but also composed different signboard maps, each may refer to a relatively small local area, to form a larger map. While the user is moving out of the current map, we zoom out of the current map and zoom into another map in which the user's location falls.

4. Conclusion

The signboard maps are generally more artistic, more stylish and more thematic than commonly used digital navigation maps. And the locations of the signboard maps are also important. We proposed the method to integrate the signboard maps in photos with digital base map to provide location based service with signboard maps on smart phones.

In this paper, we just made the experiment with the signboard maps of Kashiwa Campus at the University of Tokyo. In the future, we are going to cooperate with local governments and communities to collect and integrate more signboard maps on our proposed framework.

Keywords: Signboard Maps, Photos, Location-based Services, Relative Spatial References

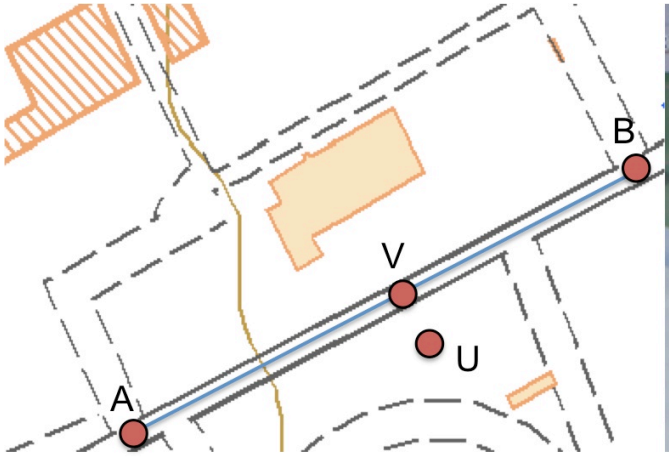

Japan Geoscience Union Meeting 2014
(28 April - 02 May 2014 at Pacifico YOKOHAMA, Kanagawa, Japan)

MTT41-P15 Room:Poster Time:April 28 18:15-19:30

Portrayal and Symbology of Global Map

ANDO, Akifumi[1] ; UBUKAWA, Taro[1] ; SAITO, Toshinobu[1*] ; YAMADA, Akiko[1] ; UEDA, Maya[1] ; SUGA, Masaki[1] ; YAMAZAKI, Satoko[1]

[1]Environmental Geography Division, Geocartographic Department

Global Map is fundamental geospatial information datasets composed of
eight kinds (Population Centre, Drainage, Transportation, Boundaries,
Land Use, Land Cover, Vegetation, Elevation) of thematic information
based on consistent specifications. It is developed under international cooperation of respective National Geospatial Infomation Authority (NGIA) around the world. Global Map version 2 (Global Version, Land Cover and Vegetation) was published in July, 2013. Analyzing Global Map with other geospatial information gives good understanding of the relationship between human activities and environmental conditions including forest distribution and land cover conditions. This poster shows our recent achievements in developing new portrayal for Global Map and tiles for WTMS.

Keywords: Global Map, Map Symbology

Japan Geoscience Union Meeting 2014
(28 April - 02 May 2014 at Pacifico YOKOHAMA, Kanagawa, Japan)

MTT41-P16 Room:Poster Time:April 28 18:15-19:30

Estimation of the Horizontal Positional Accuracy of Geospatial Data

KOSHIMIZU, Hiroshi[1*] ; MURAKAMI, Masaki[2]

[1]GSI of Japan, [2]GSI of Japan

Expectations for positioning accuracy enhancement vitalize efforts for the advancement of positioning services. For example, various driving assist service with the use of 'Authority map' (which is a large scale map that anyone can use) is being studied in the field of ITS service. It is expected that further disclosure of information about the horizontal positional accuracy of map (which should be combined with positioning information) will be required.

As for the horizontal positional accuracy of map, the threshold (upper limit value) called 'standard deviation' is prescribed in the General Standard of Operation Specifications for Public Surveys for digital topography: 1.75m in the case of the scale 1:2500 (2.50m in the case of editing pre-existing data). However, this 'standard deviation' gives no specific information about probability density functions which are inevitable for the definition of the positional accuracy. Moreover, it is pointed out that above threshold is too large in relation to actual values of public survey works and thresholds of several rules in other countries.

We therefore give the definition of the index 'standard deviation' expressing the horizontal positional accuracy of map with the use of the past research of GreenWalt-Shultz (1968), which had a crucial impact in the FGDC accuracy standards (1998). Let X, Y be random variables which have horizontal residual component values x, y as realized values which are obtained from sample points in the map. Here, 'residual value' means the difference of the observed value and the value considered to be true concerning the same point. If a set { (x,y) } contains no bias and outlier, residual value (x,y) is considered to represent positional accuracy of the point. We assume that realized values of X (Y) are normally distributed with density function fx (fy) of mean 0 and variance sxˆ2 (syˆ2). Let P(R) the probability which a sample point falls in the closed disc with radius R. P(R) is represented by the density function f which has fx and fy as a marginal density function on XxY with the use of conversion from (x,y) to polar coordinates. If sx=sy then we can easily show that P(sx)=P(sy)=0.3935, othewise P(s)=0.3935 leads an approximate expression s=0.5(sx+sy), which is shown by converting the polar coordinates expression of P(R) into the form of integral transformation of certain modified Bessel function (of the first kind) and using numerical calculation methods. If sx=sy then sx=sy=s. Therefore, we define the index 'standard deviation' by s, and call s 'Circular Standard Error' or 'CSE' for short. Estimated value of s should be calculated by { (x,y) }.

Based on this redefinition, we investigated the horizontal positional accuracy of public survey works for digital topography with the scale 1:2500. We regarded (independently) observed coordinate value of GNSS positioning as true value at the sample point, and removed the effect of bias and outlier as much as possible in advance. As a result, we obtained a rough estimate on the CSE: Estimated average value of CSE is 0.3˜0.4m, and estimated threshold (upper limit value) is 0.8m. This estimation indicates the necessity of tightning the threshold for the positional accuracy in the General Standard of Operation Specifications for Public Surveys.

Keywords: positional accuracy

Japan Geoscience Union Meeting 2014
(28 April - 02 May 2014 at Pacifico YOKOHAMA, Kanagawa, Japan)

MTT41-P17 Room:Poster Time:April 28 18:15-19:30

Effectiveness of the consecutive cross sections expression for the relief representation

ARAI, Riku[1*] ; MORITA, Takashi[2] ; KUDO, Keisuke[1]

[1]Graduate School of Engineering and Design, Hosei University, [2]Faculty of Engineering and Design, Hosei University

A map that shows the relief topography is having a lot of kinds. For example altitude tints map, and a color shaded relief map, etc. In late years, by a detailed digital altitude model, we can come to express an irregularity of the slight topography. In this way, we can recognize the topography intuitively.

However, like a contour line, it is important that we grasp ups and downs of the topography quantitatively. Therefore we stack a contour line on topography irregularity map and are effective in visualizing the ups and downs between specific two spots by beginning to talk about any section. Furthermore, we may express the topography as a map of the subject by handling shadow in the continuation section that cut and brought down a parallel section to equal distance continually. In addition, it may show former city space structure by grasping ups and downs of such slight topography.

This study made the topography irregularity map around the rich moat of topography ups and downs. Furthermore, I visualize the city space structure that watched ”Ichigaya Hachiman” from a geographic characteristic as an example by consecutive cross section expression. And I reevaluate an effect of the consecutive section expression in the topography irregularity map.

As a result, I showed city space structure and ups and downs of the slight topography by an irregularity map clearly as well as superficial contour line and color shaded relief. And the consecutive cross section expression expressed detailed topography incline to supplement an irregularity map.

Keywords: topographic map, consecutive cross sections, urban space structure, moat of a Edo castle, hilly sections of Tokyo, shrine

Japan Geoscience Union Meeting 2014
(28 April - 02 May 2014 at Pacifico YOKOHAMA, Kanagawa, Japan)

MTT42-01 Room:314 Time:May 2 09:00-09:15

Mass-independent fractionation of mercury stable isotopes in deep-sea hydrothermal systems

TAKEUCHI, Akinori[1*] ; TOMIYASU, Takashi[2] ; KODAMATANI, Hitoshi[2] ; YAMAMOTO, Masahiro[3] ; MARUMO, Katsumi[4]

[1]National Institute for Environmental Studies, [2]Kagoshima University, [3]JAMSTEC, [4]University of Toyama

It has been recognized that mercury (Hg) isotope analysis is an important new tool for identifying Hg source and tracking Hg transformations in the environment. Mass-dependent (MDF) and -independent (MIF) fractionations of Hg isotopes are caused by a wide variety of biogeochemical processes including redox reactions and volatilization. Volcanic activities and its associated hydrothermal activities are the main sources of naturally-emitted Hg in the environment. Several previous studies suggested that the naturally-emitted Hg indicated both MDF and MIF. It was thought that the MDF was caused by a process of liquid-vapor partitioning during ascending and the MIF was caused by photoreduction. It was, however, suggested that both photoreduction and volatilization could cause the MIF, and it has never been distinguish from each other in the hydrothermal systems. In this study, geological samples in active deep-sea hydrothermal systems at Izu-Bonin arc were collected and measured their Hg isotopic compositions. They indicate both MDF and MIF. The δ^{202}Hg values range from -1.0 to 0.5 ‰, indicating the liquid-vapor partitioning, whereas the calculated Δ^{199}Hg values are mostly between 0.1 and 0.2 ‰, indicating the MIF in the deep-sea hydrothermal systems without photoreduction. The linear relationship between Δ^{199}Hg and Δ^{201}Hg, ranging from 1.6 and 2.0, also indicates the nuclear volume effect. This result suggest that MDF and MIF of Hg isotopic compositions can be utilized to distinguish naturally-emitted Hg from anthropogenic Hg.

Keywords: Mercury Isotope, MIF, Deep-sea Hydrothermal Systems, CV-MC-ICP/MS

Japan Geoscience Union Meeting 2014
(28 April - 02 May 2014 at Pacifico YOKOHAMA, Kanagawa, Japan)

MTT42-02 Room:314 Time:May 2 09:15-09:30

Speciation of metal ions in water: comparison of their reactivities with oxygen-donar hard ligands

TAKAHASHI, Yoshio[1*] ; MIYAJI, Asami[1] ; TANAKA, Masato[1]

[1]Graduate School of Science, Hiroshima University

Complexation of metal cations with ligands such as hydroxide ion, carbonate ion, carboxylate ion, and phosphate ion is one of the most important factors controlling behaviors of metal ions in natural environment. Previous studies showed that these ligands were classified as ”intermediate hard ligands” having oxygen donor, which favors to form ionic bonding. However, it was found that the reactivity of these ligands depends on ionic radius and that there is a difference of the reactivity between hydroxide ion and other intermediate hard ligands such as carbonate and carboxylate. For example, among divalent alkaline earth metal ions, Mg2+ mainly precipitates as hydroxide (brucite), while Ca2+ prefers to form carbonate (calcite) or phosphate (apatite) minerals rather than hydroxide. However, quantitative discussion on the selectivity of metal cations has not been performed.

In this study, we evaluated the standard Gibbs free energy, entropy, and enthalpy for the complex formation of hydrated metal cations with these ligands based on a critical thermodynamic database. As a result, we found that the entropic contribution to the free energy was large in the case of hydroxide complex of smaller cation. In contrast, the entropic contribution to the free energy was small in the case of hydroxide complex of larger cation and other complexes. In addition, the enthalpy contribution was not significant in this reaction. In the aqueous complexation reaction, entropy was controlled by the number of water molecules replaced by the ligand, suggesting that hydroxide complex for large cation was not stable due to the small effect of dehydration.

This suggestion was confirmed by quantum mechanical calculations, which was performed with B3LYP/6-311+G∗level using Gaussian 09. We calculated distance between metal (M) in the center and oxygen (O) in the ligand with the increase of number of water molecules placed in the vicinity of the metal ion. As a result, it was found that the M-O distance for hydroxide complex is larger than that of carbonate in the case of larger cation and vice versa This means that hydroxide prefers to form outer-sphere complex for lager metal ion, which is not the case of other intermediate hard ligands. This result is consistent with what we suggested based on the thermodynamic data.

Keywords: Speciation, Entropy, Complexation, Hydrolysis, Quantum chemical calculation

Japan Geoscience Union Meeting 2014
(28 April - 02 May 2014 at Pacifico YOKOHAMA, Kanagawa, Japan)

MTT42-03 Room:314 Time:May 2 09:30-09:45

Consistency between fission-track and U-Pb ages of zircon and its implications

IWANO, Hideki[1*] ; DANHARA, Tohru[1]

[1]Kyoto Fission-Track Co.

Following the recommendation by the Fission Track Working Group of the IUGS Subcommission on Geochronology (Hurford, 1990), the fission-track method was transformed into a simplified and user-friendly dating tool. Standardization based on the common use of international age standards is what is called the zeta calibration. However, the adoption of the standardization scheme in which fission-track ages are determined against reference ages (K-Ar, Ar/Ar, Rb-Sr), and not based on physical parameters directly associated with the fission process, meant that the fission-track method lost its status as an independent geochronometer. Over the last two decades, we have investigated the problems of the absolute calibration approach, and we have finally demonstrated that it works well for zircon when using the external detector method (Danhara and Iwano, 2013). One of our conclusions is that the fission-track age for the Fish Canyon Tuff is 28.4+/-0.2 Ma. This is concordant with the recent zircon U-Pb ages (Schmitz and Bowring, 2001; Bachmann et al., 2007) and slightly older than the sanidine Ar/Ar age of 27.8+/-0.2 Ma, which is the reference age for the zeta calibration. We will discuss the consistency between fission-track and U-Pb ages of zircon from volcanic samples and give some comments on fission-track age standardization.

Bachmann et al. (2007) Chemical Geology 236, 134-166.
Danhara and Iwano (2013) Island Arc, 22, 264-279.
Hurford (1990) Chemical Geology, 80, 171-178.
Schmitz and Bowring (2001) Goechimica et Cosmochimica Acta 65, 2571-2587.

Keywords: zircon, fission-track age, U-Pb age, calibration

Japan Geoscience Union Meeting 2014
(28 April - 02 May 2014 at Pacifico YOKOHAMA, Kanagawa, Japan)

MTT42-04 Room:314 Time:May 2 09:45-10:00

Fe isotope measurement of taenite using LA-MC-ICPMS technique with Galvano scanner system

OKABAYASHI, Satoki[1*] ; HIRATA, Takafumi[1]

[1]Division of Earth and Planetary Sciences, Kyoto University

The laser ablation-multicollector-inductively coupled plasma mass spectrometry (LA-MC-ICPMS) is widely accepted as the powerful technique to reveal the isotope ratios of solid sample. This technique can achieve the in-situ analysis of micro region with swiftness. On the other hand, it is difficult to avoid the mass spectrometric and non-mass spectrometric interferences from coexistent elements in this technique because the produced sample particles by laser ablation are directly introduced into the ICP with carrier gas. Such interferences have a potential to intercept to reveal the precise and accurate isotope data. The effect on the isotope ratios of analyte from coexistent elements can be corrected by using the standard material which include same amount of coexistent elements as the sample. However, synthesis of isotopic homogeneous solid material is extremely difficult.

In this study, we have developed a technique to measure the Fe isotope ratios of taenite in iron meteorites. The Fe isotope signature of iron meteorites is one of the key information to understand the core formation of planetesimals and terrestrial planets. However, the in-situ Fe isotope measurement of taenite is difficult because of the abundant Ni (>25 wt%) in it. In order to overcome this problem, we have applied Galvano mirrors and a telecentric optical system (Yokoyama et al., 2011) for LA-MC-ICPMS technique. In this technique, pure iron (IRMM-014) and pure Ni were ablated at a time using femtosecond laser with Galvano system as the Fe isotope standard. The ablated Ni amount was adjusted to the Ni amount in the taenite sample. The Fe isotope ratios (^{56}Fe/^{54}Fe and ^{57}Fe/^{54}Fe) of taenite phases were measured using MC-ICPMS and the mass fractionation in the mass spectrometry was corrected by sample-standard bracketing technique. The precision and accuracy of Fe isotope data obtained by the presented technique will be discussed in this presentation. The isotope analytical technique developed in this study can be applied not only for taenite phase in iron meteorite but also for other sample which include coexistent elements.

Keywords: ICP-MS, laser ablation, taenite, Fe isotope, Galvano

Japan Geoscience Union Meeting 2014
(28 April - 02 May 2014 at Pacifico YOKOHAMA, Kanagawa, Japan)

MTT42-05 Room:314 Time:May 2 10:00-10:15

High-Pressure Neutron Beamline PLANET for investigating ”Water” in the Earth

HATTORI, Takanori[1*] ; SANO, Asami[1] ; ARIMA, Hiroshi[2] ; INOUE, Toru[3] ; KAGI, Hiroyuki[4] ; YAGI, Takehiko[3]

[1]Japan Atomic Energy Agency, [2]Institute for materials research, Tohoku university, [3]Geodynamics Research Center, Ehime University, [4]Geochemical Laboratory, Graduate School of Science, University of Tokyo

The PLANET is the world’s first neutron beamline specialized for high-pressure and high-temperature experiments. The most characteristic feature is the capability to investigate the state of water and hydrogen in minerals at high-pressure and high-temperatures up to 20GPa and 2000K with the multi-anvil high-pressure apparatus. The construction was started in 2008 and the experiments have been conducted since Nov. 2012. In this talk, the design and performance of the PLANET are introduced.

PLANTET is designed so as to investigate structures not only of crystalline but also of amorphous (liquid) materials. The resolution of the diffraction pattern (Delta d/d=0.6%) was found to be almost equal to the designed value(0.5%). The elimination of the background from the sample surrounding materials, which is the most important issue in the high-pressure experiments, was found to be accomplished by using the severe incident and receiving collimators. With this development, PLANET offers very clear patterns even at high pressures. This character made the PLANET one of the most innovative beamlines among several high-pressure neutron beamlines in the world.

Keywords: neutron, high pressure, beamline, hydrous

Japan Geoscience Union Meeting 2014
(28 April - 02 May 2014 at Pacifico YOKOHAMA, Kanagawa, Japan)

MTT42-06 Room:314 Time:May 2 10:15-10:30

High-pressure neutron beamline at J-PARC and applications to earth and planetary sciences

KAGI, Hiroyuki[1*] ; IIZUKA, Riko[2] ; KOMATSU, Kazuki[1] ; YAGI, Takehiko[2] ; NAGAI, Takaya[3] ; INOUE, Toru[2] ; SANO, Asami[4] ; HATTORI, Takanori[4]

[1]Graduate School of Science, University of Tokyo, [2]Geodynamic Research Center, Ehime University, [3]Graduate School of Science, Hokkaido University, [4]Japan Atomic Energy Agency

Construction of the high-pressure dedicated beamline, PLANET, in Japan Proton Accelerator Research Complex (J-PARC) has been completed in 2012 and scientific programs for general users have just started in 2014. The PLANET beamline has a focusing mirror for incident neutron and two 90-degree detector banks. Each bank has 160 pieces of Position Sensitive Detectors (PSDs) filled with 3He gas. Each bank has a detector coverage of 90 $\pm$ 11 degree against the incident beam in the horizontal direction and 0 $\pm$ 35 degree in the vertical direction. Radial collimators are attached in front of the detector banks to reduce the background. The instrumental resolution is 0.6% in Δd/d. The accessible d-spacing is normally 0.2?4.2 A and is doubled in a double-frame setup. The power of the proton beam is around 300 kW and will be increased to 600 kW in 2014. The most characteristic feature of the PLANET beamline is the multi-anvil apparatus with six independently acting 500-tonne rams (6-axis press called ATSUHIME). Using ATSUHIME, we successfully observed neutron diffraction patterns of hydrous minerals at high pressure and high temperature without any contamination from sample-surrounding materials such as pressure transmitting media, anvils, and so on. This clearly shows that the incident slit and radial collimator installed in the beamline are very effective to obtain the diffractions under high pressure.

We focus on pressure-responses on the structure of materials with hydrogen- bonding networks through neutron diffraction measurements at high pressure. These results will contribute to fundamental understanding of hydrous materials in the deep earth and icy material in the planets.

Keywords: neutron, neutron diffraction, hydrogen, water, high pressure, ices

Japan Geoscience Union Meeting 2014
(28 April - 02 May 2014 at Pacifico YOKOHAMA, Kanagawa, Japan)

MTT42-07 Room:314 Time:May 2 10:30-10:50

Geo-neutrinos for advanced earth studies

TANAKA, Hiroyuki[1*]

[1]Earthquake Research Institute, The University of Tokyo

Neutrinoes generated in Earth (geo-neutrinos) gives us information about the distribution of Uranium (U), thorium (Th), and pottasium (K) inside Earth. Beta-decays of radionuclides U/Th/K inside Earth produce low energy anti-electron neutrinos (U and Th produces 7.41x10^7 neutrinos $kg^{-1}s^{-1}$ and 1.62x10^7 neutrinos $kg^{-1}s^{-1}$ respectively (without considering neutrino oscillation)) that traverse through Earth without being disturbed due to their extremely small interaction cross section with matter. Recent geo-neutrino observations have produced results that have a potential to support and clarify the current concerns of earth science: estimating the amount of contribution to the surface heat flux; constraining existing Earth's compositional estimates; and clarifying the origin of low shear velocity regions found at the core mantle boundary (CMB). Today, there are two detectors capable of measuring geoneutrinos: KamLAND, in Japan, and Borexino, in Italy. The KamLAND research team has found 116+/-28, 27 geoneutrino candidate events (generated through the decay processes of 238U and 232Th) during 2,991 days of geoneutrino observation (Gando et al. 2013). The contribution from geonuclear reactions to the heat flow, estimated from examination of the geoneutrino flux, reached 11.2+/-7.9, 5.1 TW. Although the volume of the Borexino detector (280 t) is much smaller than that of KamLAND (1,000 t), the background from reactor neutrinos is much lower than that for KamLAND because there are no nuclear power plants in Italy. Borexino detected 14.3±4.4 geoneutrino candidates over 1353 days of observation. Both measuremet results are consistent each other, and also reject the fullly radiogrenic model, which assumes that the total Earth's surface heat flux is completely originated from radiogenic heat from U, Th and K. The upperlimit on the fully radiogenic heat flux hypothesis (Herndon 1996) was set to be 4.5 TW at 95% confidence level (Bellini et al. 2013).

Gando A, Gando Y, Hanakago H, Ikeda H, Inoue K, et al. 2013. Reactor on-off antineutrino measurement with KamLAND. Phys. Rev. D 88:033001.

Herndon JM. 1996. Substructure of the inner core of the Earth. Proc. Natl. Acad. Sci. USA 93:646-48.

Bellini, G., Ianni, A., Ludhova, L., Mantovani, F., McDonough, W.F. 2013. Geo-neutrinos, Prog.Part.Nucl.Phys. 73:1-34

Keywords: Neutrino, Uraniun, Thorium, Mantle

Japan Geoscience Union Meeting 2014
(28 April - 02 May 2014 at Pacifico YOKOHAMA, Kanagawa, Japan)

MTT42-08 Room:314 Time:May 2 11:00-11:15

Multi-range imaging mass spectrometry using laser ablation-ICP-mass spectrometry

HIRATA, Takafumi[1*] ; HATTORI, Kentaro[1] ; OHARA, Seiya[1]

[1]School of Science, Kyoto University

Time-resolved elemental and isotopic data can provide key information about the time changes of the geochemical conditions of the surface environmental of the Earth, and therefore, critical restriction for the origin or evolutional sequence of the surface environment of the Earth and the life could be derived. To obtain reliable and exclusive information from the samples, tremendous efforts have been given to develop various analytical techniques, which could provide both the higher elemental sensitivity and higher analytical throughput. Among the analytical techniques, plasma ion source mass spectrometer coupled with the laser ablation sample introduction technique (LA-ICPMS) has now become the most sensitive and user-friendly analytical tool to derive elemental and isotopic distribution among the different phases or minerals. Moreover, in the LA-ICPMS technique, atomization and ionization of the analytes were independently carried out from the sampling (i.e., post ionization technique), and therefore, the sampling and ionization conditions could be separately optimized. The post ionization technique results in the smaller contribution of the matrix effect, which could be the major source of analytical error. Furthermore, for the LA-ICPMS technique, sample was located under the atmospheric pressure sample cell, and laser induced sample aerosols were carried into the ICP ion source using a He carrier gas. This suggests that no evacuation of the sample housing is required, and therefore, biological cell or tissue samples (i.e., wet samples) can be directly subsidized to elemental imaging analysis, obviating the drying or freezing procedure for the analysis. The LA-ICPMS technique has further advantages of imaging analysis for samples with various sizes, ranging from 10 microns to >10 mm. Because of high capability for quantitative imaging of ultratrace-elements, together with high analytical capability to measure large-sized samples, the LA-ICPMS technique has blossomed to become the key analytical technique for the imaging analysis of trace-elementals and isotopes. This is very important to obtain elemental and isotopic images for not only biological samples, but also various rock or minerals. In fact, imaging data for whole rock pierces or minerals can tell us the substantial process for the elemental distribution or diffusion among the samples. We should recall that we could not see the forst for the trees. Despite the obvious success in obtaining the elemental and isotopic imaging data, neither quantitative evaluation of the detection limits for the elements nor the dependence of the analytical conditions (e.g., laser pit size, raster rate, system setup or condition for data acquisition) onto the resulting spatial resolution were made. To investigate these, we have measured imaging analyses of several trace- and ultratrace-elements from meteorite samples and biochemical samples under the various analytical conditions. In this presentation, we will described the effect of the system setup and operational settings onto the resulting spatial resolution and onto the limit of detection for the elements.

Keywords: laser ablation, ICP-mass spectrometry, imaging mass spectrometry, multi-scale imaging, trace-elements, quantitative imaging

Japan Geoscience Union Meeting 2014
(28 April - 02 May 2014 at Pacifico YOKOHAMA, Kanagawa, Japan)

MTT42-09 Room:314 Time:May 2 11:15-11:30

Cavity ring-down spectroscopy for the isotope ratio measurements of water from fluid inclusions in stalagmites

UEMURA, Ryu[1*] ; NAKAMOTO, Masashi[1] ; GIBO, Masakazu[1] ; MISHIMA, Satoru[1] ; ASAMI, Ryuji[2]

[1]University of the Ryukyus, [2]University of the Ryukyus

Oxygen isotope record in stalagmites is useful to reconstruct past environmental changes. However, the interpretation of calcite isotope record is not straightforward because it is affected by various factors affect such as amount of precipitation and temperature. Water isotope composition of fluid inclusions, and oxygen isotope difference between water and host calcite, from stalagmite are potentially important proxies to estimate the paleo-temperature. Recently, infrared spectroscopy (IRIS) has been widely used for stable isotope ratio measurement of water. Unlike traditional isotope mass spectrometer (IRMS), the IRIS does not require pre-treatment processes (e.g., high-temperature furnace or equilibration device). A limitation of IRIS is that commercially available IRIS systems need large sample volume (1 - 2 micro litres) for liquid water measurement. In this study, we developed a custom-designed device suitable for precise measurement of smaller volume (0.05 to 0.20 microlitres) of water, and tested two extraction methods (thermal extraction and mechanical crushing). Oxygen and hydrogen isotope ratios of water were measured using cavity ring down spectroscopy (WS-CRDS Picarro L2130-i). Stalagmites samples were collected in several caves in Okinawa, Japan. Pieces of stalagmites (80-300mg) subsampled from homogeneous layers, and reproducibilities of the inclusion measurement were 0.2 permil for δ^{18}O and 1 permil for δD. The measured δ^{18}O and δD of inclusion water from recently grown stalagmites agrees with modern dripwaters, indicating that our extraction technique is useful to measure isotope ratios of past inclusion water.

Keywords: Stable isotope, Fluid inclusion, Speleothem, Stalagmite, Paleoclimate, CRDS

Japan Geoscience Union Meeting 2014
(28 April - 02 May 2014 at Pacifico YOKOHAMA, Kanagawa, Japan)

MTT42-10 Room:314 Time:May 2 11:30-11:45

Coral growth-rate insensitive Sr/Ca as a robust temperature recorder at the extreme latitudinal limits of Porites

HIRABAYASHI, Shoko[1*] ; YOKOYAMA, Yusuke[1] ; SUZUKI, Atsushi[2] ; KAWAKUBO, Yuta[1] ; MIYAIRI, Yosuke[1] ; OKAI, Takashi[2] ; NOJIMA, Satoshi[3]

[1]Atmosphere and Ocean Research Institute, The University of Tokyo, [2]National Institute of Advanced Industrial Science and Technology, [3]Amakusa Marine Biological Laboratory, Kyushu University

Corals are rich archives of climatic changes with high-resolution record of seasonal change such as sea-surface temperature(SST), in tropical and sub-tropical seas during recent and distant past. Past SST are commonly reconstructed from the trace elementals present in annually-banded coral skeletons. Recently, reef building corals were found in temperate regions due to coral habitat range shifts and/or expansions. Therefore, it could be a powerful tool for reconstructing climatic changes such as global warming and ocean acidification over long period. However, because of the more stressful environment for corals in temperate region than tropic or subtropics, we have to know how to reconstruct palaeo-SST using temperate corals.

This paper was reported Sr/Ca-based SST reconstructions for temperate Porites corals collected from Kyushu, Japan, near the northern latitudinal extent of hermatypic corals. New, high-resolution Sr/Ca data, measured along the growth axes of Porites from Ushibuka, were compered to previously published $\delta\ ^{18}$O data from the same specimens (Omata et al., 2006). Results indicate that Sr/Ca variations in a low-growth coral remain independent from growth rate, in contrast to the oxygen isotope ratios of the same coral. Results clearly indicate that Sr/Ca robustly reproduces SST variations from regions along the extreme latitudinal limits of hermatypic coral habitat, independent of growth rate variations.

Additionally, Sr/Ca of the other two Porites corals collected in Ushibuka were measured and the inter-colony variation of reconstructed SST was shown. At this stage, it is difficult to reconstruct accurate SST using only one specimen of Porites in temperate region. However, we can reconstruct SST within only 1 ℃ difference from observed SST if we calibrate Sr/Ca-SST using more than two corals. It is expected that in the future the fossil temperate corals will be commonly used for paleo-SST reconstruction.

Japan Geoscience Union Meeting 2014
(28 April - 02 May 2014 at Pacifico YOKOHAMA, Kanagawa, Japan)

MTT42-11 Room:314 Time:May 2 11:55-12:15

Maximizing organic records: Recent achievements and future directions

OHKOUCHI, Naohiko[1*] ; CHIKARAISHI, Yoshito[1] ; TAKANO, Yoshinori[1] ; OGAWA, Nanako[1]

[1]JAMSTEC

Molecular isotopic record in either organisms or sediments has been proven useful for better understanding the bio(geo)chemical processes, reconstructing paleo-environment, etc. During the last decades, target molecules have been expanding from simple lipids to complex physiologically active compounds. There are two key issues to push this molecular tool more useful and more efficient: 1) Purity of the target compounds that are extracted from environmental samples (generally a complex mixture of organic compounds), and 2) sensitivity of isotope-ratio mass spectrometry (IRMS) system for precisely measuring isotopic compositions. In this presentation we will overview the recent advances in these two issues, and how these achievements contributed to the progresses in our knowledge. We also try to mention in the future challenges of molecular isotopic signatures.

Keywords: Organic molecule, isotopic composition, nitrogen, carbon

Japan Geoscience Union Meeting 2014
(28 April - 02 May 2014 at Pacifico YOKOHAMA, Kanagawa, Japan)

MTT42-12 Room:314 Time:May 2 12:15-12:30

Precise and sensitive determination of stable isotopic compositions of amino acids

CHIKARAISHI, Yoshito[1*] ; TAKANO, Yoshinori[1] ; OHKOUCHI, Naohiko[1]

[1]Japan Agency for Marine-Earth Science and Technology

Amino acids are biologically central and functional organic compounds. Their molecular and stable isotope profiles have been employed as a tool in various fields of studies, particularly for understanding of the trophic energy flow of food web ecology as well as for estimating the origin of amino acid procurers in extraterrestrial samples (e.g., meteorites). One of the most powerful techniques in the stable isotope studies of amino acids is compound-specific isotope analysis (CSIA) by gas chromatography/isotope ratio mass spectrometry (GC/IRMS), which potentially allows a rapid and precise determination of H, C, N, O, and S isotopic compositions of individual amino acids in complex mixture of samples. However, (1) isotopic fractionation and exchange during pretreatment (e.g., hydrolysis, extraction, purification, and derivatization) of samples, (2) chromatographic separation among individual amino acids, and (3) less sensitivity on GC/C/IRMS (i.e., 10-50 nmol of elements is required) are always problematic in CSIA of amino acids.

In the presentation, we will briefly review these issues on CSIA of amino acids, and show current advances in the precise and sensitive determination of C and N isotopic compositions of amino acids (i.e., within 0.4-0.8 permil for a minimum sample amount of 0.5 nmol element), based on the minimizing isotopic fractionation during HPLC purification and derivatization as well as reducing leak and background variation in GC/IRMS instrument. With this method, we can access C and N isotopic signature of wide range of samples including amino acids in bacteria and archea isolated from natural environments as well as amino acid procurers in meteorites.

Keywords: stable isotope, amino acids, food web, meteorite

Japan Geoscience Union Meeting 2014
(28 April - 02 May 2014 at Pacifico YOKOHAMA, Kanagawa, Japan)

MTT42-13 Room:314 Time:May 2 12:30-12:45

On the role of amino acid metabolism and a biogeochemical linkage

TAKANO, Yoshinori[1*] ; CHIKARAISHI, Yoshito[1] ; OHKOUCHI, Naohiko[1]

[1]JAMSTEC

Deep-sea sediments harbor a novel and vast biosphere with yet unconstrained importance in the global biogeochemical cycle. To explore these habitats is interdisciplinary challenges for the biogeochemical and geomicrobiological scientific community. The limits of deep biosphere are on-going subject, which were not yet known in terms of environmental properties, including depth, temperature, energy availability, and geologic age; however, it is known that subseafloor microbes play a significant role in chemical reactions that were previously thought to have been abiotic.

Since the novel classification by Woese and Fox (1977), Archaea, one of three domains of life, had been originally believed to exist in extreme environments including high temperature, high salinity, low oxygen concentration. However, recent advances in molecular and phylogenic approaches revealed their widespread distribution in marine and terrestrial environment including deep subsurface biosphere. The planktonic and benthic archaeal assemblages include two major phyla Euryarchaeota and Crenarchaeota. The novel phylum have been also proposed recently as Thaumarchaota, Korarchaota, and Nanoarchaeota.

In the present study, we reviewed the recent knowledge of prokaryotic ecology and biogeochemistry from molecular-specific isotopic signatures. Among these, we focused on the role of amino acid metabolism and a biogeochemical linkage mediated by deep-sea benthic archaea.

[References]

Ohkouchi, N. and Takano, Y. Organic nitrogen: sources, fates, and chemistry. Treatise on Geochemistry, 10: Organic Geochemistry (Edited by Birrer, B., Falkowski, P., Freeman, K.), Vol. 12, Elsevier, pp. 251-289 (2014).

Takano et al., Detection of coenzyme F430 in deep-sea sediments: A key molecule for biological methanogenesis. Organic Geochemistry, 58, 137-140 (2013).

Chikaraishi et al., Determination of aquatic food-web structure based on compound-specific nitrogen isotopic composition of amino acids. Limnology and Oceanography: Method, 7, 740-750 (2010).

Keywords: amino acid metabolism, deep-sea benthic archaea, a biogeochemical linkage

Japan Geoscience Union Meeting 2014
(28 April - 02 May 2014 at Pacifico YOKOHAMA, Kanagawa, Japan)

MTT42-P01 Room:Poster Time:May 2 16:15-17:30

Simple method for separation of boron from volcanic rocks for isotopic analysis by MC-ICP-MS

SHINJO, Ryuichi[1*] ; HAMADA, Yukinori[1]

[1]Univ. Ryukyus

We developed a simple and thus effective method of separation of boron from volcanic rocks.

It has been suggested that easy volatilization of boron and isotopic fractionation during evaporation step after HF decomposition of silicate rock samples; therefore procedure of evaporation at low-temperature (<80C) with mannitol (which suppress volatilization) under boron-free specific experiment environment has been utilized.

Our new method dose not require evaporation step, thus effectively preventing boron volatilization and related fractionation. Contamination opportunity can also be reduced. In our method, supernatant HF solution at sample digestion step is loaded onto mini-column cartridge of Amberlite IRA 743 (0.25mL) with no evaporation step. Recovery yield for silicate rocks was generally >80%. To evaluate our method, the GSJ rock standards (JB-2, JB-3 and JR-2) were analyzed by following the proposed method. Measured boron isotopic compositions for these rocks were in good agreement with preferred values.

Japan Geoscience Union Meeting 2014
(28 April - 02 May 2014 at Pacifico YOKOHAMA, Kanagawa, Japan)

MTT42-P02 Room:Poster Time:May 2 16:15-17:30

Development on submicron-scale U-Pb dating by Laser post-ionized SNMS

TERADA, Kentaro[1*] ; NAKABAYASHI, Makoto[1] ; KAMIOKA, Moe[1] ; TOYODA, Michisato[1] ; ISHIHARA, Morio[1] ; NAKAMURA, Ryosuke[2] ; AOKI, Jun[1] ; HINO, Yuta[1]

[1]Graduate School of Science, Osaka University, [2]Office for University-Industry Collaboration, Osaka University

In order to decipher the history of the Solar System, in-situ U-Pb dating method using SIMS (Secondary Ion Mass Spectrometry) has been used over 40 years, of which spatial resolution is 2-10 micron. In general, the secondary ion yield of SIMS is so low (less than l %) that it has been the weak point of this in-situ analysis. Here, we report the performance of Pb isotope measurement using the Laser SNMS that consist of of Ga-ion source for primary beam, femto-second laser for post-ionization, and the multi-turn TOF-SIMS for mass spectroscopy (Ishihara et al. 2010).

Keywords: U-Pb dating, mass spectrometry, in-situ analysis, isotope analysis

Japan Geoscience Union Meeting 2014
(28 April - 02 May 2014 at Pacifico YOKOHAMA, Kanagawa, Japan)

MTT42-P03 Room:Poster Time:May 2 16:15-17:30

Inhibition effect of natural organic matter on adsorption of radiocesium onto particulate matters in Pripyat River

SUGA, Hiroki[1*] ; FAN, Qiaohui[1] ; TAKEICHI, Yasuo[2] ; TANAKA, Kazuya[3] ; KONDO, Hiroaki[1] ; KANIVETS, Vladimir v[4] ; SAKAGUCHI, Aya[1] ; INAMI, Nobuhito[2] ; ONO, Kanta[2] ; TAKAHASHI, Yoshio[1]

[1]Departmeant of Earth and planetary system science, Hiroshima University, [2]Institute of Materials Structure Science, High-Energy Accelerator Research Organization (KEK), [3]Institute for Sustainable Science and Development, Hiroshima University, [4]Ukranian Hydrometeorological Institute

Radiocesium have been emitted to environment originated from nuclear weapon tests and nuclear accidents such as in Chernobyl and Fukushima. Among various sources, the nuclear accidents in Chernobyl and Fukushima have caused serious contaminations in land-surface around these areas due to the deposition of the radionuclides dispersed via. atmosphere as aerosols. Subsequently, radiocesium can be transported via rivers into oceans. In the soil- river-sediment system, radiocesium has high affinity for particulate matters, in particular for clay minerals. The high affinity has been shown to be the results of specific adsorption to frayed edge site (FES) and interlayer site in 2:1 phyllosilicate as inner-sphere (IS) complexes. However, it has been indicated that cesium adsorption to clay minerals can be blocked by natural organic matters (NOM) that adsorb on the mineral surface. NOM are ubiquitous and play various important roles on the adsorption of metal ions on particulate matters such as (i) promotion of adsorption of metal ions by the complexation with NOM and (ii) inhibition of adsorption by covering the particulate matters. High availability of Cs in soils with relatively high organic matter content was explained in terms of the blocking of access of cesium to specific adsorption sites (such as FES and interlayer site) of the clay mineral.

In river waters in Fukushima, it has been indicated that more than 70% of radiocesium is adsorbed on particulate matters. In contrast, Sansone et al. (1996) showed that more than 70% of radiocesium was in the dissolved fraction in Chernobyl. One critically important difference between the two sites is that peat, which contains large amount of NOM, is the main surface layer in the Chernobyl area. These NOM can be introduced into the Pripyat River that can coat on the particulate matters in river waters. Thus, it is possible that high content of NOM in rivers (e.g., Pripyat River) in Chernobyl can be responsible for the larger fraction of dissolved radiocesium compared with that in Fukushima due to the blocking effect by the NOM. In this study, therefore, adsorption of cesium on particulate matters collected in the Pripyat River with the characterization of the particulate matters have been conducted to study whether the blocking effect is affecting the adsorption behavior of cesium.

Here, we examined Cs LIII-edge extended x-ray absorption fine structure (EXAFS) to study the cesium species adsorbed on the particulate matters collected from Pripyat River and also on the particulate mattes after the removal of NOM by the treatment with hydrogen peroxide. To characterize the particulate matter, distribution image of organic substances on the particulate matter was analyzed by compact Scanning Transmission X-ray Microscope (cSTXM) newly developed in Photon Factory, KEK in Tsukuba, Japan. After the cSTXM imaging, characterization of NOM was conducted by near edge X-ray absorption fine structure (NEXAFS) at the C K-edge measured for the NOM by cSTXM.

From this study, blocking effect of cesium adsorption to clay minerals by humic acid was confirmed in natural particulate matter in Pripyat River, which might be related to the larger dissolved fraction of radiocesium around Chernobyl area, compared with that in rivers in Fukushima area.

Keywords: chernobyl, natural organic carbon, STXM

Japan Geoscience Union Meeting 2014
(28 April - 02 May 2014 at Pacifico YOKOHAMA, Kanagawa, Japan)

MTT42-P04 Room:Poster Time:May 2 16:15-17:30

Development of the technique for determination of I-129 in fish samples as new tracer of marine ecosystem

KUSUNO, Haruka[1*] ; MATSUZAKI, Hiroyuki[1] ; NAGATA, Toshi[2] ; MIYAIRI, Yosuke[2] ; YOKOYAMA, Yusuke[2] ; OHKOUCHI, Naohiko[3] ; TOKUYAMA, Hironori[1]

[1]School of Engineering, The University of Tokyo, [2]Atmosphere and Ocean Research Institute, The University of Tokyo, [3]Japan Agency for Marine-Earth Science and Technology

The availability of ^{129}I as a new tracer for marine ecosystem was examined.

The iodine isotopic ratio (^{129}I/^{127}I) in seawater is determined by the anthropogenic ^{129}I transferred from the atmosphere, i.e., it shows very high ratio as the order of 10^{-10} for ^{129}I/^{127}I at the surface or surface mixing layer and suddenly decreases going deeper to some of 10^{-12} or lower. Iodine isotopic ratio (^{129}I/^{127}I) of marine lives like fish should be determined by their habitats and the ways exchanging iodine with seawater. This means that the iodine isotopic ratio is potential indicator of marine ecosystem. However there have been only few studies using ^{129}I for marine ecosystem. This is because ^{129}I is so trace in the marine lives that ordinary analytical techniques cannot detect.

Recent development of analytical technique for ^{129}I using AMS (Accelerator Mass Spectrometry) enables determine trace amount of ^{129}I concentration in environmental samples.

In this study the pyrohydrolysis method was applied to extract iodine from fish samples. A freeze-dried and homogenized fish sample, 0.1g to 0.5g, was combusted in the quartz tube under oxygen and water vapor flow. Iodine was extracted into an alkaline solution. An aliquot of this solution was taken for ICP-MS analysis to determine the stable iodine (^{127}I) concentration. The remaining was, added with carrier iodine (about 1 mg), purified by solvent extraction and collected as AgI precipitation. ^{129}I/^{127}I ratio was determined by AMS. From the AMS result and the ^{127}I concentration, the ^{129}I/^{127}I ratio of the fish samples themselves can be calculated.

The extraction yield was evaluated using IAEA-414 fish standard sample. Background in the pyrohydrolysis was also examined.

The preliminary results of fish samples, collected from Suruga-bay (located on Pacific coast in the middle of Honshu, Japan) showed 1×10^{-10} to 7×10^{-10}, which was consistent with that of surface seawater.

Keywords: Iodine-129, tracer, marine ecosystem, fish, AMS

Japan Geoscience Union Meeting 2014
(28 April - 02 May 2014 at Pacifico YOKOHAMA, Kanagawa, Japan)

MTT42-P05 Room:Poster Time:May 2 16:15-17:30

Exploring the ecology of catfish through trace elements analyses of otolith by LA-HR-ICPMS to reconstruct palaeo-SST

AMEKAWA, Shota[1*] ; YOKOYAMA, Yusuke[1] ; KUBOTA, Kaoru[1] ; SAKAI, Saburo[2]

[1]Atmosphere and Ocean Research Institute, The University of Tokyo, [2]Japan Agency for Marine-Earth Science and Technology

Otoliths are incrementally precipitated aragonite biominerals found within the inner ear of all teleost fish. Previous studies show that oxygen isotopes (δ18O) of otolith aragonite precipitate in equilibrium with those of seawater regarding ambient water temperature (Campana, 1999). Therefore, (δ18O) of otolith can be used as a strong thermometer for reconstructing the past environment. In the meantime, fish habitats are necessary to be revealed before understanding the palaeoenvironments using otolith due to its nature as biomineral associated with fish. Thus we applied trace element measurements in the specimens to identify the habitable zones namely marine, brackish and freshwater. Strontium abundance in carbonate samples (Sr/Ca) is the best indicator to be employed because of distinct differences in concentration in marine and riverine waters (Walther and Thorrold, 2006). The present study is therefore aiming for identifying the past fish ecology using Sr/Ca in otoliths measured by newly developed laser ablation (ArF excimer) high resolution inductively coupled plasma mass spectrometry (LA-HR-ICPMS). The study area is the Gulf of Kutch in Gujarat district, northwestern part of India. This area is strongly influenced by Indian monsoon, which is characterized as distinct seasonal rainfall (humid summer and dry winter). Salinity distribution within the Gulf of Kutch is unusual compared with general river-estuary system. Lower salinity (˜37) is observed in the inner part, whereas higher values (>40) are observed near the mouth (Vethamony et al., 2007). In this study, we analyze both modern and fossil otoliths. Fossil otoliths were excavated from archaeological sites of Harappan Civilization located in Bagasra and Datrana. According to otolith morphology, they probably the otoliths of Siluriformes Ariidae catfish, known as marine catfish. Trace element concentrations relative to Ca (23Na, 25Mg, 55Mn, 88Sr and 137Ba / 43Ca) were measured along with growth bands of otoliths. They are measured using LA-HR-ICPMS. The system is consisted with Thermo Finnigan Element XR high resolution inductively coupled plasma mass spectrometer coupled to Resonetics 193 nm excimer laser ablation system installed at Atmospehre and Ocean Research Institute. Nine modern and 16 fossil otoliths thin sections were prepared and 6 modern and 4 fossil sections were analyzed using LA-HR-ICPMS.Abrupt changes in Sr/Ca with an amplitude of as much as 3 mmol/mol within ˜2 weeks suggest fish migration between freshwater and the seawater. From a conservative mixing model for Sr/Ca of estuarine water, the fish has migrated to riverine environment sometimes in their life since the model predicts small changes in Sr/Ca of water if salinity is higher than ˜5 unit. It is rather changes in Sr concentrations in ambient water than that for water temperature or salinity in the gulf.

Keywords: otolith, trace element, oxygen isotope, LA-HR-ICPMS, Gulf of Kutch

Japan Geoscience Union Meeting 2014
(28 April - 02 May 2014 at Pacifico YOKOHAMA, Kanagawa, Japan)

MTT42-P06 Room:Poster Time:May 2 16:15-17:30

Improved 10Be preparation to reduce analytical background for earth surface process studies

YAMANE, Masako[1*] ; YOKOYAMA, Yusuke[2] ; MIYAIRI, Yosuke[2] ; HORIUCHI, Kazuho[3] ; MATSUZAKI, Hiroyuki[4]

[1]JAMSTEC, [2]AORI, Univ. Tokyo, [3]Hirosaki Univ., [4]Grad. Sch. Eng., Univ. Tokyo

Due to advancement of Accerelator Mass Spectrometry (AMS), *in situ* produced beryllium-10 (^{10}Be) in quartz has been used for earth surface process studies, such as surface exposure dating (*e.g.* Yamane *et al*., 2011), erosion rate estimations (*e.g.* Shiroya *et al*., 2012), tectonic processes (Yokoyama *et al*., 2005) and so forth (*e.g.* Gosse and Phillips, 2001). In order to expand the applicability of this technique, the sample with low ^{10}Be concentration need to be measured with high precision. This requires reduction of background that is often affected isobars (boron-10). We have conducted several attempts and found that the length of time exposed to the ambient atmosphere during the oxidization process is the most important step to increase ^{10}Be background (Yokoyama *et al*., submitted). In this presentation, we discussed our experimental results and potential improvement of topics for understanding of earth surface process.

Keywords: beryllium-10, background, earth surface process, Accerelator Mass Spectrometry

Japan Geoscience Union Meeting 2014
(28 April - 02 May 2014 at Pacifico YOKOHAMA, Kanagawa, Japan)

MTT42-P07 Room:Poster Time:May 2 16:15-17:30

Rradiocarbon pretreatment system of AORI AMS

MIYAIRI, Yosuke[1*] ; YOKOYAMA, Yusuke[1] ; YAMANE, Masako[2] ; HIRABAYASHI, Shoko[1]

[1]Atmosphere and Ocean Research Institute, University of Tokyo, [2]Japan Agency for Marine-Earth Science and Technology

The Accelerator Mass Spectrometry(AMS)is effective in radiocarbon dating. By the conventional method, a large tandem accelerator(e.g.Accelerating voltage = 5MV) was used. However, the small accelerator(e.g.Accelerating voltage = 500kV) is used in the new AMS analysis.

The small AMS machine is handy.We installed small AMS machine in our laboratory. We will present the outline of new AMS pretreatment system and the geochemical application research using that.

Keywords: Radiocarbon, AMS, Accelerator Mass Spectrometry, 14C

Japan Geoscience Union Meeting 2014
(28 April - 02 May 2014 at Pacifico YOKOHAMA, Kanagawa, Japan)

MTT43-01 Room:311 Time:May 1 15:15-15:30

Multi-site infrasound observation around Syowa station, Antarctica

KAKINAMI, Yoshihiro[1*] ; OKADA, Kazumi[6] ; YAMAMOTO, Masa-yuki[1] ; KANAO, Masaki[2] ; MURAYAMA, Takahiko[3] ; MATSUSHIMA, Takeshi[4] ; ISHIHARA, Yoshiaki[5]

[1]Kochi University of Technology, [2]National Institute of Polar Research, [3]Japan Weather Association, [4]Institute of Seismology and Volcanology, Faculty of Sciences, Kyushu University, [5]JAXA Space Exploration Center, Japan Aerospace Exploration Agency, [6]Institute of Seismology and Volcanology, Faculty of Science, Hokkaido University

Infrasound is one of the frontier fields in geophysics to observe atmospheric events. World wide infrasound observing network has been constructed as the CTBTO (Comprehensive Nuclear-Test-Ban Treaty Organization) to detect infrasound signal from huge artificial explosions, however, the CTBTO infrasound observing stations usually catch the natural infrasonic waves generated by many geophysical events, like volcanic eruptions, earthquakes, tsunamis, etc. For example, when a huge meteorite fall was observed near Chelyabinsk, Russia in 2012, the induced infrasonic waves reached to many distant CTBTO stations more than 10,000 km apart from. In the polar region, there exists local infrasound sources generated mainly by the ice sheets on ground, ice field, and glacier motions. Icequakes have been frequently monitored by seismic stations in polar region, however, monitoring of induced atmospheric infrasonic waves through lithosphere-atmosphere coupling is still in progress. We installed an infrasound sensor at Syowa station, Antarctica in 2008 during IPY (International Polar Year) period by JARE (Japanese Antarctic Research Expedition) 49 mission. However, the direction-finding of the infrasonic waves is significant to study the comparison between the seismic data, thus, 2 sensors were added on Syowa to make a triangle sensor array in 2013 by JARE 54. In addition, 5 more sensors were installed at 5 locations around Syowa in 2013 (Murayama et al., 2013).

The infrasound data observed at Syowa can be transferred to Japan via satellite connection, however, the data recorded by data logger at the stations near Syowa cannot be obtained without visiting there. In JARE 55 mission, we obtained one-year infrasound observation data recorded at several stations around Syowa and will return them back to Japan in March 2014. In this paper, we will introduce some preliminary results obtained in Antarctica as the first multi-site infrasound observation at the frozen continent.

Keywords: ifrasound, Antarctica, multi-site observation, JARE, ice quake

Japan Geoscience Union Meeting 2014
(28 April - 02 May 2014 at Pacifico YOKOHAMA, Kanagawa, Japan)

MTT43-02 Room:311 Time:May 1 15:30-15:45

Characteristic features of infrasound waves observed at Antarctica

KANAO, Masaki[1*] ; MURAYAMA, Takahiko[2] ; YAMAMOTO, Masa-yuki[3] ; ISHIHARA, Yoshiaki[4] ; KAKINAMI, Yoshihiro[3] ; OKADA, Kazumi[5] ; MATSUSHIMA, Takeshi[6]

[1]National Institute of Polar Research, [2]Japan Weather Association, [3]Kochi University of Technology, [4]Japan Aerospace Exploration Agency, [5]Hokkaido University, [6]Kyushu University

Characteristic features of infrasound waves observed at Antarctica reveal the physical interaction involving surface environmental variations in the continent and surrounding Southern Oceans. A single infrasound sensor has been continuously recorded since 2008 at Syowa Station (SYO; 39E, 69S), the Lutzow-Holm Bay (LHB), East Antarctica. The continuously recording data clearly represent a contamination of the background oceanic signals (microbaroms) during whole seasons. In austral summer in 2013, several field stations by infrasound sensors are established along the coast of the LHB. Two infrasound arrays with different diameter size are installed at both SYO (by 100 m spacing triangle) and S16 area on continental ice sheet (by 1000 m spacing triangle). Besides these arrays, two isolated single stations are deployed at two outcrops in LHB. These newly established arrays clearly detected the propagating directions and frequency contents of the microbaroms from Southern Ocean. Microbaroms measurements are a useful tool for characterizing ocean wave climate, complementing other oceanographic and geophysical data in the Antarctic. Moreover, several kind of remarkable infrasound signals are demonstrated, such as regional earthquakes, together with a detection of the airburst shock waves generated from meteorite injection at the Russian Republic on 15 February 2013. Detail and continuous measurements of the infrasound waves in Antarctica could be a new proxy for monitoring a regional environmental change as well as temporal climate variations in high southern latitude.

Keywords: infrasound, array observations, Lutzow-Holm Bay, East Antarctica, microbaroms, surface environment

Japan Geoscience Union Meeting 2014
(28 April - 02 May 2014 at Pacifico YOKOHAMA, Kanagawa, Japan)

MTT43-03 Room:311 Time:May 1 15:45-16:00

Monitoring snow avalanches by using infrasound with an object of establishing remote detection system of snow avalanches

ARAI, Nobuo[1] ; MURAYAMA, Takahiko[1*] ; IWAKUNI, Makiko[1] ; TANIMOTO, Saki[2] ; TAKAHASHI, Daisuke[2] ; KURIHARA, Yasushi[2] ; ARAKI, Keiji[2] ; YAMAMOTO, Masa-yuki[3]

[1]Japan Weather Association, [2]Railway Technical Research, [3]Kochi University of Technology

It has been demonstrated that avalanches produce strong infrasonic vibrations in air during their movement (Bedard, 1988[1], Hejda, 1995[2]). These infrasonic vibrations propagate great distances and can follow the natural relief. This fact shows that it is possible to monitor remotely the snow avalanche by using infrasound detection system.

We aim to establishing remote detection system of snow avalanches. In order to study the feature of the signal associated with snow avalanches, as a first step, we carried out trial infrasound observation simultaneously with the video monitoring and the meteorological observation at mountainous region in Niigata Prefecture from January to April 2013. During the trial observation, some infrasound signals generated by snow avalanches were recorded. We analyzed these data and attempted to extract features from infrasound signals.

[References]

[1] Bedard, A. J. et al. 1988. On the feasibility and value of detecting and characterizing avalanches remotely by monitoring radiated sub-audible atmospheric sound at long distances. Proc. A Multidisciplinary Approach to Snow Engineering, Santa Barbara, CA.

[2] Hejda, D. 1995. Caracterisation de l'emission acoustique des avalanches, (These de diplome, E. P. F. Lausanne, Suisse.)

Keywords: Infrasound, Snow avalanches, Avalanche monitoring

Japan Geoscience Union Meeting 2014
(28 April - 02 May 2014 at Pacifico YOKOHAMA, Kanagawa, Japan)

MTT43-04 Room:311 Time:May 1 16:15-16:30

Micro-barometric variation associated with rainfall

IYEMORI, Toshihiko[1] ; SANO, Yasuharu[2*] ; HAYASHI, Taiichi[3] ; ODAGI, Yoko[1] ; AOYAMA, Tadashi[1] ; NAKANISHI, Kunihito[1]

[1]Graduate School of Science, Kyoto University, [2]Asahi University, [3]DPRI, Kyoto University

A sudden rainfall (shower) is often preceded by a micro-barometric variation. To examine quantitative relationships between them, we conducted observations of micro-barometric, rainfall and absorption of BS broadcasting radio waves and recorded the data with one second resolution.

As a result, we often observed the events where a pressure increase starts about one minute before a strong rainfall. Just after the start of the rainfall, micro-barometric variation with period about a few minutes were also observed. These results suggest that the dynamic pressure associated with the falling rain drops pushes the air and observed as a gradual increase of the pressure on the ground. If this is the case, a rarefaction waves may propagate upward over the rain cloud. In this paper, we will show the results obtained from many events.

Keywords: micro-barometric variation, gravity wave, rainfall, acoustic gravity wave

Japan Geoscience Union Meeting 2014
(28 April - 02 May 2014 at Pacifico YOKOHAMA, Kanagawa, Japan)

MTT43-05 Room:311 Time:May 1 16:30-16:45

Ionospheric disturbances by volcanic explosions: Observations with GNSS

NAKASHIMA, Yuki[1*] ; HEKI, Kosuke[1]

[1]Dept. Natural history sciences, Graduate school of science, Hokkaido Univ.

There have been numbers of reports that atmospheric waves, e.g. internal gravity waves and acoustic waves, excited by various natural or artificial phenomena on the ground, shake up the ionospheric F layer as high as 300 km [Calais et al., 1998 GJI; Heki and Ping, 2005 EPSL]. Acoustic waves from volcanic eruptions are observed as infrasound in near fields, but they also propagate upward and cause ionospheric disturbances [Heki, 2007 GRL]. We try to reveal the characteristics of ionospheric disturbances caused by volcanic explosions using Total Electron Content (TEC) data derived at the dense array of ˜1240 Global Navigation Satellite System (GNSS) stations in the Japanese GEONET.

Heki [2006] detected TEC changes of ˜0.1 TECU in the region to the south - southeast of the volcano ˜10 minutes after the explosion of the Asama Volcano, central Japan, on Sep. 1, 2004, at 11:02 UT. He estimated the atmospheric wave energy from the amplitude of TEC disturbances, and inferred the explosion energy by comparing the TEC change amplitudes with those caused by an artificial explosion with known energy [Calais et al., 1998]. Later, Dautermann et al. [2009 JGR] performed a similar study for the 2003 explosion of the volcano in the Montserrat Island, West Indies.

Here we report on the TEC disturbances caused by the explosion of the Kirishima-Shinmoe volcano, southern Kyushu, Jan. 31 2011, 22:54 UT. According to the JMA documents issued in 2011 January, this explosion induced the infrasound of ˜458 Pa, which blasted some window glasses in Kirishima-city, Kagoshima. We also detected 0.2-0.3 TECU peak-to-peak amplitude disturbances after the 2009 October explosion of the Sakurajima volcano, southern Kyushu. They appeared 10 minutes after the explosion and propagated southward with a sound speed at the F layer height. In contrast to the period of ˜4 minutes of typical coseismic ionospheric disturbances, TEC changes by volcanic explosions were found to have periods of ˜2 minutes or shorter.

In the presentation, we will compare new examples of ionospheric disturbances by volcanic explosions, such as the 2011 Shinmoe and 2009 Sakurajima cases, with older cases such as the 2004 Asama case.

Keywords: GPS, GNSS, infrasound, acoustic wave, volcanic explosion, ionosphere

Japan Geoscience Union Meeting 2014
(28 April - 02 May 2014 at Pacifico YOKOHAMA, Kanagawa, Japan)

MTT43-06 Room:311 Time:May 1 16:45-17:00

Simulation of ionospheric variations caused by acoustic waves generated in the lower atmosphere

SHINAGAWA, Hiroyuki[1*]

[1]NICT

In the lower atmosphere of the earth, acoustic-gravity waves are generated by various kinds of natural and artificial sources, such as cumulus clouds, tornados, typhoons, earthquakes, tsunamis, volcanic eruptions, meteor impacts, nuclear explosions, rocket launches, etc. Previous theoretical and observational studies have suggested that acoustic-gravity waves induced by such sources can propagate up to the upper atmosphere, producing temporal and spatial variations in the thermosphere and in the ionosphere. However, specific mechanisms of upper atmospheric variations caused by the acoustic-gravity waves have not yet been fully understood because the atmosphere-ionosphere system is an extremely complicated and nonlinear, and it is easily disturbed by many other sources in the atmosphere and in space. In order to quantitatively study the ionospheric variations caused by tsunami-driven acoustic-gravity waves of the 2004 Sumatra earthquake and 2011 Tohoku-oki earthquake, we developed a nonhydrostatic compressible atmosphere-ionosphere model. The model successfully reproduced atmospheric waves and large-scale electron density variations that are caused by tsunami-driven acoustic-gravity waves. We are now developing an atmosphere-ionosphere model with higher spatial resolution and more realistic parameters. We expect that the model is able to reproduce atmospheric-ionospheric phenomena associated with infrasonic and gravity waves produced by various kinds of phenomena. We will report previous results and future prospects.

Keywords: acoustic wave, lower atmosphere, upper atmosphere, ionosphere, simulation, model

Japan Geoscience Union Meeting 2014
(28 April - 02 May 2014 at Pacifico YOKOHAMA, Kanagawa, Japan)

MTT43-07 Room:311 Time:May 1 17:00-17:15

Low-frequency atmospheric pressure waves associated with the outer-rise earthquake on Oct. 25, 2013, 17:10 UTC.

ARAI, Nobuo[1*] ; IWAKUNI, Makiko[1] ; MURAYAMA, Takahiko[1] ; NOGAMI, Mami[1]

[1]Japan Weather Association

Sensitive microbarographs in and around Japan recorded unequivocal signals associated with the 2011 Off the Pacific Coast of Tohoku, Japan earthquake (Mw = 9.0) (*Arai et al., 2011*).

These signals retained the original shape of the tsunami and traveled in the atmosphere significantly faster than the tsunami waves in the ocean, therefore, we think that an establishment of a network of infrasound observation along the coast line facing the subduction zone would improve the tsunami warning system.

According to this idea, we deployed three (3) microbarograph stations in Ofunato City, Iwate last July as the first step of the establishment of a network of infrasound observation and are trying to observe atmospheric pressure changes continuously.

The outer-rise earthquake occurred off the Fukushima region on Oct. 25, 2013, 17:10 UTC and the tsunami waves with few tens centimeter heights observed at coastal area of Tohoku region. And some curious atmospheric pressure waves detected at our Ofunato sites. The characteristics of the observed signals are consistent with the features of the tsunami source produced by the outer-rise earthquake.

Reference:

Arai et al. , Atmospheric boundary waves excited by the tsunami generation related to the 2011 great Tohoku-Oki earthquake, Geophysical Research Letters, Vol. 38, L00G18, doi:10.1029/2011GL049146.

Keywords: Infrasound, atmospheric pressure change, outer-rise earthquake, detection of tsunami

Japan Geoscience Union Meeting 2014
(28 April - 02 May 2014 at Pacifico YOKOHAMA, Kanagawa, Japan)

MTT43-08 Room:311 Time:May 1 17:15-17:30

Examination on Numerical Simulation of Tsunami-Induced Extremely Low Frequency Sound Waves with Geospatial Information

OKUBO, Kan[1*] ; KAWASHIMA, Ken[1] ; OSHIMA, Takuya[2] ; TAKEUCHI, Nobunao[3]

[1]Graduate School of System Design, Tokyo Metropolitan University, [2]Faculty of Engineering, Niigata University, [3]Graduate School of Science, Tohoku University

Air pressure changes associated with earthquakes and/or tsunami have been investigated previously. As for air pressure changes associated with tsunami, some observation results have been reported (T. Mikumo (1964), T. Mikumo, et al. (2008) and William L. Donn and Eric S. Posmentier (1964), Y. Tamura (2011), N. Arai, et al. (2011)).

We have measured the air pressure in the terrestrial atmosphere with other meteorological parameters (temperature, humidity, etc.) continuously at Hosokura outdoor observation station (HSK) in Miyagi Prefecture, Japan. The extremely low frequency sound waves (so-called micro barometric waves) are also detected as large changes of air pressure in the 2011 off the Pacific coast of Tohoku Earthquake (M 9.0, origin time;14:46.18JST) (K. Okubo, et al. (2011)).

Although the power failure was caused by the earthquake occurrence, our observation system had been maintained by the UPS system and the private power generation. Therefore, in this earthquake, our observation system successfully observed extremely low frequency sound waves induced by tsunami. The waves were detectable at the observation point on the ground surface sufficiently early before the arrival of tsunami waves at coastal areas, because sound waves propagate faster than ocean waves (tsunami).

These results can encourage early tsunami detection (S. Iwasaki (1992), T. Izumiya (1994)) using multi-site observation and arrival time difference method. That is, detection of tsunamis might be possible by monitoring extremely low frequency sound waves at ground surface observation sites and/or sea-level observation at relatively low cost. It is important to obtain information of tsunami as soon as possible; arrival time, area and scale.

In this study we present a fundamental examination on analysis and visualization of extremely low frequency sound waves caused by tsunami using numeral approach. We employ the numerical simulation using the Finite-Difference method in Time-Domain (FDTD method) (Yee, 1966) with geospatial information for the large-scale sound wave propagation. As an elementary study, it is applied to the estimation of extremely low frequency sound waves' propagation and time-series analysis of sound pressure.

Through our study, we show the numerical results of sound pressure distribution and estimate the propagation phenomena of sound waves, compared with the observed data at HSK. This examination may help the development of the design of early tsunami detection system. In the future, further efforts can suggest new systems for early warning of destructive tsunami using a combination of other measurements.

We are grateful to Hosokura Metal Mining Co. for the maintenance of our site. This research was partially supported by a Grant-in-Aid for Scientific Research from the Japan Society for the Promotion of Science.

Keywords: Numerical Simulation, tsunami, sound field change, microbarometric wave, infrasound, numerical visualization

Japan Geoscience Union Meeting 2014
(28 April - 02 May 2014 at Pacifico YOKOHAMA, Kanagawa, Japan)

MTT43-09 Room:311 Time:May 1 17:30-17:45

Atmospheric Gravity Waves from the 2010 Maule, Chile earthquake (Mw8.8)

MIKUMO, Takeshi[1*] ; IWAKUNI, Makiko[2] ; ARAI, Nobuo[2]

[1]Kyoto University, [2]Japan Weather Service, [3]Japan Weather Service

Atmospheric pressure waves were recorded after the 2010 Maule, Chile earthquake (Mw=8.8) by microbarographs at seven International Monitoring System (IMS) stations in the distance range up to 7,680 km. By applying bandpass-filtering, we extracted low frequency gravity waves, removing atmospheric noise and higher-frequency acoustic modes, and then estimated their phase velocities around 332-341 m/s. To compare with these observations, we constructed synthetic waveforms, referring to the source dimension and coseismic vertical ground displacements based on geodetic measurements (Moreno et al., 2012), and incorporating a standard atmospheric sound velocity structure up to a height of 220 km. The comparison between the observed and synthetic waveforms provides generally satisfactory agreement, and suggests the time constant of ground displacements between 2 and 3 min in the northern and southern segments of the entire source region extending for about 500 km..

Keywords: 2010Maule, Chile earthquake, Mw=8.8, low-frequency, Atmospheric gravity waves

Japan Geoscience Union Meeting 2014
(28 April - 02 May 2014 at Pacifico YOKOHAMA, Kanagawa, Japan)

MTT43-P01 Room:Poster Time:May 1 18:15-19:30

High resolution barometer array in Palau, Western Pacific

ISHIHARA, Yasushi[1*] ; FUKAO, Yoshio[1] ; SHITO, Azusa[2] ; OBAYASHI, Masayuki[1] ; SHIROOKA, Ryuichi[1]

[1]JAMSTEC, [2]Institute for Geothermal Sciences, Kyoto University

The Variety of waves is propagating in the atmosphere, ocean and solid earth. And there are interacting between each layer. For total and integrated understanding, multi parametric measurement over different field is required. We target Palau islands, western Pacific for multi parametric measurement. We are operating broadband seismic station in a station of Pacific Geophysical Network (OHP network). And another seismic station is also under operation due to removing of seismic station. Meteorology group of JAMSTEC has their station including meteorological radar. We think that Palau is fine condition to construct integrated geophysical measurement field. So that we deployed high resolution barometric small array in Palau.

Palau locates tropical zone and its daily weather condition is similar and relative more stable than middle latitude zone and polar area that have some day's variation and passing of front. In our research, one of mail focuses is very low frequency band of barometric variation; the ambient condition has merit to get accurate detection of signal.

As for observation system, sensor is quartz oscillation type high resolution barometer and recorder is Linux Box via serial communication. We set to be sampling of 2 sps to get high resolution data. We installed Five(5) stations in Palau whose station interval is about 20km. Two stations of them locate at seismic stations and another station is same area with weather station. The array is operating from August, 2013 and is under operation.

The tentative data review shows atmospheric gravity wave is frequently recorded in longer period of 200sec. Sometimes event pulse-like signals are detected. Apparent velocity of these waves is 20 ? 30 m/s and direction of propagation varies daily. Most signal arrives from outside of this array. We report character of these wave and relation with meteorological condition.

Keywords: atmospheric gravity wave, micro seism

Japan Geoscience Union Meeting 2014
(28 April - 02 May 2014 at Pacifico YOKOHAMA, Kanagawa, Japan)

MTT43-P02 Room:Poster Time:May 1 18:15-19:30

Improvement and evaluation of optical-type infrasound sensor for multi-site observation

IKEHARA, Kousuke[1*] ; YAMAMOTO, Masa-yuki[1] ; KAKINAMI, Yoshihiro[1] ; ISHIHARA, Yoshiaki[2]

[1]Kochi University of Technology, [2]JAXA Space Exploration Center, Japan Aerospace Exploration Agency

Infrasound is applicable for remote-sensing methods for detecting geophysical phenomena in the atmosphere. There have been developed and used many types of infrasound sensors, however, typically used infrasound sensors are almost developed by foreign countries, resulting high cost situation in Japan. If we can develop low cost infrasound sensors, multi-site arrayed observation will be realized in near future.

Recently, infrasound signal generated by tsunami was clearly detected by many CTBTO infrasound stations (Arai et al., 2011), suggesting a new era for establishing a dense infrasound sensor network in every prefecture of Japan for preventing or reducing catastrophic disasters. Because the nature of pressure waves with large wavelength, amplitude of infrasound generated by tsunami might be proportional to the size of the disasters. Combination with sensor networks of seismometers on ground and ocean floor, GPS-buoy type wave recorders, and water manometers on ocean floor, establishing a dense network of infrasound sensors with arrayed configuration is desired.

Since 2006, we have been developing new sensing method of infrasound by using piezo film and PSD (Position Sensitive Detectors), achieving frequency range between 0.001 Hz and 10 Hz as well as minimum pressure level of 0.01 Pa (Yamamoto and Ishihara, 2009). In 2013, we tried downsizing the PSD type infrasound sensor developed in 2008 into a size of 0.15 m x 0.15 m x 0.25 m height with calibrating it by using space chamber (0.8 m length x 0.58 m diameter) as an accurate volume pressure reservoir (Manabe et al., 2013). Here, we improved the PSD optical-type infrasound sensor by using 3D printer technology to make many tiny parts designed with 3D CAD software.

By pushing and pulling a small amount of air by a small syringe, calibrating pressure waves with extremely weak amplitude (10 Pa to 0.01 Pa) can be generated in the space chamber, precise measurement of artificially generated infrasonic signals could be realized. The waves were measured by both of the developed PSD sensor and Chaparral Model-2.5 infrasound sensor at the same time. Comparison with output signals by two types of sensors, the downsized PSD type infrasound sensor was carefully studied. In this paper, we will introduce the new design and obtained calibrating datasets.

Keywords: infrasound, multi-site observation, sensor development, optics, measurement, low-cost

Japan Geoscience Union Meeting 2014
(28 April - 02 May 2014 at Pacifico YOKOHAMA, Kanagawa, Japan)

MTT43-P03 Room:Poster Time:May 1 18:15-19:30

Pressure sensors detected wind noise produced in wind tunnel

IWAKUNI, Makiko[1*] ; YAMAMOTO, Masa-yuki[2] ; TANIMOTO, Saki[3] ; KAKINAMI, Yoshihiro[2] ; IKEHARA, Kosuke[2] ; OKADA, Kazumi[4] ; ARAKI, Keiji[3] ; KURIHARA, Yasushi[3] ; ARAI, Nobuo[1] ; MURAYAMA, Takahiko[1] ; NOGAMI, Mami[1]

[1]Japan Weather Association, [2]Department of systems engineering, Kochi University of Technology, [3]Railway Technical Research Institute, [4]Imstitute of Seismology and Volcanology, Hokkaido University

As infrasound and pressure disturbance induced by local wind around infrasound sensors are partially in the same frequency range, amplitude of the infrasound signal is sometimes lower than that of pressure disturbance by strong wind. Thus, obtaining the infrasound signal by analyzing software from the observation data with such wind noises is one of the technical objectives to solve. Usually, some porous pipes connected with the infrasound sensors have been used in order to reduce such local wind disturbances.

To evaluate such system for wind noise reduction, we conducted experimental study by using a wind tunnel with wind speed up to 60 m/s. We used nano-resolution pressure transducer (6000-16B manufactured by Paroscientific Inc., USA) and microphone type infrasound sensors

(Chaparral physics, Model25 manufactured by Univ. of Alaska Fairbanks) in the wind tunnel of the Railway Technical Research Institute (RTRI), Japan. In this presentation, we will show the relationship between the wind speed and porous pipe configuration installed in the wind tunnel.

In this presentation, we show the relation between wind speed and pipe direction.

Keywords: Infrasound, wind noise reduction, pipe reduction system, wind tunnel

Japan Geoscience Union Meeting 2014
(28 April - 02 May 2014 at Pacifico YOKOHAMA, Kanagawa, Japan)

MTT44-01 Room:311 Time:May 2 14:15-14:30

Legacy Technology Still in Use: Lessons from FLOSS Development

BABA, Yoshihiko[1*]

[1]Ritsumeikan University

1. Introduction

In science, including geospatial and earth science, use of the Internet is becoming more and more important. Institutions provide more and more, spatial data and scientists share the information or work on a project regardless of geographical boundary. In such situation, social media will be becoming more and more important, but the popularity changes so easily. On the other hand, there are several social tools which have been around for more than 30 years, such as IRC and CVS/Subversion/git. In this paper, the advantages and disadvantages of the current and legacy social tools.

2. Underlying Philosophy

IRC and CVS/Subversion/git are very popular among free and libre open source software (FLOSS) developers. One of the most important factor of free software was revealed by Eric Raymond, who contrasted two different free software development models:

The cathedral model: source code is available with each software release, but code developed between releases is restricted to an exclusive group of software developers.

The bazaar model: the code is developed over the Internet in view of the public.

In fact, all the commercial projects and many FLOSS projects are organized in the cathedral model. The point is, only FLOSS software can be developed in the bazaar model. The most well-known project which adopted the bazaar model is perhaps Wikipedia. What can we learn from the project?

3. IRC vs twitter

There are many real time chat tools, such as IRC, Skype, Messenger, Twitter and LINE.

IRC is a communication protocol developed in 1988. In IRC, users join a server (e.g. freenode.net) using IRC clients (e.g. xchat), then joins a room (e.g. #qgis, #grass) to talk and discuss issues. It is said that there are more than 50,000 users on Freenode. The figure may be small, when compared to twitter or LINE. It is noted that the author(s) asked several Fink developers to review this article. IRC can be compared to twitter in that they are both for “short text” and real-time communication.

When using twitter, you can browse information about a certain topic using hash tag (#). However, twitter is in its essence a ”twit”, expressing one’s opinion and rarely becomes a place for conversation/discussion.

ITO (MTT38-01) discusses that the information is well organized at togetter by a coordinator. Byt the summary on togetter is often very difficult to read. On the other hand, chat logs of many IRC channels are very useful without any editing. Perhaps, something can be learned from IRC. But so far, my suggestion is to use IRC for scientific discussion.

4. Discussion

As seen in the previous section, there are several legacy tools that are still widely used, especially among FLOSS developers. One of the advantages of these legacy tools is that they have been evolved to support the ”cathedral” model explained above.

For geospatial and earth science, such tool may be useful to share the information of, say, open data. There are many institutions, public or private, which offer GIS data on the Internet. The official data, such as shape files provided at data.gov.uk or nlftp.mlit.go.jp/ksj/, would be more useful when one finds an error, fix it and report and/or redistribute it. The download pages may be more enhanced with wiki, where users can post their ways of using the data. Google maps, or its more ”open” alternative, OpenStreetMap, may be more sustainable if they learn more from legacy tools.

5. Conclusion

Several social tools for FLOSS development, which have been developed since 1980s, are reviewed. Some tools, such as IRC, are still used despite the recent advancement of newer social tools. In fact, these tools may be more advanced, in that they give more powers to users, than the recent and more popular social media, such as Facebook and twitter.

Keywords: FLOSS, IRC, CVS, Bug Tracking

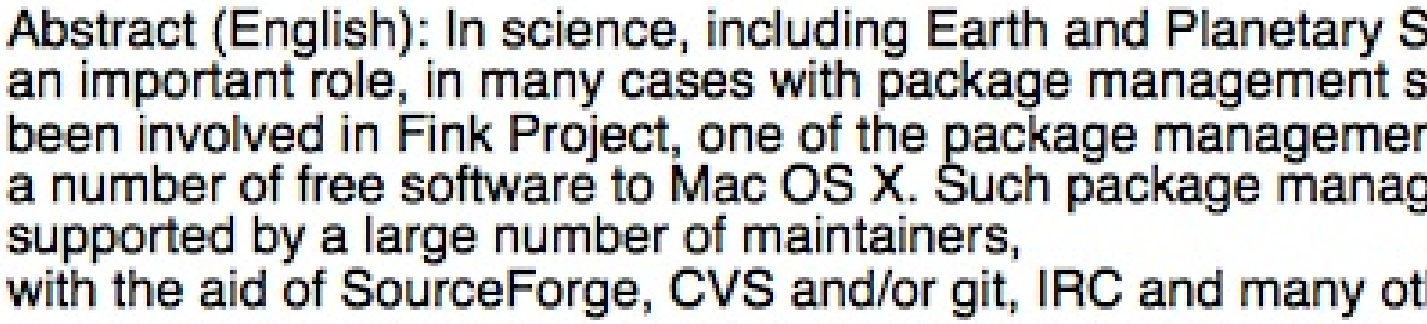
Abstract (English): In science, including Earth and Planetary S
an important role, in many cases with package management s
been involved in Fink Project, one of the package managemer
a number of free software to Mac OS X. Such package manag
supported by a large number of maintainers,
with the aid of SourceForge, CVS and/or git, IRC and many ot

Japan Geoscience Union Meeting 2014
(28 April - 02 May 2014 at Pacifico YOKOHAMA, Kanagawa, Japan)

MTT44-02 Room:311 Time:May 2 14:30-14:45

Establishing Technology of Environmental Monitoring Using Social Media

ITO, Masaki[1*]

[1]The University of Tokyo

This paper discuss the way to enable environmental monitoring using social media. Several existing approaches such as development of original software and utilizing crowdsourcing service are introduced with there advantages and disadvantages. Finally the author emphasizes the need of further research on theory and technology.

Keywords: Social Media, Environmental Monitoring, Crowdsourcing

Japan Geoscience Union Meeting 2014
(28 April - 02 May 2014 at Pacifico YOKOHAMA, Kanagawa, Japan)

MTT44-03 Room:311 Time:May 2 14:45-15:00

A Web-application for Time-dependent Observation Data for both Scientific and Social Data

MURATA, Ken T.[1*]

[1]National Institute of Information and Communications Technology

The NICT Science Cloud is one of the science clouds proposed for development of sciences. A variety of science data are collected and stored in the science cloud to be analyzed interdisciplinary. After the Internet is widely used, new concept and information technology haves shown up; semantic web and linked open data (LOD). These technologies enable information on the Internet machine readable. In many science fields, it is pointed out that the semantic web will play an important role for the interdisciplinary research works. However, there have been few ideas to be ever proposed as a methodology or roadmap to the interdisciplinary science using semantic web. Herein we present a concept of professional knowledge and academic knowledge following collective knowledge proposed as a Web 2.0. Based on the concept, we design a Web-application for interdisciplinary science. The application (named STARS touch) provides users with an environment of dynamic and light preview of any types of time-dependent data. In the demonstration, we show an example of simultaneous preview of both scientific data (satellite observation data) and social data (newspaper information).

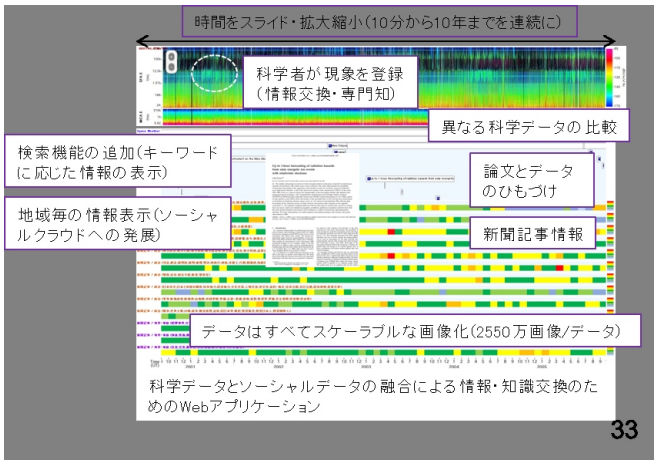

Japan Geoscience Union Meeting 2014
(28 April - 02 May 2014 at Pacifico YOKOHAMA, Kanagawa, Japan)

MTT44-04 Room:311 Time:May 2 15:00-15:15

The trial which carries out information dissemination by SNS at a high school students

AOKI, Kunihiro[1*]

[1]Nihon univ. BUZAN high school & junior high school

Even if it thinks that a teacher will take communication with a student, it is very difficult to try to be connected with a high school student.

Then, ”whether, during session, communication can be taken with a student” is important.

The method for being connected with a student in the first half is reported.

It is what ”the atmosphere which a student says easily is built for”, and ”a lesson which a student tries to hear positively that the talk is” that I take care by the lesson.

Therefore, I am made to prepare time to concentrate only for a short time several times while I accept a student’s positive remark.

As a mistake is made in being right, it catches not related to a student’s remark and its head is bowed in assent, the boundary of the mistake is clarified if behind right.

Thus, by corresponding from a student’s viewpoint, I think that a student opens the heart to a teacher.

If it comes so far, a student will be connected in SNS.

The most is a student and a graduate although the number of the followers of my Twitter is 95 now.

In order to usually disseminate the information on extension and geography of a lesson, or earth science the second half using SNS, practice using SNS is reported.

Even if it can take communication by SNS with the present condition and a student, there is no reaction in the photograph and comment related to geography.

Most of the reasons are a thing with a ”petty” photograph, and a thing with ”many” character numbers.

For example, even if it shows the photograph of a terrace, only the comment ”it is peaceful” comes.

If the number of characters exceeds 70 characters, it is tired of reading a character.

It is adiaphorous, even if the contents of the photograph also have a reaction in the direction where the scene is mixed and it shows geographical feature, vegetation, etc.

The photograph about geography is published, and since a result which is considered even if it is going to ask for a comment or is going to offer teaching materials has not come out, I would like to obtain a comment from you, although SNS is convenient.

Keywords: Twitter, Line, Lesson

Japan Geoscience Union Meeting 2014
(28 April - 02 May 2014 at Pacifico YOKOHAMA, Kanagawa, Japan)

MTT44-05 Room:311 Time:May 2 15:15-15:30

Social media as a source of innovative ideas for education and outreach in geoscience

OGUCHI, Takashi[1*] ; ISHIKAWA, Hajime[1] ; HASHIMOTO, Mari[2]

[1]CSIS, Univ. Tokyo, [2]Meiji Gakuin Univ.

Scientists are often expected to contribute to education and outreach in their specialized fields. They can provide scientifically accurate information about their fields based on deep knowledge. However, they may be much affected by the customs and common sense of their fields, and may not be good at attracting attention of people who do not have specialized knowledge in the fields. Social media contribute to the reduction of this problem, through interactions of people with various backgrounds. Scientists of a particular field often interact with those who are interested in the field but have different backgrounds including non-scientists. Such people sometimes provide scientists with novel ideas for effective education and outreach. Subsequent comments from scientists on the ideas may be useful for those who provided the ideas. In this presentation, we discuss such constructive interactions among persons in social media, with reference to geomorphological examples.

Keywords: social media, education, outreach, interaction among persons

Japan Geoscience Union Meeting 2014
(28 April - 02 May 2014 at Pacifico YOKOHAMA, Kanagawa, Japan)

MTT44-06 Room:311 Time:May 2 15:30-15:45

The possibility and current issues of sharing information with social media in geoparks

NIINA, Atsuko[1*]

[1]Regional Innovation Research Center, Tottori University of Environmental Studies

This presentation reports on the possibility and current issues of sharing information with social media in the case of San-in Kaigan Gelobal Geopark. Sharing knowledge and experiences is necessary for the development of the geopark network. Communication is one of the best ways to share them among people. There are various ways of communication; for instance, face-to-face communication, non-face-to-face communication, mass media and social media. In the case of San-in Kaigan Geopark which spans across 110 km from east to west and 30 km from north to south, social media is a complementary tool to communicate among local actors, stakeholders and shareholders in the wide territory of the geopark.

Keywords: social media, communication, sharing information, San’in Kaigan Geopark

Japan Geoscience Union Meeting 2014
(28 April - 02 May 2014 at Pacifico YOKOHAMA, Kanagawa, Japan)

MTT44-07 Room:311 Time:May 2 15:45-16:00

”San’in Kaigan Geopark ∗Fortune Cookie in Love” Project

KOYAMA, Makoto[1] ; FURUKAWA, Tomoko[1] ; MATSUBARA, Noritaka[2*]

[1]San’ in Kaigan Geopark Promotion Council, [2]Inst. Nat. Env. Sci., Univ. Hyogo

San’in Kaigan Geopark Promotion Council conducts ”Questionnaire on Recognition of San’in Kaigan Geopark” every year. In a questionnaire survey conducted at PR campaign in Keihanshin area in 2013, San’in Kaigan Geopark recognition was low among 10s (27%) and 20s (24%) compared to 70s over (68%). An issue for the future is considering ways to raise awareness of geopark activities among young people. One of the reasons why many young people are not familiar with geopark is insufficient PR activity through the use of the internet. Now the council provides information available on the official website and Facebook. The problem is that those websites are not well-known to the general public.

For this reason, San’in Kaigan Geopark undertook ”San’in Kaigan Geopark ∗Fortune Cookie in Love” Project, which local guides, tourism facilities, local residents, geopark-related officials and researchers dance along ”Fortune Cookie in Love”- by J-pop’s most popular girl group AKB48. We uploaded a video to Youtube on January 31, 2014 and promote the San’in Kaigan Geopark to the general public. There are 43 different scenes and 265 wonderful performers including mascots in about 4-minute video. Organized yet creative dancing entertains those who watch the video. We also advertise it to the media, and people who access to this video on Youtube easily exceed 10,000.

From now on, we will analyze the awareness and the effect of this project through a questionnaire and any changes in the number of visitors across the San’in Kaigan Geopark.

Keywords: sns, youtube, Fortune Cookie in Love, San’in Kaigan, geopark

Japan Geoscience Union Meeting 2014
(28 April - 02 May 2014 at Pacifico YOKOHAMA, Kanagawa, Japan)

MTT44-08 Room:311 Time:May 2 16:15-16:30

San'in Kaigan Geopark Tourism Promotion By Female Bloggers

ANDO, Kazuya[1*] ; NAKATANI, Hideaki[1] ; OOE, Seiji[1] ; ISHIGAMI, Nobuyuki[1]

[1]San'in Kaigan Global Geopark Promotion Office

While there is a strong trend among independent travelers to gather information and plan trips within Japan through the use of the internet and word-of-mouth information, there is a lack of information regarding geotourism available online. In response to this situation, a number of San'in Kaigan Geopark model tours were operated in Tottori Prefecture. These were promoted by female bloggers who are popular and influential in the independent tourism market. In 2012 and 2013, a total of 70 female bloggers established their own themes and planned trips to the San'in Kaigan Geopark. Each blogger posted their travel reports on their blog sites and on twitter. At the same time, a "San'in Kaigan Geopark Model Tours for Women" facebook page was established so that each of the travel reports could be posted and shared. As a result of this continual availability of travel information, San'in Kaigan Geopark related pages received a high number of online hits, and increased awareness and popularity regarding the Geopark was achieved.

Keywords: San'in Kaigan Geopark, Tours for Women, Geotourism, Female Bloggers

Japan Geoscience Union Meeting 2014
(28 April - 02 May 2014 at Pacifico YOKOHAMA, Kanagawa, Japan)

MTT44-P01 Room:Poster Time:May 2 16:15-17:30

Effects and issues of information transmission using the social media in a large active geopark

MATSUBARA, Noritaka[1*]

[1]Inst. Nat. Env. Sci., Univ. Hyogo

The San'in Kaigan Geopark is located in the west of Japan, spanning approximately 120km from its easternmost point, at Kyogamisaki Cape in the city of Kyotango, to its westernmost point, on the Aoyakaigan Coast in the city of Tottori, and measuring a maximum of 30km from north to south.

In terms of administrative jurisdictions, the Geopark spans a total of three cities and three towns in 3 prefectures (Kyoto Prefecture, Hyogo Prefecture, Tottori Prefecture).

Sharing and generating information is difficult in such a large active geopark. Then, we decided to use a social media to share and generate information smoothly. We created fan page of the geopark to Facebook. We have established an administrator in each area to generate regional information.

Keywords: geopark, facebook, San'in Kaigan Geopark, social media

Japan Geoscience Union Meeting 2014
(28 April - 02 May 2014 at Pacifico YOKOHAMA, Kanagawa, Japan)

MTT44-P02 Room:Poster Time:May 2 16:15-17:30

Utilization of facebook for the management of working groups in North Ibaraki Geopark

AMANO, Kazuo[1*] ; HOSOI, Jun[2] ; IBARAKI UNIVERSITY, Geological information utilizing project[1]

[1]Faculty of Science, Ibaraki University, [2]Graduate School of Science and Engineering, Ibaraki University

Exchange of information with SNS like Twitter, foursquare, facebook has been done in the North Ibaraki Geopark (Saito et al., 2010; Ito et al., 2011, 2012; Amano et al., 2012, 2013). Facbook is very useful for the management of the North Ibaraki Geopark because it has many capabilities such as file upload and event planning etc. Recently, Utilization of facebook for management of four working groups in the North Ibaraki Geopark is carried out. Members of each working group successfully discuss or communicate many things for the management of the North Ibaraki Geopark.

Keywords: SNS, geopark, North Ibaraki Geopark, facebook

Japan Geoscience Union Meeting 2014
(28 April - 02 May 2014 at Pacifico YOKOHAMA, Kanagawa, Japan)

MTT44-P03 Room:Poster Time:May 2 16:15-17:30

Study on the socialized development environment in the geospatial informations field

SETO, Toshikazu[1*]

[1]Center for Spatial Information Science, the University of Tokyo

1. Introduction

The deployment of the technology and systems for geospatial information is the spread of the open-source movement and culture since 2000, opening up of technology and information has come to be regarded as important in the GIS field (Sui, 2014). This open culture is expected to spread to social, political, and economic areas, such as Open Government. This is an important point for government that have not gone far enough to implement GIS, but the platform is beginning to be wide open.

The major features of GIS technology since the 2010s have been open source code, various code development platforms and interfaces, translation of software documentation, concept creation for application development, and cloud computing which has led to social interaction and cooperation. In this study, mainly in the Free and Open Source Software for Geospatial (FOSS4G), we examine the actual situation of the socialized open developing environment for GIS technology and consider whether that is a problem and what are its effects.

2. Platform to support the socialized developing environment

The Quantum GIS (QGIS) is a desktop open-source GIS software from the Open Source Geospatial (OSGeo) Foundation to support the development and publication of source code that has been made available through repositories such as Source-Forge. GitHub is a Web-based hosting service for software development projects, which started gaining popularity around 2010. Transifex, which was founded in 2008, has emerged as a Web-based translation platform. It provides variety and takes better advantage of the version control system than Git, and it tracks changes in programs such as forks that incorporate a user's own code as part of the development project, and it provides for fluid use of source code. In fact, we have started to migrate to system of Git from SVN, the platform for Web maps for applications such as Ushahidi. As a localization system on the Web, Transifex provides convenient visualization of progress and a translation interface. Transifex has been used to translate 20 or more OSGeo projects including QGIS software with Japanese versions of all projects. In addition, translations of QGIS user manuals can be incorporated directly into the software, and the translation of case studies of open data, such as in the use case, do not matter, because they are shared as a target.

3. Challenges that the effects of social networking bring to openness

Social networking in open-source software development, such as with Transifex and GitHub, is creating many opportunities for GIS technology. For example, Harvard University has developed an open-source package in which geospatial information from various libraries are combined based on Geonode. Also in Japan, use of platforms such as IdeaLinkData and CityData that allow social sharing of regional data is increasing, and more involvement of various actors using GIS is expected. Additionally, with increased participation opportunities for data users and developers through the Web, and to develop open data events such as Hackathon, which began recently in Japan, this trend in data and source code is also becoming a medium to provide resources directly.

However, while open-source social networking accelerates development, product development itself is being subdivided into code for individual functions and, due to different versions in the library, errors can increase. In addition, mutual information exchange between developers is spread by social networking, with smaller contributors able to lead the development as compared to developers from the English-speaking countries. Therefore, it is expected that social networking will contribute to the generation of open data as well as to software development and translation to support visualization and data manipulation of geospatial information, such as the introduction in GIS education and the creation of opportunities for participation.

Keywords: open culture, FOSS4G, crowdsourcing, GitHub

Japan Geoscience Union Meeting 2014
(28 April - 02 May 2014 at Pacifico YOKOHAMA, Kanagawa, Japan)

MZZ45-01 Room:422 Time:April 29 14:15-14:30

Edmund Naumann (1854-1927) and Mt Fuji

YAJIMA, Michiko[1*]

[1]Tokyo Medican and Dental University

Edmund Naumann (1854-1927) and Mt Fuji
Michiko YAJIMA

Mt Fuji is the highest mountain in Japan at 3776 m. In 2013 Mt Fuji was added to the World Heritage List as a Cultural Site. Japanese people, young and old, man and woman, climb Mt Fuji for religious reason since the old age. Scientific research on Mt Fuji started at the Meiji Era by the foreigners. Before 1854 Japan closed the doors to the Westerners. Once opened the door to the Westerners, Meiji Government hired many foreign teachers.

Edmund Naumann (1854-1927) came to Japan in 1875, became the first professor of Geology in the University of Tokyo, founded the Geological Survey of Japan and made the good geological reconnaissance map of Japan. He was fascinated by the Mt Fuji just when he reached Japan. At that time many westerners came on boat, the first sight of Japan is Mt Fuji. Western scientists all made the race to climb Mt Fuji. Naumann climbed the Mt Fuji in 1883. His research work is just surrounding Mt Fuji. He made clear the history of measurement of the height of Mt Fuji. He made clear the history of eruption of Mt Fuji. His most important geologic work is proposing the Fossa Magna in the central Japan. He thought the reason of Fossa Magna may be the intrusion of Mt Fuji.

After he came back to Germany he wrote even the script of Opera “ Taketorimonogatari ” that is the old Japanese tale of beautiful lady who came from the heaven and came back to the heaven at Mt Fuji with the smoke of eruption.

Keywords: Naumann, Mt Fuji, Fossa Magna

Japan Geoscience Union Meeting 2014
(28 April - 02 May 2014 at Pacifico YOKOHAMA, Kanagawa, Japan)

MZZ45-02 Room:422 Time:April 29 14:30-14:45

The Research on Seitaro Tsuboi Materials: Interpreting his Correspondence

TOCHINAI, Fumihiko[1*]

[1]Kanazawa Institute of Technology

The author has studied a large quantity of historical materials about a geologist Seitaro Tsuboi (1893-1986) (hereinafter ”Tsuboi Materials”) since 2010, which have been collected and archived by Multi-media and Socio-information Studies Archive, University of Tokyo. Tsuboi conducted researches on igneous petrogenesis with physical and chemical methods from 1920s to 1950s, which attracted positively or negatively many geologists. Combined with his position, a professor of petrology at (Imperial) University of Tokyo, he had considerable influence on the course of Japanese geological sciences.

Prior to the study of Tsuboi Materials, the author’s understanding was that Tsuboi’s influence over Japanese geological community rapidly decreased after his retirement from the professorship in 1954. However, the analysis of contents of Tsuboi Materials, such as correspondence with publishers about his books and documents about royalties on his books, suggests that his researches did attract people’s interests even in the late 1970s. The details will be introduced in the presentation.

Keywords: History of Science, History of Geology in Japan, Seitaro Tsuboi, Archive

Japan Geoscience Union Meeting 2014
(28 April - 02 May 2014 at Pacifico YOKOHAMA, Kanagawa, Japan)

MZZ45-03 Room:422 Time:April 29 14:45-15:00

The Examples of the ”puzzle-solving” in the Plate Tectonics Theory

CHIBA, Jun'ichi[1*]

[1]Yokohama School, O-hara Business College

It is generally considered that the plate tectonics theory has become a paradigm in the field of solid earth science (for instance, Miyashiro, 1998). Indeed, when I was engaged in descriptive research on the structural geology of Boso peninsula when I was studying for the doctoral degree, I would use technical terms of the accretionary prism theory, a sub-theory of the plate tectonics theory, to interpret observed facts. Also, looking at an outcrop in front of me, I was often asking myself, ”Which part of an accretionary does this piece correspond to?” in the middle of a field survey. By doing so, I was trying to integrate new observed facts into the framework of the accretionary prism theory, which can be considered in a sense as ”puzzle-solving” in normal science as referred to by Thomas Kuhn.

Tomari (2008) describes how the Japanese earth science society accepted the plate tectonics theory, apart from the memoirs of people directly involved in this process. Tomari argued that while geophysicists and seismologist accepted the plate tectonics theory in a relatively smooth manner, it took ten more years for geologists to accept it, which he described as ”a lost decade”. He ascribes it to the following causes: the geologists were interested less in application of physics and chemistry (principle of the present) than description of the respective geographical features of each region in accordance with the orogenesis theory; also, the geologists who were the leading figures in the Association for the Geological Collaboration in Japan, which accounted for the majority of the geological society in Japan at that time, harshly criticized the plate tectonics theory. Shibasaki(2011) argued against the claim of Tomari, by noting that the Japanese geological society by no means accepted the plate tectonics theory late for the following reasons: geologists who were conducting research on biostratigraphy with the use of Radiolaria fossils from the late 1970s to the early 1980s led the geological society to accept the plate tectonics theory by, for example, successfully explaining some of the problems of areal geology with the accretionary prism theory ? in particular, the problem associated with age determination of block-in-matrices (Radiolaria revolution); as such, they were able make a contribution to a theory on global movements precisely because they were engaged in research on areal geology. She also maintained that since most of the young researchers who contributed to the Radiolaria revolution belonged to the Association for the Geological Collaboration in Japan, while it is certainly true that the researchers who were the leading figures of the association were against the plate tectonics theory, their influence was limited. She then argued that it is necessary to conduct more integrated research on science history.

With regard to the question described above, I argue that it is meaningful to review when the kind of research that corresponds to the ”puzzle solving” of the plate tectonics theory began in each of the sub-fields of geology (structural geology, stratigraphy, volcanic petrology, metamorphic petrology and mineralogy, in addition to areal geology). It is because it is possible to determine whether the result of any given research corresponds to the ”puzzle-solving” of the plate tectonics theory from its theoretical structure; and by doing so, it is possible to show that the plate tectonics theory functions as a paradigm. In this presentation, I introduce some examples of the geological studies which are regarded as the ”puzzle-solving” in the plate tectonics theory.

Keywords: plate tectonics, puzzle-solving, history of science, geology

Japan Geoscience Union Meeting 2014
(28 April - 02 May 2014 at Pacifico YOKOHAMA, Kanagawa, Japan)

MZZ45-04 Room:422 Time:April 29 15:00-15:15

A history of mining, mineralogy and geology in the German literature

UENO, Fuki[1*]

[1]Graduate School of Information Science, Nagoya University

The question of organic or inorganic nature of minerals had been a subject of a debate since the ancient Greece to the Middle Ages. Thales and Pythagoreans believed that stones had souls, whereas Plato and Aristotle believed they possessed an anima. In the view of nature in the Ancient Rome, people believed that leaving mines without mining for a certain period of time would allow them to refill. In the Middle Ages, the relationship between minerals and magic was debated, and people believed stones had anima whereas jewels had magical powers. This thinking was further developed by alchemists, for whom the knowledge and understanding of minerals and jewels was essential.

The idea that minerals have supernatural power is also found in the German literature, especially that of the 18 and 19th century. A lot of novelists at the time studied mining, mineralogy and geology as they had been involved in mining business. In their writings stones have mystic powers.

However, already in the 13th century, Albertus Magnus ridiculed the idea of stones having a soul. Georg Agricola published De Re Metallica (1556) a complete and technical treatise on mining and extractive metallurgy in the 16th century, whereas Leibniz created Protogaea, an ambitious account of terrestrial history, central to the development of the earth sciences in the 17th century.

I will introduce works of romanticist (Goethe, Novalis, etc.) and philosophers (Leibniz, etc.) involved in mining business, and discuss the gap between their philosophy and reality.

Japan Geoscience Union Meeting 2014
(28 April - 02 May 2014 at Pacifico YOKOHAMA, Kanagawa, Japan)

MZZ45-05 Room:422 Time:April 29 15:15-15:30

Wang Mo’s role in the history of Japanese and Chinese geography

SHIBATA, Yoichi[1*]

[1]Institute for Research in Humanities, Kyoto University

Wang Mo is first Chinese graduate of the department of geography at Imperial University of Tokyo, and also founder of second department of geography in China. This paper examines his role in the history of Japanese and Chinese geography.

Keywords: institutionalization of geography, diffusion of geographical thought, Chinese international students in Japan, history of geography

Japan Geoscience Union Meeting 2014
(28 April - 02 May 2014 at Pacifico YOKOHAMA, Kanagawa, Japan)

MZZ45-06 Room:422 Time:April 29 15:30-15:45

Theory Change in Science - Case Study on the Solar System Formation

AOKI, Shigeyuki[1*]

[1]University of Aizu

Philosophy of science today has been particularized, just like particular sciences themselves. Philosophy of earth (and planetary) sciences was active in the 1980s-1990s following the Plate Tectonics Revolution in the 1960s, but seems to be inactive these days. Recent anthology on philosophy of science (Curd & Psillos 2013) discusses biology, chemistry, cognitive science, economy, psychology, social sciences, etc. while making no references to earth sciences. The above-mentioned literature on Plate Tectonics Revolution was based on preliminary historical studies on the earth sciences in the 1960s. In contrast to this, the synthetic process of earth and planetary sciences is not yet documented in detail, so philosophy of earth and planetary sciences has to start with digging up interesting historical data.

This presentation, drawing on Brush(1996), overviews the theoretical developments on the origin and evolution of the solar system in the 20th century, and then discusses which model best explains this process.

Keywords: Philosophy of Science, History of Science, Science Studies

Japan Geoscience Union Meeting 2014
(28 April - 02 May 2014 at Pacifico YOKOHAMA, Kanagawa, Japan)

MZZ45-07 Room:422 Time:April 29 15:45-16:00

A rudimentary consideration on anthropogenic climate change and countermeasures to it, ”geoengineering” in particular

MASUDA, Kooiti[1*]

[1]JAMSTEC

The issue called ”anthropogenic climate change” (ACC) or ”global warming” is such a chain of causes and effects that human industrial activities result in increase of concentration of greenhouse gases such as carbon dioxide in the atmosphere, enhancement of the greenhouse effects, and cause changes of climate which can be characterized by increase of global mean surface tempearture. It also have such aspects as sea level rise and changes of dryness, which have impacts on human society. The impacts are given unevenly between regions and between generations.

Since 1998 when the IPCC was established, the countermeasures to ACC has been discussed in terms
of ”mitigation” and ”adaptation”. In its 5th Assessment Reports (AR5) to be published in 2013-14, another category called ”geoengineering” is added. Here I tentatively follow the categorization of AR5.

The human society has developed within the constraint of the environment, by adapting to it. Climate, including its changes, is part of of the environment, and adaptation to it is one of basic functions of the human society. There are a few notable issues, however. Since the start of agricuture, the human society has experienced the climate of Holocene which has extraordinarily small variability in the context of the whole Quaternary era. Also, in the modern world, adaptation by migration has become difficult, since clear national baoundaries and land ownership have been developed, and population has increased so much thanks to technologies which also involve utilization of fossil fuel. In addition, with recent development of global ideas of equality between nations and humanitarianism,
people tend to valuate avoiding such fates where many people die untimely.

In the middle 20th century, it was hoped to technologically control climate
within a state favorable to human society. Development of science resulted in two pieces of understanding. One is that the climate is a complex system with large uncertainty due to nonlinarity and difficulty of observation. Another is that emission of carbon dioxide by burning of fossil fuels is an important forcing that shifts the energy balance of the climate system. Then, people tended to think a kind of ”passive intervention” by reducing the forcing that human activities already have made as the major countermeasure to the climate change. It has become customarily called ”mitigation”.

The essense of mitigation is reducing use of fossil fuels. International decision making on it has not been very successful even though 20 years have passed after the establishment of UNFCCC in 1992. It is because energy resources is fundamental to economical development.

In this context, hopes to technologically control climate, e.g. ”geoengieering” have risen again. It is still diffficult, however. The technology is not finished, and the knowledge about effects, side-effects and costs is uncertain.

Two major sub-catetories of ”geoengineering” are called ”carbon dioxide removal” (CDR) and ”solar radiation management” (SRM).

CDR is equivalent to mitigation as far as it reduces the forcing to the atmosphere, but it modifies the environment of geological formations, soil, or ocean, where the carbon dioxide is put. In addition, failure of sequestration is possible. ”How much environmental modification and possibility of accidents people can tolerate” will be a subject of social decision making. The decision making can be done within a country if the sequestration is made within its territory.

SRM can cancel the greenhouse forcing in global mean sense, but it will enhance it in some of latitude bands and seasons. Assessments of its impacts is as difficult as regional projection of ACC. The fact that this is intentional makes the issue of liability more serious. Thus, such an international governance regime that is much stronger than the current UNFCCC regime is necessary, in addition to technological feasibility, to include SRM in policy options.

MZZ45-07 Room:422 Time:April 29 15:45-16:00

Keywords: anthropogenic climate change, global warming, geoengineering, adaptation to climate change, mitigation of climate change, solar radiation management

Japan Geoscience Union Meeting 2014
(28 April - 02 May 2014 at Pacifico YOKOHAMA, Kanagawa, Japan)

MZZ45-08 Room:422 Time:April 29 16:15-16:30

Partial Commensurability: Translations between Multiple Observational Systems in Solid-Earth Physics

MORISHITA, Sho[1*]

[1]Kyoto University / JSPS

The theme of incommensurability was introduced to philosophy of science by Kuhn and Feyerabend in 1960s. This theme has been discussed as problem of translations between multiple paradigms or conceptual frameworks. However, in 90s, a philosopher of science Ian Hacking extended the problematique ontologically. He argued that incommensurability is the problem of translations between multiple ”closed systems” in experimental science [Hacking 1992].

If we apply his argument to observational science, it is outlined as below. Each observational equipments forms closed systems. That is, each equipment has the particular procedure and principle of observation which correspond to the mechanical structure of it. The data are visualized in the peculiar way and analyzed with the unique methods of correction. When observational equipment is different, the methods for articulations and the results are totally different. Therefore, a result from a particular observational equipment is difficult to translate into a result of another observational equipment.

This theme suggest the problem how we can achieve the comparison between different observational systems. In this paper, the author will call such comparison ”partial commensuration” and discuss some specific examples of solid-earth physics, such as joint-inversion.

Keywords: Incommensurability, Observational Systems, Translation

Japan Geoscience Union Meeting 2014
(28 April - 02 May 2014 at Pacifico YOKOHAMA, Kanagawa, Japan)

MZZ45-09 Room:422 Time:April 29 16:30-16:45

A Web-application of Dynamic Time-Scale Previewer and its Application for Historical Geoscience Studies

MURATA, Ken T.[1]*

[1]NICT

The NICT Science Cloud is one of the science clouds proposed for development of sciences. A variety of science data are collected and stored in the science cloud to be analyzed interdisciplinary. After the Internet is widely used, new concept and information technology haves shown up; semantic web and linked open data (LOD). These technologies enable information on the Internet machine readable. In many science fields, it is pointed out that the semantic web will play an important role for the interdisciplinary research works. However, there have been few ideas to be ever proposed as a methodology or roadmap to the interdisciplinary science using semantic web. Herein we present a concept of professional knowledge and academic knowledge following collective knowledge proposed as a Web 2.0. Based on the concept, we design a Web-application for interdisciplinary science. The application (named STARS touch) provides users with an environment of dynamic and light preview of any types of time-dependent data. In the demonstration, we show an example of simultaneous preview of both scientific data (satellite observation data) and social data (newspaper information).

Keywords: STARS touch, NICT Science Cloud, Web Application

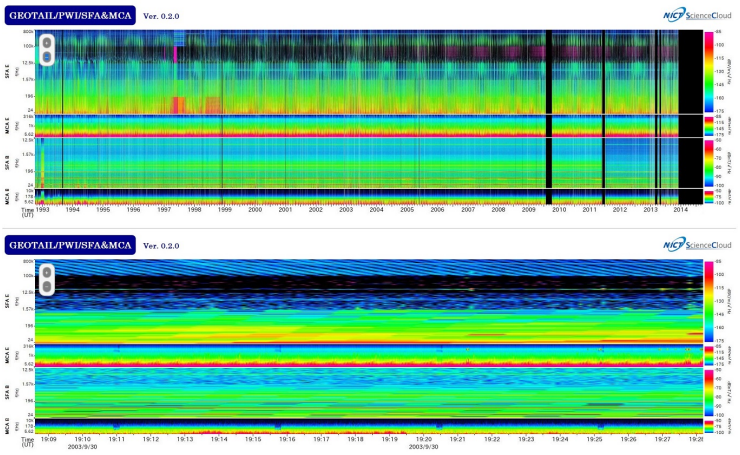

Japan Geoscience Union Meeting 2014
(28 April - 02 May 2014 at Pacifico YOKOHAMA, Kanagawa, Japan)

MZZ45-10 Room:422 Time:April 29 16:45-17:00

Science against Natural Hazard 1960-1993: Has the Natural Disaster Science Overcome the Disasters?

YAMADA, Toshihiro[1*]

[1]Post-doctoral Fellow of Pedagogy, University of Tokyo

The disastrous Ise-wan Typhoon of 1959 triggered the emergence of the field of Natural Disaster Science in Japan, which was proposed by the geophysicist Hasegawa Mankichi (1894-1970), President of Fukui University. The project, funded by the Ministry of Education and well organized especially by the geologist Matsuzawa Isao (1906-1990), Professor of Nagoya University, was continued until 1990s and provided many opportunities for the researches and activities of geoscientists. This article focuses this project considering the following contexts: 1) the post-war defense conversion in the field of earth sciences; 2) the interrelationship between the two major disciplines, geology and geophysics, in the sciences; and 3) the inclusion of the human and social sciences to cope effectively with such hazards and disasters.

Keywords: Natural Disaster Science, contemporary history of earth sciences, defense conversion, interdisciplinary domain, Hasegawa Mankichi, Matsuzawa Isao

Japan Geoscience Union Meeting 2014
(28 April - 02 May 2014 at Pacifico YOKOHAMA, Kanagawa, Japan)

MZZ45-11 Room:422 Time:April 29 17:00-17:15

The reasons why we couldn’t avoid the Okawa Elementary School disaster

HAYASHI, Mamoru[1*]

[1]University of TOYAMA

March 11, 2011. Fifty minutes after the earthquake off the Pacific coast of Tohoku region, the big tsunami hit the Okawa Elementary School at Ishinomaki city. The victims include 74 students and 10 teachers from that school, as well as 3 students from Okawa Junior High School that had come to take children home and unknown number of Okawa district residents. Only 4 children and 1 teacher survived the catastrophe. It is considered the worst tragedy under the school administration since the establishment of the school system in Meiji Restoration.

The role of Earth Planetary Science will be examined considering the fact that the comprehension about magnitude of those involved in science education is still in the 1960’s, and the problem concerning the Okawa Elementary School accident verification committee’s investigation, which is predictable and not enough to get to the truth about the tsunami catastrophe.

Japan Geoscience Union Meeting 2014
(28 April - 02 May 2014 at Pacifico YOKOHAMA, Kanagawa, Japan)

MZZ45-12 Room:422 Time:April 29 17:15-17:30

Characteristics of the modern stone industry and the regional context in each granite production areas in Japan

INUI, Mutsuko[1*]

[1]School of Science and Engineering, Kokushikan University

Japanese stone industry has been thought to have developed to supply materials for the western architectures that were introduced in Japan in the late 19th century. It is also thought that it simply reduced because the imported stone materials became inexpensive. They are true, in a way, but the fact is more intricate, according to the interview survey carried out in several granite production areas. It is important to learn and record the complexity in the industrial history of one of the Japanese undergroung resources. Characteristic Japanese manner in the stone industry is described in this article. Difference in the industrial structure and history between several production areas are then documented.

Modern quarrying and stone manufacturing industry in Japan was established shortly after the introduction of western architecture, which used stones. Before that, stone was not popular in architectures. Therefore, stone was accepted in Japanese construction as decorating or finishing material. As the result, the standard manner of stone panelling in Japan became very elaborate, which only allowed beautifully designed stone panels with perfect colors and patterns, without any irregularities. The tradition has lead to low yield ratio (high rate of waste). Japan is also unique in its market of large granite tombstone which became popular after the world war II. Religeous monuments are also popularly produced in stones. Stone materials in Japan therefore had two different markets, one for building stones, another for tombstones and religeous craftworks.

Grain size, number density and orientation of cracks seems to determine the use of the stone, for building stone or for tombstone. Coarse grained granite with less cracks and veins yields large sized blocks, which is more favorable for architectural use. Some of those granites are used in famous hitorical buildings in Tokyo (e.g. Shodoshima stone, Kitagi stone). Fine grained granites with greyish colors are favored for tombstones in Japan (e.g. Aji stone, Oshima stone). Those quarries tend to have cracks with high number density and very low yield ratio, resulting in very expensive tombstone products.

Another factors that made difference between the granite production areas are the location of the quarry. Quarries on islands had advantage when principal transportation was seaborne. The transportation however shifted onto land and the islands lost their advantage. The relation between the quarry and the town sometimes restricted the activity of the quarry, concerning the noise or the disturbance on the landscape. Ownership of the mining area seemed to affect the sense of community in the production area.

The scheme and the unique manner of the stone industry in Japan are described. The interview survey revealed the context of each several granite production areas in Japan, and demonstrated how they corresponded to the decrease of stone production in Japan.

Keywords: building stone, tombstone, headstone, granite, quarry, modern industrial history

Japan Geoscience Union Meeting 2014
(28 April - 02 May 2014 at Pacifico YOKOHAMA, Kanagawa, Japan)

MZZ45-P01 Room:Poster Time:April 29 18:15-19:30

History of marble mining in Mine, Yamaguchi Prefecture, Japan, and its use in historic buildings

INUI, Mutsuko[1*]

[1]School of Science and Engineering, Kokushikan University

Mine District, Yamaguchi Prefecture, Japan, had been the largest marble mine in Japan for several decades until around 1970. Marble of Mine have been used in many buildings built during those period, also in Tokyo. However, import of inexpensive marble started to increase and soon overwhelmed the domestic marble. Most of the domestic marble mines have closed. It is important to remember the role of Japan's marble, one of our precious natural resources, in the developing industry of Japan during those times. The knowledge is also important to assess the building properly. The assessment may determine if the historic buildings should be conserved, renovated, or conversed. The aim of this study is to describe as many Mine marbles as possible for record, concerning e.g. its color, texture, how it was called, the locality of the quarry, during what period it was mined, or in what historic building it was used.

Keywords: marble, Mine district, Japan, stone industry, quarry, historic building

Japan Geoscience Union Meeting 2014
(28 April - 02 May 2014 at Pacifico YOKOHAMA, Kanagawa, Japan)

MZZ45-P02 Room:Poster Time:April 29 18:15-19:30

Review of self-experiments on the cooperative study between EPS and philosophy of science since 2008

KUMAZAWA, Mineo[1*] ; UENO, Fuki[1]

[1]Nagoya University, [2]Nagoya University

[Decoding the Earth's evolution related to philosophy of science] Motivation of the interdisciplinary works came up during the planning of the decoding research program (1995-1997) on the whole evolution history of the Earth from its birth at 4.6 billion years ago to the present time. In that program, the Earth history is described by a sequence of several time periods separated by the characteristic big events. We have assigned the present as the 7th big event in the Earth's history, with such a notion that Homo sapiens started science to try to understand everything; life, the Earth and the World. The present time is the boundary of the two different types of research; the past as a target of historical science and the future to predict and control even ourselves so as to fit with what we shall hope. We recognize that the World started self-reference and self-intervention in a way of coevolution between the life and the Earth environments by means of science and technology. The role of science has been evolving to have more influence to social and human subject, thereby more importance is placed on meta-science or philosophy of science.

Traditional philosophy of science with their classic discipline appears helpless, since it does not refer to newer experience and knowledge and deeper thinking having been accumulated lately by science method. This situation is making the philosophers difficult to digest science, a new comer. In addition, there are serious problems on science side; usually scientists do not pay much attention to meta-science; what the science is, why science works, how science contributes to people, etc., simply because most of them are slotted into the specific roles in a big science system. This situation appears serious for the modern society in respect to its survival on such a small friable Earth, as we geoscientists know well.

To face with this difficulty, we tried self?experiments of joint research by geoscientists with Todayama and his collaborators on the subject of common interests since 2009, and some of the results have been reported at JpGU meeting. Fortunately, Todayama School has been trying to open up a new trend, 'naturalized philosophy of science', so the collaboration was really welcome. This work was supported in 2011-2013 by JSPS Grant-in-Aid for Scientific Research (23320005) headed by Dr. Shigeyuki Aoki. The outcomes of research on the history of geoscience were published in Nagoya Journal of Philosophy, Vol.10 (2013), and the works on other topics will appear in the forthcoming volumes.

[The problems recognized] The collaboration between the scientists and philosophers of science was found still difficult due to the difference in languages, cultures and even in the way of discussions. Whereas it is difficult to review objectively in detail at this moment, we shall keep trying to find out the good ways of collaboration with meta-science for our survival succession. We have obtained a bright hope along this line in the present work.

In conclusion, we found an 'indispensable minimum recipe' of approaching the problem. It is the promotion of education policy for the graduate students to take double tracks striding the boundary between science and human studies to be seamless. We have to remind that the Japanese education system appears far behind the contemporary necessity.

[The purpose of this poster presentation] We believe that the straightforward discussions are really useful among the research workers of different disciplines for activating the intellectual potential, in particular. The purpose of this presentation is to invite those who are interested in the interdisciplinary communication between science and meta-science to have discussions in front of our poster. Note: Two authors of this presentation were the acting managers of the collaboration works between Geoscience and Todayama School of philosophy of science.

Keywords: Science of Science Phenomena, Meta-Science, Philosophy of Science, Normative Science